EuropaCat XII

ABSTRACTS

KAZAN, RUSSIA

30 AUGUST – 4 SEPTEMBER, 2015

EUROPACAT XII

CATALYSIS: BALANCING THE USE OF FOSSIL AND RENEWABLE RESOURCES

Boreskov Institute of Catalysis SB RAS, Novosibirsk
Zelinsky Institute of Organic Chemistry RAS, Moscow
Lomonosov Moscow State University, Moscow
Arbuzov Institute of Organic and Physical Chemistry KSC RAS, Kazan

XII European Congress on Catalysis
”Catalysis: Balancing the use of fossil and renewable resources”

Kazan (Russia) 30th August - 4th September, 2015

ABSTRACTS

Novosibirsk - 2015

УДК 544.4 + 661.097.3 + 665.6/.7 + 620.9
ББК 24.54 + 35.514 + 31.6
Е91

Е91 EuropaCat XII. Catalysis: Balancing the use of fossil and renewable resources. European Congress on Catalysis. Kazan (Russia) 30th Aug. - 4th Sept., 2015. [Electronic resource] = ЕвропаКат XII. Катализ: сбалансированное использование ископаемых и возобновляемых ресурсов. Европейский конгресс по катализу : abstracts / ed.: V.I. Bukhtiyarov, A.Yu. Stakheev – Novosibirsk : Boreskov Institute of Catalysis, 2015 – 1 electronic optical disc (CD-R). ISBN 978-5-906376-10-7

В надзаг.: Boreskov Institute of Catalysis SB RAS
Zelinsky Institute of Organic Chemistry RAS
Lomonosov Moscow State University
Arbuzov Institute of Organic and Physical Chemistry KSC RAS

The book of abstracts includes the plenary lectures, keynote lectures, oral and poster presentations on the following topics:

- Novel catalytic materials and processes for securing supplies of raw materials
- Catalyst preparation and characterization
- Energy-related catalysis
- Catalysis and chemicals
- Catalysis and environmental protection
- XI European Workshop on Innovation in Selective Oxidation (ISO ‘15) "Selectivity in Oxidation: Key to new resources valorization"

УДК 544.4 + 661.097.3 + 665.6/.7 + 620.9
ББК 24.54 + 35.514 + 31.6

ISBN 978-5-906376-10-7

CONGRESS PATRON

Rustam MINNIKHANOV, President of the Republic of Tatarstan

ORGANIZERS

- Russian Academy of Sciences
- Federal Agency for Scientific Organizations, Moscow
- Ministry of Education and Science of Russian Federation
- NFPP "National Catalytic Society"
- Tatarstan Regional Government, Kazan
- Tatarstan Academy of Sciences
- Kazan Scientific Center, Kazan
- Boreskov Institute of Catalysis SB RAS, Novosibirsk
- Zelinsky Institute of Organic Chemistry RAS, Moscow
- Lomonosov Moscow State University, Moscow
- Arbuzov Institute of Organic and Physical Chemistry KSC RAS, Kazan
- JSF “TatNefteKhim-Invest Holding”, Kazan
- Kazan (Volga Region) Federal University, Kazan
- Kazan National Research Technological University, Kazan
- Mendeleev Chemical Society of Republic of Tatarstan

The Professional Congress Service Agency: Monomax Ltd., St.Petersburg

Russian Academy of Sciences

Federal Agency for Scientific Organizations

Ministry of Education and Science of Russian Federation

NFPP "National Catalytic Society"

Tatarstan Regional Government

Tatarstan Academy of Sciences

Kazan Scientific Center

Boreskov Institute of Catalysis SB RAS

Zelinsky Institute of Organic Chemistry RAS

Lomonosov Moscow State University

Arbuzov Institute of Organic and Physical Chemistry KSC RAS

JSC TatNefteKhim-Invest Holding

Kazan (Volga region) Federal University

Kazan National Research University

Mendeleev Chemical Society of Republic of Tatarstan

Monomax Ltd.

FINANCIAL SUPPORT

Министерство образования и науки Российской Федерации

The Ministry of Education and Science of The Russian Federation

RFBR

Russian Foundation for Basic Research, Moscow

GENERAL CONGRESS PARTNER

TATNEFT

JSC TATNEFT

TAIF-NK

TAIF-NK PSC

NIZHNEKAMSKNEFTEKHIM

PJSC "NIZHNEKAMSKNEFTEKHIM"

KAZANORGSINTEZ

PJSC KAZANORGSINTEZ

OFFICIAL PARTNER

GAZPROM NEFT

JSC GAZPROM NEFT

HONORARY CONGRESS PARTNER

CAS
A division of the American Chemical Society

CHEMICAL ABSTRACTS SERVICE

SciFinder®

CAS, SciFinder®

CONGRESS PARTNER

PJSC SIBUR HOLDING

SPECS SURFACE NANO ANALYSIS GmbH

CHROMOSIB

NOVOMICHURINSK CATALYST PLANT

PARTNER OF THE CONGRESS PROGRAM

BRUKER Ltd

PROMENERGOLAB LLC

INFORMATIVE PARTNERSHIP

Journal "Catalysis in industry"

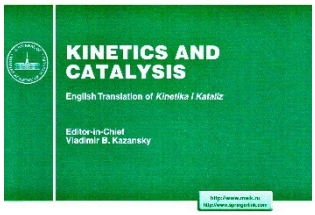

Journal "Kinetics and catalysis"

Journal "Supercritical fluids: theory and practice"

INTERNATIONAL SCIENTIFIC COMMITTEE

Chairman: Valentin PARMON, President of the Natonal Catalysis Society,
Boreskov Institute of Catalysis SB RAS

The EFCATS Council, as well as

Sergei ALDOSHIN, Presidium of RAS, Moscow
Valentine ANANIKOV, Zelinsky Institute of Organic Chemistry RAS, Moscow
Konstantin BRYLIAKOV, Boreskov Institute of Catalysis SB RAS, Novosibirsk
Valerii BUKHTIYAROV, EFCATS, Boreskov Institute of Catalysis SB RAS, Novosibirsk
Usein DZHEMILEV, Institute of Petrochemistry and Catalysis RAS, Ufa
Mikhail EGOROV, Zelinsky Institute of Organic Chemistry RAS, Moscow
Zinfer ISMAGILOV, Institute of Coal Chemistry and Material Science SB RAS, Kemerovo
Irina IVANOVA, Lomonosov Moscow State University, Moscow
Vasily KAICHEV, Boreskov Institute of Catalysis SB RAS, Novosibirsk
Salambek KHADZHIEV, Topchiev Institute of Petrochemical Synthesis RAS, Moscow
Vladimir KAPUSTIN, JSC VNIPINEFT, Moscow
Vladimir KAZANSKY, Zelinsky Institute of Organic Chemistry RAS, Moscow
Vladimir LIKHOLOBOV, Institute of Hydrocarbon Processing, SB RAS, Omsk
Valerii LUNIN, Lomonosov Moscow State University, Moscow
Ilya MOISEEV, Kurnakov Institute of General and Inorganic Chemistry RAS, Moscow
Alexander NOSKOV, Boreskov Institute of Catalysis SB RAS, Novosibirsk
Mikhail SINEV, Semenov Institute of Chemical Physics RAS, Moscow
Oleg SINYASHIN, Kazan Scientific Center RAS, Kazan
Alexander STAKHEEV, Zelinsky Institute of Organic Chemistry RAS, Moscow
Mark TSODIKOV, Topchiev Institute of Petrochemical Synthesis RAS, Moscow

ORGANIZING COMMITTEE

Shamil GAFAROV, Government of the Republic of Tatarstan (Chair)
Valerii BUKHTIYAROV, EFCATS, Boreskov Institute of Catalysis SB RAS (Chair)
Oleg SINYASHIN, Kazan Scientific Center RAS (Vice-Chair)
Alexander STAKHEEV, Zelinsky Institute of Organic Chemistry RAS (Vice-Chair)

Kazan:

Viliam P. BARABANOV, Mendeleev Chemical Society of Republic of Tatarstan
Vladimir BUSYGIN, TAIF PSC
Ilshat GAFUROV, Kazan (Volga Region) Federal University
German DYAKONOV, Kazan National Research Technological University
Andrei KARASIK, Arbuzov Institute of Organic and Physical Chemistry KSC RAS
Anzhelika KARASIK, Arbuzov Institute of Organic and Physical Chemistry KSC RAS
Nail MAGANOV, Tatneft OJSC
Akhmet MAZGAROV, Volga Research Institute of Hydrocarbon Feed
Myakzyum SALAKHOV, Tatarstan Academy of Sciences
Albert SHIGABOUTDINOV, TAIF PSC
Rafinat YARULLIN, JSC TatNefteKhimInvest Holding

Novosibirsk:

Konstantin BRYLIAKOV, Boreskov Institute of Catalysis SB RAS
Vasily KAICHEV, Boreskov Institute of Catalysis SB RAS
Ekaterina KOZLOVA, Boreskov Institute of Catalysis SB RAS
Lyudmila STARTSEVA, Boreskov Institute of Catalysis SB RAS
Tatiana ZAMULINA, Boreskov Institute of Catalysis SB RAS

Moscow:

Ekaterina LOKTEVA, Lomonosov Moscow State University
Olga PAKHMANOVA, Topchiev Institute of Petrochemical Synthesis RAS
Olga TUROVA, Zelinsky Institute of Organic Chemistry RAS

St.-Petersburg

Natalia P. AVDEENKO, Monomax Ltd.

Plenary lectures

PL-1

Catalysis in Organic Chemistry: from Butlerov to these Days

Ananikov V.P.*

Zelinsky Institute of Organic Chemistry, Russian Academy of Sciences, Moscow, Russia

* val@ioc.ac.ru

Keywords: organic synthesis, catalysis, atomic precision

Mechanistic studies have revealed fascinating nature of catalytic reactions that are now ubiquitously employed in modern organic chemistry. A variety of metal species are generated during well-known catalytic reactions [1-4]. In fact, mononuclear metal complexes, metal clusters and nanoparticles are easily accessible on catalyst activation stage or during the course of the catalytic reaction. Formation of "cocktail" of metal species in solution is not uncommon starting with wide variety of different metal precursors (pre-catalysts) [3]. Recent studies provided important evidence on unusual reactivity of small metal clusters, especially the properties connected with "superatomic" structural units [2].

Another important point is evolution of the metal catalyst during catalytic reaction. Evolution of metal complexes in homogeneous catalysis as well as evolution of supported metal catalysts under heterogeneous conditions are the processes of paramount importance. Understanding the nature of these processes is required to achieve selective transforamtions and to develop stable and recyclable catalysts.

Design of new generation of adaptive catalytic systems to facilitate transformations in organic synthesis will be presented and discussed with a focus on development of organic synthesis procedures performed with "atomic precision" [5].

References

[1] Ananikov V.P., *ACS Catal.*, **2015**, 5, 1964; doi: 10.1021/acscatal.5b00072.

[2] Eremin D.B., Ananikov V.P., *Organometallics*, **2014**, 33, 6352; doi: 10.1021/om500637k.

[3] Kashin A.S., Ananikov V. P., *J. Org. Chem.*, **2013**, 78, 11117; doi: 10.1021/jo402038p.

[4] Zalesskiy S. S., Sedykh A. E., Kashin A. S., Ananikov V. P., *J. Am. Chem. Soc.*, **2013**, 135, 3550; doi: 10.1021/ja311258e.

[5] Ananikov V.P., Khemchyan L.L., Ivanova Yu.V., Bukhtiyarov V.I., Sorokin A.M., Prosvirin I.P., Vatsadze S.Z., Medved'ko A.V., Nuriev V.N., Dilman A.D., Levin V.V., Koptyug I.V., Kovtunov K.V., Zhivonitko V.V., Likholobov V.A., Romanenko A.V., Simonov P.A., Nenajdenko V.G., Shmatova O.I., Muzalevskiy V.M., Nechaev M.S., Asachenko A.F., Morozov O.S, Dzhevakov P.B., Osipov S.N., Vorobyeva D.V., Topchiy M.A., Zotova M.A., Ponomarenko S.A., Borshchev O.V., Luponosov Y.N., Rempel A.A., Valeeva A.A., Stakheev A.Yu., Turova O.V., Mashkovsky I.S., Sysolyatin S.V., Malykhin V.V., Bukhtiyarova G.A., Terent'ev A.O., Krylov I.B., "Development of new methods in modern selective organic synthesis: preparation of functionalized molecules with atomic precision", *Russ. Chem. Rev.*, **2014**, 83, 885; doi: 10.1070/RC2014v083n10ABEH004471.

PL-2

Enhancing Catalytic Rates in Constraints – from Acid-base to Metal Catalyzed Reactions

Lercher J.A.[1,2*]

1 - TU München, Department of Chemistry, Garching, Germany
2 - Institute for Integrated Catalysis, Pacific Northwest National Laboratory, Richland, WA, USA

* johannes.lercher@tum.de

Understanding the elementary steps in acid-base and metal catalyzed organic transformations is a key for improving existing and developing new catalysts and process routes for nearly all energy related chemical conversions. Solid acids and bases with nano-pores such as zeolites act as solid Brønsted and Lewis acids being excellent model as well as industrial catalysts with well-defined acid-base sites and a well-defined reaction space around the sites. Within the pores of molecular sieves reacting molecules are constrained in a reaction space, which can be subtly adjusted via direct synthesis, as well as via the addition of cations, oxidic clusters or organic fragments. The impact of such changes on mono- and bimolecular reactions such as elimination reactions of alcohols, cracking and alkylation of hydrocarbons are discussed for gas and liquid phase reactions.

Experimental methods to define the state of the reacting molecules combined with detailed kinetic analysis and theory will be used to explain the principal contributions of the interactions and the confinement to determine reaction rates. The chemical environment in these pores also influences metal catalyzed hydrogenation and hydrogenolysis via new pathways enabled by the proximity of metals and Brønsted acid sites. Using examples for catalyzed reactions in gas and liquid phase, it will be shown that the reactivity can be drastically increased by tailoring the space around the active site.

PL-3

Fossil and Renewable Energy: the Turning Point of the Liquid Fuels Production

Bellussi G.*

Eni S.p.A, SVP Downstream R&D, San Donato Milanese – I, Italy

* giuseppe.bellussi@eni.com

Keywords: bio-fuels, renewable, heavy oil conversion, slurry hydroprocessing

Energy, as well as food and water is a basic need for survival. Over the past 150 years, the energy availability guaranteed first by coal and then by oil and gas, has supported the growth of the world population to the current level of 7 billion people. The increase of population prompted the demand of basic needs and therefore the exploitation of planetary resources, impacting on their availability and increasing the environmental pressure.

Today the availability of energy sources and the effects on the environment generated by their use, are among the main critical issues that humanity faces. The production and trade of energy resources are often linked to events with important socio-economical impact, just remember the effects generated by the discovery and exploitation of shale-gas and shale-oil and then by the fall in oil prices. The strong concern on climate change and environmental effects of entropic activity is pushing the majority of nations to react through shared actions, but the conflicting requirements of developed countries and those under development are slowing down the effectiveness of these processes. At the recent UN climate conference held in Lima last December (COP-20), weak progress have been made. It was reconfirmed the principle of common but differentiated responsibility, already introduced in the first United Nations Framework Convention on Climate Change in 1992, which states that every nation must take action to mitigate the climate change according to its own financial and infrastructural capability. It was also introduced a tool (Lost & Damage) through which developing countries particularly vulnerable to the consequences of climate change will be able to receive financial compensation for natural disasters now inevitable, but the main differences between the parties were not reconciled and the most important decisions have been postponed to the next conference in Paris in December 2015. The European Union countries are facing the consequences of these changes with the addition of local problems. The production of liquid fuels in Europe has suffered from an economical point of view from 2008 until the second half of 2014, when the drop in oil prices has given breath for the refinery industry. The problems of this sector are generated by the progressive reduction in fuel demand, by the entry of not negligible amount of bio-fuels, by the obsolescence of the European refining system, characterized by a relatively large number of medium/small refineries and by the high cost of energy. Although since 2007, 14 plants have been closed, persists in Europe overcapacity of refining that endangers other production sites. This crisis is structural in its nature and therefore major interventions targeted to balance supply and demand are required as well as new technological solutions. A reduction of refining capacity appears unavoidable, but at the same time the production of bio-fuels matching the technical and environmental needs, the efficiency improvement of refining technologies to pursue the reduction of energy consumption and the total conversion of crude oil in good quality middle distillates must be strongly pursued. The disciplines most involved by these needs are catalysis, materials science and process engineering. In this presentation some recent results related to the production of bio-fuels and to the total conversion of the oil barrel to middle distillates will be presented and discussed trying to highlight the prospects and the opportunities that science and technology can offer for the mitigation of the problems exposed.

PL-4

Catalysis Using Supported Gold and Gold Palladium Nanoparticles

Hutchings G.J.*

Cardiff Catalysis Institute, School of Chemistry, Cardiff University, Cardiff, UK

* hutch@cf.ac.uk

Gold catalysis has become a well-established field of endeavour. Much still remains to be discovered in this interesting research field, but to date much progress has been made. In this lecture recent preparation strategies to make supported nanoparticles will be described and discussed. These will involve the use of colloidal and impregnation methods. Monometallic gold catalysts will be discussed together with bimetallic gold palladium and trimetallic gold palladium platinum catalysts.

The first part of the talk will discuss the use of carbon-supported gold nanoparticles for the hydrochlorination of acetylene.[1] This is one of the original reactions where the high activity of gold catalysts was first observed.[2] Details of the catalyst characterisation will be described showing the evolution of the catalyst structure as it is exposed to the reaction conditions. Using detailed aberration-corrected STEM together with X-ray photoelectron spectroscopy the important features of this catalyst will be explored.

In the second part the preparation of bimetallic gold palladium and gold platinum catalysts will be described for the oxidation of alcohols, the activation of C-H bonds[3] and the direct synthesis of hydrogen peroxide.[4] In the final part the preparation and use of the more complex trimetallic nanoparticles will be discussed.[5] One particular example concerns the oxidation of benzyl alcohol as when using supported gold palladium nanoparticles toluene can be observed as a by-product. This by-product can be switched off in two ways. First the design of the bimetallic catalyst support is crucial and the interfacial sites are considered to be important for the selective oxidation to benzaldehyde. Oxides that maximise the interfacial contact give lower toluene formation and with MgO and ZnO in particular no toluene formation is observed although high activities for selective oxidation are observed. Secondly, addition of platinum to the gold palladium bimetallic also swiches off toluene formation. The origins of these effects will be discussed.

References

[1] M. Conte, A.F. Carley, G. Attard, A.A. Herzing, C.J. Kiely, G. J. Hutchings, J. Catal., **257**, 190-198 (2008)

[2] G.J. Hutchings J. Catal. **96**, 292-295 (1985)

[3] L. Kesavan, R. Tiruvalam, M.H. Ab Rahim, M.I. bin Saiman, D.I. Enache, R.L. Jenkins, N. Dimitratos, J.A. Lopez-Sanchez, S.H. Taylor, D.W. Knight, C.J. Kiely, G.J. Hutchings, Science **331**, 195-199 (2011)

[4] J.K.Edwards, B. Solsona, E. Ntainjua N, A.F. Carley, A.A. Herzing, C.J. Kiely, Graham J. Hutchings Science **323**, 1037-1041 (2009)

[5] J.K. Edwards, J. Pritchard, L. Lu, M. Piccinini, G. Shaw, A.F. Carley, D.J. Morgan, C.J. Kiely, G.J. Hutchings Angew. Chem. – Int Ed., **53**, 2381-2384 (2014)

PL-5

Mesoporous Metal-Organic Frameworks as Platforms for Single-site Heterogeneous Catalysts

Hupp J.T.*

Northwestern University, Evanston, IL, U.S.A.

* j-hupp@northwestern.edu

AIM (ALD In MOFs) is an emerging synthesis technique that provides access to well-defined arrays of non-aggregating, monodisperse, and organic-capping-ligand-free clusters of metal atoms, metal-oxides/hydroxides, and metal-sulfides. The technique entails adapting atomic-layer-deposition (ALD) chemistry to mesoporous metal-organic framework materials that present suitable node- or linker-based reaction sites. By using multiple, individually self-limiting, ALD growth cycles, clusters of varying, predetermined size, and clusters comprising mixed compositions can be synthesized. In some cases the obtained clusters lack stable analogues in conventional heterogeneous catalyst synthesis chemistry, in part due to a propensity for conventionally synthesized clusters to aggregate under typical conditions for catalysis of gas-phase reactions. As one might guess, the properties of AIM-synthesized clusters and the associated porous-MOF scaffolds render the clusters readily accessible to candidate molecular reactants. The clusters, in many cases, display high catalytic activity for both gas-phase and condensed-phase reactions reactions. Notably, excellent steam stability and moderate thermal stability (temperatures to ca. 350 ^{o}C) can be obtained with appropriately designed MOFs This presentation will center on one or two case studies, including AIM-MOF synthesis, structural characterization, catalytic activity, and computationally informed analysis of mechanisms of catalysis.

Because the catalytic clusters comprising nodes and subsequently installed metal atoms are monodisperse, both coordinatively and in terms of cluster size, the resulting ensembles are amenable to structural and functional characterization with a level of precision previously associated mainly with single crystal metal or metal-oxide surfaces. The porosity of the MOF scaffold, however, makes the catalyst arrays three-dimensional and greatly increases the number of active sites relative to two-dimensional arrays. In addition to boosting overall catalytic activity, the presentation of monodisperse catalysts in 3D rather than 2D arrays greatly facilitates structural and functional characterization.

This presentation will touch on catalyst characterization, including *in operando* characterization. The characterization methods include DRIFTS, EXAFS, total X-ray scattering and pair-distribution-function analysis, single-crystal X-ray diffraction, and energy-dispersive microscopy. Both structural characterization and functional characterization are facilitated by comparative computational modeling and simulations.

References

[1] "Vapor-Phase Metalation by Atomic Layer Deposition in a Metal–Organic Framework," J. E. Mondloch, W. Bury, D. Fairen-Jimenez, S. Kwon, E. J. DeMarco, M. H. Weston, A. A. Sarjeant, S. T. Nguyen, P. C. Stair, R. Q. Snurr, O. K. Farha, and J. T. Hupp, *J. Am. Chem. Soc.*, **2013**, *135*, 10294–10297

[2] "Defining the Proton Topology of the Zr_6-Based Metal–Organic Framework NU-1000," N. Planas, J. E. Mondloch, S. Tussupbayev, J. Borycz, L. Gagliardi, J. T. Hupp, O. K. Farha, and C. J. Cramer, *J. Phys. Chem. Lett.*, **2014**, *5*, 3716–3723

[3] "Metal-organic framework nodes as nearly ideal supports for molecular catalysts: NU-1000- and UiO-66-supported iridium complexes," Dong Yang, Samuel O. Odoh, Timothy C. Wang, Omar K. Farha , **2015**, DOI: 10.1021/jacs.5b02956

PL-6

Dynamics in Heterogeneous Catalysis

Schlögl R.[1,2*]

1 - Fritz-Haber-Institut der MPG, Berlin, Germany
2 - MPI Chemical Energy Conversion, Mühlheim, Germany

* acsek@fhi-berlin.mpg.de

Heterogeneous catalysis carries its name from the concept of a well-defined heterogeneous interface between the catalyst surface and the reactant environment. The processes of adsorption, desorption and reaction between adsorbates describes the overall reaction. Under conditions where adsorption dominates the overall reaction such an interface can be clearly identified and studied by many techniques.

Under conditions of high performance catalysis with significant turnover this definition becomes increasingly difficult. Strong structural modifications of the solid surface are involved in such reactive states. We identify the transformation of a sharp interface into a termination layer with substantially different structural and chemical properties than the bulk. In certain cases even the bulk underneath a sub-surface region of the solid undergoes reaction-induced transformations.

These phenomena are at the center of the so-called gaps in catalysis science. They describe catalysts as chemically dynamical systems interacting with the molecular dynamics of the reactants. Under such conditions the definition of active sites as elements of the bulk structure of a catalyst material becomes questionable as well as the concept of a surface where all constituents are active. Consequently the metrics of “activity” becomes a challenge. The often-practiced structural analysis of a catalyst outside its reaction environment describe a state of the system as far apart from the reacting state as “models” constructed from a-priori assumptions about the nature of the active state.

The contribution illustrates the role of in-situ techniques in discovering and analyzing such active states of catalysts. In consequence we may realize that the distinct difference between homogeneous and heterogeneous catalysis gradually vanishes under the unified concept of a dynamical active site resulting from catalyst-reactant interactions.

PL-7

Models for Heterogeneous Catalysts: Complex Materials at the Atomic Level

Freund H.-J.*

Fritz-Haber-Institut der Max-Planck-Gesellschaft, Faradayweg, Berlin, Germany

* freund@fhi-berlin.mpg.de

Our understanding of catalysis, and in particular heterogeneous catalysis, is to a large extend based on the investigation of model systems. The enormous success of metal single crystal model surface chemistry, pioneered by physical chemists, is an outstanding example. Increasing the complexity of the models towards supported nanoparticles, resembling a real disperse metal catalyst, allows one to catch in the model some of the important aspects that cannot be covered by single crystals alone. One of the more important aspects is the support particle interface. We have developed strategies to prepare such model systems based on single crystalline oxide films, which are used as supports for metal, and oxide nanoparticles, which may be studied at the atomic level using the tools developed in surface science.

However, those oxide films may also serve as reaction partners themselves, as they are models for SMSI states of metal catalyst. Using such model systems, we are able to study a number of fundamental questions of potential interest, such as reactivity as a function of particle size and structure, influence of support modification, as well as of the environment, i.e. ultra-vacuum or ambient conditions, onto reactivity.

The thin oxide film approach allows us to prepare and study amorphous silica as well as 2D-zeolites. Those systems, in spite of their complexity, do lend themselves to theoretical modelling as has been demonstrated.

PL-8

Fundamental Studies of Metal-Exchanged Zeolites for Selective Catalyticreduction of Nitrogen Oxides in Oxygen Excess

Skoglundh M.*

Competence Centre for Catalysis, KCK, Chalmers University of Technology, Göteborg, Sweden

* skoglund@chalmers.se

Selective catalytic reduction with ammonia (NH_3-SCR) is a well-established and effective method to eliminate nitrogen oxides (NO_x) in oxygen excess for stationary and mobile applications. For the latter case vanadia supported on titania was the first NH_3-SCR catalyst that was commercialized. This catalyst is highly effective around 350-450°C, however at lower or higher temperatures, the efficiency of the catalyst to reduce NO_x decreases. Furthermore, problems like toxicity of volatile vanadium compounds and high activity to oxidize sulfur dioxide have promoted the development of alternative catalysts. Zeolite systems are in this connection interesting candidates. Presently, iron- and copper-exchanged zeolite structures are the most attractive alternatives to the traditional vanadia-based SCR catalyst. However, several challenges arise when using metal-exchanged zeolites in exhaust gas after-treatment systems for vehicles. Two of the more important issues are the hydrothermal stability and the tolerance against chemical poisoning. Furthermore, the possibility to control the distribution of the metal species in the zeolite by thermal treatment during the preparation or after deactivation is another important aspect of metal-exchanged zeolite structures.

The first part of this lecture will focus on iron-exchanged zeolite beta, Fe-BEA, as NH_3-SCR catalyst. The deactivation of Fe-BEA after hydrothermal treatment, and phosphorous and potassium exposure has been studied experimentally and by kinetic modeling as well as activation and regeneration of the catalyst using hydrogen treatment. The fundamental mechanisms for thermal and chemical degradation of Fe-BEA will be presented and discussed. Furthermore, the activation and regeneration of the catalyst by hydrogen exposure will be discussed. The second part of the lecture will focus on copper-exchanged zeolite structures. The solid-state ion-exchange of different types of zeolite structures from copper oxides has been studied experimentally in different atmospheres. It is shown that the copperexchange is possible at unprecedented low temperatures, as low as 250°C, when facilitated by ammonia. The influence of the treatment conditions on the copper-exchange and the mechanism of the ion-exchange process will be presented and discussed. Such copperexchanged zeolite structures with high copper loading are potentially interesting catalysts for a number of technical applications.

Keynote lectures

V-KN1

Catalytic Wastewater Treatment

Descorme C.*

Institut de recherches sur la catalyse et l'environnement de Lyon (IRCELYON), UMR5256 CNRS – University of Lyon, Villeurbanne, France

* claude.descorme@ircelyon.univ-lyon1.fr

Although the water resource is not exhaustible, the water quality must be preserved, which does represent a major challenge for the coming decades. Water is extremely useful on a daily basis for many different industrial, agricultural and domestic applications. As a result of all these different uses, a wide variety of waste effluents is being produced everyday all over the world. The lecture will concentrate on such wastewater but not on the treatments involved upon the production of drinking water.

While conventional wastewater treatment plants, mainly based on biological processes, are quite efficient for the purification of low concentrated, non-toxic and biodegradable wastewater, new solutions had to be imagined for the treatment of toxic and/or non-biodegradable and/or highly concentrated effluents.

Many different approaches have been investigated, numerous combinations have been tested but none of the alternatives developed up to now might be considered as universal. None of them is really better than the other: the more tools in the toolbox, the better.

Before selecting one technology over another, many different parameters have to be considered including the composition of the effluent, the concentration of the pollutants, the physical and chemical characteristics of the wastewater (pH, ionic force, turbidity, etc.), the volumes to be treated, as well as some engineering and economical aspects, etc. The final objective of the treatment is also to be taken into account, i.e. whether the pollutants should be totally mineralized or the treated effluents should only be made biodegradable or the organic content should be recovered to produce new chemicals and/or materials.

Among the possibilities, catalytic processes may play a crucial role, especially when the reaction conditions need to be made milder and/or when the process has to be ran faster and/or whenever selectivity issues are of major concern. Again, different options have been evaluated, including both reduction and oxidation processes.

Key examples taken from the recent literature will be presented all along the lecture, trying to combine different aspects and approaches, going from the development of innovative catalytic materials till the mechanistic information. Looking at the reduction processes, both the hydrodehalogenation and the catalytic reduction reactions will be briefly reviewed and the major challenges to be overcome will be highlighted both in terms of material science or catalytic efficiency (activity and selectivity). Finally, most catalytic oxidation processes will be listed, especially the advanced oxidation processes (AOPs), involving the hydroxyl radicals as the active oxygenated species; and the catalytic wet air oxidation for the most complex type of effluents. The main achievements and the key issues in the different fields will be identified.

II-KN2

Lewis Acid-base Catalysts for the Synthesis of Fine Chemicals

Pârvulescu V.I.*

University of Bucharest, Faculty of Chemistry, Department of Organic Chemistry, Biochemistry and Catalysis, Bucharest, Romania

* vasile.parvulescu@g.unibuc.ro

Keywords: metal nano-particles, Lewis acidity and basicity, preparation method, selective and stereoselective hydrogenation

Particle size is one of the key parameters determining the electronic properties, and as a direct consequence, the catalytic behavior of the supported metals. Sub-nanometric particles were already reported to exhibit beneficial Lewis acid properties for the control of both the activity and selectivity in reactions of importance [1]. However, specific Lewis properties can also be induced in nano-supported metal catalysts.

Based on this importance, the synthesis of metal and alloy nanoparticles of controlled size and shape become a hot topic. Unique properties at the interface between molecular structures and bulk materials can be thus induced following a rational design [2]. Typically, this occurs under strong reduction conditions and requires the presence of a stabilizer able to preserve the above properties.

The aim of this lecture is to present the synthesis of different Lewis acid-base catalysts for the synthesis of fine chemicals. First part will discuss metal- (Pd, Ru, Au, Pt, Ir) and alloy- (Pd-Au) nanoparticles and their catalytic behavior, focusing on the selectivity effects induced after their immobilization onto inorganic carriers. The preparation of the catalysts exhibiting metal Lewis acidity was carried out using several routes: i) the reduction of inorganic metal salts with $Na[AlEt_3H]$ or $Na[BH_4]$ [3-8] followed by the embedding of the resulted colloids in inorganic matrix supports using the sol-gel techniques (SiO_2, ZrO_2, SiO_2-Ta_2O_5]; ii) reduction of the organometallic complexes under supercritical CO_2 conditions followed by the ionic liquid stabilization of the resulted nano-particles [9]; iii) ionic exchange and deposition/precipitation of the noble metals onto zeolites and metal oxides [10-11]; and iV) impregnation of noble metals onto oxifluoride supports [12].

Second part will consider Lewis nano-base catalysts prepared *via* hydrolysis of $Mg(OCH_3)_2$ in a methanol–toluene mixture.

The characterization of these catalysts evidenced in all the cases the presence of the Lewis acid or basic centers. The concentration of these centers was correlated with other properties as particle size and shape, dispersion, etc that were determined using an ensemble of techniques: adsorption-desortption of N_2 at 77K, *in situ* FTIR measurements, DR-UV-Vis, SAXS, XRD, XPS, SEM, TEM, Mossbauer spectroscopy, etc. [2-6].

Finally, the talk will try to associate all these characteristics with the selectivity effects. The effect of the *Lewis acidity* in nano-particles was checked in various reactions like hydrogenation of C=C bonds in simple molecules like styrene or different cycloalkenes, hydrogenolysis of complex molecules like 1,1a,6,10b-tetrahydro-1,6-methanodibenzo[a,e]cyclopropa[c] cycloheptenes, diastereoselective hydrogenation of C=O versus C=C in un-saturated aldehydes and ketones like cinnamaldehyde or prostaglandin derivatives, or reduction of nitric oxides with hydrocarbons. The modification of the supported metal nano-particles by asymmetric ligands like Synphos and cinchonidine will be also discussed comparatively with the homogeneous systems in the selective hydrogenolysis of bicyclo[2.2.2]oct-7-enes and hydrogenation of ethyl pyruvate. The effect of *Lewis basicity* was checked in transesterification reactions.

Conclusions

A correct electron density in metal nanoparticles may lead to very high selectivities, and even activities, in complex reactions. Since there are still many reactions for which the selectivity levels are un-satisfactory future developments in the preparation control of such catalysts are necessary.

Acknowledgements

The author kindly acknowledges the UEFISCDI for the financial support (grant PN-II-ID-PCE-2011-3-0060, ctr. 275/2011).

References

[1] M. Boronat, A. Leyva-Pérez, A. Corma, Acc. Chem. Res. 47 (2014) 834.
[2] Nanoparticles. From Theory to Applications (Ed.: G. Schmid),Wiley-VCH, Weinheim, 2004.].
[3] H. Bönnemann, U. Endruschat, B. Tesche, A. Rufinska, C. W. Lehmann, F. E. Wagner, G. Filoti, V. Pârvulescu, V. I. Pârvulescu, Eur. J. Inorg. Chem. (2000) 819.
[4] R. Preda, V. I. Pârvulescu, A. Petride, A. Banciu, A. Popescu and M. D. Banciu, J. Mol. Catal. 178 (2002) 79.
[5] V. I. Pârvulescu, V. Pârvulescu, U. Endruschat, G. Filoti, F. E. Wagner, C. Kübel, R. Richards, Chem., Eur. J. 12 (2006) 2343.
[6] V. I. Pârvulescu, V. Parvulescu, U. Endruschat, P. Granger, R. Richards, ChemPhysChem 8 (2007) 666.
[7] F. Neatu, A. Kraynov, V.I. Parvulescu, K. Kranjc, M. Kocevar, V. Ratovelomanana-Vidal, R. Richards, Nanotechnology 19 (2008) 225702/1.
[8] F. Neaţu, A. Kraynov, L. D'Souza, V.I. Pârvulescu, K. Kranjc, M. Kočevar, V. Kuncser, R. Richards, Appl. Catal. A: General 346 (2008) 28–35.
[9] V. Cimpeanu, M. Kocevar, V.I. Parvulescu, W. Leitner, Angew. Chem. Int. Ed. 48 (2009) 1085.
[10] M. De bruyn, S. Coman, R. Bota, V. I. Pârvulescu, D. E. De Vos, P. A. Jacobs, Angew. Chem., Int. Ed. Engl. 115 (2003) 5491.
[11] F. Neatu, Z. Li, R. Richards, P.Y. Toullec, J.-P. Genet, K. Dumbuya, J.M. Gottfried, H.-P. Steinruck, V.I. Parvulescu, V. Michelet, Chem. Eur. J. 14 (2008) 9412.
[12] A. Negoi, S. Wuttke, E. Kemnitz, D. Macovei, V.I. Parvulescu, C.M. Teodorescu, S.M. Coman, Angew. Chem. Int. Ed. 49 (2010) 8134.
[13] M. Verziu, B. Cojocaru, J. Hu, R. Richards, C. Ciuculescu, P. Filip, V.I. Parvulescu, Green Chem. 10 (2008) 373.

IV-KN3

Design of Supported Molecular Catalysts for Organic Synthesis

Jones C.W.*

Georgia Institute of Technology, Atlanta, USA

* cjones@chbe.gatech.edu

Keywords: rhodium, carbene, cyclopropanation, Rh2(DOSP)4, flow reactor, asymmetric, catalysis

1 Introduction

Molecular rhodium metal-ligand complex catalysts are a highly versatile class of catalysts used in both bulk chemical production (e.g. hydroformylation) and in the synthesis (e.g. asymmetric hydrogenation) of high value complex organic molecules, such as pharmaceuticals. In all cases, due to the cost of rhodium and in the latter case the ligands, achievement of high turnover numbers (TONs) is critical. This has led to the exploration of methodologies to increase the TONs of these catalysts by catalyst recovery and recycle. This presentation will describe our development of supported asymmetric dirhodium complex catalysts for cyclopropanations and C-H activation mediated catalytic coupling reactions [1,2]. The catalyst behavior, including reaction and substrate scope, will be initially described in batch reactions. Subsequently, a new design of a flow reactor for deployment of solid catalysts based on polymer/oxide hollow fibers will be described [3].

2 Experimental/methodology

A silica-grafted analogue of the well-known $Rh_2(DOSP)_4$ catalyst that reacts donor-acceptor diazonium compounds with various coupling partners via carbene-mediated reactions was prepared as described in the literature [2]. The obtained catalysts were used in an array of asymmetric cyclopropenation and cyclopropanation reactions, as well as coupling reactions that proceed via catalytic C-H activation, including (i) tandem ylide formation/[2,3] sigmatropic rearrangements with allylic and propargylic alcohols and (ii) combined C–H functionalization/Cope rearrangements in a batch reactor.

Cellulose acetate / oxide composite hollow fibers were also prepared as microfluidic flow reactors [3]. The oxide particles included porous silica particles as well as zeolites. To the silica particles, well-defined molecular catalysts could be grafted, and both an organocatalyst (primary aminopropyl fragments) and organometallic catalyst ($Rh_2(DOSP)_4$ analogue described above) were grafted to the silica particles within the fibers. The fibers were then used as flow reactors for an array of reaction types important in organic synthesis, including a deprotection reaction (Brønsted acid zeolite), a coupling reaction (aminopropyl catalyst), and a series of asymmetric coupling reactions (dirhodium carneoid catalysts).

3 Results and discussion

A wide array of asymmetric coupling reactions were conducted using both the silica-supported dirhodium carbenoid catalyst in batch, with product yields and ee's being comparable in most cases (Fig 1).

Three catalysts were also incorporated into composite polymer/oxide hollow fibers. The fibers containing acidic ZSM-5 zeolite are demonstrated to effect the deprotection of benzaldehyde dimethyl acetal in flow. In addition, fibers containing silica-grafted aminopropyl organocatalysts are shown to efficiently catalyse the Kneovenagel condensation of benzalde-

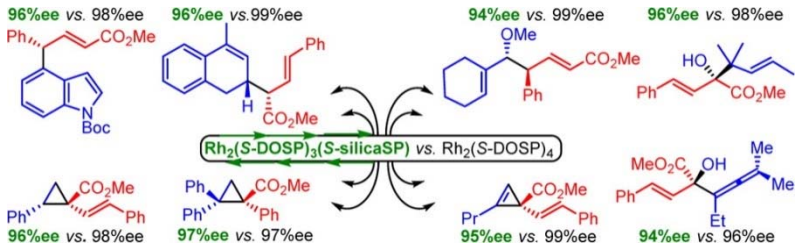

Fig 1. Array of products obtained in asymmetric cyclopropanations, cyclopropenations, as well as C-H coupling reactions catalysed by dirhodium carbenoid catalysts.

hyde and malononitrile in flow. Finally, the dirhodium carbenoid catalyst is demonstrated to catalyse some of the same reactions studied in batch in flow. Fig. 2, below, shows that excellent performance was obtained in flow even after 1000 turnovers were achieved.

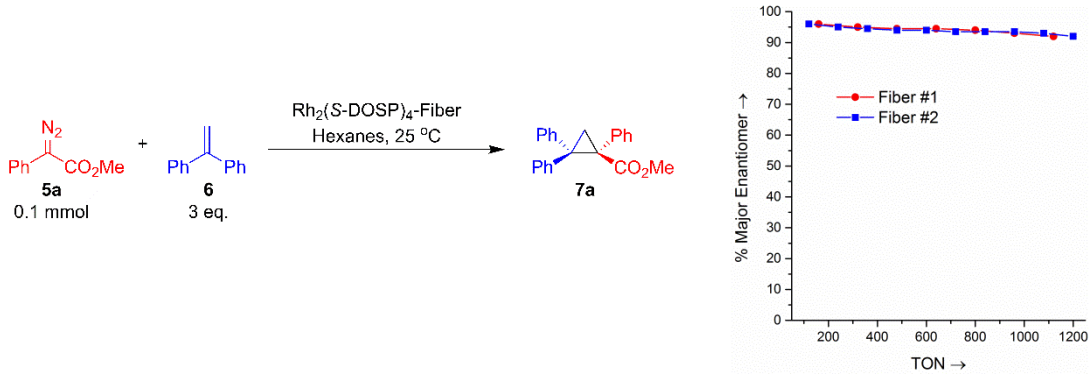

Fig 2. Asymmetric cyclopropanation in flow using dirhodium carbenoid catalyst over 1000 turnovers.

4 Conclusions

A new supported dirhodium carbenoid catalyst supported on porous silica is reported for a variety of asymmetric coupling reactions. This catalyst shows good activity and selectivity, closely paralleling the performance of the parent homogeneous catalyst, $Rh_2(DOSP)_4$. The catalyst is exploited in both batch reactions and in a novel, polymer/oxide hollow fiber microfluidic reactor. The hollow fiber reactor is demonstrated to be a new mode of facilitating catalyst-reagent contacting while carrying out organic synthesis in flow.

Acknowledgements

We thank the NSF under the Center for Selective C¬–H Functionalization (CCHF), No. CHE-1205646 for funding.

References

[1] H. M. L. Davies, R. E. J. Beckwith, *Chem. Rev*. 103 (2003) 2861.
[2] K. Chepiga, Y. Feng, N. A. Brunelli, C. W. Jones, H. M. L. Davies, *Org. Lett*. 15 (2013) 6136.
[3] E. G. Moschetta, S. Negretti, K. M. Chepiga, N. A. Brunelli, Y. Labreche, Y. Feng, F. Rezaei, R. P. Lively, W. J. Koros, H. M. L. Davies, C. W. Jones, manuscript submitted.

III-KN4

Catalysis to Produce Solar Fuels. Status and Challenges

Centi G.*, Perathoner S.

Dept. DIECII, Section Industrial Chemistry, University of Messina, ERIC aisbl and CASPE/INSTM, Messina, Italy

* centi@unime.it

Keywords: solar fuels, CO_2, utilization, artificial leaves, renewable energy, low-carbon economy, sustainable, energy, production

1 Introduction

Realize a sustainable, resource-efficient and low-carbon economy is a major current challenge for society [1,2], but there are main issues to couple the renewable energy sources with the actual energy infrastructure, even considering smart grids. All renewable energy sources except biomass still suffering of major problems of storage and transport at long distance, as well as integration in the industrial production chain. CO_2 conversion to (liquid) fuels using renewable energy sources, e.g. the production of solar fuels, appears as the preferable and more sustainable solution to above problems and to avoid very large investments. The chemical (re)use of CO_2 using renewable energy thus become a key aspect towards the more general goal of resource and energy efficiency, because combines the reuse of a waste and of a relevant carbon sources to the reduction of fossil fuel use as well as GHG and pollutants emissions [3,4]. At the same time, catalysis to produce solar fuels has a major impact in reshaping the future of chemical production and low-carbon bioeconomy. We limit discussion here to the concept of solar fuels as those deriving from the conversion of CO_2 using renewable source of energy to synthetize the products of reaction [5].

2 The impact on scenario for sustainable energy/chemical production

There are many major changes in the chemical production, necessary to respond to the request of a resource and energy efficient sustainable future and to move to a low carbon economy. The use of alternative raw materials is between these driving forces. Biomass as chemical feedstock, (re)use of CO_2, waste valorisation, use of renewable energy, use of fossil fuels alternative to oil (actually accounting for majority of petrochemistry production), from shale gas to coal, are between these driving elements [2,3]. There is a change from the current (oil-centred) petrochemistry to the future of chemical production based on a larger use of alternative raw materials and of renewable energy sources. The lecture will shortly introduce this changing scenario and the impact on moving to solar fuels in this general panorama [3,4].

Solar fuels are a key element to move to a low-carbon bioeconomy [6]. Depending on the model for biorefineries, different options may be possible to integrate bio- and solar-refineries. In the energy biorefinery, where biofuels are the characterizing element, the utilization of CO_2 and renewable energy has the main scope to decrease the carbon footprint and at the same time increase the productivity in energy products. In biorefineries where chemicals are the main product (biofactories) the scope is instead different and the target is the optimal integration of CO_2 utilization within the value chain. However, a range of different other cases are also possible. The lecture will shortly discuss some of the possibilities for new sustainable biorefineries and the opportunities to integrate renewable energy sources in the biorefinery production (solar biorefineries).

There is a changing panorama for bio-based production, with new opportunities offered by the integrated utilization of CO_2 and renewable energy to move to a sustainable and low-carbon bioeconomy.

3 Options and opportunities for solar fuels

There are four main options to implement solar fuels and realize energy efficiency:

- A resource & energy efficiency chemical production, with the objective to reduce the use of fossil fuels as raw material and energy vectors, and to introduce renewable energy in the chemical production chain [2-4].
- Import unexploited renewable energy (RE) resources, via renewable H_2 (water electrolysis) using remote RE sources and CO_2 conversion to methanol or other CO_2-derived energy vectors, and production of solar fuels and chemicals [7].
- Local storage on RE in smart grids, with the main example being power-to-gas (CO_2 to CH_4) [8].
- Develop artificial leaves, in a long-term, for distributed production [9,10].

The lecture will comment these options, their status and opportunities.

4 Moving to artificial leaves

After analysing the motivations why chemical energy storage is the key for a sustainable use of solar energy, and some of the recent progresses in producing solar fuels and related devices, the discussion will be focused on the analysis of the critical elements of artificial leaves to consider for the development of next-generation solar photoelectrocatalytic (PEC) devices [9,10]. There are many challenges to be addressed to realize with good efficiency this process, from the challenges in the electrocatalysts to the understanding of the coupling of the fast processes of charge separation with the slower (at least three order of magnitude) processes of catalytic reduction and charge transfer [11,12]. There is the need to understand this chemistry and to analyse the role of advanced design in nanomaterial to control these processes. Transport processes and reactions at the interface are often dominating the overall performances. Thus, the development of the single components should proceed in parallel with the device development, and not separate as currently. Integrated nano-engineering of materials and devices is the challenge to address properly above problem and to enable the practical implementation of artificial leaf-type devices [13-15]

References

[1] F Cavani, G Centi, S Perathoner, F Trifirò. Sustainable Industrial Chemistry, Wiley-VCH: Weinheim (Germany), 2009.
[2] S Perathoner, G Centi, *J Chinese Chem Soc*, 61 (2014) 719.
[3] P Lanzafame, G Centi, S Perathoner, *Chem. Soc. Rev*. 43 (2014) 7562.
[4] S Perathoner, G Centi, *ChemSusChem*, 7 (2014) 1274.
[5] G Centi, S Perathoner, *ChemSusChem*, 3 (2010) 195.
[6] P Lanzafame, G Centi, S Perathoner, *Catal. Today* 234 (2014) 2.
[7] G Centi, EA Quadrelli, S Perathoner, *Energy & Env. Science*, 6 (2013) 1711.
[8] EA Quadrelli, G Centi, JL Duplan, S Perathoner. *ChemSusChem*, 4 (2011) 1194.
[9] S Bensaid, G Centi, E Garrone, S Perathoner, G Saracco, *ChemSusChem*, 5 (2012) 500.
[10] G Centi, S Perathoner, Artificial Leaves, in Kirk-Othmer Encyclopedia of Chemical Technology, Wiley 2014, DOI: 10.1002/0471238961.articent.a01
[11] G. Centi, S. Perathoner, R. Passalacqua, C. Ampelli, in Carbon-Neutral Fuels and Energy Carriers, N.Z. Muradov, T. Veziroğlu (ed.s), CRC Press (Boca Raton, FL - USA) 2011, Ch. 4, 291-324.
[12] C Genovese, C Ampelli, S Perathoner, G Centi, *J. Catal*., 308 (2013) 237.
[13] G. Centi, S. Perathoner, Green Carbon Dioxide: Advances in CO_2 Utilization, John Wiley & Sons 2014, ISBN: 978-1-118-59088-1
[14] DS Su, G Centi, *J Energy Chem*. 22 (2013) 151.
[15] DS Su, S Perathoner, G Centi, *Chemical reviews* 113 (2013) 5782.

V-KN5

Carbon Dioxide as Carbon Source for the Energetic and Chemical Value Chain: Challenges and Opportunities for Catalysis

Leitner W.*

Institut für Technische und Makromolekulare Chemie, RWTH Aachen University, Aachen, Germany

* leitner@itmc.rwth-aachen.de

The finite resources of fossil feedstock together with the increase in anthropogenic emission of carbon dioxide (CO_2) are a major concern of global importance. The use of CO_2 as carbon source offers the possibility to contribute to sustainable processes at the interface of the energy and chemical supply chains.

This presentation highlights some of the key scientific challenges associated with these concepts and demonstrates how catalysis research combining molecular and engineering sciences provides key contributions to this area. The general aspects and current trends in academia and industry [1] are illustrated with examples concerning the development, application, and mechanistic understanding of catalysts and catalytic systems for the selective conversions of CO_2 to formic acid [2] and higher carboxylic acids [3], to methanol [4] and for methylation [5], and for polyurethane synthesis [6]. Possible applications include the use of CO_2 as C1-building block for fuels and polymers, as well as for chemicals and pharmaceuticals.

References

[1] M. Peters, B. Köhler, W. Kuckshinrichs, W. Leitner, P. Markewitz, T. E. Müller, *ChemSusChem* **2011**, *4,* 1216 – 1240.

[2] S. Wesselbaum, U. Hintermair, W. Leitner, *Angew. Chem.* **2012**, *51,* 8585-8588.

[3] T.G. Ostapowicz, M. Schmitz, M. Krystof, J. Klankermayer, W. Leitner, *Angew. Chem.* **2013**, *52*, 12119-12123.

[4] a) S. Wesselbaum, T. vom Stein, J. Klankermayer, W. Leitner; *Angew. Chem.* **2012**, *51,* 7499-7502;

b) S. Wesselbaum, T. vom Stein, M. Hölscher, J. Klankermayer, W. Leitner, et al. *Chem. Sci.,* **2015,** *6,* 693-704.

[5] a) K. Beydoun, T. vom Stein, J. Klankermayer, W. Leitner, *Angew. Chem.* **2013**, *52,* 9554–9557; b) K. Beydoun, G. Ghazzas, K. Thenert, J. Klankermayer, W. Leitner, *Angew. Chem.* **2014**, *53*, 11010–11014.

[6] J. Langanke, A. Wolf, J. Hofmann, K. Böhm, M. A. Subhani, T. E. Müller, W. Leitner, C. Gürtler, *Green Chem.,* **2014**, *16,*1865–1870.

II-KN6

Electron Microscopy Advances in Catalysis

Helveg S.*

Haldor Topsoe A/S, Nymøllevej 55, Kgs. Lyngby, Denmark

* sth@topsoe.dk

Keywords: electron microscopy, atomic-resolution, *in situ*, dynamics, reactivity

In recent years, electron microscopy has made significant progress for the study of solid materials at the atomic-scale. Advancements in electron optics and data acquisition methods have made electron microscopy capable of delivering images with sub-Ångström resolution and single-atom sensitivity [1-3]. Parallel developments of gas cells, sample stages and micro-electro-mechanical system devices have made high-resolution electron microscopy available for *in situ* observations of solid materials during exposure to reactive gas environments at pressures up to atmospheric levels and temperatures of up to several hundred centigrade [4-6]. It is desirable to take advantage of these emerging technologies in the study of heterogeneous catalysts because they provide unique information about surface structures and dynamics.

In this contribution, I will outline advances in electron microscopy that enable observations of catalysts at atomic-resolution and in catalytically meaningful environments. Their application will be illustrated with studies within e.g. hydrotreating, methanol synthesis and diesel automotive exhaust abatement catalysis [1-11]. Moreover, it will be discussed how the atomic-scale observations can beneficially be combined with reactivity data, calculated or measured, from simpler model systems. Hereby, the description of the dynamic functions and properties of catalysts can be extended with information that is specific to the exposed surface sites, which, in general, should contribute to the continued development of new and better catalysts.

References

[1] C. Kisielowski, Q.M. Ramasse, L.P. Hansen, M. Brorson, A. Carlsson, A.M. Molenbroek, H. Topsøe, S. Helveg, *Angew. Chemie. Int. Ed*. 49 (2010) 2708.

[2] L.P. Hansen, Q.M. Ramasse, C. Kisielowski, M. Brorson, E. Johnson H. Topsøe, S. Helveg, *Angew. Chemie. Int. Ed*. 50 (2011) 10153.

[3] Y. Zhu, Q.M. Ramasse, M. Brorson, P.G. Moses, L.P. Hansen, C.F. Kisielowski, S. Helveg, *Angew. Chemie. Int. Ed*. 53 (2014) 10153.

[4] J.R. Jinschek, S. Helveg, *Micron* 43 (2012) 1156.

[5] S. Helveg, C.F. Kisielowski, J.R. Jinschek, P. Specht, G. Yuan, H. Frei, *Micron* 68 (2015) 176.

[6] J.F. Creemer, S. Helveg, G.H. Hoveling, S. Ullmann, A.M. Molenbroek, P.M. Sarro, H.W. Zandbergen, *Ultramicroscopy* 108 (2008) 993.

[7] S.B. Vendelbo, C.F. Elkjær, H. Falsig, I. Puspitasari, P. Dona, L. Mele, B. Morana, B.J. Nelissen, R. van Rijn, J.F. Creemer, P.J. Kooyman, S. Helveg, *Nat. Mater.* 13 (2014) 884.

[8] S.B. Simonsen, I. Chorkendorff, S. Dahl, M. Skoglundh, J. Sehested, S. Helveg, *J. Am. Chem. Soc.* 132 (2010) 7968.

[9] S.B. Simonsen, I. Chorkendorff, S. Dahl, M. Skoglundh, J. Sehested, S. Helveg, *J. Catal.* 281 (2011) 147.

[10] L.P. Hansen, E. Johnson, M. Brorson, S. Helveg, *J. Phys. Chem. C* 118 (2015) 22768.

[11] C. Holse, C.F. Elkjær, A. Nierhoff, J. Sehested, I. Chorkendorff, S. Helveg, J.H. Nielsen, *J. Phys. Chem. C.* (2014) in press.

IV-KN7

Chemical Photocatalysis Using Visible Light

Koenig B.

Faculty of Chemistry and Pharmacy, University of Regensburg, Regensburg, Germany

* burkhard.koenig@ur.de

Keywords: photocatalysis, visible light, conPET, arylation reactions, photoredox catalysis, green, chemistry

The use of visible light for organic synthesis is a very old idea: More than 100 years ago the Italian chemist Giacomo Ciamician discovered and promoted the field. Recently, photoredox chemistry mediated by metal complexes, such as ruthenium-trisbipyridine, or organic dyes, such as eosin or perylenediimides, gained enormous interest for applications in organic synthesis.

We present some of the recent results using photoredox catalysis with visible light from our laboratory including photooxidations, oxidative C-C bond formation and arylation reactions utilizing one or two photons for activation.

References

[1] I. Ghosh, T. Ghosh, J. I. Bardagi, B. König, *Science* **2014**, *346*, 725 – 728;
[2] D. P. Hari, B. König, *Chem. Commun*. **2014**, *50*, 6688 – 6699;
[3] D. P. Hari, T. Hering, B. König, *Angew. Chem. Int. Ed*. **2014**, *53*, 725 – 728;
[4] P. Schroll, C. Fehl, S. Dankesreiter, B. König, *Org. Biomol. Chem*. **2013**, *11*, 6510 – 6514;
[5] D. P. Hari, B. König, *Angew. Chem. Int. Ed.* **2013**, *52*, 4734 – 4743;
[6] T. Hering, D. P. Hari, B. König, *J. Org. Chem*., **2012**, *77*, 10347 – 10352;
[7] D. P. Hari, T. Hering, B. König, *Org. Lett*. **2012**, *14*, 5334 – 5337;
[8] P. Schroll, D. P. Hari, B. König, *ChemistryOpen* **2012**, *1*, 130 -133;
[9] D. P. Hari, P. Schroll, B. König, *J. Am. Chem. Soc*. **2012**, *134*, 2958 – 2961;
[10] M. Cherevatskaya, M. Neumann, S. Füldner, C. Harlander, S. Kümmel, S. Dankesreiter, A. Pfitzner, K. Zeitler, B. König, *Angew. Chem. Int. Ed.* **2012**, *51*, 4062 – 4066.

V-KN8

Exploiting Acid-base Cooperativity in Metalloenzyme-like Lewis Acid Zeolites for Biomass Conversion

Van De Vyver S., Lewis J.D., Román-Leshkov Yu.*

Massachusetts Institute of Technology, Cambridge, Massachusetts 02139, USA

* yroman@mit.edu

Keywords: biomass conversion, Lewis acids zeolites, C-C coupling, transfer, hydrogenation

1 Introduction

In our efforts to shift away from traditional petroleum-based raw materials to supply fuels and chemicals, biomass has emerged as an attractive renewable carbon-containing feedstock. Its complex chemical diversity has created daunting challenges that require the implementation of robust, active, and selective catalysts to effectively transform it into useful products. In this lecture, new developments in the use of Lewis acid zeolites will be presented in the context of converting biomass-derived oxygenates into value-added products. Specific examples will be presented highlighting the role that catalytic pairs play in enhancing the activation of targeted functional groups, achieving cooperative catalysis, or promoting one-pot cascade reaction sequences. Lewis/Brønsted acid pairs will be discussed in the context of hydrolysis/transfer hydrogenation cascades for the conversion of furfural into gamma-valerolactone, while Lewis acid/base pairs will be discussed in the context of cooperative C-C coupling of oxygenates, including coupling of hydroxyacetone with formaldehyde to form α-hydroxy-γ-butyrolactone (HBL), i.e. a chemical intermediate used for production of pharmaceuticals.[2]

2 Experimental/methodology

Reactivity studies were performed in batch and flow reactors at between 80 and 160 °C using 1,4-dioxane, toluene, water or acetone as solvents, and a metal:oxygenate ratio of 1:100 and a oxygenate:formaldehyde ratio of 1:3 [1]. Sn-Beta was synthesized based on a procedure reported by Corma et al. [3]. Details on the characterization of the catalysts can be found in publication [4].

3 Results and discussion

As a representative example of C-C coupling, the production of HBL will be discussed in more detail. Sn-Beta zeolites effectively catalyze the C–C coupling reaction between DHA and formaldehyde, yielding up to 60 % HBL at 98% conversion after 3 h [1]. Byproducts observed were lactic acid and (1,3-dioxolan-4-yl)methanol. The conversion pathway of DHA into HBL involves consecutive aldol condensation, 1,2-hydride shift, dehydration, intramolecular hemiacetal and keto–enol tautomerization reactions. Of particular importance in this pathway is the aldol condensation step, as our reactivity studies, coupled with spectroscopic and computational analyses, corroborate a mechanism involving soft enolization of DHA followed by an aldol addition of formaldehyde to the Sn-enolate intermediate, generating erythrulose as an intermediate species. More specifically, in our proposed mechanism, the framework Sn atom polarizes the carbonyl group of DHA, resulting in a substantial increase in the acidity of the α-proton. This proton can be removed by the basic oxygen atom connected to Sn, generating a Sn-enolate

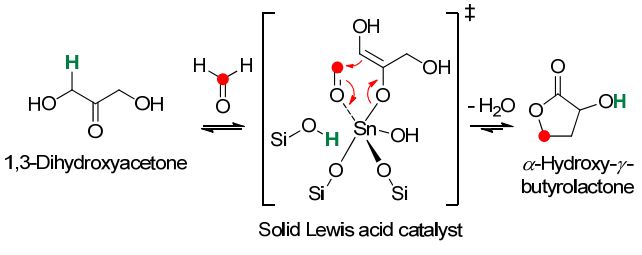

Scheme 1. Proposed soft enolization pathway for the catalytic C–C coupling between DHA and formaldehyde using Sn-Beta zeolites.

intermediate and a silanol group (Scheme 1). Coordination of the oxygen atom of formaldehyde to the Sn center induces polarization in the molecule, further enhancing its reactivity by increasing the electrophilicity of the aldehyde carbon.

Formation of the aldol addition product erythrulose as a reaction intermediate in the production of HBL was substantiated by using it as a reactant in place of DHA. A reaction of erythrulose with Sn-Beta under identical conditions as those used for DHA generated a 24% HBL yield, thus confirming that erythrulose can undergo the suggested transformation. To further support our hypothesis, isotopically labeled formaldehyde was reacted with DHA in the presence of Sn-Beta and investigated using GC-MS and 13C NMR. The mass spectrum of the product mixture agrees with that obtained from the reaction with unlabeled formaldehyde, but is shifted by m/z = 1 to higher m/z ratios. Specifically, the main fragment ion at m/z 58, corresponding to the resonantly stabilized species 13CH2=CH–CH+–OH, indicates that HBL contains the 13C label at the C4 position. This was corroborated by 13C NMR, which showed a main resonance at δ = 65.2 ppm corresponding to the C4 atom. The highly selective incorporation of 13C atoms can indeed be rationalized by considering the proposed C–C bond formation mechanism. Formation of erythrulose is calculated to proceed exothermically with a ΔG0 value of 0.4 kJ mol−1, which, although slightly positive, compares favorably to 16.8 kJ mol−1 for the previously proposed aldol condensation of pyruvic aldehyde with formaldehyde into 4-hydroxy-2-oxobutanal [4]. The estimated ΔG0 values of the ring closure and 1,2-hydride shift are -49.1 and -57.0 kJ mol−1, respectively, strengthening the feasibility of the reaction mechanism shown in Scheme 1. Although this abstract is not meant to divulge detailed spectral data, we note that we were also able to observe formation of C5 sugars, indicating the occurrence of two consecutive aldol condensation reactions

4 Conclusions

Catalytic pairs represent a powerful, yet relatively unexplored, strategy for the selective activation of oxygenates. Akin to metalloenzymes, Lewis acid zeolites can be engineered to feature catalytic pairs and catalyze reactions with high activity under mild conditions. In particular, the development of catalytic C–C bond formation schemes based on renewable substrates is of importance to define sustainable paradigms for chemical manufacture. With a few exceptions, aldol condensation reactions between biomass-derived platform chemicals using heterogeneous Lewis acid zeolites have received little attention so far.

References

[1] Van de Vyver, S., Odermatt, C., Romero, K., Prasomsri, T., Román-Leshkov, Y. ACS Catal. 5, 972 (2015).

[2] Yamaguchi, S., Motokura, K., Sakamoto, Y., Miyaji, A., and Baba, T. Chem. Commun. 50, 4600 (2014).

[3] Corma, A., Nemeth, L. T., Renz, M., Valencia, S. Nature 412, 423-425 (2001)

[4] Lewis, J. D., Van de Vyver, S., Crisci, A. J., Gunther, W. R., Michaelis, V. K., Griffin, R. G.,Román-Leshkov, Y. ChemSusChem 7, 2255 (2014).

II-KN9

Real-time Analysis of Catalytic Reactions Using Simultaneous Orthogonal Methods

Mcindoe J.S.*

Department of Chemistry, University of Victoria, P.O. Box 3065, Victoria, Canada

* mcindoe@uvic.ca

Powerful insights into catalytic mechanisms can be acquired through direct observation of intermediates while the reaction is being carried out. Numerous spectroscopic and kinetic tools have been utilized for this purpose, and our focus has been on developing real-time methodologies to allow electrospray ionization mass spectrometry (ESI-MS) to reliably perform this task in real time. Fast and sensitive and with a high dynamic range, ESI-MS is capable of handling the complex soup of components that is an evolving catalytic reaction. With the use of charged tagged substrates and continuous infusion of sample, the reactants, products, byproducts, catalyst resting state, decomposition products and abundant intermediates can be measured simultaneously and reproducibly at a sampling rate of 1 s^{-1}. However, by offloading the task of assessing reaction progress to an orthogonal method, the overall dynamic range can be increased to over 5 orders of magnitude, i.e. real time analysis of species present at part-per-million levels during reactions performed at typical concentrations (0.1 M). Examples of our approach will be presented in the context of a variety of transition-metal catalyzed reactions, including various palladium-catalyzed cross-coupling reactions and rhodium-catalyzed hydrogenation and hydroacylation reactions.

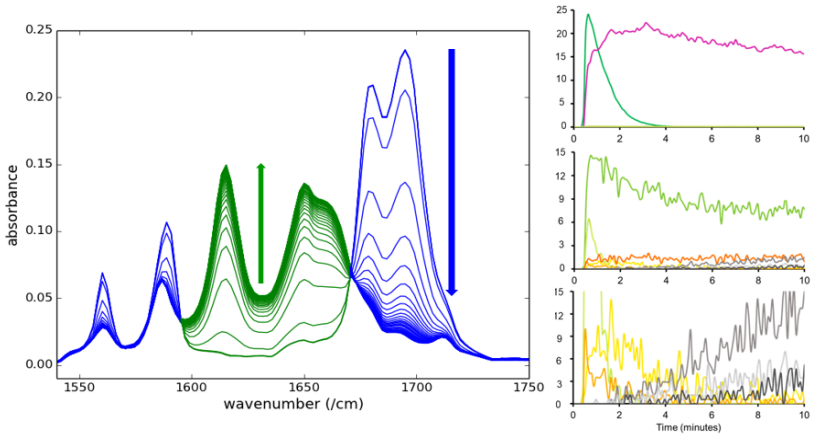

Fig. 1. Complementary real-time spectroscopic and spectrometric data from a catalytic reaction.

V-KN10

Base Metal Catalysis for Cross Coupling and Addition Reactions

Hu X.L.*

Laboratory of Inorganic Synthesis and Catalysis, Institute of Chemical Sciences and Engineering, Ecole Polytechnique Fédérale de Lausanne, Lausanne, Switzerland

* xile.hu@epfl.ch

Keywords: iron catalysis, nickel catalysis, cross coupling, alkyl, radical, alkynes, alkenes

1 Introduction

The advancement of catalysis has had a significant impact on society. As chemists strive to improve the efficiency of chemical synthesis and to enable green and renewable energy conversion and storage technologies, fundamental research in catalysis is as important today as at any time in the past. Base metal catalysis, where the catalysts contain only elements abundant in the earth's crust, offers potential advantages in cost, availability, scalability, and sometimes compatibility with health and the environment. In this talk, I will present our recent work in base metal catalyzed cross coupling reactions and functionalization of alkenes and alkynes.

2 Experimental/methodology

Cross coupling of alkyl halides is challenging because metal alkyl intermediate species are prone to unproductive beta-H elimination. We have applied Ni, Cu, and Fe-based catalysts for these reactions. We also employ well-defined metal complexes as mechanistic probes.

Alkynes and alkynes are readily available and inexpensive feedstock chemicals. We have developed Fe and Cu catalysis to transform these unsaturated molecules into higher-valued compounds through addition reactions.

3 Results and discussion

We developed a well-defined Ni catalyst, Nickamine, that catalyzes the alkyl-alkyl, alkyl-aryl, and alkyl-alkynyl Kumada coupling of activated alkyl halides, as well as direct alkylation of alkynes and heterocycles (Figure 1).[1-5] The mechanism of these reactions was thoroughly studied using radical probes, kinetics and DFT computations.[6,7] We also studied the mechanism of analogous Fe-catalyzed alkyl-aryl Kumada coupling using defined Fe pincer complexes.[8] A common bimetallic oxidative addition reaction pathway involving alkyl radical intermediates was found for these coupling reactions.

We discovered that Fe catalysts could be used to promote the 1,2-addition of perfluoroalkyl iodides to alkynes and alkenes.[9] The resulting perfluoroalkylated alkyl and alkenyl iodides could be further functionalized by cross coupling reactions. Further investigation showed that copper catalysis can be used to promote the 1,2-addition of alpha-carbonyl iodides to alkynes,[10] resulting beta,gamma-unsaturated ketones which are an important class of organic molecules.

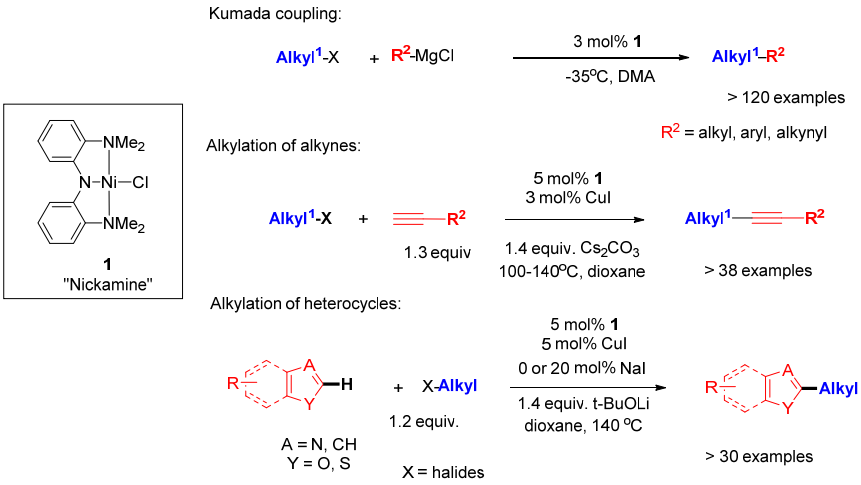

Fig. 1. Cross coupling-type reactions catalyzed by Nickamine.

4 Conclusions

We have developed efficient base metal catalysis for some important organic reactions such as cross coupling and alkene and alkyne functionalization. The complex mechanism of these reactions is started to be elucidated, showing unique features compared with precious metal catalysis.

Acknowledgements

We thank the EPFL, the Swiss National Science Foundation, and the European Research Council for financial support.

References

[1] O. Vechorkin, X. L. Hu, *Angew. Chem., Int. Ed.* **2009**, *48*, 2937-2940.
[2] O. Vechorkin, V. Proust, X. L. Hu, *J. Am. Chem. Soc.* **2009**, *131*, 9756-9766
[3] O. Vechorkin, A. Godinat, R. Scopelliti, X. L. Hu, *Angew. Chem., Int. Ed.* **2011**, *50*, 11777-11781.
[4] O. Vechorkin, D. Barmaz, V. Proust, X. L. Hu, *J. Am. Chem. Soc.* **2009**, *131*, 12078-12079.
[5] O. Vechorkin, V. Proust, X. L. Hu, *Angew. Chem., Int. Ed.* **2010**, *49*, 3061-3064.
[6] J. Breitenfeld, J. Ruiz, M.D. Wodrich, X.L. Hu *J. Am. Chem. Soc.* **2013**, *135*, 12004-12012.
[7] J. Breitenfeld, M.D. Wodrich, X.L. Hu *Organometallics* **2014**, *33*, 5708-5715.
[8] G. Bauer, M.D. Wodrich, R. Scopelliti, X.L. Hu *Organometallics* **2015**, *34*, 289-298.
[9] T. Xu, C.W. Cheung, X.L. Hu *Angew. Chem. Int. Ed.* **2014**, *53*, 4910-4914.
[10] T. Xu, X.L. Hu *Angew. Chem. Int. Ed.* **2015**, *54*, 1307-1311

I-KN11

Catalysis in Confined Space – from Zeolites and Zeotypes to Functionalized Metal-Organic Frameworks

Olsbye U.*, Lillerud K.P.

Department of Chemistry, University of Oslo, Oslo, Norway

* unni.olsbye@kjemi.uio.no

More than a decade of systematic studies of zeolite- and zeotype-catalysed reactions have revealed how confinement effects may alter the rates of individual reactions, as well as the selectivity of complex reaction networks (see e.g. [1-2]).

A parallel, large research effort is targeting another class of nanoporous solids, metal-organic frameworks (MOFs), as a next generation sorbents and catalysts. Ideally, MOFs offer a wide variety of functionalities and pore sizes. However, synthesis as well as chemical, thermal and mechanical stability issues may restrict their applicability. In this lecture, focus will be set on the Zr-MOF series developed at UiO [3-5]. Studies of chemical stability and mechanical strength, catalyst formulation and catalyst performance (ethene oligomerisation, CO_2 reduction) will be presented.

References

[1] U. Olsbye, S. Svelle, M. Bjørgen, P. Beato, T.V.W. Janssens, F. Joensen, S. Bordiga, K.P. Lillerud Angew. Chemie Int. Ed. 51 (2012) 5810-5831.

[2] R.Y. Brogaard, R. Henry, Y. Schuurman, A.J. Medford, P.G. Moses, P. Beato, S. Svelle, J.K. Nørskov, U. Olsbye J. Catal. 314 (2014) 159–169.

[3] J. Hafizovic Cavka, S. Jakobsen, U. Olsbye, N. Guillou, C. Lamberti, S. Bordiga, K.P. Lillerud J. Am. Chem. Soc. 130(42 (2008) 13850-13851.

[4] G.C. Shearer, S. Chavan, J. Ethiraj, J.G. Vitillo, S. Svelle, U. Olsbye, C. Lamberti, S. Bordiga, K.P. Lillerud Chem. Mater. 26 (2014) 4068-4071.

[5] S. Øien, G. Agostini, S. Svelle, E. Borfecchia, K.A. Lomachenko, L. Mino, E. Gallo, S. Bordiga, U. Olsbye, K.P. Lillerud, C. Lamberti Chem. Mater. 27 (2015) 1042−1056.

I-KN12

Development of New Catalytic Materials for Sustainable Production of Chemicals

Tatsumi T.*

Tokyo Institute of Technology, 2-12-1 Ookayama, Meguro-ku, Tokyo, Japan

* ttatsumi@cat.res.titech.ac.jp

Our comfortable modern life is supported by numerous chemical, in particular petrochemical, products. At present, petrochemical industry is based on lower olefins that are produced by thermal cracking of petroleum naphtha in Southeast Asia and Europe. We need to develop the methods for manufacturing chemical products from more substantial fossil resources if possible, and for the long term, preferably from renewable resources.

To develop new technologies of efficient and sustainable production of lower olefins that could replace the conventional thermal cracking process**,** we have tried to improve the catalytic performance of zeolites in catalytic naphtha cracking that occurs at much lower temperature and gives higher selectivity for propylene than thermal naphtha cracking. The critical matter is the elongation of catalyst duration time. There are two main causes for the activity loss, coke deposition and dealumination. Several methods for mitigating the deactivation have been developed.

Because of the shale gas revolution, the use of methane as chemical feedstock as well as fuels is attracting widespread attention. At this time methanol is considered as getting more available chemical feedstock. While methanol production through direct oxidation of methane is extremely difficult, it is worth challenging. In any case, methanol to olefins (MTO) reaction is a promising route to the lower olefins. In this reaction, the deactivation as a result of coke deposition is a critical problem. For the MTO reaction a large number of zeolites were screened and we have found CIT-1 (**CON**) zeolite is promising for selectively converting methanol to propylene and butenes without serious loss of activity.

While fossil fuels will be the dominant factor in the future energy and chemicals scenario for a couple of decades to come, we need to develop methods of alternative chemicals production. Compared to petroleum and natural gas, biomass has low H/C and high O/C ratios and low calorific value. Thus biomass could be useful for the production of chemical products that are not manufactured on a massive scale in the current petrochemical industry. It has long been recognized that 5-hydroxymethylfurfural (HMF) is a bio-based "platform" material for producing useful chemicals. Increasing research interest has been paid to the synthesis of HMF from sugars, particularly from glucose. We have found an effective transformation of glucose to HMF over Beta zeolite by finely tuning acid properties. The high Brønsted/Lewis acid ratio is a key factor for selective production of HMF from glucose. Meanwhile, a great deal of effort has been devoted to the production of sorbitol, as bio-based feedstock, from cellulose. For example, sorbitol can be converted to isosorbide (1,4:3,6-dianhydrosorbitol) through double intramolecular dehydration. Isosorbide can be used to produce polymers such as polyester and polycarbonate; Poly-(ethylene-co-isosorbide)- terephthalate is a bio-based alternative to polyethylene terephthalate (PET). Isosorbide can also replace bisphenol A in the production of polycarbonate and epoxy resins. We have developed highly active zeolite catalysts for the dehydration of sorbitol to isosorbide in water.

For a future sustainable chemicals scenario, it may be desirable to develop efficient methods for utilizing CO_2 by using renewable energy, which could be the ultimate goal. Photocatalytic decomposition of water by visible light, which accounts for a great majority of sunlight, is an enormous challenge and it is absolutely necessary to activate the research in this field. In Japan a 10-year METI (Ministry of Economy, Trade and Industry)-sponsored national project that

targets the recycling CO_2 by using solar H_2 started in 2012. This project is named ARPChem (Artficial Photosynthesis of Chemicals). At this moment this project focuses on the production of light olefins as chemical feedstock. We are developing the process consisting of methanol synthesis from CO_2 and H_2, followed by the MTO reaction catalyzed by zeolites.

V-KN13

Progress and Challenges in Urea/SCR Technology for Removing NOx from Diesel Engine

Nam I.-S.*

Department of Chemical Engineering/School of Environmental Science and Engineering, Pohang University of Science and Techlogy (POSTECH), Pohang, Republic of Korea

* isnam@postech.ac.kr

Keywords: NOx, reduction, Urea/SCR, Mn-Fe, bimetallic, catalyst, CuSSZ13, ESR

The advent of energy-efficient automotive diesel engine has significantly reduced its fuel consumption and CO_2 emission to atmosphere in recent decades [1]. From an environmental point of view, however, the emissions of atmospheric pollutants including nitrogen oxides (NOx) from the diesel engine become a primary concern, while CO and HCs can be readily oxidized by a diesel oxidation catalyst (DOC) commonly installed into diesel after-treatment system under lean operating condition. The abatement of NOx from the diesel engine exhaust is thus one of the critical issues for the commercial implementation of the modern energy-efficient diesel engine technology.

Among promising NOx reduction technologies currently available, the LNT and the SCR technologies are the two leading ones despite their inherent shortcomings still remaining as important technical issues to be resolved [2-3]. A practical advantage of the urea/SCR technology over the LNT rests on the fact that it does not require the use of a large amount of noble metals and complex engine controls which is the essential requirement for the LNT technology [4]. The HC/SCR technology lags behind due primarily to its insufficient low-temperature activity and narrow temperature window on top of its poor tolerance toward H_2O and SO_2 [5].

The urea/SCR technology is undoubtedly one of the commercially proven, reliable and available technologies to meet the stringent worldwide environmental regulations including EURO VI and SULEV for reducing NOx emissions from diesel engine [1,6-7]. The V_2O_5/TiO_2 catalyst has been employed as the conventional SCR catalyst especially for the removal of NOx from stationary sources [8,9]. However, V_2O_5/TiO_2 may not be active in the diesel exhaust temperature ranging from 150~250 ^oC for light duty diesel engine to 200~350 ^oC for heavy duty one, and zeolite based-catalysts including ZSM5 and SSZ13 have then been regarded as the promising urea/SCR catalyst to be directly applied to the diesel after-treatment system [10-12]. In recent years, a number of efforts for further improving the low-temperature activity as well as the stability of the urea/SCR catalysts have been underway for their implementation to the next generation vehicles equipped with the advanced diesel engines.

In this presentation, the progress and challenges in the urea/SCR technology to remove NOx from diesel engine will be reviewed in the topics ranging from the underlying catalysis to the recent research trend and commercial applications. Included in the discussion will be the promoted V_2O_5/TiO_2 catalyst by the modification of catalyst support [13,14] as well as the bimetallic catalyst systems aimed at improving the low temperature activity of the current urea/SCR catalysts and their catalytic characteristics [15,16]. In addition, the local environment of active sites in CuSSZ13, currently regarded as the most promising low-temperature SCR catalyst, will be discussed by ESR and XANES studies in order to understand its strong thermal stability [17]. Also presented will be the tolerance of CuSSZ13 toward CO_2, recently reported as a new deactivating precursor for the urea/SCR catalyst [18].

References

[1] R.M. Heck and R.J. Farrauto, Catalytic Air Pollution Control: Commercial Technology, John Wiley & Sons, Inc. New York, 2002, Chap. 8.
[2] J.-H. Park, M.S. Han, S.J. Park, D.H. Kim, I.-S. Nam, G.K. Yeo, J.K. Kil, Y.K. Youn, *J. Catal.* 241 (2006) 470.
[3] S.J. Park, H.A. Ahn, I. Heo, I.-S. Nam, J.H. Lee, Y.K. Youn, H.J. Kim, *Top. Catal.* 53 (2010) 57.
[4] W.S. Epling, L.E. Campbell, A. Yezerets, N.W. Currier, E.P. James, *Catal. Rev.* 46 (2004) 163.
[5] E. Jobson, Top. Catal., 28 (2004) 191.
[6] S, Brandenberger, O. Kröcher, A. Tissler, R. Althoff, *Catal. Rev.* 50 (2008) 492.
[7] J.H. Baik, S.D. Yim, I-S. Nam, Y.S. Mok, J-H. Lee, B.K. Cho, S.H. Oh, *Top. Catal.* 30/31 (2004) 37.
[8] P. Forzatti, Appl. Catal. A: Gen., 222 (2001) 221.
[9] H.J. Chae, S.T. Choo, H. Choi, I.-S. Nam, H.S. Yang, S.L. Song, *Ind. Eng. Chem. Res.* 39 (2000) 1159.
[10] J.H. Baik, S.D. Yim, I-S. Nam, Y.S. Mok, J-H. Lee, B.K. Cho, S.H. Oh, *Ind. Eng. Chem. Res.* 45 (2006) 5258.
[11] J.-H. Park, H.J. Park, J.H. Baik, I.-S. Nam, C.-H. Shin, J.-H. Lee, B.K. Cho, S.H. Oh, *J. Catal.* 240 (2006) 47.
[12] H.J. Kwon, Y. Kim, I.-S. Nam, S.M. Jung, J.-H. Lee, *Top. Catal.* 53 (2010) 439.
[13] S.T. Choo, S.D. Yim, I.-S. Nam, S.-W. Ham, J.-B. Lee, *Appl. Catal. B: Environ.* 44 (2003) 237.
[14] H.J. Chae, I.-S. Nam, S.-W. Ham, S.B. Hong, *Appl. Catal. B: Environ.* 53 (2004) 117.
[15] Y.J. Kim, H.J. Kwon, I.-S. Nam, J.W. Choung, J.K. Kil, H.-J. Kim, M.-S. Cha, G.K. Yeo, *Catal. Today* 151 (2010) 244.
[16] Y.J. Kim, H.J. Kwon, I. Heo, I.-S. Nam, B.K. Cho, J.W. Choung, M.-S. Cha, G.K. Yeo, *Appl. Catal. B: Environ.* 126 (2012) 9.
[17] Y.J. Kim, J.K. Lee, K.M. Min, S.B. Hong, I.-S. Nam, B.K. Cho, *J. Catal.* 311 (2014) 447.
[18] Y.J. Kim, K.M. Min, J.K. Lee, S.B. Hong, B.K. Cho, I.-S. Nam, *ChemCatChem* 6 (2014) 1186.

II-KN14

Approaching Complexity in Heterogeneous Catalysis by Density-Functional Modelling

Neyman K.M.[1,2*]

1 - Institució Catalana de Recerca i Estudis Avançats (ICREA), 08010 Barcelona, Spain
2 - Departament de Química Física & Institut de Química Teòrica i Computacional, Universitat de Barcelona, c/ Martí i Franquès, 1, 08028 Barcelona, Spain

* konstantin.neyman@icrea.cat

Keywords: nanostructures, coverage effects, subsurface species, transition metal particles, ceria

1 Introduction

Key elements of nanomaterials for current and prospective applications often consist of many thousands of different atoms and thus remain inaccessible for the first-principles (based on Density Functional Theory, DFT) computations due to their size and complexity. However, such systems could be quite realistically represented by computationally tractable smaller model nanoparticles and their aggregates, whose surface structure and reactivity reveal only weak or monotonic size dependence.

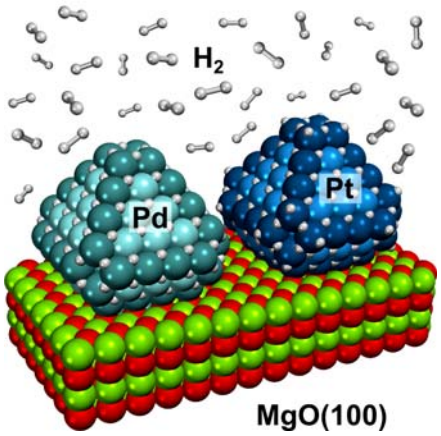

Fig. 1. Models for studies of hydrogen absorption in MgO(100)-supported 1.6 nm large Pd_{127} and Pt_{127} particles with surfaces saturated by hydrogen [8].

2 Results and discussion

We address various problems related to approaching complexity of multicomponent nanomaterials for heterogeneous catalysis and energy technologies in the frameworks of DFT electronic structure modelling.

Among the discussed questions are:
(*i*) To what extent commonly used slab models represent surface properties of metal and metal-oxide nanostructures?
(*ii*) How to design and handle more realistic models?
(*iii*) How significant are interactions at the interface of metal nanoparticles with supporting oxide materials of different kinds and degrees of ordering?
(*iv*) How important are surface coverage effects?
(*v*) Are there reliable ways to computationally optimize chemical ordering of metal components in sufficiently large bimetallic nanoparticles?

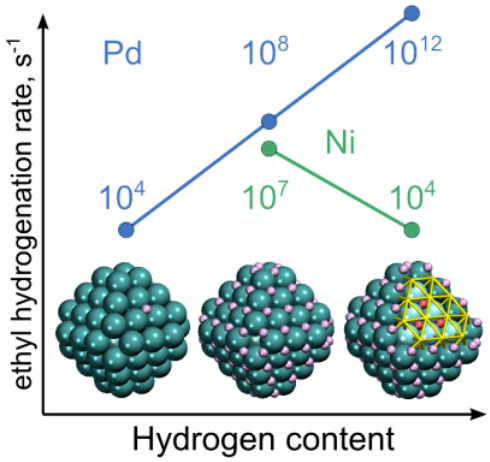

Fig. 2. Subsurface hydrogen can modify the stability and the reactivity of the adsorbed hydrogen in two different ways: in the presence of subsurface H a representative reaction of ethyl hydrogenation is calculated to be strongly accelerated on Pd (Pt), but slowed down on Ni (Rh) [7].

3 Conclusions

The presented results illustrate the current state of advanced theoretical models in heterogeneous catalysis. A general conclusion is that to provide realistic enough description of complex experimentally relevant catalytic systems and processes at affordable computing cost, the models need to be *as simple as possible, but not simpler*.

Acknowledgements

The author gratefully acknowledges financial support by the European Commission (FP7-NMP.2012.1.1-1 project ChipCAT, ref. Nº310191) and the Spanish MINECO (grant CTQ2012-34969) and thanks the Red Española de Supercomputación for provided computer resources.

References

[1] F. Viñes, C. Loschen, F. Illas, K.M. Neyman, Edge sites as a gate for subsurface carbon in palladium nanoparticles. *J. Catal*. 266 (2009) 59.
[2] F. Viñes, Y. Lykhach, T. Staudt, M. P. A. Lorenz, C. Papp, H.-P. Steinrück, J. Libuda, K. M. Neyman, A. Görling, Methane activation by platinum: Critical role of edge and corner sites of metal nanoparticles. *Chem. - Eur. J*. 16 (2010) 6530.
[3] K.M. Neyman, S. Schauermann, Hydrogen diffusion into Pd nanoparticles: Pivotal promotion by carbon. *Angew. Chem. Int. Ed*. 49 (2010) 4743.
[4] G.N. Vayssilov, Y. Lykhach, A. Migani, T. Staudt, G.P. Petrova, N. Tsud, T. Skála, A. Bruix, F. Illas, K.C. Prince, V. Matolín, K.M. Neyman, J. Libuda, Support nanostructure boosts oxygen transfer to catalytically active platinum nanoparticles. *Nature Materials* 10 (2011) 310.
[5] S.M. Kozlov, H.A. Aleksandrov, K.M. Neyman. Adsorbed and subsurface absorbed hydrogen atoms on bare and MgO(100)-supported Pd and Pt nanoparticles, *J. Phys. Chem. C* 118 (2014) 15242.
[6] A. Bruix, Y. Lykhach, I. Matolínová, A. Neitzel, K.C. Prince, F. Illas, V. Matolín, J. Libuda, K.M. Neyman et al., Maximum noble metal efficiency in catalytic materials: Atomically dispersed surface platinum. *Angew. Chem. Int. Ed*. 53 (2014) 10525.
[7] H.A. Aleksandrov, S.M. Kozlov, S. Schauermann, G.N. Vayssilov, K.M. Neyman, How absorbed hydrogen affects catalytic activity of transition metals. *Angew. Chem. Int. Ed*. 53 (2014) 13371.
[8] S.M. Kozlov, H.A. Aleksandrov, K.M. Neyman, Energetic stability of absorbed H in Pd and Pt nanoparticles in a more realistic environment. *J. Phys. Chem. C* 119 (2015) 5180.
[9] S.M. Kozlov, I. Demiroglu, K.M. Neyman, S.T. Bromley, Reduced ceria nanofilms from structure prediction. *Nanoscale* 7 (2015) 4361.
[10] P.C. Jennings, H.A. Aleksandrov, K.M. Neyman, R.L. Johnston, O_2 dissociation on M@Pt core-shell particles for 3d, 4d and 5d transition metals. *J. Phys. Chem. C* 119 (2015), 10.1021/jp511598e.

III-KN15

Operando Studies on PdZn-ZnO, (Pd-)Co_3O_4 and Ni-ZrO_2: Synergies between Surface Science Based Model Systems and Technological Catalysts

Rupprechter G.*, Rameshan C., Föttinger K., Suchorski Y., Bukhtiyarov A., Li H., Anic K., Wolfbeisser A., Lukashuk L.

Institute of Materials Chemistry, Vienna University of Technology, 1060 Vienna, Austria

* guenther.rupprechter@tuwien.ac.at

Our group´s philosophy is to study catalytic surface reactions on heterogeneous catalysts *via a two-fold approach,* employing both *surface science based planar model catalysts* as well as *industrial-grade catalysts* [1-3]. For both, the focus is on examining *active functioning catalysts* under *operando* conditions, at (near) ambient pressure and at elevated temperature (Figure 1).

In particular for ultrahigh vacuum (UHV) based model catalysts that has been a challenge, requiring application of *in situ surface spectroscopy*, such as sum frequency generation (SFG) laser spectroscopy, polarization-modulation infrared reflection absorption spectroscopy (PM-IRAS) and near ambient pressure x-ray photoelectron spectroscopy (NAP-XPS) [1]. To image ("see") ongoing surface reactions by *in situ surface microscopy*, photoemission electron microscopy (PEEM) was applied to polycrystalline samples [2]. For technological catalysts, analogous *operando* studies were performed by Fourier transform infrared spectroscopy (FTIR), x-ray absorption spectroscopy (XAS), near ambient pressure x-ray photoelectron spectroscopy (NAP-XPS), and x-ray diffraction (XRD) [3]. Most of the operando studies were performed at synchrotron sources (BESSY (DE), MaxLab (SE), SLS (CH)), and in lock-step with theory.

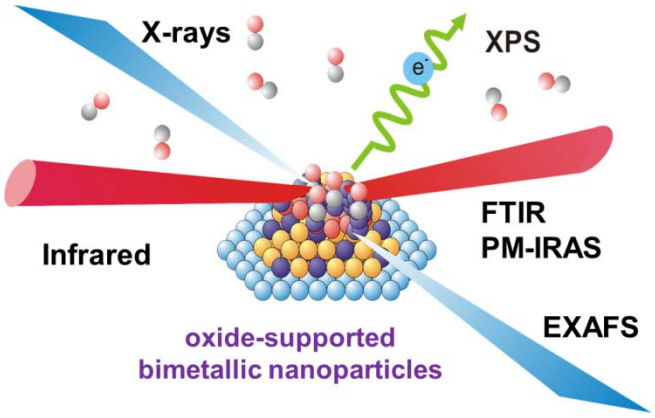

Fig. 1. Schematics of spectroscopic studies of functioning catalysts; from [3].

This two-fold approach yields a better "*holistic*" view of the catalytically relevant atomic and electronic surface structures of catalysts, as well as of molecular details that steer reaction activity and, even more important, reaction selectivity. Comparing surface science based single crystals with nanoparticle model catalysts elucidates the *materials gap*, and comparing UHV to ambient pressure studies reveals the *pressure gap*. In particular, synergisms between studies on model and technological catalysts often provide access to atomistic details.

Among the systems studied are
i) hydrogen generation by methanol steam reforming on alloy (intermetallic) catalysts, i.e. PdZn

surface alloys on Pd(111) single crystals [4] and PdZn nanoparticles supported on ZnO [3], ii) CO oxidation on noble metals [2], thin films and commercial cobalt oxides (Co_3O_4 and CoO), iii) CO and water adsorption, and methane reforming on Ni-ZrO_2, employing an ultrathin ZrO_2 trilayer (O-Zr-O) film on Pt_3Zr(0001) [5] as well as commercial ZrO_2 as support [6].

The combined studies provide detailed mechanistic insight, e.g. on i) the effect of PdZn thickness, surface corrugation and valence band structure on selectivity, ii) locally-resolved catalytic ignition, surface oxide formation/reduction, oxygen vacancy formation as well as carbon balance, iii) electronic structure of ultrathin oxides, and gas-induced oxide and nanoparticle reconstructions. Very recently, we have applied the operando NAP-XPS approach to examine electrochemical water splitting on perovskite-type electrodes under potential control, elucidating polarization-driven changes of surface composition and their effect on reaction kinetics [7].

Acknowledgements

Supported by the Austrian Science Fund (FWF SFB-F45 FOXSI, FWF DK+ Solids4Fun, and Projects ComCat and DryRef).

References

[1] G. Rupprechter, *Advances in Catalysis, 51 (2007) 133-263.*
[2] D. Vogel, Ch. Spiel, Y. Suchorski, A. Trinchero, R. Schlögl, H. Grönbeck, G. Rupprechter, *Angewandte Chemie International Edition, 51 (2012) 10041–10044.*
[3] K. Föttinger, G. Rupprechter, *Accounts of Chemical Research, 47 (2014) 3071−3079.*
[4] Ch. Rameshan, W. Stadlmayr, Ch. Weilach, S. Penner, H. Lorenz, M. Hävecker, R. Blume, T. Rocha, D. Teschner, A. Knop-Gericke, R. Schlögl, N. Memmel, D. Zemlyanov, G. Rupprechter, B. Klötzer, *Angewandte Chemie International Edition, 49 (2010) 3224-3227.*
[5] H. Li, J.J. Choi, W. Mayr-Schmölzer, C. Weilach, C. Rameshan, F. Mittendorfer, J. Redinger, M. Schmid, G. Rupprechter, *Journal of Physical Chemistry C, in press. DOI: 10.1021/jp5100846*
[6] A. Wolfbeisser, B. Klötzer, L. Mayr, R. Rameshan, D. Zemlyanov, J. Bernardi, K. Föttinger, G. Rupprechter, *Catalysis Science and Technology, 5 (2015) 967-978.*
[7] A. K. Opitz, A. Nenning, C. Rameshan, R. Rameshan, R. Blume, M. Hävecker, A. Knop-Gericke, G. Rupprechter, J. Fleig, B. Klötzer, *Angewandte Chemie International Edition, in press.*

III-KN16

Photocatalytic Overall Water Splitting: Present and Future

Li C.*

State Key Laboratory of Catalysis, Dalian Institute of Chemical Physics, Chinese Academy of Sciences, Dalian National Laboratory for Clean Energy, Dalian, China

* canli@dicp.ac.cn

This lecture presents the research progress on solar fuel productions from photocatalytic and photoelectrocatalytic (PEC) processes with the emphasis on the fundamental understanding of the semiconductor-based photocatalytic and photoelectrocatalytic water splitting for solar fuel production.

The great challenge of energy conversion photocatalysis lies in its complicated processes including light absorption (harvesting), charge separation and migration, and redox reactions. In order to gain high photon energy conversion efficiency, a photocatalyst or photocatalytic system must harmonically guarantee high efficiencies of all these three processes instead one of them. Semiconductors with appropriate phase junctions have been demonstrated to be an efficient approach for achieving efficient charge separation [1]. Cocatalysts play important roles in the assembly of efficient semiconductor photocatalyst. It has been conceptually demonstrated Pt-PdS/CdS dual cocatalyst system can achieve 93% H_2 evolution activity in the presence of sacrificial reagents under visible light irradiation (l>420 nm) [2,3]. Recently, it has been also demonstrated that electrons and holes can be spatially separated on the {010} and {110} facets of $BiVO_4$ crystal [4]. It has been demonstrated that the intrinsic nature of charge separation between different facets of $BiVO_4$ together with the synergetic effect of dual-cocatalysts plays key role in photocatalytic activity enhancement [5]. This work opens up a new avenue for the assembly of semiconductor crystal based artificial photosynthesis system by selectively loading of dual cocatalysts on the different facets.

Alternative approaches other than powdered semiconductor system should be also highly considered, such as photoelectrochemical (PEC) and solar cell coupled with water electrolysis catalyst systems. A Ta_3N_5 photoanode coated with ferrihydrite (Fh) layer on which Co_3O_4 water oxidation cocatalyst (Co_3O_4/Fh/Ta_3N_5) was deposited, could yield a photocurrent of 5.2 $mAcm^{-2}$ at a potential of 1.23 V vs. RHE under AM 1.5G simulated sunlight irradiation. And remarkably, about 94% of the initial activity could be maintained even after 6 h irradiation, which is due to the avoidance of the corrosion of Ta_3N_5 via. efficient hole storage and transfer by the Fh layer [6]. A self-biased photoelectrochemical–photovoltaic coupled system consisting of FeOOH/Mo:$BiVO_4$ photoanode and a Pt/p-Si solar-cell-based photocathode showed h_{STH} of 2.5% under parallel irradiation [7].

References

[1] X.Wang, H.X. Han, and Can Li, et al. Angew. Chem. Intd. Ed. 2012; 51: 13089–13092.
[2] H. J. Yan, J. H. Yang and Can Li, et al. J. Catal 2009; 266: 165–168.
[3] J. H. Yang, H. X. Han, and C. Li, et al., Acc.Chem.Res., 2013, 46, 1900-1909
[4] R. G. Li, F. X. Zhang and C. Li, Nature. Commun. 2013; 4: 1432.
[5] *R.G. Li, H. X. Han and C. Li,et al.* Energy Environ. Sci., 2014, 7, 1369 – 1376
[6] G. J. Liu, J. Y. Shi, and C. Li, C et al. Angew. Chem. Int. Ed. 2014; 53: 7295.
[7] C. M. Ding, J.Y. Shi, and C. Li, et al. Phys.Chem.Chem.Phys. 2014; 16: 15608.

IV-KN17

Novel Catalytic Methods for Synthesis of Organic Building Blocks and Biologically Important Heterocycles

Gevorgyan V.*

Department of Chemistry, University of Illinois at Chicago, Chicago, Illinois, USA

* vlad@uic.edu

We have developed a set of novel efficient transition metal-catalyzed annulation and cycloisomerization methodologies for synthesis of multisubstituted carbo- and heterocycles [1-22]. Traditionally, regioselective synthesis of carbo- and heterocycles possessing various functional groups is not a trivial task. We have shown, however, that incorporation of migrating step(s) in the cyclization cascade often helps solving this problem. Thus, it was found that in the presence of Cu-, Ag-, and Au catalysts, a number of groups, such as Hal-, RS-, AcO-, TsO-, Ar-, and SiR_3 could undergo 1,2- or 1,3-migration, or in some cases even double migration, which allows for expeditious synthesis of densely-functionalized carbo- and heterocycles, which are not easily accessible via existing techniques. Most of these transformations proceed via metal-stabilized carbene intermediates. The validity of vinylidene- and carbene intermediates in some of these cascade reactions was tested by means of DFT calculations. We have also developed new tri-component coupling reactions toward expeditious assembly of aminoindoline, aminoindole, and imidazopyridine cores. These methods were used for synthesis of libraries of small heterocyclic molecules for wide biological screening.

The scope of these transformations will be demonstrated and the mechanisms will be discussed.

References

[1] Kel'in, A. V.; Sromek, A. W.; Gevorgyan. V. J. Am. Chem. Soc. 2001, 123, 2074.
[2] Kim, J. T.; Kel'in, A. V.; Gevorgyan, V. Angew. Chem., Int. Ed. 2003, 42, 98.
[3] Sromek, A. W.; Kel'in, A. V.; Gevorgyan, V. Angew. Chem., Int. Ed. 2004, 43, 2280.
[4] Sromek, A. W.; Rubina, M.; Gevorgyan, V. J. Am. Chem. Soc. 2005, 127, 10500.
[5] Seregin, I.; Gevorgyan, V. J. Am. Chem. Soc. 2006, 128, 12050.
[6] Chuprakov, S.; Hwang, F. W.; Gevorgyan, V. Angew. Chem. Int. Ed. 2007, 46, 4757.
[7] Horneff, T.; Chuprakov, S.; Chernyak, N.; Gevorgyan, V.; Fokin, V. V. J. Am. Chem. Soc. 2008, 130, 14972.
[8] Dudnik, A. S.; Gevorgyan, V. Angew. Chem., Int. Ed. 2007, 46, 5195.
[9] Schwier, T.; Sromek, A. W.; Yap, D. L. M.; Chernyak, D.; Gevorgyan, V. J. Am. Chem. Soc. 2007, 129, 9868.
[10] Xia, Y.; Dudnik, A. S.; Gevorgyan, V.; Li, Y. J. Am. Chem. Soc. 2008, 130, 6940.
[11] Dudnik, A. S.; Sromek, A. W.; Rubina, M.; Kim, J. T.; Kel'in, A. V.; Gevorgyan, V. J. Am. Chem. Soc. 2008, 130, 1440.
[12] Dudnik, A. S.; Xia, Y.; Li, Y.; Gevorgyan, V. J. Am. Chem. Soc. 2010, 132, 7645.
[13] Chernyak, N.; Gevorgyan, V. Angew. Chem., Int. Ed. 2010, 49, 2743.
[14] Chernyak, N.; Gorelsky, S. I.; Gevorgyan, V. Angew. Chem., Int. Ed. 2011, 50, 2342.
[15] Chattopadhyay, B.; Gevorgyan, V. Angew. Chem., Int. Ed. 2012, 51, 862.
[16] Kazem Shiroodi, R.; Dudnik, A. S.; Gevorgyan, V. J. Am. Chem. Soc. 2012, 134, 6928.
[17] Gulevich, A. V.; Gevorgyan, V. Angew. Chem., Int. Ed. 2013, 52, 1371.
[18] Gulevich, A. V.; Dudnik, A. S.; Chernyak, N.; Gevorgyan, V. Chem. Rev. 2013, 113, 3084.
[19] Kuznetsov, A.; Gulevich, A.; Wink, D. J.; Gevorgyan, V. Angew. Chem., Int. Ed. 2014, 53, 9021.
[20] Kazem Shiroodi, R.; Soltani, M.; Gevorgyan, V. J. Am. Chem. Soc. 2014, 136, 9882.
[21] Kazem Shiroodi, R.; Koleda, O.; Gevorgyan, V. J. Am. Chem. Soc. 2014, 136, 13146.
[22] Shi, Y.; Gulevich, A.; Gevorgyan, V. Angew. Chem., Int. Ed. 2014, 53, 14191.

I-KN18

Design of Novel Hybrid Hierarchical Catalysts for Direct Synthesis

Khodakov A.Y.[1*], Ordomsky V.V.[1], Cai M.[1], Subramanian V.[1], Lancelot C.[1], Palcic A.[2], Valtchev V.[2], Nhut J.-M.[3], Pham-Huu C.[3], Moldovan S.[4], Ersen O.[4]

1 - UCCS, Université Lille 1-ENSCL-EC Lille, Bat. C3, Cité Scientifique, 59655 Villeneuve d'Ascq, France

2 - LCS, ENSICAEN, 6 Boulevard Maréchal Juin, 14000 Caen, France

3 - ICPEES, ECPM, Université de Strasbourg, 25 rue Becquerel, 67087 Strasbourg, France

4 - IPCMS, Université de Strasbourg, 23, rue du Loess BP 43, F-67034 Strasbourg, France

* Andrei.Khodakov@univ-lille1.fr

Keywords: hierarchical catalysts, syngas, dimethylether, zeolite, copper

1 Introduction

Dimethyl ether (DME) is one of the most promising environmentally optimized alternatives to conventional fossil fuels due to its high cetane index, low emission of CO, NO_x and particulates and reduced noise. DME can also be used as a substitute for liquefied petroleum gas (LPG). DME is biodegradable; it has low toxicity and does not corrode any metals. In addition, DME is an important intermediate for the production of useful chemicals (i.e. methyl acetate and dimethyl sulphate) and petrochemicals (light olefins, BTX aromatics). In the industry, DME can be produced from syngas using either two-stage or single-stage direct technologies. The two-stage technology is currently considered as the most mature route. In the first stage, syngas is converted into methanol over copper based catalysts. In the second stage, methanol is dehydrated into DME over acid catalysts. The maximum syngas conversion to methanol is limited by thermodynamics especially at high temperatures. The single-stage direct DME synthesis overcomes these thermodynamic constraints and leads to higher per-pass CO conversions and higher DME productivity. The direct DME synthesis, however, requires an efficient bifunctional catalyst. The crucial issue in catalyst design for direct DME synthesis is optimisation of the catalyst composition and interaction between methanol synthesis and methanol dehydration active phases. Direct DME synthesis faces several challenges. First, the catalyst activity can be improved for more efficient manufacturing. Second, because of very fast reaction of carbon monoxide with released water, significant amounts of CO_2 are produced. This leads to lower carbon efficiency. Third, the activity of the DME synthesis catalyst decreases with time on stream. The catalyst deactivation affects both copper and acid catalyst sites. The deactivation phenomena may include copper oxidation, sintering, coke deposition, contamination by impurities in syngas, etc.

Zeolite based catalysts have several advantages for methanol dehydration to DME relevant to more conventional oxide catalysts. However, the low back-diffusion of DME through the zeolite crystals could lead to post-reactions yielding undesirable by-products and carbonaceous residues. The latter induces plugging of the catalyst's pores and thus progressive deactivation. Therefore it is of interest to develop new zeolite catalytic system with a hierarchical porosity, i.e. micropores connected from each other with a network of meso- or macropores, in order to facilitate the reactant access and product removal.

The present work addresses design of efficient bifunctional catalysts on the basis of copper and hierarchical ZSM-5 zeolites for direct DME synthesis from syngas. In particular, the lecture is devoted to the strategies relevant to the control of catalyst activity, selectivity and stability.

2 Experimental/methodology

The $CuO–ZnO–Al_2O_3$ precursor was prepared by co-precipitation. A series of ZSM-5 zeolites were prepared from Na_2O - SiO_2 -Al_2O_3-TPAOH - H_2O systems. The hierarchical structure was created using sacrificial templates and treatment with HF_2^-. The hybrid catalysts were prepared using kneading. The catalysts were characterized both *ex-situ* using BET, SEM, TEM, XPS, TPR TPO, FTIR with adsorbed molecular probes (CO, Py, lutidine). The catalytic performance was evaluated in a fixed-bed millireactor. The *operando* XRD/XANES/EXAFS synchrotron experiments were carried out at the ESRF (SNBL beamlines) using a high pressure capillary cell with simultaneous on-line MS analysis of reaction products.

3 Results and discussion

Strategies for the activity control

DME, methanol, hydrocarbons, carbon dioxide and water are major products of carbon monoxide hydrogenation over hydride copper-zeolite catalysts. The activity depends on both concentrations of copper active phase and acid sites in zeolites. Our detailed study revealed a strong correlation between the zeolite crystallite sizes and reaction rate. At the same concentration of copper active sites, higher reaction rate is systematically observed over the catalysts containing smaller zeolite crystallites. The equilibrium of carbon monoxide hydrogenation shifts to methanol, because of rapid transfer of methanol molecules for dehydration to the acid site of the zeolite.

Strategies for the selectivity control

Our results suggest that higher concentration of Bronsted acid sites favours DME selectivity and suppress yields of methanol. Carbon dioxide is undesirable products of DME direct synthesis. Carbon dioxide produces in secondary reactions, its selectivity increases with higher carbon monoxide conversion. Two strategies are proposed to decrease the CO_2 selectivity in direct DME synthesis. The first one involves catalyst promotion which might affect the rate of elementary steps of different reactions. Promotion with tin for example resulted in a noticeable drop in carbon dioxide production. The presence of tin in the catalysts seems to considerably slow down the water gas-shift reaction leading to CO_2. The second strategy focuses on the protecting of the active sites for methanol synthesis from exposure to water. Water gas shift reaction in the bifuncntional catalysts for direct DME synthesis occurs on copper phases. Encapsulation of copper in hydrophobic silica nanospheres could result in a decrease in the CO_2 selectivities and enhanced DME productivity.

Strategies for the stability control

A combination of *ex-situ* and *operando* XAS characterization uncovered that copper is present in metallic form under a wide range of operating conditions. Copper sintering could be a major reason for the deactivation of hybrid hierarchical catalysts. The sintering phenomena are significantly accelerated in the presence of co-fed water. Copper sintering results in a decrease in the number of active sites for methanol synthesis. In addition the migration of copper nanoparticles can plug the porous structure of zeolite and reduce the concentration of acid sites for methanol dehydration. Copper sintering is accelerated by higher concentration of Bronsted acid sites on the external surface of zeolite. The *operando* experiments conducted under realistic conditions of DME synthesis did not reveal any noticeable copper oxidation. No significant carbon deposition was also observed. Catalyst deactivation can be accelerated by the heat spots, the reaction is exothermic. The strategies for the catalysts stability control developed in this work address reducing the concentration of Bronstend acid sites on the external surface of zeolite by sylilation or shaping the catalysts on silicon carbide host matrix with high thermoconductivity.

Acknowledgements

The authors gratefully acknowledge the French National Research Agency (CATSYN-BIOFUEL project ANR-12-BS07-0029) and SNBL/ESRF for use of the beamtime.

III-KN19

Understanding Photocatalytic Process: Intrinsic Properties, Morphology and Timescale

Takanabe K.*

Division of Physical Sciences and Engineering, KAUST Catalysis Center (KCC), King Abdullah University of Science and Technology (KAUST), Thuwal, Saudi Arabia

* kazuhiro.takanabe@kaust.edu.sa

Keywords: photocatalysis, water splitting, charge separation, interface, semiconductor, solar fuel

1 Introduction

Solar energy conversion is must to compensate the gap between energy production and its demand which is increasing with years [1]. A large scale energy generation from solar energy is only achieved by collection of solar spectrum at large scale. Overall water splitting using heterogeneous photocatalysts using a single semiconductor enables to directly generate H_2 from photo-reactor and is one of the most economical technologies in large-scale production of solar fuels [2]. The efficient photocatalyst materials are essential to make this process feasible for future technology. The potential scheme of photocatalytic process at different scale is depicted in Figure 1.

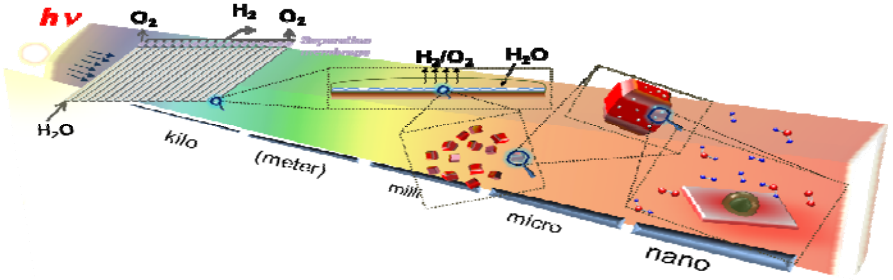

Fig. 1. A schematic of basic concept of overall water splitting at different scale.

2 Discussion

The photocatalysis involves multiple steps of the photophysical and electroccatalytic processes, as depicted by Figure 2. The photocatalytic reaction is initiated by the excited charge carriers (electrons and holes) that are generated by the absorption of the photons in the semiconductor materials (photocatalysts) [3]. Both the generated electrons and the holes move to the surface of the photocatalytic materials and subsequently initiate their respective redox reactions [3]. The photocatalytic process fully utilizes the electronic configuration occurring at the metal–semiconductor and semiconductor–electrolyte interfaces by constructing band structures (the formation of band bending and barriers) [4,5], preferably without introducing p–n junctions that generally increase the process cost. This electronic structure is essential in enhancing the charge separation and in achieving a highly efficient photocatalytic process because the photophysical process, including the generation and recombination of the excited carriers, occurs on a significantly shorter time scale (femto- to-microseconds) than surface electrocatalytic reactions, unless the process is separated effectively (microseconds to several seconds) [3]. The design of the photocatalysts should be focused on the following points [6]:

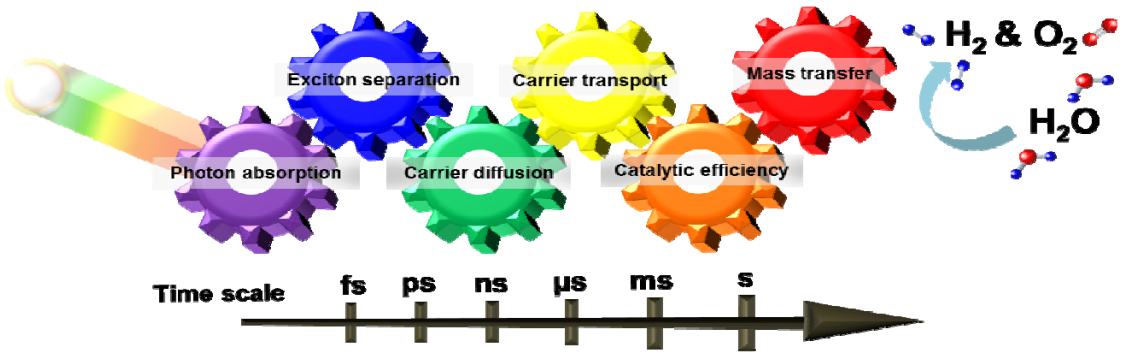

Fig. 2. Six sequential properties that require attentions to achieve efficient photocatalytic water splitting.

1) Select suitable elements to be used as photocatalysts that possess the suitable band positions and band gaps with high absorption coefficients and low exciton binding energy;

2) Synthesize highly crystalline bulk photocatalysts throughout the particle with appropriate concentrations of the majority carriers;

3) Construct band bending in such a way to improve charge separation;

4) Develop highly active cocatalysts for surface electrocatalysis;

5) Effectively locate the sites and maximize the concentrations of the reduction/oxidation cocatalysts on the photocatalyst surfaces.

6) Optimize solution condition for improved water redox reactions (pH, electrolyte etc.).

To understand the properties that affect photocatalytic process, various forms of photocatalytic materials are needed [7]. For example, thin film configuration is effective to measure absorption properties, such as absorption coefficient, refractive index, dielectric constant, and charge carrier concentration, carrier mobility, carrier lifetime and diffusion length. Calculations including density functional theory provide useful information, such as electronic structure (direct/indirect band gap), absorption coefficient, exciton binding energy, and dielectric constant. Photoelectrochemical configuration is effective to measure photoelectrochemical performance at different potential (Fermi level) and at different excitation wavelength. Semiconductor-electrochemistry is also effective to learn flat-band potential and majority carrier concentrations of the semiconductor. Measurements of the electrocatalytic performance give information of overpotential required for the respective redox reactions, and concentration gradient and diffusion of electrolyte. As a consequence of these parameters, photocatalytic powder configuration can only measure hydrogen and/or oxygen with and without sacrificial reagents [8].

To achieve efficient photocatalysis for overall water splitting, all of the parameters discussed above should be improved because the overall efficiency is obtained as the multiplication of all these fundamental efficiencies. Accumulation of knowledge from solid-state physics to electrochemistry and multidisciplinary approach to conduct various measurements are inevitable to fully understand the photocatalysis and to improve the efficiency.

References

[1] N.S. Lewis, D.G. Nocera, Proc. Natl. Acad. Sci. U.S.A., 103 (2006) 15729.
[2] B.A. Pinaud et al., Energy Environ. Sci. 6 (2013) 1983.
[3] K. Takanabe, K. Domen, *Green* 1 (2011) 313.
[4] H. Yoneyama, Crit. Rev. Solid State Mater. Sci. 18 (1993) 69.
[5] H. Gerischer, J. Phys. Chem. 88 (1984) 6096.
[6] K. Takanabe, K. Domen, *ChemCatChem* 4 (2012) 1485.
[7] F.E. Osterloh, Chem. Soc. Rev. 42 (2013) 2294.
[8] T. Hisatomi, K. Takanabe, K. Domen, Catal. Lett. 145 (2015) 95.

IV-KN20

Application of Zeolite Catalysts for the Production of Clean Fossil Fuels and Biofuels

Vasalos I.A.*

Chemical process and energy resources institute, P.O BOX 361 GR-570 01 Thermi Thessaloniki, Greece

* iacovos@vasalos.com

Keywords: Zeolite Catalysts, Biofuels, Clean fossil fuels

Transportation fuels are one of the most important energy carriers used in internal combustion or jet engines. Diesel and gasoline are the key fuels in use today and in the foreseeable future. Zeolites have played a major role in the manufacturing of both fuels for over half a century. In this presentation emphasis will be placed on Fluid Catalytic Cracking (FCC), the workhorse process for the refining industry for many years. We will briefly examine the evolution of the FCC process by reviewing the progress dictated by environmental requirements such as reduction in the carbon dioxide and sulfur dioxide emissions in the refinery and the requirements set by the clean air act for reducing the auto exhaust emissions.

Although future developments in refining catalysts have the potential to play a major role in reducing the carbon footprint of fossil fuels, it is necessary to reduce the carbon intensity (gr CO2e per MJ fuel consumed) of transportation fuels via the gradual introduction of alternative fuels such as electricity/hydrogen and biofuels. Among the biofuels of great interest are hydrocarbon type fuels, because they are compatible with existing infrastructure and internal combustion engines. Main fuels in this category include: Hydrogenated Vegetable Oil (HVO), Fischer Tropsch Liquids and transportation fuels derived from Biomass Thermal Pyrolysis or Biomass Catalytic Pyrolysis.

It will be shown that zeolite catalysts play a major role in upgrading Fischer Tropsch Liquids and producing diesel, aviation fuel and naphtha. Emphasis will be placed on the use of ZSM-5 for the Biomass Catalytic Pyrolysis process, where biomass is processed in a Circulating Fluid Bed reactor using a ZSM-5 catalyst both as heat carrier and as a catalyst for the in situ upgrading of the pyrolysis vapors. Finally, future research directions to improve the economics of biomass derived hydrocarbons will briefly be discussed.

KN21

Nanocatalyst Based on Hybrid Structured Materials: Synthesis and Application

Karakhanov E.[1*], Maximov A.[1,2], Rosenberg E.[3]

1 - Moscow State University, Chemistry Department, Moscow, Russia
2 - Institute of Petrochemical Synthesis RAS, Moscow, Russia
3 - Department of Chemistry and Biochemistry University of Montana Missoula, Montana, United States of America

* kar@petrol.chem.msu.ru

Keywords: nanoparticle, hybride structured support, selective hydrogenation, catalysis, phenols, aromatic compounds, dienes

1 Introduction

The catalyst containing nanoparticles demonstrate high selectivity and activity, recyclable and thus meet the requirements for green catalysts technological application. The principal problem arising at nanoparticles synthesis and their application in catalysis is necessity to stabilize and control their size. The main approaches to solve this problem are incorporation of metal nanoparticles in channels of solid supports with regular structure. Designing novel support materials, having a regular structure and capable of binding the substrate molecule selectively, could be considered as one of the most promising area for creating of new selective catalysts [1-3]. We report herein a number of different approaches for design new hybrid materials for hydrogenation catalysts based on metal nanoparticles and structured supports [2-5].

2 Experimental

The synthesis of hybrid mesoporous supports and catalytic experiments on hydrogenation were carried out as described in [3-6].

3 Results and Discussion

As a catalysts we synthesized a number of hybrid materials (Fig.1-2):

a) **The heterogeneous organic supports synthesized by the covalent binding of dendrimers using diepoxide and diisocianate.** Approach includes prior cross-linking of the dendrimers with subsequent encapsulation of metal nanoparticles. Depending on the generation of the dendrimer, one can obtain particles differing in size (1–4 nm), which may significantly affect the process of catalytic reactions.

b) **The microporous materials synthesized by sol-gel methods in situ using dendrimers.** The preliminary modification of the dendrimer terminal aminogroups by the silyl-containing linkers and synthesis of mesoporous silica channels in presence of a template using sol-gel method and grafting the modified dendrimers to the silica surface formed *in situ*.

c) The combination of silica polyamine composite (SPC) hybrids with dendrimers to provide an easy route to stabilization of nanoparticles on the silica surface, **E.**g. polypropyleneimine (PPI) dendrimers of the third generation that have been covalently grafted to a silica surface modified with polyallylamine (PAA) have been synthesized.

d) Organic polymers with highly ordered mesoporous structure modified by functional groups (resol based mesoporous materials and mesoporous aromatic frameworks). The nanoparticles were included into pores.

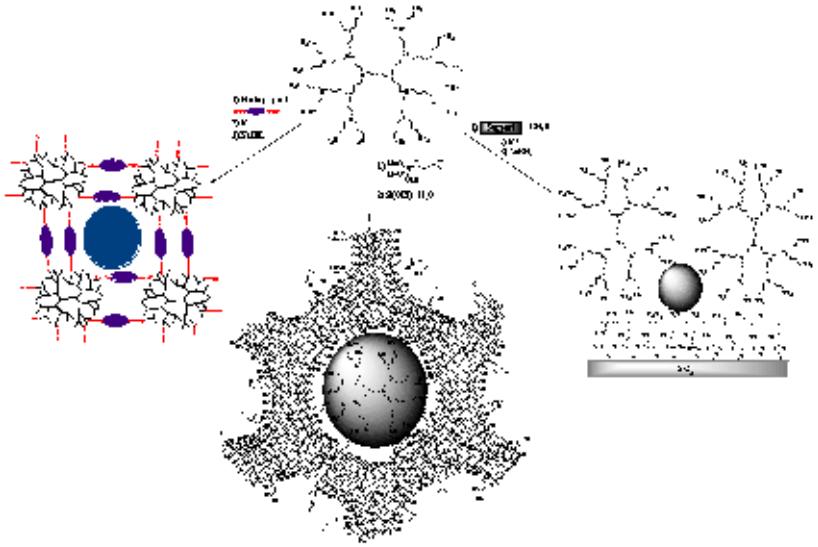

Fig 1. Preparation of hybrid catalyst on the base of dendrimers

The nanopartilces of Pd, Rh, Ru, Pt were encapsulated into the materials using impregnation- reduction method. All materials obtained were identified by the TEM, XPS, FTIR, NMR MAS methods. The size of the particles was shown to be 2-5 nm and could be regulated by the structure of support.

The catalysts synthesized showed superior activity and selectivity in the hydrogenation of different unsaturated and aromatics compounds. The Pd nanocatalysts demonstrated high efficiency in selective semihydrogenation of phenylacetylene to styrene, dienes to monoenes. The turnover number exceeded the 100000 h-1. Ruthenium and Rhodium catalysts exhibit high activity in the hydrogenation of aromatics and phenols. The hybrid catalysts displayed high resistance to metal leaching and could be widely used in green solvents

4 Conclusions

Catalysts based on metal nanoparticles encapsulated into different types of structured hybrid matrices were synthesized. The materials displayed high activity and substrate selectivity in the hydrogenation of various substrates,

Acknowledgments

This work was supported by the RFBR grant No . 14-03-00210

References

[1] E. Karakhanov, A. Maksimov, A. Zolotukhina, Y. S. Kardasheva. Russian Chemical Bulletin. 62 (2013) 1465–1492

[2] E.A. Karakhanov, A. L. Maximov, V. A. Skorkin, A. V. Zolotukhina, A. S. Smerdov, A. Yu. Tereshchenko, *Pure Appl. Chem.* 81 (2009), 2013 – 2023

[3] E. Karakhanov, A. Maximov, Yu. Kardasheva, V. Semernina, A. Zolotukhina, A. Ivanov, G. Abbott, E. Rosenberg, V. Vinokurov, *ACS Appl. Mater. Interfaces* 6 (2014) 8807−8816

[4] E. A. Karakhanov, A. L. Maksimov, E. M. Zakharian et al. *Journal of Molecular Catalysis A: Chemical*. 397 (2015) 1–18

[5] Anton Maximov, Anna Zolotukhina, Vadim Murzin, Edward Karakhanov, Edward Rosenberg. *ChemCatChem* (2015) DOI: 10.1002/cctc.201403054

[6] E.Karakhanov, A.Maksimov, I.Aksenov, V.Kuznecov, T.Filippova, S.Kardashev, D.Volkov, *Russ. Chem. Bull.*, 63, (2014), 1459-1464

Session I
"Novel catalytic materials and processes for securing supplies of raw materials"

I-OP01

Layered Zeolite SRZ-21 for Cumene Production

Wang G.W, Wei Y.L, Gao H.X, Yang W.M*

Sinopec Shanghai Research Institute of Petrochemical Technology, Shanghai, China

* yangwm.sshy@sinopec.com

Keywords: MWW-type zeolites, delaminated zeolites, benzene alkylation, cumene production

1 Introduction

The layer-structured zeolite MCM-22 was invented by Mobil in 1990[1]. Each layer of the zeolite MCM-22 includes a two-dimensional 10-membered ring sinusoidal channel system and a hexagonal-array of cups, having 12-ring openings on the external surface of the layer. The formation of the layer structure and super-cages improves diffusion behaviours of the big organic molecules in micro-pores, which benefits the macro-molecule organic reactions. However, the layer structure of MCM-22 collapses after calcination, forming a uniform three-dimensional framework structure.

Recently, several discrete products with different arrangements of the MCM-22 monolayers were prepared from the MCM-22 lamellar precursors [2-3]. ITQ-2, which is essentially made of very thin layers of MCM-22, was prepared from as-made MCM-22 by delamination in base conditions [2]. However, the serious dealumination may happen during the delamination process. Layered MCM-36 could be also prepared by pillaring as-made MCM-22 with silica but the coverage of acid sites of zeolite is inevitable during the pillaring, which results in the loss of catalytic active sites.

In the present work, a layered zeolite with MWW structure, denoted as SRZ-21, was successfully prepared by using the mixture of organic silane and inorganic silica as the raw materials. The structure of the SRZ-21 zeolite was investigated by X-ray diffraction (XRD), transmission electron microscopy (TEM) and nuclear magnetic resonance (NMR). The SRZ-21 zeolites were evaluated for the benzene alkylation reaction with propylene and the di-isopropylbenzene (DIPB) transalkylation reaction with benzene.

2 Experimental

The SRZ-21 was prepared according to the recipe described in U.S. patent 8,030,508[4]. A mixture of sodium hydroxide, sodium aluminate, silica sol, hexamethyleneimine, organic silicon and water were introduced to a stirred autoclave and held at 130-175 ^{o}C for 20-120 hours. The product was then filtered, washed and dried. The SRZ-21 zeolite with a molar ratio of SiO_2/Al_2O_3 of 42.1 was obtained.

3 Results and discussion

TEM images reveal that the thickness of the single-layer of the SRZ-21 zeolite is around 2.6 nm, which is much thinner than that of the MCM-22. The thinner layers of the SRZ-21 provide a larger pore volume compared to that of MCM-22(1.66 versus 1.20 cm^3/g), which benefits the molecular diffusion and favours the macro-molecule organic reactions. The broad peaks at 8.2, 9.5, 15.9 and 22.6^{o} of the XRD pattern (as shown in Fig. 2) confirm the highly non-uniform layer structure of SRZ-21. Figure 3 compares Si^{29}NMR spectra of the zeolites. The resonance peaks at -5 to -26 ppm observed on the SRZ-21 reveal complex chemical coordination of organic silicon in SRZ-21, while the weaker peaks at -103 and -97 ppm indicate that the addition of organic silane greatly reduces the amount of silicon hydroxyl group on layer surface and therefore suppresses further condensation of layer structure of SRZ-21.

Table 1 lists the reaction results of SRZ-21 for benzene alkylation with propylene. The catalyst was evaluated at 170°C with a benzene/propylene molar ratio of 2.5. The propylene weight hourly space velocity (WHSV) was 5.2 h^{-1}. As Table 2 indicates, after 120 hours reaction, propylene conversion maintains at 100%, cumene selectivity remains around 88% and the concentration of the n-propylbenzene (NPB) in cumene is below 330 ppm. Transalkylation reaction takes place at 190 °C with a benzene/DIPB weight ratio of 2.5. The DIPB WHSV was 2.0 h^{-1}. As Table 2 indicates, after 200 hours reaction, DIPB conversion maintains at around 60%, propyl group selectivity remains nearly 100%, and the concentration of NPB in cumene is below 550 ppm. Therefore, SRZ-21 exhibits excellent activity, selectivity and stability for benzene alkylation with propylene, and also for DIPB transalkylation. In addition, impurity NPB can be controlled at a quite low concentration.

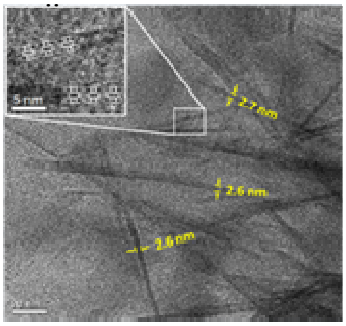

Fig. 1. TEM image of the SRZ-21

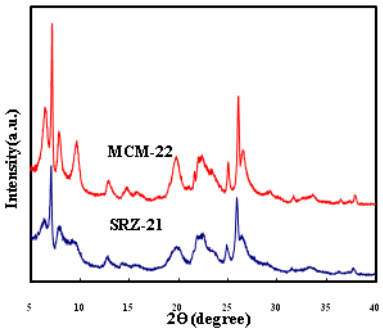

Fig. 2. XRD patterns

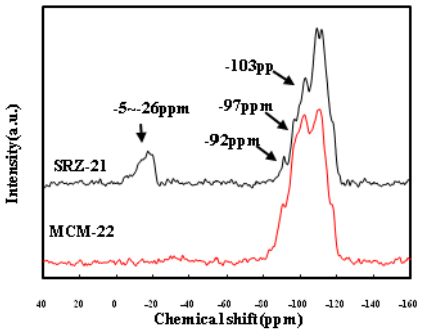

Fig. 3. Si^{29} NMR spectra

Table 1. Benzene Alkylation Reaction with Propylene over SRZ-21.

Reaction time (h)	Propylene conversion (%)	Cumene selectivity (%)	NPB/IPB (ppm)
24	~100	88.5	280
120	~100	88.7	320

Table 2. DIPB Transalkylation Reaction with Benzene over SRZ-21.

Reaction time (h)	DIPB conversion (%)	Propyl selectivity (%)	NPB/IPB (ppm)
48	59.68	~100	565
200	60.40	~100	537

4 Conclusion

Layered zeolite SRZ-21 comprising organic silicon in framework is successfully synthesized by using a mixture of the organic silane and silica sol as the silicon sources. SRZ-21 could be prepared at a wider Si/Al mole ratio range. The layer structure of SRZ-21 is stable during crystallization. The characterization results proved that the layered structure remains unchanged after calcinations and the organic silicon species mainly locates between the layers of zeolite crystal. The catalytic performances demonstrate that SRZ-21 has excellent activity, selectivity and stability for benzene alkylation reaction with propylene, and also is a good catalyst candidate for DIPB transalkylation reaction.

References

[1] M.K. Rubin, P. Chu, US. Patent 4,954,325, 1990.
[2] A. Corma, U. Diaz, V. Fornés, et al., Journal of Catalysis 191 (2000) 218-224.
[3] A. Corma, V. Fornés, J. Martínez-Triguero, et al., Journal of Catalysis 186 (1999) 57-63
[4] H.X. Gao, B. Zhou, Y.L. Wei, et al., US. Patent 8,030,508, 2011.

I-OP02

Relationship between the Crystal Morphology and Acidity of the *BEA-type Zeolites and the Resistance to Coke Formation during Ethanol to Hydrocarbons Transformation

Astafan A.[1,2], Benghalem M.A.[1], Belin T.[1], Pouilloux Y.[1], Patarin J.[2], Bats N.[3], Bouchy C.[3], Pinard L.[1*], Daou T.J.[2]

1 - Institut de Chimie des Milieux et Matériaux de Poitiers, Poitiers, France
2 - Université de Strasbourg, Université de Haute Alsace, Equipe Matériaux à Porosité Contrôlée (MPC), Institut Science des Matériaux de Mulhouse (IS2M), ENSCMu, Mulhouse, France
3 - IFP Energies nouvelles, Rond-point de l'échangeur de Solaize, Solaize, France

* ludovic.pinard@univ-poitiers.fr

Keywords: zeolite *BEA, nano-sponge, deactivation, coke, Ethano to hydrocarbons

1 Introduction

The deactivation of acid zeolites involved in hydrocarbon transformation are mainly due to the retention of carbonaceous compounds (coke) inside the pores. The creation of mesopores by post-synthesis treatments zeolites is both a simple and efficient tool to mitigate catalyst deactivation by coking. The presence of mesopores, close to the Brønsted acid sites, greatly improves the stability of such hierarchical catalyst by favoring the fast desorption of products. This enhanced stability is not due to a decrease in coke toxicity, but rather an inhibition of the growth of coke precursors, in turn related to the shorter diffusion path length (DPL) of reactants and products [1]. But, the reduction of DPL by post-synthesis treatments is limited; indeed, earlier desorption experiments evidenced a 4-fold reduction in DPL upon hierarchization of ZSM-5 zeolites by alkaline leaching, irrespective of their parent's conventional micro- and nano-crystals. The shortest DPL in zeolites can be obtained by reducing the crystal thickness up to a single unit cell dimension. In 2009, Ryoo and co-workers christened the dawn of new zeolitic materials, by using specifically designed bifunctional compounds including at least two quaternary ammonium functions directing the formation of different zeolites (MFI, *BEA), linked by an alkyl spacer, and a hydrophobic alkyl chain inhibiting a further growth of the material [2]. They obtained ultrathin zeolite structures (MFI, *BEA) with a controllable thickness combined with an ordered or desordered mesoporosity. By using gemini-type quaternary ammonium surfactants as a structure–directing agent, DPL in a MFI nano-sheets was only of 2 nm. An ultra-short DPL favors the mass transfer of products enhancing in consequence the zeolite stability in reactions sensitive to coking (e.g. methanol-to-gasoline and methanol to propylene). It should be underscored that the studies concerning the nano-sheet zeolites currently focus rather on the MFI structure than on the *BEA.

In this study, three *BEA zeolites (Si/Al ~ 20) with crystallite size ranging from micrometer to nanometer were synthesized (one micro-crystal (MC), one nano-crystal (NC) and one nano-sponge (NS)) in order to establish a relation between the textural properties of the catalyst and it's lifetime. The transformation of ethanol to hydrocarbons is a reaction highly sensitive to the texture properties of the material. Such a model reaction is therefore a good proxy to investigate the correlation between the crystal morphology of the *BEA-type zeolites and the resistance to coke formation.

2 Results and discussion

A micro-sized, nano-sized and nano-sponge H*BEA zeolites with a Si/Al ratio of 23 were synthetized and tested on ethanol-to-hydrocarbons transformation. The micro-sized *BEA

zeolite is a typical microporous material, whereas the nano-sponge material is a hierarchical material constituted of micropores interconnected to an ordered mesoporores network (Fig. 1).

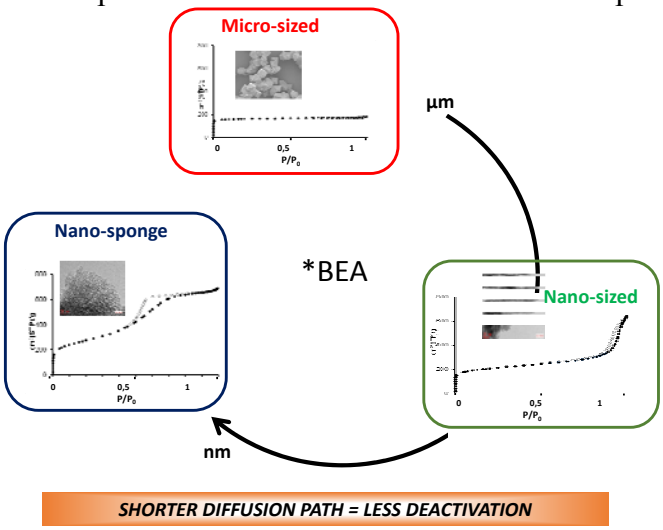

Fig.1. Scanning electronic (SEM), transmission electronic microscopy (TEM) images and Adsorption/desorption isotherms at -196 °C of micro-crystal (MC) , nano-crystal (NC) and nano-sponge (NS) *BEA-type zeolites.

The synthetize of nano-sponge zeolite material needs the use of a gemini-type quaternary ammonium surfactant. Regardless of the textural properties of *BEA zeolites, EtOH dehydrates into ethylene via diethyl-ether, and ethylene oligomerization leads to unwanted formation of coke which provokes a total pore blockage. The dehydration reaction is less affected by carbon deposition, since it occurs on weak acid sites located on the pore mouth and/or on external surface.

The coke composition depends on the shape and dimensions of the *BEA zeolite pores, the structures of molecules trapped inside the zeolite micropore are limited to polyalkyl-benzenes, -naphtene –anthracenes and –pyrenes, but their growth are related to the diffusion path length. The diminution of the crystallite size enhances the molecular traffic of reactants and products. To prevent consecutive reactions such as the autocatalytic formation of poly-aromatics compounds, the diffusion path length must be extremely short. Its dimension does not must exceed the length of few zeolite unit cells (i.e. 2 nm). It should be underscored that the desorbed coke precursor can be trapped on silanols and/or Lewis acid sites; the impact of the external coke has none impact on the catalyst stability.

Unfortunately, the extreme diminution of the crystallite size, obtained only with nano-sponge zeolite, modifies probably the electronic environment of aluminum atoms in the zeolite framework, which weakens the strength of the Brønsted acid sites. Increasing the external surface and consequently the number of pore mouth provides also a signal advantage during catalyst regeneration by coke combustion: the accessibility of reactant (e.g. oxygen) to molecule trapped inside the zeolite micropore is greatly facilitated.

Finally, the catalyst activity as well as coke oxidation rate depend on the strength of acid sites, but the weaker acid on nano-sponge *BEA zeolite is counterbalanced by a better mass transfer of reactants and products in the micropores.

Acknowledgements

The authors thank IFPEN for its financial support and Syrian government for the doctoral grant given to A. Astafan.

References

[1] M. Choi, K. Na, J. Kim, Y. Sakamoto, O. Terasaki, R. Ryoo, Nature, 461 (2009) 246.
[2] F. Ngoye, L. Lakiss, Z. Qin, S. Laforge, C. Canaff, M. Tarighi, V. Valtchev, K. Thomas, A. Vicente, J. P. Gilson, Y. Pouilloux, C. Fernandez, L. Pinard, J. Catal., 320 (2014) 118.

I-OP03

Gold-Based Yolk-Shell Nanoreactors. Enhancement of Catalytic Performance via Gold Cores Decoration with Ceria or Pd

Evangelista V.[1], Acosta B.[1], Miridonov S.[2], Pestryakov A.[3], Fuentes S.[4], Simakov A.[4*]

1 - Centro de Investigación Científica y de Educación Superior de Ensenada (CICESE), Posgrado en Física de Materia les, Ensenada, México

2 - Centro de Investigación Científica y de Educación Superior de Ensenada (CICESE), Departamento de Óptica, Ensenada, México

3 - Tomsk Polytechnic University, Department of Technology of Organic Substance and Polymer Materials, Tomsk, Russia

4 - Centro de Nanociencias y Nanotecnología, Universidad Nacional Autónoma de México (CNyN-UNAM), Departamento de Nanocatálisis, Ensenada, México

* andrey@cnyn.unam.mx

Keywords: gold decoration, palladium, nanoreactors, ceria

1 Introduction

Gold nanoparticles (Au NPs) have a great potential in many reactions important for environmental protection, such as reduction of nitro-aromatic compounds, CO oxidation, water-gas shift reaction, and different reactions of fine chemistry [1-4]. However, they easily aggregate due to their high surface energy, resulting in changes in the size and shape of the NPs during the catalytic reaction with the consequent decay in their catalytic activity [5]. Yolk-shell materials (nanoreactors, NRs) represent a new generation of heterogeneous catalysts with excellent catalytic stability due to their specific structure, which consists of a core, commonly the active phase, surrounded by a porous shell in a core@void@shell arrangement [6] which acts as a physical barrier between the nuclei preventing their agglomeration and their further deactivation by keeping them isolated from each other.

According to the commonly reported diameter of oxide shell pores (2.5-5 nm), the size of the metal core should be above 5 nm in order to prevent its free release from the porous shell [7]. A significant decrease in pore size causes diffusion problems particular for the reactions of fine chemistry including relatively large molecules. One way to enhance the catalytic performance of NRs with relatively large pores and cores is decoration/doping of their cores [8,9].

Herein, we propose to enhance catalytic performance of $AuSiO_2$ and $Au@ZrO_2$ yolk-shell NRs well presented in the literature via decoration of their Au cores with ceria or Pd.

2 Experimental

The non-decorated $AuSiO_2$, $AuZrO_2$ NRs and those decorated with Pd ($AuPd@SiO_2$ and $AuPd@ZrO_2$) were synthesized following the conventional bottom-up route [10] presented in Fig. 1. Au cores partially covered with Pd (molar ratio Au20:Pd1) were homogeneously encapsulated into silica shells to form $AuPd@SiO_2$ NRs via usage of high PVP concentration and prolonged time of nanoparticles treatment with PVP before bimetallic nanoparticles encapsulation. $Au\text{-}CeO_2@ZrO_2$ NRs (gold core encapsulated into porous zirconia shell and doped by ceria) were synthesized via a new proposed route (Fig.1) [11]. Au cores encapsulated into SiO_2 ($Au@SiO_2$) were decorated with ceria via injection of ceria precursor into a void space of silica shell (formed through surface-protected etching of silica by hot water) with its subsequent hydrolysis and thermal treatment ($Au\text{-}CeO_2@SiO_2$). $Au\text{-}CeO_2@ZrO_2$ nanoreactors were obtained using $Au\text{-}CeO_2@SiO_2$ as a template and replacement of SiO_2 by ZrO_2. The prepared NRs characterized by STEM-EDS, XPS, in situ and ex situ UV-Vis spectroscopy, and N_2 thermal ad-sorption were tested in

the reduction of nitrophenols into corresponding amino-phenols and in CO oxidation.

3 Results and discussion

The catalytic activity for decorated Au-CeO_2@ZrO_2 and AuPd@ZrO_2 NRs in the 4-nitrophenol reduction was found to be 3 and 2.6 times higher than for non-decorated Au@ZrO_2 NRs, respectively. The high affinity of ceria for the 4-nitrophenol adsorption strongly enhances the catalytic activity of the decorated Au-CeO_2@ZrO_2 NRs via activation of additional route of the 4-nitrophenol reduction through condensation of the reaction intermediates. Enhancement of the catalytic activity for decorated NRs was found in CO oxidation as well. The enhanced activity of Au-ceria or AuPd NRs in CO oxidation may be explained by activation of oxygen on ceria and by electronic interactions between Pd and Au, respectively.

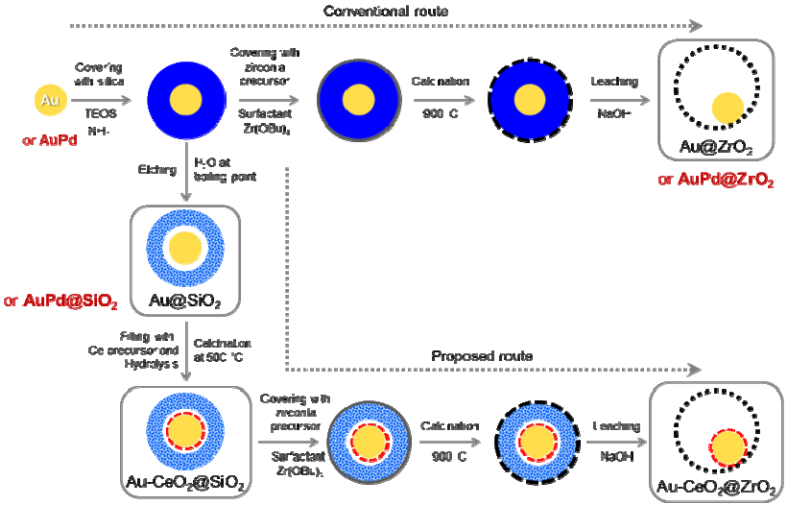

Thus, herein proposed route of nanoreactor core decoration may be successfully applied for the synthesis of nanoreactors with cores modified with different materials in order to make them highly effective for different catalytic reactions.

Acknowledgements

The authors thank O. Callejas, J. Mendoza, E. Flores, F. Ruiz, J. Peralta and M. Sainz for technical assistance. This research project was partially supported by CONACyT (México) and PAPIIT-UNAM (México) through Grants 179619 and 203813, respectively.

References

[1] M. Haruta, T. Kobayashi, H. Sano, N. Yamada, *Chemistry Letters* 16 (1987) 405–408.
[2] M. Stratakis, H. Garcia, *Chemical Reviews* 112 (2012) 4469–4500.
[3] Q. Fu, S. Kudriavtseva, H. Saltsburg, M. Flytzani-Stephanopoulos, *Chemical Engineering Journal* 93 (2003) 41–53.
[4] A. Corma, H. Garcia, *Chemical Society Reviews* 37 (2008) 2096–2126.
[5] J.A. Lopez-Sanchez, N. Dimitritos, C. Hammond, G.L. Brett, L. Kesavan, S. White, P. Miedziak, R. Tiruvalam, R.L. Lenkins, A.F. Carley, D. Knight, C.J., Kiely, J. Hutchings, *Nature Chemistry* 3 (2011) 551–556.
[6] I. Lee, M. Albiter, Q. Zhang, J. Ge, Y. Yin, F. Zaera, *Physical Chemistry Chemical Physics* 13 (2011) 2449–2456.
[7] R. Güttel, M. Paul, C. Galeano, F. Schüth, *Journal of Catalysis* 289 (2012) 100–104.
[8] R. Güttel, M. Paul, F. Schüth, *Catalysis Science & Technology* 1 (2011) 65–68.
[9] X. Fang, Z. Liu, M.-F. Hsieh, M. Chen, P. Liu, C. Chen, N. Zheng, *ACS Nano*, 6-5 (2012) 4434–4444.
[10] P. M. Arnal, M. Comotti, F. Schüth, *Angewandte Chemie International Edition* 45 (2006) 8224–8227.
[11] V. Evangelista, B. Acosta, S. Miridonov, E. Smolentseva, S. Fuentes, A. Simakov, *Applied Catalysis, B, Environmental* 166-167 (2015) 518–528.

I-OP05

Selective Catalysis with Metal Nanoparticles Encapsulated in Porous Materials

Abildstrøm J., Gallas Hulin A., Mielby J., Kegnæs S.*

Technical University of Denmark, Department of chemistry, Lyngby, Denmark

* skk@kemi.dtu.dk

Keywords: zeolites, nanoparticles, gold, encapsulation, TEM, oxidaiton

1 Introduction

In spite of the great technological, environmental and economic interests, general methods for the stabilization of metal nanoparticles against sintering are missing. Although for some specific systems it has been achieved by optimizing the interaction of nanoparticles with a support material or by encapsulation of the metal particles [1-3]. However, these known catalytic systems are in general rather expensive and difficult to synthesize and they cannot be produced in the industrial scale. Therefore, the development of novel sintering stable heterogeneous nanoparticle catalysts, which find use in the chemical industry, is of great importance.

Recently, we have developed several different catalytic systems where metal nanoparticles are confined in different porous materials. As an example gold nanoparticles were encapsulated inside of the silicalite-1 zeolite [4].

First of all, the aim with encapsulation of metal nanoparticles in a porous matrix like a zeolite is to prevent the nanoparticles from sintering during a high temperature catalytic reaction. Furthermore, the porous matrix can also contribute actively to the catalytic reaction: the presence of charge-compensating cations within the inorganic frameworks introduces additional active sites, such as acid sites for instance and their strength and concentration can to some extent be tailored for a particular application. Moreover, in our work we have shown that the metal nanoparticles encapsulated in zeolite materials are only accessible through the pores, which highly favour size-selective reactions.

Here we present the progress that has been made on the synthesis of metal nanoparticles confined in different porous materials and their application in catalysis.

2 Experimental

All the obtained materials were synthesized from commercially available chemicals. All zeolites were prepared using traditional synthesis methods known from the literature. Preparation of different recrystallized zeolites containing metal nanoparticles were based on the impregnation procedure of recrystallized silicate-1 material obtained by an alkaline dissolution-reassembly process in the presence of the surfactant [4].

We have tested all obtained materials as catalysts in the different selective oxidation and hydrogenation reactions. Furthermore, we have characterized the prepared materials with various techniques including SEM, in situ TEM, STEM, TEM tomography, XPS, XRF, BET and XRD among others.

3 Results and discussion

Here, the progress that we have made on the synthesis of metal nanoparticles confined in different zeolite materials is presented. As an example the composite material containing gold

nanoparticles trapped inside a silicalite-1 zeolite is shown in in Figure 1. The gold nanoparticles are 2–3 nm in diameter and the particles are only situated inside the zeolite. The obtained material was also characterized by X-ray photoelectron spectroscopy (XPS). The XPS also confirms that the metal particles are only located inside of the zeolite framework. Additionally, this prepared material with encapsulated nanoparticles has demonstrated to be highly active and selective for the catalytic gas-phase oxidation of ethanol to acetaldehyde.

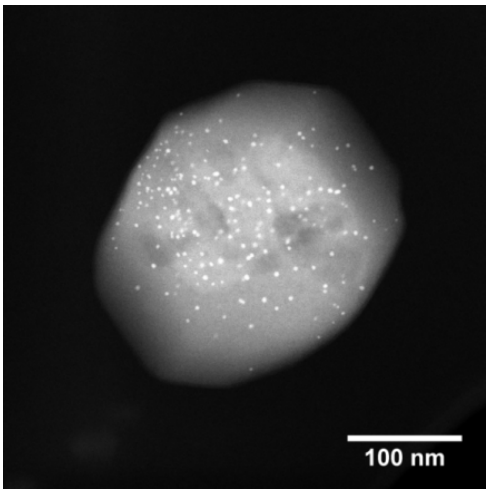

Fig. 1. STEM image of gold nanoparticles encapsulated in silicalite-1.

Furthermore, all obtained materials modified with metal nanoparticles confined in different porous materials were tested as selective catalysts in different reactions and characterized with various techniques including SEM, TEM tomography, XRF, BET and XRD among others.

4 Conclusions

In conclusion, we have developed several simple and effective methods for encapsulation of metal nanoparticles in different porous materials. The methods are cost-effective, practical, and result in a narrow size distribution of small nanoparticles that are situated inside the porous materials. Furthermore, the materials showed catalytic activity and selectivity in a number of test reactions.

Acknowledgements

The authors gratefully acknowledge the support of the Danish Council for Independent Research, Grant No. 12-127580.

References

[1] Arnal P.M., Comotti M., Schüth F., *Angew. Chem. Int. Edit.* (2006), 45, 8224; *Angew. Chem.* (2006), 118, 8404
[2] Y. Dai et al., Angew. Chem. Int. Ed. 49 (2010) 1.
[3] A. B. Laursen et al., Angew. Chem. Int. Ed. 49 (2010) 3504.
[4] Mielby J., Abildstrøm J.O., Wang F., Kasama T., Weidenthaler C., Kegnæs S., *Angew. Chem.* (2014) 126, 1-5

I-OP06

Ethene Oligomerization in Ni-based Zeolites: Experimental and Theoretical Investigations of the Reaction Mechanism

Henry R.[1*], Brogaard R.Y.[1], Ganjkhanlou Y.[2], Berlier G.[2], Bleken B. T.[1], Groppo E.[2], Olsbye U.[1], Bordiga S.[1,2]

1 - Department of Chemistry, University of Oslo, Oslo, Norway
2 - Dipartimento di Chimica and NIS, Università di Torino, Torino, Italy

* reynald.henry@smn.uio.no

Keywords: alkene, oligomerization, nickel, zeolite, reaction mechanism

1 Introduction

Ethene oligomerization is one of the major processes for producing linear and branched higher alkenes such as propene and butadiene, precursors of several commercial chemicals used in plastics, lubricants and surfactants [1]. The process is performed industrially using homogeneous catalysts in organic solvents. Heterogeneous catalysis in principle offers substantial environmental and practical benefits, avoiding use of toxic solvents and facilitating catalyst separation and reusability. However, heterogeneous catalysts for ethene oligomerization generally suffer from low activity compared to their homogeneous counterparts. Presently, Ni-containing inorganic porous materials are the most important heterogeneous catalysts for ethene oligomerization [1]. Both Ni^{+} and Ni^{2+} ions have been proposed as the active sites in the reaction [1,2], but knowledge of the reaction mechanism is quite limited.

In this work we investigate ethene oligomerization in nickel-containing zeolites, combining operando infrared (IR) spectroscopy, periodic density functional theory (DFT) calculations, micro-kinetic modeling and catalytic testing. Based on the results, we propose a catalytic cycle analogous to the traditional Cossee-Arlman mechanism used in homogeneous catalysis (shown for ethene dimerization in Figure 1 (left)).

2 Materials and Methods

The fully periodic, spin-unrestricted DFT calculations employed the BEEF-vdW functional [4] accounting for dispersion interactions and were conducted using Quantum Espresso [5]. The calculations employed the AFI framework. The super cell contains one Al/Si substitution (Si/Al = 47) balancing the positively charged extra-framework Ni species in the catalytic cycle (see Figure 1). Vibrational frequencies were calculated in the harmonic approximation and used to derive free energies and to simulate IR spectra. CatMAP [6] was used for DFT-based micro-kinetic modeling of ethene dimerization, deriving a steady-state solution.

The experiments employed Ni^{2+}-exchanged and -impregnated H-ZSM-5 (Si/Al = 51-59), both as conventional microcrystals and as nanosheets [3]. Catalytic tests were carried out in a plug-flow reactor at temperatures ranging from 50 to 300 °C under atmospheric pressure, with 0.3 bar of ethene and helium as an inert carrier gas. The effluent was analyzed by gas chromatography. Fourier Transform IR spectra were measured in transmission mode both in static and in operando conditions by dosing CO or ethene on samples activated in vacuum/O2 or He/O2 flow, respectively. The evolution of adsorbed species on the catalyst surface was followed by the IR instrument, coupled to a mass spectrometer for gas phase product analysis.

3 Results and discussion

In the IR experiments the CO probe was employed to get information on the nature and

distribution of Ni ions in the ZSM-5 zeolite channels. The results indicate the presence of Ni^{2+} counter-ions, but also of $Ni(OH)^+$ and NiO_x species, stabilized either as counter-ions or grafted to defective hydroxyl nests. When heating the catalysts in vacuum we observed a partial self-reduction of Ni^{2+} ions.

We propose a catalytic cycle as shown for ethene dimerization in Fig. 1 left, based on Ni(II) species charge-balanced by one Al/Si substitution in the zeolite framework. We calculated the corresponding free energy profile using DFT and used it for micro-kinetic modeling. The model suggests that at typical reaction temperatures, around 150 °C the dimerization rate is limited by desorption of the product alkene, indicating that it will keep growing by additional reactions with ethene until it blocks the pore system and deactivates the catalyst. This hypothesis is supported by the operando IR experiments, where long alkyl chains are observed on the zeolite catalysts, and catalytic tests showing rapid deactivation (Fig. 1 right).

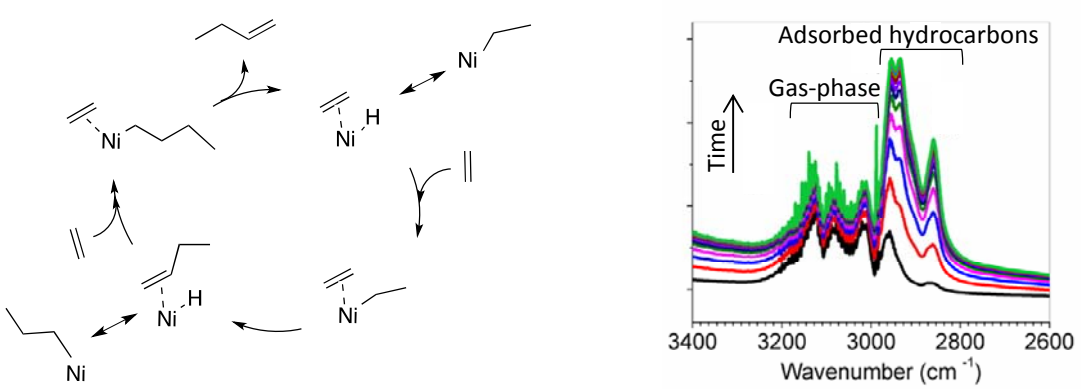

Fig. 1. (left) The catalytic cycle considered in the micro-kinetic model of ethene dimerization catalyzed by zeolite-supported Ni(II) species. (right) IR spectra in operando conditions (150 °C and 20 mL/min ethene), showing build-up of alkyl chains.

4 Conclusions

This work proposes and models a catalytic cycle of ethene oligomerization in Ni-based zeolite catalysts, which is supported by experimental observations. The work hence provides a starting point for identifying rate-limiting factors with the aim of improving the performance of nickel-based zeolite materials.

References

[1] A. Finiels, F. Fajula, V. Hulea, *Catal. Sci. Technol.* 4, 2412 (2014).
[2] A. Martínez, M. A. Arribas, P. Concepción, S. Moussa, *Appl. Catal. A* 467, 509 (2013).
[3] B.T. Bleken, D. Wragg, B. Arstad, A. Gunnæs, J. Mouzon, S. Helveg, L. Lundegaard, P. Beato, S. Bordiga, U. Olsbye, S. Svelle, K. Lillerud, *Top Catal.* 56 (2013) 558-566.
[4] J. Wellendorff, K. T. Lundgaard, A. Møgelhøj, V. Petzold, D. D. Landis, J. K. Nørskov, T. Bligaard, K. W. Jacobsen, *Phys. Rev. B* 85, 235149 (2012).
[5] Quantum Espresso suite, *http://www.quantum-espresso.org*.
[6] Medford, A. J. CatMAP, *https://github.com/ajmedford/catmap/wiki*.

I-OP07

Synthesis, Characterization and Catalytic Study of Ni Supported Apatite-Type Lanthanum Silicates in Glycerol Steam Reforming Reaction

Pandis P.[1], Charisiou N.[2], Goula M.[2], Stathopoulos V.N.[1*]

1 - Laboratory of Chemistry and Materials Technology, School of Technological Applications, Technological Educational Institute of Sterea Ellada, Psahna, Chalkida, Greece

2 - Department of Environmental and Pollution Control Engineering, School of Technological Applications, Technological Educational Institute of Western Macedonia, Koila, Kozani, Greece

* vasta@teihal.gr

Keywords: heterogeneous, catalysis, apatites, glycerol steam reforming

1 Introduction

Although rare earth apatites have attracted interest as promising solid oxide fuel cell [1-3] electrolytes, over the last years their catalytic application studies are increased. Recently research groups have reported the use of such materials as a support instead of γ-Al_2O_3 of platinum catalysts at de-NO_X by propylene or propylene oxidation [4-6]. It has been observed that the doping effect of the apatite structure with Al of Fe provides an excess of interstitial oxygen ions in the lattice which contributes to the increase of catalytic activity in the oxidative coupling of methane [7]. Recent research efforts have focused on the surplus of glycerol associated with biodiesel production in order to contribute to the need for hydrogen production from various feedstocks such as hydrocarbons, water and derivatives of biomass. The glycerol steam reforming reaction has been investigated on various catalysts and Ni appears as the most promising active metal, due to its property to promote the C–C rupture. [8].

In this study, $La_{9.83}Si_{6-x-y}Fe_xAl_yO_{26\pm\delta}$, apatites were prepared by solid state reaction and characterized for their structural properties. These materials were impregnated with Ni and were systematically studied for their catalytic activity in the glycerol steam reforming (GSRM) reaction. A comparison with Al_2O_3 supported Ni catalysts is performed.

2 Experimental

$La_{9.83}Si_{6-x-y}Fe_xAl_yO_{26\pm\delta}$ apatite materials e.g $La_{9.83}Si_{4.5}Fe_{1.5}O_{26\pm\delta}$ (LFSO) and $La_{9.83}Si_{4.5}Al_{0.25}Fe_{0.75}O_{26.5\pm\delta}$ (LAFSO) were prepared by solid state synthesis mixing stoichiometric amounts of oxides and annealing at 1000°C for 2h. The powders were mechanically milled and uniaxial pressed into pellets and sintered at 1450°C-1500°C. Crystal phases were identified by XRD and microstructure by SEM. Pellets were crashed and milled. A powder size fraction -425μm +350 μm was used as support for the Ni wet impregnation. Porosity was measured by means of the Archimedes method. The Ni catalysts were prepared by the wet impregnation method using $Ni(NO_3)_2 \cdot 6H_2O$, aqueous solutions to a final catalyst loading of Ni equal to 8 % wt. After impregnation, the catalysts were air-dried overnight and calcinated at 800°C for 4 hours. Reduced samples were produced under 50ml/min of pure hydrogen (H_2) flow for 2 hours at 800°C. Apatite oxides and catalyst (fresh, reduced and used) samples were characterized by means of the XRD and SEM. Catalytic tests were performed using a fixed bed reactor at temperatures ranging from 450°C to 750°C with a feed consisting of $C_3H_8O_3$ (20% v/v.) and H_2O in the liquid phase. The amount of catalyst used in the catalytic bed was 200 mg. Catalytic performance was studied in order to investigate the effect of the reaction temperature on (i) glycerol conversion, (ii) hydrogen yield, (iii) H_2/CO molar ratio, and (iv) gas and liquid products concentration of the produced gas mixtures at the outlet of the reactor.

3 Results and Discussion

Figure 1 shows the XRD spectra of single phase apatite supports and the catalytic results of the concentrations of gaseous products of the GSRM reaction.

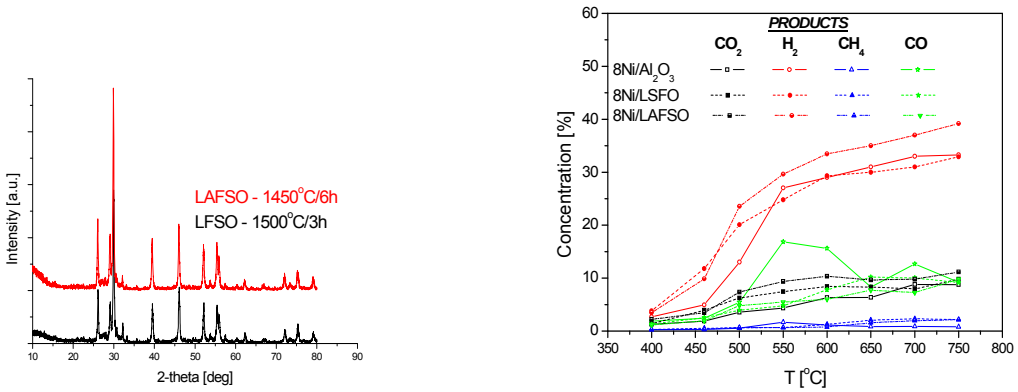

Fig. 1. XRD spectra (left) and catalytic results (right)

Ni/apatite catalysts provided a glycerol conversion close to 100% for the whole range of temperatures and a higher H_2 concentration at the gaseous products even for low temperatures, ranging between 25 and 40 % v/v for 500-750 ^{o}C. Moreover, CO_2 and CO concentrations were rather constant having the values of 10 and 5% v/v for the aforementioned temperature range, respectively. Liquid products as acetol, acetone, allyl alcohol, acetic acid and acetaldehyde were detected only for T<700 ^{o}C and at rather low concentrations.

4 Conclusions

The synthesis and the preparation of Ni/ATLS catalysts were successfully prepared through the wet impregnation technique. The performance of Ni/ATLS catalysts in the GSRM reaction exhibited higher performance in comparison with Al_2O_3 supported Ni catalysts even from lower temperatures.

Acknowledgements

Financial support by the programs Archimedes III and THALIS implemented within the framework of Education and Lifelong Learning Operational Programme, co-financed by the Hellenic Ministry of Education, Lifelong Learning and Religious Affairs and the European Social Fund, Projects: 'Synthesis, Characterization and study of properties of solid electrolytes of the apatite structure for fuel cell applications - APACELL' and 'Production of Energy Carriers from Biomass by Products. Glycerol Reforming for the Production of Hydrogen, Hydrocarbons and Superior Alcohols', is gratefully acknowledged.

References

[1] H. Gasparyan et al, ECS Trans., 25 (2009), 2681.
[2] H. Gasparyan et al, Solid State Ionics, 192 (2011) 158
[3] V.Sadykov et al, Solid State Ionics, In Press, Corrected Proof, Available online 25 November 2014
[4] A. Ono, M. Abe, S. Kato, M. Ogasawara, et al., Appl. Catal., B., 103 (2011) 149.
[5] S. Kato, T. Yoshizawa, N. Kakuta, S. Akiyama, et al., Res. Chem. Intermed., 34 (2008) 703.
[6] T. Wakabayashi, S. Kato, Y. Nakahara, M. Ogasawara, et al., Catal. Today, 164 (2011) 575.
[7] X.H. Zhang, X.Yi, J. Zhang, Z. Xie, J. Kang, L. Zheng, Inorg. Chem., 49 (2010) 10244.
[8] J.M. Silva, M.A. Soria, L.M. Madeira, Renew Sust Energ, Rev 42 (2015) 1187

I-OP08

Renewable Feedstocks for Refineries & Conventional Sulfided Catalysts

Horáček J.*, Kubička D.

Research Institute of Inorganic Chemistry, RENTECH-UniCRE, Litvinov, Czech Republic

* jan.horacek@vuanch.cz

Keywords: hydrotreating, vegetable oils, sulfided catalysts, bio-oil

1 Introduction

The higher use of renewable fuels required by the European directives 2009/28/EC and 2009/30/EC can be met only with increase in these fuels production. The directives promote in particular utilization of biofuels of the 2nd and 3rd generation and limit the use of the1st generation biofuels. The most popular conversion route is hydrothermal conversion of used cooking oils which are easy to convert in revamped common hydrotreating or hydrocracking units directly to diesel fuel. Another promising source is flash-pyrolysis bio-oil which could be obtained in significantly larger quantities than used cooking oils from a wide variety of biomass feedstocks. However, hydroprocessing of bio oils is more complicated because of its variable chemical properties and composition depending on the feedstock pyrolyzed. High water content, acidity and wide range of chemical functionalities are the key challenges. The presentation aims to compare the aspects of complete deoxygenation of the two most probable feedstocks (bio-oil and waste triglycerides) and to discuss the possibilities to improve the stability of hydroprocessing/hydrocracking catalysts.

2 Experimental/methodology

Hydrotreating and hydrocracking experiments of a model compound (rapeseed oil, food quality) were carried out in bench scale reactor with internal diameter 40 mm and overall length 110 cm. a thermowell (7 mm diameter) with thermocouples was installed in the axis of the reactor. Commercial NiW hydrocracking catalyst was crushed and sieved and the fraction 2-3 mm was used for experiments. The catalyst was activated using 1 % H_2S in hydrogen (refinery circulation gas) and feedstock with DMDS addition. Mild hydrocracking was performed at temperatures 350-390 °C and pressure 12.5 MPa. Hydrotreating was performed as coprocessing of atmospheric gas oil (AGO) with 10 % addition of rapeseed oil using a CoMo type commercial catalyst.

Hydroprocessing of bio-oil (purchased from BTG) has been investigated in bench scale reactor (id = 17 mm) at nonisothermal temperature profile using CoMo and NiMo hydrotreating catalysts. The experimental conditions used were analogous to those used in the work published by Elliott et al. [1]. The bio-oil study was focused on evaluating the feasibility of using commercial sulfide catalysts for bio-oil processing. Particle size selected for the tests was 0.5-1.0 mm. The beginning of the catalyst bed has been kept at 220 °C, the middle at 300 and the end at 370 °C. Bio-oil has been fed at WHSV = $0.2h^{-1}$. The performance of the CoMo catalyst has been investigated under hydrogen flow containing 0.08 vol. %, while in case of the NiMo catalyst hydrogen with higher sulfane content (1.6 vol.% in H_2) has been used. Samples of products were collected each 4 hours. Samples of gaseous products were also analyzed.

3 Conclusions

Hydrocracking of rapeseed oil resulted in its total deoxygenation without deactivation observed. SIMDIS (simulated distillation GC analysis) of products showed that middle distillate was the main product, containing only a minor amount of gasoline fraction. GC analyses

confirmed highly paraffinic nature of the product, which resulted in a high melting point of the middle distillate. In all the products, low sulphur content (<10 ppm) was observed.

Coprocessing of AGO with 10 % addition of rapeseed oil resulted in sulphur content bellow 10 ppm at temperatures 345 – 385 °C. Long term experiment showed slow deactivation that could be folowed by the slow change in physical parameters.

Bio-oil conversion over the CoMo catalyst produced a totally deoxygenated organic liquid. Changes in composition of the product pointed to a rapid decrease in the hydrogenation function of catalyst. Based on the observed fully coked catalyst bed (through the whole length of reactor) and rapid decrease in the hydrogenation activity, a higher dosing of sulfane donor agent was applied to improve the equilibrium [2] of competitive adsorptions to anionic vacancies. The following test, performed with a NiMo catalyst and with higher H_2S partial pressure, resulted in extending the test length (until reactor clogging) and changed deactivation specifics. All product samples consisted of clear organic and aqueous phases. The deactivation could be observed by the changing boiling point distribution (Fig. 1) during the time on stream. The change in fractions distributions [Fig. 1] shows a decrease in the cracking activity of the catalyst.

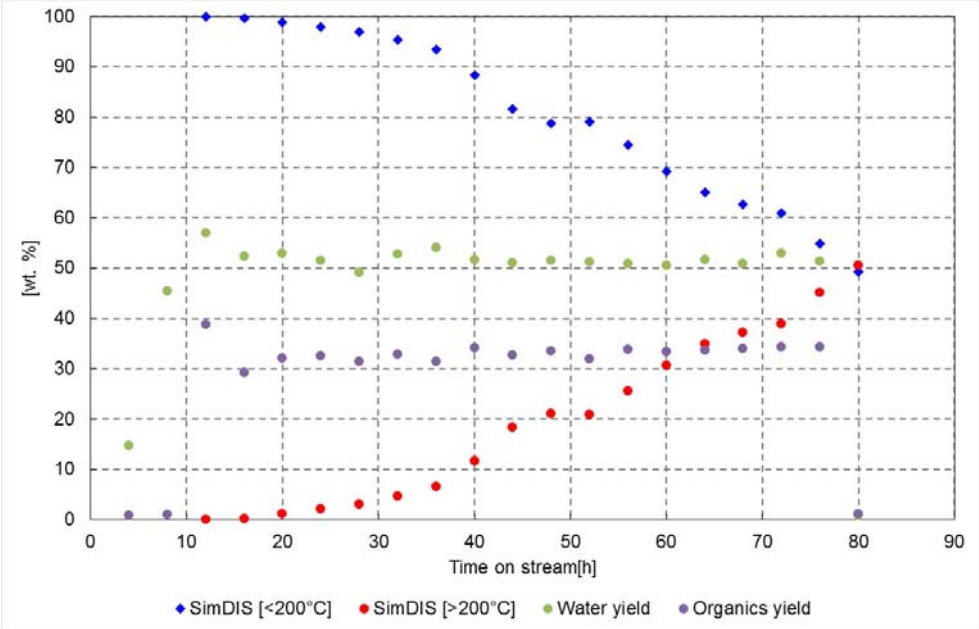

Fig. 1. Yields of products and organic phase fractions distribution

Acknowledgements

This publication was created in connection with the project Unipetrol research and education center Reg. CZ.1.05/2.1.00/03.0071, which is funded through the Operational Programme for Research and Innovation Development of the Structural Funds (specifically the European Regional Development Fund) and the state budget of the Czech Republic.

References

[1] D. C Elliott; T. R Hart; G. G. Neuenschwander; L. J. Rotness; M. V. Olarte,; A. H. Zacher; Y. Solantausta; Energy Fuels, 26, (2012) 3891−3896.

[2] E. Furimsky; F. Massoth; Catalysis Today, 17, (1993), 537-660

I-OP09

Towards Efficient Hydrodeoxygenation on Transition Metal Phosphides

Peroni M., Huang X., Lee I., Baráth E., Gutiérrez O.Y., Lercher J.A.*

Technische Universität München, Department of Chemistry and Catalysis Research Center, Germany

* Johannes.Lercher@ch.tum.de

Keywords: hydrodeoxygenation, palmitic acid, metal phosphides, citric acid

1 Introduction

Transition metal phosphides are an interesting option as catalyst for hydrodefunctionalization of biomass derived molecules, intrinsically more active than sulfides and more poison tolerant than most base or noble metals [1,2]. As newer synthesis methods have replaced the old high temperature routes, a wider variety of catalytic materials has become available [1]. In order to explore intrinsic catalytic properties of phosphides with high specific surface areas, a series of bulk phosphide catalysts (W, Mo, and Ni) was prepared by a route based on the addition of citric acid in the synthesis [3] and explored with respect to the hydrodeoxygenation of palmitic acid as a model compound for algae based feedstocks.

2 Experimental/methodology

The citrate method was adapted for the catalysts studied based on a temperature-programmed reaction (TPR). Citric acid was added during the precipitation of the precursor salts to obtain a gel, which was further treated sequentially in air and H_2 at 500°C - 650°C [3]. The materials were passivated after synthesis (1 vol.% O_2/N_2) and reactivated in situ in H_2 prior to physicochemical characterization or catalysis. The conversion of palmitic acid was performed in a trickle bed reactor at 180-300 °C and 40 bar.

3 Results and discussion

Two series of W-, Mo-, and Ni-phosphides were synthesized, one prepared by the conventional TPR techniques (denoted in the following as TPR-phosphides), the other with the citrate method described above (denoted in the following as CA-phosphides). In both cases, the phases obtained were WP, MoP, and Ni_2P according to XRD and elemental analysis. Materials synthesized using citric acid had a much higher specific surface area than the TPR-phosphides. Interestingly, the enhancement of the specific surface area depended on the nature of the transition metal, i.e., from < 5 to 11 m^2/g for WP, from 6 to 17 m^2/g for MoP, and from < 5 to 230 m^2/g for Ni_2P. Concomitant changes in the average crystal size were observed, i.e., from 35 to 27 nm for WP, from 29 to 22 nm for MoP, and from 132 to 49 nm for Ni_2P. As expected, CA-phosphides (which did not deactivate under the reaction conditions used) were much more active in the HDO of palmitic acid than the corresponding TPR-phosphides (Figure 1a). The conversion of palmitic acid follows two main routes, hydrodeoxygenation (HDO) and decarbonylation (DCO). The former is preferred and leads to hexadecanol as the main product below 300 °C (Figure 1b). The selectivity was also influenced by the preparation procedure, e.g., the DCO selectivity was lower on CA-phosphides than on TPR-phosphides. Comparing the performances of the CA-phosphides, surprisingly, the HDO activity was not proportional to the surface area of the materials. The activity increased as follows: $Ni_2P < WP \leq MoP$. This contrasting observation is related to residual carbon in the phosphides (quantified by elemental analysis), which forms a mesoporous structure (N_2-physisorption) that disperses the phosphide particles (TEM), but also decreases the available metal surface. Therefore, we conclude that two

opposite effects induced by residual carbon determine the activity. The intrinsic activity (TOF), determined from the concentration of accessible metal and the initial rates, increases with decreasing particle size. Differences in the selectivity to HDO are caused by intrinsic differences in the acid site concentrations of the studied materials.

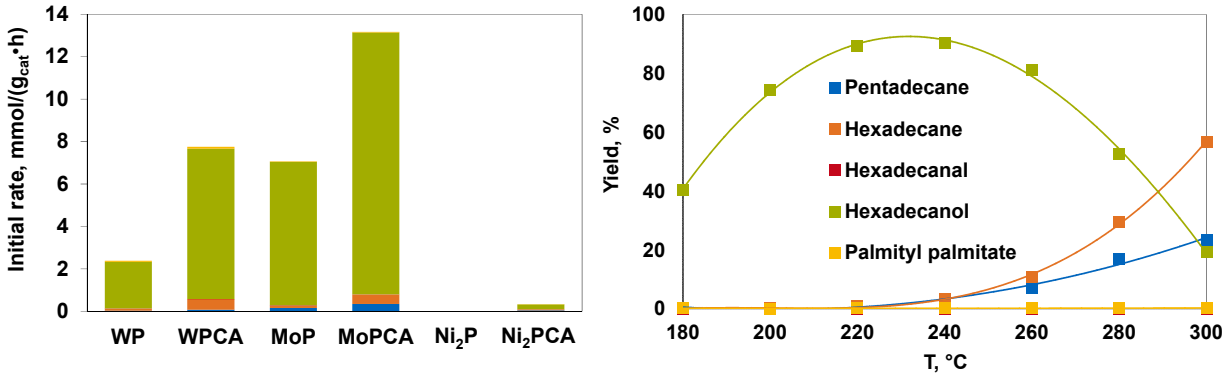

Fig. 1. (a) Comparison of the initial rate on TPR- and CA-phosphides at 240°C, 40 bar and 1h^{-1} (WHSV). (b) Product yield on CA-MoP as a function of temperature at 40 bar and 1h^{-1} (WHSV), H_2/palmitic acid molar ratio: 1000.

4 Conclusions

The use of citric acid during the synthesis leads to smaller crystals and higher specific surface areas of the CA- compared to the TPR-phosphides. This leads to higher intrinsic activity. The overall activity of the samples, however, is also influenced by residual carbon present after the CA-synthesis route. The product distribution depends on the intrinsic activity of the phosphides (Ni_2P, being the most selective material towards decarboxylation), and their acidity, which is required for key dehydration steps.

MoP CA is the most active catalysts. However, W-based phosphides are more selective to hexadecane C16 than Mo- and Ni- based phosphides.

References

[1] R. Prins, M. E. Bussell, *Catal. Lett.* 142 (2012) 1413.
[2] S. T. Oyama, *Journal of Catalysis* 216 (2003) 343.
[3] V. M. L. Whiffen, K. J. Smith, *Top Catal* 55 (2012) 981.

I-OP10

Catalytic Oxidative Desulfurization of Diesel Fuel as an Alternative to and Combination with HDS Process

Ismagilov Z.R.[1,2*], Kerzhentsev M.A.[1], Yashnik S.A.[1], Khairulin S.R.[1], Kuznetsov V.V.[1], Salnikov S.V.[1], Bourane A.[3], Jin Yaming[3], Koseoglu O.R.[3]

1 - Boreskov Institute of Catalysis SB RAS, Novosibirk, Russia
2 - Institute of Coal Chemistry and Material Science, Kemerovo, Russia
3 - Saudi Aramco, Research and Development Center, Dhahran, Kingdom of Saudi Arabia

* zinfer1@mail.ru

Keywords: oxidative desulfurization, dibenzothiophene family, deep desulfurization, Cu-Zn-Al catalyst

1 Introduction

New requirements for ultra-low sulfur content (10 ppm) in liquid motor fuels demand novel approaches for ultra-deep desulfurization. Thiols, mercaptans, thiophene and benzothiophene families are known to be removed effectively by hydrodesulfurization over sulfide $CoMo/Al_2O_3$ and $NiMo/Al_2O_3$ catalysts. The residuals sulfur (50-350 ppm) left in fuel is represented mainly by dibenzothiophene (DBT) and its derivatives. The compounds of the DBT family are rather resistant to removal by HDS. In addition, alkylsubstituted derivatives of DBT and naphtothiophene have high boiling points, resulting in their accumulation in high-boiling fractions during oil distillation.

The gas phase oxidative desulfurization (ODS) of motor fuels, initially proposed for desulfurizing petroleum fractions, may become a new promising technology for removal of refractory sulfur compounds [1]. Hydrogen peroxide, organic hydroperoxides, nitrous oxide, ozone, oxygen or air are suggested as oxidants. Some of these oxidants provide selective oxidation of heterocyclic sulfur compounds to sulfones and sulfoxides at 30-110°C and atmospheric pressure. Sulfones and sulfoxides, being polar compounds, are easily separated by extraction or adsorption from hydrocarbon fractions. It should be noted that alkylsubstituted DBT derivatives are easier subjected to oxidation in comparison with thiophene and benzothiophene, the steric hindrance becomes apparent only with an increase of the number of alkyl substituents in DBT.

We propose that the selective oxidation of sulfur-containing compounds over catalysts with oxygen is more perspective methods for diesel fuels desulfurization [2, 3]. During this process sulfide and heterocyclic sulfur-compound transform to sulfur dioxide, and hydrocarbon fragments are oxidized to carbon dioxide and water [1]. According to [4] CuZnAl-O catalysts can be promising for ODS.

The goal of this work is to study in detail ODS of heterocyclic sulfur-compounds in gas-vapor phase over CuZnAl-O and Cu/CeO_2 catalysts. The oxidant (O_2, O_3, N_2O), molar ratio O_2/S, LHSV, GHSV and temperature were varied within a wide range for the purpose of increasing sulfur removal efficiency. The data on the efficiency of the gas-phase desulfurization of hydrocarbon fuels will be compared with the literature data on peroxide oxidation of sulfur compounds dissolved in hydrocarbon fuels.

2 Experimental

The catalysts based on oxide Cu-Zn-Al and Cu-Ce compositions have been prepared by precipitation [5] or by incipient wetness impregnation with subsequent calcination at 500°C.

The catalysts were tested at 200-450°C in ODS of thiophene, dibenzothiophene (DBT) and 4,6-dimethyl dibenzothiophene (DMDBT) dissolved in octane or toluene, with oxygen as

oxidant. The optimal catalysts were also studied in ODS of straight-run diesel fraction by oxygen and in ODS of thiophene, DBT with ozone and N_2O as oxidants at 70-400°C.

Samples were studied in a flow reactor placed in a furnace with a fluidized bed of quartz sand. A loading of the catalyst granules (0.5-1.0 mm) was 2 g. The ODS tests were conducted at a ratio of O_2/S=20-240, GHSV=1500-20000 h^{-1} and WHSV=3-10 h^{-1}. Liquid products were collected in the reflux condenser cooled to 5°C. Analysis of total sulfur was performed using a sulfur analyzer ASE-2. GC analysis was performed in a GC Crystal-2000M equipped with TCD and flame photometric detector.

Physico-chemical properties of the CuZnAl-O catalyst before and after ODS reaction were studied by AAS-ICP, CSH-analysis, XRD, DTA-MS, H_2-TPR, FTIR, UV-Vis, ESR and XPS to find correlations between the properties and sulfur reactivity and make assumptions about the reaction mechanism.

3 Results and discussion

The reactivity of different sulfur containing molecules in ODS over catalysts increased in the sequence: thiophene<DBT<DMDBT. The main sulfur containing product of oxidation of these compounds was SO_2. During the ODS reactions, carbon and sulfur accumulated in the catalyst. A method for catalyst regeneration at 300-500°C was developed.

According to DTA-TG, FTIR and XPS, data, at 300-500°C ODS proceeds via the stage of adsorption of sulfur containing molecules, followed by their destruction and evolution of SO_2 into the gas phase. In case of strong interaction of sulfur-containing molecules with the catalyst active sites the accumulation of sulfur on the catalyst surface takes place in the form of metal sulfides, polysulfides and sulfates. Stronger interaction with catalyst surface is observed for thiopnene.

4 Conclusions

The gas phase oxidative desulfurization of refractory sulfur compounds of motor fuels with air was shown to be feasible at atmospheric pressure and moderate temperatures: 350-400°C, which can offer better economic solutions and incentives in fuel desulfurization.

Acknowledgements

This work was financially supported by SAUDI ARAMCO under contract No.6600022642.

References

[1] Z. Ismagilov, S. Yashnik, M. Kerzhentsev, V. Parmon, A. Bourane, F.M. Al-Shahrani, A.A. Hajji, O.R. Koseoglu. *Catal. Rev. Sci. Eng.* 53 (2011) 1.

[2] US 8,906,227 B2 - 2014-12-09. Mild hydrodesulfurization integrating gas phase catalytic oxidation to produce fuels having an ultra-low level of organosulfur compounds. A. Bourane, O.R. Koseoglu, Z.R. Ismagilov, S.A. Yashnik, M.A. Kerzhentsev, V.N. Parmon.

[3] US 8,920,635 - 2014-12-30. Targeted desulfurization process and apparatus integrating gas phase oxidative desulfurization and hydrodesulfurization to produce diesel fuel having an ultra-low level of organosulfur compounds. A. Bourane, O.R. Koseoglu, Z.R. Ismagilov, S.A. Yashnik, M.A. Kerzhentsev, V.N. Parmon.

[4] L. Gao, Y. Tang, Q. Xue, Ye Liu and Y. Lu. *Energy and Fuels* 23 (2009).

[5] WO2013015889 (A1) – 2013-01-31. Catalytic compositions useful in removal of sulfur compounds from gaseouhydrocarbons, processes for making these and uses thereof. A.Bourane, O.R. Koseoglu, Z.R. Ismagilov, S.A. Yashnik, M.A. Kerzhentsev, V.N. Parmon.

I-OP11

Hydrotreatment Catalysts for Bio-Oil and Lipids Processing into Valuable Chemicals and Biofuels

Yakovlev V.A.[1*], Khromova S.A.[1], Kukushkin R.G.[1,2], Rodina V.O.[1], Bykova M.V.[1,2], Venderbosch R.H.[3], Parmon V.N.[1]

1 - Boreskov Institute of Catalysis SB RAS, Novosibirsk, Russia
2 - Novosibirsk State University, Novosibirsk, Russia
3 - Biomass Technology Group B.V., Enschede, The Netherlands

* yakovlev@catalysis.ru

Keywords: biomass, bio-oil, biofuel, hydrodeoxygenation, hydrotreatment catalysts

1 Introduction

The new catalytic technologies of biomass processing should play a key role in the bioenergetics and chemical industry evolution. In Boreskov Institute of Catalysis (BIC) the investigations are carried out in the field of heterogeneous hydrotreatment catalysts development for competent processing of biomass derivatives into valuble chemicals and biofuels. The following catalytic systems are of primary interest: catalysts for selective hydrogenation and complete hydrodeoxygenation of bio-oil components, hydrocracking catalysts for lipids processing into green diesel and kerosene, catalysts for fatty alcohols production via selective hydrogenation of lipids derivatives. Each bio-feedstock has certain peculiarities for processing and as a result definite requirements to the catalysts are established. The latest results of catalysts investigation in the above mentioned types of biomass processing are reported about.

Hydrodeoxygenation of bio-oil (BO)

Bio-oil (BO) being a liquid product of flash pyrolysis of grinded wood is considered to be a perspective alternative feedstock for the petrol production. The main goal of the bio-oil hydrotreatment is to reduce the content of oxygen that is responsible for such negative properties of BO as high viscosity, non-volatility, aggressivity, immiscibility with mineral oil, instability, and tendency to polymerization. Since BO is a very specific aggressive feed, research activities are focused on the development of catalysts with improved stability (resistance to water and acidic medium at elevated temperatures, stability to coking, stability against sintering, etc.). The study of Ni-based catalysts in hydrodeoxygenation of BO and model compounds showed that the increase of Ni content in the catalyst leads to an increase in the H/C ratio of the reaction products, which is a positive factor for the bio-oil hydrotreatment, because of lower viscosity and molecular weight of products obtained [1]. The aspects for an improvement of catalysts stability via modification by Mo and P compounds were discussed separately [2].

Selective hydrogenation of bio-oil components

Present activities of BIC were aimed at Ni-based sol-gel catalysts [3] performance in selective hydrogenation of furfural (representing aldehyde group in pyrolysis oil reactions). The objective of this part was to investigate the effect of the reaction temperature and catalyst reduction temperature on its activity and selectivity. The reactions were carried out at a constant pressure of 6 MPa, isothermal conditions − 110, 130, 150, and 170 ^{o}C for the catalysts reduced at 250 ^{o}C (150 ^{o}C for the catalyst reduced at 300 ^{o}C), iso-propanol was used as a solvent. It was observed that the main product of furfural hydrotreatment basically was furfuryl alcohol (FA), minor components were tetrahydrofurfuryl alcohol, 2-methylfuran and isopropyl ether. The reaction scheme is proposed on the Fig. 1.

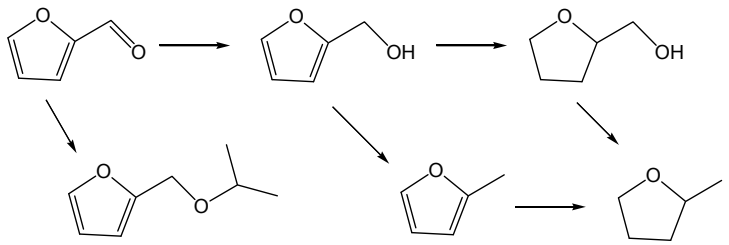

Fig. 1. Scheme of furfural conversion pathways over sol-gel Ni-based catalysts from [3].

According to the kinetic investigations and catalysts study it was concluded that metallic Cu species in the catalysts were favorable for the selective hydrogenation of furfural to FA. It was also noted that if the Ni species on the catalyst surface were reduced during the pre-reduction stage or during the reaction as well, the selectivity was shifted towards the products of further FA hydrogenation. So, the change of Ni-Cu-based catalysts pre-treatment conditions allows variation of hydrogenation processes selectivity.

Selective hydrogenation of lipids into fatty alcohols

Fatty alcohols are valuable products for chemical industry and pharmaceutics. The selective hydrogenation of lipids derivatives (fatty esters and acids) was carried out at 280-330^{o}C and 3.5-5.3 MPa of H_2 [4]. It was shown that oleic acid is a more attractive substrate for achievement of maximum yield of fatty alcohols in the presence of Ru-Sn-B/Al_2O_3. The peculiarity of the process is the presence of additional pathways of acid conversion including direct hydrodeoxygenation into n-alkanes, wax formation and wax hydrocracking to alkanes. The experimental data are correctly discibed by the proposed kinetic model. This model can be used for estimation of products distribution at the process up-scaling.

Hydrodeoxygenation of lipids into biofuels components

Lipids can be converted into fuel components by the catalytic hydrotreatment. In this respect the task is to develop stable non-sulfided catalyst. The effect of molybdenum on activity of Ni-based catalysts in hydrodeoxygenation of fatty acid esters was studied. Catalysts Ni-Cu/Al_2O_3, Ni-Mo/Al_2O_3, Cu-Mo/Al_2O_3, Mo/Al_2O_3, and Ni-Cu-Mo/Al_2O_3 with different Ni/Mo ratios were prepared and tested in hydrodeoxygenation of methyl palmitate and ethyl caprate at 300 °C, 1 MPa. It was found that the increase of Mo content (from 0% to 6.9%) in the Ni-Cu-Mo/Al_2O_3 catalysts leads to an increase of normal alkanes yield. The catalysts were characterized by X-ray photoelectron spectroscopy (XPS), temperature programmed reduction, and X-ray diffraction techniques. The XPS data showed that the increase of fatty acid esters conversion is related to the changes of ratio between different oxidation states of molybdenum (Mo^0, Mo^{4+}, and Mo^{6+}) on the Ni-Cu-Mo/Al_2O_3 catalysts surface [5].

Acknowledgements

The investigation of catalytic bio-oil conversion was carried out under the large scale collaborative project FASTCARD ("FAST Industrialisation by CAtalysts Research and Development"), European Union 7th Framework Programme, Grant Agreement No 604277.

References

[1] A.R.Ardiyanti, S.A. Khromova, R.H. Venderbosch, et al. Appl. Catal. B: Env. 117-118 (2012) 105-117

[2] M.V. Bykova, D.Yu. Ermakov, S.A. Khromova, et al. Catal. Today. 220-222 (2014) 21-31

[3] M.V. Bykova, D.Yu. Ermakov, V.V. Kaichev, et al. Appl. Catal. B: Env. 113-114 (2012) 296-307

[4] V.O. Rodina, S.I. Reshetnikov, V.A. Yakovlev. Catalysis in Industry. 4 (2014) 55-62

[5] R.G. Kukushkin, O.A. Bulavchenko, V.V. Kaichev, V.A.Yakovlev, Appl. Catal. B: Env. 163 (2015) 531-538

I-OP12

Aldol Condensation of Biomass Derived Aldehydes: Comparison of the Reactivity of Furfural and Hydroximethylfurfural

Cueto J., Faba L., Díaz E., Ordonez S.*

University Of Oviedo, Oviedo, Spain

* sordonez@uniovi.es

Keywords: 2nd generation biofuels, condensation, adducts, MgZr-mixed oxides, MgAl-mixed oxides

1 Introduction

The development of technologies for obtaining energy from renewable resources is nowadays a key scope of the research on heterogeneous catalysis. The transformation of biomass into liquid fuels is a key point in this topic, considering that this is the only renewable alternative to obtain naphtha- and diesel-grade substitutes. Despite of the different biological and thermochemical processes that have been studied, catalytic routes deserve main attention because these processes satisfy the green-chemistry principles and allow obtaining a very specific range of products. One of the most promising process implies the hydrolysis and dehydration of (hemi)cellulosic fraction, the increase of the length of the carbon chain by aldehydes cross-condensation (usually using the acetone as linking molecule) and the complete hydrodeoxygenation of the condensated adducts to obtain linear alkanes in the diesel range [1].

There are several researches about the condensation of furfural and acetone, trying to optimize the catalytic properties to enhance the C13 fraction, to identify the optimum reaction conditions and to study the reaction mechanism and kinetic [2,3]. Furfural is the aldehyde obtained by the dehydration of pentoses. However, the major aldehyde obtained in the dehydration of (hemi)cellulosic fraction is the 5-hydroxymethylfurfural (5-HMF), because the highest percentage of this fraction is hexoses. The higher complexity of this molecule increases the difficult to control its reactivity and there are very few references about its condensation. The deep knowledge of this reaction is compulsory to implement this process with real biomass. The aim of this study is to compare the results obtained in the aldol condensation of furfural and 5-HMF with acetone, identifying the discordances between optimum conditions with one and other derivative, and to relate the differences obtained with the influence of the hydroxyl group.

2 Experimental/methodology

The reactions are carried out in a batch reactor, loaded with 250 mL of aqueous solution with 2.5% of organics (initial mole rate aldehyde:acetone 1:1). The aldol condensation is studied using MgZr and MgAl as catalysts, using 0.5g of mixed oxides in each reaction. MgZr and MgAl are prepared by co-precipitation method [2]. The reactor is pressurized to 10 bar in nitrogen and the condensation temperature is fixed at 50 ºC. The evolution of reactants and products is followed for 8 hours by analysing the samples with a gas chromatograph equipped with a FID detector (Shimadzu GC2010) using ethyl acetate as organic solvent.

The presence of precipitated compounds is analysed by lixiviation experiments using ethanol as solvent and analysing the liquid phase by GC-MS. Possible changes on the catalytic surface and its properties are studied different characterization techniques.

3 Results and discussion

The evolution of aldehydes and acetone with both catalysts are shown in **Figure 1**,

observing different behaviours as function of the reactant and catalyst. MgAl is more active for the condensation of 5-HMF, with higher conversion of both, aldehyde and acetone (final values of 67 and 58 %, respectively). Opposite to this, the furfural condensation is more favoured with MgZr than with MgAl. In all the cases, the aldehyde/acetone ratio condensation is similar, despite that the ratio between C15/C9 or C13/C8 products, suggesting different influences of side-reactions and adsorption processes.

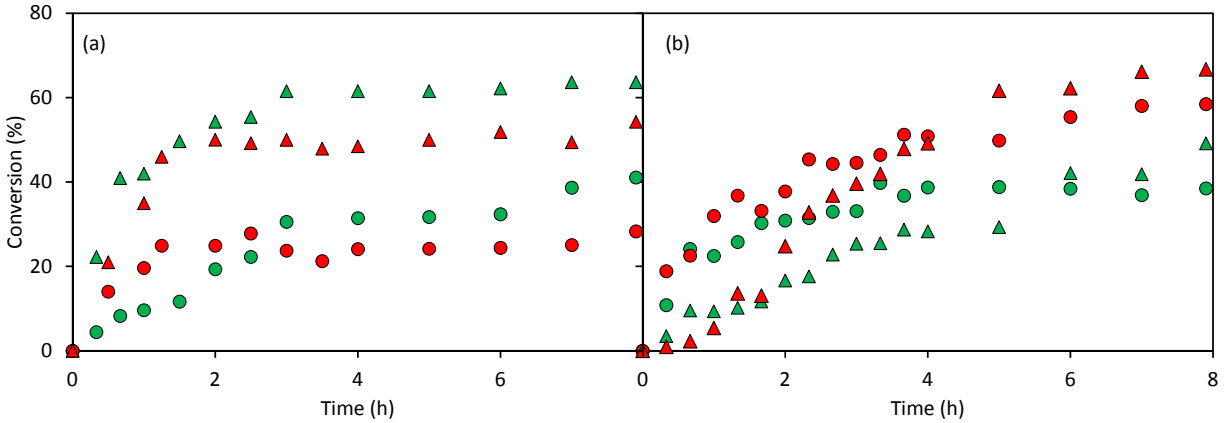

Fig. 1: Conversion evolution in the aldol condensation of acetone with (a) furfural and (b) 5-HMF when MgZr (green) or MgAl (red) are used as catalyst. Symbols: (▲) aldehyde; (●) acetone.

In the furfural condensation, the acetone self-condensation is the only side-reaction identified, obtaining mesityl oxide as by-product. This reaction is more relevant in the case of MgAl, catalyst that also enhances the furfural permanent adsorption (corroborated by analyses of spent catalysts). As consequence, the C13 selectivity with MgAl only reaches values of 11%, whereas this value is six-times higher with MgZr. The analysis of product selectivities is more difficult in the case of HMF condensation because of the low solubility of C15 adduct in aqueous phase. Consequently, only C9 is observed in the liquid phase, obtaining final selectivities of 46.9 and 19.2 % with MgZr and MgAl, respectively. The analysis of solid phase demonstrate a more complex condensation mechanism in which C15 is the major product but other side-products related to the self-reactivity of 5-HMF were also found. The comparison of these solids revealed a C15 production 10 times higher with MgAl than with MgZr. These solubility problems are prevented by carrying out the condensation in a reducing atmosphere using bifunctional catalysts (Pd/MgZr and Pd/MgAl). The partial hydrogenation of aliphatic unsaturations enhances the C15 solubility without affecting to the condensation step. Pd/MgAl is identified as the most active catalyst, selectivity of 27 % of C15 adduct (but less than 5% with MgZr). Activity results were justified by the different distribution of acid/basic sites, in such a way that MgAl distribution stabilizes the C9 adsorption, enhancing its condensation.

4 Conclusions

The condensation of HMF is mechanistically most complicated than the condensation of furfural, leading to the formation of heavier compounds. In the same way, the HMF condensation also leads to the formation of solid products.

Acknowledgements

This work was supported by the Spanish Government (contract CTQ2011-29272-C04-02).

References

[1] G.W. Huber, J.N. Chheda, C.J. Barret, J.A. Dumesic, *Science 308 (2005) 1446*.
[2] L. Faba, E. Díaz, S. Ordóñez, *Appl. Catal. B 113 (2012) 201*.
[3] I. Sádaba, M. Ojeda, R. Mariscal, R. Richards, M. López Granados. *Catal. Today 167 (2011) 77*.

I-OP13

Surfactants from Algae Derived Feedstock: Acylation of Amino Alcohols with Fatty Acids over Zeolite Beta

Tkacheva A., Dosmagambetova I., Mäki-Arvela P.*, Hachemi I., Kumar N., Eränen K., Hemming J., Smeds A., Murzin D.Yu.

Åbo Akademi University, Turku, Finland

* pmakiarv@abo.fi

Keywords: zeolite, acylation, fatty acid, amino alcohol, surfactant

1 Introduction

Algae are rich in lipids, proteins and sugars and the utilization of lipids for production of fuels has been intensively investigated. On the other hand, the use of proteins abundant in, for example *Chlorella* algae as a feedstock, for production of chemicals has been scarcely studied. The main components in proteins are amino acids, which can be catalytically hydrogenated to the corresponding amino alcohols [1]. Biocompatible surfactants, such as N-alkyl amides, have several application areas in pharmaceuticals and cosmetics [2]. According to our knowledge there is only one publication in the open literature on catalytic acylation of amino alcohols to N-alkyl amides (Fig. 1) [3]. The aim of this work is to study catalytic acylation of amino alcohols with fatty acids using different feedstock.

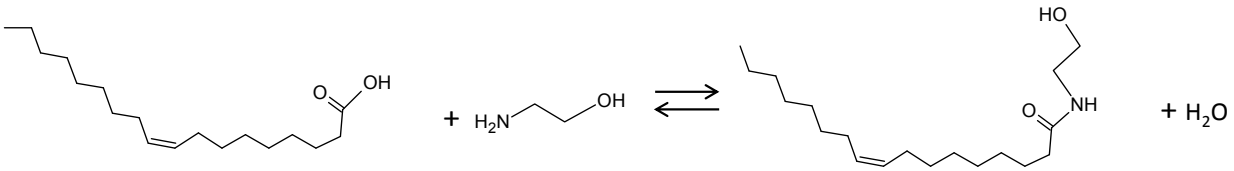

Fig. 1. The reaction scheme for production of oleoyl ethanol amide.

2 Experimental

Zeolite H-Beta-22, in which the number denotes SiO_2 to Al_2O_3 ratio. was synthesized as described in [4] and used as a catalyst. The catalyst was characterized with various physico-chemical methods (pyridine FTIR, XRD, SEM-EDXA, TEM, nitrogen adsorption). Different feedstock, i.e. stearic acid, methyl palmitate and technical grade oleic acid was tested. In addition biodiesel was used, which was prepared via in situ transesterification of algae at 60°C for 4 h with methanol and 20 wt% sulphuric acid as a catalyst. This Chlorella algae derived biodiesel contains 77% FAME (main components being methyl linolenate, linoleate and palmitate) and 7 % fatty acids. The following aminoalcohols were used as a nitrogen source: ethanolamine, alaninol and leucinol. In a typical experiment the initial concentration of the reacting acid was 0.72 M and an equimolar amount of ethanol amine in 100 ml of anhydrous hexane and 500 mg of catalyst were used under 20 bar of argon at 180°C. The kinetic experiments were performed in the kinetic regime using a small catalyst particle size (< 63 μm) and a high stirring speed (1100 rpm). The samples were withdrawn from the reactor, silylated and analyzed in GC using capillary and short GC columns. The reaction products were identified with GC-MS. The biodiesel feedstock was also characterized by ICP-MS method.

3 Results and discussion

H-Beta-22, which was used as a catalyst, exhibited high specific surface area, 686 m^2/g_{cat} and a relatively high amount of Brønsted acid sites compared to Lewis acid sites, being 167 μmol/g_{cat} and 33 μmol/g_{cat}, respectively. XRD pattern of H-Beta-22 zeolite catalysts were similar to those reported in the literature [5].

The conversion in the amidation of technical grade oleic and stearic acids was 74% and 94%, respectively within 3 h using H-Beta-22 as a catalyst. Selectivity to the desired amide was also very high, over 68% and only small amounts of aminoalkylesters were formed (Table 1). Furthermore, also alkylester amides, i.e. molecules containing 38 C atoms in the case of oleic acid and ethanolamine, when both amino- and hydroxyl groups in 2-aminoethanol react with two fatty acid molecules, were formed based on GC short column analysis. Due to a limited amount of purified Chlorella based biodiesel available, the initial biodiesel concentration was 32% of that used for amidation of other feedstock. The conversion of biodiesel was only 28% after 6 h reaction time, most probably due to its low initial concentration as well as possible presence of catalyst poisons, such as sulphur and phosphorus. The main products in the amidation of biodiesel were amides of unsaturated C18 esters.

Table 1. Results from amidation of fatty acids and esters over zeolite beta. Ethanol amine was used as a N-source. Conditions: 180°C, 20 bar total pressure, Ar atmosphere, 0.72 M acid and ethanolamine, 0.5 g catalyst, reaction time 3 h.

Reactant	Fatty acid/ester conversion (mol%)	Selectivity to amide (mol%)	Selectivity to esteramide (mol%)	Selectivity to esteramine (mol%)	Other products (mol%)
Oleic acid[a]	73	73	23	4	4
Stearic acid	94	90	4	2	4
Biodiesel[b]	28	44	n.c.[c]	traces	52[c]

[a]technical grade oleic acid (65 wt%), containing also linoleic, palmitic and palmitoleic acids as well as Me-stearate, [b] biodiesel with initial concentration 0.23 M, catalyst amount 96 mg, reaction time 6 h, [c]esteramines of several different esters were not confirmed (n.c.) by GC-MS, but lumped together with other product

4 Conclusions

Amidation of fatty acids and biodiesel from Chlorella algae was successfully demonstrated over a relatively acidic, medium pore zeolite H-Beta-22 at 180°C using initial reactant concentrations of 0.72 M for both fatty acid (or ester) and aminoalcohol. Conversion of stearic acid after 3 h was 94% giving over 90% selectivity to oleoylethanolamide. Amidation of Chlorella based biodiesel was also demonstrated. In the final work reaction kinetics and reaction mechanism will be discussed.

References

[1] F. T. Jere, J. E. Jackson, D. J. Miller, *Ind. Eng. Chem. Res*. 43 (2004) 3297.
[2] A. Pinazo, R. Pons, L. P´erez, M. R. Infante, *Ind. Eng. Chem. Res.* 50 (2011) 4805.
[3] M. Musteata, V. Musteata, A. Dinu, M. Florea, V.-T. Hoang, D. Trong-On, S. Kaliaguine, V. I. Parvulescu, *Pure Appl. Chem*. 79 (2007) 2059.
[4] J. I. Villegas, N. Kumar, T. Heikkilä, V.-P. Lehto, T. Salmi, D. Yu. Murzin, *Topics in Catal.* 45 (2007) 187.
[5] http://www.iza-structure.org/database, 5.2.2014.

I-OP14

A Novel Efficient Synthesis of Guaifenesin over Calcined Hydrotalcite

Yadav G.D.*, Bhanawase Sh.L.

Department of Chemical Engineering, Institute of Chemical Technology, Matunga, Mumbai, India

* gdyadav@yahoo.com

Keywords: catalysis, biomass, hydrotalcite, guaiacol, glycidol, green chemistry

1 Introduction

Biomass is abundant and renewable source for energy, chemicals and materials [1]. Guaiacol and glycidol have been obtained from biomass respectively by valorization of lignin and glycerol. However, lignin is waste of the paper and pulp industries and glycerol is co-product during the biodiesel production. Synthesis of guaifenesin from renewable sources should result in a greener and more sustainable process. One of the possible paths to produce guaifenesin based on biomass is from guaiacol and glycidol by using heterogeneous catalysis.

Guaifenesin is an expectorant drug in racemic form; used for treatment of coughing, asthma, gout, fibromyalgia, to facilitate conception and also used by singers to improve voice. Generally guaifenesin is synthesized by Williamson's type of etherification reaction in which nucleophile of guaiacol attacks on glycidol, epichlorohydrin, 1-chloroglycerol, glycerol carbonate, 3-bromo-1-propene and isopropylidene glycerol [2]. Homogeneous catalysts such as triethyl amine, sodium hydroxide, potassium carbonate used in stoichiometric have been reported which are corrosive, toxic, hazardous to health and not easily separated from product, and thus create pollution problems. As far as we know from literature, this reeaction with heterogeneous catalyst has not been published. Now we are reporting a novel protocol catalyzed by calcined hydrotalcite (CHT). Influences of different parameters are studied in the reaction of guaiacol with glycidol to check the activity and selectivity of CHT. Reaction mechanism and kinetics are derived. CHT is highly active and selective towards product and is reusable.

2 Experimental/methodology

2.1 Catalyst synthesis

Following catalysts were synthesized and further characterized: (1) Hydrotalcite (HT) and calcined hydrotalcite (CHT)[3], (2) 10% w/w CHT supported on hexagonal mesoporous silica (HMS); (i.e. CHT/HMS) [4], (3) 8.8% w/w potassium modified zirconium hydroxide; (i.e. K- ZrO_2) [5], (4) Aluminium oxide (Al_2O_3) was prepared by calcination of aluminium hydroxide at 450º in furnace for 6 h.

2.2 Experimental setup, reaction procedure and method of analysis

The reaction was carried in high pressure reactor (Amar Equipments, Mumbai). In a typical reaction, guaiacol (0.0081 mol) and glycidol (0.020 mol), THF (10 cm^3) and 0.03 g cm^{-3} of the catalyst were charged to the reactor. The total organic phase volume was made with THF to 30 cm^3. Then reactor was heated to attain the desired temperature, and an initial sample was collected. Reaction mass was agitated with a mechanical stirrer at desired speed, and samples were collected periodically and analyzed by HPLC (Agilent 1260 infinity HPLC system with C18 column). The reaction was carried out at 120ºC at a speed of agitation of 1000 rpm under autogenous pressure. Product confirmation was carried out by GCMS from Perkin Elmer, Clarius Model 500 on Elite-1 capillary column.

3 Results and discussion

3.1 Catalyst characterization

Prepared catalysts were characterized as reported elsewhere. [3, 4].

3.2 Efficacy of various catalysts and study of effect of various parameters

Activity of different catalysts such as CHT-HMS, K-ZrO_2, MgO, Al_2O_3, HT, and CHT were evaluated for conversion and selectivity. Order of catalysts activity was found as follows: K-ZrO_2 > CHT > HT > MgO > CHT-HMS > Al_2O_3 while order of selectivity for product was found as follows: Al_2O_3 >MgO > CHT >HT > K-ZrO_2 > CHT-HMS. K-ZrO_2 was not reusable. So CHT was found to be the best for the reaction considering activity and selectivity. CHT gave 78.5 % conversion with 88.3% selectivity towards the product. Effect of following parameters was studied: speed of agitation, catalyst loading, mole ratio, temperature, and catalyst reusability. Regenerated catalyst was characterized to verify the properties in comparison with fresh catalyst.

3.3 Reaction kinetics

A possible mechanism based on the synergistic cooperation of the weak acid sites with the basic sites is proposed. In absence of external mass transfer resistance and intraparticle diffusion resistance, Langmuir–Hinshelwood–Hougen–Watson (LHHW) model was developed with weak adsorption. Guaiacol (A) was assumed to adsorb on basic site (S_1) and glycidol (B) on acidic site (S_2). The plot of ln [(M-XA)/M (1-XA)] against t was made at different temperatures to validate the model. Apparent activation energy of reaction was calculated as 9.82 kcal mol^{-1}.

4 Conclusions

Condensation of guaiacol with glycidol was studied using various catalysts. On the basis of catalyst activity and selectivity, CHT was the best. To obtain maximum yield of guaifenesin, the reaction may be done at following conditions: speed of agitation; 1000 rpm, temperature; 120 ºC, catalyst loading; 0.03 g cm^{-3}, mole ratio of guaiacol to glycidol; 1:5. Reaction kinetics was studied and reaction is second order with activation energy is 9.82 kcal mol^{-1}. Catalyst can be reused. Overall reaction is clean and green.

Acknowledgements

G.D.Y. acknowledges support from R.T. Mody Distinguished Professor Endowment of ICT and J.C. Bose National Fellowship of DST-GOI. S.L.B. acknowledges to the University Grants Commission (UGC) for awarding the Junior Research Fellowship under its Green Technology special meritorious fellowship program.

References

[1] J. Zakzeski, P. C. A. Bruijnincx, A. L. Jongerius, B. M. Weckhuysen, *Chem. Rev.*110 (2010) 3552.
[2] A. M. Truscello, C. Gambarotti, M. Lauria, S. Auricchio, G. Leonardi, S.U. Shisodia, A. Citterio, *Green. Chem.* 15 (2013) 625.
[3] M. J. Climent, A. Corma, S. Iborra, A. Velty, *J. Catal.* 221 (2004) 474.
[4] G. D. Yadav, P. Aduri, *J. Mol. Catal. A Chem.* 355 (2012) 142.
[5] Y. Wang, W. Y. Huang, Y. Chun, J. R. Xia, J. H. Zhu, *Chem. Mater.* 13 (2001) 670.

I-OP15

Tuning the Selectivity of the Diols Produced from Cellulose with the Basic Sites of the Catalysts

Van Der Wijst C.[1], Skeie Liland I.[1], Zhu J.[1], Zhang T.[2], Wang A.[2], Chen D.[1*]

1 - Norwegian University of Science and Technology, Department of Chemical Engineering
2 - Dalian Institute of Chemical Physics, Chinese Academy

* de.chen@ntnu.no

Keywords: cellulose, conversion, Ni-Zn catalysts, basic sites, diol, distribution

1 Introduction

In complex reactions like catalytic conversion of biomass and biomass derived compounds, a better understanding of the reaction network and factors to control product selectivity is essential. The direct catalytic conversion of cellulose to diols is a complex catalytic liquefaction process. Microcrystalline cellulose must disintegrate and hydrolyze into smaller polysaccharides before the cracking, dehydration and hydrogenation steps yield the diols.

Hot-compressed water has previously been proven to be a good reaction medium for the dissolution and hydrolysis of cellulose. Water heated to 245 ^{o}C and pressurized to remain as a liquid has a high ionic product and can effectively disintegrate and hydrolyze cellulose into smaller oligo- and monosaccharides. In this process, water acts as reactant, catalyst and as a reaction medium [1]. The generated sugars undergo catalytic conversion to various products dependent on the nature of catalytic system. Nickel-tungsten based catalysts and nickel-zinc oxide based catalysts are two systems used in this process, but yield a different diol product distribution. The nickel-tungsten based catalysts yield mostly ethylene glycol (EG) and minor formation of 1,2-propandiol (PG) and 1,2-butandiol while the nickel-zinc oxide based catalysts primary products are EG and PG.

Ni-Zn catalysts supported on carbon nanotubes were selected in the present work with an aim at elucidate reaction network and controlling factors for product distribution. Carbon nanotube was selected as catalyst support to reduce the diffusion limitation in liquid phase reaction compared to conventional activated carbon. The results reveled that Ni-Zn catalysts are highly basic and the basic property of the catalysts is the key parameter for product selectivity.

2 Experimental

Nickel-zinc oxide supported on carbon nanotubes were synthesized with a 30 % nickel loading and a 26 % zinc oxide loading. Nitric acid purified multiwalled carbon nanotubes where first coated with zinc oxide using the Pechini method to ensure a uniform zinc oxide layer. Nickel particles where then impregnated using the insipient wetness impregnation. The catalysts were reduced in 63 mL hydrogen flow for five hours at temperatures of 300 °C, 350 °C, 400 °C and 450 °C. The basic sites were investigated with CO_2-TPD.

The catalytic reactions were tested in a 75 mL stirring batch reactor, using 25 mL water, 0.25 g microcrystalline cellulose, 0.075 g catalyst and an initial 60 bars of H_2. The reactor was closed and heated to 245 ^{o}C generating a pressure of 120 bars, and the system was kept at 245 ^{o}C for 150 minutes.

3 Results and discussion

As can be seen from figure 1, the reduction temperature of the catalyst effects both the amount and type of basic sites generated. The CO_2-TPD profiles are given in figure 1 a). They show that each catalyst has at least two types of sites with different basic strengths. For the

lowest reduction temperature, at 300 °C, the lowest desorption peak is observed at 470 °C, while the catalyst reduced in higher temperatures has the lowest desorption peak at 425 °C. So reducing catalyst above temperatures of 300 °C will yield sites with lower basic strength. A decrease in the amount of desorbed CO_2 with increased reduction temperature can easily be observed in figure 1b).

It was found that the change in reduction temperature of the catalysts, thus the basic sites, did not influence the total yield of diols, but changes significantly the product distribution. Figure 1c) shows the yields of the main products. Here a clear increase in C_3 product formation is observed with an increased amount of basic sites per gram catalyst. According to previous proposed reaction mechanisms for this system, C_3 products are solely produced from fructose [2], meaning that the produced glucose molecules for cellulose must be isomerized to fructose. This is a known base catalysed process. The C-C splitting of the sugars also follows a base catalysed reaction, a retro aldol condensation reaction. This mechanism limit the C-C bond breaking to between the α and β carbons to the carbonyl group of the sugar. Therefore, glucose is split into one glycol aldehyde (C_2) and one erythrose (C_4) molecule, which again splits into two glycol aldehydes and are hydrogenated to EG. Fructose spilt into glyceraldehyde and 1,3-dihydroxyacetone, both C_3 molecules. Glyceraldehyde is hydrogenated into glycerol and 1,3-dihydroxyacetone is dehydrated to acetol (HA) and hydrogenated to PG. So the increased yield of the C_3 products with increasing amounts of basic sites is likely due to the increase in the isomerization of glucose to fructose.

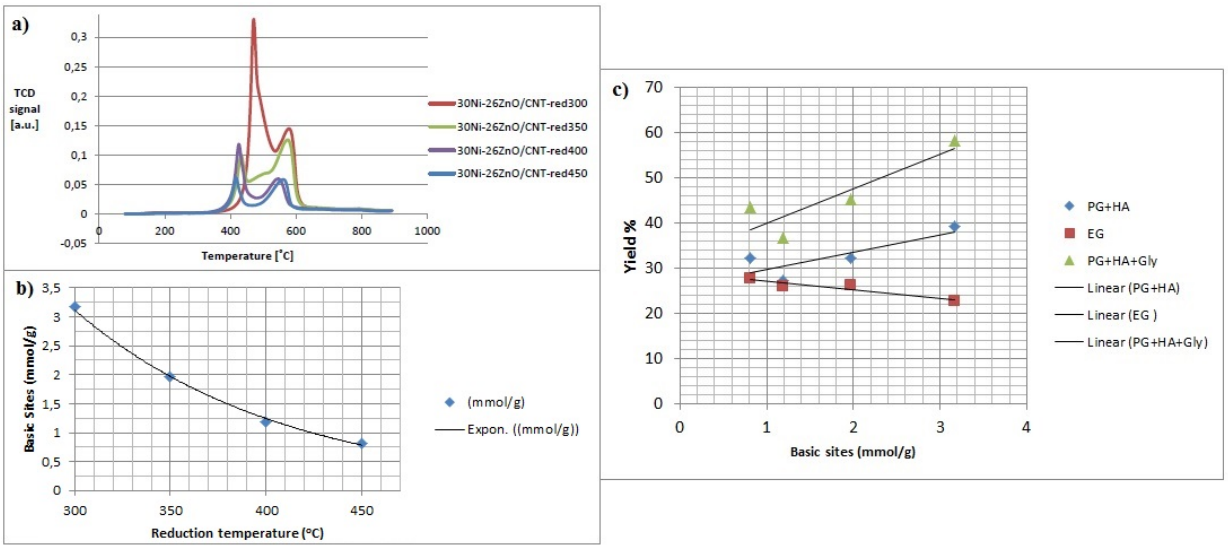

Fig. 1. a) CO_2-TPD and **b)** The amount of basic sites per gram of catalyst as a function of temperature of reduction. **c)** Yield as a function of amount of basic sites per gram of catalyst.

4 Conclusions

Results show a clear correlation between the yield of the C_3 products and the amount of basic sites per gram catalyst. The increase in C_3 yield is attributed to the increase in isomerization of glucose to fructose. This provides principles for rational design of catalysts to tune the product distribution. It rationalizes the acidic promoters such as tungsten oxides for EG synthesis.

References

[1] A. Kruse, N. Dahmen, *The Journal of Supercritical Fluids*. 96 (2015)
[2] M. Zheng, J. Pang, et al, *Chinese Journal of Catalysis*. 35 (2014)

I-OP16

Catalytic Hydrodeoxygenation of Bioderived C5 Acid into Motor Fuel Components: Kinetics and Mechanistic Study

Simakova I.L.[1,2*], Panchenko V.N.[1], Gulyaeva Yu.[1], Simonov M.[1]

1 - Boreskov Institute of Catalysis SB RAS, Novosibirsk, Russia
2 - Novosibirsk State University, Novosibirsk, Russia

* simakova@catalysis.ru

Keywords: valeric acid, Pd, Pt, metal oxides, size effect, alkane, fuel, components, FTIR *in situ*, UV-vis

1 Introduction

Lignocellulose derived C5 (valeric) acid, a product of levulinic acid conversion, can be upgraded to *n*-nonane, a green diesel component [1-3]. This work aimed to study systematically C5 acid conversion through the intermolecular coupling into 5-nonanone with CO_2 and water releasing followed by hydrodeoxygenation into *n*-nonane over Pd and Pt catalysts in reductive atmosphere. Spectroscopic methods (FTIR *in situ*, UV-Vis *in situ*) were applied to study a feasible mechanism of ketonization still debated in the literature [4-6]. Both catalytic reactions were explored separately in order to be performed thereafter in a cascade mode over the best bifunctional catalyst, which turned out to be Pt(Pd)/M_xO_y.

2 Experimental

Ketonization of valeric acid was carried out in a fixed bed flow reactor over ZrO_2 and 10 wt.%CeO_2/ZrO_2 ($m_{catalyst}$=0.5g, fr. 0.25÷0.5 mm) at 573-678K and 1 bar, both under H_2 and N_2 (10-33 cm^3/min). Hydrogenation of 5-nonanone was performed over 2 wt.%Pd/ZrO_2, and 10%CeO_2/ZrO_2 at 573-673K under P_{H2} 1-10 bar. The reaction products were analyzed by "Chromos 1000" GC (FID) with fused silica column Stabilwax-DA (50 m/0.32 mm/0.5μm) (USA) at 373-473 K with ramp 10 K/min. The catalysts were treated by hydrogen and vapors of valeric acid or 5-nonanone and analyzed using a UV-Shimadzu UV-Vis spectrometer with IRS-250A prefix diffuse reflection (UV-Vis) and a FTIR-8300 Shimadzu spectrometer with DRS-8000 prefix diffuse reflection (FTIR) at 293-423K.

3 Results and discussion

The effect of the reaction temperature, CeO_2 loading, and residence time on the C5 acid conversion and selectivity to the desired products was investigated in the decarboxylative coupling with 5-nonanone formation followed by its hydrodeoxygentaion to *n*-nonane (Fig. 1).

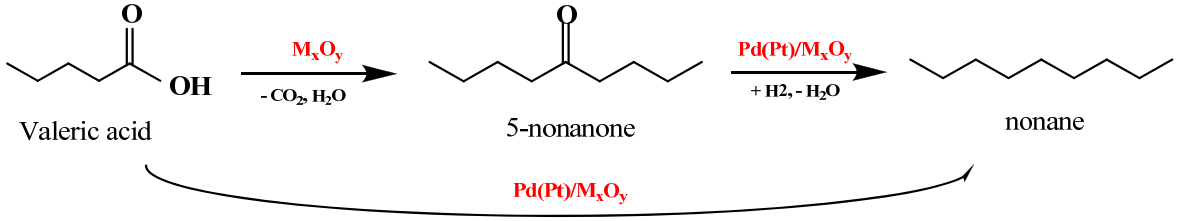

Fig. 1. Scheme of one-pot C5 acid ketonization/hydrodeoxygenation into nonane.

Regardless of the carrier gas, 10% CeO_2/ZrO_2 displayed higher catalytic activity (79% selectivity at 93% conversion) compared to neat zirconia (78% selectivity at 83% conversion) and other ceria modified zirconia, while neat ceria exhibited a very low catalytic activity. All catalysts provided higher valeric acid conversion in H_2 than in N_2 whereas selectivity to 5-nonanone was insensitive to gas atmosphere. XRD, FTIR, UV-Vis DRS, XPS, HRTEM methods

were applied to characterize catalysts in the reduced and unreduced states simulating the corresponding reaction conditions during acid ketonization [7]. Pt(Pd)/M_xO_y catalysts with the highest dispersion showed similar (85-90%) yields of *n*-nonane in deoxygenation of 5-nonanone at 628K and 6 bar. Pd/ZrO_2 catalyst was tested in one-pot transformations of the C5 acid to *n*-nonane *via* ketonization/deoxygenation at T = 628K and P = 6 bar. A correlation between catalytic activity, structural and electronic properties of catalysts was found with an aid of XPS and HRTEM.

The mechanism of ketonization on the basis of FTIR and UV-Vis in-situ study was suggested [8] being consistent with the results previously reported in [4-6]. According to the obtained spectroscopic data two approaches to the mechanism of valeric acid ketonization could be proposed differing in the carboxylate forms arisen in the first reaction stage (Fig. 2 right). After the carboxylates are formed and α-H atom is abstracted from one of them to form an anion radical the latter attacks the second carboxylate adsorbed on the same or neighboring metal species to produce β-ketoacid followed by decarboxylation to form the desired ketone.

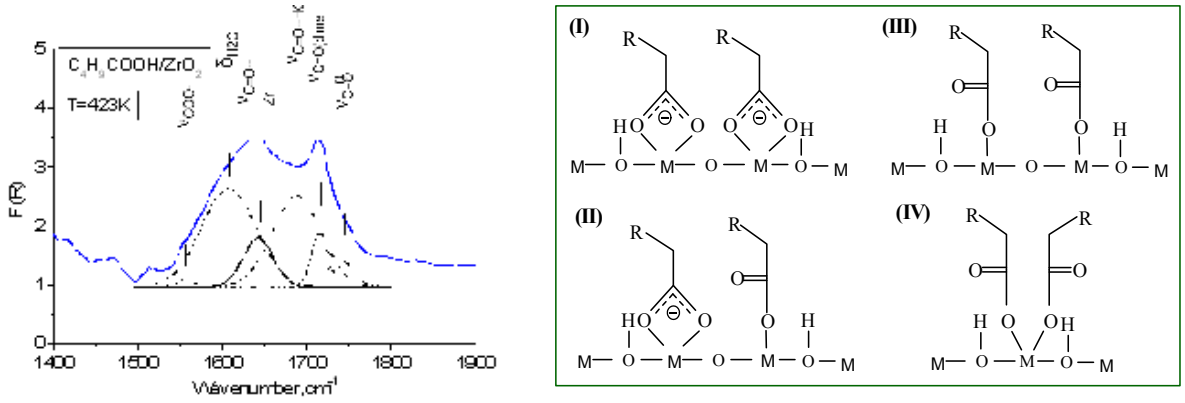

Fig. 2. FTIR spectra of valeric acid adsorbed over reduced ZrO_2 at 423K (left); valeric acid adsorption forms identified over Lewis acid sites by FTIR and UV-Vis (right).

4 Conclusions

Higher activity of ZrO_2 and CeO_2/ZrO_2 in C5 acid decaboxylative coupling in H_2 atmosphere compared to that in N_2 was found. Kinetic regularities and size effect of 5-nonanone hydrodeoxygenation over Pd and Pt on Zr and Ce/Zr oxides was elucidated. Influence of cross-reaction by-products on catalytic behaviour and product distribution was shown. FTIR and UV-Vis study allowed to identify different carboxylates adsorption forms and to reveal their key role in the ketonization mechanism. The reaction conditions were found provided C5 acid cascade mode transformation to C9 alkane with the yield more than 80%.

Acknowledgements

The authors wish to thank Prof. Zenkovets and Dr. Shutilov providing metal oxides samples. Financial support from the Russian Foundation of Basic Research (RFBR Grant No, 14-03-31571 mol_a, 15-03-09329) is gratefully acknowledged.

References

[1] A. Corma, M. Renz, C. Schaverien, *ChemSusChem*. 1 (2008) 739.
[2] J. C. Serrano-Ruiz, D. Wang, J. A. Dumesic, *Green Chem*. 12 (2010) 574.
[3] M. Renz, Eur. *J. Org. Chem.* 979 (2005).
[4] S. Sato, R. Takahashi, T.Y. Sodesawa *et al. J. Catal.* 184 (1999) 180.
[5] O. Nagashima, S. Sato, R. T. Takahashi et al, *J. Mol. Catal. A: Chem.* 227 (2005) 231.
[6] Y. Yamada, M. Segawa, F. Sato et al. *J. Mol. Catal. A: Chem.* 346 (2011) 79.
[7] Yu.A. Zaytseva, V.N. Panchenko, M.N. Simonov et al. *Top. Catal.* 56 (2013) 846.

I-OP17

K-Promoted NiMo Catalysts Supported on Activated Carbon for the Hydrogenation Reaction of CO to Higher Alcohols

Liakakou E.T.[1,2], Angeli S.D.[2], Triantafyllidis K.S.[1,3], Heracleous E.[1,4*]

1 - Chemical Process & Energy Resources Institute, CERTH, Thessaloniki, Greece
2 - Department of Chemical Engineering, Aristotle University of Thessaloniki, Thessaloniki, Greece
3 - Department of Chemistry, Aristotle University of Thessaloniki, Thessaloniki, Greece
4 - School of Science & Technology, International Hellenic University, Thessaloniki,Greece

* eheracle@cperi.certh.gr

Keywords: CO hydrogenation, higher alcohols, Ni-Mo catalyst, AC-supported, catalysts, acidity

1 Introduction

Higher alcohols have been identified as highly promising and suitable components for jet fuel [1]. These higher alcohols can be produced thermochemically in a process similar to BtL-Fischer–Tropsch, with an appropriate catalyst to drive CO hydrogenation to higher alcohols formation rather than hydrocarbons. In this study, we investigate the hydrogenation of CO to higher alcohols over K-promoted bimetallic nickel-molybdenum oxide-based catalysts supported on activated carbon (AC), focusing on the effect of acidity. Initially, we studied the role of each active metal (Ni and Mo) separately by preparing and testing monometallic catalysts supported on AC [2]. Both Mo and Ni alone proved to be inactive in CO hydrogenation under the investigated conditions, demonstrating that the Ni-Mo synergistic effect and the formation of Ni-O-Mo functionalities is mandatory in order to produce a fair amount of oxygenates. In this study, the influence of the type of the carbon used as support was examined by employing two activated carbons with significant differences in surface area. The effect of pre-treating the activated carbon with acid to remove ash prior to impregnation and form surface carbon–oxygen complexes was also investigated. Physicochemical characterization data are combined with catalytic results in higher alcohol synthesis in an attempt to identify the different functionalities of the AC support and the nature of active sites.

2 Experimental/methodology

Two activated carbons (Norit) with surface areas 600 (AC1) and 1200 (AC2) m^2/g were used as supports. The activated carbons were used either as supplied (ACXb) or after acid treatment with a 50vol% HNO_3 aq. solution at room temperature overnight (ACXa). The supported K-promoted bimetallic catalysts were prepared by a stepwise incipient wetness method, with a constant K/Ni/Mo molar ratio of 0.05/1/1, followed by drying and calcination at 575°C for 4h under N_2. The loading of the active phase was kept constant to 35wt%. Additionally, a reference NiMoK mixed oxide with the same K/Ni/Mo molar ratio was prepared by evaporation. Physicochemical characterization was conducted by ICP, BET, XRD, TGA, H_2-TPR and NH_3-TPD. Catalyst evaluation in the CO hydrogenation reaction was investigated with a high pressure bench scale unit, in the temperature range 250–280°C at 60bar, W/F ratio 0.74 g_s/cm^3 and inlet feed composition $H_2/CO=2$.

3 Results and discussion

Evaluation of the NiMo catalysts in the CO hydrogenation reaction showed that the main reaction products are dimethylether (DME), alcohols (mainly C_2-C_5), hydrocarbons and CO_2. Although the unsupported K-NiMo phase exhibited the highest activity, it mainly produced hydrocarbons and DME rather than alcohols. The use of activated carbon as support led to a minimum three-fold increase in selectivity toward higher alcohols. Characterization revealed

that the presence of the support reduces the crystallinity of the $NiMoO_4$ phase in the samples and leads to a partial transformation of this mixed oxide from the alpha to the beta-phase. Subjecting the activated carbon to acidic pre-treatment prior to active metal deposition led to double CO conversion for the K-NiMo/AC2a catalyst compared to the untreated one (K-NiMo/AC2b). This could be related to the removal of ash from the activated carbon support and the improved dispersion of the active phase, as indicated by the increased acidity of the catalyst. In terms of products, acid pre-treatment led to reduced methanol and higher alcohol selectivity as a result of the high acidity. Finally, the use of a higher surface area support led to increased CO reactivity, with the K-NiMo/AC2a exhibiting a 45% higher conversion at 280°C compared to K-NiMo/AC1a. The improvement in activity can be ascribed to better dispersion of the active phase on the higher surface area support and therefore higher exposure of active sites on the surface, as indicated by the less crystalline nature of the particles and the acidity results.

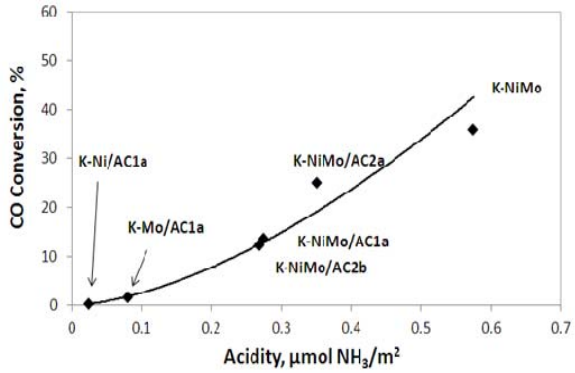

Fig. 1. Total acidity as a function of carbon monoxide conversion at 280°C for the K-promoted mono- and bi-metallic NiMo catalysts unsupported and supported on different AC supports

A clear tendency of increasing higher alcohol with decreasing acidity was evidenced, in agreement with previous results by our group on K-promoted CuZnAl catalysts for higher alcohol synthesis [3]. Moreover, a clear correlation between CO conversion and acidity was established for all catalysts, as shown in Fig. 1, indicating that Ni-O-Mo entities with acidic properties constitute the active centers for CO activation.

4 Conclusions

The use of activated carbon as support for alkali promoted NiMo catalysts was found to be beneficial for the hydrogenation of CO to higher alcohols, probably due to transformation of the active $NiMoO_4$ phase from alpha to beta. The increased activity of the higher surface area acid-treated support can be ascribed to better dispersion of the active phase on the support and therefore higher exposure of active Ni-O-Mo sites. A clear correlation between CO conversion and acidity was established for all catalysts, demonstrating that Ni-O-Mo entities with acidic properties constitute the active centres for CO activation. Overall, the K-NiMo/AC2a catalyst exhibited the optimum performance, with a space time yield of 141.5 mg/$g_{catalyst}$/h to oxygenates at 280°C, which is the highest amongst all the AC supported samples.

Acknowledgements

This study has been co-financed by the European Union (European Social Fund - ESF) and Greek national funds through the Operational Program "Education and Lifelong Learning" of the National Strategic Reference Framework (NSRF) - Research Funding Program: Thales. Investing in knowledge society through the European Social Fund (Glycerol2Energy project).

References

[1] Eurobioref Public Booklet, Available from: http://eurobioref.org/images/Eurobioref_livret_resultats_total_v4.pdf [February 2015].
[2] E.T. Liakakou, E. Heracleous, K.S. Triantafyllidis, A.A. Lemonidou, *Appl. Catal. B* 165 (2014) 296
[2] E. Heracleous, E.T. Liakakou, A.A. Lappas, A.A. Lemonidou, *Appl. Catal. A* 455 (2013) 145

I-OP18

Control of Chain Length Distribution of Hydrocarbons during Fischer-Tropsch Synthesis over Co Nanoparticles inside of Nanoreactors

Ordomsky V.V.*, Subramanian V, Khodakov A.Yu., Paul S.

Unité de catalyse et de chimie du solide, Université Lille, Lille, France

* Vitaly.Ordomsky@univ-lille1.fr

Keywords: nanoreactor, Fischer-Tropsch, chain length distribution

1 Introduction

Fischer–Tropsch (FT) synthesis recently has received a lot of attention since it is considered as an effective process to produce wide-range liquid hydrocarbon fuels and valuable chemicals from abundant resources, such as natural gas, coal and biomass, via synthetic gas. One of the main problems of the Fischer-Tropsch synthesis is too broad distribution of the produced hydrocarbons due to the Anderson-Schulz-Flory (ASF) law resulting in a non-selective formation of any hydrocarbons. Many attempts have been made to circumvent the ASF distribution and to selectively produce the necessary range of hydrocarbons. However, these methods like addition of acidic catalyst for cracking of long chain hydrocarbons or promotion with other metals are not very efficient or suffer from formation of side products.

This work aims at developing novel strategy to enhance the control of the FT synthesis by encapsulation of the metal in the nanoreactors. Variation of the size of nanoreactors should result in the restriction of the growth of the hydrocarbons with control of the chain length of the formed hydrocarbons.

2 Experimental/methodology

Silica nanoreactors with encapsulated Co nanoparticles (Co@SiO_2-nanoreactor) have been prepared by application of micelles as a matrix. Fig. 1 shows the scheme of the synthesis of Co nanoparticles encapsulated into the porous silica spheres by application of micelle synthesis. In this case cobalt nitrate present in the aqueous phase localized in the micelles formed by cetyltrimethylammonium bromide in organic phase. Reduction of the cobalt by $NaBH_4$ leads to formation of metallic Co nanoparticles. Addition of tetraethylortosilicate in the system in the presence of trimethoxy(octadecyl)silane (TMOS) leads to its hydrolysis on the surface of micelle with formation of silica spheres with pores formed by TMOS.

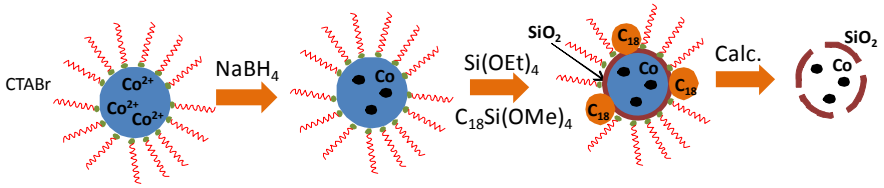

Fig. 1. Scheme of the synthesis of Co nanoparticles encapsulated in porous silica nanoreactors

The materials were characterized by elemental analysis, XPS, XRD, TEM, nitrogen adsorption and SSITKA analysis.

Catalytic experiments were carried out on the REALCAT platform in a Flowrence high-throughput unit (Avantium®) equipped with 16 parallel milli-fixed-bed reactors (d=2 mm) operating at a total pressure of 20 bar, 220°C, H_2/CO= 2 molar ratio. The gas and liquid products have been analyzed after the test by GC analysis for evaluation of the activity and selectivity to hydrocarbons.

3 Results and discussion

Analysis of the nanoreactor catalytic systems shows presence of small porous silica spheres with diameter 5-10 nm with Co nanoparticles inside (Fig. 2). FT synthesis (Fig. 2) over prepared material in comparison with Co nanoparticles prepared in the same way but without addition of TEOS and impregnated over silica support (Co@SiO_2-imp) and standard impregnated catalyst (Co/SiO_2-imp) shows that Co nanoparticles in the silica spheres provide much higher activity and stability. The high activity is the result of well dispersed Co inside of nanoreactors with low interaction with the material of support in comparison with the catalysts prepared by impregnation with high contribution of silicates. The high stability is due to the low segregation of Co nanoparticles separated by the walls of the silica spheres. Analysis of the wax products shows that encapsulation of Co nanoparticles leads to significant shift to the short chain hydrocarbons due to the restriction of the chain growth by the walls of nanoreactors with formation of the liquid hydrocarbons in comparison with solid wax over impregnated catalysts (Fig. 2). The product of the FT synthesis over nanoreactors might be directly used as diesel fuel. It means that it is possible to control the distribution of products by change of the size of the nanoreactors.

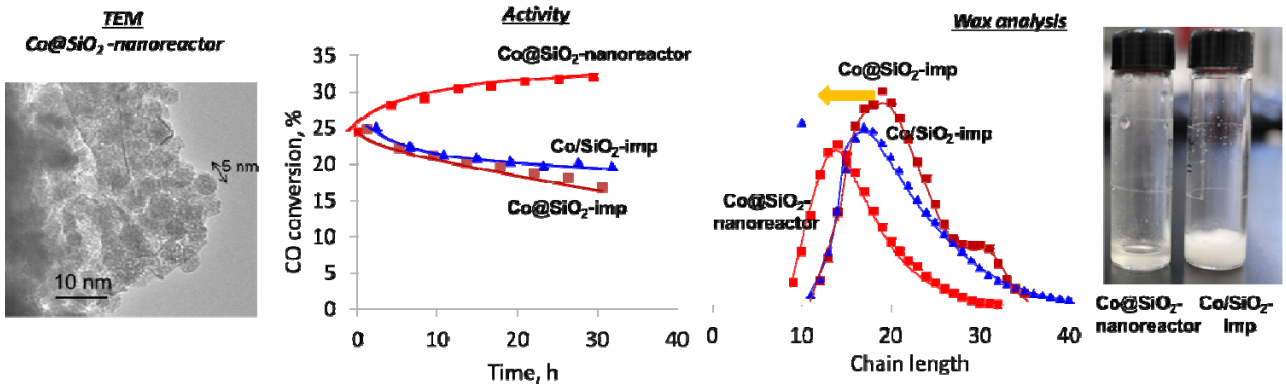

Fig. 2. Comparison of the activity and wax analysis during FT synthesis over standard impregnated Co catalyst (Co/SiO_2-imp), Co nanoparticles impregnated over silica (Co@SiO_2-imp) and Co catalysts encapsulated in nanoreactors (Co@SiO_2-nanoreactor with TEM analysis)

4 Conclusions

Thus, our results show that application of nanoreactors give significant advantages in terms of activity, selectivity and stability in FT synthesis. However, there are much more opportunities for nanoreactors in FT synthesis besides shape selectivity for combination of the processes by control of the access of chemicals in nanoreactors and variation of environment in nanoreactors to control synthesis of the other products.

Acknowledgements

The REALCAT platform is benefiting from a Governmental subvention administrated by the French National Research Agency (ANR) within the frame of the 'Future Investments' program (PIA), with the contractual reference 'ANR-11-EQPX-0037'. The Nord-Pas-de-Calais Region and the FEDER are acknowledged for their financial contribution to the acquisition of the equipment of the platform.

I-OP19

Novel Approach to Catalytic Processing of Birch Wood Biomass to Valuable Chemical Products

Kuznetsov B.N.[1,2*], Chesnokov N.V.[1,2], Levdansky A.V.[1], Garyntseva N.V.[1], Yatsenkova O.V.[1], Grishechko L.I.[1], Celzard A.[3], Pinel C.[4]

1 - Institute of Chemistry and Chemical Technology, Krasnoyarsk, Russia
2 - Siberian Federal University, Krasnoyarsk, Russia
3 - Institut Jean Lamour – UMR CNRS, Epinal, France
4 - IRCELYON, Lyon, France

* bnk@icct.ru

Keywords: wood, catalytic processing, chemical products

1 Introduction

Wood is the most abundant renewable resource for valuable chemicals and biofuels in the forest regions. Birch tree belongs to the widespread wood species in the Russia. The high content of hemicelluloses complicates the use of birch wood in pulping and hydrolysis industries but makes this wood attractive for production of valuable chemicals.

This presentation describes a novel approach to wasteless processing of birch wood biomass, based on the integration of catalytic methods of hemicelluloses, cellulose and lignin components conversion to xylose, microcrystalline cellulose (MCC), biologically active sulfates of MCC, organic and carbon aerogels.

2 Experimental/methodology

Air dry sawdust (fraction 2–5 mm) of birch wood (Betula pendula) was used as starting raw material. Birch wood composition (% wt.): cellulose – 46.5, hemicelluloses – 27.2, lignin 21.8, extractive substances – 3.6, mineral part – 0.4.

The studied integrated processing of birch wood biomass included the steps of hemicelluloses acid-catalysed hydrolysis to xylose, oxidative fractionation of prehydrolysed wood on microcrystalline cellulose (MCC) and soluble lignin, obtaining of MCC sulfates, synthesis of organic and carbon aerogels from lignin.

Kinetic of wood prehydrolysis and fractionation processes was investigated with the use of batch stirring reactor at intensive agitation. The structure of solid catalysts and products was studied by FTIR, XRD, SEM, AFM and BET methods. Sulfates of MCC, sugars from hemicelluloses and soluble products from lignin were studied by ^{1}H and ^{13}C NMR, HPLC, GC-MS, FTIR and by elemental analysis.

3 Results and discussion

The present study develops our approaches which were used for obtaining MCC and MCC sulphates from aspen-wood [1, 2] and for synthesis of aerogels from polyphenols [3].

Optimal conditions of birch-wood hemicelluloses hydrolysis to xylose were established. For complete hydrolysis with sulphuric acid catalyst the temperature 100 °C, H_2SO_4 concentration 3 % wt. and time 4 hours should be used. Solid acid catalysts (sulphated graphitized carbon and zeolite SBA-15) were less active, therefore the temperature 120 °C was used to achieve the high yield of xylose.

For the first time the kinetic regularities of oxidative fractionation of birch-wood by hydrogen peroxide in the medium of acetic acid – water in the presence of solid (1 % wt. TiO_2) and soluble (2 % wt. H_2SO_4) at the temperature range 70–100 °C were compared. Similar kinetic

parameters (reaction order, rate constant, activation energy) testify in favor of analogous mechanism of lignin oxidation for both catalysts. The optimum parameters of heterogeneous catalytic fractionation of birch-wood on cellulose and lignin were selected: temperature 100 °C, concentrations of acetic acid – 20 % wt. and hydrogen peroxide – 5 %, liquid to solid ratio – 10, time 4 h. At these conditions the effective fractionation of aspen-wood on cellulose and soluble lignin was achieved. The application of solid TiO_2 catalyst instead of sulfuric acid allows to improve the ecological safety of fractionation process and to reduce the corrosive activity of reaction medium.

The new "green" method of MCC sulfates synthesis based on the use less toxic sulfation agent – sulfamic acid in the presence of basic catalyst – urea was developed. In DMF and diglym solvents the degree of substitution of sulfated MCC reaches to 1.40–1.54. The yield of MCC sulfates prepared in diglyme was by 2.5 times higher than the yield of MCC sulfates obtained in DMF. MCC sulfates obtained by developed method have more homogeneous structure and higher anticoagulant activity as compared to sulfates prepared by conventional methods using toxic SO_3–pyridine mixtures.

New types of carbon porous materials with unique properties – carbon aerogels were prepared for the first time by carbonization of organic aerogels from lignin-formaldehyde mixtures. After carbonization at 900 °C aerogels remained fully monolithic and homogeneous despite significant (55–60 % wt.) volume shrinkage. Surface area of obtained carbon aerogels reaches 1000 m^2/g and its value depends on the amount of lignin in an initial organic aerogel. The raise of lignin amount increased the volume of macropores (> 50 nm) but decreased that of small pores (< 2 nm). The density, surface area, porosity and mechanical strength can be varied within broad limits depending on their use. Light weight carbon gels are brittle, whereas the more compact samples a much more mechanically resistant.

4 Conclusions

Main stages of integrated catalytic processing of birch-wood biomass to xylose, MCC, sulphates of MCC, organic and carbon aerogels were investigated. The first stage of studied integrated process – the hydrolysis of birch wood hemicelluloses to xylose at 120 °C was accelerated by sulfated carbon and zeolite SBA-15 catalysts. At the second stage the suspended TiO_2 catalyst was used for prehydrolized wood fractionation on MCC and soluble lignin in H_2O_2–CH_3COOH–H_2O solution at 100 °C. Biologically active sulfates of MCC were firstly obtained with the use of green sulfation agent – mixture of sulfamic acid and basic catalyst urea. Highly porous organic and carbon aerogels were firstly synthesized from soluble lignin-formaldehyde mixtures. They have good prospects for application as sorbents, catalyst supports, thermal insulators etc. Based on kinetic studies the optimal conditions of birch wood fractionation on xylose, MCC and soluble lignin were established.

Acknowledgements

The reported study was partially supported by Ministry of Education and Science of RF (project RFMEFI607 14 X0031). This work is part of GRDI "Catalytic biomass valorization" between France and Russia and the Lorraine ARCUS cooperation program.

References

[1] B.N. Kuznetsov, S.A. Kuznetsova, V.G. Danilov et al. Reac. Kinet. Mech. Cat. 2 (2011) 337.
[2] B.N. Kuznetsov, S.A. Kuznetsova, V.A. Levdansky et. al. J. Wood Sci. Technol. (2015).
[3] G. Amaral-Lubat, L. Grishechko, A. Szczurec et.al. Green Chem 14(2012) 3099.

Selective Oxidation of Methane with Hydrogen Peroxide Using Gold-Palladium Nanoparticles

Mcvicker R.U.[1*], Freakley S.J.[1], Shaw G.[1], Ab Rahim M.H[2], Forde M.M.[1], Hammond C.[1], Jenkins R.L.[1], Dimitratos N.[1], Kiely C.J.[3], Hutchings G.J.[1]

1 - Cardiff University, Cardiff, United Kingdom
2 - Faculty of Industrial Sciences and Technology, University of Malaysia, Pahang, Malaysia
3 - Lehigh University, Bethlehem, USA

* McVickerRU@cardiff.ac.uk

Keywords: heterogeneous catalysis, gold, methane oxidation

1 Introduction

Methane is our most abundant hydrocarbon. However, this natural resource is not being effectively utilised. Currently, its primary industrial use is the manufacture of methanol through the intermediate formation of synthesis gas (H_2 and CO). This is an energy intensive process requiring temperatures of up to 850 °C and pressures of up to 100 atm. Clearly, a direct method of converting methane to methanol under mild conditions would provide many advantages. Catalysis by gold-palladium nanoparticles has received significant attention in recent years as they have been shown to be highly effective at catalysing the oxidation of primary C-H bonds in toluene, benzyl alcohol oxidation and the direct synthesis of hydrogen peroxide. [1, 2] In this work gold–palladium nanoparticles are shown to be active for the oxidation of methane in water at 50 °C using hydrogen peroxide as the oxidant.

2 Experimental/methodology

Au-Pd nanoparticles were prepared by both the impregnation and the sol-immobilisation methods.[1] For both methods $PdCl_2$ and $HAuCl_4$ were used as precursors. Catalyst testing was carried out in stirred Parr autoclave reactors. Typical reactions were carried out in 10 ml of water, at 50 °C, under 30 bar methane, for 30 min and stirred at a rate of 1500 rpm. At the end of each reaction the reactor was cooled to 10 °C to minimise loss of volatile products. The reaction liquid was filtered and analysed by ^{1}H-NMR to identify all liquid phase products. D_2O (99% D) was used as a solvent and a calibrated insert containing tetramethylsilane (TMS) in deuterated chloroform (99.9% D) was used to quantify the detected products. Gas phase CO_2 was determined by GC analysis on a GC equipped with FID & TCD detectors and a methaniser. The amount of hydrogen peroxide remaining after each reaction was quantified by titration against an acidified $Ce(SO_4)$ solution of known concentration using ferroin as the indicator.

3 Results and discussion

Au-Pd catalysts prepared by the impregnation technique have been found to produce catalysts that have a low rate of hydrogen peroxide decomposition and metal particle sizes in the 5-20nm range.[3] The activity and selectivity of these catalysts are compared with those of supported and unsupported Au-Pd nanoparticles prepared by the sol-immobilisation method. As this method involves the use of a stabilising ligand it affords much greater particle size control, with a narrow particle size distribution and average particle size of 3 nm. The effect of catalyst preparation parameters is investigated with emphasis on the effect of supporting the nanoparticles and its effect on hydrogen peroxide consumption during a reaction. A variety of different supporting materials are investigated and the activity of the Au-Pd nanoparticles supported on each material is compared. The influence of the stabilising ligand on the reaction is

explored particularly in relation to reactions catalysed by Au-Pd nanoparticles prepared by sol-immobilisation.

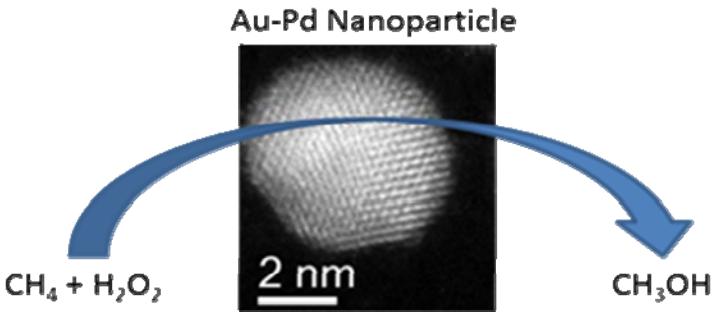

Fig. 1. TEM image of Au-Pd nanoparticles prepared by sol-immobilisation with schematic of methane oxidation reaction with H_2O_2 as oxidant.

Through time on line analysis the primary product of this reaction is shown to be methyl hydroperoxide which undergoes subsequent transformation to methanol, formic acid and carbon dioxide. [4] EPR studies have shown that methyl and hydroxyl radicles are present during the reaction and the presence of hydroperoxy radicals can be inferred from the formation of methyl hydropeorxide.

These results show that this reaction occurs *via* a radical mechanism. The reaction was found to proceed through the same mechanism regardless of whether or not the particles were supported. The reaction has been found to be highly selective for the formation of methyl hydroperoxide and methanol with optimised conditions affording an oxygenate selectivity of ca. 90%. During this presentation the effect of reaction conditions and catalyst preparation will be discussed.

4 Conclusions

Au-Pd nanoparticles have been found to be effective catalysts for the selective low temperature oxidation of methane using hydrogen peroxide as the oxidant. The primary product of the reaction is methyl hydroperoxide which is generated through the reaction of H_2O_2 and $\bullet CH_3$. The method by which the Au-Pd nanoparticles are prepared has been found to have a significant effect on catalyst activity.

References

[1] G. J. Hutchings and C. J. Kiely, *Accounts of Chemical Research*, 2013, **46**, 1759-1772.
[2] C. Della Pina, E. Falletta, L. Prati and M. Rossi, *Chem. Soc. Rev.*, 2008, **37**, 2077-2095.
[3] J. A. Lopez-Sanchez, N. Dimitratos, P. Miedziak, E. Ntainjua, J. K. Edwards, D. Morgan, A. F. Carley, R. Tiruvalam, C. J. Kiely and G. J. Hutchings, *Phys. Chem. Chem. Phys.*, 2008, **10**, 1921-1930.
[4] M. H. Ab Rahim, M. M. Forde, R. L. Jenkins, C. Hammond, Q. He, N. Dimitratos, J. A. Lopez-Sanchez, A. F. Carley, S. H. Taylor, D. J. Willock, D. M. Murphy, C. J. Kiely and G. J. Hutchings, *Angew. Chem.-Int. Edit.*, 2013, **52**, 1280-1284.

I-OP22

Ethanol Conversion into Chemicals over Au-M Containing Catalysts

Chistyakov A.V.[1,2*], Nikolaev S.A.[3], Zharova P.A.[1], Kriventsov V.V.[4], Tsodikov M.V.[1,2]

1 - Topchuev Institute of Petrochemical Synthesis RAS, Moscow, Russia
2 - Gubkin Russian State University of Oil and Gas, Moscow, Russia
3 - Lomonosov Moscow State University, Moscow, Russia
4 - Boreskov Institute of Catalysis SB RAS, Novosibirsk, Russia

* chistyakov@ips.ac.ru

Keywords: ethanol, heterogeneous catalysis, linear, alpha alcohols, gold nanoparticles, 1-butanol

1 Introduction

The first reference to gold as a catalyst dates from 1906, when Bone and Wheeler observe the oxidation of hydrogen on a heated gold gauze [1]. The recent progress in heterogeneous catalysis resulted in remarkable investigations, that revealed the high activity of supported gold nanoparticles and synergetic effect of gold with either nickel or copper in a wide range of reactions[2-4].

2 Experimental/methodology

Analytical grade ethanol (99 %) and iso-propanol (99%) were used without further purification. Catalytic tests were performed in autoclave type reactor with magnetic stirrer (Parr 5000 series) under temperature 240-295 °C and pressure 50-120 atm. Reaction products were analyzed with use of GC and MS. Au-Cu/Al_2O_3 and Au-Ni/Al_2O_3 catalysts were produced by deposition-precipitation as described in [2, 5]. As a support γ-alumina SiO_2 and TiO_2 were used. The metal content of the catalysts was determined by atomic absorption on a Thermo iCE 3000 AA spectrometer. XRD analysis was carried out on a Rigaku D/MAX 2500 instrument using Cu Kα radiation with a step size of 0.02 ° two-theta (2θ) ranging from 35 to 70 °. XPS analysis was carried out on a Kratos Axis Ultra DLD spectrometer using Al Kα radiation (1486.6 eV). TEM and EDX analysis of catalysts were carried out on a JEOL JEM 2100F/UHR microscope with 0.1-nm resolution and a JED-2300 X-ray spectrometer, respectively.

3 Results and discussion

During ethanol conversion into olefins C_3-C_8 was found that nickel oxide clusters with a size of 3.5 nm possess low TOF (0.051 s^{-1}) and low selectivity (12.73 wt.%). The TOFs of the gold clusters increases from 0.095 to 0.384 s^{-1} as the size of the gold particle decreases from 13-15.1 to 5 nm. The most probable cause of this positive size effect is the increasing amount of coordinative unsaturated atoms on the surface of the small Au^0 particles. Increasing the gold particle sizes from 5 to 13-15.1 nm results in the selectivity for C_{3+} hydrocarbons increasing from 11.69 to 29.99 mass %, which suggests the participation of multiple active centers in the conversion of ethanol into hydrocarbons. The deposition of nickel oxide particles on the Au/Al_2O_3 catalysts results in the formation of large NiO/Au aggregates consisting of small gold and nickel oxide clusters. These new NiO/Au structures have the TOF of 0.321 s^{-1} and the selectivity of 34.19 wt. %, with a total metal content of 0.13 wt. % and a Au:Ni molar ratio of 1:1. The active catalyst sites become occluded by nickel oxide as the total metal content is increased or when the molar ratio of Au:Ni > 1:1, which is manifested as a decrease in both the TOF and selectivity.

During ethanol conversion into linear alpha alcohols found that optimal temperature is 270 °C and ethanol partial pressure is > 60 atm that provides supercritical conditions. Depending on catalyst nature ethanol conversion varied from 30 to 63,5 % with selectivity on 1-butanol 58-75 %. Over Au-Ni containing catalysts ethanol converts also in hexanol-1 and octanol-1 with selectivity 21,2 and 5,6 % respectively. First time ever α-alkylation of iso-propanol with ethanol was carried out over heterogeneous Au-M containing catalysts with 3-methylbutanol-2 selectivity 55-70 % depending on catalyst composition and reaction conditions. Found that monometallic Au/Al2O3 catalyst possesses lower activity in ethanol conversion than bimetallic ones. Cu/Al_2O_3 and Ni/Al_2O_3 had no activity in butanol-1 formation. Varying of catalysts support showed that usage of TiO2 instead of Al_2O_3 increase selectivity on 10% but decreases conversion rate down to 20 %. Stability test demonstrated that during over 50 h catalysts have constant activity and selectivity.

Structural investigations explains observed synergetic effect of Au with Ni or Cu. Bimetallic catalysts have Au-MxOy nonspherical species like core-shell structures with average linear size 2-6 nm that possesses gold in both metal state and Au^+ state.

4 Conclusions

The strong synergetic effect of Au-M_xO_y containing catalysts wasdetected. Found that ethanol could be incorporated onto either olefins C_3-C_8 fraction or linear alpha-alcohols with even number of carbon atoms up to C_8. Au-Cu containing catalyst possesses the highest selectivity on 1-butanol 75 % with ethanol conversion 33 %. Au-Ni containing catalyst possesses total selectivity on 1-butanol, 1-hexanol and 1-octanol 90 % with ethanol conversion 63,5 %. First time ever α-alkylation of iso-propanol with ethanol was carried out over heterogeneous Au-M containing catalysts with 3-methylbutanol-2 selectivity 55-70 % depending on catalyst composition and reaction conditions. The optimal structural and electronic organization of Au-Cu and Au-Ni catalysts is achieved in the catalysts produced by modification of Au/Al_2O_3 with M_xO_y and implies the high concentration of special sites: $Au^{\delta+}$ atoms at the Au-M interface; partially reduced metal-oxide species at the Au-M interface; atoms with a low coordination number on the surface of nonspherical bimetallic particles.

Obtained data allow suggesting Au-Cu and Au-Ni catalysts as prospective systems for fuels components (butanol-1) producing and valorisation of ethanol into chemicals like hexanol-1 and octanol-1. Combined conversion of ethanol with iso-propanol that leads to 3-methylbutanol-2 formation may be considered as the first step of valuable monomer - isoprene production.

Acknowledgements

Authors thank for financial support RFBR (grants 13-03-12034, 15-03-06479), Council on Grants of the President of the Russian Federation for the Support of Young Scientists MK-5328.2014.3.

References

[1] W.A. Bone, R.V. Wheeler, *Phil. Trans. R. Soc. A*. 206 (1906) 1–67
[2] S.A. Nikolaev, A.V. Chistyakov, M.V. Chudakova, V.V. Kriventsov, E.P. Yakimchuk, M. V. Tsodikov, *J. Catal.* 297 (2013) 296–305
[3] W.-S. Lee, M.C. Akatay, E.A. Stach, F.H. Ribeiro, W.N. Delgass, *J. Catal.* 313 (2014) 104–112.
[4] C. Pojanavaraphan; A. Luengnaruemitchai; E. Gulari, *App. Catal. A*: *General.* 456 (2013) 135-143.
[5] S.A. Nikolaev, V.V. Smirnov, *Catal. Today* 147 (2009) 336–341.

I-OP23

Evolution and Interlayer Dynamics of Active Sites of Promoted Transition Metal Sulphide Catalysts under Hydrogen and Inert Media in the Course of Some Commercially Valuable Reactions

Kogan V.M.[1*], Nikulshin P.A.[2], Dorokhov V.S.[1], Permyakov E.A.[1]

1 - N.D. Zelinsky Institute of Organic Chemistry, RAS, Moscow, Russia
2 - Samara State Technical University, Samara, Russia

* vmk@ioc.ac.ru

Keywords: active site, alcohols, hydrodesulphurization, syngas conversion, transition metal sulphides

1 Introduction

A concept on the dynamic nature of active sites (AC) of the catalysts based on transition metal sulphides is described. The concept formed the basis of a "dynamic" model, according to which AC formed and functioning under the reaction conditions can oscillate between layers of promoted molybdenum sulphide. The model assumes the existence of "rapid" and "slow" AC and the possibility of their mutual transformation due to the reversible migration of sulphur and promoter between the crystallite layers in a hydrogen atmosphere.

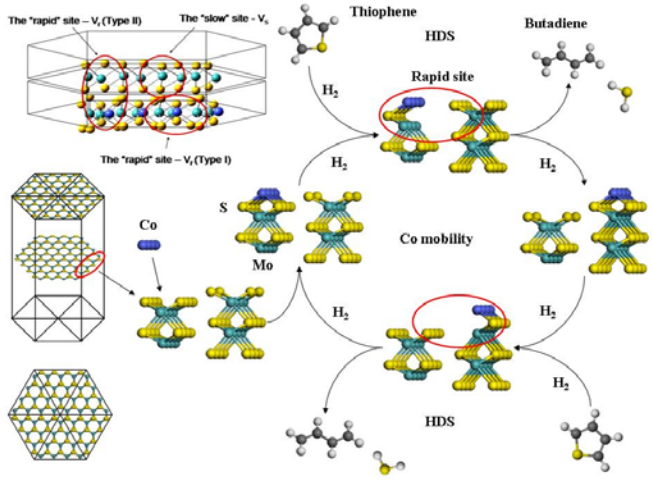

The frequency of these migrations (oscillations) determines the catalyst activity. An assumption is substantiated that the hydrogenation (HYD) and hydrodesulphurization (HDS) sites are localized at the rims of the Co(Ni)MoS_2 crystallites whereas direct desulpurization (DDS) and hydrodesulphurization (HDS) sites are localized on the edges.

Fig. 1. Dynamic model of transformations of the active sites of promoted TMS catalysts in the course of thiophene HDS.

2 Application of the dynamic model to various catalytic processes

2.1. Hydrodesuphurization of various types of crude oil.

The dynamic model explains a series of correlations structure – property that was reported in studies of the catalysts prepared under the laboratory conditions, industrial catalysts and new sulphide catalysts synthesized using heteropolycompounds, organic complexones and carbonized supports. The dependence of the catalyst activity on the number of layers and linear size was studied by the experimental and calculation methods, and the arrangement of AC of different types on the surface of molybdenum disulphide crystallites was determined.

An increase in the average linear size of the slab leads to a drop of HDS and HYD activities. The longer layers in the slabs, the fewer solid angles are, and so the higher the effect of the support. On the contrary, in the multilayered structure the support effect diminishes. The observed high HYD/DDS selectivity of the catalysts synthesized from AHM and nickel nitrate may be caused by low edge surface Ni on the MoS_2 slab which should also form the unpromoted Mo-sites responsible for the HYD reactions on the edges.

The results suggest that the catalytic activity in HDS and HYD reactions depends on the

shape of crystallites of the active phase. The results are interpreted using recently proposed concepts of interlayer dynamics. These concepts are helpful in establishing structure-activity relations for TMS

2.2. Synthesis gas conversion

Using the interlayer dynamics model for the explanation of the mechanism of syngas conversion on the sulphidized KCoMo catalysts, we obtained the general regularities governing the action of the AC of transition metal sulphides in the hydrogenolysis of sulphur containing organic compounds and syngas conversion. The role of Co is the activation of a CO molecule. Potassium stabilizes the C-O bond and prevents its cleavage, and the hydroxyl group of alcohol is formed. The ratio of the yield of alcohols to the yield of hydrocarbons decreases with temperature. This indicates that with the temperature rise the formation of alcohols becomes kinetically less favourable than the hydrogenolysis of the C-O bond and hydrogenation of the alkyl fragment to hydrocarbon. If alcohols are formed on the edges of molybdenum disulphide crystallites, the adsorbed alkyl fragment can be involved in the chain growth with another adsorbed particle localized on one of two neighbouring layers of the same edge. Therefore, the probability of carbon chain growth involving the methyl fragment on the edge is higher than that on the rim or monolayered crystallite. This statement is explained in terms of the interlayer dynamics concept by the fact that the rims contain more "slow" AC.

2.3. Alcohol conversion in hydrogen and inert media

It was found that ethanol conversion in H_2 is much smaller than in inert media such as N_2, He or Ar. Hydrogen pressure increase leads to decrease of catalytic activity whereas pressure growth of inert gases does not suppresses it. It is likely that in inert gases it takes place disproportionation of ethanol with formation of oxygenates and hydrocarbons. In contrast, hydrogen suppresses oxidative processes and shifts reaction equilibrium to reduction ones. Possible explanation of the observed phenomena is the effect of the nature and pressure of gas media on the active site structure and behavior (Fig. 2).

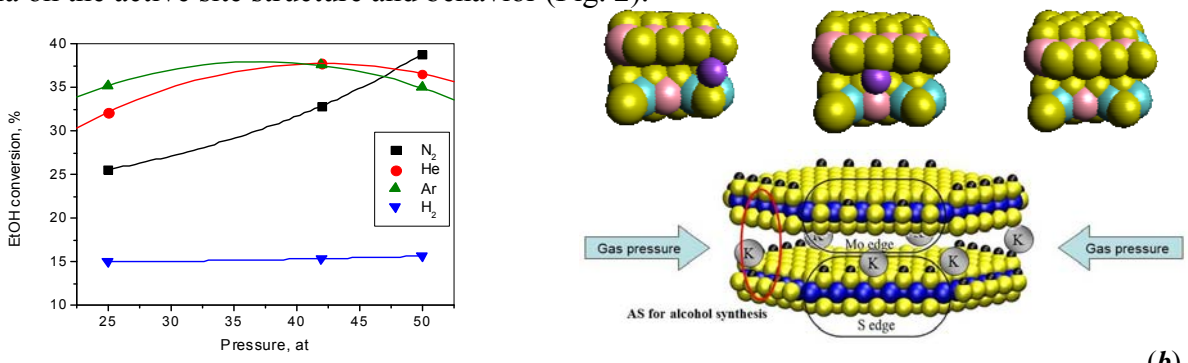

(***a***) (***b***)

Fig. 2. Ethanol conversion depending on pressure at 320°C in verious media (***a***); transfere of potussium ions in different positions between MoS_2 slab layers depending on gas medium pressure (***b***).

The obtained results allowed us to develop the methods for product selectivity control. The synthesized products could be used is additives for transportation fuels, solvents and precursors for petrochemical synthesis.

3 Conclusions

The proposed model makes it possible to develop criteria for the evaluation of the efficiency of catalytic performance for hydrodesulphurization (HDS) of hydrocarbon raw materials of various types, for syngas conversion with formation of higher alcohols and their followed conversion into wide range of oxygenates under hydrogen and inert media.

I-OP24

Taking Advantage of Mass Transfer Limitations in Egg-Shell Catalysts for Intensified Fischer-Tropsch Reactors.

Fratalocchi L.[1], Visconti C.G.[1*], Lietti L.[1], Tronconi E.[1], Rossini S.[2]

1 - Politecnico di Milano, Dipartimento di Energia, Milano, Italy
2 - Eni, San Donato Milanese, Italy

* carlo.visconti@polimi.it

Keywords: egg-shell catalysts, Fischer-Tropsch synthesis, mass transfer limitations

1 Introduction

The low temperature Fischer-Tropsch synthesis (FTS, T< 250°C, P>20 bar) aims at converting synthesis gas into long-chain hydrocarbons through the adoption of heterogeneous catalysts based on cobalt or iron. In packed bed reactors, where the adoption of "big" catalyst pellets is mandatory to limit ΔP, the performances of FTS catalysts may be significantly worsened by strong mass transfer limitations, which affect both the CO conversion rate and the C_{5+} selectivity. In the case of state-of-the-art Co-based catalysts, such restrictions occur when the characteristic length of diffusion (δ) overcomes the threshold value of 50-60 microns [1,2]. Eggshell catalysts, in which the active phase is located only in the outer region of the catalytic support, represent an engineering solution to limit both δ and pressure drops in packed-bed reactors [2]. In those catalysts, in fact, the diffusion characteristic length and the pellet diameter become two independent parameters to be optimized. In this work, a "small" Co/Al_2O_3 eggshell catalyst, to be used in compact and intensified multitubular FTS reactors, has been prepared by following an innovative preparation method. Then, its catalytic activity has been tested in a lab-scale fixed bed reactor at industrially relevant process conditions [3]. Eventually, its performances have been compared with that of a powdered catalyst. It has been found that the optimal design of the catalyst brings to outstanding C_{25+} yields, even higher than those obtained with a catalyst operating under kinetically controlled regime.

2 Experimental/methodology

The preparation method developed to synthetize a small Co/Al_2O_3 eggshell catalyst involves a few, simple steps. At first, Al_2O_3 microspheres are soaked in *n*-undecane for 40 min so to fill their pores; then, they are drained from the excess liquid and placed into a fritted glass funnel mounted on a vacuum flask. At this point, a solution of $Co(NO_3)_2{\cdot}6H_2O$ in ethanol (1.27 $ml_{ethanol}/g_{salt}$) is poured onto the microspheres and, after a short time (τ), the excess solution is removed from the flask by evacuating the system. The impregnated spheres are dried in static air at 393 K for 2 h and eventually calcined at 673 K in static air for about 12 h. By (i) using microspheres with a diameter of 600 microns, (ii) keeping τ= 2s and (iii) repeating 9 times the impregnation procedure, eggshell pellets (ES600) with a Co loading of 9 wt.% (16 wt.% in the active shell) have been obtained. A powered sample (POW100) has been obtained by grinding a fraction of the eggshell microspheres and sieving in the range 75-106 microns. Both the catalysts have been reduced in situ flowing H_2 at 400°C for 17 h and then tested at 25 barg, GHSV= 46.01 $L(STP)h^{-1}g_{Co}^{-1}$, H_2/CO molar ratio = 1.7, N_2+Ar in the feed = 24 vol.%, in the T-range 220-240°C.

3 Results and discussion

Thanks to (i) the presence of an hydrophobic liquid filling the Al_2O_3 pores, (ii) the adoption

of an hydrophilic impregnating solution and (iii) the control of the contact time between the support and the impregnating solution, the adopted preparation method allowed to obtain eggshell Co/Al_2O_3 pellets with a uniform thickness (t) of the sharp active shell region (t=75 microns). An average Co_3O_4 cry-size of 7 nm has been estimated, a value granting the optimal compromise between active phase dispersion and TOF [4] and a high reduction degree (55-67%) of the cobalt oxides upon heating the sample in H_2 up to 400°C, without the need of any promoter. When tested in the FTS, ES600 catalyst shows higher CO conversion and a slightly higher C_{5+} selectivity than POW100 sample (Figure 1), with the products containing much less olefins. According to our understanding, these results can be explained by assuming the occurrence of weak mass transport limitations in the case of ES600 catalyst, which is characterized by a value of δ (58microns) higher than POW100 (δ<15microns) and very close to the threshold limit of 50-60 microns [2,3]. The CO conversion with ES600 sample is higher than with POW100 because the local H_2/CO ratio in close proximity of the active centers is higher than in the bulk phase (H_2 diffusion in the waxes is twice as fast as that of CO), thus resulting in a speed-up of the CO conversion kinetics which is negative order with respect to CO and positive order with respect to H_2. The lower content of olefins in ES600 catalyst is related instead to the longer diffusion length, which enhances the probability of the olefins to be re-adsorbed and to undergo secondary reactions. Among these, the hydrogenation of C_n olefins to the corresponding paraffin is dominant, even though we also observed an increase of the chain growth and an increase of hydroformylation to the C_{n+1} alcohol. As a confirmation of our explanation for the observed data, while an apparent FTS activation energy of 100 kJ/mol has been estimated for POW100 sample, a value as low as 87 kJ/mol has been estimated for the ES600 catalyst.

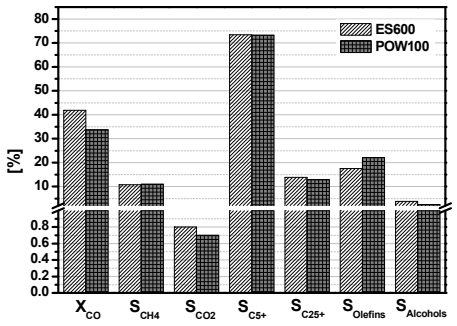

Fig. 1. CO conversion (X_{CO}) and selectivity (S_i) to the main reaction products

4 Conclusions

All the obtained results, confirming the presence of mass transfer restrictions which falsify the CO conversion kinetics for δ > 50 microns, point out that engineered eggshell catalysts suffering of "weak" mass transfer restrictions represents an optimal solution to achieve a high C_{25+} yields, while limiting the pressure drops in compact Fischer-Tropsch packed-reactors.

Acknowledgements

Sasol Germany GmbH is acknowledged for providing us with free Al_2O_3 samples.

References

[1] F. Kapteijn, R.M. Deugd, J.A. Moulijn, *Catal. Today* 105 (2005) 350-356.
[2] E. Iglesia, S. L. Soled, J.E. Baumgartner, S.C. Reyes, *J. Catal.* 153 (1995) 108-122
[3] L. Fratalocchi, C.G. Visconti, L. Lietti, E. Tronconi, U. Cornaro, S. Rossini *Catal. Today*, doi:10.1016/j.cattod.2014.09.020
[4] G.L. Bezemer, J.H. Bitter, H.P.C.E Kuipers, H. Oosterbeek, J.E. Holewijn, X. Xu, F. Kapteijn, A.J. van Dillen, K.P. de Jong, *J. Am. Chem. Soc.* 128 (2006) 3956-3964

I-OP25

Intensification of Strongly Endo- and Exo-Thermic Catalytic Processes through the Adoption of Highly Conductive "Packed Foams" Reactors

Visconti C.G., Groppi G., Tronconi E.*

Politecnico di Milano, Department of Energy, Laboratory of Catalysis and Catalytic Processes, Milano, Italy

* enrico.tronconi@polimi.it

Keywords: packed foams, structured catalysts, process intensification, heat transfer

1 Introduction

Even though it is widely recognized that spatially structured reactors are at the very heart of process intensification [1], and it has been shown that significant enhancement of radial heat transfer rates in technical multitubular catalytic reactors with external cooling can be achieved if the random packings of catalyst pellets are replaced by structured catalysts with thermally connected, highly conductive support matrices [2], some issues still exist that prevent the application of this technology at the industrial scale. For example, in the case of non-adiabatic reactors loaded with highly conductive washcoated open-cell foams (or sponges), due to the thin catalyst layer, the catalyst inventory is often insufficient, which may limit the potential advantages associated with the adoption of conductive structured reactors. Also, the catalyst loading and unloading in the reactor, as well as the replacement of the spent active phase, are particularly critical in such a technology. To overcome those issues the adoption of "packed structured" reactors has been recently proposed [3,4]. In such reactors, particularly interesting for compact scale applications (i.e. short tubes), the catalyst is loaded in the form of small pellets (e.g. microspheres) packed in the voids of highly conductive structures. Herein we investigate the concept applied to open-cell metallic foams, which has not been proposed before to our knowledge: we assess the heat transfer performances of packed sponges and compare them to those of conventional packed beds of pellets and of bare open-cell foams.

2 Experimental/methodology

Comparative heat transfer experiments have been performed in a lab-scale test rig consisting of a finned stainless steel pipe (28 mm I.D.) placed in an oven, using three different types of packings: *i)* packed beds (**PB**) of spherical pellets with **0.3** and **3** mm diameter; *ii)* bare open-cell foams (**VF**, void foams) made of two different materials (aluminium, **Al**, and FeCrAlloy®, **FeCr**), and with different geometries (cell densities 10-40 PPI and relative densities 5-6%); *iii)* packed foams (**PF**). During the experiments, carried out heating the oven at different temperatures (200-500°C), two different gases (**He** and $\mathbf{N_2}$) at different flow rates (representative of those used in compact industrial reactors) have been fed to PB, VF and PF and steady-state axial and radial T-profiles inside the packings and at the pipe skin were measured. A classical 2D two-parameters pseudo-homogeneous heat transfer model was then fitted to the experimental T-profiles to estimate the effective radial thermal conductivity of the bed, k_{er}, as well as the wall heat transfer coefficient, h_w. The overall heat transfer coefficient, U, was also calculated.

3 Results and discussion

Figure 1 shows the estimates of the overall heat transfer coefficient obtained for the different configurations using He and N_2 as flowing gas. Lines are used to group 4 different

packing configurations particularly relevant to be compared. For each configuration, a cloud of points is shown, representing data collected at different gas flow rates.

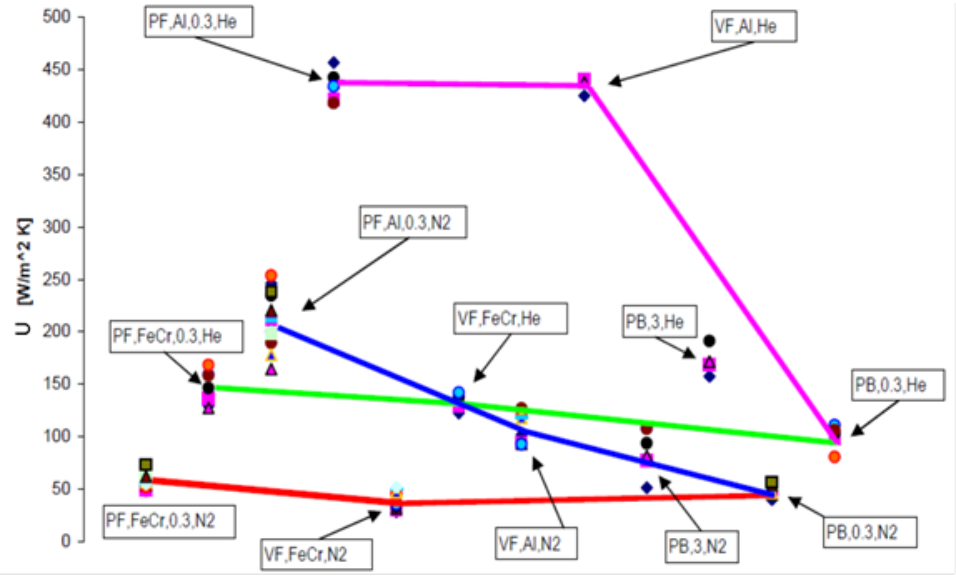

Fig. 1. Heat transfer performances of different packings upon varying the flowing gas and its flow rate

Data in Figure 1 show that at the adopted conditions heat transfer in a PB is comparable to that in a low conductive VF (FeCr). In this case, PF with a poorly conductive structured substrate performs similarly to the corresponding PB and VF. On the contrary, due to the high value of $k_{e,r}$ [2], heat transfer in a highly conductive VF (Al) is much better than in PB, which on the contrary shows higher h_w at high flow rates. In this case, a PF with a highly conductive structured substrate performs much better than both the corresponding PB and VF, due to the synergy of the enhanced conductive heat transfer in the solid structure of the foam and the convective heat transfer at the wall-bed interface of packed spheres. The former mechanism, which is flow independent, controls the effective radial conductivity. The latter one enhances the wall heat transfer coefficient and contributes to increase the overall heat transfer coefficient, particularly at high flow rates. A circuit of equivalent resistances has been identified to describe the heat transfer mechanisms within packed foams.

4 Conclusions

Our results suggest that "packed foams" may be particularly advantageous in compact reactors requiring short tubes, in view of their flow-independent, conductive heat transfer mechanism which adds to the convective heat transfer typical of packed-beds of pellets.

Acknowledgements

Funding by the Italian Ministry of Education, University and Research, Rome (MIUR, PRIN, prot. 2010XFT2BB) within the project IFOAMS ("Intensification of Catalytic Processes for Clean Energy, Low-Emission Transport and Sustainable Chemistry using Open-Cell Foams as Novel Advanced Structured Materials") is gratefully acknowledged.

References

[1] E. Tronconi, G. Groppi, C.G. Visconti, Curr. Op. Chem. Eng. 5 (2014) 55.
[2] E. Bianchi, T. Heidig, C.G. Visconti, G. Groppi, H. Freund, E. Tronconi, Chem. Eng. J. 198-199 (2012) 256
[3] D. Vervloet, F. Kapteijn, J. Nijenhuis, J.R.van Ommen, Catal. Today 216 (2013) 111
[4] Patent application WO/2010/130399

I-OP26

Microkinetics Assisted Analysis of Hydrotreating Selectivities in Fast Pyrolysis Oil Upgrading

Otyuskaya D.[1*], Lødeng R.[2], Thybaut J.W.[1], Marin G.B.[1]

1 - Laboratory for Chemical Technology, Ghent University, Gent, Belgium
2 - SINTEF Materials & Chemistry, Department of Kinetics and Catalysis, Trondheim, Norway

* Daria.Otyuskaya@UGent.be

Keywords: fast pyrolysis oil, hydrodeoxygenation, anisole, intrinsic kinetics

1 Introduction

In recent years, due to the depletion of fossil fuels and environmental concerns, biomass valorization looks as an attractive alternative route for fuels production. Among several techniques proposed for lignocellulosic biomass valorization, the most promising one is fast pyrolysis followed by catalytic upgrading to reach the desired oil quality. While a lot has already been done in the field of fast pyrolysis itself, bio-oil hydrotreatment still represents significant challenges .

A non-sulfided 15wt.%Co-3.8wt.%Mo/Al_2O_3 hydrotreating catalyst has potentially a relatively low cost in comparison to noble metal based catalysts and doesn't require sulphiding pretreatment as do conventional hydrotreating catalysts. Anisole was used as a model compound for assessing the various elementary steps by systematically varying the operating temperature, pressure and inlet composition at different space times. The obtained experimental results are expected to provide insight into the reaction mechanism, input for kinetic model construction and constitute a basis for further catalyst and process design.

2 Procedures

Intrinsic anisole HDO kinetics on a non-sulphided 15wt.%Co-3.8wt.%Mo/Al_2O_3 catalyst have been acquired in a plug flow reactor at gas-phase conditions . Off-line GCxGC-TOF-MS analysis was used for detailed product identification. For all the experiments the intrinsic kinetics regime was verified by testing the relevant criteria for mass and heat transfer limitation assessment.

3 Results and discussion

Based on the GCxGC-TOF-MS analysis of the product mixture, complemented by literature information , the following reaction network was proposed for anisole hydrotreating (Fig.1):

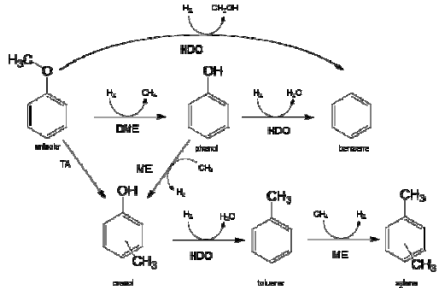

Fig. 1. Anisole HDO reaction network.

Demethylation and isomerization, including, (trans)alkylation reactions were found to occur to a significant extent. Apparently, metallic CoMo is a better isomerisation than hydrogenation or hydrodeoxygenation catalyst . The main reaction products on this catalyst were found to be

phenol and its methyl substituted analogues, c.q., cresols, while the selectivity towards benzene and toluene is less than 5% (Fig. 2).

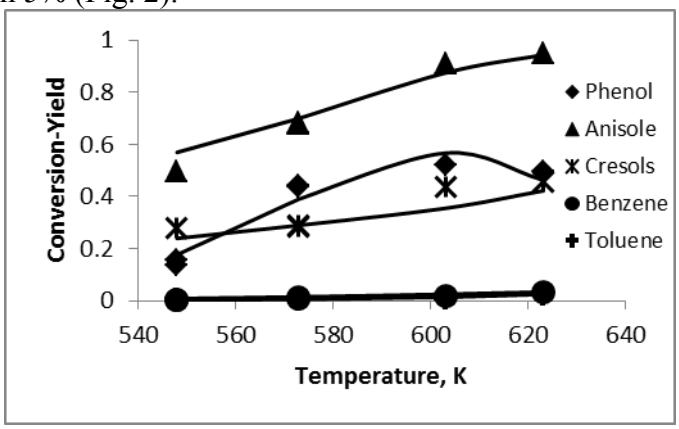

Fig. 2. Temperature effect on anisole hydrotreating conversion and product yield (symbols: experimental; lines: model simulations).

From kinetic model regression to experimental data values for activation energies and reaction rate coefficient at average temperature were estimated (Table 1). The limited hydrodeoxygenation extent is in line with the high activation energy obtained for it, compared to the other reactions.

Table 1. Parameter estimates obtained from kinetic model regression to the experimental data.

	k_{Tavr}, [mol $s^{-1}kg_{cat}^{-1}$]	Ea, [kJ mol^{-1}]
Transalkylation	$2 \cdot 10^{-6} \pm 1.6 \cdot 10^{-7}$	99±24
Methylation	$2.9 \cdot 10^{-7} \pm 1.3 \cdot 10^{-7}$	*34±40*
Demethylation	$2 \cdot 10^{-6} \pm 1.6 \cdot 10^{-7}$	55±9
Hydrodeoxygenation	$1.4 \cdot 10^{-8} \pm 0.9 \cdot 10^{-8}$	130±19

4 Conclusions and future work

A reaction network and corresponding LHHW kinetic model have been proposed for anisole hydrotreating over a non-sulphided $CoMo/Al_2O_3$ catalyst. The catalyst mainly exhibited demethylation and isomerization, rather than hydrogenation or hydrodeoxygenation behaviour, even at very high anisole conversions. The acquired data have been adequately described by kinetic model. Alternative catalysts will be explored to enhance our understanding of the determining catalyst features for the isomerization versus hydrogenation/hydrodeoxygenation selectivity. An adequate kinetics model will assist in reaching this understanding and optimizing the corresponding catalysts and process.

Acknowledgements

This paper reports work undertaken in the context of the project "FASTCARD, FAST Industrialisation by CAtalysts Research and Development". FASTCARD is a Large Scale Collaborative Project supported by the European Commission in the 7th Framework Programme (GA no 604277). For further information about FASTCARD see: http://www.sintef.no/fastcard.

References

[1] D.C. Elliott, Energy & Fuels (2007) 1792-1815.
[2] N. Navidi, J.W. Thybaut, G.B. Marin, Applied Catalysis A: General. 469 (2014) 357-366.
[3] Y. Yang, C. Ochoa-Hernández, V.A. de la Peña O'Shea, P. Pizarro, J.M. Coronado, D.P. Serrano, Applied Catalysis B: Environmental (2014). 91-100.
[4] A.L. P.Baladincz, L. Leveles, J. Hancsók, Hungarian journal of industry and chemistry 40 (2012) 45-52.

I-OP27

Stable Rh Particles on Electrosynthesized Structured Catalysts

Benito P.[1*], Nuyts G.[2], Monti M.[1], De Nolf W.[2], Fornasari G.[1], Janssens K.[2], Scavetta E.[1], Vaccari A.[1]

1 - University of Bologna, Dip. Chimica Industriale "Toso Montanari", Bologna, Italy
2 - University of Antwerp, Department of Chemistry, Belgium

* patricia.benito3@unibo.it

Keywords: Rh, RhNi, electrosynthesis, structured catalyst, catalytic partial oxidation, syngas

1 Introduction

Metal structured catalysts allow the design of more compact reactors for the conversion of fossil fuel or biomass-derived feedstocks into H_2 or syngas [1], with lower pressure drop and enhanced heat transfer. For instance, hot spots in the catalytic partial oxidation (CPO) of CH_4 are reduced. Open-cell metallic foams are optimum 3D supports, the main challenge is achieving similar performances with structured catalysts compared to pelletized ones. The catalyst performance is determined by the composition, thickness and adhesion of the coating, as well as stability of the metallic support under reaction conditions. The amount of active species (mainly Rh) is controlled by pore size, layer thickness and active phase loading; while its dispersion and stability depends on the preparation method and oxide support.

Rh catalysts, coated on FeCrAlloy foams for the CPO of CH_4, were prepared by thermal decomposition of electrosynthesized hydrotalcite-type (HT) compounds [2,3], since the latter compounds give rise to catalysts with small and stable Rh^0 particles. The FeCrAlloy foam was used as working electrode in an electrochemical cell containing Rh^{3+}, Mg^{2+} and Al^{3+} nitrates; the pH required for the HT compound precipitation on the foam surface was generated by the reduction of these nitrates. However, to balance the formation of thin layers, during the optimization of the synthesis parameters, high loaded Rh solutions were used, leading to the formation of large Rh particles [3]. Here, the metal particle size distribution, coating thickness and activity of Rh-structured catalysts were optimized by modifying the Rh/Mg/Al atomic ratio percent (a.r.%), total metal concentration and inclusion of Ni as second active phase.

2 Experimental

Electrosyntheses were performed in a three-electrode single-compartment cell on 60 ppi FeCrAlloy foam cylinders (1.0 x 1.19 cm) at -1.2 V vs SCE for 2000 s [3]. The electrolytic solution contained $Mg(NO_3)_2$, $Al(NO_3)_3$, $Rh(NO_3)_3$ or $Ni(NO_3)_2$ with 0.03M total concentration, varying the atomic ratios: Rh/Mg/Al = 11/70/19, 5/70/25, 2/70/28 a.r.% or Rh/Ni/Mg/Al = 5/15/55/25 a.r.%. Syntheses with the 5/70/25 a.r.% solution were also performed with total concentrations of 0.06 or 0.10M. Catalysts were obtained by calcination at 900 °C for 12 h. Samples were characterized by SEM/EDS, FEG-SEM and μXRF/XANES at ID21 beamline (ESRF). CPO of CH_4 tests were performed, after catalyst reduction at 750 °C for 2 h, at T_{oven}=750 °C, GHSV = 11,500-63,300 h^{-1}, CH_4/O_2/He = 2/1/20 or 2/1/4 v/v.

3 Results and discussion

The same general features were observed in electrosynthesized samples regardless of the Rh/Mg/Al a.r.% in the solution: i) the foam surface was almost entirely coated by a solid (Fig. 1a); ii) preferential precipitation on the tips of the struts, resulting in a 5-15 μm film; iii) the initial deposition of a film with a composition close to the expected one, followed by the precipitation of a film enriched in Al and Rh.

The Rh content in the precipitated solid correlated with the Rh loading in the solution. Hence, the amount of Rh species in calcined samples, identified as $Mg(Rh_xAl_{1-x})_2O_4$ by μXANES (Fig. 1b), and the Rh particle size and dispersion in spent catalysts depended both on the Rh content and layer thickness. Smaller and highly dispersed particles were observed by decreasing the Rh concentration and in thin layers. A narrow particle size distribution centred at 10 nm was measured for the spent Rh/Mg/Al = 2/70/28 a.r. % (Fig. 1c). However, the CH_4 conversion to syngas was negatively affected by the lower amount of active sites in the coating. Conversion values were 92, 85 and 72% for Rh/Mg/Al = 11/70/19, 5/70/25 and 2/70/28 a.r.%, respectively, at $CH_4/O_2/He$ = 2/1/20 v/v and 15,250 h^{-1}. The high metal support interaction that decreased the Rh reducibility, the possible oxidation of metallic particles during concentrated tests and carbon formation also determined the catalytic performances.

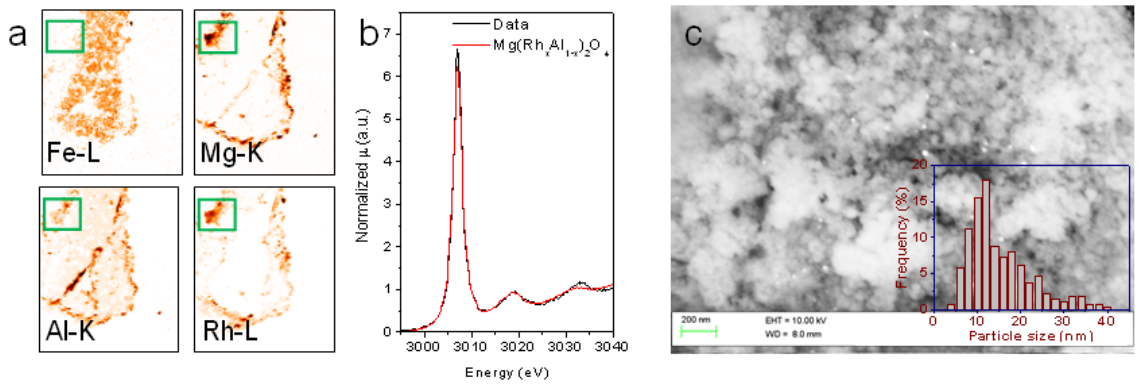

Fig. 1. Rh/Mg/Al= 2/70/28 a.r.% sample. Elemental XRF maps (a) and Rh-L_3 XANES spectrum (b) of fresh catalyst; FEG-SEM image and particle size distribution (c) of spent catalyst.

By increasing the total metal concentration from 0.03 to 0.06 M with the Rh/Mg/Al = 5/70/25 a.r.% solution a larger amount of solid containing well dispersed Rh particles was deposited and catalytic performances enhanced (Conv. CH_4 = 92 %, $CH_4/O_2/He$ = 2/1/20 v/v, 15,250 h^{-1}). On the contrary, a further increase in the concentration to 0.1M had a negative effect on coating properties.

The inclusion of Ni as second active phase produced very active RhNi bimetallic catalysts, CH_4 conversion and selectivity to syngas were above 90 % for all the reaction conditions, although it showed a lower stability with time-on-stream.

4 Conclusions

Catalysts with smaller, more dispersed and stabilized Rh metallic particles in the coating, and therefore improved catalytic performances, were prepared by tailoring the Rh content and concentration of metals in the electrolytic solution. The formation of bimetallic RhNi particles largely increased the activity, although the stability has to be still improved.

Acknowledgements

The Authors acknowledge M. Salome from ID21 Beamline of the ESRF and the financial support from the University of Bologna (FARB program).

References

[1] E. Tronconi, G. Groppi, C. Visconti, *Curr. Opin. Chem. Eng.* 5 (2014) 55.
[2] P. Benito, W. de Nolf, G. Nuyts, M. Monti, G. Fornasari, F. Basile, K. Janssens, F. Ospitali, E. Scavetta, D. Tonelli, A. Vaccari, *ACS Catal.* 4 (2014) 3779.
[3] P. Benito, M. Monti, W. De Nolf, G. Nuyts, G. Janssen, G. Fornasari, E. Scavetta, F. Basile, K. Janssens, F. Ospitali, D. Tonelli, A. Vaccari, *Catal. Today* (2014) http://dx.doi.org/10.1016/j.cattod.2014.10.003.

I-PP01

Synthesis and Characterization of Core-Shell Beta/MCM-22 Double-Microporous Composite Zeolites

Yang W.Y.*, Ling F.X., Wang S.J., Shen Z.Q., Fang X.C.

Fushun Research Institute of Petroleum and Petrochemicals,SINOPEC, Fushun, Liaoning, China

* yangweiya.fshy@sinopec.com

Keywords: Beta, MCM-22, Core-shell, Composite, zeolite, Plasma

1 Introduction

Alkylation of benzene with propylene is an industrially important reaction for the production of isopropylbenzene, an intermediate for the production of acetone and phenol. Beta and MCM-22 zeolites as solid acid catalyst, have been successfully applicated in the processes of alkylating benzene with propylene to form isopropylbenzene[1,2]. A comparative study with Beta and MCM-22 zeolites to product cumene showed that beta has a little more active and less stable than MCM-22[3], although they are excellent catalyst. Recently, composite zeolites, Y/Beta, Y/ZSM-5 and ZSM-5/SAPO-11, have been receiving much more attention especially in the field of petroleum pro-cessing and deep processing of petrochemical products, owing to its bimicroporous structures and adjustable composite acidities [4-6].

In this paper, a briefly study to obtain core-shell Beta/MCM-22 micro-microporous composite zeolites is reported. We expect it will have an advanced physical structure and exhibit higher activity and selectivity in the reaction of alkylation of benzene with propylene.

2 Experimental

Beta/MCM-22 composites were produced by conventional hydrothermal process. Chemical materials, silicasol, $NaAlO_2$, NaOH, HMI and Beta zeolites were purchased. Beta calcined in air at 300℃ for 3h, were pretreated through the Ar-H_2 plasma (50W, H_2/Ar=1.25, 70mTorr) at room temperature using Gatan 950 plasma system [7]. The typical batch composition in terms of molar ratio was: SiO_2: Al_2O_3: OH-: HMI: H_2O=1: 0.033: 0.10: 0.35: 25, Beta excluded here.

The As-synthesized powders calcined at 550℃ in air for 5h in a muffle furnace to remove organics, were charactered via various methods such as XRD, SEM, TEM, FT-IR.

3 Results and discussion

The XRD patterns of Beta, plasma-pretreated Beta, MCM-22, and Beta/MCM-22 are shown in Fig. 1. The patterns of both Beta zeolites are in good agreement with those reported previously, indicating plasma treating does not damage the crystalline structure of Beta. The patterns of Beta/MCM-22 are very complex. The peaks at 7.7°, 21.7°, 22.4°, 25.4°, 26.8° and 29.6°were assigned to the diffraction of Beta- rays, while these peaks at 7.1°, 7.2°, 8.1°, 10.0°, 14.2°, 26.1° and 28.1° can be assigned to MCM-22.

SEM and TEM results as shown in Fig. 2. The images of the composite with uniform morphology are obviously different from the Beta zeolites which look smooth (Fig. 2b). The surface morphology of the composite shows flakes similar to MCM-22 in Fig. 2c and 2d. The results of EM exhibit the Beta/MCM-22 composite core-shell structure instead of physical mixture.

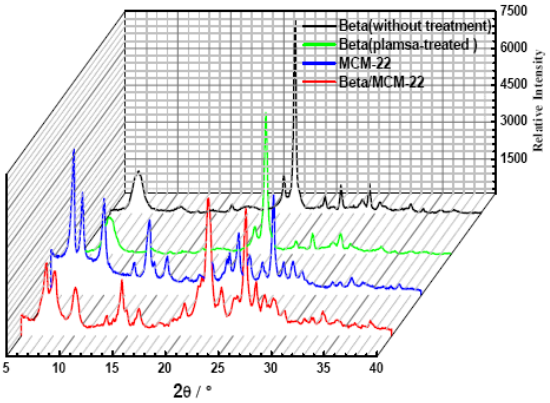

Fig. 1. XRD patterns of Beta, plasma-treated Beta, MCM-22, and Beta/MCM-22 zeolites

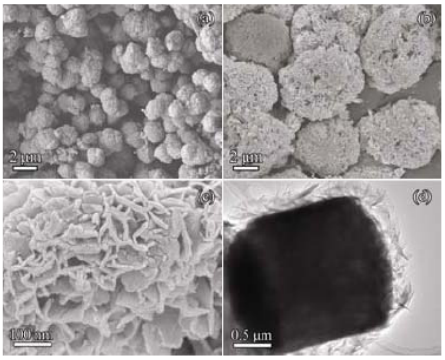

Fig. 2. SEM and TEM images of Beta (a) and Beta/MCM-22 zeolites(b, c, and d)

Brönsted acidity is a key factor controlling catalytic performance of zeolites in many technological processes. The Brönsted acid strength and distribution of the composite are shown in table 1. The total acid amounts of Beta/MCM-22 are between Beta and MCM-22. However, Medium acidity distribution of the composite reaches 40.1% higher than Beta and MCM-22, 30.0%, 38.2%, respectively. It is positively amazing for us to find CB/CL amount to13.8, which may signify the transfer of the "Al" in Beta and MCM-22 zeolites.

In brief, the reasons for our uniform Beta/MCM-22 composite zeolites attribute to the surface energy, Si-OH groups and surficial positive charges of Beta zeolites, which pre-treated by Ar-H_2 plasma.

Table 1. Acid distribution of Beta, MCM-22 and composite zeolites

Acid distribution	Beta		MCM-22		MCM-22\ Beta	
	%	$C_B\backslash C_L$	%	$C_B\backslash C_L$	%	$C_B\backslash C_L$
Total acidity (mmol/g)	0.63	1.09	0.91	3.53	0.74	2.56
160-250℃(weak)	29.0	1.27	17.4	3.27	17.7	1.76
250-350℃(medium)	30.0	1.21	38.2	5.33	40.1	13.8
350-450℃(strong)	41.0	0.99	44.4	2.71	42.2	1.64

4 Conclusions

The core-shell Beta/MCM-22 composite zeolites were successfully synthesized by hydrothermal synthesis. Beta and MCM-22 zeolites acted as core and shell, respectively. The total acid amount of Beta/MCM-22 is between Beta and MCM-22, and the medium strength distributions of the Brönsted acid are reinforced accompanying with the proportional relations of Brönsted and Lewis increased markedly to 13.80.

Acknowledgements

We gratefully acknowledge the support of this work，No.113038, 2013-2014, by China Petroleum & Chemical Corporation (SINOPEC).

References

[1] Han, M, S. Lin, et al. Applied Catalysis A: General (2003), 243(1): 175
[2] Fu, J., C. Ding. Catalysis Communications (2005), 6(12): 770
[3] Li Y., Chen B., Meng W., et al. Chinese Journal of Catalysis (2003), 24(07): 494.
[4] GUO Q., JIA W., ZHAO Z., et al. Journal of Taiyuan University of Technology(2008), 39(03): 222
[5] Pirngruber G. D., Laroche C., Maricar-Pichon M. et al.. Microporous and Mesoporous Materials (2013), 169(15): 212
[6] Wang X., Guo S., Zhao L. et al. Bull. Korean Chem. Soc, 2013, 34 (12): 3829
[7] Kameoka, S., M. Kuroda, et al. Applied Surface Science (1997), 121-122: 351

I-PP02

In Situ Hydrogenation and Desulfurization of Heavy Hydrocarbon Feedstocks with Addition of Zinc in Supercritical Water Flow

Fedyaeva O.N.*, Vostrikov A.A.

Kutateladze Institute of Thermophysics SB RAS, Novosibirsk, Russia

* fedyaeva@itp.nsc.ru

Keywords: supercritical water, hydrocarbon feedstocks, hydrogenation, desulfurization

1 Introduction

Continuous increase in energy consumption and exhaustion of natural reserves of light oils contribute to both the searching for alternative sources of hydrocarbons and the development of new energy-efficient and environmentally friendly methods of upgrading. Recently, much attention has been paid to the involvement of heavy oil and bitumen with high viscosity, high asphaltene and heteroatom content into the energy production and petrochemical synthesis. One of the ways to upgrade the heavy hydrocarbon feedstocks (HCFs) is their conversion in supercritical water (T>374°C, P>22.1 MPa).

2 Experimental

The results of investigation of effect of zinc shavings additives (the weight ratio of zinc to HCFs organic matter corresponds to an increase in H/C atomic ratio in the products and residue to ≈2) on conversion of oxygen-free bitumen [1], sulfur-rich asphaltite [2], and liptobiolith coal [3] in supercritical water flow (400°C, 30 MPa) and also the results [4] of zinc sulfidation by supercritical hydrogen sulfide without and with addition of water (400°C, P^0_{H2S}=11.8-15.2 MPa) are presented. When zinc is added, hydrogenation of HCFs is possible owing to hydrogen evolution during zinc oxidation by supercritical water. The oxidation occurred via ZnO nanoparticles formation in terms of the following reaction [5]:

$$Zn + (H_2O)_g = ZnO + H_2, \qquad \Delta H^0_{298} = -109 \text{ kJ/mol.} \qquad (1)$$

Degree of HCFs hydrogenation by hydrogen evolved during zinc oxidation by supercritical water is determined based on the hydrogen balance by means of the equations below:

$$\delta = \{([H]_L+[H]_V+[H]_R-[H_2]- [H]_0)/[H]_0\}\cdot 100\%, \qquad (2)$$

where $[H]_L$, $[H]_V$, $[H]_R$ and $[H]_0$ is the weight of hydrogen in the liquid and volatile products, conversion residue and raw HCF, respectively; $[H_2]$ is the weight of molecular hydrogen. It was found that the δ value decreases in the following series: C > A > B and corresponds to decrease in the weight ratio of metal to HCFs organic matter m_{Zn}/m_{HCF} (Table). As a whole, hydrogen and heat evolution during the reaction (1) provided for a significant increase in the yield of light hydrocarbons and increase in the oils fraction in HCFs liquid conversion products.

Table 1. Degree of hydrogenation (δ) and desulfurization (ψ) of bitumen, asphaltite and liptobiolith coal at their conversion with addition of zinc in supercritical water

HCF	Gross-formula	m_{Zn}/m_{HCF}, g/g	δ, %	ψ, %
Bitumen (B)	$CH_{1.56}N_{0.02}S_{0.006}$	1.02	13.5 ± 1.4	13 (7)*
Asphaltite (A)	$CH_{1.23}N_{0.02}S_{0.038}O_{0.02}$	1.77	30.1 ± 2.7	60 (21)
Coal (C)	$CH_{1.17}N_{0.005}S_{0.007}O_{0.04}$	1.96	36.4 ± 3.1	42 (−)

*In parentheses are the ψ values calculated for HCFs conversion without addition of zinc.

It is shown that addition of zinc shavings to sulfur-rich asphaltite resulted in significant decrease in the amount of H_2S in the volatile products during asphaltite pyrolysis (T≤400°C). During conversion of bitumen, asphaltite, and coal with addition of zinc shavings in

supercritical water flow the desulfurization degree ψ (the weight portion of sulfur atoms of raw HCFs passed into ZnS) of conversion products increases (Table). It is revealed that at supercritical water conversion of HCFs the bulk of sulfur atoms located in the aliphatic C−S bonds passes into H_2S. The desulfurization of conversion products is caused by the interaction of H_2S with zinc and zinc oxide formed by the reaction (1) in situ as a result of the following reactions:

$$Zn + (H_2S)_g = ZnS + H_2, \qquad \Delta H^0_{298} = -184 \text{ kJ/mol}, \qquad (3)$$

$$ZnO + (H_2S)_g = ZnS + (H_2O)_g, \qquad \Delta H^0_{298} = -76 \text{ kJ/mol}. \qquad (4)$$

3 Results and discussion

It is found out that ZnS nanoneedles with the diameter up to 100 nm and length up to 3 μm are synthesized at zinc sulfidation by H_2S, while the equiaxial ZnS and ZnO nanoparticles with the size up to 200 nm are formed in the presence of water. In the presence of water the average specific rate of ZnS formation calculated per unit of geometric surface of the zinc initial sample is increased by more than two orders of magnitude compared with the rate of zinc sulfidation by supercritical H_2S. This effect is caused by the fact that the rate of ZnO nanoparticles synthesis in the reaction (1) is higher than that of ZnS nanoparticles in the reaction (3). Also, it consists in the regeneration of water by the reaction (4) and its subsequent participation in ZnO nanoparticles synthesis resulting in continuous increase in the ZnO contact surface with H_2S.

Acknowledgements

This study was supported by the Russian Science Foundation (Grant no. 14-19-00801) and by the Russian Foundation for Basic Research (Grant no. 14-03-00055).

References

[1] O.N. Fedyaeva, A.A. Vostrikov, *J. Supercritical Fluids* 72 (2012) 100.
[2] O.N. Fedyaeva, V.R. Antipenko, A.A. Vostrikov, *J. Supercritical Fluids* 88 (2014) 105.
[3] O.N. Fedyaeva, A.A. Vostrikov, *J. Supercritical Fluids* 83 (2013) 86.
[4] O.N. Fedyaeva, A.A. Vostrikov, M.Y. Sokol, A.V. Shatrova, *J. Supercritical Fluids* 95 (2014) 669.
[5] A.A. Vostrikov, O.N. Fedyaeva, A.V. Shishkin, M.Y. Sokol, *J. Supercritical Fluids* 48 (2009) 154.

I-PP03

Non-Oxidative Conversion of Methane into Aromatic Hydrocarbons over Mo/ZSM-5 Catalysts

Vosmerikov A.[1*], Fedushchak T.[1], Korobitsyna L.[1], Sedelnikova O.[1], Zaykovskii V.[2]

1 - Institute of Petroleum Chemistry, Tomsk, Russia
2 - Boreskov Institute of Catalysism, Novosibirsk, Russia

* pika@ipc.tsc.ru

Keywords: catalyst, zeolite, conversion, nanoparticles, aromatization

1 Introduction

Natural and associated petroleum gases are the most important potential sources for production of valuable petrochemical products including those of organic synthesis. A development of one-step catalytic process for conversion of methane, the main component of natural and associated gases, into aromatic compounds is important to solving the problem of their rational use and environmental protection. Dehydroaromatization of methane is effective due to the use of catalytically active high silica zeolites modified with transition metal ions. Regarding that the zeolite H-ZSM-5 containing molybdenum exhibit higher CH_4 conversion and selectivity to benzene than other type's zeolites. Generally, the catalysts are produced via zeolite impregnation by metal salt solution or via mechanical mixing of a zeolite with a metal oxide. The purpose of the present investigation is to examine the influence of different Mo forms and the method for their introduction into the zeolite matrix on acidic properties, catalytic activity and stability of Mo/ZSM-5 catalysts in the process of methane dehydroaromatization (DHA) under non-oxidative conditions. Using high-resolution transmission electron microscopy (HRTEM) and energy-dispersive X-ray (EDX) spectroscopy, we studied the nature and distribution of active sites on the surface of Mo/ZSM-5 catalysts.

2 Experimental

Catalysts were prepared by mechanically mixing zeolite ZSM-5 with the molar ratio SiO_2/Al_2O_3 = 40 and nanosize powders of Mo (K-1), MoO_3 (K-2), Mo_2C (K-3) and MoO_3 reagent grade (K-4) in KM-1 vibratory ball for 2 h. Thereafter, the resulting mixtures were calcined at 540 ^oC for 4 h. The Mo nanopowder was prepared by electric explosion of wires in an argon atmosphere. MoO_3 и Mo_2C samples were prepared on the basis of Mo nanopowders. Catalyst sample (K-5) were prepared by zeolite impregnation with an acidified solution of $(NH_4)_6Mo_7O_{24}$. The concentration of Mo in the zeolite was 4.0 wt %.

The nonoxidative conversion of methane (99.99% purity) was performed in a flow setup at 750°C and atmospheric pressure. A catalyst sample (1.0 cm^3) was placed in a quartz tube reactor 12 mm in diameter. Before the onset of reaction, the catalyst was heated to 750°C in a flow of helium and kept for 20 min at this temperature; thereafter, methane was supplied at a space velocity of 1000 h^{-1}. The reaction products were determined by gas chromatography. The acid characteristics of the samples were studied by the temperature-programmed desorption (TPD) of ammonia, which allowed us to determine the strength distribution and concentration of acid sites. Specific surface area and pore volume of the samples was obtained by BET method at liquid-nitrogen temperature with a Micromeritics ASAP-2020 instrument. All the date were collected and processed by an IBM computer.

HR TEM images were obtained on a JEM-2010 electron microscope (JEOL, Japan) with a lattice resolution of 0.14 nm at an accelerating voltage of 200 kV. The high-resolution images of regular structures were analyzed using the Fourier method. Energy-dispersive X-ray analysis (EDX) on an EDAX spectrometer (EDAX Co.) equipped with a Si(Li) detector with an energy resolution of no worse than 130 eV was used to perform the local elemental analysis of the

samples. The samples for HR TEM were prepared on perforated carbon substrates fixed on copper gauzes.

3 Results and discussion

The acid characteristics of the samples show that the initial HZSM-5 has the greatest amount of acidic sites, which may be attributed to two types: weak acidic and strong acidic sites. At the introduction of Mo in a zeolite a reduction of the concentration of acidic sites of both types occurs and the decrease in the amount of strong acidic sites, especially at nanopowder of Mo, is the most marked. The decrease in the concentration of acidic sites in modified zeolites is probably determined by the interaction between OH groups connected with lattice Al and Mo forms during calcinations. Thus, the modification of a zeolite catalyst by molybdenum result in the change of its acidic properties and to the formation of novel active and inactive sites connected with different Mo forms. Comparison between the BET surface area and pore volume of the HZSM-5 and Mo/HZSM-5 indicate that the surface area and pore volume of initial zeolite are large than that of modified zeolites. Thus, it was show that the BET surface areas and the pore volumes decrease for Mo/ZSM-5 catalysts.

The methane conversion curves for Mo/ZSM-5 catalysts prepared by different method are presented in Fig.1. The catalyst prepared by zeolite mixing with the nanosized Mo powder exhibited the highest activity. With this catalyst, the methane conversion reached its maximum (16.7%) in 20 min and then gradually decreased. The catalyst obtained by zeolite impregnation with an acidified solution of $(NH_4)_6Mo_7O_{24}$ was somewhat less active, and the lowest activity was observed for the catalyst prepared by dry mixing of the zeolite with Mo_2C and MoO_3.

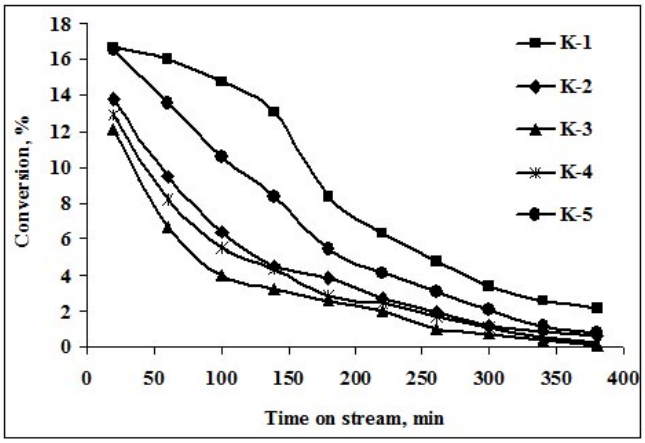

Fig. 1. Changes in the methane conversion during DHA on the 4.0% Mo/ZSM-5 catalysts

In accordance with HRTEM date in the Mo/ZSM-5 catalyst Mo is stabilized at least in two forms. The first form consists of 2-to 10-nm Mo_2C particles stabilized on the outer surface of the zeolite. The second form consists of clusters of oxidized Mo, which are detected in Mo/ZSM-5 channels.

4 Conclusions

Thus, our study showed that the method of Mo introduction into the zeolite is important for the preparation of the Mo/ZSM-5 catalysts. The most active catalyst samples were obtained with nanosized Mo powder, which is probably due to its more uniform distribution on the zeolite surface upon mechanical stirring and to its small particle size, facilitating its penetration into the zeolite channels during calcinations and during the DHA reaction.

Acknowledgements

The work was supported by grant of the Program Presidium of RAS (project № 24.44).

I-PP04

Reaction Mechanism of Dry Reforming of Methane on Rh Doped Pyrochlore Catalysts: a DFT Approach

Polo-Garzon F., Bruce D.A.*

Department of Chemical and Biomolecular Engineering, Clemson University, USA

* dbruce@clemson.edu

Keywords: dry reforming of methane, syngas, pyrochlore, DFT, reaction mechanism

1 Introduction

The dry reforming of methane (DRM) using CO_2 has long been considered a viable method for converting methane from geological or biological sources into syngas, which can then be readily used in the production of a variety of chemicals and particularly liquid fuels that can more readily be shipped via pipeline. Though DRM holds great promise, the high temperatures required for the reaction have made it very difficult to find catalysts that exhibit high activity for extended periods. To date, many catalyst materials have been investigated for this reaction. In this study, however, we have chosen to develop optimized pyrochlore catalyst materials. [1]

Pyrochlores are crystalline oxides having high thermal stability and a general formula of $A_2B_2O_7$, where *A* represents a rare-earth metal and *B* represents a transition metal. Initial experimental efforts by others showed that pyrochlores are active for DRM but the tested catalysts exhibited poor long term stability [2]; however, more recent data suggest that this trend in deactivation may not be applicable to all pyrochlores. $La_2Zr_2O_7$ (LZ) is a pyrochlore structure which has shown good long term stability, so that efforts have been made to tailor its catalytic properties, showing Rh as a promising dopant to enhance catalytic performance for DRM [3, 4]. In order to determine the role of Rh in the reaction performance and understand how the reaction proceeds, we are using first principles methods employing Density Functional Theory (DFT) to analyze structural stability, species adsorption, and calculate transition state energies for the elementary reaction steps on this catalyst material.

2 Experimental/methodology

Computational: First principles calculations were performed employing the Vienna *ab initio* simulation package (VASP), which is based on a plane-wave DFT code. The exchange correlation functional used is the generalized gradient approximation using the implementation of Perdew, Burke and Ernzerhof (GGA-PBE). Activation energies were calculated for selected elementary reactions using the climbing image nudged elastic band method (CI-NEB) and the remaining activation energies were estimated by a Bronsted-Evans-Polanyi (BEP) relation derived from our DFT data.

Experimental: The catalyst synthesis is performed using the modified Pechini method. The metal precursors (for La, Zr, Rh) were the corresponding nitrates. After the appropriate heat treatment is carried out on the material, characterization is performed by means of XRD, SEM and EDX.

3 Results and discussion

Fig. 1 shows the main reaction pathway on two different planes of the pyrochlore. These pathways were identified by means of the activation energies of a proposed reaction network (not shown). On the one hand, the plane (011) appears as inactive for DRM. More specifically, on the plane (011), the carbon atom proceeding from gaseous CH_4 is unable to fully

dehydrogenate to form CO. Thus, this plane is poisoned by unreacted carbon proceeding from CH_4, and H_2 production is limited to the point at which the catalytic sites are covered by partially oxidized carbon species.

On the other hand, the plane (111) provides a lower activation energy (ΔE_{act} = 2.38 eV) route for CHO dehydrogenation to produce CO, compared to the barrier on the plane (011) (ΔE_{act} = 3.08 eV). Along with this barrier reduction, most of the steps on plane (111) possess lower activation barriers compared to the plane (011), and more species (CH_2, CH_2O, CHO, CO, COOH) present their most stable configurations on Rh-containing active sites compared to the plane (011) (CHOH).

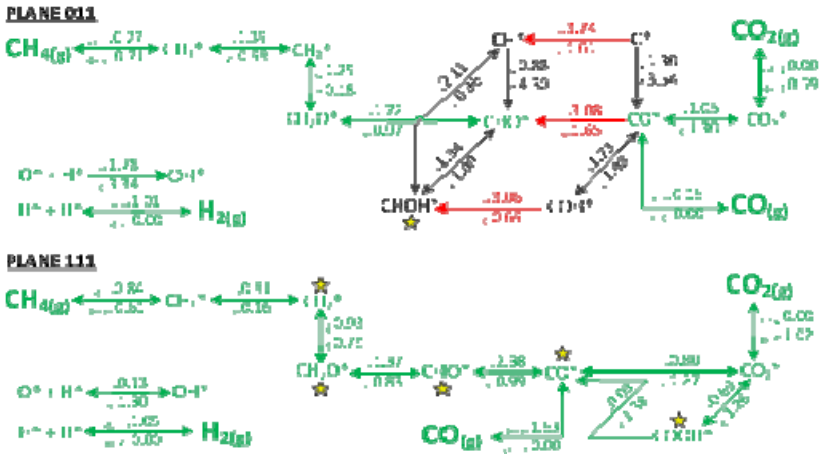

Fig. 1 Main reaction pathway on plane (011) and plane (111) for the 2 wt% Rh-substituted LZ. The values above, below and next to the arrows are activation energies in eV.

The stars (☆) represent active sites where Rh is present.

4 Conclusions

The reported CH_4 and CO_2 conversion at 550 °C at 1 atm and GHSV = 48,000 mL/g_{cat}/h, after 200 min time on stream, are 12.3% and 19.7% respectively. This difference in conversion having a stoichiometric feed is due to certain amount of CH_4 bypassing the catalytic sites, the identified reaction pathway suggests that the CH_4 dehydrogenation is a slower process compared to the CO_2 dissociation, which is reflected in the H_2 to CO ratio 44:100 found experimentally, being this ratio 1:1 theoretically. [3]. Identifying the CHO dehydrogenation as a key step and showing the importance of Rh in the reaction mechanism elucidates a way to improve the reaction performance by looking at new dopants that specifically target the CHO dehydrogenation step.

Acknowledgements

This material is based upon work supported as part of the Center for Atomic Level Catalyst Design, an Energy Frontier Research Center funded by the U.S. Department of Energy, Office of Science, Office of Basic Energy Sciences under Award Number DE-SC0001058.

We acknowledge the Clemson University high-performance computing facility, The Palmetto cluster, for providing computational resources. We thank Dr. Rachel B. Getman at Clemson University for helpful discussions.

References

[1] S. Gaur, D. Haynes, J. Spivey, Applied Catalysis A: General 403, (2011) 142.
[2] A. Ashcroft, A. Cheetham, R. Jones, S. Natarajan, J. Thomas, D. Waller, S. Clark, Journal of Physical Chemistry 97, (1993) 3355.
[3] D. Pakhare, H. Wu, S. Narendra, V. Abdelsayed, D. Haynes, D. Shekhawat, D. Berry, J. Spivey, Applied Petrochemical Research 3, (2013) 117.
[4] D. Pakhare, V. Schwartz, V. Abdelsayed, D. Haynes, D. Shekhawat, J. Poston, J. Spivey, Journal of Catalysis 316, (2014) 78.

I-PP05

Catalytic Properties of Nanoparticles of Transition Metals in the Hydrogenation Reactions

Mitina E.G.[1*], Filimonov N.S.[1], Shafigulin R.V.[1], Bulanova A.V.[1], Belyakova L.D.[2], Shishkovskiy I.V.[3], Morozov Y.G.[4]

1 - Samara State University, Samara, Russia
2 - Institute of Physical Chemistry and Electrochemistry RAS, Moscow, Russia
3 - Samara Branch of the Lebedev Physical Institute, Russian Academy of Sciences, Samara, Russia
4 - Institute of Structural Macrokinetics and Materials Science RAS, Moscow Region, Russia

* ktyfvbn@mail.ru

Keywords: nanoparticle, catalysis, hydrogenation

1 Introduction

This paper studies the catalytic activity of transition metal nanoparticles - nickel and copper obtained by different methods in the hydrogenation of unsaturated and aromatic hydrocarbons.

2 Experimental

Nickel nanoparticles were deposited on silohrom C-120. Part of the nickel nanoparticles was pretreated with AOT (sodium bis (2-ethylhexyl) sulfosuccinate) / heptane in the presence of ammonia (C-120-AOT-Ni-NH_3-D). Another part of the nanoparticles deposited on silohrom without prior impregnation (C-120-AOT-Ni-D). Specific surface of the samples are presented in Table 1.

Table 1. The specific surface area of catalysts containing nickel nanoparticles.

samples	S, m^2/g
C-120	150
C-120-AOT-Ni-D	147
C-120-AOT-Ni-NH_3-D	141

Hydrogenation of octene-1 was conducted on nickel nanoparticles with impulse method by introduction reactant into the column-reactor.

Copper nanoparticles obtained Levitation-jet [1] method were deposited to inerton. Hexyne-1 was hydrogenated with this catalyst in static. This reaction was realized with our original device that provided a direct injection to a chromatographic column.

3 Results and discussion

In this work, the rate constants and activation energies of the reactions were determined.

The rate constants were determined by changing the peak areas of reactants and products. Fig. 1 shows the chromatogram of the reaction mixture after the hydrogenation of hexyne-1 with copper nanoparticles after 10 min. from start of the reaction.

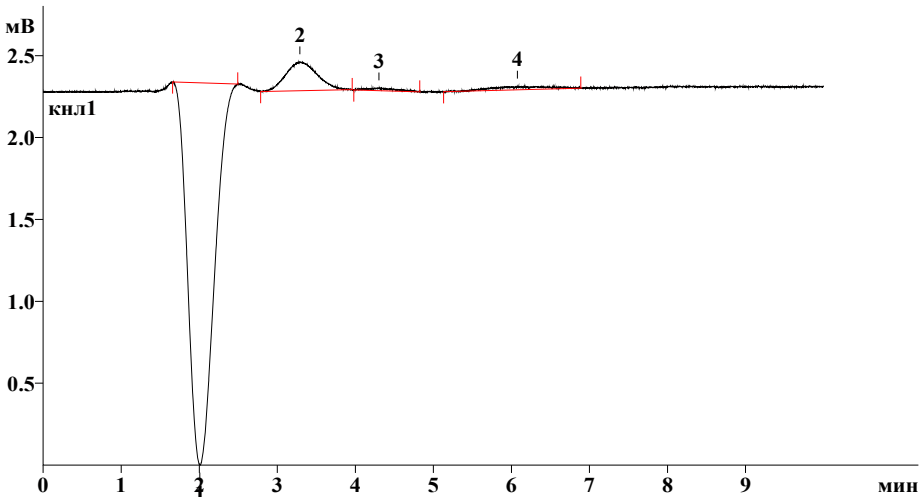

Fig. 1. Chromatogram of the reaction mixture after the hydrogenation of 1-hexyne with copper nanoparticles after 10 min. from the start of the reaction. T = 363 K. 1- hydrogen 2 - hexane, 3 – hexene-1, 4 – hexyne-1.

Table 2 shows the rate constant of hydrogenation of octene-1 with the catalysts containing nickel nanoparticles.

Table 2. Rate constant of hydrogenation of octene-1 with the catalysts containing nickel nanoparticles. (T = 423 K)

samples	k **(min^{-1}) ·10^2**
C-120	0,16
C-120-AOT-Ni-D	0,49
C-120-AOT-Ni-NH_3-D	0,90

The rate constant of hydrogenation of hexyne-1 catalyst containing copper nanoparticles at different temperatures shown the table 3

Table 3. Rate constant of hydrogenation of hexyne-1 catalyst containing copper nanoparticles.

T**, K**	k**, min^{-1}·10^2**
353	5,24
363	6,42
373	8,20

4 Conclusions

This study investigated catalysts containing copper and nickel nanoparticles. The kinetic parameters of hydrogenation of unsaturated hydrocarbons were calculated with these catalysts.

Acknowledgements

This work was supported by RFBR grant number 13-03-00465 A

References

[1] Shishkovsky I.V., Bulanova A.V., Morozov Y.G.// J.of Materials Science and Engineering B. 2012. V.12.p. 634-639.

I-PP06

Dehydration of Alcohols over Heteropoly Acid Catalysts in the Gas Phase

Alharbi W., Brown E., Kozhevnikova E., Bond G., Kozhevnikov I.*

University of Liverpool, Liverpool, United Kingdom

* kozhev@liverpool.ac.uk

Keywords: alcohol, dehydration, dimethyl ether, diethyl ether, acid catalysis, heteropoly acid

1 Introduction

Dehydration of methanol and ethanol has attracted much interest in the context of sustainable development, not only to produce hydrocarbons from non-petroleum feedstock but also to produce dimethyl (DME) and diethyl (DEE) ethers (eq. 1 and 2) [1]. These ethers, especially DME, are expected to play important role in the future energy sector as clean fuel alternatives. The dehydration reaction is usually carried out in the gas phase in the presence of solid acid catalysts such as metal oxides and zeolites.

$$2\,CH_3OH \longrightarrow (CH_3)_2O + H_2O \qquad (1)$$

$$2\,CH_3CH_2OH \longrightarrow (CH_3CH_2)_2O + H_2O \qquad (2)$$

Here we report the dehydration of methanol and ethanol at a gas-solid interface over a wide range of solid Brønsted acid catalysts based on Keggin-type heteropoly acids (HPAs), focussing on the formation of DME and DEE. The catalysts included $H_3PW_{12}O_{40}$ (HPW) and $H_4SiW_{12}O_{40}$ (HSiW) supported on SiO_2, TiO_2, Nb_2O_5 and ZrO_2, as well as bulk acidic Cs salts of HPW. Isopropanol dehydration was also studied in order to gain mechanistic insights.

2 Experimental

Details on catalyst preparation, characterization (BET, ^1H and ^{31}P MAS NMR, XRD, FTIR and NH_3 adsorption microcalorimetry) and catalyst activity testing are given elsewhere [2-4]. The dehydration of alcohols was studied in a continuous flow fixed-bed reactor in the temperature range of 90-300°C and alcohol partial pressure of 1-17 kPa in nitrogen flow.

3 Results and discussion

DME and DEE are the thermodynamically favored products and predominantly form at lower temperatures, whereas increasing reaction temperature leads to formation of hydrocarbons at the expense of ethers. Fig. 1 and 2 show the effect of temperature on alcohol conversion and product selectivity for alcohol dehydration over 15%HSiW/SiO_2. The conversion of methanol reaches equilibrium value 89% at 150°C, with a slight decline at higher temperatures probably due to catalyst coking. DME is the only product up to 200°C, with C_1-C_3 hydrocarbons also forming at higher temperatures (Fig. 1). Similarly, ethanol conversion reaches 100% at 180°C with high DEE selectivity at 90-120°C and ethane becoming the main product at higher temperatures (Fig. 2). The catalyst showed very good performance stability; no catalyst deactivation was observed at 120-150°C for at least 20 h time on stream. In these reactions, the HPA catalysts exhibit significantly higher activity than zeolite HZSM-5 due to the stronger acidity of HPA. With HPA, full alcohol conversions are reached at temperatures about 50°C lower than with HZSM-5.

The formation of DME and DEE may be represented by two different pathways termed the associative pathway and the dissociative pathway [5]. Both pathways are thought to involve

alcohol adsorption on Brønsted acid sites. Under the conditions studied, the dehydration of alcohols was zero order in alcohol, i.e., catalyst active sites were saturated with alcohol. This allowed for easy determination of catalyst turnover frequencies (TOF). The acid strength of HPA catalysts was determined by ammonia adsorption microcalorimetry in terms of the initial adsorption enthalpy. A fairly good correlation between the catalyst activity (TOF) and the catalyst acid strength was established (Fig. 3), which demonstrates that Brønsted acid sites indeed play important role in these reactions over HPA catalysts.

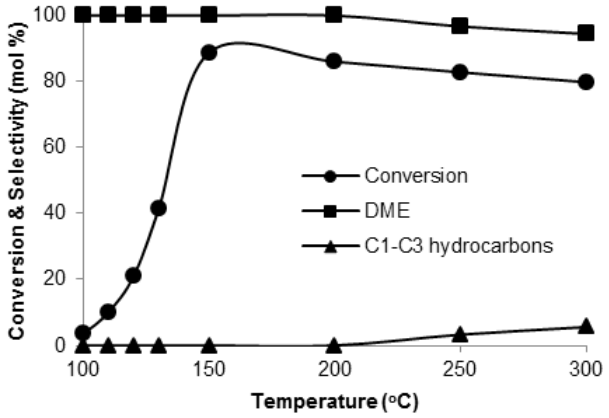

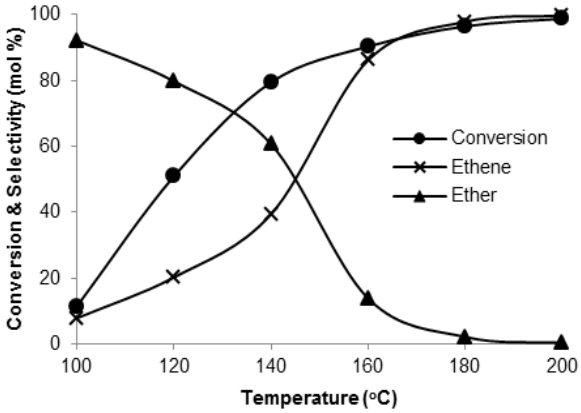

Fig. 1 (left). Effect of temperature on methanol dehydration over 15%HSiW/SiO_2 (0.2 g catalyst, 3.83 kPa MetOH partial pressure, N_2 carrier gas, 20 mL min^{-1} flow rate).

Fig. 2 (right). Effect of temperature on ethanol dehydration over 15%HSiW/SiO_2 (0.2 g catalyst, 1.48 kPa EtOH partial pressure, N_2 carrier gas, 20 mL min^{-1} flow rate) [2].

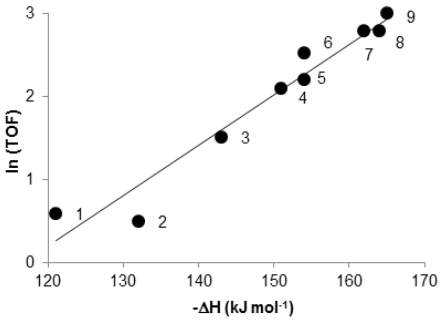

Fig. 3. Plot of ln (TOF) for ethanol dehydration (TOF in h^{-1}) over HPA catalysts at ethanol conversion range $X = 0.07 – 0.53$ vs. initial heat of NH_3 adsorption (120 °C, 0.2 g catalyst, 1.48 kPa ethanol partial pressure, N_2 carrier gas, 20 mL min^{-1} flow rate): (1) 15%HPW/ZrO_2, (2) 15%HPW/Nb_2O_5, (3) 15%HPW/TiO_2, (4) 15%HPW/Cs_3PW, (5) 15%HSiW/SiO_2, (6) 15%HPW/SiO_2, (7) $Cs_{2.25}H_{0.75}PW$, (8) $Cs_{2.5}H_{0.5}PW$, (9) 25%HPW/Cs_3PW.

Kinetics of isopropanol dehydration over HPA catalysts was also studied in order to gain mechanistic insights. The kinetic results and ^1H MAS NMR catalyst characterization point to different chemical structure of Brønsted acid sites in bulk and supported HPA catalysts, resulting in differing reaction mechanisms [4].

4 Conclusions

Solid Brønsted acid catalysts based on Keggin-type HPAs show high activity in the methanol-to-DME and ethanol-to-DEE dehydration reactions in the gas phase. The activity (TOF) of the HPA catalysts correlates with the catalyst acid strength.

References

[1] A. Corma, S. Iborra, A. Velty, *Chem. Rev*. 107 (2007) 2411.
[2] W. Alharbi, E. Brown, E. Kozhevnikova, I. Kozhevnikov, *J. Catal.* 319 (2014) 174.
[3] A. Alsalme, P. Wiper, Y. Khimyak, E. Kozhevnikova, I. Kozhevnikov, *J. Catal.* 276 (2010) 181.
[4] G. Bond, S. Frodsham, P. Jubb, E. Kozhevnikova, I. Kozhevnikov, *J. Catal.* 293 (2012) 158.
[5] P. G. Moses, J. K. Nørskov, *ACS Catal*. 3 (2013) 735.

I-PP07

Hydrodeoxygenation of Biomass-derived Ketones over Bifunctional Metal-acid Catalysts in the Gas Phase

Alharbi K., Alotaibi M., Kozhevnikova E., Kozhevnikov I.*

University of Liverpool, Liverpool, United Kingdom

* kozhev@liverpool.ac.uk

Keywords: ketone, hydrodeoxygenation, platinum, zeolite, heteropoly, acid, bifunctional catalysis

1 Introduction

Oxygen-containing organic compounds such as ketones, carboxylic acids, alcohols, phenols, etc., readily available from natural resources, are attractive as renewable raw materials for the production of value-added chemicals and biofuels [1]. For fuel applications, they require reduction in oxygen content to increase their caloric value. Much current research is focussed on the deoxygenation of organic oxygenates using heterogeneous catalysis, in particular for the upgrading of biomass-derived oxygenates obtained from fermentation, hydrolysis, and fast pyrolysis of biomass. Biomass-derived ketones can be further upgraded by aldol condensation and hydrogenation to produce alkanes that fall in the gasoline/diesel range. Hydrogenation of ketones on supported metal catalysts (e.g., Pt/C) to form alcohols is feasible, but further hydrogenation to alkanes is rather difficult to achieve on such catalysts. The ketone-to-alkane hydrogenation can be achieved much easier using bifunctional metal-acid catalysts ([2-4] and references therein).This process occurs via a sequence of steps involving hydrogenation of ketone to alcohol on metal sites followed by dehydration of secondary alcohol to alkene on acid sites and finally hydrogenation of alkene to alkane on metal sites (eq. 1).

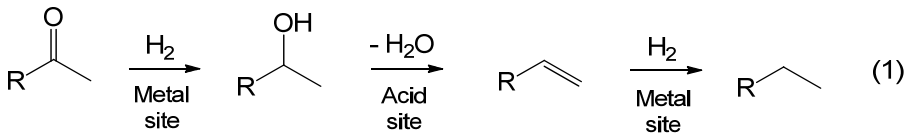

(1)

Here, we report on hydrogenation (hydrodeoxygenation) of a variety of aliphatic and aromatic ketones in the gas phase using bifunctional metal-acid catalysts comprising a metal (Pt, Ru, Ni, Cu) supported on acidic caesium salt of tungstophosphoric heteropoly acid $Cs_{2.5}H_{0.5}PW_{12}O_{40}$ (CsPW) and Pt supported on zeolites (HZSM-5, HY, HBeta). It is demonstrated that 0.5%Pt/CsPW is a highly efficient and versatile catalyst for the ketone-to-alkane hydrogenation, and an insight into reaction mechanism is gained.

2 Experimental

Details on catalyst preparation, characterization (BET, XRD, H_2-TPR and metal dispersion) and catalyst activity testing using a continuous flow fixed-bed reactor are given elsewhere [2-4].

3 Results and discussion

It was found that the activity of CsPW-supported metal catalysts in ketone hydrohenation decreased in the order: Pt > Ru >> Ni > Cu. Pt/CsPW showed the highest catalytic activity, giving in most cases almost 100% alkane yield at 100°C and 1 bar H_2 pressure (Table 1).

Table 2 shows the hydrogenation of methyl isobutyl ketone (MIBK) using Pt supported on zeolites and CsPW. Amongst the Pt/zeolite catalysts studied, Pt/H-ZSM-5 clearly stands out giving >99% selectivity to methylpentanes at 100% MIBK conversion at 200°C. The Pt/H-ZSM-5 catalyst showed excellent performance stability. It reached steady state in about 2 h and

operated without deactivation for at least 16 h [2]. 0.5%Pt/CsPW exhibited even higher activity, with stable performance for at least 14 hours on stream, yielding 99% of 2-methylpentane (2MP) at 100°C, with 100% 2MP selectivity at ≥ 99% MIBK conversion [3]. This is in agreement with the stronger acidity of CsPW compared to zeolites. Importantly, no 2MP isomerisation was observed at this temperature, thus allowing synthetically viable complete transformation of ketone to alkane without carbon backbone alteration.

Evidence was obtained that these reactions occur via the bifunctional mechanism (eq. 1), with the rate-limiting step of ketone hydrogenation on metal sites, followed by fast alcohol dehydration and olefin hydrogenation [2-4].

Table 1. Hydrogenation of ketones over 0.5%Pt/CsPW [4].[a]

Ketone	Conversion (%)	Selectivity (mol%)		
		Alkane	Alcohol	Other[b]
Acetone	98	87	9	4
2-Butanone	100	99	0	1
3-Pentanone	100	100	0	0
2-Hexanone	100	99	0	1
MIBK	100	100	0	0
Cyclohexanone	99	99	0	1
2-Octanone[c]	95	98	0	2
Diisobutyl ketone	99	93	0	7
Acetophenone	78	98	0	2[d]

[a] Reaction conditions: 100°C, 0.2 g catalyst, 2.0% ketone in H_2 flow, 1 bar pressure, 20 mL min^{-1} flow rate, 3 h time on stream, catalyst pre-treatment at 100 °C/1 h in H_2 flow. [b] C_1-C_5 cracking products together with small amount of ketone condensation products. [c] 5 h time on stream. [d] Ethylbenzene.

Table 2. Hydrogenation of MIBK over bifunctional catalysts [2,3].[a]

Catalyst	Temp. (°C)	Conv. (%)	Selectivity (%)			
			2MP	3MP	MP-ol[b]	Other
H-ZSM-5	200	20	9	0	7	84[c]
0.30%Pt/H-ZSM-5	100	94	65	0	34	1
0.30%Pt/H-ZSM-5	200	100	83	17	0	0
0.39%Pt/H-Beta	200	44	70	4	0	26[d]
0.45%Pt/H-Y	200	81	55	2	0	43[d]
0.50%Pt/CsPW	100	99	100	0	0	0
0.50%Pt/CsPW	200	95	88	12	0	0

[a] 0.2 g catalyst, 3.6% MIBK in H_2, 20 ml/min flow rate, 4 h time on stream. [b] 4-Methyl-2-pentanol. [c] C_1-C_5 cracking products and C_{6+} condensation products. [d] Mainly C_{6+} condensation products.

4 Conclusions

Aliphatic and aromatic ketones can be efficiently hydrogenated under mild conditions via metal-acid bifunctional pathway on a single bed containing 0.5%Pt/CsPW catalyst to give the corresponding alkanes a high yield.

References

[1] A. Corma, S. Iborra, A. Velty, *Chem. Rev*. 107 (2007) 2411.
[2] M. Alotaibi, E.F. Kozhevnikova, I.V. Kozhevnikov, *J. Catal.* 293 (2012) 141.
[3] M. Alotaibi, E.F. Kozhevnikova, I.V. Kozhevnikov, *Chem. Commun.* 48 (2012) 7194.
[4] K. Alharbi, E.F. Kozhevnikova, I.V. Kozhevnikov, *Appl. Catal. A* (2014), http://dx.doi.org/10.1016/j.apcata.2014.10.032

I-PP08

Ketonisation of Carboxylic Acids over Metal Oxide and Zeolite Catalysts in the Gas Phase

Bayahia H., Kozhevnikova E., Kozhevnikov I.*

University of Liverpool, Liverpool, United Kingdom

* kozhev@liverpool.ac.uk

Keywords: ketonisation, carboxylic acid, heterogeneous, catalysis, Zn-Cr oxide, silicalite

1 Introduction

Carboxylic acids, readily available from natural resources, are attractive as renewable raw materials for the production of value-added chemicals and bio-fuels [1]. Ketonisation of carboxylic acids, 2 RCOOH → $R_2CO + CO_2 + H_2O$, is employed as a clean method for the synthesis of ketones and upgrading biomass-derived oxygenates, e.g., bio-oil obtained from fast pyrolysis of biomass. Much current research is focussed on ketonisation of carboxylic acids using heterogeneous catalysis [2].

Here we report that Zn^{II}-Cr^{III} mixed oxides are active and durable catalysts for ketonisation of carboxylic acids (acetic and propionic) in the gas phase to yield acetone and 3-pentanone, respectively. Previously, Zn-Cr oxides have been used as catalysts for various reactions such as synthesis of methanol from the synthesis gas, fluorination of hydrocarbons, dehydrogenation of alcohols, etc. [3], but not for acid ketonisation so far. Additionally, we report on silicalite-1 as an environmentally benign non-metal ketonisation catalyst. Insights into reaction mechanisms are also provided.

2 Experimental

Details on catalyst preparation, characterization (BET, XRD, TG-DSC, FTIR and NH_3 adsorption microcalorimetry) and activity testing in a fixed-bed reactor are given in papers [3,4].

3 Results and discussion

Bulk Zn-Cr mixed oxides with a Zn/Cr atomic ratio of 1:1–20:1 were found to be active catalysts for the gas-phase ketonisation of acetic and propionic acids to form acetone and 3-pentanone, respectively, at 300–400°C and ambient pressure [3]. Zn-Cr (10:1) oxide showed the best performance, significantly exceeding that of the parent oxides ZnO and Cr_2O_3. The catalytic activity was further enhanced by supporting Zn-Cr (10:1) oxide on TiO_2 and Al_2O_3. With 20%Zn-Cr(10:1)/Al_2O_3, ketonisation of propionic acid occurred with 97% selectivity to 3-pentanone at 99% conversion at 380°C and stable activity for at least 24 h on stream (Fig. 1). The high activation energy (124 kJ/mol) and Weizs-Prater analysis indicate no diffusion limitations. By the yield of 3-pentanone obtained, Zn-Cr (10:1) oxide is on a par with the best ketonisation catalysts reported so far, e.g., CeO_2-Mn_2O_3.

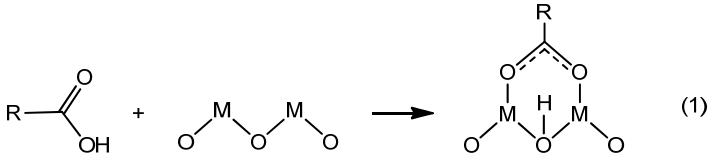

(1)

Fig. 2 shows the FTIR spectrum of acetic acid adsorbed on Zn-Cr (10:1), which is similar to those reported previously for other metal oxides. The bands at 1553 and 1462 cm^{-1} can be attributed to the antisymmetric and symmetric vibrations of the OCO group of acetate, which

indicates the bridging mode for acetate bonding (eq. 1) [3]. It is conceivable that over Zn-Cr oxides ketonisation occurs via the β-ketoacid intermediate route, which is considered to be favourable for amphoteric oxides [2].

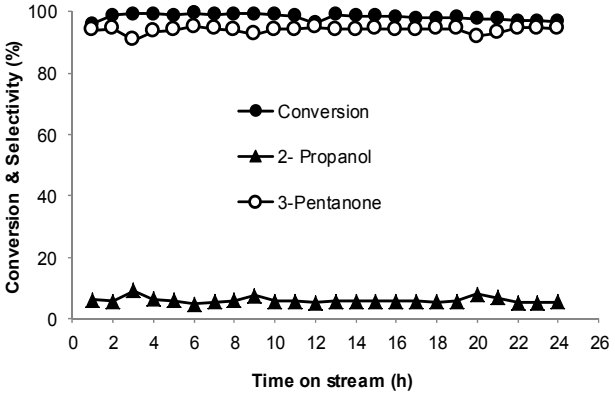

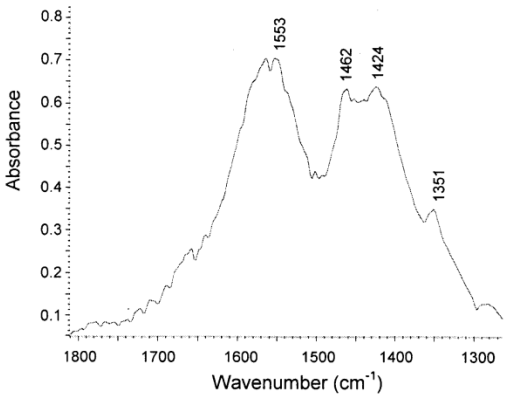

Fig. 1 (left). Propionic acid conversion and product selectivity over 20% Zn-Cr(10:1)/Al_2O_3 vs. time on stream (0.2 g catalyst, 380°C, 1 bar pressure, 20 mL/min N_2 flow rate, 2 vol% propionic acid) [3].

Fig. 2 (right). FTIR spectrum of acetic acid adsorbed on Zn-Cr (10:1) oxide after evacuation at 160°C/10^{-5} bar/1 h [3].

Amorphous silica and crystalline silicalite-1 (MFI structure) are demonstrated to be active and environmentally benign non-metal catalysts for propionic acid ketonisation at 450-500°C [4]. Silicalite-1 was particularly efficient, and its ketonisation selectivity increased by a base modification (3.7 M NH_3(aq) + 0.7 M NH_4NO_3) probably through generation of silanol nests (Scheme 1), which may be the active sites in the base-treated silicalite-1. Evidence for silanol nest formation was obtained by FTIR spectroscopy. The silicalite catalyst showed a stable performance at 500°C for at least 28 h with 84-92% 3-pentanone selectivity at 93-80% propionic acid conversion.

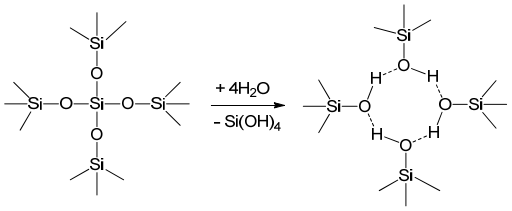

Scheme 1. Formation of silanol nest.

4 Conclusions

Bulk Zn-Cr oxides are active and durable catalysts for the gas-phase ketonisation of acetic and propionic acids at 300–400°C and ambient pressure. A mechanism for ketonisation of carboxylic acids via β-ketoacid intermediate route is proposed. Silicalite-1 is an environmentally benign non-metal catalyst for propionic acid ketonisation at 450-500°C. Ketone selectivity is increased by base treatment generating silanol nests in silicalite-1.

Acknowledgements

We thank Al-Baha University, Saudi Arabia, for PhD studentship (H. Bayahia).

References

[1] A. Corma, S. Iborra, A. Velty, *Chem. Rev*. 107 (2007) 2411.
[2] T. N. Pham, T. Sooknoi, S. P. Crossley, D. E. Resasco, *ACS Catal.* 3 (2013) 2456.
[3] H. Bayahia, E. Kozhevnikova, I. Kozhevnikov, *Appl. Catal. B* 165 (2015) 253.
[4] H. Bayahia, E. Kozhevnikova, I. Kozhevnikov, *Chem. Commun.* 49 (2013) 384.

I-PP09

The Study of Perovskite-Type Ferrites: Preparation, Characterization and Application in the Catalytic Hydrogenation of Carbon Monoxide

Dementyeva M.V.[1*], Sheshko T.F.[1], Serov Y.M.[1], Shulga A.[1], Chislova I.V.[2], Zvereva I.A.[2]

1 - Peoples Friendship University of Russia, Faculty of Science, Physical and Colloidal Chemistry Department, Moscow, Russia

2 - Saint-Petersburg State University, Saint-Petersburg, Russia

* mashadem88@mail.ru

Keywords: ferrites, hydrogenation, carbon monoxide, olefins

1 Introduction

An important task for the creation of an industrial process synthesis of olefins from carbon oxides and hydrogen is the development of high-performance and low-coked catalyst systems, as well as the study of the mechanism of this reaction. This work is devoted to the study of physico-chemical and catalytic properties of new materials - perovskite strontium ferrite gadolinium and having mixed ionic and electronic conductivity in the catalytic hydrogenation of carbon monoxide, as well as to study the influence of composition and method for producing iron on their activity and selectivity to light olefins.

2 Experimental/methodology

Studied in this work complex oxides $GdFeO_3$, $SrFeO_3$ + x, $GdSrFeO_4$, Gd_2-xSr_1 + xFe_2O_7 were prepared by solid and sol-gel synthesis. Monitor the results of the synthesis was carried out using the methods of X-ray diffraction (XRD) diffractometer ARL X'TRA with CuKα-radiation and DTA derivatograph Termoskan-2.

Determination of particle size was using the methods of X-ray diffraction of the crystals, a scanning electron microscope (Zeiss EVO®40 microscope with an accelerating voltage of 10 kV microscope Carl Zeiss Supra 40VP to 20 kV), photon correlation spectroscopy (Malvern Zetasizer Nano analyzer with a helium-neon laser capacity of 4 mW, λ = 633 nm, the algorithm Multiple Narrow Modes).

Valence state of iron atoms was studied by Mossbauer spectroscopy spectrometer Wissel (57Co in a matrix of rhodium with activity 10 mKu), isomer shifts were calculated relative to the α-Fe.

The catalytic activity is determined by feeding the gas mixture with the ratio of components [CO: H_2] = 1: 1, 1: 2 and 1: 4. Experiments were conducted in a flow apparatus at a catalytic atmospheric pressure, and space velocities 1.5 - 3.0 l / h, in the temperature range 423-723 K. Analysis of the products was carried out by chromatography on crystal device 5000 with a column of stainless steel packed poropack Q.

3 Results and discussion

Synthesized by the sol-gel and ceramic technology nanostructured perovskite ferrites $GdFeO_3$, $SrFeO_3$ + x, $GdSrFeO_4$, Gd_2-xSr_1 + xFe_2O_7 are Raddlesdena-Popper phases (An + 1BnO3n + 1, n = 1,2,3, ..., ∞) and built block architecture (Figure 1). Using the methods of XRD revealed the presence of a phase with perovskite-like layered structure for both samples obtained by solid-phase synthesis and sol-gel method.

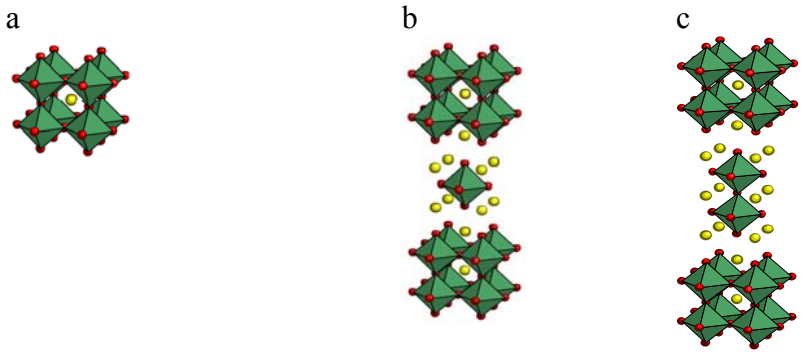

Fig. 1. Structure of the distorted perovskite ferrite GdFeO3 (a), a layered oxide $GdSrFeO_4$ (b), layered oxide Gd_2-xr_1 + hFe_2O_7 (c) (●- Sr^2 +, Gd^3 +, Fe^3 + are inside the octahedron)

Using XRD method, photon correlation spectroscopy, scanning electron microscopy revealed that the oxides synthesized by the the ceramic technology are in the microcrystalline able average crystallite size of 10 microns, and a sol-gel method - have a porous structure and crystallite length - 200 nm.

Methods of nuclear gamma resonance (Mossbauer spectroscopy) found that in complex ferrites $GdFeO_3$, $Gd_2SrFe_2O_7$, obtained by the ceramic technology, the iron atom is in a magnetically ordered state, Fe^{+3}. Increase in strontium Gd_2-xSr_1 + xFe_2O_7 lowers the symmetry of atoms Fe^{+3} (up to three fields of different symmetry), which is explained by the presence of oxygen vacancies. The Mossbauer spectra of solid solutions Gd_2-xSr_1 + xFe_2O_7, synthesized using sol-gel technology, showed that in addition to Fe + 3 in three different fields of symmetry (associated with an increase of the nanodispersion surface state) coexists in these compounds and Fe + 4.

Reaction products of the hydrogenation of carbon monoxide are hydrocarbons C_1 - C_5 basic - methane, ethylene, propylene. It is shown that the catalytic activity (rate of formation of products) affects the number of alternating layers of perovskite and it increases in the series: $SrFeO_{3-x}$ <$GdSrFeO_4$ (n = 1) <$Gd_{1,6}Sr_{1,4}Fe_2O_7$ (n = 2) <$Gd_{1,8}Sr_{1,2}Fe_2O_7$ (n = 2) <$Gd_2SrFe_2O_7$ (n = 2) <$GdFeO_3$ (n = ∞). In the temperature range 523-548 K for olefins selectivity $Gd_2SrFe_2O_7$ was 50-63%, higher values $GdFeO_3$ samples with n = ∞. Ferrites synthesized by sol-gel method had higher catalytic performance that may be associated with their nanocrystalline state with a porous structure, as well as heterovalent state iron (Fe^{+3}, Fe^{+4}), which is favorable for the activation of CO, leads to the formation of C * and CHx -radicals.

4 Conclusions

New complex perovskite ferrites was obtained (An + $_1BnO_{3n+1}$, where n = 1,2,3, ..., ∞, A = Gd, Sr, B = Fe). It was found that the oxides synthesized by the ceramic technology are in the microcrystalline state with Fe + 3 in one magnetically ordered state, and by the sol-gel method - in the nanocrystalline state and heterovalent Fe^{+3}, Fe^{+4} with oxygen vacancies. Catalytic performances are obtained in the hydrogenation of carbon monoxide. The relationship was found between the catalytic activity and physico-chemical properties of ferrites.

Acknowledgements

This work was supported by the Russian Foundation for Basic Research (№ 14-03-00940 A).

I-PP10

Influence of Pressure to the Hydrocracking Process of Goudron in the Presence of a Modificated Suspended Halloysite

Mukhtarova G.S.*, Efendiyeva N.Kh., Kasimova Z.A., Abbasov V.M., Ibrahimov H.C.

Azerbaijan NAS Institute of Petrochemical Processes, Baku, Azerbaijan

* gulermuxtarova@yahoo.com

Keywords: hydrocracking, suspended, catalyst, diesel, fraction, modificated halloysite, goudron, pressure

1 Introduction

Developmentof the existing refinery technologies and creating of new technological processes allowing to increase the depth of oil refining and to improve the quality of oil products – the urgent economical and technical problems of oil-refining industry, the solution of which is associated with the involvement in the processing of residual oil feedstock types.

Thermal and thermal-oxidative processes of oil residua refining arecharacterized by low quality of the obtainedproducts and limited possibilities to enhance the depth of oil refining and production of valuable motor fuels and feedstock for petrochemistry. Hydrocracking process is one of the most efficient processes for obtaining high-quality motor fuels from heavy oil residues (fuel oil, goudron) [1-2].

2 Experimental / methodology

The purpose of the work is to investigation the obtaining process of fuel components from low-pressure hydrocracking of the goudron obtained from Baku oils in the presence of modificatedsuspended halloysite with transition metals (Ni, Co) for obtaining additional (extra) light oil products in order to deepen the oil refining. The influence of the pressure in the range of 1.0-4 MPa at 450 ^{o}C to the processing of the goudron hydrocrackingin the presence of the modificatedsuspended high-dispersed halloysite with transition metals has been investigated. It was investigate the influence of pressure to hydrocracking process of tar.

3 Results and discussion

It was determined that with increasing of pressure from 0.5 to 4 MPa the yield of light oil products increased from 47,0 to 58% mass. So that, the yield of gasoline decrease from 30 % to 27 %, but the yield of diesel fraction increased from 16 % to 30,52 %. Further, at the increasing pressure from 4 MPa to 6 MPa the yield of light oil products increased a few, but amount of cock is decrease from 13 % to 9 %. The change of pressure also influence to the hydrocarbon composition of obtaining products. So that, with increasing of pressure from 0.5 MPa to 6.0 MPa (temperature – 430 ^{0}C) amount of sulfur, iodine number, aromatic hydrocarbons containing in the gasoline decrease. The viscosity, amount of resins, amount of sulfur and iodine number of diesel fraction are decrease.

The analysis of the quality of gasoline and diesel fractions shows that after the additional light hydrotreatment the obtained products can be recommended as component to fuels.

References

[1] E.G. Gorlov, A.S. Kotov, C.E. Gorlova / Thermocatalytic refining of oil residues in the presence of seolites and combustible shale. The chemistry of solid fuel. 1 (2009) p.31-39.

[2] A.S. Kotov, E.G. Gorlov / Thermolysis of fuel oil and goudron with the activatingadditives for obtaining light oil fractions. The chemistry of solid fuel. 3 (2009) p.30-36.

I-PP11

The New Cracking Catalysts for the Synthesis of Long Chain Paraffins α-olefins and Mixtures of Light Alkanes Conversion under Reducing Conditions

Konuspayev S.R.[1*], Dosmagambetova I.B.[1], Nurbayeva R.K.[2], Zhurtbayeva A.A.[1], Shensizbayeva A.B.[1], Bizhanov B.K.[1]

al-Faraby Kazakh National University, Almaty, Kazakhstan
A.B. Bekturov Institute of Chemical Sciences, Almaty, Kazakhstan

* srkonuspayev@mail.ru

Keywords: Olefin, Paraffin, Cracking, long-chain, Conversion, disequilibrium

1 Introduction

Development and intensification of hydrocarbon processing industry is the creation of new active and selective catalysts that can reduce energy consumption while increasing the activity and selectivity. Long chain α-olefins can be produced by the catalytic cracking of paraffins, dehydrogenation of a mixture of light olefins and alkanes obtain hydrogen. Heteropolyacid (HPA) is now widely used for various catalysts [1]. We have previously [2] proposed based catalysts decationized on natural zeolite of Shankanaysky of Almaty region, synthetic GIC and aluminum oxide. The reviews [3,4] presented provisions paraffin cracking catalyst and synthesis on the basis of long-chain α-olefins.

A mixture of light alkanes simulates passing gases and oil refinery gases fat. Creating catalysts conversion to simple olefins and hydrogen solves the problem of processing and free fatty gases. For the conversion of a mixture of light, we used the latest achievements of theoretical chemistry, in particular, we carry out the process under conditions of disequilibrium [5]. If the surface of the catalyst is to create conditions for the appearance of dissitive structures that give rise to an imbalance, the reaction shifts to the formation of reaction products. We set ourselves the task in the conversion of a mixture of light alkanes on the catalyst surface conditions of disequilibrium and unsteadiness in order to receive from alkanes olefins and hydrogen.

This article presents the data on the cracking catalysts in the synthesis of long chain paraffins α-olefins and the conversion of alkanes into a mixture of light reducing medium.

2 Experimental/methodology

Experiments were carried out in a flow reactor on stationary catalyst bed at atmospheric pressure and a temperature range of 450-550^{0}C. During the cracking of paraffins process implemented in the reaction - regeneration. Melted paraffin was supplied at a rate of 0.1-1.0 cm^3/min. Regeneration was performed with a mixture of steam-air mixture to the total absence of carbon dioxide gases in the contact. In the conversion of a mixture of light alkanes, the catalyst is pre-reduced in flowing hydrogen and the reactive gas mixture was fed to the reduced catalyst. Experiments were conducted in four modes: supplying the mixture of light alkanes to reduced catalyst; gas together with hydrogen; gas together with the water; gas together with hydrogen and water. The feed rates of the reacting gases was varied in the range of 10 - 100 h-1. When changing the modes of the catalyst was reduced in hydrogen for 30 minutes.

3 Results and discussion

Long-chain α-olefins are intermediates in the synthesis of base oils, surfactants and other

products of basic and fine chemicals. For long-chain α-olefins include catalysts based on natural zeolites, synthetic heteropolyacids (HPA) 12-molybdenum and tungsten series and Wide Pore Aluminum Silicates (WPAS). Combination of synthetic GIC with decationized natural zeolite consisting of clinoptilolite and WPAS obtained catalysts for the production of long-chain α-olfinov paraffin cracking. Cracking was carried out in a reaction-regeneration mode to the fixed bed at temperatures 450-550^{o}C and atmospheric pressure. Long-chain α-olefins were isolated by vacuum distillation of the cracking products of the wax.

A mixture of light alkanes simulating passing gases and fatty oil refinery gases are converted under reducing conditions to produce a mixture of light olefins and hydrogen disequilibrium mode. Ruthenium catalysts supported on alumina and WPAS have been used. To achieve an imbalance in the system used disequilibrium adding water and hydrogen, which are not participating in the reaction itself may be formed on the surface of the uniformly adsorbed dissipative structure, which shifts the equilibrium toward the formation of olefins and hydrogen. Were prepared and tested 3% Ru, Pt, Pd, supported on γ-Al_2O_3 in the conversion of a mixture of light alkanes into a flow system at a stationary bed of catalyst in the temperature range 350-500°C and atmospheric pressure in the four modes with clean gas and in the presence of hydrogen and water.

Catalysts certified complex physical methods to identify their physical and chemical characteristics. It was shown that surface cracking of paraffins is necessary to create additional acidic sites. To increase the conversion of a mixture of light alkanes to the surface of the catalyst necessary to create conditions for the emergence of imbalances.

References

[1] Wang De-Sheng, Yan Liang., Progress in using heteropolyacid catalysts // Fenzi Cuihua= J. Mol. Catal (China). - 2012. – V.26, №4. - P.366-375.

[2] Konuspayev S.R., Kadirbekov K.A., Nurbayeva R.K. New catalysts systems HPA-zeolite for cracking paraffins in the synthesis of long-chain α-olefins // Catalysis in industry. - 2010, №6. - P.23-28.

[3] Konuspayev S.R., Nurbayeva R.K., Batyrbekova Z.B. Hydrocarbon conversion catalysts for long chain α-olefins. // Chemical Magazine of Kazakhstan. 2014, № 2, P. 244 – 267.

[4] Shub B.R., Krylov O.V. Nonequilibrity in catalysis // M.: Chemistry, 1990. – P. 288.

[5] Konuspayev S.R., Kadirbekov K.A., Amirova A.E., The modification of rhodium catalysts by tin in dehydrogenation of light alkans mixture in reducing environment**.** //VIII Inter. Conf. Mech. of Catal. React (MCR-2009), Novosibirsk, 2009. – P.45.

[6] Konuspayev S.R., Nurbayeva R.K., Dosmagambetova I.B. et al. The conversion of light alkanes to mixtures of ruthenium catalysts.// Roscatalysis-2, Novosibirsk, 2014, V. 2, P. 112

I-PP12

One-Step Synthesis of Dimethyl-Ether from Biogenic Syngas on Mixed Metal/Alumina Mixtures

Pelaez R., Marin P., Ordonez S.*

University Of Oviedo, Oviedo, Spain

* sordonez@uniovi.es

Keywords: biomass, gasification, biofuels, thermochemical, routes, equilibrium-limited, reactions

1 Introduction

Dimethyl Ether (DME) is receiving great attention as a clean alternative fuel, owing to the increasing energy demand. DME can take the place of light naphthas due to the similar physicochemical properties. Besides, DME derivates can also be used as diesel fuel aditives of high cetane number, especially with very low soot emission in the exhaust gas from diesel engine as it has no C-C bond structure. In addition, it is quickly decomposed if leaked into the environment.

In spite of this, catalytic synthesis of DME via a high efficient route remains a great challenge, most of the efforts being paid to the synthesis from methanol. However, commercial methanol production from syngas operates under high pressure (50-150 bar) with very low one-pass reactant conversion due to severe thermodynamic limitation on this exothermic reaction. Therefore, direct DME synthesis from syngas is of great importance, where methanol synthesis from syngas is coupled in situ with methanol dehydration to DME. This scavenger effect on methanol can lower the catalyst surface concentration of the intermediate methanol and break the thermodynamic limitation on the overall CO conversion. Consequently, CO conversion in the direct DME synthesis can be up to 80% in fixed bed reactor or slurry-phase process, significantly higher than that in regular methanol synthesis such as 20% [1].

The scope of this work is to experimentally determine the efficiency of this reaction by operating with mechanical mixtures of a $CuO/ZnO/\gamma\text{-}Al_2O_3$ catalyst (the most recommended catalysts for methanol synthesis) and $\gamma\text{-}Al_2O_3$. This last material presents medium strength acid sites, active for methanol condensation into DME.

2 Experimental/methodology

Experiments were performed in a fixed bed isothermal reactor operating at 30 bar. The reactor was charged with 4 g of $CuO/ZnO/\gamma\text{-}Al_2O_3$ (ChemPack) and 2 g $\gamma\text{-}Al_2O_3$ (BASF) catalysts, ground to 250-355 μm. The catalysts were pretreated in situ with a 4% H_2/N_2 stream at a heating rate of 2 K/min until 493 K, holding for 2 h. Syngas was fed to the reactor with CO/H_2 volume ratio of 40/60.

Online analysis of the reactor feed and effluent streams were carried out using a HP 6890N gas chromatograph, equipped with HP Plot Q and MolSieve columns, and TCD and FID detectors.

3 Results and discussion

Firstly, the influence of temperature on catalyst activity and stability was studied. The reaction was carried out with a syngas flow rate of 0.5 L/min (n.t.p.), space velocity 0.22 mol/h g, at two different temperatures, 523 K and 543 K. Catalyst stability was obtained after 10 h on stream. The results show that conversion almost doubled with this increase in temperature (25-47%) while DME selectivity remained at 70%. According to these results, the following tests were done at 543 K.

Figure 1 shows the data of the catalytic test using different space velocities. The feed flow was decreased by 80% and 50%: 0.38 and 0.25 L/min (n.t.p.), respectively, 0.17 and 0.11 mol/h g. It can be seen that conversion values increase when decreasing space velocity. However, DME selectivity remained constant around 69%.

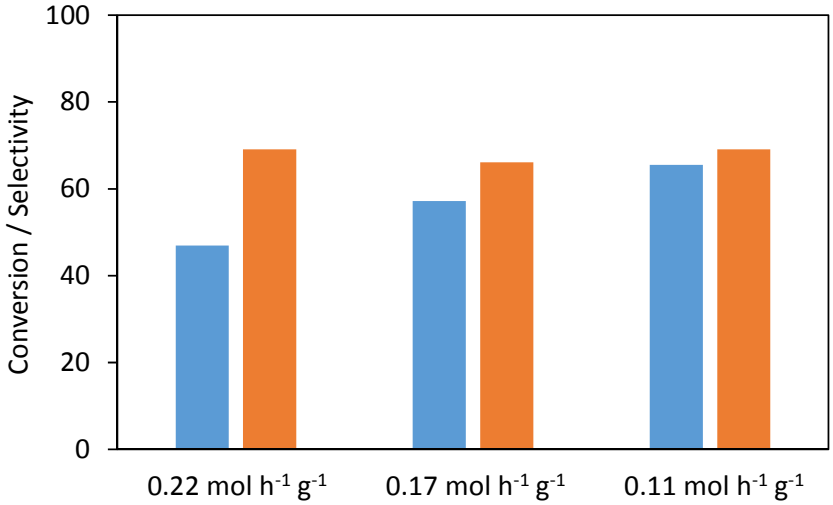

Fig. 1. Catalytic data at different space velocities (30 bar, 543K): ■ Conversion, ■ DME Selectivity

In the same way, the evolution of the reaction performance was followed for times on stream of 80 h. Although conversion decreases were observed (about 30 %), DME selectivities remain almost constant on these experiments.

Characterisation of the used catalyst (both metal oxides and alumina), suggest than the loss of activity is mainly related with chemical (copper oxidation) and morphological (copper sintering), whereas alumina does not show significant changes upon reaction, neither morphological nor chemical (distribution of acid sites).

4 Conclusions

The use of mechanical mixtures of a methanol synthesis catalysts and γ-alumina has been show as an efficient way for obtaining DME from biogenic syngas. Higher and almost constant selectivities were obtained in the reported experiment, in spite of the observed deactivation.

Acknowledgements

This work has been financed by the Principality of Asturias (GRUPIN14-078) and by the BPP company.

References

[1] V.V. Ordomskya, M. Cai, V. Sushkevich, S. Moldovan, O. Ersen, C. Lancelot, V. Valtchev, A.Y. Khodakov, *Applied Catalysis A: General* 486 (2014) 266.

I-PP13

Hydrogen Photoproduction in a Silicone Microreactor Loaded with Au/TiO_2

Castedo A.[1,2*], Llorca J.[1,2], Mendoza E.[1]

1 - Centre for Research in NanoEngineering,Universitat Politècnica de Catalunya, Barcelona, Spain

2 - Institute of Energy Technologies,Universitat Politècnica de Catalunya, Barcelona, Spain

* alejandra.castedo@upc.edu

Keywords: photoreactor, microreactor, hydrogen, gold, PDMS

1 Introduction

Hydrogen production from renewable resources offers enormous benefits for the energy sector, the environment, and the chemical industry. Photocatalytic H_2 production over irradiated semiconductors is receiving particular attention because is based on the Sun, which is a perpetual source of energy [1, 2]. Photocatalytic processes involve excitation of a semiconductor with photons of equal or higher energy than the bandgap energy producing electron-hole pairs. TiO_2–based photocatalysts are among the most attractive due to their availability, corrosion resistance, non-toxicity, low price and high photoactivity and stability. Incorporating organics such as alcohols as sacrificial electron donors into the photocatalytic process increase charge-separation efficiency and give higher H_2 generation rates. Ethanol is one of the most promising hole scavengers because it is available, easy to obtain from biomass (bioethanol) and to transport, CO_2–neutral and safe to handle. Au/TiO_2 has also the ability to increase the photoresponse of TiO_2 [1].

Slurry photoreactors facilitate mass transfer, but they are limited by poor light penetration in the suspension, no matter how active a photocatalyst, if photons are not effectively transmitted to its surface the system efficiency will be lowered. An ideally intensified photoreactor should be able to integrate both, maximized light efficiency and mass transfer simultaneously [3]. Microreactors allows a high degree of process intensification, they appear as a technology for boosting the implementation of on- site and on- demand generation of hydrogen for portable applications, thus avoiding limitations imposed by hydrogen storage [4]. In this work polydimethylsiloxane (PDMS, a silicone elastomer) microreactors were fabricated, coated with Au/TiO_2 photocatalyst and tested in the photogeneration of hydrogen from water-ethanol mixtures at room temperature under dynamic conditions. PDMS has numerous advantages, such as simple and inexpensive fabrication process, which enables rapid prototyping, and optical transparency, which is very interesting for photocatalytic process.

2 Experimental/methodology

Polydimethylsiloxane (PDMS) microreactors were fabricated from patterns made using a 3D printer (Figure 1a). Dimensions of the channels were: 500 μm (width) x 1mm (depth) x 47 mm (length) with a total volume of 0.21 cm^3.

Gold nanoparticles were loaded onto TiO_2 by impregnation from a toluene solution containing preformed Au nanoparticles [3, 4]. The Au loading was 1- 2 wt. % with respect to TiO_2. Catalysts were calcined at 673 for 2 h (2 K min^{-1}) to assure a good contact between the Au nanoparticles and TiO_2 support. A suspension of Au/TiO_2 in ethanol was prepared and deposited onto the surface of the microchannels to reach ca. 0.5 mg cm^{-2} of Au/TiO_2. The bonding between PDMS pieces was performed by corona discharge (Figure 1b).

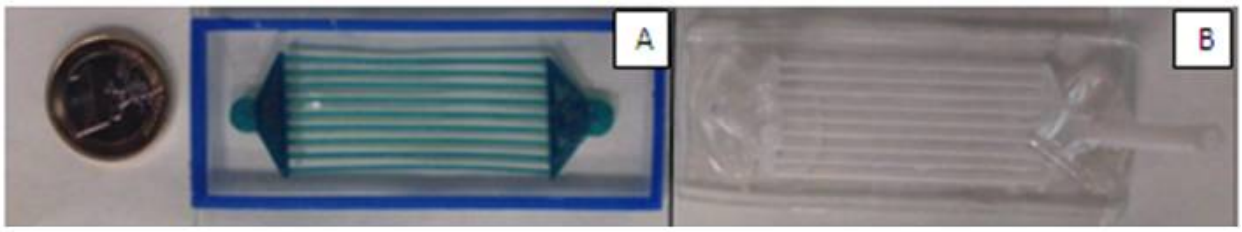

Fig.1. (a) Pattern printed with a 3 D printer. (b) PDMS microreactors loaded with Au/TiO_2.

For the photoreaction experiments, a light source consisting of two UV LEDs emitting at a wavelength of 365 nm over the microreactors was mounted. The irradiance over the microreactors was varied from 0 to 20 mW cm^{-2}. Photoreactions were carried out at 298 K. The gaseous reactants were introduced continuously by bubbling Ar through a saturator containing ethanol and water, with ethanol molar contents of 1-100% and VHSV from 5000 to 10000 h^{-1}.

The photoreactor effluents were monitored online every 2 min by gas chromatography. Blank experiments with only TiO_2 were also carried out.

3 Results and discussion

Deposition of the Au/TiO_2 photocatalyst on the microchannels was analyzed by microscopy. XRD profiles showed the presence of both anatase and rutile with a ratio of anatase:rutile 80~20. The BET surface area of TiO_2 was 90±20 m^2g^{-1} and size particle ca. 14 nm. UV-Vis reflectance spectra showed a localized surface plasmon resonance of Au at about 567 nm. Photoproduction rates of 10 μmol H_2 min^{-1} g^{-1} were obtained at 10000 h^{-1} and 15 mW cm^{-2} with a EtOH: H_2O mixture of 1:9 molar.

4 Conclusions

We have manufactured polydimethylsiloxane (PDMS) microreactors containing channels of 500 μm in diameter by designing patterns with a 3D printer. This design allows a high degree of process intensification, with an optimum mass transfer and a good light penetration. The silicone channels have been coated with ca. 0.5 mg cm^2 of Au/TiO_2 (1-2 wt% Au). Several operational conditions have been selected for the photoproduction of hydrogen, including UV dose (0-20 mW cm^{-2}), contact time (5000-10000 h^{-1}), catalyst load, and water-ethanol ratio (1-100% C_2H_5OH). The results show a very easy operation and a significant enhancement of the hydrogen photoproduction rate compared with conventional photoreactors.

Acknowledgements

This work has been funded through grant MINECO ENE2012-36368. A.C. is grateful to MINECO for a PhD grant. J.L. is Serra Húnter Fellow and is grateful to ICREA Academia program.

References

[1] Murdoch, M., et al., *Nature Chemistry*. 3 (2011) 489.
[2] Llorca, J., Cortés, V., Divins, N. J., Olivera, R., Taboada, E., in *Hydrogen from Bioethanol. Renewable Hydrogen Technologies*. Elsevier (2013) 135.
[3] Taboada, E., Angurell, I., Llorca, J., *Journal of Catalysis*. 309 (2014) 460.
[4] Taboada, E., Angurell, I., Llorca, J., *Journal of Photochemistry and Photobiology A: Chemistry.* 281 (2014) 35.

I-PP14

Influence of Suppores's Nature on the Activity of Hematin Catalysts

Memmedova M.T.*

The Azerbaijan NAS Institute of Petrochemical Processes, Baku, Azerbaijan

* memmedova-melahet@mail.ru

Keywords: natural gas, hematin, methanol, hydrogen, peroxide, aluminosilicates

1 Introduction

The production of various intermediate petrochemical products and liquid fuels from natural gas by catalytic procedures is an important problem related to high effectiveness chemical technologies. One of the pressing problems and rapidly developing domains of modern applied catalysis is oxidative activation of methane, which is main component of natural gas and the lower olefins.

Metalloporphyrin-based catalytic models of monooxygenases were used in many works. These studies showed that, monooxygenase model reactions largely occurred in nonaqueous solvents, and the active center in such reactions was hemin characterized by the formation of an H^{+}_{m} intermediate, in which the hematin form was naturally absent.

In this work, the influence of support properties on the activity of hematin-containing (biomimetic) catalysts in methane hydroxylation by hydrogen peroxide was investigated.

2 Experimental

Materials. The granulated supports used for the perparation of biomimetic catalysts were neutral and activated Al_2O_3, zeolite NaX and synthtic amorphous magnesium- and chromium-containing aluminosilicates (AlSiMg and AlSiCr, respectively).

Hemin from BDH containing 8.64% iron was used as an active center on the supports. Chemically pyre hydrogen peroxide of kh. ch. (chemically pure) grade was purified from possible impurities, in particular, stabilizers by distillation under vacuum. The row material was natunal gas containing 96% CH_4. The gas was passed through a purification system to remove small amounts of impurities.

Methods. Gas-phase hydroxylation of methane (natural gas) by hydrogen peroxide was performed in a flow quartz reactor.

Biomimetic catalysts were prepared by the adsorption of hematin on the above shown anulated neutral and activated Al_2O_3, zeolite NaX and synthtic amorphous magnesium- and chromium-containing aluminosilicates (AlSiMg and AlSiCr, respectively)

Hematin-containing catalysts were prepared by the procedure described in.

The products of the monooxygenase reaction were analyzed by gas chromatography.

3 Results and discussion

The acid-base carriers specified above were used to study the effect of the nature of an inorganic matrix on the activity of the iron protoporphyrin catalyst in methane oxidation to methanol. According to the data given in Tables 1 and 2, the biomimetic catalyst on these supports simulates both the catalase activity and the monooxygenase function of cytochrome P-450.

Table 1. Number of catalyst turnovers (n) in the catalase reaction (V_{H2O2} = 20 *ml*,*t* = 12ºC, m_{cat} = 0.5*g*, $[H_2O_2]$ = 5*wt*%); W_{H2O2} is the rate of hydrogen peroxide consumption

Sample	[Fe], mol	$W_{H_2O_2}$, $\frac{mol}{h}$	n, h^{-1}
$PP\frac{Fe3+OH}{AlSiCr}$	$0.55\cdot10^{-5}$	$0.38\cdot10^{-2}$	700
$PP\frac{Fe3+OH}{AlSiMg}$	$0.70\cdot10^{-6}$	$0.12\cdot10^{-3}$	171
$PP\frac{Fe3+OH}{Al2O3}$	$0.26\cdot10^{-5}$	$0.90\cdot10^{-3}$	347
$PP\frac{Fe3+OH}{NaX}$	$0.20\cdot10^{-5}$	$0.15\cdot10^{-3}$	75

Table 1 shows that $PPFe^{3+}OH$/AlSiCr is most active and gives 700 turnovers per hour. These results lead us to conclude that ions substantially influence the catalytic activity of supported metalloporphyrins by changing the acid-base characteristics of aluminosilicate carriers. It cannot, however, be ruled out that the ions added can themselves participate in H_2O_2 decomposition .

Table 2. Number of catalyst turnovers (n) in the monooxygenase reaction (t = 180ºC,τ = 10 *s*,$[H_2O_2]$ = 20*wt*%,N_{CH4}:N_{H2O2} = 1 : 0.5); W_{CH4} is the rate of methane consumption.

Sample	[Fe], mol	W_{CH_4}, $\frac{mol}{h}$	n, h^{-1}
$PP\frac{Fe3+OH}{AlSiCr}$	$0.30\cdot10^{-4}$	$0.13\cdot10^{-2}$	43
$PP\frac{Fe3+OH}{AlSiMg}$	$0.63\cdot10^{-5}$	$0.77\cdot10^{-3}$	122
$PP\frac{Fe3+OH}{Al2O3}$	$0.20\cdot10^{-4}$	$0.19\cdot10^{-3}$	10
$PP\frac{Fe3+OH}{NaX}$	$0.20\cdot10^{-4}$	$0.76\cdot10^{-4}$	4

Experimental data show that aluminosilicate-based biomimetic catalysts are more active in methane hydroxylation than those on Al_2O_3 and zeolite NaX (Table 2). $PPFe^{3+}OH$/AlSiCr, which is most active in the catalase reaction, shows considerably lower monooxygenase activity in comparison with $PPFe^{3+}OH$/AlSiMg. The high catalase activity of $PPFe^{3+}OH$/AlSiCr is likely to be retained in the presence of the substrate (CH_4), which makes the monooxygenase reaction less completitive . Although the alumina-based catalyst is highly active in the catalase reaction, it exhibits a moderate monooxygenase activity towards CH_4. This behavior of the biomimetic catalysts may be explained by the properties of the support proper, because the active centers ($PPFe^{3+}OH$) were the same on all supports.

I-PP15

Regeneration and Activation Studies with NiMo/(Al-MCM-41/ZSM-5) Catalyst System for Hydrocracking of Biogenic Residues

Gille T., Busse O.*, Reschetilowski W.

Technische Universität Dresden, Department of Industrial Chemistry, Dresden, Germany

* oliver.busse@chemie.tu-dresden.de

Keywords: renewables, light olefins, green chemistry, micro-/mesoporous, hydrocracking, non-food

1 Introduction

The bifunctional catalyst system can be used for the selective catalytic conversion of vegetable oil by hydrocracking. Thereby high olefin yields could be reached but deactivation of catalysts is a major problem. Accordingly, regeneration and activation of used catalyst samples are necessary. Furthermore, conversion of non-food sustainables, like biogenic residues is of particular interest.

The present work studies the influence of regeneration and activation of NiMo/(Al-MCM-41/ZSM-5) on catalytic properties in hydrocracking of biogenic residues. In this context, special attention is directed to product distribution (especially the yield of light olefins), deactivation of the synthesized catalyst sample and shortening of regeneration program.

2 Conclusion

The conversion of biogenic residue results in high yields of gaseous hydrocarbons at temperatures of 500°C, WHSV of 5 h^{-1} and pressure of 5 bars. These gaseous products consist mainly of light olefins (C_2-C_6). In this way valuable base chemicals could be produced from waste materials. The yield of olefins could keep at constant level by different regeneration programs for over 24 hydrocracking tests. Furthermore, the time of regeneration and activation steps were significantly reduced.

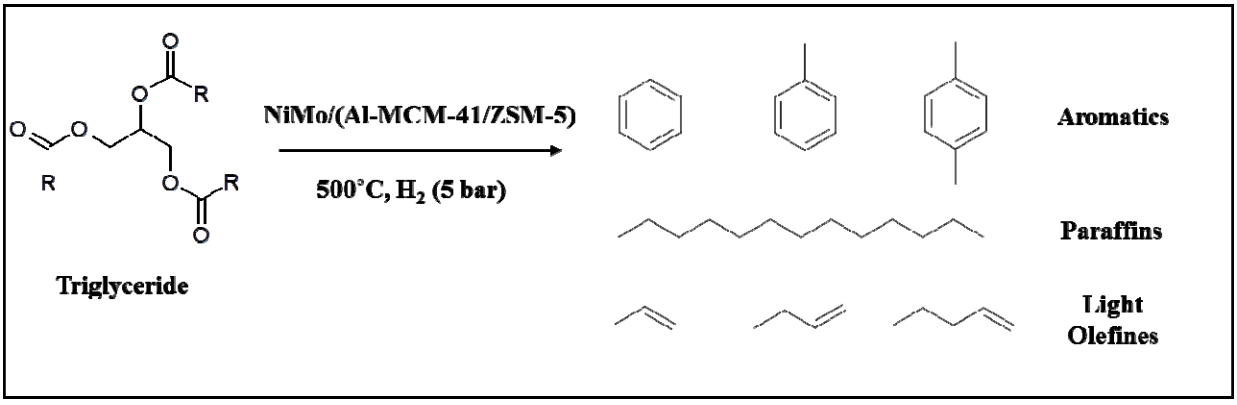

Fig. 1: Reaction scheme

Acknowledgements

We would like to thank Evonik Industries AG for the financial support.

I-PP16

Ru Nanoparticles on Acid-Modified Carbon Materials for the Hydrolytic Hydrogenation of Cellulose

Adsuar-Garcia M.D., Rufete-Beneite M, Roman-Martinez M.C.*

Department of Inorganic Chemistry, University of Alicante, Alicante, Spain

* mcroman@ua.es

Keywords: cellulose, carbon, materials, ruthenium, acidic, functionalities, sorbitol

1 Introduction

The limited supply of fossil fuels and the emissions of greenhouse gases have led to a great interest in the use of biomass as a fuel source. Cellulose is one of the most abundant compounds of biomass and it can be converted to fuels and other chemical products by means of hydrolytic hydrogenation, in which cellulose is hydrolized to glucose that is further hydrogenated to other products like sorbitol [1]. The hydrolytic hydrogenation process can be considered as composed by two steps: hydrolysis, which requires an acidic catalyst and hydrogenation for which a noble metal is necessary.

This work focuses, thus, on the preparation of bifunctional catalysts able to carry out the two mentioned steps of the process. These catalysts consist of ruthenium nanoparticles supported on carbon materials modified with acid functionalities, either created by oxidation or by the anchorage of a heteropolyacid.

2 Experimental/methodology

The carbon materials used as support are two samples of commercial multiwall carbon nanotubes of different surface chemistry named C and C_{OH}(Chengdu Organic Chemicals Co. Ltd. Chinese Academy Sciences (Timesnano)) of average outer diameter of 10-20 nm and inner diameters of 5-10 nm,and a spherical shaped activated carbon (Gun-ei Chemical Industry (Japan)), named GeA, with average diameter of 150 μm. The as-received carbon nanotubes were purified by a treatment in concentrated HCl (37wt.%) at room T for 48 h (samples identified as CD and C_{OH}D). Sample CD was treated with nitric acid solution (69%) at 120 ºC under refluxing conditions for 8 h and then named CDN. Sample GeA was oxidized with a saturated solution of $(NH_4)_2S_2O_8$ in H_2SO_4 1M at room T for 24 h (sample GeAS). The heteropolyacid $H_4O_{40}SiW_{12}$ (HPA) was anchored on support C_{OH}D according to the procedure described in the literature [2] and the sample is named C_{OH}D-HPA. HPA loading is 36wt%.

The Ru nanoparticles were prepared either by impregnation of the support with an aqueous solution of $RuCl_3$ followed by reduction with H_2 (T= 250°C 4h), or directly by solution reduction using also $RuCl_3$ as precursor and ethylenglicol[3]. Ru loading was 5 wt%.

Activity experiments were carried out in a Parr reactor (50 mL). In a typical experiment 0.500 g of ball milled cellulose, 125 mg catalyst and 25 mL water were used. The reaction conditions were 190°C and 50 bar H_2.After reaction, cellulose conversion was determined by weighting the sample and the solution was analysed by HPLC.

Characterization was carried out to analyse the chemical and textural properties of the prepared samples, using TPD and titration, and gas adsorption, respectively.

3 Results and discussion

Table 1 shows data of BET surface areas, CO_2 and CO desorption in TPD experiments and amount of acid groups determined by titration.

Table 1. Textural and chemical properties of supports.

Sample	S_{BET} (m^2/g)	V_{tot} (cm^3/g)	CO_2 (μmoles/g)	CO (μmoles/g)
CD	214	1.10	214	1507
CDN	266	1.09	1360	1916
C_{OH}D	194	0.88	290	1297
GeA	1918	0.937	327	817
GeAS	1142	0.540	3810	3105

The treatment with nitric acid increases the acidity of the CD sample with a low modification of the textural properties. As expected, sample C_{OH}D contains a large amount of oxygen groups desorbing as CO; and oxidation of sample GeA strongly increases the surface chemistry and the acidity with some reduction of the pore volume.

Table 2 shows data of catalysts acidity, cellulose conversion and selectivity to sorbitol.

Table 2. Catalytic activity in the hydrolytic hydrogenation of cellulose

Sample	*Acidity (mmol/g)*	*Conversion%*
Ru/CDN	1.00	30
Ru_d/CDN*	2.22	27
Ru_d/C_{OH}D-HPA*	1.60	42
Ru_d/GeAS*	2.48	55

*$_d$means reduction in solution

These results show that in the case of the carbon nanotubes supported catalysts the solution reduction process does not improve the catalytic activity in spite of leaving a higher acidity. However the presence of anchored HPA leads to higher activity. Support oxidation with ammonium persulfate solution leads to the most active catalyst and this is likely due to the higher development of acidity by this way.

4 Conclusions

The bifunctional catalysts prepared with acidic functionalities and Ru nanoparticles give an acceptable cellulose conversion and good selectivity to sorbitol. Among the prepared catalysts, the one with the highest developed surface chemistry is the most active.

Acknowledgements

The authors thank the financial support through public projects of reference: MAT2012-32832, PROMETEO/II/2014/01, and the UA-VIDI (grant for action research in other countries).

References

[1] H.Kobayashi, T.Komanoya, S.K. Guha, K.Hara, A.Fukuoka, *Applied Catalysis A: General* 409-410(2011)13-20.

[2] K. Inamuro,T. Ishihara, Y. Kamiya, T. Okuhara S. Yamanaka,AngewandteChemie. 2007,119,7769-7772.

[3] M. Chen, Y. Xing, Langmuir (2005) 9334.

I-PP17

Conversion of Heavy Oil into Lighter Fuels over FeOx-Based Catalyst under Sub- and Super-Critical Water Conditions

Kondoh H., Kitaguchi T., Nakasaka Y., Tago T.*, Masuda T.

Division of Chemical Process Engineering, Faculty of Engineering, Hokkaido University, Sapporo, Japan

* tago@eng.hokudai.ac.jp

Keywords: bitumen, heavy oil, FeOx catalyst, catalytic cracking, sub- and super-critical water

1 Introduction

From the perspective of diversification of energy resources, it has been required that a technological development to convert unused fossil resources into useful fuels. Oil sand bitumen (abbreviated as bitumen) is one of the promising candidates, the deposit of which is larger than that of crude oil. Consequently, we have developed iron oxide (FeOx) composite catalysts that convert heavy oil into lighter fuels in superheated steam condition [1]. In cracking system with this catalyst, the lattice oxygen in FeOx is main active sites to decompose heavy oil. When the lattice oxygen is consumed during the oxidative reaction, the crystal structure of FeOx changes from hematite to magnetite and the catalyst is deactivated. Therefore, zirconia (ZrO_2) and ceria (CeO_2) that exhibit activity to produce active oxygen species from water are loaded on FeOx, and the lack of the lattice oxygen due to the consumption was re-generated by the oxygen species [1]. Moreover, we have succeeded in improving the tolerance to sintering of FeOx by alumina (Al_2O_3) addition [2].

On the other hand, the bitumen reserved in deep layer has been produced by steam assisted gravity drainage (SAGD) method, where the bitumen with steam is obtained. Accordingly, on-site upgrading process for bitumen under sub- and super-critical water conditions is an effective approach, because the bitumen with steam thus obtained can be applied as feedstock [3]. In this study, catalytic cracking of bitumen into lighter fuels such as gas oil and vacuum gas oil (denoted as VGO hereafter) was carried out under sub- and super-critical water conditions using the FeOx catalysts. The effects of reaction atmosphere on the yields of the light fuels and the amounts of coke formed on the catalyst were examined.

2 Experimental/methodology

CeO_2-ZrO_2-Al_2O_3-FeOx catalyst (FeOx-based catalyst as here after defined) was prepared by co-precipitation method with each metal nitrates. The catalysts thus obtained were calcinated at 773 K for 2 h. The structures of the catalysts were analyzed by X-ray diffractometer.

Semisolid bitumen diluted with benzene at 10 wt% was used as a feedstock. The catalyst was confirmed in advance to be inactive to benzene. The catalytic reactions under sub-critical water (19.0 MPa) and super-critical water (26.9 MPa) atmospheres were carried out in a fixed-bed flow type reactor. The time factor, W/F (W: catalyst amount /g, F: bitumen flow rate /g h^{-1}), and F_{H2O}/F (F_{H2O}: water flow rate /g h^{-1}, F: bitumen flow rate /g h^{-1}) were 4 and 20, respectively, reaction temperature was 693 K. In addition, catalytic reaction was carried out atmospheric condition (0.1 MPa), for comparison. The obtained gaseous and liquid products were analyzed by gas chromatographs, and high-performance liquid chromatography (HPLC), respectively. The amount of coke loading on the catalyst after reaction was measured by elemental analyzer.

3 Results and discussion

Figure 1 shows the carbon yield of the catalytic cracking of bitumen under sub- and super-

critical water atmosphere over the FeOx-based catalyst. At 0.1 MPa, yield of carbonaceous materials (coke and residue) is about 40 mol%-C. In contrast, the yield of the solid products decreased to about 15 mol%-C under a high pressure condition. Specifically, a difference in the coke amount between atmospheric and high pressure condition could be observed. Under 0.1 MPa, since benzene as solvent was vaporized and bitumen was adsorbed on the catalytic surface, a heavy component (Vacuum residue: VR) in bitumen would easily change into carbonaceous residue followed by coke formation at 0.1 MPa. On the other hand, super-critical water could wash out a coke precursor from the catalytic surface, leading to suppression of coke formation.

The yield of lighter fuels such as Gas oil and VGO were increased from 35 mol%-C (Feed) to 50 ~ 70 mol%-C, and gaseous products, consisting mainly of H_2 and CO_2, were generated. Because the FeOx-based catalyst exhibits an oxidative activity, the bitumen was oxidatively-cracked, yielding the lighter fuels and CO_2. In subcritical condition of 19.0 MPa, decomposition of bitumen over the catalyst effectively proceeded as compared with super-critical water condition (26.9 MPa). The difference in the lighter component yields between sub-critical and super-critical conditions was ascribed to re-polymerization reaction of produced lighter fuels. Though the decomposition of bitumen occurred over the catalyst, it was considered that the re-polymerization reaction tended to occur with increasing the reaction pressure, leading to increase in the yields of heavy components (VR). As a result, subcritical water condition of 19.0 MPa is effective pressure for upgrading of heavy oil using FeOx-based catalyst.

Figure 2 shows the XRD patterns of the FeOx-based catalysts prior to and after the reaction of bitumen. The FeOx-based catalyst showed the peaks corresponding to hematite before reaction. This structure, however, changed into magnetite after the reaction at 0.1 MPa. This result was ascribed to insufficient re-generation of the consumed lattice oxygen in FeOx due to coke deposition on the catalyst surface. On the other hand, structure of catalyst was stable in hematite under sub- and super-critical water conditions in which the lattice oxygen of FeOx was efficiency regenerated. These results suggest that the FeOx-based catalyst is stable for upgrading bitumen under sub- and super-critical water conditions.

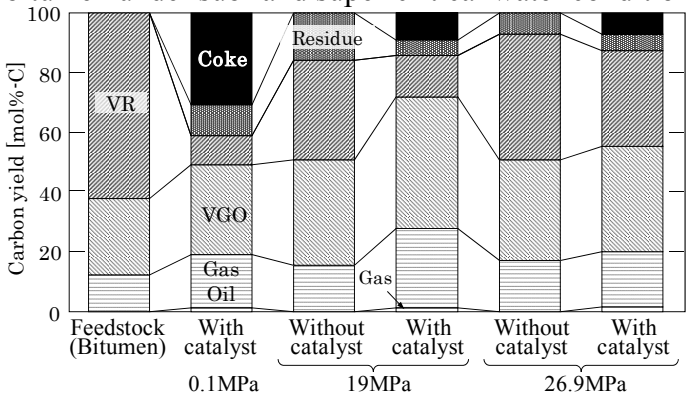

Fig. 1 Carbon yield after the catalytic of bitumen

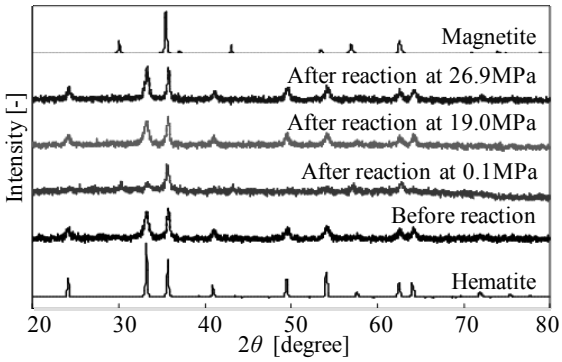

Fig. 2 XRD patterns of the catalyst before and after reaction

4 Conclusions

Bitumen was effectively decomposed over FeOx-based catalyst under sub-critical water condition. FeOx-based catalyst worked well and maintained the high activity during the upgrading of bitumen under sub-critical water.

Acknowledgements

This work was supported by the Industrial Technology Research Grant Program, from Japan Petroleum Energy Center (JPEC).

References

[1] S. Funai, T. Tago, T. Masuda, *J. Jpn. Inst. Energy*, 89, 231-236, (2010)
[2] S. Funai, E. Fumoto, T. Tago, T. Masuda, *Chem. Eng. Sci.*, 65, 60-65, (2010)

[3] A. Kishita, S. Takahashi, H. Kamimura, M. Miki, T. Moriya, H. Enomoto, *J. Jpn. Petrol. Inst.*., 46, 215-221, (2003)

I-PP18

Investigation of Furfural Hydrogenation to Furfuryl Alcohol and Tetrahydrofurfuryl Alcohol

Strigina V.A., Doluda V.Yu.*, Skvortsov A.S., Sulman M.G., Sulman E.M.

Tver Technical University, Tver, Russia

* doludav@yandex.ru

Keywords: furfural hydrogenation, catalyst, biomass

1 Introduction

The sustainable supply and use of energy for transportation represents a real challenge. Terrestrial as well as aerial mobility are strongly affected by petrol shortage. 84% of all petroleum extracted is processed as fuels, including gasoline, diesel, jet, heating and other fuel oils and liquefied petroleum gas. Burning oil releases carbon dioxide into the atmosphere contributing to global warming. The growing social, economical and political interest for the development of alternative fuel sources is not only due to general concerns of sustainability, but also related to human development and geopolitical stability. Bio-fuels are the only alternative to fossil fuels for car powering. Since the carbon backbone is ultimately produced at the expenses of photosynthesis, burning these fuels does not contribute to increase the concentration of CO_2 in the atmosphere and, consequently, to global warming [1].

Common availability of biomass (especially the non-food waste type), caused the trend for reduction of dependency from petroleum resources and increased responsibility for the environment. This factors can be the driving forces behind the development of technologies that use derivatives of furfural, which are called, not without a reason, the “sleeping giants”. One might assume that a lot of interest in furan compounds may contribute to the development of new catalytic conversion processes of furfural and its derivatives, which in the future can lower the cost of their production. This could increase the scale of production, which will result in the launch on the market beneficial alternative fuels for spark ignition engines, which are forward-looking replacement for conventional gasoline [2].

2 Experimental/methodology

This work is devoted to furfural hydrogenation under H_2 over hypercrosslinked polystyrene-supported 3% Ru catalysts. A Ru/HPS catalyst was synthesized by the impregnation method using Ru(OH)Cl3 as a precursor of Ru-containing nanoparticles with the following reduction with hydrogen. To stabilize ruthenium nanoparticles hypercrosslinked polystyreneof HPS MN 100 functionalized by amino groups was used. Furfural hydrogenation was carried out on six-cell reactor Multiple Reactor System (MRS) Series 5000 at H_2 a pressure of 6 MPa, at temperatures ranging from 363 to 403 K. 0.1 g Ru-containing catalyst, 2 ml of pure furfural and 48 ml hexane were added to the reactor. Hexane was used as the solvent. The hydrogenation was carried out under continuous stirring (800 rev/min). Samples obtained during the hydrogenation reaction were analyzed using GC-MS Shimadzu QP-2010. Chromatographic separation of sample occurred on a capillary column HP-1MS 30m×0.25mm×0.25mkm with efficiency 4300 theoretical plates for pentadekan.

3 Results and discussion

Figure 1 shows dependence of the concentration on time for furfural and furfuryl alcohol from the reaction time of furfural hydrogenation using 0.1 g of 3% Ru/HPS at 363-403 K, under H_2 pressure of 60 atm, 48 ml hexane as the solvent

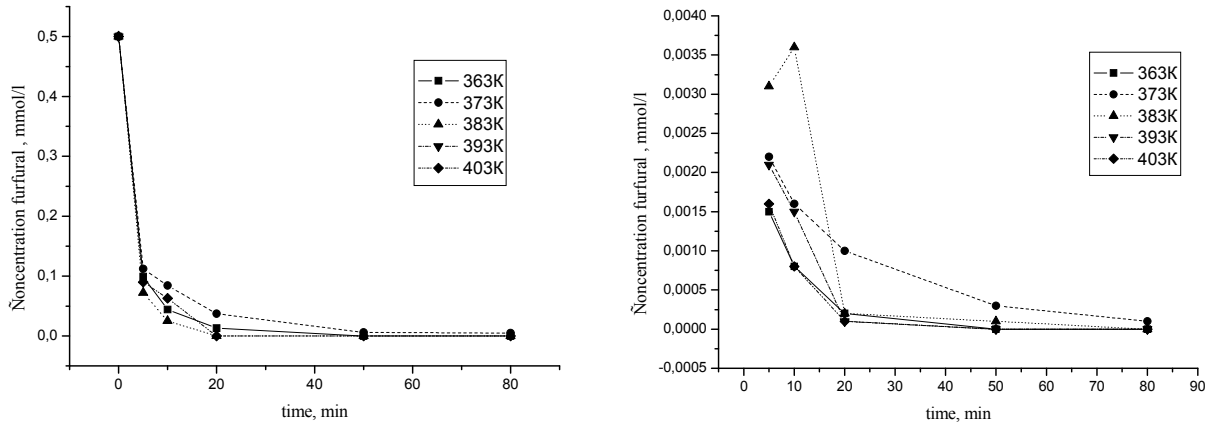

a b

Fig. 1. Dependence of the concentration on time for a) furfural b) furfuryl alcohol from the reaction time of furfural hydrogenation using 0.1 g of 3% Ru/HPS at 363-403 K, under H_2 pressure of 6 MPa, 48 ml hexane as the solvent for 80 min

During the investigation furfuryl and tetrahydrofurfuryl alcohol was found to be the main product of hydrogenation reaction, also and the intermediate products of reaction were found. The maximum conversion obtained over hypercrosslinked polystyrene-supported 3% Ru catalysts at 383 K and 6 MPa was 99.1% with 1.4% and 60.7% selectivity to furfuryl alcohol and tetrahydrofurfuryl alcohol. Increasing conversion furfural from 79.5% to 99.1% was observed in the temperature range 363 - 403 K while the formation of furfuryl alcohol decreased from 27.9 to 0%.

References

[1] C. Stamigna, D. Chiaretti, E. Chiaretti, P.P. Prosini, *Biomass and bioenergy.* 39 (2012) 478-483
[2] A. Malinowski, D. Wardzinska, *CHEMIK*. 66 (2012) 982-990.

I-PP19

Hydrodesulfurization of Dibenzothiophene and 4,6 Dimethyldibenzothiophene over NiW Catalyst Supported over Hierarchical Mordenite

Wang Y.[1,2], Sun Y.[2], Leng K.[2], Lancelot C.[1], Lamonier C.[1*], Rives A.[1], Richard F.[3]

1 - University of Lille UCCS, Villeneuve d'Ascq, France
2 - School of Chemical Engineering and Technology HIT, Harbin, China
3 - University of Poitiers IC2MP, Poitiers, France

* carole.lamonier@univ-lille1.fr

Keywords: hydrodesulfurization, NiW, hierarchical mordenite

1 Introduction

Due to the stringent demand of environmental regulations, the sulfur level in fuels must be reduced to 10 ppm in many countries, thus requiring more efficient HDS catalysts. The utilization of acidic supports has been suggested to improve the catalytic performance, in particular by enabling isomerization of the alkyl substituents in refractory compounds. Zeolites with strong acidity have thus been considered, however, due to their relatively small pore size, several problems such as rapid deactivation and diffusion limitation were generally met. To remedy this disadvantage, hierarchical zeolites have attracted much attention because of the introduction of additional mesopores. In the present work, we reported on NiW catalysts supported on mordenite and hierarchical mordenite. The catalytic performance of the obtained catalysts was evaluated in HDS of dibenzothiophene (DBT) and 4,6-dimethyldibenzothiophene (4,6-DMDBT) and compared with that of an alumina supported catalyst.

2 Experimental/methodology

Hierarchical mordenite was obtained by an acid–base–acid posttreatment method [1]. NiW based catalysts were prepared by impregnation on commercial and hierarchical mordenites and were labelled NiW/HM and NiW/HM-M, respectively (WO_3 content of 15 wt%, W/Ni molar ratio of 2.75). For comparison, a NiW/Al_2O_3 catalyst was prepared from a commercial alumina (BET surface area: 220 m^2/g, pore volume obtained by water adsorption: 0.6 cm^3/g). BET, TEM and XPS were conducted to characterize the materials. The HDS of DBT and 4,6-DMDBT was performed in high-pressure fixed-bed microreactor (length: 40 cm, inner diameter: 1.25 cm) at 613 K under 4 MPa of total pressure after in situ sulfidation of the catalyst [2].

3 Results and discussion

The catalytic performance of the catalysts were first evaluated in HDS of DBT. On NiW/Al_2O_3, products resulting from direct desulfurization (DDS) and hydrogenation (HYD) are identified [3], with a HDS reaction rate of 2.19 mmol $h^{-1}g^{-1}$. Nevertheless, lower HDS reaction rates than on alumina were measured on NiW/HM and NiW/HM-M, 0.37 and 0.98 mmol $h^{-1}g^{-1}$ respectively (as shown in Fig.1), despite the fact that these solids present higher sulfidation and promotion degree of W, as calculated from XPS. This could be attributed to the rapid deactivation of zeolite supported catalysts due to strong acidity of the support. Over NiW/HM and NiW/HM-M catalysts, alkylation (ALK) and further hydrocracking occurred due to the strong acidity of mordenite, with identical selectivities.

The catalytic performance of the solids was further evaluated in the HDS of 4,6-DMDBT, a more refractory molecule. As expected, a much lower HDS activity of NiW/Al_2O_3 (0.44 mmol h^{-}

$^{1}g^{-1}$) was found compared to HDS of DBT, attributed to the effect of steric hindrance of the methyl groups [4]. In presence of acidic supports (HM and HM-M), in addition to the products observed over conventional sulfided catalysts, isomerization products (mainly 3,6-dimethyldibenzothiophene) and their desulfurized products were obtained, allowing to maintain the same HDS reaction rates than with DBT. As a result, NiW/HM-M exhibited the best HDS rate (0.9 mmol h^{-1} g^{-1}), twice that of NiW/Al_2O_3, owing to the isomerization reactions promoted by the zeolite support. Moreover, the mesoporosity in the HM-M support appeared to be beneficial as it allows to double the HDS rate, for DBT and 4,6-DMDBT, in relation with higher developed acidity (as shown by IR-pyridine adsorption), better dispersion of the active phase (as illustrated by TEM analysis), better accessibility to large molecules and possibly to better anti deactivation ability.

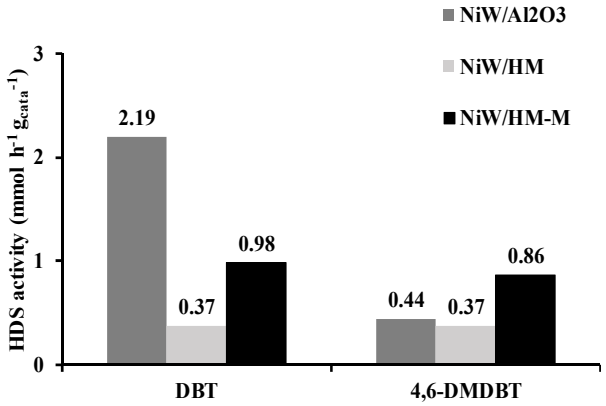

Fig 1: Activity in HDS of dibenzothiophene (DBT) and 4,6-dimethyldibenzothiophene (4,6-DMDBT) measured at 340°C under 4 MPa as total pressure, for the studied catalysts.

4 Conclusions

NiW/Al_2O_3 exhibited better HDS activity than NiW/HM and NiW/HM-M in the HDS of DBT. However, its activity was greatly inhibited in the HDS reaction of 4,6-DMDBT where NiW/HM and NiW/HM-M displayed maintained catalytic performance, probably in relation with additional reaction routes like isomerization associated to the strong acidity of the support. Furthermore, NiW/HM-M exhibited higher catalytic activity than NiW/HM in the HDS reactions of DBT and 4,6-DMDBT, showing the potential interest of hierarchical zeolites as support for deep desulfurization.

Acknowledgements

The authors acknowledge the financial support from the Fundamental Research Funds for the Central Universities (No. HIT. NSRIF. 2015046), the Scientific Research Starting Funding from HIT, the Scientific Research Foundation for the Returned Overseas Chinese Scholars State Education Ministry and the Program Caiyuanpei (N°30323NF).

References

[1] K. Leng, Y. Wang, C. Hou, C. Lancelot, C. Lamonier, A. Rives, Y. Sun, *J. Catal.* 306 (2013) 100
[2] F. Richard, T. Boita, G. Perot, *Appl. Catal. A* 320 (2007) 69.
[3] F. Bataille, J.L. Lemberton, G. Perot, P. Leyrit, T. Cseri, N. Marchal. S. Kasztelan, *Appl. Catal. A* 220 (2001) 191.
[4] F. Bataille, J.-L. Lemberton, P. Michaud, G. Pérot, M. Vrinat, M. Lemaire, E. Schulz, M. Breysse, S. Kasztelan, *J. Catal.* 191 (2000) 409.

I-PP20

"Self-Sensitization" of Photocatalytic Activity of ZnO into Visible Region

Blashkov I.*, Basov L., Lisachenko A.

St. Petersburg State University, Department of Physics, Saint-Petersburg, Russia

* slipknoter90@rambler.ru

Keywords: photocatalysis, ZnO, intrinsic defects, "core-shell" structure, spectral self-sensitization

1 Introduction

The wide-bandgap oxide ZnO is one of the most widespread converters of solar energy into chemical and electric ones. However the threshold of the band-gap excitation ($h\nu \geq 3.3$ eV) lies in UV, so less than 5% of sunlight radiation may be used. Usually it is sensitized to visible region (containing 40% of solar energy) by molecular dyes, anions/cations doping, pretreatment in plasmas of Ar, N_2 or H_2, designing composites ZnO with narrow band semiconductors.

We have developed the original "self-sensitization" methods of the wide-bandgap photocatalysts formation using intrinsic defects [1] or designing near-surface 2D structures [2].

In this report we have studied an environmentally important reaction $CO + NO \xrightarrow{h\nu} CO_2 + 1/2\, N_2$ (1) on the "self-sensitizated" ZnO photocatalyst under the activation in the visible region.

2 Experimental/methodology

The powders of ZnO grade "OSCh 12-2 ($d \sim 100$ nm), previously refined of biographical impurities, were used. Surface defects of F-type were produced by photo-reduction of the surface at low temperature. The spectro-kinetic investigation in gas phase and the analysis of adsorbed intermediate products were performed using the mass-spectrometric method. The optical and the energy parameters of the surface were determined by optical spectroscopy and UPS. Spectral features of the photo-adsorption of H_2, CO, NO and C_2H_6 molecules were measured for to determine the nature of the active centers.

3 Results and discussion

It is shown that O_2 is photo-adsorbed on electron-donor centers, while H_2, CO and C_2H_6 are photo-adsorbed on hole centers. NO is photo-adsorbed on the centers of both types giving NO^- and NO_2^- precursor states.

The reaction (1) is really photocatalytic. The spectral activation region for the reaction (1) is shifted from the UV edge (385 nm) of ZnO to the visible light up to $\lambda > 570$ nm due to the intrinsic point defects of F-type which form a near-surface 2D structure. The mechanism of the reaction kinetics and the energy schemes of the active centers are presented.

4 Conclusions

We can expect that "self-sensitization" of $ZnO/ZnO_{1-\delta}$ based photocatalysts using intrinsic point defects and near-surface 2D-nanostructures is a feasible way to optimize the design of efficient photoactive catalysts for the use of solar energy.

Acknowledgements

The research was supported by "Nanocomposite", "Centre for X-ray Diffraction studies", "Physical Methods of Surface Investigation" and "Nanophotonics" centers of St. Petersburg

State University. The work was supported by RFBR (grant № 13-03-90426) and St. Petersburg State University (grant № 11.39.1060.2012).

References

[1] Andrei A. Lisachenko, Ruslan V. Mikhailov, Lev L. Basov, Boris N. Shelimov, Michel Che. Photocatalytic Reduction of NO by CO on Titanium Dioxide Under Visible Light Irradiation. //*Journal of Physical Chemistry C.* 2007**, V.**111, P.14440-14447.

[2] Victor V. Titov, Ruslan V. Mikhaylov, and Andrey A. Lisachenko Spectral Features of Photostimulated Oxygen Isotope exchange and NO Adsorption on "Self-Sensitized" TiO_{2-x}/TiO_2 in UV−Vis Region// *J. Phys. Chem. C* 2014, 118, 21986−21994.

I-PP21

The One-Step Hydrocracking of Vegetable Oil over Platinum Catalysts with Borate-Containing Oxide Supports

Chumachenko Yu.A.*, Lavrenov A.V., Buluchevskii E.A., Gulyaeva T.I., Arbuzov A.B., Leontieva N.N., Ivashchenko O.V., Trenikhin M.V.

Institute of Hydrocarbons Processing of Siberian Branch Russian Academy of Sciences, Omsk, Russia

* juliana@ihcp.ru

Keywords: one-step hydrocracking, sunflower oil, borated alumina, borated zirconia, renewable, diesel

1 Introduction

The continuous growth of quality requirements for motor fuels and reducing hydrocarbon reserves demand participation of renewable sources based on biomass in their production. The process of production diesel fuels, based on the total hydrodeoxygenation (HDO) oils is one of the promising technologies for processing of vegetable feedstock. The resulting hydrocarbon product is characterized by increased content of C_{15}-C_{18} alkanes and the absence in the composition of sulfur compounds and aromatics. The catalysts of hydrotreating with the active phase Co(Ni)-Mo-S supported on alumina, mixed oxides (SiO_2-Al_2O_3, SiO_2-TiO_2) and zeolites are widely used in HDO. However, the cloud and pour points of the obtained diesel fuel do not reach the values stated in the current specifications. Therefore, additional hydroisomerization of fuel components over catalysts containing noble metals and acidic supports (SAPO-11, ZSM-22) are required. In addition, the stability of hydrotreating catalysts is maintained by a special introduction sulfur compounds into the reaction medium. This inclusion reduces the environmental benefits of renewable fuel production. Therefore, the development of non-sulfide hydrocracking catalysts providing one-step production of components of diesel fuels with improved low temperature properties is actual.

The main objective of this research was studying the effect of the nature oxide supports (γ-Al_2O_3, ZrO_2, B_2O_3-Al_2O_3, B_2O_3-ZrO_2) on the properties of bifunctional Pt-containing catalysts for hydrocracking of vegetable oil.

2 Experimental/methodology

The supports (γ-Al_2O_3 and ZrO_2) were prepared by calcination of pseudoboehmite and zirconia hydrate, respectively. Zirconia hydrate was obtained by precipitation from a solution of zirconium oxynitrate. The ZrO_2-Al_2O_3 support was synthesized by calcination a mixed hydroxide obtained by precipitation from a solution of zirconium and aluminum nitrate salts. Sample supports B_2O_3-Al_2O_3 and B_2O_3-ZrO_2 (20 wt.% B_2O_3) was synthesized by mixing zirconium hydroxide or pseudoboehmite with a solution of boric acid, followed by calcination. In all cases, the calcination is performed in air at a final temperature of 550 (γ-Al_2O_3, B_2O_3-Al_2O_3) or 650°C (ZrO_2, ZrO_2-Al_2O_3, B_2O_3-ZrO_2). Then, the platinum (0.5 wt. %) was introduced by impregnation of the supports with an aqueous solution of H_2PtCl_6. The obtained materials were dried at 120°C and calcined in air at 500°C. Before each experiment the catalysts were underwent to reduction treatment in hydrogen flow at 500°C. The catalysts were characterized by N_2 adsorption, XRD, TPR-H_2, chemisorption of H_2, TPD-NH_3, FTIR adsorbed CO, UV-Vis and HRTEM techniques. The catalytic tests were carried out in a continuous flow fixed bed reactor at temperature of 380°C, pressure of 4.0 MPa. The WHSV of feed was 1.0 h^{-1}. The H_2/feed ratio was 1400 (v/v). The time on stream was 20 h. The purified sunflower oil was used as the feedstock. The gaseous products of the process were determined by gas chromatograph equipped with the Porapak R column and TCD. Light gases (C_1-C_4) were analyzed by gas

chromatography using a DB-1 column and FID. Liquid hydrocarbon products were identified by GH-MS analysis. Contents of gasoline (IBP-150°C), diesel (150-350°C) and heavy gas oil (350°C-FBP) in liquid product were determined by simulation distillation.

3 Results and discussion

As can be seen from Table 1, catalysts $Pt/\gamma\text{-}Al_2O_3$ and $Pt/B_2O_3\text{-}Al_2O_3$ have the most developed porosity. Borate-containing catalysts $Pt/B_2O_3\text{-}Al_2O_3$ and $Pt/ZrO_2\text{-}B_2O_3$ are characterized by high levels of acid sites.

Table 1. Textural properties, acidity and dispersion of catalysts.

Sample	Surface area, m^2/g	Pore volume, cm^3/g	Pore size, nm	Desorption NH_3, μmol/g	Dispersion (H_2), %
$Pt/\gamma\text{-}Al_2O_3$	179	0.48	10.8	326	100
$Pt/B_2O_3\text{-}Al_2O_3$	203	0.50	9.9	498	76
Pt/ZrO_2	59	0.14	9.7	212	19
$Pt/ZrO_2\text{-}Al_2O_3$	67	0.15	9.1	187	15
$Pt/ZrO_2\text{-}B_2O_3$	150	0.16	4.4	353	7

According to the catalytic tests all systems provide complete hydrodeoxygenation vegetable oil. On the $Pt/B_2O_3\text{-}Al_2O_3$ and $Pt/ZrO_2\text{-}B_2O_3$ catalysts yield of diesel fraction reaches 81.5 wt. %. The diesel fraction include significant amounts of iso- and cycloalkanes (27.8 and 60.3 wt.% respectively, Table 2) along with the n-alkanes. That should have a positive effect on the low temperature properties of the resulting fuel components. The latter may be due to the dominance of Brønsted acid sites on the surface of borate-containing catalysts. The catalysts $Pt/\gamma\text{-}Al_2O_3$, Pt/ZrO_2, $Pt/ZrO_2\text{-}Al_2O_3$ are characterized by the Lewis type of acidity and contribute to the formation of products as almost exclusively n-alkanes (96.8 wt.% in the composition of the diesel fraction).

Table 2. Hydrocarbon composition of diesel fractions.

Compound	$Pt/\gamma\text{-}Al_2O_3$	$Pt/B_2O_3\text{-}Al_2O_3$	Pt/ZrO_2	$Pt/ZrO_2\text{-}Al_2O_3$	$Pt/ZrO_2\text{-}B_2O_3$
	Content in the diesel fraction, wt. %				
$\sum n\text{-}C_{10}\text{-}n\text{-}C_{14}$	0.7	1.0	0.9	0.9	3.7
$n\text{-}C_{15}$	5.8	3.4	7.5	7.0	3.6
$n\text{-}C_{16}$	2.1	2.7	0.9	0.9	2.9
$n\text{-}C_{17}$	66.0	41.5	77.3	77.2	21.2
$n\text{-}C_{18}$	21.1	22.7	4.4	5.0	7.5
$n\text{-}C_{19}+n\text{-}C_{20}$	1.1	0.9	2.5	2.8	0.9
The amount of n-alkanes:	96.8	72.2	93.6	93.8	39.7
The amount of iso-alkanes:	3.2	27.8	6.4	6.2	60.3

4 Conclusions

It is shown that as effective catalysts of vegetable oils hydrocracking can be used supported Pt-containing system based on both individual and borate-containing alumina and zirconia. The use of catalysts $Pt/B_2O_3\text{-}Al_2O_3$ and $Pt/ZrO_2\text{-}B_2O_3$ is more preferably due to the formation of iso- and cycloalkanes, which potentially providing good low temperature properties of diesel fuels.

Acknowledgements

The authors thank E. N. Kudrya for implementation of GH-MS analysis.

I-PP22

Stability of NiPd Bimetallic Catalysts in the Autothermal Reforming of Methane

Ismagilov I.[1*], Matus E.[1], Kuznetsov V.[1], Sukhova O.[1], Kerzhentsev M.[1], Ismagilov Z.[1,2]

1 - Boreskov Institute of Catalysis SB RAS, Novosibirsk, Russia
2 - Institute of Coal Chemistry and Material Science SB RAS, Kemerovo, Russia

* iismagil@catalysis.ru

Keywords: autothermal reforming, hydrogen production, bimetallic catalysts

1 Introduction

The decrease of anthropogenic load on the environment and transition to ecological energy production is one of urgent problems of modern society. Hydrogen energy and fuel cell technology are feasible alternatives for clean energy generation [1]. Autothermal reforming (ATR) of hydrocarbons is the most promising process for hydrogen production because of its high energy efficiency. While ATR reaction occurs at 800–900°C, the specific role of catalyst support is to provide high surface area and thermal stability, maintain dispersion of the metal particles and promote stability against sintering and carbon formation [2].The catalyst preparation method is also a key factor which can regulate the catalyst properties [3]. So the purposeful variation of support composition and preparation mode open possibility of control of state, dispersion and redox properties of the active metal, and consequently of the catalyst performance. This work is devoted to the study of the effect of support composition (x/Al_2O_3, x = CeO_2, ZrO_2, La_2O_3, $Ce_{0.5}Zr_{0.5}O_2$, $La_2O_3/Ce_{0.5}Zr_{0.5}O_2$) and preparation mode (co-impregnation, sequential impregnation) on the stability of NiPd bimetallic catalysts in the ATR of CH_4.

2 Experimental

The x/Al_2O_3 (x = CeO_2, ZrO_2, La_2O_3, $Ce_{0.5}Zr_{0.5}O_2$, $La_2O_3/Ce_{0.5}Zr_{0.5}O_2$) supports were prepared by impregnation of $(\gamma+\delta)$-Al_2O_3 granular support (0.25-0.5 mm) by an aqueous solution of salts (cerium nitrate $Ce(NO)_3 \cdot 6H_2O$, oxychloride of zirconium $ZrOCl_2 \cdot 8H_2O$, lanthanum nitrate $La(NO_3)_3 \cdot 6H_2O$) with following drying at 120°C and calcination under air at 850°C for 6 h. The content of support modifying additive (x) was varied at the range of 5-30 wt.%. NiPd bimetallic catalysts were prepared by Ni+Pd co-impregnation (CI) and Pd/Ni sequential impregnation (SI) methods. The nickel nitrate $Ni(NO_3)_2 \cdot 6H_2O$ and palladium nitrate $Pd(NO_3)_2$ were used as metal precursors. After drying at 120°C catalysts were calcined under air at 500°C for 4 h. The nominal contents of Ni and Pd metals in the prepared samples are 10 wt.% Ni and 0.2-0.5 wt.% Pd. ATR experiments were performed in a 14 mm i.d. quartz fixed bed reactor with a feed composition of CH_4: H_2O: O_2: He equal to 1: 1: 0.75: 2.5 under atmospheric pressure, at temperatures 650-950°C and gas flow rate 200 ml_N/min. Prior to each catalytic activity test, the catalysts were reduced in 30%H_2/He flow (100 ml_N/min) at 800°C for 2 h. Analysis of both inlet and outlet reaction mixtures was accomplished using the Stanford Research Systems QMS 300 mass-spectrometric gas analyzer by applying the preliminary peak intensity calibrations based on model gas mixtures.

3 Results and discussion

The ATR tests (time on stream 24 h) show that the prepared catalysts provide methane conversion of 90-100%, CO yield of 55-80% and H_2 yield of 55-85% at 850°C.The catalyst performance was significantly affected by support composition and method of catalyst preparation. An increase of H_2 yield is observed at the increase of the content of support modifying additive from 5-10 to 20-30 wt.% or using the Pd/Ni sequential impregnation method

instead of Ni+Pd co-impregnation method for the Ni and Pd precursors introduction into the support. The optimal support composition ($10Ce_{0.5}Zr_{0.5}O_2/Al_2O_3$) and preparation method (Pd/Ni sequential impregnation) were selected. The optimized catalyst $NiPd/10Ce_{0.5}Zr_{0.5}O_2/Al_2O_3$(SI) shows high activity (methane conversion of 90-100%, H_2 yield >80%) and resistance to deactivation by carbonaceous deposition during 100 h testing at 850°C in ATR of CH_4 with and without addition of H_2S (50 ppm).

In order to understand the evolution of the catalyst under reaction conditions the as-prepared and spent catalysts have been characterized by XRD, N_2 adsorption, HRTEM-EDX, DTA/TG and XPS. For as-prepared samples it was shown that average size of NiO particles increases from 6.7 to 17.5 nm in the following order of supports: La_2O_3/Al_2O_3< $La_2O_3/Ce_{0.5}Zr_{0.5}O_2/Al_2O_3$< Al_2O_3< $Ce_{0.5}Zr_{0.5}O_2/Al_2O_3$< CeO_2/Al_2O_3< ZrO_2/Al_2O_3. The type and content of nickel-containing phases (NiO, $NiAl_2O_4$, La_2NiO_4, Ni-La-Al-O) and Ni^{2+}cation reducibility are regulated by changing support composition by means of the change of strength of metal-support interaction. The content of Ni-containing species which are reduced in the high-temperature region (450-650°C) increases with: i) an increase of La content; ii) a decrease of Ce or Zr content in the support composition. The preparation method also modifies the catalyst reducibility. The use of the Pd/Ni sequential impregnation instead of Pd+Ni co-impregnation leads to formation of different types of Ni^{2+} species which are reduced in two temperature regions (300-400°C and 450-650°C). According to XRD and HRTEM-EDX data, resulting from 24-100 h on stream at 850°C in conditions of ATR of CH_4 reaction, the phase transformation of γ-Al_2O_3 to δ-Al_2O_3 and formation of Ni-Pd alloy particles (12-18 nm) occur, an increase of NiO particle size (from 10 to 25 nm) is observed, while $CeZrO_2$ particles retain their high dispersion (2-10 nm). The NiPd alloy/NiO ratio in the spent catalysts is affected by support composition and preparation mode. The formation of NiPd alloy is promoted by the use of co-impregnation method of preparation and is impeded by the presence of species with strong metal-support interaction (Ni-La-O, Ni-Al-O).

4 Conclusion

The directional regulation of Red-Ox properties, structure and particle size of Ni-containing active component by means of variation of support composition and preparation mode provides the development of an active and stable NiPd bimetallic catalyst for ATR of CH_4. Developed catalyst formulation 10wt.%Ni0.2wt.%Pd/10wt.%$Ce_{0.5}Zr_{0.5}O_2/Al_2O_3$ prepared under optimized conditions shows high activity (CH_4 conversion ~100%, H_2yield > 80%), stability (time on stream 100 h), resistance to carbon formation and resistance to deactivation by sulfur. The best ATR of CH_4 performance of the optimized catalyst can be associated with peculiarity of NiPd particles structure and the optimal ratio between Ni^{2+} species with different ability for reduction.

Acknowledgements

The authors are thankful to Dr. V.A. Ushakov, Dr. S.A. Yashnik, Dr. I.P. Prosvirin, Dr. E.Yu. Gerasimov, Dr. T.V. Larina, T.Ya. Efimenko, I.L. Kraevskaya for the assistance with catalyst characterization. Financial support of this work in the frame of the European Union 7th Framework Programme (FP7/2007–2013) under grant agreement No. 262840 is gratefully acknowledged.

References

[1] M. Ball, M. Wietschel, *Int J Hydrogen Energy.*34 (2009) 615.
[2] I.Z. Ismagilov, E.V. Matus, V.V. Kuznetsov, N. Mota, R.M. Navarro, M.A. Kerzhentsev, Z.R. Ismagilov, J.L.G. Fierro, *Catal Today*. 210 (2013) 10.
[3] I.Z. Ismagilov, E.V. Matus, V.V. Kuznetsov, M.A. Kerzhentsev, S.A. Yashnik, I.P. Prosvirin, N. Mota, R.M. Navarro, J.L.G. Fierro, Z.R. Ismagilov, *Int J Hydrogen Energy.* 39 (2014) 20992.

I-PP23

Iron Pillared Montmorillonites - Carriers of Pt-Catalysts for n-Alkanes Isomerization

Zakarina N.A., Kim O.K.*, Volkova L.D., Chanysheva I.S., Dalelkhan O., Zhumadullaev D.A., Komashko L.V.

Institute of Organic catalysis and electrochemistry after D.V. Sokolsky, Almaty, Kazakhstan

* kimolya82@mail.ru

Keywords: pillared, clays, isomerisation, Pt-catalysts, n-hexane, acid, center, (a.c.)

1 Introduction

The modern requirements to the quality of motor fuels suggest significant limitations aromatics which are ecologically dangerous components. In this connection, for the production of high-octane additives for gasoline the most promising direction is process of n-alkanes isomerization in isoparaffins and the development of new effective catalysts.

Using as a carrier of pillared layered aluminosilicate for platinum catalysts creates the opportunity for increasing of the conversion of n-alkanes, regulating of the composition and amounts of isomers at the expense of the varying acidity, dispersion of Pt particles and their distribution over the surface on the catalyst by creation of the new surface centers.

The purpose of work was the determination of the physical-chemical characteristics of the Pt-catalysts on Fe-pillared montmorillonite with varying content of platinum (0.1 and 0.35%) and their catalytic activity in the reaction of n-hexane isomerization.

2 Experimental/methodology

Methods were used: BET, XRD, TPD of ammonia, elemental analysis, electronic and IR spectroscopy. For the preparation of Pt-catalyst was used iron-pillared H-montmorillonite in Na- and Ca-forms. Pillaring was made by iron hydrocomplexes with following washing and heat treatment of the material. Platinum was introduced from H_2PtCl_6 solution by impregnation method.

The catalysts were tested in the isomerization of n-hexane at250-400^{0}C, P=1atm, molar ratio of H_2:C_6H_{14}=3.5,ω- 0.82 hour^{-1}. Analysis of the reaction products was carried out by GLC method on "3700" chromatograph with FID and the capillary column filled by squalane.

3 Results and discussion

The specific surface of iron pillared montmorillonite Fe(2.5)NaHMM and Fe(2.5)CaHMM are 166.7 and 176.6 m2 / g, accordingly. Introduction of 0.1% platinum reduces the Sss for Fe(2.5)NaHMM-contact in 1.1 times, and for Fe(2.5)CaHMM -1.2 times, with the increasing of Pt amount to 0.35% Sss of contacts is reduced in 1.6 times for Fe(2.5)NaHMM and in 1.42 times for 2 sample. It was shown that all the studied catalysts are mesoporous and mesopore maximum amount is found on the 0.35% Pt/Fe(2.5)CaHMM (90%) and 0.1% Pt/Fe(2.5)NaHMM (79.1%). Features of the porous structure of the contact lead to the concentration of platinum on the surface layers of catalyst. With the introduction of 0.35% Pt in the surface layer platinum is found 0.83% -for Fe(2.5)CaHMM and 0.97%-for Fe(2.5)NaHMM. The strength of Pt- contacts based on Fe(2.5)NaHMM is 155.5N/sm^2, and on the basis of Fe(2.5)CaHMM - 135.5 N/sm^2.

During tests of the catalysts is shown that the maximum conversion of n-hexane is 36.4%, which is observed on 0.1%Pt/Fe(2.5)NaHMM at 400^{0}C, characterized by increased amount of mesopores (79.0%). Selectivity to C_6 and C_{6+} -isomers on 0.1%Pt/Fe(2.5)NaHMM at 350 and 400^{0}C exceeds the corresponding value for the contact based on the Fe (2.5) CaHMM. Among

reaction products for catalysts of both types the insignificant quantity of C_1-C_5-products of hydrocracking and the increased content of C_{6+} isomers are noted, so that the selectivity to C_{6+} isomers is 97.8-100%. On 0.1%Pt/Fe(2.5)NaHMM disubstituted isomers of hexane and heptane in amount of 60.4% are formed. The proportion of 2,2 and 2,3dimethylbutane is 52.5% among of total amount of isomerization products. On 0.1% Pt / Fe (2.5) CaHMM proportion of 2,2 and 2,3 dimethylbutane is 66.7%, and it is 44.4%. for C_7-isomers. At the transition to the 0.35% Pt-catalysts the conversion of n-hexane increases especially at 350 and 400^0C, which is obviously connected with hydrocracking, which leads to the decreasing of selectivity to C_6 and C_{6+} isomers. The relative number of disubstituted isomers formed on 0.35%Pt-catalysts is less than on 0.1% -contacts.

Study of acid characteristics showed that total acidity of 0.35%Pt/Fe(2.5)NaHMM, which is equal to 250 mkmolNH_3/g, as the conversion of n-hexane, is more than for catalyst on the base Fe(2.5)CaHMM.The same regularity was observed on 0.1% Pt-catalysts. The acidity of Pt /Fe(2.5)NaHMM is more in 1.5 times and the activity in 1.8 times more than these values for Pt/Fe(2.5)CaHMM-contacts. Catalysts based on NaHMM markedly excel in catalysts based on CaHMM by the total amount of strong and medium a.c. (in 1.6 times). Probably for this reason, the catalysts based on NaHMM show higher activity in hydrocracking. Comparison of the data for the montmorillonite in Na- and Ca-forms, pillared iron, it can be concluded correlation between the isomerization activity of studied Pt-catalyst and total amount of a.c. and the total content of medium and strong a.c. Pt- catalysts supported on FeNaHMM have higher activity compared with the results on FeCaHMM. For identifying of acid centers type was used the method of IR spectroscopy with molecule-probe of carbon monoxide. Data on the adsorption of CO on NaHMM, Fe(2.5)NaHMM and 0.35Pt/Fe(2.5)NaHMM-contacts were compared. L.a.c. and B.a.c. with predominance L.a.c. are found on the surface of NaHMM and Fe (2.5) NaHMM. In these catalysts absorption bands of B.a.c., at vacuum after CO adsorption at 200 and 400^0C disappear. On the Pt-containing contacts after evacuation absorption bands of CO characterizing B.a.c. remain, probably due with the formation of surface water hydroxyls due to the platinum-catalyzed reaction of CO with hydrogen. It is concluded that L.a.c. and B.a.c. of different strengths in experience conditions are presented on the surface of Pt-catalyst.

Pt^0 particles with size 40-50Å are identified by TEM method on 0.1% Pt-catalysts. In addition with metal platinum particles of Pt_3Fe, αFe, FeO, and etc. are identified. With the increasing of Pt content amount of small metal particles is reduced and large Pt particles increases. The results indicate the formation of nanodispersed Pt particles on the surface of Fe-pillared MM and a strong interaction between the supported metal and carrier with formation of intermetallic compounds and oxides are observed. Because the activity the catalysts with formation of disubstituted isohexanes increases with decreasing amounts of platinum can talk about the influence of Pt particles dispersion on the direction of the isomerization process.

4 Conclusions

Conversion of n-hexane under atmospheric pressure in isomerization correlates with the total amount of strong and medium a.c. Pt-supported catalysts on FeNaHMM have more higher activity compared with the results of FeCaHMM. It has been shown that the increased acidity of Fe (2.5) NaHMM-contact leads to increased cracking and reduced selectivity by C_6-isomers. The relative number of disubstituted isomers formed on 0.35%Pt-catalysts is less than on 0.1% -contacts.The results indicate the formation of nanodispersed Pt particles on the surface of Fe-pillared MM and a strong interaction between the supported metal and carrier with formation of intermetallic compounds and oxides. It is concluded that the effect of dispersion of platinum particles on the direction of the isomerization process.

I-PP24

Acetylation of Glycerol over Mixed Zirconium Phosphate-Sulphate Catalysts

Mesrar F.[1], Testa M.L.[2], Brik Y.[1], Kacimi M.[1], Ziyad M.[1,3], La Parola V.[2], Liotta L.F.[2*]

1 - Université Mohammed V, Faculté des Sciences, Département de Chimie, Rabat, Maroc
2 - ISMN-CNR, Palermo, Italy
3 - Académie Hassan II des Sciences et Techniques, Rabat, Maroc

* liotta@pa.ismn.cnr.it

Keywords: acetylation, glycerol, phosphate, sulphate, acid, catalyst, triacetin

1 Introduction

In recent years, due to the increasing price of fossil fuel and to the environmental concern there has been a considerable interest in developing biodiesel as alternative fuel. Biodiesel is a mixture of fatty acid methyl ester (FAME) produced by the transesterification of triglycerides with methanol. One of the major problems, during the production of biodiesel, is the formation of glycerol (10% wt) as principal by-product. Different chemical transformatios of glycerol into high-value chemicals have been developed to produce propanediols, acrolein, hydroxyaceton, glyceric acid [1]. Among the different reactions, the esterification of glycerol into acetins is quite attractive due to the versatile industrial application of the final products, going from cosmetic to fuel additives [2]. Conventionally, the esterification reactions are industrially performed under batch conditions in homogeneous liquid phase catalysed by strong Brønsted acids. Efforts are being made to turn the process into "green" chemical reaction working on heterogeneous catalysts that are easier to handle and safer. Recently, some of us have reported for sulfonic acid functionalized mesoporous silicas high activity and good stability for glycerol acetylation to triacetin [3]. Metal (IV) phosphates have been successfully used as solid acid catalysts for several biomass-based components conversion to chemicals [4,5]. Proper substitution of phosphate by sulfate would increase the acidity of the catalysts.

In the present work the acetylation of glycerol over zirconium phosphates with formula $Zr_3(PO_4)_4$, α-$Zr(HPO_4)_2$ and ZrP_2O_7 was investigated. Moreover, the effect of substituting phosphate group by sulfate was also addressed.

2 Experimental

All the used catalysts were synthetized by precipitation. Zirconium phosphate with formula, $Zr_3(PO_4)_4$ and mixed zirconium phosphate-sulphate, with formula, $Zr_2(PO_4)_2SO_4$ were prepared, respectively, by adding $ZrOCl_2 \cdot 8H_2O$ aqueous solution to H_3PO_4 acid solution or to a stoichiometric mixture of H_3PO_4 and H_2SO_4 acid solutions. The obtained gel was stirred for 2 h at 80 °C until dryness, then it was dried in oven at 110 °C overnight and calcined at 500°C for 24 h. The zirconium phosphate α-$Zr(HPO_4)_2$ was prepared by adding $ZrOCl_2 \cdot 8H_2O$ aqueous solution to concentrate H_3PO_4 acid and refluxing for 48 h. The obtained gel was recovered by filtration, then, it was washed with water until pH 4.5 and dried at room temperature.

The ZrP_2O_7 was obtained by calcining at 500 °C for 24 h a portion of the α-$Zr(HPO_4)_2$ compound. The prepared samples are herein named as fresh catalysts.

Characterizations by XRD, FT-IR, NH_3-TPD were performed. Moreover, XPS analyses were carried out over the most active samples. The surface chemical composition in terms of P/Zr and S/Zr atomic ratios was monitored in the fresh and used catalysts. The glycerol acetylation reactions were performed by using a mass ratio of catalyst/glycerol equal to 5wt% and molar ratio acetic acid/glycerol corresponding to 3:1, as previously used [3]. The products

were analysed by GC-MS. Recycling experiments up to 5 cycles were performed over the most active catalysts.

3 Results and discussion

The glycerol conversion as a function of the various catalysts is displayed in Fig. 1a. Over $Zr_2(PO_4)_2SO_4$, 96% of glycerol conversion was obtained in only 1h and full conversion was reached after 3h. $Zr_3(PO_4)_4$, ZrP_2O_7 and α-$Zr(HPO_4)_2$ were less performing giving about 85-90% of glycerol conversion after 3h. The selectivity of the glycerol acetylation was oriented toward the formation of mono- and diacetin. Only in presence of $Zr_2(PO_4)_2SO_4$, after 3h of reaction, 11% of the desired triacetin was detected. The stability of the $Zr_2(PO_4)_2SO_4$, exhibiting the best catalytic performance, was investigated in recycling runs of 1h (Fig. 1b). A decreased activity was observed after the first cycle yielding about 80% of glycerol conversion in the second, third and fourth run. Further deactivation occurred in the fifth cycle, suggesting leaching of sulphate species, as confirmed by XPS analyses of the fresh and used catalyst.

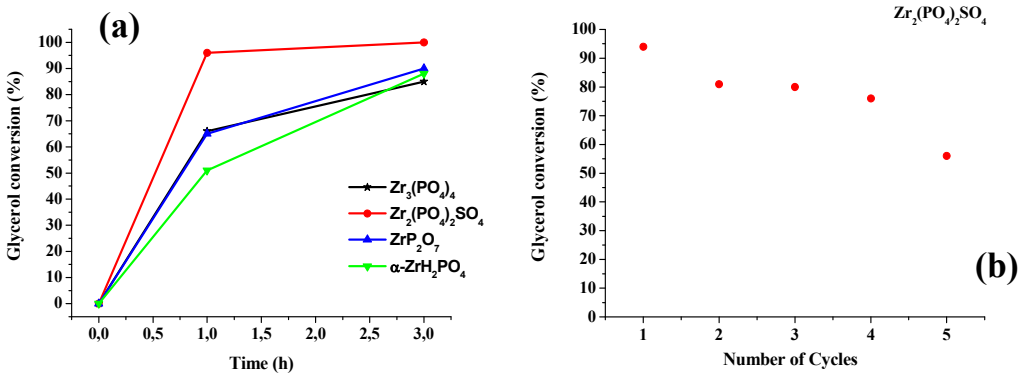

Fig. 1. (a) Conversion of glycerol over different Zr phosphates and Zr phosphate-sulphate catalysts. (b) Recycling runs over the most active catalyst, $Zr_2(PO_4)_2SO_4$.

4 Conclusions

Mixed Zr phosphate sulphate catalysts, such as $Zr_2(PO_4)_2SO_4$, appear promising for glycerol acetylation and worthy of further investigation. With this aim, glycerol acetylation over other mixed composition, $Zr_3(PO_4)_2(SO_4)_3$, $Zr_4(PO_4)_2(SO_4)_5$ and $Zr(SO_4)_2$ is in progress.

Acknowledgements

The bilateral Project CNR-CNRST (2014-2015) between Italy and Morocco is acknowledged for financial support.

References

[1] M.J. Climent, A. Corma, P.D. Frutos, S. Iborra, M. Noy, A. Velty, P. Concepcion, *J. Catal.* 269 (2010) 140.
[2] N. Rahmat, A. Abdullah, A. Mohamed, *Renewable Sustainable Energy Rev.* 14 (2010) 987.
[3] M.L. Testa, V. La Parola, L.F. Liotta, A.M. Venezia, *J. Mol. Catal. A: Chem.* 367 (2013) 69.
[4] T.F. Parangi, B.N. Wani, U.V. Chudasama, *Ind. Eng. Chem. Res.* 52 (2013) 8969
[5] B. Chen, F. Li, Z. Huang, T. Lu, Y. Yuan, G. Yuan, *ChemSusChem* 7 (2014) 202.

I-PP25

Synthesis Features of Oxide Compounds Based on Univalent Copper of Delafossite Structure

Shtertser N.V.[1,2*], Pakharukova V.P.[1,2], Khassin A.A.[2,1]

1 - Boreskov Institute of Catalysis SB RAS, Novosibirsk, Russia
2 - Novosibirsk National Research University, Novosibirsk, Russia

* nat@catalysis.ru

Keywords: copper, delafossite, synthesis, catalyst

1 Introduction

Cuprous oxide $CuMO_2$ with the structure of delafossite attracts the attention of researchers due to their physicochemical properties. Copper delafossites are p-type semiconductors transparent in the visible range of light having luminescent, thermoelectric and catalytic properties.

Well crystallized delafossite $CuMO_2$ could be prepared by solid state reaction at temperatures exceeding 1000°C [1]. However, the literature describes methods for obtaining at low temperatures, for example, synthesis using aluminum nitrate or hydrothermal synthesis [2,3]. Thermal treatment of joint co-precipitated oxyhydroxides was also studied in this research.

2 Results and discussion

Sintering of aluminum nitrate and copper oxide at 300°C doesn't give a delafossite structure, but it gives CuO phase and X-ray amorphous aluminum-containing phase. Analysis of radial distribution function of the electron density showed that aluminum cations have octahedral oxygen coordination in this compound. According to thermal analysis and XRD, the evolution of oxygen leads to the delafossite formation at temperatures as high as 990 °C (Figure 1). The final phase composition of the sample depends on the calcination and cooling atmosphere. Apparently, the cooling in the synthetic air leads to oxidation of Cu^{+1} and to the formation of spinel $CuAl_2O_4$ and copper oxide CuO phases (Table 1).

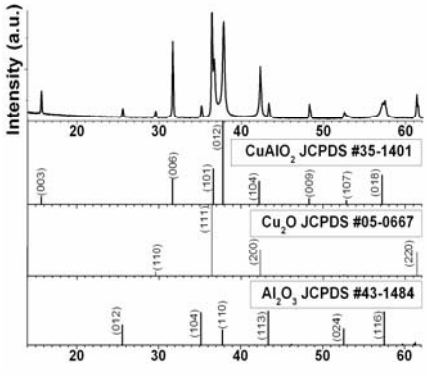

Figure 1. Diffraction pattern of the aluminum nitrate and copper oxide mixture heated at 1000°C in argon.

Table 1. Phase composition of the mixture heated to 1000 C in air and in argon.

Phase	Calcined at 1000 °C in argon		Calcined at 1000 °C in synthetic air	
	Mass fraction, %	CSD size, nm	Mass fraction, %	CSD size, nm
$CuAlO_2$	69	26	48	43

		[001]: > 100		[001]: > 100
$CuAl_2O_4$	-	-	21	45
Cu_2O	16	> 100	-	-
CuO	-	-	20	61
Al_2O_3	15	> 100	11	> 100

The copper-aluminum hydroxycarbonate obtained by coprecipitation transforms to the delafossite at 885°C. This temperature is by 100° C lower than for the samples prepared from a mixture of copper oxide and aluminum nitrate. According to thermal analysis, this process is accompanied by heat absorption and weight loss of about 1.5%.

Using the hydrothermal method of preparation, we managed to get a small amount of delafossite phase at 220°C. The best results of hydrothermal synthesis in terms of the delafossite phase yield and dispersion were obtained using Cu-Al coprecipitated compound of composition Cu:Al = 1:1 pre-calcined at 350°C. Apparently, the use of phase in which copper and aluminum ions are uniformly distributed is more preferable for delafossite phase formation under hydrothermal conditions than the use of a mixture of metal oxides and aluminum.

The significant yield of delafossite phase at a relatively low temperature (less than 420°C) has been achieved for the Co-containing sample prepared by co-precipitation method. The delafossite phase yield depends on the composition. Addition of minor amounts of aluminum improves the yield from 15% to almost 70% (Table 2).

Table 2. Phase composition of Co-containing samples.

Phase	$Cu_{0,5}Co_{0,5}$		$Cu_{0.45}Co_{0.45}Al_{0.1}$	
	Mass fraction, %	**CSD size, nm**	**Mass fraction, %**	**CSD size, nm**
$CuCoO_2$	15	22	~70	20
CuO	44	11	~18	26
CoO	37	11	-	-
Co_3O_4	4	21	~12	25

3 Conclusions

Preparation of copper oxide compounds with delafossite structure is possible at a low temperature. Dispersion suitable for the catalytic applications can be achieved. However, further research is needed to improve the phase purity of the samples.

Acknowledgements

The work was performed with the support of the Ministry of Education and Science of the Russian Federation (project no. 2211-2014/139).

References

[1] A.P. Amrute, Z. Łodziana, C. Mondelli, F. Krumeich, J. Pérez-Ramirez, *Chemistry of materials*, 25 (2013) 4423

[2] L. Torkian, M.M. Amini, *Materials Letters*, 63 (2009) 587

[3] D.Y. Shahriari, A. Barnabe, T.O. Mason, K.R. Poeppelmeier, *Inorganic Chemistry*, 40 (2001) 5734

I-PP26

Esterification-Neutralization-Transesterification of Waste Cooking Oil: *in-Situ* Three-Stage Method for Biodiesel Synthesis, Neutralization Step Optimization

Ouanji F.[1], Kacimi M.[1], Ziyad M.[1,2], Puleo F.[3], Liotta L.F.[3*]

1 - Université Mohammed V, Faculté des Sciences, Département de Chimie, Rabat, Maroc
2 - Académie Hassan II des Sciences et Techniques, Rabat, Maroc
3 - ISMN-CNR, Palermo, Italy

* liotta@pa.ismn.cnr.it

Keywords: biodiesel, three-stage method, esterification, neutralization, transesterification

1 Introduction

Biodiesel is a mixture of methyl esters of fatty acids. It is synthesized by transesterification of vegetable oils, in presence of alkaline catalysts for fast production and industrial application. Waste cooking oils (WCO) and non-edible oils, despite their high contain level of free fatty acids (FFA) and other impurities that cannot be directly converted into biodiesel, were used because of their low price [1]. It is, therefore, required to reduce the FFAs concentration in the oil below the allowed limits prior to biodiesel manufacturing. Different approaches have been attempted: neutralisation, esterification and acid or lipase catalysis transesterification. All these contribute to the increase of the biodiesel cost [1]. The synthesis using the in-situ three-stage method based on in-situ esterification, neutralization and transesterification is possible. The present work was devoted to the optimization of the neutralization step.

2 Experimental

The feedstocks (WVO) used in this study was supplied by Kilimanjaro Environment Company (Casablanca, Morocco). The WCO was filtered and heated at 115°C before using it to remove impurities and water. The oil is characterized by its high acidity developed by heating and hydrolysis (4%). The three-stage method is based on the acid-catalysis esterification of the FFA, followed by in-situ neutralization by an excess of $Ca(OH)_2$ that served as the catalyst for the followed step, e.g. transesterification. In all the stages, water was eliminated on silica traps. Esterification and transesterification reactions were performed according to literature [1].

3 Results and discussion

The calcium hydroxide material used as neutralization base and transesterification catalyst was characterized by DRX. The untreated sample exhibits a typical diagram of calcium hydroxide (portlandite) in agreement with JCPDS (N°.01-073-5492) file. The FTIR spectrum of $Ca(OH)_2$ presents a narrow absorption band at 3642 cm^{-1} due to stretching mode of O-H. TG curve showed that the dehydroxylation of $Ca(OH)_2$ occurs between temperatures 390 and 476°C, with a mass retain of about 23.5%, very close to CaO. Prior to its use $Ca(OH)_2$ was preheated at 200°C.

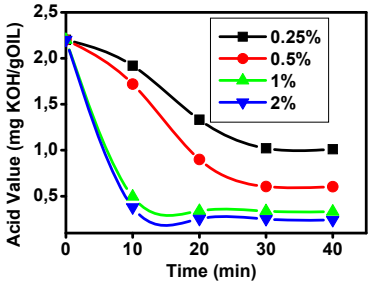

Fig. 1. Acid value variation versus time at different $Ca(OH)_2$ concentration

Preliminary studies showed that butter esterification can be completed at 60°C after 60 min using a methanol/oil ratio equal to 18:1. The achieved conversion corresponds to a residual acidity of 0.44% which is equivalent to the acidity used in the best transesterification. After the esterification, calcium hydroxide was added to the reaction mixture. Fig.1 shows that the addition of $Ca(OH)_2$ decreases the acidity of the reaction mixture denoting a neutralization of the acid catalyst. Addition of a stoichiometric amount of the base compared to the initial amount of H_2SO_4 reduces slightly the acidity.

After the neutralization, the mixture was centrifuged and the two phases were recovered. DRX characterization of the solid phase showed the formation of calcium sulfate dehydrate, e.g. $Ca(SO_4),2H_2O$ (Fig. 2) confirming an in-situ neutralization of the acid catalyst.

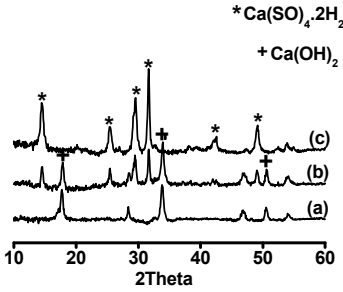

Fig. 2. DRX diagrams of $Ca(OH)_2$ (a), Excess of $Ca(OH)_2$(b) and Stoichiometric amount of $Ca(OH)_2$(c)

The transesterification was also performed immediately after the neutralization. The results show that the conversion was complete and reaches around 96 % in the three-stage method. The produced biodiesel responds reasonably to the European Standards (Table 1).

Table 1: Physicochemical properties of synthesized biodiesel

Batches		Three stages method	Classical method	Standards
Yield	**4** t.%	95.8	79	_
Ester content	**5** t.%	98	95.5	≥ 96.5
Viscosity (40°C)	**6** st	3.5	4.7	3.5-5.5
Density (15°C)	g/cm^3	0.885	0.880	0.88-0.9
Water content	ppm	348	368	500x

4 Conclusions

The optimal conditions for the transesterification reaction depend on the quality of the used cooking oil. The ^{1}H-NMR, ^{13}C-NMR, FT-IR and GC analyses of the final product confirmed that it is possible to produce biodiesel obeying European standards by the in-situ three-stage method.

Acknowledgements

The authors acknowledge Hassan II Academy of Sciences and Technology for the financial support kindly provided to this research. Our thanks go also to the CNRST for the offered open access to the facilities to perform NMR analysis. The bilateral Project CNR-CNRST (2014-2015) between Italy and Morocco is also acknowledged for financial support.

References

[1] Ana Cukalovic, J. M. Monbaliu, Y. Eeckhout, C. Echim, R.Verhé, G. Heynderickx, C.V. Stevens, *Biomass and Bioenergy* 56 (2013) 6.

I-PP27

Mechanistic Studies with Labeled $^{13}CO_2$ on Ni/ZrO_2 and Pt/ZrO_2 Dry Reforming Catalysts

Németh M.[1], Schay Z.[1], Srankó D.[1], Károlyi J.[1], Sáfrán Gy.[2], Sajó I.[3], Horváth A.[1*]

1 - Centre for Energy Research, Institute for Energy Security and Environmental Safety, Department of Surface Chemistry and Catalysis, Budapest, Hungary

2 - Centre for Energy Research, Institute for Technical Physics and Materials Science, Thin Film Physics Department, Budapest, Hungary

3 - University of Pécs, Szentágothai Research Centre, Pécs, Hungary

* horvath.anita@energia.mta.hu

Keywords: ^{13}C labeled experiments, Ni/Zr O_2, Pt/Zr O_2, DRIFTS, circulation system, dry reforming

1 Introduction

Climate change and depletion of hydrocarbon resources of the Earth are the main causes of the nowadays increased research on catalytic dry reforming (DRM: $CO_2+CH_4 \leftrightarrow 2\ CO+2\ H_2$). In our laboratory several aspects of dry reforming have been already investigated over Ni-based catalysts prepared by different methods and supported on different oxides[1,2]. In the present study the same amount of Na as catalyst promoter was used to get ZrO_2-supported Ni and Pt catalysts, applying a simple preparation method that could be feasible at larger (industrial) scale. Structural differences between the samples were investigated and the catalytic behavior was evaluated in plug flow reactor with high excess of methane and in closed loop circulation system at sub atmospheric pressure with labeled $^{13}CO_2$ reactant to be able to spoor the fate of different carbon species.

2 Experimental/methodology

ZrO_2 calcined at 600°C (denoted as Zr6) or 800°C (denoted as Zr8) was used as support for the preparation of 1%Ni/ZrO_2, 3%Ni/ZrO_2 and 1% Pt/ZrO_2 catalysts. The impregnation was done with large excess of water and with the addition of $NaHCO_3$. Dried samples were calcined in air and reduced in H_2 at 600 °C before further use. Structural investigations were carried out by TEM, HRTEM, XRD, XPS and DRIFTS methods (CO chemisorption).

Temperature programmed dry reforming experiments were done i) at atmospheric pressure in plug flow reactor and an in situ DRIFTS cell or ii) under sub atmospheric pressure (~50 mbar) in a closed loop circulation system using labelled $^{13}CO_2$. TPD in this circulation system and TPO of the retained species were used to further reveal the differences between the samples.

3 Results and discussion

The calcined and reduced fresh catalysts contained nanoparticles in the range of 2-20 nm, the Pt/ZrO_2 sample had the highest metal dispersion. The presence of Na was suggested to induce the population of unique bridged CO sites during CO chemisorption DRIFTS measurements on all the samples and to cause binding energy shift to lower values in the case of the highly dispersed Pt/ZrO_2 (XPS).

Low temperature DRIFTS measurements (shown in Figure 1 a) in the presence of dry reforming mixture showed that the carbonates/formates decomposed or could not form in a large amount on Pt/ZrO_2, while on Ni samples more and fairly stable adsorbed carbonates were detected.

On Ni samples coke formation took place during DRM reaction, as measured by the

subsequent TPO. However, most part of this carbon must reside on the support, and leave the Ni sites free, because Zr6Ni3imp despite of this coke was fairly stable and active catalyst (flow tests). CO_2 dissociation on Ni is suggested to provide the main source of active oxygen species at higher temperatures.

In contrast to Ni samples, no deposited carbon was formed on Pt/ZrO_2. The significant water gas shift activity seen during the plug flow tests and the TPD experiments after dry reforming reaction is supposed to keep the surface carbon species hydrogenated and easy to be removed in the case of Pt/ZrO_2.

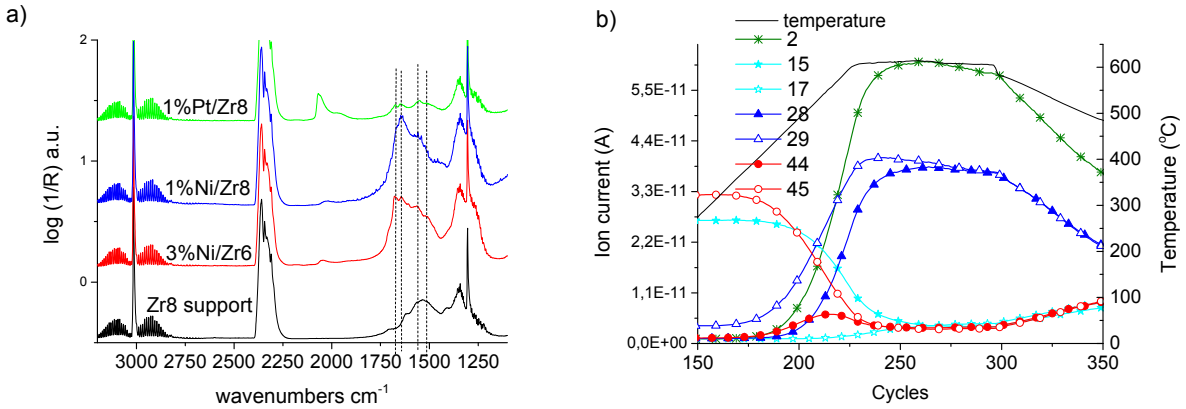

Fig. 1. a) Comparison of DRIFTS spectra of the samples obtained at 400°C in the presence of 70%CH_4:30%CO_2 mixture. b) Dry reforming reaction with 25 mbar CH_4 + 25mbar $^{13}CO_2$ in circulation system on 3%Ni/Zr8. Conditions: temperature ramp up to 600°C with 10°C/min, then 30 min isothermal part, x axis reflects time (1 MS cycle~25.8 sec).

4 Conclusions

Considering all our results, an overall mechanism for the start of reaction could be suggested that holds for Ni and Pt catalysts as well. Figure 1 b reflects, that first CO_2 is activated as $^{13}CO_{2(gas)} \leftrightarrow {}^{13}CO_{ads} + O_{ads}$ and the $^{13}CO_{ads}$ immediately desorbs. At 350-400°C, $^{12}CH_4$ dissociation happens and the surface C get oxidized by abundant active O species and desorbs as $^{12}CO_2$ together with the recombined H_2 molecules. Next, ^{12}CO appears in the gas phase because of the incomplete oxidation of surface carbon due to less available surface oxygen species and because of the $^{12}CO_2 \leftrightarrow {}^{12}CO+O$ reversible transformation on the catalyst surface. Methane dissociation is considered reversible, because methane can form from $^{13}CO + H_2$ or $^{13}CO_2 + H_2$ via surface methanation reaction that proceeds through C_{ads} intermediate species. According to our isotope labeled measurements, common reaction intermediates originating from methane and carbon dioxide do exist at 600 °C.

Acknowledgements

The authors are indebted for financial support of Era-Chemistry and the Hungarian National Research Fund (OTKA NN#107170).

References

[1] A. Horváth, G. Stefler, O. Geszti, A. Kienneman, A. Pietraszek, L. Guczi, *Catal. Today* 169 (2011) 102.

[2] A. Horváth, L. Guczi, A. Kocsonya, G. Sáfrán, V. La Parola, L. F. Liotta, G. Pantaleo, A. M. Venezia, *Appl. Catal. A: Gen.* 468 (2013) 250.

I-PP28

Mathematical Model of Catalytic Hydrodewaxing of Distillates

Belinskaya N.S.*, Ivanchina E.D., Ivashkina E.N., Nazarova G.Yu.

National Research Tomsk Polytechnic University, Tomsk, Russia

* belinskaya@tpu.ru

Keywords: catalytic hydrodewaxing, diesel fuel, mathematical model, polyfunctional catalyst

1 Introduction

One of the varieties of light hydrocracking is hydrodewaxing of distillates. It represents light hydrocracking (breakage) of n-paraffin hydrocarbons in order to produce diesel fuel with improved low-temperature properties. The purpose of the process is producing of winter arctic diesel fuel with very low freezing point (from -18 to -68 °C). A polyfunctional zeolite-containing catalyst is used in this process [1]. The work is devoted to mathematical model of the process development.

2 Methodology

While developing of the catalytic hydrodewaxing model thermodynamic analysis of reactions was made via quantum-chemical calculations of thermodynamic characteristics of reactions under technological conditions that correspond industrial unit operation. Then hydrocarbons conversion scheme was created. It includes primary reactions of long-chain n-paraffins cracking and subsequent isomerization of cracked n-paraffins through the stage of olefin and iso-olefin formation on acid sites of polyfunctional catalyst. The side reactions of hydrogenation of monoaromatic and polyaromatic compounds, cyclization of iso-paraffins are also included in the conversion scheme.

Willing to hydrocarbon conversion scheme kinetic model was developed. It represents a system of differential equations of concentrations changing under contact time:

$$\begin{cases}
\frac{dC_{N-paraffins\ C_{10}-C_{27}}}{d\tau} = -W_1 \\
\frac{dC_{N-paraffins\ C_5-C_9}}{d\tau} = 2\cdot W_1 - W_2 + W_{-2} \\
\frac{dC_{I-paraffins}}{d\tau} = W_3 - W_{-3} - W_4 + W_{-4} \\
\frac{dC_{Olefins}}{d\tau} = W_2 - W_{-2} - W_3 + W_{-3} \\
\frac{dC_{Naphthenes}}{d\tau} = W_4 - W_{-4} - W_5 + W_{-5} \\
\frac{dC_{Monoarom}}{d\tau} = W_5 - W_{-5} + 2\cdot W_6 - 2\cdot W_{-6} \\
\frac{dC_{Polyarom}}{d\tau} = -W_6 + W_{-6} \\
\frac{dC_{Hydrogen}}{d\tau} = -W_1 + W_2 - W_{-2} - W_3 + W_{-3} + W_4 - W_{-4} - 3\cdot W_5 + 3\cdot W_{-5} - W_6 + W_{-6}
\end{cases}$$

Contact time is calculated via volume of catalyst (V_{cat}) and sum of feed and hydrogen rich gas flow rate (G_R and G_{HG} respectively):

$$\tau = \frac{V_{kat}}{G_R + G_{HG}}.$$

Kinetic values of the model (preexponential factor in Arrhenius equation for each reaction) were found via solution of reverse kinetic problem using a large selection of full-scale experimental data. Rate constants of the straightforward reactions were found via Arrhenius equation and account

1.241, 1.795, 3.108 for hydrocracking of long-chain n-paraffins, dehydrogenation of short-chain n-paraffins and hydrogenation of olefins respectively. Rate constants for cyclization of iso-paraffins, hydrogenation of monoaromatic compounds, hydrogenation of polyaromatic compounds are 0.014, 0.128, 0.128 respectively.

Verification of model to the full-scale process showed a high degree of calculations accuracy in comparison to experimental values. Absolute error of calculations did not exceed 3 % wt.

3 Results and discussion

In the process of hydrocracking it is crucial to maintain the excess of hydrogen in circulating gas as fresh hydrogen, injected simultaneously with the feed, is intensively consumed in chemical reactions of hydrocracking. The hydrogen circulation rate is as higher as heavier the feed is and higher conversion degree is as well as lighter obtained products are. The hydrogen consumption rate significantly influences the exploitation expenses as well [1]. For these reasons optimal hydrogen containing gas maintenance depending on the feed composition is vital in order to achieve resource efficiency of the plant.

Using developed mathematical model hydrogen to feed molar ratio on the conversion of long-chain n-paraffins and yield of i-paraffins was investigated.

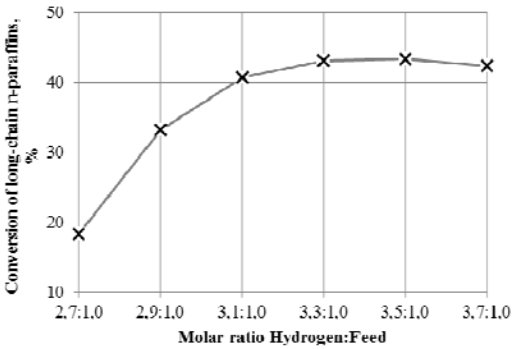

Fig. 1. Conversion of long-chain n-paraffins depending on molar ratio Hydrogen:Feed

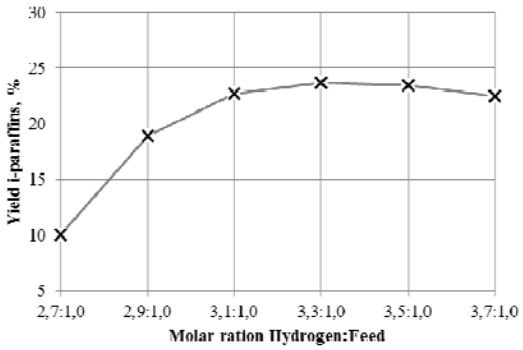

Fig. 2. Yield of i-paraffins depending on molar ratio Hydrogen:Feed

According to the fig. 1 and fig. 2 conversion of long-chain n-paraffins and yield of i-paraffins increase steadily with Hydrogen:Feed ratio increasing until 3,3:1,0 and reach 43 % and 24 % respectively for the taken feed composition. Further increasing the ratio is worthless as it leads to decreasing in long-chain n-paraffins conversion and i-paraffins yield.

4 Conclusions

The presented research showed that mathematical model is an effective instrument for analysis and optimization of complicated multifactorial re-refinery process of hydrodewaxing. Application of the model allows increasing resource efficiency of the high quality diesel fuel production on 15-20 %.

References

[1] V.M. Kapustin, M.G. Rudin. *Chemistry and Technology of oil refining*. – M.: Khimiya, 2013. – 496 p.

I-PP29

Study of Influence of Cis-Trans Isomerization on Selective Oxidations of Alkenes by Nitrous Oxide

Ivanov D.P.[1], Semikolenov S.V.[1*], Nartova A.V.[1,2], Fedorov V.S.[1,2], Babushkin D.E.[1], Dubkov K.A.[1]

1 - Boreskov Institute of Catalysis SB RAS, Novosibirsk, Russia
2 - Novosibirsk State University, Novosibirsk, Russia

* sersem@catalysis.ru

Keywords: nitrous oxide, alkenes, selective oxidation, ketones

1 Introduction

Nowadays nitrous oxide (N_2O) is considered as effective donor of oxygen. Thus recently it was discovered that nitrous oxide can lead the non-catalytic liquid-phase oxidation of alkenes into carbonyl compounds – aldehydes and ketones. These reactions run at 150-250°C with high selectivity, often close to 100% [1]. The investigation of the wide range of such reactions demonstrated that carbonyl compounds can be synthesized using different types of alkenes include linear, cyclic, heterocyclic and derivatives.

In the present work the influence of cis-trans isomerization of heptane-3 on reactivity of C=C bond of alkenes towards N_2O as well as the contribution of the reaction route with the break of the initial double bounds were studied. This knowledge is important for the understanding the oxidation reaction by nitrous oxide of double bonds of butadiene rubbers with different degrees of stereo regularity.

2 Experimental/methodology

The reaction was carried out in stainless steel Parr reactor with capacity of 100 cm^3. The composition of products was investigated by gas chromatography and NMR spectroscopy.

3 Results and discussion

On the base of obtained data the scheme of heptane-3 oxidation by N_2O was proposed. It was shown that both cis- and trans-heptane isomers perform very similar reactivity. For example the cis-isomer conversion at 240°C after 6 hours was 21.4%. In the case of trans-isomer under the same conditions conversion was 19.5%. At the same time for trans-hepten-3 the contribution of the route with C-C bound break (F_{br}) is approximately three times higher comparing with cis-heptane-3. So under such oxidation conditions trans-isomer performs higher reactivity towards bound break comparing with cis-isomer. The origin of this difference is under discussion.

It should be mentioned that conclusion on the portion of C-C bound breaks for different isomers made on the base of presented experiments well agrees with our previous studies. Thus for the oxidation of buten-2 and penten-2 F_{br} performed the intermediate value (F_{br} = 8%) [2], evidently this can be explained by the fact that these alkenes consist of the isomer mixtures. The portion of the route with C-C bound break found for cis-hepten-3 is close to F_{br} = 5% obtained for the oxidation of stereo regular cis-butadiene-1,4 rubber by N_2O [3]. At the same time the portion of the bound break for trans-heptane-3 is in good agreement with F_{br} = 15% observed for C=C bound oxidation of butadiene-nitrile rubber [4], which contains trans-butadiene-1,4

units mostly.

4 Conclusions

The presented study reveals the common regularities of the oxidation of compounds with C=C bounds by nitrous oxide. The observed difference in contribution of the reaction route with C-C bound break for the olefins confirms the results obtained for rubbers previously.

Acknowledgements

The work was supported by the Program of RFBR # 14-03-31052 mol_a.

References

[1] E. V. Starokon, K. A. Dubkov, D. E. Babushkin, V. N. Parmon, G. I. Panov, *Adv. Synth. Catal.*, 2004, 346, 268.
[2] S.V. Semikolenov, K.A. Dubkov, E. V. Starokon, D.E. Babushkin, G. I. Panov *Russ Chem Bull* (2005) 54, 4 948-956.
[3] K.A. Dubkov, S.V. Semikolenov, D.E. Babushkin, L.G. Echevskaya, M.A. Matsko, D.P. Ivanov, V.A. Zakharov, V.N. Parmon, G.I. Panov, *J. Polym. Sci., Part A: Polym. Chem*. 44 (2006) 2510-2520.
[4] S.V. Semikolenov, K.A. Dubkov, D.P. Ivanov, D.E. Babushkin, M.A. Matsko, G.I. Panov, *European Polymer Journal* 45 (2009) 3355–3362.

I-PP30

Development of New NiW Catalysts Supported on SBA-15/Zeoilte for Oil Sludge Hydrotreating

Naranov E.R.[1*], Badeeva A.S.[1], Maximov A.L.[1,2], Karakhanov E.A.[1]

1 - Department of Chemistry, Moscow State University, Moscow, Russia
2 - Topchiev Institute of Petrochemical Synthesis, Russian Academy of Sciences, Moscow, Russia

* naranov@petrol.chem.msu.ru

Keywords: hydrotreating, hydrocracking, oil sludge, micro/mesoporous materials, sulfided catalysts

1 Introduction

Incorporation of oil sludge (OS) in refining will help to solve some urgent environmental and economic problems such as energy recovery and reduction of the volume and quantity of waste. OS is the waste of oil production and sometimes refining; it consists of heavy hydrocarbons mixture (essentially, crude oil) and water [1]. Thermohydrocatalytic treatment due to particular feature of OS composition is considered to be the most reasonable way to use OS. Here we report the new synthesis of sulfided catalysts based on the micro/mesoporous systems, phys.-chemical properties of these catalysts and their catalytic activity in OS hydrotreating.

2 Experimental

In this work, an original approach for preparing NiW/SBA-15/ZSM-5 and NiW/SBA-15/zeolite-β hybrid support is presented. The adopted preparation strategy was based on the effective confinement of the suflided catalyst within the pores of an SBA-15/zeolite carrier (d_{pore} = 7.0 nm). In the course of study two different ways of synthesis micro/mesoporous aluminosilicates were applied: a) zeolitization of ZSM-5 and β in SBA-15 walls b) double templating synthesis [2]. New NiW catalysts were obtained by one-step incipient-wetness impregnation method and after that they were dried at 110 ^{o}C, calcined at 550 ^{o}C and presulfided by sulfur-toluene solution, 50 atm H_2, 400^{o}C. The supports and catalysts were characterized by various techniques including XRD, nitrogen adsorption, TEM, ^{27}Al and ^{29}Si MAS NMR, and TPD NH_3. The reactions were carried out in a steel autoclave at 50 atm. H_2 and 350-420^{o}C.

3 Results and Discussion

The results from the TEM and XRD analyses confirm incorporation of zeolites into the SBA-15 structure. Moreover, ^{27}Al MAS NMR measurements indicate that the framework aluminum species in SBA-15/zeolite is practically the same as in zeolite structure. The catalytic study shows that both SBA-15/Zeolite-β and SBA-15/ZSM-5 materials are good supports for NiW catalysts in the hydrotreating of OS. It was demonstrated that oil sludge hydrotreating gets light and middle distillate hydrocarbons and sulfur becomes less about 10 times. The experiments carrying out at 400^{o}C and higher reveal that there were a lot of gas products especially in case of NiW/SBA-15/ZSM-5 catalyst. Furthermore, it was found out that these catalysts showed higher activity than a reference NiW/SBA-15 catalyst.

4 Conclusions

In this work, NiW sulfided catalysts based on micro-mesoporous composite materials SBA-15/zeoilte-β and SBA-15/ZSM-5 were successfully synthesized. The characterization results show that the composite material possess the same mesoporous structure as SBA-15 and contain Beta (ZSM-5) zeolite crystals simultaneously. The high activity of SBA-15/zeolite supported

catalyst in oil sludge hydrotreating might be attributed to the combination of open mesoporous structure and the large amounts of acid sites.

References

[1] J. Dibble, R. Bartha, *Applied and environmental microbiology* (1979) 729
[2] R. Chal, C. Gerardin, M. Bulut, S. Donk, *ChemCatChem* (2011) 67

I-PP31

A Numerical Investigation of the Catalyst Behaviour in Fluidized Bed Circulating Reactor

Solov'ev S.A.*, Egorov A.G., Egorova S.R., Lamberov A.A., Kataev A.N., Bekmukhamedov G.E.

Kazan Federal University, Kazan, Russia

* serguei_s349@mail.ru

Keywords: fluidized bed, chemical reactor, numerical simulation, structural elements

1 Introduction

Fluidized bed reactors are widely used in the petrochemical industry, in particular for the isobutane dehydrogenation process with fine particles of the chromia-alumina catalyst. An injection of hot catalyst particles is needed for sustenance the temperature of the reaction. The main objective is effective heating of the fluidized bed region with the highest concentration of catalyst. In the large reactors the structural elements (lattice) are used for breaking gas bubbles and active mixing of gas and catalyst. In present paper the motion of solid catalyst particles with a size of 20-200 microns in isobutane dehydrogenation reactor model was investigated. Geometrically reactor is5.1 m in internal diameter and 17.4 m in height, partitioned by ten distributive lattice of angle-type with an area of free section of 30%. A vertical pipe is placed in the center part of reactor for the supplying of heated catalyst. Calculations of hydrodynamic and heat transfer processes in the reactor were carried out by numerical methods using computers with special attention to the flow near the walls in reactor.

2 Formulation of the problem

Currently, one of the ways to determine the properties of large-scale fluidized beds is numerical simulation. In a study of fluidization an Eulerian-Eulerian approach was applied, when carrier phase (gas, liquid) and discrete (solid) phase are continuous. Using kinetic theory of gases, equations (for each discrete phase) which are describing kinetic energy changes of granules in consequence of collisions was added for account of features in a fluidized bed movement.

Presented results of calculations are carried out for mono disperse catalyst (one phase of particles with 90 μm in diameter) and for poly disperse catalyst (two phases of particles with 90 μm and 30 μm in diameter). A steady fast downward flow of catalyst grains along walls of reactor and slow upward movement in the central zone was observed in calculations. This motion is providing the total intensive circulation of catalyst and gas. Any structural elements (e.g. lattice) in reactors can have a significant impact on all circulating field. Parametric calculations for different distances between lattice and reactor walls are performed in this investigation. Namely, in the calculations distance parameters as 9 cm, 5 cm and 3.6 cm were used. The main aim is to analyze catalyst and gas circulation in reactor.

3 Result of calculations

The analysis results of calculations for three cases that were described above of different distance between lattice and walls are shown in figure 1. The arrows on the lattice define the main directions for average upward and downward flows of circulating catalyst and gas in reactor. Reactor about 5 meters in diameter in cases with minor differences in structural elements of apparatus has a significant differences on the overall circulation field as it can be

seen from the figure. Catalyst rises in the central zone, and falls down in the areas closer to the external wall and in the thin layer around the central tube in case with distance 9 cm. Catalyst descends in the central zone and in a thin layer near the external wall and rises upwards in the areas closer to the outer wall in case with distance 3.6 cm. Finally, catalyst rises in almost all the reactor zones and descends in thin layers around the central tube and the external wall, but with higher velocity.

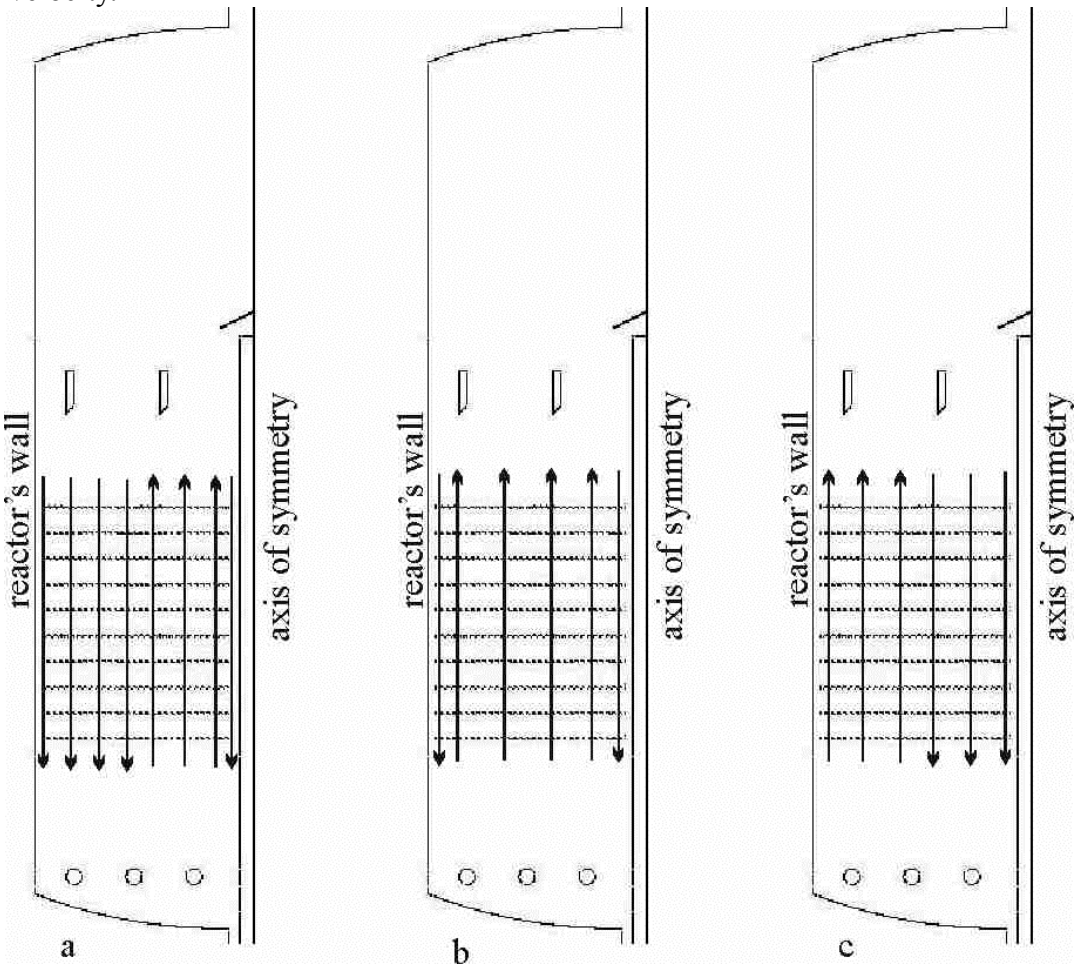

Fig. 1. Scheme of reactor and directions for average upward and downward flows of circulating catalyst and gas for different cases of distance between lattice and walls: a – 9 cm, b – 5 cm, c – 3.6 cm.

4 Conclusion

Any minor changes in the structural elements geometry can have a significant influence for hydrodynamics of the fluidized bed. Application of numerical simulation allows to predict the behavior of bed with using approximations. The researching results can be of interest for industrial applications where it is important to have a proper circulation bed.

Acknowledgements

This work was sponsored by The Ministry of Education and Science of The Russian Federation.

I-PP32

Sm, Eu Containing Hydrotalcite-Like Materials as Precursors of Catalysts for Oxidative Dehydrogenation of Light Hydrocarbons

Belomestnykh I.P.[1*], Krasnobaeva O.N.[2], Nosova T.A.[2], Elisarova T.A.[2], Danilov V.P.[2]

1 - N.D.Zelinsky Institute of Organic Chemistry, Russian Academy of Science, Moscow, Russia
2 - Kurnakov Institute of General and Inorganic Chemistry, Russian Academy of Sciences, Moscow, Russia

* belom2011@mail.ru

Keywords: paraffins, oxidative dehydrogenation, olefins, hydrotalcite, materials

1 Introduction

Layered double hydroxides (LDHs) known as hydrotalcite-like layered metal hydroxo salts, are extensively explored as precursors of various catalysts. Interest in LDHs is provided by the fact that two, three or more cations may be introduced in the brucite-like layers, besides various anions (e. g. decavanadate, paramolybdate, etc) in the interlayer space [1]. However the information on the application of such materials as multi-component catalysts for oxidative dehydrogenation (ODH) of light alkanes is still scanty. We have performed an extensive investigation of the synthesis of complex hydrotalcite-like hydroxo salts and their application as precursors of catalysts. In the present work the catalysts containing Sm and Eu were prepared using complex hydrotalcite-like layered hydroxo salts (LDHs) as precursors and tested in ODH of light alkanes (ethane, propane, isobutane) in the presence oxygen-nitrogen mixtures and CO_2.

2 Experimental

Catalysts were prepared, using complex hydrotalcite-like layered hydroxo salts (LDHs) as precursors by coprecipitation at 65°C and constant pH according to experimental procedures, described in detail earlier [1-3]. ODH of alkanes was carried out in a fix-bed quartz reactor (1.0 g of the catalyst) with on-line GC analysis. The reaction was studied varying the experimental conditions (400-650°C, atmospheric pressure, LHSV 1.0-1.5 h^{-1}). The catalyst precursor was calcinated at 500°C. The structure of the prepared precursors and calcinated materials was investigated by XRD and BET. The thermally treated samples were characterized with respect to their textural properties. The stability tests were carried out in prolonged runs of 25 and 100 hours under optimum conditions.

3 Results and discussion

Synthesized LDHs materials showed well-crystallized hydrotalcite structure. Thermal decomposition converted the precursors into mixed metal oxides characterized by developed (74 m^2/g) surface area and pore size of 200-300Å.

The optimum reaction conditions for synthesis of alkenes have been determined. Results of tests showed that ethane ODH proceeded at low temperature over catalysts containing Sm (450^0C). Ethene is formed with high selectivity (86-90%) over this catalysts but its yield is low 13.5 – 16.1%). There are data of propane and isobutane ODH over Sm-Al-Mg-O in Tables 1 and 2. The results of stability test of the Sm-Al-Mg-O catalyst for a feed with CO_2+O_2 were similar to those without O_2 addition in the feed. Thus, it seems that there is no point in using oxygen to improve the stability of the catalyst in propane and isobutane dehydrogenation with CO_2.

Table 1. Data of propane ODH over Sm-Al-Mg-O. Reaction mixture: C_3H_8:CO_2=1:1

Temperature, °C	C_3H_8 conversion, %	C_3H_6 yield, %	C_3H_6 selectivity, %
450	24.1	17.7	72.2
600	30.5	21.5	69.3

Table 2. Data of isobutane ODH over Sm-Al-Mg-O. Reaction mixture: i-C_4H_{10}:CO_2=1:1

Temperature, °C	C_4H_{10} conversion, %	(i-C_4H_8+C_3H_6) yield, %	(i-C_4H_8+C_3H_6) selectivity, %
450	23.0	20.9	90.8
600	57.0	43.0	75.6

Eu-V-Mg-O catalyst displayed a good stability during 100 hours on stream. Conversion of propane decreased gradually during the first three 3 hours on stream and became stable without any tendency to decline for following 100 hours at the average level of 20.4%. The selectivity to total alkenes remained stable during the time on stream at the average level of 76%. The propene/ethane ratio in the reaction mixtures remained constant being equal to 3/2. Conversion of isobutane and selectivity to isobutene at the presence of CO_2 and O_2 were 36.1 and 85.0 %, respectively, at 450°C over catalyst containing Eu. At 650°C conversion of isobutane and selectivity to isobutene were 65.1 and 63.0 %, respectively. Obtained data show that introduction of Sm and Eu results in an increase of olefins yield and its selectivity.

4 Conclusions

The results of complex investigation of the process of ODH of light alkane are presented. The new hydroxosalts which have a layered structure of hydrotalcite type with Sm and Eu were synthesized. These hydroxosalts were used as precursors for oxidative dehydrogenation of ethane, propane and isobutane. A strong dependence of the yield and selectivity of alkanes loading and the conditions of heat treatment were observed. The optimum reaction conditions for formation of alkenes have been determined. It was shown that introduction of Sm and Eu results in an increase of olefins yield and its selectivity.

References

[1] O.N. Krasnobaeva, I.P. Belomestnykh, T.A. Nosova, et al., *Journal Inorg. Chem*. 56 (2011) 1012.
[2] O.N. Krasnobaeva, I.P. Belomestnykh, T.A. Nosova, et al., *Journal Inorg. Chem*. 57 (2012) 1540.
[3] O.N. Krasnobaeva, I.P. Belomestnykh, T.A. Nosova et al., *Journal Inorg. Chem*. 58 (2013) 544.

I-PP33

Novel α,α-Phosphinoaminoacids: Synthesis, Properties and Catalytic Activity in the Ethylene Oligomerization Process

Fomina O.S.[1,2*], Yakhvarov D.G.[1], Sinyashin O.G.[1], Heinicke J.W.[2]

1 - A.E. Arbuzov Institute of Organic and Physical Chemistry, Kazan Scientific Center, Russian Academy of Sciences, Kazan, Russia

2 - Institute of Biochemistry Ernst-Moritz-Arndt University of Greifswald, Greifswald, Germany

* myaolechka@yandex.ru

Keywords: α,α-phosphinoaminoacids, catalytic activity, oligomerization

1 Introduction

Synthetic amino acids are of interest in various fields of chemistry, biochemistry and pharmacy.[1] The first epresentatives with a phosphanyl group were obtained by condensation of natural amino acids with secondary phosphanes and formaldehyde, usually forming bis(phosphanylmethyl) amino acids, and studied with respect to their use as ligands in rhodium-catalysed hydrogenation reactions and in complexes for radio-diagnostics.[2] The use of primary phosphanes extended the range of N-phosphanylmethyl amino acids to various P,N-heterocyclic types. The incorporation of P-alkyl instead of Pphenyl groups led to an increase in the sensitivity of Nalkyl-α-phosphanylglycines. To obtain more stable α-phosphanyl amino acids we systematically varied the nitrogen substituents of the (diphenylphosphanyl)glycines and report here on the novel N-aryl derivatives 1, their synthesis, structure and properties, and the first examples of their transitionmetal complexes and their use in homogeneous catalysis.

2 Experimental/methodology

All manipulations with air-sensitive compounds were conducted under nitrogen using Schlenk techniques. Solvents were dried by standard methods and freshly distilled before use.

I. Novel α,α-phosphinoaminoacids were all prepared by A three-component one-pot reaction of diphenylphosphine, primary amine and glyoxylic acid hydrate in diethyl ether or methanol [1,2] (Fig. 1).

II. Oligo/Polymerization of Ethylene: The various phosphanylglycines and $Ni(COD)_2$ (each ca. 100 μmol) were dissolved in THF or toluene (10 mL), cooled to 0 °C (10 min) and mixed. The resulting yellow-brown solution was stirred at room temperature for 5 min and transferred through a Teflon® tube to the argonfilled autoclave. After weighing, the autoclave was pressurized with ethylene (30–50 bar), the amount of ethylene was determined and the autoclave was placed in the silicon bath and heated overnight (15 h) at 100_5 °C. After cooling to room temperature unconverted ethylene was allowed to escape through a cooling trap (–40 °C; only trace amounts of butenes were observed). The volatiles were flash-distilled at 80 °C/4.0 mbar from the solvent product mixture. The residual waxy oligomer or polymer was treated for 1 d with methanol/hydrochloric acid (1:1), thoroughly washed with methanol and finally dried in vacuo.

3 Results and discussion

A three-component one-pot reaction of diphenylphosphine, primary amine and glyoxylic acid hydrate in diethyl ether or methanol allowed an easy access to N-monosubstituted diphenylphosphinoglycines. The reaction of nickel (0) complexes with N-monosubstituted diphenylphosphinoglycines leads to the formation of a catalytically active form of the ethylene oligomerisation catalyst via oxidative addition to O-H or O-C bond of the used phosphorus

ligand. The linear olefins with terminal methyl and vinyl groups are the main products of the catalytic ethylene oligomerisation process. The highest conversion of C_2H_4 into linear α-olefins was observed with *N*-C_6H_3-2,5-$(COOMe)_2$ phosphinoglycinate ligand.[3-5]

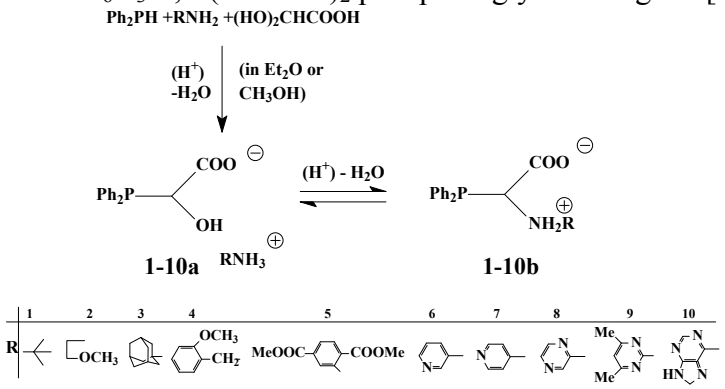

Fig. 1. Preparation of α,α-phosphinoaminoacids

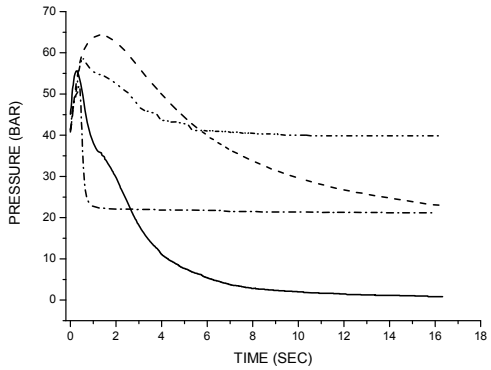

Fig. 2. Pressure time plots for consumption of ethylene (pstart 40–50 bar) in batcholigomerization tests of precatalyst complexes, formed from 4(dot dash line), 5(dotted dotted point line) , 8 (dotted line) and asolution of $Ni(COD)_2$ (each ca. 100 lmol) in THF; bath temperature 100^0C, and oligomerization tests of precatalyst complexes, formed from 4(full line) and a solution of $Ni(COD)_2$ (each ca. 100 lmol) in toluene; bath temperature 70^0C

4 Conclusions

N-Aryl-α-phosphanylglycines, novel α-phosphanyl amino acids with reduced basicity at the nitrogen atom, are easily accessible by one-pot three-component reactions of primary arylamines, diphenylphosphane and glyoxylic acid hydrate in diethyl ether at room temperature. The reaction is restricted to *N*-monosubstituted amines and was found to involve intermediate arylammonium (diphenylphosphanyl)glycolates, which reversibly condense to the slightly more stable phosphanylglycines. Highly active catalysts for oligomerization of ethylene are formed in situ from THF solutions of the phosphanylglycines and Ni(cod)2. The selectivity is the same as with the less easily accessible but hydrolytically more stable (diphenylphosphanyl) acetic acid ligand and hints at catalyst stabilization by a PO– nickel chelate backbone.

References

[1] O.S. Fomina, D.G Yakhvarov., J.W. Heinicke, O.G Sinyashin. , Uchenye Zapiski Kazanskogo Universiteta. 154 (2012).13.
[2] R.B. Kaleswara, O.S. Fomina, D.G.Yakhvarov, J. W. Heinicke, Polyhedron. 67 (2014) 306.
[3] B.R. Aluri, K. Shah, N. Gupta, O.S. Fomina, D.G.. Yakhvarov, M. Ghalib, P.G. Jones, C. Schulzke and J. W.Heinicke, European Journai of Inorganic Chemistry. (2014). 5958.
[4] M. Ghalib, J. Lach, O.S. Fomina, D.G.. Yakhvarovc, P.G. Jones, J.W. Heinicke, Polyhedron. 77(2014). 10
[5] J.W. Heinicke, J. Lach, M. Kockerling, G.J. Paim, O.S. Fomina, D.G.. Yakhvarov and O.G. Sinyashin, Phosphorus Sulfur Silicon and the Related Elements. In print

I-PP34

The Development of Integrated Technology for Oil and Vegetable Feedstock Processing to Produce Diesel Fuel for Arctic Climatic Zone and Jet Fuel

Gulyaeva L.[1*], Shmelkova O.[1], Grudanova A.[1,2], Krasilnikova L.[1], Misko O.[1], Chernysheva E.[2], Boldushevsky R.[1,2], Asaula V.[2]

1 - All-Russia Research Institute of Oil Refining, JSC, Laboratory of Hydrogenated Processes and Catalysts for Motor Fuels Producing, Moscow, Russia

2 - Gubkin Russian State University of Oil and Gas, Department of Oil Refining Technology, Moscow, Russia

** GulyaevaLA@vniinp.ru*

Keywords: biomass, pyrolysis, synthetic oil, hydroisomerization, catalyst, cold flow upgraded, motor fuels

1 Introduction

The expansion of the feedstock and the increasing of the production capacity for high quality jet fuel and diesel fuel with upgraded cold flow properties are one of the priority directions for Russian oil refining industry progress.

The production of fuels in accordance with modern environmental and operational requirements determines the need for new flexible and versatile technologies development to replace fossil fuels with alternative renewable energy sources, in particular vegetable feedstock due to wide availability, accessibility and environmental safety. We considered two processes among the modern technologies for the production of synthetic liquid fuels from plant biomass (BTL): thermochemical conversion without oxygen access (pyrolysis) and gasification to synthesis gas which is a feedstock for the Fischer-Tropsch synthesis [1, 2].

2 Experimental/methodology

At Gubkin Russian State University of Oil and Gas were carried out the investigations slow pyrolysis process of sawdust (500°C, contact time – 10-30 sec). Obtained liquid pyrolysis products contained a high water concentration, a lot of oxygenated compounds and high iodine number. Because of such characteristics pyrolysis products were unusable for use as a motor fuels component. If the feed of the process was the mixture of sawdust and black oil (the fraction boiling >350°C), pyrolysis ran with higher intensity and there was a greater liquid products yield with quality superior to products of sawdust pyrolysis. Experimentally it has been defined the best ratio between sawdust and black oil equal 1 : 3 for vegetable and oil feedstock co-processing. This ratio was used for pyrolysis to obtain the motor fuel components. Due to the high content of sulfur, nitrogen and oxygen containing compounds and aromatic hydrocarbons the pyrolysis middle fractions were subjected to hydroconversion in mixture with the straight-run diesel distillate with subsequent improvement of cold flow properties by isodewaxing.

At All-Russia Research Institute of Oil Refining (VNII NP, JSC) the samples of synthetic oil were produced by Fischer-Tropsch synthesis (low temperature, Co-catalyst). The feedstock for Fischer-Tropsch process was synthesis gas of the plant biomass steam-oxygen gasification (1200°C, 0.5 MPa). The synthetic oil boils in the kerosene and gas oil range, contains almost no aromatic and oxygenated compounds and is characterized by the absence of sulfur and nitrogen compounds.

The mixture of the synthetic oil and the hydrotreated diesel fraction was processed by isodewaxing for obtaining jet fuel and diesel fuel satisfying the requirements for use in arctic

climatic zone conditions. For this process the catalyst was developed by specialists of VNII NP, JSC.

3 Results and discussion

Hydroconversion (MPa, 350°C, 1.0 h^{-1}) of mixtures of pyrolysis middle distillate fractions and straight-run diesel distillate ran with maximum hydrogenation depth conversion of heteroatomic compounds if feedstock content up to 20% bio-component. The cold flow properties according to Russian State Standard 55475-2013 (GOST R 55475-2013) are achieved by the isodewaxing process (table 1).

Table 1. The results of the co-processing of liquid pyrolysis products and petroleum distillates.

Quality index	Value of quality index		
	Feedstock	Hydroconversion product	Isodewaxing product
Density at 15°C, kg/m^3	856	848	853
Fractional composition			
initial boiling point	180	165	140
end boiling point	360	358	357
Filterability temperature limit, °C	minus 5	minus 8	minus 32
Sulfur content, ppm	1200	16	18
Cetane number	52	50	47

Isodewaxing process of the mixture of synthetic oil obtained by the biomass gasification and hydrotreated diesel fraction resulted in yield of products with were separated on gasoline, kerosene and diesel fractions. Kerosene and diesel fractions were the main products of isodewaxing.

Isodewaxing stable product can be used as a diesel fuel for arctic conditions and meets the requirements for class 4 of EN 590:2009.

The fraction boiling in the range 135-280°C evolved from isodewaxing products on key quality indicators pass standard for aviation fuel brand JET-A1.

4 Conclusions

1. The studies shown that as a result of co-processing of pyrolysis liquid products of plant biomass and oil feedstock by processes of the hydroconversion and isodewaxing can be produced the winter diesel fuel with filterability temperature limit equal to minus 32 according to standard GOST R 55475-2013.

2. Processing of synthetic oil in a mixture with petroleum diesel distillate by isodewaxing process allows obtaining jet fuel brand JET-A1 and diesel fuel for arctic conditions of EN 590:2009 "Automotive fuels – Diesel – Requirements and test methods".

Acknowledgements

This work “The development of integrated technology for oil and vegetable feedstock processing to produce diesel fuels for arctic conditions and jet fuel” is carrying out with the Ministry of education financial support in the network of Federal target program “Research and development on the priority directions subject of scientific-technological complex of Russia for 2014-2020”. The code of agreement is № 14.579.21.0061.

References

[1] B.N. Kuznetsov, Journal of the Russian Chemical Society. 6 (XLVIII) 2003.
[2] Ya.Sh. Khakieva, V.V. Imshenetskiy, B. World of Oil Products. 5. 2006.

I-PP35

Self-Assembled Complexes of 1-Hexadecyl-4-Aza-1-Azoniabicyclo[2.2.2]Octane Bromide with Nitrates of Copper and Lanthanum as the Models of Metalloenzymes

Zhiltsova E.P.[1*], Lukashenko S.S.[1], Valeeva F.G.[1], Kashapov R.R.[1], Pashirova T.N.[1], Konovalov A.I.[1], Zakharova L.Ya.[1,2]

1 - A.E. Arbuzov Institute of Organic and Physical Chemistry, Kazan Scientific Center, Russian Academy of Sciences, Kazan, Russia

2 - Kazan National Research Technological University, Kazan, Russia

* lucia@iopc.ru

Keywords: complex, DABCO, aggregation, critical micelle concentration, solubilization

1 Introduction

The study of the chemical processes in organized media containing metallomicelles based on complexes of metals with surfactants attracts the attention of researchers due to their potentiality for the significant enhancing of the catalytic activity of systems. This is important for the creation of new materials, the decomposition of toxic substances and toxicants, as well as from the viewpoint of biomimetic aspects [1]. An important characteristic of the complexes of metals with surfactants, which determines their catalytic activity, is the ability to aggregate in solution. We have studied micelle forming, adsorption and solubilization of aqueous solutions of the complexes of 1-hexadecyl-4-aza-1-azoniabicyclo[2.2.2]octane bromide (HB-16) with nitrates of transition metals (Cu^{2+}, La^{3+}) by methods of tensiometry, conductometry, spectrophotometry (solubilization of water-insoluble dye Orange OT).

2 Experimental/methodology

Complexes 2HB-16·× $Cu(NO_3)_2$ and 2HB-16 × $La(NO_3)_3$ were obtained by the reaction of HB-16 with $Cu(NO_3)_2 \cdot 3H_2O$ and $La(NO_3)_3 \cdot 6H_2O$, respectively, in methanol. The surface tension was determined by the ring detachment method (Du-Nui). Conductivity data of solutions were obtained on CDM-2d device. Spectrophotometric measurements were carried out on a Specord 250 Plus spectrophotometer.

3 Results and discussion

The values of critical micelle concentration (CMC), adsorption characteristics at the water-air interface (the surface excess (Γ_{max}), the surface area per molecule (A_{min}), the standard free energy of interfacial adsorption at the air/saturated monolayer interface ($\Delta G_{ад}$) and standard free energy of micellization per mole of monomer unit ($\Delta G_{м}$)), the solubilizing power of aggregates were determined. It was shown that the value of CMC of the complexes by 2-3 times lower than CMC of the original HB-16 (Table 1) and its cyclic (hexadecylpyridinium bromide) (6.8 10^{-4} M, tens. [3]) and acyclic (hexadecyltrimethylammonium bromide, CTAB) (8.0 10^{-4} M, tens. [4]) analogues. The adsorption characteristics of the complexes and HB-16 are also very different. Higher area of the cross section of complexes indicates that the lower density of the surface layer of the amphiphiles occurs at the water-air interface.

Table 1. CMC of complexes in water, 25 ^{0}C

Substance	CMC × 10^4, M		
	Tensiometry	Conductometry	Orange OT solubilization
2HB-16 x $Cu(NO_3)_2$	**3.8**	2.9	3.2
2HB-16 x $La(NO_3)_3$	**3.3**	3.3	3.00
HB-16 [a]	**10.0**	10.0; 110 [b]	-

a **Data of [2];** ***b*** **CMC_2 .**

It has been established (spectrophotometry) that the solubilizing power (S) of the micellar aggregates of the complexes and the cationic surfactants with respect to the hydrophobic substrate (Orange OT) is varies at the sequence CTAB < HB-16 < [2HB-16 × $Cu(NO_3)_2$] < [2HB-16 × $La(NO_3)_3$] (Table 2), i.e. the formation by the cationic surfactant (HB-16) of the complex with copper nitrate and lanthanum nitrate facilitates its solubilization capacity. In the investigated concentration range of the complexes of copper and lanthanum the increase of the Orange OT solubility in respect of its solubility at CMC reaches 670 and 730 times, respectively. Moreover, the value S of the complexes is by 1.3-2.5 times higher than that of the original HB-16, and substantially higher (up to 3-6.5 times) than S of the acyclic analogue CTAB.

Table 2. Solubilizing power of the complexes and surfactants in water, 25 ^{0}C

Substance	S × 10^3	$S_{complex\ (surf)}$ / S_{HB-16}	$S_{complex\ (surf)}$ / S_{CTAB}
2HB-16 × $La(NO_3)_3$	**103**	**2.5**	**6.5**
2HB-16 × $Cu(NO_3)_2$	**53.2**	**1.3**	**3.3**
HB-16	**42.2**	**1.0**	**2.7**
CTAB	**15.9** [a]	**0.38**	**1.0**

a **Data of [5].**

4 Conclusions

The BH-16 complexes with copper nitrate and lanthanum nitrate are surfactants with high the aggregating capacity and the solubilizing action with respect to the hydrophobic substrate. Importantly, aggregation and solubilization capacity are main factors contributing to the catalysis of bimolecular reactions in organized solutions. It has been shown that addition of metal ions (e.g. lanthanum ions) can accelerate the cleavage of ester bonds by six orders of magnitude.

Acknowledgements

This work was supported by Russian Foundation for Basic Research, grants № 15-03-05434_a.

References

[1] J. Zhang, X.-G. Meng, X.-C. Zeng, X.-Q. Yu Coordination Chemistry Reviews 253 (2009) 2166.
[2] T.N. Pashirova, E.P. Zhiltsova, R.R. Kashapov, S.S. Lukashenko, A.I. Litvinov, M.K. Kadirov, L.Ya. Zakharova, A.I. Konovalov Russian Chemical Bulletin, International Edition 59 (2010) 1745.
[3] A. Callaghan, R. Doyle, E. Alexander, R. Palepu Langmuir 9 (1993) 3422.
[4] S.P. Moulik, M.E. Haque, P.K. Jana, A.R. Das J. Phys. Chem. 100 (1996) 701.
[5] G.A. Gainanova, G.I. Vagapova, V.V. Syakaev, A.R. Ibragimova, F.G. Valeeva, E.V. Tudriy, I.V. Galkina, O.N. Kataeva, L.Ya. Zakharova, S.K. Latypov, A.I. Konovalov J. Colloid Interface Science 367 (2012) 327.

I-PP36

Development of a General Heat Transport Modelfor Open-Cell Metal Foams

Aghaei P., Visconti C.G., Groppi G., Tronconi E.*

Politecnico di Milano, Department of Energy, Laboratory of Catalysis and Catalytic Processes, Milano, Italy

* enrico.tronconi@polimi.it

Keywords: open-cell metal foams, catalysts, carrier, tubular, reactor, heat transfer

1 Introduction

Open-cell metal foams are particularly interesting as catalyst supports in reactors with fast exo/endo-thermic reactions due to their high voidage, and thus a low pressure drop, in combination with their excellent heat transfer properties. The main goal of this work is to continue the previous works [1,2] and develop a general simulation model that is capable of describing the heat transfer properties of different open-cell metal foams with different structural properties at different operational conditions and with different gases.

2 Experimental/methodology

For this purpose, 180 steady-state heat transfer experiments using N_2 and He as flowing gasses at 300 ˚C and 500 ˚C were carried out over several different foams, FeCrAl alloy, NiCrAl alloy, aluminum, copper, and cobalt, all having a high porosity between 89 and 98% and with cell diameters varying from 0.58 to 5.09 mm. The geometrical properties of the metal foams were studied using optical microscopy and the total and hydraulic porosities were measured by a gravimetric technique. The heat transfer data were collected at three radial positions in the cylindrically shaped foams and at 11 different axial coordinates along the foam bed length, from 0 to 100 mm. First, the effective wall heat transfer parameters in the inlet zone just before the foams ($1/Bi_{w,in}$) were estimated to characterize the flow behaviour in this section. These results were then used to develop a 2D pseudo-homogeneous model based on heat transport literature correlations.

3 Results and discussion

The radial effective conductivity is composed of the sum of three contributions, i.e. conduction, convection, and radiation. The contribution by thermal conduction can be well described by the empirical correlation from Calmidi et al. [3], which considers the heat conducted through both the solid and the fluid phase. The contribution by the thermal dispersion in the foams is properly described using the model proposed by Hunt et al. [4] accounting that the dispersive contribution is directly proportional to the local flow velocity. The radiative contribution is described using the modified diffusion approximation in the Rosseland equation proposed by Glicksman et al. [5]. The wall heat transfer coefficient is estimated considering its dependency on the gas properties and also the thin gap between inner surface of the heating tube and outer surface of the sample foam [6], and additionally a contribution by radiation. All the fitting parameters in the correlation are optimized and their effects on the general fit are investigated. The simulation model based on the presented correlations showed a very satisfactory fit for all different foams and flow types tested within the range of the operational conditions covered. Among 11340 single temperature measurements, i.e. 12 foams, 15 different experimental conditions, 3 radial and 21 axial measurement points the foam bed, 91% points have temperature difference between the experimental and simulated temperature in the range of 0 to 5 °C, 8% points have the temperature difference between 5 to 10 ˚C and only 1% of the

single temperature measurement deviates more than 10 ˚C from simulations.

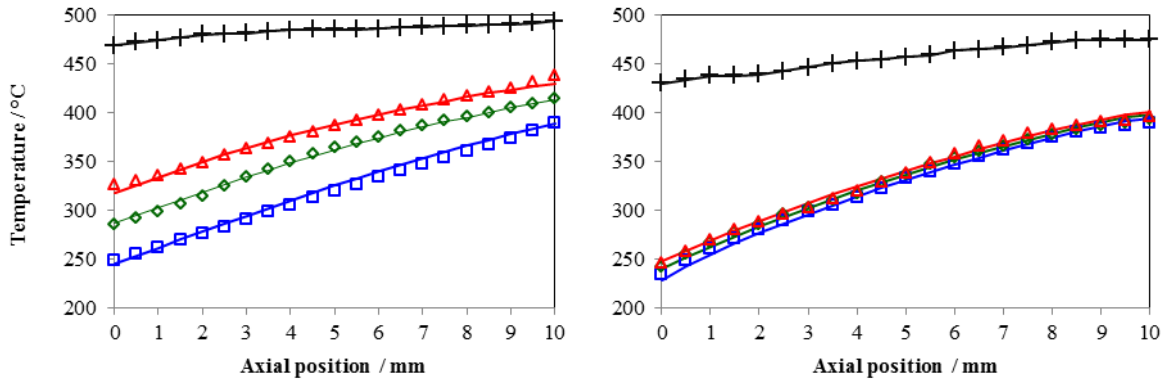

Fig. 1. Axial temperature profiles for a) NiCrAl alloy foam at 500 °C, N_2 flow rate of 35 Nl min^{-1}, cell diameter of 0.58 mm and b) Aluminium foam at 500 °C, N_2 flow rate of 35 Nl min^{-1}, cell diameter of 3.59 mm. The following abbreviations and legend are used: experimental temperature measurement at center, 0.5, 2/3 radius and heating tube wall, Exp(0) □, Exp(0.5) ◊, Exp(2/3) Δ, and Wall ┼. Fit results at centerline, 0.5, 2/3 radius, Sim(0) ▬ , Sim(0.5) ▬, and Sim(2/3) ▬.

4 Conclusions

The open-cell metal foams used in this study show a promising future as catalyst supports due to their high surface area with a small pressure drop in combination with a high effective radial thermal conductivity, varying from 0.5 W m^{-1} K^{-1} for FeCrAl and NiCrAl alloys up to 5 W m^{-1} K^{-1} for copper and aluminum foams, which can improves the heat management in catalytic reactors, resulting in higher productivity and selectivity with lower cost. By using the test results on a large number of different metal foams with various compositions, geometrical properties and porosities, at various temperatures, gas types, and gas flow rates , a general correlation was developed successfully for the effective thermal conductivity. This correlation contains a contribution by stagnant thermal conductivity accounting for conduction through both the solid and the fluid, a contribution by dispersion, and a contribution by radiation. The correlation requires as input the following foam properties: porosity, pore size, cell size, thermal conductivity of the foam solid material, and the gap size at the wall. For all foams tested the ratio of the stagnant solid conductivity of the foam and the conductivity of the dense solid material was close to one third of the relative volumetric density of the foam [1].

Acknowledgements

Funding by the Italian Ministry of Education, University and Research, Rome (MIUR, PRIN, prot. 2010XFT2BB) within the project IFOAMS (“Intensification of Catalytic Processes for Clean Energy, Low-Emission Transport and Sustainable Chemistry using Open-Cell Foams as Novel Advanced Structured Materials”) is gratefully acknowledged.

References

[1] E. Bianchi, T. Heidig, C.G. Visconti, G. Groppi, H. Freund, E. Tronconi, Chem. Eng. J., 198–199 (2012) 512–528.
[2] E. Bianchi, T. Heidig, C.G. Visconti, G. Groppi, H. Freund, E. Tronconi, Catal. Today, 216 (2013) 121– 134.
[3] V. V. Calmidi, R. L. Mahajan, J. Heat Transfer, 121(2) (1999) 466-471.
[4] M.L. Hunt, C.L. Tien, Int. J. Heat Mass Transfer, 31 (2) (1988) 301–309.
[5] L. Glicksman, M. Schuetz, M. Sinofsky, Int. J. Heat Mass Transfer, 30 (1) (1987) 187–197.
[6] J.P. Holman, Heat Transfer, McGraw-Hill, New York, 1989.

I-PP37

Selective Steam Cracking of Heavy Oil in Semibatch Reactor

Yeletsky P.M.[1,2*], Mironenko O.O.[1], Sosnin G.A.[1,3], Yakovlev V.A.[1,2]

1 - Boreskov Institute of Catalysis SB RAS, Novosibirsk, Russia
2 - UNICAT Ltd., Novosibirsk, Russia
3 - Novosibirsk State University, Novosibirsk, Russia

* yeletsky@catalysis.ru

Keywords: heavy oil, steam cracking, semibatch process

1 Introduction

The gradual depletion of light and middle crude oils with simultaneous increase of hydrocarbons consumption needs the development and upgrade of technologies on mining, transportation and processing of heavy hydrocarbon feedstock (HHCF), such as heavy oils and natural bitumens. Presently, the share of HHCF processing of total petroleum refinery processes is very low due to problems in HHCF mining, transportation and conversion. The main problems of HHCF processing are connected with high viscosity, low content of light hydrocarbons fractions, high content of tars, asphaltens, S and other heteroatoms and transition metals, mainly V and Ni. The most common approaches for HHCF processing based on two strategies: reducing carbon content by cocking and hydrogen saturation. The hydrogen saturation is usually carried out by hydrogenation and hydrocracking in the presence of Ni- and/or Mo-containing catalysts at 400 – 500 °C and high pressures of H_2 up to 200 bar and higher [1].

As an alternative source of hydrogen for HHCF cracking and hydrogenation, water can be used. Temperatures of the HHCF steam cracking are usually 420 – 500 °C, employed catalysts are Ni-based, promoted by K or Na [2] or FeO_x-based [3]. This work is devoted to investigation of process of steam cracking of high-sulfuric heavy oil (HO) from Tatarstan (Russia) in semi-flowing regime by water.

2 Experimental/methodology

For the investigation the process of steam cracking of the HO, the installation presented in Figure 1 was used. HO (200 g) and part of water (50 g) were loaded into the batch reactor with

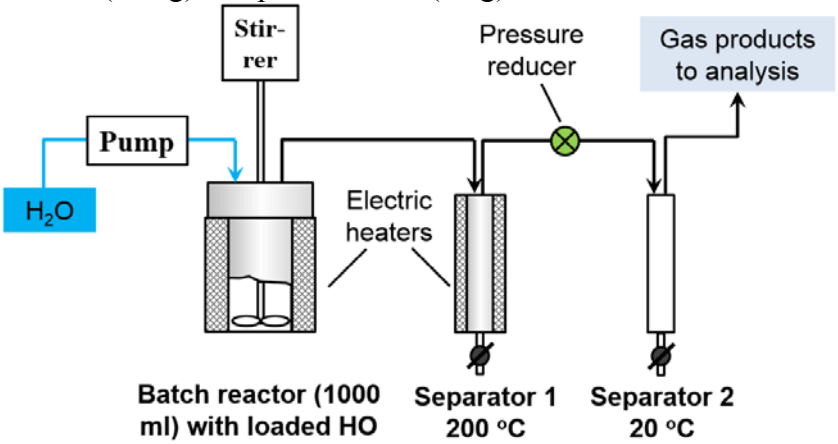

Fig. 1. The installation used for investigation the steam cracking of heavy oil (Tatarstan, Russia)

catalyst and started heating up to needed temperature (425 and 450 °C) with the rate 5 °C/min and continuous stirring 1000 rpm. When needed temperature was achieved, the water pumping (80 ml/h) was switched on. Time of the process was 2.5 h, the pressure was 20 – 25 bar. The

main part of liquid products and was being collected in the heated separator. In the case of catalytic steam cracking, the experiment was carried out with 10 % Fe_2O_3/γ-Al_2O_3 catalyst obtained by impregnation Fe from solution of $(NH_4)_3[Fe(C_2O_4)_3]$ onto γ-Al_2O_3 with following drying and calcination at 700 °C for 2 h. The analysis of fraction composition of the liquid products was carried out on a semi-automatic apparatus for distillation of petroleum products accordingly with ASTM 1160 standard. Gaseous products were studied by gas chromatography.

3 Results and discussion

Since the catalytic steam cracking is enough complex process including such subprocesses as just thermocracking (TC), steam cracking (SC) and catalytic steam cracking (CSC), the corresponding experiments on elicitation of the subprocesses have been carried out separately. In the Table 1, yields of the main products and fraction composition of liquid products are presented.

Table 1. Fraction composition of the initial heavy oil (HO) and yields of the main products of the HO thermocracking (TC), steam cracking (SC) and catalytic steam cracking (CSC).

Products	HO	TC, 425 °C	SC, 425 °C	CSC, 450 °C
	Yield, wt. %			
Liquid fractions ($T_{boil.}$ interval):	100	60.2	75.2	70.0
IBP – 200 °C	0	20.5	13.0	18.5
200 – 350 °C	20	31.1	39.9	37.3
350 – 500 °C	32	6.0	20.0	11.9
> 500 °C	48	2.6	2.3	2.3
Coke	-	25.5	15.4	18.5
Gas phase + losses:	-	14.3	9.4	11.5

In the case of TC the lowest yield of liquid products and the highest ones of coke, gaseous products and the lightest fraction were obtained. Water introducing (SC) has led to significant increase of liquid products (by 15 wt. %) and to the same total decrease of yields of coke (by 10 %) and gas (by 5 wt. %). Meanwhile, the liquid products contained lower content of fraction IBP – 200 °C and higher content of more heavy fractions. Introducing the catalyst (CSC) and increasing the process temperature from 425 to 450 °C has led to some decrease of the yield of liquid products and to increase of coke and gases yields (by ~ 5 wt % in total). The yield of gasoline (IBP – 200 °C) fraction increased by 5.5 %, the yields of more heavy fractions decreased. In the case of TC and SC, gaseous products contained low contents of H_2 (4 – 6 %) and high content of C_1-C_4 hydrocarbons. Gaseous products of CSC contained significantly more H_2 (44 %). Also in the case of SC and CSC there were traces of CO_2 (up to 2.5 %) and C_2H_4 (up to 4.0 %). H to C atomic ratio in the initial HO is 1.70, in the liquid products of TC and SC it decreased to 1.60, which seems to indicate on losses of hydrogen mainly in form of C_1-C_4 hydrocarbons. Liquid products of CSC had H to C ratio 1.78, indicating on occurring of hydrogen saturation processes in the presence of catalyst.

Acknowledgements

The work is supported by the UNIHEAT project.

References

[1] L.C. Castaceda, J.A.D. Mucoz, J. Ancheyta, *Fuel* 100 (2012) 110.
[2] US Patent 5688395, 1997.
[3] E. Fumoto, A. Matsumura, S. Sato, T. Takanohashi, *Energy & Fuels* 23 (2009) 1338.

I-PP38

Mechanochemical Synthesis of Molybdenum Carbide: New Approach for the Hydrodesulfurization Catalysts Preparation

Vasilevich A.V.*, Baklanova O.N., Lavrenov A.V., Likholobov V.A.

Institute of Hydrocarbons Processing of Siberian Branch Russian Academy of Sciences, Omsk, Russia

* vasilevich.ihcp@mail.ru

Keywords: molybdenum carbide, mechanochemical synthesis, hydrodesulfurization, dibenzothiophene

1 Introduction

In recent years, petroleum refining industry has been facing significant challenges because of the continuously decreasing allowable amount of emissions, such as SO_x, NO_x and aromatics from the combustion of fuels. With the currently used technology, the quality of fuels prescribed by the new environmental regulations can be attained by the significant modifications of refining operations [1].

Transition metal carbides are considered as the new promising catalysts and have been widely investigated in recent years because of their unique electronic structure and high performance [2]. Molybdenum carbides, with their resemblance in electronic structure to noble metals [3], have similar catalytic properties to noble metal catalysts in various organic chemical reactions [4]. It makes molybdenum carbides to be a promising substitute for noble metal catalysts in the future. These catalysts show good catalytic activity and selectivity in hydrogenation, hydrodesulfurization and hydrodenitrogenation in petroleum refining.

Molybdenum carbides were first obtained in a classical way of metallurgical process at high temperatures and the obtained material was of rather high particle sizes and low specific surface area [5]. The main method for synthesizing such molybdenum carbides currently is temperature-programmed reaction method via carbonization of molybdenum trioxide with gas hydrocarbon, such as methane, ethane, butane and their gas mixtures. In this work of molybdenum carbides were prepared using the mechanochemical synthesis. The structure and catalyst activity of the molybdenum carbides were also studied.

2 Experimental

Two series of samples were synthesized through mechanochemical synthesis both under air and inert atmosphere. Molybdenum (VI) oxide, zinc or aluminum and carbon black powders mixtures with varying molar ratio were ball milled using a AGO-2 type planetary high energy ball mill with stainless steel vials and balls under air atmosphere. The rotation speed of the mill was 1000 rpm and the ball-to-powder mass ratio was about 40:1. The second series of samples was prepared using the standard incipient wetness method. Molybdenum was impregnated at 10 wt% on carbon black using a aqueous solution ammonium heptamolybdate tetrahydrate (Aldrich, 99.98%) then the sample was dried at 120°C. Obtained sample was performed in a planetary ball mill under argon atmosphere. Samples were heat treated at 800°C for half an hour in an argon atmosphere.

3 Results and discussion

The obtained samples were characterized by means of XRD-method using a D8 Advance Bruker (40 kV and 40 mA) diffractometer with CuKα radiation (λ = 0.154 nm). The morphologies of the samples were observed by transmission electron microscopy (JEM-2100).

Fig. 1 shows the XRD patterns of samples, obtained by mechanochemical synthesis in an inert and air atmosphere. Phase Mo_2C hexagonal has sufficiently high crystallinity. In addition

to the phase Mo_2C on XRD patterns contains phases such as rhombic Al_2O_3, hexagonal FeMoO and hexagonal Fe_3C.

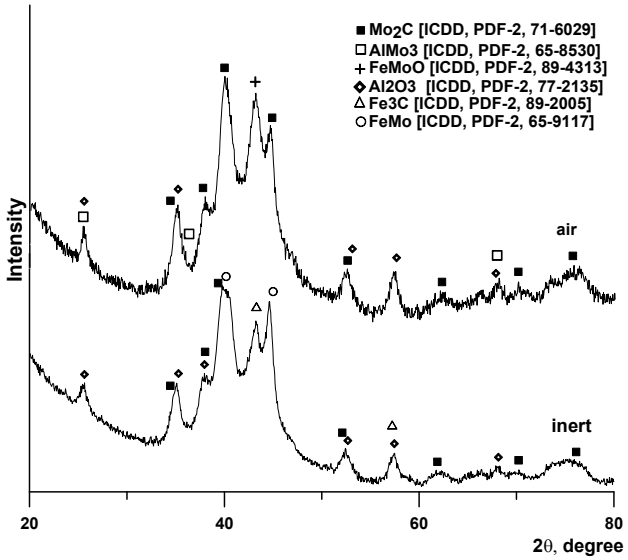

Fig. 1. XRD patterns of samples, obtained by mechanochemical synthesis in an inert and air atmosphere.

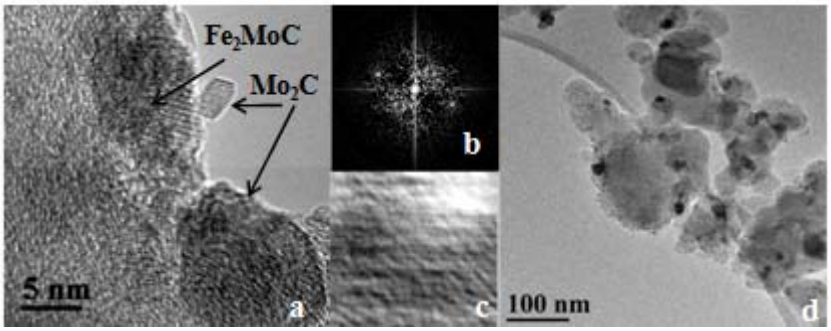

Fig. 2. (a-d) Electron-microscopic images of the samples prepared by mechanochemical synthesis and calcinations in an inert atmosphere and (b) the electron diffraction pattern and (c) image of the crystal lattice of Mo_2C obtained from a region marked with an arrow.

The model feedstock for testing of samples in the hydrodesulfurization was a heptane solution of 1 wt% and 4.7 wt% dibenzothiophene containing. The model reaction was performed at 300-320^{o}C, under a total pressure of 3.5 MPa, WHSV 2 h^{-1} and the molar ratio of hydrogen to the feedstock is 600.

4 Conclusions

Conducting testing of catalysts in the hydrodesulfurization of DBT model reactions exhibit high activity at 320^{o}C - 97.7% of DBT conversion. Analysis of the composition of the reaction products showed selectivity of the catalyst: 88.3 wt% in the composition of the reaction products accounted for cycloalkanes.

References

[1] E. Furimsky, *Appl. Cat. A: General* 240 (2003) 1.
[2] J. Guangzhou, Z. Jianhua, F. Xiuju, *Chin. J. Catal*. 27 (2006) 899.
[3] Z. Xia, Y. Shen, J. Shen, *J. Alloys Compd.* 453 (2008) 185.
[4] J. Wang, S. Ji, J. Yang, *Catal. Commun.* 6 (2005) 389.
[5] Q. Zhu, X. Zhao, Z. Zhao, *Chin. J. Catal* 26 (2005) 1047.

I-PP39

Heavy Oil Upgrading in the Presence of Organic Salts of Transition Metals under Reservoir Conditions

Foss L.E.[1,2*], Petrukhina N.N.[3], Kayukova G.P.[1,2], Tumanyan B.P.[3], Nikolaev V.F.[1], Romanov G.V.[1,2], Vakhin A.V.[2]

1 - A.E. Arbuzov Institute of Organic and Physical Chemistry, Kazan Scientific Center, Russian Academy of Science, Kazan, Russia
2 - Kazan Federal University, Kazan, Russia
3 - Gubkin Russian State University of Oil and Gas, Moscow, Russia

* iacw212@gmail.com

Keywords: catalyst, aquathermolysis, heavy oil, viscosity reduction

1 Introduction

Catalyst systems are important in chemical synthesis and technology of novel compounds, various hydrocarbon conversions and derivatives thereof, and in obtaining intermediate basic chemical raw materials. Consequently, the catalysts can be conventionally subdivided into catalysts for oil refining, catalysts for petrochemicals, gas chemistry, and organic synthesis, etc. Based on the analysis of current Russian and international research, we can define a new group of catalysts - catalysts for upgrading heavy oil under reservoir conditions [1-3].

2 Experimental/methodology

Thus, we synthesized and studied heavy oil upgrading catalysts - carboxylates of nickel and cobalt, which are organic salts of these transition metals. The obtained compounds were mixed with the heavy oil solution of tetralin as hydrogen donor. Since minerals of the oil-reservoir can influence the process of aquathermolysis [4], the experiments were carried out in the presence of kaolinite. Catalytic aquathermolysis treatment was executed in a 1 liter autoclave for 5 hours at the initial air pressure of 0,1 MPa at 250; 300 and 350°C. The product was separated to asphaltenes, hydrocarbons (HC), benzene resins (BR) and alcohol-benzene resins (ABR). To study the structural-group composition of petroleum products we calculated spectral coefficients [4]. The values of upgraded heavy oil viscosity were measured on the inclined plane rheometer at 20°C [5]. We also conducted gas chromatography/mass spectrometry (GC-MS) analysis of oil components from the initial boiling point to 125ºC.

3 Results and discussion

The results of the composition analysis of the original oil and catalytic aquathermolysis products shows significant redistribution of oil components towards increased oil content and

Table 1. Chemical composition of the original oil and the products of aquathermolysis.

The temperature of the experiment, °C	Viscosity, mPa*sec	Density at 20°C, kg/m^3	Component composition, wt %				
			HC	BR	ABR	Σ Resin	Asph
-	3390,0	960,0	55,27	25,27	13,36	38,63	6,00
250	1961,2	958,6	59,88	22,05	11,48	33,53	6,64
300	310,2	953,6	71,56	13,29	8,77	22,06	6,38
350	793,3	-	61,90	22,51	10,82	33,33	4,76

reduced resin content. Maximum redistribution of oils and resins was observed at a temperature of 300°C, due to degradation reactions of macromolecular oil components. These changes were also reflected in the decreased value of the dynamic viscosity from 3390,0 to 310,2 mPa*s and the

density from 960,0 to 953,6 kg/m^3 at 20ºC. It should be noted that this experiment showed a slight increase in asphaltene content. This is apparently due to the oxidative dehydrogenation of oils and resins in the presence of air oxygen during the catalytic aquathermolysis resulting in aromatization of hydrocarbons, and spectral coefficients testify to it. In a series of benzene, alcohol-benzene resins and asphaltenes oxydation increased respectively by 6,00; 4,81; 0,66 times and aromaticity by 1,25; 1,32; 1,48 times (Table 2). The lower temperature in the experiment (250°C) did not make it possible to achieve significant changes in the heavy oil components. If the temperature of aquathermolysis process rose to 350°C, a slight increase in the content of oil and a slight decrease in the resin content (compared with the original oil), as well as a significant reducing of asphaltenes content was observed. It could be connected with intensive hydrogenolysis and C-C bonds cracking [6]. The viscosity of the product is higher than that of the product received during the experiment conducted at 300°C. Along with a high resin content it may indicate intensified condensed reactions in an oxygen environment.

Table 2. The results of an FT-IR spectral analysis of the initial oil and the products of aquathermolysis.

Spectral indices*	Initial oil			Products after aquathermolysis, °C								
				250			300			350		
	BR	ABR	Asph	BR	ABR	Asph	BR	ABR	Asph	BR	ABR	Asph
C_1	1,62	1,87	2,07	1,26	3,53	2,81	2,03	2,47	3,07	3,65	4,35	5,80
C_2	0,06	0,16	0,05	0,04	0,43	0,25	0,24	0,77	0,33	0,04	0,44	0,26
C_3	0,53	0,61	0,74	0,55	0,64	0,76	0,62	0,67	0,78	0,57	0,70	0,75
C_4	3,36	2,45	2,06	3,49	2,11	1,82	2,50	2,39	1,70	2,89	1,77	1,30
C_5	0,16	0,53	0,29	0,15	0,49	0,35	0,30	0,42	0,34	0,17	0,60	0,37

*C_1 = D1600 / D720 (aromaticity); C_2 = D1710 / D1465 (oxidation); C_3 = D1380 / D1465 (branching); C_4 = (D720 + D1380) / D1600 (aliphaticity); C_5 = D1030 / D1465 (sulfurization).

Fraction yields from the initial boiling point to 125°C of the initial oil and of the products obtained during the experiments at 250; 300 and 350°C correlated as 1:4,3:15,0:11,6. Their analysis by GC-MS revealed that after conversion oils were enriched (compared with samples before reaction) with aliphatic hydrocarbons of isomeric structure (C4-C8) containing mono-, bis-, trismethyl-, ethyl- substituents and methyl-, ethyl- substituents of naphthenic hydrocarbons (cyclopentane, cyclohexane). A small number of aldehydes and aliphatic ethers also were found.

4 Conclusions

Thus, the role of catalysts is to intensify the reactions of hydrogen redistribution, which can involve not only the hydrogen donor but also naphthenoaromatic oil compounds, fostering the reactions of hydrogenation and hydrogenolysis of resin-asphaltene substances, and saturation of free radicals to prevent their recombination with the formation of new light components. Aquathermolysis of heavy products, which impair the stability and rheological properties of oil at a relatively high temperature, is possible. In this regard, it is important to choose the temperature of implementation of heavy oil in-situ catalytic aqauathermolysis to achieve the optimum degree of viscosity reduction at the lowest possible consumption of steam and contribution of condensed reactions.

Acknowledgements

The work is done at the expense of grants allocated under the state support of Kazan Federal University in order to improve its competitiveness among the world's leading research and education centers.

References

[1] S. Desouky, A. Al sabagh, M. Betiha, et al *International Journal of Chemical Nuclear Metallurgical and Materials Engineering*. 7 (2013) 286.
[2] Q. Wenlong, X. Zengli *Advanced Materials Research*. 608-609 (2013) 1428.
[3] S. Maity, J. Ancheyta, G. Marroquin. *Energy and Fuels*. 24 (2010) 2809.
[4] G. Kayukova, I. Abdrafikova, I. Sakhibgareyev, et al *Oil and Gas Technologies*. 5 (2012) 43.
[5] V. Nikolaev, A. Yashina, R. Ilyasov, et al *Herald Kazan Technological University*. 17 (2014) 257.
[6] Y. Yufeng, L. Shuyuan, D. Fuchen, Y. Hang *Petroleum Science*. 6 (2009) 194.

I-PP40

Influence of Catalyst Preparation Techniques on the Properties of the Cr-Mg Catalysts for Tetrachloroethylene Hydrofluorination

Simonova L.G., Zirka A.A., Isupova L.A., Reshetnikov S.I.*

Boreskov Institute of Catalysis SB RAS, Novosibirsk, Russia

* reshet@catalysis.ru

Keywords: chromium-magnesium, catalysts preparation, hydrofluorination, pentafluoroethane

1 Introduction

A wide range of solid catalysts is used for fluorination reactions: oxides, oxofluorides, and fluorides of chromium [1]. In recent decades, considerable efforts have been focused on the synthesis of chladones having zero ozone depletion potential. One of the most promising in this regard is the pentafluoroethane (Freon 125). It is well-known that the activity and selectivity of catalysts strongly depend not only on the catalysts composition, but on the method of precursor preparation as well.

In this work, we studied the effect of the Cr-Mg precursor preparation techniques on physicochemical and catalytic properties of the catalysts for the gas-phase hydrofluorination of perchloroethylene to pentafluoroethane.

2 Experimental

The catalyst samples (precursors) were prepared by using the four different techniques: wet mixing solid support. MgF_2 with $CrCl_3$ solution (sample 1) co-precipitation of metal hydrous oxides $Cr(OH)_3$ and $Mg(OH)_2$ (sample 2), mixing solid carrier MgF_2 with Cr_2O_3 slurry (sample 3) and precipitation of $Cr(OH)_3$ on solid carrier MgO (sample 4). Then, the samples were dried, heat treated in nitrogen flow at 330°C and activated by hydrogen fluoride.

Catalytic hydrofluorination of tetrachloroethylene (TCE) to pentafluoroethane was carried out in a flow reactor with a fixed catalyst bed at 330–370°C, 0.4 MPa, reactant molar ratios of HF: C_2Cl_4 = 11:1, and a contact time of 1–3 s. The activity was estimated in terms of the rate constant $k = -\ln(1 - X)/\tau$, where X is TCE conversion at the contact time τ [2].

3 Results and discussion

Most commonly used method for the Cr-Mg precursor synthesis is wet mixing of chromium chloride and magnesium fluoride [1]. As shown in the table, the sample 1, obtained by this way contains 6.1% chromium, the BET specific surface area is equal to 60 m^2/g and the reaction rate constant of the tetrachloroethylene hydrofluorination at 370°C is equal to 0.46 s^{-1}. We have found that obtaining of Cr-Mg precursors by this method with higher chromium content is difficult because the obtained pastes have poor rheological properties.

Table 1. Effect of the Cr-Mg precursor preparation techniques on the chromium content, the BET specific surface area (S_{sp}), total pore volume (V_{pore}), mean pore diameter (D_{pore}) and catalyst activity (k at 370^0C).

Sample №	Method of preparation	Cr,% (wt.)	S_{sp}, m^2/g		V_{pore}, cm^3/g	D_{pore}, Å	k_{370}, s^{-1}
			before reaction	after reaction			
1	mixing $CrCl_3$+MgF_2	6.1	60	33	0.3	400	0.46
2	co-precipitation $Cr(OH)_3$+$Mg(OH)_2$	56.1	230	3.8	0.08	70	0.04
3	mixing Cr_2O_3+MgF_2	28.9	130	35	0.4	350	0.32
4	precipitation $Cr(OH)_3$ on MgO	30.1	170	66	0.27	200	0.19

It is known that co-precipitation allows to vary the content of active component in a wide range. However, for investigated sample 2 co-precipitation of magnesium and chromium hydroxides was impossible due to a large difference in pH values for formation of hydroxides Cr (~ 5-7) and Mg (> 9). As a result, the precursor has poor textural characteristics: small volume and radius of pores, consequently, the catalyst has the low activity. The low concentration of Mg-containing support and unsatisfactory porous structure of the precursor, apparently leads to a dramatical decrease of the specific surface (from 230 m^2/g up to 3.8 m^2/g) under the reaction conditions.

Other used methods for the precursor preparation are by a mixing of solid carrier MgF_2 with a Cr_2O_3 slurry (sample 3) and by precipitation of $Cr(OH)_3$ on solid carrier MgO (sample 4), although it led to an increase in the chromium content, but did not increase the catalysts activity.

Conclusions

The effect of the chromium-magnesium precursor preparation techniques on physicochemical (the BET surface area, the total pore volume, the mean pore diameter) and catalysts activity in the gas-phase hydrofluorination of perchloroethylene to pentafluoroethane was studied. It was obtained, that more active catalyst was prepared by wet mixing of the solid carrier MgF_2 with a solution of $CrCl_3$. The precursor contained 6.1% chromium, and the BET specific surface area was equal to 60 m^2/g.

Kinetic regularities have been studied for the most active catalyst. Based on the experimental data, the pathway of perchloroethylene fluorination with HF over a 6.1% chromium–magnesium oxide catalyst was identified. The process involves several consecutive reactions for the formation of main fluorination products and parallel reactions for the formation of by-products.

Acknowledgements

This work was supported by the Russian Foundation for Basic Research, project No. 15-08-04789.

References

[1] J.M. Kemnitz, Winfield. Advanced Inorganic Fluorides. 2000. P. 367.
[2] A.A. Zirka, and S.I. Reshetnikov, Kinet. Catal. (Engl. Transl.), 49 (2008) 663.

I-PP41

Catalytic Aquathermolysis Heavy Oil in the Presence of Organometallic Complex

Sitnov S.A.[1*], Vakhin A.V.[1], Petrovnina M.S.[1], Feoktistov D.A.[1], Kayukova G.P.[2], Nourgaliev D.K.[1]

1 - Kazan (Volga region) Federal University, Kazan, Russia
2 - A.E. Arbuzov Institute of Organic and Physical Chemistry Kazan Scientific Centre Russian Academy of Sciences, Kazan, Russia

* sers11@mail.ru

Keywords: aquathermolysis, precursor of the catalyst, heavy oil, SARA-analysis, viscosity

1 Introduction

Gradually deteriorating structure of the world's hydrocarbon reserves. Research is focused on development of deposits of heavy oils. Reserves of heavy oil are comparable to reserves of traditional hydrocarbons [1]. The main obstacle in the extraction of heavy oils is their abnormally high viscosity due to the content of a significant amount of resinous-asphaltene substances. To extract heavy oil apply steam carrying thermal methods that provide viscosity reduction in the reservoir and partial conversion of heavy components as a result of aquathermolysis [2]. To increase the efficiency considering the possibility of using nanoscale or molecular catalysts, which injected into the reservoir. The search for new effective catalysts obtained by using available raw materials, is an important task for improving the energy efficiency of thermal methods of heavy oil production.

2 Experimental/methodology

Laboratory simulation of aquathermolysis on a sample of the heavy oil Ashalchinskoye field (Republic of Tatarstan) out on a laboratory autoclave (Parr Instruments, USA) with stirring was carried. In the reactor was loading of 70 g of oil and 30 g water. Precursor of the catalyst as a solution in petroleum ether on the basis 1.0 wt.% of oil was injected. Experimental conditions: temperature 250 °C, initial pressure 3 MPa, duration of the experiment 6 hours.

Hydrocarbon type content - saturated hydrocarbons, aromatics, resins and asphaltenes (SARA-analysis) based on the ASTM D4124-09 and state standards, Russian federation 32269-2013 by liquid adsorption chromatography on the aluminium oxide was determine.

The elemental analysis was performed on the analyzer PerkinElmer 2400 Series II (USA). Measurement of dynamic viscosity was carried out using a rotational viscometer FUNGILAB Alpha L.

3 Results and discussion

Aquathermolysis accompanied not only by changing the viscosity of the reservoir oil, but also a change in its composition. Commonly used molecular or colloidal catalysts are formed *in situ* from a precursor representing an organometallic compound or complex. With good solubility of the precursor of the catalyst, a hydrophobic portion of the petroleum fluid that prevents their agglomeration stabilizes the catalyst particles. The effectiveness of the catalytic process is enhanced by the association of molecules or particles of a polar (hydrophilic) catalyst with more hydrophilic asphaltenes molecules due to the considerable content of oxygen, sulfur and nitrogen functional groups, as well as associated metals such as nickel and vanadium [3]. As a result, the asphaltene fraction can be enriched with low molecular weight components, which provides an irreversible decrease in the viscosity of crude oil.

In this work the catalyst precursor has been synthesized by reacting under heating (90 to 95°C) catalyst bases - iron oxide (III) and ligand-form component - alkyl benzene sulphonic acid in a molar ratio of 1: 6.

Oil samples after aquathermolysis using different concentrations of the synthesized catalyst were examined. Found that when the content of the catalyst 1 wt.% of saturated hydrocarbons increased in 1.62 times, the amount of aromatics, resins and asphaltenes decreases in 1.12, 1.65, 1.21 times, respectively, compared with the crude oil. According to the SARA analysis determined that the asphaltene stability index (ASI) increases with increasing conversion of raw feedstock by tumors of saturated hydrocarbons. Carrying out elemental analysis of petroleum systems showed that significantly reduced sulfur content and the ratio of C/N. The viscosity of the product experience is also reduced. It is also found that the synthesized catalyst promotes the hydrogenation and hydrogenolysis reactions of the resinous-asphaltene compounds to form the light ends, hydrocarbons and non-hydrocarbon gases.

4 Conclusions

Synthesized a new catalyst for an intensification of steam carrying thermal method of heavy oil production, using available domestic raw materials. Organometallic catalyst is a complex (the precursor), based on iron oxide, soluble in polar and non-polar liquids.

Application of this catalyst showed high efficacy in the hydrogenolysis and hydrogenation of resinous-asphaltene compounds heavy oil. The catalyst promotes the formation of light fractions, thus reducing the viscosity of heavy oil.

Acknowledgements

The work is performed according to the Russian Government Program of Competitive Growth of Kazan Federal University.

This work was funded by the subsidy allocated to Kazan Federal University for the state assignment in the sphere of scientific activities.

References

[1] R. Maksutov, G. Orlov, A.Osipov, *Energy Technologies.* 6(2005). P. 36-40.

[2] J. B Hyne, J. W. Greidanus, J. D.Tyrer et al. *2nd Int. Conf. «The Future of Heavy Crude and Tar Sands»*, Caracas, Venezuela, 7–17 February 1982. — New York: *McGraw Hill*, 1984. — P. 404-411.

[3] S. K. Maity, J. Ancheyta, G. Marroquin, *Energy Fuels*. 24 (2010). P. 2809–2816.

I-PP42

Performance of Modified Nickel Catalysts in a Catalytic Membrane Reactor for Partial Oxidation of Methane

Ushakov A.E., Kozhevnikov V.L., Patrakeev M.V., Leonidov I.A., Markov A.A.*

Institute of Solid State Chemistry, Ural Branch of RAS, Ekaterinburg, Russia

* ushakov88817@gmail.com

Keywords: synthesis gas, modified nickel catalysts, membrane, reactor, partial oxidation

1 Introduction

Natural gas is broadly used as a feedstock in the production of liquid hydrocarbons via synthesis gas (syngas) as an intermediate step [2]. The industrial reforming of natural gas to syngas is dominated by catalytic steam reforming [3], which requires a large excess of the gas supply for heating. The catalytic partial oxidation (CPO) allows improvement of the reforming efficiency due to the using of the heat evolved in the CPO reaction. Further advancement in the overall performance of the gas to liquid process can be achieved by combining CPO with oxygen separation from air in a membrane reactor [4]. The long term stability and selectivity toward products of partial oxidation, i.e. CO and H_2, greatly depend on the catalyst used at the permeate side in the membrane reactor. Therefore, the aim of this work was to study the behavior of Ni based catalysts in the membrane reactor for partial oxidation of methane.

It was observed that simple Ni/Al_2O_3 catalysts degrade rather quickly because of the soot formation. In order to suppress this undesirable reaction we modified the catalysts by adding M_2O_3 oxides, where M = Mn and Fe.

2 Experimental/methodology

The preparation of the catalysts was based on co-impregnation of industrial γ-Al_2O_3 support with solutions of Ni, Mn and Fe nitrates. The BET surface area was determined by N_2 adsorption at -196°C with the help of a Micromeritics Gemini VII device. Prior to measurements the samples were pre-treated in vacuum at 300°C for 5 h. The catalytic tests were carried out in a fixed-bed flow reactor operated at atmospheric pressure. The outer shell of the reactor was made of a quartz tube. The ferrous oxygen separating membrane [4] was set inside the quartz casing in between alumina tubes that served also as in- and outlet air ducts. The membrane sizes were 1, 10 and 30 mm for wall thickness, diameter and length, respectively. The space between the membrane and the casing was filled with the catalyst. The methane conversion X_{CH_4} and selectivity S_{CO} for CO were calculated as:

$$X_{CH_4} = \frac{CH_4^{in} - CH_4^{out}}{CH_4^{in}} \times 100\% \qquad (1)$$

$$S_{CO} = \frac{CO^{out}}{CO^{out} + CO_2^{out}} \times 100\% \qquad (2)$$

3 Results and discussion

The atmospheric pressure experiments were carried out at 850-950°C for over 300 h. It should be noted that a rapid increase in the selectivity for CO was observed for both catalysts immediately after the start-up. Further increase in the methane flow was accompanied with a

decrease in the selectivity, which was more expressed for Ni/Fe_2O_3 /γ-Al_2O_3 catalyst. The selectivity attained 96 - 98% for both Fe and Mn modified catalysts (Fig.1) at methane flow values 40 – 45 ml/min whereupon a steady state was achieved (Fig.2).The methane conversion over modified catalysts was about 99 %. The after test inspections of the catalysts did not reveal any significant formation of soot or/and coke.

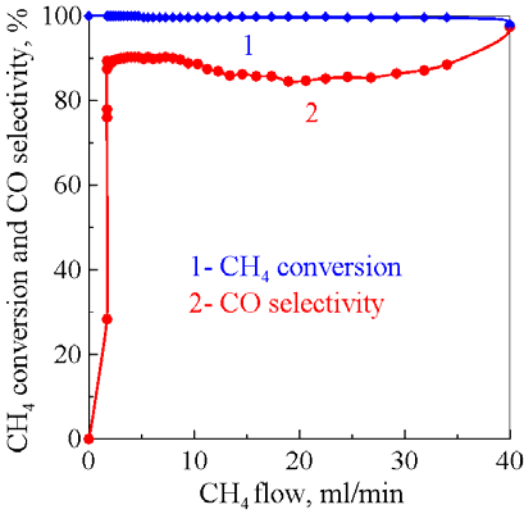

Fig. 1. CH_4 conversion and selectivity for CO at partial oxidation methane over Ni/Fe_2O_3 /γ-Al_2O_3 catalyst.

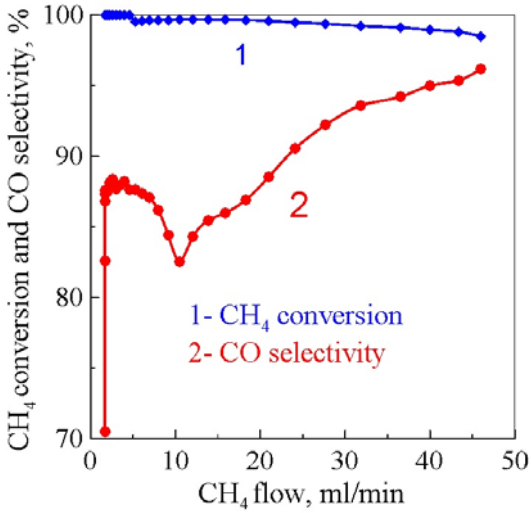

Fig. 2. CH_4 conversion and selectivity for CO at partial oxidation methane over Ni/Mn_2O_3/γ-Al_2O_3 catalyst.

4 Conclusions

The results of this work lead to the following conclusions: modified nickel catalysts were shown to exhibit high activity and stability in a catalytic membrane reactor for partial oxidation of methane.

Acknowledgements

The work was carried out under financial support of the Government of the Sverdlovsk Region and the Russian Foundation for Basic Research (Contract No. 13-08-96060-Ural).

References

[1] C. Besson, Resources to reserves, Tech. rep., IEA, 2005.
[2] B.C. Enger et al. / Applied Catalysis A: General 364 (2009) 15–26.
[3] A.S. Larimi et al / Fuel 102 (2012) 366–371.
[4] V.L. Kozhevnikov et al. / J. Solid State Electrochem. 13 (2009) 391–395.

I-PP43

Alkylphenols to Phenol and Olefins by Zeolite Catalysts: a Shape-selective Process to Valorize Raw and Fossilized Lignocellulose

Verboekend D.*, Liao Y., Schutyser W., Sels B.F.

KU Leuven, Leuven, Belgium

* Danny.Verboekend@biw.kuleuven.be

Keywords: lignin, coal, alkylphenol, dealkylation, shape-selective, zeolite

5 Introduction

The large-scale consumption of fossil fuels today will eventually lead to the depletion of the world's (cheap) oil reserves. Accordingly, an alternative source of everyday base-chemicals for the production of polymers, pharmaceuticals, and other specialty chemicals needs to be explored. Of the different types of base chemicals, aromatics represent an important building block for the (fine-)chemical industry in the manufacture of plastics, rubbers, and other synthetic fibers [1]. Ultimately, these aromatics should be derived from a sustainable source, such as plant-like materials (lignocellulose). The main constituents of raw lignocellulose are cellulose, hemi-cellulose, and lignin. Particularly the valorization of lignin is of high relevance as it is the only of the three types which comprises a substantial amount of aromatics (*ca.* 50 wt.%) [2]. Currently, a wide academic interest focusses on the extracting aromatic monomers from lignin, using a wide variety of catalyst of varying efficiency. However, the final product is often an alkylated phenol [3]. On the middle-long term the shortage of oil is likely to be (partially) compensated by the increased valorization of solid fossilized lignocellulosic resources, such as peat, lignite, and coals. Particularly on coal, the technology to isolate aromatics has been already developed decades ago [4]. Related processes primarily yield syngas, but often also up to 10 wt.% of residue (coal tar), which is rich in ethyl- and propylphenols. Although some specific applications of alkylated phenols may exist, the valorization of the substantial streams of alkylphenols is a must to fuel tomorrow's chemical industry. In this contribution we identify unmodified acidic ZSM-5 zeolites as shape-selective catalysts to convert a variety of alkylphenols selectively to phenols and olefins.

6 Experimental

Dealkylation experiments were performed in a custom-built plug-flow fixed-bed reactor equipped with 4 parallel quartz reactors. Each quartz reactor was filled with 30 mg of zeolite catalysts (H-ZSM-5, CBV 8014, Zeolyst, sieve fraction: 0.125-0.250 mm). The alkylphenol (Sigma-Aldrich, >98%) was brought to the gas phase using a nitrogen flow passed through a saturator. The same was done separately with a saturator filled with water. Afterwards, the flows were mixed and passed through the reactors. Effluent gasses where characterized using an in-line gas chromatograph equipped with a HP1 column and a FID detector.

7 Results and discussion

The most abundant alkylphenol to be derived from lignin and coal is 4-*n*-propylphenol. Initial results showed that with time on stream the catalyst deactivates rather fast (**Figure 1**). The addition of water to the feed was studied to test the catalyst ability to coop with wet streams of alkylphenols, which may originate from the streams of raw lignocellulose [5] or from the gasification of fossilized lignocellulose [4]. Unexpectedly, a full recovery of the initial

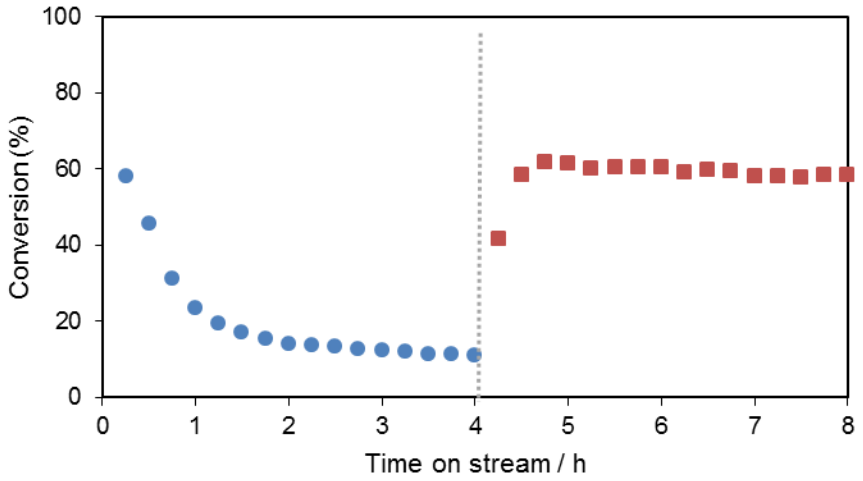

Fig. 1. Conversion of 4-*n*-propylphenol (4PP) as a function of time over a H-ZSM-5 catalyst without (0-4 h, circles) and with co-feeding water (4-8 h, squares). The selectivity was >95% at all times. The co-feeding of water completely restored the activity of the catalyst. Conditions: p = 1 bar, T = 310°C, WHSV 3.3 h^{-1}, partial pressures (0-4 h): p_{4PP} (0.02 bar) and p_{N2} (0.98 bar), partial pressures (4-8 h), p_{4PP} (0.02 bar), p_{H2O} (0.12 bar), and p_{N2} (0.86 bar).

activation occurred, hereby revealing a crucial role of the co-feeding of steam. This performance strongly differs from the dealkylation of alkylbenzenes [6], as the latter reaction requires the zeolite to be modified with metal functions or rare-earth cations, and the co-feeding of H_2 to prevent coking and maintain a stable performance. In this contribution we highlight the nature of the role water plays in the dealkylation of alkylphenols is reaction, and extrapolate it to other reactions. In addition, the influence of the length, branching, and position of the alkyl moiety is studied and related to the composition (Si/Al ratios ranging from 2.5 to 200), pore-size (0.4-0.8 nm), and pore connectivity (1D-3D) of the zeolite. Accordingly, light is shed on the exact nature of the active site, its location, abundance, and strength.

8 Conclusions

The dealkylation of alkylphenols represents a key conversion in the valorization of raw and fossilized lignocellulose. Unmodified H-ZSM-5 is a highly active catalysts and clearly displays shape-selectivity behaviour in this type of conversions. Finally, the co-feeding of water plays a crucial role in maintaining catalytic activity.

References

[1] K. Weissermel and H.-J. Arpe, Aromatics - Production and Conversion, in Industrial Organic Chemistry, Fourth Edition, Wiley-VCH Verlag GmbH, Weinheim, Germany, **2003**, pp. 316-336.
[2] G. Gellerstedt, G. Henriksson, in Monomers, Polymers and Composites from Renewable Resources (Eds.: M. N. Belgacem, A. Gandini), Elsevier, Amsterdam, **2008**, pp. 201-224; J. Zakzeski, P. C. A. Bruijnincx, A. L. Jongerius and B. M. Weckhuysen, Chem Rev 2010, 110, 3552-3599.
[3] J. S. Luterbacher, D. Martin Alonsoa, J. A. Dumesic, Green Chem., **2014**,*16*, 4816.
[4] A. W. Scaroni, M. R. Khan, S. Eser, L. R. Radovic, in Coal Pyrolysis, Ullmann's encyclopedia of industrial Chemistry, Wiley-VCH Verlag, Weinheim, **2012**, pp 407-420. T. Kaneko, F. Derbyshire, E. Makino, D. Gray, M. Tamura, K. Li, in Coal Liquefaction, Ullmann's encyclopedia of industrial Chemistry, Wiley-VCH Verlag, Weinheim, **2012**, pp 17-30.
[5] L. T. Mika, E. Cséfalvay, I. T. Horváth, **2015**, Top. Catal. doi:10.1016/j.cattod.2014.10.043
[6] J. M. Serra, E. Guillon, A. Corma, J. Catal. **2004**, 227, 459.

I-PP44

Study of Catalytic Activity of Impregnated VMgO Catalystsin the Oxidative Dehydrogenation of Ethane

Slyemi S., Barama A.*, Messaoudi H.

Laboratoire des Matériaux Catalytiques et Catalyse en Chimie Organique, USTHB, Faculté de Chimie, Alger, Algérie

* a_barama@yahoo.fr

Keywords: VMgO, $Mg_3V_2O_8$, ethane, oxidative dehydrogenation

1 Introduction

The V-Mg-O mixed oxides are known to be active and selective catalysts in the oxidative dehydrogenation of short alkanes. These good performances of VMgO catalysts are attributed to the two factors: the surface basicity which facilitates the alkene desorption and the absence of V=O species which decrease the oxidative properties of the surface [1]. Three Mg vanadate phases ($Mg_3V_2O_8$, α-$Mg_2V_2O_7$ and MgV_2O_6) can be formed in these oxides depending on several parameters, e.g., the vanadium composition, the preparation method and the calcination temperature. However, the phase responsible for the ODH selectivity in the V-Mg-O system is still a topic of debate. Most of the studies report that $Mg_3(VO_4)_2$ is the active phase and the isolated tetrahedral species (VO_4) present in this phase are responsible of the activation of the C-H bond of the hydrocarbon **[2]**. Recently, other researchers found that the biphasic V-Mg-O exhibited better catalytic performances than the pure phases **[3]**. In other words, the coexistence of $Mg_3V_2O_8$ with other phases such as MgO and α-$Mg_2V_2O_7$ could generate interactions between the different phases that improve the catalytic behavior of these mixed oxides. The formation of V_2O_5 crystallites with V=O double bond in which the V^{5+} is in octahedral coordination in these oxides favors the complete oxidation and the production of oxygenate compounds **[2]**.

2 Experimental/methodology

Two series of V-Mg-O catalysts (Mg/V=4.5) were prepared by impregnation of $Mg(OH)_2$ or commercial MgO (Merck, 97%) **,** using an aqueous hot and basic (pH=11) solution of ammonium metavanadate NH_4VO_3 (Merck, 99%). The obtained solids have been calcined at 550 and 650°C for 6 hours (5°C/mn).

3 Results and discussion

The XRD and the FTIR analysis show for all the samples, the formation of a mixture of crystalline phases: $Mg_3(VO_4)_2$, α-$Mg_2V_2O_7$ and MgO. The $Mg_3V_2O_8$ is the major phase and the α-$Mg_2V_2O_7$ is detected as traces. The MgV_2O_6 and the V_2O_5 are not observed in our catalysts. The TPR profiles, show for each of the two samples prepared by $Mg(OH)_2$ and commercial MgO, one peak of reduction observed respectively at 750 and 715°C. These two maximum peaks reduction observed at relatively high temperatures because of the high vanadium composition in our catalysts (50% of V_2O_5), indicate one step of vanadium reduction which correspond to the passage from tetrahedral coordination (V^{5+} belonging to $Mg_3V_2O_8$ phase) to a cubic spinel phase MgV_2O_4 containing V^{3+}. H_2-HT-XRD analysis effectuated for all the catalysts, show, that the lines of $Mg_3V_2O_8$ phase which is already formed at ambient temperature remained up to 625°C. Above this temperature, we note: the disappearance of $Mg_3V_2O_8$ peaks and the appearance of a cubic spinel type phase MgV_2O_4. This reduced structure of our solids is conserved after cooling the sample to the ambient temperature.

The reduction of $Mg_3V_2O_8$ phase to MgV_2O_4 indicates a change in the oxidation state of the vanadium from V^{5+} to V^{3+}. This reduction was confirmed by many researches [ref] that reported the formation of a reduced cubic phase (MgV_2O_4) containing only V^{3+} upon treatment of $Mg_3V_2O_8$ under reducing conditions.

The reactivity of the V-Mg-O samples tested in the oxidative dehydrogenation of ethane (Tr=450°C and C_2H_6/O_2=2) for 4 hours show good catalytic performances with selectivity to ethylene of 99%. These good catalytic performances are attributed to the predominance of Mg orthovanadate and to its coexistence with Mg pyrovanadate and MgO. For more precision, there may exist a cooperation between the two phases $Mg_3(VO_4)_2$ and MgO present on the catalyst surface. The higher basicity induced by the presence of MgO on the catalyst surface facilitates desorption of alkenes thus prohibiting side reactions. The significance of the role of the acid-base character of catalysts in hydrocarbon partial oxidation reactions has been pointed out in the literature. It is confirmed by this study that coexistence of $Mg_3(VO_4)_2$, MgO and α-$Mg_2V_2O_7$ is beneficial for the increased production of ethylene. It has been also established that the catalyst, prepared by commercial MgO, is less active than the solid prepared by $Mg(OH)_2$ (ethane conversion 57% against 73%). This fact allows us to say that the higher the proportion of $Mg_3V_2O_8$ detected by XRD, the higher is the conversion of ethane. The obtained results confirmed the important role of (VO_4) units present in Mg orthovanadate phase which are responsible of the activation of the C-H bond. The high activity and selectivity to ethylene obtained with the catalyst prepared via $Mg(OH)_2$ is probably due to the presence with a great proportion of isolated tetrahedral (VO_4) species on the catalyst surface.

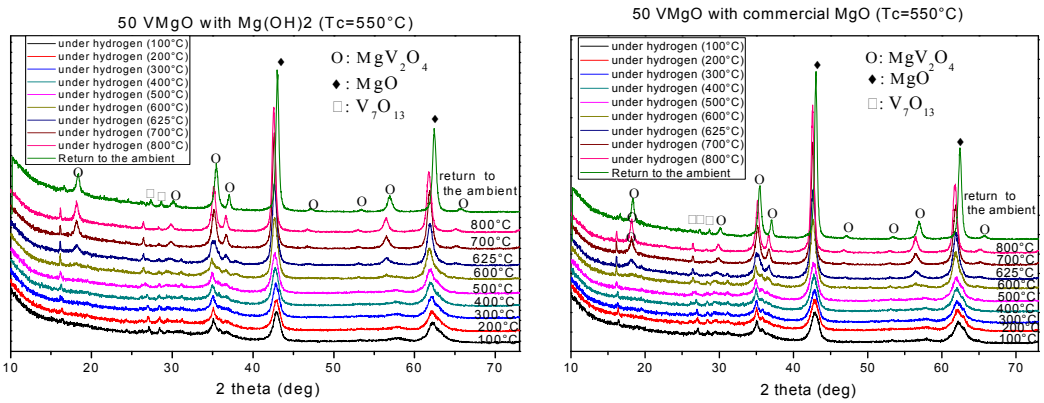

Figure: XRD patterns during reduction under hydrogen of the V-Mg-O catalysts.

4 Conclusions

The mixed oxides V-Mg-O (%V_2O_5=50%) prepared using a simple impregnation method, exhibit good catalytic performances in the ODH of ethane. The high activity and selectivity to ethylene are attributed to the high proportion of tetrahedral (VO_4) units present in Mg orthovanadate phase and to the coexistence of this phase with α-$Mg_2V_2O_7$ and MgO. These results are also due to the absence of V_2O_5 phase (confirmed by XRD and FTIR) which favors the formation of combustion products (COx). The best catalytic activity is obtained with the catalyst prepared by impregnation of $Mg(OH)_2$.

References

[1] M.A. Chaar, D. Patel, H.H. Kung, J. Catal. **109** (1988) 463–467.
[2] V. Soenen, J.M. Herrmann, J.C. Volta, J. Catal., **159** (1996) 410.
[3] M.A. Chaar, D. Patel, M.C. Kung and H.H. Kung, J. Catal., **105** (1987) 483.

I-PP45

Pt/Amorphous Silica-Alumina Catalysts for Hydroconversion of C_{20}-C_{31} n-Alkanes Mixture into Fuels with Improved Cold Flow Properties

Onishchenko M.I.[1*], Kulikov A.B.[1], Maximov A.L.[1,2]

A.V.Topchiev Institute of Petrochemical Synthesis, RAS (TIPS RAS), Moscow, Russia
Lomonosov Moscow State University, Moscow, Russia

* onishchenko@ips.ac.ru

Keywords: amorphous, silica-alumina, hydroconversion, hydrocracking, parafines, wax

1 Introduction

The growing interest in mining in cold and arctic climate is a growing need for waxy motor fuels. Traditionally, winter diesel fuel and jet fuel produced from petroleum feedstocks. However, worsening environmental problems caused by rapid technological progress has led to the need to involve the raw material that does not contain nitrogen compounds, sulfur, aromatic compounds and heavy metals. Thus, natural gas processing technology "gas to liquid" produces mostly *n*-alkanes normal structure of a wide range of composition - from light gases to heavy paraffins vacuum fraction. Long-chain *n*-alkanes processing to produce components of diesel and aviation fuels is carried out by their hydroconversion processes accompanied by hydrocracking and hydroisomerization. Bifunctional catalysts traditionally used for these processes are systems which contain a carrier, characterized by acidic properties and metal, performing hydrogenation function. Varying acidic properties of catalysts allows controlling the product distribution [1].

Zeolite catalysts tend to produce lighter products gasoline fractions [2] while the output of middle distillates is possible to increase through the use of catalyst supports with moderate acidity, which is the amorphous silica-alumina [3] and silica-alumina phosphates [4]. Moreover the developed porous structure and a large pore diameter media promotes the formation of branched alkanes inside the pores and provides a light diffusion long-chain initial alkane molecules and the conversion products. The use of platinum as the hydrogenation component is due both to the high specific activity of the metal (in comparison, for example, nickel) and the absence of catalyst poisons (like a sulfur) impurities in the feed [5].

Thus, it was investigated the behavior of Pt-containing catalysts based on amorphous silica in the hydroconversion process of the model feed containing C_{20}-C_{31} *n*-alkanes to obtain kerosene and diesel fractions having improved cold flow properties.

2 Experimental/methodology

Amorphous silica-alumina with SiO_2/Al_2O_3=10 molar ratio was synthesized in water and propanol-2 solution at room temperature using tetraethyl orthosilicate (TEOS) a as silica and alumina tri-*sec*-butoxide as an alumina sources respectively. Hexadecylamine was used as a surfactant. The prepared support was formed with Al_2O_3 (Sasol Pural SB-1) and denoted as ASA(10)-Al_2O_3. Pt was impregnated on ASA(10)-Al_2O_3 *via* the incipient-wetness method using H_2PtCl_6 aqueous solution. The Pt loading was adjusted to 0.5, 1 and 2 wt.%. The impregnated solid was dried at 100 °C overnight and reduced in H_2 flow at 350 °C for 3 h. The resulting catalysts were denoted as (X)-ASA(10)-Al_2O_3, where X is Pt content in wt.%. The samples were characterized using complex of analytical methods.

Catalytic experiments were made in a continuous flow reactor. The process parameters were varied: temperature (T) = 310-360 °C, pressure p(H_2) = 50-60 atm and liquid hour space

velocity (LHSV) = 0.5-1 h^{-1}. The composition of the feed and products was determined by gas chromatography. The cold filter plugging point (CFPP) of products was determined by ASTM D6371.

3 Results and discussion

It was shown some trends in hydroconversion of C_{20}-C_{31} *n*-alkanes with Pt-ASA(10)-Al_2O_3: increasing the reaction temperature leads to decreasing the middle distillates yield, the pressure H_2 in the range 50-60 atm doesn't make influence at products distribution and LHSV increasing resulted in conversion level decreasing. The best catalytic results were achieved by catalyst having 1 wt. % platinum content. So, the Figure 1 clearly presented the composition of the feed *(a)* and of the product *(b)* received using the sample 1%Pt-ASA(10)-Al_2O_3 at 320°C, LHSV = 0.5 h^{-1} and p(H_2) = 50 atm.

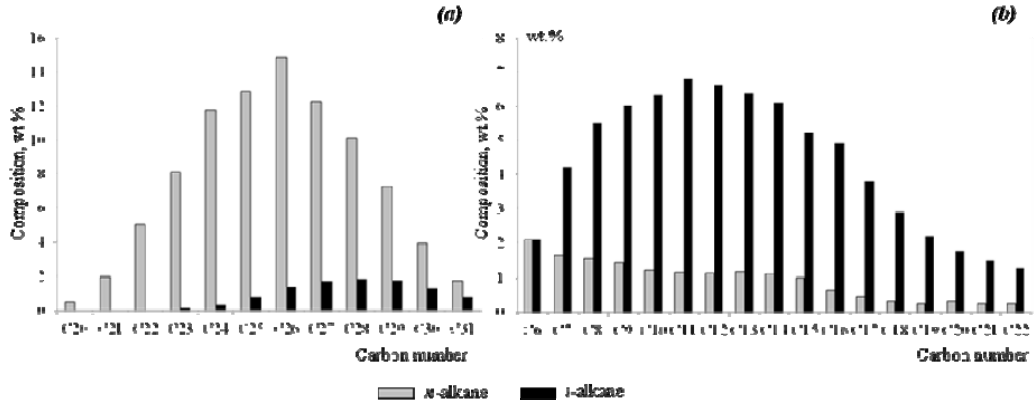

Fig. 1. Composition of the feed *(a)* and gasoline-kerosene-diesel fraction of hydroconversion product *(b)*

The cold filter plugging point determined for the diesel fraction of the product was minus 34 °C, which is a good index for the winter fuel additives.

4 Conclusions

The synthesized Pt/amorphous silica-alumina catalyst provides the formation of branched alkanes of diesel fraction from C_{20}-C_{31} *n*-alkanes that is a key factor of good cold flow fuel properties. At high conversion level up to 90% it is possible to produce up to 50 wt.% of diesel fraction.

Acknowledgements

This research was supported by the Russian Ministry of Education and Science (№ 14.607.21.0074, the Federal Target Program «The studies and development in the priority areas for Russian scientific and technological complex in 2014-2020», Project Unique Number RFMEFI60714X0074).

References

[1] C. Bouchy, G. Hastoy, E. Guillon, J. A. Martens. *Oil Gas Sci. Tech.* 64 (2009) 91-112.
[2] T. Hanaoka, T. Miyazawa, K. Shimura, S. Hirata. *Chem. Ing. J.* 263 (2015) 178-185.
[3] I. Rossetti, C. Gambaro, V. Calemma. *Chem. Ing. J.* 154 (2009) 295-301.
[4] Gy. Pölczmann, J. Valyon, Á. Szegedi, R. M. Mihályi, J. Hancsók . *Top. Catal.* 54 (2011) 1079–1083
[5] W. Bohringer, A. Kotsiopoulos, M. de Boer, C. Knottenbelt, J.C.Q. Fletcher. *Stud. Surf. Sci. Catal.* 163 (2007) 345-365

I-PP46

Tuning the Catalytic Activity of Pt and PtCo Nanoparticles by Acidic Mixed-Oxide Supports

Ly N.[1], Al-Shamery K.[1], Gervasini A.[2*], Carniti P.[2], Chan-Thaw C.E.[2], Prati L.[2]

1 - Carl von Ossietzky University of Oldenburg, Institute of Chemistry, Physical Chemistry 1, Oldenburg, Germany

2 - Università degli Studi di Milano, Dipartimento di Chimica, Milano, Italy

* antonella.gervasini@unimi.it

Keywords: Pt, CoPt nanoparticles, mixed oxides, intrinsic and effective acidity, 5-hydroxymethylfurfural

1 Introduction

The catalytic potential of metal nanoparticles (MNPs) in catalysis is well known and MNPs have been exploited in many reactions of importance for various fields [1]. Bimetallic nanoparticles can provide improved selectivity to desired products in given reactions; so the selection of given formulations (nature and relative amounts of the metal species) offers optimized systems in catalysis.

Supporting MNPs on inorganic materials gives the possibility to use these systems as effective heterogeneous catalysts, in particular maintaining the MNPs dispersion during reaction, even when severe reaction conditions have to be applied. The surface properties of the support are key factors for the optimal dispersion of the MNPs and for their stable anchorage on the surface. Among the surface properties, acidity is one of the most important. Acidity is an *intrinsic* surface property of any given material, but it can be modified by adding a second oxide component. Moreover, the acidic properties of a given material can be also modulated by means of the environment, namely the reaction solvent. Therefore, it is important to consider the actual acidity showed by the materials under the reaction conditions (*effective* acidity) [2].

Our recent advances in the catalytic application of monometallic and bimetallic nanoparticles supported on several silica mixed oxides of different acidity are here presented. Pt and Co NPs and bimetallic PtCo NPs have been synthesized and then deposited (1 wt.%) on silica modified with 5 wt.% of Al, Nb, Ti, and Zr. The obtained samples have been fully characterized by several surface techniques in order to study the textural properties (N_2 adsorption/desorption), metal dispersion, (TEM and HRTEM), and acidity properties, measured by base titrations in different liquids in order to provide measurements of both *intrinsic* and *effective* acidity [2].

The prepared samples have been used in the reaction of 5-hydroxymethylfurfural (HMF) with butan-2-ol, under H_2 pressure. From this reaction, several valuable chemicals are known to be formed [3,4], like 2,5-dimethylfuran (DMF), 2,5 dihydroymethylfuran (DHMF), 5-methyl furfural (5MF), 5-methylfuranether (5MFE), 5-hydroxymethylfuran-2-ether (HMFE), 2,5-bis(sec-butoxymethyl)furan diether (HMFDE). On the studied samples, the product of a certain reaction path and its selective formation showed to be correlated to the effective acidity of the oxide support, as measured in methanol, which provides an environment similar to the reaction one.

2 Experimental/methodology

Commercial silica (Grace) was modified at the surface with 5 wt.% of Al (Al/SiO_2), Nb (Nb/SiO_2), Ti, (Ti/SiO_2), and Zr (Zr/SiO_2) by controlled precipitation of aluminum isopropoxide, niobium ethoxide, titanium butoxide, and zirconium propoxide, respectively. The acidity of the oxide supports was determined by liquid-solid titration with phenylethylamine (PEA) basic probe dissolved in cyclohexane and methanol for the determination of the *intrinsic* and *effective* acidities, respectively [2]. Co, Pt, and PtCo NPs were deposited (1 wt.%) on the oxide supports. TEM images

of the supports with Pt, Co, and CoPt NPs have been collected with a Zeiss EM 902 electron microscope at 80 kV and HRTEM images with a Jeol JEM2100F microscope at 200 kV.

The catalytic activity was studied in an autoclave magnetically stirred (1250 rpm) at 180°C for 4-6 hours; the substrate (1.2 mmol HMF) and solvent (15 mL butan-2-ol) were loaded to the reduced catalyst sample (150 °C, 4 bars of H_2). After filtration, the reaction mixture was analyzed by gas chromatography (GC) equipped with a thermal conductivity detector (TCD).

3 Results and discussion

The synthesized mixed oxide supports possessed high surface area values (from 474 m^2/g of silica down to 352 m^2/g of Al/SiO_2, 283 m^2/g of Nb/SiO_2 and 254 m^2/g of Zr/SiO_2 and Ti/SiO_2) and good pore volume (ca. 1 cm^3/g). Silica was poorly acidic and it lost quite all its acidity in methanol. The mixed oxide supports are all more acidic than silica and they maintained lively acid sites in methanol; the following ranking of *effective* acidity in methanol was obtained (in terms of acid site density, μequiv/m^2): Al/SiO_2 >> Ti/SiO_2 ≅ Nb/SiO_2 > Zr/SiO_2 >> SiO_2.

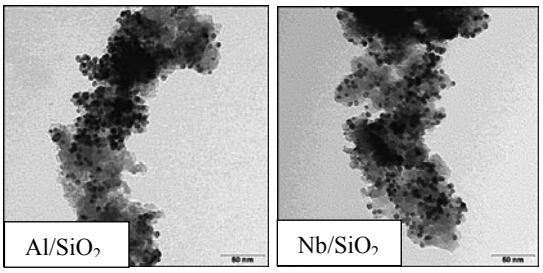

Fig. 1. TEM images of supported PtCo NPs.

Pt, Co, and PtCo NPs were deposited on the supports (1 wt.%) mainly as spherical particles of ca. 7-8 nm of size, regularly distributed, as observed from TEM images (see Figure 1, as example). The surface area values and porosity of the metal loaded samples were maintained without any remarkable differences with the relevant support.

The reaction of HMF in butan-2-ol under H_2 gave different results as a function of the *effective* acidity of the support, mediated by the nature of the metal, Pt or Co, or CoPt. The activity of the catalysts was affected by the support acidity. The bare oxidic supports had a non-negligible activity; solely SiO_2, with a very poor acidity, was completely inactive. Increasing the acidity of the support, the selectivity to ethers (HMFE and HMFDE) increased, but using the most acidic support (Al/SiO_2), high amounts of unknown products were also formed. The best compromise can be reached using Nb/SiO_2, which showed an intermediate *effective* acidity in methanol. By adding Pt, Co and PtCo nanoparticles, the activity of the catalysts generally increased, but the Co based ones appeared normally more active than the Pt counterparts. The most active catalyst (Co-Nb/SiO_2) was also the most selective toward HMFDE (77%) (Figure 2).

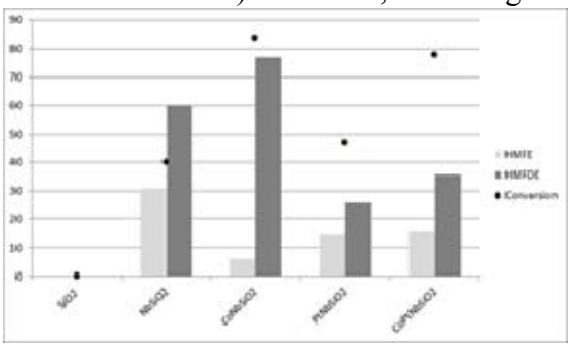

Fig. 2. Evolution of the ethers formation on MNPs on Nb/SiO_2 support.

4 Conclusions

It has been found that the support chosen for MNPs may direct the selectivity of the transformation of HMF into valuable products. Mild *effective* acidity of the support, like in the case of Nb/SiO_2, seems more suitable for enhancing the catalytic action of MNPs and depressing the production of unknown by-products.

References

[1] L. Prati and A. Villa, Accounts of Chemical Research, 2014, 47, 8553.
[2] P. Carniti, A. Gervasini, M. Marzo, *Catal. Today* 152 (2010) 42.
[3] J. Jae, W. Zheng, A.M. Karim, E. Guo, R.F. Lobo, D.G. Vlachos, *ChemCatChem* 8 (2014) 848
[4.] Y. Román-Leshkov, C.J. Barrett, Z.Y. Liu, J.A. Dumesic, *Nature* 447 (2007) 982.

I-PP47

Highly Stable and Selective Propane Dehydrogenation Catalyst

Tschentscher R.*, Akporiaye D.

SINTEF Materials & Chemistry, Oslo, Norway

* roman.tschentscher@sintef.no

Keywords: propane dehydrogenation, hydrotalcite, coking, sintering, platinum, promoters

1 Introduction

The shale gas boom has created a demand for alternative routes of propylene production, among which propane dehydrogenation is the most promising. This paper discusses the development of chromium-free catalysts with high selectivity, stability against coke formation and sintering as part of the FP7-Framework project CARENA. The work is based on earlier research on hydrotalcite-based catalyst supports.

2 Experimental

In-house made hydrotalcite-based oxide supports were used. For high dispersion the active metal phase consisting of platinum, tin and promoters was deposited by a combination of ion-exchange and precipitation. The catalysts were tested at rather severe conditions of 600 °C, without steam addition in order to rapidly screen catalysts. The optimal catalyst was tested in a wide range of conditions varying steam content, temperature and pressure. The fresh and spent catalyst was characterized by SEM, TEM, XRD, TPD and NMR.

3 Results & Discussion

Based on the screening tests a catalyst with the composition $PtZnSn/MgAlO_x$ could be identified. For propane dehydrogenation under industrial conditions the highest selectivity reported so far could be achieved (<99.5 % at 20% conversion and atmospheric pressure). Based on the high sticking coefficient of ethylene, it is expected that this byproduct has a significant role in catalyst coking by formation of oligomeric ring structures. Alloying with Zn and Sn does, thereby, reduce the size of Pt ensembles. Further, Zn poisons the acidic cracking sites. Two species of "coke" could be revealed by switching NO STEAM to STEAM during the experiment. Upon steam addition strongly adsorbed oligomeric species desorb due to competitive adsorption and hydroxylation of the support. The remaining difference in activity can be attributed to formation of high molecular weight char which can only be removed by oxidative treatment. The nature of coke is studied by NMR. Addition of steam strongly minimizes the degradation by coking. Interestingly, an increase of the steam amount above 10 vol% does not significantly change the catalyst performance. This can strongly improve the process economics compared to industrial steam concentrations of up to 60 vol%. A stable catalyst operation for several weeks can be achieved by using temperatures below 520 °C. Acceptable conversions at those temperatures could be achieved by the use of membranes removing either hydrogen or, preferably, propylene.

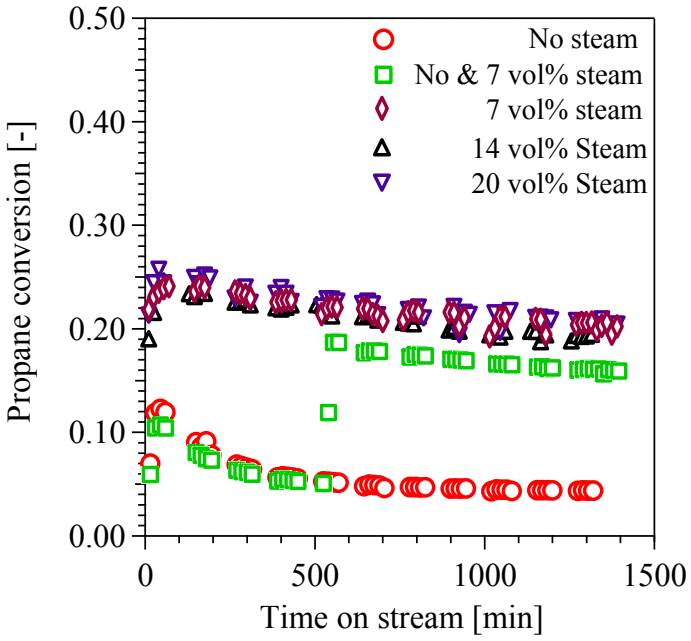

Fig. 1: Propane conversion @ 540 °C depending on steam load for 1 bar total pressure.

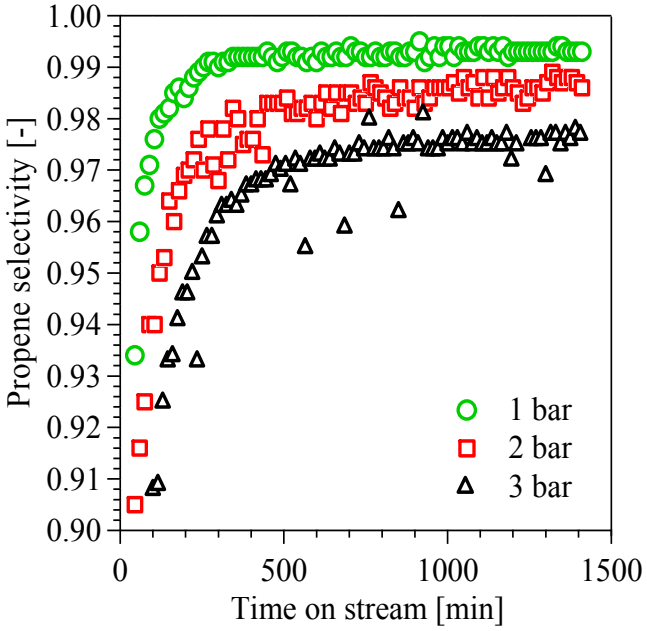

Fig. 2: Selectivity depending on pressure for 15 vol% steam.

I-PP48

Change of Phase-Dispersed Structure of Asphatenes in during the Hydrothermal-Catalytic Conversion of Heavy Oil

Kayukova G.P.[1,2*], Gubaydullin A.T.[1], Petrov S.M.[2], Rizvanov I.H.[1], Romanov G.V.[1,2], Vahin A.V.[2], Pertukhina N.N.[3]

1 - A.E. Arbuzov Institute of Organic and Physical Chemistry Kazan Scientific Centre Russian Academy of Sciences, Kazan, Russia
2 - Kazan (Volga region) Federal University, Kazan, Russia
3 - Gubkin Russian State University of Oil and Gas, Moscow, Russia

* kayukova@iopc.ru

Keywords: oil, asphaltenes, phase-dispersed structure, iron oxide, hydrothermally-catalytic processes

1 Introduction

Currently become widespread technologies aimed at mining and processing of heavy oil feedstock to produce a so-called "synthetic oil" with reduced viscosity [1]. Of interest are the processes in the environment of water vapor in the presence of sufficient available iron oxide catalysts, providing conversion of heavy petroleum residues into lighter boiling hydrocarbons [2, 3]. Elevated levels of high molecular weight components, metals and heteroelements in the heavy hydrocarbon feedstock substantially affects the processes of its production, transportation and processing. These problems are related to specific properties of asphaltenes. Asphaltenes in the oil disperse systems are in the form of supramolecular structures, which are molecules associates whose sizes vary depending on the composition and nature of oil and impact of external factors, such as temperature and pressure [4]. Therefore, in the aspects of development of deposits of heavy heavy oil and natural bitumen is important to have information about changing the composition and properties of asphaltenes in a variety of natural and anthropogenic processes.

2 Experimental/methodology

The objects of the study served as a heavy oil Ashalchinskoye field from the Permian system of Tatarstan and its conversion products. Also, its conversion products in an environment of water vapor in the presence of natural iron catalyst - hematite was obtained. Experiments were performed in an autoclave at temperatures of 210, 250 and 300 °C at various ratios of water in the reaction system. Asphaltenes from the feed oil and the products precipitated in experiments 40-fold amount of petroleum ether with Tboil 40-700° C. Deasphaltenesates were separated by liquid adsorption chromatography on silicagel ASK into components: oils and two groups of the resins: alcohol-benzene and benzene.

Asphaltenes investigated using complex physical and chemical methods: elemental and X-ray fluorescence analysis, matrix-assisted laser desorption / ionization (MALDI), ESR and IR spectroscopy. Determination of structural and dimensional parameters asphaltenes performed using X-ray powder diffraction techniques [5] and small angle x-ray scatter [6].

3 Results and discussion

The features of the processes of degradation of high-molecular components of heavy oil with a new formation of light fractions in the model of hydrothermal-catalyst system in water vapor in the presence of a catalyst - iron oxide at temperatures of 210, 250, 300°C, which lead to a change in its component, hydrocarbon, fractional and structural-group composition. The general tendency in changes in the structural and dimensional characteristics of the

supramolecular structures of asphaltenes is to increase their aromaticity factor and the distance between layers and the aromatic chain-like polymethylene moieties in their associates, as the temperature increases and experiments reduce the water content in the reaction system. This reduces size and associates itself reduces the number of aromatic layers. By small-angle X-ray scattering shows that associates the original asphaltene (before the experiment) are characterized by a heterogeneous structure, but differ in varying degrees, ordered by their location (on paracrystalline type) inside the clusters. The transition from the initial sample of asphaltenes to their transformed structure is accompanied by a shift of the maximum peak in the dispersion curves in the region of small angles up to s = 0.15 Å-1 and an increase in the interplanar spacing values to 41.2Å, due to the removal of mutual association with each other as a result of the rupture and the degradation of aliphatic chains, aromatic fringing island system. Hydrothermally catalytic treatment of heavy oil at higher temperatures (300°C) leads to a break in most of the asphaltenes of such aliphatic chains and destruction of the particles in the arrangement of correlation associates indicates that the increase in the degree of microheterogeneity at close dimensional characteristics of the particles themselves. Changes in the phase-dispersed supramolecular structure of asphaltenes accompaned by a sequence of transitions in their class in toluene insoluble substances such as carbo-carboidov further coke-like products that fall out of the dispersion medium in the form of a solid. The result of leakage is the destruction of the destructive processes supramolecular structures due to their degradation preferred alcohol-benzene resins, associated with asphaltenes, and vanadium complexes, separation of peripheral alkyl fragments, which leads to carbonisation of their structure, molecular weight decrease and increase the concentration of free radicals. Asphaltenes the conversion of heavy oil products are only those molecules and aggregates whose size is not too large to provide solubility in toluene.

4 Conclusions

Thus, it is shown the effect of temperature and water content on the formation and stability of the disperse phase in the structure of asphaltenes in the hydrothermally-catalytic processes in the presence of a catalyst - iron oxide.

Acknowledgements

The work is performed according to the Russian Government Program of Competitive Growth of Kazan Federal University.

This work was funded by the subsidy allocated to Kazan Federal University for the state assignment in the sphere of scientific activities.

References

[1] A.K. Kurochkin, S.P Toptygin, Sphere. Oil-gas. 1. (2010) 92.
[2] S.K. Maity, J. Ancheyta , G. Marroquín. Energy Fuels. 24 (2010) 2809.
[3] B.P. Tumanyan. Scientific and applied aspects of the theory of oil disperse systems. (2000). 336.
[4] V.I. Sharipov, S.B.Beregovtsova, B.N. Baryshnikov, B.N. Kuznetsov. Chemistry for Sustainable Development. 5 (1997) 287.
[5] J. W. Shirokoff, M.N. Siddiqui, M. F. Ali.. Energy & Fuels. 11(3) (1997) 561.
[6] Y.N. Xu, Y. Koga, O.P. Strausz. Fuel. 74(7) (1995) 960.

I-PP49

Catalytic Conversion of Furfural into Gasoline Components

Simakova I.L.[1,2*], Tarabanko V.E.[3], Chernyak M.[3], Morozov A.[3], Simonov M.[1,2]

1 - Boreskov Institute of Catalysis SB RAS, Novosibirsk, Russia
2 - Novosibirsk State University, Novosibirsk, Russia
3 - Institute of Chemistry and Chemical technology SB RAS, Krasnoyarsk, Russia

* simakova@catalysis.nsk.su

Keywords: furfural, propylfurfuryl, ether, acetal, octane number, hydrogenation

1 Introduction

Devising new methods for production of biofuels and fine chemicals from biomass is the main trend of the development of modern chemical industry. Such compounds are produced either by biotechnology routes (ethanol, butanol, etc.) or by chemical methods, hydrolysis, pyrolysis and others.

Furfural is the main industrial product of pentose carbohydrates hydrolysis, however development of biofuels of the furfural platform has started to be discussed only recently [1,2]. Blending research octane numbers (BRON) of ethyl-, propyl-, and butylfurfuryl ethers (110, 113 and 97, correspondingly) were determined [2,3]. 2-methylfuran was successfully tested in the mixtures with gasoline in car engines [4].

Hydrogen consumption is one of the main characteristics for furfural and other oxygenated products hydrogenation into biofuels. Alkylfurfuryl ethers are very attractive from this viewpoint (consumption of one mole of hydrogen per mole of the product). A possible way to produce such ethers is t catalytic hydrogenation of furfural dialkylacetals.

The main goal of this paper is to study furfural catalytic hydrogenation in alcohol solutions.

2 Experimental/methodology

Mesoporous carbon Sibunit-supported copper-ruthenium and platinum- (3-8 wt%) catalysts of 40-70 μm fraction were prepared by the incipient wetness impregnation method. At the end of the impregnation procedure, all catalysts were dried in an oven overnight at 100°C. The metal-containing catalysts were activated (reduced) with hydrogen *in-situ* in the reactor. Reactions were carried out in a batch reactor of 150 ml volume at 100 – 200 °C and hydrogen pressure of 1 MPa. 19.1 g of the alcohol, 0.53 g of furfural, and 0.2 – 0.4 g of the catalyst were charged in the reactor and heated during 6 hours. The products were analyzed by GLC and GC-MS (VG-7070 GC/MS and Agilent 5973N EI/PCI).

3 Results and discussion

Catalytic hydrogenation of furfural in alcohol media is accompanied by the equilibrium limited acetal formation, with furfural conversion into the corresponding acetals attaining 55-66 % (Table 1). This equilibrium leads to further hydrogenation of dipropyl- and dibutylacetals into the corresponding furfuryl ethers, which yield attains 19 %. It should be noted, that at low furfural conversions (appr. 20 %) in the presence of CuRu/C-catalyst selectivity on butylfurfuryl ether exceeds 50 % (Table 1). A similar possibility of t5-butoxymethylfurfuryl dibutyl acetal hydrogenation into the corresponding ether, 2,5-dibutoxy-methylfuran, was recently demonstrated [5,6].

Table 1. The influence of the catalyst and alcohol on the products content (mol % based on initial furfural) in furfural hydrogenation. Conditions: furfural 0.53 g, alcohol 19.2 g, catalyst 0.400 g, 110°C, 6 hours, 1 MPa H_2.

Catalyst	Alcohol	Furfural/ Furfuryl acetal	Furfuryl ether	2-Methyl-Furfural	Furfuryl alcohol
8%CuRu/C*	Butanol	43/54**	-	-	-
8%CuRu/C*	Butanol	66/13	9.3	-	11.1
8%CuRu/C	Propanol	27/54	9.5	-	8.3
3%Pt/C	Propanol	-	16.3	29.4	8.7
3%Pt+3%Ni/C	Propanol	-	18,9	27.2	30.3
3%Pt+3%Re/C	Propanol	-	15,9	34.4	20.5

*0.2 g of the catalyst. **Nitrogen atmosphere.

The yield of furfuryl alcohol in the process is 8 – 30 %. This product is not the intermediate, which upon alkylation with propanol or butanol generated alkylfurfuryl ethers. Separate experiments showed that furfuryl alcohol does not practically alkylate propanol under these conditions, and the yield of propylfurfuryl ether did not exceed 5 %. Probably, the difficulties of direct alkylation of furfuryl alcohol result from its conversion into levulinic acid and tar.

The other main product of furfural catalytic hydrogenation is 2-methylfuran, which maximum yield exceeds 30 %.

4 Conclusions

The obtained results show that furfural hydrogenation in alcohol media is accompanied by formation of acetals. Both products, furfural and furfuryl acetals, are hydrogenated, and the acetals give the corresponding ethers. In such way catalytic hydrogenation of furfuryl acetals is an alternative and promising method to produce corresponding furfuryl ethers. The products produced in the studied process, namely butylfurfuryl ether, propylfurfuryl ether, 2-methylfuran, and furfuryl alcohol offer high anti-knocking activity (BRON above 100), and they may be applied as components of biofuels.

Acknowledgements

Financial support from Russian Foundation for Basic Research (Grant No. 13-03-00754) is gratefully appreciated.

References

[1] S. Varfolomeev, I. Moiseev, B. Myasoedov, Herald of the Russian Academy of Sciences. 79 (2009) 334.
[2] J.-P. Lange, E. Heide, J. Buijtenen, R. Price. ChemSusChem. 5 (2012) 150.
[3] V. Tarabanko, M. Chernyak, A. Morozov, K. Kaygorodov, Journal of Siberian Federal University. Chemistry 7 (2014) 31.
[4] Yu. Roman-Leshkov, C. Barrett, Z. Liu, J. Dumesic. Nature 447 (2007) 982.
[5] I. Simakova, A. Morozov, V. Tarabanko, M. Chernyak, Journal of Siberian Federal University. Chemistry 7 (2014) 536.
[6] I. Simakova, V. Tarabanko, A. Morozov, M. Chernyak, South-Siberian Scientific Bulletin 3 (2014) 37.

I-PP50

Effect of Support in NiO-Based Oxygen Transfer Materials for Sorption Enhanced Chemical Looping Methane Reforming: Characterization and Reactivity Studies

Antzara A.[1], Heracleous E.[2], Ipsakis D.[1], Silvester L.[3], Bukur D.B.[3], Lemonidou A.A.[1*]

1 - Department of Chemical Engineering, Aristotle University of Thessaloniki, Thessaloniki, Greece
2 - School of Science & Technology, International Hellenic University (IHU), Thessaloniki, Greece
3 - Texas A&M University at Qatar, Chemical Engineering Program, Doha, Qatar

* alemonidou@cheng.auth.gr

Keywords: NiO-based, OTMs, support, sorption enhanced, chemical looping methane reforming

1 Introduction

Sorption enhanced chemical looping steam methane reforming is an alternative method for efficient production of pure hydrogen, combining chemical looping reforming (CLR) with in-situ CO_2 capture [1]. In this process scheme, the reformer contains, in addition to the sorbent, an oxygen transfer material (OTM) that is reduced by methane into metallic form and serves as reforming catalyst. The reforming reaction proceeds under near autothermal conditions due to the highly exothermic sorbent carbonation. In a second step the saturated sorbent is regenerated, with energy supplied by exothermic OTM re-oxidation [2]. In order for the process to be viable, it is necessary to utilize OTMs which can be easily reduced and re-oxidized without losing their stability in consecutive redox cycles [3]. In this study, the effect of support (alumina, silica, zirconia, titania) on the reduction/oxidation activity and stability of NiO-based OTMs was investigated in multiple redox cycles in a TGA unit, and under both conventional and the CLR conditions at low temperature in a fixed-bed flow unit.

2 Experimental

Four NiO-based OTMs with 40wt% NiO loading were synthesized by wet impregnation using commercial supports: (SiO_2, TiO_2, Al_2O_3, ZrO_2). The materials were characterized by BET, XRD, TPR (Micromeritics Ins., AutoChem II 2920) and XPS (Kratos Analytical, Axis Ultra DLD). Reduction in methane at 650°C followed by air oxidation at 800°C was studied in the TGA (TA SDT Q600). Conventional reforming activity of the reduced OTMs was tested at 650°C in a bench scale fixed bed flow unit with a steam/methane (S/C) ratio of 3 and GHSV=$10^5 h^{-1}$. In the second step, NiO/ZrO_2, and NiO/Al_2O_3, which exhibited satisfactory reforming activity and stability, were tested under CLR conditions (in the absence of CO_2 sorbent). The materials were initially exposed to CH_4/steam in their oxidized state at 650°C for 1h (S/C=3). At the end of reforming stage, metallic Ni was reoxidized with air at 850°C for 15min and the cycle was then repeated.

3 Results and discussion

BET results showed that the surface area of the final OTM is greatly affected by the support source, with NiO/Al_2O_3 possessing the highest surface area (117.4 m^2/g) followed by NiO/SiO_2 (56.2 m^2/g), NiO/ZrO_2 (22.9 m^2/g) and NiO/TiO_2 (16.4 m^2/g). XRD confirmed the presence of NiO phase in all OTMs, together with the identifications of mixed $NiAl_2O_4$ and $NiTiO_3$ in Al_2O_3- and TiO_2- supported OTMs, indicating a strong interaction between NiO with the corresponding supports. TPR results showed that all OTMs had a high degree of reduction (around 80%) at temperatures lower than 650°C except NiO/Al_2O_3 where a high temperature TPR peak (~751°C) was attributed to reduction of $NiAl_2O_4$, and the degree of reduction up to 650°C was ~24%.

During reduction in CH_4 in TGA experiments, a sharp weight loss was initially observed due to reduction of NiO to metallic Ni, followed by weight gain due to carbon deposition resulting from CH_4 decomposition. Highest carbon formation was observed for Al_2O_3- followed by SiO_2, ZrO_2 and TiO_2-supported OTMs. NiO/ZrO_2 and NiO/SiO_2 exhibited very high reduction degrees (>94%) while NiO/Al_2O_3 and NiO/TiO_2 showed relatively lower reducibility mainly due to the strong metal-support interaction, as detected with XRD. In terms of products, low amounts of CO_2 and H_2O from CH_4 total oxidation by NiO were first detected, followed by higher concentrations of CO and H_2 from CH_4 partial oxidation and CH_4 decomposition reaction for all four OTMs. Switching to air resulted in removal of deposited carbon, as evidenced by weight decrease and CO_2 formation. After coke removal, weight increases and reaches its initial value for all four OTMs, signifying complete re-oxidation of NiO.

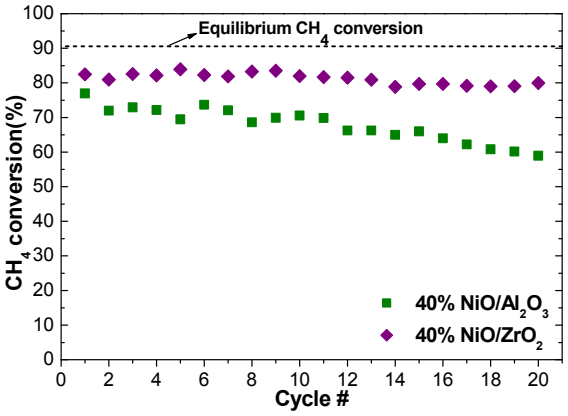

Fig. 1. Methane conversion in chemical looping reforming experiments for NiO/ZrO_2 and NiO/Al_2O_3

Experiments under conventional reforming conditions (with pre-reduced OTMs and steam in the feed) showed a satisfactory performance of NiO/Al_2O_3 and NiO/ZrO_2 at 650°C, with less than 8% deactivation after 10 h on stream. On the other hand, NiO/SiO_2 and NiO/TiO_2 were found to be inactive, with initial CH_4 conversion less than 12%. Characterization of used samples with TPO was performed to identify whether inactivity of the two latter OTMs was due to coke deposition. Carbon deposition was found to be very low and in the same range over all four supports, ruling out coke as the primary cause of deactivation. Preliminary XPS results of the used samples showed a significant amount of nickel in oxidized form over the two inactive catalysts. Further characterization is under way to confirm whether metallic Ni is easily reoxidized by steam during reforming conditions over titania and silica.

The two promising materials were then tested under CLR conditions, in the absence of CO_2 sorbent, for 20 consecutive redox cycles. Methane conversion as a function of cycles is shown in Figure 1. NiO/ZrO_2 exhibited good activity with initial CH_4 conversion around 80% and less than 2% deactivation after 20 redox cycles, corresponding to 20 hours exposure to CH_4/steam. On the contrary, NiO/Al_2O_3 even though exhibited a similar initial CH_4 conversion of 79%, deactivated quickly, leading to a CH_4 conversion of 59% in the 20th cycle. This loss of activity can be attributed to the lower hydrothermal stability of alumina compared to zirconia under steam reforming conditions.

4 Conclusions

The preliminary tests indicated that NiO/ZrO_2 is a promising OTM for sorption-enhanced chemical looping reforming, with high reforming activity and low deactivation during 20 redox cycles. The material is currently being tested with the addition of a stable synthesized CaO-ZrO_2 CO_2 sorbent to assess its full potential for the combined process.

Acknowledgements

This work was made possible by NPRP grant 5–420–2–166 from QNRF (member of Qatar Foundation). The statements made herein are solely the responsibility of the authors.

References

[1] M. Rydén, P. Ramos, Fuel Process. Technol. 96 (2012) 27.
[1] A. Antzara, E. Heracleous, D.B. Bukur, A.A. Lemonidou, Int. J Greenh Gas Control. 32 (2015) 115.
[2] L. Silvester, A. Antzara, G. Boskovic, E. Heracleous, A.A. Lemonidou, D.B. Bukur, Int. J Hydrogen Energy. DOI: 10.1016/j.ijhydene.2014.12.130

I-PP51

Aqueous Phase Reforming of Xylitol over Mono- and Bimetallic Carbon-Supported Catalysts

Godina L.I.[1], Kirilin A.V.[1], Tokarev A.V.[1], Demidova Yu.S.[2,3], Lemus J.[4], Calvo L.[4], Schubert T.[5], Gilarranz M.A.[4], Simakova I.L.[2,3], Murzin D.Yu.[1*]

1 - Åbo Akademi University, Laboratory of Industrial Chemistry and Reaction Engineering, Åbo, Finland

2 - Boreskov Institute of Catalysis SB RAS, Novosibirsk, Russia

3 - Novosibirsk State University, Novosibirsk, Russia

4 - Universidad Autónoma de Madrid, Madrid, Spain

5 - FutureCarbon GmbH, Bayreuth, Germany

* dmurzin@abo.fi

Keywords: aqueous phase reforming, sustainable, fuel production, hydrogen, carbon-supported catalysts

1 Introduction

Fuel consumption is increasing nowadays, demanding a replacement for fossil fuels. New technologies should be developed to use renewables as an energy resource. Aqueous phase reforming (APR) allows conversion of alcohols and polyols obtained from biomass to hydrogen and hydrocarbons. This process is more energy-efficient for hydrogen production compared to steam reforming, since it is performed in the liquid phase and at lower temperatures (190-250°C) [1,2].

Traditional catalysts used for oil refining are not successful for conversion of biomass, because of low hydrothermal stability and fast deactivation [3]. Thus, new catalysts should be developed. Carbon support was shown to be exceptionally stable at the APR conditions [4,5]. Different noble and transition metals were tested in the APR process [6,7]. However, catalysts were mainly supported on γ-Al_2O_3, while the reaction pathways strongly depend on the type of the support [8,9]. Thus, additional metal screening is needed for carbon-supported catalysts.

2 Experimental

Activated carbon (AC), mesoporous carbon Sibunit and carbon nano-fibers (CNF) were used as supports for preparation of two sets of catalysts, one used for metal screening and the second for catalyst optimisation. The first set of monometallic Pt, Ni, Re, Ru and bimetallic Pt-Ni, Pt-Co, Pt-Re, Pt-Ru catalysts on Sibunit was prepared via incipient wetness impregnation with Cl-containing metal precursors. The second set was prepared via impregnation of Pt colloidal nano-particles and using the micro-emulsion method with AC, CNF and Sibunit. The catalysts were tested in the APR of xylitol in a continuous set-up at 225°C and 29.7 bar. Aqueous 10 wt % solution of xylitol was fed with a flow ranging from 0.1 to 1 ml/min. Gas-phase products were analyzed online by a micro-GC (Agilent Micro-GC 3000A). Liquid-phase products were analysed via HPLC (Agilent 1100) equipped with an Aminex HPX-87H column. Carbon balance was additionally monitored via total organic carbon analysis of liquid samples, being close to 90-95%.

3 Results and discussion

Metal screening was based on such parameters as activity and selectivity to hydrogen and alkanes. All monometallic catalysts showed significantly lower activity (Ni) or deactivated very fast (Ru, Re) compared to Pt. Activity of bimetallic Pt-Ni, Pt-Co and Pt-Ru catalysts was practically en par with the monometallic one. Pt-Re catalyst was two times more active than

others. However, addition of Re or Ru to Pt shifted the reaction pathways to formation of the alkanes. Thus, the selectivity to hydrogen was rather low with Pt-Re and Pt-Ru catalysts, compared to Pt, Pt-Co, Pt-Ni. Alkanes from C1 to C7 were produced, with the ratio between different alkanes dependent on the metal (Fig.1).

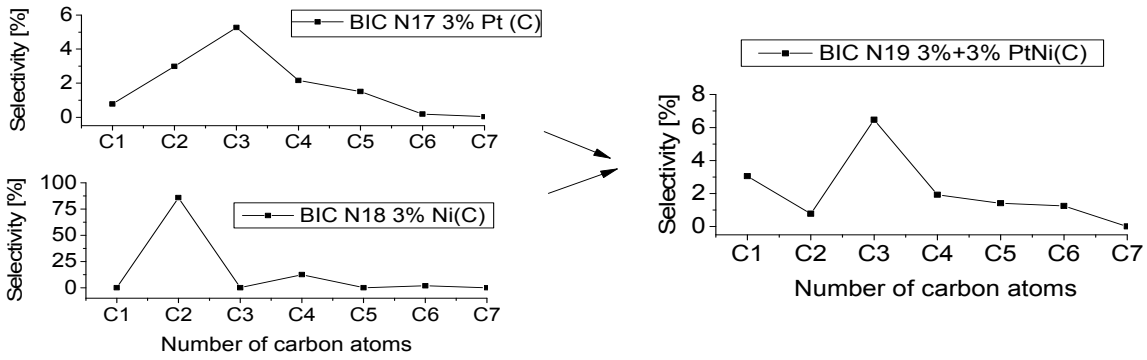

Fig. 1. Comparison of alkane distribution in APR of xylitol on Pt/C, Ni/C and bimetallic Pt-Ni/C catalysts at 225°C.

Catalysts prepared via colloidal impregnation or micro-emulsion method showed surprisingly low activity, probably due to an excess of a polymer covering catalytic sites, which leads also to leaching of Pt during long-term experiments (3-7 days).

4 Conclusions

Metal screening was performed for APR of xylitol on carbon-supported catalysts. Pt-Re was shown to be the most active and the most selective to alkanes, while monometallic Pt had the optimum combination of activity and selectivity to hydrogen among other catalysts. Alkane distribution was shown to be strongly dependent on the metal, which unravelled new insights into the reaction pathways. Stability issues were shown to be critical for the Pt catalysts prepared via impregnation of colloidal nano-particles and micro-emulsion technique.

Acknowledgements

The SusFuelCat project has received funding from the European Union's Seventh Framework Programme for research, technological development and demonstration under grant agreement No 310490 (www.susfuelcat.eu).

References

[1] R.R. Davda, J.W. Shabaker, G.W. Huber, R.D. Cortright, J.A. Dumesic, Appl. Catal. B Environ. 56 (2005) 171.
[2] B. Liu, Catalytic Generation of Hydrogen and Chemicals from Biomass Derived Polyols, ProQuest, 2008.
[3] M. Behrens, A.K. Datye, Catalysis for the Conversion of Biomass and Its Derivatives, Max Planck Research Library for the History and Development of Knowledge Proceedings, Berlin, Germany, 2013.
[4] T.-W. Kim, H.-D. Kim, K.-E. Jeong, H.-J. Chae, S.-Y. Jeong, C.-H. Lee, C.-U. Kim, Green Chem. 13 (2011) 1718.
[5] X. Wang, N. Li, L.D. Pfefferle, G.L. Haller, J. Phys. Chem. C 114 (2010) 16996.
[6] G.W. Huber, J.W. Shabaker, S.T. Evans, J.A. Dumesic, Appl. Catal. B Environ. 62 (2006) 226.
[7] J.W. Shabaker, G.W. Huber, J.A. Dumesic, J. Catal. 222 (2004) 180.
[8] H.-D. Kim, H.J. Park, T.-W. Kim, K.-E. Jeong, H.-J. Chae, S.-Y. Jeong, C.-H. Lee, C.-U. Kim, Catal. Today 185 (2012) 73.
[9] X. Wang, N. Li, J.A. Webb, L.D. Pfefferle, G.L. Haller, Appl. Catal. B Environ. 101 (2010) 21.

I-PP52

Co-Conversion of Fatty Acids and Hydrocarbons in the Conditions of Catalytic Cracking

Lipin P.V.*, Potapenko O.V., Sorokina T.P., Doronin V.P.

Institute of Hydrocarbons Processing of Siberian Branch Russian Academy of Sciences, Omsk, Russia

* lipin@ihcp.ru

Keywords: fatty acid hydrocarbon, olefin, cracking, conversion, catalyst

1 Introduction

Effective way to identify patterns of transformation real bio raw material is study the behavior of the individual compounds under catalytic cracking. Conversion various model compounds of bio-oil in conditions of cracking investigated in the works [1-3]. The authors described the direction of transformations oxygenate hydrocarbons, belonging to different classes, the distribution of the group composition of products, as well as the influence of the conditions of cracking on yield products.

The present work was aimed at studying the transformation of model oxygenate compounds (fatty acids) and various hydrocarbons under catalytic cracking.

2 Experimental/methodology

In the work as model compounds were used oleic acid, stearic acid and hydrocarbons: cyclohexane, methylcyclohexane, decalin and tetralin. The model raw material consisted of pure hydrocarbons, or mixtures of fatty acids and hydrocarbons with a ratio components of 5/95 and 25/75 respectively.

The conversions of model mixtures were investigated on a commercial equilibrium cracking catalyst. The catalyst comprised the HREY form of Y zeolite and a matrix containing amorphous aluminosilicate, aluminum hydroxide and bentonite clay [4].

Catalytic testing was performed at a lab-scale unit with a fixed-bed catalyst in the temperature of 450ºC at a catalyst-to-oil mass ratio equal to 4.

3 Results and discussion

The study of transformation oleic acid with various hydrocarbons under cracking demonstrates that the fatty acid may have a promoting effect on the conversion of hydrocarbons, and can contribute to the suppression of cracking. At low concentration (5.0 wt.%) oleic acid in mixture change of conversion of cyclohexane, methylcyclohexane and decalin substantially not observed. However, at high concentration (25.0 wt.%) oleic acid in the mixture braking effect of cracking of hydrocarbon is observed. The growth of tetralin conversion occurs regardless of the content of oleic acid for a model mixture of tetralin-oleic acid.

The promoting effect of oleic acid is connected with deoxygenation reactions and formation high molecular olefins with one or two double bonds. Olefins readily form carbocations with acid sites of the catalyst, and further carbocations interact with corresponding hydrocarbons. However, high molecular olefins are rapidly adsorbed on the catalyst surface at transformation of model mixtures with cyclohexane and methylcyclohexane. As a result, this leads to the suppression of cracking of hydrocarbons at high content oleic acid in model mixture. The proof of this fact is high content of aromatic hydrocarbons in the liquid products and growth coke on the catalyst, as olefins with two or more double bonds in the cracking conditions to undergo cyclization followed by aromatization.

In the case of the conversion of a model mixture of tetralin-oleic acid enhanced the

competitive sorption between tetralin and high molecular olefins, thus there is no suppression of cracking of tetralin.

Researching transformation various hydrocarbon with stearic acid indicates that no promotional effect of acid depends on its content in model mixture. The greatest increase of conversion cyclohexane, methylcyclohexane and decalin is observed when content of acid in the model mixture of 5.0 wt.%. For model mixture tetralin-stearic acid the greatest conversion of tetralin observes at content of acid 25.0 wt. %. As in the case of oleic acid, the promoting effect of stearic acid explains deoxygenation reactions of acid and formation paraffins and olefins containing one double bond.

In the work also presents data on the patterns of joint transformations of fatty acids and the real feedstock – hydrotreated vacuum gas oil.

4 Conclusions

The study co-conversion oleic acid with various hydrocarbons demonstrates that the unsaturated fatty acid may provide both a promoting effect on the cracking of hydrocarbons and to suppress their transformation. At a high content (25 wt.%) of acid in the model mixture define that formed high molecular olefins with two double bonds rapidly adsorbed on acid sites, thus prevent adsorption of hydrocarbons on the catalyst surface. This eventually leads to the suppression of cracking of hydrocarbons.

Researches of transformation of model mixtures type hydrocarbon-stearic acid indicate that the mechanism promoting action of fatty acid on cracking of hydrocarbons is similar as in the case of oleic acid. However, at high content (25 wt.%) of stearic acid in model mixtures sharp reduction conversion of hydrocarbon not observed.

Comparison of the distribution products of cracking indicates that products of the model mixtures with stearic acid contain gases with high content of olefins, high yield of liquid products, with simultaneous reduction of the coke on the catalyst.

Acknowledgements

The authors thank E. Kudrya for GS-MS measurements and V. Talzi for NMR studies.

References

[1] M. Bertero, G. de la Puente, U. Sedran, *Renewable Energy*. 60 (2013) 349.
[2] R. Cerny, M. Kubu, D. Kubicka, *Catalysis Today*. 204 (2013) 46.
[3] J. Asomaning, P. Mussone, D.C. Bressler, *Fuel Processing Technology*. 120 (2014) 89.
[4] V.P. Doronin, T.P. Sorokina, *Russian Journal of General Chemistry*. 77 (2007) 2224.

I-PP53

Advanced Macroporous Catalysts for Heavy Oil Hydrotreating

Semeykina V.S.[1,2,3*], Polukhin A.V.[1], Parunin P.D.[1,2,3], Parkhomchuk E.V.[1,2,3], Lysikov A.I.[1,2]

1 - Boreskov Institute of catalysis SB RAS, Novosibirsk, Russia
2 - Novosibirsk State University, Novosibirsk, Russia
3 - Scientific research centre "Energy efficient catalysis", Novosibirsk State University, Novosibirsk, Russia

* viktoriyasemeykina@ngs.ru

Keywords: macroporosity, alumina, sepiolite, heavy oils, hydrodesulfurization, hydrodemetallization

1 Introduction

Despite the evolution of alternative ways for motor oil production getting close attention for last decades crude oil production and upgrading still remains the one of the paramount practical importance on a global scale. Declining the quality of the feed oil causes enormous difficulties during the refinement due to the high content of sulfur, nitrogen, metals, asphaltens and high-boiling fractions. In heavy oil refining special attention must be given to these factors, therefore, the catalysts with the optimized texture and tuned acidic properties are required. In this paper in order to elucidate the role of these parameters we have investigated a set of CoMoNi hydrotreating catalysts: a pair of alumina-supported ones possessing a different texture with similar surface properties as well as sepiolite-supported ones having different phase composition.

2 Experimental

For the preparation of mesoporous alumina pseudobemite (Ltd. Promyshlennye katalizatory, Russia) was mixed with acidified water to produce a paste, then extruded into cylindric pellets and thermally treated. Macroporous alumina support Al_2O_3-T was prepared by the same technique with the use of polystyrene (PS) microbeads (diameter ~ 250 nm) as templates. Natural sepiolite-like mineral (Ltd. Anekst, Russia) was treated with orthophosphoric acid to adjust surface properties, extruded and calcined as well.

CoMo(Ni) supported catalysts were obtained by the incipient wetness impregnation with citric complex of Mo, Co and Ni, as described in paper [1]. For the proper control the catalysts were studied by XRD, XFS, SEM, TEM, mercury porosimetry and N_2 low-temperature adsorption methods.

Crude Tatar Oil having extremely high viscosity (360 sSt at 25°C) and sulfur content (3.4 wt.%) has been chosen as a heavy feedstock for hydrotreating experiments. Catalytic tests were carried out using a lab scale Berty reactor as described in paper [1]. Hydroprocessing parametres were as follows: T = 420 °C, P = 15 MPa, feed to H_2 volume ratio 1000, liquid hourly space velocity LHSV 1 h^{-1}, catalyst residence time under constant conditions – not less than 120 h.

3 Results and discussion

For the proper control of the texture parameters in a wide range of pore sizes all the supports and catalysts were investigated by nitrogen adsorption and Hg porosimetry (Fig.1 a). The alumina sample produced with the use of PS template showed a bimodal pore size distribution with the maximums at 12 and 113 nm referred to meso- and macropores respectively, while the reference sample represented only the mesoporous structure. According to Hg porosimetry data, introducing the PS template allowed the pore volume to increase by 2.5

times from 0.34 to 0.84 cm^3/g and the specific surface area by 20% from 168 to 194 m^2/g, with BET characteristics being almost unchanged. The sepiolite-based supports had the relatively low specific surface area in the range of 34-22 m^2/g and the high pore volume of 0.59-0.63 cm^3/g. A broaden pore size distribution in the range of 20-400 nm was observed (Fig. 1a). Enlarging the phosphorus content led to the declining of the specific surface area and the significant increasing of the pore volume.

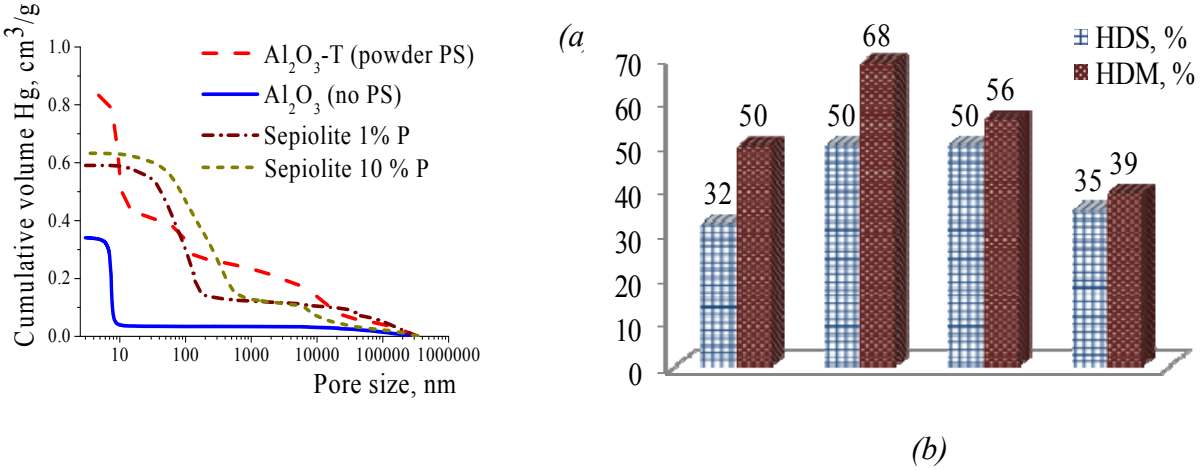

Fig. 1. (a) Mercury porosimetry data for the supports used and (b) HDS and HDM activity of the catalysts in tatar oil hydrotreating.

According to XRD data both alumina samples represented by a mixture of γ- and δ-modifications while the sepiolite-like samples had a complex multiphase composition comprised of MgO (40 wt.%) and calcium/magnesium silicates (60 wt.%) in case of Sepiolite1%P and calcium/magnesium phosphates (90 wt.%) in case of Sepiolite10%P.

The catalytic activity of the samples in tatar oil hydrotreating is evidently shown on Fig.1 b. Macro/mesoporous CoMoNi/Al_2O_3-T and CoMoNi/Sepiolite1%P performed the highest HDS and HDM efficiency among other samples, assuming the optimized texture properties make a significant contribution to the apparent activity. However, surface properties must be necessarily taken into consideration too: CoMoNi/Sep10%P despite its macroporous texture performed an unexpectedly low HDM activity (39 %) that can be accounted for the lower affinity of V-containing compounds to the phosphate surface (Fig. 1 b).

4 Conclusions

The optimized macro/mesoporous texture of the alumina support was shown to significantly affect HDS and HDM activity of the catalyst in heavy oil hydrotreating. The sepiolite-supported catalysts were found to be prospective as well due to their similar catalytic activity and basic surface properties being favourable for an enhanced catalyst lifetime. We suppose these investigations to aid in working out an effective catalyst with a high stability and an increased conversion of high molecular substrates under the heavy oil hydrotreating conditions.

Acknowledgements

The work was performed with support of the Skolkovo Foundation (Grant Agreement for Russian educational organization №1 on 28.11.2013). Also authors would like to thank Cherepanova S.V., Bulavchenko O.A., Trunova V.A., Aupov A.B. for the invaluable contribution to research.

References

[1] Parkhomchuk E.V., Lysikov A.I., Okunev A.G., Parunin P.D., Semeykina V.S., Ayupov A.B., Trunova V.A., Parmon V.N., *Industrial & Engineering Chemistry Research*. 52 (2013) 17117−17125.

I-PP54

The Role of Carrier's Carbonization Degree on the HDO Conversion of the Oleic Acid over the CoMo/C/Al_2O_3 Catalysts

Varakin A., Salnikov V., Nikulshin P.*

Samara State Technical University, Samara, Russia

* p.a.nikulshin@gmail.com

Keywords: hydrodeoxygenation, oleic acid, heteropolyanion, carbon-covered, alumina, CoMoS

1 Introduction

The oleic acid as a model compound for a component of plant oil is the most using to modeling the hydrodeoxygenation (HDO) of renewable feedstocks. The conversion of this bio-feedstock into hydrocarbons usually carried out on hydrotreating (HDT) catalysts like supported Co(Ni)MoS sulfides. The type of support has a significant impact on the morphology and composition of the active phase, and as a result on its activity and stability. The most commonly used support for HDT catalysts is alumina due to its high surface area, thermal stability, physical strength, and recoverability. But despite of all this advantages, acid and base sites on the surface of alumina may influence on properties and form of precursors, impede the sulfidation of metal oxide, and induce the rapid deactivation of the catalysts by coke formation in HDT process. The using of carbon supports with low acidity allows to achieve the well dispersed active sulfide phase and higher activity in HDT than alumina supported ones. However, carbon supports has some disadvantages that limiting their use in industry such as low thermal stability and fragility.

The interesting way to combine advantages of alumina and carbon supports is the use of carbon coated alumina [1,2]. This modification allows to decrease the interaction between the active sulphide phase and support surface, and as a result increasing the amount of so-called CoMoS-II phase (or NiMoS-II) and catalytic performance. The objective of the work was investigation of the role of Al_2O_3 carbonization on the HDO conversion of the oleic acid over the CoMoS/C//Al_2O_3 catalysts.

2 Experimental

Carbon coated carriers C_x/γ-Al_2O_3 (x = 0, 2 or 6 wt. %) were prepared by the pyrolysis of ethylene glycol and citric acid mixtures on γ-Al_2O_3 at 600 °C in N_2 flow. Carbon content was varied by changing the content of organic compounds and controlled by the DTA-TGA method.

The catalysts were prepared by conventional incipient wetness impregnation method on C_x/γ-Al_2O_3 with an appropriate aqueous solution of 12-molybdophosphoric heteropolyacid and cobalt citrate in order to obtain about 13.0 wt. % of molybdenum and 4.0 wt. % of cobalt. After impregnation the solids were dried at 80, 100, 120 °C for 2 h. Before each catalytic experiment, the catalysts were sulfided *in situ* by a mixture of dimethyldisulphide in toluene (sulfur content 6% wt.) at hydrogen pressure of 3.0 MPa and 340 °C for 24 h.

The textural characteristics of the catalysts were determined using N_2 adsorption at 77 K on a Quantochrome Autosorb-1. The HRTEM images of the active phase species were obtained on a Tecnai G2 20 electron microscope. The sulphided catalyst samples were analysed by XPS using a Kratos Axis Ultra DLD spectrometer.

Catalytic tests were performed in a bench-scale flow reactor in oleic acid (5 wt. % in toluene) HDO at 260 °C, H_2 pressure of 3.0 MPa, LHVS of 80 h^{-1}, and H_2/feed of 500 nL/L.

3 Results and discussion

The results of catalytic tests in oleic acid HDO are given in Table 1.

Table 1. Catalytic properties of $CoMo/C_x/Al_2O_3$ catalysts in oleic acid HDO

Catalyst	Conversion (%)		Rate constants × 10^4 (s^{-1})		TOF_{HDO} × 10^3 (s^{-1})	$E_A^{\#}$ (kJ·mol^{-1})
	x_{OA}	x_{HDO}	k_{OA}	k_{HDO}		
$CoMo/Al_2O_3$	41	33	10.1	7.8	7.2	65
$CoMo/C_2/Al_2O_3$	57	53	16.2	14.6	8.4	66
$CoMo/C_6/Al_2O_3$	43	41	10.8	10.1	5.7	64

Activity of the catalysts is essentially dependent on the carbon content in the support. The higher carbon content led to the higher stacking number of the CoMoS slabs. Dependence of the slab length on carbon content passed through the minimum at 2 wt. % of carbon. The $CoMo/C_2/Al_2O_3$ catalyst was the most active and has the higher C_{18}/C_{17} selectivity in all range of tested temperature (Fig. 1). Black bold curves on Fig. 2 correspond to the apparent dependence of k_{HDO} on Co content in CoMoS phase C_{CoMoS} and average particle length values; dotted lines correspond to possible correlations of k_{HDO} on C_{CoMoS} or on l.

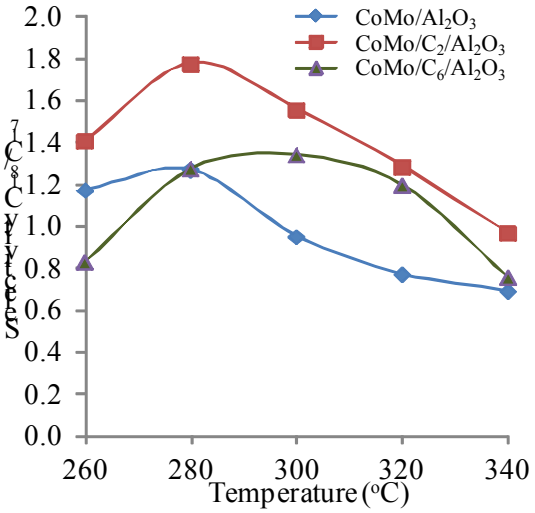

Fig. 1. The influence of process temperature on C_{18}/C_{17} ratio in oleic acid HDO

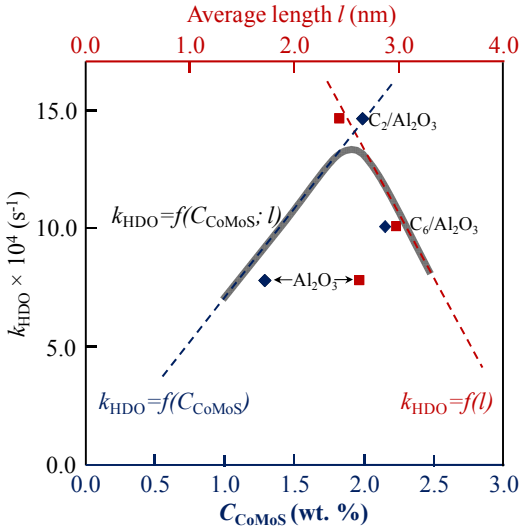

Fig. 2. Rate constants k_{HDO} correlated with cobalt content in CoMoS phase C_{CoMoS} (♦) and its average length l (■).

As a result, the $CoMo/C_2/Al_2O_3$ catalyst has optimal values of cobalt content in CoMoS phase particles and average particle length values for the highest rate constant.

4 Conclusions

The results showed that changing the carbon content it is possible to vary a stacking number/linear size ratio of the active phase particles and, thereby, to control HDO of oleic acid and C_{18}/C_{17} selectivity. $CoMo/C_2/Al_2O_3$ catalyst had optimal characteristics of active phase and highest activity and stability.

Acknowledgements

A. Varakin thanks Haldor Topsøe Company for the grant to perform his PhD work. The work was supported by Ministry of education and science of Russian Federation (project No. 2014/199) and Russian Foundation for Basic Research (project No. 14-03-97079).

References

[1] P.A. Nikulshin, N.N. Tomina, A.A. Pimerzin, A.V. Kucherov, V.M. Kogan, *Catal. Today* 149 (2010) 82.
[2] P.A. Nikulshin, V.A. Salnikov, A.V. Mozhaev, P.P. Minaev, V.M. Kogan, A.A. Pimerzin, *J. Catal.* 309 (2014) 386.

I-PP55

The Influence of Membrane Reactor Parameters on Efficiency of Hydrocarbons Dehydrogenation Process

Shelepova E.[1*], Vedyagin A.[1], Mishakov I.[1,2], Noskov A.[1,2]

1 - Boreskov Institute of Catalysis, Department of catalytic process engineering, Novosibirsk, Russia
2 - Novosibirsk State Technical University, Novosibirsk, Russia

* shev@catalysis.ru

Keywords: hydrocarbons dehydrogenation, catalytic membrane reactor, mathematical, modelling

1 Introduction

Dehydrogenation of saturated hydrocarbons is known to be the key route to yield the monomers despite on having the strong endothermic and equilibrium limitations. The oxidative dehydrogenation (ODH) is free of latter restrictions but characterized with low product selectivity. The use of the catalytic membrane reactor (CMR) with additional hydrogen oxidation permits one to combine the advantages of conventional dehydrogenation and oxidative dehydrogenation processes. In this case the endothermic and exothermic processes are supposed to take place within the different compartments of the membrane reactor (so called thermodynamically "conjugated" reactions). The impact of membrane reactor parameters on performance of dehydrogenation processes has been theoretically investigated and compared with the tubular reactor.

2 Experimental/methodology

In our research the dehydrogenation processes of ethane, propane and ethylbenzene were considered.

Ethane dehydrogenation reaction $C_2H_6 \leftrightarrow C_2H_4 + H_2$ appears to be the most strictly limited by the thermodynamics. In addition, an intensive coke formation taking place over the catalyst's surface at high temperature is worth to be noted as the main disadvantage of this process.

As in latter case, the process of propane dehydrogenation also has the similar endothermic and equilibrium limitations. This process is characterized by side products occurrence.

$$C_3H_8 \leftrightarrow C_3H_6 + H_2$$
$$C_3H_8 \leftrightarrow C_2H_4 + CH_4$$
$$C_2H_4 + H_2 \leftrightarrow C_2H_6$$

Ethylbenzene dehydrogenation is characterized by even higher number of side products, especially in case of gas mixture diluted by water vapors:

$$C_6H_5CH_2CH_3 \leftrightarrow C_6H_5CHCH_2 + H_2$$
$$C_6H_5CH_2CH_3 \rightarrow C_6H_6 + C_2H_4$$
$$C_6H_5CH_2CH_3 + H_2 \rightarrow C_6H_5CH_3 + CH_4$$
$$C_2H_4 + 2H_2O \rightarrow 2CO + 4H_2$$
$$CH_4 + H_2O \rightarrow CO + 3H_2$$
$$CO + H_2O \rightarrow CO_2 + H_2$$

The efficiency of the above mentioned dehydrogenation processes has been analyzed for the case of membrane reactor including the conjugation with hydrogen oxidation reaction.

The theoretical study was implemented by means of mathematical modeling. The membrane reactor consists of two concentric tubes, where the interior ceramic tube with catalyst bed is placed in the exterior one. The membrane is deposited as a continuous layer on the outer surface of ceramic tube. The dehydrogenation reaction is carried out over the catalyst in the tube side. Hydrogen permeates from the tube compartment of the reactor through the membrane inside the

shell compartment to be further oxidized with dioxygen. The two-dimensional type of non-isothermal stationary mathematical model of the catalytic membrane reactor for the "conjugated" dehydrogenation process has been developed. The balance equations represent a system of differential equations in partial derivatives, which were treated numerically by the method of lines and the appropriate method for ODE solving.

The dehydrogenation process was simulated at different dilutions of gas mixtures. The inlet concentration of ethane and propane in the inert gas was 10% while that of ethylbenzene was selected as 30%.

To achieve reasonable values of hydrocarbons conversion in tubular reactor one should keep the reaction temperature as high as 700°C (Fig.1). Within the high temperature region the contribution of side reaction leading to undesired products increases significantly. Selective hydrogen removal in the membrane reactor results in shifting the reaction equilibrium thus enhancing the products selectivity at lower temperatures.

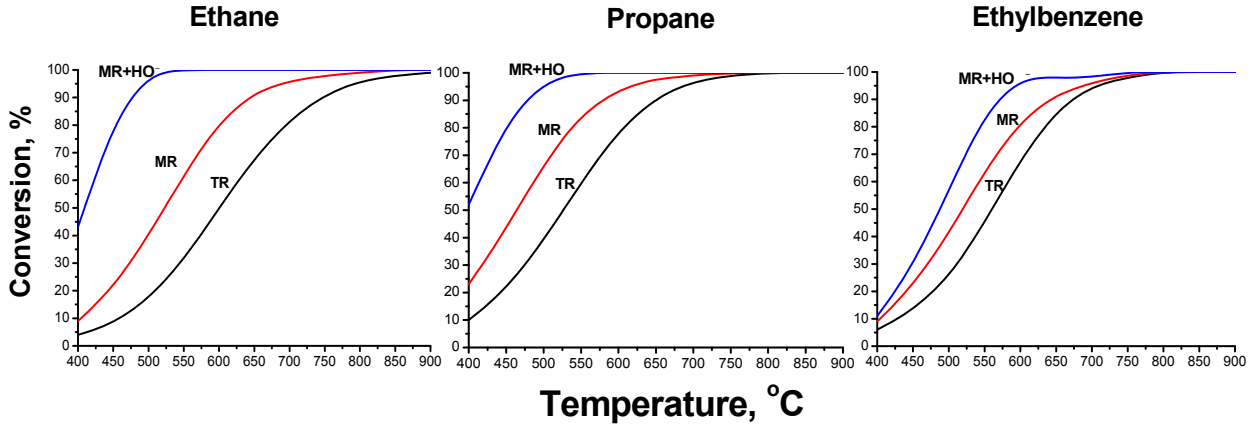

Fig. 1. Temperature dependences for ethane, propane and ethylbenzene conversions in membrane reactor (MR), tubular reactor (TR) and membrane reactor combined with hydrogen oxidation (MR+HO).

The use of the membrane reactor combined with hydrogen oxidation was found to be the most effective way to produce olefins via dehydrogenation process. Carrying out the dehydrogenation process in conjugated membrane reactor enables attainment of very high hydrocarbon conversions (98-100%) at considerably lower temperatures (500°C for ethane, 550°C for propane, and 600°C for ethylbenzene). Thus, the additional oxidation makes it possible to decrease the process temperature by 200°C for ethane and by 100°C in case of propane and ethylbenzene. Using the membrane reactor permits one to increase the conversion value by the selective hydrogen removal from the reaction zone and to shift the equilibrium towards the products.

3 Conclusions

It has been shown that the "conjugated" reaction in the membrane reactor is to be the most appropriate choice for embodiment of hydrocarbons dehydrogenation processes. The process of conjugated dehydrogenation could be realized at significantly lower temperatures as compared with conventional dehydrogenation and dehydrogenation in membrane reactor.

Acknowledgements

This work was financially supported by Russian Academy of Sciences (project V.45.3.2).

I-PP57

Self-Oscillatory Regimes of Methane Oxidation over Supported Pd Catalysts

Bychkov V.Yu.[1*], Tulenin Yu.P.[1], Slinko M.M.[1], Khudorozhkov A.K.[2], Bukhtiayrov V.I.[2], Korchak V.N.[1]

1 - Semenov Institute of Chemical Physics, Moscow, Russia
2 - Boreskov Institute of Catalysis SB RAS, Novosibirsk, Russia

* bychkov@chph.ras.ru

Keywords: self-oscillations, methane oxidation, Pd catalysts

1 Introduction

Pd catalysts are widely applied for total methane oxidation. It is known [1,2] that self-oscillations of methane oxidation rate can appear over Pd catalysts in gas mixtures with relatively high methane content, which is undesirable for practice. Earlier we have studied a mechanism of self-oscillatory methane oxidation over Pd foil and powder [3-5] using thermogravimetry and mass-spectrometry. It was shown that during the oscillations periodic oxidation-reduction of Pd takes place as well as carbon accumulation-removal in PdC_x form. Mathematical model explaining the existence of methane oxidation oscillations over Pd was proposed in paper [5]. Authors of [6] have studied oscillations of methane oxidation over Pd/Al_2O_3 using QEXAFS method and confirmed main results obtained for Pd powder. However, some significant questions such as an effect of Pd particle size on oscillation parameters and temperature range of oscillations, quantitative relationship between Pd oxidation state and catalytic activity during the oscillation cycle were still unstudied. This work is addressed to clarify these aspects.

2 Experimental/methodology

Catalysts were prepared by impregnation of γ-Al_2O_3 and α-Al_2O_3 with palladium nitrate solution at different pH to obtain Pd particles of different sizes. Pd particle size was determined by TEM. Two 1%Pd/γ-Al_2O_3 catalysts had average Pd particle sizes of 5 and 16 nm (1Pd/Al-5 and 1Pd/Al-16 later). 5%Pd/α-Al_2O_3 catalyst (5Pd/Al later) contained larger agglomerates of Pd particles with diameter of 50-60 nm and smaller Pd particles of 2-7 nm, i.e. it had bimodal particle size distribution.

Catalytic experiments were carried out in a tubular quartz flow reactor. Both reactor and catalyst temperatures were measured by thermocouples. Methane-rich mixture 41.5% CH_4, 7.5% O_2, 2% Ar, 49% He was pre-mixed for all catalytic experiments.

Thermogravimetric analysis (TGA) was performed on Setaram SETSYS EVOLUTION 16/18 instrument coupled with Pfeiffer OmniStar GSD 301 quadrupole mass-spectrometer.

3 Results and discussion

Temperature ranges of self-oscillations were studied in the tubular reactor. Oscillations of methane oxidation were observed at following temperature ranges: 345-355°C (1Pd/Al-5), 320-350°C (1Pd/Al-16), 300-360°C (5Pd/Al), i.e. decreasing of Pd particle size results in shortening of temperature range of the oscillations. An increase of oscillation period as well as significant change of oscillation waveforms were also found.

Fig.1 shows oscillations of Pd catalyst weight and O_2, H_2O and CO_2 pressures in gas phase during methane oxidation over 5Pd/Al catalyst at 360°C in thermogravimetric setup. The oscillation cycle consists of two intervals (***a-b*** and ***b-a***). To recognize the nature of the weight

oscillations the reaction process was interrupted in C, B or D points, gas phase was pumped off and the catalyst was cooled down to 30°C. Then the catalyst was heated in CO-He mixture to measure a weight drop due to PdO reduction. The results obtained allowed to conclude that the weight increase during ***b-a*** interval was caused by Pd oxidation. This Pd oxidation accompanies with an increase of methane oxidation rate. In ***a-b*** interval Pd particles are reduced and partly carbonized, and demonstrate the highest catalytic activity. Minimum catalytic activity near ***b*** point in Fig.1 corresponds to metallic Pd having chemisorbed oxygen.

Fig.2 shows a relationship between CO_2 evolution rate and Pd oxidation degree (x of PdO_x) calculated using the gravimetric results. Catalytic activity of Pd is maximum at x=0. It drops to minimum and gradually increases with x rise from 0 to 0.3.

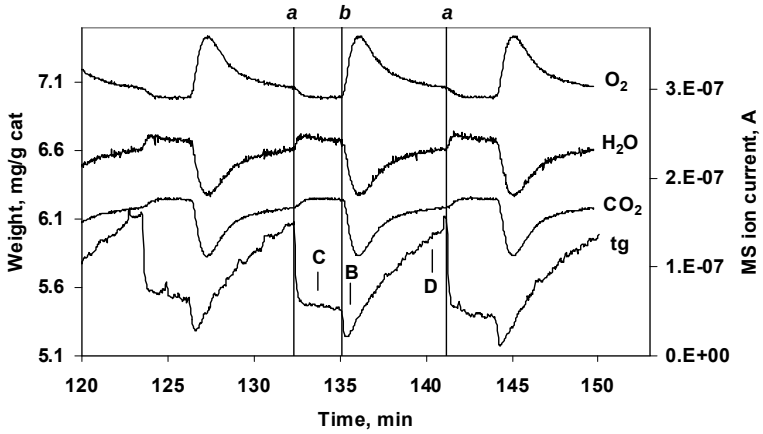

Fig.1 Oscillations over 5Pd/Al at 360°C

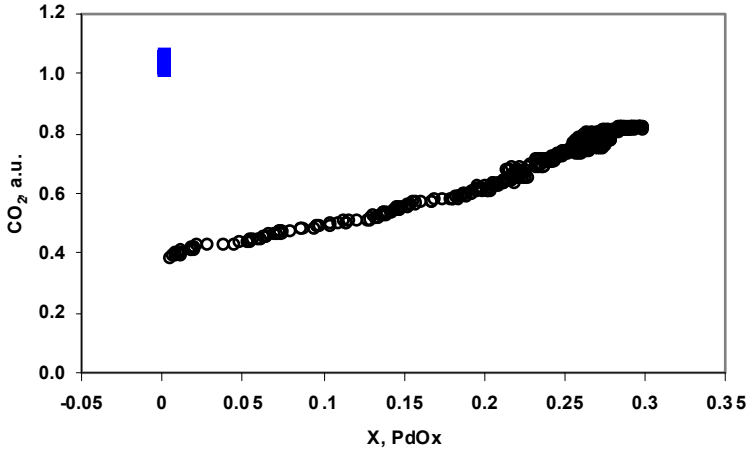

Fig.2 Effect of Pd oxidation degree on CO_2 evolution rate

Temperature hysteresis of methane oxidation rate and Pd state (Pd catalyst weight) was also studied over the Pd catalysts. The variation of Pd particle size was found to shift the temperature hysteresis interval. The nature of this phenomenon and its interconnection with the self-oscillations phenomenon are discussed.

References

[1] P. Euzen, J.-H. L. Gal, B. Rebours, G. Martin, *Catal. Today*, 47 (1999) 19.
[2] M. Lyubovsky, L.L. Smith, M. Castaldi, H. Karim, et al., *Catal. Today*, 83 (2003) 71.
[3] V.Yu. Bychkov, Yu.P. Tyulenin, M.M. Slinko, D.P. Shashkin, et al., *J. Catal*. 267 (2009), 181.
[4] V.Yu. Bychkov, Yu.P. Tyulenin, A.Ya. Gorenberg, et al., *Appl. Catal. A Gen.* 485 (2014) 1.
[5] N.V. Peskov, M.M. Slinko, V.Yu. Bychkov, V.N. Korchak, *Chem. Eng. Sci*. 84 (2012) 684.
[6] J. Stötzel, B. Kimmerle, M. Nachtegaal, J.-D. Grunwaldtz, *J. Phys. Chem. C*, 116 (2012) 599.

I-PP58

Structure Sensitivity in $La_2O_2CO_3$ and La_2O_3 Catalysts for Oxidative Coupling of Methane

Xia W.*, Hou Y.H., Han W.C., Wan H.L.

State Key Laboratory of Physical Chemistry of Solid State Surfaces, National Engineering Laboratory for Green Chemical Productions of Alcohols-Ethers-Esters, Fujian Province Key Laboratory of Theoretical and Computational Chemistry, College of Chemistry and Chemical Engineering, Xiamen University, Xiamen, China

* wsxia@xmu.edu.cn

Keywords: lanthanum oxycarbonate, lanthanum oxide, structure sensitivity, morphology effect, oxidative coupling of methane, low temperature

1 Introduction

The catalytic properties (activity and selectivity) of the solid particles could be intimately linked with the exposed crystallographic facets. For instance, the formation rate of ammonia from N_2 and H_2 on Fe crystal decreases according to the order (111) >> (100) > (110); MoO_3 shows catalytic anisotropy during propylene oxidation, with greater acrolein selectivity for the (100) plane and complete oxidation to CO_2 on the (010) facets. However, there have been rare reports upon the correlation of the catalysts for oxidative coupling of methane (OCM) with the crystallographic facets of the catalysts so far, since OCM reaction generally occurs at high temperature, and the catalysts (metal oxides) can be prepared through the calcination of metal hydroxide at high temperature that leads to the formation of sphere-shaped particles. It is found, recently, that catalysts (metal oxides) at a nanometer activate methane at lower temperatures, so it is possible that well-defined catalysts at a nanometer can be prepared via calcination at low temperatures and then used for OCM.

In the present work, we focus on the synthesis of $La_2O_2CO_3$ and La_2O_3 with a well-defined nanostructure, and explore the effects of exposed crystallographic facets or morphologies of the catalysts on the catalytic performances for OCM.

2 Experimental/methodology

Two types of $La_2O_2CO_3$ and La_2O_3 samples were synthesized.

$La_2O_2CO_3$-H: the precipitate $La(OH)_3$ obtained from the solution of $La(NO_3)_3$ was treated through a hydrothermal process, followed by desiccation and calcination in air at 500ºC.

$La_2O_2CO_3$-P: the precipitate $La(OH)_3$ was directly dried, and then calcined in air at 500ºC.

As a comparison, the referenced $La_2O_2CO_3$-H_{ref} was synthesized by a hydrothermal method too, based on the procedures reported by Shen[1].

If the $La(OH)_3$ samples are calcined in air at 700ºC, the samples are changed into La_2O_3. The related La_2O_3 samples are denoted as La_2O_3-H, La_2O_3-P and La_2O_3-H_{ref}.

The characterizations such as XRD, S(T)EM, and O_2(CO_2)-TPD were used to measure the physicochemical properties of the samples, and then the insight to the correlation of their catalytic performances in OCM with their surface structures can be given. The catalytic performances of these samples for OCM were tested at conditions: $m_{catalysts}$ = 100 mg, CH_4/O_2 = 3/1(molar ratio), GHSV = 30,000 $mL \cdot g^{-1} \cdot h^{-1}$.

3 Results and discussion

By SEM and XRD, we find that $La_2O_2CO_3$-H and $La_2O_2CO_3$-P are rod- and plate-like nanoparticles with diameters of ~20 nm, respectively. The former with the specific surface area

of ~70 $m^2 \cdot g^{-1}$ exhibits ~30% conversation of methane and ~50% C2 selectivity for OCM at 420°C, higher than the latter with the specific surface area of ~10 $m^2 \cdot g^{-1}$ (~27% conversion of methane, ~30% C2 selectivity at 500°C), displaying a shape effect of the catalysts for OCM.

For comparison of both the rod-like $La_2O_2CO_3$-H and $La_2O_2CO_3$-H_{ref} samples with almost the same specific surface area, we note that $La_2O_2CO_3$-H shows 20 times higher specific activity than $La_2O_2CO_3$-H_{ref}, which is corresponding to their O_2-TPD results. $La_2O_2CO_3$-H shows large oxygen storage capacity (OSC), in contrast, $La_2O_2CO_3$-H_{ref} almost does not adsorb any oxygen.

The further analysis illustrate that the exposed crystallographic facets of $La_2O_2CO_3$-H are significantly different from $La_2O_2CO_3$-H_{ref} (Fig. 1). For example, there are higher ratios of exposed facets with loose structures (e.g. $(1\bar{2}0)$ and $(2\bar{1}0)$) for $La_2O_2CO_3$-H than $La_2O_2CO_3$-H_{ref}, which are responsible for the difference between their catalytic performances in OCM.

Moreover, we find that the rod-like La_2O_3-H and La_2O_3-H_{ref} demonstrate similar structure sensitivity as $La_2O_2CO_3$-H for OCM. The rod-like La_2O_3-H (or -H_{ref}) has the same exposed facets as $La_2O_2CO_3$-H (or -H_{ref}), indicating that the morphologies of La_2O_3 from the decomposition of $La_2O_2CO_3$ are well kept. However, the catalytic performances (including stability) over La_2O_3 for OCM are inferior to $La_2O_2CO_3$. La_2O_3 can capture CO_2 in OCM and partially changed into carbonates, but $La_2O_2CO_3$ are stable through OCM for the tested 50 hrs.

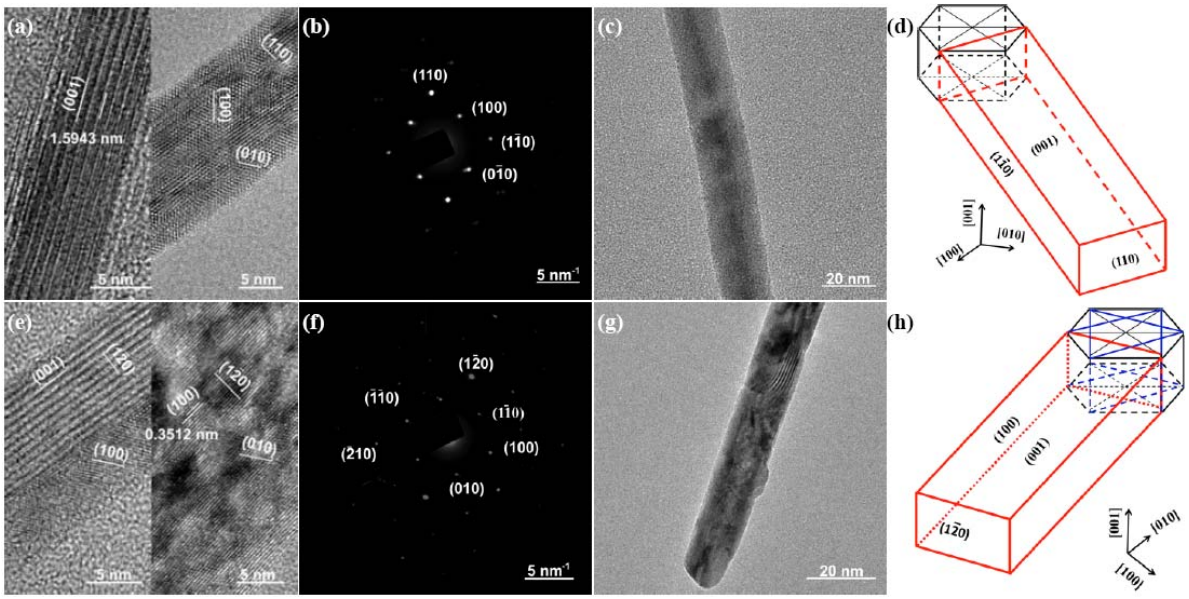

Fig. 1. HRTEM, TEM images, the selected area electron diffraction (SAED) patterns and the illustration of real shape of $La_2O_2CO_3$-H_{ref} (a-d) and $La_2O_2CO_3$-H (e-h).

4 Conclusions

The synthesized $La_2O_2CO_3$ and La_2O_3 samples for OCM exhibit significant shape effects and structure sensitivity. The catalytic performances of the rod-like sample are superior to the plate-like one, especially at low temperature (500°C below). The exposed facets with loose structure can enlarge OSC of the samples, and then enhance their activity in OCM. In addition, $La_2O_2CO_3$ is superior to La_2O_3 for OCM, and obviously more stable than La_2O_3.

Acknowledgements

Support for this research from the MOSTC (2010CB732303), NNSFC (21033006, 21373169), NFFTBS (J1310024), and PCSIRTU (IRT1036) is gratefully acknowledged.

References

[1] F. Wang, R. Shi, Z. Liu, P. Shang, X. Pang, S. Shen, Z. Feng, C. Li, W. Shen, *ACS Catalysis* 3(2013)890.

I-PP59

Mechanism of Hydrogen Transfer Reaction from Naphthenes to 1-Hexene on Y and ZSM-5 Zeolites

Potapenko O.V.*, Doronin V.P., Sorokina T.P., Krol O.V., Likholobov V.A.

Institute of hydrocarbons processing of Siberian branch of Russian academy of sciences, Omsk, Russia

* potap@ihcp.ru

Keywords: hydrogen transfer, zeolite, deuterium, olefin, naphthene

1 Introduction

Intermolecular hydrogen transfer reactions are important in the transformation of hydrocarbons in catalytic cracking, alkylation and isomerization processes. Especially developed in our organization catalytic refining process should be noted in this context [1, 2]. To determine the mechanism of hydrogen transfer from naphthene (hydrogen donor) to 1-hexene (hydrogen acceptor) transformations of mixtures containing deuterated hydrocarbons on Y and ZSM-5 zeolites were investigated.

2 Experimental

Catalytic tests were performed on lab-scale unit with fixed bed catalyst at temperatures of 350 – 550ºC, weight catalyst to hydrocarbon ratio of 1 – 5, WHSV – 10 h^{-1}. In experiments Y-type zeolites in H- and HRE-forms and zeolite ZSM-5 in the H-form were used. The feedstock was represented by mixtures of model hydrocarbons: 1-hexene, cyclohexane, methylcyclohexane. Cyclohexane-d_{12} and methylcyclohexane-d_{14} were used as deuterated compounds.

The composition of gaseous and liquid cracking products was analyzed by gas chromatography. Additionally analysis of liquid products was made on a chromato-mass spectrometer 6890/5973N (Agilent Technologies). Analysis of quantitative content of deuterium in products was performed on isotope chromato-mass spectrometer DELTA V Advantage.

3 Results and discussion

In the conversion of mixture “naphthene - hexene-1” products of hydrogen transfer reaction (Olefine + Naphtene = Parfine + Arene) may be divided into direct and apparent. Direct products are hexanes with normal and isomeric structure. Apparent are other paraffins, such as butane. Apparent products formed when a cracking reaction occur before hydrogen transfer reaction. In the presence of a hydrogen donor (source of hydride ions), and a catalyst with high activity in hydrogen transfer reactions, saturated hydrocarbons formed (hexanes, butanes), otherwise unsaturated compound formed (hexenes, butylene). Ratio of selectivity of formation saturated and unsaturated compounds with the same number of carbon atoms, for example, butanes and butenes (hydrogen transfer coefficient) [3] characterizes degree of hydrogen transfer reactions.

HREY zeolite providing bimolecular hydrogen transfer reactions has a maximal effect on the selectivity of hydrogen transfer from naphthene to olefin. The high activity of Y zeolite as compared with zeolite ZSM-5 related with a high concentration of acid sites and the absence of steric constraints for the occurrence of bimolecular reactions. HZSM-5 zeolite has a pore structure with narrow channels, which restricts the occurrence of bimolecular reactions and leads to an increase in the selectivity of the cracking reactions.

The transformation of model mixtures containing deuterated cyclohexane on zeolites Y and ZSM-5 have revealed significant differences in product composition (table 1).

Table 1. Transformation of mixture cyclohexane – 1-hexene on different type zeolites (456ºC, catalyst to hydrocarbon ratio – 3. WHSV – 10 h^{-1})

Zeolite type	HREY	HZSM-5
Naphthene conversion. % wt.	72.2	99.1
Gaseous product selectivity. %	37.1	60.5
Liquid product selectivity (w/o cyclohexane). %	37.4	28.1
Hydrogen transfer coefficient	25.3	14.5
Deuterium transfer coefficient	45.9	12.9
Arenes C_7-C_9 selectivity. %	11.4	23.1

The use of zeolite HREY as catalyst characterized by large values of hydrogen transfer coefficient (HTC) and deuterium transfer coefficient (DTC) compared to zeolite HZSM-5. In the case of HREY value DTC exceed HTC, in the case of HZSM-5 conversely. The predominance of deuterium in unsaturated compounds at transformation of mixture on HZSM-5 also point to occurrence of direct monomolecular cracking of naphthene (deuterated cyclohexane). HZSM-5 also catalyzed direct aromatization of initial hydrocarbons or intermediates – olefins and cycloolefins. It leads to increase in selectivity of the formation of aromatic compounds.

4 Conclusions

The reaction product composition is characterized by the occurrence of two competing reactions – cracking and hydrogen transfer. Cracking reactions occur predominantly at monomolecular mechanism on HZSM-5 zeolite. Bimolecular hydrogen transfer reaction from naphthene to olefin catalyzed by large pore zeolite HREY. Intermediates obtained on HZSM-5 zeolite can act as feedstock for bimolecular hydrogen transfer reactions on HREY. The mechanism of hydrogen transfer from deuterated naphthene to olefin suggests four steps: 1) activation of the olefin molecule on Brensted acid sites and carbocation formation, 2) reacting of the carbocation (on surface) with a hydrogen (deuterium) donor molecule (hydride-ion transfer step), 3) desorption of paraffin with a single deuterium atom and formation surface carbocation (from hydrogen donor molecule), 4) decomposition of the carbocation with restoration of active site.

Acknowledgements

The authors are grateful to Dr. V.P. Talsi and E.N. Kudrya.

References

[1] V.P. Doronin, T.P. Sorokina, O.V. Potapenko, M.A. Plekhanov, V.A. Likholobov. *RU Patent* 2,469,070 (2011).

[2] O.V. Potapenko, V.P. Doronin, T.P. Sorokina, V.A. Likholobov. *Fuel Processing Technology* 128 (2014) 251.

[3] F.J. Passamonti, G. de la Puente, U. Sedran. *Catalysis Today* 133–135 (2008) 314.

I-PP60

Micro-kinetic Model of Dry Reforming of Methane on Doped Pyrochlore Catalysts

Polo-Garzon F., Bruce D.A.*

Department of Chemical and Biomolecular Engineering, Clemson University, USA

* DBRUCE@clemson.edu

Keywords: syngas, pyrochlore, DFT, micro-kinetic model, reaction mechanism, dry reforming of methane

1 Introduction

The dry reforming of methane (DRM) using CO_2 has long been considered a viable method for converting methane from geological or biological sources into syngas, which can then be readily used in the production of a variety of chemicals and particularly liquid fuels. Though DRM holds great promise, the high temperatures required for the reaction have made it very difficult to find catalysts that exhibit high activity for extended periods. [1]

Pyrochlores are crystalline oxides having high thermal stability and a general formula of $A_2B_2O_7$, where *A* represents a rare-earth metal and *B* represents a transition metal. Initial experimental efforts by others showed that pyrochlores are active for DRM but the tested catalysts exhibited poor long term stability [2]; however, more recent data suggest that this trend in deactivation may not be applicable to all pyrochlores. $La_2Zr_2O_7$ (LZ) is a pyrochlore structure which has shown good long term stability, so that efforts have been made to tailor its catalytic properties, showing Rh as a promising dopant to enhance catalytic performance for DRM [3, 4]. We employed Density Functional Theory (DFT) to calculate the activation barriers for elementary reaction steps on the plane (011) and (111), concluding that the plane (111) is the catalytically active for DRM. A micro-kinetic model (MKM) is built and its predictions match experimental data which strengthens the hypothesis that the CHO dehydrogenation step is the rate determining step (RDS). This later deduced qualitatively from the activation barriers alone.

2 Experimental/methodology

Computational: First principles calculations were performed employing the Vienna *ab initio* simulation package (VASP), which is based on a plane-wave DFT code. The exchange correlation functional used is the generalized gradient approximation using the implementation of Perdew, Burke and Ernzerhof (GGA-PBE). Activation energies were calculated for selected elementary reactions using the climbing image nudged elastic band method (CI-NEB) and the remaining activation energies were estimated by a Bronsted-Evans-Polanyi (BEP) relation derived from our DFT data. The open source code SUNDIALS was modified to create the MKM for a batch reactor. The model outputs the time evolution of the partial pressure of gas phase species and the time evolution of the adsorbates coverage

Experimental: The catalyst synthesis is performed using the modified Pechini method. The metal precursors (for La, Zr, Rh) were the corresponding nitrates. After the appropriate heat treatment is carried out on the material, characterization is performed by means of XRD, SEM and EDX.

1 Results and discussion

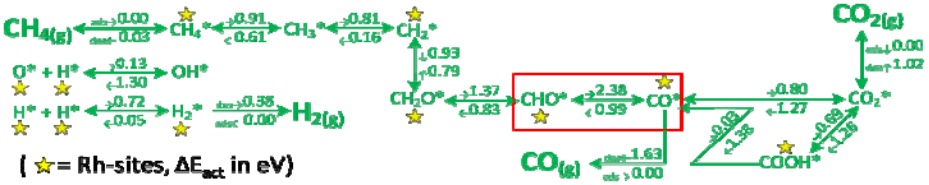

Fig. 2 Main reaction pathway on plane (111) for the 2 wt% Rh-substituted LZ. The values above, below and next to the arrows are activation energies in eV.

Fig. 1 shows the main reaction pathway on the plane (111). These activation energies, along with all other barriers for steps not as relevant (not shown in this document) are used in the MKM of a batch reactor. From Fig. 2a), it is observed how H_2 presents late desorption, suggesting that the first CO formed proceeds from CO_2 (RDS on CH_4 dehydrogenation). Additionally, the strong CO_2 decay goes along with the strong adsorption of CO_2. As seen in Fig. 2b), the MKM reproduces in great manner the experimental data for different temperatures for the 2 wt% Rh-substituted LZ, whereas it does it only in a moderate way for the 5 wt% Rh-substituted LZ, being these discrepancies probably due to neglecting the existence of Rh-Rh sites in our model, which could be present on the surface when the doping is 5%.

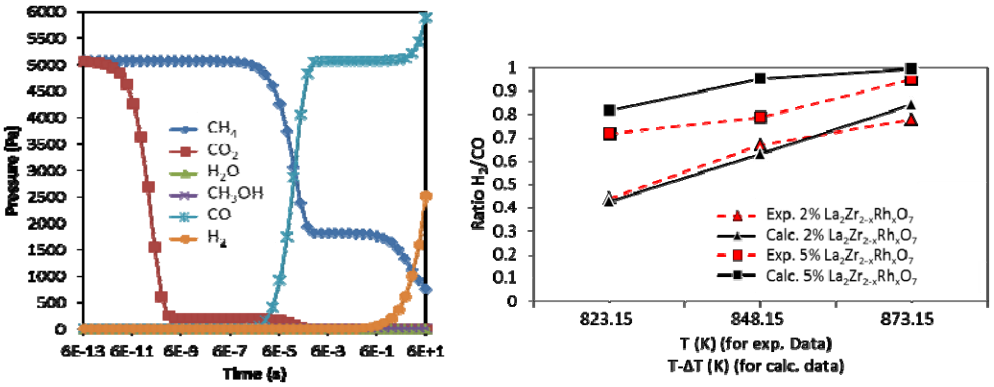

a) b)

Fig. 2 MKM outputs a) P vs. residence time in the modeled batch reactor at 823.15 K + $\Delta T_{correction}$, with $\Delta T_{correction}$ = 150 K. 2% LRhZ, b) Ratio H_2/CO vs. T. Calculated data correspond to a batch reactor after 1 min residence time. Experimental data from [3]

2 Conclusions

Our MKM model for a batch reactor successfully reproduces the experimental data for a plug flow reactor at different temperatures and a pressure of 1 atm and GHSV = 48,000 mL/g_{cat}/h, after 200 min time on stream. The model elucidates the reaction mechanism due to the pressure and coverage time evolution it outputs and furthermore it allows to quantitatively evaluate the influence of different operating conditions. DFT calculations are being performed to find what additional dopant would reduce the activation barrier for CHO dehydrogenation and then the MKM will be used to predict the net effect on the H_2/CO ratio. This catalyst will be then synthesized, characterized and tested.

Acknowledgements

This material is based upon work supported as part of the Center for Atomic Level Catalyst Design, an Energy Frontier Research Center funded by the U.S. Department of Energy, Office of Science, Office of Basic Energy Sciences under Award Number DE-SC0001058.
We acknowledge the Clemson University high-performance computing facility, The Palmetto cluster, for providing computational resources. We thank Dr. Rachel B. Getman at Clemson University for helpful discussions.

References

[1] S. Gaur, D. Haynes, J. Spivey, Applied Catalysis A: General 403, (2011) 142.
[2] A. Ashcroft, A. Cheetham, R. Jones, S. Natarajan, J. Thomas, D. Waller, S. Clark, Journal of Physical Chemistry 97, (1993) 3355.
[3] D. Pakhare, H. Wu, S. Narendra, V. Abdelsayed, D. Haynes, D. Shekhawat, D. Berry, J. Spivey, Applied Petrochemical Research 3, (2013) 117.
[4] D. Pakhare, V. Schwartz, V. Abdelsayed, D. Haynes, D. Shekhawat, J. Poston, J. Spivey, Journal of Catalysis 316, (2014) 78.

I-PP61

Catalytic Conversion of Low Molecular Alkanes with C-C Bonds Formation

Abasov S.I., Isayeva E.S., Babayeva F.A.*, Agayeva S.B., Starikov R.V., Tagiyev D.B.

The Azerbaijan NAS Institute of Petrochemical Processes, Baku, Azerbaijan

* feridan@rambler.ru

Keywords: methane, propane, benzene, alkylation, isomerization, catalyst

1 Introduction

Reactions proceeding between low molecular (C_1-C_4) alkanes with new C-C bonds formation are paid much attention lately. These are non-oxidizing methane aromatization, benzene -propane dehydroalcylation and bimolecular n-butane isomerization. Mechanisms of these reactions are not clear enough and require further researches. This report comprises the results of our studies in this field.

2 Experimental

Objects of the study were bimetal-alumina catalysts prepared by adsorptive treatment, sulfated zirconia and their mechanical mixtures with H-form of zeolites.

The samples testing were carried out by studying reactions involving the C-C bonds formation in the methane-propane and benzene-propane alkylation, as well as bimolecular isomerization of n-butane, n-hexane, and mixtures thereof.

Experiments were carried out in a flow reactor at 150-400ºC, atmospheric pressure and GHSV 350-1500 h^{-1}. The state of supported metals was characterized by diffusive reflection IR spectra of adsorbed CO as a test molecule. The role of acidic sites in the reactions was studied by selective poisoning of catalysts with ammonia.

The reaction products were analyzed by gas chromatography.

3 Results and discussion

Studies of CH_4: C_3H_8 (1: 1) mixture conversion over unreduced bimetal-alumina catalysts (see table) shown those activity in aromatization of the mixture. Products yields and distribution are temperature-dependent. As is seen from the tab.1, lower temperature facilitates an increase in yields of alkylbenzenes and C_{4+} hydrocarbons.

Lowering the temperature promotes the formation of propene and outgoing of methane, moreover methane consumption and C_{4+} hydrocarbons yields pass through a maximum. This indicates the methane involvement to the propane alkylation.

The methane substitution to benzene and application of H-form zeolites as an acid catalysts allow obtaining isopropylbenzene at 180-200ºC (see fig.). Strict hydrogen reducing of bimetal-alumina catalyst leads to irreversible catalyst deactivation during iso-C_{4+} and cumene formation. Such loss of the samples activity indicates the participation of the catalyst inner oxygen in the C-C bonds formation between those molecules.

Table1. Conversion of CH_4:C_3H_8=56:44 (%C) +10 vol.% N_2 over Ni,Cu/Al_2O_3 catalyst; GHSV=1400 h^{-1}; τ=20 min.

Temperature, °C	**500**	**550**	**600**	**650**	**680**
Conversion,%					
CH_4	1	3	2	-	-
C_3H_8	8	10	20	28	34
Contact gas,%C					
CH_4	55	53	54	58	61
C_2	2	2	4	9	12
C_3H_6	12	7	5	2	-
C_3H_8	25	27	18	19	15
i-C_{4+}	3	5	11	2	-
ArH	-	-	1	5	8
ArH composition, %C					
C_6H_6	-	-	23	63	82
C_7H_8	-	-	59	30	16
ΣC_{8+}	-	-	18	7	2

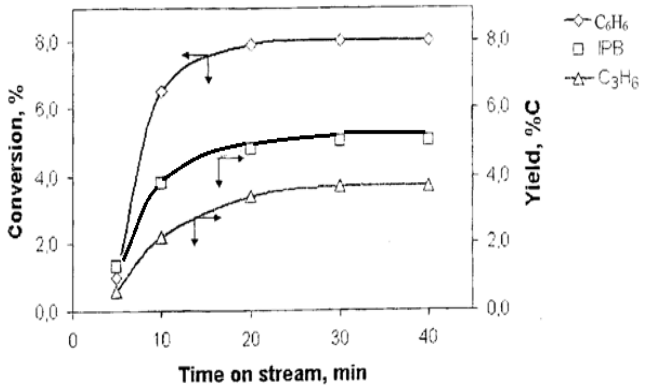

Fig. Benzene conversion and IPB and C_3H_6 yield on MC PRAC as a function of an experiment time. T=200°C, GHSV=500h^{-1}; C_6H_6:C_3H_8=1:9; MC PRAC +HM

Study of the low temperature isomerization of n-butane, n-hexane and mixtures thereof over Ni / MOR-SO_4^{2-}/ZrO_2 found that they are characterized by the higher weighted alkanes formation in contrast the original molecules (tab.2).

Table 2. Conversion of n-C_4H_{10} and n-C_6H_{14} (1:1 mole) over Ni/MOR/SO_4^{2-}/ZrO_2 H_2:CH=3:1; $T_{hydrotreatment}$=350º;GHSV=350ч$^{-1}$

Temperarute, ºC	**Conversion,* %**		**Selectivity, %**		
	n-C_4H_{10}	n-C_6H_{14}	C_1-C_3; n-C_5	i-C_4-C_6	C_7
120	18(12)	32(35)	6	64	30
170	60(32)	65(86)	49	73	18
220	88(67)	92(95)	37	59	4

This can be explained by bimolecular formation and decomposition of intermediates. SO_4^{2-}/ZrO_2 systems are known to be characterized by the presence of uncompensated positive charges that exist in the bimetal-alumina systems. Taking these into account the activation of C-C bonds formation in the studied reactions can be explained by the valence unsaturated oxygen atoms appeared in the catalytic systems, which are stabilized by pulling hydride ions from lower alkanes molecules, Based on these results a possible mechanism for the new C-C bonds formation in the studied reactions is proposed.

I-PP62

Innovative Development of Refining Sector in Azerbaijan

Asgar-Zadeh S.M.[1*], Urban O.B.[1], Javadova M.N.[1], Eldarova S.G.[1], Khudiyeva I.E.[1], Alkhasli E.A.[2], Mammadov N.A.[1]

1 - Institute of Petrochemical Processes, National Academy of Sciences of Azerbaijan, Laboratory of Complex Refining of Petroleum and Technical and Economic Researches, Baku, Azerbaijan
2 - State Oil Company of Azerbaijan Republic, SOCAR's Oil Gas Processing and Petrochemical Complex, Baku, Azerbaijan

* askerzade.saadet@gmail.com

Keywords: integration, refining, petrochemicals, refining complex, combining production, feasibility

1 Introduction

As far as the globalization of its trade and economic connections is concerned, Azerbaijan, enjoying its vast energy resources, is increasingly involved in integration processes worldwide, including those in the fuel and power sector, which is progressing in four directions: oil and gas production - refining - gas processing - petrochemicals, and is determined by a harmonic combination of adjacent industries. The decisive link in this particular chain is refining.

As a result of national economy integration into the global system, the oil industry situation is a direct consequence of global oil market prices, and amounts of oil export are defined by the capacity of domestic market and development of refining facilities. If refining industry lags behind, the involuntary export of crude and semi-products increases.

The analysis of global refining trends and market structure gives clear evidence that in conditions of unstable global energy prices and growing cost of produced resources the national economy is short to sustain itself and progress based on natural resources alone. So it comes necessary to develop conversion industries, refining and petrochemicals among them, even more so because external loans and investments cannot solve all national problems, and budget resources are not infinite.

The strategic importance of refining sector made it necessary to develop an oil strategy that has underlain the entire oil industry, refining included. Such strategy, developed in the Republic of Azerbaijan under the supervision of Heydar Aliyev, has been implemented with success.

2 Experimental/methodology

The strategy builds upon the increasing efficiency of the oil industry; it stipulates the gradual replacement (diversification) of crude export with export of high added value petroleum / petrochemical products.

The Institute of Petrochemical Processes has for many years conducted researches dedicated to developing such integrated crude refining strategy that would boost the efficiency of each individual facility and the industry as whole; these researches are targeted to set up the basis for the full-through development of the national refining industry. This plan is based on wide-scale innovations and investments that are necessary for profound modernization of the industry and development of the domestic market.

The complex refining schemes have been developed with consideration of features of Azerbaijani crudes, energy and petrochemical infrastructure, internal petroleum demand and export capabilities, prospective requirements for products with an account of environmental and economic imperatives on which a facility and market operates and structures itself.

Considering the advantage of converting crude to finished petrochemical stock, we have developed several options of integrated petrochemical industry development. To that end, both petrochemical industry development options have been studied:

- independently at petrochemical facilities, with reviewing issues of supplying feedstock to

steam crackers (gases (natural and associated) and naphtha from a refinery;

- directly at a refinery through integration between refining and petrochemical production.

3 Results and discussion

The pyrolysis unit efficiency increase and effective feedstock supply shall be attained through integration of refining, gas processing and petrochemical industries. On the other hand, integration with petrochemicals boosts the efficiency of the very oil refining. We can state an example of boosting the quality of gasolines via oxygenates ex petrochemical plant, or producing semi-synthetic oils by oil fraction alkylation with alpha-olefins plus implementing hydrocracking within the complex, which helps ramp up the resources and improve the diesel fuel quality; thus being said, it should be also noted that introduction of such hydrocracker at refineries is limited due to its high energy and capital consumption and hydrogen flow rate.

Implementing both options at the same time, we can optimize hydrocracking process in terms of CAPEX and capacity of both steam cracker and lube base oil unit. Therefore, integration between refining and petrochemicals is a win-win.

The increasingly stringent requirements for product quality call for additional conversion using costly hydrogenation processes, HC among them, which operate in severe pressure / temperature conditions, as well as new catalysts and process systems. Naturally, this results in increased refining cost and does not always solve the problem. In order to make the production of environmentally friendly petroleum products at constant market prices for oil and products profitable for a producer, we made a technoeconomic assessment of each individual process and the facility as whole when developing the said complex schemes. The technical and economic analysis has shown that such project could be feasible if hydrocracking would be used as a feedstock for SC or to produce highly viscous lubes (VI > 120).

4 Conclusions

The technoeconomic analyses of complex schemes have established that the plant integration and modernization of conversion scheme help significantly reduce operating costs, while the margin jumps 2 to 3 times compared to split crude refining at refineries and petrochemical facilities.

The study made on the premises of refining 10 MTA of crude and processing 10 BCMA of gas established that the maximum IRR of a refinery is 15-17%, while in refining-petrochemicals integration scenario it rises to 25%, and to 35% if gas processing is integrated with refining and petrochemicals.

References

[1] Гайдук И., Тенденции развития мировой нефтехимии, *Нефтегазовая вертикаль.* 17 (2001).
[2] Рустамов М.И., Аскер-заде С.М., Перспективы развития нефтеперерабатывающей промышленности Азербайджана, *Азербайджанское нефтяное хозяйство.* 14 (2008).
[3] Брагинский О., *Нефтехимический комплекс мира*, М.: Academia. (2009).
[4] В.В. Бушуев, В.А. Крюков, В.В. Саенко, *Нефтяная промышленность России – сценарий сбалансированного развития*, М.: ИД Энергия, (2010).
[5] Аскер-заде С.М., Хыдыров Б.С. и др. Энергообеспечение нефтеперерабатывающих заводов Азербайджана, *ХТММ*. 5 (2009).
[6] Рустамов М.И., Аскер-заде С.М. и др. Интеграция нефтеперерабатывающих Предприятий, *Химическая Техника*. 7 (2011).

I-PP63

Application of Tubular Reactor or High-Performance Fischer-Tropsch Synthesis

Yakovenko R.E.*, Narochnui G.B., Savost'yanov A.P.

Platov South-Russian State Polytechnic University (NPI), Novocherkassk, Russia

* jakovenko@lenta.ru

Keywords: Fischer-Tropsch synthesis, tubular reactor, heat transfer, heat-exchange coefficient

1 Introduction

In this paper, the process of heat transfer, as well as the necessary conditions for conducting high-FT process in a tubular reactor, while maintaining a quasi-isothermal mode of operation.

2 Experimental

Heat transfer is the main factor which obstructs creation of high-performance Fischer-Tropsch synthesis (FTS) by reason of high exothermicity of the process, although activity of modern FTS catalysts allow to perform the synthesis at high gas volume rates (3000-5000 h^{-1}) [1,2]. Therefore two ways are applied for intensification of the FTS. The first way supposes improvement of apparatus design (application of tubular reactors, three-phase reactors, slurry and fluidised reactors), while the second way comprises fluid-dynamic refinement [3].

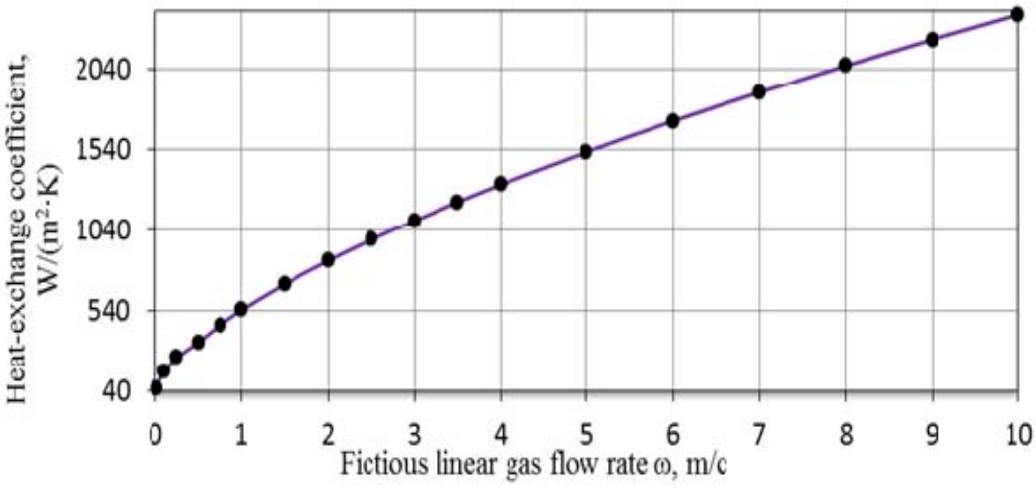

Fig. 1. Dependence of heat-exchange coefficient from fictious linear gas flow rate in tubular reactor

Heat-exchange coefficients required for distinguishing maximal conversion of CO and maintenance of stable temperature regime were calculated for reactor tubes of different diameters (20-50 mm) at gas volume rates (GVR) from 1000 to 5000 h^{-1} (see Table and Figure 2).

Table. Hydrodinamic parameters required for maintenance of quasi-isothermal regime in tubular reactor

GVR, h^{-1}	Heat-exchange coefficient, $W/(m^2 \cdot K)$	Required fictive gas rate, m/s
1000	500	1,0
2000	1000	3,0
3000	1500	5,0
4000	2000	8,0
5000	2500	>10,0

3 Results and discussion

The next parameters were applied for calculations: syngas composition (% vol.) – CO – 33, H_2 – 67; temperature – 200 °C; pressure – 2,0 MPa; catalyst particles diameter – $2{,}5 \cdot 10^{-3}$ m; porosity – 0,4. Heat-exchange coefficients were calculated by the known method [4], physical-chemical properties of reaction media were calculated by the "Technologist" software by using Peng-Robinson thermodynamic package [5].

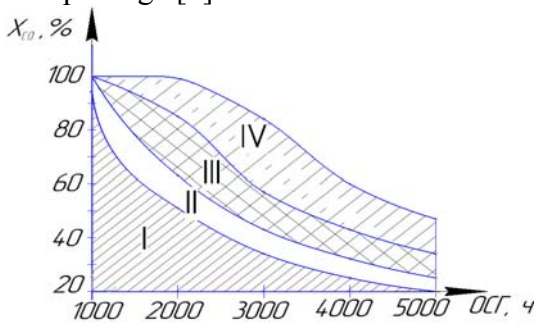

Fig. 2. Dependence of maximal conversion of CO (X_{co}) from gas volume rate at quasi-isothermal regime in tubular reactor for various diameter tubes: I – 50 mm; II – 40 mm; III – 30 mm; IV – 20 mm

4 Conclusions

Our study revealed that application of tubular reactor for the high-performance FTS is possible only at specific hydrodynamic regimes.

References

[1] LeViness S., Deshmukh S., Richard L., Robota H. // Top Catal. 2014. Vol. 57. P. 518-525.
[2] Koortzen J., Bains S., Kocher L., Baxter I., Morgan R. // Ind. Eng. Chem. Res. 2014. Vol. 53. P. 1720−1726.
[3] Savostyanov A.P., Narochnui G.B., Zemlyakov N.D., Jakovenko R.E., // The Samara Scientific cent of the Russian Academy of Sciences, 2010, V.12, № 4(3), P. 686-690.
[4] Aerov M., Todes O.M. Hydraulic and thermal basics of vehicles with fixed and fluidized granular layer. – L.: Chemistry, 1968. - 512 P.
[5] Program " Fizkhim " PPP "Tekhnolog", OOO "Tekhnosoft-kompyuternyi tsentr", Moskva.

I-PP64

Ethanol Steam Reforming on a Structured Heat-Conducting Catalytic Package: Modelling and Experimetal Perfomance

Sadykov V.[1,2], Bobrova L.[1*], Vostrikov Z.[1], Vernilovskaya N.[1,2], Mezentseva N.[1,2]

1 - Boreskov Institute of Catalysis SB RAS, Novosibirsk, Russia
2 - Novosibirsk State University, Novosibirsk, Russia

* lbobrova@catalysis.ru

Keywords: ethanol reforming, structured catalyst, Fechraloy microchannel plates, Ru+Ni/SmPrCeZrO

1 Introduction

Structured catalysts with active components supported on ceramic or metallic substrates are attractive for generation of hydrogen/syngas from biofuels in the compact reformers [1-3]. Due to a good thermal conductivity of metal substrates, formation of cool spots within the structured reactor leading to coking can be prevented [2]. In this work, experimental and numerical studies of ethanol steam reforming (ESR) over a structured package consisted of five stacked microchannel corundum – protected Fechraloy plates covered with a layer of Ni+Ru/$Sm_{0.15}Pr_{0.15}Ce_{0.35}Zr_{0.35}O_2$ active composition have been performed.

2 Experimental/methodology

The microchannel Fechraloy plates (20*50*1.5 mm, one side flat, one side with 15 channels of 0.4 mm depth provided by IMM, Germany) were protected by supporting a thin (5–10 μm) corundum sublayer by detonation spraying [2]. $Sm_{0.15}Pr_{0.15}Ce_{0.35}Zr_{0.35}O_2$ (SmPrCeZrO) oxide synthesized by Pechini route was promoted by 2% Ru+2%Ni supported by the incipient wetness impregnation using acetone solution of binuclear Ru-Ni nitrocomplex. Ru+Ni/SmPrCeZrO (4 wt.%) was supported on plates by slip casting slurries in isopropanol with polyvinyl butyral followed by drying and calcination under air at 700°C for 2 h. A structured packing consisted of five plates was tested in ESR at 500 - 900°C in concentrated feeds with the gas flow rate up to 2 m^3/h using a pilot reactor and earlier described procedures [2]. Kinetic modeling was carried out by using a pseudo-homogeneous plug-flow reactor model and a step-wise reaction scheme described in [2].

3 Results and discussion

A power-law kinetic model with effective parameters was proved to be quite sufficient to simulate reaction behavior under experimental conditions:

$$r_I\left[\frac{mol}{m^2\cdot s}\right]=k_I\cdot x_{Eth} \quad (1)$$

$$r_{II}\left[\frac{mol}{m^2\cdot s}\right]=k_{f,II}\cdot x_{CH_4}^{\alpha_{II}}\cdot x_{H_2O}^{\beta_{II}}\cdot\left[1-\frac{Q_{II}}{K_{eq,II}}\right],\ \text{where}\ Q_{II}=\frac{p_{CO}\cdot p_{H_2}^3}{p_{CH_4}\cdot p_{H_2O}}; \quad (2)$$

$$r_{III}\left[\frac{mol}{m^2\cdot s}\right]=k_{f,III}\cdot x_{CO}^{\alpha_{III}}\cdot x_{H_2O}^{\beta_{III}}\cdot\left[1-\frac{Q_{III}}{K_{eq,III}}\right],\ \text{where}\ Q_{III}=\frac{p_{CO_2}\cdot p_{H_2}}{p_{CO}\cdot p_{H_2O}}; \quad (3)$$

$$r_{IV}\left[\frac{mol}{m^2\cdot s}\right]=k_{f,IV}x_{CH_4}^{\alpha_{IV}}\cdot x_{H_2O}^{\beta_{IV}}\cdot\left[1-\frac{Q_{IV}}{K_{eq,IV}}\right],\ \text{where}\ Q_{IV}=\frac{p_{CO_2}\cdot p_{H_2}^4}{p_{CH_4}\cdot p_{H_2O}^2}. \quad (4)$$

Here, x_i and p_i are mole fractions and partial pressures (atm) of components in reactions of ethanol decomposition into CH_4 , CO and H_2 (1) followed by the reversible reactions of steam reforming (2), water-gas shift (3) and complex shift reaction $CH_4+2H_2O \leftrightarrow 4H_2+CO_2$ (4); Q_r reflects the reaction approach to equilibrium. Isothermal reactor model was applied.
Figure 1 compares the temperature dependences of experimental data with equilibrium values and those predicted by kinetic modelling with optimized kinetic parameters.

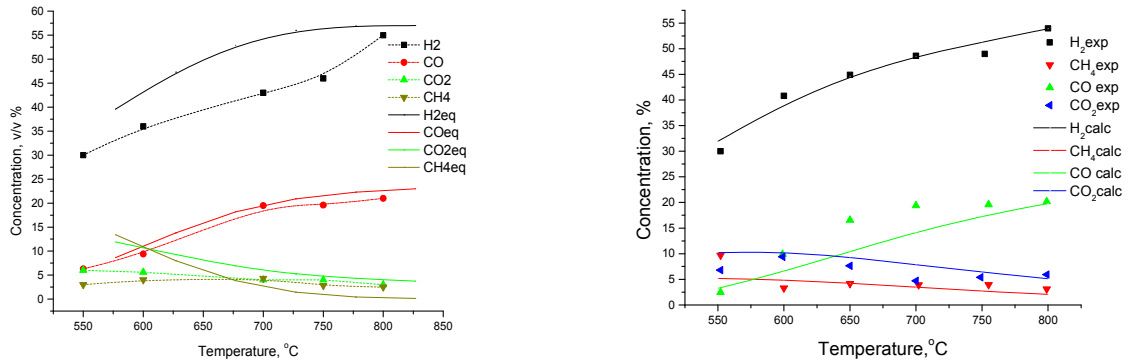

Fig. 1. Temperature dependencies of products concentration for ESR over structured package. Experimental data versus equilibrium (left) or calculated by modeling (right) values. Feed 30%EtOH+60%H_2O+N_2, contact time 0.3 s.

At high temperatures, concentrations of products approach the equilibrium level, while at lower temperatures H_2 concentration is lower due to both incomplete conversion of ethanol as well as the presence of such by-products as C_2H_4 and C_2H_6, their maximum content at 600 °C being equal to 3% and 1%, respectively. The simple reactor and kinetic models proposed in this work provide a good description of the experimental data, thus demonstrating efficient heat and mass transfer within catalytic package not limiting the catalyst performance.

4 Conclusions

The structured package comprised of five stacked microchannel corundum – protected Fechraloy plates covered with a layer of Ru+Ni/SmPrCeZrO active component has demonstrated a high performance in the ethanol steam reforming at the pilot scale. At intermediate (600-800°C) temperature range and high reagent concentrations, a high syngas yield close to equilibrium was obtained. The numerical study of the performance of the structured reactor on the base of step-wise reaction scheme with effective parameters provides a good description of the experimental data, thus demonstrating efficient heat and mass transfer within the package of microchannel catalytic plates.

Acknowledgements

Support by Russian Fund of Basic Research Project RFBR-CNRS 12-03-93115 and FP7 BIOGO Project is gratefully acknowledged.

References

[1] G. Groppi, E.Tronconi, Catal. Today 105 (2005) 297-304
[2] V. Sadykov, V. Sobyanin, N. Mezentseva et al, Fuel 89 (2010) 1230–1240
[3] E. López, N. J. Divins, A. Anzola, S. Schbib, D. Borio, J. Llorca, Int. J. Hydrogen Energy 38 (2013) 4418-4428

I-PP65

Catalytic Hydrodeoxygenation of Microalgae Biodiesel over Sulfur-Free Nickel Supported Catalyst for the Production of Biofuels

Hachemi I.*, Mäki-Arvela P., Kumar N., Murzin D.Yu.

Åbo Akademi University, Turku, Finland

* imane.hachemi@abo.fi

Keywords: hydrodeoxygenation, catalysis, nickel, chlorella microalgae, green diesel

1 Introduction

Production of sustainable energy is receiving more and more attention in the last decades. The concern about available resources has increased the interest in developing second generation biofuels from non-food feedstock as microalgae, which is highly advantageous and offers potentially great opportunities in biofuels production. From cultivation until processing, microalgae posses many advantages compared with the land feedstock [1].

A number of problems associated with the high oxygen content in fatty acids raw materials requires an upgrading step. Hydrodeoxygenation (HDO) has become a practical alternative method for the production of green diesel. In view of the foregoing, non-precious metal catalysts comprising supports other than carbon, particularly Ni on oxidic supports and hydrotalcite materials are beginning to attract attention as feasible catalysts for the conversion of lipids into fuel-like hydrocarbons via deCOx [2-6].

2 Experimental/methodology

Catalysts containing nickel supported on H-Y zeolites were synthetized by the wet-evaporation impregnation method. These materials were studied as sulfur-free catalysts for the production of green diesel. The catalytic HDO of fatty acids was performed in a semi-batch reactor at 300 °C under a total pressure of 30 bar using dodecane as a solvent. In a typical experiment 1 g of the substrate diluted in 100 ml of dodecane was injected along with 0.25 g of the catalyst with a particle size lower than 63 μm. Prior to an experiment and before injection of the deoxygenated liquid into the reactor, the catalyst was reduced at the temperature obtained from TPR. Several characterization methods were considered in order to determine the synthesized catalyst physicochemical properties. The characterization included BET, SEM, EDXA, TEM, TGA, TPR, NH_3-TPD and CO_2-TPD.

Chlorella microalgae (Fuqing King, Drarmsa Spirulina Co, Ltd, China) was used as a source of fatty acids methyl esters (FAME) in the HDO experiment. This latter was obtained from transesterification of dry algae using 20 wt% H_2SO_4 as a catalyst for 4 h at 60°C. Chlorella microalgae crude oil contains a mixture of saturated and unsaturated methyl esters plus a small fraction of acids. The composition of the saturation order of FAME is illustrated in Table 1.

Table 1. Composition of fatty acids methyl esters in *Chlorella* microalgae.

Components	Mols (%)
Unsaturated FAME	34
Saturated FAME	62
Saturated Acids	1
Unsaturated acids	3

3 Results and discussion

Nickel impregnation over H-Y zeolites permitted the preparation of a nanoparticle catalyst. TEM images show the Ni particle distribution with 4 nm as an average particle diameter (Figure 1). The metal particle size plays a major role in the HDO reaction, the small particle size facilitates a high initial catalytic activity and a high uniformity ensures high catalyst stability [7].

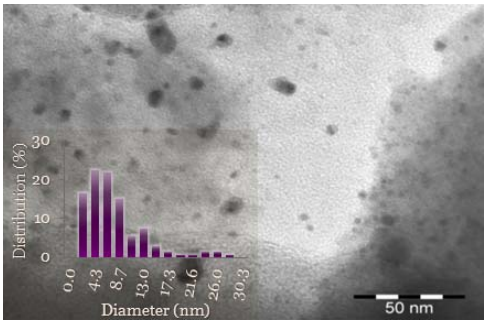

Fig. 1. TEM micrograph and metal particle distribution

Nickel supported materials were shown to be promising catalysts in the HDO of fatty acids, able to realize quantitative transformation of FAME into diesel-range alkanes as high-grade second generation biofuels under mild conditions. The conversion was moderately rapid with a total conversion attained in approximately 120 minutes, under mild operating conditions, yielding aliphatic hydrocarbons. Table 2 illustrates the yields and selectivities obtained after 6 hours of HDO of FAME over 5 wt% Ni/H-Y.

Table 2. Yield and selectivity after 6 hours of hydrodeoxygenation of fatty acids methyl esters with 94% conversion level.

	Yield (%)				Selectivity (%)				
Product	C15	C16	C17	C18	C15	C16	C17	C18	Saturated acids
FAME	14	30	19	31	14	30	19	32	4

4 Conclusions

Ni nanoparticles prepared by the wet impregnation method were investigated in the catalytic hydrodeoxygenation of fatty acids methyl esters derived from *Chlorella* microalgae. The obtained results proved the efficiency of Ni supported on H-Y zeolites in producing diesel-range hydrocarbons. This catalyst has a very interesting catalytic activity as it does not require the addition of sulfur and further purification of the products. Moreover, it was noticed that the reaction follows both hydrodeoxygenation and hydrodecarboxylation paths allowing the production of hydrocarbons with the same carbon chain as the reacting ester and one carbon shorter hydrocarbons.

References

[1] T. Shirvani, Applied Petrochemical Research, 2, 2012, 93–95.
[2] H. Zuo, Q. Liu, T. Wang, L. Ma, Q. Zhang, Q. Zhang, Energy Fuels 26, 2012, 3747–3755.
[3] B. Peng, X. Yuan, C. Zhao, J.A. Lercher, J. Am. Chem. Soc. 134, 2012, 9400–9405.
[4] Y. Yang, C. Ochoa-Hernández, V. A. de la Peña O'Shea, J. M. Coronado, D. P. Serrano, ACS Catal. 2, 2012, 592–598.
[5] B. Peng, Y. Yao, C. Zhao, J.A. Lercher, Angew. Chem. Int. Ed. 51, 2012, 2072–2075.
[6] E. S. Jimenez, T. Morgan, J. Shoup, A. E. H. Ware, M. Crocker, Catalysis Today 237, 2014, 136–144.
[7] W. Song, C. Zhao, J. A. Lercher, Chem. Eur. J., 19, 2013, 9833 – 9842.

I-PP66

Application of the Dioxo-Mo(VI) Complex Anchored on a TiO_2 in the Oxidation of DDT with Molecular Oxygen, under UV-Irradiation

Manucharova L.A.*, Bakhtchadjian R., Tavadyan L.A.

Nalbandyan Institute of Chemical Physics, National Academy of Sciences of the Republic of Armenia, Yerevan, Republic of Armenia

* loriettam@yandex.ru

Keywords: catalytic oxidation, dioxo-Mo(VI)complex, DDT, UV-irradiation

1 Introduction

Dioxo-Mo(VI) Complexes, bearing organic ligands, exhibit an oxidative capacity towards a great number of the organic compounds of the different classes (hydrocarbons, alcohols, phosphines, etc.). In the presence of the oxidant agents (such as O_2, H_2O_2, O_3 and others), enable to re-oxidize the reduced metallic centers of the complex, these reactions become catalytic. As show the investigations in recent years, the catalytic activity of these complexes rises under UV-irradiation or visible light, when they are supported on the solid surfaces or anchored on the solid matrix by chemical bonds[1].

In the present work the feasibility of the catalytic activity of dioxo-molybdenum(VI)-dichloro [4,4′-dicarboxylato-2,2′-bipyridine], anchored on TiO_2 has been tested in the oxidation reaction of DDT (1,1,1-Trichloro-2,2-bis(4-chlorophenyl)ethane) with molecular oxygen, under UV-irradiation (λ= 253.7 nm), in acetonitrile solution. DDT is a persistent organic pollutant, the direct catalytic transformation or degradation of which with O_2 by chemical methods, in our knowledge, is not known. In chemical industry the oxidation of DDT to dicofol usually is performed as a multistep process including: elimination of HCl from DDT; chlorination of DDE (1,1-bis-(4-chlorophenyl)-2,2-dichloroethene) to tetramer (dichloro diphenyl tetrachloro ethane); hydrolysis of tetramer to dicofol by para-toluene sulfuric acid). Unfortunately, the AOP technologies, successfully applied for the purification of wastewater, for several reasons, are not completely applicable in a large scale chemical transformation of DDT to dicofol.

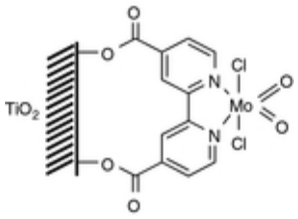

2 Experimental

The dioxo Mo-complex was fully characterized by different methods, including ^{13}C CAP NMR[2] spectroscopy. The experiments were carried out by a special protocol. Each experimental cycle was consisted of two consecutive periods: in the first period the reaction mixture (a suspension of DDT in acetonitrile, containing the anchored complex) was exposed under UV-irradiation in stirring conditions, in argon atmosphere and in the absence of molecular oxygen during about 6-7 h. Then, in the second period, the aim of which was the re-oxidation of the reduced metallic centers ($Mo^{IV} \rightarrow Mo^{VI}$), was kept without UV-irradiation and in the presence of molecular oxygen (2-2,5 h). Before the beginning of a new experimental cycle, dioxygen was thoroughly removed from the reaction mixture.

3 Results and discussion

The results show a significant increase of the consumption of DDT in the course of the first

periods of the experimental cycles in the presence of the anchored complex in comparison with the results on the "pure" TiO2 (absence of the complex). As a result of 4 consecutive experimental cycles, the amount of the consumed DDT reaches up 35% for 30h, while in the absence of the anchored complex on the "pure" TiO_2 surface, even in two time more amounts in the reaction media, it is about 13%.

In the same time, the turnover number, calculated as Δ[DDT] / [anchored complex], increases about 5.7 times becoming 3,7 for 32 h. These facts indicate the catalytic role of the anchored complex in the reaction.

The reaction products include a great number of the chlorinated and non-chlorinated organic compounds (C_2-C_{14}), as well as the products of the complete destruction of DDT, such as CO_2, H_2O, HCl. Taking into account the results of the chromatographic analyses (GC-MS) and overall amounts of Cl^- ions, determined by chemical methods, the amounts of the completely dechlorinated products are estimated as 45-47% and, correspondingly, 53-55% the partially dechlorinated or non-dechlorinated organic compounds.

The main product of the reaction is dicofol, the maximal yield of which is about 21%. The results of the chosen experimental protocol permits to conclude that the formation of dicofol, apparently, occurs via a transfer of the oxo-atom from the anchored Mo-complex to the bibenzylic carbon-atom of DDT

$$(ClC_6H_4)_2C(H)CCl_3 + O{=}Mo^{VI}(O)(Cl_2)|[L]/TiO_2 \rightarrow (ClC_6H_4)_2C(OH)CCl_3 + \\ + Mo^{IV}(O)(Cl_2)[L]/TiO_2 \quad (1)$$

where, L is 4,4′-dicarboxylato-2,2′-bipyridine ligand.

The periodical re-oxidation of the reduced complex ($Mo^{IV}(O)(Cl_2)[L]/TiO_2$) , with molecular oxygen in the "dark" reaction in the second periods of the experimental cycles may occur by the formation of oxo-peroxo moieties in Mo(VI) complexes:

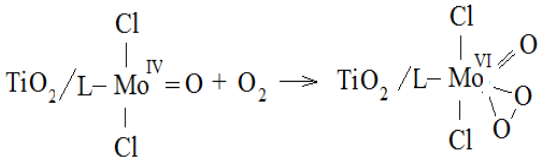

(2)

Due to the reaction (2), the amount of oxygen atoms enable to oxidize DDT (or other compounds present in the reaction mixture) may be doubled in comparison with that in the initial complex. As show the experimental data, the consumed amounts of DDT nearly are doubled, and, at the same time, the yield of dicofol is increased about 1.5 times in the first period of the second experimental cycle, after the "dark" reaction in the first experimental cycle.

The second main product of the reaction DDE (1,1-bis-(4-chlorophenyl)-2,2-dichloroethene (yield 9%) may be formed from DDT or dicofol by different channels, probably, involving also reactions of OH or HO_2 radicals, photogenerated on the TiO_2, under UV-irradiation[3]. Other reaction products, contain the chlorinated and non-chlorinated compounds not only of the oxidative decomposition (4,4'-dichlorobenzophenone (DBP), CO_2, H_2O, H^+ and Cl^- ions), but also of the reductive decomposition (DDD (1,1-dichloro-2,2-bis(p-chlorophenyl)ethane), DDM (2,2-(bis(p-chloropheny)-methane, 1,1-diphenyl methane, in overall amounts about 13-14%).

Apparently, the complex mechanism of the overall reaction include a combination of the primary oxo- or peroxo-atom transfer to DDT with a number of the further free-radical reactions. In any case, the feasibility of the direct photocatalytic oxidation of DDT with molecular oxygen opens an attractive opportunity for the elaboration of an alternative method of the oxidation of DDT in "mild" conditions, using the transition metal oxo-complexes, anchored particularly on the TiO_2 under UV- irradiation or visible light.

References

[1] H. Arzoumanian, R. Bakhtchadjian. *Chemical Journal of Armenia*, 65 (2), 2012, p.168-188.

[2] R. Bakhtchadjyan, S. Tsarukyan, J. Barrault, F. Matinez, L. Tavadyan, N. Castellanos. *Transition Metal Chemistry*, 36 (8), 2011, p. 897-900.

[3] B.Yu, J.Zeng, L.Gong, X.Yang, L.Zhang. X.Chen. *Chines Science Bulletin,* 53(1), 2008, p. 27-32.

I-PP67

Petroleum-Saturated Sands of Azerbaijan

Samedova F.I.*, Gasanova R.Z., Logmanova S.B., Badavi Y.E.

Institute of Petrochemical Processes named after acad. Y.H.Mamedaliyev, Azerbaijan NAS, Baku, Azerbaijan
** lab.21@mail.ru*

Keywords: alternative source, refining, hydrocarbon feedstock, bituminous sands, Kirmaky, basis, oil

1 Introduction

In the IPCP Azerbaijan National Academy of Sciences research on the rational use of oil-saturated earth of Azerbaijan to produce valuable petroleum products, including base oils, has been carried out.

By the method of solvent extraction from oil-saturated sand deposits of Balakhany and Mashtaga organic part was isolated, which has a high density (1143.9 kg/m^3 at 20ºC), high resin-asphaltene substances (14.2%) and low (0.906) paraffin contents. It contains Ni; Fe; Zn; Mn; Cr; Mg; Pb; Co, etc.

The problem of rational refining of the alternative sources of heavy and superheavy hydrocarbon feedstock becomes progressively urgent one. The sources for obtaining hydrocarbon feedstock are oil-bearing shales, bituminous sands, etc. The world reserves, for instance, of oil-bearing shales are estimated to be 2-3 tril. tons.

The investigations have been carried out to evaluate the properties of Azerbaijan bituminous sands of Kirmaky deposit. From the bituminous sand with extraction method there has been isolated an organic part.

As a result of the fractionation of extraction products and compounding following narrow fractions of oil products were obtained, % (w): boiling up to 180°C - 13; 180-240°C – 7.5; 240-350°C – 4.3; 350-500°C - 32.6; above 500°C - 42.6. These yields and qualities are similar to those of analogical fractions of heavy Balakhany oil except oil fraction viscosity index, which is 44 instead of 14.4 from the natural oil.

The product from petroleum-saturated sand features by high content of asphalto-resinous substances and low content of paraffin; from it the narrow fractions boiling up to 300, 300-500 and above 500°C have been isolated.

2 Experimental/methodology

By catalytic processing of oil fraction, boiling at 350-500°C, in two stages with olefins in the presence of $AlCl_3$ the possibility of using this fraction as an alternative raw material for the base oil with viscosity index 80-97 units was revealed. However, this method of processing the oil-saturated earth energy consuming and environmentally unsafe because of the use of large amounts of toxic solvent.

A new method, has been worked out which provides oil-saturated earth hydroforming without prior separation of the organic part of it, which is loaded into the reactor of pilot plant and processed with flow of hydrogen.

3 Results and discussion

Fraction 350-500°C was compared with oily fraction from Balakhany heavy oil (BHO). The investigations showed that the product from bituminous sand in quality is close to oily fraction from Balakhany heavy oil.

The comparative data of quality of oily fractions from comparable feedstock are the following:

	From petroleum-saturated sands	from Balakhany heavy oil
Bailing range, °C	350-500	360-460
Yield on feedstock, %	27.7	25.43
Density at 20°C, kg/m^3	937.3	937.7
Viscosity, mm^2/s, at		
100°C	11.1	9.22
40°C	180.6	-
Viscosity index	25	8.5
Acid number, mg KOH/g	1.82	0.56
Pour point, °C	-10	-27
Refractive index, n^{20}_D	1.5245	-

The oily fraction from a product in the amount of 27.7%, on organic part has been subjected to furfurol (300 %) selective treatment and followed by aftertreatment with gumbrine. The residue by its properties corresponded to bitumen.

The investigations showed that selective treatment fails to improve viscosity-temperature properties of a product, its viscosity index remained at low level. Viscosity at 100°C is 10.5mm^2/s, it contained 11.8% methane-naphthenic, 88.72% aromatic hydrocarbons, including 9.3% resins.

The catalytic treatment of this product has been conducted with olefins in the presence of catalyst ($AlCl_3$). The process proceeded at 60°C, contact time 3 hours.

Then from the product of catalytic treatment there has been isolated by fractionation a fraction boiling at 350-450°C with yield 19.14% on product, its viscosity at 100°C was 4.62mm^2/s, viscosity index 28.

Fraction 350-400°C isolated from reaction product was subjected to catalytic retreatment with olefins. As a result an oil has been obtained with viscosity index 96.9. The analysis of group-hydrocarbon composition of an oil obtained showed that content of methane-naphthenic hydrocarbons in oil increased from 11.8% to 66.06%, aromatic hydrocarbons decreased from 88.20% to 33.94%. Simultaneously from the residue of reaction product boiling at above 350°C (with viscosity 57-61.7mm^2/s at 100°C) by catalytic retreatment with olefins the oil has been obtained with viscosity 34.9mm^2/s at 100°C and viscosity index 89.

There has been also studied the possibility for using light fraction from the product of reaction I step boiling up to 350°C (content of olefins in it ~45%) which in a mixture with fresh olefins has been used as olefin feedstock. Using mixture as olefins provided the obtaining oil with viscosity index 80, i.e. the possibility has been established for circulation of light fraction boiling up to 350°C in catalytic treatment process.

Thus, the organic part of bituminous sand has been used as the alternative feedstock for preparation of oil products including base oils with viscosity index 80-96.9.

4 Conclusions

The group composition of oil extracted from the earth after hydroforming is similar to that of oil fields in Azerbaijan. Processing of oil fraction of hydroformed crude oil can improve viscosity index of base oils up to 100 and above.

Thus, the methods of processing the organic part of oil-saturated earth were developed, which allow to get petroleum products, including base oils, with a high degree of saturation.

References

[1] Ф.И.Самедова, Г.Н.Наджафова, В.М.Алиева и др. *Азербайджанское нефтяное хозяйство*, 1995, №5-6, с.60-64.

[2] Ф.И.Самедова, Р.З.Гасанова, Алиева В.М. и др. Тезисы докладов IV Международной Конференции по химии нефти (Томск, сентябрь, 2006).

[3] Ф.И.Самедова, А.Д.Кулиев, Р.З.Гасанова, Н.З.Кадымалиева *Нефтепереработка и нефтехимия*, 2009, №3, с. 34-36.

[4] Ф.И.Самедова, А.Д.Кулиев, Р.З.Гасанова, В.И.Алиев *Мир нефтепродуктов*, 2011, №4, с.12-15.

[5] Ф.И.Самедова, А.Д.Кулиев, Р.З.Гасанова, Н.З.Кадымалиева *Пат. Азерб. a 20080143.09.07.2008*

I-PP68

Partial Oxidation and Dry Reforming of Methane to Synthasis Gas over Complex Oxide Cobaltate-Based Catalysts

Dedov A.G.[1*], Loktev A.S.[1], Komissarenko D.A.[1,2], Mazo G.N.[3], Shlyakhtin O.A.[3], Parkhomenko K.V.[2], Roger A.-C.[2], Mukhin I.E.[1], Lijiev M.M.[1], Moiseev I.I.[1]

1 - Gubkin Russian State University of Oil and Gas, Department of General and Inorganic Chemistry, Moscow, Russia

2 - Université de Strasbourg, Institut de Chimie et Procédés pour l'Energie, l'Environnement et la Santé, Strasbourg, France

3 - M.V. Lomonosov Moscow State University, Chemistry Department, Moscow, Russia

* genchem@gubkin.ru

Keywords: methane, partial, oxidation, dry, reforming, synthesis, gas, complex, oxide, cobaltates

1 Introduction

Synthesis gas production from natural and associated petroleum gases is important stage of global petrochemistry business [1]. Syngas is traditionally produced by highly endothermic steam reforming (SRM) of natural gas [2]. However, this process provides a high H_2/CO ratio (>3), which is not suitable for Fischer–Tropsch and methanol syntheses. Syngas with a more suitable H_2/CO ratio of 2 or lower can be produced via methane partial oxidation (POM) or by dry reforming of methane (DRM). Partial oxidation and CO_2 reforming of methane have the potential to reduce the cost of syngas and can be applied in solar energy storage and/or CO_2 utilization technologies [3]. Traditional Ni-supported catalysts for POM and DRM suffer from deactivation due to the coke formation or sintering processes. An alternative approach to catalyze POM and DRM is to use the perovskite-like oxides which can produce highly dispersed active metal particles under reduction environmental and prevent the coke formation and sintering processes.

2 Experimental/methodology

Perovskite-like materials - $Nd_{2-x}Ca_xCoO_4$ (x = 1 and 0.75) and $La_{2-x}Sr_xCoO_4$ (x = 1 and 0.75) were prepared by solid-state synthesis method. The samples were characterized by XRD, SEM, HRTEM and H_2-TPR before and after catalytic test. POM and DRM tests were carried out in a flow fixed-bed quartz reactor. Prepared materials were heated from room temperature to desired one under CH_4/O_2 or CH_4/CO_2 mixture. Also the tests with preliminary reduction step under pure H_2 were performed. The outlet gas composition was analyzed by online gas chromatography with TCD.

3 Results and discussion

Results of POM experiments revealed that for all the catalysts, the conversion of methane as well as the selectivity of CO/H_2 formation increases with temperature, whereas the selectivity of CO_2-formation decreases. In the case of $NdCaCoO_4$ CO selectivity was closed to 100% with CH_4 conversion was near 90%. CH_4 conversion and CO selectivity remained constant at least for 140h under the reaction stream [4] (figure 1). $NdCaCoO_4$ catalyst was also active in DRM process. CH_4 and CO_2 conversion achieved 96 and 93%, respectively, at W=14 $l*g^{-1}*h^{-1}$ and CH_4/CO_2 =1.1. The time on stream test over $NdCaCoO_4$ catalyst revealed that CH_4 and CO_2 conversions were constant at least for 30h (W=19-25 $l*g^{-1}*h^{-1}$; CH_4/CO_2 =1) (figure 1). The activity and selectivity of La-containing catalysts in POM reaction were found significantly lower. $La_{2-x}Sr_xCoO_4$ samples catalyzed mostly deep oxidation of methane to CO_2 and H_2O.

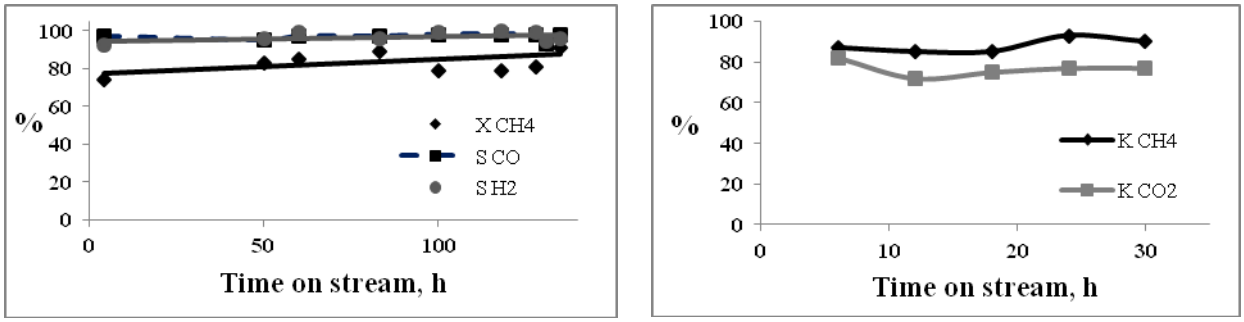

Fig. 1. Time on stream test over $NdCaCoO_4$: POM (left plot) and DRM (right plot)

The difference in the catalytic activity of synthesized materials might be clarified by H_2-TPR analysis which was performed for the fresh-prepared samples. As for the Nd-containing samples the active Co metal particles were formed at much lower temperatures compared to the $La_{2-x}Sr_xCoO_4$ catalysts. Moreover, In case of the La-containing samples the temperature of Co^0 formation was even higher than the reaction temperature zone.

The next step of the present study was to perform the POM with H_2 preliminary reduction treatment in order to create the active Co metal particles before reaction. Nevertheless, the catalysts showed the same trend – the most active material was $NdCaCoO_4$ when the less active one was $LaSrCoO_4$. XRD analysis of the spent catalysts revealed that completely reduced $LaSrCoO_4$ was partially reoxidized again to the perovskite-like structure during the POM process. These results might be explained by geometric factors. The calculated Goldschmidt tolerance factor for $LaSrCoO_4$ and $NdCaCoO_4$ are 0.97 and 0.93 respectively. These tolerance factors indicate that considering solely geometric factors lanthanum, the largest ion in the series, forms the most stable perovskite structure which is difficult to reduce to obtain active metal particles. On the other hand, once reduce stable perovskite it is much easier to reoxidize it again to the initial structure.

4 Conclusions

$NdCaCoO_4$ demonstrate high activity, selectivity and stability in both POM and DRM processes. It was found the strong relationship between reducibility and activity of perovskite-like cobaltates.

Acknowledgements

Work was supported by the Russian Foundation for Basic Research (projects 13-03-00381 and 13-03-12406), the Russian Scientific Foundation (project 14-13-01007), and by the Ministry of Education and Science of Russia within the performance of a basic unit of the state task "Organization of Carrying Out Scientific Research", questionnaire No. 1422 and the framework for the implementation of the project of the State job in the field of scientific activity, task No. 4.306.2014/K.

References

[1] K.Liu, H_2 and syngas production and purification technologies, John Wiley & Sons, Inc., (2010)
[2] J.P. van Hook, Catal. Rev. Sci. Eng. 21 (1981) 1
[3] Q.J. Yan, W.Z. Weng, H.L. Wang, H. Toghiani, *Appl. Catal. A* 239 (2003) 43-59
[4] A.G.Dedov, A.S.Loktev, D.A.Komissarenko et al., *Appl. Catal. A* 489 (2015) 140-146

I-PP69

New Polymetallic Catalysts on the Base of Shs-Intermetallides for Oxidation and Reduction Processes

Borshch V.N.[1*], Sanin V.N.[1], Pugacheva E.V.[1], Zhuk S.Ya.[1], Andreev D.E.[1], Yukhvid V.I.[1], Eliseev O.L.[2], Kazantsev R.V.[2], Kolesnikov S.I.[3], Kolesnikov I.M.[3]

1 - Institute of Structural Macrokinetics and Materials Science RAS, Chernogolovka, Moscow Region, Russia

2 - N.D.Zelinski Institute of Organic Chemistry RAS, Moscow, Russia

3 - I.M.Gubkin Russian State University of Oil and Gas, Moscow, Russia

* borsch@ism.ac.ru

Keywords: SHS-intermatallides, polymetallic catalysts, nanostructures, deep oxidation, reduction processes

1 Introduction

Complex multicomponent intermetallides produced by self-propagating high-temperature synthesis (SHS) were precursors of new polymetallic catalysts. The catalysts demonstrated high activity and selectivity in oxidation [1-3] and reduction processes [4].

2 Experimental/methodology

SHS is an energy efficient short-stage process of the general scheme:

$$\Sigma MO_X + \mu Al \rightarrow [\text{intermetallic alloy}] + \nu Al_2O_3$$

where ΣMO_X is a mixture of oxides of transition metals and rare earths, the intermetallic alloy consisted of higher and lower intermetallides with unreacted aluminum. After ignition, highly exothermic reaction passed in a combustion wave regime. The temperature reached as high as $2500^{O}C$ and higher, therefore all the products were in liquid state. The total reaction time was only a few seconds. The polymetallic alloy was leached by alkaline solution to produce the catalyst. The essential feature of the developed method was stabilization of prepared catalysts by treatment of hydrogen peroxide solution. It is necessary to prevent self-ignition of the samples in the air by removing hydrogen adsorbed during leaching and by formation of a thin oxygen layer on the catalyst surface. After that the catalysts were stable even in oxidation processes at high temperatures.

3 Results and discussions

The structure of the catalysts granules included the lower non-leached intermetallides as supports for highly disperse, disordered and partially amorphous metallic phases. Their specific surface reached more than 40 m^2/g. Oxo-metallic two-level nanostructures were observed on the surface of the all investigated catalysts. The primary levels of structure were flat hexagons of ~1 μm in diameter and less then 100 nm in thickness. The hexagons consisted of granules of 10-30 nm in size or thin unresolved geometric figures as secondary level structures (Fig.1,2).

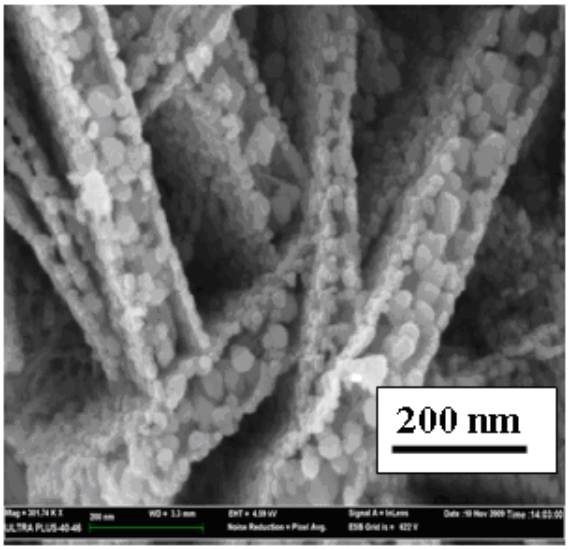

Fig. 1.SEM micrograph of surface of Fe-Mn-Ce catalyst for deep oxidation

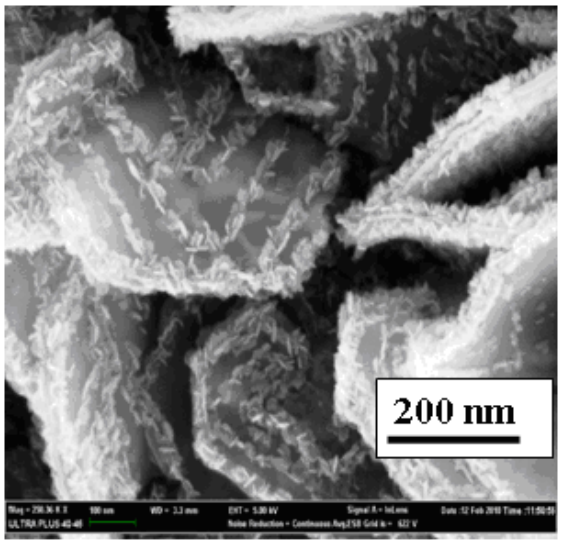

Fig. 2. SEM micrograph of surface of Co catalyst for FT process

(Ni, Fe)-Co-Mn(Ce) catalysts were highly active and stable in the deep oxidation of CO and hydrocarbons up to 450^{O}C. The temperature of 100% conversion was 150-200^{O}C for CO and 250-300^{O}C for propane under gas space velocity 120,000 h^{-1}.

Cobalt based catalysts with promoters such as V,Zr,Ce,La were tested in Fischer-Tropsch (FT) process and demonstrated high activity (~70% CO conversion) and a very high selectivity to heavy hydrocarbons (up to 94%) . The value of ASF chain growth factor **α** reached 0.94 and the product contained a large amount of solid paraffins [4]. The samples of the catalysts were not subjected to any preliminary activation by hydrogen treating at 400^{O}C in contrary to the traditional supported cobalt catalysts.

Other samples of polymetallic catalysts were tested in the process of hydrodesulfurization (HDS) of heavy oil fractions as well. Mo-Ni catalyst was very active in purification of diesel fraction at 350^{O}C, weight velocity of 1 h^{-1} and hydrogen consumption of 300 ncm^3/cm^3. The total sulfur content was reduced from initial 9900 ppm to 31 ppm. The catalyst was used without preliminary treatment by sulfur compounds and calcination.

The activation of the catalysts with formation of metallic (for FT) or sulfide (for HDS) active centers might take place at initial stages of the reactions because of light reducibility of surface nanostructures.

4 Conclusion

Therefore, the new polymetallic materials produced from SHS-intermetallides are very perspective catalysts for oxidation as well as reduction processes. We suppose that highly disordered structure of the materials with branched nanostructured surface is the main reason of extraordinary properties of the catalysts.

Acknowledgements

The work was supported by the RFBR (project No.14-08-00694).

References

[1] V. N. Borshch, E. V. Pugacheva, S. Ya. Zhuk, D. E. Andreev, V. N. Sanin, and V. I. Yukhvid / *Doklady Phys. Chem*. 419 (2008) 77.

[2] V. N. Sanin, D. E. Andreev, E. V. Pugacheva, S. Ya. Zhuk, V. N. Borshch, and V. I. Yukhvid / *Inorg. Mater.* 45 (2009) 777.

[3] E. V. Pugacheva, V. N. Borshch, S. Ya. Zhuk, D. E. Andreev, V. N. Sanin, and V. I. Yukhvid / *Int. J. SHS*. 19 (2010) 65.

[4] V. N. Borshch, O. L. Eliseev, S. Ya. Zhuk, R. V. Kazantsev, V. N. Sanin, D. E. Andreev, V. I. Yukhvid, and A. L. Lapidus / *Doklady Phys. Chem*. 451 (2013) 167.

I-PP70

Cooperation of Kazan (Volga Region) Federal University and PJSC "Nizhnekamskneftekhim" in the Development of Catalysts for the Petrochemical Industry

Lamberov A.A.*

Kazan (Volga region) Federal University, Department of Chemistry, Kazan, Russia

* Alexander.Lamberov@kpfu.ru

Keywords: petrochemical technologies, catalysts

1 Introduction

As is known, up to 90% of petrochemical and oil refining processes are implemented using catalysts which are their major scientific component. Catalysts determine the quality and cost price of the final product, they are the main core of innovative technology in these industries.

2 Experimental/methodology

Work on real catalytic processes in the Kazan University began in 2000 with the development of a catalyst for pyrolysis gasoline hydrogenation. By the time it was stopped the production of domestic catalyst KIM-1 due to its numerous disadvantages. In all reactors of the "SK" plant were loaded the catalysts produced by foreign companies «BASF» and «Shell». By 2003, this problem was solved and after a series of pilot tests, the catalyst KDO had been integrated into industrial practice PJSC "Nizhnekamskneftekhim" instead of imported analogues. In 2005 the catalyst for production of styrene from ethylbenzene had been tested successfully. This catalyst will be produced on the platform of catalyst plant after increase it capacity.

Later, in 2010-2013 this catalyst and its operation technology were the most significantly upgraded by Kazan University together with the PJSC "Nizhnekamskneftekhim". Received by that moment by the Kazan (Volga Region) Federal University funds were used to strengthen the material and technical base to create a "Laboratory of adsorption and catalytic processes". Then the laboratory was equipped with the most modern equipment for the synthesis, study and testing of catalysts. In the latter case it is unique flow catalytic reactors having a volume from 1 cm^3 to 30000 cm^3, in which may be realized industrial operating conditions of the 12 basic processes of PJSC "Nizhnekamskneftehim" on the real industrial feed.

Under the integration of PJSC "Nizhnekamskneftekhim" and Kazan (Volga region) Federal University in 2010 Research and Education Center "Petrochemistry and Catalysis" was created, and in 2013 it was opened the same name Master's Degree Program, which trains the masters and specialists for PJSC within work programs agreed by leading experts of "Nizhnekamskneftekhim".

In 2004 was designed the catalyst for dehydrogenation of isoparaffins and in 2007 together with the specialists of "L.Y. Karpov Chemical Plant" was launched the production of catalyst KDI with capacity of 1,200 tons per year on the above plant.

This catalyst after a series of pilot tests are operated at the "IM" plant of PJSC "Nizhnekamskneftekhim", but it does not cover all the needs of the company. In 2013 together with the specialists of the "Nizhnekamskneftekhim" under the Decree of the Russian Federation № 218 (III stage) was initiated an innovative project to develop the own production of the dehydrogenation catalyst KDI-M and of the modernization of the technological process of isobutylene production. To date, the plant reached its design capacity and successfully operated.

The developed technology is unique and patented in Russia. By creating a stronger contacts

between the primary particles the mechanical strength of the catalyst granules is increased, which results in low catalyst consumption rates per ton of olefin. Crystalline homogeneity of catalyst and uniform distribution of the active components in the granule determined the higher yield and selectivity of action. A low abrasive effect on reactor internals are due to close to the spherical shape of the catalyst granules and its specific granulometry.

Today, as part of this project the Kazan (Volga region) Federal University employs more than 60 researchers. Widely involved scientists of related disciplines - physics and mathematics, there is close cooperation with scientists from the University of Architecture and Construction. In the IV quarter of 2014 in the technological center of K(V)FU the experimental workshop on development of the technology of catalysts production was opened, and in 2015 the department of "Chemical industries" and the department "Industrial Catalysis" was organized for specialist training.

In close cooperation with specialists of PJSC "Nizhnekamskneftekhim" were also successfully developed: a series of catalysts for the selective hydrogenation of hydrocarbon fractions of ethylene production, the isomerization catalysts and zeolite adsorbents. All developments are protected by patents of the Russian Federation. The resulting industrial samples of these catalysts have successfully completed pilot testing in an industrial conditions and have a high degree of readiness for the introduction into commercial operation.

University not only develops the new catalysts, but also carries out works on the modernization of technological equipment producing monomers. Reactors for hydrogenation of pyrolysis gasoline were modernized, a highly efficient cyclone equipment of dehydrogenation units were developed and implemented, in a pilot plant was tested the process flowsheet of heat supply in the catalyst beds of isoamylenes dehydrogenation, taking into account the obtained results the modernization of industrial technology was started.

3 Results and discussion

Successful cooperation of PJSC "Nizhnekamskneftekhim" and K(R)FU allows to build optimistic plans for the future.

PJSC "Nizhnekamskneftekhim" requested the University to develop catalysts for the processes:

- hydrogenation of acetophenone,
- dehydrogenation of butane to butadiene,
- methyl-phenyl-carbinol dehydration.

It may be noted that all the participants of the project: scientific, technological and design centers of PJSC "Nizhnekamskneftekhim" and the laboratory of adsorption and catalytic processes of Kazan (Volga region) Federal University realized its full potential in the format of the engineering center.

I-PP71

Performance of Phase-Pure M1 $MoVNbTeO_X$ Catalysts with Different Post-Treatments for the Oxidative Dehydrogenation of Ethane

Chu B.Z.[1], An H.[1], Truter L.A.[2], Nijhuis T.A.[2], Schouten J.C.[2], Cheng Y.[1*]

1 - Department of Chemical Engineering, Tsinghua University, Beijing, China
2 - Department of Chemical Engineering and Chemistry, Laboratory of Chemical Reactor Engineering, Eindhoven University of Technology, Eindhoven, The Netherlands

* yicheng@tsinghua.edu.cn

Keywords: oxidative dehydrogenation, ethane, ethylene, mixed-metal oxide, micro-channel reactor

1 Introduction

Oxidative dehydrogenation of ethane (ODHE) is a competitive process for ethylene production currently due to its high performance in terms of ethane conversion and ethylene selectivity as well as the low risk of carbon deposition theoretically. The $MoVNbTeO_x$ catalyst has been demonstrated as promising materials in the selective oxidation of alkanes, which usually consists of M1 and M2 crystalline phases and minor amounts of other phases. The M2 phase has no activity in the ODHE process and the catalyst performance increases with the M1 phase content in the $MoVNbTeO_x$ catalyst. The phase-pure M1 catalyst is therefore ideal for obtaining a high productivity in the ODHE process.

In the present work, different post-treatment processes were applied to produce phase-pure M1 catalysts which contain different chemical compositions and surface areas. We further prepared the phase-pure M1 $MoVTeNbO_x$ catalyst on metal-ceramic complex substrates by a dip-coating method. The performance of the M1-PVA catalyst plate in a micro-channel reactor approached an ethane conversion of ~ 60% and ethylene selectivity of ~ 85% with a high catalyst productivity of 0.64 $kg_{C2H4}/kg_{cat}/h$.

2 Experimental/methodology

Figure 1 shows the general preparation procedure of $MoVNbTeO_x$ catalysts by hydrothermal synthesis and, thereafter, by various post-treatment methods. The properties of the catalysts before and after reaction were characterized by XRD, BET, ICP, XPS, SEM and TEM. These catalysts were evaluated at different temperatures (340–460ºC) with different feed composition to investigate the effect of different post-treatments on the catalyst performance (i.e., ethylene selectivity, productivity and stability) in the ODHE process.

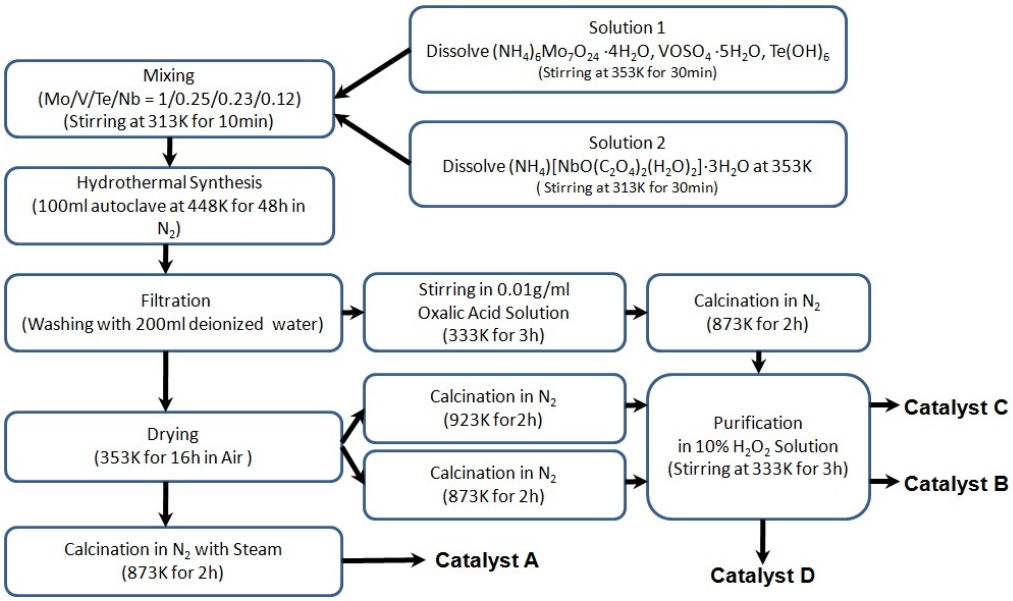

Fig. 1. Hydrothermal synthesis of phase-pure M1 catalyst

3 Results and discussion

Figure 2 shows a comparative study of M1 catalyst performance in a fixed bed and a micro-channel reactor.

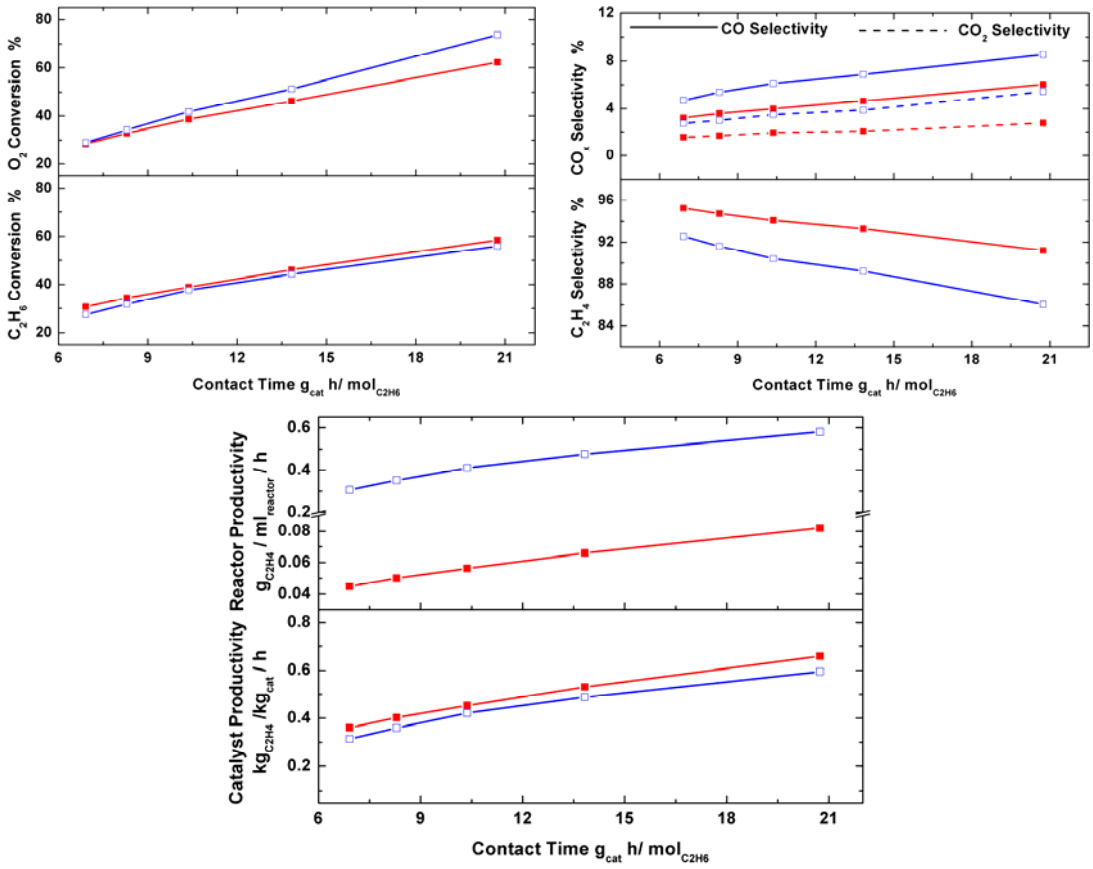

Fig. 2. Ethane and oxygen conversion, ethylene and carbon oxides selectivity, catalyst productivity and space time yield as functions of contact time for M1 catalyst in fixed-bed reactor (■) and in micro-channel reactor (□). Experiments were performed at 400 °C and 1.0 atm with a C_2H_6/O_2/He molar ratio of 30/20/50 at reactor inlet.

4 Conclusions

Catalytic performances of phase-pure M1 $MoVTeNbO_x$ catalysts can be effectively tuned by appropriate post-treatments, showing promising petentials for commercialization of the ODHE process.

Acknowledgements

Financial support from joint project supported by KNAW (The Netherlands) and Ministry of Education (China) is acknowledged.

I-PP72

Oils and Fats Conversion to the Second Generation of Biodiesel Using Pd-Containing Catalysts

Stepacheva A.A.[1*], Sapunov V.N.[2], Nikoshvili L.Zh.[1], Sulman E.M.[1], Matveeva V.G.[1]

1 - Tver Technical University, Tver, Russia
2 - Mendeleyev University of Chemical Technology of Russia, Moscow, Russia

* a.a.stepacheva@mail.ru

Keywords: biodiesel, hydrodeoxygenation, hypercrosslinked, polystyrene

1 Introduction

Last decades the development of tryglycerides (TG) conversion is geared towards the alternative of diesel fuel. The biodiesel is the second in order of inportance type of biofuels [1]. Biodiesel can be used both as pure and as mixture with petrol diesel. The synthesis of biodiesel fuel is based on two processes: (i) transestherification of TG with methanol and (ii) hydroprocessing of fatty acids. The second process allows the producing the fuel similar petrodiesel both the composition and properties [2].

The literature data shows the mechanism of the carboxylic acids conversion to the saturated hydrocarbons through two ways: direct decarboxylation and initial decarbonylation with the formation of olefine and futher hydrogenation of obtained product [3]. The process of catalytic hydrodeoxygenation (HDO) includes both of the passways.

2 Experimental

Synthesis of the Catalyst The HPS fractions with mentioned diameter 60 ~ 100 μm and mass 3 g, previously treated with acetone and dried to the constant weight, were impregnated for 8 ~ 10 min with 6 mL of solvent mixture, consisted of 4 mL tetrahydrofuran, 1 mL of methanol and 1 mL of solution of Na_2PdCl_4 in water. The treated polymers were dried at a temperature 70±2°C for 30 min. Then the obtained samples of catalyst were treated with solution of Na_2CO_3 with concentration 2,76 g/L for 15 min, washed with distilled water and dried for 1,5 hour at a temperature 70±2°C. As the result the metallopolymeric systems with Pd loading 1% (1%-Pd/HPS) were synthesized. The catalysts were previously reduced by hydrogen at a temperature 300°C for 3 hours.

The synthesized catalytic systems were analyzed by transmission electron microscopy, low-temperature nitrogen physisorbtion, X-ray photoelectron spectroscopy.

Hydrodeoxygenation of fatty acids Stearic acid (SA) (ChimMedService, Russia) was used as a model substrate for catalytic HDO. The process was carried out in stainless steel batch reactor (PARR Instrument, USA) varying the pressure 0.2-1.8 MPa, the temperature 230-260°C and SA initial concentration 0.05-0.2 mol/L. Pd-containing catalysts with metal loading varied from 1%(wt.) up to 5%(wt.) based on polymeric matrix of hypercrosslinked polystyrene were synthesized by wet impregnation method. *n*-Dodecane (Sigma Aldrich) was used as the solvent. Liquid samples were analyzed using GC-MS.

3 Results and discussion

The kinetic curves based on the experimental data (Fig.1) were investigated by the method of transformation, which consist of the linear transformation of reaction time by the multiplication of reaction time by the coefficient η [3]. So the complete conjunction of kinetic curves with the curve relevant to the maximum reaction rate was reached out. This curve was chosen as “standard” with η = 1 (see Fig.1, curve 1).

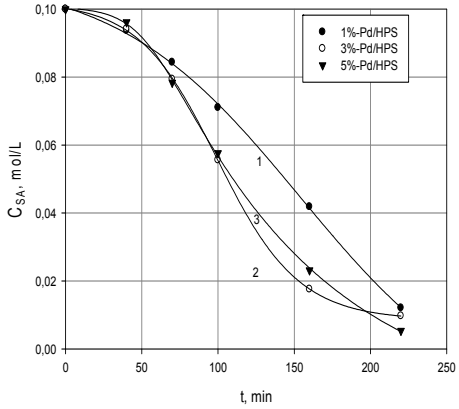

Fig. 1. Kinetic curves of stearic acid hydrodeoxygenation

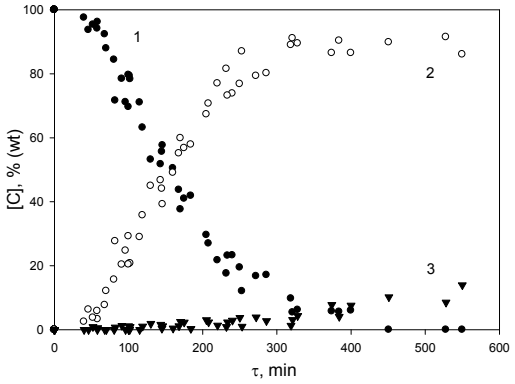

Fig. 2. Transformed curves

It is noteworthy that the linear transformation of the reaction time leads the conjunction of kinetic curves both the SA usage and reaction products formation (Fig. 2).

The data of influence of the catalyst structure on the hydrodeoxygenation rate are shown in Table 1.

Table 1. Activity and physical-chemical properties of the catalysts

Catalyst	Transformation coefficient	Conversion*, %	Selectivity**, %	S_{BET}, m^2/g	D_m, nm	Pd state
1%-Pd/HPS	1	87.9	98.9	1120.0	32.1±0.1	Pd_n (4<n<7) Pd(0)
3%-Pd/HPS	1.26	90.3	98.5	705.0	35.6±0.1	-
5%-Pd/HPS	1.27	94.6	96.2	539.0	7.6±0.1; 25.0±0.1	Pd_n (9<n<13) Pd(0)

*after 220 minutes
**regardig to n-heptadecane

4 Conclusions

Based on the experimental data, the followed conclusions can be done:

- similar mechanism of catalytic influence;
- the processes passing on the catalysts are identical because the kinetic curves of stearic acid and reaction products are completely congruent in the coordinates of concentration – adjusted time ($\tau = \eta \cdot t$);
- the calculated transformation coefficient can be used as the measure of catalytic activity.

Acknowledgements

Authors thank Russian Foundation for Basic Research (contract 12-08-00024-a) for financial support of this investigation.

References

[1] ENERS Energy Concept. Production of biofuels in the world. http://www.plateforme-biocarburants.ch
[2] M. Snare, I. Kubickova, P. Maki-Arvela, K. Eranen, D. Yu. Murzin, *Ind. Eng. Chem. Res.* 16 (2006) 5708-5719
[3] T. Kalnes, T. Marker, D.R. Shonnard, *Int. J. of Chem. React. Eng*. 5 (2007) 748-750.
[4] R. Shmidt, V. Sapunov, Informal kinetic. 1985. 264 p.

I-PP73

High Throughput Testing of Naphtha Reforming Catalysts

Kirchmann M.*, Haas A., Hauber C., Böltken T.

Hte GmbH, Heidelberg, Germany

* marius.kirchmann@hte-company.de

Keywords: naphtha reforming, refinery processes, high throughput, catalyst testing

1 Introduction

Increasing global demands for high-octane fuels, the tightening of environmental regulations and the optimization of refineries has led to an increasing demand for efficient catalyst testing capacity. Catalytic naphtha reforming as one of the key processes is a challenging application for the parallel testing of catalysts due to multi-component feeds with related complex chemistry and varying feed and product properties. Catalytic naphtha reforming is done industrially in different processes and requires for a time-efficient testing approach an accelerated decay protocol for semi-regenerative reforming (SRR) with very slow deactivation whereas continuous catalyst regeneration (CCR) needs a test protocol suitable for relatively fast catalyst deactivation. Another challenge is testing the catalysts under industrially relevant conditions to yield reformate with a constant research octane number (RON).

Herein, we present the latest developments of high throughput technology for testing catalytic naphtha reforming catalysts in 16 parallel reactors under industrially relevant conditions to yield reformate with a constant research octane number (RON). The presentation includes information on appropriate test protocols and the required analytical setup to analyse complex multi-component feeds and products. Research octane numbers (RONs) are calculated based on the distribution of Paraffins / Iso-paraffins / Aromatics / Naphthenes / Olefins (PIANO). In connection with a fully automated data evaluation it will be shown that catalysts can be precisely characterized and differentiated by activity, selectivity and deactivation. The temperature is adjusted automatically for each of the 16 parallel reactors to keep the RON of the reformate or C_{5+} at a constant specified target value for time on streams up to 1000 h.

2 Experimental/methodology

All experiments were carried out in a 16-fold parallel fixed bed reactor system. The unique process control guarantees constant pressure (2-30 barg), flow, feed concentration and temperature (up to 570°C) for very long run-times. The reactor system also allows for sequential start-up of the reactors and product analysis which means that catalysts with different deactivation time-scales can be compared at constant time-on-stream.

3 Results and discussion

The most important performance parameters for reforming catalysts are reformate or C_{5+} yield, research octane number (RON), activity (temperature) and lifetime. Complete on-line GC-analysis identifies more than 130 components in the gas phase. The hydrocarbon distribution of heavy naphtha feed and corresponding reformate is shown in Figure 1 for one exemplary catalyst. It can be seen that paraffins and naphthenes are strongly reduced and converted to aromatics and lights (C1-C4). The RON is calculated from the PIANO distribution by appropriate models and decreases during time on stream due to deactivation of the catalysts.

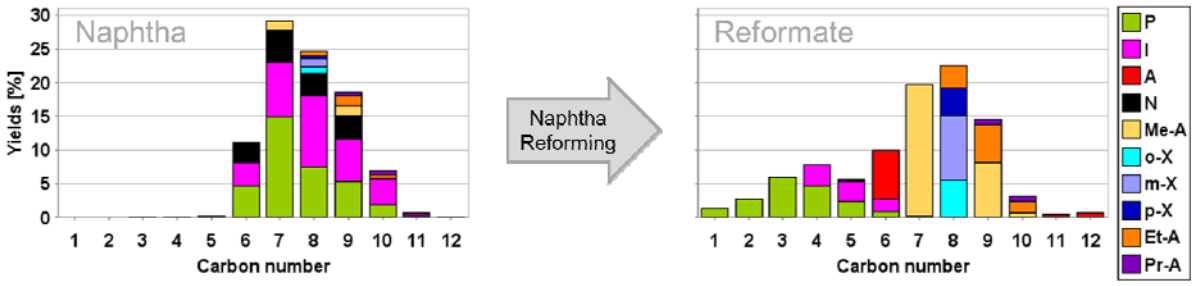

Fig. 1. Product yields of naphtha feed and resulting reformate based on complete on-line gas phase GC-analysis of more than 130 components. Me-A, Et-A and Pr-A indicate methyl-, ethyl and propyl-aromatics. The xylene isomers are abbreviated as o-, m-, and p-X.

In order to keep the octane number constant and operate under *iso*-RON conditions, the temperature is regularly adjusted for each of the 16 parallel reactors by a fully automated data evaluation process. Due to highly optimized naphtha reforming catalysts, the performance parameters of different catalysts are hard to distinguish and require statistical evaluation supported by high-throughput technology for reliable results. Since statistical significance for single-fold pilot plant testing is either limited or time consuming to obtain, high throughput testing of naphtha reforming catalysts can have a real benefit and leads to a precise catalyst differentiation with regard to activity, selectivity and lifetime under industrially relevant conditions.

4 Conclusions

Despite the various challenges, high throughput testing of naphtha reforming catalysts in 16 parallel reactors was achieved successfully under industrially relevant conditions. Detailed hydrocarbon GC-analysis with identification of more than 130 compounds allows a precise product analysis, calculation of PIANO distribution and RON calculation. Utilizing a fully automated data evaluation process, operation under *iso*-RON conditions at a constant specified RON target value is possible for time on streams up to 1000 h and more. In connection with high statistical significance of the results, high throughput testing leads to a reliable and precise catalyst differentiation with regard to activity, selectivity and lifetime.

References

[1] G. J. Antos, M. A. Abdullah, New York: Marcel Becker (2004).
[2] M. R. Rahimpour, M. Jafari, D. Iranshahi, *Applied Energy* 109 (2013) 79.

I-PP74

How Small Catalyst Crystallites Can Be: the Case of Anatase

Yatsenko D.A., Tsybulya S.V., Vorontsov A.V.*

Boreskov Institute of Catalysis SB RAS, Novosibirsk, Russia

* voronts@catalysis.ru

Keywords: nanoparticle, facets, crystallinity, XRD, DFT, DFA

1 Introduction

Building adequate models for heterogeneous catalysts is of vital importance for development of insights into the mechanisms of catalytic reactions. Since catalysis research has entered a new phase, marking the end of the era driven primarily by trial and error, theoretical models are being developed that allow not only explaining experimental results but also predicting novel catalysts and their properties. Despite vigorous developments in this field of theoretical heterogeneous catalysis, major issues concerning the effect of particle size on catalyst properties remain mainly unsolved in the small nanoscale domain, where the surfaces, edges and vertices of nanoparticles exert predominant influence on the catalytic and other properties. The present research tries to answer the question what is a minimal size of an oxide nanoparticle which is required for it to be visible as crystallite. Anatase nanoparticles of diverse sizes are taken as examples and their structure and properties are modeled and compared to experimental data.

2 Experimental

Nanoparticles (NP) of anatase with the size up to 3 nm are created by cutting them from the bulk anatase lattice with (001), (100) and (101) facets exposed. The structure of nanoparticles is optimized using density functional theory (DFT) methods as well as modern semiempirical methods for larger particles. X-ray diffraction (XRD) patterns are obtained using computer program DIANNA employing Debay equation [1].

3 Results and discussion

It is clearly demonstrated that there is a minimal size of anatase NP in order for them to show crystallinity that can be measured with XRD and EXAFS. The structure of small NP is very sensitive to the composition of their surface and distribution of hydroxyl groups over it. The crystalline core-amorphous shell structure is typical and agrees well to the experimental data. Even for ideal anatase NP, there is a strong inherent surface heterogeneity.

4 Conclusions

The results of the research can be used for further development of theoretical methods for describing heterogeneous catalytic processes on molecular and atomic scale and prediction of properties of catalytic nanoparticles in the very small domain (< 5 nm).

Acknowledgements

The support of the Russian Foundation for Basic Research via project 15-08-01936 is gratefully acknowledged.

References

[1] D. A. Yatsenko, S. V. Tsybulya, DIANNA (Diffraction Analysis of Nanopowders): Software for structural analysis of ultradisperse systems by X-Ray methods. *Bulletin of the Russian Academy of Sciences. Physics*, 76 (2012) 382-384.

I-PP75

Catalytic Decomposition of Ammonium Nitrate on Cores of Oil Breeds

Batygina M., Dobrynkin N.*, Noskov A.

Boreskov Institute of Catalysis SB RAS, Novosibirsk, Russia

* dbn@catalysis.ru

Keywords: ammonium nitrate, core of oil, breed, nitric acid, formic acid

1 Introduction

The application of oil layers heating by the chemical decomposition of a binary mixes (BM) is one of perspective technologies of oil recovery increasing [1]. In the reaction of the BM decomposition hot gases under the pressure get into the oil layers, result in a saturation of oil by gas and the oil viscosity decrease. Due to it the oil can move from the layer to a chink in a mode of the pressure head drainage and then along the chink on a surface in the lift mode. Today the level of BM technology development for oil recovery increasing does not allow carrying out an operated process of ammonium nitrate decomposition. Application of specially developed catalysts and cores of oil breeds as catalysts can become a possible method of control over the process of decomposition.

2 Experimental

The experiments were spent in a glass thermostatic reactor connected with the reflux condenser in the temperature range 40-90°C during 5 hours. Water solution containing the ammonium nitrate, formic and nitric acids was used for ammonium nitrate decomposition. Industrial reforming catalyst AP-56 (0.56% Pt/γ-Al_2O_3) and cores of oil breeds were used as catalysts. The current concentrations of ammonium ions in working solutions were defined by means of universal ionomer EV-74 with use of special ionselective electrode ELIS-121NH_4. The element composition of cores (identified with X-ray phase analysis and X-ray fluorescence analysis), the area of a specific surface (S_{BET}) and a volume of pores are presented in Table 1.

Table 1. Physical and chemical characteristics of the cores

Core	Content of elements, % wt.								S_{BET}, m^2/g	Volume of pores, ml/g
	The easy (<F)	Si	Mg	Al	K	Fe	Na	Ti		
Core - bazalt	65,01	13,53	7,20	6,35	0,20	2,74	0,73	0,33	19	0,0431
Core - clay	56,76	23,76	1,74	8,87	2,35	3,30	1,07	0,41	25	0,0634
Core - sand	65,06	23,73	0,54	6,33	1,44	0,90	1,44	0,22	15	0,0141
	Ca	**S**	**P**	**Mn**	**Ba**	**Ce**	**Sr**	**Cl**		
Core - bazalt	3,52	-	0,09	0,08	-	-	0,15	-	19	0,0431
Core - clay	0,61	0,79	0,07	0,03	0,12	0,02	0,02	-	25	0,0634
Core - sand	0,14	0,08	0,02	-	0,04	-	-	0,06	15	0,0141

3 Results and discussion

We present herein the results of catalytic activity study of cores in ammonium nitrate decomposition. It is shown that catalyst introduction in a reactionary mixture allows to raise a degree of ammonium nitrate decomposition in 3-4 times (Fig. 1) at low temperatures, whereas

the use of catalysts does not effect on ammonium nitrate conversion at high temperatures.

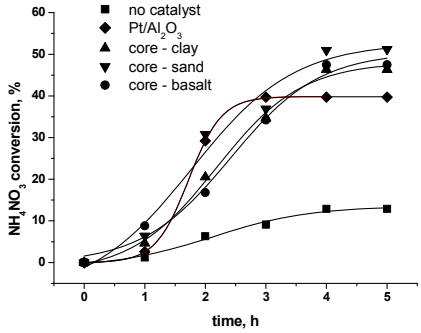

Fig. 1. Ammonium nitrate decomposition at T=51 °C (molar ratio HNO_3 : HCOOH : NH_4NO_3 = 7,8 : 3,4 : 1; HNO_3 : HCOOH = 2.3).

The influence of the ratio of used reagents on ammonium nitrate conversion is investigated at different conditions. The obtained data shows the linear growth of NH_4NO_3 conversion with increase of the content of nitric acid in solution at molar ratio HNO_3: HCOOH = 1. It has been shown that the dependence of degree of NH_4NO_3 decomposition on the ratio of nitric and formic acids represents a curve with a maximum in a point corresponding to the molar ratio HNO3: HCOOH = 2.7. The found value of the maximum is the general for various ratios of nitric acid and ammonium nitrate.

Savara and co-workers found recently [2] that ammonium nitrate decomposition can occur due to its oxidation by nitrous acid:

$NH_4NO_3 + HNO_2 \rightarrow N_2 + HNO_3 + 2H_2O$

The generator of nitrous acid is a system HNO3 - HCOOH in which there is a formation of NO and NO_2 according to the reactions [3]:

$2HNO_3 + HCOOH \rightarrow 2NO_2 + CO_2 + 2H_2O$

$2HNO_3 + 2HCOOH \rightarrow NO + NO2 + 2CO_2 + 3H_2O$

$2HNO_3 + 3HCOOH \rightarrow 2NO + 3CO_2 + 4H_2O$

Emitted NO_2 and NO just form nitrous acid at interaction with water according to the reactions [4]:

$2NO_2 + H_2O \leftrightarrow HNO_3 + HNO_2$

$2NO + HNO_3 + H_2O \leftrightarrow 3HNO_2$

The catalytic activity of core oil-bearing rocks of different nature (basalts, clays, sandstones) observed in the reaction of decomposition of ammonium nitrate for the first time. Activity of natural samples exceeds that of commercial catalyst. The observed regularities are explained on the basis of the proposed mechanism of the reaction.

Acknowledgements

Authors are grateful to Presidium of the Russian Academy of Sciences for financial support of work under the Program «Exploration fundamental scientific researches in interests of development of the Arctic zone of the Russian Federation».

References

[1] A. Merzhanov, V. Lunin, D. Lemenovskiy, E. Aleksandrov, A. Petrov, V. Lidzhi-Goryaev, *Science and technologies in the industry*. 2 (2010) 1.

[2] A. Savara, M.-J. Li, W.M.H. Sachtler, Eric Weitz. *Appl. Catal. B*. 81 (2008) 25.

[3] G.F.Vandegrift. *Technical Report ANL-00/25*. (2000) [Electronic resource] URL: http://www.ipd.anl.gov/anlpubs/2000/12/38162.pdf

[4] N. Moroz, A. Kobzev, A. Loboiko, V. Bagdasaryan, M. Vorozhbiyan, The integrated technologies and power saving. 1 (2004) 82.

I-PP76

Areas of Growth of PJSC «Nizhnekamskneftekhim»

Gilmanov Kh.Kh.*

PJSC «Nizhnekamskneftekhim», Nizhnekamsk, Russia

* shakirovams@nknh.ru

Keywords: petrochemical technologies, catalysts

1 Introduction

The level of development of the Russian Federation economy at present is determined to a wide extent by the use in its productions of the state of the art technologies and materials. Petroleum chemistry and refining, being one of the most important branches of economy until the present time maintained their dependence on overseas supplies of a variety of materials and majority of catalysts.

2 Experimental

Today, when sanctions are introduced against Russia over foreign supplies, this issue becomes particularly burning for the petrochemical productions where the majority of processes not only are running in the presence of catalysts, but also determine their economic efficiency.

For PJSC «Nizhnekamskneftekhim», in the productions of which more than 70 imported materials and catalysts are used this situation creates a real threat of shutdown of certain production units.

Therefore, the issues of substitution of import catalysts for domestic equivalents developed jointly with the specialists of R&D organizations and higher educational institutions of the Republic are being closely studied in PJSC «Nizhnekamskneftekhim».

Since 2007 PJSC «Nizhnekamskneftekhim» in collaboration with the specialists of Kazan Federal University is working on catalyst development within the frame of cooperation between high educational institutions and enterprises of real sector of economy and is creating their production facilities in its enterprise premises.

In PJSC «Nizhnekamskneftekhim» all conditions are created for the successful work in this direction – there are proprietary research and technology and design centers, there is a workshop with pilot plants for development of new types of rubbers, qualified specialists with extensive production experience and operation in petrochemical industry.

3 Results and discussion

A Research and Technology Center is a multi-profile research division which is ensuring to a great extent a successful functioning of the company. The Center is developing and introducing new technologies, allowing to provide improvement of the efficiency of operating productions. The technologies for production of chlorobutyl – and bromobutyl rubbers developed in cooperation with OAO «Yarsyntez » specialists, development of SKD-L rubber and SKD-L rubber with low dynamic viscosity, block type DSSK rubber for synthesis of ABS plastics with participation of NIISK specialists that permitted PJSC «Nizhnekamskneftekhim» to completely refuse from purchasing import rubbers for production of impact polystyrene, can serve as an example.

Since 2006, the specialists of the Centre are looking into the matter of import substitution – developing domestic inhibitors and components of catalytic systems:

- the production of neodymium neodecanoate – the main component of the catalytic system for production of SKD-N rubber - has been created in the pilot workshop,

- the technology of concentrated TIBA production has been developed which enabled the company to refuse from the imported components of catalyst for production of polyolefins,
- based on the developments of the Centre the production of more than ten grades of polyethers and polyglycols has been created and mastered.

One of the basic technologies on isoprene direct synthesis from isobutylene and formaldehyde has been developed at participation of a Reseach and Technology Center and a Design Center together with specialists of "Evrochim SPb".

In recent years PJSC «Nizhnekamskneftekhim » actively increases existing capacities of main rubber and monomer production lines and builds up production units to manufacture new product types.

PJSC «Nizhnekamskneftekhim directs significant investments for development of its own catalytic systems and establishment of their production units.

Availability of its own catalyst will provide an opportunity for the Company to solve several important tasks , including:

- energy and raw material resources reduction using more advanced catalysts ;
- provision of process utilization by its own catalyst factory;
- competitive recovery through lower end product cost due to introduction of more effective catalysts ;
- import substitution, i.e. economic security of the Company.

Together with KFU specialists a native iron oxide catalyst for isoamylene dehydrogenation has been developed, its production has been established and catalyst has been introduced into isoprene production.

This catalyst completely replaced import analogues belonging to such famous Companies as Shell and BASF, it is manufactured at PJSC «Nizhnekamskneftekhim » in quantity of 300 tons /year , totally covering demands of the Company.

Isoparaffins dehydrogenation catalyst production of IDC grade has been launched at Mendeleevsky chemical plant named after L.Ya. Karpov. Capacity of this production unit accounts for 1200 tons /year. This catalyst is a substitution of Engelhard Company's import analogue.

More effective isoparaffins dehydrogenation catalyst IDC-M for isobutylene production has been developed and its construction has been completed. Established IDC-M production unit will allow to provide the PJSC «Nizhnekamskneftekhim » Company with microspheric catalyst and replace an out-dated IM-2201.

Within the import substitution frame, developments of n-butylene isomerization catalyst in isobutylene have been carried out. Pilot scale tests (giving positive results) have been performed at one of the isomerization systems of DB and HCC plant. This catalyst has been developed instead of an import analogue of Engelhard Company.

Developments of catalyst of acetylene hydrocarbons' selective hydrogenation in ethane - ethylene fraction, vinylacetylene selective hydrogenation in butadiene fraction, pyrolysis condensate hydrogenation as well as different adsorbent grades for cleaning and drying of hydrocarbon streams are at the finalization stage.

4 Conclusion

Projections for further cooperation between PJSC «Nizhnekamskneftekhim and KFU include development of catalysts of one stage vacuum dehydrogenation of n-butane to butadiene and acetophenone hydrogenation to methyl phenyl carbinol. Particular hopes are laid by the Company on the development of a new course in Kazan (Privolzhskiy) Federal University, i.e. creation of effective native catalysts for polymerization processes. Integration of laboratory and pilot plant capabilities of Research and Technology Center with scientists of the University will allow to guarantee competiveness and economic stability of PJSC «Nizhnekamskneftekhim».

I-PP77

Sensitization of Wide-Bandgap Oxides ZnO and TiO_2 to the Visible Region Using Intrinsic Point Defects, Surface 2D Nanostructures and Composites ZnO/Si, TiO_2/Si

Lisachenko A.A.*

St. Petersburg State University, Department of Physics, Saint-Petersburg, Russia

* a.lisachenko@spbu.ru

Keywords: photocatalysis, ZnO, TiO_2, spectral sensitization, "core-shell", $(Me_x O_y)$/Si nano-composites

1 Introduction

The wide-bandgap oxides TiO_2, ZnO are known to be active in photo-activated adsorption/desorption (PA, PD) of simple molecules and in a lot of redox reactions under irradiation in the near UV. However, the UV part of the solar spectrum does not exceed 4%. Therefore the sensitization to the visible region is a key problem for improving the effectiveness of these photocatalysts. At present, several methods are used to create active sites absorbing visible light, such as molecular chromophore deposition, anion/cation doping, pretreatment in plasmas of Ar, N_2 or H_2.

Previously, we have shown that intrinsic defects of F- and V-type can be used for to "self-sensitize" wide-bandgap oxides – insulators (BeO, Al_2O_3, MgO) and semiconductors (ZnO and TiO_2). Light absorption by these centers provides photoactivity in reactions of simple molecules (H_2, O_2, CO, CO_2, N_xO_y) in the sub-bandgap region.

The present report aims to enhance the effectiveness of F- and V-type by designing the near surface 2D structures consisting of these centers. Another aim was to design the composites ZnO/Si and TiO_2/Si.

The key features of the gas–solid interface photonics are revealed and exemplified by a number of heterogeneous systems: simple molecules (H_2, O_2, CO, CO_2, NO, N_2O) adsorbed on wide-bandgap metal oxides (BeO, Al_2O_3, MgO, ZnO and TiO_2). The emphasis is focused on the sub-bandgap excitations.

We investigate the sensitization of ZnO and TiO_2 using their intrinsic colored defects, 2D "core-shell" nanostructures ZnO/ZnO_{1-x}, TiO_2/TiO_{2-x} and composites ZnO/Si, TiO_2/Si. Photocatalytic reactions of $NO + CO = 1/2N_2 + CO_2$ and photo-induced isotope oxygen, as well as photo-adsorption/desorption of simple molecules (H_2, O_2, CO, CO_2, N_xO_y) are studied.

2 Methodology

In order to reveal the mechanisms of physical and chemical steps, the *in situ* investigations were carried out in the three phases: gas – adsorbate – surface. A variety of complementary *in situ* experimental methods for step-by-step investigations were used:

– mass-spectrometry (spectro-kinetic investigation in the gas phase, thermo-desorption spectroscopy of adsorbed species);
– optical (UV-VIS-IR, FTIR spectroscopy, photo- and thermo-stimulated luminescence);
– ESR spectroscopy of active centres and of adsorbed species;
– UV(8.43eV) photoelectron spectroscopy.

SEM, XRR, XRD, XPS, UPS methods were used for samples characterization.

The photo-desorption under UHV, the photo-adsorption and the photochemical reactions in the gaseous phase were studied using the static and the "flow-through" regime. The use of the isotope enriched molecules reveals the dynamics of photo-desorption/adsorption processes [1].

3 Results and discussion

The photocatalytic reduction of NO by CO into N_2 was performed at room temperature in static regime at 0.01-0.5 Torr. It is concluded that the photocatalytic activity of nonstoichiometric TiO_{2-x} in the visible region is associated with the localized electron-donor centers (Ti^{3+} ions, F and F^+ centers).

It is shown that under VIS irradiation e^- and h^+ are generated in pairs as in the case of UV irradiation. That is possible, if the structures "core-shell" TiO_{2-x}/TiO_2 are formed on the part of the surface thus decreasing the bandgap to 2.9 eV. The surface potential in "core-shell" TiO_{2-x}/TiO_2 is the result of superposition of the Schottky barrier in the TiO_2 meso-structure and of the near-surface quantum well potential of the reduced oxide TiO_{2-x}. The latter potential decreases the E_g value on the surface that explains the VIS activity. In the near-surface energy quantum well the energy levels are discrete, that explains the long lifetimes of the excited states and as a consequence the slow processes, the "memory" effect in the photo-adsorption and the photo-reactions for this oxide. The values of the quantum yield of the process in the visible region are measured. The quantum yield of Photo-induced Oxygen Isotope Equilibration (POIEq) in the sub-bandgap absorption region is ~30 times higher than in the fundamental absorption region of TiO_2.

Nano-layers of ZnO (thickness 2–100 nm) were deposited on the surface of *p*-Si(100), SiOx/*p*-Si(100) and *n*-Si(111) using the atomic layer deposition (ALD) technique. It was found that the illumination of the ZnO/*p*-Si(100) films with visible light ($\lambda > 500$ nm) in the oxygen flow results in the release of H_2O vapor and CO_2 as evidenced by the mass-spectrometry. No release of H_2O and CO_2 was detected if the bare silicon plate was illuminated in similar conditions. Therefore, a conclusion about the photocatalytic decomposition of the surface organic contaminations under the excitation of ZnO/Si system with visible light can be drawn.

4 Conclusions

Based on the obtained results we can expect that "self-sensitization" of $ZnO/ZnO_{1-\delta}$ and TiO_2/TiO_{2-x} based photocatalysts using the intrinsic point defects and the near-surface 2D-nanostructures is a real way to optimize the design of efficient photoactive catalysts for the use of solar energy. The silicon acts as a spectral sensitizer of ZnO film to the visible light. Thus the composites ZnO/*p*-Si(100) can be used as effective photocatalyst in UV-VIS region.

Acknowledgements

The research was supported by "Nanocomposite", "Centre for X-ray Diffraction studies", "Physical Methods of Surface Investigation" and "Nanophotonics" centers of St. Petersburg State University. The work was supported by RFBR (grant № 13-03-90426) and St. Petersburg State University (grant № 11.39.1060.2012).

References

[1] Victor V. Titov, Ruslan V. Mikhaylov, and Andrey A. Lisachenko Spectral Features of Photostimulated Oxygen Isotope Exchange and NO Adsorption on "Self-Sensitized" TiO_{2-x}/TiO_2 in UV−Vis Region// J. Phys. Chem. C 2014, 118, 21986−21994

[2] V.E. Drozd, V.V. Titov, I.A. Kasatkin, L.L. Basov, A.A. Lisachenko, O.L. Stroyuk, S.Y. Kuchmiy //Structure, optical properties and visible-light-induced photochemical activity of nanocrystalline ZnO films deposited by atomic layer deposition onto Si(100). Thin Solid Films, 2014, v. 573, N 38, pp. 128-133

I-PP78

Comparing Alkylation of 3,4 Dimethylphenol with Propanols and Propenes into Oxide Catalyst

Aghayeva N.A.[1*], Taghiyev D.B.[2], Aghayev A.A.[1]

1 - Sumgayit State University, Sumgayit, Azerbaijan
2 - University of Catalysis and Inorganic Chemistry, Baku, Azerbaijan

* anazila88@gmail.com

Keywords: alkylation, 3,4 dimethylphenol, propanol-1, propene, cobalt, ferrite, catalyst

1 Introduction

Alkylation of aromatic compounds,in particular phenol with the alcohols and olefins is the most suitable method for producing their derivatives.Alkylphenols in particular propyl and isopropyl derivatives of methyl- and dimethylphenols finds its application in the preparation of medicaments, vitamins , fragrances , antioxidants and polymer materials for special purposes (ref 1)

2 Experimental

In report the results for investigation of alkylation reaction 3,4 dimethylphenol with propanol-1, proponol-2 and propene on Cobalt ferrite oxide catalyst were shown.Catalyst was synthesized by joint deposition of nitrate and oxalate salts of Co (II) и Fe (III) onto γ-Al_2O_3, followed by drying and calcination. The preliminarily found optimal content of $CoFe_2O_4$ in the catalyst is 22 wt %.Synthesized catalysts chemically homogeneous and have finely porous ferrite particles with mixed spinel structure.

The experiments carried out in reactor with fixed bed of ferrite catalyst, the volume of which is 10 cubic centimeter. Constituents of catalyst were analyzed via chromatographic and spectral methods.

3 Results

The impact of tempreture, load unit, mol ratio of initial components and hydrodynamic regime of the reactor on indicators of alkylation reaction between 3,4 dimethylphenol , propanols, and propene was investigated.

The content of produced catalyst depends on conditions of reactions and the structure of alkylation agent. The main products of alkylation reaction of 3,4 dimethylphenol with propanol-2 are 2 propyl 4,5 dimethyl and 2,6 dipropyl 3,4 dimethylphenol. In case of reaction 3,4 dimethylphenol with propanol-2 in presence of 2- isopropyl-4,5 dimethylphenols in alkyls prevails. Alkylation of dimethylphenols by propenes proceeds with low velocity and in result 2-isopropyl-4,5 dimethylphenol, trimethylphenol and ethyl-xylenol are formed.

The further regularities of comparative alkylation of 3,4 dimethylphenol with propanol and propene were identified (table)

Table1. Comparing results of alkylation of 3,4dimethylphenol with propanol and propene

Name		**Alkylation agent**		
Main product yield of the reaction per reacted 3,4 dimethylphenol %	**Propanol-1**	**Propanol-2**	**Propene ***	
-propyl ether 3,4 dimethylphenol	5.5	-	-	-
-2 propyl 4,5 dimethylphenol	83,0	-	3.5	-
2-isopropyl 4,5 dimethylphenol	-	87	70.5	73.5
3- isopropyl 4,5 dimethylphenol	-	3.5	7.4	10.8
2,6 dipropyl 3,4 dimethylphenol	7.5	-	-	-
Conversion of 3,4 dimethylphenol %	45.5	36,0	3.0	7.5

Conditions: T=330C, V=1h^{-1}, μ=1:1mol/mol

*results getting in autoclave, reaction time 3 hours.

- Alkylation ability of used agents is reduced in order :Propanol-1 > propanol- 2> propene
- selectivity of reaction of 2 propyl(isopropyl) 4,5 dimethylphenol is increased in order: Propene >propanol-2 >propanol-1
- Output of product 2 propyl(isopropyl) 4,5 dimethylphenol is increased in order: Propen >propanol-2 >propanol-1
- Alkylation of 3,4 dimethylphenol with propanol-1 is going by parallel-serial mechanism. In condition of catalyst O-(oxigen), C (carbon) alkylation of Xylenol is occurs , while in case of propanol-2 O-alkylation not present.

4 Conclusion

It was shown the high ortho-alkylation ability of Cobalt ferrite catalyst in alkylation reaction of 3, 4 dimethylphenol with propanol and low catalytic activity in reaction of 3,4 xylenol with propene.

References

[1] Dean Haymond Ernest “Cresol, xylenols and other alkylphenols” J.Chem. insight and forecasting 2012, N2, pages 17-21

[2] Taghiyev D.B, Aghayeva N.A, Nazarova M.K “Catalytic aqlkylation of cresols with propanol-1” Russian Journal of Applied Chemistry August 2013, vol.86, issue 8, pages 1252-1255

I-PP79

Knowledge Extraction for Oxidative Coupling of Methane from Publications in the Literature

Odabaşı Ç., Yıldırım R.*

Boğaziçi University, Department of Chemical Engineering, Istanbul, Turkey

* yildirra@boun.edu.tr

Keywords: oxidative coupling of methane, data mining, knowledge extraction, support vector machine

1 Introduction

The conversion of methane to more useful chemicals and fuels is a big challenge in catalysis field, and the oxidative coupling of methane (OCM) is one of the most studied processes for this purpose. OCM yield seems to depend on very large number of variables such as catalyst type, preparation and operation conditions; a huge amount of data was generated in literature to investigate the effects of these variables on the process yield. However, due to the complexity of relations among the large number of variables, the major trends and correlations in the literature cannot be effectively identified with traditional approaches. We need more systematic and effective approaches and tools to extract knowledge from such a complex literature.

Data mining is a field of computer science to extract knowledge from a database. It helps to spot the patterns that are too hard to detect with the naked eyes, and use these patterns to derive conclusions or make predictions using classification, clustering and estimation techniques. This approach could be used in the field of catalysts to extract knowledge from the publications in the literature as it was tested in previous works [1-3]. One of the most popular data mining techniques is the support vector machine (SVM), which can be used for both classification and prediction [4].

The aim of this study is to build a SVM model for the lanthanum based catalysts [5-6], which are among the promising alternatives, using the published data in the literature.

2 Experimental/methodology

I Database generation

A detailed research has been performed on the published works on OCM reaction, which can be reached online (mostly in the databases of Web of Science, Springer, Elsevier and American Chemical Society). Exactly 34 of them were found to be suitable for data extraction and used for database generation (remaining articles were not suitable to extract data that fit our purpose).Then, a database containing 525 experimental data was prepared covering the effects of various conditions on C_2 yield.

II Computational Work

Data was standardized to bring all of the variables into proportions with each other. Then, support vector machine method was implemented to extract knowledge from the database. Standardization and the organization of the database were performed in Matlab 2014a while the SVM model was build using Weka 3.7.7 which is a user-friendly data mining software.

First, the SVM parameters (C, γ) were optimized by using the whole dataset; the parameter set, which gives the minimum root mean square error (RMSE), was selected. Then, to test the predication ability of the model; the data belonging one publication was removed from the data set, a model was re-built using the remaining publications and used to predict the one publication that was removed from the data set. The same procedure was repeated for all publications.

3 Results and discussion

Parameters (C, γ) were optimized by using 5 fold cross validation on the whole dataset and the parameter set was found a (80, 0.1). The optimum parameters were used to predict the data in the whole database and the results were shown in Figure 1(a); the experimental data points could be predicted correctly with a small error percent.

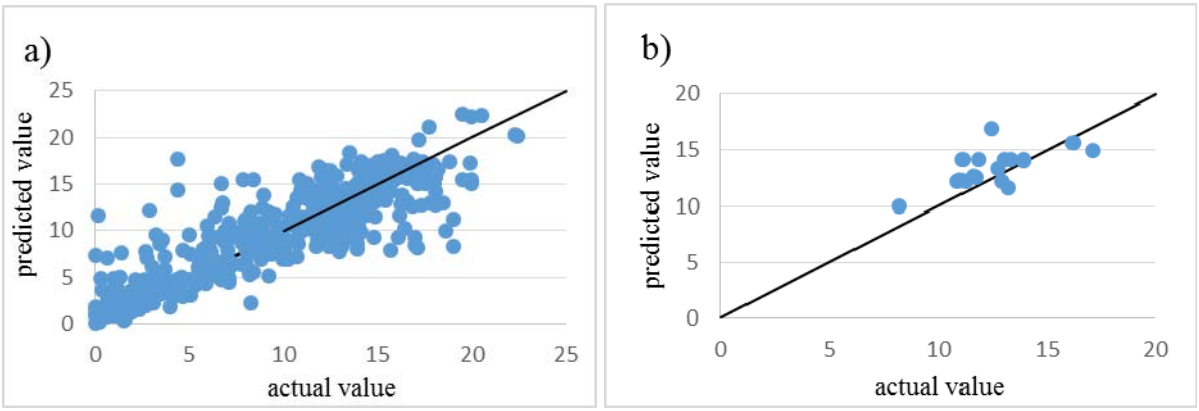

Fig. 1.a) Modelling of training set with optimal parameters (80, 0.1) b) Prediction of the unseen data points with their optimum parameters [7]

Figure 1(b) shows an example for the analysis performed for individual publications. The actual values were the C_2 yields drawn from that publication while the predicted values refer to the model predictions for the experimental conditions at which the actual results were reported. The results were quite satisfactory considering that the predictions were performed by using a model that is constructed from the other publications in the literature.

4 Conclusions

It can be concluded that data mining tools can be indeed very beneficial to analyze the past data to extract knowledge for OCM reaction as well as other similar systems with large number of publications in the literature.

Acknowledgements

The financial support is provided by Boğaziçi University Research Fund Project 7943.

References

[1] U. Zavyalova, M. Holena, R. Schlögl, M. Baerns, *ChemCatChem* 3 (2011) 1935-1947.
[2] M.E. Günay, R. Yıldırım, *Ind. Eng. Chem. Res.* 50 (2011) 12488-12500.
[3] M. E. Gunay, R. Yıldırım, *ChemCatChem* 5 (2013) 1395–1406.
[4] V. Vapnik, The Nature of Statistical Learning Theory. *Springer-Verlag*, New York, 1995
[5] V.I. Alexiadis, J.W. Thybaut, P.N. Kechagiopoulos, M. Chaar, A.C. Van Veen, M. Muhler, G.B. Marin, *Appl. Catal., B*, 150–151 (2014) 496-505.
[6] V.R. Choudhary, S. A. R. Mulla, B. S. Uphade, *Ind. Eng. Chem. Res* 37(6) (1998) 2142-2147.
[7] V.R. Choudhary, S.A.R. Mulla, V.H. Rane , *J. Chem. Technol. Biotechnol.,* 72 (1998) 125-130.

I-PP80

Pt-Sn Catalysts for Biomass Conversion into Fuel Components and Chemicals

Zharova P.A.[1*], Chistyakov A.V.[1,2], Kriventsov V.V.[3], Shapovalov S.S.[4], Murzin V.Yu.[5], Tsodikov M.V.[1,2]

1 - Topchuev Institute of Petrochemical Synthesis RAS, Moscow, Russia
2 - Gubkin Russian State University of Oil and Gas, Moscow, Russia
3 - Boreskov Institute of Catalysis SB RAS, Novosibirsk, Russia
4 - Kurnakov Institute of General and Inorganic Chemistry RAS, Moscow, Russia
5 - National research centre "Kurchatov institute", Moscow, Russia

* zharova@ips.ac.ru

Keywords: heterogeneous catalysis, vegetable oil, alkanes, olefins, algae

1 Introduction

In TIPS RAS was found that ethanol [1] and rapeseed oil [2] could be converted into a number of fuel hydrocarbons over industrial Pt/Al_2O_3 catalyst. Aim of the current work is ethanol and rapeseed oil high selective conversion into fuel components and monomers over $Pt\text{-}Sn/Al_2O_3$ catalysts with different molar ratio of active components.

2 Experimental/methodology

For catalytic experiments the original catalyst containing 0.4 wt % Pt and 0.75-1.2 wt % Sn was prepared by incipient wetness impregnation of $\gamma\text{-}Al_2O_3$ with a solution of the heterometallic complex $(PPh_4)_3(Pt(SnCl_3)_5)$ in dichloromethane [3]. Prior to each experiment, the catalyst was treated with hydrogen for 14 h at 450°C. Catalyst testing was performed in a PID Eng & Tech microcatalytic fixed-bed flow reactor unit, equipped with relevant instrumentation and control devices, under pressure 50 atm of H_2, temperature 400-480 °C, and substrates space velocity in the range of 1.2 h^{-1}. Both gaseous and liquid organic products in aqueous and organic phases were identified by GC-MS. The local structure and charge state of platinum were studied by XAFS spectroscopy.

3 Results and discussion

Over $Pt\text{-}Sn/Al_2O_3$ catalysts ethanol converts into alkanes and olefins C_3-C_8 fraction (Fig. 1). Over $1Pt\text{-}1Sn/Al_2O_3$ catalyst ethanol mainly converts into methane and carbon oxides. Total yield of hydrocarbons C_3-C_8 did not exceed 16 wt.%. Over$1Pt\text{-}3Sn/Al_2O_3$ catalyst aim fraction yield increased up to 23 wt.%. Oxygenates dominates among ethanol conversion products generally consisted of diethyl ether.

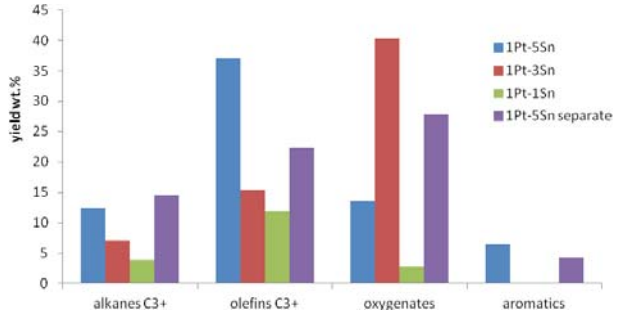

Fig. 1. Ethanol conversion products over Pt-Sn-containing catalysts.

Over 1Pt-5Sn/Al_2O_3 catalyst the maximum yield of hydrocarbons C_3-C_8 was obtained equal 50 wt.% calculated on passed carbon. Also aromatics were obtained with yield of 6 wt.%. C_1 products yield did not exceed 2.5 wt%. It should be noted that monometallic catalyst Sn/Al_2O_3 is not active in ethanol conversion into hydrocarbons. Consequently Sn content in Pt containing catalyst led to significant changes in ethanol conversion into hydrocarbon fuel components and olefins.

Rapeseed oil conversion over Pt-Sn/Al_2O_3 catalysts were investigated. Over 1Pt-5Sn/Al_2O_3 the highest yield of C_{3+} hydrocarbons was reached equal 99.5 wt.% from which 84 wt.% was C_{18} fraction and 4.5 wt.% C_3-C_4 fraction (Fig.2). Among C_{18} fraction was found 23 wt.% of olefins of which 7-10 wt.% were linear alpha olefins. Products of cracking and decarboxylation processes did not exceed 8 wt.%. Moreover, total yield of C_1 products (methane, carbon oxides) observed lower then 0,1 wt.%. Over 1Pt-1Sn/Al_2O_3 catalyst significant yield of alkane C_{17} was observed equal 30 wt.% while over 1Pt-3Sn/Al_2O_3 decarboxylation process significantly decreasing and alkane C_{17} yield was only 5 wt.% but hydrocarbons C_1-C_4 yield reaches 25 wt.%.

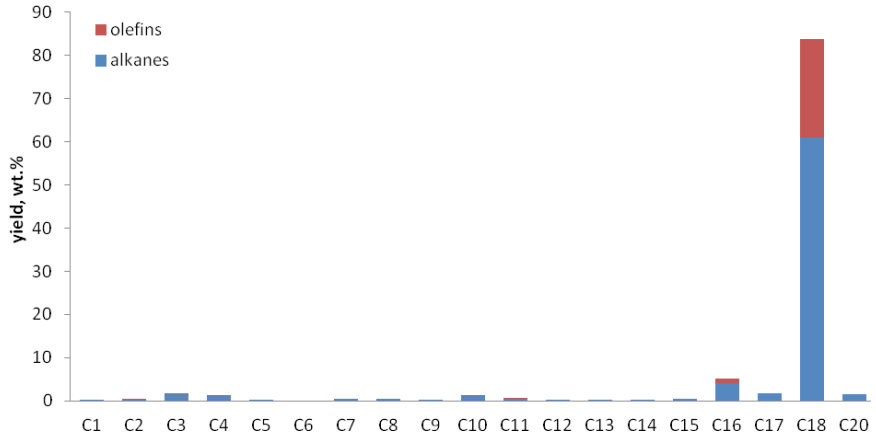

Fig. 2. Composition of the products of rapeseed oil hydrogenolysis in the presence of the 1Pt-5Sn/Al_2O_3 catalysts.

4 Conclusions

The most prospect catalyst for ethanol and rapeseed oil conversion was found to be 1Pt-5Sn/Al_2O_3. Over that carbon mass of initial oil could be converted into alkanes and olefins with only two C_{18} and C_3-C_4 fractions. So selective process may be only when oxygen of initial oil converts in water. Optimal conditions for ethanol conversion were found, that provides yield of alkanes and olefins C_3-C_8 up to 50 wt.%. Obtained results allow minimizing loss of initial carbon weight due to cancelation of carboxyl fragment of fatty acids and glycerol conversion into methane and carbon oxides.

Acknowledgements

Authors thank for financial support RFBR (grants 13-03-12034, 15-03-06479), Council on Grants of the President of the Russian Federation for the Support of Young Scientists MK-5328.2014.3.

References

[1] M. V. Tsodikov, V. Yu. Murzin, A. V. Chistyakov, F. A. Yandieva, M. A. Gubanov, P. A. Zharova, S. S. Shapovalov, O. G. Tikhonova, A. A. Pasynskii, S. Paul, F. Dumeignil, *Chemical Engineering Transactions*, 37 (2014), 583-588

[2] A. V. Chistyakov, M. A. Gubanov, M. V. Tsodikov, *Chemical Engineering Transactions*, 32 (2013), 1093-1098

[3] S.S. Shapovalov, A.A. Pasynskii, Yu.V. Torubaev, I.V. Skabitskii, M. Sheer, and M. Bodenshtainer, *Koord. Khim.*, 3 (2014), vol. 40, pp. 131–136.

I-PP81

Novel Catalytic Route for the Oxidative Dehydrogenation of Ethane and Propane over CeO_2-Based Catalysts

Kang J., Xie Q., Yu F., Zhang Q., Wang Y.*

State Key Laboratory of Physical Chemistry of Solid Surfaces, Collaborative Innovation Center of Chemistry for Energy Materials, National Engineering Laboratory for Green Chemical Productions of Alcohols, Ethers and Esters, College of Chemistry and Chemical Engineering, Xiamen University, Xiamen, China

* wangye@xmu.edu.cn

Keywords: lower alkanes, lower olefins, oxidative dehydrogenation, cerium oxide

1 Introduction

Lower olefins, mainly ethylene and propylene, are among the most important building-block chemicals. The depletion of crude oil has stimulated the development of non-petroleum routes for the production of light olefins. The production of lower olefins from lower alkanes has attracted much attention under the current background of the emergence of large quantity of shale gas. The non-oxidative dehydrogenation of lower alkanes is strong endothermic and thermodynamically limited reactions. In contrast, oxidative dehydrogenation is an exothermic reaction and can be performed at moderate temperatures. However, the selectivity of lower olefins is usually very limited at a considerable alkane conversion due to the deep oxidation, i.e., the formation of CO and CO_2 (CO_x), in the presence of O_2. To increase the olefin selectivity at a high alkane conversion is a particularly challenging task.[1, 2] We developed a new two-step route for the transformation of CH_4 into C_3H_6 via CH_3Cl and found that CeO_2 was an efficient catalyst for the oxidative chlorination of CH_4 to CH_3Cl.[3] Recently, we discovered that CeO_2 could catalyze the direct formation of C_2H_4 or C_3H_6 from C_2H_6 or C_3H_8 with high selectivity in the presence of HCl and O_2. Here, we report this new catalytic system for the oxidative dehydrogenation of C_2H_6 and C_3H_8.

2 Experimental

CeO_2 nanocrystals with different morphologies were synthesized by a hydrothermal method. The modified CeO_2 catalysts were prepared by the impregnation. The catalysts were characterized by various techniques including XRD, SEM, TEM and H_2-TPR. The catalytic reaction was performed on a fixed-bed flow reactor operating at atmospheric pressure. The products were analyzed by on-line gas chromatography.

3 Results and discussion

We first investigated the catalytic performances of various metal oxides including La_2O_3, CeO_2, Eu_2O_3, Nd_2O_3, Dy_2O_3, Tb_4O_7, Fe_2O_3, Co_3O_4, CuO, V_2O_5, Al_2O_3 for the oxidative dehydrogenation of C_3H_8 in the presence of HCl and O_2 and found that CeO_2 exhibited the highest C_3H_6 yield. Over CeO_2 nanorod catalyst, C_3H_6 yield could reach 21.3% with a C_3H_6 selectivity of 56% at 773 K. We investigated the effect of various modifiers on catalytic performances of CeO_2 nanorods. Several modifiers such as MnO_x, MgO, MoO_x, V_2O_5, CuO, could further enhance C_3H_8 conversion or C_3H_6 selectivity (Fig. 1). The C_3H_6 selectivity could be improved significantly over the MoO_x-modified CeO_2 nanorod. The C_3H_6 yield could reach 45% with a C_3H_6 selectivity of ~80% over the 8 wt% MoO_x-CeO_2 catalyst under the optimum condition. To the best of our knowledge, this is highest C_3H_6 yield achieved to date for the oxidative dehydrogenation of C_3H_8.

We clarified that HCl played a critical role in selective formation of C_3H_6. The presence of HCl not only enhanced C_3H_8 conversion but also changed product selectivity significantly over the 8 wt% MoO_x–CeO_2 catalyst (Fig. 2). CO_2 was the main product in the absence of HCl. The increase in the partial pressure of HCl significantly decreased the selectivity to CO_2 and increased that to C_3H_6. Thus, the presence of HCl is required for the selective formation of C_3H_6.

To understand the reaction pathway for the formation of C_3H_6, we investigated the effect of the contact time (*W/F*) on product selectivities at 773 K. The results showed that the selectivities to C_3H_6 and C_3H_5Cl decreased and that to CO_x increased with increasing the contact time. This suggests that C_3H_6 and C_3H_5Cl may be formed as a primary product directly from C_3H_8, and CO_x was the secondary products. Further studies are needed to clarify the C_3H_6 formation mechanism.

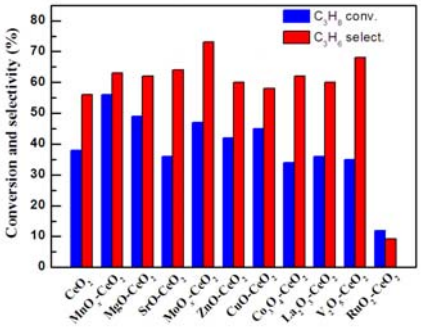

Fig. 1. Catalytic performances of the modified CeO_2 nanorods in the presence of HCl and O_2. Reaction conditions: catalyst, 0.1 g; $P(C_3H_8)$ = 18 kPa, $P(O_2)$ = 18 kPa; P(HCl) = 10 kPa; F = 48 mL min^{-1}; T = 773 K.

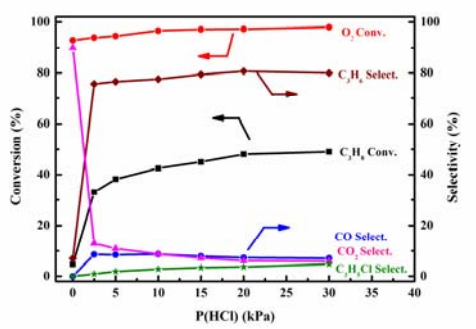

Fig. 2. Effect of HCl partial pressure on the catalytic performance of the 8 wt% MoO_x-CeO_2 catalyst. Reaction conditions: catalyst, 0.2 g; $P(C_3H_8)$ = 18 kPa; $P(O_2)$ = 9 kPa; F = 48 mL min^{-1}; T = 773 K.

We also investigated the oxidative dehydrogenation of C_2H_6 over the CeO_2-based catalyst in the presence of HCl. The yield of C_2H_4 reached ~70% over the 8 wt% MnO_x–CeO_2 catalyst at 723 K. Our catalyst was also very stable and no significant decreases in both C_2H_6 conversion and C_2H_4 selectivity were observed during a 100 h reaction.

We did not observe the formation of Cl_2 during the reaction. H_2-TPR studies showed that the reduction of Ce^{4+} to Ce^{3+} could occur under the reaction conditions. We propose that HCl is activated on catalyst surfaces, generating an active Cl species, which accounts for the selective formation of C_3H_6 or C_2H_4. We speculate that the reduction of Ce^{4+} to Ce^{3+} plays a key role in the activation of HCl to form an active Cl species. The additive, i.e., MoO_x or MnO_x may participate in the reoxidation of Ce^{3+} to Ce^{4+} by O_2.

4 Conclusions

We developed a novel catalytic route for the oxidative hydrogenation of C_3H_8 to C_3H_6 and C_2H_6 to C_2H_4 at moderate temperatures in the presence of HCl. CeO_2 was found to be an efficient catalyst and the modification of CeO_2 by MoO_x or MnO_x further enhanced the formation of C_3H_6 or C_2H_4. The 8 wt% MoO_x–CeO_2 catalyst provided the highest C_3H_6 yield, which approached 50%. We suggest that the redox between Ce^{4+} and Ce^{3+} plays a key role in the activation of HCl to form an active Cl species for lower alkane activation.

References

[1] J. Jesper, R. Javier, S. Eduardo, M. Bert, *Chem. Rev.* 114 (2014) 10613.
[2] R. Grabowski, *Catal. Rev.* 48 (2006) 199.
[3] J. He, T. Xu, Z. Wang, Q. Zhang, W. Deng, Y. Wang, *Angew. Chem. Int. Ed.* 51 (2012) 2438.

I-PP82

Single-Step Hydrotreatment of Lipids to Produce High Quality Biofuel

Wang C., Tian Z.*, Qu W., Li P., Ma H., Xu R.

Dalian National Laboratory for Clean Energy, Dalian Institute of Chemical Physics, Dalian, China

* tianz@dicp.ac.cn

Keywords: lipids, biodiesel, biojet, deoxygenation, isomerization

1 Introduction

Lipids can be converted to biodiesel or biojet fuel via hydrotreatment process. Generally, the existing technology consists of two steps, in which the deoxygenation of lipids to *n*-alkanes and isomerization of *n*-alkanes to *iso*-alkanes are carried out separately, and this will consume considerable hydrogen and energy. To combine the deoxygenation and isomerization reactions in a single step is attractive. However, big amount of water produced in the deoxygenation reaction will poison the isomerization catalyst, which make the single-step process very difficult to be carried out. In this work, a single-step hydrotreatment process for producing biodiesel or biojet fuel from lipids by using bifunctional catalysts was devised, and mechanism of the reactions and structure-activity relationship of the catalysts were also discussed.

2 Experimental

The Pt/zeolite catalysts used for the single-step hydrotreatment process were prepared by impregnation method. Zeolite such as SAPO-11, ZSM-22, ZSM-23, ZSM-5 or Beta was used as the support. The catalytic process was carried out in a 10 mL fixed-bed reactor. The soybean oil was used as feedstock, and the reaction conditions were as follows: 300-380 ^{o}C, 1-8 MPa and 0.2-30 h^{-1}(LHSV). After 3 h reaction, the products were collected and analyzed by GC-MS. The catalysts were characterized by XRD, N_2 adsorption, FT-IR, Pyridine-IR, NH_3-TPD, TPR, XPS, H_2-chemisorption and so on. For the bench-scale evaluation, a 100 mL fixed-bed reactor was used and the reaction conditions were as follows: 330-370 ^{o}C, 4-6 MPa and 1.0 h^{-1}(LHSV).

3 Results and discussion

Table 1 presented the catalytic performance of the catalysts prepared by using six zeolite supports. It can be found that high liquid yields were obtained over the mildly acidic catalyst such as Pt/S1, Pt/S2, Pt/S3 and Pt/Z3. Meanwhile, high selectivity of isomerization was obtained over Pt/S1, Pt/Z1 or Pt/Z2 with more medium and strong Brønsted acidity.

Table 1. Effect of the acidity of the catalyst

Catalyst	Str. L acidity ($\mu mol_{Py}.g^{-1}$)	Med. & Str. B acidity ($\mu mol_{Py}.g^{-1}$)	Catalytic performance			
			Liquid yield (%)	S_{alkane} (%)	$S_{isomerization}$ (%)	C17/C18
Pt/S1[a]	16.8	19.6	92.4	100	63.3	2.4
Pt/S2	7.0	6.7	93.3	100	13.4	3.3
Pt/S3	0.4	0.9	91.9	93.1	5.4	10.2
Pt/Z1	32.5	132.2	57.7	100	84.3	2.5
Pt/Z2	36.7	132.1	63.3	99.2	80.3	1.7
Pt/Z3	1.0	12.4	92.8	96.7	14.7	5.0

[a] SAPO-11 and ZSM-22 zeolite supports without treatment are named S1 and Z1, respectively. The supports after acid-treatment are named S2 and Z2, and those after alkali-treatment are named S3 and Z3.

The reaction scheme of the single-step process is illustrated as Scheme 1[1-4]. There are three parallel pathways including decarboxylation, decarbonylation and hydrodeoxygenation when

lipids are deoxygenated to *n*-alkanes. As mentioned above, water produced in the deoxygenation step is harmful to the isomerization catalyst. Therefore, pathways II and III are more favorable, since the decarboxylation and decarbonylation reactions will produce less water and consume less hydrogen. The ratio of C17 yield to C18 yield (C17/C18) was used to define the ratio of decarboxylation plus decarbonylation versus hydrodeoxygenation. As shown in Table 1 and Fig. 2, it was found that the C17/C18 was significantly influenced by the strong Lewis acidity of the catalyst. Over the catalysts with less Lewis acidity such as Pt/S3 or Pt/Z3, the C17/C18 reached more than 5, which was much higher than that over other catalysts. These results indicated that more decarboxylation (or decarbonylation), isomerization reactions and less cracking reactions will proceed over the catalyst with more medium Brønsted and less strong Lewis acidity[2].

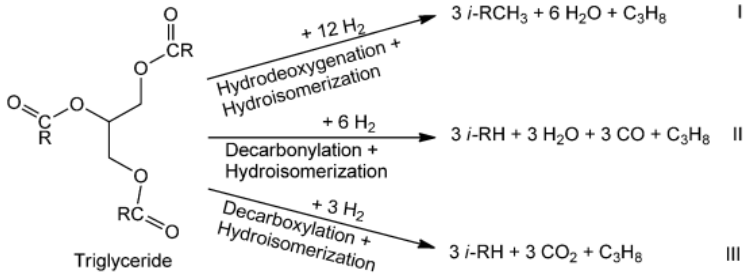

Scheme 1. Plausible reaction pathways of the single-step hydrotreatment

Based on the above results, a bi-metals/zeolite catalyst was developed, and the process was scaled-up in a 100 mL fixed-bed reactor in more than 1000h run (As shown in Fig. 3). The catalyst showed good stability and the product showed excellent properties. The freezing point and octane number of the biodiesel (>290 °C distillate) reached -30 °C and 75, respectively, while the freezing point of the biojet (130~290 °C distillate) reached less than -50 °C .

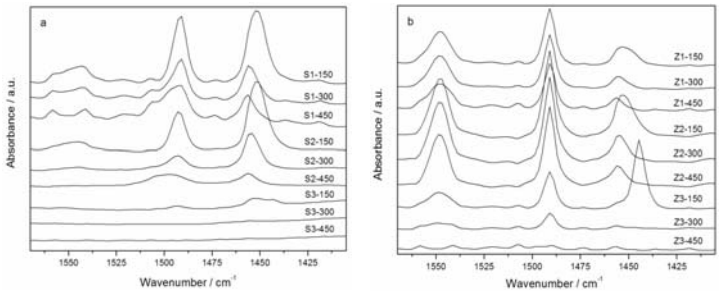

Fig. 2. Pyridine IR spectra of SAPO-11 and ZM-22 supports
S1-150 represents the S1 sample at a pyridine desorbed temperature of 150 °C

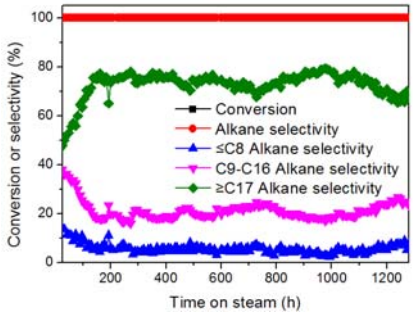

Fig. 3. 100 mL bench-scale evaluation

4 Conclusions

A single-step hydrotreatment process to produce biofuel from lipids was developed, which will perhaps overcome the main problems such as high consumption of hydrogen and energy in the existing processes[5]. Under the drive of traditional energy consumption, this processes will provide new solutions for effective conversion of biomass to liquid fuels.

Acknowledgements

The authors would like to appreciate the financial supports provided by PetroChina and BP.

References

[1] Z. Tian, C. Wang, et al, PCT/CN2012071759. 2012.
[2] C. Wang, Z. Tian*, et al, *ChemSusChem*, 5 (2012), 1974-1983.
[3] C. Wang, Z. Tian*, et al, *Chin. J. Catal.*, 34 (2013), 1128-1138.
[4] C. Wang, Z. Tian*, et al, *Catal. Today*, 234 (2014), 153-160.
[5] S. Dutta, *ChemSusChem*, 5 (2012), 2125-2127.

I-PP83

Bulk Carbonaceous Catalysts of Heavy Hydrocarbon Feedstock Processing

Morozov M.A.[1*], Akimov A.S.[1], Fedushchak T.A.[1], Zhuravkov S.P.[2]

1 - Institute of Petroleum Chemistry SB RAS, Tomsk, Russia
2 - Tomsk Polytechnic University, Tomsk, Russia

* fr0stm4n@yandex.ru

Keywords: heavy oil, restructuring, nanocatalysts, ultrasonic treatment

1 Introduction

Carbon nanomaterials - carbon nanotubes, nanofibers, 3d-metal carbides, nanodiamonds are represent the latest generation of nanosystems. Metal carbides, nanodiamonds are widely known for their ability to catalyze reactions of isomerization, aromatization, hydrogenation but has never before been used as independent catalysts of thermal cracking of heavy oil feedstocks.
At present days scientific direction that can adjust processes crude oil processing through the optimization of the structural composition of the oil disperse systems are actively developing.
The subject of this work was to determine the catalytic activity of nanocarbon systems in the process of thermal cracking of petroleum fractions and thereof residues in synchronous restructuring of oil dispersion system under ultrasonication.

2 Experimental

As an object of research were used Kaliningrad oil fractions (density 0.884 g / cm3, the total sulfur content is 0.053%).This vacuum gas oil (360-470 ° C) and heavy residue (boiling above 380 ° C).Weight of the sample of oil fraction in one experiment is 5 g.Thermal cracking of petroleum feedstock was processed in steel autoclave (volume 10 cm3) in a batch mode in an argon atmosphere at 450 ° C and pressure 0.5-0.7 MPa, the process duration was 120 or 180 minutes.As catalysts were used multilayer carbon nanotubes (catalytic gas-phase pyrolysis of ethylene), 3d-metal carbides, nanodiamonds (ND is products of recycling blasting agents), molybdenum disulfide (mechanical activation during 8 h. in inert atmosphere).Weightofthecatalystinoneexperimentis0.3g (about 6% by weight of the objects which was loaded into the reactor).Qualitative and quantitative composition of the gaseous and liquid products of the cracking of petroleum feedstock were determined by gas chromatography and the gravimetric method. Ultrasonic treatment of the samples was carried out in the ultrasonic disperser (UD-20).

3 Results and discussion

In actual conditions of an atmospheric distillation of heavy oil residue after autoclaving (thermal cracking at 450 ° C for 2 hours) there was no light fractions in temperature range 60-220 ° C.However, pretreatment of the sample in the ultrasonic, followed by autoclaving it under the conditions described above provides output of light fractions in amount of 7% by weight.At the same time, the joint ultrasonic treatment of heavy oil residue and nanocatalyst ensures the formation of light products of thermal cracking at 45-55% depending on the type of catalyst.It gives reason to suppose that the structure of heavy oil residue is changing by ultrasonic waves in the presence of nanosystems in the more favorable direction to proceeding of thermal cracking reactions, rather than under another conditions (ultrasonic treatment of heavy oil residue and subsequent addition of nanocatalyst).As can be seen from the histogram shown in

Figure 1, the highest output of light fractions, ceteris paribus, is observed in the presence of nanocatalysts ND+MoS2, and amounts to 55.2%. Slightly less output for multilayer nanotubes - 49.2%; for WC - 44,3%, for ND - 38.8%.Thus, the amount of gases produced in the specified series changes in the range of 2-5% and the amount of formed coke is less than 1%.

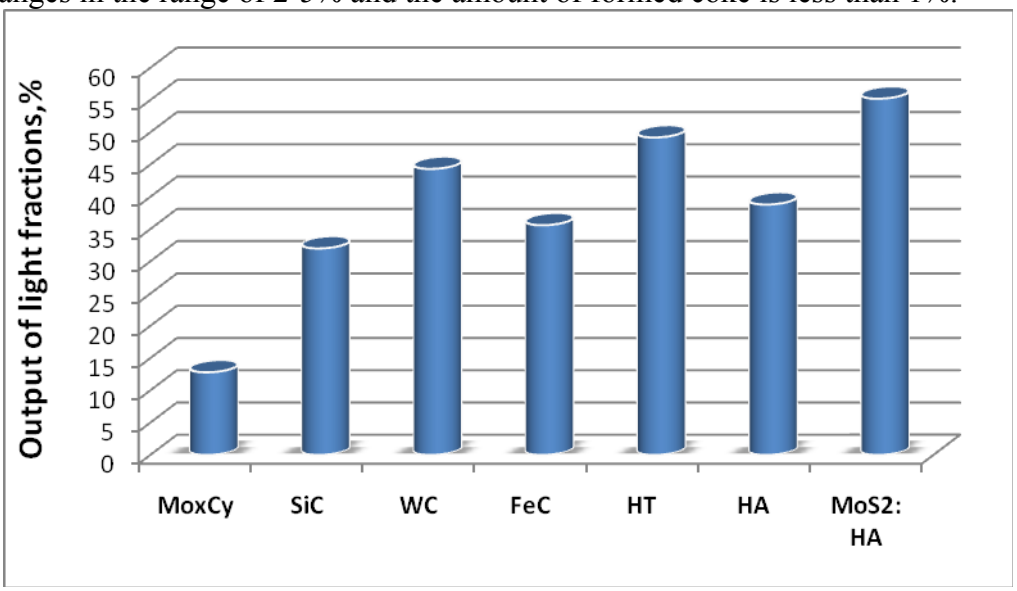

Fig 1. Activity of nanocatalysts in the thermal cracking of heavy oil residues

It is noteworthy that the use as a catalysts multilayer carbon nanotubes allow to reduce catalyst consumption by an order of magnitude; for that nanotubes was discovered the effect of "reinforcement" of heavy oil residue, making it easy to use them repeatedly and to separate from the products by simple decantation of the latter.The report also discusses the results for the thermal cracking of vacuum gas oil in the presence of listed above nanosystems with ultrasonic treatment and without it, the results of thermal analysis for residues products of thermal cracking; also discusses issues relating to the advantages of using of nanosystems for highly paraffin oil fractions (vacuum gas oil and heavy residues).

4 Conclusions

First time was demonstrated the effectiveness of joint ultrasonic treatment of oil disperse systems and nano-carbon catalysts, as a preparatory stage in the process of thermal cracking.The effect of joint treatment appears in increasing of output of light fractions.Were identified nanosystems with a high level of activity in the thermal cracking reactions with low specific consumption of catalysts (0.4 % by weight)

Acknowledgements

The authors are grateful to professors A.S. Noskov and V.L. Kuznecov for their participation in the organization of experiments, providing samples and discussion of the results.

I-PP84

Structure of the Ferrospheres Globules Active in the Total Oxidation and Oxidative Coupling of Methane

Anshits A.G.*, Fedorchak M.A., Anshits N.N., Sharonova O.M., Rabchevskii E.V., Solovyev L.A., Zhizhaev A.M.

Institute of Chemistry and Chemical Technology, Siberian Branch, Russian Academy of Sciences, Krasnoyarsk, Russia

* anshits@icct.ru

Keywords: methane, oxidation, OCM, structure of ferrospheres, ferrospinel

1 Introduction

Binary systems on the base of transition metal oxides with spinel structure are effective catalysts for deep oxidation of methane [1]. At the same time these systems practically have not been studied in the oxidative coupling of methane (OCM). In particular, it was found that the high selectivity of the formation of C_2-hydrocarbons (C2) is observed for systems on the base of zinc and calcium ferrospinels [2, 3]. In the study of the catalytic properties of ferrospheres with the content of Fe_2O_3 ($C(Fe_2O_3)$) in the range of 36–92 wt.% it was shown that at low $C(Fe_2O_3)$ < 88 wt.% the main route of methane oxidation is the deep oxidation. At $C(Fe_2O_3)$ > 89 wt.% OCM becomes the predominant process.[4]. In order to elucidate possible fundamental reasons for the different OCM performance, we thoroughly characterized ferrospheres with $C(Fe_2O_3)$ in the range of 76–98 wt.% in terms of their composition, morphology, microstructure of the iron-containing phases, and catalytic properties.

2 Experimental/methodology

The separation of narrow fractions of constant composition containing Fe_2O_3 in the range 76–98 wt.% was carried out according to [5] by using consecutive stages of grain-size classification, magnetic separation and separation by density. Fly ashes of FS and CS types from the combustion of a high calcium coals used as the raw material. The major component composition was determined by chemical analysis according to GOST 5382-91.

Catalytic activity tests were carried out in a fixed-bed 4–8 mm i.d. quarts reactor at 750°C under total pressure 1.3 at of the feed mixture CH_4:O_2:N_2 = 82:9:9 vol.% with on-line analysis of the feed and the product gases by chromotograph Agilent 7890A GC equipped by high performance columns.

Phase composition of ferrospheres characterized by X-ray powder diffraction, the full profile crystal structure analysis was done using the Rietveld method with the derivation difference minimization refinement.

SEM-EDS study of polished sections globules of ferrospheres narrow fractions was performed using a microscope TM-3000, equipped by energy-dispersive spectrometer Bruker XFlash 430H.

3 Results and discussion

Catalytic properties. Fig. 1 shows the steady-state yields of the two main products of the oxidation of methane: CO_2 ($Y(CO_2)$) and C_2-hydrocarbons (Y(C2)) as a function of $C(Fe_2O_3)$ in ferrospheres. According to the nature of the dependence $Y(CO_2)/C(Fe_2O_3)$ and $Y(C2)/C(Fe_2O_3)$ ferrospheres can be divided into two groups (Fig. 1). For the first group there is observed a monotonic reduction of $Y(CO_2)$ by one order of magnitude and a stable low value for Y(C2)

with increasing of C(Fe_2O_3) (Fig. 1a). For the second group there is a sharp increasing Y(C2) when the content of Fe_2O_3 = 89 wt.% and a subsequent certain its decrease with increasing C(Fe_2O_3). A similar dependence is observed for Y(CO_2) (Fig. 1b).

The different catalytic activity of the ferrospheres narrow fractions obviously associated with a different phase composition, structural characteristics of iron-containing phases in the ferrospheres of the different morphological types. In ferrospheres with C(Fe_2O_3) in the range of 67–88 wt.% a ferrospinel lattice parameter increases in the range of 8.344–8.396 Å and reaches a value characteristic for stoichiometric magnetite. The observed increase of the lattice parameter is explained by the substitution of ions Al^{3+} and Mg^{2+} in the structure of ferrospinel by iron ions. For ferrospheres with C(Fe_2O_3) > 89 wt.% the parameter exceeds the value 8.396 Å, which can be explained by the different levels of doping of magnetite by calcium oxide.

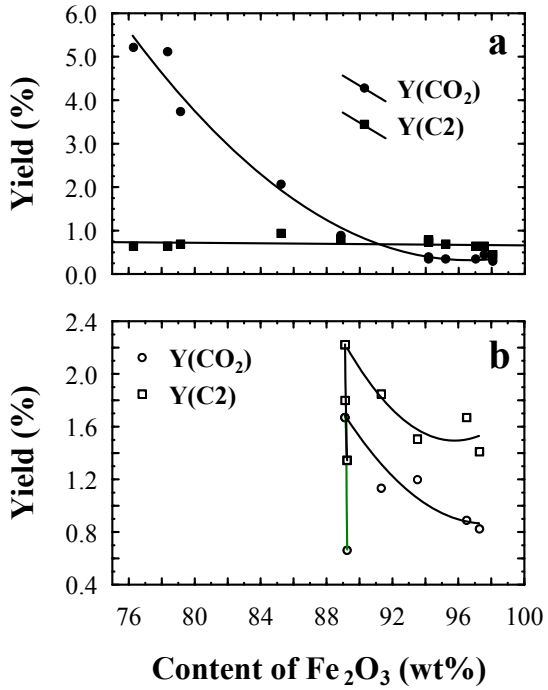

Fig. 1. The yield of the methane oxidation products at 750°C as a function of the total iron content in ferrospheres of group 1 (a) and 2 (b).

The composition of the individual globules. SEM-EDS study of the chemical compositions of polished sections of individual globules of fractions with C(Fe_2O_3) = 78.4, 93.5 and 95.2 wt.% with different activity in the OCM process and methane deep oxidation was carried out. In particular it is shown that for a fraction C (Fe_2O_3) = 78.4 wt.% with the predominant activity in methane deep oxidation the ratio of globules content of the skeletal-dendritic and block-like structures is 2:1. In fraction with C(Fe_2O_3) = 93.5 wt. % with the highest contribution in OCM the globules ratio of the skeletal-dendritic, block-like and sheet-like types is 1:6:1. The fraction with C(Fe_2O_3) = 95.2 wt.% with low activity in both reactions contains globules mainly block-like type.

4 Conclusions

The detailed analysis of the obtained results including chemical composition of individual ferrospheres of different morphological types allows us to conclude that the globules with high Al_2O_3 and MgO content and skeletal-dendritic structure are responsible for the deep oxidation of methane. The reaction OCM takes place on the sheet-like type globules with high CaO content. The block-type globules have a low activity in both reactions.

Acknowledgements

This study was supported by the grant of Russian science Fund (project No. 14-13-00289).

References

[1] G.K. Boreskov. *Catalysis. The Questions of Theory and Practice.* Novosibirsk: Nauka, 1987.
[2] Papa F., Patron L., Carp O., Paraschiv C., Ion B. *J. Mol. Catal. A. Chem*. 299 (2009) 93.
[3] Anshits A.G., Voskresenskaya E.N., Kondratenko E.V., Fomenko E.V., Sokol. E.V. *Catal. Today*. 42 (1998) 197.
[4] Vereshchagin S.N., Kondratenko E.V., Rabchevskii E.V., Anshits N.N., Solovyov L.A., Anshits A.G. *Kinet. Catal*. 53 (2012) 449.
[5] Sharonova O.M., Anshits N.N., Solovyov L.A., Salanov A.N., Anshits A.G. *Fuel.* 111 (2013) 332.

I-PP86

Production of Bio-Renewable Chemicals Using Zeolite Encapsulated Metal Nanoparticles as Bi-Functional Catalysts

Mielby J., Zacho S.L., Abildstrøm J.O., Kegnæs S.*

DTU Chemistry, Technical University of Denmark, Kgs. Lyngby, Denmark

* skk@kemi.dtu.dk

Keywords: MIBK, acetone, nanoparticles, mesoporous, recrystallization, zeolite

1 Introduction

As a consequence of the continuing depletion of fossil resources, the future chemical industry must gradually rely on renewable resources such as biomass to produce bulk and fine chemicals. An important chemical that is that is currently produced directly or indirectly from propylene is acetone. A large amount of acetone is produced via the cumene process and is therefore tied to the production of phenol. Other processes involve the direct oxidation of propylene or the hydration to isopropanol, which is then oxidized to acetone. Fortunately, acetone can also be produced by fermentation [1] and with the on-going developments in biomass processing it seems likely that bio-acetone may become an equally important platform molecule for the production of a broad range of chemicals from biomass.

One of the products that can be produced from acetone is methyl isobutyl ketone (MIBK). Traditionally, this is done in a three step process involving the base-catalyzed aldol condensation of acetone to diacetone alcohol, an acid-catalyzed dehydration to mesityl oxide and a metal-catalyzed hydrogenation to MIBK [2], see ***Scheme 1***. Heterogeneous bi-functional catalysts that contain both acid-base and metal active sites and are able to catalyze all three reactions in one step without separation of the intermediates have therefore attracted considerable interest.

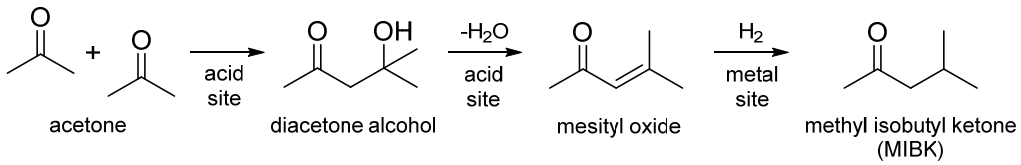

Scheme 1. One-step process for production of MIBK from acetone.

Here, we present the latest results from our on-going investigations of zeolite encapsulated metal nanoparticles and their activity and selectivity as bi-functional catalysts for the direct production of MIBK from acetone. In this reaction, the zeolite facilitates the acid catalyzed aldol condensation of acetone to mesityl oxide, while the metal nanoparticles (Ni, Pd or Pt) catalyze the following hydrogenation to MIBK.

2 Results and discussion

In order to study the effect of morphology and the close proximity between the acid and metal active sites, the metal nanoparticles (Ni, Pd and Pt) were supported on a conventional ZSM-5 zeolite as well as on a mesoporous and a recrystallized ZSM-5 zeolite. All metals were deposited by simple incipient wetness impregnation followed by drying and reduction under hydrogen.

The mesoporous zeolite was prepared by carbon-templating following the method developed by Jacobsen et al. [3] In this method, a carbon source (e.g. carbon black) is impregnated with the zeolite precursors before the material is subjected to hydrothermal crystallization. During the subsequent calcination, the carbon template is removed by combustion to leave the mesoporous catalyst.

The recrystallized zeolite was prepared by an alkaline dissolution-reassembly process performed in the presence of a surfactant [4]. The alkaline dissolution was performed in an aqueous solution of ammonium hydroxide and cetyl trimethylammonium (CTAB) at room temperature and the reassembly was performed in an autoclave under hydrothermal conditions. After the recrystallization the zeolite was washed, dried and calcined to remove the remaining surfactant. ***Figure 3***A show how the recrystallization result in the formation of intra-particles voids and mesopores that provide ideal conditions for the formation small and disperse metal nanoparticles upon simple impregnation (here shown with Ni). The nanoparticles are situated inside the zeolite rather than on the outer surface, but remain readily accessible through the inherent microporous structure. ***Figure 3***B show the N_2 physisorption isotherms of the investigated zeolites.

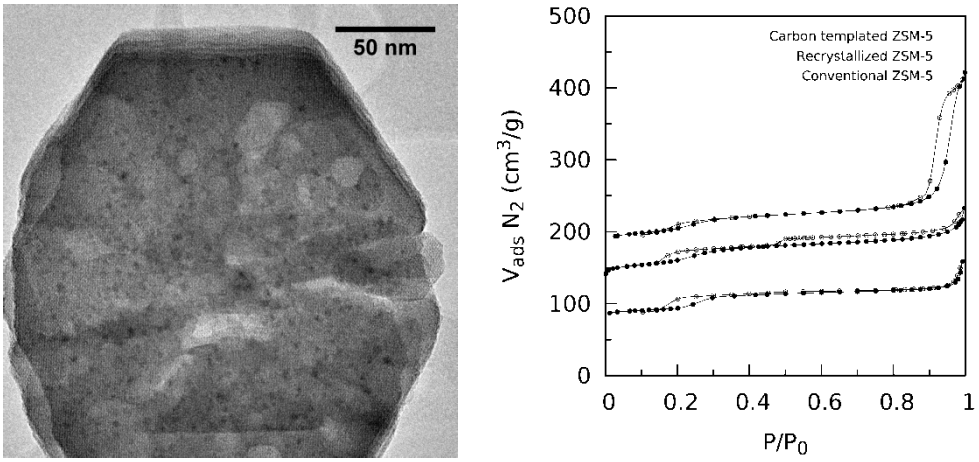

Figure 3. A) TEM image of Ni nanoparticles encapsulated in recrystallized zeolite ZSM-5. B) N_2 physisorption isotherms of the investigated zeolites at 77 K. Please note that the isotherm of the recrystallized and carbon templated and zeolite is offset by 50 and 100 cm^3/g, respectively.

3 Conclusion

In conclusion, we have investigated different zeolite supported metal nanoparticles (Ni. Pd and Pt) as bi-functional catalysts for the direct production of MIBK from acetone. Furthermore, we have developed a new and simple method to encapsulate metal nanoparticles in zeolites. Although encapsulated metal nanoparticles have many potential applications, previous attempts to encapsulate metal nanoparticles in zeolites have relied on expensive additives and complex synthetic procedures. Until now, the exploration and exploitation of zeolite encapsulated metal nanoparticles has therefore remained very limited. In contrast, our method is simple, effective and scalable and we therefore hope that impregnation of recrystallized zeolites may become a useful tool in the development of new and efficient bi-functional heterogeneous catalysts.

Acknowledgements

The authors gratefully acknowledge the support of the Danish Council for Independent Research, Grant No. 12-127580.

References

[1] Wang, Y., Janssen, H. and Blaschek, H. P. (2014) Fermentative Biobutanol Production: An Old Topic with Remarkable Recent Advances, John Wiley & Sons (2014).
[2] K. Weissermel, H.-J. Arpe, *Industrial Organic Chemistry*, Wiley-VCH Verlag GmbH (2003).
[3] K. Johannsen, A. Boisen, B. Brorson, I. Schmidt and C. J. H. Jacobsen, *Stud. Surf. Sci. Catal*. (2002), 142, 109.
[4] J. Mielby, J. O. Abildstrøm, F. Wang, T. Kasama, C. Weidenthaler and S. Kegnæs, *Angew. Chem.*, (2014), 126, 12721.

I-PP87

The Role of Cobalt Sulphide Particles in Alumina Supported CoMo HDT Catalysts

Pimerzin Al.A.*, Nikulshin P.A., Mozhaev A.V., Pimerzin A.A.

Samara State Technical University, Samara, Russia

* al.pimerzin@gmail.com

Keywords: hydrotreating, heteropolycompounds, cobalt sulphide, CoMoS, hydrogen spillover

1 Introduction

The objective of the research was to investigate the effect of the modifying alumina surface with cobalt sulphide on the physicochemical characteristics of the CoMoS active phase formed from Co_2Mo_{10}HPA as well as catalytic properties of the $Co_2Mo_{10}/Co_x/Al_2O_3$ catalysts. Moreover, the role of cobalt sulphide particles on the surface of alumina supported CoMo-catalysts and the assumption about hydrogen spillover over catalyst surface from cobalt sulphide particles to CoMoS phase crystallites were studied.

2 Experimental/methodology

Commercial sample of alumina (with specific surface area 220 m^2/g, pore volume 0.74 cm^3/g, effective pore radius 31.5 Å) was used in this work. Co-modified carriers Co_x/Al_2O_3 As well as $Co_2Mo_{10}/Co_x/Al_2O_3$ catalysts were prepared by wetness impregnation of alumina with aqueous solutions containing the required amounts of Co (II) nitrate and Co_2Mo_{10}Am, respectively.

The catalysts were analyzed using X-ray powder diffraction, N_2 physisorption, high-resolution transmission electron microscopy and X-ray photoelectron spectroscopy. The catalysts were tested in the hydrodesulphurization (HDS) of dibenzothiophene and 4,6-dimethyldibenzothiophene and the hydrodenitrogenation (HDN) of quinoline.

3 Results and discussion

The catalysts with equal Mo loading, precursor and morphology of the active phase and differ only in Co_9S_8 phase content on the surface demonstrate significant difference in catalytic properties in DBT HDS. $Co_2Mo_{10}/Co_{8.1}/Al_2O_3$ catalyst with high amount of Co_9S_8 demonstrated the same activity at 275°C as it was obtained at 300°C on no-modified catalyst previously. This result corresponds to evaluated value of spillover effect. This outcome is cautiously interpreted in favor of spillover effect due to cobalt sulphide ability to accumulate and activate molecular hydrogen.

The same trends may be observed for the HDS of 4,6-DMDBT. The increase of Co loading in support resulted in the growth of CoMoS active sites efficiency. *TOF* values increase more than twice with cobalt sulphide addition to alumina support. Reference *TOF* value is 0.13×10^4 s^{-1} while $Co_2Mo_{10}/Co_{8.3}/Al_2O_3$ catalyst demonstrate 0.47×10^4 s^{-1} *TOF* in 4,6-DMDBT HDS. $Co_2Mo_{10}/Co_x/Al_2O_3$ catalysts with Co content in alumina more than 4 wt.% demonstrate a considerable increase of *TOF* (Fig. 1). That happens due to the increase of hydrogenating activity which was confirmed by the 4,6-DMDBT HDS selectivity ratio. It grew from 5.5 to 7.5 with Co addition to alumina.

In case of Qui HDN, catalytic activity grew less than in HDS reactions. The extent of denitrogenation increased from 35 to 42 % with cobalt addition to support, whereas *TOF* almost doubled.

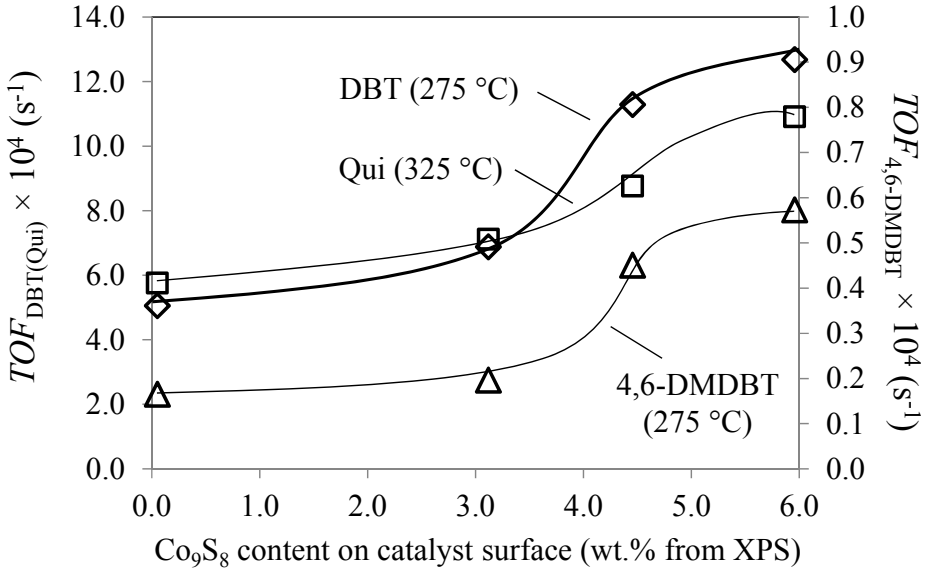

Fig. 1. Dependence of *TOF* values of DBT and 4,6-DMDBT HDS (at 275 °C, 40 h^{-1}) and Qui HDN (at 325 °C, 20 h^{-1}) reactions over $Co_2Mo_{10}/Co_x/Al_2O_3$ catalysts on Co_9S_8 content

4 Conclusions

$Co_2Mo_{10}/Co_x/Al_2O_3$ catalysts synthesized using Co_2Mo_{10}Am and Co-modified alumina had equal morphology, composition and promotion degree of the formed CoMoS active phase. Prepared samples differed from each other only in Co_9S_8 phase concentration on their surfaces, which increased with cobalt addition to the support. That is why, the investigation of the role of cobalt sulphide particles in HDT catalysts became possible.

It was shown that highly dispersed cobalt sulphide particles located on the catalysts surface exerts beneficial effect on the catalytic properties of $Co_2Mo_{10}/Co_x/Al_2O_3$ catalysts. Obtained results, also, make it possible to reassess the role of cobalt sulphide particles in HDT catalysts. The sufficient quantity of Co_9S_8 particles located on the catalysts surface can play the role of a donor of activated hydrogen, which can spill over to CoMoS active phase species over alumina surface and, thereby, increases TOF of the reactions. Therefore, cobalt sulphide entities have a positive effect on the efficiency of promoted CoMoS active sites in hydrogenolysis of heterocyclic compounds. Determined enhancements of the *TOF* values of HDS, HYD and HDN reactions on CoMoS sites are useful for developing new highly effective catalytic materials.

All presented results have been discussed in more details in [1].

Acknowledgements

Al.A. Pimerzin thanks Haldor Topsøe Company for the grant to perform his PhD paper (2012–2014). The work was supported by Ministry of Education and Science of Russian Federation (project № 2014/199).

References

[1] Al.A. Pimerzin, P.A. Nikulshin, A.V. Mozhaev, A.A. Pimerzin, A.I. Lyashenko, *Appl. Catal. B*. 168-169 (2015) 396-407.

I-PP88

Influence of Cu and Mo on Catalytic Activity of Modified Ni Based Catalysts in Hydrodeoxygenation Process of Plant Lipids

Kukushkin R.G.*, Yakovlev V.A.

Boreskov Institute of Catalysis SB RAS, Novosibirsk, Russia

* roman@catalysis.ru

Keywords: biofuel, hydrodeoxygenation, Ni-containing, catalysts

1 Introduction

Increase in energy consumption, environmental issues creates the need to develop alternative methods of energy production from biomass. Renewable biofuels are needed to partially displace petroleum derived transport fuels [1] and diversify local energy source in some region. Although the use of vegetable oils as a fuel is still considered today [2], they have certain drawbacks that lead to problems in the long-term operation of internal combustion engines [3]. Removing of oxygen from esters (biodiesel) and triglycerides by hydrodeoxygenation is required for production of hydrocarbons – biofuels competitive with conventional fossil derived fuels [4]. Ni - containing catalysts are known to be active in the hydrodeoxygenation of vegetable oils [5], Ni-Cu alloys exhibit activity in the hydrodeoxygenation of biodiesel [6], nickel-molybdenum alloys are known to have higher chemical resistance to acids as compared with monometallic nickel catalysts [7]. The aim of this study is the investigation of hydrodeoxygenation of esters in the presence of Ni-containing catalysts modified by Cu and Mo.

2 Experimental/methodology

Hydrodeoxygenation experiments were performed in continuous flow reactor over heterogeneous catalysts. The hydrodeoxygenation catalysts performance was tested at P = 1 MPa and 300 °C. The feed rates of Ar, as a carrier gas, and hydrogen were 15 and 5 L/h, respectively. Methyl palmitate and ethyl caprate mixture was used as a substrate. LHSV was 3 h^{-1}. Catalysts fraction was from 0.2 to 0.5 mm and was reduced before reaction at 520 ºC and P = 0.1 MPa by hydrogen. After reduction, the reactor was cooled to a 300 ºC and the substrate was added to the feed. The liquid phase was sampled once per hour. The gas products obtained in the hydrodeoxygenation reaction were analyzed by GC during the experiments, liquid phase was analyzed by GC and product identification was made using GC-MS technique.

3 Results and Discussion

In our work hydrodeoxygenation process was conducted over Ni - based catalysts (Ni-Cu/Al_2O_3, Ni-Mo/Al_2O_3 and Ni-Cu-Mo/Al_2O_3). In our work Ni/Al_2O_3 catalyst was modified by copper. On the one hand it was shown that increasing of copper content (Table 1) in the Ni-Cu/Al_2O_3 catalysts led to decreasing conversion of esters (Figure 1). On the other hand the increase in the copper content led also to an decrease in the production of undesired product - methane. Conversion of the esters in the presence of unmodified Ni/Al_2O_3 catalyst was higher than in the presence of catalyst modified by Cu (Figure 1).

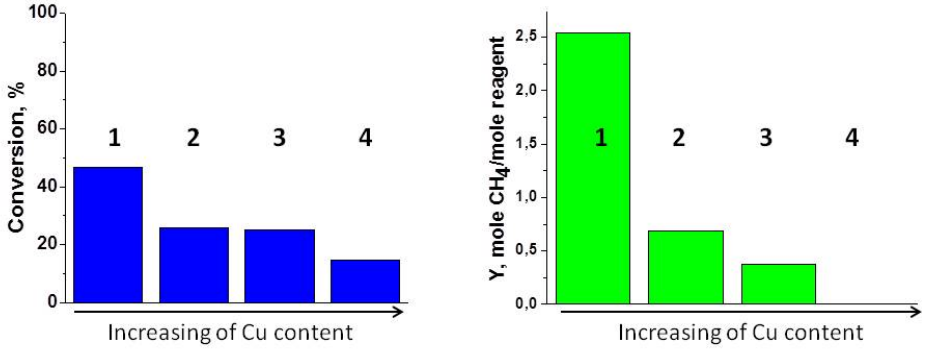

Fig. 1. Conversion and degree of methanisation in the presence of catalysts Ni-Cu/Al2O3, and Ni-Cu-Mo/Al2O3 at 300 ºC, $P_{hydrogen}$= 0.25 MPa and LHSV = 3 h^{-1}.

Alumina supported copper is not active in the reaction of esters hydrodeoxegenation and oxygen containing products only were formed in the presents of Cu/Al_2O_3 catalyst.

Table 1. Elemental analysis of nickel catalysts before reducing treatment.

Catalyst	Ni	Cu
1	10	-
2	9	1.5
3	8	2.5
4	14	-

In the next step of our investigation the influence of molybdenum on activity of Ni-based catalyst in esters hydrodeoxygenation reaction was studied. Ni-Cu catalyst were additionally modified by molybdenum. The maximal conversion of esters has been observed over Ni-Cu-6.9Mo/Al_2O_3 catalyst with alkanes as main products. Yield of alkanes increased with Mo content increasing. According to the XRD and HRTEM data, all samples after reduction contain solid solutions with different compositions [8]. It was shown by XPS that HDO increase with increasing of 4+ oxidation state of Mo on the surface of the Ni-Cu-Mo/Al_2O_3 catalysts [8]. Kinetic model of hydrodeoxygenation reaction of ester over Ni-Cu-Mo catalyst was proposed.

4 Conclusion

Correlations between molybdenum and copper content, structure and surface of the Ni based catalysts and their activity in the hydrodeoxygenation reaction of esters were observed. It was shown that catalytic activity correlate with the content of Mo^{4+} form on the surface of Ni-Cu-Mo catalysts [8] and Ni/Cu relation in the content of the Ni-Cu catalysts.

Acknowledgements

The authors acknowledge the support of RFBR (Russia) through the grant No 14-03-31844.

References

[1] R. Luque, et al., High Energy Density Phisics, 1 (2008) p.542-564.
[2] F. Jiménez Espadafor, et al., Transportation Research Part D, 14 (2009) p. 461-469.
[3] F. Ma, et al., Bioresource Technology, 70 (1999) p. 1-15.
[4] O.I. Senol, et al., Catalysis Today, 106 (2005) p. 186-189.
[5] N. Shi, et al., Catalysis Communication, 20 (2012) p. 80-84.
[6] V.A. Yakovlev, et al., Catalysis Today, 144 (2009) p. 362-366.
[7] H. Alves, et al., J.A.R. Editor-in-Chief, Editor. Elsevier: Oxford. 2010. p. 1879-1915.
[8] R.G. Kukushkin, O.A. Bulavchenko, V.V. Kaichev, V.A. Yakovlev, Applied Catal. B, 163 (2015) p. 531-538.

I-PP89

Effect of Mesoporosity and Acidity on the Hydroconversion of N-Hexadecane over Pt/Based Catalysts

Iliopoulou E.F.[1*], Heracleous E.[1,2], Lappas A.A.[1], Triantafyllidis K.S.[1,3], Linares N.[4], Garcia Martinez J.[4]

1 - Laboratory of Environmental Fuels and Hydrocarbons, CPERI/CERTH, Thessaloniki, Greece
2 - International Hellenic University, School of Science and Technology, Thessaloniki, Greece
3 - Dept. of Chemistry, Aristotle University of Thessaloniki, Thessaloniki, Greece
4 - Molecular Nanotechnology Lab., Departamento de Química Inorgánica, Universidad de Alicante, Alicante, Spain

* eh@cperi.certh.gr

Keywords: n-hexadecane, hydroconversion, Pt/ZSM-5, Pt/silica-alumina, acidity, mesoporosity

1 Introduction

Production of hydrocarbons by the gasification of biomass and subsequent Fischer–Tropsch (FT) reaction is a very promising route for renewable fuel production. The F-T process produces a high amount of F-T waxes, which are then upgraded by hydrocracking. Hydrocracking is carried out over bifunctional catalysts composed by a hydrogenating–dehydrogenating component (usually a highly dispersed noble metal) supported on an acidic carrier, which provides the cracking/isomerization function. Ideally, a balance between the two functions is required to produce a fuel with high cetane number (linear alkanes) and simultaneously good cold flow properties (branched alkanes) [1]. The purpose of the current work is to investigate the effect of acidity and mesoporosity of Pt/based catalysts supported on conventional or mesoporous ZSM-5 carrier and a commercial, amorphous, mesoporous silica/alumina support on the hydrocracking of F-T waxes using n-decahexane as the model compound.

2 Experimental/methodology

A commercial ZSM-5 zeolite (SiO_2/Al_2O_3 ratio: 30) was subjected (a) to calcination (400°C/3h/air) to transform the ammonium to the proton-form (H-ZSM-5) and (b) to alkaline treatment of H-ZSM-5 with a solution of NaOH for the desilication of the zeolitic framework and mesoporosity formation. The desilicated sample was acid treated with an HCl solution to remove the extra-framework Al debris and restore the initial Si/Al ratio. The derived sample was calcined (400°C/3h/air) to obtain the final material in its H-form (herein labeled as ZSM-5(meso)). A commercial silica-alumina was also used as a mesoporous support of moderate Brönsted acidity. Pt was impregnated on all three supports. All samples were calcined (400°C/3hr/air). Characterization was performed by BET, XRD, ICP and FTIR-pyridine adsorption for acidity measurement. Hydroconversion tests were realized on a high pressure test unit, equipped with a fixed bed reactor, using n-hexadecane as a model compound. The reaction was conducted at 30 bar, 275°C, using a weight hourly space velocity (WHSV) of $4h^{-1}$ and a H_2/HC molar ratio of 7.5. The liquid samples were analyzed with PIANO analysis, while the composition of the reaction off-gases was detected by a GC.

3 Results and discussion

Characterization results of zeolitic carriers are summarized in Table 1, while properties of silica-alumina and Pt-based catalysts are currently measured. Concerning the surface area of the materials, a slight decrease is initially observed due to the alkaline treatment (not shown here), which however is significantly increased after the acid treatment. Pore size distribution confirms that alkaline (not shown here) and acid treatments gradually lead to mesoporosity formation,

since the parent zeolite exhibits mainly microporosity. Acidity is a very important property of the zeolitic catalysts, as both hydroisomerization and undesired hydrocracking reactions take place over the acid catalytic centres. Alkaline treatment decreases the Brönsted and increases the Lewis acid sites (not shown here), simultaneously lowering the total acidity, a fact probably related with the formation of extraframework Al due to the targeted removal of Si, which can explain both the formation of Lewis centres and the decrease in total acidity. On the contrary, the further acid treatment leads to a slight restoration of the total acidity, mainly attributed to the significant increase in Brönsted acidity, derived via the dealumination of the zeolitic framework.

Table 1. Textural, acidic properties and chemical composition of the zeolitic carriers

Catalyst	Porosity characteristics			Acidic characteristics	
	Surface area (m^2/g)	Micro-porosity (cm^3/g)	Meso-Porosity (cm^3/g)	Brönsted sites (μmol/g)	Lewis sites (μmol/g)
H-ZSM-5	357	0.136	0.104	265.564	54.926
ZSM-5(meso)	600	0.141	1.149	156.071	115.507

In terms of catalytic efficiency, Pt/ZSM-5(meso) catalyst presented significantly lower activity compared to Pt/H-ZSM-5 (33.1% vs 64.5% conversion), which can be related with its quite lower Brönsted acidity. Moreover, the Pt/mesoporous zeolite catalyst favoured the production of isomers of lower C number (C_4-C_6). The higher pores sizes, due to mesoporosity incorporation, combined with the adequately retained acidity, seem to enhance undesired secondary cracking reactions, as evidenced by the drastically reduced C_7-C_{10} product components (Fig.1).

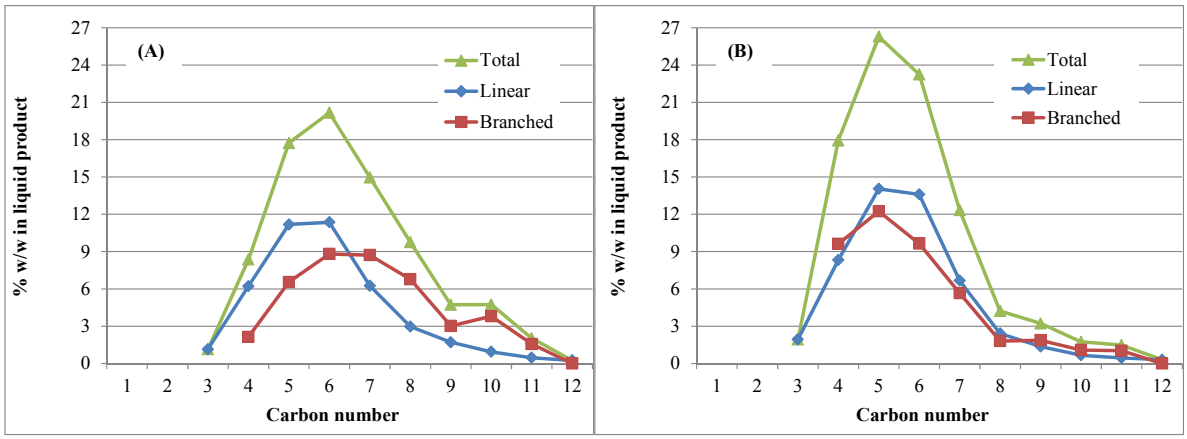

Fig. 1. Cracking product distribution on: (A) Pt/H-ZSM-5; (B) Pt/ZSM-5 (meso)

4 Conclusions

Bifunctional catalysts consisting of Pt on amorphous silica–alumina and zeolitic (ZSM-5) supports were prepared for the hydrocracking of n-hexadecane (n-$C_{16}H_{34}$). Introduction of mesoporosity in ZSM-5 was accompanied by changes in Brönsted and Lewis acid sites distribution. Evaluation of Pt/ZSM-5 catalysts performance showed significant differentiations in activity. Decreased acidity led to less active material, while the presence of mesoporosity additionally affected selectivity, slightly enhancing formation levels of C_4-C_6 products.

Acknowledgements

This work is financially supported by the CAPITA – ERANET, "WAVES:WAste bio-feedstocks hydro-Valorisation processES", 13CAPITA-13-6 Project.

References

[1] F. Regali, M. Boutonnet, S. Järås, *Cat. Today* 214 (2013) 12.

I-PP90

Hydrolysis of Carbohydrates in Green Algae Using Solid Acid Catalysts

Pezoa Conte R.[1*], Pham T.N.[2], Mäki-Arvela P.[1], Willför S.[3], Mikkola J.-P.[1,2]

1 - Industrial Chemistry and Reaction Engineering, Johan Gadolin Process Chemistry Centre, Åbo Akademi University, Åbo-Turku, Finland

2 - Technical Chemistry, Department of Chemistry, Chemical-Biological Center, Umeå University, Umeå, Sweden

3 - Wood and Paper Chemistry, Johan Gadolin Process Chemistry Centre, Åbo Akademi University, Åbo-Turku, Finland

* rpezoa@abo.fi

Keywords: solid acid catalyst, macroalgae, hydrolysis, carbohydrates, monosaccharide

1 Introduction

Nowadays the scientific community agrees that there is a need of using renewable resources, in order to keep production of chemicals and energy in the long term in a more sustainable way. Algae are organisms living in marine environments that have a huge potential to meet this challenge. Among the most outstanding properties in algae they contain substantial amount of carbohydrates, higher grow rates compared to terrestrial plants and absence of lignin which makes its carbohydrates more accessible to hydrolysis.

Hydrolysis of oligosaccharides using acid catalysts has been already reported, mainly using hemicelluloses as raw material and solid acid catalyst such as Smopex, Amberlyst and zeolites [1,2]. These works have obtained complete conversion and sugar yields up to 85 wt-% [3].
In this work, we report the catalytic hydrolysis of carbohydrates from green algae *Ulva rigida* using the catalyst Amberlyst-70 for production of sugars.

2 Experimental/methodology

175 mL of deionized water (DI, Millipore) were disposed in the 250 mL glass reactor over a heating pot. The heating pot was set up at 110°C in order to control temperature inside the reactor to be 90°C, which was monitored by a thermometer in contact with the reaction solution at all time. Once the set up temperature was achieved, 785 mg of Amberlyst-70, equivalent to 0.01 mol H+ eq./L, and subsequently 2,000 mg of previously freeze dry *U. rigida* were disposed into the reactor. The system was continuously agitated by a stirrer at 800 rpm. The reaction was carried out for 259 hours. Samples of 2.6 mL were taking at 0, 2 h and every 24 h until the end of the reaction time. Once reaction time was completed, the reactor was cooled down under a stream of running water and then filtered though a glass fiber filter. Fibers were thoroughly washed with deionized water, kept in freezer and freeze dried overnight. Samples, final solution and remaining fibers were kept in freezer prior monomer and carbohydrate analyzes in gas chromatograph as described in [4]. Several physicochemical methods such as OEC, TGA and EDXA were used to characterize the solid residue.

3 Results and discussion

Total carbohydrate content of fresh *U. rigida* resulted in 400 mg/g of dry algae reported by gas chromatography. Glucose content is high in *U. rigida*, accounting for 183 mg/g of dry algae, whereas rhamnose and xylose content were 81 and 39 mg/g of dry algae. On the contrary, cellulose content was very low; suggesting that the value of glucose reported may come from starch.

In order to quantify carbohydrate dissolution and carbohydrate hydrolysis into monomers, total carbohydrate content and total monomers content were analyzed in the liquid phase. Fig. 1 shows the carbohydrate dissolution and hydrolysis kinetics. The results show relatively fast carbohydrate release, 63.4 wt-% in 259 hours (relative to total carbohydrate contained in *U. rigida*), whereas carbohydrate hydrolysis to monomers was rather slow under these reaction conditions, achieving a maximum of 13.6 wt-%. The carbohydrate hydrolysis starts very slow during the first 100 hours of reaction, due to initial dissolution of carbohydrate species such as ulvan or starch. At 100 hours of reaction the carbohydrate hydrolysis of *U. rigida* started to increase slowly. These results clearly show that it is possible to verify monomers production by this method, although temperature is rather low to accelerate hydrolysis kinetics.

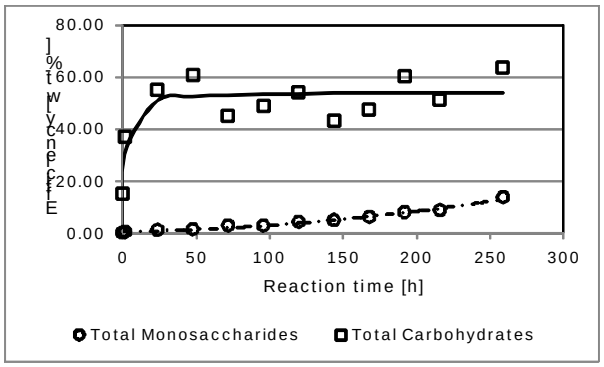

Fig. 1. Efficiency of catalytic hydrolysis of carbohydrates contained in *U. rigida*. Catalyst: Amberlyst 70 0.01 M H^+ eq., Temperature 90ºC.

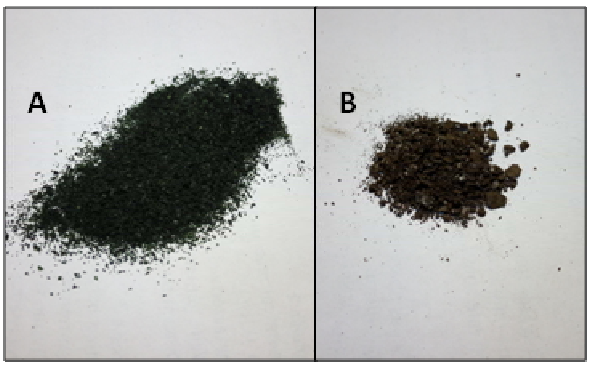

Fig. 2. (A) Pristine *U. rigida* sample. (B) Residue left after catalytic hydrolysis using Amberlyst 70 0.01 M H^+ eq. at 90ºC for 259 hours.

U. rigida samples fresh (A) and residue (B) are depictured in Fig 2a,b. The brown colour observed in the residue is related to its low carbohydrate content, accounting for 40.32 mg/g of dry treated algae, thus confirming carbohydrate removal from the pristine sample.

4 Conclusions

Catalytic hydrolysis of carbohydrate contained in macroalgae show great potential in terms of production of sugars for further applications such as biofuel production. However, more experiments are required to complement the present work and optimization of hydrolysis yields, by testing different catalyst, slightly increase of temperature and use of pressurized reactors.

Acknowledgements

This work is a part of the activities of Johan Gadolin Process Chemistry Centre (PCC), a centre of excellence financed by Åbo Akademi University. Academy of Finland is gratefully acknowledged for funding this project. In Sweden, the Bio4energy programme, Kempe Foundations (Kempe Stiftelserna) and Wallenberg Wood Science Center under auspices of Knut and Alice Wallenberg Foundation are gratefully acknowledged. Prof. Mario Edding from the Research and Technological Center in Applied Phycology Northern Catholic University is acknowledged for kindly donating algae samples.

References

[1] B. Kusema, G. Hilmann, P. Mäki-Arvela, S. Willför, B. Holmbom, T. Salmi, D.Y. Murzin, *Catalysis Letters* 141 (2011), 408-412.
[2] P. Carà, M. Pagliaro, A. Elmekawy, D. Brown, P. Verschuren, N. Shiju, G. Rothenberg, *Catalysis & Technology* 3 (2013), 2057-2061.
[3] L. Vilcocq, P. Castilho, F. Carvalheiro, L. Duarte, *Chemistry & Sustainability* 7 (2014), 1010-1019.
[4] I. Anugwom, V. Eta, P. Virtanen, P. Mäki-Arvela, M. Hedenström, M. Hummel, H. Sixta, J.-P. Mikkola, *Chemistry & Sustainability* 7 (2014), 1-8.

I-PP91

Mesoporous Zeolites Synthesised with In Situ Generated Carbon Template

Abildstrøm J.O., Gallas-Hulin A., Mielby J., Kegnæs S.*

Technical University of Denmark, Kgs. Lyngby, Denmark

* skk@kemi.dtu.dk

Keywords: mesoporous zeolites, metal, nanoparticles, bifunctional, catalyst, hydrocracking

1 Introduction

Zeolites are among the most widely used industrial catalysts. The micropores in zeolite crystals have dimensions close to those of typical reactant and product molecules in many large-scale processes, and the structure is responsible for the characteristic size and shape selectivity typical of zeolite catalysts. However, a catalyst can only be efficient if the reactant molecules are able to diffuse into the crystal and react inside the pores. Thus, for some applications, the sole presence of micropores might result in an unacceptably slow diffusion of reactants and products to and from the active sites located inside the zeolite crystals. Several different strategies have been proposed to overcome this challenge, a multitude of these require however often costly reagents or are time consuming [1].

Here, we present a versatile method for the preparation of zeolites with an additional mesoporous system. This is done using *in situ* generation of a carbon template, directly onto the silica raw material. The carbon template is later removed by combustion, leaving mesopores. This method allows for careful control of the porosity of the mesoporous zeolite, and it does not depend on the availability of specialized carbon templates. The effect of the mesoporosity generated by this *in situ* carbon templating was tested in hydrocracking of n-octane.

2 Experimental

A carbon source was deposited on zeolite precursors by leading methane gas over metal nanoparticles on silica. Afterwards the material was subjected to a hydrothermal crystallization step, where the zeolites formed around the carbon-template. During the subsequent calcination, the carbon-template was removed by combustion to leave the mesoporous catalyst. The other mesoporous sample was prepared in a similar manner, except with the carbon source being BP-2000. All catalysts were tested for both stability and activity in a plug flow reactor for the hydrocracking of n-octane [2].

3 Results and discussion

The resulting zeolite revealed presence of an additional mesoporous system from physisorption, compared to a conventionally prepared ZSM-5. XRPD proved the formation of ZSM-5 crystal structure, even with the added carbon template during synthesis. TEM image, Figure 1(a), shows the resulting mesoporous zeolites with clearly visible mesopores, as well as metal nanoparticles. Figure 1(b) shows a close up of the zeolite and the metal nanoparticles, which are in the size range of 2-10 nm.

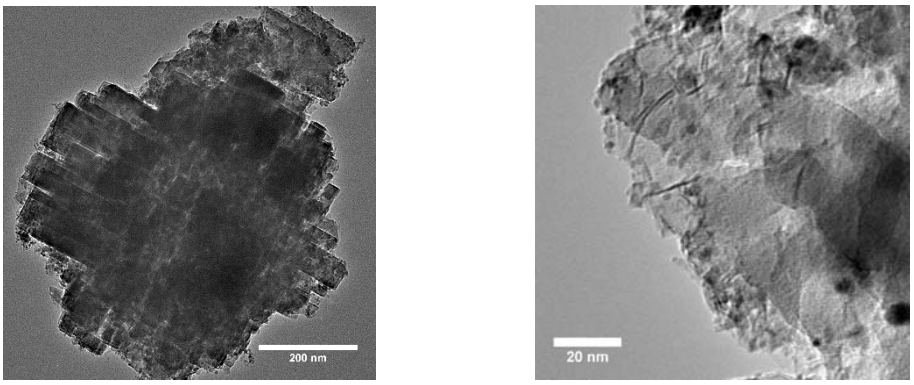

(a) (b)

Fig. 1. (a) TEM image of the *in situ* carbon templated HZSM-5. (b) TEM image close up of *in situ* carbon templated HZSM-5

By hydrocracking of n-octane, it is visible that the added generated mesopores are clearly an advantage, as there is an increase in both stability and activity compared to the conventionally prepared zeolite.

4 Conclusions

Mesoporous HZSM-5 zeolite was prepared by a cheap and innovative carbon templating method. Transmission electron microscopy and physisorption proved the existence of a secondary pore system in the zeolite, while still retaining the crystal structure. Metal nanoparticles were observed after the hydrothermal synthesis. The mesoporous zeolite showed an increase in both activity and stability compared to conventional ZSM-5 in a model reaction of cracking n-octane. Both improvements are believed to be a result of the introduced mesopore system, as it facilitates an increased mass transfer of reactants and products.

Acknowledgements

We gratefully acknowledge the support of the Danish Council for Independent Research, Grant No. 10- 093717 and Grant No. 12-127580.

References

[1] K. Möller, T. Bein, *Chem. Soc. Rev.* 42 (2013) 3689
[2] J.O. Abildstrøm et. al., submitted (2015)

I-PP92

Study of Biforming Process on CoMoNi Catalyst by Accelerator Mass Spectrometry

Lysikov A.[1,2], Parkhomchuk E.[1,2,3], Parunin P.[1,2,3*], Polukhin A.[1], Semeykina V.[1,2,3]

1 - Boreskov Institute of Catalysis SB RAS, Novosibirsk, Russia
2 - Novosibirsk State University, Novosibirsk, Russia
3 - Scientific research centre "Energy efficient catalysis", Novosibirsk State University, Novosibirsk, Russia

* parunin_pasha@mail.ru

Keywords: biforming, AMS, radioactive, methane, heavy oils, oil refining, carbon

1 Introduction

Nowadays the demand on light oil fractions (naphtha, diesel, kerosene) is constantly increasing while sources of light oil, that is reach in light fractions, are running down. Therefore, heavy oils become more and more popular in oil refining industry. Heavy oil upgrading technologies usually use two groups of methods: carbon rejection methods (delayed coking, fluid coking etc.) and hydrogen addition methods (H-Oil, LC-fining etc.). Nevertheless, there are exist some alternative ways of oil refining that look promising but are not investigated well for using in industrial scales. One of them is biforming process. Biforming (from the words *Boreskov Institute* – the place where first experiments were carried out, and word *form*) is a quite new process in oil refining that use is held with hydrocarbon gases presence. The principle of the method is in integration of methane or other hydrocarbon gases (C_2-C_5) in liquid hydrocarbon molecules. In this paper the biforming process was investigated on mesoporous CoMoNi catalyst with the presence of ^{14}C marked methane. The methane integration was analyzed by acceleration mass spectrometry (AMS) of ^{14}C content in biforming products.

2 Experimental/methodology

Carbon probe preparation was carried out on lab scale device in four steps: 1) probe burning at 800 °C in O_2 (99% purity) flow ; 2) CO_2 sorption at 25°C ; 3) CO_2 desorption at 900°C; and 4) graphitization at 550°C, 0.12MPa in electrolytic hydrogen (99.9% purity) atmosphere for 3 hours. The carbon yield is 85% from the carbon quantity in a probe. Method gives the level of ^{14}C contamination no more than 2% of ^{14}C natural content.

^{14}C determination in the graphite probes was conducted using accelerator mass spectrometry (AMS) method. The method allows detecting the ^{14}C isotope in a concentration of 10^{-15} compared with the main isotope.

Biforming experiments were carried out on the lab scale apparatus described in paper [1]. Parameters of the process were as follows: temperature 420°C for biforming experiment and 20°C for methane solution experiment, pressure 15MPa, LHSV $1h^{-1}$, gas/feed volume ratio 1000. Tatar oil (^{14}C content below accuracy of carbon probe preparation method) was used as a feed for the process. Methane (97% purity) with ^{14}C mark (in form of methane with 99% purity) was used as reagent. The catalyst used in experiment was mesoporous alumina with CoMoNi active component.

3 Results and discussion

The investigation of biforming process was carried out in three steps:

1. Tatar oil ^{14}C analysis. This experiment has been carried out as a reference. According to the AMS analysis, the ^{14}C content in tatar oil is about 1.33% of ^{14}C natural level (Fig 1.) that is

below the accuracy of carbon probe preparation method. Result showed that there is dead carbon in tatar oil only (there is only ^{12}C carbon presented in tatar oil)

2. Methane solution experiment. The aim of this experiment is to take into account the solution of methane in oil. By the AMS method there was determined that the ^{14}C content in the product was 1.29% of natural level (Fig 1.). By this way experiment showed that methane is insoluble in heavy tatar oil. This is explained by the fact that methane is more soluble in light hydrocarbons than in heavy hydrocarbons.

3. Biforming process. The AMS analysis of biforming products gave in result only 1.29% of ^{14}C natural level (Fig 1.). The 14C content in biforming products showed that there is no methane integration in oil molecules. Therefore, the biforming process do not proceed with parameters used in the experiment.

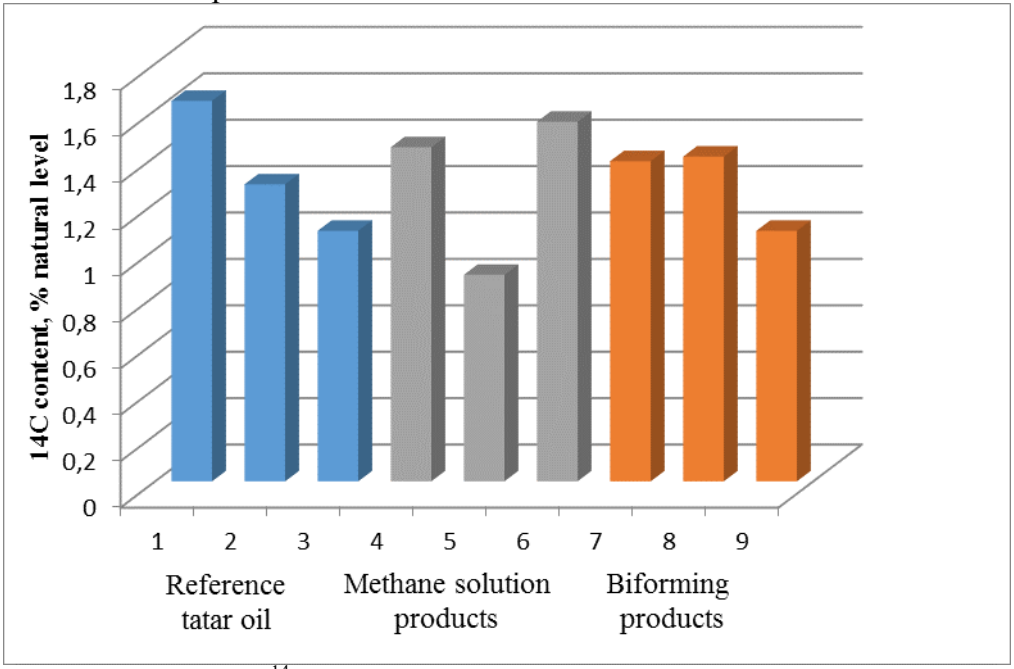

Fig 1. ^{14}C content in tatar oil and biforming products.

4 Conclusions

Method of ^{14}C analysis in oils have been set. Namely the carbon probe preparation for AMS analysis. The carbon probe preparation has level of ^{14}C contamination no more than 2% of ^{14}C natural content. The carbon yield is 85% from the carbon quantity in a liquid probe. The minimal volume of liquid probe is 30µl.

Biforming process do not proceed with parameters used in experiment : 420°C, 15MPa, LHSV $1h^{-1}$, CoMoNi mesoporous catalyst. Further studies should be conducted in this field. In the first instance, some experiments with other catalysts and hydrogen addition should be carried out.

Acknowledgements

Authors would like to thank Kuleshov D., Kalinkin P., for the invaluable contribution to research.

References

[1] Parkhomchuk E.V., Lysikov A.I., Okunev A.G., Parunin P.D., Semeykina V.S., Ayupov A.B., Trunova V.A., Parmon V.N., *Industrial&Engineering Chemistry Research*. 52 (2013) 17117−17125.

I-PP93

Synthesis of Alcohols and their Conversion in Reactive and Inert Gases on Alkali Modified Molybdenum Disulphide Catalysts

Dorokhov V.S.*, Permyakov E.A., Kogan V.M.

Zelinsky Institute of Organic Chemistry RAS, Moscow, Russia

* viktor.s.dorokhov@yandex.ru

Keywords: molybdenum, disulphide, alcohols, synthesis, oxygenates, synthesis-gas, mechanism

1 Introduction

Molybdenum-based sulphide catalytic systems are promising for production of alcohols from CO and H_2. The model of interlayer dynamic nature of the active sites of transition metal sulphide catalysts was taken as a conceptual basis for the work [1].

2 Results and discussion

We conducted investigations of structure and functioning mechanism of potassium modified MoS_2-based catalysts active phase in oxygenates synthesis reaction. We found out that potassium forms a single phase with molybdenum disulphide and substantially changes its structure. Addition of potassium increases average number of layers and average linear size of MoS_2 crystallites. As it follows from our catalytic experiments, both Co and K increases selectivity of alcohols formation [2].

It was assumed that the formation of alcohols and hydrocarbons from CO and H_2 is caused by the formation of active sites containing potassium in the active phase of the (Co)MoS catalyst. The mechanism was proposed for the formation of alcohols from synthesis-gas on the KCoMoS catalysts [3].

The addition of ethanol or ethylene to syngas substantially changes the reaction rate and composition of the products [3]. The reaction products of syngas in the presence of ethanol and ethylene contain alcohols and also ethers and esters, aldehydes, ketones, and organic acids. Therefore, the use of ethanol and ethylene additives to syngas makes it possible to obtain a wide range of compounds of different classes.

Is was also established that alcohol molecules are able to disproportionate with formation of olefins, alkanes and different oxygenates on KCoMoS-catalyst under inert atmosphere (N_2, Ar, He). We proposed mechanism for conversion of alcohols to different oxygenates on KCoMoS catalysts.

3 Conclusions

The application of the interlayer concept as a generalized approach to synthesis of alcohols makes it possible to explain the experimental structure-properties correlations and to optimize the catalyst composition for these processes. The principles were developed for the preparation of efficient sulphide catalysts based on molybdenum promoted with cobalt and modified by potassium for the synthesis of alcohols from syngas.

Acknowledgements

This work was financially supported by the Russian Foundation for Basic Research (Project No. 14 03 31769 mol_a).

References

[1] V.M. Kogan, P.A. Nikulshin, N.N. Rozhdestvenskaya, *Fuel*. 100 (2012) 2–16.
[2] V.S. Dorokhov et al, Kinetics and Catalysis. 54 №2 (2013) 243–252.
[3] V.M. Kogan et al, Russ. Chem. Bull. 63 №2 (2014) 2014. P. 332-345.

I-PP94

Glucose and Cellulose Derived Ni/C-SO_3H Catalysts for Liquid Phenol Hydrodeoxygenation

Kasakov S.[1], Zhao C.[1,2], Barath E.[1], Chase Z.A.[3], Camaioni D.M.[4], Fulton J.L.[4], Vjunov A.[4], Shi H.[4], Lercher J.A.[1,4*]

1 - Technische Universität München, München, Germany
2 - East China Normal University, Shanghai, China
3 - Washington State University, Pullman, USA
4 - Pacific Northwestern National Laboratory, Richland, USA

* stanislav.kasakov@tum.de

Keywords: carbon support, IR spectroscopy, phenol, hydrodeoxygenation, X-ray absorption,spectroscopy

1 Introduction

Effective utilization of biomass as a renewable source of energy and feedstock for conversion to useful chemicals hinges upon designing highly active and stable catalysts. [1] A one-step efficient conversion of lignin-derived phenolic oil, such as lignin waste from industrial paper production, [2] has yet to be developed. This approach requires multifunctional catalysts that have sufficient contact with reactants and high stability of the active sites under process conditions.

In this contribution, we report a novel dual-functional Ni/C-SO_3H catalyst that exhibits remarkably high activity towards phenol hydrodeoxygenation (HDO) in liquid hexadecane at mild reaction conditions (473 K, 4 MPa H_2). An in-depth *ex situ* and *in situ* characterization of sulfonated carbon supports, and Ni incorporated carbon catalysts permitted correlating catalyst properties and catalytic activity. Mutual influences of metal and acid sites anchored either on one (Ni/C-SO_3H) or physically mixed (C-SO_3H + Ni/C-SO_3H) carbon sheets have been investigated with respect to the model reaction of phenol HDO.

2 Methodology

High surface carbon materials were produced by pyrolysis of two carbon precursors, glucose and cellulose, resulting in graphitic respectively graphene like structures. The dual functional catalyst synthesized by grafting as-synthesized nickel nanoparticles supported on SO_3H-carbon was designed to fulfil a cascade reaction of four subsequent reactions of phenol hydrodeoxygenation (HDO).

The nano-sized Ni particles grafted onto sulfonated carbon support were studied in greater detail using *ex situ* transmission electron microscopy (TEM) and *in situ* X-ray absorption fine structure (XAFS) techniques.

Additionally using in situ IR spectroscopy, the rate determining step of the liquid phase phenol HDO was evaluated. Thus, phenol HDO catalysis was further improved by admixing C-SO_3H with the Ni/C-SO_3H catalyst to balance the two catalytic functions and achieving nearly quantitative conversion of phenol towards cyclohexane in 6h, at temperatures as low as 473 K.

3 Results and discussion

The representative TEM image of the Ni particles grafted on the sulfonated carbon support is shown in Figure 1a, along with the particle size distributions obtained from statistical analysis of at least 300 Ni particles from the TEM images. Ni nanoparticles on sulfonated high surface carbon (Ni/C-SO_3H) exhibited an average size of 4.2 ± 1.2 nm.

The state of Ni and its particle size in the Ni/C-SO_3H catalyst were investigated by XAS

during phenol HDO. Figure 1b contains the near-edge (XANES) portion of the spectra of the 10 wt. % Ni/C-SO_3H during HDO of 0.56 M phenol/water solution at 473 K and a total pressure of 5 MPa. To determine the concentration of both the Ni(0) and Ni(II) phase as a function of time, we simulated the XANES spectra as linear combinations of Ni foil (473 K), NiO and α-$Ni(OH)_2$ standards. Initially, the Ni particles were 100 % in the Ni(II) state, or specifically, a 20:80 mixture of NiO and $Ni(OH)_2$. The reduction to Ni(0) started after 12 min, i.e., when the temperature of 473 K was reached, and proceeded to completion within 50 min. The metallic state of Ni dominated after 30 min following the start of the reaction.

The figure 1c shows the time-resolved in situ IR spectroscopy study during phenol HDO over Ni/C-SO_3H catalyst. With increasing reaction time, the intensity of IR peaks of phenol (1224 cm^{-1} aromatic CO stretch) declined, while cyclohexanol (1067 cm^{-1} alicyclic CO stretch) increased first and then slowly dropped to a low value, indicating that cyclohexanol was still present after 180 minutes of reaction. The sharp increase of the C-H_x stretching vibration peaks (2928 cm^{-1} representing the CH_x peaks) demonstrates the high hydrogenation rates on the nano-sized Ni particles. Thus, the rate-determining step is concluded shown to be the dehydration of cyclohexanol.

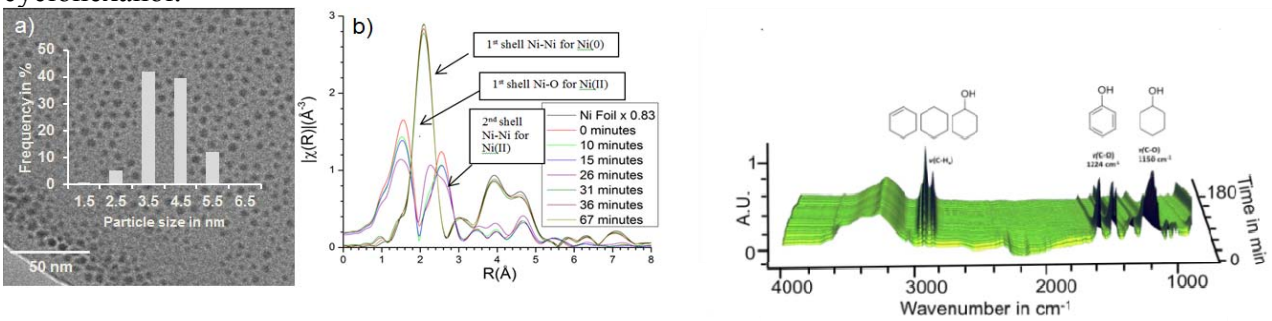

Figure 1 a) TEM image of Ni/C-SO_3H and b) Ni K-edge spectra of the χ(R) magnitude of Ni foil (black line) to that of Ni/C-SO_3H as a function of time at 473 K and 5 MPa P_{H2} and c) time-resolved *in situ* IR spectroscopy study during phenol HDO over Ni/C-SO_3H in hexadecane as solvent at 473 K and 3 MPa H_2.

Based on the insight from in situ IR studies, we attempted to accelerate the rates of cyclohexanol dehydration, the limiting step in phenol HDO in hexadecane, by adding sulfonated carbon (C-SO_3H) with the supported Ni/C-SO_3H catalyst. Interestingly, the additional amounts of sulfonated carbon influenced not only the dehydration of cyclohexanol but also the hydrogenation of phenol. The results suggest that the sulfonic acid groups interact with Ni directly or indirectly, reducing its availability for hydrogenation.

4 Conclusions

Bifunctional, highly active, and stable catalysts have been developed that combine metallic Ni nanoparticles (3–5 nm) with acidic sulfonated HS carbons derived from glucose and cellulose. *In situ* XAFS measurements demonstrate that the active metallic Ni phase in the Ni/C-SO_3H catalysts is stable in the aqueous phase under HDO conditions. The rate-determining step is shown to be the acid-catalyzed dehydration of cyclohexanol. Thus, the catalysis of HDO could be optimized by mixing additional C-SO_3H with the Ni/C-SO_3H catalyst to provide the subtle balance required for the two synergistic catalytic functions.

Acknowledgements

This work was supported by the US Department of Energy (DOE), Office of Basic Energy Sciences (BES), Division of Chemical Sciences, Geosciences & Biosciences. Pacific Northwest National Laboratory is a multi-program national laboratory operated for DOE by Battelle.

References

[1] J.M. Thomas, Angew. Chem. Int. Ed. **1999**, *38*, 3588-3628
[2] C. O. Tuck, E. Pérez, I. T. Horváth, R. A. Sheldon, M. Poliakoff, Science **2012**, *337*, 695-699.

I-PP95

Role of Nb in Formation of MoVTeNb Catalyst for Propane Ammoxidation

Ishchenko E.V.[1,2*], Kardash T.Yu.[1,2], Ishchenko A.V.[1,2], Andrushkevich T.V.[1]

1 - Boreskov Institute of Catalysis SB RAS, Novosibirsk, Russia
2 - Novosibirsk State University, NSU, Novosibirsk, Russia

* lazareva@catalysis.ru

Keywords: propane ammoxidation, MoVTe(Nb) catalyst, M1 phase, M2 phase

1 Introduction

To date, the problem of oil gas utilization and industrial processing of its components (methane, ethane and propane) is very actual. This issue is closely connected with the need to develop new power saving technologies in petrochemical industry. In light of this, the development of relevant manufacturing process of acrylonitrile from inexpensive and abundant propane instead propylene is challenging and economically is attractive. MoVTeNbO catalysts are reported [1, 2] to be the most efficient catalysts for the ammooxidation of propane to acrylonitrile. The role of Nb in the formation of the structure of these catalysts is still under debate. The work object is to elucidate of Nb effect on the phase composition and catalytic function in selective conversion of propane.

2 Experimental

The $Mo_1V_{0.3}Te_{0.23}O_n$ and $Mo_1V_{0.3}Te_{0.23}Nb_{0.12}O_m$ catalyst were synthesized from aqueous slurry using ammonium heptamolybdate, ammonium metavanadate, telluric acid and niobium oxalate. Thereafter, a lab spray-dryer (Buchi-290, T_{inlet}= 220°C and T_{outlet}= 110°C) was used for rapid drying of the crude precursors. The resulting orange solid precursors (220°C) were treated by step in interval 250–550°C under the flow of He.

XRD, IR-spectroscopy and HRTEM have been used for characterization of final catalysts.

The propane ammooxidation was carried out in a fixed-bed tubular reactor with on-line chromatographic analysis at 420°C with the feed consisting of 5% C_3H_8, 6% NH_3, 89% air.

3 Results and discussion

Mixing solutions of the initial components result to the formation of heteropoly compounds (HPC) with Anderson-type structure in MoVTe and MoVTeNb systems. These structures are preserved after spray-drying. A nanostructured M1 phase is formed after the decomposition of the HPC.

In MoVTe sample the increase in the heat treatment temperature to >450°C leads to destruction of the M1 domains and crystallization of the M2 phase, a number VMo oxides and individual oxide phases. The heat treatment of MoVTeNb results to the transformation of nanostructured particles to phases M1 and M2 (Fig.1).

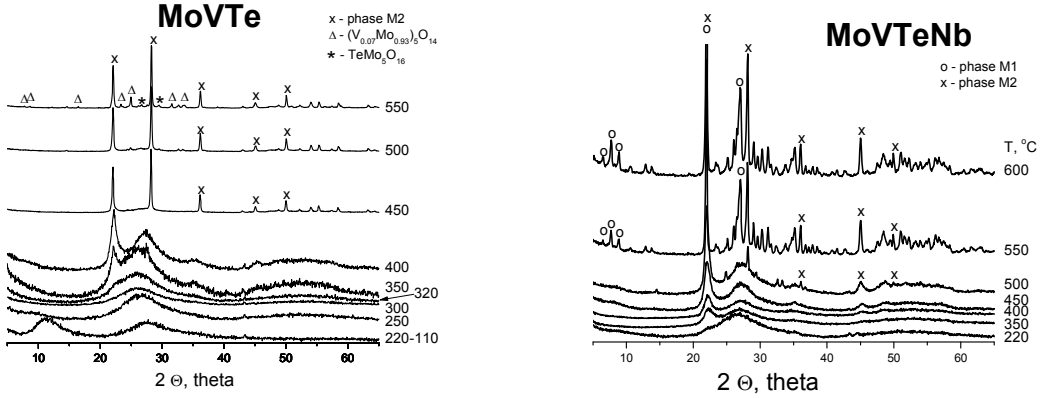

Fig. 1. XRD patterns of MoVTe and MoVTeNb catalysts

Table 1. Effect of the phase composition of $Mo_1V_{0.3}Te_{0.23}O_n$ and $Mo_1V_{0.3}Te_{0.23}Nb_{0.12}O_m$ catalyst on the catalytic properties.

Compound	T, °C*	X, %	S C_3H_3N, %	S C_3H_6, %	S CO_x, %	Phase composition
MoVTe	450	23.7	35.3	15.8	34.6	Nanostructured phases
MoVTeNb	450	28.6	36.8	13.1	37.6	Nanostructured phases
MoVTe	550	4.1	33.7	40.0	17.0	M2 (80%), $V_{0.97}Mo_{0.95}O_5$, $V_xMo_{5-x}O_{14}$, $TeMo_5O_{16}$
MoVTeNb	550	57.0	68.8	4.7	15.3	M1 (80%), M2

* Temperature of heat treatment, X - the conversion of propane, S – selectivity, τ - 2s.

Table 1 demonstrates catalytic properties and phase composition of the catalysts. It exhibits comparable behavior relating activity and selectivity of nanostructured three- and four-component catalysts.

Changing phase composition under heat treatment results to strong distinction of catalytic behavior. The activity of ternary-component catalysts containing mainly the phase M2 decrease, at this time high selectivity is preserved. In contrast to the ternary system, the four-component system transits from the low-temperature state containing highly dispersed crystallites of M1 to the well-crystallized M1 phase. This process is accompanied by an improvement of the catalytic properties as compared with ones of nanostructured sample.

4 Conclusions

So, catalytic activity is determined by the phase composition of the catalysts. Phase transformation in the ternary system result in decreasing catalytic characteristics. Contrary, in the four-component system, the transformation of nanostructured M1 phase to well-crystallized M1 phase enhances the catalytic properties. Our results provide evidence of the key role of niobium in the stabilization of orthorhombic structure of M1 phase.

References

[1] T. Ushikubo *Catal. Today.* 78 (2003) 79-84.
[2] T. Ushikubo, H. Nakamura, Y. Koyasu, S. Wajiki, *US Pat. 5.380.933* (1995).
[3] H. Watanabe, Y. Koyasu *Appl. Catal A: Gen.* 194-195 (2000) 479-485.
[4] F. Ivars, B. Solsona, S. Hernandez, J.M. Lopez Nieto *Catal. Today* 149 (2010) 260–266.

I-PP96

$CuFe_2O_4$ Magnetic Nanoparticles: An Efficient, Recyclable Catalyst for N-arylation of Indole and Imidazole with Aryl Halide under Mild Reaction Conditions

Yadav G. D.*, Nakhate A.V.

Department of Chemical Engineering, Institute of Chemical Technology, Mumbai, India

* gdyadav@yahoo.com

Keywords: spinel ferrite nanospheres, hydrothermal synthesis, magnetic separation, N-arylation, heterogeneous catalyst

1 Introduction

The C–N bond formation is one of the most important chemical reactions in organic synthesis and represents an important step in the production of nitrogen containing heterocyclic molecules which play vital role in natural products, industrial polymers, agrochemical and biologically active pharmaceutical products [1-2].

Herein, we report a simple, effective and environmentally greener protocol for synthesis of different spinel ferrite microspheres which is highly efficient, stable, well-dispersed and magnetically recyclable catalyst. The resulting catalyst was applied for *N*–aryaltion reaction of indole and imidazole with different aryl halide. The reaction afforded good to excellent yields with $CuFe_2O_4$ MNPs as catalyst under ligand-free conditions. In addition, $CuFe_2O_4$ MNPs could be reused at least six times showing no loss of catalytic activity (scheme 1). A comprehensive investigation of various parameters was accomplished for indole and a kinetic model developed and validated against experimental results. The studies were extended to other heterocycle.

2 Experimental

2.1 Preparation of $CuFe_2O_4$ particle

MFe_2O_4 (M = Cu, Co, Mg, Mn, Ni) MNPs were prepared by hydrothermal method. A mixture of the $MCl_2.2H_2O$ (5mmol), $FeCl_3.6H_2O$ (10mmol), polyethylene glycol 400 (2g) and sodium acetate (7g) in ethylene glycol was used to form a stable transparent solution. The mixture was sealed in teflon lined SS autoclave. The autoclave was maintained at 200ºC for 24 h and allowed to cool to room temperature. The black products were washed several times with ethanol and dried at 60ºC for 6 h.

2.2 General procedure for N-arylation of nitrogen nucleophiles and substrate study.

All experiments were performed in high pressure reactor. Predetermined amounts of reactants and the catalyst were charged into the autoclave and the temperature raised to the set value. Once the temperature was attained, a zero hour sample was withdrawn and sampling was done periodically. The control experiment was: iodobenzene (3 mmol), indole (2 mmol), K_3PO_4 (3 mmol), NMP (30 mL made up volume) as solvent and 0.001 g/ml catalyst. The reaction was carried out at 120 ºC with a speed of agitation (400 rpm). Products were confirmed by ^1H, ^{13}C NMR and GC-MS analyses.

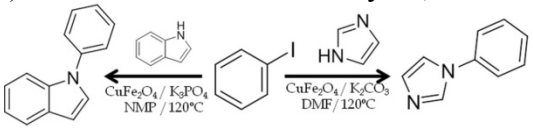

Scheme 1. Copper catalyzed *N*-arylation

3 Results and discussion

The XRD patterns of MFe_2O_4 agreement with the standard XRD patterns of JCPDS data except some pure metal impurity peak were observed [Figure 1. (a)]. TEM and SEM images,

clearly showing that the as prepared MFe_2O_4 is usually in a spherical shape with smooth surface, and has a narrow size distribution, EDXA confirmed the chemical composition of ferrite complex [Figure 2 (b-c)]. The FT-IR spectra of MFe_2O_4 showed a strong band associated with the Fe-O stretching vibration at 620-650 cm^{-1}. TGA spectra confirmed that catalyst was thermally stable. The isotherm of the MFe_2O_4 MNPs nanosphere exhibited type IV isotherm depicting characteristics of the mesoporous solid with hysteresis loops, indicating that the adsorption process was completely irreversible. In order to optimize the reaction conditions, initial studies were conducted using $CuFe_2O_4$ as a choice of catalyst for N-arylation of indole with iodobenzene as a model reaction. Different reaction parameters such as catalyst screening, solvent, base, speed of agitation, catalyst loading, molar ratio and temperature using $CuFe_2O_4$ as catalyst were studied [Figure 1(d-e)] [Figure 2 (a-e)]

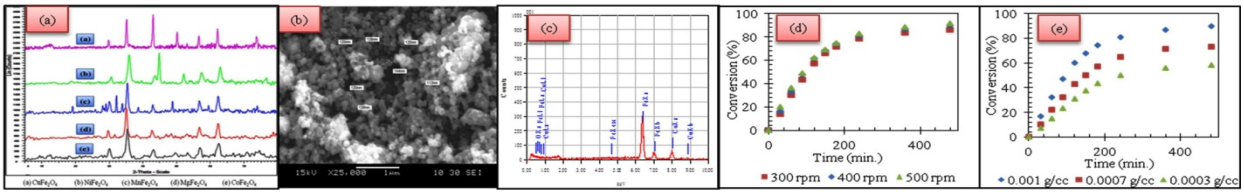

Fig.1. (a) XRD patterns of MFe_2O_4 (b) SEM image of $CuFe_2O_4$ (c) EDXA of $CuFe_2O_4$. (d) Effect of speed of agitation (e) Effect of catalyst loading

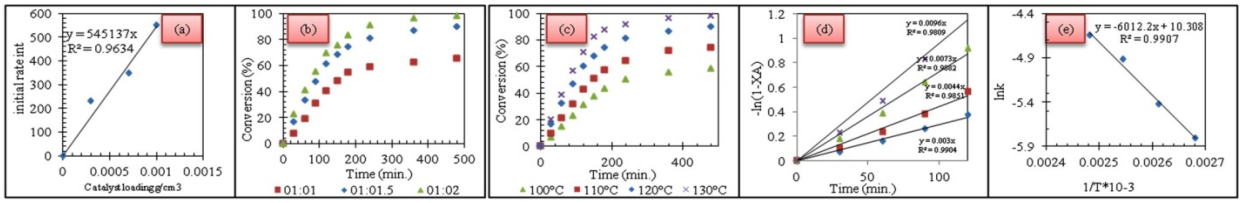

Fig.2. (a) Plot of initial rate vs. catalyst loading (b) Effect of mole ratio (c) Effect of temperature (d) plot of $\ln(1-X_A)$ vs. time (e) Arrhenius plot lnk vs $1/T*10^{-3}$

4 Conclusions

A series of ferrite complex oxides MFe_2O_4 (M = Mg, Cu, Ni, CO, Mn) microspheres were prepared by a simple and effective hydrothermal approach and characterized by using SEM, TEM, XRD, FT-IR, TGA and BET. The $CuFe_2O_4$ magnetic microsphere exhibited impressive catalytic activity under ligand free conditions producing desired products in moderate to excellent yield. . The catalyst can be reused six times with minor changes in the catalytic activity. We have reported a kinetic model for this reaction system. The reactions were found to be intrinsically kinetically controlled. The LHHW type model with weak adsorption of all species fits our data well and the system follows first order kinetic equation. The activation energy was found to be 13.06 kcal mol^{-1}.

Acknowledgements

GDY acknowledges support as J. C. Bose National Fellow from DST-GOI and from R. T. Mody distinguished Professor Endowment. AVN gratefully acknowledges the support provided by CSIR-JRF.

References

[1] S. Löber, H. Hubner, P. Gmeiner, *Bioorg. Med. Chem. Lett.* 16 (2006) 2955–2959.
[2] T. Balle, J. Perregaard, M. T. Ramirez, A. K. Larsen, K. K. Soby, T. Liljefors, K. Andersen, *J. Med. Chem.* 46 (2003) 265–283.

I-PP97

The Polypropylene Based Composites Produced by Using Pre-Adsorbed Catalyst on the Surface of Carbon Nanotubes

Kazakova M.[1,2*], Kuznetsov V.[1,2], Sergeev S.[1], Moseenkov S.[1], Selutin A.[1,2], Ischenko A.[1,2], Schmakov A.[1,2], Matsko M.[1], Zakharov V.[1]

1 - Boreskov Institute of Catalysis SB RAS, Novosibirsk, Russia
2 - Novosibirsk State University, Novosibirsk, Russia

* mas@catalysis.ru

Keywords: Ti-Mg, supported catalyst, multi-wall carbon nanotubes, polypropylene

1 Introduction

Multi-wall carbon nanotubes (MWCNTs) have been widely regarded as an attractive candidate for the use as a fillers in the composite materials. Incorporation of carbon nanotubes into the polymer matrix results in significant improvement of polymer properties – mechanical strength, electrical and thermal conductivity, fracture toughness, electromagnetic shielding properties [1-3]. These improvements can be achieved in case of the uniform distribution of the filler in the polymer matrix. The common methods for the preparation of MWCNT/polymer composites include mechanical mixing with extrusion, solution mixing, melt blending, coagulation precipitation technique and in situ polymerization. In the present work the *in situ* polymerization technique was applied for preparation of MWCNT/polypropylene (MWCNT/PP) composites with various MWCNTs loading. Original preparation procedure of catalytic species TMC/MWCNT with uniform distribution of TMC on the MWCNT surface was proposed.

2 Experimental/methodology

In this study MWCNTs (d ~ 9 nm) as produced and after oxidation pre-treatment (denoted as MWCNT-ini and MWCNT-ox, correspondingly) were used [4]. Carbon nanotube oxidation was performed by reflux of 1–2 g of MWCNTs in the excess of concentrated nitric acid (90 min). This procedure provides formation 0.8 carboxylic groups per 1 nm^2.

Catalysts preparation was carried out by (1) impregnation and precipitation of organomagnesium compound as alkoxy magnesium compounds using magnesium-titanium alkoxide complex $(Mg(OEt)_2 \cdot Ti(OEt)_4$ or $(EtMgBu + Si(OEt)_4)$ and (2) subsequent titanation of surface alkoxy magnesium compounds with titanium tetrachloride in the presence of an electron donor compound (dibutyl phthalate – DBP). The obtained catalytic systems were denoted as TMC/MWCNT - $(TiCl_4/DBP/MgCl_2)$/MWCNT).

Propylene slurry polymerization was performed in heptane; triethyl aluminum (18 mmol/L) and propyl trimethoxy silane was used as the cocatalyst (mole ratio Al/Si was 30); concentration of H_2 2 vol. % and temperature 70°C. Propylene pressure (1-6 atm) and polymerization time were selected for obtaining the desired amount of PP. The resulting product was washed with heptane and ethanol, and dried to the constant weight.

Structure and morphology of initial and oxidized MWCNTs were studied using TEM, BET surface measurements, and titrimetric analysis. TEM, XRD, DSC were used for characterization of the structure of MWCNT/PP composites.

3 Results and discussion

Using both types of MWCNTs the catalysts TMC/MWCNTs with different TMC content (from 1 to 10 wt. %) were prepared. Polymer composites were prepared with desired content of

PP using these catalysts and various polymerization conditions. Based on the catalyst active component is observed some decrease in the catalytic activity (per Ti atom) compared to a sample without the MWCNTs. At the same time we didn't observe the influence of the MWCNTs nature on the catalytic activity in polymerization. The structure of the MWCNT/PP composites was studied using TEM. The propylene polymerization results in the formation of polymer powder with MWCNT homogeneous distributed in PP matrix (Fig.1A); PP molecules demonstrate high wetting ability of nanotube surface. We succeeded to observe Ti-Mg – containing catalyst particles in the form of 2-3nm dark spots (Fig.1B).

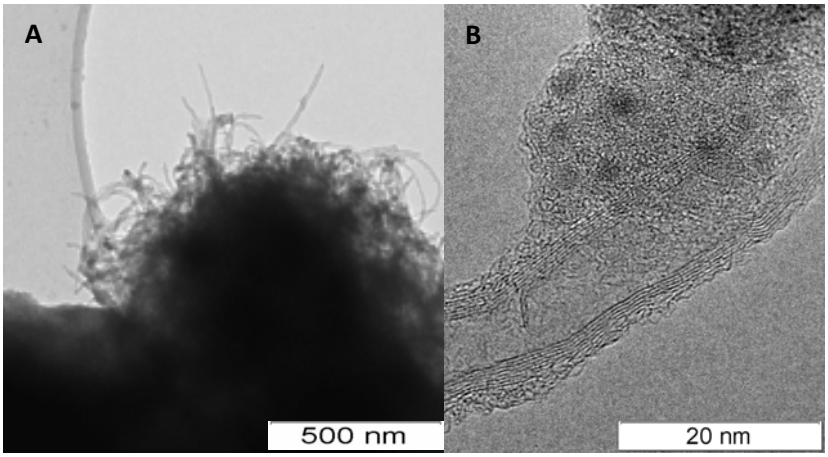

Fig. 1. TEM images of 20 wt.% MWCNT-ox/PP composite.

According to the DSC data the introduction of the nanotubes in the polymer results in the decrease of polymer's melting point (3-4°C). However, the values of the melting temperature (160-163°C) and the degree of crystallinity (50-55%) are rather high. This indicates insignificant changes in the crystal structure of the composites in comparison to pure polypropylene. According to XRD data the introduction of two types of MWCNT into polypropylene matrix does not lead to significant changes in the crystalline structure of polypropylene.

4 Conclusions

The concentrate MWCNT/PP with a uniform distribution in the polypropylene matrix of MWCNTs was obtained. PP molecules demonstrate high wetting ability of nanotube surface.

For the first time we have observed the Ti-Mg – containing catalyst species of the size 2-3 nm on the MWCNT surface, stabilized in polymer matrix. The results suggest promising directions for composite MWCNT/PP preparation via the catalyst distribution on the surface of MWCNTs followed by polymerization of propylene. MWCNT/PP composites with high concentration of homogeneously distributed nanotubes are perspective as polymer carbon nanotubes conductive masterbatches.

Acknowledgements

The work was performed as part of the grant of the Ministry of Science and Education of RFMEFI60714X0046.

References

[1] H. Xu, S. Anlage, L. Hu, G. Gruner, *App. Phys. Lett.* 90 (2007) 183119.
[2] G. Odegard, S. Frankland, T.Gates, *Aiaa Journal,* 43 (2005) 1828.
[3] Y. Yang, M. Gupta, K. Dudley, *Nanotechnology*, 18 (2007) 345701.
[4] I. Mazov, V. Kuznetsov, I. Simonova, A. Stadnichenko, A. Ishchenko, A. Romanenko, E. Tkachev, O. Anikeeva, *Applied Surface Science* 258 (2012) 6272.

I-PP98

Transition Metal Oxides on Heterogeneous Fenton-Like Systems with Thermal and Enzyme Peroxidase Catalytic Activity for Pollutant Degradation

Santana J.L.*, Cruz A., Saborit I.

Instituto Superior de Tecnologia y Ciencias Aplicadas, Havana, Cuba

* santana@instec.cu

Keywords: metal oxides, nanoparticulate, matter, magnetite, clay, composites, peroxidase enzyme, radioiodination, reaction, BSA

1 Introduction

The intrinsic enzyme-like activity of nanoparticles (NPs) or nanostructured solids has become a growing area of interest. Compared with natural enzymes, these enzyme-like NPs are stable against denaturing, low in cost, and highly resistant to high concentrations of substrate [1].Several recent studies have investigated different metal oxides and composites solid compounds in order to design new heterogeneous Fenton-like system for catalysis, clinical and technological applications. Some of the metal containing solids investigated was goethite, anatasa, clay minerals, manganese oxide and metal ferrites among others [2,3, 4]. Typical metal oxides such as anatasa, ZnO, and MnO_2 showed interesting catalytic properties on some pollutant green degradation systems. On the other hand, metallic iron, Fe^0, has been studied as a low cost and innocuous reductant in different environmental remediation processes, e.g. permeable reactive barriers [5] reduction of organochloro[6], dyes [7] .

In this work, metal oxides (MnO_2, ZnO, Fe_3O_4, and $MnFe_2O_4$) obtained by (co)-precipitation method in presence of surfactant direct micelles were evaluated as catalyst using Fenton UV heterogeneous model against methylene blue using TiO_2 as reference catalyst. These oxides were additionally evaluated for thermal degradation efficiency of methyl orange dye. Additionally, composites like Fe^0/ clay-Fe_3O_4 and Fe^0/ clay- $MnFe_2O_4$, obtained by mixed *in situ* coprecipitation and grinding methods were evaluated as peroxidase enzyme-like catalyst using radioactive iodination method of bovine serum albumin (BSA).

2 Experimental

Catalyst Preparation. In a pure water were prepared 0.02 mol/L solutions of $ZnSO_4$ or $MnSO_4$ (MercK). Pure cethyltrimethyl ammonium bromide (CTAB) was added to both reaction vessels (300 mL volume) in order to obtain 0.5 g/L surfactant solution. The mixture was vigorously stirred at room temperature for 60 minutes. To the reaction vessel were added 15 mL of diethanolamine and the system was carefully heated until 70 ^{0}C and maintained under stirring for two hours. The precipitated solids were separated (pH 10) and washed twice. After drying at 105 ^{0}C for 12 hours, the precipitated solids were heated at 600 ^{0}C for 6 hours. Using a ultrasound treated water, by which was passed a nitrogen gas flow during 2 hours was prepared a sample of pure magnetite by adding a stoichiometric mixture containing $FeSO_4 \cdot 7\ H_2O$ and $FeCl_3 \cdot 6H_2O$ (MercK) at ratio 1:2 , 1g/L of CTAB solution and 30 mL of diethanolamine. The mixture was vigorously stirred during two hours at 70 ^{0}C, pH 10. The precipitated magnetite was washed twice and dried at room temperature. The preparation of $MnFe_2O_4$ follows the same pathway and conditions but $MnSO_4$ was collocated on the initial mixture.

Magnetite and ferrite clay composites were prepared by adding prior to the before described synthesis a momtmorillonite type national clay, previously purified and micrometer sized.

Catalytic Measurements. Catalytic evaluation measurements were carried out using three models. The first one was the degradation of Methylene Blue (MB) under UV lamp in the presence of H_2O_2. In a 100 mL reaction vessel were collocated 70 mL of 0.002 mol/L solution of MB and 500 mg of each evaluated oxide. The suspension was stirred for 5 hours and the color change was determined spectrophotometrically at 695 nm. The efficiency of MB degradation was calculated. Thermal degradation of methyl orange (MO) dye was the second model in catalytic properties measurement. Arrhenius plots for MO oxidation as a function of reciprocal temperature (25, 50, 75 and 95 ^{0}C) allows calculating activation energy (Ea) for each evaluated oxide. In order to evaluate the peroxidase enzyme like activity magnetite and heterogeneous composites like Fe^0/ clay-Fe_3O_4 and Fe^0/ clay- $MnFe_2O_4$ recently mixed (0.1 mg) were putted on 2 mL Eppendorff vial. 500 µL of buffer pH 4, 200 µL of BSA solution (0.01mg/mL), 50 µL of substrate (H_2O_2 or KSCN solution) and 10 µL of radioactive solution of NaI (0.01mCi) were incubated for 30 minutes. The iodination efficiency was calculated by radioactivity measurements ratio of protein native fraction over total fractions counts after size exclusion chromatography over Sephadex G200.

3 Results and discussion

Synthesed Clay-magnetite composites

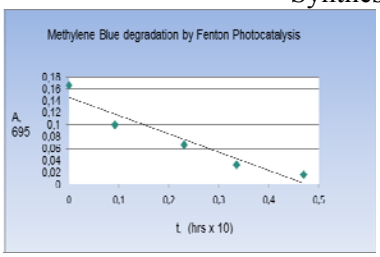

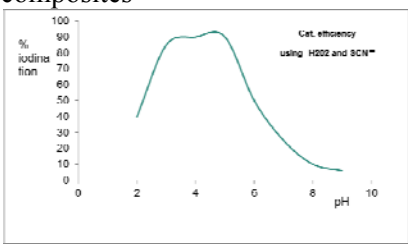

Degradation efficiency: TiO2 (anatasa) > MnO2> ZnO> $MeFe_2O_4$ (Mn, Ce)

High efficiency iodination over clay systems, Fe^0/ clay-$MnFe_2O_4$, Fe^0/clay-Fe_3O_4 were achieved.

4 Conclusions

A simple core-shell approach yields metal oxide-composite materials with catalytic and/or magnetic properties with peroxidase activity against aromatic rest of BSA. The successful radioisotope iodination substrates in absence of experimental enhancing factors such as temperature and UV radiation and with the use of rare substrate for experimental research SCN^- ion, allows affirming that oxidation mechanism can be considered artificial peroxidase enzyme activity.

References

[1] Wang, J. Feng, D.L. Yang, S. Perrett, X.Y. Nat. Nanotech-nol. 2 (2007) 577
[2] Wang, X., Zhuang, J., Peng, Q., Li, Yadong. Nature Letters. 437(2005) 121
[3] Kwan W., Voelker B., Environ. Sci. Technol.37 (2003) 1467
[4] Kwan W., Voelker B., Environ. Sci. Technol.36 (2002) 1467
[5] Lago R., Costa J., Fabris, J.et al., Catal. Commun.4(2003)525
[6] Khan F., Husain,T., Hejazi R., Environ. Manage.71(2004)95
[7] Diels, L., Dries,L., Bastiaens, D., Environ. Sci. Technol.38(2004) 2879
[8] Tratnyek,P., Mam, S., Water Res., 34(2000) 1837
[9] El-Mouhty, N., Shehab, W., Internat. J. of Basic and App. Sciences 3(2012) 260

I-PP99

Microwave-Assistant Functionalization of MOFs with Gold Nanoparticles

Butova V.V.[1*], Guda A.A.[1], Budnyk A.P.[1,2], Lamberti C.[1,2], Lomachenko K.A.[1,2], Soldatov A.V.[1]

1 - Southern Federal University, IRC Smart Materials, Rostov-on-Don, Russia
2 - University of Turin, Department of Chemistry, Turin, Italy

* vbutova@sfedu.ru

Keywords: Metal-Organic Framework, gold nanoparticles, HKUST-1, ZIF-8

1 Introduction

Metal-Organic Frameworks (MOFs) are porous hybrid organic-inorganic materials with a large surface area. Their structures can be described in terms of secondary building units (SBU) forming a characteristic topology for any given coordination network of metal ions and organic ligands [1]. This class of materials has wide range of potential applications in gas storage [2], in bio-medical studies [3], and in catalysis [4].

MOFs are typically produced by hydrothermal or solvothermal techniques. The resulted product still contains solvent molecules inside the pores. After respective activation procedure, the coordinately unsaturated metal sites inside the SBU acquire catalytic activity as Lewis acids [5]. Gold particles of 3-10 nm range are found to show remarkable catalytic activity [6], and being hosted in porous material like MOF, constitute a promising heterogeneous catalyst [7].

MOF powder can be further treated with a gold precursor looking for formation of metal nanoparticles on external surfaces of crystallites or in pores of framework. Alternatively, a gold precursor can be added already during the synthesis of MOF, allowing for growth of metal nanoclusters inside the MOF pores [8] along the formation of crystalline framework.

Present investigation is focused on development of a microwave-assistant solvothermal synthesis in order to grow gold nanoparticles inside the MOF structures – $Cu_3(BTC)_2$ [9] and Fe(BTC) [10] (BTC – benzene-1,3,5-tricarboxilic acid), and inside the ZIF-8 (zeolitic imidazolate framework) [11].

2 Experimental

The $Cu_3(BTC)_2$ (HKUST-1) MOF samples were produced in our laboratory by solvothermal technique [12] and by using microwave irradiation [13], starting from copper acetate and H_3BTC in DMF/water solutions. The commercially available Basolite C300 ($Cu_3(BTC)_2$) and its isostructural counterpart Basolite F300 (Fe(BTC)) were also used for functionalizing experiments. The ZIF-8 was produced in a microwave oven from zinc acetate and 2-methylimidazole in DMF/water solutions. The activation procedure consisted in heating in dynamic vacuum at 200 °C for 6 hours and cooling down to room temperature with finally being fluxed with dry air.

The functionalization with gold was performed on activated dry MOF powder. The water solution of 6 mg/ml $HAuCl_4$ was poured on MOF powder and the mixture has been kept under magnetic stirring for various period of time from several minutes to several days. After that, water solution of 16 mg/ml sodium citrate was added and the mixture was placed into the microwave oven to react at 100 °C for 16 minutes. After centrifugation the resulting powder was dried at 50 °C in air.

3 Results and discussion

The structures of obtained MOFs were confirmed by powder XRD measurements. For studies of gold-functionalized MOFs the TEM images were acquired, and variety of spectroscopic methods

(UV-Vis, Mid-IR, X-Ray absorption at Au L_3-edge) was used. The representative TEM images of functionalized MOFs $Cu_3(BTC)_2$ and ZIF-8 are presented in Figure 1 (marked as HKUST-1@Au and ZIF-8@Au). In the case of HKUST-1@Au the gold particles of 6-8 nm are observed to decorate the external surfaces of MOF crystals without clear evidence of penetration inside the voids. Instead, the gold particles of 5-13 nm are found to be embedded in ZIF-8 matrix as can be seen from respective TEM image.

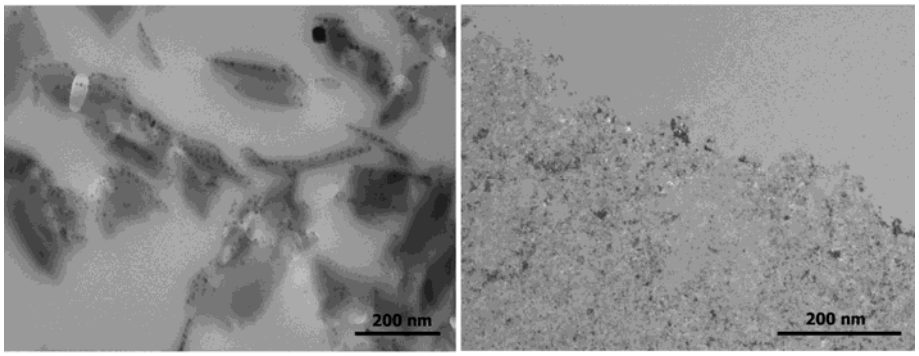

Fig. TEM images of HKUST-1@Au (left) and ZIF-8@Au (right) samples

By changing synthesis parameters, the dependence of penetration depth of gold particles inside the MOF structure with time of stirring was found. Both diffusion problems arising from pore size of MOFs and chosen conditions for formation of gold nanoparticles (interplay between gold precursor and reducing agent) might lead to different situation with MOFs functionalization. However gold nanoparticles supported on MOF crystals and embedded inside the pores are preserved against aggregation and rather stable in time.

In conclusion, we have developed the microwave-assistant solvothermal synthesis, which allowed as to functionalize three MOFs - $Cu_3(BTC)_2$, Fe(BTC), and ZIF-8 with gold nanoparticles with diameters in 5-13 nm range. Variations in time of mixing of the reagents allowing to optimize the penetration depth of gold into the porous matrix. Obtained materials have good stability and may be applied for catalytic tests.

Acknowledgements

The Mega-grant No. 14.Y26.31.0001 of the Russian Federation Government; A.A.G. and K.A.L. acknowledge the President's of Russia Grant MK-3206.2014.2 for Young Scientists.

References

[1] L. R. MacGillivray, *Metal-Organic Frameworks: Design and Application*. Wiley: 2010.
[2] M. P. Suh, H. J. Park, T. K. Prasad, D. W. Lim, *Chem. Rev.* 112 (2012) 782.
[3] P. Horcajada, R. Gref, T. Baati, P. K. Allan, G. Maurin, P. Couvreur, G. Ferey, R. E. Morris, C. Serre, *Chem. Rev*. 112 (2012) 1232.
[4] F. X. L. Xamena, J. Gascon, *Metal Organic Frameworks as Heterogeneous Catalysts*. Royal Society of Chemistry: 2013.
[5] R. Ameloot, M. Aubrey, B. M. Wiers, A. P. Gómora-Figueroa, S. N. Patel, N. P. Balsara, J. R. Long, *Chem. Eng. J.* 19 (2013) 5533.
[6] S. Sreedhala, V. Sudheeshkumar, C. P. Vinod, *Catal. Today* 244 (2015) 177.
[7] K. Sugikawa, Y. Furukawa, K. Sada, *Chem. Mater.* 23 (2011) 3132.
[8] H.-L. Jiang, B. Liu, T. Akita, M. Haruta, H. Sakurai, Q. Xu, *JACS* 131 (2009) 11302.
[9] S. S.-Y. Chui, S. M.-F. Lo, J. P. H. Charmant, A. G. Orpen, I. D. Williams, *Science* 283 (1999) 1148.
[10] H.-K. Youn, J. Kim, W.-S. Ahn, *Mater. Lett.* 65 (2011) 3055.
[11] Y.-Y. L. Xiao-Chun Huang, Jie-Peng Zhang, X.-M. Chen, *Angew. Chem. Int. Ed.* 45 (2006) 1557.
[12] K. Schlichte, T. Kratzke, S. Kaskel, *Microporous Mesoporous Mater.* 73 (2004) 81.
[13] M. Schlesinger, S. Schulze, M. Hietschold, M. Mehring, *Microporous Mesoporous Mater.* 132 (2010) 121.

I-PP100

On the Origin and State of Ni and Fe Species as Catalysts for the Initiation of Metal Dusting Corrosion

Gunawardana P.V.D.S.[1], Hwang J.[1], Walmsley J.C.[2], Svenum I.H.[2], Venvik H.J.[1*]

1 - Department of Chemical Engineering, Norwegian University of Science and Technology (NTNU), Trondheim, Norway

2 - SINTEF Materials and Chemistry, Trondheim, Norway

* hilde.j.venvik@ntnu.no

Keywords: natural gas, conversion, carbon formation, metal dusting, carbon activity, carbon filament

1 Introduction

Metal dusting corrosion constitutes a serious issue in a range of chemical industries [1–3], where a mixture of CO, CO_2, H_2, steam and hydrocarbons meets metals and alloys at elevated temperatures (T>400 ˚C) and low oxygen/steam partial pressures (P_{O_2}/P_{Steam}). The first stages of carbon formation that initiate metal dusting are analogous to carbon formation issues on heterogeneous catalysts used in the petrochemical industry. The thermodynamic driving force is hence given by the activity for carbon formation (aC), and metal dusting is prevailing for aC>1. The formation of solid carbon is nevertheless strongly controlled by kinetics; it rarely forms in the gas phase, even at very high aC. Ni and Fe are excellent catalysts for carbon formation. Unfortunately, they are also the main constituent elements of common industrial alloys. Hence their stability in alloy matrix is critical for metal dusting.

The overall objective of this study is to advance the understanding of the initiation of metal dusting corrosion. In our recent work, improved understanding of the initial carbon formation and the role of the protective surface oxide layer was obtained through a comprehensive experimental investigation, including advanced surface and bulk characterization. We have established that the surface oxide layer composition, thickness and structure, as affected by pretreatment temperature, oxidant partial pressure and sample preparation procedure, strongly affects the susceptibility to form solid carbon [4–6]. Here, we further proceed to study the nature and localization of Ni/Fe phases at the surface within and/or below the surface oxide layer formed as a result of the pre-oxidation and how they are accessed by the reducing atmosphere during syngas exposure.

2 Experimental

A set of coupon-like alloy (INCONEL® 601) samples were subjected to oxidation at different temperatures for 6 h under 10% steam/inert (at 1 bar). Then some of the pretreated samples were exposed to carburizing syngas mixtures with either *infinite* (10%CO in Ar, 1 bar) or *finite* (20% or 50% CO in H_2/CO_2/steam/Ar, 20 bar) carbon activity (aC>>1 or aC>1). The duration of the syngas exposure was also varied.

The resulting surfaces and carbonaceous products were characterized by means of optical imaging and light-optical microscopy, scanning electron microscopy (SEM), depth profile analysis by Auger Electron Spectroscopy (AES) under ion-sputtering, transmission electron microscopy (TEM) equipped with energy dispersive X-ray spectroscopy (EDS) and X-ray photoelectron spectroscopy (XPS).

3 Results and discussion

Pre-oxidation at 540 ˚C produced samples covered by a Cr and Al rich, thin oxide layer. SEM reveals carbon formation on all such samples subjected to CO exposure at *infinite a*C, increasing with exposure time as expected. The amount of carbon formed during 1 h CO exposure treatment could not be detected by visual inspection, but thin carbon filaments could be observed in high magnification covering part of the initial surface. The formation of filaments and complementary TEM/EDS results indicated the presence of metal nanoparticles containing Ni and/or Fe, and such short exposures represent a basis for an accelerated experimental protocol to reveal the origin of these particles within the surface oxide layer. Higher pre-treatment temperature under oxidizing conditions lowers the susceptibility to carbon formation, and the critical factors to and durability of this effect will be further discussed and investigated.

Under *finite a*C conditions, thick carbon deposits were obtained at 650 ˚C and 750 ˚C while no (20%CO) or little (50%CO) carbon was found after syngas exposure at 550 ˚C. Hence, under different CO concentration but a constant level of H_2, CO_2 and steam, the amount of carbon formed is clearly a function of exposure temperature and gas composition. The former clearly demonstrates the kinetic control of the (exothermic) reactions. Removal of carbonaceous deposits revealed that material degradation had taken place at higher temperatures (either '*pitting*' or '*spallation*'). As shown by Auger depth profile analysis, oxidation of the alloy matrix had proceeded alongside the reducing reactions leading to carbon formation under exposure to the 20%CO containing gas mixture at higher temperatures, while this was not the case under 50%CO. The TEM and EDS results show that the formation of filamentous carbon deposits under *finite a*C conditions was also catalyzed by metallic particles containing Ni and Fe.

XPS is currently being used to examine the oxidation states of the different species that exist in the near surface region. A next step will be detailed TEM/EDS analysis of the near surface region by a combination of carefully prepared cross-sections and micro/nano-scale samples obtained via Focused Ion Beam (FIB).

4 Conclusions

We have established protocols to investigate the catalytic properties of high temperature alloy surfaces, and factors leading to (*unwanted*) carbon formation and subsequent metal dusting, under both simplified (aC>>1, low pressure) and more industrially relevant (syngas, aC>1, high pressure) conditions. The experiments verify the kinetic nature of these phenomena and point to the importance of the structure and composition of the protective surface oxide layer that depends on the conditions of the preceding oxidative treatment. The metal dusting hence appears to be strongly linked to the inclusion of Ni/Fe species in the oxide surface layer, which subsequently reduce to facilitate carbon formation.

Acknowledgements

The financial support of Research Council of Norway through the Centre of Research-based Innovation *in*GAP (Innovative Natural Gas Processes and Products) is gratefully acknowledged.

References

1 H.J. Grabke, M. Spiegel, *Mater. Corros.* 54 (10) 2003.
[2] J. Dampc, Z. Grzesik, J. Hucinska, *Mater. Corros.* 60 (3) 2009.
[3] S. Kaewkumsai, W. Khonraeng, N, Sathirachinda, *Eng. Fail, Anal.* 27 (0) 2013.
[4] P.V.D.S. Gunawardana, J. Walmsley, A. Holmen, D. Chen, H.J. Venvik, *Energy Proc.* 26 (0) 2012.
[5] P.V.D.S. Gunawardana, J.C. Walmsley, H.J.Venvik, NACE CORROSION 2013 Conference and Expo. Paper No. 2769.
[6] P.V.D.S. Gunawardana, J.C. Walmsley, H.J. Venvik, *Ind. Eng. Chem. Res.* 53 2014.

I-PP101

Towards the Application of New Ionic Liquids Based Ru(II) Catalysts in Transfer Hydrogenation Reactions

Rafikova K.S.[1], Zazybin A.G.[1*], Bigaliyeva F.B.[1], Meric N.[2], Aydemir M.[2], Pasa S.[2], Temel H.[2], Yu V.K.[1,3]

1 - Kazakh-British Technical University, School of Chemical Engineering, Almaty, Kazakhstan
2 - Science and Technology Application and Research Center, Dicle University, Diyarbakır, Turkey
3 - Institute of Chemical Sciences, Almaty, Kazakhstan

* azazybin@yahoo.com

Keywords: SMPO, transfer, hydrogenation, phosphinites, ruthenium

1 Introduction

There is a huge demand in petrochemical industries in non-gaseous hydrogen donors for hydrogenation of organic compounds (so called transfer hydrogenation). Basically, standard industrial equipment can be used in the transfer hydrogenation process, rather than the pressurized equipment necessary when using hydrogen gas. The use of hydrogen in gas form is a much more expensive endeavor than using non-gaseous hydrogen donors, such as iso-propanol, and will make the industrial process more cost effective [1].

The popular petrochemical processes used by companies such as Shell, ARCO Chemical, Sumimoto and others more than 30 years is SMPO (styrene monomer propylene oxide) process of conversion of styrene and propene to styrene and propylene oxide that is shown in figure 1:

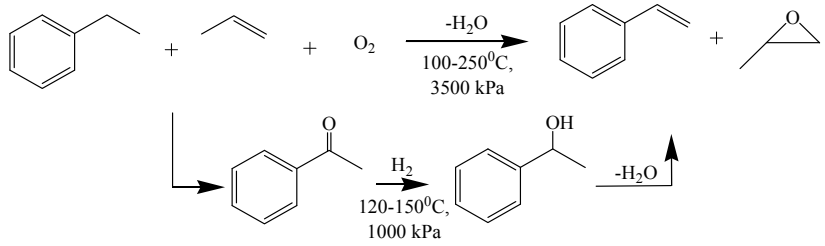

Fig. 1. SMPO process

Herein we report about significantly more mild reaction conditions (82^{0}C, atm. pressure) for the transfer hydrogenation of ketones using Ru/IL catalysts.

2 Experimental/methodology

Procedure for the catalytic hydrogen transfer reaction: a solution of complexes [Ru((Ph$_2$PO)-C$_7$H$_{14}$N$_2$Cl)(η^6-arene)Cl$_2$]Cl and [Ru((Cy$_2$PO)-C$_7$H$_{14}$N$_2$Cl)(η^6-arene)Cl$_2$]Cl (arene: benzene 1,2; *p*-cymene, 3,4) (0.005 mmol), KOH (0.025 mmol) and the corresponding ketone (0.5 mmol) in degassed iso-PrOH (5 mL) were refluxed until the reactions were completed.

3 Results and discussion

The results collected from the catalytic test reactions are listed in table 1.

At room temperature no considerable formation of 1-phenylethanol was observed. Furthermore, the precatalysts, as well as the presence of KOH, are necessary to observe appreciable conversions. The base facilitates the formation of ruthenium alkoxide by abstracting proton of the alcohol and subsequently alkoxide undergoes β-elimination to give ruthenium hydride, which is an active species in this reaction. This is the mechanism proposed by several workers on the studies of ruthenium catalyzed transfer hydrogenation reaction by metal hydride intermediates [2]. Increasing the substrate-to-catalyst ratio does not damage the conversions of

the product in most cases.

Table 1. Transfer hydrogenation of acetophenone with 2-propanol catalyzed by [Ru((Ph2PO)-C7H14N2Cl)(η6-benzene)Cl2]Cl, 1, [Ru((Cy2PO)-C7H14N2Cl)(η6-benzene)Cl2]Cl, 2, [Ru((Ph2PO)-C7H14N2Cl)(η6-*p*-cymene)Cl2]Cl, 3 and [Ru((Cy2PO)-C7H14N2Cl)(η6-*p*-cymene)Cl2]Cl, 4

Catalyst	Time[c]	Yield(%)[d]	TOF(h^{-1})[e]
1 [a]	30 min	97	194
1 [b]	48h	<5	....
2 [a]	10min	98	588
2 [b]	48h	<5	....
3 [a]	30min	95	190
3 [b]	48h	<5	....
4 [a]	10min	97	582
4 [b]	48h	<5	....

[a] Refluxing in 2-propanol; [b] At room temperature; [c] Substrate:catalyst:KOH=100:1:5 [d] Determined by GC (three independent catalytic experiments); [e] The reaction time shown in column; TOF= (mol product/mol Ru(II)Cat)*h^{-1}.A prototypical reaction using acetophenone indicated that the reaction rate not depend on the arene moieties (benzene and *p*-cymene) bound to metal center, conversely depend on the alkyl substituents on the phosphorus atom.

Encouraged by the activities obtained in these preliminary studies, we next investigated hydrogenation of substituted acetophenone derivatives (R = F, Cl, Br, 2-MeO) for the needs of petrochemistry and polymer chemistry. The introduction of electron withdrawing substituents, such as F, Cl and Br to the para position of the aryl ring of the ketone decreased the electron density of the C=O bond and the activity was improved giving rise to easier hydrogenation [3].

4 Conclusions

Results obtained from optimization studies indicate clearly that both complexes, [Ru($Cy_2POC_7H_{14}N_2Cl$)(η6-benzene)Cl_2]Cl, 2 and [Ru($Cy_2POC_7H_{14}N_2Cl$)(η6-*p*-cymene)Cl_2]Cl, 4 including Cy moiety on phosphorus atom are active and more efficient catalysts leading to nearly quantitative conversions. The catalytic activities dependent on the groups (phenyl and cyclohexyl) on the phosphorus atom, conversely not to depend on the arene moieties bound to metal center. The catalytic performance shown by both of these complexes is generally higher than that of recently reported for the related half-sandwich complexes bearing heterodifunctional P,N-ligands [4], P,O- ligands [5], and NHCs ligands [6].

Acknowledgements

The authors thank the Ministry of Education and Science of the Republic of Kazakhstan for financial support (1752/ GF4, 1318/ GF4, 0650/ GF4).

References

[1] G. Venkatachalam, R. Ramesh. *Inorganic Chemistry Communications*. 8 (2005) 1009.
[2] M. J. Palmer, M. Will. *Tetrahedron: Asymmetry*. 10 (1999) 2045.
[3] P. Pelagatti, M. Carcelli, F. Calbiani, C. Cassi, L. Elviri, C. Pelizzi, U. Rizzotti, D. Rogolino. *Organometallics*. 24 (2005) 5836.
[4] C. Standfest-Hauser, C. Slugovc, K. Mereiter, R. Schmid, K. Kirchner, L. Xiao, W. Weissensteiner. *J. Chem. Soc. Dalton Trans*. (2001) 2989.
[5] A. Caballero, F.A. Jalon, B.R. Manzano, G. Espino, M. Perez-Manrique, A. Mucientes, F.J. Poblete, M. Maestro. *Organometallics*. 23 (2004) 5694.
[6] İ. Özdemir, N. Şahin, B. Çetinkaya. *Monatshefte für Chemie*. 138 (2007) 205.

I-PP103

Syngas Production from CH_4 and CO_2 over Ni-Based Nanocomposites Catalysts at Mild Conditions

Guerrero-Caballero J.[1,2], Fang W.[1,2], Pirez C.[1,2], Paul S.[2,3], Dumeignil F.[1,2,4], Löfberg A.[1,2], Jalowiecki-Duhamel L.[1,2*]

1 - Université Lille Nord de France, Lille, France
2 - CNRS UMR8181, Unité de Catalyse et Chimie du Solide, UCCS, Villeneuve d'Ascq, France
3 - Ecole Centrale de Lille, Villeneuve d'Ascq, France
4 - Institut Universitaire de France, Maison Universités, Paris, France

* louise.duhamel@univ-lille1.fr

Keywords: hydrogen, production, syngas, methane, carbon, dioxide, nickel

1 Introduction

At the international level, the concern about the global warming and the depletion of fossil fuels has attracted much attention. Thus, several environmentally friendly technologies have been developed in the recent years. One of them is the production of high valuable syngas (a mixture of H_2 and CO) by dry reforming of CH_4 (DRM). Using CO_2 and CH_4 as reactants, gases largely involved in the global warming, is attractive in the approach of getting green processes [1]. To this purpose, Ni based catalysts are very promising candidates [2].

Following the green pathway, we report in this study the CH_4 dry reforming activity and the H_2/CO formation over Ni-based catalysts. The influence of different parameters has been studied such as the Ni loading, reaction temperature and partial pressure of the reactants.

2 Experimental/methodology

Two different series of Ni-based catalysts (Ce-Ni-O and Ni-Mg-Al-O) were prepared by coprecipitation method [3, 4]. The solids were calcined in air at 500 °C. The catalytic performance (10 – 200 mg) was conducted under the atmospheric pressure in a fixed-bed quartz reactor fitted in a programmable oven. The gas stream of CH_4/CO_2/He/Ar (5-20/5-20/x/y %v) was fed to the reactor (F_T = 100 ml/min). The stoichiometric molar ratio CH_4/CO_2 was maintained at 1 while varying the reactants concentration. The outlet gases were analyzed online by a mass spectrometer (MS).

3 Results and discussion

Very different types of Ni based composites were successfully developed and applied to syngas production from methane and carbon dioxide ($CH_4 + CO_2 \rightarrow 2\ CO + 2\ H_2$). As an example *Fig.1* shows the influence of the nickel content of cerium based compounds on CH_4 and CO_2 conversions measured at 600°C using a 5% initial concentration of each reactant. The conversion of CH_4 increases with the Ni loading, while the conversion of CO_2 presents an optimum on the catalyst with 19 wt% Ni. On this compound, the CH_4 and CO_2 conversions are about 54 and 57% respectively with the formation of about 43% (mol.) of H_2, 52% of CO and 5% of H_2O with the formation of a small amount of carbon. When Ni content increases up to 24 wt % the conversion of CH_4 is higher than the one of CO_2 which probably means that at such loading, it is easier to promote the $CH_4 \rightarrow C + 2\ H_2$ reaction. *Fig.2* presents the conversions of CH_4 and CO_2 obtained at 600ºC on a Ni-Mg-Al-O compound (10 mg) using higher concentration of the reactants (20%). In such conditions, the conversions of CH_4 and CO_2 are 58% and 66%, close to the DRM thermodynamic limitation, evidencing the high efficiency of the catalyst. The conversions remain quite stable along all the experiment, and the H_2/CO

obtained is close to 0.8. For this low temperature of 600°C, relatively good efficiency of the catalysts is observed, when comparing to recent results reported on Ni based mixed oxides catalysts [5-8] or on noble metal based catalyst [9]. The results obtained here are quite promising due to the easy catalysts preparation, the low mass of catalyst used, the low working temperature, and the relative high concentrations of the reactants used.

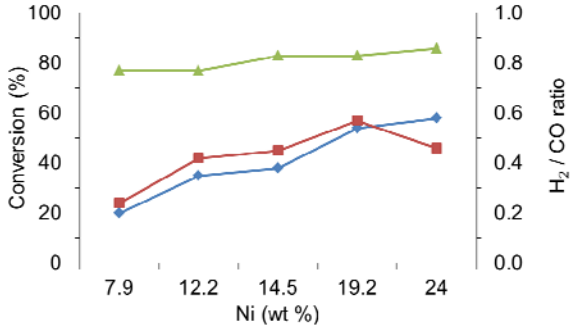

Fig. 1. CH_4 (●) and CO_2 (■) conversions and H_2/CO (▲) ratio at 600°C on Ce-Ni-O catalysts in gas stream of CH_4/CO_2/He/Ar: 5/5/10/80. (Each point after 5h).

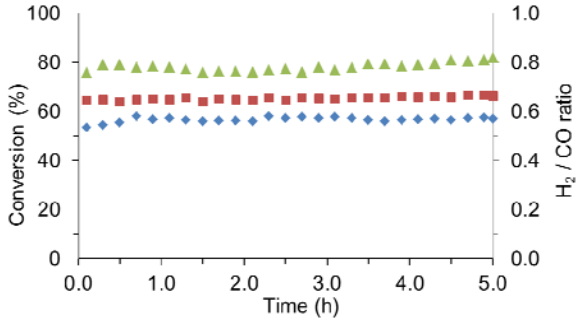

Fig. 2. CH_4 (●) and CO_2 (■) conversions and H_2/CO (▲) at 600°C on Ni-Mg-Al-O catalyst in gas stream of CH_4/CO_2/He/Ar: 20/20/20/40.

4 Conclusions

Well tuning Ni based catalysts formulation and preparation allows obtaining promising conversions of methane and carbon dioxide at mild conditions with a high selectivity for the formation of syngas (H_2 and CO).

Acknowledgements

Jesus Guerrero would like to thank for the grant of the French ministry and the University of Lille 1.

References

[1] D. Pakhare, J. Spivey, *Chem. Soc. Rev.* 3 (2014) 7813.
[2] S. Li, J. Gong, *Chem. Soc. Rev.* 43 (2014) 7245.
[3] W. Fang, C. Pirez, S. Paul, M. Capron, H. Jobic, F. Dumeignil, L. Jalowiecki-Duhamel, *ChemCatChem* 5 (2013) 2207.
[4] W. Fang, S. Paul, M. Capron, F. Dumeignil, L. Jalowiecki-Duhamel, *Appl. Catal. B* 152-153 (2014) 370.
[5] M. Yu, Y. A. Zhu, Y. Lu, G. Tong, K. Zhua, X. Zhou, *Appl. Catal. B* 165 (2015) 43.
[6] T. Odedairo, J. Chen, Z. Zhu, *Catal. Comm.* 31 (2013) 25.
[7] H. Wu, G. Pantaleo, V.L. Parola, A.M. Venezia, X. Collard, C. Aprile, L.F. Liotta, *Appl. Catal. B.* 156-157 (2014) 350.
[8] J. Dacquin, D. Sellam, C. Batiot-Dupeyrat, A. Tougerti, D. Duprez, S. Royer, *ChemSusChem* 7 (2014) 631.
[9] L. Qian, W. Cai, L. Zhang, L. Ye, J. Li, M. Tang, B. Yue, H. He, *Appl. Catal. B*. 164 (2015) 168.

I-PP104

Identification and Kinetic Tracing of Catalyst Intermediates by Complementary Spectroscopic Methods, Applied to the Resting States of Olefin-Polymerization Catalysts

Babushkin D.E.[1], Panchenko V.N.[1], Brintzinger H.-H.[2*]

1 - Boreskov Institute of Catalysis SB RAS, Novosibirsk, Russia
2 - Universität Konstanz, Konstanz, Germany

* dimi@catalysis.ru

Keywords: catalyst, speciation, resting states, olefin polymerization, UV-vis, NMR, spectroscopy

1 Introduction

The structural characterization of reactive intermediates, which arise in the course of a catalytic reaction, and the kinetic tracing of their concentration profiles are ongoing tasks in all fields of catalysis research. Magnetic resonance methods – such as NMR and EPR spectroscopy – can generally provide superb structural information concerning catalyst species present in solid or in homogeneously dissolved catalyst systems, but the time resolution of these methods is often insufficient to follow the time-course of a rapidly proceeding catalyst reaction. UV-vis spectroscopic methods, on the other hand, can generally provide only very limited structural information but these methods can, in principle, be tuned so as to provide an almost unlimited time-resolution. To elucidate catalytic processes in structural as well as kinetic terms, it would thus appear desirable to combine both of these complementary spectroscopy methods. In the following, we describe the application of this approach toward full characterization of several zirconocene-based catalyst systems used for the polymerization of α-olefins.

2 Experimental/methodology

All operations were carried out in an argon-filled glovebox or in vacuo by break-seal techniques. Solvents and liquid reagents were degassed and dried over molecular sieves (4Å) or distilled from sodium. Zirconocene complexes were obtained from MCAT Co., Konstanz, and trimethylaluminum and methylalumoxane from Aldrich Chemical Co. and used as such. Solutions for NMR experiments were prepared by dissolving ca. 1 μmol of the zirconocene dimethyl complex studied, directly in a 5-mm OD glass NMR tube, in 0.4 mL of a solution of $AlMe_3$ in C_6D_6 and then dissolving the appropriate amounts of $[Ph_3C][B(C_6F_5)_4]$ or of solid methylalumoxane in the reaction mixture. The NMR tube was transferred from the glovebox, inside an Ar-filled Schlenk vessel, to the cavity of the NMR spectrometer. After adding 1-hexene through the PTFE-lined septum closure from a PE syringe, which had also been kept inside an Ar-filled Schlenk vessel, ^1H NMR spectra were recorded on a Bruker AV 400 spectrometer, with 2.7 s acquisition time and 1 s delay time. Solutions for UV-vis experiments were similarly prepared in small (5-10 mL) sample vials. Portions of 2-2.5 mL were transferred to 1-cm UV-vis cuvettes equipped with a double-septum closure. After recording initial UV-vis spectra, 50-100 μL quantities of 1-hexene were added via a syringe through the double-septum closure and the ensuing spectral changes were recorded with a Cary 60 spectrometer, first in intervals of 12 seconds, later in 0.5- and 1-min intervals.

3 Results and discussion

In previous studies on the polymerization of 1-hexene or propene with various zirconocene-based catalysts by means of parallel ^1H NMR and UV-vis spectroscopy, we have shown that the initially predominant pre-catalyst species $[LZr(\mu\text{-}Me)_2AlMe_2]^+$ (with L = Me_2Si-bridged and/or substituted bis-indenyl ligand) is almost completely converted to cationic complexes with Zr-bound allylic chain ends, $[LZr\text{-}\eta^3\text{-}CH2CRCHR']^+$ (with R,R' = alkyl, polymeryl) [1, 2]. These polymer-carrying cationic Zr-allyl complexes, which constitute the dominant catalyst species

during ongoing polymerization catalysis, give rise to a UV-vis absorbance at ca. 560 nm. More recent kinetic studies on such a catalyst system by fast UV-vis spectroscopy provide evidence that – in addition to the two cationic complexes mentioned above and to a slowly forming decay product – an additional, short-lived intermediate arises during the first few minutes of the catalysis reaction, at the stage where most of the olefin is consumed. Since the concentration of this short-lived species appears to be proportional to the rate of olefin consumption, as obtained by parallel NMR measurements, it is likely to represent the hitherto elusive rate-determining catalyst intermediate [LZr(η^2-olefin)-polymeryl]$^+$. Its concentration appears to amount to ca. 5-10% of the total catalyst concentration.

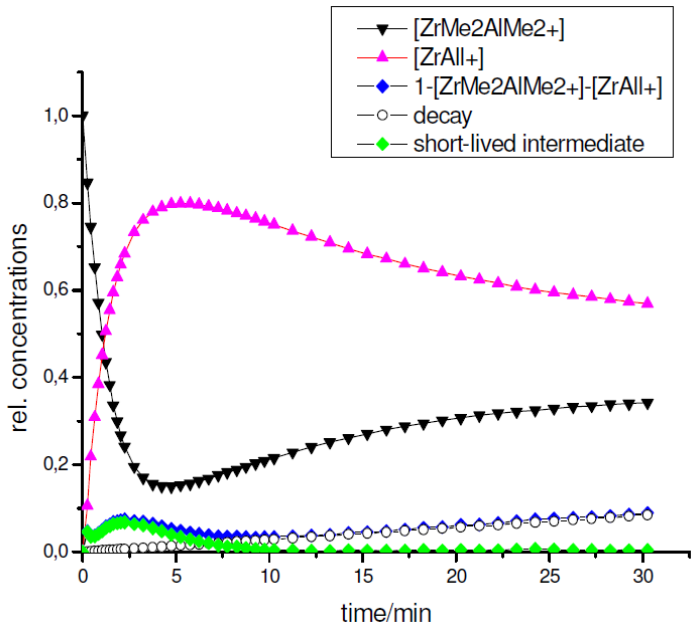

Figure 1. Concentration profiles of the pre-catalyst species [LZr(μ-Me)$_2$AlMe$_2$]$^+$ (black), of the main resting state [LZr-η^3-allyl-polymer]$^+$ (magenta), of a decay product (open circles) and of a short-lived catalyst intermediate (green), during polymerization of 1-hexene by a trityl-activated Me$_2$Si(ind)$_2$ZrMe$_2$ catalyst, determined by parallel ^{1}H NMR and UV-vis spectroscopy.

Further corroboration of the catalyst kinetics based on these UV-vis data is to be derived from ongoing NMR studies, which are aimed at a quantitative structural characterization of the polymer products with regard to internal and to chain-end unsaturations, known to arise from Zr-allyl species by olefin insertion and by their chain transfer to an alkyl-aluminum co-catalyst, respectively. Together, these spectroscopic results are expected to yield a detailed description of all relevant reaction steps involved in these catalytic polymerization reactions.

4 Conclusions

By parallel NMR and UV-vis studies, a thorough structural characterization of catalyst intermediates can be combined with a detailed kinetic elucidation of elementary reaction steps, which are responsible for the overall rate and the product distribution of a catalytic process.

Acknowledgements

The authors thank Russian Foundation of Basic Research (grant 14-03-91344) and Deutsche Forschungsgemeinschaft (grant Br 510/15-1) for financial support and Prof. E. P. Talsi and Prof. V. A. Zakharov (Boreskov Institute of Catalysis) for helpful discussions.

References

[1] D. E. Babushkin, V. N. Panchenko, H. H. Brintzinger, *Angew. Chem. Int. Ed.* 53 (2014) 9645.
[2] V. N. Panchenko, D. E. Babushkin, H. H. Brintzinger, *Macromol. Rapid Commun.* 36 (2015) 249.

I-PP106

Density Functional Theory Study of Alcohol Amination Reaction on Monoclinic Zirconia Surfaces

Martin L.[1,2], Paul J.-F.[1,2*]

1 - Unité de Catalyse et Chimie du Solide, Villeneuve d'Ascq, France
2 - Lille University, Lille, France

* jean-francois.paul@univ-lille1.fr

Keywords: DFT, calculations, oxide, surface, coadsorption, effect, alcohol amination, ethanol, ammonia

1 Introduction

In the actual environmental awareness, it is essential to develop eco-efficient processes for the synthesis of highly valuable diamine monomers (either new or already existing) using molecules obtained from biomass upgrading. Among the various processes to prepare amines, the N-alkylation of alcohols with ammonia or amines over is particularly attractive because of the availability of various types of alcohols (which can be bio-sourced diols) and the fact that water is the main by-product.

Metal-Supported Oxide catalytic family offers promising properties for alcohols amination with amines and ammonia [1]. However, the role played by the support in this amination process is not precisely understood. As the oxide supports have specific properties like Bronsted and/or Lewis acido-basic and/or redox properties, the interaction of molecules like water, ammonia, amines and alcohols with these oxide surfaces can lead to a large range of reaction.

In our study, we are interested in the catalytic reactions of ammonia and ethanol over bare and partially hydrated ZrO_2 surfaces using the Density Functional Theory (DFT). Particularly, we wanted to determine the energy barriers for different mechanisms of alcohol amination reaction and alcohol dehydrogenation process on a ZrO_2 catalyst.

2 Computational details

All calculations were performed using the plane wave DFT code VASP using the PBE functional. The electronic wave-functions were described in the Projected Augmented Wave (PAW) formalism. Reaction paths have been studied with the Nudge Elastic Band procedure (NEB) and all structures were minimized until the forces acting on each atom were less than 0.03 eV/Å.

3 Results and discussion

First, we have compared the adsorption on the exposed ZrO_2 surfaces (the (-111), (111), (011) and (001) facets were considered for the monoclinic zirconia phase [2]) of three different molecules: water, ammonia and ethanol. From our calculations, the isolated ethanol or water molecules prefer to dissociate at the zirconia surfaces due to the presence of Lewis acid Zr(s) sites and sufficiently strong Bronsted basic O(s) sites. On the contrary, ammonia is always adsorbed associatively on the Zr(s) sites. Moreover, the thermodynamic study of adsorption competition have indicated that the reactants (ammonia and ethanol) can substitute the initially adsorbed water molecules on ZrO_2 surfaces in the gas-phase conditions of the amination reaction (method proposed by Lemaire et *al.* [3] for oxide catalyst ($T_{reaction}$=200-300°C)).

Then, several possible reaction mechanisms for alcohol amination and dehydrogenation were investigated on the ZrO_2(111) plane. We demonstrated that similar catalytic behaviour was obtained for different ZrO_2 facets due to their comparable acido-basic properties. For the N-alkylation of ethanol with ammonia over zirconia, a nucleophilic substitution has been proposed

from a configuration in which the two reactants are coadsorbed on the ZrO_2(111) facet. In this Langmuir-Hinshelwood (LH) scheme (figure 1), a carbocation intermediate is formed from the adsorbed ethanol. Then the dissociated NH_3 molecule reacts with this intermediate to form the product $C_2H_5NH_2$.

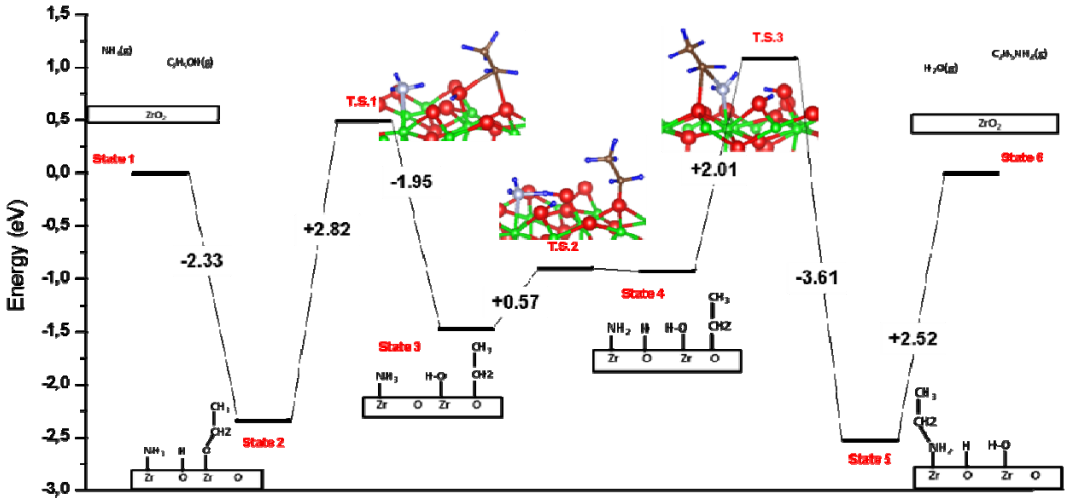

Fig. 1. An example of catalytic cycle calculated for the amination reaction in the LH case

In the Eley-Rideal (ER) mechanism, the nucleophilic NH_3 molecule does not adsorb on the surface and directly reacts on the adsorbed ethanol. In this case, we demonstrated the importance of water molecule coadsorption in a favourable configuration (hydrogen-bonded to NH_3(g) and adsorbed ethanol). Indeed, the adsorbed base [OH^-] assists the alcohol amination on ZrO_2 catalyst as it facilitates the N-H bond scission. For the ER type reaction, the calculated energy barrier is around 1.6 eV which is much smaller than those calculated for the LH mechanism (figure 1).

Finally, we also demonstrated that coadsorption of ethanol and water molecules in a specific configuration at ZrO_2(111) surface efficiently assists the ethanol dehydrogenation as it can strongly influence the C-H and O-H bonds activation.

4 Conclusions

The adsorption and reactivity of ammonia and ethanol at ZrO_2 surfaces revealed a relatively poor catalytic activity of the bare ZrO_2 surfaces for amination reaction and evidenced the crucial role played by the coadsorbed water molecule in the acide-base reactions. From our DFT calculations, we can conclude that the alcohol amination requires temperature activation to be efficient on oxide catalyst which is in agreement with previous experimental results [3]. These theoretical results highlight the importance of adding metallic particles to make this amination process more efficient.

Acknowledgements

Numerical results presented in this paper were carried out using the regional computational cluster supported by UniversitéLille1, CPER Nord-Pas-de-Calais/FEDER, France Grille, and CNRS. The project is supported by Agence Nationale de la Recherche under Contract N°ANR-13-CD2I-004 SHAPes

References

[1] K. Shimizu, *Catal. Sci. Technol.*. DOI:10.1039/c4cy01170h (2014).
[2] W. Piskorz, J. Grybos, F. Zasada, S. Cristol, J-F. Paul, A. Adamski, Z. Sojka, *J. Phys Chem C*. 115 (2011) 24274.
[3] F. Valot, F. Fache, R. Jacquot, M. Spagnol, M. Lemaire, *Tetrahedron Letters*. 40 (1999) 3689.

I-PP107

Ethylbenzene Hydroisomerization over an EU-1 Zeolite Generated in Presence of a Multivalent Surfactant Capping Agent

Marques Mota F.[1*], Jung J.[2], Ryoo R.[1,2]

1 - Center for Nanomaterials and Chemical Reactions, Institute for Basic Science (IBS), Daejeon, South Korea

2 - Department of Chemistry, KAIST, Daejeon, South Korea

* marquesf@ibs.re.kr

Keywords: EU-1 zeolite, multivalent surfactant capping agent, Ethylbenzene Hydroisomerization

1 Introduction

EU-1 (EUO topology) is a medium-pore ICI proprietary zeolite featuring deep side-pockets connected at regular distances to a tubular pore system. This intriguing microporous architecture has resulted in the industrial application of EU-1 based catalysts in the industrially relevant ethylbenzene hydroisomerization. During an initial period of fast deactivation, following the blockage by carbonaceous deposits of the access to the inner sites of the EUO micropores, solely the outer surface sites remain active and relatively insensitive to deactivation. Over the stabilized catalysts, for which only the protonic sites of large side pockets can be active, the selectivity to isomers is particularly high [1]. The quasi isolation of these acid sites is believed favorable to monomolecular one-step reactions at the expense of bimolecular reactions (e.g. ethylbenzene disproportionation and transalkylation) or of multi-step reactions (e.g. secondary cracking). As only a reduced fraction of the protonic sites can effectively participate in the acid-catalyzed reactions, up to date the challenge has been to prepare EU-1 based catalysts with a larger and easily accessible outer surface. Over the years, exploratory work has led to the synthesis of hierarchical zeolites using both top-down and bottom-up approaches. The synthesis of nanocrystalline zeolites using multi-ammonium surfactants through a capping effect has been recently reported [2]. Multivalent cationic surfactants were witnessed to be able to synthesize FAU, MOR, CHA, and MFI-type zeolite nanocrystals. In this paper, the surfactant-capping strategy was applied to the EU-1 zeolite and the resulting nanocrystalline zeolite tested in the hydroisomerization of ethylbenzene and compared with a bulk counterpart.

2 Experimental/methodology

Bulk EU-1 zeolite with Si to Al molar ratio equal to 30 was synthesized at 423 K, following a synthesis procedure described elsewhere [3]. Hexamethonium bromide (TCI) was used as the SDA. In the synthesis of the hierarchical EU-1 zeolite, $C_{18}H_{37}$-$N^+(CH_3)_2$-C_6H_{12}-$N^+(CH_3)_2$-C_6H_{12}-$N^+(CH_3)_2$-$C_{18}H_{37}$ was added to the conventional synthesis composition of EU-1 zeolite. The use of seed was pondered to reduce the necessary hydrothermal time. The obtained gel had a molar composition 60 SiO_2:1 Al_2O_3:10 SDA:1 C_{18}-N_3-C_{18}:10 Na_2O:1500 H_2O:3 seed. The bifunctional catalysts were prepared by milling the zeolite samples with 1.0 wt.% Pt/Al_2O_3, prepared by ionic exchange of □-Al_2O_3 with a hexachloroplatinic acidic solution. A corresponding weight proportion of 10:90 was used. The ethylbenzene hydroisomerization was conducted in a fixed bed stainless steel reactor at 683 K, 10 bar and a H_2/ethylbenzene=4 mol/mol. 1.0 g of catalyst with a particle size between 0.200-0.355 mm was loaded into the reactor. The catalyst was activated *in situ* at 753 K for 4 hours under H_2 flow (5 K/min, at 10 bar). The reaction was firstly carried out, at a fixed weight hourly space velocity (WHSV=15 g of ethylbenzene h^{-1} g^{-1} of catalyst), until a virtually stable conversion was obtained with increasing time-on-stream. At this point, conversion was then

determined in function of the WHSV, varied in a 2-60 h^{-1} range, by changing the reactant flow. The obtained products were analyzed online by flame ionization detector gas chromatography.

3 Results and discussion

XRD patterns of both as-synthesized EU-1 samples were in agreement with those reported in the literature. Representative scanning electron microscopy (SEM) photographs illustrated the presence of agglomerates of small granular crystals in the 20-50 nm range. The agglomerates exhibited dimensions up to 3-4 μm. SEM images confirmed the successful appliance of the surfactant-capping agent through the presence of granular crystals with decreasing particle diameters. Following nitrogen assessment, the *t*-plot method revealed an external surface of the EU-1 nanocrystals obtained in this manner of 152 m^2 g^{-1}, whereas the bulk counterpart exhibited only 62 m^2 g^{-1}. With both samples, the activity of EU-1 based catalysts was observed to decrease with TOS up to a certain extent, after which solely the outer surface sites remained active and relatively insensitive to deactivation. The results presented hereafter were obtained at the aforementioned steady state. The conversion rates of ethylbenzene were plotted for both EU-1 based catalysts as a function of the contact time, taken as the reverse of the corresponding WHSV values (Figure 1). In each case, the obtained results reveal a continuous increase of ethylbenzene conversion with the contact time. More importantly, given the significant increase of the external surface area, the catalytic activity was remarkably shifted to higher values at *iso*-WHSV values. Despite the significant increase in the catalyst activity, no detrimental effect was observed in the obtained isomerisation yields.

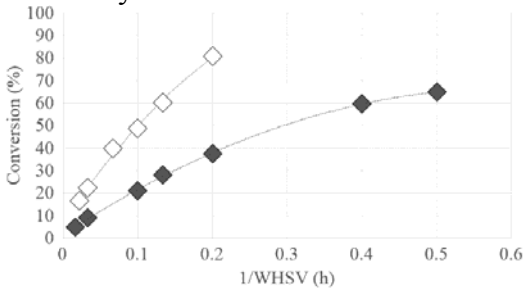

Fig. 1. Ethylbenzene conversion against contact time (taken as the reverse of WHSV) over EU-1 zeolite synthesized in presence (open diamond) and absence (closed diamond) of a capping agent.

4 Conclusions

The capping effect of a multivalent cationic surfactant was successfully used in the synthesis of EU-1 zeolite nanocrystals. Whereas the conventional template, hexamethonium bromide, was still confirmed to direct the synthesis of the zeolite crystals, the nanocrystals formation was attributed to the strongly binding effect of the surfactant molecules on the substrate surfaces. The surfactant capping was confirmed to effectively determine the crystal size in a passive manner. Preliminary catalytic results demonstrated the remarkable impact of generating an EU-1 zeolite with a larger and easily accessible outer surface, exhibiting a higher concentration of active acid sites. Current works intend to study the continuous increase of the external surface area that would allow to decrease the density of acid sites responsible for secondary and undesired bimolecular reactions.

Acknowledgements

This work was supported by the Institute for Basic Science (IBS).

References

[1] F. Moreau, P. Moreau, N.S. Gnep, *et al*, *Microporous Mesoporous Mater.* 90 (2006) 327.
[2] C. Jo, J. Jung, H. Shin, J. Kim, R. Ryoo, *Angew. Chem. Int. Ed.* 52 (2013) 10014.
[3] G.W. Dodwell, R.P. Denkewicz, L.B. Sand, *Zeolites* 5 (1985) 153

I-PP108

Catalytic Oxidation of α-Alkenes C8-C12 to Carboxylic Acids

Oleneva P.V., Berdnikova P.V., Pai Z.P.*

Boreskov Institute of Catalysis SB RAS, Novosibirsk, Russia

* zpai@catalysis.ru

Keywords: oxidation, ofterminal, alkenes, phase-transfer, catalysis, hydrogen, peroxide, peroxotungstate

1 Introduction

Monocarboxylic acids are useful products in various industries: chemical (for the production of lubricants, hydraulic fluids, paints, plastics), agrochemical (for the production of pesticides, herbicides, acaricides), food and perfume (preservatives, fragrance precursors), and pharmaceutical (drugs or their precursors).

C8-C10, C10-C12 alkene fractions and pure C8, C10 and C12 alkenes are available in oil refineries (for example, Neftekamsk Oil refinery). But effective ways of processing these fractions are limited [1]. Generally speaking, alkenes can be converted to alcohols or carboxylic acids. The results of C8-C12 terminal alkenes oxidation in two-phase system (organic phase/water phase) with phase-transfer catalysts to aliphatic carboxylic acids are shown in this study:

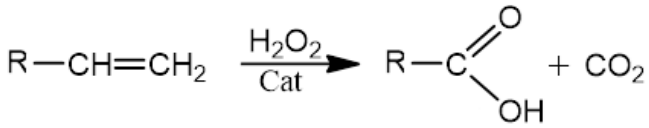

,

where R = C_4H_9, C_6H_{13}, C_8H_{17}.

2 Experimental/methodology

The available and environmentally friendly 30% aqueous hydrogen peroxide is used as an oxidant. The reaction is performed in the presence of bifunctional catalytic systems based on peroxocomplexes of tungsten in combination with quaternary ammonium cations – $Q_3\{PO_4[WO(O_2)_2]_4\}$, where Q^+ is quaternary ammonium cation [2].

The phase-transfer catalysis allows the oxidation reactions of various organic substrates to be carried out under mild conditions – at low temperature (up to 100 °C) and atmospheric pressure. The important advantage of this catalytic method is the possibility of process implementation in the absence of hazardous organic solvents. Therefore, the phase-transfer catalytic reactions can be related to the "green" chemistry. The problem of a homogeneous catalyst separation from the reaction mixture in this case is solved by separating the phases since the catalyst and the final product are in different phases – organic and aqueous, respectively.

3 Results and discussion

As shown in Figure 1, the yield of heptanoic acid (C7) in the 1-octene oxidation in the presence of $[Bu^n_4N]_3\{PO_4[WO(O_2)_2]_4\}$ catalytic complex was 18%, in the presence of $[CetPy]_3\{PO_4[WO(O_2)_2]_4\}$ catalytic complex – 90%, and in the presence of $[MeOct^n_3N]_3\{PO_4[WO(O_2)_2]_4\}$catalytic complex – 92%. The lowest activity is observed in the presence of tetra-*n*-butylammonium salt of $\{PO_4[WO(O_2)_2]_4\}^{3-}$. It is accounted for the influence of cation type on the catalytic activity as reported in [2b]. The yields of nonanoic acid (C9) in the 1-decene oxidation and the yields of undecanoic acid (C11) in the 1-dodecene oxidation in the presence of $[Bu^n_4N]_3\{PO_4[WO(O_2)_2]_4\}$ did not exceed 17-18% (Fig. 1).

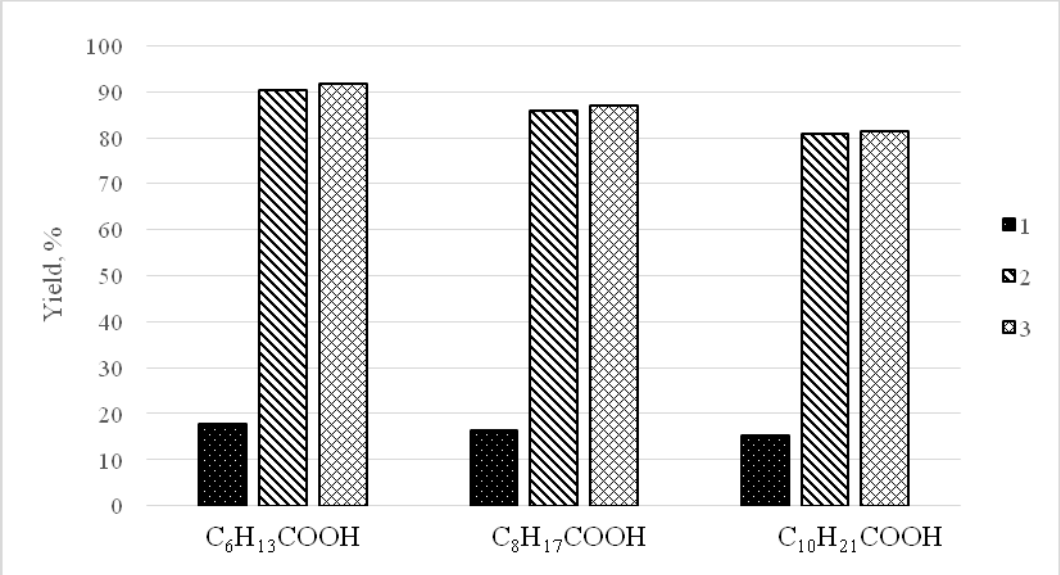

Fig. 1. Yields of carboxylic acids in α-alkenes oxidation with 30% aqueous hydrogen peroxide in the presence of catalytic complexes **1-3**.
Conditions: T = 90 °C, [Sub] / [Cat] = 200, $[H_2O_2]$ / [Sub] = 5, τ = 4 h.
1 – $[Bu^n{}_4N]_3\{PO_4[WO(O_2)_2]_4\}$
2 – $[CetPy]_3\{PO_4[WO(O_2)_2]_4\}$
3 – $[MeOct^n{}_3N]_3\{PO_4[WO(O_2)_2]_4\}$

4 Conclusions

The data obtained in the α-alkenes oxidation with 30% aqueous hydrogen peroxide in the presence of peroxopolyoxophosphotungstates $Q_3\{PO_4[WO(O_2)_2]_4\}$ demonstrate the possibility for obtaining valuable carboxylic acids (heptanoic, nonanoic and undecanoic) with high yields (more than 90%) under mild conditions (temperature < 90 °C, atmospheric pressure).

The most active catalysts are *tris*cetylpyridinium- and *tris*methyl-*n*-trioctylammonium tetrakis(oxodiperoxotungsto)phosphate.

Acknowledgements

The work was supported by the Russian Foundation for Basic Research (Project 12-03-00173-a) and Branch of General and Technical Chemistry RAS (Project 5.7.3.).

References

[1] Lakeev S.N., Karchevskii S.G., Maidanova I.O., Aleksashev V.I. Sb. materialov mezhregional'noi nauchno-prakticheskoi konferencii "Innovacionnie processi v oblasti obrazovaniya, nauki i proizvodstva" 2004, Rossiya, g. Nizhnekamsk , 4 s . (http://www.chemteq.ru/articles/olefin.html).
[2] a) Z.P. Pai, D.I. Kochubey, P.V. Berdnikova, et al., J. Mol. Catal. A: Chem., 2010, V. 332, P. 122–127; b) D.I. Kochubey, P.V. Berdnikova, Z.P. Pai, et al., J. Mol. Catal. A: Chemical: 2013, V. 366, P. 341–346.
[3] Zayavka na patent RF № 2014132335 Sposob polucheniya alifaticheskih karbonovih kislot. // P.V. Oleneva, P.V. Berdnikova, Z.P. Pai, L.V. Malysheva; prioritet 02.10.14.

I-PP109

Innovative Catalyst Design for Improved Catalytic Properties for Methanol-to-Olefins Reaction

Lefevere J.[1,2*], Protasova L.[2], Mullens S.[2], Meynen V.[1]

1 - University of Antwerp, Antwerp, Belgium
2 - VITO

* jasper.lefever@vito.be

Keywords: structured catalyst, wash coating, ZSM-5, methanol-to-olefins, robocasted catalyst

1 Introduction

Present-day catalytic research focusses often on enhancing the economic and environmental properties of existing processes. In order to do so process intensification is implied, the energy-efficiency, activity, selectivity and stability of catalysts need to be improved. By replacing packed beds of catalyst pellets or powders by a structured catalyst, the performance of the reactions that suffer from mass and heat transfer limitations can be significantly improved. However the architecture of the porous support material will have an impact on the catalytic properties of the final catalyst.

2 Experimental/methodology

By using a rapid prototyping technique the porous support was build up layer by layer [1, 2] (Figure 1). Robocasting is a solid free forming technique for the manufacture of metallic or ceramic porous structures. In this way periodic and highly reproducible support structures, with high mechanical properties and low pressure drop were synthesized [3, 4]. This technique allows to control the porosity, size of the unit cell and design of the support material. The support structures were coated by a wash coating procedure (Figure 2). After drying and sintering of the coated supports the adhesion of the coating was evaluated using ultrasonic treatment. Methanol-to-olefins (MTO), a highly economically relevant that suffers from mass and heat transfer limitations was chosen as demonstration reaction. In the present work, 3DFD support structures with different architectures were coated with ZSM-5 catalyst and compared with a packed bed of zeolite and traditional honeycomb monoliths for the conversion of methanol to olefins.

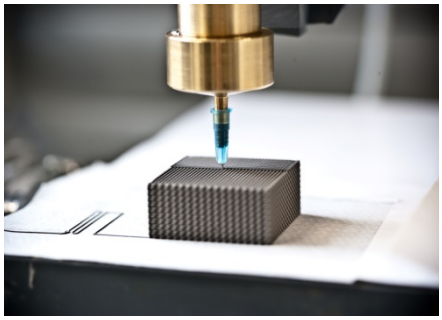

Figure 1. Synthesis of support by 3DFD

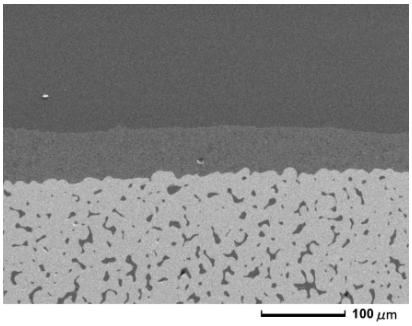

Figure 2. SEM image of coated 3DFD support

3 Results and discussion

The results of catalytic tests show an increase in activity and selectivity to the desired light

olefins (Figure 3) in case of using structured catalysts. Interestingly the 3DFD sample with zigzag channels in the direction of the gas flow shows the highest selectivity towards the desired products. It is suggested that the more tortious pathway of the reagents and products through the structure leads to the improved mass and heat transfer properties of the support resulting in better catalytic performance. Pressure drop measurements have already confirmed that the flow behaviour in the structures with different architectures is significantly different.

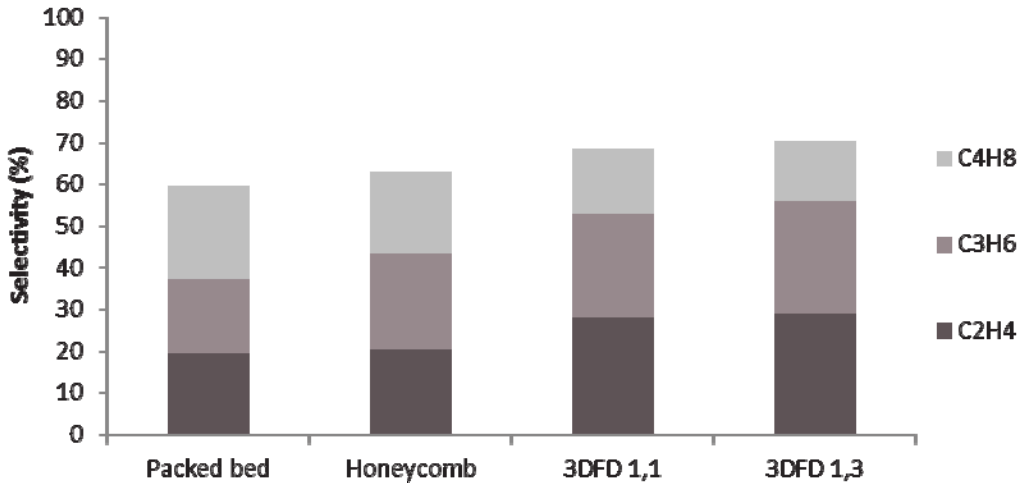

Figure 3. Selectivity to light olefins of different catalytic systems.

4 Conclusions

Robocasting could become an interesting tool for the development of innovative catalytic structures with improved mass and heat transfer properties. Further improvement can be made by optimizing the porosity, unit cell size and further design of the channels of the structures. However this implies a very large freedom of design and the input from modelling will lead to faster optimization of the design of the catalytic structure. Moreover the design of the catalyst can be altered as a function of the reaction and the desired properties of the catalyst.

References

[1] J. Stuecker, R. Ferrizz, J.C. III, J. Miller, Ind.& Eng. Chem. Res. 44 (2005) 302-308.
[2] J. Noyen, A. Wilde, M. Schroeven, S. Mullens, J. Luyten, International Journal of Applied Ceramic Technology 9 (2012) 902-910.
[3] J. Luyten, S. Mullens, I. Thijs, KONA Powd. Part. J 28 (2010) 131-142.
[4] J. Zhu, Y. Fan, N. Xu, Journal of Membrane Science 367 (2011) 14-20.

I-PP110

Development of Technology for Catalytic Neutralization of Toxic Waste Gas Impurities

Baizhumanova T.S.*, Zheksenbaeva Z.T., Tungatarova S.A., Zhumabek M., Kassymkan K.

D.V. Sokolsky Institute of Organic Catalyst and Electrochemistry, Almaty, Kazakhstan

* baizhuma@mail.ru

Keywords: oxide, catalyst, hydrocarbons, carbon, dioxide, toluene, deep oxidation

1 Introduction

The problem of chemical safety and air protection is particularly relevant due to increased emissions of industrial enterprises, which have toxic effects on the fauna and flora. Emissions of the industrial enterprises (paint, furniture, cable, pharmaceutical, printing) and transport are the main pollutants. Many chemical compounds (toluene, xylene, styrene, phenol, tricresol, white spirit, etc.), which have a negative impact on living organisms, are also harmful toxic emissions from industrial plants [1]. In this regard, the development of new-generation catalysts for deep cleaning of industrial emissions and motor vehicles which do not contain precious metals or low their content in the catalysts is relevant for the Republic of Kazakhstan.

2 Experimental/methodology

Polyoxide catalysts were prepared by incipient wetness impregnation of alumina modified by cerium with mixed aqueous solution of metal salts nitrate followed by drying at 453-473 K (4-5 h) and calcination at 873 K (1-1.5 h) in air. The spherical θ-Al_2O_3 (made at Boreskov Institute of Catalysis, Novosibirsk) with a diameter of 3-4 mm and specific surface area of 100 m^2/g, bulk weight of 0.80 g/cm^3, the mechanical strength of 150 MPa and pore volume of 0.48 cm^3/g was used as a carrier for polyoxide catalysts [2]. θ-Al_2O_3 was modified by cerium oxide, which forms the surface $CeAlO_3$ of perovskite type with alumina resistant up to 1373 K.

Deep oxidation of toluene as a model object was carried out on the flow installation. Toluene content before and after reaction was analyzed on a chromatograph Crystal-2000M with flame ionization detector on a capillary column. Column temperature - 160°C, evaporator temperature - 240°C, the hydrogen flow - 25 mL/min, air flow - 250.0 ml/min. The catalyst activity was measured in the oxidation of toluene, a substance frequently present in industrial gas emissions. The test of Ni-Cu-Cr/2% Ce/θ-Al_2O_3 catalyst was carried out at space velocity W = 5×10^3 h^{-1} in the temperature range 523-773 K and toluene concentration of 320 mg/m^3 [3].

3 Results and discussion

The obtained data showed that the nickel-copper-chromium-containing polyoxide catalysts in deep oxidation reaction of toluene at 723 K and space velocity 5×10^3 h^{-1} are arranged in the following order on the activity:

NiCuCr/2%Ce/θ-Al_2O_3(98,8%) > NiCuCr/θ-Al_2O_3 (93%) > Ni-Cu/2%Ce/θ-Al_2O_3(85%) > Ni-Cr/2%Ce/θ-Al_2O_3(76%) > Ni/2%Ce/θ-Al_2O_3(57%)

Comparison of the activity of multicomponent nickel-copper-chromium-containing catalyst supported on alumina modified by cerium with a catalyst supported on alumina without cerium showed that the conversion of toluene on the Ni-Cu-Cr/2% Ce/θ-Al_2O_3 catalyst is more high (98.8%) than on the Ni-Cu-Cr /θ-Al_2O_3 (93%) catalyst. The highest degree of conversion (up to 98.8%) of toluene was achieved on a multi-component Ni-Cu-Cr/2% Ce/θ-Al_2O_3 catalyst, and

the lowest - on the Ni/2% Ce/θ-Al_2O_3 contact.

Methods of entering the active components in composition of the nickel-copper-chromium catalyst for deep oxidation of toluene to CO_2 and H_2O were investigated. Methods for supporting of active phase indicated that sequential entering of components does not contribute to improving the effectiveness of nickel-copper-chromium catalyst. The best result was obtained at simultaneous introduction of all components in the impregnating solution. Modification by small additions of basic compounds which are introduced into impregnation solution (Na_2CO_3, KOH, NH_4HCO_3) is one of the methods for obtaining of catalysts with uniform distribution of components.

Thus, the conversion of toluene to CO_2 reaches 97.5-98.8% on the Ni-Cu-Cr/2% Ce/θ-Al_2O_3 catalyst at the temperature of 723-773 K and space velocity 5×10^3 h^{-1}.

4 Conclusions

Polyoxide Ni-Cu-Cr/2% Ce/θ-Al_2O_3 catalyst with desired properties on carriers for deep oxidation of hydrocarbons - toluene, xylene, styrene, ethyl acetate, butyl acetate, isobutanol, formaldehyde, acetone, ethanol, etc., which have a toxic effect on living organisms and flora, was developed. It has been shown that the synthesized polyoxide Ni-Cu-Cr catalyst supported on 2% Ce/θ-Al_2O_3 provides 98.8% toluene conversion up to CO_2 at space velocity 5×10^3 h^{-1}, temperature 723-773 K and content of toluene 320 mg/m^3 in the initial mixture.

Acknowledgements

This work (project No 0246/GF-4) was supported by the Ministry of Education and Science of Kazakhstan.

References

[1] K. Dossumov, N.M. Popova, Z.T. Zheksenbaeva, *Catal in Industry*. 1 (2009) 60-67.

[2] K.A. Altynbekova, N.M. Popova, L.A. Sokolova, In: Proceedings of the International Conference Regularities of deep oxidation of substances on solid catalysts. Novosibirsk, Russia, (2000) 242-247.

[3] S.A Tungatarova, Z.T. Zheksenbaeva, N.O. Omarova. In: XX International Conference on Chemical Reactors CHEMREACTOR-20. Luxemburg, December 3-7 (2012) 228-229.

I-PP111

Asphaltene Aggregation Processes in the Crude Oils

Larichev Yu.V.[1,2,3*], Martyanov O.N.[1,2,3]

1 - Boreskov Institute of Catalysis, Siberian Branch of Russian Academy of Sciences, Novosibirsk, Russia
2 - Novosibirsk State University, Novosibirsk, Russia
3 - Unicat Ltd, Novosibirsk, Russia

* larichev@catalysis.ru

Keywords: asphaltenes, deposit, crude oil, SAXS

1 Introduction

One of the most intractable problems of recovery and processing of heavy oils and their components is the formation of asphaltene deposits inside the equipment used for transport and processing of heavy oils, which lead to inefficient heat transfer, loss of energy and raw materials during the process up to a few percent of each barrel of crude oil (energy equivalent) [1]. Asphaltenes that are defined as the heaviest fractions of crude oil insoluble in normal alkanes (n-pentane, n-heptane, etc.) have the complex molecular structure. Besides alkyl-substituted aromatic structures and aliphatic chains, asphaltenes can incorporate functional groups containing heteroatoms, including sulfides and nitrogen-containing saturated structures and some carbonyl, ether, or ester groups [2]. These complex structures of asphaltenes are known to deactivate and shorten the operational lifetime of hydrotreating catalysts used for heavy oil processing because of the deposition and coke formation onto the active catalytic sites [3, 4]. This provided motivation for finding new ways for the conversion of asphaltenes into valuable chemicals.

The typical asphaltene concentrations in the heavy oils lay in the range from 1 to 15%. The asphaltene molecules can form aggregates with sizes varied from 5 to 50 nm depending on the oil type and asphaltenes structure. Asphaltene aggregates can take different shape and morphology – from disks and cylinders to the fractal-like objects [5]. The essential factor that affects the processes of asphaltene aggregation is related to the asphaltene local environment in crude oil. The composition of the surrounding fluid along with pressure and temperature play an important role in the asphaltene stability. For example, an addition of paraffin solvent changes the solubility of asphaltenes in the bulk oil because paraffin solvent properties affect interactions among asphaltenes and resins [1, 5]. The high temperatures and pressures can also change the local environment of asphaltene molecules, resulting in either an increase or decrease of asphaltene solubility in crude oil. Thus, the prediction and control of oil stability and asphaltene solubility under certain conditions requires fundamental studies of the intermolecular interactions between asphaltenes and their local environment and investigation of local rheological properties of crude oil and molecular dynamics of asphaltenes in different surroundings.

Here we report the investigation of the asphaltene aggregation process influenced by some chemical additives based on the analysis of the Small Angle X-ray Scattering (SAXS) data. The SAXS method allowed us to investigate the kinetic of the asphaltenes aggregation *in situ* and analyze the key factors that influence the aggregation processes and asphaltenes stability.

2 Experimental

The behavior of asphaltene extracted from crude heavy oil [6] according ASTM method D6560-005 [7] has been investigated. Asphaltenes density measured by He pycnometer is 1.178 g/cm^3. The asphaltenes were dissolved in toluene followed by the introduction of certain

additives into the solution. The asphaltene and the additive concentrations in solutions were 5 mass % and 20 mass % respectively. The S3 MICRO (HECUS) small angle diffractometer (Cu Kα, 50W) with a point collimation of primary beam was used for measuring scattering patterns of all samples. The scattering vector magnitude $h = 4\pi*\sin(\theta)/\lambda$ (where 2θ is the scattering angle, and $\lambda = 1.541$ Å is the radiation wavelength) was used as the scattering coordinate. The scattering intensity was measured in the range of the scattering vector magnitudes $0.01 < h < 0.6$ $Å^{-1}$. The asphaltene solutions were placed in a quartz or glass capillary with 1.5 mm external diameter. The numerical calculation of the particle size distributions based on the scattering data obtained was made via GNOM program from the ATSAS package [8].

3 Results and discussion

It was found that the asphaltene aggregates in the toluene solution without any additives have elongate shapes and wide sizes distribution with characteristic size about several nm. The influence of more than 30 chemical additives and asphaltene aggregation process has been studied. It was shown that such additives as cyclohexane, methanol, formic acid, heptane, TBAF, acetonitril, decane, hexanol-1, furfural, octen-1 tend to increase the sizes of asphaltenes aggregates. At the same time acetone, glycerol, ethylacetate, dioxane, benzyl alcohol, limonene, pinene, cycloheptatriene and ionic liquid (t-butyl imidazole tetrafluoroborate) practically do not affect the aggregates sizes. It was shown that some polar compounds (e.g. DMSO) can lead to the disaggregation of the asphaltenes.

Acknowledgements

The authors are grateful to K.V. Obida for the assistance in the measuring of the SAXS data. The study was supported by Skolkovo foundation, project No. 64 and by MES (Russia).

References

[1] A. Hammami, C.H. Phelps, T. Monger-McClure, T.M. Little, *Energy Fuels* 14 (2000) 14.
[2] Cimino, R.; Correra, S.; Bianco, A. D.; Lockhart, T. P. In Asphaltenes: Fundamentals and Applications; Sheu, E. Y., Mullins, O. C., Eds.; Springer: New York, 1995; pp 97−130.
[3] I. Gawel, D. Bociarska, P. Biskupski, *Appl. Catal. A* 295 (2005) 89.
[4] M. Idris, L.N. Okoro, *Eur. Chem. Bull.* 2 (2013) 393.
[5] Asphaltenes, heavy oils and petroleomics, edited by O.C. Mullins, Springer, NY, 2007, 669 p.
[6] F.V. Tuzikov et al, *Petroleum Chemistry* 51(4) (2011) 281.
[7] ASTM International. ASTM D6560, Standard Test Method for Determination of Asphaltenes (Heptane Insolubles) in Crude Petroleum and Petroleum Products; ASTM International: West Conshohocken, PA, 2012; http://www.astm.org/Standards/D6560.htm.
[8] P.V. Konarev et al, *J. Appl. Cryst*., 39 (2006) 277.

I-PP112

Peculiarities of MoS_2/Al_2O_3, $CoMoS/Al_2O_3$ and $NiMoS/Al_2O_3$ Catalyst's Behaviour in the Hydroconversion of Aliphatic Esters and Rapeseed Oil

Vlasova E.N.[1,2], Aleksandrov P.V.[1,2], Deliy I.V.[1,2,3], Bukhtiyarov A.V.[1,2], Gerasimov E.Y.[1,2], Paharukova V.P.[1,2], Bukhtiyarova G.A.[1*]

1 - Boreskov Institute of Catalysis SB RAS, Novosibirsk, Russia
2 - Research and Educational Center for Energy Efficient Catalysis in Novosibirsk National Research University, Novosibirsk, Russia
3 - Novosibirsk National Research University, Novosibirsk, Russia

* gab@catalysis.ru

Keywords: hydrodeoxygenation, sulfide catalyst, aliphatic ethers, rapeseed oil

1 Introduction

Hydrodeoxygenation (HDO) of triglyceride-based feedstocks such as vegetable oils and animal fats produces a mixture of C_{13}-C_{18} paraffins and is considered now as an important commercial route for the production of diesel range bio-fuels. Hydroprocessing of such feedstocks may be performed in stand-alone units or via the co-hydrotreatment of renewable feeds with petroleum-derived distillates in the existing HDS units. In both cases conventional hydrodesulfurisation catalysts (CoMo or NiMo) may be used to convert triglycerides into linear alkanes. The reaction pathways of triglyceride molecules conversion involve the elimination of oxygen through several competing routes: hydrodeoxygenation (HDO) or decarboxylation/ decarbonylation ($HDeCO_X$). The critical challenge in the developing of the new energy-efficient processes for the triglyceride-based feedstock conversion is the elucidation of peculiarities of sulphide catalyst's behaviour depending on their chemical composition.

The current work presents the results of the comparative study of MoS_2/Al_2O_3, $CoMoS/Al_2O_3$ and $NiMoS/Al_2O_3$ catalysts in the aliphatic ethers hydro conversion as well as in the hydrotreating of rapeseed oil (RSO) and its mixtures with the straight-run gasoil (SRGO). Our efforts are concentrated on the selectivity of aliphatic ether transformation depending on the active phase chemical composition and the reaction conditions; the influence of RSO content on the HDS and HDN activity of catalysts in the SRGO hydrotreating was also analyzed.

2 Experimental/methodology

The catalysts were prepared by impregnation of Al_2O_3 granules with a solution of active metals precursors, phosphoric and citric acids. The HDO of methyl heptanoate (MH) and methyl palmitate (MP) were performed in a batch reactor at 300°C and hydrogen pressure of 3.5 MPa. The reaction products were identified by GC/MS technique and quantified by gas chromatography system (Agilent 6890N) equipped with atomic emission detector (GC-AED). The hydroprocessing of RSO, SRGO and blended feeds (5-15 wt.% of RSO) was carried out in trikle-bed reactor at 3.5-7.0 MPa, 300-360°C, LHSV 1-2 h^{-1}, H_2/feed ratio 300-1000. The total S and N content in the products were determined using ANTEK 9000NS, the total oxygen content – by means of CHNSO analyzer Vario EL Cube. The quality of produced fuels (boiling range distribution, density and cetane number) was checked using the corresponding ASTM methods.

3 Results and discussion

Characterization of the catalysts in the sulfide state by means of XPS, XRD and HRTEM confirmed that the applied preparation and sulfidation procedures provide the formation of highly dispersed MoS_2, CoMoS and NiMoS nanoparticles (3-5 nm) on the alumina surface.

The comparison of catalyst's performance in MP hydroconversion let us to conclude, that the sulfided Mo/Al_2O_3, $CoMo/Al_2O_3$ and $NiMo/Al_2O_3$ catalysts revealed the same rate of the methyl palmitate conversion but the rate of the intermediate oxygenates conversion decreased in order: $CoMoS/Al_2O_3 > NiMoS/Al_2O_3 > MoS_2/Al_2O_3$. A mixture of linear saturated and unsaturated C_{15} and C_{16} hydrocarbons was produced when the oxygen-containing compounds were fully consumed. The main products obtained over the Mo/Al_2O_3 were C_{16} hydrocarbons (about 95 mol. % selectivity at 100% conversion), while $CoMo/Al_2O_3$ and $NiMo/Al_2O_3$ catalysts gave C_{16} hydrocarbons with the selectivity of 72 and 40%, respectively. So, the chemical compositions of sulphide phase effects on the contributions of the hydrodeoxygenation (HDO) and decarboxylation/decarbonylation ($DeCO_x$) pathways during the hydroconversion of methyl palmitate. The investigation of listed above catalysts in RSO hydrotreating confirmed this conclusion and elucidate the influence of reaction condition on selectivity: the rising of temperature and decrease of hydrogen pressure enhance the contribution of $DeCO_x$ pathways.

Comparing HDS rate constants for the SRGO feeds with the different RSO content showed that RSO addition (up to 15 wt. %) markedly decreased the activity of $CoMoS/Al_2O_3$ catalysts but had no effect on the activity of $NiMoS/Al_2O_3$ one. The same dependencies were observed in HDN reaction. In accordance, over $NiMoS/Al_2O_3$ catalyst ULSD can be produced from SRGO and RSO-SRGO blend at the same conditions, while the temperature increase is needed if the $CoMoS/Al_2O_3$ catalyst is used for ULSD production from RSO-SRGO blends. The hydrodeoxygenation of RSO over sulfide catalysts gave paraffins, propane, water, CO, and CO_2. It was observed in the special experiments that addition of CO to the hydrogen flow had the same effect on the HDS activity of the $CoMo/Al_2O_3$ and $NiMo/Al_2O_3$ catalysts as the addition of RSO to the SRGO feed. Thus, CO molecules formed as a result of RSO hydroconversion can be considered as a main reason of decrease of $CoMoS/Al_2O_3$ catalyst's activity. This assumption was supported by the observation that addition of benzofuran giving only water in HDO reaction had a minor influence on the activity of $CoMoS/Al_2O_3$ catalyst in HDS of SRGO. Taking into account the discovered peculiarities the reactor with multi-bed loading was proposed for the hydrotreating of RSO-SRGO mixture. The use of MoS_2/Al_2O_3 in front layer for the RSO conversion diminished the CO formation and allowed to use the $CoMoS/Al_2O_3$ catalyst in the second layer without significant decrease of HDS activity. The feasible reasons of the observed differences between $CoMo/Al_2O_3$ and $NiMo/Al_2O_3$ catalyst behavior were also discussed.

4 Conclusions

The behaviour of MoS_2/Al_2O_3, $CoMoS/Al_2O_3$ and $NiMoS/Al_2O_3$ catalysts was investigated in the HDO of aliphatic ethers and in the hydrotreating of RSO and its mixtures with the SRGO feed. It has been shown that the selectivity of aliphatic ether and RSO transformation depends on the composition of sulphide phase and the reaction conditions. The un-promoted MoS_2/Al_2O_3 catalyst turns the reaction to HDO route, avoiding the formation of C_{15} hydrocarbons and CO/CO_2 molecules. It was observed that RSO addition decreased markedly the activity of $CoMoS/Al_2O_3$ catalysts but had no effect on the activity of $NiMoS/Al_2O_3$ one in the HDS and HDN reaction. The CO molecules formed as a result of RSO hydroconversion can be considered as a main inhibitor of $CoMoS/Al_2O_3$ catalyst's activity. So, the chemical composition of sulphide phases effects strongly on the behaviour of sulfided catalysts in the hydrotreating of triglyceride-based feedstocks.

Acknowledgements

The work was performed with support of the Skolkovo Foundation (Grant Agreement for Russian educational organization №1 on 28.11.2013).

I-PP113

HMS Supported $H_4PMo_{11}VO_{40}$ Catalysts for the Isopropanol Decomposition Reaction

Salhi N.[1,2*], Benadji S.[2], Boudjeloud M.[2], Saadi A.[2], Rabia C.[2]

1 - Laboratoire LCPMM, Département de Chimie, Faculté des Sciences, Blida, Algeria
2 - Laboratoire de Chimie du Gaz Naturel, Faculté de Chimie, Alger, Algérie

* nas.salhi@yahoo.fr

Keywords: heteropolyacid, mesoporous silica, isopropanol decomposition

1 Introduction

Heteropolyacids (HPAs), $H_{3+x}PMo_{12-x}V_xO_{40}$ (x =1-3) having Kigging structure have attracted increasing interest especially for the selective oxidations of hydrocarbons. The strong Brönsted acidity of such compounds is well known to be favourable to selective oxidation reactions. However, their low surface area (<10m^2/g) is always the main drawback. In order to overcome this problem, some recent works pointed out the use of suitable supports such as mesoporous silicates (MCM-41, HMS, CMI-1, SBA-15 …), providing high thermal stability, large surface area and high pore volume.

The objective of this work is to support $H_{3+x}PMo_{12-x}V_xO_{40}$ acid (x=1) on the silicate mesoporous (HMS). These materials present the advantage to have large surface area and pore volume with uniform mesopores and high thermal stability.

2 Experimental

HPAs were supported on silicate mesopourous HMS by dry impregnation method with 3wt.% loading. Various techniques including: Elemental analysis, XRD, FT-IR-DRIFT, N_2 physisorption, TG-DTA and SEM analysis were used to characterize the fresh catalysts. Catalytic performances of supported HPAs were compared to those of HPAs bulk in the isopropanol decomposition reaction to propene, diisopropylether and acetone products at 75°C.

3 Results and discussion

The supported HPAs showed better dispersion of heteropolyacids on the HMS surface. A sensitive decrease of the HMS support surface area was observed in the presence of $H_4PMo_{11}VO_{40}$ clusters. By TG-TDA analysis, HPA-HMS catalyst showed a higher thermal stability than pure HPA.

4 Conclusion

High catalytic performances were obtained for HPA-HMS catalyst. These results could be related to the high dispersion of HPA on the support.

I-PP114

The Effect of K- and Mn- Promoters on N-Doped Carbon Nanotube-Supported Iron Nanoparticles for CO_2 Hydrogenation

Muhler M.[1*], Chew L.M.[1], Kangvansura P.[2], Ruland H.[1], Xia W.[1], Worayingyong A.[2]

1 - Laboratory of Industrial Chemistry, Ruhr-University Bochum, Germany
2 - Faculty of Science, Kasetsart University, Bangkok, Thailand

* muhler@techem.rub.de

Keywords: CO_2 hydrogenation, iron-based catalyst, N-doped carbon, nanotubes, promoter

1 Introduction

Rising concentrations of CO_2 may contribute to the increase in global temperature due to the greenhouse effect. In addition, depletion in crude oil resources and the continuous increase of its price have raised the research interest in CO_2 hydrogenation. CO_2 hydrogenation to hydrocarbons is a modification of Fischer-Tropsch synthesis (FTS), where CO_2 is used as reactant instead of CO. Recently, carbon nanotubes (CNTs) have been claimed as a promising support for catalysts used in FTS [1], because CNTs have a large outer surface area and are able to increase the dispersion of the catalytically active nanoparticles [2]. Promoters such as potassium are well known to increase the surface basicity of the catalyst. Consequently, they increase olefin selectivity and chain growth probability and suppress methane formation [2,3]. Hence, this work describes CO_2 hydrogenation to short-chain hydrocarbons over K- and Mn-promoted iron nanoparticles supported on nitrogen-functionalized CNTs (NCNTs).

2 Experimental/methodology

CNTs with inner diameters of 20-50 nm from Applied Sciences lnc. (Ohio) were subjected to nitric acid vapour treatment at 200°C for 24 h to create oxygen-functionalized CNTs (OCNTs). The OCNTs were treated at 400°C for 6 h in flowing ammonia (10 vol% NH_3 in He) to obtain NCNTs. NCNTs were added to an aqueous solution of ammonium ferric citrate to achieve a 40 wt% Fe loading. To obtain Mn-promoted iron catalyst, NCNTs were added to a mixture aqueous solution of ammonium ferric citrate and manganese (II) nitrate hydrate to achieve 10 wt% Mn and 40 wt% Fe. The mixtures were dried at 50°C overnight and calcination of the mixtures was carried out in air at 300°C for 90 min. Subsequently, the calcined samples were suspended into an aqueous solution of potassium carbonate aiming at a theoretical K loading of 1.5 wt%. CO_2 hydrogenation experiments were conducted in a fixed-bed U-tube reactor. The catalyst was first reduced in pure H_2 at 380°C and 25 bar for 5 h. Subsequently, the hydrogenation reaction was performed at 360°C and 25 bar using a mixture of 22.5% CO_2, 67.5% H_2 and 10% Ar at a total flow rate of 3.1 – 50 L g^{-1} h^{-1}. Online gas analysis was performed with a GC-TCD-FID using Ar as internal standard.

3 Results and discussion

The iron catalysts promoted with K and/or Mn showed higher degrees of conversion and more stable performance as compared to the unpromoted Fe/NCNT catalyst (Fig. 1). Potassium is known to increase the degree of carburization of iron catalysts during reaction to Hägg carbide, which is known to be the active phase in FTS [3]. It has been reported that a Mn-rich surface acts as a protective shell for an inner Fe-rich core, preventing oxidation by water formed as co-product leading to a higher stability [4]. After doping with small amounts of K, it was already possible to lower the methane selectivity from 39.9% to 5.6% and simultaneously to

enhance C_{3+} selectivity (Table 1).

Moreover, the addition of K increased the olefin selectivity significantly up to 80%. The product distribution over Mn/Fe/NCNT was almost similar to Fe/NCNT demonstrating that Mn acted as structural promoter. By increasing the residence time in the reaction zone, the selectivity towards hydrocarbons was increased while the selectivity of CO was decreased (Table 1) suggesting that CO is an intermediate being favoured at short residence times.

Table 1. Product selectivities, chain growth probabilities, olefin selectivities and CO_2 conversion.

Catalyst	Product selectivity (%)					$C_{2=}$-$C_{5=}$/C_2-C_5	α	X (CO_2) %
	CO	C_1	C_2	C_{3+}	Alcohol			
Fe/NCNT[a]	38.4	39.9	12.1	9.4	0.2	0.09	0.29	25.4
K/Fe/NCNT[a]	74.9	5.6	5.3	12.2	2.0	0.87	0.41	31.8
Mn/Fe/NCNT[a]	48.5	35.6	9.3	6.5	0.0	0.11	0.34	27.6
K/Mn/Fe/NCNT[a]	72.1	5.9	5.2	14.5	2.4	0.89	0.43	30.3
K/Mn/Fe/NCNT[b]	45.5	12.0	11.5	28.4	1.4	0.90	0.45	31.0
K/Mn/Fe/NCNT[c]	30.4	14.5	13.1	35.7	3.0	0.90	0.47	34.9

[a] total flow of 50 L g^{-1} h^{-1}, [b] total flow of 12.5 L g^{-1} h^{-1}, [c] total flow of 3.1 L g^{-1} h^{-1}.

4 Conclusions

CO_2 hydrogenation over unpromoted iron catalyst resulted in a high methanation tendency combined with a low olefin selectivity. By adding K, it was possible to suppress methane formation and to increase the olefin selectivity significantly. The stability of catalysts was improved by doping with Mn, which acts as structural promoter. The addition of both K and Mn enhanced the catalytic activity and stability of iron catalysts in CO_2 hydrogenation.

Acknowledgements

The work was conducted under the project "Sustainable Chemical Synthesis (SusChemSys)", which is co-financed by the European Regional Development Fond (ERDF) and the state of North Rhine-Westphalia, Germany, under the Operational Programme "Regional Competitiveness and Employment" 2007 – 2013.

References

[1] H.J. Schulte, B. Graf, W. Xia, M. Muhler, ChemCatChem 4 (2011) 350.
[2] R.W. Dorner, D.R. Hardy, F.W. Williams, H.D. Willauer, ACS Symposium Series 1056 (2010) 125.
[3] T. Riedel, M. Claeys, H. Schulz, G. Schaub, S.-S. Nam, K.-W. Jun, M.-J. Choi, G.Kishan, K.-W. Lee, Appl. Catal. A 186 (1999) 201.
[4] T. Grzybek, J. Klinik, H. Papp, M. Baerns, Chem. Eng. Technol. 13 (1990) 156.
[5] Ly May Chew, Praewpilin Kangvansura, H. Ruland, H. J. Schulte, C: Somsen, Wei Xia, G. Eggeler, Attera Worayingyong, M. Muhler, Applied Catalysis A: General 482 (2014) 163.

Session II
"Catalyst preparation and characterization"

II-OP01

Combining Operando Spectroscopy and Chemometrics to Understand Changes in the Active and Deactivating Species during the Methanol-to-Olefins Reaction over H-SSZ-13

Ruiz-Martínez J.[1], Borodina E.[1], Meirer F.[1], Lezcano-González I.[1], Mokhtar M.[2], Asiri A.M.[2,3], Al-Thabaiti S.A.[2], Basahel S.N.[2], Weckhuysen B.M.[1*]

1 - Utrecht University, Debye Institute for Nanomaterials Science, Inorganic Chemistry and Catalysis Department, Utrecht, The Netherlands

2 - Department of Chemistry, Faculty of Science, King Abdulaziz University, Saudi Arabia

3 - Center of Excellence for Advance Materials Research, King Abdulaziz University, Saudi Arabia

* j.ruizmartinez@uu.nl

Keywords: operando spectroscopy, methanol-to-olefins, zeolite, UV-Vis, H-SSZ-13, multivariate analysis

1 Introduction

In most of the zeolite-catalysed reactions, deposition of discrete hydrocarbon species, also known as coke, causes loss of the catalytic activity and subsequent deactivation. Understanding catalyst deactivation by coke formation, especially when catalysts are working under real reaction conditions, is highly needed for the improvement of our current zeolite catalysts. This is notoriously difficult in relevant zeolite-catalysed reaction, for example the methanol-to-olefins (MTO) reaction, where discrete hydrocarbon species are believed to be the real active sites and therefore beneficial for the catalytic reaction [1]. Methods to discriminate between deactivating coke and active coke are therefore critical to understand catalyst functioning. In this research work, we report a method to determine the role of the hydrocarbon species during the MTO reaction over zeolite H-SSZ-13. Operando UV-Vis spectroscopy in combination with a multivariate analysis allow us to reveal that the reaction temperature affects to a great extent the nature of both the hydrocarbon species active in the MTO reaction and the hydrocarbon species deactivating the catalyst material.

2 Experimental/methodology

An Al-containing H-SSZ-13 was synthesized and characterized by N_2 physisorption, scanning electron microscopy, inductively coupled plasma optical emission spectrometry, X-ray diffraction, temperature-programmed desorption of NH_3 and CO adsorption at 77 K followed by IR spectroscopy. Operando tests were performed in a fixed bed reactor coupled with an UV-Vis optical probe. The analysis of the reaction products were performed with on-line gas chromatography (GC) and UV-Vis data were analyzed with the aid of a non-negative matrix factorization method. The nature of the compounds retained after MTO reactions was determined by dissolution of the zeolite sample and analysis of the extracted hydrocarbons by GC/MS.

3 Results and discussion

Catalytic activity data show that within the range of reaction temperatures studied (i.e., 573-723 K) the induction period decreases and catalyst stability increases with the reaction temperature. During the catalytic tests, the zeolite H-SSZ-13 was continuously monitored by operando UV-Vis spectroscopy in order to obtain detailed insight into the hydrocarbons formed inside of the pores during the MTO reaction. Interestingly, the UV-Vis data show that the reaction temperature affects the dynamics and position of the characteristic UV-Vis bands. This

can be related to a change in the rate and nature of the hydrocarbon species formed inside of the zeolite micropores. For an accurate chemical assignment of the UV-Vis bands, we have combined those experiments with the analysis of the retained hydrocarbons, determined by GC-MS, after a dissolution-extraction procedure.

Due to the complexity and dynamics of the spectra, a NNMF chemometrical method was applied for the analysis of the data. Two main groups of bands (I and II) with different kinetic behaviour were identified, as shown in Figures 1a and 1c during the MTO reaction at 573 and 723 K, respectively. Figures 1b and 1d clearly show that the group I is strongly linked to the activity of the material, whereas group II increases until the catalyst is completely deactivated. These results point out that each group of bands corresponds to species responsible for the activity and deactivation of the catalyst.

Interestingly, the reaction temperature affects the nature of both groups of species, as can be observed by the different UV-Vis features in Figures 1a and 1c. More specifically, the majority of active hydrocarbon pool species at low reaction temperatures (i.e., 573-598 K) are methylated benzene carbocations, while methylated naphthalene carbocations are determined as dominant active hydrocarbon pool species at high reaction temperatures (i.e., 623-723 K). Furthermore, at low reaction temperature deactivation occurs because of pore filling with methylated naphthalene carbocations and when the temperature is higher the deactivation is related to bulkier species, such as phenanthrene, pyrene and more poly-aromatic species, blocking the porosity of the catalytic material.

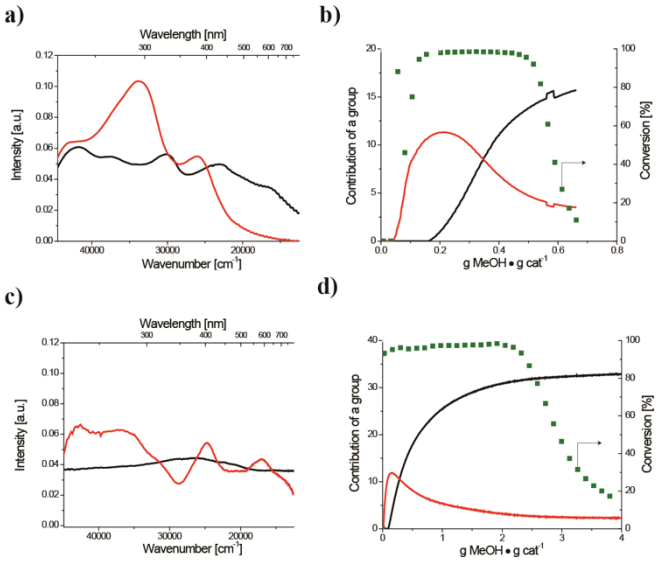

Figure 1. Deconvolution of the in-situ UV-Vis spectra collected during MTO reactions at 573 (a and b) and 723 K (c and d) on a H-SSZ-13 catalyst. The groups of bands (Eigen-spectra) for the species with different kinetics (a and c) and the evolution of every group of species as a function of methanol load on the catalyst material (b and d) were calculated by a non-negative matrix factorisation method. The red curve represents group I (active species), while the black curve corresponds to group II (deactivating species).

4 Conclusions

In this contribution we present a powerful approach to discriminate between the hydrocarbon species, which are contributing to the activity and deactivation of a H-SSZ-13 catalyst during the MTO reaction. This combines an operando UV/Vis spectroscopy setup with a chemometrical analysis of the spectroscopic data. This methodology reveals that the nature of the active and deactivating species change with the MTO reaction temperature. These results provide important fundamental insight into the MTO reaction and deactivation mechanisms.

References

[1] Olsbye, U.; Svelle, S.; Bjørgen, M.; Beato, P.; Janssens, T. V. W.; Joensen, F.; Bordiga, S.; Lillerud, K. P. *Angew. Chem. Int. Ed. 51*, 5810–5831, (2012).

[2] E. Borodina, F. Meirer, I. Lezcano-González, M. Mokhtar, A. M. Asiri, S. A. Al-Thabaiti, S. N. Basahel, J. Ruiz-Martinez, B. M. Weckhuysen, *ACS Catal.* **2015**, 992-1003.

II-OP02

Elucidation of the Mechanism of Hydrothermal Synthesis of Zeolite Catalysts Using Ex-Situ and *in Situ* Approaches

Ivanova I.I.[1,2*], Kolyagin Yu.G.[1,2]

1 - M.V. Lomonosov Moscow State University, Chemistry Department, Moscow, Russia,
2 - A.V. Topchiev Institute of Petrochemical Synthesis RAS, Moscow, Russia

* iiivanova@phys.chem.msu.ru

Keywords: zeolites, hydrothermal synthesis mechanism, *in situ*, MAS, NMR

1 Introduction

Synthesis under hydrothermal conditions is the main synthetic route leading to wide variety of catalysts such as zeolites, zeotypes, mesoporous and micro-mesoporous materials, hybrid inorganic-organic frameworks and others. The improvement of existing catalytic materials and rational design of novel ones require the profound understanding of the mechanism of their synthesis.

The traditional approach for the investigation of the mechanism of hydrothermal synthesis is based on the interruption of the synthesis at different stages, isolation of the intermediate products and their analysis by a complex of physicochemical methods. The mechanism proposals are usually made on the basis of the information about structure and composition of intermediate products. This approach is named «*ex situ*», since intermediate products are analyzed outside of the reaction system. However this method does not always provide reliable results, since the state of the reaction system during synthesis can change significantly after the interruption of the reaction and isolation of intermediate products. To obtain full and, what is the most important, reliable information about the processes occurring during the synthesis, the techniques of direct observation "*in situ*" are required. But the "in situ" studies of hydrothermal synthesis of molecular sieve catalysts are connected with a lot of experimental difficulties concerned with severe synthesis conditions (temperatures up to 220 °C, pressure up to 20 atm, alkaline media) and with the complexity of the studied system, which is usually composed of various phases: true solutions, colloid solutions, gels, amorphous precipitates nanosized crystalline intermediates and final products.

This contribution is aimed at the development of the new techniques for the investigation of the mechanism of hydrothermal synthesis based on the application of NMR spectroscopy *in situ* and at the elucidation of the mechanisms of synthesis of Al-, Zr- and Sn-BEA zeolites.

2 Experimental/methodology

The synthesis of zeolites Al-, Zr- and Sn-BEA was carried out at 140 °C under hydrothermal conditions according the procedures described in [1-3]. For the investigation of the mechanisms of synthesis two approaches were used: traditional *ex situ* approach and novel *in situ* method based on MAS NMR spectroscopy. The first approach included the investigation of the structure, the composition and properties of stable intermediates recovered during the synthesis of molecular-sieve catalysts by means of wide range of physico-chemical methods, including XRF, XRD, IR spectroscopy, low-temperature N2 adsorption, TGA-DSC analysis, SEM and TEM. The amount, strength and nature of the active sites of catalysts was investigated by means of temperature-programmed desorption and IR spectroscopy of adsorbed probe molecules. The second approach was based on the direct observation of the state of atomic nuclei, which compose the frameworks of reagents, products and intermediates, during the synthesis using solid-state NMR spectroscopy in situ. The measurements were carried out in specially

constructed autoclave-type MAS NMR cell adapted for Bruker AVANCE II 400WB spectrometer. The spectra were recorded every 4 hours for ^{1}H, ^{23}Na, ^{27}Al, ^{29}Si and ^{119}Sn nuclei. The duration of experiments was from 1 hour to several days.

3 Results and discussion

The results obtained showed that the application of *in situ* MAS NMR approach provides unique information on the dynamics of various nuclei in reagents, intermediates and final products directly during the hydrothermal synthesis. It was found out that the spectral data for ^{1}H nuclei allow to follow the changes in pH and to study the kinetics of organic templates' transformations. At the same time, ^{29}Si MAS NMR permits detecting various mobile and rigid inorganic species, gives insight into the formation of intermediate unstable phases, including protozeolitic phases, and allows to follow their transformation into solid zeolitic structures. ^{29}Si MAS NMR HPDEC spectra allows detecting mobile and disordered siliceous species, whereas CPMAS technique provides the information about silicon atoms in solids. ^{27}Al and ^{119}Sn MAS NMR spectroscopy gives detailed information about the creation of zeolite active sites. Thus, the formation of different Al and Sn sites was detected and the kinetics of their transformation during synthesis was investigated. To summarize, it has been demonstrated that the spectral data give insight into the mechanism of the main steps of synthesis, including, gel formation, gel aging, crystal nucleation, growth and recrystallation; provide information on the kinetics of each reaction step; enable detection intermediate species stable only under hydrothermal conditions. The technique can be used without interrupting the synthesis and perturbing the crystallization process, it reduces the time and minimizes the amount of sample required for mechanistic studies by several orders of magnitude and allows for isotopic labelling of specific nuclei.

The comparison of the results of *in situ* MAS NMR experiments with *ex situ* studies performed using XRD, SEM, TEM, IR and adsorption techniques outlined that the kinetic parameters obtained using both approaches are in good agreement and pointed to full identity in structure and morphology of final products. The main benefit of the *ex situ* approach is the possibility to apply the whole complex of modern physicochemical techniques, which allows to obtain comprehensive information on the structure and properties of stable intermediate products. The *in situ* MAS NMR approach makes it possible to follow the nuclei dynamics directly during the synthesis and to get additional information about the unstable intermediate products. Combination of these two approaches will lead to fast progress in understanding the mechanisms of synthesis of different solids and therefore will facilitate the development of novel advanced materials.

4 Conclusions

The potential of the *in situ* MAS NMR techniques for the unravel of the mechanism of hydrothermal synthesis of zeolite catalysts has been fully demonstrated. The technique can be used without interrupting the synthesis and perturbing the crystallization process and provides unique information on the main steps of synthesis, including, gel formation, gel aging, crystal nucleation, growth and recrystallation.

Acknowledgements

The authors thank the Russian Science Foundation for the financial support (grant 14-23-00094).

References

[1] J. Perez-Pariente, J.A. Martens, P.A. Jacobs, Appl. Catal. 31 (1987) 35.
[2] S. H. Liu, S. Jaenicke, G.-K. Chuah, J. Catal. 206 (**2002**) 321.
[3] C. Valencia, A. Corma, US Pat. No 5968473.

II-OP03

Optimizing Catalytic Performances of Oxide Catalysts via Morphology Engineering

Huang W.*

Department of Chemical Physics, University of Science and Technology of China, Hefei, China

* huangwx@ustc.edu.cn

Keywords: oxide nanocrystal catalysts, propylene partial oxidation, structure-activity, relation, reaction, mechanism

1 Introduction

Selective oxidation of propylene with molecular oxygen is of great importance and oxides are used as the catalysts. The morphology of oxide nanoparticles decides the exposed crystal planes and thus strongly affects their catalytic performances. Recently uniform oxide nanocrystals predominantly exposing one or two types of crystal planes have been successfully prepared. In this talk I will report two examples to demonstrate the morphology effect of oxide catalysts on their catalytic performances in selective oxidation of propylene: one is propylene oxidation with O_2 catalyzed by Cu_2O nanocrystals [1], the other is propylene epoxidation with O_2 and H_2 catalyzed by Au/TiO2 catalysts [2].

2 Experimental/methodology

Uniform cubic (c-Cu_2O), octahedral (o-Cu_2O) and rhombic dodecahedral (d-Cu^2O) Cu_2O nanocrystals were synthesized, characterized and used as the catalysts for propylene oxidation with O_2. 0.2 g catalyst was used and heated in a reaction gas mixture (C_3H_6 /O_2/N_2 = 4/2/44 with flow rates of 50mL/min) from RT to reaction temperature in 6 h. The products were analyzed online using a gas chromatograph (Shimazu GC-2014) equipped with a flame ionization detector and a thermal conductivity detector, attached, respectively, to a FFAP capillary column (0.32 mm×60 m) and a Porapak Q compact column (3 mm×3 m).

1wt%-Au/TiO_2 catalysts employing P25 (Au/P25), anatase TiO_2 nanocrystals predominantly exposing the {001} facets (Au/TiO_2(001)), anatase TiO_2 nanocrystals predominantly exposing the {100} facets (Au/TiO_2(100)) as the supports were synthesized, characterized and used as the catalysts for propylene oxidation with O_2 and H_2. 0.25 g catalyst was used and heated in the reaction gas mixture (C_3H_6/O_2/H_2/Ar = 1/1/1/7, GHSV = 8000 $mlh^{-1}g^{-1}_{catalyst}$) to 50 ºC at a rate of 2 ºC/min. All reaction products were analyzed using an online Shimazu GC-2014 gas chromatograph equipped with both flame ionization detectors (FID) and thermal conductivity detector (TCD). One FID was attached to a Stabilwax-DA capillary column (0.53 mm × 60m) to detect propylene and oxygenates (acetaldehyde, PO, acetone, propionaldehyde, acrolein, acetic acid, and isopropanol), and the TCD was attached to a Porapak Q (3mm × 3m) and C13x compact column (3 mm × 3m) to detect H_2 and O_2.

Propylene conversion was calculated by moles of (oxygenates + CO_2/3)/moles of propylene in feed, PO selectivity was calculated by moles of PO/moles of (oxygenates + CO_2/3), acrolein selectivity was calculated by moles of acrolein/moles of (oxygenates + CO_2/3), and CO_2 selectivity was calculated by moles of CO_2/moles of (oxygenates + CO_2/3).

3 Results and discussion

Figure 1 shows the catalytic performances of different Cu_2O nanocrystals in in propylene oxidation with molecular oxygen. Cu_2O nanocrystals exhibit distinct morphology-dependent catalytic activities. The specific reaction rate normalized to the specific surface area over various

Cu_2O nanocrystals follows the order of o-Cu_2O > d-Cu_2O > c-Cu_2O. Very interestingly, we observed that the catalytic selectivity of Cu_2O nanocrystals in propylene oxidation with molecular oxygen is also sensitively dependent in their morphology. c-Cu_2O is highly selective in catalyzing the propylene combustion reaction with the CO_2 selectivity above 80% under investigated reaction temperatures. o-Cu_2O exhibits the highest selectivity towards the partial oxidation of propylene to acrolein. d-Cu_2O exhibits comparable selectivity towards propylene oxide (20%), acrolein (40%) and CO_2 (40%). Combining operando DRIFTS results demonstrate the formation of different surface species during the propylene chemisorption and oxidation on meansurements and DFT calculations, C_3H_6(a) on Cu_{CUS} of Cu_2O(111), bridging C_3H_6(a) on neighboring Cu_{CSA} and three-coordinated O_{CUS} of Cu_2O(110) and bridging C_3H_6(a) on two neighboring two-coordinated O_{CUS} of Cu_2O(100) were identified as the active species respectively producing acrolein, PO and CO_2.

Table 1 summarizes catalytic performances of Au/TiO_2 catalysts in propylene oxidation with O_2 and H_2 at 50 ºC. The results demonstrate a distinct TiO_2-morphology-dependent catalytic performances of Au/TiO_2 catalysts. Au/P25 gives a C_3H_6 conversion of 0.50%, a PO selectivity of 98.36% and a PO formation rate of 18.1 $mmol_{PO}/h/g_{Au}$. These data are comparable to previous reported results of Au/P25. Au/TiO_2(001) is more active than Au/P25 and meanwhile keeps the similar selectivity toward PO. The C_3H_6 conversion reaches 0.69% and the PO selectivity is 97.64%, giving a PO formation rate of 25.4 $mmol_{PO}/h/g_{Au}$. However, Au/TiO_2(100) is much less active than Au/P25 and its selectivity toward PO is also poorer than that of Au/P25. The C_3H_6 conversion is only 0.14%. Besides the PO production with a selectivity of 89.44%, acetone and CO_2 were observed to form with the selectivity of 5.58% and 4.98%, respectively. Thus PO formation rate over Au/TiO_2(100) is as low as 4.2 $mmol_{PO}/h/g_{Au}$. Therefore, the PO formation rate of various Au/TiO_2 catalysts follows the order of Au/TiO_2(001) > Au/P25 >> Au/TiO_2(100), and the PO formation rate over Au/TiO_2(001) is higher than that of Au/P25 by more than 40%. The ensemble consisting of intimately-contacting $Au^{\delta-}$ species and Ti^{4+} species with weak chemisorption strength is active to catalyze propylene epoxidation with O_2 and H_2 to propylene oxide.

Above results reveal a morphology-engineering strategy of oxide catalysts not only for the innovation of both active and selective catalysts but also for the fundamental understanding of complex heterogeneous catalytic reactions at the molecular-level.

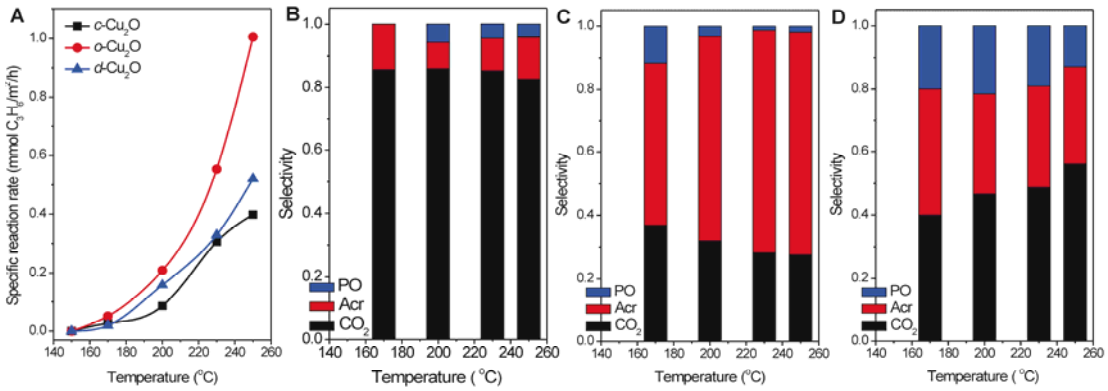

Fig. 1. (**A**) Specific reaction rate of C_3H_6 oxidation catalyzed by Cu_2O cubes (c-Cu_2O), octahedra (o-Cu_2O) and rhombic dodecahedra (d-Cu_2O). Selectivity of C_3H_6 oxidation catalyzed by (**B**) c-Cu_2O, (**C**) o-Cu_2O and (**D**) d-Cu_2O.

Catalyst (250mg)	Conversion (%)			C_3H_6 selectivity (%)			PO formation rate ($mmol_{PO}/h/g_{Au}$)	O_2 selectivity	H_2 efficiency
	C_3H_6	H_2	O_2	PO	Acetone	CO_2			
Au/P25	0.50	2.96	1.61	98.36	0.76	0.88	18.1	30.3%	16.5%
Au/TiO_2(001)	0.69	2.54	1.63	97.64	0.80	1.56	25.4	41.1%	26.5%
Au/TiO_2(100)	0.14	3.20	1.66	89.44	5.58	4.98	4.2	7.4%	3.8%

Table 1. Catalytic performances of Au/TiO_2 catalysts in C_3H_6 oxidation with H_2 and O_2 (C_3H_6: O_2: H_2: Ar =1: 1: 1: 7, GHSV = 8000 $mLh^{-1}g$-1 catalyst, T = 50 ºC).

References

[1] Q. Hua et al., Langmuir **27** (2011), 665.
[2] S. Chen et al, submitted.

II-OP04

Methane Activation on In-Modified ZSM-5 Zeolite. Solid-State NMR Characterization of the Pathways of the Alkane Transformation to Surface Species

Stepanov A.G.[1,2*], Gabrienko A.A.[1], Arzumanov S.S.[1], Moroz I.B.[1], Toktarev A.V.[1], Freude D.[2]

1 - Boreskov Institute of Catalysis, Siberian Branch of the Russian Academy of Sciences, Novosibirsk, Russia

2 - Universität Leipzig, Fakultät für Physik und Geowissenschaften, Leipzig, Germany

* stepanov@catalysis.ru

Keywords: methane activation, In/H-ZSM-5, zeolite, surface species, characterization, NMR, *in situ*

1 Introduction

In-modified zeolites are promising catalysts for methane transformation to aromatic hydrocarbons. It has been revealed that methane reacts with ethylene or benzene yielding propylene or toluene on In/H-ZSM-5 [1,2]. However, the pathways of methane activation and transformation to the surface species, which evolves further to final reaction products still unclear.

In this paper, we have analyzed in situ the kinetics of H/D exchange of methane with Brønsted acid sites of zeolite H-ZSM-5 modified with indium (In^+/H-ZSM-5 and InO^+/H-ZSM-5) by ^{1}H MAS NMR and compared this kinetics with the kinetics on the pure acid form of zeolite H-ZSM-5. Surface species formed from methane at elevated temperatures have been monitored with ^{13}C CP/MAS NMR spectroscopy. This approach to the study of methane activation on heterogeneous catalysts allowed us to establish some peculiarities of methane activation by Brønsted acid sites and by indium species of In^+/H-ZSM-5 and InO^+/H-ZSM-5 zeolites and clarify the pathway of methane involvement in the reaction with ethylene and benzene.

2 Experimental

Details of the synthesis and characterization of In-modified zeolites ZSM-5 are described in refs. [3,4]. Kinetics of the H/D exchange was analyzed in situ in a closed microreactor, representing a sealed glass tube of 5 mm diameter and 10 mm length. The reactor could be tightly inserted in 7 mm zirconia rotor to perform the reaction monitoring with ^{1}H MAS NMR at 450-570 K. The surface hydrocarbon species formed from methane in the course of the reaction at elevated temperature (300–670 K) were analyzed by ^{13}C CP/MAS NMR spectroscopy at room temperature (296 K). NMR spectra were recorded at 9.4 T on a Bruker Avance-400 spectrometer equipped with broad-band double-resonance MAS probe. 7 mm zirconia rotors for ^{1}H MAS NMR 4 mm rotors for ^{13}C MAS NMR with the inserted sealed glass tube were spun at 3-10 kHz by dry compressed air. Details of NMR experiments are provided in refs. [3,4].

3 Results and discussion

Analysis of the kinetics of hydrogen (H/D) exchange between methane-d_4 and Brønsted acid sites (BAS) for both the pure acid form zeolite (H-ZSM-5) and In- modified zeolites (In^+/H-ZSM-5 and InO^+/H-ZSM-5) has shown that the rate of exchange is two order of magnitude larger on InO^+/H-ZSM-5 than that on H-ZSM-5. The activation energy (E_a=74 kJ mol^{-1}) for the

reaction of the exchange on InO^+/H-ZSM-5 is lower than that on H-ZSM-5 (E_a=127 kJ mol^{-1}). The significant change of the kinetic parameters of the exchange for InO^+/H-ZSM-5 is rationalized in terms of involvement of both InO^+ species and BAS in activation of methane molecules on this In-modified zeolite. The shape of the kinetics (Fig. 1a) shows that besides H/D exchange methane-d_4 is involved in chemical transformation on InO^+/H-ZSM-5 to form some surface species. ^{13}C CP MAS NMR shows that this surface species exhibits the chemical shift of -29 ppm, which indicates that indium-methyl ($OIn-CH_3$) is formed from methane (-6 ppm) (Fig. 1b). H/D exchange kinetics data presume that some transient intermediate complex of methane with the zeolite InO^+ species and BAS is formed within the void of zeolite pore. This complex is either involved in the reaction of H/D exchange with BAS of the zeolite or evolves further to offer indium methyl species.

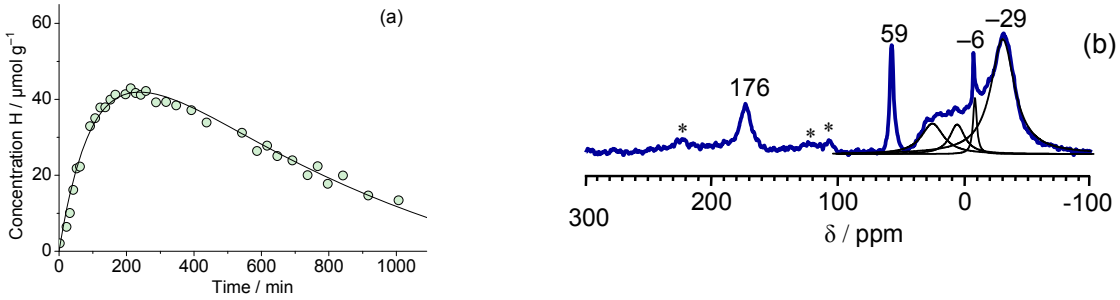

Fig. 1. (a) Kinetics of H/D exchange of methane-d_4 with BAS of InO^+/H-ZSM-5 at 445 K. (b) ^{13}C CP MAS NMR spectrum of the products of interaction of methane-^{13}C with InO^+/H-ZSM-5 at 523 K.

Further interaction of InO^+ with $OIn-CH_3$ gives methoxy species (CH_3-O-InO) with the signal at 59 ppm. Methoxy evolves to formate species (176 ppm). Acetaldehyde is further formed by interaction of the formate with $OIn-CH_3$. The interaction of methoxy with benzene produces toluene. The latter reaction can represent a pathway of methane involvement in co-aromatization with ethylene, which is transformed to aromatics itself on this zeolite catalyst.

4 Conclusions

The pathways of methane activation and transformation to surface species on In/H-ZSM-5 were characterized by solid-state NMR. The intermediate surface species were identified. The mechanism of methane involvement in the reaction of its co-aromatization with ethylene was established.

Acknowledgements

This work was supported by Russian Foundation for Basic Research (Grant No. 14-03-00040)

References

[1] T. Baba, Y. Abe, K. Nomoto, K. Inazu, T. Echizen, A. Ishikawa, K. Murai, *J. Phys. Chem. B*, 109, (2005) 4263.
[2] T. Baba, Y. Abe, *Appl. Catal*. A 250 (2003) 265.
[3] A.A. Gabrienko, S.S. Arzumanov, I.B. Moroz, I.P. Prosvirin, A.V. Toktarev, W. Wang, A.G. Stepanov, *J. Phys. Chem. C*, 118 (2014) 8034.
[4] S. S. Arzumanov, I.B. Moroz, D. Freude, J. Haase, A.G. Stepanov, *J. Phys. Chem. C*, 118 (2014) 14427.

II-OP05

Pd Size Effect in Liquid Phase Semihydrogenation of Substituted Alkynes on Supported Pd Catalysts

Stakheev A.Yu.[1*], Markov P.V.[1], Turova O.V.[1], Mashkovsky I.S.[1], Khudorozhkov A.K.[2], Bukhtiyarov V.I.[2]

1 - Zelinsky Institute of Organic Chemistry RAS, Moscow, Russia
2 - Boreskov Institute of Catalysis SB RAS, Novosibirsk, Russia

* st@ioc.ac.ru

Keywords: liquid-phase semihydrogenation, diphenylacetylene, nanoparticle, particle size effect

1 Introduction

Alkynes are versatile reagents in organic synthesis since C≡C group can be easily transformed to a cis-alkene through stereoselective addition of hydrogen molecule on Pd catalyst. This so called semihydrogenation is often an important step in industrial processes as well as in laboratory-scale reactions. However, careful selectivity control and minimization of over-hydrogenation is required.

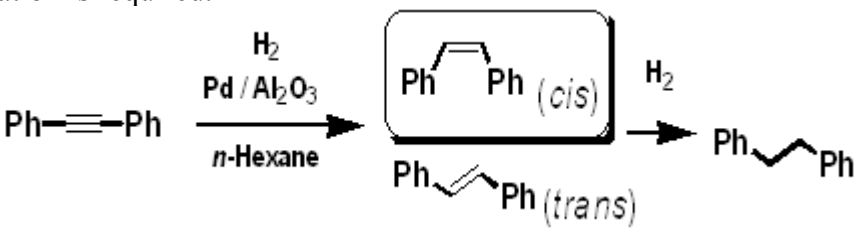

In this work we studied a relationship between the size of Pd nanoparticles (ranging from 1.5 to 22 nm) in 1%Pd/Al_2O_3 catalyst and the activity/selectivity in liquid-phase diphenylacetylene (DPA) hydrogenation.

2 Experimental/methodology

Series of Pd/Al_2O_3 catalysts was prepared by impregnation of alumina with Pd nitrate solutions followed by air calcination at 400-600°C for 3 hours and reduction in flowing H_2 at 400°C. Variation of Pd/NO_3^- ratio during impregnation and the calcination temperature enabled variation of Pd particle size from 1.5 to 22 nm with narrow particle size distribution (see below).

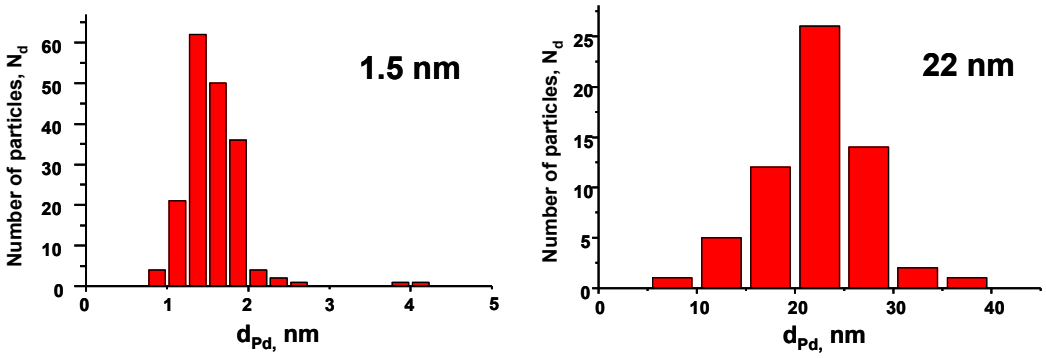

Hydrogenation was carried out in autoclave at 5 atm H_2 and room temperature. The reaction kinetics was monitored by the rate of H_2 uptake, and the reaction products were analyzed using ^{1}H-NMR.

3 Results and discussion

Catalytic data reveal a significant increase in turnover frequency (calculated per surface Pd atom) and pronounced improvement of the selectivity as Pd particle size increases from 1.5 to 22 nm (Fig. 1, (a) and (b) respectively). The observed relationship can be explained by a strong adsorption of bulky DPA molecule on low-coordinated surface atoms of small Pd nanoparticles. Strong absorption reduces TOF_{DPA} due to competition between adsorbed DPA molecules and hydrogen. As Pd particles grow in size, the percentage of low-coordinated palladium surface atoms rapidly decreases thus increasing TOF_{DPA}.

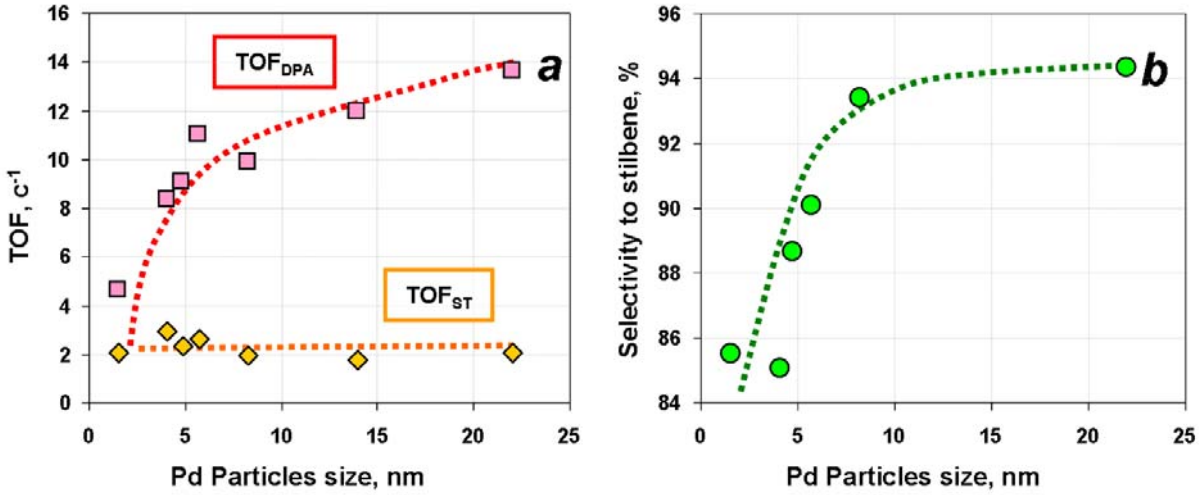

Fig. 1. Effect of Pd particle size on TOF [n(DPA)/n(Pd_{surf})*s^{-1}] (a) and selectivity toward stilbene formation (b) in the course of DPA hydrogenation over 1%Pd/Al_2O_3. Reaction conditions: P_{H2} = 5 bar, T_{react} = 25°C, [DPA]/Pd ~ 4000, n-C_6H_{14} as solvent

The strong increase in TOF_{DPA} with increasing Pd particle size indicates structure sensitivity of triple bond hydrogenation. On the other hand, $TOF_{stilbene}$ of the second hydrogenation stage (double bond hydrogenation) remains essentially independent on Pd particle size. This implies structure-insensitivity of the second stage. We suggest that the different structure sensitivities stem from the differences in rate-limiting steps: activation of triple the π-bond on the 1-st stage, vs. formation of C-H □-bond on the 2-nd stage [1].

As a result of different structure sensitivities of the 1-st and 2-nd hydrogenation stages, the ratio $TOF_{DPA}/TOF_{stilbene}$ increases with increasing Pd particle size thus improving the selectivity in alkene (stilbene) formation.

4 Conclusions

Variation of Pd particle size provides the effective tool for tuning activity-selectivity parameters in selective semihydrogenation of substituted alkynes due to different structure sensitivity of triple bond hydrogenation vs double bond hydrogenation.

Acknowledgements

Financial support by RFBR grant #13-03-12176 is gratefully acknowledged.

References

[1] R.A. van Santen, M. Neurock, S.G. Shetty, Chem. Rev. 110 (2010) 2005

II-OP06

Dispersion and Orientation of Zeolite ZSM-5 Crystallites within a Fluid Catalytic Cracking Catalyst Particle

Sprung C.*, Weckhuysen B.M.

Utrecht University, Department of Chemistry, Inorganic Chemistry and Catalysis, Utrecht, The Netherlands

* sprung@fhi-berlin.mpg.de

Keywords: zeolite ZSM-5, fluid catalytic cracking, polarisation, dispersion and orientation

1 Introduction

Fluid catalytic cracking (FCC) is of great industrial importance in crude oil refinery. The FCC catalyst particles are a complex mixture of various components (such as boehmite, kaolinite, silica, and zeolite) to ensure the catalytic performance and its resistance to chemical and mechanical deactivation. Locating the various components in a catalyst particle is challenging and may involve the degradation of the particle [1]. Confocal fluorescence microscopy (CFM) is non-destructive and has been proven to selectively image zeolite crystals within the matrix of FCC particles by selective staining [2].

The Brønsted acid catalyzed oligomerisation of 4-fluorostyrene was chosen, since their dimeric carbocationic products form elongated species, which are trapped inside the zeolite channel architecture, and, furthermore are fluorescent after excitation in the visible spectrum. Well characterized large coffin-shaped ZSM-5 crystals served as a model system to prove the principle of orientation/polarization dependent interaction of light with such anisotropic crystals [3]. This knowledge was translated for the investigation of the location, orientation, dispersion, and quantification of the zeolite component of 1-3 μm in size inside a real industrial FCC catalyst particle [3].

2 Experimental

Large coffin-shaped ZSM-5 crystals and FCC catalyst particles were impregnated at 30°C with excess of 4-fluorostyrene (the probe molecule) before the oligomerisation reaction of the probe molecule was initiated by increasing the temperature rapidly to 180°C.

An upright optical microscope from Olympus (BX 41) was employed in reflectance mode, equipped a 30 W halogen lamp. The incoming light was plane-polarized through a U-90 PO3 polarizer and the reflected light was analysed with a rotatable analyser U-AN360 from Olympus. Fluorescence microscopic investigations were performed with a Nikon ECLIPS 90*i* confocal microscope in reflectance mode. Excitation light was provided by a 561 nm laser and plane polarized by an internal polarizer/analyzer, the emission range recorded was 580 – 750 nm. FCC particles were investigated by a rotation sequence in steps of 5° [3].

3 Results and discussion

Both absorption and emission of light of elongated molecules are, of course, oriented. In preliminary experiments on large coffin-shaped ZSM-5 crystals, this principle was proven and investigated. Elongated molecules entrapped inside the zeolite channels do absorb/emit light of a certain polarisation plane, which distinguishes it from an area/volume with the same molecules, but randomly oriented.

Figure 1 shows the fluorescence images of a fresh FCC catalyst particle, containing small zeolite ZSM-5 crystallites (and the oligomerised carbocationic species of the probe molecule). The FCC catalyst particle was rotated with respect to the horizontally oriented polarisation plane

of excitation light. Depending on the orientation of the catalyst particle, hence, the zeolite component inside this catalyst particle, the fluorescence of entrapped oligomerised carbocationic species was observed or absent (exemplified highlighted by the white arrows in Figure 1). The polarisation dependence of the observed fluorescence confirms its origin from a crystalline (anisotropic) material, hence, the zeolite component. A single orientation did amount to only 20-40% of the total fluorescence observed when all images of the 5°-rotation sequence were considered.

The emitted fluorescence light was statistically analysed with respect to its intensity and dispersion. A large number of fluorescence light was observed for domains of 0.015-0.25 μm^2, which represents single zeolite crystallites or small aggregates thereof and a fairly high degree of zeolite dispersion. However, the highest amount of crystalline material was aggregated into larger domains (ca. 1–5 μm^2) with more or less similarly oriented zeolite crystallites.

A typical composition of an FCC catalyst particle was assumed, consisting of boehmite, kaolinite, and silica as binder material (composition 1:1:1), and zeolite ZSM-5 as the zeolite component. The amount of detected fluorescence light originating from the stained zeolite ZSM-5 aggregates corresponds to about 15 wt% [3].

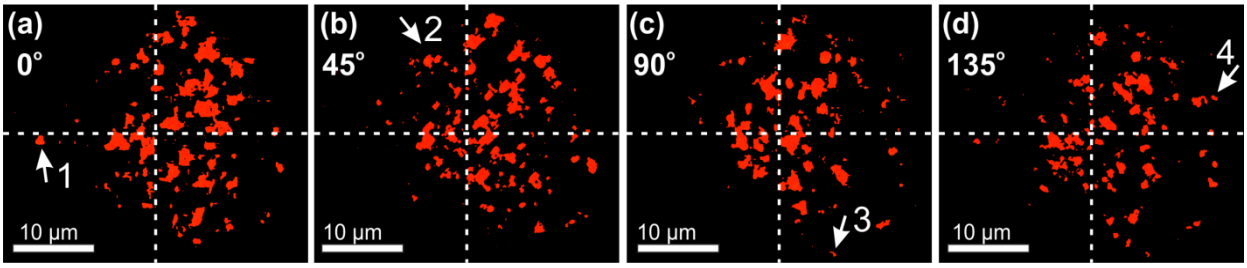

Fig. 1. Fresh FCC catalyst particle containing ZSM-5 at 180°C after 4-fluorostyrene oligomerisation; the images, which belong to an image sequence of full circumference in 5° steps, show a FCC particle rotated to orientations of (a) 0°, (b) 45°, (c) 90°, and (d) 135° with respect to the allowed vibrational path of the polarizer. The images were rotated back to the initial position for better comparison. The arrows/pointer 1 - 4 highlight exemplified areas where fluorescence signal appears/disappears.

4 Conclusions

The anisotropic nature of absorption and emission of elongated molecules entrapped inside zeolite channels was employed to selectively visualize the zeolite component within the matrix of an industrial FCC catalyst particle. Confocal fluorescence microscopy views the inner volume of the intact catalyst particle and is selective to (anisotropic) crystalline material and allows its location, size distribution, and orientation in three dimensions. This selective visualization may serve as a post-synthesis quality control on the dispersion and quantity of zeolite ZSM-5 crystallites inside a single FCC particle.

References

[1] M. A. Karreman, I. L. C. Buurmans, J. W. Geus, A. V. Agronskaia, J. Ruiz-Martinez, H. C. Gerritsen, B. M. Weckhuysen Angew. Chem. Int. Ed. 51 (2012) 1428.
[2] I. L. C. Buurmans, J. Ruiz-Martínez, W. V. Knowles, D. van der Beek, J. A. Bergwerff, E. T. C. Vogt, B. M. Weckhuysen, Nature Chem. 3 (2011) 862.
[3] C. Sprung, B. M. Weckhuysen Chem. Eur. J. 20 (2014) 3667.

II-OP07

Parahydrogen-Induced Polarization in Heterogeneous Catalytic Processes

Kovtunov K.[1*], Barskiy D.[1,2], Salnikov O.[1,2], Burueva D.[1,2], Bukhtiyarov V.[3], Koptyug I.[1,2]

1 - International Tomography Center, Novosibirsk, Russia
2 - Novosibirsk State University, Novosibirsk, Russia
3 - Boreskov Institute of Catalysis SB RAS, Novosibirsk, Russia

* kovtunov@tomo.nsc.ru

Keywords: heterogeneous hydrogenation, parahydrogen, mechanism evaluation, MRI, NMR

1 Introduction

Parahydrogen-induced polarization of nuclear spins provides enhancements of NMR signals for various nuclei of up to four to five orders of magnitude in magnetic fields of modern NMR spectrometers and even higher enhancements in low and ultra-low magnetic fields. It is based on the use of parahydrogen in catalytic hydrogenation reactions which, upon pairwise addition of the two H atoms of parahydrogen, can strongly enhance the NMR signals of reaction intermediates and products in solution. A recent advance in this field is the demonstration that PHIP can be observed not only in homogeneous hydrogenations but also in heterogeneous catalytic reactions. The use of heterogeneous catalysts for generating PHIP provides a number of significant advantages over the homogeneous processes, including the possibility to produce hyperpolarized gases, better control over the hydrogenation process, and the ease of separation of hyperpolarized fluids from the catalyst. The latter advantage is of paramount importance in light of the recent tendency toward utilization of hyperpolarized substances *in vivo* spectroscopic and imaging applications of NMR. In addition, PHIP demonstrates the potential to become a useful tool for studying mechanisms of heterogeneous catalytic processes and for in situ studies of operating catalytic reactors.

2 Experimental/methodology

Pure (>99.99%) hydrogen gas was used for the preparation of >90% p-H2 using a Bruker Parahydrogen Generator BPHG 90. High-resolution high-field NMR spectroscopy was conducted on a Bruker Avance NMR spectrometers. For ALTADENA experiments, the hydrogenation reaction was performed in a temperature-controlled reaction chamber at Earth magnetic field, and the resulting gas was transferred for detection to the NMR spectrometer via Teflon tubing. For PASADENA experiments, a small quantity (a few milligrams) of supported metal catalyst was placed at the bottom of a standard NMR tube, and the gas:p-H2 mixture was delivered to the catalyst via Teflon tubing.

High-field 3D MRI studies were conducted using a 4.7 T Varian MRI scanner (Varian, Palo Alto, California) and a custom-built 38 mm ID dual-channel MRI coil tuned to 1H frequency of 200.25 MHz. All low-field studies were carried out using a Kea2 NMR spectrometer (Magritek, Wellington, New Zealand) with a custom-built frequency optimized dual-channel RF 1H-X probe. The flow rate was not controlled in low-field MR experiments due to experimental limitations.

3 Results and discussion

Several supported metal catalysts were synthesized, characterized and tested in heterogeneous hydrogenation of propene with parahydrogen to maximize nuclear spin

hyperpolarization of propane gas using Parahydrogen Induced Polarization. The Rh/TiO_2 catalyst with 1.6 nm Rh metal particle size was found the most active and effective in pairwise hydrogen addition and robust, demonstrating reproducible results with multiple hydrogenation experiments and stability for ≥1.5 years. 3D ^1H magnetic resonance imaging (MRI) of 1% hyperpolarized flowing gas with micro-scale spatial resolution (625x625x625 μm^3) and large imaging matrix (128x128x32) was demonstrated using pre-clinical 4.7 T scanner and 17.4 s imaging scan time [1]. Moreover, propene-d_6 gas was efficiently hyperpolarized using PHIP technique and Rh/TiO_2 catalyst allowing for preparation of pure HP propane-d_6 gas. PHIP of propane-d_6 provides significant advantages for the mechanistic studies of the catalytic hydrogenation reaction, showing in particular that propene gas is hydrogenated to yield propane, which can be subsequently dehydrogenated by the catalyst studied. Propene-d_6 can also be useful for high-resolution high-field MRI of flowing HP propane-d_6 gas as demonstrated here by 3D MRI with 0.5×0.5×0.5 mm^3 and 17.7 s spatial and temporal resolution. Importantly, low-field NMR at 0.0475 T enabled efficient direct detection of PHIP hyperpolarized propane-d_6 in contrast to non-deuterated PHIP polarized propane. The feasibility of high-resolution MRI should pave the way to biomedical use of PHIP hyperpolarized propane-d_6 as an inhalable contrast agent for pulmonary imaging using proton MRI hardware and pulse sequences [2]. In the case of mechanism evaluation very recent results show that PHIP may be succesfully utilized for studying the heterogeneous hydrogenation of several unsaturated (acrolein, crotonaldehyde) and saturated (acetone, propanal) carbonyl compounds. PHIP effects were successfully observed in liquid and gas phase hydrogenations of C=C bond of acrolein and crotonaldehyde over several supported metal catalysts and bulk metals and oxides. These observations confirm the existence of the route of pairwise hydrogen addition to the C=C bond in the reaction mechanism [3,4].

4 Conclusions

Therefore, the concept of PHIP in heterogeneous hydrogenations has clearly proven its viability. While this sub-field of hyperpolarization in magnetic resonance is still in its infancy, at this point the demonstration that many types of heterogeneous catalysts have an intrinsic ability to produce PHIP is quite an important and encouraging achievement. Heterogeneous processes may have certain limitations, but they also have many advantages over their homogeneous counterparts. In particular, while it is possible in principle to remove a dissolved catalyst from solution of a hyperpolarized molecule, practical attempts to do this lead to a dramatic reduction in the levels of signal enhancement by several orders of magnitude. In this respect, PHIP appears to be a more direct way to catalyst-free hyperpolarized liquids and solutes, and quite likely the only way to utilize parahydrogen to produce hyperpolarized gases. It is also expected that PHIP could become a useful tool in the mechanistic studies of heterogeneous catalytic processes.

Acknowledgements

This work was supported by the grants from RFBR (14-03-00374-a, 14–03–31239-mol-a, 12–03–00403-a, 14-03-93183 MCX_a).

References

[1] K.V. Kovtunov, D.A. Barskiy, A.M. Coffey, M.L. Truong, O.G. Salnikov, A.K. Khudorozhkov, E.A. Inozemtseva, I.P. Prosvirin, V.I. Bukhtiyarov, K.W. Waddell, E.Y. Chekmenev, I.V. Koptyug, *Chem. Eur. J.* (2014), 20, 11636 – 11639

[2] K.V. Kovtunov, M.L. Truong, D.A. Barskiy, O.G. Salnikov, V.I. Bukhtiyarov, A.M. Coffey, K.W. Waddell, I.V. Koptyug, E.Y. Chekmenev, *J. Phys. Chem. C* 118 (2014), 28234.

[3] O.G. Salnikov, K.V. Kovtunov, D.A. Barskiy, A.K. Khudorozhkov, E.A. Inozemtseva, I.P. Prosvirin, V.I. Bukhtiyarov, I.V. Koptyug, *ACS Catalysis* 4 (2014), 2022.

[4] K.V. Kovtunov, D.A. Barskiy, O.G. Salnikov, A.K. Khudorozhkov, V.I. Bukhtiyarov, I.P. Prosvirin, I.V. Koptyug, *Chem. Commun.* 50 (2014), 875.

II-OP08

Selective Hydrogenation Processes over Novel Fiberglass Based Catalysts

Gulyaeva Yu.K.[1], Kaichev V.V.[1,2], Zaikovskii V.I.[1,2], Suknev A.P.[1], Brongersma H.H.[3,4], Bal'zhinimaev B.S.[1*]

1 - Boreskov Institute of Catalysis SB RAS, Novosibirsk, Russia
2 - Novosibirsk State University, Novosibirsk, Russia
3 - ION-TOF GmbH, Munster, Germany
4 - Eindhoven University of Technology, Eindhoven, Netherlands

* balzh@catalysis.ru

Keywords: fiberglass, palladium, nanoparticles, acetylene, hydrogenation, 13C, labeling

1 Introduction

Non-porous fiberglass (FG) textile materials of silicate origin are widely used as perfect heat and electric insulators. However, these materials are much less known in catalysis in spite of their obvious advantages, such as chemical inertness, improved hydrodynamics and ability to make the structured beds of any shape. The capability of FG to stabilize highly dispersed metals (clusters) in the bulk is responsible for excellent performance of FG based catalysts in various oxidation reactions in spite of extremely low noble metal content (0.01-0.02 wt.%) [1]. Here, we present new data on the Pd/FG catalysts preparation, their performance in selective hydrogenation of acetylene, as well as kinetic and mechanistic studies using SSITKA technique. The STEM-HAADF, XPS and HS-LEIS were used to characterize the size, charge and location of Pd species.

2 Experimental

Leached FG silicate materials modified with Al, Zr or rare earth metals were used for the catalyst preparation. Pd(II) cations were introduced into the bulk of glass via ion exchange from its amine complex. The small metal clusters Pd(v) were formed and confined in the bulk of glass by redox treatments at elevated temperatures. The ratio of metal clusters to the Pd remaining on the external surface of the fibers was controlled by the heating rate or by selective removal of surface particles. In addition, the catalyst where metal is deposited mainly on the external surface of the fibers was prepared using anionic palladium precursor (H_2PdCl_4). FG catalysts were tested in selective hydrogenation of acetylene under reaction conditions close to the tail-end process and studied by SSITKA technique using $^{13}C_2H_2$ at acetylene conversion close to 100 %.

3 Results and discussion

The key stages of FG catalyst synthesis are i) the ion exchange of Pd amine cations with the strong protons to anchor them in the bulk of glass and ii) the redox treatment at elevated temperature to decompose the Pd complexes and to form the 1 nm $Pd^{\delta+}$ clusters located in the bulk of glass at a depth of 10-20 nm. In order to increase their number at the expense of Pd particles remaining on the external surface of the fibers, the decomposition of the Pd amine complexes was carried out at a higher heating rate. Indeed, the fraction of clusters grows substantially with the heating rate, so that the catalyst calcined at 50 K/min contained mostly the $Pd^{\delta+}$ particles. In the case of Pd(s)/FG when anionic precursor was used, big palladium particles were deposited only on the external surface of the fiberglass.

The FG catalysts showed high performance in acetylene hydrogenation and their activity did not change after removal of metal particles from the external surface of the fibers. Moreover,

the Pd(v)/FG catalyst containing only $Pd^{\delta+}$ clusters showed the highest catalytic activity. These data clearly indicated that small $Pd^{\delta+}$ clusters were mainly responsible for the catalyst performance, while contribution of the surface particles to the activity was insignificant. The subsurface location of active sites did not limit the reaction rate due to fast diffusion in the bulk of glass.

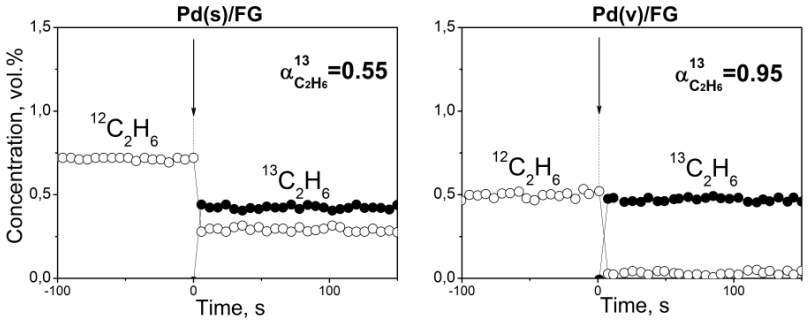

Fig. 1. ^{13}C label transfer from acetylene to ethane observed after replacement of $^{12}C_2H_2$ by $^{13}C_2H_2$ under steady state conditions. Feed gas (vol.%): 2.0 C_2H_2 + 2.0 C_2H_4 +7.0 H_2 + He for balance. Here, α^{13}_{C2H6} is the ^{13}C isotopic fraction in ethane. Arrows show the switching of isotope composition.

Unlike conventional Pd-supported catalysts, an unusual kinetics of selective acetylene hydrogenation over FG catalyst was observed: the reaction selectivity decreases very slowly with the conversion remaining quite high (*ca.* 60%) until a complete conversion of acetylene. At the same time, over Pd(s)/FG containing only metal particles on the external fiber surface, the selectivity drops sharply with acetylene conversion as for conventional monometallic catalysts [2,3]. To clarify the plateau-like dependence of selectivity *vs* conversion, the SSITKA study using double labeled $^{13}C_2H_2$ at a very high acetylene conversion of 97-99 % was carried out (Fig. 1). Surprisingly, over Pd(v)/FG ethane was produced mainly from acetylene despite a 100-fold excess of ethylene, while over Pd(s)/FG nearly half of ethane was produced from gas-phase ethylene. So, it was concluded that gas-phase ethylene was not involved in hydrogenation over the catalyst where active sites were confined in the glass bulk. This fact is related to the capability of glass to absorb selectively the polarizable molecules like acetylene, but not ethylene.

Within the proposed reaction mechanism, the turnover frequencies (TOFs) were measured and compared with the literature data. It was concluded that the reaction rate referred to the number of active sites slightly depends on Pd particles dispersion.

4 Conclusions

The effective methods of confining highly dispersed Pd particles (clusters) in the subsurface layers of glass and the increase in their concentration have been developed. These small clusters demonstrated high activity in selective acetylene hydrogenation. It was clearly shown that gas-phase ethylene was not involved in the reaction even at its very high excess and ethane, being the main by-product, was formed from acetylene only. This is caused by the ability of glass to absorb predominantly the readily polarizable molecules like acetylene (but not ethylene). As a result, high selectivity (the ethylene increment of 60 %) can be achieved at a complete conversion of acetylene, which is even higher than that of the commercial bimetallic catalyst.

References

[1] B.S. Balzhinimaev, E.A. Paukshtis, S.V. Vanag, et al., *Catal. Today* 15 (2010) 195-199.
[2] S.K. Kim, J.H. Lee, I.Y. Ahn, W. J. Kim, S.H. Moon, *Appl. Catal. A* 401 (2011) 12-19.
[3] Q. Zhang, J. Li, X. Liu, Q. Zhu, *Appl. Catal. A* 197 (2000) 221-228.

II-OP09

Dependence of Catalytic Activity of Palladium Nanoparticles on Stabilization Models

Ermolaev V.V.*, Arkhipova D.M., Miluykov V.A., Gaynanova G.A., Zakharova L.Ya., Sinyashin O.G.

A.E. Arbuzov Institute of Organic and Physical Chemistry KSC RAS, Kazan, Russia

* vadim.ermolaev@mail.ru

Keywords: nanoparticles palladium, phosphonium, ionic, liquids, Suzuki reaction, size, distribution, stabilization, mechanism

1 Introduction

Palladium nanoparticles (PdNPs) are widely used as the catalyst in cross-coupling reactions such as Suzuki reaction [1, 2]. Nanoscale catalysis combines the advantages of homogeneous and heterogeneous processes, i.e., possesses high activity and recyclability. The problem of nanoparticles aggregation could be effectively solved by using sterically hindered phosphonium ionic liquids (PILs) as stabilizers [3].

ILs are not clear homogeneous solvents but could be considered as "supramolecular" fluids [4]. Therefore, the influence of stabilizer on the catalytic reaction is crucial. Modelling of NP's stabilization process admits to find out the optimal reaction conditions.

2 Experimental

PILs with a bulky cation containing three *tert*-butyl groups and alkyl chain on the phosphorus atom were synthesized. For comparison, we have obtained similar known in the literature phosphonium salts. A number of physical chemical methods such as NMR spectroscopy, elemental analysis, ESI, TG-DSC was used for characterization of new compounds.

The range of phosphonium salts was used for stabilization of PdNPs. The size distribution of nanoparticles was evaluated by transmission electron microscopy. More over it was mentioned that nature both of anionic and cationic part of phosphonium salt has influence at size distribution. The resulting catalytic systems were tested in Suzuki cross-coupling reaction under mild condition with low palladium loading (0.36 mol%).

3 Results and discussion

We have observed the formation of aggregates of PdNPs as well as individual nanoparticles (Fig. 1).

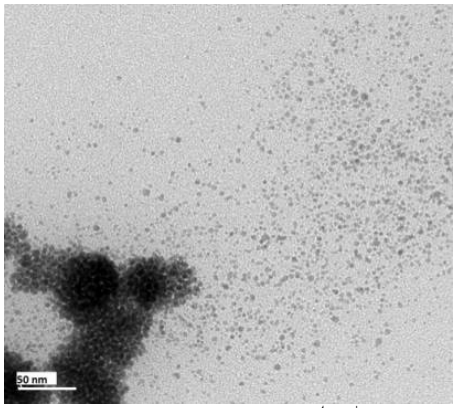

Fig. 1. PdNPs stabilized by $Bu^t_3P^+C_{10}H_{21}BF_4^-$.

PdNPs stabilized with PILs containing linear substituents were less active than sterically hindered ones. It was also found that concentration of stabilizer in the reaction mixture along with its structure has a significant effect on the catalytic activity of stabilized palladium nanoparticles. The latter is connected with represented stabilization models (Fig. 2).

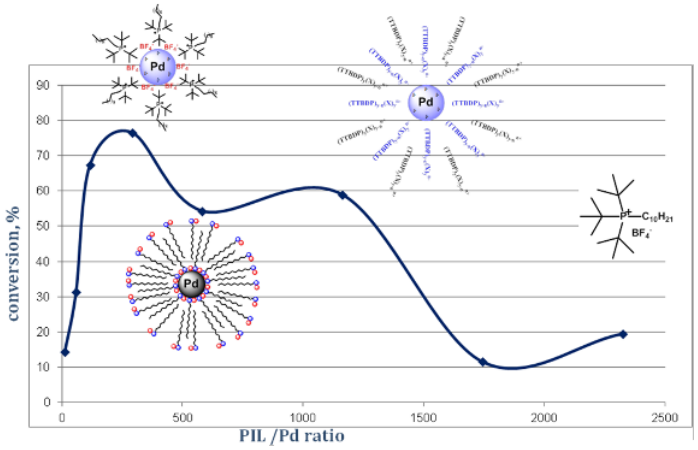

Fig. 2. Dependence of conversion on PIL/PdNPs ratio and supposed models of stabilization.

4 Conclusions

A number of synthesized PILs was tested as the stabilizers of PdNPs in Suzuki cross-coupling of 1,3,5-tribromobenzene and phenylboronic acid. Size distribution and arrangement of PdNPs are determined by nature of the coating agent as well as its concentration in reaction mixture. Rational design and concentration control of these salts allows to separate the contribution of steric and electrostatic factors in PdNPs stabilization.

Acknowledgements

Authors are grateful for the financial support to the Russian Foundation for Basic Research (13-03-12170).

References

[1] A. Balanta, C. Godard, C. Claver, *Chem. Soc. Rev.* 40 (2011) 4973.
[2] J. D. Scholten, B. C. Leal, J. Dupont, *ACS Catal*. 2 (2012) 184.
[3] V. V. Ermolaev *et al, Russ. Chem. Bull., Int. Ed*. 62 (2013) 657.
[4] J. Dupont, *Acc. Chem. Res.* 44 (2011) 1223.

II-OP10

Selective Ethylene Trimerization by Titanium Complexes Bearing Phenoxy-Imine Ligands with Pendant Arm: NMR- and EPR-Spectroscopic Study of the Reaction Intermediates

Soshnikov I.E.[1,2], Semikolenova N.V.[1], Bryliakov K.P.[1,2], Zakharov V.A.[1,2], Talsi E.P.[1,2*]

1 - Boreskov Institute of Catalysis SB RAS, Novosibirsk, Russia
2 - Novosibirsk State University, Novosibirsk, Russia

* talsi@catalysis.ru

Keywords: ethylene, trimerization, NMR, EPR, active, species, mechanism

1 Introduction

Linear α-olefins 1-hexene and 1-octene are important comonomers utilized in the copolymerization with ethylene to generate linear low-density polyethylene. They are produced predominantly via nonselective oligomerization of ethylene. This oligomerization generally yields a broad range of olefins that obey a Schulz–Flory distribution (SHOP process or the Sablin process)[1]. Therefore, catalyst systems that are selective for particular target alkenes would be of great industrial and academic interest.

In 2010 Fujita, Kawamura and coworkers prepared a titanium(IV) complex $LTi^{IV}Cl_3$ bearing a phenoxy-imine ligand with a pendant aryl-OCH_3 donor for selective ethylene trimerization (Chart 1). This complex when activated by MAO produced 1-hexene with exceptionally high activity (up to 132 kg 1-hexene (g Ti)$^{-1}$ h^{-1} bar^{-1}).[2]

The main disadvantage of titanium selective trimerization catalysts is the formation of 2-5 wt. % of high molecular weight polyethylene (PE), which can result in reactor fouling. The nature of the titanium species, responsible for the undesirable PE formation, was unclear.

The hypothetical metallacyclic mechanism of ethylene selective trimerization by the titanium catalysts is depicted in Scheme 1.[3] Unfortunately, previous attempts to isolate or spectroscopically observe Ti(IV) or Ti(II) species, responsible for ethylene trimerization, have not thus far been successful.

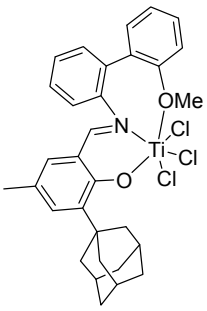

Chart 1.

This work is aimed at using NMR and EPR spectroscopic monitoring of the Ti(IV), Ti(III) and Ti(II) species formed upon the activation of titanium(IV) phenoxy-imine pre-catalyst $LTi^{IV}Cl_3$ with various activators (MAO, MMAO, $AlR_3/[CPh_3]^+[B(C_6F_5)_4]^-$, R = Me, Et, ^{i}Bu) to elucidate the possible role of the observed titanium species in ethylene trimerization and polymerization reactions.

2 Experimental/methodology

All solvents were dried before used. Complex $LTi^{IV}Cl_3$ (Chart 1) was synthesized according to published procedures.[2] Co-catalysts for the catalytic and spectroscopic experiments were purchased from Crompton, AKZO, and Aldrich and used as is.

Samples for NMR and EPR experiments were prepared in the glovebox. For the NMR-tube ethylene trimerization experiments, the break-sealed technique was used. ^{1}H and ^{13}C NMR spectra were measured on a Bruker Avance 400 MHz NMR spectrometer at 400.130 and 100.613 MHz, respectively, using 5 mm o.d. glass NMR tubes. Chemical shifts were referenced to residual solvent peak, 2.09 ppm for CD_2H proton resonance of toluene. EPR spectra were measured on a Bruker ER-200D spectrometer at 9.3 GHz.

3 Results and discussion

Using NMR and EPR spectroscopy, we have monitored transformations of the Ti species in the ethylene trimerization catalyst systems. At the initial stage of the reaction between $LTi^{IV}Cl_3$ with co-catalysts $AlMe_3/[Ph_3C]^+[B(C_6F_5)_4]^-$, MAO or MMAO, diamagnetic outer-sphere Ti(IV) ion pairs of the type $[LTi^{IV}Me_2]^+[A]^-$ ($[A]^- = [B(C_6F_5)_4]^-$, $[MeMAO]^-$ and $[MeMMAO]^-$) are formed. These ion pairs are fairly stable and gradually transform into paramagnetic Ti(III) and Ti(II) species upon storing at room temperature.

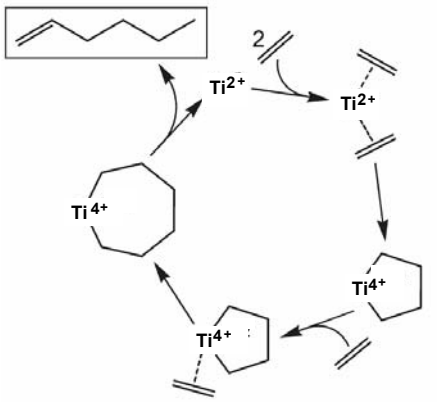

Scheme 1. Proposed metallocyclic mechanism of the selective ethylene trimerization.[3]

In the catalyst systems $LTi^{IV}Cl_3/AlMe_3/[Ph_3C]^+[B(C_6F_5)_4]^-$ and $LTi^{IV}Cl_3/MAO$, complexes with proposed structures $LTi^{III}Me_2$, $LTi^{II}Cl$ and $[LTi^{II}][A]^-$ ($[A]^- = [B(C_6F_5)_4]^-$ or $[MeMAO]^-$) were observed using EPR (Ti(III), S = ½) and NMR spectroscopy of the paramagnetic molecules (Ti(II), S = 1). According to our quantitative measurements the concentration of Ti(III) species in both systems was significantly smaller than that of Ti(II) species, and did not exceed 10 % of the overall titanium content.

In contrast, in the catalyst system $LTi^{IV}Cl_3/MMAO$, a major part of titanium (more than 50%) exist in the reaction solution in the trivalent state (complexes with proposed structures $[LTi^{III}(\mu\text{-}H)(\mu\text{-}Cl)Al^iBu_2]^+[MeMMAO]^-$ and $[LTi^{III}(\mu\text{-}Me)(\mu\text{-}Cl)Al^iBu_2]^+[MeMMAO]^-$). The system $LTi^{IV}Cl_3/MMAO$ demonstrates a lower ethylene trimerization activity than the system $LTi^{IV}Cl_3/MAO$, and produces higher amounts of polyethylene; this behavior correlates with the higher concentration of Ti(III) species in the former system. On the basis of the data obtained we propose that Ti(III) species promote undesirable PE formation.

4 Conclusions

The catalyst systems $LTiCl_3/A$ (A = activator, L = phenoxy-imine ligand) used for selective ethylene trimerization were studied by NMR and EPR spectroscopy. It was found that Ti(IV) complexes $[LTi^{IV}Me_2]^+[A]^-$ and Ti(II) complexes of the type $[LTi^{II}][A]^-$ ($[A]^- = [B(C_6F_5)_4]^-$, $[MeMAO]^-$, and $[MeMMAO]^-$) participate in the selective ethylene trimerization process, whereas Ti(III) species of the type $[LTi^{III}(\mu\text{-}H)(\mu\text{-}Cl)Al^iBu_2]^+[MeMMAO]^-$ and $[LTi^{III}(\mu\text{-}Me)(\mu\text{-}Cl)Al^iBu_2]^+[MeMMAO]^-$ can promote undesirable PE formation.

Acknowledgements

This work was supported by the Russian Foundation for Basic Research (Grant 14-03-31155).

References

[1] A. Forestiere, H. Olivier-Bourbigon, L. Saussine, *Oil Gas Sci. Technol*. 64 (2009) 649.
[2] Y. Suzuki, S. Kinoshita, A. Shibahara, S. Ishii, K. Kawamura, Y. Inoue, T. Fujita, *Organometallics* 29 (2010) 2394.
[3] H. Hagen, W.P. Kretschmer, R.F. van Buren, B. Hessen, D.A. van Oeffelen, *J. Mol. Catal. A*: *Chem*. 248 (2006) 237.

II-OP11

Chemistry of the Active Metal Center in the Selective Catalytic Reduction of NO by NH_3

Mossin S.[1*], Janssens T.V.W.[2], Rasmussen S.B.[2], Vennestrøm P.N.R.[2], Lundegaard L.F.[2], Moses P.G.[2], Giordanino F.[3], Borfecchia E.[3], Lomachenko K.A.[3,4], Bordiga S.[3], Godiksen A.[1], Beato P.[2]

1 - Department of Chemistry, Technical University of Denmark, Lyngby, Denmark
2 - Haldor Topsøe A/S, Lyngby, Denmark
3 - Department of Chemistry, NIS Centre of Excellence and INSTM Reference Center, University of Turin, Turin, Italy
4 - Southern Federal University, Rostov-on-Don, Russia

* slmo@kemi.dtu.dk

Keywords: selective catalytic reduction, Cu, chabazite, zeolite, *in-situ*, spectroscopy, active, site

NO_x emissions from power plants and mobile combustion engines are a global concern due to the detrimental effects of NO_x on the environment and public health. The current best technology for removal of NO_x from the exhaust of both types of emission sources is based upon the selective catalytic reduction of NO_x by ammonia. The commercial catalytic systems are based on the redox active metals vanadium, copper or iron, but to this point the reaction mechanism for all of the catalytic systems are still under discussion.

We present a new reaction scheme for the SCR reaction exemplified by copper exchanged zeolites and adaptable to iron exchanged zeolites and vanadia (V_2O_5) on TiO_2.

The new reaction scheme is compatible with previous suggestions [1,2,3] but is the first to fully comply with the constraints usually put upon chemically consistent reaction schemes at moderate temperatures.

1 Experimental/methodology

Transient intermediates in catalytic reactions are often impossible to trap and to investigate spectroscopically. At the same time a large number of different metal containing species are present in the activated catalysts giving a multitude of spectator sites and sites that participate in side-reactions. Recent investigations [4,5,6] have elucidated and quantified the copper species present in dehydrated Cu-SSZ-13. The method used includes Fourier Transform Infrared (FTIR), Electron Paramagnetic Resonance (EPR) spectroscopy and X-ray Absorption Spectroscopy (XAS). Using the same spectroscopic investigation techniques and the same Cu-SSZ-13 material under *in-situ* and *operando* conditions the resting states of the Cu-SSZ-13 catalyst under reducing SCR relevant conditions (NH_3 + NO) and oxidizing conditions (NO + O_2) have been identified.

2 Results and discussion

The experimental investigation identify Cu^+ bound to the zeolite framework in the reduced resting state and $Cu^{2+}NO_3^-$ in the oxidized resting state.

When connecting these resting states to a chemically consistent cycle the following constraints were applied:

1. Only stable neutral molecules are adsorbed or desorbed during the reaction.
2. The total reaction is equal to the SCR reaction:

$$4\ NH_3 + 4\ NO + O_2 \rightarrow 4\ N_2 + 6\ H_2O$$

The approach was successful resulting in a consistent reaction cycle for the SCR reaction on a mononuclear metal site. This includes two separate cycles each with an oxidation and a reduction step with the fast SCR reaction being identified as being an integral part of the SCR reaction.

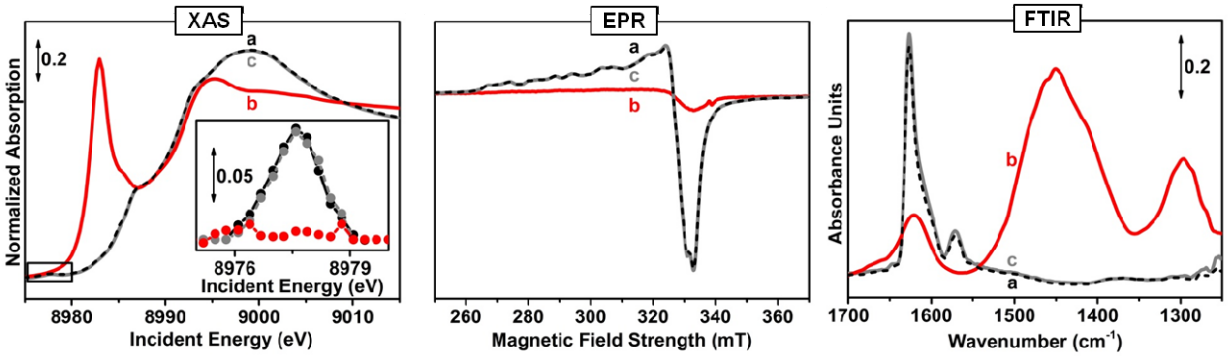

Figure 1. Spectra of Cu-SSZ-13 (Cu/Al = 0.44, Si/Al = 14) at flow conditions at 250 ºC exposed first to NO + O_2 (a) then to NH_3 + NO (b) and finally to NO + O_2 (c).

3 Conclusions

A consistent cycle for the SCR reaction of NO with NH_3 is suggested. The implications on the chemical requirements of the metal of the active site can be summarized as follows:

1. Able to perform one-electron redox reactions.
2. Able to coordinate a NO molecule in both the reduced and the oxidized state.
3. Able to support an OH^- ligand in the oxidized state under reaction conditions.

These requirements are all fulfilled by V^{5+}/V^{4+}, Cu^{2+}/Cu^{+} and Fe^{3+}/Fe^{2+}, which are active in the SCR reaction.

Acknowledgements

Carlo Lamberti and Kirill A. Lomachenko thank the support from the Mega-grant of the Russian Federation Government to support scientific research at Southern Federal University, No.14.Y26.31.0001. Susanne Mossin acknowledges financial support by the Danish Independent Research Council DFF 1335-00175 and DFF 09-070250, and Carlsbergfondet for supporting the upgrade of the EPR instrument at the Technical University of Denmark. Sachem is acknowledged for making TMAdaOH available.

References

[1] Paolucci, C.; Verma, A. A.; Bates, S. A.; Kispersky, V. F.; Miller, J. T.; Gounder, R.; Delgass, W. N.; Ribeiro, F. H.; Schneider, W. F. *Angew. Chem. Int. Ed.* **2014**, *53*, 11828.
[2] Ruggeri, M. P.; Nova, I.; Tronconi, E. *Top. Catal.* **2013**, *56*, 109.
[3] Gao, F.; Kwak, J. H.; Szanyi, J.; Peden, C. H. F. *Top. Catal.* **2013**, *56*, 1441.
[4] Godiksen, A., Stappen, F. N., Vennestrøm, P. N. R., Giordanino, F., Rasmussen, S. B., Lundegaard, L. F., Mossin, S. *J. Phys. Chem. C* **2014**, *118*, 23126.
[5] Andersen, C. W.; Bremholm, M.; Vennestrøm, P. N. R.; Blichfeld, A. B.; Lundegaard, L. F.; Iversen, B. B. *IUCrJ* **2014**, *1*, 382.
[6] Borfecchia, E.; Lomachenko, K. A.; Giordanino, F.; Falsig, H.; Beato, P.; Soldatov, A. V.; Bordiga, S.; Lamberti, C. *Chem. Sci.* **2015**, *6*, 548.

II-OP12

Novel Preparation of Reverse Model Catalyst for CO Oxidation and H_2O Dissociation

Paul R.[1,2], Gharachorlou A.[3,2], Detwiler M.D.[3,2], Delgass W.N.[3,2], Ribeiro F.H.[3,2], Reifenberger R.G.[4,2], Fisher T.S.[5,2], Zemlyanov D.Y.[1,2*]

1 - Birck Nanotechnology Center, West Lafayette, IN, USA
2 - Purdue University, West Lafayette, IN, USA
3 - School of Chemical Engineering, West Lafayette, IN, USA
4 - Department of Physics, West Lafayette, IN, USA
5 - Department of Mechanical Engineering, West Lafayette, IN, USA

* dzemlian@purdue.edu

Keywords: single, crystal, atomic, layer, deposition, CO oxidation, H_2O dissociation, surface, science

1 Introduction

The nature of the support-catalyst interaction and the influence of the boundary between a metal-catalyst and a support could be crucial for understanding the working mechanism of a catalyst. These questions can be addressed through design of a reverse catalyst, which is basically oxide particles or thin film deposited on the surface of a bulk metal catalytic support. The reverse catalysts approach allows researchers to overcome technical problems such as sample conductivity and sensitivity, which are typical for regular catalysts where small amount of interface between metal-catalyst and oxide support could be hardly detected.

The controlled preparation of a model reverse catalyst is not always straightforward. To understand the relative importance of oxide and metal-catalyst during a catalytic event, the oxide layer must be synthesized in a well-controlled manner. Oxide films are typically prepared by e-beam evaporation of desired metal in O_2. The evaporation/oxidation protocol cannot be easily transferred between experimental set-ups. Here we report a new approach to the synthesis of thin oxide films on Pt(111), Pd(111) and Cu(111) by atomic layer deposition (ALD). The advantages of this approach are that: (i) the amount of deposited material can be well controlled by adjusting the number of deposition cycles; (ii) the method can be easily used on the other system without laborious adjustments of the deposition parameters; (iii) the method can be transferred to porous materials; and (iv) the deposition can be achieved at relatively low temperatures compared to conventional evaporation deposition techniques.

Commensurate with the foregoing objectives, we study the adsorption and oxidation of trimethylaluminum (TMA) and bis(η_5-cyclopentadienyl)iron (ferrocene), which is a well-known ALD precursors for Fe and Al oxide deposition. The reactivity of reverse model catalysts FeO and Al_2O_3 Pt(111), Pd(111) and Cu(111) were tested for CO oxidation and H_2O dissociation.

2 Experimental/methodology

Samples used were Pt(111), Pd(111) and Cu(111) single crystals with orientation accuracy < 0.1°. Two experimental apparatuses were used. The first was a Surface Analysis Cluster at Birck Nanotechnology Center in West Lafayette, IN, USA, equipped with the following tools: X-ray Photoelectron Spectroscopy (XPS), Low Energy Electron Diffraction (LEED), High Resolution Electron Energy Loss Spectroscopy (HREELS), and Scanning Tunneling Microscopy (STM). The second apparatus was a synchrotron-based XPS at the ISISS (Innovative Station for In Situ Spectroscopy) beamline at the BESSY II synchrotron in Berlin, Germany, which is capable of operating at pressures up to 1 mbar.

The single crystals were prepared via multiple cycles of Ar^+ sputtering, annealing in O_2 and in

UHV. Sample cleanliness was checked with XPS, HREELS, STM, LEED. The following ALD precursors were used trimethylaluminum (97%, Sigma Aldrich), bis(η_5-cyclopentadienyl)iron (ferrocene or $Fe(Cp)_2$) (97%, Sigma Aldrich). The precursors was contained in stainless steel Swagelok mini cylinders and dosed to the preparation chamber via a system of leak valves. Prior to dosing, several cycles of freeze-pump-thaw were performed for purification.

3 Results and discussion

First, the adsorption of ferrocene and TMA was studied on Pt(111), Pd(111) and Cu(111). Ferrocene was found to adsorb dissociatively on Pt(111) at low exposures. At high exposure, molecularly adsorbed $Fe(Cp)_2$ dominated. The chemistry of TMA on Pt(111), Pd(111) and Cu(111) is governed by activity of a surface and in particularly in the carbon chemistry. TMA adsorb dissociatively to monomethyl aluminium on Pt(111), whereas dissociation to aluminium was observed on Pd(111). This difference was explained by efficient removing of hydrocarbon fragments on Pd(111), whereas, on Pt(111), the active sides were blocked by carbon. Alloying of Al and Pd was observed even t RT. No adsorption of TMA was found on Cu(111). on the other hand, TMA could adsorb on Cu(111) covered with O_{ads}. Al was immediately oxidized to form alumina on the O_{ads}/Cu(111) surface and the reaction is limited by amount of O_{ads}.

In order to prepare FeO and Al_2O_3 islands, ferrocene and TMA fragments were oxidized in O_2 and water. An example of FeO island observed by STM is shown in Fig. 1. The presence of FeO and Al_2O_3 islands was crucial for CO and H_2O adsorption. For instance, in the case of FeO/Pt(111), water was found to dissociate on the FeO islands, whereas CO adsorbed only on the Pt(111) surface. The saturated CO_{ads} could be titrated by O_2 at 300 K on FeO/Pt(111) surface, which was not possible to achieve on Pt(111) (no iron) under the same conditions. The CO_{ads} species in a bridge adsorption configuration was affected in the vicinity of the FeO and Al_2O_3 islands. Likely, this was active species in the reaction. This observation demonstrates demonstrate the importance of the boundary between oxide and metal-catalyst.

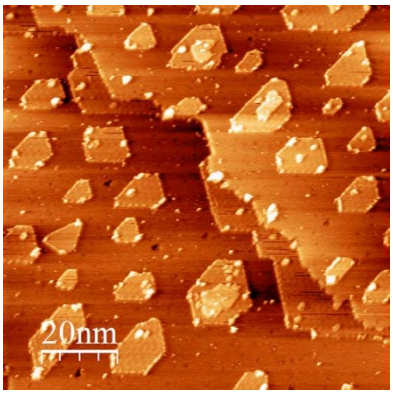

Fig. 1 FeO islands on Pt (111) observed after 3 ALD cycles.

4 Conclusions

The developed procedures of novel reverse catalysts preparation are providing the precise control of chemical composition and morphology of reverse catalysts. Application of such models in fundamental research is allowing study of the ample scope of aspects of catalysts behaviour. CO adsorbed in the vicinity of the oxide islands was identified as an active species of the $CO+O_2$ reaction lowering temperature threshold. The oxides demonstrated the critical role in water dissociation.

Acknowledgements

This material is based upon work supported as part of the Institute for Atom-efficient Chemical Transformations (IACT), an Energy Frontier Research Center funded by the U.S. Department of Energy, Office of Science, Office of Basic Energy Sciences. The authors acknowledge the Helmholtz-Zentrum Berlin for provision of synchrotron radiation beamtime at beamline ISISS-PGM of BESSY II (project 2013_1_121219) and thank the HZB/BESSY II staff members at beamline ISISS-PGM, the U.S. Air Force Research Laboratory (AFRL), and its Office of Scientific Research (AFOSR) under the MURI program on Nanofabrication of Tuneable 3D Nanotube Architectures.

II-OP13

Dynamic High-Resolution Study of the Structural Evolution of Ag Nanoparticles during Carbon Gasification within an Aberration-Corrected Environmental Transmission Electron Microscope

Cadete Santos Aires F.J.[1*], Aouine M.[1], Li S.[1], Tuel A.[1], Epicier T.[1,2]

1 - Institut de Recherches sur la Catalyse et l'Environnement de Lyon, Villeurbanne, France
2 - Laboratoire MATEIS, Villeurbanne Cedex, France

* francisco.aires@ircelyon.univ-lyon1.fr

Keywords: carbon gasification, Ag nanoparticles, dynamic high resolution, environmental TEM

1 Introduction

Gasification of carbon can be achieved, in the presence of metal catalysts supported on solid carbon materials, at high temperature in oxidative environments. Indeed, oxygen adsorbs and dissociates on the metal surface then interacts with the carbon at the interface with the metal leading to the formation of carbon dioxide; concurrently carbon is consumed and the metallic nanoparticle maintains the interface with the carbon and thus advances, forming in this way a trench on the surface of the carbon. On structured materials such as graphite or graphene these trenches tend to be rather 2D [1,2] at the surface of the material (hereafter named "pacman effect"). In this work we have studied the gasification of a non-structured material (amorphous carbon) by silver-based nanoparticles (NPs) in presence of oxygen and at variable temperatures. We were particularly interested on the dynamic structural evolution of the silver NPs observed in real-time within an environmental TEM and at atomic resolution as permitted by the imaging Cs corrector.

2 Experimental/methodology

This work was performed in the Ly-EtTEM (Lyon Environmental and tomographic Transmission Electron Microscope), a 80-300 kV TITAN objective lens C_s-corrected Environmental TEM from FEI equipped with a GATAN high resolution Imaging Filter (GIF) recently installed in Lyon.

Samples were prepared according to a synthesis described in [3]; the silver based NPs stand on the supporting carbon film and gasification of this film is observed between 400 and 500°C under variable oxygen partial pressures (between 10^{-1} and 5 mbar).

3 Results and discussion

We were able to follow in real-time the dynamics of carbon gasification and catalyst evolution by high resolution imaging (Fig.1) unlike previous studies. *In situ* EELS yields complementary information necessary to fully interpret the observed phenomena (structural changes, shrinking and coating of the catalyst, …). The mechanism deduced from our *in situ* study is schematically summarized in Fig.2 : (i) at the beginning of the gasification experiment the NP have surprisingly an hexagonal structure consistent with previously identified hexagonal forms of silver, either metallic or containing diluted oxygen (Fig.2 a-c); (ii) at a given moment during gasification the NP transforms to fcc-Ag, gasification slows down, the particle begins to shrink (surface oxide formation that decomposes) while a coating forms around it (Fig.2 d); (iii) once the particle is completely coated gasification stops and the NP shrinking stops (Fig.2 e).

The hexagonal to fcc transition (which occurs over a period of 4-5 seconds) and the

phenomenon that induces this transition remain however unexplained but most certainly related to the influence of oxygen.

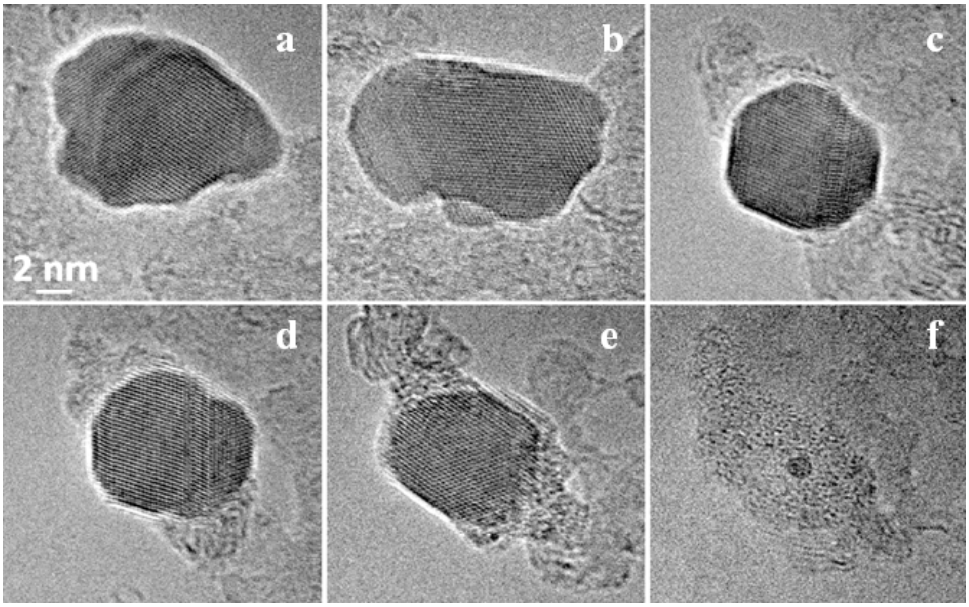

Fig. 1. Selected video frames from an HRTEM sequence recorded *in situ* at 495°C under 0.6 mbar of oxygen (see text for details).

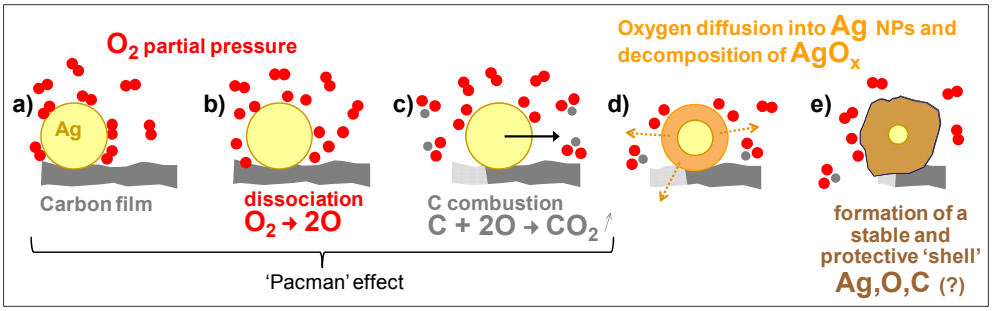

Fig. 2. Schematic interpretation of the sequence shown in Fig.1 (see text for details).

4 Conclusions

Gasification of amorphous carbon by Ag NPs was studied *in situ* (P_{oxygen}, T variables) in an ETEM. Gasification rate slows when the Ag NPs transform from initial hexagonal structure to fcc; concurrently the Ag NPs shrink rapidly. The dynamic real-time high resolution images associated with local EELS measurements allowed to propose a mechanism for the observed phenomena; however the motor behind the hexagonal to fcc transition still remains to be clarified.

Acknowledgements

The authors would like to thank the CLYM (Consortium Lyon-St-Etienne de Microscopie) for the access to the Ly-EtTEM.

References

[1] S.K. Shaikhutdinov and F.J. Cadete Santos Aires, *Langmuir* 14 (1998) 3501.
[2] T.J. Booth *et al*, *Nano Letters* 11 (2011) 2689.
[3] S. Li *et al*, *Chem. Comm.* 49 (2013) 8507.

II-OP14

Atomic-Resolution Imaging of Environmental Catalysts

Ek M.[1*], Zhu Y.[1], Brorson M.[1], Moses P.G.[1], Puig Molina A.M.[1], Ramasse Q.[2], Kisielowski C.[3], Helveg S.[1]

1 - Haldor Topsoe A/S, Kgs. Lyngby, Denmark
2 - SuperSTEM Laboratory, SciTech Daresbury Campus, Daresbury, UK
3 - NCEM, Lawrence Berkeley National Laboratory, CA, USA

* came@topsoe.dk

Keywords: transmission, electron microscopy, single-atom, sensitivity, *in-situ*, studies, HDS, SCR

1 Introduction

In recent years, electron microscopy has made considerable progress that is beneficial to heterogeneous catalysis. With advances in electron optics and in gas cells, atomic-resolution electron microscopy can now provide images of catalysts at the level of single atoms or in catalytic reaction environments. Such imaging capabilities offer unprecedented new atomic-scale information about surface structures and dynamics in catalysts and, in turn, open up new ways to improve the understanding of structure-sensitivity in catalytic processes.
Here, we demonstrate such electron microscopy advances on two catalysts for environmental purposes: Co-promoted MoS_2 on graphite for hydrodesulfurization (HDS) processes in oil refining, and V_2O_5/TiO_2 for selective catalytic reduction (SCR) of nitrogen oxides in automotive exhaust abatement. Imaging of these catalysts has long remained particularly challenging as the active phases are atomically dispersed on the support.

2 Experimental section

Observation of the catalysts in their pristine states was made possible by careful optimization of the imaging conditions and sample environment. Single-atom sensitivity imaging of the HDS catalyst was therefore done by means of low-voltage and low dose-rate scanning transmission electron microscopy (STEM) and electron energy loss spectroscopy (EELS) conducted at the SuperSTEM facility [1,2]. Likewise, for the SCR catalyst, *in-situ* observations during exposure to reactive gas environments was done by means of low dose-rate high-resolution transmission electron microscopy (TEM) and EELS at Haldor Topsoe A/S [3].

3 Results and discussion

Figure 1 shows a STEM image of a graphite-supported MoS_2 nanocrystal in a [001] orientation at single-atom sensitivity. Quantitative analysis of the image contrast was used to assign the atomic columns in the basal plane to 1Mo or 2S atoms, allowing the edge terminations of the nanocrystal to be determined. Moreover, STEM-EELS image contrast analysis of the MoS_2 edges unambiguously demonstrate that the single Co promoter atoms attach preferentially to the S-edge and are each coordinated by four S atoms. These observations are significant because the HDS catalytic activity is associated with the edges. Comparison with model studies suggests that the observed edge structures under high vacuum conditions resemble the catalytic active sites under working conditions [1,2].

Figure 2A shows EELS data of the V_2O_5/TiO_2 catalyst acquired at room temperature and high vacuum, as used in conventional electron microscopy, and at oxidizing conditions. The spectra show that the catalytically relevant V_2O_5 oxidation state is, however, only preserved during exposure to oxidizing conditions in the microscope. Under such *in-situ* conditions, atomic-resolution TEM images as in figure 2B were produced by summation of high-resolution

TEM image series in order to enhance the sensitivity toward the single atom level [3]. Hereby it was observed that the vanadia surface layer was isostructural with the anatase TiO_2 support, and that no amorphous phases were present on the particle surfaces.

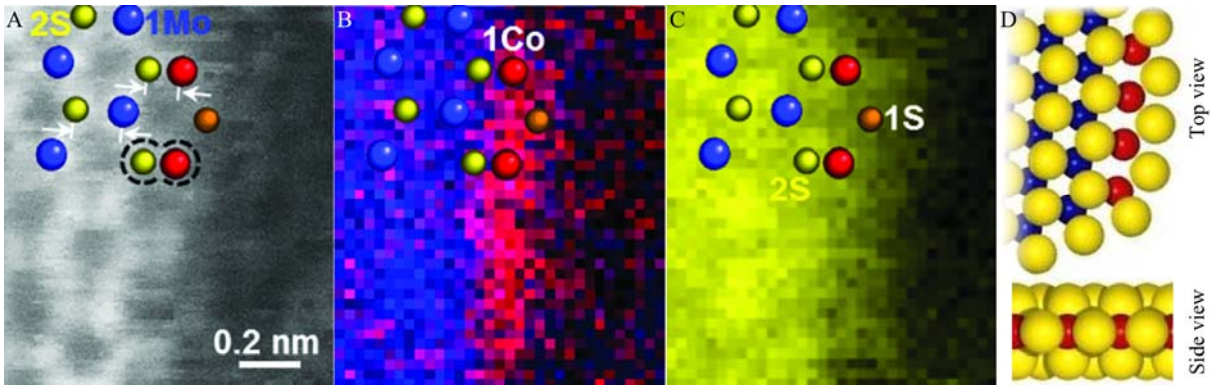

Fig. 1. (A) Atomic-resolution STEM image of the S-edge of a Co-promoted MoS_2 nanocrystal and corresponding EELS maps of the distribution of Co and Mo (B) and S (C). Each image is overlaid with an atomic model, which is also shown in its entirety in the last panel (D). Adapted from [2].

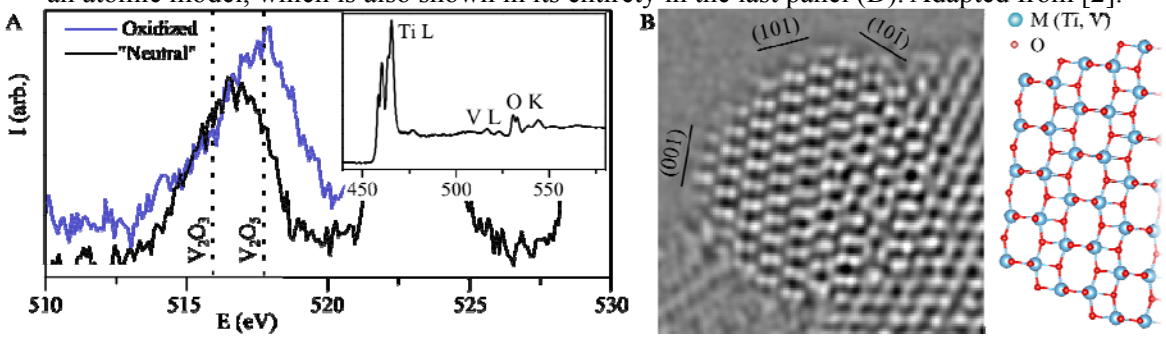

Fig. 2. (A) EELS of the V_xO_y/TiO_2 catalyst at the V $L_{2,3}$ ionization edge acquired under oxidizing (300°C, 1 mbar O_2) and conventional TEM (room temperature, vacuum) conditions. Vertical lines indicating the energy loss for two bulk vanadium oxides are included for comparison. (B) Atomic-resolution TEM image of a V_2O_5/TiO_2 particle acquired at oxidizing conditions.

4 Conclusions

The ability to observe the HDS and SCR catalysts at atomic resolution and sensitivity and in their pristine states was made possible by careful control of the imaging and sample environment. The structural information about industrial-style catalysts open up new important opportunities; the interplay with information, measured or calculated, from simple model systems, allowing the description of the catalysis to be extended with information specific to the exposed surface sites, will be discussed.

Acknowledgements

The authors would like to thank Prof. A.D. Jensen (Department of Chemical and Biochemical Engineering, DTU, Denmark) for supplying the V_2O_5/TiO_2 samples. The Danish Council for Strategic Research (grant Cat-C) is acknowledged for financial support.

References

[1] L.P. Hansen, Q.M. Ramasse, C. Kisielowski, M. Brorson, E. Johnson, H. Topsøe, S. Helveg, *Angewandte Chemie Int. Ed.* 50 (2011) 10153
[2] Y. Zhu, Q.M. Ramasse, M. Brorson, P.G. Moses, L.P. Hansen, C.F. Kisielowski, S. Helveg, *Angewandte Chemie Int. Ed.* 53 (2014) 10723
[3] S. Helveg, C.F. Kisielowski, J.R. Jinschek, P. Specht, G. Yuan, H. Frei, *Micron* 68 (2014) 176

II-OP15

Operando Spatially- and Time-Resolved XAS Andvalence-to-Core-XES for the Characterization of Fe- and Cu-Zeolite Catalystsfor NH_3-SCR of NOx

Doronkin D.E., Günter T., Carvalho H.W.P., Baier S., Boubnov A., Sheppard T., Casapu M., Grunwaldt J.-D.*

Karlsruhe Institute of Technology, Karlsruhe, Germany

* grunwaldt@kit.edu

Keywords: zeolite, NOx, reduction, X-ray, absorption, emission, spectroscopy, NEDC

1 Introduction

In the last decade, Fe- and Cu-exchanged zeolites have received significant attention due to their superior performance and thermal stability as compared to the widely used V_2O_5-WO_3/TiO_2 for selective catalytic reduction (SCR) of NOx with NH_3 [1]. Many efforts are under way for gaining a detailed understanding of the structural parameters essential for a high performance and also for enhanced hydrothermal durability. This will allow further tuning of the preparation methods and rational design of improved catalysts. Furthermore, knowledge about the reaction mechanism is essential for modelling of the exhaust aftertreatment control algorithms.

Among the different characterization methods, X-ray absorption spectroscopy (XAS) is one of the few techniques which can be applied under realistic reaction conditions without altering the process dynamics. Important information such as oxidation state, coordination geometry, type and number of nearest neighbours of a metal site including the structural changes due to interaction with reactants, can be derived by monitoring the changes occurring in the pre-edge, near edge (XANES) and extended X-ray absorption fine structure (EXAFS) of a XAS spectrum [2]. The "quick scanning" technique QEXAFS [3] allows gaining this information during transient runs with 1-10 Hz frequency. Complementary information about species reacting with the metal site can be gained using valence-to-core X-ray emission spectroscopy (V2C-XES), which allows e.g. to distinguish between atoms with close atomic numbers like O and N [2]. Importantly, due to penetration nature of X-rays we can apply XAS and XES techniques *in-situ* or *operando* employing reaction cells with a fixed bed as plug-flow reactors and realistic gas mixtures, flows, and temperatures [4].

Here we report results of a spatially- and time-resolved operando XAS study on various Fe- and Cu-zeolite catalysts and XES studies of Fe-ZSM-5 and Cu-SSZ-13 catalysts during SCR of NOx with NH_3 [5,6]. The obtained data significantly extend the understanding of the SCR reaction mechanism over zeolite-based catalysts and allowed obtaining additional input data for modeling the catalyst behavior.

2 Experimental/methodology

Fe- and Cu-zeolites were obtained either by preparation in our laboratories or as commercial samples. XRD, BET surface area, AAS, EXAFS and UV-Vis were employed for the material characterization. A quartz capillary microreactor (plug-flow reactor geometry) which allows on-line monitoring of the catalytic performance was used for the XAS/XES measurements. The catalyst bed was heated by a hot gas blower between 185 – 550 °C while dosing a gas stream containing 0 – 1000 ppm NO, 0-1000 NO_2, 0 – 1200 ppm NH_3, 5% O_2,

~1.5% H_2O in He. The simulation of the NEDC driving cycle was conducted using a Silicon etched microreactor with an integrated heater and low thermal mass. The spatially-and time-resolved XAS measurements were carried out at the X10DA SuperXAS beamline (Swiss Light Source) and the XES data were acquired at the ID26 beamline (European Synchrotron Radiation Facility). Simulated XES-spectra were calculated by DFT for comparison with the obtained experimental data.

3 Results and discussion

Strong gradients of Fe and Cu oxidation state and a decrease of coordination number have been observed along the catalyst bed for all processes involving NH_3. Inlet of the catalyst bed typically had more reduced Fe (Cu) sites with lower average coordination number. Furthermore, the gradient was stronger when both NO and NH_3 were in the reaction mixture. This indicates a reaction of NOx and NH_3 adsorbed on Fe^{3+} (Cu^{2+}) leaving Fe^{2+} (Cu^{+}) with a lower coordination number [5]. Reoxidation of metal sites by oxygen is suggested to be the rate-limiting step of the NH_3-SCR which is strongly inhibited by NH_3 at lower temperatures for Fe-zeolites. Concurrently it was observed that water inhibits the SCR reaction by coordination to the Fe-active center.

This is further supported by application of V2C-XES which provided evidence of the adsorption of NH_3 and NO (Fig. 1) in the presence of water and in combination with DFT-calculations allowed the identification of potential reaction intermediates for the SCR process on Fe- [6] and Cu-zeolites [7]. Interestingly, V2C-XES spectra of Cu-SSZ-13 uncovered different NH_3 and NO adsorption structures as compared to the case of Fe-ZSM-5 zeolite.

To supplement the steady-state data and to describe Fe and Cu oxidation state dynamics XAS measurements were done in a quick scanning mode during NH_3 concentration transients [5] as well as during temperature transients. As a result, the behavior of the metal sites was monitored during a simulated driving cycle (New European Driving cycle, NEDC) and correlated with the catalyst performance.

4 Conclusions

By application of novel *operando* spectroscopic techniques we could unravel mechanistic steps of the NH_3-SCR. Spatially-resolved XAS allowed to describe gradients of the oxidation state and coordination number of Fe and Cu active sites supporting previously proposed mechanistic schemes [5], while results of XES and QEXAFS during NEDC simulations underlined differences in adsorbed intermediates and redox dynamics of Fe- and Cu-sites in zeolite catalysts.

References

[1] I. Nova, E. Tronconi (Eds.), *Urea-SCR Technology for deNOx After Treatment of Diesel Exhausts*, Springer Science+Business Media New York (2014).
[2] E. Gallo, P. Glatzel, *Adv. Mater.* 26 (2014) 7730.
[3] R. Frahm, *Physica B* 158 (1983) 342.
[4] J.-D. Grunwaldt, M. Caravati, S. Hannemann, A.Baiker, *Phys. Chem. Chem. Phys.* 6 (2004) 3037.
[5] D.E. Doronkin, M. Casapu, T. Günter et al., *J. Phys. Chem. C* 118 (2014) 10204.
[6] A. Boubnov, H.W.P. Carvalho, D.E. Doronkin et al., *J. Am. Chem. Soc.* 136 (2014) 13006.
[7] T. Günter, H.W.P. Carvalho, D.E. Doronkin et al., submitted for publication.

II-OP16

Novel Research Platforms ISISS and EMIL at BESSY II: *in situ* Surface Characterization of Catalysts by Synchrotron Based near Ambient Pressure X-Ray Electron Spectroscopy

Hävecker M.[1,2], Heine C.[2], Eichelbaum M.[2,3], Rosowski F.[3], Trunschke A.[2], Pfeifer V.[2], Velasco Vélez J.J.[2,4], Lips K.[1], Reichardt G.[1], Knop A.[2], Schlögl R.[2,4*]

1 - Helmholtz-Zentrum Berlin für Materialien und Energy / BESSY II, Energy Materials, Berlin, Germany

2 - Fritz-Haber-Institut der Max-Planck-Gesellschaft, Inorganic Chemistry, Berlin, Germany

3 - TU Berlin, BasCat, UniCAT BASF JointLab, Berlin, Germany

4 - Max-Planck-Institut für Chemische Energiekonversion, Heterogeneous Reactions, Mülheim a.d. Ruhr, Germany

* mh@fhi-berlin.mpg.de

Keywords: selective oxidation, VPP, synchrotron, NAP-XPS, XAS, *in situ*

1 Introduction

The surface of functional materials like catalysts responds to the ambient conditions. X-ray photoelectron spectroscopy (XPS) and soft X-ray absorption spectroscopy (XAS) are one of the most versatile methods for the investigation of surfaces on the atomic scale providing quantitative information about the elemental composition and chemical specificity. Surface sensitive *in situ* spectroscopy, i.e. in the presence of a reactive environment allows studying the formation of the interface (gas/solid or liquid/solid) of a catalyst with time and thus adds a dynamic dimension to the spectroscopic characterization. The ISISS facility (Innovative Station for *In Situ* Spectroscopy) operated by the Fritz-Haber-Institut (FHI) at the synchrotron radiation source BESSY II of the Helmholtz-Zentrum Berlin (HZB) is dedicated to this kind of *in situ* studies by near ambient pressure XPS (NAP-XPS) and variable pressure soft-XAS (vP-XAS). Examples for the dynamic formation of the electronic surface structure by interaction with the ambient gas under equilibrium will be presented. Furthermore, vP-XAS studies will be discussed to investigate the pressure dependence of complex alkane oxidation reactions.

Finally, an outlook on future activities at HZB/BESSY to develop further synchrotron based ambient pressure characterisation methodologies will be given. Recently, the advent of reaction cells based on electron transparent membranes at low kinetic energy (i.e. high surface sensitivity) has found much interest [1]. First results of the application of this type of cells allowing performing XPS studies at 1000mbar gas pressure and in liquids will be presented. Currently, HZB and FHI are establishing EMIL, The Energy Materials In-Situ Laboratory Berlin at BESSY II. This novel facility includes a new laboratory building hosting beamlines providing an unusual broad photon energy range from 80eV – 8000eV in one spot and (among others) a NAP-high kinetic energy XPS endstation capable to operate at kinetic energy of photoelectrons up to 7000eV that allows studying buried layers and liquid/solid interfaces [2]. Prospects of this new facility for catalyst research will be discussed.

2 Experimental/methodology

We characterized the surface of the alkane oxidation catalyst vanadyl pyrophosphate $(VO)_2P_2O_7$ (VPP) with NAP-XPS in the mbar pressure range and with vP-soft XAS in the electron yield mode at pressures up to 1000mbar at various gas compositions at temperature up to 400°C. Simultaneously, the catalytic performance was determined by mass spectrometry.

3 Results and discussion

Analysis of NAP-XPS spectra provide evidence that details of the electronic structure like work function, core level binding energies, valence and electron affinity of the technical catalyst VPP do respond systematically on the gas phase (Fig. 1a). This indicates the formation of a dynamic surface/subsurface space charge region that has an impact on the charge transport properties of the active catalyst [3]. Additionally, the vanadium oxidation state has been extracted from the V L_3-edge XAS under O_2, C_4H_{10}, and C_4H_{10}+O_2 feed in a variable pressure XAS experiment (vP-XAS). It was found that the vanadium oxidation state changes both with the gas composition and the total pressure (Fig. 1b). The observed pressure gap is understood in terms of Gibbs free energy of the surface and its dependence on the oxygen partial pressure of the surrounding gas phase [4].

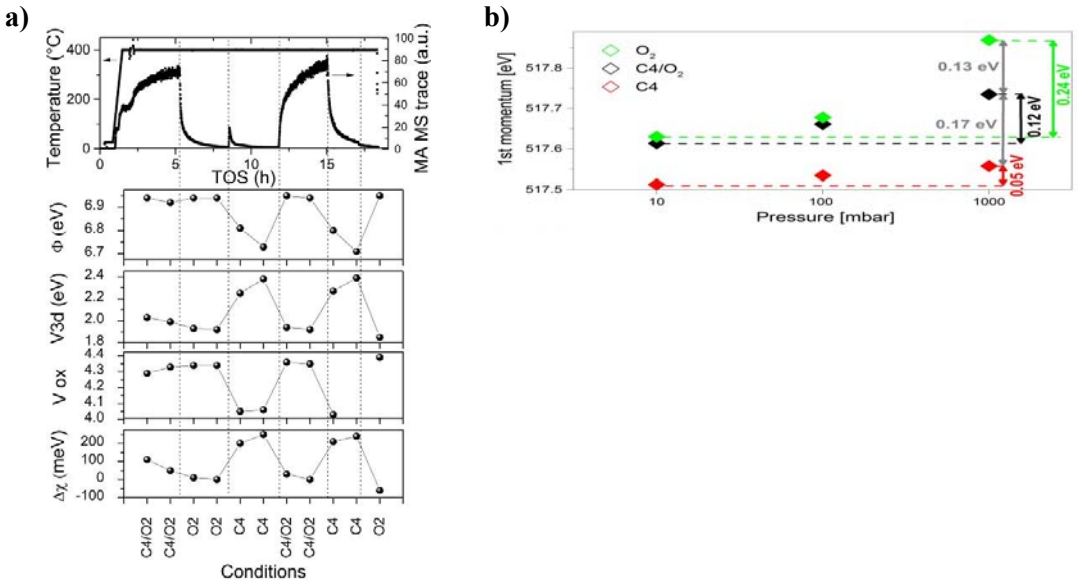

Fig. 1. a) Maleic anhydride (MA) product trace compared with work function Φ, V3d binding energy, vanadium oxidation state V_{ox} and electron affinity change Δχ of VPP at 400°C in different gas mixtures. **Fig. 1b)** 1st momentum of the VL_3-edge as a measure for the vanadium oxidation state of VPP at 400°C in different gas mixtures as a function of the total pressure.

4 Conclusions

This study demonstrates the power and versatility of NAP-electron spectroscopy methodologies to determine details of the electronic surface structure on a molecular level in various gas mixtures at relevant temperature and at total pressures up to 1000mbar. The feasibility of NAP-XPS and vP-XAS has been exemplified in the selective n-butane oxidation to MSA on the technical catalyst VPP. Vanadium oxidation state, work function, and surface dipole moment are related to the catalytic performance. Details of the pressure dependence of the vanadium oxidation state have been elucidated. Thus, both the pressure gap and the materials gap between model and technical catalysts have been tackled.

Acknowledgements

HZB/BESSY is acknowledged for providing beamtime. Part of the project has been supported by BMBF in the framework of ReAlSelOx project, grant number 033R028B.

References

[1] J. D. Stoll and A. Kolmakov, *Nanotechnology* 23 (2012) 505704.
[2] R. Follath et al. *J. Physics: Conf. Series* 425 (2013) 212003
[3] M. Eichelbaum et al., *Angew. Chem.* DOI: 10.1002/anie.201410632.
[4] C. Heine et. al. *J. Phys. Chem. C.* 118 (2014) 20405.

II-OP17

Mechanism for Selective Oxidation of Ethanol over V-Ti Catalyst

Kaichev V.[1*], Chesalov Y.[1], Saraev A.[1], Klyushin A.[2], Knop-Gericke A.[2], Andrushkevich T.[1], Bukhtiyarov V.[1]

1 - Boreskov Institute of Catalysis SB RAS, Novosibirsk, Russia
2 - Department of Inorganic Chemistry, Fritz Haber Institute of the Max Plank Society, Berlin, Germany

* vvk@catalysis.ru

Keywords: ethanol oxidation, acetaldehyde, acetic acid, vanadium oxide

1 Introduction

Over the past several years, an idea to use renewable resources in chemical industry has been becoming popular in the whole world. Especially many efforts have been focused on the development of technologies for production of alternative fuels based on bio-oil, biodiesel, or bioethanol. At the same time, bioethanol or simply "ethanol", which is produced from biomass by the hydrolysis and sugar fermentation processes, can be used as a raw material for catalytic production of various useful chemical compounds. Depending on the catalyst and reaction conditions, ethanol can be transformed to acetaldehyde, acetic acid, diethyl ether, butadiene, or ethyl acetate with a high selectivity. A special attention is paid to the development of novel catalytic technologies for the industrial production of acetaldehyde and acetic acid via one-step gas-phase conversion of ethanol. Here, we report the first results of our mechanistic study of the gas-phase selective oxidation of ethanol to acetaldehyde and acetic acid over titania-supported vanadium oxide catalysts. We used Fourier transform infrared spectroscopy (FTIR) and near ambient pressure X-ray photoelectron spectroscopy (NAP-XPS) that allowed us to study the catalyst state and adsorbed species during the oxidation of ethanol. The data are complemented by results of temperature-programmed reaction spectroscopy (TPRS) and kinetic measurements.

2 Experimental

All experiments were performed using a monolayer V_2O_5/TiO_2 catalyst, which was prepared by the impregnation as described in details elsewhere [1]. The steady-state activity of the catalyst was tested at atmospheric pressure in a differential reactor with a flow-circulating configuration. The reactor was constructed from Pyrex glass tubing with a 12-mm inner diameter and a 50-mm length. The feed consisted of ethanol, oxygen, and nitrogen in a molar ratio of 1:4:15. The concentrations of products and reactants were determined with an on-line gas chromatograph equipped with thermal conductivity and flame ionization detectors [1].

The *in situ* XPS and TPRS experiments were performed at the synchrotron facility BESSY II, Berlin, using the ISISS beamline equipped with an on-line quadrupole mass spectrometer Prizma QMS-200. The experiments were performed in a flow regime at 0.5 mbar. The *in situ* FTIR measurements were performed at atmospheric pressure on a BOMEM MB-102 spectrometer using a feed of 1.5 vol% C_2H_5OH in air flowing at 50 mL/s.

3 Results and discussion

The oxidation of ethanol was examined over the catalyst in a temperature range of 110-230 °C. Acetaldehyde (CH_3CHO), acetic acid (CH_3COOH), diethyl ether ($(C_2H_5)_2O$), ethyl acetate (CH_3-COO-CH_2-CH_3), crotonaldehyde (CH_3CH=$CHCHO$), ethylene (C_2H_4), carbon oxides (CO and CO_2), and water were detected as products. It was found that the conversion of

ethanol increases monotonically with the reaction temperature and achieves 100% at 230 °C. At low temperatures, acetaldehyde is the major product. Its selectivity is 100% at 110 °C. The selectivity toward acetaldehyde decreases with temperature, and the reaction shifts toward acetic acid. The formation of small amounts of ethyl acetate, ethylene, crotonaldehyde, CO, and CO_2 was also observed. Between 180 and 230 °C, acetic acid becomes the main reaction product. At 200 °C, its selectivity achieves approximately 60% at the conversion of ethanol near 95%. At temperatures above 250 °C, the oxidation of ethanol to CO and CO_2 predominates. Such dependence of selectivity on the reaction temperature and conversion suggests that acetic acid is formed consecutively from acetaldehyde, while carbon oxides are formed during the further oxidation of acetic acid.

The formation of adsorbed species during the oxidation of ethanol was examined by infrared spectroscopy *in situ* at 100, 150, and 230 °C. At 100 °C, the main reaction intermediate adsorbed on the catalyst surface was ethoxide, which results from the dissociative adsorption of ethanol on acid-basic surface sites (V-O). In addition, the spectrum exhibits an extra peak at 1267 cm^{-1}, which corresponds to the δ(OH) mode of adsorbed molecular ethanol, and a broad band at 3600-2800 cm^{-1} due to H-bonded hydroxyl groups. At 230 °C, the surface is mainly covered by acetate species. According to NAP-XPS data, titanium cations remain in the Ti^{4+} state, while V^{5+} cations undergo a reversible reduction under reaction conditions. It means that the selective oxidation of ethanol over vanadium oxide catalysts occurs at the redox V^{n+} sites via the Mars-van Krevelen mechanism involving the surface lattice oxygen species. We suggest that the catalytic cycle starts with the catalyst in the oxidized state. Ethanol adsorbs intact on the acid-base sites of the catalyst and further can dissociate to form the adsorbed ethoxide species and OH group. The formation of ethoxide species is accompanied with a decrease in the ν(V=O) bands appearance of a strong band due to H-bonded hydroxyl groups. We believe that the chemisorption of ethanol is a heterolytic process, during which the proton from the alcohol hydroxyl group is transferred to the vanadyl oxygen atom and the oxidation state of vanadium changes from V^{5+} to V^{4+}. Acetaldehyde is formed in a subsequent step via a transfer of a proton from a CH_2 group to the adjacent vanadyl oxygen atom, which is accompanied with the partial reduction of the next vanadium atom. The OH species ultimately recombines with another OH to form H_2O and a vanadyl oxygen species; adsorbed acetaldehyde can desorb as a product. Hence, two terminal V=O bonds are involved in the oxidative dehydrogenation of ethanol through the transfer of two electrons.

Because the selectivity toward acetic acid increases with ethanol conversion, we can speculate that the formation of acetic acid should occur as a consecutive reaction by oxidation of initially formed acetaldehyde. Thus, adsorbed acetaldehyde reacts with lattice oxygen atoms to form an adsorbed acetate species, which then desorbs as acetic acid at temperatures in the range of 170-230 °C or decomposes to CO and CO_2 at higher temperatures. The formation of acetate is accompanied with the further reduction of vanadium to V^{3+} and formation of an oxygen vacancy. It is confirmed by NAP-XPS, which indicates the high concentration of the adsorbed acetate species and V^{3+} cations observed in pure ethanol at 110°C. The catalytic cycle is finally closed by oxidizing the V^{3+} and V^{4+} cations via irreversible chemisorption of oxygen with the formation of the active sites. Therefore, the catalytic cycle for the oxidation of ethanol to acetic acid involves the transfer of four electrons.

Acknowledgements

This work was partially supported by the Russian Foundation for Basic Research (Research projects No. 13-03-00128-a) and President Grant for Government Support of the Leading Scientific Schools of the Russian Federation (grant SS-5340.2014.3).

References

[1] V.V. Kaichev, G.Ya. Popova, Yu.A. Chesalov, A.A. Saraev, D.Y. Zemlyanov, S.A. Beloshapkin, A. Knop-Gericke, R. Schlögl, T.V. Andrushkevich, V.I. Bukhtiyarov, *J. Catal.* **311** (2014) 59.

II-OP18

What are the Active Sites of Gold in CO Oxidation Reaction?

Klyushin A.Yu.[1*], Rocha T.C.R.[1], Li X.[1], Huang X.[1], Lunkeinbein T.[1], Friedrich M.[1], Hävecker M.[1,2], Bukhtiyarov A.V.[3,4], Prosvirin I.P.[3,4], Bukhtiyarov V.I.[3,4], Knop-Gericke A.[1], Schlögl R.[1]

1 - Fritz-Haber-Institute of the Max Planck Society, Dep. of Inorganic Chemistry, Berlin, Germany
2 - Helmholtz-Zentrum Berlin/BESSY II, Department of Solar Energy Research, Berlin, Germany
3 - Boreskov Institute of Catalysis SB RAS, Novosibirsk, Russia
4 - Novosibirsk State University, Novosibirsk, Russia

* klyushin@fhi-berlin.mpg.de

Keywords: Au nanoparticles, X-ray, photoemission, spectra, strong, metal-support, interaction

1 Introduction.

The discovery that gold nanoparticles (Au NPs) supported on metal oxides are active in low-temperature CO oxidation [1] has inspired a considerable amount of research focused on understanding the basis of activity of Au catalysts [2]. Various factors—such as quantum size effects, low coordinated atoms, surface ions and the support interaction [3]—have been proposed as factors that influence Au activity. Here we report the findings from our recent study on the catalytic properties of oxidized Au and Au NPs on various supports in CO oxidation reaction.

2 Experimental/methodology.

All measurements were performed in the near ambient pressure X-ray photoelectron spectroscopy (NAP-XPS) endstation at the ISISS beamline at HZB/BESSY II (Berlin, Germany) [4]. Gold containing samples (Au foil, Au NPs supported on carbon and transition metal oxides) were characterized using *in-situ* XPS and *ex-situ* techniques, such as electron energy loss spectroscopy (EELS), scanning and transmission electron microscopy (SEM and TEM). CO and O_2/O_3 were introduced to the chamber at different ratios, keeping the pressure and temperature constant, at 0.3 mbar and 100°C, respectively.

The procedure, used to prepare the Au/HOPG (highly oriented pyrolytic graphite) model catalysts, is described in detail elsewhere [5]. The procedure involves forming defects on the HOPG surface via soft Ar^+ sputtering, followed by Au deposition and surface annealing at 300°C in UHV (for Au NPs stabilization). Au NPs supported on functionalized carbon nanotubes (CNTs) were prepared using immobilization and incipient impregnation methods. Nanoscopic Au was electrochemically deposited on Au foil. Au NPs on transition metal oxides were synthesized by deposition-precipitation (Au/Fe_2O_3, Au/TiO_2) [6,7] and photochemical decomposition of intermediate gold-azido complexes (Au/Fe_2O_3, Au/Cr_2O_3) [8].

3 Results and discussion.

Our *in-situ* measurements show that the oxidation of extended Au surfaces by O_3 treatment is accompanied by the formation of meta-stable surface oxide(s) [9]. It was found that Au oxide does not directly participate in CO oxidation on Au-based catalysts. Our experiments on Au foil allow us to conclude that low-coordinated Au atoms, present on the surface after oxidation, do not possess sufficient CO conversion at room temperature. Similar to oxidized Au foil, Au NPs on oxygen-free supports (HOPG, functionalized CNTs, Au foil) do not show any catalytic activity, regardless of the NPs' size, the type of the support and the method of synthesis. Therefore, NP size reduction and/or oxidation are not sufficient to activate Au.

In contrast, the Au NPs on oxygen containing supports show high catalytic activity, which depends on the method of preparation, and can be associated with the formation of positively charged Au species (Figure 1). Indeed, only the samples prepared by deposition-precipitation methods showed significant CO conversion at low temperature. XPS revealed the presence of two Au species (Au^0 and $Au^{\delta+}$) on the surface of active Au/TiO_2 and Au/Fe_2O_3 samples. The energy shift of the $Au^{\delta+}$ peak, relatively to bulk gold (Au^0), depends on the support, and is 0.7 eV and 0.85 eV to higher binding energy for Au/TiO_2 and Au/Fe_2O_3, respectively. TEM images indicate the formation of overlayers on Au particles. EELS spectra confirm the formation of transition metal oxide overlayers on top of the Au NPs.

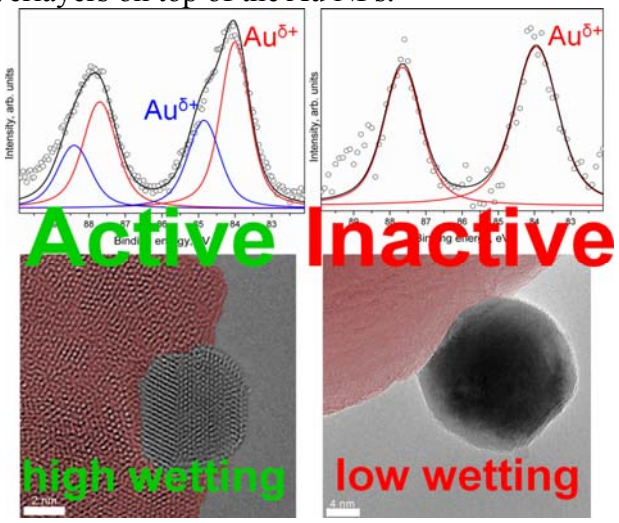

Figure 1. Au 4f XP spectrum and TEM image of Au/Fe_2O_3 synthesized by deposition-precipitation (left) and photochemical decomposition of intermediate gold-azido complex (right) method.

4 Conclusions.

Our results suggest a mechanism of Au activation via Strong Metal Support Interaction (SMSI), assuming a strong influence of the support on the electronic structure of the gold through charge transfer and stabilization of low-coordinated Au atoms. Therefore SMSI plays key role in Au activation and is more important than size reduction.

Acknowledgements.

We thank Gisela Weinberg (Fritz-Haber-Institute der Max-Planck, Berlin)for providing the SEM images of the gold foil, Rosa Arrigo (Fritz-Haber-Institute der Max-Planck, Berlin), Zailai Xie (Fritz-Haber-Institute der Max-Planck, Berlin), Yi Youngmi (Fritz-Haber-Institute der Max-Planck, Berlin) and Olaf Timpe (Fritz-Haber-Institute der Max-Planck, Berlin) for sample preparation and HZB for the allocation of synchrotron radiation beamtime.

References

[1] M. Haruta, N. Yamada, T. Kobayashi, S. Iijima, *J. Catal* , 115 (1989) 301.
[2] B.K. Min, C.M. Friend, *Chem. Rev.* 107 (2007) 2709.
[3] R. Meyer, C. Lemire, Sh.K. Shaikhutdinov and H.-J. Freund, *Gold Bulletin* 37 (2004) 72.
[4] H. Bluhm, M. Hävecker, A. Knop-Gericke, E. Kleimenov, R. Schlögl, D. Teschner, V.I. Bukhtiyarov, D. F. Ogletree, M. Salmeron, *J. Phys. Chem. B*, , 108 (2004) 14340.
[5] D. V. Demidov, I. P. Prosvirin, A. M. Sorokin, T. Rocha, A. Knop-Gericke, V. I. Bukhtiyarov, *Catal. Sci. Technol.*, 1 (2011) 1432.
[6] R.M. Finch, N.A. Hodge, G.J. Hutchings, A. Meagher, Q.A. Pankhurst, M.R.H. Siddiqui, F.E. Wagner, R. Whyman, *PCCP* 1 (1999) 485.
[7] R. Zanella, S. Giorgio, C.H. Shin, C. Henry, C. Louis., *J Catal.* 222 (2004) 357.
[8] C.M. Rienäcker, (2001): *Synthese und Charakterisierung von Gold-Azid- und Blei-Halogen-Verbindungen sowie Untersuchungen zur Schlagempfindlichkeit mittels der Fallhammermethode. Ph.D. Thesis, Ludwig-Maximilians-Universität, München, Germany.*
[9] A.Yu. Klyushin, T.C.R. Rocha, M. Hävecker, A. Knop-Gericke, R. Schlögl, *PCCP* 16 (2014) 7881.

II-OP19

Ceria Supported Gold Catalysts: Mechanistic Studies of CO Oxidation Using a Combined Operando Approach

Schilling C. M.[1,2,3], Lohrenscheit M.[1,2,3], Hess C.[1,2,3*]

1 - Technische Universität Darmstadt, Darmstadt, Germany
2 - Eduard Zintl-Institut für Anorganische und Physikalische Chemie, Darmstadt, Germany

* schilling@chemie.tu-darmstadt.de

Keywords: operando, gold, ceria, Raman, IR

1 Introduction

Gold catalysis is a research area of growing interest. Ceria supported gold catalysts show a high activity and stability in low-temperature CO oxidation. However, the influence of active support materials such as ceria on the catalytic properties of gold nanoparticles is not well understood. In this context, we prepare gold loaded ceria catalysts and employ *operando* spectroscopy to study the room temperature oxidation of CO. In particular, combined operando Raman and UV/Vis spectroscopy, *quasi in situ* X-ray photoelectron spectroscopy (XPS) as well as *operando* diffuse reflectance infrared spectroscopy (DRIFTS) are used. It will be shown that the use of complementary Raman and IR spectroscopic methods provides new insight into the mode of operation of ceria supported gold catalysts.

2 Experimental

Ceria is prepared by calcination of cerium(III) nitrate and loaded with gold via deposition precipitation. Gold loadings of 0,1, 0,5 and 1,0 wt% were deposited on the calcined (ca) and a commercial (co) ceria support (Fluka). The Au/CeO_2 catalysts are investigated in the *multi in situ*-setup.[1,2] Which allows for simultaneous Raman and UV/Vis spectroscopy under *operando* conditions plus *quasi in situ* X-ray photoelectron spectroscopy without air exposure. The activity is monitored by gas phase infrared spectroscopy. Additionally, *operando* DRIFTS measurements were performed at comparable conditions and at equal CO conversion as in the *multi in situ*-setup. The total flow rate was 100 ml/min. 25 V% O_2 in Ar for oxidative conditions, 5 V% CO and 25 V% O_2 in Ar for reaction conditions and 5 V% CO in Ar for reductive conditions. The experiments were performed at room temperature. Samples are studied as pellets and powders.

3 Results and discussion

UV-Vis data of synthesized Au/CeO_2 catalysts show a broad band in the visible region around 600 nm irrespective of the used ceria support material. This band is attributed to a reduction of ceria indicating the presence oxygen defects in ceria support. While ceria is reduced upon gold loading gold is partially oxidized. XP spectra reveal that the majority of gold particles is in a metallic state (Au^0) and only about 6% in an oxidized state (Au^+).
Fig. 1 shows the CO stretching region of the Raman spectra of 0,5 wt% Au/CeO_2 (ca) under oxidative, reaction and reductive conditions. If CO is provided in the gas phase Raman spectra indicate a band of gas phase CO at 2142 cm^{-1} as well as bands of adsorbed CO (2113 cm^{-1} and 2130 cm^{-1}), whereas the intensities of the latter bands decrease under reaction conditions. The redshift of the two bands compared to gas phase CO indicates a softening of the C-O bond upon adsorption. So far these CO-related bands have only been observed in IR experiments and have been assigned to CO adsorbed on gold; the band at 2113 cm^{-1} is also confirmed by our own IR data. Therefore, we conclude that CO is adsorbed at net electron donor gold particles. This is

consistent with partially oxidised gold particles indicated by XPS. Interestingly, when switching from oxidative to reaction conditions *operando* Raman spectra also reveal distinct changes regarding ceria phonons and peroxide species indicating the influence of the ceria support on catalysis.

Operando DRIFT spectra are depicted in Fig. 2. As indicated by the solid and dashed lines adsorbed carbonate and formate are observed, respectively. The carbonate region of a sample with 0,5 wt% gold loading on commercial ceria (co) exhibits a rapid build-up of bidendate carbonate species (solid lines, 1300 cm^{-1} and 1575 cm^{-1}) under reaction conditions, which transform into bidendate formate species (dashed lines, 1370 cm^{-1} and 1595 cm^{-1}) under reductive conditions.[3] Monodendate carbonate species (solid lines, 1395 cm^{-1} and 1465 cm^{-1}) remained unchanged upon treatment for 1h under oxidative conditions and switching to reaction conditions.

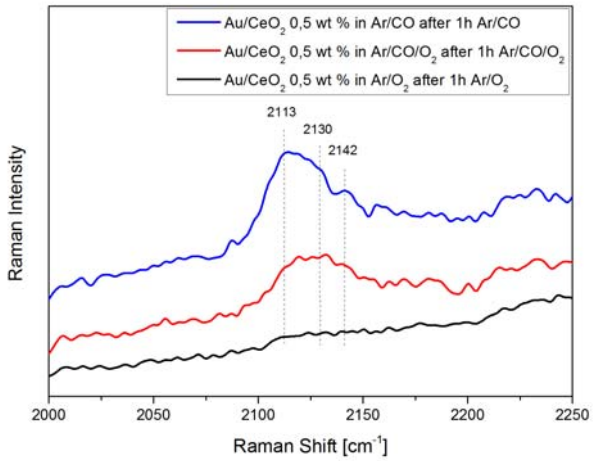

Fig. 1. *Operando* Raman spectra of 0,5 wt% Au/CeO_2 (ca) under oxidative, reaction and reductive conditions showing adsorbed CO at 2113 and 2130 cm^{-1}.

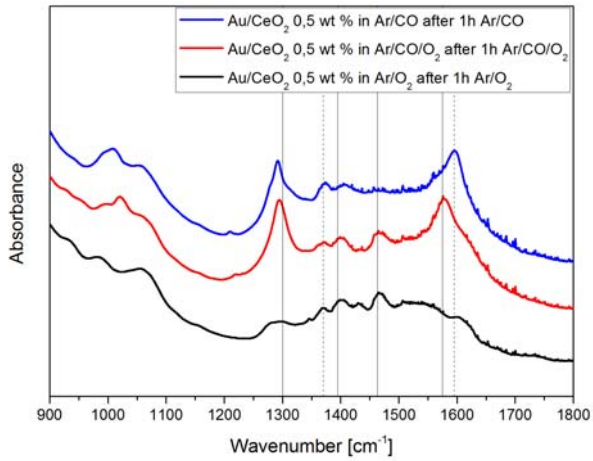

Fig. 2. *Operando* DRIFT spectra of 0,5 wt% Au/CeO_2 (co) showing a build-up of bidendate carbonate (solid) during reaction and formate (dashed) in

4 Conclusions and outlook

Operando Raman and IR data demonstrate the potential of a complementary vibrational spectroscopic approach to elucidate the mode of operation of Au/CeO_2 catalysts in CO oxidation. Depending on the gas environment (oxidative, reaction, reductive) a distinct spectral signature of adsorbed CO, carbonate, formate, hydroxyl and peroxide species as well as ceria phonons is observed allowing for new insight regarding the presence of reaction intermediates and the role of the support.

The presented combined *operando* spectroscopic approach will also be a promising strategy to elucidate the catalytic mechanism of other oxidation reaction over supported gold loaded ceria catalysts such as preferential oxidation of CO or selective oxidation reaction of organic compounds.

Acknowledgements

The authors thank Marcel Heber for his contributions and the Merck'sche Gesellschaft für Kunst und Wissenschaft e.V. for providing a research fellowship for C. Schilling.

References

[1] C. T. Nottbohm, C. Hess, *Catalysis Communications 22*, (2012) 39.
[2] C. Hess, *Topics in Catalysis 56*, (2013) 1593.
[3] R. Leppelt, B. Schumacher, V. Plzak, M. Kinne, R. J. Behm, *Journal of Catalysis 244*, (2006) 137.

II-OP20

Reactivity of Oxygen in Methanol Partial Oxidation over Au(111) Model Catalyst Surface

Vovk E.I.[1,2], Karatok M.[2], Shah S.A.A.[2], Turksoy A.[2], Bukhtiyarov V.I.[1], Ozensoy E.[3*]

1 - Boreskov Institute of Catalysis SB RAS, Novosibirsk, Russia
2 - Bilkent University, Chemistry Department, Ankara, Turkey
3 - Bilkent University, Department of Chemistry, Bilkent, Turkey

* ozensoy@fen.bilkent.edu.tr

Keywords: oxygen, gold, gold, oxide, subsurface, oxygen, methanol partial oxidation

1 Introduction

Gold is very active and selective in various partial oxidation processes and oxidative coupling reactions [1,2]. One of the crucial requirements for the selective oxidation reactions on gold is the adsorbed atomic oxygen. Atomic oxygen on gold surfaces can be prepared by various methods including ozone decomposition. Activity of the oxygen on the gold surface strongly depends on the temperature. In this contribution, we investigate the atomic oxygen overlayers on the Au(111) model catalyst surface and their reaction with methanol in an attempt to elucidate the nature of the different oxygen species and their dissimilar activities.

2 Experimental

All experiments were performed in a multifunctional ultra-high vacuum chamber equipped with Temperature Programmed Desorption (TPD) /Temperature Programmed Reaction Spectroscopy (TPRS), X-ray Photoelectron Spectroscopy (XPS), Low Energy Electron Diffraction (LEED) and Infrared Reflection Absorption Spectroscopy (IRAS) techniques. Atomic oxygen layers on the Au(111) surface were prepared by ozone exposure onto the clean gold surface.

3 Results and discussion

We have found that adsorbed oxygen layers prepared at various temperatures reveal drastically different reactivities towards methanol. Figure 1 presents the TPRS profiles recorded after ozone exposure onto the clean Au(111) surface at 460 K (Fig. 1a) or 140 K (Fig. 1b) followed by subsequent methanol adsorption at 140 K. The peaks corresponding to the m/z = 31 and 32 channels at ~ 200 K are associated with molecular desorption of unreacted methanol, which is known to desorb from the clean gold surface non-dissociatively (i.e. molecularly). The unreacted oxygen desorbs recombinatively (m/z = 32) at ~ 500 K. The oxygen prepared at 460 K and methanol desorb separately, where almost no (or extremely limited) interaction is detected, as indicated by the insignificant CO_2 (m/z = 44) production (Fig. 1a). The oxygen layer prepared at 140 K interacts with methanol with complete oxygen utilization, and unreacted oxygen is not detected (Fig. 1b). In this latter case, methanol is partially oxidized producing CO_2 (m/z = 44) desorbing at 300 K as well as methyl formate (m/z = 60) due to the oxidative coupling reaction. At higher oxygen coverages, formaldehyde can be also detected as an additional partial oxidation product.

In order to understand the nature of the oxygen species, we have performed TPD experiments of adsorbed oxygen prepared at various temperatures. The oxygen overlayers prepared at 460 K demonstrate zero-order desorption kinetics without an apparent saturation. Zero-order desorption behavior is interpreted by the formation of subsurface oxygen via diffusion/solvation. The presence of the bulk gold oxide (which can also explain zero-order kinetics) was not confirmed in XPS measurements. The formation of subsurface oxygen

explains deactivation of oxygen on the gold surface with increasing temperature (Fig. 2).

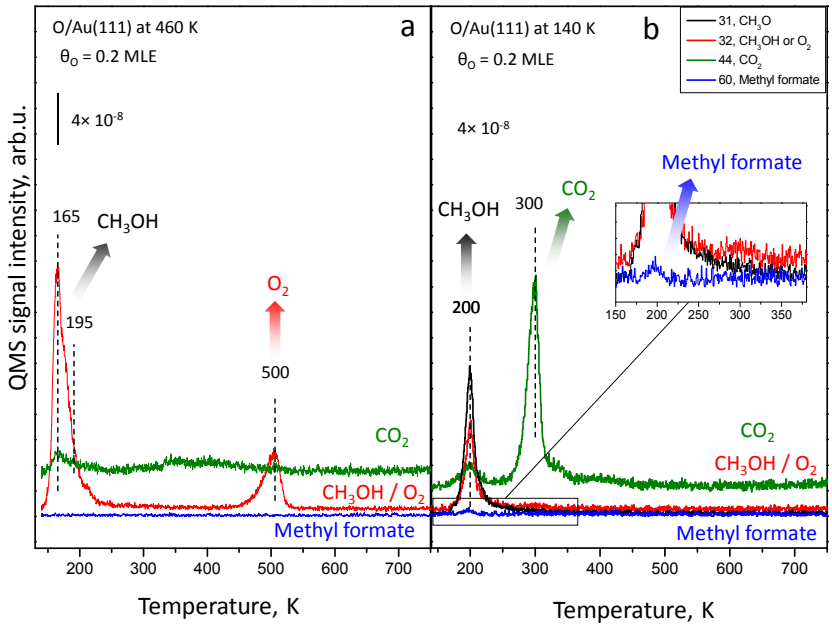

Fig. 1. TPRS profiles obtained after exposure of Au(111) to ozone at 460 K (a) or 140 K (b), followed by methanol exposure at 140 K.

4 Conclusions

In the current contribution, we have investigated the oxygen overlayers prepared at different temperatures on Au(111) model catalyst surface and their different reactivities in methanol partial oxidation. Our findings suggest that the reactivity of oxygen is closely linked to the presence/absence of oxygen diffusion into the subsurface of the gold catalyst as summarized in Fig. 2.

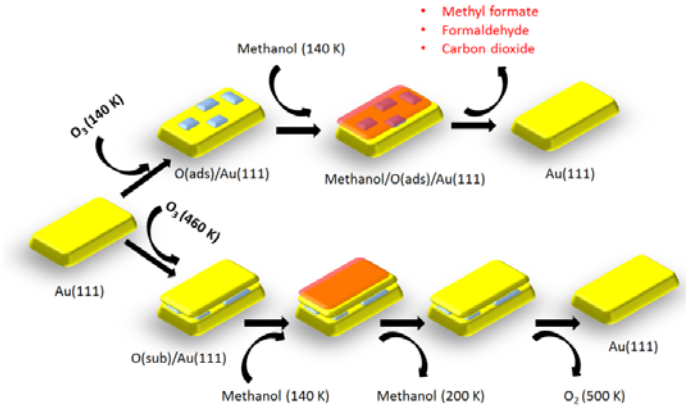

Fig. 2. Methanol interaction with oxygen layers prepared at 140 K vs. 460 K.

Acknowledgements

Authors acknowledge financial support from the Scientific and Technical Research Council of Turkey (TUBITAK) (Project Code: 112T589). E.I. Vovk acknowledges the TUBITAK support of visiting scientist program 2221.

References

[1] B. Xu, R.J. Madix, C.M. Friend, *Acc. Chem. Res.* 47 (2014) 761-772.
[2] X. Liu, L. He, Y. Liu, Y. Cao, *Acc. Chem. Res.* 47 (2014) 793-804.

II-OP21

Cu-SAPO-34 Synthesis and In Situ Characterization. Insights into DeNOx-SCR Mechanism

Cortés-Reyes M., Díaz-Rey M.R., Herrera M.C., Larrubia M.A., Alemany L.J.*

Departamento de Ingeniería Química, Facultad de Ciencias, Campus de Teatinos, Universidad de Málaga, Málaga, Spain

* luijo@uma.es

Keywords: SCR, Cu-SAPO-34, DeNOx

1 Introduction

Selective catalytic reduction (SCR) is one of the most used technologies for the NO_x abatement in stationary sources and heavy-duty vehicles. Recently, it is proposed as an advanced technology to reduce NO_x from lean-burn engines vehicles. For this purpose, copper exchanged zeolites have been reported as an excellent choice, showing suitable acidity, for ammonia adsorption, and a metal, which promotes the activation of NO_x and, subsequent H_2O and N_2 formation [1]. Due to the low hydrothermal stability of large pore zeolites, such as ZSM5 or BETA, small pores materials with a chabazite structure are being studied [2]. It is important to know the species that are involved in the process as well as its relation with the synthesis process. The aim of this contribution is to study the influence of the preparation of the Cu-SAPO-34 in its properties and its performance and possible species involved in the SCR mechanism.

2 Experimental

A series of silicoaluminophosphates was synthesized by ultrasonic assisted hydrothermal method. The molar gel composition was 2 DEA: 0.6 SiO_2:1 Al_2O_3: (0.2-0.8) P_2O_5:50 H_2O. The Cu-loading was modified from 0 to 4 wt% and was incorporated during the synthesis [3]. Materials were characterized by DRX, XPS, N_2 adsorption-desorption, TEM, SEM and Raman. NH_3 adsorption was analyzed by in situ FTIR to evaluate the acid-strength and acid-sites distribution; as well as isothermal experiments of NH_3 adsorption were carried out in a TG-MSruns. NO adsorption was studied by FTIR observing the species involved in the process. The behavior in the SCR process was analyzed in stationary experiments at different temperatures.

3 Results and discussion

From all the synthesized materials, in Table 1 the characteristics obtained by low temperature N_2 adsorption-desorption and XPS of two phosphorus content (45 and 17wt%) in the acidic form, identified as SAPO-34+1 and SAPO-34+2, respectively, and with 2wt% of copper are shown. The structural properties are modified with the gel composition. In the same synthesis conditions of temperature and time, increasing the amount of phosphorus, the zeolitic materials show higher cristallinity, an increment in the relation between metaphosphate (PO_3^-) and P_2O_5 and a stabilization of copper in oxidation state +1, as well as the formation of copper oxides. The copper incorporation increases the total pore volume since a strong cristallinity loss takes place. The samples with higher cristallinity and more metaphosphate amount show greater ammonia retention net capacity, adsorbing more NH_3 in Brönsted acid centers.

Table 1. Textural properties and copper oxidation states relation

	S_{BET} ($m^2 \cdot g^{-1}$)	V_p ($cm^3 \cdot g^{-1}$)	Cu(I)/ Cu(II)
SAPO-34+1	559	0.29	-
SAPO-34+2	439	0.59	-
2Cu-SAPO+1	556	0.43	5
2Cu-SAPO+2	456	0.63	1.5

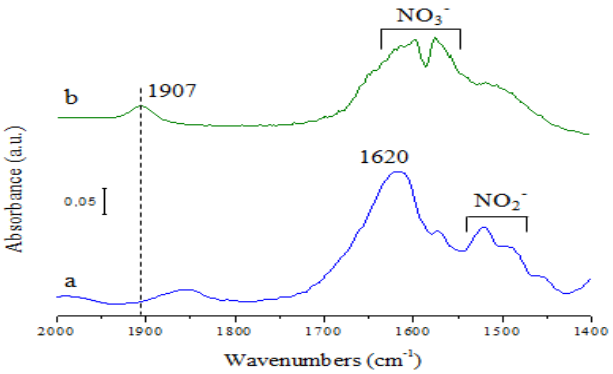

Fig. 1. FT-IR spectra of NO adsorbed (16torr) onto the samples after outgassing at 100ºC for a) 2Cu-SAPO+1 and b) 2Cu-SAPO+2

In Figure 1, the species of NO adsorbed onto the Cu-containing catalysts after outgassing at 100ºC are shown. At low Cu(I)/Cu(II) ratio, mononitrosyl-Cu^{+2} species are detected at 1907cm^{-1}, which are the active sites to the selective catalytic reduction of NO_x with NH_3, being selective to nitrogen. The predominance of copper in oxidation state +1, favours the oxidation of ammonia, decreasing drastically the NO_x conversion at temperatures above 300ºC. Nevertheless, in these conditions, the selectivity to N_2 is almost 100%. In the case of 2Cu-SAPO+2 bridged bidentate and bridged monodentate nitrate are observed; whereas 2Cu-SAPO+1 adsorb a higher amount of NO as nitrates (c.a.1620 cm^{-1}) as well as nitrite and monodentate nitrite in the framework. For that reason, the N_2O production between 250 and 350ºC is increased due to the ammonia nitrates decomposition.

4 Conclusions

The synthesis and the gel composition influence the textural properties as well as the copper oxidation states ratio in zeolitic materials. The variation of the synthesis parameters yields a material with high cristallinity, constant ammonia retention capacity in the operation window of SCR technology and a suitable Cu(I)/Cu(II) ratio to ensure the efficient selective catalytic reduction of NO_x with NH_3 and avoid co-side products.

Acknowledgements

MCR acknowledges the Spanish Ministry of Education, Culture and Sport for a FPU grant.

References

[1] B. Pereda-Ayo, U. De La Torre, M.J. Illán-Gómez, A. Bueno-López, J.R. González-Velasco, *App. Catalysis B: Environmental*. 147 (2014) 420.
[2] J. Xue, X. Wang, G. Qi, J. Wang, M. Shen, W. Li, *Journal of Catalysis*. 297 (2013) 56.
[3] M. Cortés-Reyes, M.R. Díaz-Rey, M.C. Herrera, M.A. Larrubia, L.J. Alemany (submitted)

II-OP22

Structure-Reactivity Relationships in Low-Temperature NH_3-SCR of NO over Highly Effective $V_2O_5/Ce_xZr_{1-x}O_2$ Catalysts

Vuong T.H., Radnik J., Armbruster U., Brückner A.*

Leibniz Institute for Catalysis at the University of Rostock, Rostock, Germany

* huyen.vuong@catalysis.de

Keywords: $V_2O_5/Ce_xZr_{1-x}O_2$ catalysts, low-temperature, NH3-SCR, *in situ*, UV/Vis, *in situ*, EPR

1 Introduction

The selective catalytic reduction (SCR) of nitrogen oxides by ammonia is one of the most important processes for NO_x abatement from exhaust gases [1]. While V_2O_5-WO_3/TiO_2 catalysts are industrially used in power plants, noble metals such as Pt supported on CeO_2 are part of 3-way catalysts for mobile engines. The operation of both types of catalysts is limited to high and narrow temperature windows of 400-500°C. A promising way to develop inexpensive and stable catalysts for NO_x abatement at low temperature (needed, e. g., for diesel and lean-burn engines) may be to support V_2O_5 on CeO_2, due to the high oxygen mobility and interesting redox properties of the CeO_2 support. However only a few studies exist so far which show almost total NO conversion on 5 % V_2O_5/CeO_2 at about 240 °C and low gas-hourly space velocities (GHSV) of only 12000 h^{-1} [2].

It is the aim of this study to explore the potential of catalysts containing V_2O_5 dispersed on mixed CeO_2/ZrO_2 supports for the SCR of NO by NH_3 at low temperature (100-300°C). We expect that partial replacement of Ce^{4+} by smaller Zr^{4+} ions could promote defect formation and oxygen transport within the catalyst lattice [3], which could enhance the catalytic performance. Various techniques such as XRD, XPS, EPR and UV-Vis-DRS were used, partly *in situ* under catalytic reaction conditions, to elucidate relations between structural properties and catalytic performance.

2 Experimental

Different $Ce_xZr_{1-x}O_2$ supports (x = 1, 0.9, 0.8, 0.7, 0.5, 0.3 and 0) were prepared by a citrate method, impregnated with NH_4VO_3 and calcined at 400°C to reach V_2O_5 loadings of 5 %. The SCR activity measurements of the $V_2O_5/Ce_xZr_{1-x}O_2$ catalysts were performed in a fixed-bed quartz continuous flow reactor operating at atmospheric pressure, in the temperature range from 100°C to 300°C, using reactant gas composition of 1000 ppm NO, 1000ppm NH_3, 5 vol% O_2, balance He, and a total flow rate of 100 mL/min. *In situ* UV-Vis DRS were recorded at 200 °C using the same gas composition with a flow rate of 25 mL/min after 1h pretreatment at 275 °C in air. Kinetic studies of reduction and reoxidation were performed by *in situ*-UV-vis-DRS monitoring the absorbance at 700 nm in the range of d-d-transitions of reduced V-species.

3 Results and discussion

XRD powder patterns of all catalysts indicate that ZrO_2 was incorporated into the CeO_2 lattice to form a homogeneous solid solution while maintaining the fluorite structure. No reflections of crystalline V_2O_5 were observed, pointing to high dispersion. XPS results suggest a higher surface V concentration on the mixed oxide supports compared to pure CeO_2 and ZrO_2. This may be due to the higher BET surface areas of the mixed oxides. EPR and XPS results revealed that the 5% V_2O_5/ZrO_2 catalyst contains the highest amount of V^{4+}, yet enriched in the

bulk, while the surface contains exclusively few highly dispersed V^{5+} species. In contrast, the catalyst 5 % V_2O_5/CeO_2 contains exclusively V^{4+}, while on the mixed $Ce_xZr_{1-x}O_2$ support, both V^{5+} and V^{4+} are present. *In situ* UV-Vis-DRS spectra indicate that 5% V_2O_5/ZrO_2 contains a significant amount of tetrahedral VO_4 sites while octahedrally coordinated V is dominating on CeO_2 and the mixed supports.

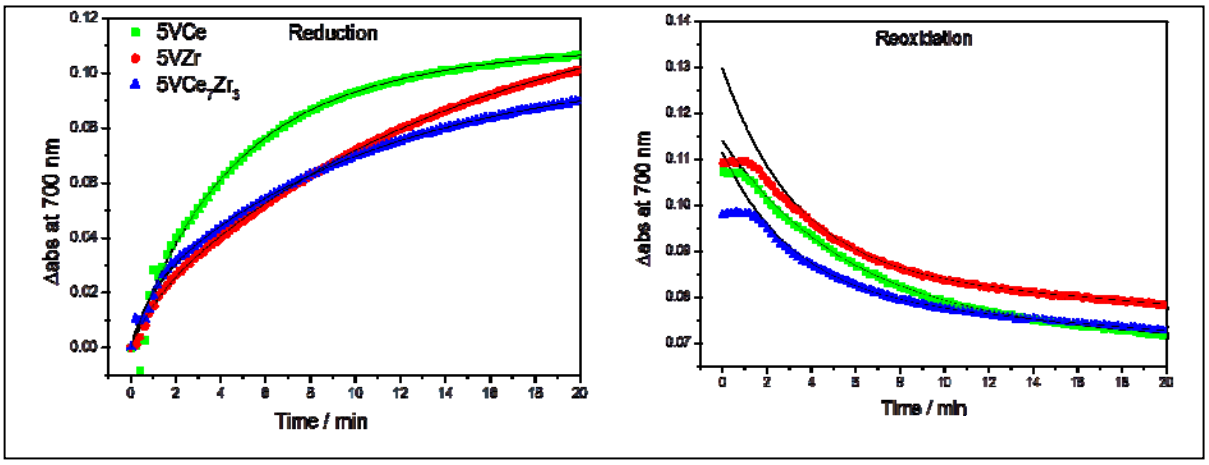

Fig. 1. Difference in absorbance at 700 nm during reduction of oxidized VO_x species by 0,1% NH_3/He and during reoxidation of reduced VO_x species by 5% O_2/He at 200 °C. Experimental data – colored filled symbols, black solid line – simulated curve according 2-sites model.

Fitting of the time-dependent redox behavior of the V sites by a first-order rate law revealed the presence of two types of oxidized and reduced VO_x species (probably on the surface and in the bulk) in all these catalysts (Fig. 1). Maximum rate constants for both reduction and reoxidation were obtained for the highly active 5 % $V_2O_5/Ce_{0.7}Zr_{0.3}O_2$ (compared to the less active catalysts supported on pure CeO_2 and ZrO_2). This suggests that the mixed oxide support might promote oxygen mobility and improve the redox behavior of the supported VO_x species which in turn raises the catalytic performance. In situ-EPR studies of $VO_x/Ce_xZr_{1-x}O_2$ under NH_3-SCR feed indicate the presence of V^{4+} in states of low activity (150°C) while exclusively V^{5+} is present in states of high activity (250°C).

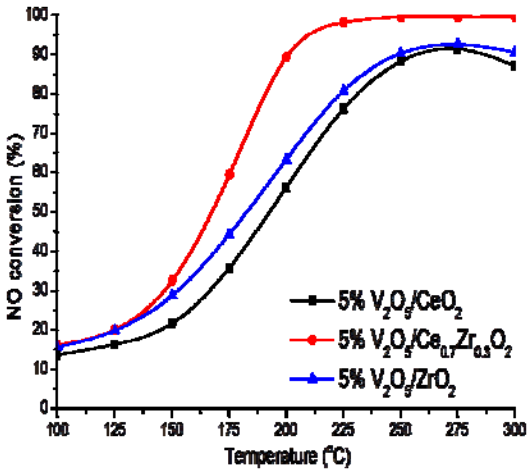

Fig. 2. Catalytic behaviour of 5% $V_2O_5/Ce_xZr_{1-x}O_2$

Highest catalytic performance was measured with catalyst 5 % $V_2O_5/ Ce_{0.7}Zr_{0.3}O_2$ which, compared to literature values [2] reached full conversion of NO at a significantly lower temperature (200 °C compared to 240 °C) and at a 5-fold GHSV of 60000 h^{-1} (compared to 12000 h^{-1}) (Fig. 2). These are the best results ever achieved with this catalytic system.

References

[1] H. Bosch, F.J.J.G. Janssen, *Catal. Today* (1988) 2369.
[2] C. Li, Q.Li, P. Lu, H. Cui, G. Zeng, *Front. Environ. Sci. Engin*. 6 (2012) 156.
[3] B. M. Reddy, P. Bharali, P. Saikia, S.-E. Park, M. W. E. Van Den Berg, M. Muhler, W. Grünert, *J. Phys. Chem. C* 112 (2008) 11729.

II-OP23

Kinetics Study of Oxychlorination Process by Combined *in-situ* Mass- and Spatial-time Resolved UV-Visible Spectrophotometry

Rout K.R.[1], Chen D.[1*], Baido M.F.[1], Fenes E.[1], Fuglerud T.[2]

1 - NTNU, Trondheim, Norway
2 - INEOS, Norway

* ranjan8109@gmail.com

Keywords: $CuCl_2/\gamma\text{-}Al_2O_3$ catalyst, UV/Vis, spectroscopy, *in situ* spectroscopy, oxychlorination, process

1 Introduction

Oxychlorination of ethylene is the most important route to produce 1, 2-dichloroethane (EDC), which is a key step for poly-vinyl chloride (PVC) [1]. In commercial ethylene oxychlorination reactors, gaseous ethylene, HCl and air react with $CuCl_2/\gamma\text{-}Al_2O_3$ catalyst at a temperature range of 217 ^{0}C-257 ^{0}C and a pressure 5-6 atm.

The $CuCl_2/\gamma\text{-}Al_2O_3$ catalyst is effective in the oxychlorination of ethylene because $CuCl_2$ can catalyze the conversion of HCl to chlorine. In the literature [2], it has been shown that by feeding the three reactants separately, the oxychlorination reaction is catalyzed by a highly dispersed $CuCl_2$ phase and thereby follows a three step redox mechanism:

Step 1. Reduction of $CuCl_2$ to CuCl. (1)
Step 2. Oxidation of CuCl to form an oxy-chloride. (2)
Step 3. Hydrochlorination of the oxy-chloride using HCl to form $CuCl_2$ and H_2O. (3)

Despite more than 30 years of great research and commercial application of oxychlorination reaction, the reaction mechanism is not fully understood [1]. However, most of the work has been performed in the past to study qualitatively the oxidation state of the $CuCl_2$ catalyst during the reaction, which is of great importance for catalyst activity and stability. It is generally agreed that the oxychlorination involves a redox process in which copper cycles between Cu^I- and Cu^{II} states [1]. One of the main challenges of this process is that the Cu^I deposits on the surface of the catalyst during the reaction thereby caused the aggregation, and loss of Cu active materials due to its low melting temperature and volatility. Hence, a spatial-time prediction of oxidation state of Cu in industrial reactors is of great importance, which requires detailed kinetics of the both reaction including catalyst active component involved in elementary reaction steps in the redox cycle.

In-situ spectroscopy is an approach to monitor online the physicochemical phenomena of the catalyst material in a reactor [3]. The results from such in-situ study at industrial relevant conditions provide detailed insight into the working principles of the catalytic material. So that it would then be possible to improve the existing catalyst formulations or design completely new catalysts, which are more active and/or selective. In this respect, it is advantageous to look on catalytic systems from different perspectives by making use of multiple characterization techniques. However, to the best of our knowledge, a spatially-time resolved systematic in-situ quantitative kinetic study on the Cu^{II}/ Cu^I of the $CuCl_2/\gamma\text{-}Al_2O_3$ catalyst in a fixed-bed reactor is still missing.

2 Experimental/methodology

A strategy of combined transient and steady-state kinetic study was employed. The transient kinetic study was performed for individual reaction steps such as the reduction- (Eq. 1), oxidation- (Eq. 2) and hydrochlorination (Eq. 3) in the catalytic cycle of oxychlorination

process. The UV-Vis spectroscopic technique in the reactor focuses on the same spot of a catalyst in a reactor under true reaction conditions and is capable of delivering sub second time resolution. However, in the overall reaction study, the UV-Vis focuses on the same spot of catalysts in the reactor first until the process reached steady-state to get the time resolved kinetic data. After that the whole catalyst bed of the reactor is scanned by UV-Vis spectroscopy to measure the active Cu^{II} along the reactor axis.

3 Results and discussion

The Cl in the catalysts gradually is reacted with ethylene to form EDC, and the amount of Cl in the catalysts decreases with time, resulted in a decrease in the reaction rate for the chlorination of ethylene cycle (Eq. 1). The selectivity to EDC is close to 100%. Based on the mass balance according to the equation (1), the uptake of removable Cl with time can be. From it, the amount of the Cu^{II} active sites of the catalyst reduced to Cu^{I} upon exposure to ethylene could be estimated. The change of Cu state from Cu^{II} to Cu^{I} has been studied by the use of UV-Vis spectroscopy, which changes in the relative conversion of ethylene or relative changes in amount of Cu^{II}. The oxidation step with oxygen transforms Cu^{I} to Cu^{II} in the form of Cu_2OCl_2. The time required for a complete reaction is much longer in the oxidation step than in the reduction step, at the identical reactant pressure. It suggests that the rate of the oxidation step (step 2, Eq. 2) is lower than the one of the reduction step (step 1, Eq. 1). It was found that the kinetics of hydro-chlorination (3) is much fast than other two steps, which is not relevant step for the kinetics of the total catalytic cycle. The steady-state experiments were performed with co-feeding of ethylene, oxygen and HCl for two different reaction conditions (condition I; one with excess of oxygen and condition II; with stoichiometric amounts). It has been found that near to the inlet of the reactor, Cu^{II} has been reduced to Cu^{I} and Cu^{I} dominates in the catalyst bed. However, near to the outlet of the reactor the reduction of Cu^{II} to Cu^{I} was not complete. At the reaction condition II, where the stoichiometric amounts of reactants were fed, the reactor was scanned after reaching steady-state (at 46 mins). It is found that Cu^{I} dominates in the whole reactor bed in the steady-state condition and they are much lower than the values at reaction condition, i.e., excess oxygen, due to the lower oxygen concentration and thus the lower oxidation rate. As a result, the conversion is higher at the higher oxygen concentration (condition I) compared to the one at the stoichiometric composition (condition II). The combined results of conversions in gas phase and Cu^{II} concentration at the catalyst surfaces at the steady-state conditions further confirmed the dynamic nature of the active sites.

4 Conclusion

We expect that the developed methodology will be generally useful for developing catalyst diagnostics strategies, in cases where the catalyst undergoes oxidation state changes, in particular in redox reactions. Therefore, the combined transient and steady-state kinetic study by the use of UV/Vis- and mass spectroscopy is a powerful tool for kinetic study of the reactions involving redox cycles. It will provide not only the kinetics of the main reactions, but also oxidation state changes of the catalyst active component.

Acknowledgements

This work is part of the inGAP Center for Research-based Innovation, which receives financial support from the Research Council of Norway.

References

[1] Lamberti C, P.G., Bordiga S, Berlier G, D'Acapito F, and Z. A, Angew Chem Int Ed 2000. 39:2138
[2] Baiker A, H.W., J. Catal., 1983. 84
[3] Bennici SM, V.B., Alexander Nijhuis T, Weckhuysen BM, Angew. Chem Int Ed, 2007. 119

II-OP24

Design and Preparation of Zeolitic Catalysts for Ethylbenzene via Vapour-Phase Benzene Alkylation

Yang W.M.*, Wang Z.D., Zhang B., Sun H.M., Huan M.Y., Xue M.W.

Sinopec Shanghai Research Institute of Petrochemical Technology, Shanghai, China

* yangwm.sshy@sinopec.com

Keywords: ethylbenzene, zeolite catalyst, alkylation, bio-ethanol, FCC, off-gas

1 Introduction

As an important bulk chemical, ethylbenzene is mainly manufactured through catalytic benzene alkylation processes, which in turn is used for the production of styrene, and then to produce polystyrene, ABS resin, SAN resin and some other products [1]. For the manufacture of ethylbenzene, liquid phase $AlCl_3$-based alkylation process was first introduced in 1950s, and then zeolite-based alkylation processes, both vapor phase and liquid phase, were developed to solve the corrosion problem of $AlCl_3$ process [2]. However, due to the oil shortage and requirements for sustainable developments, it is of great desire to develop new catalytic processes with raw materials diversity. For ethylbenzene manufacture, the challenge is how to design and prepare different catalysts suitable for different ethylation agents and the processes thereof. Herein, pure ethylene, bio-ethanol and FCC (Fluid Catalytic Cracking) off-gas were used in vapor phase benzene alkylation processes. According to the processes characteristics, three different catalysts using ZSM-5 zeolite as the major active component were designed, prepared and applied.

2 Experimental/methodology

ZSM-5 zeolites were synthesized using silica sol (40 wt %) and $Al_2(SO_4)_3$•$18H_2O$ as silicon and aluminum sources, respectively. After hydrothermal crystallization, the products were filtered, washed with deionized water and dried overnight. The obtained ZSM-5 zeolites were extruded into small pellets with 2 mm in diameter and 10mm in length. Then, calcination and ion-exchange with 1 M NH_4NO_3 solution were carried out with combinations of modification treatments with steam and/or phosphoric acid solution. Vapor phase benzene alkylation experiments were carried out in a fixed bed reactor.

3 Results and discussion

Figure 1 illustrates different vapour phase benzene alkylation processes using different ZSM-5 zeolite catalysts of nano-ZSM-5, Phosphorous modified ZSM-5 and oriented ZSM-5.

For benzene alkylation process using pure ethylene, the key point is to inhibit coke formation and reduce the main byproduct of xylene, so that catalyst with high diffusion property was needed. Nano-sized ZSM-5 zeolite was chosen as the active component, and a steam treatment procedure was needed to make a good alkylation catalyst [3].

Ethylene is usually produced from the catalytic thermo cracking of naphtha originating from crude oil. The rise of price of crude oil thus drives up the price of ethylene. Meanwhile, due to the rapid development of biochemical engineering technology, the cost for obtaining ethanol has greatly decreased. For instance, ethanol can be produced through fermentation of crops, such as maize and cassava, and crop straw. Thus, catalytic process that uses ethanol instead of ethylene for ethylbenzene manufacture has certain competitive advantages. However, either water in bio-ethanol raw material, or that produced in the alkylation reaction would cause the loss of active Al sites, result in bad performance of the catalyst. So that combination

treatments with steam and phosphoric acid solution were introduced to insure the catalyst possess a long lifetime, high selectivity and capability of converting a substantial amount of ethanol to minimize the generation of impurities such as xylene [4].

FCC off-gas contains 10-30% ethylene, which can be used as ethylene source to produce ethylbenzene. However, separation process of ethylene from FCC off-gas would increase the overall investment and running cost, and the impurities, like propylene, would cause side reactions and catalyst deactivation when FCC off-gas is directly fed. In order to meet commercial requirements, ZSM-5 zeolite with b-orientation was synthesized. Moreover, the shaped catalyst possessed abundant macro and mesopores, and combinations of hydrothermal treatment and acid leaching modification were carried out to remove the Lewis acid site to inhibit side reactions. Over the as prepared catalyst, reactants could easily diffuse through the macropores and mesopores to reach the active sites located in micropores. The catalyst showed a stable reaction level in both ethylene conversion and selectivity, while the industrial runtime went beyond 12 months [5,6]. These enhanced catalytic performances can be attributed to the decreased mass transfer limitation in the straight channels along the b-axis in zeolite and further combined modification. Since the first commercialization of this catalyst in 2009, the overall ethylbenzene capacity in 2013 was about 700 kt, and it will reach 1.3 Mt in 2015.

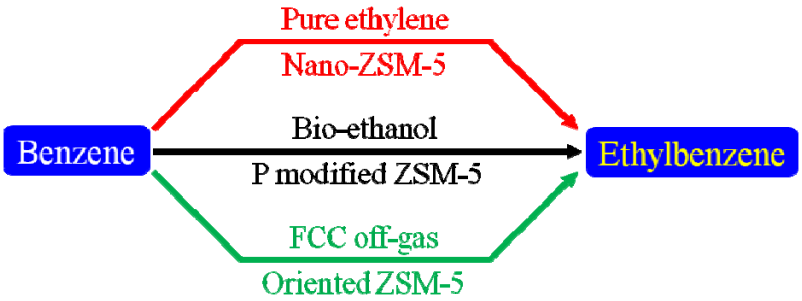

Fig. 1. SRIPT's ethylbenzene manufacture processes using different raw materials and catalysts.

4 Conclusions

Three different ZSM-5 zeolite based catalysts were designed, prepared and commercialized in vapour phase benzene alkylation processes for ethylbenzene manufacture using ethylene, bio-ethanol and FCC off-gas as raw materials by Sinopec Shanghai Research Institute of Petrochemical Technology. The key point to obtain ideal catalysts is the combination of ZSM-5 zeolites and the post-treatment procedures. New catalysts and processes for industrial and fine chemicals production are under investigation and will be commercialized in the coming future.

References

[1] J. Cejka, B. Wichterlova, *Catal. Rev.* 44 (2002) 375.
[2] T. F. Degnan Jr., C. M. Smith, C. R. Venkat, *Appl. Catal. A: Gen.* 221 (2001) 283.
[3] W. Yang, H. Sun, Q. Chen, *Adv. Fine Petrochem.* 3 (2002) 12.
[4] W. Yang, H. Sun, W. Liu, B. Zhang, Z. Shen, M. Huan, H. Zhang, *US Patent* 8519208 (2013).
[5] M. Huan, H. Sun, B. Zhang, H. Li, W. Yang, *Chem. React. Eng. Tech.* 24 (2008) 395.
[6] J. Gou, *Ind. Catal.* 22 (2014) 397.

II-OP25

Hydrotreating Catalyst Activation under Industrial Conditions

Van Haandel L., Hensen E.J.M., Weber Th.*

Inorganic Materials Chemistry, Eindhoven University of Technology, Department of Chemical Engineering and Chemistry, Eindhoven, The Netherlands

* th.weber@tue.nl

Keywords: hydrotreating, Mo S_2, activation, promoter, EXAFS

1 Introduction

Two-dimensional transition metal sulfides are chemically versatile and have a wide range of applications in catalysis, opto-electronics and batteries [1]. MoS_2 can provide a low cost alternative to Pt as hydrogen evolution catalyst and has been applied successfully for many years in oil-refining to catalytically remove sulfur from oil. In hydrodesulfurization (HDS) catalysts, the electronic properties of MoS_2 are tuned by the addition of Co/Ni, improving the intrinsic activity by about one order of magnitude. Studies on model systems, often performed under reaction conditions deviating substantially from those in industrial practice, have led to the Co-Mo-S model with Co/Ni atoms located at the edges of MoS_2 nanosheets [2]. A drawback of these model studies is that trends in model HDS reactions using thiophene or dibenzothiophene (DBT) usually do not match with those observed in industrial gas-oil HDS tests. Consequently, structure-performance relations at the lab scale are not well suited to predict performance under real HDS conditions (20-60 bar, 350-400°C, gas-oil feed).

In the present work, we follow the activation of Co-Mo HDS catalysts by *in situ* X-ray absorption spectroscopy (XAS) under conditions close to industrial practice (20 bar, 350°C, model diesel feed). We demonstrate that the temperature of the oxide-to-sulfide phase transition strongly depends on activation parameters (pressure, sulfiding agent) and the composition of the catalyst precursor. The influence of a range of organic additives with varying chelating propensity for the precursor metals on the catalytic performance in model and gas-oil HDS reactions is determined. By correlating these activity trends to the structure of the active phase, we obtain deeper insight into structure-performance relations in real gas-oil HDS.

2 Experimental/methodology

High metal loading catalyst precursors (~20 wt%), representative of commercial ones, were prepared via impregnation of γ-alumina with an aqueous solution of Co and Mo salts and various additives such as phosphoric acid (P), polyethylene glycol (PEG), citric acid (Cit) and nitrilotriacetic acid (NTA). The dried or calcined precursors were activated in a sulfur-rich feed (H_2/H_2S (10%) or H_2 and an organosulfide dissolved in n-hexadecane) at 1 or 20 bar pressure. The sulfided catalysts were characterized by XAS, X-ray photoelectron spectroscopy (XPS) and transmission electron microscopy (TEM); their performance was evaluated in thiophene, DBT and gas-oil HDS reactions. XAS experiments were performed at the Co K and Mo K edge with a homemade *in situ* cell at BM26A of the European Synchrotron Radiation Facility (ESRF, France).

3 Results and discussion

Figure 1 shows that the Co sulfide phase forms in a very short timespan (< 5 min) when Co-Mo HDS catalysts are activated under conditions similar to industry (20 bar H_2, model diesel feed). This 'ignition' is very different from the gradual sulfide phase formation, which is usually

observed under model laboratory conditions (1 bar H_2/H_2S); it emphasizes that active phase genesis should be monitored under conditions as close as possible to commercial practice [3]. The rapid phase transition can be ascribed to *in situ* generation of H_2S by the decomposition of organosulfides in the feed at elevated temperatures, where Co would already be sulfided in a conventional H_2/H_2S sulfidation procedure..

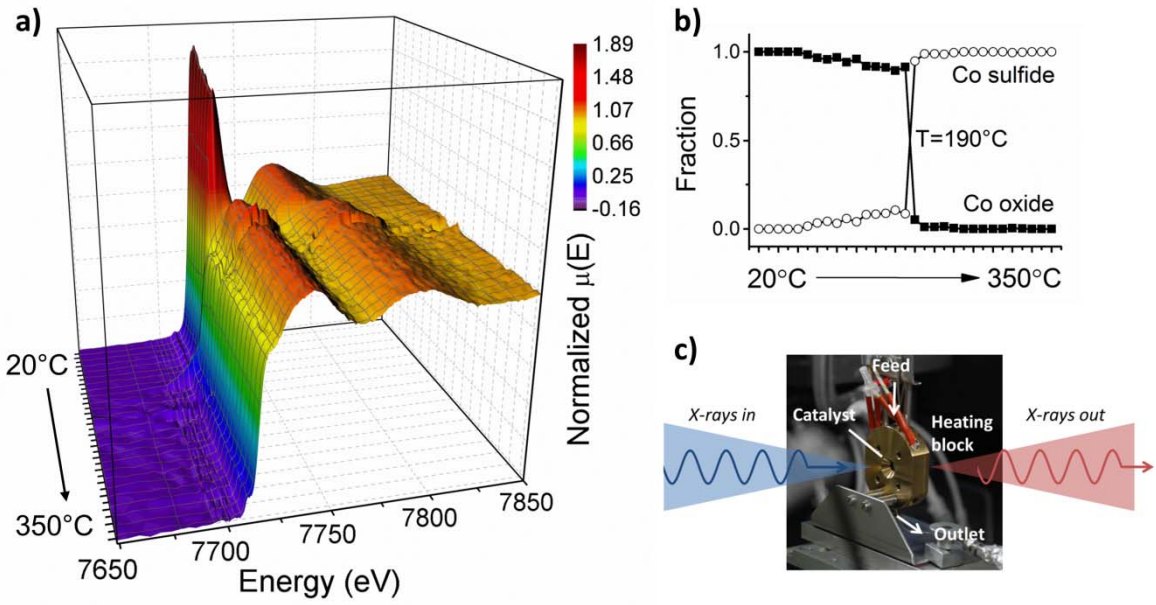

Fig. 1. a) *in situ* Co K XANES of a Co-Mo catalyst heated in a mixture of n-hexadecane/tert-nonylpolysulfide(5%) and H_2 gas (20 ml/min) at 20 bar. The time per spectrum was 5 minutes. b) composition of the catalyst as determined by linear combination fitting (LCF). c) picture of the experimental setup.

In dried and calcined catalyst precursors prepared without additives, a significant portion of the Mo remains oxidic (20-25%) and Co preferentially forms Co_9S_8, which is undesired because of its low HDS activity. Catalytic performance was strongly improved by incorporating additives in the impregnation step, which facilitated the formation of MoS_2. The use of weakly chelating additives led to the highest HDS activity in model compound reactions (DBT, thiophene), which can be ascribed to optimal Co-Mo interaction. These catalysts were found to form sulfides at temperatures as low as 50°C; this finding contradicts the general notion that delayed sulfidation of the promoter leads to catalysts with optimal Co-Mo interaction [3]. We propose that the reducibility of Mo in the precursor is the key parameter that determines the efficient incorporation of the promoter ions into the active 'Co-Mo-S' phase.

4 Conclusions

We have for the first time characterized the structure of the active phase for a suite of Co-Mo catalysts under real HDS conditions. Activation in a model diesel feed led to rapid active phase genesis , initiated by thermal decomposition of organosulfides in the feed. An optimum interaction of the promoter and the active phase was achieved for catalyst precursors prepared with weakly chelating ligands. It is proposed that the reducibility of Mo in the precursor is the key parameter that determines the efficient formation of the active 'Co-Mo-S' phase.

References

[1] M. Chhowalla et al., *Nature Chem.* 5 (2013) 263.
[2] Y. Zhu et al., *Angew. Chem. Int. Ed.* 53 (2014) 10723.
[3] R. Cattaneo et al., *J. Catal.* 191 (2000) 225.

II-OP26

Development of In Situ Techniques to Monitor Oxygen Evolving Electrocatalyst Surfaces

Pfeifer V.[1*], Arrigo R.[1,2], Velasco-Vélez J.[1,2], Haevecker M.[1,3], Stotz E.[1], Knop-Gericke A.[1], Schloegl R.[1,2]

1 - Fritz-Haber-Institut der Max-Planck-Gesellschaft, Inorganic Chemistry, Berlin, Germany
2 - Max-Planck-Institut für Chemische Energiekonversion, Heterogeneous Reactions, Mülheim a.d. Ruhr, Germany
3 - Helmholtz-Zentrum Berlin für Materialien und Energie, Catalysis for Energy, Berlin, Germany

* vpfeifer@fhi-berlin.mpg.de

Keywords: water, electrolysis, *in situ*, NAP-XPS, Iridium, Platinum, PEM

1 Introduction

Being a low carbon technology, hydrogen production from water electrolysis is especially appealing nowadays. The hydrogen generated can either be deployed for further synthesis of fuels or stored and later fed into fuel cells. For the design of suitable electrode materials for water splitting, it is crucial to understand the structural transformations of electrocatalyst surfaces upon the sluggish oxygen evolution reaction (OER). To monitor changes in the electronic structure of electrocatalysts while the OER proceeds, we have designed an electrochemical cell based on the proton exchange membrane (PEM) Nafion® that is compatible with a Near-Ambient-Pressure X-ray Photoelectron Spectroscopy (NAP-XPS) setup. The cell makes a step towards bridging the pressure gap between classical XPS measurements in UHV and electrochemical measurements in aqueous electrolytes.

2 Experimental

The electrochemical Nafion®- cell, as depicted in Fig. 1, can be integrated into the NAP-XPS setup of the ISISS beam line at BESSY II. The samples tested are sputter-coated Nafion® membranes. Nafion® serves as electrolyte and additionally as separation between liquid water and the reduced pressure measurement chamber. The OER electrocatalyst is the working electrode and faces the X-rays. The mud crack type structure of the sputtered electrodes is both water permeable and conductive. A continuous flow of water is provided through the channels on the counter electrode side. Due to the pressure difference, the water diffuses through the mud cracked electrodes as well as the Nafion® into the measurement chamber; a pressure of 10^{-2} mbar results. The water serves two purposes: First, it enables proton conductivity by hydrating Nafion®. Second, it supplies the electrodes with the molecules for the electrocatalytic reaction. The anode and the cathode are externally connected to a potentiostat that allows the application of potentials for electrochemical testing. Gas evolution is monitored by online mass spectrometry (MS). Overall, the Nafion®-cell is suitable to investigate low-temperature gas-phase water electrolysis *in situ*: while the OER proceeds, changes in the electronic structure of the working electrode catalyst can be identified via XPS measurements.

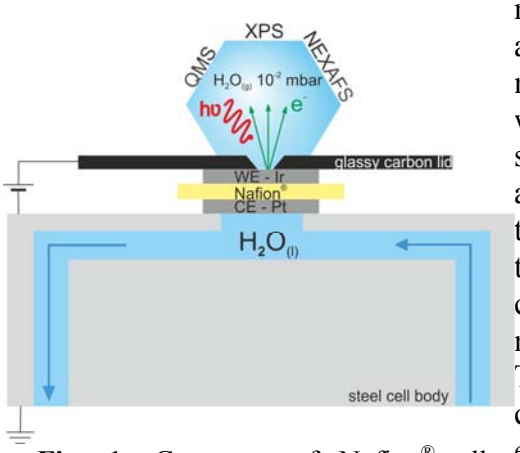

Fig. 1: Geometry of Nafion®-cell. Water penetrates the porous Pt and Ir films, diffuses through the membrane and generates a water pressure in the range of mbars in the XPS chamber.

3 Results

For Pt as model OER electrocatalysts, the Nafion®-cell enabled us to find that the active Pt surface is an electronically modified, metallic Pt surface with oxygen in the surface and surface-near region. The surface oxide layer formed is needed for water dissociation. Furthermore, we learned that a stable oxidic phase with stronger Pt-O bonds induces an overpotential and is detrimental for the OER activity.[1]

Currently, we are investigating the more active OER catalyst Ir. Figure 2a) shows the chronoamperograms at two applied potentials. The resulting gas evolution is evident in the O_2 trace of the MS. As expected, the OER rate increases when applying higher potentials. In the Ir 4f XP spectra in Fig. 2b), it is apparent that Ir is oxidized during the OER. According to the binding energy and the line shape of the formed oxidized species, it seems to be neither crystalline nor stoichiometric IrO_2 but rather hydrous Ir oxohydroxide that catalyzes the OER.

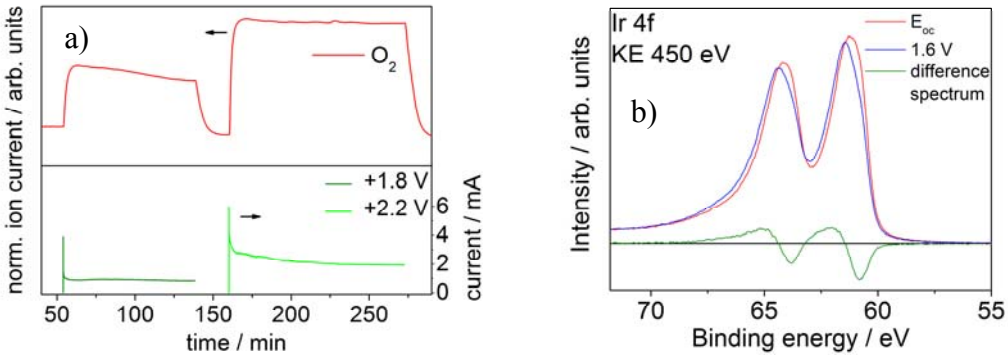

Fig. 2: a) CAs and MS O_2 trace that evidence the current flow in the Nafion®-cell and gas evolution upon voltage application. b) Ir 4f XP spectra recorded at OCP and at 1.6 V. The oxidation of Ir is clearly visible in the difference spectrum by the growing contribution at higher binding energy.

4 Conclusions and outlook

The potential of the Nafion®-cell for investigating gas-phase water electrolysis *in situ* has been demonstrated. It is a candidate for contributing to a better understanding of surface transformations of electrode materials occurring under reaction conditions. The next upgrade of the cell will be the integration of a reference electrode to work at well-defined potentials. Furthermore, another electrochemical cell based on a graphene membrane separating the liquid from the UHV is under development. This cell should finally allow us to also tackle liquid-phase water electrolysis and close the pressure gap.

Acknowledgements

The authors thank Achim Klein-Hoffmann for TEM sample preparation, Gisela Weinberg and Wiebke Frandsen for SEM/TEM measurements and HZB/BESSY II for beam time allocation.

References

[1] R. Arrigo, M. Hävecker, M. E. Schuster, C. Ranjan, E. Stotz, A. Knop-Gericke, and R. Schlögl, *Angew. Chem. (Int. Ed.)* 52, (2013)

II-OP27

CO_2 and H_2O (co)Adsorption on a ZrO_2 Thin Film

Li H.[1*], Anic K.[1], Rameshan C.[1], Bukhtiyarov A.V.[2], Prosvirin I.P.[2], Rupprechter G.[1]

1 - Institute of Materials Chemistry, Vienna University of Technology, Vienna, Austria
2 - Boreskov Institute of Catalysis, Siberian Branch, Russian Academy of Science, Novosibirsk, Russia

* hao.li@tuwien.ac.at

Keywords: ZrO_2, CO_2, H_2O, co-adsorption, *in situ* XPS, *in situ* IRAS

1 Introduction

Being a carbon source, the utilization of carbon dioxide (CO_2) became attractive from both an environmental and economical perspective. However, CO_2 is a very stable molecule, thus to induce a reaction the activation of CO_2 by catalysts is required [1]. One way of activating CO_2 is dry reforming of methane (DRM), when CH_4 is reformed by CO_2 on Ni or Pt particles supported by zirconia (ZrO_2). During DRM, CO_2 is reduced to carbon monoxide (CO) via reaction precursors or intermediates, which can further oxidize the carbon formed via CH_4 dissociation. Such activation can occur on the ZrO_2 or on the interfacial sites [2]. As a support, technical ZrO_2 powder material can activate CO_2 by forming carbonate with basic anionic sites, or by forming formate with hydroxyl groups [2]. However, due to the possible different reaction pathways, microscopic mechanisms of the functions of ZrO_2 need to be further understood via a surface science approach. We therefore conducted a systematic study of the interaction between CO_2 and a pristine ZrO_2 ultra-thin film (CO_2 adsorption on ZrO_2), as well as the interaction between CO_2 and a hydroxylated ZrO_2 ultra-thin film (CO_2 and H_2O co-adsorption).

2 Experimental/methodology

In this study the pristine ultrathin ZrO_2 film was prepared following a route described before [3,4]. The structure and the chemical composition of the films were characterized by Low Energy Electron Diffraction (LEED) and high resolution X-ray Photoelectron Spectroscopy (XPS), respectively [4]. CO_2 Temperature Programmed Desorption (TPD) was used to investigate desorption of CO_2 upon dosing at 90 K and subsequent heating. In situ XPS was employed to study the change of the electronic structure of the ZrO_2 film and the oxidation state of the accumulated carbon related species upon CO_2 or CO_2+H_2O adsorption. Infrared Reflection Absorption Spectroscopy (IRAS) was used to examine the functional groups of the formed species. In addition, formic acid (HCOOH) and formaldehyde (HCHO) were dosed on ZrO_2 and measured by IRAS in order to obtain reference data of vibrational frequencies for the measured absorption bands.

3 Results and discussion

LEED and XPS indicated the formation of a well-structured ZrO_2 film, corresponding to the (111) facet of cubic ZrO_2. After dosing at 90 K, CO_2 only weakly bonded to the ZrO_2 film and desorbed at 117 K, as shown by CO_2 TPD. Also, in situ XPS and IRAS did not detect any electronic changes of the ZrO_2 film or accumulated carbon related species upon exposure to CO_2 (from 1×10^{-6} mbar to 3×10^{-2} mbar) at 343 K. However, when ZrO_2 was subjected to a reactive mixture of CO_2 and H_2O various carbon related species were formed on the surface, as shown in Fig. 1. Specifically, species at a binding energy of 284.4 eV (elementary carbon), 285.5 eV and 286.4 eV (CH_xO) and 288.3 eV (formate) were observed in presence of CO_2 and H_2O. Except the elementary carbon, the formed features disappeared upon heating to 523 K in the reaction

mixture, but reversibly reappeared after cooling in the same gas atmosphere to 343 K. IRAS measurements confirmed the formation of CH_xO and formate species on ZrO_2 when it was exposed to CO_2 and H_2O at the same conditions. Characteristic adsorption bands for ν(C=O), ν(C-O) and CH_2 bending were observed at similar wavenumbers as obtained by measuring HCOOH and HCHO, respectively, on the ZrO_2 film as a reference. Therefore, we assume that CO_2 and H_2O codosing induces the formation of formaldehyde, dioxymethylene and formate on the surface of ZrO_2.

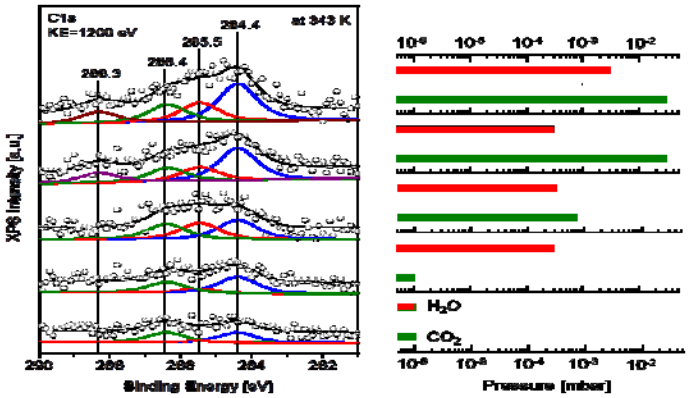

Fig. 1. C 1s spectra of the ZrO_2 ultrathin film in the presence of CO_2 and H_2O mixture (spectra taken at 343 K, KE=1200 eV)

4 Conclusions

CO_2 adsorbs only weakly on ZrO_2 ultrathin film and desorbs at low temperature. H_2O can activate CO_2 via hydrogenation and leads to the formation of formaldehyde, dioxymethylene and formate on the ZrO_2 surface.

Acknowledgements

This work was supported by the Austrian Science Fund (FWF) within SFB F45 "FOXSI" (F4502). The authors thank Dr. Jan Knudsen, Dr. Niclas Johansson and Dr. Joachim Schnadt at Max Lab (Lund University).

References

[1] N. Homs, J. Toyic, P. de la Piscina. *Acitivation of Carbon Dioxide. Chapter 1 Catalytic Processes for Activation of CO_2.*

[2] D. Pakhare, J. Spivey. *Chemical Society Reviews.* 43 (2014) 7813.

[3] M. Antlanger, W. Mayr-Schmölzer, J. Pavelec, F, Mittendorfer, J, Redinger. P, Varga, U. Diebold, M. Schmid. *Physical Review B.* 86 (2012) 03451.

[4] H. Li, J. J. Choi, W. Mayr-Schmölzer, C. Weilach, C. Rameshan, F. Mittendorfer, J. Redinger, M. Schmid, G. Rupprechter. *The Journal of Physical Chemistry C (2015),* in press.

II-OP28

Operando Raman and UV-Visible Spectroscopy of $H_3PW_{12}O_{40}$ in the Gas Phase Dehydration of Methanol to Dimethylether

Schnee J.*, Gaigneaux E.M.

Université catholique de Louvain, Institute of Condensed Matter and Nanosciences (IMCN/MOST), Louvain la Neuve, Belgium

* josefine.schnee@uclouvain.be

Keywords: heteropolyacids, dimethylether, operando, spectroscopy, coke, methanol, dehydration

1 Introduction

Heteropolyacids (HPAs) are molecular clusters possessing a very high Brönsted acidity. They are widely used as acid catalysts. For gas phase reactions, the main issue in HPA-based catalysis is their deactivation due to the formation of carbonaceous deposits called "coke" [1]. We currently investigate the catalytic activity of $H_3PW_{12}O_{40}$ (HPW12), the most acidic Keggin-type HPA, in the gas phase dehydration of methanol to dimethylether (DME). DME is nowadays seen as one of the most important and promising renewable fuels for the future [2]. Herein, we demonstrate via *operando* Raman and UV-Visible characterization that changes in the selectivity to DME over HPW12 as catalyst are related to the amount of coke produced and to the latter's degree of disorganization.

2 Experimental/methodology

The catalytic performance of HPW12 (800 mg, 100-200 µm) in the dehydration of methanol was investigated *operando* in a quartz reactor provided with optical windows. The latter allowed characterizing the catalyst *at work* throughout the reaction by Raman and UV-Visible spectroscopies. Spectra of both techniques were recorded simultaneously every 2 minutes. For Raman spectroscopy, an Nd-YAG laser with 532 nm wavelength was used. For UV-Visible spectroscopy, a deuterium-halogen light source and a temperature-resistant reflection probe were used. The catalytic tests were performed following a temperature program from room temperature to 350°C (7 steps of 2 hours at 100, 150, 200, 250, 300 and 350°C, ramps of 1°C/min in-between). The inlet gas flow was composed of 27 mL/min of nitrogen saturated with 10 vol% of methanol. The outlet gas flow was analyzed by fast GC (5.5 min/run). The catalytic activity is herein reported in terms of conversion of methanol and selectivity to dimethylether.

3 Results and discussion

As shown on Fig.1, in the here applied test conditions, the conversion of methanol on HPW12 was of 3%, 65% and 90% at respectively 100°C, 150°C and 200°C. Then it remained constant up to 350°C (with small variations). The selectivity to DME was around 90% up to 200°C. From 200°C on, it dropped (85%, 70% and 40% at respectively 250°C, 300°C and 350°C), with methane, ethylene and propylene detected as byproducts. The peak of selectivity observed after having cooled the reactor back to room temperature is considered as an artefact.

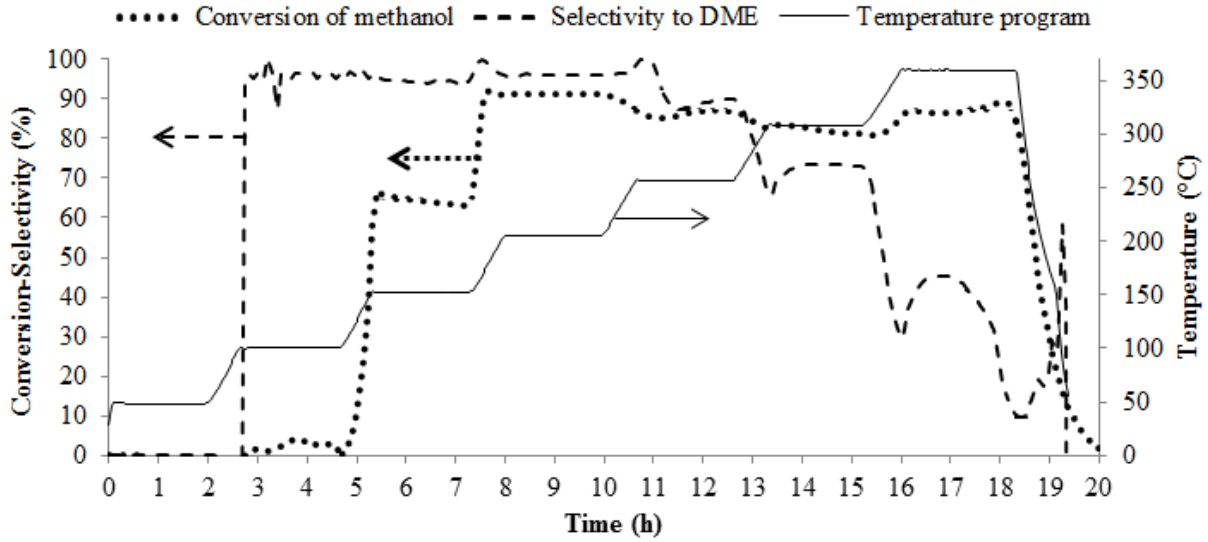

Fig. 1. Conversion of methanol and selectivity to DME during the temperature programmed reaction with HPW12 as catalyst.

Operando UV-Visible spectra reveal an increase of absorption in the visible region as soon as the reaction was started, reflecting the rapid formation of dark-colored coke. Up to 200°C, the UV absorption edge of HPW12 remained visible (O^{2-} to W^{6+} charge transfer absorption bands at 250 nm and 350 nm). At 250-300-350°C however, when the selectivity to DME was dropping, the coke's absorption in the visible region reached its maximum and completely masked HPW12's UV absorption edge. On *operando* Raman spectra, the bands of polyaromatic coke became visible at 100°C: a D1 band at 1300-1450 cm^{-1} reflecting disorganized non-graphitic coke and a D2 band at 1600-1650 cm^{-1} reflecting less disorganized coke [3]. Up to 250°C, the D2 band was more intense than the D1 one. At 300°C, the relative intensity of the D1 one started to increase with time on stream. At 350°C, both bands had nearly equal intensities. The increase of relative intensity of the D1 band, reflecting an increase of the structural disorganization of coke, here occurs together with the production of methane which is the byproduct of reactions that increase the aromaticity of coke.

4 Conclusions

The *operando* Raman and UV-Visible spectra reflect the changes in the selectivity to DME obtained with HPW12. More precisely, a drop of selectivity to DME is associated to an increased production of coke (revealed via UV-Vis) possessing an increasing degree of disorganization (revealed via Raman) and an increasing aromaticity (indicated by the production of methane).

References

[1] I.V. Kozhevnikov, *Journal of Molecular Catalysis A: Chemical*. 262 (2007) 86-92.
[2] Y. Fu, T. Hong, J. Chen, A. Auroux, J. Shen, *Thermochimica Acta*. 434 (2005) 22-26.
[3] R.W. Court, M.A. Sephton, J. Parnell, I. Gilmour, *Geochimica et Cosmochimica Acta*. 71 (2007) 2547-2568.

II-OP29

Raman Study of the Deactivation Products in the Methanol to Olefines Reaction: a Combined *in situ* - *in silico* Approach

Signorile M., Bonino F., Damin A.*, Bordiga S.

Department of Chemistry, NIS and INSTM Reference Centre, University of Turin, Italy

* alessandro.damin@unito.it

Keywords: UV-Raman, Methanol-to-Olefines, coke, aromatic-hydrocarbons, ceolites

1 Introduction

Allowing the production of valuable chemicals from a source different from oil, the Methanol to Olefines (MTO) reaction is an industrial process which relevance is continuously increasing in the last years. One of the main limitations affecting MTO is the relatively fast catalysts deactivation, due to coking [1]. Moving to a deeper insight, coke is composed by molecules belonging to the arenes and particularly to methylated benzenes (MBs) and polycyclic aromatic hydrocarbons (PAHs). Raman spectroscopy finds large application in the study of carbonaceous materials [2, 3], of which aromatic hydrocarbons are a particular subset. Each MB/PAH shows a peculiar vibrational spectrum, allowing to determine the nature of the coke species [4]. The main drawback related to the application of Raman is the fluorescence of the sample: MBs and PAHs are highly emissive in the visible region and their fluorescence can overlap the Raman signal. Generally such interference can be avoided by using an excitation wavelength falling outside of the visible [4, 5]. As most of the interesting molecules show their electronic transitions in the 200-400 nm spectral region [6, 7], a further advantage can be achieved by exciting by means of a UV radiation, that is the exploitation of the resonant Raman effect. This allows to increase of orders of magnitude the sensitivity toward the resonant species, i.e. significantly reducing their limit of detection and allowing their analysis even when diluted. Being in a real catalytic system the coke species dispersed on a porous material with high surface area, the possibility to exploit the resonance makes feasible their characterization, even *in situ*. A picture of the deactivation products has been obtained combining the experimental data with molecular simulation: the Raman spectra of MBs and PAHs have been computed and compared with experimental data. Advanced computational tools have been adopted in order to properly simulate the Raman intensities when the resonance conditions are achieved [8].

2 Experimental/methodology

To get a better knowledge in the deactivation of MTO catalysts, the characterization performed by UV Raman spectroscopy has been coupled to the simulation of the Raman spectra of the investigated species. The study can be articulated in three key steps:

1. Some selected aromatic molecules have been studied by Raman in different matter states (pure solids/liquids, in diluted solution and adsorbed from gas phase on high surface area materials) in order to build a reference database for the following step.
2. Different zeolites have been deactivated under different reaction conditions (varying e.g. the temperature, the feed,…) and their Raman spectra have been compared with ones of the reference molecules. This allowed to unambiguously recognize the main deactivation products and the effect of the zeolite topology on their formation. Wanting to avoid spurious contribution to the spectra, all the materials have been carefully activated in controlled conditions and then characterized *in situ* in order to remove the already adsorbed contaminants and avoid their re-adsorption.
3. The vibrational spectra of MBs and PAHs have been simulated by ab initio calculation: different computational approaches have been tested in order to get the better agreement

with the experimental data. Furthermore the simulation of the Resonant Raman intensities has been performed, allowing an easier understanding of the experimental data.

3 Results and discussion

An example of application is given in Figure 1: a H-ZSM-5 catalyst (Si/Al=45) has been deactivated in 100 mbar of MeOH at 350°C.

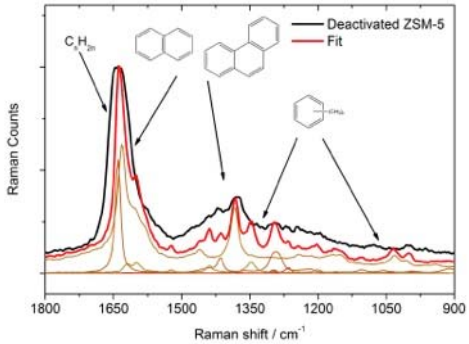

Figure 1. UV Raman spectrum of a H-ZSM-5 deactivated in 100 mbar of MeOH at 350°C (black line) and a tentative fitting based on the experimental Raman spectra of MBs and PAHs (red line).

The very complex spectrum due to deactivation products can be rationalized by comparing it with the spectra of the reference MBs and PAHs [9]. Furthermore a tentative fitting of the signal can be tried with a linear combination of their spectra: the main contributions to the Raman spectrum of deactivated zeolites can be attributed to the formation of naphthalene, phenantrene and highly methylated benzenes (mainly tetra- and hexa-MB). The further combination with computational results should help to better discriminate the observed moieties, i.e. allowing to recognize species which are difficult to obtain in a sufficiently pure form (e.g. methylated PAHs) or which can not be easily obtained outside of the reaction conditions (e.g. carbocations).

4 Conclusions

The combination of *in situ* UV Raman spectroscopy and their parallel simulation can represent an interesting tool in the characterization of the deactivation species in the MTO reaction. Starting from the fundamental insights presented in this study it is possible to extend the basic knowledge on the deactivation pathways according to the different catalysts topologies, eventually applying the same methodology to more complex experimental conditions (e.g. *operando*).

Acknowledgements

The authors would like to acknowledge dr. F. Santoro for providing the FCClasses code for the Resonant Raman simulation and prof. K. P. Lillerud and Dr. Pablo Beato for fruitful discussion and providing the catalysts samples.

References

[1] U. Olsbye, S. Svelle, M. Bjorgen, P. Beato, T.V.W. Janssens, F. Joensen, S. Bordiga, and K.P. Lillerud, *Angew. Chem.-Int. Edit.* 51 (2012)
[2] A.C. Ferrari, J.C. Meyer, V. Scardaci, C. Casiraghi, M. Lazzeri, F. Mauri, S. Piscanec, D. Jiang, K.S. Novoselov, S. Roth, and A.K. Geim, *Phys. Rev. Lett.* 97 (2006) 187401-1
[3] A.C. Ferrari, and J. Robertson, *Phys. Rev. B* 61 (2000) 14095
[4] S.A. Asher, and C.R. Johnson, *Science* 225 (1984) 311
[5] F. Fan, Z. Feng, and C. Li, *Accounts Chem. Res.* 43 (2010)
[6] J. Catalan, and J. Carlos Del Valle, *J. Phys. Chem. B* 118 (2014)
[7] J. Ferguson, L.W. Reeves, and W.G. Schneider, *Can. J. Chem.* 35 (1957)
[8] F.J. Avila Ferrer, V. Barone, C. Cappelli, and F. Santoro, *J. Chem. Theory Comput.* 9 (2013) 3597
[9] M. Signorile, F. Bonino, A. Damin, S. Bordiga, *ChemCatChem*, submitted (2015)

II-OP30

Where are the Active Sites in Zeolite Nano-Crystals? Influence on Post-Synthesis Treatment from Hard X-Ray Depth Profiling with XPS

Proff C., Fodor D., Orlando F., Van Bokhoven J.A.*

Institute for Chemical and Bioengineering, ETH Zurich and Paul Scherrer Institute, Villigen, Switzerland

* j.a.vanbokhoven@chem.ethz.ch

Keywords: hollow zeolites, quantitative aluminium distribution, base leaching, nano-reactors

1 Introduction

Framework aluminum determines the catalytic properties of zeolite crystals. Also, very often post-synthesis modification is applied to enhance the zeolite performance and the local concentration of aluminum strongly affects the outcome of such treatment. Thus, to achieve understanding of the relation between structure and performance, the aluminum distribution within a single crystal must be determined. Although aluminum enrichment at the surface is a well-known phenomenon, there is no quantitative insight into industrially relevant crystals in the size range of tens of nanometers. Non-destructive depth profiling using hard X-ray photoelectron spectroscopy (XPS) can be done at the synchrotron, based on the different penetration depth of electrons of varying kinetic energy. We quantified the aluminum distribution in ZSM-5 crystals of 50 to 100 nm in size. Slight differences in synthesis procedure lead to significant differences in the aluminum distribution within a single crystal. Moreover, the data unambiguously point to a significant redistribution of aluminum and silicon atoms within a crystal during base leaching. Thus, besides mesopore formation, base leaching additionally modifies the structure of the remaining zeolite. These data are of fundamental importance for the interpretation of the difference in catalytic performance between various zeolite batches and of the changes in performance after post-synthesis modification.

2 Experimental/methodology

ZSM-5 nano-crystals with a Si/Al ratio of 50 were synthesized as described in detail elsewhere [1]. XPS depth profiling measurements were performed at the near ambient pressure photoemission (NAPP) endstation at the PHOENIX beamline of the Swiss Light Source (SLS). Si 1s and Al 1s core level spectra were measured at photon energies between 2175 and 6860 eV, corresponding to photoelectron kinetic energies between 600 and 5000 eV. Cross-section dependency was corrected using the data from Trzhaskovskaya et al. [2]. The Al 1s and Si 1s spectra were best fitted with Gaussians and a linear background. The measurements were performed with the photon beam impinging at 60° off the surface normal, while photoelectrons were collected at 30° emission angle. The inelastic mean free path corresponding to each kinetic energy was calculated assuming a 9 eV band gap and ZSM-5 structure [3] and the composition. Concentration profiles were extrapolated from the Si/Al ratio vs. kinetic energy profiles using the maximum entropy regularization procedures presented by Weiland et al. [4].

3 Results and discussion

Figure 1 shows the aluminum distribution obtained using the XPS depth profiling of two differently synthesized batches of ZSM-5, both with tetrapropyl amine (TPA) as structure-directing agent and a Si/Al ratio of 50. ZSM-5A, of which the TPA was made in our lab, has a high surface concentration of aluminum, which rapidly decreases to zero within about 10 nm.

ZSM-5B, synthesized using commercially available TPA, has a similar decline in aluminum concentration, however, there is a remaining aluminum content in the bulk of the crystal.

Upon base leaching the material with no aluminum in its core yields hollow zeolite crystals, the other one the more typical cheese-like mesoporous structure. Also, the aluminum showed a different depth profile (not shown in the figure) in the outermost layer after this treatment, pointing to dissolution and re-insertion of silicon and aluminum in the framework during the base treatment.

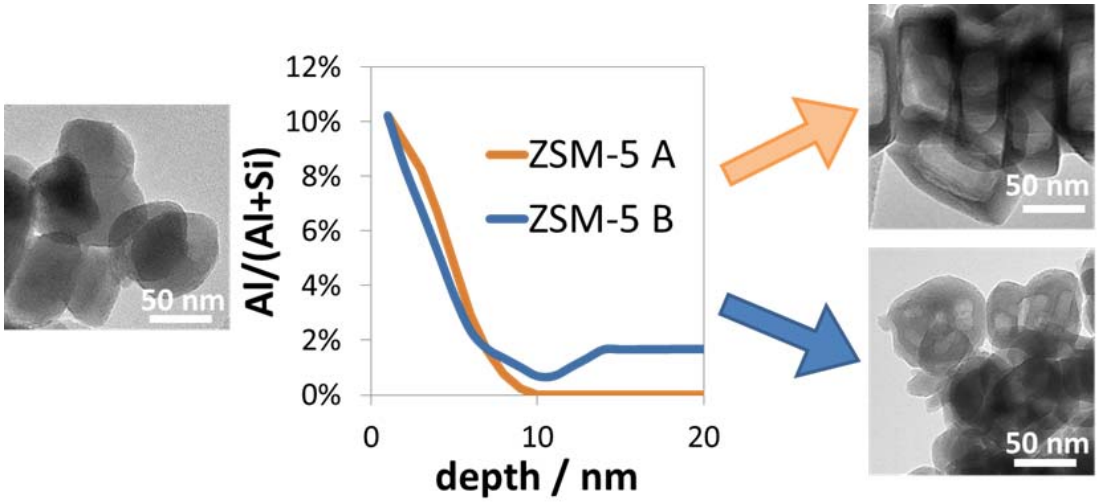

Fig. 1. Quantitative aluminum distribution in ZSM-5 crystals with Si/Al ratio of 50. Base leaching of these crystals yield very different material: the one with no aluminum in its core yields hollow zeolite crystals.

4 Conclusions

The Si/Al ratio vs depth inside ZSM-5 nanocrystals before and after NaOH leaching was quantified with synchrotron-based (XPS) depth profiling. This revealed a distinct variation of the Si/Al ratio with depth between two different materials with very similar composition, but slightly differing synthesis conditions. Leaching created hollow nano-crystals in case of one material and cheese-like nano-crystals with many pores in case of the other. An aluminum-rich surface zone is followed by an aluminum devoid zone in case of the parent material forming after leaching hollow crystals, while the other parent material exhibits after the aluminum-rich zone a low non-zero aluminum level in the bulk. The structure of the nano-crystals is well preserved after leaching as well as the crystal size. This can be attributed to the high aluminum concentration in the outer shell, protecting the outer shell of the nano-crystals from dissolution. However, even within this shell, dissolution and recrystallization occurs during base leaching changing the aluminum depth profile.

References

[1] Fodor, D., Pacosová, L., Krumeich, F. & van Bokhoven, J. A. Facile synthesis of nano-sized hollow single crystal zeolites under mild conditions. *Chem. Commun.* 50 (2014) 76–78.

[2] Trzhaskovskaya, M. B., Nefedov, V. I. & Yarzhemsky, V. G. Photoelectron angular distribution parameters for elements Z=1 to Z=54 in the photoelectron energy range 100–5000 eV. *At. Data Nucl. Data Tables* 77 (2001) 97–159.

[3] Tanuma, S., Powell, C. J. & Penn, D. R. Calculations of electron inelastic mean free paths. IX. Data for 41 elemental solids over the 50 eV to 30 keV range. *Surf. Interface Anal.* 43 (2011) 689–713.

[4] Weiland, C. *et al.* Nondestructive compositional depth profiling using variable-kinetic energy hard X-ray photoelectron spectroscopy and maximum entropy regularization. *Surf. Interface Anal.* 46 (2014) 407–417.

II-OP31

ETEM Investigation of Gold Nanoparticle Formation in Recrystallized Zeolite Silicalite-1

Agata. G.H.[1*], Thomas. W.H.[2], Jerrik J.M.[1], Søren K.[1]

1 - Technical University of Denmark, Department of Chemistry, Kgs. Lyngby, Denmark
2 - Technical University of Denmark, Centre for Electron Nanoscopy, Kgs. Lyngby, Denmark

* skk@kemi.dtu.dk

Keywords: zeolites, nanoparticles, gold, encapsulation, eTEM

1 Introduction

Supported gold nanoparticles, since the first report on their high catalytic activity in low-temperature CO reduction, have been used extensively in organic chemistry reactions [1]. However, supported nanoparticles are prone to sintering which is causing a thermal deactivation of the catalyst [2]. The stability might be improved by encapsulation of individual nanoparticles inside the porous inorganic material. Such materials were proven to be size-selective and stable under extreme temperature conditions [3].

The preparation of gold nanoparticle encapsulated zeolite silicalite-1 is reported. The zeolites are modified by a recrystallization process (desilication), which creates voids and mesopores inside the crystal structure of individual particles. This additional porosity facilitates the formation of gold nanoparticles inside the zeolite channels upon wet impregnation. Environmental Transmission Electron Microscopy (eTEM) is applied for the characterization of the material with the emphasis on the process of *in-situ* nanoparticle formation inside the zeolite channels, sintering stability at elevated temperatures, and the reactivity of the material in the simple oxidation reaction. Furthermore, the influence of degree of desilication and temperature of desilication on the recrystallized material is investigated. Variation in choice of gold precursor and water content for impregnation of the recrystallized silicalite-1 are examined in terms of size of nanoparticles and their distribution inside the zeolite framework.

2 Experimental

All the reported materials were synthesized form commercially available chemicals. Zeolite silicalite-1 was prepared using traditional synthesis method. Preparation of gold recrystallized silicalite-1 was based on impregnation of recrystallized silicalite-1 prepared by an alkaline dissolution-reassembly process in the presence of the surfactant [4]. Obtained materials were investigated using HRTEM in terms of *ex-situ* nanoparticle formation and eTEM for the *in-situ* formation under the atmosphere of hydrogen at elevated temperature. Other analytical techniques like BET, ICP-MS, and XRD were applied for the standard characterization.

3 Results and discussion

eTEM imaging of the gold recrystallized silicalite-1 was performed under elevated temperature and hydrogen atmosphere in order to investigate the *in-situ* formation of gold nanoparticles. Figure 1 depicts recrystallized zeolite crystals with encapsulated gold nanoparticles. Immediate *in-situ* formation of Au-NP was observed under the irradiation with electron beam in vacuum (right side Figure 1). In this case, nanoparticles were located at the surface of the inner voids in the crystals. Gradual reduction of metal nanoparticles was performed using blanked-beam, where specimen was exposed to the electron beam only for the time to sample an image (left side Figure 1). In this case, distribution of nanoparticles is more uniform between the voids surface and channels of the zeolite.

Stability against sintering was monitored *in-situ* in oxygen atmosphere at elevated temperatures in eTEM and showed promising results. Catalytic activity was confirmed based on simple oxidation reaction.

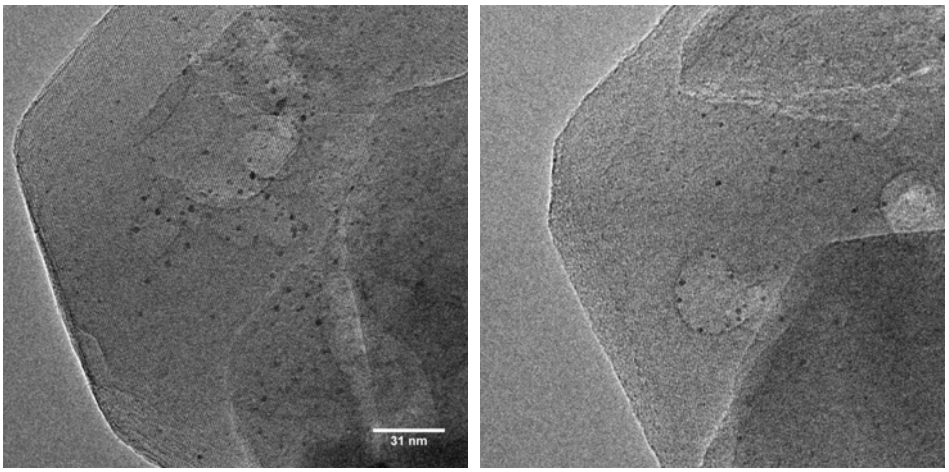

Fig. 1. eTEM image of recrystallized silicate-1 with encapsulated Au nanoparticles. Left: beam-blanked specimen; right: constant-illumination specimen. Cavities inside the zeolite crystal are visible as large voids localized in the centre of the crystal. Nanoparticles are visible in the matrix of zeolite – in the channels and at the edges of cavities. Gold nanoparticles are 3nm in size. The channels structure of silicate-1 is visible.

4 Conclusions

Environmental Electron Transmission Microscopy was used as a main tool for *in-situ* investigation of nanoparticle formation in the recrystallized zeolite silicalite-1. Various parameters influencing the characteristics of material were examined using above technique. Stability for sintering and catalytic activity were proven and observed.

Acknowledgements

The authors would like to thank Centre for Sustainable and Green Chemistry sponsored by the Danish National Research Foundation.

References

[1] M. Haruta, N. Yamada, T. Kobayashi, S. Iijima, *J. Catal*. (1989)115, 301
[2] T.W. Hansen, A.T. DeLaRiva, S.R. Challa, A.K. Datya, *Acc. Chem. Res*. (2013) 46, 1720
[3] P.M. Arnal, M. Comotti, F. Schüth, *Angew. Chem. Int. Edit.* (2006), 45, 8224; *Angew. Chem.* (2006), 118, 8404
[4] J. Mielby, J.O. Abildstrøm, F. Wang, T. Kasama, C. Weidenthaler, S. Kegnæs, *Angew. Chem.* (2014) 126, 1-5

II-OP32

Size-Dependent Redox Behaviour in Iron Observed Using Top-Down Lithography and *in-situ* Single Particle Spectro-Microscopy

Karim W.[1,2*], Kleibert A.[2], Gobrecht J.[2], Ekinci Y.[2], Van Bokhoven J.A.[1,2]

1 - ETH Zurich, Zurich, Switzerland
2 - Paul Scherrer Institute,Villigen, Switzerland

* waiz.karim@psi.ch

Keywords: top-down, nanofabrication, single particle spectroscopy, PEEM, metal, catalyst, iron, oxidation, size effects

1 Introduction

Shape and size of nanoparticles considerably affect catalytic activity. [1] Their synthesis in a controlled manner resulting in well-defined shape and size as well as their characterization at the single particle level will help gaining deeper insight into chemical mechanisms and elucidating size and shape effects. The mechanism of oxidation of iron has extensively been investigated in the past and studies have concluded that the behavior of bulk iron is different from nanoparticles but knowledge about the behavior in nanoscale is limited. [2] To determine size-dependent redox behaviour in iron, we have fabricated model systems with well-defined particle sizes using top-down nanolithography. Single particle spectro-microscopy was performed on all different sizes and effect of particle size in oxidation and reduction of iron nanoparticles has been determined.

2 Experimental/methodology

In this work, well-defined model systems consisting of ordered single iron nanodots of different sizes from 6 nm to 80 nm were realized in a 5 × 5 cm^2 field-of-view using top-down nanofabrication. This involves accurate proximity effect correction during exposure of PMMA resist using electron beam lithography (EBL), followed by optimization of resist development, thermal evaporation of iron and lift-off. X-ray photoemission electron microscopy (PEEM) enables measuring the structure of individual iron particles (schematic shown in Fig. 1a). Simultaneous microscopy and in-situ x-ray absorption spectroscopy (XAS) was performed on all different sizes under the same conditions with high elemental sensitivity through annealing and leading to the observation of a clear size effect of the controlled oxidation of the iron nanoparticle.

3 Results and discussion

The SEM image of the fabricated model system consisting of iron oxide nanoparticles of different sizes in a 5 × 5 cm^2 field-of-view is shown in Fig. 1b. Elemental contrast image at Fe L_3 edge observed during PEEM measurement is shown in Fig. 1c. XAS spectra from single particle were extracted at different stages of oxygen dosage and all different sizes were studied simultaneously under identical condition. Having the same spectra for all sizes at the initial state of metallic iron, clear size dependence was seen already in the XAS spectra after five minutes of controlled oxygen dosing at 10^{-8} mbar. The smaller nanodots oxidized much faster than the larger ones. The percentage concentration of iron(0) and evolution of different oxides over duration of oxygen dosage could be simulated for all sizes using reference spectra of each of the possible species (FeO, Fe_2O_3, and Fe_3O_4), as shown for 80 nm dot in Fig. 2a. Comparison of oxidation rates and composition for different sizes clearly indicate a size-effect. Fig. 2b shows

the plot comparing the initial rate of oxidation per unit area for all different sizes. The rate of oxidation per surface area increases exponentially for nanoparticles below 20 nm. Based on the kinetics and thermodynamic stability of different oxides, activity of different sizes is compared and a reaction mechanism for the inter-conversion of oxides in iron nanoparticles was proposed.

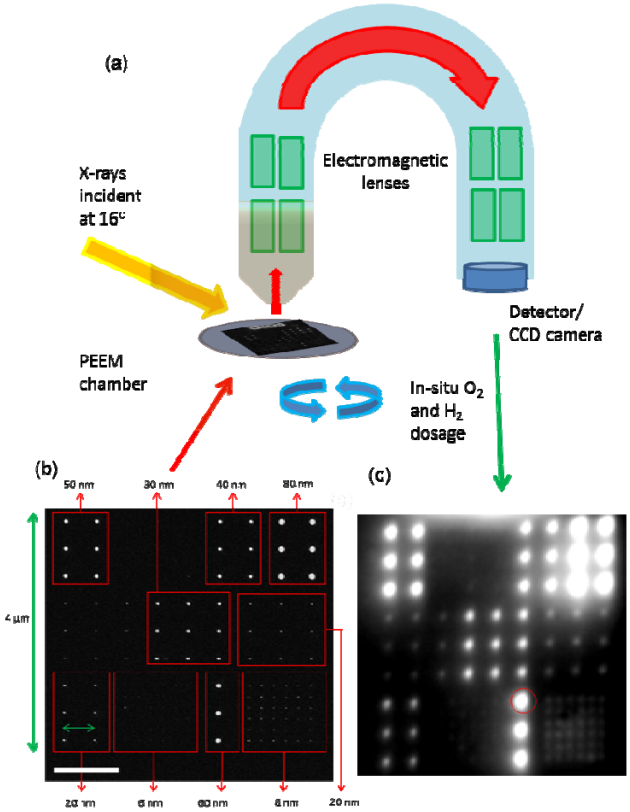

Fig. 1 (a) Schematic of PEEM setup for single particle spectroscopy. (b) SEM image of the model system consisting of particles from 6 nm to 80 nm prepared using top-down nanofabrication. (c) Elemental contrast image of the model system measured in the PEEM at the Fe L_3 edge. Nanoparticles of all different sizes were probed simultaneously.

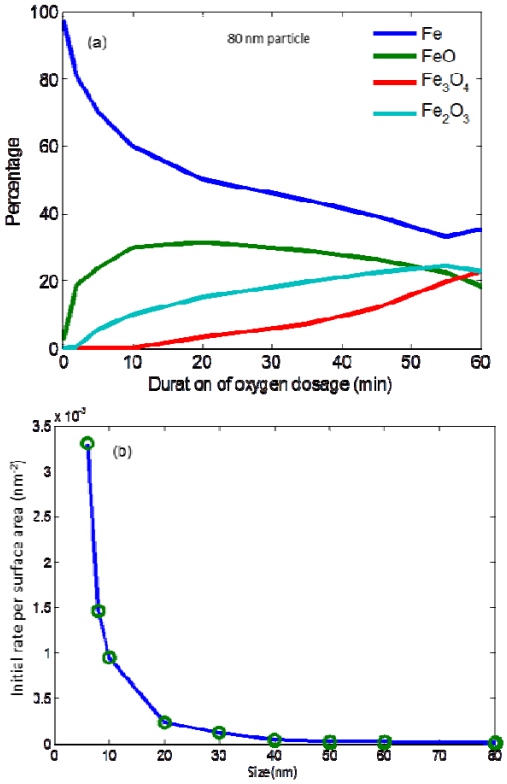

Fig. 2 (a) Change in concentration of Fe, FeO, Fe_2O and Fe_3O_4 during oxygen dosage for 1 hour observed for 80 nm sized particles. Similar analysis was performed for nanoparticle of different sizes. (b) Initial rate of oxidation per surface area compared for all sizes. The rate increases exponentially for particle size below 20 nm.

4 Conclusions

In summary, we have achieved state-of-the-art top-down nanofabrication methods enabling well-defined to fabricate novel model systems. In conjunction with in-situ spectroscopy technique to study single particles using PEEM, we have determined size effect in redox reactions of iron nanoparticles.

Acknowledgements

We would like to acknowledge the contribution of Vitaliy Guzenko for the support in handling the electron beam lithography tool at Laboratory for Micro and Nanotechnology in Paul Scherrer Institute.

References

[1] M. Shekhar, F. H. Ribeiro, Journal of the American Chemical Society 134 (2012) 4700-4708
[2] W. Feitknecht, K. J. Gallacher, Nature 228 (1970) 548-549

II-OP33

Investigating Fundamental Properties of Syngas Conversion Catalysts - a Model Approach

Fredriksson H.O.A.*, Bu Y., Dad E., Sui H., Niemantsverdriet J.W.

Eindhoven University of Technology, Eindhoven, The Netherlands

* h.o.a.fredriksson@tue.nl

Keywords: syngas, model-catalyst, UV-vis, XPS, sintering, oxidation

1 Introduction

Although both methanol synthesis and Fischer-Tropsch synthesis are well-established, commercially used processes, our understanding of the catalysts, and in particular their de-activation mechanisms is incomplete. A reason for this is of course the complexity of the reaction, including many possible side reactions. Another reason is the complexity of commercially used catalysts, containing promoter and support materials as well as three-dimensional, random distributions of the catalyst materials in pores[1, 2]. On such catalysts, it is hard to determine the relative importance of reactant and product diffusion, contact and spill-over effects between catalyst and support/promoter or changes in particle distributions. Furthermore, in larger catalytic beds it is difficult to avoid local variations in gas composition and temperature. A catalyst can therefore exhibit different properties at different locations in the catalytic bed. Post reaction analysis of catalyst can thus yield different results depending on from where in the reactor the sample is collected, making it difficult to determine well-defined catalyst properties and to correlate these with overall reactivity. This problem is elegantly circumvented by the use of flat model catalysts in micro-reactors[3]. For such systems, the gas composition and temperature of the catalyst can be precisely controlled and measured. Therefore, fundamental properties of the catalysts, such as oxidation state, stability towards sintering and contact between the various catalyst components can be conveniently studied.

2 Experimental/methodology

We have prepared well defined, flat model catalysts, supported on quartz and TEM-windows by wet-chemical methods or physical vapor deposition. The catalysts consist either of Fe or Cu nanoparticles, with various amounts of promoters. Pre- and post-reaction XPS characterization of the model catalysts were performed using a Kratos, Axis Ultra and a Thermo Scientific, K-alpha spectrometer with monochromatic Al Kα sources and TEM characterization was performed using a FEI, Tecnai G2 Sphera microscope. In addition, we have used a modified Insplorion X1 instrument (Insplorion AB, Gothenburg, Sweden) to perform in-situ UV-vis spectroscopy, nanoplasmonic sensing and mass-spectroscopy. The latter equipment allowed us to follow sintering behavior and changes in oxidation state, while simultaneously measuring the catalyst activity.

3 Results and discussion

Using the complementary techniques, XPS, TEM, UV-vis and mass spectroscopy allowed us to correlate changes in fundamental catalyst properties to changes in activity. In particular, the newly developed combination of in-situ, UV-vis spectroscopy and mass spectroscopy on model catalysts facilitates characterization of changes in the catalyst properties in real time. We have successfully demonstrated the oxidation, reduction and carburization behaviour of Cu- and Mn-promoted Fe catalysts in different gas compositions. Cu acts as a reduction promoter while Mn retards reduction but stabilizes the catalyst towards sintering. In our investigations of Cu-catalysts, we have shown how the oxidation state of the catalyst influences its reactivity in CO-

oxidation experiments. Inclusion of small amounts of oxygen in the feed gas (~1 %) leads to oxidation of the metallic copper, which is accompanied by an immediate decrease in catalyst activity. Furthermore, we show how the catalyst sintering is influenced by the gas environment. In reducing gas, sintering sets in at significantly lower temperatures than in an oxidizing environment.

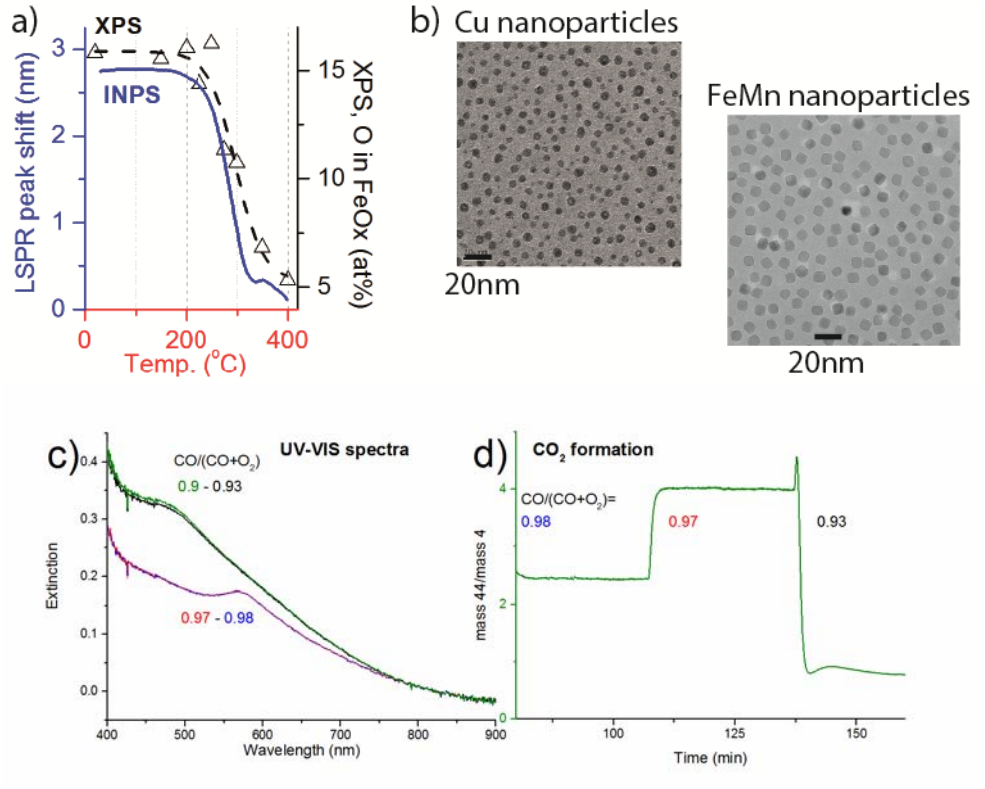

Fig. 1. a) Reduction of an Fe model-catalyst measured by in-situ nano-plasmonic sensing and XPS. The big drops in both signals indicate catalyst reduction. b) TEM images of Cu and Fe, flat model catalysts. c) Optical extinction measured from a Cu-model catalyst during CO-oxidation experiments with increasing oxygen content and d) the corresponding CO_2 formation during the experiment. The big drop in CO_2 formation when the oxygen content is increased to 7% correlates with a sharp shift in the optical spectra caused by catalyst oxidation.

4 Conclusions

Fabrication and characterization of model catalysts using XPS, TEM and in-situ UV-vis and mass spectroscopy has been demonstrated. The strength of the approach was demonstrated in several experiments including catalyst oxidation/reduction and sintering of catalysts used for syngas conversion.

References

[1] E. de Smit, B.M. Weckhuysen, *Chem. Soc. Rev.* 37 (2008) 2758.
[2] J. Schumann, T. Lunkenbein, A. Tarasov, N. Thomas, R. Schlogl, M. Behrens, *ChemCatChem.* 6 (2014) 2889.
[3] P. Thune, P. Moodley, F. Scheijen, H. Fredriksson, R. Lancee, J. Kropf, J. Miller, J.W. Niemantsverdriet, *J. Phys. Chem. C*. 116 (2012) 7367.

II-OP34

CeO_2 Carrier Shape Effects on CuO_x/CeO_2 CO-PROX Catalysis: Operando X-Ray Spectroscopy and DFT Modelling Studies

Monte M.[1], Bolívar C.L.[1], Munuera G.[2], Martínez-Arias A.[1], Conesa J.C.[1*]

1 - Instituto de Catálisis y Petroleoquímica, CSIC, Madrid, Spain
2 - Real Academia Sevillana de Ciencias, Fac. de Química, Sevilla, Spain

* jcconesa@icp.csic.es

Keywords: ceria, nanocubes, ambient, pressure, XPS, XAFS, DFT modelling, hydrogen, technology, copper, oxide

1 Introduction

CuO_x/CeO_2 is a nonexpensive catalyst with good activity and selectivity in the CO-PROX reaction. Its active centres for the CO oxidation are assumed to be located at the CuO_x-CeO_2 interface borderline [1], so that modifying that interface is expected to provide ways to tailor the catalytic properties. In recent work [2] we have shown that with a nanocube-shaped ceria support, which exposes mainly the more reactive (001) surface, the selectivity is improved. Further XANES/XPS and XAFS results coupled to DFT modelling are reported here which confirm previous data indicating that on the mentioned (001) surface a stronger oxide-oxide interaction exists together with a stabilization of a less reduced state of copper. This explains the retardation of H_2 oxidation, as the latter requires a deeper reduction of the Cu oxide phase.

2 Experimental/methodology

Copper oxide was deposited via impregnation on ceria nanospheres (NS), nanorods (NR) or nanocubes (NC) of different specific surfaces as already reported; details of the preparation, multitechnique characterization (using XRD, Raman, HRTEM, S_{BET}, H_2-TPR and EPR) and CO-PROX performance (catalytic tests and *operando*-DRIFTS measurements) of the catalysts can be found elsewhere [2,3]. We have now carried out *operando* XPS/XANES experiments ($P \leq 100$ Pa) at the ISISS station of BESSY II synchrotron in Berlin, and Cu K edge XAFS measurements at CLAESS station in synchrotron ALBA near Barcelona. DFT+U calculations on models consisting of $(CuO)_{12}$ rodlike clusters lying of CeO_2 (111) and (001) slabs were made using periodic program VASP and PAW representation of the electronic cores.

3 Results and discussion

Surface-sensitive XANES at the Cu L_3 edge of the Cu-NC and Cu-NS catalysts measured under small CO pressure at increasing temperatures show (see e.g. Fig. 1a) that copper in the nanocube-supported sample resists reduction better than in the nanosphere-supported one. Also, Cu atoms at the interface can be distinguished by an XPS feature with unusually low energy values of the Cu(2p) peak and of Auger LMM features. Furthermore, preliminary analysis of recently acquired EXAFS data at Cu K edge on the calcined catalysts (Fig. 1b) indicates that a 0.16% Cu-NC sample, which has similar surface concentration of Cu than a 1% Cu-NS sample, has a much more distorted coordination environment, i.e. the CuO particles are significantly altered by the interaction with the CeO_2 (001) surface. This agrees with the previous observation by XRD that CuO nanocrystals do not form easily on ceria nanocubes [2]. XANES data also confirm that the 0.16% Cu-NS sample is more resistant to reduction under CO-PROX reaction than the NC-supported sample having similar Cu surface concentration.

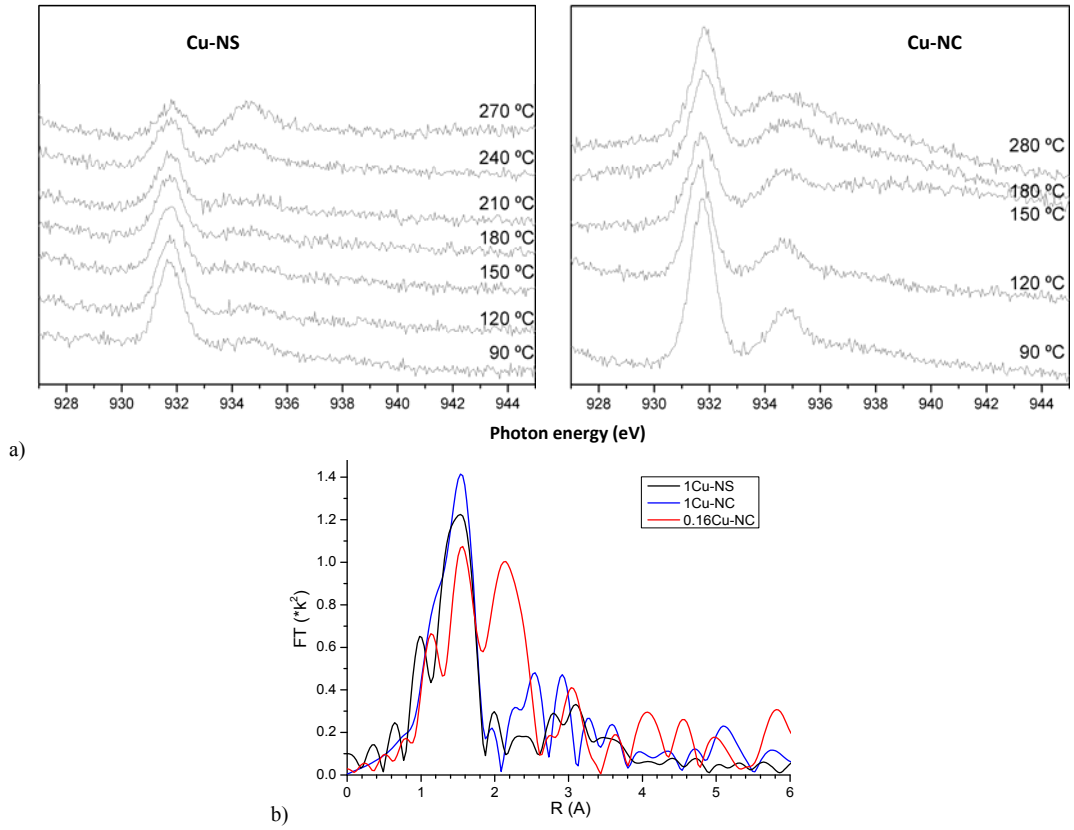

Fig. 1 a) Cu L_3 XANES spectra (recorded through the Cu LMM Auger electrons) of samples Cu-NC and Cu-NS under 0.5 mbar CO at increasing temperatures. b) k^2-weighted Fourier transforms of Cu K edge EXAFS oscillations recorded for calcined catalysts

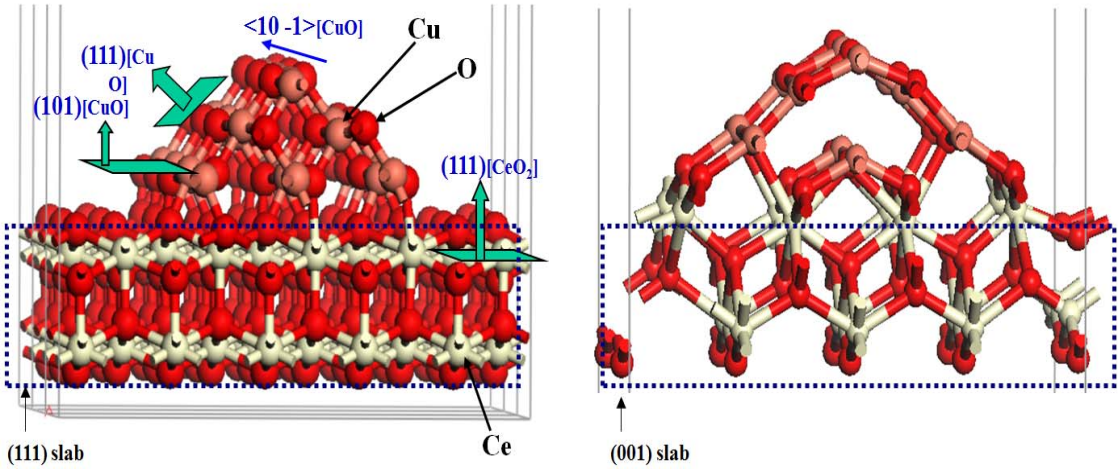

Fig. 2 Models of CuO clusters on CeO_2 surfaces. Left: (111), right: (001)

Both observations are justified by DFT+U calculations. CuO particles (represented by a CuO nanorod) become much more distorted on CeO_2 (001) (Fig. 2), due to a stronger interaction with the more reactive (001) surface (which contains less coordinated Ce ions). Adhesion energy difference between both systems in this case amounts to 0.67 eV/interface Cu atom. Furthermore, creating oxygen vacancies in both CuO and Cu_2O clusters is found to require more energy in the $CuO_x/CeO_2(001)$ case.

4 Conclusions

Synchrotron-based X-ray spectroscopies and DFT modelling confirm that CuO interacts more strongly with the (001) surface of ceria, leading to important particle distortion and to a more favoured transfer of electrons from CuO_x to CeO_2 upon reduction, which keeps copper in a more oxidized state. This explains the differences in CO-PROX selectivity between Cu-NC and Cu-NS catalysts.

Acknowledgements

Financial support from MINECO Plan Nacional project CTQ2012-32928 and European COST Action 1104 is acknowledged. Also computer centres IFCA and CTI-CSIC are thanked for their providing computing time on the parallel machines *altamira* and *trueno*.

References

[1] a) D. Gamarra, C. Belver, M. Fernández-García, A. Martínez-Arias. *J. Am. Chem. Soc.* 129 (2007) 12064; b)D. Gamarra, G. Munuera, A.B. Hungría, M. Fernández-García, J.C. Conesa, P.A. Midgley, X.Q. Wang, J.C. Hanson, J.A. Rodríguez, A. Martínez-Arias, *J. Phys. Chem. C* 111 (2007) 11026.

[2] D. Gamarra, A. López Cámara, M. Monte, S.B. Rasmussen, L.E. Chinchilla, A.B. Hungría, G. Munuera, N. Gyorffy, Z. Schay, V. Cortés Corberán, J.C. Conesa, A. Martínez-Arias, *Appl. Catal. B: Environmental* 130-131 (2013) 224.

[3] M. Monte, D. Gamarra, A. López Cámara, S.B. Rasmussen, N. Gyorffy, Z. Schay, A. Martínez-Arias, J.C. Conesa, *Catal. Today* 229 (2014) 104.

II-OP35

A Density Functional Theory Study on the Mechanism of the Cycloaddition of CO_2 and Epoxides

Offermans W.K.[1*], Gürtler C.[1], North M.[2], Leitner W.[3], Müller T. E.[1]

1 - CAT Catalytic Center, ITMC, RWTH Aachen University, Aachen, Germany
2 - Department of Chemistry, University of York, York, United Kingdom
3 - Lehrstuhl für Technische Chemie und Petrolchemie, RWTH Aachen University, Aachen, Germany

* Willy.Offermans@CatalyticCenter.RWTH-Aachen.de

Keywords: carbon dioxide utilisation, carbonates, epoxides, modelling reaction mechanism, homogeneous catalysis, DFT

1 Introduction

Depending on applied conditions and the choice of catalyst, the cycloaddition of carbon dioxide and epoxides leads to cyclic carbonates or polyethercarbonates (Scheme 1). Both possible products represent valuable, industrial compounds [1]. For example, cyclic carbonates can be used as aprotic solvents, precursors for polymers and pharmaceutical intermediates. Most current catalysts for the cycloaddition, which are used in industrial processes, require the use of high reaction temperatures and/or high pressures of carbon dioxide.

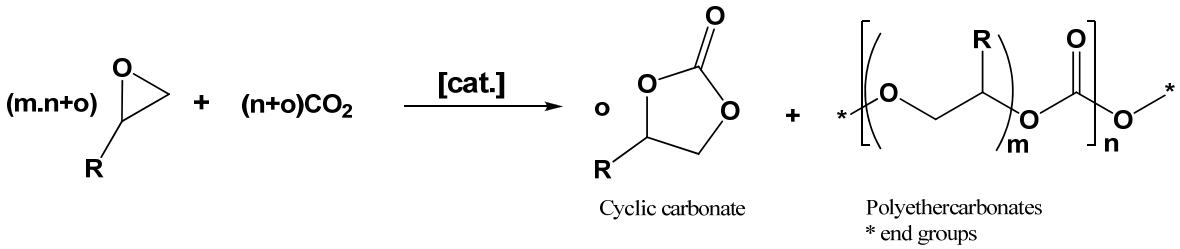

Scheme 1: Catalyzed (poly)cycloaddition of CO_2 and epoxides to polyethercarbonates and/or cyclic carbonates

Systems based on tetrabutylammonium bromide and μ-oxo bridged bimetallic aluminum complexes, such as [{Al(acen)}$_2$•(μ-O)] or [{Al(salen)}$_2$•(μ-O)], have been identified as catalysts for the cycloaddition of CO_2 and epoxides to cyclic carbonates at atmospheric pressure and close to room temperature [2]. It has been anticipated that these μ-oxo bridged bimetallic aluminum complexes act as Lewis acid [2]. A likely mechanism is proposed as follows: The epoxide coordinates to one of the aluminum centers and is ring-opened by bromide to a halogenated alkoxide. CO_2 is presumably activated by tributylamine to a zwitter-ionic carbonate, that can add to the other free aluminum atom of the adduct of [{Al(acen)}$_2$•(μ-O)] and epoxide. The carbonate and alkoxide are envisaged to react at the scaffold of the bimetallic aluminum complex to the cyclic carbonate. Inspired by this, we started density functional theory calculations to model the proposed mechanism *in silico*.

2 Experimental/methodology

Electronic structure calculations within the framework of density functional theory (DFT) were performed by using the DMol^3 program [2,3]. The Perdew-Burke-Ernzerhof functional to account for the exchange-correlation of the electrons was applied [4]. A correction for dispersion interactions, as proposed by Grimme and implemented by McNellis et al., was applied [5,6]. A double numerical basis set plus a polarization d-function on all non-hydrogen atoms and a polarization p-function on all hydrogen atoms was used to expand the one-electron Kohn-Sham eigenfunctions. Full electron, spin restricted calculations were performed. No constraints were

applied during geometry optimization. All reactant and product states were shown to be minima by a normal mode frequency analysis. The synchronous-transit method was applied to localize possible transition states [2]. These states were further optimized by following eigenvectors to gain the best predicted configuration of the transition state. Transition states were analyzed by a normal mode frequency analysis and confirmed by only one imaginary frequency for the normal mode pointing into the direction of the reaction coordinate. It was confirmed by the calculation of the minimum energy path that the transition state connected the reactant and product state on the potential energy surface.

3 Results and discussion

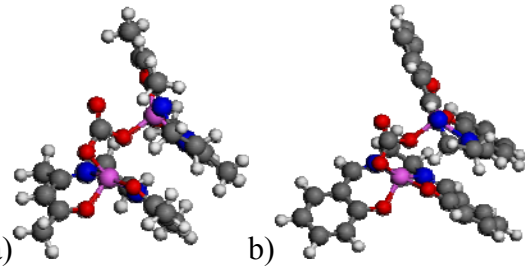

Fig. 1: Ball and stick models of predicted incorporation products of CO_2 and μ-oxo bridged bimetallic aluminum complexes: a) [{Al(acen)}$_2$(μ-CO_3)] and b) [{Al(salen)}$_2$(μ-CO_3)]. The colour coding of these carbonate complexes is intuitively: hydrogen, carbon, oxygen, nitrogen, and aluminum are white, grey, red, blue, and pink, respectively.

Already in an early stage, the modelling predicted incorporation products of CO_2 and [{Al(acen)}$_2$(μ-O)] or of CO_2 and [{Al(salen)}$_2$(μ-O)] (Figure 1), which were not considered in the reaction mechanism before. The isolation of [{Al(acen)}$_2$(μ-CO_3)] was not yet successful, but the existence of [{Al(salen)}$_2$(μ-CO_3)], its salen analogon, was proven experimentally by ESI-MS, NMR, and IR analytics. Moreover a chemical proof was found by showing that the latter carbonate complex can react with propylene oxide to produce propylene carbonate. Thus it is plausible that the carbonate complex plays a role in the catalysis.

4 Conclusions

Incorporation products of CO_2 and μ-oxo bridged bimetallic aluminum complexes were predicted by DFT modelling. Inspired by these findings, the existence of [{Al(salen)}$_2$(μ-CO_3)] was proven experimentally and this compound was shown to react with propylene oxide to propylene carbonate. Based on this we tentatively conclude that we have predicted and found interesting intermediates in the catalytic cycle of epoxides and CO_2. The focus of the modelling is now to elucidate their role in the cycloaddition of CO_2 and epoxides.

Acknowledgements

W. Offermans thanks the European Union for financial funding of the project CyclicCO2R (grant number: 309497). We further acknowledge the financial support of Bayer MaterialSience, Bayer Technology Services and RWTH Aachen University.

References

[1] M. Peters, B. Köhler, W. Kuckshinrichs, W. Leitner, P. Markewitz, and T. E. Müller, *ChemSusChem*, **4**, (2011) 1216.
[2] M. North and R. Pasquale, *Angew. Chem. Int. Ed.* **48**, (2009) 2946.
[3] B. Delley, *J. Chem. Phys*. **92**, (1990) 508.
[4] B. Delley, *J. Chem. Phys*. **113**, (2000) 7756.
[5] J. P Perdew, K. Burke, and M. Ernzerhof, *Phys. Rev. Lett*. **77**, (1996) 3865.
[6] S. Grimme, *J. Comp. Chem.* **27**, (2006) 1787.
[7] E. R. McNellis, J. Meyer, and K. Reuter, *Phys. Rev. B* **80**, (2009) 205414.
[8] N. Govind, M. Petersen, G. Fitzgerald, D. King-Smith, and J. Andzelm, *Comput. Mater. Sci.* **2003**, (2003) 250.

II-OP36

Effect of Structure and Composition of Gold and Gold-Palladium Clusters in H_2O_2 Formation

Pichugina D. A.*, Beletskaya A.V., Kuzmenko N.E.

Lomonosov Moscow State University, Department of Chemistry, Moscow, Russia

* daria@phys.chem.msu.ru

Keywords: DFT, gold, palladium, clusters, hydrogen, peroxide

1 Introduction

Hydrogen peroxide is one of the most important green oxidants. The synthesis of H_2O_2 involving a direct hydrogenation of oxygen has attracted interest as it is an environmentally friendly process. Palladium-based catalysts have high activity in direct synthesis of H_2O_2 but low selectivity due to H_2O formation as an unwanted biproduct. Using a bimetallic $AuPd/Al_2O_3$ and AuPd/C catalysts it is possible to increase the yield of H_2O_2 [1-3]. Precise information concerning the catalytic sites of Au, Pd, and AuPd particles governing H_2O_2 and H_2O formation has not been achieved yet. A quantum chemical simulation based on DFT was widely used for the study of the catalytic reaction mechanism and the nature of active sites of gold clusters [4,5]. Here we present the results of DFT simulation of H_2O_2 formation from H_2 and O_2 including the steps 1-10 (Fig. 1) on gold and gold-palladium clusters: Au_n, $Au_{n-1}Pd$ (n=8, 20, 32), Au_4Pd_4, $AuPd_7$.

2 Methodology

Structures optimization and energy calculation were performed using spin-polarized Perdew−Burke−Ernzerhof (PBE) functional of density functional theory (DFT). The Priroda code was used for an all-electron calculation in scalar−relativistic approximation, which is based on the full four component one-electron Dirac equation with spin−orbit effects separated out. The energy-optimized extended Gaussian basis set of triple-polarized quality of the large component, and the corresponding kinetically balanced basis for the small component was used: Au [30s29p20d14f/8s756d2f], Pd [26s23p16d5f/7s6p4d1f], O [10s7p3d/3s2p1d], and H [6s2p/2s1p]. We have considered the influence of cluster's structure and composition on the energy differences (ΔE) and activation energy (E_a) of the steps of H_2O_2 formation (Fig. 1). The exact structure of TS has been determined according to the procedure of eigenvector following with the Berny algorithm.

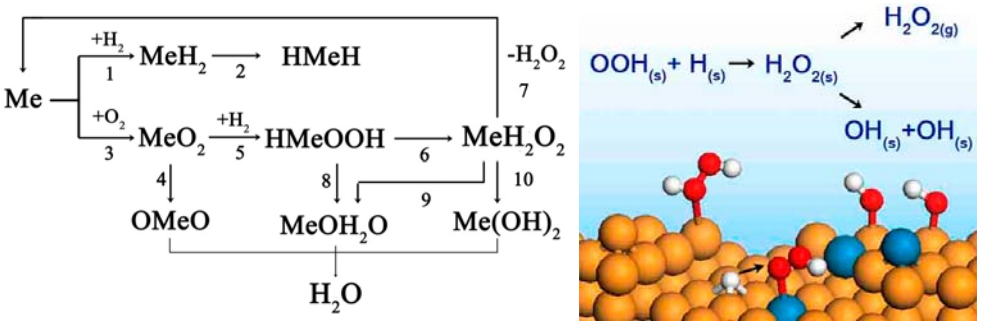

Fig. 1. The steps of the H_2O_2 formation from H_2 and O_2.

3 Results and discussion

An ambiguous mechanism is hidden behind the seemingly simplistic chemical equation ($H_2 + O_2 = H_2O_2$). According to physical chemistry formalism, the negative value of ΔE, low E_a in steps 1-3,5, and 6 favor the formation of $H_2O_{2(s)}$, and the small value of desorption energy of H_2O_2 (step 7) provides the formation of the final product, $H_2O_{2(g)}$. The formation of H_2O requires breaking of the O−O bond in at least one of the intermediates ($O_{2(s)}$, $OOH_{(s)}$, and $H_2O_{2(s)}$). Thus to increase the selectivity, steps 4, 8-10 should have high E_a, and desorption energy of H_2O_2 should be lower than the E_a of step 10. The condition of activity and selectivity is considered on Au_n, $Au_{n-1}Pd$ (n=8, 20, 32), Au_4Pd_4, $AuPd_7$ clusters which are simulated the active site of the catalyst.

Firstly, we consider H_2O_2 formation on Au_8 and Au_7Pd. The gold cluster weakly adsorb of H_2, O_2, it has high activation energies in steps (6) and (10). So, Au_8 is inert toward the H_2O_2 synthesis as well as to H_2O byproduct formation. Bimetallic $Au_{8-x}Pd_x$ (x=1, 4, 7) clusters can strong adsorb H_2 and O_2 on Pd atom and form active $H_{(s)}$ and $O_{(s)}$. The low E_a's in step (6) obtained for $Au_{8-x}Pd_x$ promote H_2O_2 formation with high activity, but low E_a in step (10) causes low selectivity due to O−O bond rupture in $H_2O_{2(s)}$. The spin conservation according to the Winger–Witmer rules from the triplet state in the intermediates to the singlet state occurs in step (5). The rate-determining step is the hydrogenation of $OOH_{(s)}$.

Influence of the cluster's structure on the H_2O_2 formation is studied on Au_n and $Au_{n-1}Pd$ (n=2, 8, 20, 32). A gold atom located on the top of Au_{20} and Au_{32} is considered as active sites. For bimetallic $Au_{19}Pd$ and $Au_{31}Pd$, we study the steps (6), (7), (10) on Pd atom located on the top of $Au_{31}Pd$ and facet of $Au_{19}Pd$. The gold clusters demonstrate low activity in hydrogen peroxide formation. Substitution of gold atoms by palladium in Au_{20} leads to an increase in the activity of a catalyst in the considered reaction of H_2O_2 formation, but low coordinated Pd atoms are also responsible lowering the selectivity because of H_2O formation. The compromise between activity and selectivity suggests that a Pd atom surrounded by gold atoms facilitates H_2O_2 synthesis.

4 Conclusions

Based on physical chemistry formalism, the conditions of the activity and selectivity of the H_2O_2 formation are supposed and tested on small Au and AuPd clusters as a model of active sites. The gold clusters demonstrate low activity in hydrogen peroxide formation. A Pd atom surrounded by gold atoms in AuPd clusters facilitates H_2O_2 synthesis.

Acknowledgements

This research was supported by the Projects RFBR 13-03-00320, RFBR 14-01-00310, and NSh 3171.2014.3.

References

[1] J.K. Edwards, E. Ntainjua, A.F. Carley, A.A. Herzing, C.J. Kiely, G.J. Hutchings, Angew. Chem. Int. Ed. 48 (2009) 8512.
[2] P. Landon, P.J. Collier, A. J. Papworth, C.J. Kiely, G.J. Hutchings, Chem. Commun. (2002) 2058.
[3] D. Gudarzi, W. Ratchananusorn, I. Turunen, M. Heinonen, Tapio Salmi, Catalysis Today. (2014) (in press).
[4] A.V. Beletskaya, D.A. Pichugina, A.F. Shestakov, N.E. Kuz'menko, J. Phys. Chem. A. 117 (2013) 6817.
[5] S.A. Nikolaev, D.A. Pichugina, D.F. Mukhamedzyanova, Gold Bulletin. 45 (2012) 221.

II-OP37

Surface Phenomena Affecting the Performance of Pd-Ag Alloys

Svenum I.-H.[1], Vicinanza N.[2], Herron J.A.[3], Peters T.A.[1], Bredesen R.[1], Mavrikakis M.[3], Venvik H.J.[2*]

1 - SINTEF Materials and Chemistry, Trondheim, Norway
2 - Department of Chemical Engineering, NTNU, Trondheim, Norway
3 - University of Wisconsin-Madison, Madison, WI, USA

* Hilde.j.Venvik@ntnu.no

Keywords: PdAg, surface, density, functional, theory, hydrogen, carbon, monoxide, adsorption, permeation

1 Introduction

Palladium based alloys have interesting catalytic properties in selective hydrogenations, and are also important in hydrogen separation membrane technology [1]. By alloying, it is possible to enhance the catalytic activity or selectivity [2], as well as to suppress the formation of hydride phases under hydrogen exposure. Pd alloyed with Ag has been heavily investigated in this respect [3], and the structure and composition of the PdAg surface will affect the bond strength of adsorbed species. On the other hand, the reactive environment may alter the surface composition through segregation [4,5]. In order to investigate adsorption and dissociation of H_2 on PdAg alloy surfaces we have performed a combined experimental and theoretical study of surface phenomena affecting hydrogen transport through PdAg membranes.

2 Methodology

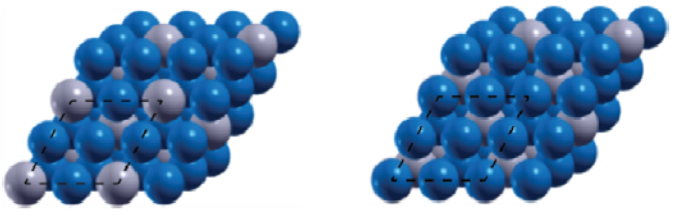

The theoretical investigations have been performed using periodic, self-consistent DFT calculations with the DACAPO code [6,7]. The exchange-correlation energy and potential are described by the generalized gradient approximation (GGA-PW91) [8]. The Pd_3Ag surface is modelled using a slab orientated in the (111) direction. Adsorption and reaction properties of $Pd_3Ag(111)$ with varying surface composition are investigated, as represented by either bulk (25% Ag) or Pd (0% Ag) termination, as displayed in Figure 1. Activation barriers for H_2 dissociation with increasing amount of CO pre-adsorbed are calculated using the climbing image nudged elastic band (CI-NEB) method [9].

Pd-23 wt% Ag thin films were prepared by a two-step magnetron sputtering technique [10,11]. Exposures and membrane permeation measurements were performed in a micro channel configuration that eliminates gas phase mass transfer limitations, before and after heat treatment in air. Competitive adsorption was investigated by addition of CO to the feed, and the PdAg thin films were further analysed through equilibrium sorption measurements and atomic force microscopy.

3 Results and discussion

Experimentally, we find that the hydrogen transport through thin Pd-Ag membranes is limited by surface phenomena below a certain thickness, which depends on how the surface has been treated (exposure and temperature) [12,13]. Exposure to air at elevated temperature is found to lift the surface limitations to the H_2 transport kinetics in the thickness range 1-5 μm, and CO poisoning effects are also reduced [14]. The hydrogen solubility remains, however, unaffected. The membrane surface generally roughens, but this cannot fully account for the observed improvements. This suggests that phenomena affecting the surface kinetics need further investigation.

The experimental data have been correlated to DFT calculations, revealing that the structure and composition of the PdAg surface is important with respect to hydrogen adsorption, dissociation, dissolution and desorption phenomena. At low coverage, H and CO favour hollow sites on bulk- and Pd-terminated $Pd_3Ag(111)$ [5]. The binding weakens upon increasing coverage, but is consistently stronger when the surface termination is Pd dominated. CO and H generally also favour the same adsorption sites, leading to inhibition of H adsorption by CO. The adsorption energetics of hydrogen is weakened in the presence of CO, and these changes depend on surface composition. A higher coverage of CO co-adsorbed with H is predicted on a Pd-terminated compared to a bulk-terminated surface. Finally, the activation barrier for hydrogen dissociation is found to increase due to adsorbed CO on the surface, but is significantly lower for the Pd-terminated surface.

4 Conclusions

Hydrogen permeation experiments and theoretical investigations can be applied to elucidate surface phenomena, i.e. adsorption, dissociation, and dissolution, on Pd alloy surfaces. The theoretical investigations explain how the surface composition may be important in this respect, demonstrating how the competitive adsorption as well as the reactivity of the Pd-Ag surface is altered by changes in the on surface composition.

Acknowledgements

The financial support from the Research Council of Norway, NTNU Thematic Strategic Area "Energy", and Statoil ASA through the NTNU-SINTEF Gas Technology Centre is thankfully acknowledged. J. A. H. and M. M. gratefully acknowledge financial support by the US Department of Energy, Office Basic Energy Sciences. Computational resources include Norwegian (NOTUR) and American supercomputer facilities.

References

[1] R. Bredesen, et al, in "Membrane Engineering for the Treatment of Gases, Volume Gas-separation Problems combined with Membrane Reactors" (E. Drioli and G. Barbieri, Eds.), p. 40, The Royal Society of Chemistry, 2011.
[2] J. K. Nørskov et al., Nature Chem. 1 (2009) 37.
[3] G.J. Grashoff et al., Platinum Met. Rev. 27 (1983) 157157.
[4] J. Greeley, M. Mavrikakis, Nature Mater. 3 (2004) 810.
[5] I-H. Svenum et al., Catal. Today 193 (2012) 111.
[6] B. Hammer et al., Phys. Rev. B 59 (1999) 7413.
[7] J. Greeley et al., Annu. Rev. Phys. Chem. 53 (2002) 319.
[8] J. P. Perdew et al., Phys. Rev. B 46 (1992) 6671.
[9] G. Henkelman et al. J. Chem. Phys. 113 (2000) 9901.
[10] R. Bredesen, H. Klette, "Method of manufacturing thin metal membranes", US Patent (2000) 6,086, 729.
[11] H. Klette, R. Bredesen, Membr. Techn. 2005 (2005) 7.
[12] A.L. Mejdell, et al. J. Membr. Sci. 307 (2008) 96.
[13] N. Vicinanza, et. al., J. Membr. Sci. 476 (2015) 602.
[14] A.L. Mejdell, et al. J. Membr. Sci. 350 (2010) 371.

II-OP38

Understanding Selectivity Issues in Rh-Catalyzed CO Hydrogenation

Filot I.A.W., Van Santen R.A., Hensen E.J.M.*

Schuit Institute of Catalysis and Institute of Complex Molecular Systems, Eindhoven University of Technology, Eindhoven, The Netherlands

* i.a.w.filot@tue.nl

Keywords: Fischer-Tropsch, density functional theory, microkinetic modelling, rhodium

1 Introduction

The hydrogenation of CO to ethanol is attractive, for instance, as an alternative route of light olefins production. Several catalysts are known to catalyse syngas conversion into alcohols. We investigated Rh nanoparticle catalysts for this purpose. Detailed analysis of the CO hydrogenation chemical network on Rh provides a better understanding of the Fischer-Tropsch reaction mechanism on other metals. The most important question to be answered are: what is the rate-limiting step and what factors determine the selectivity to ethanol vs. methane.

2 Methodology

Density functional theory calculations were performed to investigate all elementary reaction steps relevant to CO hydrogenation over Rh. These reaction include those steps necessary to produce alkanes, alkenes, oxygenates, methane and water. From the obtained dataset, rate constants were constructed using the Eyring equation and microkinetics simulations were performed as published previously.[1] In these simulations, a Degree of Rate Control analysis[2] as well as a Degree of Selectivity Control analysis were performed to investigate the propensity of the individual elementary reaction steps on the overall activity and selectivity of CO hydrogenation over Rh.

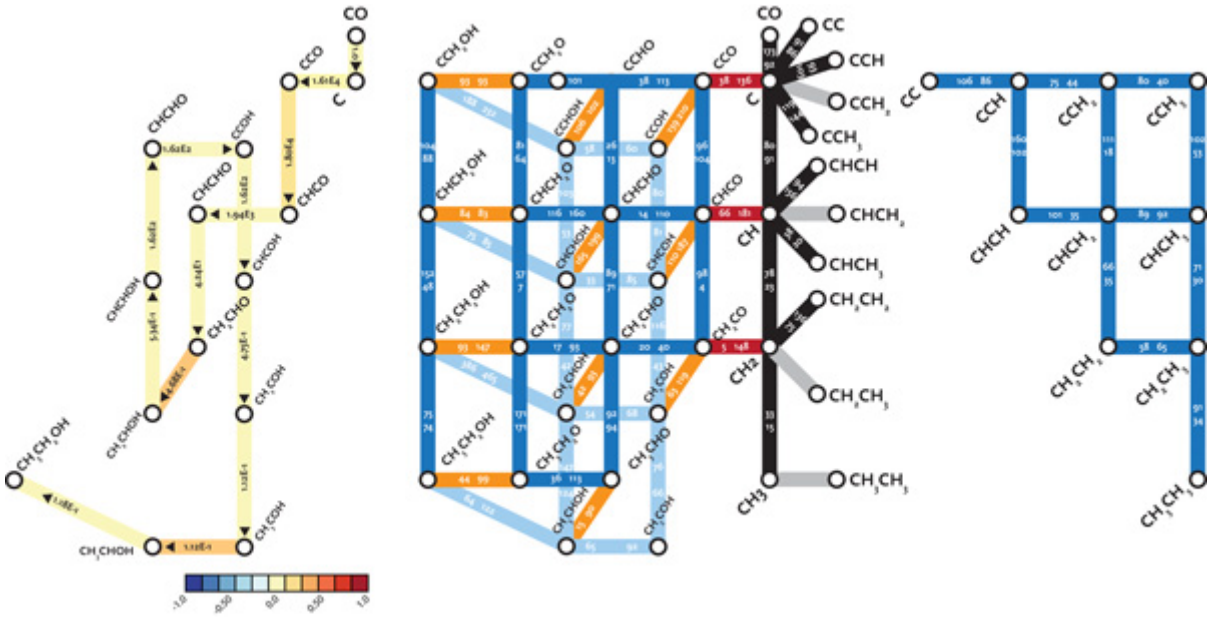

Fig. 1. (left) DRC analysis of ethanol formation.(right) CO hydrogenation reaction network diagram.

3 Results and discussion

Figure 1 shows the activation energies (both forward and backward direction) of all elementary reaction steps to form C_2 species in CO hydrogenation over Rh as well as the DRC analysis for ethanol formation. The three steps that mainly control the ethanol formation are CCO hydrogenation to CHCO, CH_3CHO hydrogenation to CH_3CHOH and CH_3COH hydrogenation to CH_3CHOH. The coupling step with the highest rate towards ethanol formation was found to be C+CO coupling (not shown here). Figure 2 shows the DSC analysis. From this analysis, we can see that ethanol production can be improved by inhibiting CH_2 and CH_3 hydrogenation.

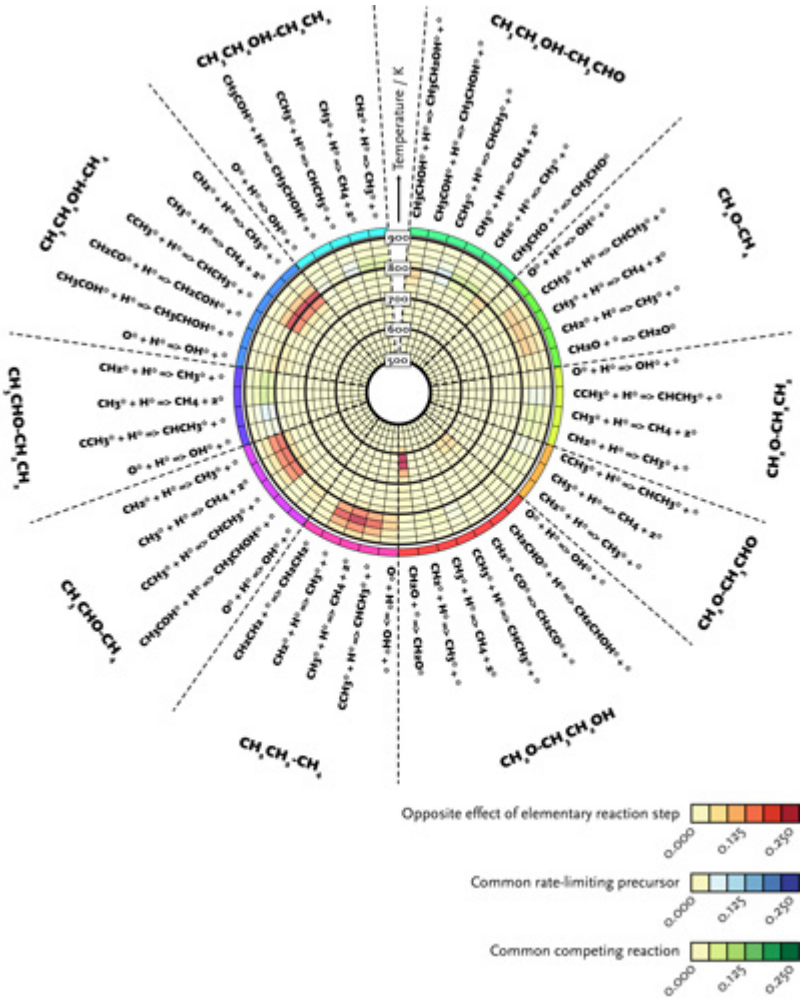

Fig. 2. Correlation between degree of selectivity control parameters showing which steps control which product selectivity as a function of temperature.

4 Conclusions

Our study reveals that (i) CO dissociation does not limit the reaction rate nor the selectivity and (ii) ethanol is formed by C+CO coupling followed by a complex series of hydrogenation and dehydrogenation reactions. Ethanol selectivity can be improved by decreasing the rate of CH_x hydrogenation that promotes methane formation. These insights will be discussed in the frame of promoter effects described in literature.

References

[1] Filot, I.A.W., van Santen, R.A., Hensen, E.J.M., *Angew. Chem. Int. Ed.,* **2014**, 53, 12746
[2] Stegelmann, C.; Andreasen, A.; Campbell, C. T. *J. Am. Chem. Soc.* **2009**, 131, 8077.

II-OP39

In silico Exploration of Bimetallic Sulfides Catalysts

Saab M., Raybaud P.*

Direction Catalyse et Séparation, IFP Energies nouvelles, Solaize, France

* mohamad.saab@ifp.fr

Keywords: density functional theory (DFT), transition, metal, sulfides (TMS), hydrodesulfurization, CoMoS, NiMoS

1 Introduction

Degradation of the crude oil properties and strengthening of environmental specifications on transportation fuels motivates the continuous improvement of hydrotreating catalysts efficiency. The industrial NiMoS and CoMoS active phases are constituted of MoS_2 nano-layers promoted either by nickel or cobalt (Figure 1) [1]. While the promotion effect of other 3d transition metals (Me) are known to be far much lower, MoS_2 nano-layers promoted by 3d metals remain poorly described. In this communication, we propose a systematic theoretical study of MeMoS phases in order to quantify periodic trends in structural, electronic, and energetic descriptors of MeMoS and better understand their catalytic activities.

2 Experimental/methodology

For total energy calculations, we use the Vienna ab-initio simulation package (VASP) [3], based on periodic plane wave density functional theory (DFT). We use generalized gradient approximation (GGA-PW91), including spin polarization corrections [2]. The cut-off energy of the plane wave basis set is fixed at 337.0 eV.

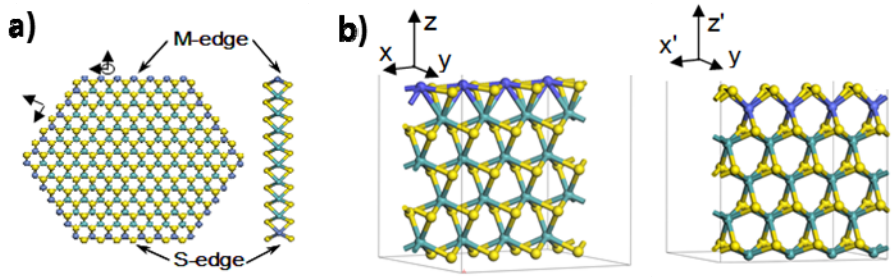

Figure 1. a) MeMoS nano-crystallite, b) $Mo_{16}Me_4S_z$ periodic slabs used to simulate the M-edge and S-edge of a promoted nano-crystallite with various promoter Me content. (Yellow balls: sulfur, green balls: molybdenum, blue balls: Me)

To determine the local structure and sulfur coverages of the two edges (M-edge and S-edge) present in HDS reaction conditions, we calculate the edge energies of the optimized slab (ionic forces smaller than 0.02 eV/Å) by using the following equations:

$$Mo_{16}Me_4S_{z_0} + (z - z_0)H_2S \rightarrow Mo_{16}Me_4S_z + (z - z_0)H_2$$

$$\Delta G = E(Mo_{16}Me_4S_z) - E(Mo_{16}Me_4S_{z0}) - (z - z_0)(\Delta\mu_s + E(S_\alpha))$$

is the stoichiometry of the slab used for simulating the promoted M- or S-edge (Figure 1) with 4 nonequivalent Me edge sites. Z represents the number of sulfur atoms which depends on the sulfidation conditions. Note: z_0=32 corresponds to the reference slab exposing M-edge with 0% S and S-edge with 100%S. $\Delta\mu_S$ represents the chemical potential of sulfur connected to (T, $p(H_2S)/p(H_2)$) conditions [4].

3 Results and discussion

Magneto-structure effects are known to play an important role in some bulk 3d TM monosulfides [5]. For MeMoS edge structures, we also found that the edge energy is influenced by the magnetic states of Me=Cr, Mn, Fe (weak effect for Co). The largest effect is revealed for the M-edge with 0%S on MnMoS exhibiting magnetism of ~3 μ_B per Mn atom (local antiferromagnetism). Moreover, this effect depends on the sulfur coverage itself. This first result shows that magnetism may be a key descriptor of these MeMoS phases.

Including spin corrections, Figure 2 shows that the S-coverage at the edge depends on HDS conditions, on the edge and on the nature of the 3d metal (Me). For the M-edge, the larger the d-band filling is, the lower the coverage of sulfur at the M-edge : Ti > Mn > Co > Ni. In HDS conditions ($-1 < \Delta\mu_S < -0.8$), the preferred S-coverage is 25% for TiMoS M-edge. By contrast, the S coverage drops to 0% S for NiMoS M-edge where Ni is stabilized in a square planar environment. Intermediate coverages and edge stabilization are found for Mn and Co. For the S-edge, Figure 2b shows that in HDS conditions, Co is strongly stabilized with 50%S leading to a tetrahedral environment as shown earlier [8]. For Ni, Ti, and Mn, the decrease of the S-coverage is also favorable as promoter, with a weaker energy stabilization.

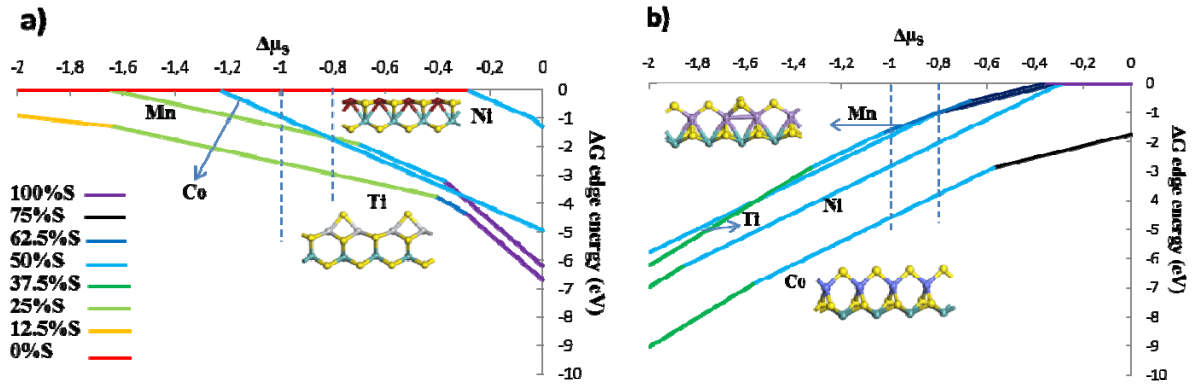

Figure 2. Edge energy diagram as a function of $\Delta\mu_S$: a) M-edge and b) S-edge. For sake of clarity we only report the results for Ti, Mn, Co and Ni.

4 Conclusions

We have determined the energy diagrams for two relevant edges of the mixed MeMoS nano-crystallites as a function of HDS reaction conditions. The nature of the 3d metal (Me) impacts differently the structure (S-coverage) and energy of the two edges. In addition, we highlight non negligible magneto-structure effects for Cr, Mn, Fe promoted systems. We will further discuss how the 3d metals influence the equilibrium shape of MeMoS nano-crystallites suspected to impact catalytic activity.

References

[1] H. Toulhoat , P. Raybaud, Catalysis By Transition Metal Sulfides, TECHNIP, Paris, 2013.
[2] J. P. Perdew, Y. Wang, Phys. Rev. B 45 (1992) 13244.
[3] G. Kresse, J. Furthmüller, Phys. Rev. B 54 (1996) 11169; G. Kresse, D. Joubert, Phys. Rev. B 59 (1999) 1758.
[4] E. Krebs, B. Silvi and P. Raybaud, Catal. Today, 130 (2008) 160.
[5] D. Hobbs and J Hafner, J. Phys.: Condens. Matter 11 (1999) 8197-822.

II-OP40

Effect of Mo Addition on Hydrotreating Activity, Stability to Corrosion, and Physicochemical Properties of Ni-Based Catalysts for Bio-Oil Upgrading

Bykova M.V.[1,2*], Rekhtina M.A.[1,2], Kaichev V.V.[1], Saraev A.A.[1], Shmakov A.N.[1], Lebedev M.Yu.[1], Venderbosch R.H.[3], Yakovlev V.A.[1]

1 - Boreskov Institute of Catalysis SB RAS, Novosibirsk, Russia
2 - Novosibirsk State University, Novosibirsk, Russia
3 - Biomass Technology Group B.V., Enschede, The Netherlands

* bykova@catalysis.ru

Keywords: bio-oil, hydrodeoxygenation, molybdenum, Ni-based catalysts, modification, stability

1 Introduction

Currently, the needs of the transport sector account for about one-third of global energy consumption, while 95% of them are covered by the refinery. The use of lignocellulosic biomass for biofuels production is believed to make a worthy alternative to fossil oil in future. One of the prospective approaches for the biomass conversion into biofuels is fast pyrolysis giving a liquid product − bio-oil (pyrolysis oil, PO). Among the different types of PO application [1] its co-processing with conventional oil refinery products on the FCC units should be outlined. But before such processing pyrolysis oil should be upgraded to reduce its polarity, corrosiveness, etc. to make its properties resemble those of non-polar conventional hydrocarbons. Catalytic hydrotreatment (HDO) is a potential way to improve bio-oil characteristics. The catalysts for this process should meet a number of requirements, such as high activity in hydrogenation/hydrodeoxygenation reactions, and high stability, which is obvious as PO is a quite aggressive reactive medium. The research activities in this field are still in progress as the development of perfect catalytic system presents an obstacle.

Recent works [2] have shown that Ni-based catalysts (with high Ni content, more than 50 wt.%) prepared by sol-gel technique with addition of Cu possess high activity in hydrotreatment of PO and its model mixtures. Nevertheless, these systems still needed an improvement as they did not show appropriate stability (active component leaching, coking, agglomeration). In latest investigations it was shown that modification of these catalysts by P-/Mo-containing agents results in the significant improvement of mechanical strength, resistance to corrosion, and lowering of coke deposition [3]. But the variation of modifiers content has not been studied yet. Thus the aim of the present research work was to study the effect of different Mo content on the catalysts performance in HDO process, their stability against leaching, and to make a correlation with their physicochemical properties.

2 Experimental

A series of Ni-based catalysts was prepared by sol-gel technique described elsewhere [4], using commercial $NiCO_3 \cdot 3Ni(OH)_2 \cdot 4H_2O$, $2CuCO_3 \cdot Cu(OH)_2$, and ethyl silicate-32. Mo-containing agent MoO_3 was added during the sol-gel preparation stage as well. The Ni/Cu mass ratio was kept constant, while Mo/Ni ratio was varied. Sol-gel stage was followed by drying (100 ^oC), calcination (500 ^oC), reduction in tubular quartz reactor (H_2 flow, 500 ^oC), and passivation (2 vol. % O_2 in N_2). The catalysts were designed as **NiCuMo(X)/SiO_2**, where X = 0, 0.04, 0.08, 0.125, 0.175, and 0.3 − Mo to Ni atomic ratio.

Samples thus prepared were tested in hydrotreatment of guaiacol (GUA) being a well-known model compound of pyrolysis oil. Hydrotreatment process has been carried out in a batch reactor at 320 °C, H_2 pressure 9 MPa (kept constant during the reaction), using 0.2 g of reduced

catalyst in powder form and guaiacol solution in hexadecane (V_{GUA}/V_{solv}=1/10). During the process the liquid samples were withdrawn from the reactor for further chemical analysis (GC and GC-MS). The catalysts stability to corrosion was studied by the glacial acetic acid treatment at severe conditions (boiling T = 118 ^{o}C, 2 hours). To characterize the catalysts a wide range of physicochemical methods was employed: X-Ray fluorescence, TPR, XRD, XPS, CO chemisorption, BET, HRTEM.

3 Results and discussion

The investigation of NiCuMo(X)/SiO_2 resistance to corrosion in glacial acetic acid have shown the gradual increase of stability with the amount of Mo in the catalyst. The best result was obtained for the sample with the highest Mo content − NiCuMo(0.3)/SiO_2 (only 1.8% mass loss in contrast to 30.9% for non-modified NiCu/SiO_2 system).

Very remarkable results were obtained during the catalysts testing in HDO process. It was observed that GUA conversion over NiCuMo(X)/SiO_2 series of catalysts proceeds by two main routs: (i) initial benzene ring hydrogenation (into methoxycyclohexanoles) followed by hydrodeoxygenation of O-containing groups (HYD-route, Fig. 1), (ii) first elimination of oxy-groups (with benzene formation) and further hydrogenation of aromatic ring (HDO-route, Fig. 1). In both cases cyclohexane was the final and the main product of GUA transformations. It was shown that increasing Mo content in the catalyst allowed higher contribution of HDO route with respect to HYD route, the latter was prevailing in the case of non-modified NiCu/SiO_2. Thus the use of Mo in Ni-based catalysts can shift the reaction routs and can be profitable in terms of hydrogen economy during the HDO process. Though this assumption needs to be checked further, using other model substrates and real feed. According to the catalysts characterization by physicochemical methods, the improvement of their resistance to corrosion and the changes in reaction selectivities during HDO process could be associated with the change of active component nature: electronic effects between Mo^0 and Ni^0, and the presence of coordinatively unsaturated species Mo^{x+} (x = 4, 5) in the catalysts composition, which can play a significant role in activation of O-containing compounds.

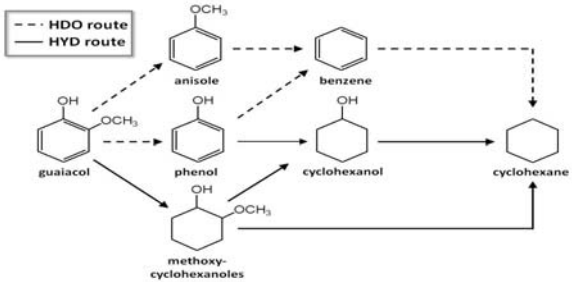

Fig. 1. Guaiacol conversion scheme over sol-gel NiCuMo(X)/SiO_2 catalysts.

Acknowledgements

This work was performed under the large scale collaborative project FASTCARD ("FAST Industrialisation by CAtalysts Research and Development", EU FP7, GA No 604277).

References

[1] S. Czernik, A.V. Bridgwater, *Energy Fuels.* 18 (2004) 590-598
[2] M.V. Bykova, D.Yu. Ermakov, V.V. Kaichev, et al. Appl. Catal. B: Env. 113-114 (2012) 296-307
[3] M.V. Bykova, D.Yu. Ermakov, S.A. Khromova, et al., *Catal. Today.* 220-222 (2014) 21-31
[4] M.A. Ermakova, D.Yu. Ermakov, *Appl. Catal. A.* 245 (2003) 277-288

II-OP41

Pd/C Catalysts Prepared by Direct Pyrolysis of Sawdust Impregnated by Palladium Nitrate for Hydrodechlorination of Chlorobenzenes

Lokteva E.S.[1,2*], Klokov S.V.[1,2], Golubina E.V.[1,2], Maslakov K.I.[1,2], Vasiliev K.Yu.[1,2], Antonova M.V.[1], Likholobov V.A.[2]

1 - M.V.Lomonosov Moscow State University, Chemistry Department, Moscow, Russia
2 - Institute of Hydrocarbons Processing of the Siberian Branch of the RAS, Omsk, Russia

* les@kge.msu.ru

Keywords: palladium, carbon support, pyrolysis, sawdust, hydrodechlorination, chlorbenzenes

1 Introduction

Hydrodechlorination (HDC) is a prospective way of polychlorinated wastes disposal due to the intrinsic absence of polychlorinated dioxins in products, reduced energy demands and possibility to reuse the hydrocarbon moiety of chlorinated compounds being disposed. Pd, supported on activated carbon, is very effective hydrogenation catalyst. High specific surface and relative inertness of active carbon provide good Pd particle size distribution in the range optimal for catalysis. Pyrolysis of sawdust in inert atmosphere at desirable temperature is the appropriate way to produce carbon support from the timber wastes. Besides, reductive atmosphere formed during pyrolysis, could provide the reduction of metal from the salt. Therefore this is promising method of one-step production of ready-to-use Pd/C catalysts. In this work Pd/C catalysts for chlorobenzene hydrodechlorination were produced by direct pyrolysis of the birch sawdust impregnated with $Pd(NO_3)_2$ in Ar flow.

2 Experimental/methodology

The catalysts were prepared by pyrolysis of sawdust impregnated with $Pd(NO_3)_2$ at 430°C in Ar (4 h) with or without pretreatment (Table). They were characterised by SEM (JSM 6490 LV, JEOL), TEM (JEM 2100F, JEOL), low-temperature N_2 adsorption-desorption (Micometrics ASAP 2000), XPS (Kratos Axis Ultra DLD), Raman spectroscopy (Horiba Jobin Yvon LabRAM HR 800 UV), TPR and DSC-TG (449PC Jupiter Netzsch, Netzsch GmbH) before and after catalytic tests in gas-phase HDC of chlorobenzene at 100-350°C (flow-type fixed bad tubular reactor, 8 mg of catalyst, H_2:chlorobenzene = 30), and tested in multi-phase HDC of hexachlorobenzene and 1,3,5-trichlorobenzene at 50°C (batch reactor, i-octane as a solvent, aliquat 336, aq.KOH, H_2).

Table. Pd/C catalysts prepared in this work

Sample	Pretreatment	S_{BET}, m^2/g	d of 90%Pd particles, nm	Pd, mas.%	CB conversion at 150°C, %
Pd/C(S)	Soaking of sawdust in water, 72 h	135	1.5-3	2	88
Pd/C(SUS)	Soaking of sawdust in water,72 h; sonification 22 kHz 2 h during soaking	146	2-7	3	80
Pd/C(HTG)	Hydrothermal treatment in H_2O vapor, 200°C, 1 h	17	2-10, 12-22	0.5	89
Pd/C(HTL)	Hydrothermal treatment in liquid H_2O, 200°C, 1 h	225	2-10	0.5	92
Pd/C(N)	No pretreatment	7	1.5-3	7	52

Pd/C(A)	HNO_3 washing	7	1.5-3	7	100

3 Results and discussion

Raman spectroscopy and XPS data for C1s electrons demonstrated that pyrolysis in Ar at 430°C transforms sawdust impregnated with $Pd(NO_3)_2$ to the material similar to activated carbon (Raman spectra contains both D and G lines), having biomorphic structure, according to SEM data. Pretreatment of sawdust makes possible to vary and increase S_{BET} (see Table) to as high as 225 m^2/g (Pd/C(HTL)), as opposed to 7 m^2/g for Pd/C(N) and Pd/C(A). By XPS it was found that Pd on the surface is in the metal state (Pd^0) in all samples. According to TEM data, the increase of S_{BET} is accompanied with broadening of Pd particle size distribution (PSD). Narrow PSD (1.5-3) was found for Pd/C(S); for Pd/C(HTG) it is the broadest one and even bimodal (see Table); in addition, large (about 500 nm) Pd-containing particles are seen in SEM images. Small fraction of PdO (15-30 nm in size) encapsulated in carbon support was found only for Pd/C(N) by TPR and electron diffraction analysis during TEM.

All prepared Pd/C catalysts provide 90-100% conversion to benzene at 250-350°C in gas-phase HDC of chlorobenzene. At 100-200°C the most active were catalysts with increased S_{BET} (Pd/C(S), Pd/C(SUS), Pd/C(HTL))(See Table). Pd/C(HTG) containing lowest fraction of 2-5 nm Pd particles was the less active in HDC of chlorobenzene at 100°C (23% conversion). The acid washing of sawdust to remove Ca and Mg (up to 0,2% in original sawdust, EDS data) (sample Pd/C(A)) decreases the CB conversion. The H_2 treatment of Pd/C(N)(280°C, 4h) leads to decrease of low-temperature CB conversion.

XPS analysis demonstrated the relative stability of the Pd/C after prolonged catalytic tests in chlorobenzene HDC: only about 10% Pd in Pd/C(S), Pd/C(SUS), Pd/C(HTL) and Pd/C(HTG) oxidized to PdO, and about 10% Pd in Pd/C(SUS), Pd/C(HTL) and about 5% Pd in Pd/C(S), Pd/C(HTG) transformed to $PdCl_2$.

Pd/C catalysts were active also in HDC of 1,3,5-trichlorobenzene and hexachlorobenzene in multi-phase batch system. Additional improvement of catalytic performance was achieved for CoPd/C catalysts, produced by pyrolysis of sawdust co-impregnated with Co and Pd nitrates. CB conversion at 150°C increases to 91% for CoPd/C (N).

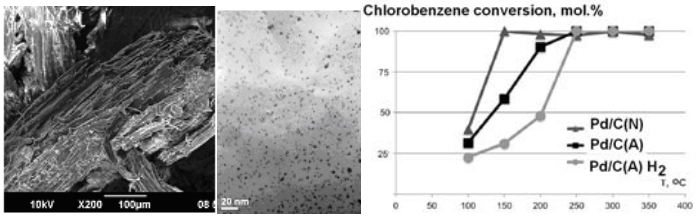

Fig. 1. TEM (a), SEM (b) images of Pd/C(N); CB conversion vs temperature

4 Conclusions

Pyrolysis of sawdust impregnated with $Pd(NO_3)_2$ in inert atmosphere is an appropriate way to produce Pd/C catalysts containing nanoparticles of Pd^0 on carbon support of biomorphic structure, active in gas-phase HDC of chlorobenzene and liquid-phase HDC of polychlorinated benzenes. Pretreatment of sawdust provides significant increase of S_{BET} (up to 225 m^2/g) at concurrent widening of Pd particle size distribution. The presence of alkali-earth metals in Pd/C and modification with Co improve catalytic properties.

Acknowledgements

This work was maintained by Russian Scientific Foundation (14-33-00018). This work was supported in part by M.V. Lomonosov Moscow State University Program of Development.

II-OP42

Formation Mechanism of Well-Dispersed Pd Nanoparticles with High Thermal Stability on SiO_2 Using $Pd(acac)_2$ as Precursor

Weng W.Z.*, Xie Y.H., Li B., Zheng Y.P., Huang C.J., Wan H.L.

State Key Laboratory of Physical Chemistry of Solid Surfaces, National Engineering Laboratory for Green Chemical Productions of Alcohols, Ethers and Esters, Department of Chemistry, College of Chemistry and Chemical Engineering, Xiamen University, Xiamen, China

* wzweng@xmu.edu.cn

Keywords: Pd/SiO_2, palladium, bis-acetylacetonate, impregnation, Sinter-resistance, preparation, mechanism

1 Introduction

Supported metal nanocatalysts with metal particles of less than 10 nm are attracting increasing attention because of their unique catalytic performance in many chemical reactions. However, maintaining the stability of metal nanoparticles on the supports in high temperature environments is usually rather difficult. Here, we report the synthesis of a well-dispersed Pd/SiO_2 catalyst with high thermal stability by using a simple impregnation method with $Pd(acac)_2$ as the Pd precursor. The interaction of $Pd(acac)_2$ with SiO_2 surface and decomposition of the $Pd(acac)_2$ on SiO_2 under air were characterized by a variety of techniques aiming at understanding the formation mechanism of the Pd nanoparticles in the above Pd/SiO_2 catalyst.

2 Experimental

The catalysts were prepared by impregnation method using $Pd(acac)_2$ (Alfa Aesar) desolved in acetylacetone as impregnation solution. The SiO_2 (Sigma-Aldrich, 430 $m^2 \cdot g^{-1}$, 35 to 60 mesh) was first treated with 20 wt% HNO_3 for 24 h followed by washed thoroughly with water, and dried overnight at 110 °C or calcined at temperature between 400 and 900 °C for 2 h before use.

TEM experiments were performed using FEI Tecnai 30 high-resolution transmission electron microscope operated at an accelerating voltage of 300 kV. Before the TEM experiments, the samples were reduced with a gas mixture of H_2/Ar = 5/95 (volume ratio) at 600 °C for 0.5 h. TG analysis was recorded on a TGA Q600-SDT apparatus. The sample (5 mg) was heated under an air flow of 100 $mL \cdot min^{-1}$ from 50 to 800 °C at a heating rate of 10 $°C \cdot min^{-1}$. The *in situ* IR experiments were carried out on a Thermo Nicolet Nexus FTIR spectrometer equipped with a liquid-nitrogen cooled MCT detector and an in-house-built high-temperature *in situ* IR cell [1]. The IR spectra were recorded at a resolution of 4 cm^{-1} and with 32 scans using the spectra of empty IR cell as references. XPS experiments were carried out by using an Omicron Sphera II hemispherical electron energy analyzer using Al Kα X-ray source as incident radiation. The binding energy of the element was reference to the Si1s peak at 103.3 eV. *In situ* XRD experiment was performed on a Panalytical X'pert PRO diffractometer equipped with a XRK-900 reactor. Cu-*Kα* radiation obtained at 40 kV and 30 mA was used as the X-ray source.

3 Results and discussion

Fig. 1 shows the TEM images of the 3wt% Pd/SiO_2 catalysts prepared by calcining a $Pd(acac)_2/SiO_2$ precursor in air at indicated temperatures followed by reducing with a H_2/Ar = 5/95 mixture at 600 °C. It can be seen that metallic Pd particles with mean size of 3.0-3.2 nm were observed over the samples calcined at temperature between 200 and 800 °C. It was also found that the size of Pd particles in the catalysts remained at approximately 3 nm even at a relatively high Pd loadings (8wt%). These results indicates that the Pd/SiO_2 catalyst prepared

using $Pd(acac)_2$ as precursor has a superior resistance against sintering at high temperatures.

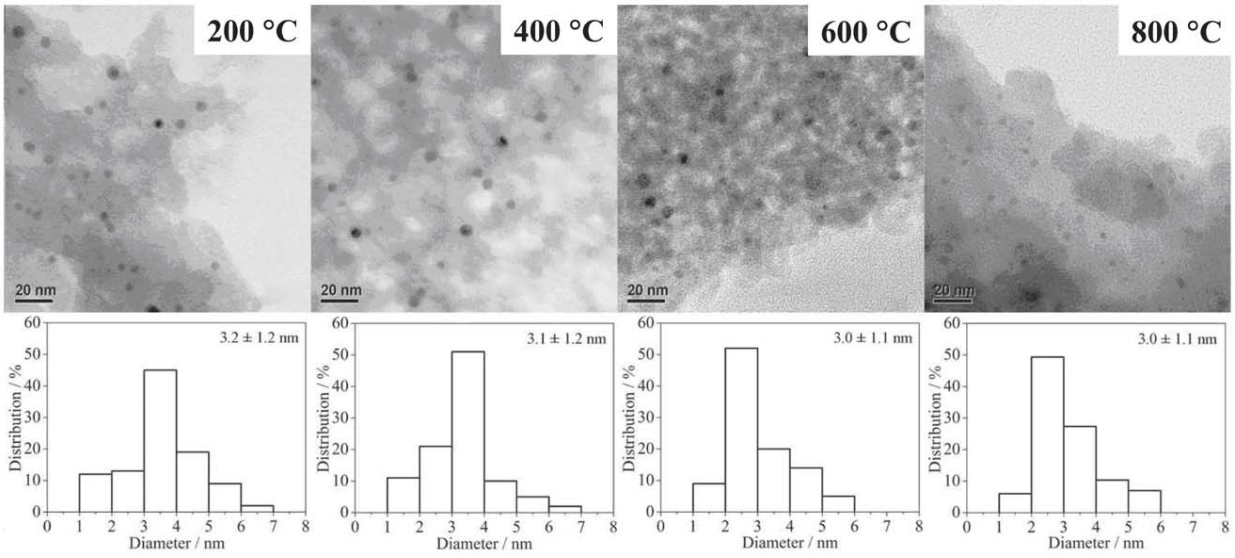

Fig. 1. TEM images and size distribution of the metallic Pd particles on the 3wt% Pd/SiO_2 calcined at different temperature.

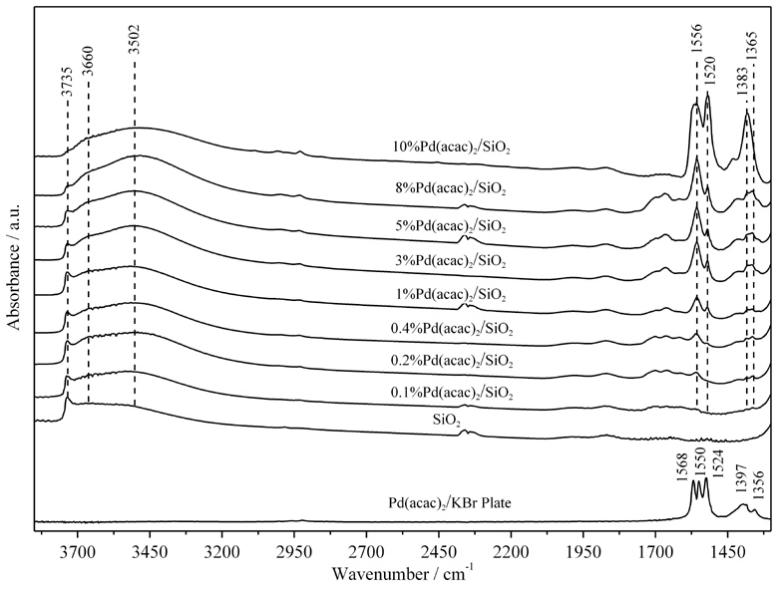

Fig. 2. IR spectra of $Pd(acac)_2$ on SiO_2 as a function of Pd loadings.

The interaction between $Pd(acac)_2$ complex and SiO_2 surface, and the thermal decomposition of the $Pd(acac)_2$ complex on SiO_2 surface under air were characterized by *in situ* IR, TG-MS, XPS and *in situ* XRD. When SiO_2 was impregnated with a solution containing $Pd(acac)_2$, the silanol groups on SiO_2 surface acted as the centers to interact with $Pd(acac)_2$ molecules, leading to the formation of hydrogen bonded $Pd(acac)_2$ single layer on SiO_2 surface (Fig. 2). Concentration of silanol groups on SiO_2 surface has a direct impact on the dispersion of $Pd(acac)_2$. On a fully hydroxylated silica surface, formation of a monolayer of $Pd(acac)_2$ on 1 g of the SiO_2 with surface area of ~400 $m^2 \cdot g^{-1}$ requires 5.7×10^{20} molecules of $Pd(acac)_2$, corresponding to ~9 wt% of Pd loadings. This is confirmed by the results of IR characterization shown in Fig. 2, in which no characteristic IR band corresponding a multiple layer of $Pd(acac)_2$ species was detected in the samples with Pd loadings below 8 wt%. When a silica supported $Pd(acac)_2$ sample was heated under air to ~200 °C, the $Pd(acac)_2$ species in the single layer on SiO_2 surface decomposed into the metallic Pd nanoparticles with average size about 2.8 nm. The

resulting Pd nanoparticles demonstrated superior stability against sintering at high temperature (Fig. 1). No significant aggregation of Pd nanoparticles was observed when the samples with Pd loadings between 0.1 and 8 wt% was heated to 800 °C in air or to 600 °C in a mixture of H_2/Ar = 5/95. In the $Pd(acac)_2/SiO_2$ samples with Pd loadings higher than 9 wt% or the samples prepared with a silica of low concentration of surface hydroxyl groups (obtained by calcining SiO_2 at temperature between 400 and 900 °C.), however, multiple layers of $Pd(acac)_2$ could also form on the SiO_2 surface, because there were no enough surface OH sites to allow all $Pd(acac)_2$ molecules to "fit" into the single layer. Decomposition of multiple layer $Pd(acac)_2$ species in air at elevated temperature result in the formation of large Pd particles on SiO_2.

4 Conclusions

A sinter-resistant Pd/SiO_2 catalyst with average Pd particle size of about 3 nm and variable metal loadings can be made using a simple impregnation method with $Pd(acac)_2$ as precursor followed by decomposition of $Pd(acac)_2/SiO_2$ in air at temperature between 200 and 800 °C. Formation of single layer of $Pd(acac)_2$ on SiO_2 surface through the hydrogen bond interaction of silanol group with $Pd(acac)_2$ is a key step towards the final formation of well-dispersed Pd nanoparticles on SiO_2. This straight forward procedure can also be used in the synthesis of other sinter-resistant metal catalysts supported on SiO_2 such as Ni/SiO_2 and $Rh\text{-}CeO_2/SiO_2$.

Acknowledgements

The work is supported by the National Natural Science Foundation of China (21473144) and the Program for Innovative Research Team in Chinese Universities (IRT_14R31).

References

[1] W. Z. Weng, M. S. Chen, Q. G. Yan, et al., *Catal. Today*. 63 (2000) 317.

II-OP43

Au-Rh and Au-Pd Nanocatalysts Supported on Rutile Titania Nanorods: Structure and Chemical Stability

Konuspayeva Z.[1], Afanasiev P.[1], Nguyen T.S.[1], Di Felice L.[1], Morfin F.[1], Nguyen N.T.[2], Nelayah J.[2], Ricolleau C.[2], Li Z.Y.[3], Yuan J.[4], Berhault G.[1], Piccolo L.[1*]

1 - Institut de recherches sur la catalyse et l'environnement de Lyon (IRCELYON), UMR 5256 CNRS & Université Claude Bernard - Lyon 1, Villeurbanne, France

2 - Laboratoire Matériaux et Phénomènes Quantiques (MPQ), UMR 7162 CNRS & Université Paris-Diderot, Paris Cedex 13, France

3 - Nanoscale Physics Research Laboratory (NPRL), School of Physics and Astronomy, University of Birmingham, Birmingham, UK

4 - Department of Physics, University of York, York, UK

* laurent.piccolo@ircelyon.univ-lyon1.fr

Keywords: nanoalloys, Au-Rh, Au-Pd, hydrogenation, thioresistance, aberration-corrected, TEM

1 Introduction

The thermodynamic properties of bulk alloys are expected to influence the structure of their nanosized counterparts. In this work, we have compared the well-known bulk-miscible Au-Pd system [1,2] to the rarely studied bulk-immiscible Au-Rh system [3] in terms of structural and catalytic hydrogenation properties. In addition, we have focused on the effect of gold on the resistance of Pd and Rh toward oxidation in air and sulfidation in catalytic conditions.

2 Experimental/methodology

TiO_2 rutile nanorods were synthesized hydrothermally from commercial TiO_2 (Degussa P25). Au-Pd and Au-Rh nanoparticles (NPs), along with their monometallic counterparts, were prepared using a colloidal chemical (co)reduction route employing chloride salts as metal precursors, polyvinyl alcohol (PVA) as surfactant, and $NaBH_4$ as reducing agent. The obtained colloids were immobilized on titania pre-acidified with HCl [4].

3 Results and discussion

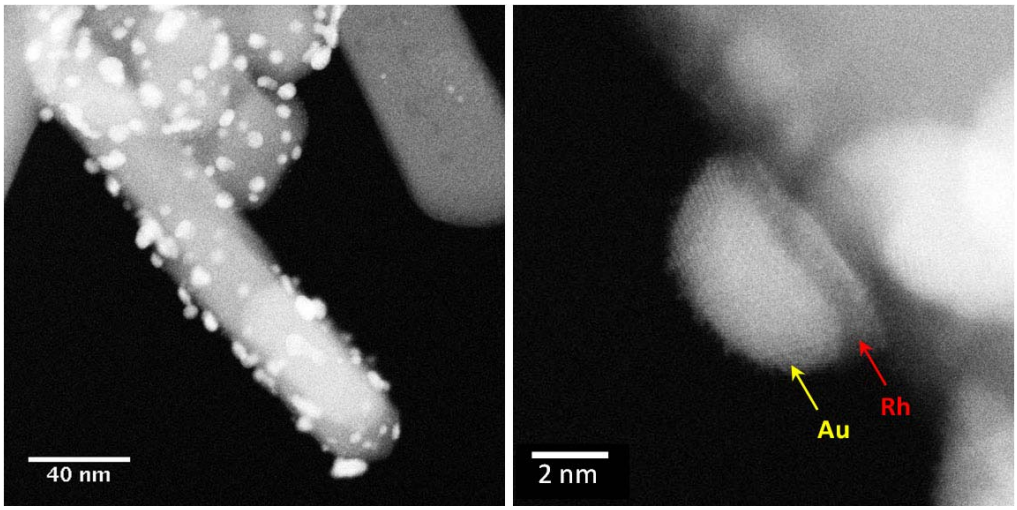

Fig. 1. STEM-HAADF images of pre-reduced $Au_{63}Rh_{37}/TiO_2$ sample.

The prepared solids were treated in H_2 flow at 350 °C, which was found efficient (as attested by FTIR) for totally removing the PVA while preserving the size (3 nm), shape and bimetallic nature of the NPs. While Au-Pd NPs are alloyed at the atomic scale, forming a solid solution, aberration-corrected scanning transmission electron microscopy (STEM) shows a well-defined segregated structure with Rh located at the interface between Au and TiO_2 (Fig. 1b).

The catalysts were evaluated in the gas-phase hydrogenation of tetralin (4 MPa of hydrogen, 24 kPa of tetralin, 350 °C) in the absence or presence of H_2S (50 ppm). Overall, gold is seen to decrease the activity of Pd- and Rh-based catalysts but it stabilizes them in the presence of sulfur, avoiding sulfidation. In the case of (Au-)Rh systems (Fig. 2), while Rh/TiO_2 is instable in S-free conditions and its activity increases upon H_2S addition to the feed, the Au-Rh/TiO_2 catalysts are much more stable and less sensitive to H_2S introduction or removal.

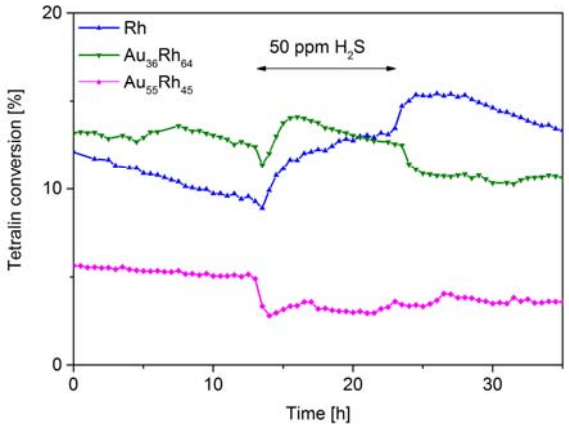

Fig. 2. Tetralin conversion to decalin on (Au-)Rh/TiO_2 catalysts without and with H_2S in the feed.

Furthermore, comparative X-ray photoelectron spectroscopy (XPS) analyses of as-prepared, pre-reduced and pre-calcined samples, supported or unsupported, show that TiO_2 and Au both stabilize Pd and Rh against oxidation in air [5].

4 Conclusions

Au-Rh/TiO_2 and Au-Pd/TiO_2 catalysts synthesized by colloidal/sol immobilization methods were characterized by (S)TEM, XPS and FTIR, and were evaluated in the hydrogenation of tetralin. While Au and Pd atoms form a solid solution, Au and Rh atoms segregate into single-phase domains within the NPs. These domains arrange in an Au/Rh/TiO_2 stacked configuration upon ligand-removal treatment at 350 °C in H_2. The presence of TiO_2 and Au is seen to inhibit surface oxidation and sulfidation of Pd and Rh, leading to improved catalyst stability.

Acknowledgements

We acknowledge the French National Research Agency (ANR-BS10-009 "DINAMIC" project) for financial support, A. Auyezov & M. Burkitbayev for ZK thesis co-supervision, and L. Massin & L. Cardenas for XPS analyses. The work in UK was supported by EPSRC grants and the STEM instrument was obtained through the Birmingham Science City project.

References

[1] G. J. Hutchings and C. J. Kiely, *Acc. Chem. Res.*, 46 (2013) 1759.
[2] F. Gao and D. W. Goodman, *Chem. Soc. Rev.* 41 (2012) 8009.
[3] L. Óvári, A. Berkó, R. Gubó, Á. Rácz and Z. Kónya, *J. Phys. Chem. C* 118 (2014) 12340.
[4] Z. Konuspayeva, G. Berhault, P. Afanasiev, T.-S. Nguyen, A. Auyezov, M. Burkitbayev L. Piccolo, *MRS Proceedings* 1641 (2014) mrsf13–1641–aa08–07.
[5] Z. Konuspayeva et al., *Phys. Chem. Chem. Phys*, submitted.

II-OP44

Defectiveness of Carbon Nanomaterials as a Key Parameter of their Effectiveness as a Support for Cobalt Catalysts in Fischer-Tropsch Synthesis

Chernyak A.S., Savilov S.V., Lunin V.V., Suslova E.V.*

Lomonosov Moscow State University, Moscow, Russia

* suslova@kge.msu.ru

Keywords: Fischer-Tropsch, synthesis, carbon, nanoflakes, carbon, nanotubes, bomb, calorimetry

1 Introduction

The Fischer-Tropsch (FT) synthesis is carried out in the presence of Co or Fe catalysts supported on carbon or oxide carriers. In recent years most of the works are devoted to the study of catalysts supported on carbon nanotubes (CNT) and other carbon nanomaterials (CNM). The catalytic activity and selectivity essentially depend on the size of Co or Fe nanoparticles which on its own is determined by the method of synthesis of catalysts, the nature of surface of CNM (morphology, degree of oxidizing, content of heteroatoms in the carbon structure) and other factors. In the present investigation the attempts to systematize the influence of surface of very wide range of CNT and CNM on the stabilization of Co nanoparticles under FT synthesis were legislated in the first time. Characteristics such as the standard enthalpy of formation and the ratio of intensities of the lines I_D/I_G in the Raman spectra were criteria selected as a universal.

2 Experimental/methodology

CNT were synthesized by pyrolytic decomposition of hexane at 750 ^oC in the presence of MgO template (S = 45 m^2/g) impregnated with aqua solution of cobalt nitrate (0.1 mol. %) and ammonium molybdate (0.03 mol. %) in the quartz tube reactor with an inner diameter of 50 mm (velocity of N_2 was 500 ml/min). Nitrogen-doped CNT (N-CNT) were observed by pyrolysis of acetonitrile under the similar conditions. Nitrogen-doped carbon nanoflakes (CNF) were synthesized by pyrolysis of acetonitrile, butylamine or pyridine in the presence of MgO (S = 140 m^2/g) at 800-900 ^oC during 15-90 min. Depending on temperature and synthesis duration N-CNT and N-CNF with different nitrogen content were observed. According to XPS data the content of nitrogen in N-CNT and N-CNF was 1.6 – 2.6 and 7.2 – 10.9 at. % respectively. Purification of the CNM from the metallic impurities was carried out by boiling in 10% hydrochloric acid solution. The surface of CNT was oxidized by nitric acid during 1, 3, 6, 9 and 15 h. According to XPS data the oxygen content was 6.48 – h 8.85 at. %.

All CNT and CNM were investigated by BET, SEM, TEM, Raman spectroscopy, XPS, TG/DSK and bomb calorimetry.

Catalysts were prepared by impregnation of carbon supports with alcoholic solution of $Co(NO_3)_2 \cdot 6H_2O$, the content of Co was 15 mass. %. FT synthesis was performed in a fixed-bed reactor under atmospheric pressure, 200-220 ^oC and $CO:H_2:N_2$ mixture (2:4:1 vol. %).

3 Results and discussion

Increasing oxidation time of CNT from 1 to 9 h led to increasing the number of oxygen-containing groups on the surface of CNTs from 6.5 to 8.9 at. %, further increasing of oxidation time had no effect on the oxygen content. The increase of the ratio of intensities of I_D and I_G lines Raman spectra and of heat of combustion from 28.027 up 28.542 kJ/g may evidence the increase of degree of «defectiveness» of CNT [1].

During the study of nitrogen-doped nanomaterials (N-CNT and N-CNF) a similar pattern was observed. The increase of the synthesis's temperature does not change the shapes of Raman spectra significantly. Nevertheless the half-width at maximum of the peaks become increase while the I_D/I_G ratio decreases, which is in good agreement with supposition about the elimination of N-atoms with temperature growth.

We assume that the role of stabilization center of cobalt nanoparticles on the surface of the CNM is played defects in carbon structure: functional groups, such as carboxyl, obtained by oxidation with nitric acid, nitrogen heteroatoms, disordering of the graphene structure of CNT and CNF formed during CNM growth [2]. By increasing the number of stabilization centers of cobalt nanoparticles can be achieved after their deposition on the surface of the CNF and catalysts will differ increased stability.

Co catalysts supported on CNM demonstrated better characteristics in the cases of more degree of «defectiveness» of CNM. However, the catalysts deposited on nitrogen-doped CNM supports demonstrated low activity: CO conversion not exceed 13 vol. %.

4 Conclusions

The proposed method of assessing the effectiveness of Co-supported catalysts for FT synthesis which is based on evaluation of defects in the CNT surface or CNM Raman spectroscopy techniques and bomb calorimetry. It was found that the most promising supports can be considered oxygen-containing CNT.

Acknowledgements

The authors thank E. Arkhipova, A. Egorov and K. Maslakov for the invaluable help in carrying out of experimental researches; «Research Priorities in Sciences» program and «Nanochemistry and nanomaterials» user facility of the Department of Chemistry at MSU for instrumental support; RFBR, RSF and RAS Presidium program for finance support.

References

[1] N. Cherkasov, S. Savilov, A. Ivanov, V. Lunin, *Carbon.* 63 (2013) 324.
[2] S. Savilov, A. Egorov, A. Ivanov, V. Lunin, *Procedia Engineering* 93 (2014) 25.

II-OP45

Proposal of a Catalytic Cooperation Model between Ru-Supported Nanoparticles in Ammonia Synthesis under Mild Reaction Conditions

Fernández C.[1], Gaigneaux E.M.[1*], Bion N.[2], Duprez D.[2], Ruiz P.[1]

1 - Université catholique de Louvain, Institute of Condensed Matter and Nanosciences - IMCN, Division «Molecules, Solids and Reactivity-MOST», Louvain-la-Neuve, Belgique

2 - Université de Poitiers, CNRS, UMR 7285, Institut de Chimie des Milieux et Matériaux de Poitiers (IC2MP), Poitiers, France

* eric.gaigneaux@uclouvain.be

Keywords: Ru nanoparticles, distribution of sizes, catalytic cooperation, low-temperature, NH_3 synthesis

1 Introduction

It has been commonly accepted that the activation of N_2 is the rate-determining step (RDS) for ammonia synthesis on metallic surfaces, and that the B_5-type sites, exposing a three-fold hollow site close together with a bridge site, are the most active sites for N_2 activation on Ru crystals. The maximum formation of these sites in Ru-supported catalysts has been found for Ru sizes of 1.8–2.5 nm [1], leading to optimal activities under high temperatures (200–500 ºC) and pressures (30–100 bar) [2]. However, under mild reaction conditions (< 200 °C, < 10 bar) the adsorption and transfer of hydrogen seem to have significant implications for the kinetics and mechanism of NH_3 synthesis. Then, additional features of the metal surface become relevant for a high catalytic activity. A broad size distribution of Ru-supported nanoparticles is required for a high activity in NH_3 synthesis under mild conditions [3], since a synergy in the catalytic activity was observed between particles of different sizes. The goal of this work is to clarify the mechanism of catalytic cooperation between Ru particles of different sizes, by separately studying the H_2 activation and transfer and the reactivity of adsorbed species on catalysts containing small and larger nanoparticles.

2 Experimental/methodology

Ruthenium catalysts (X: 1, 3 and 7 wt.% Ru) were prepared from $RuCl_3$ by a colloidal method (RuX/Al- COLL), which consists in depositing on γ-Al2O3 a colloidal suspension of RuO_2 nanoparticles prepared via hydrolysis, using H_2O_2 as oxidizing agent. A new strategy was used to prepare a Ru (10 wt.%) catalyst, by mixing the RuO_2 colloids used in the synthesis of Ru3/Al-COLL and Ru7/Al-COLL, and then depositing the resulting colloid on γ-Al_2O_3. This catalyst is denoted as Ru(7+3)/Al-COLL. Catalytic tests were carried out in a fixed-bed tubular reactor. The catalyst (400 mg) was pretreated in H_2 (80 ml/min, 200ºC/2h). The reaction was performed at 50-150ºC and 5 bar, in a N_2/H_2 mixture of 1:3 vol.% (40 ml/min, GHSV=6000 ml/h/g_{cat}). Catalysts were characterized by BET, XPS, TEM, XRD and H_2-chemisorption. Additionally, H/D isotopic exchange and 'operando' DRIFTS experiments were performed.

3 Results and discussion

The activity for NH_3 synthesis increases with the mean size of Ru particles, up to 7 nm (Fig. 1). Moreover, an enhanced catalytic performance was observed with Ru(7+3)/Al-COLL, having a broader size distribution (SD: ± 3nm) of Ru particles in the range 2–17 nm (Table 1). A reaction order of 0.05 with respect to N_2 was obtained for small Ru nanoparticles, indicating that the reaction rate depends very little on N_2 partial pressure and that the actual limiting step for the

reaction on small particles might be the release of active sites. In addition, H/D homoexchange experiments at low temperatures shown that $H_2(g)+D_2(g)=2HD(g)$ reaction is much slower on small Ru nanoparticles, and therefore, a low amount of strongly attached H atoms is expected to cover the surface. In consequence, the hydrogenation of NH_x intermediates species and the release of active sites for further N_2 adsorption may be limiting the reaction over small Ru nanoparticles, as confirmed by the study of reaction orders.

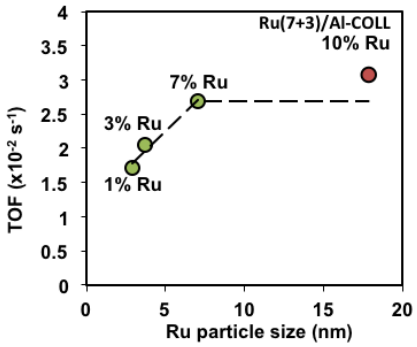

Fig. 1. TOF as a function of Ru mean size, for NH_3 synthesis at 100ºC and 5 bar

Table 1. Mean size of Ru supported particles and their activity for NH_3 synthesis at 5 bar

Catalyst	Ru loading (wt.%)	XPS Ru mean size (nm)	SD of sizes (nm)	TOF (x100 s^{-1}) 100ºC	150ºC
Ru1/Al-COLL	1	2.9	± 0.9	1.72	1.95
Ru3/Al-COLL	3	3.7	± 0.9	2.05	2.30
Ru7/Al-COLL	7	7.1	± 0.9	2.69	2.36
Ru(7+3)/Al-COLL	10	17.9	± 3	3.07	3.23

The faster H/D equilibration reaction on larger Ru nanoparticles shows that they decrease the energetic barrier for H_2 activation, ensuring an effective release of active sites. The mobility of H atoms between Ru metal particles and the alumina support was confirmed via H/D isotopic exchange experiments. Therefore, the presence of large Ru nanoparticles can influence the reaction kinetics on small particles, by activating and promoting the mobility of adsorbed H atoms. It is suggested that the catalytic cooperation mechanism between particles of different sizes involves the migration of H atoms from large to small Ru particles, promoting the hydrogenation of NH_x adsorbed on small metal particles and the release of blocked active sites.

4 Conclusions

NH_3 synthesis is better conducted on surfaces with a broad size distribution of Ru nanoparticles. Small particles contain active sites for N_2 activation, but at low temperature, they slowly activate and strongly attach H_2, affecting the hydrogenation of adsorbed NH_x and the release of active sites for N_2 adsorption. On the contrary, larger Ru nanoparticles decrease the energetic barrier for H_2 activation and allow a higher mobility of H atoms. The cooperation mechanism would involve migration of H atoms from large to small Ru particles, promoting the hydrogenation of adsorbed NH_x on small metal particles and the release of blocked active sites.

Acknowledgements

Financial support of the Belgium National Fund for Scientific Research (FSR-FNRS) and 'Becas Chile' program of CONICYT (Chile) are gratefully acknowledged.

References

[1] C. J. H. Jacobsen, Søren Dahl, Poul L. Hansen, Eric Törnqvist, Lone Jensen, Henrik Topsøe, Dorthe V. Prip, Pernille B. Møenshaug, I. Chorkendorff, *J. Molec. Catal. A.* 163 (2000) 19–26
[2] B. Lin, K. Wei, J. Lin, J. Ni, *Catal. Commun.* 39 (2013) 14–19
[3] C. Fernández, C. Sassoye, D. P. Debecker, C. Sanchez, P. Ruiz, *App. Catal. A.* 474 (2014) 194–202

II-OP46

Water-Gas-Shift and Methane Reactivity on Reducible Perovskite-Type Oxides

Penner S.P.[1*], Thalinger R.T.[1], Opitz A.O.[2], Schmidmair D.S.[3], Heggen M.H.[4]

1 - University of Innsbruck, Institute for Physical Chemistry, Innsbruck, Austria
2 - Vienna University of Technology, Institute of Materials Chemistry, Vienna, Austria
3 - University of Innsbruck, Institute of Mineralogy and Petrography, Innsbruck, Austria
4 - Forschungszentrum Jülich, Ernst-Ruska Center for Electron Microscopy, Jülich, Germany

* simon.penner@uibk.ac.at

Keywords: perovskites, electron microscopy, water-gas shift reaction, mixed conducting, SOFC-anodes

1 Introduction

A current trend in catalysis sees a re-focus on the catalytic action of the individual parts of a more complex catalyst entity. As many catalyst systems represent a combination of (noble) metals and (oxidic) supporting materials, the latter are increasingly studied with respect to their intrinsic surface reactivity. However, due to the inherent structural and electronic complexity of oxides, the identification of e.g. a catalytically active site is not straightforward. These challenges are far higher if more complex oxide systems are studied. Such complex systems may also come as a single phase binary oxide adopting a distinct crystallographic structure. A well-known example are perovskitic materials. Uses as ferroelectrica or solid oxide fuel cell (SOFC) cathodes are well-known. Catalytic applications are reported for environmentally relevant deNOx processes, diesel exhaust catalysis, total oxidation of hydrocarbons or dry reforming of methane. Specifically, also the water-gas shift reactivity on perovskite systems has been in the focus of research[1]. However, direct correlations of catalytic properties and associated structural changes still remain scarce. This is a particular pity, since e.g. hydrocarbon conversion is usually carried out at high temperatures (T > 600°C), eventually giving rise to an array of structural changes, including surface reconstruction or chemical segregation of individual atom species. Especially the surface structure and chemistry (e.g. the cation or oxygen vacancy concentration) are in a dynamical state depending on the experimental conditions (e.g. hydroxylation degree of the surface or oxygen partial pressure). Thus, surface and bulk structure and composition might significantly deviate from one another and need to be separately assessed.

To clarify this issue, a comparative study of activity for hydrogen oxidation, water-gas shift and methane reforming was performed on the two perovskite-type materials $La_{0.6}Sr_{0.4}FeO_{3-\delta}$ (LSF) and $SrTi_{0.7}Fe_{0.3}O_{3-\delta}$ (STF) with the aim of directly linking surface and bulk reactivity to catalytic properties.

2 Experimental/methodology

Structure-activity correlations in doped perovskite systeme were established using a combined approach of Electrochemical Impedance and Raman spectroscopy, structural characterization by X-ray diffraction (XRD) and aberration-corrected Scanning Transmission Electron Microscopy (STEM) as well as catalytic measurements in the (inverse) water-gas shift reaction and methane reforming.

3 Results and discussion

Impedance measurements on model-type LSF thin film electrodes revealed a comparatively

high surface activity of the material in oxidizing as well as reducing atmospheres. On powder samples the water-gas shift reactivity as well as conversion of CO_2 by the inverse water-gas shift reaction starting at about 450°C was observed on both LSF and STF. Generally, the catalytic performance for the water-gas shift equilibrium is heavily influenced by the extent of pre-reduction in hydrogen. Catalytic methane reforming reactivity or decomposition was observed on neither of the two materials, only total oxidation of methane to CO_2 with reactive lattice oxygen on initially fully oxidized powder samples. In general, the catalytic activity of both perovskite-type oxides is strongly dependent on the degree of reduction and the associated reactivity of the remaining lattice oxygen. Structure-wise, high-resolution high-angle annular dark-field electron microscopy images (Figure 1, right) show that after a catalytic reaction both perovskites still appear SrO-terminated (Figure 1, left). Raman measurements on STF reveal a reversible modification of the Fe/Ti-O structural entity upon treatment in the water-gas shift reaction mixture at 600°C as deduced from according changes in the Fe/Ti-O stretching vibration. Generally, combining XRD and Raman measurements, a clear difference in the surface and bulk reactivity of the two perovskite-type oxides results.

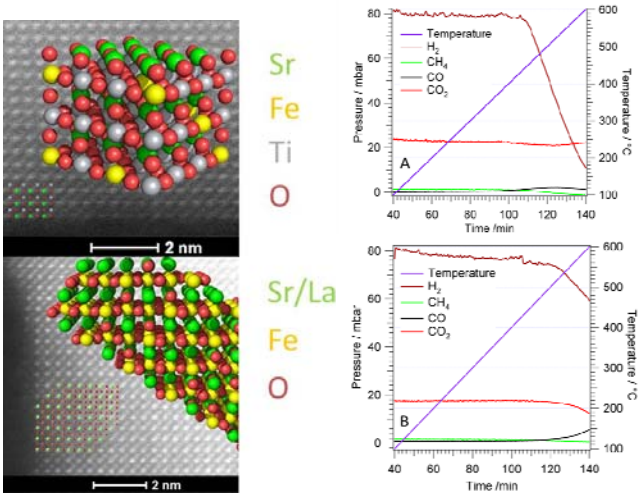

Fig. 1. Left: High-resolution STEM-HAADF images of STF (above) and LSF (below) after an inverse water-gas shift reaction (iWGSR) cycle up to 600°C with overlaid crystallographic structures showing the exact position of each atom in the structure and at the surface. Right: Reaction profiles of the iWGSR on STF without (panel A) and with (panel B) pre-reduction in hydrogen at 600°C (1 h, 1 bar).

4 Conclusions

As the most important parameter highly influencing the reactivity, the reduction degree could be determined: it controls the oxygen reactivity and the specific oxidation and reduction capability of the active sites in the working state of the perovskitic catalysts. The presented results in turn allow for the first time the direct correlation of a catalytic profile measured on a perovskite system to bulk and surface structural changes occurring during each step of catalytic pre-treatments and catalytic reaction.

Acknowledgements

We thank the FWF (Austrian Science Foundation) for financial support under the project FOXSI F4503-N16.

References

[1] M. A. Pena, J. L. G. Fierro, Chem. Rev. 101, 2001, 1981-2017

II-OP47

Facile Redispersion of Sintered Au Nanoparticlces with Controllable Size for Catalytic Application

Duan X., Tian X., Ke J., Yuan Y.*

State Key Laboratory of Physical Chemistry of Solid Surfaces and National Engineering Laboratory for Green Chemical Production of Alcohols-Ethers-Esters, College of Chemistry and Chemical Engineering, Xiamen University, Xiamen, China

* yzyuan@xmu.edu.cn

Keywords: Au, catalyst, sintering, redispersion, particle, size, acetylene, hydrochlorination

1 Introduction

Catalysis with supported gold nanoparticles (Au NPs) has become a focus of intense research, which is wildly used in energy conversion, chemicals production, *etc*. However, sintering of Au NPs is one of the most common events leading to deactivation of Au based catalysts. Although several reports have conducted to minimize or reverse the Au catalyst deactivation owing to sintering [1–3], controlling the Au particle size associated with the mechanism of redispersion is still ambiguous. Herein, we firstly established the correlation between the C–X bond dissociation energy (BDE) of alkyl halides and relative redispersion efficiency. Time-dependent XRD patterns and TEM images illustrate the procedures of redispersion, following a mechanistic discussion. The catalytic test of acetylene hydrochlorination was conducted to show the performance of regenerated Au catalysts.

2 Experimental

The catalyst 1 wt.% Au/C was prepared by the impregnation method. Analytic reagent of alkyl halides were employed to treat the sintered Au/C catalysts under established conditions. The samples before and after redispersion are characterized by means of various techniques like BET, XRD, TEM, *etc*. The acetylene hydrochlorination was carried out in a fixed bed reactor. The gas phase products were analysed on-line by GC with a FID detector equipped a GDX-301 column.

3 Results and discussion

The TEM image in Fig. 1a shows that the sintered Au/C catalyst has an average size of 30 nm. After the sintered Au/C catalyst was treated in CHI_3 at 40 °C for 5 min, the TEM image in Fig. 1b indicates that there are some smaller Au NPs in the periphery of larger particle on the catalyst surface, which likely taking place a reverse agglomeration or reverse Ostwald ripening process. After 30 min, the Au NPs can be readily redispersed to less than 3 nm (Fig. 1c). Fig. 2 (*Left*) shows plots of the redispersion efficiency against BDE of C–X (X = I, Br, Cl). CHI_3 exhibits the highest redispersion efficiency for its minimum C–I BDE. The results suggest that the C–X BDE of alkyl halides might be served as a descriptor for the reverse agglomeration of sintered Au/C.

Further experimental results indicate that the high dispersed Au NPs with mean particle sizes of *ca.* 0.8, 2.6, and 6.8 nm can be obtained after the sintered Au/C catalysts were treated with CHI_3, C_6H_5I and $C_5H_{11}I$ at 40 °C for 3-7 days, respectively. The findings may pave the way for the facile regeneration of sintered Au-based catalysts for practical applications. In fact, the regenerated Au/C catalyst can almost recover its activity for the hydrochlorination of acetylene (Fig. 2, *right*).

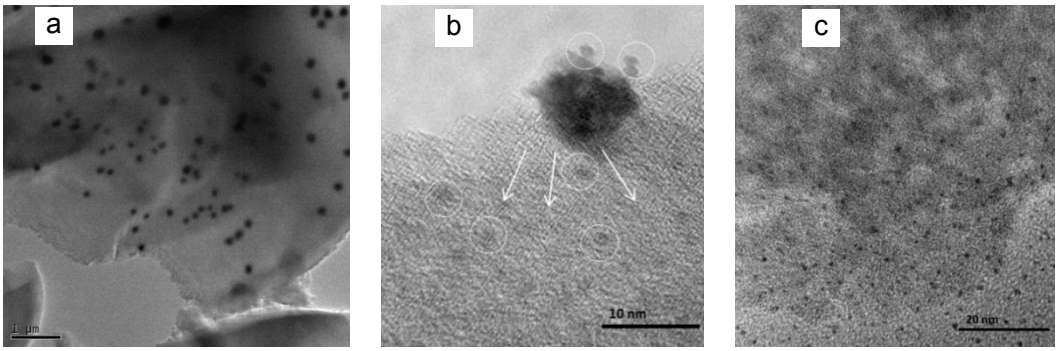

Fig. 1 TEM images of Au/C catalyst. (a) sintered Au/C; (b) and (c) the sample (a) treated in CHI_3 at 40 °C for 5 min and 30 min, respectively.

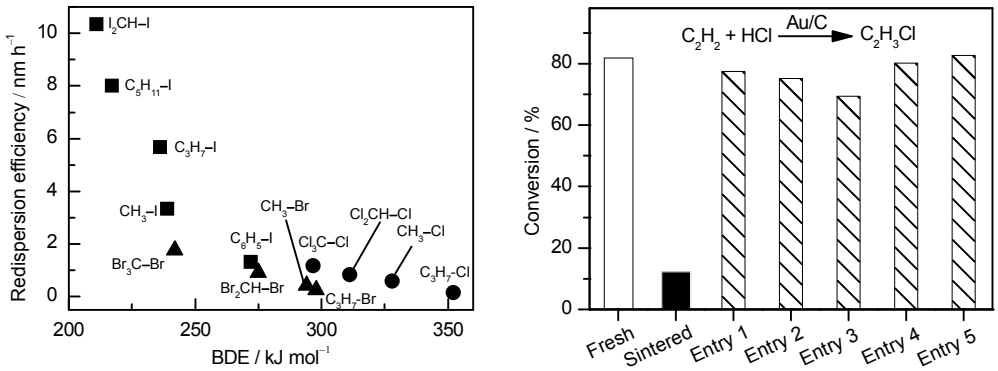

Fig. 2 *Left*: correlation between redispersion efficiency with C–X (X = I, Br, Cl) BED of alkyl halides; *Right*: acetylene hydrochlorination over the Au/C catalyst before and after reactivation. Reaction conditions: P = 0.1 MPa, T = 180 °C, GHSV (C_2H_2) = 600 h^{-1}.

4 Conclusions

We have demonstrated a facile and rapid protocol for the redispersion of sintered Au/C catalysts. The correlation of C–X BDE of alkyl halides with redispersion efficiency revealed that the alkyl halides with lower BDEs are able to redisperse the sintered Au/C efficiently. The method is also able to facilitate the redispersion and/or regeneration of Au-based catalysts until the desired sizes of Au NPs are obtained. The proposed mechanism may help formulate a molecular-level understanding of the critical interfacial events. The forthcoming work will put weight on adjusting to weaken and elongate the C–X bond with a functional donor that would benefit the dispersion efficiency and size/shape controlling of supported Au NPs.

Acknowledgements

We gratefully acknowledge the financial supports from the National Basic Research Program of China (2011CBA00508) and the Natural Science Foundation of China (21303141, 21403178 and 21473145).

References

[1] J. Sá, S.F.R. Taylor, C. Paun, A. Goguet, R. Tiruvalam, C.J. Kiely, M. Nachtegaal, G.J. Hutchings, and C. Hardacre, *Angew. Chem. Int. Ed.* 50 (2011) 8912.
[2] A. Goguet, C. Hardacre, Y. Saih, and J. Sá, *J. Am. Chem. Soc.* 131 (2009) 6973.
[3] K. Morgan, R. Burch, M. Daous, J.J. Delgado, A. Goguet, C. Hardacre, L.A. Petrov, and D.W. Rooney, *Catal. Sci. Technol.* 4 (2014) 729.

II-OP48

Shape Effect of TiO_2 on the Performance of VO_x/TiO_2 Catalysts for NH_3-SCR

Shi Q., Li Y., Zhan E., Ta N., Shen W.*

Dalian Institute of Chemical Physics, Chinese Academy of Sciences, Dalian, China

* shen98@dicp.ac.cn

Keywords: TiO_2, shape effect, nanosheets, nanospindles, VO_x/TiO_2 catalysts, NH3-SCR

1 Introduction

VO_x/TiO_2 catalysts have been industrially used for selective reduction of NO with NH_3 in abating polluting emission from power plant [1]. It is generally viewed that VO_x monolayer on titania are the most active species and their interaction with underlying TiO_2 largely determine the catalytic performance [2]. The {001} facet of TiO_2 favors a monolayer dispersion of vanadium oxide species [3], but this reactive facet grew very fast under synthetic conditions and the commonly used TiO_2 particles are dominantly enclosed by the thermodynamically stable {101} facet [4]. Here, we examined the shape effect of TiO_2 particles, in terms of the exposed crystalline facets, on the dispersion of VO_x species in VO_x/TiO_2 catalysts.

2 Experimental

TiO_2 nanosheets (TiO_2-S) and nanospindles (TiO_2-P) were prepared by a hydrothermal method with the aid of F^- and CH_3COO^-, respectively. The VO_x/TiO_2 catalysts with a V_2O_5 loading of 8.2 wt% were prepared by an impregnation method; they were calcined at 673 K in air before characterizations and catalytic tests. Structural analysis was conducted by Raman spectroscopy, XPS, NMR, XRD and TEM techniques. Selective reduction of NO with NH_3 was performed with a continuous-flow fixed-bed quartz reactor at atmospheric pressure. The typical reaction conditions are 100 mg catalyst, 1000 ppm NO /1000 ppm NH_3/ 3 vol% O_2 / He (60 mL min^{-1}), and 303-673 K.

3 Results and discussion

XRD patterns of the TiO_2 nanoparticles showed characteristic diffraction lines of anatase TiO_2. The (200) diffraction line in the TiO_2-S sample intensified remarkably while the (004) diffraction line weakened considerably, suggesting a predominant exposure of the {001} facet [5]. The TiO_2-P sample showed enhanced diffraction intensity in the (004) plane and a decrease in the (200) line, indicating the exposure of the {101} facet. TEM observation revealed that the TiO_2-S exhibited a sheet-like morphology with the thickness of 7 nm and the side length of 40 nm. It consisted of 74% {001} facet on the square surface and 26% {101} facet on the isosceles trapezoidal surface. The TiO_2-P had a spindle-like shape with 50 nm in length and 20 nm in

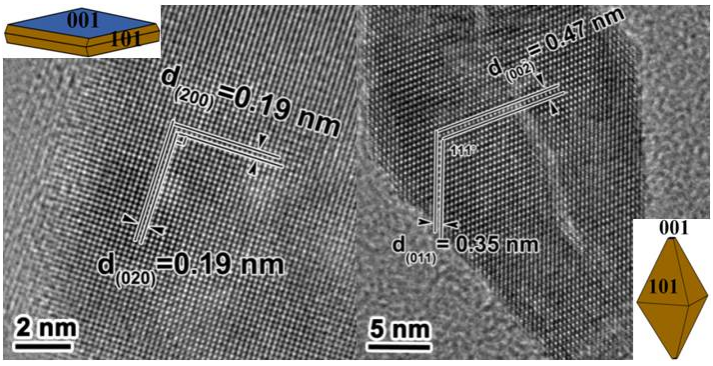

diameter; and it was enclosed by 81% {101} facet on the isosceles trapezoidal surface and 19% {001} facet on the top surface.

The VO_x/TiO_2 catalysts maintained almost the original size and morphology of the TiO_2 supports. STEM observation and EELs analysis confirmed that the VO_x species were dispersed at monolayer level in both cases but their atomic coordinations strongly depended on the shape of TiO_2. XPS profiles and Raman and NMR spectra indicated that TiO_2-S, predominantly exposed the reactive {001} facet, favored a selective deposition of vanadia species in octahedral coordination, whereas TiO_2-P, enclosed with the {101} facet, induced the generation of tetrahedral VO_x species. The {001} facet is terminated with 50% Ti_{5c} atoms and 50% Ti_{6c} atoms, whereas the {101} surface is composed by 100% unsaturated Ti_{5c} atoms [5]. Accordingly, vanadia presented as octahedral-coordinated state on the {001} facet but tetrahedral-coordinated environment on the {101} facet [6]. Therefore, it can be concluded that the dominantly exposed facets of TiO_2 nanoparticles tuned the dispersion of vanadia species and their interactions with TiO_2.

On the VO_x/TiO_2-S catalyst, the conversion of NO reached 50% at 465 K and approached 100% at 560 K. However, the temperatures for the corresponding NO conversions over the VO_x/TiO_2-P catalyst shifted to 496 at 608 K, respectively. The reaction rate on the VO_x/TiO_2-S catalyst was 1.71×10^{-6} mol g^{-1} s^{-1} at 503 K; but it decreased to 7.05×10^{-7} mol g^{-1} s^{-1} over the VO_x/TiO_2-P catalyst. The turnover frequency, based on the amount of vanadium, was 1.90×10^{-3} s^{-1} on the VO_x/TiO_2-S catalyst and 7.82×10^{-4} s^{-1} over the VO_x/TiO_2-P catalyst. TPSR of pre-adsorbed NH_3 further evidenced the superior activity of the VO_x/TiO_2-S catalyst, over which NO consumption occurred at 353-543 K with the production of significant amounts of N_2 and H_2O. On the VO_x/TiO_2-SP catalyst, however, the temperature window for NO consumption shifted to 553-673 K, forming much less of N_2 and H_2O. All these results demonstrate that vanadia species with an octahedral coordination on the reactive {001} facet of TiO_2 are intrinsically more active for the selective reduction of NO with ammonia.

4 Conclusions

Anatase TiO_2 nanosheets and nanospindles were applied to support vanadia species for selective reduction of NO with ammonia. The preferential exposure of reactive {001} crystal facet on TiO_2 nanosheets favored the selective deposition of octahedral vanadia species; whereas TiO_2 nanospindles that were dominated by the {101} facet induced the formation of tetrahedral VO_x species. This finding demonstrates the importance of morphology in the preparing efficient VO_x/TiO_2 catalysts.

References

[1] P. Granger, V. I. Parvulescu, *Chem. Rev*. **2011**, *111*, 3155-3207.
[2] I. E. Wachs, B. M. Weckhuysen, *Appl. Catal. A* **1997**, *157*, 67-90.
[3] A. Vejux, P. Courtine, *J. Solid State Chem*. **1978**, *23*, 93-103.
[4] X. Q. Gong, A. Selloni, *J. Phys. Chem. B* **2005**, *109*, 19560-19562.
[5] F. Tian, Y. P. Zhang, J. Zhang, C. X. Pan, *J. Phys. Chem. C* **2012**, *116*, 7515-7519.
[6] Y. J. Du, Z. H. Li, K. N. Fan, *Surf. Sci*. **2012**, *606*, 956-964.

II-OP49

Design and Preparation of Pt-Transition Metal Oxides (TMO) Nanoparticles Supported on 3DOM Oxides with Enhanced Catalytic Activity for Soot Combustion

Zhang X.D, Wei Y.C*, Zhao Z

State Key Laboratory of Heavy Oil Processing, China University of Petroleum, Beijing, China

* weiyc@cup.edu.cn; zhenzhao@cup.edu.cn

Keywords: 3DOM, materials, platinum, nanoparticles, TMO, core-shell, structure, soot combustion

1 Introduction

Soot particle emitted from diesel engine vehicles is one of probable precursors to damage the human health. Development of catalysts, which decrease the emission amount of diesel soot, is one of the focus research topics in the field of environmental catalysis. To design a synthesize high-performance material of catalytic activity, understanding the properties affecting catalytic performance is of great importance. The key challenge is to find effective catalysts for soot combustion that operates at low temperatures. A number of researches show that transition metal oxides (TMO: Ti, Mn, V, Cr, Fe, Co, Ni, Cu, Zn, Ce, etc.) are one of the key components in auto-exhaust treatment catalysts. 3DOM structure oxides will be a valuable and promising catalyst system not only for diesel soot combustion due to their good catalytic properties and big pore sizes but also for catalytic oxidation of hazardous macromolecule organic compounds. However, the catalytic performance is limited by the intrinsic activity of metal oxide. Noble metal nanoparticles are possible choices for enhancing the intrinsic catalytic activety of 3DOM metal oxides. Among the reported catalysts for soot oxidation, Pt-based catalysts are still the best catalytic system, and are also only currently commercialized for practical conditions. The catalytic performance of Pt nanocrystals can be finely tuned by transition metal oxides (TMO) due to the strong metal-oxides interaction. Thus, the shape-controlled synthesis of Pt-TMO nanoparticles over 3DOM Al_2O_3 support is a promising route for enhancing their catalytic activities.

2 Experimental

Synthesis of monodispersed PMMA microsphere, assembly template, and preparation of 3DOM Oxide (e.g., Al_2O_3, ZrO_2) supports by colloidal crystal template (CCT) were method described previously [1-4]. 3DOM Al_2O_3-supported Pt-TMO nanoparticle (NPs) catalysts were synthsized by one-pot process of the gas bubbling-assisted membrane reduction-precipitation (GBMR/P) method just developed in our lab. The typical preparative procedures were described as follows: 3DOM Al_2O_3 support and TMO precursor were also introduced into the H_2PtCl_6 solution (Beaker I). The mixture solution was driven by a peristaltic pump. A reductant solution ($NaBH_4$) in Beaker II was injected to the membrane reactor with two ceramic membrane tubes (Φ 3 mm × 160 mm) by a constant flow pump. Meantime, the hydrogen gas was also injected by the two other membrane tubes. The $NaBH_4$ solution was infiltrated through the abundant holes (d=40 nm) on the wall of the ceramic tubes into the glass tube reactor, where the reduction of metal ions occurred immediately when the two solutions met. After complete consumption of the $NaBH_4$ solution, the precipitation agent ($NH_3 \cdot H_2O$) was added into Beaker II and was injected to the membrane reactor same as the reductant agent by a constant flow pump. The synthesis process was stopped after complete consumption of the precipitation agent solution. The final products were calcined in an oven at 500 ^oC for 1 h and the desired 3DOM Pt-TMO/oxide catalysts were obtained.

3 Results and discussion

Fig. 1 shows SEM (A), TEM (B), STEM (C) and HRTEM (D) images of 3DOM Pt-$CeO_{2-\delta}$/oxide catalysts. The SEM image exhibits that the macroporous material contains a skeleton surrounding uniform close-packed periodic voids with the average diameter of 260±10 nm. The wall thicknesses observed from SEM images are 30±5 nm. 3DOM structures with overlapped pores can be also clearly observed by TEM and STEM images in Fig. 1(B-C). The spherical platinum nanoparticles are anchored evenly over the surface of 3DOM oxide host, and all Pt particles are highly dispersed (Fig. 1C). One Pt nanoparticles on the surface of 3DOM oxide were covered by the $CeO_{2-\delta}$ nano-sheet and formed the core-shell structural Pt-$CeO_{2-\delta}$ nanoparticles (Fig. 1D). The ordered nanostructure with Pt-$CeO_{2-\delta}$ core-shell-type nanoparticles would provide abundant catalytic active sites with low- coordinatively unsaturated ceric cation duo to the maximal contact region of $CeO_{2-\delta}$(shell)-Pt(core)-oxide (support) nanojunction system. Therefore, 3DOM Pt-$CeO_{2-\delta}$/oxide catalysts show high catalytic activities (T_{50}, 340 ^{o}C) for diesel soot combustion under the loose contact between soot and catalysts.

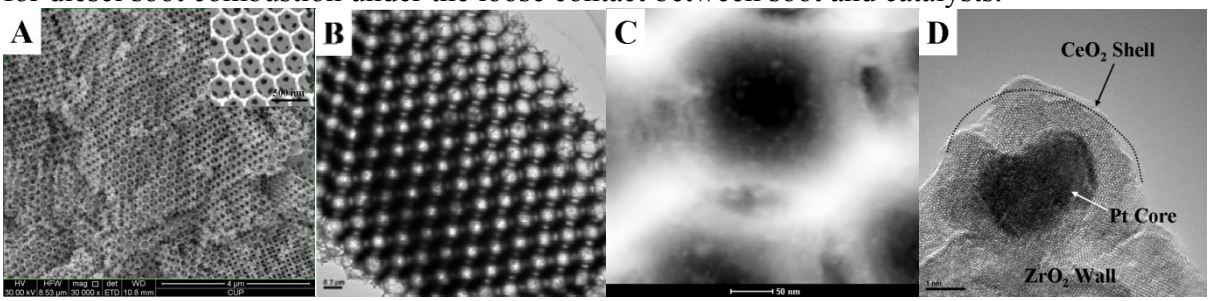

Fig. 1 SEM (A), TEM (B), STEM (C) and HRTEM (D) images of 3DOM Pt@$CeO_{2-\delta}$/oxide catalysts.

4 Conclusions

The catalysts of 3DOM oxides-supported Pt-TMO nanoparticles were synthesized successfully by one-pot GBMR/P method. The mutifunctional materials, which combine both advantages of 3DOM structure and nanoparticles with the maximal contact region of TMO(shell)-Pt(core)-oxides(support) nanojunction system, may be useful for fundamental research on metal-support synergetic effect and potential practical applications in the catalytic oxidation of solid particles.

Acknowledgements

We acknowledge the financial supports from the National Natural Science Foundation of China (No. 21177160 and 21303263, 21477164), Beijing Nova Program (No. Z141109001814072), Specialized Research Fund for the Doctoral Program of Higher Education of China (No. 20130007120011) and Science Foundation of China University of Petroleum, Beijing (No. 2462013YJRC13 and 2462013BJRC003).

References

[1] Y. Wei, Z. Zhao, T. Li, J. Liu, A. Duan and G. Jiang, *Appl. Catal. B*, 146 (2014) 57.
[2] Y. Wei, J. Liu, Z. Zhao, et al., Energy Environ. Sci. 4 (2011) 2959.
[3] Y. Wei, J. Liu, Z. Zhao, et al., Angew. Chem. Int. Ed. 50 (2011) 2326.
[4] Y. Wei, J. Liu, Z. Zhao, et al., J. Catal. 287 (2012) 13.

II-OP50

Oxidative Conversion of Methane over Gd-Sr-Co-Perovskites: Structure-Activity Relationship

Vereshchagin S.N.[1*], Solovyov L.A.[1], Shishkina N.N.[1], Dudnikov V.A.[2], Anshits A.G.[1,3]

1 - Institute of Chemistry and Chemical Technology, Siberian Branch, Russian Academy of Sciences, Krasnoyarsk, Russia

2 - L.V. Kirensky Institute of Physics, Siberian Branch, Russian Academy of Sciences, Krasnoyarsk, Russia

3 - Siberian Federal University, Krasnoyarsk, Russia

* snv@icct.ru

Keywords: methane, oxidation, OCM, perovskite, crystal, structure

1 Introduction

Substituted rare-earth perovskites with the general formula $A_xA'_{1-x}B_yB'_{1-y}O_{3-\delta}$ (A – rare-earth; A' – Ca, Sr, Ba; B, B'– Mn, Co, Fe, Ni) display a wide variety of fascinating electric, magnetic, optical and catalytic properties. They are particularly promising for total and partial oxidation of hydrocarbons, oxygen conducting media for catalytic membrane reactors, CO and hydrogen generation, electro-, photocatalysis and fuel cells.

It is known, that the perovskite structure allows a large number of ionic substitutions to form new compounds - solid solutions or complex oxide compositions. Such substitutions may result in the formation of A/B-site ordered or completely/partially disordered states giving rise to specific properties not inherent to ABO_3 perovskites. In particular, lead-based complex perovskites belong to a special family of substituted materials (called ''relaxors'') which have extraordinarily high dielectric constants due to the formation of nanoscale ordered regions in a disordered matrix [1].

As to catalytic applications it is generally accepted that the nature of B-site ions is crucial for catalysis on perovskites, while A-side ions have moderate influence on performance. That is why there are numerous papers considering the interrelation between catalytic and physico-chemical properties of B-site cation (including order–disorder phenomena on B-site) but to the best of our knowledge, there is only limited information on correlations between the peculiarities of A-site ion distribution and catalytic performance of $A_xA'_{1-x}BO_{3-\delta}$ mixed perovskites [2]. The aim of this work is the synthesis of A-site ordered and disordered Gd-Sr-cobaltates and the comparison of their catalytic properties in the reaction of CH_4 oxidative conversion.

2 Experimental/methodology

Samples of *annealed* perovskite were prepared by a conventional solid phase ceramic synthesis from Gd_2O_3 (99.99 %), Co_3O_4 (99.7 %) and $SrCO_3$ (99.99 %) powders. The compounds were ground in an agate mortar with ethanol, pressed into pellets and calcined at 1200°C for 12 h in air with intermediate re-grinding and re-pelleting. The final ceramic pellets were ground to the particle size of 100-160 microns, annealed additionally at 1200 °C in air for 1 h and cooled down with cooling rate of 2 °C·min^{-1}.

Samples of *quenched* perovskite with A-site disordered Gd^{3+}/Sr^{2+} ions were prepared from the annealed samples, which were additionally calcined at 1200 °C for 1 h in air and quenched from 1200 °C to room temperature, an estimated ramp rate from 1200 °C to 900 °C was about 30 °C·s^{-1}.

Phase compositions of perovskite catalysts were characterized by X-ray powder diffraction; the full-profile crystal structure analysis was done using the Rietveld method with the derivative difference minimization refinement [3]. Simultaneous thermal analysis (STA) experiments were

performed on a NETZSCH STA 449C analyzer equipped with an Aeolos QMS 403C mass spectrometer. The oxygen content and non-stoichiometry index δ were calculated using the value of mass loss *(Δm*, %) measured by the thermogravimetric reduction. Tests for catalytic activity were carried out in a fixed-bed 4 mm i.d. quartz reactor under atmospheric pressure with an on-line gas chromatographic analysis of the feed and the product gases.

3 Results and discussion

Crystall structure. XRD patterns of the annealed samples of $Gd_xSr_{1-x}CoO_{3-\delta}$ (x=0.8, 0.9) corresponded well to superstructures with ordered Gd^{3+}/Sr^{2+} ions over A-sites (Fig.1) and anion vacancies over O-sites, similar to that published previously for x=0.8 [4]. In situ high-temperature XRD analysis showed that above 1100°C the superstructure reflections disappeared due to a phase transition to the cubic perovskite phase with randomly distributed Gd/Sr sites and anion vacancies. DSC measurements of annealed samples (20%O_2-Ar, 10°s^{-1}) reveal reversible endo-effects with T_m temperatures at 1074, 1013 and 990 °C for x=0.5, 0.8, 0.9, respectively, which may be ascribed to the cation order–disorder transition. Quenching the samples (x=0.5-0.9) from 1200°C resulted in the preservation of the Gd/Sr-disordered cubic phase which is stable under oxidative conditions (5–20% O_2) at least up to 850°C and slowly transfers to the ordered tetragonal superstructure upon heating above 900°C.

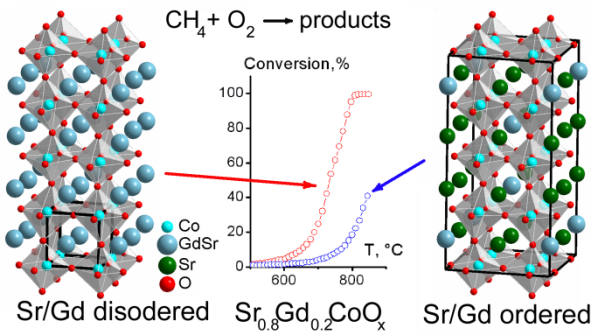

Fig.1 Ordered and disordered structures of $Gd_{0.8}Sr_{0.2}CoO_{3-\delta}$ and light-off curves for oxidation of methane. Feed, CH_4:O_2:He =27:13:60.

Catalytic activity. Thus prepared samples of $Gd_xSr_{(1-x)}CoO_{3-\delta}$ with ordered (annealed) and disordered (quenched) distribution of Gd^{3+}/Sr^{2+} ions demonstrated completely different catalytic activity in CH_4 oxidation, the quenched samples being up to 5 times more active than annealed one (Fig.1) At 360-600°C reaction of deep oxidation of CH_4 prevailed and CO_2 was the only product of CH_4 oxidation but at T>650°C reaction of oxidative coupling of methane (OCM, conversion of CH_4 to C_2-hydrocarbons) starts. The selectivity of methane conversion to ethane+ethylene was found to be higher for samples with ordered Gd^{3+}/Sr^{2+} ions distribution. Kinetic studies of methane oxidation reaction at 360-600°C, O_2 TPD and TPR in hydrogen make it possible to conclude that the observed difference in catalytic behavior of ordered and disordered structures caused by the presence of weakly bound mobile oxygen, which is responsible for deep oxidation of methane on disordered (quenched) perovskites.

4 Conclusions

Cubic perovskite phases with disordered Gd/Sr cations were found to be up to five times more active in the reaction of methane combustion and less selective in OCM than tetragonal perovskite phases with ordered distribution of Gd^{3+}/Sr^{2+} ions over the A-sites of the crystal lattice. Gd^{3+}/Sr^{2+} ion site ordering in Gd/Sr-cobaltates results in the oxygen vacancy ordering. The difference in catalytic performance is attributed to weakly bound mobile oxygen, presented on A-site disordered perovskites, and results from the structure-directed increase in both the amount of mobile oxygen and its mobility in the crystal lattice.

References

[1] A. S. Bhalla, R. Guo and R. Roy, *Mater. Res. Innovations*. 4 (2000) 3.
[2] S.N. Vereshchagin, A.L. Solovyov, E.V. Rabchevskii, *at al, Chem.Comm.* 50 (2014) 6112.
[3] L.A. Solovyov, *J. Appl. Cryst.* 37 (2004) 743.
[4] M. James, D. Cassidy, D. J. Goossens, R. L. Withers, *J. Solid State Chem.* 177 (2004) 1886.

II-OP51

In Situ XPS Study of DeNOx Reactions on Platinum Catalysts: Pressure and Material Gaps

Nartova A.V.[1,2,3*], Semikolenov S.V.[1], Bukhtiyarov A.V.[1,3], Khudorozhkov A.K.[1,3], Makarov E.M.[1,2], Kvon R.I.[1]

1 - Boreskov Institute of Catalysis SB RAS, Novosibirsk, Russia
2 - Novosibirsk National Research University, Novosibirsk, Russia
3 - Research and Educational Center for Energy Efficient Catalysis in Novosibirsk National Research University, Novosibirsk, Russia

* nartova@catalysis.ru

Keywords: *in situ* XPS, Pt/ Al_2O_3 nitric oxide neutralization

1 Introduction

The elucidation of the mechanisms of catalytic reactions as well as mechanisms of catalyst activation and deactivation can be a key to the design of the new improved catalysts. In the sphere of heterogeneous catalysis the investigation of the processes taking place under reaction conditions on the surface of the catalyst demands involving powerful *in situ* surface science techniques such as *in situ* XPS (X-ray photoelectron spectroscopy). At the same time the set of methodical issues has to be resolved when *in situ* XPS is applied. This can be done by using the special constructed systems that model real catalysts.

In the present work, the results of *in situ* XPS study of the NO involved reactions modeling processes of car exhaust neutralization are presented.

2 Experimental/methodology

Thin alumina film with thickness of 1.2 nm formed on the surface of FeCrAl alloy foil was used as support for preparation of model Pt catalysts suitable for *in situ* XPS experiments [1, 2]. γ-Al_2O_3 (specific surface area 225 m^2/g) from Sasol was used for preparation of Pt on alumina catalysts for kinetic experiments. On the surface of both model and porous alumina platinum was deposited from $H_2[Pt(OH)_6]/HNO_3$ aqueous solutions with subsequent reduction in H_2. Samples were characterized by XPS, scanning tunneling microscopy (STM) and transmission electron microscopy (TEM). Pt foil and Pt(100) single crystal were used as bulk catalyst models.

NO decomposition, NO+CO and NO+C_3H_6 reactions were chosen as model processes of NOx neutralization. *In situ* XPS experiments were performed in a VG ESCALAB HP photoelectron spectrometer equipped with a special gas cell (gas phase pressure up to 1 Pa) and a photoelectron spectrometer at the ISIS Beam Station (BESSY II, Berlin) (up to 15 Pa). STM experiments were carried out in a SPM1000 system (RHK Technology). TEM experiments were carried out on a JEOL JEM-2010. ^{15}N isotopic kinetic studies were performed in a static reactor equipped with mass-spectrometry gas phase analysis.

3 Results and discussion

XPS study of NO adsorption on the surface of Pt(100) single crystal at NO pressure 10^{-7} mbar indicates formation of the single nitrogen-containing surface state with N1s line binding energy (BE) of 400.9 eV. According to literature this state can be identified as NO_{ads} [3]. Using XPS gas cell NO pressure was raised up to 0.01 mbar, approaching to the conditions interesting from the stand point of car exhaust neutralization. At this pressure in addition to NO_{ads} the new state shifted to the higher BE at ~1.2 eV and assigned to $(NO)_{2,ads}$ was found [4]. No other nitrogen-containing surface species were observed under NO pressure up to 0.015 mbar in

temperature range from 320K to 670K.

The next step on the way of catalytic car exhaust neutralization investigation would be *in situ* XPS study of the Pt nanoparticles on porous alumina. Unfortunately due to sample charging effect XPS peaks of surface nitrogen-containing species overlap with N1s peak of gas phase when standard X-ray gun is used. As result spectrum deconvolution needs some additional information. Application of XPS with synchrotron radiation is impossible in this case due to the same surface charging effect.

So special constructed model system Pt/AlOx/FeCrAl was used for *in situ* XPS studies of NO decomposition and NO+CO, NO+C_3H_6 reactions. Obtained data were compared with results of static reactor catalytic tests. Only N_2 and N_2O were found as nitrogen-containing products of considered reactions on Pt/γ-Al_2O_3 and Pt foil under static reactor conditions up to 90-100% NO conversion. It was found that NO pre-treatment of the catalysts improves the activity of the supported catalysts, activating the systems. At the same time Pt foil was deactivating gradually after a few cycles of NO decomposition runs when Pt on alumina was still active.

According to *in situ* XPS data three nitrogen-containing surface species, described as N_{sup}, N_{ads} and N_2O_{ads}, were found on the surface of model Pt/AlOx/FeCrAl samples in the presence of NO in gas phase. Interesting that no NO_{ads} was recorded in the case of Pt/AlOx model catalyst as contrasted to Pt(100) single crystal. So the principal difference of surface layer composition between supported and bulk catalysts is found. Supposedly NO activation and decomposition take place on metal particles; N_{sup} forms by the spillover of N_{ads} on the support. Basing on obtained data it can be assumed that nitrogen-containing species of alumina support are involved into reactions. *In situ* XPS study of NO decomposition on Pt foil and Pt(100) single crystal indicates on the accumulation of oxygen (product of NO decomposition) which can be described as oxygen introduced into sub-surface layer of Pt. Used reaction temperature is not enough to remove this oxygen effectively. The observed accumulation results in the fast deactivation of Pt bulk catalysts under NO decomposition conditions.

So under reaction condition the adsorbed layer composition is completely different for supported and for bulk Pt catalysts. Results of investigation of single crystals and foils can't be applied to the real catalytic car exhaust neutralization process directly. As it was shown to get practically important information using powerful *in situ* XPS techniques special model systems should be applied bridging the gap between model and real catalysts.

4 Conclusions

On the base of comparison of *in situ* XPS data obtained for special model catalysts Pt/AlOx/FeCrAl with isotopic kinetic studies of DeNOx reactions on Pt/γ-Al_2O_3 the details of catalyst activation, deactivation and catalytic reactions were studied and the explanations of obtained effects were proposed. Applied approach bridges the pressure and material gap between model and real catalysts and provides information very useful for the practical catalysis.

Acknowledgements

Support from The Russian Science Foundation (grant 14-23-00146) is gratefully acknowledged. The authors are very appreciating to Dr. V.I. Zaikovskii for TEM data and Prof. F.H. Ribeiro and Dr. D.Y. Zemlyanov for the collaboration.

References

[1] A.V. Nartova, R.I. Kvon, E.I. Vovk, V.I. Bukhtiyarov, *Bull. Russ. Acad. Sci.: Phys.* 69, 4 (2005) 600.
[2] A.V. Nartova, R.I. Kvon, *Kinet. Catal.* 45, 5 (2004) 730.
[3] H. P. Bonzel, G. Brodén, G.Pirug, *J. Catal.* 53, 1, (1978) 96.
[4] T. Herranz, X. Deng, A. Cabot, Z. Liu, M. J. Catal. 283 (2011) 119.

II-OP52

Synthesis of Hierarchical Zeolites Using a Mono-Quaternary Ammonium Surfactant as the Mesoporogen

Zhu X.[1], Rohling R.[1], Filonenko G.[1], Mezari B.[1], Hofmann Jan P.[1], Asahina S.[2], Hensen E.J.M.[1*]

1 - Inorganic Materials Chemistry group, Eindhoven University of Technology, Eindhoven, The Netherlands

2 - JEOL Ltd., Akishima, Tokyo, Japan

* e.j.m.hensen@tue.nl

Keywords: zeolite, SSZ-13, mesopore, surfactant

1 Introduction

Porous materials with the chabazite pore topology containing 6.7 Å × 10.9 Å-sized cavities interconnected by 8-membered rings with pore apertures of 3.8 Å are the preferred catalysts for the Methanol-To-Olefins (MTO) process. Industrially, the Si-substituted AlPO form is used. The use of the more acidic/active aluminosilicate SSZ-13 would be beneficial in practice, if rapid coke formation could be suppressed. One of the approaches to improve stability of SSZ-13 in the MTO reaction is to introduce mesopores in the crystals. Wu et al. [1] succeeded in this by combining TMAdaOH and an expensive diquaternary ammonium type surfactant $C_{22\text{-}4\text{-}4}Br_2$, and the lifetime of mesoporous SSZ-13 was three times higher than that of conventional SSZ-13.
In this study, we present a much simpler, cheaper and industrially scalable dual-templating strategy [2]. It is based on a simple-to-prepare amphiphilic surfactant containing a single N-methylpiperidine head group as quaternary ammonium center (C_{16}MP). We show how it can be used in concert with conventional zeolite structure-directing agents (SDAs) to efficiently downsize microporous domains in SSZ-13 zeolite. This approach is not only very effective as only small amounts of the template need to be added to the synthesis gel, but it also leads to materials with the highest catalytic MTO performance reported so far.

2 Experimental/methodology

In a typical synthesis of conventional SSZ-13 (denoted by SSZ-13-bulk), Ludox AS40, $Al(OH)_3$, NaOH (50 wt%), TMAdOH (25 wt%), and distilled water were mixed to obtain a gel composition of 20 TMAdOH : 7.5 Na_2O : 2.5 Al_2O_3 : 100 SiO_2 : 4400 H_2O. The resulting gel was stirred at room temperature for 2 h and crystallized at 160 °C for 8 days. The hierarchical SSZ-13 (named by SSZ-13-C_{16}MP) was synthesized by the same way, the calculated amount of C_{16}MP was added into the gel and stirred for 2 hours, the final gel was transferred to the autoclave and crystallized statically at 160 °C for 8 days. After crystallization, the zeolite product was filtered, washed with distilled water and dried at 110 °C. The product was calcined at 550 °C for 10 h under flowing air and ion-exchanged three times with 1.0 M NH_4NO_3 solutions followed by calcination at 550°C for 4 h in order to obtain its proton form. Methanol-to-olefins was performed in a fixed-bed reactor at 350°C at a WHSV of 0.8 g $g^{-1}h^{-1}$. The products were analyzed by online gas chromatography.

3 Results and discussion

As shown in Fig. 1, low-voltage scanning electron microscopy (LV-SEM) images show the decreased size of the microporous domains in SSZ-13-C_{16}MP. The zeolite consists of particles with dimensions in the range of 200−500 nm made up from stacked three-dimensional intergrowths of cubic crystals with sizes much smaller than 100 nm. These images also show

mesoporous voids between the primary particles. The mesopores can also been seen by TEM. On contrary, SSZ-13-bulk consists of micrometer-sized crystals with very smooth surfaces.

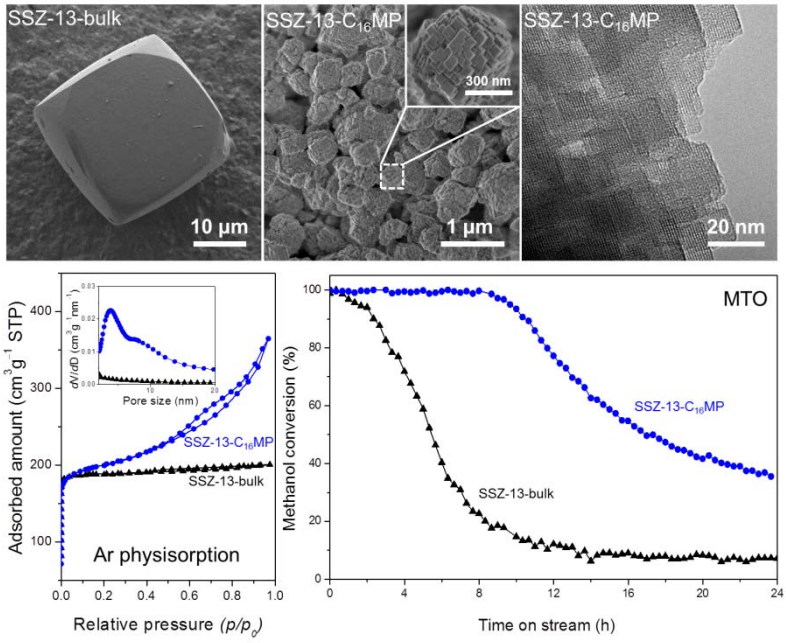

Fig. 1. Morphology, textural, and catalytic properties of SSZ-13-bulk and SSZ-13-C_{16}MP.

The Ar physisorption isotherm of SSZ-13-bulk has the usual type I shape of microporous materials. The additional presence of mesoporosity in SSZ-13-C_{16}MP is evident from the type IV shape of isotherm. The potential of mesoporous SSZ-13-C_{16}MP in acid catalysis was evaluated in the MTO reaction. The catalyst lifetime is defined as the time to reach 50 % of methanol conversion. Initially, all catalysts convert the methanol feed completely. Deactivation of bulk SSZ-13 was rapid and its lifetime was only 5 h. For SSZ-13-C_{16}MP methanol conversion only started decreasing after 9 h. The rate of deactivation was much slower and the lifetime of SSZ-13-C_{16}MP was 17 h. The greatly improved performance is attributed to the smaller microporous domains in the hierarchical zeolite, effectively reducing molecular trafficking distances. Catalyst lifetime of SSZ-13-C_{16}MP was also substantially better than for other mesoporous SSZ-13 reported earlier by us [1]. The total methanol conversion capacity improved from 6 to 24 $g_{methanol}/g_{catalyst}$ for SSZ-13-bulk and SSZ-13-C_{16}MP. Further synthesis efforts show that the C_{16}MP mesoporogen can also be used to generate mesoporosity in ZSM-5 zeolite using diaminohexane as the SDA. However, with tetrapropylammonium as SDA bulk zeolite is obtained. Molecular modeling is used to explain this subtle difference.

4 Conclusions

Hierarchically structured SSZ-13 zeolite has been successfully synthesized using the novel mono-quaternary ammonium surfactant as mesoporogen. The resulting zeolite is highly mesoporous and thus exhibits the highest catalytic performance in the MTO reaction reported so far. Our approach should be generally applicable to other zeolite topologies.

References

[1] L. Wu, V. Degirmenci, P.C.M.M. Magusin, B.M. Szyja, E.J.M. Hensen, Chem. Commun. 48 (2012) 9492.

[2] X. Zhu, R. Rohling, G. Filonenko, B. Mezari, J. P. Hofmann, S. Asahina, E.J.M. Hensen, Chem. Commun. 50 (2014) 14658.

II-OP53

Evidence of Remarkable Redox Behaviour of Ce-Doped Ordered Mesoporous Alumina at Moderate Temperature

Fonseca J.[1], Bion N.[2*], Licea Y.E.[3], Morais C.[2], Rangel M.C.[1], Duprez D.[2], Epron F.[2]

1 - GECCAT Grupo de Estudos em Cinética e Catálise, Instituto de Química, Universidade Federal da Bahia, Campus Universitário de Ondina, Salvador, Brazil

2 - University of Poitiers, CNRS, Institut de Chimie des Milieux et Matériaux de Poitiers (IC2MP), Poitiers, France

3 - LABCATH(Laboratório de Catálise Heterogênea) DFQ, Instituto de Química, Universidade Federal de Rio de Janeiro, Rio de Janeiro, Brazil

* nicolas.bion@univ-poitiers.fr

Keywords: cerium, ordered mesoporous alumina, redox, catalysis, isotopic, exchange

1 Introduction

Cerium-based materials are extensively studied because of their remarkable properties that make them interesting for a wide scope of catalytic applications [1]. The importance of CeO_2 is linked to its oxygen storage capacity and mobility, due to the two stable valence states of the Ce^{4+}/Ce^{3+} couple. These properties are improved when the crystallite size of ceria decreases since over pure ceria the phenomenon is limited to the surface and sub-surface layers. In the present study, we performed a series of cerium-doped mesoporous alumina employing the Evaporation Induced Self Assembly (EISA) route [2] and we particularly investigated the redox behaviour of these large surface mixed oxides by using advanced characterization techniques.

2 Experimental/methodology

The materials (Al_2O_3 and CeXAl where X represents the $n_{Ce}/(n_{Ce}+n_{Al})$ molar ratio and correspond to 2, 5, 10, 15 and 20%) were prepared employing a methodology close to the one described by Yuan et al. [2]. The as-synthesized materials were calcined at 400°C under air atmosphere. High surface ceria provided by Rhodia was studied as reference material for comparison.

The samples were characterized by: ICP-OES, XRD, TEM, low temperature N_2 adsorption/desorption isotherms. Redox behaviour and oxygen mobility was evaluated by temperature-programmed-reduction (TPR), oxygen storage capacity complete (OSCC), oxygen isotopic exchange $^{18}O/^{16}O$ techniques, High Field Solid State NMR and X-ray Absorption Near Edge Structure (XANES).

3 Results and discussion

BET surfaces and contents of Ce are reported in Table 1. Pure Al_2O_3, with 322 $m^2\ g^{-1}$ BET surface exhibits mesoporous morphology with hexagonal symmetry as characterized by N_2 adsorption/desorption isotherms and low angles XRD patterns. CeXAl mixed oxides also display amorphous walls and high specific surface area values which decrease when the content of Ce increases. Up to 20 wt% Ce, the mesoporosity is preserved although the hexagonal symmetry of the mesopores disappears progressively on diffractograms and TEM pictures.

Table 1. BET surface area and Ce loading of the CeXAl samples.

Samples	Al_2O_3	Ce2Al	Ce5Al	Ce10Al	Ce15Al	Ce20Al
S_{BET} (m^2 g^{-1})	322	355	350	316	254	256
Ce content (wt%)	-	6.0	11.0	20.8	29.3	35.5

The values of H_2 consumption during TPR as well as the values of CO_2 produced during OSCC are significantly superior to the ones expected based on the behavior of commercial high surface ceria. However the mobility of the oxygen in these samples does not match with the behavior of pure cerium oxide. Combining $^{17}O/^{16}O$ isotopic exchange technique and ^{17}O solid state NMR (Fig.1), we demonstrate that the mobility of oxygen atom from the alumina lattice is improved by the presence of cerium. EXAFS and XANES analyses permit to propose a hypothesis to explain the strong reducibility based on a reversible reaction between amorphous mesoporous Al_2O_3 and very small ceria crystallites (Fig.2).

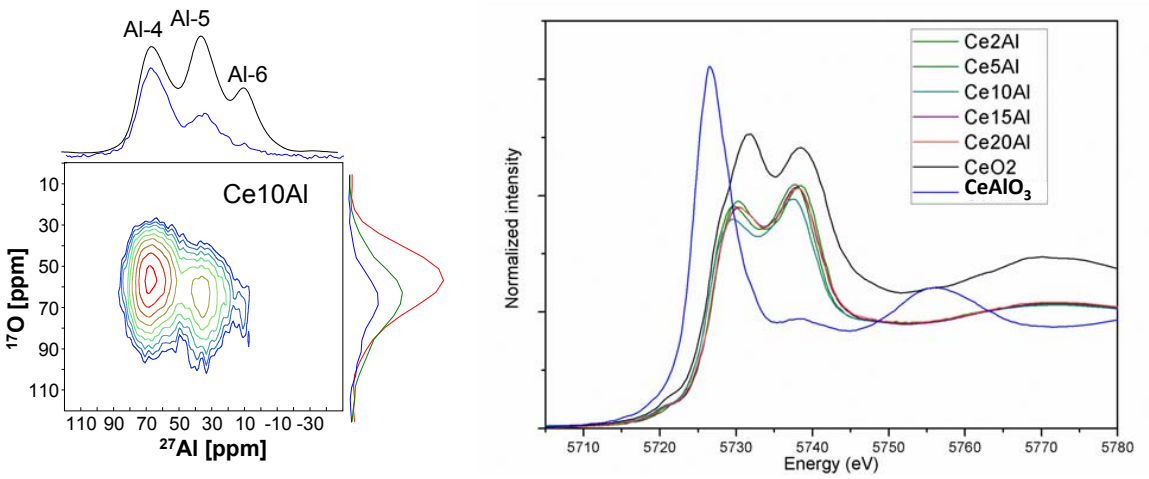

Fig. 1. ^{27}Al-^{17}O heteronuclear correlation spectra of ^{17}O-exchanged Ce10Al sample; b) XANES spectra for the CeXAl samples under oxidation (5%O_2/He) atmosphere.

4 Conclusions

In the present work, cerium-doped large surface alumina samples have been produced. We demonstrated by XANES and OSCC techniques that the high reduction rate of the solids observed at 400°C is reversible. Such properties make these mixed oxides very interesting supports of catalysts for selective oxidation reactions.

Acknowledgements

The authors thank the CAPES/COFECUB (Ph 603/08) and CNPq for the financial support. Financial support from the TGIR RMN THC Fr3050 for conducting NMR experiments is gratefully acknowledged.

References

[1] A. Trovarelli and P Fornasiero, eds, *Catalysis by Ceria and Related Materials,*2nd ed., Imperial College Press, London, (2012) pp. 1-879.

[2] Q. Yuan, A.-X. Yin, C. Luo, L.-D. Sun, Y.-W. Zhang, W.-T. Duan, H.-C. Liu., C.-H. Yan, *J. Am. Chem. Soc.* 130 (2008) 3465.

II-OP54

Support Functionalization to Retard Copper Particle Growth in the Methanol Synthesis Reaction

Van Den Berg R.[1*], Parmentier T.E.[1], Elkjaer C.F.[2], Gommes C.J.[3], Sehested J.[2], Helveg S.[2], De Jongh P.E.[1], De Jong K.P.[1]

1 - Utrecht University, Debye Institute for Nanomaterials Science, Inorganic Chemistry and Catalysis, Utrecht, Netherlands
2 - Haldor Topsoe A/S, Lyngby, Denmark
3 - University of Liege B6A, Department of Chemical Engineering, Liege, Belgium

* r.vandenberg1@uu.nl

Keywords: support functionalization, particle, growth, methanol synthesis

1 Introduction

Metal particle growth is one of the main reasons for catalyst deactivation in commercial copper catalysts for methanol synthesis. The extent of particle growth depends next to the reaction conditions upon the characteristics of the catalysts, e.g. initial metal particle size, support geometry and metal-support interaction [1, 2]. It is difficult to decouple the effects of these characteristics on particle growth, especially for commercial-like catalysts under industrial conditions. In our contribution we report on the sole effect of support functionalization on copper particle growth in the methanol synthesis reaction.

2 Experimental/methodology

Non-porous silica spheres of 30-50 nm in diameter were synthesized and subsequently functionalized with aminopropyltriethoxysilane (APTES) [3, 4]. One weight percent of copper was deposited via incipient wetness impregnation of copper nitrate followed by drying and calcination in N_2 (A) or 2% NO/N_2 (B) gas flow [5]. The extent of surface functionalization was determined with diffuse reflectance infrared spectroscopy (DRIFTS) and ICP. Copper oxide particle sizes were determined with TEM. The temperature at which the copper oxide particles were reduced to metallic copper was determined with temperature programmed reduction (TPR). The wetting of the copper particles was investigated with *in-situ* TEM. The catalytic performance of the copper catalysts in the methanol synthesis reaction was investigated at 40 bars at 260 °C for 10 days. Second order deactivation fits were used to calculate the deactivation constants ($K_{D,2}$).

3 Results and discussion

Functionalization of silica with APTES led to the introduction of amine groups and a loss of free silanol groups on the silica surface as shown by DRIFTS and ICP. Incipient wetness impregnation with copper nitrate followed by calcination led, for the functionalized silica, to a higher copper dispersion. Similar copper particle size distributions for the unfunctionalized and the amine-functionalized silica were, however, obtained when the N_2 flow during calcination of the former was changed to a 2% NO/N_2 flow for the latter catalyst (Figure 1B, D). The subsequent reduction of the copper oxide particles to metallic copper was retarded from 180 to 230 °C in the presence of amine groups, indicating a strong interaction between the copper oxide particles and the support. The wetting of the copper particles after reduction, determined with *in-situ* TEM was identical, indicating similar adhesion of the particles to the support.
The initial activity of both catalysts in the methanol synthesis reaction was similar, but copper on functionalized silica remained more active over time (Figure 1A). Electron microscopy on

the spent catalysts showed significant particle growth for copper on unfunctionalized silica and very limited particle growth for copper on functionalized silica (Figure 1C, E). The most probable particle growth mechanism for these catalysts was Ostwald ripening, since the particles were small (2-3 nm) and relatively distant (>5 nm) to each other [2]. Since the thermodynamic driving force for particle growth was the same for both catalysts, it was concluded that either the formation of mobile copper species or their mobility was slowed down due to the presence of amine groups.

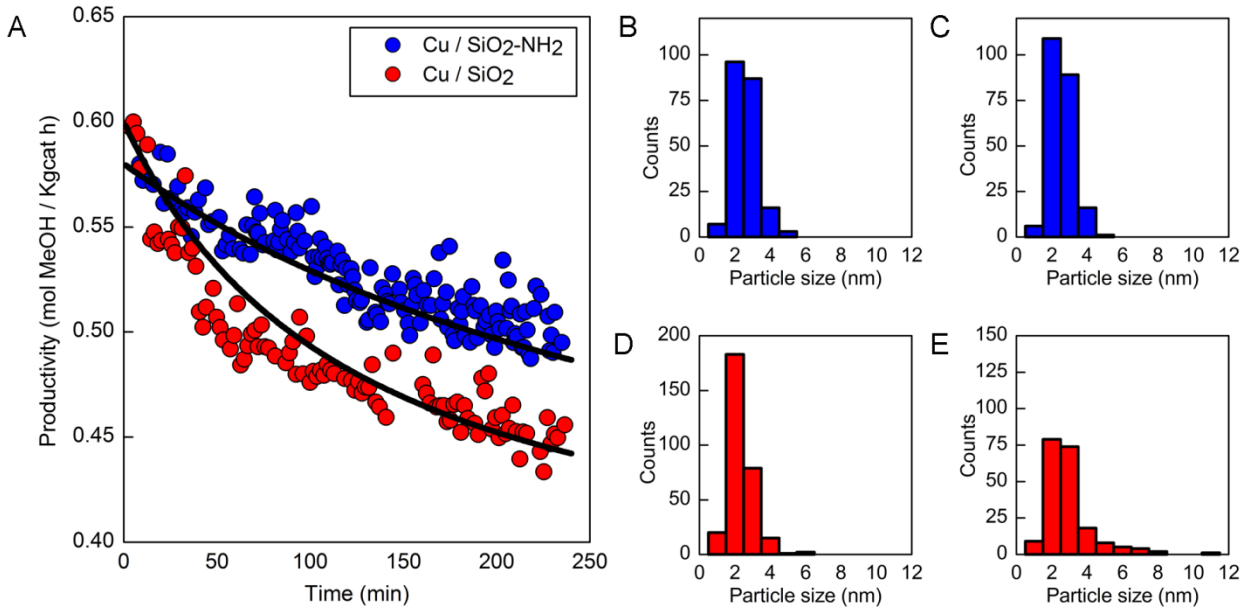

Fig. 1. (A) Catalytic performance of copper on silica (red) and copper on amine-functionalized silica (blue). (B, C) Copper particle size distributions of copper on silica before and after methanol synthesis reaction. (D, E) Copper particle size distributions of copper on functionalized silica before and after methanol synthesis reaction.

4 Conclusions

Functionalizing a silica support with amine groups retarded copper particle growth in the methanol synthesis reaction.

Acknowledgements

The authors would like to thank Haldor Topsøe A/S for funding.

References

[1] C.T. Campbell, J.R.V. Sellers, *Faraday discuss*. 162 (2013) 9.
[2] G. Prieto, M. Shakeri, K.P. de Jong, P.E. de Jongh, *ACS nano*. 8 (2014) 2522.
[3] W. Stöber, *J. Colloid Interface Sci*. 26 (1968) 62.
[4] R.L. Oliveira, P.K. Kiyohara, L.M. Rossi, *Green Chem*. 12 (2010) 144.
[5] P. Munnik, M. Wolters, A. Gabrielsson, S.D. Pollington, G. Headdock, J.H. Bitter, P.E. de Jongh, K.P. de Jong, *J. Phys. Chem. C*. 115 (2011) 14698.

II-OP55

Selective Hydrotreating of FCC Gasoline on K_x-CoMoS/Al_2O_3 Catalysts

Ishutenko D.I.*, Nikulshin P.A., Pimerzin A.A.

Samara State Technical University, Samara, Russia

* dasha.ishutenko@gmail.com

Keywords: FCC gasoline, KCoMoS, HDS/HYD, selectivity hydrotreating, octane, number

1 Introduction

Nowadays in Russia the ecological requirements are moving towards limiting the amount of benzene and aromatic hydrocarbons in gasoline what leads to redistribution of fractions in gasoline pool – the amount of catalytic reforming product decrease and the amount of fractions coming from FCC.

FCC gasoline is characterized by great amount of olefins (to 40 wt.%) and high level of sulfur content (to 1.5 wt.%) [1]. One of the most efficient way of upgrading FCC gasolines is hydrotreating. But unsaturated hydrocarbons are quite reactive in hydrotreating conditions what leads to hydrogenation and reduction of octane number consequently. The solution of this problem is selective hydrodesulfurization which allows to reduce total sulfur content and to minimize octane loss. Conventional hydrotreating (HDT) catalysts, sulfided Co(Ni)Mo/Al_2O_3, possess both HDS and HYD activities which levels are high. So HDS/HYD selectivity of such catalysts is low and does not satisfy the requirements for hydrotreating of FCC gasoline. Therefore, design of catalyst with high HDS and low HYD activities (i.e. with high HDS/HYD selectivity) is greatly desired. One of the effective method to improve HDS/HYD selectivity of TMS catalysts is modification with alkali metalls [2].

The aim of the work was the comparison of catalytic properties of industrial and laboratory (K)-CoMoS/Al_2O_3 catalysts synthesized with the use of molybdenum heteropolycompound (HPC) in HDS of FCC gasoline.

2 Experimental

Catalysts were synthesized by means of the incipient wetness technique via impregnation of the alumina with the aqueous solutions of precursors ($H_3PMo_{12}O_{40}$, $CoCO_3$, citric acid and KOH) with following drying and liquid-phase sulfidation.

Physical-chemical characteristics of catalysts were determined with the use of the following techniques: low-temperature nitrogen adsorption, Raman spectroscopy, X-ray photoelectron spectroscopy (XPS), high-resolution transmission electron microscopy (HRTEM), NH_3-TPD, H_2-TPR.

Catalytic activity examination was carried out in a bench-scale flow reactor in hydrotreating of heavy fraction of FCC gasoline under the following conditions: temperature of 240-320 °C, pressure of 1.5 MPa, LHSV of 4.5-10.0 h^{-1}, H_2/feed ratio of 100 nl/l. The performance of synthesized catalysts was estimated with conversions of sulfur and olefinic compounds and HDS/HYD selectivity that calculated as a ratio of HDS and HYD rate constants.

3 Results and discussion

Modifying catalyst with potassium leads not only to significant changes in physical-chemical properties but also to considerable changes in catalytic activity and HDS/HYD selectivity. Thus, with the growth of the process temperature we observed increase of both HYD

and HDS activity on all catalysts, but process temperature over modified sample impacted less significant than for unmodified and industrial ones. Besides sulphur conversion levels on K-$CoMoS/Al_2O_3$ catalyst were comparable with the results obtained on industrial and unmodified samples, whereas HYD activity was sufficiently lower. That resulted in maximum of HDS/HYD selectivity at 280°C over modified catalyst. Meanwhile industrial sample showed HDS/HYD selectivity around laboratory $CoMoS/Al_2O_3$ catalyst and about 2.5 times lower than modified one.

For all three catalysts kinetic characteristics such as reaction order, activation energy and preexponential factor were calculated (Fig.1). It was established that in hydrotreating of FCC gasoline on CoMo catalysts HYD reactions are described by first order kinetic equation, whereas HDS reactions are described by kinetic equation of 1.33 order what is in agreement with data published earlier [3]. Both activation energy and preexponential factor of HDS as well as HYD for unmodified catalyst were higher than similar for industrial sample, what can indicates the formation of active centres with different nature during preparation stage. Modifying with potassium led to decrease of activation energy and preexponential factor of HDS and HYD, so it can be conclude, that using alkali metal promotes changing the nature and amount of both types of active sites.

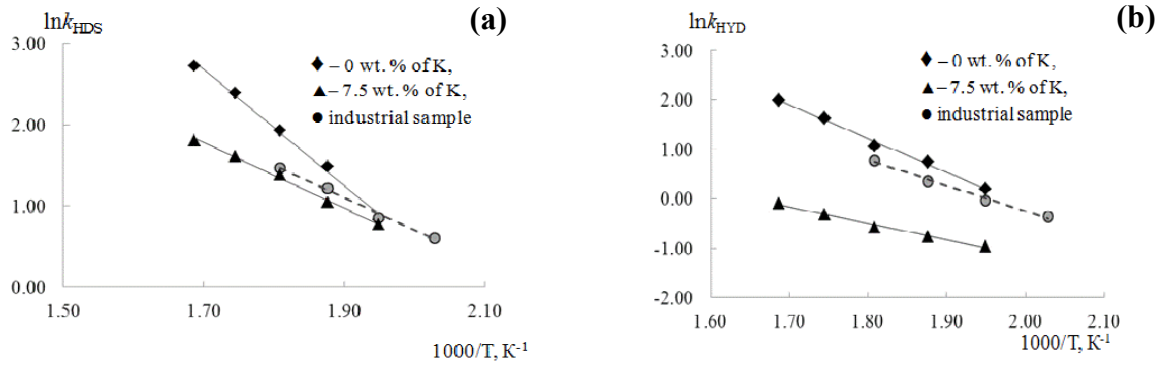

Fig. 1. Arrhenius plots of rate constants of HDS (k_{HDS}, wt.$^{-0.33}$·% h^{-1}) (**a**) and HYD (k_{HYD}, h^{-1}) (**b**) over K_x-$CoMoS/Al_2O_3$ catalysts

Changing the strength of HDS and HYD active sites connected with the reduce of apparent activation energy for both reactions what evidently is a result of donor properties of alkali metal. Decreasing the active centers amount is conformed with the reduction of preexponential factor for K-$CoMoS/Al_2O_3$ catalyst in comparison with $CoMoS/Al_2O_3$ sample. Besides, it can be mentioned that apparent activation energy and preexponential factor of HDS reactions for modified catalyst is similar to industrial sample whereas for HYD reactions all that characteristics are lower.

4 Conclusions

Modifying TMS catalysts with alkali metal leads not only to changing of physical-chemical characteristics but also catalytic properties and kinetic characteristics as well. Using potassium in catalyst synthesis results in changing of both active sites nature and amount.

Acknowledgements

The work was supported by Ministry of education and science of Russian Federation (project No. 14.577.21.0152)

References

[1] S. Brunet, D. Mey, G. Perot, C. Bouchy, F. Diehl, *Applied Catalysis A: General*. 278 (2005) 143.
[2] Y. Fan, J. Lu, G. Shi, H. Liu, X. Bao, *Catalysis Today*. 125 (2007) 220.
[3] Patent 4149965 USA,1979

II-OP56

Immobilized Grubbs Catalysts on Mesoporous Materials: New Insights into Support Characteristics and their Impact on Catalytic Activity and Product Selectivity

Dewaele A., Van Berlo B., Dijkmans J., Jacobs P., Sels B.*

Center for Surface Chemistry and Catalysis, KU Leuven, Leuven, Belgium

* bert.sels@biw.kuleuven.be

Keywords: heterogeneous, catalysis, ring-opening, ring-closing, metathesis, ruthenium, mesoporous materials, macrocycles

1 Introduction

Since the discovery of ordered mesoporous silica (OMS), this research area has developed greatly over the years leading to materials with unique opportunities for applications in heterogeneous catalysis, including the immobilization of Ru metathesis catalysts. Recently a new and practical immobilization strategy of Hoveyda-Grubbs complexes on silica supports by non-covalent adsorption was reported by Van Berlo *et al*. [1]. Later, this adsorption concept was studied and expanded successfully by others on OMS (e.g. MCM-41, SBA-15) [2-7]. Despite the evaluation of some silica materials as support structure for the physisorbed immobilization of Grubbs complexes in different studies, no profound study concerning the influence of the different textural and structural characteristics of mesoporous silica and of the immobilization process on the catalytic performance has been done since. In search for the ideal catalyst for the ring-opening ring-closing metathesis (RO-RCM) of cyclooctene to form macrocycles, we here extent this research area by systematically investigating in detail the impact of several textural and structural parameters of the support like pore size, pore architecture, surface area and morphology on the catalytic activity and product selectivity of the immobilized Hoveyda-Grubbs 2nd generation catalyst (HG 2). The optimal support-catalyst system is used to unravel the reaction pathways of RO-RCM of cyclooctene to cyclic oligomers under heterogeneous catalysis conditions.

2 Experimental/methodology

Immobilization of the mesoporous support was performed by adding a solution of HG 2 in toluene (1.57 mM, 2.5 mL) to the support (0.1 g). After 30 min. of stirring, the heterogeneous catalyst was thoroughly washed with hexane and dried. RO-RCM reactions of cyclooctene (0.05M) were performed in glass reactor vials in hexane (5 mL) with 50 mg of the immobilized catalyst at 35 °C. The reaction mixture was analysed by GC and GPC.

3 Results and discussion

The best support characteristics for immobilization of the HG 2 catalyst were defined to obtain a maximal activity in the RO-RCM of cyclooctene. This was accomplished by scrutinizing on one hand textural and structural parameters of the support, as well as investigating surface properties like surface adsorption, silanol density and catalyst loading. Hereby typical heterogeneous aspects such as pore diffusion limitations were examined. Immobilized ordered mesoporous silica MCM-41 and TUD-1 were found to answer these conditions best, and resulted in highly active catalysts. The activity of both supports was greatly improved by a temperature treatment prior to immobilization in order to obtain a high amount of free surface silanols, which are used as anchoring points during the immobilization. Among

these two supports, TUD-1 has a higher affinity for HG 2 than MCM-41 at low Ru loadings due to a greater fraction of geminal silanols on the former structure. Furthermore, since MCM-41 has smaller pores, it is more prone to diffusion limitations compared to TUD-1 at high Ru loadings. This phenomenon originates from linear polymer obstruction and is even more pronounced in cage-like pore systems. As a consequence, this affects product selectivity.

With an optimized catalytic system the ideal conditions to obtain a high selectivity to C16-C56 cyclic oligomers, valuable intermediates in *e.g.* lubricant and fragrance industry, under batch conditions were investigated. Unraveling the reaction pathways of the RO-RCM of cyclooctene, the mechanistic understanding led to optimal conditions for synthesizing macrocyclic oligomers (Fig. 1). At low monomer concentrations (0.05 M), performing reactions under a kinetic regime (low Ru loadings of 0.3 wt%), and at full conversion, selectivities of 70 % to the C16-C56 cyclic oligomeric fraction were obtained.

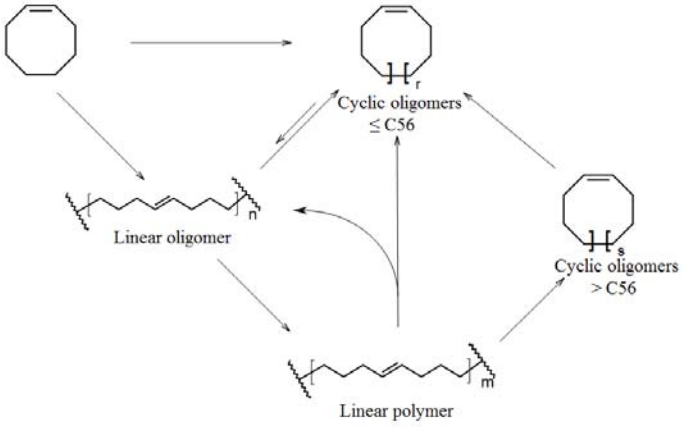

Fig. 1. Proposed reaction scheme for the ring-chain equilibrium of cyclooctene with HG 2/MCM-41.

4 Conclusions

Screening of OMS and study of the immobilization process brought on one hand new insights into the support characteristics and treatment needed for an economically favorable RO-RCM reaction. On the other hand it led to a better understanding of the reaction mechanism of the RO-RCM of cyclooctene under heterogeneous conditions to direct the reaction to the desired end product.

Acknowledgements

FWO-Flanders is thanked for its financial support. The authors are grateful to J. Martens for general financial support through Methusalem. K. Houthoofd is thanked for NMR measurements, I. Cuppens for ICP-AES, S. Kerkhofs and G. Brabants for the SAXS measurements and W. Vermandel for his help with the continuous experiments.

References

[1] B. Van Berlo, K. Houthoofd, B. Sels, P. Jacobs, *Adv. Synth. Catal.* 350 (2008) 1949.
[2] H. Yang, Z. Ma, Y. Wang, L. Fang, *Chem. Commun.* 46 (2010) 8649.
[3] H. Balcar, T. Shinde, N. Zilkova, Z. Bastl, *Beilstein J. Org. Chem.* 7 (2011) 22.
[4] T. Shinde, N. Zilkova, V. Hankova, H. Balcar, *Catal. Today* 179 (2012) 123.
[5] W. Solodenko, A. Doppiu, R. Frankfurter, C. Vogt, A. Kirschning, *Aust. J. Chem.* 66 (2013) 183.
[6] M. Bru, R. Dehn, J.H. Teles, S. Deuerlein, M. Danz, I.B. Müller, M. Limbach, *Chem. Eur. J.* 19 (2013) 11661.
[7] J. Cabrera, R. Padilla, M. Bru, R. Lindner, T. Kageyama, K. Wilckens, S.L. Balof, H.-J. Schanz, R. Dehn, J.H Teles, S. Deuerlein, K. Müller, F. Rominger, M. Limbach, *Chem. Eur. J.* 18 (2012) 14717.

II-OP57

Effect of Nucleus and Shell on the Mechanism of the 4-Nitrophenol Reduction over AuPd Based Nanoreactors

Acosta B.[1*], Evangelista V.[1], Miridonov S.[2], Pestryakov A.[3], Fuentes S.[4], Simakov A.[4]

1 - Centro de Investigación Científica y de Educación Superior de Ensenada (CICESE), Posgrado en Física de Materiales, Ensenada, México

2 - Centro de Investigación Científica y de Educación Superior de Ensenada (CICESE), Departamento de Óptica, Ensenada, México

3 - Tomsk Polytechnic University, Department of Technology of Organic Substance and Polymer Materials, Tomsk, Russia

4 - Centro de Nanociencias y Nanotecnología, Universidad Nacional Autónoma de México (CNyN-UNAM), Departamento de Nanocatálisis, Ensenada, México

* bracosta@cnyn.unam.mx

Keywords: nanoreactors, 4-nitrophenol, mechanism, AuPd, nucleus, shell

1 Introduction

The selective hydrogenation of the nitro groups is an important transformation since many produced aromatic amines have multiple industrial applications. Among different tested catalytic systems, Au-based catalysts showed high performance in the reduction of 4-nitrophenol (4NP) into 4-aminophenol (4AP) [1, 2]. It has been reported a catalytic enhancement in this reaction when Pd and Au are combined [3]. On the other hand, the encapsulated nanoparticles (nuclei) into porous matrices (shells) have become attractive due to their high catalytic stability. These relatively new structures have been called as nanoreactors (NRs) and are encoded as nucleus@shell [4]. There are only few reports in the literature dedicated to the encapsulation of AuPd NPs into porous oxide shells [5, 6]. Till now, no data about the reduction of nitro compounds over AuPd@Oxide NRs is presented in the literature.

This paper is devoted to the analysis of the 4NP reduction into 4AP over AuPd-based NRs.

2 Experimental protocol

The bottom-up route was used for the synthesis of AuPd-based nanoreactors with shells of PVP, SiO_2 or ZrO_2. Briefly, free AuPd NPs with different Au:Pd molar ratios (20:1 and 3:1) were prepared using Au NPs as seeds as in [7]. AuPd@PVP NRs were obtained by AuPd NPs treatment in PVP (Mw=10,000). AuPd@SiO_2 composites, synthesized using a modified Stöber method to encapsulate AuPd NPs into silica, were exposed to a surface protecting etching with a concentrated base for the synthesis of AuPd@SiO_2 NRs or used as a hard template for AuPd@ZrO_2 NRs [8].

The reduction of 4NP was carried out under magnetic stirring at 25°C in a quartz cuvette (1 cm of optical path) placed into temperature controlled holder (CUV-UV/VIS-TC, Avantes). UV-Vis spectra were recorded every 2 seconds using set-up including light source (AvaLight- DHS, Avantes) and UV-Visible spectrometer (Ava- Spec-2048, Avantes). Before injection of aqueous suspension of nanoreactors (28-100 µL, 7.1 10^{-3} µmol Au) the reaction mixture of 4NP (10 µL, 30 mM), $NaBH_4$ (3.7 mL, 1 mM) and H_2O (290 µL) was stirred during 15 min. The individual spectral components were resolved by the principal component analysis method [9] from the experimental UV-Vis spectra collected during the reaction.

3 Results and discussion

It was revealed that the reduction of 4NP over obtained NRs (Fig. 1, left) proceeds through:

1) direct reduction to 4AP and 2) indirect reduction via condensation of intermediates of 4NP partial reduction with their consequent reduction to 4AP. Kinetic constants (Fig. 1, right) were estimated by the fitting of experimental profiles for 4NP, 4,4-azobiphenol and 4AP with simulated ones. The deposition of Pd on the surface of Au NPs favored the steps of reduction. Encapsulation of NPs into the PVP shells affected the mass transport in particular for Au-based NRs. PVP diminished the contribution of the indirect route while ZrO_2 shell drastically increased it. Interestingly, activity for Au_3Pd_1@PVP NRs was higher than that for free Au_3Pd_1 NPs. The latter seems to be related with the partial surface reconstruction of Au_3Pd_1 nuclei due to the contact with PVP shell.

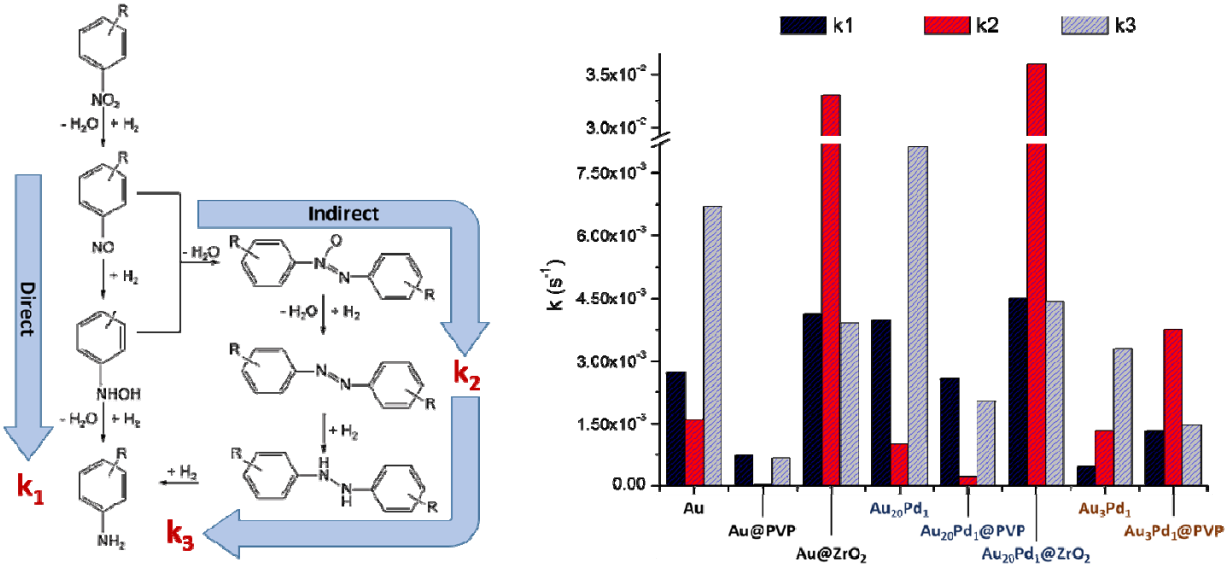

Fig. 1. Reaction scheme for the reduction of aromatic nitro compounds proposed by Haber [10] (left). Estimated reaction rate constants (k_1, k_2 and k_3 for scheme on left) for the 4NP reduction over free NPs, NPs@PVP and NPs@ZrO_2 NRs (right).

4 Conclusions

The presence of AuPd species on the surface of nanoreactor's nuclei favors the reduction steps while oxide shell participates in the reaction mechanism provoking indirect route of the 4-aminophenol formation through condensation of intermediates.

Acknowledgements

The authors would like to thank E. Flores, F. Ruiz, J. Peralta and M. Sainz for technical assistance. This research project was supported partly by CONACyT (Mexico) and PAPIIT-UNAM (Mexico) through grants 179619 and 203813, respectively.

References

[1] S. M. El-Sheikh, A. Ismail, J. Al-Sharab, *New Journal of Chemistry* 37 (2013) 2399-2407.
[2] K-I. Shimizu, Y. Miyamoto, T. Kawasaki, T. Tanji, Y. Tai, A. Satsuma, *Journal of Physical Chemistry C* 113 (2009) 17803-17810.
[3] A. Azetsu, H. Koga, A. Isogai, T. Kitaoka, *Catalysts* 1 (2011) 83-96.
[4] X. Huang, C. Guo, J. Zuo, N. Zheng, G. Stucky, *Small* 5-3 (2009) 361-365.
[5] A. Samanta, T. Rajesh, N. Devi, *Journal of Material Chemistry A* 2 (2014) 4398-4405.
[6] X. Fang, Z. Liu, M. F. Hsieh, M. Chen, P. Liu, C. Chen, N. Zheng, *ACS Nano* 6-5 (2012) 4434-4444.
[7] X.W. Lou, L.A. Archer, Z. Yang, *Advanced Materials* 20 (2008) 3987-4019.
[8] P.M. Arnal, M. Comotti, F. Schüth, *Angewandte Chemie International Edition* 45 (2006) 8224-8227.
[9] F. G. Halaka, G. T. Babcock, J.L. Dye, *Biophysical Journal* 48 (1985) 209-219.
[10] F. Haber, *Zeitschrift fur Elektrochemie, Angewandte Physikalische Chemie* 22 (1898) 506.

II-OP58

Direct Conversion of Ethylene to Propylene: Strategy of Catalyst Preparation

Lavrenov A.V., Sayfulina L.F.*, Buluchevskiy E.A.

Institute of Hydrocarbons Processing of Siberian Branch Russian Academy of Sciences, Omsk, Russia

* luiza@ihcp.ru

Keywords: ethylene, propylene, palladium, oxide, rhenium, oxide, sulfated, zirconia, direct, conversion

1 Introduction

Today the necessity for propylene is rapidly increasing due to the increasing demand of polypropylene, propylene oxide, etc. Today increased propylene production is one of the most significant objectives in petroleum chemistry. Deep-cracking [1], metathesis of ethylene and 2-butenes [2] and the direct conversion of ethylene to propylene are applied and suggested for solving this problem. Direct conversion of ethylene to propylene without any addition of other hydrocarbons is the most desirable route, but no single catalyst with high ethylene conversion and propylene selectivity has been found so far. In our previous reports, NiO-Re_2O_7/B_2O_3-Al_2O_3 and PdO-Re_2O_7/B_2O_3-Al_2O_3 bimetallic catalysts [3, 4] showed good performance for direct conversion of ethylene to propylene with high propylene selectivity. The explanation was given by a mechanism that consist of three steps in which ethylene dimerization on Ni or Pd sites affords 1-butene that can be isomerized to 2-butene on acidic sites as the first and the second steps followed by metathesis reaction of the 2-butenes and non-reacted ethylene on Re sites. In earlier reports [5] it was shown that supported PdO catalysts can be highly active in ethylene dimerization at low temperatures (25°C). This fact is determined by the Pd application in the preparation of catalysts for the direct conversion of ethylene to propylene. The aim of our studies is preparation a new PdO-Re_2O_7 catalyst, based on SO_4^{2-}/ZrO_2 for the direct conversion of ethylene to propylene at mild conditions (reaction temperature up to 100°C, atmospheric pressure). Special attention is paid to the influence of the supported metal oxide (PdO, Re_2O_7) content, to the support nature and to the several the preparation procedures of PdO-Re_2O_7/SO_4^{2-}/ZrO_2 catalysts: impregnation with aqueous solutions of H_2PdCl_2 and $HReO_4$ in different order.

2 Experimental

A series of supported PdO catalysts with different Pd loading (between 0.2 and 5 wt. %) were prepared by the impregnation of SiO_2-Al_2O_3 (12% Al_2O_3) with an aqueous solution of H_2PdCl_4, followed by calcination in air at 550°C. A series of catalysts based on supports with different supports nature (SiO_2, t-ZrO_2, γ-Al_2O_3, B_2O_3-Al_2O_3, SO_4^{2-}/Al_2O_3, SO_4^{2-}/ZrO_2) containing 1 wt. % PdO were prepared also by the impregnation and were characterized by HRTEM/EDX, TPR and XPS. Ethylene dimerization over supported PdO catalysts was carried out in a fixed bed reactor at 50 and 100°C, atmospheric pressure and WHSV of 0.5 h^{-1}. Three series of catalysts for direct ethylene to propylene conversion were prepared by impregnation of SO_4^{2-}/ZrO_2 with aqueous solutions of H_2PdCl_4 and $HReO_4$ in different order, each impregnation being followed by calcination in air at 550°C. These series of catalysts are loaded 1 wt. % of PdO and 2, 5, 10 wt. % of Re_2O_7 (in nominal). Direct conversion of ethylene to propylene over PdO-Re_2O_7/SO_4^{2-}/ZrO_2 catalyst was also carried out in a fixed bed reactor at 40 and 80°C, atmospheric pressure and WHSV of 0.5 h^{-1}. The products of the reaction were analyzed with online gas chromatography.

3 Results and discussion

At 1 wt. % PdO loading, ethylene conversion and 2-butene selectivity over PdO/SiO_2-Al_2O_3 had

maximum: 80.0 % and 20.0 %, respectively. Considering this data, influence of supports nature for the dimerization and isomerization functions on Pd-containing catalysts was studied. The PdO/SiO_2, PdO/Al_2O_3 and PdO/ZrO_2 showed low conversion (at the most of 4-6 %) in ethylene dimerization. As well as PdO/SiO_2-Al_2O_3 catalyst, the catalysts based on anion-modified supports ($PdO/SO_4^{2-}/Al_2O_3$, PdO/B_2O_3-Al_2O_3, $PdO/SO_4^{2-}/ZrO_2$) indicated high ethylene conversion: from 60.0 to 79.0 %. High ethylene conversion can be attributed to stable Pd cationic form and highly-dispersed Pd-containing particles on the surface with different supports nature (XPS, and TPR analysis data). Maximum selectivity of 2-butene (up to 90%) is achieved with $PdO/SO_4^{2-}/ZrO_2$ catalyst. Thus, SO_4^{2-}/ZrO_2 support was used for preparing a new catalyst for the direct conversion of ethylene to propylene at mild conditions. Influence of the preparation method and Re_2O_7 content in the PdO-$Re_2O_7/SO_4^{2-}/ZrO_2$ system was studied. Optimal method of catalyst preparation is impregnation of support by solution of palladium precursor and then by solution of rhenium precursor, each impregnation being followed by calcination in air at 550°C (a series of Pd-Re catalysts). The maximum yield of propylene (62.1 wt. %) was achieved on the PdO-$Re_2O_7/SO_4^{2-}/ZrO_2$ catalyst with 4.1 wt. % Re_2O_7 at the temperature of 80˚C (Table 1).

Table 1. Catalytic performance of PdO-$Re_2O_7/SO_4^{2-}/ZrO_2$ catalysts (at 80°C).

Catalyst	Composition (wt.%)			Reaction time (h)	Conversion of ethylene (%)	Yield of propylene (wt.%)	Selectivity (%)		
	Re_2O_7	PdO	SO_4^{2-}				Propylene	2-butene	C_{5+}
Pd-Re-10	4.1	1.1	7.3	0.2	81.9	62.1	75.8	10.1	14.0
				1	48.9	17.9	36.6	46.6	16.8
Pd-Re-5	3.6	1.1	7.3	0.2	81.9	49.8	60.8	7.2	32.0
				1	56.3	25.3	44.9	37.7	17.4
Pd-Re-2	1.9	1.1	7.3	0.2	86.1	56.3	65.4	26.5	8.0
				1	62.6	27.9	44.6	38.1	17.4

4 Conclusions

A series of Pd-Re catalysts, which was prepared with the impregnation of support by solution of palladium precursor and then by solution of rhenium precursor, exhibited ethylene conversion, lower than for other two series. But at that a series of Pd-Re catalysts showed high propylene yield (42.4-55.2 wt. % at 40°C and 49.8-62.1 wt. % at 80°C), and that the initial activity depends on the Re_2O_7 content in the catalysts. Thus, PdO-$Re_2O_7/SO_4^{2-}/ZrO_2$ catalyst exhibits a higher propylene yield in the direct conversion of ethylene to propylene at mild conditions (reaction temperature up to 100°C, atmospheric pressure).

Acknowledgements

This work was supported by the Russian Fund for Basic Research, Grant No. 13-03-12258 ofi_m. We would like to thank Omsk Collaborative Center Siberian Branch Russian Academy of Sciences for measurements.

References

[1] J. Knight, R. Mehlberg, *Hydrocarbon processing*. 9 (2011) 91.
[2] D. Soni, M.R. Rao, G. Saidulu, D. Bhattacharyya,V.K. Satheesh, *Petroleum Technology Quaterly (PTQ)*. Q4 (2009). 95.
[3] Pat. 2427421 (RU). 2011.
[4] E. Buluchevskiy, M. Mihkailova, A. Lavrenov, *Chemistry for Sustainable Development*. 21 (2013) 55.
[5] Pat. 3758626 (US). 1973.

II-OP59

Design of Highly Efficient Catalysts for Catalytic Membrane Reactors: Study within the Framework of DEMCAMER Project

Ismagilov I.[1*], Matus E.[1], Kuznetsov V.[1], Sukhova O.[1], Kerzhentsev M.[1], Ismagilov Z.[1,2], Mota N.[3], Navarro R.[3], Fierro J.[3], Koekkoek A.[4], Gerritsen G.[4], Abbenhuis H.[4]

1 - Boreskov Institute of Catalysis SB RAS, Novosibirsk, Russia
2 - Institute of Coal Chemistry and Material Science SB RAS, Kemerovo, Russia
3 - Instituto de Catálisis y Petroleoquímica, CSIC, Madrid, Spain
4 - Hybrid Catalysis B.V., Eindhoven, the Netherlands

* iismagil@catalysis.ru

Keywords: autothermal, reforming, oxidative coupling of methane, DEMCAMER

1 Introduction

Process Intensification (PI), which is defined as "any chemical engineering development that leads to a substantially smaller, cleaner, safer and more energy efficient technology", is likely to be the next revolution of the chemical industry [1]. The technology of membrane reactor plays an important role in PI and is based on a device combining a membrane based separation and a catalytic chemical reaction in one unit. DEMCAMER - DEsign and Manufacturing of CAtalytic Membrane Reactors by developing new nano-architectured catalytic and selective membrane materials" is a large scale collaborative project including 18 European organizations as consortium participants. The aim of DEMCAMER is to develop innovative multifunctional Catalytic Membrane Reactors (CMR) based on new nano-architectured catalysts and selective membrane materials to improve their performance, durability, cost effectiveness and sustainability (lower environmental impact and use of new raw materials) over four selected chemical processes for pure hydrogen, liquid hydrocarbons and ethylene production [1]:

- Autothermal Reforming, (ATR)
- Fischer-Tropsch Synthesis, (FTS)
- Water Gas Shift, (WGS)
- Oxidative Coupling of Methane, (OCM)

DEMCAMER will bring the proof of concept of these novel CMRs by the set-up and validation of pilot prototypes relevant for each process [1]. The research activity of the team from Boreskov Institute of Catalysis (BIC) focused on the development of novel catalyst materials for ATR of CH_4 and OCM processes as well as quantum-chemical modeling. These studies will be applied to understand the structure-property-performance relationships.

2 Experimental

For each process four different catalyst generations have been developed. For each catalyst generation, 8-10 catalyst formulations have been prepared varying the type of support, the nature of the active phase, the addition of promoters and/or the method of preparation. The effect of following parameters on the physicochemical properties of catalysts and their performance in the reaction were studied:

ATR of CH_4:

- active component (Ni, Pt, Rh, Pd)
- support composition (La_2O_3, $Ce_xZr_{1-x}O_y$, $Ce_xGd_{1-x}O_y$, $La_2O_3/Ce_{0.5}Zr_{0.5}O_2/Al_2O_3$,)
- promoter type (Mo, Re, Sr, Sn, Pt, Pd)
- method of preparation (citrate sol-gel method, Pechini method, impregnation)
- calcination, pre-treatment and ATR reaction conditions

OCM:

- type of catalyst system (catalysts based on tungsten and promoted with manganese and rare earths and supported on conventional silica carrier; catalysts based on rare earth and alkaline earth metal oxides)
- metal contents
- promoter type (La, Ce, Zr, S, P, Cl)
- preparation mode (citrate sol-gel method, sequential impregnation, mixture slurry method)
- calcination, pre-treatment and OCM reaction conditions.

Moreover, some catalysts have been also prepared by the POSS® nanotechnology implemented by Hybrid Catalysis. In order to identify the Red-Ox, textural, surface and structural characteristics of catalysts influencing catalytic activity and stability detailed characterization of catalyst systems in both fresh and used state has been performed by a complex of methods (N_2 adsorption, XRD, TPR, HRTEM-EDX, TG-DTA, XPS and ESDR). The design and assembling of the kinetic setup for the studies of catalytic activities in ATR and OCM process have been done. The screenings of prepared catalysts as well as stability tests (up to 100 h) have been carried out. The optimal reaction conditions to achieve the maximum efficiency in the hydrogen production from ATR and C_2 hydrocarbon production from OCM were determined.

3 Results and discussion

Detailed physicochemical characterization of fresh and used catalysts combined with catalytic activity measurements have allowed to determine the correlation between composition, preparation conditions and activity and stability of the developed catalysts [1-4]. From catalyst screenings and durability tests in the laboratory set-up, the final optimal catalyst composition and preparation mode were selected, with emphasis on the catalyst nanostructure control, as final catalyst generation for scale-up and conformation for testing at pilot scale. For ATR of CH_4 the $NiPd/Ce_{0.5}Zr_{0.5}O_2/Al_2O_3$ catalyst prepared by Pd/Ni sequential impregnation showed high activity (methane conversion > 90%, hydrogen yield > 80% at 850^{o}C), resistance to carbon formation and deactivation by sulfur during 100 h of operation under reaction feed containing 50 ppm of H_2S. $MnNaWLa/SiO_2$ catalyst prepared by sequential impregnation method at optimized conditions showed high activity (methane conversion > 50%, C_2 yield > 18%) during 24 h of the OCM reaction at 800^{o}C.

4 Conclusion

The rational preparation procedures and perspective composition of catalysts for ATR of CH_4 and OCM have been developed. Final catalyst generation developed for each processes showed high values of activity, selectivity and stability in compliance with the DEMCAMER targets.

Acknowledgements

Financial support of this work in the frame of the European Union 7th Framework Programme (FP7/2007–2013) under grant agreement No. 262840 is gratefully acknowledged.

References

[1] http://www.demcamer.org
[2] I.Z. Ismagilov, E.V. Matus, V.V. Kuznetsov, N. Mota, R.M. Navarro, M.A. Kerzhentsev, Z.R. Ismagilov, J.L.G. Fierro, *Catal Today*. 210 (2013) 10.
[3] I.Z. Ismagilov, E.V. Matus, V.V. Kuznetsov, S.A. Yashnik, I.P. Prosvirin, M.A. Kerzhentsev, Z.R. Ismagilov, N. Mota, R.M. Navarro, J.L.G. Fierro, *Appl. Catal. A.* 481 (2014) 104.
[4] I.Z. Ismagilov, E.V. Matus, V.V. Kuznetsov, M.A. Kerzhentsev, S.A. Yashnik, I.P. Prosvirin, N. Mota, R.M. Navarro, J.L.G. Fierro, Z.R. Ismagilov, *Int J Hydrogen Energy.* 39 (2014) 20992.

II-OP60

A Kinetic Fingerprint for Distinguishing Porous Diffusion

Fushimi R.[1,2*], Redekop E.[3], Nyapete C.[4], Korakianitis T.[1], Gleaves J.[5], Yablonsky G.[2]

1 - Idaho National Laboratory, Idaho Falls, USA
2 - Parks College of Engineering, Aviation and Technology, Saint Louis University, Saint Louis, USA
3 - Department of Chemistry, University of Oslo, Oslo, Norway
4 - Department of Chemistry, Saint Louis University, Saint Louis, USA
5 - Department of Energy, Environmental and Chemical Engineering, Washington University in Saint Louis, Saint Louis, USA

* Rebecca.fushimi@inl.gov

Keywords: TAP, Reactor, MOFs, intraparticle, diffusion, porous, transport, transient, kinetics

1 Introduction

Metal organic frameworks (MOFs), formed from metal complexes joined by organic linking structures, are a distinctive class of nanoporous material with high surface area and pore volume. While zeolites have greater thermal and chemical stability, MOFs offer a greater degree of flexibility for pore size and surface chemistry according to the selection of the linking molecule. The TAP (Temporal Analysis of Products) vacuum pulse response technique [1,2] offers a unique characterization of adsorption kinetics and intraparticle transport in nanoporous materials [3,4] with a number of advantages. In particular, the measurement is made at low pore occupancy where molecules can freely diffuse and processes occurring on the external surface can be distinguished from processes that take place in the porous confines. Here we present a probe molecule filtering that results under TAP conditions where only molecules that have a finite surface lifetime gain access to the pore. This offers an advanced tool for materials characterization that can distinguish properties that are not observable with conventional techniques.

2 Experimental/methodology

A TAP pulse response experiment, described elsewhere [5], starts with a very small (10 nmol) pulse of probe molecule/inert molecule mixture at the entrance of a microreactor packed in three zones with two larger sections of inert (SiC) particles separated by a thin zone of active material. At the exit of the microreactor (10^{-8} torr) a mass spectrometer collects the pulse response. 6 mg of a commercial sample of the HKUST-1, $Cu_2(C_{12}H_4O_8)$, MOF produced by BASF under the tradename Basolite®C300 was tested in the TAP reactor using various probe molecules (methane, ethane, propane, propene, butane, butene, krypton, etc.). The reactor temperature was slowly (2 °C/min) decreased from 200 – 20 °C while pulsing every 10.1 seconds. The evolution of the pulse response curves with temperature was collected. Data was analyzed using the moment-based technique and applied to an adsorption model of porous diffusion using the basic kinetic coefficient approach to the state-defining experiment as described by Shekhtman et al. [6].

3 Results and discussion

Due to the low number of collisions in the gas phase during a TAP experiment, when the kinetic diameter of the diffusing species is similar to the pore diameter, only molecules with a finite lifetime on the external surface will have the opportunity to enter the intraparticle space. The evolution of reactor residence time is shown in Figure 1 when propene, propane and krypton are pulsed over the HKUST-1 material in separate experiments as the temperature changes. At temperatures above 180 °C the reactor residence time for propane and krypton is

similar and is generally governed by diffusion through the particle bed: $D \propto \sqrt{8RT/\pi M_w}$. Propane and propene, being of similar molecular weight should exhibit similar Knudsen transport but the presence of a double bond results in a much higher reactor residence time. As the temperature decreases the residence time for krypton follows the dependence for Knudsen transport through the reactor but the residence time for propane dramatically increases indicating a kinetic process. The dependence for propene is characterized by two plateaus that can be explained by a strong interaction of the double bond with the catalyst and a significant contribution of intraparticle diffusion.

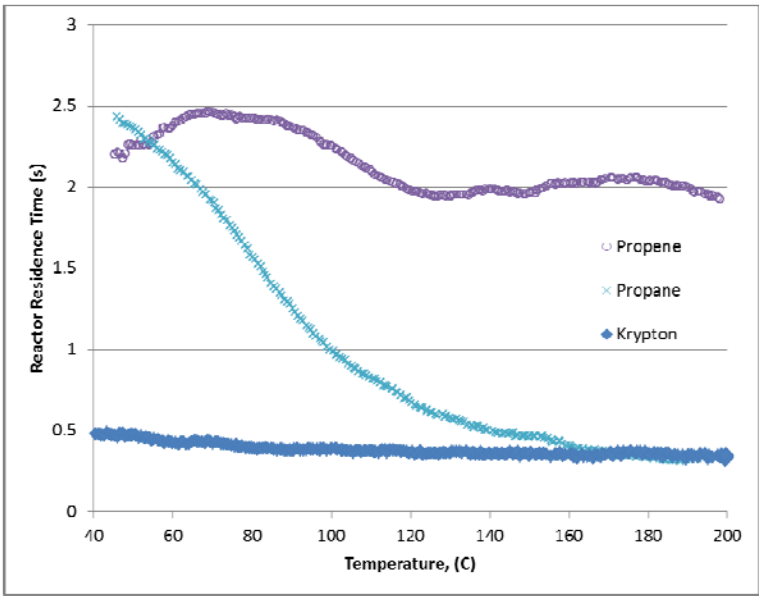

We present a kinetic model describing the competing processes of entering the pore and desorbing from the external surface. Applying this kinetic model to the TAP experimental configuration we can distinguish time delays in pulse response curves that are due to the residence time in pores from those caused by adsorption on the external surface.

Fig. 1. Reactor residence time as a function of temperature for different probe molecules (propene, propane and krypton) pulsed over the HKUST-1 material.

4 Conclusions

Under TAP pulse response conditions, when the size of the probe molecule is similar to that of the pore size, an energy barrier exists for entrance to the porous confines that can be described as a kinetic process. This enables a measurement of properties *intrinsic* to the material structure and surface chemistry that are not observable under standard conditions. Characteristics unique to the external surface and internal confines can be used to better distinguish different candidate materials for applications development.

Acknowledgements

The authors would like to acknowledge Saint Louis University's President's Research Fund (#8718) for supporting this work.

References

[1] J. Perez-Ramirez and E. V. Kondratenko, *Catal. Today*, 121 (2007) 160-169.
[2] J. Gleaves, G. Yablonsky, X. Zheng, R. Fushimi, and P. Mills, *J. Molec. Catal. A: Chem.* 315 (2010) 108-134.
[3] O. P. Keipert and M. Baerns, *Chem.Eng.Sci.*53 (1998) 3623-3634.
[4] J. Delgado, T. Nijhuis, F. Kapteijn, and J. Moulijn, *Chem.Eng.Sci.* 59 (2004) 2477-2487.
[5] J. Gleaves, G. Yablonskii, P. Phanawadee, and Y. Schuurman, *Appl. Catal., A*, 160 (1997) 55-88.
[6] S. Shekhtman, G. Yablonsky, J. Gleaves, and R. Fushimi, *Chem. Eng. Sci.* 58 (2003) 4843-4859.

II-PP01

Capped Co-promoted Pd/AlOOH Catalysts in Dehydrogenation of Formic Acid for Hydrogenation of Maleic Anhydride

Choudhary H., Nishimura S., Ebitani K.

School of Materials Science, Japan Advanced Institute of Science and Technology, Nomi, Japan

* ebitani@jaist.ac.jp

Keywords: CoPd/AlOOH catalysts, Capping agent, Formic acid, Hydrogenation, Succinic acid

1 Introduction

In the current era of energy crisis, researchers are striving to develop technologies to maintain a balance between conventional petroleum feedstock and renewable biomass resources through catalytic approaches. Various studies on the catalytic dehydrogenation of formic acid (FA) into hydrogen is an appreciable contribution to these developments [1]. FA, a convenient hydrogen storage material [2], can be obtained from biomass in high yields [3]. Despite of amazing research attainments in FA dehydrogenation, limited efforts were made to substitute dangerous and difficult-to-handle H_2 under greener conditions. The Pd-based catalysts were found to be effective in promoting the dehydrogenation of FA [4], where the dehydrogenation catalysis can be enhanced by doping a transition metal (such as Co) to promote the 2-electron oxidation pathway of FA [5]. It has also been understood that the chemical, physical and geometrical properties of metallic NPs can be considerably influenced in the presence of capping agents to have a marked impact on their catalyses [6]. In this contribution, we demonstrate the synthesis of boehmite (AlOOH) supported capped CoPd NPs for the hydrogenation of maleic anhydride (MAn) using FA as a hydrogen source [7].

2 Experimental

Material synthesis: A homogeneous solution containing requisite amounts of $Co(OAc)_2 \cdot 4H_2O$ and/or $Pd(OAc)_2$ with/without capping agent were added to AlOOH (S_{BET}: 465 $m^2\ g^{-1}$) dispersed in water. A hydrothermal treatment of the resulting mixture at 453 K afforded mono-/bi-metallic catalysts after drying *in vacuo* overnight at room temperature.

Catalytic activity: In a general reaction procedure, maleic anhydride (MAn, 0.5 mmol) in deionized water (5 mL) and catalyst (25 mg) were weighed in a Teflon vessel (50 mL). After addition of FA (1.9 mmol), the autoclave was sealed and heated at 353 K for 3 h. The conversion and yields were determined with a calibration curve method by HPLC (Waters 600 using Aminex HPX-87H column).

As-prepared catalysts were characterized minutely using TEM, XRD, XPS and XAS [KEK-PF (2013G586): BL-9C (Co K-edge) and BL-9A (Pd L_3-edge); SPring-8 (2013B1478 and 2014B1472): BL01B1 (Pd K-edge)] to explain their catalytic performances.

3 Results and discussion

We found that among various CoPd catalysts, *N*,*N*-dimethyldodecylamine *N*-oxide (DDAO)-capped bimetallic CoPd NPs supported on AlOOH (CoPd-DDAO/AlOOH) exhibited superior catalysis for the hydrogenation of MAn to succinic acid (SA) using FA as a sustainable hydrogen source (Table 1, entries 1-4). CoPd-DDAO/AlOOH emerged as a robust catalyst and can be reused effectively by preventing the cobalt leaching as compared to non-capped CoPd/AlOOH (entries 1-2). The catalysis did not progress in the absence of either catalyst or FA (entries 5-6). The supported CoPd NP catalysts were characterized thoroughly to comprehend their catalytic activity. The electron microscopy confirmed the uniform distribution of Co and Pd

within each CoPd NP throughout the CoPd-DDAO/AlOOH catalyst. XRD, XPS and XAS supported the Co-Pd interactions, whereas, XPS and XAS advocated the electron exchange in Co-Pd-capping to control the electron density on Pd in the CoPd catalysts. Also, the composition of CoPd NP was deciphered as CoPd alloy along with cobalt oxides from XPS and XAS analyses. The absence of any widely-used reducing agent during the preparation of catalyst was considered as the main reason for the presence of cobalt oxides. From these results, it was expected that the alloying of Co with Pd in the presence of DDAO, afforded electron rich Pd (that enhanced the adsorption/dissociation of substrates) and modified the Pd-Pd bond distance to facilitate the better alignment of metal d-orbital with the carbonyl π-orbitals onto the catalyst surface.

Table 1. Hydrogenation of Maleic anhydride (MAn) using Formic acid (FA).

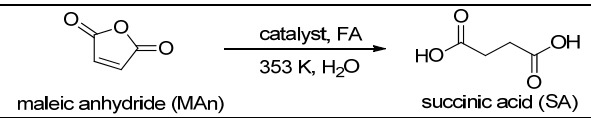

Entry	Catalyst	Co[a] / wt%	Pd[a] / wt%	Conv.[b] / %	Yield[b] / %
1	CoPd-DDAO/AlOOH	0.75, 0.71[c]	2.53, 2.52[c]	>99, >99[c]	>99, >99[c]
2	CoPd/AlOOH	0.94, 0.39[d]	2.44, 2.41[d]	72	56
3	CoPd-CTAB/AlOOH	0.63	2.49	52	36
4	CoPd-PVP/AlOOH	0.55	2.51	49	35
5[e]	CoPd-DDAO/AlOOH	0.75	2.53	0	0
6	blank	0	0	0	0

Reaction conditions: MAn (0.5 mmol), FA (1.9 mmol), Catalyst (25 mg), H_2O (5 mL), 353 K, 3 h, Teflon lined autoclave. [a]Determined by ICP-AES analysis. [b]Calculated by HPLC. [c]After 5th catalytic run. [d]After 1st catalytic run. [e]Without FA. CTAB; cetyltrimethylammonium bromide. PVP; poly(*N*-vinyl-2-pyrrolidone).

4 Conclusions

In conclusion, we found that CoPd-DDAO/AlOOH acts as a robust catalyst for the hydrogenation of MAn using FA as hydrogen source without additive/base. The characterization of various capped CoPd catalysts evidences the superior catalysis of CoPd-DDAO/AlOOH because of enhanced stability (metal leaching inhibition) and electronic/geometric modifications in Pd states in the presence of Co and DDAO.

Acknowledgements

HC extends his thanks to Japan Society for the Promotion of Science (JSPS) for fellowship. This work is partially supported by JSPS KAKENHI Grant Numbers 26-12396 (Grant-in-Aid for JSPS Fellows) and 25820392 (Grant-in-Aid for Young Scientists (B)), and the Mitani Foundation for Research and Development, Japan.

References

[1] V. Mazumder, S. Sun, *J. Am. Chem. Soc.* 131 (2009) 4588; A. Boddien, D. Mellmann, F. Gartner, R. Jackstell, H. Junge, P.J. Dyson, G. Laurenczy, R. Ludwig, M. Beller, *Science* 333 (2011) 1733.
[2] T.C. Johnson, D.J. Morris, M. Wills, *Chem. Soc. Rev.* 39 (2010) 81.
[3] J.J. Bozell, *Science* 329 (2010) 522; H. Choudhary, S. Nishimura, K. Ebitani, *Appl. Catal. B: Environ.* 162 (2015) 1.
[4] J.S. Yoo, F. Ablid-Pedersen, J.K. Norskov, F. Studt, *ACS Catal.* 4 (2014) 1226.
[5] V. Mazumder, M. Chi, M.N. Mankin, Y. Liu, Ö. Metin, D. Sun, K.L. More, S. Sun, *Nano Lett.* 12 (2012) 1102.
[6] For example, H. Zhang, T. Watanbe, M. Okumura, M. Haruta, N. Toshima, *Nat. Mater.* 11 (2012) 49; D. Tongsakul, S. Nishimura, K. Ebitani, *J. Phys. Chem. C* 118 (2014) 11723.
[7] H. Choudhary, S. Nishimura, K. Ebitani, *submitted*.

II-PP02

In-Situ TEM and Electron Tomography: Revealing the Location and the Mechanism of Formation of Copper Particles

Van Den Berg R.[1*], Elkjaer C.F.[2], Gommes C.J.[3], Sehested J.[2], De Jongh P.E.[1], De Jong K.P.[1], Helveg S.[2]

1 - Utrecht University, Debye Institute for Nanomaterials Science, Inorganic Chemistry and Catalysis, Utrecht, Netherlands
2 - Haldor Topsoe A/S, Lyngby, Denmark
3 - University of Liege B6A, Department of Chemical Engineering, Liege, Belgium

* r.vandenberg1@uu.nl

Keywords: particle formation, *in-situ* TEM, electron, tomography

1 Introduction

Two of the main industrial routes to synthesize supported metal catalysts are incipient wetness impregnation and co-precipitation followed by calcination and reduction. It is unclear, however, how metallic particles form during the reduction of a co-precipitated sample and which of the two routes leads to a more thermally stable catalyst. Two advanced TEM techniques, namely *in-situ* TEM and electron tomography (ET), were employed to unravel the mechanism of formation and to determine the exact location of the metal nanoparticles with respect to the support for Cu/SiO_2 methanol synthesis catalysts.

2 Experimental/methodology

Copper on silica catalysts were synthesized via incipient wetness impregnation with copper nitrate followed by drying, calcination and reduction, and via reduction of a co-precipitated copper phyllosilicate [1, 2]. The formation of an ensemble of metallic copper particles during reduction of the copper phyllosilicate was imaged in real time with *in-situ* TEM. The number, size and location of the emerging copper nanoparticles were tracked over time. For both catalysts, the 3D location of the copper particles after reduction with respect to the silica support was determined with electron tomography. The stability of the copper catalysts was investigated in the methanol synthesis reaction at 40 bars at 260°C for 10 days.

3 Results and discussion

In-situ TEM showed that copper particles forming during the reduction of a co-precipitated copper phyllosilicate were not mobile, indicating that growth occurred via diffusion of copper species to the nucleated particles (Figure 1). As soon as a new particle appeared it grew first very fast and then slower, expectedly as the copper ion concentration in the surrounding copper phyllosilicate was gradually depleted. As a result, particles that nucleated early during reduction grew, on average, larger than particles that nucleated later.

Electron tomography revealed the 3D location of the copper particles with respect to the silica support. After reduction of the copper phyllosilicate, the particles were partially entrapped in the silica, since the copper particles and the silica support were formed at the same time (Figure 2A). For copper on silica gel, prepared via incipient wetness impregnation of an existing support, the copper particles were located on the surface of the silica (Figure 2B).

Copper on silica, prepared via reduction of a co-precipitated copper phyllosilicate, showed an improved stability in the methanol synthesis reaction compared to copper on silica prepared via incipient wetness impregnation. Both catalysts had similar initial particle size distributions and particle-particle distances.

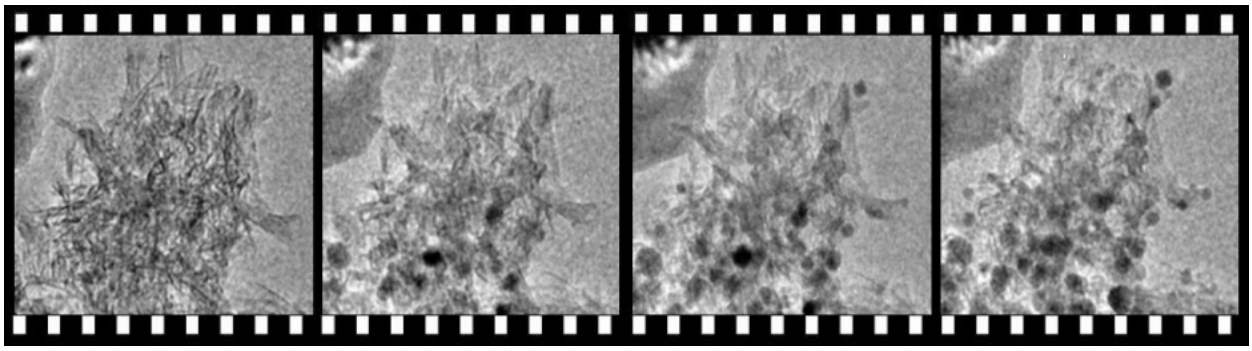

Fig. 1. *In-situ* TEM images (170 x 170 nm) taken of the same location during reduction of a co-precipitated copper phyllosilicate.

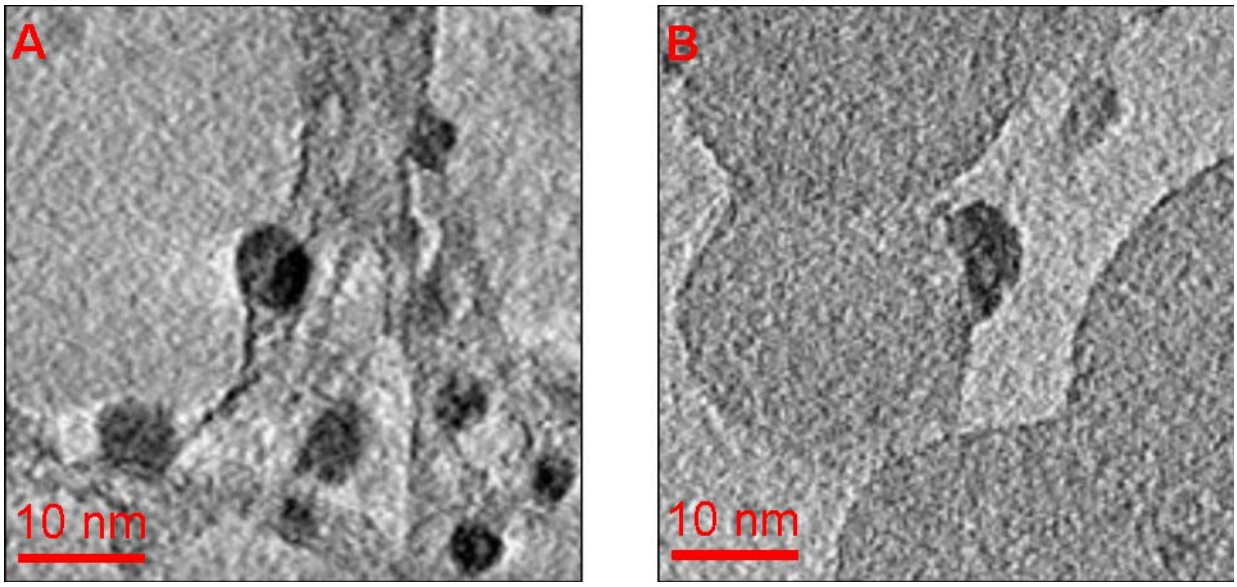

Fig. 2. TEM tomogram sections of copper on silica prepared via co-precipitation followed by reduction (A) and via incipient wetness impregnation of copper nitrate (B).

4 Conclusions

Copper particles formed during reduction of a co-precipitated copper phyllosilicate were partially entrapped in the silica support. These entrapped particles proved more stable against growth in the methanol synthesis reaction compared to a Cu/SiO_2 catalyst prepared via incipient wetness impregnation where copper particles were located on the convex surface of the silica spheres.

Acknowledgements

The authors would like to thank Haldor Topsøe A/S for funding.

References

[1] C.G. van der Grift, P.A. Elberse, A. Mulder, J.W. Geus, *App. Cat*. 59 (1990) 275.
[2] P. Munnik, M. Wolters, A. Gabrielsson, S.D. Pollington, G. Headdock, J.H. Bitter, P.E. de Jongh, K.P. de Jong, *J. Phys. Chem. C*. 115 (2011) 14698.

II-PP03

Effect of the PdFe Alloy in the Catalysis of Water Gas Shift Reaction

Arroyo-Ramirez L.[1*], Doan-Nguyen V.[2], Murray C.B.[2,3], Gorte R.J.[1,3]

1 - University of Pennsylvania, Department of Chemical and Biomolecular Engineering, Philadelphia, USA

2 - University of Pennsylvania, Department of Chemistry, Philadelphia, USA

3 - University of Pennsylvania, Department of Materials Science and Engineering, Philadelphia, USA

* lisandra@seas.upenn.edu

Keywords: palladium, iron, alloy, TEM, WGS

1 Introduction

Nano-sized particles continue to attract interest for heterogeneous catalysis, especially alloy nanoparticles, due to their unique catalytic properties. These nanomaterials have been studied to improve the catalytic activity in reactions for hydrogen production. We report the synthesis of Pt@ZnO and Pd@ZnO core-shell nanostructure that form alloy after mild reduction [1]. For the methanol steam reforming, the formation of the PtZn and PdZn alloy increase the CO_2 selectivity compare to the metal catalysts. Another, important reaction is the water gas shift ($CO + H_2O \rightarrow CO_2 + H_2$). The addition of Fe was found to increase WGS rates of Pd catalysts but not for other metals such Pt and Rh [2]. The enhancement associated with addition of Fe to Pd catalysts is due to the PdFe alloy.

In this work, we present the synthesis of Pd/Al_2O_3 and $PdFe/Al_2O_3$ nanocatalysts. We studied the effect of adding Fe to Pd in the catalysis of water gas shift reaction. The PdFe alloy improve the rates of the WGS reaction compared to Pd catalyst. Also, the $PdFe/Al_2O_3$ catalysts have similar activation energy than Pd/CeO_2 [2]. These findings are important for tailor the alloys synthesis for applications in heterogeneous catalysis.

2 Experimental/methodology

The controlled synthesis of the PdFe alloy nanoparticles were done by co-reduction of $Pd(acac)_2$ and $Fe(acac)_2$, similar to previously reported procedures [3]. The PdFe alloy nanoparticles were deposited on Al_2O_3 support for a metals loading of 1-wt%. Also, Pd nanoparticles were prepared by reduction of $Pd(acac)_2$ and deposited on Al_2O_3 support. For comparison, conventional Pd/Al_2O_3 and $PdFe/Al_2O_3$ catalysts with 1-wt% metal were prepared by impregnation of the support with aqueous solutions of $(NH_3)_4Pd(NO_3)_2$ and $Fe(NO_3)_3 \cdot 9H_2O$, respectively. The dried powders were calcined in air at 773 K for 6 h. The catalysts were characterized by TEM and CO chemisorption. The water gas shift reaction rates were measurement by placing 0.10 g of the sample in a tubular reactor and flowing CO and H_2O at a partial pressures of 25 torr and 25 torr, respectively, with He as carrier.

3 Results and discussion

The 1-wt% Pd/Al_2O_3 and 1-wt% $PdFe/Al_2O_3$ catalysts were prepared to study their catalytic activity towards water gas shift (WGS) reaction. TEM images of the PdFe alloy show uniform nanoparticles of approximately 5 nm in diameter. In the CO chemisorption measurements, the $PdFe/Al_2O_3$ show low palladium dispersion that can be due the formation of alloy. The $PdFe/Al_2O_3$ catalyst show higher rates compared to Pd/Al_2O_3 catalysts. It is noteworthy that these catalysts have the same particles sizes, so the increase in the catalytic

activity for the $PdFe/Al_2O_3$ catalyst can be attribute to the Fe present in the sample.

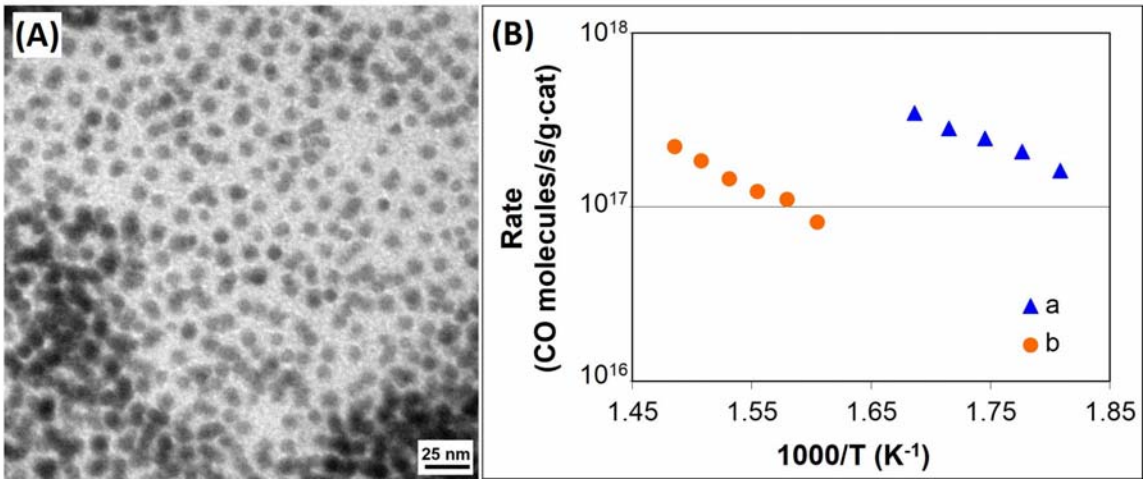

Fig. 1. (A) Transmission electron microscopy (TEM) image for the PdFe alloy nanoparticles. (B) Rates for the water gas shift (WGS) reaction over (a) $PdFe/Al_2O_3$ and (b) Pd/Al_2O_3 catalysts.

4 Conclusions

We successfully demonstrated the synthesis of PdFe alloy nanoparticles and deposited on alumina. The addition of Fe to Pd catalysts increase the rates for WGS reaction compared to Pd catalysts. These findings were important because can lead to better understanding of the alloy effect in catalytic reactions.

Acknowledgements

We acknowledges financial support from the University of Pennsylvania Provost Academic Diversity Fellowship, U.S. Department of Energy (Project DE-SC0009440), Department of Energy, Office of Basic Energy Sciences, Chemical Sciences, Geosciences and Biosciences Division (Grant No. DE-FG02-13ER16380) and the Richard Perry University Professorship.

References

[1] L. Arroyo-Ramírez, C. Chen, M. Cargnello, C. B. Murray, P. Fornasiero, R. J. Gorte, *J. Mater. Chem. A* 2 (2014) 19509.

[2] R. J. Gorte, S. Zhao, *Catal. Today* 104 (2005) 18.

[3] S. Sun, S. Anders, T. Thomson, J. E. E. Baglin, M. F. Toney, H. F. Hamann, C. B. Murray, B. D. Terris, B.D. *J. Phys. Chem. B* 107 (2003) 5419.

II-PP04

Architecting Acid-Mediated Synthesis of Ordered Mesoporous Aluminosilicates

Nunna V.K., Parasuraman S.*

National Centre for Catalysis Research and Department of Chemistry, Indian Institute of Technology, Chennai, India

* selvam@iitm.ac.in

Keywords: ordered mesoporous aluminosilicates, intrinsic, hydrolysis, method, moderate, solid, acids

1 Introduction

Ordered mesoporous aluminosilicates (OMAs) with moderate Brønsted acidity have great potential as heterogeneous acid catalysts. However, the synthesis of acid-mediated OMAs such as H-AlSBA-15 and H-AlIITM-56 is difficult owing to: (i) existence of trivalent aluminium under acidic conditions; (ii) differences in the hydrolysis rates of both silicon and aluminium sources and (iii) easy dissociation of Al–O–Si bonds. Hence, it is a big challenge to incorporate trivalent aluminium in the tetrahedral silicate framework [1,2]. For this purpose, we have developed a novel (intrinsic) hydrolysis method in which the hydrolysis rates of source materials are matched using precursors.

2 Experimental

A 4.0 *g* of Pluronic P123/ Brij-56 surfactant was added to 30 *mL* of water and stirred till a clear solution was obtained. Thereafter, 70 *mL* of 0.086 *M* HCl was added and stirred for 2 *h* and *p*H was adjusted to 1.5. Then, 8.30 *g* of TEOS and aluminium citrate was added at 2 *h* interval to this mixture and the resultant gel was stirred at 40°*C*/50°*C* for 22 *h*. The mixture was transferred to a teflon-lined autoclave for hydrothermal treatment (100°*C* for 24 *h*). The obtained precipitate was filtered, washed, dried at 60°*C* for 6 *h* and calcined at 550°*C* for 1 *h* in nitrogen, and 5 *h* in air with a heating rate of 1°*C* min^{-1}. The final samples were designated as H-AlSBA-15/H-AlIITM-56 [3]. Scheme 1 illustrates the methodology for the preparation.

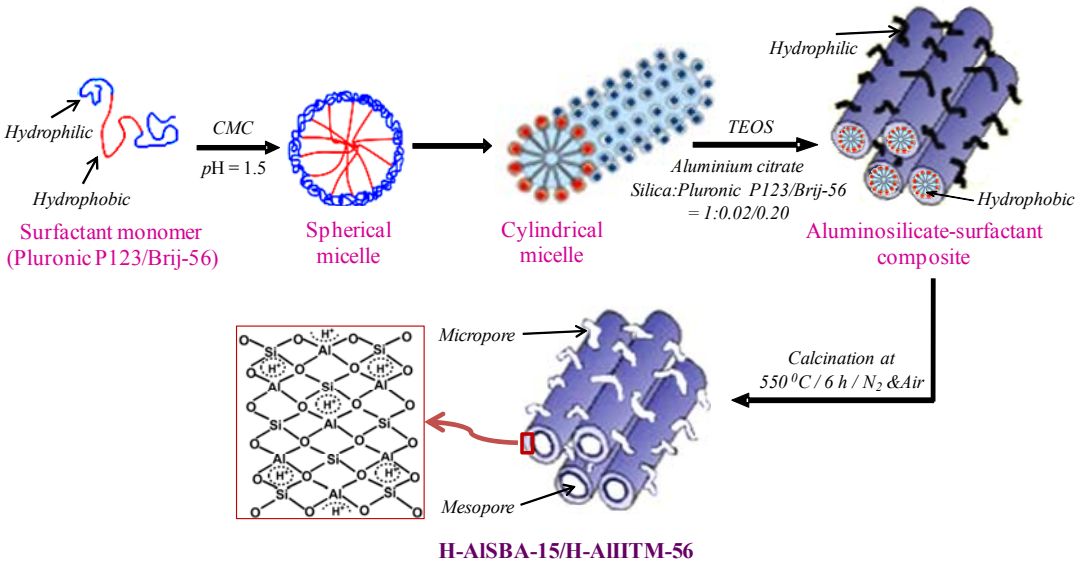

Scheme 1. Acid-mediated synthesis of OMAs by intrinsic hydrolysis method.

3 Results and discussion

Figure 1 depicts XRD, N_2 sorption isotherms and ^{27}Al MAS-NMR spectra of OMAs. It can be seen from this figure that a well-ordered, narrow-pore sized and tetrahedral coordinated H-AlSBA-15/H-AlIITM-56 could be achieved with our novel intrinsic hydrolysis method. In addition, for the first time, this method allows us to incorporate high aluminium content in the silicate matrix. Table 1 summarized the structural and textural properties of the samples.

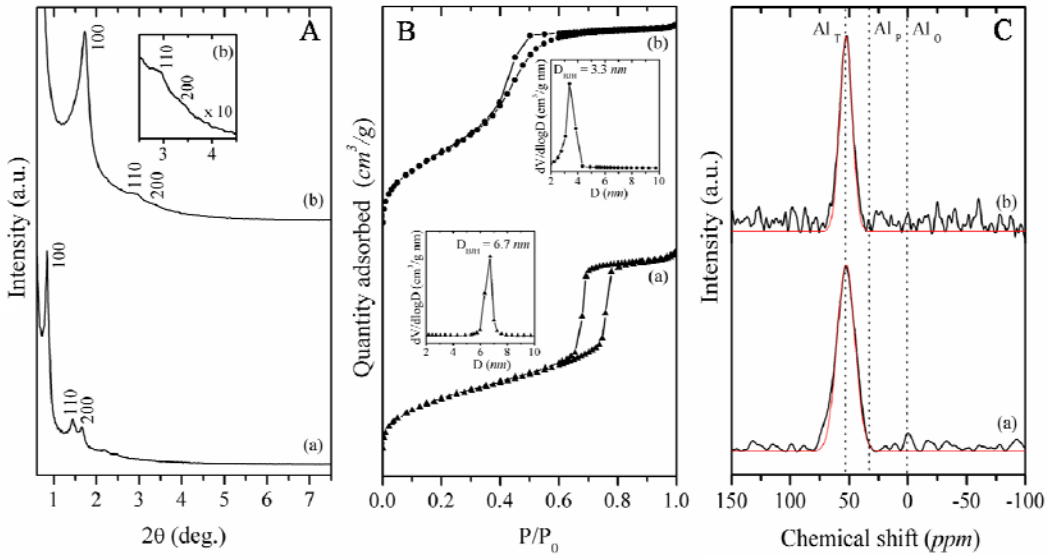

Fig. 1 Low angle XRD patterns (A), N_2 sorption isotherms (B), and ^{27}Al MAS-NMR spectra (C) of: (a) H-AlSBA-15; (b) H-AlIITM-56.

Table 1. Structural, textural and compositional characteristics of acid-mediated OMAs.

Material	a_o (nm)		n_{Si}/n_{Al}[a]		S_{BET} ($m^2\ g^{-1}$)	D_{BJH} (nm)	V_p ($cm^3\ g^{-1}$)	h_w[b] (nm)
	as-syn.	calc.	gel	product				
H-AlSBA-15	12.4	12.0	30	85	599	6.7	0.76	5.3
H-AlIITM-56	6.2	6.0	30	80	818	3.3	0.79	2.7

[a] n_{Si}/n_{Al} determined by XRF; [b] Wall thickness, $h_w = a_0 - D_{BJH}$.

4 Conclusions

For the first, we could successfully achieve the incorporation of trivalent aluminium in the ordered mesoporous silicate matrix under acidic condition. The catalysts, viz., H-AlSBA-15 and H-AlIITM-56, exhibit moderate acidity and show promise for acid catalysed reactions, e.g., tertiary butylation of phenol [4].

Acknowledgements

The authors thank Department of Science and Technology, New Delhi for funding NCCR, IIT-Madras; Prof. B. Viswanathan for the interest in the work.

References

[1] D. Zhao, Q. Huo, J. Feng, B. F. Chmelka, G.D Stucky, *J. Am. Chem. Soc.,* 120 (1998) 6024.
[2] P. Selvam, N. V. Krishna, B. Viswanathan, *J. Indian Inst. Sci.,* 90 (2010) 271.
[3] N. V. Krishna, P. Selvam, *Adv. Porous Mater.,* 2 (2014) 106.
[4] P. Selvam, N. V. Krishna, A. Sakthivel, *Adv. Porous Mater.,* 1 (2013) 239.

II-PP05

Atomic Scale Understanding of Hydrodesulfurization Catalysis Using High-Pressure Scanning Tunneling Microscopy

Mom R.V.[1*], Frenken J.W.M.[1,2], Groot I.M.N.[1]

1 - Huygens-Kamerlingh Onnes Laboratory, Leiden, The Netherlands
2 - Advanced Research Center for Nanolithography, Amsterdam, The Netherlands

* mom@physics.leidenuniv.nl

Keywords: hydrodesulfurization, scanning tunneling microscopy, model, catalyst, *operando* studies

1 Introduction

During hydrodesulfurization (HDS), sulfur is removed from crude oil using hydrogen over a Co or Ni promoted MoS_2 catalyst, typically supported on Υ-Al_2O_3. The catalyst is generated *in situ* from a MoO_3 precursor using a sulfur-rich feedstock (sulfidation). In recent years, the requirements on sulfur levels in fossil fuels have become stronger while the quality of crude oil is decreasing. This has inspired continuing interest in improved understanding and rational design of the catalyst.

While a combination of spectroscopy and microscopy methods has generated a good understanding of the atomic structure of the catalyst and its precursor, little is known about their dynamics under reaction conditions. *Ex situ* studies reveal that the precursor is highly dispersed, with single MoO_3 units being the dominant species [1]. During sulfidation, small crystalline islands of MoS_2 are formed. Studies using model systems have shown that several stable edge structures exist [2], and that these are the active sites for HDS.

Here, we show our efforts to extend the model approach for hydrodesulfurization. We have developed a new model system, MoO_3 on an alumina film on NiAl(110), which allows us to study the detailed nature of the MoO_3–alumina bond using a scanning tunnelling microscope (STM). With our high-pressure STM [3], we have performed *operando* experiments, following the dynamics of the atomic structure of the catalyst under reaction conditions.

2 Experimental

In order to create well defined model catalysts, we prepared single-crystal supports under ultra-high vacuum conditions (see figure 1). We have employed NiAl(110) and Au(111) crystals. Both were cleaned by cycles of Ar^+ bombardment and annealing, after which they were checked

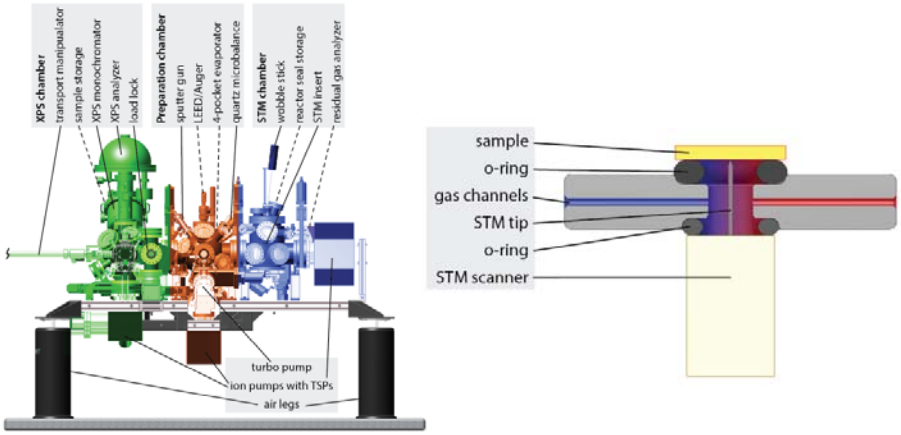

Fig. 1. The ReactorSTM [3]. Left: Ultra-high vacuum apparatus Right: Reactor geometry with STM

for impurities using X-ray photoelectron spectroscopy (XPS) and low-energy electron diffraction (LEED). To grow an alumina film on NiAl(110), the NiAl sample was exposed to a controlled amount of oxygen. This resulted in an alumina film thickness of 0.5nm. Thickening of the alumina film was accomplished by subsequent exposure to NO_2. The crystallinity of the film was checked using LEED and STM. MoO_3 was deposited onto the substrate by heating a Mo evaporation source in the presence of oxygen. MoS_2 could be deposited on Au(111) in a similar fashion, by Mo deposition in the presence of H_2S.

After preparation the catalysts were characterized by XPS and transferred to the STM chamber. By pressing the sample onto a polymer o-ring on top of the STM, the sample and STM scanner are sealed off from the ultrahigh vacuum environment, enclosing the reactor volume (see figure 1). With this geometry, experiments at pressures up to 6bar and temperatures up to 300 ºC can be performed. A dedicated gas supply system was used to control the composition, flow and pressure in the reactor (not shown in figure 1).

3 Results

We have established that the Al_2O_3/NiAl(110) model support is stable under high-pressure conditions, although some sensitivity towards H_2O was found. The deposition of MoO_3 on Al_2O_3/NiAl(110) results in a highly dispersed catalyst precursor (see figure 2). Polymerized MoO_3 coexists with the expected isolated MoO_3 species. *Operando* studies using the model catalysts will be discussed.

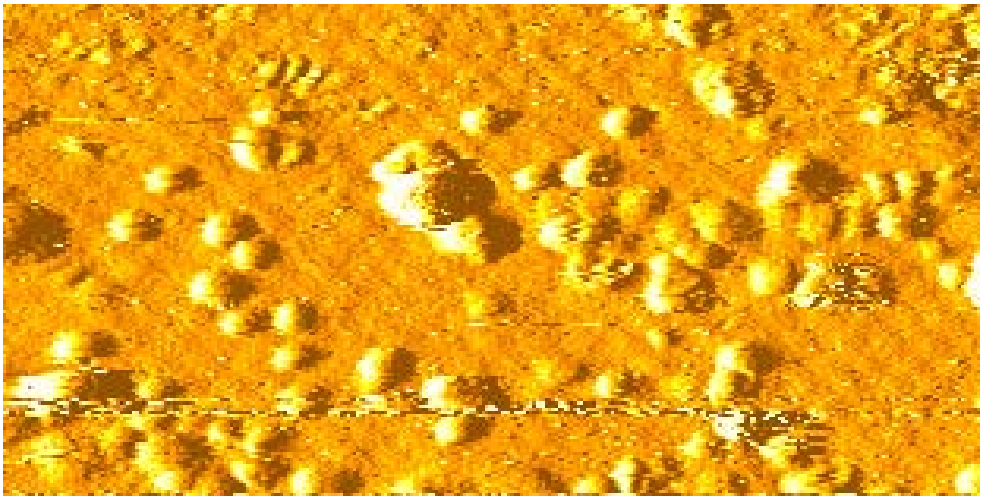

Fig 2. Differentiated STM image of MoO_3 on Al_2O_3/NiAl(110). Size 12 nm x 24 nm

Acknowledgements

The authors would like to thank NIMIC, a public-private partnership, for funding this work and Peter van der Tuijn, Mirthe Bergman, Fred Schenkel, Gertjan van Baarle, Marcel Rost, Peter van Veldhuizen and Ko Koning for technical support.

References

[1] S. Boghosian *et al., Catal. Sci. Technol.* 3 (2013) 1869
[2] J.V. Lauritsen *et al., J. of Catalysis* 221 (2004) 510-522
[3] C.T. Herbschleb *et al., Rev. Sci.Instr.* 85 (2014), 083703

II-PP06

A Novel Synthesis Strategy in Supercritical CO_2 for the Preparation of Nanostructured Ce-Pr Mixed Oxide with Enhanced Catalytic Properties

Parres-Esclapez S.[1], Rico-Perez V.[2], Bueno-López A.[2], Pescarmona P.P.[1,3*]

1 - COK, University of Leuven, Leuven, Belgium
2 - Inorganic Chemistry Department, University of Alicante, Alicante, Spain
3 - Chemical Engineering Department, University of Groningen, Groningen, The Netherlands

* p.p.pescarmona@rug.nl

Keywords: nanostructured, catalysts, Ce-Pr mixed oxide, supercritical, carbon dioxide, green solvent, CO oxidation

1 Introduction

The synthesis of materials using supercritical carbon dioxide (scCO2) has received growing attention in recent years [1]. The specific properties of scCO2, which include tuneable density, gas-like viscosity, low surface tension and high diffusivity, can enable the synthesis of nanostructured materials with unique morphologies and features [2, 3]. Moreover, CO2 is a green solvent, since it is renewable, inexpensive, non‐toxic and can be easily removed from the reaction mixture upon depressurisation, thus enabling the straightforward separation from the products. Here, we present the synthesis of nanoscaled Ce-Pr mixed oxide by using a novel method employing supercritical CO2 as reaction medium, and the application of these materials as heterogeneous catalysts for the oxidation of CO.

2 Experimental

Ce-Pr mixed oxide was prepared with a new methodology based on a tailored design of the reactor that allows bringing in contact a solution containing the metal precursors [$Ce(NO_3)_3$ and $Pr(NO_3)_3$, in ratio 3:1] with an aqueous alkaline solution, only in the presence of supercritical CO_2 fluid. The two solutions are originally placed in separate vessels and they mix only once the supercritical CO_2 conditions are reached. For comparison, the same mixed oxide was prepared with conventional methods, or in $scCO_2$ but in a single vessel. Also pure CeO_2 and PrO_2 were prepared as references. All materials were calcined at 500 □C. The oxides were characterised by means of TEM, XRD, N_2-physisorption and H_2-TPR. The catalytic oxidation of CO was performed in a cylindrical fixed-bed reactor at atmospheric pressure and with a total flow rate of 50 ml/min (1000 ppm CO + 5 % O_2 + He balance; GHSV = 12000 h^{-1}), operated in the range 25-500 ºC. The gas composition was analysed by GC.

3 Results and discussion

The novel synthesis method developed in this work employs supercritical CO_2 as a solvent to bring in contact two solutions, containing the metal precursors and a base, respectively. Under these conditions, the precipitation of the oxide occurs when the two solutions come in contact. The supercritical CO_2 medium promotes the formation of a highly-dispersed precipitate with an intimate contact between the two metal species by:

(i) creating a homogeneous, low-density solution of the two metal precursors

(ii) favouring the rapid precipitation of the oxides, due to their low solubility in $scCO_2$.

The obtained Ce-Pr mixed oxide ($Ce_{0.75}Pr_{0.25}O_2$_$scCO_2$) consists of interconnected nanoparticles with a typical size of 6-7 nm (see TEM in Fig. 1) and presents much higher surface area

compared to its counterparts synthesised with conventional methods or in $scCO_2$ but in a single vessel (Fig. 1). The H_2-TPR profile of $Ce_{0.75}Pr_{0.25}O_2$_$scCO_2$ shows a single peak at relatively low temperature (below 500 ºC, see Fig. 1), indicating that the desired high dispersion of Pr within the mixed oxide was achieved. These features are promising for the catalytic properties of the Ce-Pr mixed oxide in the oxidation of CO. Indeed, $Ce_{0.75}Pr_{0.25}O_2$_$scCO_2$ displayed much superior catalytic performance compared to pure CeO_2 and PrO_2 synthesised with the same approach, and also compared to oxides with the same composition but prepared with a conventional synthesis method, or in $scCO_2$ but in a single vessel (Fig. 1).

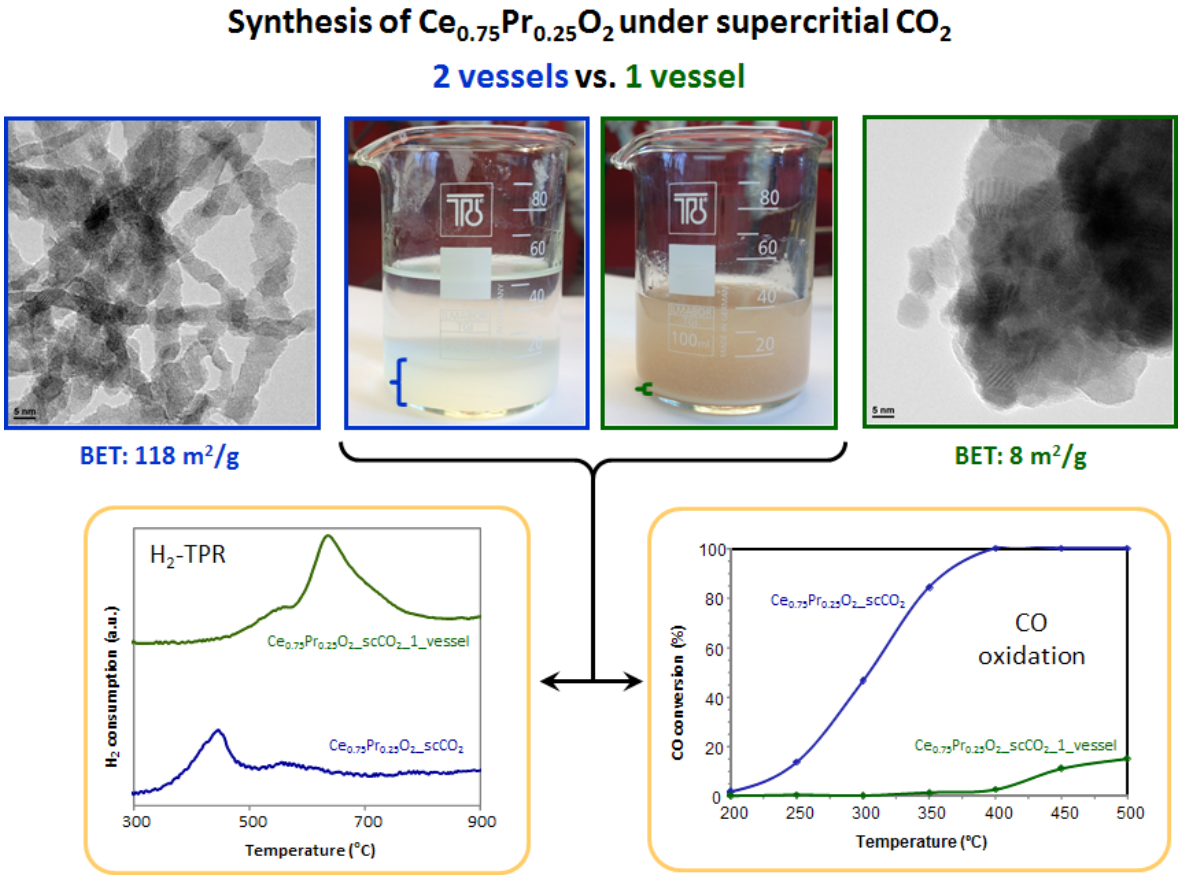

Fig. 1. Comparison between Ce-Pr oxides prepared in $scCO_2$ using a 2-vessel or 1-vessel reactor design.

4 Conclusions

The use of supercritical CO_2 as reaction medium was coupled to a tailored reactor design to produce a nanostructured Ce-Pr mixed oxide with high surface area and with enhanced catalytic activity in the oxidation of CO. This novel synthesis method is of general applicability and, therefore, is also promising for the preparation of other mixed oxide catalysts.

References

[1] Z.-R. Tang, S. A. Kondrat, C. Dickinson, J. K. Bartley, A. F. Carley, S. H. Taylor, T. E. Davies, M. Allix, M. J. Rosseinsky, J. B. Claridge, Z. Xu, S. Romani, M. J. Crudace, G. J. Hutchings, *Catal. Sci. Technol.*, 1 (2011) 740.

[2] F. Cansell, B. Chevalier, A. Demourgues, J. Etourneau, C. Even, Y. Garrabos, V. Pessey, S. Petit, A. Tressaud, F. Weill, *J. Mater. Chem.*, 9 (1999) 67.

[3] J. Jammaer, C. Aprile, S.W. Verbruggen, S. Lenaerts, P.P. Pescarmona, J.A. Martens, *ChemSusChem,* 4 (2011) 1457.

II-PP07

Synthesis and Regeneration of Differentcatalysts with the Supercritical Fluid Technology

Bilalov T.R.[1], Zakharov A.A.[1], Jaddoa A.A.[1,2], Gabitov F.R.[1], Gumerov F.M.[1*]

Federal State Budgetary Educational Institution of Higher Professional Education "Kazan National Research Technological University", Kazan, Russia
Technological University, Baghdad, Iraq

* t.bilalov@yandex.ru

Keywords: supercritical fluids, catalist, synthesis, regeneration

1 Introduction

Supercritical fluid technologies based on the use of working environments in sub- and supercritical fluid states are currently one of the most promising innovative scientific and technological areas. Supercritical fluids, while combining the advantages of gaseous and liquid states of working environments, greatly intensify heat and mass transfer processes. Diffusivity (binary diffusion, self-diffusion) of supercritical fluid media is 1-2 orders of magnitude higher than the figure for the same liquid organic solvents. In the case of supercritical fluid media, there are no phase boundary, surface tension, and, therefore, capillary effect. This define their high penetrability into the porous structure and important perspectives, including within the objectives of the synthesis and regeneration of heterogeneous catalysts. The effectiveness of this approach has been repeatedly confirmed not only by numerous studies, but also by industrial implementations.

2 Experimental/methodology

Synthesis of a palladium chloride benzonitril complex is carried out according to the method described in work [17]. For synthesis the following materials are used: carbon dioxide with 99.995% volume maintenance of CO_2 (GOST 8050-85, certificate of quality № 2052); palladium chloride purity of 99.99% and the pure for analysis benzonitril with the main component maintenance not less than 99.7%. Kinetics research of SC-CO_2-impregnation process and aluminum oxide impregnation by a benzonitril complex on the basis of palladium chloride has been carried out on experimental unit, described in [1]. Supercritical fluid CO2-impregnation process in the static mode is described in [1]. Activity of the prepared catalysts samples study has been carried out on the microcatalytic experimental unit of flowing type which has been described in [2, 3].

Regeneration of the spent catalyst was performed at supercritical fluid extraction system that allows performing the regeneration in a dynamic mode [4]. Spent catalyst, used in present work, was nickel-molybdenum catalyst deposited on alumina "Criterion514" and "DN 3531" brands, manufactured by *"Criterion Catalyst and technology"*. Carbone dioxide, used in regeneration process, was with 99.995% volume maintenance of CO_2 (GOST 8050-85, certificate of quality № 2052).

3 Results and discussion

Results of impregnation process, compared with solubility of palladium chloride benzonitrile complex at T=308.15 K is given in Figure 1. The results confirm results of earlier carried out research of palladium chloride benzolnitrile complex solubility in supercritical carbon dioxide [2, 3]. The study shows, that preferable range of SC-CO_2-impregnation process parameters are 19.0 - 21.0 MPa and 313.15˚K - 318.15˚K.

Another important task is regeneration of spent catalyst with the use of supercritical fluids. In this work the spent "Criterion514" and "DN 3531" catalysts manufactured by *"Criterion Catalyst and technology"* were regenerated with the use of pure and modified supercritical carbon dioxide. The regeneration process was held at temperatures range from 323,15 to 383,15 K and pressures 20 and 30 MPa. Results are shown in Figure 2.

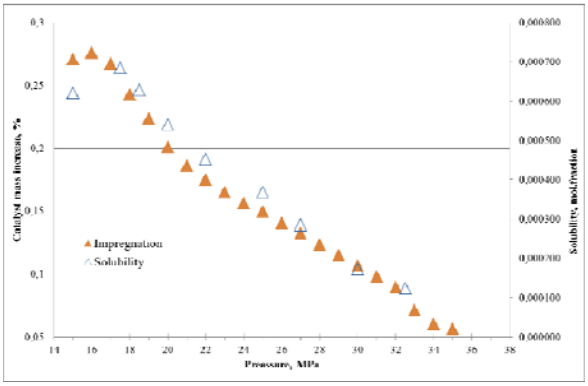

Fig. 1. Increase in mass of the catalyst carrier as a result of implementation SC-CO2-impregnationprocess. Comparison to nature of impregnation material solubility change in supercritical carbon dioxide at a temperature T = 308,15 K

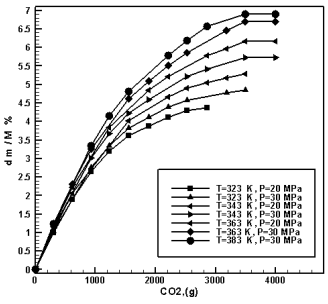

Fig. 2. Nickel-molybdenum catalyst mass change - pure SC-CO_2 mass relationship

4 Conclusions

The data obtained suggest that the synthesis and regeneration using supercritical carbon dioxide modified with various polar additives allows getting various types of catalysts, with characteristics that are not inferior to industrial counterparts. In this case, the regeneration is carried out at significantly lower temperatures as against the commonly used methods of regeneration, which has a beneficial effect on the overall performance of catalysts and on the energy consumption associated with regeneration thereof, which ultimately leads to lower cost of the finished products.

Acknowledgments

The authors of this study are grateful to the Russian Science Foundation (RSF) for financial support in the form of the respective grant (contract No. 14-19-00749).

References

[1] A.A. Zakharov, Ameer Abed Jaddoa, F.M. Gumerov Synthesis of the palladium catalyst with the SC-CO_2-impregnation method realized in the static mode // International Journal of Analytical Mass Spectrometry and Chromatography, Vol. 2, No.4, 2014, p. 113-122

[2] Bilalov, T.R., Gumerov, F.M., Gabitov, F.R., Kharlampidi, Kh.E., Fedorov, G.I., Sagdeev, A.A., Yarullin, R.S. and Yakushev, I.A. (2009) The Synthesis and Regeneration of Palladium Catalysts with the Use of Supercritical Carbon Dioxide. Russian Journal of Physical Chemistry B, 3, 80-92. http://dx.doi.org/10.1134/S1990793109070094

[3] Bilalov, T.R. and Gumerov, F.M. (2011) The Manufacturing Processes and Catalyst Regeneration, Thermodynamic Basis of Production Processes and Regeneration of Palladium Catalysts Using Supercritical Carbon Dioxide. LAP LAMBERT Academic Publishing GmbH & Co. KG., Dudweiler Landstr, 153 p.

[4] Zakharov AA, Ameer Abed Jaddoa, Bilalov TR Gumerov FM The solution of some environmental problems of catalytic chemistry using supercritical fluid medium // V All-Russian Conference of Young Scientists "Supercritical fluid technology to solve environmental problems", 2014. - P. 76-79

II-PP08

Solvation Shell of Platinum Complexes in Solutions According to EXAFS Data

Kanazhevskiy V.*, Chesalov Yu., Kochubey D.

Boreskov Institute of Catalysis SB RAS, Novosibirsk, Russia

* v.kanazhevskiy@mail.ru

Keywords: EXAFS, Raman, spectroscopy, solvation, shell, hexachloroplatinate, water, solution, DMSO

1 Introduction

Using EXAFS and Raman spectroscopy the structure of the solvation shell of hexachloroplatinate complexes in dimethylsulfoxide (DMSO) and water solutions over a wide range of concentration and aging time up to six months were studied. The experimental results clearly reveal that chlorine atoms are in the platinum atoms surrounding. Hydrolysis processes and direct interactions of platinum atoms are not observed. The Pt-Cl bond length is 2.3 Å. The chlorine coordination number is 6. No metal-metal bonds through bridging chlorine atoms are also observed. A tightly bound solvation shell covers the platinum complexes. Regardless of the solvent origin, solution concentrations and aging times, EXAFS curves of radial distribution function (RDF) exhibit maximums in the region 3.7-4.4 Å. These maximums belong to oxygen atoms of the solvation shell. The shell is likely to contain cations H_3O^+, $H_5O_2^+$ and molecules of DMSO, depending on the solvent type and platinum concentration.

2 Experimental/methodology

Two sample series were studied: solutions of a hexachloroplatinate acid in water (concentration from 0.0031 up to 0.4 M) and DMSO (0.02 and 0.2 M).

The samples were prepared using H2PtCl6×6H2O (pure grade), distilled water, benzene (chemically pure) and DMSO (chemically pure). The initial commercial complexes were used without additional purification or modifications. Solutions of hexachloroplatinate were treated in a shaded room; the samples were stored and aged away from light to prevent hydrolysis (photolysis).

Aqueous solutions were prepared immediately before spectra recording. Hexachloroplatinate was preliminary dissolved in water to achieve an initial sample concentration of 0.4 M. The rest samples in the series were prepared by successive two-times dissolution of the previous sample at each step.

To prepare solutions in DMSO, a hexachloroplatinate sample was preliminary flood with benzene in order to reduce water content of the complex. EXAFS spectra suggest that platinum complexes do not dissolve in benzene. On standing in benzene, orange crystals of H2PtCl6×6H2O converted to yellow “needles” of H2PtCl6×2H2O. After 7 days, benzene was decanted from the two-phase mixture. Raman spectra confirm a decrease in a number of the water molecules coordinated to the complex, resulting from drying of the initial complex placed into benzene. Dried hexachloroplatinate was dissolved in DMSO to a concentration of 0.2 M. The following dilution resulted in a 0.02 M H2PtCl6 solution. According to Raman spectra, the as-prepared solutions contain small amounts of benzene.

The solutions were held in DMSO away from sunlight, at standard conditions during 5 month and at 80°C during 5 hours.

Sharp EXAFS maximum at 2.32 Å and three vibrational lines at 343, 320,161 cm-1 indicated regular Oh-symmetry of [PtCl6]2- ion clearly showed the absence of the hydrolysis (photolysis) in water and DMSO solutions studied.

3 Results and discussion

EXAFS and vibrational spectroscopy were used to study the structure of complexes H_2PtCl_6 in water and DMSO solutions in the wide range of concentrations and ageing times to 5 months.

Our data confirm the earlier suggestion that platinum atoms are surrounded by chlorine atoms. The Pt-Cl bond length is approximately 2.3 Å. The chlorine coordination number is six. No traces of hydrolysis (photolysis) were observed in the studied samples. Platinum atoms are not directly bound to each other. There are no metal-metal bonds through bridging chlorine atoms.

We were the first to show that the platinum complexes are surrounded by a tightly bound (>10 kcal/mole) solvation shell. The EXAFS RDF curves exhibit maximums in the range 3.7-4.4 Å irrespective of solvent type, solution concentration and ageing time. These peaks belong to the atoms involved in the solvation shell. It is likely that the solvation shell of the complex used in prepared platinum solutions is formed by H_3O^+, $H_5O_2^+$ and DMSO molecules, depending on the solvent type and platinum concentration. For DMSO solutions, the solvation shell involves cations H_3O^+, $H_5O_2^+$, "crystal" water and solvent molecules. The number of oxygen atoms, which were related by EXAFS to the solvation shell of the complex in a DMSO solution, is small due to inclusions of larger solvent molecules in it.

Studied changes in concentration of the water solutions do not yield alterations in nuclearity of the complex. For several solution concentrations, we observed a hints of the solvation shell reconstruction manifested as a change in symmetry of the platinum surrounding with chlorine.

After a half-year storage of the solutions in DMSO at normal conditions, the symmetry of the coordination surrounding of platinum with chlorine decreases, which is associated with an effect of the solvation shell. It was established that the solvation shell radius decreases after a semi-annual sample storage. The reasons of "tightening" of the solvation shell call for additional investigations. Note that after storage of solutions for 5 hours at 80°C, the surrounding of platinum with chlorine does not change.

Probable binding of platinum complexes into associates by a solvation shell is not excluded with our data. In this case, Pt-Pt distances should approach the detection limit of EXAFS and be missed in spectra for two reasons: first, the distance between two atoms should exceed 6 Å; second, intensity of the maximum should be low due to high lability of the complex [1].

4 Conclusions

Using EXAFS and vibrational spectroscopy a tightly bound solvation shell of H_2PtCl_6 in DMSO and water solutions is established. The shell contains H_3O^+, H_5O^{2+} and DMSO molecules, depending on the solvent type. EXAFS suggests O-atoms of the shell are located at a distance of 3.7-4.4 Å from Pt. Complexes' structure was studied in wide concentration range DMSO and water solutions. The complexes are mononuclear and unhydrolyzed. Combining via the shell is possible.

Acknowledgements

The authors are grateful to professor E.V. Boldyreva and A.F. Achkasov from the Research and Educational Centre "Molecular Design and Ecologically Safe Technologies" Novosibirsk State University for assistance in recording the ATR-IR spectra.

References

[1] D.I. Kochubey, N.B. Shitova, S.G. Nikitenko, *Kinet Catal+*. 43 (2002) 555.

II-PP09

Synthesis of Catalytically Active Mesoporous Aluminosilicates without the Use of Templates

Agliullin M.R.[1*], Talipova R.R.[1], Grigor'eva N.G.[1], Kutepov B.I.[1], Dmitrieva A.A.[2], Rahimov M.N.[2]

1 - Institute of Petrochemistry and Catalysis RAS, Ufa, Russia
2 - Ufa State Petroleum Technological University, Ufa, Russia

* maratradikovich@mail.ru

Keywords: mesoporous aluminosilicates, sol-gel, synthesis, oligomerization of 1-octene

1 Introduction

In the last time in heterogeneous catalytic conversion of the acid-base type of various organic substances intensively studied the catalytic properties of mesostructured mesoporous aluminosilicate [1]. Their synthesis base on coprecipitation of the inorganic component with surfactant. They were supposed to be used for the catalytic conversion of large organic molecules. However, despite the fact that since the first report on the synthesis of these materials [2] has been more than 20 years in the literature, in practice, there is no information on their use as industrial catalysts and carriers for them. This situation is explained by the fact that the synthesis of catalytically active mesoporous materials is complex and multistage. In this case, use the templates expensive.

More accessible way to prepare the mesoporous catalytically active aluminosilicates can be sol-gel synthesis using silicon alkoxides and aluminum. The method allows to adjust the porous aluminosilicate structure in a wide range and provides a uniform distribution of Al^{3+} cations in the silica matrix [3].

The present work deals to method of sol-gel synthesis of catalytically active mesoporous aluminosilicates with a narrow pore size distribution.

2 Experimental/methodology

Mesoporous aluminosilicates are prepared by sol-gel synthesis using oligomeric esters of orthosilicic acid (ES-40) and an alcoholic solution of aluminum nitrate. Synthesis was carry out in two stages. The first stage is gelation at pH = 3, the second at pH = 10.

The phase composition of the obtained aluminosilicate was characterized by: X-ray diffraction; IR spectroscopy and MAS NMR ^{27}Al and ^{29}Si.

The acidity of the surface was characterized by TPD of NH_3 and IR spectroscopy of CO adsorption of probe molecules.

The porous structure was characterized by low-temperature nitrogen adsorption-desorption and transmission electron microscopy.

Catalytic properties of the obtained mesoporous aluminosilicates tested in the oligomerization reaction of 1-octene. The reaction is carried out continuously in rotating autoclaves under the following conditions: the content of catalyst per olefin is 10-30 wt%, T = 150-200 °C, τ = 3-5 h. Qualitative and quantitative analysis of the products of the oligomerization reaction of 1-octene was carried out by high performance liquid chromatography and ^{1}H and ^{13}C NMR spectroscopy.

3 Results and discussion

In this paper we study the effect of the ratio of SiO_2/Al_2O_3, SiO_2/H_2O and the pH of the precipitation on the porous structure, phase composition and surface acidity. It has been shown

that carrying out synthesis in acidic medium before gelation point and then to the alkaline allows synthesizing mesoporous aluminosilicate (SiO_2/Al_2O_3 = 20) with relatively narrow pore size distribution of from 3 to 5 nm of Fig. 1 and a high proportion embedded in an aluminum silicate framework (Fig.2). When this change of the specific surface area of 450 to 720 m^2/g, specific pore volume - from 0.5 to 1.2 cm^3/g, a pore diameter - from 0.17 to 7 nm and a total acidity of ammonia - ranging from 100 to 750 μmol / g.

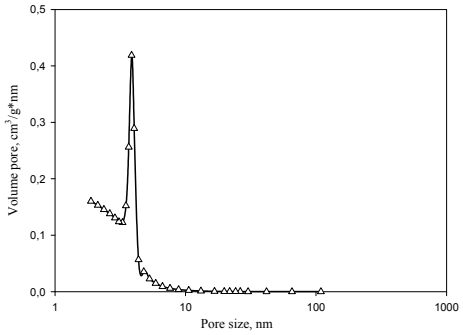

Fig. 1. The pore size distribution

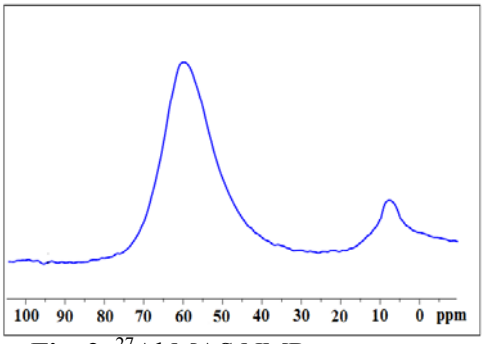

Fig. 2. ^{27}Al MAS NMR spectrum

It was found that the conversion of 1-octene in conditions studied achieves 90%, the selectivity to dimers - 40 ÷ 55%, trimers - 25 ÷ 38%, tetramers - 5 ÷ 17%. Products oligomerization of 1-octene in the presence of mesoporous aluminosilicates catalysts are oligomers with a degree of oligomerization n = 2-4. The formation of higher molecular weight products not were detected.

4 Conclusions

Developed a method of sol-gel synthesis of mesoporous aluminosilicate based on the use of oligomeric esters of orthosilicic acid (ES-40) and an alcohol solution of aluminum nitrate. The method allows to obtain mesoporous aluminosilicates having a narrow pore size distribution. Obtained aluminosilicates exhibit high catalytic activity in the oligomerization of 1-octene with a high yield of trimers.

Acknowledgements

The work was supported by Russian Foundation for Basic Research RFBR Project 14-03-97021 r_povolzhie_a

References

[1] D. Trong On, D. D. Giscard, C. Danumah, S. Kaliaguine, Appl. Catal. A: Gen. 222 (2001) 299.
[2] C.T. Kresge, M.E. Leonowicz, W.J. Roth, J.C. Vartuli, J.S. Beck, Nature 359 (1992) 710.
[3] C.J. Brinker, G.W. Scherer, Sol-Gel Science, the Physics and Chemistry of Sol-Gel Processing, Academic Press, 1990.

II-PP10

Tuning of the Copper-Zirconia and Palladium-Zirconium Phase Boundary for CO_2-Selective Methanol Steam Reforming

Mayr L.[1*], Klötzer B.[1], Zemlyanov D.[2], Penner S.[1]

University of Innsbruck, Institute for Physical Chemistry, Innsbruck, Austria
Purdue University, Birck Nanotechnology Center, West Lafayette, USA

* l.mayr@uibk.ac.at

Keywords: Cu, Zr, inverse, model, system, methanol steam reforming, water, activation, surface, redox, chemistry

1 Introduction

To prepare an active "inverse" methanol-reforming Zr^0-(pre)-catalyst on Pd- and Cu-metal substrates, a novel ALD/CVD approach was followed and compared to results of previous experiments using a self-developed sputter device . The latter, sputter-based experimental series already showed that H_2O activation sites exist in the Zr(ox)-Cu system, combining Zr redox activity ($ZrO_2 \leftrightarrow ZrO_{2-x}$) with water activation . The ALD/CVD technique using organometallic Zr precursors was originally used to prepare thin insulating layers of ZrO_2, aiming to scale down microelectronic devices. This ALD/CVD system was now adopted for inverse model catalyst synthesis. However, different kinds of interaction between precursor, Zr and catalytically active substrate have been observed for different metals leading to various active sites for MSR.

2 Experimental/methodology

ALD/CVD preparation of Zirconium-t-butoxide (ZTB) was investigated on Cu(111) and Pd(111) single crystals using in-situ and ex-situ XPS, STM, HREELS and LEED. The aim was to prepare a metallic Zr (sub-) monolayer film on a metal substrate as an inverse pre-catalyst to maximize potential bi-functional sites induced by ZrO_x segregation under reaction conditions. Alternatively, a ZrO_2/ZrOH layer with a high number of active interface sites can already be formed via organic precursor hydrolysis and/or oxidation. The Zr results were compared with Al on Pd(111), using tri-methyl-aluminum (TMA) as a precursor. Differences in particle topography and size result in significant differences in redox activity of Al and Zr.

3 Results and discussion

Temperatures between 300°C and 550°C are required for Zr^0 deposition via decomposition of the volatile ZTB compound on Pd(111). The organic moieties of the precursor can easily be removed by heating in vacuum, leading to subnanometer Zr^0 clusters of a few atoms. These clusters behave very different as bulk Zr^0 with respect to redox activity. The subnano-Zr can be oxidized or hydroxylated reversibly and, by annealing in vacuum at 400°C, it can be very easily reduced to Zr^0 again. This highly redox active state has been characterized with in-situ XPS and was also found to be active for methanol decomposition. The unusual Zr-redox behavior on Pd was not observed for Al, according to STM, because no sub-nano Al-clusters but rather big particles were formed on Pd(111).

4 Conclusions

In the Cu-Zr "real" and "inverse" UHV model catalyst study with high pressure catalysis experiments not only "good" but also "bad" active sites that trigger methanol dehydrogenation

towards CO have been identified. To design a CO_2-selective catalyst these sites need to be avoided, while simultaneously active sites for water activation need to be provided. We showed that the degree of hydroxylation of Zr is crucial for catalyst stability and CO_2-selectivity.

Fig 1.: Scheme of product pattern observed on Cu/ZrO_xH_y "inverse" and "real" model catalysts in methanol steam reforming

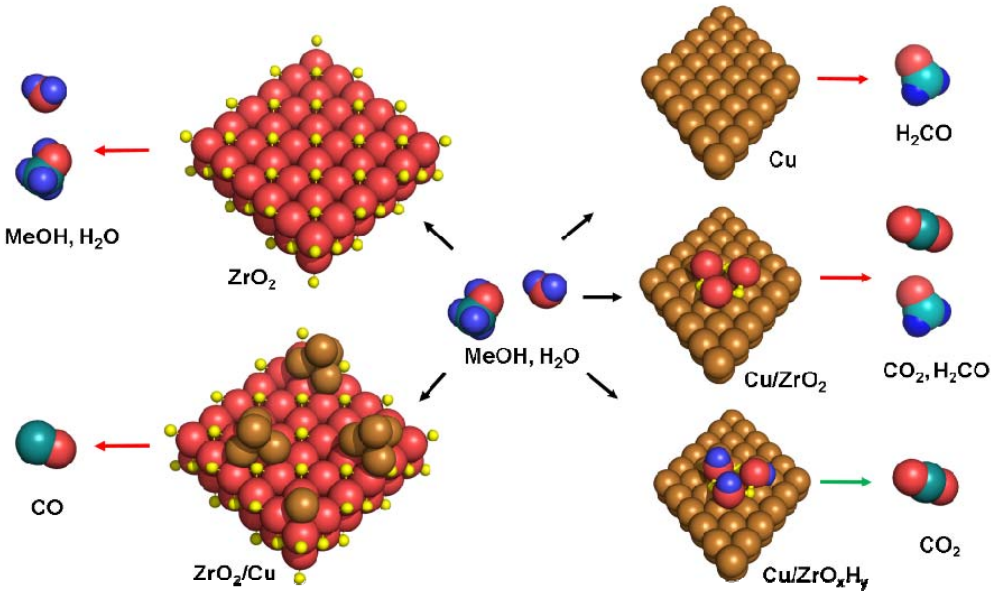

References

[1] L. Mayr, N. Köpfle, A. Auer, B. Klötzer, S. Penner, An (ultra) high-vacuum compatible sputter source for oxide thin film growth, Rev. Sci. Instrum., 84 (2013) -.

[2] L. Mayr, B. Klötzer, Z. Dmitry, S. Penner, Steering of methanol reforming selectivity by zirconia-copper interaction, J. Catal., accepted in Oct 2014 (2014).

II-PP11

Activated Reactive Synthesis, a Flexible Route to Produce Manganese Oxides with Improved Textural, Redox and Catalytic Properties

Averlant R.[1], Lebedeva A.[1], Lamonier J.-F.[1*], Giraudon J.-M.[1], Royer S.[2], Alamdari H.[3]

1 - Université Lille1, Villeneuve d'Ascq, France
2 - Université de Poitiers, Poitiers, France
3 - Université Laval, Department of Mining, Metallurgical and Materials Engineering, Québec, Canada

* jean-francois.lamonier@univ-lille1.fr

Keywords: manganese oxide, reactive, mechanical, grinding, catalytic oxidation, VOC

1 Introduction

Seeking for effective and low cost materials for low temperature Volatile Organic Compounds (VOCs) removal remains an important industrial challenge. Manganese oxides have been identified as promising materials for the total formaldehyde (HCHO) oxidation [1]. Recent attentions have been paid to the tunnel-type structures, due to their excellent catalytic performances for VOCs oxidation. Among these structures, cryptomelane (α MnO_2) showed the best catalytic activity in VOCs oxidation [2], underlining the important effect of the material morpho-structural properties. Specific surface area and porosity, crystal size, surface reducibility, *etc.* are parameters to control to maximize material catalytic performance [1]. Great efforts have been made to produce metal oxides with low particle size and high surface area. A promising synthesis route, recently reported for the preparation of mixed metal oxides, is to use the activated reactive synthesis (ARS) process [3,4]. This solvent free synthesis process involves the restructuring of a pre-crystallized metal oxide *via* reactive grinding process, to generate nanostructured materials with high surface area. In the present work, the advantages of the reactive mechanical grinding process, applied to the pure cryptomelane, are presented.

2 Experimental

Commercial α-MnO_2 (Mn_C), cryptomelane-type oxide, from Sigma Aldrich, was used for the synthesis of activated oxides by ARS process. The process involves two successive steps, including a first high energy ball milling (Mn_HEBM materials), and a second low energy ball milling (Mn_ LEBM materials). The first step was conducted under 2 hours of milling time using SPEX laboratory mill, whereas the second step was performed under different milling times (0.5, 1 and 2 h), using attrition mill.

XRD, N_2 physisorption, TEM, XPS and H_2-TPR experiments were conducted to elucidate structural, textural, surface and redox properties of materials obtained at the different synthesis stages. Total catalytic oxidation under air of two VOCs (formaldehyde and toluene) was studied to assess the benefit of reactive mechanical grinding process for manganese oxides activation.

3 Results and discussion

XRD analyses confirmed the presence of the cryptomelane phase (α-MnO_2, PDF n°44-0141) for the Mn_C, Mn_HEBM and Mn_LEBM samples.

After the high-energy ball milling, XRD reflections became less intense and more broadened. The average crystal size decreased from 19 nm (Mn_C) to 10 nm (Mn_HEBM). The specific surface area was not significantly improved (10 $m^2.g^{-1}$), despite the decrease in crystal

domain size. The generation of micron-size aggregates, exhibiting a high degree of agglomeration after high-energy ball milling treatment, is awaited.

The crystallite size remained constant after the low energy ball milling, whatever the milling time applied. However the second milling step was efficient to increase the specific surface area of the Mn_HEBM sample. After only 30 min of the LEBM treatment, the specific surface area value was two times higher than that of the untreated sample, this value being still increasing with the milling time (Fig. 1).This result can be related to the de-agglomeration of the aggregates (Fig. 2), resulting in substantial increase of the accessible surface area.

The Average Oxidation Number of Mn was not significantly modified by the ARS process. Values of 3.2 and 3.6 were obtained from H_2-TPR and XPS analyses, respectively, suggesting that the surface was more oxidized than the bulk cryptomelane. Redox properties were found to be affected by the material microstructure since the reduction of Mn species in Mn_HEBM and Mn_LEBM was promoted at low temperature.

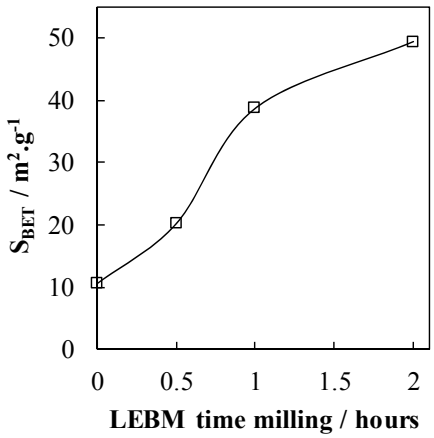

Fig. 1. SSA evolution with LEBM time.

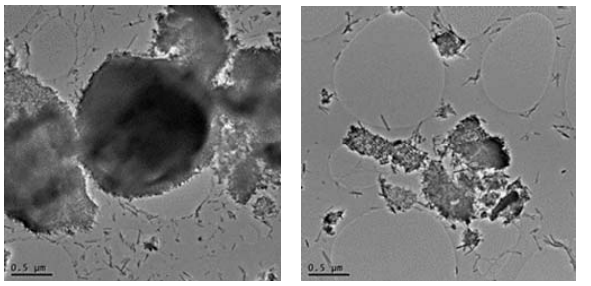

Fig. 2. TEM images recorded on the initial sample, and after 2 h of HEBM.

Specific activity of cryptomelane in formaldehyde or toluene oxidation was enhanced when the LEBM process was applied to the catalyst. The specific activity can be ranked as follows : Mn_LEBM > Mn_HEBM ~ Mn_C. Increase of low energy ball milling time led to an increase in specific activity, owing to the improvement of textural and redox properties of the corresponding materials.

4 Conclusions

The activated reactive synthesis process has been successfully applied for the cryptomelane activation. Improved textural, redox and catalytic properties have been measured, especially after particles de-agglomeration step occurring during the low energy ball milling.

Acknowledgements

The Region “Nord-Pas de Calais” and the French Agency for the Sustainable Development, ADEME, are acknowledged for the financial support of this work through Ph.D. grant (Rémy Averlant) and CORTEA convention n°11-81-C0108.

References

[1] J. Quiroz Torres, S. Royer, J.-P. Bellat, J.-M. Giraudon and J.-F. Lamonier, ChemSusChem, 6 (2013) 578.
[2] V.P. Santos, S.S.T. Bastos, M.F.R. Pereira, J.J.M. Orfao and J.L. Figueiredo, Catalysis Today, 154, (2010) 308
[3] S. Laassiri, D. Duprez, S. Royer and H. Alamdari, Catal. Sci. Technol. 1 (2011) 1124.
[4] S. Laassiri, N. Bion, D. Duprez, S. Royer and H. Alamdari, Phys. Chem. Chem. Phys.16 (2014) 4050.

II-PP12

Ternary and Quaternary Interstitial Nitrides for Ammonia Synthesis

Hargreaves J.S.J.[1*], Mcfarlane A.R.[1], Hector A.L.[2], Cook J.[2], Levason W.[2], Sardar K.[2], Bion N.[3], Can F.[3], Richard M.[3]

1 - School of Chemistry, Joseph Black Building, University of Glasgow, Glasgow, U.K.
2 - Department of Chemistry, University of Southampton, Southampton, U.K.
3 - University of Poitiers, CNRS UMR 7285, Institut des Milieux et Matériaux de Poitiers (IC2MP), Poitiers, France

* Justin.Hargreaves@glasgow.ac.uk

Keywords: interstitial nitrides, ammonia synthesis, isotopic, exchange

1 Introduction

Interstitial metal nitrides are a range of materials that are increasingly of interest as heterogeneous catalysis[1,2]. For ammonia synthesis, some literature exists on the application of ternary metal nitrides including Co_3Mo_3N and Ni_2Mo_3N which have been reported to display high efficacy [3]. Of these two systems, it seems that Co_3Mo_3N is the more active, however there has been little investigation into rationalizing these findings within the context of structure/activity relationships. A theoretical study has invoked a synergy between Co and Mo for N_2 adsorption where one species binds N too strongly and the other too weakly – resulting in a material that has the optimal N_2 adsorption enthalpy [4]. This study also suggests surface sensitivity. The activity of Ni_2Mo_3N could also be rationalized in a similar manner. In addition, the extension of the ternary Co_3Mo_3N and Ni_2Mo_3N systems to yield quaternary systems is also of interest for possibly further improving activity and also improved understanding of the origin of enhanced activity. Previous work has examined Ni_2Mo_3N for ammonia synthesis [5]. The synthetic route employed – ammonolysis of a nickel molybdate precursor - created Ni_2Mo_3N with a residual nickel metal impurity, as dictated by stoichiometry. The ammonia synthesis reaction activity was poor. Accordingly sol-gel based routes aimed both at the preparation of phase pure Ni_2Mo_3N which is free from the presence of Ni and also well-defined quaternary $Ni_{2-x}Co_xMo_3N$ systems have been developed in this study. A specific advantage for the ternary nickel molybdenum system is that it can be prepared by direct reaction of the oxide precursor with N_2/H_2 by-passing the ammonolysis step necessary for the cobalt system[6].

2 Experimental/methodology

Ni (M) + Ni_2Mo_3N was prepared by drop-wise addition of 400 ml of a 0.25 M aqueous solution of $Ni(NO_3)_2.6H_2O$ to a 150 ml solution of $Na_2MoO_4.(H_2O)_2$. The resulting precipitate was then calcined at 700 ^oC for 6 hours under a flow of nitrogen gas (5 ml min^{-1}). Nitridation was performed by exposing the calcined material to a high space velocity flow of NH_3 and then heating using the following procedure; ambient to 357 ^oC at 5.6 ^oC min^{-1}, 357 – 447 ^oC at 0.5 ^oC min^{-1}, 447 – 785 ^oC at 2.1 ^oC . The furnace was held at this temperature for 5 hours.

Sol-gel derived precursors were synthesised by calcination of a gel obtained from stoichiometric amount of $(NH_4)_6Mo_7O_{24}.4H_2O$, $M(NO_3)_2.6H_2O$ (M = Ni or Co), citric acid monohydrate (79.35 g) and 600 cm^3 of 8-10 % aqueous HNO_3. The gel was calcined in air at 500 °C (heating rate 60 °C min^{-1}) for 2 hours to obtain the precursor. The precursor was nitrided under NH_3 at 5 °C min^{-1} to the target temperature (600 or 700 °C) and maintained for at least 6 hours, before cooling at 10 °C min^{-1}.

Ammonia synthesis tests involved pre-treating the nitrides at 700 °C with the reactant gas ($3H_2$:$1N_2$) for 2 hours before cooling to the reaction temperature, 400 °C. Ammonia synthesis rates were analysed by flowing the exhaust gas through a solution of H_2SO_4 and measuring the conductivity change of the solution as a function of time.

3 Results and discussion

The powder x-ray diffraction patterns of the Ni_2Mo_3N systems prepared by N_2/H_2 pretreatment of the oxide precursors are presented in Figure 1. Both patterns evidence Ni_2Mo_3N as major phases but in the case of the sample prepared from $NiMoO_4$, the large phase fraction of Ni is clearly visible (*).

Figure 2 presents conductivity plots representing the ambient pressure NH_3 synthesis activities of both systems. In the case of the phase pure Ni_2Mo_3N the rate of ammonia synthesis measured was 330 µmol hr^{-1} g^{-1} (b) whereas it was only < 15 µmol hr^{-1} g^{-1} for the Ni containing sample (a). Nitrogen isotopic exchange pathways have been investigated and related to performance for these systems[6]. This will be discussed within the context of their catalytic performance. In addition, a range of $Ni_{2-x}Co_xMo_3N$ materials have been prepared and screened for activity and the results will be considered in terms of composition-performance relationships.

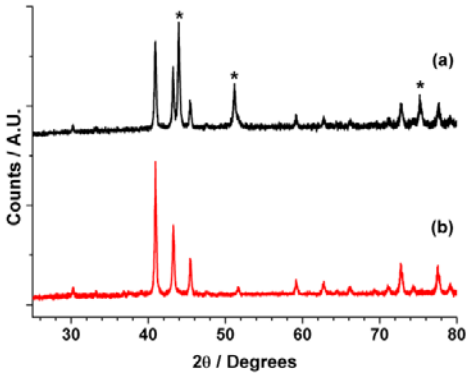

Figure 1. XRD comparison of Ni+Ni_2Mo_3N (a) and Ni_2Mo_3N (b).

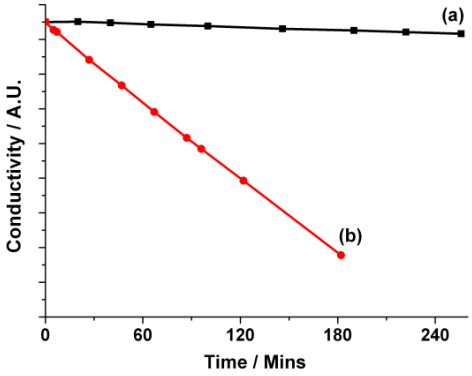

Figure 2. Reaction profiles of Ni+Ni_2Mo_3N (a) and Ni_2Mo_3N (b).

4 Conclusions

This study has shown that different synthesis routes can be employed for successful preparation of Ni_2Mo_3N materials. In particular, the sol-gel route results in a pure-phase Ni_2Mo_3N which is highly active for the ammonia synthesis reaction at ambient pressure. This presentation will also outline the application of N_2/H_2, as opposed to NH_3, for nitridation performance which would be highly beneficial if large-scale synthesis was desired. Furthermore, the access to high quality phase pure quaternary systems demonstrated in this study will provide further insight into the origin of the high activity exhibited by interstitial nitride catalysts.

References

[1] S.T. Oyama, G.L. Haller, Catalysis Special Periodic Report 5, 1982, p 333.
[2] S. M. Hunter, D. H. Gregory, J. S. J. Hargreaves, M.. Richard, D. Duprez, N. Bion, *ACS Catal.*, **2013**, *3* (8), pp 1719
[3] C.J.H Jacobsen, *Chem. Commun*., (2000), 1057.
[4] C. J. H. Jacobsen, S, Dahl, B. S. Clausen S. Bahn, A. Logadottir, J. K. Norskov, *J. Am. Chem. Soc.* 123 (2001) 8404.
[5] J.S.J. Hargreaves, D. McKay, *J. Mol. Cat: A*, 305 (2009) 125.
[6] N. Bion, F. Can, J. Cook, J. S. J. Hargreaves, A. L. Hector, W. Levason, A. R. McFarlane, M. Richard, K. Sardar, *Appl. Catal. A: Gen.,* in press

II-PP14

Kinetic Classification for the Coupled Reactions. New Oportunities of Catalytic Systems Design

Bruk L.G.*, Temkin O.N.

Moscow State University of Fine Chemical Technology, Moscow, Russia

* lgbruk@mail.ru

Keywords: coupled reactions, kinetic classification, mechanism, catalytic system design

1 Introduction

The phenomenologic Shilov's theory of coupled reactions [1] and modern kinetic theory of multiroute reactions allowed us to formulate the principle of kinetic conjugation (PKC) [2,3]. The aproach to catalytic systems design on the base of PKC includes purposeful selection of catalytic systems using information about probable mechanisms of reactions resulted in desirable products formation from available starting reagents [2]. The primary (basic) reaction (according Shilov's terminology) may be source of key intermediate or catalyst which is necessary to obtain desirable products.

2 Experimental/methodology

The kinetic classification of coupled reactions is proposed. This classification includes one-route and multiroute mechanisms. A one-route coupled reaction mechanism includes consecutive elementary steps leading to two (or more) different products. This reaction is described by one stoichiometric equation. The reaction including carbon monoxide oxidation and acetic acid dehydratation [3] may be used, for example:

$$Pd(OAc)_2 + CO = CO_2 + Pd(0) + (Ac)_2O$$

$$Pd(OAc)_2 \xrightarrow{CO} Pd(OAc)(COOAc) \xrightarrow{-CO_2} Pd(OAc)(Ac) \rightarrow Pd(0) + (Ac)_2O$$

Multiroute coupled reactions are described by a number of independed stoichiometric equations and may be chain and non-chain processes. The example of chain coupled reaction is H_2SO_3 and H_3AsO_3 oxidation:

Initiation: $2\ SO_3^{2-} + 0{,}5\ O_2 + 2\ H^+ \rightarrow 2\ SO_3^{\cdot -} + H_2O$

Chain termination: $2\ SO_3^{\cdot -} \rightarrow S_2O_6^{2-}$

The first route of chain propagation:

$$SO_3^{\cdot -} + O_2 \rightarrow SO_5^{\cdot -}$$

$$SO_5^{\cdot -} + SO_3^{2-} \rightarrow SO_4^{\cdot -} + SO_4^{2-}$$

$$SO_4^{\cdot -} + SO_3^{2-} \rightarrow SO_3^{\cdot -} + SO_4^{2-}$$

Stoichiometric equation: $2\ SO_3^{2-} + O_2 = 2\ SO_4^{2-}$

The second route of chain propagation:

$$SO_3^{\cdot -} + O_2 \rightarrow SO_5^{\cdot -}$$

$$SO_5^{\cdot -} + AsO_3^{3-} \rightarrow SO_4^{\cdot -} + AsO_4^{3-}$$

$$\underline{SO_4^{\cdot -} + SO_3^{2-} \rightarrow SO_3^{\cdot -} + SO_4^{2-}}$$

Stoichiometric equation: $SO_3^{2-} + AsO_3^{3-} + O_2 = SO_4^{2-} + AsO_4^{3-}$

The example of multiroute reaction in the catalytic system $PdBr_2$-$CuBr_2$-THF was designed using PKC [4]. Stoichiometric equations of the routes:

$$CO + O_2 + H_2O \rightarrow CO_2 + H_2O_2$$

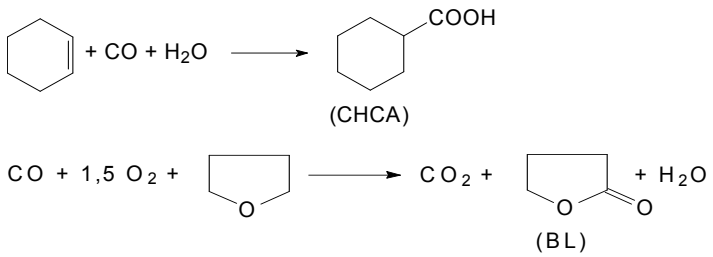

Fig.1. Mechanism of the coupled reactions

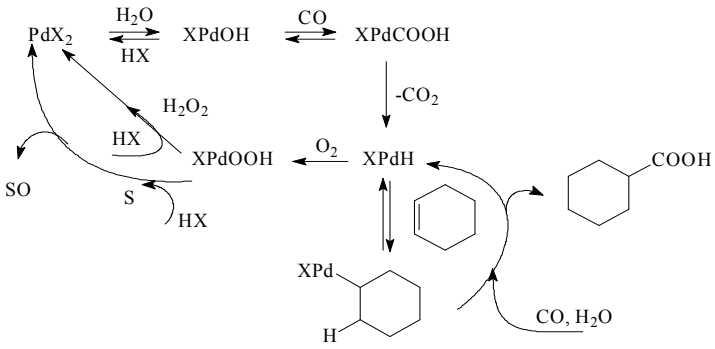

3 Conclusions

The oxidation of different substances (RH, ROH, RCHO, H_2, CO) is the most often used as primary reaction. The mechanisms of the coupled reactions are discussed.

Acknowledgements

This study was supported by Russian Foundation for Basic research, grant no 14-03-00052

References

[1] N.A. Shilov. O soprjajennikh reaktsijakh okislenija (About coupled oxidation reactions). Moscow, 1905, 304 p.
[2] L.G. Bruk, O.N. Temkin et al. *Kinet. Catal*., 51 (2010) 702.
[3] T.A. Stromnova, M.N. Vargaftik, I.I. Moiseev *Russ. Chem. Bull.*, 1983. No 1. P. 31.
[4] L.G. Bruk, I.V. Oshanina, S.N. Gorodskii, O.N. Temkin *Ross. Khim. Zhurn. (Zhurn. Ross. Khim. ob-va im. D.I. Mendeleeva)*. 50 (2006), no 11. P. 103.

II-PP15

Tailored Synthesis of Palladium Nanoparticles on Carbon Nanofibers for Different Catalytic Applications

Podyacheva O.[1,2*], Suboch A.[1,2], Bulushev D.[1], Zacharska M.[3], Eremenko N.[4], Eremenko A.[4], Kibis L.[1,2], Boronin A.[1,2], Stonkus O.[1,2], Slavinskaya E.[1,2], Ismagilov Z.[1,4]

1 - Boreskov Institute of Catalysis SB RAS, Novosibirsk, Russia
2 - Novosibirsk State University, Novosibirsk, Russia
3 - University of Limerick, Limerick, Ireland
4 - Institute of Coal Chemistry and Material Science, Kemerovo, Russia

* pod@catalysis.ru

Keywords: palladium nanoparticles, CNFs, nitrogen, doped, formic, acid, nitrobenzene

1 Introduction

Graphite-like carbon nanomaterials have a great potential for practical application in nanoelectronics and catalysis, for the development of advanced composite materials, gas or biosensors and sorbents. Carbon nanofibers (CNFs) having a large number of graphite edges are of specific interest to be used as catalyst supports [1]. Doping of CNFs by nitrogen (N-CNFs) allows to change electrophysical properties of CNFs and create new anchoring sites for catalyst precursors [2-3]. The current paper is devoted to the development and study of the different procedures of the palladium nanoparticles stabilization by means of CNFs and N-CNFs and elucidation of the correlation between particle size, electronic state of Pd and catalytic activity in CO oxidation, formic acid decomposition and hydrogenation of nitrobenzene.

2 Experimental/methodology

CNFs and N-CNFs were synthesized by a procedure described in [2]. Palladium (1-2% Pd) was deposited by incipient wetness impregnation of the carbon nanofibers with palladium nitrate, palladium acetate or a mixture of palladium acetate with triphenylphospine (PPh_3) solutions followed by calcination in hydrogen. The catalysts were characterized by XRD, XPS, TEM and N_2 adsorption methods. The activity of the catalysts was tested in CO oxidation reaction (0.2%CO, 1%O_2, 0.5%Ne and He) by TPR-CO+O_2 method with GHSV = 240000 h^{-1}. Formic acid (2 vol.%) decomposition was investigated in a flow reactor with a catalyst loading of 6.8 mg and total flow rate 51 cm^3. Hydrogenation of nitrobenzene was investigated in a steel reactor loaded by 10 mg of catalyst and 0.3 ml of nitrobenzene at atmosphere pressure under stirring.

3 Results and discussion

The palladium particle size in the catalysts depends on the type of carbon nanofibers and precursor giving bimodal or monomodal distribution and mean particle sizes from 1.5 to 13 nm, Fig. 1. According to XPS, in all catalysts palladium was found in the main metallic (E_b(Pd3d5/2) = 335.6–335.8 eV) and oxidized (E_b(Pd3d5/2) = 337.3-337.8 eV) states.

The catalysts testing showed that activity in CO oxidation reaction did not depend on the type of carbon nanofibers, particle size and palladium content; the temperature of 50% CO conversion changed within the interval of 190-200°C that was typical for palladium supported on alumina. Meantime, a type of the support and precursor strongly influences the activity of catalysts in formic acid decomposition and hydrogenation of nitrobenzene, Table 1. The highest value of activity was demonstrated by the catalysts with the smallest Pd nanoparticles deposited on nitrogen doped carbon nanofibers. The use of N-CNFs led to an increase of selectivity

towards hydrogen formation from formic acid. The best 2%Pd/7%N-CNFs exceeded the activity of Pd/C catalysts in hydrogenation of nitrobenzene reported in literature (~ 2 L H_2/g Pd ·min) by ~ 6 times. Combination of HAADF-STEM and EELS showed that Pd nanoparticles are attached to the surface of N-CNFs via nitrogen species. A study of N-CNFs by XPS allowed to conclude that mainly pyridinic nitrogen atoms are responsible for this binding.

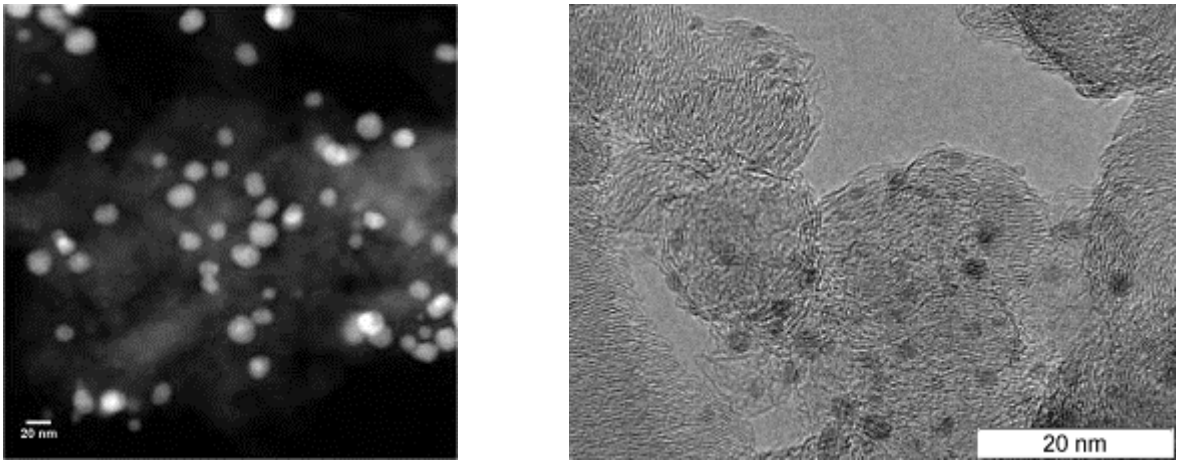

Fig.1. HAADF/STEM image of 1%Pd/7%N-CNFs ($Pd(NO_3)_2$) and STEM image of 2%Pd/7%N-CNFs ($Pd(CH_3COO)_2/PPh_3$).

Table 1. The Pd particle size and activity of catalysts in hydrogenation of nitrobenzene at 40°C and formic acid decomposition reactions (R- reaction rate, T_{50} – temperature of 50% conversion).

Sample	Mean particle size, nm	Precursor	Nitrobenzene hydrogenation R, L H_2/g Pd·min	Formic acid decomposition T_{50}, °C
2%Pd/0%N-CNFs	2	$Pd(CH_3COO)_2/PPh_3$	11.6	
2%Pd/7%N-CNFs	1.5	$Pd(CH_3COO)_2/PPh_3$	13.2	
1%Pd/0%N-CNFs	2.3	$Pd(CH_3COO)_2$		185
1%Pd/7%N-CNFs	2.3	$Pd(CH_3COO)_2$		155
1%Pd/0%N-CNFs	9	$Pd(NO_3)_2$	2.1	255
1%Pd/7%N-CNFs	13	$Pd(NO_3)_2$	3.4	180

4 Conclusions

A combination of a proper precursor and N-CNFs allowed to control the size of supported Pd nanoparticles and improve the activity of catalysts in reactions of formic acid decomposition and hydrogenation of nitrobenzene.

References

[1] J. Zhu, A. Holmen, D. Chen, *ChemCatChem.* 5 (2013) 378.
[2] Z. Ismagilov, A. Shalagina, O. Podyacheva et al., *Carbon*. 47 (2009) 1922
[3] O. Podyacheva, Z. Ismagilov, *Catalysis Today*. doi.org/10.1016/j.cattod.2014.10.033.

II-PP16

Synthesis of Bimetallic PdAg Nanoparticle Arrays by the Diblock Copolymer Micelle Approach: a Way to Synthesize Supported Catalysts with Controlled Size, Composition and Spacing

Ehret E.[1], Beyou E.[2], Mamontov G.V.[3], Bugrova T.A.[3], Domenichini B.[4], Prakash S.[1], Aouine M.[1], Cadete Santos Aires F.J.[1,3*]

1 - Institut de Recherches sur la Catalyse et l'Environnement de Lyon, UMR 5256 CNRS/UCB Lyon 1, Villeurbanne, France

2 - Ingénierie des Matériaux Polymères, UMR 5223 CNRS/UCB Lyon 1/INSA Lyon/UJM Saint-Etienne, Bâtiment POLYTECH-Lyon, Villeurbanne, France

3 - National Research Tomsk State University, Laboratory of Catalytic Research, Tomsk, Russia

4 - Laboratoire Interdisciplinaire Carnot de Bourgogne, UMR 6303 CNRS/Université de Bourgogne, Dijon, France

* francisco.aires@ircelyon.univ-lyon1.fr

Keywords: diblock, copolymer micelles, ordered, nanoparticle arrays, PdAg

1 Introduction

Bimetallic nanoparticles (NPs) display unique properties drastically different from those of the corresponding single-component particles. These properties are assumed to result from both the electronic and structural effects of the bimetallic NP. As these properties depend also on the preparation conditions, the synthesis of bimetallic NPs with accurately controlled structures and compositions is essential to obtaining advanced materials for electronic, magnetic, optic and catalytic properties. In the present study, 2D ordered arrays of bimetallic PdAg NPs were successfully synthesized via the copolymer micelle approach and characterized by various spectroscopic and microscopic characterization methods. A special focus was laid on the influence of the type of reduction treatments on the chemical nature and the stability of the PdAg NPs. A comparison with the synthesis of single metal (Pd and Ag) NPs obtained by the same method was made.

2 Experimental/methodology

A series of polystyrene-b-poly(4-vinylpyridine) (PS-b-P4VP) diblock copolymers of various compositions and molecular weights was synthesized by nitroxide mediated radical polymerization using an alkoxyamine unimolecular initiator (Styryl-SG1). Intermolecular interactions between the $PdCl_2$ and/or $AgNO_3$ salts and P4VP micellar core and formation of nanoparticles from the micellar complex were investigated by various spectroscopic (UV-vis, XPS) and microscopic (AFM, HRTEM/EDX) characterization methods.

3 Results and discussion

Once the base solutions were made, three ways to produce the final arrays of bimetallic NPs were investigated (Fig. 1). One consisted in using an oxygen-plasma treatment after dip-coating of the SiO_2 surface (Fig. 1a); this method uses the large amount of electrons generated by the plasma to reduce the metallic cations and lead to the formation of the NPs that eventually oxidize under the oxygen-plasma. A second method consisted in introducing a reducing agent (hydrazine) to the base solution (Fig. 1b-path1). The third method consisted on flowing a vapour of the reducing agent (hydrazine) over the film after dip-coating of the SiO_2 surface (Fig. 1b-

path2). Spectroscopic and microscopic characterization of the resulting films before and after reduction showed that the two first methods consistently lead to the formation of rather regular arrays of NPs. In the case of the films before reduction we observe that, for the three methods, the metallic loaded micelles preferentially arrange to form a quasi-hexagonal pattern on the carbon coated copper grid; a close observation of the P4VP cores revealed a fine grain substructure inside every micelle corresponding to ultrasmall (bi)metallic NPs (Fig. 2e). After reduction either by oxygen-plasma or by hydrazine in the solution (Fig. 2) we obtain rather organized arrays of bimetallic NPs. The NPs have uniform sizes (Fig. 2d-insert) and compositions. Unlike the NPs obtained by oxygen plasma, those obtained by hydrazine in the solution are not oxidized. A full characterization of the physicochemical properties of the NPs was enabled by the use of different methods (ICP, AFM, HRTEM/EDX, XPS, UV-Vis).

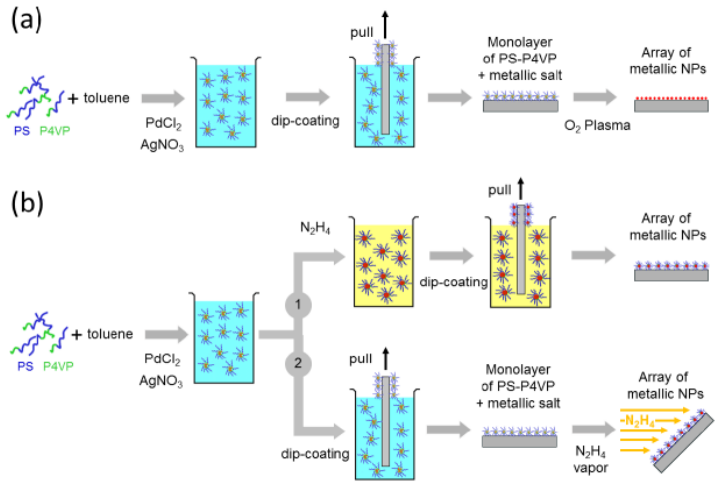

Fig. 1. Methods used to produce the arrays of PdAg nanoparticles: (a) oxygen-plasma; (b) Hydrazine in solution or hydrazine vapour. (see text for details)

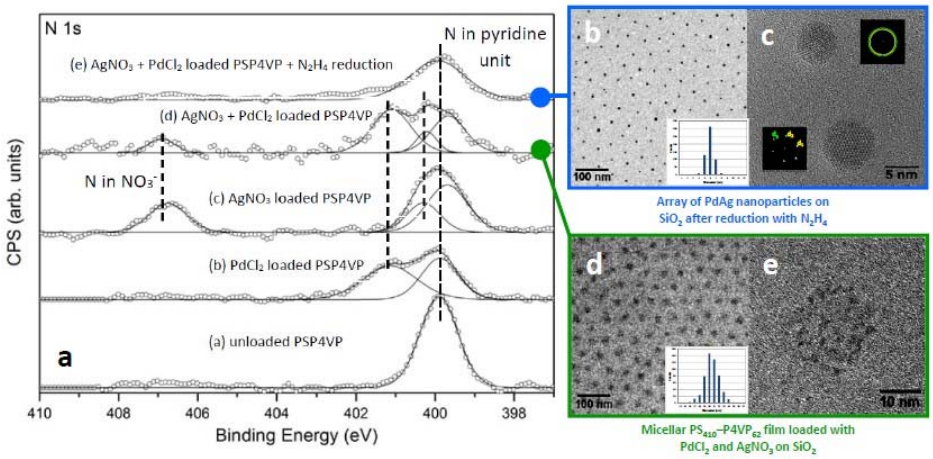

Fig. 2. XPS (a) and TEM (b-e) results for the arrays of PdAg NPs supported on SiO_2 obtained by the method using hydrazine as reducing agent in the solution.

4 Conclusions

The copolymer micelle approach is an excellent method to obtain ordered arrays of bimetallic nanoparticles supported on flat surfaces with controlled sizes, spacing and compositions. These collections of NPs can thus be used as model catalysts (for COV abatement in the case of PdAg) where important parameters that influence their catalytic behaviour can be finely monitored and modulated.

II-PP17

Influence of Platinum Anion Complexes Composition on their Anchoring on Magnesium – Aluminum Layered Hydroxides

Stepanova L.N.[1*], Belskaya O.B.[1,2], Likholobov V.A.[1,3]

1 - Institute of Hydrocarbons Processing SB RAS, Omsk, Russia
2 - Omsk State Technical University, Omsk, Russia
3 - Omsk Scientific Centre, Omsk, Russia

* Lchem@yandex.ru

Keywords: layered double hydroxides, platinum anion complexes, anchoring, propane, dehydrogenation

1 Introduction

$Pt/MgAlO_x$ is promising catalytic system for light alkanes dehydrogenation to corresponding alkenes that have high industrial demand. These catalysts could be an alternative to chromia-alumina catalysts that have bad environmental characteristics, and to used nowadays platinum catalysts that have insufficient stability. Layered double hydroxides (LDH) are used as the support precursor for $Pt/MgAlO_x$. The structure of LDH is similar to the structure of brucite where part of magnesium ions is replaced by aluminum ions. The presence of trivalent cations induces excess positive charge of layers, which is compensated by anions located in the interlayer space, where water molecules are also present. The important feature of LDH is moderate and easy adjustable basicity. $Pt/MgAlO_x$ catalysts synthesis is a multistage process, and stage of interaction of platinum complexes with support has a significant effect on properties of resulting platinum sites. Since supported platinum atoms are active sites of alkanes dehydrogenation, to obtain an active catalysts requires understanding of what factors during catalyst synthesis influence the dispersion and electronic state of the platinum sites.

This study investigates the anchoring of platinum complexes with different composition and geometry ($[PtCl_6]^{2-}$, $[PtCl_4]^{2-}$, $[Pt_3(CO)_6]_n^{2-}$) on magnesium – aluminum layered hydroxides with different Mg/Al ratio (Mg/Al = 2, 3, 4). Catalytic properties of $Pt/MgAlO_x$ were tested in propane dehydrogenation.

2 Experimental

LDH-MgAl-CO_3 (with CO_3^{2-} - anions in interlayer space) was synthesized by co-precipitation. LDH-MgAl-OH (with OH^- - anions in interlayer space) was obtained after calcinations of LDH-MgAl-CO_3 at 550 °C and subsequent hydration of mixed oxides in water. Structural features of the synthesized samples of LDH and $MgAlO_x$ mixed oxides were studied by XRD (D8 Advance, Bruker). Elemental analysis of LDH was made by ICP-AES on Varian 710-ES spectrometer, thermal analysis was performed on STA-449C Jupiter (Netzch). Scanning electron microscope (SEM) study performed on JSM-6460 LV (JEOL) microscope equipped with an energy-dispersive X-ray spectrum (EDS).

Anchoring of platinum chloride complexes was carried out on LDH-MgAl-OH and anchoring of platinum carbonyl complexes – on $MgAlO_x$. Chemical composition of adsorbed complexes was investigated by ^{195}Pt NMR and diffuse reflectance electron (DRE) spectroscopy. Platinum dispersion was determined by hydrogen chemisorptions. Transmission electron microscopy (TEM) was recorded on JEM-2100 (JEOL).

Catalytic properties of $Pt/MgAlO_x$ was investigated in propane dehydrogenation under the following conditions: catalyst loading 0.50 g., T = 550 °C, atmospheric pressure, WHSV 8 h^{-1} and H_2/C_3H_8 molar ratio of 0.25. Before reaction, samples were calcined at 550 °C and reduced in hydrogen at 550 °C.

3 Results and discussion

Study of adsorption of $[PtCl_6]^{2-}$ complexes on LDH-MgAl-OH showed that LDH with Mg/Al = 2 and 3 have the largest of adsorption capacity equal to 0.8 – 1.17 mmol/g (16 – 20 wt. % of adsorbed platinum). The intercalation of $[PtCl_6]^{2-}$ complexes into LDH interlayer space was confirmed by XRD and thermal analysis with mass spectrometric identification of the products. According to ^{195}Pt NMR and DRE spectroscopy adsorption of the complexes on LDH (regardless of the Mg/Al ratio) did not lead to significant hydrolysis of the complexes. It was assumed that complexes $[PtCl_6]^{2-}$ fixated in interlayer space by electrostatic interaction with positively charged LDH layers.

When $[PtCl_4]^{2-}$ complexes anchore on LDH-MgAl-OH the greatest number of complexes adsorb on the most basic LDH with Mg/Al = 4. Adsorption capacity equal to 1.37 mmol/g exceeds stoichiometric value. Therefore part of complexes hydrolyzes upon contact with basic support and fixes on its external surface. Absence of signals in the ^{195}Pt NMR spectra for supported complexes suggests the possibility of coordination of $[PtCl_4]^{2-}$ with hydroxyl groups of the LDH-MgAl-OH. According to DRE spectroscopy complexes adsorption leads to their hydrolysis to $[Pt(H_2O)Cl_3]^-$ on the surface. Inversion of intensity of the 003 and 006 peaks on the diffraction pattern of the supported systems indicates to increase in the electron density in interlayer space due to $[PtCl_4]^{2-}$ presence in interlayer space.

No adsorption of platinum carbonyl complexes $[Pt_3(CO)_6]_n^{2-}$ occurred on LDH-MgAl-OH owing to steric difficulties. During adsorption complexes on $MgAlO_x$ their anchoring occurred with saving of structure of mixed oxides (solvent - acetone) as well as with recovery of LDH structure (solvent - acetone + 5 vol. % H_2O). DRE spectroscopy of platinum carbonyl complexes supported on $MgAlO_x$ indicates a decrease in the size of complexes at their contact with basic support.

0.3%Pt/$MgAlO_x$ catalysts obtained using different platinum complexes were investigated in propane dehydrogenation. Propane conversion and propylene yield decrease with increase Mg/Al ratio for catalysts made from chloride precursors. Platinum dispersion decrease with increase Mg/Al ratio too. Herewith catalysts obtained from $[PtCl_4]^{2-}$ were 20-30% more active in comparison to the samples obtained from $[PtCl_6]^{2-}$ due to the larger platinum dispersion. Propane conversion, platinum dispersion and stability of catalysts obtained from platinum carbonyl complexes were above respective characteristics for samples, made using chloride precursors.

4 Conclusions

Composition and geometry of platinum complexes $[PtCl_6]^{2-}$, $[PtCl_4]^{2-}$, $[Pt_3(CO)_6]_n^{2-}$ as well as Mg/Al ratio in LDH-MgAl have a significant effect on anchoring of complexes onto support and on dispersion, electronic state of the platinum sites and their activity in propane dehydrogenation.

Acknowledgements

This work was supported by a grant from the President of the Russian Federation for young scientists and leading scientific schools of the Russian Federation (project no. NSh_3631.2014.3).

II-PP18

An Acidity Study of Encapsulated Heteropolyacids in a Sol-gel Silica Matrix for a Green Friedel-Crafts Alkylation

Pezzotta C.*, Müller K., Gaigneaux E.

Université catholique de Louvain, IMCN Institute of Condensed Matter and Nanosciences, Louvain-la-Neuve, Belgium

* chiara.pezzotta@uclouvain.be

Keywords: Friedel-Crafts alkylation, green chemistry, fine chemistry, pyridine, adsorption and TPD, heteropolyacids, Brönsted, acidity

1 Introduction

Friedel-Crafts alkylation is a key reaction widely used in pharmaceutical and polymer industry for the production of substituted aromatic compounds. Traditionally performed through homogeneous catalysis and in strong acidic conditions, it presents several inconveniences as pollution, difficult product separation, diffuse equipment corrosion and use of hazardous and toxic materials. To solve these problems the transition from homogeneous to heterogeneous catalysis has been attempted [1].

In this work Keggin type tungstophosphoric acid (HPW) was encapsulated in a silica matrix using the sol-gel method. The catalyst obtained was characterized in order to understand the nature of the interaction between HPW and the silica matrix. Then, the samples were tested in the Friedel-Crafts alkylation of resorcinol with methyl-tert-butyl ether to produce 4-tert-butylresorcinol and 4,6-di-tert-butylresorcinol.

Acidity measurements were performed using pyridine adsorption and temperature programmed desorption. The data obtained show the existence of a correlation between acidity and catalytic activity.

2 Experimental/methodology

Preparation: The preparation of the catalysts followed the procedure explained by Kukovecz [2] with some modifications. In a three neck round bottom flask 14 ml of tetraethoxy silane (Sigma-Aldrich, ≥ 99.0%) was added to a mixture of 10 ml of absolute ethanol (Normapur), 7.5 ml of ethylene glycol (Fluka, ≥ 99.5%) and 6 ml of distilled water. A calculated mass of HPW was then added in order to reach 11, 20, 30 and 40% of the total sample mass. The mixture was then magnetically stirred for one hour at 80°C under nitrogen atmosphere. 10 mL of HCl (Sigma-Aldrich, 37% w/w) was then added in order to allow the sol-gel transition to occur after approximately one hour. The transparent gel was then removed from the flask and put in a crystallizer to be dried in air for one day. After that, the catalyst was dried under vacuum at 140°C for three hours and calcined in air for six hours at 450°C. The powder obtained was grinded and sieved to obtain particles between 100 and 200 µm. Before the catalytic test the samples are washed overnight in ethanol in a Soxhlet extractor and dried under vacuum at 100°C for 2h. The catalysts were named: SG (sol-gel) – HPW – XX (HPW weight % on the total sample weight (SiO_2 + HPW)). SG – SiO_2 was the silica matrix without HPW.

Catalytic test: The resorcinol (7 g, Sigma-Aldrich, 99%) alkylation with methyl-tert-butylether (45 ml, Sigma-Aldrich ≥ 99.0%) was carried in air in a three neck round bottom flask connected with a Liebig condenser. After resorcinol dissolution, 0.6 g of catalyst was added and the mixture stirred at 60°C for 21h. The mixture was analysed every 120 minutes with a GC-FID Varian 3800 equipped with an ID-HT5 column. As internal standard 2,4-di-nitrobenzene (Aldrich 97%) was used.

Characterization: Pyridine adsorption and TPD was performed in order to measure the samples surface acidity and to distinguish the nature of the acid sites. Pyridine adsorption was carried on using a wafer of pure catalyst placed in a Pyrex cell equipped with a NaCl window. The wafer was degassed at 300°C and under vacuum for 3h. Then a fixed amount of pyridine vapor was put in contact with the sample. After adsorption, the wafer was left under vacuum for 30 minutes to remove the physisorbed pyridine. After that the sample was heated at 100, 150, 200 and 250°C to desorb the pyridine. A spectrum was taken for each temperature. For the determination of the relative amount of Lewis and Brönsted acid sites, the area of the bands at 1450 cm^{-1} and 1540 cm^{-1} of the spectrum taken at 100°C were integrated.

The interactions between the HPW and the silica matrix were investigated using IR spectroscopy performed with the same instrument.

3 Results and discussion

Although silica is known to have a very high absorption coefficient that can sometimes hide the presence of other compounds, fig. 1 shows the bands related to the W=O and W-O-W vibrations of encapsulated HPW. The weak intensity of these bands could be due to a deep HPW encapsulation into the support pores. Beside this, almost no leaching of HPW in ethanol was observed by UV-vis spectroscopy after the Soxhlet extraction, suggesting that the Keggin structure was firmly incorporated into the silica matrix.

The maximum amount of Brönsted acid sites (55% of the total acidity) was reached in the SG-HPW-30.

Catalytic tests showed activity for all the samples. The SG-SiO2 was tested as reference and showed no activity. The resorcinol conversion increases as the HPW loading increases with the exception of the SG-HPW-40. In that case a drop in the activity was observed. From fig.2 it is visible that in spite of the highest HPA loading, this sample shows a low amount of Brönsted acid sites on its surface. This suggests that the Keggin structures, due to excess loading, may form clusters that reduce the dispersion and consequently the acid sites number on the surface.

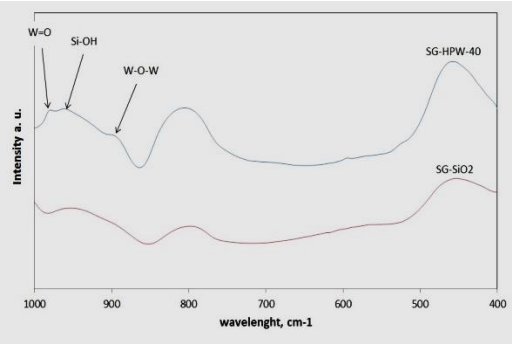

Fig.1 FTIR spectra showing WO band of encapsulated HPW.

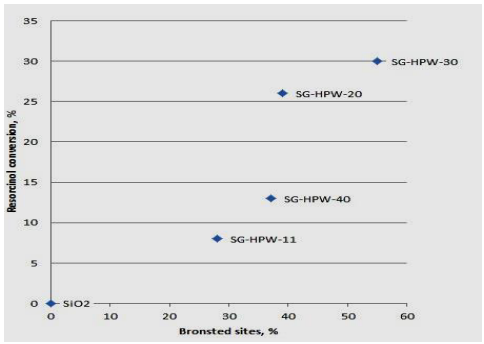

Fig.2 Resorcinol conversion vs Brönsted acidity.

4 Conclusions

A heterogeneous acid catalyst active in the Friedel-Crafts resorcinol alkylation was prepared. The catalytic activity was found to increase with the number of Brönsted acid sites. The heterogenization of HPW using the encapsulation in a silica matrix was successful and led to leaching resistant catalysts that possess promising features for further developments.

References

[1] G. Sartori, R. Maggi, *Advances in Friedel-Crafts acylation reactions: catalytic and green processes* (2010) CRC Press.

[2] Á. Kukovecz et al., *Synthesis, characterisation and catalytic applications of sol–gel derived silica–phosphotungstic acid composites, Applied Catalysis A: General* 228 (2002) 83 – 94.

II-PP19

Carbide and Graphene Growth, Suppression and Dissolution in Ni Model Systems Studied by *in-situ* XPS and SXRD

Rameshan R.[1,2*], Mayr L.[1], Penner S.[1], Franz D.[3], Vonk V.[3], Stierle A.[3], Klötzer B.[1], Knop-Gericke A.[2], Schlögl R.[2]

1 - Institute of Physical Chemistry, University Innsbruck, Innsbruck, Austria
2 - Department of Inorganic Chemistry, Fritz-Haber-Institute of the Max-Planck-Society, Berlin, Germany
3 - Department of Photon Science, Deutsches Elektronen Synchrotron DESY, Hamburg, Germany

* raffael.rameshan@uibk.ac.at

Keywords: nickel, graphene, carbide, *in-situ* X-ray photoelectron spectroscopy, surface X-ray spectroscopy, heterogeneous catalysis

1 Introduction

Carbon chemistry represents one of the fastest evolving and expanding research areas primarily due to the extraordinary physicochemical properties of its modifications, especially graphene and carbon nanotube materials [1]. In catalysis, the activity and selectivity of the entire catalytic entitity can be modified by carbon in connection with metal-support interaction [2]. Furthermore, the stability of Ni-based anode materials in Solid Oxide Fuel Cells (SOFC) can be enhanced by carbon management, when they are exposed to hydrocarbon rich fuel gas. Carbon managment requires the understanding of the adsorption, migration, dissolution and resegregation of carbon on the catalyst, as well as of the structural and electronical properties of different scenarios of C-distribution. In particular, the role of the clock-reconstructed Ni(111) surface carbide regarding further C-growth and dissolution is tested and experimental data are compared to the structural models proposed in the literature[3].

2 Experimental

In our work, we focus on the behavior of Carbon on different Nickel systems in the temperature region of 300K to 800 K. The samples were exposed to methane and ethylene under different pressure and temperature condition to observe carbide and graphen/ite formation and dissolution.

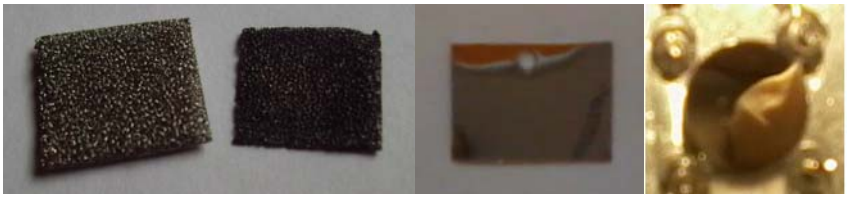

Fig. 1. Ni-Foam(left), -foil(middle) and Ni(111) single crystal(right) used to investigate carbon chemistry.

Experiments were performed at the following beamlines and UHV-systems:

I. In-situ XPS at the beamline ISISS-PGM of BESSY II, Berlin
II. SXRD at the ID03 beamline of ESRF, Grenoble
III. Additional ex-situ experiments in UHV system, Innsbruck [4]

3 Results and discussion

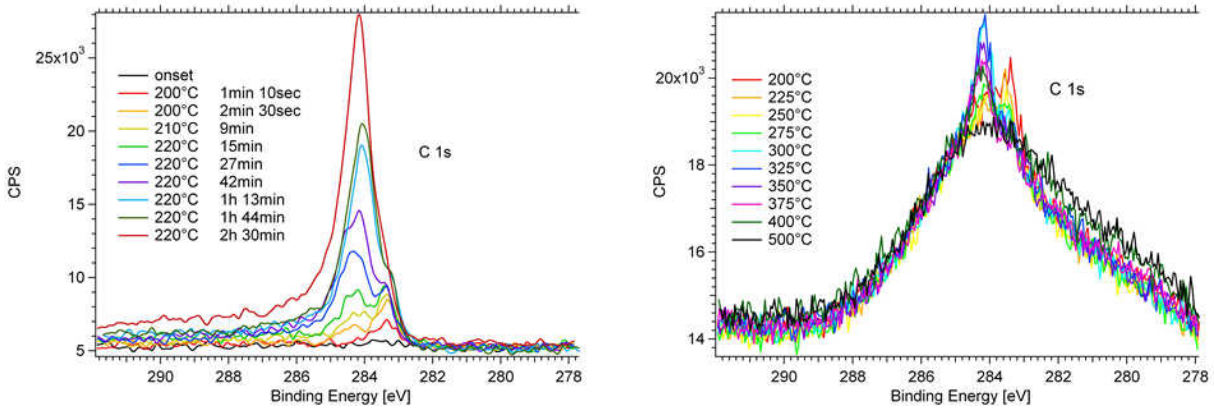

Fig. 2. In-situ XPS spectra of carbide and graphene/ite growth on Ni-foam(left) and Ni-foil(right)

4 Conclusions

As shown in Fig 2, sequential formation of carbide and graphene/ite could be observed both on Ni foam and Ni foil, whereby more amorphous carbon was observed on the latter. In addition, the coexistence of surface carbide and graphene/ite in a certain temperature region was observed as well as the preferential dissolution of the surface carbide at >= 670 K.

Carbide was moreover grown on Ni(111) and the subsequent graphene/ite formation was observed, using similar experimental conditions as on foam/ foil. After thermal dissolution of the carbidic clock-reconstructed $(39)^{1/2}$R16.1°x$(39)^{1/2}$R16.1°phase at 700 K, as indicated by the loss of the related diffraction intensities, the presence of epitaxial and unrotated graphene domains is indicated by the absence of rotated graphene reflections, together with a strong alteration of the specular reflectivity of the surface. These results complement recent structural investigations by STM [5, 6]. Structure modelling of SXRD data to confirm the most plausible configurations of unrotated graphene on Ni(111) will be presented.

Acknowledgements

We would like to thank our Co-workers at BESSY II, the ERSF and DESY. Especially we want to thank for financial support by the Fritz-Haber-Institut der Max-Planck-Gesellschaft.

References

[1] S.J. Tauster, S.C: Fung, R.T.K. Baker, J.A. Horsley. *Science, 211*(4487), 1121.
[2] A. Rinaldi, J.P. Tessonnier, M.E. Schuster, R. Blume, F. Girgsdies, Q. Zhang, R. Schloegl *Angewandte Chemie International Edition,* 50(14) 3313
[3] F.Mittendorfer, er al., *Phys. Rev. B* (2011) 201401
[4] L. Mayr, er al, *Review of Scientific Instruments* 85.5 (2014) 055104
[5] L. Patera, C. Africh, R. Weatherup, R. Blume, S. Bhardwaj, C. Castellarin-Cudia, A. Knop-Gericke, R. Schloegl, G. Comelli, S. Hofman, C. Cepek, *ACS Nano,* (2013) 7(9) pp7901-7912
[6] P. Jacobson et al., *ACS Nano* (2013) 6(4), pp3564-357

II-PP20

Effect of the Preparation Method of $La_{1-x}Sr_xFeO_3$ Perovskites on N_2O Decomposition

Margellou A.*, Petrakis D., Pomonis P.

Department of Chemistry, University of Ioannina, Ioannina, Greece

* amargel@cc.uoi.gr

Keywords: Perovskites $La_{1-x}Sr_xFeO_3$, chiral silica, N_2O decomposition

1 Introduction

N_2O decomposition has been extensively studied over many simple oxides but less over perovskites [1-2]. In this work, the N_2O decomposition has been studied over perovskites $La_{1-x}Sr_xFeO_3$ synthesized through two different methods: (i) sol-gel auto-combustion using glycine as fuel and (ii) wet impregnation of metal nitrates on chiral silica as a substrate.

2 Experimental/methodology

The perovskites $La_{1-x}Sr_xFeO_3/SiO_2$ (x= 0, 0.25, 0.50, 0.75 and 1.0) were prepared using the wet impregnation method of metal nitrates on chiral silica [3]. For the wet impregnation, pre-estimated amounts (mmoles M) of metal nitrates were mixed with citric acid and impregnated on chiral silica. In order to find the optimum amount for the N_2O decomposition, three perovskites $xLaFeO_3/SiO_2$ were synthesized with 0.5, 2.5 and 5.0 mmoles $LaFeO_3$ per g SiO_2. For the sol-gel auto-combustion method, the metal nitrates were dissolved in distilled water and glycine was added with molar ratio Gly/M=1. The solution was heated at 100°C to evaporate the H_2O and then at ~250°C in order to initiate the combustion. All catalysts were calcined at 600°C for 6h and characterized by XRD, N_2 porosimetry and SEM. The catalytic experiments were held in a PFR reactor with total flow 60.0 cc/min and WSHV≈18.000h^{-1}. The analyses of the reactants and products took place in a gas chromatograph GC-15A Shimadzu.

3 Results and discussion

In the $La_{1-x}Sr_xFeO_3/SiO_2$ samples, the XRD patterns at low angles show a peak of MCM-type hexagonal mesostructure. Comparing the impregnated samples with the pure chiral silica, the mesostructure is partially destroyed as the perovskites amount increases and the perovksite phase is formed as seems at XRD patterns at high angles. The calculated d_{100} values from Bragg equation for the synthesized materials are shown on Table 1 and are lower than the pure silica. The substitution of La with Sr is not influence the d_{100}. For the perovskites $La_{1-x}Sr_xFeO_3$ prepared with glycine the XRD pattern confirms the perovskites structure. The crystallite size calculated via the Scherrer's equation (D_{cryst}) shown on Table 1. It seems that the crystallite size is influenced from the Sr addition as it initially decreases with substitution x=0.25, 0.50 and later increases as x=0.75, 1.00.

The N_2 adsorption-desorption isotherms for the $La_{1-x}Sr_xFeO_3$ materials from sol gel auto combustion method correspond to non porous and low specific surface area solids with ssa=12-28 m^2/g. The isotherms of the impregnated correspond to mesoporous materials with high ssa equal to 697m^2/g for $0.5LaFeO_3/SiO_2$, 577m^2/g for $2.5LaFeO_3/SiO_2$ and between 300-500m^2/g for $5.0La_{1-x}Sr_xFeO_3/SiO_2$.

In the SEM images the perovskites system $La_{1-x}Sr_xFeO_3$ prepared with glycine shows a compact

and shapeless structure whereas the impregnated samples maintain the morphology of the chiral silica which does not influenced by the addition of perovskites

Table 1. Properties and catalytic activity of the synthesized materials.

Material	d_{100} XRD (nm)	T_{50} (°C)	Ea (kJ/mol)	Material	D_{cryst} (nm)	T_{50} (°C)	Ea (kJ/mol)
SiO_2	4.1	-	-	$LaFeO_3$	31	507	133
$0.5LaFeO_3/SiO_2$	3.8	-	-	$La_{0.75}Sr_{0.25}FeO_3$	17	487	148
$2.5LaFeO_3/SiO_2$	3.9	612	124	$La_{0.5}Sr_{0.5}FeO_3$	14	495	137
$5.0LaFeO_3/SiO_2$	3.7	587	130	$La_{0.25}Sr_{0.75}FeO_3$	15	500	152
$5.0La_{0.75}Sr_{0.25}FeO_3/SiO_2$	3.8	555	137	$SrFeO_3$	19	533	129
$5.0La_{0.5}Sr_{0.5}FeO_3/SiO_2$	3.8	560	131				
$5.0La_{0.25}Sr_{0.75}FeO_3/SiO_2$	3.6	606	125				
$5.0SrFeO_3/SiO_2$	3.8	640	149				

In the N_2O decomposition the $0.5LaFeO_3/SiO_2$ did not show any activity and the $2.5LaFeO_3/SiO_2$ was less active compare to the $5.0LaFeO_3/SiO_2$ as a result the substitution of La with Sr happened to $5.0LaFeO_3/SiO_2$. The most active catalysts were $5.0La_{0.75}Sr_{0.25}FeO_3/SiO_2$ and $La_{0.75}Sr_{0.25}FeO_3$ (Fig. 1A). From the temperature T_{50} where 50% of N_2O has been converted (Table 1 and Fig. 1B), it can observed that the perovskites synthesized through the sol gel auto combustion method are more active catalysts compared to the impregnated perovskites. The activation energies for all the samples in the range of 130-150 kJ/mol.

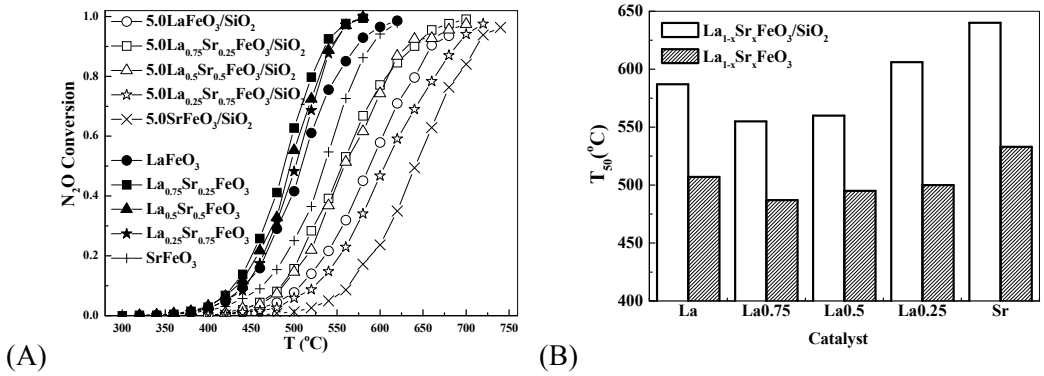

(A) (B)

Fig.1.(A) Temperature profiles and (B) Temperature T_{50} of the prepared materials.

4 Conclusions

Perovskites $La_{1-x}Sr_xFeO_3$ were used as catalysts in the N_2O decomposition. The non porous perovskites prepared through the simple, fast and easy method of auto-combustion show high activity towards the N_2O decomposition whereas the mesoporous catalysts $La_{1-x}Sr_xFeO_3/ SiO_2$ showed lower activity. The higher specific surface area and the chiral morphology of the silica support did not improve the catalytic properties of the system $La_{1-x}Sr_xFeO_3$.

Acknowledgements

This research has been co-financed by the European Union (European Social Fund – ESF) and Greek national funds through the Operational Program "Education and Lifelong Learning" of the National Strategic Reference Framework (NSRF)-Research Funding Program: THALES. Investing in knowledge society through the European Social Fund.

References

[1] N. Russo, D. Mescia, D. Fino, G. Saracco, V. Specchia, Ind. Eng. Chem. Res., 46 (2007) 12 4226
[2] F. Kapteijn, J. Rodriguez-Mirasol, J. A. Moulijn, Applied Catalysis B: Environmental, 9 (1996) 25
[3] Giung-Ling Lin, Yi-Hua Tsai, Hong-Ping Lin, Chih-Yuan Tang and Ching-Yen Lin, Langmuir 23 (2007) 4115.

II-PP21

Hidden Resources of Electron Scattering at Surface and in the Bulk of a Solid: an Exploratory Research

Cholach A.R.[1*], Asanov I.P.[2]

1 - Boreskov Institute of Catalysis SB RAS, Novosibirsk, Russia
2 - Nikolaev Institute of Inorganic Chemistry, Novosibirsk, Russia

* cholach@catalysis.ru

Keywords: core level excitation, coupled electron transitions

1 Introduction

The resonant core level excitation makes a crucial impact on an atom and results in specific responses disclosing intrinsic properties of a system which part of an atom is. A fine structure in extended and near above the threshold X-ray absorption spectra revealing the short-range atomic geometry and the density of vacant states were particularly detected and became the grounds of EXAFS and XAS, respectively, while the fine structure in soft X-ray emission spectra near below the threshold disclosing the valence states of a target atom is known as XES [1, 2]. The report highlights similar effects discovered by ordinary techniques of Disappearance Potential Spectroscopy (DAPS) and X-ray Photoelectron Spectroscopy (XPS). Fine structures in extended DAPS spectra reveal the valence states of near-surface atoms and plasmon oscillations, while those in C_2F XPS spectra above both, C and F K-edges are in agreement with the total Density of States (DOS) structure. Events are regarded as a novel route for energy dissipation at surface and in the bulk, the Conjugate Electron Excitation (CEE) which includes a set of independent shake-off and shake-up electron transitions, each coupled with the core level excitation.

2 Methodology

DAPS traces the threshold core level excitations of target atoms by an electron beam of time-based energy [3]. Whenever accelerating *potential* overcomes the core level energy a part of scattered electrons *disappears* from elastic current providing the spectral dip. The capability of DAPS to reveal *any* channel of elastic electron consumption, particularly that related to coupled electron transition has been exploited. DAPS measurements were made on the Pt(100) single crystal of 99.999% purity and (1x1) surface structure around the Pt4d core level [4]. XPS studies were performed on a Phoibos 150 Specs spectrometer under Al K_α excitation. The fluorinated graphite of C_2F stoichiometry was prepared by treating the highly orientated pyrolytic graphite with saturated vapors of a solution BrF_3 in Br_2 [5]. Pt DOS was calculated by the Quantum Espresso package within a *12x12x12* grid. Core electrons were treated with the Perdew-Burke-Ernzerhof ultrasoft pseudopotential [6]; the plane waves were used for a basis set of the valence electron wave function [4].

3 Results and discussion

Spectral features in Fig. 1(a) fit 1π, 5σ and 4σ valent states of the adsorbed CO molecule. Furthermore, a perfect agreement between experimental and theoretical spectra within 5-12 eV gives evidence that CEE readily affects the substrate atoms. Fig. 1(b) displays close similarity between higher energy "tails" in C1s and F1s XPS spectra of C_2F. The satellite at ~ 5 eV corresponds to CEE shake-up $\pi \rightarrow \pi^*$ transition and naturally accompanies the primary C1s peaks since π bond is localized exclusively at the carbon atom. Meanwhile finding similar satellite above F1s seems incredible because F atom has nothing to do with the π bond, but this finding is in line with CEE expectations. The other spectral features are in agreement with the

total DOS structure of C_2F. CEE phenomena developed by DAPS and confirmed by XPS emphasize the strong community of core and outer shell electronic structures and enables to believe that both inelastic scatterings, at surface and in the bulk of a solid follow similar rules.

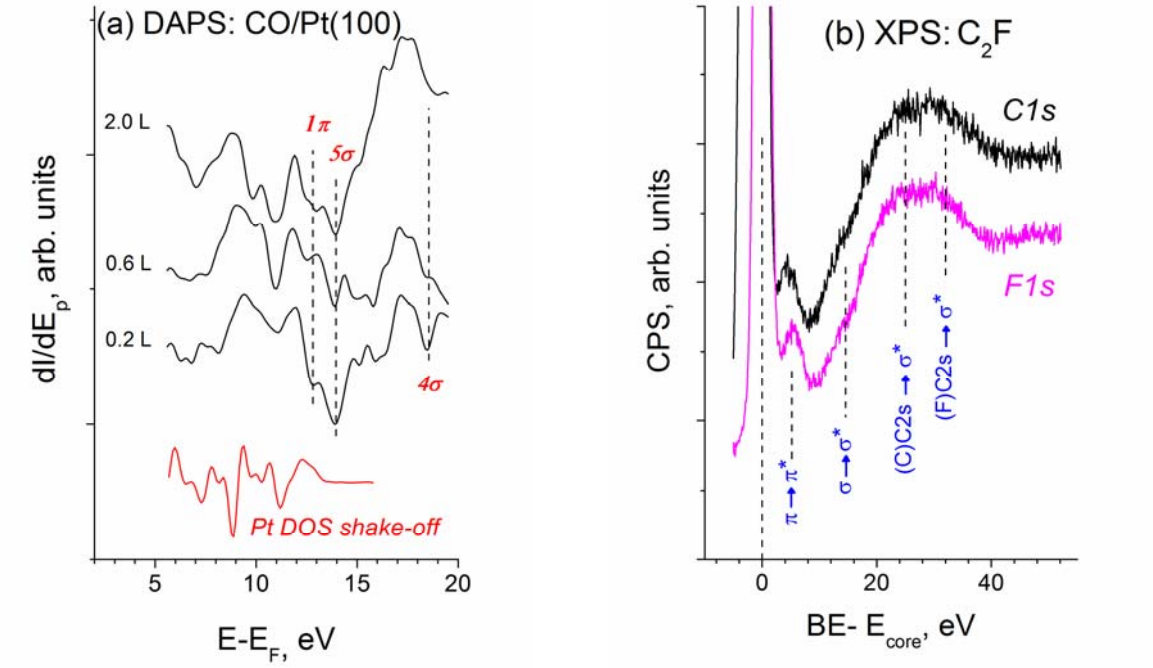

Fig. 1. (a) DAPS spectra (in black) obtained after exposure of Pt(100) surface to CO and theoretical DAPS spectrum corresponding to shake-off transition of the Pt valence band to vacuum level; (b) Interband transitions above F and C K-edge (C is bound to F) according to total DOS of C_2F.

4 Conclusions

A unified electronic structure of chemically bound atoms at surface, including adsorbed species or in the bulk originally holds a set of cells for the resonant energy absorption such as intra- and interband transitions, plasmon oscillations, ionization of valent states, etc. It becomes a common occurrence that the core level excitation is accompanied by using those cells to form an additional multichannel route for the nonradiative energy dissipation. An event comes true on condition that both, the primary and coupled electrons belong to the same configuration.

Acknowledgements

The work has been supported by the Russian Foundation for Basic Research under Grants Nos. 14-03-00285 and 13-03-01155.

References

[1] G. Bunker, *Introduction to XAFS: A Practical Guide to X-ray Absorption Fine Structure Spectroscopy*, Cambridge University Press, Cambridge, 2010.
[2] T. Schiros, K.J. Andersson, L. G. M. Pettersson, A. Nilsson, H. Ogasawara, *J. Electron Spectrosc. Relat. Phenom.* 177 (2010) 85.
[3] J. Kirschner, *Electron-excited core level spectroscopes*, Springer, Berlin, 1977.
[4] A. Cholach, V. Tapilin, *J. Chem. Phys.* 138 (2013) 104201 http://dx.doi.org/10.1063/1.4794141
[5] I.P. Asanov, L.G. Bulusheva, M. Dubois, N.F. Yudanov, A.V. Alexeev, T.L. Makarova, A.V. Okotrub, *Carbon* 59 (2013) 518.
[6] P. Giannozzi, S. Baroni, N. Bonini, et al. *J. Phys.: Condensed Matter* 21(2009) 395502.

II-PP22

Surface Defects: Evaluation the Gap between Structure and Catalytic Activity

Cholach A.R.*, Matveev A.V., Bulgakov N.N.

Boreskov Institute of Catalysis SB RAS, Novosibirsk, Russia

* cholach@catalysis.ru

Keywords: surface defect, structure, catalytic activity

1 Introduction

Surface imperfections often make a strong influence on heterogeneous catalytic reaction. The surface defect may serve as an active center accelerating the rate limiting step; and on the contrary, it can accumulate impurities thus inhibiting the reaction [1]. The wave nucleation observed by Field Emission Microscopy during $NO+H_2$ reaction on a Rh twin tip [2] and in $CO+O_2$ reaction at Pt(110) and Pt(210) surfaces [3] are truly governed by structural defects, while stabilization effect ~ 50-80 kJ/mole of low-coordinated sites at edges and corners of Pt nanoparticles against Pt(111) plane was reported for CH_n species [4]. Anyway, surface defects take there a direct part in the reaction process. The specific behaviour of surface imperfections is usually interpreted at qualitative level and the lack of quantitative considerations encouraged the present study highlighting a simple model bridging up the structure and activity of surface defects as specific centres for adsorption and catalytic reactions.

2 Theoretical

Thermodynamic investigation of the adsorbed species was performed by semi-empirical Method of Interacting Bonds (MIB). MIB does not predict coordination, bond angles and other particular features, but empowers a perfect comparative accuracy. An equality of operating parameters, i.e. an identity of chemical bond nature in reference molecules and in a substance being examined is the only condition for high quantitative reliability of calculations [5].

3 Results and discussion

The sum of Lost Bonds by adjacent atoms (*LB*) forming a given adsorption site as compared with bulk atoms is taken for evaluation the local surface imperfection, while the heat of hydrogenation in the adsorbed layer $N + H \rightarrow NH$ at that site is considered as a measure of activity, in regard to a particular case [2]. Model calculations within the *LB* range of 1-20 have shown that *N* atom expectedly prefers defective adsorption sites of larger *LB* at basic planes of the transition and noble metals, whereas *NH* formation exhibits an opposite behaviour; Fig. 1 shows typical data on Fe as an example. As it turned out, surface defects are responsible for the formation of weakly bound, but inclined to hydrogenation atomic nitrogen as well as the larger by 5-8 orders equilibrium *NH* coverage against perfect terraces. Just these peculiarities force *N* atoms to recombine and desorb at a particular spot between (111) terraces and (100) steps at the Rh(533) single crystal [6] and make an extended defect of the grain boundary to be the center for surface wave nucleation in the $NO+H_2$ reaction on a Rh tip [2].

The model was further tried in examination the optimal catalytic center for NH_3 synthesis assuming the maximum activity corresponds to maximal *NH* coverage θ_{NH} under equilibrium θ_H, θ_N and θ_{NH}. So far as θ_{NH} is a function of *LB*-dependent equilibrium constants K_N, K_{NH} at invariable K_H, then the required sum of *LB* on a volcano curve $\theta_{NH}(K_N, K_{NH})$ is provided by $\partial\theta_{NH} / \partial(LB) = 0$. The latter equation comes true on condition that $K_N = \alpha/(\beta - 1)$, where α

and β are the slopes in opposite linear dependences for heats of *N* adsorption and *N+H* reaction vs. *LB* in Fig. 1, respectively. In these terms an optimal site for *Ru* at typical conditions of NH_3 synthesis ($P_{N_2} \sim 10^2$ atm.; $T \sim 800$ K) was found to consist of 2 atoms at (110)-(2x1) FCC plane, while *Rh* is an unpromising catalyst due to unrealistic *LB* values. Analogous consideration has revealed the coincidence between an optimal sum of *LB* predicted for catalytic center of *Fe* atoms in Fig. 1 and that related to *"C_7"* center in Fig. 2 as responsible for largest activity of the Fe(111) single crystal among others in NH_3 synthesis [7].

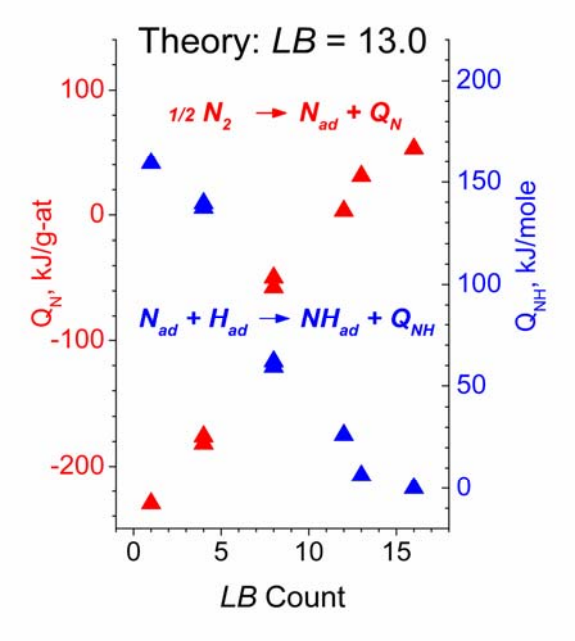

Fig. 1. Heats of indicated reactions at various adsorption sites of basic Fe BCC planes and 0.5 monolayer coverage.

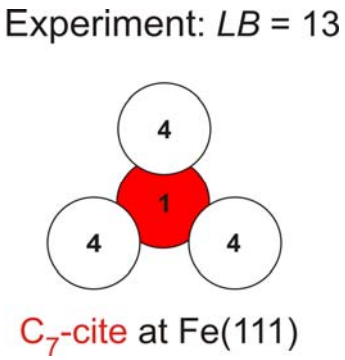

Fig. 2. LB numbers for atoms composing the "C_7"-cite, where "7" originally means the number of nearest neighbors around the middle atom [7].

4 Conclusions

The sum of bonds lost by atoms forming an adsorption site as compared to bulk atoms is a handy and useful measure of local surface imperfection close to physical meaning of the matter. This statement has been specifically confirmed by the following points: the reason of advanced activity of the grain boundary in chemical surface wave nucleation becomes clearly understood; the sum of lost bonds predicted for optimal catalytic center in NH_3 synthesis and formed by various atoms is close to experimental data, and this especially concerns C_7-cites as responsible for largest activity of the Fe(111) single crystal among others. The same approach can be applied to any other adsorption or catalytic process exhibiting high surface sensitivity.

Acknowledgements

The work has been supported by the Russian Foundation for Basic Research under Grant No. 14-03-00285.

References

[1] F. Liu, H. He, Z. Lian, W. Shan, L. Xie, K. Asakura, W. Yang, H. Deng, *J. Catal.* 307 (2013) 340.
[2] A. R Cholach, M.F.H. Van Tol, B.E. Nieuwenhuys, *Surf. Sci.* 320 (1994) 281.
[3] R. Imbihl, *Surf. Sci.* 603 (2009) 1671.
[4] F. Vines, Y. Lykhach, T. Staudt, M.P.A. Lorenz, C. Papp, H. P. Steinrueck, J. Libuda, K. M. Neyman, A. Goerling, *Chem. – Eur. J.* 16 (2010) 6530.
[5] A.R. Cholach, N.N. Bulgakov, *Catal. Lett.* 143 (2013) 817.
[6] F. Esch, A. Baraldi, C. Comelli, S. Lizzit, M. Kiskinova, P.D. Cobden, B.E. Nieuwenhuys, *J. Chem. Phys.* 110 (1999) 4013.
[7] D.R. Strongin, J. Carrazza, S.R. Bare, G.A. Somorjai, *J. Catal.* 103 (1987) 213.

II-PP23

Design of Ceramometal Cu-Al Catalyst with Egg-Shell Microstructure for Water-Gas Shift Reaction

Tikhov S.[1*], Minyukova T.[1], Valeev K.[1], Cherepanova S.[1], Salanov A.[1], Kaichev Yu.[1], Saraev A.[1], Andreev A.[1], Lapina O.[1], Sadykov V.[1,2], Gerasimov K.[3]

1 - Boreskov Institute of Catalysis SB RAS, Novosibirsk, Russia
2 - Novosibirsk State University, Novosibirsk, Russia
3 - Institute of Solid State Chemistry and Mechanochemistry SB RAS, Novosibirsk, Russia

* tikhov@catalysis.ru

Keywords: Cu-Al ceramometals, microstructure, water-gas shift reaction

1 Introduction

Water-gas shift reaction (WGS) is one of the primary industrial reactions of hydrogen production. One of the main problem of low temperature shift is the low activity of conventional catalyst per volume of the catalyst bed [1]. The possible way to increase the volume activity is the use of ceramometal catalysts with enhanced real and loading density [2]. The aim of the presented work is development of new CuAl-based catalyst prepared through the stage of mechanical alloying of Cu-Al powders and its detailed characterization.

2 Experimental

Aluminum powder with platelet-shaped particles and electrolytic copper powder of dendritic shape were used as starting materials. The powders were mixed in the weight ratio Al:Cu = 13:87 and mechanically milled (MA) in an APF mill (65 g acceleration) under air for 3, 6, 9 and 12 min (denoted as CuAl(3)- CuAl(12)). The details of MA procedure are presented in [3]. The procedure of porous cermets preparation from the MA product included next steps:

a) loading of the MA product into a stainless steel die specially designed to ensure a free access of water and hydrogen release;

b) hydrothermal treatment (HTT) of the loaded die in boiling water for few hours.

This stage provides formation of strong monoliths due to conjugation of the red-ox reaction of aluminum oxidation and formation of contacts between the particles due to crystallization of aluminum hydroxides. Similar to the stage of MA, oxidation of Al at HTT stage diminishes the extent of the exothermic reaction of Me-Al interaction at the stage of calcination.

c) Removing the monolithic product of HTT from the die followed by drying for 1 hour at 120°C and thermal treatment under air at 550°C.

The cermets before and after WGS testing were studied by XRD, NMR, SEM with an energy-dispersive spectroscopy unit EDX INCA, XPS. Compressing (crushing) strength, textural properties as well as thermal conductivity and coefficient of the thermal expansion (CTE) were determined as well. Catalytic activity of samples in the water gas shift reaction was estimated using a flow system in the temperature range of 160-270°C at atmospheric pressure. The tests were performed in the reaction mixture CO : H_2O : H_2 = 8 : 42 : 50 on a catalyst fraction of 0.14– 0.25 mm mixed with quartz fraction of the same particle size in 1:1 ratio. Before the tests, the catalyst was activated in 5% H_2 in He for 2 h at 270°C.

3 Results and discussion

According to XRD the initial cermets consist of CuO, Al_4Cu_9 intermetallide and solid solution of aluminium in copper Cu(Al). Alumina was not detected but by ^{27}Al NMR. After catalytic tests Cu, Cu(Al), Al_4Cu_9 were found. With the time of preliminary milling the

structural properties of cermets are changing non-monotonously. The amount of Al_4Cu_9 passes through the maximum, while that of amorphous alumina – through the minimum.

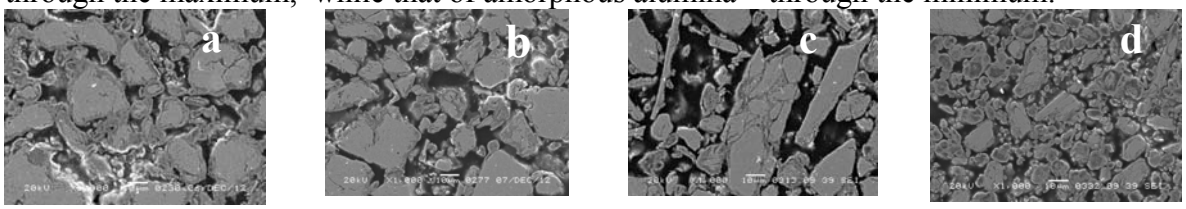

Fig. Microstructure of Cu-Al cermets: (a) – 3 min; (b) – 6 min; (c) – 9 min; (d) – 12 min.

SSA and mesopore volume pass through the minimum, while macropore volume (pore size – up to few microns, see Fig.) - through the maximum (Table). Large amount of open macropores provide improved permeability of cermet monoliths.

Table . Properties of Cu-Al cermets.

Sample	Time MA, min	SSA, m^2/g	V_{meso}, cm^3/g	V_{macro}, cm^3/g	Compress. Strength, MPa	$\rho_{catal.bed}$, g/cm^3	k', s^{-1}	Cu (Cu+Al)	TOF, s^{-1} (240°C)
CuAl(3)	3	14.4	0.02	0.05	10.5	~2.3	2.8	0.59	0.3
CuAl(6)	6	9.9	0.01	0.06	9.9	~2.2	3.3	0.51	0.4
CuAl(9)	9	9.0	0.02	0.07	7.7	~2.1	4.8	0.52	0.6
CuAl(12)	12	15.7	0.04	0.04	9.7	~2.0	7.8	0.59	0.5
$Cu_{50}Zn_{20}Al_{30}O$	-	121	-	-	-	~1.0	9.1	0.39	0.3

The microstructure of initial cermets has an egg-shell character with metallic phases in cores randomly distributed in the oxide matrix (Fig). A large amount of metallic phases provides cermets enhanced loading density (Table), thermal conductivity (1.8-2.4 W/(m·K)), and CTE ($9 \div 15 \cdot 10^{-6}$ K^{-1}) compared to conventional porous ceramics used in WGS catalysis. This makes possible to connect ceramometals with metallic elements to provide regular structure of the catalyst bed and to increase its loading density.

The cermets catalyst possesses a higher concentration of copper on the surface. But the first order WGS rate constants estimated with taking into account the difference or real density of cermet catalysts were found to be lower than for conventional oxide catalyst prepared by precipitation method due to much higher SSA of the latter (Table). The TOF values of some cermet catalyst were found to be higher than for mixed oxide catalyst, having the same order of magnitude like other active CuZnAl oxide catalyst [4]. The specific nature of Cu active sites on the surface of cermets probably related with the surface structure of intermetallic Al_4Cu_9 phase is discussed.

4 Conclusions

The detailed study of the structural, textural, surface and other physical properties in comparison with catalytic properties of cermet CuAlO/CuAl catalysts has been carried out. It was found that TOF values of some cermet catalyst are higher than for CuZnAl oxide catalyst. The structure sensitivity of cermets has been discussed.

Acknowledgements

This work was supported in part by RFBR grant #14-08-00251 and FP7 Project BIOGO.

References

[1] C.Ratnasamy, J.P.Wagner, *Catal.Rev.-Sci.Eng.,* 51 (2009) 325.
[2] S.Tikhov, V.Sadykov, K.Valeev et al., *Catal.Today,* (2015) [DOI: 10.1016/j.cattod.2014.12.009].
[3] D.V.Dudina, O.I.Lomovskii, K.R.Valeev, S.F.Tikhov et al., *J.Alloys Comp,* (2015) [DOI:10.1016/j.allcom.2014.12.120].
[3] M.J.L.Ginés, N.Amadeo, M.Laborde, C.R.Apesteguía, *Appl.Catal. A.,* 131(1995) 381.

II-PP24

Parahydrogen-Induced Polarization (PHIP): a Superior Tool for Mechanistic Studies of Heterogeneous Catalytic Reactions

Salnikov O.G.[1,2*], Kovtunov K.V.[1], Barskiy D.A.[1,2], Burueva D.B.[1,2], Koptyug I.V.[1,2]

1 - International Tomography Center, SB RAS, Novosibirsk, Russia
2 - Novosibirsk State University, Novosibirsk, Russia

* salnikov@tomo.nsc.ru

Keywords: hydrogenation, parahydrogen-induced polarization, mechanisms of catalytic reactions

1 Introduction

Parahydrogen-Induced Polarization (PHIP) is a very informative method for mechanistic and kinetic investigations of catalytic reactions involving hydrogen. Parahydrogen is a nuclear spin isomer of hydrogen with a total zero nuclear spin. PHIP technique is based on the use of parahydrogen-enriched gas mixtures in hydrogenation reactions. If the reaction mechanism allows addition of two atoms from the same hydrogen molecule to the same substrate molecule (i.e., pairwise hydrogen addition) than the usage of parahydrogen-enriched gas results in hyperpolarized (non-equilibrium) nuclear spin states of reaction product molecules. Consequently, the corresponding NMR signals of product molecules are significantly enhanced, allowing detection of short-lived reaction intermediates and minor products. Moreover, the characteristic anti-phase line shape of hyperpolarized NMR signals clearly indicates the existence of pairwise hydrogen addition route. Thus, the PHIP technique can provide unique information about reaction mechanisms which cannot be obtained with other methods.

So far, mostly investigations of homogeneous hydrogenations catalyzed by transition metal complexes benefited from the use of PHIP technique. However, in 2007-2008 it was found that PHIP effects can be observed in heterogeneous hydrogenations catalyzed by both immobilized metal complexes and supported metal nanoparticles. Thereafter PHIP was used for mechanistic studies of heterogeneous hydrogenations of hydrocarbons (propene, propyne, 1,3-butadiene, 1-butyne) over supported metal catalysts [1].

2 Experimental/methodology

Parahydrogen-Induced Polarization (PHIP) technique was used for mechanistic and kinetic studies of catalytic hydrogenations. H_2 gas was enriched with parahydrogen up to 50 % by passing it through the spiral tube with FeO(OH) powder maintained at liquid N_2 temperature or up to 92 % with the use of Bruker Parahydrogen Generator BPHG 90. The mixtures of parahydrogen-enriched H_2 and various substrates were used in hydrogenation experiments carried out in the gas phase at atmospheric pressure both inside and outside the NMR probe. The reaction products were analyzed by ^{1}H NMR spectroscopy.

3 Results and discussion

In this work PHIP technique was used for investigation of heterogeneous hydrogenation of α,β-unsaturated carbonyl compounds [2] and vinyl acetate. The existence of route of pairwise hydrogen addition to C=C bonds of acrolein, crotonaldehyde and vinyl acetate over several supported Pt, Pd and Rh catalysts was demonstrated. In hydrogenation of acrolein over Pd-Sn/Al_2O_3, Pd-Sn/TiO_2, Pd-Zn/TiO_2 and Pd/TiO_2 catalysts with parahydrogen the proton of CHO group of propanal was also polarized. This can be explained by C(O)-H bond dissociation which represents a side process on the catalysts surface. In hydrogenation of acrolein and vinyl acetate over Rh catalysts the formation of hyperpolarized 2-butene was observed. We assume that this

by-product is formed as a result of dimerization and hydrogen addition to adsorbed vinyl species which are formed by decarbonylation of acrolein or hydrogenolysis of vinyl acetate C-O bond. In hydrogenation of acetone and propanal the hyperpolarized NMR signals of propane resulting from C=O bond hydrogenolysis were observed. All these observations of side reactions products became possible only due to the high NMR signal enhancement provided by PHIP. This again demonstrates the unique possibilities of PHIP technique. It is notable that in our experiments with carbonyl compounds we never observed PHIP effects in C=O bond hydrogenation. This suggests that C=O bond is probably hydrogenated exclusively in non-pairwise manner.

Also for the first time deuterated precursor (propene-d6) was used in heterogeneous hydrogenation with parahydrogen [3]. In case of Rh/TiO_2 catalyst PHIP effects were observed not only for the hydrogenation product propane-d6 but also for the reactant. It means the occurrence of H/D-exchange via hydrogen addition with subsequent dehydrogenation.

In this work it was demonstrated for the first time that PHIP effects can be successfully observed in heterogeneous hydrogenations catalyzed by bulk metals (Pt, Rh) and metal oxides (CaO, Cr_2O_3, CeO_2, PtO_2, PdO, Rh_2O_3). This result indicates the existence of pairwise hydrogen addition route on both types of catalysts [4].

For the first time PHIP technique was used for kinetic studies of heterogeneous hydrogenations. It was found that in propene hydrogenation over Pt/Al_2O_3 catalyst the reaction orders with respect to H_2 are different for the non-pairwise and the pairwise hydrogen addition [5]. Therefore, different types of active sites on catalyst surface are responsible for these two routes of hydrogenation reaction. Also the evaluation of activation energies for both pairwise and non-pairwise routes of H_2 addition to propyne hydrogenation over Pd/aluminosilicate fiberglass catalyst was carried out [6]. It was found that at 175-275 °C the activation energies have similar values (about 60-70 kJ/mol) for both reaction routes. However, at 275-350 °C the rate constant for pairwise hydrogen addition is practically temperature-independent, while the rate constant for non-pairwise hydrogenation continues to grow with increasing temperature.

4 Conclusions

Our results clearly demonstrate that PHIP is a superior method providing unique information about mechanisms of not only homogeneous but also heterogeneous catalytic hydrogenations.

Acknowledgements

This work was supported by RFBR (14-03-00374-a, 14–03–31239-mol-a, 12–03–00403-a). Also we thank Prof. V.I. Bukhtiyarov and his group for catalysts preparation and characterization.

References

[1] K.V. Kovtunov, V.V. Zhivonitko, I.V. Skovpin, D.A. Barskiy, I.V. Koptyug, *Top. Curr. Chem.* 338 (2013), 123.

[2] O.G. Salnikov, K.V. Kovtunov, D.A. Barskiy, A.K. Khudorozhkov, E.A. Inozemtseva, I.P. Prosvirin, V.I. Bukhtiyarov, I.V. Koptyug, *ACS Catalysis* 4 (2014), 2022.

[3] K.V. Kovtunov, M.L. Truong, D.A. Barskiy, O.G. Salnikov, V.I. Bukhtiyarov, A.M. Coffey, K.W. Waddell, I.V. Koptyug, E.Y. Chekmenev, *J. Phys. Chem. C* 118 (2014), 28234.

[4] K.V. Kovtunov, D.A. Barskiy, O.G. Salnikov, A.K. Khudorozhkov, V.I. Bukhtiyarov, I.P. Prosvirin, I.V. Koptyug, *Chem. Commun.* 50 (2014), 875.

[5] O.G. Salnikov, K.V. Kovtunov, D.A. Barskiy, V.I. Bukhtiyarov, R. Kaptein, I.V. Koptyug, *Appl. Magn. Reson.* 44 (2013), 279.

[6] O.G. Salnikov, D.A. Barskiy, D.B. Burueva, Y.K. Gulyaeva, B.S. Balzhinimaev, K.V. Kovtunov, I.V. Koptyug, *Appl. Magn. Reson.* 45 (2014), 1051.

II-PP26

Biomorphous $CeZrO_2$and $CuO\text{-}CeZrO_2$ Catalysts for Low-Temperature CO Oxidation

Kaplin I.Y.[1,2*], Lokteva E.S.[1,2], Golubina E.V.[1,2], Voronova L.V.[2]

1 - Lomonosov Moscow State University, Chemistry Department, Moscow, Russia
2 - Institute of Hydrocarbons Processing of the Siberian Branch of the RAS, Omsk, Russia

* kaplinigormsu@gmail.com

Keywords: template, sawdust, CTAB, ceria-zirconia, copper oxide, CO oxidation

1 Introduction

Ceria-zirconia catalysts modified with CuO are promising systems for low-temperature CO oxidation. Developing of the mesoporous system of such catalyst increases the amount of adsorption sites and provides good transportation of reagents and products. In this work both organic surfactant (cetyltrimethylammoniumbromide, CTAB) and pine sawdust were compared as templates to create mesoporous structure for $CeO_2\text{-}ZrO_2$ and $CuO\text{-}CeO_2\text{-}ZrO_2$ catalysts. Catalytic tests were performed in CO oxidation in the range of from 100 to 450°C.

2 Experimental/methodology

The catalysts were prepared by impregnation of pine sawdust (0,25 – 0,5 mm) with the solution of $ZrO(NO_3)_2{\cdot}H_2O$ and $(NH_4)_2[Ce(NO_3)_6]$ together with $Cu(CH_3COO)_2{\cdot}H_2O$ ($CuO/Ce_xZr_{1-x}O_2$) or without it ($Ce_xZr_{1-x}O_2$) with further drying at 120°C and calcination at 600 - 630°C. On the base of literature data [1] the amount of modifier CuO was chosen to be about 20-25 mol.%.

Comparative systems were prepared using CTAB by slow addition of the solution of the same salts (0.01 mol/100 ml) and 0.05 M citric acid in water to 0,005 M ethanol solution of CTAB with subsequent aging during 3 h, drying at 120°C and calcination at 600 - 630°C.

The catalysts were characterised by SEM (JSM 6490 LV, JEOL), XRD (Bruker D8 Advance ($Cu\ K_\alpha$, using database ICDD JCPDS PDF1, low-temperature N_2 adsorption-desorption (Micometrics ASAP 2000), XPS (Kratos Axis Ultra DLD), TPR and DSC-TG (449PC Jupiter Netzsch, Netzsch GmbH).

Catalytic tests were performed by pulse microcatalytic method using the mixture of 2 vol.% CO and 1 vol.% O_2, balance He, pulse value 1 ml, with GC analysis of products.

3 Results and discussion

Ce:Zr mole ratio in the prepared samples varied from 1:1 to 4:1, the content of CuO was about 20-25 mol.%. The samples based on sawdust denoted as (SD), the others as (CTAB).

SEM investigation demonstrated biomorphic structure for the samples prepared using sawdust as a template (Fig.1a). Both morphology and S_{BET} depends on temperature ramp-up during calcination. Slow temperature increase in the range 150-250°C promotes the saving of biomorphic structure in final complex oxide, fast process promotes material sintering. The samples prepared using CTAB were also characterized by porous structure (Fig. 1b).

XRD diffractograms of $CeZrO_2$ and $CuO/CeZrO_2$ prepared using CTAB or SD contain ceria-circonia phase reflexes (28.8, 33.3, 47.9) broadened slightly for $CeZrO_2$ (SD) and strongly for $0.25CuO/CeZrO_2$ (SD). Separate CuO phase is present in all Cu-containing samples. The weak reflex at 2theta = 60° is characteristic for the presence of Cu_2O phase.

The presence of both CuO and Cu_2O was confirmed by XPS, where the shoulder at 932.5 eV characteristic for Cu^+ was present in Cu 2p spectra near the peak of Cu^{2+} at 934 eV for $0.25CuO/CeZrO_2$ (SD) and $0.25CuO/CeZrO_2$ (CTAB) samples. Local EDS analysis gives $0{,}23CuO/Ce_{0{,}44}Zr_{0{,}56}O_2$ formula for the

surface of 0.25CuO/$CeZrO_2$ (SD). TPR demonstrated the presence of two hydrogen absorbtion peaks: small one with maximum at 240°C and broad one with maximum at 360°C assigned to Cu reduction from oxides.

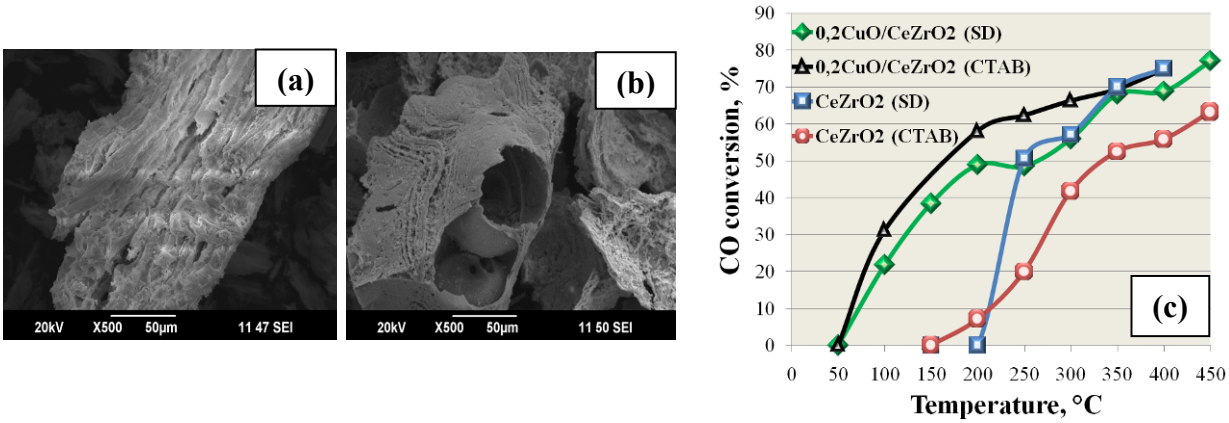

Fig. 1. SEM images of 0.2CuO/$CeZrO_2$ (SD) (a) and 0.2CuO/$CeZrO_2$ (CTAB) (b); CO conversion vs temperature for different samples (c)

All prepared catalysts are active in CO oxidation (Fig. 1c). The addition of CuO to $CeZrO_2$ (SD) leads to the significant decrease of the reaction temperature: the CO conversion at 200°C was 0 on $CeZrO_2$ (SD) and 62% on 0.2CuO/$CeZrO_2$ (SD); at 100 and 150°C it was 25 and 50% respectively. 0.2CuO/$CeZrO_2$ (CTAB) has even better catalytic performance, at 100 and 200°C CO conversion was 30 and 58% respectively. According to [1], it could be explained by better crystallinity of 0.2CuO/$CeZrO_2$ (CTAB) seen from XRD data, that facilitate the transfer of lattice oxygen from the bulk to the surface. However the difference could be connected also with the difference in Cu:Ce:Zr ratio in the samples prepared using CTAB or SD.

4 Conclusions

1. The sawdust which is the waste in timber industry could be effectively used as the template for active ceria-zirconia catalysts instead of organic templates. The application of bio-template and careful tuning of calcination conditions helps to form the biomorphic structure in $CeZrO_2$ and CuO/$CeZrO_2$.

2. The phase composition of $CeZrO_2$ and CuO/$CeZrO_2$ produced using sawdust and CTAB as template is similar, both contain mixed ceria-zirconia oxide and separate phase of CuO with the traces of Cu_2O. However the extent of crystallinity of ceria-zirconia oxide is higher for the CuO/$CeZrO_2$ (CTAB) and lower for CuO/$CeZrO_2$ (SD).

3. Modification of $CeZrO_2$ with Cu oxide leads to the significant decrease of the temperature of CO oxidation, from 250 to 100°C and less. CuO/$CeZrO_2$ prepared using CTAB or SD provide comparable conversion of CO to CO_2, however the first was slightly more active than 0.2CuO/$CeZrO_2$ (SD) possible due to higher crystallinity facilitating the transfer of lattice oxygen from the bulk to the surface.

Acknowledgements

This work was maintained by Russian Foundation for Basic Researches (13-03-00613). This work was supported in part by M.V. Lomonosov Moscow State University Program of Development.

References

[1] J. Luo et al., *Appl.Catal. A : General* 423-424 (2012) 121.

II-PP27

Ethanol Steam Reforming over RhPd Supported on Nanoshaped CeO_2

Soler L.[1*], Divins N.J.[1], Casanovas A.[1], Xu W.[2], Senanayake S.D.[2], Wiater D.[3], Trovarelli A.[3], Llorca J.[1]

1 - Institute of Energy Technologies, Universitat Politècnica de Catalunya, Barcelona, Spain
2 - Chemistry Department, Brookhaven National Laboratory, Upton, New York, USA
3 - Dipartimento di Chimica, Fisica e Ambiente, Università di Udine, Udine, Italy

* lluis.soler.turu@upc.edu

Keywords: nanoshaped ceria, ethanol steam reforming, operando XRD, ceria-supported, noble metals

1 Introduction

One of the challenges of ethanol steam reforming (ESR) to produce hydrogen (H_2) is how to employ lower temperatures and improve the efficiency of ESR [1], in order to scale down the ESR for diverse forthcoming applications. In the last two decades, a myriad of supported metals have been investigated as potential catalysts for ESR [2]. Among them, the bimetallic Rh-Pd system supported over CeO_2 pioneered by the Idriss' group in 2008 [3] has shown an outstanding catalytic performance for ESR. The synergic effect of Rh that provides C-C bond cleavage with Pd that promotes H_2 recombination and the simultaneous dissociation of H_2O and oxygen mobility provided by CeO_2 leads to a highly active, selective and stable catalyst for the ESR. Recent advances on RhPd/CeO_2 catalysts demonstrated their functionality in several applications, for instance, catalytic membrane reactors to yield high purity H_2 [4], steam reformer for direct PEM fuel cell feeding [5] or microreactors to generate H_2 by bio-ethanol reforming [6]. Earlier last year, Llorca's group illustrated for the first time strong restructuring of the ceria-supported RhPd nanoparticles that takes place under ESR conditions, inducing strong changes to the behavior of the catalyst [7].

Here we report a systematic study of the ESR reaction over RhPd nanoparticles supported on ceria with different morphologies (nanocubes, nanorods and nanopolyhedra), analyzing their catalytic performance and using several characterization tools (operando X-ray diffraction, electron microscopy, etc.) in order to investigate the role of the oxide morphology and the importance of the size and synthetic routes to load RhPd nanoparticles onto ceria supports.

2 Experimental/methodology

Nanoceria supports with different morphologies were fabricated by a hydrothermal method in the range of 373-453K as reported elsewhere in detail [8,9]. Briefly, ceria nanocubes (CeO_2-C) were prepared mixing $Ce(NO_3)_3 \cdot 6H_2O$ and NaOH under vigorous stirring. After precipitation, the suspension was heated for 24h at 453K in an autoclave. Ceria nanorods (CeO_2-R) were synthesized similarly, but heating for 24h at 373K. Conventional nanopolyhedral ceria (CeO_2-P) was prepared by precipitation of an acidic solution of $Ce(NO_3)_3 \cdot 6H_2O$ with a base. Noble metals (3% w/w total with respect to the ceria support, Rh:Pd=1:1 molar) were loaded onto the nanoceria using two different procedures: (i) wetness impregnation, using $PdCl_2$ and $RhCl_3$ solutions and (ii) deposition of core-shell RhPd@dodecanethiol preformed nanoparticles. The ESR reaction tests were performed at 600-1050K.

3 Results and discussion

The H_2 production by catalytic ESR at low temperature (<700 K) over RhPd/CeO_2-C is higher than RhPd/CeO_2-R catalyst and both perform better than a conventional RhPd/CeO_2-P

catalyst, as illustrated in Fig. 1.

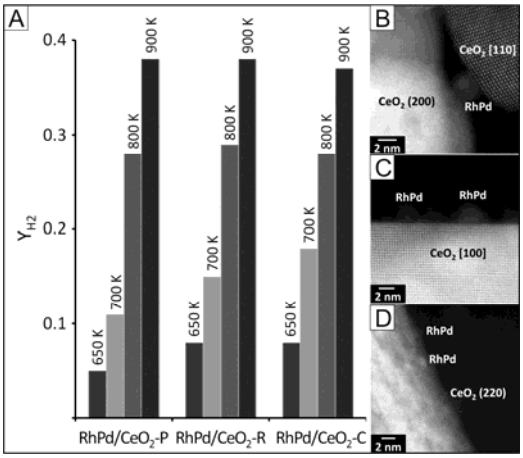

Fig. 1. (A) Hydrogen yield (Y_{H2}, between 0 and 1) obtained at different temperatures over RhPd/CeO_2 catalysts prepared by impregnation from chloride salts. STEM images of RhPd/CeO_2-P (B), RhPd/CeO_2-R (C) and RhPd/CeO_2-C (D). Adapted from [10].

According to operando XRD results, we further show that the reorganization of RhPd nanoparticles is much easier on CeO_2-C and CeO_2-R than CeO_2-P, where the XRD profiles do not show significant variations. Ongoing experiments with preformed RhPd nanoparticles will show the influence of the morphology of the nanoceria support on the performance of the ESR.

4 Conclusions

We have demonstrated the effect of the morphology of the nanoceria support to enhance H_2 production by ESR reaction. The use of RhPd/CeO_2-nanocubes catalyst at low temperature (<700 K) showed a better performance than other morphologies, such as nanorods or nanopolyhedral ceria. The behaviour observed in these catalytic systems can be understood by considering the metal reorganization over {100} and {110} crystallographic planes of ceria compared with over the low surface energy {111} planes of ceria.

Acknowledgements

Authors thank financial support from grant MINECO ENE2012-36368. J.L. is Serra Húnter Fellow and is grateful to ICREA Academia program. L.S. acknowledges the Beatriu de Pinós Program for financial support through Project No. 2013 BP-B 00007.

References

[1] N. Bion, D. Duprez, F. Epron, *ChemSusChem*. 5 (2012) 76-84.
[2] J. Llorca, V. Cortés, N.J. Divins, R. Olivera, E. Taboada, *Renewable Hydrogen Technologies*, Eds. L.M. Gandía, G. Arzamendi, P.M. Diéguez, Elsevier, Amsterdam, 2013; Ch. 7, pp. 135–169.
[3] M. Scott, M. Goeffrey, W. Chiu, M.A. Blackford, H. Idriss, *Top. Catal*. 51 (2008) 13-21.
[4] E. López, N. J. Divins, J. Llorca, *Catal. Today* 193 (2012) 145–150.
[5] R. Koch, E. López, N.J. Divins, M. Allué, A. Jossen, J. Riera, J. Llorca, *Int. J. Hydrogen Energ*. 38 (2013) 5605–5615.
[6] N. Divins, E. López, A. Rodríguez, D. Vega, J. Llorca, *Chem. Eng. Process.* 64 (2013) 31–37.
[7] N.J. Divins, I. Angurell, C. Escudero, V. Pérez-Dieste, J. Llorca, *Science* 346 (2014) 620–623.
[8] H.-X. Mai, L.-D. Sun, Y.-W. Zhang, R. Si, W. Feng, H.-P. Zhang, H.-C. Liu, C.-H. Yan *J. Phys. Chem. B* 109 (2005) 24380-24385.
[9] E. Aneggi, D. Wiater, C. de Leitenburg, J. Llorca, A. Trovarelli, *ACS Catalysis* 4 (2014) 172–181.
[10] N.J. Divins, A. Casanovas, W. Xu, S.D. Senanayake, D. Wiater, A. Trovarelli, J. Llorca. *Cat. Today* (2015) DOI: 10.1016/j.cattod.2014.12.042

II-PP28

Design and Synthesis of Supported Vanadium Catalysts for Oxidative Dehydrogenation of Hydrocarbons

Kharlamova T.S.[1*], Sadykov V.A.[2,3], Vodyankina O.V.[1]

1 - Tomsk State University, Tomsk, Russia
2 - Boreskov Institute of Catalysis SB RAS, Novosibirsk, Russia
3 - Novosibirsk State University, Novosibirsk, Russia

* kharlamova83@gmail.com

Keywords: catalyst, design, vanadium, lanthanum, silicate, co-precipitation, formation, mechanism

1 Introduction

Lower alkenes as well as styrene are important materials for chemical industry. Thereby, production of these hydrocarbons is of increasing interest. Oxidative dehydrogenation (ODH) of alkanes is believed to be promising reaction for their production [1,2].

Catalyst based on supported vanadia showed promising results for the ODH reaction [1,2]. However, the outlook of ODH of propane and other hydrocarbon shows that new concepts for catalyst design are required [2]. Previous investigations have shown that various parameters, including oxidation state, coordination number, aggregation state, reducibility of vanadium species, vanadium content, support nature etc., are required to be considered to account for the catalytic behavior observed for the selective ODH, with the factors that govern the catalytic performances of the surface VO_x species still being debated [1,2].

The presence of isolated tetrahedral vanadium oxide species is commonly supposed to be essential for maintaining high conversion and selectivity in the ODH of lower alkenes, whereas polymeric vanadium species could favor undesired combustion reaction pathways [1-4]. The vanadium incorporation into the support structure was shown to allow stabilizing isolated VO_4 species [3,4]. Using of complex oxides containing isolated VO_4 units in their structure could be an alternative way to development of new active and selective catalysts for ODH.

Lanthanum orthosilicates with an apatite structure can be a possible matrix for isolated tetrahedral vanadium oxide species [5,6]. However, a tailor-made design of materials with desired properties requires developing of controlled synthesis method based upon understanding general physicochemical regularities at each stage of the selected preparation technique. In the present work, the peculiarities of genesis of the structure and texture of lanthanum orthosilicates in the course of synthesis by co-precipitation as well as preparation of vanadium catalysts on the basis of lanthanum silicates are considered.

2 Experimental

Undoped and doped lanthanum silicates were produced by co-precipitation method. To clarify the features of the structure and texture genesis of lanthanum silicates in the course of synthesis, the local structure, phase composition and textural characteristics of undoped and Al- and Fe-doped samples were studied at different stages of their synthesis by XRD, thermal analysis, low-temperature adsorption of N_2, IR spectroscopy, ^{27}Al and ^{29}Si MAS NMR spectroscopy, UV-Vis DR spectroscopy and TEM with EDXA.

3 Results and discussion

Some features of genesis of the structure and texture of apatite-type lanthanum silicates in the course of synthesis via co-precipitation were elucidated, which can be interpreted in terms of formation of amorphous precipitates of slightly soluble hydroxides and their crystallization via

the mechanism of "oriented accretion" [7]. Thus, according to IR, UV-Vis DR, ^{27}Al and ^{29}Si MAS NMR spectroscopy as well as TEM with EDXA data, an amorphous lanthanum silicate with the local structure typical for the orthosilicate, containing Al or Fe atoms in the polymeric structure in the case of doped samples, is formed already at the stages of co-precipitation, ageing and drying of the residue. This indicates that the interaction between constituents under precipitation occurs at the level of hydroxocomplexes or at the molecular level in the step of polycondensation. The polycondensation of La polyhydroxocomplexes in the presence of Si and Al ones during co-precipitation was assumed to result in the formation of primary particles with the polymeric structure similar to that of $La(OH)_3$ hydroxide with columns to be partially filled by Si and Al. It is also interesting from a catalytic point of view that, according to ^{27}Al MAS NMR and UV-Vis DR spectroscopy data, only a part of dopant atoms is present as four-coordinated AlO_4 or FeO_4 units located in the volume of primary particles, while another part is present as six-coordinated AlO_6 or FeO_6 units, being situated at the surface of primary particles forming the amorphous precursor.

Besides, according to low-temperature N_2 adsorption and TEM data, the growth of size of primary particles forming precipitate as well as crystallization of the amorphous lanthanum silicate does not occur in the course of precipitate aging in mother solution at ambient conditions as well as drying up to 120 ºC, but only in the course of the subsequent temperature treatment of the xerogel up to 800 ºC, with intermediate and final products of ageing preserving a "memory" about the initial sample structure. According to the TEM data, irregular-shaped crystalline and partially crystallized lanthanum silicate particles as well as amorphous ones of the precursor are simultaneously present in the sample during its crystallization. Thus, one can assume that the formation of the crystalline structure of the lanthanum orthosilicate occurs inside primary particles formed via the rearrangement of their polymer structure during subsequent thermal treatment in accordance with the mechanism of "oriented accretion" [7]. The irregular shape of formed crystalline particles, in turn, indicates that the formation rate of secondary crystal during crystallization is higher than the ones of crystallization centers and nuclei. In general, textural characteristics of produced crystalline lanthanum silicates were shown to be determined by those of amorphous precursor, which structure formation begins at the early synthesis stages and is mainly completed during thermal treatment in the range of 120-500 ºC.

4 Conclusions

Peculiarities of genesis of the structure and texture of lanthanum silicates in the course of synthesis by co-precipitation were examined. The possible mechanism of the apatite-type lanthanum silicate formation is considered. Given the peculiarities of their formation via co-precipitation, the vanadium catalysts based on amorphous and crystalline lanthanum orthosilicates will be prepared by co-precipitation as well as wetness impregnation methods. Their structure peculiarities and catalytic properties in ODH of propane will be examined.

Acknowledgements

This research was supported by "The Tomsk State University Academic D.I. Mendeleev Fund Program" grant.

References

[1] E.M. Mamedov, V. Cortes Corberan, *Appl. Catal. A,* 127 (1995) 1.
[2] O.V. Buyevskaya, M. Baerns, *Catal.*, 16 (2002) 155.
[3] Y. Lio, W. Feng, T. Li, H. He, et al, *J. Catal.,* 239 (2006) 125.
[4] K. Chalupka, C. Thomas, Y. Millot, F. Averseng, S. Dzwigaj, *J. Catal.,* 305 (2013) 46.
[5] E. Kendrick, M.S. Islam, P.R. Slater, *J. Mater. Chem.*, 17 (2007) 3104.
[6] T.S. Kharlamova, A.S. Matveev, A.B. Ishchenko, A.N. Salanov, *Kinet. Catal.*, 55 (2014) 361.
[7] R.A. Buyanov, O.P. Krivoruchko, React. Kinet. Catal. Lett., 35 (1987) 293.

II-PP30

The Interaction of Model NSR Catalysts BaO/MO_2 and $Pt\text{-}BaO/MO_2$ (MO_2 = TiO_2, ZrO_2, TiO_2-ZrO_2) with NO_2

Smirnov M.Yu.*, Kalinkin A.V., Toktarev A.V., Bukhtiyarov V.I.

Boreskov Institute of Catalysis SB RAS, Russia, Novosibirsk, Russia

* smirnov@catalysis.ru

Keywords: NOx storage, nitrate, nitrite, Pt, oxidation

1 Introduction

NSR (NO_X storage-reduction) catalysts are used for nitrogen oxides neutralization in automobile exhaust gases by NO_x storage in the form of nitrites and nitrates followed by their reduction to nitrogen. A disadvantage of the NSR-catalysts containing Ba-substances supported on γ-Al_2O_3 as a NO_x absorbing component is their high susceptibility to poisoning by sulfur oxides. The stability of the NSR catalysts to poisoning can be improved by replacing the traditional support material (γ-Al_2O_3) on TiO_2 or ZrO_2. In this paper we studied the interaction of model NSR-systems BaO/MO_2 and $Pt\text{-}BaO/MO_2$ (M = TiO_2, ZrO_2, TiO_2-ZrO_2) with NO_2 using XPS.

2 Experimental

The most of stages of the preparation of the model NSR-catalysts, their reactions with NO_2, and XPS spectra acquisition were carried out in SPECS spectrometer ($P < 5 \times 10^{-9}$ mbar, Mg Kα radiation). Samples of the catalysts were prepared in the form of thin films on substrates made of FeCrAlloy plates coated with an alumina layer. The support films of ~10-15 nm in thickness were deposited by evaporation in vacuum (TiO_2, ZrO_2) or by hydrolysis of titanium or/and zirconium complexes (TiO_2, ZrO_2, TiO_2-ZrO_2). BaO (~3.5-5.5 monolayers) was deposited by evaporation of barium from $BaAl_4$ alloy, followed by annealing in oxygen at 500°C. Platinum was deposited by evaporation of metallic Pt. Treatment in NO_2 was performed in a preparation chamber of the spectrometer at pressure of 3×10^{-6} mbar and a sample kept at room temperature. NO_2 was produced by lead nitrate decomposition.

3 Results and discussion

BaO/MO_2. At the initial NO_2 exposures, the line with the binding energy of ~ 403.5-404 eV appears in the N 1*s* region that is attributable to barium nitrite species (Fig. 1). With increasing exposure, the intensity of this line is reduced, and simultaneously the line with the binding energy of 407-407.5 eV belonging to barium nitrate species starts to grow. At the initial stage, the reduction of NO_2 molecules into the nitrite species is accompanied by the oxidation of surface carbon that is confirmed by spectra recorded in the C 1*s* region. The formation of barium nitrate occurs more efficiently when the support contains ZrO_2 (Table 1). Apparently, barium titanates are present in the sample BaO/TiO_2 that are less reactive than BaO with respect to NO_2.

$Pt\text{-}BaO/MO_2$. After platinum deposition, an asymmetric shape of the Pt $4f_{7/2}$ and Pt $4f_{5/2}$ lines in the Pt 4*f* region and the binding energy BE($Pt4f_{7/2}$) ~72 eV indicate that the samples contain small platinum particles in the metallic state. The interaction of these samples with NO_2 also leads to the successive formation of barium nitrite and barium nitrate. The total amount of NO_2 absorbed is greater than in the case of BaO/MO_2 samples, mainly due to a more efficient formation of nitrite (Table 1). Two new states of platinum are formed in the reaction with NO_2 (Fig. 2a). The first state, which is characterized by a doublet of asymmetric lines (drawn in

green) and BE(Pt4$f_{7/2}$) increasing monotonically with NO_2 exposure, belongs to metallic platinum particles with dissolved oxygen [1]. With the further exposure increase, the second doublet appears and grows, which lines (drawn in red) have a symmetric shape, and BE(Pt4$f_{7/2}$) ~72 eV corresponds to PtO_2.

Pt 4*f* spectra of the samples annealed in vacuum at 500ºC reveal that the annealing makes Pt particles larger. Again, the reaction with NO_2 leads to the successive formation of barium nitrite and barium nitrate, but with the preferential formation of nitrate (Table 1). In this case, spectra in the Pt 4*f* region (Fig. 2b) show that PtO_2 is formed in very small quantities and only after the largest NO_2 exposures. The result is not surprising, since larger Pt particles are oxidized more difficult [2].

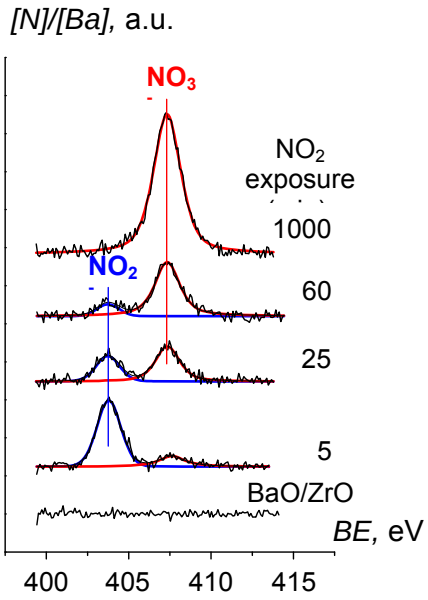

Fig. 1. N 1*s* spectra for BaO/ZrO_2 sample under its reaction with NO_2.

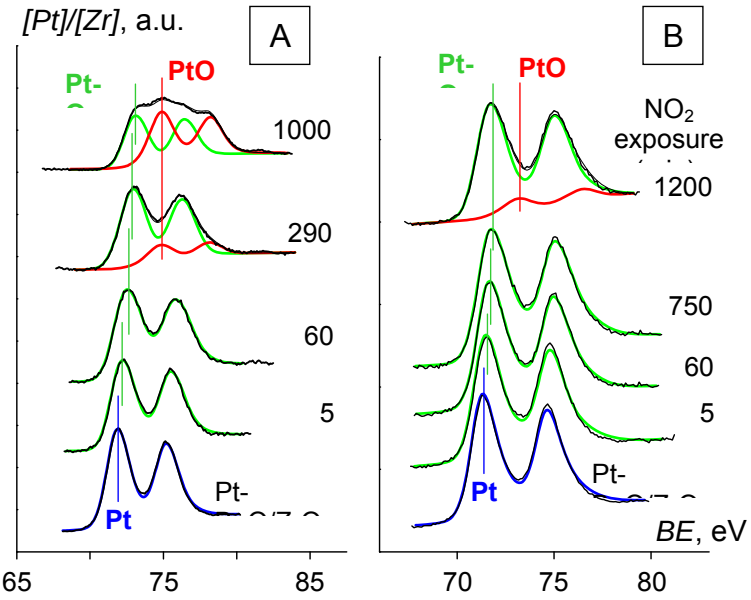

Fig. 2. Pt 4*f* spectra for fresh (A) and annealed (B) Pt-BaO/ZrO_2 samples under its reaction with NO_2.

Table 1. The nitrate ($[NO_3^-]/[Ba]$) and total NO_x^- ($[NO_x^-]/[Ba] = [NO_2^-]/[Ba]+[NO_3^-]/[Ba]$) concentrations achieved in the reactions of the model NSR catalysts with NO_2.

Model catalyst	BaO/TiO_2	BaO/ZrO_2	BaO/TiO_2-ZrO_2	Pt-BaO/TiO_2-ZrO_2, fresh	Pt-BaO/TiO_2-ZrO_2, annealed
$[NO_3^-]/[Ba]$	0.18	0.38	0.41	0.43	0.58
$[NO_x^-]/[Ba]$	0.21	0.38	0.41	0.56	0.58

Acknowledgements

The authors thank Russian Science Foundation (grant 14-23-00146) for financial support.

References

[1] M.Yu. Smirnov, E.I. Vovk, A.V. Kalinkin, A.V. Pashis, V.I. Bukhtiyarov, *Kinetics and Catalysis*. 53 (2012) 117.

[2] M.Yu. Smirnov, A.V. Kalinkin, E.I. Vovk, A.M. Sorokin, V.I. Bukhtiyarov, *XIth European Congress on Catalysis*, Lyon, 2013, S5-T2-OR-04.

II-PP31

Location, Toxicity and Growth Mechanism of Coke on Hierarchical MOR Zeolites

Chouati M.[1,2], Soualah A.[2], Pouilloux Y.[1], Pinard L.[1*], Astafan A.[1]

1 - Institut de Chimie des Milieux et Matériaux de Poitiers, UMR 7285 CNRS, Poitiers France
2 - LPMC, Laboratoire de Physico-chimie des Matériaux et Catalyse Université A.MIRA, Béjaia, Algérie

* ludovic.pinard@univ-poitiers.fr

Keywords: Mordenite, desilication, coke, deactivation, regeneration

1 Introduction

The presence of regular pores of molecular dimensions in zeolite can have multiple effects on the catalyst lifetime. In favourable cases, the microporous shape selectivity can prevent formation of bulkier molecules that block pores and thus dramatically slow down catalyst deactivation. In many cases however, depending on pore shapes and dimensionality of zeolite system, bulky molecules, usually called "coke", can accumulate inside the porous network and impede diffusion of reactants/products to/from active sites by pore blocking or poisoning, leading to a rapid deactivation [1].

The size and shape of micropores, channel intersections, external surface apertures determine the shape and the maximum size of trapped coke molecules [1-2]. Moreover, the zeolite dimensional channel system affects catalytic consequences of deactivation. On a three-dimensional system like MFI, deactivation occurs mainly by acid site poisoning; i.e. one coke molecule poisons one active site. Contrariwise, deactivation occurs only through pore blockage on one-dimensional zeolite system; i.e. on MOR more than 20 Brønsted acid sites can be deactivated by only one coke molecule [1].

The creation of mesopores on MOR zeolite crystal, through demetallation treatments, leads to a three-directional porous system that could reduce considerably the coke toxicity. The degree of the three dimensionality of the hierarchical MOR zeolite is related to the interconnection between mesopores with micropores.

The aim of this work is to establish a relation between the textural properties of different hierarchical HMOR zeolites and the toxicity, location composition of coke formed during the propylene oligomerisation.

2 Experimental/methodology

A commercial Mordenite was used as a starting material (MOR structure type and Si/Al = 10) in protonic form (**MOR**). Three hierarchical zeolites were prepared by alkaline treatment using aqueous sodium hydroxide (0.2M, 70 °C, 2h); **MOR D** was prepared by desilication with NaOH, **MOR DL** by desilication followed by acid leaching with aqueous of HCl (0.5 M, 10 min, 30 °C) in order to remove all fragments formed during alkaline treatment, susceptible to block the micropore access, and **MOR LDL** by acid leaching before and after desilication. The table 1 reports some selected properties of the catalysts.

Table 1: Selected properties of commercial and hierarchical mordenite zeolites

Catalyst	MOR	MOR D	MOR DL	MOR LDL
V_{micro}[a] ($cm^3.g^{-1}$)	0.20	0.19	0.23	0.20
V_{meso}[b] ($cm^3.g^{-1}$)	0.15	0.25	0.20	0.34
$[PyH^+]$[c] ($\mu mol.g^{-1}$)	1056	621	680	784
[PyL][d] ($\mu mol.g^{-1}$)	31	162	133	130

[a]micropore volume calculated by using *t*-plot method; [b] Mesopore volume $=V_{total}-V_{micro}$ (V_{total}: volume adsorbed at $p/p_0=0.99$) ; [c,d] Measured by pyridine adsorbed on Brønsted (PyH^+) and Lewis (PyL) acid sites, respectively, after evacuation at 150 °C.

3 Results and discussion

The evolution of carbonaceous deposits was monitored by gravimetric measurements during conversion of propene at 623 K under pressure of 1 bar, by conventional microbalance instrumentation. The coking rate is very fast on MOR, after 4 min all the access of micropores were blocked to nitrogen. Initially, all coke molecules are soluble in methylene chloride after dissolution of the zeolite matrix, but insoluble coke appeared during the coking time. Soluble coke molecules can be lumped in four families according to their number of aromatic rings: naphthalene, anthracene, benzoflorene and chrysene. It should be underscored that the degree of alkylation of coke molecule is low, it does not exceed 4. On Hierarchical MOR zeolite, an additional porosity leads to a supplementary coke uptake. This additional coke leads to insoluble coke as the expense of the soluble coke. Detailed coke features, in term of molecular structure, have been obtained by combining a large range of techniques: matrix-assisted laser desorption/ionization time of flight mass spectrometry (MALDI-TOF MS) directly on the spent catalyst. From these data a schematic build-up of carbonaceous residues will be proposed.

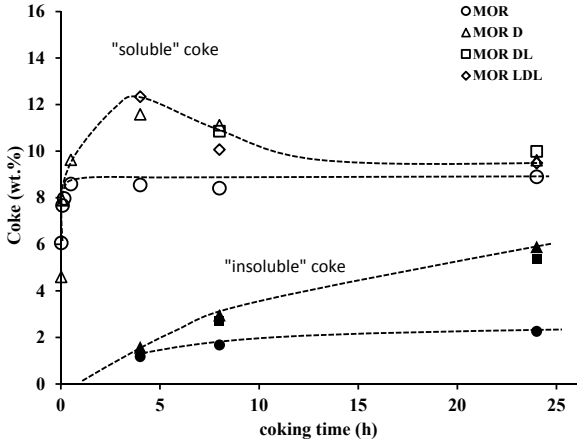

Fig. 1. (a): Content of soluble and insoluble coke deposited on mordenites samples during propylene oligomerisation.

Acknowledgements

Nourrdine Chouati thanks Algerian government for the doctoral grant.

References

[1] M. Guisnet, F. Ramôa Ribeiro (eds), Deactivation and Regeneration of Zeolite Catalysts, Imperial College Press, London, 2011.

[2] F. Ngoye, L. Lakiss, Z. Qin, S. Laforge, C. Canaff, M. Tarighi, V. Valtchev, K. Thomas, A. Vicente, J. P. Gilson, Y. Pouilloux, C. Fernandez, L. Pinard, J. Catal., 320 (2014) 118.

II-PP32

Computational Investigation of Palladium Supported Boron Nitride Nanotube Catalysts

Schimmenti R.*, Prestianni A., Ferrante F., Duca D.

Università degli Studi di Palermo, Dipartimento di Fisica e Chimica, Palermo, Italy

* roberto@cccp.unipa.it

Keywords: metal supported, catalysts, oxygenate, adsorption, DFT, calculations, ONIOM

1 Introduction

Boron nitride based nanotube (BNNT) derivatives showed really interesting properties such as high chemical and thermal stability as well as great mechanical strength and high thermal conductivity. [1] These features make them especially suitable for high temperature technologies and catalysis: as an example, the lack of acidic sites and their peculiar thermal properties, should reduce the sintering of disperded metals. Metal supported on BNNTs have been studied as catalysts for the selective oxidation of lactose, showing high activity and selectivity. [2] For this and other related reactions, namely carbohydrates oxidation, it has been showed that the chemical nature of the support could affect the degree of dispersion and dimension of the dispersed nanoparticle, ruling the reaction activity and selectivity. [3] A computational study could elucidate effectively how the interactions between metals and BNNTs affect the growth of metal clusters. Since it has been showed that the presence of edge and corners on the metal nanoparticle could exert a detrimental effect on the global activity of the above mentioned reactions, the modelling of high dimension metal clusters showing different surfaces should be addressed.

In this study the interactions of small palladium clusters (Pd_2, Pd_3 and Pd_4) with a single walled BNNT were modelled. Since it has been previously demonstrated to be a representative model for a range of relevant sites, [4] a Pd_{30} cluster was chosen in order to investigate the interaction of a larger cluster with the BNNT support. Finally, the oxygenate D-glucopyranose adsorption on the Pd_{30}/BNNT system was analysed to model medium-complex biomass derived molecules.

2 Computational details

Calculations were performed by the Gaussian 09 code package. A QM/MM approach, exploiting the 2-layer ONIOM method was employed. The UFF molecular mechanics was selected as the low level (real system) while the high level (model system) was defined in the framework of the DFT, employing the Coulomb-attenuated CAM-B3LYP hybrid exchange-correlation functional. The Los Alamos LANL2 effective core potential and the corresponding double ζ basis set were used for the Pd atoms, while for the lighter atoms (H, B, N, C, O) the D95V basis set was adopted.

3 Results and discussion

The interaction energy and the geometry of the calculated most stable structures are reported in Figure 1. On the whole, the adsorption processes seem to be favoured, increasing the size of the cluster. This can be outlined taking into account the most stable spin state of the clusters, which in almost every case is the triplet one. The geometrical features of the optimized structure can be rationalized considering a balance between both the Pd–Pd and the metal–support interactions.

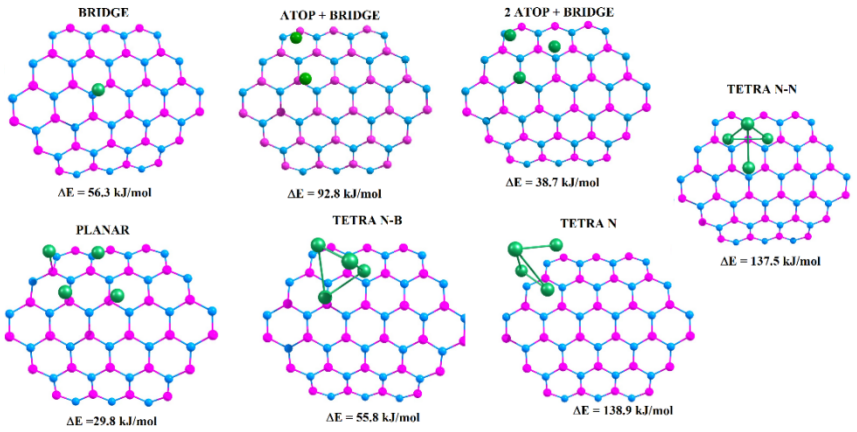

Fig. 1. Optimized structures and interaction energies, characterizing Pd_n/BNNT systems

These peculiar interactions are particularly significant in the Pd_4 planar structure in which a mixed endo/exocyclic coordination of the cluster with the BNNT surface is observed. Simulation of a massive Pd_{30} cluster suggests that the BNNT could decisively affect the geometry of the supported particles: indeed, the global effect of the adsorption onto the BNNT can be described as a screw displacement of the [100] plane toward the [111]. Moreover, the BNNT support exerts an electron donating effect on the cluster. The effects above would seem to be important in the description of the catalytic properties of the BNNT systems. As an example, the adsorption process of one D-glucopyranose molecule on the cluster is less favoured if the Pd_{30} is supported on the BNNT. With respect of this, it is thus reasonable to infer that the negative charge, which might be confined on the Pd_{30} cluster is pretty limited hence the BNNT support could consistently affect the adsorption of electron donating species on the same cluster.

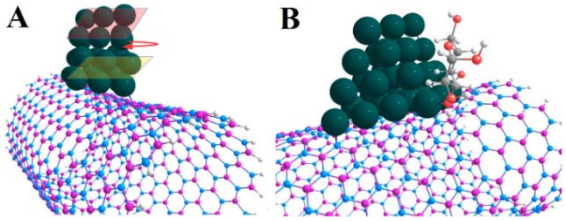

Fig. 2. **A**) "Screw" displacement of the 100 plane of the cluster toward the 100; **B**) Optimized structure of a D-glucopyranose molecule on the supported Pd_{30}

4 Conclusions

The interaction of Pd_2, Pd_3, Pd_4 and Pd_{30} clusters with BNNT surface was studied by means of a computational approach. It has been showed that the adsorption process is moderately exoergic; the geometry of the clusters is largely depending on the considered spin state. Furthermore, the BNNT clearly affects the supported metallic cluster structures, which results quite different with respect of those unsupported, *i.e.* optimized *in vacuum*. This effect is much more relevant for the larger clusters. On the latter, indeed, i) a rearrangement of the [100] and [111] planes and ii) a negative charge enrichment occur. These phenomena could promote a detrimental effect on the adsorption of the D-glucopyranose molecule on the Pd_{30} cluster.

References

[1] M. Terrones, J. M. Romo-Herrera, E. Cruz-Silva, F. López-Urías, E. Muñoz-Sandoval, J. J. Velázquez-Salazar, H. Terrones, Y. Bando, D. Golberg, *Mater. Today*, 10 (2007) 30.
[2] N. Meyer, D. Pirson, M. Devillers, S. Hermans, *Appl. Catal. A.* 467 (2013) 463.
[3] N. Meyer, M. Devillers, S. Hermans, *Catal. Today*. 241 (2015) 200.
[4] A. Prestianni, M. Crespo-Quesada, R. Cortese, F. Ferrante, L. Kiwi-Minsker, D. Duca, *J. Phys. Chem. C* 118 (2014) 3119.

II-PP33

Peculiarities of Controlled Synthesis of Highly Efficient Cu-Containing Catalyst for Methanol Synthesis

Minyukova T.P.[1], Khassin A.A.[1,2], Yurieva T.M.[1*]

1 - Boreskov Institute of Catalysis SB RAS, Novosibirsk, Russia
2 - Novosibirsk State University, Novosibirsk, Russia

* min@catalysis.ru

Keywords: Cu catalysts, methanol synthesis

1 Introduction

Catalytic methanol synthesis from carbon oxides and hydrogen is a key step of natural gas conversion to valuable organic compounds and polymers. Nowadays the world production of methanol is over 60 million tons per year. The composition and the method of preparation of the Cu-Zn-Al methanol synthesis catalysts are almost unchanged during last 50 years and close to the initially proposed by ICI. However, the structure of the catalyst and its active state, as well as the mechanism of methanol synthesis are still the challenges further investigation. This paper reports the experimental data about the nature of the active component, the structural features of precursors and the active state of Cu-Zn-containing methanol synthesis catalysts.

2 Experimental/methodology

CuZnAl(Cr) catalysts precursors of different composition have been obtained by coprecipitation method, that provides complete chemical interaction of the components in the form of hydroxocompounds (HOCs) and high reproducibility of their properties. HOCs and the products of their thermal treatment and reductive activation were thoroughly studied with a large set of modern physico-chemical methods: XRD, including *in situ* XRD, DTA, EM, IR. Catalytic behaviour was tested in the laboratory flow reactor at 1 atm.

3 Results and discussion

The results presented in Table 1 evidence that both in Al- and Cr-containing samples HOCs of different structure are formed. The conditions of coprecipitation and quantitative ratio of the components determine the composition and structure of HOC. The chosen composition and conditions provided obtaining of homogeneous model samples of hydrozincite, aurichalcite and hydrotalcite structure. Their thermal decomposition results in the oxide compounds formation, which are solid solutions on the base of anion-modified oxides - ZnO* (wurtzite-type) and spinel*. The reductive activation of solid solutions leads to the formation of Cu^0 nanoparticles on the surface of hard-to-reduce oxides. As it is seen from Table 1, the catalytic activity of these Cu^0 nanoparticles differ significantly. The most active are the catalysts on the base of aurichalcite-type precursor. The same catalysts are the most stable.

The detailed study of the products of thermal decomposition and reductive activation of CuZnAl(Cr) HOCs of aurichalcite structure has been performed. Figure 1 presents the micrograph of reduced at 220^0C in hydrogen CuZnO sample. Nanoparticles Cu^0, epitaxially bonded to the ZnO surface, are clearly visible. Their stability in reductive atmosphere depends on the Al(Cr) presence and restricted to 380-400^0C.

Table 1. Cu^0 species and hydroxo- and oxo- precursors compounds, methanol synthesis rates at 220^0C, 1 atm, reaction gas CO : CO_2 : H_2 = 20 :5 : 75 ($C_{MeOH} = 1 \cdot 10^{-3}$ vol.%).

Hydroxo- and oxo precursor (at.fraction)	Cu-mode	W, mmol MeOH/g/h
Hydrozincite ($Cu_{0.08}Zn_{0.92}$) ── CuZnO* (W)	Cu^0/ZnO	5.5
Hydrozincite ($Cu_{0.20}(Al/Cr)_{0.15}Zn_{0.65}$) ──CuZnO(Al/Cr)* (W)	Cu^0/ZnO(Al,Cr)	8.0
Aurichalcite ($Cu_{0.40}(Al/Cr)_{0.15}Zn_{0.45}$) ── CuZnO(Al/Cr)* (W)	Cu^0/ZnO(Al, Cr)	16.0
Hydrotalcite ($Cu_{0.33}Al/Cr_{0.67}$) ── $Cu(Al/Cr)_2O_4$* (spinel)	Cu^0/spinel	0.3

*- a.m.ZnO solid solution;
W - wurtzite type ZnO

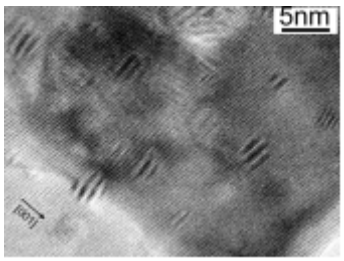

Fig.1 HR-TEM micrograph of metallic Cu nanoparticles epitaxially bonded to ZnO (note the characteristic Moire fringes due to mismatch of interatomic distances in the epitaxial phases) in the Cu-Zn oxide after its reduction in hydrogen at 220^0C.

4 Conclusions

The obtained results and recently published data suggest that the active state of Cu-Zn-containing methanol synthesis catalysts is an extremely complicated system, which includes defective metallic particles that strongly interact with the supporting defective ZnO phase in the form of epitaxial bonding and are at least partially decorated by amorphous oxide overlayer [1, 2]. Both the metallic nanoparticles and the oxide support have mixed (Cu-Zn) composition and are defective. $Al^{3+}(Cr^{3+})$ cations are not merely structural promoter, however, directly affect the specific activity of the active sites.

The intimate interaction of Cu-Zn species may only be possible as the result of their genesis from mixed Cu-Zn oxide phases. Solubility Cu^{2+} in ZnO* can be dramatically increased by anionic modification of the mixed oxide structure. Promotion of the oxide structures by small quantities of $Al^{3+}(Cr^{3+})$ cations can further expand solubility ranges and thermal stability of the catalyst. Evolution of anionic admixtures due to overheating the mixed oxide beyond the threshold of their thermal stability (*ca.* 380-400^0C) leads to decomposition and recrystallization of mixed oxides, causing the decrement of the catalytic activity in methanol synthesis. The most natural way for production of anion-modified mixed oxide is decomposition of mixed hydroxycarbonates at moderate temperatures.

Acknowledgements

Programme of Presidium of Russian Academy of Sciences #V.45.8.11 and basic research project V.45.3.6 of RAS for financial support. Prof. L.M.Plyasova, Dr. V.I.Zaikovskii, Mrs.M.P.Demeshkina for their help.

References

[1] A.A. Khassin, T.P. Minyukova, T.M. Yurieva. *Mendeleev Commun.,* 24(2) (2014) 67.
[2] M.Behrens, F.Studt, I.Kasatkin, S.Kühl, M.Hävecker, F.Abild-Pedersen, S.Zander, F.Girgsdies, P.Kurr, B.-L.Kniep, M.Tovar, R.W.Fischer, J.K.Nørskov, R.Schlögl // *Science*. 336 (2012) 893.

II-PP34

Effect of Catalyst Preparation on the Selective Hydrogenation of Canola Oil Over Low Percentage Pd/Diatomite Catalysts

Auyezov A.B.[1*], Toshtay K.[1,2], Yeraliyeva A.T.[1], Bizhanov Zh.A.[1], Toktasinov S.K.[1], Kudaibergen B.[1], Nurakyshev A.[1]

1 - DSE «Scientific Technology Park», RSE «Al-Farabi Kazakh National University», Almaty, Republic of Kazakhstan

2 - Kazakh-British Technical University, Almaty, Republic of Kazakhstan

* auyezov_ali@mail.ru

Keywords: hydrogenation, diatomite, trans-isomers, Pricat-9910, palladium, catalyst, canola oil

1 Introduction

The hydrogenation of vegetable oils is an important practice in the modifications of fats and oils. Catalytic hydrogenation of vegetable oil has seen a lot of advances recent years, especially regarding efforts to reduce the *trans*-fatty acids (TFA). High intake of TFA has been associated with increased risk of coronary heart disease, diabetes mellitus and decrease HDL-cholesterol and promote inflammation [1-2]. Nowadays, Ni-catalysts are most commonly used for vegetable oils hydrogenation in industrial hydrogenation. It is carry out high temperature (180-230°C), this conditions of hydrogenation using Ni catalysts promote the formation of *trans*-isomers and products of thermal decomposition of fatty acids. Nickel tend to be dissolved in the oil to form corresponding salts, its salts may lead to the cause product toxicity. For hydrogenation vegetable oils reaction many researches shows that nickel catalysts are not very active below 130°C. Palladium catalysts are active at low temperature of 70°C and decreased *trans*- fatty acids in hydrogenation of vegetable oils. Therefore, the main challenge in developing new technologies obtain pure product is to the replacing the nickel catalyst with palladium catalyst can be more efficient and real prospects [3-6].

In this research work new low content palladium catalysts supported on diatomite were synthesized, investigated for good support qualities, and tested for their hydrogenation activity on vegetable oil in laboratory and experimental-industry testing. The results are compared to those obtained over a commercial nickel catalyst (Pricat-9910).

2 Experimental/methodology

In this study, we choose a catalyst support using diatomite. The raw diatomites obtained from Aktobe/Kazakhstan and chemical treatment was performed with hydrochloric acid. Then, 0.2% palladium supported on diatomite was prepared by the adsorption method, investigated for good support qualities, and tested for their hydrogenation activity on canola oil. Pilot testing hydrogenation process carried out in 10t of capacity batch reactor at 90°C and pressure of hydrogen 0.5MPa by using 0.2% Pd/D catalyst and compared to commercial nickel catalyst (Pricat-9910) at 150°C and 0.5MPa. The fatty acid composition of the hydrogenated canola oil was determined by gas chromatography (GC). Iodine values and melting point were determined. Solid fat content (SFC) determined using nuclear magnetic resonance (NMR) spectrometry, taking readings from samples in at temperature 10, 20, 30 and 40°C.

3 Results and discussion

The commercially refined and bleached canola oil used in this work. The calculated iodine value (IV) was 133. Acid value - 0.26±0.01 mg KOH/g, peroxide value - 8.7±0.2 meq. of

oxygen/kg, and content of phosphorus - 5±1 mg/kg of oil.

It was canola oil used in industrial pilot hydrogenation. Pilot testing of palladium catalyst for hydrogenation of canola oil was carried out on LTD "Maslo-Del" (Almaty city) oil and fat factory. The fatty acid composition at hydrogenation process is listed in table 1 and solid fat content figure 1.

Table 1. The composition of fatty acids partial hydrogenated canola oil over low percentage palladium catalyst and commercial Ni catalyst

Catalysts	T, °C	IV*	Melting point, °C	Fatty acid composition, %					*Trans*-isomers, %
				$C_{16:0}$	$C_{18:0}$	$C_{18:1}$	$C_{18:2}$	$C_{18:3}$	
Feedstocks	-	128.9	-	6.6	3.0	38.5	33.2	14.1	1.4
Pricat-9910	150	78.5	33.0	9.5	8.8	65.6	11.3	-	20.5
0.2% Pd/D	90	72.4	32.6	8.7	9.9	67.5	5.6	-	13.4

On table 1, pilot tests and analysis of products shows that low percentage palladium catalyst is able to carry out the process at lower temperature than the commercial nickel catalyst. Hydrogenation at lower temperature and pressure can minimizes the isomerization of a *cis*- to *trans*-isomer double bond conformation. The results of the chromatographic analysis of products show that *trans*-isomers content was reduced at 1.5 times as palladium catalyst is compared with nickel catalyst.

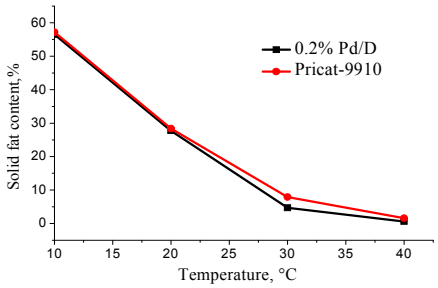

Fig.1. Hydrogenated canola oil SFC curve depending on the temperature

Figure 1 shows physical parameters of products such as solid fat content obtained from both catalysts are the same. Also, other parameters like melting point and iodine values are the same too.

4 Conclusions

A low percentage of palladium catalyst is more effective and highly selective in hydrogenation of canola oil. Palladium catalysts are active at low temperature of 90°C and decreased *trans*-fatty acids in hydrogenation of vegetable oils than nickel catalyst.

References

[1] A. Valenzuela, N. Morgado. *Biol Res*. (1999); 32:273-287.
[2] D. Mozaffarian, M.B. Katan, A. Ascherio. Engl. J. Med. 354 (2006) 1601–1613.
[3] K. Belkacemi, A. Boulmerka, J. Arul, and S. Hamoudi, Catal., (2006). vol. 37, p. 113–120.
[4] M. Plourde, K. Belkacemi, J. Arul, Ind. Eng. Chem. Res. 43 (2004) 2382–2390.
[5] M. Plourde, K. Belkacemi and J. Arul, Ind. Eng. Chem. Res., (2004). 43: p. 2382-2390.
[6] B. Nohair, C. Especel, G. Lafaye, J. Mol. Catal. A: Chem., (2005). 229 (1-2): p. 117-126.

II-PP35

Metal-Free N-Doped Carbon Networks as Hydrogenation Catalysts: a Computational Study

Cortese R.*, Ferrante F., Duca D.

Università degli Studi di Palermo, Dipartimento di Fisica e Chimica, Palermo, Italy

* remedios.cortese@unipa.it

Keywords: metal-free, hydrogenation catalysts, N-doped carbon, frameworks, DFT

1 Introduction

The development and assessment of a future industry more environmentally-friend will include the use of metal-free catalysts. Most of the reported metal-free catalysts are homogeneous and, as a consequence, their recycle is often difficult. Therefore, the development and investigation of heterogeneous metal-free catalysts is of great interest both theoretically and experimentally. N-doped nanotubes and graphene sheets were recently synthesized. [1,2] With respect of these, it was demonstrated that the incorporation, within the carbon structures, of nitrogen atoms causes a larger electron mobility and introduces more active sites for catalytic reactions. The nitro- and cyano-moieties were experimentally compared toward hydrogenation catalyzed by these new-generation doped materials, founding that although the former is in any case hydrogenated the latter does not show any reactivity [3]. The present investigation is aimed at elucidating the main features of the hydrogen fragmentation over these carbon frameworks and subsequently the hydrogenation mechanism potentially involved when nitro- and cyano-moieties over N-doped carbon networks are considered.

2 Experimental/methodology

Several models and different theoretical approaches were employed in this study, to characterize the structural and energetic properties of nitrogen pyridinic moieties framed within a carbon network, commonly classified as pyridinic defects. Two different kinds of pyridinic defect configurations within a carbonaceous environment, here referred as 4N and 3N sets of defects were studied. The species belonging to the 4N set were obtained by removing two carbon atoms from the carbonaceous framework and substituting the four unsaturated carbon atoms formed by an equivalent number of nitrogen atoms. To form a 3N defect, conversely, one carbon atom was removed and the resulting three unsaturated carbon atoms were replaced by three nitrogen atoms. Three different model classes were employed in the here investigation. The classes above may be identifiable as molecular, truncated nanotubes, and periodic nanotubes.

The calculations on the first and second class of models were carried out by employing the Gaussian 09 code package whereas the third one was managed using the SIESTA method as implemented in the homonymous code. Molecular models were analyzed within the density functional theory (DFT) framework, using as exchange-correlation functionals both the hybrid B3LYP and the new-generation hybrid M06-2X joined with the correlation-consistent polarized double zeta basis set cc-pVDZ. Truncated nanotube models were finally treated employing a hybrid QM/MM approach using the ONIOM energy extrapolation scheme. DFT was employed as higher level, by using the same computational specifications employed for the molecular models, and UFF as lower level.

3 Results and discussion

The title study can be here summarized into three main issues: i) the analysis of hydrogen fragmentation on N-doped carbon network models, bearing 3N and 4N defects, [4] ii) the

adsorption of nitro- and cyano-moieties on hydrogenated N-doped carbon networks models containing 3N defects and, finally, iii) the search of the catalytic hydrogenation pathways involving the C_6H_5-NO_2 and C_6H_5 -CN molecules (see Fig. 1).

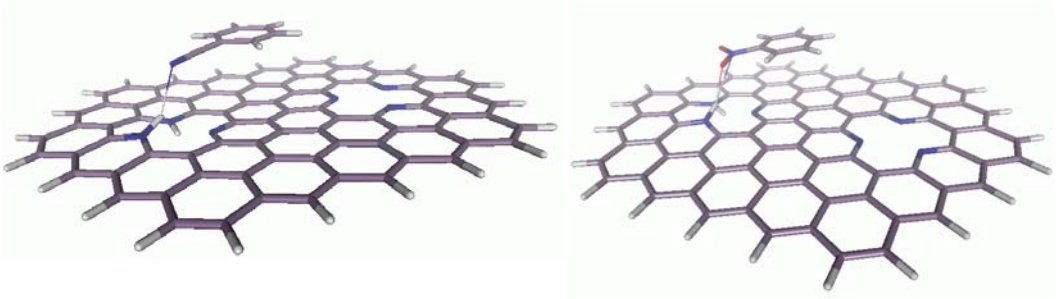

Fig. 1. Adsorption of C_6H_5 -CN and C_6H_5-NO_2 on hydrogenated 3N carbon framework models.

The H_2 fragmentation ergonicity was studied on all the carbon networks models containing 4N as well as 3N defects. This analysis was performed studying the ergonicity as a function of both i) the size of the π-system, surrounding the N-defect and ii) the curvature of the carbon network. On the ground of the performed analyses, it was found that all the N-defect arrangements considered give rise to largely exergonic H_2 fragmentation while the characteristics of the π-systems, surrounding the N-defects, affect the H_2 activation and chemisorption processes, increasing the transformation exergonicity with increasing the size and regularity of the aromatic environment. Moreover, the different N-defect topologies influence the H_2 fragmentation and activation processes while the carbon framework curvature seems to have only limited influence on the energetics. Concerning the reactivity of C_6H_5-NO_2 and C_6H_5 -CN molecules, it was found that the adsorption process of the two molecules is largely different: a more pronounced adsorption energy on the hydrogenated N-doped carbon network was indeed found for the C_6H_5-NO_2 with respect to the C_6H_5-CN molecule. These adsorption properties very probably are related to the occurrence of their pretty different reported reactivity.

4 Conclusions

The H_2 fragmentation was analyzed on different carbon networks containing pyridinic defects. The influence of the π-system characteristics as well as of the nanotube curvature on the ergonicity associated to the H-H cleavage on these metal-free catalysts was investigated and important insights within the hydrogenation reactions of the C_6H_5-CN and C_6H_5-NO_2 were gained.

Acknowledgements

This work was supported by the POLYCAT project funded by the 7th Framework of the European Community: G.A. No CP-IP 246095; http://polycat-fp7.eu/

References

[1] H. Wang, T. Mayalagan, X. Wang, ACS Catal. (2012) 1052
[2] H. Xingbang, Z. Zheng, L. Qiuxing, W. Youting, Z. Zhibing, Chem. Phys. Lett. (2011) 287
[3] A. Wolf, M. Volker, J. Assman, L. Mleczko, DE102008028070 pat. (2009)
[4] R. Cortese, F. Ferrante, S. Roggan, D. Duca, Chem. Eur. J. doi:10.1002/chem.201405896

II-PP36

Enhanced Catalytic Performance of Ni-Fe Alloy in Methane Dry Reforming: Role of Fe

Theofanidis S.A.*, Galvita V.V., Poelman H., Marin G.B.

Ghent University, Laboratory for Chemical Technology (LCT), Ghent, Greece

* StavrosAlexandros.Theofanidis@UGent.be

Keywords: Ni-Fe alloy, effect of Fe, methane dry reforming, *in-situ* XRD, carbon formation

1 Introduction

Methane reforming processes are currently used to produce syngas or hydrogen. Due to increasing demands for H_2 and syngas applications, the role of these processes has recently become more important. Methane dry reforming ($CH_4 + CO_2 \leftrightarrow 2CO + 2H_2$) converts two greenhouse gases into valuable chemicals and offers the attractive advantage of a H_2/CO molar product ratio close to one, suitable for widespread use in many industrial processes (Fischer-Tropsch synthesis, etc) [1].

Conventional catalysts for methane dry reforming are Ni supported over oxides such as Al_2O_3, SiO_2, MgO. Despite the large variety of catalysts currently in use, the rapid deactivation caused by sintering of the active metal and by carbon formation remains the major challenge of this reaction. Carbon deposition results from methane decomposition ($CH_4 \rightarrow C + 2H_2$) and/or Boudouard reaction ($2\ CO \rightarrow C + CO_2$). Alloying Ni with other metals can improve the catalytic performance and one suitable modifier is Fe [2]. Iron species have good redox properties, like CeO_2 [3]. Previously an improved performance was reported in the steam reforming activity of Ni–Fe/Al_2O_3 catalysts, due to Ni–Fe alloy formation [4].

In order to investigate the effect of Fe on Ni/$MgAl_2O_4$, a series of Fe-Ni /$MgAl_2O_4$ catalysts are tested. One aspect that awaits clarification is whether and how the Ni-Fe alloy contributes to the elimination of carbon deposition during methane reforming. Further, the mechanism for dry reforming over a Ni-Fe catalyst is not clear. These questions are addressed in this study by performing in-situ X-ray diffraction (XRD) characterization of Ni-Fe/$MgAl_2O_4$ catalysts during H_2 temperature-programmed reduction (H_2-TPR), CO_2 temperature-programmed oxidation (CO_2-TPO) and dry reforming. Alternate pulses are also applied by switching the flow between CO_2, inert He and CH_4 over a Ni/$MgAl_2O_4$, Fe/$MgAl_2O_4$ and Fe-Ni/$MgAl_2O_4$ catalysts.

2 Experimental

Catalyst preparation. Four Ni-Fe catalysts were prepared by incipient wetness impregnation on the support ($MgAl_2O_4$) using an aqueous solution of corresponding nitrates. The catalysts were dried at 393 K for 12h and subsequently calcined in air at 1023 K for 4 h. The Ni loading was maintained at 8wt%, while the Fe loading was varied from 0 to 5, 8 and 11wt% as it is shown at Table 1.

In-situ time resolved XRD. In-situ XRD measurements were performed in a home-built reaction chamber housed inside a Bruker-AXS D8 Discover apparatus (Cu Kα radiation of 0.154 nm). The reactor chamber had a Kapton foil window for X-ray transmission. The setup was equipped with a linear detector covering a range of 20^o in 2θ with an angular resolution of 0.1^o. The pattern acquisition time was approximately 10 s.

3 Results

During H_2-TPR, Fe_2O_3 and NiO were reduced above 973K to form a Ni-Fe alloy (Figure 1A), which constitutes the active phase for the methane dry reforming reaction. This

alloy remained stable in a flowing gas stream of CO_2 during re-oxidation (Figure 1B), until 900 K, but was decomposed to metallic Ni and Fe_3O_4 above this temperature.

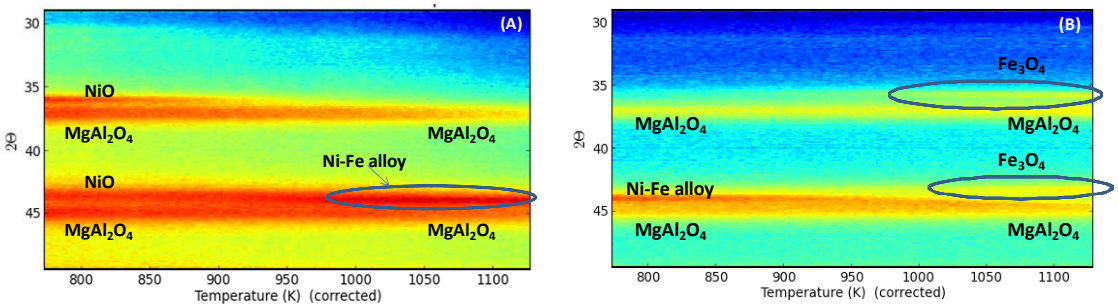

Figure 1. 2D XRD pattern for Ni/Fe=0.7 (A) Alloy formation during H_2-TPR. Conditions: maximum temperature= 1123 K, heating rate: 30 K/min, flow rate: 60 ml/min, 10%H_2/He. (B) Alloy decomposition during CO_2-TPO. Conditions: maximum temperature=1123 K, heating rate: 30 K/min, flow rate: 60 ml/min

The effect of Fe addition to the activity of a Ni/$MgAl_2O_4$ catalyst, under methane dry reforming reaction conditions was found to depend on the employed Ni/Fe ratio. Activity measurements indicated that Fe/Ni=0.7 mol/mol presented a high selectivity towards CO and a CO/H_2 ratio close to unity. Even though lower Ni/Fe ratios led to lower CO/H_2 values, the latter were still higher than those resulting from Ni/$MgAl_2O_4$. Furthermore, the implementation of regeneration cycles showed that the catalyst activity can be restored. Lower amounts of accumulated carbon were observed after reaction on Fe-promoted samples compared to the Ni/$MgAl_2O_4$ sample.

Alternate CH_4 and CO_2 pulses in combination with in-situ XRD allowed to determine the mechanism of methane dry reforming over Ni-Fe catalyst. Mars-Van Krevelen mechanism can describe this reaction where CO_2 oxidizes Fe to FeO_x (Eq. 1), and CH_4 is activated on Ni sites to form H_2 and surface carbon (Eq. 2). The latter was reoxidized by lattice oxygen from FeO_x, producing CO (Eq. 3).

$$Fe + CO_2 \rightleftharpoons FeO_x + CO \quad (1)$$

$$CH_4 \xrightarrow{Ni} C + 2H_2 \quad (2)$$

$$FeOx + C \rightleftharpoons xCO + Fe \quad (3)$$

Acknowledgements

This work was supported by the FAST industrialization by Catalyst Research and Development (FASTCARD) project, by the "Long Term Structural Methusalem Funding by the Flemish Government" and the Interuniversity Attraction Poles Programme, IAP7/5, Belgian State – Belgian Science Policy. The authors acknowledge support from Prof. C. Detavernier with the in situ XRD equipment (Department of Solid State Sciences, Ghent University) and from Dr. Vitaliy Bliznuk (Department of Materials Science and Engineering, Ghent University) for the HRTEM measurements.

References

[1] D. Pakhare, and J. Spivey, Chemical Society Reviews 43 (2014) 7813-7837.
[2] J. Ashok, and S. Kawi, ACS Catalysis 4 (2014) 289-301.
[3] A.S. Bobin, V.A. Sadykov, V.A. Rogov, N.V. Mezentseva, G.M. Alikina, E.M. Sadovskaya, T.S. Glazneva, N.N. Sazonova, M.Y. Smirnova, S.A. Veniaminov, C. Mirodatos, V. Galvita, and G.B. Marin, Topics in Catalysis 56 (2013) 958-968.
[4] L. Wang, D. Li, M. Koike, S. Koso, Y. Nakagawa, Y. Xu, and K. Tomishige, Applied Catalysis A: General 392 (2011) 248-255.

II-PP37

Hybrid SILP Catalysts Based on Carbon Materials

Rufete-Beneite M, Roman-Martinez M.C.*, Adsuar-Garcia M.D., Linares-Solano A.

Department of Inorganic Chemistry. University of Alicante, Alicante, Spain

* mcroman@ua.es

Keywords: SILP, catalysts, carbon materials, Rh, complex, hydrogenation, hybrid catalysts

1 Introduction

SILP ("Supported Ionic Liquid Phase") catalysts constitute a way to prepare hybrid catalysts in which the active phase (frequently a metal complex) is dissolved in a supported IL phase, avoiding thus important chemical or geometrical modifications. The hybrid condition arises from the combination of significant properties of homogeneous and heterogeneous catalysis. In brief, the advantages of SILP catalysts are [1]: (i) concomitant use of ILs, (ii) high catalytic activity owing to a uniform distribution of catalytic active species within the SILP, and (iii) easy separation from the reaction products for further reusability. Carbon materials have proved to be suitable catalysts supports [2] and they can also be appropriate for SILP systems [3]. This is because they can be prepared with large surface areas, tuned porosity and surface chemistry, and variable morphology. This allows, thus, a broad variety of arrangements and interactions of the IL within the support surface. The present work deals with the preparation of SILP catalysts with a Rh complex as active species, using several carbon materials as support and different IL loadings. The purpose is to study the effect of the support properties and of the amount of IL in the catalysts activity and stability, tested in the hydrogenation of cyclohexene.

2 Experimental/methodology

The carbon materials used in this work are: i) GeA: Spherical shaped activated carbon (Gun-ei Chemical Industry (Japan)), with average diameter of 150 μm. ii) KA: Spherical shaped activated carbon (Kureha Corporation (Japan)), with average diameter of 780 μm. iii) T: Carbon black T-10157 from Columbian Chemical Company (USA) and iv) SA: Powder activated carbon SA-30 from MeadWestvaco (USA).The ionic liquid used in this work is 1-butyl-3-methyl-imidazolium hexafluorophosphate ([bmim][PF_6]) supplied by Solvionic and the Rh complex was chloro(1,5-cyclooctadiene)rhodium(I) (RhCOD).

The catalysts were prepared inside a Schlenk system as follows: about 0.5 g of the carbon material were degassed in vacuum at 150 °C for 5 h; after cooling, variable amounts of ionic liquid and the required amount of Rh complex to obtain 1 wt% Rh, mixed with 2 mL acetone, was added to the outgassed solid and the system was kept under Ar atmosphere and stirring until the sample took on a dry aspect.

Conditions of the activity experiments are: 10 mL of 5 vol% cyclohexene in toluene, 30 mg catalyst, 10 bar $H_2$and 333 K. Reusability tests were performed under the same conditions with the catalysts recovered by filtration. Homogeneous and biphasic tests were carried out dissolving the required amount of the RhCOD complex in toluene or in the amount of IL equivalent to that loaded in the hybrid catalysts, respectively. Analysis was carried out by gas chromatography.

3 Results and discussion (font style: Times New Roman bold 12pt)

Figure 1 shows conversion data obtained with some of the catalysts prepared and with homogeneous and biphasic systems having a similar amount of Rh complex.

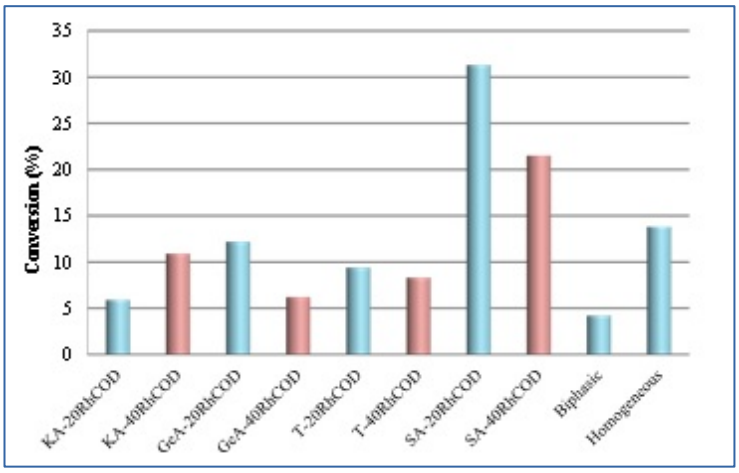

It can be observed that the biphasic system is less active than the homogeneous one, meaning that the ionic liquid hinders the access to the active phase. However, the SILP catalysts are more active than the biphasic system. It is interesting that there is a very important effect of the support and it must be pointed out that the two SA based catalysts (with 20 a 40% IL)are more active than the complex in homogeneous phase. Regarding the IL loading, it seems that 20% gives better results than 40%, and this is agreement with the mentioned effect of the IL to hinder the access to the active phase.

Upon use, the catalysts lose a certain amount of IL, higher in the catalysts with 40% IL and also dependent on the support. Rh leaching is negligible and thus it can be concluded that the reaction takes place with the heterogenized complex. Table 1 includes data about IL leaching. The catalysts were tested in two consecutive catalytic runs and they showed to be recyclable.

	leaching(%)		**leaching(%)**
Catalyst	**IL**	**Catalyst**	**IL**
KA20-RhCOD	48	KA40-RhCOD	65
GeA20-RhCOD	25	GeA40-RhCOD	72
SA20-RhCOD	17	SA40-RhCOD	24
T20-RhCOD	5	T40-RhCOD	45

Table 1. IL leaching after use in cyclohexene hydrogenation.

4 Conclusions

Hybrid SILP catalysts prepared with carbon materials as support have shown to be active and reusable in the hydrogenation of cyclohexene, being with a given support much more active than the homogeneous one. There is a notable effect of the support properties on the catalytic activity.

Acknowledgements

The authors thank the financial support through public projects of reference: MAT2012-32832 and PROMETEO/II/2014/01

References

[1] T. Selvam, A. MacHoke, W. Schewieger, *Applied Catalysis A* 445-446 (2012) 92-101.
[2] E. Auer, A. Freund, J. Pietsch, T. Tacke, *Applied Catalysis A* 173 (1998) 259-271.
[3] M. Rufete-Beneite, M.C. Román-Martínez, A. Linares-Solano, *Carbon*77 (2014) 947-957.

II-PP38

Influence of the Support Nature on Palladium Activity in Liquid-Phase Hydrogenation of C=C Bond in Molecules with Polar and Non-Polar Substituents

Kulagina M.A.[1,2*], Simonov P.A.[1,3], Romanenko P.A.[1], Kvon R.I.[1], Gerasimov E.Yu.[1]

1 - Boreskov Institute of Catalysis SB RAS, Novosibirsk, Russia
2 - Research and Educational Center for Energy Efficient Catalysis in Novosibirsk National Research University, Novosibirsk, Russia
3 - Novosibirsk National Research University, Novosibirsk, Russia

* kulagina_ma92@mail.ru

Keywords: supported palladium, liquid-phase hydrogenation, maleic, acid, cyclohexene, support effect

1 Introduction

The phenomenon of metal-support interaction and its influence on the performance of supported metal catalysts is commonly associated with an electron transfer between the metal and the support. However, for the case of liquid-phase reactions, their specific activity (i.e. turnover frequency – TOF) seems to be also affected by the liquid-solid interface structure which is dependent on both the nature of the catalyst constituents and the solution composition [1]. In our first paper [2], we succeeded in preparing a set of highly dispersed palladium catalysts supported on different inorganic powders (oxides, carbons, salts) with low specific surface areas (less than 20 m^2/g) to avoid diffusion limitations in their pores during catalytic testing. We revealed the TOF values for palladium nanoparticles in hydrogenation of C=C bond of maleic acid (**MA**) in water at 50°C to decrease with increasing effective charge of the cations forming oxide supports. Though this fact could be attributed (from the classical point of view) to modification of metal electronic state under action of the cation's electric field, an influence of the catalyst-solution interface structure on the catalytic activity remained unclear.

This work aims at investigating the catalytic effects caused by the existence of the electric double layer (EDL) at the catalyst surface, which is formed due to the difference between aqueous solution pH and pH_{IEP} of the supports. This layer might hamper the diffusion of ionized MA molecules to the active sites of the catalyst. For comparison, catalytic hydrogenation of non-polar unsaturated molecules (cyclohexene – CH) in solvents with relatively low dielectric constants (aliphatic alcohols) was also investigated. This reaction is known to be structure insensitive [3] and no EDL formation can be expected under its conditions.

2 Experimental/methodology

Supports' texture properties (pore volume, S_{BET}) were investigated by low-temperature N_2-adsorption. Zetasizer Nano ZSP was used to measure ζ-potential values for the support particles in water. Procedure of the supported palladium catalysts (0.5 wt% Pd) preparation by hydrolysis of H_2PdCl_4 in basic media was described in ref. [2]. Dispersion of Pd particles was determined by XRD, TEM and CO-chemisorption methods. The electronic state of the supported metal was characterized by XPS using SPECS and ESCA HP spectrometers.

Catalytic tests were carried out in 100 ml jacketed glass reactor under static conditions at 2°C (CH)/50°C (MA) and P_{H2} = 1 atm (1200 rpm, 7-40 mg of the charged catalyst, 6 ml of the substrate solution). Concentration of CH in anhydrous methanol or 96% ethanol was 0.32 M and MA in water 0.2-1.5 M. The catalysts were pre-reduced in the reactor with 2 ml of the solvent at 50°C before testing. The reaction rate values were calculated from the time-dependences of H_2 uptake.

3 Results and discussion

1. No explicit interrelations between electronic state of Pd particles (according to XPS), pH_{IEP} of the supports and TOFs of the catalysts in CH and MA hydrogenation were found.

2. TOF values of the palladium catalysts in CH hydrogenation depend on the support nature but not the solvent (Table 1).The latter fact agrees with conclusions previously mentioned in ref. [3]. Otherwise the support-dependence has been revealed for the first time and now it cannot be strictly attributed to Pd particle size or support material type. Also within alumina-supported catalysts decrease of TOFs with increasing S_{BET} of the supports (Table 1, samples nos. 7-9) for both CH and MA hydrogenation reactions is observed. Note that the apparent activation energy of the reaction falls down to zero for the porous aluminas. Addition of up to 10 wt% water in alcohol solvent in CH hydrogenation doesn't result in changing of TOFs.

3. Unlike to regularities of MA hydrogenation in water, TOF values of the Pd catalysts in CH hydrogenation in alcohols don't regularly vary with effective charges of oxide supports'cations, emphasizing that their electric field is not the only TOF-determining factor.

4. For both catalytic processes, TOF values of the related catalysts don't depend on Pd dispersion if the catalysts are subjected to low-temperature reduction (<150°C) with H_2, however, sintering of Pd in H_2 at 400°C leads to structure sensitivity of CH hydrogenation, probably due to the manifestation of the strong metal-support interaction.

Table 1. Catalytic activity of 0.5% Pd/Support catalysts in hydrogenation reactions in different solvents.

No.	Support	S_{BET}, m^2/g	d_s (Pd), nm	TOF values (s^{-1})		
				CH hydrogenation		MA hydrogenation
				ethanol	methanol	water [2]
1	In_2O_3	3.9	6.0	11.8	10.3	0.6
2	TiO_2	1.9	8.3	9.0	9.0	2.9
3	Kieselguhr (SiO_2)	1.7	5.1	7.4	7.4	3.1
4	Carbon Black T-900	8.0	5.1	3.5	3.3	7.3
5	Sibunit 159	11.6	3.3	6.2	7.4	8.6
6	ZrO_2	14.3	1.5	2.9	2.0	0.9
7	α-Al_2O_3	10.6	2.0	6.6	3.7	3.0
8	γ-Al_2O_3Reachim	105	1.2	2.3	2.1	1.4
9	γ-Al_2O_3Puralox	200	1.4	1.3	0.9	1.2

4 Conclusions

Palladium catalysed liquid-phase hydrogenation of C=C bonds of CH and MA is governed by the nature of the catalyst support. Electronic state of Pd apparently isn't a parameter directly influencing the catalyst activity. As hydrogenation of non-polar molecule (CH) occurs without EDL formation the cause of its support-dependence could be found in different wettability of support material surface by solvent molecules. The structure sensitivity of the reactions occurs only after high-temperature reduction of Pd with H_2 at 400°C.

Acknowledgements

The authors are grateful to the Russian Foundation for Basic Research for providing financial support (Project 13-03-00689). The work was also supported by the Skolkovo Foundation (Grant Agreement for Russian educational organization №1 on 28.11.2013).

References

[1] V. Ponec, G.C. Bond, *Stud. Surf. Sci. Catal,* 95(1995).

[2] M.A. Kulagina, E.Yu. Gerasimov, T.Yu. Kardash, P.A. Simonov, A.V. Romanenko, *Catal. Today* doi:10.1016/j.cattod.2014.07.048.

[3] E.E. Gonzo, M. Boudart, *J. Catal.* 52 (1978) 462-471.

II-PP39

Electrochemical Alternating Current Synthesis of Composite Materials for Catalysis

Smirnova N.V.[1*], Kuriganova A.B.[1], Leontyeva D.V.[1], Novikova K.S.[1], Barbashova A.A.[1], Doronkin D.E.[2]

1 - Platov South-Russian State Polytechnic University (NPI), Novocherkassk, Russia
2 - Karlsruhe Institute of Technology, Karlsruhe, Germany

* smirnova_nv@mail.ru

Keywords: electrochemical synthesis, alternating current, electrocatalyst, disel, oxidation, catalyst, photocatalyst

1 Introduction

At present composition materials containing nanoparticles of metals or metal oxides are widely used in catalysis. Pt/C or Pd/C catalysts are used as electrocatalysts for anode and cathode for low temperature fuel cells, for electrolysis of water. Pt/Al_2O_3 diesel oxidation catalysts apply for removing of diesel engines pollutants. Powder oxides of tin, nickel, titan or copper are well known as effective nanomaterials for different hetero- and photocatalytic processes. The electronic structure, bonding, surface energy, and chemical activities of the materials are directly related to their morphology, and the shapes are directly related to their properties and stabilities. The development of micro- or nano- composite materials with special size and well-defined shape may open new opportunities for exploring materials catalytically properties. The proposed "one-pot" electrochemical method of nanocatalysts synthesis is based on phenomena of oxidation and dispergation of metals under alternating current.

2 Experimental

The method of preparation of composite materials (Pt/C, Pt/SnO_x-C, Pt/NiO-C, Pt/Al_2O_3, Cu_2O-ZnO) based on metal oxidation and dispergation under alternating current was used. This method has been utilized in our previous works, in which highly efficient Pt/C [1] and Pt/SnO_x-C [2] catalyst for low temperature fuel cells and NiO/C composite for supercapacitors [3] have been successfully prepared.

The electrochemical cell has two metal foil electrodes with surface area 3 cm^2 and 0.25 mm thick immerged into the aqueous solution containing alkaline cations. The electrodes are connected to pulse ac source operating at 50 Hz. Finally, the prepared catalysts was carefully washed with bidistilled water to a neutral pH and dried at 80 ^oC for 1 hour.

The crystal structure of the products was characterized by X-ray powder diffraction (XRD, X-ray diffractometer ARL X'TRA («Thermo Scientific», Switzerland) with Cu Ka radiation (l = 1.540562Å) . The morphology, particles sizes and microstructure were performed using scanning electron microscope (SEM, Quanta 200), transmission electron microscope (TEM, JEOL JEM-EX-1200). The specific surface areas of oxide materials were measured by the Brunauer-Emmett-Teller (BET) method on a ChemiSorb 2750. Electrocatalytic properties of the as-prepared Pt/C, Pd/C and Pt/MO_x-C catalysts were evaluated by means of polarization measurements in modeling conditions and membrane-electrode assembles using a potentiostat ELINS P-30S. UV-vis adsorption spectrophotometer (Shimadzu 1800) was used to detect the absorbance of the dye solution during the photocatalytic processes in the wavelength of 300 – 600 nm.

3 Results and discussion

A method of electrochemical synthesis of materials for hetero- and electrocatalysis was

developed. The method is based on a phenomena of metal oxidation and dispergation in non-stationary conditions of electrolysis. The process of metals oxidation/partial reduction of oxides is periodic and accompanied by intensive gas evolution (oxygen appears during anodic impulse, hydrogen appears during cathodic impulse). This fact and a high current frequency in the whole allow obtaining the highly dispersed structures.

The effect of the essential technological parameters (current asymmetry and density, composite and temperature of electrolyte) on the process rate was investigated. The main technological parameters, which define a structure of composite materials on a base of platinum and palladium nanoparticles or copper, tin and nickel oxides, are a composite of electrolyte and current density. The highly dispersed metals or metal oxides are formed in the electrolytes containing chlorides (for Cu and Sn) and hydroxides (for Pt, Pd and Ni) alkaline metals. Increasing the current density in the range of 0.1 to1.0 A/cm^2 was found to result in formation of more defective disordered structures with high values for dispersion. The temperature varying from 30 to 80 °C does not have any influence on the structure of materials. Asymmetry of alternating current defines a process rate but not a type of oxide structure.

Electrocatalytic properties of composite materials on the base of produced oxides and Pt nanoparticles Pt/MO_x-C (M=Sn, Ni) with catalytic activity towards the oxidation of aliphatic alcohols (methanol and ethanol), which are prospective fuels for low-temperature fuel cells, were investigated. Oxide component of MO_x-C composite promotes adsorption of oxygen-containing particles on catalyst and contributes to the reaction of adsorbed alcohol molecules oxidation via the Langmuir-Hinshelwood mechanism providing the reaction rate increase by 20% compared to the one on Pt/C catalyst and anode potentials decrease that result in reduction of anode overpotential in low-temperature fuel cells.

Pt/γ-Al_2O_3 diesel oxidation catalysts prepared by electrochemical dispergation technique demonstrate high catalytic activity and reasonable hydrothermal stability.

Prepared Cu_2O nanocrystallites and nanocomposite Cu_2O/ZnO exhibited superior photoactivities in a very small irradiation time.

4 Conclusions

The possibility of application of electrochemical metal oxidation and dispergation as an operation technique for the production of composite catalysts materials was evaluated. The method is easy-to-use and inexpensive. As-prepared materials can be effectively used as electrocatalysts in fuel cells, diesel oxidation catalysts and photocatalysts in technologies of purification of water as well as in the processes of organic compounds oxidation.

Acknowledgements

This work was supported by the Russian Science Foundation (project nr. 14-23-00078).

References

[1] I. Leontyev, A. Kuriganova, Y. Kudryavtsev, B. Dkhil, N. Smirnova, *Appl.Catal. A: Gen.* 431-432 (2012) 120.

[2] A. B. Kuriganova, N. V. Smirnova Pt/SnOx-C composite material for electrocatalysis, Mendeleev Commun. 24 (2014) 351.

[3] D.V. Leontyeva, I.N. Leontyev, M.V. Avramenko, Yu.I. Yuzyuk,Yu.A. Kukushkina, N.V. Smirnova, *Electrochim. Acta.* 114 (2013) 356.

II-PP40

On Combined Reactivity and Thermogravimetric Study of CO and CO_2 Hydrogenation to Methanol over Cu Based Catalyst

Tarasov A.V.*, Frei E., Schumann J.

Fritz-Haber Institut der Max-Planck Gesellschaft, Dapartment of Inorganic Chemistry, Berlin, Germany

* tarasov@fhi-berlin.mpg.de

Keywords: methanol synthesis, thermogravimetry, adsorbates, CO and CO_2 hydrogenation

1 Introduction

Catalysts for conversion of CO_2 into chemicals and fuels are an important building block for sustainable usage of energy resources and feedstock in chemical industries. This work aims to illustrate the potential of the thermogravimetric technique combined with activity measurements in studying reaction intermediates and mechanistic aspects. One of the promising reactions of industrial relevance used for CO_2 conversion is methanol synthesis over Cu – based catalyst.

$$CO_2+3H_2 \rightleftarrows CH_3OH+H_2O$$

The instant study elucidates the working principle of two realistic high performance catalysts with respect to the adsorbates accumulated during the steady state under reaction conditions (30bar, 250°C) in CO or CO_2 gas feeds.

2 Experimental/methodology

A number of combined experimental techniques were applied for obtaining data for the catalysts under realistic working conditions. The continuous weight measurement of a catalyst while exposing it to a reactive atmosphere under controlled ambient or high-pressure conditions provides important information about chemical reactions and structural changes of the solid sample material. *In-situ* high pressure thermogravimetry coupled with mass-spectrometry was used to examine the catalyst surface coverage with adsorbed species in different feeds. The reactivity measurements in steady and transient state in combination with surface titration experiments were performed for the analysis of stable surface intermediates and exploring the nature of the active catalytic site with respect to the specific catalyst.

3 Results and discussion

Two limiting cases for Cu-based catalyst are considered: copper nanoparticles supported on irreducible MgO (Cu/MgO) and Cu particles of comparable size and shape supported on ZnO (Cu/ZnO). For both systems the reactivity measurements indicate the presence of a sticky adsorbate layer in CO and CO_2 feed which might be removed as methanol by continues purging in H_2 (see Figure 1). For the Cu/ZnO catalyst the total amount of methanol formed under transient state during purging in H_2 after CO exposure under steady state is 6 times less than the one estimated after CO_2 exposure. This data are in good agreement with catalysts performance under steady state. On the opposite Cu/MgO system showed in transient state the same amount of accumulated mobile adsorbates in CO as well as in CO_2 feed. However the activity in CO_2 hydrogenation is 100 times less than in CO hydrogenation. This behavior supports the presenceof significant amounts of adsorbed carbon formed on the catalyst under steady state, e.g. in a formate-derived adsorbate layer which in the absence of carbon in the feed can still be hydrogenated to methanol, but not converted in a catalytic cycle under reaction conditions.

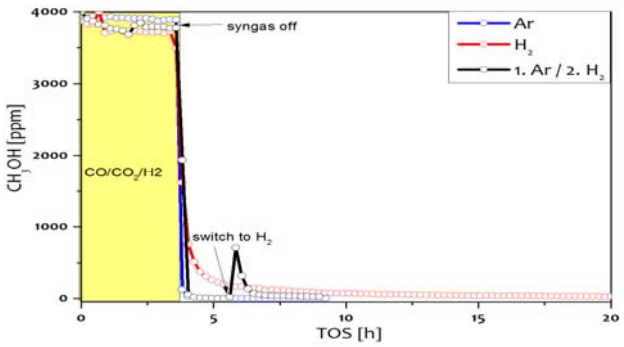

Fig. 1. Variation of methanol concentration over Cu/ZnO catalyst (GC data) by switch from syngas $CO_2/CO/H_2/He$ (6/8/59/27) to argon, pure hydrogen and argon with subsequent purging with hydrogen.

A gravimetric *in situ*-measurement under methanol synthesis reaction conditions showed that Cu - based catalysts gain mass in CO_2-containing feed and reversibly lose that weight when the feed is switched to CO only indicating the same type of adsorbates for the different Cu catalysts. The total amount of adsorbed species under steady state varies for the different catalytic systems. The Cu/ZnO system possesses a weight gain of 1.9wt% and 1.2wt% in CO_2 and CO respectively, while Cu/MgO catalyst showed a total weight increase due to adsorbates of 0.39wt% and 0.27wt% (see Figure 2) in the corresponding feeds.

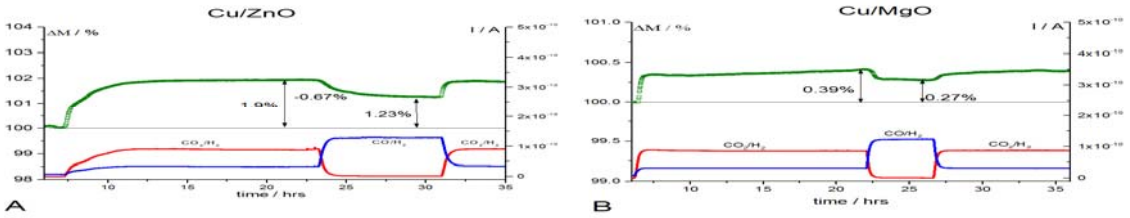

Fig. 2. In situ-thermogravimetry at 30 bar, 250°C in different gases (A) Cu/ZnO and (B) Cu/MgO

4 Conclusions

Analysis of the catalyst performance and the surface titration data provide evidence that CO hydrogenation requires isolated Cu-sites whereas the prerequisite for the successful CO_2 hydrogenation is the presence of ZnO decorated Cu surface [1]. This Cu/ZnO interface can be realized for instance as a graphitic ZnO overlayer [2], which hinders at the same time a successful CO hydrogenation.

References

[1] Behrens, M.et al. *Science* **2012,** *336* (6083), 893-897.
[2] Lunkenbein, T. et al. *Angew. Chem. Int. Ed.,* **2015,** accepted, DI: 10.1002/anie.201411581

II-PP41

Alumina Exsiccates Prepared via CTA Technology

Isupova L.A.*, Danilevich V.V., Danilova I.G., Paukshtis E.A., Ushakov V.A., Parmon V.N.

Boreskov Institute of catalysis SB RAS, Novosibirsk, Russia

* isupova@catalysis.ru

Keywords: alumina, desiccant, preparation

1 Introduction

Due to stability in humid atmospheres and high capacity alumina exsiccates are widely used for natural gas exsiccation [1, 2]. Their properties depend on a phase composition, acid and base properties of alumina and granules porosity, that depend on exsiccates preparation details. For example, the exsiccates based on eta alumina prepared via energy and resources reserving CTA (centrifugal thermal activation) technology are characterized with higher capacity as compared with that based on gamma alumina [3-5]. At that these exsiccates differ in porosity and acid and base properties. One of the ways to influence the acid and base properties of alumina is modification with different electrolytes. The modification may be done by impregnation of calcined exsiccates or f.e. during plastic paste preparation stage.

The main goal of the paper is investigation of eta and gamma based alumina exsiccates (phase composition, acid and base properties, porosity and durability of granules, static and dynamic capacities) prepared via CTA technology depending on row hydroxides (bayerite or pseudo boehmite structured) and nature of electrolytes (acid or base) used for pastes preparation.

2 Experimental

As the raw material the product prepared by centrifugal thermal activation of gibbsite in the pilot flash-reactor TSEFLAR^{TM} (CTA-product) was used [5]. The hydration of CTA- product was carried out in alkaline or acid solutions to prepare bayerite (Ba) or pseudo boehmite (Pbe) containing hydroxides [3]. As prepared hydroxides as powders were placed in a mixer for peptization at alkaline (NaOH, KOH) or acid (HNO_3, H_2SO_4) modulus of 0.07-0.1. The prepared plastic pastes were forced through the draw die of a ram extruder with a hole diameter of 4 mm to obtain extrudates. Finally the extrudates were calcined in a tubular furnace in flowing dry air at 420^{o}C (obtained from bayerite) and 500^{o}C (obtained from pseudo boehmite) for 4 hours.

The dynamic capacity of as prepared adsorbents was determined as the mass of water absorbed by a 100 cm^3 of adsorbent (at dew point of dry gas -40^{o}C). Static water capacity of the adsorbents was determined as the mass of water adsorbed by a 100 g of adsorbent (25^{o}C, relative humidity of 10% and 60%). The type and concentration of acidic and basic sites on sample surfaces were studied by FTIR spectroscopy of adsorbed CO and $CDCl_3$, correspondingly. [6]. X-ray diffraction (XRD) was performed on an HZG-4 diffractometer. Because of the complexity of the quantitative determination of individual phases in a multiphase system (due to the similarity of their parameters), the phase composition of the products was characterized in terms of (γ+η)-Al_2O_3, χ-Al_2O_3 and χ-like Al_2O_3 + X-ray amorphous phase. Textural data were obtained via nitrogen adsorption.

3 Results and discussion

In the Table 1 there are data on alumina exsiccates prepared via CTA technology with using of different row hydroxides (bayerite or pseudo boehmite) and electrolytes (HNO_3, H_2SO_4, NaOH, KOH). Using of H_2SO_4 and especially NaOH and KOH as compared with HNO_3 during

preparation lead to decrease of specific surface areas of exsiccates of both series (based on eta or gamma alumina) and changing their porosity. Such textures changing are more expressed for exsiccates based on gamma alumina. So using of H_2SO_4 leads to decrease of mezopores volume without change in micropores volume, that result in decrease of mean pore size, while using of base electrolytes lead to increase the mezopores volume and micropores disappearance, that result in increase of mean pore size. Such changing in texture does not strongly influence the static capacity but influence the dynamic capacity of exsiccates.

Preparation	Static capacity, %		Dynamic capacity, g/100 cm^3	S_{sp}, m^2/g	V_{micro*}, cm^3/g	V_{mezo}^{**}, cm^3/g	$\sum V$, cm^3/g	D^{***}, nm
	10%	60%						
Ba-HNO_3	-	21.59	5.29	379	0.15	0.13	0.28	2.9
Ba- H_2SO_4	-	21.19	5.59	313	0.13	0.13	0.26	3
Ba-NaOH	7.6	17.9	4.8	272	0.11	0.17	0.28	3.5
Ba-KOH	7.9	17.5	4.1	269	0.05	0.18	0.23	3.7
Pbe- HNO_3	-	21.13	2.9	346	0.20	0.25	0.45	4.1
Pbe- H_2SO_4	-	23.10	5.25	327	0.16	0.10	0.26	2.7
Pbe-NaOH	7.8	21.5	4.8	263	0.005	0.41	0.415	6.4
Pbe-KOH	7.6	20.3	4.4	314	-	0.39	0.39	5.5

Table 1. Properties of exsiccates

It is interesting that increase in dynamic capacity of exsiccate based on gamma alumina due to using of H_2SO_4 occurs simultaneously with decrease of mean pore size while due to using of NaOH(KOH) – simultaneously with increase of mean pore size.

Investigation of acid and base properties of exsiccates with probe molecules (CO and $CDCl_3$) has shown that using of H_2SO_4 leads to increase of Lewis acidity while using of NaOH(KOH) leads to appearance of strong basic sites without change of Lewis sites concentration. Hence the increase in dynamic capacity of based on gamma alumina exsiccates due to modification with alkaline is mainly due to appearance of basic sites while increase in pore size may decrease the effect.

4 Conclusions

Using of acid (H_2SO_4) and base (NaOH, KOH) electrolytes instead of HNO_3 during preparation lead to strong increase the dynamic capacity of gamma alumina based exsiccates up to level of eta alumina base exsiccates mainly due to decrease of mean pore size (H_2SO_4) or appearance of basic sites (NaOH, KOH).

Acknowledgements

The work was supported by by grant of the RAS, project № 5.7.1.

References

[1] Sircar S., Rao M.B., Golden T.C., Studies in Surface Science and Catalysis. Elsevier, 99 (1996) 629.
[2] Стайлз Э. Носители и нанесенные катализаторы. Теория и практика. М.: Химия, 1991, 24.
[3] L.A. Isupova, Yu.Yu. Tanashev, I.V. Kharina, et al., Chem.eng. J., 107/1-3 (2005) 163.
[4] V. V. Danilevich, L. A. Isupova, A.P. Kagyrmanova, I.V. Kharina, D.A. Zyuzin, A.S. Noskov, Kinetics and Catalysis, 53/5 (2012) 673 (russian).
[5] V. V. Danilevich, L. A. Isupova, E. A. Paukshtis, V. A. Ushakov, Kinetics and Catalysis, 55/3 (2014) 391(russian).
[6] Paukshtis E.A., IR spectroscopy in heterogeneous acid-base catalysis. Novosibirsk, Nauka, 1992, 255p (russian).

II-PP42

Textural and Transport Properties of Hydrotreatment Catalysts (γ-Aluminas) Characterised by ^{129}Xe-NMR Spectroscopy

Weiland E.[1,2*], Springuel-Huet M.-A.[1], Nossov A.[1], Guenneau F.[1], Quoineaud A.-A.[2], Gédéon A.[1]

1 - Sorbonne Universités, UPMC Univ Paris 06, UMR 7574, Laboratoire de Chimie de la Matière Condensée de Paris, Paris, France

2 - IFP Energies nouvelles, Etablissement de Lyon – Rond-point de l'échangeur de Solaize , Solaize, France

* erika.weiland@gmail.com

Keywords: Xe-NMR, γ-alumina, porosity, connectivity, diffusion

1 Introduction

During last decades, the environmental legislation became more severe, a sulfur level lower than 10 ppm is required on the produced diesel fuel. Those levels can only be reached by hardening the working temperature conditions or by using more active catalysts. In both cases the activity and selectivity of hydrotreating catalysts play an important role in petroleum industry, from an economic and a technologic point of view. Catalysts used for hydrotreating are widely composed of sulfur molybdenum promoted by nickel or cobalt phase supported on high surface alumina (200–250 m^2/g).

The characterization of textural and transport properties of catalytic materials is decisive to better understand the impregnation processes of metal salt solutions or chelating agents into the pores and improve active phase. ^{129}Xe NMR is a spectroscopic technique able to characterize pore size and tortuosity for zeolites, mesoporous solids and MOF.

The xenon atom has significant highly-polarizable electron cloud, very sensitive to its environment and ^{129}Xe NMR has proved to be very useful to study the porosity of micro and mesoporous solids [1]. In this study we show that ^{129}Xe NMR is an alternative technique to porosimetry or electron microscopy 3D transmission experiments.

2 Experimental/methodology

Different types of ^{129}Xe NMR experiments have been performed on a Bruker DSX 300 spectrometer: i) measurements of the chemical shift of adsorbed xenon under chosen conditions in order to correlate the chemical shift to the pore size of catalysts, ii) 2D exchange NMR (EXSY) to study the connectivity between pores of different sizes in catalysts presenting multi modal porosity.

To minimize the effect of strong adsorption sites existing at the alumina surface on the chemical shift of adsorbed Xe, the samples have been pretreated at 573 K overnight and the chemical shift has been measured at P ≈ 600 Torrs. In these conditions, the chemical shift is expected to depend on the pore size only. The porosity of all alumina samples (≈ 20) has also been characterized by N_2 adsorption at 77 K.

In 2D EXSY spectra, off diagonal peaks arise from the exchange of Xe atoms between two environments, characterized by the diagonal peaks, during the so-called mixing time (t_{mix}). The variation of the intensity of the off-diagonal peaks as a function of the mixing time allows determining an exchange rate which characterizes the pore connectivity.

3 Results and discussion

As it has been already obtained with zeolites [2] and silicas [3-5], we have established a correlation between the measured chemical shift, corresponding to the interactions of the Xe atoms with the pore surface solely, and the pore size (Figure 1). Considering that the measured chemical shift, δ_S, arises from the chemical exchange between adsorbed and bulk phase, it can be expressed as [3]:

$$\delta_s = \frac{\delta_a}{1 + \frac{V}{K_{ads} \cdot S \cdot R \cdot T}}$$

where δ_a is the chemical shift of a Xe atom interacting with the surface, V and S are the pore volume and the pore surface area, respectively. K_{ads} is the Henry adsorption constant. The V/S ratio is equal to D/η, D being the pore size and η a parameter depending on the pore geometry. Fitting the experimental results with equation gives δ_a = 117 ppm and K_{ads} = 2.2×10^{14} $Torr^{-1}m^{-2}$. These values are very similar to those obtained for silicas [3] and allow us to use the variation of the chemical shift for silicas as a reference to determine the value of the geometric factor, η, describing the complex pore geometry in aluminas.

In the example given Figure 2, the 2D EXSY spectrum shows an exchange between the two types of pores and between the larger pores and the gas phase outside of the pellet.

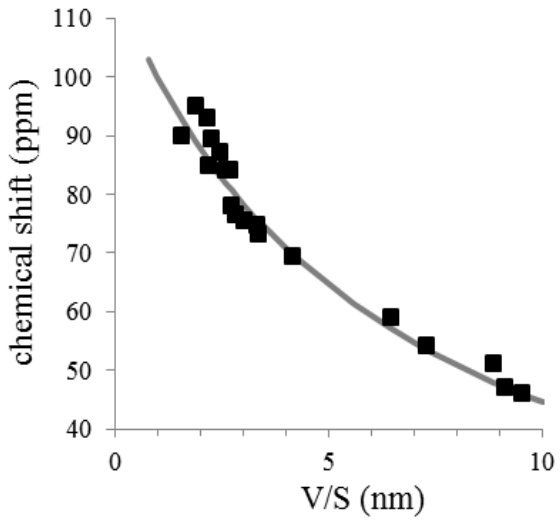

Figure 1 : Chemical shift variation versus the volume-to-surface ratio of pores for different aluminas.

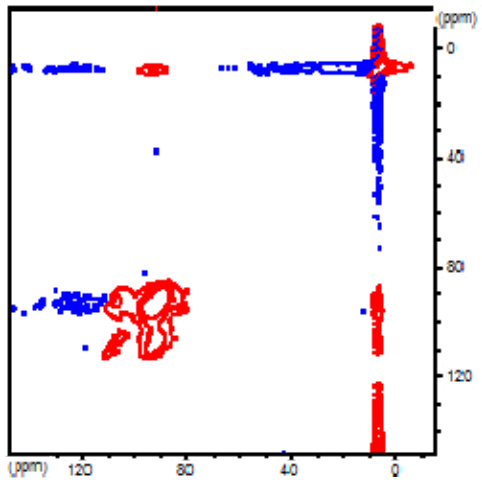

Figure 2: 2D EXSY **spectrum** of an **alumina** with **bimodal porosity**, $\mathbf{P_{Xe}}$ **= 10 bars**, T = **293 K**, $\mathbf{t_{mix}}$**=30 ms**

4 Conclusion

Xe NMR technique has allowed us to establish a correlation between the chemical shift and the pore size for aluminas, to obtain information on the connectivity between different porosities (EXSY) in order to characterize the tortuosity of the porous network.

References

[1] J.-L. Bonardet, J. Fraissard, *Catal Rev,* 41 (1999) 115-225.
[2] J. Fraissard, T. Ito, M. Springuel-Huet, *Stud Surf Sci Catal* 28 (1986) 393-400.
[3] V. Terskikh, I. Moudrakovski, *Langmuir,* 18 (2002) 5653-56
[4] F. Cros, J.-P. Korb, *Langmuir,* 16 (2000) 10193-97
[5] A. Julbe, L. De Ménorval, *J. Porous Mater,* 6 (1999) 41-54

II-PP43

Organoboron Nanoparticles Catalityc Properties: the Substrate Effect

Kharitonov V.A.*, Grishin M.V., Gatin A.K., Slutsky V.G., Shub B.R.

Semenov Institute of Chemical Physics, Russian Academy of Sciences, Moscow, Russia

* vch.ost@mail.ru

Keywords: substrate effect, organoboron nanoparticles, charging, ammonia, decomposition

1 Introduction

Currently, there is not enough information to fully describe the effect of the substrate on the heterogeneous catalytic processes involving nanoparticles. In general, the substrate can prevent coalescence of the nanoparticles or contribute in opposite process, modify the shape, structure and charge of the nanoparticles, bring in the nanoparticle-padded catalytic system additional active sites (which can be for example, oxygen vacancies or nanoparticle-substrate interface in oxide substrates), stabilize the intermediate reaction products. As a result of the interaction effects described above the nanoparticle chemical properties may vary within wide limits.
Our purpose was to compare the catalytic properties of organoboron nanoparticles (OBN) deposited on substrates of various nature (conductors and semiconductors), on the example of the ammonia decomposition.

2 Experimental/methodology

Experiments were performed in ultrahigh vacuum setup equipped with a scanning tunneling microscope (STM), Auger and mass spectrometers, additional accessories. The residual gas pressure in the setup chamber didn't exceed $P = 2 \times 10^{-8}$ Torr.

Organoboron nanoparticles (OBN) with an average size of 14.6 nm and composition $(C_2B_{10}H_4)_n$ synthesized by high-temperature pyrolysis of the vapor carborane $C_2B_{10}H_{12}$ in the flow type setup with an initial vapor pressure $P = 6.35 \times 10^{-3}$ MPa and temperature T = 1273 K [1]. Samples were prepared by depositing lyosol (1 mg of OBN per 2 ml of CCl_4) on several substrates: high-oriented pyrolythic graphite (HOPG) plate, oxidized silicon wafer, and oxidized aluminum plate and dried at room temperature. Taking into account the self-substrate and setup catalysis the measurements on the cells with substrates without OBN were also made.

The measurements were carried out at a temperature of 750 K.

Determining the structure and electronic structure of the OBN coating was carried out by atomic force and scanning tunneling microscopy.

3 Results and discussion

OBN formed individual clusters of on the substrates surfaces. Clusters size varied from 4-5 micron laterally with 140 nm altitude which is about 10 nanoparticles layers down to single nanoparticles.

Mass spectra of the gaseous medium components in the vacuum chamber exhibit a number of lines corresponding to the starting substances and their decomposition products. Lines with M/e = 2 and 28 correspond to H_2^+ and N_2^+, ions formed from NH3 decomposition products, M/e =17 – mainly correspond to NH_3^+ ions, formed from NH_3 reactant. The degree of ammonia decomposition achieved by OBN coverage was determined by comparing NH_3 conversion in the OBN-on-substrate experiment with the control experiment on substrate without OBN. Thus obtained ammonia conversions due OBN are 2.8%, 2.3% and 1.2% for HOPG, Al_2O_3 and SiO_2 substrates respectively.

State of the OBN coverage before and after reaction was determined by scanning tunneling microscopy and spectroscopy. To do this, we measured the current-voltage characteristics (CVC) of STM tunneling nanocontact, including OBN deposited on the substrate, or a substrate area containing no OBN. These data showed that the OBN physical characteristics do not undergo changes during the interaction with NH_3. At the same time, shape of the CVC curves for OBN on substrates of various natures varies considerably. OBN/HOPG sample CVC matches CVC formed by conductors (S-shaped relationship), while CVC for OBN/Al_2O_3 and OBN/ SiO_2 samples are both diode-like as they demonstrate sharp asymmetry of positive and negative voltage branches. Wherein the CVC measured on OBN coverage are shifted relative to CVC measured on pure substrates in 0.2 V and 0.6 V for Al_2O_3 and SiO_2. Such a shift indicates potential difference between OBN and the substrate due to the transition of electrons in OBN.

Thus, it can be argued that there is a correlation between the catalytic ability of OBN and their potential against the substrate. This result can be explained as follows. The NH_3 decomposition is a straight-chain process with radicals generated by the ammonia decay $NH_3 \rightarrow NH_2\bullet + H\bullet$, which occurs under pretty high activation energy (750 K). Carborane easily transforms into a diradical $C_2B_{10}H_{12}\bullet\bullet$. The two-stage formation of radicals in the $NH_3/C_2B_{10}H_{12}$ system $C_2B_{10}H_{12}\bullet\bullet + NH_3 \rightarrow C_2B_{10}H_{12}H\bullet + NH_2\bullet$, $C_2B_{10}H_{12}H\bullet \rightarrow C_2B_{10}H_{12} + H\bullet$ should occur at a higher rate than single-stage $NH_3 \rightarrow NH_2\bullet + H\bullet$. OBN consist of interconnected partially dehydrated $C_2B_{10}H_{12}$ molecules, so diradicals can be easily generated on the surface of OBN, accelerating the $NH_2\bullet$ and $H\bullet$ radicals emergence, which explains the catalytic properties of OBN in the decay of ammonia. The presence of relative to the substrate negative potential on the OBN causes OBN negative charging. Surplus electrons fill upper energy orbitals of OBN and prevent the formation of diradicals as their presence implies an OBN valence electron transition to higher free energy level. Thus, the higher the OBN potential, the smaller will be the OBN surface diradicals concentration and, accordingly, less catalytic effect, as is observed experimentally.

4 Conclusions

The substrate effect on catalytic properties of organoboron nanoparticles was investigated on the example of ammonia decomposition reaction. OBN deposited on HOPG achieve the highest rate of the ammonia decomposition. Catalytic activity ratio for OBN on HOPG, Al_2O_3, SiO_2 substrates is 1.00 : 0.82 : 0.43 relatively. Correlations between substrate nature and its influence on the catalytic properties were discovered. The difference in the substrates influence was explained by OBN charging. Reaction mechanism elucidating the OBN catalytic effect on different substrates was presented.

Acknowledgements

The research group would like to thank RFBR for grants 14-03-31068, 14-03-00156, 14-03-90012, 13-03-00391, 15-03-00515.

References

[1] V.G. Slutskii, M.V. Grishin, V.A. Kharitonov, A.K. Gatin, B.R. Shub, and S.A. Tsyganov, *Russ. J. Phys. Chem. B*, **7**, (2013), 343.

II-PP44

The Influence of Support Properties on State of Supported CrO_x and Activity of Chromium Oxide Catalysts in Dehydrogenation of Hydrocarbons

Bugrova T.A.[1*], Litvyakova N.N.[1], Biryukova K.A.[1], Santos Aires F.J.C.[1,2], Prakash S.[2], Mamontov G.V.[1]

1 - Tomsk State University (TSU), Tomsk, Russia
2 - Institut de Recherches sur la Catalyse et L'Environnement de Lyon (IRCELYON), Villeurbanne cedex, France

* bugrova.tatiana@gmail.com

Keywords: chromia containing catalysts, mixed supports, hydrocarbons, dehydrogenation, isobutane

1 Introduction

Dehydrogenation of saturated (C_3-C_5) hydrocarbons is a large-scale process to produce olefins (propylene, n-butenes, isobutylene, etc.) in the world petrochemical industry. These products are widely used for production of synthetic rubbers, plastics and other valuable chemical products. Catalytic dehydrogenation is the widely used method of olefin production.

Currently, Cr-containing catalysts are the main type of materials for dehydrogenation of C_3-C_5 hydrocarbons. Support properties and preparation conditions define the state of supported chromium and its catalytic properties. The state of active component may be controlled by changing of support nature or by introduction of modifying additives. Alumina (especially γ-Al_2O_3) is the most widely used support due to low cost, stability at high temperatures, high porosity and surface area, ability to stabilize active component in highly dispersed active state. The main problems of alumina application are formation of inactive chromium aluminate and side reactions leading to reduction of catalyst activity. Besides, there are chromium oxide catalysts supported on ZrO_2, SiO_2, TiO_2 [1, 2]. Typical silica supports have high specific surface area and pore volume as well as insignificant proper catalytic activity. The pore size of silica can be varied in a wide range. However, the use of silica instead of Al_2O_3 is limited by inability to stabilize active component in desirable state, and thus, low activity. The highest activity in dehydrogenation reactions shows chromia catalysts supported on ZrO_2 [3] because of chromia stabilization in highly dispersed state. However, high cost, low surface area and low stability of zirconia at high temperatures limit its use.

Thereby, the purpose of the present work is to develop systems on mixed supports and study the effect of support properties on the state and activity of the active component (CrO_x) in isobutane dehydrogenation.

2 Experimental/methodology

Cr-containing catalysts with loading of Cr corresponding to one monolayer (5 at_{Cr}/nm^2) were prepared by incipient wetness impregnation method using water solution of H_2CrO_4 and KNO_3 (K/Cr molar ratio was 1:5). The catalysts were dried at room temperature for 12 h and calcined at 600 °C for 4 h. ZrO_2, SiO_2, $nZrO_2/SiO_2$, Al_2O_3 and $nZrO_2/Al_2O_3$ (n = 0.5, 1.0, 2.0 monolayer of zirconia, 5 at_{Zr}/nm^2) were used as supports. $nZrO_2/Al_2O_3$ and $nZrO_2/SiO_2$ supports were prepared by incipient wetness impregnation method using water solution of $ZrO(NO_3)_2 \cdot H_2O$ stabilized by citric acid (molar ratio Zr:citric acid = 1:2). Catalysts were studied by low temperature N_2 sorption, XRD, TPR, UV-vis spectroscopy, XPS, TEM and tested in reaction of isobutane dehydrogenation in a fixed bed reactor.

3 Results and discussion

The results of investigation of support structure by N_2 sorption show that ZrO_2 is characterized by low value of surface area (34 m^2/g). Modification of the Al_2O_3 and SiO_2 supports (surface area 176 and 102 m^2/g, respectively) by means of zirconia leads to reduction of the volume of large mesopores. In spite of this the obtained supports have high values of surface area (110-157 m^2/g) with developed system of wide transport mesopores, which make them promising to be used as supports for Cr-containing catalysts.

The absence of reflexes of Cr-containing phases for Cr/ZrO_2 and Cr/Al_2O_3 catalysts in XRD patterns indicates on small particle sizes (less than 3 nm) or covering distribution of chromia on the surface of these supports. Cr(VI) species were determined by TPR and UV-vis spectroscopy for Cr/ZrO_2 and Cr/Al_2O_3 catalysts. The formation of highly dispersed Cr_2O_3 clusters (UV-vis and XRD results) due to reduction of Cr(VI) species was observed. The formation of large Cr_2O_3 particles (29 nm according XRD results) was shown for Cr/SiO_2 catalyst. Figure 1 shows possible models of formation of Cr-containing phase depending on interaction with different supports. Increasing amount of Cr(VI) species was observed for $Cr/nZrO_2/SiO_2$ and $Cr/nZrO_2/Al_2O_3$ catalysts.

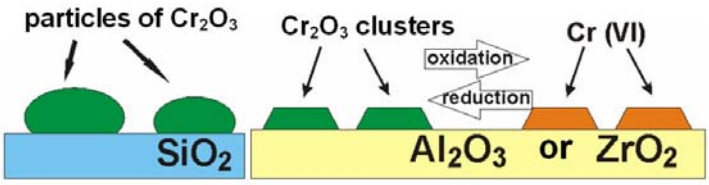

Fig. 1. The model of CrO_x phase formation on the surface of different supports

The testing of catalysts in the isobutane dehydrogenation shows that Cr/ZrO_2 catalyst has the highest specific catalytic activity. The reducing of Cr(VI) in Cr/ZrO_2 during catalytic process leads to formation of dispersed Cr_2O_3 clusters, having high activity in the dehydrogenation reaction. The highest activity of Cr/ZrO_2 catalysts also may be explained by specific interaction of Cr with ZrO_2. The formation of large α-Cr_2O_3 particles observed for Cr/SiO_2 catalyst causes low activity of this catalyst. The activity of Cr/Al_2O_3 catalyst was lower than the one of Cr/ZrO_2 but higher than the one of Cr/SiO_2. Modification of silica support with zirconium oxides leads to significant increase in activity of Cr-containing catalyst compared to initial Cr/SiO_2 catalyst. It is connected with increasing of the share of Cr(VI), which is stabilized by ZrO_2 in highly dispersed state.

4 Conclusions

It was shown that states of chromium depend on the nature of support. The combination of properties in mixed supports allowed us to control the state and activity of supported chromium, which can be considered as the foundation for the preparation of efficient Cr-containing catalysts for dehydrogenation of hydrocarbons.

Acknowledgements

This work was supported by the Russian Federal Target Program "Research and development in the priority fields of scientific and technological complex of Russia in 2014-2020" (State Contract No. 14.578.21.0028).

References

[1] M.A. Vuurmar, I.E. Wachs, D.J. Stufkens, et al., *J. Mol. Catal*. 80 (1993) 209.
[2] J. Sloczynski, B. Grzybowska, A. Kozlowska, et al., *Catal. Today.* 169 (2011) 29.
[3] S. De Rossi, M. P. Casaletto, G.Ferraris, *Appl. Catal. A. General* 167 (1998) 257.

II-PP45

Characterization and Mobility of the Different Protonic Species in Anhydrous and Hydrated 12-Tungstophosphoric Acid Studied by Solid State 2H NMR

Kolokolov D.I.[1,2*], Luzgin M.V.[1,2], Jobic H.[3], Stepanov A.G.[1,2]

1 - Boreskov Institute of Catalysis, Siberian Branch of Russian Academy of Sciences, Novosibirsk, Russia

2 - Novosibirsk State University, Faculty of Natural Sciences, Department of Physical Chemistry, Novosibirsk, Russia

3 - Institut de Recherches sur la Catalyse et l'Environnement de Lyon, CNRS, Université de Lyon, Villeurbanne, France

* kdi@catalysis.ru

Keywords: hydroxonium, heteropolyacid, acid, protons, mobility, 2H NMR, proton, conduction, ion

1 Introduction

Heteropolyacids (HPAs) represent a promising class of solid acids with a particularly high catalytic activity in acid-type reactions such as hydration, dehydration, alkylation, isomerization, and sulfhydration and good proton conduction properties for PEM fuel cells. For each case, the functionality of the system based on HPA is governed by the structure and the mobility of its protonic species [1-2]. In the anhydrous state the latter are represented by surface protons with superacidic properties. When hydrated by interaction with water new active species the $[H_3O]^+$ and the $[H_5O_2]^+$ ions are formed. The location and mobility of these protonic species play a crucial role in any dynamical process running in the system, being it an acid-type catalytic reaction or a charge transfer in PEM fuel cells. Among the family of HPAs, 12-tungstophosphoric acid with Keggin-type heteropolyanion structure ($H_3PW_{12}O_{40}$ or the TPA) exhibits the strongest acidity and overall stability, thus being of major interest for industrial applications. Despite good knowledge of the TPA primary and secondary structures both in the hydrated and dehydrated states, even the location of the acidic protons on the surface of the Keggin anion in anhydrous TPA until recently was actively debated. The possible migration of the acid sites in the anhydrous TPA received only qualitative estimations. Location and dynamics of protonic species in hydrated TPAs was studied in details for only high water concentrations (> 10 water molecules per Keggin unit) leaving the mechanism of interaction of TPA with water somewhat uncertain.

Considering the practical and fundamental importance of the problem, in the present work, we have performed the analysis of both ^{2}H NMR line shape and the evolution of T_1, T_2 relaxation with temperature for the deuterated analogue of the solid 12-tungstophosphoric acid (TPA × nH_2O) at different hydration levels ($0 < n < 6$) in wide temperature range of 103−503 K. This allowed us to characterize in detail the mobility of different protonic species, including acidic OH groups, water molecules, and hydroxonium ions.

2 Experimental

Details of preparation of HPA hydrate with a certain amount of water are given in refs. [3]. ^{2}H NMR experiments were performed at 61.424 MHz on a Bruker Avance-400 spectrometer using a high power probe with a 5 mm horizontal solenoid coil. All ^{2}H NMR spectra were obtained by Fourier transformation of the quadrature-detected phase-cycled quadrupole echo arising in the pulse sequence. The duration of the π/2 pulse was 1.8-2.1 μs. Inversion-recovery experiments were carried out to derive spin-lattice relaxation times (T_1) and CPMG pulse sequence was used to derive spin-

spin relaxation times (T_2).

3 Results and discussion

Analysis of the ^{2}H NMR spectra line shape temperature dependence for anhydrous TPA showed, that in the absence of water, there are two types of surface protons. The ones rapidly flipping, being localized on the bridged oxygen sites, and the ones involved into relatively fast migration over the surface oxygens of the Keggin anion. While below 423 K the population of fast migrating protons is low, almost all surface protons are rapidly diffusing over the Keggin-anion surface at T > 503 K by hopping between neighboring oxygens. The temperature dependences of the two-site fliping and the isotropic reorientation by diffusion over the Keggin anion show that both motions follow the Arrhenius law. The activation barrier for the localized two-site flips is E_f = 72 kJ mol^{-1} with a pre-exponential factor of k_{f0} = 3.2 x10^{13} s^{-1}; the isotropic deuteron migration is characterized by an activation barrier of E_D = 78 kJ mol^{-1} with a pre-exponential factor of k_{D0} = 1.2 x10^{13} s^{-1}. Such observation evidences that in anhydrous TPA deuterons exhibit motional modes with rates higher than 1 kHz ($t_C < 10^{-3}$ s) already at 423 K. Moreover, at the temperatures of chemical reactions mediated by TPA (T > 373 K) the major fraction of deuterons is mobile and migrating ($t_C<10^{-4}$ s) over the Keggin-anion surface. This means that the acidic protons are not localized at certain terminal or bridging surface oxygens at the respective reaction temperatures, that is, the acidic protons can be regarded as being delocalized on the time scales of the catalytic reactions.

At low hydration levels (n < 6) the TPA surface protons interacts with water to form $[D_3O]^+$ and $[D_5O_2]^+$ ions. The analysis of the evolution of spin relaxation times with temperature for different spectral species allowed quantify the kinetic parameters of the $[D_3O]^+$ ion formation/decomposition and to characterize the mobility of the OD, D_2O, and $[D_3O]^+$ species. The water molecules and the $[D_3O]^+$ ions were concluded to exhibit fast internal rotations about their symmetry axes, and these motions are not influenced by the water concentration for the case of a low hydration level of TPA × nD_2O (n < 10, i.e., when the secondary structure remains cubic with Keggin anions directly attached to each other). The hydroxonium ion is additionally involved in a wobbling motion on the surface of the Keggin anion. This motion may be related to the mechanism of decomposition of the ion back to water hydrogen bonded to the TPA surface acid protons. The proton (deuteron) diffusion and the charge transfer mechanism in the TPA hydrates might be defined by the $[D_3O]^+$ ions formation and migration between neighboring TPA Keggin units. The rate constant of the latter process depends on the water concentration as the higher hydration levels favors the formation of the $[D_5O_2]^+$ ion which itself is not diffusing, we have found that the barrier associated with the process gradually increases from 24 kJ mol^{-1} for n = 3 to 30 kJ mol^{-1} for n = 5.2 and to ~ 35 kJ mol^{-1} for n = 14).

4 Conclusions

Location and mobility of the active protonic species in $D_3PW_{12}O_{40}$ x nD_2O (0<n<6) hydrates were successfully characterized by ^{2}H NMR solid state spectroscopy.

Acknowledgements

This work was supported by the Russian Foundation for Basic Research (grant no. 12–03–31108)

References

[1] A. V. Ivanov, E. Zausa, Y. Ben Taarit, N. Essayem, *Appl. Catal. A*, 256 , (2003), 225.
[2] R. C. T. Slade, G. B. Hix, B. Ducourant, *Solid State Ionics, 99,* (1997), 233
[3] D.I. Kolokolov, M.S. Kazantsev, M.V. Luzgin,H. Jobic, A.G. Stepanov, *J. Phys. Chem. C*, 118, (2014), 30023

II-PP46

Differences in the Location of Guest Molecules within Zeolite Pores as Revealed by Multilaser Excitation Confocal Fluorescence Microscopy: Which Molecule is Where?

Sprung C.*, Weckhuysen B.M.

Utrecht University, Dept. of Chemistry, Inorganic Chemistry and Catalysis, Utrecht, The Netherlands

* sprung@fhi-berlin.mpg.de

Keywords: zeolite, ZSM-5, confocal, fluorescence, microscopy, polarisation, location of guest, molecules

1 Introduction

Zeolites are an important group of heterogeneous catalysts, which are for example employed in the Fluid Catalytic Cracking (FCC) process (such as zeolite Y and ZSM-5) [1]. Their internal pore architecture makes these catalysts selective for reactants, products, and transition states. Large coffin-shaped zeolite ZSM-5 crystals are an ideal model system to investigate industrially relevant topics at the scale of a microscope [2]. In order to make this possible a Brønsted acid catalysed oligomerisation reaction was employed to form elongated molecules inside the zeolite channels. Their location (i.e. type of channel) and spectroscopic fingerprints are recorded in 3 dimensions and parent, as well as post-synthesis steamed zeolite crystals making use of multi-laser excitation confocal fluorescence microscopy.

Large coffin-shaped ZSM-5 crystals were strictly oriented with respect to the recorded polarisation plane of emission light and elongated molecules have been formed due to the acid catalysed oligomerisation of the probe molecule. In this respect, the cyclic and linear dimeric carbocation are of main interest. Steric constraints of the zeolite channels locate these dimeric carbocationic species in certain positions, which were used to determine visual and spectroscopic features of large coffin-shaped ZSM-5 crystals [3].

2 Experimental

Large coffin-shaped ZSM-5 crystals were used in its acid form and impregnated at 30°C with excess of 4-fluorostyrene (the probe molecule). Subsequent rapid heating to 180°C induced the oligomerisation reaction of the probe molecule inside the zeolite channels.

A Nikon Eclips 90*i* confocal microscope was used for fluorescence investigations. Eighteen focal planes were recorded, of which each image was a composition of 32 real colour images. For each set of focal planes, three dimensional fluorescence spectra were extracted. Three crystal batches (parent, steamed 500°C, and steamed 700°C) were positioned in roof or gable position under the microscope, and oriented to 0°, 45°, and 90° with respect to the incoming and recorded polarisation plane of excitation light (405, 457, 488, 514, 561, 642 nm) and emission light, respectively. An overview of the investigation principle is illustrated in Fig. 1 [3].

3 Results and discussion

The highest fluorescence intensity was observed for emission polarised parallel to the crystal's short axis, which coincides with the crystallographic orientation of the straight channels. This emission vanished completely when the crystal was turned 90° away from this orientation. However, fluorescence from a different location, i.e. a rim around the whole crystal was observed. In absence of the intense fluorescence light of oligomeric carbocationic species situated inside the straight zeolite channels, it was possible to observe emission from such species inside the sinusoidal channels. The increased emission from sinusoidal channels with

increasing post-synthesis steaming temperature was the onset of pore structure degradation, starting from the outer surface of the crystal.

The multilaser excitation approach was employed to specifically excite the cyclic and linear dimeric carbocation species, respectively. Their absorption bands were determined in preliminary experiments by UV/Vis microspectrsoscopy [2]. The recorded fluorescence maps revealed different polarisation dependences in accordance to the applied excitation wavelength.

In addition to the polarisation dependent observation of emission light, fluorescence spectra in a range of 320 nm with a resolution of 10 nm were extracted and translated into the third dimension (cf. Fig. 1). In addition to the location/orientation of dimeric carbocationic species inside these ZSM-5 crystals they could be distinguished by their spectroscopic features. Cyclic and linear dimeric carbocations inside sinusoidal zeolite channels revealed an additional fluorescence band shifted by 40 and 20 nm (for 561 and 488 nm excitation) to longer wavelength, respectively, compared to the same dimeric carbocation inside the straight zeolite channels.

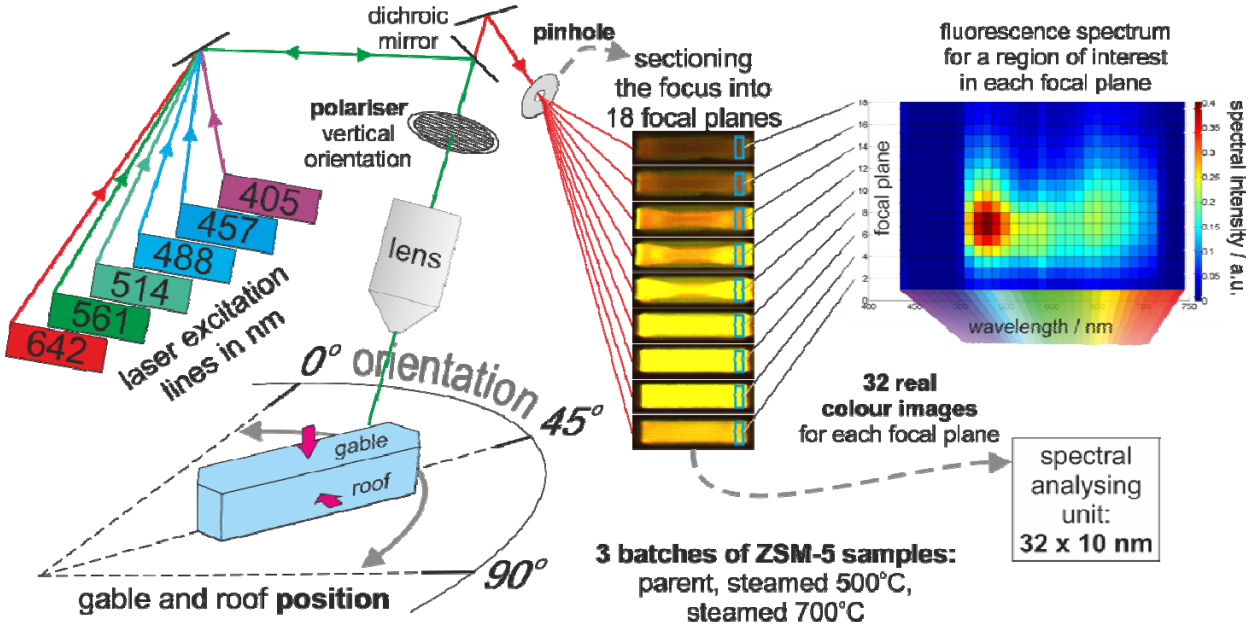

Fig. 1. Overview of the investigation and evaluation principle for the polarised fluorescence confocal microscopy on three sets of large coffin-shaped ZSM-5 crystals.

4 Conclusions

A systematic polarised fluorescence confocal microscopic investigation was presented for three batches of large coffin-shaped ZSM-5 crystals. The observation of polarised emission was linked to structural features of such crystals, and the location of dimeric carbocationic species inside straight and sinusoidal zeolite channels was distinguished. Fluorescence spectra were extracted (translated into the third dimension) from which it was possible to discriminate the same dimeric carbocationic species situated inside straight and sinusoidal zeolite channels, respectively, based on their spectroscopic features.

References

[1] G. Jiménez-García, R. Aguilar.Lóppez, R. Maya-Yescas, Fuel 90 (2011) 3531.

[2] E. Stavitski, M. H. F. Kox, B. M. Weckhuysen, Chem. Eur. J. 13 (2007) 7057.

[3] C. Sprung, B. M. Weckhuysen J. Am. Chem. Soc. (2015) DOI: 10.1021/ja511381f.

II-PP48

Active Cu Structure for Water-Gas-Shift Reaction

Zhang Z., Huang W.*

University of Science and Technology of China, HeFei, China

* huangwx@ustc.edu.cn

Keywords: Cu nanocrystals, Water-Gas-Shift reaction, active structure, reaction mechanism

1 Introduction

Water-gas-shift (WGS) reaction a very important industrial catalytic reaction involving Cu/ZnO as the catalyst, and copper is believed to the active component but the active copper structure is not clear. Here we report the successful synthesis of uniform Cu nanocrystals with various shapes preferentially exposing different crystal planes and their catalytic activity in the WGS reaction. Our results clearly demonstrate that the Cu(100) surface is the active structure for the WGS reaction. Via the combination of in-situ experimental measurements and DFT calculations, the reaction mechanism of the WGS reaction on the Cu surface was revealed.

2 Experimental/methodology

The synthesis of uniform Cu nanocrystals with different morphologies followed those reported in Ref. 1. The structures of Cu nanocrystals were characterized by SEM, TEM/HRTEM, in-situ XRD, XPS, operando-DRIFTS, TPRS, and the catalytic activity of Cu nanocrystals in the WGS reaction were evaluated by using a fixed-bed flow reactor employing an online GC-14 gas chromatograph to analyze the composition of the effluent gas.

3 Results and discussion

Figure 1 shows SEM, TEM, SEAD and HRTEM images of as-synthesized Cu nanocrystals. Cu cubes, octahedra and rhombic dodecahedra are quite uniform, but resulting from the synthesis methods, they are all with very large pores. The HRTEM and ED results demonstrate that Cu cubes, octahedra and rhombic dodecahedra are single crystals and respectively expose the {100}, {111} and {110} crystal planes. These are also verified by the CO adsorption results. The BET surface areas of Cu cubes, octahedra and rhombic dodecahedra are 1.17m^2/g, 2.35m^2/g and 3.33m^2/g, respectively.

Figure 2A shows the catalytic performances of Cu cubes, octahedra and rhombic dodecahedra in the WGS reaction and the corresponding Arrhenius plots. The catalytic activity follows the order of Cu cubes >> Cu rhombic dodecahedra >> Cu octahedra. The apparent activation energies calculated from the Arrhenius plot is 52.98±1.96 kJ/mol for Cu cubes and 71.62±4.87 kJ/mol for Cu rhombic dodecahedra. These results clearly demonstrate that the Cu{100} surface is the active Cu structure for the WGS reaction. Operando DRIFTS, TPRS experimental results and DFT calculation results demonstrate that moderate adsorption energies of all surface intermediates involved the WGS reaction on Cu(100) offer its high catalytic activity.

4 Conclusions

Uniform Cu cubes, octahedra and rhombic dodecahedra respectively exposing the {100}, {111} and {110} crystal planes were successfully synthesized and used as the catalysts for the WGS reaction. Cu cubes enclosed with the Cu{100} crystal planes were identified the active structure and the reaction mechanism was revealed. These results not only significantly deepen the fundamental understanding of Cu-involved catalysts for the WGS reaction but also provide

the guidelines to synthesize highly active for Cu-involved catalysts for the WGS reaction.

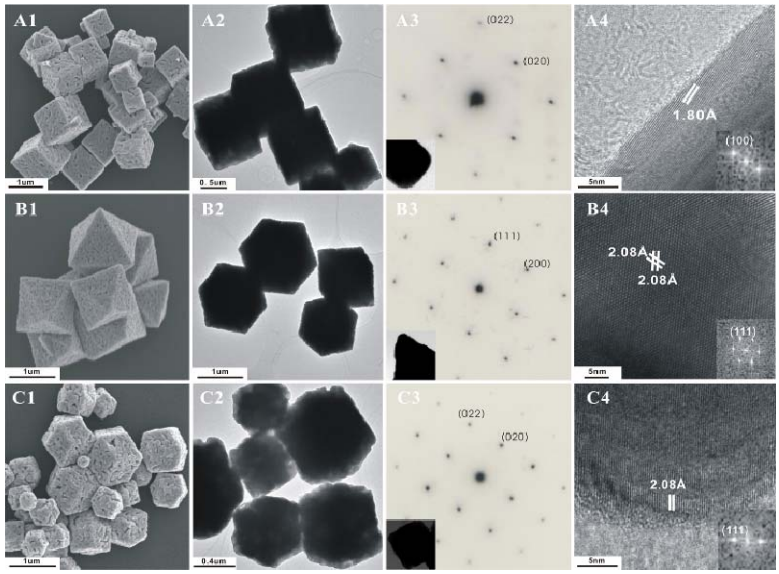

Fig. 1. SEM, TEM, SEAD and HRTEM of c-Cu(A1, A2, A3, A4), o-Cu(B1, B2, B3, B4) and d-Cu(C1, C2, C3, C4).

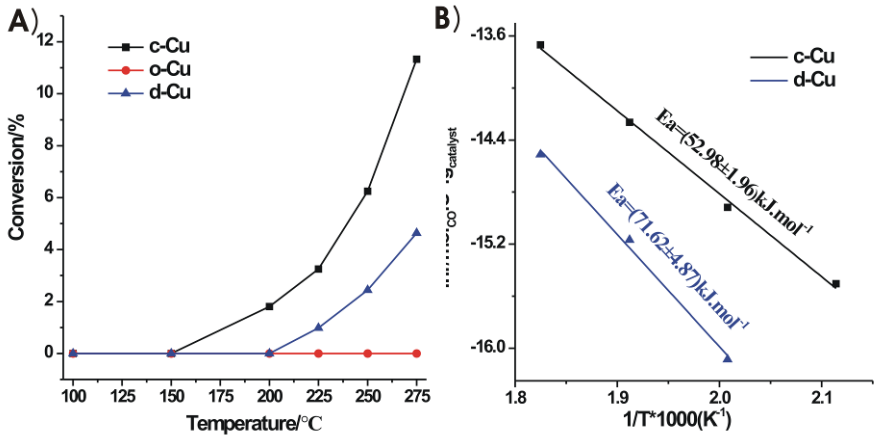

Fig. 2. A) Catalytic performance of c-Cu, o-Cu and d-Cu in the Water-Gas-Shift reaction. B) The Arrhenius plot of the WGS reaction catalyzed by c-Cu and d-Cu.

Acknowledgements

This work was financially supported by the National Basic Research Program of China (2013CB933104, 2010CB923301) and the National Natural Science Foundation of China (21173204, U1332113).

References

[1] Z. H. Zhang, W. X. Huang et al., manuscript submitted.

II-PP49

Enhancing Catalytic Performance of Au/TiO_2 Catalyst in Propylene Epoxidation with O_2 and H_2 via Tuning TiO_2 Morphology

Chen S.[1], Zhang B.[2], Su D.[2], Huang W.[1*]

1 - Hefei National Laboratory for Physical Sciences at Microscale, CAS Key Laboratory of Materials for Energy Conversion, Department of Chemical Physics, University of Science and Technology of China, Hefei, China

2 - Shenyang National Laboratory for Materials Science, Institute of Metal Research, Chinese Academy of Sciences, Shenyang, China

* huangwx@ustc.edu.cn

Keywords: nanocatalysis, surface, chemistry, oxide, nanocrystals, metal-oxide, interaction, active, site

1 Introduction

Propene epoxide (PO) is an essential industrial chemical material intermediates produced by the partial oxidation of propylene. The current manufacturing processes such as chlorohydrin process and Halcon process are environmentally unfriendly and unsustainable. Gas-phase epoxidation of propylene with O_2 is a highly desirable green process for PO production but remains as a great challenge. Hayashi et al. firstly reported that gold nanoparticles highly dispersed on TiO_2 catalyzed propylene epoxidation with O_2 and H_2 to produce PO with selectivity above 90%,[1] and then this system has been extensively studied as a promising green route to produce PO. We prepared Au/TiO_2 catalysts employing TiO_2 nanocrystals with different morphologies as the supports and studied their structures catalytic performances in propylene epoxidation with O_2 and H_2. Strong morphology effects were observed, resulting in different Au-TiO_2 interaction, structures and catalytic performances of Au/TiO_2 catalysts. Au/TiO_2(001) are most active in producing PO and its PO yield is greatly enhanced over traditional Au/P25 catalyst by more than 40%. Meanwhile, the ensemble of intimately-contacting $Au^{\delta-}$ and Ti^{4+} on anatase TiO_2 {001} and {101} facets was identified as the active structure catalyzing propylene epoxidation with O_2 and H_2 to PO. There results demonstrate morphology-engineering of oxides as an effective strategy to optimize the catalytic performance and understand the fundamental catalysis of oxide-involved catalysts.

2 Experimental/methodology

Propylene epoxidation with O_2 and H_2 experiment. The catalytic performance of Au/TiO_2 nanocatalysts in propylene epoxidation with O_2 and H_2 was evaluated in a quartz tubular microreactor of 8 mm diameter and 300 mm length. The catalyst experienced no pretreatment prior to the catalytic reaction. 250 mg catalyst (particle size: 280–450 μm) was used and heated in the reaction gas mixture to 50 °C at a rate of 2 °C/min. All reaction products were analyzed using an online Shimazu GC-2014 gas chromatograph equipped with both flame ionization detectors (FID) and thermal conductivity detector (TCD). Operando DRIFTS measurements were performed on a Nicolet 6700 FTIR spectrometer equipped with an in-situ low-temperature DRIFTS reaction cell (Harrick Scientific Products, INC) and a MCT/A detector. Temperature control of the catalysts is performed via a combination of resistive heating and liquid-N_2 held in an externally attached Dewar container in the range 120-773K.

3 Results and discussion

The results are summarized in Table 1 and demonstrate a distinct TiO_2-morphology-dependent catalytic performances of Au/TiO_2 catalysts. $Au/TiO_2(001)$ is more active than Au/P25 and meanwhile keeps the similar selectivity toward PO. The C_3H_6 conversion reaches 0.69% and the PO selectivity is 97.64%, giving a PO formation rate of 25.4 $mmol_{PO}/h/g_{Au}$. However, $Au/TiO_2(100)$ is much less active than Au/P25 and its selectivity toward PO is also poorer than that of Au/P25. The C_3H_6 conversion is only 0.14%. Besides the PO production with a selectivity of 89.44%, acetone and CO_2 were observed to form with the selectivity of 5.58% and 4.98%, respectively. Thus PO formation rate over $Au/TiO_2(100)$ is as low as 4.2 $mmol_{PO}/h/g_{Au}$. Therefore, the PO formation rate of various Au/TiO_2 catalysts follows the order of $Au/TiO_2(001)$ > Au/P25 >> $Au/TiO_2(100)$, and the PO formation rate over $Au/TiO_2(001)$ is higher than that of Au/P25 by more than 40%. Fig.1 shows that the weaker adsorption ability of Ti_{5c} sites on $Au/TiO_2(001)$ and Au/P25 than that of Ti_{5c} sites on $Au/TiO_2(100)$ facilitates the desorption of PO from the surface to avoid its further oxidation. Thus $Au/TiO_2(001)$ and Au/P25 catalysts are much more active and selective in catalyzing propylene epoxidation with H_2 and O_2 than $Au/TiO_2(100)$ catalyst. The significantly-enhanced PO yield of $Au/TiO_2(001)$ over Au/P25 could be attributed to its larger number of active $Au^{\delta-}$-Ti^{4+} ensemble due to the large specific surface area of $TiO_2(001)$ and the fine size of Au particles.

Table 1. Catalytic performances of Au/TiO_2 catalysts in C_3H_6 oxidation with H_2 and O_2 (C_3H_6: O_2: H_2: Ar =1: 1: 1: 7, GHSV = 8000 $mL \cdot h^{-1} \cdot g^{-1}$ catalyst, T = 50 °C.

catalyst	Conversion (%)			C_3H_6 selectivity (%)			PO formation rate ($mmol_{PO}/h/g_{Au}$)	O_2 selectivity	H_2 efficiency
	C_3H_6	H_2	O_2	PO	Acetone	CO_2			
Au/P25	0.50	2.96	1.61	98.36	0.76	0.88	18.1	30.3%	16.5%
$Au/TiO_2(001)$	0.69	2.54	1.63	97.64	0.80	1.56	25.4	41.1%	26.5%
$Au/TiO_2(100)$	0.14	3.20	1.66	89.44	5.58	4.98	4.2	7.4%	3.8%

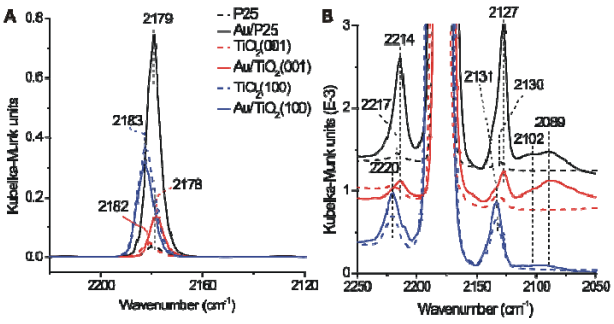

Fig. 1. Operando DRIFTS spectra of CO adsorption on TiO_2 and Au/TiO_2 samples at 120 K with P_{CO} = 2.5 mbar.

4 Conclusions

In summary, employing anatase TiO_2 nanocrystals predominantly enclosed the {001} facets, anatase TiO_2 nanocrystals predominantly enclosed the {100} facets, and P25 predominantly enclosed the {101} facets, we have successfully demonstrated the morphology/crystal plane effect of TiO_2 support on the structure and catalytic performance of Au/TiO_2 catalysts for propylene epoxidation with H_2 and O_2. $Au/TiO_2(001)$ catalyst contains the largest amount of active $Au^{\delta-}$-Ti^{4+} ensemble and thus is most active in propylene epoxidation reaction with a propylene oxide yield of more than 40% higher than traditional Au/P25 catalyst. There results demonstrate morphology-engineering of oxides as an effective strategy to optimize the catalytic performance and understand the fundamental catalysis of oxide-involved catalysts.

References

[1] Hayashi, T.; Tanaka, K.; Haruta, M. *J. Catal.* 1998, 178, 566-575.

II-PP51

Oxidative Dehydrogenation of Propane over Hydroxyapatites Substituted with Mg^{2+} and SiO_4^{4-} Ions

Rasskazova L.[1*], Zhuk I.[1], Korotchenko N.[1], Kovalev E.[2], Glazneva T. [2], Larina T.[2], Paukshtis E.[1,2], Bal'zhinimaev B.[2], Parmon V.[1,2], Kozik V.[1]

1 - National Research Tomsk State University, Tomsk, Russia
2 - Boreskov institute of catalysis SB RAN, Novosibirsk, Russia

* ly_2207@mail.ru

Keywords: hydroxyapatite, magnesium and silicon ions, surface, properties, oxidative dehydrogenation of propane

1 Introduction

Nowadays, $Ca_5(PO_4)_3OH$ hydroxyapatite (HA) is actively studied as a catalyst for many processes including dehydration and dehydrogenation of alcohols, acrylic acid production from lactic acid, levulinic acid hydrogenation to γ-valerolactone. It is known that HA has the structural flexibility due to the ability of ions in its structure to be replaced by various cations and anions. Ion substitution of Ca^{2+} ions by the cations and PO_4^{3-} ions by the anions allow changing the acid-base and catalytic properties of HA. In this study, the synthesis of HA modified by Mg^{2+} and SiO_4^{4-} ions was performed to determine the modifying effect of ions on the acid and catalytic properties for oxidative dehydrogenation of propane.

2 Experimental/methodology

Liquid-phase synthesis of HA was performed via microwave assisted approach according to the technique described elsewhere [1, 2]. Synthesis of $Ca_{9.9}Mg_{0.1}(PO_4)_6(OH)_2$ (MgHA) and $Ca_{10}(PO_4)_{5.4}(SiO_4)_{0.6}(OH)_{1.6}$ (SiHA) powders was performed via the same route adding magnesium nitrate and tetraethoxysiloxane to the stock solutions. The samples were then calcined at 600°C in air. X-ray diffraction analysis of HA, MgHA, and SiHA samples was performed on Shimadzu XRD 6000 diffractometer. FTIR spectra of the samples diluted in BaF_2 matrix were registered on Shimadzu FTIR-8300 spectrometer. The acidity of the surface was determined by FTIR spectroscopy of adsorbed CO. The catalytic activity of the samples was studied in the oxidative dehydrogenation of propane at 350-550°C in a flow unit equipped with a tubular reactor (the inner diameter of 4 mm). The reactor was charged with 0.5 g of catalyst in the form of grains of 0.2-0.5 mm. The composition of reaction mixture was 27% C_3H_8 + 5.5% O_2 + He. Before testing, the catalysts were calcined in a helium flow at 350°C.

3 Results and discussion

Table 1 summarizes the specific surface of the obtained samples as well as their catalytic properties. It can be seen that only the sample modified with magnesium revealed good selectivity in the reaction of oxidative dehydrogenation.

Table 1. Specific surface and catalytic data obtained at 550°C for studied hydroxyapatites

Sample	HA	SiHA	MgHA
S_{BET}, m^2/g	85	83	72
Propane conversion, %	9.4	9.3	17.1
Selectivity of propylene + ethylene formation, %	17	13	57

XRD method showed the presence of a single phase of $Ca_5(PO_4)_3OH$ hydroxyapatite in the samples. The impurity phases were not detected also by IR method (Fig. 1) which would allow to reveal the impurities of amorphous silica. The bands of stretching and deformation vibrations of the phosphate groups in the frequency range of 580-650 and 960-1080 cm^{-1} as well as isolated (surface) hydroxyl groups at 3560 cm^{-1} and hydrogen-bonded (bulk) hydroxyl groups at 3400 cm^{-1} were observed in the spectra.

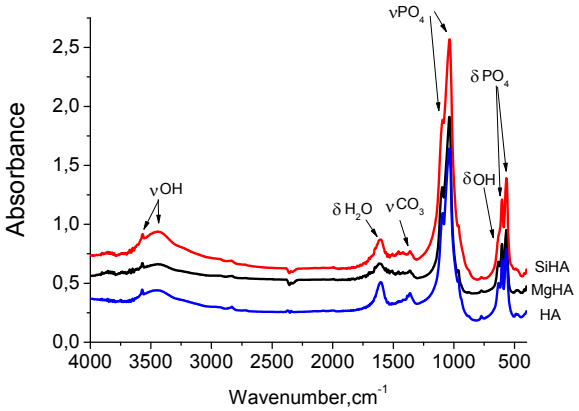

Fig. 1. FTIR spectra of HA, MgHA, and SiHA samples.

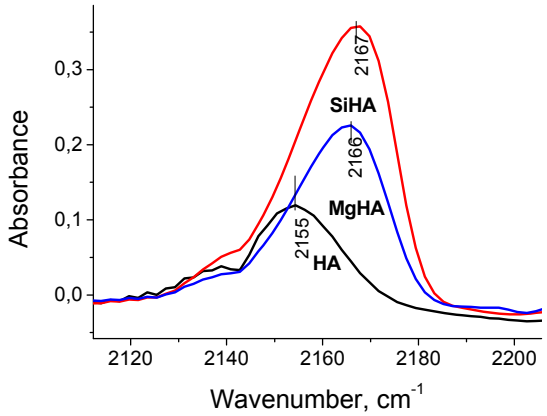

Fig. 2. FTIR spectra of CO adsorbed on the surface of HA, MgHA, and SiHA samples.

Low-temperature CO adsorption revealed the presence of Lewis acid sites (LAS) and the coordinately unsaturated Ca^{2+} and Mg^{2+} cations on the surface of HA, MgHA, and SiHA samples characterized by absorption bands in the region of 2150-2170 cm^{-1}. The strength of LAS in the samples decreases in the following order: SiHA > MgHA > HA (Fig. 2). The row of activity does not coincide with the row of site strength, which may indicate that the oxidative dehydrogenation of propane occurs with participation of acid-base pairs. The expected row of strength of basic sites is MgHA > HA > SiHA, and this row correlates well with the one of catalytic activity.

4 Conclusions

The samples of magnesium- and silicon-substituted HA were synthesized, their surface properties and catalytic activity were studied. It was found that the introduction of Mg^{2+} and SiO_4^{4-} ions into the structure of HA did not alter the hydroxyapatite structure, but it led to increased surface acid properties. The sample modified by magnesium showed the highest activity and selectivity in the oxidative dehydrogenation of propane. The achieved total selectivity in the formation of ethylene and propylene at 550°C over this catalyst was 57% at conversion of 17%.

Acknowledgements

The work was performed within the scope of the Russian Ministry of the Education task (project number of 11.801.2014/K).

References

[1] L.A. Rasskazova, N.M. Korotchenko, V.V. Kozik, V.K. Ivanov, L.P. Shilyaeva, Theor. Found. Chem. Eng. 48 (2014) 682.
[2] L.A. Rasskazova, N.M. Korotchenko, G.M. Zeer, J. Appl. Chem. 86 (2013) 744.

II-PP52

Evolutions of the Surface Structure and Catalytic Performance of PtRu/C and PtRu/Al_2O_3 during Thermal Treatments

Zhang H., Ma C.J., Zheng J.B., Zhang N.W.*, Li Y.H., Chen B.H.*

Dept. of Chemical and Biochemical Engineering, National Engineering Lab. for Green, Productions of Alcohols-Ethers-Esters, College of Chemistry and Chemical Engineering, Xiamen University, Xiamen, China

* zhnw@xmu.edu.cn, chenbh@xmu.edu.cn

Keywords: surface structure, thermal treatment, PtRu, bimetallic, catalyst, preferential, oxidation of CO, selective oxidation of benzyl alcohol

1 Introduction

As one of the most important and typical bimetallic catalysts, supported PtRu nanoparticles are widely used in electrooxidation and catalytic oxidation. In order to get better performance, thermal treatment under specified conditions is often conducted before being used in reactions. However, structure evolution of the supported nanoparticles during the treatment is complicated and less studied, and more research is needed to reveal its influence on the catalytic performance thus the structure-performance relationship with the purpose of designing catalysts in a more scientific way. We have recenctly studied the surface structure evolutions of PtRu bimetallic nanoparticles during thermal treatment under H_2, and obtained the influences of their surface structure on the catalytic properties via preferential CO oxidation and selective oxidation of benzyl alcohol as model reactions.[1]

2 Experimental/methodology

PtRu/C and PtRu/Al_2O_3 was prepared by a one-pot surfactant-free polyol process and then treated under H_2 at different temperatures.The samples treated at 200 ºC, 300 ºC, 400 ºC, 500 ºC, 700 ºC are labeled as PtRu-200H, PtRu-300H, PtRu-400H, PtRu-500H, PtRu-700H, respectively. The catalysts were characterized by TEM, ICP, XPS, HS-LEIS and in situ DRIFTS. Preferential oxidation of CO experiments were performed in a fixed-bed lab reactor at atmospheric pressure. The reaction mixture consisted of 1% CO, 0.5% O_2, 50%H_2 and N_2 balance. The weight hourly space velocity (WHSV) of total gaseous reactant was 40,000 $mL \cdot g^{-1} \cdot h^{-1}$. Selective oxidation of benzyl alcohol was performed in a Teflon-lined reactor. The reaction conditions are as follows: 100 mg catalysts, 20 mL benzyl alcohol, 1MPa O_2, 100 ºC, 8h.

3 Results and discussion

Figure 1 shows the TEM results of the as-prepared PtRu/C. As can be seen, the size of the bimetallic nanoparticle is about 2 nm, and the structure can also be proved as a nano-alloy.The compositions of the samples were measured by ICP and XPS, and the results are shown in table 1.The bulk Pt/Ru mole ratio, as determined by ICP, is about 1.66. The Pt/Ru mole ratio on the surface determined by XPS increased monotonously from 1.48 to 2.53 with the increase in the thermal treatment temperature. This means Pt would migrate to the surface during the thermal treatment and this can also be proved by the HS-LEIS results.

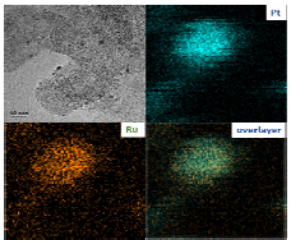

Fig. 1.TEM results of

Table 1. Summary of some characterization data

sample	size /nm	Pt/Ru Mole Ratio	
		by ICP	by XPS
PtRu-200H	1.67±0.40	1.66	1.48
PtRu-300H	1.63±0.39	1.66	1.53
PtRu-400H	1.79±0.34	1.66	1.63
PtRu-500H	1.84±0.37	1.66	1.79
PtRu-700H	3.06±1.05	1.66	2.53

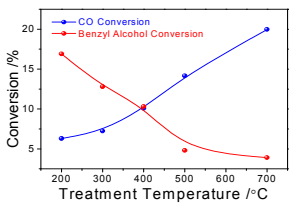

Fig. 2. Conversion of CO or benzyl alcohol at 100 ºC over different catalysts.

The influence of thermal treatment on PtRu catalytic properties was studied through the catalytic oxidation of CO and benzyl alcohol, and the results are shown in figure 2. It's clearly that the conversions of CO increase with the treatment temperature. This means a Pt rich surface is of benefit to the CO oxidation. However, the highest conversion of benzyl alcohol was obtained over PtRu-200H, which is about 17.5% and it will decrease with the increase in the treatment temperature.

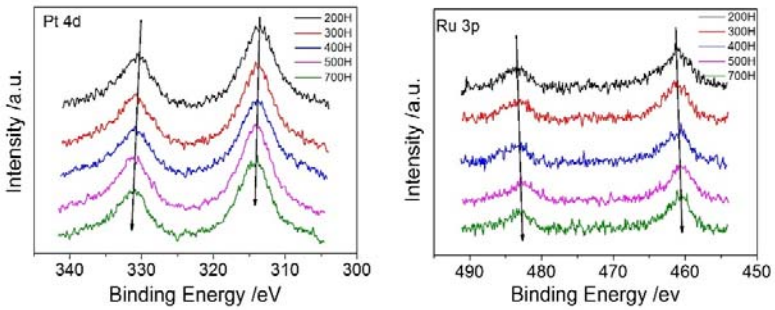

Fig. 3. XPS analysis for $PtRu/Al_2O_3$ treated at different temperatures

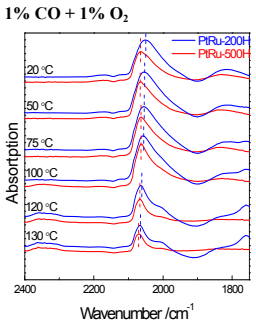

Fig. 4. In situ DRIFTSfor CO oxidation

In order to understand the opposite relationships between the activity and treatment temperature for the oxidation of CO and benzyl alcohol, we then studied the catalysts by XPS and in situ IR. Due to the black colour of carbon, it cannot be used in the IR study and thus we then supported the PtRu on Al_2O_3. The size of the bimetallic nanoparticle is also about 2 nm, and the segregation of Pt to the surface can be also proved as indicated by the XPS results. The activity towards CO oxidation also increases with the treatment temperature. This means $PtRu/Al_2O_3$ treated under different temperature resulted in similar structure to the corresponding PtRu/C. The $PtRu/Al_2O_3$ was then studied by XPS and in situ DRIFTS. As the treatment temperature increased, it can be observed from figure 3 that the binding energies of Pt 4d were shifted to higher values while that of Ru 3p were shifted to lower values.These results indicates the electronic interactions between Pt and Ru get strengthened with increased treatment temperatures, and the electrons are transferred from Pt to Ru. As shown in the figure 4, significant blue shift of the peak for linearly adsorbed CO can be observed for the sample treated at 500 degrees, as compared with that at 200 degrees. This means Pt atoms on the catalysts treated at higher temperature will be more easily oxidized during the reaction. We believe this is because the electrons of Pt are transferred to Ru as supported by the XPS results.

Based on these, the reasons for the reverse relationships between the activity and treatment temperature for the two reactions can be explained. For CO oxidation, oxidized Pt species, on which the adsorption of CO is much weaker, can work as O_2 activation sites and enhance the activity towards CO oxidation, so its activity increased with the treatment temperature. On the other hand, as for the selective oxidation of benzyl alcohol, the rate-determined step is the dehydrogenation of the alcohol. Metallic Pt species can work as hydrogen acceptors and help to accelerate the dehydrogenation step. As the metallic Pt decreased with the increase of treatment temperature, the activity for the oxidation of benzyl alcohol will also decrease.

4 Conclusions

In summary, the surface structure of PtRu nanoparticles with identical bulk composition has been successfully tuned by thermal treatment under H_2 at different temperatures. According to the XPS and LEIS characterizations, we found Pt will migrate to the surface and the electronic interactions between Pt and Ru get strengthened with the increase of treatment temperatures. Such changes lead to the Pt atoms on the catalysts treated at higher temperature more easily to be oxidized during the reaction. It was observed that oxidized Pt species is favorite to CO oxidation, while metallic Pt to oxidation of benzyl alcohol respectively.

References

[1] Zhang, H.; Zheng, Z.; Ma, C.; Zheng, J.; Zhang, N.; Li, Y.; Chen, B. H. *ChemCatChem* **2015**, *7*, 245.

II-PP53

Photoactive Coatings Based on Titanium Dioxide Formed by Plasma-Electrolytic and Anodic Oxidation

Kondrikov N.B.*, Vasilyeva M.S., Andreev A.A., Stepanov I.V., Lapina A.S., Runov A.K.

Far Eastern Federal University, Department of Physical and Analytical Chemistry, Vladivostok, Russia

* kondrikov.nb@dvfu.ru

Keywords: titanium dioxide, plasma-electrolytic oxidation, anodic oxidation, photoactive coating

1 Introduction

Improving the photoactive and photocatalytic properties of titanium dioxide (TDO) is an important task, especially in the environmental aspect, and there, in the foundations, in two directions: the formation of nanostructured film coatings TDO and its doping for regulation of the phase and chemical composition.

There governmental capabilities in these areas are methods of plasma-electrolytic oxidation (PEO) [1] and anodic oxidation (AO) .The .first lets through the implementation of the regime of microplasma discharges form the oxide not only oxidizing metal (Ti), but also include a film component of forming electrolyte. The second lets a way to form and regulate nanotubular structures TDO and use it as a photocatalyst or a template for modify its photoactive properties [2].

2 The experimental

When PEO titanium samples are formed carbonate-silicate electrolites used with different contents of sodium vanadate, sodium tungstate and europium oxide (electrolyte- suspension). The formation of the coating occurred at the selected voltage, currents and times. Anodic oxidation of titanium was conducted in fluorinated aqueous [3] and non-aqueous [4] electrolytes in the constant voltage mode (20-40 V). Morphology of surface, phase and elemental composition were investigated by SEM, XRD, energy-dispersive X-ray spectroscopy (EDX). Definition photoactivity of samples was conducted under the photocurrent generated by exposure of UV-radiation in a three-electrode quartz cell on the potentiostat "AUTOLAB PGSTAT-302N".

3 Results and discussion

Under the conditions of formation of coatings by the PEO-method volume of generated photocurrents) is a linear function of the concentration of content of dopants (given by EDX – analysis data) in coatings with correlation coefficients close to 1. Maximal quantity of dopant is disclosed under formation coating with the addition of tungsten salt – up 5.6 at%. Photocurrents generated on the undoped sample of TDO and in the presence of dopant differ by more than an order of magnitude Figure 1.

When generating a photocurrent samples of nanotubular TDO and doped Pt observed similar dependences, but the emergence of the photocurrents due here in the introduction of platinum nano-particles of titanium dioxide nanotubes with decrease recombination of photogenerated of electrons and holes, which should contribute to the efficiency of photo-catalysis. The highest photocatalytic activity in the decomposition of methyl orange showed by coating doped by maximum amount of tungsten, the degree of degradation of up to 93%.

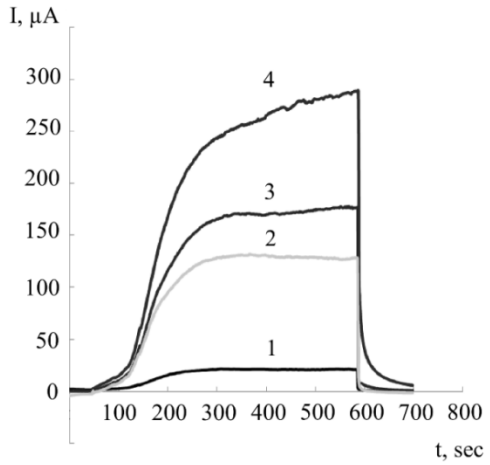

Fig. 1. The dependence of the photocurrents generated by samples of titanium dioxide coatings: undoped –1 and modified by additives of Eu_2O_3 – 2, $NaVO_3$ – 3, Na_2WO_4 – 4 from the time of UV-irradiation.

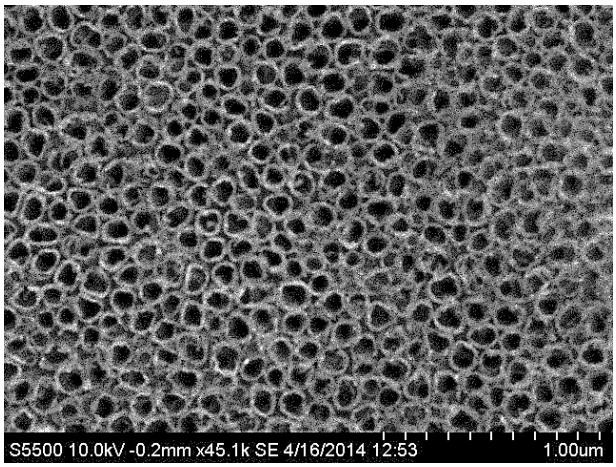

Fig. 2. SEM-image of nanotubular coating TiO_2 formed by anodic oxidation.

4 Conclusion

The photoactivity of film coatings TDO formed by PEO as well as AD, as well as the influence of dopants and nanostructures on their photocatalytic properties are showed.

Highest photoactivity for PEO-coating is disclosed for film formed in presense of tungsten salt as doping component. under bigger its concentration in electrolyte. The coatings formed by anodic oxidation in fluorine-containing electrolytes characterised by one-dimensial (nanotubular) nanostructures which-must more efficiency in photocatalysis due for specific surface area, faster electron mobility. Those factors will be investigated in future.

Acknowledgements

The work was supported by the "Research Fund of Eastern Federal University", Agreement 12-03-13003 / 13 and Government Order of Ministry of Education and Science of Russian Federation, - project 179.

References

[1] M.S. Vasilyeva, N.B. Kondrikov et.al, Protection of Metals and Physical Chemistry of Surfaces, v.50, (2014), N4, P.499-507.
[2] A.N.Banerjee, Nanotechnology, Science and Applications, v.4 (2011), P. 35-65.
[3] R.Beranek, H. Hildebrand, P.Shmuki, Electrochem. Solid –State Lett. 6, (2003), B12-B14.
[4] Y.Lai, H.Zhuang, Z.Chen at al. Electrochimica Acta , V.54, (2009), P.636-645.

II-PP54

The Role of Etch Pits in Catalytic Etching of Platinum Catalyst Gauzes in Ammonia Oxidation

Salanov A.N.[1,2*], Suprun E.A.[1], Serkova A.N.[1], Sidelnikova O.N.[3], Sutormina E.F.[1], Isupova L.A.[1], Parmon V.N.[1,2]

1 - Boreskov Institute of Catalysis, SB RAS, Novosibirsk, Russia
2 - Novosibirsk State University, Novosibirsk, Russia
3 - Institute of Solid State Chemistry and Mechanochemistry, Novosibirsk, Russia

* salanov@catalysis.ru

Keywords: platinum gauzes, ammonia oxidation, catalytic, etching

1 Introduction

Ammonia oxidation with air on platinum catalyst gauzes is widely used in chemical industry for synthesis of nitric acid [1]. It is well known that the gauzes undergo deep structural rearrangement of the surface layers (catalytic etching) during this process. It results in the formation of pits, facets and crystals, platinum loss and decrease of the catalytic activity [2-5]. Two possible mechanisms of the catalytic etching are usually discussed. They are related to increased surface mobility of metal atoms due to the influence of adsorbates [2-3] and to the formation of volatile platinum oxides (PtO_2, etc.) [4-5]. To determine regularities in the formation of pits, facets and crystals, and their role in the catalytic etching of platinum catalyst gauzes during the NH_3 oxidation, we carried out detailed investigation of the surface microstructure of platinum catalyst gauzes treated in air and in the reaction medium (NH_3+O_2).

2 Experimental/methodology

Catalytic oxidation of NH_3 in air was carried out in a laboratory flow reactor made of quartz tube with the inner diameter 11.2 mm at feed (~10% NH_3 in air) flow rate 880-890 l/h, gauze temperature 860±5 °C and total pressure ~3.6 bar. The platinum catalyst gauzes used in the study were made from a wire with d ~100 μm, which had the following chemical composition (in wt.%) 81% Pt, 15% Pd, 3.5% Rh and 0.5% Ru. The gauzes were treated in the reactor for 50 hours both in the reaction mixture and in air. The surface microstructure was studied using a scanning electron microscope (SEM) JSM-6460 LV (Jeol). The surface chemical composition of the studied samples was determined by Energy Dispersive X-ray Microanalysis (EDS).

3 Results and discussion

To determine the role of pits, facets and crystals in catalytic etching of platinum catalyst gauzes during the NH_3 oxidation, we analyzed in detail the surface morphology of regions/fragments of gauzes with different degrees of etching. Grains with 1-13 μm diameter separated by boundaries containing pores with the diameter of 200-400 nm were observed on the fragment of the surface with minimum etching (Fig. 1a). Crystallite plains with the height ~ 100 nm and many pits with the diameter of 50-150 nm were observed on the surface of the grains as dark spots. Some of the pits have pyramidal shape of the etch pits at places where screw dislocations come to the surface. The concentration of these pits is 4.5 10^8 cm^{-2}, which is close to the density of dislocations in platinum estimated in [3]. Larger pores were observed in grain boundaries and on the grain surface on the wire fragments with intermediate etching degree (Fig. 1b). The concentration of the etch pits decreased by a factor of 3-4 in comparison with the fragments having minimum etching (Fig. 1a).

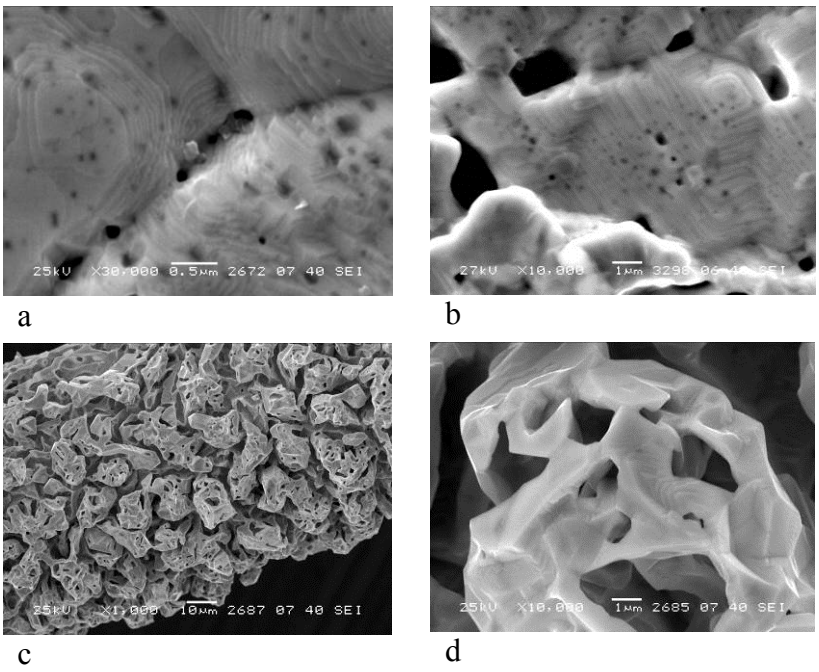

Fig.1. Scanning electron image of fragments of the platinum catalyst wire treated in reaction mixture (~ 10% NH_3 in air) at 860 °C for 50 h.: a, b – fragments with minimum and intermediate catalytic etching; c, d – fragments with maximum catalytic etching.

The fragments of the wire with maximum etching have developed surface morphology (Fig. 1c, 1d). Figure 1c shows a continuous layer of crystallites with the size of 3-16 μm separated by voids with the width of 1-10 μm. An image of such crystallite in higher magnification is shown in Fig. 1d. Voids between grains and penetrating pores in the crystallites were observed. They can be formed by merging of growing etch pits in grain boundaries and on the surface of grains. Treatment of platinum catalyst gauzes in air at 860 °C results only in the formation grain boundaries. No formation of pits, facets, crystals or other surface structures, i.e. surface etching, was observed.

4 Conclusions

Detailed investigation of the surface microstructure of platinum catalyst gauzes after 50 hours of treatment in the NH_3+O_2 reaction mixture revealed fragments of wires with different etching degrees demonstrating the formation, growth and merging of etch pits resulting in catalytic etching. We believe that the NH_3 oxidation on metal atoms located on surface defects (grain boundaries, dislocations) results in weakening of bonds between these atoms. As a result, the mobility of the atoms increases, they migrate and are gradually incorporated into crystal plains on the grain surfaces. Due to these processes, the etch pits formed at the surface defects gradually grow and merge forming voids between and inside the formed crystallites. These processes may result in catalytic etching of the surface of platinum catalyst gauzes.

References

[1] L. Lloyd, Handbook of Industrial Catalysis, Springer Science+Business Media, LLC 2011
[2] M.R. Lyubovsky, V.V. Barelko, J. Catal. 149 (1994) 23.
[3] R.W. McCabe, T. Pignet, L.D. Schmidt, ,J. Catal, 32 (1974) 114.
[4] A.R. McCabe, C. Wong, H.S. Woo, Platinum Met. Rev. 30 (1986) 54
[5] O. Nilsen, A. Kjekshus, H. Fjellvag, Appl. Catal., A: General 207 (2001) 43

II-PP55

Solid-Phase Synthesis of Intercalated Compounds of Molybdenum Disulfide

Fedushchak T.A.[1*], Akimov A.S.[1], Morozov M.A.[1], Uimin M.A.[2], Petrenko T.V.[1], Vosmerikov A.V.[1], Zhuravkov S.P.[3]

1 - Institute of Petroleum Chemistry SB RAS, Tomsk, Russia
2 - Institute of Metal Physics UB RAS, Ekaterinburg, Russia
3 - Tomsk Polytechnic University, Tomsk, Russia

* taina@ipc.tsc.ru

Keywords: solid phase, synthesis, intercalation, molybdenum disulfide, hydrodesulfurization

1 Introduction

Earlier in the process of constructing of massive 1-, 2-, 3-, 4-component sulfidehydrotreating catalysts we have developed methods [1] that were based on the solid-phase direct combination of catalytic components.The catalysts were prepared from molybdenite (MoS2 as dimensional inorganic precursor of the active component), 3d-metal powders (as promoters), electroexplosivepseudobohemite, nanodiamonds, carbon nanotubes and nanofibers (as structurants and binders).Thus was shown the possibility of obtaining a hydroprocessing catalysts which have a high level of activity, easily and simple - in a single step and without using of aqueous solutions or organic solvents [2]. It is known that the activity of the two-component Co-MoS_2/Al_2O_3 systems is largely increasing subject to pre-intercalation of active phase - nanocrystallites of potassium [3].Significant activity in model hydrogenolysis reactions were shown by catalysts which were obtained by monolayer dispersion (exfoliation).Previouslyintercalationandexfoliationwasn'tobservedinsolid-phaseconditions.

The subject of this work was researching of possibility of intercalation during mechanical activation of molybdenum disulfide in the presence of polar liquids, as well as the determination of the activity of catalysts in the model reaction of hydrogenolysis of DBT.

2 Experimental

Catalysts were prepared from the purified coarse molebdenite in the presence of trace amounts of polar liquids (water, methanol; 100 and 200 μL) under conditions of mechanical activation (4, 8 and 12 hours) in a vertical vibration mill in vacuo.Experiments to test the activity of the catalysts were made in an autoclave type «AUTOCLAVEENGINEERS» reactor with a volume of 100 ml at a pressure of 3.4 MPa and temperature of 340 ° C ($S_{initial}$ = 500 ppm).Composition of the hydrodesulfurization products was identified by results of gas chromatography-mass spectrometry analyzes using magnetic chromatography-mass spectrometr DFS "ThermoScientific"(Germany).The rate constants of DBT hydrogenolysis were defined assuming pseudo-first order of that reaction :$C_{DBT} = C^0_{DBT} \cdot e^{-kt}$. From tangent of angle of slope of the dependenceln (C^0_{DBT}/C_{DBT}) from t were obtained the corresponding values of the rate constants.Samplesfromthereactorwerecollectedat 0.5, 1, 2, 3, 4, 6 and 7 hours.

Activity of the catalysts was assessed by the level of residual sulfur (sulfur analyzer OXFORD InstrumentsLab - X 3500 SCL) in the final hydrogenation products taking into account the values of the rate constants for the conversion of DBT (initial sulfur content of 500 ppm).Catalyst samples MoS_2 + CH_3OH "before" and "after" the model reaction was analyzed by synchronous thermal analysis and mass spectrometry (TGA/DSC + MS) on the instrument STA-449C ("Netzsch") combined with a quadrupole mass spectrometer QMS 403C.

Heating was carried out in air (flow rate 20 ml / min) to 650^0C at a heating rate of 10 ° C /

min.For processing the results of thermogravimetry (TGA) and differential scanning calorimetry (DSC) was used in the program "ProteusAnalysis".

3 Results and discussion

The greatest activity in the hydrogenolysis model reaction has been demonstrated with catalyst MoS2 + 100 μL of CH_3OH; residual sulfur content decreased from 500 ppm to 2 ppm.As can be seen from the TEM images shown in Figures 1 and 2, after mechanoactivating (8 hours), both samples were heavily milled and crystallites were aggregated.At the same time, in nanocrystallite packs of molybdenum disulfide (Figure 1) the distance between the layers remain close to 0,615 nm.Figure 2 shows a sample of MoS2 wich was mechanoactivated in the presence of 100 μLCH3OH and that picture reflecting crystallographic shifts and rotations of the layers, the additional formation of defects, nanocrystallitessplitted to separate layers.
In other words, intercalation occurs with partial exfoliation in the experimental conditions and in a presence of trace amounts of methanol.

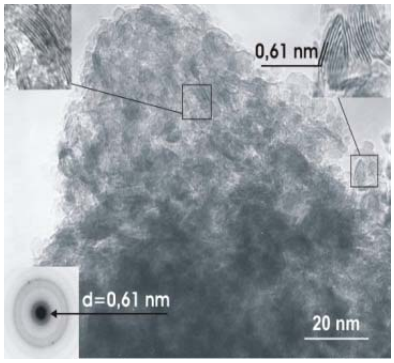

Fig. 1. TEM picture of MoS2 after mechanoactivation (8 h.)

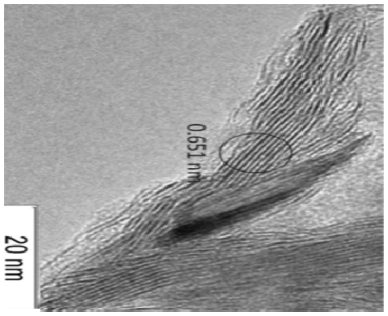

Fig. 2. TEM picture of system MoS_2+ 100 μL of CH_3OH after mechanoactivation (8 h.)

The paper discusses the results of XPS, XRD, synchronous thermal analysis with mass spectrometry for catalysts "before" and "after" their participation in the model reaction.

4 Conclusions

For the first time, was carried out method of direct solid-phase combination of coarse MoS2 with microscopic quantities CH3OH received catalyst with high activity for hydrodesulfurization structures for dibenzothiophene's series. Intensive increasing of activity can be attributed to the formation of new active sites during intercalation and partial exfoliation.

Acknowledgements

The authors are grateful to professors A.S. Noskov and V.I. Zaikovskii for their participation in the organization of experiments and discussion of the results.

References

[1] T. Fedushchak, T. Petrenko, A. Vosmerikov, D. Kanashevich, L. Velichkina, S. Zhuravkov Russian Journal of Physical Chemistry A. 2012. V. 86. 3. P. 375-379.
[2] T. Fedushchak, M. Uimin, A. Ermakov, A. Akimov, N. Shegoleva, T. Petrenko,S. Zhuravkov, A. Vosmerikov.ChemistryforSustainableDevelopment. – 2013. V.6.P.683-685
[3] V. Dorokhov, D. Ishutenko, P.Nikulshin, O. Eliseev, N. Rozhdestvenskaya, V. Kogan, A. Lapidus, DokladyChemistryJuly 2013, Volume 451, Issue 1, P. 191-195

II-PP56

Interactions in Catalytic System Ru-Rb-C (Sibunit) for Low-Temperature Ammonia Synthesis Investigated by EXAFS

Smirnova N.S.[1*], Iost K.N.[1], Temerev V.L.[1], Borisov V.A.[1], Kochubey D.I.[2], Tsyrul'nikov P.G.[1], Kriventsov V.V.[2]

1 - IHP SB RAS, Omsk, Russia
2 - BIC SB RAS, Novosibirsk, Russia

* everinflame@gmail.com

Keywords: low-temperature ammonia synthesis, sibunit, ruthenium, rubidium, EXAFS-spectroscopy

1 Introduction

It is known that ruthenium-alkali metals-carbon support system is highly active in ammonia synthesis [1, 2]. In our case the carbon-carbon composite Sibunit was used as effective carrier for Ru-Rb components. Sibunit is the mesoporous support which combines electrical conductivity with high mechanical strength.

The preparation of modified Ru/Sibunit catalysts is a complex multi-stage process, so catalytic activity depends on processes occurring on each preparation step. The aim of this work is the investigation of structural changes in the Ru-Rb-Sibunit system, which take place on different stages of catalyst preparation. The main advantage of using the Ru-Rb/Sibunit catalysts for investigation by the EXAFS and XANES spectroscopy is the possibility to study local environment not only for ruthenium but for rubidium, which acts as catalyst promoter.

2 Experimental

Supported ruthenium catalyst was prepared by impregnation of Sibunit (S_{BET} = 320 m^2/g, particle size was 0.4 – 0.8 mm) with aqueous solution of $[Ru(NH_3)_nCl_m](OH)_p$ (n =5-6, m=0-1, p=1-2) complex, followed by drying at 120 °C for 3 h (air) and reduction in hydrogen flow at 450 °C for 4 h (H_2 flow was 60 ml/min, heating rate 10 °C/min up to 450 °C). Obtained 4%Ru/Sibunit catalyst was impregnated by aqueous $RbNO_2$ solution, followed by drying at 120 °C for 3 h and activation in argon flow (60 ml/min, 350 °C, 2 h, heating rate 5 °C/min). The sample after activation was reduced in H_2 at 350 °C, 2 h, heating rate was 5 °C/min. Derived 4%Ru-8.5%Rb/Sibunit (mas. %) catalyst was flowed by Ar. The part of the catalyst was taken for EXAFS-spectroscopy after each step of synthesis.

Determination of catalytic activity in reaction of ammonia synthesis was carried in flow reactor under pressure of gaseous mixture H_2:N_2 (molar ratio 3:1) 0.7 MPa and 350 °C. The amount of outlet ammonia was determined by absorption of NH_3 with sulfuric acid solution followed by titration of the H_2SO_4 excess with NaOH solution.

Ruthenium and rubidium K-edge EXAFS spectra were measured on an EXAFS spectrometer at the Siberian Synchrotron Radiation Center. The spectra were obtained using synchrotron radiation at electron energy of EXAFS 2 GeV in the VEPP-3 storage ring, and a current of 70 mA employing a cut-off Si (111) crystal as a monochromator. All spectra were recorded in the transmission mode with a step of 2.5 eV. The resulting spectra were processed using the Viper software following the standard procedure in [3]. The spectra were processed as $k^2\chi(k)$ in a wave number range of 2.50–12.00 $Å^{-1}$. The data on the structure of the compounds were taken from the Inorganic crystal structure database (ICSD).

3 Results and discussion

List of examined samples is presented in table 1.

Table 1. List of samples

№	Sample	Preparation
1	4%Ru/Sibunit	Sibunit impregnation by $[Ru(NH_3)_nCl_m](OH)_p$ complex, dried 120°C 3 h
2	4%Ru/Sibunit	Sample № 1 reduced H_2 450°C 4 h
3	4%Ru-8.5%Rb/Sibunit	Sample №2 impregnated by $RbNO_2$, dried 120°C 3 h
4	4%Ru-8.5%Rb/Sibunit	Sample № 3 activated in Ar 350°C 2 h
5	4%Ru-8.5%Rb/Sibunit	Sample №4 reduced in H_2 350°C 2 h, final
6	4%Ru-8.5%Rb/Sibunit	Sample №5 after NH_3 synthesis

According to EXAFS data, ruthenium in Ru/Sibunit catalyst after drying (sample №1) presents as initial complex. The spectrum of the sample after hydrogen treatment (№2) has only one distance Ru-C of 2.08 Å, which refers to the distance from ruthenium to support carbon. Absence of distances corresponding Ru-Ru, Ru-O-Ru or Ru-C-Ru, means that after reduction ruthenium presents in monatomic state. After impregnation by $RbNO_2$ solution and drying the peak attributed to distance Ru-C (2.08 Å) is remaining. The other peaks in the spectra of sample 3 have low intensities that indicate the absence of an ordered structure.

EXAFS spectra for samples 4% Ru-8.5% Rb/Sibunit after activation in argon (sample №4) and subsequent reduction in hydrogen (№5) are almost identical. The RDF curve in each case exhibits three peaks corresponding to the first (2.69 Å), second (3.79 Å) and third (4.69 Å) coordination spheres of metallic ruthenium.

In all cases the presence of peak at 1.8 Å (in the R-δ scale) in the RbK spectra is related with processes of two-electron excitation in alkali metals [4] and does not refer to actual interatomic distance. The next peak corresponds the Rb-C or Rb-O distance with ~2.9 Å.

4 Conclusions

It is shown that ruthenium in Ru-Rb/Sibunit catalyst after reduction presents in metallic state. Absence of Ru-Rb distance indicated that ruthenium and rubidium are located mainly separate from each other.

Acknowledgements

Physicochemical studies were partially performed in the Omsk Regional Center for collective use of SB RAS (Omsk). This work was supported by the Russian Foundation for Basic Research, projects № 14-03-90032-Bel_a and 14-33-50345-mol_nr, RFBR(140301066).

References

[1] Patent British Petroleum № 4600571 (1986) 6.
[2] Aika K.-i., Kawahara T., Murata S., Onishi T. *Bull. Chem. Soc. Jpn.* 63 (1990) 1221.
[3] D.I. Kochubey. EXAFS spectroscopy in catalysis (in russian), Nauka (1992) 145.
[4] De Panfilis S., Di Cicco A., Filipponi A. et al.// *J. Synchrotron Rad.* 8 (2001) 764.

II-PP57

Influence of Carbon Nanotubes Oxidation on the Co/CNT Structure and Catalytic Activity in CO Hydrogenation

Chernyak S.A.*, Suslova E.V., Ivanov A.S., Egorov A.V., Savilov S.V., Lunin V.V.

Lomonosov Moscow State University, Moscow, Russia

* madseryi@kge.msu.ru

Keywords: carbon nanotubes, CO hydrogenation, oxidation process

1 Introduction

Carbon nanotubes (CNT) possess unique set of properties such as high thermal conductivity and stability, large surface area and chemical inactivity, which allow to use this material as effective support for various catalytic processes [1]. However, pristine CNT are usually unsuitable for metal coating due to the absence of surface stabilization sites. Therefore, different methods are used to stabilize and disperse metal particles on the surface of CNT. The most common methods are surface functionalization, partial substitution of carbon atoms by heteroatoms and controlled formation of surface defects. In this study we considered the influence of CNT oxidation on the morphology and catalytic activity of Co/CNT catalysts.

2 Experimental

Multiwall CNT were synthesized using catalytic chemical vapor deposition method (CCVD). Hexane was used as carbon source, the temperature was 650°C. Complex oxide Co-Mo/MgO was used as growth catalyst. Synthesized material was annealed at 400°C in air flow, washed by HCl and distilled water to remove amorphous carbon and metal impurities.

Washed CNT were boiled in nitric acid during 1, 3, 6, 9, 12 and 15 h. BET Surface area and pore radius were determined by nitrogen adsorption; oxygen content was measured by XPS (surface content) and TGA-MS (volume content); the intensity ratio of the D to the G band (I_D/I_G) from Raman spectra was used to estimate the amount of disorder or defects present in the structure of the CNTs. Samples were denoted as CNT-n, where n means hours of oxidation.

Catalysts were obtained using impregnation of Co nitrate ethanol solution for the Co loading of 15 wt. %. CO hydrogenation was performed in a fix-bed reactor. *In situ* reduction of catalysts (H_2, 400°C, 4 h) was carried out before catalytic tests. Reduced samples were tested in CO hydrogenation conditions (220°C, 1 bar, H_2:CO=2.1:1, 70 h). Reduced and treated catalysts were studied by TEM.

3 Results and discussion

CNT-n characteristic are given in table 1. Maxima of the defectiveness, BET surface area, surface oxygen content (degree of functionalization) are obtained at 9 h oxidation, while total oxygen content has a maximum at 15 h.

Table 1. CNT supports features depending on the oxidation time.

CNT oxidation time (h)	BET surface area (m^2/g)	Average pore radius (nm)	Content of O bounded with C (at.%, XPS)	Total content of O (wt.%, TGA-MS)	I_D/I_G
0	192	18.8	0.3	-	1.13
1	229	12.7	6.5	4.3	1.03
3	233	12.9	8.0	5.0	1.07
6	237	9.8	8.6	4.8	1.38

9	249	1.8	8.9	5.2	1.36
12	246	1.8	8.7	5.5	1.29
15	232	1.8	8.8	6.2	1.17

TEM images of the reduced catalysts reveal CNT destruction in case of long-time oxidation (fig. 1a). It was found that Co particle size decreases and metal dispersion increases with increase of oxygen content. Particles with average diameter 4 nm mixed with huge agglomerates of Co were detected in the sample which contains 6.5 at. % of O (fig. 1b). Otherwise, no large particles were found in the sample with 8.8 at. % of O (fig. 1c).

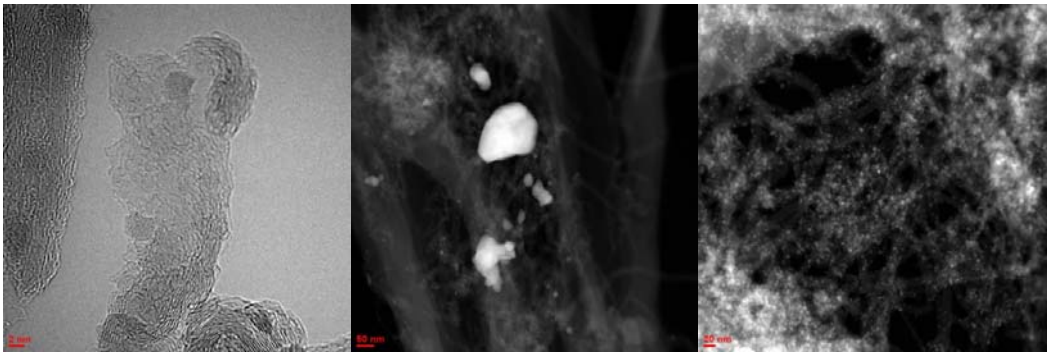

Fig. 1. TEM images of cobalt catalysts supported on CNT: a, c – Co/CNT-15; b – Co/CNT-1.

The dependences of catalytic activity and selectivity from Co/CNT-n structure were obtained in present work. Fig. 2 shows increase of CO conversion with surface oxygen content in CNT growth. The correlation between C_{5+} selectivity and defectiveness was also discovered.

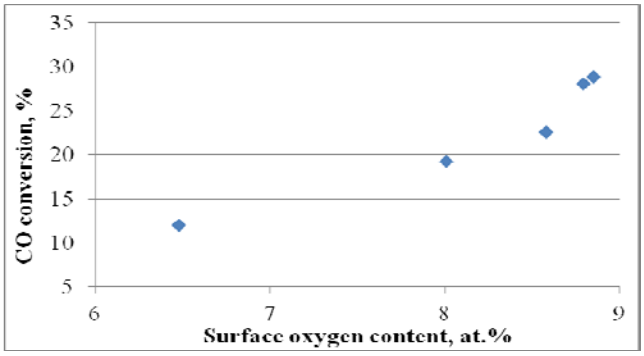

Fig. 2. Change of CO conversion with CNT-surface oxygen content.

Acknowledgements

The authors kindly acknowledge E.A. Nesterova (XPS), N.E. Strokova (TGA-MS), O.Y. Isaikina (Raman spectroscopy).

References

[1] A. Tavasoli, K. Sadagiani, F. Khorashe, A.A. Seifkordi, A.A. Rohani, A. Nakhaeipour, *Fuel Proc. Tech.* 89 (2008) 491.

II-PP59

Hydrothermal Treatment of Gamma Alumina: Mechanisms and Effects on Catalytic Properties

Mukhambetov I.N.*, Lamberov A.A.

Kazan (Volga region) Federal University, Kazan, Russia

* hello_@bk.ru

Keywords: hydrothermal treatment, gamma alumina, skeletal, isomerization of n-butenes, boehmite, lewis, acidity, solid, phase, transition

1 Introduction

Gamma alumina is one of the most commonly used materials as catalysts and their supports. For some catalytic processes it is necessary to increase the acidity of γ-alumina for the synthesis of catalysts with perfect activity. It is known that hydrothermal treatment is an alternative method for the modification of alumina acidity. This process accompanied by a formation of boehmite, however, the cause of the additional active sites have not been identified.

The purpose of this work were: study of structure transformations alumina during hydrothermal treatment, mechanism of the acidity increasing and its influence on catalytic properties in skeletal isomerization of n-butenes and 1-phenylethanol dehydration.

2 Experimental/methodology

The hydrothermal treatment of aluminum oxide was performed in an autoclave at 150°C and heating/cooling rate of 7 deg min^{-1}. On being kept for a certain time, the autoclave was cooled to room temperature and the sample was extracted, dried at 120°C for 2 h.

Hydroxyl groups of alumina and boehmite were studied by IR spectroscopy (Vertex 70) after the evacuation (residual pressure 10^{-3} mbar). The acid centers of the samples were studied by the method of temperature-programmed desorption (TPD) of ammonia on a Quantachrome ChemBET Pulsar TPR/TPD instrument and also via IR spectroscopy (Vertex 70) of adsorbed pyridine.

The catalytic activity of the samples in the course of skeletal isomerization of n-butenes was tested in an isothermal flow-through laboratory reactor in the continuous mode at a temperature of 540°C, raw material : steam molar ratio of 1 : 4. For 1-phenylethanol dehydration – 280°C and raw material : steam molar ratio of 1 : 10.

The porous structure of the samples was studied by the method of low-temperature adsorption of nitrogen with a Quantachrome Autosorb IQ instrument.

The differential-thermal analysis (DTA) was made with an MOM Q-1500 D derivatograph (Hungary) in the temperature range 24–1000°C at a heating rate of 10 deg min^{-1} in argon.

Micrographs of the samples were obtained with a Zeiss EVO-50XVP scanning electron microscope (SEM).

3 Results and discussion

Shown that the transition alumina→boehmite occures in solid phase. In the process of hydrothermal treatment takes a linear accumulation of boehmite, thus sizes of boehmite microcrystals change nonlinearly (Figure 1).

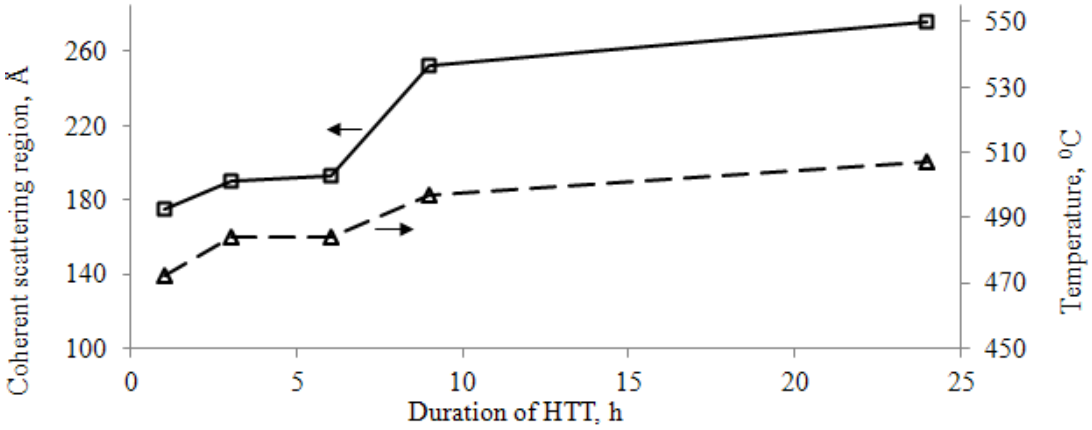

Fig.1. Resizing CSR of boehmite along the [120] and a maximum of thermal decomposition to alumina during the HTT.

After 1–3 h of hydrothermal treatment, secondary aggregates of the starting aluminum oxide are dispersed, which leads to an increase in the specific surface area. In the process, the content of acid centers and the activity of the samples in the skeletal isomerization of *n*-butenes on strong Lewis acid centers also grow. At a long treatment duration (>6 h) the specific surface area and acidity of aluminum oxide decrease.

We analyzed the change of the hydroxyl cover and it is assumed that boehmite forms layer by layer from surface of alumina primary particles (Figure 2). From this viewpoint, the pore structure and acidity distribution changes attributed.

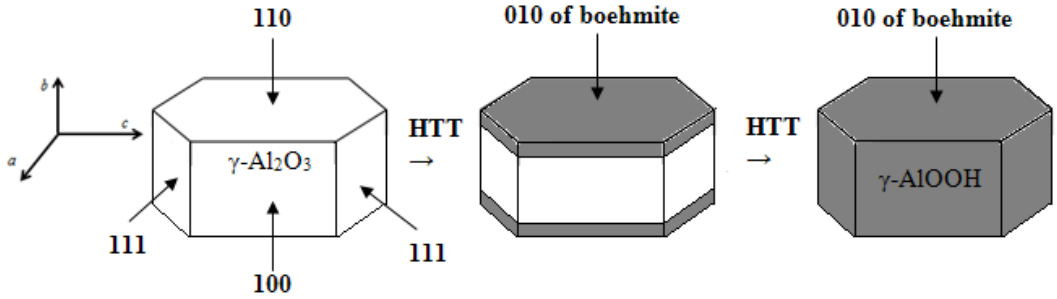

Fig.2. The scheme of conversion of primary particles during the HTT.

4 Conclusions

- Shown mechanism of the transition alumina→boehmite during hydrothermal treatment.
- Interpretated the increase in acidity.
- Catalytic activity of alumina in skeletal isomerization of n-butenes can be improved by hydrothermal treatment from 30 to 33 % at the same selectivity.

II-PP60

Multifunctional Bimetallic Transition Metal Catalysts for Stable and Selective Methane Dry Reforming

Aw M.S.[1], Dražić G.[2], Zorko M.[2], Djinović P.[1*], Pintar A.[1]

1 - Laboratory for Environmental Sciences and Engineering, National Institute of Chemistry, Ljubljana, Slovenia

2 - Laboratory for Materials Chemistry, National Institute of Chemistry, Ljubljana, Slovenia

* petar.djinovic@ki.si

Keywords: transition metal catalysts, ordered mesoporous, alumina, methane dry reforming, syngas, iron, nickel

1 Introduction

Biogas, a mixture of CH_4 and CO_2 is formed in large quantities as a result of anaerobic digestion of organic material, wastes and energy crops. Its production in Europe is growing exponentially in the last decades [1]. CH_4/CO_2 gas mixtures can be directly catalytically converted to syngas via methane dry reforming reaction. If CH_4-CO_2 reforming reaction is to become a complimentary pathway for syngas production, transition metal catalysts which exhibit good activity and especially high resistance to coke accumulation are essential. The latter requirement is difficult to achieve due to high thermodynamic driving force for coke formation and catalyst fouling by its accumulation.

The following rationale was utilized in this work: active transition metal clusters were deposited within the pores of ordered mesoporous alumina to prevent their sintering and growth. The function of neighboring CeO_2-ZrO_2 clusters was to supply oxygen species and gasify the coke, prevent its accumulation and ensure continuous catalyst self-regeneration. This study demonstrates stable and selective reforming of CH_4 with CO_2 over extended time with bimetallic transition metal catalysts containing Ni, Co, W and Fe.

2 Experimental

Ordered mesoporous Al_2O_3 was prepared by evaporation-induced self-assembly method [2] using Pluronic P123, anhydrous ethanol and aluminum isopropoxide. CeO_2 and ZrO_2 (4 mol. % relative to Al_2O_3, Ce:Zr = 4:1) were deposited over the Al_2O_3 using wet-impregnation technique, dried and calcined for 4 h at 350 ^oC (sample denoted as AlCZ). A total of 3 wt. % metals (NiFe, NiW, CoFe and CoW) was wet-impregnated over the AlCZ support. The weight ratio of Ni or Co to Fe or W was equal to 1 to 4 in all cases. The samples were calcined for 4 h at 650 ^oC and are denoted by: NiFe/AlCZ, NiW/AlCZ, CoFe/AlCZ and CoW/AlCZ. Prior to catalysis, samples were activated *in-situ* (20 % H_2/N_2) at 750 °C. Catalytic tests were performed in a tubular quartz reactor at 750 ^oC. Equimolar reactant feed of CH_4 and CO_2 (50 NmL/min each) was fed into the reactor at WHSV = 30 L/(g_{cat}·h). Prepared catalysts were characterized by XRD, N_2 sorption, HR TEM-EDX, H_2-TPR, Raman and UV-Vis techniques.

3 Results and discussion

N_2 sorption showed that AlCZ supports exhibit type-IV isotherm with H1-type hysteresis loop and pore size distribution between 5 and 10 nm. TEM characterization confirmed ordered mesoporous structure of AlCZ support (Fig. 1a). Fig. 1b shows TEM image of the CoFe/AlCZ catalyst with corresponding elemental mapping. These images reveal that after active metal deposition, the ordered mesoporous structure of catalysts was maintained. Also, high dispersion of active metals clusters (below 5 nm) over the surface of the alumina matrix was achieved. Deposited active phase did not form alloys, but instead consisted of single metal clusters.

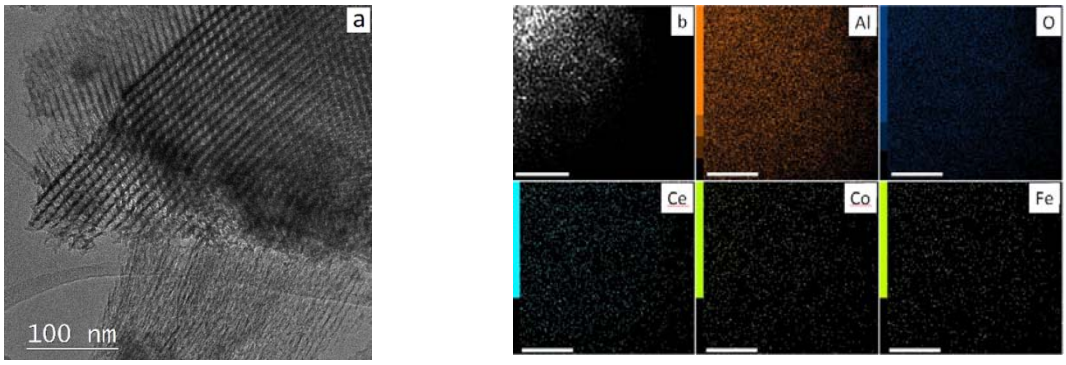

Figure 1. Ordered mesoporous morphology of the (a) AlCZ support and (b) TEM-EDX mapping of CoFe/AlCZ catalyst. Scale bar = 100 nm.

Results of catalytic tests for the most promising catalysts, NiFe/AlCZ and CoFe/AlCZ are presented in Fig 2 and Table 1. These materials exhibited stable activity during the 20 h TOS and H_2/CO ratios which are very close to the equilibrium values. On the other hand, a noticeable deactivation of NiW/AlCZ and CoW/AlCZ catalysts was identified. Also, a significantly lower H_2/CO ratio over these catalysts indicates the dominance of WGS reaction, which consumes a substantial part of H_2 to produce water.

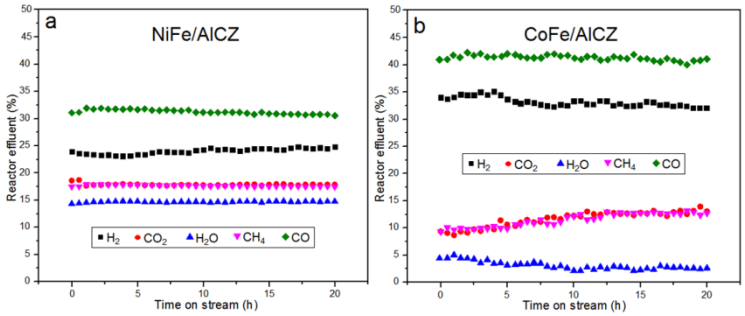

Figure 2. Reactor effluent as a function of time on stream for supported (a) NiFe and (b) CoFe catalysts.

Table 1. BET specific surface area, total pore volume of synthesized bimetallic catalysts along with achieved CH_4 and CO_2 conversions, H_2/CO ratio and accumulated carbon during 20 h catalytic tests.

Catalyst	BET specific surface area, m^2/g	Total pore volume, cm^3/g	X CH_4, %	X CO_2, %	H_2/CO ratio, /	C content, wt. %
NiFe/AlCZ	196	0.29	82	80	0.88	0.6
NiW/AlCZ	228	0.50	86	90	0.68	0.8
CoFe/AlCZ	256	0.57	89	91	0.84	1.2
CoW/AlCZ	220	0.49	87	78	0.56	4.7

4 Conclusions

The employed strategy of depositing bimetallic clusters within the pores of ordered alumina matrix in close proximity to reducible CeO_2-ZrO_2 nanoclusters proved a successful strategy for the development of stable and selective NiFe and CoFe catalysts for CH_4-CO_2 reforming reaction. The presence of W resulted in more pronounced deactivation and undesired WGS activity.

Acknowledgements

The authors gratefully acknowledge the financial support of the Ministry of Education, Science, Culture and Sport of the Republic of Slovenia through Research program P2-0150.

References

[1] 2011 AEBIOM Annual Statistical Report (http://www.aebiom.org), retrieved 29.12.2014
[2] S.M. Morris, P.F. Fulvio, M. Jaroniec, *J. Am. Chem. Soc.* 130 (2008) 15210.

II-PP61

Magnetically Separable Metal Nanoparticles as Effective Reusable Hydrogenation Catalysts

Nikoshvili L.[1*], Lyubimova N.[1], Matveeva V.[1], Sulman E.[1], Shifrina Z.[2], Bronstein L.[2,3,4]

1 - Tver Technical University, Tver, Russia
2 - A.N. Nesmeyanov Institute of Organoelement Compounds of Russian Academy of Science, Moscow, Russia
3 - Indiana University, Indiana, USA
4 - King Abdulaziz University, Jeddah, Saudi Arabia

* nlinda@science.tver.ru

Keywords: magnetic, nanoparticles, palladium, selective, hydrogenation, alkynols

1 Introduction

Recently, magnetic nanoparticles (MNPs) attracted considerable attention as catalytic supports. They allow easy separation of catalysts from reaction mixtures and their repeated uses, resulting in energy conservation, more environmentally friendly processes and cheaper target products [1-4]. While developing magnetically separable catalysts, two important requirements should be taken into account: (i) narrow MNP size distribution due to the dependence of magnetic properties of NP size; (ii) in most cases the surface of MNPs should be functionalized due to the necessity of attachment of catalytic species to NP surface.

Monodisperse MNPs can be prepared by thermal decomposition of iron acetylacetonates or carboxylates in high-boiling solvents containing surfactants. However, surfactants can be replaced by functional ligands including polymers.

In this work we report several approaches to synthesis of iron oxide MNPs and their use as support for palladium-containing catalysts of alkynol hydrogenation (Fig. 1): thermal decomposition of iron-containing precursor [5]; ligand exchange method using functional acids containing multiple double bonds [6]; functionalization of MNP surface with polyphenylenepyridyl dendrons or dendrimers [7, 8].

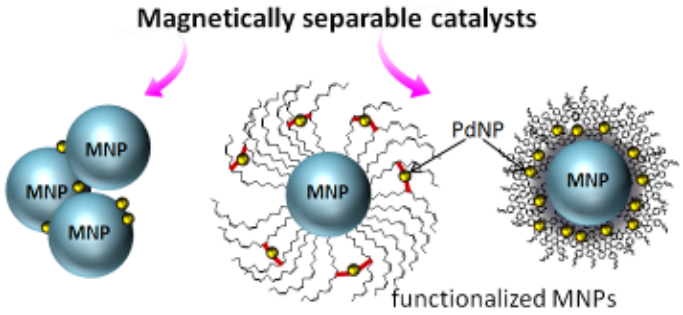

Fig. 1. Schematic representation of used catalytic systems

2 Experimental

In the present work $Pd(acac)_2$, $Pd(oac)_2$, $PdCl_2$ or $(CH_3CN)_2PdCl_2$ were used as Pd sources, and well-defined iron oxide NPs of different compositions as an iron source. Iron oxide NPs were prepared via the thermal decomposition of iron oleate in octadecane and eicosane as solvents, which were chosen to control the reaction temperature and achieve the desired NP size. In the case of MNPs functionalized with polyphenylenepyridyl dendrons/dendrimers of functional acids, $Fe(acac)_3$ was used as iron source. Synthesis was carried out either via ligand

exchange method or in the presence of desired dendrons/dendrimers. It is noteworthy that dendrons/dendrimers served for interdendrimeric stabilization of MNPs and at the same time for encapsulation of catalytically active Pd NPs.

Catalytic testing was carried out in selective hydrogenation of 2-methyl-3-butyn-2-ol (dimethylethynylcarbinol) to 2-methyl-3-buten-2-ol (dimethylvinylcarbinol), which is intermediate of such industrially important compounds as linalool and isophytol, and vitamins E and K, in isothermal glass batch reactor at ambient hydrogen pressure varying the solvent type, temperature and substrate-to-catalyst ratio.

3 Results and discussion

All the synthesized Pd/MNPs catalysts were shown to be promising in alkynol hydrogenation (up to 98% of selectivity at 95% of a substrate conversion, along with extremely high activity were achieved).

It important to note that in some cases, e.g. MNPs covered with functional acids containing multiple double bonds, two types of Pd NPs formation were found: intraparticle and interparticle. The latter was found to result in aggregation. Such an aggregation allowed fast magnetic separation which is necessary for the development of efficient magnetically separable catalysts. In the case of dendron/dendrimer functionalized NMPs, for certain dendron/dendrimer concentrations and structures, well-dispersible, multi-core, flower-like crystals were formed. Besides, aggregation also took place while adding palladium species and the shape and density of aggregates were found to depend on the rate of palladium addition.

Even when no functionalization of MNPs was performed aggregation of MNPs in the presence of Pd NPs occurred that was likely due to polarization forces.

It is noteworthy that independently of the type of functionality on MNP surface, for all the catalytic systems, it was found that samples, which were preliminarily reduced with hydrogen, were much more active and selective in comparison with unreduced samples as well as in comparison with traditional Lindlar catalyst.

4 Conclusions

The magnetic composites containing Pd species have been synthesized and tested in a model reaction of selective hydrogenation of dimethylethynylcarbinol. *Easy magnetic recovery of the catalysts, high selectivity and activity along with stability of their catalytic performance make them promising for a commercial use.*

Acknowledgements

Financial support was provided by the FP7 project *POLYCAT* (*CP-IP 246095-2*), the Ministry of Education and Science of the Russian Federation and the Russian Foundation for Basic Research **and** the Deanship of Scientific Research (DSR), King Abdulaziz University, Jeddah, under grant no.(GR-33-7).

References

[1] D. Wang, D Astruc, *Chem. Rev.* 114 (2014**)** 6949.
[2] Z. Wang, B. Shen, A. Zou, N. He, *Chem. Eng. J.* 113 (2005) 27.
[3] Y. Zhu, S.C. Peng, A. Emi, Z. Su, Z. Monalisa, R.A. Kemp, *Adv. Synth. Cat.* 349 (2007) 1917.
[4] V. Polshettiwar, R. Luque, A. Fihri, H. Zhu, M. Bouhrara, J.-M. Basset, *Chem. Rev.* 111 (2011) 3036.
[5] **R. Easterday,** et al.**,** *ACS Appl. Mater. Interfaces,* 6 (2014) 21652.
[6] S.H. Gage, et al.**,** *Langmuir,* 29 (2013) 466.
[7] N.V. Kuchkina, et al.**,** *Macromolecules*, 46 (2013) 5890.
[8] E.Yu. Yuzik-Klimova, et al.**,** *RSC Adv.*, 4 (2014) 23271.

II-PP63

Characterization of Electron-Acceptor Sites on the Surface of Sulfated and Chlorinated Alumina by EPR Using Spin Probes

Shuvarakova E.I.[1,2*], Bedilo A.F.[1,2]

1 - Boreskov Institute of Catalysis SB RAS, Novosibirsk, Russia
2 - Novosibirsk Institute of Technology, Moscow State University of Design and Technology, Novosibirsk, Russia

* Katerina.shuv@gmail.com

Keywords: electron-acceptor sites, EPR, sulphated alumina, chlorinated alumina

1 Introduction

Aluminum oxide is widely used as a catalyst support. The surface of Al_2O_3 is known to have both acid and base sites of different types. Deposition of sulfates or chlorides on the γ-Al_2O_3 surface is known to lead to a substantial increase of its acidity and catalytic activity in acid-catalyzed reactions. The catalytic properties of sulfated alumina generally resemble those of sulfated zirconia, which is more widely known due to its higher acidity and catalytic activity. Meanwhile, low cost, high surface area, wide availability, and reasonable thermal stability make sulfated alumina an attractive catalyst for acid-catalyzed processes that do not require very high acid strength.

Spontaneous ionization of aromatic molecules is known since the 1960s. The presence of the active surface sites of different strength, capable of ionizing the aromatic molecules was suggested. Conventionally, they are divided into strong, medium and weak. Electron-acceptor sites of different strength can be characterized using aromatic probes with different ionization potentials [1, 2]. Our recent results suggest that such sites are most likely responsible for decomposition of halocarbons [3] and ethanol dehydration [4]. This study was devoted to analysis of relations between the concentrations of electron-acceptor sites and modifying components and mechanisms of processes taking place on different sites and adsorption of the used aromatic donor molecules.

2 Experimental/methodology

Sulfated Al_2O_3 samples with the different concentrations of SO_3 (2, 4, 8, 12, 16 wt.%) and chlorinated samples with Cl contents of 1, 2, 4, 8 wt.%. were studied. Two experimental techniques were used for characterization of electron-acceptor sites [2]. The former was to study changes of the concentration of paramagnetic particles over time at room temperature. The first measurement was carried out immediately after the activation of the sample. The following measurements were carried out every 24 hours for one week. The second technique was to study the changes in the concentration of paramagnetic particles after heating the activated samples with probes for 18 hours at 80°C.

3 Results and discussion

It was found that the concentration and the strength of electron-acceptor sites significantly grow with an increase of the sulfate concentration (Fig. 1). The strongest electron-acceptor sites tested with toluene immediately after adsorption were only detected with a concentration of SO_3 not less than 4%. The weakest sites tested with perylene presented on the surface of all the samples, with their concentration on 12% SO_3 sample being 3×10^{19} g $^{-1}$.

The study of chlorinated samples showed that there were no strong sites on their surface. Chlorination only led to minor growth of the concentration of the weak sites. Their concentration tested using perylene or anthracene after the heat treatment at 80°C increased only

by a factor of 2 on the sample 4% Cl^- compared to the unmodified support.

Recommendations on the use of spin probes for testing electron-acceptor sites with different strength are suggested. A mechanism of the polycondensation of aromatic probes on the surface electron-acceptor sites explaining experimental results and possible structures of such sites were proposed.

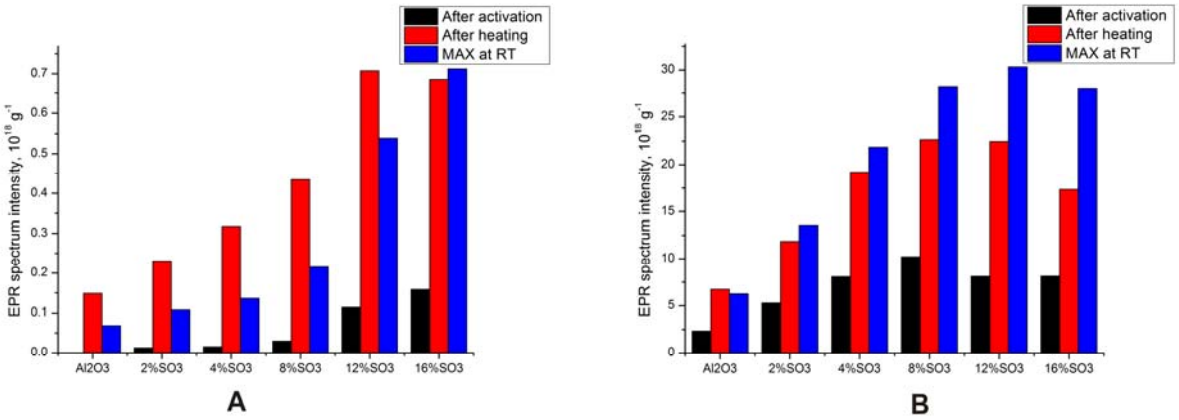

Fig. 1. Comparison of the EPR spectra intensities observed on alumina samples with different sulfate concentrations immediately after spine probe adsorption, after heating at 80 °C for 18 h and maximum concentration achieved at room temperature: A – toluene adsorption on strong sites, B – perylene adsorption on weak sites.

4 Conclusions

Alumina modification with sulfates was found to result in a gradual increase of the concentration of electron-acceptor sites characterized using the formation of radical cations from aromatic molecules with different ionization potentials. The strongest electron-acceptor sites tested with toluene immediately after adsorption were detected only on sulfated alumina with a concentration of SO_3 not less than 4%. Al_2O_3 chlorination only led to minor growth of the concentration of the weak sites.

Measuring the concentration of radical cations generated immediately after adsorption of a donor appears to be the most direct way of estimating the concentration of electron-acceptor sites with the corresponding strength. Apart from fast generation of primary radical cations on strong electron-acceptor sites and their following transformations, slow formation of EPR signal attributed oligomeric hydrocarbon species is observed. The rate of their formation depends on the concentration of sulfates and the used electron donor. This process seems to take place on weak electron-acceptor sites of the alumina surface and can be used to characterize them.

Acknowledgements

This study was supported in part by Russian Foundation for Basic Research (Grants 13-03-12227-ofi_m and 15-03-08070-a).

References

[1] A.F. Bedilo, A.M. Volodin, *Kinet. Catal.* 50 (2009) 314.
[2] A.F. Bedilo, E.I. Shuvarakova, A.A. Rybinskaya, D.A. Medvedev, *J. Phys. Chem. C* 118 (2014) 15779.
[3] A.F. Bedilo, E.I. Shuvarakova, A.M. Volodin, E.V. Ilyina, I.V. Mishakov, A.A. Vedyagin, V.V. Chesnokov, D.S. Heroux, K.J. Klabunde, *J. Phys. Chem. C* 118 (2014) 13715.
[4] R.A. Zotov, V.V. Molchanov, A.M. Volodin, A.F. Bedilo, *J. Catal.* 278 (2011) 71.

II-PP64

X-Ray Diffraction Methods for Nano-Scale Structural Studies of Catalytic Materials

Pakharukova V.P.[1,2*], Yatsenko D.A.[1,2], Nikulina O.S.[1,2], Bulavchenko O.A.[1,2], Pakharukov I.Yu.[1,2], Tsybulya S.V.[1,2]

1 - Boreskov Institute of Catalysis, SB RAS, Novosibirsk, Russia
2 - Novosibirsk State University, Novosibirsk, Russia

* verapakharukova@yandex.ru

Keywords: structural, characterization, Ga_2O_3 oxide, Pt/γ- Al_2O_3 catalysts, DFA, PDF method

1 Introduction

The key aspect in catalysis research is understanding any structure–performance relationships. Characterization of catalytic materials is related with an ability to study nano-scale structures. There is significant drawback with common XRD methods, since they probe well-crystallized materials. Bragg peaks from nanocrystalline phases are broadened. Moreover, additional diffuse scattering is missed in standard XRD analysis, whereas it contains information on the local structure and defects. Alternative effective approaches take into account both the Bragg and diffuse scattering. Calculation of full profile of XRD pattern by means of Debye Function Analysis (DFA) allows modelling XRD pattern for crystallites of any size and shape [1-2]. Analysis of radial distribution function (RDF) of electron density or pair distribution function (PDF) is directed on atomic-scale structural studies [3]. This method is based on integral analysis of the full XRD pattern and reveals distribution of interatomic distances up to 1-3 nm. The possibilities of these methods to probe structure of catalytic materials are shown for some examples: 1) structural study of nanocrystalline γ-Ga_2O_3 oxide; 2) determination of local atomic structure of supported platinum in Pt/γ-Al_2O_3 catalysts.

2 Experimental

Calculations of XRD patterns were performed by the DFA method using the DIANNA software [2]. Experimental XRD patterns were obtained at a Bruker D8 Advance diffractometer (Cu $K_{\square}$ radiation, λ=1.5418Å) and at diffractometry stations (λ=0.703 Å and λ=0.368 Å) in the Siberian Synchrotron and Terahertz Radiation Centre (Novosibirsk, Russia). The RDFs or PDFs were obtained by the Fourier transformation of normalized scattering intensity [3].

3 Results and discussion

γ-Ga_2O_3

Nanocrystalline Ga_2O_3 oxides have been used as supports or catalysts. Gallia has a polymorphism somewhat similar to that of alumina. There is limited information on structure of the γ-Ga_2O_3 phase. High dispersion complicates structure solving. The XRD pattern of the γ-Ga_2O_3 oxide under study exhibits broadened and unresolved peaks (Fig. 1). The modelling by DFA method showed that the XRD pattern corresponds to a spinel type structure with vacancies in tetrahedral 8a and octahedral 16d cation positions and with additional cations in nonspinel 8b, 16c, 48f positions. The best fit was obtained for crystallites of a parallelepiped shape with dimensions of 0.8×1.6×1.6 nm (Fig.1). Analysis of PDF confirmed that area of atomic arrangement in the oxide did not exceed 1.5-2 nm in size; correlations in atomic arrangement fade at longer distances (Fig.1). Observed atomic correlations differed from those characteristic for the ideal spinel structure. Proposed model of defect spinel with filling spinel and nonspinel sites was more appropriate for describing the observed atomic ordering.

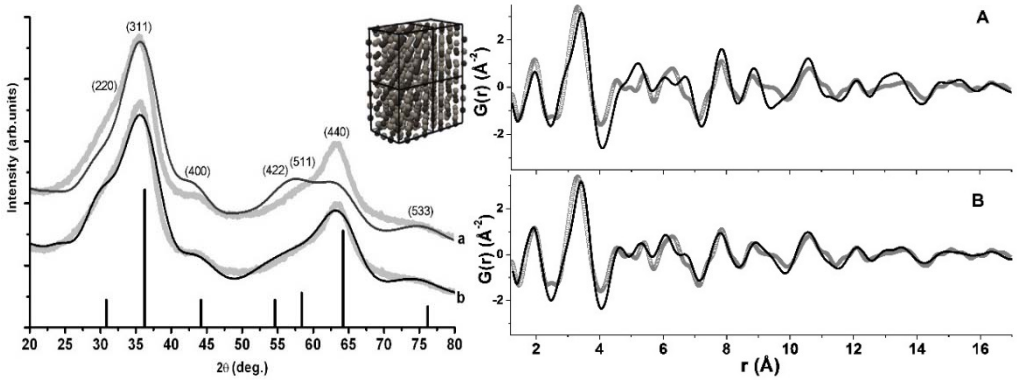

Fig. 1. Left side: experimental (gray line) and model (black line) XRD patterns for the γ-Ga_2O_3 oxide. Right side: experimental (gray circles) and model (black line) PDFs for the γ-Ga_2O_3 oxide. **a** - ideal spinel, **b** – cation deficient defect spinel.

Pt/γ-Al_2O_3

Analysis of differential curves (d-RDFs) between RDFs of the catalysts and support allows the local structure of supported nanoparticles to be determined. The atomic structure of supported platinum in the 0.75 wt % Pt/γ-Al_2O_3 catalysts was studied [4]. Both the metal Pt^0 and oxide PtO_x species were detected depending on catalyst preparation conditions (Fig.2). The data provided an insight into the structure of highly dispersed PtO_x species. The results supported recent suggestions about interaction between the platinum and alumina. The Pt atoms had atomic correlations with support atoms. In particular, the Pt atoms seemed to be strongly anchored to the cation vacancies in the γ-Al_2O_3 surface.

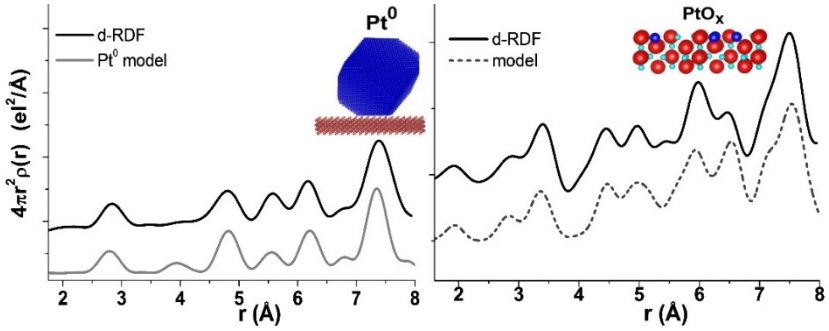

Fig. 2. Experimental d-RDFs describing the Pt local arrangement in the Pt/γ-Al_2O_3 catalysts in comparison with RDFs calculated for the Pt^0 phase and model of atomic ordering at insertion of Pt atoms into cation vacancies in the alumina surface.

4 Conclusions

The DFA and PDF methods are complementary powerful techniques for structural diagnostics of nanocrystalline catalytic materials. The PDF method allows one to reveal structure of supported nanoparticles, when it is applied on heterogeneous catalysts.

Acknowledgements

This work was supported by the RSCF project №14-23-00037.

References

[1] P. Debye, *Ann. Physik.* 46 (1915) 809-823.
[2] S.V. Tsybulya, D.A. Yatsenko, *Journal of Structural Chemistry* 53 (2012) 150-165.
[3] E.M. Moroz, V.P. Pakharukova, A.N. Shmakov, *Nucl. Instrum. Methods A* 603 (2009) 99.
[4] V. Pakharukova, I. Pakharukov, V. Bukhtiyarov, V. Parmon Appl. Catal. A: Gen. 486 (2014) 12-18.

II-PP65

Design of Active and Selective Catalyst Systems on the Basis of Clinoptilolite for Hydrocarbon Cracking

Kadirbekov K.A.[1,2*], Zhambakin D.K.[1], Nurbaeva R.K.[2], Aitureev A.U.[2], Kadirbekov A.K.[2], Imanbekov K.I.[2]

1 - LLP «Kazatomprom-Sorbent», Almaty, Kazakhstan
2 - JSC «A.B. Bekturov Institute of chemical sciences», Almaty, Kazakhstan

* kkairati@mail.ru

Keywords: natural zeolite, clinoptilolite, modification, mineral acids, organic acids, heteropolyacids

1 Introduction

It is known that hydrocarbon cracking is carried out on acidic centers, therefore ideal catalysts for this process are solid acids [1,2]. Zeolites, as solid acids are the main catalysts for the cracking of hydrocarbons.

2 Experimental/methodology

As the object of research natural zeolites of Shankanay field (Kazakhstan) was taken, in which the major rock-forming mineral is acid- and heat-resistant clinoptilolite.

Catalysts based on natural zeolite of Shankanay field were synthesized by modification with mineral acids, organic acids, and heteropolyacids (HPA).

Modification of natural zeolite samples (Kl) was performed by the method of Kerr in a Soxhlet apparatus. All samples were dried in an oven and calcined at 500 ° C for 4 hours in a muffle furnace. An acid modification conditions: 1.6-2 mm fraction of the zeolite, the ratio S:L of 1:10 (wt.), processing temperature 94-98ºC, the contact time to 10 hours. After a predetermined time, the samples were washed thoroughly from residual acid, dried to air-dry state.

3 Results and discussion

Modification of natural zeolite sample with various acids leads to structural changes of clinoptilolite. Acid activation of clinoptilolite increases its surface and pore volume, decreases average pore diameter, which in turn directly affect the properties of the active acid sites of the zeolite, as well as their distribution on the catalyst surface.

The study found that the catalysts obtained by modification of natural zeolite with various by nature acids, by the specific surface area starting from the lowest arranged in a row:

Kl > H4EDTA/Kl > HKl-1 > H4EDTA/HKl-1 > HSal/HKl-1 > PW12-HPA/HKl-1

Special attention deserves the abnormal growth of the surface when the modification with 10% PW12-HPA to 257.0 m2/g, since this value is much higher than for pure zeolite and HPA. Obviously, when HPA applied on the surface of the zeolite there is a deep interaction occurs. In addition, there is formation of new nanostructures that have been shown by TEM and SEM.

By volume of pores the catalysts starting from the lowest may be arranged in a row:

Kl > HKl-1 > HSal/HKl-1

The pore distribution on the catalyst surface shifts toward micropores, or in other words, on the surface mainly micropores are found.

Obviously, the growth surface of the catalyst is due to the formation of new micropores.

Determination of surface micropores (Smc) also shows their growth from 2.49 to 38.07 m^2/g after modification with hydrochloric acid and to 67.84 m^2/g with sulfosalicylic acid.

As a result of the XPS study it was found that when impregnating heteropolyacids of molybdenum and tungsten series, the zeolite framework partially decomposed with the formation of individual and Al-O- and Si-O- structures. Since conditions of the main elements of the zeolite varies a little. Molybdenum and tungsten in catalysts are in present as Mo (6+) and W (6+), respectively, which evidence of retaining heteropoly-like structure.

Morphology and microfeatures, elemental composition in the observed point, the distribution pattern of elements on the surface of initial clinoptilolite and its acid-modified forms examined by SEM (JSM-6X80) and TEM HR (JEM–2010) (Fig. 1.).

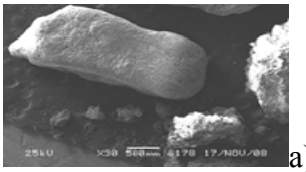
a)
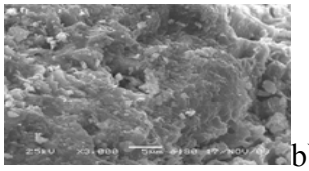
b)
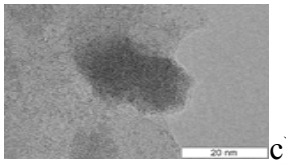

c)

Fig. 1. – Electron-microscopic image of zeolite samples: granules of natural zeolite; HKl-1, PW12-HPA/HKl-1.

According to electronic images of natural zeolite granules are irregular in shape (Fig. 1a) and are characterized by a specific structure consisting of irregularities and cracks, which causes the penetration of relatively large cations.

Surface of decationized clinoptilolite HKl-1 (Fig. 1b), characterized by inhomogeneity and the presence of multiple shallow channels, which have a layered structure.

When modification of zeolite with decationized HPA of Tungsten 12 series, there is a sharp increase in the specific surface area of the catalyst. Obviously, when HPA impregnated on the surface of the zeolite there is a deep interaction. Thus on the TEM HR images of catalyst homogeneous structures of HPA interspersed into the pores of the zeolite are visible. The dimensions of these structures are a few nanometers. Obviously, the occurrence of these nanostructures alters the catalytic properties, particularly cracking activity of the catalyst considerably increases, consequently the yield of liquid products of the cracking reaction, constituting mainly of the long-chain α-olefins increase.

By means of CO adsorption method of strength and concentration of acid sites were identified. In the series starting from lowest: HKl > 10%HSal/HKl > 10% PW12-HPA/HKl. There is a significant increase in the proportion of strong and very strong Bronsted acid sites. Strong acid sites are found at 10% PW12-HPA/HKl and HKl. Bronsted centers of the second type on 10%PW12-HPA/HKl by the shift are greater than HKl, although the concentration is less. Acid sites of the third type on the catalysts, approximately the same amount, but they obviously do not determine the activity of the cracking catalyst. The total concentration of strong acid sites on 10%PW12-HPA/HKl and sum of shifts at 340 cm^{-1} and 320 cm^{-1} is higher than on HKl. It should be noted that the increase in acidity correlates with high silicate modulus (SiO_2/Al_2O_3) of the zeolite sample.

4 Conclusions

Thus, by modification of natural zeolite with various acids, active hydrocarbon cracking catalysts for the synthesis of long chain α-olefins were designed. Due to low cost and availability of natural zeolite developed catalysts can be used on an industrial scale.

References

[1] Kadirbekov K.A. Chem. journal of Kazakhstan. 2010, #3 – pp. 103-120.

[2] Konuspayev S. R., Kadirbekov K. A., Nurbayeva R.K., and Sarsekova A.T. Catalysis in Industry. 2011, Vol. 3, No. 1, pp. 76–80.

II-PP66

Effect of Oxygen Bulk Diffusion in Nickel on Self-Sustained Oscillations in the Catalytic Oxidation of Methane

Ustyugov V.[1*], Finkelstein E.[2], Lashina E.[1], Chumakova N.[1], Gornov A.[2], Kaichev V.[1], Bukhtiyarov V.[1]

1 - Boreskov Institute of Catalysis SB RAS, Novosibirsk, Russia
2 - Institute for System Dynamics and Control Theory, Irkutsk, Russia

* ustugov@catalysis.ru

Keywords: self-sustained oscillations, methane, oxidation, oxygen bulk diffusion, nickel

1 Introduction

Nonlinear behavior, like self-sustained oscillations in the reaction rate, is an unusual and, nevertheless, well-known phenomenon in the heterogeneous catalysis. Sinusoidal or harmonic oscillations, relaxation-type oscillations, and chaotic behavior have been observed to date in approximately 40 catalytic reactions in a wide pressure range, from ultrahigh vacuum up to atmospheric pressure, over all types of catalysts, including single-crystals, polycrystalline foils, wires, and supported catalysts. Several mechanisms describing the rate oscillations for different reactions were proposed. However, the most of them is based on the Langmuir-Hinshelwood mechanism and do not take into account the diffusion in subsurface layers of catalysts. This study is devoted to theoretical analysis of the influence of the diffusion of oxygen atoms into nickel on the self-sustained rate oscillations in the catalytic oxidation of methane.

2 Methodology

The microkinetic scheme for the oxidation of methane over nickel was published elsewhere [1]. Parameters of elementary reactions, such as enthalpies and activation energies, were determined using a phenomenological approach suggested by E. Shustorovich [2]. Pre-exponential factors of elementary steps were evaluated in the framework of the transition state theory [3]. The diffusion coefficients of oxygen atoms in nickel were determined on the basis of experimental data. The mathematical model of the reaction consists of a system of ordinary differential equations and takes into account concentrations of surface intermediates, an oxygen concentration in subsurface layers, and the heat balance.

3 Results and discussion

The model of the catalytic oxidation of methane over nickel was amended with a step of the diffusion of oxygen atoms from the nickel surface into subsurface layers. It allows us to study the influence of this step on the characteristics of the oscillatory behavior. In full agreement with previous study [1] the model without the oxygen diffusion under certain parameters has oscillatory solution (fig. 1). In this case the oscillations starts without any delay. In contrast in the model with the oxygen diffusion we found a long induction period before arising the self-sustained oscillations. Similar effect was observed experimentally. Also we found that the concentration of oxygen in the subsurface layers of nickel oscillates synchronously with the concentrations of reaction products in the gas phase.

In both cases we found the partial pressure oscillations of products and reactants as well as the concentration oscillations of main intermediates on the catalyst surface. Simultaneously the catalyst temperature oscillated with the amplitude of several Celsius degrees. Typical oscillations are presented in fig. 1.

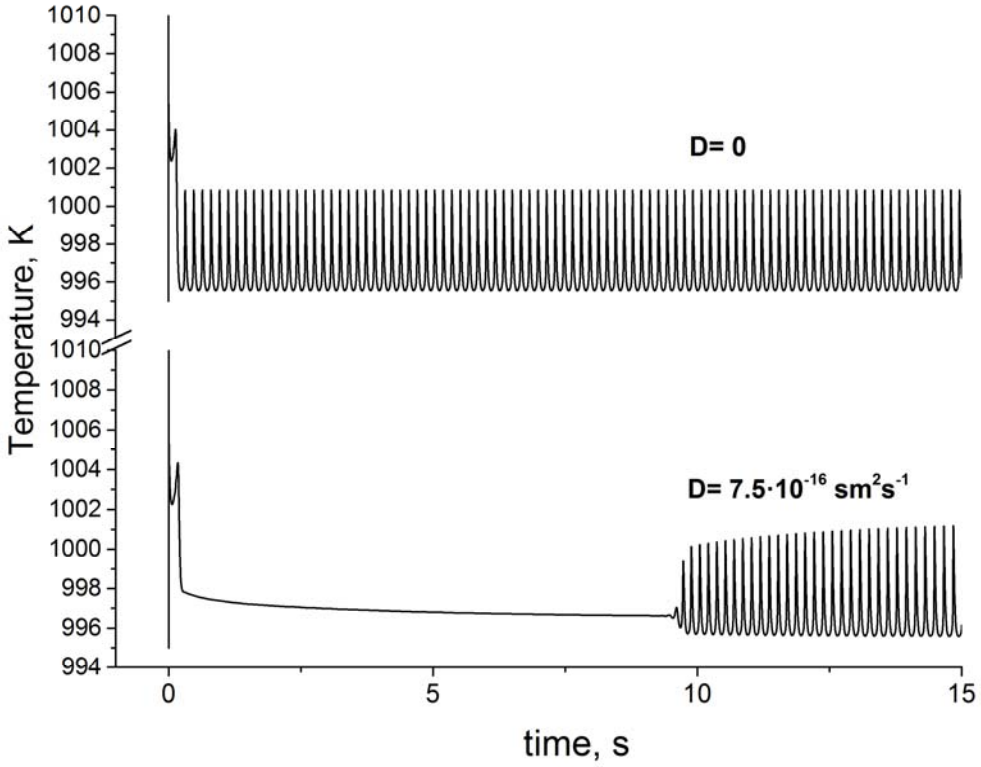

Fig. 1. Oscillations of catalyst temperature in the models of methane oxidation without (top) and with (bottom) oxygen diffusion. D is coefficient of oxygen bulk diffusion.

4 Conclusions

The addition of the oxygen diffusion into the model leads to the appearance of an induction period before the self-sustained rate oscillations. The concentration of oxygen in the subsurface layers of nickel oscillates synchronously with the concentrations of reaction products in the gas phase.

Acknowledgements

The work was partially supported by the Grant of President of Russian Federation for government support of Leading Scientific Schools (SS-5340.2014.3).

References

[1] E.A. Lashina, V.V. Kaichev, N.A. Chumakova, V.V. Ustyugov, G.A. Chumakov, V.I. Bukhtiyarov, *Kinet. Catal*. 53 (2012) 374.
[2] E. Shustorovich, in: D.D. Eley, H. Pines, P.B. Weisz (Eds.), *Adv. in Catal.* 37 (1990) 101.
[3] J.A. Dumesic, D.F. Rudd, L.M. Aparicio, J.E. Rekoske, A.A. Trevino, The Microkinetics of Heterogeneous Catalysis. American Chemical Society, Washington, 1993.

II-PP67

SEM and EDX Characterization of $Mn/Na_2WO_4/SiO_2$ Catalyst for Oxidative Coupling of Methane

Leba A., Dusova-Teke Y., Avci A.K., Yildirim R.*

Bogazici University, Department of Chemical Engineering, Istanbul, Turkey

* yildirra@boun.edu.tr

Keywords: OCM, oxidative coupling of methane, SEM-EDX

1 Introduction

The demand for chemicals and energy has been continuously increased in recent years as the result of industrial development and increasing concerns for greenhouse gas emissions. One of the promising alternatives for the production of basic chemicals and liquid fuels from natural gas is the oxidative coupling of methane (OCM) process, which converts methane into valuable hydrocarbons such as ethane and ethylene [1]. Although this process has been well-known for a few decades, there is still some scientific challenge to achieve a commercial OCM catalyst. Therefore, a great attention has been still paid on this issue by many researchers. Numerous attempts has been made utilizing various catalyst types, forms, reactors and operating conditions in order to enhance the OCM process. The silica supported active metals such as Mn and Na_2WO_4 as in $Na_2WO_4/Mn/SiO_2$ catalyst is one group of catalyst that has been suggested for this purpose [2]. In this work, SEM characterization of various forms of $Na_2WO_4/Mn/SiO_2$ catalyst for OCM reaction has been investigated to support the work performed to determine the most suitable catalyst form for this important reaction.

2 Experimental/methodology

The various structures such as particulate catalyst, wash coat monoliths and single monolithic structures of 2wt.%Mn/5wt.%Na_2WO_4/SiO_2 catalyst were prepared through three different methods (incipient to wetness to impregnation method, sol-gel method and direct hydrothermal synthesis method (MCM-41)). Scanning electron microscopy (SEM) coupled with energy dispersive X-ray spectroscopy (EDX) analysis was performed with Philips XL 30 ESEM-FEG instrument in our research center to observe the surface morphology of fresh and used catalysts.

3 Results and discussion

SEM results showed that Mn and Na_2WO_4 metals were uniformly dispersed on the surface of particulate catalyst prepared with incipient to wetness to impregnation method, while these metals were disorderly dispersed on the one prepared by sol-gel method; EDX results also verified these findings. Figure 1 shows the catalyst loadings on MCM-41 catalysts. As it is seen in Figure 1.b, there are large porous structures filled by Na (light color) as also verified by EDX analysis. Mn metals were also observed as grey stripes. EDX results also showed that Mn and WO_4 were better dispersed than Na metals.

Figure 2 shows SEM results of monosil structured catalysts. It is clearly seen that a good porous structure was obtained, and the catalyst (the white dots that was identified as NAby EDX analysis) was well dispersed on the cross sectional area normal to flow (Figure 2.c). On the other hand, it was found that these metals did not well diffuse into the monosil structure as it is seen from Figure 2.d, which shows a surface inside the monolith parallel to flow direction; the number of white dots are much smaller than that was observed in Figure 2.c. Both catalysts

performed slightly lower than the particulate catalysts in the reactions tests (at 700 °C with a CH_4/O_2 ratio of 10), and resulted about 10% C_2 (ethane and ethylene) yield as compare to 14% obtained with particulate catalyst.

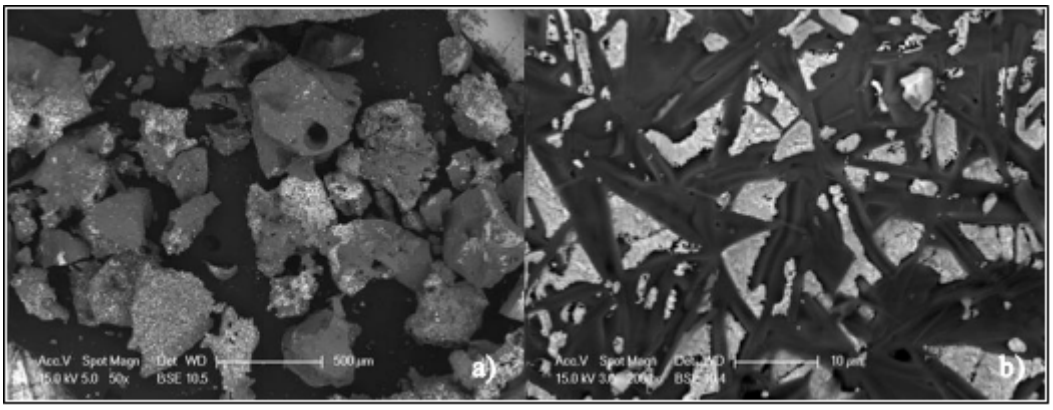

Fig. 1. SEM images of MCM-41 catalyst over 2wt.%Mn/5wt.%Na_2WO_4/SiO_2: a) 500 µm, b) 10 µm.

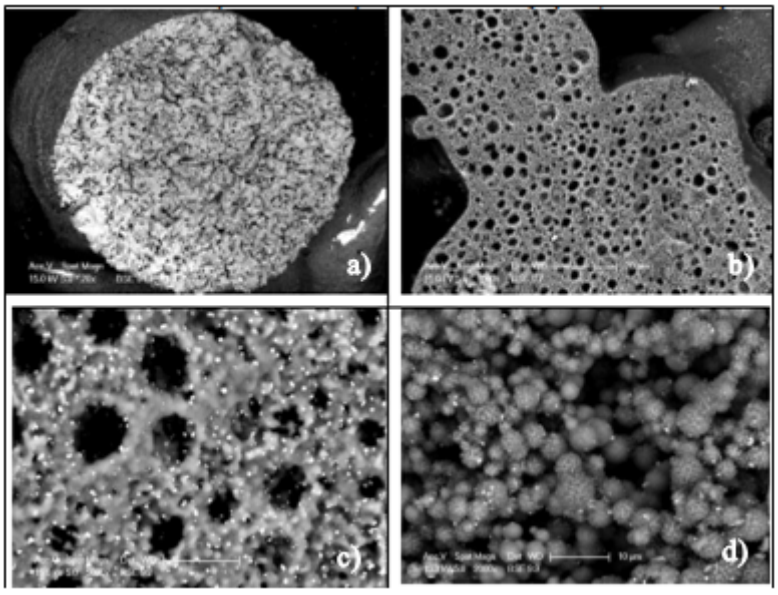

Fig. 2. SEM images of monosil catalyst over 2wt.%Mn/5wt.%Na_2WO_4/SiO_2: a) 1 mm, b) 20 µm in cross section normal to flow, c) 5 µm in cross section normal to flow, d) 10 µm in cross section parallel to flow.

4 Conclusions

SEM and EDX characterization of 2wt.%Mn/5wt.%Na_2WO_4/SiO_2 showed that the dispersion of Mn and Na_2WO_4 metals were quite different in different forms of the catalysts; this difference seems to affect the catalytic activity and therefore C_2 (ethane and ethylene) yield.

Acknowledgements

The financial support for this work was provided by TÜBİTAK through project 112M714.

References

[1] M. R. Rahimpour, M. R. Dehnavi, F. Allahgholipour, D. Iranshahi, S. M. Jokar, *Applied Energy.* 99 (2012) 496-512.

[2] M. R. Lee, M. J. Park, W. Jeon, J. W. Choi, Y. W. Suh, D. J. Suh, *Fuel Processing Technologies.* 96 (2012) 175-182.

II-PP68

Significant Enhancement Effect of PVP Capping Ligands on Catalytic Activity of Cu_2O Octahedra in CO Oxidation

Cao T.[1,2,3], Hua Q.[1,2,3], Zhang Z.[1,2,3], Huang W.[1,2,3*]

1 - Department of Chemical Physics, University of Science and Technology of China, Hefei, China
2 - Hefei National Laboratory for Physical Science at the Microscale, Hefei, China
3 - CAS Key Laboratory of Materials for Energy Conversion, Hefei, China

* huangwx@ustc.edu.cn

Keywords: cuprous, oxide, capping ligands, CO oxidation

1 Introduction

In the synthesis process, surfactant is often employed to provide the growth of nanoparticles and stable a certain crystal plane. Although several capping ligands were found to enhance the catalytic selectivity for some catalytic reactions, concerning the catalytic activity, all previously-reported capping ligands exert the surface-blocking effect to decrease the number of active surface sites accessible to reactants and subsequently the catalytic activity. [1,2] We comparatively studied the catalytic performances of Cu_2O octahedra with different amounts of PVP capping ligand in CO oxidation. Very unexpectedly, PVP was found to significantly enhance the catalytic activity of Cu_2O octahedra, and the relevant mechanism was revealed.

2 Experimental/methodology

We have synthesized PVP-protected octahedral Cu_2O nanocrystals (denoted as o-Cu_2O-PVP). o-Cu_2O-PVP were treated in the stream of mixed gas (C_3H_6:O_2:Ar=2:1:22) at 200°C for 30min and 120min and then cooled down to room temperature with Ar gas stream to acquire partial PVP-protected Cu_2O octahedra (denoted as o-Cu_2O-partial PVP) and PVP-free Cu_2O octahedra (denoted as o-Cu_2O) respectively. The catalyst diluted with SiO_2 was used to evaluate the catalytic activity and the reaction gas consisting of 2% CO and 1% O_2 balanced with N_2 was fed at a rate of 20 mL/min. The conversion of CO was calculated from the change in CO concentration of the inlet and outlet gases. XPS measurements were performed on an ESCALAB 250 high performance electron spectrometer using monochromatized Al Kα (hν = 1486.7 eV) as the excitation source. DRIFT spectra were measured on a Nicolet 6700 FTIR spectrometer equipped with an in-situ DRIFTS reaction cell with 64 scans and a resolution of 4 cm^{-1} using an MCT/A detector. The catalyst was heated at various temperatures with the reaction gas stream, and the chemisorption process was in-situ studied by the DRIFTS measurements performed till the chemisorption saturated.

3 Results and discussion

We have successfully developed a novel controlled-oxidation strategy to selectively remove full or part of the capping ligands on o-Cu_2O-PVP without the change of their composition, morphology, size, and surface structure. Fig. 1 (A) and (B) shows the catalytic performance of various Cu_2O nanocrystals in CO oxidation with stoichiometric oxygen (2% CO and 1% O_2 balanced with N_2). Very evidently, the capping agents on octahedral Cu_2O nanocrystals controls their catalytic performance in which o-Cu_2O-PVP is the most catalytically active among these nanocatalysts. The activity order is o-Cu_2O-PVP>o-Cu_2O-partial PVP>o-Cu_2O. The reaction mechanism of various Cu_2O octahedra is the same. In Fig. 1 (C) and (D), the intensities of o-Cu_2O-PVP in N 1s spectra are the same, however, the C-N bond at 287.6eV in C 1s spectra in o-

Cu_2O-PVP partially broke after reaction to form a N-CH-CH_2 moiety, which enhanced the O_2 adsorption on Cu_2O surface to increase the reaction activity. Fig. 2 shows the DRIFTS spectra acquired for the chemisorption of CO+O_2 on various Cu_2O catalysts at various temperatures. At 30°C, CO chemisorbs on coordinatively unsaturated Cu only at 2104 cm^{-1}. As the temperature increases, the chemisorption at 2184 cm^{-1} arises. CO and O_2 co-chemisorbs evidently on coordinatively saturated Cu at 2184 cm^{-1}, which is the intermediate species of CO reaction. At 140°C, the chemisorption of o-Cu_2O-PVP at 2184 cm-1 is the strongest. While o-Cu_2O-partial PVP, and o-Cu_2O have no catalytic activity at 140°C, the chemisorption at 2184 cm-1 weakened, which follows the activity order.

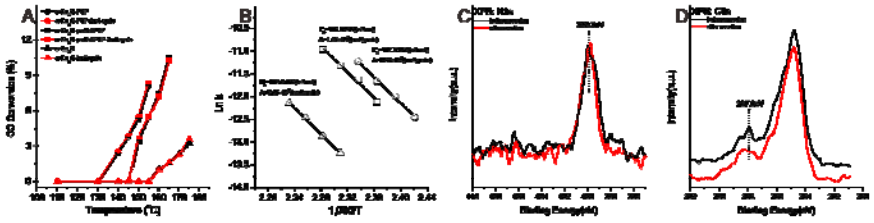

Fig. 1. (A) Catalysis performance, (B) Arrhenius plots of various Cu_2O octahedra in CO oxidation, (C) N 1s spectra, and (D) C 1s spectra of o-Cu_2O-PVP before and after reaction.

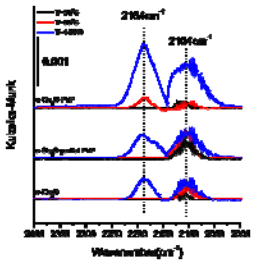

Fig. 2. DRIFTS spectra of CO+O_2 chemisorption on various Cu_2O octahedra at various temperatures. The gas CO adsorption is deducted.

4 Conclusions

We report the first time that PVP capping ligands on Cu_2O octahedra can significantly enhance their catalytic activity in CO oxidation. PVP partially decomposes with the breaking of the N-C bond of the N-CH-CH_2 moiety and the remaining group can enhance the O_2 adsorption on the Cu_2O octahedra surface. CO oxidation mechanism on the Cu_2O octahedra surface is identified to be the LH mechanism. This work shows that proper capping agent introduced in the catalyst synthesis can markedly improve the catalytic activity of gas-phase catalytic reactions, and it is of great significance to discover and research more high-effective catalysts and opens a new window to research the catalysis of nanocrystals.

References

[1] S. T. Marshall, M. O'Brien, B. Oetter, A. Corpuz, R. M. Richards, D. K. Schwartz and J. W. Medlin, *Nat. Mater.* 9 (2010), 853.

[2] K. Chen, H. T. Wu, Q. Hua, S. J. Chang and W. X. Huang, *Phys. Chem. Chem. Phys.* 15 (2013) 2273.

II-PP69

Development of Hybrid Nanocomposites by Immobilization of Metal Nanoparticles on the Supramolecular and Polymer Matrices of Resorcinarene Derivatives

Ziganshina A.Y.[1*], Sultanova E.D.[1], Sergeeva T.Yu.[1,2], Mukhitova R.K.[1], Nizameev I.R.[1], Kadirov M.K.[1], Salnikov V.V.[3], Zuev Yu.F.[3], Zakharova L.Ya.[1], Konovalov A.I.[1], Atlanderova A.A.[2]

1 - A.E. Arbuzov Institute of Organic and Physical Chemistry, Kazan Scientific Center, Russian Academy of Sciences, Kazan, Russia

2 - Kazan (Volga region) federal university, Kazan, Russia

3 - Kazan Institute of Biochemistry and Biophysics, Kazan Scientific Centre, Russian Academy of Sciences, Kazan, Russia

* az@iopc.ru

Keywords: hybrid nanocomposites, resorcinarenes, cavitands, metal nanoparticles

1 Introduction

Metal nanoparticles have attracted much attention over the last decade due to their unique catalytic properties [1]. The properties of metal nanoparticles are strongly depended on the size, shape and support materials. Metal nanoparticles assembled in the cluster show higher catalytic activity due to high surface to volume ratio [2]. Although metal nanoparticles on solid supports have been successfully employed in catalysis, most systems undergo from shortcomings such as passivation of the surface, lack of long-term stability, low dispersibility which limit their capacity and applications [3]. Macrocyclic compounds are attractive compounds for the construction of supporting matrix for metal nanoparticles due to their easy modification, rich host-guest complexation properties and ability to self-assemblies both in solutions and on the surface. We have used aggregates of water-soluble resorcinarenes as templates for the synthesis of metal nanoparticles with different size and shape. The catalytic properties of the hybrid nanocomposites obtained will be discussed in the presentation.

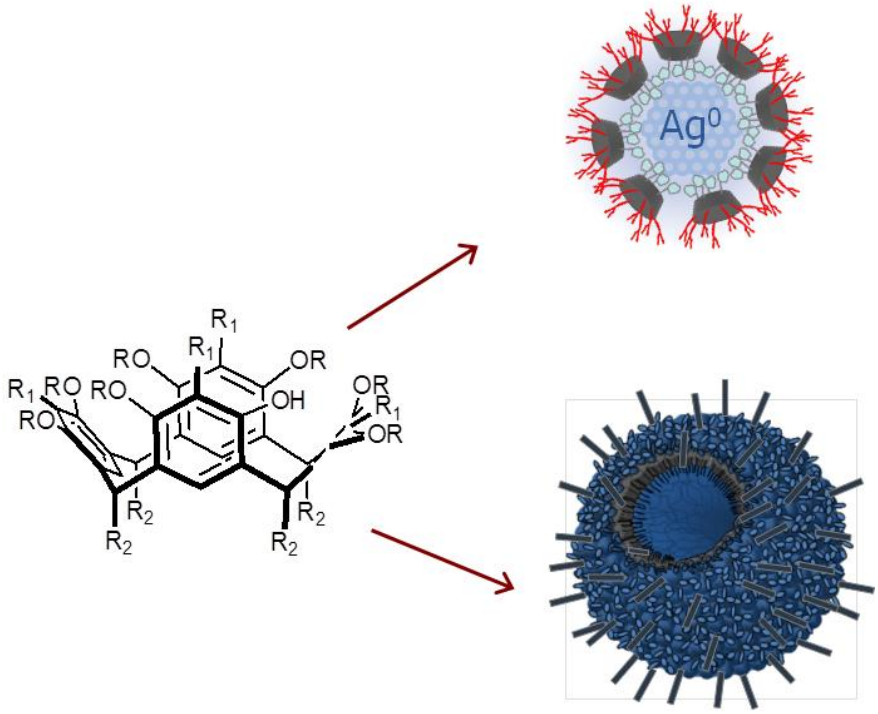

Scheme 1. Hybrid nanomaterials using metal nanoparticles and resorcinarene assemblies.

Acknowledgements

This study was supported by the Russian Foundation for Basic Research (grant nos. 15-03-04999).

References

[1] B. Corain, G. Schmid, N. Toshima, *Metal Nanoclusters in Catalysis and Materials Science: The Issue of Size Control*. Elsevier, Amsterdam (2008).
[2] L. L. Chng, N. Erathodiyil, J. Y. Ying, *Acc. Chem. Res.* 46 (2013) 1825.
[3] T-D. Nguyen, C-T. Dinh, T-On Do, *Chem. Commun*. 51 (2015) 624.

II-PP70

Kinetically Modelled Temperature Programmed Desorption of CO_2 as a Powerful Tool for Identification and Quantification of Sites of Copper/Ceria Catalysts for CO-PROX

Barbato P.S.[1], Di Benedetto A.[2], Landi G.[1*], Lisi L.[1]

1 - Research Institute on Combustion, CNR, Naples, Italy
2 - DICMAPI, University of Naples Federico II, Naples, Italy

* landi@irc.cnr.it

Keywords: CO-PROX, CuO/CeO_2 catalysts, CO_2, TPD, TPD model

1 Introduction

Copper-ceria systems have been investigated as possible catalysts for CO preferential oxidation, proposed as purification step of H_2-rich streams for PEMFC application. The good performance of this class of materials has been related to synergistic interaction between copper and cerium oxide, the activity towards CO oxidation being essentially addressed to the copper oxide-ceria interfacial sites [1,2].Copper dispersion and interaction with ceria is affected both by CuO load and by catalyst preparation method [2,4,5], nevertheless a quantitative analysis of the extent of this phenomenon has never been attempted.

In this work we applied a combined (experimental/modelling) technique, we named Kinetically Modelled Temperature Programmed Desorption (KM-TPD) using CO_2 as probe molecule, to identify and quantify the active sites of copper-ceria catalysts with different Cu load prepared by wet impregnation or by solution combustion synthesis. The results of the KM-TPD showed that the model succeeded in quantitatively identifying the active sites for both CO and H_2 oxidation providing a good correlation with the catalytic activity and selectivity of the catalysts.

2 Experimental/methodology

Wet impregnated (CuCe-I) samples with a nominal CuO load equal to 0.5, 4 and 8 wt. % CuO and a solution combustion synthesized (CuCe-S) catalyst containing 4 wt. % CuO were prepared and calcined in air at 450°C for 2h.

The lab-scale set-up used for CO-PROX experiments was described elsewhere [6]. Catalytic tests were conducted at fixed contact time. H_2, CO and O_2 concentrations were fixed at 50, 0.5 and 0.9 vol.% respectively. Reaction temperature ranged from 80 to 200 °C.

The KM-TPD is based on experimental tests and modelling analysis of TPD, here applied to CO_2 desorption. Experimental CO_2 TPD tests were carried out by using a Micromeritics Autochem II 2020 analyzer. After contacting the sample for 45 min at room temperature with a 15 vol.% CO_2/He mixture and purging, it was heated at 10°C/min up to 300°C. The TPD model was developed to identify the number and the type of CO_2 species desorbing from different surface sites. In [6] more details on the governing equations and approximations used in the model are given.

3 Results and discussion

The CO_2 sorption capacity of the support is comparable to that of the CuO/CeO_2 catalysts suggesting a significant contribution of ceria. For impregnated copper/ceria catalysts [6] three different sites can be identified through CO_2 KM-TPD, associated respectively to i) cerium centres deeply modified by the strong interaction with copper active towards CO oxidation (θ_1), ii) not modified cerium centres (θ_2) and iii) copper centres in supported copper oxide active for H_2 oxidation (θ_3), respectively. The θ_2 sites are those more significantly affected by copper

coverage. Indeed, by increasing the CuO loading the amount of CO_2 adsorbed over these sites decreases up to the monolayer coverage (4 wt % CuO) suggesting that copper deposition partially covers these ceria sites not sufficiently balanced by new copper adsorption sites. On the other hand, the amount of H_2 oxidation centres increases exceeding the monolayer coverage.
The same sites were identified for the CuCe-S sample and a lower value of the activation energy of the CO_2 desorption step from the sites associated to CO-oxidation centers was found. Moreover, a more homogeneous distribution of copper sites was obtained for this sample compared to the impregnated catalyst with the same CuO load with an evident dominance of CO oxidation sites, likely promoted by a stronger interaction with ceria (figure 1).

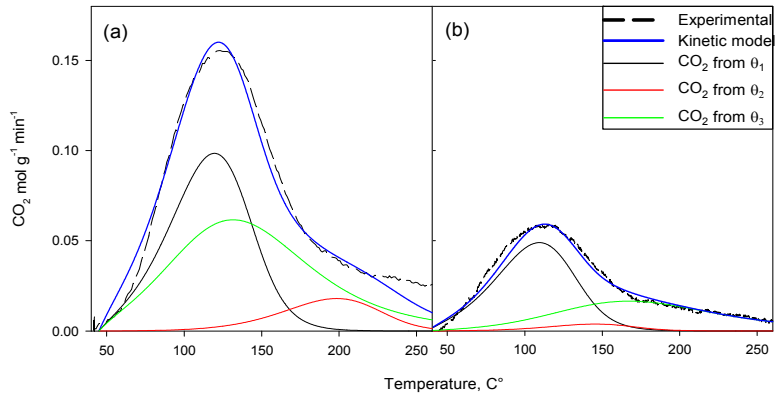

Fig. 1. CO_2-TPD profiles over CuCe-I (a) and CuCe-S (b) catalysts. Overall experimental and model profiles, CO_2 desorbed from each site as obtained by the model.

Both conversion and selectivity (not reported) are in agreement with the results of KM-TPD which well explain the different performances of the catalysts investigated in this work. In particular, the relative amount and the temperature range of sites assigned to CO and H_2 oxidation account for the activity and the selectivity found in the CO-PROX tests.

4 Conclusions

A technique based on the coupling between modelling and experiments of temperature programmed desorption of CO_2 is applied to determine the sites distribution of copper ceria catalysts prepared by different techniques and with different CuO load. The qualitative and quantitative evaluation of sites active for CO and H_2 oxidation very well agrees with the catalytic performance in CO-PROX of catalysts suggesting that this technique may be useful for kinetic study.

Acknowledgements

This work was financially supported by Italian MIUR (FIRB2010 “Futuro in Ricerca”, project n° RBFR10S4OW).

References

[1] A. Matinez-Arias, M. Fernandez-Garcia, O. Galvez, J.M. Coronado, J.A. Aderson, J.C. Conesa, J. Soria, G. Munuera, *Journal of Catalysis*, 195 (2000), 207.
[2] Sedmak, G., Hocevar, S., and Levec, J., *Journal of Cataysis.*, 213(2003) 135.
[3]G. Avgouropoulos, T. Ioannides. *Applied Catalysis A, General* 244(2003)155.
[4]W. Yang, D. Li, D. Xu, X. Wang. *Journal of Natural Gas Chemistry* 18(2009) 458.
[5] R. Prasad, G. Rattan. *Bulletin of Chemical Reaction Engineering & Catalysis*. 5(2010) 7.
[6]A. Di Benedetto, G. Landi, L. Lisi, G. Russo, *Applied Catalysis B, Environmental* 142-143 (2013) 169.

II-PP71

Photocatalytic Activity of Al-Doped TiO_2

Murzin P.D.[1*], Murashkina A.A.[2], Rudakova A.V.[1], Emeline A.V.[1], Ryabchuk V.K.[2], Tsyganenko A.A.[2], Bulanin K.M.[1]

1 - Laboratory "Photoactive Nanocomposite Materials", Saint-Petersburg State University, Saint-Petersburg, Russia

2 - Saint-Petersburg State University, Saint-Petersburg, Russia

* murzinpetrff@gmail.com

Keywords: photoactivity, doped TiO_2, phenol, decomposition, characterization

1 Introduction

Titanium dioxide is a well-known material widely used for a variety of purposes as a photocatalyst [1]. In order to improve the photocatalytic activity of titania doping and co-doping by metallic and non-metallic impurities are used [2].

Activity enhancement of titania by aluminum addition has been poorly studied, and the results obtained by different authors are rather inconsistent. [3]

It has been shown [4] that the optimal metal dopant concentration for a photocatalyst of a given particle size varies from 0.01 at% to 1 at% independently on the metal dopant nature.

In the present work a series of Al-doped titanium dioxide samples synthesized by sol- gel method was studied.

2 Experimental/methodology

Seven samples with different aluminum content (0, 0.1%, 0.3%, 0.5%, 0.7%, 0.9% and 1.1%) were prepared. Photocatalytic activity was evaluated by the decomposition of phenol under irradiation by Xe lamp in aqueous suspension. Phenol concentration was determined by means of high-performance liquid chromatography.

Surface characterization was carried out by SEM, Raman spectroscopy, X-ray phase analysis, FTIR spectroscopy of adsorbed CO, specific surface area was measured by BET method.

3 Results and discussion

Figure 1 shows the dependence of initial phenol decomposition rate for the samples on the weight percentage of aluminum dopant. The dependence manifests a maximum at 0,5% of Al content.

The well-known decrease of particle size and increase of specific surface area of Al-doped samples from ~ 800 nm up to 50 nm and from 1.7 m^2/g up to 28 m^2/g, respectively, have been observed. The growth of dopant concentration leads to higher uniformity of grains, *i.e.* lower degree of aggregation.

No significant correlation between activity and selectivity (towards formation of phenol products such as hydrochinon and catechol) has been found.

These facts lead us to the conclusion that different types of active centers account for the activity enhancement with the increase of dopant concentration. The highest activity seems to be due to the optimal balance between particle size and aluminum concentration. Some of such active sites can be associated with the coordinately unsaturated Ti^{4+} or Al^{3+} cations detected by FTIR spectra of adsorbed CO.

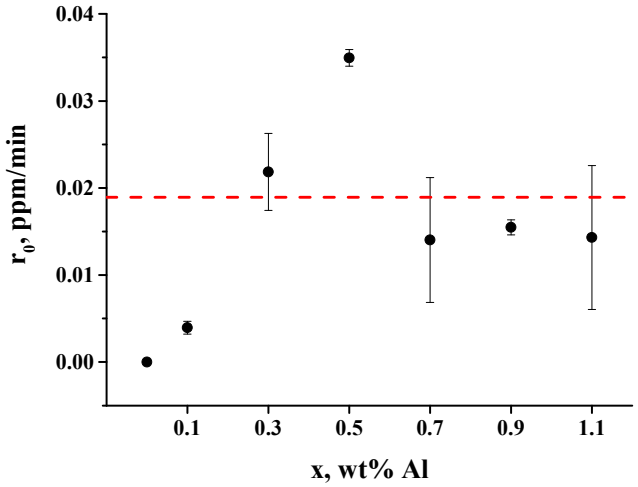

Fig. 1. The dependence of initial rate of phenol photodegradation reaction (r_o) for the x-Al-TiO_2 samples on the weight percentage of aluminum dopant (x). Dashed line marks the value of initial rate of phenol photodegradation for commercial TiO_2 Degussa P25.

Regardless to the mechanism of aluminum dopant effect on photocatalytic activity of titania, the results obtained let one to consider that the inconsistence results of different authors on the properties of Al-doped titania, might be caused by various balance between particle size and aluminum concentration.

4 Conclusions

The study of photocatalytic activity of Al doped TiO_2 sensitized by sol-gel method shows the existence of a maximum in the dependence of phenol degradation initial rate on aluminum dopant concentration near 0.5 %.

Aluminum doping seems to be a promising way to improve the quality of titania based photocatalysts.

Acknowledgements

The study was performed within the Project "Establishment of the Laboratory "Photoactive Nanocomposite Materials" supported by a grant of the Government of Russian Federation No. 14.Z50.31.0016. We are grateful to the Resource Centres "Nanophotonics", "Nanotechnology", "Chemical Analysis and Materials Research Centre", "X-ray Diffraction Studies", "Optical and Laser Materials Research" of the Research Park of St.Petersburg State University for the assistance in synthesis and sample characterization.

References

[1] Chen, X., Mao, S.S., Chem. Rev. 2007, 2891-2959
[2] Chen, X.; Mao, S.S., Surf. Sci. Rep. 2008, 63, 516−582; Pelaez M, Nolan N.T., Pillai S.C. , Seery M.K., Falaras P., Kontos A.G., Dunlop P.S.M., Hamilton J.W.J., Byrne J.A., O'Sheaf K., Entezari M.H., Dionysiou D.D., Applied Catalysis B: Environmental. 2012. Vol. 125. P. 331– 349; Choi, J. ; Park, H., Hoffmann, M.R., Phys.Chem. C. 2010. 114 (2), pp. 783-792.
[3] Liu, S.; Liu, G.; Feng, Q., J. Porous Mater. 2010. 17. p. 197–206
[4] Bloh J.Z., Dillert R., Bahnemann D.W., J. Phys. Chem. C 2012. Vol. 116. P. 25558−25562

II-PP72

On the Physics of Intercalation of Hydrogen into Surface Nanoblisters in Pyrolytic Graphite & Epitaxial Graphene: Relevance to the Hydrogen Storage Problem

Nechaev Yu.S.[1*], Filippova V.P.[1], Tomchuk A.A.[1], Sundeev R.V.[1], Yurum A.[2], Yurum Y.[3], Veziroglu T.N.[4]

1 - P. Bardin Central Research Institute for Ferrous Metallurgy, G. V. Kurdjumov Institute of Metals Science and Physics, Moscow, Russia
2 - Sabanci University, Nanotechnology Research and Application Centre, Istanbul, Turkey
3 - Sabanci University, Faculty of Engineering and Natural Sciences, Istanbul, Turkey
4 - International Association for Hydrogen Energy, Miami, USA

* yuri1939@inbox.ru

Keywords: pyrolytic graphite, epitaxial graphene, atomic hydrogen, intercalation (without catalysts), surface graphene nanoblisters, thermal-elastic thermodynamic equilibrium

1 Introduction

There is a number of recent data on the surface nanoblister formation in highly oriented pyrolytic graphite (HOPG, Fig. 1) and epitaxial graphene (Fig. 2) under hydrogenation in atomic gaseous hydrogen (without catalysts). The process physics has been yet not enough studied.

2 Experimental/methodology

The thermodynamic analysis [1-3] of some recent experimental data (Fig. 1) has been done.

3 Results and discussion

Figure 1 shows the results of hydrogenation (**at 300 K and P(Hgas) ≈ 0.1 mPa, without any catalyst**) of surface layers of HOPG samples.

Similar STM, AFM and other data of different researchers for the epitaxial graphenes (Figure 2) have been also analyzed in [1-3] (the "open access" Journals).

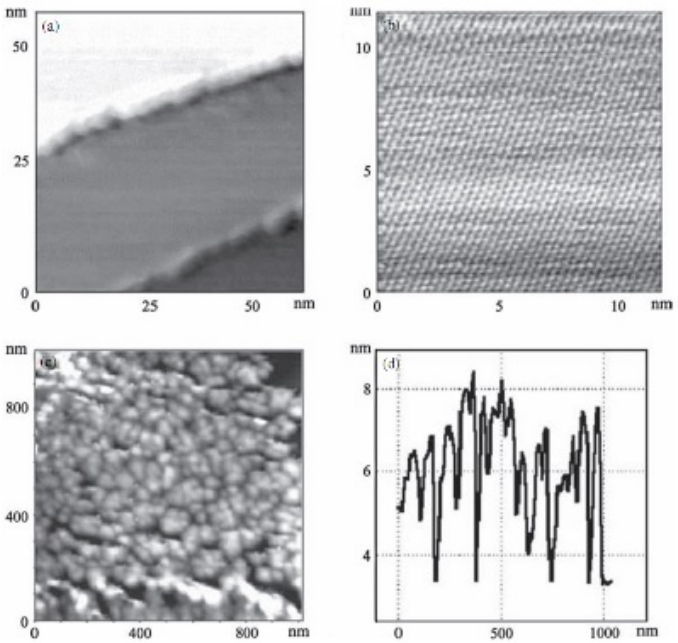

Fig. 1. STM and AFM data {Waqar (2007)} showing the hydrogen accumulation (intercalation) in HOPG with forming blister-like surface nanostructures; hydrogenation was done at 300 K and P(Hgas) ≈ 0.1 mPa, without any catalyst. The pressure of the molecular gaseous hydrogen (H2), "captured" inside the surface graphene nanoblisters, is of P(H2gas) ≈ 100 MPa); the compression effect is of 12 orders (from 0.1 mPa to 100 MPa), at the expense of the energy of association of hydrogen atoms to molecules "captured" inside the graphene nanoblisters (the quantitative interpretation) [1-3].

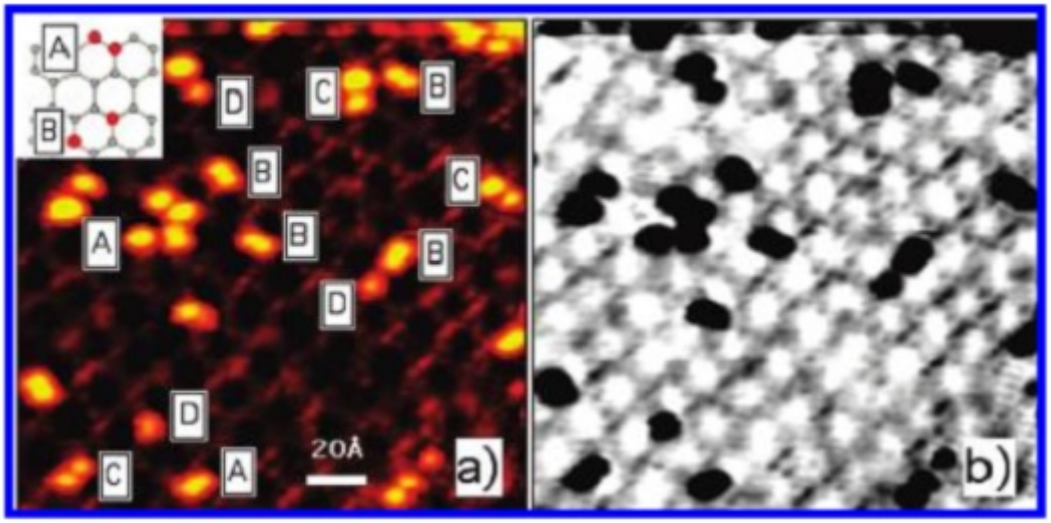

Fig. 2. (a) STM image of hydrogenated graphene/SiC {Balog et al. (2009)}. (b) Same image as in (a) with inverted color scheme, giving emphasis to preferential hydrogen adsorption on the SiC surface. Hydrogen dose at T(beam) = 1600 K, t = 5 s, F = 1012 – 1013 atoms/cm2s (P(Hgas) ≈ 0.1 mPa).

The very recent experimental data {Geim et al. (2014)} show that a hydrogen atom can not pass through a perfect graphene network. The analysis [1-3] of a number of experimental data (Figs. 1, 2) show that a hydrogen atom can pass through permeable defects in graphene, i.e. grain boundaries, their triple junctions and/or others.

4 Conclusions

The "thermodynamic forces" and energetics of forming of graphene nanoblisters (under atomic hydrogen treatment, without catalysts) in the surface HOPG layers (Fig. 1) and epitaxial graphenes (Fig. 2) have been quantitatively described, particularly, the conditions of the thermal-elastic thermodynamic equilibrium [1-3]. The physics of intercalation of H2 gaseous nanophase of a high density into graphene nanoblisters have been revealed [1-3]. It can be used for solving of the very current problem of the hydrogen on-board efficient and safety storage.

Acknowledgements

The reported study has been supported by the RFBR (Project #14-08-91376_CT) and the TUBITAK (Project #213M523).

References

[1] Yu. S. Nechaev, Alp Yurum, Adem Tekin, Nilgun Karatepe Yavuz, Yuda Yurum, T. Nejat Veziroglu, "Fundamental open questions on engineering of super hydrogen sorption in graphite nanofibers: Relevance for clean energy applications", *American Journal of Analytical Chemistry,* Vol. 5 (2014) P. 1151-1165.

[2] Yu. S. Nechaev, V. P. Filippova, Alp Yurum, Yuda Yurum, T. Nejat Veziroglu, "The reversible hydrogenation-dehydrogenation of membrane and epitaxial graphenes", *Journal of Chemical Engineering and Chemical Research*, Vol. 2, # 1 (2015) P. 421-456.

[3] Yu. S. Nechaev and T. Nejat Veziroglu, "On the hydrogenation-dehydrogenation of graphene-layer-nanostructures: Relevance to the hydrogen on-board storage problem", *International Journal of Physical Sciences*, Vol. 10, Iss. 2 (2014) P. 1-36.

II-PP73

On the Spillover Effect Manifestation when the Solid Hydrogen Intercalation into Hydrogenated Graphite Nanofibers: Relevance to the Hydrogen Storage Problem

Nechaev Yu.S.[1*], Filippova V.P.[1], Tomchuk A.A.[1], Sundeev R.V.[1], Yurum A.[2], Yurum Y.[3], Veziroglu T.N.[4]

1 - P. Bardin Central Research Institute for Ferrous Metallurgy, G. V. Kurdjumov Institute of Metals Science and Physics, Moscow, Russia
2 - Sabanci University, Nanotechnology Research and Application Centre, Istanbul, Turkey
3 - Sabanci University, Faculty of Engineering and Natural Sciences, Istanbul, Turkey
4 - International Association for Hydrogen Energy, Miami, USA

* yuri1939@inbox.ru

Keywords: graphite nanofibers, hydrogenation, solid hydrogen, intercalation, storage, spillover effect

1 Introduction

The spillover effect manifestation in hydrogenated carbon-based nanomaterials has been not enough studied up to nowadays, particularly, relevance for solving the current problem of the hydrogen on-board efficient storage.

2 Experimental/methodology

The thermodynamic analysis [1-3] of the related experimental data (Figs. 1, 2) has been done.

3 Results and discussion

Figure 1 shows the two steps ((a) and (b)) of hydrogenation (**at 300 K and $P_{(Hgas)}$ ≈ 0.1 mPa, without any catalyst**) of surface layers of a high oriented pyrolytic graphite (HOPG).

Similar STM, AFM and other data of different researchers for the epitaxial graphenes have been also analyzed in [1-3].

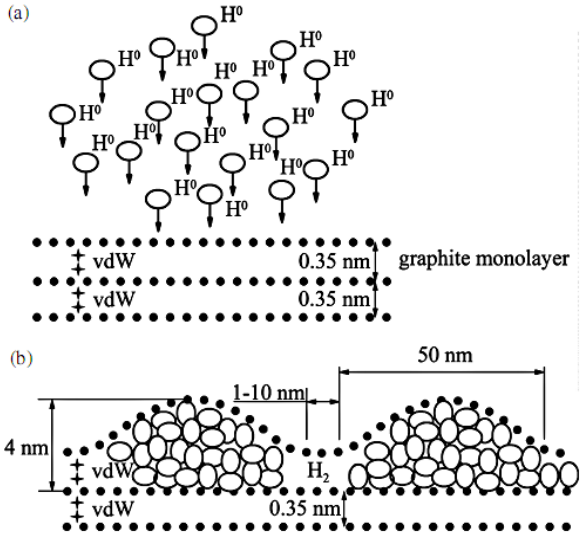

Fig. 1. Model {Waqar (2007) from STM and AFM data} showing the hydrogen accumulation (intercalation) in HOPG with forming blister-like surface nanostructures; **hydrogenation** was done **at 300 K and $P_{(Hgas)}$ ≈ 0.1 mPa, without any catalyst**. (a) Pre-atomic hydrogen (**$P_{(Hgas)}$ ≈ 0.1 mPa**) intercalation step. (b) Molecular gaseous hydrogen (H2), "captured" inside the surface graphene nanoblisters (**$P_{(H2gas)}$ ≈ 100 MPa**), after the intercalation step. Sizes are not drawn exactly in scale. **The compression effect is of 12 orders (from 0.1mPa to 100 MPa), at the expense of the energy of association of hydrogen atoms to molecules "captured" inside the graphene nanoblisters.**

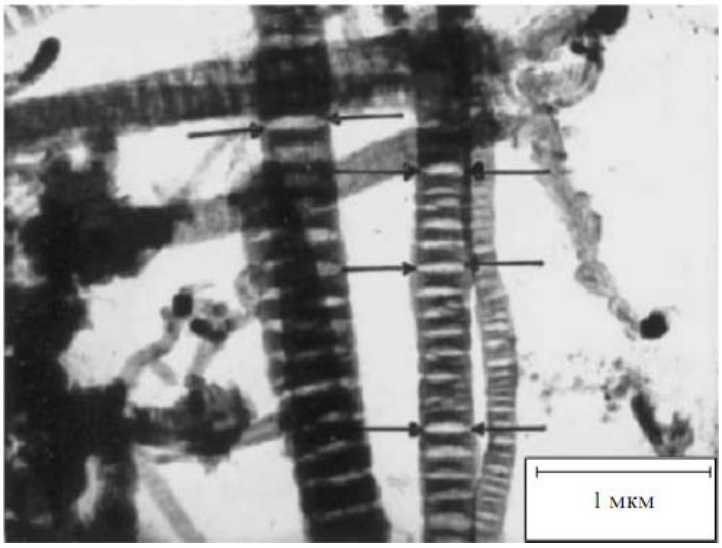

Fig. 2. Micrographs {Gupta et al. (2004)} of hydrogenated graphite nanofibers (**at 300 K and $P_{(H2gas)}$ ≈ 8 MPa,** with **Pd-catalyst**) after release from them (at 300 K, for 10 min {Park et al. (1999)} of intercalated high-density hydrogen (17 mass. % - the gravimetrical reversible hydrogen capacity). The arrows in the picture indicate some of the slit-like closed nanopores of **the lens shape**, where the **intercalated molecular solid hydrogen** nanophase (under pressure of **50 GPa**) was localized [1-3].

4 Conclusions

In the light of analysis [1-3], the spillover effect is obviously manifested in data {Gupta et al. (2004)} (Figure 2) and data {Park et al. (1999)}.

Acknowledgements

The reported study has been supported by the RFBR (Project #14-08-91376_CT) and the TUBITAK (Project #213M523).

References

[1] Yu. S. Nechaev, Alp Yurum, Adem Tekin, Nilgun Karatepe Yavuz, Yuda Yurum, T. Nejat Veziroglu, "Fundamental open questions on engineering of super hydrogen sorption in graphite nanofibers: Relevance for clean energy applications", *American Journal of Analytical Chemistry,* Vol. 5 (2014) P. 1151-1165.

[2] Yu. S. Nechaev, V. P. Filippova, Alp Yurum, Yuda Yurum, T. Nejat Veziroglu, "The reversible hydrogenation-dehydrogenation of membrane and epitaxial graphenes", *Journal of Chemical Engineering and Chemical Research*, Vol. 2, # 1 (2015) P. 421-456.

[3] Yu. S. Nechaev and T. Nejat Veziroglu, "On the hydrogenation-dehydrogenation of graphene-layer-nanostructures: Relevance to the hydrogen on-board storage problem", *International Journal of Physical Sciences*, Vol. 10, Iss. 2 (2014) P. 1-36.

II-PP75

Oxidation of n-Heptane over Sphere Catalysts with a Composition of TiO_2-SiO_2-M_xO_y, where M is Co or Ni

Shamsutdinova A.[1*], Zharkova V.[1], Brichkov A.[1], Glazneva T.[2], Bobkova L. [1], Larina T.[2], Paukshtis E.[1,2], Parmon V.[1,2], Kozik V.[1]

1 - National Research Tomsk State University, Tomsk, Russia
2 - Boreskov institute of catalysis SB RAN, Novosibirsk, Russia

* selenet_1408@mail.ru

Keywords: sol-gel method, titania, silica, n-heptane, transformation, hollow, sphere catalysts, microtomography, UV-Vis DRS

1 Introduction

The preparation technique of new composite catalytic materials in the form of hollow spheres was developed. TiO_2-SiO_2 composites were modified by nickel and cobalt. After annealing, the spatial structure of sphere samples was studied by X-ray microtomography on a digital 3D microtomograph. The state of the cations of transition elements and titanium was characterized by UV-Vis DR spectroscopy. The catalysts were tested in the oxidation of n-heptane.

2 Experimental/methodology

A spherical material with the composition of TiO_2-SiO_2-M_xO_y, where M is Co (TSC-1 sample) and Ni (TSN-1 sample), obtained by sol-gel method, was used as a catalyst. Before testing, the catalyst was annealed at 400°C in air. The samples after annealing were named as tTSC-1 (with cobalt) and tTSN-1 (with nickel). The catalytic properties were studied in the model oxidation reaction of n-heptane oxidation. The flow set-up with a quartz tube reactor (the inner diameter of 4 mm) was used. The reactor was charged with 0.2 g of catalyst, the diameter of the catalyst spheres was 0.2-0.5 mm. The mixture containing 0.8% n-heptane in air was passed through the catalyst. The ratio of n-heptane to oxygen in the feed gas was 1/25. Feed space velocity was 4.5 L/h. The reaction temperature was varied from 110°C to 600ºC. Product analysis was performed on a Shimadzu FTIR-8300 spectrometer.

3 Results and discussion

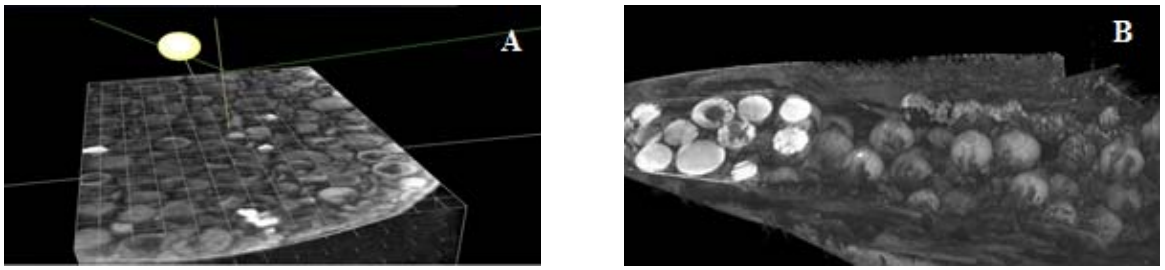

Fig. 1. Cross-sections of tTSC-1 (A) and tTSN-1 (B) sphere catalysts obtained by computer microtomography.

After annealing, the material represent a hollow spheres of a layered structure with the inner part of d-metal oxides coated by the layer with a composition of 70 mol.% Ti_xO_y + 30 mol.% Si_xO_y. Fig. 1 shows the examples of the cross-section of computer microtomography of tTSC-1 and tTSN-1 samples. Two structures are visually distinguished for tTSC-1 sample (Fig. 1-A): a dark color refers to the air-filled cavity of sphere, a lighter color refers to a complex oxide

framework with a composition of Ti_xO_y-Si_xO_y. Fig. 1-B shows that the inner part of tTSN-1 sample for the most part of spheres is filled, although there are individual hollow particles.

The UV-Vis spectra of both samples contain a band gap in the region of 28 000-32 000 cm^{-1} characteristic for TiO_2. The spectra of the samples in the visible region are characterized by absorption bands due to *d-d*-transitions of Co^{2+} and Ni^{2+} cations. The band at about 15 000 cm^{-1} for tTSC-1 sample refers to the Co^{2+} cations in tetrahedral oxygen coordination and, probably, corresponds to Co_3O_4 phase. The absorption band at about 14 000 cm^{-1} for tTSN-1 sample corresponds to Ni^{2+} cations in octahedral oxygen coordination in the state, probably, close to NiO.

Fig. 2 shows that the oxidation reaction for tTSC-1 sample starts at 250°C. The process goes predominantly in the direction of deep oxidation. Attention is drawn to the increase in the selectivity of olefins formation on this sample as the temperature rises above 500°C. The oxidation over tTSN-1 sample starts at 400°C, and the partial oxidation is observed at 400-450°C. The selectivity towards the partial oxidation products reaches 63% (the absorption bands used for products identification are given in Table 1). A deep destructive oxidation of n-heptane starts at temperatures above 550°C. The maximum conversion of heptane at 600°C over tTSC-1 sample is 80%. For tTSN-1 sample, the n-heptane conversion does not exceed 50%. For both samples, the cracking products (in particular, methane) are detected at temperatures above 500°C.

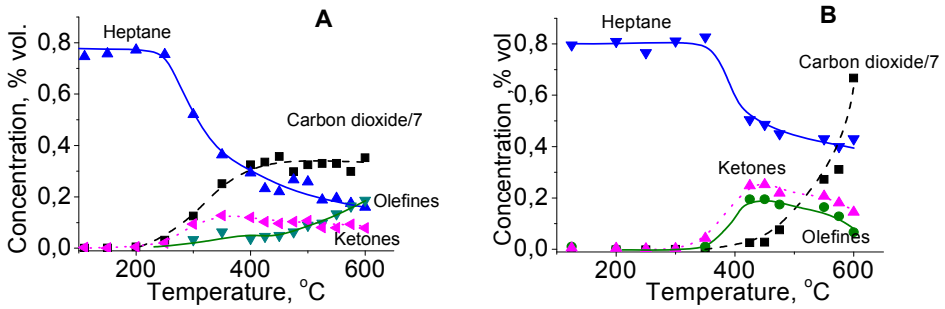

Fig. 2. Temperature dependences of n-heptane concentration over tTSC-1 (A) and tTSN-1 (B) samples.

Table 1. Characteristic IR absorption bands for products identification.

Wavenumber, cm^{-1}	Structural fragments	Vibration modes
3016	Methane	νCH stretching
1745	Ketones	νC=O stretching in ketones
1100, broad	alcohol ethers	νC-O-C stretching in complex ethers
945	HRC=CR'H	δC=CH bending, nonplanar

4 Conclusions

The technique of preparation of new composite catalytic materials in the form of hollow spheres was developed. The resulting catalysts were characterized by physical methods and tested in the oxidation of n-heptane. It was found that besides the destructive oxidation, the oxidative dehydrogenation of n-heptane and formation of partial oxidation products such as ketones and esters took place.

Acknowledgements

The work was performed within the scope of the Russian Ministry of the Education task (project number of11.801.2014/K).

II-PP76

C-C Bond Activation in Acetaldehyde Oxidation on Au(111)

Karatok M.[1], Vovk E.I.[1,2], Shah S.A.A.[1], Turksoy A.[1], Ozensoy E.[1*]

1 - Bilkent University, Chemistry department, Ankara, Turkey
2 - Boreskov Institute of catalysis, Novosibirsk, Russia

* ozensoy@fen.bilkent.edu.tr

Keywords: gold, oxidative coupling, partial oxidation, acetaldehyde, methyl, acetate

1 Introduction

Gold has been considered as a relatively inactive metal in catalysis for a long time. However, pioneering studies in the last few decades demonstrated the unusual catalytic properties of the gold nanoparticles in oxidation reactions [1,2]. Furthermore, structurally-tuned heterogeneous gold catalysts demonstrate high selectivity in partial oxidation reactions [3]. In order to optimize the performance of these uniquely active and unusually selective catalytic materials, mechanisms of the catalytic reactions on the gold surfaces need to be understood at the molecular level. Selective oxidation and oxidative coupling reactions of alcohols and aldehydes result in the production of commercially valuable partial oxidation products such as esters which are of high demand by the chemical industry. In the current work, partial oxidation reaction of acetaldehyde on the Au(111) model catalyst surface is investigated and the formation of acetic acid and methyl acetate which can be formed due to C-C bond activation is demonstrated.

2 Experimental/methodology

Experiments were performed in a custom-made ultra-high vacuum (UHV) chamber which is equipped with X-ray Photoemission Spectroscopy (XPS), Low Energy Electron Diffraction (LEED), Infrared Reflection Absorption Spectroscopy (IRAS) and Temperature Programmed Desorption (TPD)/ Temperature Programmed Reaction Spectroscopy (TPRS) capabilities. Atomic oxygen on the Au(111) model catalyst surface was formed by ozone decomposition.

3 Results and discussion

Figure 1 shows TPRS results of acetaldehyde on the oxygen pre-covered Au(111) surface. In the current experiment, 0.004 L (Langmuir) of O_3 was initially dosed onto the clean Au(111) surface at 140 K followed by 0.4 L acetaldehyde exposure at 90 K. Desorption channels for anticipated products (i.e. m/z = 18, 28, 29, 32, 43, 44, 45 and 59) were simultaneously monitored during the temperature-programmed reaction. In the figure, desorption peaks at 141 K in the m/z = 28, 29, 43, and 44 channels are associated with the chemisorbed acetaldehyde. This assignment is in agreement with acetaldehyde desorption from the clean (oxygen-free) Au(111) surface. Desorption features located at 171 K in the figure, particularly for the m/z= 29, 43 and 59 desorption channels can be predominantly assigned to methyl acetate (MA), the oxidative coupling product. Desorption temperature and fragmentation pattern of MA were also confirmed by temperature programmed desorption (TPD) spectrum of chemisorbed MA on the clean Au(111) surface. In order to form MA, C-C bond in acetaldehyde molecule must be broken and the formation of MA demonstrates that oxygen pre-covered Au(111) surface activates C-C bond. On the other hand, desorption signals appearing at 226 K in m/z = 29, 43, 44, 45 channels indicate acetic acid desorption. Intensive desorption signals appearing at higher temperatures are attributed to decomposition of polymerization products of acetaldehyde.

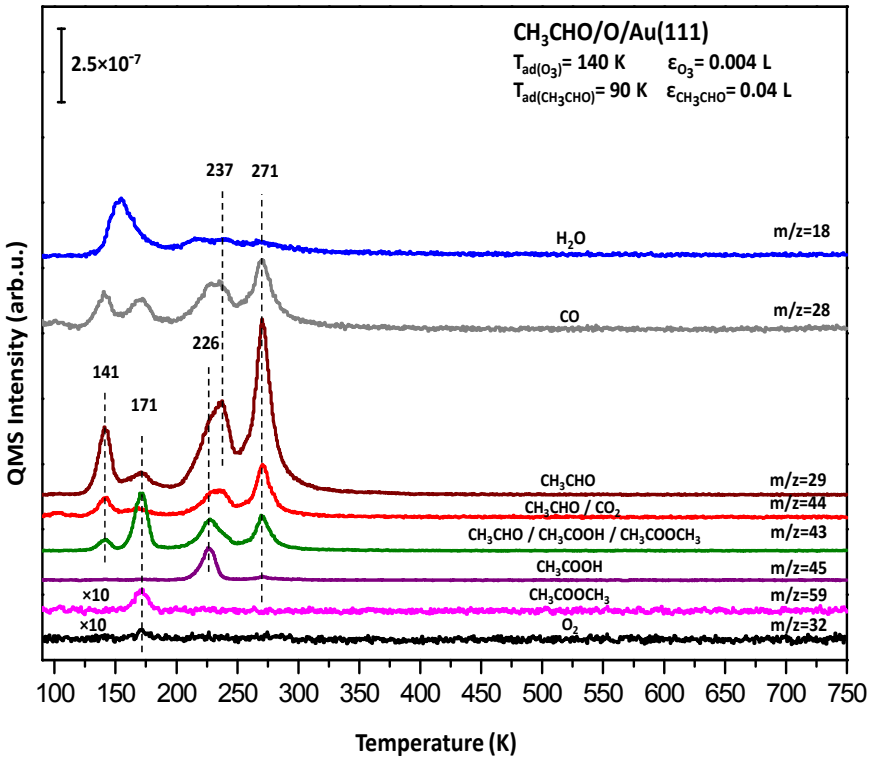

Fig. 1. TPRS profiles for the selected desorption channels obtained after 0.004 L ozone exposure on the clean Au(111) model catalyst surface at 140 K followed by 0.04 L acetaldehyde exposure at 90 K.

4 Conclusions

In the current work, partial oxidation of acetaldehyde on the oxygen pre-covered Au(111) model catalyst surface is investigated. We show that for low oxygen coverages, two different partial oxidation products namely, methyl acetate and acetic acid can be generated without the formation of significant quantities of carbon dioxide. Since the formation of methyl acetate implies C-C bond cleavage; the experimental detection of methyl acetate among the products of acetaldehyde oxidation demonstrates that oxygen pre-covered Au(111) model catalyst surface can activate C-C bonds.

Acknowledgements

Authors acknowledge the financial support from the Scientific and Technological Research Council of Turkey (TUBITAK) (Project Code: 112T589). E.I. Vovk acknowledges the financial support from the Scientific and Technological Research Council of Turkey (TUBITAK) (Program Code: 2221).

References

[1] M. Haruta, T. Kobayashi, H. Sano, N. Yamada, *Chem. Lett.* 16 (1987) 405.
[2] J. Gong, B. Mullins, *Acc. Chem. Res.*42 (2009) 1063.
[3] A. Wittstock, V. Zielasek, J. Biener, C. M. Friend, M. Baumer, *Science* 327 (2010) 319.

II-PP78

Commercial Experience of Operating FCC Unit with Low Catalyst-To-Feed Ratio and the Reduced REO Content in the Catalysts

Levinbuk M.I.[1,2*], Maksimov I.S.[2]

1 - A.V. Topchiev Institute of Petrochemical Synthesis RAS, Moscow, Russia
2 - Gubkin Russian State University of Oil and Gas, Moscow, Russia

* levinbuk.mi@gmail.com

Keywords: FCC, catalyst-to-feed ratio, rare earth oxides, microspherical, catalysts, feed, conversion

1 Introduction

FCC units operated worldwide differ by the quality of feed, feed space velocity, catalyst-to-feed mass ratio and contact time. Significant increase of capital investments is defined by the material changes in these parameters. Therefore, when increasing the unit capacity, one needs to select an individual catalysts type for every existing FCC unit, which provides the required product yields and quality of the target products.

2 Experimental/methodology

The constructional features of the Unit provide the optimal yield of gasoline when using traditional catalysts with reduced capacity compared to its design value.

During the period from 2000 to 2011 the average daily load of the Unit was gradually increased by approximately 20 %. Special selection of cracking catalysts have maintained a high gasoline yield 54.0 wt% as well as high yields of olefins C_3 (5.5 wt%) and C_4 (7.0 wt%), while the catalyst-to-feed ratio was steadily reduced to 4.6 without an extensive modernization of the existing Unit equipment.

In the period from 2000 to 2011 the zeolite surface area of equilibrium cracking catalysts was increased from 60 to 114 m^2/g, and at the same time REO content was decreased from 1.50 to 0.97 wt%.

The refiner operating the Unit has developed plans to increase the processing depth. The planned reconstruction of the crude oil distillation units will increase the production of vacuum gas oil. Therefore the designed Unit capacity will be increased by 20 %.

A group of specialists with BASF support has conducted the research aimed at the selection of catalysts that can be operated at a new value of catalyst-to-feed ratio. Having taken into account the long experience in this field, a new catalyst composition was proposed.

Some catalyst samples were synthesized for testing. The zeolite surface area of tested samples was 134 m^2/g, and REO content was 0.78 wt%. The activity of the samples was determined on an ACE unit (Advanced Cracking Evaluation unit) at the conditions typical for commercial FCC units.

3 Results and discussion

The experimental results obtained on the industrial catalyst used in 2011 together with the two synthesized catalyst samples are presented in Fig. 1,2. Using the trends shown in Fig. 1 it is possible to choose a cracking catalyst which allows not only to maintain but also to increase the gasoline yield, at decreased catalyst-to-feed ratios. Similar trends for the feed conversion are shown in Fig. 2.

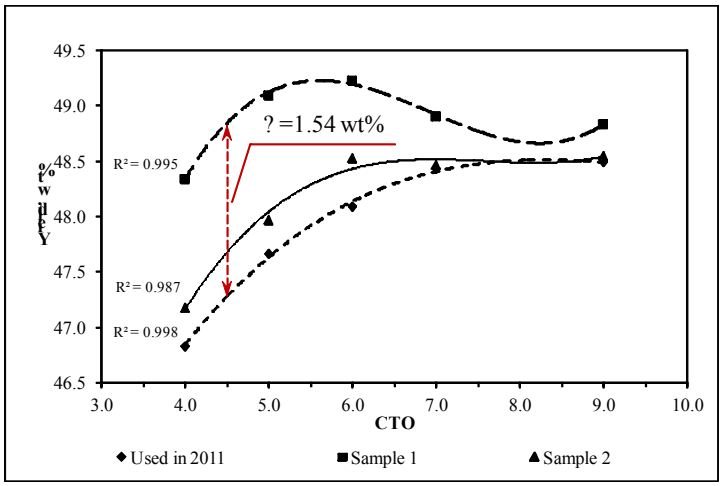

Fig. 1. Gasoline yields for analyzed samples on ACE unit

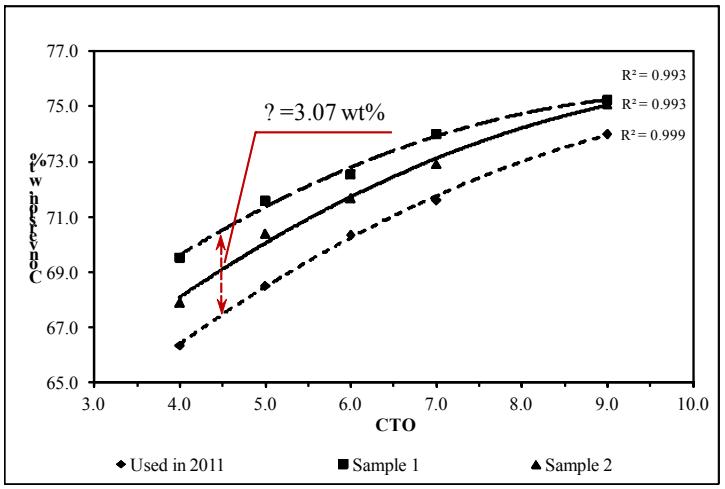

Fig. 2. Conversion change for analyzed samples on ACE unit

4 Conclusions

Enhancement of the FCC Unit capacity led to the development of catalysts with reduced REO content and increased quantity or quality (modulus) of zeolite component in the sample for the purpose of maintaining constant basic product yields at low catalyst-to-feed ratio without considerable reconstruction of the Unit equipment.

Decrease the REO content could be balanced by the increased zeolite content in the catalyst. Therefore, the stability of active zeolite as well as zeolite matrix durability start to play a dominating role.

When choosing a catalytic cracking catalyst, it is crucial to consider the catalyst-to-feed ratio, conditioned by the design of the FCC unit. By defining the interrelation of catalyst-to-feed ratio and catalyst properties the use of existing equipment can be effectively maximized.

For the development of FCC catalysts without REO it is necessary to carry out a set of studies on special modification of Y zeolite.

Acknowledgements

Authors are grateful to BASF for their assistance in the synthesis and laboratory testing of cracking catalyst samples.

II-PP79

Tuning the Catalytic Activity of Palladium Nanoparticles by Modification Phosphonium Ionic Liquid Structure

Arkhipova D.M.[1*], Ermolaev V.V.[1], Miluykov V.A.[1], Islamov D.R.[2], Kataeva O.N.[1], Sinyashin O.G.[1]

1 - A.E. Arbuzov Institute of Organic and Physical Chemistry KSC RAS, Kazan, Russia
2 - Kazan (Volga region) Federal University, Kazan, Russia

* arkhipova-daria@mail.ru

Keywords: palladium nanoparticles, phosphonium ionic liquids, stabilization, Suzuki reaction

1 Introduction

Palladium nanoparticles (PdNPs) stabilized by ionic liquids (ILs) have been successfully used in catalysis [1, 2]. Among the myriads of ILs the phosphonium salts especially sterically hindered ones have been less studied.

Catalytic activity of PdNPs depends on their size as well as on their environment in the solution. The interactions between nanoparticle and stabilizer molecules are important for understanding the mechanism of the nanoparticle stabilization. Varying structure (nature) of stabilizer we can influence on type of stabilization and as a consequence on catalysis efficiency.

2 Experimental

A series of sterically hindered phosphonium ionic liquids (PILs) with different length of alkyl chain was synthesized according to the previously reported technique [3]. The structure of obtained phosphonium salts was proved by X-Ray analysis (Fig. 1). There was found that alkyl chain elongation leads to the ordering of the PIL packing.

PdNPs were obtained *in situ* by stirring palladium acetate in ethanol in PIL presence without any additional reducing agents.

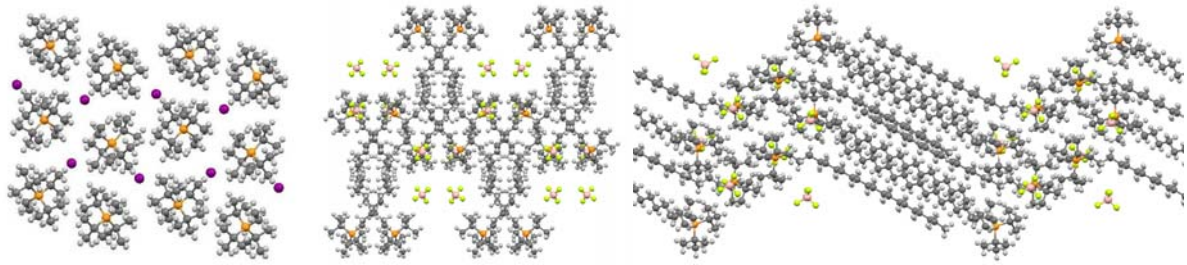

Fig. 1. Crystal packing of PILs.

Suzuki cross-coupling of 1,3,5-tribromobenzene and phenylboronic acid (Fig. 2) was chosen as a model reaction. Sterically hindered PILs allow carrying out the coupling reaction in mild conditions.

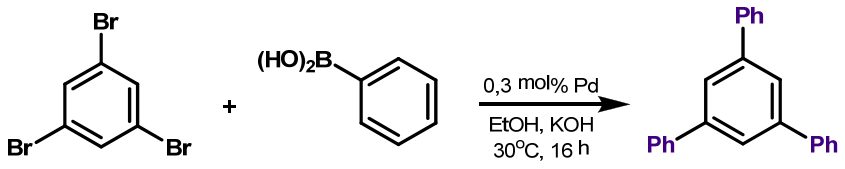

Fig. 2. Suzuki cross-coupling reaction.

3 Results and discussion

We have found that varying the length of the linear alkyl substituent of the sterically hindered phosphonium salt allows tuning catalytic activity of PdNPs. The structure and supramolecular organization of PIL determine its behaviour in solution and the efficiency of the catalytic composition.

PILs contained short linear alkyl substituents provide predominantly electrostatic stabilization of PdNPs, PILs with long alkyl chains – steric stabilization. Catalytic system on both of them demonstrate low activity that can be explained by high stability of formed PdNPs. Phosphonium salts contained medium length linear alkyl chains realize the balance between electrostatic and steric types of stabilization that favours the best combination of stability and activity of PdNPs.

4 Conclusions

Sterically hindered PIL contained alkyl chain of medium length allow to reach optimal combination of stability and activity of formed PdNPs. Achieved balance between electrostatic and steric types of nanoparticle stabilization is necessary condition for the effective catalysis.

Acknowledgements

Authors are grateful for the financial support to the Russian Foundation for Basic Research (13-03-12170).

References

[1] A. Balanta, C. Godard, C. Claver, *Chem. Soc. Rev*. 40 (2011) 4973.
[2] (a) J. Durand, E. Teuma, F. Malbosc, Y. Kihn, M. Gomez, *Catal. Commun*. 9 (2008) 273;
(b) J. D. Scholten, B. C. Leal, J. Dupont, *ACS Catal*. 2 (2012) 184.
[3] V. Ermolaev et al, *Dalton Trans.* 39 (2010) 5564.

II-PP80

Advantages of Ultrasonic Spray Pyrolysis to Prepare Catalysts for Carbon Nanofiber Synthesis

Krasnikova I.V.[1*], Mishakov I.V.[1,2], Vedyagin A.A.[1]

1 - Boreskov Institute of Catalysis, Siberian Branch of RAS, Novosibirsk, Russia
2 - Novosibirsk State Technical University, Novosibirsk, Russia

* tokareva@catalysis.ru

Keywords: ultrasonic spray pyrolysis, catalyst preparation, CNF

1 Introduction

At present, carbon nanomarerials (carbon nanotubes and nanofibers) are of great value due to its exceptional properties. Most commonly they are characterized via chemical resistance, mechanical strength, large surface area and high aspect ratio. Carbon nanofibers (CNF) are known to be successfully applied as modifying agents in diverse composites and materials.

Chemical vapour deposition (CVD) of hydrocarbons is widely used for CNF synthesis. The process is implemented on dispersed particles of the iron subgroup metals (Fe, Co, Ni) and their alloys with other elements. There are different techniques for catalyst preparation such as mechanochemical activation of metal oxides, co-precipitation of precursor salts, and impregnation of supports. Unfortunately, all listed methods are known to have the certain drawbacks concerning ecological and environmental aspects as well as difficulties in obtaining active particles with controllable size and distributions. From the other hand, all issues mentioned should be addressed when developing technology for scaled-up synthesis of CNF.

From this point of view, one of the most interesting and prospective approaches is related to using an ultrasonic spray pyrolysis (USP) of precursor solutions. USP offers a great flexibility in a continuous flow process for the synthesis of novel materials on large scale. Additionally, the controllable size and composition of active particles along with high purity grade should be noted as advantages of this preparation method [1]. Usually the process involves the following procedures: atomization of precursor solution (suspension) by ultrasonic nebulizer; drying of sprayed droplets in a preheated chamber; collection of formed particulate matter by a cyclone, filter bag or electric field precipitator [2].

2 Experimental/methodology

A series of Ni-Cu-Mg-O catalysts have been prepared using ultrasonic spray pyrolysis. A piezoelectric element (1.7 MHz, 30 W) of a domestic humidifier was used as an ultrasonic generator. More detailed description of the experimental setup is given in [3]. The precursor aqueous solution contained the dissolved nitrates of nickel, copper, and magnesium. The total concentration of salts was varied in the range of 0.1–5 wt.%. The aerosol particles were transferred by the air flow to the furnace preheated to 250°C. The fast drying of micron droplets of the solution in the furnace resulted in the formation of very fine particles (including those of submicron size); the particles were trapped using a domestic electric precipitator.

The USP-prepared samples were heated at 550°C; the treatment resulted in decomposition of nitrates and formation of the corresponding oxides. Two different heating procedures were used: (1) the sample was placed in a muffle and treated at 550°C for 30 min; (2) the sample was heated from room temperature to 550°C at a rate of 5°C/min. All prepared catalysts were tested in the synthesis of CNFs by propane decomposition at 700°C. Catalyst samples and synthesized CNF material were analyzed by scanning electron microscopy (JSM-6460). The morphology of the carbon product was examined by TEM using a JEM 1400 instrument, Jeol (Japan).

3 Results and discussion

Results of the performed studies are schematically presented in Fig. 1. It can be seen that the concentration of salts in precursor solution plays a defining effect on formation of spherical particles of the catalyst being synthesized. At the minimum concentration of solution (0.1%) the smallest (> 1 μm) dense spherical particles with rather narrow size distribution were formed. The increase in a concentration leads to enlargement of particle diameter accompanied with widening of the size distribution. One more important factor to be mentioned is related to a heat treatment conditions. Heating of samples in mild conditions with slow T-ramping rate makes it possible to preserve spherical shape and initial dispersion of particles upon decomposition of nitrates into mixed oxides. On the contrary, rapid elevation of calcination temperature results in considerable sintering of spheres into fused porous system. Treatment regime was found to affect the morphology and texture of synthesized CNFs. Thus, USP sample prepared from low-percentage solution catalyzes the growth of carbon fibers of close diameter with preferable feather-like morphology. Other USP catalysts encouraged the formation of carbon fibers in wider range of diameters with a decreased morphological purity.

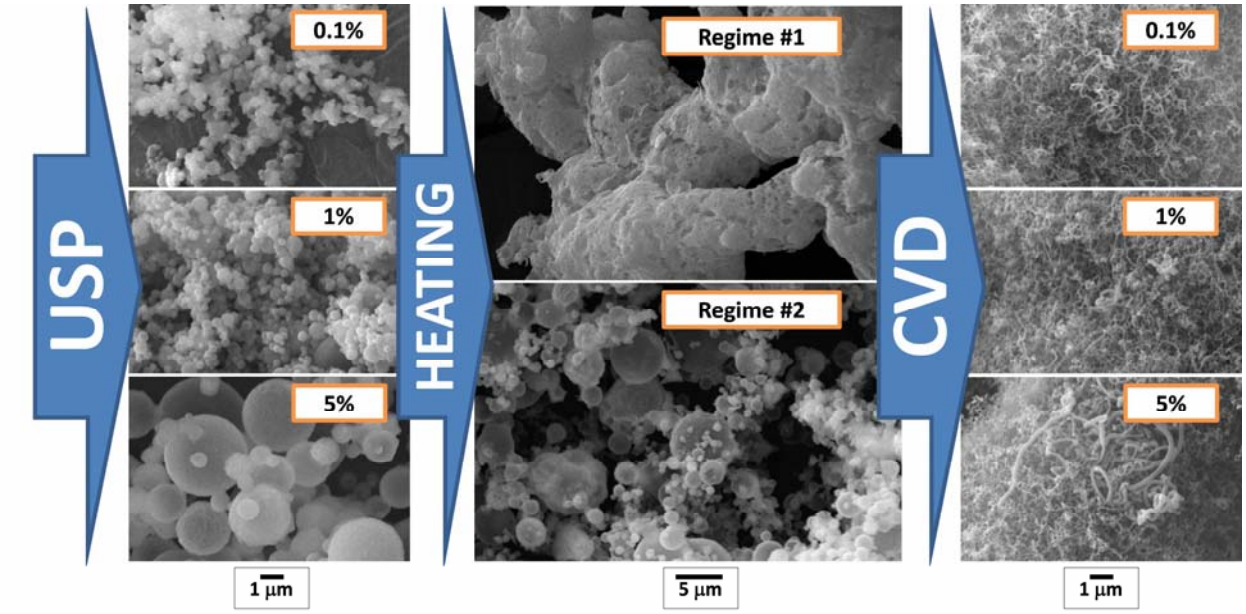

Fig.1. Principle scheme for USP catalyst preparation and CNF synthesis.

4 Conclusions

An alternative method of catalyst preparation for synthesis of carbon nanofibres was proposed on the basis of ultrasonic spray pyrolysis. The simplicity of setup installation along with easy control of particle size of synthesized catalysts makes such method very attractive. The regime of the heat treatment was found to have a significant effect on particle size distributions and, ultimately, upon the textural and morphologic features of CNF.

This study was supported by Russian Academy of Sciences (project № V.45.3.5).

References

[1] J. Bang, K. Suslick, *Adv. Mater.* 22 (2010) 1039.
[2] K. Okuyama, M. Abdullah, I. Lenggoro, F. Iskandar, *Advanced Powder Technol*. 17 (2006) 587.
[3] Strel'tsov et. al., *Nanotechnologies in Russia.* 9 (2014) 715.

II-PP81

Modification by Sn as a Key Factor in Thermal Stability of Pd-Ceria Based Catalysts for Low-Temperature CO Oxidation

Stonkus O.A.[1,2,3*], Slavinskaya E.M.[1,3], Gulyaev R.V.[1,3], Zadesenets A.V.[1,4], Shubin Yu.V.[1,4], Korenev S.V.[1,4], Zaikovskii V.I.[1,3], Boronin A.I.[1,3]

1 - Novosibirsk State University, Novosibirsk, Russia
2 - Research and Educational Center for Energy Efficient Catalysis, Novosibirsk State University, Novosibirsk, Russia
3 - Boreskov Institute of Catalysis, Novosibirsk, Russia
4 - Nikolaev Institute of Inorganic Chemistry, Novosibirsk, Russia

* stonkus@catalysis.ru

Keywords: low-temperature CO oxidation, coprecipitation, palladium ceria, tin, oxide

1 Introduction

At present, palladium-ceria based catalysts are widely used for many catalytic processes, including neutralization of industrial harmful gases and exhaust gases of vehicles. Among these gases one of the most toxic is carbon monoxide, which is necessary to neutralize in a wide temperature range – from room temperature up to 1000 °C. These conditions increase the requirements for thermal stability of CO oxidation catalysts. In this work we present physico-chemical study of Pd-ceria catalysts modified by tin which are capable to be active in CO oxidation at 0 °C after the calcination procedure at 1000 °C.

2 Experimental/methodology

The synthesis of Pd/CeO_2 catalysts was performed by coprecipitation of Pd and Ce nitrates by NaOH, while catalysts Pd/CeO_2-SnO_2 were prepared by oncoming precipitation using precursors $(NH_4)_2[Ce(NO_3)_6]$ and $Pd(NO_3)_2$ (acidic solution) with $Na_2[Sn(OH)_6]$ (alkaline solution). After the precipitation the samples were dried and calcined in air in a wide temperature range (at 450 - 1000 °C).

A complex of physical methods (HRTEM, XRD, XPS, Raman spectroscopy) was used to establish the microstructure, composition and electronic state of components in the prepared catalysts after their calcination or after their treatment in the reaction media. The catalytic properties of the samples were examined by temperature programmed reaction in $CO+O_2$ (TPR-$CO+O_2$ or light-off method) and in CO (TPR-CO) using plug flow reactor with mass-spectrometric analysis of the gas mixture.

3 Results and discussion

The coprecipitation synthesis with subsequent calcination at high temperatures was shown to give the formation of two palladium states: PdO nanoparticles ($E_b(Pd3d_{5/2})$ = 336.5 eV) and Pd^{2+} ionic state in the form of $Pd_xCe_{1-x}O_{2-\delta}$ solid solution ($E_b(Pd3d_{5/2})$ = 338.0 eV) [1]. The ratio between PdO and $Pd_xCe_{1-x}O_{2-\delta}$ phases depends on the calcination temperature due to their strong interaction and dissolution of PdO nanoparticles inside ceria lattice. Also, TPR-CO showed the formation of low-temperature high reactive oxygen state, which was attributed to the surface compounds of palladium and ceria PdO_x(s)/Pd–O–Ce(s) characterized by $E_b(Pd3d_{5/2})$ = 336.1 eV. High catalytic activity is provided by highly dispersive palladium states, which are not stable at T> 800-900°C, turning into Pd°, PdO and CeO_2 nanoparticles.

Introduction of tin into the catalysts structure led to enhancement of the catalytic properties after thermal activation at 900-1000 °C as it can be seen from Fig. 1 (a) comparing Pd/CeO_2 and

Pd/CeO_2-SnO_2 catalysts activity. Investigation of the Pd/CeO_2-SnO_2 samples showed that the high reaction rate correlates with the presence of highly dispersive palladium states in these catalysts attributed to surface palladium compounds and ionic palladium in the composition of $Pd_xCe_{1-x-y}Sn_yO_{2-x-\delta}$ solid solution, respectively. The higher thermal stability of such palladium states was explained by increasing the stability of the defective structure of the support. TEM investigations showed existence of smaller support particles in modified catalysts owing to formation of a microdomain structure representing a fluorite phase particles ($Ce(Sn)O_2$) stabilized on the surface of $Sn(Ce)O_2$ particles with rutile structure (Fig. 1 b-c).

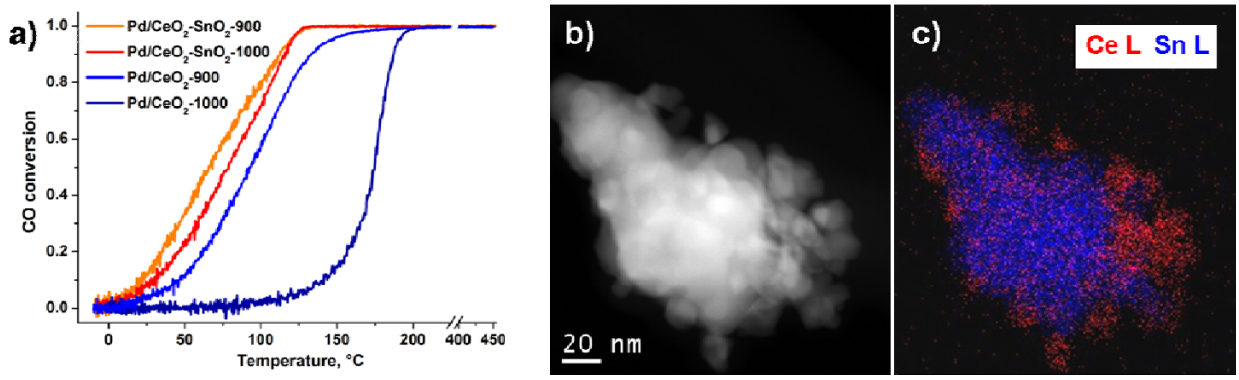

Fig. 1. (a) Temperature dependences of CO conversion of Pd/CeO_2 and Pd/CeO_2-SnO_2 (Sn/Ce = 50:50) catalysts calcined at 900 and 1000 °C; (b-c) HAADF-STEM image and corresponding EDX-mapping pattern (CeL signal is shown in red, SnL signal is shown in blue) of the Pd/CeO_2-SnO_2-900 catalyst.

XPS investigation allowed us to establish that in the case of Pd/CeO_2-SnO_2 catalyst the thermal activation effect was related to segregation of Pd^{2+} ions to the subsurface layers of fluorite phase providing formation of surface species PdO_x(s)/Pd–O–Ce(s). Discussing mechanism of low-temperature CO oxidation, the coincidence of activation energies in CO oxidation for both catalysts suggests the same nature of the active sites and the reaction mechanism. Thus, the Pd-ceria surface species PdO_x(s)/Pd–O–Ce(s) are believed to determine CO oxidation rate in low-temperature region.

4 Conclusions

Using the procedure of oncoming precipitation the Pd/CeO_2-SnO_2 catalysts for low temperature CO oxidation were synthesized for the first time. These catalysts are characterized by high activity with unusually high thermal stability at temperatures up to 1000 °C. Formation of microdomain structure is shown to provide high thermal stability of catalytically active phases including the surface PdO_x(s)/Pd–O–Ce(s) species which determine the reaction rate.

Acknowledgements

This work was supported by the Ministry of Education and Sciences of Russian Federation (target grant for state support of leading universities of the Russian Federation #074-U01) and Skolkovo Foundation (Grant Agreement for Russian educational organizations no. 3 of 25.12.2014).

References

[1] E.M. Slavinskaya, R.V. Gulyaev, A.V. Zadesenets, O.A. Stonkus, V.I. Zaikovskii, Yu. V. Shubin, S.V. Korenev, A.I. Boronin, *Applied Catalysis B: Environmental* 166–167 (2015) 91–103.

II-PP82

Application of the Nanopowders of Ni, Co and their Alloy Prepared by a Method of Plasma-Mechanochemistry for the Reaction of the Carbon Dioxide Conversion of Methane

Tavadyan L.A.[1], Grigoryan R.R.[1], Arsentev S.D.[1*], Aloyan S.G.[2]

1 - Institute of Chemical Physics, Academy of Sciences of Armenia, Yerevan, Armenia
2 - Institute of General and Inorganic Chemistry, Academy of Sciences of Armenia, Yerevan, Armenia

* arsentiev53@mail.ru

Keywords: catalysis, nanopowder, mechanochemistry, methane

1 Introduction

Because of their small sizes, nanopowders show a number of unique properties, which are of interest for researchers in various areas of modern science [1, 2], particularly, in the development of active and stable catalysts for the process of the carbon dioxide conversion of methane (CDCM) [3, 4]:

$$CH_4 + CO_2 = 2H_2 + 2CO \ (\Delta H° = 247 \text{ kJ/mol}).$$

The product of CDCM is synthesis gas, which serves as a raw material for the production of valuable organic compounds and motor fuels. Furthermore, CDCM can be an effective method for the utilization of methane and carbon dioxide, which produce the greenhouse effect [5, 6].

2 Experimental

Fig. 1 shows the reaction module designed for the synthesis of nanomaterials. It consisted of two cylindrical mechanoreactors (*1*, *2*) with an inside diameter of 50 mm and a length of 100 mm made of corrosion resistant steel.

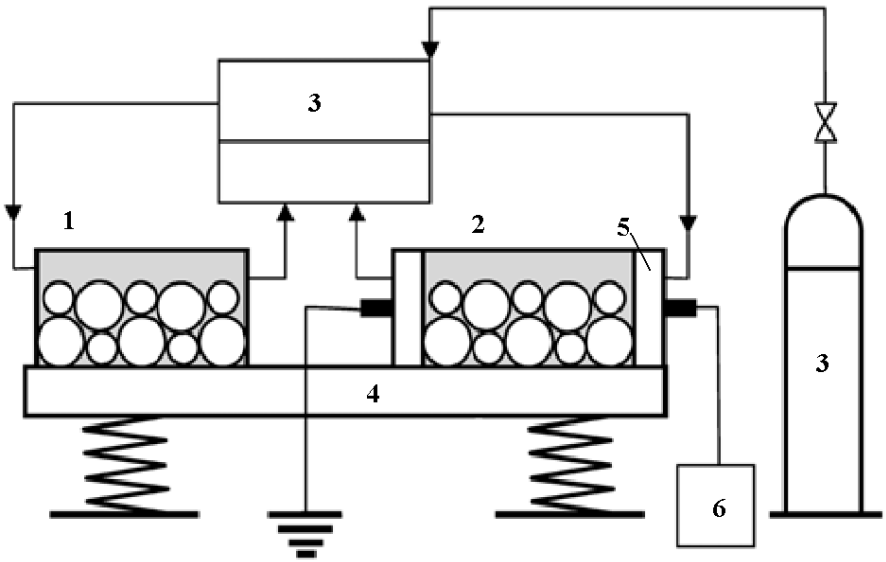

Fig. 1 - Reaction module: (*1, 2*) reactors, (*3*) gas inlet and outlet system, (*4*) vibrating mill, (*5*) end disks with electrodes, and (*6*) highvoltage pulse generator.

Metal balls (R6M5 steel) 8 mm in diameter were used as grinding bodies, which filled 3/4 of the reactor volumes. Crushing was performed in an atmosphere of argon in vibrating mill *4* at

a vibration frequency of 25 Hz and an amplitude of 4 mm in the following two regimes: mechanochemical (reactor *1*) and plasma-mechanochemical (reactor *2*). For supplying high voltage, reactor *2* was equipped with two end teflon disks with central metal hollow electrodes *5*. High voltage (30 kV; 50 Hz; current, ~200 μA) was generated with the converter *6*.

3 Results and discussion

The experiments performed under analogous conditions showed that CDCM did not occur in a reactor filled with a quartz glass up to a temperature of 960°C. With the use of nickel nanopowder as a catalyst, the reaction began at 500°C. The degrees of CH_4 and CO_2 conversion were similar in the test temperature range, and at 830°C they reached 99.4 and 99.7%, respectively. A few hours after the beginning of the reaction, the balance on carbon (the amount of CO formed at a specified conversion of methane and CO_2) was disrupted because of the formation of condensation products (coke formation) on the catalyst surface and the catalytic activity of nickel nanopowder decreased.

On Co nanopowder, the reaction began at 550°C, and the conversion of CH_4 at 850°C did not exceed 30%; that is, this nanopowder was less active than the nickel sample. In this case, in contrast to the nickel catalyst, the cobalt catalyst did not lose its activity for a long time, and it gradually decreased only 300 h after the onset of reaction because of the coking of the surface. Thus, the cobalt catalyst is less active than the nickel one, but it is more resistant to poisoning by condensation products.

The reaction on the Ni-Co alloy obtained by the mechanochemical method came into play at 400°C and the degrees of CH_4 and CO_2 conversion at 870°C were 65 and 70%, respectively. However, the sample lost its catalytic activity after 5 h. With the use of a Ni-Co alloy prepared by the plasma-mechanochemical method, the process also began at 400°C, but the conversions of CH_4 and CO_2 at 870°C were as high as 90 and 99.5%, respectively, at the product ratio H_2 : CO = 1.2–1.4, which is close to the results given in [3].

Thus, a comparison between the results obtained on the Ni-Co alloys shows that the nanopowder, obtained by the plasma-mechanochemical method, has higher catalytic activity and retained it for a long time.

We also studied the possibility of regenerating a catalyst based on the Ni–Co alloy coked upon CDCM with hydrogen at a temperature of 400°C. The results, obtained using X-ray diffraction analysis showed that regeneration with hydrogen at 400°C for several hours leads to the disappearance of the peak of graphite. At this the restoration of the initial catalyst activity takes place. In the course of reduction with hydrogen, the formation of methane was detected, which became less significant with time.

4 Conclusions

Thus, in this work, we studied the catalytic activity of the nanopowders of Ni, Co and their alloys in the process of the carbon dioxide conversion of methane. Nickel nanopowder was found the most active but unstable CDCM catalyst, which rapidly loses its activity as a result of the formation of condensation products on its surface. The nanopowder of the Ni-Co alloy synthesized by the plasma-mechanochemical method is an active, selective and stable CDCM catalyst. The regeneration of the Ni-Co alloy catalyst with hydrogen at a temperature of 400°C for several hours leads to the restoration of its initial activity.

References

[1] Tret'yakov, Yu.D., *Nanotekhnologii* (Nanotechnologies), Moscow: Fizmatlit, 2009.

[2] Gusev, A.I., *Nanomaterialy, nanostruktury, nanotekhnologii* (Nanomaterials, Nanostructures, and Nanotechnologies), Moscow: Fizmatlit, 2007.

[3] Krylov, O.V., *Ross. Khim. Zh.*, 2000, vol. 44, no. 1, p. 19.

[4] Ma, J., Sun, N., Zhang, X., Zhao, N., Xiao, F., Wei, W., and Sun, Y., *Catal. Today*, 2009, vol. 148, p. 221.

[5] Fan, M.S., Abdullah, A.Z., and Bhatia, S., *Int. J. Hydrogen Energy*, 2011, vol. 36, no. 8, p. 4875.

[6] Arutyunov, V.S., *Ross. Khim. Zh.*, 2001, vol. 45, no. 1, p. 55.

II-PP83

Effective Acidities of Heterogeneous Catalysts in Various Liquids in Relation with their Catalytic Activity

Carniti P., Prati L., Gervasini A.*

Università degli Studi di Milano, Dipartimento di Chimica, Milano, Italy

* antonella.gervasini@unimi.it

Keywords: solid acid catalysts, acid catalysis, intrinsic acidity, effective acidity, liquid, chromatography

1 Introduction

Acid catalysis is by far one among the most important area of catalysis by industries in all sectors of chemical manufacturing. Solid acid catalysts are applicable to a *plethora* of acid-promoted processes in organic synthesis, material transformation, depollution reactions, and so forth with well-known advantages over the gas or liquid acid catalysts. Solid acids can be described in terms of their Brönsted/Lewis acid sites, strength and number of these sites. High product selectivity can depend on the fine-tuning of these properties selectivity. For example, hydrolysis reactions generally require medium acid strength sites, while dehydration, esterification and alkylation reactions require strong acid sites [1,2].

In this context for all the liquid-solid catalytic reactions, particular attention has to addressed to the reaction solvent. The nature and properties of the solvent (polarity, proticity, hydrophlicity, solvating ability, etc.) can affect the acidity of the catalyst surface by interaction (coordination, H-bond, chelation, etc.) with the present Brönsted/Lewis acid sites. The nature of the acid sites and the relative proportion between Brönsted/Lewis surface sites can be modified upon the solvent-surface interaction. Moreover, due to solvent-surface interaction, the acid strength of the sites can be altered; generally, it decreases, with consequences on the activity and selectivity of the catalyst.

For all that has been said above, the determination of the *effective* acidities of acid catalysts measured in different liquids is of high importance for the correct choice of the *best* acid catalyst (in terms of amount of acid sites and site strength) for given liquid solid acid-reactions. For example, only few solid acids are known to be able to maintain lively acid sites in water [3] and only few catalysts are suitable for valorization reactions of polysaccharides to obtain useful chemicals, like 5-hydroxyfurfurol, furfural, levulinic acid, etc.

We would like to present here our recent results on the study of *effective* acidities of several catalysts and supports measured in various liquids, like water, methanol, 2-propanol, hydro-alcoholic mixtures, among others, and the observed relations with catalytic activity in some liquid-solid reactions of biomass valorization, running in the same liquids.

For such measurements, basic solutions of 2-phenylethylamine (PEA), chosen as molecular probe, in the selected liquid, have been used. The measurements can carry out according with a complete recirculation mode or according with a pulse method [4]. The numerical treatment of the collected data permitted obtaining not only the amount of the *effective* acid sites with evaluation of the fraction of strong acid site in a given liquid, but also thermodynamic or kinetic parameters relevant to the acid-base adsorption phenomenon.

2 Experimental/methodology

The sample studied are both bulk and supported acid catalysts: niobium oxide (NBO) and niobium phosphate (NBP) (kindly furnished by CBMM from Brasil); and other synthesized catalytic materials: a ternary compound containing Nb_2O_5, 2.5 wt.%; P_2O_5, 2.5 wt.% and SiO_2, 95 wt.% (NbPS), niobia supported on silica, and on silica-zirconia oxides (Nb, 10 wt.%); metal

nanoparticles (Pt, Co, and PtCo) deposited on acidic mixed-silica oxides (silica-alumina, silica-niobia, silica-titania, and silica zirconia (with 5 wt.% Al, Nb, Ti, and Zr).

The liquid-solid acid-base titrations have carried out by using 2-phenylethylamine (PEA) as basic probe in a modified liquid-chromatographic (HPLC) composed of a pump and an UV-detctor; the sample powder was put at the place of the chromatographic column (Fig. 1A). With the line, it was possible to operate in complete recirculation mode, and a typical step-chromatogram was obtained from the titrations (Fig. 1B), or in dynamic mode obtaining a tipycal pulse-chromatogram (Fig. 1C).

The choice of liquid used to dissolve the basic probe affects the result of the titrations. Cyclohexane with apolar and aprotic characteristics was chosen to determine the *intrinsic* acidity of the samples, due to complete absence of interaction with the surfaces functionalities. With the other liquid used (water, methanol, 2-propanol, hydro-alcoholic mixtures), which are able to coordinate, solvate, and make interactions with the acid sites of the surfaces, *effective* acidities of the samples were determined.

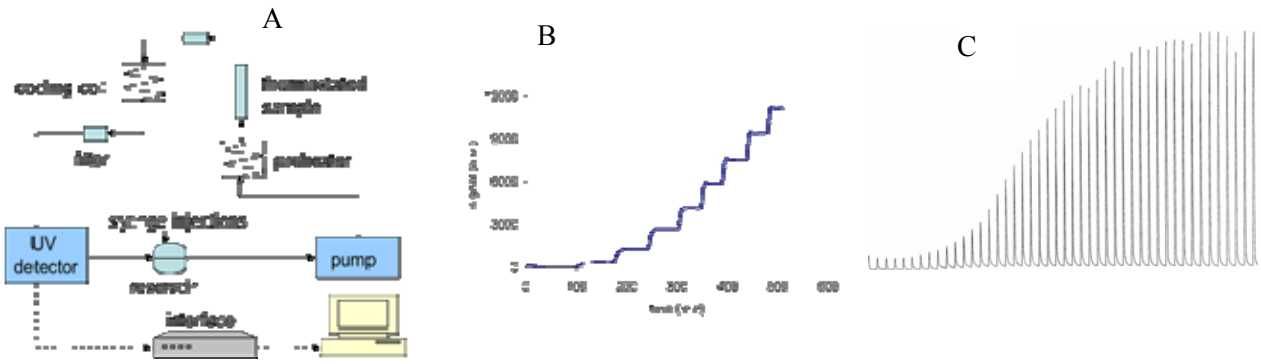

Fig. 1. Scheme of the HPLC line used for the liquid-solid titrations (A); chromatograms obtained for experiments in total recirculation mode (B) and in pulse mode (C).

3 Results and discussion

On several catalysts, examples of *effective* acidity measured in the same reaction solvent in relation with their catalytic activity will be presented.

For example, NBO and NBP are known water-tolerant acid catalysts, for this, they have been used in reactions of disaccharide (sucrose, cellobiose, maltose), and polysaccharide (inulin) hydrolysis and sugar (fructose) dehydration [5]. NbPS is more acidic than NBO and NBP, when it is titrated in cyclohexane (0.600, 0.403, and 0.207 mequiv/g for NbPS, NBP, and NBO, respectively), while in water NBP and NBO have higher *effective* acid sites than NbPS (0.192, 0.350, and 0.126 mequiv/g on NBO, NBP, and NbPS, respectively). As expected, NbPS loses part of its acidity in water due to the presence of silica that does not possess any acidity in water. This behaviour has consequences on the catalytic activity, as observed in the studied reactions.

Niobia dispersed on an acid support (silica-zirconia) is effective for the acid conversion of xylose to furfural, due to the water-tolerant acid properties of the niobia phase. As higher the niobia dispersion (prepared by sol-gel) as better the catalytic performances, which could be associated with the highest amount of strong *effective* acid sites.

References

[1] G. Busca, Chem. Rev. 107 (2007) 5366.
[2] P. Gupta, S. Paul, Catal. Today 236 (2014) 153.
[3] T. Okuhara, Chem. Rev. 102 (2002) 3641.
[4] P. Carniti, A. Gervasini, M. Marzo, Catal. Today 152 (2010) 42.
[5] M. Marzo, A. Gervasini, P. Carniti, Carbohydrate Res. 347 (2012) 23.

II-PP84

New Heterogeneous Catalysts for Free Radical Generation

Krugovov D.[1*], Mengele E.[1], Kasaikina O.[1], Berezin M.[2]

1 - N.N. Semenov Institute of Chemical Physics, Russian Academy of Sciences, Moscow, Russia
2 - Institute of Problem Chemical Physics, Russian Academy of Sciences, Moscow region, Russia

* kagur1982@mail.ru

Keywords: surfactants, acetylcholine, montmorillonite, cellulose, chitosan, oxidation, polymerization

1 Introduction

The phenomenon of micellar catalysis has been known for a rather long time and applied in many processes, but the significant influence of surfactants on the mechanism of hydrocarbon oxidation was found and studied only in recent decades [1-3]. Surfactants (S) form with hydroperoxides (LOOH) mixed micelles {*n*LOOH–*m*S} and the behavior of hydroperoxides in these mixed micelles determines the influence of the surfactants on oxidation. Cationic surfactants (S+) are found to catalyse decomposition of hydroperoxides into free radicals.

For the combinations of different hydroperoxides and S+ it has been established that {*n*LOOH–*m*S+} systems generate radicals rather actively at moderate temperatures in both organic and aqueous media [2,4,6], according to the following sequence:

$$nLOOH + mS+ \Leftrightarrow \{nLOOH–mS+\} \rightarrow LO_2^{\cdot}$$

Thus, mixtures S+ and LOOH can be used as a lipophilic and hydrophilic initiating system.

In this study the development of catalytic systems for radical generation based on this property of cationic surfactants is presented. The possibility of heterogeneous catalysts, prepared by adsorption of S+ on solid carriers, has been explored as free radical initiating systems for oxidation and radical polymerization processes.

2 Experimental/methodology

The carriers (M) - montmorillonite (Cloisite Na, USA), (MC)-microcrystalline cellulose (Evalar, RF), and (CH)-chitosan (Fortex, RF) were used as purchased. The well known S+ - cetyltrimethylammonium bromide (CTAB, Fluka) was taken to prepare catalysts as follows: a solid carrier was placed into the CTAB solution of known concentration in chloroform for 10 hours under stirring; then a carrier was separated from solution, washed out with clean chloroform and all the chloroform fractions were combined. The washed solid residue was dried under the flow of warm air. The CTAB residue, obtained after evaporation of chloroform, was weighted to determine CTAB adsorption (Γi) on a carrier.

The model chain reaction of limonene oxidation [2,3] was used to estimate the catalytic activity of heterogeneous catalysts in hydrocarbon oxidation. The polymerization of styrene, containing 0.05 M cumene hydroperoxide (CHP), was a model reaction to examine the catalysts in radical polymerization. The rates (R) of both chain reactions are described by the equation: $R = a\,[LH]R_i^{0,5}$, where R_i is the radical initiation rate, $a = k_p/(2k_t)^{0,5}$ is the ratio of rate constants for chain propagation (k_p) and termination (k_t). Oxygen uptake was measured by volumetric method in limonene oxidation; the polymerization rate was determined by microcalorimetry using DAC-1-1. With known rate constants for both processes [2,4,7] the initiation rate was calculated according to: $R_i = (R/([LH]\cdot a)^2$.

We studied the possibility of polymerization on the surface of glass covered by CTAB monolayer as well. The property of polymer layer obtained was determined by AFM method using Bruker AFM FastScan in ScanAsyst+PeakForceQNM mode.

3 Results and discussion

Table 1 demonstrates the adsorption of CTAB on montmorillonite, cellulose, and chitosan as well as the rates of initiation, calculated on the base of measured rates of styrene polymerization and limonene oxidation carried out in the presence of 4%(weight) heterogeneous catalysts.

Table 1. Adsorption CTAB on carries and radical generation rates during polymerization of styrene and oxidation of limonene, catalyzed by heterogeneous catalysts (4%); 60°C.

Catalyst	Adsorption, Mol/g	$R_i \cdot 10^7$, Mol/(L·s) Styrene polymerization	$R_i \cdot 10^7$, Mol/(L·s) , Limonene oxidation
-	-	0.42	0.58
M/CTAB	$5{,}71\ 10^{-4}$	0.76	2,54
MC/CTAB	$1{,}85\ 10^{-4}$	7.5	20,2
CH/CTAB	$1{,}72\ 10^{-5}$	4.8	0,82

So far as hydroperoxides are potential source of radicals, cumene hydroperoxide (0.05M) was used in styrene polymerization and limonene hydroperoxide (0.2M) was added to limonene (2M) in chlorobenzene.

Unlike a less adsorption of CTAB on cellulose and chitosan the polymerization rates with these catalysts were found to be in several times higher than that with M/CTAB. The rates of free radical generation via catalytic limonene hydroperoxide decomposition decrease in the sequence: MC/CTAB > M/CTAB >CH/CTAB. The increase of catalytic effect of cationic surfactant on the cellulose surface and the role of hydroperoxide nature in colloid catalytic system are discussed.

By means of AFM the adsorption of CTAB on glass surface and properties of polystyrene layer formed on the surface immersed in the solution of tert-butyl-hydroperoxide in styrene were studied. At AFM image of the surface, which was immersed in styrene, well-marked areas of the polystyrene film with the characteristic Young's modulus, was detected, while, on the AFM image of the surface, not in contact with styrene, only traces of preparation - the areas covered with CTAB and free glass were found.

4 Conclusions

All heterogeneous carriers, covered with CTAB monolayer, catalyse the decomposition of hydroperoxides into free radicals and initiate radical chain processes in olefins containing hydroperoxides. It can be used for covering of complicated heterogeneous surface by polymer layer and for production of nanocomposites by the vinyl monomer radical polymerization initiated with the colloid heterogeneous system of LOOH and a nanodispersed carrier hydrophobizated with a cationic surfactant.

Acknowledgements

The authors thank the company Bruker for help in the study of samples by AFM. This work is partly supported by grants RSF 14-23-0018 and RFFI 14-03-00757

References

[1] Kasaikina, O.T., Kortenska, V.D., Kartasheva, Z.S., et al., Coll. Surf. A: Physicochem. Eng. Asp., (1999) 149 (1), 29.
[2] Kasaikina, O.T., Kartasheva, Z.S., Pisarenko, L.M.,Rus. J. Gen. Chem. (Engl) (2008), 78(8), 1533.
[3] Krugovov, D.A., Pisarenko, L.M., Kondratovich, et al., Petr. Chem. (Engl.) (2009) 49(2), 120
[4] . Kasaikina O.T., Golyavin A.A., Krugovov D.A. Mosc.Univ. Chem. Bul. (2010) 65(3), 206.
[4] Patent RF № 2348608 (2009)
[5] Kancheva V.D., Kasaikina O.T. Cur. Med. Chem. (2013) 20**,** 4784,
[6] Trunova, N.A., Kartasheva, Z.S., et al., Colloid. J. (Engl. Transl.) (2007), 69(5), 655.
[7] Denisov E.T., Denisiva T.G Handbook of antioxidants: bond dissociation energies, rate constants, activation energies and enthalpies of reactions. Boca Raton: CRC press, (2000).

II-PP85

High Active Cr-Al Oxides Catalyst for the Ozone Friendly Freons Synthesis: Pretreatment Conditions and Kinetic Study

Isupova L.A., Simonova L.G., Zirka A.A., Larina T.V., Reshetnikov S.I.*

Boreskov Institute of Catalysis, Novosibirsk, Russia

* reshet@catalysis.ru

Keywords: pretreatment, chromium–aluminum catalyst, chladones, kinetics

1 Introduction

In recent decades, considerable efforts have been focused on the synthesis of chladones having zero ozone depletion potential. The most promising in this regard are chladones of the ethane row (HFC-134a, HFC-125). Numerous patents are devoted to the processes of production of HFC-125 and the catalysts [1-3] containing usually chromium (III) compounds. These catalytic systems can be used and for synthesis of the chladone of the next generation HFC-1234yf (2,3,3,3-tetrafluoropropene) having zero ozone depletion (ODP) and low global warming (GWP) potentials [4]..

In Boreskov Institute of catalysis the high active Cr_2O_3/γ- Al_2O_3 catalyst in comparison with the industrial (Russia) Cr-Mg catalyst was developed. It is well-known that the activity and selectivity of catalysts strongly depend not only on the catalysts composition, method of precursor preparation but n pretreatment conditions as well.

In this work, we studied the influence of the pretreatment conditions (temperature and gas composition) on the physicochemical and catalytic properties of the chromium–aluminum catalysts. Kinetic study of most active catalysts in pentafluoroethane (HFC-125) sinthesis by the gas-phase hydrofluorination of tetrachloroethylene.

2 Experimental

Catalyst (precursor) containing 95 wt % chromium oxide (on Cr_2O_3 basis) and 5 wt % Al_2O_3 were prepared by the addition of a mixture of $CrCl_3$ and $AlCl_3$ solutions to a solution of ammonia (9%) at a constant pH and a temperature. After the completion of precipitation, the suspension was aged for 1 h, washed with distilled water, filtered, and dried in air at 110–120°C for 12 h.

The catalytic activity of samples in the fluorination of tetrachloroethylene to pentafluoroethane was determined using a flow reactor with a fixed catalyst bed (grain size of 0.25–0.5 mm) in the kinetically controlled region at 320–370°C, 0.4 MPa, reactant molar ratios of HF: tetrachloroethylene = (10–20) : 1, and a residence time of 1–3 s. The activity was estimated in terms of the first-order reaction rate constant $k = -\ln(1 - X)/\tau$, where X is the tetrachloroethylene conversion (in mole fractions) at the residence time τ [5].

3 Results and discussion

The prepared catalyst sample (precursor) was heattreated between 165 and 600°C using two different procedures: in nitrogen or in air. The thermal behavior of the Cr–Al samples in nitrogen and air in the temperature range 110–600°C were studied by thermal and X-ray diffraction analyses, uv-vis diffuse reflectance spectroscopy, and specific surface are measurements.

It was obtained that the temperature and gas composition of pretreatment strong effect on the specific surface area and activity of the catalysts (Fig.1). As the temperature of heat treatment in nitrogen is increased, this sample undergoes gradual dehydration and, at ~300°C,

when the residual water content decreases to ~10 wt % (~0.5 (mol H_2O/Cr^{3+}), S_{sp} begins to increase. At 400°C, the residual water content is 4.7% and S_{sp} is close to its maximum. As the temperature is raised to 500°C, S_{sp} remains approximately invariable. The increase in S_{sp} due to the dehydration of the sample is accompanied by an increase in catalytic activity. This is in agreement with the view that the thermolytic loss of hydroxyl groups results in the formation of coordinately unsaturated, catalytically active surface species (Cr^{3+} and O^{2-}).

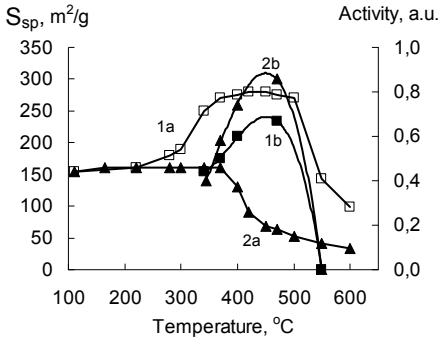

Fig. 1. Influence of the treatment temperature on the specific surface area and activity of the catalysts: (*1a*) S_{sp}, N_2; (*1b*) activity, N_2; (*2a*) S_{sp}, air; (*2b*) activity, air.

The dehydration of chromium hydroxide and the highly exothermic oxidation of Cr^{3+} to oxides with $CrO_{1.9}$ stoichiometry occur in the temperature range from 200 to 370°C (the heat treatment in air). Between 370 and 400°C, $CrO_{1.9}$ decomposes to less oxidized forms $CrO_{1.5}$. Very exothermic rystallization yielding coarse α-Cr_2O_3 crystals occurs at 410–420°C. The oxidation–decomposition processes $CrO_{1.5} \leftrightarrow CrO_{1.9}$ are reversible for noncrystallne fine_particle chromium oxides. Coarse α-Cr_2O_3 crystals contain no reversibly oxidizable chromium species that are the most active in the catalytic hydrofluorination of chloroalkanes. The oxides having reversibly oxidizable chromium exhibit high activity in hydrofluorination, but they are unstable and decompose readily to $CrO_{1.5}$ above 370°C. The highly active catalyst should have a large specific surface area and low concentrations of deactivating impurity anions and water along with the optimal oxidation state of chromium. This can be explained by the following processes occurring in the oxidation medium:

$$Cr_2O_3(am.) \xrightarrow{200-370^0 C} Cr\,O_{1.9}(am.) \xleftrightarrow{370-400^0 C} Cr\,O_{1.5}(am.) \xrightarrow{410-420^0 C} \alpha\text{-}Cr\,O_{1.9}(cr.)$$

4 Conclusions

The physicochemical properties of the Cr_2O_3/γ- Al_2O_3 catalysts obtained by heat treatment of the sample (precursor) in nitrogen and air between 110 and 600°C and their influence on the catalytic activity in tetrachloroethylene hydrofluorination was studied by the TA, TPD, X-ray diffraction, BET, and DRS methods. It was shown that the temperature and gas composition of precursor pretreatment strong effect on the specific surface area and activity of the catalysts. The $CrO_{1.9}$ compounds are more active than $CrO_{1.5}$. For more active catalyst sample kinetic study was performed.

References

[1] E. Lacroix, J.-P. Schirmann: Patent EP 847801, 1998.
[2] F. Rinaldi, P. Cuzzato, L. Bragante, S. Ausimont: Patent US 5919728, 1999.
[3] S.K. Sheremet'ev, I.G. Trukshin, V.G. Barabanov, S.N. Mikhajlov, N.I. Samsonova, I.P. Uklonskij, V.F. Denisenkov: Patent RU 2141467, 1999.
[4] Patent RU 2418782 (DuPont). 2007.
[5] L.G.Simonova, S.I.Reshetnikov, A.A.Zirka at al. Patent RU 2402378, 2009.
[6] A.A. Zirka, and S.I. Reshetnikov, Kinet. Catal. (Engl. Transl.), 49 (2008) 663.

II-PP86

A Computational Approach to Understand the Promotional Effect in Ni-Fe Bimetallic Catalyst

Ray K.[1*], Pandey D.[1], Singh B.[2], Prasad R.[2], Deo G.[1]

1 - Department of Chemical Engineering, Indian Institute of Technology Kanpur, Kanpur, India
2 - Department of Physics, Indian Institute of Technology Kanpur, Kanpur, India

* koustuvr@iitk.ac.in

Keywords: Ni-Fe bimetallic catalyst, Ni-Fe, alloy, CO_2 hydrogenation, density of states (DOS)

1 Introduction

Supported Ni-Fe bimetallic catalysts with a specific Ni to Fe ratio was found to possess superior catalytic activity for CO_2 hydrogenation to CH_4 compared to supported monometallic Ni catalyst [1]. It was proposed that the formation of suitable alloy played a dominant role in the enhancement in catalytic activity. In the present communication computational (DFT) and experimental studies were undertaken to gain insights into the enhancement due to metal alloys.

2 Methodology

Catalyst synthesis, characterization and testing during the CO_2 hydrogenation reaction were similar to those reported previously, except that the total metal was 15 weight percent [1]. The rate for CO_2 conversion was converted to TurnOver Frequency (TOF). The surface-slab model and closed packed (111) surface were chosen for computational studies. The three synthesized catalysts, $100Ni/Al_2O_3$, $75Ni25Fe/Al_2O_3$ and $50Ni50Fe/Al_2O_3$, were represented by Ni(111), $Ni_3Fe(111)$ and NiFe(111) surfaces. The theoretical calculations were performed within density functional theory framework using CASTEP code [2]. The generalized gradient approximation was used to include the exchange-correlation effects. The surface relaxations play an important role due to lower coordination in the surface layers, and thus, we have relaxed top two layers of all slabs until the residual forces were less than 0.01 eV/Å. The Brioullin-Zone sampling was done using 4×4×1 k-mesh within Monkhorst-Pack scheme [3]. The plane wave cut-off energy of 360 eV was employed.

3 Results and discussion

Characterization and reactivity data of the three catalysts and surfaces are presented in Table 1. The shift in the XRD 2θ values was indicative of Ni-Fe alloy formation. Table 1 also revealed that the rate significantly increased for the supported Ni-Fe catalysts.

Table 1. Characterization (experimental and theoretical) of catalysts

Catalyst	XRD		H_2-TPD (µmole/g)	Rate (µmole/g.s)	ε_d of surface Ni atoms (eV)	w_d of surface Ni atoms (eV)
	hkl	2θ				
$100Ni/Al_2O_3$	Ni(111)	44.5°	82	51	-1.28	-2.25
$75Ni25Fe/Al_2O_3$	$Ni_3Fe(111)$	44.2°	115	162	-1.31	-2.28
$50Ni50Fe/Al_2O_3$	NiFe(111)	44.0°	124	124	-1.33	-2.30

Four properties were considered for electronic characterization of the DOS of d electrons: the d-band center ($\boldsymbol{\varepsilon_d}$), d-band width ($\mathbf{w_d}$), upper d-band edge ($\boldsymbol{\varepsilon_u}$) and DOS at Fermi level (E_F) [4-6]. The $\boldsymbol{\varepsilon_d}$ and $\mathbf{w_d}$ of surface Ni atoms were calculated and the values are given in Table 1. The $\boldsymbol{\varepsilon_d}$ gradually decreased and shifted further away from E_F compared to pure Ni. The $\boldsymbol{\varepsilon_u}$ and DOS at E_F of Ni_3Fe and NiFe shifted significantly from Ni and a small difference of these two properties

between Ni_3Fe and NiFe is also existed. Furthermore, the ε_u of the surface Ni atoms for Ni_3Fe and NiFe was below E_F. As previously reported shifting of ε_d away from E_F also resulted in lowering of DOS at E_F [7]. The lowering of ε_d (and DOS at E_F) and ε_u suggested higher filling and weaker chemical bonding between the adsorbate and surface Ni atoms [4, 5]. Thus, the adsorption was expected to be weaker on the bimetallic catalyst compared to Ni.

To correlate the reactivity and electronic characterization data the TOF of catalysts was plotted as a function of ε_u and DOS at E_F as shown in Fig. 1. The results reveal that there exists an optimum value of these two properties that maximizes the TOF. Such variations suggest that the key reactant and other intermediate species have an optimum adsorption bonding on the surface giving rise to a maximum TOF for the $75Ni25Fe/Al_2O_3$ catalyst.

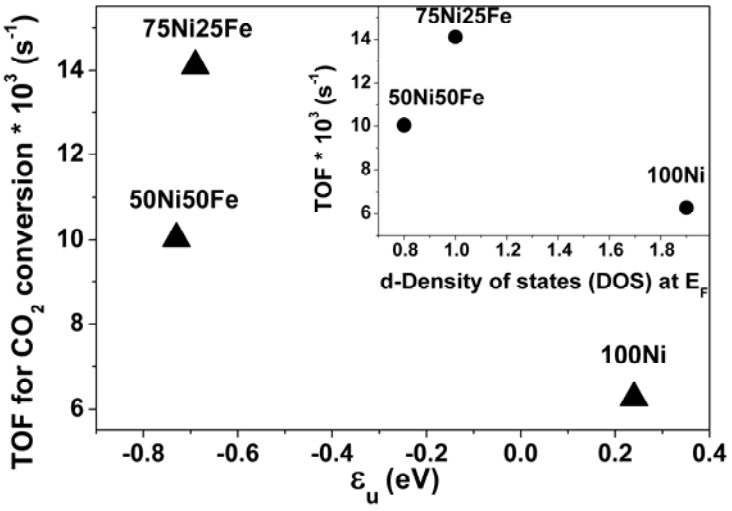

Fig. 1. Plot of TOF vs. ε_u and (inset) TOF vs. d-DOS at E_F (considered at 0.0 eV). Reaction conditions: T = 523 K, P = 1 atm, CO_2:H_2 = 1:24, W/F_{CO2} = 10.3 kg_{cat}-h/kg-$mole_{CO2}$

4 Conclusions

The enhancement in catalytic activity for two bimetallic catalysts over pure Ni was due to the formation of alloy. For the alloys the electronic nature of the surface Ni atoms gets perturbed. An optimum value of ε_u and DOS at E_F of the surface Ni atoms appears to be the cause for the improved catalytic activity of the Ni-Fe bimetallic catalyst of a specific Ni to Fe ratio.

Acknowledgements

The support from the Council of Scientific and Industrial Research (CSIR), Project No. 22(0634)/13/EMR-II, is gratefully acknowledged.

References

[1] D. Pandey and G. Deo, Journal of Molecular Catalysis A: Chemical, 2014, **382**, 23-30.
[2] S. J. Clark, M. D. Segall, C. J. Pickard, P. J. Hasnip, M. I. J. Probert, K. Refson and M. C. Payne, Z. Kristallogr., 2005, **220**, 567-570.
[3] H. J. Monkhorst and J. D. Pack, PHYSICAL REVIEW B,1978, **13**, 5188-5192.
[4] H. Xin, A. Vojvodic, J. Voss, J. K. Nørskov and F. Abild-Pedersen, PHYSICAL REVIEW B, 2014, **89**, 115114-115119.
[5] B. HAMMER and J. K. NØRSKOV, ADVANCES IN CATALYSIS, 2000, **45**, 71-129.
[6] M. K. Sabbe, L. Lain, M.-F. Reyniers and G. B. Marin, Phys. Chem. Chem. Phys., 2013, **15**, 12197-12214.
[7] R. Hirschl, Y. Jeanvoine, G. Kresse and J. Hafner, Surface Science, 2001, **482-485**, 712-717.

II-PP87

Origin of the Spontaneous Formation of Cobalt Nano-Islands under Fischer Tropsch Conditions and Mechanistic Consequences

Banerjee A.[1], Gunasooriya G.T.K.K.[2], Saeys M.[2*], Otyuskaya D.S.[2]

1 - Department of Chemical and Biomolecular Engineering, 4 Engineering Drive 4, National University of Singapore, Singapore

2 - Laboratory for Chemical Technology, Ghent University, Gent, Belgium

* Mark.Saeys@UGent.be

Keywords: Fischer Tropsch synthesis, reconstruction, nano-islands, B5 step sites, CO activation

1 Introduction

Fischer-Tropsch synthesis transforms synthesis gas, a mixture of CO and H_2, to long-chain hydrocarbons and water. In recent years, interest in Fischer-Tropsch synthesis as an attractive route to convert natural gas, coal and biomass to clean transportation fuels, has surged. Supported cobalt catalysts are often preferred due to their high activity, selectivity towards long chain hydrocarbons, and low CO_2 selectivity. The structure and coverage of catalyst surfaces under reaction conditions differs dramatically from ideal clean surfaces. To begin to elucidate catalyst activity and selectivity, computational catalysis needs to build realistic surface models and consider coverages under reaction conditions. Cobalt catalysts undergo a massive reconstruction under Fischer-Tropsch (FT) conditions as observed by STM [1] creating defect sites that play a key role in activity and selectivity [2].

2 Methodology

To build realistic models, the thermodynamic stability of various surface structures was modelled using density functional theory with the revised Perdew-Burke-Ernzerhof-Van der Waals functional, and taking into account the effect of temperature, pressure and coverage. With this approach, the site preference and CO adsorption is accurately described on several transition metal surfaces [3]. Transition-state structures were obtained with the climbing-image Nudged Elastic Band method, and vibrational frequencies confirmed the nature of the transition states.

3 Results and discussion

Though surface carbon atoms are thermodynamically unstable on Co terraces under Fischer Tropsch conditions (+40 kJ/mol), they adsorb very strongly at B5 step sites. The unique stability of these square-planar carbon species can be attributed to the local aromaticity of the Co_4C unit [4]. The presence of square planar carbon oxidizes the neighbouring Co with a calculated Co 2p binding energy of 780 eV, and therefore enhances CO adsorption at those sites [5]. The oxidation of a small fraction of the surface Co has been correlated with FT activity [6], but was never attributed to the formation square-planar carbon. The synergistic adsorption of carbon and CO and the high CO coverage make it thermodynamically favourable to break up Co terraces and create step sites (Figure 1a), driving the formation of islands [5]. The size and shape of the nano-islands follows from a detailed balance between favourable step creation and unfavourable corner creation. The calculations predict that, under FT conditions, triangular islands of ~1.8 nm and containing 28 Co atoms are the most stable, in agreement with STM data [1]. The reconstruction is sensitive to the reaction conditions and our model explains why no reconstruction was observed in a recent study under mbar conditions [7]. Electron count

arguments related to the local aromaticity furthermore limit the coverage of square-planar carbon at the B5 sites to 50%, leaving B5 sites available for reaction (Figure 1b).

C-O scission is a key step in the FT mechanism, and occurs either by direct cleavage of CO at defect sites, via a hydrogen-assisted pathway, or after formation of a C-C bond via the CO insertion mechanism. Our kinetic study [2] shows that the propagation mechanism for the CO insertion mechanism is consistent with available experimental kinetic data [8,9]. However, the initiation and termination steps for the CO insertion mechanism remain to be elucidated. In this work, we analyse various reaction paths for the formation of the chain-initiating CH species at the edge sites of the nano-islands. The calculations suggest that C-O activation proceeds with an overall barrier of about 120 kJ/mol and has a rate in line with experimental kinetic data.

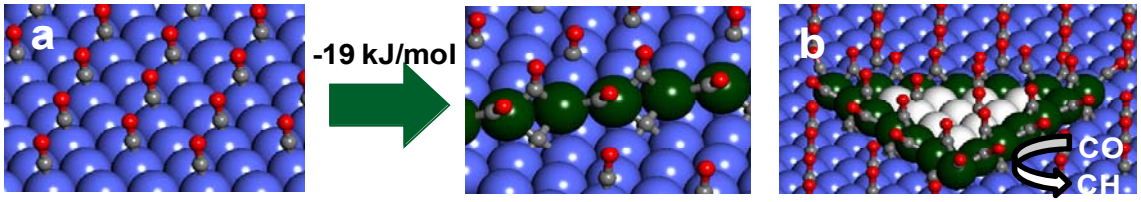

Fig. 1. (a) Break-up of CO-covered terraces to form C and CO-covered step sites is favourable with a Gibbs free energy of -19 kJ/mol Co step sites. (b) CO dissociation at the B5 sites of the Co28 nano-islands is kinetically fast, creating chain-initiating CH species.

4 Conclusions

Cobalt catalysts undergo a massive surface reconstruction under Fischer-Tropsch conditions to form nano-islands. Though the energy penalty to create step sites is substantial, the unusual stability of square-planar carbon at the B5 steps and the increased CO adsorption energy and high CO coverage at the step sites together make it highly favourable to create step sites under Fischer-Tropsch conditions. The most stable nano-islands contain 28 Co atoms and have a diameter of 1.8 nm. The edges of these nano-islands are not fully covered, leaving active sites for facile CO dissociation.

Acknowledgements

This work was supported by Shell Global Solutions and by a Faculty Strategic Funding Initiative form the National University of Singapore.

References

[1] J. Wilson, C.de Groot, *J. Phys. Chem.* 99 (1995) 7860.
[2] M. Zhuo, A. Borgna, M. Saeys, *J. Catal.* 297 (2013) 217.
[3] G.T.K.K. Gunasooriya, H.P.C.E. Kuipers, S.van Bavel, M. Saeys *submitted.*
[4] A. Nandula, T. Q. Thang, M. Saeys, A. N. Alexandrova *to be submitted.*
[5] A. Banerjee, H.P.C.E Kuipers, S. Van Bavel, M. Saeys *submitted.*
[6] N. E. Tsakoumis, A.Voronov, M. Ronning, W.van Beek, O. Borg, E. Rytter, A. Holmen, *J. Catal.* 291 (2012) 138.
[7] M. Ehrensperger, J. Wintterlin,. *J. Catal.* 319 (2014) 274.
[8] Schweicher J.; Bundhoo A.; Kruse N.; *J. Am. Chem. Soc.*, 134 (2012) 16135.
[9] Tuxen, A.; Carenco, S.; Chintapalli, M.; Chuang, C; Escudero, C.; Pach, E.; Jiang, P.; Borondics, F.; Beberwyck, B.; Alivisatos, A. P.; Thornton, G.; Pong, W.; Guo, J.; Perez, R.; Besenbacher, F.; Salmeron, M.; *J. Am. Chem. Soc.*, 135 (2013) 2273.

II-PP88

Instrumentally Induced Differential Charging Effect in XPS – Turning Drawback to Advantage

Kvon R.I.[1*], Bukhtiyarov A.V.[1,2], Nartova A.V.[1,3,2], Makarov E.M.[1,3,2], Kulagina M.A.[1,3], Shterk G.V.[1,3,2], Bukhtiyarov V.I.[1,3,2]

1 - Boreskov Institute of Catalysis SB RAS, Novosibirsk, Russia
2 - Research and Educational Center for Energy Efficient Catalysis in Novosibirsk National Research University, Novosibirsk, Russia
3 - Novosibirsk National Research University, Novosibirsk, Russia

* kvon@catalysis.ru

Keywords: XPS, charging effects, metal nanoparticles catalyst support

1 Introduction

X-Ray photoelectron spectroscopy (XPS) is the universal and very informative tool of catalysts investigations. Due to the extremely small depth of analysis (from units to tens of nanometers) it provides the information about the uppermost layers of the catalyst and – when *in situ* mode is applied – about the adsorbed layer composition. The data on the elemental analysis, oxidation states of observed elements, chemical composition of adsorbed moieties, etc. obtained from XPS measurements are widely used in the studies of the preparation, activation, exploitation and ageing of the model and industrial catalysts.

The detection of the chemical state alterations of the small fraction of the element(s) of interest by the registration of subtle changes of the shape and/or position of photoelectron peaks is probably most beguiling capability of XPS techniques for the exploration of the supported metal catalysts. Yet there is important instrumental drawback when metal nanoparticles at oxide supports are studied by XPS. Namely, under X-Ray irradiation the surface of poorly conductive samples accumulates the positive charge (so-called "surface charging") that directly affects the kinetic energies of emitting photoelectrons and, therefore, the positions of XPS peaks. The magnitude of such "charging shift" can be comparable or even exceed the values of chemical shifts tabulated for the metals in different oxidation states. The effect becomes more prominent when the monochromatic primary excitation is used due to the substantially lower flux of the background (inelastically scattered) electrons generated by X-Ray source. For instance, when compensating flux is absent, tantalum oxide sample exhibits the surface charging shift of Ta4f peak for more than 60 eV.

It is obvious that in such cases the conventional spectra processing by using the position of C1s peak from adventitious carbon for re-calibration is hardly acceptable. Instead, the instrumental charge neutralization is recommended by XPS experts. Yet by variation of flood gun (charge neutralizer) parameters one can arbitrarily achieve any position of the chosen photoelectron peak within the some limited range on the binding energy (BE) scale. On one hand, it raises another experimental problem: how to determine the proper or "correct" level of the charge compensation. But on the other, it gives to the scholars the new spectroscopic tool to probe the specimen surface.

2 Experimental/methodology

The XPS experiments were performed on a SPECS spectrometer equipped with PHOIBOS-150 MCD-9 hemispherical energy analyzer, monochromatic AlKα X-ray gun and FG 15/40 flood gun. Various flood gun parameters (emission current and electron flux energy) were used to achieve the different charge neutralizing modes.

The set of various supports (Sibunit, alpha-alumina, carbon coated alumina, Si, Zr, Ta, W oxides with relatively low specific area (ca. 10 m^2/g) as well as Pt and Pd model catalysts

prepared using these supports were investigated to elucidate the influence of surface conductivity and uniformity on the efficiency of the charge neutralizing.

3 Results and discussion

The data show that the magnitude of the charge shift depends on the power balance between X-ray and electron beam (flood gun) sources. The variation of low energy electron flux density at constant X-Ray Gun power shifts the photoelectron peaks of non-conductive support elements as expected. However, the spectral behavior of the same supports but covered with metal nanoparticles is more complicated. The support spectra are usually consists of two components: one responds to the changing flood gun power like the clean support does, but another reveals substantially lower value of "charging shift". Moreover, the fraction of the latter component in the spectra correlates with both the amount of the metal detected by XPS at the surface of the support and the surface resistivity of the support material. Then, for alumina supported Pd catalyst (0.5% wt) such spectral feature of Al2p signal is as low as 10% of total intensity while for 0.5% wt Pd/WOx sample the whole signal of W4f line shifts evenly when flood gun power is changed.

Thus, the deposition of metal particles on the surface of the non-conductive supports corrupts its homogeneity (in terms of conductivity) so that it becomes possible to elucidate the patches of the specimen surface with different affinity to electron. Literally, metal particles act like "antennas" receiving beta-radiation from outer source – most likely due to the sharp distortion of the equipotential lines of electrostatic field. Therefore, some additional information on the surface density (population) of the metal particles at the support surface could be derived by the variation of charge neutralizer power – thus turning the surface charging from enemy to the ally of the scholar.

4 Conclusions

The induced differential charging of the surface of supported metal catalysts is proved to provide the additional information on the properties of the supported metal catalysts. It becomes possible to evaluate the population density of metal nanoparticles at the support surface, and therefore, to estimate the average size of such particles directly from the spectroscopic data.

Acknowledgements

The research is kindly supported by The Russian Science Foundation (grant 14-23-00146).

II-PP89

Kinetics of Activation Fischer-Tropsch Iron-Based Catalysts under CO and CO/H_2 Flows

Kazak V.O.*, Chernavskii P.A., Pankina G.V.

MSU, Faculty of Chemistry, Moscow, Russia

* vladislavkazak@gmail.com

Keywords: iron, nanoparticles, Fischer-Tropsch synthesis, kinetics of carburization

1 Introduction

Fischer-Tropsch synthesis (FTS) is an alternative method to produce a variety of chemicals as hydrocarbons and oxygenate from syngas [1]. Both cobalt and iron are used as FTS catalysts, but iron is more preferable because of their low cost, high resistance to poisons and possibility to work under low H_2/CO ratio. It is known that iron carbides are active phases in FTS iron-based catalyst [2]. Recently, it was established that activity and selectivity of iron catalyst depend on the composition of the mixture by which catalyst activated [3-5], but the reasons are still unclear.

In our research, we investigated the kinetics of carburization FTS iron catalysts in the atmosphere of both carbon monoxide and syngas ($CO:H_2$ = 1:1) by *in situ* magnetometric method.

2 Experimental

Both samples were obtained by incipient wetness impregnation of iron nitrate ($Fe(NO_3)_3 \cdot 9H_2O$) aqueous solution. Two different commercially available (CARiACT, Fujisilysia Chemical Ltd.) silica gels namely Q-15 and Q-50 with average pore size 15 and 50 nm respectively were used as supports. After impregnation procedure catalysts were dried 4 h in air flow under 80°C and then they were calcined 4 h in air flow under 400°C.

Elemental analysis of prepared catalysts carried out by energy-dispersive X-ray microanalysis (EDX). X-ray diffraction spectroscopy (XRD) was used for determination of phases and average particles size of calcined samples.

Kinetic measurements were conducted by *in situ* magnitometric method [6]. All experiments were made under isothermal conditions. 20 mg of sample was heated up to desired temperature (250 or 350°C) in argon flow and then argon flow was changed to a selected activation mixture (CO or $CO+H_2$). During experiment sample's magnetization was detected.

3 Results and discussion (font style: Times New Roman bold 12pt)

It was shown by EDX microanalysis that content of iron is 14.8 and 15.4 wt. % for Fe/Q-15 and Fe/Q-50 respectively. Only hematite (Fe_2O_3) phase was detected by XRD analysis of prepared samples. Average particle size of hematite calculated from Scherrer equation is 11 and 30 nm for Fe/Q-15 and Fe/Q-50 respectively.

Results of kinetic measurements are given in Fig 1. Kinetic curves of the activation process under 250°C have a sigmoid form for both CO and $CO+H_2$ flows. On the contrary, magnetization sharply rises up, then passes through a maximum and finally slowly decreases in the case of the activation under 350°C. Kinetic curves obtained under 350°C are described in a proper manner by a simple model of consecutive irreversible processes (Table 1):

$$Fe_2O_3 \xrightarrow{k_1} Fe_3O_4 \xrightarrow{k_2} \chi - Fe_5C_2$$

$$C_{Fe_3O_4} = C^0_{Fe_3O_4} \times \frac{k_1}{k_1 - k_2} \times \left[\exp\left(-k_2 t\right) - \exp\left(-k_1 t\right)\right]$$

It should be noted that these processes are a number of topochemical reactions and both k_1 and k_2 are effective constants of complex processes. Obtained data have shown that rates of both processes and final magnetization are lower in the case of $CO+H_2$ activation than in the case of CO activation. It's known that wustite (FeO) might be generated during reduction of hematite (Fe_2O_3) in the presence of hydrogen. We assumed that in the case of activation by $CO+H_2$ wustite produces and reacts to silica gel with formation of paramagnetic iron silicate (Fe_2SiO_4). Moreover, the effect of the presence of hydrogen in activation mixture is stronger for smaller hematite nanoparticles.

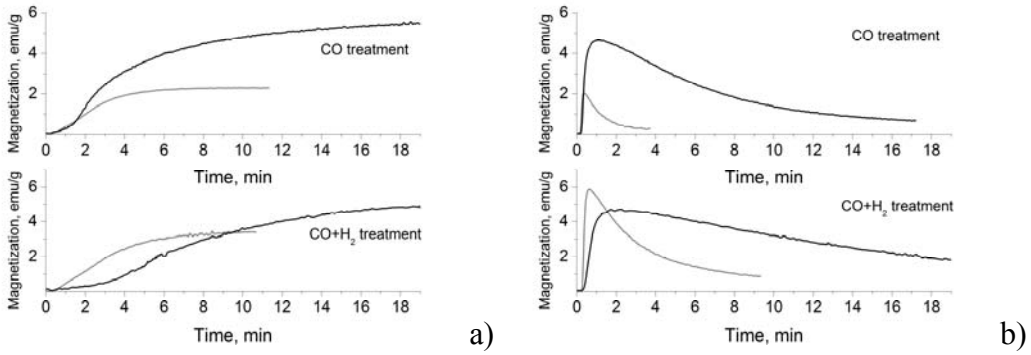

Fig. 1. Kinetic curves of Fe/Q-15 (gray lines) and Fe/Q-50 (black lines) activation under 250°C (a) and 350°C (b).

Table 1. Results of least square fitting of kinetic curves obtained under 350°C by suggested model.

Catalyst	k	in CO flow	in $CO+H_2$ flow
Fe/Q-15	k_1	0.17	0.135
	k_2	0.0138	0.0045
Fe/Q-50	k_1	0.0646	0.0283
	k_2	0.00229	0.00099

4 Conclusions

Kinetics of carburization FTS two iron catalysts with different particle size was investigated. It was shown that the composition of activation mixture dramatically effects on the kinetics of carburization FTS iron-based catalysts. The size effect of activation processes was established.

References

[1] M. E. Dry, *Catalysis today*. 71 (2002) 227.
[2] M. E. Dry, *Stud. Surf. Sci. Catal.* 152 (2004) 533.
[3] M. Luo, H. Hamdeh, B. H. Davis, *Catalysis Today*. 140 (2009) 127.
[4] T. Herranz, S. Rojas, F. J. Pérez-Alonso et al., *J. Catal.* 243 (2006) 199.
[5] J. Xu, C. H. Bartholomew, *J. Phys. Chem. B.* 109 (2005) 2392.
[6] P. A. Chernavskii, B. S. Lunin, R. A. Zakharyan et al., *Instrum. Exp. Tech.* 57 (2014) 78.

II-PP90

Gold Nanoparticle-Loaded Filter Paper: a Recyclable Dip-Catalyst for Real-Time Reaction Monitoring by Surface Enhanced Raman Scattering

Zheng G.[1], Polavarapu L.[1], Pastoriza-Santos I.[1], Pérez-Juste J.[1*], Liz-Marzán L.M.[1,2]

1 - Departamento de Química Física, Universidade de Vigo, Vigo, Spain
2 - Bionanoplasmonics Laboratory, CIC biomaGUNE, San Sebastián, Spain

* juste@uvigo.es

Keywords: *in-situ*, monitoring, SERS, filter papers, recyclable dip-catalyst

1 Introduction

The use of NPs for catalyst in solution is usually limited by the need to maintain their colloidal stability, as well as reusability, under typically harsh reaction conditions. One general approach that is often applied to overcome this limitation comprises the integration of NPs within various kinds of solid supports, leading to nanocomposites with greater stability and recyclability. Recently, we and other research groups have introduced ordinary filter paper as a suitable support material for NPs as it offers several advantages apart from particles stability, such as low-cost, biodegradability, flexibility and availability. Additionally, since the nanoparticle-paper interaction is mainly driven by electrostatics, surface charge further hinders high surface loadings and therefore prevents the nanoparticle self-assembly. These limitations could be overcome if the doping process is promoted from non-aqueous NP dispersions. We report a fast strategy that can easily be extended to large scale fabrication of robust and recyclable "dip-catalysts" with the ability to exhibit strong SERS activity. Furthermore, "dip-catalysts" can be also used to probe the progress of the reaction on the catalytic surface by monitoring the fingerprint signals of reactants and products through SERS.

2 Experimental/methodology

Firstly, fabricate the monodisperse and high concentration of gold NPs as the previous method. Then, the filter paper were cut into the designed area, and dipped into the solution of the gold NPs while dried soon by the hair drier. "dip catalysts" was dried in the hoven at 60^{o}–C overnight. Finally, after evaluation and characterization of the "dip catalysts", we have in-situ monitored the conversion of nitrothiophenol (4-NTP) into animothiophenol(4-ATP) on the surface of the "dip catalysts" through surface enhanced raman scattering (SERS).

3 Results and discussion

In the Fig.1, the time evolution of the Raman scattering modes of 4-NTP (1343 cm^{-1}) and 4-ATP (1593 cm^{-1}) allowed us to quantify the fraction of reactant (4-NTP) and product (4- ATP) at various reaction times. The reaction kinetics were treated as a pseudo-first order reaction ($NaBH_4$ concentration is in large excess with respect to 4-NTP) and we applied the steady-state approximation (since the evidences show that the intermediate reacts very fast).The steady-state approximation requires that the reaction rate of the second step will be larger than the first one, and therefore the formation of the intermediate 4,4'-dimercapto-azobenzene (4,4'-DMAB) should be the rate determining step. The fit of the exponential decrease of the 1343 cm^{-1} band to a first order equation resulted in a rate constant for the first step (k_R) of 5.09×10^{-3} s^{-1}. Therefore, the product formation, i.e. the band located at 1593 cm^{-1}, should show an exponential increase with time, also with a first order rate constant (k_P) similar to that for the first step (k_R). The good agreement between both reaction rates (5.09×10^{-3} s^{-1}vs.6.57×10^{-3} s^{-1} for k_R and k_P, respectively)

indeed demonstrate that no formation of the intermediate.

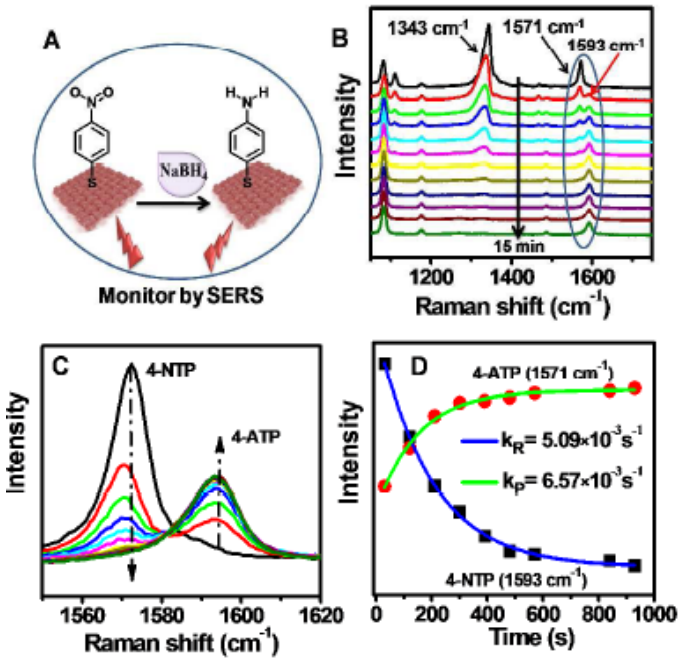

Fig.1. shows the scheme of the While acting as catalysts, Au NP-loaded paper composites display excellent surface enhanced Raman scattering (SERS) efficiency, allowing the real-time monitoring of chemicalreactions. [1]

4 Conclusions

In conclusion, we report a new type of bifunctional "dip-catalyst" based on Au NPs loaded on filter paper, which can be prepared by simple dip-coating of paper in concentrated Au NPs dispersions in toluene. The catalyst shows excellent recyclability with unchanged catalytic efficiency for more than 20 consecutive cycles. In addition, the catalytic substrate exhibits high SERS efficiencies that allow us to monitor the progress of reactions occurring on catalytic surfaces through the detection of SERS signals of reactants and products. The present work is expected to open new ways of application of multifunctional NP-loaded paper, not only for heterogeneous catalysis but also for monitoring reaction progress by SERS.

Acknowledgements

This work was supported by the Spanish MINECO (MAT2013-45168-R and CTQ 2010-1639)and by the Xunta de Galicia/FEDER (GPC2013-006). G. Z. acknowledges financial support from China Scholarship Council. G. Zheng and L. Polavarapu equally contributed to this work

References

[1] Guangchao Zheng, Lakshminarayana Polavarapu, Luis M. Liz-Marzán, Isabel Pastoriza-Santos, and Jorge Pérez-Juste, *chemcomm*. 2015, DOI: 10.1039/C4CC09466B.

II-PP91

Graph Machine Based Advanced Data Modelling for High-Throughput Zeolite Catalyst Screening

Goulon A.[1], Faraj A.[1], Leflaive P.[2*]

1 - IFP Energies nouvelles, Rueil-Malmaison, France
2 - IFP Energies nouvelles, Solaize, France

* philibert.leflaive@ifpen.fr

Keywords: high-throughput, structural, encoding, QSAR, neural networks, zeolite, adsorption, enthalpies

1 Introduction

Zeolites are widely used as catalysts in the refining and petrochemical industries. However the lack of accurate models for predicting hydrocarbons adsorption on molecular sieves prevents using these models for statistical learning together with high throughput experimentation.

This work aims at developing a QSAR (Quantitative Structure Activity Relationship) model for zeolite catalysis having a new structure. This model is used within a high throughput iterative screening loop to determine hydrocarbons adsorption enthalpies on different molecular sieves.

2 Model construction

In a classical Quantitative Structure-Activity Relationship (QSAR) approach, molecules and catalysts are generally described using vectors composed of a large set of molecular and catalysts descriptors. In this work, an alternate approach is used as we suppose that all the required information for the molecule (reactant) encoding is contained within its structure, which is mathematically coded as a graph and further as a function (called Graph Machine) with the same mathematical structure. A description of this approach can be found in [1]. Since no molecular descriptors are used, the collection, computation and selection of these descriptors, which is often a major issue in QSAR applications, is no longer required.

In this previous work, Graph Machines (GM) were only associated with the molecules, then only allowing the prediction of the adsorption enthalpies of other molecules on the same solid. In this work, these functions were changed so that they both characterize the reactants and the zeolite catalysts. The solids have been characterized by one or more descriptors, considered in GM as external data : one or more tag(s) which take(s) the value(s) of the descriptor(s) associated with the solid is added at each node of the graph. The obtained GM function characterizes then both the molecule and the solid. Four descriptors were used : Unit Cell Size (UCS), Sanderson's intermediate electronegativity, the number of cations and their ionic radius.

3 Virtual high-throughput screening of zeolite catalyst

The new GM/QSAR model was applied in a virtual high-throughput screening to determine the adsorption enthalpy at zero coverage of 12 hydrocarbons (9 alkanes and 3 aromatics) on 10 cation exchanged faujasites with various Si/Al ratios. Experiments are carried out by series of 12 experiments. The experimental data used are those published by Canet et al. in [2,3].

The developed model is first used to choose an initial set of experiments (3 series of 12 experiments). The experimental results are then used as a training set for the model. The system then enters within a high throughput iterative process where the model is used for both the design of a new series of 12 experiments and result (adsorption enthalpy of a given molecule on a given solid) prediction. Figure 1 shows the variation of the mean and max. error values between experimental data and model prediction for the complete experimental space. It can be seen that with only 50% of the total number of experiments, adsorption enthalpies can be accurately

predicted with a mean error as low as 3 kJ/mol.

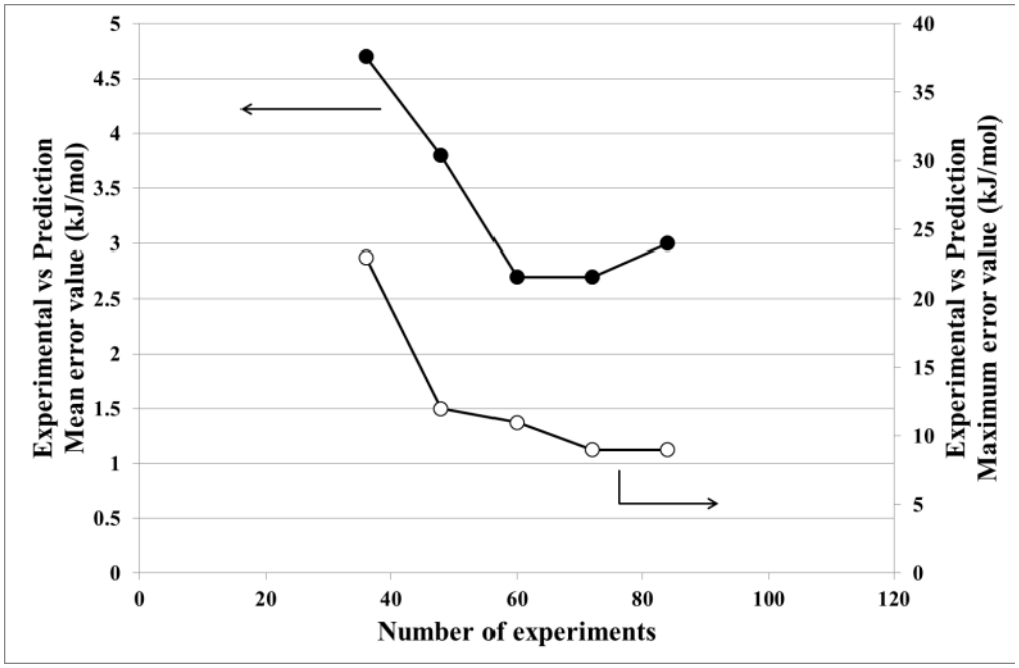

Fig. 1. Evolution of the mean and max. error values (kJ/mol) between experimental data and model prediction for the complete experimental space (120 experiments).

Finally, the predictive ability of the QSAR model was tested using a "leave one out" derived methodology by successively removing one solid after the other from the experimental data base. The results, reported in table 1, were satisfactory for all solids but prediction was better for alkanes than for aromatics.

Table 1. Error values (kJ/mol) between experimental data and model prediction after removal of one solid from the experimental data base. The adsorption enthalpies of the different hydrocarbons on the removed solid are estimated with model trained with all the other experimental data.

Molecule	CsY	KLSX	KY	LiLSX	LiY	Na LSX	NaX	NaY 2,4	NaY 3,4	RbY	Mean molecule error value
2-methylbutane	7.97	2.33	1.19	2.38	8.56	1.85	0.52	0.19	7.48	7.27	**3.97**
n-pentane	0.18	1.58	0.92	0.98	0.63	0.50	0.15	4.32	1.16	6.40	**1.68**
cyclohexane	8.24	1.61	0.48	1.83	9.17	4.60	1.93	0.09	6.24	3.84	**3.80**
2-methylpentane	0.56	3.34	0.45	2.65	4.89	0.76	1.44	4.56	5.35	2.33	**2.63**
3-methylpentane	1.07	1.50	0.77	1.15	7.46	1.39	1.28	0.91	9.16	2.25	**2.69**
2,3-dimethylbutane	2.22	2.82	4.72	0.79	3.39	0.35	0.26	2.58	1.66	2.08	**2.09**
n-hexane	1.38	2.84	1.23	0.21	2.27	1.25	1.58	2.42	1.70	0.06	**1.50**
n-heptane	2.00	4.46	2.29	0.83	0.30	0.30	2.00	7.16	5.41	0.43	**2.52**
2,2,4-trimethylpentane	3.74	4.74	3.74	1.45	3.10	0.87	3.56	11.63	4.28	2.17	**3.93**
toluene	6.65	0.13	3.27	9.31	4.89	6.30	0.00	5.01	0.67	3.67	**3.99**
m-xylene	4.73	11.30	11.35	2.72	17.94	11.64	1.79	8.20	1.07	11.86	**8.26**
p-xylene	0.79	2.08	12.34	4.54	8.76	10.91	3.82	1.65	0.43	0.30	**4.56**
Mean solid error value	**3.29**	**3.23**	**3.56**	**2.40**	**5.95**	**3.39**	**1.53**	**4.06**	**3.72**	**3.55**	**3.47**

References

[1] A. Goulon, A. Faraj, G. Pirngruber, M. Jacquin, F. Porcheron, P. Leflaive, P. Martin, G.V. Baron, J.F.M. Denayer, *Catal. Today* 159 (2011) 74
[2] X. Canet, F. Gilles, B-L. Su, G. de Weireld, M. Frère, *J. Chem. Eng. Data*. 52 (2007) 2117
[3] X. Canet, F. Gilles, B-L. Su, G. de Weireld, M. Frère, P. Mougin, *J. Chem. Eng. Data*. 52 (2007) 2127

II-PP92

Catalytic Methane Decomposition Using Iron-Lanthanum Catalysts: Effect of Fe Loading on Activity Performance

Ibrahim A.*, Al-Fatesh A., Khan W., Fakeeha A., Abasaeed A.

Chemical Engineering Department, College of Engineering, King Saud University, Riyadh, KSA

* aidid@ksu.edu.sa

Keywords: conversion, Fe-loading, lanthanum, methane decomposition

1 Introduction

The catalytic methane decomposition ($CH_4 \rightarrow C+H_2$) produces carbon oxides–free hydrogen and carbon nanomaterial [1]. Hydrogen is presently seen for halfway point as a promising energy route in both power generation and transport sectors [2,3]. The conventional processes: steam reforming, partial oxidation, and auto-thermal reforming of natural gas incur excessive costs in purification of hydrogen from coproduced carbon oxides [4,5]. In the present work, thermo-catalytic methane decomposition was studied to promote the catalytic activity and stability for simultaneous production of pure hydrogen and elemental carbon. The produced nanotubes avail in numerous new technologies. Iron supported on Lanthanum catalyst was used to measure the activity performance. Effect of different active metal loadings on hydrogen and carbon yield at 700□C was investigated.

2 Experimental/methodology

Iron supported over lanthanum catalysts were prepared by wet impregnation technique. Various iron loading 20%, 30 and 40% were used. The samples were prepared under constant stirring and fixed temperature of 80°C for 3 h. After that, cooled and dried overnight at 120°C. The samples were then subjected to calcination pretreatment at 500°C for 3 h before taking them to the reactor. The experiments were performed in a fixed bed micro tubular reactor at 700°C, atmospheric pressure and F/W= 66 $mL.min^{-1}.g_{cat}^{-1}$. For each run the catalyst was first activated under H_2 flow (40 $mL.min^{-1}$) at 500°C for 2 h. For composition determination, the outlet gases were passed through online gas chromatography. Catalysts were characterized by BET and TGA techniques.

3 Results and Discussion

The catalytic performance of iron supported catalysts Fe//La_2O_3 at 700°C for 3 h time-on-stream (TOS) is presented in Fig. 1. The supported Fe catalysts with various Fe loading were tested at atmospheric pressure. The activity measurement was obtained from the conversion of methane and the textural and characterization properties of the catalysts were measured by BET and TGA. Fig. 1 depicts that the initial methane conversion increased with the increase of the Fe loading as result of the increase in the active sites. Therefore, 11.0, 33.6 and 42.0% conversions were obtained using 20%, 30% and 40% Fe/La_2O_3 catalysts respectively. The activity performance of 20%Fe/La_2O_3 was the least and decreased progressively with time due to the carbon formation while, the activity for 30 and 40% Fe/La_2O_3 increased as time of reaction increased. The final conversion values for 30% and 40% Fe/La_2O_3 became 62.5 and 65.0 %. The increase of conversion with reaction time was attributed to the deposition of the carbon that affected the space velocity of the outlet gases. Hence, it was apparent from results that the 40% Fe catalyst showed relatively high methane conversion compared with both 20% and 30% Fe catalysts.

Table 1 shows the results of specific surface areas and amount of coke deposits over spent catalysts The BET surface area of fresh Fe/La_2O_3 and therefore activity enhancement were increased with the increase of Fe loading. On the other hand the surface area of the spent catalysts increased

after reaction as result of carbon deposition. The carbon formation also increased with the increase of Fe loading. The activity test and characterization results revealed that the catalyst containing 40wt% Fe over La_2O_3 support presented relatively better catalytic performance among all the tested catalyst.

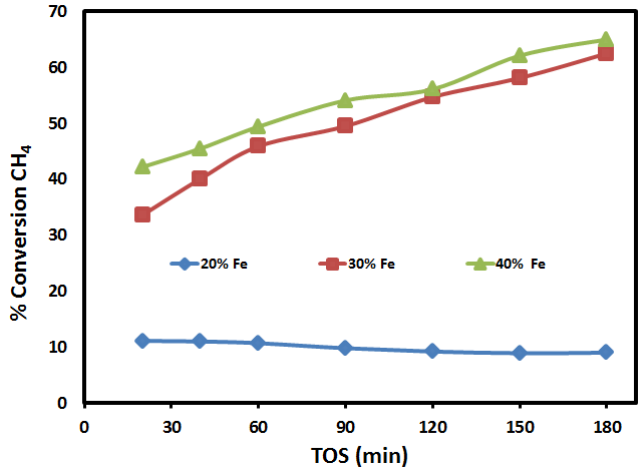

Fig. 1. CH_4 conversion for Fe-La catalysts at 700°C

Table 1. BET surface area and Carbon formation (TGA)

Catalyst loading	Fresh S_{BET} (m^2g^{-1})	Used S_{BET} (m^2g^{-1})	Carbon (%)
20%Fe/La	6.1	10	9.9
30% Fe/La	15.5	42.3	61.8
40% Fe/La	20.1	51.8	75.4

4 Conclusions

In the present study, Catalytic methane decomposition using Fe based catalysts supported over La_2O_3, has been investigated. The results revealed that Fe supported catalysts produced pure hydrogen and nanotubes. 40% Iron catalysts gave relatively better conversion and stability performances.

Acknowledgements

The authors gratefully acknowledge their appreciations to King Saud University for funding this work

References

[1] A. A. Ibrahim, A. H. Fakeeha, A. S. Al–Fatesh, A. E. Abasaeed, W. U. Khan, *International Journal of Hydrogen Energy*, in press. (2014) 1.
[2] T. H. Ortmeyer, P. Pillay, *Proc IEEE* 89 (2001) 1837.
[3] P. P. Edwards, V. L. Kuznetsov, W. I. F. David, N. P. Brandon, *Energy Policy,* 36 (2008) 4356.
[4] D. J. Roddy, *Applied Thermal Engineering*, 53 (2013) 299.
[5] P. M. Sforza, A. Castrogiovanni, R. Voland, *Applied Thermal Engineering*, 49 (2012) 154.

II-PP93

Temperature-Programmed vs. Isothermal Pulsed Oxidation of Graphene Formed on Pt/Mg(Al)O_x Dehydrogenation Catalysts

Redekop E.A.[1], Prieto I.[2], Galvita V.[1*], Marin G.B.[1]

1 - Laboratory for Chemical Technology, Ghent University, Zwijnaarde, Belgium
2 - Department of Chemical Engineering and Environmental Techonolgy, University of Valladolid, Valladolid, Spain

* Vladimir.Galvita@UGent.be

Keywords: graphene, TPO, TAP, catalyst, regeneration, dehydrogenation

1 Introduction

Minimizing the deactivation of supported metal catalysts by coke is a major challenge for the catalytic science, which can have a far-reaching impact on many industrial applications. Coke deposits are typically formed from deeply dehydrogenated hydrocarbon precursors either by polymerization/aromatization reactions or by the growth of graphitic carbon from C1 species. Moreover, the graphitic carbon can grow via different mechanisms, depending on the solubility of carbon in the active metal. In this study, the grapheme formation and burning is investigated on Pt/Mg(Al)O_x catalysts. Due to the basicity of the support and low solubility of carbon in Pt, the coke deposits formed on these catalysts are comprised exclusively of grapheme sheets which are continuously shifted from Pt nanoparticles onto the support surface. It is demonstrated herein that the process of burning off these chemically-uniform graphene deposits is rather complex, and its kinetics is governed by the reaction/transport interplay.

2 Experimental/methodology

Pt/Mg(Al)O_x catalysts were prepared by wet impregnation of $Pt(acac)_2$ onto calcined Mg(Al)O_x precursors [1]. In atmospheric flow TPO experiments, freshly reduced catalysts were coked in a 60 ml/min atmospheric pressure flow of 5% C_3H_8 in He for 15 minutes at 923 K. After coking, the catalyst was cooled to room temperature in He and then heated up to 873 K in the flow of 100% O_2 with a linear temperature ramp. Experiments were repeated with the ramps of 5, 7, 10, and 15 K/min to evaluate the activation energies using Kissinger plots. Spent catalysts after coking and after partial burn-off of coke were analysed ex-situ using HRTEM imaging and Raman spectroscopy. In TAP pulse-response experiments, freshly reduced catalysts were subjected to a series of C_3H_8 pulses at 923 K until no changes were observed in the conversion of propane and the yield of propylene. The coke formed during this pulse-sequence was burned-off at a constant temperature by pulsing pure O_2 while monitoring the CO_2 signal.

3 Results and discussion

When fresh catalysts were exposed to the propane feed, a short period of extrinsic relaxation was observed, during which the selectivity towards propylene was low and the main product was methane [1]. By the end of the relaxation period, non-selective hydrogenolysis sites were mostly blocked by coke, and the reaction proceed with near 95% selectivity towards propylene. The coke deposited under reactive conditions for 15 minutes was subjected to TPO, resulting in two CO_2 peaks at ~660 K and ~808 K. The activation energies of carbon burn-off were estimated as 107 and 185 kJ/mol, respectively. In another experiment, the TPO treatment was discontinued after the exhaustion of the first, low-temperature peak, and the catalyst was quenched to room temperature. Both, completely coked and partially regenerated samples were examined by HRTEM and Raman, which confirmed the deposition of graphene sheets on Pt

nanoparticles and support (Fig 1D).

From TPO patterns, it was reasonable to suggest that the low-temperature peak corresponds to coke on Pt sites, while the high-temperature peak corresponds to coke on the support. However, HRTEM revealed that coke burned within the low-temperature peak included the coke from both locations. The remaining coke corresponding to the high-temperature peak was located in tight encapsulating layers around large nanoparticles [2] and in the pockets of the support surface devoid of small Pt nanoparticles (Fig 1C,D).

During the burn-off of coke deposits in the isothermal pulse mode (TAP), the CO_2 response exhibited two distinct peaks. The earlier peak appears at the same time throughout the pulsing sequence (Fig 1A,B). The later peak drifts to much later times, as more and more coke was burned. These results suggest that a transport process of either oxygen or carbon is involved in the production of CO2 corresponding to this later peak.

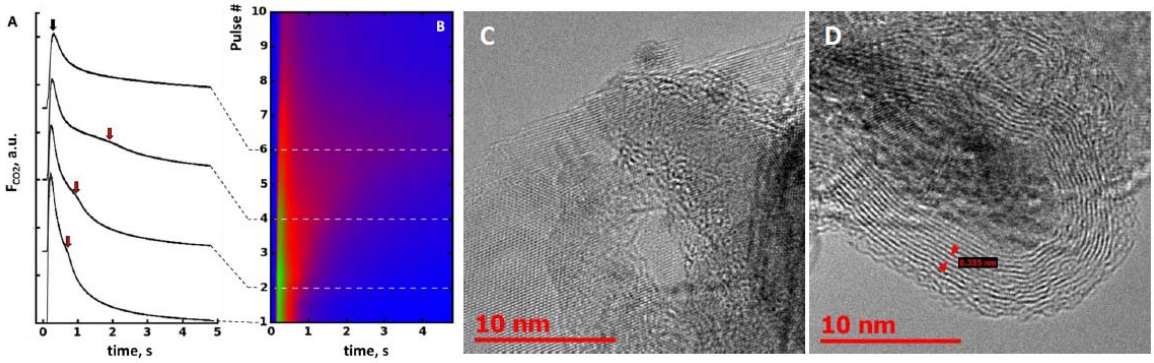

Fig. 1. Oxidation of graphene on Pt/Mg(Al)O_x catalysts: (A) CO_2 response during pulsed oxidation in TAP. Notice the evolution of the slower peak marked with red arrow; (B) Overview of the entire oxidation pulse sequence. CO_2 intensity as a function of time (x-axis) and pulse number (y-axis); (C) Residual coke in Pt-poor regions after burning of the low-temperature peak in TPO experiments; (D) Residual coke encapsulating large Pt nanoparticles.

4 Conclusions

The deposition and oxidation of graphene sheets were investigated by TPO, isothermal pulsed oxidation in TAP, HRTEM, and Raman spectroscopy. Based on our findings it can be concluded that even chemically-uniform graphene deposits on the surface of supported Pt catalysts may result is a complex oxidation behaviour controlled by a transport/reaction interplay. The assignment of distinct TPO peaks is not straightforward and does not follow simplified concepts such as coke on metal vs coke on support. Instead, the peaks are distinguished based on a commensurate availability of oxygen and carbon within the complex landscape of the catalyst surface. This results will contribute to better understanding of the coking process and to optimizing the catalyst regeneration protocols.

Acknowledgements

This work was supported by the 'Long Term Structural Methusalem Funding by the Flemish Government'. E. A. Redekop acknowledges the Marie Curie International Incoming Fellowship granted by the European Commission (Grant Agreement No. 301703). The authors also express their gratitude to V. Bliznuk for acquisition of the TEM images.

References

[1] E.A. Redekop, V.V. Galvita, H. Poelman, V. Bliznuk, C. Detavernier, G.B. Marin, *ACS Catal.* 4 (2014), 1812

[2] Z. Peng, F. Somodi, S. Helveg, C. Kisielowski, P. Specht, A.T. Bell, *J. Catal.* 286 (2012) 22.

II-PP94

The Role of Electron-Acceptor Sites during Catalytic Dehydrochlorination of 1-Chlorobutane over Metal Oxides

Shuvarakova E.I.[1,2*], Bedilo A.F.[1,2], Akimova T.N.[3], Chesnokov V.V.[1,3], Kenzhin R.M.[1]

1 - Boreskov Institute of Catalysis SB RAS, Novosibirsk, Russia
2 - Novosibirsk Institute of Technology, Moscow State University of Design and Technology, Novosibirsk, Russia
3 - Novosibirsk State Technical University, Novosibirsk, Russia

* Katerina.shuv@gmail.com

Keywords: electron-acceptor sites, EPR, 1-chlorobutane dehydrochlorination, MgO, Al_2O_3

1 Introduction

One of the most intriguing properties of many heterogeneous acid catalysts is their ability to generate spontaneously organic radical cations upon adsorption of aromatic electron donors [1]. ZSM-5 zeolites and sulfated zirconia materials possessing exceptionally strong electron-acceptor sites capable of ionizing compounds with very high ionization potentials, such as benzene (IP = 9.2 eV) [1]. The existence of weaker electron-acceptor sites with electron affinities ~ 7 eV in large quantities on the surface of many conventional oxides is no less remarkable. Electron-acceptor sites of different strength can be characterized using aromatic probes with different ionization potentials [1, 2].

It was shown earlier that the catalytic activity in dehydrochlorination of 1-chlorobutane over nanocrystalline MgO substantially increases with time due to the MgO conversion to $MgCl_2$ [3]. This increase coupled with a surface area decrease indicates that more active sites are formed on the surface during this reaction. Recently we reported that weak electron-acceptor sites formed due to the MgO halogenation might be responsible for solid-state reaction between nanocrystalline MgO and CF_2Cl_2 [4]. In this study we characterized weak electron-acceptor sites formed during 1-chlorobutane dehydrochlorination using perylene and anthracene as spin probes, and found a good correlation between their concentrations and the catalytic activity.

2 Experimental/methodology

Nanocrystalline and commercial MgO and Al_2O_3 samples were studied in catalytic dehydrochlorination of 1-chlorobutane. The samples were placed in an EPR sample tube, activated in an argon flow for 1 h at the reaction temperature, and subjected to reaction with 1-chlorobutane. 1-Chlorobutane conversion to a mixture of butenes was monitored by gas chromatography. After the reaction was carried out for the desired time, the sample was quickly cooled down to room temperature and filled with a 2×10^{-2} M solution of perylene or anthracene in toluene. The concentration of electron-acceptor sites was determined by integration of the EPR spectra registered immediately after the spin probe adsorption and after additional heating at 80°C for 18 h.

3 Results and discussion

The catalytic activity of nanocrystalline aerogel-prepared MgO was found to increase significantly during the 1-chlorobutane dehydrochlorination reaction, which is accompanied by modification of the MgO surface and bulk with chloride ions. No electron-acceptor sites were observed on the surface of initial MgO samples. They appeared only during the reaction. Their concentration normalized per unit mass gradually increased during the reaction due to the surface chlorination. A good correlation was observed between the catalytic activity and the

concentration of weak electron-acceptor sites (Fig. 1). Commercial MgO sample was substantially less active and showed much lower concentration of electron-acceptor sites.

Al_2O_3 samples are characterized by substantial concentrations of electron-acceptor sites [2]. This made this material much more active, so that similar chlorobutane conversion was achieved at temperature lower by 50°C than on nanocrystalline MgO. The catalytic activity and the concentration of electron-acceptor sites increased during the first 20 min on stream due to the surface chlorination that is known to increase the concentration of electron-acceptor sites [5]. Again a good correlation was observed between the catalytic activity in dehydrochlorination of 1-chlorobutane and the concentration of weak electron-acceptor sites.

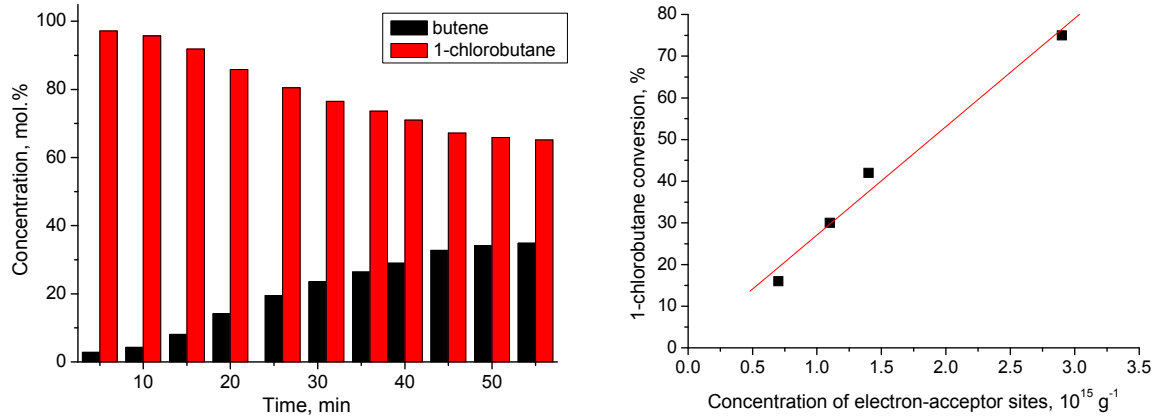

Fig. 1. Concentrations of butene and 1-chlorobutane vs. time on stream for 1-chlorobutane dehydrochlorination over nanocrystalline MgO at 250°C (left) and correlation between the catalytic activity and intensities of EPR spectra observed immediately after perylene adsorption (right).

4 Conclusions

This is the first study where the concentrations of electron-acceptor sites were measured during a catalytic reaction. It is shown that the concentration of weak elector-acceptor sites correlates with the catalytic activity. The obtained results indicate that weak electron-acceptor sites tested using perylene may be the active sites accounting for 1-chlorobutane dehydrochlorination in the active state of the catalysts. It seems to be very important to study possible correlations between the concentrations of electron-acceptor sites and catalytic activity of various catalytic reactions believed to take place on surface acid sites to elucidate the possible role of electron-acceptor sites in these reactions.

Acknowledgements

This study was supported in part by Russian Foundation for Basic Research (Grants 13-03-12227-ofi_m and 15-03-08070-a).

References

[1] A.F. Bedilo, A.M. Volodin, *Kinet. Catal.* 50 (2009) 314.
[2] A.F. Bedilo, E.I. Shuvarakova, A.A. Rybinskaya, D.A. Medvedev, *J. Phys. Chem. C* 118 (2014) 15779.
[3] I.V. Mishakov, A.F. Bedilo, R.M. Richards, V.V. Chesnokov, A.M. Volodin, V.I. Zaikovskii, R.A. Buyanov, K.J. Klabunde, *J. Catal.* 206 (2002) 40.
[4] A.F. Bedilo, E.I. Shuvarakova, A.M. Volodin, E.V. Ilyina, I.V. Mishakov, A.A. Vedyagin, V.V. Chesnokov, D.S. Heroux, K.J. Klabunde, *J. Phys. Chem. C* 118 (2014) 13715.
[5] R.A. Zotov, V.V. Molchanov, A.M. Volodin, A.F. Bedilo, *J. Catal.* 278 (2011) 71.

II-PP96

Surface Electron-Acceptor Sites: their Structure and Role in Catalytic and Solid-State Reactions

Bedilo A.F.[1,2*], Shuvarakova E.I.[1,2]

1 - Boreskov Institute of Catalysis SB RAS, Novosibirsk, Russia
2 - Novosibirsk Institute of Technology, Moscow State University of Design and Technology, Novosibirsk, Russia

* abedilo@bk.ru

Keywords: electron-acceptor sites, acid catalysts, destructive, sorption, EPR

1 Introduction

One of the most intriguing properties of many heterogeneous acid catalysts is their ability to generate organic radical cations upon adsorption of aromatic electron donor molecules [1]. ZSM-5 zeolites and sulfated metal oxides posses exceptionally strong one-electron acceptor sites capable of ionizing compounds with very high ionization potentials, such as benzene (IP = 9.2 eV) [1, 2]. The existence of weaker electron-acceptor sites with electron affinities ~ 7 eV in large quantities on the surface of alumina and some other metal oxides is no less remarkable [2].

Catalysts possessing the strongest electron-acceptor sites show outstanding activity in acid-catalyzed reactions. Earlier we suggested that such strong acceptor sites might be responsible for skeletal isomerization and cracking of light alkanes over sulfated zirconia [3]. We also reported that the catalytic activity of doped alumina catalysts in such conventional acid-catalyzed reaction as ethanol dehydration correlated with the concentration of weaker acceptor sites [4].

In the current communication the properties of electron-acceptor sites of acid catalysts will be explored and their possible structure will be analyzed using DFT quantum chemical simulations. The concentrations of electron-acceptor sites of different strengths were measured for the first time in the course of reaction with the catalytic activity and performance in solid-state destructive adsorption processes. Recommendations on the use of spin probes for testing electron-acceptor sites with different strength will be suggested.

2 Experimental/methodology

Nanocrystalline and commercial MgO, VO_x/MgO and Al_2O_3 samples were studied in catalytic dehydrochlorination of 1-chlorobutane and destructive sorption of CF_2Cl_2. The samples were placed in an EPR sample tube, activated in an argon flow for 1 h at the reaction temperature, and subjected to reaction with the flow containing either the CF_2Cl_2 or 1-chlorobutane at desired temperature. 1-Chlorobutane conversion to a mixture of butenes was monitored by gas chromatography. After the reaction was carried out for the desired time, the sample was quickly cooled to room temperature and filled with a 2 x 10^{-2} M solution of perylene or anthracene in toluene. The concentration of electron-acceptor sites was determined by integration of the EPR spectra registered immediately after the spin probe adsorption and after additional heating at 80°C for 18 h. Quantum chemical simulations were carried out by DFT method using Gaussian 09 software, B1B95 hybrid functional and 6-31+G(d,p) basis set.

3 Results and discussion

The electron-acceptor strength of conventional acid sites usually believed to exist in acid zeolites is below 1 eV and is definitely not sufficient to account for their experimentally observed electron-acceptor properties. We simulated stronger acid/electron-acceptor sites by increasing the distance between the acidic proton and its counter ion. Our simulations show that

such polarization sites are stronger than the conventional sites, but their electron affinity never exceeds ~ 6 eV. This value was obtained for sites where the proton is moved away from the compensating framework ion sufficiently far that it no longer feels the presence of the counter ion. Their acidity is comparable with those of hydronium ions and conventional strong liquid acids. In fact, our calculations show that the strength of such sites is just right for protonating ethanol. So, such sites may account for the activity of conventional solid acid catalysts such as catalytic activity of Al_2O_3 in ethanol dehydration reported to correlate with the concentration of weak electron-acceptor sites [4].

Stronger acceptor sites with electron affinity approaching the experimentally observed value for the strongest electron-acceptor sites (~ 9 eV) could be simulated only as superelectrophilic sites containing two adjacent extra protons solvated by the oxide matrix. Their acidity is sufficient for protonation of light alkanes similar to the one observed in liquid superacids. So, they are likely to account for the activity of sulfated zirconia in this reaction.

Weak electron acceptor sites were found to be formed on the surface of nanocrystalline MgO destructive adsorbents during their solid-state reactions with CF_2Cl_2. This reaction is characterized by an unusual long induction period [5]. Their activity was observed to correlate with the concentration of weak electron-acceptor sites tested by anthracene or perylene.

The catalytic activity of nanocrystalline aerogel-prepared MgO was found to increase significantly during the 1-chlorobutane dehydrochlorination reaction, which is accompanied by modification of the MgO surface and bulk with chloride ions. No electron-acceptor sites were observed on the surface of initial MgO samples. They appeared only during the reaction due to the surface chlorination. A good correlation was observed between the catalytic activity and the concentration of weak electron-acceptor sites. Substantial concentrations of electron-acceptor sites present on Al_2O_3 surface [2] made this material much more active in dehydrochlorination. Similar chlorobutane conversion was achieved at temperature lower by 50°C than on nanocrystalline MgO. Again a good correlation was observed between the catalytic activity in dehydrochlorination of 1-chlorobutane and the concentration of weak electron-acceptor sites.

4 Conclusions

According to the results of our simulations, the experimentally observed high electron affinity of solid acid catalysts can be explained assuming that dissociation to the positive and negative charges occurs on their surface during activation. The resulting sites are remarkably similar in their properties to the species resulting from the electrolytic dissociation of strong homogeneous acids and superacids and accounting for their reactivity. For the first time the concentrations of electron-acceptor sites were measured during catalytic and solid-state reactions. The experimental correlations between the concentrations of the electron-acceptor sites and the catalytic activity in reactions catalyzed by acids suggest that these reactions are likely to occur on such sites rather than on more abundant traditional acid sites. Such sites also seem to be responsible for at least some bulk solid-state reactions.

Acknowledgements

This study was supported in part by Russian Foundation for Basic Research (Grants 13-03-12227-ofi_m and 15-03-08070-a).

References

[1] A.F. Bedilo, A.M. Volodin, *Kinet. Catal.* 50 (2009) 314.
[2] A.F. Bedilo, E.I. Shuvarakova, A.A. Rybinskaya, D.A. Medvedev, *J. Phys. Chem. C* 118 (2014) 15779.
[3] A.F. Bedilo, A.S. Ivanova, N.A. Pakhomov, A.M. Volodin, *J. Mol. Catal. A.* **158** (2000) 409.
[4] R.A. Zotov, V.V. Molchanov, A.M. Volodin, A.F. Bedilo, *J. Catal.* 278 (2011) 71.
[5] A.F. Bedilo, E.I. Shuvarakova, A.M. Volodin, E.V. Ilyina, I.V. Mishakov, A.A. Vedyagin, V.V. Chesnokov, D.S. Heroux, K.J. Klabunde, *J. Phys. Chem. C* 118 (2014) 13715.

II-PP97

Direct Imaging of Octahedral Distortion in a Complex Molybdenum Vanadium Mixed Oxide

Lunkenbein T.*, Girgsdies F., Noack J., Wernbacher A., Eichelbaum M., Trunschke A., Schlögl R., Willinger M.G.

Fritz-Haber-Institut der Max-Planck-Gesellschaft, Berlin, Germany

* lunkenbein@fhi-berlin.mpg.de

Keywords: chemical, electron microscopy, annular bright field, M1, phase, beam, sensitive, heterogeneous catalysis

1 Introduction

"It would be very easy to make an analysis of any complicated chemical substance; all one would have to do would be to look at it and see where the atoms are. The only trouble is that the electron microscope is one hundred times too poor." With this statement R. Feynman has already highlighted the future importance of transmission electron microscopes (TEMs) in 1959.

Nowadays Cs corrected TEMs are powerful enough to obtain point resolution below 50 pm.[1,2] However, direct imaging of light elements next to heavy elements remains complex. In probe corrected scanning transmission electron microscopy (STEM) recent developments tackle this challenge, resulting in the revival of the annular bright field (ABF) detector. In contrary to the contrast detected by the high angle annular dark field (HAADF) method, the ABF detector is also sensitive to light elements.[3,4]

2 Results and discussion

Using the ABF detector, we investigated orthorhombic (Mo,V) oxides crystallized in a structure analog to the M1 structure (ICSD no. 55097) of MoVTeNb oxide. The obtained micrographs were compared with Rietveld refined X-ray diffraction (XRD) and electron paramagnetic resonance (EPR) data. Figure 1 shows an ABF image where the oxygen atoms brighten up. Furthermore we directly measured metal-oxygen bond angles and discussed the oxidation states of the metal centers. Our results prove Feynman´s prediction.

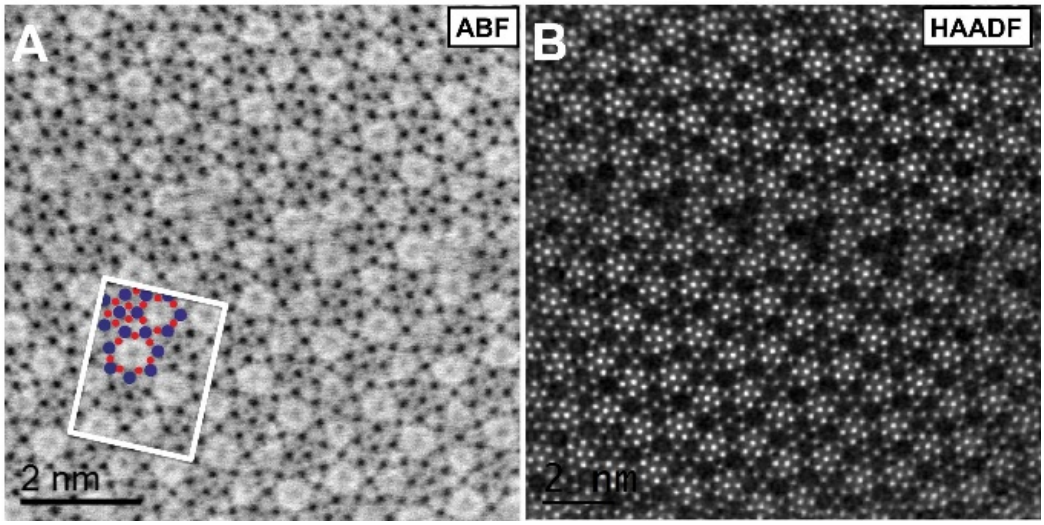

Fig. 1. (A) ABF-STEM image of $(Mo,V)O_x$. The white rectangle displays the orthorhombic unit cell. Metal sites are highlighted blue and oxygen atoms are labeled red. (B) Corresponding HAADF image.

3 Conclusions

Seeing where the atoms are, generates in particular in heterogeneous catalysis a deeper understanding of the functionality of materials on the way towards tailor-made catalysts.

References

[1] Erni R, Rossell MD, Kisielowski C, Dahmen U, *Phys. Rev. Lett.* 2009; 102: 096101.
[2] Takayanagi K, Kim S, Lee S, Oshima Y, Tanaka T, Tanishiro Y, Sawada H, Hosokawa F, Tomita T, Kaneyama T, Kondo Y, *J. Electron Microsc.* 2011; 60: S239-S244.
[3] Batson PE, *Nat Mater* 2011; 10: 270-271.
[4] Findlay SD, Shibata N, Sawada H, Okunishi E, Kondo Y, Ikuhara Y, *Ultramicroscopy* 2010, 110: 903-923.

II-PP98

State and the Catalytic Properties of Cu/ZSM-5 in Selective NO Reduction with Propane

Shutilov R.*, Zenkovets G., Gavrilov V.

Boreskov Institute of Catalysis SB RAS, Novosibirsk, Russia

* shutilov@catalysis.ru

Keywords: Cu/ZSM-5, state and location of copper containing component, SCR of NO with propane

1 Introduction

One of the most common methods of removing nitric oxide from gaseous emissions is the selective catalytic reduction (SCR) of NO to N_2 with propane, over Cu/ZSM-5 catalysts. Is spite of the extensive investigations of the physicochemical and catalytic properties of Cu/ZSM-5 catalysts for a long time, the optimal characteristics of these catalysts have not been determined. Significant factors in the catalytic properties of Cu/ZSM-5 catalysts are the state of copper ions and their location in the zeolite structure. A promising line of investigation of the Cu/ZSM-5 catalysts in order to improve their catalytic properties is to successively study and optimize the main catalyst formation stages with various copper containing precursors. Here, we report the state of copper in the Cu/ZSM5 supported catalysts prepared with ammonia solutions of copper nitrate of different structure and the catalytic properties of these catalysts in the SCR of NO with propane.

2 Experimental

Cu/ZSM-5 catalysts were prepared by ion exchange of the HZSM-5 with Si/Al =17 with aqueous ammonia solution of copper nitrate with NH_4OH/Cu = 23 and 2, which were prepared by dissolving of $Cu(NO_3)_2$ $3H_2O$ (Aldrich) in aqueous ammonia with a preset ammonia concentration. The zeolite was immersed into a solution with a given NH_4OH/Cu ratio and stirred at room temperature for 24 h. The copper concentration in all cases was 10 g/L, the ratio of solution volume to zeolite weight was 10.

Catalysts were investigated with UV-Vis (DRS), IR, ESR, H_2-TPR. Activity measurements in SCR of NO with propane were carried out in fixed-bed quartz flow reactor under steady state conditions. Temperature was measured in the 200–500 °C range, GHSV was 42000 h^{-1}. The reaction mixture was 340 ppm NO, 0.15 vol % C3H8, and Ar as the balance. The NO conversion rate at reaction temperatures of 300 and 400 °C were calculated.

3 Results and discussion

It was shown in [1] that at NH_4OH/Cu = 23 in aqueous ammonia solutions of copper nitrate tetraammine copper association species axially bonded by hydroxyl groups and a weak exchange interaction between Cu^{2+} ions (CC I) are formed. At NH_4OH/Cu = 2–3, Cu^{2+} association yields species with hydroxyl groups in the equatorial plane, water and ammonia molecules in the axial positions, and a strong exchange interaction (CC III) (Fig. 1).

The amount of sorbed copper on zeolite under equilibrium conditions was much larger for CC III than for CC I (3.25 wt % against 1.72 wt %). Investigation of the distribution of copper in the pore space of zeolite by sorption methods and IR spectroscopy of adsorbed CO demonstrated the location copper species mainly on the surface of mesopores formed by the packing of zeolite nanocrystallites. In the Cu/ZSM-5 sample prepared using CC I, the total copper concentration determined by IR spectroscopy is close to the concentration determined by chemical analysis (97%). In the catalyst obtained using CC III, the total copper concentration

determined by IR spectroscopy is 59% of the concentration determined by chemical analysis. This distinction due to CC III yielding larger clusters in which only part of the copper ions is accessible to CO being chemisorbed [2].

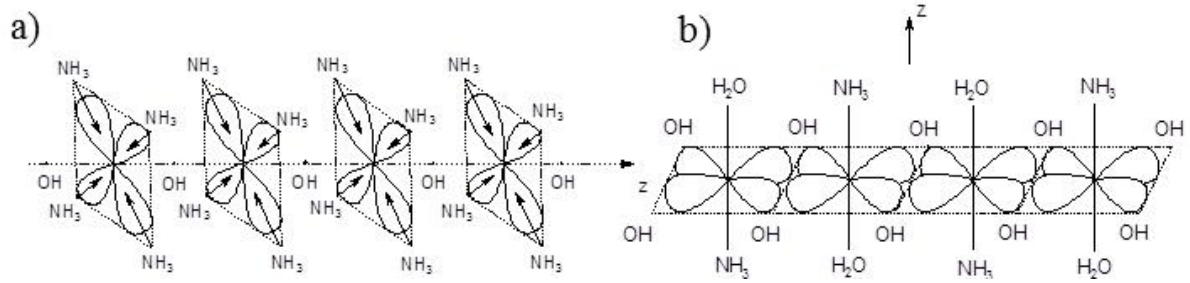

Fig.1 The structure of copper complexes CC I (a) and CC III (b).

The activity of Cu/ZSM-5 obtained using CC I increase with an increasing copper content from 0.5 to 1.72 wt %. The catalyst with 3.15 wt % Cu/ZSM-5 prepared using the CC III is more active than the best of the sample based on CC I (Tabl. 1). The reaction rate per gram of Cu for the catalysts prepared using CC I changes only slightly as the copper content increased. For the catalyst prepared using CC III, the reaction rate is lower than the W values for the catalysts obtained using CC I [3].

Table. 1 Catalytic properties of the Cu/ZSM-5 samples prepared by ion exchange using the CC I and CC III solutions (reaction rates W_m and W were calculated for 275°C)

Cu, wt. %	Type of CC	$T_{X=50\%}$, °C	W_m, 10^{-7} mol NO $g_{cat}^{-1}min^{-1}$	W, 10^{-5} mol NO $g_{Cu}^{-1}min^{-1}$
0.5	CC I	368	2.0	3.9
1.05	CC I	310	3.3	3.6
1.72	CC I	284	6.5	3.8
3.15	CC III	267	9.5	2.9

The main factors determining the catalytic properties of Cu/ZSM5 in the SCR of NO with propane is the optimum size of the copper species located on the zeolite surface that ensures the highest accessibility of the active component to the reactants and the optimum degree of covalence of the Cu–O bond in the species.

4 Conclusions

Catalytic properties of the Cu/ZSM-5 catalyst prepared by ion exchange of the HZSM-5 with aqueous ammonia solution of copper nitrate can be tuned by varying the nature of copper precursor (CC I or CC III). These factors have a significant effect on the copper species located on the surface of zeolite. In the SCR of NO with propane the highest reaction rate per gram of Cu attainable on the catalyst prepared from CC I. This due to the optimum size of Cu^{2+} oxide clusters, which ensures that a large proportion of the active component is have an optimum degree of covalence for the given process involved in the reaction and the copper–oxygen bonds.

Acknowledgement

This work was supported by the RFBR grant №14-03-31372.

References

[1] V.F Anufrienko, R.A. Shutilov, G.A. Zenkovets, V.Yu. Gavrilov and al., *Rus. J. Inor. Chem.* 57 (2012) 1285.
[2] R.A. Shutilov, G.A. Zenkovets, E.A. Paukshtis, V.Yu. Gavrilov, *Kinet.Catal*. 55 (2014) 243.
[3] R.A. Shutilov, G.A. Zenkovets, V.Yu. Gavrilov, and al., *Kinet.Catal*. 55 (2014) 620.

II-PP99

In situ XRD Study of Oscillations during the Methane Oxidation over Palladium and Nickel Foils

Saraev A.A.*, Vinokurov Z.S., Shmakov A.N., Kaichev V.V., Bukhtiyarov V.I.

Boreskov Institute of Catalysis, Novosibirsk, Russia

* asaraev@catalysis.ru

Keywords: oscillations, *in situ* XRD, methane oxidation, nickel, palladium

1 Introduction

One of the most interesting and unusual phenomena of catalysis is the rate self-sustained oscillations [1]. To date approximately 70 oscillating heterogeneous catalytic systems are known. Among them are oscillations in the oxidation of light alkanes over transition metals which attract special attention in the last years due to practical importance [2]. The understanding of the origin and the mechanism of these oscillations can open the possibility to perform the catalytic processes more effectively using the unsteady-state operation.

A number of different mechanisms that predict and interpret oscillations in the different heterogeneous catalytic reactions have been developed over the last 30 years [1]. Unfortunately, these findings were mainly based on UHV studies and cannot be directly transferred to technical catalysis. Also the mechanism of originating oscillations at the atmospheric pressure was suggested for methane oxidation over Pd and Ni [3,4]. Nevertheless, in the last case the mechanisms are discussed without any direct evidence. Here we present the first results of an in situ study of the oscillations in the methane oxidation over Pd and Ni foils at the atmospheric pressure. We used time-resolved XRD in situ technique, i.e., while oscillations take place, simultaneously with mass-spectrometry and catalyst temperature measurements.

2 Experimental

The kinetic experiments were performed in a flow quartz reactor. A palladium or nickel foil catalysts were placed in the reactor, and the reactor was inserted and heated in a tubular furnace. The catalyst temperature was measured by a K-type thermocouple spot welded to the center of nickel or palladium foils. The reaction was carried out under atmospheric pressure in a feed gas mixture ($Ar/CH_4/O_2$). The output gas composition was analyzed with a mass spectrometer SRS UGA-100, which was connected to the end of the reactor through a heated stainless steel capillary provided for the pressure reducing. The mass spectrometry data and the catalyst temperature were simultaneously recorded by a real-time data acquisition software. The methane, oxygen, and argon flows were regulated separately with mass-flow controllers Horiba SEC-Z500.

In situ XRD-MS experiments were carried out at the “High Precision Diffractometry” station at Siberian Synchrotron and Terahertz Radiation Center (Novosibirsk, Russia). The diffractometer was equipped with high temperature reaction chamber Anton Paar XRK-900, which allows measuring diffraction patterns within temperature range from RT to 900°C at different environments. The time-resolved XRD experiments were performed using position sensitive parallax-free linear OD-3M detector. X-ray wavelength of 1.724 Å was set by a single reflection from flat perfect crystal monochromator Ge(111). The methane, oxygen, and argon flows were regulated separately with mass-flow controllers Sierra SmartTrak-50. The catalyst temperature was measured by a K-type thermocouple.

3 Results and discussion

The relaxation oscillations in the methane oxidation over palladium were observed in a temperature range of 350-500°C. In case of a nickel foil used as a catalyst the oscillations were observed in a higher temperature range of 650-900°C. It is worth noting that in both cases the oxygen deficient gas mixture was used. The periodic changes in the reactant concentration were accompanied by synchronous variations of the catalyst temperature. In case of Pd during the oscillations the periodic evolution of CO_2 and H_2O and no changes of CO and H_2 signals were observed. It means that the total methane oxidation take place. In case of Ni the products of both the partial and total methane oxidation were detected. The regular oscillations appeared after an induction period, which are characterized by a very low activity of the catalysts. The activated catalyst did not have the induction period. According to SEM the operation of the catalysts under reaction conditions resulted in a development of a rough and highly porous surface structure due to strong restructuring of both the palladium and nickel foils.

Using in situ XRD allows us to find that the phase (and chemical) composition of the surface layer of the palladium and nickel catalysts changes during the oscillations. The periodic changes of XRD reflex intensities corresponding to Pd, PdO, and "PdC_x-like" phases were accompanied by synchronous variations of the catalyst temperature. In the low active state the catalyst surface was oxidized, and transition to the high active state occurred simultaneously with the formation of metallic phase on the catalyst surface. The rise of metallic reflex was accompanied by rising the additional reflex corresponded to a different phase with the larger lattice parameter than the one of metallic phase. We consider that this reflex is due to the formation of "PdC_x-like" phases (a small amount of carbon dissolved into subsurface layers).

On the contrary, for the nickel catalyst no nickel carbide features was detected by XRD. Only XRD reflexes corresponding to Ni and NiO were observed, their intensities were changing in antiphase. It is evident that in the high active state the surface layer of nickel is metal; a transition to the low active state is accompanied by the formation of a surface layer on NiO.

The using in situ techniques for the characterization of catalyst during a reaction under study is more preferable than a classic ex situ approach because it is able to reveal information about the active and inactive catalyst states. This information is invaluable for developing the reaction mechanism.

4 Conclusions

Thus, our study has clearly confirmed that the originating of oscillations in the catalytic oxidation of methane over Pd as well as Ni is determined by the periodic oxidation/reduction of palladium/nickel surface. It was previously shown that a similar mechanism for the self-sustained oscillations is realized in the oxidation of propane on Ni in a deficiency of oxygen at pressures of about 1 mbar [2]. To the best of our knowledge, it is the first direct experimental evidence for the redox mechanism of triggering rate in the oxidation of light alkanes over a transitional metal in the kinetic oscillations.

Acknowledgements

This work was supported by the President Grant for Government Support of the Leading Scientific Schools of the Russian Federation (grant SS-5340.2014.3). XRD experiments were carried out with involvement of equipment belonging to the shared research center "SSTRC".

References

[1] R. Imbihl, G. Ertl, Chem. Rev. 95 (1995) 697.
[2] V. Kaichev, A. Gladky, I. Prosvirin, A. Saraev, M. Havecker, A. Knop-Gericke, R. Schlogl, V. Bukhtiyarov, Surf. Sci. 609 (2013) 113.
[3] X. Zhang, C. Lee, D. Mingos, D. Hayward, Appl. Catal. A 240 (2003) 183.
[4] X. Zhang, D. Hayward, D. Mingos, Catal. Lett. 86 (2003) 235.

II-PP100

Temperature Behayiour of the Silane and Germane Molecule Fractures Adsorbed by a Growth Surface in an Epitaxial Process

Orlov L.[1,2], Ivin S.[2*]

1 - Institute for Physics of Microstructures, Russian Academy of Sciences, Nizhni Novgorod, Russia
2 - Nizhny Novgorod Alexeev State Technical University, Nizhni Novgorod,Russia

* orlov@ipm.sci-nnov.ru

Keywords: silane, germane, pyrolysis, kinetics disintegration, growth process, hydrogen

1 Introduction

The effects of the interaction of hydride molecular beams with an epitaxial surface and accompanying phenomena at the gas–solid interface underlie the molecular_beam epitaxy method which is used to solve various problems of microelectronics and nanoelectronics. In the high vacuum layer epitaxy method using high purity chemical compounds as molecular sources, layers are grown under conditions of surface-bond saturation with decomposition products of carrier gas molecules in a relatively wide range of growth temperatures. Under these conditions, the epitaxial_growth process is closely related to trapping mechanisms and features of the pyrolysis of molecules adsorbed by the epitaxial surface. It is clear that it is impossible to achieve the required result in the technology without a detailed understanding of the entire set of processes occurring on the growth surface. Therefore, not only heightened interest in the purely practical problems associated with the fabrication of perfect epitaxial structures has been recently observed in publications, but also particular attention has been paid to an analysis of phenomena occuring on the growth surface of silicon wafers and the layer growth and doping mechanisms. This problem, even in the simplest case of a single component system, is strongly complicated when using molecular flow sources due to the specificity and the diversity of physic-chemical processes in the vicinity of the two phase boundary.

2 Methodology

We discussed the kinetic models of silicon and germanium hydride molecule decomposition on a surface under conditions of epitaxial SiGe layer growth and determined the characteristics of the main kinetic constants responsible for the molecule decomposition rate on the growth surface. A relatively simple technique was developed, which allows not only estimation of the concentrations of molecule fragments adsorbed by the surface, but also an analysis of the dependence of the main kinetic parameters on the gas temperature and pressure in the reactor [1]. Kinetic analysis is most commonly performed using monomolecular pyrolysis models simplified as much as possible. Physicochemical and kinetic models based on this approximation provide quite acceptable understanding of the basic mechanisms of processes and reactions on a wafer surface and allow the possibility of determining the most important kinetic constants, but have also some disadvantages. In this work we are studying the layer growth models considering details of molecule pyrolysis on the growth surface which involve more than one radical fractions by the surface at different sorption process. The difficulties arising in the case of unambiguous description of the corresponding kinetic and temperature dependences are most often associated with the necessity to involve additional experimental data (if such are available), in particular, on the surface concentrations of individual molecule fragments adsorbed by the growth surface. In some cases, problems can also be caused by the cumbersomeness of numerical calculations based on analysis of a set of nonlinear kinetic equations, including a large number of independent parameters [2].

3 Results and discussion

The objective of this study is to derive relations allowing calculation of the disintegration rates of molecule fragments adsorbed by a silicon-germanium growth surface during its interaction with a molecular beams, based on the data of performed technological experiments and kinetic equations. It seems also important to determine the interrelation of the adsorbed molecule decomposition rate to other kinetic coefficients and to understand the effect of selection of the molecular decomposition model on the temperature dependences of the corresponding kinetic coefficients. In contrast to previously considered decomposition models of monosilane SiH_4 and disilane Si_2H_6 [2] molecule with one stable radical on a silicon_wafer surface, in the present study we assume that the hydride molecule is decomposed into at least two different surface radicals, which corresponds to the experimental data obtained by infrared (IR) spectroscopy [3] and mass spectrometry [4]. These results allowed us to study also the peculiarities of the kinetics molecule disintegrations of the gas silane-germane mixture on the SiGe growth surface and to determine the basic kinetics parameters in this process for the temperature range of 450–800°C. The effect of the mechanism of the adsorption of hydrogen atoms and various conditions of their transfer from the molecule to the growth surface on the temperature dependences is considered too. For the disilane pyrolysis, we showed that the disintegration model on two nonidentical fractions (Si_2H_6=SiH_3+SiH_2+H) is best at all hydrogen atoms transfer with molecule on the Si surface. Artifacts which arise on the studied dependences in a high temperature region at use of the one component model (Si_2H_6 = 2SiH_3) [2] for two component model vanish. The characteristic temperature dependences for the disintegration rate of molecule fragments for the disilane (a) and gas mixture (SiH_4+GeH_4) (b) have been studied. We determined the molecular disintegration rates for silane-germane mixture that is shown on figure 1.

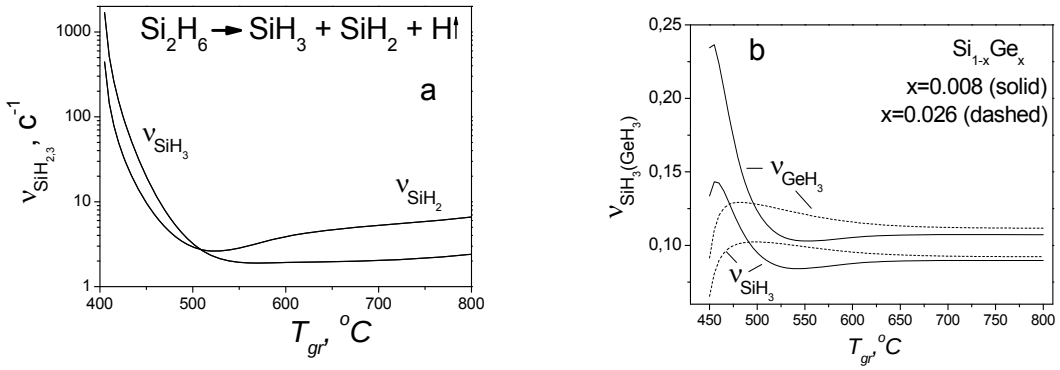

Fig. 1. Temperature dependences of the decomposition rates of the Si_2H_6 molecule fragments $\nu_{SiH2,3}$ on the Si surface for $\theta_{SiH3}/\theta_{SiH2}$ = 3 at disilane disintegration (a) and SiH_4, GeH_4 fragments from gas mixture at $Si_{1-x}Ge_x$ layer growth(b) by UHVCVD method.

Acknowledgements

The work was supported by the RFBR grant, project № 14-03-00364.

References

[1] A.V. Potapov, L.K. Orlov, S.V. Ivin, *Thin Solid Films,* 336 (1999) 191.
[2] Orlov L.K., Ivina N.L., T.N. Smyslova, *Russ. Journal General Chem.*, 83 (2013) 2240.
[3] M. Shinohara, A.Seyama, et.al., *Physical review B*, 65 (2002) 075319 (2002).
[4] S.M. Gates, C.M. Greenlief, D.B. Beach, *J. Chem. Phys.,* 93 (1990) 7493.

II-PP101

Model Systems for Co Fischer-Tropsch Catalysts

Strømsheim M.D.[1], Svenum I.H.[2], Borg A.[3], Venvik H.J.[1*]

1 - Department of Chemical Engineering, Norwegian University of Science and Technology (NTNU), Trondheim, Norway
2 - SINTEF Materials and Chemistry, Trondheim, Norway
3 - Department of Physics, Norwegian University of Science and Technology (NTNU), Trondheim, Norway

* hilde.j.venvik@ntnu.no

Keywords: single crystals, cobalt, alkali metal, scanning tunneling microscopy

1 Introduction

In Fischer – Tropsch synthesis (FTS) [1], natural gas, biomass or coal are converted to liquid fuels via synthesis gas. With respect to Co based catalysts, issues such as the nature of the active site(s), factors controlling the selectivity (C_{5+}, olefin/paraffin), support and promotor effects, and deactivation remain under dicussion. Despite the many investigations applying supported Co catalysts, relativively few model system investigations exist in the literature compared to e.g. precious metals, partly related to difficulties in working with (clean) Co single crystals having a hcp→fcc phase transition at ~420ºC. Investigations of γ-Al_2O_3-supported Co–Re powder catalysts with alkali impurity loadings up to 1000 ppm reported a decrease in catalyst activity during FTS, while the H_2 chemisorption properties [2] and the H_2 and CO differential heats of adsorption [3] remained unaffected. In this project, we investigate the deposition of submonolayer amounts of alkali metals on Co surfaces, and their effect on restructuring and FTS relevant adsorbates.

2 Experimental/methodology

Scanning Tunneling Microscopy (STM) and Low Energy Electron Diffraction (LEED) has been utilized to investigate the adsorption of alkali metals (AM), CO and hydrocarbons on cobalt single crystal surfaces. The AM was deposited from a SAES Getter source at a current of 6.5 A. All measurements were performed at room temperature (RT) and under ultra high vacuum (UHV) conditions. Complementary Density Functional Theory (DFT) investigations of the relevant Co surfaces have been carried out with the Vienna Ab initio Simulation Package (VASP) [4], which utilizes pseudo-potentials and plane wave basis sets.

3 Results and discussion

Figure 1a) and b) compares the clean surface of Co(11-20) with the (n x1) CO-reconstructed surface obtained at saturation level (~6 L). STM images of this surface restructuring was previously reported by Venvik et al.[5], who concluded that migration of Co was involved to give a (3x1) structure in well ordered areas. This provides a starting point for investigating the effect of catalyst poisons and promotors on the surface structure. Figure 1 c) shows the Co(11-20) surface after deposition of submonolayer amounts of K. The LEED images obtained after deposition of K showed a (1x1) structure. Changes to the step edges have been observed during the adsorption of FTS relevant adsorbates on the alkali-precovered surface. It is therefore conjectured that K may be decorating the step edges, as was observed for adsorption of K on the Ni(100)(2×2)p4g-N surface [6]. Results from adsorption experiments on alkali-precovered Co will be presented and discussed along with relevant comparison to modelling investigations.

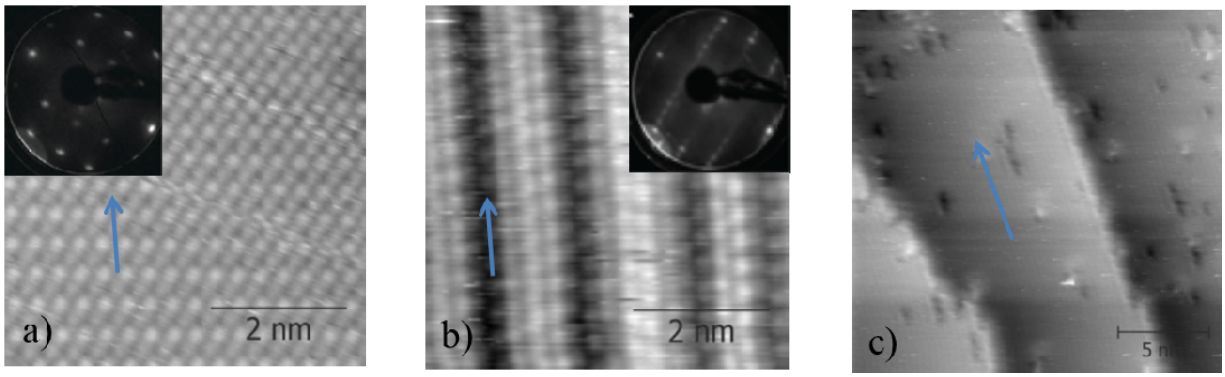

Fig.1. 53x50 Å^2 STM image of the a) clean and b) CO-reconstructed (~6.5 L) Co(11-20) surface with corresponding LEED patterns, and c) 200x200 Å^2 STM image of the Co(11-20) surface after evaporating submonolayer amounts of K from a SAES Getter Source. The [0001]-direction is indicated.

4 Conclusions

Investigations with STM have been carried out on cobalt single crystal surfaces. The preliminary results indicate that submonolayer amounts of deposited K affect the adsorption phenomena occuring during exposure to FTS relevant adsorbates. Further research is required to establish precisely the distribution of K on the single crystal surfaces.

Acknowledgments

The financial support of Research Council of Norway through the Centre of Research-based Innovation (SFI) inGAP (Innovative Natural Gas Processes and Products) is gratefully acknowledged.

References

[1] T.F. Fischer H., Berichte Der Dtsch. Chem. Gesellschaft 59 (1926) 832.
[2] C. Balonek, A. Lillebø, S. Rane, E. Rytter, L. Schmidt, A. Holmen, Catal. Letters 138 (2010) 8.
[3] E. Patanou, A.H. Lillebø, J. Yang, D. Chen, A. Holmen, E.A. Blekkan, Ind. Eng. Chem. Res. 53 (2013) 1787.
[4] G. Kresse, J. Hafner, Phys. Rev. B 47 (1993) 558.
[5] H.J. Venvik, A. Borg, C. Berg, Surf. Sci. 397 (1998) 322.
[6] A.G. Norris, M.J. Scantlebury, A.W. Munz, T. Bertrams, E. Dudzik, P. Finetti, P.W. Murray, R. McGrath, Surf. Sci. 424 (1999) 74.

II-PP102

Synthesis of Zeolites from Fly Ashes for Potential Applicationin Environmental Problems

Arroyave M.J., Arboleda E.J.*, Echavarría I.A., Hoyos D.A.

Universidad de Antioquia, Medelín, Colombia

* johana.arboleda@udea.edu.co

Keywords: fly ash, zeolites, alkaline fusion, chromium

1 Introduction

The amount of fly ashes released by factories and thermal power plants has been increasing throughout the world. Several new approaches for disposing this have been taken to reduce the cost of disposal or to minimize environmental impact. Preparation of zeolites from fly ash is one of the approaches which have been receiving a lot of attention as potential replacements for the effective but expensive commercial synthetic materials [1]. One of the most important properties of zeolites are ion exchange capacity that are effective for metal ion adsorption [2]. The properties and chemical composition of fly ashes vary depending on the source and power-plant operation [1,3]. Now, it is particularly important understanding the succession of zeolite formation of different types of fly ashes to provide useful information for the selection of raw fly ashes to synthesize zeolites. Finally we center attention in the environmental significance, of the chromium adsorption onto surface of zeolites synthetized through fly ashes of different sources.

2 Experimental/methodology

Zeolites were prepared by alkaline fusion followed by hydrothermal synthesis. The raw materials were three fly ash from Colombian industry. The fusion process began with mixing fly ash with NaOH powder (fly ash/NaOH 0.8333 in weight) and treating the resulting mixture in air at 700 °C for 3 h at a heating rate of 1 °C/min. After fusion, the powder was dissolved in distilled water (fused fly ash/H_2O 0.2046 g/ml) and sodium aluminate ($NaAlO_2$), followed by aging with stirring for 24 hours at room temperature. The crystallization of the gel was carried out at 100 °C at two different temperatures (24 and 7 hours). Batch processes for chromium adsorption were performed by shaking different amounts of each zeolite (0.01-0.5 g) and 100 mL of chromium solutions with different concentrations. Materials characterization by X-ray diffraction in Panalytical Empyiria 2012 served for identifying phases. Chemical composition were obtained by X-ray fluorescence analysis in Axios MAX (PANalytical). Additionally the materials were characterized by SEM, Surface areas, and thermal analysis. Chromate analyses were determined by atomic absorption spectrophotometry using the Thermo Scintific iCE 3000.

3 Results and discussion

The XRD patterns of the raw fly ashes (Figure 1) consisted mainly of quartz (SiO_2), mullite ($Al_6Si_2O_{13}$) and hematite (Fe_2O_3) as crystalline phases. However diffractogram show evidence ofamorphous phase in the 2θ range of 20-35°. Table 1 shows the elemental composition of fly ashes used in this study which can be classified as Class F according to ASTM C618. The raw fly ashes has 70% SiO_2+ Al_2O_3+Fe_2O_3, with a SiO_2/Al_2O_3 between ratio = 1.47, and low contents of major impurities, such as Fe, Ca and S.

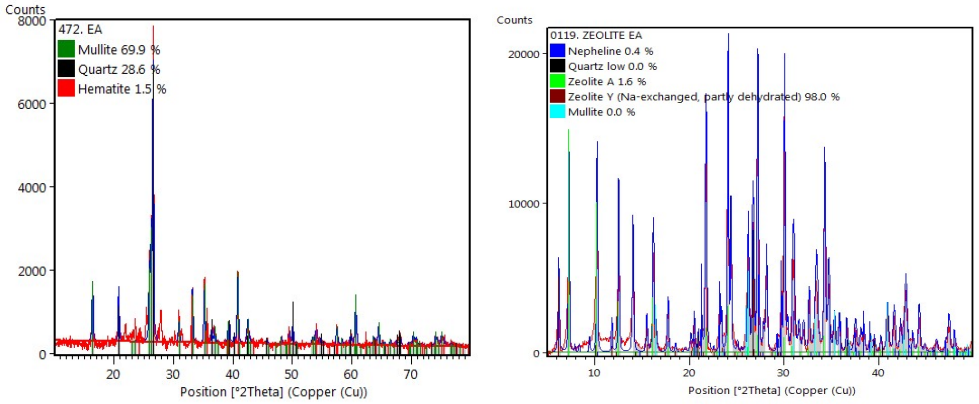

Figure 1. XRD patterns (right:fly ash (EA), left: quantitative refinement of EA/Zeolite Y)

All samples were characterized by X-ray powder diffraction to identify the structure phase and determine the effect of the crystallinity of the structure. Its comparison of peak positions of XRD spectra with reference from PDF4 DATABASE indicating the presence of LTA or FAU phases. As a representative, the X-ray diffraction (XRD) pattern of Slag from food industry (EA) (Figure 1), clearly show XRD pattern of zeolite A without the formation of faujasite. On the other hand, when the fused fly ash solutions were mix with sodium aluminate, faujasite was formed. Furthermore, it was observed that the adsorption percentage of Chromium onto the zeolites synthesized from Colombian fly ashes increased rapidly with increasing adsorbent concentration, as expected.

Table 2 Chemical Compositions and Mean Particle Size of Untreated Fly Ashes

	Slag from food industry (EA)	**Residue from manganese extraction (JMn)**	**Fly ash from textile industry (CTBI)**
SiO_2	46.97	46.78	44.78
Al_2O_3	31.90	15.62	33.63
Fe_2O_3	4.51	14.98	7.16
Na_2O	1.07	---	0.56
K_2O	1.79	2.74	1.41
Other*	13.7	19.82	12.463

* Others include Ti, Mg, P, and S oxides

4 Conclusions

The performed investigations show that a general fusion method can convert several fly ashes with wide variations in composition into zeolite FAU and LTA. Furthermore, the zeolites synthetized were found to successfully remove chromium ions from single aqueous solution.

Acknowledgements

The authors would like to thanks to Universidad de Antioquia and Colciencias for the financial support.

References

[1] Chang, H. & Shih, W. A General Method for the Conversion of Fly Ash into Zeolites as Ion Exchangers for Cesium. *Ind. Eng. Chem. Res.* **5885,** 71–78 (1998).

[2] Basaldella, E. I., Vázquez, P. G., Iucolano, F. & Caputo, D. Chromium removal from water using LTA zeolites: Effect of pH. *J. Colloid Interface Sci.* **313,** 574–578 (2007).

[3] Ríos, C. C., Williams, C. D. & Roberts, C. L. A comparative study of two methods for the synthesis of fly ash-based sodium and potassium type zeolites. *Fuel* **88,** 1403–1416 (2009).

II-PP103

Spin Probes for Characterization of Active Sites on the Surface of Oxide Catalysts and Prediction of their Catalytic Activity

Volodin A.M.[1*], Bedilo A.F.[1,2]

1 - Boreskov Institute of Catalysis SB RAS, Novosibirsk, Russia
2 - Novosibirsk Institute of Technology, Moscow State University of Design and Technology, Novosibirsk, Russia

* volodin@catalysis.ru

Keywords: spin probes, EPR, electron-donor sites, electron-acceptor sites, oxygen, radicals

1 Introduction

Obtaining information on the nature of active sites of heterogeneous catalysts for prediction of their catalytic activity is one of the main goals of physical methods used for investigation of catalysts. Active sites of oxide catalysts are located on their surface, usually are not paramagnetic and in most cases consist of some surface low-coordinated structures. The concentration of such sites is not high. EPR spectroscopy is one of the few physical methods that can reliably deal with such low concentrations. If the active sites are not paramagnetic, their investigation by EPR requires the use of some spin probes forming paramagnetic species after adsorption.

In this communication we shall present the results of the studies carried out at Boreskov Institute of Catalysis SB RAS on application of spin probes for characterization of diamagnetic surface active sites of oxide catalysts. The main goal of these studies is to develop spin probe techniques for determination and characterization of surface active sites that account for catalytic activity of oxide catalysts.

2 Experimental/methodology

To determine a correlation between the concentration of active sites detected by the spin probe method and the catalytic activity, it is necessary to study many samples. Therefore, it is particularly desirable to develop express techniques that do not require "in situ" experiments or vacuum treatment of the samples. In this study we used donor molecules with different ionization potentials (chlorobenzene, toluene, anthracene, perylene) for characterization of electron-acceptor sites with different strengths. Acceptor molecules with different electron affinities (nitrobenzene, 1,3,5-trinitrobenzene) were used for characterization of electron-donor sites. Lewis acid sites were studied using adsorption of stable nitroxyl radicals TEMPO and TEMPONE from toluene solutions. Before the experiments, the catalyst samples were dehydrated in air in quartz EPR tubes at 200-700 °C. Then, they were cooled to room temperature and filled with a solution of the used spin probe. The maximum concentration of the formed radical species corresponded to the concentration of the detected active sites on the surface of the studied catalyst. Some experiments were carried out in an EPR "in situ" installation with adsorption of reagents from the gas phase. Detailed description of the used express techniques and some of their applications were reported in our earlier publications [1-5].

3 Results and discussion

1. It is demonstrated that radical cations formed after adsorption of aromatic molecules with different ionization potentials can be used to determine the concentrations of active sites on the surface of acid catalysts. Using a spin probe with high ionization potential (chlorobenzene), it is possible to detect active sites of sulfated zirconia accounting for isomerization and cracking of light

alkanes [1]. Spin probes with lower ionization potentials (e.g. anthracene) can be used for characterization of active sites on Al_2O_3 accounting for alcohol dehydration [2].

2. Intrinsic electron-donor sites of Al_2O_3 support have been shown to participate in stabilization of atomically dispersed ionic forms of supported Pd. These are the sites accounting for high activity of Pd/Al_2O_3 catalysts in CO oxidation. The activity of such catalysts can be predicted by determining the concentration of electron-donor sites of the surface of such catalysts by measuring the concentration of radical anions formed after adsorption of 1,3,5-trinitrobenzene [5].

3. For characterization of electron-donor and electron-acceptor sites during catalytic and solid-state reactions we developed a novel procedure when the reactions were carried out directly in tubes suitable for EPR measurements. The obtained results indicate that such sites are indeed present during the catalytic reactions and can be measured quantitatively. A good correlation was observed between the rate of the CF_2Cl_2 destructive sorption on nanocrystalline MgO and the concentration of weak electron-acceptor sites characterized using anthracene as a spin probe [4].

4. The concentration of strong Lewis acid sites on the surface of acid catalysts was efficiently measured by titration using adsorption of TEMPONE nitroxyl radical from toluene solution.

5. NO is another spin probe successfully applied by us using "in situ" experiments under vacuum. This paramagnetic molecule proved to be a convenient spin probe for characterization of Lewis acid sites on the surface of oxides where it can be adsorbed at liquid nitrogen temperatures. It was also used for revealing Fe(II) ions, which have even spin and are not observed by EPR, by forming readily observable complexes with S = 3/2 [6].

6. EPR silent oxygen radical anions O^- on the surface of MgO and CaO were revealed using the formation of complexes with molecular oxygen, which are reliably detected by EPR [6]. Characterization of oxygen radical anions is of great interest due to their possible role in photocatalytsis and selective oxidation reactions. It was recently demonstrated by quantum chemical calculations that EPR silent oxygen radical anions might be present under catalytic conditions on the surface of VO_x/TiO_2 catalysts widely used for selective oxidation of various organic substrates [7].

4 Conclusions

The obtained results demonstrate that the spin probe method has great potantial for identification of the active sites of various oxide catalysts. It is shown that in many cases such information can be obtained under relatively simple experimental conditions.

Acknowledgements

Financial support by the Russian Foundation for Basic Research (Grants 13-03-00988-a and 15-03-08070-a) is acknowledged with gratitude.

References

[1] A.F. Bedilo, A.M. Volodin, *Kinet. Catal.* 50 (2009) 314.
[2] R.A. Zotov, V.V. Molchanov, A.M. Volodin, A.F. Bedilo, *J. Catal.* 278 (2011) 71.
[3] A.F. Bedilo, E.I. Shuvarakova, A.A. Rybinskaya, D.A. Medvedev, *J. Phys. Chem. C* 118 (2014) 15779.
[4] A.F. Bedilo, E.I. Shuvarakova, A.M. Volodin, E.V. Ilyina, I.V. Mishakov, A.A. Vedyagin, V.V. Chesnokov, D.S. Heroux, K.J. Klabunde, *J. Phys. Chem. C* 118 (2014) 13715.
[5] A.A. Vedyagin, A.M. Volodin, V.O. Stoyanovskii, I.V. Mishakov, D.A. Medvedev and A.S. Noskov, *Appl. Catal. B* 103 (2011) 397.
[6] A.M.Volodin, S.E.Malykhin, G.M.Zhidomirov, *Kinet. Catal.* 52 (2011) 605.
[7] V.I. Avdeev, A.F. Bedilo, *J. Phys. Chem. C.* 117 (2013) 14701.

II-PP104

Cr-Doped Silica Porous Monolith as a Model for Experimental and Theoretical Studies of Phillips Catalyst

Budnyk A.[1,2], Damin A.[2*], Bordiga S.[2]

1 - Southern Federal University, IRC "Smart Materials", Rostov-on-Don, Russia
2 - University of Turin, Department of Chemistry, NIS Centre, Turin, Italy

* alessandro.damin@unito.it

Keywords: Phillips catalyst, Cr-doped porous silica, glass, ethylene polymerization

1 Introduction

The Phillips catalyst is a highly versatile Cr/SiO_2 system accounting for the production of several types of polyethylenes [1]. It is still the subject of an intense industrial and academic research, both from an experimental [2] and theoretical point of view [3]. The determination of the structure of the active sites of the real catalysts remains difficult, although constitutive knowledge about Cr/SiO_2 system has been accumulated on simplified model systems. The sol-gel methods allowing to obtain optically transparent monoliths displaying a high surface area. Both properties facilitate the spectroscopic investigation of the structure and the catalytic activity of metal centres in transmittance geometry in whole UV-Vis-NIR and Mid-IR regions.

Prior to ethylene polymerization, the Phillips-type catalysts have to be "activated" by calcination in air at elevated temperature. During this step Cr ions in the oxidized state (+6) react with the hydroxyl groups at the silica surface and remain anchored in the form of chromates or, less probably, dichromates and polychromates. Simultaneously, molecular water is released through the condensation of surface hydroxyl groups and the formation of strained siloxane bridges; the dehydroxylation process increases with the rise of temperature. A clear relationship between silica hydroxylation degree, properties of the Cr sites, and catalytic activity, is still missing. In the present work we report an experimental study of catalytic activity of the Cr/SiO_2 model systems with different Cr content and the dehydroxylation state of the silica support. The experimental results were then used for validating theoretical models of the Cr/SiO_2 catalyst based on a cluster approach.

2 Experimental/methodology

Tetraethyl orthosilicate (TEOS) was added to a mixture of ethanol and distilled water in molar ratio of 1:4:20, respectively, under stirring at room temperature (RT) [4]. The pH was adjusted to ~1-2 by addition of diluted nitric acid. A proper amount of CrO_3 in water was added to get a set of samples with Cr loading in the 0.01-0.5 wt% range. The mixtures in sealed plastic vessels were kept at 50 °C for 2-3 days until occurrence of gelation. The treatment was followed with a week of aging at 80 °C and that of drying, when vessels were pin-holed and the temperature was gradually rising up to 120 °C. The dry xerogels were calcined at 600 °C for 1 h in air.

The activation procedure consisted of a few successive steps: thermal activation under dynamic vacuum at chosen temperature (550, 650 or 750 °C) for 1 h; oxidation in pure O_2 (100 mbar) for 1 h time of contact with subsequent cooling to 350 °C in the presence of oxygen and evacuation. This allows to prepare three $Cr(VI)/SiO_2$ samples; in order to prepare the corresponding $Cr(II)/SiO_2$ systems, the samples are further treated in presence of CO at 350 °C for 1 h time of contact and evacuation. Then samples are cooled down to RT under dynamic vacuum.

The produced samples were characterized by BET analysis, X-Ray Powder Diffraction, UV-Vis-NIR, FTIR and Raman spectroscopies. The DFT calculations were performed by adopting a cluster approach and Gaussian 09 software.

3 Results and discussion

Fig.1 presents some experimental results (a-d) together with clusters of $Cr_A(II)$ and $Cr_B(II)$ sites adopted to model $Cr(II)/SiO_2$ systems in their highly dehydroxylated form (e) [5].

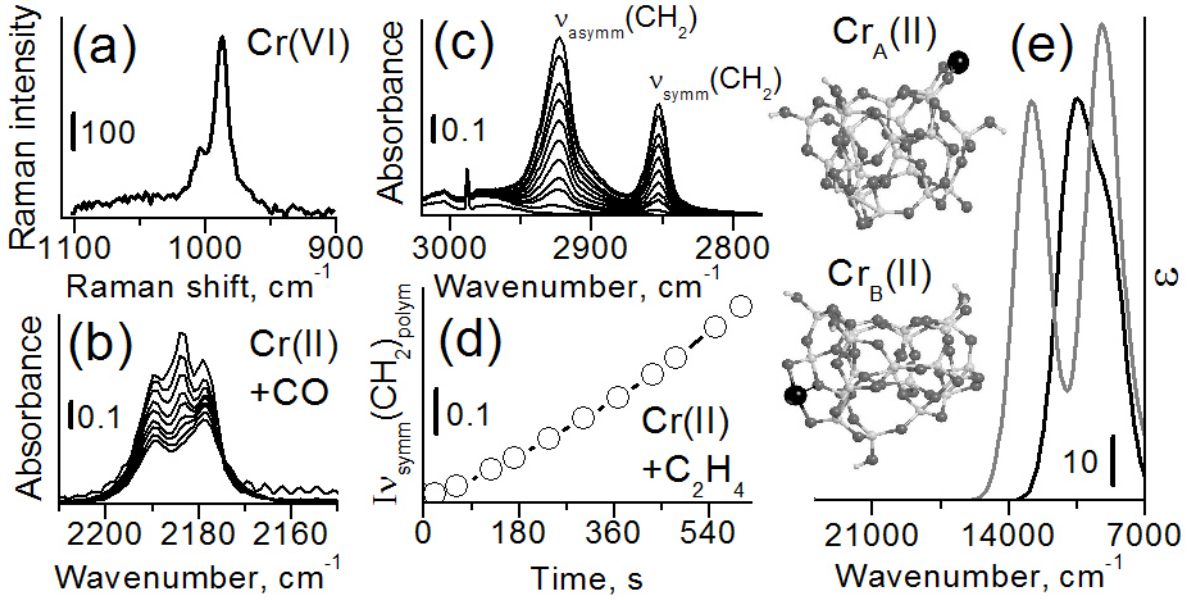

Fig. 1. Experimental results on Cr 0.1 wt% activated at 650 °C: (a) Raman spectrum (325 nm laser line) in air, (b) CO (100 mbar) adsorption on $Cr(II)/SiO_2$ at RT, (c) FTIR of polymerization of C_2H_4 (100 mbar) at RT, (d) the kinetics of C_2H_4 polymerization followed at 2853 cm^{-1}, and graphical representation of $Cr_A(II)$ and $Cr_B(II)$ clusters and computed UV-Vis spectra for both models (e).

4 Conclusions

The Cr-doped silica mesoporous monoliths with high surface area have been synthesised by one-pot sol-gel method. They were employed as a model of Phillips catalyst for fundamental studies on the structure and activity of Cr catalytic centres. Despite extremely low Cr loading, the FTIR of CO probes revealed the families of surface Cr sites, already described for more concentrated Cr/SiO_2 systems. These species readily react at RT with ethylene condensed into the pores, causing a fast growth of polyethylene. A systematic investigation of the hydroxylation state of the surface on the $Cr(II)/SiO_2$ sample as a function of the activation temperature in the 550–750 °C interval was performed in terms of distribution of fully isolated and weakly interacting hydroxyl groups. Experimental observations allowed for development of cluster models of Cr_A and Cr_B sites, which satisfactory reproduce the main experimental data.

Acknowledgements

The financial support provided by FIRB grant No. RBAP115AYN (Italy) and by the Mega-grant No. 14.Y26.31.0001 (Russia) are highly appreciated.

References

[1] M.P. McDaniel, *Adv. Catal.*, 53 (2010) 123.
[2] E. Groppo, C. Lamberti, S. Bordiga, G. Spoto, and A. Zecchina, *Chem. Rev.* 105 (2005) 115.
[3] A. Damin, J.G. Vitillo, G. Ricchiardi, S. Bordiga, C. Lamberti, E. Groppo, and A. Zecchina, *J. Phys. Chem. A* 113 (2009) 14261.
[4] A. Budnyk, A. Damin, C. Barzan, E. Groppo, C. Lamberti, S. Bordiga, and A. Zecchina, *J. Catal.* 308 (2013) 319.
[5] A. Budnyk, A. Damin, E. Groppo, A. Zecchina, and S. Bordiga, *J. Catal.* (2015) accepted.

II-PP105

Rational Design of Cu-Based Catalyst of Oxychlorination Process by Combined In-Situ Mass- and Spatial-Time Resolved UV-Visible Spectroscopy.

Baidoo M.F.[1], Rout K. R.[1], Fenes E.[1], Fuglerud T.[2], Chen D.[1*]

1 - Norwegian University of Science and Technology,Chemical Eng. Dept, Trondheim, Norway
2 - Technology and Projects, INEOS ChlorVinyl,Herre, Norway

* de.chen@ntnu.no

Keywords: rational design, doped, CuCl2/γ- Al_2O_3 catalyst, oxychlorination, UV/Vis spectroscopy, *in situ* spectroscopy

1 Introduction

Oxychlorination of ethylene is the most important route to produce 1, 2-dichloroethane (EDC), which is a key step for poly-vinyl chloride (PVC) [1]. In commercial ethylene oxychlorination reactors, gaseous ethylene, HCl and air react with $CuCl_2/\gamma$-Al_2O_3 catalyst at a temperature range of 217 ^{0}C-257 ^{0}C and a pressure 5-6 atm.

The $CuCl_2/\gamma$-Al_2O_3 catalyst is effective in the oxychlorination of ethylene because $CuCl_2$ can catalyze the conversion of HCl to chlorine. In the literature [2], it has been shown that by feeding the three reactants separately, the oxychlorination reaction is catalyzed by a highly dispersed $CuCl_2$ phase and thereby follows a three step redox mechanism:

Step 1. Reduction of $CuCl_2$ to CuCl.
Step 2. Oxidation of CuCl to form an oxy-chloride.
Step 3. Hydrochlorination of the oxy-chloride using HCl to form $CuCl_2$ and H_2O.

In-situ spectroscopy is an approach to monitor online the physicochemical phenomena of the catalyst material in a reactor [3]. The results from such in-situ study at industrial relevant conditions provide detailed insight into the working principles of the catalytic material. So that it would then be possible to improve the existing catalyst formulations or design completely new catalysts, which are more active and/or selective. In the past [4], an operando XANES and EXAFS have been performed to monitor the Cu^{II} to Cu^{I} transformation in the ethylene oxychlorination environment on the $CuCl_2/\gamma$-Al_2O_3. It has been found that the rate determining step of the overall process (1) is the CuCl oxidation (3). It is noted that the XANES and EXAFS are performed in transition mode, i.e., the catalyst layer is very thin and the space velocity is very high. Therefore, it is difficult for the detailed kinetic study. Hence, we developed an operando set-up to study kinetics of the reaction including catalyst active component involved by combined UV/Vis- and mass spectroscopy, where the reaction conditions and flow can be well controlled in the normal fixed bed reactor.

2 Experimental/methodology

A strategy of combined transient and steady-state kinetic study was employed. The transient kinetic study was performed for individual reaction steps such as the reduction, oxidation and hydrochlorination steps in the catalytic cycle of oxychlorination process. The UV-Vis spectroscopic technique in the reactor focuses on the same spot of a catalyst in a reactor under true reaction conditions and is capable of delivering sub second time resolution. However, in the overall reaction study, the UV-Vis focuses on the same spot of catalysts in the reactor first until the process reached steady-state to get the time resolved kinetic data. After that the whole

catalyst bed of the reactor is scanned by UV-Vis spectroscopy to measure the active Cu^{II} along the reactor axis.

3 Results and discussion

First experiments have been performed by using $CuCl_2/\gamma\text{-}Al_2O_3$ catalyst for individual steps of the oxychlorination process. The change of Cu state from Cu^{II} to Cu^{I} has been studied by the use of UV-Vis spectroscopy, whereas the reaction rate, conversion has been calculated by Mass spectroscopy. It has been found that the rate determining step of the overall process is the CuCl oxidation step. Results obtained from oxychlorination of ethylene on $CuCl_2/\ \gamma\text{-}Al_2O_3$ catalyst, showed a lower reaction rate on the oxidation step (step2) than the reduction step (step1), which leads to deactivation of catalyst due to the excess amount of intermediate (CuCl). Therefore, CeO_2 is used as promoter to enhance the catalytic performance of the reaction by reducing the reaction rate at the reduction step (step1) in one hand and increasing the oxidation rate on the other hand. Various weight percentages of Ceria (1, 3 and 5 wt %) doped with $CuCl_2/\ \gamma\text{-}Al_2O_3$ is been used in several cycles.

4 Conclusions

UV-VIS and Mass Spectroscopies, combined with laboratory techniques made it possible to have a good understanding in kinetic behaviour of the active phase and effects of CeO_2 as promoter for the catalyst. Results show that even low concentrations of ceria in $CuCl_2/\gamma\text{-}Al_2O_3$ can highly enhance catalytic performance of the catalyst however high concentration of CeO_2 has negative impacts on activity of the catalyst.

Acknowledgements

This work is part of the inGAP Center for Research-based Innovation, which receives financial support from the Research Council of Norway.

References

[1] Lamberti C, P.G., Bordiga S, Berlier G, D'Acapito F, and Z. A, Angew Chem Int Ed 2000. **39:2138**
[2] Baiker A, H.W., J. Catal., 1983. **84**
[3] Bennici SM, V.B., Alexander Nijhuis T, Weckhuysen BM, Angew. Chem Int Ed, 2007. **119**
[4] Muddada NB, O.U., Caccialupi L, Cavani F, Gianolio D, and L.C. Bordiga S, PCCP 2010. **12:5605**

II-PP106

Controllable Metal Dusting of Ni-M Alloys: New Opportunities for Design of Self-Organized Catalysts and Synthesis of Carbon Nanomaterials

Mishakov I.V.[1,2*], Bauman Yu.I.[1], Shubin Yu.V.[3,4], Rudnev A.V.[3], Vedyagin A.A.[1], Buyanov R.A.[1]

1 - Boreskov Institute of Catalysis, Novosibirs, Russia
2 - Novosibirsk State Technical University, Novosibirsk, Russia
3 - Nikolaev Institute of Inorganic Chemistry, Novosibirsk, Russia
4 - Novosibirsk State University, Novosibirsk, Russia

* mishakov@catalysis.ru

Keywords: metal dusting, Ni alloys, self-organized catalysts, carbon, fibers, dichloroethane, precursor

1 Introduction

Metal dusting (MD) of bulk metals and alloys (based on Ni, Co or Fe) is well known as catastrophic form of corrosion, which leads to disintegration of initial fabrics into a powdery mixture of graphitic carbon and metal dust. MD occurs in strongly carburizing atmosphere (CO, CO_2, hydrocarbons) at intermediate temperatures of 400-800°C. In the same time, MD process is now considered to be low-cost and efficient route to produce such valuable products as carbon nanomaterials (CNM) including nanotubes and nanofibers [1]. During the process, Fe or Ni nanoparticles which catalyse the growth of CNM, are produced spontaneously from the bulk metal precursors (steel, nichrome, etc.).

In this research we have implemented an earlier developed approach for catalyst preparation which was based on the phenomenon of MD of the standardized bulk Ni-M alloys used as precursors [2]. Being exposed to aggressive reaction medium containing chlorinated hydrocarbons and H_2, the bulk Ni and its alloys undergo very fast disintegration under action of MD resulting in emergence of equivalent active particles catalyzing the growth of nanostructured carbon filaments. Thus prepared self-organized catalytic system was fond to be characterized by very high activity in decomposition of 1,2-dichloroethane (superior to that known for analogous supported catalysts), extreme resistance to deactivation and huge productivity towards carbon nanomaterial exceeding 500 g/g_{Ni} [3].

In the presented study, the bimetallic alloys Ni-M (M=Co, Cu, Fe, Cr, Mo; x=0.01÷0.5) have been synthesized by various methods to be further explored as precursors for preparation of self-organized catalysts active in production of carbon nanomaterials.

2 Experimental/methodology

First series of $Ni_{1-x}M_x$ precursor alloys was synthesized by the coprecipitation technique. The resulted samples of mixed Ni-M hydroxocarbonates were reduced in H_2 flow at 800°C for 30 min to obtain the metallic $Ni_{1-x}M_x$ alloys. Second series of bimetallic Ni-M samples was prepared via mechanochemical activation of the corresponding metallic powders in planetary ball mill AGO-2 at various activation time (τ=0.2÷15 min). Carbon material (Sibunit, S_{BET} = 350 m^2/g) in amount of 5 wt. % was used as a loosening agent.

All Ni-M samples prepared have been tested in quartz flow reactor equipped with McBain balances to study the kinetics of MD in $C_2H_4Cl_2/H_2/Ar$ reaction mix. Reaction temperature was varied in the range of 550-675°C. Physicochemical characterizations of resulted self-organized catalysts as well as the morphology and texture of carbonaceous product were analyzed using microscopy (SEM, TEM), EDX and adsorption method (BET).

3 Results and discussion

XRD patterns revealed that single-phase Ni-M samples were obtained in each case. Shift of the reflexes compared to the position of Ni reflexes (inset) proved the alloys formation (Fig.1).

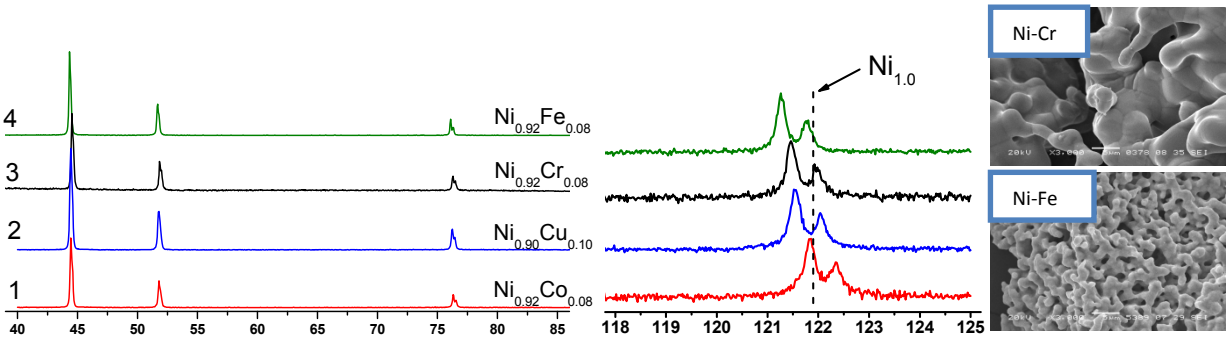

Fig.1. XRD patterns and SEM images for $Ni_{1-x}M_x$ precursor alloys prepared by coprecipitation method. All samples were reduced in H_2 at 800°C.

Results of kinetic studies showed that process of MD of synthesized Ni-M samples is characterized by rather short induction period (less than 30 min) which makes their preliminary activation not necessary. Ni-Mo precursor was found to give the most active catalyst while the best stabilizing effect was elucidated for the addition of Cr. Regardless to initial concentration of Cr added, the resulted disperse Ni particles contained only 0.4-0.6 at. % of chromium.

Disintegration of starting alloys in reaction mixture results in formation of the active metallic sites catalyzing the multi-directional growth of carbon fibers (Fig.2). The grown fibers were found to have submicron diameter and segmented morphology as prevailing. Due to poorly packed and defective structure, the obtained carbon product is characterized with sufficiently high surface area (up to 400 m^2/g) and porosity (0.5-0.8 cm^3/g).

The effect of M and its concentration in Ni-M precursor upon catalytic activity and structural peculiarities of CNM product being formed will be discussed in details.

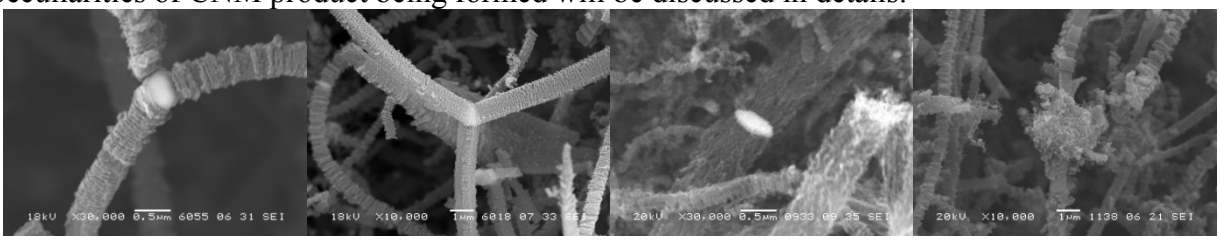

Fig.2. SEM images of active Ni-M particles resulted from disintegration of corresponding alloyed Ni-M precursors (*from left to right*: Ni-Cr, Ni-Fe, Ni-Cu, Ni-Mo). Reaction mix: $C_2H_4Cl_2/H_2/Ar$, 600°C.

4 Conclusions

Metal dusting of Ni-based alloys in aggressive reaction medium can be considered as a new platform for rather simple and effective method to prepare self-organizing catalysts for synthesis of nanostructured carbon materials. Suggested approach is expected to give the great opportunities for purposeful design of catalytic systems with desired properties and unlimited operating durability.

Acknowledgments

This study was financially supported by Russian Foundation for Basic Research (project No. 14-03-00411-a) and Russian Academy of Sciences (project No. V.45.3.5).

References

[1] J. Chang, H. Tsai, W. Tsai // *J. Phys. Chem. C*. 112 (2008) 20143.
[2] I. Mishakov et al. // *Topics in Catalysis*. 56 (2013) 1026.
[3] Yu. Bauman et.al. // *Nanotechnologies in Russia*. 9 (2014) 380.

II-PP108

Characterization of the Catalysts with Atomically Dispersed Pd and Rh on Alumina

Vedyagin A.A., Volodin A.M., Stoyanovskii V.O., Kenzhin R.M.

Boreskov Institute of Catalysis SB RAS, Novosibirsk, Russia

* stoyn@catalysis.ru

Keywords: noble metal, cations, UV–vis, EPR, luminescence, ethane, hydrogenolysis

1 Introduction

Recent experimental studies have demonstrated that atomically dispersed or sub-nanometer sized ionic clusters of precious metals show the highest activity in a number of oxidation reactions. The nature of oxide support is believed to play the defining role in stabilization of such species in active state. Concentration of intrinsic centers on a surface of γ-Al_2O_3 that are capable to stabilize the supported precious metals in atomic and cluster forms is not that great and usually does not exceed 0.5 wt. % by metal. In the case of Pd and Rh containing catalytic systems there are two main processes known to be responsible for catalyst deactivation. The first one refers to the sintering of dispersed Pd while another process is related to the bulk diffusion of Rh ions into support. The present study aims in a developing of spectroscopic optical, EPR and catalytic (ethane hydrogenolysis) methods for characterization of Pd and Rh state on alumina-based catalysts containing ultra-low concentrations (as low as 0.02 wt. %) of the supported metals.

2 Experimental/methodology

Incipient wetness impregnation was used for the synthesis of Pd and Rh containing catalysts. H_2PdCl_4 (Merk), $RhCl_3 \cdot 4H_2O$ (Merck) and γ-Al_2O_3 (Condea, SSA = 205 m^2/g) were used as the starting materials. After impregnation, the samples were dried and then calcined in air at 630 °C for 12 h [1, 2]. Different concentrations of H_2PdCl_4 and $RhCl_3 \cdot 4H_2O$ in the impregnation solutions were used to obtain the 0.01–0.5 wt. % loadings of the supported metal. The thermal aging of the samples was carried out in air at 830 °C (12 h) and 1000 °C (12 h). In this study, a spin probe technique was used for quantitative and qualitative analysis of the electron-donor sites on the alumina surface. The surface concentrations of Rh and Pd were determined using ethane hydrogenolysis as a test reaction [1, 2].

3 Results and discussion

Deposition of palladium on intrinsic sites on alumina surface which are capable to stabilize Pd in isolated and cluster ionic leads to selective modification of the alumina electron-donor sites. These sites are responsible for appearance and stabilization of TNB radical anions, which could be detected by EPR thereby characterizing the sites. The data presented in Fig.1 show that Pd deposition on Al_2O_3 results in a substantial increase in the concentration of radical anions registered by EPR after TNB adsorption. This increase is readily detectable even at low concentration of deposited palladium (0.06 wt. %, Fig.1).

The diffuse reflectance spectra are known to be sensitive for the Rh state changes during the thermal treatment. Surface Rh^{3+}complexes and Rh^{3+}:γ-Al_2O_3 have d-d bands at 326 and 424 nm, and charge transfer band with the edge at 250 nm. As rhodium leaves the surface, the band becomes narrower without changing its position. Charge transfer bands towards shorter wavelengths as well as d-d shifts were observed in case of bulk Rh^{3+} ions in α-Al_2O_3 indicating a significant increase in magnitude of crystal field for Rh^{3+} in corundum.

Luminescence was observed for Rh^{3+} ($4d^6$) ions occupying low-spin octahedral positions in α-Al_2O_3 only among other transition phases of alumina [1]. The excitation spectrum Rh^{3+}:α-Al_2O_3 consists of two well-resolved bands at 390 and 320 nm corresponding to allowed transitions $^1A_{1g} \rightarrow {}^1T_{1g}$, $^1T_{2g}$ and charge transfer band with the edge at 215 nm (Fig. 2.) Analysis of the concentration of corundum phase in samples with 0.01–0.5 wt. % loadings of Rh after calcination at 1000 °C has suggested a promoting effect of Rh in the formation α-Al_2O_3.

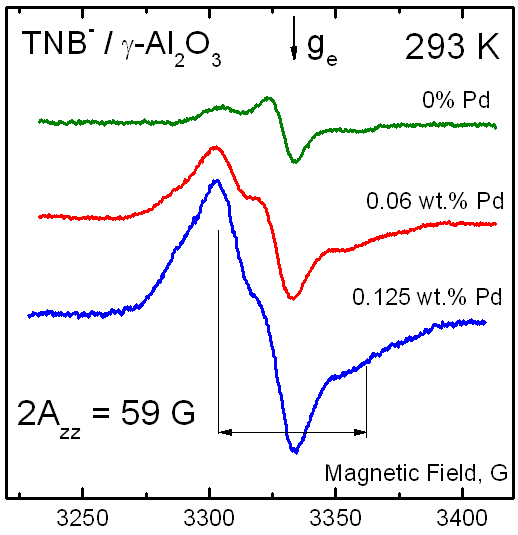

Fig. 1. EPR spectra observed after TNB adsorption on samples with Pd concentrations 0-0.125 wt. %.

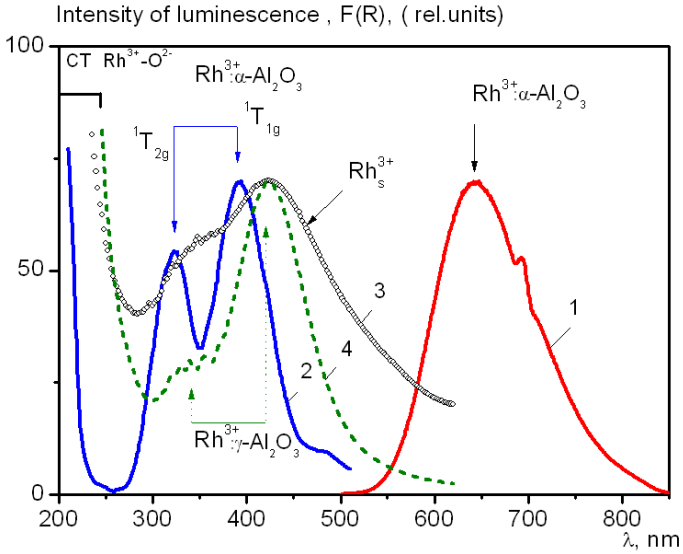

Fig. 2. Luminescence (1) and excitation (2) spectra of Rh^{3+}:α-Al_2O_3. Amplitude normalized diffuse reflectance UV-VIS spectra of Rh/Al_2O after calcination at 600 (3) and 800 °C (4).

The activity of the both Pd and Rh catalysts in ethane hydrogenation correlates with the specific surface area of metal that is proportional to its surface concentration. It was shown that after thermal aging at 830 °C only 9.9% of Rh initial concentration left on the surface. Further treatment at 1000°C resulted in a slight decrease in the concentration down to 8.5% of the initial level.

4 Conclusions

The original highly sensitive spectroscopic optical, EPR and catalytic techniques for characterization of catalysts with atomically dispersed Pd and Rh on alumina will be discussed in details. The methods developed allowed us to investigate such systems with ultra-low concentrations (0.02–0.03 wt. %) of supported metal. In addition to mentioned, these approaches can be successfully applied to study the Pd and Rh state in binary Rh–Pd/Al_2O_3 catalysts [3, 4].

Acknowledgements

Financial support by the Russian foundation for Basic Research (Grant No. 13-03-00988-a) is acknowledged with gratitude.

References

[1] A.A. Vedyagin, A.M. Volodin, V.O. Stoyanovskii, I.V. Mishakov, D.A. Medvedev, A.S. Noskov, *Appl. Catal. B: Env.* 103 (2011) 397.
[2] V.O. Stoyanovskii, A.A. Vedyagin, G.I. Aleshina, A.M. Volodin, A.S. Noskov, *Appl. Catal. B: Env.* 90 (2009) 141.
[3] A.A. Vedyagin, M.S. Gavrilov, A.M. Volodin, V.O. Stoyanovskii, E.M. Slavinskaya, I.V. Mishakov, Y.V. Shubin, *Top Catal* 56 (2013) 1008.
[4] A.A. Vedyagin, A.M. Volodin, V.O. Stoyanovskii, R.M. Kenzhin, E.M. Slavinskaya, I.V. Mishakov, P.E. Plyusnin, Y.V. Shubin, *Catalysis Today* 238 (2014) 80.

II-PP109

Novel Catalysts for Selective C≡C Bond Hydrogenation Based on Metal-Organic Framework MIL-53(Al) as a Host Matrix for Pd Nanoparticles

Isaeva V.I.*, Markov P.V., Turova O.V., Mashkovsky I.S., Stakheev A.Yu, Kustov L.M.

ND Zelinsky Institute of Organic Chemistry RAS, Moscow, Russia

* sharf@ioc.ac.ru

Keywords: metal-organic frameworks, palladium nanoparticles, semihydrogenation, diphenylacetylene

1 Introduction

Selective semihydrogenation of an acetylenic function is a demanding task. Not only does the stereoselectivity (E/Z ratio) need to be controlled, but the hydrogenation of the resulting olefin to alkane must be suppressed as well. During the last decade the metal-organic framewoks (MOFs) received a considerable attention as metal carriers for heterogeneous catalysis, which enable fine tuning the activity and selectivity of the resulted heterogeneous systems [1]. In this study we explored the catalytic performance the novel catalysts on the basis of Pd nanoparticles encapsulated in microporous metal-organic framework MIL-53(Al) in the hydrogenation of diphenylacetylene (DPA) in a liquid phase as the model substrate. Al^{3+}-derived microporous phenylenecarboxylate frameworks, i.e. MIL-53 (Al(OH)bdc, bdc = benzene-1,4-dicarboxylate) was utilized for Pd deposition. MIL-53 (Al) was chosen as a support because of its exceptional thermal stability: the framework crystalline structure remains intact at temperature as high as 450°C [2]. In addition, the aromatic moiety of the framework pore surface facilitates the encapsulation of metal NPs inside the pores. An important task of this research was the elucidation of the impact of the preparation procedure of Pd NP nanocomposites on their catalytic performance. The synthesized palladium-containing catalysts were characterized by a combination of the physico-chemical methods: SEM, DRIFT, selective CO chemosorption, and volumetric N_2 adsorption. The dispersion and location of Pd nanoparticles were examined by XRD, TEM, and XPS.

2 Experimental

Preparation of the Pd@MIL nanocomposites includes the synthesis of metal organic supports and introducing Pd followed by reduction.

MIL-53 Support Preparation. The samples were prepared by hydrothermal reaction between the nitrate salt of the metal ion ($Al(NO_3)_3 \times 9H_2O$) and terephthalic acid (1,4-benzenedicarboxylic acid, H_2bdc) in a Teflon-lined stainless steel Parr autoclave at 220°C for 3 days. To remove the solvent/H_2bdc molecules from MIL-53 pores, further activation treatments of samples were performed by calcinations according to procedure 1 (72 h, 330°C) or procedure 2 (3 h, 450°C) in air.

Catalyst Preparation. Pd (1 wt. %) was deposited by mixing 0.5 g of the parent samples with a $Pd(acac)_2$ solution in absolute chloroform (5.0 mg in 0.30 mL). The 1%Pd@MIL-53 samples were prepared by heating under vacuum at 423 K (4 h). Before reaction the catalyst was additionally activated at 150°C or 300°C in flowing 5%H_2 + Ar.

Characterization of MIL-53 materials.

The samples were characterized by a number of physicochemical methods: XRD, SEM, and volumetric N_2 adsorption/desorption. The composition and surface areas of the synthesized MOF supports are given in Table. N_2 adsorption data were obtained at -196°C. The powder XRD pattern were measured in a transmission mode using a Huber G670 Guinier camera diffractometer (CuK_α radiation) at 22°C. Scanning electron microscopy (SEM) studies were performed using a LEO 1455 VP with an XR microanalyzer (Carl Zeiss).

Catalytic tests. The catalysts were tested in the liquid-phase hydrogenation of diphenylacetylene (DPA) at 5 bar of H_2 pressure, room temperature (25°C), using *n*-hexane as a solvent. Substrate/Pd ratio was ~ 4000. Typically, the catalyst (2.5 mg), substrate (170 mg), and solvent (6 ml) were placed into a stainless autoclave, purged by He and pressured with H_2. Stirring was switched on (700 rpm) to start the reaction. H_2 consumption was calculated on the basis of H_2 pressure drop, measured by electronic pressure sensor. The reaction was periodically stopped and the reaction mixture was analyzed by NMR.

3 Results and discussion

XRD and SEM investigation confirmed the retention of crystalline structure of MIL-53(Al) framework upon the Pd NPs introducing and during the reaction. XRD revealed also the significant effect of the introduction procedure of the Pd nanoparticles in the network topology for several samples. Textural properties of microporous metal-organic framework were strongly modified by palladium insertion, leading to significant changes in N_2 sorption properties. TEM and XRD study revealed the average diameter of immobilized Pd nanoparticles of 2-5 nm. Dispersion and location of Pd nanoparticles affected strongly both by MIL-53(Al) activation conditions and reduction procedure of palladium-containing catalyst.

The semihydrogenation of diphenylacetylene proceeds according to consecutive route over Pd/MIL-53(Al) samples (Scheme 1): DPA hydrogenation followed by stilbene hydrogenation. The catalysts demonstrate high activity in this reaction (Table 1).

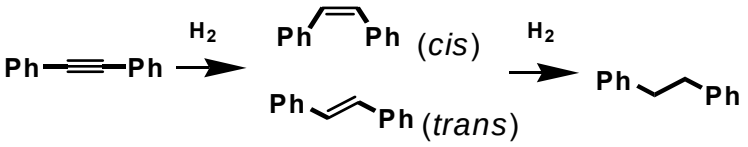

Scheme 1.

Selectivity in alkene (stylbene) formation exceeds 90% at dipehylacetylene conversion as high as 95%. The catalysts also show high stereoselectivity (E/Z ratio) toward formation of cis-isomer and favorable stability (Table 1).

Table 1. TONs and selectivity parameters in DPA hydrogenation in *n*-C_6H_{14} over Pd/MIL-53(Al) nanocomposites. P_{H2} = 5 bar, T_{react} = 25°C, [DPA]/Pd ~ 4000.

Catalyst, T reduction, ^{0}C	TON_{DPA}, s^{-1}	TON_{DPE}, s^{-1}	r_{DPA}/r_{DPE}	S_{DPE}**	$S_{cis/(cis+trans)}$**
Pd@MIL-53(1*), 150^{0}C	2.5	0.4	6.5		
Pd@MIL-53(2*), 150^{0}C	2.1	0.3	7.0	91%	95%
Pd@MIL-53(1*), 300^{0}C	3.5	0.7	6.2		
Pd@MIL-53(2*), 300^{0}C	5.3	0.8	6.0	85%	94%

* Metal-organic framework activation procedure (Experimental part).
** Selectivity to alkene and cis-isomer at DPA conversion of 95%.

4 Conclusions

Effective catalysts for selective hydrogenation of DPA to *cis*-stilbene has been developed using the phenylenecarboxyate framework MIL-53(Al) as a host matrix for Pd nanoparticles immobilization. It was found that Pd@MIL-53(Al) catalysts showed favorable activity and selectivity in semihydrogenation even after mild reduction at 150°C. Selectivity of diphenylacetylene transformation into *cis*-stilbene exceeds 94%. Our study revealed a strong impact of parent framework activation conditions on the catalytic performance of Pd@MIL-53(Al) nanocomposites.

Acknowledgements

Financial support by RFBR grant No13-03-12176 is gratefully acknowledged. The research was also supported by the Russian Science Foundation (Grant No. 14-50-00126).

References

[1]D. Farrusseng, S. Aguado, C. Pinel, *Angew. Chem. Int. Ed.,* 48 (2009) 7502.
[2]C.Serre, F.Millange,C.Thouvenot, M.Nogues, G.Marsolier, D.Loűer, G.Ferey, *J.Am.Chem.Soc*.124 **(**2002) 13519.

II-PP110

Effect of the Synthesis Route on NOx Storage over Ceria/Zirconia Based-Mixed Oxides in LNT Applications

Say Z., Samast Z.A., Ozensoy E.*

Department of Chemistry, Bilkent University, Ankara, Turkey

* ozensoy@fen.bilkent.edu.tr

Keywords: DeNOx, CeO_2, ZrO_2, TPD, LNT, Pt

1 Introduction

CeO_2 can be used as apromoter and/or as a support materialin Three-Way Catalysis (TWC) and Lean NOx Trap (LNT) systems. The primary function of ceria-based stems from theirfavorable redox properties as well thier high oxygen storage and transport capacity [1-3]. ZrO_2can be used together with CeO_2in order to modify surface properties of heterogeneous catalysts that may enhance thermal stability, change surface acidity and improve metal particle dispersion [4,5]. Moreover, ZrO_2 is a promising additive due to its onboard H_2 generation ability via steam reforming reactions [6]. Inthe current study, structural evolution of ternary ($CeO_2/ZrO_2/Al_2O_3$) mixed oxides was followed as a function of temperature by means of XRD, Raman and BET surface area analysis. Moreover, NOx adsorption capabilities of these materials were investigated by means ofin-situ FTIR and TPD techniques [7].

2 Experimental/methodology

Pt/Ce/Al, Pt/Zr/Al, Pt/Ce/Zr/Al and Pt/(Ce-Zr)/Al mixed oxides were synthesized by incipient wetness impregnation method as described in our former reports[2,3]. While subsequent wetness impregnation was used for Pt/Ce/Al, Pt/Zr/Al and Pt/Ce/Zr/Al systems; Pt/(Ce-Zr)/Al catalyst was synthesized via co-impregnation.

3 Results and Discussion

The effect of the synthesis protocol on NO oxidation and relative NO_x adsorption capacity as well as nitrate/nitrite decomposition pathways were studiedvia TPD analysis (Figure 1). Thermal stability of nitrates on Pt/Zr/Al was found to be much higher than that of Pt/Ce/Al, however Pt/(Ce-Zr)/Al revealed the highest NO_x adsorption capacity among all of the investigated materials including the conventional Pt/20BaO/Al benchmark catalyst(Table 1). In other wrords,simultaneous impregnation of CeO_2 and ZrO_2 led to the formation of a mixed oxide(Pt/(Ce-Zr)/Al)that had a superior NOx adsorption ability as compared to the systems where subsequent impregnation was used (*i.e.*Pt/Ce/Zr/Al).Furthermore, CO adsorption experiments via in-situ FTIR spectroscopy(data not shown)indicated a higher dispersion of Pt particles over Pt/(Ce-Zr)/Al as compared to that of Pt/Ce/Zr/Al.It is also worth mentioning that nitrate/nitrite decomposition on Pt/(Ce-Zr)/Al resulted in much higher quantities of N_2 and N_2O compared to that of the other currently investigated catalysts, indicating a greater capability of NO_x reduction. These results indicate that mixed-oxide catalytic systems prepared via co-impregnation method reveal superior catalytic properties as they exhibit higher NO_x storage capability, better Pt dispersion as well as enhanced NO_x reduction ability.

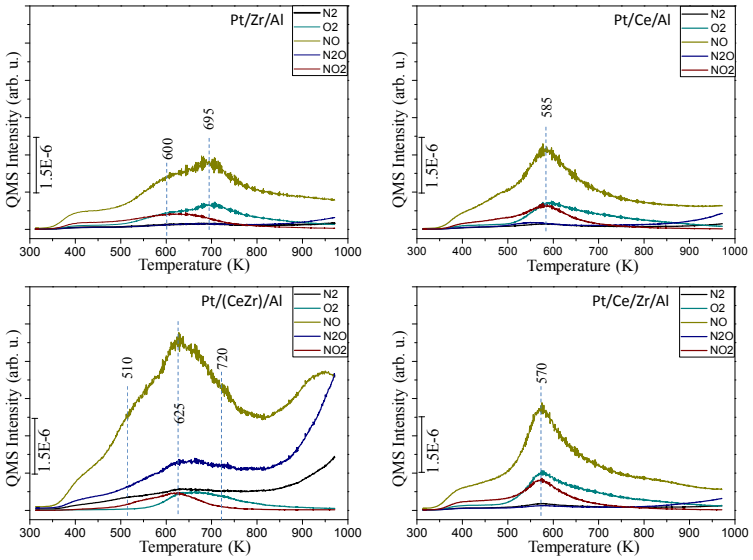

Figure 1. TPD profiles obtained from synthesized materials after adsorption and saturation with NO_2(g) at 323 K for 10 min.

Materials	S_{BET} (m^2/g)	Total integrated areas under NOx-related desorption features in TPD (arb. units)	Total integrated areas under NOx-related desorption features in TPD (arb. units)
Pt/Ce/Al	133	10.2	0.077
Pt/Zr/Al	152	10.3	0.068
Pt/(CeZr)/Al	142	39.1	0.276
Pt/Ce/Zr/Al	136	11.0	0.081
Pt/Ba/Al	132	25.5	0.193

Table 1.BET specific surface area values of the investigated catalysts; total integrated areas under NO_x-related desorption features in TPD; and normalized version of these latter values per specific surface area (detailed calculations can be found in Ref.[3]).

4 Conclusions

It is a great challenge to modify surface characteristics of materials in order to achieve superior NOx storage performance. In this study, we investigated the effect of the synthesis route of theternary (CeO_2/ZrO_2/Al_2O_3) mixed oxides on the LNT catalytic properties. The catalyst synthesized viasimultaneous impregnation(i.e. Pt/(CeZr)/Al)revealed superior characteristics with a promising potential in LNT applications.

Acknowledgements

We acknowledge the financial support from the Scientific and Technological Research Council of Turkey (TUBITAK) (Project Code: 111M780).

References

[1] M. Casapu, J. Grunwaldt, M. Maciejewski, M. Wittrock, U. Gobel, A. Baiker,Applied Catalysis B: Environmental 63 (2006) 232.
[2] Z. Say, E.I. Vovk, V.I. Bukhtiyarov, E. Ozensoy, Topics in Catalysis 56, 950 (2013).
[3] Z. Say, E.I. Vovk, V.I. Bukhtiyarov, E. Ozensoy, Applied Catalysis B: Environmental 142, 143, 89 (2013).
[4] V. Perrichon, L. Retailleau, P. Bazin, M. Daturi, J.C. Lavalley, Applied Catalysis A: General 260 (2004) 1.
[6] H. Zhu, J. Kim, S. Ihm, React. Kinet.Catal.Lett 97 (2009) 207.
[7] Z. Say, Z.A. Samast, E. Ozensoy (in preparation 2015)

II-PP111

Choice and Validation of the Promoting Additives on the Zeolite Catalysts of Isobutane Alkylation

Alexandrova J.V.[1], Vlasov E.A.[1], Maltseva N.V.[1], Murzin D.U.[2], Postnov A.U.[1*]

1 - St. Petersburg StateTechnological Institute (Technical University), Department of General Chemical Technology and Catalysis, St. Petersburg, Russia
2 - Abo Akademi University, Turku, Finland

* julia_alex84@bk.ru

Keywords: alkylate, alkylation of izobytane, zeolite, dekationation, dealyuminizing, cationic exchange

1 Introduction

Alkylate is one of the most important components of synthetic motor fuel and represents the mix of isoparaffin hydrocarbons with octane number more than 90-94 which is almost not containing aromatic and unsaturated hydrocarbons and possessing stability and detonation firmness in comparison with other components of gasolines. Alkylation of isobutane belongs to the acid catalyzed processes and is traditionally carried out in the presence of the concentrated H_2SO_4 and HF acids. However in connection with strengthening of economic and ecological requirements to industrial processes intensive development of new types of heterogeneous catalysts of alkylation of isobutane which the most perspective are zeolites are conducted now. The gasoline received with application the zeolites of catalysts doesn't contain such polluting impurity compounds as sulfur, nitrogen, oxygen, and also the resinous substances and unsaturated hydrocarbons which are present when cracking oil fractions.

2 Experimental/methodology

Increase of activity of zeolites NaY is conducted, increasing values of the module silicate SiO_2/Al_2O_3 by a dealyuminizing, and changing of molecular sieve, acid and main properties by method by ionic exchange for cations NH_4^+, or 2nd and 3rd valent metals. For optimization technology of synthesis, increase stability and activity, and also decrease in processes of coke production as the promoting additives are chosen: **Cs^+, La^{3+}, Ca^{2+}, Ce^{3+}, Ni^{2+}, Zr^{4+}.** The HCaLa-USY catalyst in a polycationic form on the basis of NaY with the entered ions $Ca^{2+}$and La^{3+} received by methods:

1) 3-stages dekationation of NaY → NH_4Y (fraction of 100-200 microns at mechanical hashing subjected to influence during 1 h in 1,5 M solution $(NH_4)_2SO_4$ with the subsequent washing at 70 °C during 1ch. Further granules filtered and dried at t = 120 °C 4 h).

2) dealyuminizing NH_4Y → H-USY by the method of consecutive deaminization (removal of molecules of NH_3) and thermosteam processing (TSO) at t = 550 °C

3) 2-stages cationic exchange with consecutive replacement of part of the acid centers for Ca^{2+} ions and La^{3+} in 0.75M $CaCl_2$ and $La(NO_3)_3$ solutions respectively at t = 60 °C, washing (t = 120 °C, 4 h), a filtration and TSO: ***H-USY →HCa-USY→HCaLa-USY***

3 Results and discussion

Dealyuminizing and dekationation of ultrastable NaY to H-USY led to decrease in Sud with 898 to 727 m2/g, and also with noticeable change of integrated function of Gammet H0I 11,3→7,7, respectively. About change of a ratio of the silicate module Si/Al illustrating shift of

an intensive strip ~1000 cm-1, characteristic for zeolites, and Si-O-Al relating to antisymmetric valent fluctuations follow from the analysis of IR spectrums. Upon transition from NaY→H-USY there is a decrease in amount of atoms of Al in an elementary lattice of NaY with 55 to 37, raising Si/Al practically in twice with 1,5→2,7. Broadening of a structural and sensitive strip ~ 1000 cm-1 and change of its integrated intensity from 77% (NaY) to 87 (samp. HCaLa-USY), in comparison with an intensive narrow strip of HY-Al-Zr (118%), indicates a rupture of communications and growth of concentration of defects in structures of zeolite.

Table 1. Characteristics of the synthesized samples on the basis of high-silica zeolites

Sample	V_Σ	Vmakro	Vmezo	H_{oI}	Sud	$P_\square$	x,
	cm^3/g				m^2/g	MPas	%
Series on the NaY in polycationic form (NaY + % promotor,2)							
HCaLa-USY	0,56	0,40	0,16	7,3	510	0,6	9,0
HCaLa-USY-Ni	0,52	0,39	0,13	7,1	500/13**	0,8	6.5
HCaCe-USY	0,49	0,33	0,16	7,2	490	0,7	11,0
HCaCe-USY-Ni	0,42	0,33	0,12	7,4	480/13**	0,7	10.5
Series on the NaY + PB + % promotor Me							
HY-Al-Zr	0,49	0,21	0,28	5,8	144	1,1	98,6
HY-Al- Ce	0,41	0,32	0,20	7.6	141	1,0	34.5
HY-Al-Cs	0,39	0,16	0,28	7.8	150	1,3	23,0

Impregnation by ions of Ca2+-La3+, Ca2+-Ce3+ doesn't influence on the acid properties of the H-USY, but conducts to some growth of extent of conversion with 3,5 to 9,5%, thus all samples in the polycationic form are characterized by close VΣ values = 0,42 - 0,56 cm3/g with prevalence of Vmakro 0,33-0,40 cm3/g, with an obvious tendency to coking up - falling of Sud with 480-500 to 13 m2/g. Change of Si/Al in samples of HY and HCaLa-USY with 2,7 to 7,3 speaks about high degree of ionic exchange, and also ability of cations to settle down in zeolite cavities, impregnation of Ni2+ not considerably affects Si/Al values, acidity and activity.

Use as a binding psevdoboehmit PB (10-30% of mas.) increased durability (P□) it is model more than by 1,5 times (tab. samp. HY-Al-Me). In the studied samples there is a reorganization of porous structure due to growth of volume of mesoporous Vmezo=0,25-0,28 and reduction of Vmakro=0,16-0,32 cm3/g. Sample HY-Al-Cs different low x=23%, is characterized by the developed Vmakro, and neutral range of H0I = 7.8 that apparently is connected with features of an arrangement cations of Cs+ mainly in the centers of six-membered rings of three-dimensional structure. Lower Si/Al value in a sample of HY-Al-Zr (4,6) with amount atoms of Al in a zeolite 30 lattice that in comparison with samples in a polycationic form (Si/Al =7,3, number of atoms Al =10) is connected with additional introduction cations of Al in the form of PB in structure of the catalyst, influencing H0I = 5,8 and activity.

4 Conclusions

Thus, introduction of a certain type of a cation (monocationic form of the catalyst), and also a combination introduction of two and more cations (polycationic form), operating availability of porous structure (a dekationation, a dealyuminizing), it is capable to influence formation of the active centers the zeolitecontaining catalysts, the acid and main characteristics, and activity, modeling the direction and selectivity of process. It is established that conversion of isobutane on the HY-Al-Zr catalyst, makes 98,5% thus the maintenance of C5-C8 fractions in alkylate = 82,7% of masses that testifies to prospects of further researches.

Acknowledgements

Work is performed within the State contract № 14.Z50310013 from March 19, 2014.

II-PP112

In situ and *ex situ* Studies of Bimetallic Catalysts Activation for Multiwalled Carbon Nanotubes Growth

Kuznetsov V.L.[1,2], Krasnikov D.V.[1,2], Shmakov A.N.[1,2*], Lapina O.B.[1], Andreev A.S.[1,2], Ishchenko A.V.[1], Prosvirin I.P.[1], Kalinkin A.V.[1], Zakharov D.N.[3], Kazakova M.A.[1,2]

1 - Boreskov Institute of catalysis SB RAS, Novosibirsk, Russia
2 - Novosibirsk State University, Novosibirsk, Russia
3 - Brookhaven National Laboratory, Upton, USA

* kuznet@catalysis.ru

Keywords: carbon nanotube growth, bimetallic catalyst, *in situ* methods, activation

1 Introduction

Multi-walled carbon nanotubes (MWCNTs) are known as one of the most perspective components for numerical composite materials due to their remarkable mechanical, chemical, and electronic properties [1]. Properties of MWCNTs significantly depend on their structure (defectiveness, diameter distribution, morphology of agglomerates, concentration of impurities etc.) which in turn depends on the type of catalyst (nature and dispersion of active metals, nature of support and promoters) and on reaction conditions used during nanotube production. It was found that bimetallic catalysts are more effective than monometallic. In the present paper, we study the formation of the active component of various bimetallic catalysts (Fe-Co, Co-Mn, Fe-Mo, Co-Mo) during MWCNT growth using *in situ* synchrotron radiation X-ray diffraction analysis (SRXRD) and *in situ* XPS in combination with *ex situ* and *in situ* high speed HRTEM, solid-state ^{59}Co NMR, and gas chromatography. HRTEM, Raman data, thermal dependence of conductivity and magnetoresistance measurements were used to characterize relationship between MWCNT defectiveness and catalyst composition.

2 Experimental/methodology

Bimetallic oxide catalysts containing Fe-Co, Co-Mn, Fe-Mo, Co-Mo were produced via polymerized complex route based on the Pechini-type method [2,3], which provides the production of highly dispersed oxide systems containing homogeneously distributed metal ions of active components and support. MWCNTs were synthesized in a flow integral reactor via ethylene decomposition on the catalyst surface at 600-680ºC (C_2H_4 : Ar mixture 1:1, 15–60 min). Active metal particles were generated *in situ* on the surface of oxide matrix during catalyst reduction by ethylene.

Catalyst structural changes and MWCNT morphology were monitored by HRTEM and SEM. *In situ* SRXRD measurements at 20–700ºC were carried out with XRK-900 reactor chamber (Anton Paar, Austria) equipped with fast, parallax-free one-coordinate X-ray detector OD-3M-350 in Siberian Synchrotron and Terahertz Radiation Centre. *In-situ* XPS spectra were obtained by a SPECS X-ray photoelectron spectrometer with PHOIBOS-150-MCD-9 analyzer at 600-700 ºC in 5-10^{-6} Torr C_2H_4. ^{59}Co NMR experiments were performed on Bruker Avance II NMR spectrometer outside of magnet using high power broadband probe. The Raman spectra of MWCNT powders have been measured with a Jobin Yvon S-3000 spectrometer (Ar–Kr laser, 514.5 nm) in microscopic configuration with the spectral resolution of 2 cm^{-1}.

3 Results and discussion

According to the XRD data, catalyst active components (alloyed metal particles) are solid or at least contains crystalline core during CNT growth. At the same time alloy particles smaller

than 5-7 nm are roentgen-amorphous in the conditions of the reaction. Sintering rate of active metal particles during catalyst activation is an important factor, which determines the diameter distribution of growing MWCNTs.

For the first time we have obtained data confirming a stepwise formation of bimetallic alloy. It was found that cobalt particles are formed at the first stage of catalyst reduction (Fe-Co catalysts). These primary particles promote (via spillover of activated hydrogen) the reduction of Fe species with the subsequent formation of the alloy. Fig.1A shows in situ XPS data demonstrating different rates of reduction of components of bimetallic Fe-Co/Al_2O_3 catalyst.

Using comparative studies of MWCNTs with HRTEM, Raman data, thermal dependence of conductivity and magnetoresistance measurements it was shown that each type of catalyst promotes formation of MWCNTs with specific properties. Fig. 1B demonstrates almost a linear dependence of a ratio of intensities of 2D (two-phonon scattering) and D (disorder-induced) bands (I_{2D}/I_D) on the mean diameter of MWCNTs produced with two different types of catalysts. It should be mentioned that each type of catalyst provides the linear dependence with its own specific slope. The difference in slope can be explained in terms of differences in kinetics and energy parameters of the main steps of MWCNT growth for different type catalysts. The graphene fragments have been proposed to form a mosaic structure of nanotubewalls .

The obtained data can be used to provide the process kinetic model development and optimize the synthesis conditions to produce MWCNT with controlled properties.

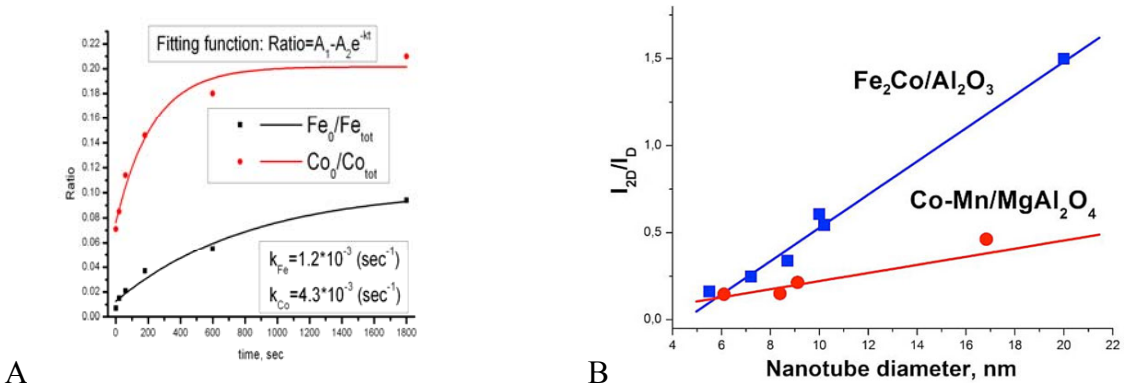

Fig. 1. A. *In situ* XPS data on the activation Fe-Co catalysts demonstrating higher reduction rate of Co vs. Fe. B. A dependence of I_{2D}/I_D intensity ratio on the diameter of nanotubes produced with different catalysts.

Acknowledgements

This study was partially supported by grant of the Ministry of Science and Education of RFMEFI60714X0046. Research carried out in part at the Center for Functional Nanomaterials, Brookhaven National Laboratory, which is supported by the U.S. Department of Energy, Office of Basic Energy Sciences, under Contract No. DE-SC0012704.

References

[1] Satoru Suzuki (ed.) "Syntheses and Applications of Carbon Nanotubes and Their Composites", ISBN 978-953-51-1125-2 (2013).

[2] V.L. Kuznetsov, D.V. Krasnikov, A.N. Schmakov, K.V. Elumeeva, *Phys. Status Solidi B* 249 (2012), 2390.

[3] V.L. Kuznetsov, S.N. Bokova-Sirosh, S.I. Moseenkov, et al., *Phys. Status Solidi B*, 251 (2014), 244.

II-PP113

Catalytic Activity of $PC_{sp3}P$ Pincer Iridium Hydride Complexes in Olefines Hydroformylation and Acceptorless Alcohols Dehydrogenation: DFT and Spectroscopic Study

Silantyev G.A.[1], Filippov O.A.[1], Belkova N.V.[1*], Kozinets E.M.[1], Musa S.[2], Gelman D.[2], Shubina E.S.[1]

1 - A.N.Nesmeyanov Institute of Organoelement Compounds RAS, Moscow, Russia
2 - The Hebrew University of Jerusalem, Institute of Chemistry, Edmond Safra Campus, Jerusalem, Israel

* nataliabelk@ineos.ac.ru

Keywords: iridium hydride, structure, reaction, mechanism, molecular, spectroscopy, DFT

1 Introduction

A variety of recently developed catalysts operate via different ligand-metal cooperating mechanisms and new "non-innocent" ligands and their complexes keep appearing in the literature [1-3]. Reversible switching between different coordination modes found in these compounds opened new practical reactivity patterns in non-oxidative (i.e. alternative to the conventional oxidative addition/reductive elimination sequence) activation and formation of polar and non-polar bonds. At that, many such systems contain stereochemically rigid pincer ligands and keep their geometry during the catalytic runs.

The dibenzobarrelene-based $PC_{sp3}P$ pincer iridium complex **1** is catalytically active in acceptorless dehydrogenation of alcohols (Scheme 1). The intramolecular interaction of hydride with the dangling CH_2OH group that leads to facile hydrogen release was hypothesized as the origin of its high catalytic activity [4]. Indeed, the role of proton-hydride interactions is well recognized in chemistry of transition metal hydrides [5-7]. Herein we present the recent results on the intra- and intermolecular interactions involving hydride ligand and hydroxymethyl groups of **1** and their role in the complex structure and reactivity.

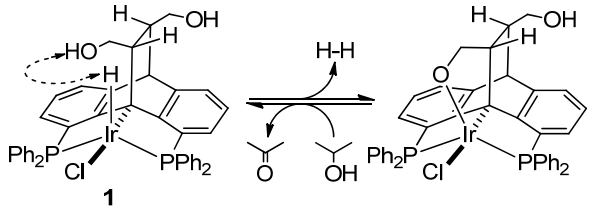

Scheme 1.

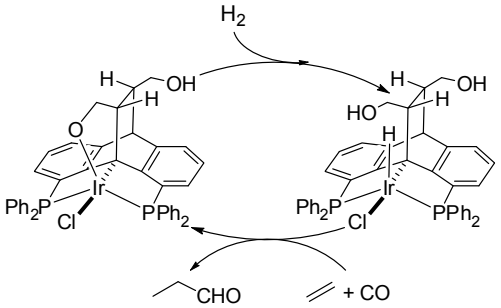

Scheme 2.

2 Experimental/methodology

Calculations were performed with the Gaussian09 package at the DFT/M06 level without any ligand simplification and symmetry restrictions. Effective core potentials (ECP) and its associated SDD basis set supplemented with f-polarization functions (SDD(f)) were applied to the Ir atom. The first coordination sphere of Ir (P, H, Cl and C1 atoms), OH and CO groups and all atoms of reactants (C_2H_4, and CO) were described with 6-31++G(d,p) basis set, the rest of atoms - with a 6-31G basis set. The nature of all of the stationary points on the potential energy surface was confirmed by vibrational analysis.

All manipulations were performed under an argon atmosphere using standard Schlenk tech-

nique. NMR investigations were carried out on Bruker AVANCE 600 NMR spectrometers supplied with a specially designed low temperature dual probe-head (SEI, 5 mm tube size). The IR spectra of solutions were measured on Nicolet 6700 FTIR spectrometer in CaF_2 cells using home modified cryostat Carl Zeiss Jena for variable temperature measurements.

3 Results and discussion

The structure of complex **1** differs from that of many other catalysts with "non-innocent" or bifunctional ligands: the hydroxymethyl group is formally far away from the metal. The results of variable temperature IR and NMR (^1H, ^{31}P) analysis of **1** and its analogue – COOEt substituted complex **2** in different media (dichloromethane, toluene, DMSO, and mixed solvents) in combination with the quantum chemical (DFT/M06; AIM) calculations imply flexibility of the dibenzobarrelene-based scaffold [8] unprecedented for conventional pincer ligands. Both the complex **1** and its counterpart **2** prefer facial configuration of the PCP ligand with P-Ir-P angle of ca. 100º. Such geometries are dictated by stabilizing Ir···O interaction and differ by the mutual arrangement of the H and Cl ligands. The complexes show dynamic equilibrium between two most stable *fac*-isomers, which can be transformed into the meridional ones in the presence of coordinating additives (CH_3CN, DMSO or CO, but not Et_3N), some of which have been used as auxiliary base in catalytic alcohols dehydrogenation [4].

A series of stoichiometric and catalytic experiments showed complex **1** is capable of promoting olefin hydroformylation via the metal-ligand cooperating mechanism (Scheme 2) [9]. DFT optimization of some proposed intermediates have been carried out for both hydrogenation and hydroformylation reactions. The mechanism of the H_2 activation and C-H bond formation involves unprecedented intramolecular cooperation between the structurally remote functionality and the metal center. Interestingly the most probable catalytic cycle for hydroformylation/hydrogenation operates via *fac*-form. Model IR studies of *i*PrOH dehydrogenation show higher activity of *fac*-isomer relative to *mer*-one which is further facilitated by addition of Et_3N.

4 Conclusions

The hemilabile CH_2OH group of **1** does not only stabilize active species through the reversible coordination to iridium (Ir···O interaction) but its presence is crucial for catalytic activity. The catalytic reaction mechanism involves intramolecular CH_2OH – Ir cooperation and proceeds without the change of the metal oxidation state.

Acknowledgements

The authors thank the Russian Foundation for Basic Research (RFBR, projects No. 14-03-00594 and 14-03-31828) and the ISF Petroleum Alternatives.

References

[1] C. Gunanathan, L. J. W. Shimon, D. Milstein, *J. Am. Chem. Soc.* **2009**, *131*, 3146-3147.
[2] M. Käß, A. Friedrich, M. Drees, S. Schneider, *Angew. Chem. Int. Ed.* **2009**, *48*, 905-907.
[3] D. Gelman, S. Musa, *ACS Catal.* **2012**, *2*, 2456-2466.
[4] S. Musa, I. Shaposhnikov, S. Cohen, D. Gelman, *Angew. Chem. Intern. Ed.* **2011**, *50*, 3533-3537.
[5] N. V. Belkova, E. S. Shubina, L. M. Epstein, *Acc. Chem. Res.* **2005**, *38*, 624-631.
[6] O. A. Filippov, N. V. Belkova, L. M. Epstein, A. Lledós, E. S. Shubina, *Comput. Theoret. Chem.* **2012**, *998*, 129-140.
[7] S. Marincean, J. E. Jackson, *J. Phys. Chem. A* **2010**, *114*, 13376-13380.
[8] G. A. Silantyev, O. A. Filippov, S. Musa, D. Gelman, N. V. Belkova, K. Weisz, L. M. Epstein, E. S. Shubina, *Organometallics* **2014**, *33*, 5964-5973.
[9] S. Musa, O. A. Filippov, N. V. Belkova, E. S. Shubina, G. A. Silantyev, L. Ackermann, D. Gelman, *Chem. - Eur. J.* **2013**, *19*, 16906-16909.

II-PP114

Manifestation of Resonance Dipole-Dipole Interactions in Spectra of Adsorbed Strongly Absorbing Molecules

Dobrotvorskaia A.N.*, Gatilova A.V., Kolomiitsova T.D., Shchepkin D.N., Tsyganenko A.A.

St. Petersburg State University, Department of Physics, St. Petersburg, Russia

* a.dobrotvorskaya@spbu.ru

Keywords: adsorption, IR, spectroscopy, dynamic interaction, SF6, CF4, NF3

1 Introduction

Lateral interactions, studied in detail by IR spectroscopy for CO adsorbed on metals and oxides , affect greatly the adsorption and catalytic properties of solid surfaces. The method of isotopic dilution enables us to distinguish two kinds of interactions: static effect and the dynamic interaction, referred also as resonance dipole-dipole interaction (RDDI). The former affects the strength of surface sites, while the latter modifies the positions, shapes and widths of absorption bands in the adsorbed molecule spectra, thus distorting the information about surface active sites and the geometry of adsorbed layer. It accounts also for the surface vibrational energy transfer and, thus, plays an important role in catalytic and photocatalytic reactions.

The RDDI manifests itself in vibrational spectra of molecular systems when molecules have large derivative of the dipole moment, i.e. high absorbance. This should be taken into account when the spectra of strongly absorbing molecules are investigated. The aim of this study was to find out the manifestations of the RDDI in spectra of SF_6, CF_4 and NF_3 molecules adsorbed on the surface of amorphous or crystalline oxide adsorbents.

A previous study has shown that the position and band shapes depend critically on the mutual transition dipole moment orientation in the laboratory frame. For the flat oxide surfaces the structure of studied systems can be considered as a 2D adsorbed layer in XY plane perpendicular to Z axis. For SF_6 and CF_4 two collective modes arise in the ν_3 region with the in-plane and perpendicular to the surface orientations of dynamic dipoles. The latter should have a higher frequency and is more sensitive to the influence of the surface.

In adsorbents with channel- like pores the confined molecules form chains that can be considered as 1D (1-dimentional) linear structures. Such model can be used to describe adsorption in silicalite-1, pure siliceous zeolite with ZSM-5 structure. For SF_6 chains the calculated spectrum in the region of ν_3 mode has also a doublet of two components, but with the separation about twice smaller as compared with the spectra of flat layers of the same molecules.

2 Results and discussion

Figure 1 shows the experimental spectra of SF_6 adsorbed on pressed powder samples: ZnO, MgF_2 and CaO, where of 2D adsorbed layers should be formed, as well as on silicalite-1, where 1D chains could be anticipated. For comparison, spectra of solid film of SF_6 on cell windows is also presented. The latter can be considered as a 3D system of interacting molecules.

The spectra of three systems with 2D layers can be considered as a superposition of a couple of two components 44- 62 cm^{-1} apart with one more band at about 944 cm^{-1}. The latter is more intense in the spectra run at higher temperatures and lower coverages, is close to the position of ν_3 band of gaseous SF_6 (949 cm^{-1}) and can be attributed to not interacting single molecules ("2D gas"). Such a band in the spectrum of silicalite-1 appears at 937 cm^{-1}. Its intensity decreases on lowering the temperature, while sharp bands of interacting molecules grow at 949, 929 and 927 cm^{-1} (fig.1 b). Thus, the band becomes split by 20-22 cm^{-1}, the low-

frequency component itself consists of two peaks about 2 cm^{-1} apart.

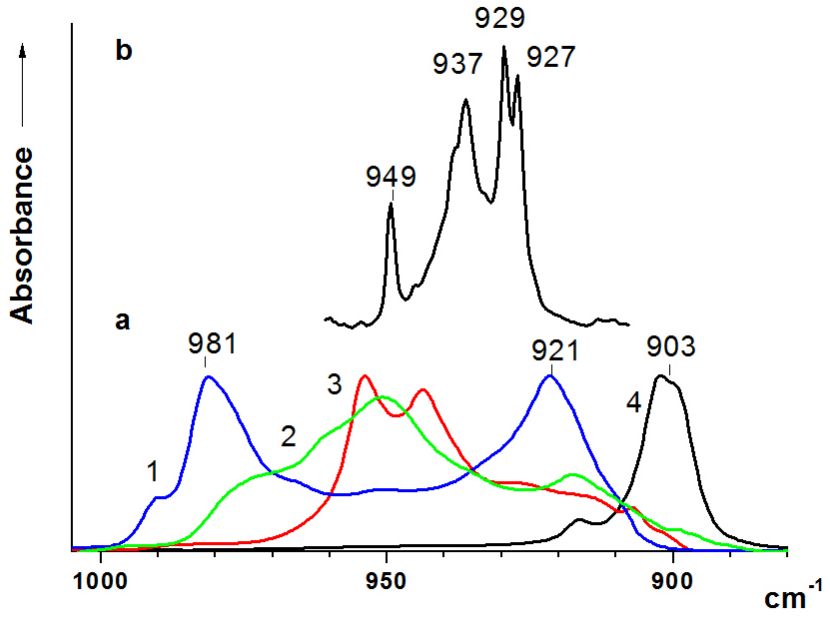

Fig. 1. The region of ν_3 vibration in FTIR spectra of SF_6 adsorbed on: (a) ZnO (1), MgF_2 (2), CaO (3), a solid film on the cell windows (4) and (b) silicalite-1. The spectra were registered with the resolution of 4 cm^{-1} (a) and 1 cm^{-1} (b) at 77K. The presented spectra correspond to maximum surface coverage.

The spectra do not depend seriously on the pretreatment conditions. Two components almost at the same positions were observed for ZnO pretreated at 723 or 773 K, although in the latter case the spectra of adsorbed CO do not reveal the presence of Lewis sites, rather abundant after treatment at lower temperature [5].

Analogous spectra were obtained for ν_3 band of CF_4 adsorbed on ZnO and zeolites. NF_3 molecule has two highly intense IR bands of ν_1 and ν_3 vibrations near 1100 and 900 cm^{-1} [6]. Both the bands of molecules adsorbed on ZnO were found to be distorted by RDD interaction. The observed spectra were consistent with the model, where the molecular axes are perpendicular to the surface.

Thus, this is the RDDI and not the specific adsorption interaction that accounts for the observed bandshape. Moreover, different splitting values for 2D systems and comparison of the observed and calculated spectra enable us to conclude that the intermolecular distances in the adsorbed layers or chains are sensitive to the lattice parameters of the adsorbents, and thus, the adsorbates form rather commensurate layers, than the close packed structures at the surfaces. The bandshape in the IR spectra of adsorbed molecules bears information on the geometry of catalyst surfaces.

References

[1] A. Politano, G. Chiarello, J. Phys. Chem. C 115 (2011) 13541.
[2] A. Zecchina, D. Scarano, S. Bordiga, G. Spoto, C. Lamberti, Advances in catalysis, 46 (2001) 265.
[3] A.A. Tsyganenko, S.M. Zverev, React. Kinet. Catal. Lett., 36 (1988) 269.
[4] V. Buch, L. Delzeit, C. Blackledge, J. P. Devlin, J. Phys. Chem. , 100 (1996) 3732.
[5] A. Dobrotvorskaia, T. Kolomiitsova, S. Petrov, D. Shchepkin, A. Tsyganenko. Spectrochim. Acta Part A. 2015.
[6] T. D. Kolomiitsova, D. N. Shchepkin, K. G. Tokhadze, W. A. Herrebout, B. J. van der Veken, The J. Chem. Phys., 121 (2004) 1504.

II-PP115

Novel Surface Oxide on Pt(111) as the Active Phase for NO and CO Oxidation

Van Spronsen M.A.*, Frenken J.W.M., Groot I.M.N., Mom R.V.

Huygens-Kamerlingh Onnes Laboratory, Leiden University, Leiden, The Netherlands

* spronsen@physics.leidenuniv.nl

Keywords: platinum, surface, oxide, CO oxidation, NO oxidation, operando, STM

1 Introduction

To understand catalytic reactions on surfaces, we need both chemical and structural information on an atomic level of the interface between catalyst and reactants. The surface structure present under reaction conditions is dictated by thermodynamics and the high chemical potential of the gas phase cannot be ignored. Although a high chemical potential can also be achieved by cooling the system to lower temperatures, this will not automatically result in an identical structure. This limitation is most pronounced when atomic mobility is needed to reconstruct the catalytic surface atoms.

Recent developments in instrumentation allow the use of several surface-sensitive techniques at high temperatures and at or near high-pressure conditions. Most of these recently developed tools, such as scanning tunneling microscopy (STM) and surface X-ray diffraction (SXRD), have been used to study CO oxidation over noble metal catalysts [1]. After studying this model catalytic reaction, the focus has shifted towards more complex reactions, such as the oxidation and reduction of NO [2,3], which is of major importance in pollution control.

2 Experimental/methodology

STM is essentially pressure insensitive. We have constructed a complete experimental setup, which integrates a small (0.5 mL) reactor flow cell within an STM. In this microscope, the specimen surface is pressed on an elastomer ring and acts as the top wall of the reactor. The reactor cell with the microscope is housed inside an ultrahigh vacuum system. The vacuum environment allows for traditional surface science preparation and characterization. This reactorSTM enables us to image surfaces and nanoparticle ensembles with high resolution during chemical reactions at high pressures (6 bar) and elevated temperatures (600 K) [4].

3 Results and discussion

Platinum finds its main application as a car catalyst to control the emission of exhaust gases. When the catalyst operates in excess oxygen, platinum catalyzes the oxidation of CO, NO and residual hydrocarbons. Despite platinum's wide use for catalytic oxidation, the active surface phase under oxygen-rich reaction conditions is still highly debated. Traditionally, it was believed that the bare metallic surface was the most reactive. But the recent development of new operando surface science tools has enabled the identification of phase transitions to states of higher activity for CO oxidation. Models, introduced to explain this, range from the formation of a hyperactive oxygen-covered surface to the presence of surfaces oxides or even the growth of a bulk oxide.

For the Pt(111) surface, the facet lowest in energy, it is also not clear what the relevant structure is under oxygen-rich reaction conditions. Both a surface oxide and bulk α-PtO_2 have been found to be stable in different experiments. With the high-pressure, high-temperature reactorSTM, we have studied the oxidation of Pt(111) and have found a stable surface oxide that

assembles in a 'spoke wheel' superstructure at 1 bar O_2 at 430 K as shown in Fig 1A and Fig 1B. Fig 1C shows a proposed structural model of the surface oxide on Pt(111). This surface oxide was also studied during NO oxidation and CO oxidation under reaction conditions.

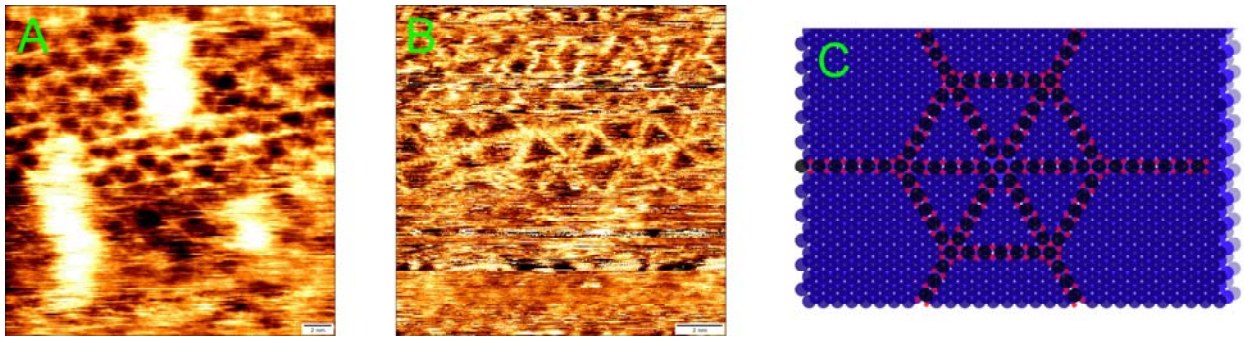

Fig. 1. Two STM images of the surface oxide on Pt(111) under 1.0 bar O_2 and 0.2 bar Ar at 420 K, 24 nm × 24 nm (A) and 15 nm × 15 nm (B). The proposed model, (C), consist of linear change of oxidized Pt rows. O atoms are depicted in red and oxidized Pt atoms in black. The remaining Pt atoms are visualized in blue.

4 Conclusions

We report the formation of surface oxide on Pt(111) that has not been observed previously. This surface oxide forms at high O_2 pressure and at elevated temperature (1.0 bar, 420-520 K). This surface oxide was studied under both NO and CO oxidation and it is believed to be the active phase in these reactions.

Acknowledgements

This work is supported by NanoNextNL, a micro and nanotechnology consortium of the Government of the Netherlands and 130 partners.

References

[1] B.L.M. Hendriksen, *et al.*, *Nature Chemistry* 2 (2010), 730
[2] C.T. Herbschleb, *et al.*, *Catal. Today* 154 (2010) 61
[3] M.A. van Spronsen, *et al.*, *Catal. Today* 244 (2014) 85
[4] C.T. Herbschleb, *et al.*, *Rev. Sci. Instrum.* 85 (2014) 083703

II-PP116

Thermally Stable Multicomponent Manganese Catalyst for Deep Oxidation of Methane

Baizhumanova T.S.*, Tungatarova S.A., Zheksenbaeva Z.T., Kassymkan K., Zhumabek M.

D.V. Sokolsky Institute of Organic Catalyst and Electrochemistry, Almaty, Kazakhstan

* baizhuma@mail.ru

Keywords: methane deep oxidation, manganese catalyst, flameless, combustion

1 Introduction

Gaseous hydrocarbons (methane, ethane, and propane) have special significance among the organic fuels. They are mainly used in the form of household and motor fuel or burned in the composition of waste gas in the "torch". Each year, approximately 403 million m^3 of dilute gases (0.5 - 1.0 % CH_4) of coal mines in Kazakhstan is released into the atmosphere without processing. In this case, a potential source of energy is lost and ozone layer of the Earth is destroyed. In this regard, the problem of their efficient processing and optimal use for various technological purposes (production of heat and electricity, as well as organic synthesis) is relevant.

Catalytic oxidation of CH_4 to CO_2 to produce heat is a promising way of utilization of mine, ventilation and burnt in flares methane. Calculating the cost of heat in Gcal produced during deep methane combustion in a pilot plant showed that at the concentration of CH_4 0.6-0.85% it is 0.5-0.6 USD which is below the cost of coal-fired boiler heat. Catalytic combustion is different from thermal combustion, as occurs on the surface of solid catalysts without flame selectively to CO_2 at significantly lower temperatures which avoids the formation of nitrogen oxides and other harmful substances. Unfortunately, most of the known oxide and mixed catalysts other than hexa-aluminate lose activity in the case of overheating (up to 1473K) at methane combustion in heat generators, gas turbines due to their interaction with carriers. Therefore, the development of catalysts complete combustion of CH_4, aimed at improving the thermal stability of oxide contacts due to modification of carriers through the synthesis of perovskites and hexaaluminates is particularly relevant. Development of active polyoxide Mn catalysts and the study of their thermal stability for deep oxidation of lean mixtures of methane to CO_2 for use in catalytic heat generators is the aim of this work.

2 Experimental/methodology

New approaches to the synthesis of thermally stable multicomponent oxide catalysts were used for the development of catalysts for combustion of methane and propane-butane in heat generators. The rare earth elements (REE - La, Ce) and alkaline earth elements (AEE - Ba, Sr) were entered into the composition of supported polyoxide catalysts based on 3d metals (Ni, Cu, Cr, Mn) for the formation of perovskite-like structures and spinels on the surface. The granulated θ-Al_2O_3 (S = 100 m^2/g) modified with cerium, which forms resistant surface $CeAlO_3$ perovskite up to 1373 K was used as a carrier. The oxide catalysts have been promoted with platinum and palladium (0.05 %) to improve the activity and thermal stability.

Catalysts were prepared by capillary impregnation of alumina by mixed aqueous solution of nitrates by incipient wetness, followed by drying at 453-473 K (4-5 h) and calcination at 873 K (1-1.5 h) in air. Activity of catalysts was determined at oxidation of methane by air in flow installation at 673-973 K. Investigation of deep oxidation of CH_4 (0.5-4 %) on catalysts was

carried out by varying the space velocity from 10×10^3 h^{-1} to 20×10^3 h^{-1} and the O_2 concentration from 2 % to 20 %.

3 Results and discussion

It was carried out oxidation of 0.5 % CH_4 in air at GHSV =10×10^3 h^{-1} on the synthesized catalysts after heating at 873 K and 1473 K. Initial contacts allow to obtain 85-99 % conversion at 973 K after heating of catalysts at 873 K for 1 h. Catalysts heated at 873 K for 1 h can be arranged in series according to the degree of oxidation at 973 K: AP-56 (100 %), NiCuCr + Pd (99 %), NiCuCr + Pt (96 %), MnREEAEE/2 % Ce/θ-Al_2O_3 (92 %), NiCuCr/2 % Ce/θ-Al_2O_3 (91 %), MnREEAEE + Pd (90 %), MnREEAEE + Pt (85 %). Contact based on Ni-Cu-Cr/2 % Ce/θ-Al_2O_3 is the most effective catalyst for oxidation of methane at 973 K. This catalyst is similar to the known industrial Pt contact AP-56 (0.56 % Pt). Synthesized contacts were heated in air at 873 K for 1 h, then sequentially at 1073 K, 1273 K, 1373 K and 1473 K for 5 h at each temperature due to the fact that catalysts may be subjected to significant overheating (1473 K) and lose activity during combustion of CH_4.

Heating at high temperatures affects in different ways on the degree of oxidation of CH_4 on different catalysts. Heating of catalysts at 1473 K resulted in a significant decrease in the surface of catalysts. High temperature heating had no negative effect on the degree of oxidation of CH_4 on MnREEAEE catalysts up to 1373 K. Slight decrease in the degree of conversion of CH_4 (not more than 10 %) was observed only in the case of heating at 1473 K in contrast to Pt/Al_2O_3 (AP-56) catalyst the efficiency of which dramatically decreased after 1373 K. As a result, α_{CH4} reached 60 % at 973 K and only 10 % - at 773 K. The activity of MnREEAEE catalyst decreased slightly for the initial and heated samples at 973 K (not more than 2-7 %). A sharp decrease in the degree of conversion of methane occurred after heating starting from 1373 K and especially at 1473 K for Ni-Cu-Cr catalyst. It reached 63 % at 973 K and decreased to "zero" at 773 K. Specific oxidation rate of methane remains constant for MnREEAEE catalyst even as result of heating at 1373-1473 K in contrast to Ni-Cu-Cr catalyst.

It has been shown that MnREEAEE/2 % Ce/θ-Al_2O_3 catalyst is the most thermally stable up to 1473 K in comparative studies of oxide catalysts for the combustion of methane to CO_2. It provided 88-92 % methane oxidation at 973 K and a GHSV of 10×10^3 h^{-1}. The results indicate the greater thermal stability (up to 1473 K) of the Mn-containing contacts with the addition of Ce, La, Ba, and Sr at combustion of methane. It was found that part of oxides form perovskite according to research carried out by ESDR, TPD.

4 Conclusions

It was established that MnREEAEE catalyst supported on 2 % Ce/θ-Al_2O_3 has a higher thermal stability (up to 1473 K) and specific activity in the reaction of deep oxidation of methane, compared to known catalysts (IC-40 and Ni-Cu-Cr/2 % Ce/θ-Al_2O_3) which are used for purification of gases from organic substances and combustion of CH_4. The results indicate the real possibility of practical use of thermally stable up to 1473 K MnREEAEE/2 % Ce/θ-Al_2O_3 catalyst for utilization of lean mixtures of CH_4 in catalytic heat generators. The developed catalyst does not concede to known analogues both in activity and thermal stability, where perovskites and manganese hexaaluminates were used.

Acknowledgements

This work (project No 0245/GF-4) was supported by the Ministry of Education and Science of Kazakhstan.

II-PP117

Thermostable Cu-Containing Catalyst with Grafted Active Component for the Dehydrogenation of Cyclohexanol to Cyclohexanone

Vanchourin V.I.[1*], Dzhumamukhamedov D.Sh.[1], Pavlov U.L.[1], Marachuk L.I.[2], Dulnev A.V.[3]

1 - D.Mendeleev University of Chemical Technology of Russia, Moscow, Russia
2 - JSC "Grodno Azot",Grodno, Republic of Belarus
3 - LLC "NIAP-KATALIZATOR", Novomoskovsk, Russia

* vanchourin@mail.ru

Keywords: grafted catalyst, thermostability, cyclohexanol dehydrogenation

1 Introduction

The dehydrogenation of cyclohexanol to cyclohexanone is a necessary stage for obtaining the monomer in the caprolactam production. The process is carried out at low temperature Cu-containing catalysts.

Better selectivity of H3–11 catalyst made by foreign company BASF [1] reaches 99.5% at the experiment temperature of 240 – 250 °C, but its activity does not exceed 50% and is very sensitive to the possible overheating. On exposure to elevated temperatures the copper particles easily migrates along the support surface, sintered to agglomerates, which leads to a reduction of the active surface. The best of native K-CO catalysts [2] are more active, but less selective (97 - 98%) than the H3-11catalyst.

In the Mendeleev University together with LLC "NIAP-Katalizator" there is developed the technology of catalyst dehydrogenation of MAK-K cyclohexanol with grafted nano-structured active component on the surface of silica support.

The technology was tested at the factory. The pilot batch of MAK-K catalyst was prepared.

2 The methods of experiment

The samples of MAK-K catalyst prepared by depositing the active component (AC) from an aqueous solution of ammonium carbonate complex of copper on the carrier under the conditions of intense heat and mass transfer. As the catalyst carrier was used the white carbon powder and active aluminium hydroxide in the form of boehmite, in a weight ratio of 3:1. The finished catalyst contains 20-22 wt. % of CuO and represents the light turquois cylindrical granules with the diameter of 4.5-5.5 mm and a length of 5-12 mm. Measurement of the activity and selectivity of catalyst samples were carried out in a multi-flow type setting at 220 - 250 °C, atmospheric pressure and volumetric feed rate of 1.0 h^{-1}, mounted at JSC "Grodno Azot". Thermostability of catalyst was estimated by the reduction degree of activity after overheating under reaction mixture at volumetric flow rate of 0.5 h^{-1} and a temperature of 350 °C during 16 hours. The total duration of catalyst test sample was 64 hours. Analysis of the reaction mixture was performed by chromatography.

The specific surface area (S_{BET}) was measured by chromatographic method via thermal desorption of nitrogen. The average size of nanostructured crystallite AC ($d_{cr,}$) calculated according to the X-ray phase analysis [3] and by the formula [4]. The mechanical strength (σ) of the samples was estimated by the value of destructive effort on the corn of catalyst.

3 Results and discussion

Selectivity, activity, textural properties and the mechanical strength of MAK–K and H3–11 catalyst samples are shown in the table 1.

Table 1. Characteristics of MAK–K and H3–11 catalysts

Catalyst	Selectivity, %	Activity, %	σ, kg/corn	S_{BET}, m^2/g	d_{cr}, nm
H3–11	99,5 (100 *)	50,0 (29,8*)	75 (10*)	125 (80*)	13 (28*)
MAK–K	99,1 (100 *)	56,6 (48,1*)	30 (36*)	220 (215*)	3,5 (4*)

* values of the catalysts after overheating

It can be seen that both catalysts have approximately equal initial selectivity, high value of which maintained after their thermostability experiment. H3-11 catalyst activity reduces from 50.6% to 29.8% (a change of 41 rel.%) after overheating at 350 °C. Under the same experiment conditions the MAK–K catalyst activity reduces by 15 rel.% from 56.6% to 48.1%. According to the petrography and electron microscopy analyses the particle morphology of AC in the MAK-K remain unchanged in the form of nanoscale clusters associated or included in the structure of the silica. On the contrary, in the H3−11 catalyst the irreversible changes happen associated with reduction of S_{BET} and aggregation of the AC nanoparticles. Their high mobility and lightweight surface migration are due to the weak interaction of the copper component with crystalline silica carrier. According to IR-spectrometry at synthesis MAK catalyst changes the surface properties of the silica component of the carrier due to the enrichment of its hydroxyl group associated with aluminum. As a result, there is a chemical interaction and binding of AC with carrier to form the grafted phase in the stable nanostructured state. The initial strength of the H3−11 catalyst is larger than the strength of MAK−K catalyst, but after overheating and the resulting effects of polymorphic transformation of the carrier is sharply reduces. Mechanical strenght of MAK-K, on the contrary, increase by 15-20% due to the formation of layers of crystallized phase consisting AC (intergrain hardening effect) around the periphery of the grains of the amorphous carrier.

4 Conclusions

The technology of Cu-containing MAK−K catalyst based on the combined aluminum-silica carrier was developed, that provides a uniform distribution of the active component in a stable nano-structured state.

A selectivity of MAK−K corresponds a selectivity of better industrial H3−11catalyst, and its activity and thermostability significantly higher.

References

[1] D. Heinecke. R. Meissner, M. Hesse, H. Gerken, The method of obtaining oxide catalysts containing copper with oxidation state more than zero, RF Patent 2,218,987, 2003.

[2] I.L. Kozlov, F.V. Kalinchenko, A.J. Kalinevich, L.G. Daniel, The method of obtaining catalyst for carbon monoxide conversion by steam, RF Patent 2157279, 1999.

[3] A. Guinier X-ray crystal. Theory and practice. Translated from French by E. Belova, SS Kvitki, VP Tarasova edited by Academician NV Belov. M .: Nauka. (1961) 604.

[4] K.G. Jonah, A.P. Karnaukhov, E.E. Quo, *Kinetics and Catalysis*. 12 (1971) 457.

II-PP118

Hydrogenation of Benzene in the Presence of Nickel Nanocatalysts Immobilized on Chitosan

Taghiyev D., Zeynalov N.*

Institute of Catalysis and Inorganic Chemistry named after academician M.Nagiyev of NAS of Azerbaijan, Baku, Azerbaijan

* zeynalovnizami3@gmail.com

Keywords: nickel nanoparticles immobilization, chitosan, hydrogenation of benzene, carrier, cyclohexane

1 Introduction

Hydrogenation of aromatic compounds is one of the most important processes both in modern petrochemical industry and thin organic synthesis. In this regard, an essential object is to develop highly-active and selective hydrogenation catalysts providing appropriate results even under low loads and permitting us to regenerate and recycle them. The systems based on nanoparticles of metals are perspective in this respect.

Materials containing metal particles of nanometer size show unique physical-chemical properties and in recent years they have been the object of intensive researches. The use of them as catalysts is of particular interest, because in such systems the share of surface atoms in relation to total number of atoms in a particle is very great and by varying the sizes of nanoparticles we can manage their catalytic properties. Zerovalent complexes and nanoparticles of nickel are more commonly known as effective and selective catalysts of many organic reactions. The basic problem is aggregative instability of metal nanoparticles and their tendency to coarsening. Thus, nanoparticles are fixed on carriers (oxides of metals, zeolites, carbon and et.) or stabilized by adding ligands, including polymers of various types. In the majority of cases it is necessary to find a balance between interaction of nanoparticles with carrier and stabilization of their sizes.

2 Results and discussion

The purpose of our researches is to use chitosan matrix for the synthesis of nickel nanoparticles and evaluation of its catalytic properties in hydrogenation of benzene. To produce nanocomposites of chitosan-metal we used a chemical method which consists of the reduction of metals to the zero state from solutions of their salts with polymer matrix. Because of its specific and high sorption properties; possibilities of developing active surface in the reaction, chitosan is a convenient matrix for chemical reduction of metals in it. It is possible to perform reduction processes with high rate, to produce a considerable amount of reduced metals, to regulate the arrangement (on chitosan or in its volume) and sizes of formed metal particles. N,N´-methylene-bis-acrylamide was used as a cross-linking agent. The stage of depositing metal was performed in the water due to a good solubility of nickel salts in it and ability to swelling of polymers containing amine groups. It was established that because of regular structure of a carrier we can obtain immobilized nanoparticles with narrow size distribution.

We determined the reduction conditions of ion Ni (II) from the solutions of its salts to Ni(0) by using sodium borohydride and hydrazine as a reduction agent in non-soluble chitosan matrix. It was shown that when reducing $NaBH_4$, nickel particles with 12-15 nm radius were formed, but when using hydrazine it is found to be 26 nm. Sizes of particles were determined by X-ray phase analysis.

One of the main requirements to efficiency of catalysts is a high swelling capacity in

reaction media which contributes to the distribution of active centers throughout all the volume. The catalyst obtained by us swells well in reaction medium, during hydrogenation not only its surface but also all its volume operates.

Synthesized nickel nanoparticles were filtered and washed out with water (from unreacted salts of metal and non-complexing polymers) and dried under vacuum at room temperature. Before using the catalyst was activated by gaseous hydrogen. Regeneration of the catalyst must be always carried out in conditions higher than the reaction temperature. Reaction products were analyzed by gas-liquid chromatography method.

Hydrogenation of benzene with chitosan-nickel nanocatalyst was performed at room temperature and atmospheric pressure. The obtained polymer-immobilized nickel nanoparticles show high activity in hydrogenation reaction of benzene and maintain it in repeated cycles. Catalytic properties of nanocomposites depend on producing conditions which impact on the size of the formed nickel nanoparticles.

Cross-linking agent largely determines the sizes of cavities and pores of the material, and therefore, the size of particles and possible diffusion limitations, occurring during the reaction.

We have studied the influence of cross-linking degree on the size and character of distribution of nickel nanoparticles, as well as activity and selectivity of synthesized materials in hydrogenation of benzene in detail.

It is shown that the catalysts based on matrix with high cross-linking degree also showed high activity in hydrogenation of benzene. The selectivity by end product (cyclohexane) turned to be a few per cent more than for analogues with low cross-linking degree.

The influence of the reaction time on selectivity in hydrogenation of benzene with catalyst chitosan-nickel was investigated. It is shown that at an early stage of hydrogenation reaction of benzene (1-1.5 h.) the mixture containing cyclohexadiene, cyclohexene, cyclohexane and benzene was obtained. Then the first two products are partially converted to cyclohexane with overall conversion of benzene to 35-40%. It was found out that up to 50.2% of cyclohexane is produced in the presence of chitosan-nickel nanocatalyst during hydrogenation of benzene for 5 h.

3 Conclusion

The use of nanostructured systems based on cross-linked chitosan carrier permits us to synthesize catalysts of hydrogenation of benzene based on nickel nanoparticles. Variation of cross-linking degree of a carrier permits us to regulate the size of nanoparticles, their activity in hydrogenation of benzene and to influence on substrate selectivity of the process. The studied nanocomposites keep catalytic activity when carrying out repeated cycles of the reactions on them and the fact that they are in immobilized form enables to detect them easily from reaction medium and reuse.

II-PP119

Key Magnetic Intermediates in Rhenium-Based Olefins Metathesis Catalytic Systems

Abbasov Y.[1], Ismailov E.[1*], Tagiyev D.[2]

1 - Institute of petrochemical Processes, Physical and Physical-Chemical Investigations department, Baku, Azerbaijan

2 - Institute of Catalysis and Inorganic Chemistry, Department of Heterogeneous Catalysis, Baku, Azerbaijan

* etibar.ismailov@gmail.com

Keywords: magnetic intermediates, rhenium complexes, metathesis of olefins

1 Introduction

In the last 20 years metathesis has become one of the most powerful method for construction of chemical carbon-carbon bond and is used in chemistry of organic, mono- and polymer materials [1-3]. Three types of metathesis - cross metathesis in which two different alkenes undergo an intermolecular transformation to produce a new olefinic product; ring opening metathesis polymerization, a procedure that involves the opening of cyclic alkenes to give polymeric compounds. ring closing metathesis, which enables the formation of cyclic compounds [4,5]. Although the molecular structures of the active sites in different systems are characterized for a lot olefin metathesis catalytic systems, there is no information about the nature of these sites during catalyst activation and olefin metathesis. The absence of direct characterization during catalyst activation and olefin metathesis prevents accessing fundamental information about the reaction intermediates and reaction mechanism. The absence of direct observation measurements of the catalytic active sites and reaction intermediates during olefin metathesis is one of the primary reasons for the lack of scientific progress in this important field of catalysis.

In this report the results of studies of magnetic intermediates and reactions with their participation in rhenium-based catalytic systems of olefin metathesis are given. Three of the most active metals used in classical olefin metathesis are molybdenum, tungsten and rhenium. However, none of the known compounds of these metals showed activity in the metathesis reaction in the absence of a co-catalyst or activator.

2 Experimental/methodology

It is shown that electron paramagnetic resonance (EPR) technique allow to identify complexes of rhenium with nonzero spin and get sufficient information about the nature of rhenium intermediates and reactions with their participation in catalytic systems of the above processes. Rhenium complexes with nonzero electron spin are identified in olefin metathesis catalyst systems based on complexes of mono-, bi-, hexa -nuclear compounds of different valence of rhenium: $Re(CO)_5X$**;**$Re_2X_4(CH3COO)_4 \cdot 2H_2O$, $[DMFAH]_2Re_6X_{14}$, where (X=Cl, Br).

Figure 1 shows a characteristic paramagnetic rhenium complexes registered in the systems for olefins metathesis based on rhenium complexes and aluminiumorganic compounds.

EPR signals with magnetic resonance parameters (MRP): g_o =2.070, A_o (^{185,187}Re) =321 G at 300K and $g_{\parallel}$=2.135, $g_{\perp}$=2.067, $<g_o>$ =2.098, $A_{\parallel}$ (^{185,187}Re) =469 G, $A_{\perp}$ (^{185,187}Re) =271 G, $<A$ (^{185,187}Re)$>$ =337 G at 77K are registered for the products of the reaction of $Re(CO)_5Br$ with $(C_2H_5)_3Al$ in n- heptane solution. These values of MRP belong to low spin complexes of rhenium with total spin S=1/2 and square-pyramidal structure of a local environment. Results of this work show that in all cases the interaction of rhenium complexes with aluminiumorganic

compounds in solution leads to stable at room temperature paramagnetic complexes with total spin S=1/2 and highly covalent Re-C bond. The formation of paramagnetic rhenium complexes with $Re=CH_2$ bond and total electron spin S = 1/2 is established. The presented spectra are the first direct observation of paramagnetic rhenium intermediates in the catalytic systems for olefin metathesis.

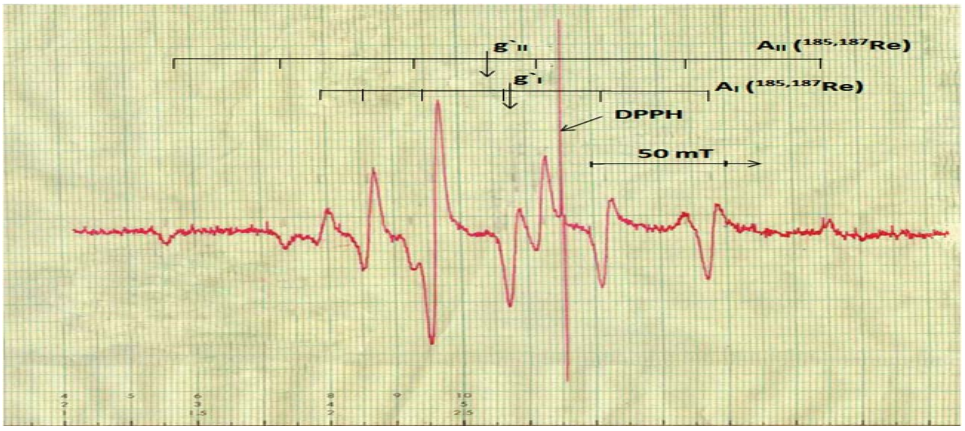

Fig. 1. EPR spectrum at 77K of the $Re(CO)_5Br+Et_2AlCl$ in n-heptane solution after 10 min interaction at room temperature.

3 Conclusions

It is shown that the used electron paramagnetic resonance (EPR) technique allows to identify complexes of rhenium with nonzero spin, to establish the structure of rhenium intermediates and study the reactions with their participation in catalytic systems for olefins metathesis. Rhenium complexes with nonzero electron spin are identified in olefin metathesis catalyst systems based on complexes of mono-, bi-, hexa -nuclear compounds of different valence of rhenium. The formation of paramagnetic rhenium complexes with an electron spin S = 1/2 and paramagnetic complexes with $Re=CH_2$ bond is established. We can also note that in this report the first direct observation of paramagnetic rhenium intermediates in olefin metathesis systems is given. The reactions of intermediates with C_2-C_4 olefins are studied and catalytic cycle involving these intermediates in the metathesis of olefins in these catalyst systems are discussed. The results have methodological value also: the detected signals in the EPR spectra of paramagnetic complexes of rhenium in the Ziegler type catalyst systems consisting of mono-, (bi-, hexa-) nuclear rhenium complexes of different valence and aluminum organic compounds was used to identify paramagnetic rhenium complexes in other systems. Used approaches apparently also render a possibility to understand the nature of rhenium based catalysts activity in olefin metathesis and open for broad and successful future use of rhenium catalysts for this purpose.

Acknowledgements

We are grateful to the Fund of Science Development administrated by the Council of Azerbaijan President for the support.

References

[1] R. Schrock, Acc. Chem. Res.23 (1990) 158.
[2] R. Schrock, A. Hoveyda, Angew. Chem. Int. Ed. 42 (38) (2003) 4592.
[3] R. Grubbs, "Olefin metathesis". Tetrahedron 60 (34), (2004), 7117.
[4] C. Samojłowicz, K.Grela, Chem. Rev. 109 (8) (2009). 3708.
[5] K.Grela, (Ed"Progress in metathesis chemistry)". Beilstein J. Org. Chem. **6**. (2010). 1089.

II-PP120

Dibenzothiophene Hydrogenolysis on Zinc Modified Ni-MoW/Al_2O_3 Hydrotreating Catalysts

Tomina N.N.[1*], Antonov S.A.[2], Maximov N.M.[1], Pimerzin A.A.[1]

1 - Samara State Technical University, Samara, Russian Federation
2 - United Research and Development Centre, Moscow, Russian Federation

* tominann@yandex.ru

Keywords: dibenzothiophene hydrogenolysis, hydrotreating catalyst

1 Introduction

Ni-MoW/Al_2O_3 catalysts, applied for oil fractions hydrotreating, have high hydrogenation, but haven't enough hydrodesulfurization (HDS) activities. Introduction a low concentration of ZnO into hydrotreating catalysts lead to increase in HDS activity [**1, 2**]. This method of modification by transition metal additives is very perspective, like it should be concluded from rare scientific works [**3**]. The growth of HDS up to 20 wt. % of ZnO in work [**3**] in opposite to [**1**] was shown. So, the optimal amount of ZnO, increased HDS, wasn't found. The effect of modification wasn't explained.

2 Experimental/methodology

γ-Al_2O_3 carrier was synthesized from AlOOH (TH-60, «Sasol»). Pore structure was determined by adsorption of nitrogen at 77K (S_{BET} = 205 m^2/g, V =0,682 cm^3/g, $R_{eff.}$ = 48 Å). A line of Ni-MoW/Al_2O_3 catalysts was synthesized by means of wetness impregnation method from aqua solution of Ni, Mo and W compounds ($Ni(NO_3)_2 \cdot 6H_2O$, $H_3PMo_{12}O_{40} \cdot 17H_2O$, $H_3PW_{12}O_{40} \cdot 29H_2O$). Introduction of ZnO was carried out with different methods (**Table 1**). Catalysts were sulphided before catalytic tests. The HR TEM images of active phase were recorded for samples 1-4 after sulphidation. Catalytic activity was determined in a bench-scale flow reactor unit in the hydrogenolysis of dibenzothiophene under the next conditions: hydrogen pressure of 3.00 ± 0.04 MPa, model mixture volume feed of 10.0 ± 0.2 cm^3/h, hydrogen feed of 40 cm^3/min, temperature of 250 ± 1 ^0C. 0.300 ± 0.005 g catalyst with particle size 0.50-0.25 mm was loaded in reactor. Model mixture contained dibenzthiophene (DBT) and isooctane. Every catalytic test was carried out twice. Relative deviation of parallel tests was ± 0,8 %. Hydrogenated products were analyzed by means of gas-liquid chromatography. Identification of products was carried out by combined gas chromatography mass-spectrometry method.

3 Results and discussion

Three lines of Ni-MoW/Al_2O_3 catalysts were synthesized. Samples № 2-4 and № 5-7 had a different order of component introduction. Carriers of samples № 2-4 were prepared by means of Al_2O_3 impregnation with aqua solution of $(CH_3COO)_2Zn \cdot 2H_2O$, than dried (120°C) and calcined at 500°C for 1 hour. Modified ZnO-Al_2O_3 carrier was impregnated with aqua solution of Ni, Mo and W compounds and than dried. Al_2O_3 carriers of catalysts № 5-7 were impregnated with aqua solution of Ni, Mo and W compounds, dried, impregnated with aqua solution of $(CH_3COO)_2Zn \cdot 2H_2O$ and dried again. Catalysts № 8-10 were impregnated with aqua solution of Ni, Mo, W and Zn compounds and dried. Comparison sample was Ni-MoW/Al_2O_3 catalyst without ZnO (№1).

Catalysts have approximately the same loads of NiO, MoO_3, WO_3 and different amounts of ZnO (**Table 1**). Results of catalytic test are presented in **Fig. 1**.

ZnO modification of Al_2O_3 surface changes the morphology of NiMoW(S)/Al_2O_3 catalysts sulfide phases. The increase of sulfide phase slab length from 4,1 to 4,6 and 4,3 nm and number

of layers from 1,5 to 1,9 and 1,7 was found for NiMoW/ZnO-Al_2O_3 catalysts, modified with 0,5 and 1 % ZnO, respectively.

Table 1. Properties of synthesized catalysts

№	Catalyst	Content, wt. %				Synthesis method
		NiO	MoO_3	WO_3	ZnO	
1	NiMoW/Al_2O_3	5,9	13,7	6,0	-	1. Impregnation of γ-Al_2O_3 by solution of Ni, Mo and W compounds.
2	NiMoW/ZnO-Al_2O_3	5,1	14,1	6,0	0,5	1. Impregnation of γ-Al_2O_3 by solution of $(CH_3COO)_2Zn$, drying and calcination. 2. Impregnation of Al_2O_3-ZnO by solution of Ni, Mo and W compounds.
3		5,0	13,4	6,0	1,0	
4		5,4	13,3	6,0	3,0	
5	Zn/NiMoW/Al_2O_3	5,1	13,6	6,0	0,5	1. Impregnation of γ-Al_2O_3 by solution of Ni, Mo and W compounds, drying. 2. Impregnation of NiMoW/Al_2O_3 by solution of $(CH_3COO)_2Zn$, drying.
6		5,8	13,9	6,0	1,0	
7		5,7	13,8	6,0	3,0	
8	NiMoWZn/Al_2O_3	5,7	13,7	6,0	0,4	1. Impregnation of γ-Al_2O_3 by solution of Ni, Mo, W, Zn compounds, drying.
9		5,3	14,2	6,0	0,8	
10		5,8	14,6	6,0	2,4	

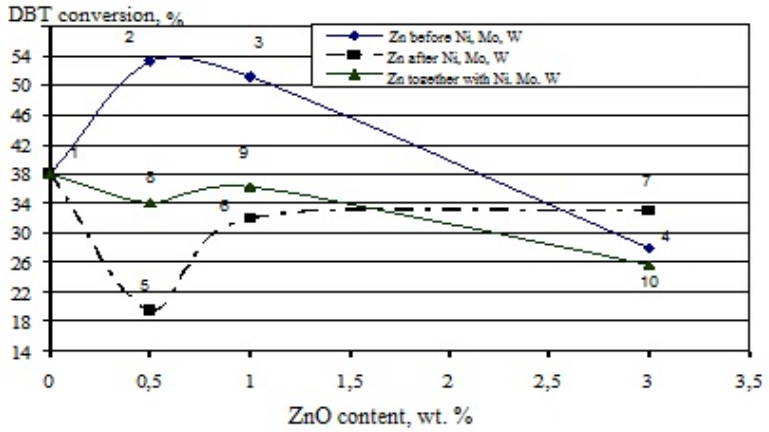

Fig. 1 Relationships between DBT conversions, amounts of ZnO and introduction method (numbers on the curves correspond to samples numbers in Table 1)

The number of multilayer slabs has a linear correlation with DBT HDS activity. Too high dispersion of sulfide phase particles isn't good for DBT HDS activity.

4 Conclusions

Modification of Al_2O_3 with ZnO in amounts of 0.5-1.0 wt. %, followed by introduction of active phase precursors, increases DBT HDS activity from 38 to 54%. Impregnation of dried NiMoW/Al_2O_3 catalysts with solution of $Zn(CH_3COO)_2$ decreases the activity (the minimum of activity in this case was found for NiMoW/Al_2O_3 modified with 0.5 wt.% of ZnO). Parallel introduction of Zn, Ni, Mo and W decreases the catalysts activities in all cases.

Acknowledgements

The work was supported by Russian Federal target program «Investigations and developments of priority directions of scientific-technological complex progress of Russia for 2014-2020 years» (project № 14.577.21.0140).

References

[1] Linares C.F., Fernandez M. *Catal. Lett*. 126 (2008) 341.
[2] Strohmeier B.R., Hercules D.M. *J. Catal*. 86 (1984) 266.
[3] Jacono M.L., Schiavello M. *Science and Catalysis*. 1 (1976) 473.

II-PP121

Hydrotreating of Vacuum Gas Oil on NiMo/P-γ-Al_2O_3 Catalysts

Maximov N.M.*, Tomina N.N., Solmanov P.S., Pimerzin A.A.

Samara State Technical University, Samara, Russian Federation

* maximovnm@mail.ru

Keywords: hydrotreating, vacuum gas oil, phosphorus

1 Introduction

Analysis of works in period of 2009-2014 years showed, that the most frequently method of hydrotreating catalysts modification was introduction of phosphorus on carrier surface. These catalysts have mild acidity (good resistance to deactivation by coking) and high hydrogenation activity in hydrogenation reactions for aromatic hydrocarbons and heterorganic compounds. So, investigations in the field of hydrotreating catalysts, modified by phosphorus, are actual ones.

2 Experimental/methodology

Modification of hydrotreating catalysts carrier was carried out with phosphoric acid water solution by wetness impregnation method (P_2O_5 content 0,5, 1, 2 and 5 wt. %), followed by draying and calcination. Modified carrier was impregnated with water solution of active phase precursors (Mo, Ni(Co)) on the second stage of synthesis.

NH_3 TPD analysis of synthesized catalysts was carried out with TPDRO 1100 analyzer. NH_3 adsorption was performed in flow of NH_3/N_2 (1:1 vol.) for 30 minutes. Temperature range of desorption was 25-1000°C. The catalytic activity of the samples was determined in a bench-scale flow reactor unit in the hydrotreating process of vacuum gas oil.

3 Results and discussion

Catalyst, contained 2 wt. % P_2O_5, showed the maximum of activity in hydrodesulphurization (HDS) reactions (1,0 order kinetic model) and sample with 5 wt. % P_2O_5 demonstrated the highest hydrogenation degree (HYD) in reactions of polycyclic aromatic hydrocarbons (PAH) and olefins (**Fig. 1-3**). The situations of minimum were different for HDS and HYD curves.

P_2O_5 introduction at 0.5 wt. % reduces a number of acidic centers, desorbed NH_3 in temperature range of 550-820 °C (**Fig. 4**). P_2O_5 introduction at 5.0 wt. % increases total acidity in the range of 550-820 °C (**Fig. 4**).

Authors **[1]** showed that the usage of carbon carriers for hydrotreating catalysts synthesis had significant limitations. A large number of strong Lewis centers on synthesized catalysts, adsorbed polycyclic aromatic hydrocarbons more intensive than sulfur-organic compounds. It's well known that the adsorption of sulfur-, nitrogen-organic and polycyclic aromatic compounds are competitive reactions, so the catalyst had a low HDS activity.

HDS reactions, when carrier has a low number of strong adsorption centers, passes in a low degree, but inhibits in less degree by nitrogen-organic and polycyclic aromatic compounds. This is the source of the first minimum of activity in HDS (**Fig. 1**). The introduction of larger amount of P_2O_5 result in increase of strong adsorption centers number, which get an optimum for HDS activity at 2.0 wt. % of P_2O_5.

Further increasing of P_2O_5 amount causes a lot of strongest centers, which fast and irreversible adsorb polycyclic aromatic hydrocarbons. In this way, HDS reactions are effectively inhibited on catalysts with amount of P_2O_5 more than 2 wt. % (the second minimum of activity in HDS (**Fig. 1**).

The curves of hydrogenation of polycyclic aromatic hydrocarbons and olefins have one

minimum, which corresponds to minimum of catalysts acidity (**Fig. 2-4**).

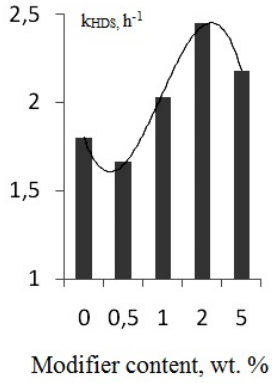

Fig. 1. Relationship between k_{HDS} and P_2O_5 content for NiMo/P-γ-Al_2O_3 catalysts

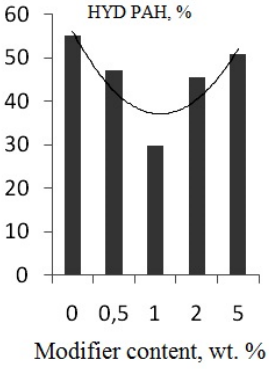

Fig. 2. Relationship between HYD PAH and P_2O_5 content for NiMo/P-γ-Al_2O_3 catalysts

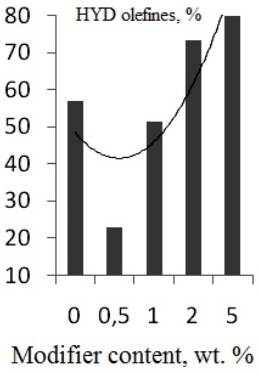

Fig. 3. Relationship between HYD olefines and P_2O_5 content for NiMo/P-γ-Al_2O_3 catalysts

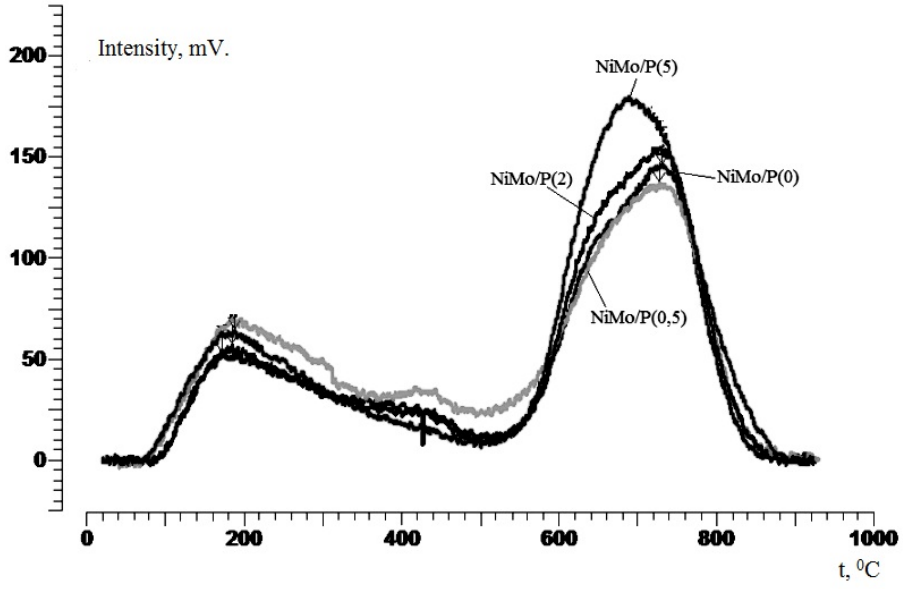

Fig. 4. NH_3 TPD curves for NiMo/P catalysts

4 Conclusions

The optimum amount of P_2O_5 for modification of vacuum gas oil hydrotreating catalyst was found. The relationships between HDS, HYD PAH, HYD olefins and P_2O_5 content for NiMo/P-γ-Al_2O_3 catalysts were determinated. The maximum of HDS activity was found for catalyst, contained 2.0 wt. % of P_2O_5.

Acknowledgements

The work was supported by Russian Federal target program «Investigations and developments of priority directions of scientific-technological complex progress of Russia for 2014-2020 years» (project № 14.577.21.0140).

References

[1] Dugulan A.I., van Veen J.A.R., Hensen E.J.M. *Applied Catalysis B: Environmental*.142 (2013) 178.

II-PP122

Progress in the SAXS Study of Supported Metal Catalysts and Porous Composite Materials

Larichev Yu.V.[1,2*]

1 - Boreskov Institute of Catalysis, Siberian Branch of Russian Academy of Sciences, Novosibirsk, Russia

2 - Novosibirsk State University, Novosibirsk, Russia

* ylarichev@gmail.com

Keywords: SAXS, masking liquids, supported catalysts, functional materials

1 Introduction

Determination of particle sizes is an important and complicated problem in heterogeneous catalysis. At present, TEM, XRD and CO chemisorption are conventionally used for solving this problem. The Small Angle X-ray Scattering (SAXS) potentially has great advantages compared to these traditional methods. First of all, unlike transmission electron microscopy, SAXS yields information about particle sizes from a macroscopic amount of sample. Second, unlike XRD, SAXS allows for obtaining a particle size distribution instead of an average value of particle sizes. Also SAXS can be applied for study of amorphous and soft samples. However, SAXS is rarely used for determination of particle sizes in heterogeneous catalysts. The reason of low interest is the problem of distinguishing a weak scattering signal originating from supported metal particles from the huge background scattering signal of a porous support. One of the ways for effective separation these signals is a using of liquids with high density for masking support scattering (Fig. 1) [1].

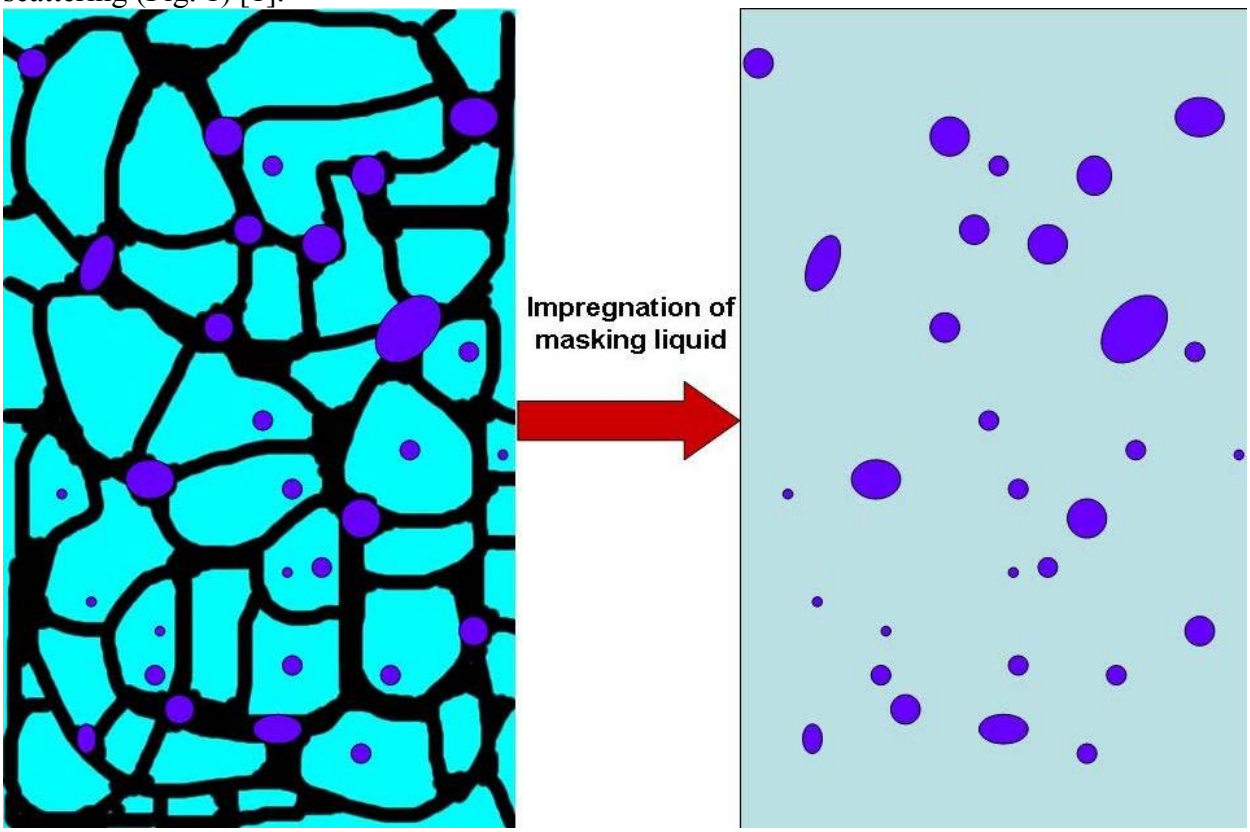

Fig. 1. Principal scheme of parasitic scattering background removal from support pores and particles.

The main barrier for application this concept is extremely high absorbance of X-ray radiation for typical high dense liquids (such as $CHBr_3$ or CH_2I_2). Despite on the opposite requirement to the masking liquids we design high-density liquid mixtures with relatively low X-ray absorbance. The main compounds of these mixtures are fluorocarbons which has good compromise properties between high density and low absorbance. Using this technique it is possible to mask parasitic scattering signal from any phases with density less 2.8 g/cm^3.

2 Experimental

The S3 MICRO (HECUS) small angle diffractometer (Cu Kα, 50W) with a point collimation of primary beam was used for measuring scattering patterns of all samples. The scattering vector magnitude $h = 4\pi*\sin(\theta)/\lambda$ (where 2θ is the scattering angle, and $\lambda = 1.541$ Å is the radiation wavelength) was used as the scattering coordinate. The scattering intensity was measured in the range of the scattering vector magnitudes $0.01 < h < 0.6$ Å^{-1}. A powder sample was placed in a quartz or glass capillary with 1.5 mm diameter. Then, a masking liquid was added using a special syringe with a thin needle. In all cases, the quantity of the masking liquid exceeded the pore volume in the sample. Calculation of the particle size distributions from scattering data were based on the GNOM program from the ATSAS package [2].

3 Results and discussion

In presentation will be discussed prospects and restrictions of new technique, examples of their application to study some catalysts and porous composites. Application of masking liquids for SAXS study of supported catalysts has been revealed advantage of this method versus TEM and XRD. Using this method we can get particle sizes distribution in the wide size range and analyze bulk inactive metal particles more effectively comparing to TEM and XRD. Also in presentation will be shown results of study amorphous carbon-mineral composites. These composites have been prepared from renewable resources (such as rice husk and sapropels). It has been found that shape of silica-contained template particles their behavior depends on the nature of initial precursor. In the case of composites prepared from rice husk has been found that inorganic template have a small particles with smooth shapes near to spheres. Increasing of the temperature treatment are increasing sizes of template particles. In the case of composites prepared from sapropels mineral template have large particles with fractal shape which partially destroyed after heat treatment.

SAXS with using this technique became a highly effective method for study different types of supported catalysts or porous composites. The main limitation in current version is a medium level of material density which could be effectively masking. Nevertheless even current density range which we plan to expand contains a lot of type's different materials and catalysts.

Acknowledgements

The author is grateful to P.M. Yeletsky, O.I. Krivonos for samples preparation and K.V. Obida for assistance in the investigations of the samples. The reported study was supported by RFBR, research project No. 14-03-31851 mol_a and by MES (Russia).

References

[1] Yu.V. Larichev et al, *J. Appl. Cryst.*, 46(3) (2013) 752.
[2] P.V. Konarev et al, *J. Appl. Cryst*., 39 (2006) 277.

II-PP123

Silica Poisoning Effect on HDT Catalysts Processing Light Coker Naphtha

Pérez-Romo P.*, Aguilar-Barrera C., Navarrete-Bolaños J., Fripiat J.

Instituto Mexicano del Petróleo, México, México

* pperezr@imp.mx

Keywords: silica poisoning, HDT alumina catalyst, silicon compounds, deactivation

1 Introduction

Delayed coking process is a thermal cracking process that upgrades crude oil vacuum distillation bottoms into gas and liquid products such as gas oil and naphthas, leaving behind a solid concentrated carbon material known as petroleum coke. Delayed coking units use silicon polymers (antifoaming) that are added to the coker drums in order to suppress foaming that is generated by the light gases that are produced. As a consequence of the high temperatures that prevail in DC operation, silicon polymers decompose to form lighter silicon compounds that distill mainly with the naphtha product. Deactivation of industrial HDT catalysts by silicon deposition was studied by Kellbergs et al [1] and found that catalysts have relative short lifetimes because of the accumulation of silicon species on the surface and concluded that the silicone oil in the naphtha feed is transformed into silica gel species.

The aim of the present contribution is to further both the knowledge of the silicon deposition mechanism under different concentrations and the interaction of silicon with the alumina support of a commercial HDT catalyst.

2 Experimental/methodology

Samples of fresh and industrially spent $NiMo/Al_2O_3$ HDT commercial catalyst were used.

Linear polydimethylsilane (PDMS) $(CH_3)_3SiO[SiO(CH_3)_2]_nSi(OCH_3)_3$, which is currently used as an antifoaming product in delayed coker operations, was dissolved into the coker naphtha feed with different concentrations. This stream was treated at 427°C and 1 kg/cm^2 in a stainless steel, ¾" O.D., reactor that was heated by automatic temperature control.

In order to produce the Si-doped catalysts, a reactor test unit was used. The reactor was packed with 13.9 g of fresh NiMo HDT commercial catalyst, which was dehydrated in N_2 stream at 150°C for 2 h, then sulfided at 315°C by dimethyl-disulfide diluted in a straight run naphtha stream to reach the sulfide phase. Three catalysts were treated (labeled as DNA, DNB and DNC) with the Si-doped naphtha at 240, 260 and 280°C and 55 kg/cm^2.

3 Results and discussion

Table 1. Silicon content in feedstock and in the final catalyst.

Sample	Si in thefeed (ppm)	Theoretical Si (%)	Si deposited on the catalysts (%)
DNA	383	6.9	3.5
DNB	223	4.0	3.2
DNC	98	1.8	1.6

The silicon content in the naphtha and Si-doped HDT catalysts was analyzed by atomic absorption and the results are shown in Table 1. Theoretical Silicon, defined as the % silicon that

should be deposited on the catalyst assuming a complete removal of silicon from the stream, was calculated from the silicon content in the feedstock, the naphtha flux and the time on stream. Silicon deposited on the catalyst was lower than theoretical silicon in different amounts, as shown in Table 1. The difference between them was wider as the silicon concentration in the feed was higher too (Table 1). This suggests that the Si deposition on the catalyst is controlled by the accessibility and availability of active sites on the catalyst surface.

In DNA and DNB samples (Figure 1), the peak attributed to dialkyl silicon species at -22 ppm is clearly observed, whereas the peak assigned to monoalkyl and inorganic silicon compounds are detected in all the Si-doped catalysts. The highest content was found for Q species, followed by T species, while dialkyl structures were found in minor content in all samples. The DNA and DNB samples showed a similar content and distribution of Si species in spite of the different content of silicon in naphtha with which was doped. It is important to note that in these two catalysts, the amount of T and Q species was comparable while in DNC, the proportion of them was increased from species type D to T and finally to Q. The results of the species distribution in the deactivated industrial catalyst suggest that silicon species in the coker naphtha are adsorbed and converted on the surface of HDT catalyst, releasing CH groups from dialkyl to monoalkylsilylated structures. The next steps in the transformation are the formation of silanol species and, finally, the siloxanes groups. In this case, the conversion is constant and the accumulation is observed at the end of the path. It is important to note that this behavior is valid when a few ppm of silicon are put in contact with the catalyst. When higher concentrations of silicon are used, rapid saturation is observed. An accumulation process was detected, which begins with species T and excess of silicon cannot be retained. It is a suggested explanation for the distribution of T and Q species and for the total amount found in the DNA and DNB catalysts.

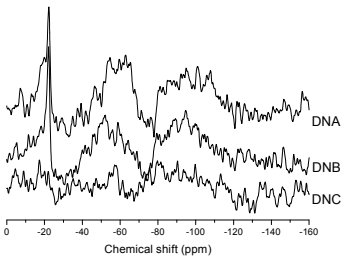

Fig. 1. 29Si MAS NMR spectra of samples doped with different silicon contents.

4 Conclusions

Because of its affinity for silica, the alumina surface is extremely sensitive to the poisoning of the catalyst. On the alumina surface there is a finite available amount of active sites that could be retaining silicon compounds from antifoam additives. The adsorption reaction rate is controlled by the transformation of D into T silicon species. The amount of deposited silicon plays a major role in the catalytic activity for hydrodenitrogenation and hydrogenation reactions)

Acknowledgements

This work was supported by IMP (D.00501 project).

References

[1] L. Kellberg, P. Zeuthen, J. Jakobsen, *J. of Catal.* (1993) 45.

II-PP124

Optimizing the Controlled Synthesis of PVP-Based Carbon Supported Ru Nanoparticles: Synthesis Approaches and Characterization

Simakova I.[1,2*], Demidova Yu.[1,2], Prosvirin I.[1], Glaesel J.[3], Etzold B.[3], Schubert T.[4], Simakov A.[5], Murzin D.Yu.[6]

1 - Boreskov Institute of Catalysis, Novosibirsk, Russia
2 - Novosibirsk State University, Novosibirsk, Russia
3 - Friedrich-Alexander Universität Erlangen-Nürnberg, Erlangen, Germany
4 - FutureCarbon GmbH, Bayreuth, Germany
5 - Centro de Nanociencias y Nanotecnología, UNAM, Ensenada, México
6 - Åbo Akademi University, PCC, Turku/Åbo, Finland

* simakova@catalysis.ru

Keywords: Ru colloidal NPs, synthesis, effect of reduction temperature, PVP/Ru ratio, reducing agent, metal content, microwave assistance

1 Introduction

Nowadays nanosized metal nanoparticles (NPs) attract a lot of attention due to their unique chemical and physical properties. Among different applications of metal NPs a special attention is focused on catalysis. In particular, a colloidal method based on immobilization of colloidal metal NPs over different types of supports is an effective alternative approach to the synthesis of supported metal catalysts with well-defined particles. A precise control over size and shape of NPs at the nanometer scale by varying the synthesis conditions is expected to allow prediction of their catalytic performance as well as to give possibility to tune material properties with high accuracy and reproducibility. The purpose of the current work is to explore regularities of ruthenium NPs formation via polyol reduction and to determine key parameters for the synthesis of Ru NPs with a controllable particle size allowing further preparation of heterogeneous catalysts for different catalytic application, e.g. aqueous phase reforming (APR) of bioderived sugar and sugar alcohols. The influence of different synthesis parameters, such as reduction conditions, the ratio between Ru and stabilizing agent (PVP), and the Ru concentration on the particle size was studied.

2 Experimental

A series of colloidal Ru NPs were synthesized by the polyol method using $RuCl_3 \cdot nH_2O$ and ethylene glycol (EG) as a metal precursor and a reducing agent, respectively [1]. As a general procedure, $RuCl_3 \times nH_2O$ and PVP (mol Ru/mol monomers PVP = 1/1 – 1/50) were dissolved in EG under stirring followed by heating up to a predetermined temperature (170÷198°C) in a sand bath or in the microwave oven. In the case of $NaBH_4$ reduction was performed by addition of the stoichiometric amount of $NaBH_4$ under efficient magnetic stirring.The Ru NPs formation as well as their stability after immobilization over mesoporous Sibunit, carbon nanofibers of platelet structure and TiC carbide-derived carbon under reaction conditions simulating APR were monitored by physical methods, including UV-Vis, XRD, TEM, XPS.

3 Results and discussion

In order to develop an approach to the synthesis of Ru NPs with a controllable particle size the regularities of PVP-stabilized Ru NPs formation from $RuCl_3$ through the polyol method were studied (Fig. 1). The effect of the PVP/Ru, Ru concentration, reduction temperature and

the reducing mode on the mean diameter and size distribution of Ru-NPs was investigated. The particle size prepared by the current polyol technique does not depend strongly on the Ru/PVP ratio and reduction temperature varied in the range 1/1-1/50 and 170-198ºC, respectively, while an increase in the metal concentration in the solution favoured NPs growth. The hundred-fold increase in $RuCl_3$ concentration in the solution was shown to result in a particle size growth from 1.7 to 2.6 nm. A relatively simple method was developed for the synthesis of Ru NPs under microwave irradiation providing small Ru NPs with a narrow size distribution (Fig.2). The synthesis of Ru colloids with Ru/PVP ratio 1/5 under microwaves was found to afford the particle size of about 2.1 nm, which is similar to the one obtained under reflux conditions. However, the method developed under such microwave assistance is rather simple and leads to a fast formation of small Ru NPs with a narrow size distribution due to faster attainment under microwave of the required reduction temperature (Fig. 2a). Faster reduction by $NaBH_4$ at an ambient temperature was found to result in formation of smaller NPs of ca 1.8 nm compared to that reduced by EG (Fig. 2b). According to UV-Vis and XPS data the Ru NPs were found to be in the metallic state independent on the PVP/Ru ratio, the reducing agent and the heating mode. Highly concentrated Ru colloids with a controllable NPs size were immobilized over different carbon supports.

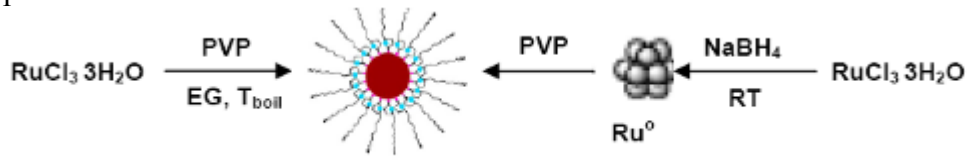

Fig. 1. Different approaches of PVP-stabilized ruthenium nanoparticle synthesis.

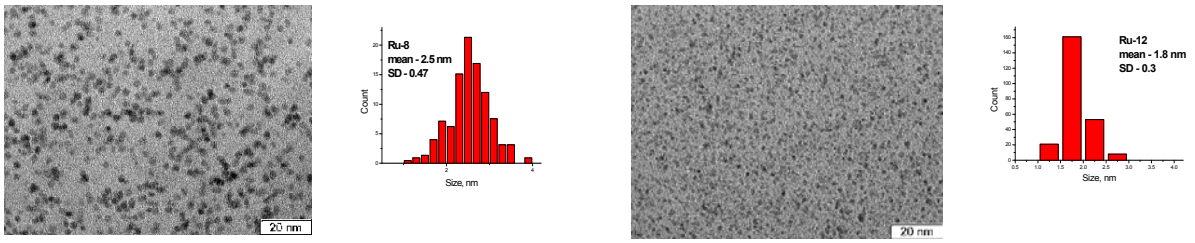

a **b**

Fig. 2. TEM images (left) and the corresponding particle size distribution (right) of PVP-stabilized Ru NPs reduced by a) EG under microwave irradiation b) by $NaBH_4$.

4 Conclusions

Different strategies to prepare Ru NPs of different size with narrow particle size distribution were applied. Stable Ru NPs with mean diameters 1.7÷2.8 nm and a narrow distribution were prepared by reduction of $RuCl_3$ with EG as well as PVP as a stabiliser in the temperature range 170 ÷198^{o}C. As an effective alternative approach Ru NPs synthesis using microwave assistance along with $NaBH_4$ reduction at room temperature was developed. The effect of heating conditions, Ru/PVP ratio, reducing agent and initial Ru precursor concentrations on the particle size was studied.

Acknowledgements

The SusFuelCat project has received funding from the European Union's Seventh Framework Programme for research, technological development and demonstration under grant agreement No 310490 (www.susfuelcat.eu).

References

[1] A. Gual, J.A. Delgado, C. Godard, S. Castillón, D. Curulla-Ferré, C. Claver, *Top.Catal.* 56 (2013) 1208-1219.

II-PP125

Sulfated Perfluoropolymer on Carbon Nanofibers Composites: Preparation, Acidity and Catalytic Activity in the Gas-Phase Benzene Nitration

Koskin A.P.[1*], Kenzhin R.M.[1], Mishakov I.V.[1,2], Vedyagin A.A.[1,2]

1 - Boreskov Institute of Catalysis SB RAS, Novosibirsk, Russia
2 - Novosibirsk State Technical University, Novosibirsk, Russia

* koskin@catalysis.ru

Keywords: gas-phase nitration, sulfated perfluoropolymer, polymer-carbon composite, nitrobenzene

1 Introduction

In industry the aromatics nitration is carried out in the liquid phase with a mixture containing nitric and sulfuric acids [1]. The sulfuric acid medium has two functions: it acts as a homogeneous nitration catalyst and at the same time as a dehydrating agent. A major problem of this technology is associated with diluting of the nitration mixture by water formed as one of the reaction products [2]. Another disadvantage of homogeneous benzene nitration is related to contamination of nitrobenzene (NB) with a high concentration of nitrophenols (NPs, more than 2000 ppm) formed as by-products [3]. Heterogeneous catalytic nitration processes could be regarded as an alternative to the industrial homogeneous nitration technique.

In this study we developed synthetic methods for Nafion deposition on carbon nanofibers and studied the catalytic properties in the gas-phase benzene nitration, durability and acidity of the obtained materials. Our main goal was to achieve higher nitrobenzene selectivity to meet the market demand (total NPs content < 400 ppm).

2 Experimental/methodology

Carbon nanofibers (CNF-*x*, where *x* is the CNF specific surface area) were selected as a catalyst support due to the highly-defective structure of their graphite layers, which is convenient for synthesis of a durable Nf/CNF composite. CNF were prepared by decomposition of methane (or propane-butane mixture) on supported Ni-Cu/Al_2O_3 catalyst at 500-700° [4]. The sulfated perfluoropolymer was deposited on the surface of the support either by wet mixing (wm) or by wet impregnation (wi) methods [5].

Gas-phase benzene nitration reaction was carried out in accordance with proved technique using nitric acid water azeotropic solution as a nitrating agent (160°-170°C, feeds: Benzene/ HNO_3/N_2 = 1/0.42/21.3 (molar ratios)) [5]. The yield of NB was determined by GC (Crystall-2000M, HP-5, TCD); concentration of NPs by HPLC (Agilent-1200, the column SE-30, UVD). Catalytic activity of samples was represented by calculation of the STY_{NB} parameter, by $mg_{NB}/g_{cat}/h$.

The pore volume, average pore diameter and specific surface area of the samples were measured by low-temperature nitrogen adsorption (Micrometrics ASAP-2400). Chemical analyses of the materials were carried out by AAS. Pyridine adsorption experiments were carried out by saturating Nf/CNF in solution containing the already known concentration of pyridine in THF. GC was used to quantify the amount of pyridine adsorbed on the catalyst.

3 Results and discussion

The most active and stable catalysts were synthesized by the wet impregnation method. The best results were obtained for the catalyst containing 20 wt.% Nafion prepared by multi-step wet impregnation (ms, STY_{NB} = 327 mg_{NB} g_{cat}^{-1} h^{-1}, benzene (nitric acid) conversion were 36.2 (38%)). Its good performance can be explained by a combination of high surface area with high concentration of acid sites.

Total amount of the Nf/CNF acid groups were estimated via sulfur element analysis, because each sulfonic group constitutes a potential acid site (0.164 mmol/g for 20% Nf/CNF). Elemental analysis data are well consistent with the polymer loadings used in the catalyst preparation. The experiment on the pyridine adsorption reveal that 0.181 mmol/g are adsorbed on 20% Nf/CNF and 0.021 mmol/g on the ion-exchanged Na^+-20% Nf/CNF form. The accessibility of the H_3O^+-Nf/CNF acid sites (in swelling form) was estimated by EPR [6]. Radical cations are formed by anthracene adsorption on the H_3O^+-Nf/CNF sites. We observed an increase in the concentration of cation radicals when the amount of deposited Nafion was increased. No acceptor sites were found on the CNF support or on dry Nafion. Overall, a good correlation was observed between the concentration of the acceptor sites on the surface of the composites measured by EPR and their catalytic activity in the gas-phase nitration of benzene.

Table 1. Catalytic properties of H_2SO_4/SiO_2, Nafion/SiO_2 and Nafion/CNF composites in gas-phase benzene nitration.

#	Sample, preparation method	S, m^2/g	N^I, 10^{16} g^{-1}	STY_{NB}, mg_{NB} g_{cat}^{-1} h^{-1}		Nitrophenol content, ppm[4]
				5 h	12 h	
1	Nf-H (pure)	0.02	0	340	trace	252
2	10% H_2SO_4/SBA-15	770	25	375	211	377
3	20% Nf/CNF-318, wm	121		293	130	181
4	10% Nf/CNF-318, wi	234	16	280	111	203
5	20% Nf/CNF-318, wi	169	40	327	320	291
6	50% Nf/CNF-318, wi	60		270	265	243

[1]Concentration of radical cations generated from anthracene adsorbed from 0.04 M benzene solution on the samples activated at 120°C for 16 h followed by heat treatment at 80°C for 32 h.

4 Conclusions

In summary, the best catalyst exhibits 99.9% selectivity to nitrobenzene with concentration of by-products (mainly nitrophenols) less than 300 ppm. The prepared Nf/CNF catalysts containing supported perfluoropolymer were shown to have sufficiently high catalytic activity and acceptable resistance to the sulfuric acid leaching, which is typical for all known H_2SO_4/Silica catalysts.

Acknowledgements

The authors are grateful to the Russian Foundation for Basic Research (№ 14-03-31833) for financial support.

References

[1] G.A. Olah, R. Malhotra, S.C. Narang, Nitration Methods and Mechanism, VCH, New York, 1989.
[2] O.V. Bakhvalov, Chem. for Sust. Devel. 11 (2003) 439.
[3] O.V. Kozlova, A.G. Bazanov, N.G. Zubritskaya, Russ. J. of Org. Chem. 46 (2010) 1095.
[4] I.V. Mishakov, R.A. Buyanov, V.I. Zaikovskii, I.A. Streltsov, A.A. Vedyagin, Kinet. Catal. 49 (2008) 868.
[5] A.P. Koskin, R.M. Kenzhin, A.A. Vedyagin, I.V. Mishakov, Cat. Comm. 53 (2014) 83.
[6] R.A. Zotov, V.V. Molchanov, A.M. Volodin, A.F. Bedilo, J. Catal. 278 (2011) 71.

II-PP126

Characterization and Methane Dry Reforming Performance of CeO_2 Prepared by Modified Precipitation Route

Rotaru C.G.[1], Postole G.[2], Florea M.[1*], Matei-Rutkovska F.[2], Pârvulescu V.I.[1], Gelin P.[2]

1 - University of Bucharest, Faculty of Chemistry, Department of Organic Chemistry, Biochemistry and Catalysis, Bucharest, Romania

2 - Université Lyon 1, CNRS, UMR 5256, IRCELYON, Institut de recherches sur la catalyse et l'environnement de Lyon, Villeurbanne, France

* mihaela.florea@chimie.unibuc.ro

Keywords: ceria, hydrogen, peroxide, precipitation method, dry reforming of methane

1 Introduction

Cerium oxide was suggested as a promising candidate for anode component in Solid Oxide Fuel Cells (SOFCs), due to its catalytic activity in reforming and enhanced resistance against coke formation [1-2]. This capability has been attributed to some unique properties, such as oxygen storage capacity, oxygen mobility and ability of cerium to switch easily between oxidized and reduced states ($Ce^{3+} \leftrightarrow Ce^{4+}$). The preparation method affects properties such as the surface area, defects concentration and thermal stability. As an example the addition of H_2O_2 during the preparation steps of ceria nanomaterials led to an improvement of the surface area and redox properties [3].

The present work aims at studying the effect of adding H_2O_2 during the synthesis, alone or with cetyltrimethylammonium bromide (CTAB), a template agent, on morphologic, structural and catalytic properties of ceria. The samples were characterized by powder X-ray diffraction (PXRD), scanning electron microscopy (SEM), isotherms of adsorption-desorption of nitrogen at -196 ^{o}C, thermogravimetric and differential thermal analysis (TG-DTA), Raman spectroscopy, and temperature programmed reduction experiments in CH_4 (TPR-CH_4) or H_2 (TPR-H_2). Catalytic properties in methane dry reforming were investigated in view of the potential use of ceria as SOFC anodes operating on CH_4+CO_2 mixtures such as in biogas.

Experimental

Samples were synthesized using an aqueous solution of $Ce(NO_3)_3 \cdot 6H_2O$ (0.1 mol/L) and adding to it H_2O_2, CTAB, or H_2O_2/CTAB. NH4OH was the added drop-wise ammonium hydroxide until the pH reached the value of 9 to obtain the precipitate (stirring at 60 °C for 1 h). The precipitate was separated by centrifugation, washed in water and ethanol, and dried. Samples were further calcined in air at 500 and 900 °C (5h). The samples were denoted in relation with the additive used: CeO_2; CeO_2_CTAB; CeO_2_H_2O_2; CeO_2_CTAB_H_2O_2.

Dry methane reforming reaction was carried out in a continuous flow system at atmospheric pressure using mixtures containing 0.5% CH_4 - 0.5% CO_2 and 0.25% CH_4 - 0.75% CO_2 in He as balance (stoichiometric and oxidizing conditions, respectively). The total flow rate was equal to 60 mL/min. The conversion was measured within the temperature range of 750 - 900 °C.

Results and discussion

Samples were all active in the conversion of CH_4/CO_2 mixtures, CO and H2 being produced. H_2/CO ratios much lower than unity were obtained. This was explained by the contribution of the reverse water gas shift reaction which becomes predominant above 850 °C in the experimental conditions used. Table 1 shows methane conversion rates at 900°C in stoichiometric and oxidizing conditions. Samples prepared by H_2O_2 addition were found to be

slightly more active, which can be only partly correlated with their higher surface area.

Table 1. Comparison between the surface areas of the CeO_2 powders calcined at 900 °C and the specific methane conversion rates obtained at 900 °C in CH_4/CO_2 reaction mixtures

Sample	CH_4 consumption rate (mmol/h.g)		Surface area (m^2/g)
	Stoichiometric	Oxidizing	
CeO_2	5.6	4.0	5.6
CeO_2_CTAB	5.2	3.4	7.6
CeO_2_H_2O_2	6.8	4.6	13.7
CeO_2_CTAB_H_2O_2	6.7	4.5	20.1

TPO experiments after catalytic testing indicated that no graphitic carbon formed during the reaction on CeO_2_H_2O_2 and CeO_2_CTAB_H_2O_2 while 7.3 and 0.2 µmol C per g of sample was measured on CeO_2 and CeO_2_CTAB, respectively. For all samples bands at 600 and 667 cm^{-1} were observed by Raman (figure 1), being consistent with the presence of Ce^{3+} associated or not with oxygen vacancies in the ceria lattice. With respect to the conventional preparation or CTAB use, the H_2O_2 addition in the synthesis step favors the formation of stable bulk defects (oxygen vacancies) as shown by XRD, and improves bulk reducibility as determined by TPR-H_2. It is also observed that the ultimate OSC measured by TPR-CH_4 is about twice lower than that of CeO_2 and does not change upon successive TPR/TPO cycles. When CTAB is used as additive, the ceria structure suffers modifications upon cycles as for CeO_2. However, while a stable structure is reached for CeO_2 after only one cycle, this evolution is inhibited by the presence of CTAB. The effect is suppressed when CTAB is used with H_2O_2. Physicochemical properties of various samples are discussed and tentatively correlated with catalytic performances.

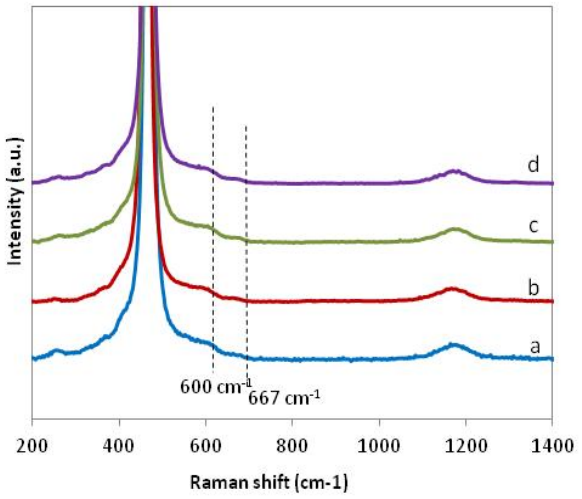

Fig. 1. Raman spectra of CeO_2 samples calcined at 900 °C. (a) CeO_2, (b) CeO_2_CTAB, (c) CeO_2_H_2O_2, (d) CeO_2_CTAB_H_2O_2_.

Conclusions

Compared to materials synthesized conventionally or by using CTAB, the use of H_2O_2 during synthesis mitigates surface loss under high temperatures operation (e.g. 900 °C), improves bulk redox properties when alternating between oxidizing and reducing treatments, and highest catalytic activity and resistance to deposition of graphitic carbon. CeO_2_CTAB_H_2O_2, while not exhibiting improved catalytic properties, presents the highest surface area upon calcination at 900 °C and can find application in catalytic processes where this property is of special importance.

Acknowledgements

The authors kindly acknowledge the UEFISCDI and ANR for the financial support (grant POLCA/2013).

References

[1] S.C. Singhal, Solid State Ionics 135 (2000) 305-313.
[2] L. Fan, C. Wang, M. Chen, B. Zhu, J. Power Sources 234 (2013) 154-174.
[3] J. Rebellato, M. M. Natile, A. Glisenti, Appl. Catal. A: Gen. 339 (2008) 108–120.

II-PP127

Precisely Controlled Synthesis of PVP- Capped Ni and Co Metal Nanoparticles

Demidova Yu.[1,2], Simakova I.[1,2*], Prosvirin I.[1], Glaesel J.[3], Etzold B.[3], Schubert T.[4], Simakov A. [5], Murzin D.Yu.[6]

Boreskov Institute of Catalysis, Novosibirsk, Russia
Novosibirsk State University, Novosibirsk, Russia
Friedrich-Alexander Universität Erlangen-Nürnberg, Erlangen, Germany
FutureCarbon GmbH, Bayreuth, Germany
Centro de Nanociencias y Nanotecnología, UNAM, Ensenada, México
Åbo Akademi University, PCC, Turku/Åbo, Finland

* simakova@catalysis.ru

Keywords: nickel, cobalt, nanoparticles, reduction temperature effect, atmosphere effect

1 Introduction

Development of effective approaches for controlled synthesis of metal nanoparticles (NPs) is of great fundamental and practical interest due to a wide range of applications in different fields, including electronics, optics, magnetic devises and catalysis. In fact, the NPs size and shape strongly affect their chemical and physical properties. In this connection, there are numerous investigations devoted to the synthesis and detail studies of key parameters determining formation of nanostructured materials [1, 2]. A rational control of NPs characteristics can be achieved through regulation of the synthesis conditions. Ni is widely used as an industrial hydrogenation/hydrotreating catalyst while Co exhibits appreciable activities for C–C bond scission, water–gas shift reaction, and Fischer–Tropsch synthesis [3]. Supported Ni and Co metal NPs are anticipated also to be of potential interest as inexpensive catalytic materials for aqueous phase reforming (APR) of bioderived sugar and sugar alcohols resulting in a mixture of hydrogen and alkanes [4]. In the present work it is demonstrated that Ni and Co NPs with controllable sizes can be prepared in bench scale quantities by a facile modified polyol method utilizing sodium borohydride ($NaBH_4$) as a reducing agent and polyvinylalcohol as a capping agent with a high metal/PVP ratio.

2 Experimental

Co and Ni NPs were prepared by the modified polyol method. Solutions of Co or Ni chloride in ethylene glycol with PVP (Ru/PVP = 1:5) were used as initial mixtures. The reduction was performed by a stoichiometric amount of $NaBH_4$ under an efficient magnetic stirring at the temperature varied from 7 to 170°C during 1 h. Ni NPs were synthesized under both Ar and air atmosphere, whereas Co colloids synthesis was performed only under inert atmosphere. Ni and Co colloids as well as NPs immobilized on the carbon supports (mesoporous Sibunit, carbon nanofibers, and TiC carbide-derived carbon) were analyzed by a variety of state of the art physical methods including TEM, XPS, XRF, UV-Vis.

3 Results and discussion

In order to find out the operating parameters of the polyol synthesis determining a controllable formation of Ni and Co NPs the role of the reduction temperature under an inert gas atmosphere was studied. Changes in the reduction temperature were suggested to affect the reduction rate allowing particle size regulation. The reduction temperature was varied from 23 to 170°C for Ni NPs and from 7 to 23ºC for Co NPs. TEM date shown that the average diameter

of Ni NPs size increased from 2.6 to 3.2 nm when the reduction temperature increased from 23 to 140ºC. With respect to Co NPs the temperature increase from 7 to 23ºC resulted in the increase in Co NPs size from 1.8 to 2.6 nm, whereas further change from 23 to 100ºC affected less significantly the metal particles size. The results presented above indicate that the size of the base metal NPs increases with elevation of the synthesis temperature. To investigate the role of gas atmosphere on the formation of Ni NPs the gas-dependent evolution of the NPs size was carried out in air or in Ar at 140ºC. As a result, the size of NPs formed at 140ºC in air was 5.4 nm compared to 3.2 nm formed in Ar. When the temperature was increased to 170 C, the Ni NPs size increased to 9.8 nm. Thus, a tendency of the particle size to increase with an increase in the reduction temperature was observed for base metal colloids synthesized by the modified polyol method. In the case of Ni colloids an oxidative atmosphere promoted formation of larger NPs with a wider particles size distribution compared to those formed in the inert gas atmosphere.

Table 1. Average size of Ni and Co NPs synthesized by a modified polyol method.

Me	Atmosphere	T_{red}, °C	d_n, nm	SD
Ni	Ar	23	2.6	0.6
Ni	Ar	140	3.2	0.9
Ni	air	140	5.4	2.7
Ni	air	170	9.8	6.9
Co	Ar	7	1.8	0.5
Co	Ar	23	2.6	0.6
Co	Ar	100	2.8	0.5

4 Conclusions

A series of Co and Ni NPs with the average particle sizes 1.8÷2.8 and 2.6÷9.8 nm, respectively, were synthesized by the modified polyol method. The influence of reducing temperature and gas atmosphere was studied. Parameters determining formation of Co and Ni NPs by the polyol method with a controlled size were found. Increase of reduction temperature and application of an oxidative atmosphere were found to increase nanoparticles size favouring the NPs growth versus nucleation.

Acknowledgements

The SusFuelCat project has received funding from the European Union's Seventh Framework Programme for research, technological development and demonstration under grant agreement No 310490 (www.susfuelcat.eu).

References

[1] G. Schmid, *Chem. Rev.* 92 (1992) 1709-1727.
[2] R.G. Finke, J.D. Aiken III, *J. Mol. Catal. A: Chem.* 145 (1999) 1-44.
[3] R.R. Davda, J.W. Shabaker, G.W. Huber, R.D. Cortright, J.A. Dumesic, *Appl. Catal. B.* 43 (2003) 13-26.
[4] A.V. Kirilin, A.V. Tokarev, H. Manyar, C. Hardacre, T. Salmi, J.-P. Mikkola, D.Yu. Murzin, *Cat. Tod.* 223 (2014) 97-107.

II-PP128

Syngas Production via Dry Reforming of Methane over $NiAl_xFe_{2-x}O_4$ Oxides: Synthesis, Characterization and Reactivity Study

Benrabaa R.[1,2*], Löfberg A.[3], Guerrero Caballero J.[3], Rouibah K.[1,4], Boukhlouf H.[1,5], Vannier R.N.[3], Bordes-Richard E.[3], Rubbens A.[3], Barama A.[1]

1 - Laboratoire de Matériaux Catalytiques et Catalyse en Chimie Organique, Faculté de Chimie, USTHB, Alger, Algérie

2 - Université 20 Août-Skikda, Faculté de Technologie, Département de Pétrochimie &Génie des Procédés, Alger, Algérie

3 - Unité de Catalyse et de Chimie du Solide, UMR CNRS 8181, Université Lille 1, Sciences et Technologies, Bât, Villeneuve d'Ascq, France

4 - Université Mohamed Seddik Ben Yahia-Jijel, Faculté des Sciences et Technologie, Alger, Algérie

5 - Entreprise Nationale Sonatrach, Institut Algérien du Pétrole, Alger, Algérie

* rafikemp@gmail.com

Keywords: dry reforming of methane, spinel, reducibility, $NiFe_2O_4$, $NiAl_2O_4$

1 Introduction

The reforming of methane to syngas using CO2 instead of steam is an attractive route, including from the point of view of sustainability because it uses two greenhouse gases. Compared to noble metals, Ni-catalysts are cheap but very easily deactivated by coking. Ni-based mixed oxides structurally well-defined like perovskites and spinels are being studied because they possibly make solid solutions and allow to vary the composition and thus the catalytic properties. In this study, the textural, structural and catalytic properties of nickel ferrite aluminate samples prepared by coprecipitation method, using nitrates and chlorides salts as precursor, are presented.

2 Experimental/methodology

The catalysts $NiAl_xFe_{2-x}O_4$ (x = 0; 0.5; 1; 1.5; 2) were prepared by coprecipitation route using nitrates and chlorides salts as precursors and sodium hydroxide as precipitating agent. The precursors were calcined at 800 °C. Samples were characterized by B.E.T, XRD, Raman, SEM-EDS and XPS. Their reducibility was investigated by in situ methods (H_2-TPR and H_2-HTXRD), at various temperatures. The catalytic performance in DRM was measured in a fixed bed reactor, at 1 atm, CH_4/CO_2/He/Ar = 20:20:10:50 (total flow 100 mL/min) and 650–800°C range. After experiment, the catalyst was reoxidized under 2% O_2 in He (50 mL/min) at 700 °C for 30 min to quantify the coke deposition.

3 Results and discussion

The surface area as well as the surface Ni/Fe atomic ratio (EDS and XPS), varied according to the Al percentage (Table 1). According to EDS and XPS, the surface Fe/Ni ratio was more or less close to stoichiometry (Fe/Ni = 2). Raman spectroscopy and XRD (Figure 1) patterns showed the presence of the spinel as majority phase in all synthesized oxides [2,3], traces of free NiO are observed in all case excepted $NiFe_2O_4$ case. The catalytic activity in DRM of the spinel samples showed that aluminate spinel is more active (with the CH_4 and CO_2 conversions ~ 90 mol%) than ferrite spinel (whose the CH_4 and CO_2 conversions not exceed 3 and 6 mol% respectively). This could be related to the high reducibility and the high specific surface area observed for aluminate samples. For $NiFe_2O_4$, a significant contribution of reverse water gas shift reaction was observed. At higher reaction temperatures (above 700°C), aluminate spinel

catalysts showed substantial carbon deposition (20%).

Table 1. Textural, structural and surface properties of $NiAl_xFe_{2-x}O_4$ catalysts

Catalyst	S_{BET}	EDS data		XPS data				
(x=)	(m^2/g)	Fe/Ni	Al/Ni	BE[a] Fe	BE[a] Al	BE[a] Ni	Fe/Ni	Al/Ni
00	10	2.3	---	710.9	---	855.2	2.6	---
0.5	25	0.6	0.5	---	---	---	---	---
1.0	38	1.0	0.5	---	---	---	---	---
1.5	45	1.0	0.4	---	---	---	---	---
2.0	101	---	2	---	74.2	855.7	---	5

[a] BE: Binding energy (eV).

00025166028825165926 4

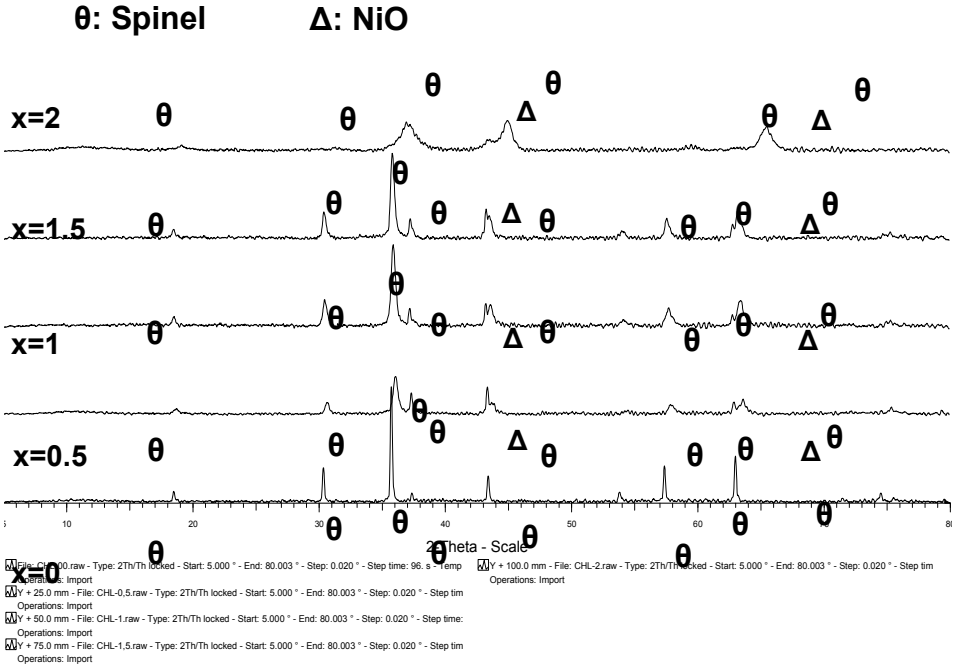

Figure 1. XRD patterns of $NiAl_xFe_{2-x}O_4$ catalysts prepared by coprecipitation method

4 Conclusions

The obtained results show that all aluminate spinel is more active than ferrite spinel in CO_2-reforming of methane. A significant contribution of reverse water gas shift reaction was observed in ferrite spinel case. A good correlation between textural and structural properties and reducibility of catalysts with catalytic performance is observed.

Acknowledgements

L. Burylo, N. Djelal, O. Gardoll and M. Frère are acknowledged for XRD, ATG-ATD, TPR and XPS experiments, respectively.

References

[1] R. Benrabaa, A. Löfberg, C. Lancelaut, E. Bordes-Richard, R. N. Vannier, A. Barama, *Catal Today*. 203 (2013) 188.

[2] R. Benrabaa, H. Boukhlouf, A. Löfberg, A. Rubbens, R-N. Vannier, E. Bordes-Richard, A. Barama, *J of Nat Gas Chem*. 21 (2012) 595.

II-PP129

Preparation of Cu Loaded Magnetic Nanoparticle Catalyst and its Catalytic Activity for Degradation of Azo Dyes

Kurtoglu K., Gubbuk I.H.*

Selcuk University Faculty of Sciences Department of Chemistry, Konya, Turkey

* ihilalg@gmail.com

Keywords: dye degradation, magnetic, nanoparticle, methylene blue

1 Introduction

Magnetic separation using magnetically recoverable nanoparticles offers a promising approach that can meet the requirements of high accessibility with improved reusability. Therefore, magnetically separable catalysts have attracted increasing attention in recent years [1]. The development of more efficient and stable catalysts has been an increasingly important goal for chemists and material scientists for both economic and environmental reasons [2].

In this study, Fe3O4@SiO2 - Cu nanoparticles for catalytic reduction of azo dye pollutants are prepared. This nanoparticles exhibit enhanced catalytic reduction efficiency for azo dyes compared with those of pure Cu or Fe3O4 nanoparticles, and can also be rapidly separated from aqueous solution using a magnet. Synthesized magnetic nanoparticles were characterized by different techniques including X-ray diffraction (XRD), Scanning electron microscopy (SEM), Fourier transform infrared (FT-IR) spectroscopy and thermal analysis (TGA). The degradation efficiency was found to depend essentially on initial dye concentration, solution pH and the catalyst loading.

2 Experimental/methodology

All chemicals were analytical reagent grade: copper nitrate (Merck), sodiumborohydride and azo dyes (all from SigmaeAldrich). Water used for the preparation of all solutions was deionised by reverse osmosis. FeCl3 and FeCl2 were purchased from Sigma Aldrich.

The magnetic nanoparticle, Fe3O4, was prepared by a precipitation method. Briefly, 60mL of FeCl2 and FeCl3 aqueous ethanol solution with a concentration ratio of 5:1 was prepared, 1.0 mol/L ammonia solution was added drop by drop with vigorous stirring until pH 10, and a black product was obtained. Then, the black product was crystallized under 50 ◦C water bath for 3 h. Subsequently, separated with magnet, the obtained black magnetite particles were washed with ethanol for 3 times, dried at 50 ◦C for 12 h [3].

Fe3O4 spheres were coated by SiO2 films, by using TEOS as a precursor. The resulting Fe3O4@SiO2 particles were loaded with Cu nanoparticles. The material showed better performance than a conventional Fe3O4 catalyst in catalytic reduction of azo dyes with NaBH4. It can be separated from the reaction mixture by a magnet and be recycled without obvious loss of catalytic activity [4].

Catalytic activity of Fe3O4@SiO2 - Cu was investigated by means of degradation of azo dyes by sodium borohydride in aqueous solutions. Typically, 300 mL of the 1x10-4 mol L-1 dye solution was mixed with 0.010 g of Fe3O4@SiO2 - Cu. Thereafter, 5 mL of the sodium borohydride solution was added to the dispersion and the reaction was monitored by UV-VIS spectrometry. Study of the catalytic activity of Fe3O4@SiO2 - Cu was conducted at the laboratory temperature.

3 Conclusions

We have demonstrated that it can be used as magnetic recoverable nanocatalysts. The magnetic nanocatalyst exhibits an enhanced performance towards the decomposition of organic azo dyes.

In this study, Fe3O4@SiO2‐Cu composites have been synthesized by a chemical method, with Fe3O4 as a substrat, copper nitrate as a metal precursor and TEOS as a stabilizator. These composites accessible and highly dispersed Cu nanoparticles, thus resulting in high catalytic activities in the degradation of azo dyes.

Acknowledgements

This research was supported under Selcuk University BAP Projects funding. Authors gratefully acknowledge the financial support of the Selcuk University.

References

[1] C. An, X. Ming, J. Wang, S. Wang, *J. Mater. Chem*., 2012, 22, 5171
[2] J. Ji, P. Zenga, S. Ji, W. Yanga, H. Liua, Y. Li, *Catalysis Today* 158 (2010) 305–309.
[3] Q. Chang, K. Deng, L. Zhu,G. Jiang, C. Yu, H. Tang, *Microchim Acta* (2009) 165:299–305
[4] Y. Chi, J. Tu, M. Wang, X. Li, Z. Zhao, *J Colloid and Interf. Sci.* 423 (2014) 54–59.

II-PP130

The Photocatalytic Hydrogen Evolution by Alloyed CdTeS Nanocrystals

Aslan E.[1], Baslak C.[1], Hatay Patir I.[1], Kus M.[2], Ersoz M.[1*]

1 - Department of Chemistry, Selcuk University, Konya, Turkey
2 - Department of Chemical Engineering, Selcuk University, Konya, Turkey

* ersozm@gmail.com

Keywords: hydrogen, evolution, quantum, dots, photocatalysis

1 Introduction

Energy and environmental issues at a global level are vital topics. Because of its environmental friendliness and high energy capacity, hydrogen has been described as a potential energy carrier. Conversion of sunlight into chemical energy in the form of hydrogen (H_2) is one of the crucial issue of 21st century chemistry. The key issue for approaching this target is to develop highly efficient and cheap catalytic systems. Since the discovery of hydrogen evolution through the photoelectrochemical splitting of water on n-type TiO_2 electrodes [1]. In recent years, photocatalytic water splitting using solar energy has become a promising approach to the production of clean, environmentally friendly and low-cost hydrogen. So far, numerous active semiconductor-based photocatalysts and their composites have been developed for photocatalytic hydrogen production reactions because of their suitable physical and photochemical properties. Among the various semiconductor photocatalysts, the hydrogenase-CdTe hybrid-nanostructures [2, 3] and water-soluble CdTe quantum dots (QDs) [4,5] have recently attracted considerable attention for their high photocatalytic activity under visible-light irradiation. In this study, photocatalytic generation of hydrogen by using 3-mercaptopropionic acid capped CdTe and CdTeS alloy nanocrystals have been investigated under visible-light irradiation in the aqueous solution by using at the pH 4.65 ascorbic acid solution as a sacrificial electron donor and $CoCl_2.6H_2O$ as an artificial catalyst.

2 Experimental/methodology

Synthesis of nanocrystals

In the synthesis, all reactions were carried out in oxygen-free water under nitrogen. The $Cd(MPA)_2$ precursor was prepared by mixing n moles $CdCl_2$. $5/2H_2O$ with 2n moles MPA in 200 ml of water. pH of the solution was adjusted to 12 with 0.1 mol. L^{-1} KOH. The prepared solution of Cd-thiolate complex was loaded in a three-necked flask. It was deaerated by bubbling of nitrogen for 30 min and heated at 100 °C. At the 80 °C of temperature, 10.0 ml of fresh NaHTe aqueous solution prepared from $NaBH_4$ and Te powder (0.2 mmol) and to prepare the sulphur precursor thiourea (0.2 mmol) with 2 ml of fresh NaHTe aqueous solution under nitrogen were used. The precursor solutions were injected into the reaction system under vigorous stirring using two syringes; the solution was then refluxed at 100 °C. Part of the refluxing solution was taken out at regular intervals for further characterizations. The prepared CdTeS QDs were precipitated and washed with 2-propanol more than three times. The QDs were dried overnight at room temperature. CdTe core nanoparticles were synthesized using only Cd and S precursor and MPA capping agent.

Photocatalytic hydrogen evolution

Ascorbic acid (3×10^{-2} M) and $CoCl_2.6H_2O$ (2×10^{-4} M) solution was prepared in the flask and

bubbled with N_2 to remove O_2. Nanocrystals (CdTe and CdTeS) was taken a reaction cell (total volume 135ml) and then, both electron donor solution and nanocrystals were taken in the glove box system. Solution and catalyst was mixed in the glove box. Catalysts are dissolved easily in the sacrificial solution. And then this mixture was stirred vigorously under the visible light source (Solar Light – XPS 300TM) and at room temprature. Then gas sample took periodically in the headspeace, which is above the solution. The gas in the headspace was analyzed using a Shimadzu GC-2010 Plus gas chromatograph (detector, TCD; column temperature, 323 K; column, RESTEK molecular sieve 5A porous layer open tubular capillary column 30 m 0.53 mmID 50 um df; Ar as a carrier gas) to determine the produced hydrogen.

3 Results and discussion

CdTeS alloy nanocrystals exhibits the hydrogen evolution rate of 8 $mmolg^{-1}h^{-1}$, which is about two times higher than that of CdTe. When a sample of CdTe and CdTeS alloy nanocrystals is irradiated in ascorbic acid/Co^{+2} solution for 12 h, they produce a total of 49 $mmolg^{-1}$ and 88 $mmolg^{-1}$ of H_2. Remarkably, the photocatalytic hydrogen evolution on as-prepared nanocrystals proceeds for longer than 12 h without any noticeable decrease in the activity, indicating that catalysts are stable and are not photocorroded in the aqueous medium.

4 Conclusions

In summary, we have successfully developed the 3-mercaptopropionic acid capped CdTe, and CdTeS alloy nanocrystal photocatalysts. The higher photocatalytic activity obtained for CdTeS alloy nanocrystals as compared to the CdTe.

Acknowledgements

This research was supported under Selcuk University BAP Projects funding. Authors gratefully acknowledge the financial support of the Selcuk University. This work carried out under the umbrella of the TUBITAK (The Scientific and Technological Research Council of Turkey) (211T185) project and the COST Action (MP1106).

References

[1] A. Fujishima, K. Honda, *Nature* 238 *(*1972) 37.
[2] K. A. Brown, S. Dayal, X. Ai, G. Rumbles, P. W. King, *J. Am. Chem. Soc.*, 132 (2010) 9672–9680.
[3] F. Wang, W. Wang, X. Wang, H. Wang, C. Tung, L. Wu, *Angew. Chem. Int. Ed.*, 50 (2011) 1 – 6.
[4] Z. Li, X. Li, J. Wang, S. Yu, C. Li, C. Tung, L. Wu, *Energy Environ. Sci.*, , 6 (2013) 465-469.
[5] X. Mathew, A. Bansal, J. A. Turner, R. Dhere, N. R. Mathews, P. J. Sebastian, *J. New Mat. Electrochem. Systems*, 5 (2002) 149-154.

II-PP131

Ruthenium Nanoparticles Supported on Carbon – an Active Catalyst for the Hydrogenation of Lactic Acid to Form 1,2-Propane Diol

Iqbal S.[1], Schonmakers D.[1], Lu L.[2], Kondrat S.A.[1], Jones D.R.[1*], Wells P.P.[3], Gibson E.K.[3], Morgan D.J.[1], Kiley C.J.[2], Hutchings G.J.[1]

1 - Cardiff Catalysis Institute, School of Chemistry, Cardiff University, Cardiff, UK
2 - Department of Materials Science and Engineering, Lehigh University, Bethlehem, USA
3 - The UK Catalysis Hub, Research Complex at Harwell, Harwell, UK and University College London, Kathleen Lonsdale Materials, Department of Chemistry, London, UK

* JonesDR7@cardiff.ac.uk

Keywords: lactic acid, 1,2-propanediol, biomass, hydrogenation, Ru catalyst

1 Introduction

1,2-propanediol (PDO) is an attractive commodity chemical, frequently used as a de-icing fluid and anti-freeze, as well as in the production of cosmetics and pharmaceuticals[1]. The production of PDO currently involves the selective oxidation of propene and involves environmentally unfriendly processes. An efficient synthesis of 1,2-propanediol from lactic acid is an area of great interest in modern day green chemistry. Ru-C catalysts are the most widely studied system for this reaction[2-4], but most of the literature is focussed on using commercially available Ru/C materials for characterizing reaction parameters or comparing different promoters. In this study, we report that various different types of carbon can be used for supporting the Ru nanoparticles and they show different activity under moderate reaction conditions and compare the activity with a commercial carbon-supported Ru catalyst. We also show the effect of preparation method on the catalyst, comparing the use of impregnation *vs*. sol immobilisation and investigate the stability of each catalyst.

3 Experimental/methodology

Wet impregnation method: Asolution of the Ru nitrocyl nitrate (5 wt% with respect to activated carbon) was added to the support in order to obtain a paste. The catalyst was dried (110 °C, 16 h) and heated in N_2 (400 °C, 3h, 20 °C/min heating rate).

Sol immobilisation method: Catalysts were prepared starting from a solution of PVA (10 mg) and ruthenium chloride (0.04g) in water (800 ml). Freshly prepared solution of $NaBH_4$ ($RuCl_3/NaBH_4$ = 1/3.3 mole %) was added to generate the sol. After 30 min the activated carbon (1.98g) was added and the solution was acidified to pH 2 with sulphuric acid. The catalyst was then filtered and dried (110 °C, 16 h).

Characterisation: XRD, TPR, TEM, XPS, and EXAFS were all employed to characterise the samples in this study.

Catalyst testing: The reactor was charged with lactic acid (5% in H_2O, 10 g) and catalyst (0.025 g). The autoclave was sealed, pressurised with hydrogen (35 bar) and stirred (1000 rpm) for 2.5-32 hours at 120 ^{O}C. The reaction mixture was analysed by HPLC (Agilent Technologies 1260 Infinity with a Varian MetaCarb 67H capillary column (0.65 x 30 cm) and a refractive index detector). Products were identified by comparison with authentic samples.

4 Results and discussion

The commercial Ru/C catalyst was more active than those prepared supported on different carbons, as shown in Table 1.

Table 1: LA conversion to PDO with Ru supported on different carbons, wet impregnation method of preparation. Reaction conditions*:* 5 wt.% substrate (0.5M ML, 0.6M LA) in water, 120 ^{o}C, 35 bar H_2 pressure, and 2.5 h reaction time

Catalysts (Ru/C)	LA conversion (%)	PDO Selectivity (%)
Commercial catalyst	19	100
Wood derived carbon	13	100
Coconut shell derived carbon	10	100
Activated carbon	9	100
Graphene oxide	2	100
Carbon black	15	100

The BET surface areas of the carbon supports and the Ru/C were determined along with the the pore size distributions of the two most active catalysts. The addition of Ru did not affect the overall surface area and that there are significant variations in surface areas and pore size distributions that do not correlate with observed catalyst activity. XRD patterns for the Ru-catalysts supported on various carbons show that no reflections can be assigned to Ru.

TPR measurements show that the support has an effect the reduction behaviour of ruthenium, which can have an effect on its activity. Graphene oxide supported Ru, for example, has a higher reduction temperature, which explains its poor activity under reaction conditions. The more active catalysts showed a peak around 90 ^{O}C and another Ru species that reduced at around 200 ^{O}C. The activated carbon and the wood derived carbon showed only one reduction peak at 100 ^{O}C.

XPS and EXAFS measurements also point toward well dispersed ruthenium nanoparticles on the surface being the most

5 Conclusions

We have prepared a series of 5wt.% Ru/C catalysts and compared then with a commercial Ru/C catalyst and carried out characterisation to determine the reason for the activity of these catalysts. The commercial catalyst was the most active, followed by the catalyst prepared on VXC72. These carbon supports facilitate a greater dispersion of ruthenium on the surface, upon which the activity relies.

References

[1] Corma, A.; Iborra, S.; Velty, A. *Chem. Rev.* **2007**, *107*, 2411
[2] Maki-Arvela, P.; Simakova, I. L.; Salmi, T.; Murzin, D. Y. *Chem. Rev.* **2014**, *114*, 1909
[3] Zhang, Z.; Jackson, J. E.; Miller, D. J. *Appl. Catal., A* **2001**, *219*, 89
[4] Chen, Y.; Miller, D. J.; Jackson, J. E. *Ind. Eng. Chem. Res.* **2007**, *46*, 3334

II-PP132

First Principles Study of Oxygen Adsorption and Dissociation on Au-Ag Clusters in the Propylene Epoxidation Reaction

Polynskaya Y.G.*, Pichugina D.A., Kuz'menko N.E.

M.V. Lomonosov Moscow State University, Moscow, Russia

* julia.g.snyga@gmail.com

Keywords: oxygen, activation, Au-Ag clusters, propylene epoxidation

1 Introduction

The development of nanostructured catalysts of selective oxidation is of exceptional significance for science and chemical technology. It is generally accepted that gold is inert, however nanostructured gold exhibits high catalytic activity [1,2]. The electronic properties of gold nanoparticles change with doping heteroatoms [3]. In particular, in gold nanoparticles, the replacement of Au atoms by Ag atoms creates $Au^{\delta+}$ sites. It is known that gold and silver nanoparticles have been used as catalysts for propylene edoxidation. However, silver nanoparticles have very poor selectivity for the epoxidation reaction of propylene. In the case of gold catalysts, shape and size of gold nanoparticles have influence on selectivity of this reaction. One of the key questions for this study is how doping of gold clusters with silver will affect the mechanism of the propylene epoxidation. Another key question is how the structure of gold-silver clusters in general and the structure of active centers in particular will affect on oxygen adsorption and activation.

2 Methodology

Geometry optimizations were performed within the spin-polarized approach (PBE functional) [4]. The Priroda program [5] was used for the all-electron calculations within the scalar-relativistic approach, which was based on the full four-component one-electron Dirac equation with separation of the spin-orbit effects. The initial coordinates of the tetrahedral Ag_{20} and Au_{20} clusters were taken from previous studies [6–8]. The true TS structures were determined according to the Berny algorithm [9]. Calculations or the intrinsic reaction coordinate through the single imaginary mode of the TS were performed to validate the TS structures.

3 Results and discussion

In the present work we considered tetrahedral Au_{20} and Ag_{20} clusters, their mono-doped analogs ($Au_{19}Ag$ and $Ag_{19}Au$), as well as core-shell clusters Au_4Ag_{16} and $Au_{16}Ag_4$. After optimizations, all clusters preserved tetrahedral structure. It should be noted, that silver tends to occupy atoms with high coordination number (facet atoms) in $Au_{19}Ag$, while gold tends to occupy atoms with low coordination number (edge, top) in $AuAg_{19}$. We have previously calculated ionization potentials (IP), electron affinity (EA), energy of HOMO-LUMO gap (E_{H-L}), and average atomic binding energy (E_b) [10]. It was shown that values of all these parameters decrease with an increasing number of silver atoms in cluster. Then we considered three type of oxygen adsorption: molecular (O_2^-), peroxide (O_2^{2-}) and dissociative (atomic O). We obtained that pure gold cluster does not interact with molecular oxygen. It must be emphasized that oxygen dissociation on Au_{20} is endothermic process. Upon replacement of gold atoms with silver atoms in clusters oxygen adsorption became exothermic. In $Au_{19}Ag$ O_2 prefers bonding the apex gold atoms than the facet silver atoms [10]. Only molecular or peroxo-like oxygen adsorption can be formed on the core-shell $Au_{16}Ag_4$ cluster. Two sites of oxygen

adsorption were found on the Au_4Ag_{16} cluster: on the silver atoms located on the edges and on the gold atoms placed on the centre of the facets. Molecular and peroxo-like adsorption is more favorable on the edge sites in the Au_4Ag_{16}. We considered O_2 adsorption on the three isomers of $AuAg_{19}$ having gold atom on apex, edge and facet ($AuAg_{19}$_1, $AuAg_{19}$_2, $AuAg_{19}$_3). The heat of adsorption slightly depends on the location of gold atom, and it is close to 31 kJ/mol for all isomers. E_{ad} of oxygen calculated for Ag_{20} are equal to the E_{ad} calculated for $AuAg_{19}$. Oxygen adsorption on the top atoms of Ag20 is the most favorable [10].

4 Conclusions

The model tetrahedral $Au_{20-x}Ag_x$ (x = 0, 1, 4, 16, 19) clusters having different composition are proposed and examined in the reaction with oxygen. The stability and reactivity are predicted by the calculation of IP, EA, E_b and HOMO−LUMO gap. With the increase of the silver content in the bimetallic Au−Ag clusters values of IP, EA, and HOMO−LUMO gap decrease. Silver tends to occupy the facet position in the bimetallic cluster and gold tends to occupy the apex position. Strong correlation between the cluster activity in oxygen activation and the content of silver atoms in cluster is observed. Oxygen activation and dissociation on Au−Ag clusters are more favorable on edge atoms.

Acknowledgements

This research was supported by the Russian Federation Foundation for Fundamental Research through the Project 13-03-00320, 14-01-00310, and 11-01-00280, and by the Council for Grants of the Russian Federation President Project MK-92-2013-3 and NSh-3171.2014.3. The reported study was supported by the Supercomputing Centre of M.V. Lomonosov Moscow State University [11].

References

[1] S. Chretien, S. Buratto, H. Metiu, *Curr. Opin. Solid State Mater. Sci.* 11(2007) 62.
[2] Y. Zhang, X. Cui, F. Shi, Y. Deng, *Chem. Rev.* 112(2012) 2467.
[3] S. L. Christensen, M. A. Macdonald, A. Chatt, P. Zhang, 116(2012) 26932.
[4] J. P. Perdew, K. Burke, M. Ernzerhof, *Phys. Rev. Lett.* 77(1996) 3865.
[5] D.N. Laikov, Yu. A. Ustynyuk, *Russ. Chem. Bull. Int. Ed.* 54 (2005) 820.
[6] Z. W. Wang, R. E. Palmer, *Nanoscale* 4 (2012) 4947.
[7] D. Y. Zubarev, A. I. Boldyrev, *J. Phys. Chem. A* 113 (2009) 866.
[8] M. Chen, J. E. Dyer, K. Li, D. A. Dixon, *J. Phys. Chem. A* 117 (2013) 8298.
[9] H. B. Schlegel, *J. Comput. Chem.* **3** (1982) 214.
[10] Y. G. Polynskaya, D. A. Pichugina, N. E. Kuz'menko, *Comput. Theor. Chem.* 1055(2015) 61.
[11] V. Sadovnichy, A. Tikhonravov, Vl. Voevodin, and V. Opanasenko, "Lomonosov": Supercomputing at Moscow State University. *In Contemporary High Performance Computing: From Petascale toward Exascale* (2013) 283.

II-PP135

The Effect of Hydrolysis Temperature on the Textural Properties of Nanoscale Rutile

Shikina N.V.[1], Bessudnova E.V.[1], Mel'gunov M.C.[1], Rudina N.A.[1], Ischenko A.V.[1], Ismagilov Z.R.[1,2]

1 - Boreskov Institute of Catalysis, Novosibirsk, Russia
2 - Institute of Coal Chemistry and Materials Science, Kemerovo, Russia

* shikina@catalysis.ru

Keywords: rutile, nanoscale, $TiCl_4$, thermolysis, texture

1 Introduction

Porous TiO_2 nanopowders are widely used in solar cells, lithium-ion batteries, photocatalysis, nanobiotechnologies and catalysis [1-2]. The porous structure is important for all the listed fields because it determines the specific surface area, the pore system of a material, and in most cases makes it possible to enhance the functional properties of a material. In catalysis, the porous structure of a material is of special importance because the catalytic processes require pores of a certain size and shape to provide an access of reactants to the active component. Features of the porous structure are determined by the particle size, packing and morphology, i.e. by the texture of a material. In this work, the effect of $TiCl_4$ hydrolysis temperature on the textural properties of the resulting nanoscale rutile and on the changes of these properties upon calcination were studied.

2 Experimental

Nanoscale titanium dioxide with the rutile structure was synthesized by thermolysis of titanium tetrachloride in a 0.5 M solution of hydrochloric acid at a temperature of 50, 60, 70, 80, 90°C and a constant ratio $[H_2O]/[Ti] = 39$ in 0.5 M HCl. After the synthesis, the finished product was purified by dialysis against distilled water, dried at 100°C and calcined at 300, 500, 700 and 1000°C.

The textural properties (specific surface area, pore volume and pore size distribution) of the samples synthesized at different temperatures with subsequent calcination were studied by low-temperature nitrogen adsorption on an ASAP-2400 (Micrometrics) instrument and by mercury porosimetry on an AutoPore IV 9500 V1.09 (Micromeritics) device. TEM studies were carried out on a JEM-2010 (JEOL, Japan) electron microscope. SEM studies were performed on a JSM 6460LV (JEOL, Japan) scanning microscope.

3 Results and discussion

As shown by the study of the textural properties of the starting dried rutile powders synthesized at different hydrolysis temperatures, materials with a high specific surface area of 110-140 m^2/g and a pore volume of 0.09-0.12 cm^3/g are produced over the entire temperature range [3]. According to the low-temperature nitrogen adsorption data, the samples synthesized at low temperatures (50-70°C) contain 33-41% of micropores. As the temperature of hydrolysis is raised, the fraction of micropores decreases to 18-21% and, accordingly, the fraction of mesopores increases, which is indicated also by a growing hysteresis loop on the adsorption isotherms (Fig. 1).

Fig. 1. Nitrogen adsorption-desorption isotherms for rutile samples synthesized at different temperatures.

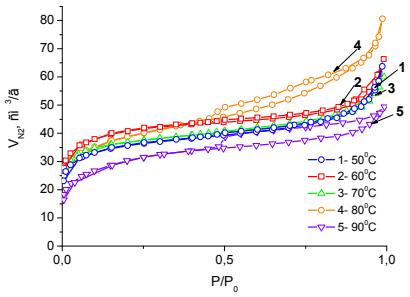

Calcination of the rutile samples is accompanied by a decrease in the specific surface area and pore volume. A decrease in the specific surface area upon calcination up to 300°C is related to the sintering of micropores and the growth of crystallites. Further elevation of the temperature produces even a greater increase in the crystallite sizes, increases the size of mesopores and decreases their volume. Sintering of mesopores and a decrease in their size and volume are observed for the samples calcined at 1000°C. These samples are virtually non-porous. As shown by the BET study, rutile synthesized at 90°C is most stable to sintering.

According to the TEM data, the coherently intergrown rutile crystallites form the filaments that agglomerate into the fan-like structures. Raising the synthesis temperature increases the length of filaments and the density of agglomerates. Upon calcination of the rutile samples, size of the particles increases and their shape changes from filamentary crystals at 100°C to elongated 10-30 nm plates at 300-500°C, and then to 50-70 nm octahedra at 700°C and more than 300 nm octahedra at 1000°C. In addition, elevation of the calcination temperature decreases the number of interparticle boundaries, decreases the number of defects in the samples and increases their crystallinity. The TEM data agree well with the results obtained by the BET study of the calcined samples.

The morphological features of nanorutile powders in dependence on the synthesis and calcination temperatures were revealed by the SEM method. It was shown that a low synthesis temperature (50-70°C) leads to conglomerates of underdeveloped globules consisting of the fan-like agglomerates. As the synthesis temperature is raised to 80°C, the globules start to separate from each other to form the spheres with a better energy compensation; this process is completed at 90°C. The size of conglomerates increases with raising the hydrolysis temperature and remains virtually unchanged during the calcination.

4 Conclusions

The BET, TEM and SEM studies of nanoscale rutile have demonstrated that the particle morphology is characterized by a hierarchical packing: the coherently intergrown crystallites form the filaments that are aggregated into the “open fan” structures, such fan-like aggregates are packed in conglomerates represented by the intergrown or separated globules in dependence on the synthesis temperature. The temperature mode is the key factor that produces changes at different packing levels and determine features of the porous structure of nanoscale rutile.

Acknowledgements

This work was supported by grant of Program of the Ministry for Education and Science of the Russian Federation (Project No. 14.583.21.0004)

References

[1] Kohei Seki. Development of RuO_2/Rutile-TiO_2 catalyst for industrial HCl oxidation process. *Catal. Surv.Asia.* 14 (2010) 168-175. DOI: 10.1007/s10563-010-9091-7.

[2] Levina A.S., Repkova M.N., Ismagilov Z.R., Shikina N.V., Malygin E.G., Mazurkova N.A., Zinov’ev V.V., Evdokimov A.A., Baiborodin S.I. High-performance method for specific effect on nucleic acids in cells using TiO_2~DNA nanocomposites. *Scientific Reports* (2012) |2:756| DOI: 10.1038/srep00756.

[3] Исмагилов З.Р., Бессуднова Е.В., Шикина Н.В., Ушаков В.А. Исследование влияния температуры синтеза на свойства наноразмерного рутила с высокой удельной поверхностью. *Российские Нанотехнологии.* 8 (2013) 14-18.

II-PP136

Propene Epoxidation with Molecular Oxygen over Gold-Silver Catalysts: Density Functional Calculations

Polynskaya Y.G.*, Pichugina D.A., Kuz'menko N.E.

M.V. Lomonosov Moscow State University, Moscow, Russia

* julia.g.snyga@gmail.com

Keywords: propene, oxidation, gold-silver, cluster, bimetallic system, density functional theory

1 Introduction

Propylene oxide is important product in chemistry industry, because it is used in the productions of glycols, polyurethanes and different type of plastics. Currently there are two main industrial methods for propylene oxide production. Organic hydroperoxide process and chlorhydrin process have been used for commercially produce propylene oxide [1, 2]. However, these methods are not appropriate from the view of "green chemistry". Recently, considerable progress has been made in the epoxidation of propene with molecular oxygen over coinage metal catalysts such as Au and Ag [3, 4]. However, both gold and silver catalysts have some problems in propene epoxidation. Thus, use of silver in reaction has been difficult because of the low conversation of propylene and a low selectivity towards propylene oxide. Some features of mechanism using a silver catalyst have not been established. In the case of gold catalysts, gold supported on TiO_2 or titanium silicate zeolites converts propene to propylene oxide with a high selectivity (≈90%), but selectivity of gold particles is sensitive to their size and shape [4].

The main goal of this study was to investigate of the structure of the active centre of the silver and gold-doped silver clusters on the reaction mechanism.

2 Methodology

Geometry optimizations were performed within the spin-polarized approach (PBE functional) [5]. The Priroda program [6] was used for the all-electron calculations within the scalar-relativistic approach, which was based on the full four-component one-electron Dirac equation with separation of the spin–orbit effects. The initial coordinates of the tetrahedral Ag_{20} cluster were taken from previous studies [7]. Mono-doped $Ag_{n-1}Au$ clusters have been generated by substituting one Ag atom with a Au atom in the Ag_{20} clusters at relatively low-coordinated sites. The true TS structures were determined according to the Berny algorithm [8]. Calculations of the intrinsic reaction coordinate through the single imaginary mode of the TS were performed to validate the TS structures.

3 Results and discussion

A key step of oxidation process is the interaction of molecular oxygen with catalysts and the formation of active oxygen (superoxide O_2^-, peroxide O_2^{2-}, and atomic $O_{(ad)}$). The type of adsorbed oxygen species affects the rate and the mechanism of the catalytic reactions, and in the beginning of our research the quantum chemical analysis of the structure and electronic properties of $Au_{20-x}Ag_x$ (x = 0, 1) and influence of heteroatoms in Ag_{20} on the oxygen adsorption and dissociation was performed. The oxygen activation was determined by such parameters as heat of adsorption (Q_{ads}), metal−oxygen distance, oxygen-oxygen distance and vibration frequency ω(O-O). We calculated all these parameters and identified that increase of distance O-O and decrease vibration frequency occur with increasing oxygen activation on metal. According to quantum chemical calculation oxygen interacts with atoms with low coordination number [9].

The next step was to investigate mechanism of reaction of propylene oxidation on silver and

bimetallic $AuAg_{19}$ clusters. Before the search of the reaction mechanism, we calculated propylene adsorption on oxidized complexes $Ag_{20}O_2$ and $AuAg_{19}O_2$. Than we selected the most stable structures (Figure 1): (a) where propylene bonds with defect silver atom with adsorption energy (E_{ads}) about -110 kJ/mol and (b) where propylene bonds with not defect silver atom with E_{ads}=-70 kJ/mol. Modeling of the oxidation reaction has shown that the reaction goes through the formation of a five-membered oxametallacycle consisting of two metal atoms and a −O−C−C− fragment and four-membered oxametallacycle including a single metal atom and −O−C− fragment, that results agree with experiment data.

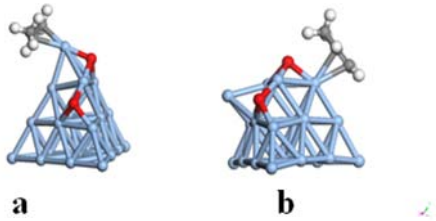

Fig. 1. Optimized structures of $Ag_{20}O_2C_3H_6$

4 Conclusions

Three type of oxygen adsorption was observed: molecular, bridge, and dissociation. The most oxygen activation was observed in case of dissociative adsorption. Oxygen adsorption leads to marked deformation of the clusters as compared to the bare neutral structure.

Simulation the pathway of propylene oxidation has shown that the reaction goes through the formation of a five-membered oxametallacycle consisting of two metal atoms and a −O−C−C− fragment and four-membered oxametallacycle including a single metal atom and −O−C− fragment.

Acknowledgments

This research was supported by the Russian Federation Foundation for Fundamental Research through the Projects 13−03−00320, 14-01-00310, and 11−01−00280, and by the Council for Grants of the Russian Federation President Projects MK−92−2013−3 and NSh−3171.2014.3. The reported study was supported by the Supercomputing Center of M.V. Lomonosov Moscow State University [10].

References

[1] F. Cavani, J.H. Teles, ChemSusChem 2 (2009) 508.
[2] T.A. Nijhuis, S. Musch, M. Makkee, J.A. Maulijn, Appl. Catal. A 196 (2000) 217.
[3] M. Boronat, A. Pulido, P. Concepción, A. Corma, Phys. Chem. Chem. Phys. 16 (2014) 26600.
[4] S. Lee *et. al.*, Angew. Chem. Int. Ed. 48 (2009) 1467.
[5] J. P. Perdew, K. Burke, M. Ernzerhof, Phys. Rev. Lett. 77 (1996) 3865.
[6] D. N. Laikov, Y. A. Ustynyuk, Russ. Chem. Bull. Int. Ed. 54 (2005) 820.
[7] M. Chen, J. E. Dyer, K. Li, D. A. Dixon, J. Phys, Chem. A 117 (2013) 8298.
[8] H. B.Schlegel, J. Comput. Chem. 3 (1982) 214.
[9] Y.G. Polynskaya, D. A. Pichugina, N.E. Kuz'menko, Comp. Theor. Chem. (in press).
[10] V. Sadovnichy, A.Tikhonravov, Vl. Voevodin, V. Opanasenko, Chapman & Hall/CRC Computational Science; Boca Raton, USA, CRC Press (2013) 283.

II-PP137

A Comparative Study of Methanol Conversion to Light Olefins over SAPO-34 Prepared via Conventional and Ultrasound Assisted Hydrothermal Methods

Ibragimov H.J.[1], Babaeva F.A.[1], Ahmadova R.H.[1], Rodemerck U.[2], Kondratenko E.V.[2*]

1 - Azerbaijan National Academy of Sciences, Institute of Petrochemical Processes named after Yu.G. Mamedaliev, Department of "Chemistry and technology of oil and gas", Baku, Azerbaijan

2 - Leibniz Institute for Catalysis at the University of Rostock, Department of "Catalyst discovery and reaction engineering", Rostock, Germany

* rena_ax@rambler.ru

Keywords: SAPO-34, hydrothermal, ultrasound, methanol, light olefins

1 Introduction

Because of growing demand for light olefins and the shortage of petroleum resources in the future, the methanol-to-olefin (MTO) technology, regarded as an alternative process for the production of light olefins from nonpetroleum sources, has received strong significant academic and industrial attention [1]. Silicoaluminaphosphate molecular sieves (SAPOs), with CHA framework, have been widely used in many chemical processes, especially in methanol-to-olefin (MTO) process. The SAPO-34 catalyst shows higher selectivity for lower olefins and the complete conversion of methanol in the MTO reaction. Chemical and structural properties of SAPO-34 can affect the methanol conversion and product distribution in MTO process. Thus, optimization of effective parameters in catalyst synthesis is very important steps for development of MTO process [2]. In this study we investigated influence of synthesis method of catalyst to its activity.

2 Experimental/methodology

The SAPO-34 catalyst was synthesized via conventional (HT) and ultrasound assisted hydrothermal (SONO) methods. For synthesis of HT-SAPO-34 the final gel was stirred for 25 h, for synthesis of SONO-SAPO-34 the gel was sonicated for 30 min. In the case of HT-SAPO-34 the synthesis was accomplished at two temperatures for 12 h – 120^0C with further increasing to 200^0C, but in the case of SONO-SAPO-34 at 200^0C for 48 h. Then samples were centrifugated and washed followed by-drying at 110^0C for 12 h and calcination at 550^0C for 12 h. Catalytic tests were conducted at 450^0C-, and 0.125 MPa-, for 5 h on stream using $CH_3OH:N_2$=60:40 feed with a contact time of 2.05 $mg_{cat}\cdot min\cdot ml^{-1}$ with respect to methanol.

3 Results and discussion

C_2-C_4 low olefins were main products of reaction, while C_1-C_4 alkanes were formed in a low amount. Methanol conversion was complete during the process. Figure 1 shows the yield of C_2-C_4 olefins as function of time on stream. Difference in catalytic activity of HT-SAPO-34 and SONO-SAPO-34 was observed during catalytic tests.A short glance on the figure confirms the positive effect of ultrasound pretreatment of gel on catalyst activity and stability. Perfect crystalline structure of SONO-SAPO-34 makes it stable catalyst with longer life time. This conclusion is supported by the fact based on XRD analysis (the average crystallite size calculated for HT-SAPO-34 and SONO-SAPO-34 are 33 and 27 nm, respectively). The effectiveness factor of SONO-SAPO-34 can be explained with less crystal size. The low stability of HT-SAPO-34 can be addressed by its improper crystallinity.

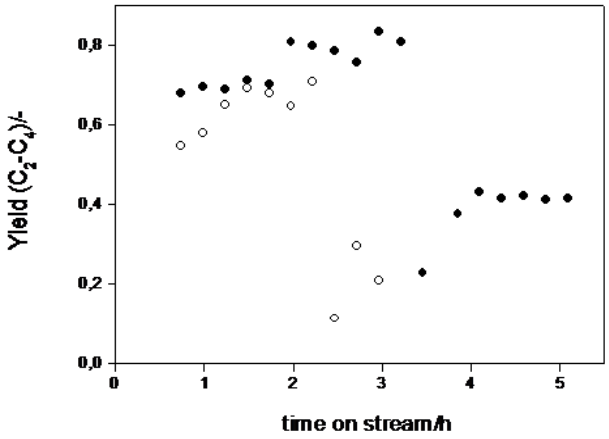

Fig. 1. Time-on-stream yield of C_2-C_4 olefins over HT-SAPO-34- ○ and SONO-SAPO-34- ●

In both cases, with rapidly deactivation of catalysts dimethyl ether is formed in high amounts.

4 Conclusions

The catalytic performance study reveals that SONO-SAPO-34 is a suitable catalyst for MTO process due to its high activity and stability in comparison to HT-SAPO-34.

References

[1] J. Cejka, A.Corma, S.Zones, *Zeolites and catalysis: Synthesis, reactions and applications.* Wiley-VCH, Weinheim (2010), 687-712

[2] S. Askari, R. Halladj, M. Sohrabi, *Microporous and Mesoporous Materials*. 163 (2012) 334-342.

II-PP138

Stabilization of Transition Metal Ions in Unstable Oxidation State in the Matrix of Layered Double Hydroxides with the Structure of Hydrotalcite

Ryltsova I.G.[1*], Saenko R.N.[1], Nestroynaya O.V.[1], Lebedeva O.E.[1], Danshina E.P.[2]

1 - Belgorod State National Research University, Department of Biology and Chemistry, Belgorod, Russia

2 - Belgorod State National Research University, Shared Facilities Center "Diagnosing the Structure and Properties of Nanomaterials", Belgorod, Russia

* ryltsova@bsu.edu.ru

Keywords: layered double hydroxide (LDH), hydrotalcite, unstable oxidation, state, nickel

1 Introduction

Layered double hydroxides (LDHs) of the hydrotalcite family are layered materials of the general formula $\left[M^{2+}_{1-x} M^{3+}_{x} (OH)_2 \right]^{x+} (A^{n-})_{x/n} \cdot mH_2O$. Interest in LDHs is due to the presence of a number of unique properties typical forgiven class of compounds: magnetic, optical, redox properties, etc. The papers discussing the synthesis and properties of LDHs with cations of different nature and rather complicated mixtures of cations are rather common [1, 2]. However the papers are mainly focused on the introduction of those cations, for which valences 2 and 3 are the most stable ones (iron, copper, zinc, chromium, bivalent nickel, cobalt, gallium, and others). Attempts of stabilization of unstable valence states of the cations in the lattice of LDH are poorly described. At the same time such systems may exhibit unusual redox, catalytic and other properties therefore their synthesis might be of interest. The present article is concerned with the study of systems of co-precipitated hydroxides of magnesium (II), aluminum (III) and nickel (III).

2 Experimental

LDHs containing Ni^{3+} ions in the structure of metal hydroxide layers were synthesised by co-precipitation from the aqueous solutions of mixtures of magnesium, aluminium and nickel salts in oxidizing media. Sodium hypochlorite was used as the oxidizing agent. After synthesis the samples were transformed to carbonate form by ion exchange. The phase composition of samples were studied by X-ray diffraction (XRD) using Rigaku diffractometer (CuK_α - radiation with scanning step 2θ 0,5°). Chemical analysis of the samples was performed using scanning electron microscope QUANTA 3D equipped with a detector of the characteristic X-ray dispersive energy photons (20 kV). Content of Ni^{3+} in the samples was determined by iodometric titration.

3 Results and discussion

Atomic ratio Al^{3+}:Ni^{3+}in the co-precipitated samples was varied in a wide range. Fig. 1 displays XRD patterns for the samples prepared. In the absence of aluminum hydrotalcite-like phase is not formed, only the formation of individual brucite and nickel (III) hydroxide with the structure of brucite was observed. In the systems Mg/AlNi-1:3 and Mg/AlNi-1:1 the coexistence of brucite, Ni (III)-containing layered hydroxide and nickel (III) hydroxide was proved. Only a product obtained from a solution with cations ratio Mg:Al:Ni = 12:3:1is represented by a single phase with a structure similar to hydrotalcite. The formula of synthesized LDH was calculated on the base of the results of chemical analysis: $Mg_6Al_{1,52}Ni_{0,48}(OH)_{15,97}Cl_{0,03}CO_3 \cdot 3{,}5H_2O$. The

presence of chlorides not replaced by carbonate anions is probably due to the fact that in the course of synthesis Cl^- is able to substitute some OH^--groupsin metal hydroxide layers in the structure [3].

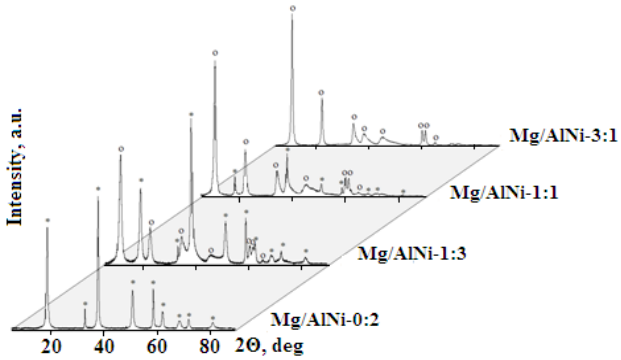

Fig.1. X-ray diffraction of the synthesized samples (* - brucite, o - hydrotalcite)

The content of Ni^{3+} in LDH sample was monitored for 12 months (Fig. 2). For comparison Ni^{3+}content was determined in the synthesized sample of nickel hydroxide ($Ni_2O_3 \cdot xH_2O$). The values of m_t/m_0(the ratio of mass fractions of Ni^{3+}in the sample after the storage and the as-precipitated samples) for the samples demonstrate that $Ni^{3+}$is much more stable in the matrix LDH than in the nickel (III) hydroxide.

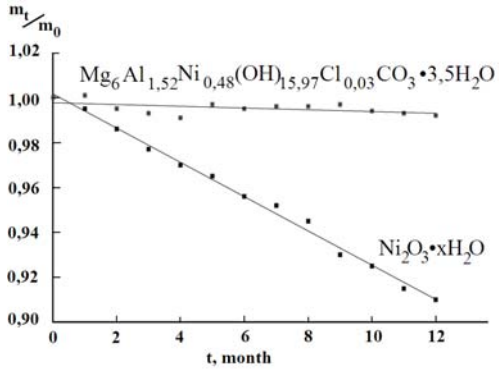

Fig.2. Decrease of Ni^{3+}content in the samples

4 Conclusions

LDH containing Ni^{3+} ions in the structure of metal hydroxide layers was synthesised. The formation of single phase product was shown to be possible with a substitution of up to 25% aluminium ions for nickel in the structure of hydrotalcite. Thus the introduction of cations in the structure of hydrotalcite allows to stabilize them in unstable oxidation state.

Acknowledgements

This research was performed as part of the State task of BelSU 2014 N 420-154.

References

[1] F.Cavani, F.Trifiro, A.Vaccari, *Catal. Today*, 11(1991), 173-301.
[2] C.Forano, T.Hibino, F. Leroux, C.Taviot-Gueho, *Handbook of Clay Science* 1(2006), 1021 - 1098.
[3] V.R.L.Constantino, T.J. Pinnavaia, *Inorg. Chem.*, 34(4) (1995), 883-892.

II-PP139

Modeling the Mechanism of Surface Stages of Vapor Phase Catalytic Oxidation of 4-Methylpyridine

Vorobyev P.B., Michailovskaya T.P., Saurambaeva L.I., Yugay O.K.*, Serebryanskaya A.P.

A.B. Bekturov Institute of Chemical Sciences, JSC, Almaty, Kazakhstan

* yu.ok@mail.ru

Keywords: oxidation, catalyst, vanadia, 4-methylpyridine, cluster approach, modeling

1 Introduction

Heterogeneous vapor phase catalytic oxidation of 4-methylpyridine is a new efficient and ecology friendly technology of isonicotinic acid, feedstock for the synthesis of a number of antituberculosis drugs. [1]

2 Experimental

Maximum selectivity of isonicotinic acid is 57% on vanadia at a temperature of 350°C. Pyridine-4-carbaldehyde is contained in the reaction products together with isonicotinic acid. Vanadia catalyst promotion of additives of metal oxides of groups IV-VI of the Periodic System reduces the content of pyridine-4-carbaldehyde in the reaction products and increases selectivity of isonicotinic acid (Fig.) .

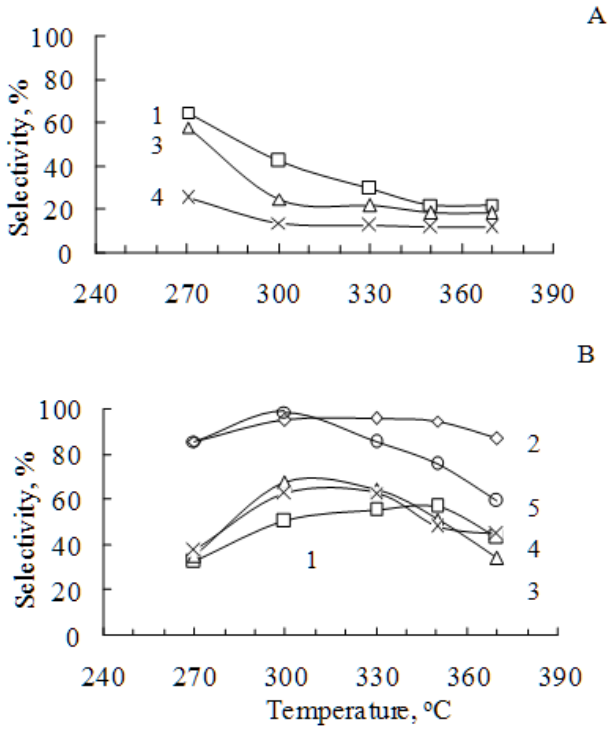

Volumetric feed rate of 4-methylpyridine-35 г·л$^{-1}_{кат.}$·ч$^{-1}$. molar ratio 4-methylpyridine:O_2:H_2O=1:14:26.
Catalysts: 1 – V_2O_5, 2 – V_2O_5-TiO_2, 3 – V_2O_5-Al_2O_3, 4 – V_2O_5-Fe_2O_3, 5 – V_2O_5-ZrO_2.
Fig. Dependence of selectivity of pyridine-4-aldehyde (A) and isonicotinic acid (B) formation from temperature of 4-methylpyridine oxidation on various catalysts

During oxidation of 4-methylpyridine corresponding aldehyde is formed with a higher yield than during oxidation of 3-methylpyridine. The reason for this is the lower the basicity of the pyridine-4-carbaldehyde compared to 3-isomer. Pyridine-4-carbaldehyde kept weaker on the acid sites surface, it does not have time to oxidize into isonicotinic acid and therefore desorbed into the gas phase. Quantum chemical calculations of the basicity of the pyridine-3- and pyridine-4-aldehydes in the gas phase and experimental data on the influence of water on kinetics of oxidation of 4-methylpyridine confirm this hypothesis (table). At a chemisorption on a catalyst surface water creates the new acid centers capable to interact with heteroatom of nitrogen of a substratum.

Table. Effect of water concentration on the rate constants of stages of 4-methylpyridine oxidation on the V-Ti-Zr-oxide catalyst at a temperature of 245°C. The initial concentrations: [4-methylpyridine] = 1,1 • 10-4, [O2] = 9,4 • 10-3 mol • L-1

Stage №	Stage of reaction	k_i, c^{-1}					
		$[H_2O] \cdot 10^3$, mol/l					
		0	1,3	2,45	5,1	8,9	15,2
1	4-Methylpyridine→ 4-PyCHO	1,788	1,970	2,799	3,891	4,269	4,241
2	4-PyCHO → 4-PyCOOH	1,713	1,968	3,790	6,249	6,389	9,571
3	4-PyCOOH →Py	0,290	0,126	0,080	0,088	0,078	0,056
4	4-Methylpyridine → CO_2	0,084	0,276	0,485	0,316	0,118	0,161
5	4-PyCOOH → CO_2	0	0	0	0,667	0,434	0,514
6	4-PyCHO → 4-PyCN	0,164	0,597	0,814	1,079	0,862	0,650

3 Results and discussion

Kinetic calculations show that isonicotinic acid arise via stage of forming 4-pyridine carbaldehyde. At the stage 3 part of the acid is decarboxylated until pyridine.
When water concentration increases the velocity constant of the aldehyde conversion into acid dramatically rises. 4-cyanopyridine is present in the reaction products. Nitrogen donor for the pyridine-4-aldehyde conversion to 4-cyanopyridine in the stage number 6 are nitrogen moieties of deep oxidation initial 4-methylpyridine (stage number 4) and isonicotinic acid (stage number 5) [2].

4 Conclusion

The cluster approach and the program Gaussian-09 W were used to model both the 4-methylpyridine chemisorption on the vanadia and vanadium binary catalysts surface. It is shown that the promotional effect of the modifier oxide on the vanadia catalytic activity is caused with increasing of nucleophilicity (proton affinity) of vanadium bonded oxygen and reduction enthalpy of deprotonation of the oxidized methyl group of the chemisorbed 4-methylpyridine. An interesting fact is that the avulsion of a proton from the methyl group and its transfer to the vanadyl oxygen of cluster to form a new bond ≡V-O-H requires less energy than heterolytic breaking C-H bond of the methyl group chemisorbed substrate. This can be explained by the fact that "when moving along the reaction path the energy required to break the old bonds, compensated by the energy released in the formation of new" [3].

References

[1] Mashkovskij M.D. Lekarstvennye sredstva. V 2-h tomah. T. 2. Har'kov: Torsing, 1997. 592 s.
[2] Suvorov B.V., Bukejhanov N.R. Okislitel'nye reakcii v organicheskom sinteze. M.: Himija, 1978. 200 s.
[3] Boreskov G.K. Sushhnost' kataliticheskogo dejstvija // Zhurnal VHO im. D.I. Mendeleeva. 22, 5(1977) 495-505.

II-PP140

Effect of the Preparation Method of Nano-Titanium Pyrophosphate on Catalytic Properties: the Conversion of n-Butane

Mokrane E.[1,2*], Messaoudi H.[1], Slymi S.[1], Barama S.[1], Taufiq-Yap Y.H.[3], Pinard L.[4], Barama A.[1]

1 - LMCCCO, Faculty of Chemistry,USTHB, Algiers, Algeria
2 - Chemistry Department, Faculty of Sciences, UHBC, Chlef, Algeria
3 - Catalysis Science and Technology, Universiti Putra Malaysia, Serdang, Malaysia
4 - IC2MP, Université de Poitiers, Poitiers cedex, France

* zinamokrane@gmail.com

Keywords: pyrophosphate, phosphate, TiP_2O_7, ODH, n-butane, nano-catalyst

1 Introduction

Titanium pyrophosphates (TiPO) are used in the conversion of n-butane. TiPO catalysts were prepared, by used several methods [1-3] then characterized and tested in ODH of n-butane. Catalyst were characterized by means of X-ray diffraction (XRD), Fourier transformed infrared (FT-IR), Thermal gravimetric analysis (TGA), Brunner-Emmett-Teller surface area measurement (BET) and temperature-programmed desorption of ammonia (NH_3-TPD), Field Emission Scanning Electron Microscopy (FE-SEM) to characterise and describe structural and textural surfaces properties. The effect of the preparation method in conversion of n-butane into butenes and butadiene has been investigated.

2 Experimental

Catalysts preparation:

1. Method A: precipitation-concentration A: done in two steps, 1) is to synthesize titanium oxide TiO2 by coprecipitation of $Ti(OH)_4$ hydroxides. 2) Titanium dioxide and stoichiometric amount of phosphoric acid (85%) are agitated at 80°C, then dried, crushed and calcined [1].

2. Method B: Method coprecipitation B: A sodium pyrophosphate $Na_4P_2O_7$ 0.1M is added in Drop Count in stoichiometric ratios to a 0.1M solution of titanium chlorides $TiCl_4$ in hydrochloric acid 6M (HCl 37%). The precipitate is filtered and washed then dried overnight. Then crushed and calcined too [2].

3. Method S: Solid phase method S: Titanium dioxide TiO2 is mixed in stoichiometric amounts with diammonium hydrogen phosphate $(NH_4)_2HPO_4$. The mixture is grind vigorously and then dried at 120 ° C for one a week, then calcined [3].

Characterization:

The TGA analysis was carried out on a Perkin Elmer Thermal Analyzer. Powder X-ray diffraction patterns were recorded employing CuKα radiation (λ = 1.5418 Å). FTIR analyses were determined using KBr method. The specific surface area of the catalyst sample was measured by BET method. The TPD-NH_3 analysis was done. The acidity and the acidic strength distribution of the catalyst were studied. The morphology surface images of nanostructures of TiPO catalysts were acquired by using (FE-SEM).

Catalytic activity:

The catalytic tests were performed in a fixed bed reactor in the reaction temperature range of 400-500°C, Gas feeds: air/butane= 5/1. The reaction products were analyzed by gas chromatography.

3 Results and discussion

The P:Ti ratios obtained from chemical analysis were close to the theoretical ones for both solids. The specific areas and porosities are shown in Table1. The FTIR spectrum shows titanium pyrophosphate frequencies observed in similar compounds are examined [1-2].

Table 1. Physico-chemical properties of bismuth pyrophosphate catalysts.

Catalyst	Specific surface area ($m^2.g^{-1}$)	Pore volume (10^{-2} cm3.g^{-1})	Particle size* (nm)	Acidity (mmol.g^{-1})	Conv (%)	Sel (%)	Yield
TiPO-2-A	6.51	3.46	41.23	0.38	**25.2**	**45.59**	11.47
TiPO-2-B	6.46	1.8	51.8	1.71	**46.3**	**10.6**	4.9
TiPO-2-S	3.20	2.12	56.42	0.15	**28.1**	**42.95**	**12.07**

***** FE-SEM calculated particle size.

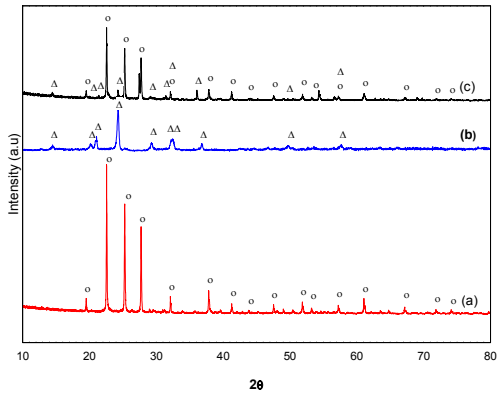

Fig.1. X-ray diffraction patterns of TiPO samples:
a) TiPO-2-A, b) TiPO-2-B, c) TiPO-2-S

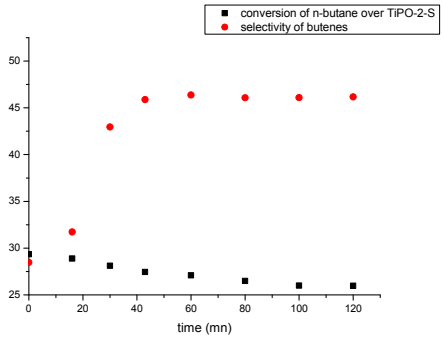

Fig. 2. Conversion of n-butane and butenes selectivity of TiPO-2-S catalyst

In XRD spectra (Fig.1) we identify the phase TiP_2O_7 (JCPDS 00-038-1468) in samples TiPO-2-A and TiPO-2-S. The DTA/TG curves show that samples are stable up 600°C. FE-SEM showed condensed nanoparticles. The major product under this reaction condition is trans-2-butene. The ODH reaction of n-butane gives the best yield (12.07) obtained over TiPO-2-S catalyst, with a conversion of 28.12% and selectivity of 42.95%; which is inversely related to the acidity of the catalyst.

4 Conclusions

The conversion of n-butane and selectivity in ODH are stable in the early measures. For the three catalysts, the best performance is observed at the same temperature 450 °C and for the same reaction time (35 min). All catalysts are activated over time.

Acknowledgements

We gratefully acknowledge the IC2MP, UP, France and The PutraCat, UPM, Malaysia.

References

[1] I.-C. Marcu, I. Sandulescu, J.M. Millet, Applied Catalysis A: General 227 (2002) 309-320.
[2] T. Masui, H. Hirai, N. Imanaka, G. Adachi, Journal of Alloys and Compounds 408-412 (2006) 1141-1144.
[3] H. Mahmoud, B. Louati, F. Hlel, K. Guidara, Ionics 17 (2011) 223-228.

II-PP141

Relationship between Surface Acid/Base Sites of Solid Catalysts and their Catalytic Activity in Biomass Derived Reactions

Bennici S., Auroux A.*

Université Lyon 1, CNRS, UMR 5256, IRCELYON, Institut de Recherches sur la Catalyse et l'Environnement de Lyon, Villeurbanne, France

* aline.auroux@ircelyon.univ-lyon1.fr

Keywords: acidity/basicity, adsorption calorimetry, fructose dehydration

1 Introduction

Among other parameters, the catalytic activities of solid materials are dependent on the accessibility of active sites to reactant molecules. Relative acid strengths of solid catalysts depend markedly on whether a solvent is present, on the nature of the solvent, and may vary as the medium in which the acidity is measured is changing [1,2].

2 Experimental/methodology

A series of acid materials such as zeolites (MFI), silica-alumina (Si-Al), niobium oxide (NBO), niobium phosphate (NBP), and resin (Nafion) have been studied in terms of number, strength and activity of their acid sites. In gas phase adsorption calorimetry the acidity was determined using ammonia as basic probe. In water, acidity of samples was estimated through the adsorption of a typical basic probe molecule, phenylethylamine diluted in water; and using a differential titration microcalorimeter for the determination of the strength and UV-vis spectroscopy for the determination of the number of acid sites, both performed in similar conditions. The equilibrium isotherm and heats of adsorption are the critical design variables in estimating the performance of an adsorption process. Their shapes proved significant information on the nature and the strengths of solvate-solvent and sorbate-solvent interactions and also the degree of energetic heterogeneity of the solid surfaces under study.

The same samples were probed as catalysts for the dehydration of fructose to 5-HMF, a reaction which has attracted much attention because of the demand of renewable resources, such as biomass, as substitutes for petroleum chemicals [3].

3 Results and discussion

Correct evaluation of reliable experimental data from titration calorimetry for systems with well-defined initial state and with controlled addition of a base titrant results in differential heats of surface processes. Results allowed to discriminate the active acid sites of catalysts in water by their strength and to assess that their relative acid strength is changing with reaction medium (gas phase or liquid medium).

Figure 1 represents the conversion of fructose (after 6 h reaction in water medium at 130 °C in an autoclave) as a function of the number of strong acid sites at the surface of the various catalysts, as determined in aqueous and gas phases. A nearly linear relationship can be observed in both cases for conversion of fructose except for Nafion sample. When the number of acid sites is determined by NH_3 gas phase adsorption, the Nafion sample (Brønsted sites only) displays a much lower sites number than in liquid phase and does not fit with the other samples

which possess both Brønsted and Lewis acid sites.

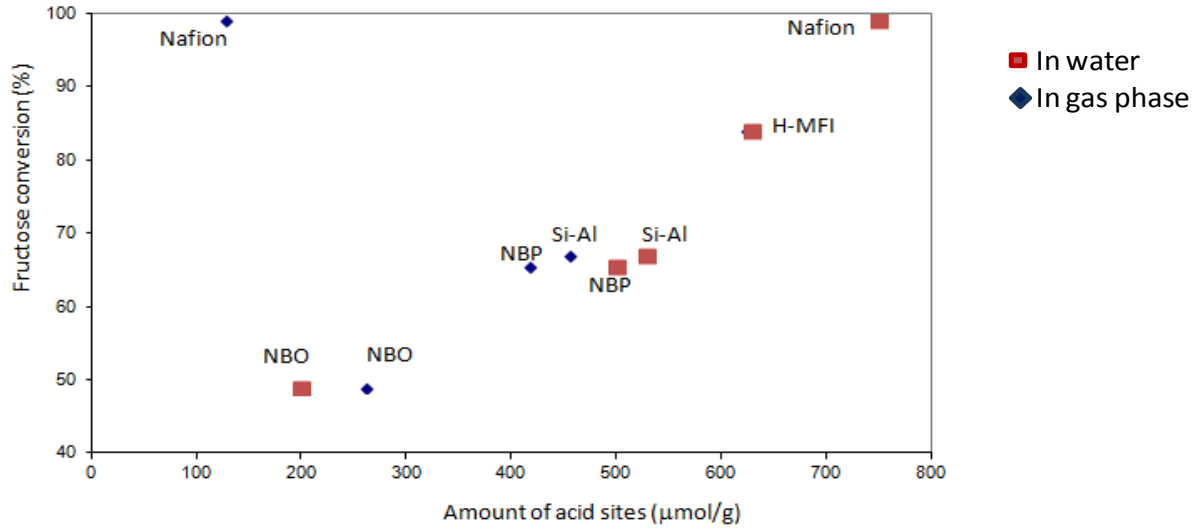

Fig. 1. Fructose conversion over various catalysts vs. acidity in gas and water phases

4 Conclusions

The determination of the acid-base properties of solid catalysts in the same media as used during the catalytic reaction is fundamental to correlate the catalytic activity to the surface properties.

This work has well demonstrated that for reactions performed in water or any other liquid solvent the number and the strength of accessible acidic/basic sites can be different, depending strongly on the solvent-solid bondings.

Acknowledgements

The authors thank Dr. O.Otman for his experimental help.

References

[1] A. Gervasini, A. Auroux A. *Thermochimica Acta*, 2 (2013) 1993
[2] R. Kourieh, S. Bennici, M. Marzo, A. Gervasini, A. Auroux. *Catalysis Communications* 19 (2012) 119
[3] R. Kourieh, V. Rakic, S. Bennici, A. Auroux. *Catalysis Communications* 1 (2013) 5

II-PP142

Selective Hydrogenation of Phenylacetylene to Styrene over Pd-Fe/SiO_2. Effect of Catalyst Preparation

Kirichenko O.A., Shesterkina A.A.*, Kozlova L.M., Mishin I.V., Kapustin G.I., Kustov L.M.

N.D. Zelinsky Institute of Organic Chemistry, Russian Academy of Sciences, Moscow, Russia

* anastasiia.strelkova@mail.ru

Keywords: iron-palladium catalysts, phenylacetylene hydrogenation

1 Introduction

Selective hydrogenation of alkynes to alkenes, without further reduction to alkanes, is of particular importance in the production of polymers [1]. Modifications of the Pd-based catalysts by alloying resulted in active and selective catalysts [2-4]. The Pd-Fe_3O_4/SiO_2 catalyst shows the reasonably high conversion and selectivity [4], yet alloyed Pd-Fe NPs exhibit a decrease in TOF as compared with Pd NPs [5]. Therefore, it seems of particular interest to evaluate the effect of Pd and Fe state on the catalytic activity in the hydrogenation of phenylacetylene (PhA) to styrene.

2 Experimental/methodology

The catalysts were prepared by simultaneous or consecutive deposition of the metal precursors on the silica carriers with a specific surface area of 340 m^2g^{-1} (HS) or 30 m^2g^{-1} (LS). $(NH_4)_3Fe(C_2O_4)_3$, Pd acetate, and $[Pd(NH_3)_4]Cl_2$ were used as precursors. Then a different thermal treatment was applied. The samples were characterized by XRD, TEM, TPR. The catalytic activity of prepared samples was tested in the selective hydrogenation of PhA to styrene at the following reaction conditions: 0.1-0.4 M PhA in ethanol, 10-50 mg of a catalyst, 1 atm H_2 , 20-60ºC, molar ratio PhA : Pd = 200-1000.

3 Results and discussion

The XRD analysis revealed the formation of the Pd^0, α-Fe_2O_3, and Fe_3O_4 phases after calcination of the samples at 240–260ºC (Fig. 1). All Pd-Fe calcined or reoxidized samples exhibited the H_2 consumption below the starting reduction temperature of Fe oxides indicating the strong interaction between Fe oxide and Pd species. Formation of the Pd-rich alloys and the Fe^0 phase after reduction at 400ºC was confirmed by XRD (Fig. 1).

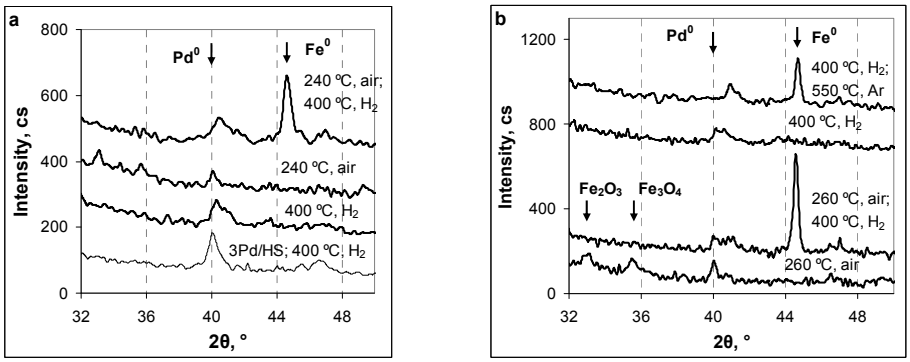

Fig. 1. XRD patterns of the samples 3Pd8Fe on HS (a) and on LS (b) supports after thermal treatment at different conditions

There was no peak of hydrogen release at 50-70ºC on the TPR curves of the samples reduced at 400ºC, which indicated the absence of pure Pd^0 particles and the formation of the Pd–Fe alloy particles suppressing the β-PdH formation at ambient temperatures.

The samples prepared by consecutive deposition of Pd acetate on the Fe precursor surface were active in PhA hydrogenation (Table 1, sample 3Pd7Fe/HS-R), yet fast deactivated. The simultaneous deposition of the Fe precursor and $[Pd(NH_3)_4]Cl_2$ resulted in the more active and stable samples after the precursor reduction (Table 1, sample 3Pd8Fe/HS-R). However, their selectivity was low due to further hydrogenation to ethylbenzene. Intermediate calcination before reduction significantly enhanced the catalytic activity and selectivity, with the catalytic behavior strongly depending on the Pd particle size, alloying and the support texture (Table 1). The styrene yield was comparable or even higher than for the Pd catalyst. The shape of the conversion and selectivity curves (Fig. 2) indicated the different mechanisms of hydrogenation for the samples on the different carriers.

Table 1. The initial rate, selectivity to styrene and its yield at the complete PhA conversion.

Sample[a]	**Fe, %**	**Pd, %**	***d*(Fe^0) nm**	***d*(Pd) nm**	r_0, $mol_{PhA}\ mol_{Pd}^{-1}\ s^{-1}$	r_0, $mol_{H2}\ mol_{Pd}^{-1}\ s^{-1}$	**S_{100}, %**	**Yield, g g_{ct}^{-1} h^{-1}**
3Pd7Fe/HS-R	6.9	3.3	nd	nd	0.034	0.036	-	-
3Pd8Fe/HS-R	7.6	3.0	nd	15 (3)	0.08	0.07	56	2.0
3Pd8Fe/HS-CR	7.6	3.0	19	10	0.23	0.19	86	9.4
3Pd8Fe/LS-CR	7.8	3.2	33	20	0.063	0.065	82	7.7

[a]The prepared samples are denoted as xPdyFe/A-B, where x and y are referred to the Pd and Fe loading (mass %), A was the support abbreviation, and B denotes the sample treatment (C - calcined, R - reduced at 400ºC).

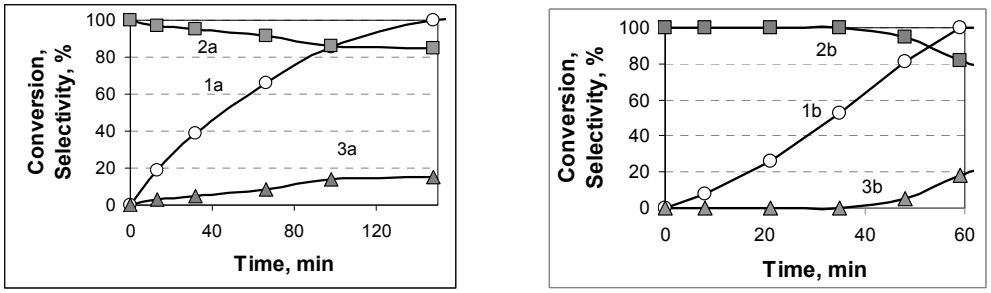

Fig. 2. PhA conversion (1), selectivity to styrene (2) and to ethylbenzene (3) over 3Pd8Fe/HS-CR (a) and 3Pd8Fe/LS-CR (b). Reaction conditions: 23ºC, 0.16 M PhA, PhA:Pd = 940 (a) and 330 (b).

4 Conclusions

The catalytic behavior of the Pd-Fe/SiO_2 system is strongly dependent on the catalyst preparation variables that change the Pd particle size and Pd-Fe alloying, with the Pd^0 NPs of the size 10 nm being preferable.

References

[1] S. A. Nikolaev, L. N. Zanaveskin, V. V. Smirnov, V. A. Averyanov, K. L. Zanaveskin, *Russ. Chem. Rev.*78 (2009) 231.
[2] S. Domínguez-Domínguez, Á. Berenguer-Murcia, B.K. Pradhan, Á. Linares-Solano, D. Cazorla-Amoros, *J. Phys. Chem. C* 112 (2008) 3827.
[3] X. Chen, A. Zhao, Z. Shao, C. Li, C. T. Williams and C. Liang, *J. Phys. Chem. C* 114 (2010) 16525.
[4] K. H. Lee, B. Lee, K. R. Lee, M. H. Yi and N. H. Hur. *Chem. Commun.* 48 (2012) 4414.
[5] S. Domínguez-Domínguez, Á. Berenguer-Murcia, D. Cazorla-Amorós, Á. Linares-Solano, *J. Catal.* 243 (2006) 74.

II-PP143

Bimetallic PdRu Nanocatalysts for the Hydrogenation of Phenols

Maximov A.L.[1,2], Zolotukhina A.V.[1*]

1 - Moscow State University, Chemistry Department, Moscow, Russia
2 - Institute of Petrochemical Synthesis RAS, Moscow, Russia

* anisole@yandex.ru

Keywords: hydrogenation, catalysis, phenols, bimetallic PdRu nanoparticles

1 Introduction

Hydrogenation is one of the most important processes in the petrochemical industry and organic synthesis. In particular, hydrogenation of phenol is used to obtain cyclohexanone and cyclohexanol, the main intermediates for the nylon-6 and adipic acid production [1,2]. Another, novel application in the hydrogenation of phenolic compounds is a biofuel production from lignin [3,4]. Therefore, it is the actual problem to develop high-efficient and selective catalysts for the hydrogenation of phenols. The particular interest is referred to the bimetallic nanoparticles and alloys, whose activity and selectivity can be tuned changing the metals ratio and their nature [5,6]. Here we report the synthesis of the bimetallic PdRu nanoparticles, encapsulated into cross-linked dendritic matrix, and their application in the hydrogenation of phenols.

2 Experimental

The synthesis of the heterogeneous networks, based on the poly(propylene imine) (PPI) dendrimers of the 3rd generation, cross-linked with 1,6-diisocyanatohexane, is described elsewhere in literature [7].

The synthesis of dendrimer-encapsulated PdRu nanoparticles was carried out according to the following procedure. The desired amounts of the dendritic carrier (dendrimer cont. ~ 55%) and water were placed in the round-bottom flask of the volume required, equipped with the magnetic stirrer and reflux condenser. Then, $RuCl_3$ and $Pd(OAc)_2$ were added to the resulting suspension at stirring. The molar Pd : Ru ratio was 1 : 1, and (Pd + Ru) : dendrimer ratio was 10 : 1. The reaction was carried out for 12 h at 70 ^{0}C and vigorous stirring. After that the reaction mixture was evaporated *in vacuo*, resulting in the dark, black-brown powder. At the next stage the precursor obtained was reduced, using the 10-fold molar excess of $NaBH_4$ in the water-ethanol mixture. The reaction was carried out for 12 h at room temperature and vigorous stirring. After the time passed, the reaction mixture was centrifuged several times with water and ethanol, and the residue was dried in the air, resulting in the black powder.

The catalytic experiments were carried out according to the following procedure.

The catalyst and the substrate in the desired ratio were placed into a thermostated steel autoclave equipped with the glass vial-insert and magnetic stirrer. Water was added according to the proportion of 1 mg or 1 μl of substrate per 1 μl of water. The autoclave was sealed, pressurized with hydrogen to a pressure up to 10 or 30 atm. and connected to the thermostat. The reaction was carried out at 90ºC for the required time, after which the reactor was cooled below room temperature and depressurized. The reaction products were analyzed by gas-liquid chromatography.

3 Results and Discussion

A method of co-complexation was used to prepare bimetallic PdRu catalyst [3]. A complex

formation between metal ions and the dendrimers tertiary aminogroups was the driving force of the reaction. Coordination of both Pd and Ru ions with the same types of the donor atoms was suggested to favour to their nearby arrangement and the formation of the bimetallic nanoparticles at the reduction stage [3]. The mean particles diameter according to the TEM data was 2-2.5 nm.

The catalyst obtained was tested in hydrogenation of phenol, its ethers and substituted phenols. It should be noted, that the hydrogenation of phenol in presence of the bimetallic platinum group catalysts has not well developed yet, and there are only few works, dealing with similar systems [8,9], including PdRu nanoparticles [9]. Also there was no any communications concerning the synthesis of the PdRu nanoparticles, encapsulated into the polyamine dendrimers.

Our research revealed, that PdRu catalysts based on the cross-linked PPI dendrimers were active in the liquid-phase hydrogenation of phenol and similar compounds. Varying the reaction time, hydrogen pressure and substrate to catalyst ratio, the high selectivity on cyclohexanone (up to 100%) can be achieved, while the analogous monometallic Ru catalyst yielded only cyclohexanol. Replacement of phenol to more hydrophobic anisole and then to phenethole resulted in the drastical decrease in conversion and the formation of the hydrogenolysis (benzene, cyclohexane) and deoxygenation (phenol) products, which total portion among the reaction products was 10-40% and increased with the increasing the reaction time and decreasing the substrate to catalyst ratio. Introducing the alkylic substituents to the aromatic ring of phenol also led to the decrease in conversion. The main reaction products were corresponding substituted derivates of cyclohexanol. The polar hydrophilic hydroquinone and resorcinol, vice versa, were converted faster than phenol. The latter gave *trans*-1,3-cyclohexanediol as the main reaction product with the selectivity up to 95%, while the former underwent deoxygenation during the reaction, giving up to 50% of the cyclohexanol and phenol. Their portion, as for phenolic ethers, increased, when increasing the reaction time and catalyst amount.

4 Conclusions

Hybrid bimetallic catalyst based on the PdRu nanoparticles encapsulated into the cross-linked dendritic matrix was synthesized. The material obtained appeared to be active in the hydrogenation of phenol and its derivates. For phenol, 100% selectivity on the cyclohexanone can be achieved. Introducing the hydrophobic substituents to the hydroxyl-group or the aromatic ring of phenol led to the conversion decreasing. The formation of the hydrogenolysis and deoxygenation by-products was typical of the hydroquinone and phenolic ethers.

Acknowledgments

This work was supported by the RFBR grant No 14-03-31531.

References

[1] W.K. Chwang, J.N. Vicent, T.T. Tidwel, *J. Am. Chem. Soc.* 99 (1977) 7233.
[2] K. Weissermel, H.-J. Arpe. *Industrial Organic Chemistry*, VCH Verlagsgesellschaft, Weinheim (1993) 457 p.
[3] J.M. Pepper, W.F. Steck, R. Swoboda, J.C. Karapally, *Adv. Chem.* 59 (2009) 238.
[4] N.A. Vasyunina, A.A. Balandin, S.V. Chepigo, G.S. Barysheva, *Bull. Acad. Sci. USSR Div. Chem.* Sci. 9 (1960) 1224.
[5] Y.-M. Chung, H.-K. Rhee, *J. Mol. Catal. A: Chem.* 206 (2003) 291.
[6] M. Murata, Yu. Tanaka, T. Mizugaki, K. Ebitani, K. Kaneda, *Chem. Lett.* 34 (2005) 273.
[7] E.A. Karakhanov, A.L. Maximov, A.V. Zolotukhina, S.V. Kardashev, *Petr. Chem.* 50 (2010) 1.
[8] J.A. Baeza, L. Calvo, J. J. Rodriguez, E. Carbó-Argibay, J. Rivas, M. A. Gilarranz, *Appl. Catal. B: Envir.* 168 (2015) 283.
[9] Ch. Huang, X. Yang, H. Yang, P. Huang, H. Song, Sh. Liao, *Appl. Surf. Sci*. 315 (2014) 138.

II-PP144

Hybrid Bimetallic RhRu and PdRh Nanocatalysts: Synthesis and Application

Maximov A.L.[1,2], Zolotukhina A.V.[1*], Karakhanov E.A.[1]

1 - Moscow State University, Chemistry Department, Moscow, Russia
2 - Institute of Petrochemical Synthesis RAS, Moscow, Russia

* anisole@yandex.ru

Keywords: hydrogenation, catalysis, phenols, bimetallic, nanoparticles, PdRh, RhRu

1 Introduction

Immobilization of metal complexes and nanoparticles on the surface of heterogeneous carriers is one of the most prospective trends for the high-efficient catalysts development, allowing to combine properties of both homogeneous (high activity and selectivity) and heterogeneous catalysts (stability and recyclability) [1-3]. A particular interest has an application of bimetallic nanoparticles in catalysis, allowing to carry out various processes with higher rate and selectivity [4,5]. Here we propose a new approach for immobilization of bimetallic PdRh and RhRu nanoparticles in channels of mesoporous silica, prepared by sol-gel method and modified by poly(propylene imine) (PPI) dendrimers, and their use in the hydrogenation of phenols.

2 Experimental

The synthesis of hybrid mesoporous carrier was carried out similarly to the following procedure. The PPI dendrimer of the 2nd generation, preliminarily modified by the (3-glycidoxy)propyltrimethoxysilane, was placed in the aqueous solution of the Pluronic 123. After that tetraethoxysilane, preliminarily hydrolyzed by aqueous HCl was added. After the mixture had been vigorously stirred, an aqueous NH_3 solution was added for gelation. The material obtained was heated at 100 ^{0}C, centrifuged with water and ethanol and then dried at air. The synthesis of dendrimer-encapsulated PdRh and RhRu nanoparticles was carried out according to the following procedure. The desired amounts of the heterogeneous hybrid carrier (dendrimer cont. ~ 18.5%) and solvent were placed in the round-bottom flask of the volume required, equipped with the magnetic stirrer and reflux condenser. Then, the metalloprecursors were added to the resulting suspension at stirring. For the PdRh catalyst, the molar Pd : Rh ratio was 0.35 : 0.65, and (Pd + Rh) : dendrimer ratio was 3 : 1. For the RhRu catalyst, the molar Ru : Rh ratio was 0.3 : 0.7, and (Pd + Rh) : dendrimer ratio was 4 : 1. After 12 h the reaction mixture was evaporated *in vacuo*, resulting in the dark, black-brown powder. At the next stage the precursor obtained was reduced, using the 10-fold molar excess of $NaBH_4$. The catalytic experiments were carried out according to the following procedure. The catalyst and the substrate in the desired ratio were placed into a thermostated steel autoclave equipped with the glass vial-insert and magnetic stirrer. Water was added according to the proportion of 1 mg or 1 μl of substrate per 1 μl of water. The autoclave was sealed, pressurized with hydrogen to a pressure up to 10 or 30 atm. The reaction was carried out at 80ºC for the required time. The reaction products were analyzed by gas-liquid chromatography.

3 Results and Discussion

The synthesis of catalysts was carried out in 3 stages: 1) preliminary modification of the dendrimer terminal aminogroups by the silyl-containing linkers; 2) formation of mesoporous silica channels in presence of a template using sol-gel method and grafting the modified

dendrimers to the silica surface formed *in situ*; 3) encapsulation of the bimetallic nanoparticles using a co-complexation method similar to the literature procedures [6,7]. Thus, PdRh and RhRu hybrid catalysts were prepared. Both of the catalysts prepared were examinated in the phenols hydrogenation. It was found out, that RhRu catalyst gave selectivity on cyclohexanone near to 100% even at long reaction times and high catalyst loading, proving a deeper conversion (up to 80%). The similar results were found for the PdRh catalyst. Using anisole or phenethole instead of phenol led to the dramatic downfall in conversion. Also hydrogenolysis (phenol, cyclohexanol, cyclohexanone) and deoxygenation (benzene, cyclohexane etc.) by-products were formed. Their total portion reached up to 50% and decreased when the reaction time and catalyst loading decreased. Introducing the alkylic substituent into the aromatic ring of phenol also resulted in the decrease in conversion in comparison with phenol. Formation of a small quantity (up to 10-15%) of the hydrogenolysis by-products was typical for the both catalysts. At the same time the activity of the RhRu catalyst in the alkyl-substituted phenols hydrogenation did not depend on the substrates size and geometry, whereas for PdRh decrease in activity with the substrate size increased was observed. Both of the catalyst synthesized showed high activity in the hydrogenation of polar hydroquinone and resorcinol, and poor activity for pyrocathechol with *ortho*-position for the hydroxylic groups. Also the formation of the hydrogenolysis by-products (up to 20%, especially for hydroquinone) was observed in presence of the both catalysts. Their portion, as for phenolic ethers, increased, when the reaction time and catalyst amount increased. Generally, synthesized bimetallic catalysts were found to be less active, but more selective in comparison with corresponding monometallic Ru and Rh catalysts.

4 Conclusions

Hybrid bimetallic catalysts based on the PdRh and RhRu nanoparticles encapsulated into the PPI dendrimers, grafted on the mesoporous silica surface, were synthesized. The materials obtained appeared to be active in the hydrogenation of phenol and its derivates. For phenol, 100% selectivity on the cyclohexanone can be achieved for the both catalysts. Introducing the hydrophobic substituents to the hydroxyl-group or the aromatic ring of phenol led to the conversion decreasing. The formation of the hydrogenolysis and deoxygenation by-products was typical of the hydroquinone and phenolic ethers.

Acknowledgments

This work was supported by the RFBR grant No 14-03-31531.

References

[1] E. Karakhanov, A. Maximov, *Metal Complexes and Metals in Macromolecules*, Wiley-VCH, Weinheim (2003) 457 P.
[2] A.D. Pomogailo, Catalysis by Immobilized Complexes, Nauka, Moscow (1991) 448 P.
[3] E. Karakhanov, A. Maximov, Yu. Kardasheva, V. Semernina, A. Zolotukhina, A. Ivanov, G. Abbott, E. Rosenberg, V. Vinokurov, *ACS Appl. Mater. Interfaces* 6 (2014) 8807−8816.
[4] J. Meurig Thomas, B.F.G. Johnson, R. Raja, G. Sankar, P.A. Midgley, *Acc. Chem. Res.* 36 (2003) 20-30.
[5] Ch. Huang, X. Yang, H. Yang, P. Huang, H. Song, Sh. Liao, *Appl. Surf. Sci*. 315 (2014) 138.
[6] Xi. Peng, Q. Pan, G.R. Rempel, Sh. Wu, *Catal. Commun*. 11 (2009) 62.
[7] Ya. Wang, Xi. Peng, *Nano-Micro Lett.* 6 (2014) 55.

II-PP145

Peroxocomplexes Contaning Rare Earth Elements as Effective Catalysts of Oxidation Reaction of Mono and Bicyclic Unsaturated Hydrocarbons with Hydrogene Peroxide

Dadashova N.R.*, Alimardanov H.M., Sadiqov O.A., Qaribov N.I., Quliyev A.D., Huseynova M.E., Aghabayli G.B.

Institute of Petrochemical Processes of NASA, Baku, Azerbaijan

* dadasova_17@hotmail.com

Keywords: peroxocomplexes, liquid-phase, oxidation, hydrogen peroxide, unsaturated hydrocarbons

1 Introduction

A series of peroxotungsten and molybdenum complexes of rare earth elements (REE) (Gd, Nd, Pr, La) in the induced oxidation reaction of unsaturated hydrocarbons with cyclohexene and norbornene fragments was synthesized and studied.

The oxidation reaction of unsaturated hydrocarbons is one of the important directions of obtaining oxygen-containing compounds with the given structure. The catalytic processes based on the use of oxidants and heterogeneous catalysts based on transition metals are of great interest. To create heterogenized peroxo complexes of transition metals as catalysts for the oxidation of unsaturated compounds with the air oxygen and hydrogen peroxide, is the focus of researchers' attention. In this aspect, the development of peroxotungsten and molybdenum complexes of REE, finding conditions for the formation of these complexes, determination of the structure and composition, as well as their use as catalysts for the stoichiometric oxidation of unsaturated alicyclic compounds remains an urgent task.

2 Experimental/methodology

To study the structure of the samples of peroxocomplexes of phospohotungsten and molybdenum- $X\{PO_4[MeO(O_2)_2]_4\}$, (where X=Gd, Nd, Pr,La, Me= Mo,W) FTIR, EPR, XRD and TGA methods of analysis have been used.

In the IR spectra of the obtained peroxocomplexes, the intense bands correspond to the crystallization water (3450-3200 cm^{-1}), ion PO_4^{3-} (1089, 1023 cm^{-1}), the double bond Me = O (955, 935 cm^{-1}), and O-O bond (850 and 858 cm^{-1}). The broad band is characteristic for the seven-coordination diperoxocomplexes at 575 cm^{-1} and the band of medium intensity for symmetric and asymmetric vibrations of Me fragment at 625 and 968 cm^{-1}. The intense bands are characteristic at 414 $cm^{-1}$and at 464 $cm^{-1}$for GdO^+ and NdO^+ fragments,respectively.

Thermograms of complexes are characterized by an endothermic effect associated with the lost of water and by an exothermic effect associated with the decomposition of peroxo compounds and release of oxygen (140 ° C). This proves the assumption that water enters the inside sphere and dimer (or tetramer) forms of peroxotungstate (peroxomolybdate) complexes containing gadolinium and neodymium are formed.

3 Results and discussion

The results of the studies on oxidation of vinylcyclohexene (VCH), tetrahydroindene (THI) and norbornene (NB) show that the reaction products are the corresponding oxiranes and vicinal diols.

In the presence of the samples of diperoxophosphate complexes containing (Nd, Pr, La) the selectivity by the epoxide of VCH and THI at 40ºC is 68-72%, and by that of vicinal diol it is

selectivity of vicinal diol is 10-15 %(at the conversion of hydrocarbons 14-20%) .But in the case of a sample containing gadolinium, yield of VCH and THI epoxide is 75-78%, and vicinal diol 18-22% (at the conversion of VCH and THI 17-23%). This proves that the peroxocomplex of gadolinium as compared with the peroxocomplex of Nd, Pr, and La is more active.

II-PP146

Silver Modified $MgNi/SiO_2$ Catalysts for Vegetable Oil Hydrogenation

Krstić J.[1], Gabrovska M.[2*], Radonjić V.[1], Lončarević D.[1], Stanković M.[1], Nikolova D.[2], Bilyarska L.[2], Jovanović D.[1]

1 - University of Belgrade, Institute of Chemistry, Technology and Metallurgy, Department of Catalysis and Chemical Engineering, Belgrade, Republic of Serbia
2 - Institute of Catalysis, Bulgarian Academy of Sciences, Sofia, Bulgaria

* margo@ic.bas.bg

Keywords: $MgNi/SiO_2$, catalyst, water, glass, silver modification, sunflower oil hydrogenation

1 Introduction

Hydrogenation of vegetable oils is a traditional oleochemical process aiming to change the physical properties of the oils as well as to enhance the oxidation and thermal stability of the hydrogenated products. In the view of high activity, inert nature of the metal relative to the oil, availability and economic consideration, metal nickel, supported on different sources of silica, is the most appropriate catalyst for the reaction. Despite intensive research activity in this field, the role of additives or modifiers on the catalytic performance of the vegetable oil hydrogenation catalysts is quite scarce in the literature [1,2]. The aim of the present study is to elucidate the effect of the silver content in $MgNi/SiO_2$ system on the activity and the composition of the fatty acids obtained during the sunflower oil hydrogenation.

2 Experimental/methodology

A series of silver modified Mg-Ni materials with composition Mg/Ni = 0.1 and SiO_2/Ni = 1.15, differing in Ag content (Ag/Ni = 0.0025, 0.025 and 0.1) was prepared by the precipitation-deposition on SiO_2 derived from water glass used as a source of silica support. The designation of the samples corresponds to the Ag/Ni molar ratio, i.e. 0.0025AgNi, 0.025AgNi and 0.1AgNi. The preliminary reduction of the as-synthesized precursors after drying at 105°C was performed in a laboratory set-up using a quartz reactor by means of a "dry reduction" method at 430°C for 5 h with H_2 at a flow rate of 10 dm^3/h and a heating rate of 1.5°C/min. After cooling down to room temperature, the precursors were impregnated with pure paraffin oil in order to prevent the exceptional pyrophority of the Ni^0. The partial hydrogenation of sunflower oil was carried out up to 230 min and was performed in a 1.5 dm^3 glass reactor Series 5100, computer coupled with Mass Flow Controller F-201C and Pressure Meter F-502C under the following conditions: catalyst concentration - 0.03 wt. % of Ni with respect to the amount of oil; stirring rate - 1200 rpm; hydrogenation temperature - 150°C and H_2 pressure - 0.2 MPa. The activity of the catalysts was evaluated by measuring the changes in the Refraction Index at 50ºC of the starting oil, and periodically collected partially hydrogenated oils. The fatty acids content in the starting refined sunflower oil and the fractions of hydrogenated oils were determined after their conversion into fatty acid methyl esters according to IUPAC method II.D.19. The analysis was performed on gas chromatograph SHIMADZU GC-9A with FID detector and capillary GC column Agilent HP-88 (100 m x 0.25 mm I.D., 0.20 μm film thicknesses).

3 Results and discussion

The hydrogenation activity is estimated by the changes in the Refraction Index (RI) values and the quantity of the consumed hydrogen as function of hydrogenation time for the studied

catalysts. A diminution of RI value of the crude oil (1.46368) downs to the level of 1.45688 (0.1AgNi), 1.45721 (0.025AgNi) and 1.46081 (0.0025AgNi) is registered, reviling the low activity of the catalyst with the lowest silver amount. The results obtained are in accordance with the quantity of the consumed hydrogen (dm^3) at the end of the reaction, namely: 0.1AgNi (51.2) > 0.025AgNi (46.3) >> 0.0025AgNi (20.7).

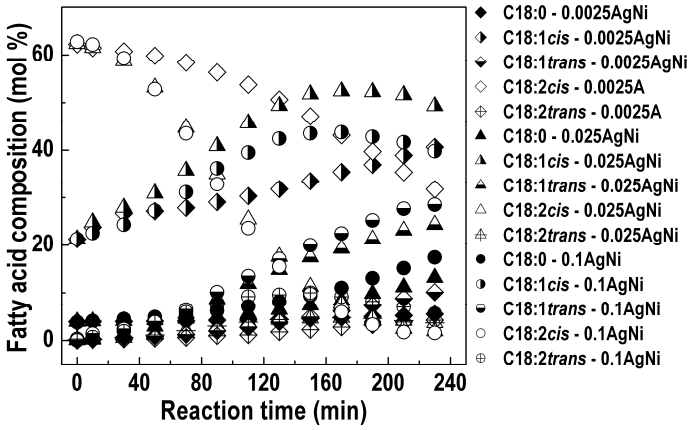

Fig. 1. Fatty acid composition of the studied catalysts

The differences in the activity of the catalysts reflect on the different fatty acid profiles and different composition of the fatty acids obtained during the sunflower oil hydrogenation (Fig. 1). Concomitant with the hydrogenation (partially or fully saturation of double bonds), the catalytic isomerization of naturally occurring *cis* fatty acids to *trans* fatty acids takes place. The overall hydrogenation involves consecutive saturation of linoleic acid (C18:2*cis*) to oleic acid (C18:1*cis*), and subsequent saturation of C18:1*cis* to stearic acid (C18:0) as well as parallel reversible isomerization of C18:2*cis* to C18:2*trans* and C18:1*cis* to C18:1*trans* [1].
It may be seen a decrease of C18:2*cis* (mol %) in the follow order: 0.1AgNi (1.4) < 0.025AgNi (2.0) << 0.0025AgNi (32.0) at the end of the reaction, as well as an increase of C18:0 in a reverse order, both related to the hydrogenation of the double bonds. The results demonstrate high selectivity of 0.025AgNi and 0.1AgNi catalysts toward C18:2*cis* hydrogenation turns it almost entirely into C18:1*cis*. It is well known that C18:2*cis* is one of the ‘‘essential’’ fatty acids, thus its presence is necessary for human nutrition. Therefore, small amounts of it are allowed in the edible hydrogenated oils.

Comparison of the performance of the active 0.025AgNi and 0.1AgNi catalysts permits to be recommended as an appropriate for selective edible sunflower oil hydrogenation the catalyst with intermediate silver content (0.025AgNi). This finding is based on the demonstrated similar hydrogenation activity, higher content of C18:1*cis* formation and lower amounts of harmful for the human health C18:1*trans* and C18:0 fatty acids in the hydrogenated derivatives.

4 Conclusions

It may be concluded that the careful changing the content of silver modifier offers a possibility to control as the hydrogenation activity as well as the composition of fatty acids in the hydrogenated edible oils.

Acknowledgements

This study is supported by the Ministry of Education, Science and Technological Development of the Republic of Serbia (Project No. III 45001).

References

[1] J. Veldsink, M. Bouma, N. Schöön, A. Beenackers, *Catal. Rev. - Sci. Eng.*, 39 (1997) 253.
[2] M. Balakos, E. Hernandez, *Catal. Today*, 35 (1997) 415.

II-PP147

New Insights on Active Sites of Key Catalyst Materials Using Microcalorimetry at Close to the Reaction Conditions

Wrabetz S[1*], Teschner D[1], Amakawa K[2], Frank B[1], Perez-Ramirez J[3], Trunschke A[1], Schlögl R[1]

1 - Fritz-Haber-Institut der Max-Planck-Gesellschaft, Dept. of Inorganic Chemistry, Berlin, Germany
2 - BASF SE, Ludwigshafen, Germany
3 - ETH Zurich, Zurich, Switzerland

* wrabetz@fhi-berlin.mpg.de

Keywords: adsorption, adsorption, enthalpy, active sites, reversibility, reactivity, quantitative

1 Introduction

Heterogeneous catalysis involves specific chemical interactions between the surface of a solid and the reacting gas (or liquid phase) molecules. The catalytic cycle is generally composed of absorption/desorption steps, and surface reaction processes. The 1st step is the activation of the reacting molecules by adsorption. Thus, the study of adsorption phenomena plays an important role. Knowledge about the heat of adsorption of reactants on the surface of a catalyst as well as the number of adsorption sites, energetic distribution of adsorption sites, adsorption constants and the specific surface area can contribute to a better understanding of complex microkinetics. Moreover, quantitative data provide a basis for theoretical modeling. Since perhaps only a minor fraction of all surface atoms form active centers, the determination of their number and strength requires a sensitive analytical method. We focus on adsorption microcalorimetry. To facilitate the correlation of microcalorimetric results with the catalytic performance, a molecule similar to the reactant, or the reactant itself, is used. $T_{ads.}$ is chosen lower than $T_{reaction}$ to separate the adsorption process from the catalytic reactions or closely related to $T_{reaction}$ to study the surface chemical events during reaction.

2 Experimental

Microcalorimetric experiments were carried out in a Calvet calorimeter (SETARAM MS70) combined with a high vacuum system, which enables the dosage of probe molecules within a range of 0.04 □mol. The required pretreatment of the catalysts (reduction, oxidation, dehydration) is conducted in a separate chamber connected to the calorimetric cell. Subsequently the cell is cooled to room temperature ($p_{final} = 10^{-7}$ mbar), placed inside the calorimeter, and connected to the micro-calorimetric gas-adsorption system. Then, the selected probe molecule is dosed stepwise at selected T_{ads}. Pressure, $T_{ads.}$ and the heat signals were recorded during all dosing and desorption steps. Desorption is performed at $T_{ads.}$ under UHV. A positive energy corresponds to an exothermic process. Furthermore, a procedure was developed to characterize the adsorption sites on the surface of a catalyst in any stage along the reaction profile by quasi *in situ* adsorption microcalorimetry.[1,2] The calorimeter cell can be used as a fixed bed reactor containing the catalyst under e.g. propane oxidative dehydrogenation reaction conditions. [2]

3 Results and discussion

In this work, we will demonstrate how structure-activity correlations can be established by combining microcalorimetry with electron microscopy, spectroscopic techniques, DFT calculations and catalytic test reactions. The power of these complementary methods will be illustrated by choosing the following examples:

(i) Propylene metathesis over MoOx/SBA-15 (Fig. 1) [3]
The surface of MoOx/SBA-15 – active in propylene metathesis at 50°C – was probed by propylene adsorption at $T_{reaction}$ in order to trace the initiation step of C_3H_6 metathesis. Catalytic activity is directly correlated with the strength of the propylene interaction with the active surface site. The quantification implies that ca. 1% of Mo atoms formed active sites. The most active catalyst is characterized by strong and irreversible adsorption of propylene, the highest amount of MoO_x adsorption sites for propylene, and a homogeneous distribution of the energy of these adsorption sites.

(ii) Three-phase semi-hydrogenation of 1-hexyne over TiO_2-supported ceria at 80°C (Fig. 2) [4]
In order to correlate the catalytic performance with characteristic properties of ceria, the chemisorption of 1-hexyne at $T_{reaction.}$ was studied on two 20wt%CeO_2/TiO_2 catalysts that show different activity. The more active catalyst is characterized by a higher amount of adsorption places for 1-hexyne. Regeneration of the latter catalyst with H_2 is facilitated. Furthermore, the obtained results indicate that under reaction conditions a significant portion of the surface sites is covered by dehydrogenated species and is not available for hydrogenation. This is in line with DFT calculations of acetylene adsorption on CeO_2(111) showing that the most preferred adsorption mode is dissociative with respect to the C–H bond. [5] Nevertheless, the remaining small number of surface sites is active and highly selective in alkyne hydrogenation.

(iii) Oxidative dehydrogenation (ODH) of propane and ethylbenzene (EB)
The reaction is considered as the model reactions to establish a mechanistic model for carbon-catalyzed ODH. [2] From the mechanistic point of view, quinone groups (C=O, nucleophilic oxygen) are believed to be the active site. It was found that the redox cycle of surface C=O and C-OH groups is the key process, which includes only a small fraction of surface O species and favourably occurs at the zigzag-termination of sp^2 carbon planes. Higher activation barriers in the reduction step correlate with the higher stability of the aliphatic C-H bond in propane over the benzylic C-H bond in EB.

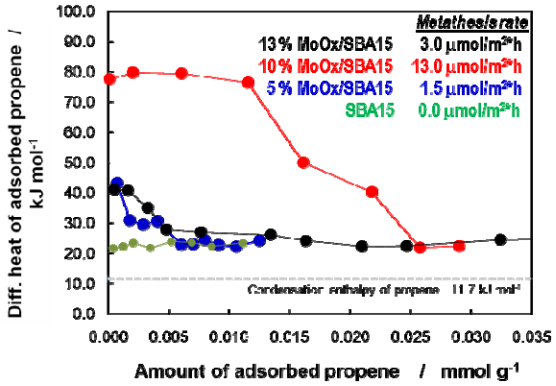

Fig.1: Differential heat of propene adsorbed on MoO_x/SBA-15 and SBA-15 at $T_{reaction}$=50°C.

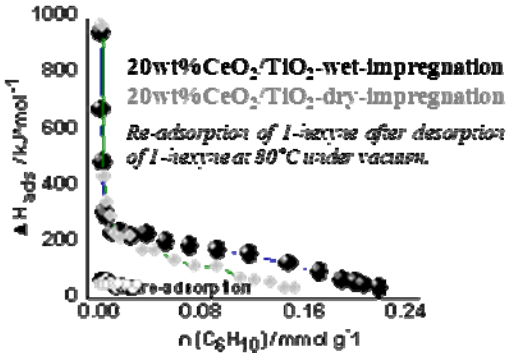

Fig. 2: Differential heat of adsorption of 1-hexyne on CeO_2/TiO_2 at $T_{reaction}$=80°C.

References

[1] S. Wrabetz, X. Yang, G. Tzolova-Müller, R. Schlögl, F. C. Jentoft, J. Catal. 269 (2010) 351.
[2] B. Frank, S. Wrabetz, O.V. Khavryuchenko, R. Blume, A. Trunschke, R. Schlögl, ChemPhysChem 12 (2011) 2709.
[3] Amakawa, K., Wrabetz, S., Kröhnert, J., Tzolova-Müller, G., Schlögl, R., Trunschke, A.; J. Am. Chem. Soc., 134 (2012) 11462.; K. Amakawa, J. Kröhnert, S. Wrabetz, B. Frank, F. Hemmann, C. Jäger, R. Schlögl, and A. Trunschke, ChemComm., submitted.
[4] G. Vilé, S. Wrabetz, L. Floryan, M.E. Schuster, F. Girgsdies, D. Teschner, J. Pérez-Ramirez, ChemCatChem, 6 (2014) 1928.
[5] J. Carrasco, G. Vilé, D. Fernández-Torre, R. Pérez, J. Pérez-Ramírez, M. V. Ganduglia-Pirovano, J. Phys. Chem. C 118 (2014) 5352.

II-PP148

Influence of Ruthenium Content in Co-Al Fischer-Tropsch Catalyst on Kinetics of Cobalt Reduction

Kungurova O.A.[1,2,3*], Shtertser N.V.[1,2], Demeshkina M.P.[2], Khassin A.A.[1,2]

1 - Research and Educational Center for Energy Efficient Catalysis in Novosibirsk National Research University, Novosibirsk, Russia
2 - Boreskov Institute of Catalysis, Novosibirsk, Russia
3 - Tomsk State University, Tomsk, Russia

* olya-sky@inbox.ru

Keywords: Fischer-Tropsch synthesis, cobalt-alumina catalysts, kinetics of reduction, ruthenium

1 Introduction

Cobalt-alumina Fischer-Tropsch catalysts prepared by DPU (deposition by precipitation during urea decomposition) method are highly active and have good C_{5+} selectivity [1]. However the activation temperature is high for these catalysts exceeding 500°C, which makes the activation procedure and equipment expensive.

Introduction of tiny amount of noble metal facilitates cobalt reduction and decreases the required activation temperature [2]. Promoted with 0.2 wt. % of ruthenium Co-Al catalysts have reduction temperatures by 50−85 °C lower than those of unprompted ones [3,4]. Increasing ruthenium content shifts the reduction temperature further (ΔT = 100−110 °C). In cited works authors note rising of reducibility and dispersion of promoted catalysts. Ru was also reported to improve the activity of catalyst, prepared by impregnation of alumina and silica [5,6].

Noble metals may serve as sites for activation of hydrogen and also as nuclei for formation of metallic cobalt phase. Studying the reduction kinetics of Ru-promoted Co-catalysts can help to understand the mechanism of the metallic cobalt particles formation and the role of ruthenium in this process. Meanwhile the kinetic studies data on cobalt reduction are missing in literature. The studying of kinetics in non-isothermal conditions can be carried out by means of thermal analysis. By this poster presentation we report the effect of ruthenium content on the process of reductive activation of Ru-promoted Co-Al catalyst as well as the catalytic activity and selectivity these catalysts in the Fischer-Tropsch synthesis.

2 Experimental/methodology

Cobalt-alumina catalyst was prepared by DPU method using δ-Al_2O_3. Co loading is 9.2 wt. %. Ruthenium was introduced by impregnation with aqueous solutions of $RuNO(NH_3)_2(NO_3)_3$ complex and consequent drying under IR lamp. Ru concentration in the impregnating solutions corresponded to Ru loading of 0.2, 0.5 and 1 wt. % (samples were designated as $Ru_{0.2}$Co-Al, $Ru_{0.5}$Co-Al, $Ru_{1.0}$Co-Al).

Reduction behavior and kinetic parameters of reduction were studied by thermal analysis at varied heating rates using Netzsch STA 449. Reduction was performed in H_2 and Ar gas mixture, composed by pure hydrogen flow fed to the sample chamber and pure argon flow fed to the balance chamber and passed through the balance chamber to the sample chamber. Fischer-Tropsch synthesis was carried out at 190 °C, 2.1 MPa, feed ratio H_2:CO:N_2 = 6:3:1 in a single row fixed bed reactor using 4 mm catalyst grain. Catalytic activity and selectivity were measured at CO conversion being in the range of 8−15 %.

3 Results and discussion

Ru promotion lowered significantly the cobalt reduction temperature. Figure 1 shows that

the temperature maximum which corresponds to formation of metallic Co particles shifts to lower temperature range from 530 °C for Co-Al to 350, 290 and even 280 °C for $Ru_{0.2}$Co-Al, $Ru_{0.5}$Co-Al, $Ru_{1.0}$Co-Al respectively.

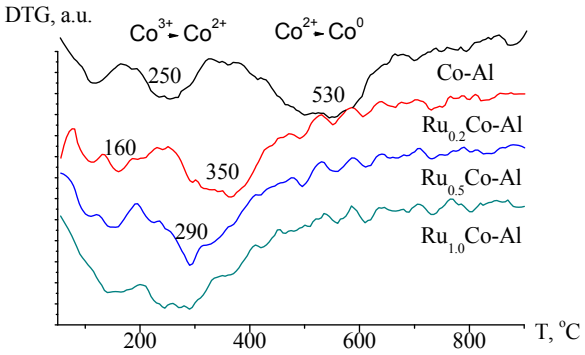

Fig. 1. DTG-profiles of Co-Al and Ru_xCo-Al catalysts in flow of H_2 and Ar gas mixture

Therefore, the activation temperatures for Ru-promoted catalysts are lower by 200 °C than that for Co-Al. The study on kinetics of cobalt reduction is in progress and the results will be reported at the poster.

Table 1. Catalytic properties of Co-Al and Ru_xCo-Al catalysts

Catalyst	Co-Al	$Ru_{0.2}$Co-Al	$Ru_{0.5}$Co-Al	$Ru_{1.0}$Co-Al
$T_{reduction}$, °C	500	350	330	330
W CO, mmol/g_{cat}·h	4.26	3.45	3.41	4.31
W CH_2, mg/g_{cat}·h	59.7	48.3	47.7	60.4
S(C_{5+}), %	78	76	79	79
S(CH_4), %	10.0	9.5	9.3	9.9

Table 1 summarizes some of the parameters of the catalytic performance of Co-Al and Ru_xCo-Al catalysts in the Fischer-Tropsch synthesis at 190 °C, 2.1 MPa. Activation temperature was selected accordingly to the thermal analysis data. The activity and selectivity of promoted catalysts are almost as high as that of unpromoted catalyst.

3 Conclusions

Addition of small amounts of Ru to alumina-supported cobalt catalysts significantly lowers the temperature of cobalt reduction. The promoted catalysts exhibit high catalytic activity and selectivity in the Fischer-Tropsch synthesis, which is comparable with unpromoted catalyst.

Acknowledgements

We are thankful to Prof. V.A. Emelyanov for providing us $RuNO(NH_3)_2(NO_3)_3$ complex.

This work was performed with support of the Skolkovo Foundation (Grant Agreement for Russian educational organization №1 on 28.11.2013).

References

[1] I.I. Simentsova, A.A. Khassin, T.P. Minyukova, L.P. Davydova, A.N. Shmakov, O.A. Bulavchenko, S.V. Cherepanova, G.N. Kustova, T.M. Yurieva. *Kinet. Catal.* 53 (2012) 497.
[2] G. Jacobs, T.K. Das, Y. Zhang, J. Li, G. Racoillet, B.H. Davis. *Appl. Catal. A-Gen.* 233 (2002) 263.
[3] G. Jacobs, P.M. Patterson, Y. Zhang, T. Das, J. Li, B.H. Davis. *Appl. Catal. A-Gen.* 233 (2002) 215.
[4] S.-H. Song, S.-B. Lee, J.W. Bae, P.S. Sai Prasad, K.-W. Jun. *Catal. Commun*. 9 (2008) 2282.
[5] A. Kogelbauer, J.G. Goodwin, Jr., R. Oukaci, *J. Catal.* 160 (1996) 125).
[6] N. Tsubaki; S. Sun, K. Fujimoto. *J. Catal.* 199 (2001) 236.

II-PP149

Novel Catalyst Supports with Lamellar and Hierarchical Porosity

Papa E.[1], Benito P.[1,2*], Vaccari A.[1,2], Medri V.[1], Landi E.[1]

1 - National Research Council of Italy, Institute of Science and Technology for Ceramics (CNR-ISTEC), Faenza, Italy

2 - Department of Industrial Chemistry "Toso Montanari", Alma Mater Studiorum Università di Bologna, Bologna, Italy

* patricia.benito3@unibo.it

Keywords: geopolymer, ice-templating, hierarchical porosity, lamellar porosity, catalyst support

1 Introduction

Geopolymers are synthetic alkaline alumino-silicates [1] that may be regarded as the amorphous counterpart or precursor of crystalline zeolites. At the atomic scale, the geopolymer network is formed by SiO_4 and AlO_4 tetrahedra connected by oxygen corners: the tetrahedra form Si-O-Al-O rings of various sizes and endow the geopolymer matrix with ion exchange properties [2]. These materials show properties ranging from those characteristic of ceramics, cements, zeolites or refractories [1]. Geopolymers are intrinsically mesoporous and a hierarchical pore system may be obtained combining meso and macropores [3]. Water-based freeze casting (or ice-templating) may be used to prepare porous materials with main unidirectional oriented pores and a high open porosity, where the final component results in a lamellar structure [4]. The aim of this study is to produce and characterize novel catalyst supports of different geometries and dimensions, with lamellar macroporosity and geopolymer intrinsic mesoporosity.

2 Experimental

Geopolymer slurries were prepared by mixing metakaolin (M1200S, AGS Minéraux) with KOH/K_2SiO_3 aqueous solutions (Aldrich) at high (H_2O:K_2O=23.0) and low (H_2O:K_2O=13.5) dilutions under mechanical stirring [3]. After a maturation step at r. t., distilled water (50 vol. %) was added to the slurries, then mechanically mixed. The mixtures were cast in pre-cooled rubber molds to produce monoliths, cylinders and plates up to 15 cm side. Then cast slurries were frozen at -40°C and sublimated at P= $8 \cdot 10^{-2}$ torr for 24h (Edwards MFD01). After demolding, the samples were rinsed in deionized water and then dried at 100°C.

The morphological and microstructural features were examined by environmental Scanning Electron Microscopy (E-SEM). The bulk density of the samples was determined by weight-to-volume ratio. Ultra-macro-porosity was investigated by image analysis. Pore size distribution in the range 0.0058–100 μm was analyzed by porosimetry by Hg intrusion. Measurements of specific surface area, pore volume and pore size distributions in the 2-500 nm range were carried out by N_2 adsorption/desorption at −196 °C. The Si/Al and K/Al molar ratios in the final consolidated samples were determined by X-Ray Fluorescence (XRF) analysis.

3 Results and discussion

Figure 1 shows how basic (due to the presence of K) catalyst supports, with different size and geometry and a lamellar macroporosity may be prepared by ice-templating. The porosity and stoichiometry may be altered by varying the dilution of the starting geopolymer slurry (Table 1). A broad mesopore distribution was detected between 4 to 100 nm, with maximum from 5 to 7 nm. While, the pore size distributions measured by Hg intrusion porosimetry are bi-

and tri-modal, respectively for low and high dilution. The results account for the intrinsic porosity of the geopolymer matrix (pores ranging from 0.0058 to 1 μm) [3], suitable for the inclusion of a catalytic active phase to prepare bifunctional catalysts. The smallest macro-pores due to ice-templating may decrease the mass-transfer phenomena. In details, water is the reaction medium in geopolymerization, but it does not enter into the geopolymer framework; it gives rise to a steric hindrance acting as a pore forming agent upon its removal during setting. Consequently the starting dilution of the geopolymer slurry greatly affects the intrinsic porosity and the textural characteristics in term of lamellar pore width.

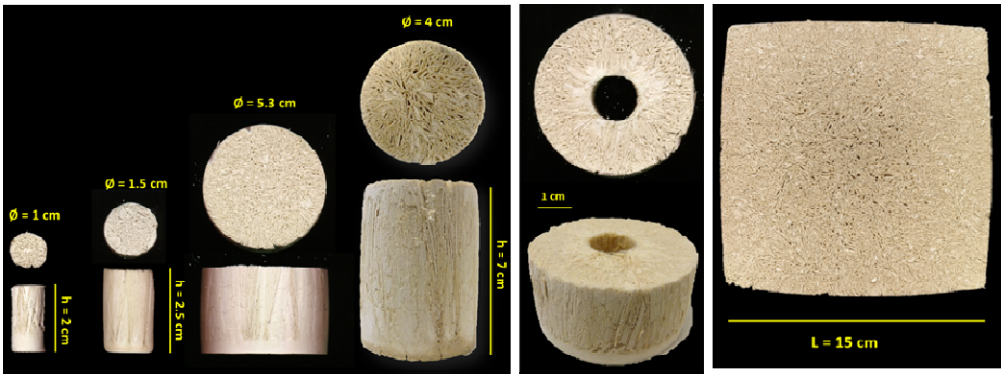

Fig. 1. Some catalyst supports of different size and geometry a with lamellar macroporosity

Table 1. Characteristics of the catalyst supports prepared with low diluted (LD) and high diluted (HD) geopolymer slurries added with 50 vol% of water.

Sample	Bulk density $g \cdot cm^{-3}$	Total porosity (%)	Lamellar Pore width, μm	Total pore volume $mm^3\ g^{-1}$	S_{BET} $m^2\ g^{-1}$	V_p $cm^3\ g^{-1}$	Si/Al	K/Al
LD	0.7	70	15-100	853	39.4	0.115	1.87	0.36
HD	0.5	80	20-250	1404	26.0	0.091	1.69	0.37

4 Conclusions

Unidirectional lamellar catalytic supports with different geometries and large dimensions may be easily produced by the ice-templating of geopolymer slurries. Hierarchically porous materials are realized with textural characteristics depending on the starting dilution of the geopolymer slurries. Due to the alkaline properties and textural features, these novel supports may be useful to prepare tailor-made bifunctional catalysts. Catalytic tests are ongoing to assess the suitability of these systems.

Acknowledgements

This work was supported by the Flag project RITMARE –La Ricerca Italiana per il Mare (coordinated by the National Research Council of Italy) and by the Ministero Italiano per l'Università e la Ricerca (MIUR Roma).

References

[1] J. Davidovits, in Geopolymers Chemistry and Applications, Davidovits J. Ed., Institut Geopolymere, Saint-Quentin, France, 2008.
[2] J. Dedecek, Z. Tvaruzkova, Z. Sobalik, *J. Am. Ceram. Soc.* **91** (2008) 3052.
[3] E. Landi, V. Medri, E. Papa, J. Dedecek, P. Klein, P. Benito, A. Vaccari, *Appl. Clay Sci.* **73** (2013) 56.
[4] S. Deville, *Adv. Eng. Mater.* **10** (2008) 155.

II-PP150

Synchrotron Based *operando* Study of Structure Activity Relationships of Model Electrocatalysts for Water Splitting

Goryachev A.[1*], Carla F.[2], Drnec J.[2], Onderwaater W.[2], Krause P.P.T.[3], Wonders A.H.[1], Hensen E.J.M.[1], Hofmann J.P.[1]

1 - Technische Universiteit Eindhoven, Inorganic Materials Chemistry, Eindhoven, Netherlands
2 - European Synchrotron Radiation Facility, Grenoble, France
3 - Justus-Liebig-Universität Giessen, Physikalisch-Chemisches Institut, Gießen, Germany

* a.goryachev@tue.nl

Keywords: *operando* synchrotron, Pt(111), roughening, on-line electrochemical mass-spectrometry, electrocatalysis

1 Introduction

Solar hydrogen produced by (photo)electrochemical water splitting (PWS) is a promising alternative to conventional fossil energy resources. Mostly, photocatalysts are complex multicomponent semiconductor based systems. However, even the most active photocatalytic materials are not able to drive PWS without electrocatalyst due to interfacial energy losses. In order to design optimal electrocatalysts, structure-activity relationships are needed. Platinum as the best-performing and best-known H_2 evolution catalyst has thus been chosen as a model catalyst to setup a novel technique combination enabling to simultaneously track structural changes together with reaction products detection and electrochemical characterization.

2 Experimental/methodology

In our experiments an OLEMS (on-line electrochemical mass-spectrometry) tip [1] was implemented to an *in-situ* electrochemical cell designed at ID03 (ESRF, Grenoble) [2] (Fig. 1a). The tip was approached at 20 μm distance to working electrode surface with piezo stage driver (Thorlabs), fine positioning has been done by maximizing hydrogen response. 0.1 M $HClO_4$ degased solution was used as electrolyte. Alongside the OLEMS product characterization, surface X-ray techniques were utilized to follow changes in surface morphology and crystallography. GISAXS (Grazing-Incidence Small-Angle X-ray Scattering) and XRR (X-Ray Reflectivity) could provide information on surface roughening, while SXRD (Surface X-Ray Diffraction) was used to determine the surface crystal structure. As a showcase to validate the combined OLEMS–[SXRD/GISAXS/XRR] setup for *operando* studies of electrode transformations, we chose H_2 and O_2 evolution reactions (HER and OER) on Pt(111).

3 Results and discussion

During the combined XRR-OLEMS experiment, the Pt(111) electrode was repeatedly switched between OER (1.6 V, 10 s) and HER (−0.4 V, 10 s) potentials with intermittent resting potential (0.3 V, 10 s). XRR was continuously recorded at the point of maximal intensity change at fixed angular position together with simultaneous mass spectrometric analysis of the produced gases by OLEMS. The combined dataset shown in Fig. 1b comprising structural and reactivity data demonstrates the strength of the multi-technique approach to study reactivity trends of electrocatalytic model surfaces under *operando* conditions. Complementary GISAXS and SXRD data obtained under identical conditions can provide additional insight into structural development of the surface as well as oxide formation finally arriving at solid *operando* structure-activity relationships for electrocatalytic (model) systems.

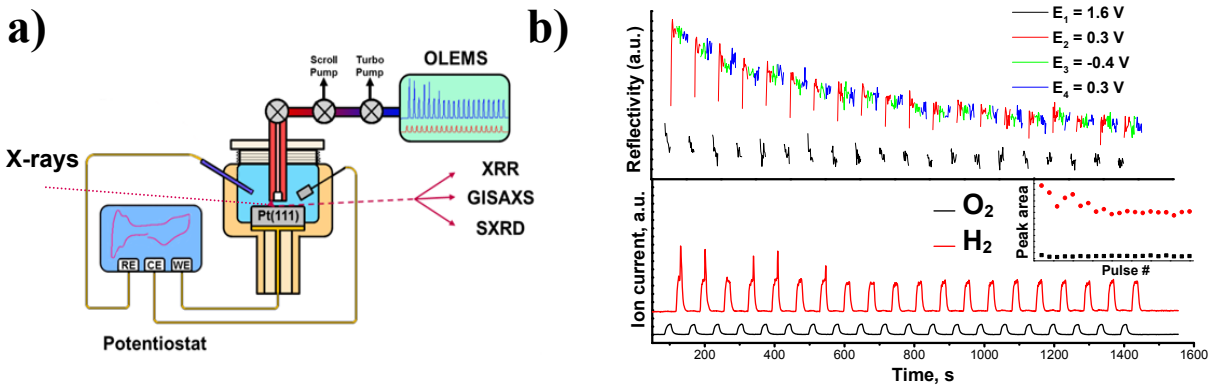

Fig. 1. a) Scheme of combined OLEMS-[SXRD/GISAXS/XRR] setup; b) XRR-OLEMS curves upon switching between OER and HER potentials.

4 Conclusions

The ultimate combination of electrochemical and surface x-ray characterization techniques have been applied to study structure-activity relationships on example of model electrocatalyst Pt(111).

Acknowledgements

This work is sponsored by NRSC-C. The experiments were performed at European Synchrotron Radiation Facility (Grenoble, France) at ID03 beam line. I would like to thank the staff of ID03 (Francesco Carla, Jacub Drnec, Willem Onderwaater), Ad Wonders, Jan Philipp Hofmann and Philipp Krause for their tremendous help with experiments.

References

[1] Wonders, A. H., *et al. J. Appl. Electrochem*. 36 (2006) 1215–1221
[2] Foresti, M. L., *et al. Electrochim. Acta*. 51 (2006) 5532–5539

II-PP151

The Problem of Correct Interpretation of Catalyst Acidity by the TPD NH_3 Curves

Solomonik I.G.[1,2], Mordkovich V.Z.[1,2*]

1 - Department of New Chemical Technologies and Nanomaterials, Technological Institute for Superhard and Novel Carbon Materials, Moscow, Russia
2 - INFRA Technology Ltd., Moscow, Russia

* solomonik@tisnum.ru

Keywords: Fischer–Tropsch synthesis, catalyst, zeolite, TPD NH_3

1 Introduction

The way the catalyst functions is determined by the specific genesis of the system, including formation and activation modes. Thus, the mere use of literature data on the individual components when considering the behavior of the composite in different experimental conditions can not be entirely correct.

A Fischer-Tropsch process is well known [1] to have the surface acidity effect on the hydrocarbon synthesis, hydrocarbon isomerization, and olefin formation. A study [2,3] on the acid properties of the catalyst carriers by spectroscopic methods using probe molecules allows the identification of Lewis and Bronsted centers of different nature and strength both on the outer surface of the particles and inside the pores. At the same time, it is complicated to quantify the correlation due to the difficulty in determining the extinction coefficients. Simpler thermodesorption methods allow us to determine the total acidity of the samples (e.g., ammonia desorption). However, the correlation of the observed desorption peaks with the centers of a certain type, as well as their identification based only on the thermal desorption curves, is hampered. In this study, we use a TPD NH_3 method (detector - TCD) to investigate the acidic properties of the Fischer-Tropsch reaction molded catalysts with Raney cobalt as an active component based on the metal aluminum-containing composites, varying only in the type of their constituent zeolite.

2 Experimental/methodology

The catalysts were prepared by [4] by extrusion of a paste containing powders of Al°, binder (boehmite), dispersed Co° [5], and the corresponding zeolite (H-beta, mordenite, H-ZSM5, HY, Vegobond) in a ratio of 50:20:20:10 in the calculation of the dry mixture.

Thermal desorption of ammonia was registered (by an Autosorb-1C Quantachrome Instr. with a katharometer) after pretreatment of a granular catalyst formed "as is" in a vacuum (300° C, 4 hours), or without pretreatment for a full compliance of the activated catalyst with the system undergoing the acidity test.

The sample after (or without) pretreatment was heated (10°/min) in a stream of pure H_2 to 400°C, and was recovered at this temperature for 1 hour and cooled to 40°C. Then, at this temperature, the surface was cleaned by evacuation of recovery products for 0.5h, and ammonia was sorbed (0.5 hours, 40°C, 1%NH_3/N_2). Further, ammonia was desorbed (20°/min) in a stream of helium.

Thus, the acidic properties of the experimentally obtained system correspond to the acidic properties of a Fischer-Tropsch catalyst after reductive activation. The control experiments (without evacuation after recovery) confirmed the adequacy of the hydrate-hydroxyl cover of the emerging surface existing in the real conditions of the catalyst surface. The modeling compounds (individual zeolites, γ-Al_2O_3, boehmite gel after acid treatment) were activated

similarly to the functioning catalysts.

3 Results and discussion

For zeolites proper, ammonia desorption acidity is shown in Fig.1. Apparently, Vegobond has the lowest total acidity, while mordenite has the greatest number of strong centers.

The total intensity of a TPD curve of the zeolite-based catalyst (Fig. 2, an exemplary system with Hβ) differs significantly from the curve of individual zeolite introduced into its structure.

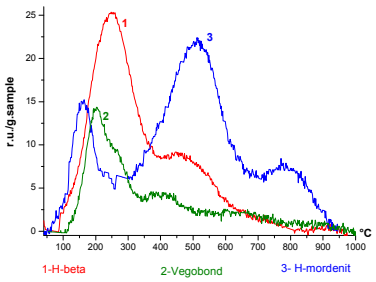

Fig.1 TPD NH_3 for individual zeolites

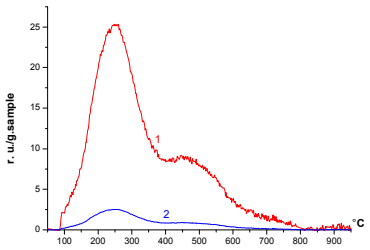

Fig.2 TPD NH_3 for an Hβ-based catalyst (1) and Hβ (2) in 10% of the catalyst weight

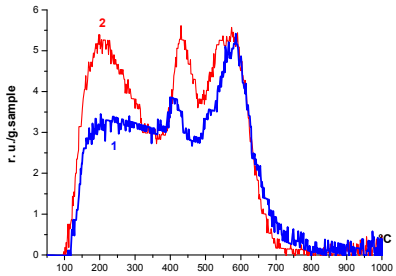

Fig.3 TPD NH_3 for a zeolite-free catalyst (1) and a catalyst with an Hβ zeolite (2)

A careful study of the initial catalyst and model systems, upon activation by a thermal vacuum treatment, with modification by nitric acid and potassium hydroxide, and a number of binder (boehmite) treatments, showed that the high-temperature peak with a maximum at 600°C is caused not only by desorption of ammonia, and the release of water in the conversion of the binder in the already molded catalyst may contribute up to 50% in the signal intensity. A 410-430°C maximum is mainly due to ammonia desorption from the unreduced cobalt oxide phase, wherein the catalyst has no more than half of $Co^{\delta+}$ ions initially introduced with Raney cobalt available for adsorption. Modification of systems allows a purposeful removing of the weak acid sites (thermal vacuum treatment, acid treatment) and strong acid sites (alkali treatment).

3 Conclusions

It is shown that the TPD curves are very similar for catalysts containing different zeolites; at the same time, the effects are significantly different from the respective ones in individual zeolites. The observed TPD curve peaks are determined not only by the desorption of ammonia, but also by the hydroxyl removal in the processes of phase transformations of aluminum oxide, formed from the binder or due to zeolite lattice destruction. A correct comparison of acidity and catalytic activity of composites is possible only for the systems subjected to the same effects.

References

[1] R. J. Gormley, V. U. S. Rao, R. R. Anderson, R. R. Schehl,R. D. H. Chi, J. of Catal.,113(1988)193
[2] L. Damjanovic´ and A. Auroux, Zeolite Characterization and Catalysis, 2009,p.107
[3] E.A. Paukshtis. Infrakrasnaya spektroskopiya v geterogennom kislotno-osnovnom katalize. Novosibirsk, Nauka, 1992
[4] RU Patent No 2405625, 2010
[5] Solomonik I.G., Gryaznov K.O., Mordkovich V.Z. II Russian Congress on Catalysis, 2(2014) 83

II-PP152

XPS Study of Au/C Model Samples Oxidation by NO_2

Kalinkin A.V.*, Smirnov M.Yu., Bukhtiyarov V.I.

Boreskov Institute of Catalysis SB RAS, Novosibirsk, Russia

* avkalinkin@mail.ru

Keywords: supported, gold, graphite, oxidation, NO_2

1 Introduction

Gold catalysts exhibit high activity in a number of oxidative processes. Nevertheless, it is believed that gold cannot adsorb an oxidant from the gas phase without its specific activation (atomization, microwave discharge, etc.). As a result, the mechanism of action of gold catalysts is currently the subject of debate. Previously, we have shown that nitrogen dioxide produced by the decomposition of lead nitrate directly in a vacuum chamber of an XPS spectrometer possesses the ability to selectively oxidize fine particles of platinum with the formation of a mixture of oxides of Pt(II) and Pt(IV). In the present study, this technique was used to study the possibility of oxidation of gold deposited on highly oriented pyrolytic graphite (HOPG).

2 Experimental

This work was performed using an X-ray photoelectron spectrometer (SPECS, Germany) equipped with a hemispherical analyzer and a 9-channel detector. Photoelectron spectra were recorded using monochromated X-ray radiations Al Kα ($h\nu = 1486.7$ eV) and Ag Lα ($h\nu = 2983.4$ eV). HOPG was preannealed for 1 h in ultrahigh vacuum. Photoelectron spectra of these samples contained only photoelectron and Auger lines of carbon. Gold was deposited onto the HOPG surface kept at room temperature with the use of an EFM3 evaporator by heating a premelted gold wire with an electron beam. Two type samples were prepared for the study. In the first case, gold was directly evaporated onto a clean, atomically smooth HOPG surface (Au/HOPG); in the second case, gold was deposited onto a preactivated surface (Au/HOPGA). The activation consisted in a short sputtering of the HOPG surface with low energy Ar ions (1 s, 500 eV) in order to produce defects. The gold coverage was evaluated by comparing the intensities of Au 4f and Au $3d_{3/2}$ peaks from the model samples with those from an Au foil. To treat the samples, NO_2 at a total pressure of $3 \cdot 10^{-5}$ Torr was produced directly in the chamber of the SPECS spectrometer by thermal decomposition of $Pb(NO_3)_2$. The sample temperature during this treatment was near 300 K.

3 Results and discussion

During the deposition of gold on the smooth surface of HOPG, the FWHM (full width at half maximum) for the doublet Au 4f and the binding energy (BE) Au $4f_{7/2}$ were constant and characteristic of a gold foil in the whole range of gold coverages. During the deposition of gold on the activated surface with coverage $\Theta(Au) \geq 0.1$ML, the spectral characteristics of the doublet Au 4f also corresponded to bulk gold. At lower coverages, the doublet Au 4f broadened and its BE increased. For example, at $\Theta(Au) = 1.2 \cdot 10^{-2}$ ML, the BE was 84.8 eV. Figure 1 shows the spectral region Au 4f for the samples Au/HOPG and Au/HOPGA with similar coverages Θ(Au). It is assumed that the deposition of gold on the smooth surface of HOPG leads to the formation of 3D gold particles a few nm in size. The BE(Au $4f_{7/2}$) of the 3D particles does not depend on the particle size and equals 84.0 eV. For the HOPGA samples, the deposition of gold leads to the formation of not only 3D particles but also isolated atoms of gold. The Au atoms in

this case can stabilize on surface defects with the formation of a bond Au-C_n with one or several atoms of carbon. In this case, the electron density of the Au atom transfers to the carbon atoms, thereby increasing the BE(Au $4f_{7/2}$) relative to bulk gold. Superposition of different Au-C_n states leads to the broadening of the doublet Au 4f.

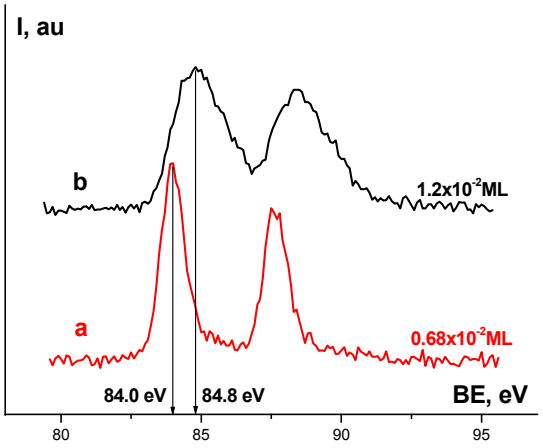

Figure 1. Au 4f core-level spectra of samples Au/HOPG (a) and Au/HOPGA (b).

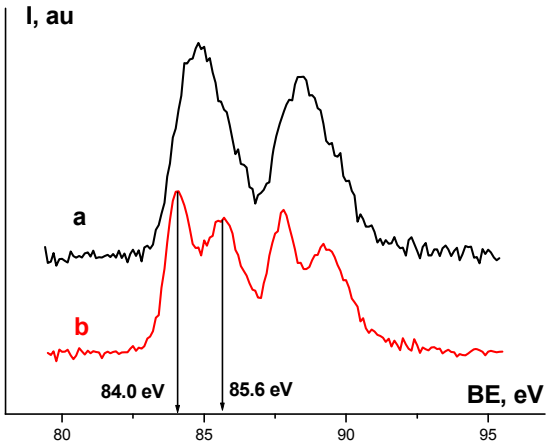

Figure 2. Au 4f core-level spectra of the sample Au/HOPGA with Θ(Au) = $1.2 \cdot 10^{-2}$ ML before (a) and after (b) treatment in NO_2 for 150 min.

The prepared samples were treated with nitrogen dioxide. It was shown that this treatment does not lead to any changes in the region of Au 4f for the samples Au/HOPG with any Θ(Au) and for the samples Au/HOPGA with Θ(Au) ≥ 0.1 ML. This result suggests that 3D gold particles are resistant to NO_2. The treatment in NO_2 of the sample Au/HOPGA with Θ(Au) < 0.1 ML resulted in the oxidation of gold. Fig. 2 shows the Au 4f spectra of the sample Au/HOPGA with Θ (Au) = $1.2 \cdot 10^{-2}$ ML before and after the treatment in NO_2. As is seen, the doublet Au 4f after this treatment changes into a superposition of two narrow doublets with the BE(Au $4f_{7/2}$) equal to 84.0 and 85.6 eV. The state with BE = 84.0 eV corresponds to 3D particles of metallic gold. The state with BE = 85.6 eV presumably corresponds to Au(III) in the surface compound (C–Au=O), which is formed during the oxidation of bound gold atoms Au-C_n with nitrogen dioxide. Thus, gold atoms that are chemically bound to the support can be oxidized under relatively "mild" conditions and hence can act as the active sites in the oxidation catalysis.

4 Conclusions

The deposition of gold on the atomically smooth surface of HOPG results in the formation of 3D gold particles with the BE(Au $4f_{7/2}$) = 84.0 eV. The form of gold deposited on the surface activated with argon ions (HOPGA) depends on coverage Θ(Au). At low coverages, the deposition leads to the formation of isolated gold atoms. The atoms are stabilized on the graphite surface by chemical bonding with carbon with the formation of surface compounds Au-C_n. The 3D gold particles are resistant to oxidation with nitrogen dioxide at a pressure $3 \cdot 10^{-5}$ torr. The isolated atoms of gold under these conditions are oxidized to form the state Au(III) stabilized on the surface of graphite. The stabilized gold atoms may act as active sites of gold catalysts.

Acknowledgements

The authors are grateful to the Russian Science Foundation (project 14-23-00146) for financial support.

II-PP153

Effect of Chemical Composition on the Structural Peculiarities and Catalytic Behavior of Cu-Spinels in Water Gas Shift Reaction

Plyasova L.M[1], Minyukova T.P.[1*], Molina I.U.[1], Shtertser N.V.[1,2], Larina T.V.[1], Kriventsov V.V.[1], Kustova G.N.[1], Simentsova I.I[1], Zaikovskii V.I.[1,2], Yurieva T.M.[1]

1 - Boreskov Institute of Catalysis SB RAS, Novosibirsk, Russia
2 - Novosibirsk State University, Novosibirsk, Russia

* min@catalysis.ru

Keywords: Cu-spinels, physico-chemical studies, WGSR

1 Introduction

Studies of spinel-type catalysts for WGSR attract great attention last years because of their high activity and high resistance to adverse factors of the reaction medium - high temperature and high steam content [1]. Although the study of these catalysts continues for a long time, the impact of the chemical composition and the ratio of trivalent cations on the distribution of copper cations in the oxide and its catalytic properties is still unclear. In the present paper we report the results of the study of the effect of chemical composition on the structural peculiarities and catalytic properties of mixed CuFeCr, CuFeAl and CuCrAl oxides of spinel structure.

2 Experimental

The samples were obtained by thermal decomposition of mixed hydroxocarbonates. Coprecipitation method at constant pH=6.6-6.8 and temperature 70-75°C was applied for hydroxocarbonates synthesis, using 10% nitrates and 6% sodium carbonate aqueous solutions. Precipitants were washed with distilled water and air dried under an IR lamp at 90°C for 12 hours. Netzsch STA-409 station was used for studying the process of decomposition in Ar flow at a temperature rise rate of 10 K/min. XRD studies were performed on D-8 diffractometer (Bruker) using Cu-K_α–irradiation (graphite monochromator in the reflected beam). Electron microscopic study of high resolution (HREM) of the samples was performed on a transmission electron microscope JEM-2010 (JEOL) (resolution 0.14 nm, the accelerating voltage of 200 kV). To determine the appropriate concentrations and ratios of elements the local energy-dispersive X-ray microanalysis (EDX-analysis) was used. Samples for studies were supported to the Al- grid. IR adsorption spectra are recorded on a Fourier transform spectrometer Bomem MB-102 in the region 250-4000 cm^{-1} and Bruker spectrometer in the region of 100-300 cm^{-1}. Samples were prepared by pressing in CsJ and polyethylene, respectively. Electronic spectroscopy of diffuse reflectance (ESDR) was used for the characterization of the electronic state of copper in studied spinels. Shimadzu spectrophotometer UV-2501 PC with diffuse reflectance attachment with ISR-240 A was used. Samples in powder form were placed in a quartz cuvette with a pathlength of 2mm and diffuse reflectance spectra were recorded relative to a standard sample reflection - $BaSO_4$ in the wavelength range 190-900 nm (11 000-53 000 cm-1). The catalytic activity of the samples in the water gas shift reaction was measured in a catalytic flow system over a temperature range of 150-210°C at a near atmospheric pressure. The tests were performed in a reaction mixture CO : H_2O : H_2 = 8 : 42 : 50 on a catalyst fraction of 0.14– 0.25 mm mixed with quartz glass of the same particle size in a ratio of 1:1.

Before the onset of the tests, the catalyst was activated in 5% H_2 in He for 2 h at 270°C.

3 Results and discussion

It is shown that depending on the Fe^{3+}/Cr^{3+} (Al^{3+}/Cr^{3+}) ratio the formed spinels exist in two structural modifications - a cubic and tetragonally distorted cubic. To follow the connection of composition and structure the tetragonal distorted spinels were examined in non-standard space group $F4_1/ddm$. Crystallographic relation between the cubic and tetragonal distorted cubic spinel phases was analyzed. It is shown that the distribution of cations on the crystallographic positions, the nature and extent of tetragonal distortion CuFeCr, CuAlCr spinel depends on the ratio of Fe^{3+}/Cr^{3+} (Al^{3+}/Cr^{3+}). Taking into account the energy preference of cations and mixed spinel structure the expected cation distribution was calculated. Dependence between the Fe^{3+}/Cr^{3+} (Al^{3+}/Cr^{3+}) ratio and the cation distribution was confirmed by spectral methods - IR, ESDR, EXAFS. Cu^{2+} ions are placed in tetrahedral positions in $CuCr_2O_4$ and the amount of tetrahedrally coordinated Cu^{2+} reduces with Fe^{3+}/Cr^{3+} growth in CuFeCr spinels. CuFeAl spinels structure remains cubic and partially reversed for all compositions.

Figure 1 shows a dependence of apparent activation energy (E_a) of WGSR from the mole fraction of Fe for CuFeCr and CuFeAl. For partially reversed CuFeAl spinels we didn't observe a dependence between Cu ions distribution and E_a (Fig.1 curve 1). In accordance with estimated cations distributions for CuFeCr spinels E_a changes from 8 kcal/mol for $CuCr_2O_4$ to 24 kcal/mol for $CuFe_2O_4$ (Fig.1 curve 2). Such a dependence correlates with Cu ions amount in octahedral positions (Fig.1 curve 3).

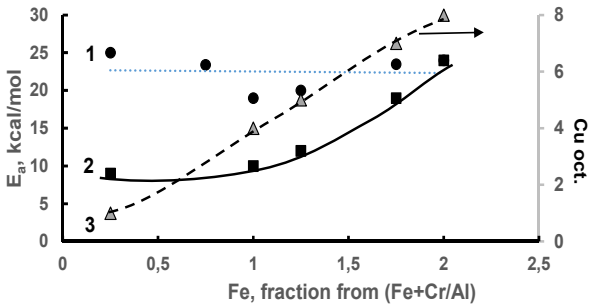

Fig. 1. Dependence of apparent activation energy (E_a) of WGSR from mole fraction of Fe for: (1) CuFeCr; (2) – CuFeAl; (3) Cu^{2+} in octahedral positions of CuFeCr spinels

4 Conclusions

The effect of chemical composition and Fe/Cr (Fe/Al) ratio on the extent of spinel structure tetrahedral distortion and on distribution of cations between tetrahedral and octahedral positions was systematically studied. The correlation between distribution of copper ions and catalytic behavior in low temperature WGSR was experimentally confirmed.

Acknowledgements

The authors thank RFBR (project # 13-03-00469 «a») and basic research project V.45.3.6 of RAS for financial support. The authors are grateful to M.P. Demeshkina and Dr.N.A.Baronskaya for their help.

References

[1] C. Ratnasamy, J.P. Wagner, *Catal. Rev*. 51 (2009) 325.

II-PP154

Influence of Ag-CeO_2 Interfacial Interaction on Activity of Ag/CeO_2 Catalysts in Oxidative Reactions

Grabchenko M.V.[1], Mamontov G.V.[1*], Zaikovskii V.I.[2,3], Vodyankina O.V.[1]

1 - Tomsk State University, Laboratory of Catalytic Research, Tomsk, Russia
2 - Institute of Catalysis SB RAS, Novosibirsk, Russia
3 - Novosibirsk State University, Novosibirsk, Russia

* GrigoriyMamontov@mail.ru

Keywords: silver, cerium, oxide, strong, metal-support, interaction

1 Introduction

Catalytic activity of supported catalysts depends on both particle size of the active component and interaction between active component and support. Several strategies have been developed to control the interfacial interactions. Nevertheless, it is very difficult to get insight into the interfacial roles in catalytic system and control the interfacial interaction to designing new materials. Thus, obtaining of strong metal-support interaction (SMSI) and its discovery has awakened interest [1].

The aim of the present work was to study the interfacial interaction of silver nanoparticles with cerium oxide and the effect of this interaction on the activity in low-temperature oxidation of organic compounds.

2 Experimental/methodology

Two series of Ag/CeO_2 catalysts prepared by impregnation and co-deposition methods were compared. Cerium oxide was prepared by deposition method using $Ce(NO_3)_3$ as ceria precursor and ammonia solution as precipitant. Ag/CeO_2 catalysts (loading of silver was 10% wt.) were prepared by two methods: impregnation and co-deposition. Aqueous solution of silver nitrate was used for impregnation of CeO_2 support (Ag/CeO_2-imp catalyst). Co-deposition method was used to prepare catalyst with increased interfacial interaction between Ag and CeO_2 support (Ag/CeO_2-coDP catalyst). Aqueous ammonia solution was slowly dropped into mixture of cerium (III) and silver nitrates aqueous solution at room temperature to precipitate and provoke red-ox reaction:

$$Ce(OH)_3 + Ag(NH_3)_2^+ + 2\ H_2O = Ce(OH)_4 + Ag^o + NH_4^+ + NH_4OH$$ [2, 3]

Discoloration to darker tones was an indicator of this reaction.

Specific surface area (S_{BET}) and pore size distribution of samples were determined according to low-temperature N_2 sorption using TriStar II 3020 analyser (Micromeritics, United States). XRD patterns were recorded with Shimadzu XRD-6000 diffractometer using CuKα in the range from 10 to 80º (2θ). Structure of samples and features of Ag-CeO_2 interfaces were studied by TEM HR using the JEM-2200FS microscope (JEOL). The oxidative ability of catalyst was studied by TPR H_2 and TP reaction of CO oxidation using ChemiSorb 2750 (Micromeritics, United States).

3 Results and discussion

Cerium oxide prepared by deposition methods had specific surface area of 66 m^2/g and pore size of 2-10 nm. According to XRD data, cerium oxide average partical size was ~ 12 nm. TEM result showed CeO_2 particle size distribution in the range of 5-16 nm.

The interaction of ceria with silver nanoparticles was observed by TPR H_2, which is the main

way to control the SMSI effect [4]. TPR profile of CeO_2 (Fig. 1a) is characterized by hydrogen consumption at 350-650 °C and over 700 °C, which can be associated with reduction of surface and bulk of CeO_2, respectively. The main H_2 consumption was observed at 50-300 ^oC for Ag/CeO_2 catalysts. These peaks were associated with simultaneous reduction of dispersed silver and ceria oxides, which characterized the $Ag\text{-}CeO_2$ interaction. The high peak intensity at 218 ^oC for Ag/CeO_2-coDP catalyst may be a result of strong interaction between Ag particles and CeO_2 support.

The features of the interaction of silver particles with surface of CeO_2 were explained by TEM HR results. The epitaxy of silver particles on cerium oxide was observed for Ag/CeO_2-coDP catalyst. The transition of lattice of well-faceted silver nanoparticles (111) (d_{111}=2.3Å) to lattice of CeO_2 with d_{111}=3.1Å is shown in TEM HR image for this catalyst (Fig.1 b). While silver clusters with size of 0.5-3 nm were observed for catalyst prepared by impregnation method (Fig.1c). The epitaxy of silver on the ceria surface may indicate on strong metal-support interaction. The formation of small cluster might be result of weak interaction of silver with ceria support.

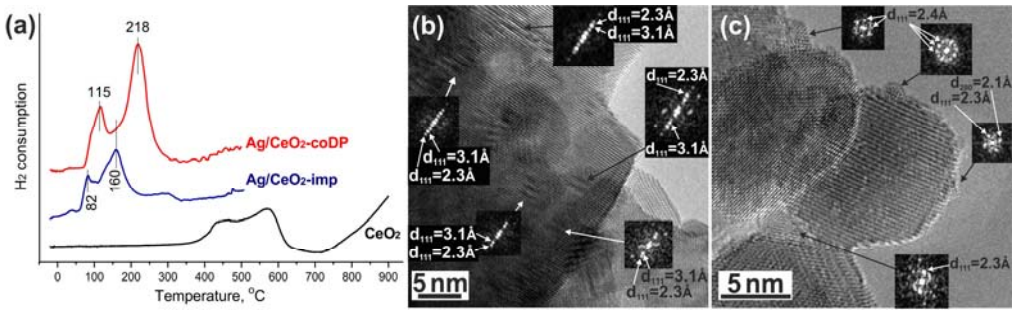

Fig. 1.TPR H_2 profile of Ag/CeO_2 catalysts (a), TEM images of Ag/CeO_2-coDP (b) and Ag/CeO_2-imp (c)

CO oxidation over Ag/CeO_2 catalysts was observed over 20 ^oC and temperature of 50 % CO conversion was 297, 204 and 107 ^oC for CeO_2, Ag/CeO_2-coDP and Ag/CeO_2-imp, respectively. The highest activity of Ag/CeO_2-imp catalyst may be associated with cluster state of supported silver or weak interaction of silver with ceria support. The strong metal-support interaction in Ag/CeO_2-coDP catalyst was not favourable for low-temperature CO oxidation.

4 Conclusions

Thus, it was shown that distribution of active component on support surface and their interaction depend on preparation method . It was shown that Ag/CeO_2 catalysts prepared by co-deposition had strong support-metal interaction expressed in epitaxy of silver on the ceria surface and more intensive simultaneous reduction of silver and cerium oxides in TPR. Weak interaction of silver clusters with ceria support was observer for catalyst prepared by impregnation method. The activity of supported small silver cluster in CO oxidation was higher in comparison with silver particles strongly bonded with ceria support.

Acknowledgements

This research was supported by "The Tomsk State University Academic D.I. Mendeleev Fund Program" grant.

References

[1] S.J. Tauster, *Accounts of Chemical Research*. 20 (1987) 389.
[2] J. Zhang, L. Li, X. Huang, G. Li, *J. Mater. Chem.* 22 (2012) 10480.
[3] T. Mitsudome, Y. Mikami, M. Matoba, T. Mizugaki, K. Jitsukawa, K. Kaneda, *Angew. Chem. Int. Ed.* 51 (2012) 136.
[4] N. Acerbi, S.C.E. Tsang, G. Jones, S. Golunski, P. Collier, *Angew. Chem. Int. Ed.* 52 (2013) 7737.

II-PP155

Well-Defined and Atomically Dispersed Supported Palladium Catalysts for Carbon-Carbon Coupling Reactions

Dachwald O.H.[1*], Wirth A.S.[1], Köhler K.[1], Goh S.L.[2], Högerl M.P.[2], Boch F.J.[1], Basset J.-M.[2]

1 - Catalysis Research Center, Department of Chemistry, Technische Universität München, Garching, Federal Republic of Germany

2 - KAUST Catalysis Center, King Abdullah University of Science & Technology, Thuwal, Kingdom of Saudi Arabia

* Oliver.Dachwald@tum.de

Keywords: grafting, single-site catalysis, coupling reactions, surface science

1 Introduction

In order to prepare supported metal catalysts, precursors are in most cases immobilised via ion exchange or impregnation techniques. These methods are often based on electrostatic interactions between the metal ion and the support. Grafting has been established as a method to obtain catalysts with atomically dispersed active sites.[1] During grafting, chemical bonds between the precursor and the functional groups of the support are formed (see Scheme 1).

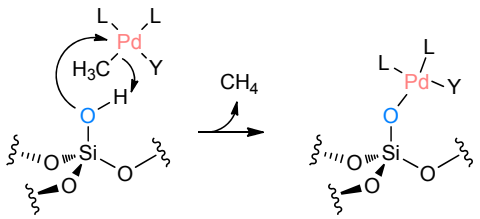

Scheme 1: Grafting: reaction between the functional group of the support surface (silanol for silicon dioxide) and the reactive methyl ligand of the metal precursor complex.

Up to now, only a few contributions about grafting of palladium have been reported.[2,3] The synthesis procedure was optimised based on a methodology already successfully applied for platinum catalysts.[4] As prepared materials were applied as model catalysts in coupling of deactivated aryl halides such as chlorides or donor-substituted bromides in HECK and SUZUKI-MIYAURA reactions. Isolated surface metal complexes depict the highest possible metal dispersion, namely a single atom under ideal conditions and mark a versatile starting point for various material-scientific investigations in working catalysts.

2 Experimental/methodology

The materials were synthesised by methods which are mostly used in surface organometallic chemistry. Applied methods comprise classical organometallic and complex chemistry as well as high vacuum technique for support preparation.

Silicon dioxide in 100 – 300 µm grain size was calcined at 500 °C prior to use. High vacuum treatment at this temperature leads to isolated and vicinal silanol groups on the surface. The grafting reaction was performed in aprotic solvents (benzene, toluene).

The precursor dimethyl-(bis-(diphenylphosphino)-ethane)-palladium(II) was prepared according to modified literature procedures.[7] Any treatment subsequent to dehydroxylation of the support was carried out under aprotic and dry conditions in order to preserve the homogeneous surface properties.[5] The palladium surface species were investigated by IR spectroscopy, CO chemisorption and temperature programmed reaction techniques.

3 Results and discussion

Organometallic precursors for grafting generally comprise basic ligands for the actual

grafting reaction (leaving groups) and stabilising spectator ligands. Noble metals seek towards an oxidation state of zero which is well known for preparing and handling their complexes; a phenomenon generally referred to as 'self-reduction'. The key was to find a balance between reactivity of the leaving ligand and the overall stability of the metal complex. Alkanides are strong BRØNSTED-bases ($pK_a(CH_4)$ = 49) and react readily with protons of surface hydroxyl groups on oxidic support materials. Silica was thermally treated *in vacuo* to generate only isolated and vicinal silanol groups on the surface.

The grafted materials with highly (atomically) dispersed palladium species were tested in C-C coupling reactions of SUZUKI-MIYAURA and HECK type. They showed excellent catalytic activity in conversion of demanding substrates and hence outperform supported palladium nanoparticles prepared by common methods. The materials allow the investigation of leaching phenomena during the catalytic reaction und thus acquiring deeper understanding of mechanistic details. It has been and still is subject of discussion what is the actual active species in catalytic carbon-carbon (CC) coupling reactions by immobilised catalysts. The catalysts obtained by grafting show superior activity in CC coupling reactions when compared to materials synthesised by conventional methods. The release of the required amount of palladium into the solution to perform the reaction takes place under conditions when rather inert substrates (aryl chlorides) can be successfully activated (see Fig. 1). Eventually, re-deposition of palladium affords a material which, regarding its surface species is chemically altered compared to the fresh catalyst.

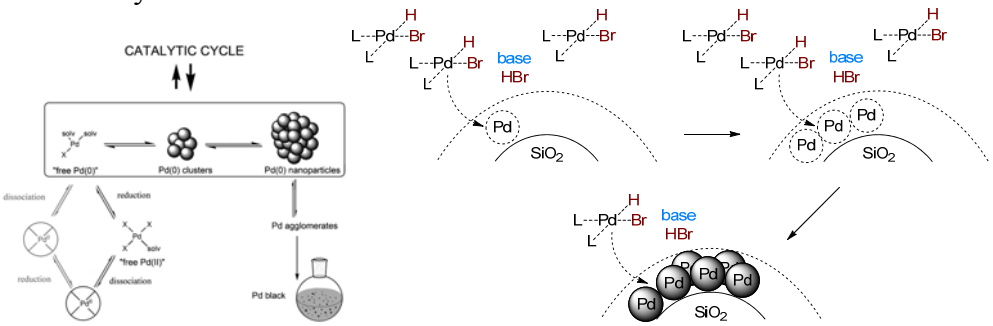

Fig. 1: Reaction mechanism in 'heterogeneous' HECK reactions (left)[6] and proposed re-deposition of the active species after running out of substrate.

4 Conclusions

Even though grafted metal complexes provide the highest possible dispersion (of 100 %), a molecular surface mechanism in CC coupling reactions seems unlikely due to sterical hindrance. However, the catalysts are capable of readily providing highly active palladium species in the required amount, which makes them a versatile tool in converting rather inert substrates in CC coupling reactions. Additionally, the highly dispersed palladium centres provide a starting point in for vast studies in catalyst degradation, their long-term stability and applicability.

Acknowledgements

We are thankful to both KAUST and the "Studienstiftung des deutschen Volkes" for financial support.

References

[1] C. Copéret, M. Chabanas, R. Petroff Saint-Arroman, J.-M. Basset, *Angew. Chemie Int. Ed.*, **2003**, *42*, 156
[2] M. K. Richmond, S. L. Scott, H. Alper, *J. Am. Chem. Soc.*, **2001**, *123*, 10521
[3] M. K. Richmond, S. L. Scott, G. P. A. Yap, H. Alper, *Organometallics*, **2002**, *21*, 3395
[4] K. Chatziapostolou, M. Albert, J. Samson, J. Zheng, A. I. Frenkel, M. Tromp, V. D'Elia, S. Ould-Chikh, K. Köhler, *submitted*.
[5] B. A. Morrow, A. J. McFarlan, *Langmuir*, **1991**, *7*, 1695
[6] C. Röhlich, K. Köhler, *Adv. Synth. Catal.*, **2010**, *352*, 2263

[7] G. S. Hill, M. J. Irwin, L. M. Rendina, R. Puddephat, *Inorg. Synth.*, **1998**, *32*, 170

II-PP156

Synthesis and Redox Behavior of Oxide Supported Isolated Nickel Complexes

Boch F.J.[1*], Haeßner C.[1], Köhler K.[1], Högerl M.P.[2], Goh S.L.[2], Basset J.-M.[2]

1 - Catalysis Research Center, Department of Chemistry, Technische Universität München, Garching, Federal Republic of Germany

2 - KAUST Catalysis Center, King Abdullah University of Science & Technology, Thuwal, Kingdom of Saudi Arabia

* florian.boch@tum.de

Keywords: grafting, single-site catalyst, model catalyst, redox properties, EPR

1 Introduction

Heterogeneous catalysts with a high number of uniform and isolated active sites offer advantages over supported metal particles, in particular as model catalysts. Due to their higher dispersion, these materials are expected to possess enhanced catalytic activities and offer the possibility of getting better insights into reaction mechanisms.[1] During grafting, chemical bonds between the metal center of the precursor and the functional groups of the support are formed, leading to single-site catalysts. In contrast to early transition metals and to the 4d and 5d homologues there are only few contributions for grafting of nickel.[2-4] Especially the oxidation state and the redox properties of grafted nickel species are an interesting field of investigation, as the oxidation state of the catalytic site is expected to be crucial for its activity and often a matter of discussion.[5]

2 Experimental/methodology

Oxidic supports were pre-treated thermally under high vacuum conditions, in order to generate isolated and vicinal silanol groups on the surface of the support, whereupon the number of hydroxyl groups can be adjusted by the pretreatment temperature.[6] These hydroxyl groups serve as binding site for the isolated metal centers on the surface. Organometallic complexes were reacted with the hydroxyl groups on the support. The obtained catalysts were characterized by the means of elemental analysis, IR, NMR and EPR spectroscopy.

3 Results and discussion

Different organometallic complexes with basic ligands, such as alkanides, and stabilizing spectator ligands were used as precursors for the grafting procedure. Amongst the tested precursors dimethyltris(trimethylphosphine)nickel(II)[7] meets the requirements regarding precursor reactivity under optimized conditions in the best way. It showed the best performance to strike the balance between high reactivity towards the acidic surface hydroxyl groups and sufficient stability to handle the complex without premature decomposition. The precursor was reacted with a carefully pretreated and highly specified silica surface (Scheme 1).

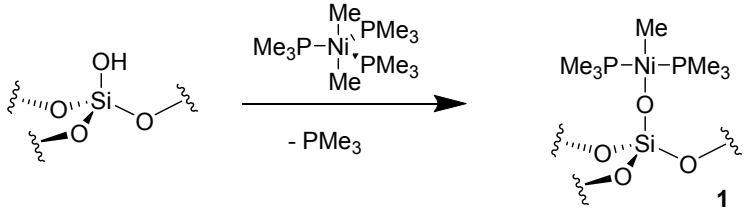

Scheme 1: Grafting reaction of dimethyltris(trimethylphosphine)nickel(II)[7] with silica

The as-obtained single-site catalysts were characterized by IR-spectroscopy, solid state NMR and elemental analysis. The results prove that isolated nickel species were formed. The results of the elemental analysis indicate that one phosphine ligand of the precursor is released during the reaction. The molar ratio Ni/P is 1:2 and the carbon and hydrogen analyses indicate an elemental composition matching the structure of **1**. Solid state NMR-investigation support the proposed structure as two signals occur in the ^{1}H-spectrum at δ = 1.30 ppm and -1.28 ppm with a ratio of 18:3. The ^{13}C-spectrum shows two signals at δ = 11.66 and δ = -27.83 ppm. The ^{31}P-spectrum shows one signal at δ = -18.78 ppm.

The oxidation state of the precursor before and after the reaction was monitored by means of NMR and EPR spectroscopy. A change of the oxidation state of the nickel centers from II to I was observed. Surprisingly, isolated paramagnetic NiI species were found as well as sharp NMR signals which are caused by diamagnetic NiII species. The EPR spectra show the hyperfine structure of an axial d9 NiI system with g values $g_{\parallel}$ = 2.265 und $g_{\perp}$ = 2.079. The hyperfine coupling constants were A1= 98.0 G and A2=49.5 G indicating that the two phosphine ligands are not equivalent due to the distortion caused by the bulky surface in the metal ion's coordination sphere.

These results indicate that two different isolated species, a diamagnetic and a paramagnetic one, were formed on the surface. The reactions of the catalysts towards different reducing and oxidizing agents were investigated by temperature programmed reduction and EPR. The calcined catalysts could only be reduced at temperatures above 550 °C. The reduction was accompanied by agglomeration of the nickel species to particles. The agglomeration was monitored via transmission electron microscopy.

In order to get a better insight into the occurring processes on the surface, additional model experiments were performed in solution with tris-(*tert*-butoxy)silanol as model for a silica surface.

4 Conclusions

Supported catalysts with isolated nickel centers were synthesized by grafting procedures. These catalysts exhibit a very interesting redox behaviour. Diamagnetic Ni^{II} as well as paramagnetic Ni^{I} species could be detected after the grafting procedure. This feature predestines these catalysts as model system for investigating the relation of the oxidation state and the catalytic activity for alkene oligomerization reactions on isolated metal centers.

Acknowledgements

We thank Dr. Gabriele Raudaschl-Sieber (TUM) and Edy Abou-Hamad, Ph.D. (KCC) for recording the solid state NMR spectra.

References

[1] C. Copéret, M. Chabanas, R. Petroff Saint-Arroman, J.-M. Basset, *Angew. Chemie Int. Ed.*, **2003**, *42*, 156
[2] A. Dorcier, N. Merle, M. Taoufik, F. Bayard, C. Lucas, A. de Mallmann, J.-M. Basset, *Organometallics*, **2009**, *28*, 2173
[3] M. K. Richmond, S. L. Scott, H. Alper, *J. Am. Chem. Soc.*, **2001**, *123*, 10521
[4] M. K. Richmond, S. L. Scott, G. P. A. Yap, H. Alper, *Organometallics*, **2002**, *21*, 3395
[5] A. Brückner, U. Bentrup, H. Zanthoff, D. Maschmeyer, *J. Catal.,* **2009,** *266*, 120–128
[6] B.A. Morrow, A. J. McFarlan, *Langmuir*, **1991**, *7*, 1695
[7] H.-F. Klein und H.H. Karsch, *Chem. Ber.*, **1972**, *105*, 2628-2636

II-PP157

Surface Composition of the Industrial Dehydration Alumina Catalyst

Vasilyev V.A.*, Oparkin A.V., Karalin E.A., Kharlampidi Kh.E.

Kazan national research technological university, Kazan, Russia

* viktormemfis@mail.ru

Keywords: alumina, styrene, dehydration, alkali metals, alkali earth metals

1 Introduction

Sodium is the only one of alkali and alkali earth metals, the content of which is regulated by the state standards of Russian and Foreign manufacturers of alumina (excluding high-purity alumina of Sasol company [1]). However, a qualitative analysis of the outer surface of the industrial dehydration catalysts of 1-phenylethanol to styrene, that we carried out by XRD (X-ray fluorescence analysis), showed the presence of the potassium and calcium – catalytic poisons for solid acids (like sodium) [2].

2 Experimental/methodology

Determination of the content of cations on the surface of alumina were carried out by flame photometry in the low-temperature multi-channel flame photometer BWB - XP (BWB Technologies, UK); multi-point calibration.

3 Results and discussion

The results of quantitative analysis of samples of industrial alumina AOK-63-22K (JSC SCTB "Katalizator", Novosibirsk, Russia) from various serials (production 2008 - 2013), industrial alumina AOA (Dnipropetrovsk, Ukraine) from various serials (production 2009 - 2010), and several samples of aluminum oxide produced in non-CIS countries (samples 3-6) are shown in Table 1.

Table 1. Average surface concentration of elements

Catalysts sample	Concentration, μmol/g		
	Na	K	Ca
AOK catalyst	33,4	3,70	1,8
AOA catalyst	7,1	0,12	3,9
Sample № 3	1,6	0,06	0
Sample № 4	1,2	1,90	0
Sample № 5	49,0	2,74	12,4
Sample № 6	24,2	1,67	7,4

As shown in Table 1, the content of potassium and calcium at the surface of some samples is sufficiently high and reaches (in total) 60% of the sodium concentration (alumina AOA).

It should also be noted, that we detected an intense oscillations of the contents of these elements in the composition of the alumina, produced during one calendar year at one factory (Table 2).

Table 2. Surface concentration of elements, alumina AOA

Production date, serial number	Concentration, μmol/g		
	Na	K	Ca
2009, № 1	4,9	0,13	2,5
2009, № 2	4,9	0,13	4,4

2009, № 3	17,7	0,14	11,4
2009, № 4	4,1	0,12	3,3
2009, № 5	15,9	0,18	10,7
2010, № 1	15,9	0,17	9,0
2010, № 2	3,6	0,11	0,5
2010, № 3	4,0	0,12	0,8
2010, № 4	3,6	0,07	0,0
2010, № 5	4,4	0,09	0,1

4 Conclusions

Based on the experimentally observed reduction effect of K^+ and Ca^{2+} cations on dehydrating activity of catalyst, we conclude that it is reasonable for consumer perform incoming inspection of the content of these elements in the alumina industry serials.

Acknowledgements

This research was supported by the Ministry of Education and Science of Russian Federation as part of the state contract (“PNIL 02.14”, base part).

References

[1] http://www.sasolgermany.de/

[2] V. Vasilyev, D. Vafin, K. Paraschuk, E. Karalin, *Herald of Kazan Technological University*. V. 15, № *16* (2012) P. 48 - 49.

II-PP158

Characterization of V-Al PILC Clay Surfaces after Modification by Cu-Zn Impregnation

Marcos F.C.[1], Lucredio A.F.[1], Assaf J.M.[2], Assaf E.M.[1*]

1 - São Paulo University, São Paulo, Brazil
2 - Federal University of São Carlos, São Carlos, Brazil

* eassaf@iqsc.usp.br

Keywords: pillared, clays, montmorillonite, catalysts, copper, zinc

1 Introduction

The development of a new bifunctional catalyst, containing two types of active sites (metallic and acid), can be the key to improve performance of the catalysts in catalytic reactions in one-step. Metallic copper is the active site, often being used in methanol synthesis. ZnO is used to increase Cu dispersion in the sample, thus providing a high number of active sites exposed to gaseous reactants [1]. Pillared clays (PILC´s) have been studied as acid catalysts due their performance and low cost. The introduction of aluminum polycations in the clays leads to a significant modification in their acidity. The acidity modification is due to two factors: (a) increase in the specific area and (b) appearance of new acid sites in the pillars molecular introduced and the binding sites between the pillars and the lamellae [2].

The goal of this study is production of a new bifunctional catalyst, which can be applied in the future for direct conversion of syngas to dimethyl-ether (STD-process).

2 Experimental/methodology

The clay used was Volclay (region Wyoming (EUA)) montmorillonite. The synthesis of the aluminum-pillared clay was carried out from a pillaring agent, which was prepared from the hydrolysis of an $AlCl_3.6H_2O$ 1M solution with NaOH 0.4 M (OH^-/Al^{3+} = 2.0). A montmorillonite aqueous suspension of 2 % (w/v) was prepared and stirred for 3h. The pillaring agent was added drop wise while stirring, then this mixture was stirred for a further 3 h and left to settle for 24h. The solid was calcined at 500 ^oC/2h at a heating rate of 3 °C.min^{-1}, obtaining V- Al PILC.

Cu-Zn catalysts supported on V-Al PILC were prepared by the impregnation method using 5wt% and 10wt% of Cu and 5wt% Zn. The catalysts were named 5%Cu V-Al PILC, 5%Cu 5%Zn V- Al PILC and 10%Cu 5%Zn V- Al PILC.

The materials were analyzed by X-ray diffraction (XRD), energy dispersive spectroscopy (EDS), N_2 adsorption/desorption isotherms, temperature-programmed reduction (TPR) and X-ray absorption near edge structure (XANES). The acidity studies were performed using FTIR after pyridine adsorption.

3 Results and discussion

XRD pattern for natural clay showed an intense reflection for the basal spacing d_{001}=9.4Å and XRD patterns for V-Al PILC indicated that the pillaring procedure was successful due to the increase of the basal spacing, d_{001}= 16.7 Å. XRD patterns for the bifunctional catalysts showed two peaks at 2θ values of 35.57º and 38.73º and are related to the monoclinic structure of CuO (JCPDS card Nº. 05-0661), and other peaks at values of 2θ= 31.73º, 34.37º, 36.21º, 47.48º, 56.53º and 67.86º, related to hexagonal structure of ZnO (JCPDS card Nº. 89-1397).

Analysis by EDS for natural clay compared to V-Al PILC showed a significant decrease in the amount of Na and Ca. This is indicative of exchange of these ions by aluminum polycation.

The bifunctional catalysts showed Cu and Zn real values close to nominal. It was observed in the TPR profiles of bifunctional catalysts, that ZnO did not improve the reduction of CuO, when compared to the catalyst without ZnO. It was observed that the pillaring process increased the specific surface area. After impregnation of Cu-Zn, it a decrease was observed in the specific surface area and pore volume. This may be due to Zn covering the pores of the V-Al PILC, however the higher Cu content impregnated increased the specific surface area and pore volume. N_2 adsorption isotherms of the bifunctional catalysts have a combination of shapes I and IIb, with hysteresis cycles of the Type H3 and H4 [3].

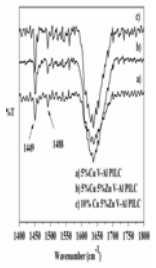

Fig. 1. FT-IR spectra of adsorbed pyridine on bifunctional catalysts.

Table 1. XANES- Quantification of oxide species Cu K-edge under H_2 flow at 300 °C.

Catalysts	Molar ratios	
	CuO	Cu_2O
5%Cu	6.0 ± 1.3	19.0 ± 2.1
5%Cu 5%Zn	17.0 ± 0.7	21.0 ± 1.0
10%Cu 5%Zn	3.0 ± 1.5	23.5 ± 2.5

FTIR spectra with pyridine adsorbed are shown in Fig 1. The bifunctional catalysts showed two bands characteristic of pyridine adsorbed in the acids sites. The band at 1449 cm^{-1} is characteristic of physisorbed pyridine, related to Lewis acids sites. The band at 1488 is associated with both Brønsted and Lewis acid sites [4]. XANES results (Table 1) demonstrated that Cu local order under the temperature studied is composed of a mixture of phases: CuO, Cu_2O and Cu^0, with Cu^0 phase in higher quantities. ZnO did not favored the reduction of Cu, as already discussed in the TPR analysis, when the 5%Cu and 5%Cu5%Zn samples are compared.

4 Conclusions

The 10%Cu5%Zn-V-Al PILC catalyst can be the most promising to the STD-process, this is due the presence of Lewis and Brønsted acids sites and higher specific surface area and Cu^0 molar ratios.

Acknowledgements

The authors thank the FAPESP (grant number 2012/17957-3) for financial support and the LNLS (Campinas, Brazil) for XANES analyses.

References

[1] W. Chen, B. Lin, H. Lee, M. Huang, *Applied Energy*. 98 (2012) 92.
[2] A. Romero-Pérez, E. Roca Jali, K. Sapag. *Catalysis Today.*187 (2012) 88.
[3] E.Jalil *et al*., *Applied clay science*. 87 (2014) 245.
[4] T. Kamegawa *et al*., *Physical Chemistry Chemical Physics*. 15 (2013)13326.

II-PP159

Impact of the Additives on the Texture Properties of Re/γ-Al_2O_3 as Catalysts for Water-Gas Shift Reaction in the Presence of Sulphur-Containing Gases

Nikolova D.[1*], Edreva-Kardjieva R.[1], Gabrovska M.[1], Serwicka E.M.[2]

1 - Institute of Catalysis, Bulgarian Academy of Sciences, Sofia, Bulgaria
2 - Jerzy Haber Institute of Catalysis and Surface Chemistry, Polish Academy of Sciences, Krakow, Poland

* dimi@ic.bas.bg

Keywords: sulphided, Re catalyst, Co, Ni additives, N_2 sorption, WGS reaction, sulphur presence

1 Introduction

The water-gas shift (WGS) reaction ($CO + H_2O \leftrightarrow CO_2 + H_2$) is keeping up its key position as an integral stage of ammonia and methanol synthesis as well as hydrogen production. Alumina-supported Re-based catalysts have been used in various reactions as hydrogenation, metathesis, reforming as well as hydrodesulfurization and hydrodenitrogenation process [1, 2]. To our knowledge, such catalysts have not yet been investigated in the WGS reaction conditions in the presence of S-containing gases. This promoted us to study the activity of Re_2O_7/γ-Al_2O_3 system in the WGS reaction over preliminary sulphided samples using Ni, Co and K as additives. The alkali character of K provokes a question about its effect on the pore texture of an amphoteric support like γ-Al_2O_3 after addition as a second or third component. The present study provides information how the deposition of K, Ni and Co additives on Re/γ-Al_2O_3 affects the catalyst texture after the calcination procedure and after activity test in WGS reaction.

2 Experimental/methodology

The single-component Re (15.3 wt.% Re_2O_7), Ni (3 wt.% NiO), Co (3 wt.% CoO) and K (5 wt.% K_2O) samples were prepared by incipient wet impregnation of the γ-Al_2O_3 support with aqueous solutions of the corresponding metal salts followed by drying at 105°C and calcination at 450°C. Ni and Co was added as second component and K was introduced either as a second or a third component to single-component Re sample, following the same preparation procedure of drying and calcination. The synthesized bi- and tri-component samples were denoted as KRe, NiRe, CoRe, KNiRe and KCoRe. The weight content of the Re_2O_7 corresponded to a surface density of 2 atoms Re/nm^2 support. The calcined samples were pre-sulfided *in situ* (6 vol.% H_2S in H_2 at 400°C for 2 h) in continuous-flow reactor. The WGS reaction was carried out at: 2 vol.% H_2S, 7.8 vol.% CO, 90 vol.% Ar gaseous mixture; atmospheric pressure; 180-400°C temperature range; GHSV 4000 h^{-1}; 0.3 steam/gas ratio.

Multipoint BET surface areas (S_{BET}) of the support and the samples were estimated using N_2 sorption at –196ºC (Quantochrome Autosorb Automated Gas Sorption System), according to the BET equation. Evacuation at 200ºC for 18 h was performed prior to sorption analysis. Adsorption-desorption isotherms were used to calculate multipoint BET surface areas, pore size distribution (PSD), using Barrer, Joyner and Halenda (BJH) method, and total pore volumes (V_{tot}) at a relative pressure P/P_o=0.995±0.001 [3].

3 Results and discussion

The sorption isotherms of the calcined and tested γ-Al_2O_3 support and promoted Re-containing samples are of type IV, typical for mesoporous structure with the hysteresis loops of

H2 type, related to the interconnected network of pores with different size and shape according to IUPAC classifcation.

The BET surface area of the calcined support decreases after component deposition in the order: CoRe ≈ NiRe ≈ KCoRe ≈ Re > KRe > KNiRe. The trend is different for the corresponding tested samples: Re > KRe ≈ NiRe ≈ CoRe > KNiRe > KCoRe.

The total pore volume does not change practically, being in range of 0.4-0.6 m^3/g for the calcined samples and 0.3-0.6 m^3/g for the tested ones. The Re deposition on γ-Al_2O_3 leads to the formation of new micro pores - S_{micro} increases by 85 %. The addition of Ni (NiRe sample) and K (KRe, KNiRe and KCoRe) results in the diminution of the amount of the micro pores. The reaction conditions cause the increase of S_{micro} in all samples. The values are in 15-21 m^2/g range, the most significantly being in KRe, NiRe and KNiRe (with 67%, 100% and 320%, respectively).

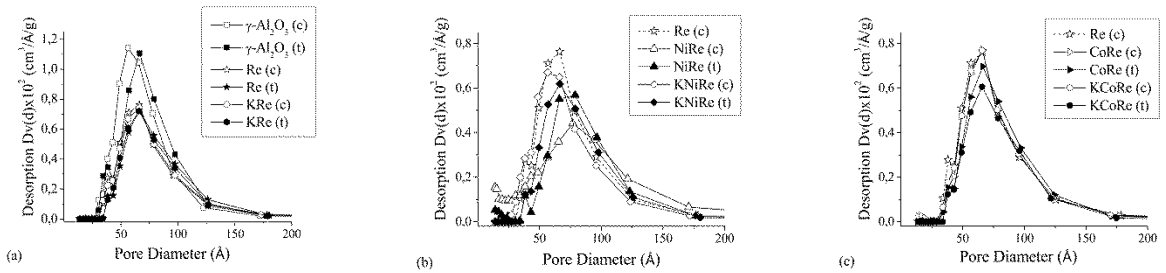

Fig. 1. Pore size distributions

The overall view on pore size distribution in the γ-Al_2O_3 support and in the calcined samples demonstrates mainly a bimodal distribution of the free mesopores in the range 30-180 Å. The data clearly show that after calcination and after test the mesoporous texture of the γ-Al_2O_3 support is preserved (Fig. 1a). The impregnation of the Re active component leads only to filling of pores by the surface species formed. The deposition of Ni on calcined Re sample induces greater changes (Fig. 1b) in the PSD than the K and Co do (Fig. 1a,c). The addition of K causes the redistribution of the pores in the tri-component KNiRe sample, whereas the PSD remains the same in the tri-component KCoRe sample. Only filling and/or partial blocking as well as unblocking of the carrier pores is registered after activity test in WGS reaction because of generated migration of the surface species.

4 Conclusions

Contrary to our expectations, introduction of K to calcined Re, NiRe and CoRe samples does not exert a strong impact on the primary mesopore texture of γ-Al_2O_3, and neither does addition of Co. Greatest changes in the catalyst texture are induced by Ni deposition.

Acknowledgements

D.N., R.E.-K., and M.G. are grateful to the National Science Fund of Bulgaria for partial financial support.

References

[1] J. Räty, T. A. Pakkanen, Catal. Lett., 65 (2000) 175.
[2] N. Escalona, J. Ojeda, R. Cid, G. Alves, A. López Agudo, J.L.G. Fierro, F.J. Gil Llambías, Applied Catalysis A: General, 234 (2002) 45.
[3] F. Rouquerol, J. Rouquerol, K. Sing, in Adsorption by Powders and Porous Solids, Principle, Methodology and Applications, Academic Press, 1999.

II-PP160

Application of Sodium Octacarboxylate Resorcinarenes in Synthesis of Silver Nanoparticles

Sergeeva T.Yu.[1,2*], Sultanova E.D.[2], Mukhitova R.K.[2], Nizameev I.R.[2], Kadirov M.K.[2], Ziganshina A.Y.[2], Konovalov A.I.[2]

1 - Kazan (Volga region) federal university, Kazan, Russia
2 - A.E. Arbuzov Institute of Organic and Physical Chemistry of Kazan Scientific Center of Russian Academy of Sciences, Kazan, Russia

* tanechcka11@mail.ru

Keywords: hybrid, nanomaterials, resorcinarene, silver nanoparticles

1 Introduction

Metallic nanoparticles (Au, Ag, Pd, Pt) show unique optical, electric and catalytic properties [1,2] and, therefore, are of a great interest for researchers. Silver nanoparticles have been applied in electronics, optoelectronic [3] and in medicine [4]. We have used amphiphilic derivatives of resorcinarenes with decyle ($C_{10}H_{19}$-CA), decynyl ($C_{10}H_{21}$-CA), methyl (CH_3-CA) and ferrocene (Fc-CA) groups at the lower rim as stabilizers in the synthesis of the monodisperse silver nanoparticles (AgNPs). The resorcinarenes prevent the aggregation of AgNPs and influence the size and shape of the silver nanoparticles produced.

2 Experimental/methodology

Stable colloidal silver nanoparticles have been obtained in aqueous media using common methods in the presence of $C_{10}H_{19}$-CA, $C_{10}H_{21}$-CA, CH_3-CA as stabilizers and sodium borohydride as a reducing agent. In the case of Fc-CA, the reducing agent was not used, the ferrocene groups act as reducing agents.

AgNP were characterized by the data of UV-vis and IR spectroscopies, static and dynamic light scattering (SLS and DLS), atomic force microscopy (AFM), scanning electron microscopy (SEM) and transmission electron microscopy (TEM) and thermogravimetry (TG).

3 Results and discussion

The influence of the length of the hydrophobic tail of the size and shape of AgNPs is investigated. The silver particles of different sizes are formed using of methyl-resorcinarene CH_3-CA. while the assembled resorcinarenes $(C_{10}H_{19}\text{-CA})_n$ and $(C_{10}H_{21}\text{-CA})_n$ produce monodispersed AgNPs of about 30 nm. The average size of hybrid systems Ag@$C_{10}H_{21}$-CA and Ag@$C_{10}H_{19}$-CA is about 85 nm, and the hydrodynamic diameter is about 90 nm. Hybrid nanosystems stable in water for a long time, and turbidity of the solutions is observed only after several months of storage.

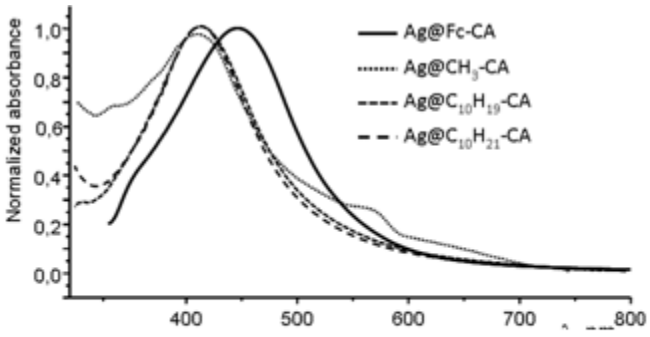

Fig.1. UV-Vis spectra of hybrid nanoparicles Ag@Fc-CA, Ag@$C_{10}H_{19}$-CA, Ag@$C_{10}H_{21}$-CA and Ag@CH3-CA.

In the synthesis of silver nanoparticles was also used ferrocene-resorcinarene. It acts not only as a template and stabilizer, but also as a reductant. Formation of Ag(0) is due to the

reduction of silver ions ferrocene groups resorcinarene by followed the organization in hybrid nanoparticles Ag@Fc-CA.

In the case of Ag@Fc-CA the average size of AgNPs is slightly larger and it is about 35-40 nm. The diameter of the hybrid nanoparticle Ag@Fc-CA is slightly smaller than Ag@$C_{10}H_{19}$-CA and Ag@$C_{10}H_{21}$-CA. At the data of AFM and SEM mean diameter of Ag@Fc-CA is about 60 nm, and the hydrodynamic diameter is about 80 nm. Evidently, the ferrocene-resorcinarene forms thinner organic cover in Ag@Fc-CA, as compared with the Ag@$C_{10}H_{19}$-CA and Ag@$C_{10}H_{21}$-CA.

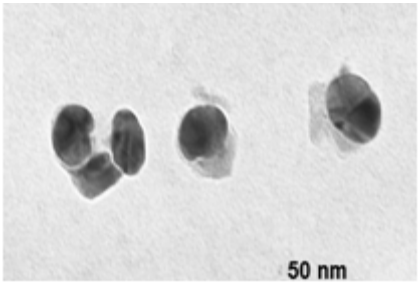

Fig.2. TEM image of Ag@Fc-CA.

Catalytic properties of the hybride nanosystems Ag@CA were studied in the common used reaction of reduction of p-nitrophenol with sodium borohydride in water. The results shows that sodium borohydride does not reduce nitrophenol in pure water. The addition of 40 nanomole of Ag@CA rapidly accelerates the reaction, and it is finished in a few minutes. The highest catalytic activity is observed for Ag@$C_{10}H_{19}$-CA. The lowest activity is detected for Ag@Fc-CA due to the lower surface area of metal nanoparticles or formation of dense packing of Fc-Ca molecules on the silver surface.

The synthesis and characteristics of Ag@CA will be discussed in the presentation.

Table 1. Observed rate constants and normalized rate constant of reduction reaction p-nitrophenol using hybrid nanoparticles Ag@CA.*

Catalyst	**Rate constants, k, s^{-1}**	**Normalized rate constant, k_{cat}, Ag-$mol^{-1}s^{-1}$**
Ag@Fc-CA,	0,0029	72500
Ag@$C_{10}H_{21}$-CA	0,0045	112500
Ag@$C_{19}H_{19}$-CA	0,0128	320000

*n(Ag@CA) = 40 × 10^{-9} M, C(*p*-nitrophenol) = 0,113 mM, C($NaBH_4$) = 5 mM, H_2O, 25 °C.

4 Conclusions

Thus, amphiphilic resorcinarenes with carboxylic groups on the upper rim were used as templates for the creation of silver-containing hybrid organic-inorganic nanoparticles Ag@CA. The hybrid nanoparticles exhibit high catalytic activity, which was demonstrated by the reduction reaction of nitrophenol in water.

Acknowledgements

This work was supported by the Russian Foundation for Basic Research (grant 12-03-00379)

References

[1] P. Herves, M. Perez-Lorenzo, L.M. Liz-Marzan, J. Dzubiella, Y. Lu, M. Ballauff *Chem. Soc. Rev.* 41 (2012) 5577-5587
[2] P. Taladriz-Blanco, J. Herves, J. Perez-Juste *Top. Catal.* 56 (2013)1154 – 1170
[3] G. V. Hartland *Chem. Rev.* 111 (2011) 3858 –3887
[4] S. Boudebbouze, A. W. Coleman, Y. Tauran, H. Mkaouar, F. Perret, A. Garnier, A. Brioude, B. Kim, E. Maguin, M. Rhimi *Chem. Commun.* 49 (2013) 7150 –7152

II-PP161

A Theoretical Study on the Effect of Active Centers of SiO_2 Surface on O_2 Interaction with Small Supported Silver Clusters

Ivanova-Shor E.A.*, Laletina S.S., Shor A.M., Nasluzov V.A.

Institute of Chemistry and Chemical Technology SB RAS, Krasnoyarsk, Russia

* shor-elena@rambler.ru

Keywords: density, functional, theory, silver, oxygen, adsorption, supported cluster, silica

1 Introduction

Silica plays important role in heterogeneous catalysis as a support for variety of metal clusters with a size from few to some thousands atoms. Many properties of silica as a support depend on the nature of its surface. The clean dehydroxylated surfaces of crystalline silica or silica film as well as hydroxylated surfaces of amorphous silica are rather inert toward binding of metal clusters. However, various imperfections and point defects being in abundance on real silica surface can act as sites for trapping metal clusters. The physical and chemical properties of supported metal clusters strongly depend on the existence and the nature of such defects. Among various defects of SiO2 surface, paramagnetic surface centers such as silicon dangling bond, ≡Si▪ (E□), and nonbridging oxygen, ≡Si–O▪ (NBO), [1] are considered as the most essential for effective trapping of metal clusters [2].

In the current work we report the results of theoretical study on how properties of NBO and E□ adsorption sites affect the interaction of O2 with small silver clusters (Agn, n=3,4) attached to these SiO2 defects. Ability of silver to activate oxygen is the key factor determining its catalytic activity in many oxidation reactions. It is well known that silver clusters of nanometer size supported on oxide surface are effective catalysts in such important industrial processes as epoxidation of ethylene and oxidation of methanol. At the same time, small supported Ag clusters containing few atoms (<10) attract growing attention as, in particular, perspective catalysts of propylene epoxidation and selective catalytic reduction of NO by hydrocarbons.

2 Experimental/methodology

The calculations were performed using all-electron scalar relativistic density functional method and accurate quantum mechanics/molecular mechanics (QM/MM) scheme of embedding QM clusters in an elastic polarizable environment described at the MM level [3]. The SiO2 surface was modeled as idealized structure of the walls that form the hexagonal channels of mesoporous silicalite MCM-41.

3 Results and discussion

Attaching neutral Ag3 and Ag4 clusters to E□ centers results in formation of the covalent Si–Ag bond. A transfer of electron density from support to metal clusters is observed, yielding a small negative effective charge, about -0.1e. In contrast, adsorption at NBO centers results in the partial oxidation of silver clusters and formation of the polar covalent O-Ag bond. The spin state of unsupported Ag3 and Ag4 clusters are exchanged upon adsorption at NBO and E□ centers [4]. In line with these changes, silver trimers and tetramers anchored at NBO centers feature ability to adsorb O2 similar to those of their gas-phase cationic counterparts [5]. At Ag3/NBO site O2 is stabilized in the terminal form only with small binding energy, BE < 12 kJ/mol. Similarly to gas-phase cation Ag4+, bridge (two-end) orientation of O2 is the most stable O2 adsorption form at Ag4/NBO site. It is accompanied by 2D→3D transformation of the silver tetramer and characterized by substantial binding energy (BE=97 kJ/mol). The interaction of O2 with Ag3/E□ center results in formation of two adsorption forms with terminal and bridge orientations of oxygen molecule. The

calculated interaction energies of these two forms fall in the narrow interval of 39-42 kJ/mol. Similarly to Ag4/NBO, the bridge orientation is the most stable O2 adsorption form at Ag4/E□ site; 2D→3D transformation of the metal moiety is also observed. O2 adsorption energy at Ag4/E□ site is notably smaller, BE=59 kJ/mol.

The positively charged bare Agn clusters attached to NBO defects interact with negatively charged regular oxygen centers of SiO2 surface due to electrostatic forces. Molecular adsorption of O2 results in transfer of electron charge density from metal moieties to oxygen and, as a consequence, further increases the oxidation state of the silver clusters supported at NBO centers and partially oxidizes them on E□ defects. The value of the charge transfer correlates with the O2 interaction energy: it is minimal for the O2 adsorption at the Ag3/NBO complex and maximal for the O2/Ag4/NBO system. In turn, the increased positive charge on silver cluster strengthens its electrostatic interaction with support and additionally stabilizes O2 adsorption forms. This effect is most pronounced for Ag4/NBO site, where the adsorption of molecular O2 is almost twice as strong as that on free cation Ag4+. For such small unsupported clusters as Ag3 and Ag4 dissociative O2 adsorption is not favorable process [6]. At variance, for the Ag4/NBO and Ag4/E□ centers a strong electrostatic interaction with silica surface makes dissociative mode the most preferable form of O2 adsorption with the binding energies 123 and 75 kJ/mol, respectively. At Ag3/E□, the stability of O2 dissociative and molecular adsorption forms is similar. O2 dissociation is unfavorable at Ag3/NBO site.

To elucidate the O2 dissociation mechanism on supported silver clusters various transition states (TS) with respect to breaking of O–O bond were located. The ability of silver clusters to dissociate O2 depends on their ability to activate adsorbed molecule. This activation, in general, occurs as electron charge transfer from metal cluster to O2. It works better for the metal cluster with unpaired electron and higher electron density. Indeed, the activation barriers of O2 dissociation are reduced on going from supported closed-shell Ag3 to open-shell Ag4 clusters and from positively charged Agn/NBO to neutral Agn/E□ systems. As a consequence, the lowest activation barrier, 142 kJ/mol, was calculated for O2 dissociation at Ag4/E□ site, whereas the dissociation at Ag3/NBO centers is characterized by the highest activation barrier, 316 kJ/mol. O2 dissociation barrier at Ag4/NBO and Ag3/E□ clusters has the intermediate value of the activation barriers, 175 kJ/mol. Besides the main reasons mentioned above, the heights of the barriers are also determined by the metal cluster reconstruction along reaction path. The calculated activation barriers are by 78-304 kJ/mol higher than O2 adsorption energies.

4 Conclusions

Therefore, it is supposed that any attempts to overcome these barriers will lead to O2 desorption rather than its dissociation. This manifests that small SiO2 supported silver clusters studied in this work are very stable with respect to oxidation.

Acknowledgements

This work was supported by the Presidium of the Russian Academy of Sciences (Project no. 45 of the Priority program no. 24). The calculations were carried out at the Siberian Supercomputer Center of the Siberian Branch of the Russian Academy of Sciences (Novosibirsk, Russia).

References

[1] V.A. Radzig, in: L.I. Trakhtenberg, S.H. Lin, O.J. Ilegbusi (Eds.), Physico-Chemical Phenomena in Thin Films and at Solid Surfaces, Thin Films and Nanostructures, vol. 34, Elsevier, London, 2007, p. 231.
[2] G. Pacchioni, N. Lopez, F. Illas, Faraday Discuss. 114 (1999) 209.
[3] A.M. Shor, E.A. Ivanova Shor, V.A. Nasluzov, G.N. Vayssilov, N. Rösch, J. Chem. Theory Comput. 3 (2007) 2290.
[4] A.M. Shor, E.A. Ivanova-Shor, S.S. Laletina, V.A. Nasluzov, N. Rösch, Surf. Sci. 604 (2010) 1705.
[5] A.M. Shor, S.S. Laletina, E.A. Ivanova Shor, V.A. Nasluzov, V.I. Bukhtiyarov, N. Rösch, Surf. Sci. 630 (2014) 265.
[6] S. Klacar, A. Hellman, I. Panas, H. Grönbeck, J. Phys. Chem. C 114 (2010) 12610.

II-PP162

Hydroprocessing of Heavy Crude Oil

Schacht P.*, Díaz-García L., Portales B., Ramirez S.

Instituto Mexicano del Petróleo Eje Central Lázaro Cárdenas Norte, México, México

* pschacha@imp.mx

Keywords: heavy crude oil, supported catalyst, upgrading viscosity

1 Introduction

The objective of the hydrotreating processes is to convert high molecular weight hydrocarbons in lighter fractions and upgrade the crude oil (1). In the presence of hydroprocessing catalyst loaded with metal transitions supported on alumina and hydrogen donor it is induced simultaneous hydrocracking, hydrodesulphurization and asphaltenes conversion to minimize the sulfur, nitrogen and metal content of the heavy oil at high hydrogen pressure (2). In the present work, a comparative study of four hydrotreating catalysts, namely, MoNi, NiW, CoMoP and, CoMoNiWP supported on alumina, were synthesized and evaluated in a batch reactor of 500 ml, at 673 K during 1 hour.

2 Experimental Section

All of the catalysts were prepared by successive impregnation on γ Al_2O_3 and dried at room temperature overnight, and finally calcined at 773 K for 2 h, the catalysts were characterized by Elemental Analysis, Textural properties and Temperature-programmed reduction (TPR).

A: Ni-W: [$Ni(NO_3)_2.6H_2O$ Aldrich 98%] and [$(NH_4)_{12}W_{12}O_{40}$].
B: Mo-Ni: [$(NH_4)_6Mo_7O_{24}$ Aldrich 99%], and [$Ni(NO_3)_2.6H_2O$ Aldrich 98%].
C: Co-Mo-P: [$(NH_4)6Mo_7O_{24}$, Aldrich 99%], [$Co(NO_3)_2$), Aldrich 98%], [H_3PO_4, Baker 86 %].
D: Co-Mo-Ni-W-P: [$Co(NO_3)_2$), Aldrich 98%], [$(NH_4)6Mo_7O_{24}$, Aldrich 99%],[$Ni(NO_3)_2.6H_2O$ Aldrich 98%], [H_3PO_4, Baker 86 %], and [$(NH_4)_{12}W_{12}O_{40}$].

The Activity Tests of heavy crude oil were carried out in a Parr batch reactor, physical and chemical properties of the feed and products were characterized according to the ASTM methods.

3 Conclusions

In this paper, it was shown a comparative study of four different hydrotreating supported alumina catalysts, formulation: NiMo, NiW, CoMoP and NiCoMoWP. We determine that the catalyst D showed the best catalytic behavior measured as API gravity increase and the lower asphaltenes content, 1.5 wt%. However, the CoMoP catalyst showed the higher aromatic content taking account the lower metal loading (13 wt%).

Table 1. Physical and chemical properties of the catalysts

Catalysts	**A**	**B**	**C**	**D**
	NiW	**NiMo**	**MoCoP**	**MoWNiCoP**
Surface area, m^2/g	179	183	190	171
Pore volume, cm^3/g	0.49	0.35	0.55	0.39
Mean pore diameter, Å	86	78	75	75
Metal content wt %				

Co	-	-	3.5	2.4
Mo	-	10.33	12.7	13.4
Ni	4.4	3.16	-	4.0
P	-	-	1.5	2.0
W	13.6	-	-	2.0

Table 2. Physical and chemical properties of the products

	Feed	**Products**			
Properties		A	B	C	D
API gravity	12.6	18.4	21.5	21.2	24.5
Sulfur, wt%	5.13	3.2	2.42	1.7	1.5
C_5 insolubles, wt%	26.7	17.73	15.8	7.1	6.1
Ramsbotton Carbon, wt%	16.15	12.56	11.46	7.3	6.8

References

[1] Nick A. Owenn, Oliver R. Inderwildi, David A. King, Nassar, 2010; Nassar Energy Policy 38 (2010) 4743–4749.

[2] J. Sayyad Amin, E. Nikooee, M.H. Ghateec, Sh. Ayatollahib, A. Alamdari, T. Sedghamiz. App. Surface Sc. 257 (2011) 8341– 8349.

II-PP163

In-situ EPR Spectroscopy of the NH_3-SCR Mechanism of Copper Chabazite

Godiksen A.[1*], Vennestrøm P.N.R.[2], Rasmussen S.B.[2], Lundegaard L.F.[2], Mossin S.[1]

1 - Technical University of Denmark, Department of Chemistry, Centre for Catalysis and Sustainable Chemistry, Lyngby, Denmark
2 - Haldor Topsøe A/S, Lyngby, Denmark

* anigo@kemi.dtu.dk

Keywords: EPR, Cu-CHA, NH_3-SCR, zeolites, SCR-mechanism, copper

1 Introduction

Selective Catalytic Reduction (SCR) is one of the most effective ways to reduce the environmentally harmful NO_x gasses emitted from combustion process. The NH_3-SCR process uses ammonia as the reducing agent, and copper exchanged zeolites have proven to be a good catalyst for this process [1]. Especially the small pore zeolite chabazite (CHA) have received increasing attention due to its high stability [2]. The knowledge of the mechanism of this process can improve the understanding of the role of the reactants and intermediates and lay the foundation of future catalyst systems.

Very recently a mechanism for the NH_3-SCR process catalyzed by Cu-CHA was proposed, with a key step involving the formation of a copper nitrate species [3]. This species and the whole mechanism are investigated using *in-situ* Electron Paramagnetic Resonance (EPR) spectroscopy.

2 Experimental

Samples investigated consisted of a series of Cu-CHA with constant Cu/Al ratio of 0.5 and varying Si/Al ratio in the range 15-30 and a series with constant Si/Al ratio of 15 and varying Cu/Al ratio in the range 0.1 to 0.6.

EPR spectra were collected on an X-band Bruker EMX EPR Spectrometer. Samples were fractioned to 150-300 μm before placed in a quartz tube and positioned using quartz wool. Time resolved EPR spectra were recorded during heating to maximum 300 ^{o}C under flow conditions (GHSV = 400,000 h^{-1}). The exit gas content of NO, NO_2 and NH_3 was measured using a Thermo Electron Corporation Ammonia Analyzer.

3 Results and discussion

The black trace in Figure 1 left shows the dehydrated Cu-CHA with the two distinct EPR active species corresponding to copper sites located in 6 membered ring sites as described by Godiksen et al. [4]. Starting from the dehydrated sample the flow is changed from He/O_2 to $NO/O_2/He$. A species with an EPR spectrum described with the parameters: $g_{||}$ = 2.28 and A = 462 MHz emerges which is assigned to a Cu(II)-nitrate species [5].

By removal of nitrogen monoxide from the feed gas the EPR signal assigned to Cu(II)-nitrate disappears (Figure 1 right), which could be related to the equilibrium between NO, O_2 and $(2\,NO + O_2 \rightleftharpoons 2\,NO_2)$ NO_2 . The resulting spectrum is similar to the spectrum recorded on dehydrated Cu-CHA, which indicates that no new EPR active sites are present.

A flow of ammonia together with nitrogen monoxide results in almost complete disappearance of the EPR signal (Figure 1 right).The disappearance of EPR signal can originate from reduction of Cu(II) to Cu(I), from ferromagnetism (coupling of Cu(II)) or the Pseudo Jahn-

Teller effect [4]. XANES spectra confirm that Cu(II) is reduced to Cu(I) [2], and thus the EPR signal loss is ascribed to reduction.

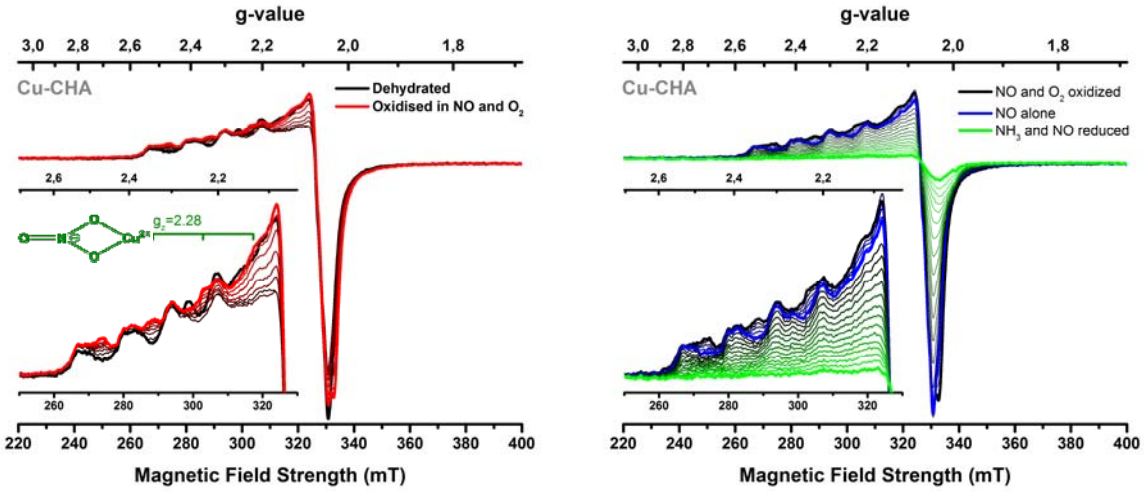

Fig. 1. Left: In-situ EPR spectra of Cu-CHA dehydrated in oxygen at 200 °C (black) and intermediate spectra when flow changed to NO and O_2 (red). In the last spectra of the series (red) a new copper species is seen with $g_{||} = 2.28$ which corresponds to a Cu(II)-nitrate, illustrated in green. Right: In-situ EPR spectra of Cu-CHA starting from the species oxidised in NO and O_2 (black), then removing oxygen from the flow results in the collapse of the EPR active Cu(II)-nitrate, and results in the blue spectra which is similar to the dehydrated spectrum. Finally the flow is changed to ammonia and nitrogen monoxide, whereby the EPR signal disappears almost completely (green).

4 Conclusions

EPR spectroscopy is a very specific and sensitive method for the analysis of the coordination environment and oxidation state of copper. In this work *in-situ* EPR is used to identify steps of the NH_3-SCR mechanism. A Cu(II)-nitrate species is observed in a flow of nitrogen monoxide and oxygen, which disappears upon removal of oxygen in the flow. The EPR signal disappears in a flow of ammonia and nitrogen monoxide, which indicates an almost complete reduction of the copper, and thus loss of the EPR activity.

Acknowledgements

Thanks to the Danish Independent Research Council (DFF − 1335-00175 and DFF− 09-070250) for financial support of the project. Carlsbergfonden is acknowledged for supporting the upgrade of the EPR instrument at Department of Chemistry, DTU.

References

[1] J. H. Kwak, R. G. Tonkyn, D. H. Kim, J. Szanyi, C. H. F. Peden, *J. Catal.* 275 (2010) 187-190.
[2] S.J. Schmieg, S. H. Oh, C. H. Kim, D. B. Brown, J. H. Lee, C. H. F. Peden, D. H. Kim, *Catal. Today* 184 (2012) 252–261.
[3] T. Janssens, H. Falsig, L. Lundegaard, P. N. R. Vennestrøm, S. B. Rasmussen, P. G. Moses, F. Giordanino, E. Borfecchia, K. A. Lomachenko, C. Lamberti, S. Bordiga, A. Godiksen, S. Mossin, P. Beato, '*A consistent reaction scheme for the selective catalytic reduction of nitrogen oxides with ammonia'* [submitted].
[4] A. Godiksen, F. N. Stappen, P. N. R. Vennestrøm, F. Giordanino, S. B. Rasmussen, L. F. Lundegaard, and S. Mossin, *J. Phys. Chem. C* 118 (2014) 23126-23138.
[5] A. V. Kucherov, J. L. Gerlock, H.-W. Jen, M. Shelef, *Zeolites* 15 (1995) 15-20.

II-PP164

In situ EMR / GC Study of the Conversion of Ethanol into Hydrocarbons on Fe-Zr/Al2O3 Catalysts

Aliyeva N.M.*, Mammadov E.E., Huseynova F.I., İsmailov E.H.

Institute of petrochemical processes, Azerbaijan National Academy of Sciences, Baku, Azerbaijan

* elcanm@bk.ru

Keywords: ethanol, hydrocarbons, Zr-Fe-Al, oxide, catalysts, *in situ* EMR/GC

1 Introduction

The conversion of ethanol to hydrocarbons over solid catalysts is one of the most studied reactions in heterogeneous catalysis [1-5]. At the Institute of Petrochemical Processes of Azerbaijan National Academy of Sciences the system based on Jeol JES-PE-3X ESR spectrometer, LXM 80 (Russia) chromatograph and flowing micro-catalytic reactor is constructed and used to obtain the simultaneous kinetic and spectral data directly about magnetic sites of catalysts and reaction products [6].

The aim of this work is monitoring of the state of active components by in-situ EMR in combination with simultaneous GC analysis of gas phase products of ethanol to hydrocarbons conversion over Fe-Zr/γ-Al_2O_3 catalyst with different content (1-5 wt%) of iron and zirconium, identification of the magnetic species and study of their role in the activity and selectivity control of this reaction.

2 Experimental/methodology

The catalysts were prepared by wet impregnation technique of γ-alumina support with the $ZrOCl_2$ $8H_2O$ and $FeCl_3$ $2H_2O$ solutions. The prepared samples of catalysts were dried at 393K and then calcined in the presence of flow of purified air at 673K for six hours. These catalysts are tested in the conversion of ethanol to hydrocarbons at 473-573K and atmospheric pressure. Element composition on the surface and phase composition of the samples are determined by X-ray fluorescence microscopy and X-ray diffraction methods using XGT 7000, Horiba, Japan, microscope and XRD TD3500, China diffractometer, respectively. The composition of elements on the surface and the phase composition of catalyst before and after conversion of ethanol are studied.

3 Results and discussion

The catalytic conversion of ethanol was studied at reaction temperature range from 473 to 573°K. The hydrocarbons was not detected at 473 K by GC. For monometallic Fe and Zr/ γ-Al2O3 catalysts, the main reaction products consisted of ethane, propane and hexane at all reaction temperatures, benzene and toluene start to appear at reaction temperature 523K, and xylene - as traces at 573K also detected. Maximum values of the yield of ethane (70.6%) and propane (2.8%) detected at reaction temperature 553K for Fe/γ-alumina and at reaction temperature 523K (38.5 and 2.0%, respectively) for Zr/ γ-alumina catalysts. The yield of hexane hydrocarbons at all reaction temperatures is higher for Zr catalyst than for Fe one. Benzene and toluene appear as traces at reaction temperature 523K and increase with increasing the reaction temperature up to 573K. At the same time the yield of hexane hydrocarbons decreases with the increase in reaction temperature. The same trend is observed for aromatic compounds, which are obtained in higher yield on Zr catalyst.

In the simultaneously recorded EMR spectra for these catalysts two different by nature signals are observed: belong to ferromagnetic/superparamagnetic FeOx for Fe/γ- Al2O3 (or

their modified by Zr forms) catalysts with effective g-factor g=2.14-3.65 and line width ΔH=110 -320 mT and paramagnetic carbon deposits with g=2.003 and ΔH= 0.5-0.7 mT. The formation of hydrocarbons is accompanied with the appearance of signals at g=2.14–2.15 and ΔH= 125–131 mT in the EMR spectra. The increase of the hydrocarbons (ethane as well as propene, propane, butenes and butanes) yields at the reaction temperatures of 553 and 573 K is accompanied by an increase of the EMR signals at g=2.14–2.15. The temperature dependence of EMR spectra of samples is investigated for catalysts with different contents active elements in the range 293-573K. It was established that the dependence of the intensity of the EMR signals on concentration of iron in samples at different temperatures of reaction is correlate with the yield of hydrocarbons. It was established that the catalytic activity of samples in ethanol to hydrocarbon conversion correlate with the concentration of magnetic particles. Active catalyst are characterized with the symmetrical ESR signal, due to super-paramagnetic particles of the size 15-20nm. The Scherrer formula was used to evaluate from diffractogram the grain size of identified phases of active elements for this catalyst (35-45 nm).

4 Conclusions

In situ EMR under flow conditions and on-line GC analysis of gas-phase products were successfully used to study the conversion of ethanol over Fe-Zr/γ-Al2O3 catalyst and constructed system can be enough effective for investigation of reaction ability, catalytic activity of magnetic particles for many other reactions.

The conversion of ethanol on Fe-Zr/γ-Al2O3 catalysts leads to formation of ethane, propane, butane, pentane, hexane – aliphatic hydrocarbons and benzene, toluene and xylene - aromatic hydrocarbons. The conversion of ethanol to aromatics increases as the Zr loading increases, which indicate that the active sites necessary for formation of aromatics is the Zr ion based structures, phases (ZrFeO3, ZrO2) in vicinity with γ-alumina acid sites that facilitate the formation of aromatic compounds. The detected ZrO2 and ZrFeO3 phases in the samples can catalyze secondary reaction of products formed initially by the acid sites of alumina. It is established that in the conversion of ethanol to hydrocarbons Zr active sites prefer the formation of aromatic compounds and FeOx species prefer the cracking reaction. At these sites, it is possible the activation and dimerization of the alkenes. The mechanism of reaction with participation of these structures and influence of Zr on the state of magnetic particles are discussed.

Acknowledgements

The authors would like to thank The Fund of Science of the State Oil Company of Azerbaijan Republic for financial support of these studies.

References

[1] R. Le Van Mao, T. M.Nguyen, and G. P. McLaughlin, Applied Catalysis, 48 (1989) 265-277
[2] S. N. Chaudhuri, C. Halik, and J. A. Lercher, Journal of Molecular Catalysis, 62 (1990) 289–295
N. R. C. Fernandes Machado, V. Calsavara, N. G. C. Astrath, A. M. Neto, and M. L. Baesso, Applied Catalysis A: General, 311 (2006) 193–198
[3] K. Murata, M. Inaba, and I. Takahara, Journal of the Japan Petroleum Institute, 51 (2008) 234–239
[4] M. Riad and S. Mikhail, J.Petroleum Technology and Alternative Fuels. 2(4) (2011) 55-62
[5] E.H.Ismailov, D.B.Tagiyev, M.I.Rustamov. Operando - II, Toledo, Spain. Book of Abstracts, (2006) 142-143

II-PP165

DFT Studies of Adsorbed N_2O and NH_3 on Pd(110)

Bryliakova A.A.*, Tapilin V.M.

Boreskov Institute of Catalysis, Russian Academy of Science, Novosibirsk, Russia

* bryliakova@catalysis.ru

Keywords: nitrous oxide, ammonia, density functional theory, Pd(110), adsorption, reduction

1 Introduction

Nitrous oxide and ammonia are undesired byproducts in the catalytic reduction of NO with H_2 occurring in automotive catalytic converters. Because of the need to remove these agents, it is necessary to understand how they are formed and to know the positions of adsorbate atoms. Automotive three-way catalyst is based on Pt, Rh or Pd catalysts. The reconstructed Pd(110)-1×2 surface formed from very short close-packed terraces and edges is often used as a model for real palladium catalyst, which has rough irregular surface. Recently, several experimental studies dealing with angular distribution of desorbing products in NO reactions over palladium have been reported [1, 2]. Theoretical consideration of N_2O and NH_3 adsorbing states and direction of their vibrations promotes interpretation of the experimental data and is the required step for subsequent calculations of reaction paths for the reduction of NO over Pd(110).

In this contribution, we have performed density functional theory (DFT) calculations in order to determine the adsorption structures and stretching vibrations of the N_2O and NH_3 molecules on the Pd(110)-1×2 surface.

2 Methodology

First-principles calculations for the structure relaxations and calculations of vibration frequencies were performed using the generalized gradient approximation (GGA) of Perdew-Burke-Ernzerhof (PBE). The interactions between the ionic cores and the electrons are described by ultrasoft pseudopotentials. The simulations have been done using the PWSCF package [3].

The Pd(110)-1×2 surface was modelled by a seven-layer thick slab, and the N_2O or NH_3 molecule was adsorbed on one side of the slab. Each layer of the slab contains four atoms, except the topmost one containing two atoms. This corresponds to coverage of 0.25ML (using the symmetry of the unreconstructed surface).

3 Results and discussion

Our calculations show that adsorbed species are bound to the surface by terminal nitrogen atom of N_2O and nitrogen atom of NH_3. Four different adsorption configurations are found stable for the N_2O molecule. In the most stable configurations, the molecule is monocoordinated to a Pd atom of the topmost layer along the $[1\bar{1}0]$ and $[001]$ directions, respectively. Two two-fold bridge forms of adsorbed N_2O lying along the same directions are slightly less stable then monocoordinated on-top forms. Adsorbed NH_3 molecule occupies on-top sites over the ridge and over the side surface (facet on-top form) of Pd atomic rows (Fig.1). Small lengthening of the N-N bond and change of intermolecular vibration modes of the N_2O molecule indicate weakening of the N-N bond as a result of N_2O adsorption. A decrease in the frequency of the NH_3 symmetric deformation mode from that for free (1132 cm^{-1}) and little flattening of the molecule allow assuming a little weakening of N-H bonds of adsorbed NH_3.

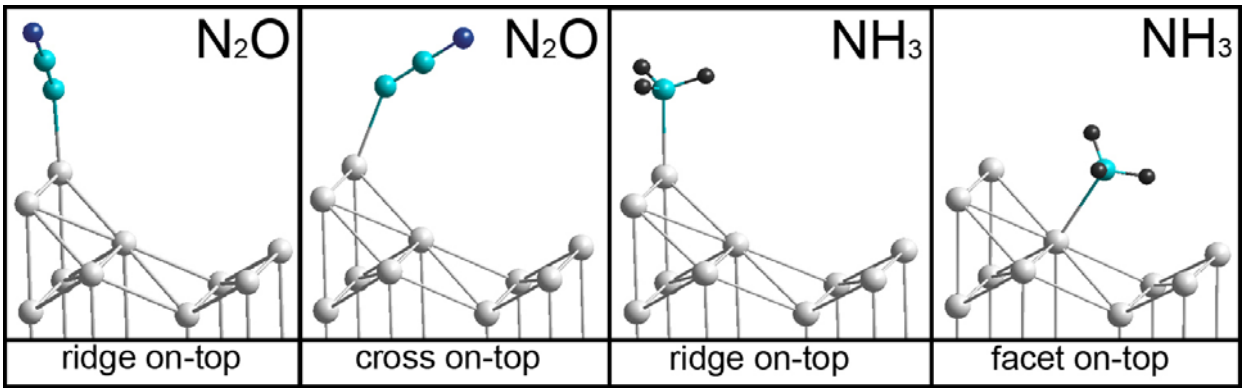

Fig. 1. Model of the most stable N_2O and NH_3 adsorption structures over Pd(110)-1×2 surface.

Table 1. Calculated energetic, structural and vibrational data of the isolated and adsorbed N_2O and NH_3.

	Site	E_b *(eV)*	$d_{Pd\text{-}N}$ *(Å)*	$d_{N\text{-}N}$ *(Å)*	$d_{N\text{-}O}$ *(Å)*	$\angle_{Pd\text{-}NN}$ *(deg)*	$\angle_{NNO}$ *(deg)*	ν_{int} *(cm^{-1})*	$\nu_{Pd\text{-}N_2O}$ *(cm^{-1})*
N_2O	ridge on-top	0.31	2.11	1.15	1.20	53	179	2287, 1258, 550, 521	309, 209 203
	cross on-top	0.31	2.11	1.15	1.20	34	179	2302, 1258 559, 502	308, 235
	ridge bridge	0.25	1.71	1.16	1.20	86	178	2222, 1223 520, 372	234, 230
	cross bridge	0.23	1.73	1.16	1.20	51	178	2302, 1258, 559, 502	308, 235
	gas phase			1.14	1.20		180	2172, 1310, 558, 558	
		E_b *(eV)*	$d_{Pd\text{-}N}$ *(Å)*	$d_{N\text{-}H}$ *(Å)*	$d_{H\text{-}H}$ *(Å)*		$\angle_{HNH}$ *(deg)*	ν_{int} *(cm^{-1})*	$\nu_{Pd\text{-}NH_3}$ *(cm^{-1})*
NH_3	ridge on-top	0.75	2.18	1.02	1.67		109, 109, 110	3560, 3553, 3405, 1598, 1588, 1051	517, 494, 344, 262
	facet on-top	0.70	2.18	1.02	1.68		109, 109, 110	3551, 3482, 3308, 1569, 1559, 1073	570, 546, 365, 261
	gas phase			1.02	1.65		107	3565, 3565 3434, 1727, 1727, 1132	

E_b is the binding energy calculated as the total energy difference between the separated and combined systems. The $d_{Pd\text{-}N}$ label stands for the adsorbate-surface distance. The $d_{N\text{-}N}$, $d_{N\text{-}O}$, $d_{N\text{-}H}$, $d_{H\text{-}H}$, $\angle_{Pd\text{-}NN}$, $\angle_{NNO}$, $\angle_{HNH}$ labels stand for the distances and the angles between corresponding atoms. The ν_{int} and $\nu_{Pd\text{-}N_2O}$, $\nu_{Pd\text{-}NH_3}$ labels stand for intermolecular and adsorbate-surface vibrations.

4 Conclusions

DFT simulation predicts that N_2O binds weakly to the ridge of the Pd(110)-1×2 surface in two on-top an two bridge stable forms, NH_3 adsorption occurs in two on-top forms: on the ridge and on the rows' side surface of the Pd(110)-1×2. The geometry of N_2O and NH_3 is almost unchanged upon adsorption.

References

[1] Yu. Ma and T. Matsushima, J. Chem. Phys. 124 (2006) 144711.
[2] Yu. Ma and T. Matsushima, J. Phys. Chem. B 109 (2005) 1256.
[3] P. Giannozzi, et al J. Phys.: Condens. Matter, 21 (2009) 395502.

II-PP166

Supporting Surfactant-Hybridized $H_3PW_{12}O_{40}$ on TiO_2 to Obtain Highly Dispersed Entities for Acid Catalysis: the Undesired Coking Effect of Burning the Surfactant

Schnee J.*, Bourdoux S., Raj G., Gaigneaux E.M.

Université catholique de Louvain, Institute of Condensed Matter and Nanosciences (IMCN/MOST), Louvain la Neuve, Belgium

* josefine.schnee@uclouvain.be

Keywords: supported, heteropolyacids, organic-inorganic, hybrid, acid catalysis, polyaromatic, coke

1 Introduction

Heteropolyacids (HPAs) are well defined molecular clusters possessing a very strong Brönsted acidity. Although widely used in acid catalysis, bulk HPAs have a low surface area (1 to 5 m^2/g) [1]. Supporting them on a suitable material allows a better dispersion and thus a better accessibility of their protons during catalytic reactions. Wet impregnation does not allow a precise control of the dispersion. It indeed often leads to crystalline HPA aggregates on the support's surface [1]. To address this problem, Raj *et al*. have investigated a novel strategy [2]: the hybridization of $H_3PW_{12}O_{40}$ (HPW12) with an organic surfactant (dimethyldioctadecyl ammonium bromide - DODA), and subsequent burning of the surfactant, allows obtaining highly isolated HPA entities on a HOPG surface. In our work, we have tried to apply this strategy to synthesize real HPW12/TiO_2 powder catalysts with high HPW12 dispersion. Herein, we demonstrate that the limiting factor therein is the formation of coke during the combustion of DODA, which induces a decrease of HPW12's catalytic activity.

2 Experimental/methodology

HPW12-DODA hybrids were prepared by mixing an ethanolic solution of HPW12 (0.5g HPW12/50mL) with an ethanolic solution of DODA (0.514g in 100 mL) for 2 hours at room temperature. HPW12-DODA/TiO_2 samples resulted from mixing a given volume (depending on the desired HPW12 loading on TiO_2) of the HPW12-DODA solution with a suspension of TiO_2 (2.5 g of P25 from Degussa - 50 m^2/g - in 100 mL ethanol) for 2 hours. The solid was recovered by rotary evaporation of ethanol (40°C, vacuum). Samples with different HPW12 loadings were prepared. The loading is expressed as a percentage of the amount of HPW12 that is required to form one complete monolayer on TiO_2 (%TM). DODA was eliminated by an exposure to UV-O_3 or by calcination under O_2 at 290, 350 or 450°C. Reference HPW12/TiO_2 catalysts were prepared with the same procedures but without DODA (classical wet impregnation). All samples were characterized by X-ray diffraction (XRD), NH_3 temperature programmed desorption (NH_3-TPD), FT-IR and Raman spectroscopies. Their catalytic activity was tested in the dehydration of methanol.

3 Results and discussion

XRD and NH_3-TPD show that non-hybridized HPW12 starts to form crystalline aggregates on TiO_2 at a loading of 63%TM. The latter is thus the minimum loading at which it makes sense to investigate the DODA-hybridization as a way to enhance the dispersion of HPW12. The HPW12-DODA/TiO_2 containing this HPW12 loading of 63%TM has first been subjected to various treatments in order to determine the most efficient way to eliminate the surfactant, and

so to finally isolate the HPW12 entities. According to FT-IR spectroscopy, DODA is destroyed by exposing the sample to UV-O_3 or by calcinating it for 2 hours under pure O_2 at 290 or 350°C. However, the Raman spectra after those treatments show the bands of polyaromatic coke at 1350-1600 cm^{-1} (see Fig. 1. A. for a typical spectrum). The latter hides the main peak of HPW12 at 1000 cm^{-1} and the signal of TiO_2 between 300 and 800 cm^{-1} visible on the spectrum of HPW12(63%TM)/TiO_2 prepared without DODA. Thus, although DODA has been destroyed as such, recalcitrant carbonaceous deposits are formed. This is likely due to the strong acidity of HPW12. The calcination under pure O_2 at 450°C is the only treatment leading to the complete elimination of this coke. As a counterpart, it induces the thermal decomposition of HPW12. Indeed, the FT-IR spectrum after such treatment does no longer show the fingerprint of HPW12. In the case of the three previously mentioned treatments (UV-O_3 and calcination under pure O_2 at 290 or 350°C), FT-IR spectra still show intact HPW12. The XRD patterns after those three non HPA destructive treatments do not show the diffraction peaks of HPW12 crystals, indicating that the dispersion of HPW12 has been enhanced via the DODA-hybridization. However, likely as a consequence of the formation of coke from the combustion of DODA, the catalytic methanol dehydration activity of the HPW12(63%TM)-DODA/TiO_2 sample after the various DODA-elimination procedures is always lower than the activity of the HPW12(63%TM)/TiO_2 reference sample prepared by classical wet impregnation without DODA (see Fig. 1. B.).

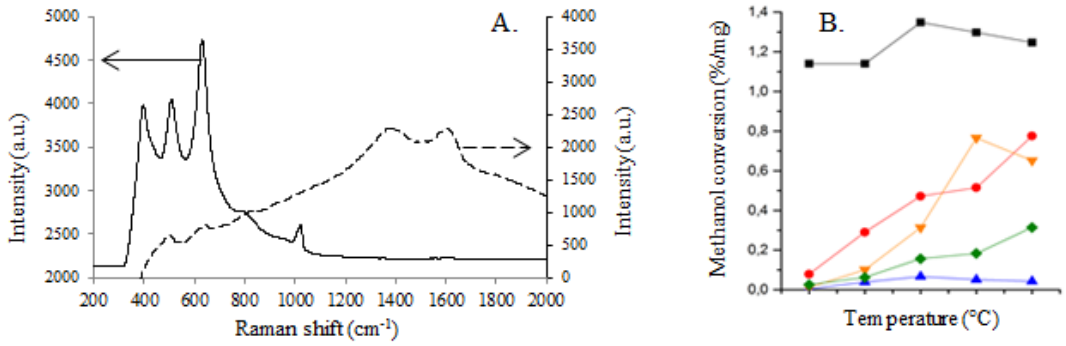

Fig. 1. (A) Raman spectra of HPW12(63%TM)/TiO_2 (–) and of HPW12(63%TM)-DODA/TiO_2 after DODA elimination trial under O_2 at 350°C (– –) / (B) Methanol conversion (%/mg catalyst) obtained with HPW12(63%TM)/TiO_2 reference catalyst (–▪–) and with HPW12(63%TM)-DODA/TiO_2 after DODA elimination trial under O_2 at 290°C (–•–), at 350°C (–▲–) and at 450°C (–▼–), and after the same treatment under O_2 at 290°C than previously followed by an exposure to UV/O_3 in addition (–◆–).

4 Conclusions

In agreement with the previous work of Raj *et al*. [2], hybridizing HPW12 with DODA prior to supporting it on TiO_2 leads to a better HPW12 dispersion. However, the aim of enhancing the dispersion, namely allowing a better accessibility of HPW12's acid sites to reactants, could not be achieved by such a DODA-based strategy. Indeed, on one hand, at HPW12-friendly temperatures, the complete elimination of DODA induces the formation of polyaromatic coke on HPW12. On the other hand, at temperatures which allow burning that coke, HPW12 is thermally decomposed and so loses acidity. Further improvements of the approach are currently under investigation.

References

[1] R. Fazaeli, S. Tangestaninejad, H. Aliyan, *Applied Catalysis A: General*. 318 (2007) 218-226.
[2] G. Raj, C. Swalus, A. Guillet, M. Devillers, B. Nysten and E.M. Gaigneaux, *Langmuir*. 29 (2013) 4388-4395.

II-PP167

Effect of Dopant Nature on Low-Temperature WGS Activity of Cu-Mn Spinel Oxide Catalysts Prepared by Combustion Method

Tabakova T.[1*], Papavasiliou J.[2], Ivanov I.[1], Idakiev V.[1], Avgouropoulos G.[2,3]

1 - Institute of Catalysis, Bulgarian Academy of Sciences, Sofia, Bulgaria
2 - Foundation for Research and Technology-Hellas (FORTH), Institute of Chemical Engineering Sciences (ICE-HT), Patras, Greece
3 - Department of Materials Science, University of Patras, Rio Patras, Greece

* tabakova@ic.bas.bg

Keywords: Cu-Mn spinel oxide, urea, combustion method, WGSR, doping effect

1 Introduction

The Water-Gas Shift Reaction (WGSR) is a well-established industrial process for hydrogen generation by conversion of CO in hydrogen-rich gas streams. The need of high-purity hydrogen for fuel cell applications stimulates a great activity in the design of novel, highly active and stable WGS catalysts. Copper is often used as an active component in low-temperature (LT) WGS catalysts. The problem with the tendency of Cu to deactivate could be tackled by development of new catalytic formulations. Recently, we have reported that the urea-nitrates combustion method is an attractive technique for preparation of Cu-Mn catalysts with favorable characteristics and catalytic properties for WGSR [1]. Catalytic measurements carried out under both idealized and realistic reformate feeds and comparison with the performance of commercial $CuO-ZnO-Al_2O_3$ catalyst demonstrated the superior performance of these catalysts. It was proposed that the catalysts' stability was related to the higher resistance of copper nanoparticles to sintering, which maintain their small size after WGS reaction. The aim of present work was to examine the effect of the nature of some doping oxides, namely, CeO_2, Fe_2O_3 and Al_2O_3 on the physicochemical properties and activity of Cu-Mn spinel oxides in the WGSR at low temperature.

2 Experimental/methodology

Doped Cu-Mn-M (M = Ce, Fe or Al) catalysts with Cu/(Cu+Mn+M) atomic ratio of 0.30 were prepared by single-step urea-combustion method. The selection of this atomic ratio was based on the results reported in a previous study [2]. The combustion synthesis involved autoignition of a mixed solution of urea with nitrates of copper, manganese and dopant (75% excess of urea) in an open muffle furnace (preheated at 400–500 ^oC) and further heating at 550 ^oC for 1 h. The catalysts were characterized by N_2 physisorption, XRD, H_2-TPR and XPS. The WGS activity was evaluated in a conventional flow reactor at space velocity of 4000 h^{-1} within a temperature range of 140–240 °C. The influence of reaction gas mixture, including idealized and realistic reformate, H_2O/CO ratio and contact time on the activity were also investigated.

3 Results and discussion

The temperature dependence of CO conversion over doped Cu-Mn oxide catalysts during LT WGSR with an idealized reformate feed is illustrated in Fig. 1. The catalytic activity of Cu-Mn oxide sample was improved in the presence of dopants. The following activity order was observed: $Cu_{0.30}Ce_{0.07}Mn_{0.63} \approx Cu_{0.30}Fe_{0.07}Mn_{0.63} > Cu_{0.30}Al_{0.07}Mn_{0.63} > Cu_{0.30}Mn_{0.70}$. The catalytic tests under a realistic reformate feed demonstrated better performance of the Fe-doped

Cu-Mn catalyst at 240 °C, whereas at lower temperature (220 °C) $Cu_{0.30}Al_{0.07}Mn_{0.63}$ exhibited slightly higher activity. The effect of space velocity on CO conversion was studied at 180 °C. The increase of water partial pressure (from 5 to 10 kPa) caused an increase of CO conversion over all catalysts and this effect was more pronounced over doped by Ce and Fe samples. It was observed that all doped catalysts exhibited good tolerance towards a high concentration of water. It is known that high H_2O/CO ratios are typical under fuel processor conditions for low-temperature shift reactors and the resistance to the presence of a high amount of steam could be considered as an important feature.

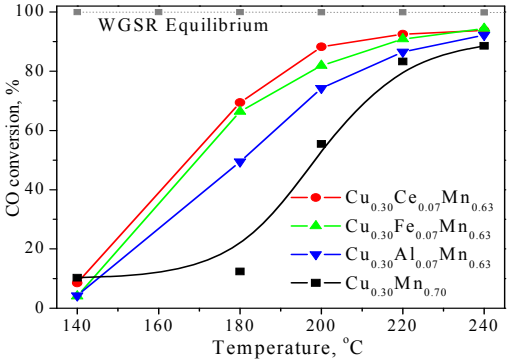

Fig. 1. Temperature dependence of CO conversion over doped Cu-Mn oxide catalysts

The measurements of BET surface area showed more significant increase of specific surface area of Fe and Al-doped samples and slight increase in the case of Ce-doped sample in comparison with undoped Cu-Mn catalyst. XRD patterns of fresh catalysts correspond to the spinel phase $Cu_{1.5}Mn_{1.5}O_4$ and Mn_3O_4/ Mn_2O_3. No detectable diffractions of third metal (except reflections of CeO_2) can be distinguished in doped catalysts most probably due to fine dispersion or/and incorporation of some amount in the spinel oxide structure. The analysis of XP spectra indicated that Mn(III), Mn(IV), Cu(II) and Cu(I) species were simultaneously present in the fresh, oxidized samples. Doping metals were presented in the Cu-Mn samples in a fully oxidized state, i.e. Ce^{4+}, Al^{3+} and Fe^{3+}. An enrichment of the surface with dopant species was also observed. The reduction profile of Cu–Mn catalyst was characterized by a broad peak centered at about 400 °C with shoulder at higher temperature side. The addition of dopants shifted the T_{max} of the peaks to lower temperature and altered their shape. Well visible shoulder was registered at lower temperature side. It was ascribed to reduction of highly dispersed copper oxide particles.

XRD and XPS measurements of the samples after catalytic tests are in progress in order to gain new insight on the effect of different dopants on WGS activity.

4 Conclusions

It was found that doping of Cu-Mn spinel oxide catalysts prepared by combustion method could be an efficient approach for design of novel, highly active and stable WGS catalysts.

Acknowledgements

T. T., I. I. and V. I. gratefully acknowledge the financial support by the Bulgarian National Science Fund (Projects E-01/07-2012 and DFNI E-02/2-2014).

References

[1] T. Tabakova, V. Idakiev, G. Avgouropoulos, J. Papavasiliou, M. Manzoli, F. Boccuzzi, T. Ioannides, *Appl. Catal. A*, 451 (2013) 184.
[2] J. Papavasiliou, G. Avgouropoulos, T. Ioannides, *J. Catal.* 251 (2007) 7.

II-PP168

Catalytic Dehydration of Methyl Lactate to Acrylic Acid

Chernyshev D.O., Suslov A.V., Varlamova E.V., Staroverov D.V.*, Suchkov Yu.P., Shvets V.F.

D. Mendeleyev University of Chemical Technology of Russia, Moscow, Russia

* stardv@muctr.ru

Keywords: methyl lactate dehydration, acrylic acid, calcium-phosphate-silica, catalysts, structure

1 Introduction

Development of the production of multifunctional organic acids in low-cost, high-efficiency fermentation processes makes available a new route to chemical production from biomass. Lactic acid is approaching large-scale production via fermentation and show particularly excellent promise as feedstocks for catalytic conversion routes such as hydrogenation, dehydration, or condensation (Figure 1).

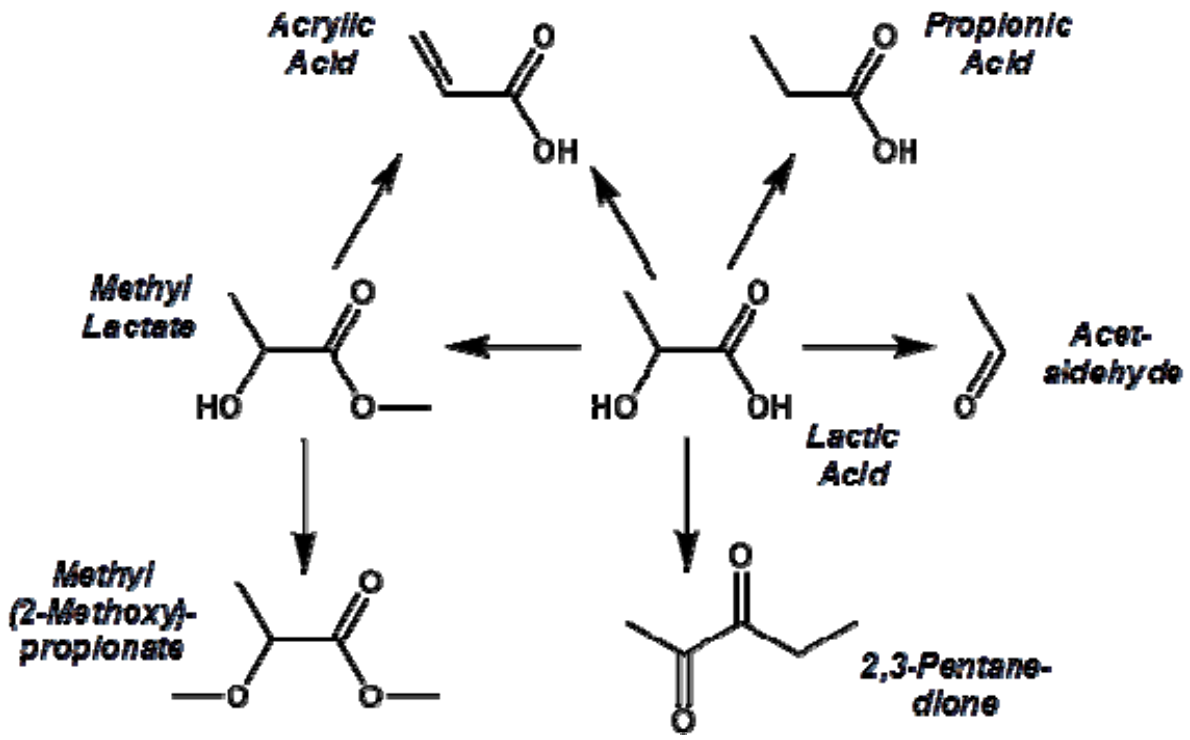

Fig. 1. Possible scheme for chemicals based on lactate feedctocks.

In particular, it looks attractive at least partial redirecting of producing conventional petrochemicals such as acrylate monomers to renewable feedstocks. A bottle neck for implementing this technology is the development of effective catalysts of lactate materials dehydration. This study investigated methyl lactate dehydration over various calcium-phosphate-silica catalysts under various conditions [1].

2 Experimental

Sampling procedures

Catalysts $Ca_3(PO_4)_2/SiO_2$, $CaHPO_4/SiO_2$, $Ca(H_2PO_4)_2/SiO_2$ и $Ca_2P_2O_7/SiO_2$ with different

ratio of corresponding calcium phosphate component vs silica (from 90/10 to 60/40 wt.%) was prepared by precipitation method followed by water rinsing to remove soluble impuritgies. Samples obtained was dried at 120°C and then calcined at 480°C in air.

Characterization and evaluation methods

Catalysts obtained were characterized by XRD and FTIR methods and the specific surface areas and pore volumes of catalysts were measured.

The dehydration of methyl lactate over the catalysts was carried out in a fixed-bed quartz reactor operated at 350-420°C and atmospheric pressure. The feedstock (20–50 wt.% aqueous solutions of methyl lactate) was pumped into the preheating zone of reactor and driven through the catalyst bed by nitrogen. Regulating the nitrogen flow rate it was maintained hold-up time 0.5-1 s.

Analysis of the products was carried out by GC and GC-MS methods.

3 Results

The data of experiments on dehydration of methyl lactate showed that, regardless of the structure of calcium phosphate component, the highest efficiency is typical for samples with ratio 'Ca-PO_x/SiO_2' = 80/20 wt.%. The methyl lactate conversion over the catalyst $Ca_2P_2O_7/SiO_2$ (80/20%масс.) at 390°C, methyl lactate content in feedstock 20 wt.% and hold-up time 1 c was 74,7% and acrylates selectivity was 48,8%.

Side reactions of condensation and polymerization lead to coke deposition, resulting in catalyst deactivation. Complete catalyst regeneration and activity recovery is achieved by calcination it in air at 480°C.

From XRD and FTIR data was found that freshly prepared catalysts based on calcium hydrophosphates decomposed during calcination to form ultimately pyrophosphate structure. During the regeneration of these catalysts as well as $Ca_2P_2O_7/SiO_2$ pyrophosphate structure is preserved.

4 Conclusions

We investigated methyl lactate dehydration to acrylates over calcium-phosphate-silica catalysts. Catalysts with ratio 'Ca-PO_x/SiO_2' = 80/20 wt.% exhibited highest efficiency.

Catalysts on base of hydrophosphate precursors passed into pyrophosphate form under preparing and perfomance conditions.

Deactivated catalysts was completely restored its activity by calcining in circulating air at 480°C.

Acknowledgements

This work was supported by the Ministry of Education and Science of Russia (the project ID RFMEFI57714X0037).

References

[1] Jong-Min Lee, Dong-Won Hwang, Young Kyu Hwang, Shiva B. Halligudi, Jong-San Chang, Yo-Han Han. Efficient dehydration of methyl lactate to acrylic acid using $Ca_3(PO4)_2$–SiO_2 catalyst, *Catal. Commun*. 11 (2010) 1176.

II-PP169

Synthesis of Zr-BEC Zeolite Catalyst with Strong Lewis Acidity

Kots P.A.[1], Sushkevich V.L.[1], Tyablikov O.A.[1], Ivanova I.I.[1,2*]

1 - Department of Chemistry, Lomonosov Moscow State University, Moscow, Russia
2 - A.V. Topchiev Institute of Petrochemical Synthesis, Russian Academy of Science, Moscow, Russia

* iiivanova@phys.chem.msu.ru

Keywords: polymorph, degermanation, BEC, germanosilicate, Zr-Beta, Lewis acidity, FTIR, CO

1 Introduction

In past decade, use of germanium as a silicon substituent in zeolite synthesis led to a discovery of new large-pore molecular sieves structures. One of them is the polymorph C of zeolite Beta (BEC), which was synthesized for the first time by Corma et al [1]. But unfortunately, the use of such materials is strongly limited due to their low catalytic activity and poor thermal stability, because of strong tendency of Ge-O-Si bonds to hydrolyze. This drawbacks can be overcome by the replacement of Ge atoms in the framework with other atoms [2]. This contribution is aimed to elaborate post-synthetic method to incorporate Zr in framework of BEC. Zirconium-containing Beta zeolite is a perspective material possessing unique water-tolerant Lewis acidity associated with Zr atoms in framework position.

2 Experimental

BEC-type germanosilicate synthesis was performed according to previously reported procedure [3]. Stabilization of as-made BEC materials with TEOS was based on the procedure proposed by Wu et al. [4]. Stabilized materials were treated with $ZrOCl_2$ in aqueous or DMSO solutions of HCl.

3 Results and discussion

Fig. 1a shows XRD pattern of as-made BEC germanosilicate. Material obtained is highly crystalline and no impurities were detected by XRD. Based on results of Tuel et al. [5] as-made BEC could be easily degermanated under acidic pH at 70°C. But, direct treatment in the presence of $ZrOCl_2$ leads to complete amorphization (Fig. c). Treatment with $ZrOCl_2$ in DMSO also leads to significant decrease in crystallinity, but not as prominent as in the case of water. According to XRF analysis, presented in Table 1, water-treated sample losses approx. 65% GeO_2. Thus, amorphization may be coupled with germanium extraction from the framework.

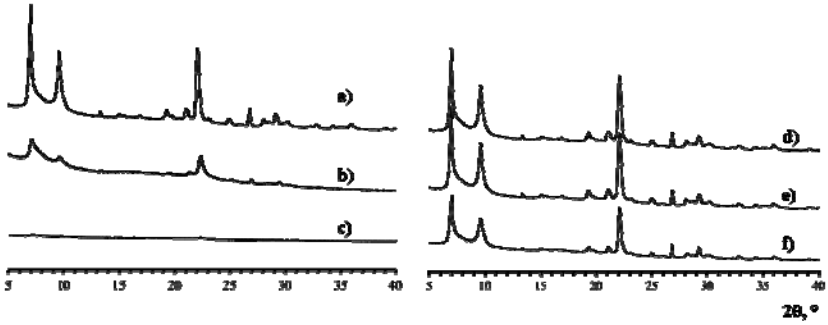

Fig. 1. XRD patterns of as-made BEC-type germanosilicate (a), after treatment with $ZrOCl_2$/HCl at 70°C for 12h in DMSO (b) and in water (c), after stabilization at 170°C with TEOS (d), subsequently treatment in $ZrOCl_2$/DMSO/HCl at 70°C for 12 h (e), after subsequent calcination in air at 550°C for 6 h (f).

Because the direct treatment was the recently established by Wu et al. stabilization procedure was chosen. XRD pattern of stabilized BEC-Si (Fig. 1d) indicate the preservation of

original crystallinity (Table 1). Stabilized samples were treated with $ZrOCl_2$ in DMSO under acidic pH and material obtained showed high crystallinity (Fig. 1e and Table 1).

Table 1. XRF data and crystallinity analysis.

Sample	Si/Ge	(Si+Ge)/Zr	cryst., %
as-made BEC	2.4	-	100
$ZrOCl_2$/water/HCl	11.5	22	20
$ZrOCl_2$/DMSO/HCl	4.9	97	50
TEOS	3.5	-	80
TEOS+$ZrOCl_2$/DMSO/HCl	4.5	55	75

As shown in Table 1 the elaborated synthetic procedure leads to highly crystalline material with high amounts of Zr ($^{Si+Ge}/_{Zr}$ =55). Changes in local structure of Si were examined via ^{29}Si solid-state NMR spectroscopy confirms the formation of Si(3Si,1Zr) domains. Lewis acidic properties of calcined Zr-BEC were examined with FTIR of adsorbed CO and acetonitrile-d_3. FTIR spectra of adsorbed CO indicates high content of strong Lewis acid sites associated with Zr^{4+} cations (band at ca. 2196 cm^{-1}) in the sample obtained. The comparison of the results obtained over novel Zr-BEC catalyst with traditional Zr-BEA samples points, that the procedure elaborated allows for much higher degrees of Zr incorporation.

4 Conclusions

The post-synthetic procedure for incorporation of Zr-heteroatom in germanosilicate with BEC structure was developed for the fist time. The procedure involves: 1) stabilization of the parent structure via solvotermal treatment with TEOS; 2) incorporation of Zr in 0.01M HCl solution in DMSO. The data obtained clearly show, that Zr-BEC in highly crystalline, thermally stable material with strong Lewis acidity. Comparing with conventional Zr-BEA sample, our Zr-BEC posses higher density of Lewis acid sites.

Acknowledgements

The authors thank the Program №14-23-00094 of Russian Science Foundation for the financial support.

References

[1] G. Sastre, J. Vidal-Moya, T. Blasco, J. Rius, J.L. Jorda, M.T. Navarro, F. Rey, A. Corma, *Angew. Chem. Int. Ed.* 41 (2002) 4722.
[2] M. El-Roz, L. Lakiss, A. Vicente, K. N. Bozhilov, F. Thibault-Starzyk, V. Valtchev, *Chem. Sci.*, 5 (2014) 68–80.
[3] L. Tosheva, N. Mahé, V. Valtchev. *Studies in Surface Science and Catalysis*, 170 (2007), 616.
[4] H. Xu, J. Jiang, B. Yang, L. Zhang, M. He, P. Wu, *Angew. Chem*, 126 (2014) 1379.
[5] X. Liua, N. Kasiana, A. Tuel, *Microporous and Mesoporous Materials* 190 (2014) 171.

II-PP170

Bimetallic Copper Catalysts Supported on Activated Carbon Fibers for Ethanol Dehydrogenation

Ponomareva E.A.*, Tolulope O., Parastaev A.S., Egorova E.V.

Lomonosow Moscow University of Fine Chemical Technology, Moscow, Russia

* katerinaii@inbox.ru

Keywords: ethanol dehydrogenation, activated carbon, fibers, copper catalyst

1 Introduction

Copper is a well-known catalyst for the ethanol dehydrogenation reaction. However, its utility is often limited by rapid loss of activity. One of the probable reasons for deactivation of copper catalyst is sintering due to the inherently low melting point of bulk copper. Thus, instead of bulk copper, the supported copper catalyst has become prevalent in practice. Earlier it was shown that activated carbon fiber (ACF) is suitable for the role of a carrier and 5%Cu/ACF was proved to be more active compared with other copper catalysts supported on carbon materials [1]. ACF, consisting of arranged microfilaments, represents a valuable alternative to randomly packed beds of granulated carbons. It has important advantages due to a high specific surface area, low pressure drop and suppressed mass transfer limitations.

Introduction of an additional compound into copper based on carbon catalysts could bring to its higher stability. Different oxides were used for this purpose and Cr2O3 is one of the most prevalent. Moreover, some extra effects can appear. For example, Cu-ZrO2 system was proved to be selective for ethylacetate formation [2], while copper supported catalyst mainly generates acetaldehyde. In this work, activities of Cr-Cu/ACF and Zr-Cu/ACF catalysts for ethanol dehydrogenation were studied.

2 Experimental

Commercial activated carbon cloth ACF (AW1101, KoTHmex Taiwan Carbon Technology CO) was used as a support. SSABET of the carrier (measured by N2 adsorption–desorption at −196 ˚C via ASAP 2020, Micromeretics) was ~ 1050 m2/g. The catalysts were prepared by wetness impregnation with water solution of appropriate salt with following drying at 100 ˚C for 1 h. Cu(NO3)2·3H2O, Cr(NO3)3·9H2O, ZrCl4 were used as metal precursors. The loading of every metal was 5 wt%. When bimetallic catalyst prepared two technics were tested – co-impregnation and consequent impregnation. The second technic included calcination of a sample at 300 ˚C for two hours before the impregnation with copper salt water solution.

The ethanol conversion experiments were carried out at atmosphere pressure using a conventional quartz reactor. 0,5 ml of a sample was used in every test. Liquid flow rate of ethanol (93 wt%,) was 32 h-1. Received products were analyzed by gas chromatography. Prior to the reaction, every sample was calcined in situ in a stream of argon and then reduced in a stream of hydrogen.

The catalysts were characterized with help of scanning electron microscope TescanMira LMU equipped with a secondary electron detector and X-Max EDS detector. XRD analysis was carried out as well.

3 Results and discussion

Zirconium and chromium presented in the form of their oxides (ZrO2 and Cr2O3 respectively) created some areas of films on the surface of ACF, which were also observed in bimetallic systems. Without copper both components were proved to be almost inactive in the

process studied. Conversion of ethanol didn't exceed 2 %.

Activities of bimetallic catalyst compared with copper supported catalyst are represented on figure 1. It is shown that addition of Zr leads to remarkable decrease in conversion. However the maximum of conversion was observed at 375 ˚C while over the other catalysts it was reached at 350 ˚C. Such small activity of Cu-Zr/ACF catalyst can be explained by bad distribution of copper particles (fig. 2a) as well as binding of the active component (Cu) with zirconium oxide.

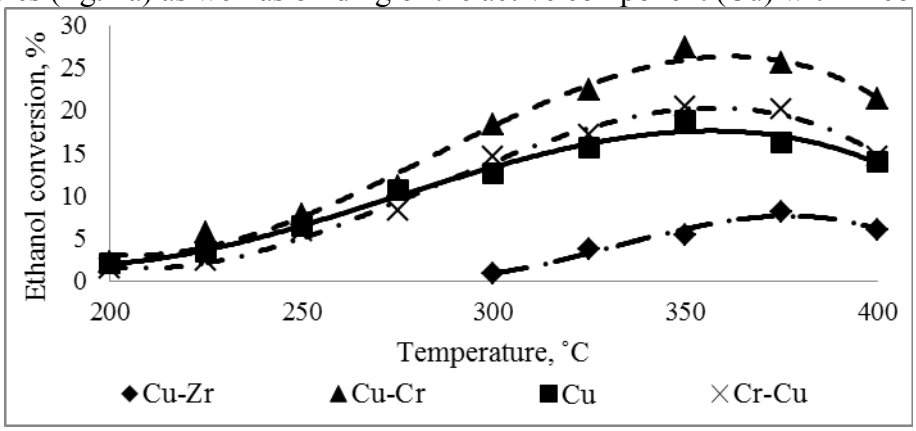

Fig. 1. Ethanol conversion over copper containing catalysts

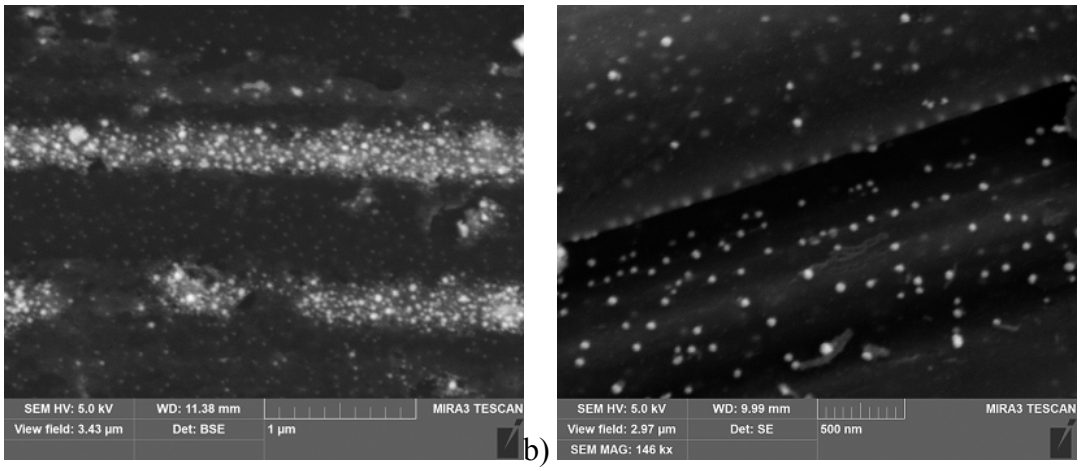

a) b)

Fig. 2. SEM images of Cu-Zr /ACF (a) Cr-Cu/ACF (b) catalysts

Cr-Cu/ACF catalyst, prepared by consequent impregnation technic (fig. 2b) shows better distribution of Cu particles, that is similar to Cu/ACF catalyst [1]. Hence Cu-Cr/ACF, prepared by co-precipitation, was more active (fig.1). Test for stability for both copper-chromium system showed an improvement compared to copper supported catalyst.

4 Conclusions

It was shown that addition of Zr to copper supported on activated carbon fibres decreases the activity of catalytic system, while addition of Cr has positive impact. Moreover, the way of preparation of a sample has an influence.

References

[1] E. Ponomareva, E. Egorova, D. Bokarev, A. Parastaev. *Vestnik MITHT.* 6 (2013) 23
[2] A. Sato, D. Volanti, I. C. de Freitas, E. Longo, J. C. Bueno. *Catalysis Communications.* 26 (2012) 122

II-PP171

Oxidative Activation of Methane over MnNaW/SiO_2 Catalysts: Models for Active Sites

Ismagilov I.[1*], Shubin A.[1], Zilberberg I.[1], Matus E.[1], Kerzhentsev M.[1], Ismagilov Z.[1,2]

1 - Boreskov Institute of Catalysis SB RAS, Novosibirsk, Russia
2 - Institute of Coal Chemistry and Material Science SB RAS, Kemerovo, Russia

* iismagil@catalysis.ru

Keywords: methane activation, MnNaW/SiO_2, quantum-chemical, modeling

1 Introduction

The oxidative coupling of methane (OCM) is a promising process for direct production of ethane and ethylene. The MnNaW/SiO_2 is one of suitable OCM catalysts that show both high product yield and long-term stability. The complex reaction mechanism of OCM and multicomponent composition of MnNaW/SiO_2 catalyst complicate the elucidation of the role of different components of this catalyst. The surface cluster species WO_4 with one W=O and three W-O-Si bonds was one of the first model of the active site suggested for this reaction [1, 2]. The Mn_2O_3 species were proposed to act as the active sites responsible for the methane activation, while Na^+ and oxo anion (WO_4^{2-}, MoO_4^{2-}, SO_4^{2-}, PO_4^{3-}or $P_2O_7^{4-}$) affect the formation of the specified Mn species [3]. A modified mechanism based on two metal (W-Mn) site has been presented: activation of CH_4 is suggested to take place on W^{6+} sites while the activation of O_2 - on the Mn^{3+} sites [4]. Both Na-O-Mn and Na-O-W species were identified as active sites of the catalysts for OCM [5]. Thus, the structure of the active center for the OCM reaction is still a matter of discussion. In the present study quantum-chemical modeling of the active center of MnNaW/SiO_2catalyst were performed. To clarify the OCM mechanism the following tasks were considered: (i) optimization of structure for possible W and Mn oxide species on the surface of α-cristobalite; (ii) determination of barrier energy for the abstraction of hydrogen from methane at isolated and supported W(+6) and W(+4) species; (iii) optimization of structure for possible polynuclear W and Mn species on the surface of α-cristobalite.

2 Experimental

All calculations have been performed at the B3LYP level using the LANL2TZ(F) and 6-311G** basis sets for tungsten and lighter atoms, respectively.

3 Results and discussion

The models for active sites for the MnNaW/SiO_2 catalyst have been considered assuming (1) α-cristobalite form of the SiO_2 oxide and (2) five-coordinated W(+6) complex having single terminal W=O group bonded to the α-cristobalite (111) surface through bridged oxygen centers (≡WO(OH)). It was shown that various tungsten species (=$WO(OH)_2$,-$WO(OH)_3$,$WO(OH)_4$) on the SiO_2 surface relatively easily transform to each other due to hydrolysis of the W-O-Si bonds by water molecules. According to the energy diagram for described hydrolysis process the most stable structures are the water-coordinated tungsten species attached to the surface via one or two oxygen centers of support while adsorbed at the cristobalite surface $WO(OH)_4$ complex appears to be quite labile to migration and can achieve easily the other tungsten oxide species or manganese oxide to form a dimer.

The first step of the oxidative coupling of methane is the hydrogen abstraction.

Corresponding C-H bond cleavage includes two quite different routes - heterolytic and homolytic – which determine all further reaction steps. The abstraction of hydrogen from methane at isolated $WO(OH)_4$ to form $W(OH)_5$ is predicted to require quite high energy of about 70 kcal/mol. Surprisingly, the heterolytic dissociation at this model goes through a barrier of about 49 kcal/mol. Taking into account that the hydrogen abstraction by $WO(OH)_4$ complex requires about 50-70 kcal/mol it is concluded that oxo-center should be somehow activated to facilitate the reaction.

It is found that oxygen vacancy formation followed by W(+6)-to-W(+5) or or W(+6)-to-W(+4) reduction substantially decreases the energy required to dissociate methane at tungsten complex. The lower barrier of about 37 kcal/mol takes place for supported four-coordinated W(+4) complex without topmost oxygen ligand. The final state for this process is a six-coordinated tungsten complex having both the hydrogen and the methyl group. Homolytic methane dissociation at this center goes over a higher barrier of about 52 kcal/mol.

The activation of $WO(OH)_4$ complex through creation of the oxo-center of radical character has been considered. This is achieved by charging the $WO(OH)_4$ complex. It was found that crucial drop of CH_4 dissociation barrier to about 5 kcal/mol takes place for charged model complex $WO(OH)_4^+$, for which the terminal oxo-center (which abstracts hydrogen from C-H bond) possesses radical character as one may judge from oxygen Mulliken spin density of about 0.88 e.

To find less energetically demanding scenario of the C-H bond dissociation for OCM the investigation of polynuclear tungsten-containing complexes on the silica support has been performed. It is shown that there is a multiplicity of tungsten W-Mn polynuclear complexes (from dimer to tetramer) between two neighboring “nests” on cristobalite. Stable Mn(+5) and Mn(+3) species are predicted, coupled to support by three bridge oxygen in the neighborhood of the W(+6) complex. The Mn(+5) complex contains terminal atomic oxygen ligand with distinct radical character in the state with the spin projection of 1. It is supposed that the latter center should be as active in the C-H activation as the radical oxo-center of $WO(OH)_4^+$ complex.

4 Conclusions

The optimization of mono- and polynuclear W and Mn species on the surface of α-cristobalite has been performed and values of barrier energy for the abstraction of hydrogen from methane were determined. The barriers of the methane dissociation at oxo-centers provided by the W(+4) and W(+6) species on α-cristobalite appear to be as high as 40-70 kcal/mol. All the oxygen centers in these systems are of closed-shell configuration. Heterolytic mechanism is preferable over homolytic for such centers. Situation is qualitatively changed when oxygen center possesses radical character. The barrier of C-H activation drops to about 5 kcal/mol for $WO(OH)_4^+$ model center. Based on this result one may guess that the true OCM active center is that associated with Mn (+5) complex having terminal oxygen ligand with a radical character.

Acknowledgements

Financial support of this work in the frame of the European Union 7th Framework Programme (FP7/2007–2013) under grant agreement No. 262840 is gratefully acknowledged.

References

[1] Z.C. Jiang, C.J. Yu, X.P. Fang, S.B. Li, H.L. Wang, *J. Phys. Chem.* 97 (1993) 12870.
[2] H.C. Chen, J.Z. Niu, B. Zhang, S.B. Li,Acta. Phys.Chim.Sinica. 17 (2001) 111.
[3] S. Hou, Y. Cao, W. Xiong, H. Liu, Y. Kou, *IndEngChem Res*. 45 (2006) 7077.
[4] Z.C. Jiang, H. Gong, S.B. Li, *Stud.Surf. Sci.Catal.* 112 (1997) 481.
[5] S. Ji, T. Xiao, S. Li, C. Xu, R. Hou, K.S. Coleman, M.L.H. Green, *Appl.Catal. A*. 225 (2002) 271.

II-PP172

The Investigation of Structure of Biocatalyst Used in the Vegetable Oils Transesterification

Doluda V.*, Sulman E., Matveeva V., Lakina N., Burmatova O., Stepacheva A.A.

Tver Technical University, Tver, Russia

* doludav@yandex.ru

Keywords: biodiesel, magnetic, nanoparticles, lipase, FTIR, spectroscopy

1 Introduction

Last years the attention of the scientific society is forwarded to the methods of ecological fuels production. One of these types of fuels is biodiesel which is presented by fatty acids esters. The biodiesel is produced by the transesterification reaction of oils in the presence of catalyst. The most prospective catalysts are the biocatalysts on the base of hydrolytic enzyme lipase immobilized on the modified surface of magnetic nanoparticles (MNPs).

The use of MNPs as the enzyme support gives some advantages as easy biocatalyst separation from reaction media (due to magnetic properties) and simplicity of modification [1].

In this work the biocatalysts on the base of lipase immobilized on the surface of MNPs modified by sodium citrate and aminopropyltrietoxysilane were synthesized. Moreover the comparative characterization of the synthesized biocatalysts was done using FTIR spectroscopy.

2 Experimental

In this work the MNPs were used as the enzyme support. MNPs were prepared as follows. 5.2 g $FeCl_3 \cdot 6H_2O$ and 8.8 g $FeSO_4 \cdot 7H_2O$ were dissolved in 25 mL of azoted water. This mixture was drop-wise added to 250 mL of NaOH 1.5 M. The particles obtained were washed by distilled water to pH=7, than the 98% ethanol was added while the solution volume reached to 50 mL. The mixture was treated with ultrasound 10 min [1]. The synthesized nanoparticles were dried in the vacuum.

The pancreatic lipase (L3126 Type II, 100-400 un/mg) immobilization was carried out by two ways: (i) the pretreatment of 0.1 f of MNPs with sodium citrate ($Na_3C_6H_5O_7$) 0.1 mg/mL, glutaric dialdehyde (Glu) 0.01 mg/mL and lipase (Lip) 0.005 mg/mL, (ii) the treatment of MNPs with (3-aminopropyl)trietoxysilane (APTS) 0.005 mg/mL, glutaric dialdehyde 0.01 mg/mL and lipase 0.005 mg/mL.

The activity of the immobilized lipase was determined using the modified method of Ota-Yamada [2]. The investigation of the biocatalysts structure was done using FTIR spectrophotometer IR Prestige 21 equipped with direct reflection device which allows analyzing of impure samples in the spectral range 7800-350 cm^{-1} with high accuracy.

3 Results and discussion

The comparative analysis (Fig.1) of results obtained in the experiments carried out at atmospheric pressure and in the supercritical CO_2 media showed that the activity of native lipase decreased by 1.4 times, the activity of biocatalysts Fe_3O_4/APTS/Glu/Lip and $Fe_3O_4/Na_3C_6H_5O$/Lip by 1.2 and 1.3 times relatively. So it can be concluded that in the media of supercritical CO_2 the synthesized biocatalysts reserve their catalytic activity for a longer time and have better stability in comparison with atmospheric pressure.

To investigate the structure of biocatalysts samples the FTIR analysis was done. The results show the presence of covalent bonds between the functional groups of modifying agents and lipase (Fig.1).

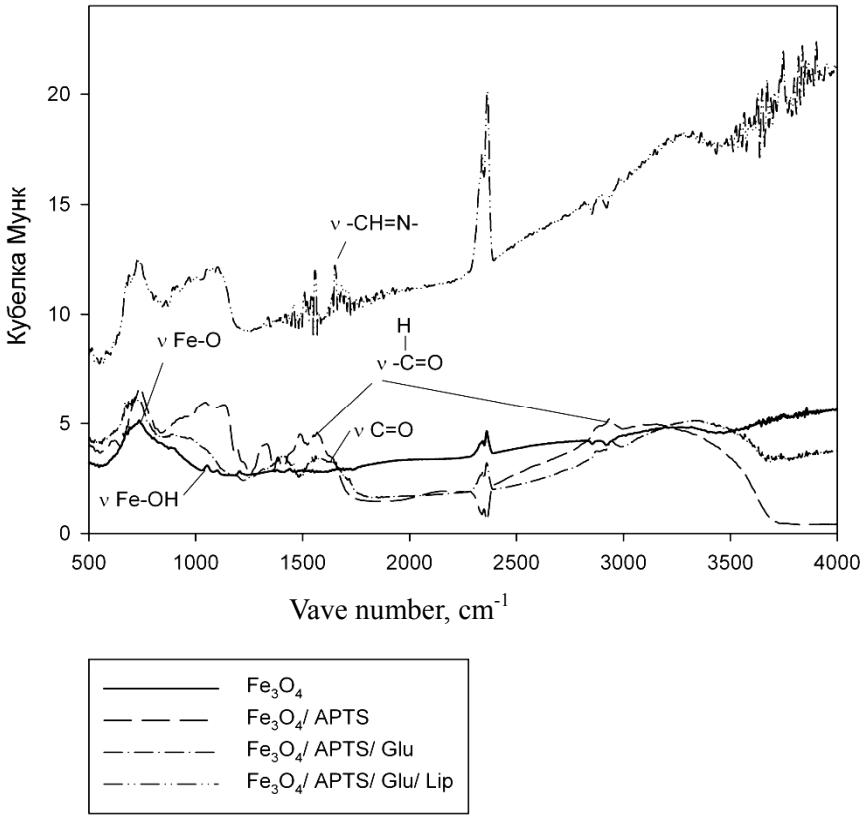

Fig.1. IR-spectra of biocatalysts samples, modified by APTS

4 Conclusions

The data obtained in the work devoted to the formation of active and stable biocatalysts used in the vegetable oils transesterification reaction shows the great prospective. The pancreatic lipase immobilization on the modified surface of MNPs passes through the covalent bonds that provides high stability of biocatalysts in supercritical CO_2 media.

Acknowledgements

Authors thank the Ministry of education and science of Russian Federation for financial support (grant RFBR № 13-08-00831 A).

References

[1] A.E. Ghaly et al. *Am. J. of Biochemistry and Biotechnology*. 6 (2010) 54
[2] M. Tudorache et al. *Applied Catalysis A: General*. 437 (2012) 90.

II-PP173

Enlargement of the Surface Area of Highly Porous Catalysts

Sulman E.M.[1*], Shumilov V.V.[2,1], Shimanskaya E.I.[2]

1 - Tver Technical University, Tver, Russia
2 - Tver State University, Tver, Russia

* sulman@online.tver.ru

Keywords: ceramic, catalysts, alumina, surface, area, wash-coating

1 Introduction

Highly porous cellular catalysts are a specific class of porous materials which consist of large cells with linear dimensions from5 mm to 10 mm and have geometry approximately corresponding to a cuboctahedron.

Highly porous ceramic structures can be produced in various forms from a variety of materials and exhibit such qualities as high porosity and good interconnectivity. Due to their specific geometry and other properties these materials can be used in a wide range of engineering problems [1].

2 Experimental

In this paper, method of polyurethane matrix replication was used for the production of highly porous cellular material. The technology involves thermal decomposition of polyurethane foam structure after its soaking in ceramic slurry. Polyurethanesample of predetermined shape is first processed by the slurry. The slurry contains alumina as filler, with addition of components imparting compressive strength, acid and alkali resistance, defoamers and other additives (2%).

Particular attention in this study is paid to increasing the surface area of the obtained samples. Ceramic carrier created by replication method from the α-alumina is processed in slurry containing γ-alumina as filler. The alternative can be precipitation of extra amount of γ-alumina from hot solution of aluminum nitrateon samples.

Presently, extensive research of samples' surface area is carried out. The obtained data confirm the absence of micro- and mesopores in samples produced from α-alumina. The data also indicate that mesopores occur after applying γ-alumina (applying methods specified above).Surface area significantly increases if a combination of methods is applied.

The next step is to apply a catalytically active component (Platinum).On this stage of the studies measurements of catalytic activity were carried out; the example can be the reaction of separation of optical isomers obtained in the ethylbenzeneformate racemisation reaction. Strength and macroporosity of the catalyst system were studied as well [2].

3 Results and discussion

By varying the composition of slurry a new catalytic system with extended surface area can be obtained. Development of optimum sintering temperature mode allows to avoid catalyst structure destruction.

One sample having platinum on the foam support is shown in Figure 1.

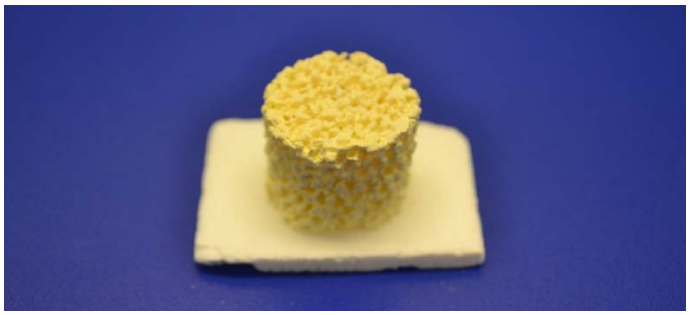

Figure 1. Alumina foam with catalytically active platinum layer at the surface

4 Conclusions

The advantages of porous catalysts are large surface area and high permeability for gas and liquid flow, which results in high rates of mass and heat transfer. This allows to produce catalyst systems of small volume.

References

[1] Shumilov V.V. *«Physics, chemistry and new technologies», XXI Karginsky readings* (Tver, 27 march 2014)

[2] Shumilov V.V. *Master's Thesis*, Abo Akademy (Finland, Turku, 2014)

II-PP174

CO Oxidation on the Bimetallic Pd-Au/HOPG Catalysts: *in-situ* XPS and MS Investigation

Bukhtiyarov A.V.[1,2*], Prosvirin I.P.[1,3], Saraev A.A.[1], Klyushin A.Yu.[4], Knop-Gericke A.[4], Schlogl R.[4], Bukhtiyarov V.I.[1,2,3]

1 - Boreskov Institute of Catalysis, Novosibirsk, Russia
2 - Research and Educational Center for Energy Efficient Catalysis in Novosibirsk National Research University, Novosibirsk, Russia
3 - Novosibirsk State University, Novosibirsk, Russia
4 - Fritz-Haber-Institute der Max Planck Society, Berlin, Germany

* avb@catalysis.ru

Keywords: Pd-Au catalysts, *in-situ* XPS, CO oxidation

1 Introduction

Bimetallic systems attract the great interest of many scientific groups due to its ability to induce the significant improvement of catalytic properties compared to monometallic catalysts [1-2]. Among these systems the Pd-Au catalysts is one of the most frequently studied ones because they have exhibited high catalytic activity in a number of industrially important reactions. Although a large number of publications devoted to study of bimetallic Pd-Au systems has been published in recent years, the reasons of synergistic effects in different catalytic reactions have not be rationalized.

One of the most evident proposals, which have been supported by many researchers, is the key role of surface composition of bimetallic particles. It is well known that not only the ratio of the introduced metals, but also temperature of calcination will affect the surface composition causing the big difference between Au/Pd atomic ratios in the bulk and surface [1-2]. It is also evident that surface composition can be varied under the influence of reaction mixture due to enrichment of the surface with one of the metals. Thus the detailed study of surface structure and composition of bimetallic Pd-Au catalysts is necessary to understand the nature of active sites and help to optimize the catalyst composition for the best activity, selectivity and stability.

Success in such a study is impossible without development of procedures for synthesis of bimetallic Pd-Au catalysts with controlled particle size and Au:Pd ratio. Furthermore, low loading of the active component (< 1-2wt. %) and complex composition of the high surface area supports of a noble metal on high surface area supports in “real” supported catalysts limits the application of surface sensitive techniques. Using of model catalysts, where metal particles deposited on the planar support, could help to solve those problems and get more reliable data concerning surface structure and chemical composition of active metals depending on different treatments [3-4].

2 Experimental/methodology

XPS/STM study of the formation of Pd-Au bimetallic particles with controlled size and Au:Pd atomic ratio supported on Highly Oriented Pyrolytic Graphite (HOPG). This investigation was performed at RGBL station at the Berlin synchrotron radiation source BESSY II [5]. Then, the prepared Pd-Au/HOPG bimetallic catalysts were investigated in CO oxidation with combination of *in-situ* XPS and MS at ISISS beamline (Berlin, Germany) located also at BESSY II [6].

3 Results and discussion

Pd-Au bimetallic particles formation

Initially the set of samples with different size of gold particles supported on the HOPG surface were prepared using original three-step procedure developed by us for preparation if the Ag/HOPG model catalysts preparation [**7**]. All prepared Au/HOPG samples were characterized by STM and XPS. STM indicates that all samples are characterized by quite narrow particle size distribution (PSD) with the mean particle size of 4-7 nm depending on the sample. Then the Au/HOPG samples were used as templates for preparation of Pd/Au/HOPG bimetallic samples. The Pd amount was varied by variation of deposition time. The XPS and STM investigation shows that using this procedure a set of bimetallic Pd/Au/HOPG samples with various particle density, size distribution and Pd/Au atomic ratio were prepared. Two types of particles on the surface of HOPG in those freshly prepared samples were identified: "core-shell" bimetallic Pd/Au particles and monometallic Pd particles with smaller size.

XPS study of subsequent annealing of the samples in UHV conditions at different temperatures (from RT to 500°C) indicates that "core-shell" Pd/Au particles transform to the Pd-Au alloy ones during heating from 200 to 400°C. Annealing at 500°C sinters the particles.

CO oxidation

It was shown that the prepared Pd-Au/HOPG samples started to be active in CO oxidation reaction at 100°C. The redistribution of Au and Pd atomic concentration on the surface in the course of the reaction was investigated using *in-situ* XPS. It has been shown that the Au/Pd atomic ratio enhances when the sample is active in CO oxidation.

4 Conclusions

Formation of the model bimetallic Pd-Au/HOPG catalysts has been investigated with XPS and STM. The optimal temperature for the Pd-Au alloy formation is 400°C. Variation of Au/Pd atomic ratio on the particle surface is regulated by variation of the amount of deposited Pd and the temperature of annealing. Samples prepared using the proposed procedure is stable against sintering until 500°C.

The prepared Pd-Au/HOPG samples are active in CO oxidation reaction. The Au/Pd atomic ratio varies together with activity in CO oxidation.

Acknowledgements

The authors would like to thank Russian Foundation of Basic Research (grant 14-53-12004) and grant of President of Russian Federation for government support of Leading Scientific Schools (grant SS-5340.2014.3) for support. The work was performed in the framework of the joint Research and Educational Center for Energy Efficient Catalysis (Novosibirsk State University, Boreskov Institute of Catalysis).

References

[1] C. W. Yi, K. Luo, T. Wei and D. W. Goodman, J. *Phys. Chem. B*. 109 (2005) 18535.
[2] Aiqin Wang, Xiao Yan Liu, Chung-Yuan Mou, Tao Zhang, *Journal of Catalysis* 308 (2013) 258.
[3] Demidov, D.V., Prosvirin, I.P., Sorokin, A.M., Rocha, T., Knop-Gericke, A., Bukhtiyarov, V.I., *Kinetics and Catalysis*. 52 (2011) 855.
[4] A. V. Bukhtiyarov, R. I. Kvon, A. V. Nartova, and V. I. Bukhtiyarov, *Russian Chem. Bull.* 60 (2011) 1977.
[5] http://www.bessy.de/rglab/index.html
[6] www.helmholtz-berlin.de
[7] Demidov, D.V., Prosvirin, I.P., Sorokin, A.M., Bukhtiyarov V.I., *Catal. Sci. Technol.* 1 (2011) 1432.

II-PP175

Reduction of Catalysts Based on Mn-Zr Oxides: *in situ* XPS and XRD Study

Bulavchenko O.A.[1,2*], Vinokurov Z.S.[1,2], Afonasenko T.N.[3], Tsyril'Nikov P.G.[3], Tsybulya S.V.[1,2], Saraev A.A.[1,2], Kaichev V.V.[1,2]

1 - Novosibirsk State University, Novosibirsk, Russia
2 - Boreskov Institute of Catalysis SB RAS, Novosibirsk, Russia
3 - Institute of Hydrocarbon Processing SB RAS, Omsk, Russia

* isizy@catalysis.ru

Keywords: manganese oxide, zirconium oxide, solid, solution, *in situ* XRD, *in situ* XPS, reduction

1 Introduction

ZrO_2 is used as a support with high thermal resistance. Moreover, solid solutions based on ZrO_2 exhibit high catalytic activity in a number of practically important reactions. Mn-Zn mixed oxides can effectively catalyze the gas-phase oxidation of hydrocarbons or chlorcarbons. Although there is agreement that the catalytic activity of these catalysts is determined by their redox properties, the exact mechanism of these oxidation reactions is not clear yet. Mn cations can enter the lattice of ZrO_2 with the formation of solid solutions $Zr_{1-y}Mn_yO_2$, in which lattice oxygen possesses sufficiently high mobility and hence high reactivity. On the other hand, some authors suppose that the active species in oxidation reactions is mobile oxygen that is incorporated in disperse MnO_x rather than lattice oxygen of the solid solution

One of the main ways to study redox properties of catalysts is the method of temperature-programmed reduction (TPR). On the basis of its results, it is possible, to draw some conclusions about the presence in the catalysts of various forms of manganese oxides MnO_x. However, the TPR technique is an indirect method that allows monitoring only the absorption of hydrogen rather than the change in structural characteristics of catalysts or in the charge state of Mn and Zr. The aim of this work was to investigate the reduction of Mn-Zn mixed oxides by hydrogen in a wide temperature range in order to elucidate the origin of active species that catalyze the oxidation of hydrocarbons and chlorcarbons.

2 Experimental/methodology

A series of catalysts based on mixed Mn-Zr oxides with different molar ratios Mn/Zr have been prepared by coprecipitation of manganese and zirconium nitrates, calcined at 650 ^oC for 4 h.

TPR-H_2 was performed in a quartz reactor using a flow setup with a thermal conductivity detector. The flow rate of 10 vol % of H_2 in Ar was 40 mL/min. The heating rate was 10 °C/min.

Catalysts were characterized by a powder XRD technique using a D8 Advance diffractometer (Bruker). The reduction of the catalysts was studied in situ using synchrotron radiation at the Siberian Synchrotron and Terahertz Radiation Center (Novosibirsk, Russia). The in situ diffractometer was equipped with a high-temperature reactor chamber XRK-900 (Anton Paar) The heating rate was 5 °C/min; the total flow rate (H_2) was 150 mL/min.

In situ XPS experiments were performed at the ISISS (Innovative Station for In Situ Spectroscopy) beamline at the synchrotron facility of BESSY II (Berlin, Germany). The experimental station was described in detail elsewhere [1]. In these experiments, Zr*3d*, Mn*2p*, O*1s*, and C*1s* core-level spectra of sample were recorded under a H_2 flow at 140, 350, 500, 620^oC. The total pressure of H_2 was 0.5 mbar. All the spectra were obtained with a photon energy of 860 eV.

3 Results and discussion

It has been found that at low Mn/Zr ratios, when the Mn content is below 30 atom %, the catalysts are single-phase solid solutions ($Mn_yZr_{1-y}O_{2-\delta}$) based on a ZrO_2 structure. According to XPS data, manganese in these solutions exists mainly in the Mn^{4+} state. An increase in the Mn content mostly leads to an increase in the number of Mn cations in the structure of the solid solutions, but a part of manganese form Mn_2O_3 and Mn_3O_4 in crystalline and amorphous states.

Reduction of these catalysts with hydrogen was studied by a TPR, in situ XPS and XRD, 100 to 700 °C. Figure 1 shows a series of diffraction patterns recorded during the reduction of the sample with Mn/Zr=1. At room temperature, the sample contains two phases: a solid solution $Mn_yZr_{1-y}O_4$ and Mn_2O_3. The reduction of this sample leads to a change in the lattice parameter of the solid solution $Mn_yZr_{1-y}O_4$, which is indicated by the shift of corresponding peaks to larger angles. Besides, the reduction leads to transformations of manganese oxides. The XRD data illustrates the two-stage reduction of manganese: $Mn_2O_3 \rightarrow Mn_3O_4 \rightarrow MnO$.

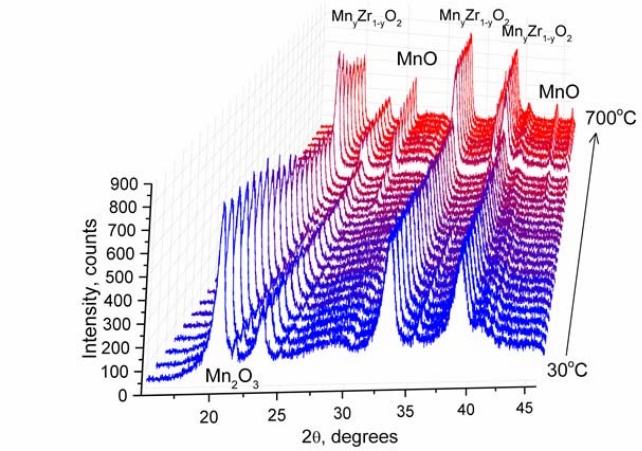

Fig. 1. Series of in situ diffraction patterns (λ = 1.0157 Å) recorded during reduction of the sample Mn/Zr=1 with hydrogen in the ranges from 30 to 700 °C

According to TPR data and to data on the change in the lattice parameter the reduction of solid solutions proceeds in two steps. In the first stage, at temperatures of 100-500°C, manganese cations undergo partial reduction to Mn^{2+}, whose presence is confirmed by XPS measurements. The lattice parameter of $Mn_yZr_{1-y}O_2$ in this case varies because of changes in the oxidation state of manganese cations in the bulk of solid solution. In the second stage, at temperatures of 500-700°C, manganese cations exit from the bulk of the solid solution and segregate on its surface. The lattice parameter at this stage increases because of the decrease in the number of Mn cations in the oxide.

4 Conclusions

Mn-Zr oxide catalysts were obtained by coprecipitation of corresponding nitrates, and their physical and chemical characteristics were studied. The reduction of mixed oxides in hydrogen was studied by in situ XRD, TPR, and in situ XPS. It has been shown that the reduction of the solid solutions proceeds in a wide temperature range 100-700 °C via two steps. At the first step, at 100-500 °C, Mn cations, which constitute a solid solution, undergo partial reduction. At the second step, at 500-700°C, Mn cations irreversibly exit to the particle surface.

Acknowledgements

This work was supported by the RSCF project №14-23-00037.

References

[1] A. Knop-Gericke, E. Kleimenov, M. Hävecker et all *Adv. Catal.* 52 (2009) 213

II-PP176

Ionic liquid Supported on Diatomic Powder as Catalist of Benzene Alkylation with 1-Octene

Akhmedyanova R.A.[1], Miloslavskii D.G.[1], Kharlampidi H.E.[1,2], Zhavoronkov P.A.[1*]

1 - Kazan National Research Technological University, Department Of Synthetic Rubber, Kazan, Russia

2 - Kazan National Research Technological University, Department of General Chemical Engineering, Kazan, Russia

* queendael07@mail.ru

Keywords: ionic liquids, aluminum chloride, benzene alkylation, 1-octene

1 Introduction

To date in the industry process of alkylation benzene with olefins is using catalyst systems based on aluminum chloride. Advantage of such systems is to use a smaller excess of benzene and the possibility to conduct of alkylation and transalkylation processes in a single reactor. However, the catalytic systems, based on aluminum chloride, have a number of disadvantages: corrosiveness, the need to remove them from the reaction mass, a large amount of wastewater.

An alternative is to use catalytic systems - ionic liquids (IL) based on aluminum chloride, including supported on solid supports.

Chemical and mineralogical composition and structure of diatomite powder - a sedimentary rock provide all the prerequisites for its use as such a solid carrier.

2 The experimental

The ionic liquid is a salt of tetramethylammonium chloride and aluminum chloride with a melting point of 50°C.

Drawing of IL on diatomite powder was carried out by impregnation of of the calcined support by an ionic liquid in medium of methylene chloride, followed by solvent removal and drying.

The degree of ionic liquid coating on diatomite powder was evaluated by the nitrogen content determined by elemental analysis, as well as in terms of bulk density.

3 Results and discussion

It is shown that with increasing amount of ionic liquid in the mixture, the nitrogen content increases in the catalyst component, and bulk density increases. It was also found that, irrespective of the mass ratio of the original IL, degree of ionic adsorption is 52-54% of its original amount.

If the content of IL increases in the initial mixture, the total pore volume and specific surface of the catalyst decrease (Table).

Table - Surface structural characteristics of the samples of catalyst - ionic liquid TMAX - aluminum chloride supported on diatomite powder.

The ratio of IL: Diatomite powder wt%	Specific surface, m^2 / g	Total pore volume cm^3 / g	Average Pore Diameter, nm
0.0:100.0	23,0	0,088	15,4
20.0:80.0	9,6	0,034	14,2
33,3:66,7	3,4	0,017	19,6
50.0:50.0	2,9	0,016	21,5

The resulting samples were used as the catalysts in the alkylation of benzene by octene-1. The temperature of the alkylation process was 80 ° C, duration - 3 hours.

4 Conclusion

The ionic liquid applied to the diatomite powder in a weight ratio of 20:80 was active in the alkylation process of benzene by 1-octene and provided satisfactory conversion of 1-octene.

Aknowledgements

This work was financially supported by the Russian Ministry of Education within the basic part of the state task

II-PP177

Influence of Acid-Base Characteristics of the Alumina on Properties of the Supported Palladium Particles and their Catalytic Activity

Boretskaya A.V.[1*], Il'yasov I.R.[1], Lamberov A.A.[1], Boretskiy K.S.[1], Bikmurzin A.Sh.[2]

1 - A.M. Butlerov Institute of Chemistry, KFU, Kazan, Russia
2 - Association "Nizhnekamskneftekhim", Nizhnekamsk, Russia

* ger-avg91@mail.ru

Keywords: palladium, catalysts, γ- Al_2O_3, butadiene-1,3, hydrogenation

1 Introduction

The supported palladium catalysts are widely used in large industrial processes of hydrogenation of acetylene and diene compounds. These processes are realized in the preparation of monomers for the production of synthetic rubber and plastics with the usage of the imported catalytic systems. Despite sufficient activity, these catalysts do not provide a high selectivity and a long service cycle operation, so that it requires a detailed analysis of the active phase formation of supported palladium particles at all stages of catalyst synthesis. Thus, the properties of the supported metal particles in the catalyst systems are mainly determined by two factors: the size of the particles and interaction "metal - support". The latter occurs in the step deposition of the metal complex and its attachment to the acid-base surface of the alumina support. The results about the regularities of the palladium particles formation during application of palladium complex on alumina characterized by the different acid-base properties are obtained in this work. The influence of the concentration and strength of the acid-base centers on the formation of the charge state, dispersion and geometrical characteristics of the supported palladium particles on alumina is established. The obtained data will be used in the synthesis of the supported metal particles with set properties and creation of new catalysts of selective hydrogenation not conceding or surpassing in the operational characteristics of import catalytic systems.

2 Experimental

2.1 Support preparation and characterization

Modification of aluminum hydroxide was carried out by weak organic acids. It were oxalic, citric and acetic acids. This samples was calcined at 550 ^{0}C for preparation γ-Al_2O_3. Differential thermal analysis (DTA) under argon and air was performed on samples by derivatograph system «F.Paulik, J. Paulik and L. Erdey Q-1500 D» in the temperature range from 20 to 1000 ^{0}C. The phase analysis of the samples was carried out on an automatic X-ray diffractometer DRON-based serial-2 using long-wave radiation $CuK_{\alpha.}$ The surface areas of supports, pore volume, distribution of pore volume and pore diameter were determined by the ASAP 2400 analyzer company, Micromeritics AutoChem (USA). Thermo-programmed desorption of ammonia was carried out in a quartz reactor with a thermal programmable temperature rise from 100-600 ^{0}C on the instrument AutoChem Micromeritics (USA).

2.2 Catalyst preparation and characterization

The catalysts were prepared by chemisorption impregnation. The palladium was deposited onto γ-Al_2O_3 unmodified and modified by organic acids with usage 0.5 wt % solution of palladium acetylacetonate as metal precursor. The catalysts were dried for 12 h at 80 ^{0}C.

Interaction of the metal with a support was measured by means of temperature-programmed

reaction experiments in the temperature range 50-700 ^{0}C on a Micromeritics AutoChem.

2.3 Catalytic tests

Hydrogenation of Butadiene-1,3 was performed in gase phase in laboratory conditions on a flow-circulation installation of a fixed bed catalyst. One gram of catalyst initially was reduced in the reactor for 1 h under H_2 at 160 ^{0}C. Analysis of the reactants and the reaction products of hydrogenation was carried out by gas chromatography with a flame ionization detector and a thermal conductivity detector on the Chromos GCh – 1000.

3 Results and discussion

According to the data of DTA, the formation of the low-temperature modification of γ-Al_2O_3 for all samples of pseudoboehmite alumina was observed in the temperature range of 200-462 ^{0}C and the decomposition of aluminum salts in an air stream to a temperature of 531 ^{0}C. Thus for formation of alumina without organic residues was carried out heat treatment of all aluminum hydroxides at 550 ^{0}C. The formation of γ-Al_2O_3 at a given heat treatment was determined by XRF method.

According to the results of the texture analysis, modification of aluminum hydroxide with organic acids results in an increase in surface area and pore volume. The total acidity of the alumina samples estimated by the method of temperature programmed desorption of ammonia showed an increase in the acidity of the samples treated with acid approximately in 1,2 times compared with the original one. It is due to the growth of defects in the crystal oxide structure estimated by helium pycnometry. It was showed a decrease in the density of the modified samples as a result of a less dense coordination of primary crystallites of corresponding hydroxide and aluminum oxide.

On the basis of the results of the temperature programmed reduction with hydrogen the increase acidity of the supports leads to the stronger interaction of acid-base centers modified carrier with supported palladium particles. It leads to the formation of electron-deficient atoms surface of the active component.

According to the catalytic tests, the catalysts based on the modified supports showed a higher conversion of 1,3-butadiene, up to 94%, while the selectivity of 1-butene slightly decreased and amounted to 31-42%.

4 Conclusions

Thus, modification of aluminum hydroxides by weak organic acids leads to changes of texture characteristics, accompanied by an increase in surface area and decrease in pore volume; and increase in of the acidity of the supports with higher percentages of strong acid centers. The growth of 1,3-butadiene conversion probably occurs due to the high dispersivity of the metal on the surface of the acidic support and decrease in selectivity to butene-1 explained by the presence of the charged palladium particles that cause the deeper hydrogenation of 1,3-butadiene in butane.

II-PP178

Genesis of HDT Catalysts Prepared with the Use of Co_2Mo_{10}HPA and Cobalt Citrate: Study of their Gas and Liquid Phase Sulfidation

Nikulshin P.A.[1*], Mozhaev A.V.[1], Maslakov K.I.[2], Pimerzin A.A.[1], Kogan V.M.[3]

1 - Samara State Technical University, Samara, Russia
2 - Chemistry Department, M.V. Lomonosov Moscow State University, Moscow, Russia
3 - N.D. Zelinsky Institute of Organic Chemistry, RAS, Moscow, Russia

* p.a.nikulshin@gmail.com

Keywords: hydrotreating, heteropolycompounds, CoMoS, genesis, deactivation

1 Introduction

Production of clean fuels with less than 10 ppm sulfur content is one of the most important and claiming the attention problem in recent petroleum refinery. It is known that the active phases of the HDS catalysts are the MoS_2 or WS_2 nanocrystallites promoted by cobalt or nickel, deposited on a high specific surface area supports. Activation procedure such as sulfidation is an important step to improve catalytic properties of sulfide catalysts. Two different routes are commonly used for sulfidation of HDS catalysts: (i) with a H_2/H_2S mixture, carried out in gas phase and most practiced in laboratory experiments, and (ii) with spiked feedstock, in which sulfiding is mainly done by the sulfur of the organosulfide agents (also called "spiking" agents). It is known that conversion of the oxidic catalyst structure into the sulfided phase during gas or liquid phase sulfidation methods determines the final structure and performance of the catalyst. There is no consensus on which of sulfidation method is better. Thus for new precursors and HDS catalysts it is necessary to investigate both sulfidation methods. The objective of the research was to study sulfidation mechanisms of the HDS catalysts prepared with the use of Co_2Mo_{10}HPAand cobalt citrate.

2 Experimental/methodology

Catalysts were prepared by means of the incipient wetness technique via impregnating the γ-Al_2O_3 with mixed water solutions of precursors (Co_2Mo_{10}HPA and cobalt or nickel complexes with citric acid (CA)). Then the catalysts were dried at 110^0C (4 h). Catalysts were subjected to gas phase sulfidation. For this purpose, catalyst samples were placed into a separate glass reactor where sulfidizing process was carried out under a flowing H_2/H_2Smixture (85/15 v/v %, 50 ml/min, 0.1 MPa) at 20, 100, 200, 300 and 400^0C for 1 h. Samples were then cooled down to room temperature at a rate of 20–25^0C/min under the reactive mixture. Liquid phase sulfidation was carried out in bench-scale flow reactor for the $Co_3(CA)_{4.5}$-Co_2Mo_{10}HPA/Al_2O_3 catalyst. Straight run gas oil (SRGO) with DMDS (2 wt.%) was used as a feedstock. The catalysts were soaked with this sulfiding feed in hydrogen atmosphere (3.5 MPa) at 140◦C, using a liquid hourly space velocity (LHSV) of 4 h^{-1}. Then the LHSV was decreased to 2 h^{-1} (with H_2/oil = 300 NL/L) and the bed temperature was raised to 230^0C at a rate of 25^0C/h and stabilized for 8 h. The final temperature of sulfidation was 340^0C (ramping rate of 20^0C/h) and it was stabilized for 9 h. In each sulfidation experiment catalyst sample was cooled down to room temperature at a rate of 15–20^0C/min under the reactive mixture and an organic solvent. The catalysts have been studied by N_2 adsorption, XRD, HRTEM and XPS methods and tested in diesel HDT.

3 Results and discussion

The XPS and HRTEM measurements of the synthesized catalysts confirmed the formation of

multilayer slabs of type II CoMoS phase after gas and liquid phase sulfidations. Fig. 1 shows the models of genesis of the active phase of the $Co_3(CA)_{4.5}$-Co_2Mo_{10}/Al_2O_3 catalyst in gas or liquid phase sulfidation [1].

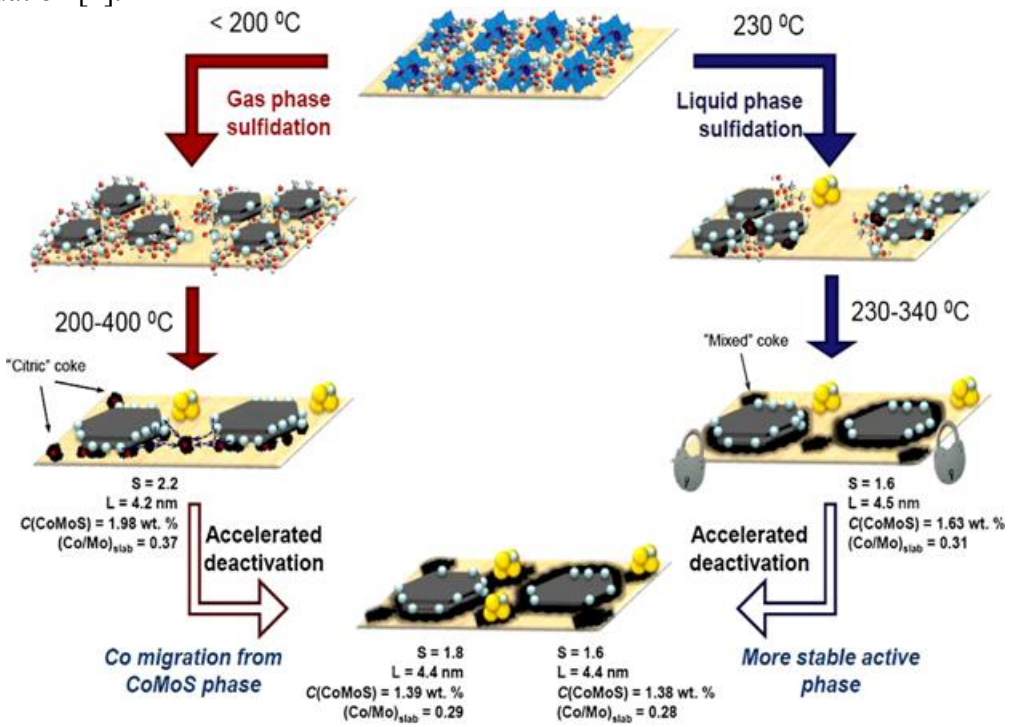

Fig. 1. CoMoS phase formation mechanisms during gas and liquid phase sulfidation of the $Co_3(CA)_{4.5}$-Co_2Mo_{10}/Al_2O_3catalyst (*S* – average stacking number, *L* – average length were found from TEM; Co content in CoMoS phase and $(Co/Mo)_{slab}$ were found by XPS).

4 Conclusions

Mechanisms of the active phase formation from Co_2Mo_{10}HPA and cobalt citrate precursors during gas and liquid phase sulfidation processes have been established. The first step of gas phase sulfidation is formation of MoS_2 nanoclusters from Co_2Mo_{10}HPAwith the deficiency of promoter atoms. The second step is destruction of cobalt citrate at higher temperatures and fixing of the Co atoms on the edges of MoS_2 crystallites. In liquid phase sulfidation, both metals (Co and Mo fromCo_2Mo_{10}HPA and Co from citrate) are sulfided simultaneously with the formation of nuclei of CoMoS phase II type at low temperature (230^0C). At high temperature (340^0C) the increase of particle size of CoMoS phase is occurred.

Gas phase sulfidation of the catalyst leads to formation of active phase with higher Co content in CoMoS and promoter ratio than liquid sulfidation. Initial activity in diesel HDT of the gas sulfided catalyst was higher than activity of the sample sulfided by the liquid phase method.

Study of behavior of the catalysts in accelerated deactivation revealed that the liquid phase sulfided sample was more resistant to the deactivation. This occurred probably due to stabilization of active phase particles by coke formed during liquid phase sulfidation. This effect prevents loss of Co atoms from CoMoS phase.

Acknowledgements

The work was partly financially supported by the Russian Foundation for Basic Research (grant 14-03-31901).

References

[1] P.A. Nikulshin, A.V. Mozhaev, K.I. Maslakov, A.A. Pimerzin, V.M. Kogan, Appl. Catal. B 158–159 (2014) 161–174

II-PP179

Different Preparation Method of WTi-Pillared Clay: Catalytic Application in the n-Hexane Isomerisation

Ferjani W.*, Khalfallah B.L.

Laboratoire de Chimie des Matériaux et Catalyse, Département de Chimie, Faculté des Sciences de Tunis, Tunis, Tunisie

* ferjani_wiem@hotmail.fr

Keywords: tungsten, titanium, pillared clay, isomerisation, n-hexane

1 Introduction

Pillaring layered compounds with inorganic species is a well route in preparing porous materials. The potential advantages of pillared interlayer clays lie in the possibility of achieving larger pore sizes and sufficient acidic functions: Lewis and Bronsted acid sites. Generally, metals are deposited on pillared clays by means of ionic exchange, incipient wetness, or dry impregnation of samples. The number of chemical reactions for which the potential application of pillared clay (PILC), whether as catalysts or as catalyst supports, has been evaluated and is continuously increasing [1, 2]. The Ti-pillared clays have been explored in various applications, especially those requiring acid sites [3-5]. However, the difficulties of its preparation have made its use less interesting comparing to other pillared clays. So far, there has not been any published work describing a method for the preparation of WTi-PILC or studying the effect of tungsten amounts on the physico-chemical properties of Ti-PILC nor discussing the catalytic activity of the WTi-pillared clays. For this reason, it has been interesting to investigate the effect of preparation method and tungsten amounts added to the clay during the synthesis of WTi-PILC. All the materials were characterized by different technique then tested in the n-hexane isomerisation, reaction widely utilized to evaluate the surface acidity of heterogeneous catalysts.

2 Experimental/methodology

The intercalated Ti-solution solution was prepared by slowly adding $TiCl_4$ into HCl (6M) under vigorous stirring. The tungsten solution was prepared by dissolving ammonium metatungstate $(NH_4)_6H_2W_{12}O_{40}$ in distilled water (10^{-2} M).

For the first method, the intercalated Ti-solution and W-solution were simultaneously added to the suspension of the initial clay under vigorous stirring. After 24h, the solid fraction was separated by centrifugation and dried at room temperature. The second method is the tungsten addition by incipient wetness of the intercalated Ti-clay. The samples were also dried at room temperature and finally calcined at 400 °C.

3 Results and discussion

The catalytic activity of the samples is strongly dependent of the preparation method. Furthermore, the selectivity toward isomers is mainly function of the tungsten amounts added to the clay during mixed intercalation (Fig. 1). In fact, the highest selectivity observed for tungsten-titanium-pillared clay (WTi-PILC) is directly related to the content of tungsten retained by the clay and essentially to the homogeneous pillars distribution. In all cases, products distributions revealed that mono-branched isomers form the major proportion of products while di-branched isomers were the minor products.

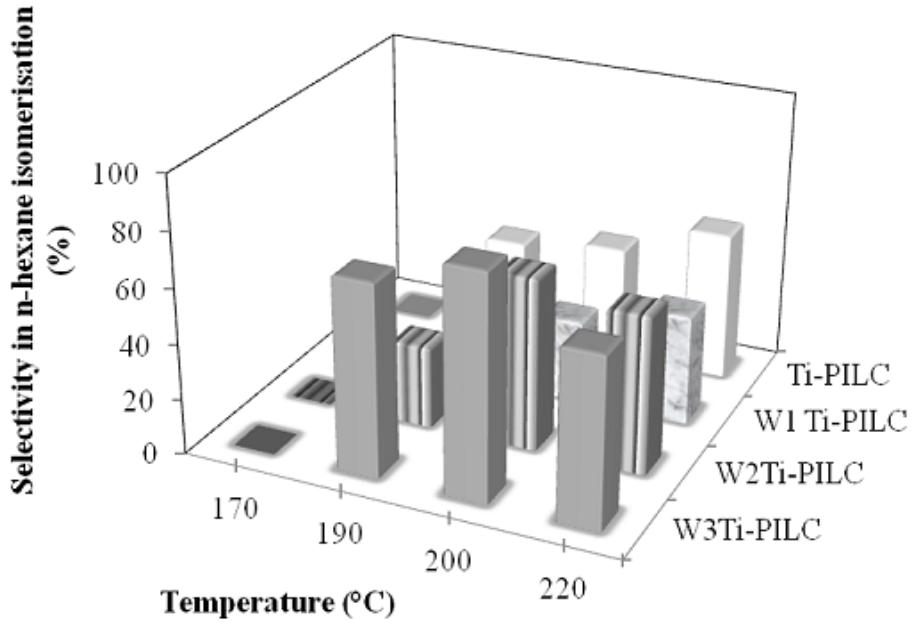

Fig. 1 : Selectivity towards isomers products at different temperature reaction.

4 Conclusions

The structural, textural and catalytic properties of tungsten-titanium pillared clay are largely influenced by the preparation method and the tungsten amounts added to the clay during intercalation process. The use of two methods induced dissimilar textural, structural and catalytic properties of the samples. Enhanced porosity by pillaring allows selective catalysis in the n-hexane isomerisation.

References

[1] L. M. Gil, Gandia, Catal. Rev-Sci. Eng. 42(1&2) (2000) 145-212.
[2] G. Centi, S. Perathoner, Microp. Mesop. Mater. 107 (2008) 3-15.
[3] L. Khalfallah Boudali, A. Ghorbel, P. Grange, Catal. Lett, 86/4 (2003) 251.
[4] L. Khalfallah Boudali, A. Ghorbel, P. Grange, F. Figueras, *Appl. Catal. B* 59 (2005) 105.
[5] J. Arfaoui, L. Khalfallah Boudali, A. Ghorbel, G. Delahay, Catal. Today 142 (2009) 234.

II-PP180

Vanadium Supported on [WTi]-Pillared Clay: Catalytic Application in the Selective Catalytic Reduction of NO by NH_3

Ferjani W.[1*], Khalfallah Boudali L.[1], Delahay G.[2], Petitto C.[2]

1 - Laboratoire de Chimie des Matériaux et Catalyse, Département de Chimie, Faculté des Sciences de Tunis, Tunis, Tunisie

2 - Institut Charles Gerhardt Montpellier, UMR 5253, CNRS-UM2-ENSCM-UM1, Equipe MACS, Ecole Nationale Supérieure de Chimie, Montpellier Cedex 5, France

* ferjani_wiem@hotmail.fr

Keywords: vanadium, tungsten, titanium, pillared clay, SCR-NO

1 Introduction

The removal of nitrogen oxide from outgases is one of the most challenging problems of these days. So far the only process of NO removal from stationary sources used on industrial scale has been selective catalytic reduction (SCR) with ammonia. Therefore, a great deal of effort has been made for the development of new catalysts and several researchers have published reviews that cover the various range of SCR-NO by ammonia [1, 2]. The most frequently used catalyst is V_2O_5 and WO_3 or MoO_3 supported on TiO_2 [1]. However, the use of TiO_2 as support is limited by the fact that it possesses low specific surface area and porosity, only Lewis acid sites and low resistance to sintering compared to Titanium pillared clay (Ti-PILC), characterized by large surface area, high porosity, good thermal stability, a sufficient amount of Bonsted with Lewis acid sites. Recently, considerable effort has been made to investigate layered clays and their SCR behaviour [3]. In our previous work, we have compared Ti-PILC and sulphated Ti-PILC either unpromoted or promoted with V_2O_5 [4-6]. We have also demonstrated that the promoting effect of tungsten in the presence of sulphate was not found [7]. For this reason, it has been interesting to investigate SCR-NO by ammonia over vanadium supported on WTi-PILC prepared in absence of sulfate. To the best of our knowledge, this is the first report of vanadia supported on WTi-PILC prepared with different amounts of tungsten and vanadium then tested in the SCR-NO by ammonia.

2 Experimental/methodology

The tungsten solution, prepared by dissolving ammonium metatungstate $(NH_4)_6H_2W_{12}O_{40}$ in distilled water (10^{-2} M), was simultaneously added with the intercalated Ti-solution to the clay suspension under vigorous stirring. After 24h, the solid fraction was separated by centrifugation and dried at room temperature. Vanadium supported on mixed WTi-pillared clay were prepared by incipient wetness impregnation of the support with a solution of ammonia vanadate NH_4VO_3 (0.1M) dissolved in water acidified by oxalic acid. All the samples were dried at 80°C.

3 Results and discussion

Textural, structural and catalytic properties of WTi-PILC supports are largely influenced by the tungsten content incorporated in the clay and essentially by the amount of vanadium added to the support. The SCR activities of the investigated supports doped with 2% of vanadium are shown in Fig. 1. The V/WTi-PILC catalyst that exhibits better activity between 200°C and 400°C is the sample having homogeneous distribution of pillars, good porosity and an adequate total acidity.

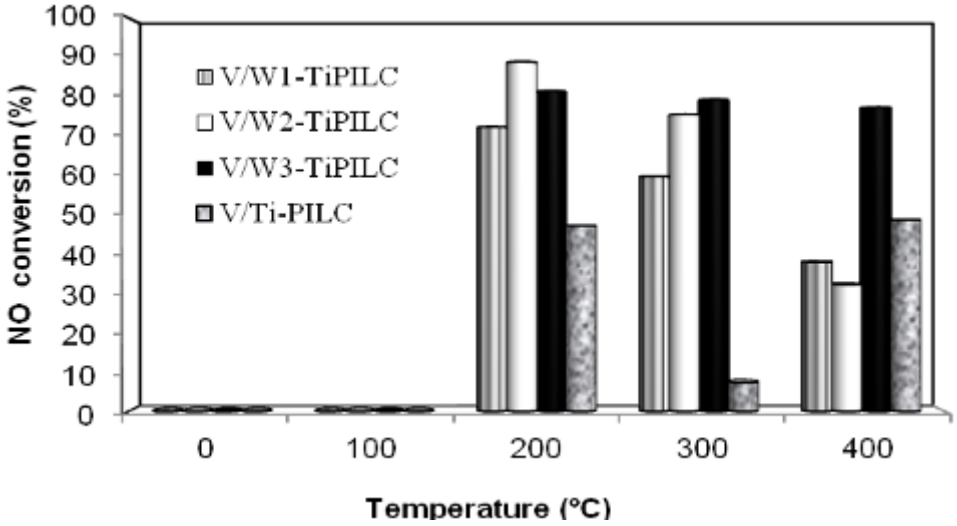

Fig.1: NO conversion for SCR-reaction.

4 Conclusion

The efficiency of vanadium supported on mixed WTi-PILC catalyst is related to essentially the homogenous pillar distribution in the support. Based on the results, it can be concluded that the incorporation of an appropriate amount of tungsten on Ti-PILC is a key factor for obtaining a good support of vanadium to catalyze the SCR-NO reaction by ammonia.

References

[1] G. Busca, L. Lietti, G. Ramis, F. Berti, Appl. Catal. B 18 (1998) 1.
[2] P. Grange, V.I. Parvulescu, Chem. Rev. 111 (2011) 3155.
[3] T. Grzybek, Catal. Today. 119 (2007)125-132.
[4] L. Khalfallah Boudali, A. Ghorbel, P. Grange, Catal. Lett, 86/4 (2003) 251.
[5] L. Khalfallah Boudali, A. Ghorbel, P. Grange, F. Figueras , *Appl. Catal. B* 59 (2005) 105.
[6] J. Arfaoui , L. Khalfallah Boudali, A. Ghorbel, G. Delahay, *Catal. Today* 142 (2009) 234.
[7] L. Khalfallah Boudali , A. Ghorbel, P. Grange, Compt. Rend. Chim., 12 (2009) 779-786.

II-PP181

Isomerization of Light Hydrocarbons over the ZSM-5 Zeolites

Velichkina L.*, Kanashevich D., Vosmerikov A. , Fedushchak T.[1]

Institute of Petroleum Chemistry, Siberian Branch of the Russian Academy of Sciences, Tomsk, Russia

* mps@ipc.tsc.ru

Keywords: ZSM-5, modification, n-alkanes, gasoline, isomerisation, coke

1 Introduction

According to the current literature, isomerization of light hydrocarbon raw materials follows two main routes: over the chlorinated [1] or sulphated [2] oxide catalysts, both having numerous disadvantages. On the other hand, it is much more reasonable to use zeolites that allow to converting n-alkanes under extraordinary conditions, i.e., without feeding the hydrogenous gas to the reaction medium at atmospheric pressure and without any use of noble metals and superacid additives, which would favor cost reduction of the final product [3-5].

The aim of this work is to investigate the catalytic activity and stability of the pentasil zeolite with the silica modulus 40 and its nickel-containing analog in the course of a hydrogen-free isomerization of C_5-C_8 n-alkanes and straight-run gasoline oil fraction.

2 Experimental/methodology

The high-silica ZSM-5 zeolite with SiO_2/Al_2O_3 molar ratio of 40 was manufactured by hydrothermal synthesis. Modification of ZSM-5 with a nanosized nickel powder obtained by the gas-phase method in the amount of 0.5% by weight of the nickel oxide was carried out by dry mixing in a vibrating mill for 2 hours, followed by compressing the resulted mixture into pellets, refinement of 0.5-1.0 mm fraction and its sampling. The average particle size of nickel nanopowder was 50 nm.

The catalytic activity of the initial and the Ni-containing zeolite was studied in the conversion reactions of normal pentane, hexane, heptane and octane, an artificial mixture of n-pentane: n-hexane = 1: 2, and straight-run gasoline fraction (low-boiling fraction boiling out at a temperature of 90 °C). The tests of catalytic activity of zeolites were carried out in a flow installation at the reaction temperatures of 280-360 °C, volumetric feed rate of 2 h^{-1} and atmospheric pressure. The dynamics of deactivation of zeolite catalysts was investigated in the course of conversion of the hydrocarbon raw materials under study during 16 hours of their continuous operation at 320 °C and 2 h^{-1}. The amount and nature of the coke deposits were determined by differential thermal analysis. The composition of the initial feedstock and its conversion products were analyzed by gas chromatography.

3 Results and discussion

The gaseous products of conversion of all types of the hydrocarbon raw materials under study over zeolite catalysts are mainly presented by C_1-C_4 alkanes, whose largest fraction are propane, n- and isobutanes. As the process temperature increases from 280 to 360 °C, the conversion of the initial feedstock also increases, thus resulting in a higher intensity cracking reaction and gives rise to an increased yield in the gaseous products, whose hydrocarbon composition varies slightly.

The major liquid products of isomerization over zeolite catalysts under study are n- and isoalkanes, C_4-C_8 alkylbenzenes, and a minor amount of olefins and naphthenes. An increase in the process temperature from 280 to 320 °C results in the increased total yield of hydrocarbons with isometric structure, while further increase in temperature to 360 °C – in the reducing of

their concentration. The dependence of the individual isoalkane yield on the process temperature is identical to that of the total yield – the maximum amount of C_4, C_6, C_7 and C_8 isoalkanes is also formed at a temperature of 320 °C and that of C_5 isoalkanes only at 340 °C. The fraction of hydrocarbons with isometric structure having number of carbon atoms 9 and 12 in a catalyzate increases with a rise in process temperature.

The content of gaseous alkenes increases over the entire temperature range in the course of zeolite modification with a nickel nanopowder. Their maximum is reached at 300 °C, while the yield in C_1-C_4 alkanes, n- and C_{5+}iso-alkanes is slightly decreased. It is important to note that the yield of catalyzates with a prevailing content of isometric hydrocarbons significantly increases during the conversion over Ni-ZSM-5 zeolites.

Noteworthy is also the relationship between the type of hydrocarbon raw materials and the yield in catalyzate resulting from its processing over the zeolite catalyst: the lighter are the hydrocarbon raw materials, the lower is the yield of liquid product but it is typical only for the use of individual hydrocarbons. In the case of use of pentane-hexane mixture the yield of liquid product increases considerably compared with the individual hydrocarbons.

The highest selectivity towards a formation of isoalkanes for 16 hour's reaction is observed for the Ni-ZSM-5 sample and it remains practically unchanged during the whole period of operation of the catalyst.

The maximum amount of carbon deposits with a dense structure is formed during the conversion of n-octane, while the minimum amount – n-pentane, which is due to the greater thermodynamic stability of alkanes with lower molecular weight.

The nickel-containing zeolite catalyst exhibits a higher stability during conversion of various hydrocarbons and their mixtures as compared to the initial sample, which is due to the presence of nickel-containing active centers in this catalyst system. Their involvement into the hydrogenation-dehydrogenation reactions results in a decreased rate of formation of condensed molecules being coke precursors. The catalyst deactivation is thus slower compared to the initial zeolite.

4 Conclusions

The use of different types of hydrocarbons in the course of isomerization of unmodified and nickel-containing ZSM-5 zeolites allowed to reveal the main trends in the distribution of the reaction products and to determine the optimal reaction conditions for the formation of the maximum amount of iso-alkanes and the minimum amount of coke.

References

[1] T.V. Vasina, L.V. Kustov, I.A. Novakov, B.S. Orlinson, *Russian Journal of Physical Chemistry.* 87 (1) (2013) 24

[2] M.D. Smolikov, L.I. Bikmetova, D.I. Kiryanov, et al. *Catalysis in Industry*. 5 (2014) 44

[3] L.M. Velichkina, D.A. Kanashevich, L.N. Vosmerikova, A.V. Vosmerikov, *Chemistry for Sustainable Development.* 22 (3) (2014) 241

[4] A.F. Gisetdinova, T.P. Kiseleva, O.M. Posokhova, et al. *Catalysis in Industry.* 5 (2014) 38

[5] M.D. Smolikov, V.A. Shkuryonok, S.S. Yablokova, et al. *Catalysis in Industry.* 2 (2014) 51

II-PP182

A GGA+U DFT Investigation of Silver Atom, Trimer and Tetramer Supported by a Nanosized Particle $Ce_{21}O_{42}$

Nasluzov V.A.[1*], Laletina S.S.[1], Ivanova-Shor E.A.[1], Shor A.M.[1], Neyman K.M.[2,3]

1 - Institute of Chemistry and Chemical Technology SB RAS, Krasnoyarsk, Russia
2 - Institucio Catalana de Recerca i Estudis Avancats (ICREA), Barcelona, Spain
3 - Departament de Quimica Fisica & IQTCUB, Universitat de Barcelona, Barcelona, Spain

* shor-elena@rambler.ru

Keywords: density, functional theory, nanostructured, ceria, silver, cluster, oxygen, adsorption

1 Introduction

Ceria supported transition metals (TM) are known for activity in catalytic oxidation reactions. In this relation active sites on surface of nanosized cerium oxide particles are of particular interest. To characterize such structural features we considered localization of monomer, trimer and tetramer silver species on a $Ce_{21}O_{42}$ cluster (Fig. 1, [1]). Effect of support on these TM species is quantified via adsorption of O_2 probe molecule. All calculations are done using PW91+4 pseudopotential density functional approximation [1].

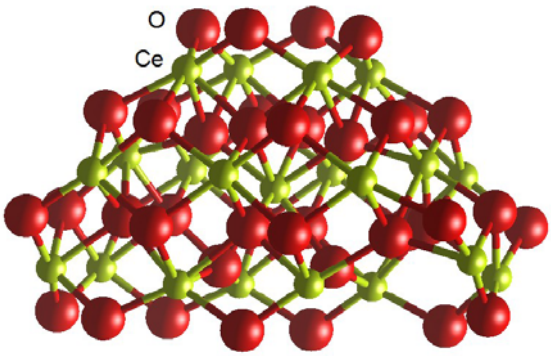

Fig. 1. Nanosized particle $Ce_{21}O_{42}$

2 Results and discussion

Surface of the $Ce_{21}O_{42}$ particle exposes small (111) and (100) facets as well as edge sites at their intersections. There are three- and two-coordinated oxygen atoms, O^{3c} and O^{2c} centers, and six- and five-coordinated cerium atoms, Ce^{6c} and Ce^{5c} centers. On interaction with ceria surface Ag_n moieties are oxidized. Each Ag and Ag_3 adsorbates donate to the substrate particle one electron. Ag_4 clusters in rhombus and tetrahedron configurations donate one and two electrons, respectively. Each donated electron is localized on just one cerium center, reducing it from Ce(IV) to Ce(III). Such centers are recognized via their magnetization of generally ≥0.7 μB and via increment of involved average Ce-O bond lengths by ~10 pm. Somewhat more stable structures are formed when donated electrons are localized on Ce^{6c} atoms.

Most stable $Ag_n/Ce_{21}O_{42}$ complexes are formed for adsorption on (100) facets, via interaction with O^{2c} atoms. The binding (adsorption) energies of Ag, Ag_3 and Ag_4 are calculated to 2.2, 2.9 and 3.0 eV, respectively. Silver atom in the most stable isomer of $Ag/Ce_{21}O_{42}$ system is in a hole position and interacts with four O^{2c} atoms (the so-called O_4-pocket [2]). Silver trimer in the $Ag_3/Ce_{21}O_{42}$ complex is in upright position. An $Ag_3/Ce_{21}O_{42}$ isomer with parallel to (100) facet orientation is ~0.5 eV less stable. The most stable $Ag_4/Ce_{21}O_{42}$ complex features tetrahedral structure of silver tetramer. The isomer with parallel to (100) facet silver rhombus is ~0.7 eV less stable. Still less stable is isomer with upright orientation of silver rhombus.

Ag_n adsorption on the (111) facets results in less stable complexes with binding energies of ~1.2 eV for $Ag/Ce_{21}O_{42}$, 1.7–2.5 eV for $Ag_3/Ce_{21}O_{42}$ and 1.6–2.0 eV for $Ag_4/Ce_{21}O_{42}$. In the $Ag/Ce_{21}O_{42}$ complex silver atom is localized in a hollow position between one O^{2c} and two O^{3c} atoms. In the most stable $Ag_3/Ce_{21}O_{42}$ complex on (111) facet, silver trimer is in upright position with O^{2c} and O^{3c} atoms bound to two silver atoms in the base of the Ag_3 triangle. $Ag_3/Ce_{21}O_{42}$ complexes with parallel to (111) surface Ag_3 plane are 0.3–0.4 eV less stable. Binding energies for $Ag_3/Ce_{21}O_{42}$ complexes with upright silver trimers bound to two O^{3c} atoms are calculated to 1.7–1.9 eV. Binding energies for complexes with Ag_4 located on (111) facet are calculated to be 2.0 and 1.6 eV with tetrahedral and rhombus silver tetramers, respectively.

Binding of O_2 molecule on the discussed above supported silver species are strongly dependent on the nature of supporting surface site. O_2 binding energies to silver atoms supported on (100) facets are small, 0.2–0.3 eV. In contrast, binding to silver atoms localized at (111) facets is rather strong, 0.7 eV for terminal adsorption mode and 1.3–1.4 eV for bridging adsorption mode. Molecular and dissociative O_2 adsorption on silver trimer supported at the (100) facet are calculated to be 0.2 and 0.4 eV, respectively. Binding energies for molecular and dissociative adsorption on silver trimer supported on (111) facets are slightly larger: 0.6 and 0.7 eV, correspondingly. O_2 binding energies for molecular adsorption on silver tetramers supported on (100) facets are 0.4–0.6 eV. Molecular adsorption on tetrahedral isomer of silver tetramer supported on (111) facets is again 0.5 eV more profitable than for such isomer on (100) facets.

For Ag_4 complexes on (100) facets O_2 binding energy for dissociative adsorption is in a range 1.2–1.5 eV. So, binding energy for molecular and dissociative adsorption on $Ag_4/Ce_{21}O_{42}$ is much more different than for $Ag_3/Ce_{21}O_{42}$ complexes.

Results for molecular silver clusters on $Ce_{21}O_{42}$ are compared with those calculated for similar clusters on MgO [3,4] and SiO_2 surfaces [5,6].

Acknowledgements

This work was supported by the Presidium of the Russian Academy of Sciences. The use of the computational resources of HPC Research Department of the Siberian Federal University (Krasnoyarsk, Russia) is gratefully acknowledged.

References

[1] A. Migani, G.N. Vayssilov, S.T. Bromley, F. Illas, K.M. Neyman. *Chem. Commun*. 46 (2010) 5936.
[2] A. Bruix, Y. Lykhach, I. Matolínová, A. Neitzel, T. Skála, N. Tsud, M. Vorokhta, V. Stetsovych, K. Ševčíková, J. Mysliveček, R. Fiala, M. Václavů, K.C. Prince, S. Bruyère, V. Potin, F. Illas, V. Matolín, J. Libuda, K.M. Neyman, *Angew. Chem. Int. Ed*. 53 (2014) 10525.
[3] C. Inntam, L.V. Moskaleva, K.M. Neyman, V.A. Nasluzov, N. Rösch, Appl. Phys. A 82 (2006) 181.
[4] C. Inntam, L.V. Moskaleva, I.V. Yudanov, K.M. Neyman, N. Rösch, Chemical Physics Letters 417 (2006) 515.
[5] A.M. Shor, E.A. Ivanova-Shor, S.S. Laletina, V.A. Nasluzov, N. Rösch, Surf. Sci. 604 (2010) 1705.
[6] A. M. Shor, S. S. Laletina, E. A. Ivanova Shor, V. A. Nasluzov, V. I. Bukhtiyarov, N. Rösch, Surf. Sci. 630 (2014) 265.

II-PP183

Quantum-Chemical Investigation Ligand-Stabilized Gold Clusters in Oxidation Reaction

Golosnaya M., Pichugina D., Kuz'menko N.*

M.V. Lomonosov Moscow State University, Moscow, Russia

* mashagolosnaya@gmail.com

Keywords: gold catalysis, gold-protected nanoclusters, phosphine, ligands

1 Introduction

Gold (Au) nanoparticles have been found to be capable of catalyzing a variety of reactions, such as selective oxidation and hydrogenation [1]. The main problem in the preparation of metals NP is that they are unstable in solution and tend to agglomerate to form larger aggregates. For stable NPs to provide there must use stabilizing agents, namely organic ligands, which are adsorbed on the particle surface, prevent their association.Ligand-protected gold nanoclusters have been widely studied due to their interesting optical, electronic, and charging properties, as well as potential applications in catalysis, biomedicine, and nanoelectronics[2].

Studying and revealing the well-defined atom packing structures of metal nanoclusters is of critical importance for understanding the quantum size and shape effects in nanoclusters. The synthesis of metal clusters with phosphine ligands has been extensively researched since the 1960s [3]. However, the structures, which was provided, were difficult to identify. In the past decades, because of the development of computational techniques, the number of synthesized and successfully identified nanoclusters is significantly increased. Over the past few years, a number of thiolate-protected gold nanoclusters gold atoms have been reported. However, with respect to phosphine-protected gold nanoclusters, much fewer have been attained [4]. We have analyzed the structural stability and electronic properties of the recently reported structurally known tetranucleargold cluster with phosphine ligands - $Au_4[P(CH_3)_2PCH_3(CH_2)_2P(CH_3)_2]_2^q$(q=+2, -2, 0), by using density functional theory. The cluster has synthesized and defined recently by NMR spectroscopy and X-ray spectroscopy [5]. It was shown, that the cluster exhibit size-specific physical and chemical properties, including photoluminescence, which are not observed in bulk metals.

Despite significant progress in the area catalytic properties of clusters, mechanism of formation as well as the phosphine ligands influence on the catalytic properties of have not been fully understood. Therefore, the main goal of this study is quantum-chemical study catalytic properties of gold-based catalysts, namely ligand-stabilized, in oxidation reactions.

2 Methodology

Geometry optimizations was performed within the spin-polarized approach (PBE functional) [6]. The Priroda program [7]was used for the all-electron calculations within the scalar-relativistic approach, which was based on the full four-component one-electron Dirac equation with separation of the spin-orbit effects.

2 Results and discussion

In present work we investigated the structure and electronic properties of cluster $Au_4[P(CH_3)_2PCH_3(CH_2)_2P(CH_3)_2]_2^q$(q=+2, -2, 0) as well as the catalytic activity of this cluster toward molecular oxygen adsorption.The high value of the HOMO-LUMO gap energy is typical for the cationic cluster. The charge strongly influences on the structure of the cluster. Gold atoms in the cationic cluster formed an elongated rhombus. The neutral model is

characterized by distortion of the structure. In addition, we observed breaking of Au-Au bonds in the anionic structure(fig. 1). The structure of the cationic cluster is in good agreement with X-ray data [1]. The modelling of oxygen adsorption on $Au_4[P(CH_3)_2PCH_3(CH_2)_2P(CH_3)_2]_2^q$ have indicated that molecular type of oxygen adsorption is most favourable in the cluster.

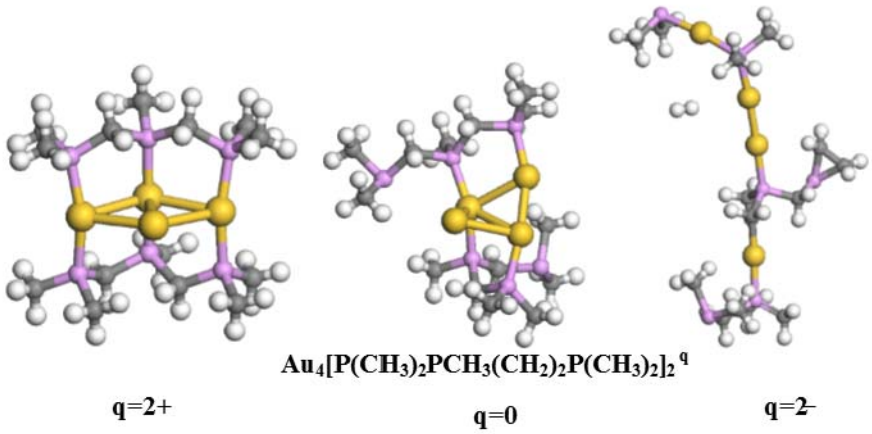

Fig. 1. The structure of $Au_4[P(CH_3)_2PCH_3(CH_2)_2P(CH_3)_2]_2^q$cluster (color labels: violet = P; yellow = Au; white = P; grey = C).

3 Conclusions

In summary, we have analysed the structural stability and electronic properties of a newly crystallized cluster $Au_4[P(CH_3)_2PCH_3(CH_2)_2P(CH_3)_2]_2^q$ by using DFT. The study of the cluster has provided much important information concerning the stability, structure and physical properties of phosphine protected metal clusters with ultra-small metal cores.

Acknowledgements

This research was supported by the Russian Federation Foundation for Fundamental Research through the Project 13-03-00320, 14-01-00310, and 11-01-00280, and by the Council for Grants of the Russian Federation President Project MK-92-2013-3 and NSh-3171.2014.3. The reported study was supported by the Supercomputing Centre of M.V. Lomonosov Moscow State University [8].

References

[1] M. Haruta,M. Date, Appl. Catal. A. 222 (2001) 427.
[2] R. Sardar,A.M. Funston,P. Mulvaney, R. W. Murray, *Langmuir.* 25(2009) 13890
[3] M. McPartlin, R. Mason, L.Malatesta, J. *Chem. Soc. D.*7(1969) 334.
[4] A. Das,T. Li,K. Nobusada, Q. Zeng,N. L. Rosi, R. Jin, *J. Am. Chem. Soc.* 134(2012) 20286.
[5] T. M. Dau, Y.-A. Chen, A. J. Karttunen, E. V. Grachova,S. P. Tunik, K.-T. Lin, W.-Y. Hung,P.-T. Chou, T.A. Pakkanen, I. O. Koshevoy, *Inorg. Chem*. 53(2014) 12720
[6] J. P. Perdew, K. Burke, M. Ernzerhof, *Phys. Rev. Lett.*77(1996) 3865.
[7] D.N. Laikov, Yu. A. Ustynyuk, *Russ. Chem. Bull. Int. Ed.* 54 (2005) 820.
[8] V. Sadovnichy, A.Tikhonravov, Vl. Voevodin, V. Opanasenko, Chapman & Hall/CRC Computational Science; Boca Raton, USA, CRC Press (2013) 283.

II-PP184

Preparation Approach to the Control of Rhodium Dispersion for TiO_2 and Al_2O_3 Supported Catalysts

Kovtunova L.M.[1,2*], Khudorozhkov A.K.[1], Prosvirin I.P.[1], Bukhtiyarov V.I.[1]

1 - Boreskov Institute of Catalysis SB RAS, Novosibirsk, Russia
2 - Novosibirsk State University, Novosibirsk, Russia

* kovtunova@catalysis.ru

Keywords: rhodium, supported catalysts preparation, size control, nanoparticles

1 Introduction

Nowadays catalysts play a major role in modern industrial and economic structures. Noted, that more than 80% of the petrochemical products and chemicals produced by industry with heterogeneous catalysis and therefore with supported catalysts. The main advantage of using heterogeneous catalysts is that they can be removed easily from the reaction products. Furthermore, high thermal stabilities and high activities of supported nanoparticles allow to utilized them in many industrial processes. It is well known that supported catalysts may be successfully used not only in heavy industrial chemistry like synthesis of NH_3 or petrochemistry but also in fine chemistry for asymmetric hydrogenation for instance. The heterogeneous catalyst preparation methods include co-crystallization, ion-exchange or impregnation result in formation of metal particles dispersed on an oxide support such as Al_2O_3, SiO_2 or TiO_2. Subsequent oxidation and/or reduction steps can cause aggregation of the supported metal nanoparticles, resulting in changes in particle size and thus in size-dependent properties such as activity and selectivity.

Nowadays rhodium typically used for the production of automotive catalysts. Careful attention should therefore be paid during catalyst preparation to produce highly efficient catalysts with low metal loading, high metal dispersion and a long lifetime without deactivation. Different impregnation methods are available for catalyst preparation such as wet, incipient-wetness and dry impregnation or impregnation with interactions (e.g. ion exchange and adsorption methods). . Generally for the preparation of metal supported catalysts the final metal loading and the metal dispersion depends on the preparation technique used and on the final treatments to bring the catalyst in the active form [1, 2].

2 Experimental/methodology

The commercially available $RhCl_3*3H_2O$ was used as the start material for rhodium catalyst preparation. The catalysts were prepared via wet impregnation of Al_2O_3 or TiO_2 support with rhodium nitrate or acetic aqueous solutions.

Rhodium hydroxide was prepared by precipitation of $RhCl_3$ with sodium hydroxide. Rhodium precursors were obtained by dissolution of rhodium hydroxide in HNO_3 or HOAc. As a result, rhodium nitrate (III) solutions with varying relative concentrations of nitric acid and Rh were prepared. Next, both rhodium nitrate solution and rhodium acetic solution were used for the supported rhodium catalysts preparation.

To determine the influence of temperature pretreatment on the active component dispersion level, and therefore particle size distribution, the reduction of catalysts by hydrogen at 300 °C for 3 hours was performed after calcinations at different temperatures (400 °C for 4 hours, 600 °C for 2 hours).

3 Results and discussion

The procedure of supported rhodium catalysts (Rh/TiO_2 and Rh/Al_2O_3) preparation by using rhodium nitrate and acetate precursors was shown. It was found that the sizes of rhodium nanoparticles are strongly dependent from the preparation procedure and it allows to receive supported rhodium nanoparticles with particles size from 1 to 10 nanometers, that was examined by CO-chemisorption, TEM and XPS methods. It was found that the major mechanism for control of dispersion degree of the active component is the nature of the rhodium complexes (precursors). It was shown that the utilization of nitrite-nitrate complexes of rhodium leads to formation of highly dispersed rhodium (1-5 nm) nanoparticles, whereas usage of rhodium acetic complexes causes formation of relatively big metal particles up to 5-10 nm. The support pre-treatment is also highly important. It was shown, that modification of the TiO_2 or Al_2O_3 with HOAc solution leads to enlargement of Rh particle size for Rh/TiO_2 and Rh/Al_2O_3 supported catalyst.

It was shown that rhodium supported catalysts with different particle sizes are very active in heterogeneous hydrogenation of propylene to propane. Based on previously reported results demonstrating that metals supported on titanium oxide (TiO_2) generally exhibit higher levels of parahydrogen-induced polarization effects compared to other oxide supports, a number of metal catalysts supported on TiO_2 were tested in heterogeneous gas phase hydrogenation of propene with parahydrogen. All Rh/TiO_2 catalysts studied were very active in heterogeneous hydrogenation of propene to propane and, importantly, produced strongly polarized as detected by high-resolution NMR spectroscopy. The maximum signal at 9.4 T was observed with 1.6 nm particles. This catalyst yielded polarized propane with significant signal enhancement compared to the thermally polarized propane. Therefore, this catalyst was selected for further MRI studies [3].

4 Conclusions

Preparation methods for size selective synthesis of supported rhodium nanoparticles were developed. It was shown that the nature of rhodium precursors, calcination temperature and support modification may significantly effect on the sizes of rhodium nanoparticles. All supported rhodium catalysts are very active in heterogeneous hydrogenation of unsaturated gaseous compounds and lead to formation of strong polarization when parahydrogen was used.

Acknowledgements

This work was financially supported by the Russian Science Foundation (Project No. 14-23-00146).

References

[1] Se H. Oh, Carolyn C. Eickel, *Journal of Catalysis.* 128 (2) (1991) P.526
[2] Z.L. Zhang, V.A. Tsipouriari, A.M. Efstathiou, X.E. Verykios, *Journal of Catalysis.* 158 (1) (1996) P.51
[3] K. Kovtunov, D. Barskiy, A. Coffey, M. Truong, O. Salnikov, A. Khudorozhkov, E. Inozemtseva, I. Prosvirin, V. Bukhtiyarov, K. Waddell, E. Chekmenev, I. Koptyug, *Chem. Eur. J.* 20 (2014) 11636.

II-PP185

The Nature of Carbon Supports Action on the Palladium Electronic State and Catalytic Properties

Kochubey D.I.[1*], Smirnova N.S.[2], Temerev V.L.[2], Iost K.N.[2], Tsyrul'nikov P.G.[2], Radkevich V.Z.[3], Khaminets S.G.[3], Samoilenko O.A.[3], Kriventsov V.V.[1]

1 - Boreskov Institute of catalysis SB RAS, Novosibirsk, Russia
2 - Institute of Hydrocarbons Processing SB RAS, Omsk, Russia. Lavrentieva
3 - Institute of Physical Organic Chemistry NAS of Belarus, Minsk, Belarus

* radkevich_vz@ifoch.bas-net.by

Keywords: carbon supports, electronic state of palladium, XANES, CO oxidation

1 Introduction

Carbon supports may have great differences in the structure and electrophysical properties. It is known that carbon materials are narrow band semiconductors, so the effect of strong metal-support interaction may be observed on them. Previously this effect was actively studied for the metals supported on the transition metal oxides. Often strong interaction metal-metal oxide leads to the metal nanoparticles decoration with metal suboxides. This decoration may lead to almost total encapsulation of active compound nanoparticles and decrease of their catalytic activity. But for the suboxides with electro conductivity exchange of the electrons between metal and support becomes possible which could lead to increase of catalytic activity. This effect was observed for rhodium catalyst on titanium suboxide [1]. For the carbon supports that effect takes place even without decoration. Moreover, modification of the electron configuration for Pt catalysts on carbon support, due to transition of part *d* electrons into *p* or *s* states was observed [2].

2 Experimental

The influence of the carbon supports, including graphite-bearing material (sibunit) and carbon-base fibers (busofit, karbopon), on the electronic state of palladium and catalytic activity Pd/C systems were studied in this work. 1%Pd/busofit and 1%Pd/karbopon catalysts were prepared by means of the ion exchange method from H_2PdCl_4. The 1%Pd/sibunit catalysts were prepared via impregnation method. Prepared catalysts are dried in He for 1 h. and reduced in H_2 at 300^{o}C 2h.

3 Results and discussion

The NIR-VIS spectra (fig.1) were measured for supports. Forbidden band width was calculated from spectra derivative using Tauc theory [3]:

$$d[\ln(D(h\nu)*h\nu)]/d(h\nu)=k/(h\nu - Eg)$$

(D - optic density; hν - optical photons energy; Eg - forbidden band width).

The maximums at 0.8 and 1.0 eV are needed additional analysis. Spectra analysis has shown two forbidden bands with width of 1.3 and 2.0 eV for busofit, one forbidden band with 1.2 eV for carbopon, sibunit don't have forbidden bands with width more than 1 eV (fig. 1a).

According to HREM data the average Pd particle size for all catalysts is 1.7 nm. Radial distributions of atoms (RDA) around Pd have Pd-Pd distance for metal and Pd-C distance from carbon atoms of support was observed. The coordination numbers for first Pd-Pd distance in metal determined from EXAFS data are too low. The structure distortion due to support action may be reason of that.

Catalytic activities for 1%Pd/sibunit, 1%Pd/busofit and 1%Pd/karbopon were determined in the CO oxidation reaction (dry reaction mixture (0,3 vol.% CO in air), 5,5 mg of Pd in catalyst

loading, 3300 h^{-1}). Experiments results have shown increase of catalytic activity with the increase of forbidden band width (fig.1).

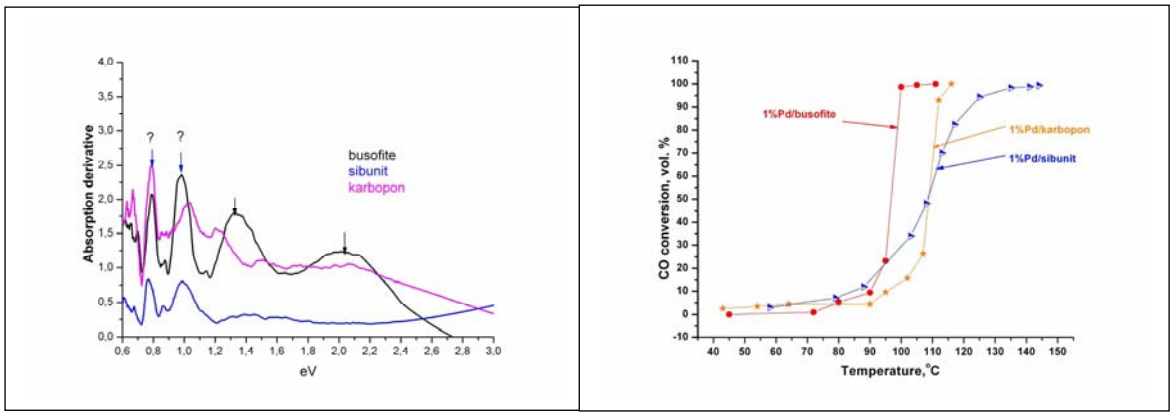

Fig. 1. a) The width of forbidden bands for carbon supports b) Catalysts activity in CO oxidation reaction

Additional information was obtained from XANES spectra. The shift of the spectrum edge in the region of greater energy indicate the increase of electron deficiency on the metal nanoparticles. Catalytic activity of the samples with greater electron deficiency is higher was determined (Table 1).

Table 1. Edge position for Pd catalysts

Catalysts	1%Pd/ busofit	1% Pd/ karbopon	1%Pd/sibunit
E, keV	24.3938	24.3914	24.3926

4 Conclusions

The correlation of the Pd catalysts activity in CO oxidation reaction and forbidden band width of the carbon supports was determined. Catalytic activity also correlated with electron deficiency metal Pd nanoparticles. Nanoparticles with greater electron deficiency are more active.

Acknowledgements

This work was supported by the Russian Foundation for Basic Research, project № 14-03-90032-Bel_a, RFBR(140301066) and the Belarusian Republican Foundation for Fundamental Research Grant No X14P-090.

References

[1] O.V. Netskina, D. I. Kochubey, I. P. Prosvirin, D. G. Kellerman, V.I. Simagina, O. V. Komova, *J. Mol. Cat. A: Chem.,* 390 (2014) 125.

[2] S.G. Khaminets, L. L.Potapova, B. Z.Radkevich, D. I. Kochubei, Yu. G. Egiazarov, *Russian J. of Phys. Chem. A,* 84 (2010) 561.

[3] P. V. Morozov, E. I. Grigor'ev, S. A. Zav'yalov, V. G. Klimenko, A. A. Nesmelov, A. Y. Vdovichenko, S. N. Chvalun, *Tech. Phys. Russian J. Appl. Phys*. 58 (2013) 408.

II-PP186

Mössbauer Spectroscopy Investigation of Iron-Cerium Oxide Systems as Catalyst in the Reaction of the Methylbutene Dehydrogenation

Bochkov M.A.[1*], Kharlampidi Kh.E.[1], Akhmerov O.I[1], Pyataev A.V.[2]

1 - Kazan National Research Technological University, Kazan, Russia
2 - Kazan Federal University, Kazan, Russia

* m.a.bochkov@gmail.com

Keywords: iron oxide, cerium, Mössbauer spectroscopy, dehydrogenation

1 Introduction

Investigations of dehydrogenation catalysts are carried out for a long time. However a question about a nature of catalyst active component is still discussed. Also, there is no consensus on the phase and chemical transformations in the system of iron – oxygen that occur during this system synthesis and working.

2 Experimental/methodology

Samples of iron oxide and iron-cerium oxide systems as catalysts for the dehydrogenation reaction of methylbutenes are studied by Mössbauer spectroscopy method. Samples were prepared by initial magnetite (S_A / S_B ~ 1,1) solution impregnation of cerium salt (III), followed by drying, molding and burning in air at 650 ° C. The formed granules of polycrystalline samples were placed in the reactor as a catalyst in the dehydrogenation reaction of methylbutenes. The catalytic activity of the samples in the reaction of isoprene synthesis from isoamylenes was determined on flow microcatalytic laboratory setting under the conditions of catalyst loading amount of 1 cm3, molar feed steam dilution 1:20, at the temperature of 580ºC. Analysis of the reaction products was carried out by chromatography.

3 Results and discussion

Mössbauer transmission spectra of obtained samples were largely similar to spectra of standard model of α-Fe_2O_3 in the parameters of hyperfine interactions. In case of magnetite the yield of isoprene for decomposed hydrocarbons (YD) is 77%. The introduction of cerium into the magnetite composition increases the selectivity of catalyst, i.e. YD to 84%. To elucidate the mechanism of interaction between the catalyst system and the reaction medium, Mössbauer measurements were carried out after the catalyst system staying in the reactor in transmission geometry at room temperature. The spectrum of the oxide system after the reactor is a magnetite like system which is characterized by parameters of hyperfine interactions close to founded in chemically pure Fe_3O_4 samples. The ratio of the partial areas S_A / S_B ~ 1,9.

4 Conclusions

During the catalytic reaction in oxide system conversion from α-Fe_2O_3 to Fe_3O_4 like system occurs which is attended with the changes in A and B positions populations in the spinel structure in the direction of S_A / S_B ratio increasing with respect to the initial magnetite. By Mössbauer spectroscopy method insignificant role of cerium in the formation of magnetic microstructure in initial iron-cerium oxide system and in the system after working in the reactor was revealed. Increasing of the catalyst selectivity is apparently connected with the formation of the respective solid solutions on the surface of the iron oxide polycrystallites. These results

require further investigations of granules thin surface layer composition and its changes during the reaction.

Acknowledgements

This work was supported by the Ministry of Education and Science of the Russian Federation within the base part (AMRL 02.14).

II-PP187

EPR and DFT Study of the Oxygen Radicals Formation on Oxide Surfaces Due to Homolytic Splitting of Water

Malykhin S.E.[1,2*], Bedilo A.F.[1,3], Volodin A.M.[1], Avdeev V.I.[1]

1 - Boreskov Institute of Catalysis, Novosibirsk, Russia
2 - Novosibirsk State University, Novosibirsk, Russia
3 - Novosibirsk Institute of Technology, Moscow State University of Design and Technology, Novosibirsk, Russia

* malykhin@catalysis.ru

Keywords: surface, oxygen, radicals, oxides, EPR, DFT

1 Introduction

Long-distance separation of electron-hole pairs is usually assumed to be the first stage of various thermal and photochemical processes resulting in the formation of ion radicals on the surface of oxides. A common feature of all such processes is the generation of isolated paramagnetic species with S=1/2 stabilized on the surface, which can be detected by EPR [1]. However, long-distance charge separation with participation of the conductivity or valence bands is unlikely for wide band-gap dielectrics, such as MgO with the band gap 7.8 eV. Still, the experiments show that the radicals can be effectively generated under illumination with soft UV light with 4.1 eV (303 nm) photon energy [1, 2]. A viable alternative to the physical charge separation mechanism is a "chemical" mechanism ascribing the generation of the ion radicals to the formation of mobile radical species [2, 3]. Radicals H• and OH• formed from the fragments of chemisorbed water H^+ and OH^-, respectively, are the most likely candidates for such species.

In this communication we shall demonstrate that the chemical and spectroscopic properties of O^- radicals formed as hole and electron sites seem to be exactly same. This is possible only if these species are not charged and are formed due to the homolytic splitting of chemisorbed water molecules. Quantum-chemical simulations supporting this hypothesis will be discussed.

2 Experimental/methodology

ESR experiments were conducted in our high-vacuum EPR "in situ" installation. The standard sample pretreatment included alternating oxygen-vacuum treatments at 500°C in a vacuum line with a trap cooled by liquid nitrogen. ERS-221 spectrometer was used for registration of X-band ESR spectra at variable temperatures. The EPR samples were subjected to the illumination directly in the spectrometer cavity. A monochromator used made it possible to study spectral characteristics of the photoreactions in the energy range of 1 - 5 eV.

The Mg_9O_9 cluster was used as a model of an MgO nanoparticle, see Figure 1, left. The energetics of the processes was estimated using spin-polarized density functional theory (DFT) b3lyp/6-31g(d) in the Gaussian 09 quantum-chemical package. Steps and kinks on the surface of MgO particles are common surface defect sites. For these we adopted MgO (410) facet shown in Figure 1, right. The energetics and optimal structures were obtained by spin-polarized PW91 DFT functional. Plane-wave basis set restricted to kinetic energies below 25 Ry. Core electrons were approximated using ultrasoft pseudopotentials. Periodic structure calculations were carried out using Quantum Espresso 4.3 package.

3 Results and discussion

MgO illumination by UV light in the presence of N_2O was shown to result in the formation of spectroscopically indistinguishable O^- radicals both on electron and hole sites. So the total

concentration of such radicals proved to be higher than after illumination in oxygen when such radicals are formed only on hole sites. Chemical properties of the O^- radicals formed on the electron and hole sites in reactions with O_2, CO and ethylene were found to be the same as well. This is possible only if these species are formed by the transfer of uncharged radical species formed from homolytic splitting of water.

The oxygen radical O^- obtained after UV-illumination and O^- produced due to N_2O decomposition on electron-rich F-centre according to our scheme are almost the same species, see Fig. 1, left. So, it is not surprising that their EPR spectra have no differences at all. According to quantum-chemical simulations, the homolytic water dissociation on the oxide surface has the energetic barrier 2.75-3.39 eV, depending on the nature of radical stabilization sites. Thus, it becomes clear why soft UV illumination with photon energy about 4 eV is sufficient for generation of the radicals. Note that complete water removal is feasible under experimental conditions, for example, by heating the sample up to 1200 K. Molecular oxygen or nitrous oxide are able to stabilize radical sites by shifting the equilibrium towards further production of the oxygen radicals as it is shown by our DFT calculations.

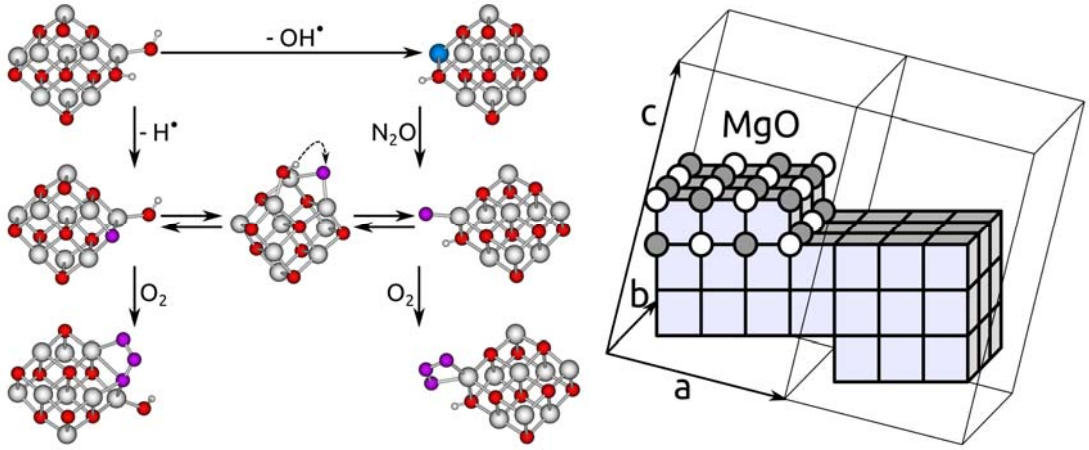

Fig. 1. Quantum-chemical models of radicals on the MgO surface simulated using the molecular cluster approach (left) and the MgO step simulated using a periodic MgO (410) surface slab (right).

4 Conclusions

In conclusion, let us emphasize that under real experimental conditions the surface of oxides always contains some chemisorbed water. So, generation of ion radicals on partially hydroxylated oxide surface due to homolytic dissociation of chemisorbed water seems to adequately describe the mechanisms of many thermal and photostimulated processes resulting in the formation of ion radicals on oxide surfaces.

Acknowledgements

This study was supported in part by Russian Foundation for Basic Research (Grants 14-03-01110 and 15-03-08070).

References

[1] A.M. Volodin, S.E. Malykhin, G.M. Zhidomirov, *Kinet. Catal.* 52 (2011) 605.
[2] S.E. Malykhin, A.M. Volodin, A.F. Bedilo, G.M. Zhidomirov, *J. Phys Chem C* 113 (2009) 10350.
[3] M. Chiesa, M.C. Paganini, E. Giamello, C. Di Valentin, G. Pacchioni, *Angew. Chem.* 42 (2003) 1759.

II-PP188

Design of Novel Copper(I) Complexes of Pyridyl Substituted 1,5-Diaza-3,7-Diphosphacyclooctanes

Strelnik I.D.*, Musina E.I., Karasik A.A., Sinyashin O.G.

A.E. Arbuzov institute of organic and physical chemistry KSC RAS, Kazan, Russia

* igorstrelnik@mail.ru

Keywords: aminomethylphosphine, copper(I), P,N-ligands

1 Introduction

Coordination systems based on copper halides show a remarkable structural diversity, [1] which arises from the many possible variation of coordination numbers (two, three and four) available for copper(I) and for the geometries that can be adopted by the halide ions and phosphine ligands. The development of the catalytic systems based on phosphine copper(I) complexes is not so intensive as for palladium complexes, but it still presents a perspective area due to the cheapness and availability of the first one [2]. Mostly these catalysts show moderate activity, which is generally surpassed to complexes based on "hard" N and/or O donors. Thus in several years a row of the works dedicated to the catalytic properties of the phosphine copper(I) complexes for the C-N bond formation [3], hydrosilylation [4] and ketalization [5] reactions were published. The system based on the R_2P-N-PR_2 ligand showed the best activity for the amination reactions among the Cu(I) phosphine complexes [3]. The effectiveness of these copper(I) complexes with the additional nitrogen donor center for the C-N cross-coupling reactions motivated us for the construction of the row of novel copper(I) complexes on the basis of pyridylsubstituted 1,5-diaza-3,7-diphosphacyclooctanes coordinated in P,P-bridge, P,N- or P,P-chelate modes and containing at least one uncoordinated nitrogen atom.

2 Results and discussion

New 1,5-diaza-3,7-diphosphacyclooctanes **1-2** were smoothly obtained in the good yields by the condensation reaction of corresponding primary pyridylphosphines, paraformaldehyde and primary amines. The following interaction of **1-2** with copper (I) iodide in dichloromethane at ambient temperature (Scheme 1) readily led to the complexes **3-6.** The ligands steric effect determinates the formation of complexes with various structure. Thus the reaction of **1a** with CuI (1 eq) leads to the P,P-bridged complex **5a**, while the same reaction of **1b** with the bulky chiral α-methylbenzyl substituents gives the dimeric P,P-chelate complex **4b**.

It should be mentioned that the ligands with the *ortho*-pyridyl substituents directly linked to phosphorus atoms show P,P-coordination modes (**3a,b, 4b, 5a)**, while the insertion of the linker between phosphorus atoms and pyridyl groups allows to reach P,N-chelate coordination of the metal (**6a-c**).

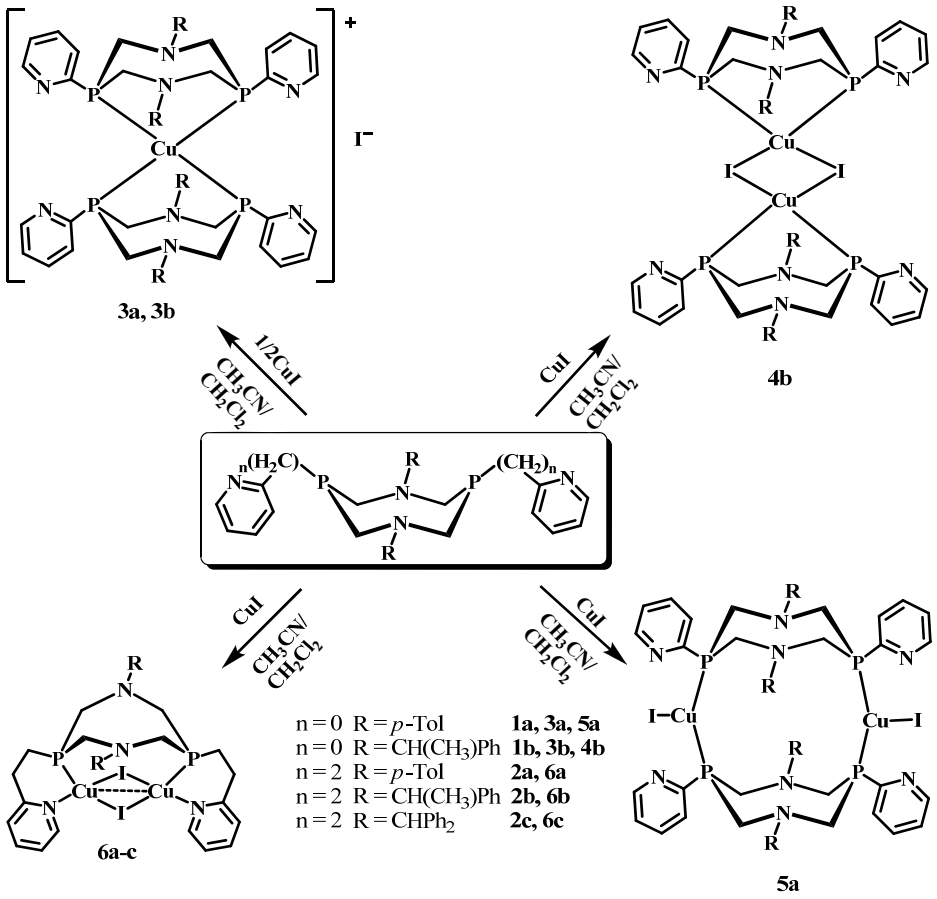

Scheme 1.

All obtained complexes have donor atoms in the secondary coordination spheres, which are localized nearly to the metal core, which makes them perspective as catalysts of the hydrosilyilation or amination reactions. Compounds **3-6** will be tested in the C-N cross-coupling reactions in the near future.

3 Conclusions

The row of novel aminomethylphosphines copper(I) iodide complexes with various coordination modes were obtained. It was found that the steric effects of ligands determinates the copper complex structures.

Acknowledgements

The work is supported by the RFBR (13-03-00563_a) and NSh (4428.2014.3) research grants.

References

[1] R. Peng, M. Li, D. Li, *Coord. Chem. Rev.*, 2010, 254, 1.
[2] I.P. Beletskaya, A.V. Cheprakov, *Coord. Chem. Rev.* 2004, 248, 2337.
[3] S. Daly, M.F. Haddow, D.F. Wass et al., *Organometallics,* 2008, 27, 3196
[4] S. Diez-Gonzalez, S.P. Nolan, *Acc. Chem. Res.,* 2008, 41, 349
[5] X. Tan, L. Li, J. Zhang et al., *Chem. Mater.* 2012, 24, 480
[6] A.A. Kelkar, N.M. Patil, R.V. Chaudhari, *Tetrahedron Lett.,* 2002, 43, 7143.

II-PP189

SiO_2 Modified with ZrO_2 as a Complex Support for Cr-Containing Catalysts for Dehydrogenation of Hydrocarbons

Litvyakova N.N., Bugrova T.A., Mamontov G.V.*

Tomsk State University (TSU), Tomsk, Russia

* GrigoriyMamontov@mail.ru

Keywords: complex supports, chromia-containing catalysts, hydrocarbons dehydrogenation

1 Introduction

Many industrial catalysts are composed of one or more active components supported on the surface of support. State and dispersion of active components influence on catalytic properties and depend on many factors. The introduction of the active component on the support surface is the determinative step of the catalyst preparation. Distribution of active component on the surface of support and its state may be controlled by changing of properties of support surface, porosity, the precursor nature and amount of the component introduced.

Silica is one of the most widely used supports for heterogeneous catalysts because of its high specific surface area and pore volume. However, the application of silica supports is limited by complexity to stabilize active component in desirable state. Therefore, the modifying of silica by transition metal oxides with suitable surface properties is one of the ways to improve the properties of catalysts.

The aim of this work is to study the distribution of zirconia modifier and active component CrO_x on the surface of silica, depending on the amount of oxide introduced, silica pre-treatment conditions as well as activity of prepared Cr-containing catalysts in the isobutane dehydrogenation. Silica with wide mesopores (10-50 nm) was used as a primary support, providing the desired porous structure of catalyst, while zirconium oxides were used as a secondary support, providing the required functional properties for active component stabilization.

2 Experimental

Mesoporous silica (KSKG) was used as a primary support. A series of $nZrO_2/SiO_2$ supports where n was 0.5, 1 or 2 monolayers (one monolayer corresponds to 5 Zr atoms per nm^2 of support) were prepared by impregnation method using aqueous solution of $ZrO(NO_3)_2*2H_2O$ stabilized with citric or hydrochloric acids. Then the samples were dried at 80°C for 12 hours and calcined at 600°C for 4 hours. Cr-containing catalysts were prepared by impregnation of initial silica and ZrO_2/SiO_2 supports by aqueous solution of H_2CrO_4 and KNO_3 (Cr/K molar ration was 5/1). The content of chromium oxides was 1 monolayer (5 Cr atoms per nm^2) that corresponds to 6.1-7.0 %wt. of Cr_2O_3. CrO_x/ZrO_2 catalyst was prepared as a reference.

Pore structure of the supports and catalysts was studied by low-temperature N_2 sorption. Chemical state of Cr was studied by electron diffuse reflectance spectroscopy (UV-vis), TPR, XRD and XPS. Catalytic properties of the prepared catalysts were measured in isobutane dehydrogenation in a bed fixed reactor at ambient pressure.

3 Results

On the basis of N_2 sorption results it was shown that the nature of acid (citric and hydrochloric) stabilizing the zirconia precursor influence on its distribution in pores of silica. A series of ZrO_2/SiO_2 mixed support with specific surface area of 100-120 m^2/g and pore volume

of 0.6-1.0 cm^3/g had mesopores with sizes of 2-60 nm.

Formation of α-Cr_2O_3 particles was observed by XRD and UV-vis for CrO_x/SiO_2 catalyst. Addition of ZrO_2 onto silica surface led to decreasing of Cr_2O_3 loading and increasing of amount of Cr(VI) species.

Results of catalytic tests are shown in Fig. 1. The activity of Cr/ZrO_2 (rate of isobutene conversion per 1 mol of chromium) is higher in comparison with the one of CrO_x/SiO_2 catalyst. Addition of zirconia in CrO_x/SiO_2 catalyst led to significant increasing of catalytic activity. It was associated with increasing of amount of Cr(VI) species in the presence of zirconia (UV-vis and TPR).

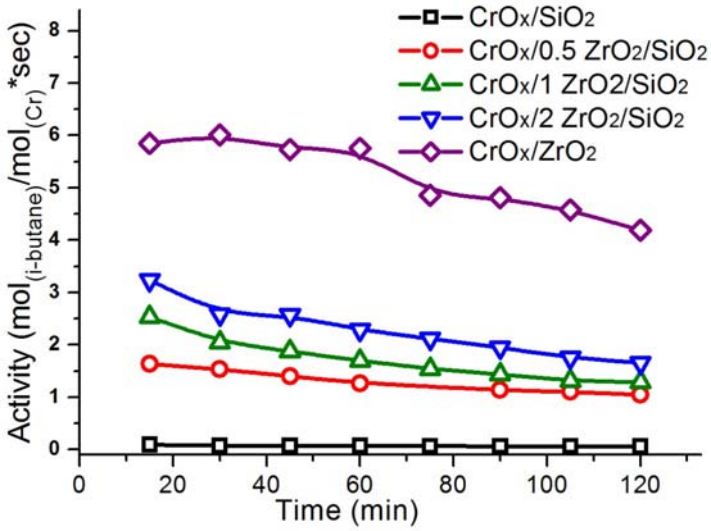

Fig. 1. Activity of Cr-containing catalysts in isobutene dehydrogenation

4 Conclusions

Thus, new approach to develop mixed ZrO_2/SiO_2 supports for Cr-containing catalyst for dehydrogenation of hydrocarbons was suggested. It was shown that ZrO_2/SiO_2 supports with high specific surface area and porosity may be prepared by simple impregnation technique and used as supports for Cr-containing catalyst. Elevated activity of $Cr/ZrO_2/SiO_2$ catalysts is associated with increasing of amount of Cr(VI) species stabilized by ZrO_2 surface.

Acknowledgements

This work was supported by the Russian Federal Target Program "Research and development in the priority fields of scientific and technological complex of Russia in 2014-2020" (State Contract No. 14.578.21.0028).

II-PP190

Rh-CeO_2-Al_2O_3 Catalysts for the Partial Oxidation of Methane

Benito P.[1*], Ballarini A.[2], Valentini L.[1], Fornasari G.[1], Scelza O.[2], Vaccari A.[1]

1 - University of Bologna, Dip. Chimica Industriale "Toso Montanari", Bologna, Italy
2 - Universidad Nacional del Litoral, Instituto de Investigaciones en Catálisis y Petroquímica "José Miguel Parera", FIQ-UNL-CONICET, Santiago del Estero, Argentina

* patricia.benito3@unibo.it

Keywords: ceria, alumina, rhodium, catalytic partial oxidation, natural gas, syngas

1 Introduction

The catalytic partial oxidation (CPO) of CH_4 to syngas is an exothermic process that achieves high CH_4 conversion and selectivity to syngas at short contact times and autothermally [1]. However, the harsh reaction conditions may lead to catalyst deactivation. A lot of efforts have been devoted to develop active and stable catalysts also reducing the formation of hot spots [2]. Rh is the most active metal and its performances are related to the support and preparation route. γ-Al_2O_3 shows large specific surface area, making it possible to obtain highly dispersed metallic particles. On the other hand, its acidic character promotes carbon formation and it suffers from phase changes at high temperatures, leading to the sintering and deactivation of the catalyst. The stabilization of γ-Al_2O_3 by addition of Ce is well-known [3] and the chemical role of Ce in the evolution of CPO was reported [4]; however the modification of the performances due to the changes in surface area and Rh dispersion could not be investigated. In this work, we studied the role of Ce content (0, 5, 10 and 20 wt.%) on chemical-physical and catalytic properties of Rh-CeO_2-Al_2O_3 catalysts (0.25 wt.% Rh) under harsh CPO reaction conditions.

2 Experimental/methodology

Precursors of Rh-CeO_2-Al_2O_3 catalysts were prepared by coprecipitation at constant pH (9.5) of an aqueous solution of $Ce(NO_3)_3$, $Al(NO_3)_3$ and $Rh(NO_3)_3$. Catalysts were obtained by calcination at 900ºC for 12h and were labelled Rh*x*CeAl_2O_3, where x is the Ce wt.% (0, 5, 10 and 20 wt.%). Samples were characterized by PXRD, N_2 adsorption/desorption, Micro-Raman Spectroscopy, TPR, HRTEM, XPS and Cyclohexane Dehydrogenation (CHD) test reaction.

CPO tests were performed, after catalyst reduction, with a natural gas mixture (90 % v/v CH_4, 7 % v/ C_2H_6 and 3 % v/v C_3H_8) at 1.2-1.4 bar, τ= 5 ms and C/O = 1. The oven temperature (T_{oven}) was set at 500 and 750ºC, modifying the gas mixture ($C/O_2/N_2$= 2/1/20 and 2/1/4 v/v).

3 Results and discussion

A mixture of γ-, η- and δ-Al_2O_3 phases were identified in Rh-Al_2O_3; while Rh*x*CeAl_2O_3 samples contained both Al_2O_3 and CeO_2 fluorite-type phases. The intensity of CeO_2 lines increased with the Ce loading; but their broadness suggested a high CeO_2 dispersion in the Al_2O_3 support. Nevertheless the presence of large amounts CeO_2 reduced the surface area, it decreased from 142 to 116 m^2g^{-1} in 5 and 20 wt.% Ce-loaded samples, respectively.

Three different Rh species were identified by TPR in $RhAl_2O_3$: segregated Rh_2O_3, well dispersed Rh^{3+} species, and rhodium aluminate. Rh*x*CeAl_2O_3 samples showed the reduction profile characteristic of CeO_2-Al_2O_3 based catalysts, with H_2 consumption peaks related to the reduction of Rh^{3+} species, surface and bulk CeO_2, and formation of $CeAlO_3$. The higher the Ce loading, the more intense the $CeAlO_3$ peak and the higher the reduction temperature.

The presence of a small amount of Ce (5wt.%) increased the number of available Rh^0, as evidenced by CHD. Moreover, HRTEM images indicated the formation of Rh nanoparticles in

all reduced samples, although the size slightly increased with the Ce loading. XPS confirmed the formation of Rh^0 during the catalyst pretreatment. On the other hand, the oxidation state of Ce depended on its content, while in $Rh20CeAl_2O_3$ reduced sample both Ce^{3+} and Ce^{4+} species were identified, XPS suggested that in $Rh5CeAl_2O_3$, Ce^{4+} was completely reduced to Ce^{3+}.

CPO tests evidenced that the differences in chemical-physical properties of the samples determined the catalytic performances (Fig. 1). In the initial test, T_{oven} = 500ºC and 2/1/20 v/v mixture, similar conversion values were achieved with $RhAl_2O_3$ and $Rh5CeAl_2O_3$ samples, while increasing the Ce content the activity decreased. The differences were smoothed during tests at 750ºC with a concentrated 2/1/4 v/v mixture; however, conversion was still lower over $Rh20CeAl_2O_3$ and this sample deactivated with time-on-stream. Selectivities in H_2 and CO were high and followed a similar trend than conversion.

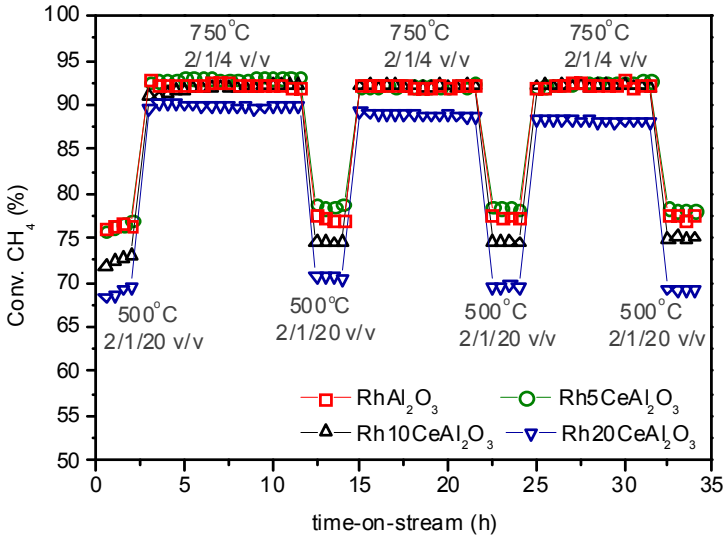

Fig. 1. Evolution of conversion of CH_4 with time-on-stream for all the catalysts studied

The characterization of spent catalysts revealed that the transition from metastable Al_2O_3 to α-Al_2O_3, taking place in $RhAl_2O_3$, was inhibited in all the Ce-containing catalysts. CeO_2 was not detected by XRD, while $CeAlO_3$ was only identified in the highest Ce-loaded sample. A loss of area occurred in $RhAl_2O_3$ and $Rh20CeAl_2O_3$, while for the 5wt.% Ce sample surface area values before and after tests were quite similar. Lastly, Raman spectroscopy confirmed the presence of carbon only in the $RhAl_2O_3$ and the full reduction of CeO_2 during CPO tests.

4 Conclusions

CeO_2 was dispersed in Al_2O_3 modifying the surface area, Rh dispersion, γ-Al_2O_3 stability and catalytic performances. A high Rh dispersion and catalytic performances, can be achieved by addition of 5 wt.% Ce, also avoiding both carbon deposition and α-Al_2O_3 formation. Contrarily a further increase in the Ce content affected negatively to the chemical physical properties and catalytic performances.

Acknowledgements

The financial support by the Ministero per l'Universita e la Ricerca (MIUR, Italy) and the Universidad Nacional de Litoral (CAI+D, Argentina) are gratefully acknowledged.

References

[1] L.E. Basini, A. Guarinoni, *Ind. Eng. Chem. Res.* 52 (2013) 17023.
[2] B. Enger, R. Lødeng, A. Holmen, *Appl. Catal. A* 346 (2008) 1.
[3] A. Piras, A. Trovareli, G. Dolcetti, Appl. *Catal. B* 28 (2000) 77.
[4] A. Donazzi, B. Michael, L. Schmidt, *J. Catal.* 260 (2008) 270.

II-PP191

Stereoselective Conversion of 14-Membered to 7-Membered Cyclic Aminomethylphosphines – a New Route to Ni(II) Electrocatalysts of Hydrogen Transformation

Fesenko T.I.*, Musina E.I., Karasik A.A., Sinyashin O.G.

A.E. Arbuzov Institute of Organic and Physical Chemistry, Kazan Scientific Center, Russian Academy of Sciences, Kazan, Russia

* fesenko@iopc.ru

Keywords: dissociation, acid catalysis, Ni(II), complexes, P,N–ligands, cyclic aminomethylphosphines

1 Introduction

The expanded use of energy from intermittent renewable energy sources such as solar and wind will require the ability to efficiently convert electricity to chemical energy for storage as fuels. [1] Nickel and cobalt diphosphine complexes that incorporate a positioned base in the ligand have been found to be active electrocatalysts for hydrogen production in acidic acetonitrile solutions.[2] The amine base positioned near the metal center has been proposed to function as a proton relay that facilitates the formation or cleavage of the H-H bond. Ni(II) complexes of 1-aza-3,6-diphosphacycloheptanes were found to be very effective catalysts for hydrogen production.[5]

2 Results and discussion

Here we report the synthesis of novel seven-membered cyclic P,N-ligands with alkyl substituents on the nitrogen atoms and their Ni(II) complexes. Unexpectedly reaction of the bis(phenylphosphino)etane with formaldehyde and iso-propylamine gives 14-membered 1,8-diaza-3,6,10,13-tetraphosphacyclotetradecane (**1**) [4,5] instead of expected 7-membered 1-aza-3,6-diphosphacycloheptanes. However macrocyclic Ni(II) complexes of **1** (Scheme 1) did not show the noticeable catalytical activity for the electrochemical hydrogen oxidation or production.

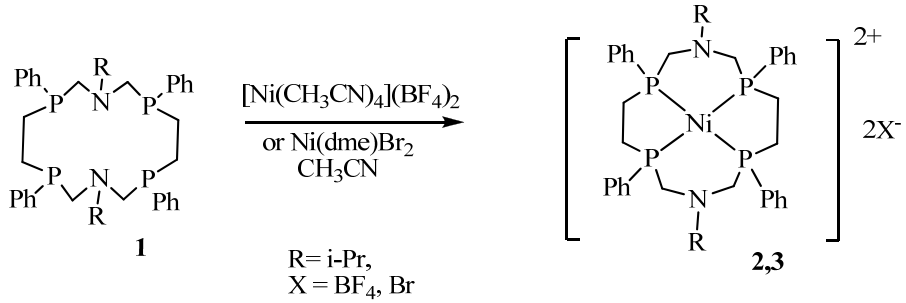

Scheme 1 Synthesis of complexes **2**, **3**

We found that 14-membered aminomethylphosphine **1** was unstable in the solution and underwent nearly quantitative the interconversion to desired 1-aza-3,6-diphosphacycloheptanes 4**a**, 4**b** (Scheme 2).

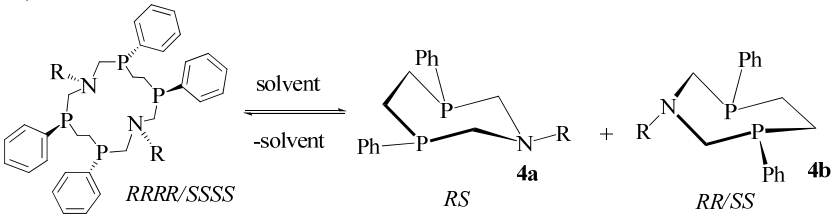

Scheme 2 The dissociation of 14-membered aminomethylphosphine **1**

We supposed that the rate of the dissociation of **1** will be increased by an acid catalysis. Indeed if 10 mol% CH_3PhSO_3H was added the rate of dissociation increased. Under the acid-free conditions the dissociation proceeds during 650 hours (Fig.1a), while the acid-catalyzed dissociation reached the final point after 150 hours (Fig.1b).

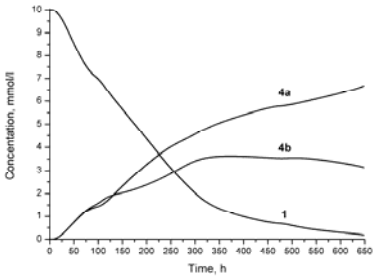

Fig.1a Dissociation in normal conditions

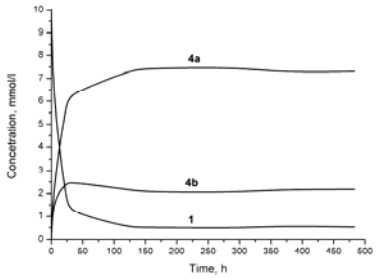

Fig.1b Dissociation with addition of CH_3PhSO_3H

The complexes **5**, **6** were obtained by the reaction of 7-membered aminomethylphosphines **4a, 4b** with Ni (II) complexes (Scheme 3) in dichloromethane. The structure of the complex **5** was established by X-ray diffraction analysis (Fig.2)

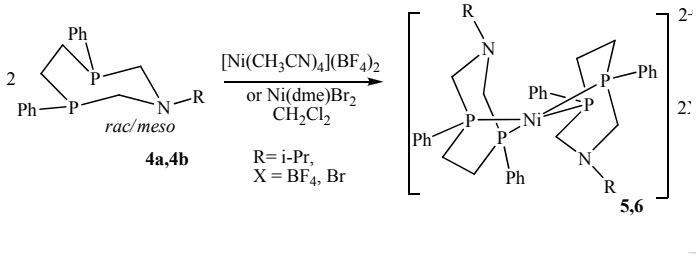

Scheme 3 Synthesis of complexes **5**,**6**

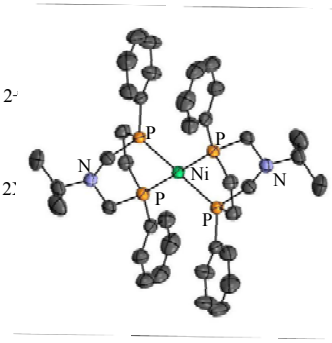

Fig. 2 Complex **5** cation

It should be mentioned that structure of obtained complexes **5** and **6** are similar to that of described effective potential catalysts of electrochemical H_2 production [3].

Acknowledgements

This work was supported by President's of RF Grant for the support of leading scientific schools (No.NSh-4428.2014.3) and Programmes of Russian Academy of Sciences

References

[1] R. M. Bullock, Ed.; 1st ed.; *Catalysis without Precious Metals*, Wiley-VCH: New York, (2010).
[2] D. L. DuBois, R. M. Bullock, *Eur. J. Inorg. Chem.* (2011) 1017.
[3] M.L. Helm, M.P. Stewart, D.L. DuBois et al. *Science*. 333 (2011) 863.
[4] E.I. Musina, A.A. Karasik et al. *Phosphorus, Sulfur, and Silicon*. 186 **(**2011) 761.
[5] R.N. Naumov, E.I. Musina, T.I. Fesenko et al. *Dalton Trans*. 43 (2014) 12784.

II-PP192

Core/Shell and Hollow Metal-Oxide Nanoparticles Supported on ZSM-5: Synthesis and Properties

Yashnik S.A.[1*], Zaikovskii V.I.[1], Sharafutdinov M.R.[2], Saraev A.[1], Kaichev V.V.[1], Ismagilov Z.R.[1,3], Parmon V.N.[1]

1 - Boreskov Institute of Catalysis, Novosibirsk, Russia
2 - Institute of Solid State Chemistry and Mechanochemistry, Novosibirsk, Russia
3 - Institute of Coal Chemistry and Material Science, Kemerovo, Russia

* yashnik@catalysis.ru

Keywords: Cu-ZSM-5, hollow particle, core-shell particle, nanoscale, Kirkendall effect

1 Introduction

In the past decade zeolites with different morphology are considered as matrix for stabilization of oxide and metal nanoparticles of transition and noble metals, e.g., Cu, Ag, Au and others [1, 2]. Nanoparticles are known to possess unique optical, magnetic, redox and catalytic characteristics.

Current communication is devoted to study of oxidation processes of metal (Cu, Ni, Co) nanoparticles supported on ZSM-5 zeolite, aiming to find correlation between structures of metal-oxide particles, such as core/shell, hollow and bulk, and oxidation conditions. The TPR-H_2, XRD in situ, HRTEM, XPS, UV-Vis DR, and the optical spectra modeling were used to confirm the hypothesis about the structure of metal-oxide particles over zeolite. The CO and NO oxidation as well as NO SCR by propane were employed to examine catalytic characteristics of different metal-oxide particles.

2 Experimental

The Cu-, Ni- and Co-containing ZSM-5 samples were reduced in hydrogen-containing mixture at 200 - 700^{o}C; and then subjected to oxidation at 25, 100, 300, 500 и 700^{o}C in air, dry oxygen or moist oxygen stream. Metal content was 2.5 wt%.

The TPR-H_2 experiments were conducted with mixture 10% H_2 in argon and heating rate 10^o/min, before and between experiments the samples were pretreated in situ in oxygen at the temperature specified above. DR UV-Vis spectra were obtained at room temperature using a "Shimadzu" UV-2501 PC spectrophotometer equipped with a diffuse reflectance accessory (ISR-240 A). HRTEM images were obtained using a JEOL Model JEM-2010 electron microscope with an accelerating voltage of 200 kV and a lattice resolution of 0.14 nm. Chemical composition of sample surface were studied using a photoelectron spectrometer (SPECS Surface Nano Analysis GmbH) equipped with a high-pressure cell that allowed us the heating of samples at 200 - 400^{o}C in H_2 or O_2 containing mixtures. The sample XRD composition during Reduction/Oxidation were registered on the station of time-resolved diffraction (station ''5b'' at the VEPP-3 storage ring, BINP, Novosibirsk).

CO (0.1 vol%) and NO (400 ppm) oxidation tests were carried out as TPR mode. Heating rate was 10^{o}C/min. Selective catalytic reduction of NO (NO-SCR) by propane (320 ppm NO, 1500 ppm C_3H_8, 3.2 vol.% O_2 in N_2) was studied using a flow reactor at 42000 h^{-1} and temperatures 200–550 ^{o}C.

3 Results and discussion

Nanoscale Kirkendall effect is illustrated with reference to 2.85%Cu-ZSM-5 sample (Fig.1). The phenomenon was revealed at low-temperature (up to 100^{o}C) oxidation of 10-20 nm Cu^0

particles located on a surface of zeolite crystallites. Hollow metal-oxide nanoparticles (Fig.1B) are formed from core/shell nanoparticles containing the 3-5 nm Cu_2O layer on a surface of a copper nanoparticle (Fig.1A) due to different diffusion coefficients. At oxidation temperatures 300°C and above, bulk CuO particles near 40 nm are only formed (Fig.1C). When size of Cu^0 particles is 40-50 nm and higher, the core/shell nanoparticles are resistant to further oxidation. The Cu^0-Cu_2O-CuO transformations are identified by XRD in situ and XPS.

The core/shell, hollow and bulk Cu-oxide particles have different optical, redox and catalytic properties. DR UV-Vis spectra showed a shift of plasmon absorption from 17500 to 15800-16500 cm^{-1} at oxidation of Cu^0 to core/shell particles. A fundamental absorption edge (FAE) of Cu_2O nanoparticles (22200 cm^{-1}) and an adsorption bands corresponding d-d transition (13000-15700 cm^{-1}) and a ligand-metal charge-transfer (CTB) of square-planar copper(II)-oxide clusters (29500 cm^{-1}) were observed in spectra of samples with hollow CuOx particles. The 40-50 nm CuO nanoparticles are shown blue-shift of optical band gap compared with bulk CuO phase (2.3-3.1 against 1.85eV).

The core/shell and hollow CuO_x particles are more reducible in H_2-TPR experiment compared with CuO nanoparticles and CuO phase, 165 – 185°C against 235°C.

Catalytic performance of the core/shell and hollow CuO_x particles supported on ZSM-5 in oxidation of CO, NO and propane are found to correlate well with their redox behavior. While in NO-SCR by propane the core/shell and hollow CuO_x particles supported on ZSM-5 were less active in comparison with the Cu-substituted ZSM-5.

Similar nanoscale effects are also observed during oxidation of the Ni and Co nanoparticles supported on ZSM-5 zeolte. Kirkendall effect for Ni nanoparticles was detected at low-temperature oxidation, while the core/shell and hollow CoO_x particles were formed at higher temperatures.

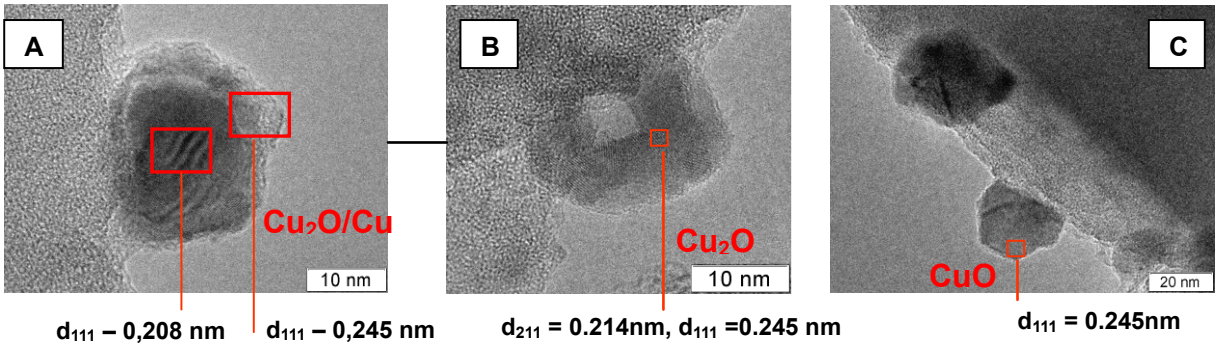

Fig.1. TEM images of copper nanoparticles formed during oxidation of 10-20 nm Cu^0 at different temperatures: core/shell Cu^o/Cu_2O-CuO (A), hollow Cu_2O (B) and bulk CuO (C).

4 Conclusions

2D and 3D metal-oxide nanoparticles are formed at oxidation of nanoparticles of Cu, Ni and Co. Their structures and properties are found to significantly depend on oxidation temperature.

Acknowledgements

This research was supported by Presidium of RAS (Grant №24-35).

References

[1] S.A.Yashnik, V.F. Anufrienko, V.I. Zaikovskii, et.al. *Stud. Surf. Sci. Catal.*, 174A (2008) p.177-180.
[2] S.A. Yashnik, Z.R. Ismagilov, V.F. Anufrienko, *Catal. Today*, 110 (2005) 310-322.

II-PP193

The Synthesis and Characterization of Co Nanoparticles Supported on Multi-Wall Carbon Nanotubes for Catalytic Applications

Kazakova M.[1,2*], Andreev A.[1,2], Ishchenko A.[1,2], Lapina O.[1,2], Kuznetsov V.[1,2]

1 - Boreskov Institute of Catalysis, SB RAN, Novosibirsk, Russia
2 - Novosibirsk State University, Novosibirsk, Russia

* mas@catalysis.ru

Keywords: Co supported catalyst, multi-wall carbon nanotubes, internal field, ^{59}Co NMR

1 Introduction

Over the last few years, the interest to carbon nanostructures has grown enormously that mostly relates to the numerous searches of possible industrial applications. Among large variety of carbon nanomaterials, carbon nanotubes (CNTs) attract a special attention. Due to unique mechanical properties, large specific surface area, high electrical and thermal conductivity, and chemical stability, CNTs can be considered as a key component in different composites, in various electrochemical devices (lithium-ion batteries, supercapacitors) and for different applications in catalysis as supports. CNTs could be utilized as supports for various catalytic processes. For instance, one of the promising directions is Fischer-Tropsch synthesis (FTS) in the form of cobalt catalysts supported on CNTs [1]. High thermal conductivity of MWCNTs makes them also attracting as supports for the development of new catalysts of FTS avoiding overheating of the catalyst bed. In the present work, the structure of cobalt systems based on the perspective carbon supports, functionalized multi-wall carbon nanotubes (MWCNTs), has been investigated. The special attention has been applied to characterize Co species fixed on the surface of MWCNTs by the internal field (IF) ^{59}Co NMR.

2 Experimental/methodology

MWNTs were synthesized by CVD of ethylene decomposition over the bimetallic Fe-Co catalysts at 680°C. We have used functionalized MWCNTs containing surface carboxylic groups (0.76 groups per 1 nm^2) produced via boiling concentrated nitric acid (denoted as MWNT-Ox-NA) [2]. Co-containing samples were prepared by impregnation of MWCNTs (surface area of 305 m^2/g, average particle diameter of 9.4 nm) with the aqua solutions of Co (II) salts followed by calcination under an inert atmosphere and reduction in a stream of hydrogen at the temperature of 350°C. The samples with Co concentrations: 3.5, 7.3, 11.7 and 14.5 wt. % were obtained. The structure and morphology of pure and Co-containing MWCNTs was monitored by TEM. The structure of the cobalt metal in the catalyst after the reduction was investigated by IF ^{59}Co NMR providing information about the structural (FCC, HCP, and stacking faults - sfs) and magnetic (magnetic domains and domain walls) features.

3 Results and discussion

The sample 3.5% Co/MWCNT-Ox-Na mainly contains Co-oxide particles within the channels of MWCNTs of 3-5 nm in the size. The particle size is not increased after the reduction in hydrogen. The increase of Co content (within the range 3.5 up to 14.5 wt. %) leads to the growth of Co^0 particle sizes from 5-10 nm to 50-80 nm. The studied samples show both types of Co metal particles as inside the MWCNTs with certain diameter of 5 nm as maximum and various lengths, and Co metal particles located on the surface.

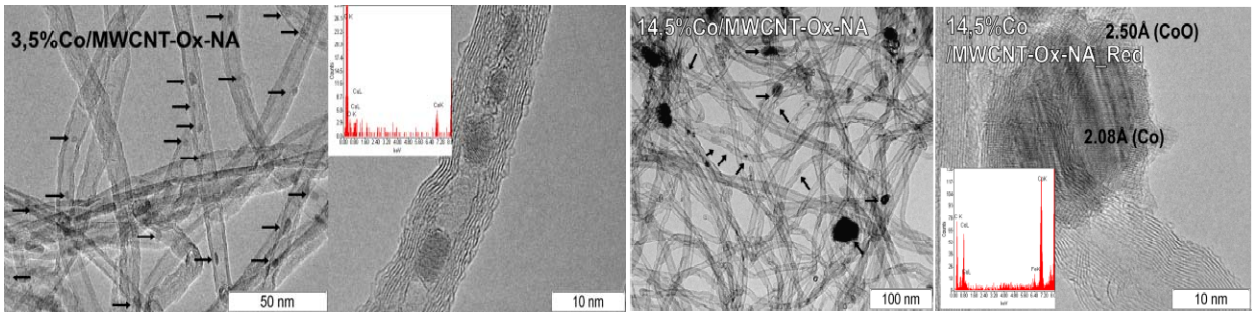

Fig. 1. TEM images of 3.5 and 14.5 wt.% Co/MWCNT-Ox-NA, correspondingly. Arrows show Co particles inside and outside nanotube channels.

The IF ^{59}Co NMR data shown in Fig 2 allow to discern 5 different signals in spectra (2D distribution helps determining the number of resonances) from HCP and FCC Co metal stacking, magnetic domains and domain walls (d.w.). The d.w. resonances state the existence of large Co particle of more than 70 nm in size [3]. Returning to the present work, the d.w. reflects filled with Co metal MWCNTs where diameter is restricted by internal tube size (~5 nm), however the length reaches 100 nm.

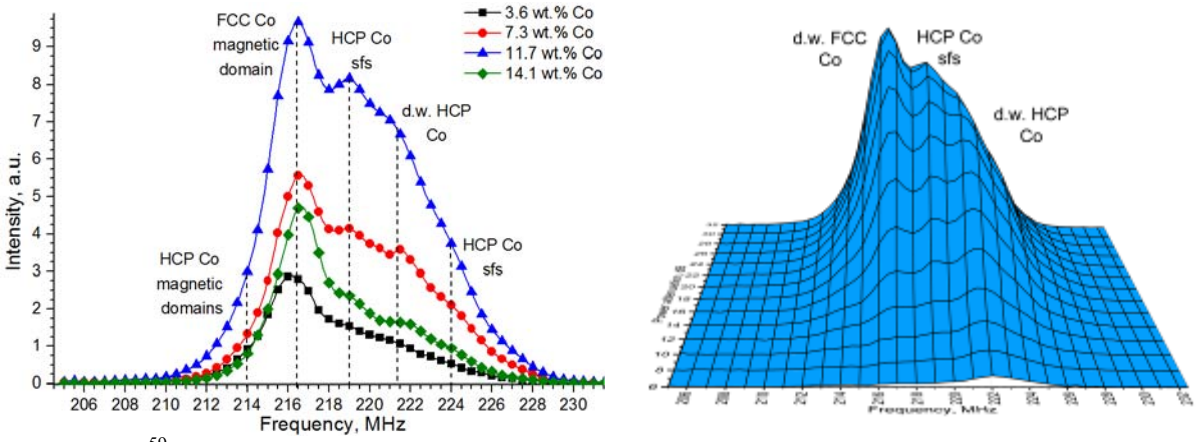

Fig. 2. IF ^{59}Co NMR spectra of studied samples (left) and 2D spectrum (right).

4 Conclusions

Varying the deposition conditions gives cobalt particles both inside the internal channels of the tubes and on the external surface. Co particles inside the channels of MWCNTs have an elongated and rounded shape and the average diameter of 2–3 nm. IF ^{59}Co NMR gives five different types of metallic Co particles. The increase of Co concentration leads to the decrease in the relative content of Co in a cubic stacking, resulting the increase of the HCP/FCC ratio from 1.0 to 1.7. The increase of the portion of magnetic domain walls of HCP suggests the presence of elongated particles up to 100 nm inside the MWCNTs.

Acknowledgements

The reported study was supported by RFBR, research project № 14-03-31684 mol_a.

References

[1] A. Tavasoli, K. Sadagiani, F. Khorashe, A.A. Seifkordi, A.A. Rohani, A. Nakhaeipour, *Fuel Processing Technology.* 89 (2008) 491.
[2] I. Mazov, V. Kuznetsov, I. Simonova, A. Stadnichenko, A. Ishchenko, A. Romanenko, E. Tkachev, O. Anikeeva, *Applied Surface Science* 258 (2012) 6272.
[3] A. S. Andreev, O.B. Lapina, S.V. Cherepanova, *Applied Magnetic Resonance* 45 (2014) 1009.

II-PP194

Gallium Oxides Catalysts for Light Paraffins Conversion

Agafonov Yu.A.[1*], Gaidai N.A.[1], Botavina M.A.[1,2], Martra G.[2], Lapidus A.L.[1]

1 - N.D.Zelinsky Institute of Organic Chemistry RAS, Moscow, Russia
2 - University of Torino, Department of IPM Chemistry and NIS Centre, Torino, Italy

* plassey@mail.ru

Keywords: paraffins, dehydrogenation, olefins, carbon, dioxide, gallium oxides catalysts

1 Introduction

Gallium supported oxides are effective catalysis for dehydrogenation of light paraffins. Side processes, such as cracking and coke formation, decrease yield of olefins. Silica framework using as support is characterized by good resistance to coke formation. This work devoted to the comparison of gallium catalysts prepared by wet impregnation on silica and direct one-pot synthesis embedding Ga species in the siliceous mesoporous framework of MCM-41 for process of propane dehydrogenation. The process was also studied in the presence of CO_2 which can interact with hydrogen, forming at propane dehydrogenation, what results in the shift of reaction equilibrium, and partly oxidizes coke and catalyst surface.

2 Experimental

Catalysts were prepared by wet impregnation of silica (KSKG) from water solutions of gallium nitrates and direct one-pot synthesis embedding Ga species in the siliceous mesoporous framework of MCM-41. Catalysts under investigation are contained 5.0-40.0%Ga on SiO_2 and 1.0-3.0%Ga in MCM-41. Catalyst structure and adsorption properties were controlled by X-ray diffraction, N_2 adsorption, TPR-H_2 and FTIR. Long-duration tests of catalysts were carried out in a flow reactor at 600°C, volume space velocity 200 h^{-1}, atmospheric pressure and at initial reaction composition (%, vol.): (C_3H_8) (15), CO_2 (30), N_2 (55). Before the reaction all catalysts were activated in O_2 flow at 600°C for 6 hours. The reaction products were analyzed by GC methods using two columns – molecular sieves 5A (H_2, N_2, CH_4, CO) and Porapak-Q (CO_2, hydrocarbons C_1-C_3). After each experiment the catalysts were regenerated in O_2 flow at 600°C for 10 hours. Unstationary phenomena were investigated using the transient response method in the flow reactor of small volume connected with mass-spectrometer. Relaxation curves describing a transition of the system to a new steady state were obtained by a jump change of the corresponding concentrations. The partial pressures of C_3H_8 and CO_2 were changed in the limits 0.125-0.33 and 0.30-0.75 atm., respectively, temperature was 600°C. Some adsorption-desorption tests of the reaction components and experiments on replacement of C_3H_6 by CO_2 and opposite had been also done at 200°C. For all the experiments the relaxation time was lower than the turnover time. Thus, it allows characterizing all observed relaxations as own ones.

3 Results and discussion

Results of investigations on propane dehydrogenation in the presence of CO_2 over studied catalysts showed (Fig. 1) that catalysts prepared by one-pot method demonstrate considerably more high specific activity and stability in propene formation than the catalysts made by wet impregnation. According to TPR-H_2 data, catalysts Ga-MCM are characterized by high dispersity. It was shown in [1] that high metal dispersity (Ni) in silica framework is accompanied by an intense decrease of coke formation. We observed the analogical effect. One of reasons of it can be a decrease of possibility for interaction between adsorbed olefins and further growth of chain because of an increase of distance between centers of their adsorption.

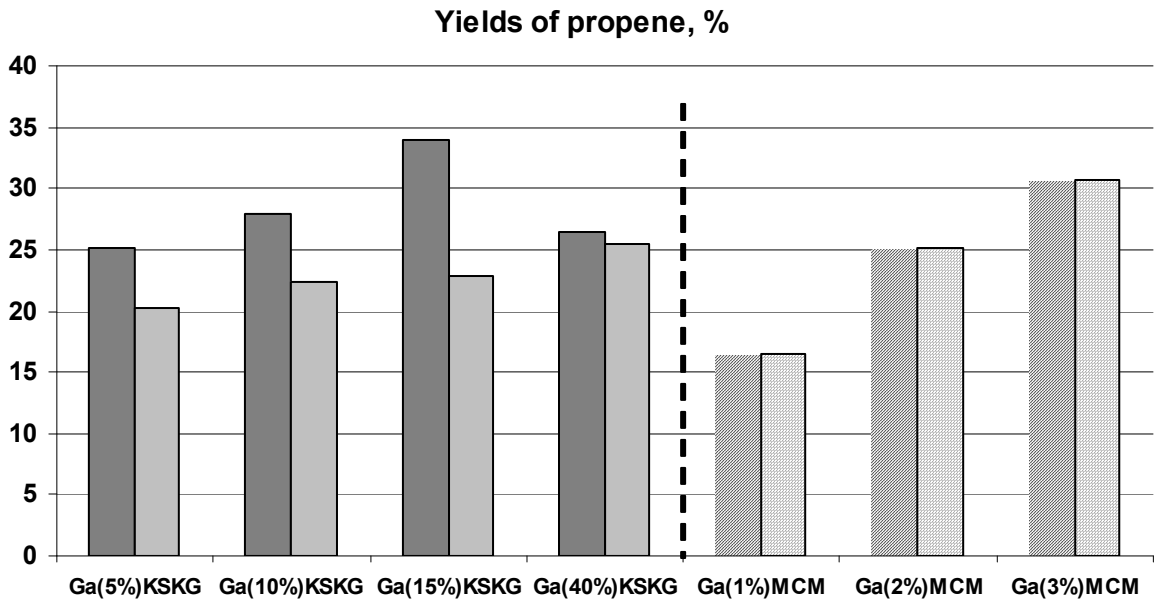

Fig. 1. The initial yields of propene (d after 300 min of work ( ) at dehydrogenation of propane over Ga-catalysts prepared by different methods

Dehydrogenation of propane over gallium catalysts proceeds through heterolytic dissociation reaction pathway with the formation of Ga-hydrides [2]. In this case CO_2 would have the negative influence on this process due to its oxidized properties and can inhibit the hydride formation. Really, this effect is detected in stationary and unstationary experiments: the propene yield was more high in the CO_2 absence for all studied catalysts.

The comparison of responses $(He+C_3H_6)/(He+CO_2)$ and $(He+CO_2)/(He+C_3H_6)$ at 200°C per the time of replacing one component by another showed that CO_2 is tied more firmly than C_3H_6. It was shown that amounts of cracking products are decreased in CO_2 presence also over all catalysts. Also it is shown that the delay of C_3H_6 appearance in gas phase is increased in the following row of responses: $[He/(C_3H_8+He)] < [He/(C_3H_8+CO_2)] < [(He+CO_2)/(C_3H_8+CO_2)]$. Thus, CO_2 precludes the interaction of propane with an active surface.

4 Conclusions

The advantages of Ga-catalysts, prepared by direct one-pot method before catalysts obtained by wet impregnation, are demonstrated in this work. The specific activity and stability of Ga-MCM catalysts are higher but coke formation is less because of high dispersity and strong bond of active phase with the support.

It was shown that the use of CO_2 at paraffin dehydrogenation is limited because of it precludes an interactions of paraffins with active centers reducing an yield of olefin.

Acknowledgements

This work was financially supported by the Division of Chemistry and Materials Science (Program No. 1)

References

[1] Zhicheng Liu et al, *Applied Catalysis B: Environmental.* 125 (2012) 324
[2] Sebasti´an E. Collins et al, *Journal of Catalysis.* 211 (2002) 252

II-PP195

Synthesis and Catalytic Activity of the Polymer-Stabilized Palladium Nanoparticles

Sultanova E.D.[1*], Salnikov V.V.[2], Mukhitova R.K.[1], Zuev Yu.V[2], Zahkarova L.Ya[1], Ziganshina A.Yu.[1], Konovalov A.A.[1]

1 - A.E. Arbuzov Institute of Organic and Physical Chemistry, Kazan Scientific Center, Russian Academy of Sciences, Kazan, Russia

2 - Kazan Institute of Biochemistry and Biophysics, Russian Academy of Sciences, Kazan, Russia

* elsultanova@iopc.ru

Keywords: palladium nanoparticles, nanocapsules, catalysis, viologen

1 Introduction

The results of last years show that the nanosized metal particles demonstrate higher catalytic activity compare to bulk metal due to larger surface to volume ratio. It involves many researches to create new catalytic nanosystems with different shape and properties. [1] The most promising systems showing high stability and catalytic activity are nanocomposites on base of polymer and metal nanoparticles. [2]

In this presentation, we will demonstrate our last results concerning the creation of new catalytic hybrid nanocomposites of palladium nanoparticles stabilized on the surface of polymeric nanocapsules.

2 Experimental/methodology

Polymeric nanoparticles was synthesized as described in [3]. The nanocomposite Pd@p(MVCA^{8+}-co-St) was obtained using the modified method [4]. Pd@p(MVCA^{8+}-co-St) was characterized by the physical and chemical method of IR-, NMR- spectroscopy, transmission electron microscopy (TEM), scanning electron microscopy (SEM), Energy-dispersive X-ray spectroscopy (EDX), dynamic light scattering DLS.

NMR spectroscopic experiments were carried out with an Avance 600 spectrometer (Bruker, Germany) equipped with a pulsed gradient unit capable of producing magnetic-field pulse gradients in the z direction of about 56 Gcm^{1}. D_2O was used as a solvent in all experiments. Chemical shifts were reported relative to HDO (d= 4.7 ppm) as an internal standard. UV/Vis spectra were recorded with a Perkin–Elmer Lambda 25 UV/Vis spectrometer. Fluorescence emission spectra were recorded with a Cary Eclipse fluorescence spectrophotometer (USA). Imaging of the polymer nanocapsules with and out palladium nanoparticles probe microscope (Veeco). The morphology of the implanted structured silicon surfaces were characterized in plan-view by scanning electron microscopy (SEM) using high-resolution microscope Merlin Carl Zeiss combined with ASB (Angle Selective Backscattering) and SE InLens (Secondary Electrons Energy selective Backscattering) detectors, which was also equipped for energydispersive X-ray spectroscopy (EDX) analysis with AZTEC X-MAX energy-dispersion 5 spectrometer from Oxford Instruments.

3 Results and discussion

For the creation of new catalytic nanocomposite, the polymeric nanoparticles decorated with viologen groups (p(MVCA^{8+}-co-St)) were chosen. p(MVCA^{8+}-co-St) effectively binds with negative charged metal complexes $PdCl_4^{2-}$ due to electrostatic forces. The soft reduction of $PdCl_4^{2-}$ leads to the formation of Pd nanoparticles stabilized with p(MVCA^{8+}-co-St)

(Pd@p(MVCA^{8+}-co-St)) (Scheme 1). The TEM image (Fig. 1A) show that Pd nanoparticles with the size about 10 nm decorate the surface of the polymer nanoparticles p(MVCA^{8+}-co-St) to form the flower like nanocomposite Pd@p(MVCA^{8+}-co-St).

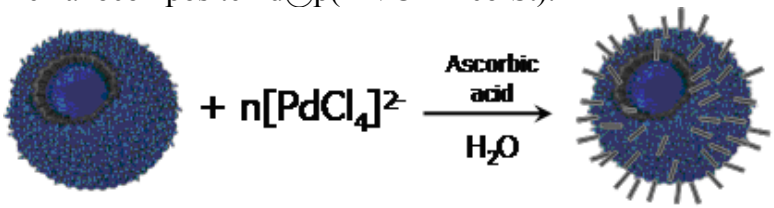

Scheme 1. Synthesis of p(Pd@MVCA8+-co-St).

The catalytic properties the nanocomposites were examined on the reaction of reduction of *p*-nitrophenol by $NaBH_4$ in water. The reduction of *p*-nitrophenol is a conventional reaction for the evaluation of catalytic activity. [5] The results show that Pd@p(MVCA^{8+}-co-St) shows very high catalytic activity. Six nanomoles of palladium in Pd@p(MVCA^{8+}-co-St) is enough for the completely reduction of nitrophenol during 10-15 minutes.

The synthesis, characterization and catalytic properties of Pd@p(MVCA^{8+}-co-St) nanocomposited will be discussed in the presentation.

A B

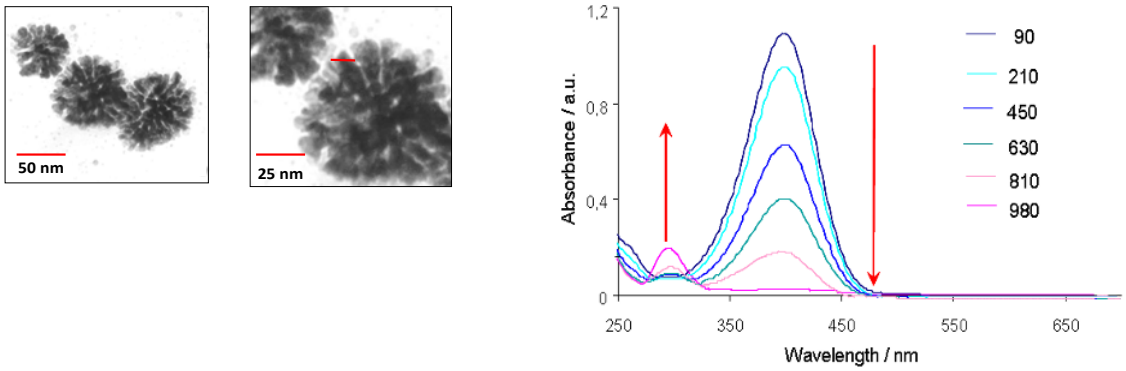

Fig. 1. A) TEM images of Pd@p(MVCA^{8+}-co-St). B) UV−vis spectra of Pd@p(MVCA^{8+}-co-St) at various reaction times.

4 Conclusions

We demonstrated a new method to prepare new hybrid nanomaterials. The Pd@p(MVCA^{8+}-co-St) obtained, exhibits a high catalytic activity. In the future, we plan to investigate this catalyst in other reactions.

Acknowledgements

This study was supported by the Russian Foundation for Basic Research (grant nos. 15-03-04999).

References

[1] K. R. McCrea, J. S. Parker, G. A. Somorjai, J. *Phys. Chem. B*, 106 (2002), 10854.
[2] R. U. Islam, M. J. Witcomb, M. S. Scurrell, E. Lingen, W. Otterloc, K. Mallick, *Catal. Sci. Technol*. 1 (2011), 308.
[3] E. D. Sultanova, E. G. Krasnova, S. V. Kharlamov, G. R. Nasybullina, V. V. Yanilkin, I. R. Nizameev, M. K. Kadirov, R. K. Mukhitova, L. Y. Zakharova, A. Y. Ziganshina, A. I. Konovalov, *ChemPlusChem* DOI: 10.1002/cplu.201402221
[4] A. Mohanty, N. Garg, R. Jin *Angew. Chem. Int. Ed.* 49 (2010), 4962.
[5] P. Lu, T.Teranishi, K.Asakura, M.Miyake, N.Toshima, *J. Phys. Chem. B* 103 (1999), 9673.

II-PP196

Cu(111) Chlorination on Atomic Scale: Adsorption, Diffusion, and Desorption

Pavlova T.V.*, Zhidomirov G.M., Eltsov K.N.

A.M. Prokhorov General Physics Institute RAS, Department Of Technologies And Measurements On Atomic Scale, Moscow, Russia

* pavlova@kapella.gpi.ru

Keywords: reaction, dynamics, thermal desorption, atomic structures, chlorination, DFT

1 Introduction

In heterogeneous catalysis, 3d metals are often used as catalysts and halocarbons - as promoters. After dissociation of adsorbed halocarbon molecules, all steps of surface transformations for molecule radicals and halogens are needed to understand. In particular, halogens desorption process is rather interesting. For copper as catalyst and for chlorine as promoter, we have contradictory information about desorption process. Conclusion that chlorine desorbs as atoms is made on the base of thermal desorption spectroscopy (TDS) experiments [1] and Density Functional Theory (DFT) calculations [2]. On the other hand, only cooper chloride was detected in thermal desorption spectra for chlorinated Cu(111) and Cu(100) in [3,4]. Taking into account that chlorinated cooper surface is catalyst in 1,2-dichloroethane production as a part of industrial oxychlorination reaction, the resolution of this contradiction is important.

2 Calculation details

To understand surface processes at the atomic level, we carried out detailed *ab initio* theoretical study of different steps of Cu(111) chlorination: Cl_2 adsorption, Cl and Cu atoms diffusion, surface structure transformations, and thermal desorption of reaction products. All DFT calculations were carried out with Vienna Ab initio Simulation Package (VASP) [5]. Energy barriers are evaluated with Nudged Elastic Band (NEB) method [6]. Range of chlorine coverage on Cu(111) was used from separate atoms to saturated monolayer. In contrast to the previous study [2], we consider Cl atoms not only on perfect Cu(111) surface, but also near defects like Cu adatoms and step edges. All atomic structures were modeled in accordance with experimental STM images obtained in [3]. Several scenarios have been tested.

3 Results and discussion

The most energetically favorable adsorption sites for chlorine are steps, where the Cl atom is attached to two Cu atoms on the step edge, directly above one Cu atom from terrace. On terraces, Cl adsorption is preferred at surface defects like adatoms. Ideal (111) surface is occupied by Cl in fcc sites, coupled Cl in fcc-hcp sites in the form of chains, and Cl in the ordered $(\sqrt{3}x\sqrt{3})R30°$ structure that undergoes a continuous uniaxially compression with domain walls formation at Cl coverage increasing up to saturated submonolayer. Our analysis shows that the latter structure is thermodynamically most stable followed by CuCl film, in a good agreement with experimental observations [3,7]. In contrast to the previous theoretical work [2], we report about a variety of thermodynamically stable structures on Cl/Cu(111).

Figure 1 shows activation energies for Cl_2 adsorption, Cl and Cu adatoms diffusion, and desorption of different species (Cl, Cl_2, CuCl, Cu). It was found that Cu(111) have strong catalytic effect on Cl_2 dissociation canceling the activation barrier at both perpendicular and parallel orientations of the molecule axis. Cooper and chlorine atoms have negligible small diffusion barriers on Cu(111), allowing effective surface structure transformations at T > 30 K.

However, modification of step edges is possible at significantly higher temperatures, T > 282 K.

At Cl/Cu(111) annealing to remove chlorine, CuCl molecules desorb first from step edges, with activation energy of 2,47 eV (T ~ 802 K). It is in accordance with the TPD experiment [4], where CuCl molecules were detected in mass-spectrometer at around (700 - 850) K with peak maximum at 800 K. Even after chlorine removing from step edges, this sites will be almost immediately occupied by Cl due to the energetically gain in adsorption energy in combination with small diffusion barrier of Cl atoms. This highlights the important role of step edges as the most active sites on Cu(111).

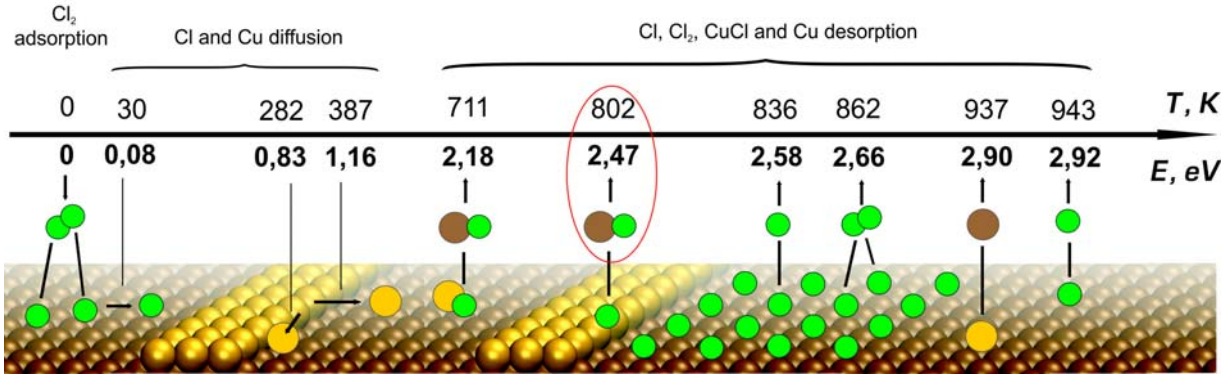

Fig. 1. Activation energies for Cl_2 adsorption, adatoms diffusion, and desorption of different species. Temperatures were evaluated from activation energies by Polanyi-Wigner equation.

4 Conclusions

We have computationally studied the reaction of cooper chlorination on ideal and defective (111) surface. The consistent theoretical description of the whole reaction allows us to make following conclusions:

- Cl_2 dissociation occurs spontaneously;
- Cl atoms prefer to be adsorbed at step edges;
- Cl atoms easily diffuse on surface via bridge positions;
- CuCl molecules are desorbed species;
- CuCl molecules are desorbed from step edges.

Acknowledgements

The reported study was supported by RFBR, research project 15-02-99607 A. We thank the Joint Supercomputer Center of RAS for the use of their computational facilities.

References

[1] P.J. Goddard, R.M. Lambert, *Surf. Sci.* 67 (1977) 180.
[2] S. Peljhan, A. Kokalj, *J. Phys. Chem. C.*113 (2009) 14363.
[3] B.V. Andryushechkin, K.N. Eltsov, *Proceeding of the Prokhorov General Physics Institute*, Vol. 59 - Moscow: Nauka, 2003. P. 106.
[4] K.N. Eltsov at al., *Surf. Sci.* 251/252 (1991) 753.
[5] G. Kresse, J. Furthmuller, *Phys. Rev. B.*54 (1996) 11169.
[6] G. Henkelman, B.P. Uberuaga, H. Jonsson, *J. Chem. Phys.* 113(2000) 9901.
[7] B.V. Andryushechkin at al., *Surf. Sci.* 470 (2000) L63.

II-PP197

Combustion Synthesis of Perovskites from Solid Organometallic Glycine-Based Precursors

Simagina V.I.*, Mukha S.A., Komova O.V., Netskina O.V., Odegova G.V., Derbilina A.V.

Boreskov Institute of Catalysis SB RAS, Novosibirsk, Russia

* simagina@catalysis.ru

Keywords: perovskite, catalyst, organometallic precursor, self propagating, high-temperature synthesis

1 Introduction

Complex oxides with a perovskite structure are known to be catalysts for a wide range of redox processes. They are characterized by a high activity, considerable oxygen mobility, thermal stability of their structure, a unique diversity of their properties and chemical compositions. Volume combustion synthesis (VCS) [1] based on igniting gel-like (viscous) organometllic precursors prepared by concentrating aqueous solutions of metal nitrates and organic compounds (amino acids, urea, citric acid and others) has been the most wide-spread method of their preparation. But this method requires a stage of a prolonged high temperature (~1000^{o}C) calcination of the resulting product to decompose the thermo-stable phases of lanthanum carbonates and to complete the formation process of the perovskite phase.

This study has been undertaken for an improvement of the glycine-nitrate combustion method which would allow to obtain easily dryable and grindable solid organometallic complex precursors and to conduct the perovskite synthesis both in the VCS regime and in the course of self-propagating high-temperature synthesis (SHS). An analysis of the combustion products of the organometallic precursors depending on the combustion regime is given and an energy-efficient approach to perovskite synthesis is proposed. It should be noted that there are only few studies devoted to SHS synthesis of perovskites and to comparison of combustion products from VCS and SHS regimes.

2 Experimental/methodology

The organometallic precursors of the perovskites (OMPP) – LaMGlyOx (M–Fe^{3+}, Co^{2+}, Ni^{2+}, Cu^{2+} and others, Gly–glycine, Ox–oxidant) were prepared by interacting aqueous solutions of glycine and nitrates in the presence of sodium hydroxide (series I) or ammonia (series II) using stoichiometric quantities. The synthesis was conducted at room temperature, under continuous stirring and gradual addition of the base. The solvent was removed in a rotary evaporator after which the complexes were dried in a vacuum box and ground.

Combustion synthesis of the perovskite was conducted in VCS and SHS regimes. In the case of VCS a quartz glass with a thin layer of OMPP powder was heated at 500 ^{o}C for 5–10 min. Its combustion produced a loose solid residual. In the case of SHS a pellet of OMPP was ignited with a lighter. The lighter was removed as soon as the burning started. As the reaction went on "serpentines" of the layered perovskite growing in lengths were formed [2].

Physicochemical methods of investigation: TGA, IR, FTIR, XRD, X-ray fluorescence, S_{BET}, HR TEM, differential dissolution [2].

3 Results and discussion

The formation of OMPP in the presence of alkali was studied. Alkali addition to the glycine-nitrate mixture was found to promote glycine coordination to the metal which results in the formation of a neutral solid compound whose structure contains an oxidant (series I–$NaNO_3$, series II–NH_4NO_3). According to IR and thermal analysis data this oxidant does not exist as a

separate phase but is chemically bound to the ligand and enters into the structure of a complex X-ray amorphous complex compound. The presence within the structure of the synthesized OMPP along with the fuel component (glycine) also of an oxidant makes them able to undergo exothermal decomposition and combustion. It was shown that the nature of the transition d-metal cation and the oxidant together and the regime of the burning are the most significant factors determining the process of their decomposition.

The OMPP of series I was found to be little acceptable for perovskites synthesis because of the higher temperatures required for their decomposition (Fig.1) as well as the presence of impurities of sodium compounds in the final product. On the contrary, the burning of OMPP of series II proceeds efficiently in both regimes (VCS, SHS) with a high degree of gasification at lower initiation temperatures. Phase composition of the perovskites from both combustion regimes has been investigated (IR (Fig.2), XRD, TGA, XRD, TEM (Fig.3), S_{BET}, differential dissolution). The combustion regime of the precursor plays an important role in the resulting phase composition, dispersion and crystallinity of the product. It was found that in the SHS regime the perovskite content in the combustion product was as high as 90% without the additional stage of calcination. The observed phase homogeneity and high crystallinity degree of the resulting perovskites may indicate that a higher combustion temperature has been reached in the SHS regime. Under such conditions, the lanthanum carbonate phase decomposes and the formation of carbonaceous residues becomes unlikely. This observation was common for all OMPK of series II studied.

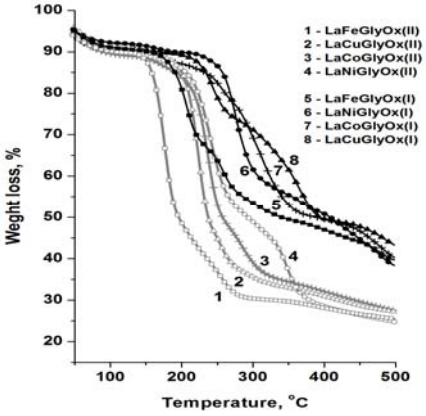

Fig. 1. TG curves of OMPP of I and II series.

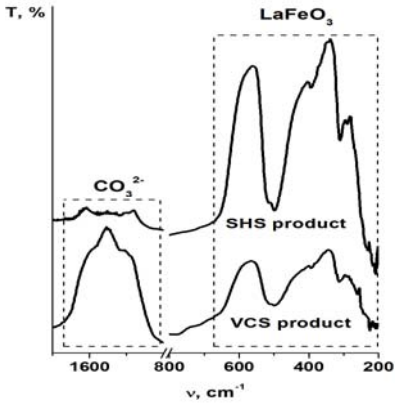

Fig. 2. FTIR spectra of products of VCS and SHS from LaFeGlyOx(II).

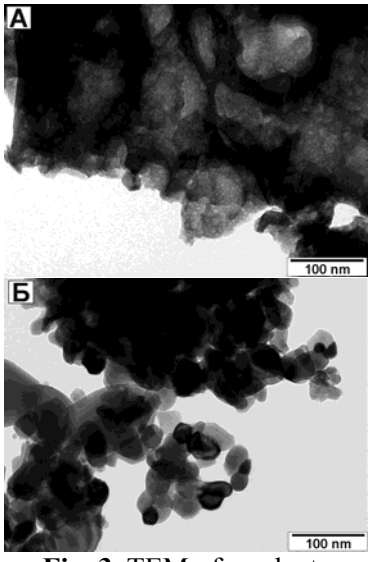

Fig. 3. TEM of products of VCS (A) and SHS (B) from LaFeGlyOx(II).

4 Conclusions

Thus, solid organometallic complex precursors of perovskite catalysts have been synthesized which are capable of forming perovskite phase in the energy-saving self-propagating high-temperature synthesis without the additional stage of calcinations.

References

[1] A.S. Mukasyan, C. Costello, K.P. Sherlock, D. Lafarga, A. Varma, *Sep. Purif. Technol.* 25 (2001) 117-126.

[2] O.V. Komova, S.A. Mukha, O.V. Netskina G.V. Odegova, A.A. Pochtar`, A.V. Ishchenko, V.I. Simagina, *Ceram. Int.* 41 (2015) 1869-1878.

II-PP198

The Characterization of Ziegler Type Ti-Based Catalysts of Ethylene Polymerization by XPS

Nizovskii A.I.[1,2*], Kalinkin A.V.[1], Koshevoy E.I.[1], Mikenas T.B.[1], Bukhtiyarov V.I.[1]

1 - Boreskov Institute of Catalysis SB RAS, Novosibirsk, Russia
2 - Omsk State Technical University, Omsk, Russia

* alexniz@inbox.ru

Keywords: supported Ziegler-Natta type catalysts, XPS

1 Introduction

The supported Ziegler-Natta type catalysts of α-olefin polymerization represent catalytic systems of the composition $(Me_x^{(n+)}L_y)/MgCl_2$, where Me - transition metal, usually Ti, in degree of oxidation from (2+) to (4+), L - Cl, OR-groups. The most effective support for an active component of the catalyst is «the activated» waterless (hydrophilic) magnesium chloride with the developed surface, modified by various additives (electron donor or acceptor compounds). The features of composition and structure of polymerization catalysts possessing high sensitivity to H_2O, O_2 and other polar compounds demand use of the inert atmospheres at all stages of work with these systems: synthesis, research of an active component, test in polymerization reaction.

One of the most used physical methods allowing obtain information about electron state of the active centers of the catalysts is the XPS method. However, for studying the systems that actively interact with atmospheric gases (oxygen and water vapor), its facilities are very limited. Working with such materials requires special chambers with controlled atmosphere, the glove box, and transport of the samples to the spectrometer is an important problem because the ordinary commercial devices involve loading the samples in contact with atmospheric gases. In this work, the samples were loaded into the spectrometer using a specially designed glove box docked to the XPS spectrometer (Fig. 1).

2 Experimental

XPS spectra of supported Ziegler-Natta type catalysts were obtained on a SPECS (Germany) photoelectron spectrometer as described in [1]. Powder samples were fixed on a sample holder using a double-side conductive adhesive tape. Samples were loaded in the spectrometer via fast entry lock system. XPS measurements were carried out in a UHV analyzer chamber at a base pressure of 5×10^{-9} Torr.

Figure 1. Download the sample into the SPECS spectrometer using «home made» glove box.

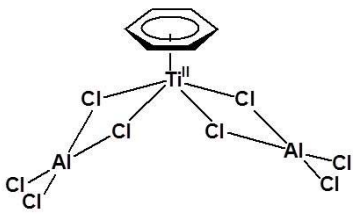

Figure 2. [η^6-Benzene$TiAl_2Cl_8$]

Before the measurements, the binding energy (BE) scale was calibrated against the characteristic lines of metallic gold and copper — $Au4f_{7/2}$ at 84.0 eV and $Cu2p_{3/2}$ at 932.6 eV, respectively. To take into account the charging effect appeared for non-conducting substances as a result of photoemission under MgK_α irradiation, the C1s line with the BE of 284.8 eV was used as internal reference.

3 Results and discussion

In the study of divalent titanium complex of [η6-BenzeneTiAl2Cl8] composition (initial compound for preparation of TMC with Ti(II)), in the XPS spectra, the lines corresponding to Ti(+2) as well as Ti(+3) were observed in the region of Ti2p. After recording the spectra, the sample was moved into lock chamber of the spectrometer that was filled atmosphere. After this procedure, the spectra of all the regions were recorded again as for the initial sample. As can be seen in Fig 3 (a), the lines corresponding to Ti(+2) and Ti(+3) were disappeared and the line corresponding to Ti(+4) was observed at the spectrum (Fig 3 (b)). At the same time, the intensity of the Ti2p line increased by an order.

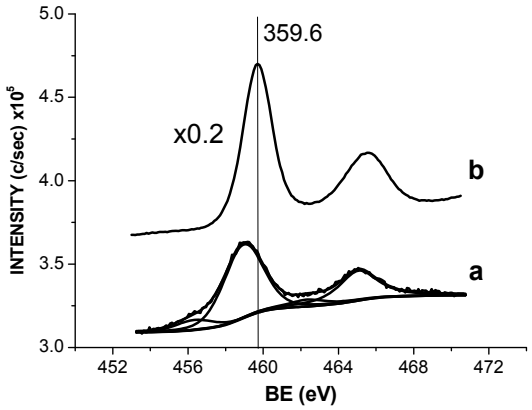

Figure 3. Ti2p core-level spectra of samples: initial (a) and after exposure to air (b).

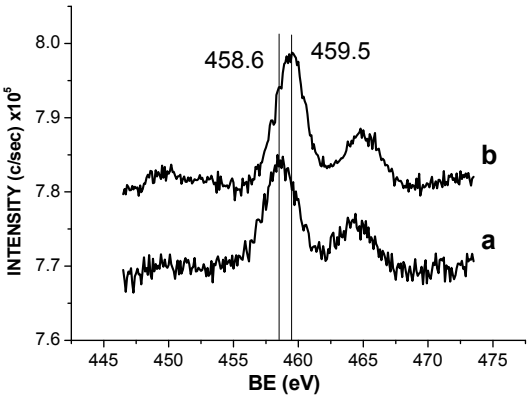

Figure 4. Ti2p 4f core-level spectra of the $Ti/MgCl_2$ samples: initial (a) and after exposure to air (b).

The samples with low concentration of supported titanium (at. ratio Ti/Mg = 0.02) were also studied. As for the previous sample, spectra were recorded for the initial sample and for the sample after exposure to the atmosphere. It is seen from the spectra in the region of Ti2p (Fig. 4) that in the initial sample, oxidation state of titanium corresponded to (+3) and after oxidation treatment, the surface of the sample contained Ti(+4).

4 Conclusions

It has been shown that the «home made» glove box system developed in Boreskov Institute of Catalysis allowed to study the supported Ziegler-Natta type catalysts by XPS effectively.

Acknowledgements

The work was supported by the grant of the President of the Russian Federation for the state support of the leading scientific schools of the Russian Federation (NSh-5340.2014.3).

II-PP199

New Possibility for Investigation of Supported $Pt/MgAlO_x$ Catalysts by XPS with Use of Monochromatic AgL_α Irradiation

Nizovskii A.I.[1,2*], Kalinkin A.V.[1], Smirnov M.Yu.[1], Belskaya O.B.[3,2], Bukhtiyarov V.I.[1]

1 - Boreskov Institute of Catalysis SB RAS, Novosibirsk, Russia
2 - Omsk State Technical University, Omsk, Russia
3 - Institute of Hydrocarbons Processing, Siberian Branch of Russian Academy of Sciences, Omsk, Russia

* alexniz@inbox.ru

Keywords: platinum supported Pt/MgAlOx catalysts, XPS, monochromatic AgLa

1 Introduction

The capabilities of XPS to study heterogeneous catalysts are severely restricted for supported $Pt/MgAlO_x$ catalysts. When XPS spectra from these catalysts are taken with the standard AlKα or MgKα irradiations, the Pt4f doublet line is masked by a strong Al2p line as well as by the additive lines-satellites from Mg2s line. A possible solution of this problem could be the use of AgLα irradiation with the photon energy of 2984.3 eV for excitation of $Pt3d_{5/2}$ and Al1s lines.

2 Experimental

All measurements were performed with a SPECS (Germany) photoelectron spectrometer equipped with two X-ray sources. One source with a double Al/Mg anode works without a monochromator, whereas another source, with a double Al/Ag anode, was used with a monochromator. Application of the monochromator narrows essentially the energy width of the exciting irradiation and, hence, the width of the photoemission lines. For each sample, spectra were recorded using non-monochromatic MgKα (hν = 1253.6 eV) and monochromatic AgLα (hν= 2984.3 eV) irradiations.

3 Results and discussion

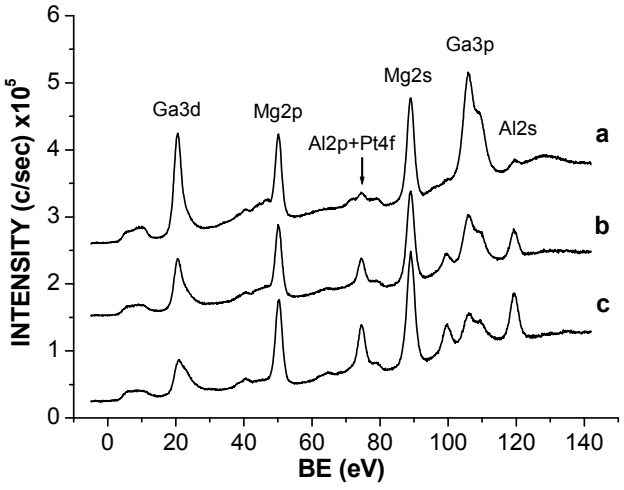

Figure 1. XPS spectra of Pt/MgAlO*x* catalysts with various Ga/Al ratios in support: 10% Al (a); 50% Al (b); 70% Al (c).

A Full Width at Half Maximum (FWHM) is an important characteristic of photoelectron spectra. The smaller is the FWHM, the better is the spectra resolution and, therefore, the more accurate is the determination of the positions and areas of spectral components belonging to different chemical states of an element.

FWHM of the $Pt3d_{5/2}$ line in the studied compounds and catalysts is higher than that of the MgKα-excited $Pt4f_{7/2}$ line by approximately 1.5 eV. The higher value of the $Pt3d_{5/2}$ FWHM makes this line less useful for the characterization of most platinum containing substances than the Pt4f line. Nevertheless, the use of AgLα irradiation for measurement of the $Pt3d_{5/2}$ spectra might be very helpful for the Pt/Al_2O_3 catalysts and many other particular systems where the Pt4f doublet line is strongly screened by the Al2p line, so the researchers have to analyze the broad $Pt4d_{5/2}$ line (FWHM of 4.5 – 5.0 eV) instead.

When AgLα irradiation is used for study the supported $Pt/MgAlO_x$ catalysts, need arises, as well as when the conventional X-ray sources are used, the calibration of the spectral lines because of their shift due to surface charging. Usually, for supported catalysts, as a standard the internal standard is used that is the value of binding energy of the line of the support, for example, Al2p, Mg2p and others as well as the value of binding energy of C1s line from residual organic contaminents on the surface of samples. In this case, under transition to a more hard X-ray irradiation region (hν=2984.3 eV) than traditional sources, the intensity of Al2p, Mg2p lines significantly reduced. This is due to two factors, namely a decrease in the photoionization cross sections for these levels compared with AlKα or MgKα irradiations and an overall reduction in the intensity of the X-ray source as AgLα source is used only in monochromatic regime.

In this work, the following method of calibration was used. Firstly, the values of binding energies of the most intense lines (O1s, Mg1s, $Ga2p_{3/2}$) were calibrated relative to C1s line (284.8 eV). Then, these lines were recorded also at AgLα irradiation along with the lines for Pt3d, Al1s, Mg1s and others. This procedure allows to create a specific set of internal standards for different oxide supports using proposed radiation.

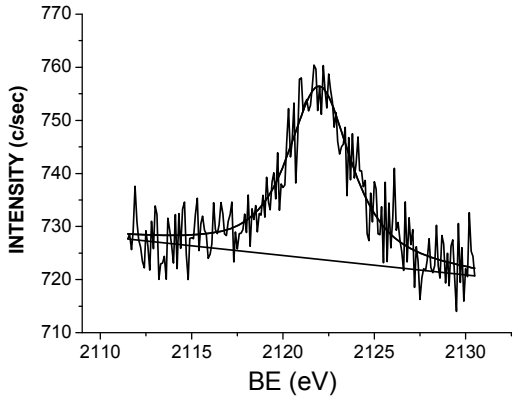

Figure 2. $Pt3d_{5/2}$ core-level spectra of $Pt/MgAlO_x$ (2% wt. Pt).

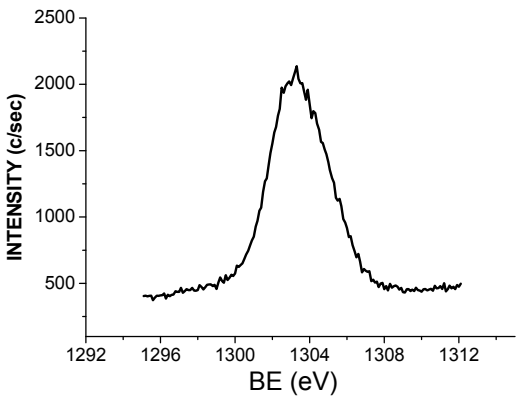

Figure 3. Mg1s spectra of Pt/MgAlO*x* catalysts.

4 Conclusions

AgLa irradiation is an useful tool for investigation of supported Pt-alumina catalysts. The values of $Pt3d_{5/2}$ binding energy can be used for determination of the oxidation state of platinum in supported $Pt/MgAlO_x$ catalysts and other systems containing both platinum and aluminum.

Acknowledgements

The work was supported by the grant of the President of the Russian Federation for the state support of the leading scientific schools of the Russian Federation (NSh-5340.2014.3).

II-PP200

Modeling and Optimization of Sol-Gel Process Parameters to Synthesize Nanostructured Boria-Alumina Catalyst Supports: Response Surface Methodology Approach

Özcan O.[1,2*], Dusova-Teke Y.[3], Kibar M.E.[1,2], Seçkin C.[3], Yonel-Gumruk E.[3], Akın A.N.[1,2]

1 - Kocaeli University, Department of Chemical Engineering, Kocaeli, Turkey
2 - AYARGEM, Alternative Fuels R&D Center, Kocaeli University, Kocaeli, Turkey
3 - Turkish Petroleum Refineries Corporation, R&D Department, Izmit, Turkey

* orhan.ozcan@kocaeli.edu.tr

Keywords: sol-gel, boria-alumina, response surface methodology

1 Introduction

Recently, nanostructured metal oxides as catalyst support materials have gained much attention for their unique physicochemical properties like high surface area, high pore volume and high pore size [1].

Alumina-based mesoporous materials are well suited catalytic materials. Alumina is an amphoteric metal oxide and has a wide range of applications in heterogeneous catalysis both as catalysts and supports. The acidity on the alumina surface can be tuned by surface modification with supported oxides. Among alumina-based materials, boria-alumina mixed oxides have been considered as important acid catalysts in many industrial applications such as catalytic reforming, cracking and hydrotreating reactions [2,3,4]. Boron addition to the alumina support is known to increase Bronsted acid sites and improves catalytic performance by decreasing metal-support interaction [5,6,7].

In literature, B_2O_3-Al_2O_3 mixed oxide catalyst supports are mostly prepared by impregnation on γ-alumina with boric acid [1,7] and precipitation technique using ammonium hydroxide [3,8]. The design, synthesis and modification of binary oxide materials need to be well controlled. For this purpose, the sol-gel route seems convenient since it allows the formation of the active phase directly in the catalyst lattice [9,10].

In this study, a sol-gel process was used to prepare mesoporous B_2O_3-Al_2O_3 supports with high BET surface area around 500 m^2/g. Response surface methodology (RSM) has been studied in order to optimize the process variables like boria content and hydrolysis ratio to achieve high surface area and mesoporous structure. For the characterization of sol-gel prepared binary oxide supporting materials XRD, BET, FTIR, TPD, SEM and TEM techniques were used.

2 Experimental/methodology

The sol-gel precursors for Al_2O_3 and B_2O_3 are aluminum isopropoxide (AIP) and sodium tetraborate decahydrate, respectively. Desired amount of precursors were dissolved in 1-propanol and well stirred to prepare a medium for hydrolyzing step. Sodium tetraborate decahydrate was dissolved in given amount of water which was then used to complete hydrolysis at 85 ^oC under reflux. All prepared samples were aged for 2 days to grow the network encapsulating the solution and dried in an oven at 100 ^oC for 24 hours. Calcination step was done at 500 ^oC for 3 hours in a muffle furnace.

3 Results and discussion

Optimum sol-gel process parameters to synthesize B_2O_3-Al_2O_3 (1-5 wt% B_2O_3) catalyst supports are defined by utilizing response surface methodology approach. Due to the face centered composite design, four parameters and their experimental values are summarized in Table 1. According to experimental design points, 30 runs were performed which included 6 repeating runs on the centered levels. BJH adsorption/desorption isotherms and pore size distributions of the samples were investigated by structural and catalytic point of view. TEM images and XRD patterns were interpreted to analyze the crystalline size using Scherrer equation. The acidity of boria-alumina supports with increasing B_2O_3 content were defined by TPD and FTIR results. The effect of aging, drying and calcination process to the textural properties of final product were also discussed.

Table 1. Experimental design points

Name	Units	Low Actual	Mean	High Actual	Low Coded	High Coded
HNO_3	mol HNO_3/mol AIP	0,1	0,5	0,9	-1	1
AIP	Molarity	0,4	0,7	1	-1	1
R	mol H_2O/mol AIP	15	57,5	100	-1	1
B_2O_3	% weight	1	3	5	-1	1

Maximum BET surface area of the sol-gel prepared boria-alumina support has been reached 538 m^2/g under the conditions listed in Table 2. It was concluded that the addition of boria to the alumina support at low hydrolysis ratio was increasing total surface area by effecting the pore structure slightly.

Table 2. Experimental conditions

Name	Units	Level
HNO_3	mol HNO_3/mol AIP	0,1
AIP	Molarity	1
R	mol H_2O/mol AIP	15
B_2O_3	% weight	5

Acknowledgements

This work was funded by Turkish Petroleum Refineries Corporation and TUBITAK (ARDEB 1003) with project number 213M194.

References

[1] F. Rashidi, T. Sasaki, A. M. Rashidi, A. N. Kharat, K. J. Jozani, *Journal of Catalysis*. 299 (2013) 321-335.
[2] T. Xiu, J. Wang, Q. Liu, *Microporous and Mesoporous Materials*. 143 (2011) 362-367.
[3] C. Flego, W. O. Parker Jr., *Applied Catalysis A: General*. 185 (1999) 137-152.
[4] S. A. El-Hakam, E. A. El-Sharkawy, *Materials Letters*. 36 (1998) 167-173.
[5] Usman, T. Kubota, I. Hiromitsu, Y. Okamoto, *Journal of Catalysis*. 247 (2007) 78-85.
[6] P. Torres-Mancera, J. Ramires, R. Cuevas, A. Gutierrez-Alejandre, F. Murrieta, R. Luna, *Catalysis Today*. 107-108 (2005) 551-558.
[7] F. M. Bautista, J. M. Campelo, A. Garcia, D. Luna, J. M. Marinas, M. C. Moreno, A. A. Romero, *Applied Catalysis A: General*. 170 (1998) 159-168.
[8] Y.-W. Chen, M.-C. Tsai, *Catalysis Today*. 50 (1999) 57-61.
[9] A. Martyla, B. Olejnik, P. Kirszensztejn, R. Przekop, *International Journal of Hydrogen Energy*. 36 (2011) 8358-8364.
[10] L. Forni, G. Fornasari, C. Tosi, F. Trifiro, A. Vaccari, F. Dumeignil, J. Grimblot, *Applied Catalysis A: General*. 248 (2003) 47-57.

II-PP201

Investigation of the Microstructure Features of the Solid Solutions $La_{1-x}Ca_xCoO_{3-\delta}$ in Different Gas Environment

Gerasimov E.Yu.[1,2*], Vinokurov Z.S.[1,2], Kulikovskaya N.A.[1], Isupova L.A.[1], Tsybulya S.V.[1,2]

1 - Boreskov Institute of Catalysis, Novosibirsk, Russia
2 - Novosibirsk State University, Novosibirsk, Russia

* gerasimov@catalysis.ru

Keywords: perovskite, planar, defects, XRD, HRTEM, oxidation

1 Introduction

Complex oxides $La_{1-x}Ca_xMO_{3-\delta}$ (M = Mn, Fe, Co) with perovskite-type structure intensively studied over the years, due to the unique combination of magnetic and electronic properties. In particular, the compounds of this class are used in catalysis in high temperature oxidation processes. The catalytic properties of these solutions depend on the preparation methods and the degree of substitution of calcium cations. Increasing of Ca^{2+} content enhances the mobility of the O^{2-} anion, which positively influences on the catalytic activity of the samples, but in some cases, limits the region of existence of the solid solutions and may cause decomposition of the solid solutions in high-temperature processes.

This work studies the characteristics of the formation of the microstructure of perovskite oxides of $La_{1-x}Ca_xCoO_{3-\delta}$ by XRD and HRTEM methods and compare the microstructure features of solid solutions $La_{1-x}Ca_xCoO_{3-\delta}$, with the previously studied series of $La_{1-x}Ca_xMO_{3-\delta}$(M = Mn, Fe).

2 Experimental/methodology

The samples $La_{1-x}Ca_xCoO_{3-\delta}$ were synthesized by dissolving in water the corresponding nitrate salts in the appropriate ratio followed by evaporation and annealing of the product at 900° for 4 hours (the Pechini method). High resolution electron microscopy (HRTEM) images were obtained on a JEM-2010 (Japan) with resolution 1.4 Å. X-ray microanalysis (EDX) of elemental composition of the samples was carried out using energy-dispersive spectrometer with a Si-(Li) detector with an energy resolution of 130 eV. In situ XRD experiments were carried out at the "High Precision Diffractometry" station at Siberian Synchrotron and Terahertz Radiation Center (Novosibirsk, Russia). The diffractometer was equipped with high temperature chamber Anton Paar HTK2000 and position sensitive parallax-free linear OD-3M detector. X-ray wavelength of 1.01 Å was set by a single reflection from flat perfect crystal monochromator Si(200).

3 Results and discussion

According to XRD, in a series of $La_{1-x}Ca_xCoO_{3-\delta}$ the presence of morphotropic transition R-3c ($0 \le x \le 0.2$) → Pm3m ($0.3 \le x \le 0.4$) reported, associated with a gradual increase of the content of Ca cations. Samples with $x \ge 0.5$ are multiphase, the main component of those is based on the perovskite phase $La_{0.6}Ca_{0.4}CoO_{3-\delta}$. According to HRTEM samples with $x \le 0.5$ are almost single-phase solid solutions with the perovskite structure, while containing a small proportion of simple oxides CaO and Co_3O_4.

Application of the samples as the CH_4 oxidation catalysts at 600T^oC (?) leads to partial phase decomposition of solid solutions and formation of planar vacancies in the perovskite structure in the direction of the planes (101). An interesting feature is the presence of irregularities in the crystal structure of the perovskite matrix. Thus, formation of alternating perovskite-brownmillerite structures are occurred after performing of methane oxidation reaction(Fig. 1). Also, as the result of reaction partial formation of nanostructures in orthorhombic perovskite matrix are occurred. Apparently, this nanostructures lead to the further formation of brownmillerite structure in perovskite.

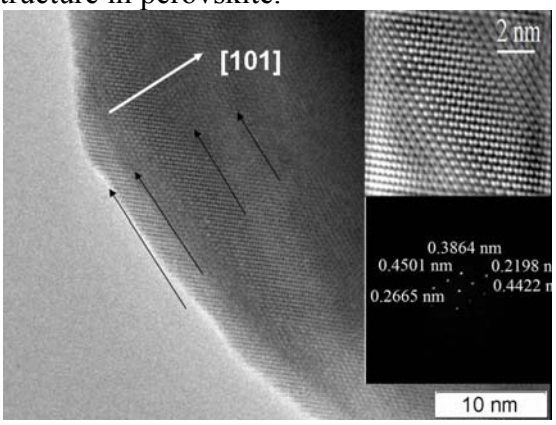

Fig. 1 HRTEM image of $La_{0.6}Ca_{0.4}CoO_{3-\delta}$ microstructure after CH_4 oxidation reaction. In inserts FFT image and Fourier–cleaned image are shown.

To examine the thermal stability of the solid solutions *in situ* testing of samples was performed in the high temperature chamber using synchrotron radiation. Calcination of the samples in air has virtually no effect on the structure and microstructure of $La_{1-x}Ca_xCoO_{3-\delta}$ solid solutions. Heating of perovskite oxides under vacuum, conversely, results in a partial decomposition of the solid solutions. For example, in $La_{0.6}Ca_{0.4}CoO_{3-\delta}$ there is an allocation of oxides CaO and Co_3O_4 on the surface of $La_2Co_2O_5$, wherein the particle sizes of formed phases are in the range of 50 - 100 nm.

4 Conclusions

In this work the solid solutions $La_{1-x}Ca_xCoO_{3-\delta}$ synthesized by polymerized complex precursor (Pechini) method were studied. XRD and HRTEM show the formation of X-ray single-phase solid solutions in the range of replacement parameter $0.5 \geq x \geq 0$. According to XRD, structure of the samples seemed to be almost unaffected after the CH_4 oxidation reaction, but HRTEM data indicate the formation of nanoheterogeneous sites on perovskite surface. Increase of the substitution parameter (x = 0.2, 0.4) lead to formation of simple oxides of Co and La particles on the surface of the initial phase. Furthermore, there is a formation of planar defects in the direction of the crystallographic planes (101). As a result of the reaction medium in the sample $La_{0.6}Ca_{0.4}CoO_{3-\delta}$ areas are formed with alternating elements of the perovskite structure and brownmillerite.

It is shown that the calcination in air samples does not change the structure of the sample, and calcination in vacuum conversely leads to separation of the solid solutions. Whereby it can be concluded that the decomposition of the solid solution caused by the partial removal of oxygen.

Acknowledgements

The reported study was supported by RSF, research project No. 14-23-00037. In situ XRD experiments were carried out with involvement of equipment belonging to the shared research center *"*SSTRC*"*.

II-PP202

Deactivation Mechanism of Molybdenum Catalysts

Yelimanova G.G.[1*], Smolin R.A.[2], Batyrshin N.N.[1], Kharlampidi Kh.E.[1]

1 - Kazan national research technological university, Kazan, Russia
2 - United research and development center, Kazan, Russia

* yelimanova@mail.ru

Keywords: molybdenum catalyst, organic hydroperoxide, hydrogen peroxide, deactivation, epoxidation

1 Experimental/methodology

Thermal stability of catalysts was studied on change of concentration of the dissolved molybdenum in the range of temperatures 90 - 120 ° C, using the ampoules method. Concentration of the dissolved molybdenum was defined by titration method [1].

Oxidation was carried out in the reactor of the manometrical installation allowing to fix change of oxygen volume absorbed during reaction as function of time. Catalyst PMKZh was allocated in a firm look, and dissolved in a dimetilformamid (DMFA).

2 Results and discussion

As a result of experiments it is established that at temperatures close to working temperatures in the industrial reactor of epoxidation of GPEB propylene (110 ºC), there is a fast decrease in the content of the dissolved molybdenum in catalysts.

The catalysts, synthesized on organic hydroperoxides, CMC and MC are losing 85% of the dissolved molybdenum at temperatures of 110, 120 ºC already through 15 minutes, and ~45% initial metal are remained in PMCZh.

It is known that derivatives of ortovanadiyevy acid thermally are decomposed by the radical way [2] since compounds of molybdenum and vanadium behave similarly in epoxidation reactions and decomposition of hydroperoxides,, it is possible that the compounds of molybdenum which are a part of catalysts also are decomposed by the homolytic way

The fact of decomposition substance with free radicals can be detect experimentally to acceleration a radical chain reaction. In this work we used standard reaction of liquid-phase oxidation of styrene oxygen, kinetic characteristics by which are repeatedly checked and described in literature [3].

Styrene mixed with DMFA oxidised very slowly. In the presence of a molybdenum catalyst, the rate of oxidation of styrene is increased depending on the temperature on the order of 2-4 (at T=80°C with $8{,}97 \cdot 10^{10}$ to $5{,}39 \cdot 10^{6}$ mol/l·c). Moreover, the oxidation begins immediately without the induction period.

3 Conclusions

Thus, it is experimentally proved that the molybdenum catalyst deactivation begins with homolytic decomposition. Based on this fact, as well as based on the composition of products of decomposition molybdenum catalysts, are proposed scheme of the mechanism of deactivation.

Acknowledgements

This research was supported by the Ministry of Education and Science of Russian Federation as part of the state contract ("PNIL 02.14", base part).

References

[1] Busev A.I. Analytical chemistry of molybdenum. - M .: USSR. 1962. 306 p.
[2] Batyrshin, N.N. Turning vanadyl acetylacetonate in the process of liquid-phase oxidation of hydrocarbons / N.N. Batyrshin, G.V. Koshkin, H. E. Kharlampidi // Petrochemicals. - 1982. - T.22. - S. 637 – 642.
[3] Emanuel, N.M. The order of testing of chemical compounds as stabilizers in polymeric materials / N.M. Emanuel, G.P. Gladyshev, E.T. Denisov, V.F. Tsepalov et al. - Chernogolovka: USSR Academy of Sciences, 1976.

II-PP203

Plasma-Arc Synthesis of PdCeSnC Composites for Preparation of Highly Active Pd/CeO_2-SnO_2 Catalysts for Low-Temperature CO Oxidation

Boronin A.I.[1,2*], Slavinskaya E.M.[1,2], Gulyaev R.V.[1,2], Zaikovskii A.V.[3], Smovzh D.V.[3], Novopashin S.A.[3]

1 - Novosibirsk State University, Novosibirsk, Russia
2 - Boreskov Institute of Catalysis, Novosibirsk, Russia
3 - Kutateladze Institute of Thermophysics, Novosibirsk, Russia

* boronin@catalysis.ru

Keywords: plasma-arc synthesis, low-temperature CO oxidation, composite, Pd/CeO_2, Pd/SnO_2

1 Introduction

Catalysts based on cerium oxide and palladium are among the most promising catalysts used for oxidation of carbon monoxide and other harmful gases. The development of new effective catalysts for neutralization of carbon monoxide is tightly bound with necessity to form highly dispersed states of active components Pd and CeO_2. These states are required to be stable in a wide temperature range and under the action of reaction medium. Perspective way to create new effective catalysts of CO oxidation is an application of nanocomposite precursor materials prepared by plasma-arc synthesis (PAS). This method is based on sputtering of the separate components as a highly dispersed nanoparticles forming complicated nanostructured composites. During the subsequent calcination in air the burning of carbon occurs which facilitate the transformation of the composite precursors to dispersed metal-oxide catalytic systems [1]. For the implementation of this new approach, in this work the composite Pd/CeO_2-SnO_2 catalysts were prepared from PdCeSnC composite precursors obtained by PAS. The step-by-step calcination of this PdCeSnC composite allowed us to investigate the process of the component phase transitions and to obtain highly active CO oxidation catalysts.

2 Experimental/methodology

In the presented work, the PdCeSnC composite precursors were prepared by PAS for the first time. The synthesis of Pd/CeO_2-SnO_2 catalysts was carried out in two steps: step 1 – direct synthesis of the PdCeSnC composite in the plasma-arc chamber, and step 2 – calcination of the composite in air at 450°C - 1000°C resulting in carbon burning from composite material and formation of the catalyst. HRTEM, XRD, XPS, Raman spectroscopy were used to investigate the microstructure, composition and electronic state of the composite components after the high-temperature calcination step. The catalytic testing was performed by the temperature programmed reaction in $CO+O_2$ (TPR-$CO+O_2$) using plug flow reactor with mass-spectrometric analysis of the gas mixture.

3 Results and discussion

Figure 1a shows that the high activity (low T_{10} and T_{50} values) is observed for the 1%Pd/CeO_2 catalysts after calcination at 600-800°C, while calcination at T = 900°C results in decrease of activity with the further dramatic deactivation after calcination at 1000°C. Introduction of Sn to the catalyst composition results in better catalytic performance compared to Pd/CeO_2. As it can be seen from Fig. 1b the Pd/CeO_2-SnO_2 catalyst is characterized by

excellent activity after calcination at 600-900°C. Calcination at 1000°C results in increase of T_{50} value, but this deactivation effect is less pronounced compared to Sn-free sample. These data demonstrate the strong thermal activation effect and the high thermal stability of catalysts doped by tin. HRTEM and XRD data indicate extremely high dispersed states of palladium and other components of modified catalysts.

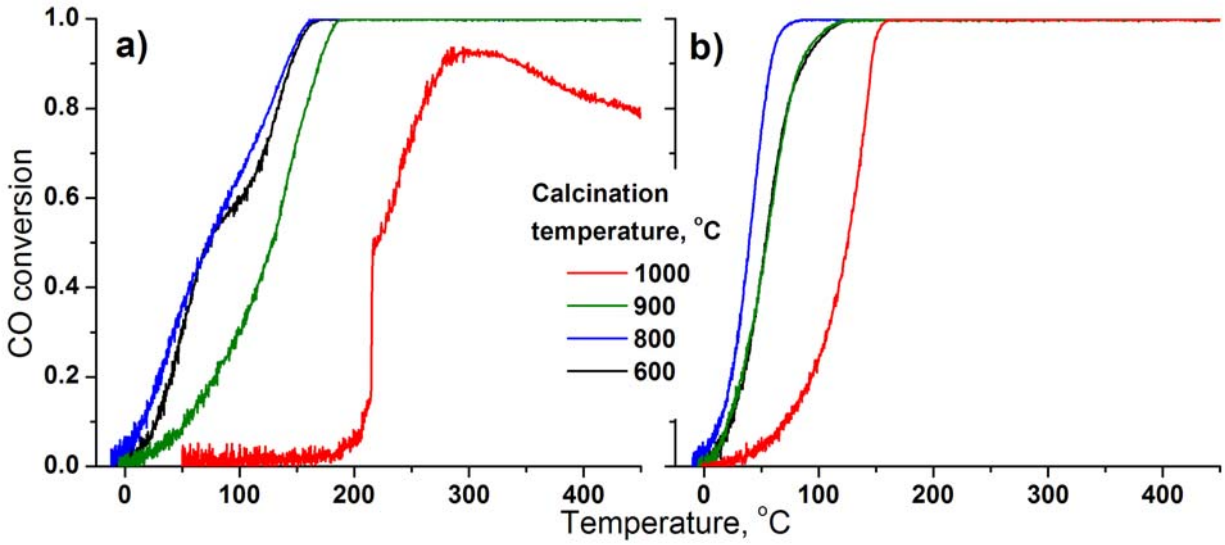

Fig. 1. Temperature dependences of CO conversion for CO oxidation reaction using 1%Pd/CeO_2 (a) and 1%Pd/CeO_2-SnO_2 (b) catalysts calcined at 600°C-1000°C.

The XPS data show the presence of sp^2- and sp^3- carbon nanostructures which are mixed with the components in the initial PdCeC or PdCeSnC composites. These carbon nanostructures play a key role in the formation of the high-defect solid solution of palladium in the CeO_2 structure ($Pd_xCe_{1-x}O_{2-\delta}$). Introduction of tin to the initial composite leads to formation of small SnO_2 nanoparticles after calcination. Together with the residual carbon structures the SnO_2 nanoparticles prevent sintering of $Pd_xCe_{1-x}O_{2-\delta}$ particles during calcination.

4 Conclusions

The plasma-arc method was applied to synthesize the PdCeC and PdCeSnC composites which can be effectively used as precursors for preparation of Pd/CeO_2 and Pd/CeO_2-SnO_2 catalysts with high activity in CO oxidation reaction. The obtained Pd-ceria based catalysts modified with tin represent a very promising catalytic system, which has a unique combination of high thermal stability and activity in CO oxidation starting at low temperatures.

Acknowledgements

This work was supported by the Russian Foundation of Basic Research (Grant 14-03-01088) and Ministry of Education and Sciences of Russian Federation (target grant for state support of leading universities of the Russian Federation #074-U01).

References

[1] R.V. Gulyaev, E.M. Slavinskaya, S.A. Novopashin, D.V. Smovzh, A.V. Zaikovskii, D.Yu. Osadchii, O.A. Bulavchenko, S.V. Korenev, A.I. Boronin, *Applied Catalysis B: Environmental,* 147 (2014) 132.

II-PP204

Catalytic Performance of MFI Zeolite Synthesized with Cetyltrimethylammonium Cation as SDA

Campos A.F.P., Borges D.G., Cardoso D.*

Universidade Federal de São Carlos, São Carlos, Brazil

* dilson@ufscar.br

Keywords: MFI zeolite, cetyltrimethylammonium cation, transesterification reaction

1 Introduction

An alternative to overcome diffusional restrictions relative to application of zeolite materials is by using in the form of nanocrystals (crystal sizes below 100 nm). These zeolites can be synthesized through the use of specific structure-directing agents, such as bifunctional surfactants [1]. Based on this concept, several studies have explored the ability of cationic amphiphilic surfactants commonly used to obtain mesoporous materials as zeolite structure-directing agents, for example, alkyltrimethylammonium surfactants ($C_nH_{2n+1}N^+(CH_3)_3Br^-$, n = 6, 8, 10, 12, 14 e 16) [2,3]. In this study, we have evaluated the performance of cetyltrimethylammonium cation as structure-directing agent to obtain zeolites, as well as, the activity and catalytic stability study of these zeolitic materials in the catalytic transesterification.

2 Experimental/methodology

The chemical composition of the reaction mixture used to synthesis of zeolites was 1 SiO_2: 0,125 Na_2O: 0,01 Al_2O3: 0,05 CTMABr: 40 H_2O[2]. The syntheses were conducted at temperature of 150 ºC and different hydrothermal treatment time (1-6 days). The zeolites were characterized through X-ray diffraction, scanning electron microscopy (SEM), thermogravimetric and chemical analysis. The catalytic tests were performed using the catalytic transesterification between methanol and ethyl acetate (2:1). The catalytic reactions were conducted in the presence of 4 % (w/w) catalyst at 50 ºC and 0,5 hours of reaction time. After the reaction, the catalysts were filtered, dried and reused several times. The conversion of ethyl acetate was quantified by gas chromatography.

3 Results and discussion

As shown in Figure1-a, the XRD patterns of the materials synthesized with $CTMA^+$ cation from hydrothermal treatment of 2 days are of MFI structure.

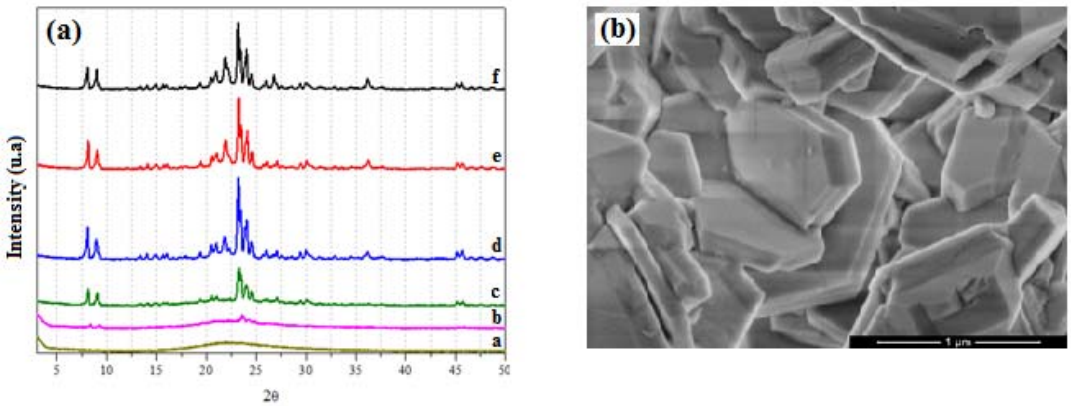

Fig. 1. (a) XRD power patterns of materials obtained from CTMA+ cations at 150 ºC after (a) 1, (b) 1,5, (c) 2, (d) 3, (e) 4 and (f) 6 days. (b) SEM image of MFI formed after 6 days at 150 ºC.

The elongated cations $CTMA^+$ affected the morphology of the MFI crystals and after 6 days it was obtained hexagonal plates crystals (Figure 1-b). These cations fit within ten-membered ring straight channels of MFI structure and it should restrict the growth of crystals in direction of straight channels [1].

Due to the presence of the cations inside the zeolite channels, these as-synthesized materials exhibited catalytic activity to transesterification reaction (Fig. 2-a). The organic cations present in these zeolites are associated to siloxy anions ($\equiv SiO^-$) and the catalytic reaction takes place through these anions present on the surface of catalytic material [4]. The loss of catalytic activity as function of catalytic uses is related to leaching of organic $CTMA^+$ cations associated to these siloxy anions. These assumptions are supported by the thermal analysis (Figure 2-b).

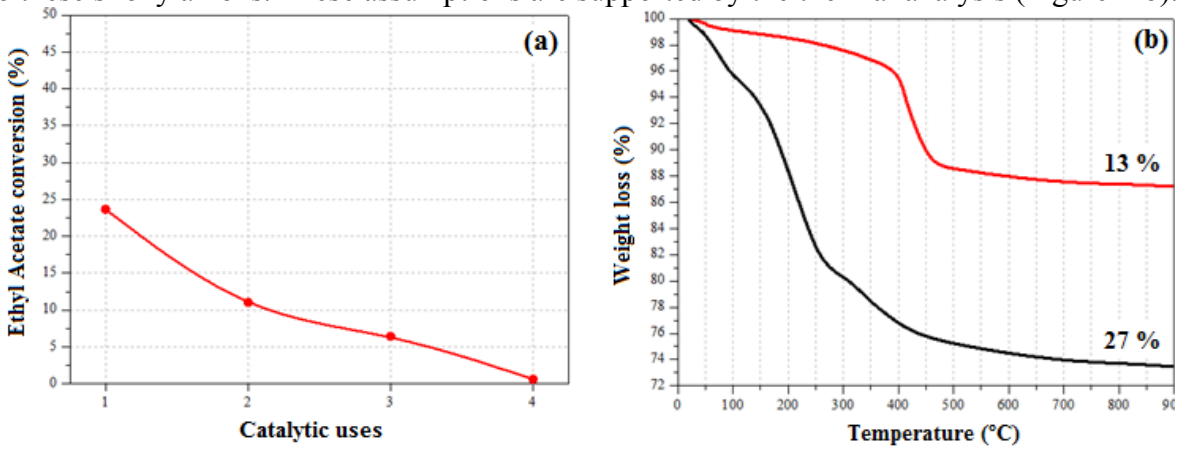

Fig. 2. (a) Ethyl acetate conversion as function of catalytic uses and (b) thermal analyses of the MFI-zeolites before (black line) and after successive catalytic uses (4th use – red line).

Figure 2-b presents the thermal analyses of the zeolites before and after successive catalytic uses (4th use). Before the material was used catalytically, there was a weight loss of 27 % that can be attributed to the following events: (1) below 100 ºC, the desorption of water molecules and (2) between 100 and 300 ºC, the combustion of organic CTMA+ cations. After the fourth catalytic use of the zeolite, the weight loss was only 13 %, associated mainly to the decomposition of organic CTMA+ cations.

4 Conclusions

The results confirmed the formation of MFI-type zeolite through organic $CTMA^+$ cation from 2 days at 150 ºC. The zeolitic materials obtained were catalytically active for the transesterification reaction and it is believed that the low catalyst stability is related to leaching of $CTMA^+$ cation present on the surface of these materials.

Acknowledgements

Thanks to CNPQ for the financial support.

References

[1] M.Choi, Nature. 461 (2009).
[2] S. Che, D. Xu, J. Feng, *Dalton Trans*. 43 (2014).
[3] T. Moteki, S.H. Keoh, T. Okubo, *Chem. Commun*. 50 (2013).
[4] L. Martins; T. J. Bonagamba; R Azevedo; P Barfiela; D. Cardoso, Applied Catalysis. A, General, v. 312, p. 77-85, 2006.

II-PP205

New High Porosity Endogas Production Catalyst on Foam Substrate for Low-Carbon Steel Heat Treatment

Makarov A.A.*, Fotin D.V.

ECAT Company, Perm, Russia

* makarov@ecocatalysis.com

Keywords: catalyst endogas, porous catalysts, steel carbonization

1 Introduction

Carbonization is one of the most widely used methods of friction and high-load metal parts performance characteristics improvement. This process involves diffusion saturation of low-carbon steel in controlled atmosphere with a mixture of carbon oxide and hydrogen (**endogas**) derived from natural gas and air mixture. Reactions of partial oxidation of hydrocarbon (including endogas production) proceed on solid nickel or platinum catalyst. Specialized cementation furnaces with premixed ($CO:H_2$) atmosphere or furnaces with built-in **endogas** generator are used for carbonization [1].

The challenge of low-carbon steel carbonization and endogas generation is the difference in process temperatures. Low-carbon steel (18ХГТ/HGT grade of alloy structure steel with 0.17-0.23% C, 0.17 – 0.37% Si, 0.8-1.1 Mn, up to 0.3% Ni, up to 0.035% S, up to 0.035 P, 1 – 1.3% Cr, 0.03 – 0.09 Ti and up to 0.3% Cu content) carbonization proceeds at temperatures of 850-950°C, while endogas generation occurs at 1020-1050°C. Carbonization velocity in most cases is 0,1mm/h with process time amounting to 8-12 hours. These conditions have a negative impact on overall carbonization process cost. From the chemical performance prospective, GIAP type catalysts currently in use allow to generate atmospheres with relatively high carbon residue content (2-3% vol.), which leads to low process performance timing-wise and easy decomposability of microcrystalline state of carburized case[1, 2].

The goal of this research work was development of catalyst that would allow to lower endogas generation temperature and consequently generate atmosphere with low carbon residue content (not exceeding 1%). One more significant goal was stabilization of catalyst phase composition and minimization of solid-state transformations between catalyst components at high temperatures [3]. Achievement of these goals would allow to reduce carbonization process time and improve its quality, as well as achieve process velocity amounting to 0,2-0,3 mm/h.

2 Experimental/methodology

γ-Al_2O_3 / Pt system was used as catalyst body to be applied on heat resistant high-porosity material with the following composition: Fe-Ni-Cr-Al. It was selected because it is well-characterized and easily accessible. Besides these catalysts are less toxic than their analogues with NiO active component. Other reasons why platinum was selected as catalyst of choice are as follows a) complex platinum compounds can be evenly distributed on the surface of aluminum oxide b) platinum crystallite size can be controlled c) partial oxidation reaction proceeds efficiently and selectively on platinum [4].

Heat resistant Fe-Ni-Cr-Al alloy was selected not only because of its thermal stability, but its structural properties as well. First, open cell high porosity (95-98%) structure gives an opportunity to blend gas-air mixture (hydrocarbon: air) homogeneously and completely. Secondly, catalyst microstructure allows to avoid local overheating that can be caused by high exothermicity of partial hydrocarbons oxidation reaction.

Thirdly, high surface area creates maximum adhesion with γ-Al_2O_3/Pt system. γ-Al_2O_3 stabilization was performed at 85-950^oC by means of doping 0,5% rare-earth oxide (either La or Pr or Nd). X-ray phase and BET-method analysis demonstrated that atoms of rare-earth element embedded into γ-Al_2O_3 crystalline grid stabilize its phase and prevent phase transistions γ-Al_2O_3 / δ- Al_2O_3 / θ- Al_2O_3 / α- Al_2O_3. Surface area of γ-Al_2O_3 doped with rare-earth oxide and heat treated at 950^oC amounted to 90-105m^2/g.

Catalyst was manufactured in 2 stages. In the first stage catalyst substrate Fe-Ni-Cr-Al was impregnated with γ-Al_2O_3 / La_2O_3 suspension and then heat treated at 1000^oC. In the second stage, the catalyst was impregnated with platinum complex compound solution followed up by deliquification and heat treatment under hydrogen at 950^oC. Pulsed chemisorption method of CO was used to establish that platinum content on the surface amounts to 65-77%. Size of 87% of platinum particles falls within 2 to 11 nm range. Catalyst samples 34 mm in diameter and 32 mm in height were manufactured for test purposes.

Endogas was generated by means of passing 35 litres/hour of propane/butane mixture and 400 litres/hour of air through synthetized heterogeneous catalysts at 930^oC. Content of generated gas mixture was as follows: CO 23,84%vol.; CO_2 0,09%vol.; CH 0,88%vol.; H_2 30,63%vol. The catalyst recovered after tests did not change its dimensions and did not have any soot on the surface.

18ХГТ/HGT grade alloy structure steel sample was carbonized at 920^oC under generated endogas for 4 hours after temperature equalization. Then the sample was cooled down to room temperature, after that heating for hardening at 830-840^oC was performed followed by temper hardening in base oil Е120А/И20А at 200^oC for 2 hours. Test results demonstrated that carburized case thickness amounted to 1,2 mm, thickness of efficient layer with thickness exceeding 500HV0,1 amounted to 0,7 mm.

3 Results and discussion

1. High conversion rate in 800 to 940°C temperature range (residual methane content not exceeding 0,91% vol.);

2.Addition of rare-earth elements oxides allows to stabilize aluminum oxide structure and maintain high surface area at high temperatures;

3. Low levels of soot formation on catalyst surface lead to absence of necessity in forced catalyst burning;

4. Endogas generation is maintained in the required gas-air mixture delivery volume range from 0,4 to 1,5 m^3/hour;

5. End result – steel carbonization process is high velocity, easy to control and is characterized by high quality of microstructure.

4 Conclusions

Catalyst samples were successfully tested in ZAO "Nakal – Promyshlenniye Pechi".

References

[1]. Lakhtin Y.M. Heat Treatment in Manufacturing Engineering. Mashinostroenie:1980.
[2]. Zimmermman R., Günther K. Materials Science & Metallurgy. Reference Book. Metallurgiya:1982.
[3]. Pakhomov N. A. Scientific foundations of catalyst preparation: introduction to theory and practice. SB RAS: 2011. 262p.
[4].Krylov O.V. Heterogenous catalysis: Textbook. Academkniga: 2004. 679 p.

II-PP206

Spherical Aluminum Oxide for Synthesis of Supported Catalysts

Murzin D.Yu.[1], Shishkova M.L.[2*], Shvarts T.V.[2]

1 - Laboratory of Industrial Chemistry, Process Centre, Abo Academi University Fin-2050, Turku/Abo, Finland

2 - The Department of General Chemical Technology and Catalysis, and Laboratory of Catalytic Technologies, St. Petersburg State Technological Institute (Technical University), Saint-Petersburg, Russia

* margolen239@gmail.com

Keywords: impregnation, the active ingredient, carrier of active alumina, formation

1 Introduction

Spherical alumina are widely used in chemical and petrochemical industry as an adsorbent, desiccant, media and catalyst for various processes. Spherical catalyst has an optimum range in size, provides the most dense packing of grains has a maximum ratio of volume to external surface of the grain. It has a maximum surface loading. Due to the increased mechanical strength of such a catalyst has a long life[1]. The development of modern and advanced catalytic and adsorption processes with moving and fluidized and fixed layers of particles requires the development of methods of producing mechanically strong ball and the resulting pellet catalysts and sorbents, resistant to abrasion and impact loads[2]. In the manufacture of oxide catalysts widely used method of applying active ingredients to the finished porous base. The technology of producing such catalysts involves two separate processes: getting media and the actual catalyst. In the process of obtaining media includes such stages as the preparation of raw material, its molding, drying and heat treatment. Introduction components may make the active components of the coagulation of pseudosasa; impregnation of the finished spherical granules media. Upon receipt of spherical granules distributed way using hydrocarbon-ammonia or liquid molding processes, including chemical peptization pseudoboehmite hydrogel (PB), and the coagulation of droplets pepsirefresh PB. This technology is versatile and productive, guarantees of phase and structural uniformity of spherical granules, allows to carry out the process continuously, that is rational in heavy industries.

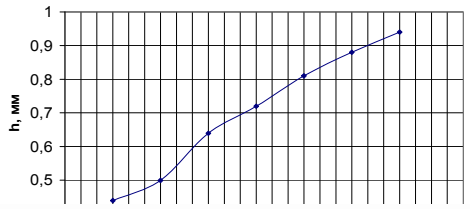

Fig. 1 - The dependence of the depth of diffusion impregnation of salt from time

2 Experimental/methodology

Earlier in the study process of impregnating a porous support γ-Al_2O_3 with a solution containing compounds of the active component, were used cylindrical granules of γ-Al_2O_3 carrier brands AOA-1 and A-64. In this work, using Sol-gel technology samples were obtained spherical granules of γ-Al_2O_3 with a homogeneous texture (d_{gr}=4-5 mm) for subsequent synthesis catalysts. As a source of raw materials used presidency aluminum hydroxide pseudoboehmite structure with a specific surface area of at least 200 m^2/g and a content of impurities of sodium-0,03;iron(III)-0,035; sulfur(VI)-0,02 in terms of oxides, % mass. In the introduction of the active component was carried out by impregnation stage coagulation of the catalyst granules of γ-Al_2O_3 using aqueous solutions: $(NH_4)_2CrO_4$, $(NH_4)_2Cr_2O_7$. Molding paste was produced using a cylinder, with holes at the bottom. Drops fell into the tank with a two-

layer fluid, the upper layer kerosene, lower - solution of chromate (bichromate) ammonium. In the upper layer drops took a spherical shape, and the lower coagulate and saturated with dissolved salt. All stages of preparation and molding were carried out in optimal conditions (in accordance with [3]):

• peptization equivalent of nitric acid, HNO_3: 30 mg acid in 1 g-mol of Al_2O_3;
• pH of sol: pH of 3.2 to 3.8 and its density is: ρ=1,25-1,3 g/cm^3;
• the size of the dosing channel: d =5 mm;
• the height of the layers of kerosene h =30 mm and ammonia solution h=220 mm;
• the concentration of ammonia in neutralizing the solution C=18% mass. and time stay granules t=180 sec;
• temperature and time of drying (110 ^oC - 4 h) and annealing (550 ^oC - 4 h).

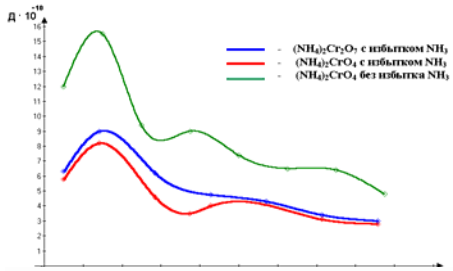

Fig. 2 - Change of the diffusion coefficient depending on time

3 Results and discussion

Investigated the increase of time of impregnation of the granules from 30 to 240 sec. The dependence of the depth of diffusion impregnating salt h, mm time is presented in figure 1. Found that the rate of diffusion of NH_4^+ (as indicator used phenolphthalein) inside the granules exceeds the diffusion rate of chromate ions, probably due to the smaller size of the ions NH_4^+ (1,43 Å) compared with the chromate ions CrO_4^{2-} (5,41 Å). Determined the effect of the concentration of ammonia solution to the diffusion rate of chromate and bichromate ions. The diffusion coefficient defined by the equation calculation time full response interdiffuse in the field[3]. Considering the dependence of diffusion coefficient on the depth of the granules (Fig.2) for the different nature of the solutions of the complexes, it can be noted that the diffusion coefficient with increasing time of impregnation increases to some maximum value and then decreases, with an excess of ammonia causes a considerable decrease of the diffusion coefficient ceteris paribus. The decrease of the diffusion coefficient caused by the formation of the shell of the granule layer of aluminum hydroxide increased density. The obtained structural-mechanical properties of the synthesized samples are shown in table 1.

Table 1 - characteristics of samples of spherical carrier of γ-Al_2O_3 catalyst

	$P_\circ$, MPa	**V_Σ, см^3/г**	**Sуд, m2/g**
The carrier	4,5	0,6	230
The catalyst	4,5	0,4	190

4 Conclusion

Thus, in this work was done a method for producing spherical granules Al_2O_3 by sol-gel transition peptized pseudoboehmite alumina hydroxide, and the introduction of the active catalyst component in the step of coagulation; properties of the synthesized samples correspond to the optimum values for this type of catalysts.

Acknowledgements

The work was performed as part of the State contract № 14.Z50.31.0013 on March 19, 2014

References

[1] Lamberov A. A., Ilyasov I. R. and others // Catalysis in industry. 2008. No. 5.
[2] Pakhomov, N. A. Scientific bases for the preparation of catalyst / H.A. Pakhomov // Textbook for chem.-technology. spec. higher education institutions. Novosibirsk: Izd.Department of catalysis SB RAS, 2011. – p.280.
[3] Grachev, A. Comparison of effective diffusion coefficients in porous catalysts. - Kinetics and catalysis,1971,T. 12,V. 5, p. 1301-1305.

II-PP207

In-situ XPS Study of Active Component of Pd/Al_2O_3 Catalysts in Total CH_4 Oxidation

Prosvirin I.P.[1,2*], Chetyrin I.A.[1,2,3], Khudorozhkov A.K.[1,3], Bukhtiyarov V.I.[1,2,3]

1 - Boreskov Institute of Catalysis SB RAS, Novosibirsk, Russia
2 - Novosibirsk State University, Novosibirsk, Russia
3 - Research and Educational Center for Energy Efficient Catalysis in Novosibirsk National Research University, Novosibirsk, Russia

* prosvirin@catalysis.ru

Keywords: *in-situ* XPS, methane oxidation, Pd/Al2O3 catalysts, active component

1 Introduction

It is well known that the charge state of the active component of catalyst may change under the influence of the reaction medium. This can lead to the formation of new catalytically active sites on the surface differing significantly from those in thus prepared samples. Catalytic combustion is widely used for the abatement of methane emissions from methane- or natural gas combustion devices, including natural gas vehicles and the significant effect of active component particle size on the activity was already revealed for many catalytic systems. Palladium supported on alumina is a common catalyst used for the oxidative removal of small amounts of hydrocarbons from gaseous or liquid streams [1]. In the present study we performed *in-situ* XPS study of the reaction of total oxidation of methane over alumina-supported palladium catalysts, depending on the Pd initial state and the particle size of the active component.

2 Experimental/methodology

In-situ experiments were carried out on the photoelectron spectrometer VG ESCALAB "High Pressure" which allows measuring spectra at a pressure of the reaction mixture up to 0.1 mbar [2]. In our case the experiments were performed at 0.02 mbar, with variation of temperature from 30 to 450 ^oC and oxygen to methane ratio – from 4/1 to 1/1. The methane and oxygen flows were regulated separately with Horiba-Z500 mass flow controllers. Total pressure in the high-pressure gas cell was measured with a MKS type 121A baratron.

3 Results and discussion

Samples with close particle size (4-5 nm) but different initial state of Pd (metal or oxidic, Fig.1a) were chosen to reveal the state of active component under the reaction conditions. It was shown that Pd state doesn't change at samples exposing to the reaction mixture at $O_2/CH_4 = 4/1$ and room temperature. Temperature increase up to 430^oC at $O_2 + CH_4$ mixture presence resulted in methane and O_2 consumption accompanied by CO_2 appearance in the gas phase. At that, independently on the initial Pd state in the sample, both oxidic and metallic state of palladium formed on the surface that follows from the position of Pd3d core level spectrum at 335.8 ± 0.1eV. Peak fitting of these spectra was performed supposing presence of both components and showed that the relative content of Pd^{2+} and Pd^0 states in these samples is very close (Fig.1b). Variation of the temperature and reaction mixture composition showed that both these parameters affect Pd^{2+}/Pd^0 ratio.

Study of redox capability of palladium showed that full reduction of PdO to Pd^0 by methane occurs at temperatures 200-300 °C, whereas oxidation of the metallic phase to PdO in the

oxygen atmosphere for 6 hours, even at 400 °C, leads to the formation of the mixed metal-oxide phase with E_b = 335.8 ± 0.1 eV, which indicates its high stability.

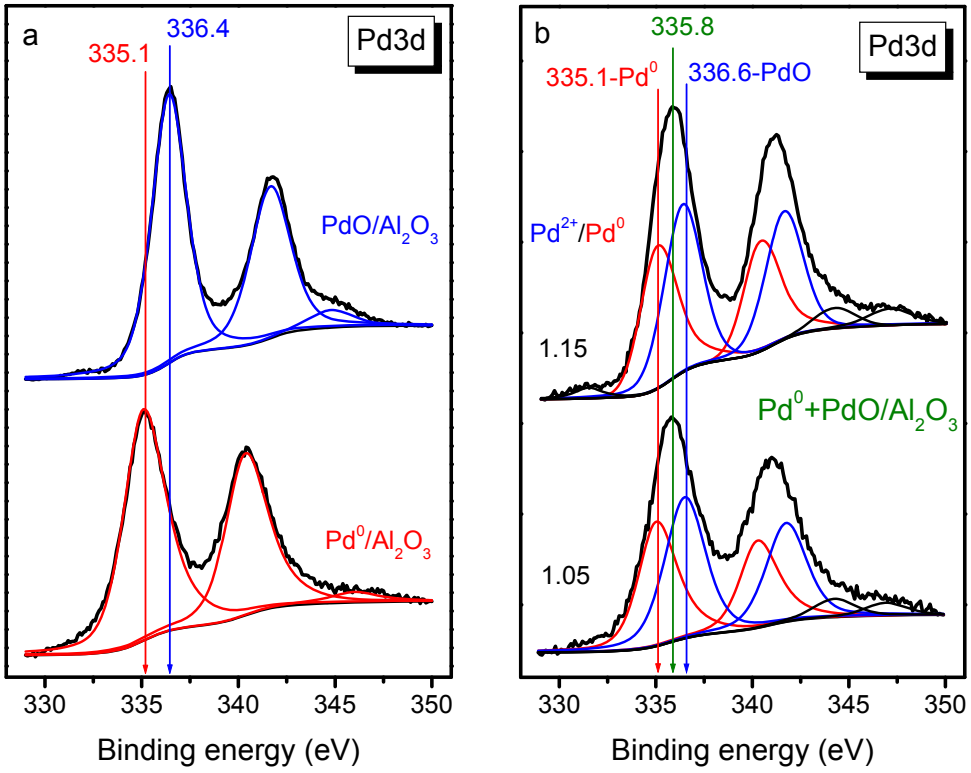

Fig. 1. Pd3d core level spectra of Pd/Al_2O_3 samples characterized by different Pd state (Pd^0 and PdO) recorder under the reaction mixture (O_2 / CH_4 = 4/1, P = 0.02 mbar) at T = 30 °C (a) and 430 °C (b).

4 Conclusions

Mixed metal-oxide state of Pd characterized by E_b = 335.8 eV forms on the surface of $1\%Pd/Al_2O_3$ samples under reaction conditions independently of the initial state of Pd in as prepared samples. Ratio between Pd^0 and PdO therein depends on both temperature and O_2 to CH_4 ratio in the reaction mixture.

Acknowledgements

Financial support of this work was provided by the Russian Science Foundation (grant 14-23-00146).

References

[1] R. Burch, F.J. Urbano, *Appl. Catal. A*, 1995, 124 (1995) 121.
[2] V.I. Bukhtiyarov, V.V. Kaichev, I.P. Prosvirin, *Topics Catal.* 32 (2005) 3.

II-PP208

Effect of Synthesis Method and Doping Metals (M: Pt, Ce) in Ni-M/SBA-15 Based Catalysts for Dry Reforming of Methane

Rodriguez-Gomez A.*, Pereñiguez R., Caballero A.

Inst. Ciencia de Materiales de Sevilla and Universidad de Sevilla, Seville, Spain

* albrodgom@icmse.csic.es

Keywords: Ni catalysts, SBA-15, dry reforming of methane, impregnation, deposition-precipitation, carbon deposition

1 Introduction

Dry reforming of methane (DRM) has awake the interest in the last decades due to its double application, in production of synthesis gas (syngas, $CO+H_2$) used for several liquid hydrocarbon production, and in obtaining pure H_2 by purification of syngas, promising to become one of the major sources of energy in the near future. The coke formation during DRM is one of the substantial problems to be solved for catalyst stability, and it is related with the nature of the active phase (metal), its dispersion over the support employed, and other factors as the high temperature reaction and activation of CO_2 [1]. Nickel is one of the promising alternatives to the active and stable noble metals used as Pt, Rh or Ir, due to its good catalytic performances for a low cost material. Some studies for avoiding the coke deposition in Ni based catalysts are related with doping with noble metals (Pt) or by oxidative effect promoted by CeO_2 [2] due to the ability of this oxide to change between Ce^{3+}/Ce^{4+} oxidation states. The aim of this study is to combine both alternatives using mesoporous SBA-15 as a support, since it has a high specific surface area for helping better dispersionand smaller size of the metallic particles. In this context we have used different synthesis methods to evaluate the properties of Ni-M/SBA-15.

2 Experimental

Firstly, the SBA-15 used as support was prepared by the method described elsewhere [3]. After that, the 10%Ni-M/SBA-15 systems were prepared by three methods: [Im] using a conventional incipient wetness impregnation method, and calcining in air at 550 ºC; [ImU] consisting in a modification of the method described in [4], enhanced by ultrasound treatment and heating in Ar at 500 ºC; and [DP] deposition-precipitation, described by *Liu et al*. [5] and modified by us adjusting some parameters as the decomposition temperature of urea. Basically, a solution of the metallic precursor (Ni or Ni-Ce) together with nitric acid is added to the SBA-15 under stirring at 55 ºC. Then the urea was added, and the solution is heated for 2 h.The Pt-doped catalyst was prepared by adding 1% Pt by the ImU method over the previously calcined Ni/SBA-15 DP. Additionally, a Ni/SiO_2 catalyst was prepared as a reference, using a high surface commercial support (Aldrich-CAS: 112926-00-8, $600m^2/g$) by DP-method. The physicochemical state of the powders was characterized by means of BET, TEM, XRD, TPR, XPS, Raman and XAS. The measurements of the catalytic performance for the DRM reactions were accomplished in an atmospheric flow reactor using 20 mg of catalysts pre-reduced *in situ* at 750 ºC in H_2 5% vol. in He for 1h. The feed gas was a CH_4:CO_2 (1:1) mixture with a space velocity of 240000 ml/h·g and the temperature for reaction was 750 ºC.

3 Results and discussion

The BET results for calcined SBA-15 show surface area about $650m^2/g$ which decrease up to 250-300 m^2/g in the catalysts prepared by DP method (calcined and reduced systems).

According to our results, this effect must be related with the formation of $Si(OH)_4$ in SiO_2 during the treatment, acting as the precipitant agent of Ni^{2+} which results in formation of a nickel phyllosilicate phase detected by XRD in the calcined samples.

In the case of Im and ImU systems, the BET values present differences between the calcined and the reduced samples, with values around 450 and 350m^2/g respectively. Temperature programmed reduction (TPR) for Im, ImU and DP Ni/SBA-15 samples shows very different profiles (Fig.1) where the maximum of H_2 consumption varies from temperatures of 350 ºC for Ni-Im to 650 ºC for Ni-DP. It is also clear from these profiles that the modification applied in the Ni-ImU method results in different reducibility properties of the nickel phase. Ce and Pt doped catalysts present similar behavior under TPR than the monometallic Ni-DP, with a slight shift to lower temperatures. The high temperature of reduction for Ni/SBA-15 DP is associated with the formation of a nickel phase strongly interacting with the SBA-15 support, maybe related with the phyllosilicate phase detected in that sample.

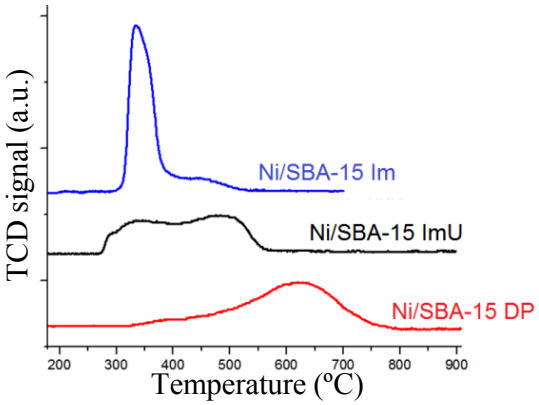

Fig. 1. TPR profile for Ni/SBA-15 monometallic systems.

The wider reduction peak observed for Ni-DP and Ni-ImU compared with Ni-Im, could be ascribed to a high dispersion of the metallic active phase, resulting in smaller particles with a better homogeneous size distribution (3-4 nm), as reflected in Fig. 2. Also, metallic particles inside the mesoporous structure can be easily detected.

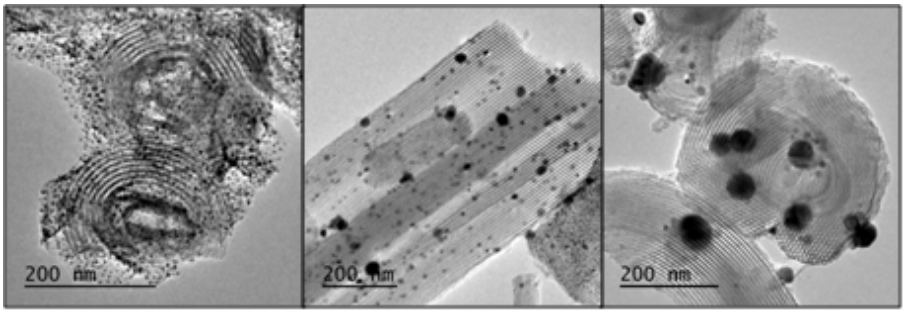

Fig. 2. TEM images for reduced samples: Ni/SBA-15.

Catalytic testduring 40h in DRM at 750 ºC, shown significant differences between the systems studied (Table 1). Thesamples prepared by DP present the most promising results based on a higher stability, together with a lower carbon deposition, as detected by ATD and Raman spectroscopy after DRM. This catalytic performance is promising even for Ni monometallic system, with improved conversions by adding 1%Pt and 10%CeO_2. Unexpectedly, in these doped systems the amount of coke detected after reaction were much higher. These data prove the singularity of our Ni/SBA-15 DP catalyst, where the outstanding performance, specially the high stability in reaction, seems to be related with the metal-support interaction described before

Table 1. CH_4 and CO_2 conversion for DRM at 750 ºC.

Sample	**CH_4 conversion (%) Initial/1000/2500min**	**CO_2 conversion (%) Initial/1000/2500min**
Ni/SiO_2 DP	61 / 36 / 20	73 / 46 / 31
Ni/SBA-15 DP	60 / 60 / 60	73 / 73 / 73
Ni/SBA-15 Im	43 / 23 / -	53 / 33 / -
Ni/SBA-15 ImU	29 / 18 / 15	40 / 29 / 24
Pt/Ni/SBA-15 DP	75 / 71 / 67	81 / 79 / 76
Ni-CeO_2/SBA-15 DP	70 / 59 / 53	81 / 73 / 66

References

[1] D. Pakhare, J. Spivey, *Chem. Soc. Rev*. 43 (2014) 7813.
[2] V.M. Gonzalez-DelaCruz, J.P. Holgado, R. Pereñiguez, A.Caballero, *J.Catal.* 257 (2008) 307; V.M.Gonzalez-Delacruz, F. Ternero, R. Pereñiguez, A. Caballero, J.P. Holgado, *App.Catal. A.* 384(2010) 1.
[3] A. I. Acatrinei,M. A. Hartl,J. Eckert,et al., *J. Phys. Chem. C*. 113 (2009) 15634.
[4] S. Zhang, S. Muratsugu, N. Ishiguro, M. Tada, *ACS Catal*. 2013, 3, 1855-1864.
[5] H. Liu, H. Wang, J. Shen, Y. Sun, Z. Liu, *App.Catal. A: Gen.* 337 (2008) 138.

II-PP209

1-Alkyne Selective Hydrogenation with Pd/AC Catalysts. Effect of Precursor Salt

Lederhos C.[1*], Miranda C.[2], Betti C.[1], Badano J.[1], Maccarrone J.[1], Carrara N.[1], Coloma-Pascual F.[3], Cagnola E.[1], Quiroga M.[1]

1 - Instituto de Investigaciones en Catálisis y Petroquímica – Facultad de Ingeniería Química (CONICET- UNL), Santiago del Estero, Argentina

2 - Grupo de Catálisis, Departamento de Química, Universidad del Cauca,Cauca, Colombia

3 - Servicios Técnicos de Investigación, Facultad de Ciencias, Universidad de Alicante, Alicante, España

* clederhos@fiq.unl.edu.ar

Keywords: alkyne selective hydrogenation, alkene, activated carbon, palladium, supported catalysts

1 Introduction

The carbonaceous materials are widely used as catalyst supports in different industrial reactions. The catalysts supported on activated carbon (AC) have advantages over other material: low cost, stability, mechanical strength, high surface area, ability to modify their surface chemistry, etc. [1]. Olefins obtained by hydrogenation of alkynes, are of great academic and industrial interest, either for the synthesis of biologically active compounds, in the production of margarine industry for lubricants, plastic, etc., also presenting fine chemical applications. The objectives of this work are: a) to prepare low loading palladium catalysts supported on activated carbon, using chloride and nitrate as precursor salts, and b) to evaluate them as catalyst during the liquid phase selective hydrogenation of 1-heptyne to 1-heptene.

2 Experimental

Palladium was supported on activated carbon (Norit CNR-115, S_{BET}: 1503 $m^2\ g^{-1}$, micropore volume: 0.738 g mL^{-1}) by incipient wetness impregnation. Aqueous acidic solutions (pH = 1, HCl or HNO_3 0.1N) of $PdCl_2$ or $Pd(NO_3)_2$ used as precursor salts, were deposited on CNR to prepare the PdCl/CNR or PdN/CNR catalysts, with 0.4 wt% Pd. Samples were dried 24 h at 373 K and reduced in H_2 at 393 K. The metal content was determined by ICP in OPTIMA 21200 Perkin Elmer equipment. The hydrogen chemisorptions were determined at 303 K using a Micromeritics AutoChem II in 2920 instrument. Fourier transform infrared spectroscopy (FTIR) spectra were recorded on a Thermo Nicolet Model IR-200 spectrometer from 400 to 4000 cm^{-1} in transmission mode. To obtain the disk, 0.5 mg AC was mixed with 100 mg of KBr and then pressed. The electronic state of surface species and their atomic ratios were obtained by X-ray Photoelectron Spectroscopy (XPS) on a VG-Microtech Multilab Equipment. Binding energies (BE) of Pd $3d_{5/2}$, N 1s and Cl $2p_{3/2}$ were analyzed. C 1s signal was used as a reference. The catalyst evaluations were carried out in a stirred tank reactor of stainless steel equipped with a magnetic stirrer operated at 800 rpm, 303 K, 150 kPa H_2 pressure and using 0.75 g catalyst. 75 mL of 1-heptyne in toluene (5%) was used as feed solution. Reactants and products were analyzed by Gas Chromatography with Flame Ionization Detector (FID) and a capillary column.

3 Results and discussion

Table1. Metal loading, Dispersion values, XPS results and TOF

Catalysts	Metal loading (%)	D (%)	XPS			TOF (s^{-1})
			Pd $3d_{5/2}$ (eV)	Pd/C ($^{at}/_{at}$)	Cl or N/Pd ($^{at}/_{at}$)	
PdN/CNR	0.39	48	335.2	0.074	2.04	$1.7.10^{-1}$
PdCl/CNR	0.42	62	335.2	0.006	1.56	$6.4.10^{-2}$

Table 1 shows the metal loadings, dispersions (determined by hydrogen chemisorption technique), XPS results and TOF values for PdCl/CNR and PdN/CNR. As shown in Table 1, PdCl presents higher dispersion than PdN. XPS revealed that both catalysts have the same position for the Pd BE at 335.2 eV, indicating the presence of Pd° species on the surface [2]. The Pd/C atomic ratios show a markedly greater amount of palladium on the PdN catalyst surface. Cl/Pd and N/Pd atomic ratios indicate the presence of chloride and nitrogen on the surface due to the low reduction temperature used. Such temperature does not permit the complete elimination of precursor salts that remains on the surface of the carbon support. IR profile of PdN/CNR showed a main peak at 3444 cm^{-1} assigned to O–H stretching due to water absorbed on the surface of the material, and to hydroxylated groups. In this region, for PdN also appears an overlapping signal of N-H stretching due to the treatment with nitric acid. Besides, in PdCl/CNR the broad signals at 3444 cm^{-1} were observed but with less intensity indicating only O-H vibration remains, but the C–H vibrations of methyl and methylene groups are no longer discernible indicating a decrease in the aliphatic character of the material [3]. Both catalysts have a band at 1635 cm^{-1} which is a characteristic peak for carbon materials [4] and is probably ascribable to carbonyl groups which are highly conjugated in the graphene layer such as quinone and/or ion radical structure C=O. This is more intense for PdN/CNR caused by the treatment with HNO_3 during preparation steps.

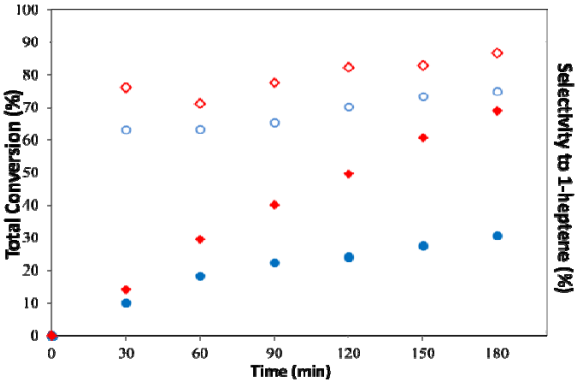

Fig. 1. 1-heptyne Total Conversion (%) (filled symbol) and Selectivity to 1-heptene (%) (open symbol) as a function of time for PdN/CNR (□,□) and PdCl/CNR (□,□)

Fig. 1 shows 1-heptyne total conversion and selectivity to 1-heptene for both catalysts. It can be seen the best performance of PdN/CNR catalyst, presenting at 180 min c.a. 70 % of 1-heptyne total conversion (55% higher than PdCl/CNR) with c.a 80% of selectivity to 1-heptene. In Table 1 the high TOF number indicates that PdN/CNR sample is the most active catalyst. Although PdN/CNR is low dispersed, it has an abundance of active species on the catalyst surface, as shown by XPS. It is possible that in PdCl/CNR, the superficial remaining chlorine interacts as a poison, decreasing the total conversion.

4 Conclusions

Two palladium catalysts were synthesized from different precursor salts (chloride and nitrate) on activated carbon with 0.4 wt% Pd. PdN/CNR showed the best performance in activity and selectivity during the selective hydrogenation of 1-heptyne to 1-heptene. The characterization results show that the treatment with HNO_3 during the preparation step of PdN/CNR modified the support surface. The best performance of PdN/CNR can be attributed to the high concentration of active species Pd° on the surface of the support catalyst. It is possible that the remaining chlorine in PdCl/CNR interacts as a poison, decreasing the total conversion.

Acknowledgements

The financial assistance of UNL, CONICET and ANPCyT are greatly acknowledged by authors.

References

[1] A. Dantas Ramos et al, *Applied Catalysis A: General* **277** (2004) 71
[2] NIST X-ray Photoelectron Spectroscopy Database NIST Standard Reference Database 20, Version 3.5. National Institute of Standards and Technology, USA, 2007. http://srdata.nist.gov/xps/
[3]V. Alves, S. Borges, N. Coelho, *International Journal of Analytical Chemistry*. **2011**, Article ID 765746, 8.
[4] M. Akhter, J.Keifer, A. Chughtai, D. Smith, *Carbon* **23** (1985) 589.

II-PP210

Investigation of Activity of Supported Block Catalysts in Oxidation of Light Alkanes into Hydrogen-Containing Compositions

Baizhumanova T.S.*, Tungatarova S.A., Zheksenbaeva Z.T., Zhumabek M., Kassymkan K.

D.V. Sokolsky Institute of Organic Catalysis and Electrochemistry, Almaty, Kazakhstan

* baizhuma@mail.ru

Keywords: activity block catalysts, carrier, alkanes, hydrogen

1 Introduction

It was previously determined optimal activation conditions: concentration ≥ 0.2%, the ratio of elements Pt : Ru (2 : 1, 1 : 1) on a carrier in the comparative study of low-percentage disperse Pt, Ru and Pt-Ru/2% Ce/(θ+α)-Al_2O_3 catalysts in the oxidation of the methane of natural gas. The process conditions are τ = 4 msec, T = 1173K, 1.6% CH_4 : 0.8% O_2 = 2 : 1 in argon to produce synthesis gas with a ratio of H_2 / CO = 2.0 without the formation of CO_2, which is the most suitable for use in the synthesis of methanol and hydrocarbons by the Fischer-Tropsch process [1]. The study by physical and chemical methods has shown that oxygen on the surface of Pt-, Ru- and Pt-Ru/2% Ce/(θ+α)-Al_2O_3 catalysts is adsorbed in 2 forms (T_1 = 273 - 573 and T_2 = 573 - 1173 K). Introduction of ruthenium into the platinum catalyst with the ratio Pt : Ru = 2 : 1 and 1 : 1 increases the adsorption of oxygen in the second temperature range. Evolution of the structural oxygen (which is required for the selectivity of process) at temperatures from 973 to 1173 K, i.e. at temperature corresponding to temperature of syngas production with high selectivity was determined. It is assumed that the reaction of selective catalytic oxidation of CH_4 on the Pt : Ru (2 : 1, 1 : 1) catalysts is carried out by the direct mechanism with participation of reduced Pt-Ru clusters having the highest adsorption capacity of atomic hydrogen [2]. It is known that catalyst stability is one of the most important characteristics. The test of catalyst operation was performed on optimal catalysts Pt : Ru = 1 : 1 and 2 : 1 in the selective catalytic oxidation of methane to syngas at the millisecond contact times in prolonged terms. It was found that the synthesized catalyst was active and selective for 410 h [3].

2 Experimental/methodology

The block ceramic catalyst having supported active phase consisting of 1% (Pt+Ru)/2% Ce/(θ+α)-Al_2O_3, was prepared for the research. The active phase of catalyst was prepared by sequentially supporting of elements on the (θ+α)-Al_2O_3 100-200 microns, S_{sp} = 57.7 m^2/g) from the aqueous solutions of metal salts $Ce(NO_3)_3 \times 6H_2O$, $Ru(OH)Cl_3$, and $H_2PtCl_6 \times 6H_2O$ by capillary wetness impregnation followed by heating in air at 873 K for 3 h. Microspherical 1% Pt-Ru/2% Ce/(θ+α)-Al_2O_3 catalyst was supported on the block ceramic honeycomb carrier (fragments of blocks d = 10 mm; h = 20 mm, the channel size 1.0 × 1.0 mm, wall thickness 0.5 mm). Layering of the active phase of catalyst with binder on the blocks in several steps is the essence of process.

Tests of the ceramic block catalysts in oxidation of CH_4 were conducted in flow apparatus at atmospheric pressure in a quartz reactor with internal diameter of 0.025 m. The prepared catalyst block is wrapped in fiberglass and placed in a reactor. Initial reaction mixture was introduced at a rate of 50 ml/min after purging the system with inert gas (Ar) for 30 min at varying the ratio of reaction gases CH_4 and O_2 in a mixture from 1 : 1 to 4 : 1 and gradually

increasing the temperature from 700 to 875°C and volume rate from 1000 to 10000 h^{-1}.

3 Results and discussion

The process of oxidative conversion of hydrocarbon mixtures which are close to real while gradually increasing the reaction temperature from 700 to 875°C was investigated. Increase of methane conversion from 28 to 48% is observed with the growth of temperature. The amount of the produced H_2 increases from 33% to 84% at 850°C and again decreases to 70.2% at 875°C. A small amount of CO is formed at a temperature 700°C which increases with increasing temperature from 0.6 to 40.5%. Formation of C_2H_4 is observed at a reaction temperature 750°C in an amount of 13.0% and with the growth of temperature is lowered to 4%. Thus, the temperature 850°C is optimal for the formation of hydrogen, and 875°C and 750°C - for CO and C_2H_4, respectively. Effect of space velocity on direction of oxidative conversion of hydrocarbon mixture, which is close to the real, at variation of space velocity from 1000 to 10000 h^{-1} was studied. It was found that the hydrogen yield was 40.5% at 1000 h -1. Amount thereof increased to 84.0% at 5000 h^{-1} and then reduced to 45.1% with increasing space velocity up to 10,000 h^{-1}. The same dependence is observed for the formation of CO and ethylene. The amount of CO is increased from 10.5% to 38.0% and ethylene - from 7.8% to 13.0% at 5000 h^{-1}. Product yield gradually decreases with further increase in space velocity to 10000 h^{-1}. Increasing the space velocity from 1000 h^{-1} to 5000 h^{-1} positively affects on the conversion of initial mixture to desired products. 5000 h^{-1} is optimal space velocity for the formation of desired products. Thus, optimum ratios of main gases in the reaction mixture were also determined.

4 Conclusions

Thus, optimization of technological modes of oxidative conversion of hydrocarbon mixture was carried out. Effect of varying the reaction temperature, space velocity and ratio of gases for selective production of desired products was investigated. The temperature ranges of 725-875°C and space velocity 5000 h^{-1} are optimal process parameters to produce hydrogen compositions. It is determined that the oxidative conversion of methane to hydrogen-containing mixture is carried out at the optimum ratio of components $CH_4 : O_2 = 2 : 1$ at a concentration of gases (50% : 25%), respectively.

Acknowledgements

This work was supported by the Ministry of Education and Science of Kazakhstan.

References

[1] K. Dosumov, N.M. Popova, T.S. Baizhumanova, S.A. Tungatarova, *Petroleum Chemistry*. 6 (2010) 455.

[2] S.A. Tungatarova, T.S. Baizhumanova, I.A. Shlygina, A.A. Shapovalov, M. Zhumabek, K. Kassymkan, *Journal of Chemistry and Chemical Engineering.* 12 (2013) 1111.

[3] S.A. Tungatarova, T.S. Baizhumanova, M. Zhumabek, K. Kassymkan, L.V. Komashko, *International Research Journal.* 4 (2014) 84.

II-PP211

Synthesis of C/Al_2O_3 and SO_4^{2-}/Al_2O_3 Aerogels and their Catalytic Activity in Dehydrochlorination Reactions

Bedilo AF[1,2*], Shuvarakova EI[1,2]

1 - Boreskov Institute of Catalysis SB RAS, Novosibirsk, Russia
2 - Novosibirsk Institute of Technology, Moscow State University of Design and Technology, Novosibirsk, Russia

* abedilo@bk.ru

Keywords: aerogels, sulfated alumina, dehydrochlorination, electron-acceptor, sites, EPR

1 Introduction

Aerogels are materials obtained by a sol-gel process followed by supercritical drying of the latter. The obtained materials have high surface areas and pore volumes [1]. Deposition of sulfates on γ-Al_2O_3 is known to lead to a substantial increase of its acidity and catalytic activity in acid-catalyzed reactions [2, 3]. High surface area, wide availability, and reasonable thermal stability make sulfated alumina an attractive catalyst for variety of acid-catalyzed processes that do not require very high acid strength. However, one-step synthesis of sulfated alumina aerogels has not been reported yet. In the current communication we shall discuss the effect of various organic and acidic modifying agents, including sulfates, on the textural properties of alumina aerogels and their performance in reactions with chlorinated hydrocarbons.

2 Experimental/methodology

For preparation of modified Al_2O_3 aerogels, aluminum isopropoxide (Aldrich) was dissolved in a desired amount of ethanol and/or other solvent. A solution of the modifying agent was quickly poured into the reaction vessel with aluminum isopropoxide solution and the resulting mixture was stirred for 10 min. Then, a stoichiometric amount of hydrolysis water dissolved in same solvent was added. The resulting gel was aged for 2 hours, subjected to supercritical drying in an autoclave at 265°C and by calcination either under vacuum or in air.

Dehydrochlorination of 1-chlorobutane was performed in a flow reactor. 99% 1-chlorobutane used in the experiments was introduced into the reactor by saturation of the argon flow with C_4H_9Cl vapor at room temperature. Experiments on decomposition of (2-chloroethyl)ethyl sulfide (2-CEES) were carried out in a 25 ml three-necked flask under argon with stirring. Ten ml pentane, 15 ml decane used as internal standard, 200 mg of powder sorbent and 15 ml 2-CEES were placed in the flask. Electron-acceptor sites of the synthesized aerogels were studied by EPR using spin probes according to an earlier developed procedure [2].

3 Results and discussion

The highest specific surface areas of alumina aerogels after supercritical drying exceeding 1200 m^2/g that are 4-5 times higher than those of typically used alumina materials were obtained for the samples prepared with an ethanol-toluene mixture used as the solvent. After activation under vacuum at 500°C the surface area of the alumina aerogels without the organic modifying agents was typically between 600 and 700 m^2/g. The surface areas of the carbon-coated aerogels was typically somewhat lower, about 400-500 m^2/g. HRTEM data showed that the carbon-coated alumina nanoparticles were nanocrystalline with typical dimensions of several nanometers and covered with several layer of graphitic carbon. XRD data did not show any clear peaks indicating that the aerogels even after calcination remained amorphous to x-rays.

Sulfated alumina aerogels were synthesized by a similar procedure with sulfuric acid used as a modifiying agent. The sulfuric acid addition results in a substantial decrease of the pore volume, whereas the high surface area of the Al_2O_3 aerogels is preserved. The surface areas of the sulfated alumina aerogels after calcination at 600°C usually required to make active acid catalysts were about 600 m^2/g. This value appears to the highest ever reported for sulfated alumina catalysts and is 2-3 times higher than those reported in the literature.

We found that the activity of high surface area nanocrystalline alumina materials in dehydrochlorination of 1-chlorobutane compared favorably with that of other nanocrystalline metal oxides. The temperature of 1-chlorobutane decomposition decreased by ca. 100°C in comparison with MgO aerogel studied in detail earlier [4] while maintaining 98% selectivity to butenes. Sulfated alumina had even higher activity due to its higher acidity.

2-CEES is a mustard gas mimic commonly used to characterize the performance of materials developed for destruction of poisonous chlorinated compounds. We found that alumina and carbon-coated alumina aerogels chemisorbed 2-CEES at room temperature from pentane solution even more efficiently than MgO aerogels or conventional Al_2O_3. Sulfated alumina aerogels showed even better performance in the destructive sorption. 2-CEES conversion rate in pentane solution at room temperature over sulfated aerogel alumina was 3 times higher than on Al_2O_3 aerogel and 8 times higher than on MgO aerogel. This reaction was exceptionally fast over all sulfated oxides, both aerogel and conventionally prepared, so almost maximum conversion was reached in the first 2 minutes. Furthermore, the high surface area of the developed sulfated alumina aerogels made it possible to achieve the absolute highest conversion.

Earlier the activity of alumina and sulfated alumina in ethanol dehydrogenation was found to correlate with the concentration of weak electron-acceptor sites [3]. Their concentration was much higher on the aerogels than on conventional alumina catalysts due to high surface area. The catalytic activity of the synthesized materials in dehydrochlorination of 1-chlorobutane and 2-CEES seems to correlate with the concentration of weak electron-acceptor sites.

4 Conclusions

We have demonstrated that the textural parameters of alumina aerogels can be effectively controlled by selection of the solvents and modifying agents. Carbon-coated Al_2O_3 with permeable carbon coating can be prepared by adding modifying agents with bulky organic groups during gelation followed calcination under vacuum. Typical dimensions of the alumina nanoparticles synthesized by this method do not exceed few nanometers. The activity of high surface area nanocrystalline alumina materials in dehydrochlorination of (2-chloroethyl)ethyl sulfide (2-CEES) and 1-chlorobutane compared favorably with that of other nanocrystalline metal oxides and correlates with the concentration of weak electron-acceptor sites.

Acknowledgements

This study was supported in part by Russian Foundation for Basic Research (Grants 13-03-12227-ofi_m and 15-03-08070-a).

References

[1] E.V. Ilyina, I.V. Mishakov, A.A. Vedyagin, S.V. Cherepanova, A.N. Nadeev, A.F. Bedilo, K.J. Klabunde, Micropor. Mesopor. Mater. 160 (2012) 32.
[2] A.F. Bedilo, E.I. Shuvarakova, A.A. Rybinskaya, D.A. Medvedev, *J. Phys. Chem. C* 118 (2014) 15779.
[3] R.A. Zotov, V.V. Molchanov, A.M. Volodin, A.F. Bedilo, *J. Catal.* 278 (2011) 71.
[4] I. V. Mishakov, A. F. Bedilo, R. M. Richards, V. V. Chesnokov, A. M. Volodin, V. I. Zaikovskii, R. A. Buyanov, K. J. Klabunde, *J. Catal.* 206 (2002) 40.

II-PP212

Hydrogen and Oxygen Interaction with Single Supported Gold Nanoparticles

Grishin M.V., Kirsankin A.A.*, Gatin A.K., Shub B.R., Dohlikova N.V.

Semenov Institute of Chemical Physics RAS, Moscow, Russia

* kirsankin@mail.ru

Keywords: nanoparticles, adsorption, scanning, tunnelling, spectroscopy

1 Introduction

In recent years, scanning tunnelling microscopy (STM), which ensures resolution at the atomic level, has been widely used for the study of supported metallic nanoparticles. It was found that surface structures and adsorption properties of supported metallic nanoparticles are determined by their shapes which in turn strongly depend on the nature of the support. At the same time, such low coordinated sites as edges and kinks strongly affect the interaction of a surface with adsorbed species. The use of STM for the analysis of surface structures of metallic nanoparticles seems promising, in that this method allows *in situ* analysis of surface structures, i.e., in the course of a reaction.

Scince demonstrating by Haruto their catalytic activity [1] three decades ago gold nanoparticles retains attention of many scientists. Gold nanoparticles which, in contrast with the bulk metal, manifest catalytic activity in certain reactions. In this study we demonstrated dependence of adsorption properties of single gold nanoparticles on the nature of the substrate. High ordered pyrolytic graphite (HOPG) and silicon covered oxide (SiO_2/Si) were used as substrate.

2 Experimental/methodology

Morphology and electronic structure of gold nanoparticles were determined by scanning tunneling microscopic technique by Omicron. The residual gas pressure in the setup chamber didn't exceed $P = 2 \times 10^{-8}$ mbar. Local changing of the surface state of gold nanoparticles was defined by current-voltage dependence of tunneling contact including single gold nanoparticle (*I(V)*-curves).

Gold nanoparticles were prepared by a deposition method. Chloroauric acid with a gold loading of 5 wt % was first dissolved in distilled water and after deposited on the surface of substrate (HOPG and SiO_2/Si). Substrate with acid was dried and then calcined in ultrahigh vacuum (10^{-10} mbar) at 500 K for 6 h.

3 Results and discussion

Single gold nanoparticles supported on HOPG (Au/HOPG)

The formation of gold nanoparticles occurs near the lattice defects of graphite surface. Both isolated nanoparticles of 4-5 nm and large agglomerates with lateral sizes of 40-100 nm consisting of individual 5 nm particles on the graphite surface were observed. The current-voltage dependence of tunneling contact consisting gold nanoparticles corresponds to the metallic conduction.

To study the interaction of hydrogen with gold nanoparticles at room temperature sample was kept over 500 seconds at room temperature in molecular hydrogen at a pressure of $P = 2 \times 10^{-6}$ mbar (exposure 1000 L). The hydrogen exposure doesn't lead to shape and sizes changing of gold nanoparticles. The band gap with width of 0.8 V on the *I(V)*-curves was observed after hydrogen exposure. Hydrogen-gold binding energy lower limit was measured by thermodesorption method and is equal to 1.7 eV. Based on the results of quantum-chemical calculation made by us the

hydrogen adsorption on Au_{13}-H_{12} clusters is characterized by breaking of H-H bond and formation of Au-H bond with binding energy of 3 eV.

The oxygen adsorption can be determined only after the preliminary exposure of gold nanoparticles in hydrogen. Current-voltage dependence of tunneling contact of Au/HOPG with adsorbed oxygen and hydrogen doesn't differ from these of gold nanoparticles coated by hydrogen only. Perhaps oxygen adsorption occurs without breaking of O-O bond.

Au/HOPG sample, coated firstly by hydrogen and then by oxygen, were exposed into the hydrogen for evaluation of Au/HOPG reactivity. The measured current-voltage dependence exhibit multiple local maxima located almost symmetrically with respect to the coordinate origin. The voltage differences corresponding to the position of peaks on the experimental curves was 0.41 and 0.25 V between adjacent peaks which is accurate within a dimensional factor corresponds to quanta of electron-vibration excitation of the O-H bond and the deformation vibration of the water molecule.

Single gold nanoparticles supported on SiO_2 (Au/ SiO_2)

The lateral diameter of single gold nanoparticles supported on SiO_2 is 4-5 nm. The comparison of gold nanoparticles diameters into SiO_2 and HOPG allows making a conclusion that type of substrate doesn't have a significant influence on the morphology of gold nanoparticles.

Au/HOPG and Au/Sio_2 equally interact with hydrogen. Hydrogen is chemisorbed on gold nanoparticles supported on SiO_2 at room temperature as well as on gold nanoparticles supported on HOPG. However at the following puffing of oxygen the formation of water molecules on the surface of gold nanoparticles was observed. Thus, it was found that water is formed at the gases puffing by H-O-H scheme on Au/HOPG and by H-O scheme on Au/SiO_2.

4 Conclusions

The conditions of hydrogen and oxygen adsorption on Au/HOPG and Au/Sio_2 were determined by methods of scanning tunneling microscopy and spectroscopy. Production of water molecules on gold nanoparticles was observed. It was shown that, application of semiconductor as a substrate dramatically increases the reactivity of gold nanoparticles.

Acknowledgements

The research group would like to thank RFBR for grants 14-03-00156, 14-03-90012, 13-03-00391, 15-03-02126.

References

[1] M Haruta, N Yamada, T Kobayashi, S Iijima J. Catal. 115 (1989) 301

II-PP214

Cu(I) and Rh(I) Complexes of Novel Pyridyl-Containing Phospholanes

Shamsieva A.V.*, Musina E.I., Karasik A.A., Sinyashin O.G.

A.E. Arbuzov Institute of Organic and Physical Chemistry of Kazan Scientific Center of Russian Academy of Sciences, Kazan, Russia

* shamsieva.aliya@mail.ru

Keywords: phospholanes, P,N ligands, Rh(I) complexes

1 Introduction

The correlation of stereoelectronic effects in tertiary phosphine ligands with the reactivity of their coordination complexes is key to understanding their efficiency in homogeneous catalysis. Cyclic phosphines are in special interest for coordination chemistry and catalysis due to their relatively rigid structrure. However the chemistry of phosphorus heterocycles is much less developed than the analogous nitrogen chemistry [1]. Cyclic phosphines have been shown to be excellent ligands for catalysis and particularly hydroformylation catalysis [2-5]. There are only two works focused on studying rhodium-catalysed hydroformylation of 1-octene using phenyl or *tert*-butyl substituted cyclic phosphines [6] and bidentate cyclic bisphosphines with ring size from 5 to 7 [7].

It was demonstrated that the catalyst activity decreases with increasing phosphacycle ring size and the most active catalyst system was based on the rhodium complex with ligand with smaller ring (**L_5**).

Herein we describe the synthesis of new phosphalanes containing pyridyl moiety on phosphorus atom and their complexes with transition metals.

2 Results and discussion

A novel pyridyl containing tertiary cyclic phosphines – 1-(pyridine-2'-yl)phospholane **1** and 1-(4'-methyl-pyridine-2'-yl)phospholane **2** were obtained in good yields in reaction of corresponding primary pyridylphosphines with 1,4-dichlorobutane in superbasic medium according Scheme **1:**

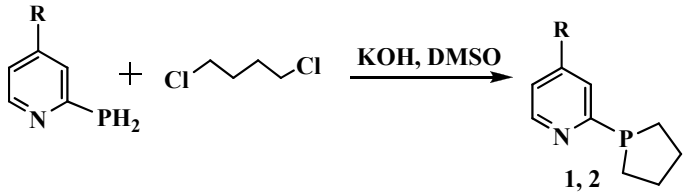

Scheme 1.

Reaction of **1** and CuI led to the formation of complex **3** with "butterfly" shaped Cu_2I_2 halide core and bidentate P,N-bridge coordination of one ligand molecule and P-monodentate coordination mode of two others (Scheme **2**).

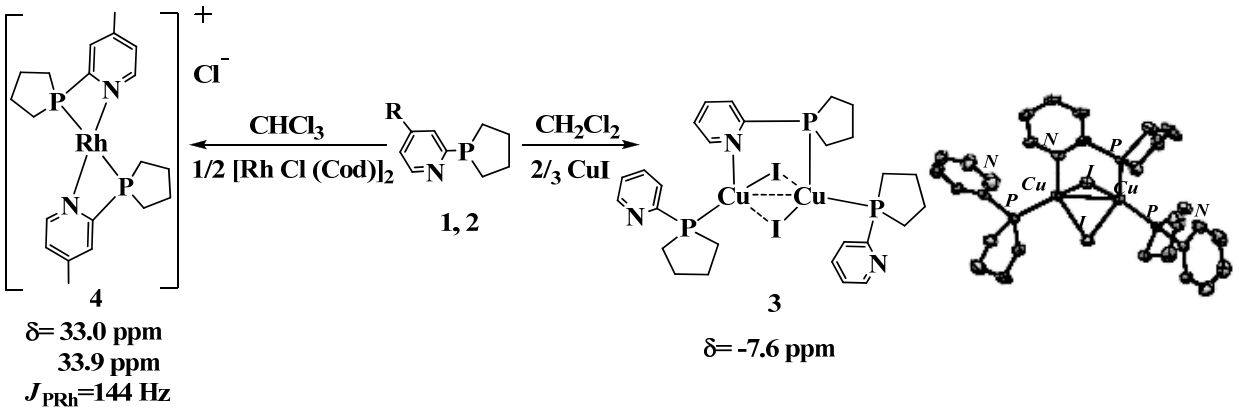

Scheme 2.

The abillity of the ligand **1** to form the P,N-coordinated complexes motivated us to test it coordination with rhodium, which is catalytic active metal. Thus, the reaction of **2** with $[RhCl(Cod)]_2$ led to bis-P,N-chelate complex **4**, the spectral parameters of complex **4** are similar to that of described catalyst [8], which makes it perspective to test in hydroformylation reactions.

Acknowledgements

This work was supported by RFBR (No. 14-03-31302_mol_a).

References

[1] (a) F. Mathey, In *Phosphorus-Carbon Heterocyclic Chemistry*; Pergamon Press: Oxford, U.K., 2001; (b) R. Doherty, M.F. Haddow, Z.A. Harrison, *et all Dalton Trans*. 2006, 4310 and references therein.
[2] (a) R.F. Mason, J.L. van Winkle, *U.S. Patent* 3 400 163, 1968 (to Shell); (b) J. P. Steynberg, K. Govender, P.J. Steynberg, *World Patent WO* 14248, 2002 (to Sasol).
[3] T. Mackewitz, W. Ahlers, E. Zeller, M. Roper, R. Paciello, K. Knoll, R. Papp, *World Patent WO* 00669, 2002 (to BASF).
[4] B. Breit, E. Fuchs, *Chem. Commun*. (2004) 694.
[5] R.A. Baber, M.L. Clarke, K. Heslop, A.C. Marr, A.G. Orpen, P.G. Pringle, A. Ward, D.E. Zambrano-Williams, *Dalton Trans.* (2005) 1079.
[6] (a) G. Gruttner, M. Wiernik, *Chem. Ber.* 48 (1915) 1473. (b) G. Gruttner, E. Krause, *Chem. Ber.* 49 (1916) 437.
[7] J.H. Davies, J.D. Downer, P.J. Kirby, *Chem. Soc. C* 1966, 245.
[8] K. Wajda-Hermanowicz, Z. Ciunik, A. Kochel, *Inorg.Chem.* 45 (2006) 3369.

II-PP215

Development of Stable Catalysts for Debenzylation of Hexaazaisowurtzitane Derivatives

Malykhin V.V.*, Sysolyatin S.V.

Institute for Problems of Chemical and Energetic Technologies SB RAS, Biysk, Russia

* astro-78@mail.ru

Keywords: catalytic debenzylation, Pd catalyst, hexaazaisowurtzitane, derivatives

1 Introduction

In the field of high-energy materials, great attention has been paid over the last decade to studying the properties and searching for effective synthesis methods of 2,4,6,8,10,12-hexanitro-2,4,6,8,10,12- hexaazaisowurtzitane (HNIW, CL-20, HAW), a powerful explosive [1].

HAW has not received wide application due to its high cost and complexity of the industrial synthetic method. One of the known synthetic routes to HNIW is depicted in the scheme below [2,3]:

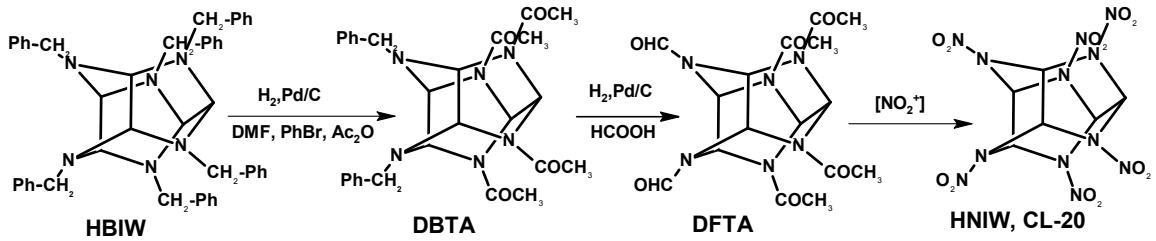

At the present time, the synthetic methods of the polycyclic cage are fairly well studied, as are DFTA nitration techniques [3,4], and they can be applied without any difficulty. However, the two catalytic stages of the process (HBIW→DBTA→DFTA), which are more complicated and are price determinative in the entire synthesis method of HAW, have been much less studied. A Pd catalyst is used sequentially at the two stages of debenzylation. The key problem in the practical realization of these stages is that the expansive Pd/C catalyst would be rapidly deactivated, not allowing its multiple reuse. The known techniques to regenerate Pd catalysts do not permit the catalyst activity to be recovered to the initial level—which is necessary for exhaustive reaction of hydrodebenzylation. The catalyst recycling may reduce the HAW production cost.

2 Results and discussion

The effects of the catalyst preparation methods on the catalyst activity were studied. The reducing agent nature was found to considerably influence the catalytic properties while the surface finishing technique and support dispersion had little impacts. The activities of the differently obtained catalysts were evaluated under model and relatively near-real conditions.

The possibility of the multiple separate use of the catalyst at the synthesis stages of DBTA and DFTA was investigated and demonstrated. Optimum catalyst loadings that enable the catalyst recycling up to 10 times at the first stage of debenzylation and up to 14 times at the second were identified.

The catalyst deactivation character at the two process stages was studied by TEM microscopy. The catalyst deactivation at the debenzylation stages is essentially caused by the irreversible enlargement of the palladium particles (Fig. 1).

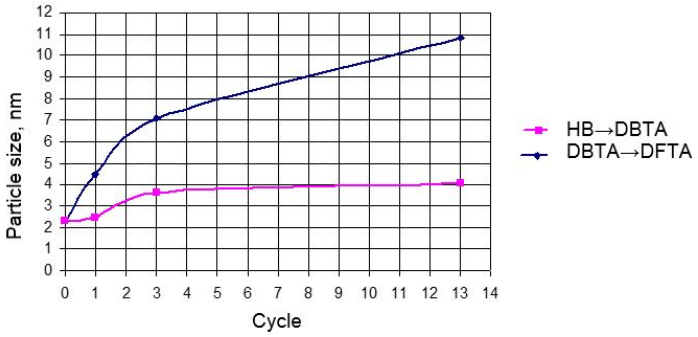

Fig.1. Variation of the mean Pd particle size upon recycling the catalyst at the debenzylation stages

The different characters of deactivation at the debenzylation stages do not enable recycling the catalyst sequentially in the two-stage process (HB→DBTA→DFTA). The key solution to the multiple reuse of the catalyst at the debenzylation stages of HB is separately using the catalyst: the first process (HB→DBTA) employs one sample of the catalyst and the second process (DBTA→DFTA) uses another one (freshly prepared or the spent one from the first stage) [5].
Based on the studies conducted, a technology has been developed for the two-stage catalytic debenzylation of HB with multiple reuse of the catalyst, which allows the catalyst consumption to be appreciably reduced.

4 Conclusions

The technology for the two-stage catalytic debenzylation of HB permits the Pd catalyst consumption to be decreased by a factor of five.

The study results have been corroborated in the course of working out the regimes on a pilot setup at IPCET SB RAS.

Acknowledgements

The research was supported by the RFBR grant No.13-03-12193.

References

[1] US Patent 5693794
[2] Nielsen A. T., Chafin A. P, Christian S. L., et al., Tetrahedron. 54 (1998 – №39) 11793.
[3] S.V.Sysoliatin, A.A.Lobanova, Y.T.Chernikova, G.V.Sakovich, Rus. Chem. Rev. (Engl. Transl.). 74. (2005) 757.
[4] Nielsen A.T., Nissan R.A., Vanderah D.J.,et al., J.Org.Chem. 55 (1990) 1459.
[5] Sergey V. Sysolyatin, Alexander I. Kalashnikov, Valeriy V. Malykhin, Irina A. Surmacheva, Gennady V. Sakovich, International Journal of Energetic Materials and Chemical Propulsion. 9. (2010- №4) 365.

II-PP216

Molybdenum-Containing Catalyst Production for Olefins Epoxidation with Using 1,1'- Dioxydicyclohexylperoxide

Gayfullin A.A.*, Tuntseva C.H., Kharlampidi Kh.

Kazan National Research Technological University, Chair "General Chemical Technology", Kazan, Russia

* gaifullin@kstu.ru

Keywords: the catalyst molybdenum, 1,1'- dioxydicyclohexylperoxid, epoxidation, propylene

1 Introduction

Researches on improvement of propylene hydroperoxide epoxidation of are carried on beginning from introduction of joint receiving styrene and propylene oxide at Public Joint-Stock Company «Nizhnekamskneftekhim» (Russia, Tatarstan). However today's actual problems are increasing molybdenum solubility, decreasing ethyl benzene hydroperoxide (EBHP) consumption in the catalyst preparation, increasing catalyst stability, and also development of new catalyst with the best technological and technical-and-economic indicators.

The analysis of both scientific and technical literature and also the patent publications connecting with receiving molybdenic catalysts for olefins epoxidation shows that for the catalyst synthesis the various hydroperoxide compounds can be used (hydrogen peroxide, peracids, ethyl benzene hydroperoxides, cumene hydroperoxides, I tretbutit hydroperoxides, I tretamit hydroperoxides and so on).

We developed the way of receiving peroxide derivative of cyclohexanone based on reaction between the cyclohexanone and hydrogen peroxide that is contained in sewage of ethyl benzene oxidation shop in production of styrene and oxide of propylene [1]. The result of interaction is the 1,1 '-dioxydicyclohexylperoxide.

In literature sources there are no data on using this peroxide in synthesis of the molybdenic catalyst for epoxidation. Therefore it was very interesting to study possibility of the catalyst preparation on the basis of 1,1 '- dioxydicyclohexylperoxide received with using the peroxide-containing sewage.

2 Experimental/methodology

In the researches the ethyl alcohol (State standard specification 18300-72), powdery metal molybdenum (TC 48-19-316-92) and 1,1 '- dioxydicyclohexylperoxide with the content of active oxygen – 6,9%, melting temperature – 69,1 °C and molar weight – 230,1 was used.

The epoxidation catalyst was prepared by dissolution of powdery metal molybdenum in alcohol solution of 1,1 '- dioxydicyclohexylperoxide in the thermostatically controlled reactor with a mixer at the temperature of 50 °C within 2 hours. For preparation of catalysts the peroxide alcohol solutions with concentration of 0,4 - 1,68 mol/l was used. The molybdenum content in catalytic solution was 0,7 - 4,0% mass. Peroxide concentration was determined by method of iodinemetric titration. The content of the dissolved molybdenum in catalytic solution was determined by a vanadatometric method.

3 Results and discussion

The researche was carried on in two directions. At the first stage the composition and also the catalyst preparation conditions was optimized. The analysis of the obtained data showed that the most convenient method of the molybdenum-containing catalyst synthesis is the way based on dissolution of metal molybdenum powder in alcohol solution 1,1 '-

dioxydicyclohexylperoxide. After experimental studying of various factors influencing activity of the received catalyst samples the optimum compounding and also synthesis optimum conditions were developed. At the second stage the pilot production tests of propylene epoxidation by ethyl benzene hydroperoxide on the basis of the received optimum catalyst were carried out. The tests of process of propylene epoxidation showed the high selectivity of reaction of propylene oxide formation and also product yield exceeding similar indicators for the industrial catalyst.

The results received during the pilot production tests were used for development of basic data for design of set for molybdenic catalyst synthesis on the basis of 1,1 '- dioxydicyclohexylperoxide.

4 Conclusions

The catalyst received with using 1,1 '- dioxydicyclohexylperoxide has following advantages in comparison with industrial one: it allows to exclude the ethyl benzene hydroperoxide from catalyst synthesis process, it allows considerably to decrease a consumption of ethyl alcohol. The main ecological advantage is the utilization of peroxide-containing sewage.

References

[1] A.A. Gayfullin, S. N. Tuntseva, R. A. Gayfullin, Kh.E.Kharlampidi. Herald of Kazan Technological University V. 15, № 23 (2012) P. 26 - 30.

II-PP217

Synthesis and Characterization of Novel Ru(II)-Diimine-Layered Double Hydroxide Nanocomposites as a Light-Responsive Water Oxidation Electrocatalyst

Srankó D.F.[1*], Horváth Zs.E.[2], Chamam M.[1], Kerner Zs.[1], Pap J.S.[1]

1 - Institute for Energy Security and Environmental Safety, Centre for Energy Research, Hungarian Academy of Sciences, Budapest, Hungary

2 - Institute of Technical Physics and Materials Science, Centre for Energy Research, Hungarian Academy of Sciences, Budapest, Hungary

* sranko.david@energia.mta.hu

Keywords: water oxidation, layered double hydroxide, photosensitizers

1 Introduction

Water oxidation has a key role in the field of hydrogen production. In the recent years, several new concepts appeared to design potential novel catalysts, *e.g.*, LDHs with high activity for water oxidation, improving the appealing of this area[1]. Although the intercalation of LDHs with photosensitive compounds is described in the literature for obtaining sensors with high stability, the effect of the intercalated photosensitizer on the LDH's photocatalytic activity is less known. Moreover, in the literature, there is example for the electron transfer between the lattice sites of the positively charged LDH and adsorbed $[Ru(bpy)_3]^{2+}$ $[Fe(bpy)_3]^{2+}$ and $[Os(bpy)_3]^{2+}$ cations[2]. The unique combination of properties of $[Ru(bpy)_3]^{2+}$ (bpy = 2,2'-bipyridine) and of its modified versions, like chemical stability, redox properties, excited-state reactivity and excited state lifetime made it interesting as photosensitizer. In practice, the bipyridine-type Ru(II) complexes as photosensitizers, can be a part of photocatalytic molecular devices.

2 Experimental/methodology

Synthesis of $[Ru(2\text{-}pyridyl\text{-}2'\text{-}benzothiazole)_2](Cl^-)_2$ - RuPBT - complex provides potential photosensitizer that can be built into a composite system for catalysis. The active substrate, NiFe−LDH was synthesized with 3:1 ratio of the divalent and trivalent metals. RuPBT was characterized using ESI-MS, and FT-IR spectroscopy and its light absorption was measured by UV-VIS spectrophotometry. Since RuPBT is positively charged like the NiFe-LDH layers, terephtalate anion was used as a link, attaching the complex to the surface of the LDH. The successful synthesis of the molecular-photosensitizer-on-functional-LDH composite was proved by using a variety of techniques (XRD, FT-IR, cyclic voltammetry and XPS). Furthermore, catalytic activity of the host material was studied in oxygen evolving reaction (OER).

RuPBT was synthesized by reacting $RuCl_3 \bullet xH_2O$ with the 2-pyridyl-2'-benzothiazol ligand with the ratio of 1:3 at 80 ˚C in dimethyl-formamide. The obtained metal complex has a broad absorbtion band with λ_{max} at 480 nm.

NiFe-LDH was synthesized via co-precipitation method, from nitrate salts. The structure of the obtained material was characterized by XRD. The basal distances of the LDHs (d_{003} = 7.9 Å) were the same even when different surface modification methods were applied. In the gallery space of the NiFe-LDH CO_3^- anions were added to avoid the possible modification of the composition during OER. Na-therephthalate (TT) and the 2:1 mixture of Na-therephtalate and RuPBT (TT-RuPBT, c = 3 M) were disolved in a water:ethanol:NaOH 5:1:1 solution in the presence of NiFe-LDH. After stirring for 24 h at 60 ˚C the residue was filtered and cleaned by washing. No changes in the basal distances of the LDH occured during the modification of the surface.

3 Results and discussion

Surface concentration of Ru on LDH was determined by X-ray photoelectron spectroscopy (XPS). The peaks present at 283.2 eV and 287.4 eV were assinged to Ru 3d, while those at 463.3 eV and 466.8 eV to Ru 2p. The Ru/Ni ratio is 0.0112.

For the electrochemical measurements (cyclic voltammetry and chronoamperometry) a thin film of the LDH or LDH-TT-RuPBT was fabricated on the surface of an ITO (indium doped tin oxide) electrode. 0.1 g of a 10 g/dm^3 suspension was layered on the surface obtaining 1 mg of the dry, thin layer LDHs. The CVs were recorded at pH 9.0 in borate buffer in the presence or absence of 0.1 mM of RuPBT in the bulk solution. Importantly, a new cathodic peak is present when LDH-TT-RuPBT is tested. Note that an electrocatalytic anodic wave is present either way with the onset potential being at ~0.97 V.

Electrocatalytic water oxidation (*e.g.* OER) tests were conducted in pH 9.0 borate buffer setting 1.25 V at the ITO against the AgCl/Ag ref. electrode, either in the dark or under continous irradiation (>360 nm, 300 W Xe-lamp). The NiFe-LDH on ITO showed much higher O_2 production rate when irradiated. Importantly, the charge (Q)/evolved n(O_2) ratio corresponds to ~100% efficiency. Irradiating the samples with light at λ = 480 nm wavelenght only the NiFe-LDH-TT-RuPBT composite system showed oxygen production rate.

4 Conclusions

RuPBT was successfully synthesized. The obtained metal complex was immobilized on the surface of NiFe-LDH with terephtalate anions. Several techniques proved the presence of the RuPBT on the surface of the LDHs. Furthermore CV measurements showed significant difference in the electrochemical properties of the organic-inorganic composite material.

Our experiments demonstrate the potential of NiFe-LDH as light-responsive water oxidation electrocatalyst. RuPBT (as an archetype of robust molecular photosensitizer) was successfully attached to the LDH causing no detectable structural changes. Therefore we think that LDHs can be applied as host-catalyst bifunctional materials to accomodate photosensitizers that in turn may allow their photoactivation in the visible range. Further investigations will aim to explore this field.

References

[1] M. Gong, Y. Li, H. Wang, Y. Liang, J. Z. Wu, J. Zhou, J. Wang, T. Regier, F. Wei, H. Dai, Journal of American Chemical Society 135 (2013) 8452–8455

[2] R. Roto, G. Villemure, Journal of Electroanalytical Chemistry 601 (2007) 112-118

II-PP218

Synthesis of Zeolite Membranes of the Type MCM-22 and Y for Use in the Separation Process Oil/Water

Barbosa A.S.*, Rodrigues M.G.F.

Federal University of Campina Grande, Academic Unit of Chemical Engineering, Campina Grande, Brazil

* antoniellybarbosa@yahoo.com.br

Keywords: zeolite MCM-22, zeolite, zeolite membrane, α-Al2O3, oil-in-water

1 Introduction

Oily wastewater from industry and domestic sewage is one of the main pollutants to the environment in the world. With the production of crude oil and natural gas, an aqueous stream named "produced water" is normally accompanied due to the hydraulic fracturing process. The produced water, which contains dispersed oils, suspended particles and dissolved solutes, constitutes the largest waste stream from oil and gas manufacturing industries [1]. Many have been made in the treatment of oily different membranes with effluents. Ceramic membranes have been known for years, and used in many different applications, depending upon their numerous advantages: stability at high temperature and pressure resistance, good chemical stability, high mechanical strength, good durability and antifouling properties. Ceramic MF membrane may be made from alumina, mullite, cordierite, silica, spinel, zirconia and other refractory oxides [2]. The aim of this work is the use of thin zeolite membranes (MCM-22 and Y) (rubbing and mechanics mixture) for the separation of suspensions of oil-in-water.

2 Experimental/methodology

The methodology used in the synthesis of materials: zeolites MCM-22 and Y, α-alumina ceramic membranes and the membranes zeolite Y and MCM-22, followed by methods described [3] e [4].

3 Results and discussion

The results of XRD of samples of MCM-22 zeolite, ceramic membrane, MCM-22 zeolite membrane, Y zeolite, ceramic membrane, Y zeolite membrane are shown in Fig. 1.

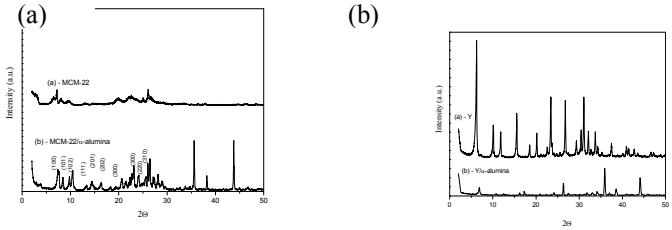

Figure 1. XRD patterns of the samples: (a) MCM-22 zeolite and zeolite Membrane MCM-22 and (b) Y zeolite and zeolite Membrane Y.

Two distinct phases can be identified as a constituent of the zeolitic membrane structure: MCM-22 zeolite and clay (α-Al_2O_3) membranes are shown in Fig. 1(a). The XRD pattern showed that the MCM-22 zeolite synthesized on the ceramic membrane (α-alumina) showed crystalline structure as described by Yang et al. [5] without evidence of other crystalline phases (impurities). The formation of MCM-22 zeolite on the surface of the porous (α-Al_2O_3) membrane can be confirmed by observation of characteristic peaks in the regions corresponding to 2θ = 12–25˚ and 2θ = 26–29˚; the peaks have good intensity [6]. From the XRD pattern

(Figure 1b), it was found that the material obtained has characteristic peaks of zeolite Y, with the peaks corresponding to 2θ values of 6,2º; 10,3º; 12.5 °; 15,8º; 17,6º; 20,0º; 21,7º; 26,0º; 27,9º; 31,0º and 34,0º, which according to the standard IZA (International Zeolite Association) and a JCPDS card 43-0168, peaks are typical sodium Y zeolite (NaY) and can also observe the presence of the crystalline phase stable α-alumina (standard record JCPDF 10-0173), thus confirming the formation of zeolite membrane Y.

Figure 2 shows the SEM images obtained for MCM-22 zeolite membrane and Y zeolite membrane.

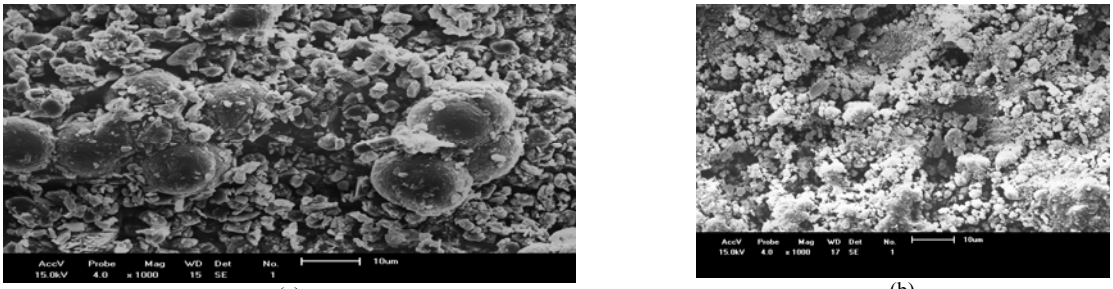

(a) (b)

Figure 2. Micrographs of samples: (a) zeolite membrane MCM-22 (b) zeolite membrane Y

Figure 2a provides an example of a zeolite membrane MCM-22 that was prepared. Two different morphologies on the surface of zeolite membrane MCM-22 was observed. Upon close examination of the cross-section (Figure 2b), the membrane has grown a zeolitic film composed of crystals of MCM-22 and there is the morphology of the ceramic (α-alumina) support, the image displayed by this layer is according to, referring to the ceramic α-alumina support [3].

Through the micrograph (Figure 2b), there is the formation of a heterogeneous surface with no cracks and surface defects. It was found that the support was covered with zeolitic material. It was also possible to observe the presence of grain boundaries similar to those of zeolite Y [4].

Conclusions

The XRD pattern showed that the MCM-22 zeolite membrane and Y zeolite membrane obtained by the method of secondary growth synthesized on the ceramic support crystalline structure showed no evidence of other phases characterized as impurities. A SEM micrograph of the membrane zeolite MCM-22 and Y zeolite membrane showed the formation of a zeolite layer over the ceramic support, which spherical particles grown on the surface of the ceramic support.

Acknowledgements

The authors thank Petrobras for financial support and to improve CAPES (Coordenação de Aperfeiçoamento de Pessoal de Nível Superior) for the scholarship granted.

References

[1] S. Zhang, W. Peng, F. Xiuzhu, C. Tai-Shung, Sustainable water recovery from oily waste water via forward osmosis-membrane distillation (FO-MD), Water research, 52 (2014) 112–121.

[2] L. Yanga, A. Thongsukmaka, K. K. Sirkara, K. B. Grossb, G. Mordukhovich. Journal of Membrane Science**,** 378 (2011) 138–148.

[3] Antonielly S. Barbosa, Antusia S. Barbosa, Meiry G.F. Rodrigues. Desalination and Water Treatment, (2015) 1-8.

[4] Ana P. Araújo, Meiry G.F. Rodrigues. Avances en Ciencias e Ingeniería, 3 (2012) 51-58.

[5] F. H. Tezel, P. Li, Adsorption separation of N_2, O_2, CO_2 and CH_4 gases by β-zeolite, Microporous and Mesoporous Materials, 98 (2007) 94-101.

[6] M. W. Ackley, U. Rege, H. Saxena, Application of natural zeolites in the purification and separation of gases, Microporous and Mesoporous Materials, 61 (2003) 25–42.

II-PP219

Membrane Zeolite MCM-22/γ-Alumina Applied to the Adsorption Capacity of the Gasoline

Barbosa A.S.*, Rodrigues M.G.F.

New Materials Development Laboratory, Federal University of Campina Grande, Campina Grande, Brazil

* antusiasb@hotmail.com

Keywords: membrane zeolite MCM-22/γ-alumina, adsorption

1 Introduction

Industrial processes generate effluents contaminated with organic substances and they have to be treated before disposal without harming the environment. An efficient and sustainable process for purification or for the remediation of groundwater have to meet environmental legislation while operating cost [1]. The zeolite membranes belong to the group of microporous inorganic materials, which are a promising technology. They have advantages over polymeric membranes, especially in respect to chemical resistance, biological stability and resistance to high temperatures and pressures, and over traditional methods of separation (distillation, centrifugation, etc.), such as low power consumption energy, long life, light physical space occupation and ease of cleaning [2]. The preparation and characterization of zeolite membranes is still an innovative subject in Brazil. Within this context, this work is to synthesize zeolite membranes of the MCM-22 type on the γ-alumina ceramic supports, using the secondary growth technique (rubbing), to evaluate the performance in the test adsorption capacity in gasoline.

2 Experimental/methodology

For the synthesis of the ceramic support (γ-alumina) was initially carried out thermal decomposition of aluminum sulfate (Al_2 (SO_4) $_3.16H_2O$) P.A., in a muffle furnace at a temperature of 1000°C using a heating rate of 5°C/min and 2 hours threshold. Then 200ml prepared dispersion having the following composition: 40% of alumina obtained above; 0.2% PABA para-amino benzoic acid (dissolved in ethanol); 0.5% oleic acid (lubricant) and 59.3% ethyl alcohol. The mixture was ground for 1 hour in a ball mill and then placed in an oven for 24 hours at 60°C; umidificou with 7% water, allowed to stand for one day. Was weighed 3 g of the material and placed in the mold. The pressing was performed with 4 tons. The compressed material was subjected to sintering at 700°C for 1 hour.

The zeolite membrane was prepared using the technique of secondary growth (rubbing) [3]. One solution to the synthesis of MCM-22 zeolite membrane was prepared. The methodology used was based on the procedure described in [4]. It is initially hydrolyzed tetraethyl orthosilicate in the aqueous hydrochloric acid solution under heating to obtain the synthesis gel. Later there was prepared an aqueous solution consisting of: sodium aluminate, sodium hydroxide, hexamethyleneimine, to this solution was added the previously hydrolysed gel synthesis, where it was kept under stirring at room temperature for 20 h. The solution was then placed in Teflon crucible and placed in stainless steel autoclaves, where the γ-alumina ceramic substrates with the seeds of zeolite MCM-22 were deposited by rubbing immersed. The hydrothermal synthesis for the growth of the zeolite layer on the support surface occurred at 150°C for 4 days. The synthesis product obtained was washed with distilled water to neutral pH and dried in an oven at 60°C for 24 hours.

3 Results and discussion

Figure 1 shows the XRD pattern of zeolite MCM-22 obtained membrane / γ-alumina in Table 1 and its adsorption capacity for gasoline.

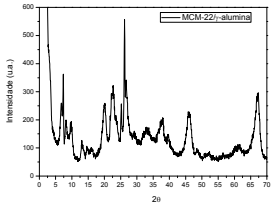

Fig. 1. XRD pattern of zeolite membrane MCM-22/γ-alumina.

Table 1. Adsorption capacity of the samples

Samples	Capacity (g gasoline / g sample)
MCM-22/γ-alumina	22,01

The peaks relating to the XRD patterns of zeolite membrane MCM-22 / γ-alumina synthesized with secondary growth method (rubbing), have similar peaks to those found for the zeolite powder [5, 6] together with the characteristic peaks of ceramic support [7], which indicates that typical zeolite membranes MCM-22 / γ-alumina were successfully obtained. High adsorption capacity values of the gasoline zeolitic membrane (MCM-22 / γ-alumina) were observed in table 1. Studies carried out in the laboratory development of new materials [8, 9] show that organophilic clays to adsorb gasoline values 5.13 and 5.62 respectively. By comparing the results of this study with the literature [8, 9] it can be seen that the adsorption capacity values were much higher than for gasoline, demonstrating that the zeolite membranes are very promising materials for gas adsorption capacity.

4 Conclusions

In conclusion, the formation of zeolite membranes on the γ-alumina ceramic support was investigated. Based on the results of X-ray diffraction, it was verified that the preparation method used to sow the ceramic support, (Rubbing), was effective in obtaining the zeolite membrane MCM-22/γ-alumina as well as the adsorption of gasoline.

Acknowledgements

The authors would like thank CAPES Coordenação de Aperfeiçoamento de Pessoal de Nível Superior, Petrobras for their financial support to this research.

References

[1] L. Xiaobing, Z. Chunjuan, L. Jiongtian, Mining Science and Technology. 20 (2010) 778–781.
[2] J. Caro, N. Noack, P. Kölsch, R. Schäfer, Microporous and Mesoporous Mat. 38. (2000) 3-24.
[3] M. P. Titus, Thesis doctoral, Universitat de Barcelona, Barcelona, 2006.
[4] Y. Wu, X. Ren, J. Wang. Materials Chemistry and Physics. 113 (2009) 773–779.
[5] J. H. Lawton, D. E. Bignell, B. Bolton, G. F. Bloemers, P. Eggleton, P. M. Hammond, M. Hodda, R. D. Holt, D. S. Srivastava & A. D. Watt. 39 (1998) 72–76.
[6] Y. Wu, X. Ren, Y. Lu, J. Wang. Materials Letters. 62 (2008) 317–319.
[7] A.S. Barbosa, A.S. Barbosa, M.G.F. Rodrigues. 9th Ibero-American Congress on Membrane Science and Technology. (2014).
[8] M.F. Mota; J.A. Silva, M.B. Queiroz, H.M. Laborde, M.G.F. Rodrigues, Brazilian Journal of Petroleum and Gas. 5 (2011) 97-107.
[9] G.C. Oliveira, M.F. Mota, M.M. Silva, M.G.F. Rodrigues, H.M. Laborde, Brazilian Journal of Petroleum and Gas. 6 (2012) 171-183.

II-PP220

Study of Adsorption of Hydrogen and Ethane on Bimetallic Platinum and Iridium Nanoclusters Using Quantum-Chemical Calculations

Garifzianova G.G.*, Shamov A.G.

Kazan National Research Technological University, Department of Catalysis, Kazan, Russia

* garifz@kstu.ru

Keywords: platinum, iridium nanocluster, DFT

1 Introduction

One of the most promising directions in the field of catalysis is the use of catalysts containing several atoms of metal and deposited on an inert support. A large number of works devoted to the study of physical and chemical properties of nanoclusters of platinum group, as well as bimetallic clusters based on them [1-2]. Modern quantum-chemical methods are widely used along with modern experimental techniques for exploration of geometry and electronic structures.

Understanding the mechanism of interaction between hydrogen and platinum-iridium clusters is of fundamental scientific and practical interest, since the adsorption of hydrogen is an essential stage in many industrially important catalytic processes, such as hydrogenation and dehydrogenation of hydrocarbons.

2 Results and Discussion

The Structure of nanoclusters Pt_nIr_m (n,m=1 ÷ 3) were studied using DFT with different basis sets. The calculations were performed using the Gaussian 09 program [3]. The geometry structures of nanoclusters were obtained for states with different spin multiplicities.

We studied adsorption of hydrogen molecule on the bimetallic nanoclusters Pt_nIr_m (n,m =1 ÷3). For this purpose, potential energy surface (PES) scan calculations with geometry optimization at each point were performed. Inspection of the geometry structure of resulting Pt_3IrH_2 cluster (method B3LYP/LanL2DZ) showed that position of hydrogen on top of the platinum is more favorable than bridge position. A similar study of the mechanism of hydrogen adsorption was conducted for rhombic cluster Pt_2Ir_2. Results of the latter study showed that adsorption of hydrogen on the clusters Pt_nIr_m (n,m =1 ÷ 3) is barrierless reaction. Relative stability of Pt-Ir clusters is strongly affected by the presence of hydrogen, thus, Pt_2Ir_2 cluster transformed from the cluster with diamond-shaped flat structure into three-dimensional tetrahedral cluster.

The activation energy of the ethane hydrogenolysis on these bimetallic Pt-Ir clusters is smaller than on monometallic iridium and platinum clusters [1]. Potential energy profiles and activation barriers were calculated for key stages of the ethane conversion on bifunctional $PtIr_m$ (m =2 ÷ 3) catalysts. Geometrical parameters of the transition states TS1 on the clusters $PtIr_3$ is shown in Figure. The activation enthalpy for this process is 42.9 kJ/mol.

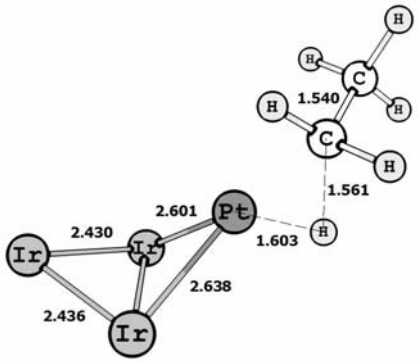

Figure. Optimized geometries of transition state TS1 structure reaction of the ethane hydrogenolysis on these bimetallic $PtIr_3$ cluster. Bond lengths are given in Å.

3 Conclusions

Results of the latter study showed that adsorption of hydrogen on the clusters Pt_nIr_m (n,m =1 ÷ 3) is barrierless reaction. Geometrical parameters of the optimized structures of nanoclusters and transition states of the ethane hydrogenolysis on these bimetallic Pt-Ir clusters were also obtained.

References

[1] O.B. Yang, S.I. Woo, R. Ryoo, *J. of Catalysis. Journal*. 137 (1992) 357
[2] M.-L. Yang, Y.-A. Zhu, C. Fan, Z.-J. Sui, D. Chen, X.-G. Zhou, *Phys. Chem. Chem. Phys.* 13(2011) 3257
[3] M. J. Frisch, et all. Gaussian 09, Revision A.1, Gaussian, Inc., Pittsburgh PA, 2009

II-PP221

Influence of Zink on the Formation and Properties of Catalysts Pt/Mg(Zn)AlO$_x$ Obtained from the Layered Hydroxides

Belskaya O.B.[1,2*], Stepanova L.N.[1], Erenburg S.B.[3], Trubina S.V.[3], Nizovskii A.I.[4,2], Kalinkin A.V.[4], Bukhtiyarov V.I.[4], Likholobov V.A.[1,2]

1 - Institute of Hydrocarbons Processing SB RAS, Omsk, Russia
2 - Omsk State Technical University, Omsk, Russia
3 - Nikolaev Institute of Inorganic Chemistry SB RAS, Novosibirsk, Russia
4 - Boreskov Institute of Catalysis SB RAS, Novosibirsk, Russia

* obelska@ihcp.ru

Keywords: zinc containing, layered double hydroxides, platinum, catalysts, alkane, dehydrogenation, EXAFS

1 Introduction

Platinum catalysts supported on aluminum–magnesium oxide materials are widely used in base-catalyzed reactions and in the conversion of hydrocarbons. The formation of the properties of the catalysts may depend considerably on the structure and composition of the precursor of the oxide support, namely, layered double hydroxide (LDH). The general formula of LDHs is $M^{2+}_{1-x}M^{3+}_x(OH)_2[(A^{n-})_{x/n}\bullet mH_2O]$, and they consist of brucite-like layers in which part of the divalent cations (M^{2+}) is isomorphically substituted by trivalent cations (M^{3+}) that have a similar ionic radius. The excess positive charge of the layers is compensated by hydrated A^{n-} anions located in interlayer spaces. A unique feature is that with this type of hydroxide precursor, the M^{2+} and M^{3+} cations undergo uniform distribution during the subsequent formation of the mixed oxide phase. The introduction of special modifiers to adjust the properties of supported platinum to the demands of a particular reaction to obtain target product with high selectivity is an effective approach. The novelty of this work was to introduce the modifier cation (zinc) in the structure of the support during the LDH synthesis. Formation of zinc-containing LDH is poorly described in the literature but it is known that zinc modifies the properties of the supported platinum. In particular, in the presence of ZnO, the dispersion of Pt grows and dehydrogenation activity of supported catalysts increases. Our study examined the effect of zinc in LDH on the formation of active sites of the catalysts Pt/Mg(Zn)AlO$_x$, their composition, adsorption and catalytic performance. Catalytic properties were tested in propane and n-decane dehydrogenation.

2 Experimental/methodology

LDH-Mg(Zn)Al-CO_3 (with CO_3^{2-}-anions in interlayer space) was synthesized by co-precipitation, M^{2+}/Al=2. LDH-Mg(Zn)Al-OH (with OH^--anions in interlayer space) was obtained after calcinations of LDH-Mg(Zn)Al-CO_3 at 550 °C and subsequent hydration of mixed oxides in water. Anchoring of platinum chloride complexes was carried out on LDH-Mg(Zn)Al-OH. Elemental analysis was made by ICP-AES (Varian 710-ES). Structural features of LDH and mixed oxides were studied by XRD (D8 Advance, Bruker). Adsorption–desorption isotherms of nitrogen at 77.4 K were measured using a static volume vacuum system ASAP-2020M (Micromeritics). CO and H_2 pulse chemisorption (AutoChem II 2920, Micromeritics) and transmission electron microscopy (JEM-2100, JEOL) were used to estimate the particle size of platinum. X-ray photoelectron spectroscopy (XPS) was carried out on a spectrometer SPECS, Germany. EXAFS and XANES spectra of the PtL_{III} absorption edge were measured at the ID26-beamline of the European Synchrotron Radiation Facility (ESRF, Grenoble, France). Catalytic properties of Pt/Mg(Zn)AlO$_x$ were investigated under the following conditions: T = 550 °C, atmospheric pressure, WHSV 8 h^{-1} and H_2/C_3H_8 molar ratio of 0.25 (in propane dehydrogenation); T=460°C, pressure 0.2 МПа, WHSV 17 h^{-1}, $H_2/C_{10}H_{22}$ molar ratio of 7 (in decane

dehydrogenation).

3 Results and discussion

Study of the LDH showed that hydrotalcite-like structure was saved when a partial or complete replacement of Mg to Zn took place as well as the introduction of Pt(IV) anionic complexes in the interlayer space of Mg(Zn)Al-OH. Calcination of zinc-containing LDH with adsorbed platinum complexes led to an interaction between zinc and platinum with a significant modification of platinum properties. In zinc-containing samples the particles of platinum had different morphology and smaller sizes in comparison with $Pt/MgAlO_x$. In accordance with the EXAFS data for $Pt/Mg(Zn)AlO_x$ there are no peaks in the spectra corresponding to platinum-platinum bonds (fig. 1a). Therefore it can be assumed that platinum atoms surrounded only by zinc atoms. The results of XPS showed that the Pt/Al atomic ratio for all the samples was close to ~ 0.007. The value of binding energy $Pt3d_{5/2}$ for sample with Zn/(Mg+Zn)=0.1 (2122.7 eV) was significantly higher, than for the samples Zn/(Mg+Zn)=0.5, 0.7. For the latter, the energy was close to that of the metallic state of platinum (and even slightly lower) and was equal 2121.4 eV. From the EXAFS and XPS results it can be concluded that platinum in these samples is in the Pt-Zn alloy particles with a relatively low platinum concentration.

The resulting catalysts are characterized by a higher propane conversion (close to the equilibrium at a Zn/(Mg+Zn)=0.1) with a selectivity in the propylene formation 99% (fig. 1b). When Zn/(Mg+Zn)>0.1, there is some decrease in activity while maintaining high selectivity. This may be result of decreased specific surface area and changes in the pore space of the oxide support due to the formation of additional phase enriched by zinc. Modifying of platinum in the presence of zinc also has been shown in the transformation of higher alkanes. Decrease in the content of dienes in the products of n-decane conversion may be a consequence of the weakening of the C_{10}-olefin adsorption on platinum. Thus their further dehydrogenation to dienes becomes impossible. This behaviour is usually explained by the formation of alloys and the electron transfer to the platinum atoms.

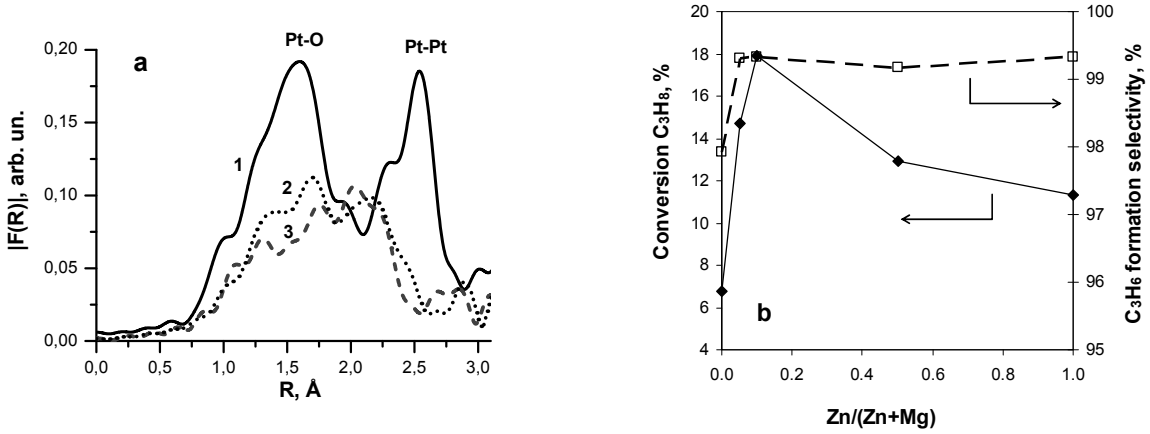

Fig. 1. a) Fourier transform magnitude |F(R)| of kχ(k) function in the 3–18 $Å^{-1}$ region for the PtL_{III} EXAFS spectra of samples 1.0%Pt/Mg(Zn)AlO_x, Zn/(Mg+Zn)=0, 0.5, 0.7 (curves 1, 2, 3, respectively); b) propane conversion and propylene formation selectivity for 0.3%Pt/Mg(Zn)AlO_x, Zn/(Mg+Zn)=0, 0.05, 0.1, 0.5, 0.7, 1.0.

4 Conclusions

The work illustrated the effect of platinum modifying with zinc when it is introduced into the structure of the support during the synthesis of LDH. The changes in the chemical composition, morphology and sizes of supported metal particles were detected. Supported platinum in catalysts $Pt/Mg(Zn)AlO_x$ was characterized by the adsorption and catalytic properties providing selective producing of olefins from light and higher alkanes.

Acknowledgements

This work was supported by a grant from the President of the Russian Federation leading scientific schools of the Russian Federation (project no. NSh-3631.2014.3).

II-PP222

Textural Properties of Iron-Based Catalysts Supported on Mesoporous Silica SBA-15 Synthesized with Different Silica Source

Eduardo R.S.[1*], Rodrigues J.J.[1], Rodrigues M.G.F.[1], Cruz M.G.A.[2], Fernandes F.A.N.[2]

1 - Federal University of Campina Grande, Campina Grande, Brazil
2 - Federal University of Ceará, Ceará, Brazil

* raphael_leahpar17@hotmail.com

Keywords: catalyst, iron, copper, potassium, Fischer-Tropsch synthesis, rice, husk, ashes

1 Introduction

SBA-15 is a new class of mesoporous silicate that has a high thermal and hydrothermal stability when compared to materials belonging to the M41S family, due to the greater thickness of the walls of the pores [1]. The evaluation and the influence of the support as the surface area and the pore size in the mesoporous structure materials enable higher metal dispersion and the reactants and products access to the pores of the catalyst, providing a higher catalytic activity [2]. The rice husk ash may be used in the synthesis of mesoporous materials because it is amorphous, and only becomes crystalline silica when heated to high temperatures [3]. Among various fields iron oxides are applied highlight the processes involving adsorption and catalysis, which have attracted great interest due to redox and textural properties [4]. Two metals are normally present in the iron catalysts, potassium and copper. Potassium acts on the activity and selectivity. Copper has a significant influence on the speed which iron catalyst achieves maximum activity, although there are questions about the impact on other properties of the catalyst [5]. This work aims to evaluate the textural properties of the catalyst Fe/Cu/K/SBA-15RHA.

2 Experimental/methodology

The catalyst Fe/Cu/K/SBA-15RHA was prepared with the molecular sieve SBA-15RHA synthesized by hydrothermal method [6] using Pluronic P123 as template, hydrochloric acid and rice husk ash as silica source, treated previously by heat and chemical processes [7]. The catalyst Fe/Cu/K/SABA-15 was prepared using nitrates of iron and cupper and potassium bicarbonate as metals precursors. The incorporation of metals was taken by simultaneous wet impregnation with solutions from metals precursors. The catalyst was prepared with molar ratio 100Fe/5Cu/18K/139SiO_2. The catalyst was submitted to heat treatment under nitrogen and synthetic air flow for conversion of nitrates to oxides. The textural properties from SBA-15 and catalyst were obtained by characterization by nitrogen adsorption, evaluated by adsorption N_2 isotherms and desorption isotherms at -196°C using equipment Micromeritics ASAP 2020 a relative pressure range (p/p_0) ranging from 0.02 to 1.0.

3 Results and discussion

Figures 1 (a) and (b) show the N_2 adsorption/desorption isotherms at 77 K of the calcined SBA-15RHA and catalysts Fe/Cu/K/SBA-15RHA.

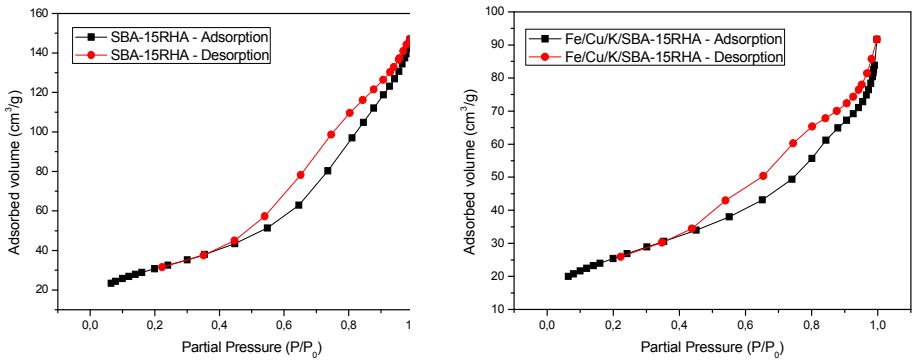

Fig. 1. N_2 adsorption/desorption isotherm at 77 K for calcined SBA-15 (a) and catalyst Fe/Cu/K/SBA-15 (b)

The isotherms for the calcined SBA-15 sample were of type IV and H1 hysteresis type, comprising two vertical branches over a range of 0.5 to 0.8 (P/P0) on the abscissa axis. This behavior is characteristic of mesoporous materials of which the SBA-15 is part [6]. The patterns on adsorption and desorption pressures were maintained in the catalyst Fe/Cu/K/SBA-15RHA, having the three phases of condensation (monolayer, capillary condensation and external multilayer) and H1 hysteresis type associated with the difference between the pressures on the adsorption and desorption. The textural analysis of the calcined SBA-15RHA support and the catalysts is presented in Table 1.

Parameter	S_{BET} (m^2/g)	Specific pore volume (cm^3/g)	Average pore diameter (nm)
SBA-15RHA	112	22.3	7.6
Fe/Cu/K/SBA-15RHA	91.7	12.8	7.8

Table 1. Textural properties of molecular sieve SBA-15RHA and Fe/Cu/K/SBA-15RHA catalyst.

There was a decrease in pore volume of 42.6%, and 18.1% in surface area when compared to the synthesized molecular sieves, used as supports. With the inclusion of metals in used rate, it was expected that reduction of these properties.

4 Conclusions

By the results from specific surface area, total pore volume there were changes in the support (SBA-15), since there was a reduction of its specific surface area, already small, and total volume of pores after impregnation. This would mean that some pores are blocked with iron, copper and potassium species.

Acknowledgements

The authors would like thank Coordenação de Aperfeiçoamento de Pessoal de Nível Superior (CAPES), Petrobras for their financial support to this research.

References

[1] M. M. A. Reza; R, S. S. M. Jafar; K. D. Ajay. *Fuel Processing Technology*. 90 (849-856) 2009.
[2] A. Griboval-Constanta; A. Y. Khodakov; R. Bechara; V. L. Zholobenko. *Studies in Surface Science and Catalysis*. 144 (609-616) 2002.
[3] C. Real; M. Alcala; J. Criado. Journal of the American Ceramic Society. 79 (2012-2016) 1996.
[4] U. Schwertmann; R. M. Cornell; *Iron Oxides in the Laboratory*, 2nd ed., VCH: Weinhein, 2000.
[5] B. H. Davis. *Catalysis Today*, 84 (83–98) 2003.
[6] D. Zhao; Q. Huo; J. Feng; B. F. Chmelka; *Journal of American Chemical Society*, 120 (6024-6036) 1998.
[7] L. A. Cano; M. V. Cagnoli; N. A. Fellenz; J. F. Bengoa; N. G. Gallegos; A. M. Alvarez; S. G. Marcjetti. *Applied Catalysis A: General*, 379 (105) 2010.

II-PP223

Soybean Oil Transesterification Applying Iron-Based Catalysts Supported on Mesoporous Silica SBA-15

Eduardo R.S*, Lima E.G, Rodrigues J.J, Rodrigues M.G.F

Federal University of Campina Grande, Campina Grande, Brazil

* raphael_leahpar17@hotmail.com

Keywords: catalyst, iron, copper, potassium, transesterification soybean oil

1 Introduction

The transesterification has emerged as the best option for obtaining biodiesel, since the process is relatively simple; combined with this technique, researchers seek to lower the biodiesel manufacturing process using reusable catalysts, developing studies on heterogeneous catalysts that are reused in the manufacture of fuel [1]. Studies with heterogeneous acid catalysts have been developed for the transesterification reaction. These catalysts can transesterified the triglycerides esterified the free fatty acids and suffer little influence of water that perhaps may be present in the raw material. Such catalysts use primarily solid with basic or acidic characteristics [2]. Mesoporous materials SBA-15 type silica compounds essentially, have several properties which make them potential acid catalysts, emphasizing their high surface areas. In addition, these materials have thicker walls of the pores, resulting in a higher hydrothermal stability. However, to make them catalytically active by their structures are basically formed of silica, the introduction of metal is required [3]. The factors considered important in the dispersion of the active phase on the support of the metal ions are the oxidation states and the character of the atomic radius, and those related to the selectivity and activity of the catalysts. The wide applicability of VIII group metals as catalysts is partly because of these having variable oxidation state and high activity for breaking C-C links [4].

2 Experimental/methodology

The catalyst Fe/Cu/K/SBA-15 was prepared with the molecular sieve SBA-15 synthesized by hydrothermal method [3] using Pluronic P123 as template, hydrochloric acid and Tetraethylorthosilicate as silica source. The catalyst Fe/Cu/K/SABA-15 was prepared using nitrates of iron and cupper and potassium bicarbonate as metals precursors. The incorporation of metals was taken by simultaneous wet impregnation with solutions from metals precursors. The catalyst was prepared with molar ratio 100Fe/5Cu/18K/139SiO_2. The catalyst was submitted to heat treatment under nitrogen and synthetic air flow for conversion of nitrates to oxides. The materials were characterized by XRD and N_2 adsorption. *Transesterification of reaction:* The prepared catalysts were subjected to the reaction test using a high pressure chemical reactor with a temperature of 200ºC and with 2 hours. The reaction was conducted at a molar ratio of 1:12 oil/methanol with 5% (w/w). After the reaction, mixture was washed and the final product submitted to gas chromatography. *Ester Content:* The analysis of the methyl esters were determined by gas chromatography, using a gas chromatograph Varian450c with flame ionization detector, capillary column stationary phase Varian Ultimetal "Select Biodiesel Glycerides + RG" (0.32 mm x 15m x 0.45 um.).

3 Results and discussion

The Figure 1 shows the isotherms of X-ray diffraction pattern of catalyst Fe/Cu/K/SBA-15 (a) and your N_2 adsorption-desorption at -196°C (b), and The textural analysis of the calcined SBA-15 support and the catalysts is presented in Table 1.

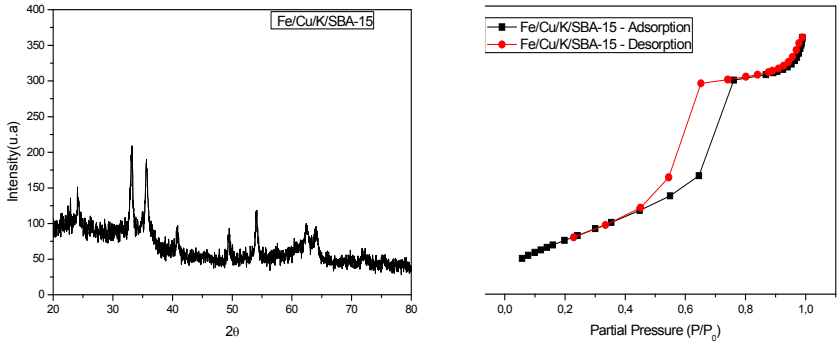

Fig. 1. XRD patterns of the catalysts Fe/Cu/K/SBA-15 (a) and N_2 adsorption/desorption isotherm at 77 K for calcined catalyst Fe/Cu/ K/SBA-15 (b).

Table 1. Textural analysis of catalyst Fe/Cu/K/SBA-15.

Parameter	S_{BET} (m^2/g)	Specific pore volume (cm^3/g)	Average pore diameter (nm)
SBA-15	490	74.7	6.0
Fe/Cu/K/SBA-15	253	37.4	6.3

The iron should be well dispersed throughout the structure of the molecular sieve SBA-15, which favors the thermal stability of the catalyst. The catalyst presented evidence of crystalline formation. It is found through analysis of N_2 adsorption-desorption isotherms of type IV and H_1 hysteresis type, comprising two vertical branches over a range of 0.5 to 0.8 (P/P0) on the abscissa axis. This behavior is characteristic of mesoporous materials of which the SBA-15 is part [3]. There was reduction of the specific surface area and total volume of pores after impregnation. This would mean that some pores are blocked with iron, copper and potassium species.

The analysis by gas chromatography provided satisfactory result of Conversion of the of soybean oil to esters applying the catalyst Fe/Cu/K/SBA-15. The value of conversion to ester of the soybean oil was 65.38%. It can be said that there was median conversion and average yield of esters.

4 Conclusions

The catalyst Fe/Cu/K/SBA-15 showed characteristic peaks phases of the oxides of iron and copper by XRD and characteristic patterns of mesoporous materials by nitrogen adsorption analysis.The transesterification reaction of soybean oil with ethanol carried out in this study had a median conversion of 65.38% with the catalyst Fe/Cu/K/SBA-15.

Acknowledgements

The authors would like thank Coordenação de Aperfeiçoamento de Pessoal de Nível Superior (CAPES), Petrobras for their financial support to this research.

References

[1] D. Y. C. Leung; X. Wy; M. K. H. Leung. *Applied Energy*. 87 (108-1095) 2010.
[2] S. J. Clark; L. Wangner; M. D. Strock; P. G. Piennaar. Journal of the American Oil Chemists' Society. 61(1632 1638) 1984.
[3] D. Zhao; Q. Huo; J. Feng; B. F. Chmelka; Journal of American Chemical Society, 120 (6024-6036) 1998.
[4] R. R. Davda; J. W. Shabaker; G. W. Huber. *Applied Catalysis*. 56 (171- 186) 2004.

II-PP224

Ni-XMo(W,V)/Al_2O_3 Catalysts Comparative Investigation in Hydrotreating of Light Coker Gasoil

Tomina N.N.*, Maximov N.M., Bajanova A.S., Moiseev A.V., Pimerzin A.A.

Samara State Technical University, Samara, Russia

* tominann@yandex.ru

Keywords: hydrotreating, diesel fuel, light coker gasoil, phosphorus

1 Introduction

In the recent years hydrotreating tungsten-containing catalysts attracted a lot of interest. These catalysts are active in hydrogenation processes and have stability at high temperatures. The sulfidation of WO_3 into WS_2 has a problem like more high temperature, than MoO_3 one. In the same time it's well known, that mixed system WO_3+ MoO_3 is more easily sulfide. In this way, we chose Mo and (W+Mo) mixed systems for active phase design, and promoted catalysts with Ni [**1**].

2 Experimental/methodology

A line of catalysts Ni-XMo(W,V)/Al_2O_3 (X = Si, P, V) was synthesized. Amounts of Ni and (Mo+W) were constant. Ni was introduced from organic salt, Mo and W were introduced from heteropolyacids (HPA) ($SiMo_{12}$-, PMo_{12}-, $PVMo_{11}$-, VMo_{12}-, SiW_{12}- and PW_{12}-HPA) by means of wetness impregnation method. Ni-AHM/Al_2O_3 and Ni-AHW/Al_2O_3 (AHM – ammonium heptamolybdate, AHT – ammonium heptotungstate) samples were applied as comparative patterns. The impregnation was carried out in two steps: a part of Mo was introduced in the first and a part of Mo or W was introduced in the second one. After each impregnation catalysts were dried at temperatures of 60, 80, 110ºC for 2 hours. Before catalytic tests catalysts were sulfided.

The catalytic activity of the samples was determined in a bench-scale flow reactor unit in the hydrotreating process of light catalytically cracked gas oil (LCGO). Contents of sulfur and polycyclic aromatic hyrocarbones (PAH) in mixture were 2,06 and 14,32 wt. % respectively.

The hydrodesulfurization (HDS) activity and hydrogenation (HYD) activity were estimated like HDS and HYD degree, respectively.

3 Results and discussion

The results of catalytic tests are showed in **Table 1** and **Fig. 1**.

Table 1. Relative HDS activities and contents of spent Ni-XMo(W,V)/Al_2O_3 catalysts

Catalyst	Coke content on spent catalyst, wt. %	Relative HDS degree: HDS/(Ni-AHM/Al_2O_3 HDS) at temperature, °C			
		340	360	390	410
Ni-AHM/Al_2O_3	3.00	1.00	1.00	1.00	1.00
Ni-SiMo/Al_2O_3	-	1.26	1.02	0.99	0.90
Ni-PMo/Al_2O_3	1.95	1.22	1.11	1.17	1.09
Ni-PVMo/Al_2O_3	1.70	1.35	1.27	1.28	1.06
Ni-VMo/Al_2O_3	-	1.41	1.28	1.19	1.09
Ni-AHT/Al_2O_3	-	1.36	1.13	1.20	1.06
Ni-SiMoW/Al_2O_3	-	1.40	1.15	1.25	1.08
Ni-PMoW/Al_2O_3	-	1.57	1.38	1.21	1.09

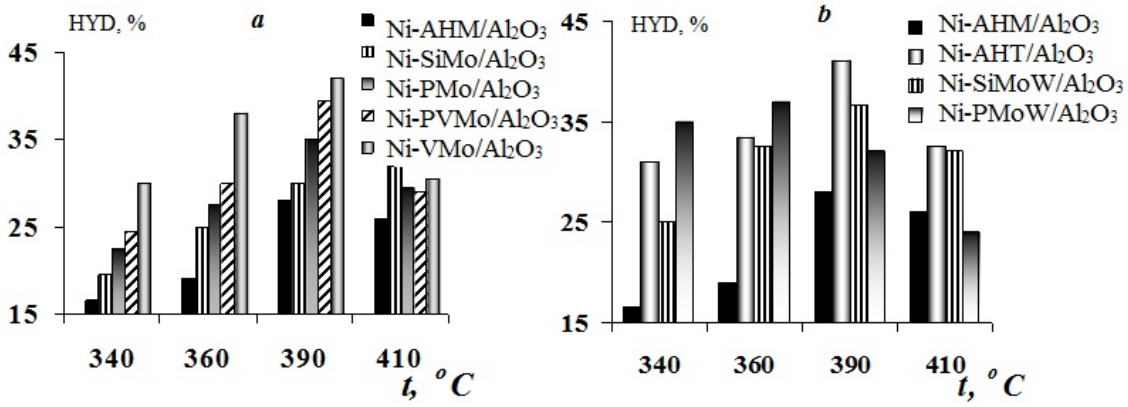

Fig. 1 Relationsips between HYD and temperature of process:
a - Ni-***X***Mo/Al_2O_3 catalysts, ***X* = *Si, P, V;* *b*** - Ni-***X***MoW catalysts, ***X* = *Si, P***
Process conditions: hydrogen pressure – 3.5 MPa, LHSV – 2.5 h^{-1},
hydrogen/feed ratio – 450 nm^3/m

The maximums of PAH HYD and HDS of sulfur compounds were found for catalysts on the bases of $PVMo_{11}$ - and VMo_{12} – HPA. Ni-VMo/Al_2O_3 catatalyst HYD degrees at temperatures of 340-390°C are higher twice than Ni-AHM/Al_2O_3 ones. Ni-AHT/Al_2O_3 catatalyst HDS degrees are higher than Ni-AHM/Al_2O_3 ones. Catalysts with higher hydrogenation activities Ni-PVMo/Al_2O_3 and Ni-VMo/Al_2O_3 have a low content of coke than others.

4 Conclusions

In this way, the best precursors for synthesis of high active hydrogenation Ni-XMo(W,V)/Al_2O_3 catalysts are $PVMo_{11}$ - and VMo_{12} – HPA. The catalysts, which contained W, showed a better HDS and HYD activities than without W ones.

Acknowledgements

The work was supported by Russian Federal target program «Investigations and developments of priority directions of scientific-technological complex progress of Russia for 2014-2020 years» (project № 14.577.21.0140).

References

[1] Tomina N.N., Pimerzin A.A., Moiseev I.I. *Russian Chemical Journal*. 52 (4) (2008) 41-52.

II-PP225

Influence of Morphology of Ni Surface on Emergence of Self-Sustained Oscillations in the Oxidation of Propane

Gladky A.Yu.[1*], Kosolobov S.S.[2], Saraev A.A.[1], Sherstyuk O.V.[1], Kaichev V.V.[1], Bukhtiyarov V.I.[1]

1 - Boreskov Institute of Catalysis, Novosibirsk, Russia
2 - Rzhanov Institute of Semiconductor Physics, Novosibirsk, Russia

* gladky@catalysis.ru

Keywords: self-sustained oscillations, propane oxidation, nickel

1 Introduction

Self-sustained rate oscillations in the oxidation of light hydrocarbons over transition metals are a well known phenomenon. Recently, we have shown that the regular kinetic oscillations arise during the oxidation of propane over Ni foils and wires [1-3]. The oscillations were observed in a temperature range 650-750□C under oxygen-lean conditions when the propane/oxygen molar ratio ranges from 3/1 to 15/1. The oscillations were of the relaxation type, which can be described as a fast change between "low-active" and "high-active" states. The driving force for the self-sustained kinetic oscillations was shown to be the periodic reoxidation of nickel. According to an *in situ* XPS study [3], the high-active state of the catalyst surface is metallic nickel, whereas during the inactive state, the surface is covered with a thick layer of NiO. Here, we present the results of our further study. We focus on studying the influence of morphology of the catalyst surface on the emergence of self-sustained oscillations.

2 Experimental

Three types of samples were used in our study: rectangular pieces of a Ni foil (0.125 mm thick, purity 99.99%, Advent Research Materials Ltd.), thin Ni films (1 μm thick) deposited on a Si substrate by magnetron sputtering, and thick Ni films (20 μm thick). In the last case, the thick Ni films were electrochemically deposited on the thin Ni/Si films.

The kinetic measurements were performed in a vacuum apparatus equipped with a fused silica flow reactor and a quadrupole mass spectrometer [1,3]. The surface morphology was studied using a scanning electron microscope LEO 1430 (Carl Zeiss) and a focused ion beam (FIB) system LEO 1540XB Crossbeam (Carl Zeiss).

3 Results and discussion

First, we studied the propane oxidation over the thick Ni foil and found that the appearance of regular oscillations is preceded by a long induction period. The duration of the induction period depends on pressure and temperature of the reaction mixture and varies in a range from a few tens of minutes to several hours. During the induction period, a rough and porous structure of the catalyst surface developed because of its strong reconstructing. The thickness of the reconstructed layer was approximately 10-20 μm. This process was accompanied with at least an 80-fold increase in the effective surface area compared with a clean, not-treated nickel foil, which undoubtedly led to a drastically increase in the number of active sites. We believe that it is the main reason for the induction period, which is always observed before the appearance of self-sustained oscillations in the catalytic oxidation of light hydrocarbons over catalysts with a low specific surface area (single crystals, foils, or wires). Moreover, without such reconstructing, the oscillations cannot arise due to low activity of these catalysts.

Indeed, over thin Ni/Si films, oscillations in the oxidation of propane under the same conditions

do not appear. In contrast, over the thick Ni/Si films, the regular kinetic oscillations arise after an induction period similar to that obtained for the Ni foil. According to SEM, over the thick Ni/Si film, a rough and porous structure developed under reaction conditions. Typical SEM images are presented in Fig. 1. The thin Ni/Si film transforms to separated agglomerates over the surface of silicon substrate. We believe that in this case the effective surface area is not enough for the emergence of self-sustained oscillations.

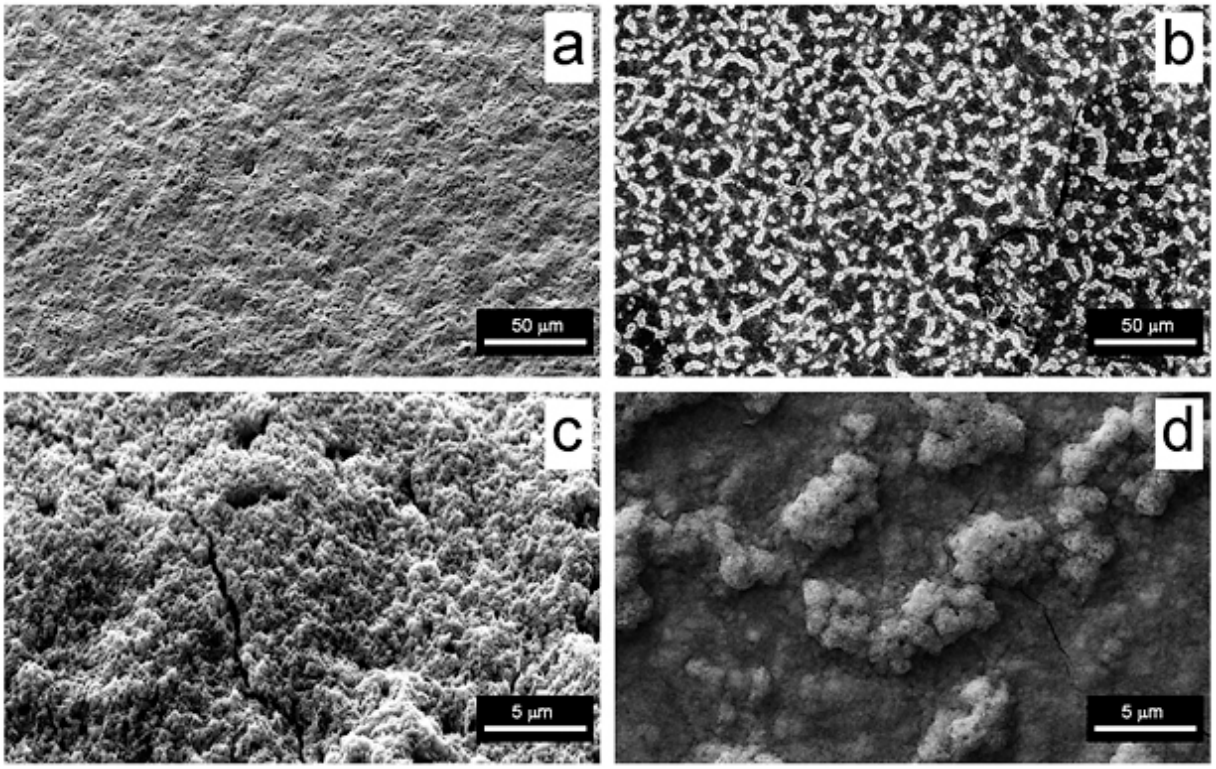

Fig. 1. Typical SEM images of the thick Ni/Si film (a, c) and thin Ni/Si film (b, d) used as catalysts of the oxidation of propane.

4 Conclusions

The main reason for the induction period observed before the appearance of self-sustained oscillations in the catalytic oxidation of light hydrocarbons over catalysts with a low specific surface area (single crystals, foils, or wires) is the formation of porous structure on the catalyst surface. Without such reconstructing, the oscillations cannot arise due to low activity of these catalysts.

Acknowledgements

The work was partially supported by the Grant of President of Russian Federation for government support of Leading Scientific Schools (SS-5340.2014.3).

References

[1] A.Yu. Glagky, V.K. Ermolaev, V.N. Parmon, *Catal. Lett.* 77 (2001) 103.
[2] A.Yu. Glagky, V.V. Kaichev, V.K. Ermolaev, V.I. Bukhtiyarov, V.N. Parmon, *Kinet. Catal*. 46 (2005) 251.
[3] V.V. Kaichev, A.Yu. Gladky, I.P. Prosvirin, A.A. Saraev, M. Havecker, A. Knop-Gericke, R. Schlogl, V.I. Bukhtiyarov, *Surf. Sci.* 609 (2013) 113.

II-PP226

Study of the Catalytic Effect of Nanosilica and Polycarboxylate on Cement Hydration and Mechanical Properties of Cement Mortars

Benmounah A.*, Samar M., Saidi M., Safi B., Kheribet R.

Research Unit: Materials, Processes and Environment (UR/MPE), Boumerdes University, Boumerdes, Algeria

* benmounah2000@yahoo.fr

Keywords: cement paste, nanosilica, superplasticizer, hydration, fluidity, mechanical strengths

1 Introduction

Given that the nanosilica particles (NS) and the polycarboxylate superplasticizer (PCE) have shown respectively a great pozzolanic activity and a best fluidity for cement pastes as have been demonstrated in previous studies [1-3]. Based on these results, the catalytic effect of mixture nanosilica (silica nanoparticles) and PCE-superplasticizer on hydration of different cements has been investigation in this study. The PCE addition to a cement paste can increase the flowability thus reducing the water demand and accelerated the setting time process of the different cements studied. The obtained results show that the PCE has played as a deflocculating agent of the cement particles reducing the particle size of the agglomerates through a steric hindrance mechanism. Also, Mechanical strengths of studied cements were improved by the mixture presence of NS and PCE. Indeed, it was found that the nanosilica particles have played a catalyst role of cements hydration reactions and thus causing the formation of new calcium hydrosilicates that contribute to the improvement of mechanical resistances. The optimum attained in the combined effect of the mixture (NS and PCE) that involved relevant microstructural modifications as proved by pore size distributions and SEM observations. These phenomenon are highlighted by measuring the mechanical strengths of the cements studied and also, by the DTA, TGA, and XRD.

2 Experimental study

Four cement types (C1: CEM II 42.5 based on pozzolan, C2: CEM II 42.5 based on blast furnace slag, C3: CEM II 42.5 based on limestone and C4: CEMI 52.5 ES) were used in this work. The superplasticizer used is based on polycarboxylate (PCE) containing the nanoparticles of silica Fume with a high content of silica approximately 83% with an estimated loss on ignition of 13.7%. To conduct the experimental work a prismatic 40x40x160 mm3 samples were manufactured for each mixture. All the specimen of mortars were mixed and prepared using a mortar mixer with a vertical axis and a capacity of 5L Also, the setting times were determined of all cement pastes with a superplasticizer presence Three-point bending test and uniaxial compression are carried out at 2, 7 and 28 days on water stored samples (under 21±1°C).

3 Results and discussion

The obtained results show that the PCE and NS have played a catalyst agent of the cement particles reducing the setting times of cement hydration (fig.1). Also, Mechanical strengths of studied cements were improved by the mixture presence of NS and PCE. Indeed, it was found that the nanosilica particles have played a catalyst role of cements hydration reactions and thus causing the formation of new calcium hydrosilicates that contribute to the improvement of mechanical strengh (fig. 2). The optimum attained in the combined effect of the mixture (NS

and PCE). The results indicate also the effectiveness of NS and PCE-superplasticizer in producing high bulk density and in accelerating the pozzolanic activity to produce more C-S-H gel by consuming calcium hydroxide Ca (OH) 2 according the reaction (1), in order to improve the mechanical properties of cement pastes [4-6].

$$Ca(OH)_2 + H_4SiO_4 \rightarrow Ca^{2+} + H_2SiO_4^{2-} + 2\,H_2O \rightarrow CaH_2SiO_4 \cdot 2\,H_2O \text{ (C-S-H)} \qquad (1)$$

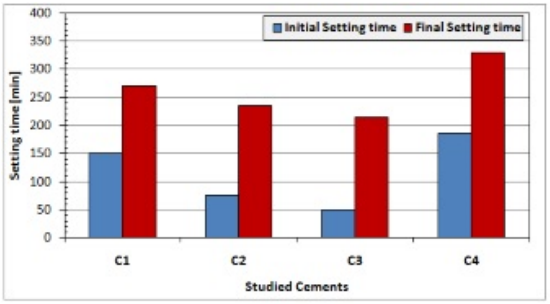

Fig. 1. Setting times of studied cements in a presence of NS and PCE

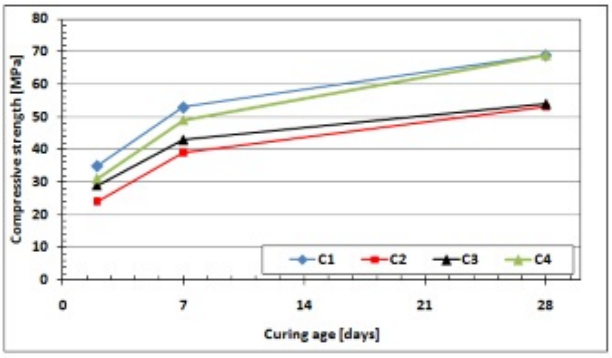

Fig. 2. Compressive strength evolution of the mortars based on C1, C2, C3 and C4

4 Conclusions

Catalytic effect of NS and PCE on the cement hydration has been investigated in this work. It can be concluded that the nanosilica particles in PCE presence, have played a catalyst role of cements hydration reactions and thus causing the formation of new calcium hydrosilicates which have contributed to the improvement of mechanical strength of the studied cements [6-7]. The results indicate also the effectiveness of NS and PCE-superplasticizer in producing high bulk density and in accelerating the pozzolanic activity to produce more C-S-H gel by consuming calcium hydroxide Ca (OH)2 in order to improve the mechanical properties of cement pastes.

References

[1] Banfill, P. F. G., a review, 11th International Cement Chemistry Congress, Durban, May, 2003
[2] UchikawaH, Hanehara,S, Shirasaka.T,. Cem. Concr. Res. (1992) 1115- 1129.
[3] Kamal H., Khayat K. H., Atcin P-C. An Overview, ACI International Workshop on Silica Fume in Concrete 1991.
[4] L. Soriano, J. Monzó, M. Bonilla, M.M. Tashima, J. Payá, M.V. Borrachero, Cement & Concrete Composites 42 (2013) 41–48
[5] J. Payà, J. Monzo, M.V. Borrachero, S. Velazquez, Cement and Concrete Research 33 (2003) 603–609
[6] Sabir B.B, Wild S, Bai J. a review. Cem Concr Compos 2001;23:441–54.
[7] Hassan AAA, Lachemi M, Hossain KMA, Khandaker MA. Cem Concr Compos 2012;34:801–7.

II-PP227

Functionalized Graphene-Containing Mesoporous Materials as Catalysts in Acid-Catalyzed Reactions

Topolyuk Yu.A.[1,2*], Kulikov A.B.[1], Maximov A.L.[1,3]

1 - A.V.Topchiev Institute of Petrochemical Synthesis, RAS, Moscow, Russia
2 - Gubkin Russian State University of Oil and Gas, Moscow, Russia
3 - Moscow State University, Dep. of chemistry, Moscow, Russia

* topolyuk@ips.ac.ru

Keywords: grapheme, functionalized graphene oxide, mesoporous, silica, SBA-15, catalysis

1 Introduction

Graphene-based hybrid materials have shown many applications in the fields of nanoelectronic and energy storage devices, advanced optical materials and catalysis due to their outstanding thermal and mechanical stabilities, superior electrical conductivity, rich chemical functionality of the surface [1]. The hexagonal SBA-15 silicas functionalized via framework incorporation different heteroatoms as well as via chemical bonding of organosilanes exhibits interesting catalytic performance [2]. The development of graphene-containing mesoporous materials (GCMM) in a form of 3D-graphene aerogels and ordered mesoporous carbons as well as and their application in electrochemical capacitors has been reported [3]. Probable combination of the unique properties of carbon nanomaterials with graphene structure and mesoporous silicates in the same material looks highly promising for its application in catalysis.

2 Experimental/methodology

Graphene oxide (GO) was synthesized via modified Hummers method [4] from pristine graphite (UPV-1-TMO) and followed by graphite oxide ultrasonication in DW for 1 h to produce a suspension of GO sheets. Functionalized graphene sheets (FGS) was obtained via GO facile covalent functionalization with (3-aminopropyl) triethoxysilane from hydroxyl groups by a coupling reaction. Graphene-containing mesoporous materials (GCMM) was prepared in sol-gel process using tetraethylorthosilicate (TEOS) as the silica source, the triblock copolymer (Pluronic P123), as the surfactant and GO or FGS, as the graphene source, in acidic condition. Following experimental GCMM- samples were prepared: SBA-15-GO (Al-SBA-15-GO), SBA-15-FGS (Al-SBA-15-FGS). Chemical surface modification of GCMM-samples was carried out by treatment in the presence of sulfuric acid and aluminum chloride at selected conditions.

3 Results and discussion

Experimental samples were characterized by XRD, TEM, N_2 adsorption-desorption methods. Elemental C, H, S, N-analysis showed that the weight content of elements in the graphene oxide, (wt.%): C (67,34 ± 0,2), H (1,47 ± 0,5), O (31,04 ± 1,0), S (0.15); the molar content of C/O~2,9/1. Based on the results obtained by x-ray diffraction studies (Fig. 1b), the appearance of graphene oxide peak centered at $2\Theta = 11.6^{o}$, corresponding to the (001) inter-planar spacing of 7.59 Å. Calculated thickness of GO layer was about 2.5 nm, what indicated that we had graphene oxide with multilayer structure. The peak in 43^{o} (Fig. 1b,c) corresponded to the disordered carbon materials. The disappearance of the (001) diffraction peak (Fig. 1c) was due to fact that the GO can be reduced in direct esterification reaction during the synthesis of silica mesoporous structure. XRD of reduced graphene showed a broad peak in the region of $20–30^{o}$ The XRD pattern of SBA-15-GO-sample indicated the hexagonal mesoporous structure

was obtained as supported by low angle XRD peak at 1,76°. The formation of this type of structure was confirmed by the results of the TEM-analysis (Fig. 2a,b).

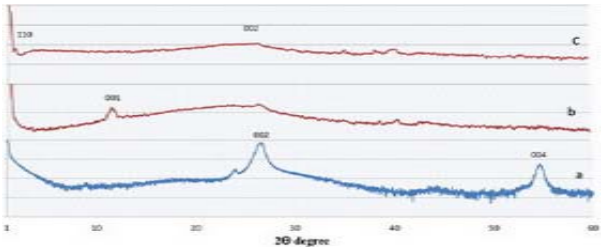

Fig. 1. XRD patterns of graphite (UPV-1-TMO) (a), GO(b) and SBA-15-GO(FGS) (c)

After modifications of the samples the XRD patterns indicated that all the samples retained the characteristic patterns of the hexagonal mesostructure. Figure 2 (c,d) shows the N2 adsorption–desorption isotherms and the BJH pore size distribution curves of SBA-15-GO-sample.

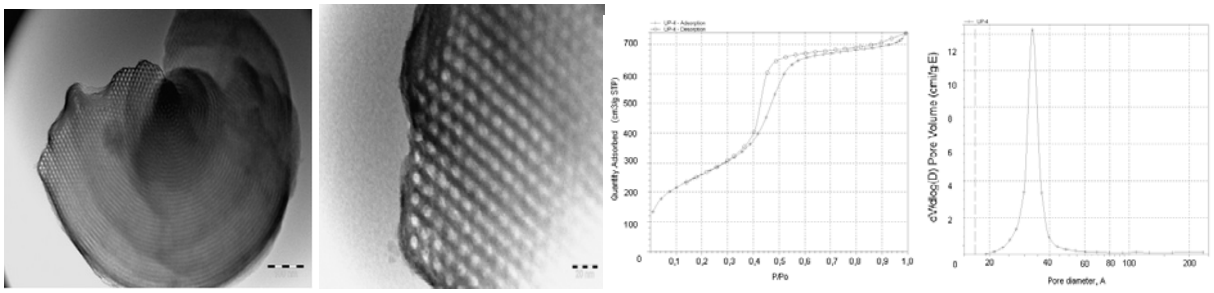

a) b) c) d)

Fig.2. TEM micrograph of SBA-15-GO (a,b), N2 adsorption–desorption isotherms (c) and the pore distribution of SBA-15-GO (d)

The sample has a BET surface area of 956 $m^2g^{-1}$and pore volume of 1.1 cm^3 g^{-1}. Textural properties of the synthesized graphene-containing mesoporous materials were similar and fit into a narrow range. The reactions of dehydration of butanol-1 and oligomerization of n-decene-1 were performed as the test reaction for investigating the catalytic activity of the functionalized GCMM. The samples obtained with FGS, as the graphene source, showed greater activity in the reaction of oligomerization of n-decene-1.

4 Conclusions

In this work, we demonstrate a hydrothermal synthesis of graphene-containing mesoporous materials with well-ordered SBA-15 structure, high surface areas (~956 m^2 g^{-1}) and large pore volumes (~1.1 cm^3 g^{-1}). The functionalized graphene-containing mesoporous material showed good catalytic efficiency in test reactions of dehydration of butanol-1 and oligomerization of n-decene-1.

Acknowledgements

Financial supports from the Russian Academy of Science Program 8 Reg № 01201352582 are greatly appreciated.

References

[1] Cancan Huang, Chun Li and Gaoquan Shi., Energy Environ. Sci., 2012, 5, 8848.
[2] Dongyuan Zhao, Jinyu Sun, Quanzhi Li and Galen D. Stucky, Chem. Mater. 2000, 12, 275-279.
[3] Zhong-Shuai Wu, Yi Sun, Yuan-Zhi Tan, Shubin Yang, Xinliang Feng and Klaus Müllen, J. Am. Chem. Soc. 2012, 134, 19532−19535.
[4] N.I.Kovtyukhova, P.J.Ollivier, B.R.Martin, T.E.Mallouk, S.A.Chizhik, E.V.Buzaneva, A.D.Gorchinskiy, Chem. Mater.,11, 771 (1999).

II-PP228

Preparation and Characterization of MOR Catalysts, Mo- MOR Ni-MOR and for Application in the Transesterification of Soybean Oil

Silva F.M.N.*, Lima E.G., Rodrigues M.G.F.

Development of New Materials Laboratory-LABNOV, Federal University of Campina Grande, Department of Chemical Engineer, Campina Grande, Brazil

* fabymedeirosquimica@hotmail.com

Keywords: mordenite, Mo-MOR, Ni-MOR, transesterification, biodiesel

1 Introduction

The current energy production in the world comes mostly from non-renewable sources which consequently increases the environmental impact. These facts have stimulated the alternative sources for fossil fuel development. One of the most promising sources is biodiesel, an alternative diesel fuel derivate from renewable sources with high quality, which allows the substitution of fossil diesel oil without engine modifications [1]. Heterogeneous catalysis is widely applied in industry due to important advantages it offers to chemical processes such as improved selectivity and easy catalyst separation from reaction mixture, reducing process stages and wastes. This is the reason why nowadays heterogeneous catalysts are being developed to produce biodiesel [2]. This work aims at the synthesis of heterogeneous catalysts MOR, Mo-MOR and Ni-MOR, for application in the transesterification reaction of soybean oil, aiming at the preparation of biodiesel.

2 Experimental

Synthesis of zeolite MOR: The mordenite zeolite was synthesized hydrothermally according to the methodology proposed by Kim and Ahn [3]. The composition of the reaction mixture was: $6Na_2O:Al_2O_3:30SiO_2:780H_2O$. In a typical synthesis, the sodium hydroxide was dissolved in deionized water, and then added to the sodium aluminate dissolved in water to the starting solution at room temperature. To this mixture was added Aerosil 380 silica slowly. Then the gel was transferred to a stainless steel autoclave and brought to the oven, where it remained for 72 hours at a temperature of 170°C (hydrothermal treatment). After this time, the solid was recovered by filtration, washed and dried at 80°C for a period of 24 hours. *Synthesis of Catalysts:* The catalysts were prepared by wet: Mo-MOR (2.5% MoO_3) being used as precursor ammonium heptamolybdate ($(NH_4)\ 6Mo_7O_{24}.4H_2O$) and Ni-MOR (2.5% NiO) and the precursor nitrate nickel ($Ni\ (NO_3)_2.6H_2O$, supported on MOR. the impregnated catalysts after calcined were subjected to a dispersion of oxides sore support in a muffle furnace at 500°C for 6 hours with a heating rate of 5 °C/min. *Biodiesel Synthesis:* The prepared catalysts were subjected to the reaction test using a high pressure chemical reactor with a temperature of 200 ºC and 2 hours. The reaction was conducted at a molar ratio of 1:12 oil/methanol with 5% (w/w) of catalysts. After the reaction mixture was washed and the final product submitted to gas chromatography.

2 Results and discussion

The XRD patterns of the MOR zeolite and their respective catalysts Mo-MOR and Ni-MOR synthesized are shown in Fig. 1. XRD patterns of MoO_3-MOR (Mo-MOR) and NiO-MOR (Ni-MOR) catalysts are shown in Fig. 1, all catalysts exhibit the characteristic peaks (2θ = 9.8, 22.4, 25.8, 26.4, 27.7 and 27.9◦) of mordenite, indicating preservation of the zeolite framework after

impregnation of metals. The diffraction peaks of bulk MoO_3 (2θ = 12.7, 23.3, 25.6, 27.3 and 38.9◦) and NiO (2θ= 40º, 46.58º, 44.58º and 43.38º) are not clearly observed in the patterns. This suggests that Mo and Ni species exist as highly dispersed surface species, as is observed in the literature [4]. Faherazzi et al. [5] have reported peaks Ni (cubic) and NiO (hexagonal) at the 2θ values of 40º, 46.58º, 44.58º and 43.38º, respectively. In this case, there is the presence of the 46.5 peak, some peaks are missing, and hence the size of the particles might be below the detection limit of XRD [6].

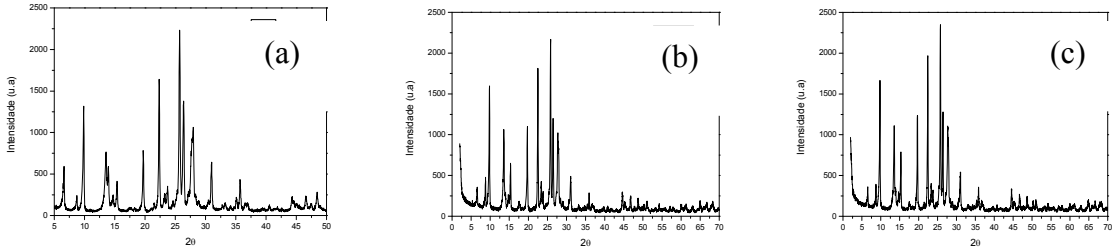

Fig. 1. Diffractograms of the samples: (a) zeolite MOR, (b) catalyst Mo-zeolite MOR and (c) Ni- zeolite MOR.

The amount of ester is a parameter considered very important for the quantification of product formed in the reaction. After the catalytic tests, biodiesel was subjected to characterization to check the conversion reaction. This parameter was evaluated by determining the ester content by gas chromatography as described in Table 1.

Table 1. Conversion results in the reaction of transesterification.

Catalysts	Conversion (%)
Zeolite MOR	22.57
Ni-Zeolite MOR	69.70
Mo-Zeolite MOR	75.35

Zeolite MOR is a natural zeolite with the content silicon [3]. The result of chromatography was satisfactory for the test with zeolite MOR, the conversion to esters obtained was 22.57%, this is can explained due acidic sites. However, deposition of metal (Ni or Mo) on the surface of the zeolite MOR renders acidity to it, and therefore this would be an efficient alternative to increase the acidity of solid catalysts (Ni-Zeolite MOR and Mo-Zeolite MOR). This can be confirmed by chromatography in the analysis of catalysts Ni-Zeolite MOR and Mo-Zeolite MOR, which provided satisfactory results as the percentage of total esters.

3 Conclusions

The transesterification reaction of soyebean oil with ethanol showed in this work presented efficient conversion of 69.70% with Ni-Zeolite MOR catalyst and 75.35% Mo-Zeolite MOR.

Acknowledgements

The authors would like thank Coordenação de Aperfeiçoamento de Pessoal de Nível Superior (CAPES), Petrobras for their financial support to this research.

References

[1] C.C. Enweremadu., M. M. Mbarawa. Renewable and Sustainable Energy Reviews 13 (2009) 2205–24.
[2] M.E. Borges., L. Díaz. Renewable and Sustainable Energy Reviews 16 (2012) 2839–2849.
[3] G. J.Kim., W. S. Ahn. Zeolites. 11 (1991) 745-750.
[4] S. Huang., H. Liu., L. Zhanga., S. Liu., W. Xin., X. Li., S. Xie., L. Xu. Applied Catalysis A: General 404 (2011) 113–119.
[5] G. Faherazzi., A. Benedetti., A. Martorans., S. Giuliano., D. Duca., G. Deganello., Catal. Lett. 6 (1990) 263.
[6] D. Karthikeyan., N. Lingappan., B. Sivasankar., N. J. Jabarathinam. Applied Catalysis A: General 345 (2008) 18–27.

II-PP229

Preparation and Characterization of Mo Catalysts Supported on Clay for the Transesterification of Soybean Oil

Lima E.G.*, Eduardo R.S., Barbosa A.S., Rodrigues M.G.F.

Development of New Materials Laboratory-LABNOV, Federal University of Campina Grande, Department of Chemical Engineer, Campina Grande, Brazil

* erigenuino@hotmail.com

Keywords: catalyst, soybean oil, transesterification, hard green clay

1 Introduction

Biodiesel is an attractive alternative to fossil based fuels on the basis of its biodegradability, non-toxicity and low C emission characteristics [1-2]. Biodiesel is generally produced using four different methods involving base-catalyzed transesterification, acid-catalyzed transesterification, enzyme-based transesterification and non-catalytic transesterification under supercritical alcohol conditions and transesterification of refined oils via homogeneous alkaline catalysts [3]. Use of heterogeneous catalysts provides many advantages in comparison to employing homogeneous catalysts including the recoverability and reusability of the catalyst particles and easier separation and purification of the glycerol (above 99%) and methyl esters. Clays such as dolomite, kaolin, and bentonite are abundant, inexpensive and have relatively high surface to volume ratios to allow them to serve as catalyst supports for the transesterification of oils with methanol to biodiesel [4]. The present work focuses on application of Mo catalysts supported of production biodiesel by transesterification of soybean oil.

2 Experimental/methodology

A hard green clay, provided by Boa Vista City (Brazil), was used. *Preparation of Catalysts*: The Mo/HGC catalyst was impregnated with molybdenum oxide generated from ammonium molybdate [(NH4)6Mo7O24 . 4 H2O] (Merck) as the source of molybdenum. The deposition on the substrates is held with a percentage of 5 % for the catalyst by wet impregnation each employing the aqueous solution of Mo. The solution remained under stirring at room temperature for 30 minutes. Subsequently, the mixture intended to drying in an oven at 100 ° C for a period of 24 hours [5]. catalyst Mo-HGC. *Transesterification of reaction:* The prepared catalysts were subjected to the reaction test using a high pressure chemical reactor with a temperature of 200 ºC and with variation of 2 and 4 hours. The reaction was conducted at a molar ratio of 1:12 oil/methanol with 5% (w/w). After the reaction, mixture was washed and the final product submitted to gas chromatography. *Ester Content:* The analysis of the methyl esters were determined by gas chromatography, using a gas chromatograph Varian450c with flame ionization detector, capillary column stationary phase Varian Ultimetal "Select Biodiesel Glycerides + RG" (0,32 mm x 15m x 0.45 um.).

3 Results and discussion

The XRD patterns of the hard green clay pure and catalyst Mo-HGC prepared are shown Figure 1. XRD patterns of hard green clay pure Fig. 1a makes a reference bentonite clay from type with crystallographic phases of the smectite group (5.79º), kaolinite (12.17º, 20.15º and 26.14º), indicating (24,94º, 34,87º e 61,84º) a crystallographic phase quartz. In a Fig. 1b shown the XRD of Mo-HGC catalyst, it was still observed the peaks characteristic of clay, with a reduction in intensity due to the thermal treatment subjected to the impregnation and appearance

in 54,21º related to the peak of the molybdenum oxide present in the catalyst (Mo-HGC).

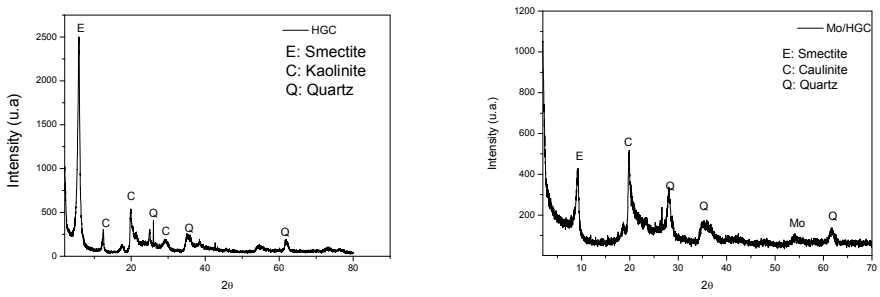

(a) (b)

Fig. 1. Diffractograms of the samples: (a) hard green Clay (HGC), (b) Mo-HGC.

The activities of the catalyst were studied the investing effects of metal (Mo) present in the support hard green clay (Table 1). The metal (Mo) present in the surface of the catalyst (Mo-HGC) showed great importance, improving the catalytic activity of the hard green clay support, providing a significant increase in conversion due to the formation of active sites generated by the presence of the metal support. The most important factor in transesterification is the reaction time. The conversion will increase the amount of reaction time, due to increased contact time with the active sites of the catalyst [6]. This effect caused by the reaction time, and the presence of the active sites with high temperature can be checked on the results.

Table 1. Results of catalytic test

Catalysts	**Conversion (%) (2h)**	**Conversion (%) (4h)**
Hard Green clay (HGC)	5.50	9.50
Mo-HGC	62.07	85.68

4 Conclusions

The XRD showed the crystal composition of the clay, that is a bentonite clay and observed the insertion of the molybdenum oxide phase after the impregnation process. In the catalytic test, the more activity was observed in the impregnated catalyst with a longer reaction, the reaction time and the presence of active sites generated by the presence of the metal (Mo) on the support (HGC) surface.

Acknowledgements

The Coordenação de Aperfeiçoamento de Pessoal de Nível Superior (CAPES) and Petrobras for their support and financial incentive.

References

[1] Y.C. Sharma, B. Singh, *Renewable Sustainable Energy Reviews* 13 (2009) 1646–1651.
[2] R. Alcantara, J. Amores, L. Canoria, E. Fidalgo, M.J. Franco, A. Navarro, *Biomass and Bioenergy* 18 (2000) 515–527.
[3] Y. Wang, S. Ou, P. Liu, Z. Zhang, *Energy Conversion and Management* 48 (2007) 184.
[4] N. Degirmenbasi, N.Boz, D. M. Kalyon, *Applied Catalysis B: Environmental* 150 (2014) 147-156.
[5] J. J. Rodrigues, L. A. Lima, W. S. Lima, M. G. F. Rodrigues, F. A. N. Fernandes, Brazilian Journal of Petroleum and Gas, 5 (2011) 149-157.

II-PP230

Structural and Textural Properties of Modified Montmorillonite Derived from an Al_{13}-Macrocation, Acid and Nickel Activations

Lahoues N.[1], Barama S.[1*], Djellouli B.[2], Barama A.[1], Massiani P.[3]

1 - Laboratoire des Matériaux Catalytiques & Catalyse en Chimie Organique, Faculté de Chimie, USTHB, Alger, Algérie

2 - Laboratoire de Génie des Procèdes Chimiques, Faculté des Sciences de l'Ingénieur, Université Ferhat Abbas – Sétif, Sétif, Algérie

3 - CNRS-UMR 7197 UPMC, Laboratoire de Réactivité de Surface, Paris, France

* siham_barama@yahoo.com

Keywords: catalysis, pillared, clays, montmorillonite, Al_{13}-macrocation, acid activation, basal, distance

1 Introduction

Considerable attention has been paid to the study of pillared clays in the context of the development of new materials, and that has attracted great interest for many years [1]. Currently, the Al_{13}-macrocation is a common treatment accorded to layer-silicates, in industrial operations as well as in research laboratories, this involved processes have been widely studied, especially for smectites like the montmorillonite and bedellite type clays. The montmorillonite (labeled MMT or B: bentonite) is a natural lamellar silicate utilized in the preparation of nanocomposites because of its high aspect ratio, high expandable capacity between lamellas, natural availability and low cost. On the other hand, the platinum catalysts are used for the oxidative catalytic reactions because they play an effective and crucial role in the hydrogen production, but platinum is nevertheless an expensive, for this reason, a recent research has shown how to get the same kind of reactivity using nickel [2] and cobalt that are a thousand times less expensive than platinum. In our work, new materials based on montmorillonite intercalated by Al_{13} and activated by acid treatment were successfully prepared. These obtained materials are modified by impregnation (doping) of nickel, cobalt and platinum which are introduced with weight percentages between 1 and 10%, but only nickel catalysts will be studied in the present work.

2 Experimental/methodology

Natural clays MMT-type are provides from Maghnia region (west of Algeria). Firstly, natural clay (BN) was mixed with an appropriate amount of water for minerals-sedimentation separation. In the second step, through Stokes-method (aggregates fraction<2micrometer), a sodic purification was realized (to remove substantial amounts of impurities) with 1N concentration of sodium chloride solution, to obtain the sodic-montmorillonite (sodic-MMT). The resulting suspension was centrifuged and precipitate was repeatedly washed to remove chloride ions. Finally, three different principal materials were prepared: (1) the exchanging of sodic-MMT by aluminum oxo-polycomplex macrocation "Al_{13}-macrocation", followed by calcination at 400°C (noted BAl_{13}), (2) the treating of sodic-MMT with sulfuric acid (noted BAc) [3], (3) the treating of sodic-MMT with sulfuric acid followed by Al_{13}-macrocation (noted $BAcAl_{13}$). These three materials were modified by impregnation with 1-10%W/W of nickel. Synthesized nanoparticles have been characterized by various physicochemical techniques such as: X-ray diffraction, SAXS (2theta<8°), TGA/DTA analysis, X-ray fluorescence, SEM, determination of specific surface area by BET method; porosity analysis and FT-IR.

3 Results and discussion

The structural and textural properties of supports and catalysts (1%w/w) are presented in

Fig.1. It can been seen that properties are highly dependent on treatments and changes undergone by different modification of samples (acid treatment, macrocation and nickel impregnation) in agreement with literature [3]. The nitrogen adsorption/desorption isotherms (Fig.1-Left) showed type-IV characteristic of mesoporous systems and the quantities of adsorbed N_2 vary in the order: Ni/BAl_{13}>BAl_{13}>$Ni/BAcAl_{13}$; this result indicates important adsorptive properties that depending on different supports. The Al_{13}-macrocation was confirmed by XRD patterns (Fig.1-Right), by observing the increase of basal line.The nanostructure of different systems were analyzed by Small Angle X-ray Scattering (SAXS). The interlayer distance d_{001} (2theta), observed for BAc, Ni/BAc, BAl_{13}, Ni/BAl_{13}, $BAcAl_{13}$ and $Ni/BAcAl_{13}$ samples, were respectively 14.62Å (6.03°), 11.5Å (7.6°), 17.52Å (5.04°), 15.7Å (5.60°), 17.8Å (4.95°) and 15.7Å (5.62°). The SAXS-calculations showed, for each solid, a decreasing of d_{001} after impregnation of support by nickel element. This result could be attributed to a decreasing of crystallinity degree which is probably related to the consequence of nickel particles dispersion as shown with the results of Table.1. The catalytic activity of these materials is evaluated in degradation of organic pollutants. Work is in progress.

Fig. 1. (Left) N_2 adsorption-desorption isotherms of supports and nickel samples (Right) XRD patterns at room temperature of nickel catalysts and supports.

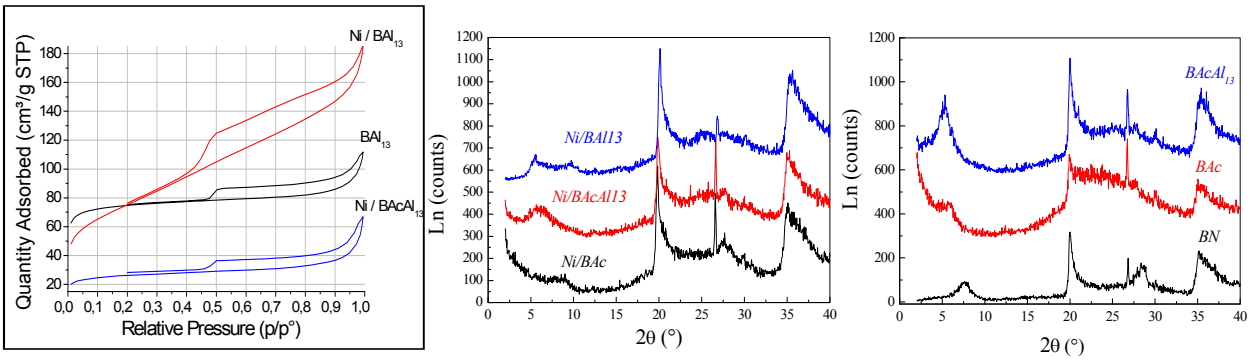

Table 1. SAXS-calculations parameters of sheets.

Catalysts/Supports	Degree of crystallinity	Number of sheet/particle
BAc	3.83	4.2
Ni/BAc	2.08	2.0
BAl_{13}	20.0	4.3
Ni/BAl_{13}	6.75	1.4
$BAcAl_{13}$	11.25	1.5
$Ni/BAcAl_{13}$	2.92	1.2

4 Conclusions

This report studies the effect of different modifications in nanoscopic structure of MMT, corresponding to macrocation by Al_{13} nanocomposites, by nickel impregnation and by acid treatment of sheets. SAXS experiments were able to provide a better idea regarding the size of the interlamellar spacing (mesopores localizations) and average lamellar distance. Nickel containing clay modified with Al_{13}-macrocation displayed higher increase of the interlayer spacing indicating higher modification, which could be interesting for our study.

References

[1] C. Marcilly et J.P. Franck (IFP), « la préparation des catalyseurs » (deuxième édition), Revue de l'institut Français du pétrole, 39, 3 (1984).

[2] S. Barama, C. Dupeyrat-Batiot, M. Capron, E. Bordes-Richard and O. Bakhti-Mohammedi, Cata.Today 141 (2009) 385–392.

[3] J. Temuujin, "Characterisation of acid activated montmorillonite clay from Tuulant (Mongolia)", Ceramics international, 30 (2000) 251-255.

II-PP231

Characterization and Activity in Dry Reforming of Methane over Alumina Supported Transition Metal Catalysts Prepared by Microemulsion and Sol-Gel Method

Halouane M.[1,2], Menad S.[2], Kouachi K.[3], Khiar C.[2*]

1 - Département de Chimie, Faculté des Sciences et Sciences Appliquées, Université Akli Mohand Oulhadj de Bouira, Bouira, Algeria

2 - Laboratoire de Chimie Appliquée et Génie Chimique, Université M. Mammeri de Tizi-Ouzou, Tizi-Ouzou, Algeria

3 - Faculté des Sciences de la Nature et de la Vie, Département des Troncs Communs, Université de Bejaia, Bejaia, Algeria

* halouane_mou@yahoo.fr

Keywords: Ni catalysts, Co catalysts, Cu catalysts, methods of prepartion catalysts, dry reforming of methane, microemulsion method

1 Introduction

A number of techniques have been used for the production of the nanoparticles, such as coprecipitation, sol-gel, hydrothermal and microemulsion [1].

In this paper, Alumina-supported Ni, Co and Cu (25 wt.%) were prepared by two different preparation techniques and have been tested in the reaction of reforming of methane by carbon dioxide at the temperature of 923 K. The two different catalyst preparation methods are the sol-gel (SG) and the microemulsion (ME). The physicochemical characteristics of the prepared catalysts were investigated by means of X-ray powder diffraction (XRD), temperature programmed reduction (TPR), transmission electronic microscopy (TEM-EDS) and BET surface area techniques.

2 Catalyst preparation

The M/Al_2O_3 (M = Ni, Co and Cu [25wt %]) catalysts were prepared by sol-gel (SG) and water-in-oil microemulsion (WO) methods. WO and SG catalysts was prepared using $M(NO_3)_2.xH_2O$ as source of metal (M) and aluminum nitrates as source of Al_2O_3.

The WO catalyst was prepared by the following procedure. Two different emulsions (WO1 and WO2) were prepared WO1 and WO2 have the same components and ratio of cyclohexane, CTAB, 1-butanol with the exception of the Water phase was put in WO1 precursors of the metal and the support and in WO2 was put the precipitating agent (NH_4OH). Then the WO2 was added dropwise into the WO1. The system was kept under stirring for 24 h. he precipitate is filtered and washed with methanol. The obtained powders were dried at 110 ° C and calcined at 900 ° C for 2 h with 3°C/ min.

The Sol-gel catalysts were prepared using the following procedure. Suitable amounts of metal and support precursors were dissolved in the appropriate amount of citric acid solution. Then the solvent was evaporated under continuous stirring at 80 ° C until a gel was obtained. After the resulting gel was dried at 110°C for 24 h, and then calcined at 900°C for 2h with 3°C/min.

3 Results and discussion

The Comparison of BET areas (Table 1) shows whatever the metal studied, that specific areas are significantly higher for the samples prepared by WO compared to those prepared by SG. The results are in agreement with literature the BET surface areas followed the order ME >

SG [2].

The diffraction X-ray analysis of all the catalysts showed the presence of characteristic lines of the MAl_2O_4 spinel phase (M: Ni, Co, Cu) crystallized in a cubic structure. In addition the comparison of MAl_2O_4 crystallite size (Table 1), according to the technique of preparation, shows that the size is smaller on the catalysts prepared by WO. On the other hand the TEM-EDX observations of Ni/Al_2O_3 catalyst prepared by WO show a uniform MAl_2O_4 particle distribution (Figure 1). In contrast, this same catalyst prepared by SG revealed that most of the particles are in the form of two-dimensional cluster.

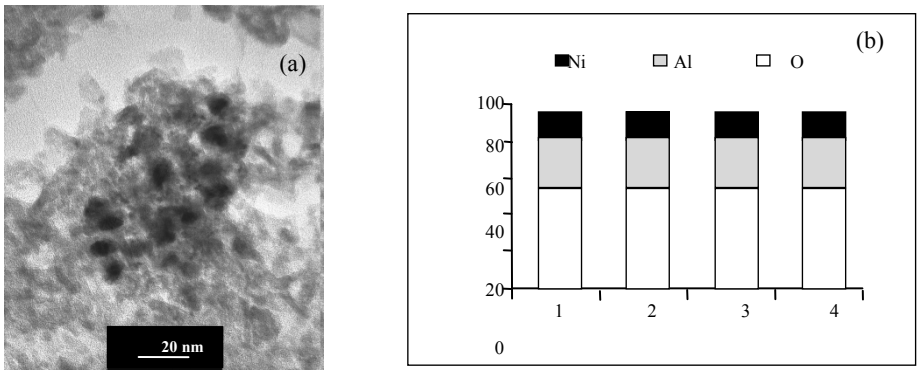

Figure 1. (a) TEM image and (b) EDX elementary distribution of NiAl-ME catalyst calcined at 923 K

ME-prepared samples reveal a positive effect on the catalytic activity and stability of catalysts. It should be noted that the better performances were recorded on the NiAl-ME catalyst (Table 1). This behavior may be related to the presence of a strong metal-support interaction and good dispersion of the particles on the support.

Table 1. Physicochemical properties and catalytic performances in the reforming methane by carbon dioxide (after 10 hours) of all catalysts prepared by microemulsion and sol-gel method.

Catalyst	BET area ($m^2.g^{-1}$)	D_{XRD} (nm)	Activity ($\mu mol.g^{-1}.s^{-1}$)		Selectivity (%)		Carbon resistance (%)
			CH_4	CO_2	H_2	CO	
NiAl-ME	123.8	8.5	175.7	260.4	87.0	93.4	93.4
CoAl-ME	144.0	11.3	128.2	154.4	82.2	86.3	91.8
CuAl-ME	126.3	13.8	99.6	112.8	65.5	71.1	95.5
NiAl-SG	42.8	15.6	149.5	195.8	86.7	91.3	95.2
CoAl-SG	19.4	23.9	114.4	136.0	81.5	86.4	95.4
CuAl-SG	18.3	23.7	91.9	101.2	52.7	74.3	85.6

4 Conclusion

The alumina supported nickel prepared by ME technique appears as the best catalysts compared than the other metal catalysts. The higher activity and stability of this catalyst in CDR is mainly related to the metal-support strong interaction, the small metallic Ni particles and dispersion of nickel that should be ascribed to the high BET surface area.

References

[1] K. Kouachi, G. Lafaye, C. Especel, O. Cherifi et P. Marécot, J. Mol. Catal A. 308 (2009) 142-149.
[2] Shan Xu, Rui Zhao, Xiaolai Wang, Fuel Processing Technology 86 (2004) 123-133.

II-PP232

Synthesis and Parameters of the Thermal Degradation of Fullerene-Containing Polymers of Norbornenes Series

Mikheev V.V.[1], Biglova Yu.N.[1*], Zagitov V.V.[1], Torosyan S.A.[2], Mustafin A.G.[1], Miftakhov M.S.[2]

1 - Bashkir State University, Department of Chemistry, Ufa, Russia
2 - Institute of Chemistry of RAS, Ufa, Russia

* bn.yulya@mail.ru

Keywords: Grubbs, 1'st generation, catalyst, fullerene-containing, norbornenes, thermal degradation

1 Experimental/methodology

New norbornenes with the covalently bonded fullerene C_{60} have been prepared as monomers for ring-opening metathesis polymerization. Under the Grubbs catalyst these monomers smoothly enter homopolymerization as well as copolymerization reactions with the parent 'non-fullerene' monomers [1].

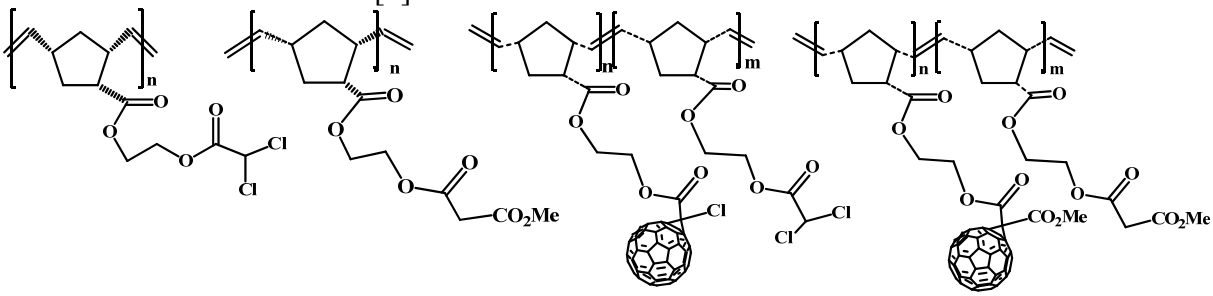

I II III IV

The thermal degradation of synthetic homo- (**I**, **II**) and copolymers (**III**, **IV**) of the norbornene series was studied. The temperature of intensive thermal degradation start (T_i), the final temperature of the mass loss (T_f) (calculated by the method of tangents), the temperature corresponding to the reduction of the weight of the polymer thermal destruction at 1% ($T_{1\%}$) and temperature of maximum rate of thermal degradation (T_{max}) are given in Table 1.

Table 1. Parameters of the thermal degradation of polymers of norbornene series

Polymer	$T_{1\%}$, °C	T_i, °C	T_{max}, °C	T_f, °C	*ΔH, kJ/g*
I	118.7	236.9	368.7	437.9	3.65
III	275.9	376.4	395.6	413.8	7.48
II	99.7	262.9	366.0	511.2	8.42
IV	270.0	415.8	449.4	487.1	13.63

2 Results and discussion

Presented in Table 1 parameters of thermal degradation of homo- and co-polymers of norbornene series demonstrate the following. In comparing the data for the homo- (**I**, **II**) and fullerene copolymers (**III**, **IV**), in the case of the latter has been a shift values ($T_{1\%}$, T_{max}, T_i) in the high temperature region. Thus the presence into macromolecule covalently bound fullerene increases the thermal stability of the polymer. Values of parameters of thermal degradation of chlorinated macromolecular compounds **I**, **III** are lower than that of the corresponding

compounds **II**, **IV**. Presumably, this is due to the presence in the macromolecule in addition to bonds C-Cl, the dissociation energy, which is lower than that for C=O, and other C-C bonds and, ultimately, reduces the chemical thermal stability of the structural member.

Acknowledgements

This work was supported by the Russian Foundation for Basic Research (grants № 14-03-31610 mol_a, 14-02-97008).

References

[1] M.S. Miftakhov, V.V. Mikheev, S.A. Torosyan, Yu.N. Biglova, F.A. Gimalova, V.M. Menshov, A.G. Mustafin, *Tetrahedron*. 70 (2014) 8040.

II-PP233

Nanoheterogeneous Catalysis in Electrochemically Induced Olefin Perfluoroalkylation

Dudkina Yu.B.[1*], Gryaznova T.V.[1], Davydov N.A.[1], Mustafina A.R.[1], Vicic D.A.[2], Budnikova Yu.H.[1]

1 - A.E.Arbuzov Institute of Organic and Physical Chemistry, Kazan Scientific Center of Russian Academy of Sciences, Kazan, Russia
2 - Department of Chemistry, LehighUniversity, Bethlehem, USA

* dudkinayu@iopc.ru

Keywords: heterogeneous catalysis, silica, nanoparticles, nickel, complex, perfluoroalkylation

1 Introduction

The present study unites the advantages of two different approaches — nanoheterogeneous catalysis (easy catalyst recycling) and electrocatalysis (generation and regeneration of the catalyst active form on the electrode surface without any additional molecular reductant) — to develop a new effective catalytic technique that is both green and atom economical.

2 Experimental/methodology

Preparative electrolyses were carried out using a B5-49 dc source at a current strength of 100 mA h^{-1} in 30-mL three-electrode cell. Synthesis of the silica nanoparticles (SNs) and their decoration by 3-[2-(2-aminoethylamino)ethylamino]propyltrimethoxysilan (AEPTS) were performed as described in [1-5]. The quantitative analysis of amino-groups at the surface of silica nanoparticles was carried out due to the fluorescent procedure with the use of fluorescamine [6]. The quantity of [(bpy)$NiBr_2$] bound with the AEPTS-SNs was calculated from the difference between the Ni(II) concentration before and after the mixing with aqueous colloids of the nanoparticles and the phase separation by atomic absorption spectroscopy.

3 Results and discussion

The overall goal of this work is to develop a nanoheterogeneous catalyst for olefin fluoroalkylations and to find ways to control the product ratio (monomer/dimer) in the reactions. α-Methylstyrene was used as the organic substrates, $H(CF_2)_6I$ was used as the perfluoroalkyl source, [(bpy)$NiBr_2$] complex was used as the catalyst as it was previously found to be very effective for similar electrocatalytic reactions [7,8].

Table 1. Perfluoroalkylation of α –methylstyrene.

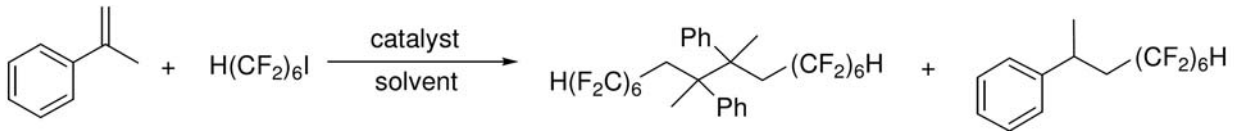

Solvent	Catalyst	Dimer/Monomer ratio	Total yield %
DMF:H_2O (8:1)	(bpy)$NiBr_2$ (1%) on AEPTS-SNs	1.0 : 1.7	48
DMF:H_2O (4:1)	(bpy)$NiBr_2$ (1%) on AEPTS-SNs	1.0 : 1.4	45
DMF:H_2O (4:1)	(bpy)$NiBr_2$ (1%) + added AEPTS-SNs	1.0 : 2.7	46
DMF:H_2O (2:1)	(bpy)$NiBr_2$ (1%) + added AEPTS-SNs	1.0 : 4.1	29
DMF	(bpy)$NiBr_2$ (1%) on AEPTS-SNs	1.0 : 0.8	53
DMF:H_2O (4:1)	(bpy)$NiBr_2$ (1%)	1.0 : 3.8	44

The data presented in Table 1 reveal the immobilization of [(bpy)$NiBr_2$] on the AEPTS-SNs is

one more factor affecting the monomer-dimer ratio in electrocatalytic perfluoroalkylation reactions. This tendency suggests an impact of coordination bonds versus physical and/or electrostatic adsorption in the immobilization of [(bpy)$NiBr_2$] complex on the AEPTS-SNs. Immobilization of the [(bpy)$NiBr_2$] complex through outer-sphere coordination with amino groups at the SNs surface is suggested to hinder access of water to coordination site that can be the reason of the aforementioned different monomer:dimer ratio.

The immobilized catalyst was tested in several reaction cycles. The results in Table 2 demonstrate that the yields of product from reactions run with recycled catalyst do not vary, supporting a heterogeneous reaction process. After each of the rounds in Table 3, the reaction mixture was centrifuged to separate the immobilized catalyst that was washed with DMF-water mixture (4:1), dispersed in water and used directly for the next synthesis. Triple use of such catalyst led only to negligible decrease in the products yield and no loss of the catalytic activity of the immobilized catalyst was observed.

Table 2. Use of recycled [(bpy)$NiBr_2$] catalyst (1 %) immobilized on AEPTS-SNs.

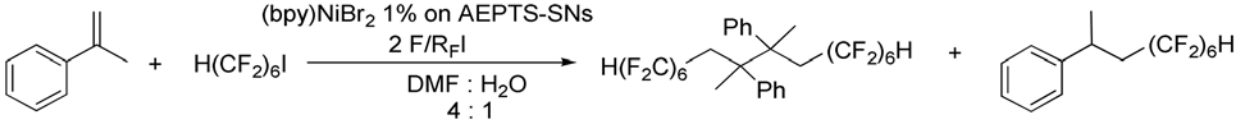

Number of repeats	Dimer/Monomer ratio	Total yield %
1	1.0 : 1.4	45
2	1.0 : 1.1	42
3	1.0 : 0.8	42

4 Conclusions

The present work employs inner-sphere coordination of [(bpy)$NiBr_2$] through amino-groups fixed on the surface of the amino-decorated silica nanoparticles as an efficient tool to switch from homogeneous to heterogeneous perfluoroalkylation catalysis. The introduced heterogeneous catalyst preparation provides sustained immobilization of the complex on AEPTS-SNs. After easy and quantitative separation from the reaction mixture the catalyst retains its high catalytic activity and can be reused. The results indicate that the addition of water to the reaction mixture increases the monomer/dimer ratio significantly.

Acknowledgements

This work was supported by a RFBR grant 14-03-31774.

References

[1] A. R. Mustafina, S. V. Fedorenko, O. D. Konovalova, A. Y. Menshikova, N. N. Shevchenko, S. E. Soloveva, A. I. Konovalov, I. S. Antipin, *Langmuir* 25 *(*2009) 3146.
[2] F. J. Arriagada, K. Osseo-Asare, *J. Colloid. Interface Sci.* 211 (1999) 210.
[3] R. P. Bagwe, C. Yang, L. R. Hilliard, W. H. Tan, *Langmuir*, 20 (2004) 8336.
[4] . P. Bagwe, L. R. Hilliard, W. Tan, *Langmuir* 22 (2006) 4357.
[5] N. Davydov, A. Mustafina, V. Burilov, E. Zvereva, S. Katsyuba, L. Vagapova, A. Konovalov, I. Antipin, *ChemPhysChem.* 13 (2012) 3357.
[6] H. Ritter, D. Brühwiler, *J. Phys. Chem.* 113 (2009) 10667.
[7] D. Y. Mikhaylov, Y. H. Budnikova, T. V. Gryaznova, D. V. Krivolapov, I. A. Litvinov, D. A. Vicic, O. G. Sinyashin. *J.Organomet. Chem.* 694 (2009) 3840.
[8] D. Mikhaylov, T. Gryaznova, Yu. Dudkina, M. Khrizanphorov, Sh. Latypov, O. Kataeva, D. A. Vicic, Yu. Budnikova, O. G. Sinyashin. *Dalton Trans.* 41 (2012) 165.

II-PP234

ZrO_2-Based Oxide Supports for Pd-Containing Catalysts for Hydrodechlorination of Chlorinated Organics

Golubina E.V.*, Lokteva E.S., Kavalerskaya N.E., Turakulova A.O.

Lomonosov Moscow State University, Moscow, Russia

* golubina@kge.msu.ru

Keywords: oxide support, metal-support, interaction, hydrodechlorination, chlorbenzenes

1 Introduction

Hydrodechlorination (HDC) is a remarkable environment friendly and cost saving alternative to the traditional methods for utilization of chlorinated pollutants. At present the structure of active site for many reactions is known but the problem of its synthesis still exists. Some reactions, for example, HDC reaction, are known to be sensitive to electronic state of supported metal. An active site of Pd-containing HDC catalysts should contain both metallic and partially oxidized Pd [1]. Since the reduction is a necessary step during catalysts preparation, is it difficult to control an oxidation state of active metal. Metal-support interaction provides useful instrument for tuning of oxidation state of active metal in the catalysts on oxide supports and could result in enhanced catalytic activity. Another important fact is an accessibility of active sites for large chlororganic molecules due to steric factor and diffusion limitations. At this point of view supplying of optimal pore size is important as well.

In this work the comparison of different types of binary oxide supports for Pd -containing catalysts was made using (1) mixed or egg-shell Al_2O_3@ZrO_2, and (2) yttria or gallia stabilized ZrO_2. In order to obtain various pore size template synthesis was used. The catalysts were tested in gas and liquid phase hydrodechlorination of chlorinated benzenes.

2 Experimental/methodology

Catalysts from 0.5 up to 5 wt.% Pd loading were prepared by impregnation or deposition-precipitation from corresponding chlorides or nitrates solutions. Individual and mixed oxides supports (ZrO_2, Y_2O_3, Ga_2O_3 and ZrO_2-M_2O_3 (M = Al, Y, Ga)) were prepared by precipitation with ammonia at pH 10. Egg-shell support Al_2O_3@ZrO_2 was prepared by deposition of ZrO_2 on Al_2O_3. In modified zirconia the content of second oxide was 1; 5 and 10 %. In some cases the synthesis was performed using templates, namely cetyltrimethylammonium bromide (CTAB), gelatin, polyethylene glycol (PEG).

Catalysts were investigated by SEM (JSM 6490 LV, JEOL, Japan), TEM (JEM 2100F, JEOL, Japan), low-temperature N_2 adsorption-desorption (Micometrics ASAP 2000), TPR (5%H_2/Ar), DSC-TG (449PC Jupiter Netzsch, Netzsch GmbH, Germany), IR spectroscopy of adsorbed CO (Bruker Equinox 55/s), AAS (Thermo Fisher Scientific iCE 3000). Catalytic HDC tests were performed under multi-phase conditions (50°C, batch reactor, hexachlorobenzene (HCB) or 1,3,5-trichlorobenzene (TCB), isooctane as a solvent, Aliquat 336, KOH aq., H_2).

3 Results and discussion

Since HDC is sensitive to electronic state of supported metal, an active site should contain both metallic and partially oxidized Pd. For Pd- containing catalyst the presence of partially oxidized metal was provided due to chemical interaction with zirconia. It was found that only Pd/ZrO_2 prepared by deposition-precipitation (DP) was active in HDC. Pd/ZrO_2 prepared by wet impregnation shows no catalytic activity. The reason is that DP technique, in contrast to

traditional impregnation, provides the formation of bifunctional active sites comprising both Pd^0 and $Pd^{\delta+}$. The presence of $Pd_xZr_yO_z$ in DP Pd/ZrO_2 was observed by TPR. Oxidized Pd was also observed by IR-spectroscopy of adsorbed CO. But activity of Pd/ZrO_2 was still insufficient: 80 % conversion of 1,3,5-trichlorobenzene was achieved within 150 min at 2% Pd loading.

To increase the efficiency of catalyst on zirconia support two ways of support structure improvement were tested: (1) precipitation of ZrO_2 on alumina to increase surface area of final oxide support; (2) modification by yttria, alumina or gallia to stabilize ZrO_2 tetragonal phase.

Modification that involves covering of Al_2O_3 surface with zirconia both to increase the surface area of ZrO_2 and to modify its properties due to interaction with alumina was found to be not successive. The samples with different degree of surface coverage of Al_2O_3 granules with zirconia (theta = 0.1; 0.5 and 1) were prepared. Nonlinear dependence of catalytic activity on coverage degree was observed for Pd-containing catalysts in liquid phase TCB hydrodechlorination. The best catalytic performance in multiphase HDC of TCB was obtained for 2% $Pd/Al_2O_3@ZrO_2$ (theta = 0.1). SEM-EDX analysis shows that Pd and ZrO_2 are separated from each other on alumina surface. Therefore the aggregation of zirconia prevents the uniform coverage of Al_2O_3 surface.

Much more successive was modification of zirconia by small amounts of Al_2O_3, Ga_2O_3 or Y_2O_3 (up to 10%), that results in the increase of catalysts stability. In the presence of most active catalyst (2% $Pd/(1\%Al_2O_3+ZrO_2)$) complete TCB hydrodechlorination in liquid phase was achieved within 60 min. The processing of 500 Mol TCB/1 Mol Pd was performed on this catalyst. TPR analysis reveals the dependence of PdH formation on the nature and amount of modifying oxide. Stable hydrogen consumption/evolution peaks corresponding to PdH formation/decomposition were observed for $Pd/(Y_2O_3+ZrO_2)$ during several cycles of cooling/heating in TPR cell. TPR analysis shows that Ga_2O_3 addition leads to the decrease of PdO reduction temperature from 80°C to RT. The addition of Al_2O_3 to ZrO_2 did not significantly influence on PdO reduction.

Template synthesis was used in order to improve catalytic activity of 2% Pd/ZrO_2 in HDC of large organic molecules e.g. hexachlorobenzene. ZrO_2 with pore size 3.5; 6 and 9 nm were prepared using various templates. Strong correspondence of activity on pore size was established: hexachlorobenzene HDC reaction rate increases with the increase of pore size. Mesoporous mixed oxide supports were studied as well. The best result was observed for the catalyst on mesoporous $Y_2O_3+ZrO_2$ support. Catalytic activity of 2% $Pd/Y_2O_3+ZrO_2$ in HDC of TCB increases: 100% TCB conversion was reached within 40 min, whereas the catalyst on microporous support provides the same TCB conversion only after 80 min.

4 Conclusions

The addition of yttrium or gallium oxide to ZrO_2 used as a support for Pd catalysts leads to the improvement of catalytic efficiency (activity and stability) in liquid and gas phase hydrodechlorination of chlorobenzenes, because of the presence of both metallic and oxidized Pd. Improvement of catalytic performance in HDC of polychlorinated benzenes was achieved also by optimization of pore size both for individual and modified zirconia supports.

Acknowledgements

This work was maintained by RFBR (13-03-00613) and in part by M.V. Lomonosov Moscow State University Program of Development.

References

[1] L.M.Gomez-Sainero, X.L.Seoane, J.L.G.Fierro, A. Arcoya, J. Catal. 209 (2002) 279

II-PP235

Quantum and Chemical Research of Nickel(II) Formazanates - Catalysts for Ethylene Oligomerization

Maslakov P.A.*, Pervova I.G.

Urals State Forestry Engineering University, Physico-Chemical Technology of Environmental Protection, Yekaterinburg, Russia

* pashalx@gmail.com

Keywords: benzothiazolylformazanates, catalysts, ethylene oligomerization

1 Introduction

Mononuclear nickel(II) benzothiazolylformazanates as catalysts have been tested while ethylene oligomerizating. The complexes are different in both nature of a substituent R1 in inter-position and a number of chlorine atoms in aryl substituent in original formazane ligand. General formula for complexes 1-3 (figure 1) and their characteristics are presented in the table 1. As it was shown earlier [1] the complex 1 is the most effective to produce highest olefines while ethylene oligomerizating.

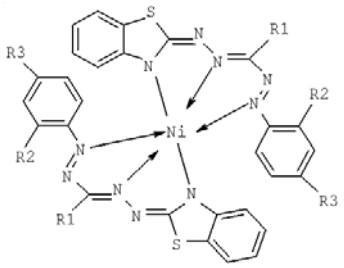

Fig. 1. Complexes, general formula

Table 1. Complexes 1-3 and their characteristics

Complexes, composition	E_0 (kJ/mol)	HOMO energy value (kJ/ mol)	LUMO energy value (kJ/ mol)	E_Σ, energy gap value (kJ/ mol)
Complex 1: R1=C_4H_9, R2=Cl, R3=H	-36668,3	-697,762	10,61081	708,3726
Complex 2: R1=C_4H_9, R2= H, R3= Cl	-45558	-664,949	-0,37399	664,5753
Complex 3: R1=C_7H_{15}, R2=Cl, R3=Cl	-35966,7	-685,628	-3,49771	682,1299

2 Experimental/methodology

PM3 method incorporated into HyperChem has been used for quantum and chemical calculation because it is the method that both shows formazanates molecule geometry and supply us with data comparable to X-ray analysis data [2].

3 Results and discussion

All of above mentioned Ni(II) complexes based on tridentate chlorine-containing

benzothiazolylformazanes are characterized by similar composition NiL_2 and pseudo-octahedral structure of MN_6 coordination unit in according to the quantum and chemical calculation. The calculation also showed a formazane is situated in both imino-form and EZE-configuration.

To establish the correlation between catalytic activity and structure in the nickel complexes as it was shown [3], energy characteristics (Highest Occupied molecular orbital energy value (HOMO), Lowest Unoccupied molecular orbital energy value (LUMO), and Energy gap value $E_{\sum}$) have been defined. According to the data presented in the table both the energy gap and HOMO energy values for complexes 1-3 are almost equal to each other and estimated as > 5 eV (482 kJ/ mol). It is evidence of geometric configuration sustainability in these complexes [4].

At the same time abnormal catalytic activity of formazanate 1 while ethylene oligomerizating resulting to butene yield can be explained by the difference in LUMO energy values. It was calculated it is the complex 1 is so-called «nucleophile» though complexes 2, 3 are «electrophiles».

4 Conclusions

The research showed such approach can be offered to predict catalytic activity for different heterocyclic nickel formazanates.

References:

[1] A.V. Zaidman, I.G. Pervova, I.N. Lipunov, R.R. Kayumov, G.P. Belov, Kh.E. Kharlampidi Petroleum chemistry. 6 (2010) 450.
[2] P.A. Maslakov, I.G. Pervova Book of abstracts of the II International conference «Applied physico-inorganic chemistry». Sevastopol. September, 23-26 (2013) 99.
[3] M.M. Eshankhogaeva Thesis of PhD. Tashkent, (1999) 378 p.
[4] V.M. Potekhin, V.V. Potekhin The theoretic base of chemical processes for organic compounds and petroleum technology. St-Petersburg: Khimizdat, (2007) 944 p.

II-PP236

Mechanism of Propane Oxidative Dehydrogenation on Surface Oxygen Radical Sites of VO_x/TiO_2 Catalysts

Avdeev V.I.[1], Bedilo A.F.[1,2*], Shuvarakova E.I.[1,2]

1 - Boreskov Institute of Catalysis SB RAS, Novosibirsk, Russia
2 - Novosibirsk Institute of Technology, Moscow State University of Design and Technology, Novosibirsk, Russia

* abedilo@bk.ru

Keywords: VOx/TiO2 catalyst, oxidative dehydrogenation, oxygen radicals, propane mechanism, DFT

1 Introduction

Oxidative dehydrogenation (ODH) of light alkanes over transition metal oxides is of great interest for synthesis of light olefins as a practicable alternative to non-oxidative dehydrogenation. Supported vanadia catalysts are among the most promising materials for this reaction. However, despite many experimental studies and theoretical simulations the nature of the active and selective surface sites in supported vanadia catalysts is still poorly understood.

Propene ODH over VO_x/TiO_2 catalysts is characterized by low activation energies about 60 kJ/mol [1]. Despite so low activation energy, the propane ODH on VO_x/TiO_2 catalysts typically takes place at 450°C or higher temperatures. The occurrence of a reaction with low activation energy at so high temperatures means that the pre-exponential factor in the reaction rate equation must be quite low. In our opinion, this fact clearly indicates that the reaction is initiated on few very active sites rather than on abundant vanadium species present in high concentration.

We have recently shown by DFT calculations that oxygen isotopic exchange on titania-supported vanadia might be initiated on surface oxygen radicals [2]. Recently such species were experimentally observed by STM and shown to be catalytically active in methanol ODH [3]. These results suggest that oxygen radicals may be present on the surface of oxidation catalysts under catalytic conditions and account for the catalytic activity of VO_x/TiO_2 catalysts. The main objective of this study is to analyze the possible role of the oxygen radicals in oxidative dehydrogenation of propane to propene on VO_x/TiO_2 catalysts using periodic DFT calculations.

2 Experimental/methodology

The structure of VO_3 species on the surface of VO_x/TiO_2 catalyst with distinct oxygen-radical character on experimentally observed (1x4)-reconstructed anatase-TiO_2(001) surface was built by isomorphic replacement of the top Ti atoms by V ones followed by reoxidation of the reduced surface V^{4+} site by an oxygen atom. The calculations were performed using the QUANTUM ESPRESSO code based on the spin-polarized DFT using Vanderbilt Ultrasoft pseudopotentials with exchange-correlation PBE functionals. The reaction pathways of the propane ODH were studied by the Climbing Image Nudged Elastic Band method (CI-NEB). Eleven to seventeen images (including 10÷16 movable ones) were specified to locate the saddle points along the minimum energy path.

3 Results and discussion

The complete pathway for propane ODH over oxygen radicals VO_3/TiO_2 in a uniform energy scale is presented in Figure 1. The first hydrogen abstraction reaction appears to be the rate-determining step of the overall ODH process. Our computations prove that the surface oxygen radical species forming on the supported vanadium oxide catalyst VO_x/TiO_2 are very reactive and can abstract hydrogen atoms from propane with low activation energy E* = 0.56 eV (54 kJ/mol). In our calculation the energetic barrier of the second stage was slightly lower. Still

both values are very close. So, their relative importance may depend on the used model and DFT functional.

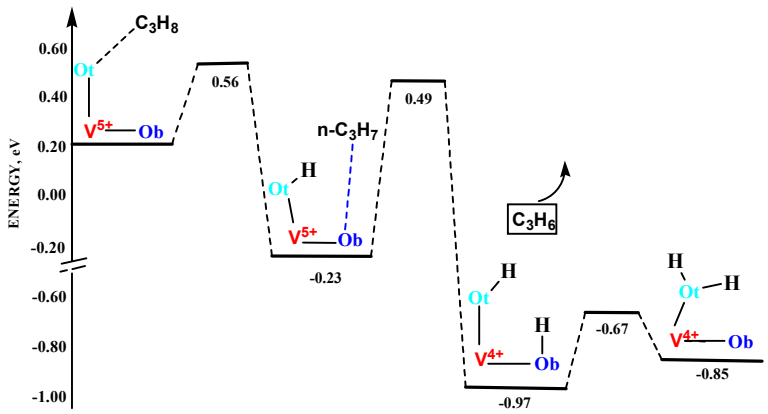

Fig. 1. Energy diagram of propane conversion to propene on the VO_3/TiO_2 active site.

We believe that high temperatures are required for generation of the active radical species in sufficient concentrations. For the reaction to take place above 450°C with relatively low experimental activation energy, the concentration of the active sites should be low. Therefore, oxygen radicals generated in low concentrations at elevated temperatures are quite capable of acting as such active sites.

It is exceptionally important, that the concentration of oxygen radical sites on the surface is low. So, the released propene, which is more susceptible to oxidation than propane, should not be immediately involved in further oxidation, unless it reaches another radical site after migrating on the surface. All these factors combined suggest that propene oxidative dehydrogenation on the oxygen radical species on the surface of VOx/TiO_2 catalyst simulated in this study should be a selective process. On the contrary, if conventional vanadyl groups commonly believed to be the active sites were the places where this reaction takes place, the released propene molecule would be involved in further oxidation processes immediately upon migrating to any adjacent V^{5+} site present in high concentration on the surface. This would make the desired high selectivity practically unachievable.

4 Conclusions

The results presented in this paper demonstrate that oxidative dehydrogenation of propane can proceed over oxygen radicals stabilized on the surface of VO_x/TiO_2 catalysts with low activation energies (~54 kJ/mol) matching the experimentally observed values. The obtained data suggest that oxygen radical species can be the active sites in this and other heterogeneous selective oxidation reactions. Further studies of reaction mechanisms with the emphasis on possible participation of such radicals in various catalytic reactions seem to be very important.

Acknowledgements

This work was supported in part by Russian Foundation for Basic Research (Grants 14-03-01110 and 15-03-08070).

References

[1] C. A. Carrero, R. Schloegl, I. E. Wachs, R. Schomaecker, *ACS Catal.* 4 (2014) 3357.
[2] V.I. Avdeev, A.F. Bedilo, *J. Phys. Chem. C.* 117 (2013) 14701.
[3] S.P. Price, X. Tong, C. Ridge, H.L. Neilson, J.W. Buffon, J. Robins, H. Metiu, M.T. Bowers, S.K. Buratto, *J. Phys. Chem. A.* 118 (2014) 8309.

II-PP237

Fickian Spillover Models: Validation and Parameter Estimation

Uner N.B.*, Uner D., Singh D.

Middle East Technical University, Chemical Engineering Department, Ankara, Turkey

* nuner@metu.edu.tr

Keywords: spillover, chemisorption, diffusion, parameter estimation

1 Introduction

The phenomenon and mechanism of spillover process is being discussed for many years and accepted as an important step in understanding the dynamics of catalysts and improving their performance [1]. Although the characterization and the theory of surface diffusion on perfect crystals has been treated to a good extent [2], the effect of spillover and surface diffusion on the performance of regularly synthesized supported catalysts is still vague.

In our previous studies on hydrogen chemisorption on Ru/Vulcan catalysts [3,4], the spillover process could be described sufficiently well by a Fickian surface diffusion mechanism following the formalism of the model presented by Kramer and Andre (KA) [5]. The model is used to predict the contribution of the support to both adsorption and desorption. Careful experiments on sequential adsorption and desorption were done to elucidate characteristics of the diffusion on the support. Such understanding would then be expected to shed light on the surface diffusion-influenced catalysis as new generation of nanostructured catalysts are being synthesized [6].

2 Experimental methodology

Spillover experiments were performed in a handmade glass manifold described in Uner et al [7]. 1 wt% Pt/Al_2O_3 was prepared by incipient wetness method, dried and calcined. The catalyst was placed into glass manifold and evacuated at 150°C for 30 min, this will removed the moisture present in the sample. Catalyst was further heated up to 350°C under 100 Torr H_2 pressure. At 350°C, system was evacuated for 10 min, then 100 Torr pressure was added every half an hour followed by 10 min evacuation for 4-5 times. After reduction process, system was kept under evacuation for 1 hr and then cool down to room temperature. At room temperature it was filled with desire H_2 Pressure, after that, sample valve was opened, to record pressure change and time. The adsorption isotherms were also measured on the same catalyst by dosing hydrogen at a desired pressure and allowing 10 min for equilibration. At sufficiently high pressures a considerable amount of spilled over hydrogen will have accumulated despite short equilibration periods. The system is evacuated for different durations and after which isotherms were measured.

3 Results and discussion

The time dependent uptake curve for the first adsorption is given in Figure 1a. For long times, the data can be converted into rates of diffusion on the support, and the KA model can be fitted. The result of the fit is given in Figure 1b. The KA model can be modified for desorption and it also captures a good trend for desorption, but slightly over predicts. The isotherms collected as described in the experimental methodology section were used to determine the desorbed hydrogen amounts. The experimental data of the desorbed hydrogen amounts and the model fit of the desorption process shown in Figure 1c are in good agreement.

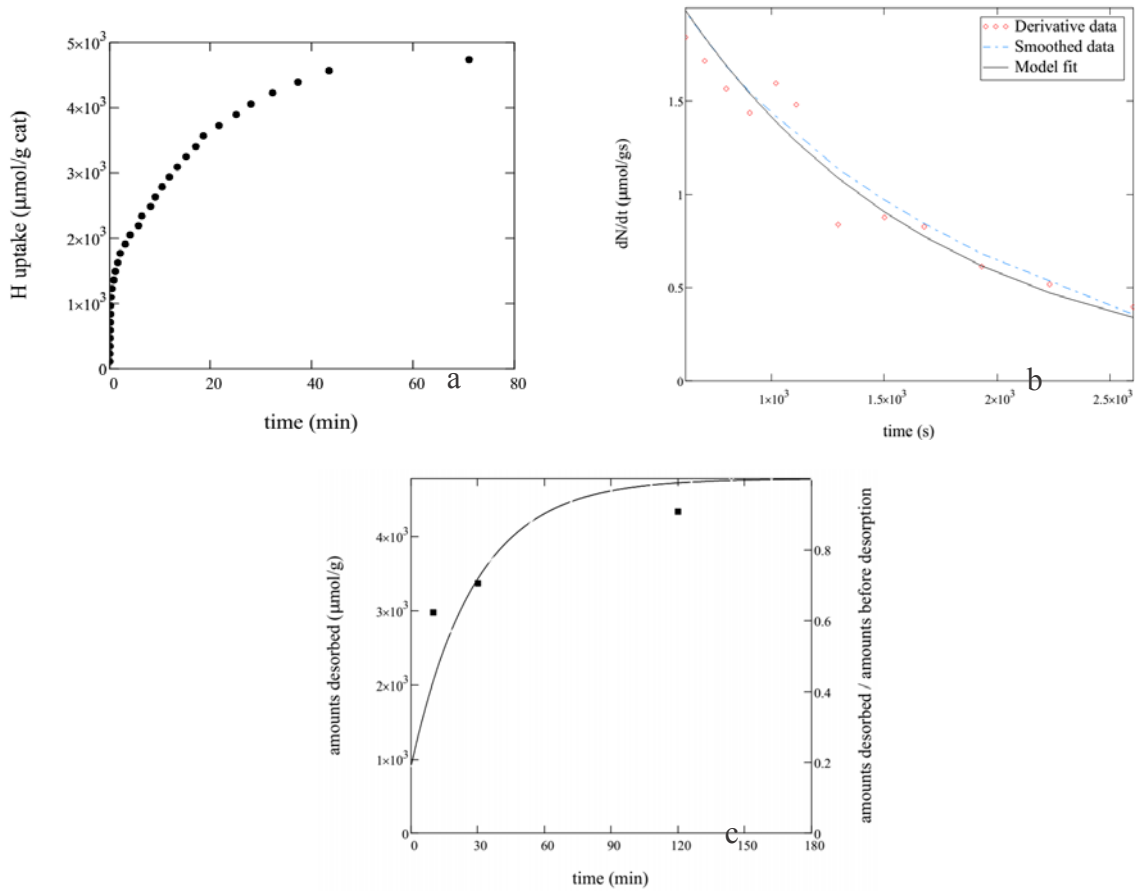

Fig. 1. a) Sample time dependent chemisorption data on Pt/Al_2O_3. b) The quality of fit of the KA model. c) Desorption rate: model versus experiment.

4 Conclusions & Outlook

In this paper, we present a methodology for determining the surface diffusion coefficient of spilled over hydrogen by volumetric chemisorption technique. Experiments are in progress to make these measurements at different temperatures and by changing the metal loading while keeping the particle size constant. The available data will be used to explore the use of spilled over hydrogen in hydrogenation reactions where simple microkinetic reaction models are available.

Acknowledgements

Financial support from TUBITAK (grant no 213M006) under the project leadership of Dr. Serkan Kincal is gratefully acknowledged.

References

[1] International Conference on Spillover, *New aspects of spillover effect in catalysis: for development of highly active catalysts*. Amsterdam; New York: Elsevier, 1993.

[2] A. Naumovets and Y. Vedula, "Surface diffusion of adsorbates," *Surf. Sci. Rep.*, vol. 4, no. 7–8, pp. 365–434, May 1985.

[3] M. Y. Aslan, "Supported Ru based ammonia synthesis catalysts," M.S., Middle East Technical University, Ankara, 2012.

[4] D. Uner, M. Y. Aslan, and N. B. Uner, "Does Spilled-over Hydrogen Inhibit Ammonia Synthesis Reaction over Ru/C Catalyst?," presented at the EUROPACAT 11, Lyon, 2013.

[5] R. Kramer and M. Andre, "Adsorption of atomic hydrogen on alumina by hydrogen spillover," *J. Catal.*, vol. 58, no. 2, pp. 287–295, Jun. 1979.

[6] S. K. Beaumont, S. Alayoglu, C. Specht, N. Kruse, and G. A. Somorjai, "A Nanoscale Demonstration of Hydrogen Atom Spillover and Surface Diffusion Across Silica Using the Kinetics of CO $_2$ Methanation Catalyzed on Spatially Separate Pt and Co Nanoparticles.," *Nano Lett.*, vol. 14, no. 8, pp. 4792–4796, Aug. 2014.

[7] D. Uner, N. A. Tapan, İ. Özen, and M. Üner, "Oxygen adsorption on Pt/TiO2 catalysts," *Appl. Catal. Gen.*, vol. 251, no. 2, pp. 225–234, Sep. 2003.

II-PP238

Mixed Spinel-Type Ni-Co-Mn Oxides: Synthesis, Structure and Catalytic Properties

Frolov D.D.[1], Fedorova A.A.[1*], Morozov I.V.[1], Sadovskaya E.M.[2], Sadykov V.A.[2]

1 - Lomonosov Moscow State University, Department of Chemistry, Moscow, Russia
2 - Boreskov Catalysis Institute, SB RAS, Novosibirsk, Russia

* fedorova@inorg.chem.msu.ru

Keywords: spinel, ethanol steam reforming, oxygen isotope exchange

1 Introduction

The ethanol steam reforming reaction is still in great interest as a way of hydrogen production. Different type of catalysts were used for ESR reaction: noble metals (Rh, Ru, Pt, Pd, Ir), non-noble metals (Co, Ni), simple oxides (ZnO, CuO), perovskites ($LaNiO_3$) and many others. Spinels are also among this catalysts: monometallic Co_3O_4 , two-component systems (NiM_2O_4, where M=Al, Fe, Mn ; MAl_2O_4, where M=Zn, Ni, Cu ; ZnM_2O_4, where M=Al, Co, Fe) and some other systems. One of reasons of such interest is the attempt to replace currently used noble metal and rare-earth containing catalysts for something cheaper and assessable. All works note that spinels show 100 % conversion of C_2H_5OH at the temperatures over 600 °C.

2 Experimental

We have studied ESR reaction catalyzed by mixed spinel-type oxides $Co_{1.8}Mn_{1.2}O_4$, $Ni_{0.33}Co_{1.33}Mn_{1.33}O_4$ and $Ni_{0.6}Co_{1.2}Mn_{1.2}O_4$. Spinels were prepared by thermal decomposition of the mixture of corresponding metal nitrates hydrates followed by annealing at 700 °C.

The samples were characterized by X-ray diffraction, X-ray absorption $L_{2,3}$-edges, BET and oxygen isotope exchange.

For ESR reaction 110 ml/min flow (GSHV = 51000 h^{-1}) with 10 vol % of ethanol was passed through reactor.

3 Results and discussion

According XRD results all initial catalysts have spinel structure with no admixtures found. Surface areas measured by BET were about 5 m^2/g for all samples. To determine the cation distribution in the samples X-ray absorption spectroscopy was used. To interpretate XAS spectra obtained some samples with known structure were studied. We chose Co_3O_4 ($Co^{2+}[Co^{3+}_2]O_4$), $CoCr_2O_4$ ($Co^{2+}[Cr^{3+}_2]O_4$), NiO, Mn_2O_3, MnO_2 as standards. Square brackets represent cations which occupy octahedral site. The latter two samples have Mn only in octahedral site as the Ni in NiO. The results obtained by analysis of spectra are presented in Table 1. According to these data, the $Co_{1.8}Mn_{1.2}O_4$ modification mechanism by replacement Co to Ni is the following: Ni^{2+} replaces Co^{3+} in octahedral sites thus making the part of Mn^{3+} to become Mn^{4+} to keep electroneutrality.

Table 1. Revealed cation distribution in Ni-Co-Mn-O spinel-type oxides from XAS experiments.

Oxide	Cation distribution
$Co_{1.8}Mn_{1.2}O_4$	$Co^{2+}[Co^{3+}_{0.8}Mn^{3+}_{1.2}]O_4$
$Ni_{0.33}Co_{1.33}Mn_{1.33}O_4$	$Co^{2+}[Co^{3+}_{0.33}Ni^{2+}_{0.33}Mn^{3+}_{1.2}Mn^{4+}_{0.33}]O_4$
$Ni_{0.6}Co_{1.2}Mn_{1.2}O_4$	$Co^{2+}[Co^{3+}_{0.2}Ni^{2+}_{0.6}Mn^{3+}_{0.6}Mn^{4+}_{0.6}]O_4$

Heterogeneous oxygen isotope exchange was discovered on all samples under

investigation. Exchangeable oxygen fraction is found to be 100 % of total lattice oxygen for all samples.

By use of numeric modeling surface exchange (R) and diffusion (D) rates were estimated (Table 2). As the exchange was limited by diffusion only the lower bound for R could be determined. It was revealed that diffusion rate correlates with Mn^{4+} content.

Table 2. Isotope exchange parameters estimated from numeric modeling.

Sample	R*10², mol/g*min	D_{eff}*10³,1/s	Mn^{4+} (see Table 1)
$Co_{1.8}Mn_{1.2}O_4$	>7	5	0
$Ni_{0.33}Co_{1.33}Mn_{1.33}O_4$	>7	9	0.33
$Ni_{0.6}Co_{1.2}Mn_{1.2}O_4$	>20	20	0.6

Study of ESR reaction revealed the same trend. The most effective catalyst was $Ni_{0.6}Co_{1.2}Mn_{1.2}O_4$. Ethanol conversion reached 100% at 700 °C (conversion rate $6 \cdot 10^{-5}$ mol·g^{-1}·s^{-1}). Experimental results for this catalyst are presented at Fig. 1.

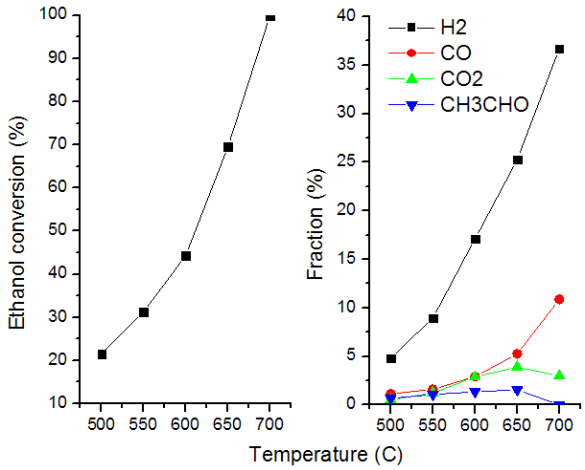

Fig. 1. Catalytic performance for the ESR reaction over the $Ni_{0.6}Co_{1.2}Mn_{1.2}O_4$ catalyst.

4 Conclusions

Ethanol steam reforming (ESR) reaction catalyzed by spinel-type mixed oxides $Co_{1.8}Mn_{1.2}O_4$, $Ni_{0.33}Co_{1.33}Mn_{1.33}O_4$ and $Ni_{0.6}Co_{1.2}Mn_{1.2}O_4$ was studied. Catalytic activity both in ESR and isotope exchange reaction rises up with Mn^{4+} content in the row $Co_{1.8}Mn_{1.2}O_4$ > $Ni_{0.33}Co_{1.33}Mn_{1.33}O_4$ > $Ni_{0.6}Co_{1.2}Mn_{1.2}O_4$.

Acknowledgements

This study was supported by the Russian Foundation for Basic Research (RFBR, Grant for young scientists no. 14-03-32056).

References

[1] V.A. de la Peña O'Shea, N. Homs, E.B. Pereira, R. Nafria, P. Ramírez de la Piscina, Catalysis Today. 126 (2007) 148-152.
[2] H. Muroyama, R. Nakase, T. Matsui, K. Eguchi, International Journal of Hydrogen Energy. 35 (2010) 1575-1581.
[3] M.N. Barroso, M.F. Gomez, L.A. Arrúa, M.C. Abello, Catalysis Letters. 109 (2006) 13-19.
[4] S. Hull, J. Trawczyński, International Journal of Hydrogen Energy. 39 (2014) 4259-4265.

II-PP239

Catalytic Activity of Palladium Complexes Based on Tridentate Ligands with Ancillary Sulfur Donor Groups in the Suzuki Cross-Coupling

Aleksanyan D.V.[1], Churusova S.G.[1], Vasil'ev A.A.[2], Kozlov V.A.[1*]

1 - N. Nesmeyanov Institute of Organoelement Compounds, Russian Academy of Sciences, Moscow, Russia

2 - N. D. Zelinsky Institute of Organic Chemistry, Russian Academy of Sciences, Moscow, Russia

* aleksanyan.diana@ineos.ac.ru, fos@ineos.ac.ru

Keywords: tridentate ligands, sulfur donors, palladium complexes, Suzuki cross-coupling

1 Introduction

Among a plethora of palladium-catalyzed cross-coupling reactions, the Suzuki cross-coupling is one of the most powerful methods for the C–C bond construction. Functionalized carboxamides have been the objects of intense research in coordination chemistry for many years, since the introduction of ancillary donor centers both into acid and amine parts enables the realization of different coordination modes, allowing fine-tuning of physicochemical properties of the resulting complexes. As a rule, such multidentate ligands contain nitrogen and phosphorus donor groups, while their analogs based on thioether-substituted acids are scarcely studied. The known examples represent mercaptoacetic acid derivatives with additional coordination-active groups [1]. To the best of our knowledge, there are no literature data on catalytic activity of the complexes based on these multidentate ligands. At the same time, recently we have shown that S,N,O-palladium(II) complexes of functionalized amides with (thio)phosphoryl pendant arms provide moderate activity in the Suzuki cross-coupling of aryl bromides with phenylboronic acid [2]. Therefore, it seemed interesting to obtain novel amide ligands with ancillary sulfur donor groups and investigate catalytic activity of their palladium complexes in the Suzuki cross-coupling.

2 Experimental

Novel multidentate ligands with the central amide moiety and ancillary sulfur donor groups were readily obtained by the condensation of *o*-thiophosphorylaniline and amino-substituted nitrogen-containing heterocycles with mercaptobenzoic, mercaptoacetic, and mercaptopropionic acid chlorides (Fig. 2).

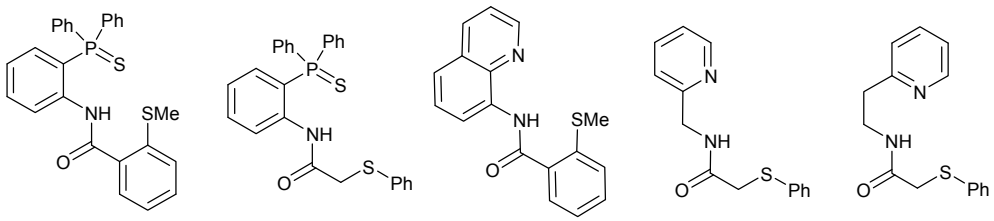

Fig. 2. Selected ligands obtained in the present study

Taking into account an important role of week sulfoxide donor ligands in transition metal chemistry, some of the resulting sulfide ligands were oxidized with H_2O_2 to the corresponding sulfoxide derivatives.

Upon complexation with the Pd(II) ions, the ligands derived readily formed S,N,X-palladium complexes, in all cases adopting a tridenate monoanionic coordination mode.

3 Results and discussion

Catalytic activity of the novel palladium(II) complexes was tested in the Suzuki cross-coupling of several aryl bromides with phenylboronic acid (Scheme 1). For correct comparison of the results, all the experiments were carried out under the same conditions. Fig. 3 demonstrates the results of catalytic experiments on the coupling of 4-bromoacetophenone with $PhB(OH)_2$ for some of the palladium complexes based on functionalized carboxamides.

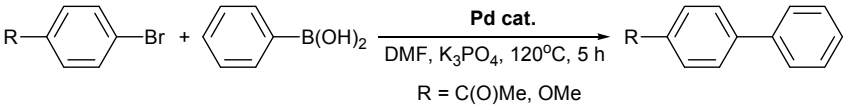

Scheme 1. Suzuki cross-coupling catalyzed by the novel palladocycles

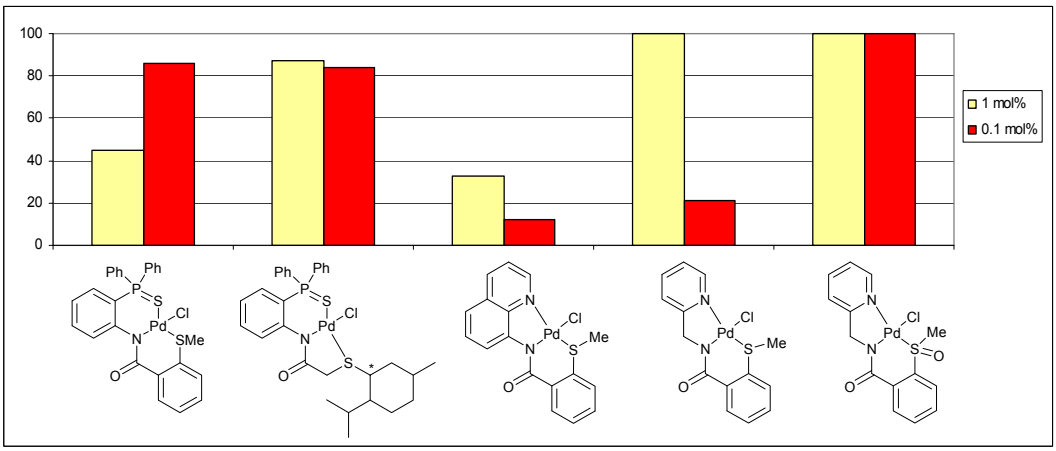

Fig. 3. Catalytic activity of selected palladocycles under study in the coupling of 4-bromoacetophenone with $PhB(OH)_2$

Taking into account the results obtained, the following regularities in the catalytic activity of the complexes under study can be outlined. N,N,S-Palladocycles are generally more active than their S,N,S-analogs based organothiophosphorus ligands, which can be associated with their hemilabile nature. Alkyl sulfides provide higher level of activity than their phenyl sulfide counterparts. The catalytic performance strongly depends on the flexibility of the ligand framework. And, finally, the sulfoxide derivatives are much more active (pre)catalysts than the corresponding sulfide-based palladium complexes.

4 Conclusions

Palladium complexes of functionalized carboxamides based on thioether-substituted acids were tested for the first time as (pre)catalysts for the Suzuki cross-coupling. The main regularities in the structure–activity relationships were established.

Acknowledgements

This work was supported by the Russian Foundation for Basic Research (project no. 14-03-31237-mol-a) and the Grant of the President of the Russian Federation for young scientists (project no. MK-382.2014.3).

References

[1] (a) P. J. Toscano, L. G. Marzilli, *Inorg. Chem.*, 22 (1983) 3342; (b) P. J. Toscano, K. J. Fordon, D. Macherone, S. Liu, J. Zubieta, *Polyhedron*, 9 (1990) 2375; (c) E. L. Klein, M. A. Khan, R. P. Houser, *Inorg. Chem.*, 43 (2004) 7272; (d) M. J. Al-Jeboori, H. H. Al-Tawel, R. M. Ahmad, *Inorg. Chim. Acta*, 363 (2013) 1301.

[2] A. A. Vasil'ev, V. Yu. Aleksenko, D. V. Aleksanyan, V. A. Kozlov, *Mendeleev Commun.*, 23 (2013), 344.

II-PP240

Synthesis and Characterization of Spinel and Perovskite Structures with Transitions Metals

Djaidja A.[1,2*], Messaoudi H.[1], Slyemi S.[1], Barama A.[1]

1 - Laboratoire des Matériaux Catalytiques et Catalyse en Chimie Organique, USTHB, Faculté de Chimie, Alger, Algérie

2 - Laboratoire des Procédés pour Matériaux, Energie, Eau et Environnement, Faculté des Sciences et des Sciences Appliquées, Université de Bouira, Algérie

* a_djaidja@yahoo.fr

Keywords: sol-gel, nickel, manganese, spinal, perovskite

1 Introduction

Spinal and perovskite structures are oxides with chemical formula AB_2O_4 and ABO_3 respectively. They are of great interest because of the variety of properties exhibited by these materials depending on the choice of the elements A and B. In the spinal structure oxides, cationic sites tetrahedral and octahedral form with the oxygen a face centered cubic lattice. The perovskite structure is conveniently described by a cubic lattice, as the cation A is often alkaline earth occupant dodecahedral position, the cation B is generally a transition element 3d, 4d or 5d [1] and is the center of an octahedral site formed by six oxygen atoms. There are several spinals which are used in heterogeneous catalysis, by citing examples: $ZnCo_2O_4$ spinal that can acts as catalyst in various reactions: CO oxidation [2], combustion of hydrocarbons [3] or the selective oxidation and reduction of several organic molecules [4]. The $ZnAl_2O_4$ spinal is very active in methanol synthesis and selective reduction of NO_x with the addition of copper [5]. There is also the spinal $MgAl_2O_4$ which has very interesting properties such as very high melting point (about 2135°C), good mechanical strength and a low dielectric constant. Therefore, it is used in many industrial applications, for example, the preparation of ceramics [6]. In catalysis, the spinal $MgAl_2O_4$ is used because of its low acidity, high heat resistance and good interaction with the metal phase. This material is used as a carrier in catalytic dehydrogenation [7] and in applications for petroleum methods [8]. Similarly, it is widely used as a support or a catalyst for reforming methane reactions [9]. Perovskites also form a large class of catalytic systems for reforming and oxidation of hydrocarbons [10]. For example, the catalysts $LaMO_3$ (M: Ni, Co, Cr) were used in the partial oxidation reaction of methane [11] as well as in the hydrogenation reactions of alkenes [12]. In our work, we have prepared spinal and perovskite materials based on magnesium, nickel, aluminum, lanthanum and manganese.

2 Experimental/methodology

Nitrates of various components were dissolved with citric acid (CA / (metal ions)) = 0.5. The pH of the solution is adjusted to 6 using aqueous ammonia (25%). The mixture is heated to 120°C until a gel. The obtained gel was dried at 180°C and calcined at 800°C for 4heurs (5°C/min).

3 Results and discussion

For both $Ni_{0.1}Mg_{0.9}Al_2O_4$ and $Mn_{0.1}Mg_{0.9}Al_2O_4$ solids, we are observed the formation of spinal phase $MgAl_2O_4$, Ni or Mn is probably introduced in the spinal structure. While for the $Ni_{0.1}Mg_{0.9}Al_{0.5}La_{0.5}O_3$ material, we are noted the presence of a mixture of oxides: MgO and/or NiO and La_2O_3. Finally, the diffractogram of $Mn_{0.1}Mg_{0.9}Al_{0.5}La_{0.5}O_3$ solid revealed the presence of MgO and perovskite phase $LaAlO_3$.

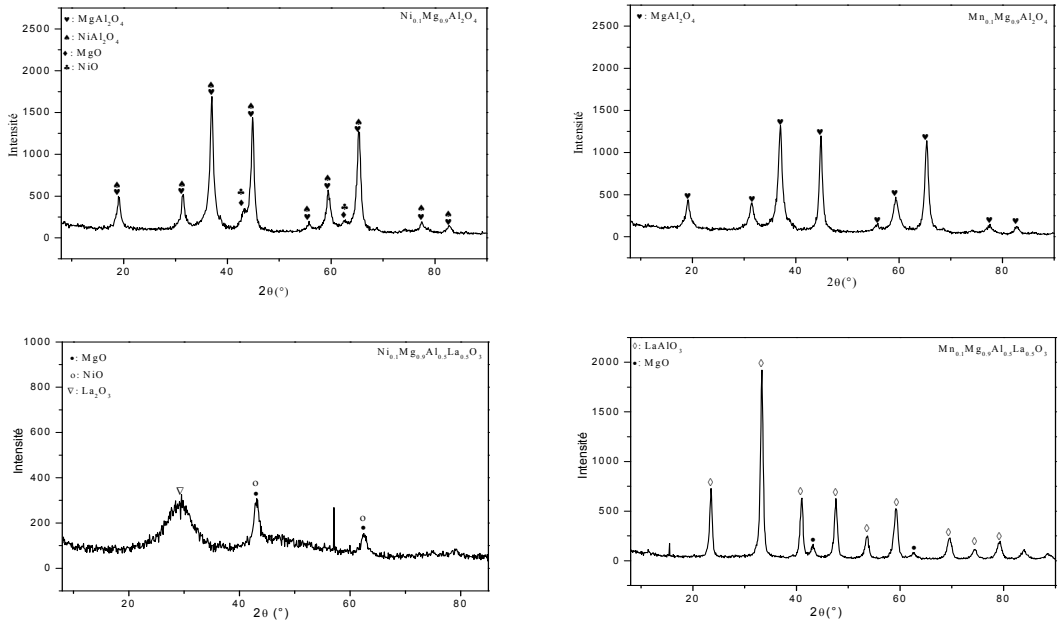

Fig. 1. XRD patterns of the elaborated solids.

Additional, themogravimetric analysis of the precursors of our catalysts are showed three main thermal events due to the elimination of free water at 100-150°C, the decomposition of ammonium nitrate between 260-290°C and the decomposition of citrate complex at 410°C. Furthermore, comparison of FT-IR spectra of various solid before and after calcination is showed a decrease of the intensity of the characteristic bands of H_2O and nitrates after heat treatment (800 °C). Likewise, characteristic bands of the metal oxides (M-O), between 450-700cm^{-1} are observed in the case of calcined solids. Otherwise, scanning electron microscopy is revealed spinal grain size of about 150 µm for the catalyst containing manganese, against about 60µm for the nickel based solids. For the perovskite structure, the grain size is estimated at about 20 µm for catalysts with manganese, and about 40 to 60µm for the solid containing nickel.

4 Conclusions

XRD analysis of the catalysts calcined at 800°C is showed the formation of different phases. The thermal analysis of the various precursors studied is revealed a similar decomposition as a function of temperature. However, relative stability is observed from 500°C for both spinal and perovskite structures. SEM analysis is showed an acceptable homogeneity of the surface of these catalysts.

References

[1] S-S.Lim, H-J.Lee, D-J.Moon, J-H.Kim, N-C.Park, J-S.Shin, Chem.Eng. J., 152 (2009) 220-226.
[2] J.Ghose and K.S.R.C.Murthy, J. Catal. 162 (1996)359.
[3] N.Guilhaume et M.Primet, J. Chem. Soc. Faraday Trans. 90(1994)1541.
[4] J.Sloczynski, J.Zió Ikowski, B.Grzybowska, R.Grabowski, J. Catal. 187(1999)410-418.
[5] F.Le Peltier, P.Chaumette, J.Saussey, M.M.Bettahar, J. Mol. Catal.A. Chem. 122(1997)131.
[6] L.Guang, L.Ikegami, L.Jong-Heum and T.Mori, J.Am.Ceram.Soc. 83(2000) 2866-2868.
[7] S.A.Boucanegra, A.D.Ballarini, O.A.Scelza, Mat. Chem and Phy. 111(2008)534-541.
[8] C.O.Areán, Colloids and Surfaces A: Physicochemical and Engineering Aspects. 180(2001)253.
[9] H.Özdemir, International Journal of Hydrogen Energy. 35(2010)12147-12160.
[10] R.M.Navarro, M.C.Alvarez-Galvan, Appl.Catal.B: Environmental. 73(2007)247-258.
[11] V.R.Choudhary, B.S.Uphade and A.A.Belhekar, J.Catal. 163(1996)312.
[12] J.O.Pentuchi, M.A.Ulla, J.A.Marcos and E.A.Lombardo, J.Catal. 70(1981)536.

II-PP241

Photocatalysis of Hydrogen Evolution from Water by Used Thioxanthene Dyes

Ponyaev A.I.*, Glukhova Y.S.

Saint Petersburg State Institute of Technology (Technical University), Saint-Petersburg, Russia

* ponyaev2002@mail.ru

Keywords: photocatalysys, thioxanthene, hydrogen, water, radical, triplet

1 Introduction

Photocleavage of water into hydrogen and oxygen is one of the most attractive ways of accumulation of solar energy and the simplest model of natural photosynthesis. A.E. Shilov et al. proposed catalytic cycle decomposition of water to hydrogen consisting of a dye-sensitizer (plays the role of chlorophyll in green plants), an electron carrier and a metal catalyst [1].

2 Experimental/methodology

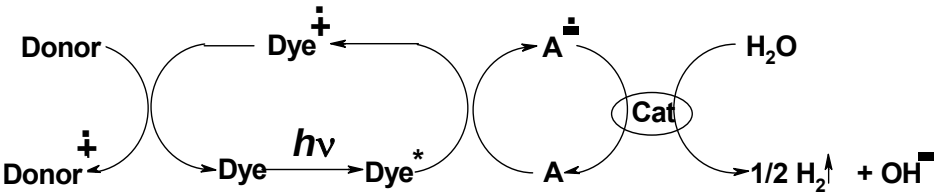

In the photocatalytic systems by decomposition of water to hydrogen was investigated a number of important xanthene dyes [2]. Xanthene dyes decomposition of water without intermediate electron acceptor in two-component scheme:

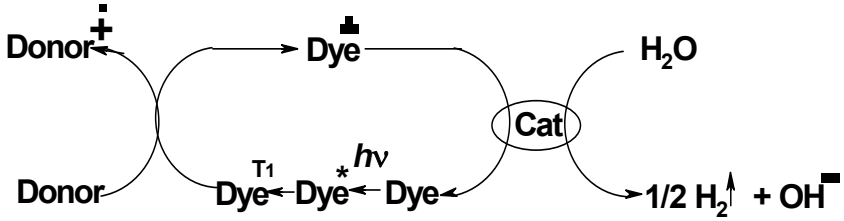

The efficiency of sensitization by xanthene dyes of reaction photocleavage of water is determined mainly by the efficiency of yield triplets and radicals.

Spectral-kinetics parameters of the radicals and triplet state xanthenes dyes has been studied with use setup of flash photolysis with time resolution 10 μs.

3 Results and discussion

The results of spectral and kinetic studies of new thioxanthene anionic dyes and kinetics of photocleavage of water into hydrogen in a homogeneous two-component photocatalytic system has been performed. It is shown that replacing the oxygen atom in xanthene moiety by a sulfur atom (***1-3***) increases the quantum yield of triplet and photohydrogen. Replacement of the carboxyl group of the phthalic fragment on sulfonic group (***4.5***) does not affect the photophysical and photocatalytic properties of the dye, and appears only in the nature of the interaction with the surfactant.

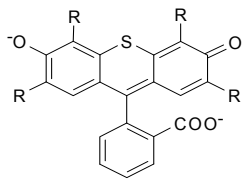
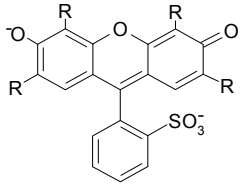

1	***2***	***3***	***4***	***5***
R=H	**Br**	**J**	**R=H**	**Br**

It is shown that replacing the oxygen atom in xanthene moiety by a sulfur atom (***1-3***) leads to a bathochromic shift of the absorption spectrum dianionic form of the dye. With the introduction of four bromine atoms in the molecule thiofluoresceine (***2***) there is a small bathochromic shift in the absorption spectrum and dramatically increases strength of the oscillator of long-wavelength band, which corresponds to the large dipole moment of the transition (table 1).

The quantum yield of triplet φ_T of the tetraiodinethiofluorescein (***3***) had 2-fold less than that of the dye (***1***). Dye (***3***) practically no luminescent unlike compounds (***1,2***) and the main channel that energy dissipation of the dye (***3***) is thermal deactivation. Obviously, this effect is due to the joint presence of heavy atoms of sulfur and iodine. Because of the low quantum yield of triplet formation, tetraiodinethiofluorescein (***3***) has low photocatalytic activity in the reaction of photoreduce water into molecular hydrogen in the system consisting of a dye, catalyst and electron donor.

Table 1. Photophysical parameters of xanthene dyes (***1-5***) in 0.1 N. NaOH

Parameters	**Fluorescein**	***1***	***2***	***3***	***4***	***5***
λ_{max} abs., nm	490	513	525	541	500	525
λ_{max} fluor., nm	528	533	545	560	530	570
λ_{max} T-T, nm	560	600	615	600	570	590
φfluor.	0.92	0.12	0.01	<0.001	0.95	<0.35
φ_T ±15%	0.05	0.75	0.9	0.4	0.05	0.6
λ_{max} $Dye^{-\bullet}$, nm	394	400	410	395	395	410
λ_{max} $Dye^{+\bullet}$, nm	430	430	450	420	430	430
$\tau_T \cdot 10^4$, s	0.9	0.5	1.5	0.6	0.9	0.6

The influence of the components of the photocatalytic system on the spectral, fluorescent, kinetic characteristics of intermediate products and photocatalytic activity has been studied (table 2). The data obtained allowed to construct a two-component photocatalytic system based on the tetrabromthiofluorescein that effectively worked hundreds of hours to the initial quantum efficiency of 15%.

Table 2. Influence of photocatalytic component on efficiency of hydrogen evolution

System	**Three Etha-nolamine**	**Colloid Platinum**	**Ethanol**	**H_2PtCl_6**	**Velocity 10^{-13} mol/s**
A	+	+	+	-	**60**
B	+	-	+	+	**46**
C	+	-	-	+	**2**
D	-	+	+		**1.2**
E	+	-	+		**0**

At the output of hydrogen affected by the presence of internal triplet sensitizers, heavy atoms, surfactants, certain rare-earth ions, and organic solvents.

Acknowledgements

The study was supported by the Russian Ministry of Education and Science (State task 1789, Contract 14.574.21.0002 unique identifier RFMEFI57414X0002) and Russian Foundation for Basic Research (Project 13-08-01425 a).

References

[1] Koryakin B.V., Dzhabiev T.S., Shilov A.E. // Dokl. Akad. Nauk SSSR. 1977. Vol. 233. No.4. P.620-622.

[2] Hashimoto K., Kawai T., Sakata T. // Chem. Lett. 1983. P.709-712.

II-PP242

Hydrotreating of Diesel Fractions and Light Coker Gasoil Mixtures on Phosphorus Modified Ni(Co)Mo/Al_2O_3 Catalysts

Tomina N.N.*, Maximov N.M., Solmanov P.S., Moiseev A.V., Pimerzin A.A.

Samara State Technical University, Samara, Russia

* tominann@yandex.ru

Keywords: hydrotreating, diesel fuel, light coker gasoil, phosphorus

1 Introduction

Carrier surface modification of hydrotreating catalysts is one of the methods of catalysts activity increasing **[1,2]**. Investigations, which described combined modification of carrier surface and applying of heteropolyacids, are not numerous. This made investigation in that field an actual one. Phosphorus compounds introduction in alumina changes a number of OH-groups on surface, which affect on strengths of carrier and active phase precursors bonds and, respectively, on their activity.

2 Experimental/methodology

A line of catalysts with different amounts of phosphorus was synthesized. Modifier was introduced on the first stage of two stages synthesis by wetness impregnation method from phosphoric acid water solution. After impregnation modified carrier was calcined at temperature of 550ºC. Modified carrier was impregnated with water solution of active phase precursors (Mo, Ni(Co)) on the second stage of synthesis. Properties of synthesized catalysts are listed below in **Table 1.**

Table 1. Characteristics of Co(Ni)Mo/P-Al_2O_3 catalysts

Catalyst	Content, wt. %			Catalyst	Content, wt. %		
	MoO_3	CoO	P_2O_5		MoO_3	NiO	P_2O_5
CoMo/P(0)	18,5	4,6	-	NiMo/P(0)	18,2	4,7	-
CoMo/P(0,5)	18,3	4,7	0,5	NiMo/P(0,5)	18,6	4,9	0,5
CoMo/P(1)	18,2	4,7	1,0	NiMo/P(1)	18,7	4,9	1,0
CoMo/P(2)	18,5	4,5	2,0	NiMo/P(2)	18,4	4,8	2,0
CoMo/P(5)	18,6	4,6	5,0	NiMo/P(5)	18,4	4,8	5,0

The catalytic activity of the samples was determined in a bench-scale flow reactor unit in the hydrotreating process of light catalytically cracked gas oil (LCGO) and straight-run gas oil (SRGO) mixture (1:9 by volume). Contents of sulfur and polycyclic aromatic compounds in mixture were 0,80 and 5,14 wt. % respectively.

3 Results and discussion

The relationships between hydrodesulfurization (HDS) constant (1,5 order kinetic model) and content of P_2O_5 are presented in **Fig. 1** and **3**. The relationships between hydrogenation degrees (HYD) and content of P_2O_5 are presented in **Fig. 2** and **4**. In all cases relationship curves have a complicated character. Samples with P_2O_5 content of 5,0 wt. % were the most active.

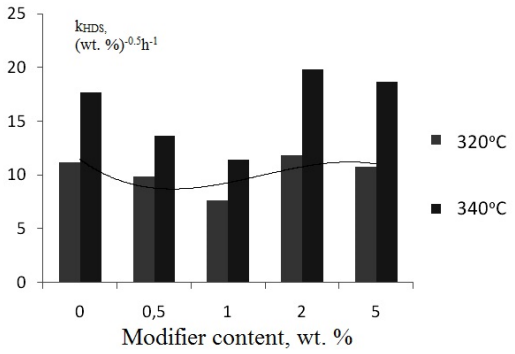

Fig. 1. Relationship between k_{HDS} and P_2O_5 content for CoMo/P catalysts

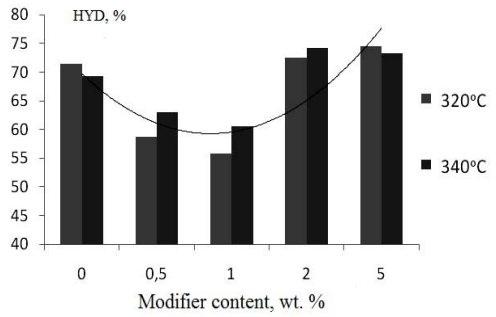

Fig. 2. Relationship between HYD and P_2O_5 content for CoMo/P catalysts

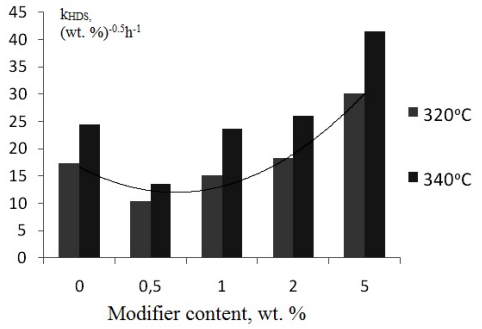

Fig. 3. Relationship between k_{HDS} and P_2O_5 content for NiMo/P catalysts

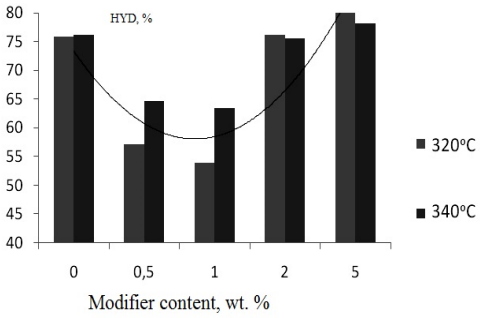

Fig. 4. Relationship between HYD and P_2O_5 content for NiMo/P catalysts

It should be mentioned, that HDS and HYD activities minimum were found for P_2O_5 content of 0,5-1,0 wt. %. The similar relationships were found in **[3]**. Authors explained this phenomenon took into account structure characteristics of modified carrier surface.

4 Conclusions

In this way, modification of carrier with P_2O_5 amounts of 2-5 wt. % get a positive effect on catalytic activities in HDS and HYD reactions. In CoMo catalysts line the maximum of activity was found for CoMo/P(2) sample and in NiMo one – NiMo/P(5).

Acknowledgements

The work was supported by Russian Federal target program «Investigations and developments of priority directions of scientific-technological complex progress of Russia for 2014-2020 years» (project № 14.577.21.0140).

References

[1] TopsøeH., ClausenB. S., MassothF. E. *Catalysis - Science and Technology*. 11 (1996) 310.
[2] Startsev A.N. Hydrotreating sulfide catalysts: synthesis, structure, properties. Novosibirsk: «GEO», 2007. – 206 p.
[3] Maity S.K., Ancheyta J., Rana M.S., Rayo P. *CatalysisToday*. 109 (2005) 42.

II-PP243

Hydrotreating of Oil Fractions on Ni_6-$PMo_nW_{(12-n)}(S)/Al_2O_3$ Catalysts

Tomina N.N.*, Moiseev A.V., Solmanov P.S., Maximov N.M., Samsonov M.V., Pimerzin A.A.

Samara State Technical University, Samara, Russia

* tominann@yandex.ru

Keywords: hydrogenolysis, oil fractions, catalyst, hydrotreating

1 Introduction

Intensity of Mo-W systems investigations increased in the last years [**1-4**]. The main works decided to catalytic tests in dibenzthiophene and 4,6 – dimethyldibenzthiophene hydrogenolysis reactions [**1, 4**]. A larger part of investigations carried out with model compounds. So, the catalytic tests of Ni-MoW/γ-Al_2O_3 catalysts with real feed are an actual ones. In this work the results of Ni_6-$PMo_nW_{(12-n)}(S)/Al_2O_3$ catalysts (mole ratio Mo:W) investigations in hydrotreating of diesel and vacuum gasoil fractions are presented.

2 Experimental/methodology

γ-Al_2O_3 carrier was synthesized from AlOOH (TH-100, «Sasol»). Pore structure was determined by adsorption of nitrogen at 77K (S_{BET} = 175 m^2/g, V = 0.901 cm^3/g, $R_{eff.}$ = 87 Å). A line of Ni-MoW/Al_2O_3 catalysts was synthesized by means of wetness impregnation method from aqua solution of Ni, Mo and W compounds ($(Ni(OH)_2)_2$*$NiCO_3$, $H_3PMo_{12}O_{40}\cdot 17H_2O$, $H_3PW_{12}O_{40}\cdot 29H_2O$). Impregnation solution also contained a citric acid as chelating agent. Catalysts were dried at 60, 80 and 110°C for 2 hours. The mole ratios of Mo:W were 1:0, 2:1, 1:1, 1:2 and 0:1 (catalysts denoted as Ni-Mo_nW_{12-n}). Catalysts were sulfided before catalytic tests in flow of H_2/H_2S = 30/70 vol. (5 l/h) at 500ºC for 2 hours. Catalytic activity was determined in a bench-scale flow reactor under hydrogen pressure in the hydrotreating of straight run diesel fraction and light coker gasoil mixture (sulfur content – 0.798 wt. %, polycyclic aromatic hydrocarbons (PAH) content – 5.14 wt. %, Iodine number – 2.4 g/100 ml) and vacuum gasoil (sulfur content – 2.07 wt. %, PAH content – 9.61 wt. %). Hydotreating of straight run diesel fraction and light coker gasoil mixture was carried out under the next conditions: hydrogen pressure of 4.00 ± 0.04 MPa, LHSV = 2.0 h^{-1}, H_2/feed = 600 nm^3/m^3, temperatures of 320 and 340 ± 1 ^{0}C. Hydotreating of vacuum gasoil was performed in the next conditions: hydrogen pressure of 5.00 ± 0.04 MPa, LHSV = 1.0 h^{-1}, H_2/feed = 1000 nm^3/m^3, temperatures of 360 and 390 ± 1 ^{0}C. HR TEM images were recorded for catalysts in sulfide form.

3 Results and discussion

Geometric characteristics of active phase were determinate on the base of HR TEM images [**5**]. The active phase morphology (length of slab – L and number of layers in slab – N) of sample with Mo:W=1:1 was notable different from others. As it assumed in [**6**], active centers (coordinatively unsaturated atoms of Mo and S) are located on the edges of slabs. Hydrogen is able to react with sulfur atoms and form anion vacancies (HDS reaction catalytic centers).

Results of straight run diesel fraction and light coker gasoil mixture hydrotreating are shown in **Fig. 1**. Catalyst with Mo/W = 1/1 demonstrated the highest hydrodesulphurization (HDS) activity.

Results of vacuum gasoil hydrotreating are shown in **Fig. 2**. Catalyst with Mo/W = 1/1

demonstrated the highest hydrodesulphurization (HDS) and hydrogenation (HYD) activities.

Table 1. Active phase characteristics of Ni-Mo_nW_{12-n}(S) catalysts

Parameter of active phase	Ni-Mo_{12}(S)	Ni-Mo_6W_6(S)	Ni-W_{12}(S)	Ni-Mo_6W_6(S) after catalytic test
Average slab length, L, nm	4,0	5,0	3,9	4,1
Average number of layers in slab, N	2,1	2,5	1,6	1,7
% atoms of Mo(W) at edge positions, f_e	24,4	20,8	24,9	23,8
% atoms of Mo(W) at corner positions, f_c	5,2	3,3	5,5	4,8

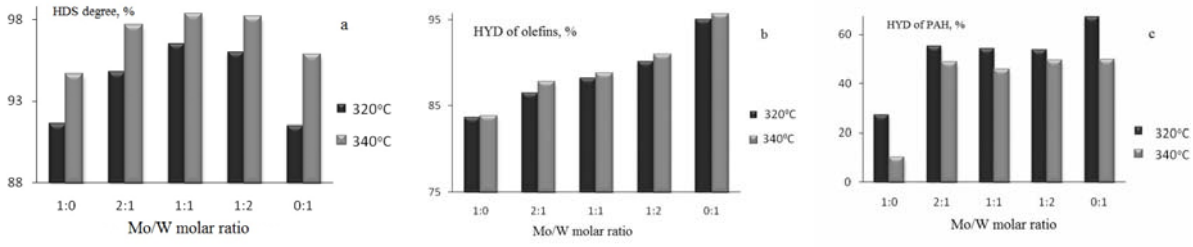

Fig. 1. Relationships between HDS degree **(a)**, HYD degrees of olefins **(b)** and PAH **(c)** of straight run diesel fraction and light coker gasoil mixture and molar ratio Mo/W

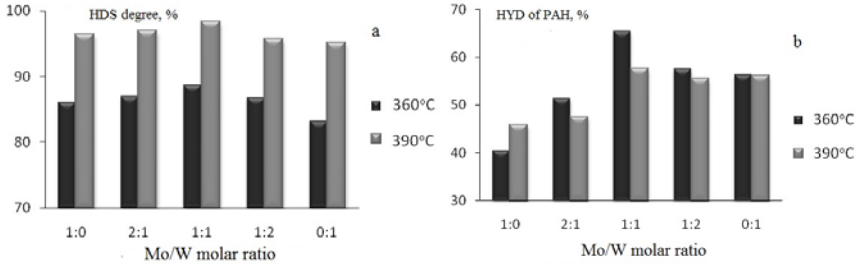

Fig. 2. Relationships between HDS degree **(a)**, HYD degree of PAH **(b)** of vacuum gasoil and molar ratio Mo/W

4 Conclusions

A line of trimetallic Ni-Mo_nW_{12-n} catalysts was synthesized and tested in hydrotreating of oil fractions. Catalyst with Mo/W = 1/1 demonstrated the highest hydrodesulphurization (HDS) activities in hydrotreating of straight run diesel fraction and light coker gasoil mixture and vacuum gasoil. Catalyst with Mo/W = 1/1 also demonstrated the highest hydrogenation (HYD) activity in hydrotreating of vacuum gasoil. Morphologies of active phases were investigated by means of HR TEM. Sulfide phase of Ni-Mo_6W_6(S) had the highest number of edge and corner Mo(W) atoms. It should be mentioned, that catalytic behavior of Ni-Mo_nW_{12-n} catalysts can't be explained in the view of active phase morphology. The Ni-Mo_nW_{12-n} catalysts are very perspective, like it was concluded from catalytic tests.

Acknowledgements

The work was supported by Russian Federal target program «Investigations and developments of priority directions of scientific-technological complex progress of Russia for 2014-2020 years» (project № 14.577.21.0140).

References

[1] Guzmán M.A., Huirache-Acuña R., Loricera C.V., et. al. *Fuel*. 103 (2013) 321.
[2] Lan L., Ge Sh., Liu K., et. al. *J. Nat. Gas Chem*. 20 (2) (2011) 117.
[3] Cervantes-Gaxiola M. E., Arroyo-Albiter M., Maya-Yescas R. *Fuel.* 100 (2012) 57.
[4] Mendoza-Nieto J.A., Vera-Vallejo O., Escobar-Alarcón L., et. al. *Fuel*. 110 (2013) 268.
[5] Mingfeng L., Huifeng L., Feng J., Chu Y., Nie H. *Catal. Today*. 149 (2010) 35.
[6] Paul J.-F., Payen E. J. Phys. Chem. B. 107 (2003) 4057.

II-PP244

Crucial Role of the Graphene Edges for CNT formation during the Preparation of Metal/Carbon Catalysts

Gordeev E.G.*, Pentsak E.O., Ananikov V.P.

N. D. Zelinsky Institute of Organic Chemistry, Russian Academy of Sciences, Moscow, Russia

* gordeev_e@ioc.ac.ru

Keywords: carbon, nanotubes, quantum-chemical, calculations, metal/carbon catalysts

1 Introduction

Usually carbon support in M/C catalysts is considered as an inert material, which is not involved in chemical transformations. However, recently we have found that interaction between metal particles and carbon support significantly changes the morphology of M/C catalysts [1].

2 Experimental/methodology

A variety of processes have been observed, where of particular interest are pitting/etching and nanotube growth under microwave irradiation (Fig. 1).

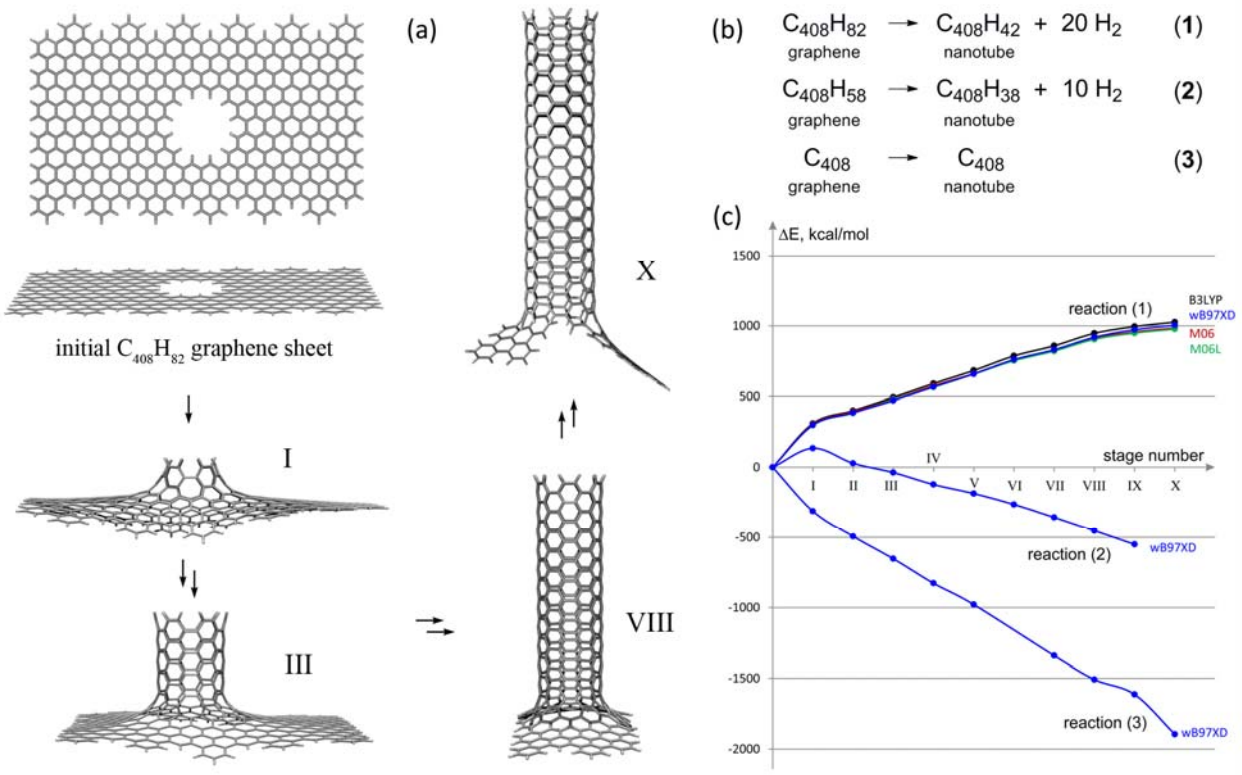

Fig. 1. (a) – Stepwise transformation of a $C_{408}H_{82}$ graphene sheet to a (6,6) nanotube; (b) – summary of nanotube formation reactions for the $C_{408}H_{82}$, $C_{408}H_{58}$, and C_{408} graphene sheets; (c) – relative energies of reactions (1−3) calculated at DFT level.

3 Results and discussion

A detailed computational study has been carried out to study the mechanism of possible modification of the carbon surface.

The nanotube formation process is strongly dependent on the state of the graphene edges: calculated energy change of +2.5; -1.5; -4.6 kcal/mol per one carbon atom was found for $C_{408}H_{82}$, $C_{408}H_{58}$ and C_{408} model graphene sheets, correspondingly. This result suggests a possibility to control CNT formation during the preparation of Metal/Carbon catalysts by changing the reaction conditions.

Acknowledgements

Financial support of the Russian Science Foundation is acknowledged (RNF Grant 14-13-01030). The Supercomputing Center of Lomonosov Moscow State University is acknowledged for usage of computational resources.

References

[1] E.O. Pentsak, E.G. Gordeev, V.P. Ananikov, *ACS Catalysis,* 4 (2014) 3806; doi:10.1021/cs500934g.

II-PP245

MnO_2 Catalyst Prepared with Microwave Assistance

Boytsova O.[1,2*], Baranchikov A.[1], Ivanov V.[1]

1 - Kurankov Institute of General and Inorganic Chemistry RAS, Moscow, Russia
2 - Lomonosov Moscow State University, Moscow, Russia

* boytsova@gmail.com

Keywords: manganese dioxide, microwave-assisted method, environmental catalysis

1 Introduction

Present-day electrochemistry trends and advances belong to processes of energy storage and conversion; they also include the related materials exploring. The exploiting alternative catalytic materials for oxygen reduction reaction (ORR) have triggered dynamic research interests. The main efforts focused on compounds providing considerable catalytic activity, nontoxicity, low cost and abundance. Manganese dioxide is a juicy system and dominant competitor in ORR field. However, the electrochemical activity of MnO_2 is correlated with its crystallographic structure and specific surface area. Manganese dioxide exists in a number of structural forms, where the basic structural element consists of MnO_6 octahedra forming layers and channels [1]. The pyrolusite (β) and ramsdellite (γ) are relatively pure forms of MnO_2. Other ones, such α, δ, contain ions like Na^+or K^+ within the lattice. A number of synthetic methods are known for the preparation of MnO_2 with desired crystal structure and morphology including sol-gel method, electrochemical deposition, precipitation, and hydrothermal synthesis, also a few papers on the synthesis of MnO_2 nanostructures with microwave irradiation [1, 2]. The last approach doesn't need high pressure, temperature, vacuum, catalysts or templates. The microwave-hydrothermal (MWHT) method was used to produce various multifunctional nanomaterials such as zeolites, metal oxides, with intriguing morphologies such as nanopheres, nanowires, and nanoporous networks. Ming et al. demonstrated a methodological approach for utilizing microwave heating during the hydrothermal process to obtain birnessite-type MnO_2. However, the employed process whether the morphology of as-prepared MnO_2 powders can be controlled by simply adjusting the process conditions was not illustrated. These work actually duplicated Xiao et al research who did α- and δ-MnO_2 with hydrothermal synthesis. It still remains debated containing K^+ ions aspect, which are inevitably inside channels from MnO_6 octahedra in α-MnO_2 and between layers in δ-MnO_2 in default, and its influence to electrochemical activity [3]. We report a strategy in microwave-hydrothermal processes that permits exquisite control over the crystal structure and morphology of MnO_2 nanostructures by temperature, time, acidity.

2 Experimental/methodology

Manganese dioxide nanostructures were synthesized by high-yield MWHT technique under mild conditions through redox reaction between permanganate and nitrite ions. In a typical synthesis, $KMnO_4$ and $NaNO_2$ with molar ratio 2:3 were added to 40 ml deionized water to form a homogeneous solution. Different amount of 0.5M H_2SO_4 were then added dropwise into the stirred solution. After stirring for 20 min, the 20 ml obtained suspension was transferred to a 30 ml Teflon vessel. The autoclave was sealed and heated to different reaction temperatures (90, 110, 150, and 170˚C) with holding time of 8, 12 or 25 min in an Berghof MWS-3* microwave digestion system. After the autoclave was cooled down to room temperature, the products were collected by centrifugation and washed with deionized water and absolute ethanol several times to remove the impurities, and dried in air at 70˚C for 12 h. All reactions under the microwave irradiation get a quantitative yield (around 99% and more) while shortening the reaction time.

Different amount of H_2SO_4 was added to initial solution, while keeping other conditions constant. The obtained products were tested by XRD, SEM, BET, EDX.

3 Results and discussion

In the absence of H_2SO_4 in initial solution the sample is only MnO_2 nanoflowers (Figure). As the amount of acid is up to 2 ml, the morphologies of particles are mixture of nanograins attached onto the nanorods. Using 3.5 ml, the sample is almost pure nanorods (Figure). A further increasing H_2SO_4 amount doesn't influence on morphology of MnO_2.

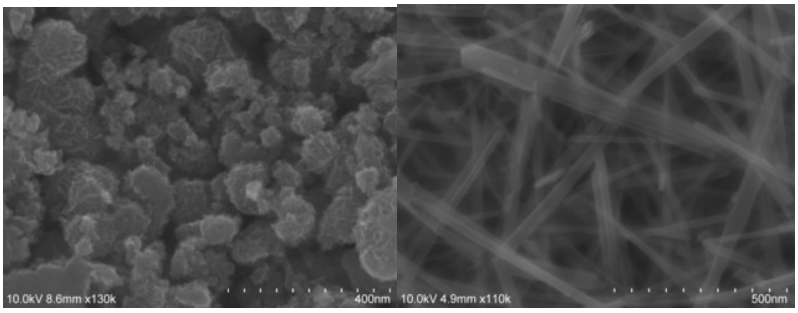

Fig. 1. SEM Images of δ-MnO_2 Nanoflowers (left), MnO_2-Pyrolusite Nanorods (right).

The coherent scattering domain sized (D csd) were calculated by the Shelyakov-Scherrer formula $Dcsd = \lambda/\beta\cos\theta$, were $\lambda Cu = 1.54178Å$ and β is the intrinsic broadening of diffraction maximum, θ - the angle of the reflection. Under acidic conditions, as the H_2SO_4 amount is increased, crystal size (domain size) is essentially constant for the samples with layered structure produced (40-50 nm). In a critical point, where H^+ dominate on K^+ion (in the present case), pyrolusite β-MnO_2 is established as the preferred phase and a structural transition is observed on XRD patterns, crystal size increases dramatically (around 100-200 nm), perhaps reflecting the thermodynamic stability of this phase.

Pyrolusite is obtained as large rod, with octahedral cross-section, a diameter of 100-200 nm and length of 1-2μm (Figure). MnO_2 nanorods grow in the (001) direction, the axis [110] is perpendicular to the side walls. These conclusions were confirmed by TEM and SAED measurements. The shape of β-MnO_2 and the favored growth along a defined direction are generated mainly under thermodynamically preferential crystal growth process.

4 Conclusions

In this work we proved that crystal structure and morphology of MnO_2 can be controlled by varying reaction time and temperature under microwave assistance as well as the amount of acid. Future work will be focused on electrochemical activity.

Acknowledgements

Authors acknowledge financial support from RFBR (project #14-29-04100)

References

[1] Xu M.-W. et al; *Energy Storage in the Emerging Era of Smart Grids*; In tech: 12 (2011).
[2] Ming B.et al; *J. of Power Sources* 198 (2012).
[3] Donne S.W. *J. of Power Sources* 195 (2010).

II-PP246

DRIFTS Studies of Support Effects on CO Adsorption and CO + O_2 Reaction over $Ce_{1-x-y}M_xCu_yO_{2-d}$ (M = Zr, Hf, Th)

Bera P.[1*], Baidya T.[2]

1 - Surface Engineering Division, CSIR-National Aerospace Laboratories, Bangalore, India
2 - Solid State and Structural Chemistry Unit, Indian Institute of Science, Bangalore, India

* partho@nal.res.in

Keywords: adsorption, CO oxidation, DRIFTS, Cu-CeO_2, doped with Zr, Hf, Th

1 Introduction

In recent years, CeO_2 and TiO_2 based noble metal ionic catalysts have been found to show significant enhancement of CO oxidation and NO reduction at a lower temperature [1,2]. It has been demonstrated that substituted noble metal ions on CeO_2 matrix are catalytically more active than dispersed fine metal particles on Al_2O_3. Pd^{2+}, Pt^{2+}, Rh^{3+}, Cu^{2+}, Ag^{+} and Au^{3+} are the active sites for several important catalytic reactions. Structural studies show that metal ions are incorporated into CeO_2 substrate to a certain limit in the solid solution form of $Ce_{1-x}M_xO_{2-\delta}$ ($x \leq 0.05$). Among the transition metals, Cu based catalysts have been found to be very active for CO oxidation, NO reduction and CO-PROX reaction [3,4]. In our previous study, it has been found that Pd^{2+} ion substituted in different CeO_2 based supports show different activities [5]. It has been observed that activation energy for CO oxidation decreases with increasing ionic character of Pd^{2+} in CeO_2 based catalysts. Therefore, it would be worthwhile to study other metal substitution in different CeO_2 supports and investigate the variation of their catalytic activities. This could give a more general outlook into how active metal ion can be activated by choosing suitable support. In this sense, it would be interesting to study the variation of catalytic activities of Cu^{2+} ion in different Cu doped CeO_2 catalysts.

Diffuse reflectance infrared Fourier transform spectroscopy (DRIFTS) is a versatile tool to get information about the nature of adsorbed species on the surface of catalyst during reaction [6]. It can also provide the trends of reaction with respect to the temperature. The present work focus on DRIFTS study to understand CO adsorption at room temperature as well as CO oxidation by O_2 at different temperatures over different Cu substituted $Ce_{1-x}M_xO_2$ (M = Zr, Hf, Th) catalysts. The effect of supports on the substituted Cu^{2+} ions toward CO adsorption/oxidation behavior has been studied.

2 Experimental/methodology

Cu^{2+} substituted $Ce_{1-x}M_xO_2$ (M = Zr, Hf, Th) were prepared by solution combustion method. BET surface areas, XRD patterns and XPS of these catalysts were carried out using Quantachrome Autosorb Automated Gas Sorption System (Quantachrome Instruments), PANalytical X'Pert PRO diffractometer and Thermo Fisher Scientific Multilab 2000 spectrometer, respectively.

CO adsorption at room temperature and in-situ DRIFT spectra of the CO + O_2 reaction as a function of temperature over Cu substituted $Ce_{1-x}M_xO_2$ (M = Zr, Hf, Th) catalysts were recorded with an accumulation of 20 scans at a resolution of 4 cm^{-1} using a FTIR spectrometer from Thermo Scientific Nicolet 380 FTIR with a liquid N_2 cooled high sensitivity MCT detector and a DRIFTS cell.

3 Results and discussion

XRD patterns of the Cu substituted $Ce_{0.75}M_{0.25}O_2$ (M = Zr, Hf, Th) catalysts are indexed to fluorite structure. XPS studies show that Cu, Ce, Zr, Hf and Th are present in +2, +4, +4, +4 and +4 oxidation states, respectively. CO derived products such as carbonates, bicarbonates and formates are formed when CO is interacted with these catalysts at room temperature. When CO is introduced over the catalyst, surface Cu species in +2 oxidation state gets partially reduced by CO and consequently, CO derived species such as carbonates are formed over the CeO_2 based supports. Therefore, frequencies related to Cu and CO interaction in these catalysts are ascribed for Cu^+–CO species whose positions are shifted to higher frequencies in Zr, Hf and Th doped catalysts. The effect of support can be observed when CO adsorption shows variation in the intensity of Cu^+–CO in different supports in similar conditions. Variation of Cu^+–CO peak intensities during CO oxidation have been accepted as probe to find the differences in supports and it is shown in Figure 1. The observed intensities of Cu^+–CO peaks increase with the following substitutions: CeZr < Ce < CeTh ~ CeHf. As all the substituents are non-reducible, only electron withdrawing power as determined by effective nuclear charge (Zeff) can influence the activity. Zeff of Hf4+ and Th4+ is more due to f electron indicating lattice oxygen is more polarized towards Hf4+ and Th4+. Therefore, Hf/Th doped catalysts are more reducing in nature. Therefore, transformation of more Cu2+ to Cu+ occurs significantly in case of Hf and Th. This also affects CO oxidation activities of these catalysts, because because localized charge on Cu2+ induces more +ve charge on 'C' atom end of the adsorbed CO molecule while reacting with lattice oxygen. This explains lowest activity of Zr substituted Cu/CeO2 among all these in Ce0.93Cu0.07O2 and catalysts.

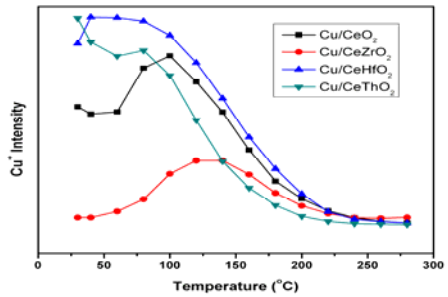

Figure 1. Cu+□CO intensity vs Temperature (°C) $Ce_{0.68}M_{0.25}Cu_{0.07}O_{2-\delta}$ (M = Zr, Hf and Th) catalysts.

4 Conclusions

Effect of electron withdrawing property of supports on CO adsorption and oxidation activities in $Ce_{0.93}Cu_{0.07}O_{2-\delta}$ and $Ce_{0.68}M_{0.25}Cu_{0.07}O_{2-\delta}$ (M = Zr, Hf, Th) catalysts.

Acknowledgements

Authors would like to thank Prof. M. S. Hegde, Indian Institute of Science, Bangalore for providing DRIFTS and XPS facilities.

References

[1] M. S. Hegde, K. C. Patil, G. Madras, *Acc. Chem. Res.* 42 (2009) 704.
[2] P. Bera, M. S. Hegde, *Catal. Surv. Asia* 15 (2011) 181.
[3] P. Bera, K. R. Priolkar, P. R. Sarode, M. S. Hegde, S. Emura, R. Kumashiro, N. P. Lalla, *Chem. Mater.* 14 (2002) 3591.
[4] A. Martínez-Arias, D. Gamarra, M. Fernández-García, A. Hornés, P. Bera, Zs. Koppány, Z. Schay, *Catal. Today* 143 (2009) 211.
[5] T. Baidya, G. Dutta, M. S. Hegde, U. V. Waghmare, *Dalton Trans.* 455 (2009).
[6] D. D. Miller, S. S. C. Chuang, *Catal. Commun.* 10 (2006) 1313.

II-PP247

Synthesis of ZSM-5 Zeolite from Fly Ash by Hydrothermal Method

Bedoya J.C., Arroyave J.C., Echavarría A., Hoyos D., Arboleda J.*

Department of Chemistry, University of Antioquia, Medellin, Colombia

* johana.arboleda@udea.edu.co

Keywords: ZSM-5 zeolite, fly ash, zeolite synthesis, hydrothermal method

1 Introduction

The synthesis of high silica zeolite ZSM-5 was reported in 1972 by Mobil [1]. ZSM-5 is a medium pore zeolite formed by 10-membered rings, which possesses a pore dimension of 0.54-0.56 nm. Its unique pore structure has excellent shape selectivity and tunable acidity, which makes an interesting material for catalyzing organic reactions. Since its discovery, extensive work has been carried out on the synthesis and applications of ZSM-5. High crystalline ZSM-5 can be synthesized within a period of about 168 h in autoclave at 120–180°C under autogenous pressures. The crystallization time can be reduced to 4–6 h under high pressures and temperatures (about 40–60 atm and 230–250°C) [2]. The possibility of synthesizing ZSM-5 at temperatures between 90–100°C and atmospheric pressure has also been reported [3-4]. These methods make available the study of the crystallization mechanism since it require a long induction period. Among the several templates used for the synthesis of ZSM-5, the most common is tetrapropylammonium bromide (TPABr). Previously, almost all the fly ash was disposed by landfill, which became expensive and caused an environmental problem. Mostly fly ash can be used as building materials according to its pozzolanic properties [5–6]. However, due to the fluctuation demand, the alternative uses of fly ash were focused as raw material for zeolite synthesis. The synthesis of zeolites from fly ash can be classified into direct and non-direct synthesis [7-8]. This work is concerned with the synthesis and characterization of ZSM-5 from different fly ashes of the Colombian Industry by the hydrothermal method.

2 Experimental/methodology

Several fly ashes from Colombian Industry were used as raw materials for ZSM-5 zeolite synthesis, by hydrothermal method. The fly ash was subjected to calcination at 700°C for 3 hours as a pretreatment, to weaken the crystallinity of the quartz phase, which is silicon oxide. To adjust the high ratio SiO_2/Al_2O_3 of the zeolite, a suspension of silicon oxide (30% LUDOX) was used and TPABr was added as the structure-directing ofZSM-5 zeolite synthesis. The synthesis through of the hydrothermal method was carried out at crystallization temperature of 190°C for 24 hours in stainless steel reactor with Teflon lining, after which the gel was left to stir for 5 hours. Finally, the material was calcined at 550°C for 5 hours to remove excess humidity and organic compounds into the structure.

3 Results and discussion

Characterization by X-ray fluorescence (F-XRD) in the fly ash identified a high content of silicon oxide (SiO_2) and aluminum oxide (Al_2O_3) in a molar ratio SiO_2/Al_2O_3 close to 1 and low content of otherwise oxides. An analysis by X-ray diffraction (XRD) determined the phases present in the feedstock and thermogravimetric analysis (TGA) allowed to determine the thermodynamic behavior of the material under consideration and defined optimal conditions to calcination.

The zeolite was characterized by several techniques, including an analysis of X-ray diffraction, where the presence of ZSM-5 stage was confirmed; chemical analysis by atomic absorption determined the Si/Al relation and the Na^+ cations percentage. Trough of analysis by scanning electron microscope (SEM) was determined the structural properties of the material and the particle size of the grains formed. Thermogravimetric analysis (TGA) succeeded for identifying the thermodynamic behavior of the zeolite and the thermal stability at high temperatures. Finally, analysis of BET surface area was use for determining the textural characteristics of the catalyst.

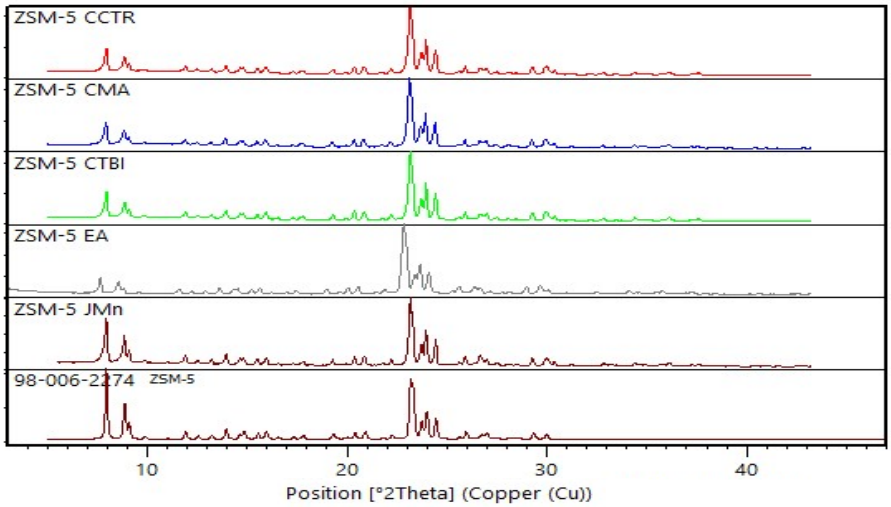

Fig 1. DRX for different zeolites ZSM-5 trough of fly ash.

4 Conclusions

The alternative use of fly ash for the synthesis of zeolite ZSM-5 by hydrothermal method was possible. The textural and crystallographic properties were examined identifying key characteristics of the material. Fly ash exposed to heat pretreatment and hydrothermal process at 190 °C and autogenous pressure for 24 hours, allowed to crystallize a MFI phase.

Acknowledgements

The authors thank the University of Antiqouia and colciencias for economic support.

References

[1] R.J. Argauer, G.R. Landolt, US Patent 3702886, Mobil Co (1972).
[2] S.J. Kulkarni, P. Srinivasu, N. Narender, K.V. Raghavan, Fast and efficient synthesis of ZSM-5 under high pressure, Catal. Commun. 3 (2002) 113–117.
[3] W.J. Kim, M.C. Lee, D.T. Hayhurst, Synthesis of ZSM-5 at low temperature and atmospheric pressure in a pilot-scale batch reactor, Micropor. Mesopor. Mater. 26 (1998) 133–141.
[4] J. Yang, S. Yu, H. Hu, Y. Zhang, J. Lu, J. Wang, D. Yin, Synthesis of ZSM-5 hierarchical microsphere-like particle by two stage varying temperature crystallization without secondary template, Chem. Eng. J. 166 (2011) 083–1089.
[5] J. Majling, D.M. Roy, Am. Ceram. Soc. Bull. 72 (1993) 77.
[6] L.D. Chen, Y. Shen, J. Su, X. Wu, Cem. Concr. Res. 30 (2000) 881.
[7] C.F. Lin, H.C. Hsi, Environ. Sci. Technol. 29 (1995) 1109.
[8] X.S. Zhao, G.Q. Lu, H.Y. Zhu, J. Porous Mater. 4 (1997) 245.

II-PP248

In Situ X-ray Absorption Spectroscopy and X-ray Powder Diffraction for Temperature- and Pressure- Dependent Hydride Phase Formation in Supported Pd Nanocatalysts

Bugaev A.L.[1,2*], Guda A.A.[1], Lomachenko K.A.[1,2], Lazzarini A.[2], Srabionyan V.V.[1], Groppo E.[2], Dmitriev V.P.[3], Pellegrini R.[4], Van Bokhoven J.A.[5,6], Soldatov A.V.[1], Lamberti C.[1,2]

1 - Southern Federal University, Rostov-on-Don, Russia
2 - Department of Chemistry, University of Torino, Torino, Italy
3 - ESRF, Grenoble, France
4 - ChimetSpA, Arezzo, Italy
5 - ETH Zurich, Zurich, Switzerland
6 - PSI, Villigen, Switzerland

* abugaev@sfedu.ru

Keywords: EXAFS, XANES, XRD, PdH, XAS, nanocatalysts

1 Introduction

Palladium nanoparticles play an important role in various fields such as catalysis, medicine, chemistry, biology, etc. In a number of industrial application supported palladium nanoparticles are used to catalyze reactions of hydrogenation when hydride phase of the palladium nanocatalysts may be formed. The understanding of the conditions of the hydride phase formation and obtaining a phase diagram of the nanocatalyst is an important step in order to investigate the active phase of the catalysts. In our study we used industrial Pd nanocatalysts (ChimetSpA) with average particle size about 3 nm deposited on carbon. Pressure-composition isotherms for palladium hydride nanoparticles were obtained using simultaneous in situ X-ray Absorption Spectroscopy (XAS) and X-ray Powder Diffraction (XRPD) measurements.

2 Experimental/methodology

Pressure composition isotherms were obtained for Pd Hydride nanoparticles with average particle size about 3 nm deposited on carbon. Experiments were carried out at Swiss-Norwegian Beamline of ESRF. Pd/C nanoparticles were packed in a 1mm thick capillary connetted to a pressurized system enabling to control hydrogen pressure. Vaccum pump was connected to the system for outgassing. Gas blower positoned above the sample was used to controll the temperature. Initial pretreatment of the sample was done at 125 °C in 200 mbar of hydrogen during 30 minutes. Pd foil and Pd black were used as reference samples.

In situ X-ray Absorption and X-ray Powder Diffraction data were collected at -10, 20, 50, 80 and 110 °C in a pressure range from 0 to 10000 mbar. X-ray Absorption Spectra at Pd K-edge were obtained in the transmition mode in the continuous scanning mode in the energy of the incoming photons from 24.1 to 25.4 keV. Pd foil was measured simultaneously for energy callibration. Single-shell EXAFS analysis was performed in Demeter package.

X-ray diffraction images was collected by CMOS-Dexela 2D detector. The photon wavelength was set as 0.50544 Å. The values of wavelength and sample-to-detector distance were optimized using silicon poweder and lanthanum hexaboride. The geometry of the experimental setup resulted in a 2θ angles from 0 to 52 degrees. For better statistics 5 images and 5 dark images with time acquisition of 10 seconds were collected at each of the experimental points. Rietveld refinement was performed in Jana2006 code giving the cell parameters and concentration of α- to β- hydride phases.

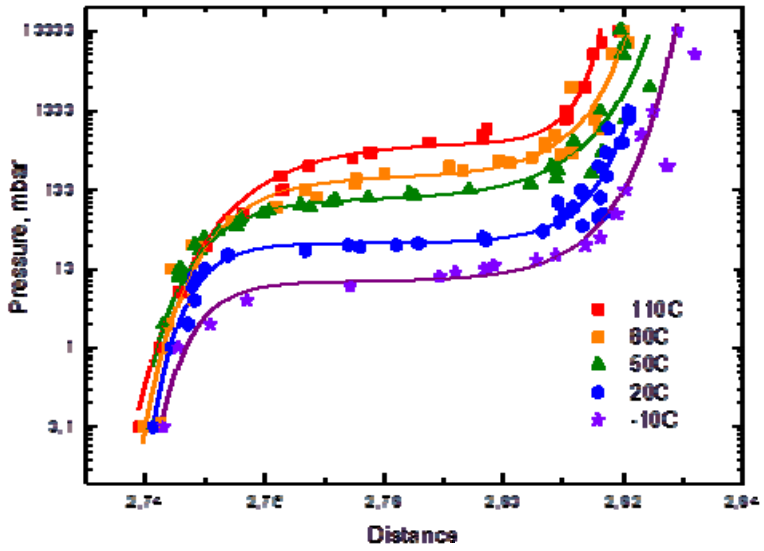

Fig. 1. Pressure-composition isotherms for Pd-H nanoparticles obtained from EXAFS.

3 Conclusions

We have performed a detailed investigation of hydride phase formation in Pd nanocatalysts using different complementary techniques: EXAFS, XANES, XRPD and volumetric measurements. The average cell parameters obtained from EXAFS and XRPD are in excellent agreement, but Rietveld analysis of diffraction data allows to separate two coexisting hydride phases, while EXAFS shows only averaged Pd-Pd distance with increased Debye-Waller parameter. The obtained results indicate that a transition from α- to β- phase occurs similarly to that in bulk Pd. XANES spectra are influence directly be hydrogen atoms and the performed fitting of XANES provides quantitative information on the amount of hydrogen absorbed in Pd nanoparticles, which correlates with volumetric measurements.

Acknowledgements

AVS and CL acknowledge the Ministry of Education and Science of the Russian Federation for funding the research (14.Y26.31.0001). ALB, AAG and KAL acknowledge the Grant of the President of Russia for Young Scientists (MK-3206.2014.2).

References

[1] Bugaev, A. L., Guda, A. A., Lomachenko, K. A., Srabionyan, V. V., Bugaev, L. A., Soldatov, A. V., Lamberti, C, Dmitriev, V.P., van Bokhoven, J. A. (2014). Temperature-and Pressure-Dependent Hydrogen Concentration in Supported PdH x Nanoparticles by Pd K-Edge X-ray Absorption Spectroscopy. The Journal of Physical Chemistry C, 118(19), 10416-10423.

II-PP249

Catalytic Performance of a Polyoxometalate/Reduced Graphene Oxide Composite in Degradation of Methylene Blue

Ucar A.[1], Findik M.[1], Gubbuk I.H.[2], Bingol H.[3], Kocak N.[1*]

1 - Necmettin Erbakan University A.K. Education Faculty, Department of Science Education, Konya, Turkey

2 - Selcuk University, Science Faculty, Department of Chemistry, Konya, Turkey

3 - Necmettin Erbakan University A.K. Education Faculty, Department of Chemistry Education, Konya, Turkey

* nkocak@konya.edu.tr

Keywords: polyoxometalate, graphene, degradation, methylene blue

1 Introduction

Dyes in water are a major class of synthetic organic compounds released by many industries such as paper, plastic, leather, food, cosmetic, textile and pharmaceutical industries. These effluents result in significant environmental pollution impact on human and animal healt[1,2]. In recent years, different type of polyoxomatalates(POMs) have been studied as novel catalysts for dye degradation of organic dyes due to their diverse properties in molecular composition, redox potential, and solubility [3,4]. However POMs are usually soluble in many polar solvents, causing difficulties in the recovery, separation, and recycling of the catalysts. These significant aspects have prompted researchers to anchor POM on a support material such as silica, metal cations (Cs, Co, Fe, etc.), zeolite, positively charged polymer chains, nanoparticles, and carbon[5-7].

In this study, we have prepared a facile way to fabricate rGO-POM composite with high stability and good catalytic properties. In our method, POM was combined with the graphene structure. The catalytic property of rGO-POM was investigated by reducing methylene blue (MB) with $NaBH_4$ as the reducing agent. The extent of dye decomposition was monitored using UV-Vis spectroscopy technique.

2 Experimental/methodology

Graphene oxide (GO) and reduced reduced graphene oxide GO was prepared to literature[8]. The reduced graphene oxide was dispersed and sonicated in DI water. In this step, ethylene glycol was added to the reduced graphene oxide solution to disperse POM on the graphene sheet. An aqueous solution of Silicotungstic acid was added to the rGO solution and mixed, filtered and washed with DI water and then dried[5]. Catalytic activity of rGO-POM composite was investigated by means of degradation of methlylene blue by sodium borohydride in aqueous solutions and the reaction was monitored by UV-VIS spectrometry.

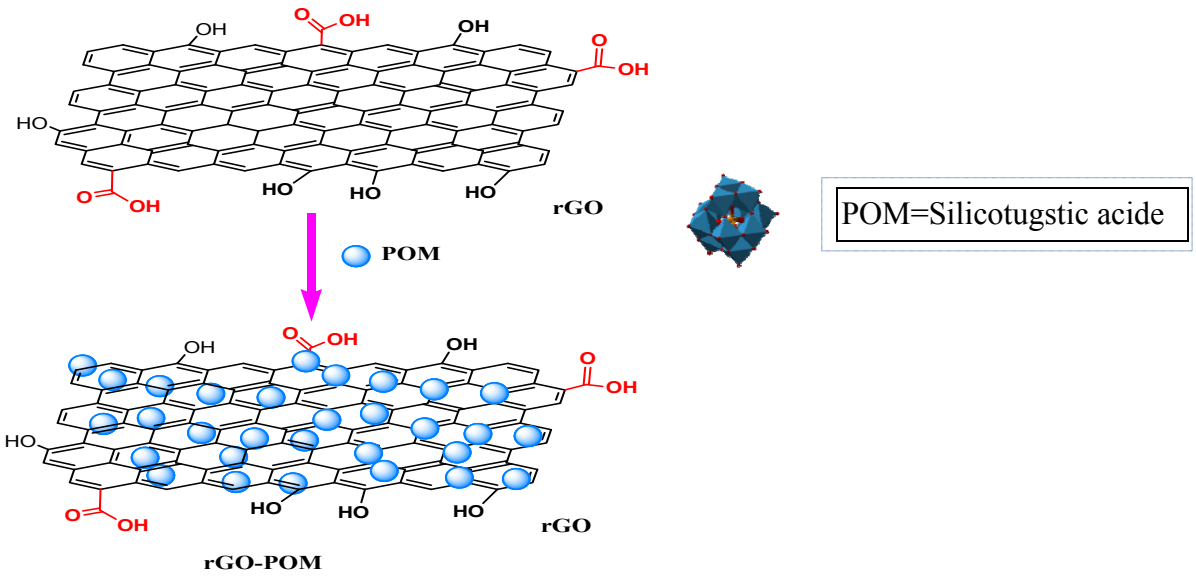

Scheme 1. rGO, POM and rGO-POM composite

3 Conclusions

This report has showed that the textile dye of MB in water can be degraded by $NaBH_4$ in the presence of rGO-POM composite.

Acknowledgements

This research was supported under Selcuk University and Necmettin Erbakan University BAP Projects funding. Authors gratefully acknowledge the financial support of the Selcuk University and Necmettin Erbakan University.

References

[1]V.K. Vidhu, Daizy Philip, Micron 56 (2014) 54–62.
[2] Wang X., Tian H., Yang Y., Wang H., Wang S., Zheng W., Liu Y., Journal of Alloys and Compounds 524 (2012) 5– 123.
[3] Wang J., Lu X., Fan S., Zhao W., Li W., Journal of Alloys and Compounds 632 (2015) 87–93.
[4]Yang, H., Shan, B., Zhang, L., "A new composite membrane based on Keggin polyoxotungstate/poly(vinylidene fluoride) and its application in photocatalysis", RSC Adv., 4, (2014) 61226–61231.
[5] Kim Y. and Shanmugam S., ACS Appl. Mater. Interfaces (2013), 5, 12197−12204.
[6] Pan D., Chen J., Tao W., Nie L. and Yao S., Langmuir (2006), 22, 5872-5876.
[7] Zheng X., Zhang L., Li J., Luo S. and Cheng J.,Chem. Commun., (2011), 47, 12325–12327.
[8] Zor E;, Saglam ME , Akin I, Saf, AO, Bingol, H. Ersoz, M , RSC ADVANCES (2014), 4, 24 12457-12466.

II-PP250

Porous Nickel Based Catalysts for the Dry Reforming of CH_4 to Synthesis Gas

Fedorova Z.A.*, Danilova M.M., Zaikovskii V.I., Porsin A.V., Kirillov V.A., Krieger T.A.

Boreskov Institute of Catalysis SB RAS, Novosibirsk, Russia

* sabirova@catalysis.ru

Keywords: nickel catalysts, CH_4, dry reforming, epitaxial binding

1 Introduction

The reforming of CH_4 with CO_2 has attracted much attention in recent years. This process produces synthesis gas with low H_2/CO ratio which can be converted into liquid hydrocarbons in the Fisher-Tropsch reaction or in the production of methanol. Nickel is preferred metal for the catalysis the CO_2 reforming of CH_4 due to its inherent availability, low cost and high activity. However, the major problem encountered with the reaction of CO_2 reforming of methane is the coke formation leading to the catalyst deactivation. For carrying out the endothermic reactions of dry reforming of CH_4, intensive heat transfer to the reaction zone is required. Therefore, the catalyst must have a high thermal conductivity. It is most promising to use catalyst on metallic supports. This work was aimed to the studying of the nickel catalysts supported on the porous nickel ribbon with MgO underlayer for dry reforming of CH_4 to syngas.

2 Experimental

In the supported nickel catalysts the MgO underlayer (~6 wt. %) was prepared by impregnating the nickel ribbon support with a $Mg(NO_3)_2$ solution followed by drying and then by calcination at 550°C in air (support I) or flowing H_2 (support II). Catalysts I and II were prepared by supporting of nickel on supports I and II via their impregnation with $Ni(NO_3)_2$ solution or a mixture of $Ni(NO_3)_2$ and $Mg(NO_3)_2$ solutions. All the catalysts were dried, calcined at 450°C in a N_2 flow and then reduced in H_2 flow at 900°C for 1 h. The catalysts were characterized by XRD, low-temperature adsorption of nitrogen, SEM and TEM HR in combination with EDX microanalysis. Catalytic activity in CO_2 reforming of CH_4 was determined by a flow method (750°C, 1 atm, m_{cat} = 0,40 g, reaction mixture flow rate – 25 l/h).

3 Results and discussion

X-ray diffraction data showed that the reduced nickel catalysts contain the phases of metallic nickel and NiO in MgO solid solution. HRTEM data show that supported nickel catalysts have the dispersed nickel particles (3-10 nm) epitaxially bound with MgO underlayer (Fig.1).

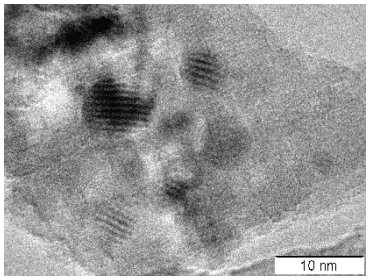

Fig.1. HRTEM image of the catalyst 2.7% Ni/(pNirb+ 6.0 % MgO) (I), 900°C, H_2.

Table shows the activity of prepared nickel catalyst in dry reforming of CH_4. The activity of nickel support with the MgO underlayer was low and decreased during the reaction (Table),

probably due to carbonization. Additional supporting of nickel onto supports with the MgO underlayer increased the catalytic activity (Table). With the increase in the content of supported nickel, the catalyst activity increased, which may result from an increase in the surface area of metallic nickel per unit weight of the catalyst. The activity of the supported nickel catalysts with high content of MgO was more stable; decreasing of conversion during the test period (9 h) was 18-20% (for the ratio CO_2/CH_4 = 1) (Table).

Table Catalytic activity of nickel catalysts in dry reforming CH_4
(750°C, 1 atm, CH_4:CO_2:N_2 = 1:1:0,86, initial mixture flow rate – 25 l/h).

Catalyst	CH_4 conversion, %	
	initial	after 9 h
pNirb+ 6.0 % MgO (II)	23	12
2.5% Ni/(pNirb+ 6.0 % MgO) (I)*)	45	22
2.3% Ni/(pNirb+ 9.0 % MgO) (I)	43	30
2.3% Ni/(pNirb+ 9.0 % MgO) (II)	53	42
4.0% Ni/(pNirb+ 11.0 % MgO) (II)	78	64

*) The catalyst was prepared by supporting of nickel on support via the impregnation with $Ni(NO_3)_2$ solution.

Figure 2 shows the methane conversion versus time-on-stream in the dry reforming of CH_4 at the various CO_2/CH_4 ratio over the catalysts reduced in H_2.

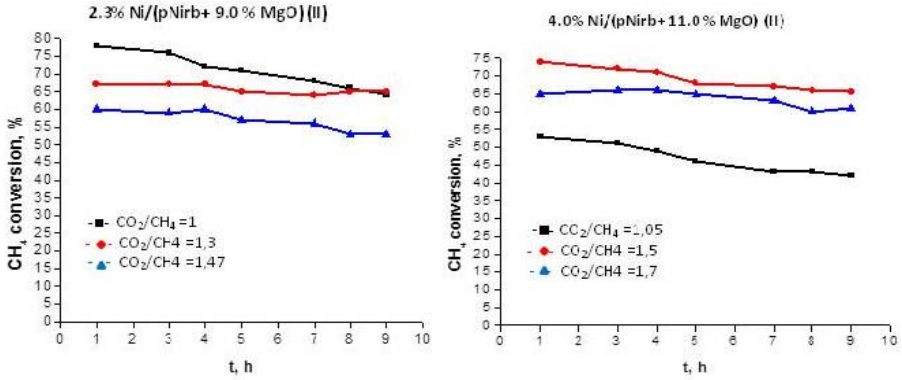

Fig.2. Methane conversion versus time-on-stream in the dry reforming of CH_4 over the reduced nickel catalysts (p = 1 atm, T = 750°C, m_{cat} = 0,40 g, V = 25 l/h) at various CO_2/CH_4 ratios.

The catalytic tests of supported nickel catalysts showed that for the catalyst 2.3% Ni/(pNirb+ 9.0 % MgO) (II) at CO_2/CH_4 ratio = 1,3 in the reaction mixture and for the catalyst 4.0% Ni/(pNirb+ 11.0 % MgO) (II) at CO_2/CH_4 ratio = 1,7 the conversion of methane was stable during the test period (Fig.2). In agree with HRTEM data some part of dispersed nickel particles (3-10 nm) epitaxually bound with MgO underlayer were in the nickel catalysts tested in the dry reforming of CH_4. It should be noted that in the catalyst 4.0% Ni/(pNirb+ 11.0 % MgO) (II) at CO_2/CH_4 ratio = 1,7 some nickel particles were extracted from the MgO underlayer and their sintering took place in the supported nickel catalysts tested in reaction.

TEM data show that carbon filaments (d ~ 50 nm) were found in the supported nickel catalysts tested in the reaction.

4 Conclusions

The nickel catalyst based on porous nickel ribbon were prepared and studied in the dry reforming of methane. At the CO_2/CH_4 ratio = 1,3 for the catalyst 2.3% Ni/(pNirb+ 9.0 % MgO) (II) and at CO_2/CH_4 ratio = 1,7 for the catalyst 4.0% Ni/(pNirb+ 11.0 % MgO) (II) in the reaction mixture the activity was stable.

Acknowledgements

This work was supported by the Russian Foundation of Basic Research (grant 15-03-04001).

II-PP251

B18 Capabilities for XAS In Situ Experiments in Catalysis

Gianolio D.[1*], Cibin G.[1], Parry S.A.[1], Dent A.J.[1], Kroner A.B.[2], Gibson E.K.[3], Wells P.P.[3]

1 - Diamond Light Source Ltd, B18 beamline, Harwell Science and Innovation Campus, Didcot, UK
2 - Diamond Light Source Ltd, Idustrial Liaison Group, Harwell Science and Innovation Campus, Didcot, UK
3 - UK Catalysis Hub, RCaH, Harwell Science and Innovation Campus, Didcot, UK

* diego.gianolio@diamond.ac.uk

Keywords: *in situ* XAS experiments, combined spectroscopies

1 Introduction

A proper understanding of structural end electronical chracteristic of the active sites plays a central role in the design and discovery of novel catalysts. To achieve this goal it is important to be able to measure the materials under the same in-situ conditions of temperature, pressure, and atmosphere that they would experience in their performance environments. In order to facilitate such experiments, B18 beamline in collaboration with Industrial Liaison Group and Research Complex at Harwell has developed several sample environments that allow the remote control of temperature and gas flow through the sample, monitoring of the reaction products and the combination of several characterization techniques combined with X-ray Absorption Spectroscopy measurements.

2 Experimental/methodology

The element-selectivity of XAS and the capability to obtain information about both electronical configuration (XANES) and atomic structure in short range (EXAFS) make this technique a valuable tool to investigate the properties of catalysts. Furthermore the time resolution of few seconds that can be achieved with continuous scanning of the monochromator in quick EXAFS mode, allows following oxidation state or coordination geometry changes during a chemical reaction. For this reason a big effort has been put to develop sample environments that allow to perform reactions and a contemporaneous data acquisition and to control the reaction parameters remotely. Currently several options are available: a capillary reactor with hot air blower to measure powders, furnaces to measure sample in pellet form and liquid cells with cartridge heating to measure solutions. Furthermore a gas mixing rig setup formed by 8 mass flow controllers and 8-port valves provides the possibility to flow through the samples complex gas mixtures and to quickly alternate between oxidizing and reducing conditions by means of a fast switching valve. Finally a mass spectrometer can be connected to the outlet to monitor the reaction products coming out of the experimental cell.

Moreover, experience shows that considerable value is added to the XAS experiment if it is possible to combine techniques to obtain complementary informations. Therefore a mythen detector is available to measure x-ray diffraction at the same time increasing the understanding on the long range order in the sample and monitoring the changes between different crystalline or amorphous phases and the formation/destruction of intermediate species during the reaction. Recently In collaboration with the Catalysis Hub the B18 team has successfully incorporated the first Raman/XAS and DRIFTS/XAS systems on the beamline. Thus it is now possible to combine the electronical and structural information provided by XAS with vibrational information achievable by Infrared or Raman Spetroscopy which can play a main role in understanding the interactions of the gases with the material.

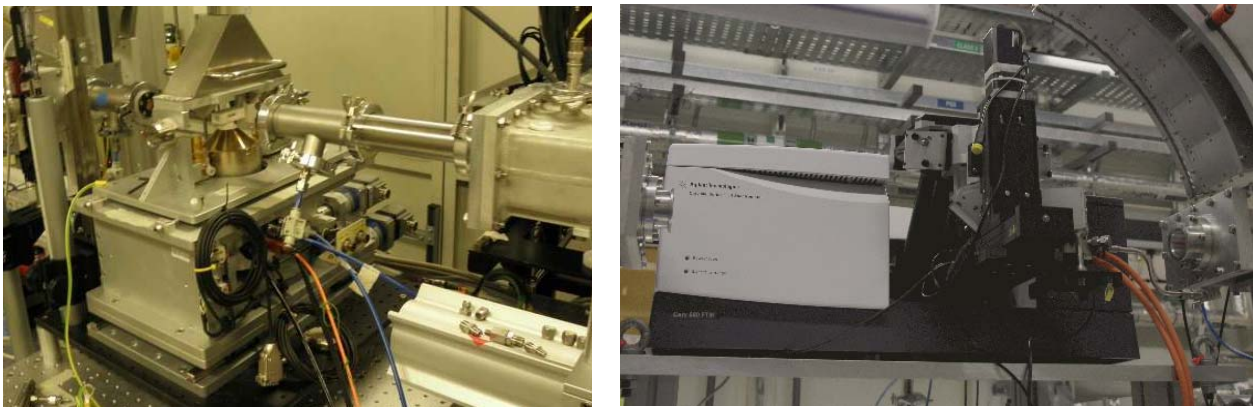

Fig. 1. a) Capillary reactor with hot air blower, on the B18 beamline b) FTIR spectrometer with Da Vinci arm and Harrick DRIFTS cell attached, on the B18 beamline.

3 Conclusions

B18 beamline at Diamond Light Source have recently developed in collaboration with Industrial Liaison Group and Research Complex at Harwell sample environments which allow the in situ study of catalysts and combination of X-ray absorption spectroscopy, diffraction and other spectroscopic techniques such as IR and Raman. B18 sum up the time resolution (in the order of few seconds) provided by quick-EXAFS scanning mode with the integrated control of catalytic conditions in capillary reactor, furnaces or heated liquid cells. A gas mixing rig setup is available to allow introducing complex gas mixtures in situ and a Mass Spectrometer to monitor the reaction products.

II-PP252

Methane and Propane Oxidation over Pd(111): Temperature Hysteresis, Induced by Oxide Formation

Matveev A.V.[1,2*], Kaichev V.V.[1,2], Saraev A.A.[1], Knop-Gericke A.[3], Bukhtiyarov V.I.[1,2]

1 - Boreskov Institute of Catalysis of the Siberian Branch of the Russian Academy of Sciences, Novosibirsk, Russia

2 - Novosibirsk State University, Novosibirsk, Russia

3 - Department of Inorganic Chemistry, Fritz Haber Institute of the Max Plank Society, Berlin, Germany

* matveev@catalysis.ru

Keywords: palladium, propylene, oxidation, temperature hysteresis

1 Introduction

Palladium is used in various catalytic applications because of its high intrinsic activity and its relatively low price compared with other noble metals. In particular, Pd-based catalysts are used for the purification of automotive exhaust gases that contain significant amounts of unburned fuel and other hydrocarbons formed by pyrolysis. Many studies have been devoted to the combustion of hydrocarbons over Pd-based catalysts [1-2]. However, the mechanism for the oxidation of hydrocarbons over palladium is still not fully understood. The mechanism is complex and the catalyst activity and selectivity are influenced by variations in the process pressure, temperature, and the gas mixture composition. Moreover, under oxidizing conditions, Pd-based catalysts can exhibit an interesting dynamic behavior, including hysteresis phenomena, self-sustained rate oscillations, spatial pattern formation, and deterministic chaos; a fast deactivation of palladium is frequently observed as well [4-13]. It is obvious that in all these cases a change in the chemical state of palladium determines the catalytic performance, causing the critical phenomena or catalyst deactivation. To develop more-effective Pd-based catalysts with a high activity in a wide temperature range, the reasons that cause these phenomena have to be understood.

2 Experimental/methodology

The TPRS and XPS experiments were carried out at the synchrotron radiation facility, BESSY II (Berlin, Germany) using the ISISS (Innovative Station for *In Situ* Spectroscopy) beamline. The experimental station was described in detail elsewhere [14]. Its key feature is a differentially pumped electrostatic lens system of a hemispherical analyzer, which allows analysis of the sample in the low mbar pressure region.

3 Results and discussion

During TPRS studies the presence of thermal hysteresis has been revealed. TPRS profiles obtained during the heating exhibit peaks of CO, CO_2, H_2 and H_2O formation with a maximum near 700 K, while during the cooling peaks are absent. According to *in situ* XPS data, the peaks of products of complete and partial oxidation of methane during the heating is determined by the formation of a surface layer of PdO. This is confirmed by the appearance in the spectra of Pd$3d_{5/2}$ intense peak at 336.65 eV at 673 K, the intensity of which increases significantly after heating to 723 K. Further heating to 823 K leads to the recovery of palladium, the surface of the Pd(111) is partially covered by a layer of surface oxide Pd_5O_4 characterized by the Pd$3d_{5/2}$ peak at 335.55 eV. Subsequent cooling to 723 K does not lead to the formation of PdO, and as a result, the cooling curve in the TPR spectra has no peaks at all. It is important to note that the

activity of PdO in a small excess of oxygen (CH_4:O_2 = 1:2.5) at 700 K exceeds the activity of metallic palladium, partially or completely covered by the surface oxide Pd_5O_4 at 850 K. This fact clearly indicates that the PdO is more active in the reaction of complete oxidation of methane than palladium in metallic state. The obtained data are in good correlation with earlier observed oxide formation during methane oxidation [15, 16]

Oxidation of propane. The influence of the reaction media resulted in a significant surface reconstruction of palladium: before starting the experiments, the surface of the single crystal was mirrored, after heating in the reaction mixture, the surface became opaque due to significant changes in roughness. In accordance with the TPRS experiments, both in excess and in deficiency of oxygen H_2, CO, H_2O and CO_2 were observed as the products of reaction. Propylene, acetone, acetaldehyde and acetic acid were not observed. TPR spectra for the ratio C_3H_8:O_2 = 1:5 and 1:25 show that the reaction starts at 650-700 K, the main product is CO. In the excess of oxygen the conversion of propane decreases, and the release of H_2 significantly reduces, being oxidized to H_2O. TPRS data and XPS spectra obtained in the step-wise heating in the reaction media at C_3H_8:O_2 =1:1 show that the reaction starts on PdO covered surface, which reduces with increasing temperature to Pd_5O_4.

4 Conclusions

In the reactions of oxidation of saturated hydrocarbons (methane and propane) on Pd(111) it was found that the active component of the catalyst is a three-dimensional palladium oxide PdO, which formation is a prerequisite for activation of the catalyst.

Acknowledgements

The financial support of Grant of President of Russian Federation for government support of Leading Scientific Schools (grant SS-5340.2014.3) and Support of the Russian Science Foundation (grant 14-23-00146) is highly appreciated.

References

[1] D. Ciuparu, M.R. Lyubovsky, E. Altman, L.D. Pfefferle, A. Datye, Catal. Rev.–Sci.Eng.44(2002) 593
[2] K. Eguchi, H. Arai, Appl. Catal. A 222 (2001) 359.
[3] Y. Deng, T.G. Nevell, J. Mol. Catal. A 142 (1999) 51.
[4] G.W. Graham, D. König, B.D. Poindexter, J.T. Remillard, W.H. Weber, Top. Catal. 8 (1999) 35.
[5] X. Zhang, C.S.-M. Lee, D.M.P. Mingos, D.O. Hayward, Appl. Catal. A 240 (2003) 183.
[6] V.Yu. Bychkov, Yu.P. Tyulenin, M.M. Slinko, V.N. Korchak, Catal. Lett. 141 (2011) 602.
[7] P. Salomonsson, S. Johansson, B. Kasemo, Catal. Lett. 33 (1995) 1.
[8] J.-D. Grunwaldt, N. van Vegten, A. Baiker, Chem. Commun. (2007) 4635.
[9] G. Centi, J. Mol. Catal. A 173 (2001) 287.
[10] H. Gabasch, E. Kleimenov, D. Teschner, S. Zafeiratos, M. Hävecker, A. Knop-Gericke, R. Schlögl, D. Zemlyanov, B. Aszalos-Kiss, K. Hayek, B. Klötzer, J. Catal. 242 (2006) 340.
[11] H. Gabasch, A. Knop-Gericke, R. Schlögl, W. Unterberger, K. Hayek, B. Klötzer, Catal. Lett. 119 (2007) 191.
[12] H. Gabasch, K. Hayek, B. Klötzer, W. Unterberger, E. Kleimenov, D. Teschner, S. Zafeiratos, M. Hävecker, A. Knop-Gericke, R. Schlögl, B. Aszalos-Kiss, D. Zemlyanov, J. Phys. Chem. C 111 (2007) 7957.
[13] V.V. Gorodetskii, A.V. Matveev, E.A. Podgornov, F. Zaera, Top. Catal. 32 (2005) 17.
[14] A. Knop-Gericke, E. Kleimenov, M. Hävecker, R. Blume, D. Teschner, S. Zafeiratos, R. Schlögl, V.I. Bukhtiyarov, V.V. Kaichev, I.P. Prosvirin, A.I. Nizovskii, H. Bluhm, A. Barinov, P. Dudin, M. Kiskinova, Adv. Catal. 52 (2009) 213.
[15] R.S. Monteiro, D. Zemlyanov, J.M. Storey and F.H. Ribeiro, J. Catal. 201 (2001) 37
[16] J. Han, D. Zemlyanov, F.H. Ribeiro, Cat. Tod. 117 (2006) 506

II-PP253

Copper Oxides (I, II) as Catalytic Precursor in C-S Cross-Coupling Reactions

Panova Y.[1], Kashin A.[2], Vorobev M.[3], Ananikov V.[1,2*]

1 - Saint-Petersburg State University, Institute of Chemistry, Saint-Petersburg, Russia
2 - N.D. Zelensky Institute of Organic Chemistry, Russian Academy of Sciences, Moscow, Russia
3 - Saint-Petersburg State University, Saint-Petersburg, Russia

* val@ioc.ac.ru

Keywords: cross-coupling, copper, oxide, catalyst, morphology, polymeric, complex

1 Introduction

Methods of C-S bond formation are valuable tools in the synthetic chemistry. Copper oxide-mediated Ullmann reaction is one of the important and wide spread technique for this purpose [1, 2]. Despite the huge number of known protocols in the field of Cu_2O- or CuO-catalyzed C-S cross-coupling reactions still it is not obvious what is exactly happened with copper oxides during catalytic reaction.

2 Experimental/methodology

Detailed NMR, ESI-MS, FE-SEM, cryo-SEM, DLS, XRD patterns studies were carried out to evaluate the role of the copper center, its oxidation state and arrangement. Ligand-free copper oxides (I, II)-catalyzed reactions of thiophenol with 4-iodotoluene were chosen as a model reactions.

3 Results and discussion

In order to study the impact of the size and shape of CuO and Cu_2O in the coupling reaction a set of copper oxide nanoparticles was synthesised. There is no size and morphology influence of catalyst on sulfides yields. It is worth to note the CuO and Cu_2O surface dramatically changes after catalysis. It was revealed Ph-SH-nucleophile has strongly effected on the shape of catalyst. The treatment of copper oxides with thiophenol results in formation of polymeric homoleptic copper (I) phenylthiolate $[CuSPh]_n$ (figure 1) [3]. Use of stoichiometric amount of $[CuSPh]_n$ and 4-iodotoluen leads to formation of desirable product of C-S cross-coupling. Moreover polymeric copper(I) complex shows catalytic activity.

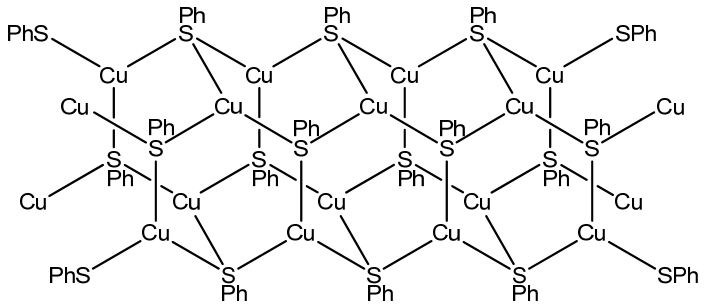

Fig. 1. Schematic drawing of polymeric complex $[CuSPh]_n$.

4 Conclusions

Indeed, whatever the copper source Cu(I) or Cu(II), copper (I) complex is the active catalyst [4]. Herein we demonstrate that CuO and Cu_2O are the precursor of Cu(I)-thiolate active complex in ligand-free C-S cross-coupling reaction.

Acknowledgements

P.Y. acknowledges Saint-Petersburg State University for postdoctoral fellowship (12.50.1560.2013).

The research was supported by research centres "Magnetic Resonance Research Centre", "Centre for X-ray Diffraction Studies", "Chemical Analysis and Materials Research Centre", "Centre for Optical and Laser Materials Research", "Nanotechnology Interdisciplinary Centre", "Molecular and cell technologies centre" of St. Petersburg State University.

References

[1] L. Rout, T. K. Sen, T. Punniyamurthy, *Angew.Chem.Int.Ed.* 46 (2007) 5583.
[2] K. Reddy, V. Reddy,A. Kumar, G. Kranthi, Y.V.D. Nageswar, Beilstein J. Org. Chem. 7 (2011) 886.
[3] C.-M. Che, C.-H. Li, S. S.-Y. Chui, V. A. L. Roy, K.-H. Low, *Chem. Eur. J.* 14 (2008) 2965.
[4] A. Casitas, X. Ribas, *Chem. Sci.*, 4 (2013) 2301.

II-PP254

Nature and Structure of Extraframework Al Species in Zeolite: NMR Study on Selective H/D Exchange between Bronsted Acid Sites and Benzene

Al-Mutairi S.[1], Mezari B.[2], Magusin P.[3], Pidko E.[2], Hensen E.[2*]

1 - SABIC, Oxygenates & Aromatics Global Technology, Jubail, Saudi Arabia
2 - Schuit Institute of Catalysis, Laboratory of Inorganic Materials Chemistry, Eindhoven University of Technology, Eindhoven, The Netherlands
3 - University of Cambridge, Department of Chemistry, Cambridge, UK

* e.j.m.hensen@TUE.NL

Keywords: faujasite, zeolite, extraframework, Al, acidity, H/D exchange, NMR

1 Introduction

Zeolite Y has the faujasite topology and is widely used as an acid catalyst for hydrocracking processes in oil refineries. However, because of the high concentration of aluminium in the lattice of as-synthesized zeolite Y, it exhibits only weak acidity and limited hydrothermal stability. Both the acidity and hydrothermal stability of such zeolites can be improved by dealumination. Ultrastable zeolites Y (USY) are typically prepared by steam calcination of the low-silica NH_4Y zeolite at high temperature. During this process, part of the Al atoms (FAl) are extracted from their framework positions. The intrinsic Brønsted acidity of the resulting dealuminated zeolite is usually higher than that of the parent material because of the increased concentration of isolated aluminum framework (AlF) atoms. The Al atoms extracted from the framework are part of the extraframework aluminium (EFAl) phase. These species are thought to strongly influence the acidity and reactivity of steam-calcined faujasite zeolites.

2 Experimental/methodology

Commercial Steam-calcined zeolite EFAl (USY) and free-EFAl dealuminated zeolite (AHFSY) was used in this study. Dealuminated Y zeolite, AHFSY was prepared by treatment with $(NH_4)_2SiF_6$ (AHFSY). The USY and AHFSY zeolites were first heated to 500 ^oC at a heating rate of 2 ^oC/min and then kept at this temperature for dehydration overnight at a total pressure of less than 10-5 mbar. The dehydrated samples were deuterated by exposure to 10 mbar D_2O gas for 30 min at 150 ^oC, followed by evacuation. This procedure was repeated two times and, finally, the samples were evacuated at 450 ^oC overnight.

Benzene (C_6H_6) H/D exchange was done by loading the deuterated D-USY and D-AHFSY in a 4-mm zirconia NMR rotor in a glove box under N_2 atmosphere. The rotor was placed in a glass tube, connected to the manifold setup and evacuated for 2 hours. Thereafter, the tube containing the sample rotor was cooled to -40 ^oC and the sample was brought in contact with 4 mbar benzene gas for 1 min. The rotor was then tightly closed with a boron nitrate cap and transferred, under low temperature conditions, to the precooled (-30 ^oC) NMR probe.

3 Results and discussion

The effect of extraframework Al (EFAl) species on the Brønsted acid sites in steam-calcined USY zeolite was studied by in situ H/D exchange between benzene and deuterated zeolite using NMR spectroscopy. The spectroscopic results in combination with model periodic density functional theory calculations indicate that EFAl species are preferentially stabilized in the faujasite sodalite cages in the form of multinuclear oxygenated and hydroxylated cationic Al

clusters. No direct interaction between adsorbed benzene and EFAl is observed. The H/D exchange reaction involves only the zeolite Brønsted acid sites (BAS), whereas the AlOH and SiOH moieties due to zeolite defects remain intact upon contacting with benzene. A much higher reactivity of BAS is observed for the EFAl-containing USY zeolite. An important finding is that in the absence of EFAl species NH_4Y zeoilite treated by ammonium hexafluorosilicate (AHFS-Y), all BAS are equally reactive towards C_6H_6, whereas in the case of USY zeolite, the rates of H/D exchange with the sodalite cage hydroxyl groups is much higher than with the accessible supercage BAS Fig.1. This evidences the selective enhancement of only a fraction of zeolitic BAS neighbouring the Lewis acidic extraframework Al species stabilized inside faujasite sodalite cages.

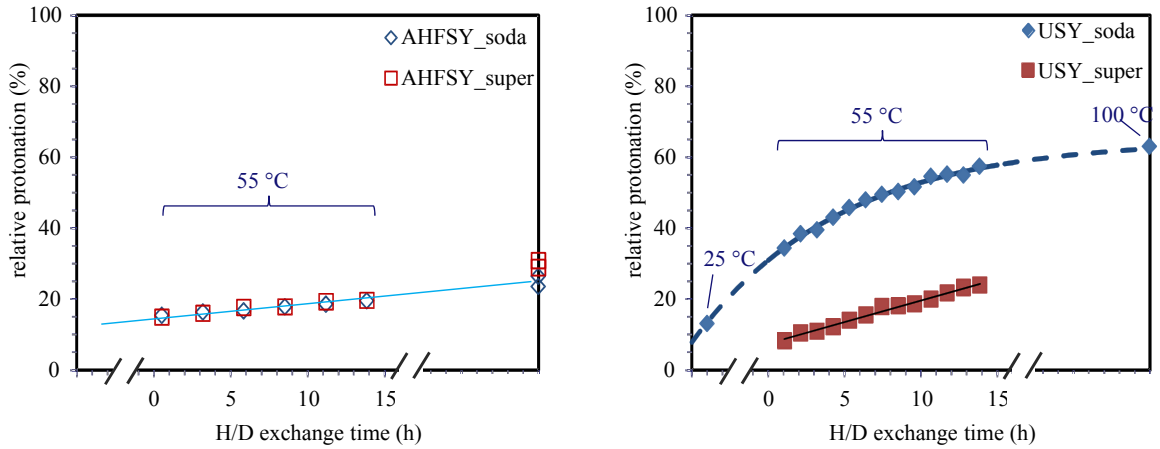

Figure 1. Plots of the relative protonation of hydroxyl sites in AHFSY (left) and USY (right) proton NMR spectra, recorded at 55 °C during H/D exchange of D-USY with C_6H_6.

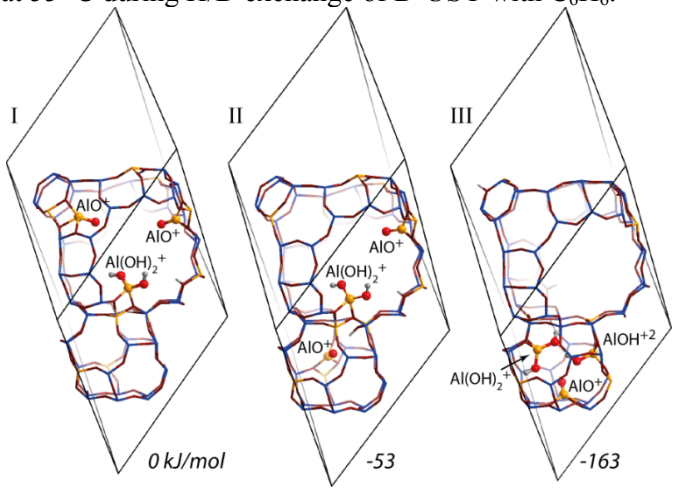

Figure 2. Optimized structures of HUSY-8 models with all EFAl species present as isolated mononuclear cations located in (I) faujasite supercage only, (II) both sodalite cage and supercage and (III) exclusively faujasite sodalite cage. Relative stabilities (italic) are given for all structures in kJ/mol with respect to the model (I) having all isolated mononuclear EFAl species stabilized exclusively at the supercage cation sites.

II-PP255

Catalytic Performance in Isopropanol Decomposition over $H_{3+X}PMO_{12-X}V_XO_{40}$ Heteropolyacids Supported on Mesoporous Molecular Sieve HMS

Salhi N.[1,2*], Benadji S.[2], Boudjeloud M.[2], Saadi A.[2], Rabia C.[2]

1 - Laboratoire LCPMM, Département de Chimie, Faculté des Sciences, U.Blida, Blida, Algérie
2 - Laboratoire de Chimie du Gaz Naturel, Faculté de Chimie, USTHB, Alger, Algérie

* nas.salhi@yahoo.fr

Keywords: heteropolyacid, mesoporous, silica, isopropanol decomposition

1 Introduction

Molybdenum and vanadium containing heteropolyacids (HPAs), $H_{3+x}PMo_{12-x}V_xO_{40}$ (x =0-3) are widely known to possess a strong Brönsted acidity and redox ability. The substitution of one or more molybdenum atoms in the primary structure of the Keggin anion by vanadium atoms leads to an enhancement of the oxidation potential of the HPA. However, owing to their small surface area (<10 m^2/g), their catalytic performances are limited. Many studies have been carried to overcome this drawback by supporting HPAs on suitable mesoporous materials (HMS, MCM-41, SBA-15 …). Such compounds offer high thermal stability, large surface area and high pore volume.

The objective of this work is to support 30 wt.% $H_{3+x}PMo_{12-x}V_xO_{40}$ (x=0-3) Keggin-type heteropolyacids on mesoporous HMS silicate material and evaluate their catalytic properties in isopropanol decomposition reaction.

2 Experimental

30wt.% $H_{3+x}PMo_{12-x}V_xO_{40}$ (x=0-3) HPAs were supported on HMS by dry impregnation method. Several physico-chemical techniques(elemental analysis, X-ray diffraction, transmission and diffuse reflectance (DR) FT-IR, Raman and X-ray photoelectron spectroscopies, nitrogen physisorption, thermal analysis (TG-DTA) and scanning electron microscopy (SEM)) were used to characterise fresh catalysts. The catalytic performances of supported HPAs were compared to those of pure one and tested in the isopropanol decomposition reaction to propene, diisopropylether and acetone products at 75°C and atmospheric pressure.

3 Results and discussion

The physico-chemical characterization of the supported HPAs showed mainly undegraded primary Keggin structure and high dispersion of heteropolyacids on the HMS surface. The BET surface area (S_{BET}) and the pore volume (Vp) of HMS decrease strongly in the presence of HPAs. The TG-DTA analysis showed that the obtained mesostructures HPA-HMS have a higher thermal stability than the HPA bulk. $H_{3+x}PMo_{12-x}V_xO_{40}$ heteropolyacids with x=0-3 supported on mesoporous HMS appear to be more active than $H_{3+x}PMo_{12-x}V_xO_{40}$ on bulk.

Otherwise, the substitution of molybdenum by vanadium atoms gives higher activity in isopropanol decomposition to propene, diisopropylether and acetone reaction especially for $H_4PMo_{11}V_1O_{40}$.

II-PP256

Speciation of Extraframework Aluminium Species in Faujasite Zeolite: a Theoretical Perspective

Liu C., Li G., Hensen E.J.M., Pidko E.A.*

Inorganic Materials Chemistry group, Eindhoven University of Technology, Eindhoven, The Netherlands

* e.a.pidko@tue.nl

Keywords: aluminium, self-organization, acidity, DFT

1 Introduction

Zeolite Y with faujasite topology is widely used as acidic catalyst for fluid catalytic cracking (FCC) and hydrocracking in the oil refinery [1]. The catalytic activity of zeolite Y strongly depends on its Brønsted acidity. However, the as-synthesized faujasite with high Al concentration in its lattice framework only shows low Brønsted acidity and stability. Further steaming calcination to form extraframework Al-containing (EFAL) species in the zeolite matrix can significantly improve its catalytic activity and hydrothermal stability [2]. The enhancement of Brønsted acidity of the steamed zeolite is often associated with the synergy between the EFAL species and neighbouring Brønsted acid sites (BAS) in zeolite pores [3]. However, the nature of these EFAL species and their intrinsic interaction mechanism with BAS are still not understood well yet. In this study, the structure, stability and location of EFALs in faujasite zeolite have been thoroughly investigated by a comprehensive periodic DFT method combined with *ab initio* thermodynamic analysis. The dominated EFAL species at the experimental conditions of catalyst activation were identified based on these investigations.

2 Methodology

DFT calculations were performed using VASP. The PBE functional and dispersion-corrected DFT-D2 was used. The electron-ion interactions were described with projected augmented waves method. The Brillouin zone sampling was restricted to the Γ point. The energy cut-off was set to 500 eV. The EFAL was introduced in different cationic sites, and full geometry optimizations were performed with fixed cell parameters. The convergence was assumed to be reached when the forces on each atom were below 0.05 eV Å-1.

3 Results and discussion

The mononuclear EFALs may potentially be present in faujasite matrix as cationic species, e.g. $[Al(OH)_2]^+$, $[AlO]^+$, $[Al(OH)]^{2+}$, and Al^{3+} neutral complexes e.g. $Al(OH)_3(H_2O)_3$, $Al(OH)_3$, and AlOOH. The neutral EFALs show no significant preference towards specific location in faujasite structure. For the cationic complexes, a direct interaction with lattice charge-compensating $[AlO_2]^-$ units is necessary for their high stability. The stability of $[Al(OH)_2]^+$ interactive with single framework $[AlO_2]^-$ does not depend on Al distribution in the framework. The cationic species bearing a higher formal charge, e.g. $[Al(OH)]^{2+}$ and Al^{3+} show a strong preference for the stabilization in a supercage SII site.

We further considered the self-organization of mononuclear EFAL to multinuclear clusters (Figure 1). The assembly of two or three separated $[Al(OH)_2]^+$ into $[Al_2O_4H_4]^{2+}$ or $[Al_3O_6H_6]^{3+}$ is strongly thermodynamically favored (ΔE = -87 and -79 kJ/mol, respectively). The self-organization of AlOOH into $[Al_4O_6]$ is also highly exothermic (ΔE = -175 kJ/mol). Although the binuclear EFAL complexes shows similar stability at faujasite's supercage and sodalite cage, a strong preference for the migration into small sodalite cages has been identified for larger tri-

and tetranuclear cations. The $[Al_2O_4H_4]^{2+}$, $[Al_3O_6H_6]^{3+}$ and $[Al_4O_6]$ clusters can be transformed to other types of multinuclear clusters by dehydration and proton transfer processes with the assistance of vicinal BAS. The dehydration is always strongly endothermic, while the energetics of proton transfer reactions is controlled by the electronic properties of the target EFAL.

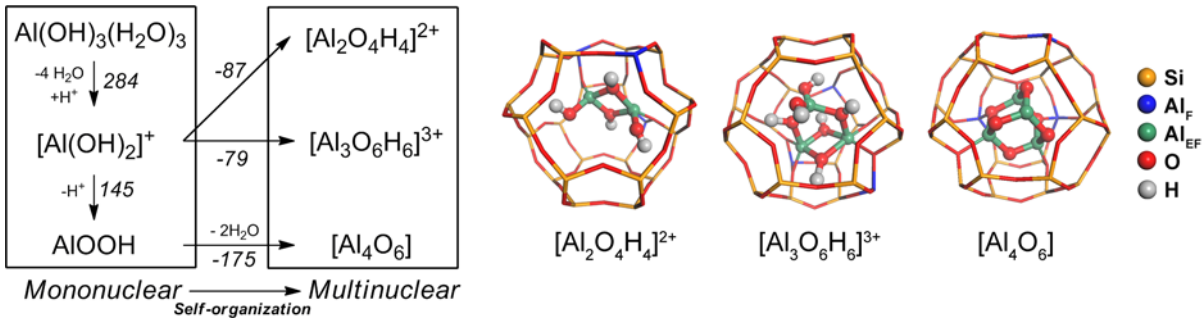

Figure 1. Interconversion of EFALs in faujasite zeolite.

To clarify the effect of temperature and the presence of water on the stability of EFALs, a statistical thermodynamic method is used. Under the typical experimental condition of hydrothermal treatment (800 K, 1 atm), the trinuclear $[Al_3O_4H_4]^{4+}$ stabilized in sodalite cage shows the highest stability. However, the reaction free energy differences among different multinuclear clusters are not very significant which indicates their stabilities are very close and different multinuclear EFALs can coexist or interconvert with each other in the system. The multinuclear EFALs with large cluster size show strong preference for the sodalite cage, which provides a better confined environment for the stabilization of these clusters due to its smaller void compared to the supercage. It is proposed that the multinuclear oxygenated and hydroxylated cationic clusters located in sodalite cage are the dominant EFAL species in faujasite zeolite. These multinuclear EFAL species may act as hubs for the proton transfer and thereby tune the charge equilibrium and modify the acidity and reactivity of zeolite.

4 Conclusions

The structural property and stability of EFALs in faujasite zeolite are studied by periodic DFT calculations combined with *ab initio* thermodynamics. The results point to a strong preference of mononuclear EFALs towards self-organization into multinuclear species. This effect is shown to be a general phenomenon for a wider range of oxygenated extraframework cations and zeolite topologies. The resulting tri- and tetra-nuclear clusters are preferentially located in sodalite cages of the faujasite structure. A*b initio* thermodynamic analysis points to the predominant formation of such species under experimentally relevant conditions. It is proposed that multinuclear oxygenated and hydroxylated EFALs located in sodalite cage are dominant species in faujasite zeolite after high-temperature steaming treatment.

Acknowledgements

The authors would like to thank the China Scholarship Council (CSC) for financial support. NWO-NCF (SH-170) is acknowledged for providing access to the supercomputer facilities.

References

[1] A. Primo, H. Garcia, *Chem. Soc. Rev.* 43 (2014) 7548.
[2] S. M. T. Almutairi, E. A. Pidko, E. J. M. Hensen et al., *ChemCatChem* 5 (2013) 452.
[3] S. Li, C. Ye, F. Deng et al., *J. Am. Chem. Soc.* 129 (2007) 11161.

II-PP257

Preparation and Characterization of Sr, Ca and Mg Doped Ceria Electrolyte for Solid Oxide Fuel Cells

Çalış B., Özdemir H., Sarıboğa V., Öksüzömer M.A.F.*

Department of Chemical Engineering, Istanbul University, Istanbul, Turkey

* fufu@istanbul.edu.tr

Keywords: fuel cell, sofc, electrolyte, doped-CeO_2

1 Introduction

Fuel cell systems are the fundamental subject of energy technologies which provide most important part of energy requirement of the world [1]. Amongst them, polymer electrolyte membran (PEM) and solid oxide (SOFC) fuel cells have come forth due to their advantages []. In these fuel cells, the most important part is electrolytes which effects fuel cell performance substantially. The most important problem in SOFC systems is the requirement of high temperatures (>800°C) in order to obtain high ionic conductivity with traditional electrolyte materials (i.e. 8YSZ) [2]. Thus, development of new electrolyte materials those give high ionic conductivity with stable performance at lower temperatures than 800°C is highly important. It is known that rare earth metals (Sm, Gd, Nd) doped CeO_2 structures show superior ionic conductivity, but they have a high cost [3]. Hence in this study cheap, readily accessible and which may be stable at lower temperatures Mg, Sr and Ca doped CeO_2 electrolytes were prepared and characterized. These compounds were prepared by citrate–nitrate combustion method and characterized by using XRD, SEM and impedance spectroscopy.

2 Experimental/methodology

Different amounts of Sr, Ca and Mg included cerium oxide electrolyte synthesized by using citrate nitrate combustion method. Starting chemicals used for the synthesis of powders were ceria oxide, magnesium nitrate, calcium nitrat, strontium nitrate, and citric acid. The appropriate amounts of cerium nitrate hexa hydrate, metal nitrates and deionized water were dissolved in 50 ml aqueous solution in which total metal ion concentration is 1 M. The solution was vigorously mixed and vaporized on an hot plate at 70°C, whereupon it became a transparent gel. The gel was heated until it turned into a black viscous mass, which on continued heating burned due to a vigorous exothermic reaction. Pale-yellowish ashes obtained after combustion were treated at 250°C. Obtained powders were calcined at 1400°C for 5h. The product was pressed into pellets and finally the pellets were sintered at 1400°C for 10h.

3 Results and discussion

In pre-experiments of this study, at two different concentrations (%5 and %10) of Sr doped ceria electrolyte were prepared. According to XRD results(Figure 1), no impurity peaks were observed in x = 0.05, and it is clear that there is precipitation of a second phase SrO in addition to the fluorite phase for composition with x> 0.10, in the present work. Therefore, future studies will focus on 0.05<x<0.1 Sr content.

Figure 2 shows SEM photographs of the sintered samples 1400°C. The surface photographs of electrolyte pellets sintered at 1400 °C show good densification, as shown in Figure 2 (a) and (b).

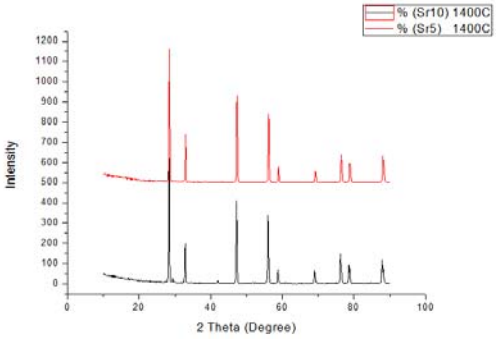

Figure 1. XRD patterns of the % 5 and % 10 Sr doped ceria

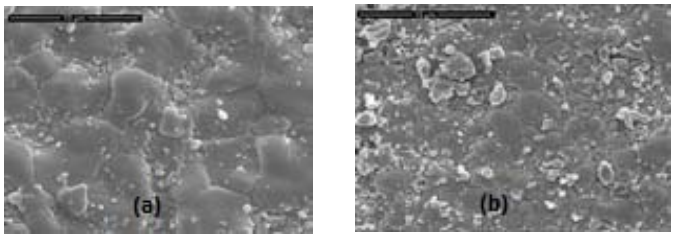

Figure 2. Surface SEM images of electrolyte sample pellets, sintered at different molar ratio of Sr (a) %5 (b) %10.

No pores are present on the surface of the pellets, which is in accordance with the relative density of the sintered pellets and beneficial for the oxygen ion transportation of the electrolyte

The O^{2-} ionic conductivities of two samples were measured by electrochemical impedance spectroscopy technique. For %5 Sr doped ceria 2.85 S m^{-1} and for %10 Sr doped ceria1.4 S m^{-1} conductivities were measured at 800 ^{o}C. Since %10 Sr doped ceria sample includes SrO insulator phase (shown in XRD pattern) which was not dissolved in ceria main phase, the conductivity of %5 Sr doped ceria shows almost two times better conductivity value than %10 Sr doped ceria. Also, %5 Sr doped ceria shows higher performance than %10 Gd doped ceria materials when compared our previous studies [8] .

4 Conclusions

In preliminary studies, the resulting conductivity results are promising. The same experiment will be done for Ca and Mg electrolytes. We will be found that CaO, MgO, SrO could not dissolve into the ceria matrix after the exact value. And conductivity of the electrolyte is measured at the exact value. Other conclusions are going to be presented at EuropaCat XII.

References

[1] YU, ZHIQIANG, 2007, *Transient Studies of Ni-,Cu Based Electrocatalysis in CH4 Solid Oxide Fuel Cell,* L, Thesis (PhD),The University of Akron

[2] STAMBOULI A.B., TRAVERSA, E., 2002, Solid oxide fuel cells (SOFCs): a review of an environmentally clean and efficient source of energy, *Renewable and Sustainable Energy Reviews* ,6 (2002) 433–455

[3] Liu YY, Li B, Wei X (2008) Citric-nitrate combustion synthesis and electrical conductivity of the Sm3+ and Nd3+ co-doped ceria electrolyte. *J Am Ceram Soc* 91:3926–3930

[4] Arai H, Kunisaki T, Shimizu Y, Seiyama T (1986) Electrical properties calcia doped ceria with oxygen ion conduction. *Solid State Ionics* 20:241-248

[5] Xu, Q., Huang, D.-P., Chen,W., Lee, J.-H.,Wang, H. andYuan, R.-Z., Citrate method synthesis, characterization and mixed electronic–ionic conduction properties of La0.6Sr0.4Fe0.2Co0.8O3 perovskite-type complex oxides. *Scr. Mater.*, 2004, 50, 165–170.

[6] Hernandez, T. and Bautista, M. C., The role of the synthesis route to obtain densified TiO2-doped alumina ceramics. *J. Eur. Ceram. Soc.*, 2005, 25, 663–672.

[7] Epifani, M., Melissano, E., Pace, G. and Schioppa, M., Precursors for the combustion synthesis of metal oxides from the sol–gel processing of metal complexes. *J. Eur. Ceram. Soc.*, 2007, 27, 115–123.

[8] M.A.Faruk Öksüzömer, Göknur Dönmez, Vedat Sariboğa, Tuba Gürkaynak Altinçekiç, Microstructure and ionic conductivity properties of gadolinia doped ceria electrolytes for intermediate temperature SOFCs prepared by the polyol method, *Ceramics International* 39 (2013) 7305–7315.

II-PP258

From *In situ* to *Operando* Mode: Experience on Synchrotron X-Ray Diffraction at SSTRC

Shmakov A.[1,2*], Vinokurov Z.[1,2], Saraev A.[1,2], Kaichev V.[1,2]

1 - Boreskov Institute of Catalysis SD RAS, Novosibirsk, Russia
2 - Novosibirsk National Research State University, Novosibirsk, Russia

* A.N.Shmakov@inp.nsk.su

Keywords: X-ray diffraction, synchrotron, radiation, heterogeneous, catalyst, structure, phase, composition

1 Introduction

The X-ray diffraction (XRD) technique seems to be main source of information on the atomic structure and phase composition of functional materials, including heterogeneous catalysts. In contrast to the conventional XRD that describes structure under static conditions, the dynamical studies of the phase and structure transformations under high temperature and reaction environment look much more attractive. Time resolution of these experiments which are usually carried out with synchrotron radiation (SR XRD) rises to submicrosecond range. Most of catalytic processes have relatively low rates and one surely doesn't need such an excellent resolution. The principal advantage of SR XRD for heterogeneous catalysis is the ability to detect structure evolution of catalyst *In Situ* within the reactor cell under reaction conditions [1]. Equipping the reactor cell with gas analyzer on the inlet and outlet of the cell one can register also activity and selectivity of catalyst along with its structure and phase composition. This is an approach to *Operando* mode. However, difficulties may arise on this way.

2 Experimental

At Siberian Synchrotron and Teraherz Radiation Center XRD experiments are executed on five beamlines, one of them is mostly dedicated to studies of catalysts and catalytic processes. The beamline consists of fixed energy monochromator with set of Si and Ge crystals which determine working photon energies, and position sensitive X-ray detector providing simultaneous registration of XRD patterns in 2Θ angular range of 30°. High temperature reactor cell mounted on the diffractometer allows the experiments with oxidation or reduction environment over the sample at temperature range from room up to 900°C and gas pressure from 0.1 mbar to 10 bars to be performed.

To analyze the gas phase composition and therefore to estimate the efficiency of catalyst the quadrupole mass-spectrometer SRS UGA-100 is attached to outlet port of reactor cell. The instrumental configuration described has been applied for several experiments including self-oscillations of the reaction rate in oxidation of methane over metal catalysts, growth of nitrogen doped carbon nanofibers from ethylene-ammonia mixture over Ni-Cu alloy catalyst, etc. The results of these attempts with respect to *Operando* mode realization are considered in the report.

3 Results and discussion

Transformation of *In Situ* to *Operando* experimental mode is intended to simulate within the laboratory reactor cell the behavior of catalyst under real working conditions including the efficiency of catalyst with respect to different gas parameters (reaction mixture composition, gas pressure, gas flow rate, etc). The first experiments with *Operando* mode detected good correlations of phase composition of catalyst with gas phase content of product. Nevertheless, it

is hardly possible to estimate the conversion of initial reagents since the products are strongly diluted with initial reagents at the outlet port of reactor. It may be caused by cell volume which is much greater then sample volume, and even the conversion is high, the portion of target product in mixture is rather low whereas gas analyzer registers total ratio of components. Although the molar amount of gas and solid components are of same order of magnitude, small surface area of solid makes total conversion to be small.

The arrangement of gas flow to penetrate through the sample should be a solution in this case. It is good idea for powder sample but looks impossible when the sample is a piece of foil. Another way is to develop a reactor cell with small volume but problems may arise with uniform heating of sample and with cell windows that should be heat, pressure and reaction medium resistant and transparent for X-rays. Perhaps there should be more permanent solution.

4 Conclusion

Finally, simple attachment of gas analyzer to reactor cell isn't enough for *Operando* mode to be realized. Besides that, the first experiments on SR XRD applying *Operando* mode have demonstrated that it seems hardly possible to use any universal reactor cell for different tasks as it is widely spread for *In Situ* experiments. To succeed in *Operando* studies one should create for individual task an individual cell, which however could be suitable for solving of other problems as well.

Acknowledgement

The work is supported by Russian Science Foundation, grant No. 14-23-00037.

References

[1] K.T.Møller, B.R.S.Hansen, A.-C.Dippel, J.-E. Jørgensen, T.R.Jensen, *ZAAC*. 640 (2014) 3029.

II-PP259

Mechanistic Insights into CO Oxidation and Preferential CO Oxidation over Cobalt Oxide and Promoted Cobalt Oxide Catalysts

Lukashuk L.[1*], Kolar E.[1], Rameshan C.[1], Teschner D.[2], Knop-Gericke A.[2], Föttinger K.[1], Rupprechter G.[1]

1 - Institute of Materials Chemistry, Vienna University of Technology, Vienna, Austria
2 - Department of Inorganic Chemistry, Fritz-Haber-Institute of the Max-Planck-Society, Berlin, Germany

* liliana.lukashuk@tuwien.ac.at

Keywords: CO oxidation, preferential CO oxidation, *operando* XAS, *operando* NAP-XPS

1 Introduction

In recent years much attention has been paid to the development of catalysts for CO oxidation and preferential CO oxidation (PROX) that are able to lower the temperature required for CO oxidation. In particular, Co_3O_4 has turned out to be a promising catalyst[1]. Interestingly, its combination with noble metals or other reducible oxides, e.g. CeO_2, has enhanced the catalytic activity [2-4]. However, the origin of this enhancement as well as the nature of the active sites and reaction mechanisms is not fully understood, mainly because current understanding of this reaction system is mostly based only on ex situ analyses of the catalysts and kinetic experiments[1,4]. Therefore, comprehensive in situ/operando studies on the structural and electronic changes of cobalt oxide and promoted cobalt oxide are crucial.

In the present work, we combined operando infrared spectroscopy (IR), in situ near ambient pressure X-ray photoelectron spectroscopy (NAP-XPS) and operando X-ray absorption spectroscopy (XAS) to study the structural and electronic changes of catalysts with the aim to understand the promotional effect of PdO and CeO_2 on the activity of Co_3O_4 in the CO oxidation and PROX, the nature of the active sites of the catalysts and the reaction pathways.

2 Experimental/methodology

Surface sites of the catalysts, i.e., 10 wt% CeO_2 on Co_3O_4, 2 wt% of PdO on Co_3O_4, and Co_3O_4, were investigated by operando IR spectroscopy and in situ NAP-XPS. In situ NAP-XPS was performed at the ISISS beamline at BESSY II in Berlin, Germany. The O1s, Co2p, C1s, Ce3d, Pd3d core-levels were recorded under working conditions; the total pressure was kept at 0.50 mbar. Operando XAS at the Co K edge and the Ce L_3 edge were performed at the l811 beamline at the MAX-lab II in Lund, Sweden. The temperature-dependent CO oxidation, PROX and the steady-state experiments were also performed in a fixed-bed flow reactor and an operand IR flow cell.

3 Results and discussion

Our operando IR spectroscopy results show that CO does not adsorb on Co^{3+} and Co^{2+} ions of Co_3O_4 catalyst but forms surface carbonate species (bidentate and monodentate), while during CO oxidation (CO/O_2=1/2) and PROX ($CO/O_2/H_2$=1/1/50) the amount of the carbonates decreases. We detected carbonate formation upon exposure of Co_3O_4 to CO also in NAP-XPS measurements (C1s at 288.2 eV). In addition, we observed elementary carbon at the surface (C1s binding energy at 284.7 eV) which indicates that Co_3O_4 dissociates CO already at RT ($2CO \rightarrow CO_2 + C$) depositing carbon at the surface. Interestingly, no significant reduction of Co_3O_4 was observed at RT. Upon heating the Co_3O_4 in CO atmosphere to 200 °C the elementary carbon

grows, and Co_3O_4 starts to get reduced (Fig.1). During the CO oxidation reaction (CO/O_2=1/2) over Co_3O_4 only a small amount of carbonates and carbon is observed between RT and 150 °C with NAP-XPS. Thus, a possible mechanism of CO oxidation proceeds via CO disproportionation or carbonate formation. The deactivation of Co_3O_4 at RT seems to be rather related to elementary carbon deposition than to the reduction of Co^{3+} to Co^{2+}. Interestingly, during PROX (CO/O_2/He=1/1/12) only slight cobalt reduction was observed even at 300 °C with in situ NAP-XPS, and formation of carbonates and elementary C likewise to CO oxidation on Co_3O_4 was detected. The low reducibility of Co_3O_4 in PROX reaction compared to pure H_2 that was revealed by in situ NAP-XPS and operando-XAS might exclude the Mars-van-Krevelen mechanism (redox mechanism) for PROX on the Co_3O_4.

Promotion of Co_3O_4 with PdO decreases the temperature of CO oxidation for PdO/Co_3O_4 ($T_{50\%}$ = 74 °C) compared to Co_3O_4 ($T_{50\%}$ = 105 °C). According to our in situ NAP-XPS experiments, Pd^{4+} species beside Pd^{2+} are present under reaction conditions (CO/O_2=1/2). In the C1s region we observed elementary carbon (284.7 eV) and carbonates (288.2 eV) that indicates CO dissociation during CO oxidation on PdO/Co_3O_4. Operando FTIR shows that on the PdO/Co_3O_4 a surprisingly small amount of CO was adsorbed to Pd upon CO exposure at RT and did not grow further with increasing temperature, whereas no CO peaks at all were observed during the reaction with carbonates being the only surface species present. Promotion of Co_3O_4 with CeO_2 increases the activity in PROX compared to pure Co_3O_4; selective oxidation of CO to CO_2 starts at 100 °C, when the reduction of Ce^{4+} to Ce^{3+} is observed by the Ce 3d XPS.

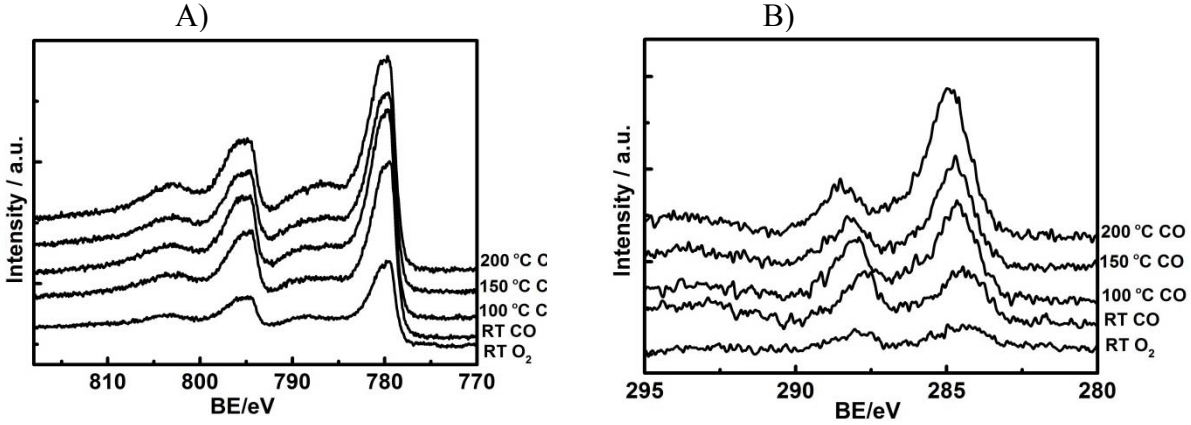

Fig. 1. XPS spectra of Co_3O_4 during CO adsorption: A) Co2p (hv=1015 eV), B) C1s (hv=465 eV)

4 Conclusions

Promotion of Co_3O_4 with PdO and CeO_2 improves the catalytic activity of cobalt oxide catalyst by enhancing CO adsorption and O_2 activation. A possible mechanism of CO (preferential) oxidation proceeds via CO disproportionation or carbonate formation.

Acknowledgements

This work was supported by the Austrian Science Funds (FWF) in the framework of the Doctoral School "Building Solids for Function" (Solids4Fun, project W1243). The authors acknowledge the beamtime granted at BESSY II at the ISISS beamline and support by the BESSY team and the beamtime granted at MAX-lab II at the l811 beamline.

References

[1] X. Xie, Y.Li, Z. Liu, M. Haruta, W. Shenm, *Nature* 458 (2009) 746.
[2] J. Yang, L. Lukashuk, J. Akbarzadeh, M.Stöger-Pollach, H. Peterlik, K. Föttinger, G. Rupprechter,U. Schubert, *Chem. Eur. J.* 21, 2 (2015) 885.
[3] K. An, S. Alayoglu, N. Musselwhite, S. Plamthottam, G. Melaet, A. Lindeman, G. Somorjai, *J. Am. Chem. Soc.* 135, 44 (2013) 16689.
[4] M. P. Woods, P. Gawade, B. Tan, U. S. Ozkan, *Appl.Catal. B* 97 (2010) 28.

Session III
"Energy-related catalysis"

III-OP01

Spinel Mn-Co Oxide in N-Doped Carbon Nanotubes as Bifunctional Electrocatalyst

Muhler M.[1,2*], Zhao A.[1,2], Xie K.[1,2], Masa J.[1,3], Xia W.[1,2], Schuhmann W.[1,3]

1 - Ruhr-University Bochum, Bochum, Germany
2 - Laboratory of Industrial Chemistry, Ruhr-University Bochum, Bochum, Germany
3 - Analytical Chemistry and Center of Electrochemistry, Ruhr-Universität Bochum, Bochum, Germany

* muhler@techem.rub.de

Keywords: carbon nanotubes, oxide, electrocatalysis, oxygen, reduction and evolution, reaction, bifunctional

1 Introduction

Decentralized supply of energy from renewable sources strongly relies on the efficient conversion and storage of energy in different forms, for example, in the form of H_2 by electrolysis of water and recovery of the energy during the reverse process in fuel cells, and in rechargeable metal air batteries. While the reversibility of the electrochemical reactions involving H_2 is efficient, the main challenge lies with improving the efficiency of the oxygen reduction reaction (ORR) and the oxygen evolution reaction (OER). Recently, transition metal-based catalysts such as Mn and Co oxides have attracted enormous interest as low-cost alternatives to noble-metal catalysts capable of catalyzing both the ORR and the OER. However, these oxides have high electrical resistance, which fortunately can be mitigated by the use of conductive additives such as graphene and carbon nanotubes (CNTs). In particular, N-doped carbon materials have been widely used not only to promote electron transfer but also to serve as complementary sites for the ORR thereby enhancing the ability of the materials to electrocatalyze both the ORR and the OER.

In this work, we demonstrate the synthesis of spinel Mn-Co oxide nanoparticles partially embedded in N-doped CNTs (NCNTs), which were used as bifunctional electrocatalysts for both ORR and OER under alkaline conditions. The synthesis was achieved by catalytic growth of NCNTs using Co-Mn oxides as catalyst and subsequent oxidative treatments.

2 Experimental

The synthesis of the spinel Mn-Co catalysts partially embedded in NCNTs was achieved by catalytic growth of NCNTs followed by oxidative treatment in the gas phase. Either Co-Mn-Mg-Al mixed oxide or Co-Mn mixed oxide were used as catalysts for the NCNT growth with pyridine or ethylenediamine as carbon and nitrogen precursors. The diameter of the obtained NCNTs ranges from 10 to 20 nm mostly. The catalyst nanoparticles exist in two different forms, either at the tip of the NCNTs or enclosed inside the NCNTs, where the nanoparticles are intimately in contact with carbon, or scattered over the NCNT agglomerates without intimate contact with the carbon surface due to explosion-like fragmentation of the initial catalyst particles during the rapid growth. Long-time washing of the NCNTs with dilute HNO_3 at room temperature removed the exposed metal species that were not in intimate contact with carbon. Subsequently, the washed NCNTs still containing the encapsulated catalyst nanoparticles were thermally treated under flowing air by moving the reactor into a heated furnace and withdrawing it from the heating zone after 5 min. This process causes opening and rupture of the CNTs through oxidation and thermal stress. Different temperatures from 300 to 600 °C were applied, and the heating process was repeated three times at each temperature. The obtained samples are designated as NCNT-300, NCNT-400, NCNT-500 and NCNT-600. In a separate experiment, the oxidative treatment was performed in HNO_3 vapor at

200 °C, which oxidizes both the residual growth catalysts and the NCNTs leading to a more hydrophilic surface.

3 Results and discussion

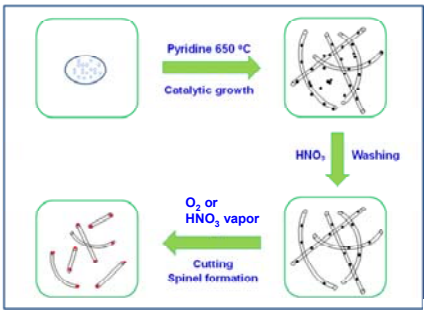

Fig. 1. The synthesis of spinel Mn-Co oxide nanoparticles partially embedded in NCNTs.(1) catalytic growth of NCNTs using the Co-Mn-Al-Mg catalyst; (2) removal of exposed catalyst nanoparticles with poor contact with carbon by washing in dilute HNO3; (3) formation of spinel oxide partially embedded in NCNTs by short exposure to air or HNO_3 vapor at elevated temperatures [1].

Fig. 1 illustrates the synthesis of the electrocatalysts. XRD and TEM studies confirmed the presence of Mn-Co spinel nanoparticles partially embedded in NCNTs. The electrocatalytic activity was evaluated in 0.1 M KOH with a catalyst loading of 210 µg cm^{-2}. The thermal oxidative cutting of NCNT drastically enhanced the ORR activity of the catalysts as indicated by the linear sweep voltammograms in Fig. 2a. Besides the nitrogen-modified carbon species, which are well known to catalyze the ORR, the spinel Mn-Co oxides formed by oxidative cutting are also expected to contribute active sites for the ORR. The ability of the obtained catalysts to catalyze both ORR and OER, that is, to serve as bifunctional catalysts, was investigated by RDE voltammetry and compared with the state-of-art catalysts: Pt/C (20% Pt on Vulcan carbon), RuO_2 and IrO_2. Studies of the OER revealed that NCNT-500 had the best activity (Fig. 2b). Remarkably, NCNT-500 showed higher ORR activity than IrO_2 and RuO_2 and very similar OER activity to RuO_2 (Fig. 2c). These results therefore underscore the huge potential of thermal oxidative cutting for synthesizing excellent bifunctional catalysts for oxygen electrodes.

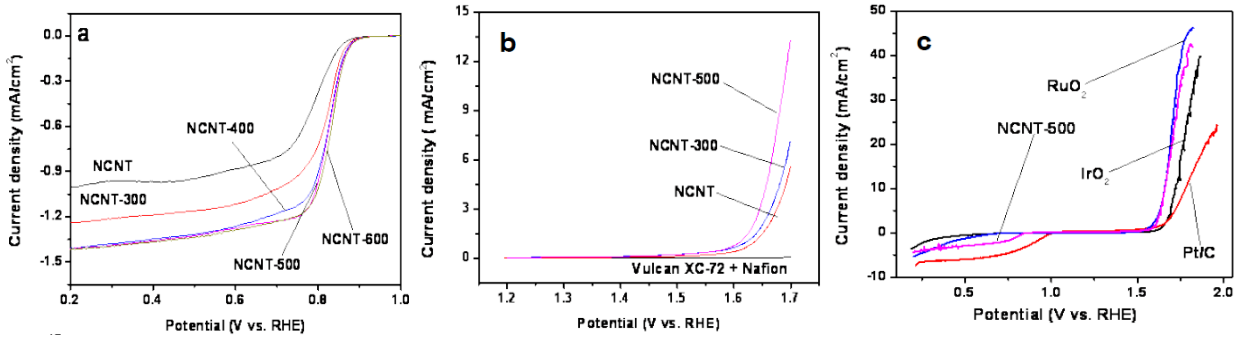

Fig. 2. (a) LSVs at 100 rpm and 5 mV s^{-1}; (b) OER current densities of blank experiment(Glassy carbon), NCNT, NCNT-300 and NCNT-500 at 1 mV s^{-1}; (c) ORR and OER activities of NCNT-500, Pt/C, IrO_2 and RuO_2 at a scan rate of 5 mV s^{-1}. Voltammograms recorded in O_2-saturated 0.1 M KOH.

4 Conclusions

Thermal oxidative treatment of catalytically grown NCNTs, in which residual Co and Mn oxide nanoparticles are buried, simultaneously ruptures the NCNTs and oxidizes the Co and Mn oxide nanoparticles forming spinel Mn-Co oxides nanoparticles partially embedded in the NCNTs. Due to a cooperative effect from the nitrogen groups in NCNT and the spinel Mn-Co oxide particles, the capability of the resulting catalysts to electrolyze both the ORR and the OER becomes tremendously enhanced producing exceptionally active bifunctional catalysts for reversible oxygen electrodes.

References

[1] A. Zhao, J. Masa, W. Xia, A. Maljusch, M. Willinger, G. Clavel, K. Xie, R. Schlögl, W. Schuhmann, M. Muhler, J. Am. Chem. Soc. 136 (2014) 7551.

III-OP02

Efficient Nanostructured InP Photocathodes for Water Reduction through Optimization of Interface Energetics and Structure

Gao L.[1], Hofmann J.P.[1], Bakkers E.P.A.M.[2], Emiel E.J.M.[1*]

1 - Laboratory of Inorganic Materials Chemistry, Department of Chemical Engineering and Chemistry Eindhoven University of Technology, Eindhoven, The Netherlands

2 - Photonics and Semiconductor Nanophysics, Department of Applied Physics, Eindhoven University of Technology, Eindhoven, The Netherlands

* l.gao@tue.nl

Keywords: photoelectrochemistry, water, splitting, buried, junction, antireflection, layer

1 Introduction

As solar energy is an intermittent energy source, energy harvested from the sun needs to be efficiently converted into chemical fuels that can be stored, transported, and used upon demand. The "Holy Grail" of solar energy conversion and storage is efficient photoelectrolysis of water using semiconductors to store solar energy in the simplest chemical bond, namely that of H_2. Indium Phosphide (InP) with a bandgap well-matched to the solar spectrum is a good candidate for photoelectrochemical (PEC) hydrogen production from water. The promise of this material is clear from the photo-conversion efficiencies (η) around 14 % for planar p-type InP (p-InP).[1,2] Herein, we show how the surface energetics and structures can be optimized towards efficiencies that compete with InP solar cells.

2 Experimental/methodology

A 1 µm-thick homoepitaxial, Zn-doped p-InP films was grown on a (100)-oriented InP wafer by Metalorganic Chemical Vapor Deposition. A 200 nm-thick heavily doped n^+-InP film was grown on the top of InP epilayer to create a buried junction (pn^+-InP). A moth-eye-like antireflection layer was created on top of pn^+-InP substrate by soft nanoimprint lithography followed by Inductively Coupled Plasma Reactive Ions Etching. Photoelectrochemical measurements were performed in a three-electrode electrochemical cell with a saturated calomel reference electrode and a Pt foil counter electrode in 1 M $HClO_4$ electrolyte. I-V curves and electrochemical impedance spectroscopy were measured by an Autolab 302N. Mott-Schottky measurements were conducted at a frequency of 10 kHz with 10 mV ac amplitude. AM 1.5G illumination was provided by a 300 W Xenon Lamp with AM 1.5G filters (Newport). Pt was photoelectrochemically deposited from a solution of 10 mM H_2PtCl_6 at a constant potential of 0.3 V vs. SCE under AM 1.5G illumination. A deposition charge of 60 $mCcm^{-2}$ was controlled for both *p*-InP and pn^+-InP electrodes (abbreviated as *p*-InP/Pt and pn^+-InP/Pt, respectively).

3 Results and discussion

Interface energetics was changed by depositing a thin layer of highly doped n^+-InP on top of a p-InP substrate (pn^+-InP). This layer forms an ohmic contact with the electrolyte on one side and a p-n junction on the other side. X-ray photoelectron spectroscopy (XPS) and Mott-Schottky measurements prove that the band-edge shifted to positive potential after n^+-InP layer deposition in vacuum and in electrolyte, respectively. As a consequence, the onset potential (V_{os}) increases from 0.7 to 0.8 V (Figure 1).

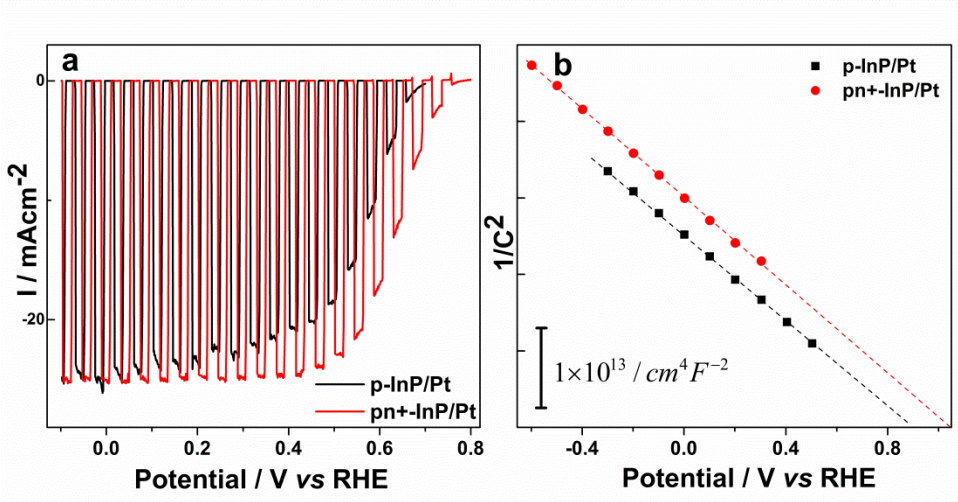

Fig. 1. (a) The current-potential (I-V) curves of *p*-InP/Pt (black line) and pn^+-InP/Pt (red line) photocathode in 1M $HClO_4$ under chopped AM1.5G illumination. (b) Mott-Schottky plots of *p*-InP/Pt (black squares) and pn^+-InP/Pt (red circles) photoelectrodes in 1M $HClO_4$ in dark. The linear fits of experimental data (solid lines) show a positive shift of band-edge after adding the n^+ layer.

The nanopillar arrays created as a moth-eye-like antireflection layer on top of pn^+-InP, are approximately 250 nm in diameter, 100 nm in height and arranged on a square lattice with center-to-center pitch of 500 nm (Figure 2). The total reflectance of pn^+-InP with antireflection layer is between 10 to 20% in the range of visible light, which is much lower than that of planar samples (above 30%). As a result, the short-circuit current (I_{sc}) of pn^+-InP_{AR} increases up to 28 $mAcm^{-2}$. Taken together, these modifications led to a photoelectrode efficiency of 15.5%, which is the highest η for water reduction by single-junction PEC cells so far.

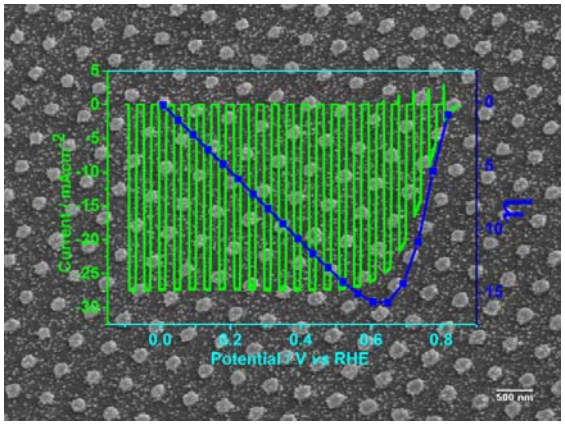

Fig. 2. 45°-tilt SEM image and I-V/efficiency curves of pn^+-InP/Pt with moth-eye antireflection layer.

4 Conclusions

A recorded photocathode conversion efficiency of water reduction by single junction PEC cells was achieved through rational design of the interface energetics and structure.

Acknowledgements

This work is supported by a NWO-VICI grant and Biosolar cells program.

References

[1] Lee, M. H. *et al*. *Angew. Chem. Int. Edit.* 51 (2012) 10760-10764
[2] Munoz, A. G. *et al*. *ECS J. Solid State Sci. Technol.*, 2 (2013) Q51-Q58

III-OP03

Novel Photocatalysts Based on $Cd_{1-x}Zn_xS/Zn(OH)_2$: Activation during the Hydrogen Evolution from Aqueous Solutions of Ethanol

Kozlova E.A.[1,2,3*], Cherepanova S.V.[1,2,3], Markovskaya D.V.[1,2], Parmon V.N.[1,2]

1 - Boreskov Institute of Catalysis SB RAS, Novosibirsk, Russia
2 - Novosibirsk State University, Novosibirsk, Russia
3 - Educational Center for Energoefficient Catalysis in Novosibirsk State University, Novosibirsk, Russia

* kozlova@catalysis.ru

Keywords: photocatalysis, hydrogen, production, $Cd_{1-x}Zn_xS$

1 Introduction

Rapid depletion of natural raw hydrocarbons (oil, gas, and coal) determines an acute need to identify and develop alternative energy sources [1]. The unique properties of hydrogen make it a versatile and environmentally friendly chemical energy carrier, suitable for use in all types of heat engines and power generation devices. The photocatalytic splitting of water using the energy of visible part of solar light is a very attractive way for the hydrogen production. In recent years, there has been a tendency to use available organic substances as electron donors for the photocatalytic hydrogen evolution. The application of organic substances as electron donors is more advantageous from a practical point of view because most of water pollutants are organic compounds, and the production of hydrogen in this case can be combined with the purification of water. To the best of our knowledge, there are only few articles that describe photocatalytic evolution of hydrogen from aqueous solutions of organic compounds under visible light. Recently, we showed that composite photocatalysts $Pt/Cd_{1-x}Zn_xS/ZnO/\varepsilon\text{-}Zn(OH)_2$ possess a significant activity in the hydrogen evolution from aqueous solutions of ethanol and the photocatalytic activity grows with the content of $\varepsilon\text{-}Zn(OH)_2$ [2]. However, zinc hydroxide is believed to have a low stability in the photocatalytic process. Thus, the aim of present research was to study the stability of composite photocatalysts $Pt/Cd_{1-x}Zn_xS/ZnO/\varepsilon\text{-}Zn(OH)_2$ in the hydrogen evolution under visible light.

2 Experimental/methodology

The composite photocatalysts $Pt/Cd_{1-x}Zn_xS/ZnO/\varepsilon\text{-}Zn(OH)_2$ were synthesized according to the method described in detail elsewhere [2].

Photocatalytic hydrogen evolution from ethanol aqueous solution was carried out by the following method. The aqueous suspension with the catalyst and substrate was placed in a sealed reactor, purged with Ar and illuminated by a 450-nm LED (40 mV/cm^2) under continuous stirring. The photocatalyst concentration was 0.5g/L, C_2H_5OH concentration was 10% (vol.), NaOH concentration was 0.1M, temperature was 20 °C. Hydrogen was analyzed by means of gas chromatography.

3 Results and discussion

Fig. 1a shows four consecutive runs of hydrogen evolution for four photocatalysts A-D. The properties and activities of photocatalysts A-D are represented in Table 1.

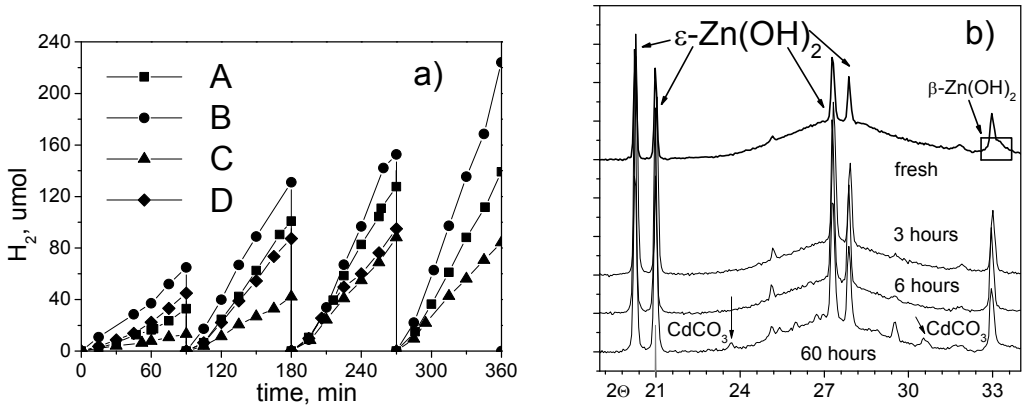

Fig. 1. Kinetics of the hydrogen evolution for photocatalysts A-D (a) and the transformation of XRD patterns of photocatalyst A during the hydrogen production (b).

Table 1. The properties and the activities of the synthesized photocatalysts.

Photocatalyst	**Phase composition after 6 h of reaction**	**Initial rate, μmol (H_2)/min**	**Highest rate, μmol (H_2)/min**	**Φ**
A $Cd_{0.6}Zn_{0.4}S$/ZnO/ε-β-$Zn(OH)_2$	$Cd_{0.6}Zn_{0.4}S$/ZnO/ε-$Zn(OH)_2$	0.54	1.70	9.4
B $Cd_{0.8}Zn_{0.2}S$/ZnO/β-$Zn(OH)_2$	$Cd_{0.8}Zn_{0.2}S$/ZnO/ε-$Zn(OH)_2$	0.72	2.63	14.5
C $Cd_{0.6}Zn_{0.4}S$/ ZnO/β-$Zn(OH)_2$	$Cd_{0.6}Zn_{0.4}S$/ZnO/ε-$Zn(OH)_2$	0.18	1.04	5.7
D $Cd_{0.5}Zn_{0.5}S$/ZnO/β-$Zn(OH)_2$	$Cd_{0.5}Zn_{0.5}S$/ZnO/ε-$Zn(OH)_2$	0.75	1.07	5.9

One can see that the rate of H_2 evolution grows with the cycle number for all photocatalysts. Thus, instead of deactivation of the photocatalysts, their activation is observed. Long-term experiments for photocatalyst A shows that the deactivation is achieved after 60 h of H_2 evolution only. XRD patterns of photocatalysts after each cycle of the hydrogen production were obtained. Fig. 1b shows the XRD pattern of fresh photocatalyst A as well as patterns of this photocatalyst after 3, 6, and 60 h of the reaction. One can observe that the content of ε-$Zn(OH)_2$ grows with the reaction time until 6 hours and then remains practically unchanged. Additionally, the $CdCO_3$ peaks appear in the XRD pattern after 60 h of reaction. For photocatalyst B, C, and D the appearance of the ε-$Zn(OH)_2$ phase after 6 h of the reaction is obsereved. XRD analysis shows that for all photocatalysts the β-$Zn(OH)_2$ phase is transformed into the ε-$Zn(OH)_2$ one during the photocatalytic reaction. The highest achieved photocatalytic activity was 2256 μmol H_2 g^{-1} h^{-1}; the estimated highest quantum efficiency (Φ) was 14.5% in respect to 450 nm.

4 Conclusions

Novel composite photocatalysts Pt/$Cd_{1-x}Zn_xS$/ZnO/$Zn(OH)_2$ with a high activity under visible light were proposed. The activation of the photocatalyst during the photocatalytic hydrogen evolution from alkaline aqueous solutions of ethanol was observed. The activation is likely caused by formation of ε-$Zn(OH)_2$ in a basic media.

Acknowledgements

The work was performed with support of the Skolkovo Foundation (Grant Agreement for Russian educational organization №1 on 28.11.2013), RF President Grant (МК-3141.2015.3) and RFBR (research project No. 15-33-20458 mol_a_ved).

References

[1] K.I. Zamaraev, V.N. Parmon, Catal. Rev. Sci. Eng. 22 (1980) 261.
[2] E.A. Kozlova, D.V. Markovskaya, S.V. Cherepanova, A.A. Saraev, E.Yu. Gerasimov, T.V. Perevalov, V.V. Kaichev, V.N. Parmon, Int. J. Hydrogen Energy 39 (2014) 18758.

III-OP04

The Role of Co-Catalysts in Photoelectrochemical versus Photocatalytic Water Splitting: CoO_x on $LaTiO_2N$

Landsmann S., Mägli A., Pokrant S.*, Trottmann M.

Laboratory Materials for Energy Conversion, Dübendorf, Switzerland

* simone.pokrant@empa.ch

Keywords: hydrogen, renewable, fuel, photoelectrochemical, water splitting, photocatalytic water splitting, co-catalyst

1 Introduction

Since the demonstration of photocatalytical water splitting by Fujishima and Honda using TiO_2 in 1972 [1], the idea to produce environmentally friendly fuel by direct conversion of solar energy into hydrogen gained increasing attention. During the last years this trend became even stronger, especially since the growing awareness about the damaging effects of greenhouse gas emissions combined with the knowledge of the limited availability of fossil energy resources like oil or coal triggered an intensive search for alternatives. Shining light on a photocatalyst leads to absorption of photons and the generation of electron-hole pairs. The generated holes and electrons, that escape recombination, diffuse and migrate to the surface of the photocatalyst particle and are consumed by the oxidation of O^{2-} to O_2 or the reduction of H^+ to H_2, respectively [2]. Hydrogen has the potential to serve as next generation fuel [3]. For this purpose the implementation of water splitting in a technological large-scale solution is desirable. Several concepts have been proposed [4]: One of them is the use of photocatalytically active particles to produce H_2 and O_2, while the photocatalyst particles are either suspended in a liquid or deposited on a film. Another concept is based on the photoelectrochemical (PEC) cell in which oxidation and reduction take place on physically separated electrodes, with the advantage that the evolving gases can be separated more easily. Today, solar light is often used to produce O_2 on the photoanode [2], while the cathode can be either photocactive or a standard electrode (mostly Pt) for H_2 production. One of the well-studied photocatalysts for O_2 production (photoanode) is $LaTiO_2N$ (LTON) [2]. To enhance the performance of the photocatalyst co-catalysts were used in both, photocatalytic and the photoelectrochemical setups. For O_2 evolution Co oxides were found to be very active co-catalysts []. However, it is not entirely clear, whether co-catalysts act on the kinetics of the oxygen evolution reaction or facilitate the charge separation process by enhancing the band bending at the solid-electrolyte interface. In this contribution, we investigate whether CoO_x co-catalysts deposited on LTON (LTON/Co) serve the same function in a photocatalytic setup compared to a photoelectrochemical setup. For this purpose we compare the photocatalytic and the photoelectrochemical activity of four morphologically different LTON and LTON/Co samples.

2 Experimental/methodology

The preparation and characterization of LTON, LTON/Co and the photocatalytic activity measurements were conducted as published previously []. LTON is synthesized in four different morphologies called PC-LTON, SS-LTON, PC-LTON-FX and SS-LTON-FX, which vary in particle size, surface area and crystalline quality. These morphologies are treated with $Co(NO_3)_2$ leading to the samples PC-LTON/Co, SS-LTON/Co, PC-LTON-FX/Co and SS-LTON-FX/Co. The LTON and LTON/Co photoanodes were fabricated by electrophoretic deposition and necked as described in [8]. The PEC measurements were conducted in a three electrode configuration with the LTON film as working electrode, an Ag/AgCl (3M) reference electrode and a Pt wire as counter electrode. The

experimental details are listed in [8]. Photocurrents were acquired on a VersaSTAT 4 potentiostat at a scan rate of 10mV/s under backside illumination.

3 Results and discussion

Figure 1a shows the photocatalytic activity of LTON and LTON/Co measured by oxygen evolution of particles suspended in a scavenger solution containing $AgNO_3$, while Figure 1b displays the PEC activity of LTON and LTON/Co represented by the photocurrent obtained at a bias of $1.23V_{RHE}$. For bare LTON samples the photocatalytic and the PEC activity are

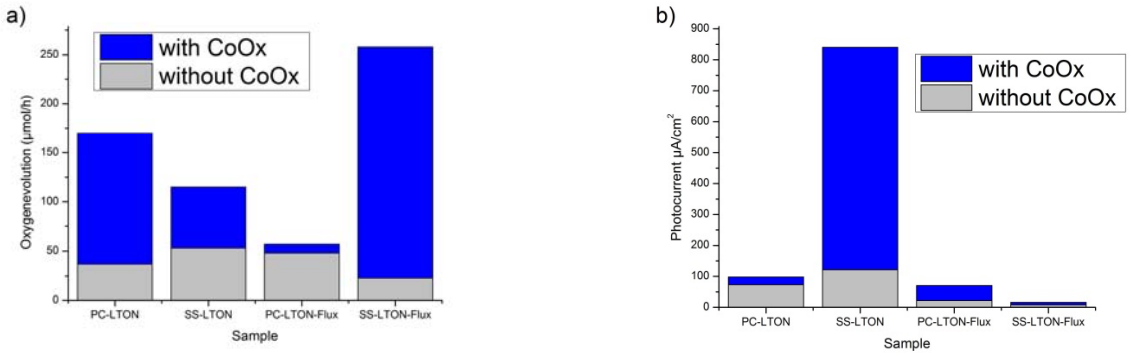

Fig. 1. a) photocatalytic activity versus b) PEC activity of LTON and LTON/Co samples

are comparable, while the effect of Co addition results in a highly different increase for both processes. The enhancement of the photocatalytic activity correlates to the surface area of the CoO_x co-catalyst nanoparticles, while for PEC electrodes large co-catalyst particles are favourable.

4 Conclusions

Our results clearly demonstrate that the co-catalyst CoO_x on LTON does not induce the same effect, if LTON/Co is used in photocatalysis or as PEC electrode. In photocatalytical experiments the co-catalysts seems to lower the kinetic barrier, while we propose that it induces enhanced band bending in the PEC case.

Acknowledgements

The Swiss National Science Foundation is gratefully acknowledged for funding this research via the PrecoR project 20PC21_155667.C. Battaglia is thanked for proof-reading.

References

[1] A. Fujishima and K. Honda, Nature 238 (1972) 37.
[2] T. Hisatomi, J. Kubota and K. Domen, Chem. Soc. Rev. 43 (2014) 7520.
[3] Y. Tachibana, L. Vayssieres and J. R. Durrant, Nature Photonics 6 (2012) 511.
[4] B. A. Pinaud, J. D. Benck, L. C. Seitz, A. J. Forman, Z. Chen, T. G. Deutsch, B. D. James, K. N. Baum, G. N. Baum, S. Ardo, H. Wang, E. Miller and T. F. Jaramillo, Energy Environ. Sci. 6 (2013) 1983.
[5] F. F. Abdi, L. Han, A. H. M. Smets, M. Zeman, B. Dam and R. van de Krol, Nat Commun 4 (2013).
[6] A. E. Maegli, S. Pokrant, T. Hisatomi, M. Trottmann, K. Domen and A. Weidenkaff, J. Phys. Chem. C 118 (2014) 16344.
[7] S. Pokrant, M. C. Cheynet, S. Irsen, A. E. Maegli and R. Erni, J. Phys. Chem. C 118 (2014) 20940.
[8] S. Pokrant, A. Maegli, M. Trottmann, L. Sagarna, E. Otal, T. Hisatomi, L. Steier, M. Grätzel and A. Weidenkaff, edited by D. Jones, 4th European PEFC & H2 Forum 2013, Luzern, 2013. A09, 5.

III-OP05

Photocatalytic Overall Water Splitting Using Ga_2O_3 with Various Phase Compositions Loaded with Rh-Free Co-Catalysts

Muhler M.[1*], Weide P.[1], Busser G. W.[1], Mei B.[2], Lukic S.[3], Winterer M.[3]

1 - Laboratory of Industrial Chemistry, Ruhr-University Bochum, Bochum,Germany
2 - Department of Physics, Technical University of Denmark, Kongens Lyngby, Denmark
3 - Nanoparticle Process Technology, University of Duisburg-Essen, Duisburg, Germany

* muhler@techem.rub.de

Keywords: photocatalysis, gallium, oxide, water splitting, chemical vapor synthesis, noble metal-free co-catalysts

1 Introduction

Direct photocatalytic water splitting using inorganic semiconductor particles is a promising way to convert sunlight into chemical energy in addition to (photo)electrochemical methods [1]. Ga_2O_3 is one of the very few materials that has the ability to perform the simultaneous stoichiometric evolution of H_2 and O_2, i.e. the overall water splitting reaction, from pure H_2O. Although this oxide has a large band gap, it is highly suitable to evaluate the properties of novel co-catalyst materials and to study charge carrier separation processes in photocatalysts with various phase compositions and structures. An improved charge carrier separation at α/β-Ga_2O_3 phase junctions was recently reported for mixed-phase Ga_2O_3 loaded with NiO as a co-catalyst [2]. Additionally, the influence of different co-catalyst systems on the performance of the two main Ga_2O_3 structures was discussed [3]. The effect of the co-catalyst composition and loading on the overall water splitting has already been demonstrated by our group using the step-wise photodeposition of Rh and Cr on commercial β-Ga_2O_3 [4]. In this contribution phase-pure α- and β-Ga_2O_3 as well as mixed phase α/β-Ga_2O_3 photocatalysts were systematically synthesized and novel binary CuO_z/CrO_y [5] and ternary $CuO_z/CrO_y/MoO_x$ [6] non-noble metal co-catalyst systems were investigated.

2 Experimental

Ga_2O_3 photocatalysts were synthesized by chemical precipitation leading to α-GaOOH followed by subsequent calcination at various temperatures between 400 °C and 900 °C. Additionally, Ga_2O_3 was synthesized in the gas phase by chemical vapor synthesis (CVS) to obtain highly crystalline materials with very well defined nanoparticles. A quantitative determination of the phase composition was achieved by X-ray diffraction and Rietveld refinement. UV-vis spectroscopy was used to determine the band gap of the materials. The synthesized samples were tested in overall water splitting using the co-catalyst systems mentioned above synthesized by photodeposition. Photocatalytic direct water splitting was performed in a semi-continuous double-walled glass reactor with a 500 W Hg-lamp (inner irradiation type) connected to an on-line gas analyzer.

3 Results and discussion

Ga_2O_3 samples obtained by precipitation and subsequent calcination exhibit various phase compositions from α- to mixed α/β- to β-Ga_2O_3, whereas the commercial Ga_2O_3 and the materials obtained by CVS are pure β-Ga_2O_3. The results of the overall water splitting confirm a significant influence of the phase composition and crystalline structure on the charge carrier separation and the activity. Figure 1 shows the H_2 and O_2 evolution rates measured for Ga_2O_3 obtained by precipitation, CVS and a commercial β-Ga_2O_3 loaded with Rh(0.1 wt%)/CrO_y(0.09 wt%) as co-catalyst.

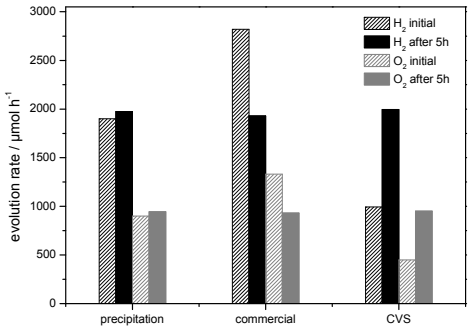

Fig. 1. H_2 and O_2 evolution rates for Ga_2O_3 obtained by precipitation, CVS and a commercial sample.

All samples produce H_2 and O_2 from pure H_2O in stoichiometric amounts. The precipitated and the CVS sample are highly active and stable during overall water splitting, whereas the commercial Ga_2O_3 significantly deactivates with time. Using a Cu_z/CrO_y co-catalyst on commercial Ga_2O_3 a maximum activity was observed for the composition CuO_z(0.66 wt% Cu)/CrO_y(0.09 wt% Cr)/β-Ga_2O_3. Different photodeposition procedures, in which the order of the CuO_x and CrO_y deposition was changed, show that the formation of a Cr_2O_3 shell on CuO_x cores is rather unlikely. Additional photodeposition of MoO_x renders the photocatalyst more active and regenerable.

4 Conclusions

Ga_2O_3 materials with various phase compositions and structures have been synthesized by precipitation and CVS and compared to commercial β-Ga_2O_3. A significant influence of the structural properties on the overall water splitting performance was determined. Synthesized Ga_2O_3 materials are as active or more active than commercial Ga_2O_3 and exhibit a significant higher stability. A ternary non-noble metal co-catalyst was found to be comparably active to a Rh-containing photocatalyst.

Acknowledgements

Financial support by the Mercator Research Center Ruhr (Mercur) and the Fonds der Chemischen Industrie (FCI) is gratefully acknowledged.

References

[1] A. Kudo, Y. Miseki, *Chem. Soc. Rev.* 38 (2009) 253-278.
[2] X. Wang, Q. Xu, M. Li, S. Shen, X. Wang, Y. Wang, Z. Feng, J. Shi, H. Han, C. Li, *Angew. Chem. Int. Ed.* 51 (2012) 13089-13092.
[3] Y. Sakata, T. Nakagawa, Y. Nagamatsu, Y. Matsuda, R. Yasunaga, E. Nakao, H. Imamura, *J. Catal.* 310 (2014) 45-50.
[4] G.W. Busser, B. Mei, M. Muhler, *ChemSusChem* 5 (2012) 2200-2206.
[5] G.W. Busser, B. Mei, A. Pougin, J. Strunk, R. Gutkowski, W. Schuhmann, M.-G. Willinger, R. Schlögl, M. Muhler, *ChemSusChem* 7 (2014) 1030-1032.
[6] G.W. Busser, B. Mei, P. Weide, P.C.K. Vesborg, I. Chorkendorff, K. Stührenberg, M. Bauer, X. Huang, M.-G. Willinger, R. Schlögl, M. Muhler, *submitted for publication*

III-OP06

Synthesis and Reactivity of Au/g-C_3N_4/TiO_2 Nanocomposites for Water-Splitting under Solar Light Illumination

Caps V., Keller N., Keller V., Marchal C.*

ICPEES, Institut de Chimie et Procédés pour l'Energie, l'Environnement et la Santé, CNRS/Université de Strasbourg, Strasbourg Cedex, France

* clement.marchal2@etu.unistra.fr

Keywords: photocatalysis, water-splitting, TiO_2, g-C3N4, gold, hydrogen, production

1 Introduction

Nowadays, the global energy demand continues to increase, in contrast to natural energy resources (fossil fuels) that decrease year by year. The major challenge is to find new environmentally friendly ways to produce energy that may cover the global consumption. The direct conversion of solar energy though an energy carrier (fuel), storable and usable upon request, appears as an interesting alternative [1]. Photocatalysis is an innovative and promising way to produce pure hydrogen from renewable energy sources. Indeed, the water dissociation (water-splitting) highlighted by Fujishima and Honda in a photoelectrocatalytic cell opened a promising way to produce hydrogen from light energy [2]. Hydrogen (H_2) is a selective energy carrier due to its high specific energy density [3].

In our study, we will focus on a photocatalytic titanium dioxide-based system (TiO_2), a cheap and common semi-conductor, associated with graphitic carbon nitride (g-C_3N_4). g-C_3N_4 appears as a very promising photocatalyst semi-conductor since it has been revealed that its band gap of 2.7 eV allows the valorization of an important part of the visible light spectra in the context of water splitting [4], contrary to the well studied TiO_2. Novel composite compounds such as Au/g-C_3N_4/TiO_2 will be synthesized and compared to the reference commercial titanium dioxide (Evonik, P25) and to titanium dioxide synthesized by a standard "sol-gel" process.

2 Experimental/methodology

Titanium dioxide (TiO_2) powder is obtained via a standard "sol-gel" process [5]. Firstly, titanium isopropoxide precursor [$Ti(OCH(CH_3)_2)_4$] was mixed with ethanol at room temperature. Then, water (adjusted to pH = 9 by addition of ammonia) was added dropwise to this solution. Secondly, the solution was evaporated under stirring until dry paste was obtained which was further dried overnight at 110°C. Then, the sample was thermal-treated for 3h in air at 400°C.

Graphitic-carbon nitride (g-C_3N_4) was obtained via a thermal polycondensation reaction of specific nitrogen-containing precursors [6]. First, an equimolar blend of melamine ($C_3H_6N_6$) and dicyandiamide ($C_2H_4N_4$) was mixed into an alumina covered crucible. The covered crucible was further heated at 550°C with a rate of 5°C/min during 3h.

g-C_3N_4/TiO_2 nanocomposites were obtained by introducing g-C_3N_4 (as synthesized) during the sol-gel synthesis of TiO_2 followed by a final calcination step at 400°C for 3h.

Gold nanoparticles were synthesized - directly onto the TiO_2, the g-C_3N_4 and the g-C_3N_4/TiO_2 support – by chemical reduction at room temperature of the $HAuCl_4$ precursor in an excess of $NaBH_4$ followed by final rinsing and filtration steps.

3 Results and discussion

From **Fig.1a** it can be observed that an homogeneous dispersion of well-defined spherical Au nanoparticles were obtained onto the g-C_3N_4 support. Au particles exhibited a monomodal distribution centered around 3,9 ± 0,9 nm. The same tendancy was observed with the TiO_2 and g-C_3N_4-TiO_2 (not shown here) supports. The Au deposition yield was higher than 80%.
A detailed study of the synthesis of g-C_3N_4/TiO_2 nanocomposites revealed modifications in their structural characterizations compared to the bare g-C_3N_4 and TiO_2 materials (**Fig.1b**). Without calcination, TiO_2 was entirely amorphous contrary to the composite which showed the presence of anatase phase of TiO_2 already at room temperature. However, XRD in temperature showed that in the composite, the crystallization of TiO_2 is unfavoured compared to pure TiO_2, accompanied by smaller crystallites sizes. To this, an increase of specific surface area (between 1.5 to 2 times higher than TiO_2) was also observed.

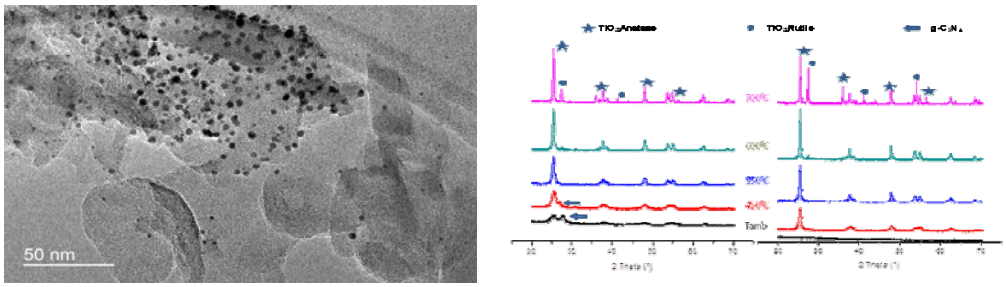

Figure 1: (a) TEM picture of Au/g-C_3N_4 sample; (b) XRD in temperature of 50wt.% g-C_3N_4/TiO_2 (left) and pure

Water-Splitting tests were carried out into a quartz reactor containing 900mL of Ultra-pure water and 250mg of sample under flowing N_2 at 100cc/min and irradiated with a 150 W halide lamp. Methanol (from 0.1 to 1 vol. %) was used as a sacrificial agent in order to increase yields of hydrogen production. The sample activity (amount of H_2 produced) was measured by a gas phase µGC. The first set of measurements of the activity of Au/g-C_3N_4 samples showed optimal gold concentration around 0.3wt.% with a hydrogen production yield of 25µmol/h after stabilization. Hydrogen production decreased to 15µmol/h for sample with 2% wt. gold. The first test on 0.3wt.%Au/50wt.%g-C_3N_4/TiO_2 composite showed a significant production of hydrogen. Compared to 0.3wt.% Au/TiO_2, a higher H_2 production is obtained (above 30 µmol/h) with 2 times less TiO_2.

4 Conclusions / Perspectives

The synthesis of new nanostructured composites allowed us to achieve better hydrogen production yield than the reference Au/TiO_2 and Au/g-C_3N_4 samples. Furthermore best hydrogen production was obtained with a gold loading of 0.3 wt. %. Future goals are to find the optimal amount of Au on the Au/g-C_3N_4/TiO_2 composites but also the optimal amount of g-C_3N_4. In the presentation, the influence of g-C_3N_4/TiO_2 ratio, as well as of Au loading will also discussed.

Acknowledgements

The authors would like to thank Thomas Cottineau for his scientific contribution and Thierry Dintzer for XPS and SEM imaging.

References

[1] K. Rajeshwar, R. McConnell, S. Licht, “Solar Hydrogen Generation” *Springer: New York*, (2008)
[2] A. Fujishima, K. Honda, *Nature* 238, (1972) 37
[3] A. Valdes, J. Brillet, M. Grätzel and al., *Phys. Chem. Chem. Phys.*14 (2012) 49
[4] X. Wang, K. Maeda, G. Xin, J.M. Carlsson, K. Domen, W. Xinchen, M. Antonietti, *Nature vol 8*, (2009) 76
[5] G. Colon, M.C. Hidalgo, J.A. Navio, *Catalysis Today* 76 (2002) 91
[6] A. Thomas, A. Fischer, F. Goettmann, M. Antonietti, J.O. Müller, R. Schlögl, J.M. Carlsson, *J. Mater. Chem.* 18 (2008) 4893

III-OP07

Efficient Solar Production of Methane from CO_2 and H_2 Using Nickel Catalysts

Puga A.V.[1,2*], Sastre F.[1,2], Liu L.C.[1,2], García H.[1,2], Corma A.[1,2]

1 - Instituto de Tecnología Química, UPV-CSIC, Valencia, Spain
2 - Instituto de Tecnología Química, Valencia, Spain

* a.puga@csic.es

Keywords: solar fuels, carbon, dioxide, photocatalysis, p-type semiconductors, nickel catalysts

1 Introduction

The production of fuels by reduction of carbon dioxide using sunlight as the energy source is a potential solution to both alleviate our dependence from fossil resources and minimise the greenhouse effects caused by the current atmospheric accumulation of such gas. This strategy would also close the carbon cycle efficiently. Unfortunately, the activation of CO_2 is an extremely challenging task, due to both thermodynamic and kinetic energy barriers involved in its reduction processes.

Based on previous research carried out in our laboratories on analogous photocatalytic CO transformations, it was proven that n-type semiconductors are more active for the water gas shift reaction, which entails CO oxidation to CO_2,[1] whereas p-type semiconductors catalyse the reduction of CO to CH_4, using either H_2 or H_2O (although to a lesser extent for the latter) as reducing agents.[2] These intriguing results encouraged the investigations presented herein, focusing on the sunlight-induced reduction of CO_2 by H_2 using a series of n- and p-type semiconductors as potential photocatalysts.

2 Experimental/methodology

Photocatalysts were commercial samples, with the exception of the following NiO samples. NiO nanoparticles (diameter 12−50 nm) were prepared by a sol−gel method from nickel acetate tetrahydrate (0.5 g in ethanol, 50 mL) and oxalic acid (0.23 M in ethanol, 100 mL), followed by drying (80−110 °C, 24 h) and calcination (500 °C, 3 h). NiO nanoplates (diameter 120−200 nm, thickness 20−50 nm) were prepared by hydrothermal treatment of the solid obtained from nickel acetate tetrahydrate (0.5 g in water, 50 mL) and aqueous NaOH (5 mL, 1.25 M) at 175 °C for 16 h.

Irradiations were carried out on a uniform thin bed of powdered semiconductor (250 mg) under a mixture of CO_2 (3.7 mmol, 15%), H_2 (17 mmol, 70%), and N_2 (3.7 mmol, 15%) for 1 h, unless otherwise stated, using a solar simulator (Newport, Oriel Instruments 69921, coupled with an AM1.5 filter). Gaseous products were analysed using a three-channel Bruker gas chromatograph. The amounts of elemental carbon on the photocatalyst after irradiation were determined by elemental analysis.

3 Results and discussion

A series of nanoparticulate transition metal oxides were tested for the reduction of CO_2 by H_2 with simulated sunlight as the source of energy (see Table 1). Whereas classical n-type semiconductor such as TiO_2 proved inactive for the reaction, CO_2 undergoes efficient reduction to CH_4 on p-type semiconductors. Among these, nickel-based materials were the most active photocatalysts.[3] Particle size is an important factor regarding photoactivity, as reflected in Table 1 by the decreasing conversion observed for a series of NiO materials. Using nanopowdered NiO or $Ni/SiO_2{\cdot}Al_2O_3$ photocatalysts, the conversion of CO_2 is essentially quantitative under

simulated solar light at short reaction times (≤ 1 h). Furthermore, the selectivity to CH_4 approaches 100%. Since the reaction is exothermic, the possible effects of local heat evolution on activity could not be overlooked. In this line, dark thermal experiments were conducted and photoactivity spectra were recorded, proving that light absorption by the nickel catalysts is actually initiating the reactions. Moreover, the presence of the silica-alumina support profoundly improves photoactivity and prolongs the lifetime of the photocatalyst.

Table 1. Photocatalytic activity for CO_2 reduction on metal oxide nanopowders.

catalyst	particle size (nm)	conversion (%)	molar balance (%)	selectivity (%)[a]		
				CH_4	CO	C_2H_6
TiO_2	20–30	0	99.0	-	-	-
Fe_2O_3	< 50	51.0	99.9	4.3	95	0.7
CoO	< 50	27.4	99.1	38.7	60.5	0.8
NiO	7–30	89.8	91.9	100	-	-
NiO	12–50	15.0	89.4	88.1	11.9	-
NiO	120–200	1.9	98.2	100	-	-
$Ni/SiO_2{\cdot}Al_2O_3$[b]	7−16	94.9	89.1	97.2	2.8	-

[a] Calculated by considering exclusively the products in the gas phase. [b] Irradiation time: 0.25 h.

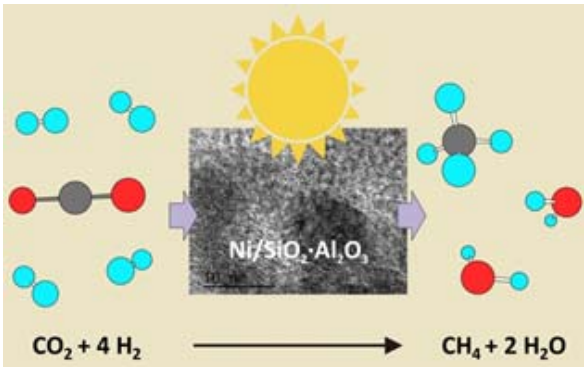

Fig. 1. Schematic representation of the sunlight-driven photocatalytic reduction of CO_2 to CH_4 on a nickel-based material, $Ni/SiO_2{\cdot}Al_2O_3$ (TEM micrograph shown in the inset).

4 Conclusions

A reaction that could potentially impact solar fuel production, namely the photocatalytic reduction of CO_2 to CH_4 with sunlight proceeds at high conversion and selectivity in short times on nanopowdered nickel catalysts. The use of a high surface area insulating support such as silica−alumina increases the efficiency and durability of the photocatalyst, due to an increase in metal dispersion and stability. The reported process can also take place under UV-free visible light.

Acknowledgements

Financial support by the Spanish Ministry of Economy and Competitiveness (Severo Ochoa and CTQ2012-32315) and by the Generalitat Valenciana (Prometeo 2012/013) is gratefully acknowledged.

References

[1] F. Sastre, M. Oteri, A. Corma and H. Garcia, *Energy Environ. Sci*. 6 (2013) 2211.
[2] F. Sastre, A. Corma and H. Garcia, *Angew. Chem., Int. Ed*. 52 (2013) 12983.
[3] F. Sastre, A.V. Puga, L. Liu, A. Corma and H. García, *J. Am. Chem. Soc.* 136 (2014) 6798.

III-OP09

$IrNiO_x$-Based Oxide Thin-Films and Metal-Oxide Hybrid Core-Shell Nanoparticles as Efficient Electrocatalysts of Oxygen Evolution

Nong H.N.[1], Reier T.[1], Oh H.-S.[1], Gan L.[1], Willinger E.[2], Teschner D.[2*], Strasser P.[1]

1 - Technical University Berlin, Department of Chemistry, Berlin, Germany
2 - Fritz-Haber Institute, Department of Inorganic Chemistry, Berlin, Germany

* teschner@fhi-berlin.mpg.de

Keywords: IrNi, core-shell, electrocatalysts, thin-films, oxygen evolution, reaction, oxide support, corrosion, resistance

1 Introduction

Water electrolysis, combined with renewable electric power generation technologies, such as solar electric, solar-thermal, hydro, or wind power plants, is expected to emerge as a low-emission method for storing excess electricity and for producing hydrogen fuel as part of a solar refinery. The challenge in electrocatalytic water splitting is the high overpotential required for the anodic oxygen evolution reaction (OER). Relatively low overpotential is attainable in acid electrolyzers using RuO_x and IrO_x-based electrocatalysts, however they are expensive and of limited sustainability. In this contribution, we address the challenges related to noble metal content and durability of water splitting catalysts by presenting a low-Ir content OER catalyst on a corrosion-stable oxide support with excellent electrochemical performance and durability.[1]

2 Experimental

IrNi-based homogenous thin films were prepared by spin-coating onto Ti substrates and calcination at various temperatures. Supported core-shell $IrNi@IrO_x$ nanoparticles on mesoporous antimony-doped SnO_2 (meso-ATO) were synthesized from $IrNi_x$ (x=3.3 to 3.8) metallic precursor alloys by applying potential cycles in acidic medium. The $IrNi_x$ metallic precursor alloys were synthesized using the polyol method in the presence of oleic acid and oleylamine as capping agents.[2] Meso-ATO powder was introduced into the reaction mixture before starting the metal reduction to form the precursor alloy. High surface area meso-ATO was synthesized by a combination of sol-gel synthesis and hydrothermal treatment.[3] The samples were characterized using a wide array of techniques involving synchrotron-based XPS, TPR, XRD, high-resolution imaging and mapping by STEM. The OER reactivity and stability of the electrocatalysts were evaluated using linear sweep voltammetry and chronopotentiometry.

3 Results and discussion

We found a strong impact of the Ir to Ni ratio on the electrocatalytic OER activity of IrNi mixed oxide films, with a maximal Ir mass based activity being 38 times higher than that of pure Ir oxide. The observed improvement in the OER activity was partially caused by the increased surface area; however, the intrinsic activity (activity per active surface area) was improved as well. Within the first electrocatalytic OER measurement the active catalyst state was obtained after leaching a certain amount of Ni selectively, though Ni was not completely removed. Above 21% initial Ni content, XRD measurements indicate an X-ray amorphous state for all mixed oxide compositions, and TPR suggested the presence of only one mixed-oxide phase. The amorphous mixed oxide state was conserved below the highest calcination T. XPS experiments of the IrNi mixed oxide films prior and after OER indicated a massive transformation of the

sample from an X-ray stable oxide into a labile, highly hydroxylated state with a fraction of incorporated water.

The preparation of metallic alloy nanoparticles supported on redox active oxides and the removal of surfactants require a balanced annealing protocol in order to maintain the chemical state of alloy and support. In this study, the materials were annealed at different temperatures (T = 180, 250, 300, 400, 500 °C) in inert N_2 gas to prevent the reduction of ATO support. XRD and XPS experiments indicated that high T annealing is detrimental, as it leads to phase separation.

After annealing, the supported precursor alloy nanoparticles were dealloyed and oxidized by applying potential cycles in acidic medium. Upon dealloying, the homogeneous Ir-Ni distribution yields a core shell type structure (EDX line scan with two symmetric Ir shell peaks at the particle edges). Interestingly, the morphology of the dealloyed nanoparticles strongly depended on particle size, while smaller nanoparticles favored Ni-richer core-shell structures, larger nanoparticles appear to undergo severe Ni leaching in their transition to core-shell structures (Fig.1 left).

The activity and stability of oxidized $IrNiO_x$/meso-ATO electrocatalysts were assessed in OER in comparison with IrO_x/C and IrO_x/commercial-ATO reference materials (Fig.1 right). $IrNiO_x$/meso-ATO calcined at T ≤ 300 °C (and particularly the one at 180°C) were the most active catalysts (Fig.1 right a,b); meanwhile their long-term stability were also excellent (Fig.1 right c,d). Further details to characterization, activity and stability will be discussed.

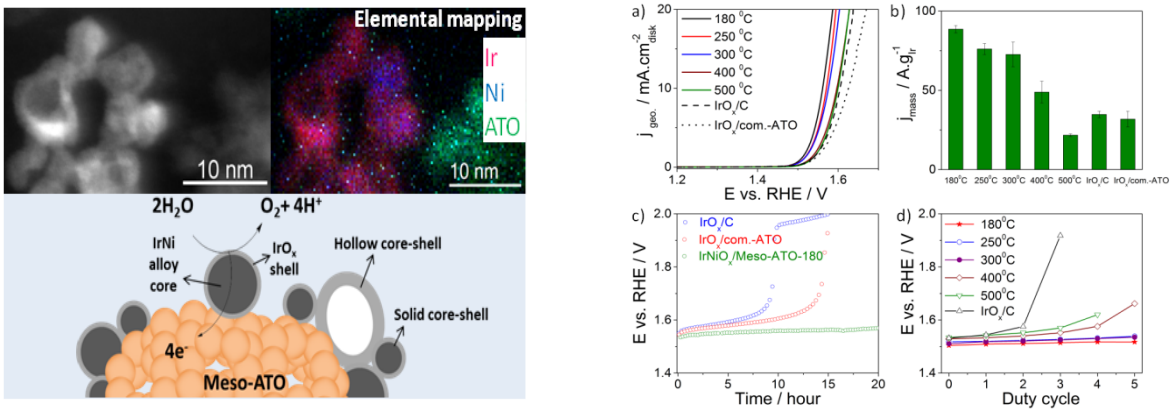

Fig. 1. Left: STEM image and EDX mapping of $IrNiO_x$/meso-ATO-180, with a schematic representation of the catalyst. Right: OER activity comparison (a,b) and stability tests (c,d).

4 Conclusions

Supported Ir-Ni oxide nanoparticles on meso-ATO with IrNi@IrO_x core-shell architectures enable low precious metal loading with excellent electrochemical performance and durability.

References

[1] Nong, H. N.; Oh, H.-S.; Reier, T.; Willinger, E.; Willinger, M.-G.; Petkov, V.; Teschner, D.; Strasser, P., Oxide-supported $IrNiO_x$ core-shell particles as efficient, cost-effective, and stable catalysts for electrochemical water splitting. Angewandte Chemie International Edition 2015, in press

[2] Nong, H. N.; Gan, L.; Willinger, E.; Teschner, D.; Strasser, P., IrO_x core-shell nanocatalysts for cost- and energy-efficient electrochemical water splitting. Chem. Sci. 2014, 5 (8), 2955-2963.

[3] Oh, H.-S.; Nong, H. N.; Strasser, P., Preparation of Mesoporous Sb-, F-, and In-Doped SnO_2 Bulk Powder with High Surface Area for Use as Catalyst Supports in Electrolytic Cells. Adv. Funct. Mater. 2015, in press

III-OP10

Partial Oxidation of Methane to Methanol with Bismuth-Based Photocatalysts

Murcia S.[1*], Villa K.[1], Andreu T.[1], Morante J.R.[1,2]

1 - Catalonia Institute for Energy Research (IREC), Sant Adrià de Besòs, Spain
2 - University of Barcelona (UB), Department of Electronics, Barcelona, Spain

* smurcia@irec.cat

Keywords: Bi_2WO_6, $BiVO_4$, selective oxidation, photocatalysis, nitrite ion

1 Introduction

The direct transformation of methane into oxygenated products is a challenging alternative for its exploitation. A wide number of catalytic approaches have been reported for the direct oxidation of methane into products like methanol, formaldehyde and longer chain compounds. In this sense, the photocatalytic approach might become a good alternative for carrying out processes at milder conditions than other catalytic paths [1]. Some materials as TiO_2, NiO, WO_3 [2], mesoporous silicas and zeolites have been studied as photocatalysts for the selective oxidation of methane into methanol with several oxidizers as water, NO or O_2.

Bismuth ternary oxides can be interesting candidates for this reaction in comparison to simple oxides, because of the hybridized band structure created by the Bi 6s orbitals, which might move the band edges to more negative potentials, increase the carrier mobility and decrease the band gap value [3]. Bi_2WO_6 and $BiVO_4$ have been synthesized, characterized and evaluated in the photocatalytic oxidation of methane to methanol for the first time. Moreover, the effect of several reaction conditions and the presence of additives have also been studied.

2 Experimental/methodology

The synthesis of Bi_2WO_6 and $BiVO_4$ was carried out by a facile hydrothermal treatment at 140ºC for 20h. Solutions of $Bi(NO_3)_3$ in acetic acid and Na_2WO_4 and $NaVO_3$ in H_2O were used as precursors. Both materials were calcined at 300ºC.

XRD, SEM and BET analysis were performed. Finally, the samples were evaluated in a commercial photochemical reactor with a medium pressure mercury lamp (450W), connected to a Shimadzu GC with TCD and FID. The gas composition was analyzed at certain intervals. For each test, a suspension of Milli-Q water with 1 $g \cdot L^{-1}$ of photocatalyst was added to the reactor and stirred, while continuously sparging a CH_4/He mixture. The temperature was kept at ca. 348K.

3 Results and discussion

The most photoactive crystalline phases were obtained for both materials: russelite orthorhombic phase for Bi_2WO_6 and the scheelite monoclinic one for $BiVO_4$. In a similar manner, the two samples presented band gap values close to the expected ones (~2.8 for Bi_2WO_6 and 2.4 eV for $BiVO_4$), with BET areas of 30 and 2 $m^2 \cdot g^{-1}$, respectively, which can be explained from the difference in crystallite sizes. Bi_2WO_6 exhibited the typically reported morphology, consisting in 3D hierarchical structures formed from self-assembled nanoplates. $BiVO_4$, on the other hand, consisted of large faceted polyhedron.

Three main products were detected during the photocatalytic tests: CH_3OH, CO_2 and C_2H_6. An initial blank test with water showed that methane can be oxidized through a photolytic process in which ·OH radicals are produced from H_2O. Though, when a photocatalyst is present, different product distributions and higher conversions are observed. Figure 1 shows the rates of products obtained during the tests. There, it is possible to observe that Bi_2WO_6 led to the highest

rates of CO_2, indicating that this material is more oxidizing than $BiVO_4$. This effect can be explained from the differences in the band edges between both materials, as the valence band of Bi_2WO_6 has more positive potential than $BiVO_4$. Thus, higher selectivity values were obtained with the latter, which is an important aspect to consider for this process.

Other reaction conditions were also evaluated. For instance, the use of additives as electron or ·OH scavengers and other oxidant species as O_2 were considered. Fe^{3+} probed to have a negative effect on the selectivity, despite a significant increase in the methane oxidation probably through a photo-Fenton mechanism in which more ·OH radicals can be generated. Nitrite ion (NO_2^-) on the other hand, had a positive effect on the selectivity by completely inhibiting the C_2H_6 formation and decreasing the complete oxidation to CO_2, thanks to a double mechanism in which it acts as UV filter and ·OH scavenger. This way, through a combination of $BiVO_4$ in a solution of (1mM) NO_2^-, enhancements in the CH_3OH selectivity from ~40 to 90% can be achieved.

Lower CH_4 conversions were obtained in additional tests carried out in presence of commercial TiO_2-P25 and rutile.

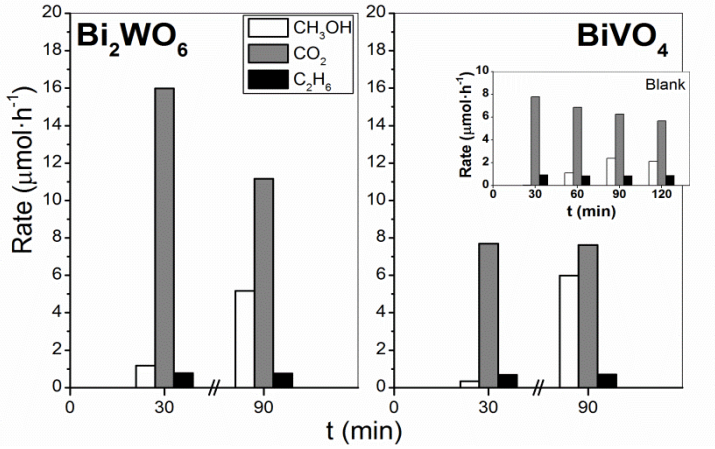

Fig. 1. Rates of products obtained during the photocatalytic tests (in the inset, the photolytic path).

4 Conclusions

$BiVO_4$ has proved to be a good candidate as photocatalyst for the selective oxidation of methane, displaying higher methanol selectivity than Bi_2WO_6, which is a more oxidizing material. The presence of low concentrations of nitrite anion might enhance the selectivity towards methanol and inhibit the ethane formation, while the addition of electron scavengers as Fe^{3+} species favors the complete oxidation path to CO_2.

Acknowledgements

This work was partially supported by the European Regional Development Funds (ERDF, FEDER Programa Competitivitat de Catalunya 2007-2013), Ministerio de Economía y Competitividad (CSD2009-00050) and the Framework 7 program under the project CEOPS (FP7-NMP-2012-309984).

References

[1] L. Yuliati, H. Yoshida, *Chem. Soc. Rev.* 37 (2008) 1592.
[2] A. Hameed, I.M.I. Ismail, M. Asiam, M.A. Gondal, *Appl. Catal. A,*470 (2014) 327.
[3] C. Belver, C. Adán, M. Fernández-García, *Catal. Today* 143 (2009) 274.

III-OP11

Photocatalytic Hydrogen Evolution from Aqueous Solutions of Na_2S/Na_2SO_3 under Visible Light Irradiation of Nonstoichiometric Silver Sulfide Nanoparticles

Rempel A.A.[1,2*], Sadovnikov S.I.[1], Kozlova E.A.[2,3], Gerasimov E.Yu.[3]

1 - Institute of Solid State Chemistry, Ural Branch of the RAS, Ekaterinburg, Russia
2 - Ural Federal University, Ekaterinburg, Russia
3 - Boreskov Institute of Catalysis, Siberian Branch of the RAS, Novosibirsk, Russia

* rempel@ihim.uran.ru

Keywords: photocatalysis hydrogen, production, silver sulfide, nanoparticles, nonstoichiometry

1 Introduction

Semiconductor nanocrystalline materials are widely used in photocatalytic processes. Selective photocatalytic reactions for organic synthesis [1], photocatalytic oxidation of organic compounds [2], and photocatalytic hydrogen production have become of special significance [3]. Taking this into account, the undersanding of very details of photocatalytic hydrogen evolution from aqueous solutions of Na_2S/Na_2SO_3 under visible light irradiation is very important nowadays [4]. So, in present work the synthesis of nonstoichiometric silver sulfide nanoparticles and study of their photocatalytic activity in Na_2S/Na_2SO_3 were undertaken.

2 Experimental

The powders of nonstoichiometric silver sulfide nanoparticles with excess of silver (nano-Ag_2S/Ag) were synthesized by chemical bath deposition from aqueous solution of silver nitrate $AgNO_3$ (50 mM) and sodium sulfide Na_2S (25 mM) containing either sodium citrate $Na_3C_6H_5O_7$ (Na_3Cit) or sodium salt of ethylenediaminetetraacetic acid $Na_2H_2(CH_2OO)_4(CH_2N)_2$ (EDTA) as complexing or stabilizing agents. The concentrations of sodium citrate or EDTA in the reaction mixtures were varied from sample to sample in the range between 25 and 50 mM in order to get silver sulfide nanoparticles with different stoichiometry.

The size (hydrodynamic diameter) of nanoparticles in the as-synthesized colloid solutions was determined by dynamic light scattering (DLS). Phase composition of the samples after drying and filtration was analyzed by X-ray diffraction (XRD) using CuK_{alpha} radiation. The XRD patterns were recorded in the 2theta range from 20 to 95° with a step of 0.02° and high statistics at each point. The XRD reflexes were separated from each other and average crystallite sizes were determined with the use of Williamson-Hall technique.

The samples were studied using high resolution transmission electron microscopy (HRTEM) with accelerating voltage of 200 kV and resolution of 140 pm. The local elemental composition was analyzed with an energy-dispersive X-ray (EDX) spectrometer equipped with a detector having energy resolution of 130 eV.

The photocatalytic evolution of hydrogen from the aqueous solution of Na_2S/Na_2SO_3 was studied by the method described earlier [5]. Before the reaction, a water suspension with a catalyst, Na_2S, and Na_2SO_3 was treated in an ultrasonic bath for 10 min and purged with argon for 20 min to remove oxygen. After that, the suspension of powdered samples was placed into a sealed thermostated reactor and illuminated with a 450 nm wavelength light emitting diode (LED) with the intensity of the irradiation of 8 mW/cm^2. The concentration of hydrogen was measured with a gas chromatograph equipped with a thermal conductivity detector and a zeolite column; argon was used as the carrier gas.

3 Results and discussion

The chemical (EDX), structural (XRD, HRTEM) and morphological (SEM, TEM) characterization of silver sulfide samples synthesized with help of sodium citrate or EDTA has shown nearly the same silver enriched chemical composition with about 2 at. % deviation from stoichiometry and nearly the same size of nanoparticles of about 50 nm.

Atomic structure of nanoparticles (XRD, HRTEM) in both cases is monoclinic acanthite-like. The only difference in structure of silver impurities was found. Silver nanoparticles in samples synthesized with EDTA has cubic closed-packed crystalline structure but in samples stabilized with sodium citrate is amorphous.

High activity of nonstoichiometric nanosized silver sulfide under visible light (450 nm) for both types of synthesis samples is found but the stability of photocatalytic activity was found exclusively for samples synthesized with help of EDTA. Silver nanoparticles can act for charge separation in the system Ag_2S/Ag and increase the activity of stoichiometric silver sulfide. Taking into account that the only difference in structure for these samples is crystalline impurities of silver phase it should be concluded that this could be the reason for stable photoactivity of samples synthesized with EDTA.

4 Conclusions

A method for the synthesis of nonstoichiometric silver sulfide nanoparticles which are catalytically active under visible light irradiation (450 nm) has been suggested and explored. High catalytic activity of nonstoichiometric silver sulfide nanoparticles was measured by the photocatalytic evolution of hydrogen from the aqueous solution of Na_2S/Na_2SO_3. Higher photostability of nonstoichiometric silver sulfide nanoparticles stabilized by EDTA in compare to non-stabilized nanoparticles were found. This effect can be explained by nonstoichiometry and crystalline silver impurities on the surface of stabilized silver sulfide nanoparticles.

Acknowledgements

This study was supported by the Russian Science Foundation (grant no. 14-23-00025) through the Institute of Solid State Chemistry of the Ural Branch of the RAS.

References

[1] V. P. Ananikov, L. L. Khemchyan, Y. V. Ivanova, V. I. Bukhtiyarov, A. M. Sorokin, I. P. Prosvirin, S. Z. Vatsadze, A. V. Medved'ko, V. N. Nuriev, A. D. Dilman, V. V. Levin, I. V. Koptyug, K. V. Kovtunov, V. V. Zhivonitko, V. A. Likholobov, A. V. Romanenko, P. A. Simonov, V. G. Nenajdenko, O. I. Shmatova, V. M. Muzalevskiy, M. S. Nechaev, A. F. Asachenko, O. S. Morozov, P. B. Dzhevakov, S. N. Osipov, D. V. Vorobyeva, M. A. Topchiy, M. A. Zotova, S. A. Ponomarenko, O. V. Borshchev, Y. N. Luponosov, A. A. Rempel, A. A. Valeeva, A. Y. Stakheev, O. V. Turova, I. S. Mashkovsky, S. V. Sysolyatin, V. V. Malykhin, G. A. Bukhtiyarova, A. O. Terent'ev and I. B. Krylov. *Russ. Chem. Rev.* 83 **(**2014) 885–985.

[2] E.A.Kozlova, N.S.Kozhevnikova, S.V.Cherepanova, T.P.Lyubina, E.Yu.Gerasimov, V.V.Kaichev, A.V.Vorontsov, S.V.Tsybulya, A.A.Rempel, V.N.Parmon. *J. Photochem. Photobiol.* A 250 (2012) 103-109.

[3] J.A. Turner, Sustainable hydrogen production. *Science.* 305 (2004) 972–974.

[4] D. V. Markovskaya, S. V. Cherepanova, A. A. Saraev, E. Yu. Gerasimov, E. A. Kozlova *Chemical Engineering Journal* 262 (2015) 146–155

[5] T.P. Lyubina, E.A. Kozlova, New photocatalysts based on cadmium and zinc sulfides for hydrogen evolution from aqueous Na2S-Na2SO3 solutions under irradiation with visible light, Kinet. Catal. 53 (2012) 188–196.

III-OP12

CO_2 Conversion Into Solar Fuels

Pastrana-Martínez L.M., Silva A.M.T., Fonseca N.N.C., Figueiredo J.L., Faria J.L.*

LSRE-LCM, Departamento de Engenharia Química, Faculdade de Engenharia da Universidade do Porto, Porto, Portugal

* jlfaria@fe.up.pt

Keywords: CO_2, photoreduction, methanol, graphene, oxide, TiO_2, solar fuels

1 Introduction

Since 1751 approximately 337 billion metric tonnes of carbon have been released to the atmosphere from the consumption of fossil fuels and cement production [1]. The latest estimates point-out to the occurrence of all time highs every year. Liquid and solid fuels are responsible for the majority of emissions, while gas and cement contribute to lower extent, with a significant decrease of gas flaring in recent years. This massive release of CO_2 to the atmosphere is believed to result in considerable climate changes, therefore a great deal of effort is being made to reduce its concentration in the atmosphere and to prevent its emissions. Different strategies include the adsorption of CO_2 into new/functionalized materials, the increase of the quantity of green carbon sinks (plants, phytoplankton, and algae containing chloroplasts), the increase of the level of dissolved carbonate and its salts in sea water; or even the capture and transfer of CO_2 to the bottom of the sea in a supercritical state [2]. The most obvious reasonable solution is to develop an efficient process for CO_2 conversion into something valuable, but without spilling other chemicals into the Earth's ecosystems, that might damage their functions. One option lies in using solar energy, which is an abundant, clean and sustainable resource [3], to photocatalytically convert CO_2 into a solar fuel [4]. Solar fuels derived from CO_2 can contribute to neutralize the carbon balance into the atmosphere and can be converted into easily transportable liquid chemicals, such as CH_3OH [5].

In this work, composites prepared from graphene oxide (GO) and titanium dioxide (TiO_2) are applied to the photocatalytic water reduction of CO_2 into renewable fuels. The effect of copper metal as co-catalyst will be assessed and its influence on the photocatalytic reaction inferred.

2 Experimental

GO was synthesized from graphite (particle size ≤ 20 μm, from Sigma-Aldrich) by a modified Hummers method [6]. GO-TiO_2 (hereafter referred as GOT) composites were synthesized by the liquid phase deposition method at room temperature, as described elsewhere [6]. The Cu-loaded GOT photocatalysts were prepared by adapting the procedure described in the literature for Cu-loaded TiO_2 [7]. Additional TiO_2-Cu_2O composites were prepared following the same procedure but without the addition of GO.

Thermogravimetric (TG) analysis of the composites was performed using a STA 490 PC/4/H Luxx Netzsch thermal analyser. The morphology of the materials was studied by scanning electron microscopy (SEM) using a FEI Quanta 400FEG ESEM/EDAX Genesis X4M microscope. The optical properties of the samples were analyzed by UV/Vis diffuse reflectance spectroscopy using a JASCO V-560 UV/Vis spectrophotometer, equipped with an integrating sphere attachment (JASCO ISV-469). X-ray photoelectron spectroscopy (XPS) was performed in a Kratos AXIS Ultra HSA using a monochromatic Al Kα X-ray source (1486.7 eV).

The photocatalytic runs were carried out in a cylindrical glass immersion photo-reactor (250 mL) with a Heraeus TQ 150 medium-pressure mercury vapor lamp located axially in the reactor

and held in a quartz immersion tube. The pH of the solution was controlled by adding NaOH. The photocatalyst load was typically 1 g L^{-1}.

The gaseous products were analyzed on-line, while methanol and ethanol were determined from liquid aliquots, using a gas chromatograph (DANI GC-1000).

3 Results and discussion

A higher absorption in the visible spectral range is clearly observed for GOT and Cu-loaded GOT composites when compared to GO-free materials, i.e., P25, TiO_2_Cu_2O, TiO_2_$Cu(NO_3)_2$ and TiO_2_$CuCl_2$. The increase in the absorption promoted by GO has been ascribed both to the capacity of the carbon phase to absorb light and also to the creation of an electronic inter phase interaction between GO and TiO_2, as previously observed for other carbonaceous materials combined with TiO_2 [6].

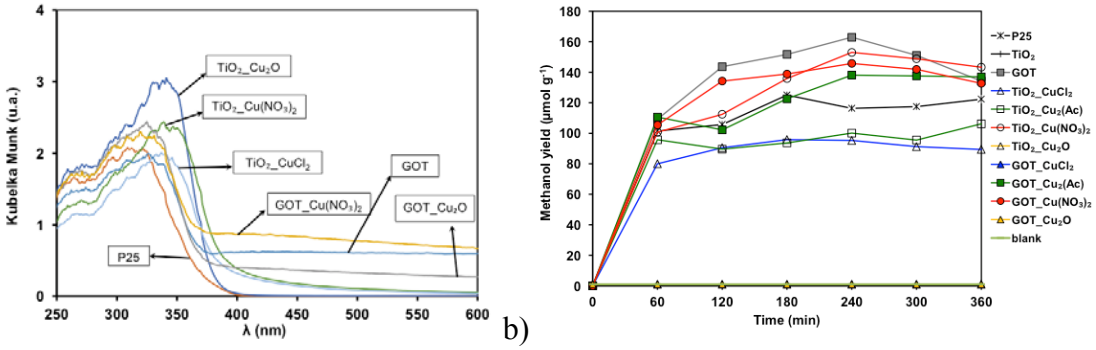

a) b)

Fig. 1. a) DRUV spectra of used photocatalysts; b) Methanol yield for photocatalytic water reduction of CO_2.

The evolution of methanol and ethanol yields during the photocatalytic experiments was measured for ten synthesized photocatalysts as well as for the commercial TiO_2 sample. In general, the photocatalysts were efficient for methanol generation with the exception of bare TiO_2, GOT_$CuCl_2$ and the catalysts prepared using Cu_2O as copper precursor (i.e., TiO_2_Cu_2O and GOT_Cu_2O, respectively).

4 Conclusions

The selectivity towards methanol formation is linked to the presence of Cu on the photocatalysts, while the visible light photo-response is assigned to the presence of GO.

Acknowledgements

This work was co-financed by FCT and FEDER under Program COMPETE (Project UID/EQU/50020/2013); LMPM by FCT grant SFRH/BPD/88964/2012 and FCT Investigator 2014 Program (IF/01248/2014); AMTS by FCT Investigator 2013 Program (IF/01501/ 2013). Support from the ESF and the HPOP. SEM analysis by Dr. Carlos Sá and CEMUP.

References

[1] T.A. Boden, G. Marland, R.J. Andres. Global, Regional, and National Fossil-Fuel CO_2 Emissions. CDIAC, Oak Ridge National Laboratory, U.S. D.O.E., (2010). doi 10.3334/CDIAC/00001_V2010.
[2] N. Ahmed, Y. Shibata, T. Taniguchi, Y. Izumi, J. Catal., 279 (2011) 123.
[3] P.D. Tran, L.H. Wong, J. Barber, J.S.C. Loo, Energy Environ. Sci. 5 (2012) 5902.
[4] A. Dhakshinamoorthy, S. Navalon, A. Corma, H. Garcia, Energy Environ. Sci. 5 (2012) 9217.
[5] H. Sun, S. Wang, Energy Fuels 28 (2013) 22.
[6] L.M. Pastrana-Martínez, S. Morales-Torres, V. Likodimos, J.L. Figueiredo, J.L. Faria, P. Falaras, A.M.T. Silva, Appl. Catal. B: Environ. 123–124 (2012) 241.
[7] J.C.S. Wu, H.-M. Lin, Int. J. Photoener. 7 (2005) 115.

III-OP13

Photocatalytic Pathways for Hydrogen Production from Biomass over UV- and Visible-Light Responsive Materials

Sanwald K.E.*, Berto T.F., Eisenreich W., Gutiérrez O.Y., Lercher J.A.

Department of Chemistry and Catalysis Research Center, Technische Universität München, Garching, Germany

* kai.sanwald@tum.de

Keywords: photocatalysis, hydrogen, biomass, TiO_2, ZnO, polyols

1 Introduction

Sunlight-driven hydrogen production from readily-available biomass-derived resources ('photocatalytic reforming') is a promising route to supply a non-polluting, carbon-neutral energy storage medium [1]. The technology has the potential to provide a simplified pathway compared to overall water splitting as the thermodynamically favored back-reaction during water splitting (i.e. water formation from H_2 and O_2) and the technically difficult separation task imposed by the latter gas mixture, are avoided.

Aiming at a comprehensive and general understanding of the reaction pathways of the anodic half-reactions over co-catalyst decorated semiconductors [2] (that have mostly been hypothesized to occur on the semiconductor surfaces), we have conducted a systematic study of the kinetics of photocatalytic reforming of a series of alcohol and polyol compounds (e.g. methanol, ethylene glycol and glycerol). By comparison of TiO_2-based photocatalysts and visible-light responsive oxynitride photoabsorbers (e.g. GaN:ZnO solid solutions [3]), we furthermore establish the impact of the nature of the semiconductor on reaction pathways and selectivities. The latter semiconductors having been unexplored with respect to solar biomass reforming.

2 Experimental

Oxynitride semiconductors were obtained from nitridation of corresponding oxide precursors. If necessary, the semiconductors were subjected to an additional thermal treatment in synthetic air. Co-catalyst loading was done via wet impregnation with appropriate precursors followed by drying and calcination. TiO_2-based photocatalysts loaded with co-catalysts were prepared from commercial TiO_2 under otherwise identical synthesis conditions.

The physicochemical properties of the photocatalysts were characterized by XRD, HR-SEM/EDX, TEM, BET, UV-Vis spectroscopy and elemental analysis (ICP-AES).

Kinetic experiments were conducted in a top-irradiation Pyrex photoreactor connected to a closed gas-circulation system. Photocatalyst suspensions (75 mg of catalyst suspended in 100 ml of a typically 20 mM aqueous reactant solution) were irradiated using a 300 W Xe lamp. The reactions were monitored by quantitative analysis of both gas- and liquid-phase species.

3 Results and discussion

We have deduced the reaction pathways from the photoreforming kinetics of compounds representative for biomass-derived feeds (and associated intermediates). Throughout all reaction sequences no hydrogen production in absence of irradiation was detected. Fig. 1 depicts photocatalytic hydrogen production from glycerol over 1 wt.% Rh/TiO_2. Initial glycerol conversion involves parallel dehydrogenation (the dominant reaction path) and dehydration (a side reaction) resulting in the formation of e.g. glyceraldehyde and hydroxyacetone, respectively.

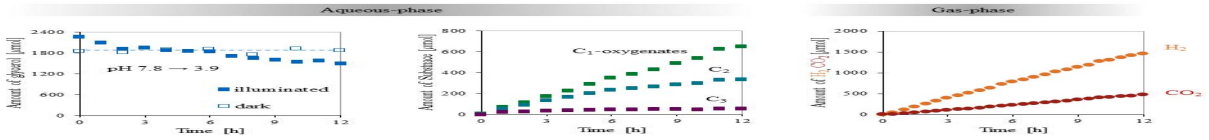

Fig. 1. Temporal profiles of liquid- and gas-phase species generated during photocatalytic hydrogen production from aqeous glycerol solution over Rh/TiO_2.

We have furthermore tracked the consecutive reactions generating C_2 and C_1 intermediates via subsequent C-C cleavage steps and followed the anodic degradation towards full mineralization (formation of CO_2). Investigations with systematically varied reactant structure (e.g. from methanol via ethylene glycol, glycerol to higher molecular weight compounds) revealed a common set of intermediates. In contrast to TiO_2-based systems, comparative investigations on oxynitride photocatalysts provide indication that multiple reaction pathways are operable. We discuss our kinetic results relating the physicochemical properties of the photocatalysts to reaction selectivities and address conceivable mechanisms for C-C cleavage.

4 Conclusions

We have compiled the reaction networks of photocatalytic hydrogen evolution from biomass model compounds over co-catalyst decorated TiO_2-based and oxynitride photocatalysts. We identified and evaluated the existence of multiple reaction pathways coupling into a joint reaction network and correlated kinetic parameters with the physicochemical properties of the photocatalyst systems.

Acknowledgements

This work is financially supported by the Federal Ministry of Education and Research (BMBF) project iC^4 (project no. 01RC1106A). Moreover, we would like to thank *Clariant* for financial support and fruitful collaboration. K.E.S. gratefully acknowledges the Fonds der Chemischen Industrie for financial support through a PhD scholarship.

References

[1] R.M. Navarro, M.C. Sánchez-Sánchez, M.C. Alvarez, F. del Valle, J.L.G. Fierro, Energy & Environmental Science 2 (2009), 35.
[2] P. Panagiotopoulou, E.E. Karamerou, D.I. Kondarides, Catalysis Today 209 (2013) 91.
[3] K. Maeda, T.Takata, M. Hara, N. Saito, Y. Inoue, H. Kobayashi, K. Domen, Journal of the American Chemical Society 127 (2005) 8286.

III-OP14

Surface Dynamics of Ni^0 and Coke during Ethanol Steam Reforming on a Ni/La_2O_3-alphaAl_2O_3 Catalyst

Montero C., Ochoa A., Bilbao J., Gayubo A.G., Castaño P.*

Department of Chemical Engineering, University of the Basque Country (UPV/EHU), Bilbao, Spain

* pedro.castano@ehu.es

Keywords: ethanol steam reforming, nickel, coke, evolution, hydrogen

1 Introduction

Steam Reforming of Ethanol (SRE) is an attractive route for H_2 production because ethanol is renewable, the increasing demand of H_2, and due to the growing prospects of obtaining ethanol from lignocellulosic biomass (second-generation) favored by the rapid technological development of enzymatic hydrolysis. Several supported catalysts have been studied in the SRE process and among them; Ni^0 has an outstanding C-C and C-H bond-breaking activity and a relatively low price. On the other hand, Ni^0 phases are not completely stable in the reaction conditions and they promote parallel reactions of coke formation and growth [1]. These dynamics foster the catalytic deactivation and the decrease in H_2 production rate. In this work, we have studied the morphologic and compositional dynamics of Ni and coke phases on a Ni/La_2O_3–αAl_2O_3 catalyst during the SRE process. Our aims are establishing a relationship among these dynamics and contribute to the understanding of the catalyst deactivation.

2 Experimental/methodology

The catalyst (with 10 wt% Ni and 9 wt% La_2O_3 nominal contents) was prepared by incipient wetness impregnation method [2], and it was equilibrated by means of a reaction-regeneration cycle [3] in order to achieve a reproducible kinetic behavior. The experiments were carried out in a fluidized bed reactor, with online analysis of reaction products by means of a micro-GC Agilent 3000. The SRE runs were performed at 500 ºC, steam/ethanol molar ratio = 3, W/F_0 = 0.09 g_{cat}·min/g_{EtOH} and time on stream (TOS) values of 1.5, 4, 8, and 20 h. Prior to the SRE, the catalyst was reduced in situ at 700 °C for 2 h by using a H_2–He flow (5 vol% H_2). The dynamic changes of composition and morphology of Ni and coke were characterized by XRD, XPS, Temperature-Programmed Oxidation (TPO), SEM and TEM microscopy, FTIR and Raman spectroscopy.

3 Results and discussion

The evolution of the conversion and product yields allows establishing 3 differentiated stages in the dynamics of the catalyst performance: Stage 1 (TOS < 4 h), with almost steady ethanol conversion values (> 90 %) and a steady H_2 yield (~ 40 %); stage 2 (4 < TOS < 8 h), with a severe drop in ethanol conversion (~ 49 %) as well as in CH_4 and CO yields, and less severe hydrogen yield drop; stage 3 (TOS > 8 h), with a steady and slow decrease in ethanol conversion. These stages of catalyst performance can be correlated with similar stages of coke growth schematized in Fig. 1: In Stage 1, the formation of filamentous coke is observed, which is incipient for TOS < 1.5 h. This type of coke does not block the accessibility of Ni^0 and contributes to increasing the surface area of the catalyst. The origin of this filamentous coke is CH_4 decomposition and Boudouard reaction, and its formation involves a decrease in the Ni^0 particle size due to the formation of Ni-carbides [4]. In Stage 2, there is a change in the mechanism of coke formation due to the change in the composition of the reaction medium

(decreasing amount of CH_4 and CO with parallel increase of ethanol) which originates a change in the composition of coke: the growth of filamentous coke occurs with a simultaneous formation of pyrolytic coke that fills the voids created by the filamentous coke and it is also deposited on the Ni^0 particles. This pyrolytic coke is originated from the decomposition of oxygenates, particularly ethanol and acetaldehyde, and its formation is the main responsible for the fast catalyst deactivation observed in this stage, together with the simultaneous decrease of Ni^0 particle size due to the formation of Ni-carbides. In Stage 3, the growth of filamentous coke slows down in favour of a faster growth of pyrolytic coke with high graphitization, Ni^0 particle size decrease even further and ethanol conversion reaches a value similar to these obtained without catalyst (with an inert solid) in a thermal decomposition process.

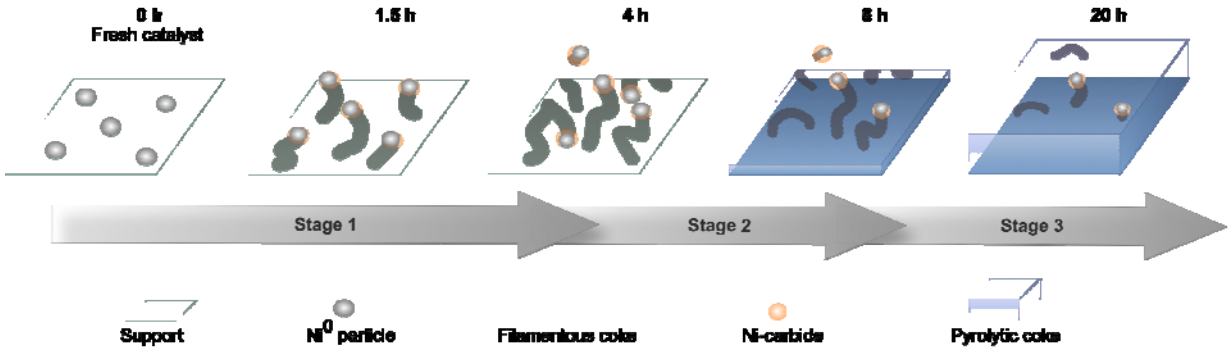

Fig. 1. Surface dynamics and deactivation stages of the Ni/La_2O_3-αAl_2O_3 catalyst during ethanol steam reforming.

4 Conclusions

The deactivation performance of the Ni/La_2O_3–αAl_2O_3 catalyst in the SRE process is strongly correlated with the surface dynamics of Ni^0 and coke, whose growth depends on the concentration of reactants and products in the gaseous phase. Three stages are differentiated during a kinetic run with Ni/La_2O_3–αAl_2O_3 catalyst (almost steady performance, followed by a severe drop in ethanol conversion and finally a steady and slow decrease in ethanol conversion), whose duration depends on the operating conditions (temperature, space time, steam/ethanol molar ratio) and that occur in parallel with the growth of Ni-carbides, filamentous and pyrolytic coke.

Acknowledgements

This work has been carried out with financial support from the Ministry of Science and Technology of the Spanish Government (CTQ2012-35263 and CTQ2013-46172-P). C. Montero and A. Ochoa are grateful for their Ph.D. grants from the National Secretariat of Higher Education, Science, Technology and Innovation of Ecuador-SENESCYT (20110560), and the Basque Government (PRE_2014_1_8), respectively.

References

[1] J. Vicente, C. Montero, J. Ereña, M.J. Azkoiti, J. Bilbao, A.G. Gayubo. Int J Hydrogen Energ 39 (2014) 12586-96.
[2] B. Valle, B. Aramburu, A. Remiro, J. Bilbao, A.G. Gayubo. Appl Catal B: Environ. 147 (2014) 402-10.
[3] C. Montero, B. Valle, J. Bilbao, A.G. Gayubo. Chem. Eng. Transac. 37 (2014) 481-486.
[4] S. Takenaka, H. Ogihara, K. Otsuka, J. Catal. 208 (2002) 54-63.

III-OP15

CO-Cleanup of Hydrogen-Rich Stream for LT PEM FC Feeding: Catalysts and their Performance in CO Preferential Oxidation and Methanation

Snytnikov P.V.[1,2*], Sobyanin V.A.[1,2]

1 - Boreskov Institute of Catalysis, Novosibirsk, Russia
2 - Novosibirsk State University, Novosibirsk, Russia

* pvsnyt@catalysis.ru

Keywords: preferential CO oxidation and CO methanation, CO clean-up, hydrogen

1 Introduction

In the last two decades, CO preferential oxidation (CO PROX) and CO preferential methanation (CO MET) are assumed as the most feasible reactions for CO removal from H_2-rich reformate for low temperature polymer electrolyte membrane fuel cells (LT PEMFC) feeding applications. Despite the existing advantages and disadvantages, both processes provide CO-cleanup to 10 ppm.

The present report summarizes the results obtained during a systematic study of catalysts, their performances and fundamental principles of the preferential CO oxidation and preferential CO methanation reactions. The most attention is concentrated on Cu/CeO_2 catalysts and their operation in a micro-channel reactor in preferential CO oxidation [1,2], and on Ni/CeO_2 catalysts and their operation in a milli-channel reactor [3,4].

2 Experimental/methodology

CO PROX was studied over supported noble mono-metal based catalysts, supported bimetallic systems prepared with the use of double complex salts, and copper-ceria catalysts [5-7]. CO MET was studied over nickel-based catalysts. The role of nickel precursor was investigated and the positive effect of chlorine on the catalyst selectivity was demonstrated. The catalysts were characterized by BET, XRD, XPS, TEM, EDX, TPR and TPD techniques.

Catalytic performance of the prepared systems in a form of grains in the fixed-bed continuous flow reactor was studied. The Cu/CeO_2 catalysts were coated on the surface of microchanel reactors and investigated in CO PROX. The structured Ni/CeO_2 catalysts supported over corrugated metal gauzes were studied in CO MET reaction in milli-channel reactor.

The effect of internal diffusion was estimated and the optimum grain size/coating thickness was found [8].

3 Results and discussion

Fig. 1a exemplifies the typical effect of temperature on the CO outlet concentration at CO PROX over 5 wt.% CuO/CeO_2 in the single micro-channel reactor at various WHSV. It is seen that the catalyst provides CO outlet concentration below 10 ppm in a wide temperature interval. An assembly comprised of 26 micro-channel reactors (Fig. 1b) demonstrated efficient operation with realistic reformate stream (containing CO_2 and H_2O) supplied at space velocities sufficient for feeding a ~100We portable LT PEM FC. The outlet CO concentration attained ~10 ppm at 100% O_2 conversion.

The temperature dependencies of the CO outlet concentration at CO MET, presented in Fig. 2a, illustrate the excellent performance of 10 wt.% Ni/CeO_2 catalyst and its ability to clean up CO to below 10 ppm in a wide temperature interval. The milli-channel reactor with structured

10 wt.% Ni/CeO_2 catalyst (Fig. 2b) provided CO deep removal from a gas stream fed to a 20 We LT PEMFC.

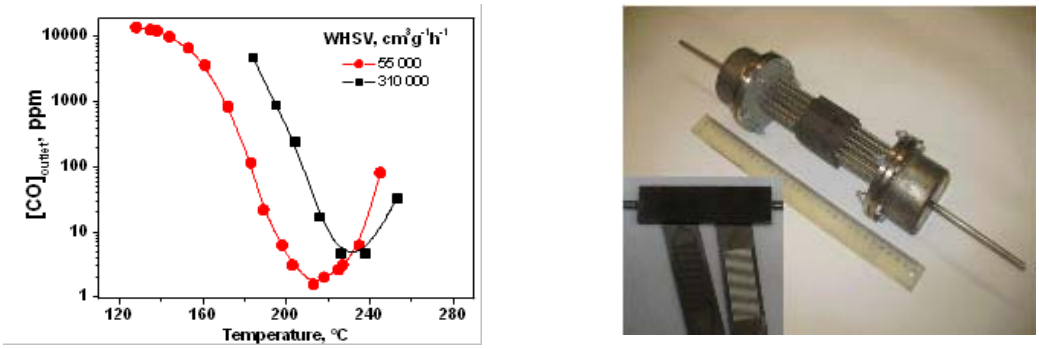

Fig. 1. The temperature dependencies of the CO outlet concentration at CO PROX over 5 wt.% CuO/CeO_2 (a), single and assembly of micro-channel reactors (b). The inlet gas mixture composition (vol.%): 1.5 CO, 2.25 O_2, 20CO_2, 10H_2O, H_2 – balance.

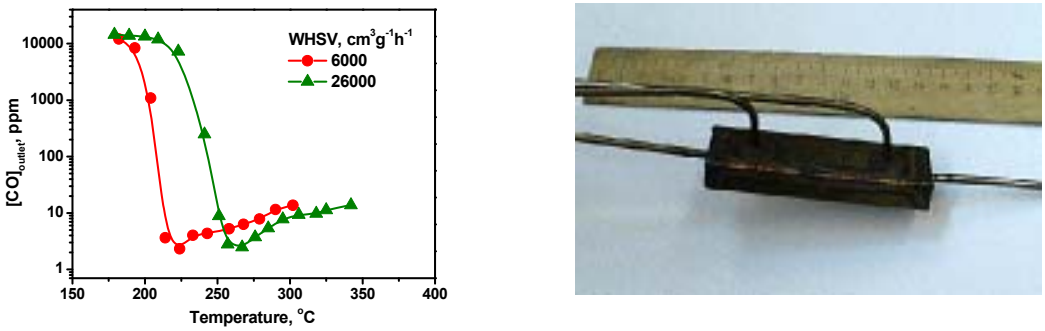

Fig 2. The temperature dependencies of the CO outlet concentration at CO MET over 10 wt.% Ni/CeO_2 (a) and general view with scheme of milli-channel reactor with structured 10 wt.% Ni/CeO_2 catalyst. The inlet gas mixture composition (vol.%): 1.5CO, 20CO_2, 10H_2O, H_2 – balance.

Based on the results obtained, the composition and structure of the catalysts' active components were determined, and reasonable suggestions on the reaction mechanisms of CO PROX and CO MET were made. The CO PROX and CO MET efficiencies were discussed comparatively.

4 Conclusions

The selected copper and nickel-ceria based catalyst provides efficient CO cleanup of H_2-rich gas streams suitable for feeding power generating units on the base of LT PEMFC.

Acknowledgements

The work was partially supported by MES (Russia), and RFBR Grant 14-03-00457-a.

References

[1] P.V. Snytnikov, M.M. Popova, et al., *Appl. Catal. A.* 350 (2008) 53.
[2] P.V. Snytnikov, D.I. Potemkin, et al., *Chem. Eng. J.* 160 (2010) 923.
[3] M.M. Zyryanova, P.V. Snytnikov, et al., *Chem. Eng. J.* 176-177 (2011) 106.
[4] M.M. Zyryanova, P.V. Snytnikov, et al., *Chem. Eng. J.* 238 (2014) 189.
[5] P.V. Snytnikov, V.A. Sobyanin, et al., *Appl. Catal. A: General* 239 (2003) 149.
[6] D.I. Potemkin, Yu.V. Shubin, et al., *Catal. Today* 235 (2014) 103.
[7] P.V. Snytnikov, S.D. Badmaev, et al., *Int. J. Hydrogen Energy* 37 (2012) 16388.
[8] D.I. Potemkin, P.V. Snytnikov, et al., *Kinet. Catal.* 52 (2011) 139.

III-OP16

Catalyst with "Core/ Shell" Structure for Steam Methane Reforming Resistant to Presence of H_2S in Gas Mixture

Konstantinov G.I.[1*], Tsodikov M.V.[1], Kurdymov S.S.[1], Bukhtenko O.V.[1], Maksimov Yu.V.[2], Murzin V.Yu.[3]

1 - A.V.Topchiev Instiute of Petrochemical Synthesis, RAS, Moscow, Russia
2 - N. N. Semenov Institute of Chemical Physics, RAS , Moscow, Russia
3 - National Research Center "Kurchatov Institute" , Moscow, Russia

* konstantinov@ips.ac.ru

Keywords: steam reforming, methane, hydrogen, Ni, H_2S, core-, shell

1 Introduction

The steam reforming of hydrocarbons is the most economically efficient way to obtain hydrogen and syngas required for ammonia production and petrochemical industy. Hydrogen is also a promising feed for proton exchange membrane fuel cells and solid oxide fuel cells [1].

The current steam reforming catalysts are mainly nickel supported on refractory alumina and ceramic magnesium aluminate. These supports provide high crush strength and stability [2]. However, coke formations and sulfur poisoning are two major problems associated with nickel catalyst. Nowadays, the general tendency is using the noble metals (Rh, Ru, Pt) as active catalytic components. They are less sensitive to deactivation due to carbon deposition and sulfur poisoning. However, the price of such catalysts 100-150 times higher than Ni-containing catalysts [3].

2 Experimental/methodology

The support was prepared at the room temperature by alkali precipitation of a mixed oxide obtained from acidic etching solution of vermiculite [4]. Granules formed from precipitation were dried in air for 48 h., then dried in a desiccator for 6 h. at 120°C, and finally calcined in a furnace with a fixed heating rate 10°C/min and isothermal exposure 1 h. at 600°C, 4 h. at 800°C, 2 h. at 850°C, 1 h. at 900°C. As a result, the mixed (Mg, Al, Fe, Si) oxide was obtained and used as the catalyst support.The support was impregnated by $Ni(NO_3)_2$ solution yielding 10 wt.% Ni. Wet granules were dried with the above drying procedure and then calcined at 500°C for 5 h.

The steam methane reforming was carried out on a laboratory setup with a flow reactor. 20 cm^3 of the catalyst was loaded in the reactor and reduced by hydrogen for 6 hours at 800°C. Then a mixture of hydrogen and pre-heated water vapor was supplied until 800°C temperature was reached. After that, the hydrogen feed was terminated and methane/vapor mixture was supplied (H_2O:CH_4= 2:1, P= 2.0 MPa, VHSV= 6000 h^{-1}). A part of resulting gas products was passed to a gas chromatograph Crystal-4000M where CO, CO_2, CH_4 и H_2 concentrations were measured. The activity of the catalyst was defined as the ratio between the observed methane conversion and equilibrium value for the operation temperature (800°C).. Thereafter all samples were sent to the structure analysis.

The structure and the phase composition of catalytically active components before and after reaction were investigated by XAFS, XRD, EDX, TEM and Moessbauer spectroscopy

3 Results and discussion

The catalytic tests of the Ni-containing catalyst held in the absence of sulfur compounds in the gas-vapor mixture show high activity in the SMR process. Concentrations of all products practically reached the equilibrium and remained stable during the whole operation time.

The Ni-containing catalyst shows high activity and stability in the SMR process also in the presence of H_2S in the gas-vapor mixture. For this purpose a series of tests with different concentrations of hydrogen sulfide (5.0 - 30.0 ppm) in the initial gas mixture were conducted. The increase of H_2S concentration didn't affect the catalyst activity during the experiment.

The XANES spectra indicated that nickel after calcinations stage was presented in the charge state Ni^{+2} and had a surrounding similar to that in NiO and iron was completely oxidized and was most likely located in the spinel structure of maghemite, γ-Fe_2O_3.

The most important changes occur upon the catalyst reduction in H_2 at 800°C. The phases of Mg_2SiO_4 and $Mg(Fe,Al)_2O_4$ spinel become larger in size. Nickel oxide was transformed into a metallic Ni structure but with shifted parameters that could indicate to a partial substitution of nickel atoms by iron and formation of Fe-Ni alloy. By TEM core/shell clusters with size of ~17 nm was found. The core consists of metallic clusters (both FeNi alloys and α-Fe) surrounded by the shell of 1–4 nm superparamagnetic γ-Fe_2O_3

After the catalyst test in the steam reforming of methane, containing 30.0 ppm H_2S the average size of particles of active components grew up from 17 nm (after reduction) to 40 nm. the core/shell configuration of the particle remained the same: the core consists of a FeNi alloy surrounded by a γ-Fe_2O_3 shell. The total size increase of the hybrid particle occurs due to the core growth, whereas the shell size remains in the range 1–4 nm. It should be mentioned that no elemental sulfur was found in the particle composition.

The next step in development of SRM catalysis was creation of synthetic catalytic systems based on γ- Al_2O_3. The main goal was to find optimal synthesis conditions to create catalysis which must repeat composition of catalyst from acidic etching solution of vermiculite. For this purpose series of samples was produced. They were tested in steam reforming of methane process. It was established that concentrations of all products practically reached the equilibrium during the whole operation time.

4 Conclusions

Nanoscale Ni-containing catalysts supported on spinel $Mg(FeAl)_2O_4$ show high activity in steam methane reforming (SMR) and partial oxidation of 30ppm H_2S in gas mixture.

The structural studies of the SMR catalyst by XAFS, XRD, EDX, HRTEM methods and Mossbauer spectroscopy reveal that after addition of Ni as an active ingredient and reduction in H_2 the hybrid cluster system with a core (γ-Fe_2O_3) /shell (FeNi) configuration is formed. In this case the core of the hybrid system, consisting of nano-sized particles of FeNi alloy, provides activity in the SMR process, while the γ-Fe_2O_3 clusters of the shell are the active component for the decomposition of hydrogen sulfide into elemental sulfur

Acknowledgements

This work was financially supported by the State contract of Department of Sciences (Ministry of education and sciences RF, Contract N14.577.21.0064), the Russian Foundation for Basic Research (projects nos. ofi_m 13-03-12034; 13-03-00697; 12-03-00007).

References

[1] J.N. Armor, *Appl. Catal*. 176 (1999).
[2] P. Gangadharan, K. Kanchi, H. Lou, *Chem. Eng. Res. Des*. 90 (2012)
[3] H.F. Rase, *Handbook of Commercial Catalysts: HeterogeneousCatalysts*, 2000
[4] Tsodikov M.V. Kurdyumov S.S., Buhtenko O.V., T.N., *RF Patent № 2483799,* 2013
[5] Perederij M.A., Tsodikov M.V., Karaseva M. S., Smirnov V.V., Maksimov Ju.V., Gurko A.A., *RF Patent № 2350387*, 2009.

III-OP17

Mechanistic Implications on Low Temperature Steam Reforming of Methane over Ni/La/CeO_2-ZrO_2

Angeli S.D., Lemonidou A.A.*

Department of Chemical Engineering, Aristotle University of Thessaloniki, Thessaloniki, Greece

* alemonidou@cheng.auth.gr

Keywords: steam reforming, methane, ceria-zirconia, mechanism, nickel

1 Introduction

Industrial steam reforming of methane for hydrogen production is accompanied by significant GHG emissions, mainly from the burner used to supply heat to the endothermic reaction. Low temperature steam reforming can lead to significant environmental and process benefits, such as reduced energy needs, milder material stability requirements and considerably simplified process layouts. On the other hand, methane steam reforming at low reaction temperature (400-550 ^oC) results in low CH_4 conversions due to thermodynamic limitations, which, however, can be surpassed by using hydrogen-selective membrane reactors.

Previous studies showed that Ni/La/CeO_2-ZrO_2 is highly active in the low temperature range as well as coke resistant even in the presence of hydrocarbon-type impurities [1] . The performance can be ascribed to CeO_2-ZrO_2 due to the active role in the redox mechanism and the gasification of carbon depositions through the mobility of surface oxygen species. Moreover, the presence of La enhances the oxygen storage capacity and the thermal stabilization of the catalyst.

In this work, we report mechanistic implications of low temperature steam reforming of methane over Ni/La/CeO_2-ZrO_2. The mobility of surface/lattice oxygen species, which may participate in the reaction scheme, is determined by isotope oxygen hetero-exchange. Methane decomposition, which has been reported as the rate determining step over nickel catalysts [2], is investigated.

2 Experimental

The catalyst containing 10wt% Ni was prepared via wet impregnation. The metal was deposited on a support containing 78%ZrO_2, 17% CeO_2 and 5%La_2O_3 that was provided by Mel Chemicals. After the deposition and the removal of the solvent the sample was dried and finally calcined at 800^oC for 5h. Basic characterization of the catalyst was realized through XRD, and H_2-TPR. Oxygen mobility was measured by temperature programmed ^{18}O isotopic exchange experiments in prereduced sample (T_{red} = 550 ^oC). The experiments took place in a U-shape reactor in a transient unit coupled with MS detector. The kinetic isotope effect of methane decomposition in 1.7%CH_4/He or 1.7%CD_4/ 15%Ar/balance He was investigated in temperature programmed mode in a heating rate of 10^oC/min.

3 Results and discussion

XRD of the sample Ni/La/CeO_2-ZrO_2 showed peaks corresponding to the Ni in oxidic form and the crystal phase of mixed $Zr_{0.84}Ce_{0.16}O_2$. No peaks of lanthana were detected implying that the dopant is finely dispersed. The reduction of Ni can be achieved at relatively mild conditions, important for the application of the low temperature steam reforming concept, with T_{max} at 480^oC.

Figure 1a depicts the evolution of the rate of oxygen exchange as a function of temperature. Consumption of $^{18}O_2$ with onset at 220 ^oC, not accompanied initially by evolution of $^{16}O_2$ or

$^{16}O^{18}O$ is attributed to reoxidation of the reduced sample. Both simple and multiple oxygen hetero-exchange are triggered at 360 °C with multiple hetero-exchange being dominating up to 500 °C. Maximum rates of $^{16}O_2$ and $^{18}O^{16}O$ evolution were observed within the temperature range of interest for the steam reforming reaction (400-550 °C). High surface/lattice oxygen mobility may play an active role in the redox mechanism by oxidizing CH_x fragments and also prevent the accumulation of carbon species on the catalytic surface.

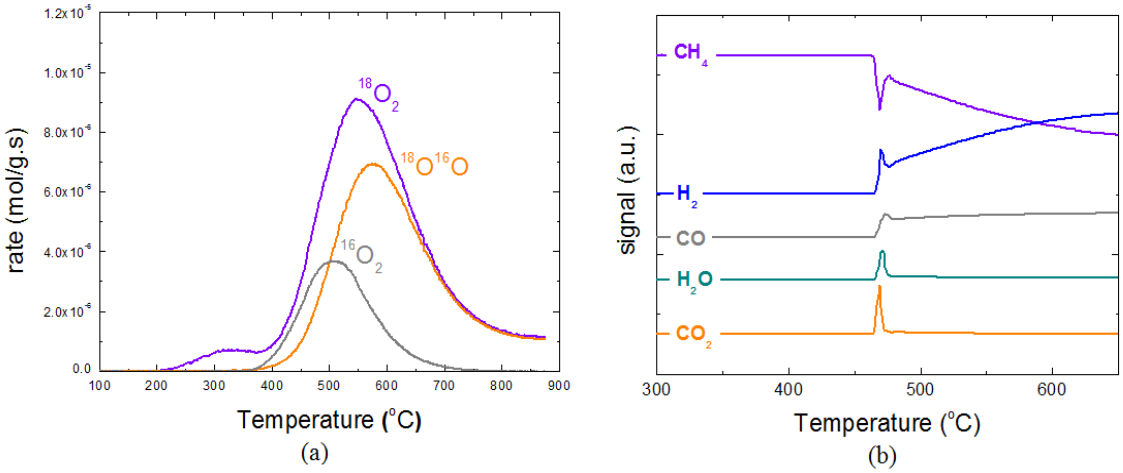

Fig. 1. (a) ^{18}O isotopic exchange profile over prereduced Ni/La/CeO_2-ZrO_2 (b) gas responses during temperature programmed methane decomposition over Ni/La/CeO_2-ZrO_2.

Methane decomposition produces hydrogen and solid carbon. However, at the onset temperature (455 °C), consumption of CH_4 leads to instant formation of H_2O and CO_2 and later to CO along with H_2 (Figure 1b). The production of oxygen-containing products in the absence of gaseous oxygen is attributed to the participation of support oxygen species in the reaction scheme. Additional experiments in methane decomposition using CD_4 instead of CH_4, which are currently in progress will allow the determination of the kinetic isotope effect and provide information about the rate-determining step. Steam reforming reaction experiments using CH_4 and CD_4 and the calculation of the kinetic isotope effect in the presence of steam, constitutes important aspects of the mechanistic study and will be conducted in the near future.

4 Conclusions

The mechanism of methane steam reforming in the low temperature range (<550 °C) is investigated over Ni/La/CeO_2-ZrO_2. H_2-TPR showed that the catalyst can be fully reduced within the temperature range of operation allowing the reduction process being conducted without the need of further heating of the reactor. At the same temperature range the catalyst showed maximum oxygen mobility as determined by oxygen isotopic exchange tests, which might contribute to the high activity and coke resistance of the catalyst. Temperature programmed methane decomposition showed that lattice oxygen of the partially reduced support participates in the reaction scheme.

Acknowledgements

This work has received funding from the European Union's Seventh Framework Programm (FP7/2007-2013) for the Fuel Cells and Hydrogen Joint Technology Initiative, for CoMETHy project under grant agreement n° 279075.

References

[1] S.D. Angeli, F.G. Pilitsis and A.A. Lemonidou, *Catal. Today.* 242 (2015) 119.
[2] J. Wei and E. Iglesia, *J. Catal.* 224 (2004) 370.

III-OP18

Mechanism of Ethanol Steam Reforming over Pt/(Ni+Ru)-Promoted Oxides by FTIRS *in situ*

Sadykov V.[1,2*], Chub O.[1], Chesalov Yu.[1], Mezentseva N.[1,2], Pavlova S.[1], Arapova M.[1,3], Roger A.-C.[3], Parkhomenko K.[3], Van Veen A.C.[4]

1 - Boreskov Institute of Catalysis, Novosibirsk,Russia
2 - Novosibirsk State University, Novosibirsk,Russia
3 - University of Strasbourg, Strasbourg, France
4 - University of Warwick, Warwick, UK

* sadykov@catalysis.ru

Keywords: ethanol, steam reforming, syngas, complex oxides, Pt/Ni+Ru, mechanism, FTIRS *in situ*

1 Introduction

Nanocomposites based on bulk/supported fluorite-like/perovskite-like complex oxides promoted by Pt/Ni+Ru etc are known to be efficient and stable to coking catalysts of ethanol steam reforming (ESR) [1, 2]. Optimization of their composition is to be based upon knowledge of the detailed mechanism of catalytic reaction. FTIRS *in situ* is a powerful tool for identification of the nature of surface species and estimation of the rates of their transformation required for this purpose [3, 4]. This work presents results of such studies for two types of catalysts based on bulk fluorite-like oxide and supported on alumina perovskite-like oxide.

2 Experimental/methodology

$Pr_{0.15}Sm_{0.15}Ce_{0.35}Zr_{0.35}O_2$ fluorite-like oxide (Catalyst I) was prepared by polymerized complex precursor (Pechini) route and calcined in air at 900°C for 2 h [5]. Pt (1.4wt.%) was supported via incipient wetness impregnation with H_2PtCl_6 solution. 10wt.% $LaNi_{0.95}Ru_{0.05}O_3$/Mg-alumina catalyst (Catalyst II) was prepared using as a source a high purity γ-alumina prepared by decomposition of aluminium hydroxide "Disperal" (Sasol) under air at 700 °C. 10 wt. % MgO and 10wt.% $LaNi_{0.95}Ru_{0.05}O_3$ were successively supported by incipient wetness impregnation with inorganic salts solution followed after each step by calcination under air at 700 °C for 2 h. Catalysts pressed into pellets were studied in the flow IR cell with NaCl windows using a CARY 660 (Agilent) FTIR spectrometer. After standard pretreatment in the stream of 20%O_2 in He at 450 °C the catalysts were cooled in He to room temperature, and ethanol was adsorbed from the flow of 1% C_2H_5OH in He. After purging cell by He, samples were heated in the He stream by steps of 50 °C up to 500 °C with spectra recording. Dynamics of the surface species transformation under contact with the stream of 2% H_2O in He was studied in the isothermal mode in the same temperature range. Gas composition at the cell outlet was analyzed by FTIR spectrometer and on-line IR absorbance, electrochemical and polarographic gas sensors [5].

3 Results and discussion

After ethanol adsorption at room temperature, bands corresponding to molecularly adsorbed ethanol (1280 cm^{-1}), water (1600 cm^{-1}) and ethoxy species (1450, 1380-1400, 1341, 1082-1100, 1046-1052 cm^{-1}, several types of terminal and bridging forms) formed by dissociative adsorption of ethanol are observed. Desorption into the stream of He with the step-wise increase of temperature is accompanied by the decrease of intensity of bands corresponding to ethanol and ethoxy species disappearing completely at T> 250 °C. Bands corresponding to acetate species (1430-1434 and 1550-1575 cm^{-1}) emerge at ~ 200 °C, their intensity growing to the maximum at 350 °C with subsequent slow decline.

Under contact with the stream of 1%H_2O in He, ethanol and ethoxy species are consumed, acetaldehyde is formed and then consumed, while acetate species are accumulated. Estimation of efficient first-order rate constants (Table 1) revealed that ethoxy groups are very reactive, so their transformation into acetaldehyde by dehydrogenation is not the rate-determining stage (rds). Transformation of acetaldehyde via C-C-bond rupture on Me sites with CH_4 as by-product is rds of ESR [4]. Acetates are spectators formed by slow acetaldehyde oxidation [4]. At T~400 ^oC only acetates are observed on the surface of catalysts in steady-state conditions being able to react with water at these temperatures. Estimation of the efficient first-order rate constant of acetates consumption by reaction with H_2O at 400 ^oC gives value ~ 10^{-3} s^{-1}, which is much lower than the rate constant of ethanol consumption This agrees with conclusion on the step-wise red-ox scheme of ESR on these catalysts with CH_4 as by-product [5]. For Catalyst II with a lower red-ox ability transformation of ethoxy species on acid sites is also accompanied by formation of such by-products as C_2H_4 and $(C_2H_5)_2O$ via dehydration route.

Table 1. Efficient rate constants of adspecies transformation for Catalyst I.

T, ^oC	k, s^{-1} (n=1)			
	Acetaldehyde consumption	**Ethoxy consumption**	**Ethanol consumption**	**Acetate formation**
	Absorption band, cm^{-1}			
	1710	**1145**	**1036**	**1436**
150	0.043	2.125	0.058	0.0055
200	0.075	2.457	0.079	0.0103
250	0.119	-	-	0.0172
300	-	-	-	0.0262

4 Conclusions

For $Pt/Pr_{0.15}Sm_{0.15}Ce_{0.35}Zr_{0.35}O_2$ and $LaNi_{0.95}Ru_{0.05}O_3$/Mg-alumina catalysts *in situ* FTIRS studies revealed that in ESR reaction transformation of ethoxy species by dehydrogenation is a fast step, while the rate-determining stage is the C-C bond rupture in thus formed acetaldehyde. Acetate species are spectators, while transformation of ethoxy species on acid sites of alumina-supported catalysts produces C_2H_4 and $(C_2H_5)_2O$ via dehydration route.

Acknowledgements

Support by Russian Fund of Basic Research Project RFBR-CNRS 12-03-93115, FP7 Project BIOGO (NMP-LA-2009-604296) and the Ministry of Education and Science of the Russian Federation is gratefully acknowledged.

References

[1] V. Sadykov, L. Bobrova, S. Pavlova, V. Parmon et al,. *Syngas Generation from Hydrocarbons and Oxygenates with Structured Catalysts*. Nova Science Publishers, Inc, New York (2012), 140p.
[2] V. Sadykov, N. Mezentseva, M. Simonov, S. Pavlova et al, *Int. J. Hydrogen Energy* (2015), http://dx.doi.org/ 10.1016/j.ijhydene.2014.11.151
[3] S. M. de Lima, I. O. da Cruz, G. Jacobs, B. H. Davis et al, *J. Catal.* 257 (2008) 356
[4] G. P. Szijjártó, Z. Pásti, I. Sajó, A. Erdoőhelyi et al., *J. Catal.* 305 (2013) 290
[5] V. Sadykov, N. Mezentseva, Yu. Fedorova, A. Lukashevich et al. *Catal. Today.* (2014) http://dx.doi.org/ 10.1016/j.cattod.2014.10.045

III-OP19

Iron Oxide-Type Structured Catalyst for Water Gas Shift Reaction

Watanabe R., Watanabe S., Fukuhara C.*

Department of Applied Chemistry and Biochemical Engineering, Graduate school of Engineering, Shizuoka University, Shizuoka, Japan

* tcfukuh@ipc.shizuoka.ac.jp

Keywords: iron oxide structured catalyst, water gas shift reaction, redox

1 Introduction

The importance of hydrogen production, mainly from natural gas steam reforming, as a clean energy source is increasing year by year. The reformed gas contains hydrogen as well as carbon monoxide. For producing more hydrogen with removing carbon monoxide, the water gas shift (WGS) reaction is an effective approach.

$$CO + H_2O \rightleftarrows CO_2 + H_2 \qquad \Delta H^0 = -41.2\ kJ \cdot mol^{-1} \qquad (eq.1)$$

In the industrial processes, the WGS reaction is performed with a two-stage catalytic processes: a high temperature shift (HTS) with a Fe_2O_3-Cr_2O_3 catalyst and a low temperature shift (LTS) with a Cu/ZnO/Al_2O_3 catalyst. The Fe_2O_3-Cr_2O_3 catalyst has an insufficient activity at low temperatures. Furthermore, Cr, which is contained in the catalyst, is a highly toxic to humans and the environment. The Cu/ZnO/Al_2O_3 catalyst is deactivated by an oxidizing atmosphere. Therefore, the catalyst with a high activity at a low temperature and stable in an oxidative atmosphere are required. The previous work revealed that the Fe_2O_3 catalyst modified by Pd and K showed a significantly higher activity than the industrial HTS catalyst at 573 K [1].

For further enhancement of the catalytic activity, we focused on a plate-type catalyst on a metal substrate. The plate-type catalyst, which is commonly called a structured catalyst, is composed of a regularly arranged catalyst on the metal plate. The structured catalyst could overcome the disadvantage of a poor heat conductivity of the iron oxide-type material, and high activity would be obtained at a low temperature due to the effective utilization for the external heat energy.

In this study, the iron oxide-type structured catalyst was developed on a metal substrate. The WGS performance of the plate-like iron oxide-type catalyst was investigated. In addition, the effects of Pd and K supported on the iron oxide-type structured catalyst on the performance were examined for enhancing the WGS activity.

2 Experimental

The structured iron oxide-type catalyst was prepared by a hydrothermal synthesis as follows; the aluminum substrate (JIS A1100P) was activated by NaOH *aq*. and HCl *aq*. at 293 K for 5 and 2.5 min. The activated substrate was then immersed in the iron precursor solution, which was prepared with $FeCl_3$ and urea in distillated water. Subsequently, the hydrothermal synthesis was performed at 368 K for 11 h to form the iron oxide on the aluminum plate. The iron oxide-type structured catalyst was then prepared by calcinating at 573 K for 2 h under N_2 atmosphere. For loading the promoter, the structured catalyst was immersed in the CH_3COOK solution. After immersing, the structured catalyst was calcined at 773 K for 2 h. Subsequently, the promoted catalyst was immersed in the $PdCl_2$ solution, and calcined at 773 K for 2 h.

Activity tests were performed at 573–823 K after setting the structured catalyst at the center of the quarts tube. Reactants of CO and H_2O were supplied to the catalyst at 5.0 and 10.0 ml min^{-1}, respectively. The gaseous reactants and products, such as CO, CO_2 and CH_4, after the

trapping of steam in the effluent gas through the cold trap were collected by a gas-tight syringe, then injected into the off-line thermal conductivity detection gas chromatograph (GC-8A; Shimadzu Co., Ltd., Japan).

3 Results and discussion

Figure 1 shows the surface images of the prepared iron oxide structured catalyst measured by FE-SEM. From these images, the circular sheets were observed on the surface of the catalyst. The diameter of the circular sheet is about 3 μm, and the thickness of the sheet is a few tens of nanometers. Such micro-sheet is stacked in a random manner on the aluminum plate. Figure 2 denotes the elemental mapping of the micro-sheet. From the mapping, the micro-sheet was composed with aluminum and iron components. The aluminum came from the aluminum substrate because the iron precursor solution does not include the aluminum component. Namely, the aluminum component was dissolved from the aluminum substrate and was incorporated in the micro-sheet during the hydrothermal synthesis. The structure of the micro-sheet was not confirmed by the XRD measurement (not shown in this proceeding). The result meant that an amorphous phase of the iron-oxide might be formed on the aluminum substrate.

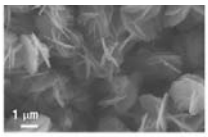

Figure 1 FE-SEM image for the iron structured catalyst.

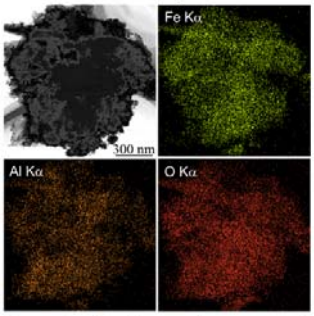

Figure 2 the elemental mapping of the micro-sheet.

Figure 3 denotes CO conversion at from 573 to 823 K over the iron oxide-based structured catalysts. To promote WGS activity, potassium and palladium were loaded on the iron oxide structured catalyst (abbreviated as Pd/K/FeO_x/Al-plate). The WGS activity over the Pd/K/FeO_x/Al-plate was obtained about 10%-conversion at low temperature of 573 K. On the other hands, other catalysts did not show any activity at 573 K. These results were satisfied with the previous study [1]. Namely, Pd, K, and Fe were necessary to show the WGS activity, and their synergetic effect was important for the WGS reaction.

Figure 4 shows the comparison of the activity of the structured catalyst with that of the Cu/ZnO/Al_2O_3 catalyst. The catalytic activity of the Pd/K/FeO_x/Al-plate increased with reaction time, while the Cu/ZnO/Al_2O_3 catalyst showed a deactivation behavior. The developed iron oxide structured catalyst had a higher stability than the commercial Cu-based catalyst.

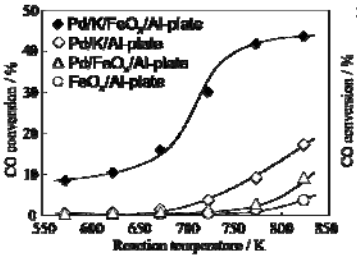

Figure 3 WGS performances of the various catalysts.

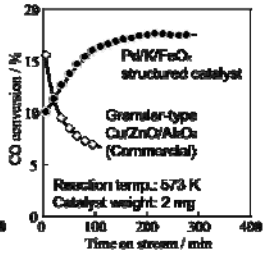

Figure 4 WGS activity of the structured and Cu-based catalysts.

4 Conclusions

The prepared iron oxide on the aluminum substrate had the characteristic morphology; the micro-sheet of iron oxide was formed on the substrate. To promote the WGS performance, Pd and K was loaded on the iron oxide structured catalyst. High activity was obtained over the Pd/K/FeO_x/Al-plate catalyst. The prepared catalyst had a superior stability to the Cu-based catalyst.

Acknowledgement

This study is supported by JSPS KAKENHI Grant-in-Aid for Scientific Research (A) (26709059).

Reference

[1] R. Watanabe Y. Sakamoto, K. Yamamuro, S. Tamura, E. Kikuchi, Y. Sekine, *Appl. Catal. A: Gen.,* 457 (2013) 1.

III-OP20

Low Temperature CH_4 Oxy-Reforming Coupled with Pd-Based Membrane for an Energy-Efficient Process for Syngas Production

Abate S.[1], Basile F.[2], Fornasari G.[2], Lombardi E.[2], Mafessanti R.[2*], Vaccari A.[2]

1 - Department of Electronic Engineering, Chemistry and Industrial Eng. – DIECII - University of Messina, Messina, Italy

2 - Department of Industrial Chemistry "Toso Montanari", Alma Mater Studiorum - University of Bologna, Bologna, Italy

* rodolfo.mafessanti2@unibo.it

Keywords: hydrogen, syngas, oxy-reforming, $Rh/Ce_{0.5}Zr_{0.5}O_2$, Pd-based membrane, H_2 purification

1 Introduction

The possibility to produce H_2 and syngas from methane at relative low temperature (700-750°C) is faced by two combined approach: 1) coupling reforming and CPO reactions using low residence time in a so–called oxy-reforming with low oxygen contents and S/C ratios. The oxy-reforming allows low external heat supply, low oxygen consumption and good control of the temperature profile which avoid sintering; 2) coupling the oxy-reforming with separation by Pd dense membrane aiming to produce pure H_2 or, in case of high pressure, syngas with a second conversion step after separation. In the present experimental configuration low radial and axial ΔT (30-50°C at 150-36 ms) are present allowing the possibility of reliable catalysts comparison, enhancing catalysts differences at low residence times. Catalyst selection have been carried out on the base of activity data and their stability against carbon formation, favored by the low S/C and O_2/C (0.7, 0.2 respectively). New catalysts based on $Rh/CeZrO_2$ have been developed using inverse microemulsion synthesis, aimed to obtain the specific $Ce_{0.5}Zr_{0.5}O_2$ phase. The coupling of oxy-reforming with a Pd thin dense membrane, placed downstream the reactor for H_2 selective separation, was studied at different S/C ratios, GHSV and P, investigating the permeability and stability of the system.

2 Experimental/methodology

Catalytic tests are carried out in a plant using the operative conditions reported in Table 1.

Table 1. Catalytic tests carried out without and with the membrane placed downstream of the reactor.

Operative Parameters	Without Membrane	With Membrane
T_{oven} [°C]	750	750 ($T_{memb.}$ = 400°C)
P [atm]	1; 3; 5; 10; 20	3; 5
GHSV [h^{-1}]	24000; 50000; 100000	24000; 100000
Steam to Carbon ratio (S/C)	0.7-1	0.7 – 1
Feed composition (CH_4; O_2; $H_2O_{(v)}$) [%v/v]	52; 11; 37	45.5; 9; 45.5

The catalysts used were Ceria-Zirconia mixed oxides obtained by inverse microemulsion (Ce/Zr-m) synthesis [1] and co-precipitation (Ce/Zr-cp) with Ce/Zr 75/25 and 50/50 a.r.. The samples were calcined at 750°C and impregnated with Rh (1 wt%). The catalysts were characterized using XRD, TPR/O, Raman, SEM, TEM-EDX and porosimetry.

The research part regarding the membrane for H_2 separation was carried out in collaboration with the University of Messina, where the actual membrane preparation was performed following the Electroless Plating Deposition (EPD) technique.

3 Results and discussion

The synthesis of the $CeZrO_2$ support carried out by microemulsion showed (by TEM-EDX) a

Ce/Zr ratio significantly more homogeneous than which obtained by co-precipitation both with Ce/Zr 75/25 and 50/50. The Ce/Zr-m 50/50 allows to obtain the specific $Ce_{0.5}Zr_{0.5}O_2$ phase detected by XRD, compatible with the tetragonal *t''* phase as confirmed by Raman spectra. Otherwise the co-precipitation lead to a XRD pattern with reflections centred on $Ce_{0.6}Zr_{0.4}O_2$ phase. Furthermore both microemulsion samples have particle and pore size with a sharp mono-modal distribution leading to a very good dispersion of the Rh after impregnation (2-3 nm).

The catalytic activity of the sample characterized by the Ce/Zr-m support, calcined at 750°C and impregnated with 1wt% of Rh (Rh1IWI_CZO-m750) is shown in figure 1. Regardless the reaction conditions, this sample shows an high activity with CH_4 conversions equal (at $24000h^{-1}$) to those calculated at the thermodynamic equilibrium. At higher GHSV, experimental data do not reach equilibrium even at 5 atm, while an higher S/C ratio slightly improve the CH_4 conversion, as shown from the data recorded at 3 atm and 100000 h^{-1}. Increasing pressure up to 10 and 20 atm the equilibrium is always reached, even at high GHSV values. The samples obtained by co-precipitation give lower conversion than those prepared by microemulsion both comparing the Ce/Zr 75/25 and 50/50, probably due to the better dispersion of the Rh in the Ce/Zr-m support. The effect of the support is also clear studying the deactivation phenomena. After 30 h time-on-stream the $Ce_{0.5}Zr_{0.5}O_2$ is very stable and no carbon formation is observed. Otherwise, different deactivation grades occur in the other samples with the following scale of stability: 50/50-m > 50/50-cp and 75/25-m > 75/25-cp, demonstrating the importance of the $CeZrO_2$ phase and its homogeneity. The peculiar properties of the $Ce_{0.5}Zr_{0.5}O_2$ are most likely due to the high oxygen mobility [2].

Feeding the outlet reformate gas to the membrane module ($T_{memb.}$ = 400°C) the gas mixture is separated using a thin Pd membrane on ceramic support for which the permeability rate (125 $mL \cdot cm^2/min$) have been previously determined with pure H_2 at 400°C and different pressures. The results of the dry gas (DG) compositions before the membrane and those relative to the permeate and the retentate streams are reported in figure 2 (a) and (b). The high H_2 permeability value of these Pd membrane allows to reach an high grade of separation together with a selectivity equal to 100% and good stability (20-25h time-on-stream). Regardless the GHSV values, the H_2 permeation is limited by the H_2 partial pressure (p_{H_2}) in the retentate that reach 1atm at the exit of the membrane ($\Delta p_{H_2} = 0$). The test at 5 atm allows to obtain a lower H_2 content in the retentate (< 30% on DG basis) which can further decrease by increasing the Δp_{H_2} using a sweep gas in the permeate side.

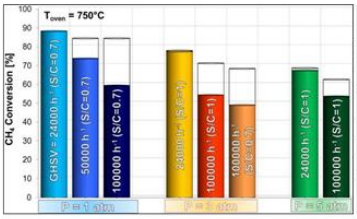

Fig. 1. Catalytic activity of Rh1IWI_CZO-m750 in function of P, GHSV and S/C ratio

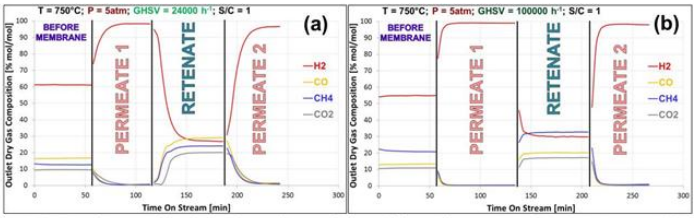

Fig. 2. DG outlet composition before the membrane and those relative to the permeate and retentate streams at: (a) $24000h^{-1}$; (b) $100000h^{-1}$

4 Conclusions

Inverse microemulsion is an interesting method for support preparation, leading to an high homogeneity both in terms of the particle size and the nature of the crystalline phase. $Rh/Ce_{0.5}Zr_{0.5}O_2$ shows the best activity due to the high Rh dispersion related with the homogeneous pore size of the support, and an high stability due to the enhanced oxygen mobility of the $Ce_{0.5}Zr_{0.5}O_2$ phase. The process for hydrogen production and separation have been demonstrated by using oxy-reforming and a downstream thin Pd membrane, which showed to be effective to obtain 100% H_2 stream, limited only by Δp_{H_2} which can be easily increased.

References

[1] V. Ballesteros, J. C. Conesa, M. Fernandez-Garcia, A. Martinez-Arias, C. Otero, L. N. Salamanca, and J. Soria, *Langmuir* **15** (1999) 4796

[2] O. Cherifi, P. Ferreira-Aparicio, A. Guerrero-Ruiz, S. Menad, and I. Rodrìguez-Ramos, *Catalysis Letters* **89** (2003) 63

III-OP21

Effect of Ni-Cu-Based Catalysts Composition and Support Structure on Hydrogen Production by Methanol Steam Reforming

Lytkina A.A.[1*], Zhilyaeva N.A.[1], Orekhova N.V.[1], Ermilova M.M.[1], Yaroslavtsev A.B.[1,2]

1 - A.V. Topchiev Institute of Petrochemical Synthesis of the Russian Academy of Sciences, Moscow, Russia

2 - Kurnakov Institute of General and Inorganic Chemistry of the Russian Academy of Sciences, Moscow, Russia

* lytkina@ips.ac.ru

Keywords: hydrogen production, methanol steam reforming, bimetallic catalyst, Cu-Ni, ZrO_2

1 Introduction

Hydrogen is considered as a perspective fuel because of its high calorific value and complete absence of toxicity because the only product of its oxidation is water. It can be efficiently utilized by combining with fuel cells, which can directly convert the chemical energy into electricity. Methanol has some advantages as a hydrogen source because it is one of the commodity chemicals [1] and it can be easily transformed into hydrogen at low temperatures. Methanol steam reforming (MSR) is an efficient process for maximizing the hydrogen production and minimizing the carbon monoxide formation. A lot of works was devoted to the investigation of an appropriate catalyst. Traditionally, copper-based catalysts distinguished by high activity and selectivity are applied in the MSR reaction. It is known also, that the most active catalysts in dehydrogenation processes are bimetallic supported systems [2]. But this issue is still of current importance for catalytic science and industry.

The aim of this work was to investigate influence of a support – ZrO_2 structure and composition of Ni-Cu bimetallic catalysts in process of methanol steam reforming.

2 Experimental/methodology

ZrO_2 was prepared by precipitation method and annealed at two different temperatures. Obtained support was promoted by Y_2O_3 and La_2O_3 to stabilize a cubic structure. Bimetallic catalysts were prepared by sequential impregnation of oxide supports (ZrO_2, ZrO_2-Y_2O_3, ZrO_2-La_2O_3) by Cu and Ni salts to achieve metal ratio 1:4 and 4:1. Obtained catalysts were tested in MSR reaction for H_2 production at different temperatures. Catalysts were characterized by DSC/TGA, BET, SEM, XRD, TEM.

3 Results and discussion

According to XRD data obtained ZrO_2 had three different modifications. Samples annealed at 350º C had an amorphous structure, and at 400º C were monoclinic. ZrO_2 doped with Y_2O_3 and La_2O_3 had cubic modification. Maximum hydrogen yield (≈2 mol per 1 mol of methanol) was achieved with the use of $Ni_{0.2}$-$Cu_{0.8}$/amorphous ZrO_2 catalyst. Presence of amorphous ZrO_2 provides high active sites concentration, which greatly improves water adsorption and composite activity. Increase of ZrO_2 support crystallinity results in the decrease of a surface area, reduction of sorption properties and the drop of catalyst activity.

It was determined that selectivity of copper-based catalysts is higher than nickel-based. It can be ascribed to change of methanol adsorption mechanism on the catalyst surface. Single-center alcohol adsorption is more preferable on catalysts with a high copper content. This in turn

reduces the CO output. A lower Fermi level of the copper-based catalysts also can promote deeper methanol oxidation to CO_2. Figure 1 shows a dependence of hydrogen yield on catalyst type and a typical TEM image of Cu-Ni/ZrO_2 catalyst. The obtained data enables to conclude that the most probable mechanism of MSR process is bifunctional and includes simultaneous water adsorption on ZrO_2 support and alcohol adsorption on metal catalyst.

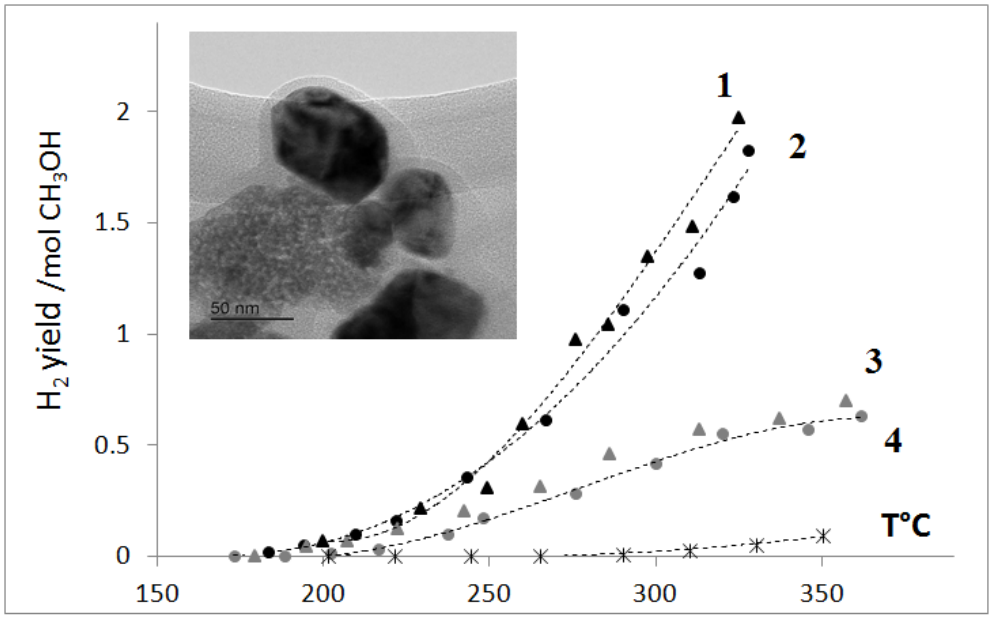

Fig. 1. Typical TEM image and hydrogen yield in SRM reaction on: 1) $Cu_{0.8}$-$Ni_{0.2}$/ amorphous ZrO_2; 2) $Cu_{0.2}$-$Ni_{0.8}$/ amorphous ZrO_2; 3) $Cu_{0.8}$-$Ni_{0.2}$/ monoclinic ZrO_2; 4) $Cu_{0.2}$-$Ni_{0.8}$/ monoclinic ZrO_2 catalysts

4 Conclusions

New catalysts ($Ni_{0.8}$-$Cu_{0.2}$/ZrO_2, $Ni_{0.2}$-$Cu_{0.8}$/ZrO_2) were developed for the methanol steam reforming process. It was confirmed that obtained catalysts are active in MSR reaction. Catalysts showed good stability without apparent deactivation during the testing. It was shown also, that support structure has the main influence on composites activity, while the nature of a dominant metal affected on the selectivity of the resulting catalysts. The influence of support structure on the mechanism of MSR reaction was discussed. The most active and selective catalyst was the amorphous sample $Ni_{0.2}$-$Cu_{0.8}$/ZrO_2. The most probable mechanism of MSR process is bifunctional and includes simultaneous water adsorption on ZrO_2 support and alcohol adsorption on metal catalyst.

References

[1] A. Iulianelli, P. Ribeirinha, A. Mendes, A, Basile, *Renewable and Sustainable Energy Rev.* 29 (2014) 355-368.

[2] E.Yu. Mironova, A.A. Lytkina, M.M. Ermilova, M.N. Efimov, L.M. Zemtsov, N.V. Orekhova, G.P. Karpacheva, G.N. Bondarenko, D.N. Muraviev, A.B. Yaroslavtsev *Int. J. Hydrogen Energy* http://dx.doi:10.1016/j.ijhydene.2014.11.082

III-OP22

Stability and Activity Promoters in Medium Temperature Water Gas Shift Catalysts

Lucarelli C.[1], Faure R.[2], Fornasari G.[3], Gary D.[2], Molinari C.[3], Schiaroli N.[3], Vaccari A.[3*]

1 - Dipartimento di Scienza e Alta Tecnologia, Como, Italy
2 - Centre de Recherche Claude-Delorme, Jouy-en-Josas, France
3 - Dipartimento di Chimica Industriale "Toso Montanari", Alma Mater Studiorum - Università di Bologna, Bologna, Italia

* angelo.vaccari@unibo.it

Keywords: medium temperature water gas shift, Cu/Zn/Al catalysts, Zr, La, Ce

1 Introduction

H_2 is widely considered as the main clean fuel of the future and is also a relevant raw material in chemical and petrochemical industry. One of the largest sources of H_2 is the Water Gas Shift (WGS) reaction, performed after hydrocarbon steam reforming (SR) of biomass gasification reactors to reduce the CO content in the final gas stream or to adjust the H_2/CO ratio for further processes (methanol and/or higher molecular weight alcohols or hydrocarbon Fischer-Tropsch syntheses). Currently, the WGS reaction is performed in two steps to achieve highest productivity: High Temperature Shift (HTS, T > 350 °C) followed by a Low Temperature Shift (LTS, T = 230-250 °C) [1]. More recently, the industrial interest moved towards new catalysts able to operate at medium temperature (MTS, T = 300°C ca.) with high activity, selectivity and stability with time-on-stream, that allow to operate in only one reactor and with low steam/dry gas ratio (S/DG). In a previous patent [2] it was reported the doping of traditional LTS Cu/Zn/Al catalysts by Ce, La, Zr, to enhance the thermal and hydrothermal stability, although only surface area values were reported. Aim of this paper was to shed light on the effects of these elements on surface and bulk properties and catalytic activity of Cu/Zn/Al MTS catalyst.

2 Experimental

The Cu/Zn/Al/X (X= Ce, Zr or La; Cu = 20 wt.%;) catalysts were obtained by coprecipitation at 60 °C and pH = 9.0 of hydrotalcite-type (HT) precursors from the nitrates of the elements, followed by calcination at 550 °C for 6 h and reduction in programmed temperature feeding a H_2/N_2 gas mixture [3]. The catalytic tests were performed in a fixed-bed reactor (INCOLOY), operating at 1.5 MPa and 250-350°C, feeding a $CO/CH_4/CO_2/H_2$: 18.8/4.6/4.6/72.0 (v/v) gas mixture. H_2O was introduced in a preheater by using a Jasco HPLC pump, operating with two S/DG ratio (0.55 or 0.25) and contact time (τ) values (0,5 and 1.0 s). The effect of the dopants on the structure and on the performance of the catalyst before and after the reaction tests was investigated by X-ray diffraction (XRD), N_2 adsorption/desorption, H_2-TPR and N_2O titration.

3 Results and discussion

To evaluate the thermal stability of the La, Ce, Zr-containing catalyst, the dried precursors were calcined at increasing temperatures (360, 460 and 550 °C) and the BET surface area values were compared to a reference Cu/Zn/Al catalyst without promoters (CAT ref). Table 1 shows the positive effect of the promoters on the thermal stability of the catalysts, evidencing a remarkable increase of the thermal stability for all the catalysts in comparison to the reference one, with a similar trend also for Cu surface area and dispersion. Catalytic tests were carried out

on the La and Zr-containing catalysts, that showed the higher surface area values. The results obtained are summarized in figure 1, with experimental CO conversion values compared to calculated CO conversions at the thermodynamic equilibrium for corresponding outlet temperature.

Table 1. Values of specific surface area and porosity and N_2O titration as a function of the calcination temperature (in brackets). The pore volume and diameter and the Cu surface area are referred to the samples calcined at 550 °C for 6 h.

	BET S.A (m^2/g) [360 °C]	BET S.A (m^2/g) [460 °C]	BET S.A (m^2/g) [550°C]	Cu S.A. (m^2/g_{CAT})	Pore volume (cm^3/g)	Pore diameter (nm)
CAT ref	**57**	**62**	**48**	**5**	**0.35**	**28**
CAT La	95	94	70	9	0.36	16
CAT Ce	89	82	58	8	0.35	19
CAT Zr	94	91	76	9	0.39	20

The activity was similar for both promoted catalysts, with better CO conversion values than that of not promoted catalyst in all the reaction conditions investigated. In particular, for S/DG = 0.55; τ = 0.5 s, T = 250 °C the promoted catalysts showed the highest increase of activity. At the higher contact time value (τ = 1.0 s, S/DG= 0.55), both promoted catalysts reached the equilibrium values regardless of the temperature, while the decrease of the S/DG ratio to 0.25, worsened dramatically the activity of all the catalysts, with the worst results observed at 250 °C.

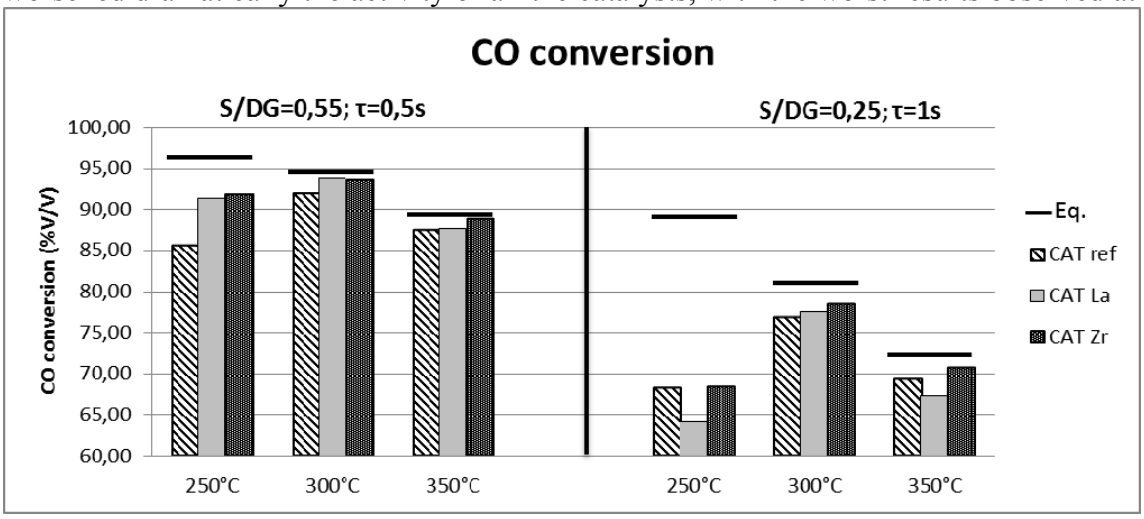

Figure 1. CO conversion for Cu/Zn/Al/La (CAT La) and Cu/Zn/Al/Zr (CAT Zr) catalysts, compared to the not promoted catalyst (CAT ref); the full lines show the CO conversion values at the thermodynamic equilibrium.

4 Conclusions

The addition of a small amount of La and Zr in a Cu/Zn/Al (Cu = 20 wt.%) catalyst promoted the surface properties and thermal stability, reflecting also on the catalytic activity in the WGS reaction at medium temperature. Significant increases of CO conversion were observed in condition of industrial interest, with a good stability with time-on-stream

References

[1] T.L. Le Valley, A.R. Richard, M. Fan, *Int. J. Hydr. Energy* **39** (2014), 16983.
[2] R.M. Sambrook, US 4,835,132 (1989) to Dyson Refractories GB.
[3] F.Basile, G. Brenna, R. Faure, G. Fornasari, D. Gary, A. Vaccari, WO 079,323 A1 (2013) to Air Liquide.

III-OP23

Effect of Nitrogen Doping of Carbon Supports for Hydrogen Production from Formic Acid Decomposition over Noble Metal Clusters and Atoms

Bulushev D.[1,2*], Zacharska M.[2], Podyacheva O.[1], Jia L.[2], Kibis L.[1], Boronin A.[1], Shlyakhova E.[3], Bulusheva L.[3], Guo Y.[2], Chuvilin A.[4], Beloshapkin S.[2], Okotrub A.[3], Ramasse Q.[5], Bangert U.[2]

1 - Boreskov Institute of Catalysis, SB RAS, Novosibirsk, Russia
2 - University of Limerick, Limerick, Ireland
3 - Nikolaev Institute of Inorganic Chemistry, SB RAS, Novosibirsk, Russia
4 - CIC nanoGUNE Consolider, San Sebastian, Spain
5 - STFC Daresbury Laboratories, Warrington, United Kingdom

* dmitri.bulushev@catalysis.ru

Keywords: hydrogen production, formic acid, noble metals clusters, carbon, atomic, resolution, STEM

1 Introduction

Formic acid can be produced from cellulose of biomass by hydrolysis or oxidation. It can be used for hydrogen storage or directly for hydrogenation reactions instead of molecular hydrogen. The effective catalysts should perform the formic acid decomposition in mild conditions with high selectivities for H_2 production. We used nitrogen-doped and undoped supports in the form of carbon nanofibers (CNFs) and mesoporous graphene like carbon (C_M) for stabilization of metal (Pt, Pd, Ru) clusters of less than 3 nm size and showed that N-doping of the supports improves considerably the hydrogen production from formic acid.

2 Experimental/methodology

The N-doped supports with 6-7 at.% of nitrogen were synthesized by catalytic growth from a NH_3/C_2H_4 mixture or from CH_3CN while the undoped materials - from C_2H_4 or CH_3OH. Noble metals were deposited by incipient wetness impregnation from salts or by deposition-precipitation method to get 1 wt.% content. The samples were reduced in H_2 at 573 K and characterized by N_2 adsorption methods, XPS and atomic resolution STEM (Nion Ultrastem 100, Titan 60-300). Regular STEM (JEM-2100F) was used to determine the mean metal particle sizes. Vapor phase formic acid decomposition (2.0 vol.% HCOOH/He, 51 mL min^{-1}) was performed in a fixed bed reactor as described earlier [1]. Turnover frequencies (TOFs) were calculated basing on the total number of metal atoms for the supported catalysts as a considerable part of metal was in the state invisible by the regular STEM and basing on the surface number for the Pt powder.

3 Results and discussion

Fig. 1 compares turnover frequencies for the formic acid decomposition over the N-doped and undoped Pt, Pd and Ru/CNFs catalysts with the mean particle sizes of 1.1, 1.5 and 2.3 nm and Pd/C_M catalysts with - 2.6 nm, respectively. The Pd catalysts showed high activities and intermediate selectivities (94-98%) as compared to the other metals. This was valid for the catalysts supported on both CNFs and C_M supports. The selectivities for the Ru catalysts were the lowest (83 and 91%) as well as the activity.

It is important that N-doping provides a considerable increase of the TOFs for all samples (Fig. 1). The effect is the most strong for Pt (10 times), but smaller for other metals (<3 times).

The TOFs for the N-doped Pt catalyst were also considerably higher than the TOFs for an unsupported Pt powder (9.3 nm), but comparable to the TOFs for the N-doped Pd catalysts. Moreover, this Pt catalyst showed improved resistance to CO inhibition and the selectivity of 99.5% at 50% conversion as compared to 96.2% for the undoped catalyst.

The strongest effect of nitrogen for Pt can be related to the smallest metal particle sizes and, therefore, the highest contribution of isolated metal atoms and clusters with a few atoms to the total content of surface metal sites. The presence of a considerable content of such species as well as Pd particles was clearly seen by atomic resolution STEM even for the Pd/C_M catalyst with the lowest dispersion of 43% (Fig. 1). These species can be active for the formic acid dehydrogenation, but only if the support is doped by nitrogen.

An XPS study showed the presence of 3 different nitrogen species in the N-doped samples. The metal clusters exist in an electron-deficient state as a considerable shift of the binding energies towards higher values was observed for the N-doped catalysts as compared to those for the undoped catalysts (by 0.6 eV for Pt) and bulk metals (by 1.5 eV for Pt). Pyridinic nitrogen stabilizes the electron-deficient clusters and isolated atoms providing their location on the open edge sites of the CNFs and C_M supports. Formic acid can be activated on the interface of these species with the support forming a surface adduct ($>NH^+HCOO^-$) with basic pyridinic nitrogen; this can be further dehydrogenated on the neighbouring clusters and isolated atoms of metals.

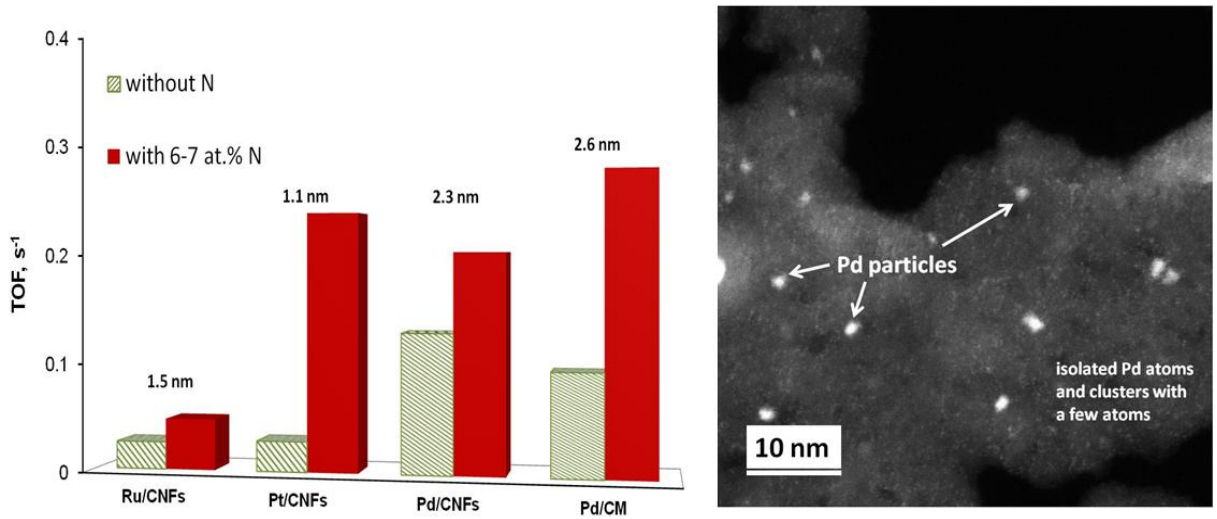

Fig. 1. Turnover frequencies of the formic acid decomposition at 398 K and atomic resolution STEM image of the 1 wt.% Pd/C_M catalyst (multiple small white dots correspond to isolated Pd atoms and Pd clusters with a few atoms).

4 Conclusions

N-doping of carbon supports for noble metals catalysts provides a considerable increase of the formic acid decomposition rate, selectivity to hydrogen and resistance to CO inhibition. This could be related to the presence of electron-deficient clusters and isolated atoms of metals stabilized by pyridinic nitrogen on the open edge graphene sites; these species can dehydrogenate the intermediate adduct of formic acid with pyridinic nitrogen to give hydrogen and carbon dioxide.

References

[1] Jia, L., Bulushev, D.A., Podyacheva, O.Yu., Boronin, A.I., Kibis, L.S., Gerasimov, E.Yu., Beloshapkin, S., Seryak, I.A., Ross, J.R.H., Ismagilov, Z.R. *J. Catalysis*. 307 (2013) 94.

III-OP24

Going Heterogeneous in the Additive-Free Hydrogen Production from Formic Acid at Room Temperature

Bulut A.[1], Yurderi M.[1], Say Z.[2], Kivrak H.[3], Gulcan M.[1], Kaya M.[4], Ozensoy E.[2], Zahmakiran M.[1*]

1 - Department of Chemistry, Yuzuncu Yıl University, Van, Turkey
2 - Department of Chemistry, Bilkent University, Ankara, Turkey
3 - Department of Chemical Engineering, Yuzuncu Yıl University, Van, Turkey
4 - Department of Chemical Engineering and Applied Chemistry, Atilim University, Ankara, Turkey

* zmehmet@yyu.edu.tr

Keywords: Pd, Ag, MnO, HCOOH, FTIR, STEM

1 Introduction

Hydrogen (H_2) is considered to be a promising energy carrier due to its high energy density (142 MJ/kg), which is almost three times higher than that of natural gas (55 MJ/kg) [1,2]. However, controlled storage and release of hydrogen are still among the critical technological barriers faced by the hydrogen economy [1-2]. In this context, formic acid (HCOOH, FA), which is one of the major stable and non-toxic products formed in biomass processing, has recently attracted significant attention as a potential hydrogen carrier for fuel cells designed towards portable use [4,5]. In the presence of metal catalysts, FA can catalytically be decomposed via dehydrogenation (1) and/or dehydration (2) pathways [3,4].

$$HCOOH(l) \rightarrow H_2(g) + CO_2(g)\ \Delta G_{298K} = -35.0\ kJ/mol\ (1)$$

$$HCOOH(l) \rightarrow H_2O(l) + CO(g)\ \Delta G_{298K} = -14.9\ kJ/mol\ (2)$$

In this study, we have focused on facile synthetic route for obtaining PdAg alloy and MnOx nanoparticles (NPs) supported on 3-aminopropyl functionalized silica ($PdAg\text{-}MnO_x/N\text{-}SiO_2$) to be used in the selective dehydrogenation of FA at room temperature in the absence of ant additives.

2 Experimental/methodology

Synthesized materials were characterized by a wide range of characterization techniques such as, ICP-OES, XRD, HRTEM, STEM, HAADF-STEM, XPS, in-situ FTIR, BET analysis and UV-Vis spectroscopy. The catalytic activity of $Pd\text{-}MnO_x/SiO_2\text{-}NH_2$ in the additive free FA dehydrogenation (*af*-FAD) was determined by volumetric measurement of the rate of hydrogen evolution. The selectivity of $PdAg\text{-}MnO_x/N\text{-}SiO_2$ catalyst in the decomposition of formic acid was investigated by GC analysis and NaOH-trap experiments.

3 Results and Discussion

Herein, we present a new heterogeneous catalyst system facilitating the liberation of hydrogen at room temperature through the dehydrogenation of formic acid in the absence of any additives with unprecedented activity, converging to that of the existing state of the art homogenous catalysts. Currently utilized heterogeneous $PdAg\text{-}MnO_x/N\text{-}SiO_2$ catalyst revealed a record activity (330 mol H_2 mol catalyst^{-1} h^{-1}) as well as excellent conversion (> 99 %) close to that of the existing state of the art homogenous catalytic systems available for *af*-FAD in the literature. Incorporation of the Ag sites into the Pd lattice leads to the formation of bimetallic PdAg alloys, decreasing the CO adsorption strength and increasing the tolerance against CO poisoning. MnO_x addition leads to the generation of sacrificial CO anchoring sites where CO can strongly bind in the form of carbonates. As a result, PdAg sites remain available for FA

dehydrogenation for an extended duration of time. MnO_x domains may influence the surface composition of the PdAg bimetallic alloys and decrease the number of Ag sites exposed on the surface of the bimetallic nanoparticles. MnO_x incorporation to the catalyst composition results in additional adsorption sites for FA and enhances the extent of formate creation even after extensive CO exposures.

Entry	Catalysts	T (K)	Conv. (%)	TOF (h^{-1})	Ref.
1	Ag@Pd	293	36	63	5
2	AgPd	293	10	72	5
3	Au@Pd	298	89	98	6
4	CoAuPd/C	298	91	37	7
5	CoAuPd/r-GO	298	51	45	8
6	CoAuPd-DNA	298	96	85	8
7	AuPd	298	28	41	9
8	AgPd	298	52	110	10
9	Pd-MnO_x	298	63	150	11
10	**PdAg-MnO_x**	**298**	**~ 99**	**330**	**this study**

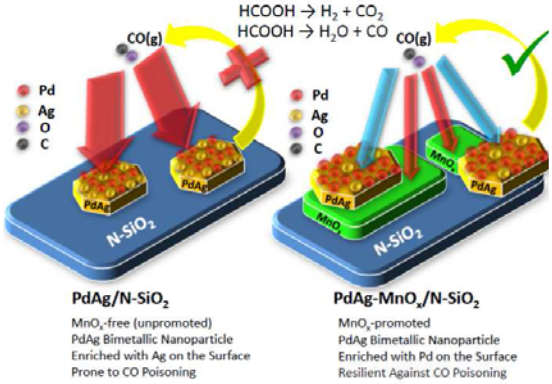

Table 1. Comparison of the catalytic performance data for the Pd-MnOx/SiO_2-NH_2 catalyst with the prior best heterogeneous catalyst systems reported for the dehydrogenation FA in the absence of any additives at low temperatures. **Scheme 1.** CO poisoning during the formic acid decomposition on PdAg/N-SiO_2 and PdAg-MnOx/N-SiO_2 catalysts and the promotional effect of MnO_x.

4 Conclusions

Currently presented superior catalytic system enables facile catalyst recovery and very high stability against agglomeration, leaching and CO poisoning. Through a comprehensive set of structural and functional characterization experiments, mechanistic origins of the unusually high catalytic activity, selectivity and stability of Pd-MnO_x/SiO_2-NH_2 were elucidated. Current heterogeneous catalytic architecture presents itself as an excellent contender for clean hydrogen production via room-temperature additive free dehydrogenation of formic acid in on-board hydrogen fuel cell applications.

Acknowledgements

MZ acknowledges Research Fund of Yüzüncü Yıl University, TUBA and FABED for financial support.

References

[1] Momirlan, M.; Veziroglu, T. N. Int. J. Hyd. Energ. 2005, 30, 225-237.
[2] Schlapbach, L.; Zuttel, A. Nature 2001, 414, 353-358.
[3] Enthaler, S.; Langermann, J. V.; Schmidt, T. Energy Environ. Sci. 2010, 3, 1207-1217
[4] Yadav, M.; Xu, Q. Energy Environ. Sci. 2012, 5, 9698-9704.
[5] Tedsree, K.; Li, T.; Jones, S.; Chan, C. W. A.; Yu, K.M.K.; Bagot, P. A. J.; Marquis, E. A.; Smith, G. D. W.; Tsang, S. C. E. Nat. Nanotech. 2011, 6, 302-307.
[6] Wang, Z. L.; Yan, J. M.; Wang, H. L.; Ping, Y.; Jiang, Q. J. Mater. Chem. A 2013, 1, 12721-12725.
[7] Wang, Z. L.; Yan, J. M.; Ping, Y.; Wang, H. L.; Zheng, W. T.; Jiang, Q. Angew. Chem. Int. Ed. 2013, 52, 4406.
[8] Wang, Z. L.; Wang, H. L.; Yan, J. M.; Ping, Y.; Li, S. J.; Jiang, Q. Chem. Commun. 2014, 50, 2732-2734.
[9] Metin, O.; Sun, X.; Sun, S. Nanoscale 2013, 5, 910-912
[10] Zhang, H.; Metin, O.; Su, D.; Sun, S. Angew. Chem. Int. Ed. 2013, 52, 3681-3684.
[11] Bulut, A., Yurderi, M., Karatas, Y., Zahmakiran, M., Kivrak, H., Gulcan, M., Kaya, M. App. Cat. B: Env. 2015, 164, 324-333.

III-OP25

Cr-Doped Alumina as Support for NiMo Vacuum Residue Hydroprocessing Catalyst

Puron H.[1], Pinilla J.L.[1], Yeletsky P.[2], Yakovlev V.A.[2], Saraev A.A.[2], Kaichev V.V.[2,3], Millan M.[1*]

1 - Department of Chemical Engineering, Imperial College London, London, UK
2 - Boreskov Institute of Catalysis, Novosibirsk, Russia
3 - Novosibirsk State University, Novosibirsk, Russia

* marcos.millan@imperial.ac.uk

Keywords: Cr-DOPED, ALUMINA

1 Experimental/methodology

Mesoporous alumina was doped with Cr using a coprecipitation method in order to prepare a support for hydrocracking catalysts. NiMo catalysts were prepared by impregnation on alumina (NiMo/Al2O3) and Cr-doped alumina (NiMo/Al2O3-Cr) and characterised. The presence of Cr in the support led to a better dispersion of NiMo and lower metal reduction temperatures as determined by temperature-programmed reduction (TPR) and X-ray photoelectron spectroscopy (XPS). As a consequence, a larger number of metal active sites was available in reduced form at operating conditions. The textural properties remained relatively unaffected by the coprecipitation of Cr together with the alumina. The catalysts were tested in their activity towards hydrodeasphaltenisation reactions using vacuum residue as feed in a batch reactor in two successive one-hour experiments involving reutilisation of the catalysts with fresh feed.

2 Results and discussion

It was found that Cr not only aided metal dispersion in catalyst synthesis but also coke dispersion during reaction, leading to sustained catalytic activity despite NiMo/Al2O3-Cr having a larger amount of coke deposits. Spent catalysts had a reduction in surface area and pore volume when compared to the fresh materials. Spent NiMo/Al2O3 catalysts had a decrease in average pore diameter (APD) whereas NiMo/Al2O3-Cr maintained the fresh material APD. NiMo/Al2O3-Cr could accommodate higher coke yields without significant variation in its textural properties.

III-OP26

The Dynamic Nature of ZnO in Industrial $Cu/ZnO/Al_2O_3$ Methanol Catalysts: From Minutes to Month

Frei E.[1*], Schumann J.[1], Kandemir T.[2], Friedrich M.[1], Trunschke A.[1], Schlögl R.[1], Lunkenbein T.[1]

1 - Fritz-Haber- Institute of the Max-Planck-Society, Department of Inorganic Chemistry, Berlin, Germany
2 - Technical University Hambur-Harburg, Institute of Chemical Process Engineering, Hamburg, Germany

* efrei@fhi-berlin.mpg.de

Keywords: methanol catalysts, $Cu/ZnO/Al_2O_3$ dynamics, layered ZnO dynamics, TOS, deactivation

1 Introduction

Methanol is one of the most important chemicals worldwide (2014 ~ 70 MMT) and is produced from syngas ($CO/CO_2/H_2$) under elevated pressures and temperatures (50-90 bar and 220-290 °C) [1]. The demand of methanol will further increase, in particular as a synthetic fuel based on the hydrogenation of CO_2, and can potentially seen as one of the key compounds for the energy supply of the future. The industrial most relevant catalyst consists mainly of $Cu/ZnO/Al_2O_3$.The role of Cu, its defective structure and influence on the active site of the catalysts, is very well understood [2]. The synergy between Cu and ZnO is crucial for the activity of the catalyst under CO_2 containing gas feeds and unique for the Cu-based catalysts [3]. Therefore ZnO can be seen as an equally important part of the catalyst. In the present work, we report on the behaviour of ZnO under different conditions and time scales, from the synthesis of the precursor until the testing of the catalysts under industrial relevant conditions. To monitor the dynamic character of ZnO in the catalyst like wetting under reducing conditions, the transformation into different modifications and deactivation relations, various in- and ex-situ techniques were used like HR-TEM, neutron diffraction, DRIFT and ambient pressure NEXAFS spectroscopy.

2 Experimental/methodology

The precursor materials were prepared by a co-precipitation route in aqueous solutions of Cu^{II}, Zn^{II} and Al^{III} nitrate and Na_2CO_3, under defined and controlled conditions (pH=6.5, T=65 °C) in a LabMax® system. The obtained zincian malachite phase was calcined in a rotating furnace at 330 °C (1 °C/min, 90 min dwell time) [4]. Additionally, we investigated commercially available catalysts.

The neutron diffraction measurements (wavelength 1.3091 Å) were conducted at BER-II at the neutron source of the HZB (Berlin, Germany).

NEXAFS and (NAP)-XPS spectra were recorded at the BESSY II facility (Berlin, Germany) at the ISISS beamline.

DRIFTS measurements at different temperatures (- 196 °C until 250 °C) with CO as a probe molecule were conducted on a Graseby Specac "Selector" attachment with environmental chamber placed in a Bruker IFS 66.

HRTEM images were taken on a FEI Titan 80-300 equipped with a Cs corrector at 300 kV. Prior to TEM investigation, the sample was reduced at 523 K and transferred to the microscope with a vacuum transfer holder under inert atmosphere.

3 Results and discussion

The influence of ZnO on the catalyst starts with the formation of the zincian malachite

precursor, in which the Zn occupies the lattice sites of higher symmetry. This leads in the calcination step to the formation of the corresponding metal oxides, homogeneously distributed and nanostructured. During the reduction of the catalyst ZnO shows an overgrowth on the metallic Cu particles and a parallel phase transformation into a graphite-like ZnO modification. Figure 1(a1) shows the layered character of this ZnO [5]. The DRIFT spectra (b) show at -196 °C a CO band at 2113 cm^{-1} confirms the presence of such a thin ZnO-layer in industrial relevant $Cu/ZnO/Al_2O_3$ catalyst. The detected vibration is assignable to CO molecules located at Zn^{II-x} cations, with a red shift of ~70 cm^{-1} compared to ZnO(10-10) [6]. Under the exposure to the electron beam of the HRTEM apparatus, a further change is observable; the layered ZnO forms a rock-salt and finally a wutzite-type ZnO structure (a2+a3). The neutron diffraction pattern of a methanol catalyst after 148d TOS shows intensive crystalline ZnO reflections (27-33 and 50-55 2Θ / °), which were formed under this long reaction time. A comparison of the other patterns (0d, 15d, 30d, 50d, 102d) give an impression of the phase transformation and deactivation mechanism of an industrial relevant catalyst. Additionally, these samples were investigated by HRTEM and other surface sensitive methods, to compare the deactivation behaviour of the catalysts with the corresponding ZnO modification and surface structure and properties.

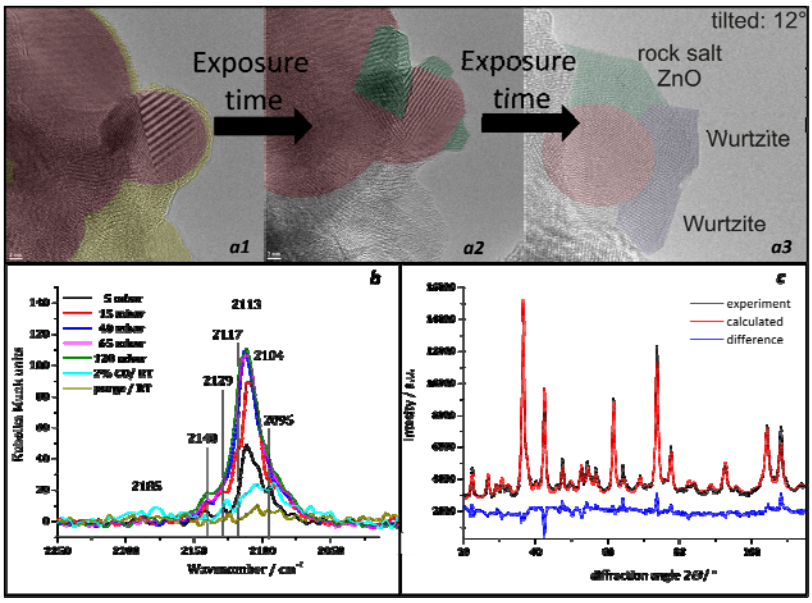

Fig. 1. (a1-a3) Aberration corrected HRTEM images of ZnO in the $Cu/ZnO/Al_2O_3$ catalyst. (b) DRIFT spectra of the $Cu/ZnO/Al_2O_3$ catalysts at – 196 °C and different CO partial pressures. (c) Insitu neutron diffraction pattern of the $Cu/ZnO/Al_2O_3$ after 148 days TOS.

4 Conclusions

This work shows with different, complementary methods detailed the enormous importance of ZnO as part of the $Cu/ZnO/Al_2O_3$ system, as an electronic and structural promoter. Fig. 1 shows exemplarily the ZnO modifications and its occurrence in different states of the catalyst. The knowledge of the dynamics at each step of the synthesis and testing procedure enables the development of new, highly stable catalysts.

References

[1] G. A. Olah, A. Goeppert, G. Prakash, *The Methanol Economy* (Wiley-VCH, Weinheim, 2006)
[2] M. Behrens, R. Schlögl et al., *Science*, 2012, 336, 893–897
[3] M. S. Spencer, *Top. Catal.,* 1999, 8, 259
[4] J. Schumann, T. Lunkenbein et al., *ChemCatChem*, 2014, 6, 2889–2897
[5] T. Lunkenbein, M. Willinger et al., *Angew. Chemie*, accepted, DOI: 10.1002/anie.201411581
[6] Wöll et al., *Angew. Chem*., 2013, 52, 11925-11929

III-OP27

Studies on Au/Cu-Zn-Al Catalyst for Methanol Synthesis from CO_2

Petrov L.A..[1,2*], Pasupulety N.[1,2], Alhamed Y.[2,3], Alzahrani A.[2,3]

1 - Sabic Chair of Catalysis, Jeddah, Saudi Arabia
2 - King Abdulaziz University, Jeddah, Saudi Arabia
3 - Chemical and Materials Engineering

* lpetrov@kau.edu.sa

Keywords: CO_2 hydrogenation, methanol, Cu-Zn-Al system, deposition, precipitation

1 Introduction

Methanol is one of the global chemical commodities which have the expected demand of 100 million metric tons for the fiscal year 2014-2015, as a chemical feedstock and transportation fuel. Industrially methanol is produced from synthesis gas ($CO+H_2$) on Cu-Zn-Al catalyst at high pressures (~ 10 Mega Pascal (MPa)). The synthesis gas predominantly produced from natural gas via catalytic steam reforming. The steam reforming products ($CO+CO_2+H_2$) catalytically converted in to methanol. However, this process yields surplus amount of hydrogen as a byproduct, which facilitates external CO_2 usage to produce additional methanol to improve the process efficiency by adding minimal capital cost [1]. Recently, the same Cu-Zn-Al system was studied for CO_2 hydrogenation reaction [2]. However, these conventional methanol synthesis catalysts are quite sensitive towards water poisoning and also the process efficiency in terms of methanol yield and selectivity has to be greatly improved [3]. Therefore, the present study emphasizes the improvement of the catalytic performance of the base Cu-Zn-Al catalyst by changing the Cu:Zn:Al ratio and also by the addition of Au. Further, our working hypothesis is focused on to reduce the reaction selectivity to CO and to study the resultant effect on methanol yield and selectivity in the presence of Au-Cu-Zn-Al system.

2 Experimental/methodology

$Cu(NO_3)_2.3H_2O$, $Zn(NO_3)_2.6H_2O$, $Al(NO_3)_3.9H_2O$, Na_2CO_3 precursors were obtained from Acros chemicals (assay ≥ 98.0%) and $AuCl_3$ (Alfa Aesar, assay ≥ 99.99%, 64.4% Au) were used without further purification.

Cu-Zn-Al samples were prepared by co-precipitation method. Gold supported catalysts were prepared by deposition precipitation (DP) method using Mettler Toledo Labmax reactor. All the dried powders were calcined at 350 ºC for 12h under static air. The base catalysts were designated as: C_2ZA, C_4ZA and C_6ZA. Here 'C' stand for copper, 'Z' for zinc and 'A' for alumina and the subscript represents the moles of copper present in these catalysts. The gold supported catalysts were named as: $0.5Au/C_4ZA$, $1Au/C_4ZA$ and $3Au/C_4ZA$. Here, the prefix 0.5, 1 and 3 correspond to the gold loading weight percentage on C_4AZ base.

Catalytic activity studies were performed using PID Eng & Tech micro reactor equipped with gas flow meter and temperature controllers. Catalytic activity tests were carried out in the temperature range of 200-260 ºC with 20ºC step size in the applied pressure range of 2-6 MPa and GHSV 7000 or 13200 h^{-1}.The reaction stream at each temperature directed to Agilent micro GC (equipped with TCD detector with column CP-Sil 5&8 CB and Pora Plot Q) to record the activity data for 30 minutes after accomplishing the steady state for 30 minutes. The calibrated results were within the sample standard deviation of ± 0.1% for CO/methanol yield and ±1.0% for CO_2 conversion.

3 Results and discussion

Fig.1a summarizes the effect of Au content in Au/C_4ZA on CO_2 conversion and CO selectivity at H_2:CO_2 6:1, GHSV 7000 h^{-1} and 4.0 MPa. Among the gold supported catalysts it seems 1wt% loading leads to promising results. The base C_4ZA showed the maximum CO_2 conversion of 25% mass with 50% of CO selectivity at 260 ºC. A slight increase (2-3%) in the CO_2 conversion was observed for 1Au/C_4ZA over base catalyst. On the other hand, the CO selectivity was reduced from 5-10% mass on 1Au/C_4ZA compared to base catalyst. The decrease in the CO selectivity on 1Au/C_4ZA might be associated with direct hydrogenation of CO to methanol on Au-Cu-Zn-Al surface where the hydrogen spill over established by TPR studies. The reduction behaviour of calcined C_4ZA and 1Au/C_4ZA were presented in Fig.1b. The base C_4ZA shows a broad signal with front shoulder at 300 ºC and a back shoulder at 325 ºC attributed to Cu^{+2} to Cu^{+1} and Cu^{+1} to Cu^0 [4]. After the addition of gold (1wt%), the reduction profile of C_4ZA shifted forward to a lower temperature. The front shoulder became more distinct and appeared at 275 ºC and the back shoulder more prominent at 325 ºC for 1Au/C_4ZA. Nano Au particles have been reported to absorb-dissociate hydrogen and further spills over to neighbouring copper oxide [5]. Hence, the addition of Au to Cu-Zn-Al lead to lower reduction temperature of neighbouring copper oxide, as observed in Fig. 1b.

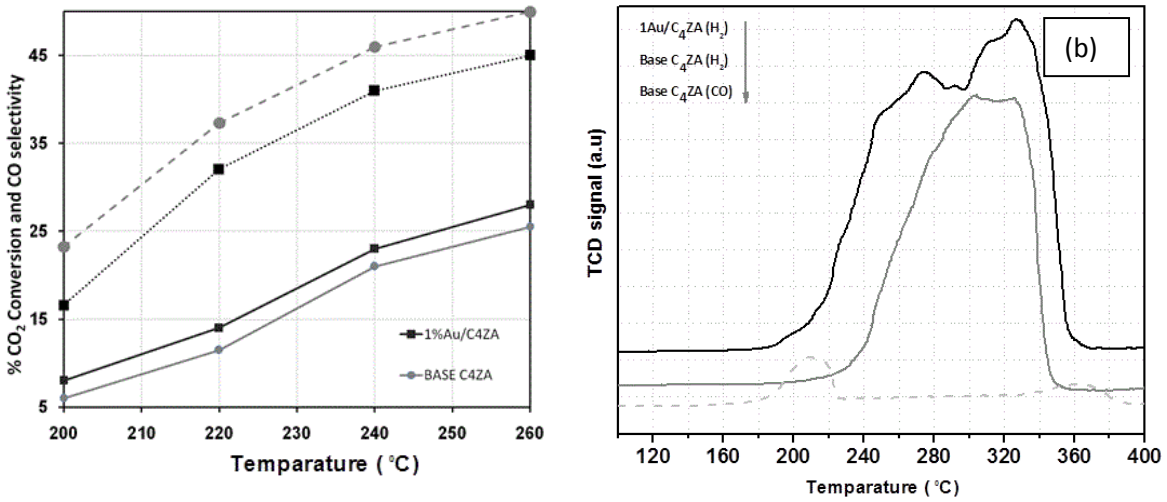

Fig.1. (a) Solid lines indicate CO_2 conversion and dotted lines indicate CO selectivity on base C_4ZA and 1Au/C_4ZA (b) TPR profiles of the calcined catalysts. Gas treatment atmosphere mentioned in brackets

4 Conclusions

Au plays a significant role in decreasing the reaction selectivity towards CO by improving the methanol yield is due to; i) spilling over the H_2 to neighbour Cu species ii) improved the adsorption capacities for H_2 and CO at Au-Cu interface.

Acknowledgements

This work is supported by Deanship of Scientific Research, King Abudulaziz University, KSA.

References

[1] www.methanol.org.
[2] A. Bansode, A. Urakawa, J. Catal., 309 (2014) 66.
[3] C. Li, X. Yuan, K. Fujimoto, Appl. Catal. A: Gen., 469 (2014) 306.
[4] L.J.Pettersson, B. Lindstrom, P.G. Menon, Appl Catal A: Gen., 234 (2002) 111.
[5] C. Kartusch, J.A. Bokhoven, Gold Bull., 42 (2009) 343.

III-OP28

CO_2 Methanation on Iron Based Catalysts

Kirchner J.[1,2], Kureti S.[1,2*]

1 - TU Bergakademie Freiberg, Freiberg, Germany
2 - Institute of Energy Process Engineering and Chemical Engineering, Freiberg, Germany

* johann.kirchner@iec.tu-freiberg.de

Keywords: CO_2 methanation, iron catalysts, structure-activity, correlation

1 Introduction

The increasing emission of CO_2 is worldwide discussed in the context of global warming. Therefore, many efforts have been made to remove CO_2 by fixation, for instance by conversion into chemicals [1]. Following a modified SNG approach (substitute natural gas) our study focuses on the hydrogenation of carbon dioxide to methane and water (Eq. 1).

$$CO_2 + 4\ H_2 \rightleftharpoons CH_4 + 2\ H_2O \qquad \Delta_R H^0 = -\ 165\ kJ/mol \qquad \text{(Eq. 1)}$$

In the methanation of carbon oxides supported Ni catalysts are currently applied. However, these catalysts suffer from several disadvantages such as Ni sintering, coke formation and leaching of nickel carbonyl [2]. Iron catalysts have been reported to be active in CO_x hydrogenation (Fischer-Tropsch synthesis) as well as water-gas shift reaction [3]. Due to its relatively low price and toxicological harmlessness we have evaluated the potential of iron based catalysts for CO_2 methanation. It is well known that iron catalysts undergo complex phase changes during hydrogenation of carbon oxides. Several iron phases such as iron oxides or metallic iron have been found to coexist. Moreover, deposited carbon may react to iron carbides or bulk carbon species with different structures [4].

2 Experimental

In the present study, different iron oxide precursors were systematically characterized by N_2 physisorption, scanning electron microscopy, X-ray diffraction and Moessbauer spectroscopy and were subsequently tested towards CO_2 methanation to correlate structure and activity. The catalytic performance was evaluated between 250 and 450°C, whereas the H_2/CO_2 ratio was varied using CO_2 fractions from 0.1 to 20 vol.%. Prior to the methanation, the catalysts were activated by reduction or carburization. The carbonaceous species formed on the catalysts in CO_2 methanation were investigated by temperature-programmed hydrogenation (TPH). Additionally, the change in phase composition and morphology was examined by using in situ X-ray diffraction.

3 Results and discussion

The catalytic study demonstrated in Fig. 1a indicates CO_2 conversion above 75 % and CH_4 selectivity up to 85 % at 400°C when using a nano-scaled y-Fe_2O_3 precursor. This original iron oxide phase is inactive for methanation, but is activated during the exposure to CO_2/H_2. The activation implies formation of metallic iron and iron carbides, e. g. Fe_3C, whereas the former reveals highest efficiency as derived from the CH_4 formation rate (Fig. 1b). Furthermore, TPH analyses made after CO_2 methanation shows production of carbon species, whereas their nature strongly depends on the physical-chemical properties of the precursor (Fig. 2). From our studies we derive high methanation activity of nano-scaled iron oxide precursors due to the presence of reactive carbonaceous species (Cα type), whereas the deactivation by graphitic bulk carbon is suppressed.

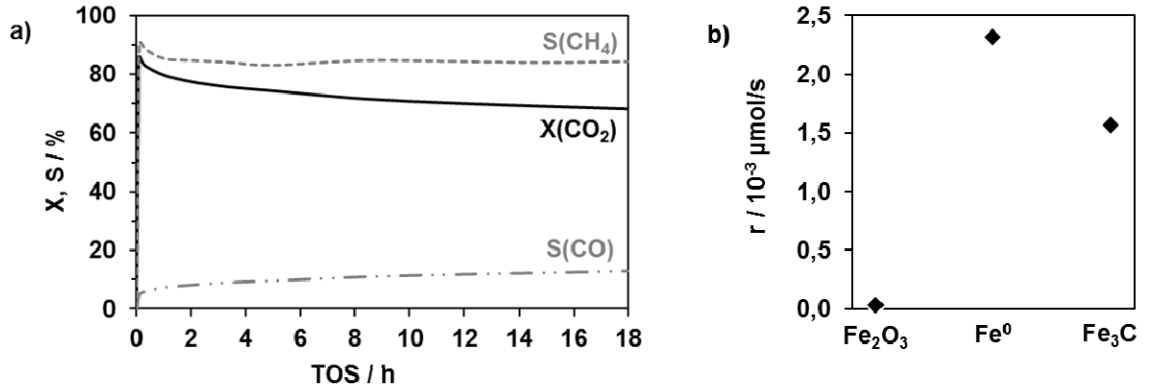

Fig. 1. Methanation activity of Fe catalysts: a) CO_2 conversion, CH_4 and CO selectivity on γ-Fe_2O_3 at 400°C, $y(CO_2)/y(H_2)=200$, GHSV=120000 h^{-1}. b) CH_4 formation rates at 350°C of Fe_2O_3, Fe and Fe_3C.

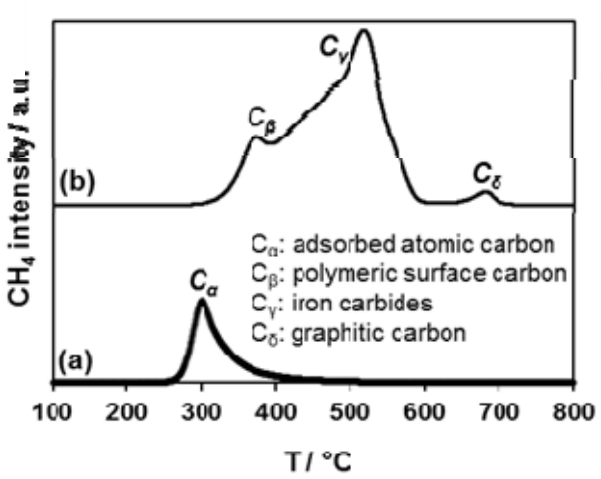

Fig. 2. TPH profiles of (a) nano-scaled Fe_2O_3 and (b) micro-scaled Fe_2O_3 used in methanation [4].

4 Conclusions

In the present study, Fe based samples were identified as promising catalysts for CO_2 methanation in order to substitute traditional Ni catalysts. The structure-activity correlation showed highest activity for metallic iron among iron oxide and iron carbide phases. CH_4 yield up to 64 % was achieved at relatively high CO_2/H_2 ratio, whereas the activity decreases with inclining CO_2 fractions.

References

[1] C. Song, *Catal. Today* 115 (2006) 2
[2] J. Barrientos, M. Lualdi, M. Boutonnet, S. Järas, *Appl. Catal. A* 486 (2014) 143
[3] E. de Smit, B. M. Weckhuysen, *Chem. Soc. Rev.* 37 (2008) 2758
[4] C. H. Bartholomew, *Appl. Catal. A* 212 (2001) 17

III-OP29

Changes in the Oxidation States of Cobalt Oxides for the OER Studied by XPS and their Correlation to the Electrochemical Activity

Weidler N.*, Kaiser B., Jaegermann W.

Technical University Darmstadt, Institute of Material Science, Darmstadt, Germany

* nweidler@surface.tu-darmstadt.de

Keywords: oxygen evolution reaction, water-splitting, chemical vapor deposition, electrocatalysis

1 Introduction

Due to the decreasing amount of fossil fuels the interest in the field of renewable energies has increased considerably. However, energy from wind and sun has the disadvantage that it is not available on a continuous basis, i.e. it is necessary to store the generated energy employing appropriate technologies. Water electrolysis represents one possibility to convert and store electric energy in chemical energy in the form of hydrogen. One of the major obstacles, which make the process uneconomical at this time, is the overvoltage loss for the oxygen evolution reaction (OER). In terms of overpotential, IrO_2 and RuO_2 are still the best dark water oxidation catalysts but they are rare and highly priced. Our work focuses on the one hand on the production of economically competitive and highly active cobalt based catalysts for the OER and on the other hand on the development of a low temperature deposition technique for their precipitation directly onto solar devices. Fundamental studies focus on the influence of the deposition parameters on the oxidation state of the Co sites and the changes therein during the electrochemical water-splitting. The change in oxidation states can be correlated to the formation of oxo-, hydroxo-, peroxo-adsorption intermediates and their effect onto the kinetics.

2 Experimental/methodology

Catalysts are prepared by chemical vapor deposition onto different electrode substrates (e.g. Titanium, Nickel). The CVD deposition process must be optimized with respect to several parameters like temperature, gas flow, precursor material etc. For chemical and structural characterization X-ray photoelectron spectroscopy (XPS) and high-resolution electron microscopy (HREM) are employed. The electrochemical investigation is perfomed by cyclic voltammetry, impedance spectroscopy and finally stability measurements. These experiments can also be done in an in-situ cell that allows a direct sample transfer into an ultra-high-vacuum system for further investigation by XPS.

3 Results and discussion

Two CVD methods were used to synthesize pure Co-Oxide on Ti from $Co(acac)_2$ precursor material. In a thermal CVD process the deposition and oxidation of $Co(acac)_2$ take place at the same time in an Ar/O_2 atmosphere at substrate temperatures between 290 and 430°C. In a plasma-enhanced CVD process, the decomposition of the precursor occurs in an oxygen plasma during the deposition. Both methods lead to different oxidation states in the catalyst and to different amounts of carbon contamination. Thermally deposited Co-Oxide/Ti shows a high content of Co(II)-states as well as a high carbon contamination, while plasma deposited Co-Oxide/Ti shows mixed valences of Co(III)/Co(II) and a low carbon contamination. While the plasma-oxidized catalysts show a higher electrochemical activity from the beginning of the reaction, the thermally oxidized CoOxides/Ti show an increase in electrochemical activity with

proceeding OER. To understand this difference in activity, we treated the as prepared catalysts in 0.1M KOH or 1M KOH under potentiostatic control at 1.7V vs. RHE or galvanostatic control at 10mA/cm^2 for 10minutes and investigated the change in oxidation state directly with XPS.

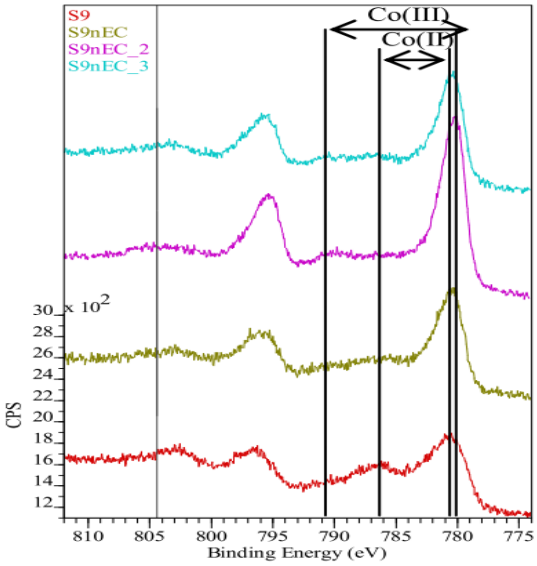

As an example**, Figure 1** shows the XPS spectra for thermally deposited Co-Oxide/Ti for the as prepared sample (S9) and the electrochemical treated samples (nEC, nEC2, nEC3).The red spectrum of the as prepared sample S9 shows the typical signal for Co(II), which consists of the main peak and its satellite in a distance of 6eV. After the first electrochemical treatment, S9nEC, the intensity of the satellite decreases and the Co(III) satellite in a distance of 11eV to the main peak starts to appear. After the second electrochemical treatment nEC2 the satellite of Co(III) is increased. Also a shift of the main peak is observed. The formation of Co(III) can be due to the formation of the adsorption intermediate Co-OOH, which has to be stabilized by the catalyst for good catalytic activity.[1] This observed change in oxidation states of CoOxide/Ti comes along with an increase in electrochemical activity, for a current density of 2mA/cm^2 the overvoltage decreases in the range of 90-100mV. We could show, that in dependency of the preparation method (thermal vs. plasma-enhanced-CVD) the catalysts show a different electrochemical behavior.

4 Conclusions

The correlation of the electrochemical activity with the oxidation state of the catalysts could be helpful to develop a fundamental mechanistic understanding. Beside the studies of the pure Co-Oxides, studies on pure Ni-Oxide and the binary Co-Ni-Oxide system will be presented. The mixed metal catalysts show even higher electrochemical activity compared to the monometallic systems.

Acknowledgements

(A part of) this work was financed by Evonik Industries AG, partially funded by the German Federal Ministry of Education and Research within the project “Sustainable Hydrogen” (FKZ: 03X3581A).

References

[1] Man, I. C.; Su, H.-Y.; Calle-Vallejo, F.; Hansen, H. A.; Martínez, J. I.; Inoglu, N. G.; Kitchin, J.; Jaramillo, T. F.; Nørskov, J. K.; Rossmeisl, J., Universality in Oxygen Evolution Electrocatalysis on Oxide Surfaces. *ChemCatChem* **2011,** *3* (7), 1159-1165.

III-OP30

Reactivity of Metals on Perovskites ($La_{0.6}Sr_{0.4}FeO_{3-d}$ (LSF) and $SrTi_{0.7}Fe_{0.3}O_{3-d}$ (STF)) Regarding Possible SOFC Usage

Thalinger R[1], Heggen M[2], Schmidmair D[3], Klötzer B[1], Penner S[1*]

1 - Institute of Physical Chemistry, University of Innsbruck, Innsbruck, Austria
2 - Ernst Ruska-Centrum for Microscopy und Spectroscopy with Electrons, Forschungszentrum Jülich, Jülich, Germany
3 - Institute of Mineralogy and Petrography, University of Innsbruck, Innsbruck, Austria

* ramona.thalinger@uibk.ac.at

Keywords: perovskite, methanereforming, nickel, rhodium, water gas shift reaction, SOFC

1 Introduction

Perovskites are currently the most popular material for SOFC cathodes [1-2]. Regarding their abilities as mixed ionic and electronic conductors (MIECs), transporting both oxygen ions and electrons effectively, they can also be used as anode materials. With this the triple phase boundary can be enlarged enormously. At the TPB the following reaction takes place:

$$CH_4 + 4O^{2-} \rightarrow CO_2 + 2H_2O + 8e^-$$

Two different perovskites, LSF ($La_{0.6}Sr_{0.4}FeO_{3-d}$) and STF ($SrTi_{0.7}Fe_{0.3}O_{3-d}$), have been selected as promising materials regarding methane chemistry and water gas shift activity. For improvement of catalytic activity and selectivity they were subsequently impregnated with various metals (Ni, Rh and Co) and investigated concerning their methanation and methane reforming activity.

2 Experimental

All measurements were done in a quartz batch reactor. The reaction mixture (CO_2, H_2 and H_2O for methanation and CH_4 and H_2O for the methane reforming reaction) was investigated up to 600 °C, after an oxidative (1 bar O_2, 1h, 400 °C) or reductive (1 bar H_2, 1h, 600°C) pretreatment. The gas phase composition was monitored continuously by mass spectrometry/ gas chromatography - mass spectrometry.

3 Results and discussion

For the pure perovskites no methanation or methane reforming activity could be observed. The fully oxidized perovskites can be reduced with methane and CO, producing CO_2. Water gas shift reaction starts for both STF and LSF at 300°C, the inverse reaction was observed above 500 °C.

For Ni-STF the methanation reaction starts at 250 °C. The methane is formed up to 400 °C. Above this temperature methane reforming yields increasing amount of carbon monoxide. Also for Ni-LSF, methanation activity can be monitored, starting at 300 °C. At 370 °C methanation competes with the inverse water- gas shift reaction and carbon monoxide is formed. Above 550 °C the methane is reformed.

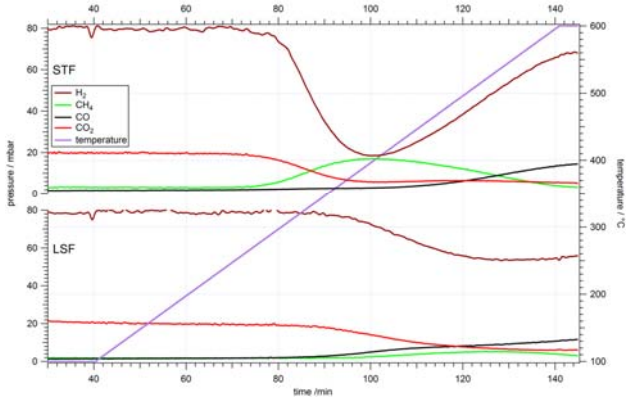

Fig. 1.: Reaction profiles of methanation reaction on Ni-STF (top) and Ni-LSF (bottom)

4 Conclusion

Both perovskites show water gas shift reactivity. Methanation / methane reforming reactivity on perovskites can only be achieved after impregnation with metals whereby STF shows better performance regarding methane production.

Acknowledgement

Ramona Thalinger acknowledges financial support via FWF SFB "FOXSI" project part F4503-N16.

References

[1] McIntosh, Steven, and Raymond J. Gorte. "Direct hydrocarbon solid oxide fuel cells." Chemical reviews 104.10 (2004): 4845-4866.

[2] Menzler, Norbert H., et al. "Materials and manufacturing technologies for solid oxide fuel cells." Journal of materials science 45.12 (2010): 3109-3135.

III-OP31

Redox Catalysts for Electrochemical CO_2 Reduction: the Role of Local Proton Source

Nervi C.*, Gobetto R., Minero C., Franco F., Cometto C., Sun C., Nencini L., Sordello F.

University of Turin, Department of Chemistry, Turin, Italy

* carlo.nervi@unito.it

Keywords: carbon, dioxide, redox catalyst, electrochemical reduction, organometallic complexes

1 Introduction

The reduction of CO_2 emissions and the need for a green and sustainable energy source are among the most important world's strategic research topics. The conversion of CO_2 into "Solar Fuels" [1] via the so-called artificial photosynthesis proceed by the photoactivation of a dye that generates a electron–hole pairs, which provides the thermodynamic driving force for the subsequent electron transfer reactions. A convenient approach is to optimize separately the catalytic and light-harvesting properties. This is possible because the photocatalytic mechanism usually proceed via a reductive quenching pathway [2], i.e. the real catalyst is the reduced form produced in situ; thus the search of an efficient catalyst for CO_2 reduction and its study can be pursued using electro-chemical techniques. To reduce the large overpotentials required for CO_2 reduction, the use of catalyst able to take advantage of proton-assisted processes [2] is mandatory [1]. In this communication we would like to show our recent findings on the use of Re and earth-abundant transition metals (Mn, Mo, W) organometallic complexes as redox catalyst for CO_2 electrochemical reduction.

2 Experimental/methodology

The complexes were synthesized and characterized in our laboratory [3]. Cyclic Voltammetry experiments were performed normally in 1 mM MeCN solutions, containing tetrabutylammonium hexafluorophosphate ($TBAPF_6$) as supporting electrolyte (0.1 M). Brønsted acids with different strength (MeOH, H_2O, CF_3CH_2OH) were added to test the proton-assisted ability of the catalysts. Photocatalytic measurements were performed in a Pyrex cell filled with a mixture of dimethylformamide and triethanolamine (DMF/TEOA 5:1 v/v; 6 mL) with the catalyst (2 mM). Experiments were carried out whilst stirring and with a constant flow of CO_2. The cell was irradiated with a Philips PLS 9 W/52 lamp. CO and H_2 were detected and quantified by GC. A Smart Trak 100 (Sierra) flow controller C100L was used during the electrochemical and photocatalytic experiments. Formic acid production was evaluated with ion chromatography.

3 Results and discussion

The effect of an antenna on Re^I complex catalytic properties has been explored and contrasting results have been observed. For example, the covalently linked non-conjugated Ru^{II}–Re^I dyad is a superior catalyst to the corresponding mixture of Ru^{II} and Re^I complexes; however, the Zn–porphyrin and Re^I complex mixture seems to be a better catalyst than the corresponding covalently linked dyad [4]. We herein compare the redox and photochemical catalytic properties of a series of Re^I carbonyl complexes that contain α,α-diimine ligands covalently linked to a highly delocalized 4-piperidinyl-1,8-naphthalimide (PNI) moiety for the CO_2 reduction process. The photochemical data parallel reasonably well the electrochemical one. But the most interesting catalytic features has been obtained in homogeneous solutions with a Mn^I catalyst carrying a local proton source. While the Re^I catalysts can work in CO_2 reduction also in

absence of Brønsted acids, the Mn^I catalysts normally cannot. However, the Mn^I catalysts **1**, characterized also by single crystal X-ray diffraction, showed a substantial catalytic activity in anhydrous media induced by the presence of a local proton source [3]. Bulk electrolysis at the end of the catalytic plateau (–1.8 V) under CO_2 showed an unusual change in selectivity for CO_2 reduction by the Mn(I) catalyst, giving a mixture of CO and HCOOH.

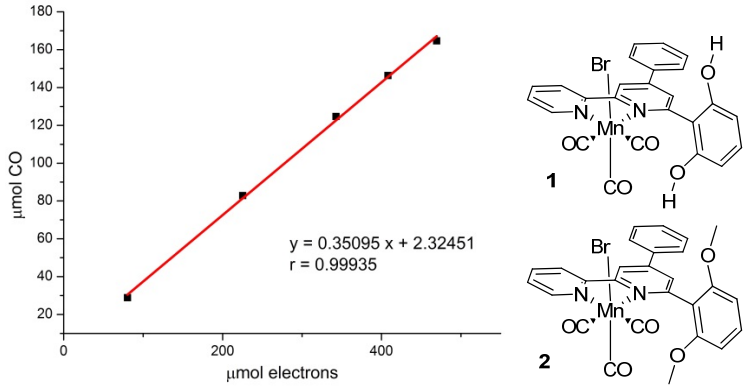

Fig. 1. CO production against the charge passed during bulk electrolysis at –1.8 V vs. SCE of a 1 mM solution of **1**. The slope of about 0.35 corresponds to a faradic efficiency of 70%.

The catalytic activity is inhibited in **2**, where the two local protons are substituted by methyl groups. We also performed a series of controlled potential electrolysis with different Brønsted acids, showing that their strengths can drive the selectivity of the catalyst towards the formation of CO or formic acid.

4 Conclusions

The introduction of a PNI group in certain Re^I complexes allowed a second electron transfer to occur at much less negative potentials than the corresponding parent derivative. For these redox catalysts, the two-electron reduction mechanism might also proceed as the formal $[PNI]^-$ group worked as an electron reservoir. The importance of local factors is evidenced by the strong catalytic activity of Mn^I complex **1**. This represents the first reported experimental evidence of an intramolecular proton-assisted catalytic process for a Mn^I catalyst, in which the key factor is the spatial closeness of protons to the active site rather than their bulk concentration in solution.

References

[1] J. Rongé, T. Bosserez, D. Martel, C. Nervi, L. Boarino, F. Taulelle, G. Decher, S. Bordiga, J. A. Martens, *Chem.Soc.Rev.* 43 (2014) 7963-7981.

[2] a) J. M. Saveant, *Chem. Rev.* 108 (2008) 2348–2378; b) C. Costentin, M. Robert, J. M. Saveant, *Chem. Soc. Rev.* 42 (2013) 2423–2436.

[3] a) F. Franco, C. Cometto, C. Garino, C. Minero, F. Sordello, C. Nervi,R. Gobetto, *Eur. J. Inorg. Chem.* (2014) DOI: 10.1002/ejic.201402912; b) F. Franco, C. Cometto, F. Ferrero Vallana, F. Sordello, E. Priola, C. Minero, C. Nervi, R. Gobetto, *Chem. Commun.* 50 (2014) 14670-14673.

[4] a) B. Gholamkhass, H. Mametsuka, K. Koike, T. Tanabe, M. Furue, O. Ishitani, *Inorg. Chem.* 44 (2005) 2326–2336; b) Z. Y. Bian, S. M. Chi, L. Li, W. Fu, *Dalton Trans.* 39 (2010) 7884–7887; c) C. D. Windle, M. V. Campian, A. K. Duhme-Klair, E. A. Gibson, R. N. Perutz, J. Schneider, *Chem. Commun.* 48 (2012) 8189–8191.

III-OP32

Hydrogen Electrode Reactions over Nickel-Based Catalysts in Alkaline Medium: Influence of Composition and Structure of Ni Particles

Oshchepkov A.G.[1,2,3*], Bonnefont A.[3], Simonov P.A.[2], Cherstiouk O.V.[2], Pronkin S.N.[1], Parmon V.N.[2], Savinova E.R.[1]

1 - ICPEES UMR 7515-CNRS-Université de Strasbourg, Strasbourg, France
2 - Boreskov Institute of Catalysis SB RAS, Novosibirsk, Russia
3 - IC UMR 7177 CNRS-Université de Strasbourg, Strasbourg, France

* alexandr.oschepkov@gmail.com

Keywords: electrocatalysis, nickel, hydrogen oxidation, hydrogen evolution, alkali

1 Introduction

Electrocatalytic hydrogen oxidation and hydrogen evolution reactions (HOR/HER) for many years have attracted strong research interest due to their fundamental and applied significance. An increasing interest in low-temperature alkaline membrane fuel cells and electrolyzers gives a new impetus to the development of efficient and stable electrocatalysts for the HOR/HER in alkaline media. The main advantage of an alkaline medium in comparison with acid one is the possibility to use non-noble metal catalysts, among which Ni seems to be the best candidate due to its relatively high activity in the HER as well as its low cost [1]. However, Ni is passivated with time under a moist air atmosphere or in an alkaline solution when supposedly irreversible β-$Ni(OH)_2$ is formed, which blocks active sites and thus decreases of the HOR/HER activity [2]. On the other hand, several scientific groups [3, 4] suggested that the addition of Ni oxide/hydroxide to metal electrodes results in a strong increase of their HER activity, supposedly due to more facile dissociative adsorption of water. In order to provide deeper insight into the influence of the composition and structure of Ni particles on their activity in the HOR/HER, in this work we study electrodeposited Ni nanoparticles with different sizes and compare them with polycrystalline Ni disk electrode, as well as carbon-supported NiCu particles. We also developed a kinetic meanfield model which provides some insights into the mechanism of the hydrogen electrode reactions.

2 Experimental/methodology

Electrodeposition technique was applied for fabrication of a set of model supported Ni catalysts of various particle size. Glassy carbon electrodes were used as supports for a 3 step (E_1 = -0.77; E_2 = -0.20; E_3 = -0.52 V vs. reversible hydrogen electrode) deposition of Ni from the 0.01 M $NiSO_4$ + 0.10 M $(NH_4)_2SO_4$ solution at 25 ^oC. The size of Ni particles was controlled by varying the duration of different deposition stages. Ni/C and NiCu/C (with different Ni:Cu molar ratio) catalysts were prepared by the incipient wetness impregnation of the support (carbon black Vulcan XC-72) with $Ni(OAc)_2$ and $Cu(OAc)_2$ solution followed by drying and reduction with H_2 at 300 ºC.

The composition and structure of Ni based catalysts were studied by various physicochemical and electrochemical methods. Kinetics of the HOR/HER was studied in H_2 saturated 0.10 M NaOH solution at very low sweep rate of 2 mV s^{-1} in order to minimize the influence of non-stationary processes.

For kinetic modelling we used Langmuir isotherms for the adsorption step and Butler-Volmer kinetics for the charge transfer processes, assuming that the hydrogen electrode reactions follow Tafel-Volmer mechanism.

3 Results and discussion

Study of the properties of polycrystalline Ni disc electrode in alkaline media using different electrochemical techniques revealed several important features. It is known that after contact with air the surface of metallic Ni is oxidized to form several layers of NiO covered by α-$Ni(OH)_2$ [2]. It was found that air-formed NiO/α-$Ni(OH)_2$ can be easily reduced electrochemically by applying potential at which hydrogen evolution occurs. However prolonged contact of α-$Ni(OH)_2$ with alkaline or even water solution results in its transformation into β-$Ni(OH)_2$, which cannot be fully reduced even by applying strong cathodic polarization. So β-$Ni(OH)_2$ blocks the surface resulting in a decrease of the specific catalytic activity of Ni electrode. On the other hand, it was found that the formation on the surface of Ni of such reducible species as NiO/α-$Ni(OH)_2$ increases its activity in the HOR/HER several times, even if the specific surface area does not change noticeably. Studying of electrodeposited Ni nanoparticles with varying sizes revealed the influence of the size on their activity most likely due to the differences in oxophilicity of the particles. The latter results in higher activity of small Ni nanoparticles in comparison with the polycrystalline Ni disc electrode.

Preparing of bimetallic Ni-based materials provides another way of increasing the activity of Ni in the HOR/HER. NiCu/C catalysts studied in this work revealed, that addition of Cu (less than 50 wt%) during the synthesis results in an increase of the specific surface area of Ni as well as its specific activity in the HOR/HER.

Kinetic meanfield model was applied taking into account the Ni oxide formation and reduction as well as the hydrogen electrode reactions. A good agreement between the experiment and modeling was obtained. We propose that formation of α-$Ni(OH)_2$ goes through the formation of intermediate NiOH species. We also suggest that the mechanism of the HOR over the Ni surface comprises a reaction between NiH_{ad} and $NiOH_{ad}$ species.

4 Conclusions

Formation of reducible Ni oxide/hydroxide species on the Ni surface leads to significant increase of its activity in the HOR/HER at potentials below 0.20 V vs. RHE. At higher potentials Ni oxide/hydroxide species inhibit the HOR activity;

Electrodeposition technique allows to prepare glassy carbon-supported Ni nanoparticles with controllable size and higher HOR/HER activity in comparison with that of a polycrystalline bulk Ni electrode;

Addition of Cu allows to considerably change mass-weighted and specific catalytic activity of Ni in HER/HOR as well as its specific surface area;

Mean-field modeling using Tafel-Volmer mechanism can reproduce qualitatively the experimental HOR/HER data on Ni electrodes.

Acknowledgements

The authors are grateful to Dr. Zaikovski V. I., Dr. Kardash T. Yu., Dr. Kvon R. I. and Dr. Simonov A. N. for their help in the characterization of materials and for useful discussions. Financial support from the grants ERA.Net RUS №208, NSh 1183.2014.3, and Russian UMNIK program № 10U/01-13 is gratefully acknowledged.

References

[1] W. Sheng, MNZ Myint, J. G. Chen, Y. Yan, *Energy Environ. Sci.* 6 (2013) 1509.
[2] D.S. Hall, C. Bock, B.R. MacDougall, *J. Electrochem. Soc.* 160 (2013) F235.
[3] D. Strmcnik, M. Uchimura, C. Wang, R. Subbaraman, N. Danilovic, D. van der Vliet, A. P. Paulikas, V. R. Stamenkovic, N. M. Markovic, *Nat. Chem.* 5 (2013) 300.
[4] M. Gong, W. Zhou, MS Tsai., J. Zhou, M. Guan, MC Lin, B. Zhang, Y. Hu, DY Wang, J. Yang, S.J. Pennycook, BJ Hwang, H. Dai, Nat. Comm. 5:4695 (2014).

III-OP33

Gas-Phase Partial Oxidation – Catalytic Carbonylation Conception for Small-Scale GTL

Arutyunov V.[1*], Savchenko V.[2], Sedov I.[2], Fokin I.[2], Makaryan I.[2], Nikitin A.[1], Strekova L.[1]

1 - Semenov Institute of Chemical Physics, Russ. Acad. Sci., Moscow, Russia
2 - Institute of Problems of Chemical Physics, Russ. Acad. Sci., Chernogolovka, Russia

* arutyunov@chph.ras.ru

Keywords: natural gas, syngas, GTL, partial oxidation, oxy-cracking, carbonylation

1 Introduction

Despite the significant progress in industrial GTL technologies, even the world class GTL plants have only marginal limits of profitability. Manufacturing of GTL products remains extremely expensive. The main reason is the high expenditures for syngas production, which is the most energy intensive step of traditional GTL that comprises more than 50% of the total GTL capital cost. Therefore, there are no expectations of the significant increase of traditional GTL in the nearest future. To increase the possibilities for practical application of gas chemistry two alternatives can be suggested. The first one is decreasing the cost of syngas, e.g. by matrix conversion of hydrocarbon gases [1]. But the more evident is the developing of alternative "without syngas" GTL routes via direct partial oxidation or oxy-cracking of hydrocarbons with subsequent catalytic carbonylation and/or oligomerization of oxidation products [2,3].

2 Results and discussion

Direct partial oxidation and oxy-cracking of hydrocarbon gases give, respectively, mixtures of oxygenates, mainly methanol, with carbon monoxide and light olefins, mainly ethylene, with carbon monoxide. But the assortment of chemicals obtained from natural gas by partial oxidation can be significantly enlarged by means of subsequent catalytic carbonylation and/or oligomerization of oxidation products including co-polymerization of ethylene and CO.

The most perspective for the alternative GTL processes are the addition reactions of CO to the low-molecular substrates, such as carbonylation of methanol to acetic acid and methyl acetate; production of ethylidenediacetate; hydroformulation of ethylene to propanal; formation of methyl propanoate during ethylene methoxycarbonylation and vinyl acetate by reaction of ethylene with acetic acid; co-oligimerization of ethylene and CO with the formation of oligoketones and oligoesters. A number of carbonylation processes operate industrially in the presence of platinum group metals based catalysts (PGM catalysts).

By special experiments both for high pressure low temperature partial oxydation of natural gas to oxigenates and low pressure high temperature oxy-cracking of complex hydrocarbon mixtures that imitate real natural and associated gases it was shown the possibility to regulate in a wide range the ratio of main products depending on stohiometic ratio necessary for subsiquent carbonylation.

Of especial importance is that the specific activity of carbonylation catalysts 2-3 orders of magnitude higher than that of Fisher-Tropsch processes, which let to significantly decrease reactor's dimensions and cost.

The common scheme of new type of GTL-processes, some of possible chemicals that can be thus obtained, most effective catalysts and reaction conditions are presented in Fig. 1.

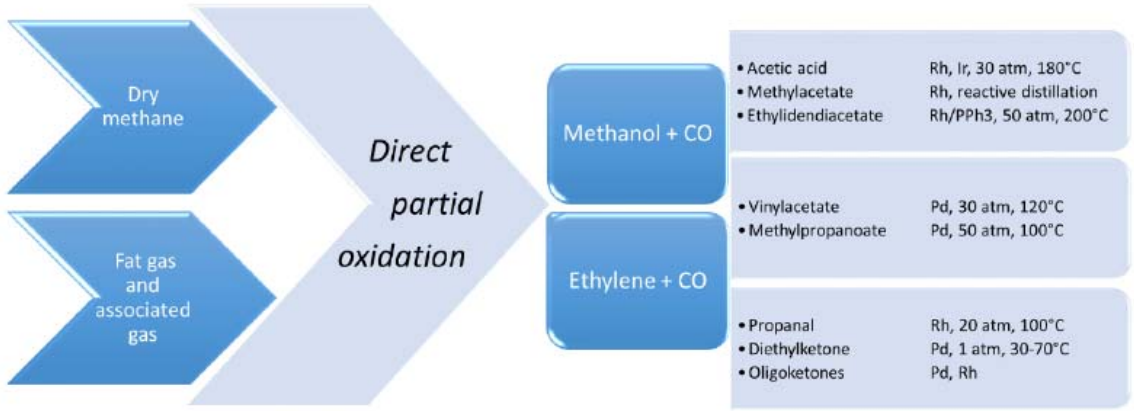

Fig. 1. New type of GTL-processes based on the carbonylation and/or oligomerization of products of partial oxidation and selective oxy-cracking of natural gas.

The first step of alternative GTL processes consists of direct oxidative conversion (for example, the partial oxidation methane to methanol); the partial oxidation of heavy components of associated petroleum gas to methanol and CO; or the oxidative cracking of heavy components of associated petroleum gas to form ethane and CO. The further processing of gas-vapor mixtures of methanol, ethene and CO (final step of alternative GTL) may give a broad assortment of high value-added marketable products. Moreover, the process simultaneously gives dry fuel gas with high methane index (Fig. 2).

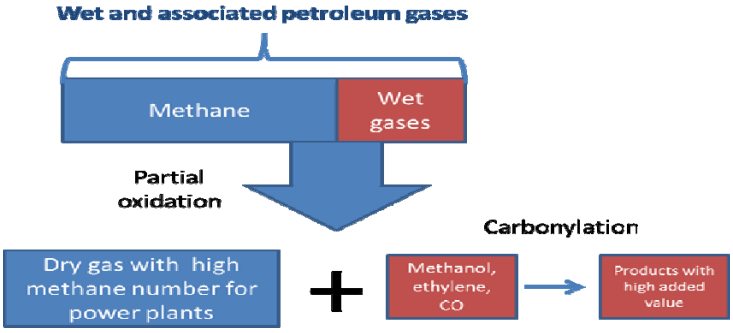

Fig. 2. Conversion of wet natural gas or associated petroleum gas yield high value-added petrochemical products and dry fuel gas with high methane index.

3 Conclusions

Direct partial oxidation of wet natural or associated petroleum gas with subsequent carbonylation and/or oligomerization of oxidation products can be considered as an alternative route for Gas-To-Liquids processes which let to avoid syngas production - the most costly and energy consuming stage of traditional GTL.

Acknowledgements

This work was supported by the Department of General Chemistry and Material Sciences of the Russian Academy of Sciences (Program No.7)

References

[1] V.S. Arutyunov, V.M. Shmelev, A.N. Rakhmetov, and O.V. Shapovalova, *Ind. Eng. Chem. Res.*, **53** (2014) 1754.
[2] V.I. Savchenko, I.A. Makaryan, I G. Fokin, I V. Sedov, R N. Magomedov, M.G. Lipilin and V.S. Arutyunov, *Neftepererabotka i Neftechimiya*, **8** (2013) 21.
[3] I.A. Makaryan, I.V. Sedov, V.I. Savchenko, *Johnson Matthey Technol. Rev.*, **59** (2015) 11.

III-OP34

Progress in the Catalysts for Small-Scale Hydrogen Generators Based on Boron-Containing Hydrides

Simagina V.I.[1*], Netskina O.V.[1], Ozerova A.M.[1], Komova O.V.[1], Odegova G.V.[1], Kochubey D.I.[1], Kellerman D.G.[2]

1 - Boreskov Institute of Catalysis SB RAS, Novosibirsk, Russia
2 - Institute of Solid State Chemistry UrB RAS, Ekaterinburg, Russia

* simagina@catalysis.ru

Keywords: hydrogen, storage, hydrogen generation, sodium, borohydride, ammonia, borane, catalyst

1 Introduction

Electronic devices (electronic tablets, navigators, communicators and others) have become indispensable in today's every-day life. For their safe operation, energy sources are needed with an energy-storage capacity exceeding that of the usual batteries. A promising solution to the problem is use of portable PEM fuel cells. However this would require creation of systems for storage and generation of high-purity hydrogen. Boron-containing hydrides – sodium borohydride ($NaBH_4$) and ammonia borane (NH_3BH_3) containing 10.5 and 19.3 wt. % of hydrogen, respectively, belong to compounds most rich in hydrogen. Their interaction with water in the presence of catalysts produces hydrogen at ambient temperatures without supply of heat. There may be two variants of the catalytic hydrogen generators: (I) using a flow reactor and (II) a batch reactor. Each type of reactor imposes its own requirements on the geometry, size, composition and strength of the catalysts. This work presents the results of our study of catalysts used in flow-reactor hydrogen generator and of the catalysts added to the "hydrogen" pellets used in batch-reactor hydrogen generator.

2 Experimental/methodology

All granular catalysts were prepared by incipient wetness impregnation of supports using aqueous solutions of corresponding metal chlorides and reduced directly in the reaction medium of boron-containing hydride solutions (*in situ*). The powder catalysts were synthesized from cobalt chloride and cobalt oxide under *in situ* conditions.

Catalytic hydrolysis of hydrides was performed in two ways.

Hydrogen generator with a flow reactor – solution of boron-based hydrides: The process of hydrogen generation was studied using a 15 wt% solution of $NaBH_4$ stabilized by sodium hydroxide or a 15 wt% solution of NH_3BH_3 at 20°C. The catalysts were tested in a flow apparatus at a feed rate of the solution of 1 cm^3/min.

Hydrogen generator with a batch reactor – solid $NaBH_4$-based pellet: At 20°C a solid-state $NaBH_4$ pellet (0.0465 g of $NaBH_4$ with the powder cobalt catalyst) was placed into a batch reactor and then 10 mL of distilled water was added. The volume of the produced hydrogen gas was measured with a 100 mL gas burette.

HRTEM with EDX analysis, FTIR spectroscopy, XRD, magnetic susceptibility, neutron scattering and EXAFS were used for characterization of *in situ* formed catalysts.

3 Results and discussion

Hydrogen generator with a flow reactor - solution of boron-containing hydrides:

Generation of large amounts of hydrogen over a prolonged period of time is best achieved in a hydrogen generator with a flow reactor [1] where a concentrated solution of hydride passes through a fixed bed of granular catalyst. The catalytic activity of VIII group metals on

granulated Sibunit, TiO_2, Al_2O_3 supports has been studied. The activity of the metals was found to decrease in the series Rh>Ru>Pt>Co>Ni on each of the studied supports, Rh/TiO_2 showing the highest activity. Its calcination (300°C) considerably accelerates $NaBH_4$ decomposition thanks to the formation in the reaction medium of electron-deficient nanoparticles of rhodium on the TiO_2 surface [2]. Among the non-noble metal catalysts the most active in $NaBH_4$ and NH_3BH_3 hydrolysis were cobalt catalysts reduced *in situ* in a medium of hydrides. Using EXAFS, neutron scattering and magnetic susceptibility it was established, for the first time, that the catalytically active phase of cobalt catalysts represents tetramers of cobalt atoms with Co-Co distances of 2.33 and 2.48 Å imbedded in a B-O-H matrix. Such a model has been called a "jelly".

It was shown that in an alkaline reaction medium the catalytically active phase of the cobalt catalysts gets destroyed to form non-active Co^0 and $Co(OH)_2$ [3]. This leads to a drop in H_2 generation rate during long-term stability tests. For a better stability of the cobalt catalyst it was modified by ruthenium as a result of which the Ru-Co catalyst becomes as stable and active as is highly effective rhodium system. According to HRTEM data the active component of the modified catalyst represents cobalt-ruthenium particles of an average size of 3.2 nm consisting of a cobalt core and a shell enriched in ruthenium. This leads to an enhanced activity of the catalytic system and prevents cobalt deactivation in the alkaline medium during the long-term stability tests [4].

Hydrogen generator with a batch reactor - solid $NaBH_4$-based pellet

Such type of hydrogen generator is needed for a short-time (to two hours) generation of hydrogen at a low generation rate which is important when charging batteries of portable devices in the field. Here the source of hydrogen is a "hydrogen" pellet representing a compressed mixture of solid hydride and a powder of active cobalt catalyst [5]. It was found that the rate of hydrogen generation upon addition of water to the $NaBH_4$-based pellet is determined by the hydride/catalyst/water ratio, the nature of the catalyst and the content of different specialized additives. It was shown also that no hydrogen losses occur during a prolonged storage of $NaBH_4$ pellets.

4 Conclusions

The obtained results show a promise for employing granulated cobalt-ruthenium catalysts in flow-reactor hydrogen generator and of powders of cobalt catalysts in batch-reactor hydrogen generator operating with $NaBH_4$-based pellets. The structure of the catalytically active phase of cobalt-containing catalysts which form *in situ* in the reaction medium under the action of hydrides has been established and the influence of different factors were determined.

Acknowledgements

The Russian Foundation for Basic Research (grant № 14-22-01045) is acknowledged for financial support.

References

[1] O.V. Netskina, R.V. Fursenko, O.V. Komova, E.S. Odintsov, V.I. Simagina. *Journal of Power Sources*. 273 (2015) 278.

[2] O.V. Netskina, D.I. Kochubey, I.P. Prosvirin, D.G. Kellerman, V.I. Simagina, O.V. Komova. *Journal of Molecular Catalysis A: Chem.* 390 (2014) 125.

[3] V.I. Simagina, O.V. Komova, O.V. Netskina. *Metal Nanopowders: Production, Characterization, and Energetic Applications*. Eds. A.A. Gromov, U. Teipel. Wiley-VCH. 2014. 199.

[4] V.I. Simagina, A.M. Ozerova, O.V. Komova, G.V. Odegova, D.G. Kellerman, R.V. Fursenko, E.S. Odintsov, O.V. Netskina. *Catalysis Today*. 242 (2015) 221.

[5] O.V. Netskina, A.M. Ozerova, O.V. Komova, G.V. Odegova, V.I. Simagina. *Catalysis Today*. DOI: 10.1016/j.cattod.2014.05.029 (in press).

III-OP35

Dry Reforming of Propane over NiO-CeO_2 Loaded Anodized Aluminum Oxide(AAO) Catalysts

Jayakodi Karuppiah J., Young Sun Mok Y.S*

Jeju National University, Department of Chemical Engineering, Jeju, South Korea

* smokie@cheju.ac.kr, smoke@jejunu.ac.kr

Keywords: anodic alumina oxide, synthesis gas, dry reforming, carbon deposition, CeO_2

1 Introduction

Synthesis gas (syngas), a fuel gas mixture consists of hydrogen and carbon monoxide is important intermediate for production of value-added oxygenated chemicals and liquid fuels [1]. Recently, it has been proven that the noble metals are less sensitive for carbon deposition on the surface therefore it is more important to develop novel catalyst with desired catalytic performance as compared to the noble metals. Among various metals nickel is catalytically active for the reforming reaction. However the deposition excess carbon on metal surface degrades their catalytic activity. Therefore, much attention has been focused on the development for Ni-based catalysts or metal oxide as well as changing supports, suppressing the carbon deposition. In order to reduce the carbon deposition, the metal-support is the key factor and needed to be improved. Recently, anodic oxidation technology was applied to produce monolith-like catalyst support which offers strong metal-support interaction. Porous anodic alumina oxide (AAO) template, are one of the most interesting structures, due to their unbranched, regular, controllable and nearly parallel pores. The above benefits of AAO show advantages for mass and heat transfer. Topology of the catalyst pore structure 10 nm–100 nm can influence reagent flow, the sequencing of catalytic active sites, and the contact time between reacting gas and catalyst. Hence, AAO is a highly promising support structure for the application in catalytic reforming reaction. In this investigation simultaneous loading of Ni and CeO_2 on AAO was studied as the catalyst for propane dry reforming reaction.

2 Experimental

Catalysts preparation

AAO templates with ordered pores were prepared by an anodization process using freshly prepared oxalic acid solution [2]. Nickel and ceria were loaded onto the AAO supports by impregnating the plates with aqueous solutions of Ni $(NO_3)_2$ and Ce $(NO_3)_3$ dissolved in 250 ml de-ionized water to keep the molar ratio changed from 0.2 to 1. Then the prepared catalysts were calcined at 450°C. The loaded metal oxide concentration was about to 4 wt% (obtained by measuring the weight of the support before and after catalyst loading) with respect to support weight.

Catalytic reaction and characterization

The dry reforming of propane with CO_2 was carried out in a thermo-catalytic reactor packed with catalyst plate (10 g, 5 × 6 cm) was cut into pieces with a size of 2–3 mm^2 and loaded into the reactor. The catalytic activity was studied in the temperature range of 480–580°C for all the catalysts. The reactant gases were fed into the reactor at the proportion of 10:30:60 ($C_3H_8/CO_2/N_2$). The total flow rate was fixed at 300 ml min^{-1} throughout this work. During the reforming reaction, the concentrations of relevant components were analyzed by a gas chromatograph equipped with a thermal conductivity detector (TCD). Numerous techniques, such as N_2 adsorption–desorption isotherm, X-ray diffraction (XRD), field emission scanning electron microscopy (FESEM) and transmission electron microscopy (TEM), and Temperature

programmed reduction (TPR) and temperature programmed oxidation (TPD) were applied for characterization of fresh and spent catalysts.

3 Results and discussion

The catalytic performance of AAO supported catalysts with various nickel and Ceria loadings at different reaction temperatures. The obtained results show that both C_3H_8 and CO_2 conversions increased with increasing ceria loading up to 80 %(0.8M) and 20 % (0.2M) NiO/CeO_2-AAO catalysts showed the highest activity for dry reforming reaction.

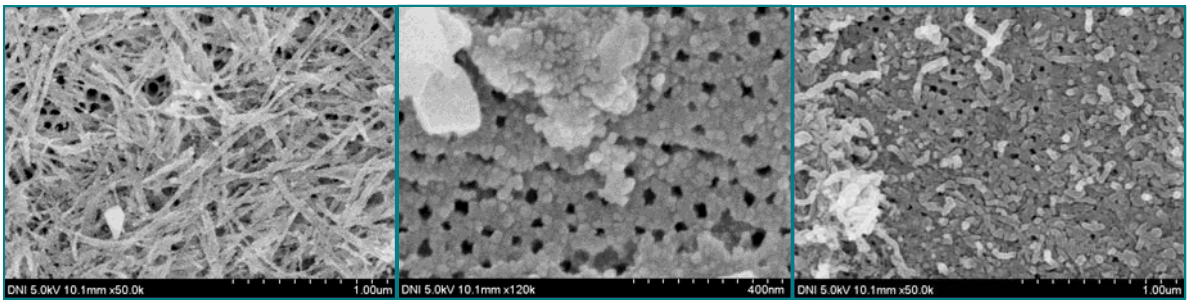

Fig. SEM images of (a) $NiO_{(0.2M)}$-$CeO_{2(0.8M)}$/AAO, (b) (b) $NiO_{(0.8M)}$-$CeO_{2(0.2M)}$/AAO catalysts and (c) $NiO_{(0.8M)}$-$CeO_{2(0.2M)}$/AAO after the reforming.

The results of catalyst testing revealed that the catalysts with higher ceria loading catalyst (0.2M NiO+0.8M CeO_2) have superior catalytic performance for activity and stability than other loading. After 12 h under stream at 540^{o}C, CeO_2 catalysts, showed a stable operation in presence of a deposited amorphous carbon. Carbon deposition on spent catalysts was analyzed by the temperature programmed oxidation (TPO). The structural and phase modification of the catalysts after the reforming reactions were further examined with XRD, SEM, TEM and TPO.

4 Conclusions

It is then noted that, the use of electroless deposition to prepare bimetallic oxides of AAO catalysts for DR provides a useful technique for synthesizing highly functional metallic catalytic systems. The main advantage of a plated catalyst is effective heat exchange and the formation of the NiO and CeO_2–bimetallic oxides on AAO support, which brings about the improvement in catalytic activity. The plated catalyst made from an equimolar concentration of metal solution forms a better NiO-CeO_2 interaction over AAO and leads to higher propane conversion and high H_2/CO ratio. High dry reforming activity of CeO_2-promoted and exhibited good stability for anti-sintering and coke resistance.

Acknowledgements

This work was supported by the research grant of Jeju National University in 2013, and by Basic Science Research Program through the National Research Foundation of Korea (NRF) funded by the Ministry of Science, ICT and future Planning (Grant No. 2013R1A2A2A01067961).

References

[1] J. Karuppiah, Y. S. Mok, *International Journal of Hydrogen Energy*. 29 (2014) 16329.
[2] P. Ciambelli, V. Palma, E. Palo, *Catalysis Today*. 155 (2010) 92.

III-OP36

Impact of Hydrocracking on Fischer-Tropsch Synthesis Selectivity: Mesoporous ZSM-5-Supported Cobalt Nanoparticles for Selective Production of C_{5-11} Isoparaffins

Cheng K., Kang J., Zhang L., Peng X., Zhang Q., Wang Y.*

Collaborative Innovation Center of Chemistry for Energy Materials, State Key Laboratory of Physical Chemistry of Solid Surfaces, National Engineering Laboratory for Green Chemical Productions of Alcohols, Ethers and Esters, College of Chemistry and Chemical Engineering, Xiamen University, Xiamen, China

* wangye@xmu.edu.cn

Keywords: Fischer-Tropsch synthesis, bifunctional catalyst, mesoporous zeolite, selectivity control, isoparaffins, hydrocracking

1 Introduction

Fischer-Tropsch (FT) synthesis is a crucial process in the transformation of non-petroleum carbon resources into clean hydrocarbon fuels via syngas. Over conventional FT catalysts, the products generally follow the Anderson-Schulz-Flory (ASF) distribution, which is wide (C_{1-80}) and unselective. The integration of acidic zeolite and conventional FT catalyst can lead to high C_{5-11} selectivity (gasoline-range) without resorting to very complex designs. However, the selectivity of light hydrocarbon (C_{1-4}) is generally unacceptably high over zeolite-supported catalysts, probably due to the diffusion limitation and the overcracking caused by the narrow and long micropores. Using mesoporous zeolites as the supports of Ru catalysts, we succeed in suppressing the C_{1-4} selectivity.[1,2] Herein, we report our recent studies on the development of highly selective mesoporous H-ZSM-5 (H-meso-ZSM-5)-supported Co catalysts by coupling Co nanoparticles with uniform particle sizes and mesoporous ZSM-5 with tunable mesopore sizes and acidities for FT synthesis. The hydrocracking of *n*-hexadecane, a model compound of heavier hydrocarbons, will also be investigated to provide deeper insights.

2 Experimental

Mesoporous ZSM-5 was prepared by post-treating a Na-ZSM-5 (Si/Al = 18) using NaOH aqueous solutions. The obtained Na-form meso-ZSM-5 was exchanged to H-meso-ZSM-5 by an ion-exchange method. Co nanoparticles were loaded onto H-meso-ZSM-5 by an impregnation with $Co(NO_3)_2$ aqueous solutions, followed by heat treatment in NO/He and H_2 reduction. The catalysts were characterized by various techniques including XRD, N_2-physisorption, H_2 chemisorption, H_2-TPR, TEM, NH_3-TPD, pyridine-adsorbed FT-IR and pulse oxidation. FT synthesis was performed on a high-pressure fixed-bed reactor at 513 K with a syngas (H_2/CO = 1/1) pressure of 2 MPa. Hydrocracking of *n*-hexadecane was operated in the same reactor at 513 K with a H_2 pressure of 2 MPa. The products were analyzed by gas chromatography.

3 Results and discussion

Fig. 1a shows that the synthesized ZSM-5 possesses a sheet-like morphology, which may be beneficial to mass transport. After post-treatment by NaOH aqueous solutions, abundant mesopores were generated over the ZSM-5 crystals (Fig. 1b).

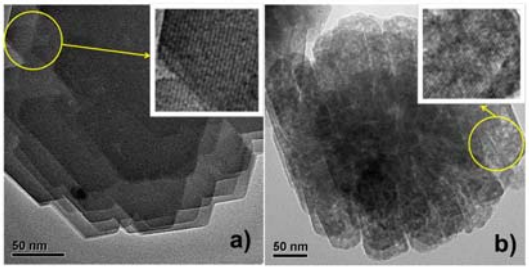

Fig. 1. TEM images of a) H-ZSM-5 and b) H-meso-ZSM-5-0.5M.

Crystalline fringes could be observed in the HRTEM images of the H-meso-ZSM-5, indicating that the crystalline structure was maintained. We clarified that the size and pore volume of mesopores increased with an increase in the concentration of NaOH aqueous solution.[3] Our pyridine-adsorbed FT-IR and NH_3-TPD studies revealed that the density of Brønsted acid sites decreased gradually with an increase in the concentration of NaOH solution.

We clarified that the post-treatment of the $Co(NO_3)_2$/H-ZSM-5 composites affected the size distribution of Co particles loaded and found that the heat treatment under NO/He could provide uniform sizes of Co particles.[3] TEM measurements further revealed that the mean sizes of Co particles loaded on H-meso-ZSM-5 with different mesopore sizes were in a range of 7.7-10.5 nm, which were beneficial to FT synthesis.[4]

Fig. 2a shows that the Co/H-meso-ZSM-5 exhibits significantly lower CH_4 and C_{2-4} selectivities and higher C_{5-11} selectivity than the Co/H-ZSM-5. The selectivity to CH_4 decreased from 22% to 8% and that to C_{5-11} increased from 51% to 70% when an optimized concentration of NaOH (0.5-0.8 M) was used for H-meso-ZSM-5 synthesis. It is also of interest that the main products in C_{5-11} are isoparaffins. The conversion of *n*-hexadecane verified that our bifunctional catalysts could catalyze the hydrocracking of *n*-hexadecane under the conditions similar to those used for FT synthesis. Fig. 2b shows the selectivity to middle-distillate products, in particular, C_{7-11}, increases significantly by using Co/H-meso-ZSM-5 instead of Co/H-ZSM-5, which mainly produced lighter hydrocarbons. The ratio of isoparaffins to n-paraffins in the cracking products was high. It can be concluded that the increment of C_{5-11} isoparaffins in FT synthesis stems from hydrocracking/isomerization of C_{12+} hydrocarbons formed on Co nanoparticles.

We further studied the roles of acidity and mesoporosity through a series of studies using meso-ZSM-5 with different mesopore sizes and different H^+-exchanging degrees. We clarified that the Brønsted acidity accounted for the hydrocracking of heavier hydrocarbons, whereas the mesoporosity mainly contributed to suppressing the formation of lighter hydrocarbons.

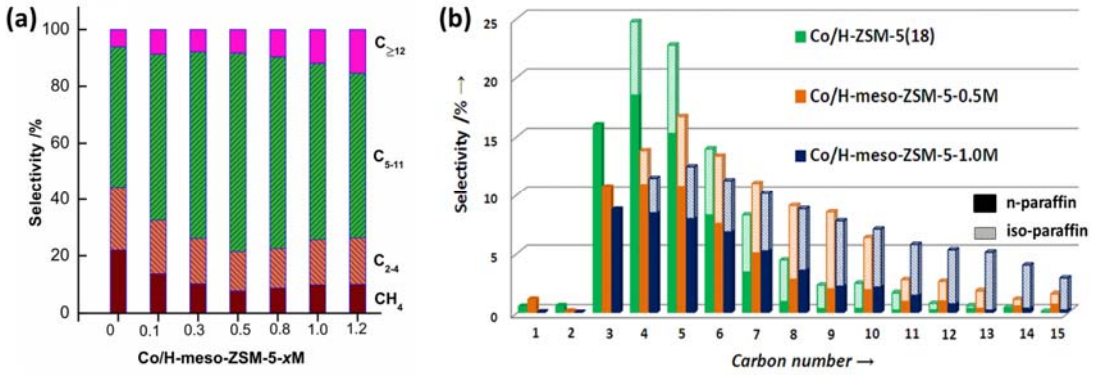

Fig. 2. Product distributions. (a) FT synthesis, (b) *n*-hexadecane hydrocracking.

4 Conclusions

The coupling of mesoporous H-ZSM-5 and uniform-sized Co nanoparticles significantly increased the selectivity to $C_{5–11}$ gasoline-range hydrocarbons (70%) with a high fraction of isoparaffins. The Brønsted acidity was required for the hydrocracking of heavier hydrocarbons (C_{12+}), whereas the presence of mesoporosity contributed to suppressing the formation of lighter hydrocarbons. Using *n*-hexadecane as a model compound, we confirmed the roles of Brønsted acidity and mesoporosity in hydrocracking/isomerization and in determining the selectivity.

References

[1] J. Kang, K. Cheng, L. Zhang, Q. Zhang, Y. Wang, et al., *Angew. Chem. Int. Ed.* 50 (2011) 5200.
[2] K. Cheng, J. Kang, S. Huang, Z. Yoo, Q. Zhang, Y. Wang, et al., *ACS Catal.* 2 (2012) 441.
[3] K. Cheng, L. Zhang, J. Kang, X. Peng, Q. Zhang, Y. Wang, *Chem. Eur. J.* 21 (2015) 1928.
[4] G. L. Bezemer, J. H. Bitter, H. P. C. E. Kuipers, H. Oosterbeek, J. E. Holewijn, X. Xu, F. Kapteijn, A. J. van Dillen, K. P. de Jong, *J. Am. Chem. Soc.* **2006**, *128*, 3956-3964.

III-OP37

CO Activation on Cobalt Fischer-Tropsch Catalyst

Chen W.*, Zijlstra B., Filot I.A.W., Ligthart D.A.J.M., Van Hoof A.J.F., Pestman R., Hensen E.J.M.

Laboratory of Inorganic Materials Chemistry, Eindhoven University of Technology, Eindhoven, The Netherlands

* E.J.M.Hensen@tue.nl

Keywords: cobalt catalyst, CO activation, transient kinetics, microkinetic modeling

1 Introduction

Fischer-Tropsch (FT) synthesis is not only the enabling technology that can convert a wide range of carbon sources into liquid fuels, but also presents an entry into the synthesis of organic intermediates [1]. It is of fundamental importance to understand the mechanism underlying the FT reaction. CO hydrogenation and FT share the same CO dissociation step that initiates the surface polymerization process and production of other chemicals with C-C bonds [2]. Modern insights into the relation between surface topology and reactivity dictate that direct CO dissociation can only occur with reasonable activation barrier on step-edge sites of transition metals such as Co, Rh and Ru [3]. Hydrogen assisted CO dissociation has been recently explored as an alternative route for less reactive planar surfaces [4]. In the present work, transient experiments combined with theoretical calculations were employed to understand CO hydrogenation on Co catalysts.

2 Materials and Methods

The catalyst containing 20 wt% Co and 0.04 wt% Pt was prepared by incipient wetness impregnation on SiO_2 (Shell). The turn over frequencies (TOF) were determined based on hydrogen chemisorption (ASAP 2000). $^{13}C^{16}O$ (Cambridge Isotope Laboratories, ^{13}C 99%, ^{18}O 95%) and $^{13}C^{18}O$ (^{13}C 99%, ^{18}O <2%) isotopes are used in transient experiment and $^{12}C^{16}O/^{13}C^{18}O$ scrambling experiment, respectively.

Plane wave density functional theory (DFT) calculations with projector-augmented wave (PAW) method were performed using Vienna ab initio simulation package (VASP) to determine all activation energies of elementary surface reactions. The microkinetic modeling (MKM) was carried out by an in-house written C++ software suit for heterogeneous catalysis. Transient data fitting was performed by Matlab (MathWork).

3 Results and discussion

The mechanism of CO activation was studied by a new approach that combines transient techniques (Fig. 1), *i.e.*, steady state isotopic transient analysis (SSITKA)and chemical transient analysis. Together with the first-principle based MKM (Fig. 2), these transient data can be interpreted in terms of the mechanism of both direct and H-assisted CO dissociation. Degree of rate control analysis of MKM suggests that CH_2O dissociation controls the methanation rate for Co(0001) surface, and CO dissociation and CH_3 hydrogenation contribute to the rate control on Co(1121). Combined transient data show better correspondence of direct CO dissociation with the kinetics than hydrogen assisted CO dissociation does. Transient data fitting based on direct CO dissociation mechanism is in agreement with first-principles calculation. By $^{12}C^{16}O/^{13}C^{18}O$ isotope scrambling experiments [5], we found that the CO scrambling TOF is close to that of the methanation rate, indicating that direct CO dissociation is the main mechanism of CO activation.

Combined, these results highlight the importance of direct CO dissociation on Co nanoparticles.

Fig. 1. Modeling of normalized methane response throughout transient experiments. Points are experimental results; lines are modeling results. The different feeds are shown on top.

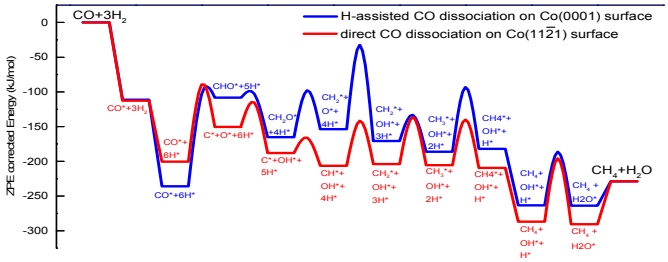

Fig. 2. Reaction energy diagram for hydrogen assisted CO activation on the Co(0001) surface (blue) and direct CO activation on the Co(1121) surface (red)

4 Conclusions

Transient kinetic experiments (SSITKA, CTKA and $^{12}C^{16}O/^{13}C^{18}O$ isotope scrambling) were combined with first-principles based microkinetics approaches to investigate the mechanism of CO activation that initiates the Fischer-Tropsch reaction. The results provide strong support for the importance of direct CO dissociation for obtaining CH_x building blocks relevant to methanation and the Fischer-Tropsch reaction.

Acknowledgements

The authors acknowledge the National Research School Combination Catalysis Controlled by Chemical Design (NRSC-Catalysis) for financial support.

References

[1] B. List, *Angew. Chem. Int. Ed.* 53 (2014) 8528.
[2] A. J. Markvoort, R. A. van Santen, P. A. J. Hilbers, and E. J. M. Hensen, *Angew. Chem. Int. Ed.* 51 (2012) 9015.
[3] S. Shetty, A. P. J. Jansen, and R. A. van Santen, *J. Am. Chem. Soc.* 131 (2009) 12874.
[4] M. Ojeda, R. Nabar, A. U. Nilekar, A. Ishikawa, M. Mavrikakis, E. Iglesia, *J. Catal.* 272 (2010) 287.
[5] C. Strebel, S. Murphy, R. M Nielsen, J. H. Nielsen, I. Chorkendorff, *Phys. Chem. Chem. Phys.* 14 (2012) 8005.

III-OP38

Ethanol Acts as Capping Agent and Formaldehyde Scavenger to Promote Efficient Lignin Depolymerization to Aromatics

Huang X.[1], Korányi T.I.[1], Boot M.D.[2], Hensen E.J.M.[3*]

1 - Schuit Institute of Catalysis, Inorganic Materials Chemistry, Eindhoven University of Technology, Eindhoven, The Netherlands

2 - Combustion Technology, Department of Mechanical Engineering, Eindhoven University of Technology, Eindhoven, The Netherlands

3 - Schuit Institute of Catalysis, Inorganic Materials Chemistry, Eindhoven University of Technology, Eindhoven, The Netherlands

* E.J.M.Hensen@tue.nl

Keywords: biomass, lignin, supercritical, ethanol, depolymerization, alkylation, Guerbet reaction

1 Introduction

Lignocellulosic biomass is a low-cost renewable feedstock that is uniquely suited for the production of sustainable liquid fuels. One approach to valorize the carbohydrate fraction is to convert the constituent sugars to ethanol by fermentation. Different from cellulose and hemicellulose, technologies to upgrade lignin into useful products are in early stage of development. Cellulosic ethanol production is approaching commercial practice. A considerable issue associated with large-scale ethanol production from lignocellulosic biomass is the co-production of large amounts of lignin; these amounts exceed both the internal energy needs of biorefineries and the world market for lignin-derived specialty products by a large margin. Therefore, new processes to add value to lignin beyond its combustion heat are needed. We have earlier reported a one-step valorization of soda lignin in supercritical ethanol using a $CuMgAlO_x$ catalyst, resulting in 23 wt% monomer yield (300 °C, 8 h) without char formation [1]. Alkylation was found to play an important role in suppressing repolymerization[1]. In the present work, we will reveal evidence for the role of ethanol to suppress repolymerization, explaining high monomer yield.

2 Experimental/methodology

Three types of lignin (Soda, Alcell, Kraft) were used as feedstock. The reactions were conducted in a batch reactor under supercritical ethanol using a mixed non-noble-metal oxides catalyst ($CuMgAlO_x$). A comprehensive workup procedure was developed to distinguish the smaller (THF-soluble) and larger (THF-insoluble) lignin fragments and char. GC-MS, GPC, ^{1}H-^{13}C HSQC NMR and elemental analysis (CHO) techniques were used to characterize the lignin products. In addition, phenol and guaiacol were also used as model reactant in order to understand the mechanistic insights during lignin depolymerization.

3 Results and discussion

We compared the solvent effect of lignin reaction using methanol and ethanol as solvents. It was found that much less monomer (8 wt% vs 17 wt%) and much more THF-insoluble lignin residue (39 wt% vs 18 wt%) were formed in methanol than in ethanol after reaction at 300 °C for 8 h. It indicates that catalytic depolymerization of lignin is much more effective in ethanol than in methanol. To understand the role of the solvent, we compared the conversion of phenol into high-molecular-weight products in methanol and ethanol. Consistently, we found that polymerization of phenol took place in methanol, but not in ethanol. This is because methanol can be readily dehydrogenated to form formaldehyde, which easily reacts with phenol to form

resins. This explains why the use ethanol is significantly more effective in producing monomers and avoiding char than the use of methanol. Furthermore, we proved that ethanol also acts as formaldehyde scavenger that reacts with the formaldehyde formed from methoxy group cleavage from the lignin during supercritical ethanol-mediated reactions. This explains the absence of char formation in ethanol. After optimizing the reaction conditions, we found that monomer yields between 60 wt% and 86 wt% (depends on the lignin used) can be obtained after reaction of lignin in ethanol at 380 °C for 8 h.

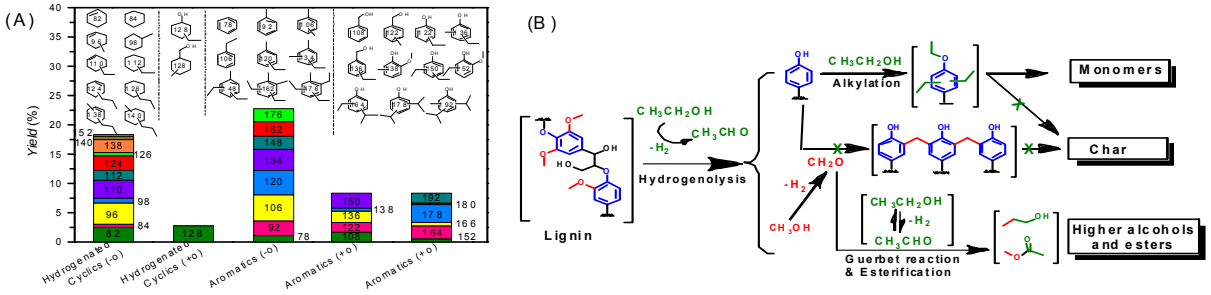

Figure 1(A). Monomeric product distribution following (soda) lignin reaction at 380 °C for 8 h over the $CuMgAlO_x$ catalyst in ethanol solvent. **Figure 1(B).** The roles of alkylation, the Guerbet reaction, and esterification on suppressing char formation during lignin depolymerization over the $CuMgAlO_x$ catalyst in ethanol solvent.

4 Conclusions

We have demonstrated high-yield production of monomeric aromatics from lignin using a $CuMgAlO_x$ catalyst in supercritical ethanol with little char formation. The monomeric products are mainly composed of alkylated aromatics and cycloalka(e)nes. The oxygen-free aromatics can be used as chemical building blocks and as octane boosters when blended with gasolines. Oxygenated aromatics may serve as valuable compounds for the chemical and polymer industry. They can also be used as low-sooting diesel fuel additives [2]. Different types of lignins, including sulfur-containing Kraft lignin, can be used as the feedstock. Importantly, we revealed new mechanistic insights about lignin depolymerization and highlighted the role of alcohol solvents. Ethanol is effective as a capping agent and formaldehyde scavenger, suppressing repolymerization and char-forming reactions. We believe that these insights provide new impetus for the design of better processes to valorize lignin.

Acknowledgements

This work was funded by the "New Energy House" project of the Eindhoven Energy Institute in collaboration with the Knowledge and Innovation Community InnoEnergy of the European Institute of Innovations and Technology.

References

[1] X. Huang, T. I. Korányi, M. D. Boot, E. J. M. Hensen, *ChemSusChem.* **7**(2014) 2276.
[2] L. Zhou, M. D. Boot, B. H. Johansson and J. J. E. Reijnders, *Fuel*, **115** (2014) 469-478.
[3] X. Huang, T. I. Korányi, M. D. Boot, E. J. M. Hensen, Submitted for publication.

III-OP39

Biofuels Production from Glycerol and TBA Using an Innovative Catalytic Membrane Reactor

Cannilla C.*, Bonura G., Feminò G., Drago Ferrante G., Frusteri F.

National Council of Research, CNR-ITAE, Messina, Italy

* catia.cannilla@itae.cnr.it

Keywords: glycerol, biofuels, membrane reactor, diesel additives, acid solid catalysts

1 Introduction

Glycerol *poly*-*tert*-butyl ethers can be produced by etherification of glycerol with *tert*-butyl alcohol by employing an acid catalyst. This synthesis represents a new route for the production of oxygenated additives for diesel fuels [1]. Since the reaction is controlled by equilibrium and water is formed as *by*-product, irrespectively from the catalyst used, the reaching of high glycerol conversion and *poly*-ethers yield is limited by thermodynamic constraints. A study regarding the optimization of the reaction conditions is here reported by exploiting an innovative batch reactor coupled with a permselective membrane to remove the water from the reaction medium and to promote the formation of *poly*-ethers. The attention has been addressed on the obtainment in one step of a mixture, containing a low amount of *mono*-ether suitable to be added to the diesel fuel.

2 Experimental/methodology

Etherification reaction of glycerol was carried out by using both a commercial acid ion resin A-15 and a acid catalyst, H730/SiO_2, prepared by impregnation of a microspherical silica with Hyflon® Ion S4X perfluorosulphonic ionomer. The reaction was performed at 80°C in liquid phase in a stainless steel reactor coupled with a permeoselective tubular membrane (furnished by Pervatech) used to remove the water formed during the reaction by recirculation of gas phase. The liquid phase was analyzed *off line* by a gas chromatograph provided with a capillary HP Innowax column.

3 Results and discussion

The etherification of glycerol generates a set of consecutive equilibrium reactions and, at the same time, secondary reactions could occurs too; in particular, when TBA is the *O*-alkylant agent, the following scheme should be considered.

Main consecutive reactions with TBA		*Main consecutive reaction with IB produced by eq.4*	
Gly + TBA ⇆ Mono + H_2O	(1)	Gly + IB⇆ Mono	(7)
Mono + TBA ⇆ Di + H_2O	(2)	Mono + IB ⇆ Di	(8)
Di + TBA ⇆ Tri+ H_2O	(3)	Di + IB ⇆ T	(9)
Secondary reactions		*Secondary reactions with IB produced*	
TBA ⇆ IB+ H_2O	(4)	IB + IB ⇆ DIB	(10)
Mono + Mono ⇆ GLY + Di	(5)	IB + DIB ⇆ TRIM	(11)
Di + Di ⇆ Tri + Mono	(6)	DIB + DIB ⇆ *poly*-isobutene	(12)

In a recent paper [1], it has been reported that with A-15, an acid-exchange resin, the best results in the etherification reaction were obtained at 70°C, with a glycerol conversion (X_{Gly}) of 80% and a selectivity to *mono*-ethers of 70%. By increasing the reaction temperature to 80°C, the X_{Gly} decreased to 67% likely due to faster accumulation of water which prevents the activation of glycerol by competitive absorption on the acid sites of the catalyst.

Then, once the equilibrium is reached, reaction no longer goes on towards *tri*-ethers

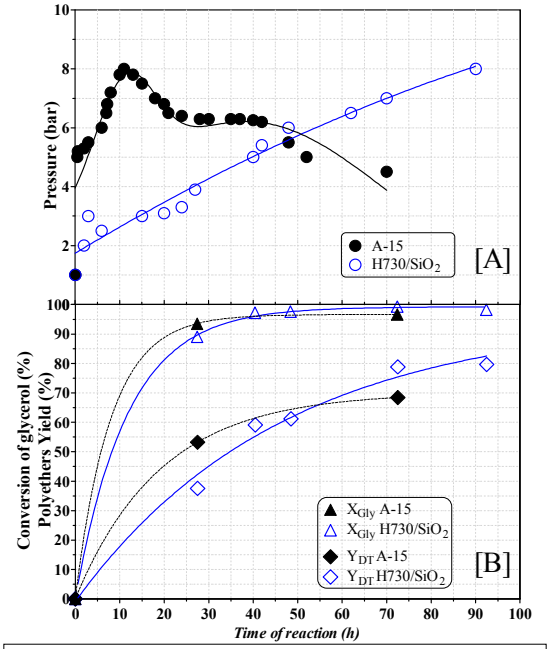

Fig. 1. Etherification reaction as a function of reaction time. T_R=80°C; $R_{cat/gly}$= 7.5 wt.% with respect to glycerol weight; $R_{TBA/gly}$= 8 mol/mol

formation; rather the dealkylation reaction of *poly*-ethers to *mono*-ethers becomes significant [2]. Therefore, the water produced affects the thermodynamic equilibrium preventing the formation of *poly*-ethers and consequently the total glycerol conversion [2]. The results previously obtained also showed that to perform the etherification of glycerol, the catalyst should be characterized by a not excessive acidity in order to avoid the occurrence of secondary reactions. Furthermore, the surface properties must be adequate to allow a high accessibility of acid sites for the activation-desorption of reaction intermediates featured by high steric hindrance. Fig. 1 shows results obtained in the etherification of glycerol with TBA both in presence of A-15 and H730/SiO_2 catalysts in terms of glycerol conversion, reaction pressure and yield to *poly*-ethers (Y_{DT}) along the time using the batch reactor coupled with the membrane. With A-15, the reaction pressure drastically increases up to 5 bar in 30 min thus confirming that the dehydration of TBA to IB takes place at high rate; pressure reaches a maximum value after 10h and then it decreases with time. On the contrary, in case H730/SiO_2 catalyst is used, the reaction pressure linearly increases with time thus suggesting that IB is formed at a lower rate, reaching higher values after very long reaction time. This result is mainly linked to the difference between the rates of IB production and consumption and confirms that, with H730/SiO_2, IB slowly accumulates into the reactor; besides χ_{Gly} progressively increases with time reaching almost the total conversion after 25h while the Y_{DT} increases up to 80% after 70h. Differently, with A-15, χ_{Gly} never reaches values higher than 96% and Y_{DT} value remains lower (68%) than that obtained with the H730/SiO_2 system. This is due to the fact that the lower rate of IB formation observed with H730/SiO_2 doesn't promote the production of byproducts by IB oligomerization (eqs.10-12) which, in case of A-15, negatively reflect on the cumulative Y_{DT}.

4 Conclusions

The use of a novel batch reactor assisted by a permselective membrane resulted to be a winning idea to produce ethers from glycerol by etherification with TBA. In fact, the removal of water allowed to shift the equilibrium towards the *poly*-ethers formation. By setting the appropriate reaction parameters and employing a proper solid catalyst (Hyflon/SiO_2), it was possible to carry out the etherification of glycerol with alcohol (TBA) to obtain a clean ethers mixture without glycerol and containing about 80 wt.% of *di*- and *tri*-ethers.

Acknowledgements

This work was financially supported by Italian Research Fund (PON R&C 2007-2013, PON02_00451_3362376) through the "BIO4BIO" project, Biomolecular and Energy valorization of residual biomass from Agroindustry and Fishing Industry.

References

[1] C. Cannilla, G. Bonura, L. Frusteri, F. Frusteri *Environ. Sci Technol*. 48 (2014) 6019.
[2] C. Cannilla, G. Bonura, L. Frusteri, F. Frusteri, *Cent. Eur. J. Chem*, 12(12) (2014) 1248.

III-OP40

Catalytic C-O Cleavage and Hydrogenation of Diaryl Ethers in Aqueous and Apolar Phase

He J.[1], Renges H.[1], Barath E.[1], Mei D.[2], Lercher J.A.[1,2*]

1 - Department of Chemistry, Technische Universität München, Garching, Germany
2 - Institute for Integrated Catalysis, Pacific Northwest National Laboratory, Richland, USA

* jiayue.he@mytum.de

Keywords: diphenyl, ether, lignin, C-O cleavage, solvent, hydrogenolysis, hydrolysis

1 Introduction

Catalytic cleavage of the C-O bond in aromatic ethers of lignin is a critical process for the conversion of lignin to fuels, and chemicals [1]. Diphenyl ether is commonly chosen as the simplest model compound for exploring the mechanism of catalytic conversion of 4-O-5 ether bond in lignin, which has the highest bond dissociation energy. Considering the higher tolerance to water and the easier application for industrial utilizations, Ni-based catalytic system in the aqueous phase were intensively studied by various groups [2,3]. These recent advances towards C-O bond cleavage in lignin model compounds have been focused exclusively on the development and screening of catalysts [4]. Much less attention has been to the influence of substituted groups and solvents. In this contribution, we will systematically explore the influence of solvents (H_2O and *n*-hexane) on the reaction pathway (hydrogenolysis, hydrolysis and hydrogenation) and kinetic parameters (initial TOFs, apparent activation energies, reaction orders) of three di-aryl ethers with various substituted groups like di-*p*-tolyl ether (-CH_3), diphenyl ether (-H) and 4,4'-dihydroxyldiphenyl ether(-OH)) on Ni/SiO_2 at 393 K and 0.6 MPa H_2. In addition, the adsorption heats of diaryl ethers on Ni surface were calculated in different environments. Furthermore, DFT calculation was also applied to determine the sequence of reaction rate of C-O bond cleavage and hydrogenation of all three diaryl ethers in apolar phase and in aqueous phase.

2 Experimental

Reagents. All the chemicals used in this study were obtained from commercial suppliers. Ni/SiO_2 catalyst was synthesized *via* deposition precipitation (DP) method.

Kinetic methods. In a typical experiment, the substrates were converted in a Parr autoclave reactor (Series 4848, 300 mL Hastelloy) in H_2O and *n*-hexane, respectively, at 393 K in the presence of 0.6 MPa H_2. Diphenyl ether (0.010 mol), 57 wt.% Ni/SiO_2 (0.30 g, 2.91×10^{-3} mol Ni in H_2O or 0.15g, 1.45×10^{-3} mol Ni in *n*-hexane), and solvent (H_2O or *n*-hexane, 80 mL) were added into the autoclave.

3 Results and discussion

Figure 1 shows the reaction proceed *via* hydrogenolysis and partial/full hydrogenation in the apolar phase. In contrast, hydrolysis appeared as a new major reaction pathway in aqueous phase. Furthermore, the full hydrogenation of diphenyl ether was not observed in water. In aqueous phase the reaction rates (C-O cleavage or hydrogenation) showed the order of $TOF_{\text{4,4'-dihydroxyldiphenyl ether}} > TOF_{\text{diphenyl ether}} > TOF_{\text{di-}p\text{-tolyl ether}}$. In aqueous phase the reaction rates (C-O cleavage or hydrogenation) followed the order of $TOF_{\text{di-}p\text{-tolyl ether}} > TOF_{\text{diphenyl ether}} > TOF_{\text{4,4'-dihydroxyldiphenyl ether}}$. In a comparison to aqueous phase, the apolar solvent will greatly enhance the selectivity to hydrogenation in a competition between hydrogenation and hydrogenolysis.

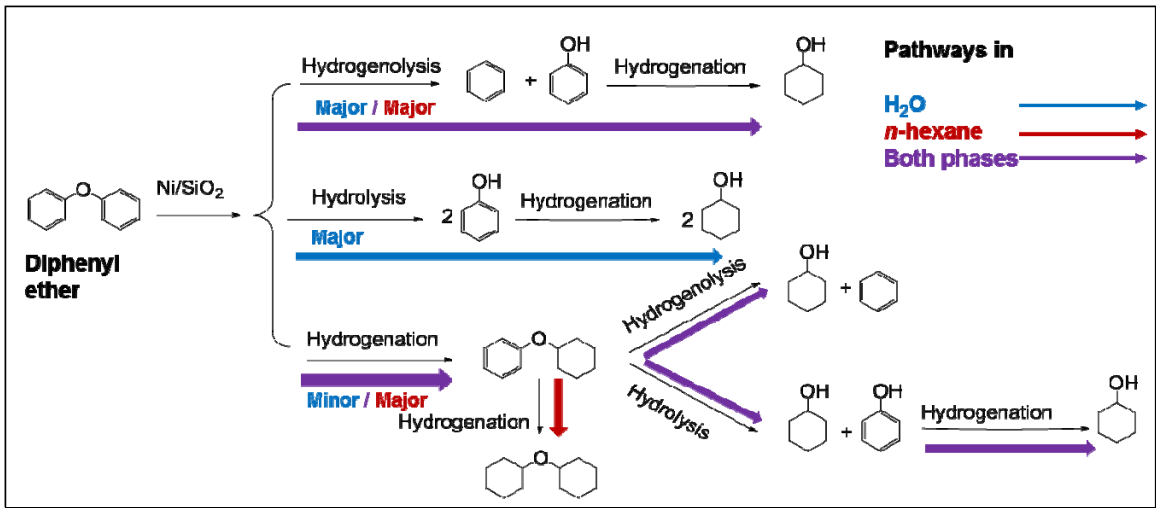

Fig. 1. The proposed reaction pathways for diphenyl ether in water and *n*-hexane.

4 Conclusions

The catalytic conversion of three di-aryl ethers with different substituted groups (diphenyl ether (-H), di-p-tolyl ether (-CH_3) and 4,4'-dihydroxydiphenyl ether (-OH)) have been explored over Ni/SiO_2 in aqueous and apolar phase (*n*-hexane). C-O bond cleavage and hydrogenation were two competitive parallel reactions over Ni/SiO_2 in the reaction conditions. Substituted groups and solvents influenced not only reaction pathway and selectivity to C-O bond cleavage and hydrogenation, but also the rates of catalytic C-O bond cleavage and hydrogenation of diaryl ethers by altering the reactant solubilities, solvent-reactant interactions, as well as by competitive solvent/reactant adsorption on the Ni surface.

Acknowledgements

J.H. gratefully acknowledges for the support from Technische Universität München and the Elite Network of Bavaria. D.M. and J.A.L. thank for the support from the US Department of Energy, Office of Basic Energy Sciences, Division of Chemical Sciences, Geosciences & Biosciences.

References

[1] P.C.A.Bruijnincx,, B.M. Weckhuysen, *Nature Chemistry* 6 (2014) 1035
[2] J. He, C. Zhao, D. Mei, J.A. Lercher, *Journal of Catalysis* 309 (2014) 280
[3] J. He, C. Zhao, J.A.Lercher, *Journal of the American Chemical Society* 134 (2012) 20768
[4] A. Rahimi, A. Ulbrich, J.J.Coon, S.S.Stahl, *Nature* 151 (2014) 249

III-OP41

The Effects of Methanol or Dimethyl ether as Methylating Agent during Zeolite Catalysed Benzene Methylation

Martinez-Espin J.S.[1,2*], Westgård Erichsen M.[1], De Wispelaere K.[3], Van Speybroeck V.[3], Beato P.[2], Svelle S.[1], Olsbye U.[1]

1 - Centre for Materials Science and Nanotechnology, Department of Chemistry, University of Oslo, Oslo, Norway
2 - Haldor Topsøe A/S, Lyngby, Denmark
3 - Center for Molecular Modeling, Ghent University, Zwijnaarde, Belgium

* juansm@smn.uio.no

Keywords: zeolites, methylation, dimethyl ether, methanol, MD, simulations, methanol-to-hydrocarbons

1 Introduction

Methylation of benzene and other aromatics are key reactions in several important industrial processes such as methanol conversion to gasoline or olefins (MTG/MTO) [1] and xylene production from toluene [2]. Microporous acid materials such as zeolites are commonly used as catalysts in these processes. This work combines experiments and theory to investigate the behaviour of methanol and dimethyl ether (DME) during benzene methylation over catalysts with different structures (MFI and AFI) and acid strength (AFI). Previous studies have revealed higher methylation rates for DME than methanol over H-ZSM-5 [3], but the methylation mechanisms are usually assumed to be similar. This study not only confirms a difference in methylation rates, but also reveals large differences in selectivity towards secondary products for methanol and DME.

2 Experimental/methodology

Catalytic experiments were performed in a fixed bed quartz reactor with 5 mg catalyst powder diluted in 40 mg quartz (particle size 250-420μm). Typically, 60 mbar of benzene was co-reacted with 60 mbar of either methanol or DME at differential conversion (WHSV = 205-375 h^{-1}, conversion < 2%) at 250-300 °C. The effluent was monitored continuously by on-line MS and a detailed analysis was performed by on-line GC-FID/MS after 10 minutes of reaction.

Ab initio molecular dynamics calculations were carried out with the CP2K simulation package to sample all relevant configurations of the guest molecules in the pores. The periodic DFT-D3 calculations were performed in a 1x1x2 H-SSZ-24 and H-SAPO-5 super cell and H-ZSM-5 unit cell, at 350 ºC and 1 bar. Rare event sampling was enhanced with a metadynamics approach [4].

3 Results and discussion

Net product formation rates obtained during benzene methylation at 250°C are shown in Figure 1. In agreement with previous studies on H-ZSM-5 [3], the use of DME led to higher total product formation rates than methanol. Furthermore, Figure 1 shows that the product distribution varied significantly based on the choice of methylating reactant. While DME predominantly yielded (sequential) methylation and dealkylation products (toluene, polymethylbenzenes and alkenes), the use of methanol led to a high selectivity towards diphenylmethane (DPM) and its methylated analogue. Similar trends were observed at 300°C for H-ZSM-5 and H-SSZ-24. DPM has previously been suggested as an intermediate during methylbenzene transmethylation reactions [5]. Preliminary results indicate a larger release of H_2 during the reaction when using methanol, indicating that DPM may be formed by phenylation of

toluene accompanied by loss of H_2.

Figure 2 illustrates the proposed reaction scheme, where formed toluene is either methylated further or phenylated to form DPM. The reaction mechanisms and kinetics of toluene phenylation are currently under investigation. In addition, ab initio molecular dynamics simulations of co-adsorption and reaction of methanol and DME with benzene, toluene and xylene have been performed in order to obtain a deeper understanding of the experimental observations. Important differences in the stability and reactivity of different co-adsorption complexes formed between methanol or DME and aromatics with an increasing degree of substitution may be possibly linked with the observed selectivity and reactivity differences.

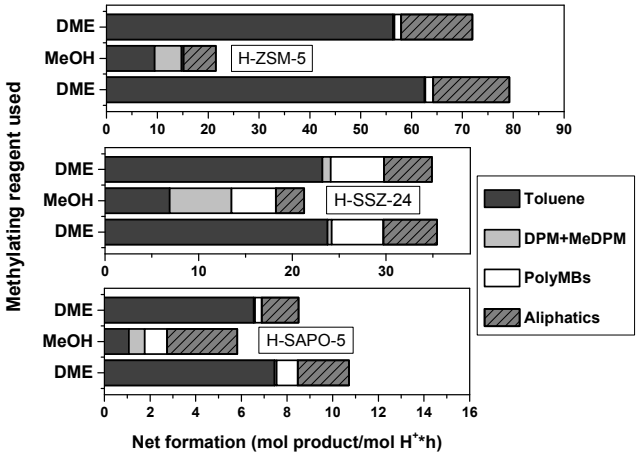

Fig. 1. Net product formation rates during benzene methylation over H-ZSM-5 (top), H-SSZ-24 (middle) and H-SAPO-5 (bottom) at 250°C. Experiments were run sequentially (e.g. DME-MeOH-DME).

4 Conclusions

This study shows that use of methanol or DME in benzene methylation led to different reaction rates and product distributions. Similar behaviour was observed irrespective of catalyst topology or acid strength. Compared to DME, the use of methanol led to lower rates of methylation and significantly higher yields of diphenylmethane. In depth experimental and theoretical studies are in progress to elucidate the reason for the observed selectivity differences and will be presented.

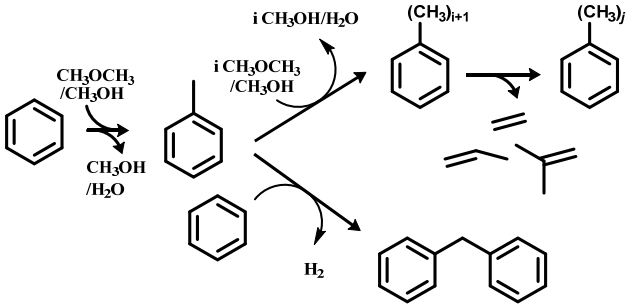

Fig. 2. Proposed reaction scheme for benzene methylation and successive reactions.

Acknowledgements

Financial support is received via the European Industrial Doctorates project "ZeoMorph" (FP7 ITN-EID), part of the Marie Curie actions. We thank the Foundation of Scientific Research - Flanders (FWO) and the European Research Council. Computational resources and services used in this work were provided by the Stevin Supercomputer Infrastructure of Ghent University and by the Flemish Supercomputer Center (VSC), funded by the Hercules Foundation and the Flemish Government – department EWI.

References

[1] U. Olsbye, et al., Angew. Chem. Int. Ed., 51 (2012) 5810.
[2] M.C. Clark, et al., Alkylation of Aromatics, in: Handbook of Heterogeneous Catalysis, Wiley-VCH Verlag GmbH & Co. KGaA, 2008, pp. 3172.
[3] S. Svelle, et al., J. Phys. Chem. B, 109 (2005) 12874.
[4] S.L.C. Moors, et al., ACS Catalysis, 3 (2013) 2556.
[5] S. Svelle, et al., J. Am. Chem. Soc., 128 (2006) 5618.

III-OP42

Kinetic Analysis and Raman Surface Characterization in the CPO of Propane, Propylene and n-C_8H_{18}

Beretta A.[1*], Donazzi A.[1], Pagani D.[1], Lucotti A.[2], Tommasini M.[2], Groppi G.[1], Castiglioni C.[2]

1 - Politecnico di Milano, Dipartimento di Energia, Milano, Italy
2 - Politecnico di Milano, Dipartimento di Chimica Materiali e Ingegneria Chimica, Milano, Italy

* alessandra.beretta@polimi.it

Keywords: kinetics, characterization, CPO, Raman, coke, logistic, fuels

1 Introduction

The Catalytic Partial Oxidation (CPO) of hydrocarbons is a promising solution for the small-scale and on-board production of H_2 or CO/H_2 mixtures (syngas). The reaction is highly exothermic and extremely fast, and is typically carried out under autothermal conditions, in compact reactors, at millisecond contact time. Fuel flexibility is a major goal for the success of CPO: the reactor should be able to process fuels spanning from NG and LPG (CH_4, C_3H_8 and C_4H_{10}) up to logistic (gasoline and diesel) and biomass-derived fuels. The main drawbacks hampering a wide-range use of hydrocarbons (larger than C_1-C_3) are the high temperatures reached in the reactor (>1000°C) and the formation of C-deposits, which lead to catalyst deactivation even when noble metal are employed. Depending on the nature of the fuel, high temperatures also enhance the activation of gas-phase cracking reactions, which form coke-precursor intermediates, such as C_2H_6, C_3H_6 and C_2H_4. In this work, we analyze the CPO of C_3H_8 (representative of LPG), C_3H_6 (C_{2+} coke-forming fuel) and n-C_8H_{18} (logistic fuel): focus is given to the reaction kinetics and the coke formation tendency. The formation of C-species as a function of temperature is followed by combining kinetic investigations performed in an annular micro-reactor with Raman measurements of the catalyst surface.

2 Materials and Methods

2 wt% $Rh/\alpha Al_2O_3$ catalysts were prepared by dry impregnation of $Rh(NO_3)_3$ of the αAl_2O_3 support (10 m^2/g BET SA). The CPO experiments were performed in an annular micro-reactor, at 1 atm, between 300 and 850°C, at high space velocity, under isothermal conditions. A MicroGC (Agilent 3000) was used to analyze the composition of the inlet and outlet gas streams. Ex-situ Raman measurements were carried out with a Raman i-Raman BWTEK instrument (785 nm laser excitation, 5 cm^{-1} resolution, 175 – 3250 cm^{-1} spectral range, TE Cooled 2048 Pixel CCD detector). The Raman measurements were taken at room temperature according to the following procedure: after stable conditions were achieved in the annular reactor at a significant temperature, the reaction was quenched under inert N_2 flow to room temperature; the reactor was extracted from the furnace and kept under inert flow; the Raman signal was measured by focusing the beam directly on the catalyst layer through the quartz wall of the reactor.

3 Results and discussion

Previous experimental and microkinetic studies on CH_4 and C_3H_8 CPO [1] pointed out strong analogies regarding the nature of the active sites and the rate determining step in the activation of these fuels. Under oxidative conditions (O_2/C = 0.5-1), the C-H bond breaks on O*-O* pairs, i.e. on a Rh surface saturated by adsorbed O* (Regime I, as defined in Ref. [2]). In the absence of O_2, under reforming conditions, the C-H bond breaks on a free Rh site pair *-* (Regime IV). Coherently, Raman characterization suggests that the Rh surface maintains

reasonably clean in C_3H_8 CPO and CH_4 CPO: very weak signals of C-structures (amorphous and graphitic) appear only in the spectra collected at T > 600°C. As well, the fuel conversion curve measured as a function of T shows a smooth transition between the oxidative and the reforming regime, around 400°C in the case of C_3H_8 (■ in Fig. 1a and b).

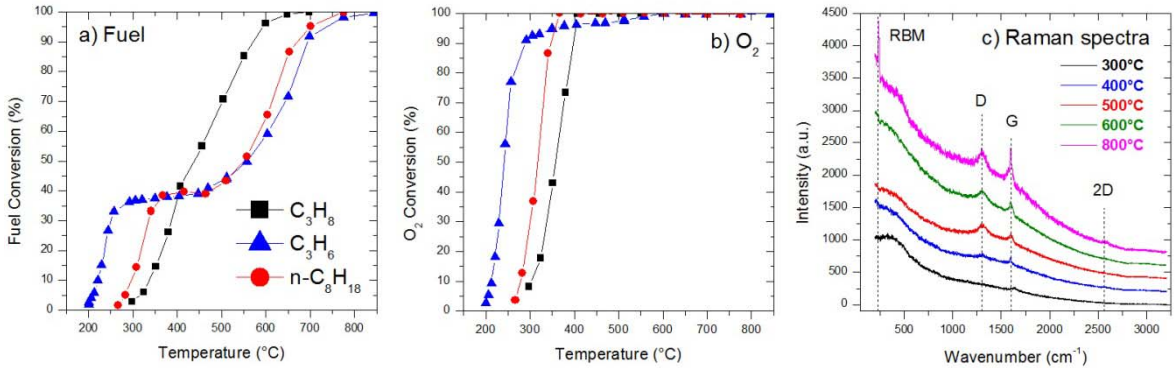

Fig. 1 - Panel a and b: CPO of C_3H_8 (■), C_3H_6 (▲) and n-C_8H_{18} (●). Panel c: Raman spectra in n-C_8H_{18} CPO at increasing T. $O_2/C = 0.56$, $O_2 = 1.7\%$, GHSV = $2*10^6$ Nl/kg_{cat}/h

Much different features characterize the kinetics of C_3H_6 CPO (▲ in Fig. 1a and b). C_3H_6 has a very high oxidation activity (O_2 is completely consumed at ~250°C), followed by a flat plateau in C_3H_6 conversion (300 – 450°C) and by a delayed onset of the reforming activity (T > 450°C). Kinetic analyses [3] indicate that the oxidation rate has an inverse dependence on O_2 and a positive quadratic dependence on C_3H_6 concentration, suggesting that C_3H_6 activation occurs on a surface only partially saturated by O* and that the dissociative adsorption of C_3H_6 on a O-* pair is the determining step (Regime II). In the absence of O_2, C_3H_6 strongly adsorbs on the surface, forming different C-species, as detected by Raman. These C-species do not partake in the reforming process and lead to surface C-poisoning and to kinetic inhibition. A positive dependence on H_2O is found for the rate of reforming, as a consequence of the beneficial effect of H_2O gasification in contrasting the accumulation of carbon.

The results of n-C_8H_{18} CPO show an intermediate behavior. Total oxidation is fast, the consumption of O_2 starts at ~250°C and completes at ~325°C (● in Fig. 1a and b). Kinetic tests indicate that the oxidation rate is directly proportional to n-C_8H_{18} concentration and independent of O_2, fully in line with C_3H_8 and with the activation of n-C_8H_{18} on O*-O* site pairs (Regime I). Instead, similar to C_3H_6 CPO, a plateau is observed in n-C_8H_{18} conversion between 300 and 450°C, with a delay of the reforming activity to high T. Inhibition by n-C_8H_{18} adsorption and C-poisoning are again suggested, and supported by Raman spectra (Fig. 1c): in the presence of O_2, the surface is almost free of C, whereas, once O_2 is consumed, amorphous deposits and graphitic-like platelets form (G, D, 2D lines) with nanotubes (sharp G component, RBM and 2D lines) gradually growing at increasing T.

4 Conclusions

Combined application of Raman characterization and kinetic tests in the annular reactor allows to individuate the nature of site active for the fuel activation (O*-O*, O*-* or *-* pairs) as well as the tendency of the fuel to stick on the catalyst surface and form C-species.

References

[1] D. Pagani et al., Catalysis Today, 197 (2012) 265.
[2] M. Garcia-Diéguez et al., Journal of Catalysis, 285 (2012) 260.
[3] D. Pagani et al., Industrial & Engineering Chemistry Research, 53 (2014) 1804.

III-OP43

Low Temperature In-Situ Hydrogen Production by Ammonia Decomposition Using Cobalt-Based Catalysts

Bell T.E.[1,2*], Hill A.K.[1,2], Torrente-Murciano L.[1,2]

1 - Department of Chemical Engineering, University of Bath, Bath, UK
2 - Centre for Sustainable Chemical Technologies, University of Bath, Bath, UK

* T.Bell@Bath.ac.uk

Keywords: ammonia decomposition, cobalt, alumina, nanorods, nanoparticle, stabilisation

1 Introduction

The use of chemical molecules, such as ammonia, as hydrogen vectors has the potential to unlock a pseudo hydrogen economy overcoming the transport and storage issues associated with in-situ use of hydrogen in fuel cells.1 Ammonia has traditionally been used for agricultural fertilisers and refrigerants, with an existing distribution infrastructure becoming a promising alternative fuel associated to its carbon-free high hydrogen content (17.6 wt.%).2 In addition, ammonia has a small explosive range and can be liquefied at room temperature under mild pressure or stored in solid metal ammine complexes.3

Based on the substantial catalytic research carried out on the synthesis and decomposition of ammonia during the last decades, this work aims to design a catalytic system from first principles able to release the potential of ammonia as a hydrogen storage medium using readably available metals such as Fe, Ni, Pt, Ir, Pd, Co as alternative to Ru-based catalysts, which, are currently the most active systems for this reaction.4

2 Experimental/methodology

Commercial carbon nanotubes (CNTs), microporous Ax-21 carbon and γ-Al2O3 nanorods (NR) are used as catalytic supports. One dimensional γ-Al2O3 nanorods are synthesised by hydrothermal treatment using Al(NO3)3·9H2O) and 1M NaOH solution at 200 ºC for 20 hours, followed by calcination at 500ºC for 3 hours.5 Cobalt is loaded by incipient wetness impregnation (IWI) followed by reduction at 450 ºC. NH3 decomposition reactions are carried out in a plug flow reactor through a packed-bed of 25 mg catalyst using 2.77 nml/min NH3 and 5 nml/min He over a range of temperatures up to 850 K.

3 Results and discussion

The decomposition of ammonia on ruthenium nanoparticles is believed to take place on B5 active sites, a specific arrangement of five ruthenium atoms. The concentration of such sites is optimum on particle sizes between 2-4 nm. This specific particle size range is selectively stabilised on CNTs support and in combination to their high conductivity, constitute the best catalytic system for ammonia decomposition reported in the literature to the date.1 Figure 1 shows that such systems can decompose ammonia at temperatures above 640 K without further optimisation. Substitution of ruthenium for more readily available cobalt on CNTs is translated in a considerable loss of ammonia decomposition activity, especially at low temperatures.

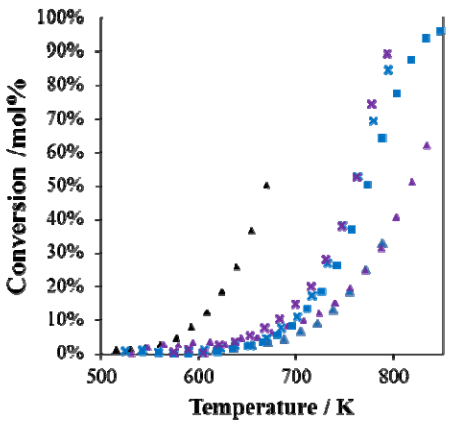

Fig. 1. Activity of ammonia decomposition catalysts. ▲- 7 wt. % Ru/CNT, ▲- 7 wt. % Co/CNT, ▲- 7 wt. % Co 7 wt. % Cs /CNT, ■ - 15 wt. % Co/ NR-γ-Al_2O_3, X – 14 wt. % Co/Ax21, X – 14 wt. % Co 14 wt. % Cs/Ax21.

However, interestingly, the use of microporous carbon support (Ax21) with a mean pore size of 2.3 nm leads to a considerable enhancement of the cobalt system, with activities at temperatures as low as 670 K. The optimization of active cobalt-based catalysts depends on the stabilisation of small particle sizes (< 2 nm), well below the optimum size previously observed for ruthenium-based systems.

High aspect ratio 1D nanostructured materials are well-known to be able to stabilise small metal nanoparticles by a combination of spatial confinement on their outer surface and specific metal-support interaction.6 Here, we present the use of γ-Al2O3 nanorods as a suitable support for cobalt nanoparticles with ammonia decomposition activity at similar temperatures as for cobalt supported on microporous carbon supports (670 K). Spatial confinement allows tuneable metal particle sizes by variation of the cobalt loading and the metal particle : support diameter ratio.

The addition of Cs to Ru/CNT catalysts has been reported to electronically modify the ruthenium particle size enhancing its activity for low temperature ammonia decomposition.1 Interestingly, this promotion effect is not applicable to the cobalt based systems. Further studies related to the effect of alkali-metals in cobalt based systems with a focus on cobalt accessibility blockage will be reported.

Table 1. Pore size, specific surface area, activation energy (E_a) and turnover frequency (TOF) at 700 K.

Support	Metal loading	Pore size / nm	S_{BET} / m^2/g	E_a / kJ/mol	TOF / mol_{NH3} $mol_{Cat}^{-1}s^{-1}$ (@700 K)
CNT	7 wt.% Ru	27.3	250	102.8	0.0366
γ-Al_2O_3 rods	15 wt.% Co	N/A	100	40.1	0.0024
Ax21	14 wt.% Co	2.3	2200	66.9	0.0039
Ax21	14 wt.% Co – 14 wt.%Cs	2.3	2200	44.3	0.0050

4 Conclusions

Cobalt is presented as an abundant and cheaper alternative to ruthenium-based catalysts for ammonia decomposition for in-situ production of H_2. Stabilisation of small particles with sizes below 2 nm is crucial to reveal its potential. High aspect ratio γ-Al_2O_3 nanostructured supports are presented to successfully stabilise cobalt nanoparticles with tuneable sizes to guide future catalyst design in this field.

Acknowledgements

The authors would like to acknowledge the UK Engineering and Physical Science Research Council for funding, the DTC in the Centre for Sustainable Chemical Technologies and SASOL UK.

References

[1] A. Hill and L. Torrente Murciano, *Int. J. Hydrogen Energy*, 2014, **39**, 7646–7654.
[2] C. Zamfirescu and I. Dincer, *Fuel Process. Technol.*, 2009, **90**, 729–737.
[3] A. Wojcik, H. Middleton, I. Damopoulos and J. Van Herle, *J. Power Sources*, 2003, **118**, 342–348.
[4] S. F. Yin, B. Q. Xu, X. P. Zhou and C. T. Au, *Appl. Catal. A Gen.*, 2004, **277**, 1–9.
[5] T. E. Bell, J. M. Gonzalez-Carballo, R. P. Tooze and L. Torrente-Murciano, *J. Mater. Chem. A*, 2015.
[6] L. Torrente-Murciano, Q. He, G. J. Hutchings, C. J. Kiely and D. Chadwick, *ChemCatChem*, 2014, **6**, 2531–2534.

III-OP44

Na-Modified Cu-Co-Based Catalysts for Higher Alcohol Synthesis: Influence of Surface Composition and CoC_2 Formation

Muhler M.[1,2*], Anton J.[1,2], Nebel J.[1,2], Froese C.[1,2], Kleinschmidt R.[3], Quandt T.[4], Ruland H.[1,2], Kaluza S.[5]

1 - Ruhr-University Bochum, Bochum, Germany
2 - Laboratory of Industrial Chemistry, Ruhr-University Bochum, Bochum, Germany
3 - ThyssenKrupp Industrial Solutions, Germany
4 - Evonik Industries, Essen, Germany
5 - Fraunhofer UMSICHT, Germany

* muhler@techem.rub.de

Keywords: higher alcohols synthesis, synthesis, gas, copper, cobalt, Na, promoter

1 Introduction

Higher alcohol synthesis (HAS) via hydrogenation of carbon monoxide is a promising route for providing important basic chemicals, alternative fuels and additives in gasoline blends. Although Rh is well known to be highly active in HAS, catalysts based on non-noble metals such as Cu, Co and Fe are considered promising systems for large-scale application. As Co and Fe adsorb CO dissociatively, while the adsorption on Cu occurs molecularly, both functions combined in one bimetallic catalyst may provide a cost-efficient alternative to precious metal-based systems [1]. Doping of modified methanol synthesis or modified Fischer-Tropsch (FT) synthesis catalysts with basic promoters such as alkali compounds is known to increase the selectivity towards higher alcohols.

Institute Français du Pétrole (IFP) first reported on selective alkali-doped Cu-Co-based catalysts in HAS [2]. However, the activity was moderate and large-scale application has not yet been realized. Our recent results indicate that these catalysts undergo severe structural changes during the reduction of the oxide precursor and during the first hours under reaction conditions. Therefore, the thorough characterization of the spent catalyst after activation and/or after HAS provides important information to further adjust the optimum reaction conditions and catalyst compositions to enhance product selectivities and the degree of conversion. The present contribution describes structure-activity correlations of high relevance for HAS revealed by thorough characterization of the catalysts in the reduced state.

2 Experimental

Cu-Co-based catalysts were prepared similar to the coprecipitation method described by IFP. The activated and spent catalysts with different Na loadings were characterized by X-ray photoelectron spectroscopy (XPS), temperature-programmed techniques (TPR, TPD), reactive frontal chromatography (RFC) and X-ray diffraction (XRD). Activation and HAS were performed in a 4-fold parallel test facility, which allows the transfer of the activated and spent catalyst under inert conditions excluding re-oxidation and contamination by air. The catalytic tests were performed at 280 °C, 60 bar and a ratio of $H_2/CO = 1$.

3 Results and discussion

An initial deactivation was observed for the samples with low Na loadings within the first 10 h in HAS. In contrast, for samples with higher Na loading the initial degree of conversion

remained essentially constant. Additionally, the product distribution strongly depends on the alkali loading since the selectivity to higher oxygenates increases significantly with increasing Na content. The XPS analysis of the spent catalyst revealed major modifications of the surface composition compared with the reduced catalyst. The main observation is a decreased Cu/Co surface ratio. The decrease in the surface Cu concentration is assumed to be caused by the migration of Cu into the bulk. The surface modification during reaction was more pronounced for Na-free samples, whereas the decrease of the Cu/Co ratio was rather low in presence of Na. Characteristic reflections of ZnO and metallic Cu were found in the XRD patterns of all spent catalysts. The degree of crystallinity increases with increasing Na loading indicating larger particles. Moreover, with increasing Na loading the intensity of reflections assigned to Co_2C increases, while these reflections are not observed for the Na-free catalyst.

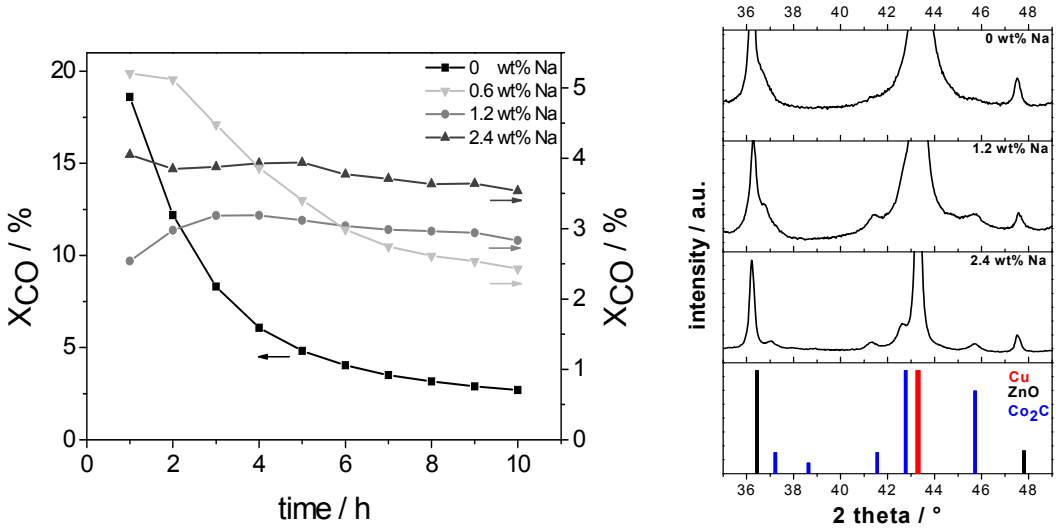

Fig. 1. CO conversion during the first 10 h on stream (left)and XRD pattern of the spent catalysts with different Na-loadings (right).

4 Conclusions

Na-modified bimetallic Cu-Co-based catalysts for HAS were successfully prepared by coprecipitation and subsequent alkali loading by incipient wetness impregnation. The thorough characterization of the reduced and spent state enabled the evaluation of different catalyst properties and their correlation with the performance in HAS. The initial deactivation observed for the Na-free catalysts is explained by strong surface modifications under reaction conditions. In contrast, the surface composition is stabilized in the presence of the Na promoter resulting in a constant degree of conversion and a constant product distribution during HAS. Obviously, the presence of alkali promoters favors the carbidization of Co, which is assumed to improve the catalyst properties with respect to deactivation and product distribution.

Acknowledgements

The work was part of the project "Bioethanol from synthesis gas - BETSY", funded by the Ministry for Economy, Energy, Building, Habitation and Transportation of NorthRhine-Westphalia within the program Ziel2.NRW financed by the European Union through the European regional development fund ERDF.

References:

[1] J. J. Spivey, A. Egbebi, *Chemical Society Reviews* **2007**, *36*, 1514–1528.
[2] P. Courty, D. Durand, E. Freund, A. Sugier, *Journal of Molecular Catalysis* **1982**, *17*, 241-254.

III-OP45

Effect of Ni on the Hydrogenation Mechanism of Polyaromatic Hydrocarbons over (Ni-)MoS_2/Al_2O_3

Schachtl E.[1], Gutiérrez O.Y.[1], Yoo J.S.[2], Studt F.[2], Lercher J.A.[1*]

1 - Technische Universität München, Department of Chemistry and Catalysis Research Center, Garching, Germany

2 - SUNCAT Center for Interface Science and Catalysis, SLAC National Accelerator Laboratory, California, USA

* Johannes.Lercher@ch.tum.de

Keywords: hydrogenation, phenanthrene, (Ni-)MoS_2/γ-Al_2O_3, isotopic, H-D exchange, DFT

1 Introduction

Transition metal sulfides, particularly MoS_2 promoted with Ni, have been extensively studied as hydrotreating catalysts. Especially for hydrodesulfurization, detailed reaction pathways and models for active sites exist [1]. Hydrogenation of polyaromatic hydrocarbons has been less investigated despite its growing relevance for heavy oil conversion. The present contribution investigates the hydrogenation of phenanthrene as a model aromatic compound aiming at a deeper insight into the hydrogenation mechanisms on (Ni-)MoS_2/Al_2O_3.

2 Experimental

Ni-MoS_2/γ-Al_2O_3 was prepared by impregnation and thermal treatment in H_2/H_2S and characterized by a series of standard and advanced techniques as reported elsewhere [2]. The catalytic activity was explored in the hydrogenation of phenanthrene (Phe), or dihydrophenanthrene (DiHPhe) at differential and integral conditions in a trickle-bed reactor at 60 bar, 553-583 K, and in the presence of H_2S.

The energetics of adsorption of the hydrocarbon on MoS_2 and Ni-MoS_2 were determined by density functional theory calculations using the QUANTUM ESPRESSO code employing ultrasoft pseudo-potentials to represent the core electrons. The BEEF-vdW [3] exchange correlation functional was used throughout.

3 Results and discussion

MoS_2/Al_2O_3 and Ni-MoS_2/Al_2O_3 with similar Mo content, the bimetallic catalyst having a molar Ni/(Mo+Ni) ratio of 0.3, were studied. The Phe hydrogenation network given in Figure 1A was derived from experiments at integral conditions with Phe and DiHPhe as reactants. The mechanism is identical for MoS_2/Al_2O_3 and Ni-MoS_2/γ-Al_2O_3. However, the contribution of the deep-hydrogenation pathway (k_2, k_4, k_5) is significant only in the presence of Ni, which also increases the Phe and DiHPhe consumption rates by a factor of 2.2.

The reaction order in Phe (see Fig. 1B), around ~0.65, was not influenced by the presence of Ni while the H_2 reaction order (see Fig. 1C) increased from 0.68 for MoS_2/Al_2O_3 to 1.2 for Ni-MoS_2/Al_2O_3. Interestingly, the presence of H_2S had no effect on the reaction over MoS_2/Al_2O_3 (zero order in H_2S) whereas it has a negative impact over Ni-MoS_2/Al_2O_3 (reaction order of -0.2). Combining the kinetic analysis and characterization of SH groups at the sulfide surface by IR-spectroscopy (which evidenced an acid character), allows to conclude that the hydrogenation of Phe occurs via stepwise proton addition and electron transfer in concerted mode. The rate determining steps are the first and second addition of hydrogen pairs for DiHPhe and tetrahydrophenanthrene (TetHPhe), respectively.

Combined IR and isotopic H-D exchange experiments showed that the concentration of

active surface hydrogen increased by 30% in presence of Ni. This may explain the increased rate of DiHPhe formation. However, it does not account for the dramatic increase of TetHPhe production rates and the concomitant change in rds. Deep hydrogenation is concluded to occur on the Ni-decorated MoS_2 edges (characterized by IR-spectroscopy of CO) where DiHPhe and TetHPhe are formed at comparable rates.

In line with this proposal, DFT calculations indicate that Phe adsorbs strongly on the basal planes of MoS_2, where it may tilt towards the edge and undergoes hydrogenation without the participation of exposed cations. In contrast, the restructured Ni-decorated MoS_2 edges offer adsorption modes that lead to the activation and multiple hydrogenation of the terminal rings of Phe.

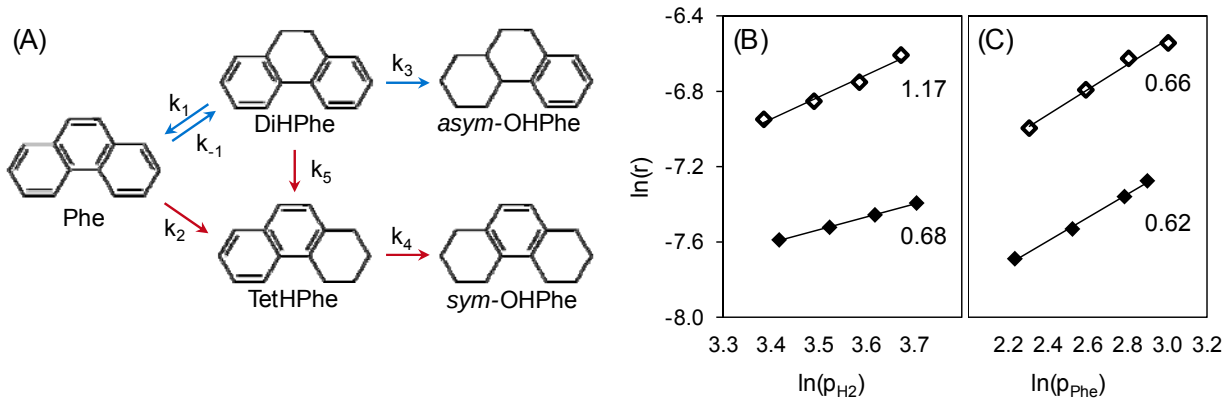

Fig. 1. (A) Reaction network for the hydrogenation of phenanthrene. The blue arrows denote steps occurring on MoS_2/Al_2O_3 and Ni-MoS_2/Al_2O_3 while red arrows denote steps occurring only on the latter. (B) Reaction order in H_2 and (C) reaction order in phenanthrene during the hydrogenation of phenanthrene on MoS_2/Al_2O_3 (◆) and Ni-MoS_2/Al_2O_3 (◇) at 573 K and 60 bar.

4 Conclusions

The promotion of MoS_2/γ-Al_2O_3 with Ni increases the concentration of active surface hydrogen and changes the rate determining step of hydrogen addition. Moreover, the combination of IR spectroscopy with DFT calculations points to a particular adsorption mode of phenanthrene on the Ni-promoted edge of MoS_2 which leads to multiple hydrogenation of the terminal rings of Phe. Thus, Ni increases the hydrogenation rates of polyaromatic hydrocarbons and modifies the surface concentration of the most abundant reaction intermediates.

Acknowledgements

Dr. Jinyi Han, Dr. Axel Brait and Dr. Alexander Kuperman are acknowledged for fruitful discussions and Chevron Energy Technology for the financial support.

References

[1] Moses, P. G.; Hinnemann, B.; Topsøe, H.; Nørskov, J. K. J. Catal. 248, 188 (2007).
[2] Schachtl, E.; Wuttke, E.; Gutiérrez, O.; Lercher, J. Mechanism and active sites of phenanthrene hydrogenation on supported NiMoS catalysts; paper presented at the 23rd North American Meeting of the North American Catalysis Society (NAM), Kentucky, USA, 2013.
[3] J. Wellendorff, K. T. Lundgaard, A. Møgelhøj, V. Petzold, D. D. Landis, J. K. Nørskov, T. Bligaard, K. W. Jacobsen, Phys. Rev. B 2012, 85, 235149.

III-OP46

Structured Catalytic Honeycombs Based on Copper/Ceria for CO Preferential Oxidation in H_2-Rich Streams

Barbato P.S.[1], Di Benedetto A.[2], Landi G.[1*], Lisi L.[1]

1 - Research Institute on Combustion – CNR, Naples, Italy
2 - DICMAPI, University of Naples Federico II, Naples, Italy

* landi@irc.cnr.it

Keywords: CO-PROX, monolith, hydrogen, copper/ceria

1 Introduction

Hydrogen to be fed to PEM fuel cell requires ultra-low CO content (10 – 50 ppm); consequently, if H_2 is produced via a reforming process, a purification step as preferential oxidation of CO (CO-PROX), in addition to WGS is required [1]. Especially for mobile applications, compactness, robustness and low pressure drops are required[2], thus suggesting the use of monolithic reactors. Indeed, although monoliths have been widely used in exhaust gas cleaning, their application in PROX process is at the early stage and only few papers have been published on this topic especially concerning copper/ceria catalysts [3-5]. Despite of the interest, the effect of the preparation method and geometrical features has not been systematically addressed. In this work our aim is to cover this lack of knowledge by reporting the effect of the preparation method, of geometrical features (as cell density) and of the thermal conductivity of the substrate material on the activity of monolithic catalysts towards CO-PROX reaction.

2 Experimental/methodology

Structured catalysts were prepared from commercial honeycomb monoliths of extruded cordierite (200 , 400, 600, 900 cpsi) and SiC (200 cpsi) cut in the desired shape and dimensions. A ceria washcoat was deposited onto monolith walls by modified dip coating procedure. Subsequently, copper oxide was supported by wet impregnation in an aqueous solution of copper acetate monohydrate (Sigma-Aldrich); drying at120°C for 1 h and calcination in air at 450°C for 2 h were carried out to obtain copper oxide. The nominal CuO load was about 4 wt.% with respect to the active layer. Different slurries were prepared to study the effect of the ceria particle size distribution by changing the milling procedure. Slurries S1 and S2 correspond to dry and wet milling respectively. We also studied the effect of colloidal ceria (Nyacol Nano Technologies Inc.) used as the only ceria precursor (slurry S4) or added to finely milled CeO_2 (slurry S3). Hereafter, monoliths will be labelled as Sx-y, where Sx and y indicate the used slurry and the cell density respectively (i.e. S1-400 is a 400 cpsi monolith prepared by dip coating in the slurry S1).

Slurries and monoliths were fully characterized by N_2 adsorption at 77K (BET and pore distribution by BJH method), Hg intrusion porosimetry, ICP-MS analysis, SEM, adhesion tests by sonication. The lab-scale set-up used for CO-PROX experiments was described elsewhere [31]. Catalytic tests were conducted at fixed flow rate or contact time. H_2, CO and O_2 concentrations were generally fixed at 50, 0.5 and 0.9 vol.% respectively; the effects of O_2 concentration and CO_2 and H_2O addition were also studied. Reaction temperature ranged from 80 to 200 °C to explore the whole temperature range of interest for CO-PROX.

3 Results and discussion

With respect to S1 slurry, wet milling and colloidal ceria addition reduce the mean particle dimension of the powder used to prepare the slurry and improve the specific surface area. The

last feature results in a larger copper dispersion, while the presence of ultra-fine particles, dominant in colloidal ceria, results in a partial intrusion of the washcoat into the cordierite macropores. The above structural modifications affect the catalytic performance. Figure 1 shows CO conversion and selectivity as a function of the reaction temperature for monoliths prepared starting from different slurries; powder catalyst performance is reported as reference. The partial intrusion of the catalyst into the cordierite macropores causes a reduction of the catalyst amount available for the reaction and, consequently, S1-400 shows the best catalytic activity. On the other hand, a larger copper dispersion is related to improved selectivity of monoliths different from S1-400. It is worth noting that at high conversion monoliths show better performance than powder, suggesting that internal diffusion is not limiting on structured catalysts. The results of experiments carried out on monoliths with different cell density and thermal conductivity (not reported) showed that high cell density and thermal conductivity lead to improved performance in terms of process intensification, selectivity, temperature control (by reducing hot spots).

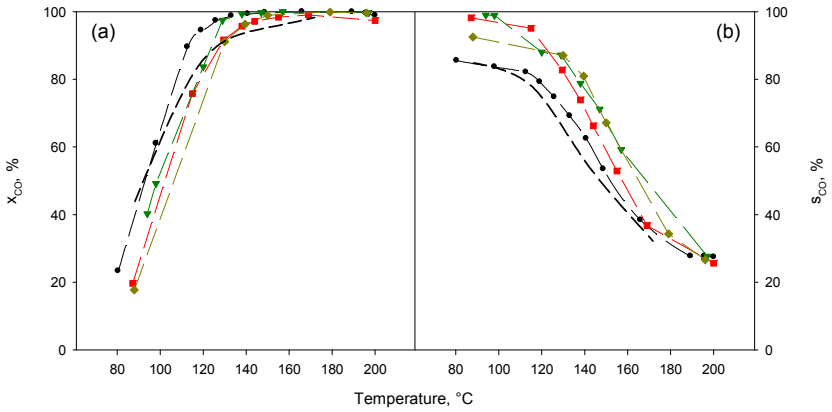

Fig. 1. CO conversion (a) and selectivity (b) as a function of the reaction temperature for monoliths: S1-400 (°); S2-400 (□); S3-400 (▼); S4-400 (□). Powder catalyst (short dashed line). $CO/H_2/O_2$=0.5/50/0.9; N_2 as balance.

4 Conclusions

CuO/CeO_2 monoliths were successfully prepared and tested in CO-PROX reaction. At high conversion (i.e. under the most interesting reaction conditions) monoliths show improved performance with respect to powder catalyst, providing higher catalyst efficiency. Slurry composition affects structural features of the washcoat and, consequently, catalytic layer adhesion and activity towards CO-PROX. The monolith performance can be optimized by engineering the catalytic systems and, in particular, by increasing the cell density and thermal conductivity of the substrate.

Acknowledgements

This work was financially supported by Italian MIUR (FIRB2010 “Futuro in Ricerca”, project n° RBFR10S4OW).

References

[1] O. Goerke, P. Pfeifer and K. Schubert, *Appl. Catal. A Gen*. 263 (2004) 11.
[2] Q. Zhang, L. Shore, R. J. Farrauto. *International Journal of Hydrogen Energy* 37 (2012)10874;
[3] C. Gu, S. Lu, J. Miao, Y. Liu, Y. Wang. *International Journal of Hydrogen Energy* 35 (2010) 6113.
[4] J.L. Ayastuy, N.K. Gamboa, M.P. Gonzalez-Marcos, M.A. Gutierrez-Ortiz. *Chemical Engineering Journal* 171 (2011) 224.
[5] O.H. Laguna, E.M. Ngassa, S. Oraá, A. Álvarez, M.I. Domínguez, F. Romero-Sarria, G. Arzamendi, L.M. Gandía, M.A. Centeno, J.A. Odriozola, *Catalysis Today* 180 (2012) 105.

III-PP01

Kinetic Analysis of Decomposition of Ammonia over Nickel and Ruthenium Catalysts

Takahashi A.*, Fujitani T.

Research Institute for Innovation in Sustainable Chemistry, National Institute of Advanced Industrial Science and Technology (AIST), Tsukuba, Japan

* at-takahashi@aist.go.jp

Keywords: ammonia, decomposition, hydrogen, production, kinetic model, catalysis, reaction, kinetics

1 Introduction

Hydrogen (H_2) is a promising energy resource and can be utilized in high-efficiency power generation systems such as fuel cells. However, the transport and storage of H_2 are obstacles for its practical use. Ammonia (NH_3) is a good candidate as an alternative H_2 carrier because of its high H_2 storage capacity and facile liquefaction under mild conditions [1]. Because high-purity H_2 is required to generate electricity with a fuel cell, a high-performance catalyst for producing H_2 from decomposition of NH_3 is needed when NH_3 is used as a H_2 carrier.

Previous studies indicated that Ru catalysts have the highest catalytic activity [1,2]. However, because precious metals are very expensive, alternative inexpensive Ni-based catalysts for decomposition of NH_3 have been widely investigated [3,4]. Nevertheless, the catalytic activity of Ni does not reach that of the Ru catalyst. Furthermore, it is unclear why there is a difference between the catalytic activities of the Ru and Ni catalysts.

In this study, the decomposition of NH_3 over Ni and Ru catalysts was investigated by using a kinetic model based on a reaction mechanism consisting of kinetically important elementary steps. The origin of the difference between the catalytic activities of the Ni and Ru catalysts was clarified.

2 Experimental

MgO-supported Ni and Ru catalysts were prepared by an impregnation method using aqueous solutions of $Ni(NO_3)_2$ and $RuCl_3$, respectively, followed by drying and calcination. The loading of metals was set at 30 wt % for Ni and 5 wt % for Ru.

The NH_3 decomposition reaction was carried out in a continuous-flow fixed-bed quartz tubular reactor at atmospheric pressure. The reaction products were analyzed by means of an on-line gas chromatograph equipped with a thermal conductivity detector and a Shincarbon ST column (Shinwa Chemical Industries Ltd., Kyoto, Japan) for N_2 and H_2. The NH_3 conversion was calculated on the basis of the production of H_2.

3 Results and discussion

A kinetic model for decomposition of NH_3 was constructed on the basis of the reaction mechanism including the following elementary steps: NH_3 adsorption⇆desorption (Eq. (1)), dehydrogenation of adsorbed NH_3 (Eq. (2)), recombinative N_2 desorption (Eq. (3)), and recombinative H_2 desorption⇆adsorption of gas-phase H_2 (Eq. (4)).

$$NH_3(g) + s \underset{k_{-1}}{\overset{k_1}{\rightleftarrows}} NH_3(a) \quad (1)$$

$$NH_3(a) + 3s \xrightarrow{k_2} N(a) + 3H(a) \quad (2)$$

$$2N(a) \xrightarrow{k_3} N_2(g) + 2s \quad (3)$$

$$2H(a) \underset{k_{-4}}{\overset{k_4}{\rightleftharpoons}} H_2(g) + 2s \quad (4)$$

The 6 unknown constants were estimated by fitting the model equations with the experimental results. The fitted results were in good agreement with the experimental data. Estimated values of the constants are listed in Table 1. Recombinative N_2 desorption (Eq. (3)) has been suggested to be the rate-determining step in the decomposition of NH_3 over most catalysts [1], and several research groups have reported values of the activation energy for recombinative N_2 dissociation. The estimated activation energy for recombinative N_2 dissociation, k_3, on the Ni and Ru catalyst are in agreement with these reported values.

Table 1 Estimated values of constants in the model

Constant	Ni catalyst		Ru catalyst	
	Pre-exponential factor, A	Activation energy, E_a / kJ·mol^{-1}	Pre-exponential factor, A	Activation energy, E_a / kJ·mol^{-1}
k_1 [mol·s^{-1}]	7.55×10^{1}	0	8.36×10^{1}	0
k_2 [mol·s^{-1}]	7.54×10^{15}	144.0	1.34×10^{14}	105.8
k_3 [mol·s^{-1}]	3.12×10^{6}	127.8	6.26×10^{5}	123.5
k_4 [mol·s^{-1}]	3.92×10^{4}	109.0	7.18×10^{2}	67.8
K_1 [–]	2.26×10^{-14}	-79.4	3.49×10^{-13}	-64.0
K_4 [–]	4.13×10^{6}	109.0	1.51×10^{4}	67.8

Furthermore, the experimental results in the high-conversion region (20–100% conversion of NH_3) at various NH_3 partial pressures and space velocities (SVs) under high-temperature conditions were compared with simulated results. The simulated lines were in good agreement with the experimental results over a wide range of reaction temperatures, NH_3 partial pressures, and space velocities (SVs). Thus, the proposed model can predict the catalytic activities of both the Ni and the Ru catalysts under a remarkably wide range of reaction conditions.

4 Conclusions

Using the minimum numbers of elementary steps necessary to understand the chemistry on the catalyst surface, the kinetic analysis presented herein has clarified the true reaction step governing the decomposition of NH_3 on Ni and Ru catalysts. Thus, the kinetic approach described herein should be a useful tool for designing new high-performance catalysts.

Acknowledgements

This work was supported by the Cross-ministerial Strategic Innovation Promotion Program (SIP) of the Cabinet Office, Government of Japan.

References

[1] S. F. Yin, B. Q. Xu, X. P. Zhou, C. T. Au, Appl. Catal. A 277 (2004) 1.
[2] T. V. Choudhary, , C. Sivadibarayana, D. W. Goodman, Catal. Lett. 72 (2001) 197.
[3] J. Zhang, H. Xu, X. Jin, Q. Ge, W. Li, Appl. Catal. A 290 (2005) 87.
[4] H. Muroyama, C. Saburi, T. Matsui and K. Eguchi, Appl. Catal. A 443-444 (2012) 119.

III-PP02

Hybrid Membrane-catalytic Reactor for Synthesis Gas and Pure Hydrogen Co-production by Dry Reforming of Methane and Ethanol

Antonov D.[1*], Fedotov A.[1], Tsodikov M.[1], Yaroslavtsev A.[1], Uvarov V.[2]

1 - A.V. Topchiev Institute of Petrochemical Synthesis, Russian Academy of Sciences, Moscow, Russia
2 - Institute of Structural Macrokinetics and Materials Science, Russian Academy of Sciences, Chernogolovka, Russia

* d.antonov@ips.ac.ru

Keywords: porous ceramic converter, Pd-containing membrane, reforming, hydrogen, syngas

1 Introduction

Original hybrid reactor consisted of Ni-Co-containing converter with integrated Pd-alloy membrane was developed. The construction allowed to carry out simultaneous processes of highly efficient dry reforming of methane (DRM) and ethanol (DRE) into syngas and in situ hydrogen separation. Removal of hydrogen decreased reaction temperature and shifted equilibrium of process.

2 Experimental/methodology

Porous ceramic membrane-catalytic converters (PCMCC) produced by self-propagating high-temperature synthesis were used for investigation. The precursors included a Ni metal powder containing 5 mass % of aluminum and a cobalt oxide (II, III) powder. The ready PCMCC contained of the Ni(Al) and Co_3O_4 active components in the ratios (mass %) 80 : 20. The PCMCC material also contained traces of carbon of the graphite press mold in which the PCMCC sintering took place. The PCMCC were porous gas permeable tubes with one end being sealed off and the other end having a round cap of larger diameter for being mounted inside the reactor. The length of the work area (tube) of the PCMCC was 160 mm, the outer diameter was 22 mm, the wall thickness was 4 mm, the average pore diameter determined by mercury porosimetry method and the bubble point method was 1–3 μm, and the material porosity was 40–60%.

Pd-containing membrane was made as a hollow fiber and was fixed in a PCMCC outlet channel. Carrier gas Ar was used for removal hydrogen from inner side of the catalytic converter.

The dry reforming of methane was carried out under the following conditions: $CH_4 : CO_2 = 1 : 1$, T = 550°C, W = 5–10 L/h, P_{inlet} = 1.1 atm, P_{outlet} = 1 atm.
The dry reforming of ethanol was conducted under the following conditions: $EtOH/CO_2$=1:5, T=200-600°C, W = 30 l/h, P_{in}=1.1 atm., P_{out} = 1 atm.

The compositions of the initial gas mixture and the reaction products were determined on-line by gas chromatography on a CHROM5 chromatograph with a thermal conductivity detector, high purity argon as the carrier gas (99.998 vol %, flow rate of 30 mL/min), and two chromatographic columns packed by SKT activated carbon. The gas concentrations were determined using Ecochrom software.Results and discussion

It was demonstrated that in DRM selective hydrogen removal from reaction zone using Pd-alloy membrane allowed to increase methane conversion up to 15% in comparison with equilibrium value. Feeding the substrate at a rate of 9 L/h and T=550°C hydrogen productivity was 3.7 L/h, including 50% of ultrapure hydrogen.

It was found that in DRE selective removal of ultrapure hydrogen decreased methane

containing in products and increased the total yield of hydrogen. It was determined that feeding the substrate at a rate of 30 L/h and T=600°C hydrogen productivity was 9 L/h, including 1.6 L/h of ultrapure hydrogen.

3 Conclusions

It was demonstrated a principal possibility of simultaneous processes of highly efficient production of syngas and ultrapure hydrogen with high performance and rate of extraction up to 50% in dry reforming of methane and ethanol using hybrid reactor.

Acknowledgements

This work was supported by the Ministry of Education and Science of the Russian Federation (agreement no. 14.607.21.0033) and RFBR 15-03-08753 A.

III-PP03

Solution Combustion Synthesis of Noble Metal-Loaded Ceria Catalysts and Application to Hydrogen Production and Purification for Fuel Cells

Nguyen T.S., Postole G., Morfin F., Piccolo L.*

Institut de recherches sur la catalyse et l'environnement de Lyon (IRCELYON), UMR 5256 CNRS & Université Claude Bernard - Lyon 1, Villeurbanne, France

* laurent.piccolo@ircelyon.univ-lyon1.fr

Keywords: solution combustion synthesis, ceria, Pt-group, metals, SRM, PROX

1 Introduction

Due to its excellent redox properties, ceria is extensively used in heterogeneous catalysis, where it can act as an oxygen buffer in oxidation reactions or prevent coking of metal phases in reforming reactions. Solution combustion synthesis is a simple and inexpensive method for preparing reducible oxides possibly loaded with noble metals in a single step [1, 2] (Fig. 1).

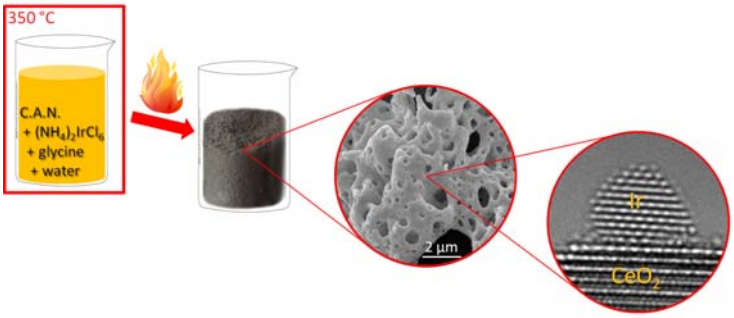

Fig. 1. Illustration of the Ir-CeO_2 catalyst preparation by SCS.

2 Experimental/methodology

Mesoporous ceria powders doped with up to 2 wt% platinum-group metals (PGMs: Pt, Pd, Ir, Rh, Ru) were synthesized by the ambient air combustion of an aqueous solution of ceric ammonium nitrate (CAN), chloride or nitrate metal precursor, and glycine or oxalyl dihydrazide used as fuels (Fig. 1). The structural properties of the powders, and the influence of such parameters as metal loading and thermochemical post-treatments, were investigated combining N_2 volumetry, aberration-corrected HRTEM, SEM, *in situ* XRD, XPS, DRIFTS, and Raman spectroscopy. The powders were employed as catalysts for the the steam reforming of methane (SRM) in water-deficient conditions (CH_4/H_2O = 10, 1 atm, 750 °C), and for the CO oxidation and preferential oxidation of CO (PROX) in H_2 excess ($H_2/CO = H_2/O_2$ = 24, 1 atm, 20-400 °C).

3 Results and discussion

The materials, whose texture appeared spongy at the micrometer scale and depended on the fuel nature, exhibited *ca.* 30 nm-sized ceria crystallites with a layered structure at the nanoscale. Comparisons with pure ceria showed that the metal inhibited ceria grain coarsening.

For SRM, 0.1 wt% Ir-CeO_2 exhibited the best performances. Due to its higher Ir dispersion and stronger Ir-CeO_2 interaction, the combustion-synthesized material was more active and stable than its conventionally prepared counterpart [3, 4]. Moreover, it was not permanently

deactivated by the introduction of H_2S in the reactant feed [4]. After reducing treatments, Ir nanoparticles anchored at the surface of ceria grains were imaged (Fig. 1), and their size (*ca.* 2 nm) and morphology did not evolve upon further heating at up to 900 °C. A complete picture of the Ir-CeO_2 interface could be established, with the presence of Ir^{x+}-O^{2-}-Ce^{3+} entities along with oxygen vacancies [3].

For CO oxidation and PROX, systematic comparisons between the samples, which exhibited similar metal nanoparticle sizes, allowed us to rank the Pt-group metals for the first time in the same conditions (Fig. 2) [5]. Rh-CeO_2 appeared as the most active system in H_2-free CO oxidation. The presence of H_2 boosted the CO oxidation activity of all the catalysts, except that of Rh-CeO_2, which promoted the decomposition of CO and the subsequent formation of methane. Pt-CeO_2, which was the most active and selective PROX catalyst, was further investigated by changing the nature of the fuel and the metal precursor. Although the catalyst activities were influenced by such parameters, the selectivities were strikingly unaffected.

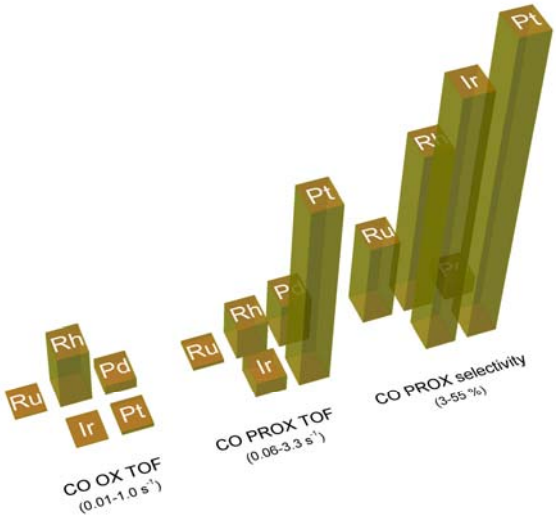

Fig. 2. Comparison of the Pt-group metals' CO oxidation and PROX performances at 140 °C.

4 Conclusions

The SCS method allowed us to prepare a series of PGM-CeO2 catalysts with high activity and high thermal stability in SRM and CO oxidation/PROX. For SRM, Ir-doped CeO2, which was synthesized for the first time by this method, is promising as catalytic layer for gradual internal reforming in solid oxide fuel cells fed with natural gas or biogas for the production of hydrogen [3, 4]. In the case of PROX, the comparison of our results with trends established from DFT calculations provides useful mechanistic insights relevant to hydrogen purification for proton-exchange membrane fuel cells [5].

Acknowledgements

We acknowledge the French National Research Agency (ANR-BS10-009 "DINAMIC" project) for financial support, S. Loridant (Raman), J.L. Rousset (PROX), F. Bosselet (XRD), and L. Massin & L. Cardenas (XPS) for analyses and discussions.

References

[1] V. M. Gonzalez-Delacruz *et al*., *Appl. Catal. A* 384 (2010) 1.
[2] M. S. Hegde *et al*., *Acc. Chem. Res.* 42 (2009) 704.
[3] T.S. Nguyen *et al*., *J. Mater. Chem. A* 2 (2014) 19822.
[4] G. Postole *et al*., *Appl. Catal. B* 166-167 (2015) 580.
[5] T.S. Nguyen *et al*., *Catal. Today* (2015), in press.

III-PP04

Syngas Production via Combined H_2O and CO_2 Reforming of Coke Oven Gas over La-Promoted $Ni/MgAl_2O_4$ Catalyst

Koo K.Y., Park J.E., Jung U.H., Yoon W.L.*

Yonsei University, Department of Environmental Engineering, Wonju, Republic of Korea

* wlyoon@kier.re.kr

Keywords: coke oven gas, combined H_2O and CO_2 reforming, syngas, sinter-stability, Ni-La/Mg Al_2O_4

1 Introduction

Coke oven gas (COG) composed of H_2 (55-60%), CH_4 (23-27%), CO (5-8%), N_2 (3-6%), and CO_2 (<2%) is a by-product of the coking process in steel industry [1]. Recently, direct reduction iron (DRI) production technology has been developed using syngas as a reducing agent in place of coke [2]. When syngas can be produced through the reforming of COG for use as a reducing gas in DRI, CO_2 emissions are reduced as the amount of coke used is minimized. In this study, syngas has been produced by combined H_2O and CO_2 reforming (CSCR) of COG. Different H_2/CO ratios can be obtained by controlling the feed ratio of H_2O and CO_2 in CSCR. CSCR is an economical and energy efficient process to supply reducing gas (H_2+CO) of DRI without an additional H_2/CO adjustment unit [3]. In general, Ni-based reforming catalysts are extensively used in commercial reforming processes because of their high activity and relatively low cost in comparison with noble metal catalysts. Ni-based catalysts often suffer from deactivation due to coke deposition and particle sintering at high reaction temperatures. However, in the reforming of COG, very little coke is formed because of coke hydrogenation by the excess hydrogen present in COG. Therefore, the development of catalysts that have high activity and good sinter-stability is a top priority in CSCR of COG. We have investigated the La promotion effect on the activity and sinter-stability of $Ni/MgAl_2O_4$ catalyst in CSCR of COG for syngas production.

2 Experimental/methodology

Ni-xLa/$MgAl_2O_4$ catalysts were prepared by a co-impregnation method using the mixture solution of $Ni(NO_3)_2{\cdot}6H_2O$ and $La(NO_3)_3{\cdot}6H_2O$. MgO-Al_2O_3 mixed oxide (MgO=30%, SASOL) was employed as a precursor of support after the pre-calcination at 800 °C for 6h in air. And then, an as-prepared catalysts were calcined at 800 °C for 6h in air. The Ni content of catalysts was fixed at 10 wt% and the La content was varied from 0 to 5 wt%. To compare the sinter-stability of Ni-xLa/$MgAl_2O_4$ catalysts, the aging treatment was carried out at 900 °C for 50 h in $H_2/H_2O/N_2$ (=20/200/25 ml/min) flow. The characterization as to surface area, metal dispersion, Ni crystallite size and reduction temperature of prepared catalysts was analysed by BET, H_2-chemisorption, XRD and TPR. The CSCR of COG was carried out at 900 °C under 5 atm for 40 h. The feed ratio was CH_4 : H_2O : CO_2 : CO : N_2 = 1 : 1.2 : 0.4 : 0.3 : 0.3 and the space velocity(SV) was fixed at 4,680,000 ml/g_{cat}·h. Before the reaction, the catalysts were reduced in 50% H_2/N_2 flow at 900 °C for 1.5 h under 5 atm. The effluent was analysed with an on-line micro gas chromatograph (Agilent 3000) equipped with TCD detector. The morphology and elemental mapping images of used catalyst were observed by TEM analysis.

3 Results and discussion

Table 1 summarizes the BET surface area, Ni dispersion, and Ni surface area of La-

promoted Ni/$MgAl_2O_4$ catalysts. For the fresh catalysts, BET surface area was gradually decreased with increasing La content. The Ni dispersion and Ni surface area were similar each other in La content of 0-2.5 wt%. However, it is noteworthy that La-promoted catalysts showed higher surface area, Ni dispersion, and Ni surface area than Ni/$MgAl_2O_4$ catalyst after aging treatment at 900°C for 50 h in $H_2/H_2O/N_2$ flow. These results demonstrate that La promotion prevents the sintering of Ni particles during the aging treatment.

CSCR of COG was conducted to examine the performance and stability of the aged catalysts. The Ni-xLa/$MgAl_2O_4$ catalysts exhibited better catalytic activity than Ni/$MgAl_2O_4$ catalyst with time on stream (data not shown here). This is in agreement with Ni dispersion and Ni surface area of the catalysts after the aging treatment. In particular, Ni-2.5La/$MgAl_2O_4$ catalyst showed the highest catalyst activity and stability for 40 h in CSCR of COG due to high Ni dispersion and surface area. TEM analysis showed that the Ni-2.5La/$MgAl_2O_4$ catalyst exhibited highly uniform dispersion of small Ni particle compared with Ni/$MgAl_2O_4$ catalyst in Fig. 1.

Table 1. Characteristics of La-promoted Ni/$MgAl_2O_4$ catalysts.

La content (%)	BET surface area (m^2/g)		Ni dispersion (%)		Ni surface area (m^2/g)	
	Fresh	Aged	Fresh	Aged	Fresh	Aged
0.0	94.3	8.8	5.2	0.28	3.5	0.18
1.0	90.3	17.0	5.4	0.28	3.6	0.18
2.5	89.0	20.0	5.3	0.36	3.5	0.22
5.0	85.0	16.6	4.2	0.30	2.8	0.20

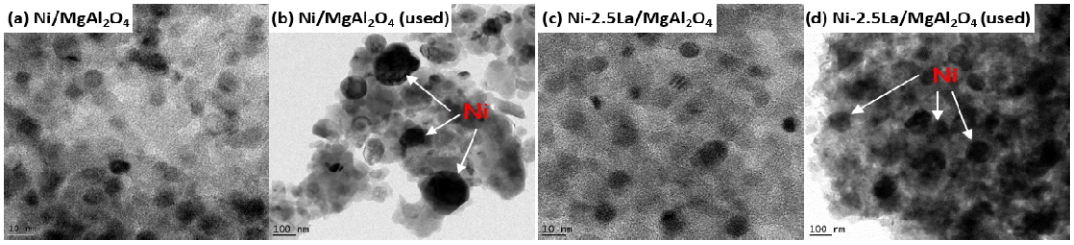

Fig. 1. TEM images of reduced and used catalysts; (a, b) Ni/$MgAl_2O_4$, (c, d) Ni-2.5La/$MgAl_2O_4$.

4 Conclusions

The La promotion to Ni/$MgAl_2O_4$ catalyst has significant effect on the Ni dispersion and surface area after the aging treatment. La-promoted catalysts had higher Ni dispersion and Ni surface area due to the enhancement of metal dispersion and SMSI. The catalyst with 2.5 wt% La, which is optimum to achieve highly dispersed Ni particles, showed the best catalytic activity and stability in CSCR of COG.

Acknowledgements

This work was supported by the New & Renewable Energy Core Technology Program of the Korea Institute of Energy Technology Evaluation and Planning (KETEP), granted financial resource from the Ministry of Trade, industry & Energy, Republic of Korea. (20123010040010)

References

[1] J.M. Bermúdez, A. Arenillas, R. Luque, J. A. Menéndez, *Fuel Process. Tech*. 110 (2013) 150.
[2] M.T. Johansson, M. Söderström, *Energy*. 36 (2011) 191.
[3] K.Y. Koo, H.-S. Roh, Y.T. Seo, D.J. Seo, W.L. Yoon, S.B. Park, *Int. J. Hydrogen Energy*. 33 (2008) 2036.

III-PP05

Hybrid DFT Study of Fe:NiOOH O_2 Electroevolution Catalyst

Conesa J.C.*

Instituto de Catálisis y Petroleoquímica, CSIC, Madrid, Spain

* jcconesa@icp.csic.es

Keywords: solar fuels, photocatalysis, water splitting, electronic structure, electrocatalysis, nickel hydroxide

1 Introduction

The layered compound NiOOH, especially when Fe-doped, is one of the best catalysts for evolution of O_2 in photo/ electrocatalytic water splitting, the mechanism involving probably Fe^{4+} or Ni^{4+} species [1]. That compound is however not well understood, as the protons in it are disordered and its electronic structure is not well clarified. The only DFT studies made, at the GGA+U level [2], assume that all OH groups are at the same side in each layer and propose a location of Fe for the most active site. Here the electronic structure of the bulk system, Fe-doped or not, is modelled with a hybrid DFT method of PBE0 type, but with the fraction α of Fock exchange taken, on the basis of GW theory concepts, as the inverse of the optical dielectric constant ε_∞, determined self-consistently by the same method. This method (named here PBE0α) gives accurate bandgap values for very different semiconductors [3].

2 Models and methodology

Several models with different stackings of the NiOOH layers were studied. Since the simple 1H stacking of $Ni(OH)_2$ is known to be changed upon oxidation to NiOOH, those of type 2H, 3H or that reported in [4], here called 2M, are tested, in all cases having 50% of protons at each layer side to avoid unphysical effects on the ε_∞ result. Calculations (spin-polarized) use periodic code VASP. First the NiOOH lattices were relaxed with a GGA+U+vdW functional; then the thus relaxed structures were used, with atoms fixed, to obtain the electronic structure data with method PBE0α. With the structures giving lowest energies supercells were constructed with 8 formula units/cell; one Ni atom in them was substituted by Fe, a new GGA+U+vdW relaxation was carried out and in the resulting configuration the electronic structure was computed with fixed geometry with the same PBE0α method as in the undoped system.

3 Results and discussion

After relaxation all Ni ions appear with distorted octahedron coordination, with 2 longer Ni-O bonds in *trans* position. Ni^{3+} ions (low spin) show ferromagnetic order, the antiferromagnetic one having slightly higher energy. For all three stackings considered (which gave similar energies, explaining the high stacking disorder experimentally observed) the preferred OH situation has a mixture of Ni atoms having $O_4(OH)_2$ and $O_2(OH)_4$ coordinations of centrosymmetric type, rather than the average $O_3(OH)_3$ one (which is anyway not far in energy). The bandgap obtained with the PBE0α method varies somewhat depending on the stacking, going from ~0.95 eV to 1.45 eV; a value of 1.28 eV is found for a 3R-type stacking presenting the mentioned *trans* $NiO_2(OH)_4$ and $NiO_4(OH)_2$ coordinations (which gives the lowest energy; Fig. 1). These gap values are much larger than predicted with the GGA+U

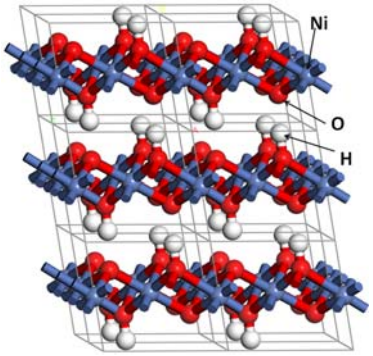

Fig. 1. Relaxed 3R-type NiOOH structure

DFT method, but are not unreasonable given the jump feature observed at 1.45 eV in the UV-Vis-NIR absorption spectrum [5]. The DOS curves (see e.g. Fig. 2a) show that the gap edges are formed by Ni 3d (e_g) states.

Substitution of Ni by Fe may give Fe^{3+} with some filled 3d states close to the valence band edge (Fig. 2b), but in some cases produces an electron transfer such as

$Ni^{3+} + Fe^{3+} \rightarrow Ni^{2+} + Fe^{4+}$

which explains some EXAFS observations of Fe^{4+} [6]; this is reflected in the DOS curves (Fig. 2c) where the Fe states at the valence band edge are replaced by Ni states. Jump of protons from the O atoms of the Fe coordination sphere to other O atoms around Ni can then be observed. Both effects indicate an easy mobility of electrons and protons between Ni and Fe species, in agreement with the conductivity increase observed upon Fe doping [1].

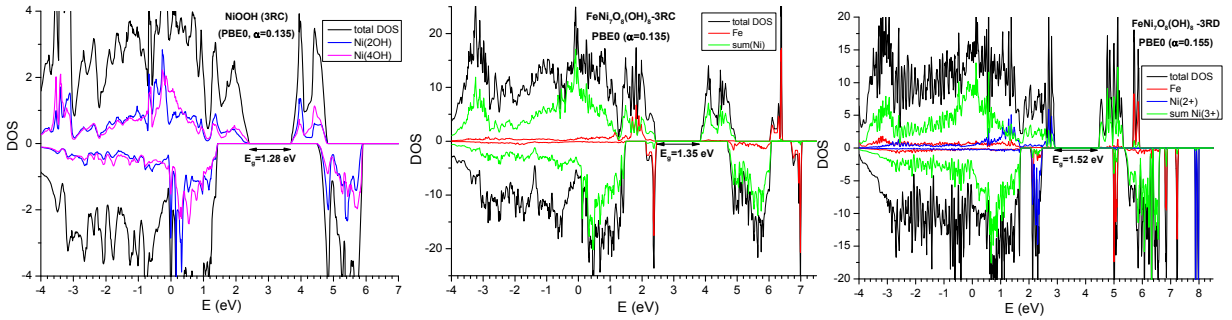

Fig. 2. DOS curves (incl. cation projections) given by PBE0α functional for a) NiOOH configuration with lowest energy (stacking 3R); b) Fe-doped NiOOH (with Fe as Fe^{3+}, coordinated to 4 OH groups); c) Fe-doped NiOOH in which electron transfer producing Fe^{4+} and Ni^{2+} has occurred.

4 Conclusions

DFT results justify the disordered character of NiOOH and predict for it a gap somewhat above 1 eV. Insertion of Fe in it gives a similar gap but facilitates proton and electron transfer in the bulk, which may explain the good electrocatalytic activity of the material.

Acknowledgements

Funding from project BOOSTER (ENE2013-46624-C4-1-R of Plan Estatal de I+D) and programme MADRID-PV (S2013/MAE-2780 of Comunidad de Madrid) as well as computing time provided at computers *altamira* and *trueno* (of Red Española de Supercomputación and CSIC, respectively) are acknowledged.

References

[1] L. Trotochaud, S. L. Young, J. K. Ranney, S. W. Boettcher, *J. Am. Chem. Soc*. 136 (2014) 6744.
[2] Y. F. Li, A. Selloni, *ACS Catalysis* 4 (2014) 1148.
[3] E. Menéndez-Proupin, P. Palacios, P. Wahnón, J. C. Conesa, *Phys. Rev. B* 90 (2014) 045207 and references therein.
[4] M. Casas-Cabanas, J. Canales-Vázquez, J. Rodríguez-Carvajal, M. R. Palacín, *J. Am. Chem. Soc*. 129 (2007) 5840.
[5] A. J. Varkey, A. F. Fort, *Thin Solid Films* 235 (1993) 47.
[6] M. Balasubramanian, C. A. Melendres, S. Mini, *J Phys. Chem. B* 104 (2000) 4300.

III-PP06

Solid Solutions for Heterogeneous Photocatalytic Hydrogen Evolution from Water - Using POM/TiO_2 Composites

Striegler K.[1*], Kasprick M.[1], Benndorf G.[2], Bertmer M.[2], Gläser R.[3]

1 - Universtät Leipzig, Faculty of Chemistry and Mineralogy, Institute of Chemical Technology, Leipzig, Germany

2 - Universtät Leipzig, Faculty of Physics and Earth Science, Institute for Experimental Physics II, Leipzig, Germany

3 - Universtät Leipzig, Faculty of Chemistry and Mineralogy, Institute of Chemical Technology, Leipzig, Germany

* karl.striegler@uni-leipzig.de

Keywords: heterogeneous, photocatalysis, solar fuel, hydrogen, evolution, TiO_2, POMs

1 Introduction

In order to respond to the rising energy demand and the fossil fuels limitation, the interest in developing new ways of supplying solar fuel is growing [1]. The discovery of the *Honda-Fujishima effect* proved that water can be split photochemically [2]. Due to the advantages of heterogeneous catalysis during the conversion of harvested light energy into utilizable fuels, focus is placed on the identification of new materials, composites and reaction pathways [3]. Nevertheless, suspended catalysts compared to photo-electrochemical cells have the advantage of a larger density of active sites and shorter diffusion lengths for charge carriers. Unfortunately, most of the suspended photocatalysts need a chemical bias in order to evolve H_2 *or* O_2 [4]. For a functional catalyst, light harvesting semiconductors and composites as well as promoters for H_2 *and/or* O_2 evolution will have to be developed [5].

2 Methodology

In order to overcome the shortcomings in the photocatalytic H_2 evolution from water, it was investigated how solid solutions of polyoxometalates (POM) in the semiconductor TiO_2 can enhance the catalytic activity of TiO_2. Hence, several synthesis routes were followed to incorporate $H_3PW_{12}O_{40}$ into the framework of TiO_2 without destroying the Keggin-structure of the POM.

I. Synthesis. The incorporation of POM into the TiO_2 was achieved by different synthesis strategies, i.e.,sol-gel method with and without a template (Pluronic P123) and hydrothermal approaches using conventional and microwave-assisted synthesis.

II. Material Characterization. The resulting materials were thoroughly characterized with N_2-sorption, elemental analysis, diffuse reflectance UV/Vis, XRD, photoluminescence, TGA, TPD and solid state MAS NMR. Thus, detailed information about the kind of incorporation of the POM was obtained for interpretation of the photocatalytic activity.

III. Catalytic Testing. A 150 W Hg-medium-pressure lamp was used to irradiate a 380 ml aqueous suspension of 100 mg catalyst (incl. 0.5wt.-% Pt^0) in 10 vol-% MeOH. The resulting gases were analyzed every 2.5 min by gas chromatography to monitor the hydrogen evolution over time.

3 Results and discussion

So far, there were no reports of a possible application of POM/TiO_2 composited for photocatalytic H_2 generation. The incorporation of intact Keggin-$PW_{12}O_{40}^{3-}$-clusters into a TiO_2 material was successful via a conventional and a microwave-assisted hydrothermal synthesis as

proven by ^{31}P-MAS NMR analysis. The materials prepared via a sol-gel method revealed the decomposition of the Keggin-cluster during preparation. No XRD reflexes were found for the Keggin structure, but both strategies prove the successful synthesis of rutile or anatase.

The left side of Figure 1 shows photoluminescence spectra of pure TiO_2 from a sol-gel synthesis as a reference material and a hydrothermally synthesized POM/TiO_2 (HT-20%PW_{12}/TiO_2) composite. Obviously, the luminescence of the reference material is magnitudes higher than that of the composite. This behavior indicates that the rate of the electron-hole recombination is lower in the composite material.

This might explain the results which are depicted in the right side of Figure 1 which shows the hydrogen evolution over time. Thus, the composites have a higher photocatalytic activity compared to the pure TiO_2 which was prepared by the same route. Hence, the incorporation of POMs into TiO_2 enhances the photocatalytic activity; most probably by altering the charge carrier recombination.

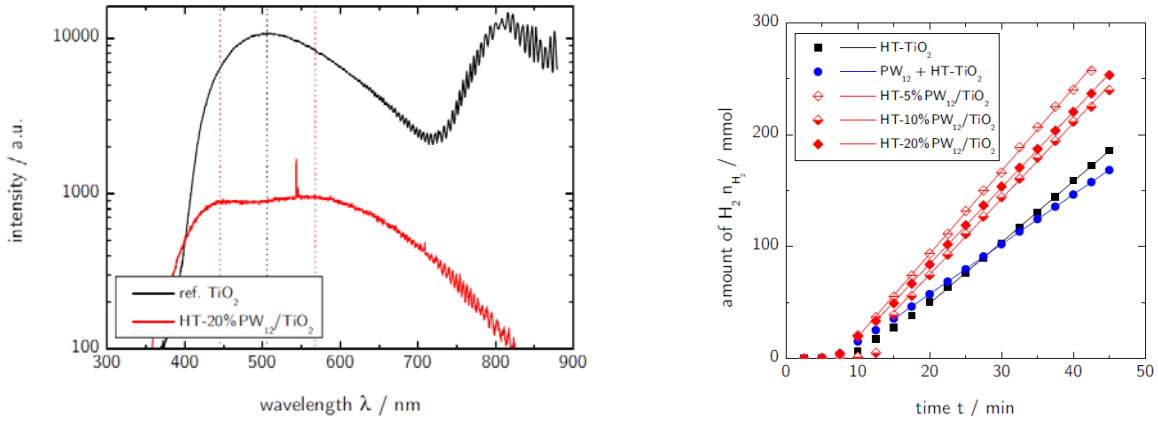

Fig. 1. Left: Photoluminescence spectra of HT-20%PW_{12}/TiO_2 and a TiO2 reference (synthesized by a sol-gel method), the dotted lines mark the maximum of the corresponding luminescence bands. Right: Amount of H_2 formed during UV irradiation of TiO_2 over time – TiO_2 samples are modified and unmodified with different amounts $H_3PW_{12}O_{40}$ (in wt.-%).

4 Conclusions

Composites of polyoxometalates $H_3PW_{12}O_{40}$ and TiO_2 exhibit a higher photocatalytic activity for hydrogen evolution in water than TiO_2 alone. Using solid state ^{31}P-MAS NMR it was proven that the Keggin structure was incorporated into TiO_2. A composite-strategy can improve the photocatalytic activity of semiconductors. Apparently, a composite strategy based on solid solutions might lead to higher photocatalytic activities due to a charge separating effect.

Acknowledgements

The authors would like to thank the ESF for financial support and research group Echem Leipzig for advices.

References

[1] F.E. Osterloh, *Chem Soc Rev.* 42 (2013) 2294.
[2] A. Fujishima, K. Honda, *Nature.* 238 (1972) 37.
[3] J.G. Rowley, T.D. Do, D.A. Cleary, B.A. Parkinson, *ACS Appl Mater Interfaces.* 6 (2014) 9046.
[4] J. Schneider, D.W. Bahnemann, *J. Phys. Chem. Lett*. 4 (2013) 3479.
[5] R. Marschall, *Adv. Funct. Mat.* 24 (2014) 2421.

III-PP07

Electrophysical Properties of Cathode Materials $Pr_{2-X}Sr_XNi_{1-Y}Cu_YO_4$ for Intermediate-Temperature Solid Oxide Fuel Cells

Gilderman V.*, Antonov B.

Institute of High-Temperature Electrochemistry of the Urals Branch of the Russian Academy of Sciences, Yekaterinburg, Russia

* V.Gilderman@ihte.uran.ru

Keywords: electrical, conductivity, $Pr_{1,85}Sr_{0,15}Ni_{1-X}Cu_xO_4$

1 Introduction

Currently, studies are being conducted on materials with mixed-conductivity Ln_2NiO_4(Ln=La,Pr)[1-2], which can be used to mean-temperature electrochemical devices as cathodes.

This paper presents the results of researches, coefficients of thermal expansion, conductivity $Pr_{1,85}Sr_{0,15}Ni_{1-X}Cu_xO_4$(X=0.0;0.1;0.5;0,9 and 1.0), Pr_2NiO_4 and Pr_2CuO_4 in the interval 293-1273K in air

2 Experimental

Samples were prepared by solid phase synthesis. The starting materials served as $Pr(OH)_3$,PrO_2,Cu_2,NiO and $SrCO_3$. Mixture of oxides and carbonic strontium mixed in alcohol medium a mortar during 1 hours were pressed pills under the pressure 67 Mpa.

The compositions were synthesized in the air during 1-11 hours at temperature 1373-1473K.

Roentgen phase analyses was performed on a Rigaku D_{max}-2200, in the copper Kα-radiation. Synthesized samples had the structure of Layered Perovskite A_2BO_4 except for composition Pr_2NiO_4, $Pr_{1,85}Sr_{0,15}NiO_4$ and $Pr_{1,85}Sr_{0,15}Ni_{0,9}Cu_{0,1}O_4$. That had impurity phase $Pr_{11}O_6$,$Pr_{11}O_6$ and PrO_2, respectively.. The thermal coefficient of linear expansion of samples was measured with quartz dilotometer. The electrical conductivity was measured by DC four probe method with Platinum electrodes. Thermal coefficient of linear expansition of $Pr_{2-Y}Sr_YNi_{1-X}Cu_XO_4$ is in the range (11.2-16,6)$\times 10^{-6}deg^{-1}$and (11.6-16,3)$\times 10^{-6}deg^{-1}$ for temperature intervals 298-973K 298-1173K,respectively.

3 Results and discussion

The total electrical conductivity of Pr_2CuO_4 is higher the electrical conductivity of Pr_2NiO_4 and $Pr_{1,85}Sr_{0,15}NiO_4$ in air at temperature above 603K(fig.1).

Praseodymium in Pr_2NiO_4 replacement for strontium leads to an increase in conductivity. Electrical conductivity of Pr_2CuO_4 has a large activation energy than σ(Pr_2NiO_4)and σ($Pr_{1,85}Sr_{0,15}NiO_4$). At temperature above 623K maximum conductivity has the $Pr_{1,85}Sr_{0,15}Ni_{0,1}Cu_{0,9}O_4$(fig.2). At temperature above 833K the conductivity of $Pr_{1,85}Sr_{0,15}CuO_4$ is higher the electrical conductivity of $Pr_{1,85}Sr_{0,15}NiO_4$, $Pr_{1,85}Sr_{0,15}Ni_{0,9}Cu_{0,1}O_4$ and $Pr_{1,85}Sr_{0,15}Ni_{0,5}Cu_{0,5}O_4$

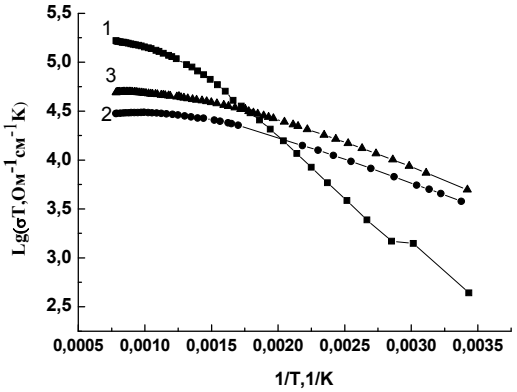

Fig.1 Temperature dependence of electrical conductivity of Pr_2CuO_4(1), Pr_2NiO_4(2) and $Pr_{1,85}Sr_{0,15}NiO_4$(3) in the air.

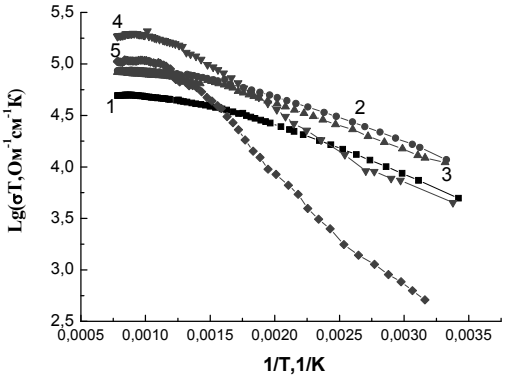

Fig.2 Temperature electrical conductivity of the samples $Pr_{1,85}Sr_{0,15}Ni_{1-X}Cu_xO_4$ in the air.1-X=0,0;2-0,1;3-0,5;4-0,9and 5-1,0.

4 Conclusions

Calculation of the activation energy of electrical conductivity in terms of the $\sigma_T = \frac{\sigma_0}{T}\exp(-\frac{E_a}{RT})$ showed that the compositions Pr_2CuO_4, $Pr_{1,85}Sr_{0,15}CuO_4$ and $Pr_{1,85}Sr_{0,15}Ni_{0,1}Cu_{0,9}O_4$ have a large activation energy of conductivity in comparison with compositions Pr_2NiO_4, $Pr_{1,85}Sr_{0,15}NiO_4$, $Pr_{1,85}Sr_{0,15}Ni_{0,9}Cu_{0,1}O_4$ and $Pr_{1,85}Sr_{0,15}Ni_{0,5}Cu_{0,5}O_4$.. The activation energy is small and is in the range (E_a=0,01—0,23 eV). This is typical of hopping conduction mechanism. Because the activation energy of σ(Pr_2NiO_4) less Ea σ (Pr_2CuO_4) it should be that the jup of e-holes is easier for nickel than for copper.

References

[1] S.Nishimoto, S. Takahashi, Y. Kameshima, M. Matsuda and M. Miyake. J. Ceram. Soc. Jap. 119 (2011) 246

[2] V.Gil'derman,B.Antonov, Seventh Russian Conference.Physical problems associated with hydrogen energy.St.Peterburg,Russia.(2011)80.

III-PP08

Foil of the Pd-In-Ru Alloy for the Membrane Technology of Preparing High-Purity Hydrogen

Chistova T.V.[1], Didenko L.P.[2*], Savchenko V.I.[2], Chizov P.E.[2], Bikov L.A.[2]

1 - Baikov Institute of Metallurgy and Materials Science, Russian Academy of Sciences, Moscow, Russia

2 - Institute of Problems of Chemical Physics, Russian Academy of Sciences, Chernogolovka, Russia

* ludi@icp.ac.ru

Keywords: hydrogen, flux, palladium alloy, foil, hydrogen separation, CO negative effect, carbon, deposits

1 Introduction

Demand in high-purity (99.9999 vol.%) hydrogen is being increased sharply due to the fast development of hydrogen power engineering. Among existing methods for hydrogen purification, membrane processes are characterized by lowest operating and capital outlays. The most promising membrane materials are palladium alloys. It is important to develop palladium alloys with high parameters of strength, plasticity, and hydrogen permeance; low thermoconcentration dilation for the operation in hydrogen; and high corrosion resistance to aggressive components of gas mixtures, because the composition of the mixtures substantially affects the productivity of the membrane and service resource. This paper presents the technological characteristics of Pd-6 wt.% In -0.5 wt% Ru alloy and the results of the study the specific permeability and the separation performance of a membrane unit based on a foil 28 μm thick from the specified alloy.

2 Experimental/methodology

The alloy composition is optimal, where a Pd–6 wt.% In solid solution corresponds to the maximum hydrogen permeability, and the addition of 0.5 wt.% Ru to Pd-In matrix increases the strength of the alloy and its operation in a hydrogen-containing atmosphere without any changes to the composition of its surface, which were observed in the Pd-6 wt.% In alloy. To exclude the formation of impurity inclusions and defects, the purity of the used materials was not lower than 99.95 wt.%. The alloy was melted in a protective atmosphere in an electric-arc furnace. The foil of the indicated alloy was prepared by cold rolling on a four-high rolling mill with intermediate vacuum annealings. The obtained foil did not require additional purification prior to experiments.

The H_2 flux through the membrane was studied in membrane unit (MU) based on a foil 28 μm thick of the Pd–In–Ru alloy. The main part of the MU is a hydrogen-permeated disc 58 mm in diameter placed between two stainless steel grids, which have 130 μm thickness and average pore radius of 2.0 μm, that provided its high mechanical strength. Graflex was used as a material for unit sealing. Filtering characteristics were studed at the temperature range of 573 to 823 K.

3 Results and discussion

The alloy Pd–6 wt.% In–0.5 wt.% Ru possesses an optimum complex of the properties. The alloy has high strength and high ductivity (H_v = 114 kg/mm^2, σ_B = 48 kg/mm^2, $\delta \approx 26\%$ (annealed)), sufficient specific hydrogen permeance, egual at 873 K to 2.2 m^3·mm/(m^2·h·MPa$^{0.5}$), and high corrosion resistance in hydrogen-containing gas mixtures obtained by hydrocarbon fuel conversion [1]. The ternary alloy withstands prolonged operation

in a hydrogen atmosphere and is stable during thermal cycling and in corrosive media (methane, CO_2, H_2S (up to 1.5 vol.%)). The technology was developed for the preparation of a membrane module based on the PdInRu foil (membrane diameter 50 mm, thickness 30 μm). The productivity of the membrane module for H_2 separation from the mixture, whose composition is identical to that of the products of natural gas conversion, is 0.3 Nm^3/h at the following parameters of the process: $P_{inlet\ mixture}$ = 2 MPa, P_{outlet} = 0.15 MPa, T = 873 K, and degree of hydrogen separation η = 0.8 [2].

The hydrogen flux through the foil (thickness 28 μm) with the composition Pd–6 wt.% In–0.5 wt.% Ru is more than twice as large as that through the foil of the Pd–23 wt.% Ag alloy. The membrane has high parameters of thermal stability and mechanical strength. The study of the dependence of the H_2 flux on the difference of the partial hydrogen pressures in the gas phase from the retentate and permeate sides of the membrane unit indicates that the permeation of hydrogen in the Pd–In–Ru foil is controlled by the diffusion of atomic hydrogen in the membrane bulk. The apparent activation energy of the hydrogen permeance is 18.7 kJ/mol. The influence of impurities (CO, N_2, Ar) on the hydrogen flux is studied using both a sweep gas (N_2) and transmembrane pressure. No negative effect of CO is observed in experiments using a sweep gas. The decrease in the H_2 flux with an increase in the impurity content in the hydrogen is due to the dilution of the mixture only. When the transmembrane pressure is used, CO exerts a negative effect on the H_2 flux, and this influence decreases with increasing temperature from 573 to 773 K. Contact of the foil with pure CO at 673 and 773 K results in an insignificant formation of carbon deposits on the membrane surface, which exerts almost no effect on the H_2 flux. No carbon deposits are formed on contact of the foil with the mixture H_2-22.5 % CO at 773 K due to CO methanation with the formation of CH_4 and H_2O.

4 Conclusions

The results of the present study show that palladium–6 wt.% indium–0.5 wt. % ruthenium alloy possesses an optimum complex of high technology characteristics. The foil of the ternary alloy is a good material for membrane technology of preparing high-purity hydrogen. The H_2 flux more than 2 times exceeds the corresponding parameter for the traditionally used foil of the Pd–23 wt.% Ag alloy. The membrane has high parameters of thermal stability and mechanical strength. The optimal temperature for H_2 separation from CO-containing mixtures is 773 K, since the inhibition of the separation process because of the reversible adsorption of CO molecules becomes lower, and the efficiency of the catalytic reaction on the membrane surface resulting in carbon deposits formation is insignificant.

Acknowledgements

This work was financially supported by the Russian Foundation for Basic Research, project nos. 13-03-12419 and 13-08-12408.

References

[1] G. S. Burkhanov, N. B. Gorina, N. B. Kolchugina N. R. Roshan, D. I. Slovetskiy, and E. M. Chistov. *Platinum Metals Rev.* 2011. V. 55(1). P.3-12.

[2] D. I. Slovetskiy and E. M. Chistov, Hydrogen-permeable membrane, filtering unit, and membrane unit, *Patent RF* 2, 416460 (2011).

III-PP09

Fischer–Tropsch Synthesis on Cobalt-Based Catalysts with Different Heat-Conductive Additives

Asalieva E.Yu.[1,2*], Sineva L.V.[1,3], Gryaznov K.O.[1,4], Kulchakovskaya E.V.[1], Mordkovich V.Z.[1,3]

1 - Technological Institute for Superhard and Novel Carbon Materials, Moscow, Russia
2 - Lomonosov Moscow State University, Moscow, Russia
3 - INFRA Technology Ltd, Moscow, Russia
4 - Lomonosov Moscow State University of Fine Chemical Technologies, Moscow, Russia

* e.asalieva@tisnum.ru

Keywords: Fischer–Tropsch synthesis, cobalt, heat-conductive additive, copper, aluminum, zinc

1 Introduction

The technology for producing high-quality synthetic oil and fuels from carbon-containing feedstock — the so-called XTL (X-to-liquids) technology — is attracting increasing attention as an alternative to the use of dwindling oil reserves. Fischer–Tropsch synthesis (FTS) is the main stage of XTL technology, which allows converting natural gas, shale gas, coal and biomass and even helps solving ecological problems such as associated gas utilization [1, 2].

Cobalt FTS catalysts convert synthesis gas into clean sulfur-free synthetic liquid hydrocarbons, mostly linear paraffins, although both branched and unsaturated hydrocarbons may also occur [2, 3]. The product does not contain undesirable aromatics nor oxygenates and satisfies petrochemical quality requirements.

Since the contemporary XTL technology is rather expensive, the prospects of its widespread industrial adoption are related with improvement of all the technological stages of the process, especially with the performance of FTS catalyst. The combination of FTS catalyst with zeolite in a composite material leads to formation of bifunctional catalyst producing high-quality synthetic oil in one step by eliminating the hydrotreating stage [4]. The main role of zeolite is the decrease in average molecular weight of produced hydrocarbons by cracking on acid sites.

The use of metallic additives in the composition of FTS catalyst provides such advantage as intensified heat conductivity, which is particularly important for FTS due to strong exothermal nature of Fischer–Tropsch reaction [2]. Catalysts of low thermal conductivity tend to get overheated during the synthesis, which may cause enlargement of the active component crystallites and decrease theproductivity and selectivity of the process.

The purpose of this work was to study the effect of heat-conductive additives (aluminum, copper or zinc metal powder) introduction to cobalt-based catalyst.

2 Experimental/methodology

The investigated catalysts were produced by the extrusion of pastes. Pastes were prepared by the techniques described elsewhere [5, 6]. All the paste samples contained 50 wt.% of heat-conductive component (Al flakes, Al spheres, Cu or Zn metal powder — HB-Al1, HB-Al2, HB-Cu and HB-Zn samples, respectively), 20–35 wt.% of binder (boehmite) and 15–30 wt.% of zeolite Beta in H-form. One sample was prepared as a reference and did not contain heat-conductive component (HB sample).Cobalt was used as an active component. The introduction of the active component into the samples was conducted by two-step impregnation with a $Co(NO_3)_2 \cdot 6H_2O$ aqueous solution.

The catalyst was activated in pure hydrogen (3000 h^{-1}) at 400˚C and 0.1 MPa for 1 hr.After activation the catalyst was heated in a synthesis gas stream at 2 MPa, raising the temperature from 170 to 230˚C. Synthesis gas (molar ratio of $H_2/CO=2$ with 5 vol.% of N_2 as balance and internal reference) was supplied at gas-hour space velocity (GHSV) of 1000 h^{-1} while the temperature was raised and optimized and then GHSV was increased stepwise up to 6000 h^{-1}. Temperature was

optimized for every GHSV so that the productivity was maximum possible.

3 Results and discussion

The introduction of different heat-conductive components into cobalt-based catalyst influenced the main catalytic properties such as CO conversion, selectivity of C_{5+} hydrocarbons formation and productivity (Fig. 1): the GHSV increase resulted in appearance of strong differences in catalysts behaviour.

The introduction of dispersed aluminum (both flakes and spheres) influenced positively the main catalytic properties and led to increase in CO conversion — by 17–25%, C_{5+} selectivity — by 7–10% and productivity — 1.1–2.7 times, compared to the reference sample. The introduction of copper powder had almost no effect on CO conversion, but resulted in C_{5+} selectivity drop to about 20% and productivity decrease in 2.4 times. The introduction of zinc was not effective as well: CO conversion did not differ much from the reference sample, but C_{5+} selectivity and productivity were noticeably lower.

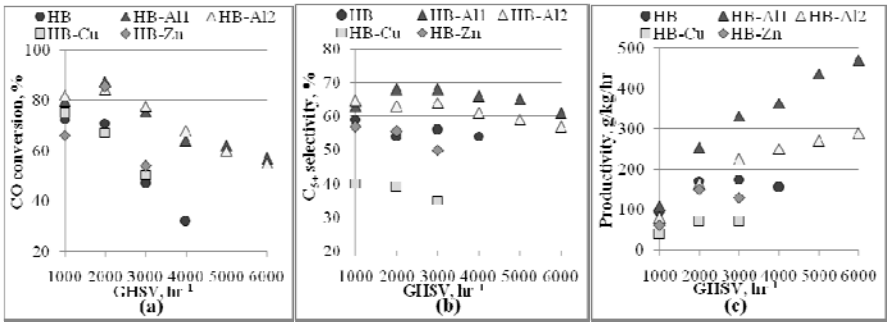

Fig. 1. The influence of GHSV on the main catalytic properties: (a) CO conversion, (b) selectivity of C_{5+} hydrocarbons formation and (c) productivity

Product composition and chain growth probability depend on heat-conductive component and on its catalytic activity (Table 1).The composition of product obtained in the presence of catalysts containing Al is the closest to those obtained in the presence of reference sample. So we suggest that Al provides heat transfer while manifesting no own catalytic activity in FTS condition. The introduction of Cu or Zn leads to drastic change in the product composition, which indicates that these metals are catalytically active in FTS conditions.

Table 1. The influence of catalyst composition on C_{5+} hydrocarbons composition (GHSV 3000 h^{-1})

Sample	C_{5+} hydrocarbons composition, wt.%			Chain growth probability (α)
	Olefins	N-paraffins	Iso-paraffins	
HB	29	32	39	0.74
HB-Al1	32	38	30	0.69
HB-Al2	31	39	30	0.72
HB-Cu	19	31	50	0.54
HB-Zn	8	77	15	0.80

4 Conclusions

Aluminum is the most promising metal for heat transfer intensification and provides significant improvement of main catalytic properties. The introduction of copper or zinc to these catalysts does not result in heat transfer intensification; moreover these metals influence the FTS parameters and thus change the group composition of the product.

References

[1] R.C. Baliban, J.A. Elia, C.A. Floudas, *AIChE Journal*. 59 (2013) 505
[2] Greener Fischer–Tropsch Processes, Ed. by P.M. Maitlis and A. de Klerk (Wiley–VCH, Weinheim, 2013)
[3] M. Dry and A. Steynberg, Fischer–Tropsch Technology. Studies in Surface Science and Catalysis, Elsevier, Amsterdam, 2004
[4] G. Espinosa, J.M. Domínguezetal, *Catal. Today*. 166 (2011) 47
[5] RU Patent 2414300, 201 [6] RU Patent 2422202, 2011

III-PP10

Gold Catalysts on Y-Modified Ceria for CO-Free Hydrogen Production via WGSR and PROX

Gencheva L.[1*], Petrova P.[1], Ivanov I.[1], Pantaleo G.[2], Liotta L.F.[2], Zanella R.[3], Boghosian S.[4], Kaszkur Z.[5], Sobczak J.W.[5], Lisowski W.[5], Venezia A.M.[2], Tabakova T.[1]

1 - Institute of Catalysis, Bulgarian Academy of Sciences, Sofia, Bulgaria
2 - Istituto per lo Studio di Materiali Nanostrutturati, CNR, Palermo, Italy
3 - Universidad Nacional Autónoma de México, México, Mexico
4 - Department of Chemical Engineering, University of Patras, Patras, Greece
5 - Institute of Physical Chemistry, Polish Academy of Sciences, Warsaw, Poland

* luilieva@ic.bas.bg

Keywords: gold catalysts, Y-modified ceria, WGSR, PROX

1 Introduction

Hydrogen has a great potential as clean and high efficient energy carrier. After the conversion via steam reforming of hydrocarbons (from natural or renewable materials) into ‘‘syn gas’’, the mixture contains CO with concentration of about 10 vol%. The preferred process for increasing the H_2 amount is the water gas shift reaction (WGSR), lowering the CO concentration to about 0.5–1 vol%. However, for the development of fuel cell technology, the concentration of CO should be below 10 ppm because of the high sensitivity of the Pt anode towards CO in polymer electrolyte membrane fuel cells. The catalytic oxidation of CO in hydrogen-rich gas streams (PROX) appears to be the simplest and the most cost effective for this purpose. Nano-gold catalysts have been proven very efficient both for WGSR at low temperatures (200–300 ^{o}C) and PROX at the fuel cell operating temperatures (80–120 °C). Beside the gold dispersion the support plays a decisive role for a good performance. Doping of ceria by metals of lower valence (< 4+) causes oxygen vacancies formation and thus increases the oxygen capacity of the ceria-based catalysts. The aim of the present study was to compare the effect of different preparation methods and the amount of Y as dopant on the WGS and PROX activity of Au/CeO_2 catalysts.

2 Experimental

Two different synthesis routes: impregnation (IM) and co-precipitation (CP) were used for preparation of Y-modified ceria supports (1, 2.5, 5 and 7.5 wt% Y_2O_3). Gold catalysts (3 wt% Au) were prepared by deposition-precipitation method. The samples were characterised by means of BET, XRD, HRTEM/HAADF, XPS, H_2-TPR and Raman spectroscopy. The WGS activity was evaluated under the following conditions: gas mixture of 4.5 vol% CO in Ar + 25 vol. % H_2O, catalyst bed volume=0.5 cm^3, space velocity (GHSV)=4000 h^{-1}. The measurements of the PROX activity, expressed as the degree of CO conversion and selectivity toward CO_2, were carried out using 60% H_2 + 1% CO + 1% O_2 and He as balance (WHSV of 60 000 mL g^{-1} h^{-1}). Tests with CO_2 and water addition to the gas feed were carried out over selected samples. For both reactions the effect of pre-treatment (reductive or oxidative conditions) and stability of the best performing catalysts was also studied.

3 Results and discussion

The catalytic tests showed better WGS performance after pretreatment in air at 350 ^{o}C than at 200 ^{o}C. In Fig. 1 (A and B) the obtained results after pretreatment at 350 ^{o}C are compared. The results revealed very high activity of all catalysts. The samples on IM supports exhibited

better performance as compared to those on CP supports. A clear trend of decreased WGS

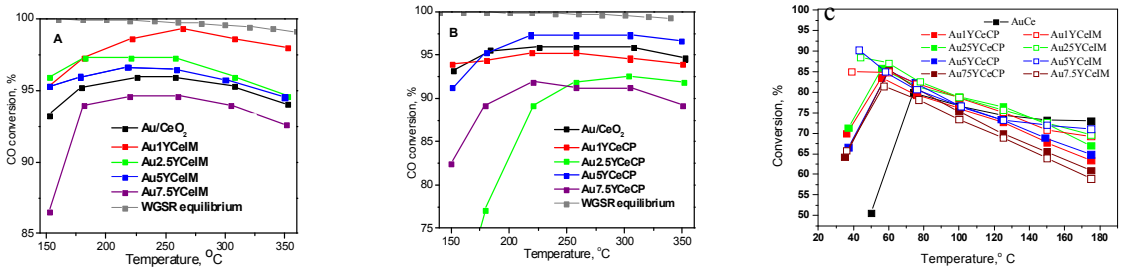

Fig. 1. WGS activity of Au samples supported on Y-doped CeO_2 prepared by IM (A) and CP (B); PROX activity of the studied gold catalysts (C)

activity with increased Y content was registered for IM samples. The best CO conversion exhibited Au1YCeIM (>98% in the range 275-300°C). The activity in PROX (higher using reductive pretreatment) is illustrated in Fig. 1 (C). At room temperature the CO conversion was significantly higher over the catalysts on IM supports as compared to those on CP ones and bare ceria. However, in the interval 80-120 °C the activity and the selectivity to CO_2 (not shown) are relatively high and they did not differ substantially, regardless the synthesis procedure and Y-amount. Slightly higher activity exhibited Au2.5YCeIM (relatively good selectivity of about 40%). The drop in activity and selectivity after CO_2 and water addition to the feed over this catalyst was not very significant, in contrast to the substantial deactivation over Au2.5YCeCP sample. The better resistance toward CO_2 deactivation using IM method could be due to the separate Y_2O_3 phase on ceria grains (confirmed by HRTEM) leading to decreased surface basicity. The differences in the catalytic behaviour was not connected to gold dispersion but it was likely related to support features. The size of gold particles seems to be independent of the synthesis procedure (XRD and HRTEM data). Y-doping of ceria by both preparation methods is favoring the high dispersion of gold particles and their stability during the catalytic operation in both reactions (HRTEM data of average size of gold particles 2.2 - 3.5 nm for all fresh and spent samples). Ceria particles were in the range of 4-8 nm (XRD data). Differences in the reducibility of ceria surface layers were visible in the TPR spectra of the initial supports. Gold causes a significant shift to lower temperature of the TPR peaks assigned to ceria surface reduction. The differences in the reducibility of all gold catalysts seems not so substantial. The relative amount of oxygen vacancies (Raman data) increased linearly with the Y-amount, to a large extent for the CP preparation. In the case of IM supports the relative concentration of oxygen vacancies is almost equal for all samples and it is significantly lower as compared to the corresponding CP supports. These results suggest that CP preparation method leads to in depth distortion of ceria structure, whereas the IM method causes predominantly surface ceria modification.

4 Conclusions

Adding yttrium to ceria had generally a positive effect on the WGS activity of the supported gold. Moreover, when yttrium was added by IM procedure the effect was inversely dependent on its amount and it was also larger than in the case of the CP procedure. At the temperature of interest for fuel cells application the catalytic activity in PROX did not differ significantly over all studied samples; the IM preparation method was beneficial for PROX at real conditions improving the resistance toward CO_2 deactivation. The comparison of present WGS and PROX results with our previous findings about the effect of different rare earths as dopants of ceria used as support of gold catalysts reveal a promising role of Y-doping.

Acknowledgements

Thanks to the COST Action CM1104 and the projects: E-01/07, E-02/2 (Bulgaria) and CONACYT 130407, PAPIIT 103513, UNAM (Mexico).

III-PP11

Gallium-Promoted Nickel/Cerium Catalysts for Hydrogen Production from Steam Reforming of Acetic Acid as a Model Compound of Bio-Oil

Nogueira F.G.E., Assaf P.G.M., Tremiliosi Filho G., Assaf E.M.*

São Paulo University, São Paulo, Brazil

* eassaf@iqsc.usp.br

Keywords: hydrogen, bio-oil, acetic acid, gallium, cerium, nickel

1 Introduction

A renewable biomass may be use as an alternative energy source, due to the large variety of feedstock available, such as sugar cane residues (tops, leaves and bagasse), grass, straw, sludge, organic domestic waste and industrial wood waste. The use of biomass reduces CO_2 emissions compared to using fossil fuels because it is a CO_2 neutral energy source besides reducing emissions of NOx and SO_X [1-2].

Hydrogen can be produced from biomass via thermochemical processes, such as flash pyrolysis, which produces mainly liquids (bio-oils), and then the bio-oils can be converted to hydrogen by catalytic steam reforming . Nevertheless, bio-oil is a very complex organic mixture like acids, ketones, alcohols, phenols and guaiacols [3-4].

Therefore, designing efficient catalyst requires the use of model oxygenated components for preliminary tests. Acetic acid (HAc), which is soluble in water, is chosen as a model compound because it is one of the most representative constituents of bio-oil. Thus, the aim of this work was to study the performance of nickel catalysts promoted with gallium (Ga) supported on CeO_2 to convert acetic acid into hydrogen.

2 Experimental/methodology

Ni catalysts supported on CeO_2 and promoted with Ga were prepared by the impregnation method. First, the Ga-CeO_2 supports were synthesized using the coprecipitation method with loadings of 1 and 3 wt. % of Ga. Ga/CeO_2 supports were then impregnated with the solution of $Ni(NO_3)_2.6H_2O$ under stirring at 70 ^oC and then dried overnight in air at 110 ^oC. The dried powder was finally calcined at 650 ^oC for 3h to obtain the NiO/Ga-CeO_2. All the nickel catalysts were prepared with a load of 5 wt.% Ni. The samples were characterized by X-ray diffraction (XRD), temperature-programmed reduction (TPR) and thermogravimetric analysis (TGA). The catalysts were named 5Ni1Ga/CeO_2 and 5Ni3Ga/CeO_2. The unpromoted catalyst, 5%Ni/CeO_2 was also prepared for comparison and was named 15Ni/Ce.

The catalytic tests for the acetic acid steam reforming were carried out using a tubular quartz reactor, containing 100 mg of catalyst. Before the reactions, the catalysts were reduced with hydrogen (30 mL min^{-1}) at 750 ^oC for 1h, to activate the catalyst. Aqueous solution of acetic acid 2:1 (H_2O: CH_3COOH) molar ratio was fed by a piston pump resulting in a flow of 2.5 $mL.h^{-1}$. The reactions were carried out at temperatures of 600 °C. The product composition was recorded over 6h of reaction.

3 Results and discussion

Figure 1A shows a XRD of 5Ni/CeO_2, 5Ni1Ga/CeO_2 and 5Ni3Ga/CeO_2 catalysts. The main phase observed in the diffraction patterns was CeO_2 with a fluorite structure (ICDD 34-0394). Diffraction peaks related to the Ga_2O_3 and NiO crystallites were not observed in the

XRD patterns of these samples. Figure 1(B) shows the H_2-TPR curves of catalysts. The catalysts present two redox peaks between t 410 ^oC and 858 ^oC which correspond to the reduction of NiO and CeO_2.

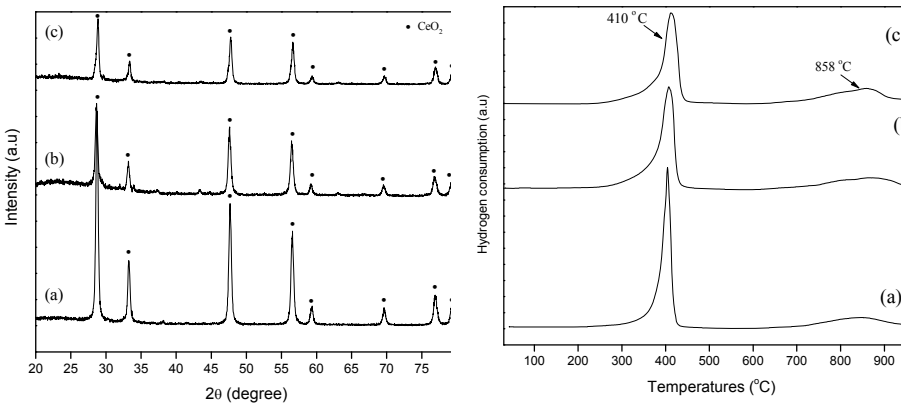

(A) (B)

Fig.1 (A) DRX of (a) 5Ni/CeO2 (b) 5Ni1Ga/CeO2 and (c) 5Ni3Ga/CeO2 catalysts and (B) H2 - TPR profiles of catalysts (a) 5Ni/CeO2 (b)5Ni1Ga/CeO2 and (c) 5Ni3Ga/CeO2

All catalysts showed conversion above 90% for acetic acid at 600 ^oC. It is noteworthy that the addition of Ga as promoter did not affect the conversion of acetic acid. The selectivity for H_2 for $5Ni/CeO_2$, $5Ni1Ga/CeO_2$ and $5Ni3Ga/CeO_2$ catalysts was ~3.5 mol H_2/mol $CH3COOH_{conv.}$ at 600 ^oC for all catalysts. However, with addition of 3% Ga the rate of coke was 0,0098 g_c $gcat^{-1}h^{-1}$, while the rate of coke formation for $5Ni/CeO_2$ and $5Ni1Ga/CeO_2$ catalysts was 0,0295 and 0,0179 g_c $gcat^{-1}h^{-1}$, respectively. This shows that addition of Ga prevents the formation of coke on the catalyst surface.

4 Conclusion

The present study demonstrates that the catalysts containing $5Ni3Ga/CeO_2$, showed the lower rate of coke formation when compared with catalysts $5Ni/CeO_2$ and $5Ni1Ga/CeO_2$.

Acknowledgements

The authors thank the FAPESP (process 2014/08934-5) and CNPq for the financial support.

References

[1] D. Johansson, P. Franck, T. Berntsson, *Energy* 38 (2012) 212.
[2] S.K. Hoekman, C. Robbins, *Fuel Processing Technology* 96 (2012) 237.
[3] M.C. Ramos, A.I. Navascués, L. Garcia, R. Bilbao, Industrial *& Engineering Chemistry Research* 46 (2007) 2399.
[4] Z. Li, X. Hu, L. Zhang, G. Lu, *Journal of Molecular Catalysis A: Chemical* 355 (2012) 123.

III-PP12

Effects of Mg Content on Ni/MgO-SiO_2 Catalyst for Ethanol Steam Reforming

Thyssen V.V., Georgetti F., Assaf E.M.*

São Paulo University, São Paulo, Brazil

* eassaf@iqsc.usp.br

Keywords: ethanol steam reforming, H_2, production, nickel, catalyst, magnesia, silica

1 Introduction

Industrially, the metal of choice for catalysts applied in several types of reactions is Ni, due to its high availability and lower cost compared to noble metals. [1,2]

Commercial silica is often used as a support due to its high specific area, which provides the reaction environment a greater contact area and possibly a greater number of active sites for the tested reaction to take place. [2]

MgO is known by the possibility of solid solution formation with the NiO. NiO-MgO is an interesting system of solid solution; they form the "ideal" model of solid solution - in which the NiO becomes part of the mesh of the support with a strong interaction with MgO - and exhibit unique catalytic properties for many reactions. [3]

Thus, the aim of this study was to prepare, characterize and tested Ni catalysts supported on MgO-SiO_2 matrices in ethanol steam reforming, and observe the influence of the Mg content on the structural and physic-chemical properties of the catalysts.

2 Experimental/methodology

Catalysts were prepared by impregnation method [2] using 10wt% of Ni supported on SiO_2, MgO and MgO-SiO_2 (10, 30 and 50wt%Mg) and named: NS, NM, N10MS, N30MS and N50MS.

The samples were characterized by EDS, surface area (BET), XRD, TGA, and H_2-TPR.

The catalysts were tested in ethanol steam reforming for initial results, using a mixture of ethanol:H_2O with feed molar ratio of 1:6 flowing at 2.5mlh^{-1}, in a period of 5h at 600^{o}C.

3 Results and discussion

The compositions obtained by EDS for Mg and Ni were close to nominal values (10, 30 and 50wt% of Mg; and 10wt% of Ni): 11, 29 and 48 wt% Mg for mixed supports (10MS, 30MS and 50MS, respectively); 11, 13, 12, 12 and 11 wt% Ni for catalysts (NS, N10MS, N30MS, N50MS and NM, respectively).

The specific surface areas showed that the addition of Mg or Ni on the S-support caused a decrease in its area: 324, 129, 56, 40 and 212 m^2g^{-1} for S-support, 10MS, 30MS, 50MS and NS, respectively. However, the addition of Ni over the M and MS-supports caused an increase in them areas: 13 m^2g^{-1} for M-support; 206, 170, 64 and 41 m^2g^{-1} for N10MS, N30MS, N50MS and NM, respectively.

XRD (Figure 1a) analysis of the supports presented diffraction peaks of amorphous SiO_2, MgO, $Mg(OH)_2$ and magnesium silicate hydrate (MSH). The catalysts showed, besides the peaks found in the supports, peaks related to NiO and $MgNiO_2$ (solid solution). [4,5]

TGA experiments (not shown here) were carried out to observe the weight loss of the 30MS and 50MS supports, and confirm the presence of MSH and $Mg(OH)_2$ on these samples. The MSH loses molecular water at 80-200^{o}C, and both supports presented a peak at this temperature range. Weight loss due to $Mg(OH)_2$ decomposition appears around 450^{o}C and was

more evident on 50MS support.[4]

Literature reports that the MgO samples hydrate to some extent by exposure to the air forming $Mg(OH)_2$ species, and when MgO or $Mg(OH)_2$ is in contact with amorphous silica and water (air) the MSH is formed in a relatively short period at room temperature.[4,5]

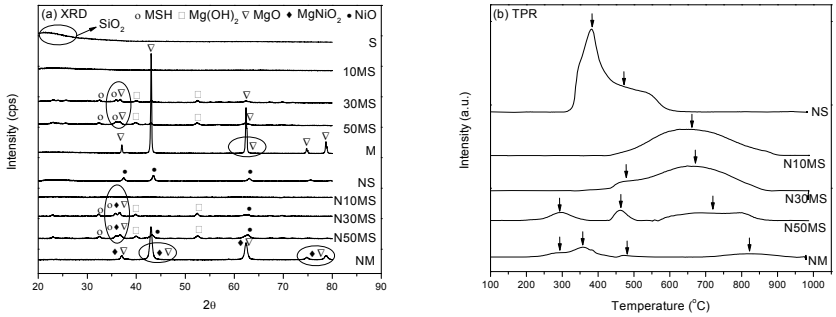

Figure 1. (a) XRD and (b) H_2-TPR.

Since the supports present no reduction, the peaks showed in TPR (Figure 1b) profiles were assigned to the reduction of NiO species present on the catalysts surface. The reduction profiles could be deconvoluted into several contributions, corresponding to different intensity of metal-support interaction: at 250-300°C signal can be attributed to the reduction of isolated NiO; the signals at 350-550°C were assigned to NiO with weak interaction with the support. It is possible to distinguish that the temperature at the maximum of the reduction peak, which was related to the NiO with moderate interaction with the support, increased from 660 to 720°C as Mg content increases between 10 and 50wt%. It would be possible to attribute the increment in the reduction temperature as Mg content increases to a greater interaction between NiO and MgO. The peak of reduction that appears at 820°C can be related to the NiO species with strongly interaction with the support.[6]

The catalysts were tested in ethanol steam reforming, and they presented activity and selectivity to gaseous products (H_2, CO, CO_2 and CH_4). All the catalysts showed total conversion of ethanol and it was observed that with the increase of Mg content on the support, the carbon deposition decreases. N30MS and N50MS catalysts showed the best H_2 selectivity.

4 Conclusions

It can be concluded that the Mg content influences the catalytic properties; it was observed that the catalysts presented different species of Mg and Ni in them surfaces: MgO, $Mg(OH)_2$, MSH, NiO and $MgNiO_2$. The catalytic tests showed that with the increase of Mg content on the support, the carbon deposition decreases.

Acknowledgements

The authors thank the CNPq, CAPES, NAP-USP-CiTecBio and FAPESP for financial support; and the LabCat at UFSCar for XRD analyses.

References

[1] S.R Kirumakki et al., *J Catal.* 242 (2006) 319.
[2] V.V. Thyssen, T.A. Maia, E.A. Assaf, *Fuel.* 105 (2013) 358.
[3] M.S. Batista et al., *J Power Sou.* 124 (2003) 99.
[4] F. Jin, A. Al-Tabbaa, *Cem Concr C*. 52 (2014) 27.
[5] T. Zhang, C.R. Cheeseman, L.J. Vandeperre, *Cem Concr R.* 41 (2011) 439.
[6] M.L. Dieuzeide, M. Jobbagy, N. Amadeo, *Catal Today*. 213 (2013) 50.

III-PP13

Ni/ZrO-ZnO Catalysts Applied in Ethanol Steam Reforming for H_2 Production

Elias K.F.M., Assaf E.M.*

São Paulo University, São Paulo, Brazil

* eassaf@iqsc.usp.br

Keywords: ethanol steam reforming, hydrogen, nickel catalyst, ZnO, ZrO_2

1 Introduction

Ethanol is a product derived from biomass and it can be transformed by steam reforming (ESR) in products with higher added value, as hydrogen fuel, it can be used in electrochemical cells that generate electricity [1]. The conversion of ethanol and products distribution are related to the composition of the catalyst and the reaction conditions. Nickel-based catalysts have been more extensively studied due to high activity and low cost. It was found that ZnO supported catalysts showed good performance because its redox and basic properties [2]. ZrO_2 is a good catalyst support for methane and methanol reforming, and it is also a good promoter for ZnO-supported catalysts in the steam reforming of methanol, but to the best of our knowledge, there has been no previous report concerning the simultaneous use of ZnO and ZrO_2 in a catalyst for ESR. The goal of this study was to evaluate the effect of adding ZrO_2 in NiZnO catalysts applied to ESR in order to produce hydrogen.

2 Experimental/methodology

NiZrOZnO catalysts containing 10wt% of Ni and 0%, 10%, 20% and 30% of ZrO2 were prepared by coprecipitation of the respective nitrates and tested in ethanol steam reforming. All samples were calcined at 700°C / 2h. The materials were characterized by temperature programmed reduction (TPR), specific surface area by the BET method and energy dispersive X-ray spectroscopy (EDX). The catalytic tests (ESR) were carried out using 150 mg of catalyst and with molar ratio ethanol: water 1:6, and total feed flow of 2.5 ml h^{-1} at 600 °C. Before the tests, the catalysts were reduced in situ with H_2 (30 mL min^{-1}).

3 Results and discussion

According to Table 1 a low surface area was observed for the 10NiZnO catalyst, as previously literature reports [3]. The addition of ZrO2 to the system favoring an increase in the area of the catalysts, however, with a high content (30%) the area returns to decrease. It is observed that there was a difference between the calculated values and real values found by EDX. This is related to small errors in handling the reagents at the time of synthesis. Table 2 shows the reactions results. A high conversion was observed for all the catalysts and it occurred because temperatures above 500 °C and high ratio water:ethanol promote high conversion. It was observed that the ethanol steam reforming was the predominant reaction, and the CO and CH_4 contents were minimized [4]. Furthermore, it was noted that increasing of ZrO_2 content, the H_2 selectivity improved, from 2.3 moles of H_2 in the catalyst 10NiZnO up to 4.4 moles of H_2 in the catalyst 10Ni30ZrZn. This effect of the ZrO_2 is according to literature, where is observed that the surface hydroxyl groups contribute significantly to the steam reforming and improving the thermal resistance of the material [5]. Moreover, it was observed by TPR analysis, which are not shown here, that increasing the ZrO2 content, there was a higher nickel-support interaction, displacing the main reduction peak of nickel to higher temperatures, an important feature for

that there is no sintering of the metal phase.

Table 1. Surface area and composition by EDX

Catalyst	Surface Area (m2 g-1)	%Ni calculated	%Ni Real*	%Zr calculated	%Zr Real*
ZrO_2	25	----	----	----	----
10Ni/ZnO	13	10	10.3	----	----
10Ni/10ZrZnO	27	10	9.6	10	7.9
10Ni/20ZrZnO	23	10	9.6	20	16.3
10Ni/30ZrZnO	12	10	9.2	30	23.8

Table 2. Conversion (%) and selectivity (mol produced/ mol of ethanol converted)

Catalyst	Conv.	H_2	CH_4	CO	CO_2
10Ni/ZnO	99	2.35	0.09	0.19	0.56
10Ni/10ZrZnO	99	3.60	0.12	0.38	0.94
10Ni/20ZrZnO	99	3.09	0.16	0.32	0.79
10Ni/30ZrZnO	99	4.42	0.23	0.46	1.23

4 Conclusions

The catalyst with 30wt% ZrO_2 exhibits superior H_2 selectivity compared to others catalysts for ESR at 600 ^oC. Therefore, the NiO/ZrO2/ ZnO catalyst is promising and could be a good choice for application in ethanol steam reforming.

Acknowledgements

The authors thank CNPQ and NAP-USP-CiTecBio for financial assistance, and DEQ/UFSCar for XRD.

References

[1] J.L. Contreras, J. Salmones, J.A. Colín-Luna, L. Nuño, B. Quintana, I. Córdova, B. Zeifert, C. Tapia, G.A.Fuentes, Int J Hydrogen Energ 188 (2014) 18835.
[2] X. Denga, J. Sun, S.Yua, J. Xi, W. Zhua, X. Qiua, Int J Hydrogen Energ. 33 (2008) 1008.
[3] J. Llorca, N. Homs, J. Sales, P. R. La Piscina, J. Catal. 209 (2002) 306.
[4] P. D Vaidya, A. E Rodrigues, Chem Eng J. 117 (2006) 39.
[5] G. Nahar, V. Dupont, Renew Sust Energ Rev. 32, (2014) 777.

III-PP14

Co Catalysts for the Dry Reforming of Methane: Effect of Support

San Jose-Alonso D., Roman-Martinez M.C.*, Illan-Gomez M.J.

Department of Inorganic Chemistry, University of Alicante, Alicante, Spain

* mcroman@ua.es

Keywords: Co catalysts, dry reforming, alumina, spinel, carbon nanotubes, magnesium, titanate

1 Introduction

The dry reforming of methane (DRM) is nowadays an attractive reaction to obtain synthesis gas with a H_2/CO ratio close to 1(very suitable to obtain different valuable products) which implies the consumption of two greenhouse gases (CO_2 and CH_4) and allows the use of biogas [1-3]. All metals from 8, 9 and 10groups (excepting Os) are able to catalyse the DRM reaction but, for industrial application, only Co and Ni are convenient from an economical point of view. The main drawback of these two metals is the high carbon deposition during reaction. Several variables have been investigated with the purpose of diminishing carbon deposition. In this work, the effect of the support in the DRM performance (activity and carbon generation) of a series of cobalt catalysts has been analyzed.

2 Experimental

Five catalysts, with a 9 wt.% nominal Co content have been prepared by excess solution impregnation using the following supports: Al_2O_3, $MgAl_2O_4$, Mg-Al_2O_3 (Mg impregnated alumina), carbon nanotubes (C) and $MgTiO_3$. After impregnation, the catalysts were dried at 100 ºC for 12 h.

Catalysts characterization was done with the following techniques: i) ICP-OES, to determine metal content, ii) TEM to study particles size distribution and the morphology of deposited carbon, iii) H_2–TPR, to analyze the catalysts reducibility and iv) OTP, to determine the amount of deposited carbon.

Prior to the catalytic activity tests, the catalysts were activated in situ by treatment with H_2 (60ml/min) at 500ºC for 90 minutes. DRM experiments were carried out in a fixed-bed quartz reactor at 700 ºC for 6 h with a 50:50 CH_4:CO_2 gas mixture (60ml/min) and 0.18 g of catalyst (20.000 h^{-1} space velocity). A gas chromatograph (HP 5890 series II with two packed columns Porapak Q and MolSieve 13X) was used for analysis.

3 Results and discussion

Table 1 shows the CH_4 and CO_2 conversion data (at ½ h and 6 h), the deactivation percentage and the amount of deposited carbon, expressed as molar percentage (moles of deposited carbon respect to the total converted carbon) and as mg of deposited carbon per g of catalyst. It is observed that the support determines the initial activity, the stability and also, the amount of deposited carbon. The catalyst supported on $MgTiO_3$ features the lowest initial conversion of methane and the lowest stability as it loses its activity after 90 minutes.The catalyst supported on carbon nanotubes and on Mg-Al_2O_3 show intermediate values of methane conversion, a constant deactivation during 6 h reaction and, the amount of deposited carbon is high. Finally, the catalysts supported on $MgAl_2O_4$ and on Al_2O_3 present high methane conversion values during the 6 h reaction, being Co/$MgAl_2O_4$ the one which shows the lowest amount of deposited carbon.

Table 1. Activity data for Co catalysts during DRM reaction at 700ºC.

	Conversion (%)				Deposited Carbon (6h)	
	CH_4, at ½ h	CH_4 at 6 h	CO_2 at 6 h	Deactivation[a] (%)	%molar[b]	mg/g[c]
Co/Al_2O_3	73	72	81	1	0.57	290
$Co/MgAl_2O_4$	63	64	74	-1	0.25	135
$Co/Mg\text{-}Al_2O_3$	51	41	52	20	0.42	230
Co/C	37	27	38	27	0.80	440
$Co/MgTiO_3$	30	0	0	100	0.04	20

[a] Deactivation, calculated as the difference between conversion at 30 minutes and 6h divided by conversion at 30 minutes and multiplied by 100.
[b] (mol of deposited carbon/mol of converted carbon)*100 (at t=6h)
[c] mg of carbon deposited per gram of catalyst

To explain the observed differences, the used (after DRM reaction) catalysts were characterized by TEM. The average size of Co particles is 14.1, 7.8, 10.2, 15.7 and 22.2 nm in catalysts supported on Al_2O_3, $MgAl_2O_4$, $Mg\text{-}Al_2O_3$, carbon nanotubes and $MgTiO_3$, respectively. This indicates that the support has a clear influence on the particle size and as a consequence on the initial catalytic activity. Thus, excepting catalyst Co/Al_2O_3, methane conversion increases as the average size of cobalt particles decreases, that is as the metal dispersion increases. The higher acidity of Al_2O_3 favors the fragmentation of methane (rate limiting step) and this could explain the higher activity of the Co/Al_2O_3 catalyst. On the other hand, the lower amount of carbon deposited on $Co/MgAl_2O_4$ respect to Co/Al_2O_3 seems to be related, also, with the lowest acidity of the $MgAl_2O_4$ support, which determines the decomposition of methane that mainly causes the carbon deposition.

4 Conclusions

The support strongly influences the catalysts activity of Co catalysts (9 wt%) in DRM. It affects the size of the loaded Co particles and, as consequence, the number of active sites on the catalyst surface. The acid/basic properties of the Al_2O_3 and $MgAl_2O_4$ supports justifies the high activity of the former and the low amount of deposited carbon of the latest catalyst, respectively.

Acknowledgements

The authors thank the financial support to the Generalitat Valenciana (Project PROMETEOII/2014/010).

References

[1] D. Deublein, “Biogas from waste and renewable resources: an introduction”, Wiley-VCH (2008).
[2] J. Xu, W. Zhou, Z. Li, J. Wang, J. Ma, Int. J. Hydrogen Energy34 (2009) 6646.
[3] M. Harasimowicz, P. Orluk, G. ZakrzewskaTrznadel, A.G. Chmielewski, J.Hazard. Mater.144 (2007) 698.

III-PP16

Iron Based Catalysts Supported on KL Zeolite for Fischer-Tropsch Synthesis

Silva J.F.[1], Bragança L.F.F.P.G.[2], Pais Da Silva M.I.[1*]

1 - Pontificia Universidade Católica do Rio de Janeiro, Rio de Janeiro, Brazil
2 - Universidade Federal Fluminense, Niteroi, Brazil

* isapais@puc-rio.br

Keywords: KL zeolite, Fischer-Tropsch synthesis, iron catalysts

1 Introduction

Fischer-Tropsch synthesis (FTS) produces clean fuels and chemicals from syngas generated from natural gas. Iron and cobalt metals have been found to be suited for FTS. Also, it has been reported that iron based catalysts generate more oxygenates and high olefin selectivity [1]. Here, we propose studying the catalytic behaviors on FTS of iron based catalysts supported on KL zeolite with different metal content (1 and 5 wt %).

2 Experimental/methodology

The KL zeolite was obtained from Toyo Soda. The catalysts were synthesized by the incipient wetness impregnation method using an aqueous solution of iron nitrate so as to prepare catalysts containing 1 and 5 wt % of Fe metal on KL zeolite support. Following impregnation, the catalysts were dried for 24 h at 353 K and calcined at 723 k in air (30 mL/min) for 4 h. The amount of incorpored metal was analyzed by Atomic Absorption Sprectroscopy (AAS). Nitrogen isotherms at 77 K were measured using a Micromeritics ASAP2010 apparatus. The X-ray diffraction (XRD) measurements were performed in a X'Pert PHILIPS equipment with Cu Kα radiation (40 kV, 30 mA) in the 2Θ range of 5°-80°. The catalytic performance in FTS was evaluated in a fixed bed microreactor under controlled conditions (543 K and 20 bar).

3 Results and discussion

The chemical composition and the textural properties of KL support and calcined supported catalysts are listed in Table 1. The results indicated that the measured metal contents approach the nominal values expected from catalysts preparation. The structural properties showed a higher total pore volume for 1 wt % Fe/KL sample and similar values for specific surface area for both catalysts. The BET area decreased after introduction of iron to KL support about 16% for both samples probably due to blocking of some zeolite pores. The XRD patterns of the KL zeolite support and catalysts are shown in figure 1. It is possible to verify that the KL zeolite structure was maintained after iron impregnation for both samples. The performances of the catalysts in FTS are presented in Table 1. According to the data obtained a higher conversion of CO was observed for 5 wt % Fe/KL. It could be attributed to the amount of iron in the support. The majority of CO was converted to C_2-C_4 and C_{5+} products for 1 and 5 wt % Fe/KL. A low content of heaviest fraction C_{19+} was observed for both catalysts showing a narrow hydrocarbons distribution from C_2 to C_{19}.

Table 1. Chemical composition, textural properties and FTS results for Fe/KL catalysts.

Samples	Metal (wt. %)	BET area (m2/g)	TPV (cm3/g)	CO conversion (%)	CH_4	C_2-C_4	C_{5+}	C_{19+}
KL	-	346	0.22	-	-	-	-	-
1wt % Fe/KL	1.1	292	0.22	19	16.5	28.8	54.8	5.7
5wt % Fe/KL	4.1	293	0.18	32	18.2	34.9	46.9	12.3

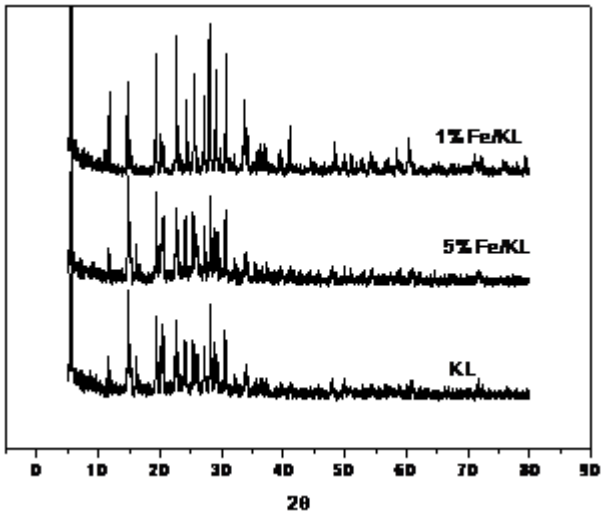

Fig. 1. XRD patterns

4 Conclusions

The characteristic pattern of the KL zeolite structure was retained after addition of metallic iron. However, the introduction of iron in the KL zeolite decreased the specific superficial area for both catalysts.

The increase of total metal content from 1 to 5 wt % indicated an increasing in CO conversion and CH_4 production.

A high (C_2-C_4) hydrocarbons distribution was observed proving that iron catalysts favour the light hydrocarbons formation.

The heaviest fraction was low for Fe catalysts indicating mainly the formation of lighter liquid hydrocarbons fractions (gasoline and diesel).

References

[1] H. Schulz, Appl. Catal. A: Gen. 186, 3 (1999).
[2] L. F. F. P. G. Bragança, M. Ojeda, J. L. G. Fierro, M. I. Pais da Silva, Appl. Catal. A: Gen. 423, 146 (2012).

III-PP17

Highly Dispersed Ni Catalysts over Cerium Modified Mesoporous MCM-41 for Hydrogen Production by Ethanol Steam Reforming

Tovar Rodríguez J.[1,2*], Ramírez Hernández G.Y.[1], Galindo Esquivel I.R.[1], Fratini E.[2], De Los Reyes Heredia J.A.[3]

1 - Universidad de Guanajuato, División de Ciencias Naturales y Exactas, Guanajuato, México
2 - Università degli Studi di Firenze, Dipartimento di Chimica e CSGI, Firenze, Italia
3 - Universidad Autónoma Metropolitana, División de Ciencias Básicas e Ingeniería, México, México

* tovar@csgi.unifi.it

Keywords: nickel catalyst, hydrogen, ethanol reforming, MCM-41

1 Introduction

Hydrogen has attracted much attention as an alternative energy carrier due to its non-polluting nature. Nevertheless, the current main sources of hydrogen are still oil-based hydrocarbons, since most of the hydrogen on Earth is found as constitutive part of larger molecules [1]. In this sense, the Ethanol Steam Reforming reaction (ESR) could be a very promising production route [2], particularly when ethanol is obtained from renewable sources. Although the use of mesoporous materials can find a versatile and broad range of applications, they still seem to be a preferred and unique source of catalytic supports for various active phases and their application shifts towards the catalysis of more selective reactions. For this purpose, Ce modified mesoporous MCM-41 could provide a better catalytic support for a Ni active phase in the ethanol steam reforming reaction to produce H_2.

2 Experimental

Cerium modified mesoporous silica MCM-41 was prepared in a hydrothermal direct synthesis approach (100ºC, 24h, following calcination at 550ºC) using 0.02, 0.04, 0.06 and 0.08 as Ce/Si molar ratios. Hexadecyltrimethylammonium bromide was used as structure directing agent; Ammonium hydroxide was used as mineralizing agent; Cerium nitrate was used as cerium precursor and Tetraethyl orthosilicate as Si source. Ni catalysts were prepared by dry impregnation method with loadings of 10% wt of Ni, using a solution of $Ni(NO_3)_2 \bullet 6H_2O$. The resulting solids were dried at room temperature for 24h and calcined at 550°C for 2h. All materials were characterized by means of Small Angle X-Ray Scattering, N_2 physisorption, Scanning Electron Microscopy and MAS Nuclear Magnetic Resonance. The ESR reaction was performed in a micro-reactor with 10mm of internal diameter and a length of 50cm at 500ºC, atmospheric pressure, a weight hourly space velocity of 0.192 cm^3/g_{cat}*min and molar ratio water/ethanol = 3. The catalysts were reduced in-situ at 546ºC for 2h with a H_2 flow of 50cm^3/min. The composition of the reactor effluent was analyzed by two gas chromatographs Clarus 580 Perkin Elmer equipped with a capillary column, one with an FID detector and the other with a TCD detector.

3 Results and discussion

The use of ultrasound irradiation in the stage preceding the hydrothermal treatment resulted in a successful incorporation of Cerium in the mesoporous structure. The hexagonal arrangement of the materials is decreased as a consequence of isomorphic Cerium substitution, with an interplanar distance ranging from 4.59 to 5.11nm. Surface area decreases from 828 to

546m^2/gr and the pore sizes enlarges from 3.56 to 4.39nm. The proportion of isolated silanol (Q_3) and total silanol groups (Q_3+Q_2) decreases at higher Ce/Si molar ratios. Figure 1 shows the well-dispersed Ni species over the MCM-41 support. The presence of cerium promoted a reduced particle size, decreasing from an average of 18nm to smaller and better-dispersed particles with sizes of 5nm.

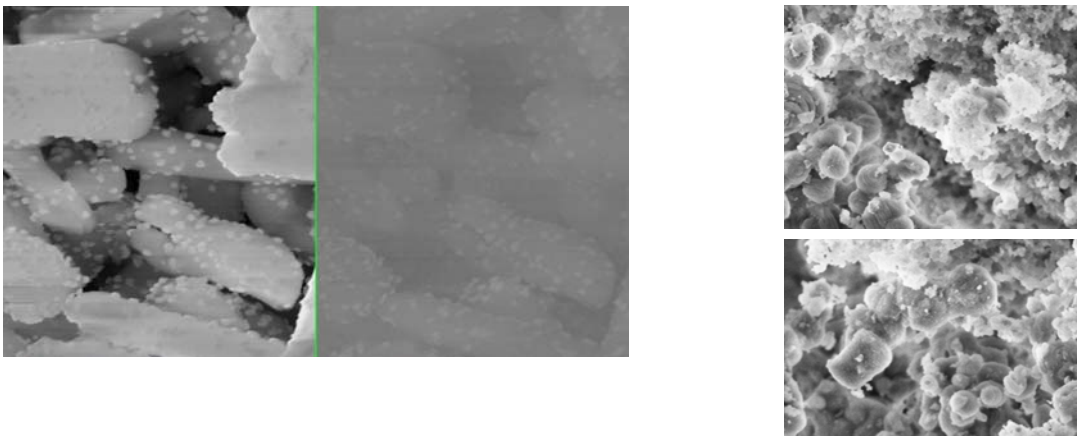

Figure 1 SEM Micrographs for 10%Ni/MCM-41: Left) Image obtained using the In-lens detector; Center) Z-contrast image acquired using the Backscattered Electron Diffraction; Right) 10%Ni/0.02CeMCM-41 catalyst (Bar length = 200nm, magnification 50kX)

When unmodified bare silica MCM-41 was used as catalytic support, the Ni/MCM-41 catalyst presented a markedly deactivation after 6h on stream, from 55% to a final value of 40% in ethanol conversion and correspondingly, hydrogen production dropped from 56% to 38%. While the composition values for CO, CH_4 and CO_2 (5, 2 and 15% respectively) remained constant, after 1.5h the Ni/MCM-41 catalyst presented formation of C_2H_4 and $C2H_4O$, which is associated to a decrease in H_2 production and coke formation by ethylene polymerization [3]. Although the production distribution was not dependant on Ce content, the CeMCM-41 proved to be a better support since the Ni/xCeMCM-41catalysts series are highly selective towards H_2, CO_2, CO and CH_4 as main gas products without ethylene formation. Complete conversion of ethanol was obtained for these catalysts during 6h on stream and no catalyst deactivation occurs.

4 Conclusions

Cerium modified mesoporous MCM-41 results in a better catalytic material for the ESR reaction compared to the support composed solely by silica since it promotes an enhanced dispersion and smaller particle size for a Ni active phase. Furthermore, the Cerium modified silica increases hydrogen production and constitutes a better catalytic support since no catalyst deactivation is evident after 6h on stream.

Acknowledgements

The authors wish to acknowledge the National Council of Science and Technology (CONACYT México, project CB-2010-158193) and the "Consorzio per lo Sviluppo dei Sistemi a Grande Interfase" (CSGI), for providing financial support.

References

[1] K. Liu, C. Song, V. Subramani, Hydrogen and Syngas Production and Purification, Wiley-VCH, 2010.
[2] G. Huber, S. Iborra, A. Corma, Chem. Rev. 2 (2006) 4044.
[3] A. Haryanto, S. Fernando, N. Murali, S. Adhikari, Energy & Fuels 19 (2005) 2098.

III-PP18

Palladium-Lead Membranes for the Separation of High-Purity Hydrogen from Hydrogen-Containing Gas Mixtures

Gorbunov S.V.*, Roshan N.R., Chistov E.M., Burkhanov G.S.

Baikov Institute of Metallurgy and Materials Science, Russian Academy of Sciences, Moscow, Russia

* Merciles@mail.ru

Keywords: membrane, hydrogen energy, palladium alloys, gas mixtures

1 Introduction

Due to the rapid progress of the hydrogen power engineering and a number of science intensive technologies, the demand for high-purity hydrogen (≥99.9999 vol %) is increased abruptly. Such high-purity hydrogen can be prepared only by its separation from hydrogen-containing gas mixtures via hydrogen diffusion through palladium-alloy membranes.

In the first place, the problem of production of commercial low-cost high-purity hydrogen requires the development of high-variety highly efficient membrane palladium-based alloys, which are intended for the preparation of efficient membrane elements for the separation of high-purity hydrogen from different hydrogen-containing gas mixtures.

Traditional palladium-silver membrane alloys cannot be used for the operation at high temperatures (773-973 K).

2 Experimental/methodology

The palladium alloys characterized by high strength, plasticity, and hydrogen permeability can be prepared via the alloying of palladium to form palladium-based solid solutions. The palladium-lead system is characterized by a wide palladium-based solid solution region (up to 20 wt % Pb). Palladium alloys with 5, 8, 12, 16, and 20 wt % Pd were prepared in the form of foils 50 μm thick by cold rolling with intermediate vacuum annealings, and their physical and mechanical properties and hydrogen permeability have been studied. Lead additions substantially strengthen palladium, whereas it plasticity decreases slightly. The hydrogen permeability was measured using an original technique, which is based on filling a calibrated volume with hydrogen, and a high-temperature cell. The Pd -8 wt % Pb alloy has the maximum specific hydrogen permeability among the Pd-Pb alloys. At 723 K, it is 2.6 $m^3 \cdot mm \cdot m^{-2} \cdot ч^{-1} \cdot MPa^{-0,5}$ and exceeds twice the hydrogen permeability of commercial B1 alloy (Pd-15 Ag-2,5 Au-0,7 Pt- 0,7 Ru-0,3 Al wt.%) at the same temperature [1].

The composition Pd - 8 wt.% Pb, which is characterized by the maximum hydrogen permeability and high strength characteristics, was selected for further studies.

Main problems of reliable operation of membranes for deep hydrogen purification and separation of gas mixtures are related to the corrosion resistance of membrane alloys, structural changes and degradation of their hydrogen permeability during operation in gas mixtures. The composition of gas mixtures affects both the possibility itself to separate high-purity hydrogen, performance, and life time.

Because of thermoconcentrational dilatation, the heating and cooling of membranes during their operation in gas mixtures are performed in vacuum or an inert atmosphere. We studied the effect of composition of synthetic gas for conversion of hydrocarbon fuels on the hydrogen permeability of Pd – 8 wt % Pb membrane, namely, on changes its hydrogen permeability during heating and cooling in one of components of conversion products, i.e., CO_2. The absence of structural changes and stable hydrogen permeability magnitudes show that the membrane can be heated to a temperature of ~300°C in the CO_2 atmosphere that subsequently changes to

operating gas mixture. This makes the membrane technology of high-purity hydrogen separation from gas mixtures of hydrocarbon fuel conversion simpler and cheaper.

3 Results and discussion

To efficiently apply the Pd-8 wt % Pb alloy in membrane elements, the alloy was evaluated for the most importance key parameter, namely, the corrosion resistance during operation in working mixture, which is identical to that of natural gas conversion, i.e., in the 60 vol % H_2 + 31 vol % CO_2 + 9 vol % CO gas mixture at temperatures of 573-773°K. It was showed that the hydrogen permeability of membrane remains unchanged, and the membrane is pressure-tight. To study the producing capacity of the Pd – 8wt%Pb membrane in the aforementioned mixture, membrane elements with membranes 50 mm in diameter and 50 μm thick have been prepared. The producing capacity (Q) of such a membrane element at $P_{input\ mix}$ = 2 MPa ($P_{H2\ part}$=1,5MPa), P_{output}=0,15 MPa, T = 773 Kand hydrogen separation ratio η = 0.8 is 0,25nm^3/h that exceeds the producing capacity of membrane element with the B1 alloy under the same conditions.

4 Conclusions

The Pd-8 wt % Pb composition is optimum and alloy shows promise for application in membrane elements for separation of high-purity hydrogen from products of the hydrocarbon fuel conversion.

Acknowledgements

This work was financially supported by the Russian Foundation for Basic Research, project nos. 13-08-12408.

References

[1] G. S. Burkhanov, N. B. Gorina, N. B. Kolchugina, N. R. Roshan, D. I. Slovetskii, and E. M. Chistov, Palladium-Based Alloy Membranes for Separation of High-Purity Hydrogen from Hydrogen-Containing Gas Mixtures, Platinum Metals Rev., 2011, 55,(1), 3-12.

III-PP19

Structural Characterization of Nanostructured Pt-Ni Alloy Electrocatalysts for Methanol Electrooxidation

Nassr A.B.A.[1], Sinev I.[2*], Pohl M.-M.[3], Grünert W.[2], Bron M.[1]

1 - Martin-Luther-University Halle-Wittenberg, Halle, Germany
2 - Ruhr-University Bochum, Bochum, Germany
3 - Leibniz-Institut für Katalyse e.V. an der Universität Rostock (LIKAT), Rostock, Germany

* ilya.sinev@techem.rub.de

Keywords: methanol electrooxidation, direct methanol fuel cell, platinum, nickel, polyol method

1 Introduction

Fuel cells powered by hydrogen or small organic molecules, e.g. methanol, may have the potential to meet requirements for energy sources with high efficiency and low emissions. Although Pt-based catalysts are still considered as optimal catalysts for fuel cell applications, substantial research has been conducted to improve them in terms of activity and stability. It was found, in particular, that adding a less noble element (Fe, Sn, Ni, Ru, etc.) can significantly improve catalyst resistance towards poisoning with intermediate CO. Two different mechanisms were proposed to be responsible for the performance enhancement. First, so-called bi-functional mechanism, explains decrease in poisoning by oxygen activation on the second metal (or its oxide). The second, electronic mechanism or ligand effect, assumes that the second metal can modify the electronic properties of Pt destabilizing the interaction between the CO molecules and the Pt surface and hence weakens the Pt−CO bonding.

In this study, we report on the preparation and comprehensive characterization of PtNi nanocatalysts supported on oxygen functionalized carbon nanotubes (FCNTs) by the polyol method in which ethylene glycol (EG) is used as solvent and reducing agent at the same time.

2 Experimental

PtNi catalysts with different Pt:Ni ratios (1:1, 2:1, 3:1, 3:2) were prepared by the polyol method. FCNTs support was mixed with required amount of metal salts (H_2PtCl_6, $Ni(NO_3)_2$) dissolved in ethylene glycol. The resulting slurry was stirred and sonicated and then split in two series for further treatment. Two essentially different approaches were used for metal ion reduction and later alloy formation. A first set of samples was refluxed in an oil bath at 160°C for 6 h after which it was allowed to cool down to room temperature under stirring and the solid product was centrifugated and washed and dried at 80°C. The resulting solid product was then heat treated in N_2 flow at 200 and 400°C. The second series was prepared using microwave (MW) radiation for metal reduction. The CNTs and metal salts containing slurry was transferred into a microwave reactor where it was irradiated at 700 W either continuously for a defined time or in a pulsed mode with pulse duration of 20 s (10 s on and 10 s off) for a specific number of pulses. The microwave step was followed by aging of the catalyst under stirring overnight. Two reference samples were prepared, one without aging and one with pH modification during the aging step by the addition of 250 mL of 0.1 M HNO_3.

All samples underwent a set of characterization techniques including inductively coupled plasma-optical emission spectrophotometry (ICP-OES) to determine bulk composition, X-ray diffraction (XRD), X-ray photoemission spectroscopy (XPS), Ion Scattering spectroscopy (ISS), X-ray absorption spectroscopy (XAS), Transmission Electron Microscopy (TEM), including state-of-the-art high resolution (HR) aberration-corrected TEM coupled with energy-dispersive X-ray-spectrometry (EDXS) for elemental mapping. The catalysts were tested toward methanol electrooxidation activity in 1M CH_3OH/0.5 M H_2SO_4 solution using cyclic voltammetry (CV) and

chronoamperometry. CO stripping was used to determine the electrochemical surface area (ECSA).

3 Results and discussion

Both XPS and XAFS studies reveal that the platinum state in the catalysts under study is metallic, with clear indications of alloy formation [1, 2]. However, besides metallic Ni significant Ni oxide contributions are also detected, and after heat treatment oxides are the only Ni species detectable by XPS. In accordance, XRD detects the presence of alloys with the degree of alloying decreasing, however not completely vanishing, after heat treatment. Oxidic species, however, are not detected by XRD. The XPS-derived near surface Pt:Ni atomic ratios, are considerably different from the bulk ones obtained by ICP-OES, indicating thus a PtNi alloy core surrounded by a Pt enriched shell with some Ni oxides present outside. The ISS depth profiles are in line with this conclusion, showing rapid drop of Pt signal comparing to Ni towards deeper sample layers. Further Pt segregation occurs during heat treatment and aggravated by stirring the catalyst in HNO_3.

Methanol electroxidation measurements with heat-treated catalysts have clearly shown their superior tolerance toward CO poisoning as well as higher activity comparing to industrial Pt/C (ETEK). In particular, for PtNi(2:1), PtNi(3:1) and PtNi(3:2) catalysts, the activities are close to each other, which is due to similar atomic Pt to Ni ratios of 3:1 as determined with ICP-OES analysis, with PtNi(3:1) providing the highest activity among all catalysts. Additionally, the mass specific activities (MSA) found by us [1] are higher than those reported in literature [3, 4]. Heat treatment at 200°C results in higher catalytic activity for most of the PtNi/FCNTs in terms of mass activity than the as prepared catalyst which can be attributed to a cleaning of the catalyst surface from adsorbed organic residuals. However, after treatment at 400°C the surface and mass specific activity decreases dramatically for all catalysts. This can be attributed to the catalyst restructuring upon heat treatment.

For the samples prepared using microwaves, the continuous mode of irradiation is more effective in preparing nanoparticle catalysts than the pulsed mode. In general, the optimized catalysts reported in this study showed higher MSA, up to 1.5 fold [2] than that obtained with PtNi catalysts with the same atomic ratio prepared by thermal post-treatment and also higher than the activity of PtNi catalysts reported recently by other groups.

4 Conclusions

PtNi/FCNTs with different Pt:Ni ratios have been prepared with ethylene glycol as reducing agent (polyol method). The catalysts display the Pt fcc structure with indications for alloy formation but also proofs for the presence of Ni oxides. A model based on the combination of advanced characterization techniques is suggested where Ni-rich phases form close to the FCNTs which are surrounded by a Pt-rich alloy. The highest catalytic activity was found for a Pt/Ni ratio of 3, which could be attributed to the availability and proper population of active Pt sites required for methanol adsorption and the easy removal of intermediate CO. Phase separation by heat treatment leads lower catalytic activity. For MW assisted catalyst preparation the irradiation mode influences both the metal loading and the activity of the prepared catalysts where catalysts prepared under continuous irradiation show higher electrocatalytic activity.

References

[1] A.B.A.A. Nassr, I. Sinev, W. Grünert, M. Bron, Appl. Catal. B: Environmental 142– 143 (2013) 849.
[2] A.B.A.A. Nassr, I. Sinev, M.-M. Pohl, W. Grünert, M. Bron, ACS Catal. 4, 2449−2462 (2014)
[3] C. Xu, J. Hou, X. Pang, X. Li, M. Zhu, B. Tang, Int. J. Hydrogen Energy 37 (2012) 10489.
[4] B. Lu, S. Xu, X. Yan, Q. Xue, Electrochem. Comm. 23 (2012) 72.

III-PP20

Effect of Pt Addition on Methane Oxidation Activity of Pd-Mn-Hexaaluminate Catalysts

Yashnik S.A.[1*], Kuznetsov V.V.[1], Chesalov Yu.[1], Ishchenko A.[1], Kaichev V.V.[1], Ismagilov Z.R.[1,2]

1 - Boreskov Institute of Catalysis, Novosibirsk, Russia
2 - Institute of Coal Chemistry and Material Science, Kemerovo, Russia

* yashnik@catalysis.ru

Keywords: Methane, oxidation, Mn-hexaaluminate, Pt-catalyst, Pd-catalyst

1 Introduction

Wide interest to the catalytic combustion chamber (CCC) of gas turbines [1,2] stimulates further researches on development of Pd-based catalysts with respect to decrease of the light-off temperature, increase of the efficiency in the hydrocarbon fuel combustion and thermal stability. Mn-hexaaluminates and aluminas modified by manganese cations have high thermal stability, sufficient specific surface area and high hydrocarbon oxidation reactivity and are considered both as catalysts for high-temperature combustion of natural gas, and as thermally stable supports for deposition of Pt-group metals [2-4]. We also observed a non-additive increase of the catalytic activity in the high-temperature oxidation of methane over Mn-alumina catalysts after their modification by Pd [5], resulting in a decrease of the light-off temperature. Here we studied an effect of Pt addition to improve the catalytic performance of the high-temperature Pd-Mn-hexaluminate in the oxidation of methane, especially in SO_2 and water presence, and compared them with the properties of Pd/Al_2O_3 catalysts. The redox properties, particle morphology, XRD-composition and active sites of the initial and spent PtPd-Mn-hexaluminates were examined in order to find a reason of high efficiency and thermal stability of the catalysts.

2 Experimental

The Mn-hexaaluminate catalyst with $MnLaAl_{11}O_{19}$ phase was prepared according to the procedure described elsewhere [5]. Its low-temperature precursor was doped with Pd and Pd by incipient wetness impregnation with chloropalladic/chloroplatinic acid or palladium/platinum nitrates followed by calcination at 1000°C. Pt+Pd content was 1.0 wt%, Pt/Pd atomic ratio was in a range 0.1-1.0.

The catalysts were tested in the methane oxidation at conditions typical to Small Gas Turbine Power Plants: 670°C and 10000 h^{-1}. Gas feed was 5 vol%CH_4, the coefficient of oxygen excess over the stoichiometric value was 3. After achievement of steady value of CH_4 conversion, 3 wt% H_2O and 1000 ppm SO_2 were introduced in the feed, CH_4 conversion was measured again. The composition, particles morphology and structures of active site in Pd- and Pt(Pd)-hexaaluminate catalysts were studied by XRD, H_2-TPR, O_2-TPR, FTIR, XPS, HRTEM.

3 Results and discussion

The Pt-doped Pd-Mn-hexaaluminate catalysts provided deep methane oxidation at 670°C and 10000 h^{-1} (Fig.1). At the same content of noble metals, substitution of part of Pd by Pt to the atomic ratio of Pt/Pd equal to 0.25-0.27 had no impact on the efficiency of methane oxidation, at a further increase of Pt fraction the tendency of a reduction of the methane oxidation efficiency was observed. The ex-nitrate catalysts were more active as compared with ex-chloride catalysts. Besides, for the ex-chloride samples the weak tendency to deactivation was observed eventually.

The presence of water vapor had a weak deactivating effect on the catalytic activity of

unmodified and Pd-modified Mn-hexaaluminate catalysts. The deactivating influence of water was amplified with sulfur dioxide addition to the air-fuel feed, so methane conversion in their presence decreased from 99% to 85-87% and 82-83% over Mn-hexaaluminate and Pd-Mn-hexaaluminate catalysts, respectively (Fig.1, c.1,2). The Pt-doped Pd-Mn-hexaaluminate catalyst with Pt/Pd=0.27 was the most stable to water vapor and sulfur dioxide (Fig.1, c.3). Note, that this catalyst was resistant to deactivation at lower temperatures also (500°C) at which high deactivation of PdO/Al_2O_3 is usually observed [6]. However, a further increase of Pt loading in the catalyst (to Pt/Pd=1.1) caused a decrease of its stability, so CH_4 conversion at 670°C falled from 99% to 90% and 30% after water and water with sulfur dioxide addition, respectively.

XRD and O_2-TPR study of the Pd-Mn-hexaaluminate and Pt-doped samples showed that the positive effect on the methane oxidation activity is due to increase in a PdO fraction and its high thermal stability (Fig.2). A PtPd-alloy formation, that was observed in spite of PdO by H_2-TPR, O_2-TPR, and XPS in the catalyst with Pt/Pd=0.27, well correlates with its high water tolerance. PdO is less stable in the presence of water in comparison with metallic Pd [6].

The FTIR absorption bands at 1145 and 1065 cm^{-1} confirmed sorption of sulfate-groups on the surface of the Mn-hexaaluminate samples. The sulfate content (thermogravimetric DTA) in them depended on the catalyst composition and increased as: $PtPd(0.27)/MnLa\text{-}Al_2O_3$ < $Pd/MnLa\text{-}Al_2O_3$ < $PtPd(1.1)/MnLa\text{-}Al_2O_3$ < $MnLa\text{-}Al_2O_3$. XRD and HRTEM indicated that structure of the aluminate phase in the spent samples does not change, interplanar distances characteristic for $MnLaAl_{11}O_{19}$ remain. EDX data showed there is sulfur which mainly settles down on large particles of aluminate phase while the sulfur is not present on Pd particles.

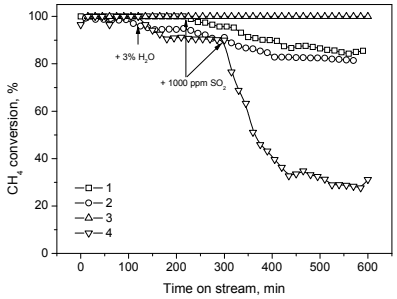

Fig. 1. Methane conversion over $MnLa\text{-}Al_2O_3$ (1), $Pd/MnLa\text{-}Al_2O_3$ (2), $PtPd(0.27)/MnLa\text{-}Al_2O_3$ (3); $PtPd(1.1)/MnLa\text{-}Al_2O_3$ (4) in water (3 wt%) and SO_2 (1000 ppm) presence. Temperature of the catalyst bed was 670°C and GHSV is 10000 h^{-1}.

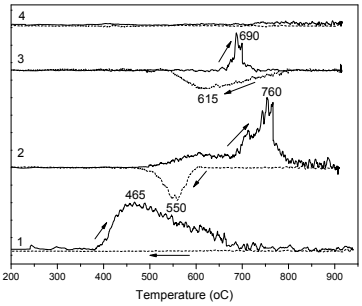

Fig. 2. Oxygen elimination and consumption during heating and cooling ramp of O_2-TPR with $MnLa\text{-}Al_2O_3$ (1), $Pd/MnLa\text{-}Al_2O_3$ (2), $PtPd(0.27)/MnLa\text{-}Al_2O_3$ (3); $PtPd(1.1)/MnLa\text{-}Al_2O_3$ (4).

4 Conclusions

The addition of Pt to Pd-Mn-hexaaluminate catalyst up to Pt/Pd ratio close to 0.25 improves its stability in the methane oxidation in water and sulfur dioxide presence without decreasing the high-temperature methane oxidation activity. Such performance of $PtPd(0.27)/MnLa\text{-}Al_2O_3$ can be explained by the formation of both PdO and PtPd-alloy in the catalyst.

Acknowledgements

This work has financial support of the Russian Fond of Basic Research (grant 15-03-05459).

References

[1] L.D. Pfefferle, W.C.L.D. Pfefferle, *Catal. Rev. Sci. Eng.* 29 (1987) 219.
[2] Z.R. Ismagilov, M.A. Kerzhentsev, et.al. In: I. Gurrapa (ed) Gas Turbines, Chapter 4:79-108. Sciyo.
[3] S.A. Yashnik, N.V. Shikina, Z.R. Ismagilov, et.al., *Catal Today* 147S (2009) 237.
[4] Z.R. Ismagilov, N.V. Shikina, S.A.Yashnik, et.al., *Catal. Today* 155 (2010) 35.
[5] S.A. Yashnik, Z.R. Ismagilov, V.V. Kuznetsov, et.al., *Catal Today* 117 (2006) 525.
[6] L. Pfefferle, *Appl.Catal. A* 216 (2001) 209.

III-PP21

The Nickel Electrocatalysts $[Ni(P^{R}_{2}N^{R'}2)_{2}]^{2+}$ (where R=Ph or o-Py) for Hydrogen Evolution

Khrizanforova V.V.*, Spiridonova Yu.S., Strelnik I.D., Musina E.I., Karasik A.A., Morozov V.I., Gerasimova T.P., Katsuba S.A., Sinyashin O.G., Budnikova Yu.H.

A.E.Arbuzov Institute of Organic and Physical Chemistry, Kazan Scientific Center of Russian Academy of Sciences, Kazan, Russia

* Khrizanforovavera@yandex.ru

Keywords: electrocatalysis, nickel, hydrogen evolution, biomimetic, cyclic, voltammetry

1 Introduction

The [FeFe]-hydrogenase enzyme can both produce and oxidize H2 at turnover frequencies of ≥9000 s^{-1}. Recent advances in Ni-based bio-inspired catalysts, such as [Ni(PR2NR'n)2]2+, demonstrated the possibility of cleaving H2 or generating H2 heterolytically with turnover frequencies comparable or superior to those of hydrogenase enzymes. In these catalysts the transformation between H2 and protons proceeds via an interplay between proton, hydride and electron transfer steps, and involves the interaction of a dihydrogen molecule with both a Ni(II) center and pendent amine bases incorporated in six-, seven or octa-membered rings, which function as proton relays. The catalysts with ligand 8-membered ring achieved the high electrocatalytic H2 production rates, up to 1540 s-1 in dry acetonitrile and up to 6700 s-1 in water-acetonitrile solutions with [(DMF)H]OTf acid as proton source.

2 Results and discussion

We report new data on the unexpectedly high activity of nickel complexes with 8-membered ring 1,5-diaza-3,7-diphosphacyclooctane ligands with the *ortho*-pyridyl substituents at the phosphorus atoms vs. phenyl with the same substituents at nitrogen (Scheme 1). These complexes demonstrate similar two reversible one-electron reductions, but have different electrocatalytic behavior in the presence of proton source [1-4]. We have observed a unique reactivity of pyridine-substituted analogue, its effectiveness exceeding that of all known relative complexes under the selected conditions. The introduction *o*-Py substituents at phosphorus as additional basic center is caused by the changing of voltage-current picture and significantly catalytic current enhancement. For example, TOFs being 100 and 15200 s^{-1} for benzhydryl substituents at nitrogen and Ph or o-Py at phosphorus respectively (Figure 1).

In situ EPR investigating of the Ni(I) state forming at the potential Ni(II/I) was performed for all nickel complexes. The formation of Ni(I) complex bound with four phosphorus atoms during the reduction of Ni(II) complexes was detected by ESR spectra in CH_3CN at room temperature under spectroelectrochemical conditions, g-factor values close to known literature values, for example for $Ni^{+1}(P^{Ph}_{2}N^{C6H4CH2P(O)(OEt)2}_{2})_{2}$ or $Ni^{+1}(P^{Ph}_{2}N^{Ph}_{2})_{2}$ [5-6]. The increasing ESR spectra intensity after temperature could be explained by formation of dimeric structure of NI(I) in CH3CN. This conclusions supported by DFT calculations.

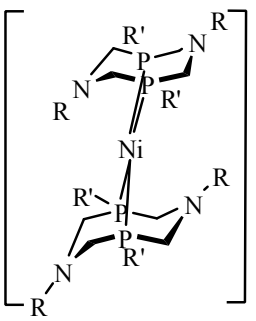

1	R'=o-Py	R=CH_3(CH)Ph;
2	R'=o-Py	R=p-Tol;
3	R'=*o*-Py	R=Ph(CH)Ph;
4	R'=*o*-Py	R=Bn;
5	R'=Ph	R=CH_3(CH)Ph;
6	R'=Ph	R=p-Tol;
7	R'=Ph	R=Ph(CH)Ph;
8	R'=Ph	R=Bn

Scheme 1. Studied nickel complexes.

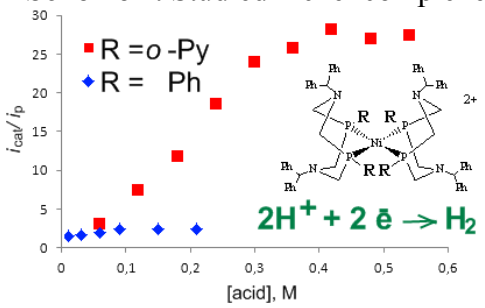

Figure 1. Plots of the i_{cat}/i_p vs. acid concentration for nickel complexes with Ph and o-Py substituents at phosphorus.

4 Conclusions

Thus, the new nickel catalysts with high catalytic hydrogen evolution rates in dry acetonitirile was obtained. Behavior and activity of catalysts were found to differ strongly for the complexes with Ph and *o*-Py substituents at the phosphorus atom at the same substituent at the nitrogen (Ph(CH)Ph). The introduction of *o*-Py substituent at the phosphorus atom causes significant TOFs increasing and changing the voltage-current picture in the acid presence. The different behavior of $[Ni(^{Po\text{-}Py}{}_2N^{Ph(CH)Ph}{}_2)_2]^{2+}$ in catalytic reaction caused by pre-protonation of *ortho*-pyridyl substituent in the acid presence.

Acknowledgements

This research was supported by Russian Science Foundation **№ 14-23-00016.**

References

[1] M.E. Carroll, B.E. Barton, T.B. Rauchfuss, P.J. Carroll, J. Am. Chem. Soc. 134 (2012) 18843−18852.
[2] S. Yao, Y. Xiong, C. Milsmann, E. Bill, S. Pfirrmann, C. Limberg, M. Driess, Chem. Eur. J. 16 (2010) 436-439.
[3] A. Kochem, F. Neese, M. Gastel, J. Phys. Chem. C 118 (2014) 2350-2360.
[4] E.I. Musina, V.V. Khrizanforova, I.D. Strelnik, M.I. Valitov, Yu.S. Spiridonova, D.B. Krivolapov, I.A. Litvinov, M.K. Kadirov, P. Lönnecke, E. Hey-Hawkins, Yu.H. Budnikova, A.A. Karasik, O.G. Sinyashin, Chem. Eur. J. 20 (2014) 3169-3182.
[5] S.C. Silver, J. Niklas, P. Du, O.G. Poluektov, D.M. Tiede, L.M. Utschig, J. Am. Chem. Soc. 135 (2013) 13246-13249.
[6] K. Fraze, A.D. Wilson, A.M. Appel, M. Rakowski DuBois, D.L. DuBois, Organometallics 26 (2007) 3918-3924.

III-PP22

Effect of CH_4 Flow Rate and Catalyst Load on the Activity Stability of Mo/HZSM-5 in the Methane Dehydroaromatization at 1073 K in an Integral, Fixed-Bed Reactor

Xu Y., Song Y., Suzuki Y., Zhang Z.-G.*

National Institute of Advanced Industrial Science and Technology (AIST), Tsukuba-shi, Japan

* z.zhang@aist.go.jp

Keywords: methane, benzene, Mo/HZSM-5 catalyst, catalyst load, CH_4 flow rate

1 Introduction

The worldwide shale-gas revolution and the increasing benzene demand in chemical industry are expected to motivate more R&D activities on the Mo/HZSM-5-catalyzed non-oxidative methane dehydroaromatization. Case studies have suggested this reaction should be operated at temperatures not lower than 1073 K and a CH_4 space velocity as high as possible to gain a performance-acceptable CH_4 conversion and a high hourly benzene formation yield simultaneously. Since the space velocity here is not a simple variable but a combined value by dividing a given CH_4 flow rate with a given catalyst load, there is a need to clarify which of these two operating factors is more crucial for maximizing the catalytic performance of the catalyst. For the reaction, the aromatics formation rate is most likely limited by mass transfer, and the secondary coke reactions of products could occur in the upper part of the catalyst bed to speed up the catalyst deactivation there and lower the catalytic efficiency of the whole bed [1,2]. This suggests there must exists a suitable combination of CH_4 feed rate and catalyst load (bed height) for the system to reach its maximum performance. Additionally, knowing limitations on both catalyst load and superficial gas rate is also essential for design of real reactors.

2 Experimental

A certain amount of fluidizable 6%Mo/HZSM-5 catalyst sample ranging from 50 mg to 1600 mg was charged into an up-flow fixed bed reactor (i.d. 8 mm) for each test. The sample was carburized in-situ in a CH_4 stream at 923 K for a pre-determined period. Subsequently, the carburized catalyst was heated to 1073 K in a H_2 stream and kept there for 5~80 min to remove most of the coke accumulated in the carburization period. Finally at the same temperature the catalyst was subjected to a CH_4 flow of 13.7~90 mL/min to start the reaction. The reaction last until the sample lost all its benzene formation activity. CH_4 conversion and the benzene concentration in the reacted stream were measured on-line using two gas chromatographs.

3 Results and discussion

Fig. 1 shows the effect of catalyst load on the time-dependence of the formation rate of aromatics at 1073 K for four different CH_4 flow rates. At each CH_4 flow rate, the catalyst lifetime for aromatic formation increases with increasing the catalyst load. This can be a consequence of the increase of active sites in the bed. However, the obvious increase in the liftime aromatics yield only ocuured in a low range of catalyst load at each CH_4 feed rate. As the catalyst load exceeds a cretain level the lifetime aromatics yield slows down its increasing pace and approaches to a fixed level. This suggests that there exists a proper catalyst load for a given CH_4 feed rate to maximize the catalytic effciency of the test catalyst and the overloaded part would not play their catalytic role in the conversion of methane to aromatics. The data in Fig. 2 provide further support for this.

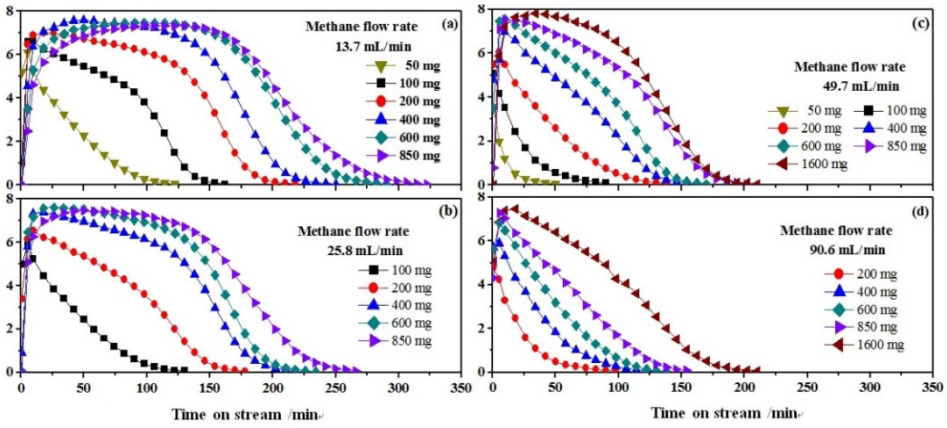

Fig. 1 Effect of catalyst load on the aromatic formation rate obtained over Mo/HZSM-5 catalyst at 1073 K.

As shown in Fig. 3, the four tests were conducted at the four different CH_4 space velocities from 6400 to 8220 mL/g/h, which were realized by reducing both CH_4 flow rate and catalyst load simultaneously. The catalyst stability does decrease, not increase with decreasing CH_4 space velocity. This is against our anticipation. It suggests that rather than catalyst load the superficial gas flow rate might be more crucial for maintaining the activity stability. While a lowered gas feed leads surely to a lower hourly aromatics production, a too high CH_4 flow rate could result in preferential coke formation in the near-surface layers of catalyst particles and/or of crystal agglomerates inside the particles [2] and speed up the catalyst deactivation. Therefore, there must exists a suitable combination of CH_4 feed rate and catalyst load (bed height) for the system to reach its maximum performance. As for the height of catalyst bed, as it is increased, catalyst particles in the upper portion of the bed might be severely deactivated prior to playing their catalytic role for more rapid coke formation originated from the decomposition of C2 species coming from the bottom portion of the bed. TG measurements of four spent samples (850 mg) collected after the reaction confirmed that the amount of coke formed in the bottom of catalyst bed was the largest and that in the upper of catalyst bed was the smallest.

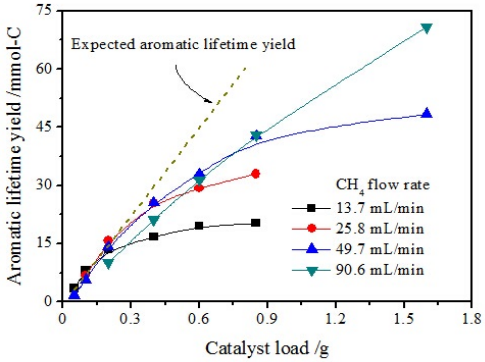

Fig.2 Effects of CH_4 flow rate and catalyst load on benzene lifetime yield over Mo/HZSM-5 catalyst at 1073 K.

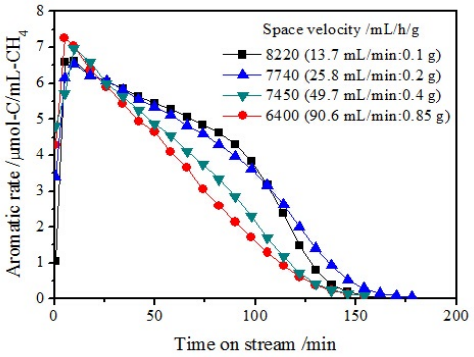

Fig.3 Time-dependence of aromatic formation rate obtained over Mo/HZSM-5 catalyst at 1073 K.

References

[1] Y. Cui, Y. Xu, Y. Suzuki, Z.-G. Zhang, Catal Sci Technol. 1 (2011) 823.
[2] Y. Xu, Y. Song, Y. Suzuki, Z.-G. Zhang, Catal Sci Technol. 3 (2013) 2769.

III-PP23

Preparation and Characterization of Pt-Sn/C Electrocatalysts for Direct Methanol Fuel Cells

Veizaga N.S.*, Rodriguez V.I., Scelza O.A., De Miguel S.R.

INCAPE, Mexico, Mexico

* nveizaga@fiq.unl.edu.ar

Keywords: carbonaceous supports, Pt-Sn catalysts, direct methanol fuel cell

1 Introduction

Low temperature Direct Alcohol Fuel Cells (DAFCs) are extremely attractive as power sources for transportation, mobile and portable applications [1]. Methanol oxidation has been reported to involve the adsorption of CH_3OH followed by successive dehydrogenation steps, yielding linearly bonded CO. At sufficiently anodic potentials, the adsorbed carbon monoxide CO_{ads}, is belived to react with an adsorbed OH_{ads} intermediate. In general, it has been shown that pure Pt systems are not efficient catalysts for the oxidation of methanol because Pt is rapidly poisoned by the CO species produced as oxidation intermediates. For this reason, the modification of Pt electrode with other metals including Ru, Sn, Mo and Sb has been investigated extensively [2].

2 Experimental/methodology

The used supports were Vulcan carbon (VC) and multiple-wall carbon nanotubes (NT). The metallic precursors were $H_2PtCl_6.6H_2O$ and $SnCl_2.2H_2O$. Catalysts were prepared by deposition-reduction technique in liquid phase (called RB) using $NaBH_4$ as reducing agent. The catalysts were characterized by: temperature programmed reduction (TPR), X-ray photoelectron spectroscopy (XPS), H_2 chemisorption, benzene hydrogenation reaction, transmission electron microscopy (TEM), CO stripping, chronoamperometry measurements and finally tested in a DMFC cell.

3 Results and discussion

TPR profiles of Pt-Sn catalysts prepared by deposition-reduction in liquid phase by sodium borohydride and supported on VC and NT do not show practically any reduction peak in the zone where Pt is reduced in the impregnated catalysts (at about 230ºC). This would indicate that the major fraction of Pt would be in metallic state (Pt^0). However, nothing can be said about the reducibility state of Sn.

In order to find more information about the Pt and Sn reducibilities of the bimetallic catalysts supported on VC and NT, a XPS characterization was done. In each case, the concentration of the Pt surface oxidized species was lower than 35%, this meaning that most of Pt surface species (>65%) are in metallic state. XPS of Sn3d shows that Sn forms oxidized species and only a small proportion of Sn^0 (10-15%) was found, this small metallic fraction perhaps forming alloys with metallic Pt.

The bimetallic catalyst supported on VC showed chemisorption values higher than those of the corresponding monometallic catalyst, the similar catalyst supported on NT showed similar values to the corresponding monometallic one.

Benzene hydrogenation is a structure-insensitive reaction, which can be carried out one active metallic site. The activation energy value of the Pt-Sn catalyst is higher than the corresponding monometallic one only in the case of the series supported on VC. This would indicate that electronic effects are more important in the Pt-Sn/VC catalyst.

The cyclic voltammograms of CO stripping corresponding to mono and bimetallic catalysts

supported on VC and NT shows an important promoting effect (the beginning of the CO oxidation is shifted to lower potentials) of Sn over Pt. It can be observed that the Pt-Sn catalyst supported on VC does not modify these values of electrochemically active specific surface (EASS) with respect to Pt/VC one, while the EASS values for bimetallic catalyst supported on NT show a decrease that would be caused by the geometric effect of Sn over active Pt sites.

Electrocatalysts were also tested in a real cell fed with methanol. When tested in the DMFC, these Pt-Sn catalysts supported on VC and NT gave a better power density than a commercial one only at low current densities (Figure 1).

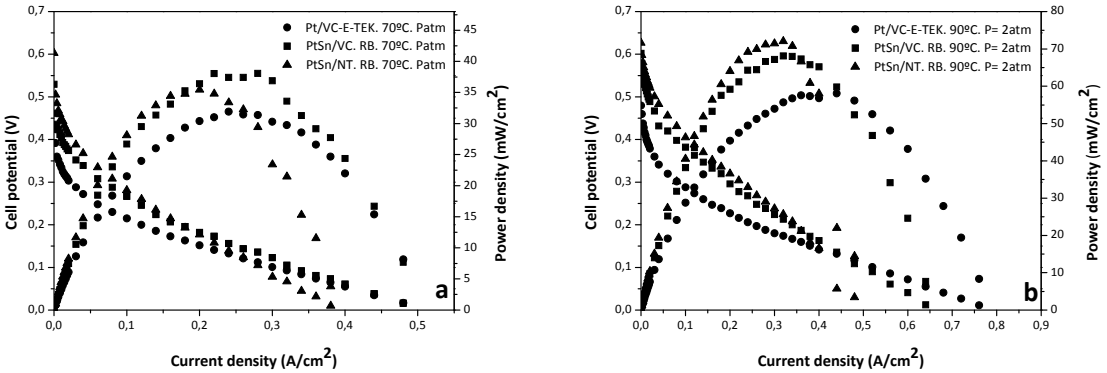

Fig. 1. Polarization and current density curves in a DMFC for Pt-Sn/VC. RB and Pt-Sn/NT. RB anodic catalysts compared to commercial Pt/VC (E-TEK 20 %wt) catalyst. As cathodic catalyst it was used a Pt/VC (E-TEK 30 %wt) one. a) 70 ºC, 1atm O_2 pressure, b) 90 ºC, 2 atm O_2 pressure. 2M methanol solution. The Pt loading was 1 mg cm^{-2} for both the anode and cathode.

Finally, Pt-Sn catalysts prepared on VC and NT were characterized by TEM showing that the presence of Sn modifies Pt during the deposition-reduction with $NaBH_4$, reducing the particle size and leading to a narrow particle size distribution than the corresponding monometallic catalysts supported on VC and NT.

4 Conclusions

The liquid phase deposition-reduction method with $NaBH_4$ (RB) to prepare bimetallic Pt-Sn catalysts gives a good Pt reducibility, and shows the presence of oxidized Sn species. A small fraction of the second metal (10-15%) stays in zerovalent state probably forming alloys.

For VC and NT as supports, it was found a low Pt-second metal electronic interaction but an important geometric effect that causes the promoting effect of Sn over Pt.

As Sn is found in the vicinity of small Pt particles, it produces an important promoting effect that makes CO electrochemical oxidation easier since it shifts the onset potential to lower values.

When tested in a DMFC, these Pt-Sn catalysts supported on VC and NT gave a better power density than a commercial one only at low current densities.

Acknowledgements

This work was made with the financial support of Universidad Nacional del Litoral (Project CAI+D), CONICET (Project 970/09) and ANPCYT (Project PICT 2097, PAE 36985).

References

[1] F. Colmati, E. Antolini, E. R. Gonzalez, *App. Catal B*. 73 (2007) 106.

[2] M. Carmo, M. Brandalise, A. Oliveira Neto, E. V. Spinacé, A. D. Taylor, M. Linardi, J. R. G. Poco, *Int. J. Hydrogen Energy*. 36 (2011) 14659.

III-PP24

The Use of Mixed SiW_nMo_{12-n} Heteropolyanions for Preparation of Ternary Transition Metal Sulfide Hydrotreating Catalysts

Kulikova M.[1], Pimerzin Al.[1], Mozhaev A.[1], Nikulshin P.[1*], Lamonier C.[2], Fournier M.[2], Lancelot C.[2], Blanchard P.[2], Payen E.[2]

1 - Samara State Technical University, Samara, Russia
2 - Université Lille1, UMR 8181 CNRS, UCCS, Villeneuve d'Ascq, France

* p.a.nikulshin@gmail.com

Keywords: hydrotreating, heteropolyanion, NiMoWS, HDS, HYD, HDN

1 Introduction

It is a world-wide tendency that more stringent environmental regulations require the production of higher quality fuels with lower sulfur concentration. The challenge is now to develop more active HDS catalysts for the ''deep refining'' of petroleum feedstocks to meet the new strict standards. Traditionally, bimetallic sulfide catalysts based on Mo or W, promoted by Ni or/and Co and supported on Al_2O_3 are used in the HDS processes. These catalysts exhibit high activity in removing sulfur from thiophene, benzothiophene, and some non-refractory dibenzothiophenes compounds. However, their activity is very low in removing sulfur from 4,6-dibenzothiophenes. Taking into account the specificity of the Mo and W based catalysts, the development of mixed Mo/W transition metal sulfides based catalysts can yield more efficient catalysts. The aim of the work was the preparation and characterization of alumina supported mixed SiW_nMo_{12-n} heteropolyanions (HPAs). For comparison purposes, catalysts based on separate $SiMo_{12}$HPA and SiW_{12}HPA were also prepared and studied.

2 Experimental

$H_4[SiMo_1W_{11}O_{40}]$ and $H_4[SiMo_3W_9O_{40}]$ HPAs were synthesized. Elemental composition and XRD determination confirmed their preparation. Catalysts with the same surface density of metals - d(Mo+W) expressed by $at.nm^{-2}$ - were synthesized by the incipient wetness method via impregnation of the supports with aqueous solutions containing the required amounts of $SiMo_{12}$HPA, SiW_{12}HPA, $SiW_{11}Mo_1$HPA, SiW_9Mo_3HPA, Ni carbonate and citric acid with molar ratio Ni/(W+Mo) = 0.5 and citric acid/Ni = 1.5/1 for promoted series. All impregnated solids were aged at room temperature overnight and subsequently air-dried at 110 ºC for 10 h without any further calcination. Chemical composition of the Ni promoted catalysts is shown in Table 1.

Table 1. Chemical composition of prepared catalysts

Catalyst	MoO_3, /wt. %	WO_3, /wt.%	NiO, /wt. %	d(Mo), /at.nm $^{-2}$	d(W), /at.nm $^{-2}$	d(Mo+W), /at.nm $^{-2}$
Ni-$SiMo_{12}$HPA/Al_2O_3	18.0	-	4.7	4.2	-	4.2
Ni-SiW_{12}HPA/Al_2O_3	-	26.2	4.2	-	4.2	4.2
Ni-$SiW_{11}Mo_1$HPA/Al_2O_3	1.4	24.2	4.3	0.4	3.9	4.2
Ni-SiW_9Mo_3HPA/Al_2O_3	4.2	20.1	4.3	1.1	3.2	4.2
Ni-$SiMo_{12}$HPA+SiW_{12}HPA/Al_2O_3 (a)	1.4	24.2	4.3	0.4	3.9	4.2
Ni-$SiMo_{12}$HPA+SiW_{12}HPA/Al_2O_3 (b)	4.2	20.1	4.3	1.1	3.2	4.2

[a] catalyst was prepared using co-impregnating solution of $SiMo_{12}$HPA and SiW_{12}HPA with molar W/Mo ratio 11/1,
[b] catalyst was prepared using co-impregnating solution of $SiMo_{12}$HPA and SiW_{12}HPA with molar W/Mo ratio 9/3.

The prepared samples were characterized by IR, Raman spectroscopies as well as by N_2 adsorption and H_2-TPR methods. The hydrotreatment activities were measured on a model feed (1000 ppm of sulfur, 3 wt. %. of naphthalene, 0.46 wt. % of quinoline and toluene as a solvent) in a bench-scale flow reactor under pressure of hydrogen. Before testing, the catalysts were activated by sulphidation. A mixture of DMDS (2 wt. % of **S**) and decane at 3.5 MPa was used in a stepwise procedure conducted over 10 h at 240 ºC and 8 h at 340 ºC. The conditions of the tests were the following: temperature 280^0C; pressure 3.0 MPa; feed space velocity 40 and 80 h^{-1}; a H_2 feedstock ratio 500 NL/L; catalysts volume 0.3 cm^3. The liquid product compositions of the samples collected every 0.5 h were determined using a GCMS-QP2010 Ultra. The HDS reaction was allowed to proceed for 10 h to evaluate the deactivation of the catalyst. To evaluate the catalytic performances, rate constants of the DBT HDS, naphthalene HYD and quinoline HDN reactions were determined [1]**.**

3 Results and discussion

Table 2 shows the hydrotreating results for the mixture of DBT, naphthalene and quinoline over the prepared samples.

Table 2. Performances of the catalysts in hydrotreating of DBT, naphthalene and quinoline

Catalyst	Conversion (%)						Rate constants ($\times 10^{-4}$ mol h^{-1} g^{-1})		
	DBT HDS		Naphthalene HYD		Quinoline HDN [a]				
	LHSV, h^{-1}						k_{HDS}	k_{HYD}	k_{HDN}
	40	80	40	80	40	80			
Ni-$SiMo_{12}HPA/Al_2O_3$	68	43	0.5	1	10	0.5	28	2	1
Ni-$SiW_{12}HPA/Al_2O_3$	65	44	14	10	3	1	27	12	2
Ni-$SiW_{11}Mo_1HPA/Al_2O_3$	78	53	14.2	7.9	3	4	37	19	3
Ni-SiW_9Mo_3HPA/Al_2O_3	72	48	8	10	2	2	31	9	2
Ni-$SiMo_{12}HPA$+$SiW_{12}HPA/Al_2O_3$	70	44	7	5	15	12	29	11	4
Ni-$SiMo_{12}HPA$+ $SiW_{12}HPA/Al_2O_3$	60	36	4	2	8.5	1.8	22	5	1

[a] conversion of quinoline and its N-containing products.

The conversion of all substrates during the tests varied from 0.5 to 78%. Conversions of reactants depending on the reaction type increased in the order HDN < HYD < HDS that correlated with the reactivity of the chosen compounds. It appeared that Ni-$SiW_{11}Mo_1HPA/Al_2O_3$ catalyst was the most active in all studied reactions. Ni-SiW_9Mo_3HPA/Al_2O_3 catalyst presented also interesting HDS activity but with lower hydrogenating property. Comparison of catalysts with same metal contents prepared with mixed $SiMo_nW_{12-n}HPAs$ and with the two separate HPAs ($SiMo_{12}HPA$ and $SiW_{12}HPA$) with the same metal content allowed us to conclude that the close interaction of both metal in the mixed HPA precursor is at the origin of the catalytic improvement.

4 Conclusions

It was found that the use of mixed $SiW_nMo_{12-n}HPAs$ as starting precursor yield high-efficient ternary transition metal sulfide HDT catalysts. This can originate from the close presence of both metals in the active sulfide phase as H_2-TPR results evidenced a modification of the metal oxides reduction. HRTEM are now in progress in order to evidence any change in the morphology of the sulfide active phase.

Acknowledgements

The work was supported by Russian Foundation for Basic Research (project 15-03-01845).

References

[1] P.A. Nikulshin, D.I. Ishutenko, A.A. Mozhaev, K.I. Maslakov, A.A. Pimerzin, *J. Catal.* 312 (2014) 152.

III-PP25

Production of Palladium Filters with Using of Diffusion Welding

Burkhanov G.S.[1], Roshan N.R.[1], Chistov E.M.[1], Fedorova E.S.[2], Lyushinskiy A.V.[2*]

1 - Russian Academy of Sciences, Metallurgy and Material Science Institute named after Baikov A.A., Moscow, Russia

2 - JSC «Ramenskoye Design Company», Moscow Region, Russia

* nilsvarka@yandex.ru

Keywords: diffusion, welding, palladium alloy foil, construction, materials, membrane element

1 Introduction

Due to rapid development of hydrogen power engineering and science intensive technologies there is a growing demand in use of high-purity hydrogen that puts a question about creation of effective, reliable and inexpensive industrial membrane elements and modules for its extraction and purification

2 Experimental/methodology

Comparative analysis of membrane elements designs showed that a construction of membrane filtering elements developed by us is the most perspective for industrial use. In our design flat membranes in the form of 50-150 mm diameter disks made out of palladium alloy foil of depth 50 – 10 micron. Due to membrane element flat design there is significant decrease of quantity of joints between membrane and constructions elements, it is important as joint leaktightness is one of the main problems of creating reliable membrane elements with increased operation life [1].

For extraction of high-purity hydrogen we have considered technology peculiarities of palladium filters production. Filter element consists of two walls, separating element and a branch pipe for removal of pure hydrogen. The wall represents a framework made of stainless steel with membrane made of palladium alloy. For fastening a membrane to framework were used technologies of soldering and welding by fusion, however such methods are labor-intensive and low-output.

Technology of the diffusion welding is the most appropriate method to obtain a joint of high quality which meets the above-mentioned requirements. Soldering technology requires a complex fitting; due to flowing of solder the last one may appear on the palladium foil and it can not be allowed; besides the whole process itself is hardly efficient. Fusion welding (argon-arc welding, laser welding and etc.) cannot be used by reason of appearing fragile phases of $FePd_3$ in welded joint, which reduce the strength of joint, due to joint melting of steel 12X18H10T and palladium.

By using an intermediate layer made of chrome-nickel alloy the quality will be slightly improved. Besides, fusion welding for this product is also hardly efficient process.

3 Results and discussion

Diffusion welding technology provides a full-strength and tight joint of membrane with framework and it is the most optimal. For this purpose an intermediate layer made of nickel is put between membrane and framework to exclude a formation of fragile phases in welding zone and to intensify a process of diffusion mass exchange between connected materials. Diffusion

welding optimal parameters: temperature T= 950^{o}C, welding pressure P= 2 kilogram-force /mm^{2}, release time - 30 min. Process is implemented in vacuum. Yield (hermetically sealed wall on helium) with welding of stainless steel framework (thickness 0.5 mm) and palladium alloy foil (thickness 30 micron) is up to 85%.

4 Conclusions

The use of diffusion welding in the manufacture of palladium filters allowed to make a vacuum-tight full-strength connection of stainless steel with foil of palladium alloys and manufacture helium sealed wall of the membrane element with prospective to its use in industrial scale to produce high-purity hydrogen need for which has been growing steadily.

Acknowledgements

This work was financially supported by the Russian Foundation for Basic Research, project nos. 13-08-12408.

References

[1] G. S. Burkhanov, N. B. Gorina, N. B. Kolchugina, N. R. Roshan, D. I. Slovetskii, and E. M. Chistov, Palladium-Based Alloy Membranes for Separation of High-Purity Hydrogen from Hydrogen-Containing Gas Mixtures, Platinum Metals Rev., 2011, 55,(1), 3-12

III-PP26

Mn-Based Water Oxidation Catalysts Supported on Tin Oxide

Massue C.[1*], Frei E.[1], Ranjan C.[2], Schlögl R.[1]

1 - Fritz-Haber-Institute of the Max-Planck-Society, Berlin, Germany
2 - MPI for Chemical Energy Conversion, Mülheim-an-der-Ruhr, Germany

* cmassue@fhi-berlin.mpg.de

Keywords: water splitting, electrocatalysis, sacrificial, agent, manganese

1 Introduction

The growing political will behind an energy transition towards renewable energy sources (RES) is highlighting the need for efficient and economically viable energy storage solutions. For hydrogen production through water splitting, good electrocatalysts are needed for the anodic oxygen evolution reaction (OER), where most of the overpotentials limiting the process efficiency occur. PEM-electrolyzers require acidic conditions and so far only expensive Ir-based OER-catalysts are stably active under these conditions. Thus, activity and stability enhancement of earth-abundant OER-catalysts like Mn or Fe would be a major step towards making water splitting a commercially relevant energy storage solution. In this regard, El-Monein et al. have reported a significant activity and stability enhancement in electrodeposited Mn/Sn-mixed oxides.[1] SnO_2-based anodes are known for their high corrosion resistance in acidic conditions[2], which make Mn/Sn mixed oxides promising candidates for low-cost and efficient OER-electrocatalysts.

We report a facile co-precipitation synthesis for Mn/Sn-precursors. After calcination, the precursors form active Mn-based OER-catalysts supported on tin oxide. OER-activities were assessed via detection of O_2-evolution in a standard sacrificial agent test. OER-tests using $(NH_4)_2Ce^{IV}(NO_3)_6$ as sacrificial agent have been proven to be suitable mimics of real water oxidation.[3] We show that Mn-specific OER-activity strongly depends on Mn/Sn-ratios and that with increasing tin content, the OER-activity could be preserved over increasing calcination temperatures. This indicates that the active OER-sites of Mn-oxides are preserved in the presence of tin. Also, temperature programmed reduction (TPR) experiments confirmed that low-temperature reduction features correlating with higher activity are preserved over calcination in tin-rich samples. As resistance against thermal decomposition is usually correlated with corrosion resistance, Mn/Sn-systems are promising candidates for water oxidation catalysis.

2 Experimental/methodology

Samples are produced via -co-precipitation at constant pH in an automated Labmax reactor system (Mettler-Toledo). A $KMnO_4/SnCl_4$-solution is constantly added to a Mn(II)-nitrate solution, while the pH is maintained neutral via the controlled addition of base. After washing and drying, samples are calcined at temperatures ranging from 300 to 700 °C. Characterization was performed using standard techniques available at FHI like XRD, BET, SEM-EDX, XRF and TG-MS. Sample were thoroughly studied by TPR experiments. OER-activity assessment was performed in a liquid batch reactor using cerium ammonium nitrate (CAN) as a sacrificial electron acceptor in solutions of pH below 1. The air-tight reactor was kept under constant Ar-stream and outlet gas were analysed via mass spectrometry in order to detect oxygen evolution. Initial rates were used as an element of comparison between the samples.

3 Results and discussion

The products of the co-precipitation synthesis are amorphous, highly hydrated Mn/Sn-hydroxides. TG-MS shows that upon calcination to 300 °C, samples loose up to 10% in mass due to water and hydroxyl group removal. At 300 and 400 °C, no XRD-patterns can be distinguished, except for broad features attributed to SnO_2. At 500/600 °C, for Mn-contents above 67%, clear crystallisation of an α-MnO_2 is observed via XRD. SEM-EDX shows the concomitant appearance of segregated Mn-rods, characteristic for the α-polymorph of MnO_2 (Fig. 2). Below 67% of Mn, the Mn-phase remains XRD-amorphous up to 700 °C.

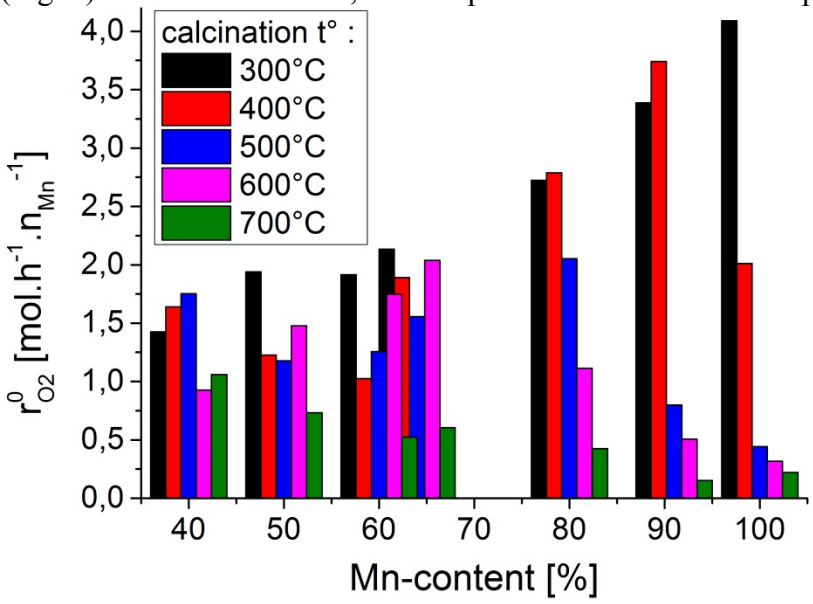

Fig. 1. Initial O_2-evolution rates for Mn/Sn OER-catalysts with varying Mn/Sn ratios and calcination temperatures with respect to the Mn-content

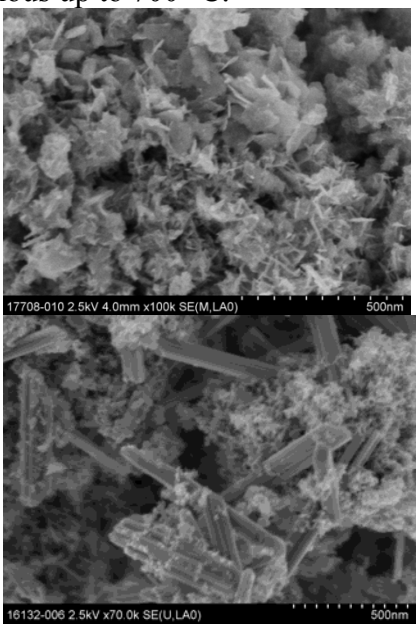

Fig. 2. SEM-image of 80%-MnO_x/SnO_2 calcined at 400°C (top) and 600°C (bottom)

Even though α-MnO_2 is sometimes reported as the most active MnO_2-polymorph, its appearance at 500 °C for samples with high Mn-content correlates with a sharp loss of activity (see Fig. 1). The XRD-amorphous Mn-phase obtained below 400 °C was identified as the active phase. Higher stability towards thermal decomposition is achieved by increasing Sn-contents. This behaviour correlates with low-temperature reduction profiles attributed to Mn-oxides in TPR and that are still observed after higher calcination temperatures in Sn-rich samples. First tests using repeated sacrificial agent injections indicate that the thermal resistance correlates with resilience against corrosion.

4 Conclusions

We conclude that for Sn-loadings above 33% there exists a synergetic effect of Mn- and Sn-oxides, that stabilizes the active OER-sites of an amorphous Mn-oxyhydroxide towards thermal decomposition. First tests suggest that this synergy correlates with resilience against corrosion. Thus Mn/Sn-based OER-catalysts are promising candidates for OER-electrocatalysis.

Acknowledgements

We would like to thank the Bundesministerium für Wirtschaft und Energie, which finances the Ekolyzer project in the framewok of which this research is being conducted. Further we would like to thank the technical staff at FHI for its kind help with sample characterization.

References

[1] A, E.-M.; N, K.; K, A.; K, H. *Mater Trans* **2005**, *46*, 309.
[2] Cachet, H.; Froment, M.; Zenia, F. *J. Electrochem. Soc.* **1996**, *143*, 442.
[3] Parent, A. R.; Crabtree, R. H.; Brudvig, G. W. *Chem. Soc. Rev.* **2013**, *42*, 2247.

III-PP27

Investigation of Co-Effect of 12-Tungstophosphoric Heteropolyacid, Nickel Citrate and Carbon-Coated Alumina in Preparation of Niw Catalysts for HDS, HYD and HDN Reactions

Minaev P.[1], Nikulshin P.[1*], Mozhaev A.[1], Maslakov K.[2], Kulikova M.[1], Pimerzin A.[1]

1 - Samara State Technical University, Samara, Russia
2 - Chemistry Department, M.V. Lomonosov Moscow State University, Moscow, Russia

* p.a.nikulshin@gmail.com

Keywords: hydroprocessing, heteropolyanion, NiWS, ULSD, HDS, HDN

1 Introduction

Production of clean fuels with less than 10 ppm sulphur content is one of the most important and claiming the attention problem in recent petroleum refinery. In years to come, hydrotreating will remain the largest scale process of petroleum refining, and its role will continue to grow. This trend requires more active catalysts, thus spurring intensive research both in industry and academia.

It is known that carbon as a support is reportedly preferable to alumina because of its high surface area and low acidity. However, carbon supports have a significant disadvantage: their low packing density, which limits their application in commercial hydrotreating catalyst formulations. The objective of this work was to investigate the co-effect of 12-tungstophosphoric heteropolyacid (HPA), nickel citrate and carbon-coated alumina (CCA) in preparation of NiW catalysts for HDS, HYD and HDN reactions. The HDS of dibenzothiophene (DBT), HYD of naphthalene and HDN of quinoline were the reactions selected to evaluate the catalytic properties of the materials. The results of this study should provide a better understanding the W based catalysts' structure and their HDS, HYD and HDN performances.

2 Experimental

A synthesis of CCA supports was carried out by the pyrolysis of a mixture of *iso*-propanol with glycerin on alumina in a bench-scale flow reactor at 600 ºC in N_2 atmosphere. The Ni_6-$PW_{12}S/C_x/Al_2O_3$ catalysts were prepared by the incipient wetness technique via impregnating the support with aqueous solutions containing the required amounts of $H_3PW_{12}O_{40}\times 3H_2O$, $NiCO_3$ and citric acid with molar ratio citric acid/Ni = 1.5/1. All impregnated solids were aged at room temperature overnight and subsequently air-dried at 110 ºC for 10 h without calcination. The contents of W and Ni in the catalysts were 15 and 3.9 wt. %, respectively.

The prepared samples were studied by N_2 adsorption, Raman spectroscopy, XRD, H_2-TPR, HRTEM and XPS methods. Catalysts were tested in a hydrotreating of model feed (1000 ppm of sulfur, 3 wt. %. of naphthalene, 0.46 wt. % of quinoline and toluene as a solvent) in a bench-scale flow reactor under pressure of hydrogen. The conditions of the tests were the following: temperature 280^0C; pressure 3.0 MPa; feed space velocity 40 and 80 h^{-1}; a hydrogen : feedstock ratio 500 NL/L; catalysts volume – 0.3 cm^3.

3 Results and discussion

Using the CCA as supports of the Ni_6-$PW_{12}S/C_x/Al_2O_3$ catalysts altered the morphology and structure of the NiWS active phase. With the rise of carbon content in the CCA up to 5 wt. %, reducible reactivity, sulphidation degree, average length and stacking number of $NiWS_2$

crystallites in the catalysts increased. Observed changes can be explained by weakening interaction between metal oxide species and carbon-coated support. Therefore, covering alumina surface by coke is beneficial to tuning the metal-support interactions, which causes easier reduction of tungsten. This property allows the CCA supported catalysts to be deeper sulphided compared with the Ni_6-$PW_{12}S/Al_2O_3$ reference.

The increase of carbon content led to the rise of the average slab length and the average stacking number of the $NiWS_2$ crystallites from 4.4 to 5.6 nm and from 1.7 to 2.3, respectively. It was shown that the increase of carbon content in the CCA allowed to essentially increase the Ni content in NiWS phase, that led to producing of high-effective catalysts. Full promotion of NiWS edges by nickel was achieved in the catalysts supported on CCA with carbon content equal 0.3 wt. % and more. Activities of the catalysts in DBT HDS, naphthalene HYD and quinoline HDN were essentially depended on the carbon content in the CCA-support (**Fig. 1**).

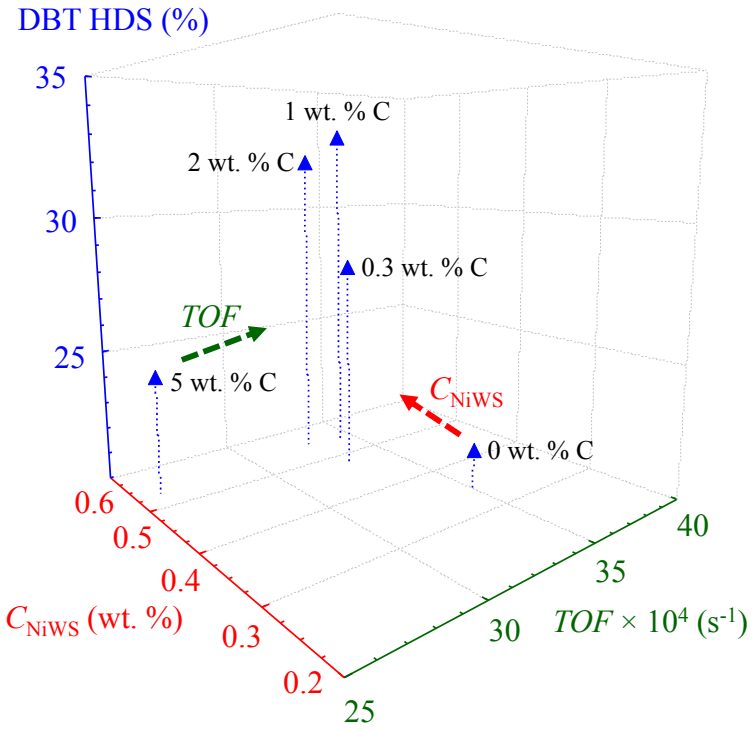

Fig. 1. 3D dependence of DBT conversion in HDS on effective Ni content in NiWS phase and TOF number for Ni_6-$PW_{12}S/C_x/Al_2O_3$ catalysts (legends at markers correspond to the carbon content in the CCA). Dotted lines show the ways of increasing DBT conversion.

Ni_6-$PW_{12}S/C_1/Al_2O_3$ catalyst showed maximal conversions of the substrates in studied reactions. This result achieved due to an optimal balance between TOF value of the active sites and their content.

4 Conclusions

Comparing the active phase morphology, the $(Ni/W)_{edge}$ ratio and catalytic properties of the Ni_6-$PW_{12}S/C_x/Al_2O_3$ catalysts it was found that TOF numbers in HDS, HYD and HDN linearly increased with the decrease of both the average length of the species of the active phase and the $(Ni/W)_{edge}$ ratio. Further improvements of supported NiW catalysts may be achieved by increasing the dispersion of the active phase species and optimizing the $(Ni/W)_{edge}$ ratio.

Acknowledgements

The work was supported by Ministry of education and science of Russian Federation (project 10.1516.2014/K) and Russian Foundation for Basic Research (project 15-03-01845).

III-PP29

Non-Noble Metal Based Carbon Electro-Catalysts for CO_2 Reduction to Fuels in Liquid and Gas Phase Conditions

Marepally B.C.*, Ampelli C., Papanikolaou G., Genovese C., Perathoner S., Centi G.

University of Messina, Dep. of Electronic Engineering, Industrial Chemistry and Engineering, Messina, Italy

* bmarepally@unime.it

Keywords: CO_2 reduction, carbon catalysts, non-noble metals, metal nano-particle (NP), renewable fuels

1 Introduction

The continuous rise in the global energy need, falling fossil fuel reserves and the drastic rise in CO_2 levels in the atmosphere creates a great opportunity towards the research for production of renewable fuels 0. This is high time that we take up this problem and develop a viable long term solution and start repairing the damage already caused to a balanced cycle. As a tiny contribution towards renewable carbon fuels, we report on the non-noble metal loaded carbon based electro-catalytic reduction of CO_2 for the production of liquid fuels under gas and liquid phase conditions 0. The experiments were performed in different homemade electro-catalytic (EC) cells for gas and liquid phases, designed on purpose to maximize the electro-catalytic area and reduce the volume of the aqueous solution. Initially, experiments were conducted using Cu thin film electrodes. Then, metal nano-particle (NP) based catalysts (using Fe, Cu, Co deposited on carbon-based substrates) were synthesized in order to improve the productivity and fine tune the selectivity in achieving longer chain hydrocarbon fuels. NMR analysis is used to determine the fuel productivities and also a comparative study with gas phase results was carried out.

2 Experimental

Preparation of metal-doped carbon layer

Carbon black (Vulcan XC-72) and commercial Carbon Nano-tubes (cup-stacked CNT from Pyrograph Inc, PR-24XT) were used as starting material for the synthesis of the electro-catalysts. Different types of oxygen functionalities were generated by suspending 1 g of carbon black/CNT in 50 mL HNO_3 (65 % Sigma Aldrich) and treated in reflux at 100 °C for 3 h, followed by rinsing to neutral pH, filtering, and drying overnight.

Then, metal NPs (Fe Cu and Co) were deposited on carbon black and CNTs by incipient wetness impregnation methodology using an ethanolic solution containing the appropriate metal precursor, $Fe(NO_3)_3{\cdot}9H_2O$, $Cu(NO_3)_2{\cdot}3H_2O$ and $Co(NO_3)_2{\cdot}6H_2O$, respectively. After drying at 60 °C for 24 h, the samples were annealed for 2 h at 350 °C. The total amount of metal loaded onto the carbon black and CNT surface was 10 wt. %. It is a good comparison to that of the metal loading used in the electro-catalysts for PEM fuel cells (usually 10-20 wt. %), which corresponds to a metal loading in the final catalyst of about 0.5 mg/cm^2.

Finally, an ethanol suspension of functionalized carbon black/CNT impregnated with metal NPs was deposited on a commercial gas diffusion layer (SIGRACET GDL 25BC, supplied by SGL Group) based on carbon fibres. To complete a working electrode, a Nafion membrane is attached with active phase (direct contact for Gas phase/ indirect for Liquid phase). The goal is to obtain C-based nanostructured electrode which can be assembled to form a multilayered composite with good proton mobility and electron conductivity and also, an improved fuel

production efficiency.

3 Results and discussion

The multi-electron processes underlying the CO_2 electrochemical reduction can lead to a large variety of products ranging from CO to various oxygenates such as alcohols, aldehydes and carboxylic acids by a complex multistep mechanism that is probably quite different comparing gas and liquid phase conditions.

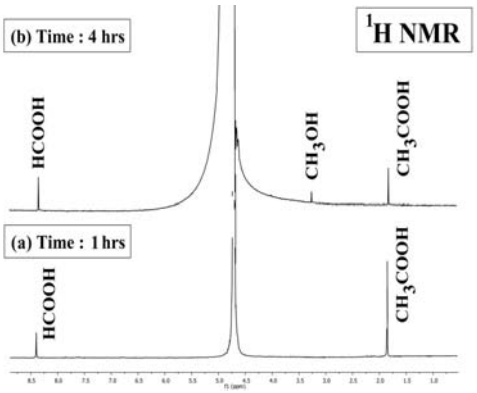

Fig. 1: NMR spectra for Fe/C showing products at times 1hr & 4 hr.

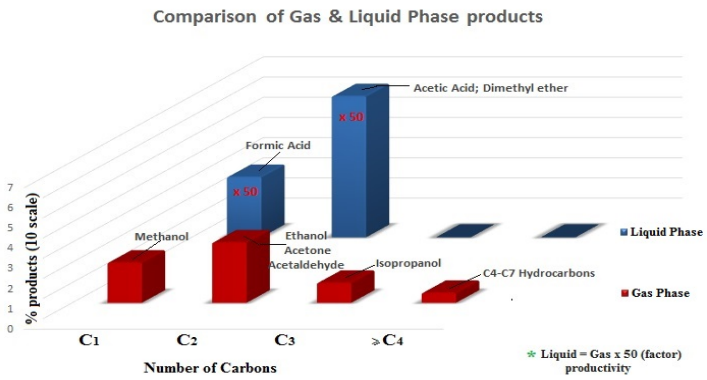

Fig. 2: Comparison of types of products in the gas & liquid phase CO_2 reduction

Fig. 1 shows the NMR spectra (using Varian NMR 500) of products for Fe based carbon catalyst under liquid phase conditions with molar concentrations of Acetic Acid and Formic Acid of $5.6*10^{-4}$ M and $6.3*10^{-4}$ M, respectively. Fig. 2 provides a comparative study on the various products formed under gas and liquid phase conditions. The ratio of the total productivities in liquid and gas phase conditions were measured to be in the range of (25-75):1, respectively for different non-noble metal based carbon electrodes experimented.

4 Conclusions

With the base motive of CO_2 reduction, the reactions performed under gas and liquid phase conditions cropped in the understanding of the improvements of the electro-catalytic activity for various non-noble metals on carbon. A notable point of interest, is that non-noble metals yielded in good fuel productivities in-place of the costly metals like platinum, gold etc. Much work needs to be done to cover all the non-noble metals and arrive at a conclusive statement, but from current work we can deduce that Fe based catalyst showed better activity than Cu followed by Co. The productivities were observed to be better in liquid phase but the gas phase yielded in better formation of oxygenates and higher chain hydrocarbons.

Acknowledgements

The authors would like to thank the co-funding through a SINCHEM grant i.e. a Joint Doctorate program Erasmus Mundus Action 1 (FPA 2013-0037) and University of Messina, Italy.

References

[1] C. Ampelli, S. Perathoner and G. Centi, CO_2 utilization: an enabling element to move to a resource and energy efficient chemical and fuel production, *Philosophical Transactions of the Royal Society A: Mathematical, Physical and Engg. Sc.*, (2015) - DOI: 10.1098/rsta.2014.0177, (in press)

[2] C. Genovese, C. Ampelli, S. Perathoner, G. Centi, Electrocatalytic conversion of CO_2 on carbon nanotube-based electrodes for producing solar fuels, *J. Catal.*, 308, 237-249, (2013)

III-PP30

Operando X-ray Absorption Spectroscopy Studies of Co_3O_4 and CeO_2-Co_3O_4 Catalysts during Preferential CO

Lukashuk L.[1*], Li H.[1], Yigit N.[1], Mcdermott E.[1], Carlson S.[2], Föttinger K.[1], Rupprechter G.[1]

1 - Institute of Materials Chemistry, Vienna University of Technology, Vienna, Austria
2 - MAX IV Laboratory, Lund University, Lund, Sweden

* liliana.lukashuk@tuwien.ac.at

Keywords: PROX, operando XAS, PEMFC, XANES reduction

1 Introduction

The hydrogen-fueled proton exchange membrane fuel cell (PEMFC) is an attractive pollution-free and energy-saving power source for portable and stationary applications. An efficient operation of PEMFC requires a high-purity H_2. Even ppm concentrations of CO severely poison the Pt anode catalyst, therefore, very deep H_2 purification for obtaining CO-free H_2 is crucial. In this regard, catalytic preferential CO oxidation (PROX), i.e., $CO+H_2+0.5O_2 \rightarrow CO_2+H_2$, is a key reaction for removing traces of CO from the H_2-rich stream.

Promising and frequently investigated catalysts for PROX are known to be supported noble metal (Pt, Rh, Ru, Ir) catalysts [1]. Due to the price and the limited availability of noble metals, increasing attention in recent years has been paid to noble-metal-free alternatives, i.e, transition metal oxides. Among these oxides especially cobalt oxide and cobalt oxide-cerium oxide have turned out to be perspective catalysts for PROX [2-4]. However, the current understanding of PROX over these catalysts is based only on the pre- and post-catalyst characterization. Open questions that often arise are: what is the electronic and geometric structure of Co and Ce during PROX, what are the active sites and reaction pathways. In this study, we aimed to shed a light on these questions and boost the understanding of PROX over cobalt based oxide catalysts.

2 Experimental/methodology

Operando X-ray absorption spectroscopy studies (XAS) at the Co K (7709 eV) and Ce L_3 (5723 eV) edges were carried out in transmission geometry at the l811 beamline at the Max-lab II in Lund, Sweden in the reaction cell designed by Max-lab II. Typically, 2.5 mg of the catalyst diluted with 10 mg of BN was loaded into the cell and pretreated in 20 %vol O_2 in He at 400 ^oC for 30 min (total flow 50 mL/min). The sample was then cooled to RT and purged with helium at RT for 15 min before the PROX reaction mixture of 1 %vol CO, 1%vol O_2, 50 %vol H_2 (total flow 50 mL/min) was introduced. The XAS spectra were recorded at RT and during subsequent heating to 350 ^oC. The reaction products were monitored with a mass spectrometer. In addition to PROX, CO- and H_2-tempearture programmed reduction experiments were performed. XAS data were analyzed using the IFEFFIT software package. The XAS experiments were complemented by in-depth catalyst characterization and catalytic tests in a flow reactor.

3 Results and discussion

The operando Co K edge X-ray absorption near-edge (XANES) spectra of Co_3O_4 catalyst during heating from RT to 350 ^oC in the PROX reaction mixture are shown in Fig. 1. (A). The analysis of XANES reveals that from RT to 250 ^oC the phase of the catalyst doesn't change in the PROX reaction mixture and that cobalt oxide is present as Co_3O_4. In the temperature region starting from around 70 ^oC, CO oxidation takes place; however, at around 200 ^oC water

production begins. Interestingly, methane production starts at 250 °C and increases with the increase of temperature, even though the bulk structure of the catalyst is Co_3O_4. However, the surface might have already a defective/reduced structure. Only at 300 °C Co_3O_4 is partially reduced to CoO and further heating to 350 °C induces complete reduction of cobalt oxide to Co metallic. The comparison of operando XANES spectra during PROX with CO-TPR and H_2-TPR XANES spectra demonstrates that the reduction temperatures of Co_3O_4 in CO/He and H_2/He atmospheres are lower than in the PROX reaction mixture. Reduction of cobalt oxide in H_2/He starts directly after 250 °C, and at 300 °C the catalyst is already metallic, whereas in CO/He atmosphere reduction starts at 250 °C but at 300 °C cobalt carbide is present in addition to the cobalt oxide phase. Moreover, CO-TPR XAS analysis of Co_3O_4 in combination with mass spectrometry analysis reveals three pathways of CO-TPR: CO removal of lattice oxygen, surface water-gas shift reaction and CO disproportionation. Delayed reduction of Co_3O_4 in the PROX reaction mixture in comparison to H_2/He or CO/He atmospheres might be because of the: 1) strong adsorption of CO and O_2 to the surface of Co_3O_4 (also evidenced by CO- and O_2-temperature programmed desorption) that prevents H_2 adsorption and reduction of Co_3O_4; 2) CO disproportionation on the catalyst surface and coverage by elementary carbon (also evidenced by in situ X-ray photoelectron spectroscopy) that hinders H_2 adsorption. Based on these results, we can exclude the redox Mars-van-Krevelen mechanism of PROX on the Co_3O_4.

Detailed analysis of operando XANES spectra at the Co K edge and Ce L_3 edge of CeO_2-Co_3O_4 during PROX, CO- and H_2-TPR demonstrates that the reduction temperatures of CeO_2-Co_3O_4 in CO/He and H_2/He atmospheres, likewise to Co_3O_4, are lower than in the PROX reaction mixture. When comparing operando XANES of CeO_2-Co_3O_4 to Co_3O_4 during PROX, an increase of the reduction temperature of cobalt oxide for CeO_2-Co_3O_4 was found as shown in Fig. 1 (B) which might explain the superior activity of CeO_2-Co_3O_4 in PROX.

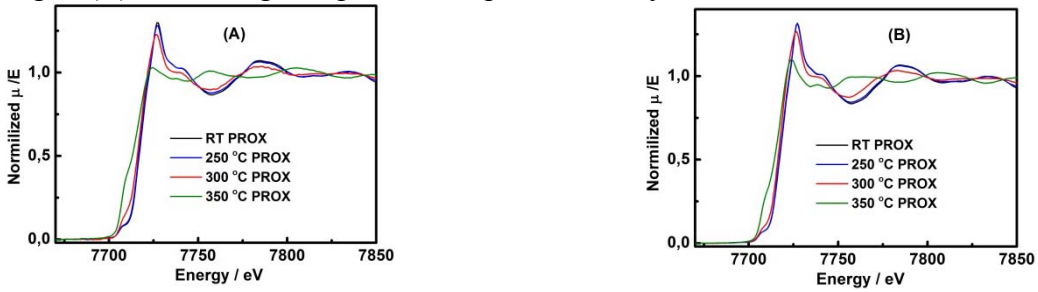

Fig. 1. Operando XANES spectra at the Co K-edge of Co_3O_4 (A) and CeO_2-Co_3O_4 (B) during PROX

4 Conclusions

Our operando XAS results demonstrate that the electronic structure of Co and Ce for Co_3O_4 and CeO_2-Co_3O_4 catalysts does not change in PROX when CO oxidation is the dominant reaction. The Mars-van-Krevelen mechanism for PROX on these catalysts is rather excluded.

Acknowledgements

This work was supported by the Austrian Science Funds (FWF) in the framework of the Doctoral School "Building Solids for Function" (Solids4Fun, project W1243). The authors acknowledge the beamtime granted at Max-lab II at the l811 beamline.

References

[1] K. Liu , A. Wang, T. Zhang, *ACS Catalysis* 2, 6 (2012) 1165.
[2] G. Marbán , I. López, T. Valdés-Solís, A. B. Fuertes, *International Journal of Hydrogen Energy* 33, 22 (2008) 6687.
[3] M. P. Woods, P. Gawade, B. Tan, U. S. Ozkan, *Applied Catalysis B: Environmental* 97,1-2 (2010) 28.
[4] P. Gawade, B. Bayram, A.-M. C. Alexander, U. S. Ozkan, *Applied Catalysis B: Environmental* 128, 11 (2012) 21.

III-PP31

Supported Gold Nanoparticles for Formic Acid Dehydrogenation

Choong C.[1], Soh M.[2], Ng J.[1], Poh C.K.[1], Chen L.[1,2*]

Institute of Chemical and Engineering Sciences, ASTAR , Singapore
Department of Materials Science and Engineering, National University of Singapore, Singapore

* chen_luwei@ices.a-star.edu.sg

Keywords: formic, acid, dehydrogenation, hydrogen, production, gold, catalysis

1 Introduction

Hydrogen can be efficiently used to generate electricity in fuel cells, releasing only water as by product. Traditionally, hydrogen is produced from natural gas or coal via intense CO_2 emission processes. Therefore, developing methods to produce hydrogen economically from renewable energy resources could lead to substantial reductions in fossil fuel consumption as well as global CO_2 emissions.

Recently, researchers have identified formic acid as one of the most promising materials for hydrogen storage because formic acid is a liquid that contains 4.4 wt.% of hydrogen with a volumetric capacity of 53.4 g/l at standard temperature and pressure [1]. CO-free H_2 can be produced via formic acid (HCOOH) dehydrogenation (Eqn. 1). It is a convenient way of producing H_2 for fuel cells designed for portable use. However, undesired reactions such as dehydration of formic acid (Eqn. 2) also occur during reaction.

$$HCOOH \rightarrow H_2 + CO_2 \quad (1)$$

$$HCOOH \rightarrow H_2O + CO \quad (2)$$

Trace amount of CO in H_2 will severely deactivate the Pt-based catalysts that are used as the anodes of fuel cells. The aim of this work is to develop new catalysts which are not only active for formic acid decomposition, but also extremely hydrogen selective. In particular, the relationship between the performance of Au/Al_2O_3 and the Au particle size was investigated.

2 Experimental

Au/Al_2O_3 (1 wt. %) was prepared via two methods; (1) sonochemical and (2) deposition-precipitation. In the sonochemical technique, $HAuCl_4.xH_2O$ and the capping reagent (lysine) were added to the catalyst support. The pH of the suspension was adjusted to 5-6 with NaOH solution. Freshly prepared reducing agent, $NaBH_4$, was introduced into the solution as it was being sonicated to facilitate the deposition of Au colloids on the support. After the reaction, the suspension was washed with deionised water for five times with a centrifuge. The suspension was then dried at 100°C and finally calcined at 250°C for 4 h. This sample is denoted as Au/Al_2O_3-S. In the deposition-precipitation method, aqueous solution of $HAuCl_4.xH_2O$ was added to suspension of Al_2O_3 at 80°C and a pH of 7, moderated by NaOH under constant stirring for 1 h. The sample was rinsed with deionised water and dried at 100°C and finally calcined at 600°C for 2 h. The catalyst is denoted as Au/Al_2O_3-DP.

The samples were characterized using X-ray diffraction (XRD), transmission electron microscopy (TEM), UV-vis and diffuse reflectance infrared fourier transform spectroscopy (DRIFTS) of formic acid. Dehydrogenation of formic acid (10 vol%) was performed in a fixed

bed reactor from 100°C to 300°C at atmospheric pressure. The catalysts were reduced at 250°C for 1 h prior to the reaction.

3 Results and discussion

The catalytic performances of the Au catalysts were evaluated at different temperatures for their activities in formic acid dehydrogenation. Fig. 1(a) shows that Au/Al_2O_3-S has a higher formic acid conversion than Au/Al_2O_3-DP. At 300°C, formic acid is fully converted over Au/Al_2O_3-S catalyst while the conversion for Au/Al_2O_3-DP is only 90.1%. The CO_2 selectivity of Au/Al_2O_3-S has a maximum value of 99.0% at 250°C, following which dehydration occurs, resulting in a decrease in CO_2 selectivity to 98.2% at 300°C (Fig. 1(b)). The CO_2 selectivity of 96.8% and 93.3% is smaller over Au/Al_2O_3-DP at 250°C and 300°C, respectively. These results indicate that Au/Al_2O_3-S has a more superior catalytic activity than Au/Al_2O_3-DP in formic acid dehydrogenation. Preliminarily, the higher catalytic activity of Au/Al_2O_3-S is likely to be related to the particle size of Au. TEM micrographs in Fig. 2 show the high resolution image of metal Au particles. The mean particle size of Au/Al_2O_3-S and Au/Al_2O_3-DP is 6 nm and 20 nm, respectively. Smaller Au particle size gives a higher activity in formic dehydrogenation, a finding in agreement with Ojeda et al. [2].

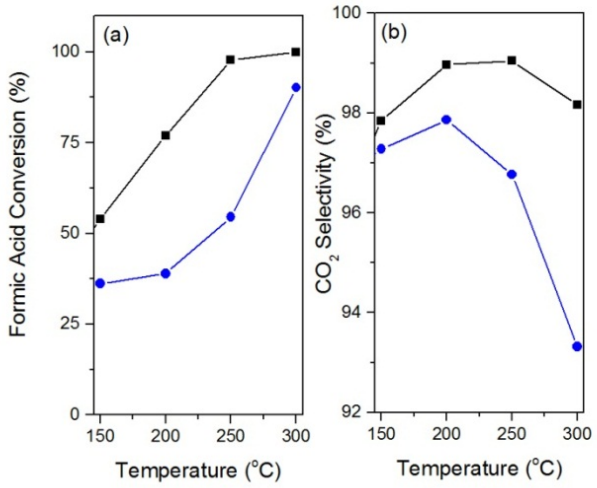

Fig. 1. Formic conversion (a) and CO_2 selectivity (b) over Au/Al_2O_3-S (■) and Au/Al_2O_3-DP (●).

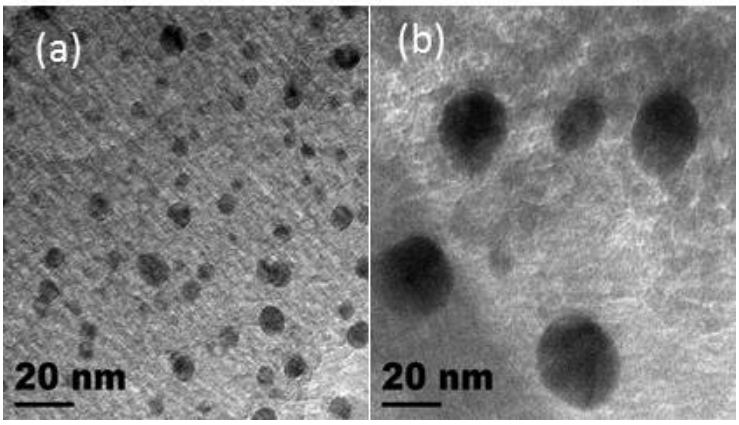

Fig. 2. TEM micrographs of (a) Au/Al_2O_3-S and (b) Au/Al_2O_3-DP.

4 Conclusions

Gold nanoparticles were deposited via sonochemical technique and deposition-precipitation method. TEM reveal that sonochemical method produces small gold nanoparticles. Catalyst

activity for formic acid dehyrogenation and selectivity to hydrogen is increasing with decreasing gold particle size.

Acknowledgements

We gratefully acknowledge the financial support from the Agency of Science, Technology and Research (A*STAR), Singapore.

References

[1] M. Grasemann, G. Laurenczy, *Energy Environ. Sci.* 5 (2012) 8171.
[2] M. Ojeda, E.Iglesia, *Angew. Chem. Int. Ed.* 121 (2009) 4894.

III-PP33

Iron(II) Clathrochelates as Homogeneous Electrocatalysts of Hydrogen Production at Low Ph

Dolganov A.V.*, Novikov V.V., Nelyubina Yu.V., Lebed E.G., Voloshin Ya.Z.

A.N.Nesmeyanov Institute of Organoelement Compounds of Russian Academy of Sciences, Moscow, Russia

* dolganov_sasha@mail.ru

Keywords: clathrochelates, iron complexes,eElectrocatalysis, hydrogen production

1 Introduction

Increasing energy demands of an ever-growing population calls for new energy sources, one of them being molecular hydrogen. To make hydrogen-based economics a reality, highly efficient and chemically stable catalysts for hydrogen production that do not contain precious platinum group metals need to be designed. For this purpose, we suggest to use iron(II) clathrochelate complexes with functionalizing pyridinyl substituents, which emerged as effective homogeneous electrocatalysts for hydrogen evolution at low pH; we expected the protonation of these complexes to increase their solubility in water due to the formation of salts (Scheme 1).

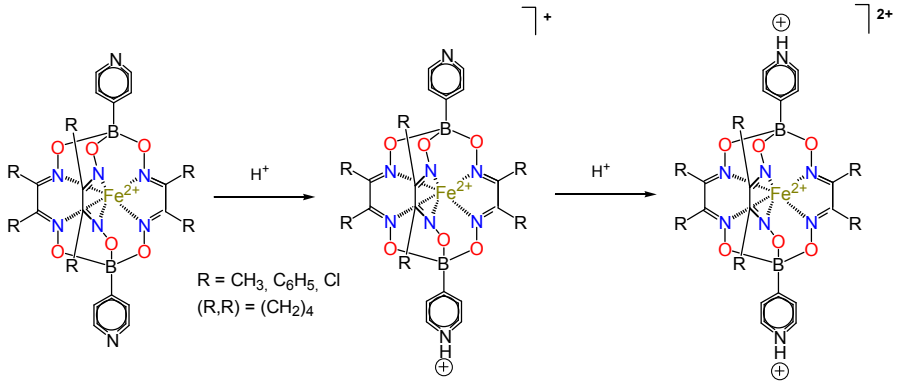

Scheme 1

2 Experimental

2.1. Cyclic voltammetry: cyclic voltammetry experiments were carried out in acetonitrile solutions with 0.1 M $((n\text{-}C_4H_9)4N)BF_4$ as a supporting electrolyte using a model Parstat 2273 (Prinston Applied Research, USA) potentiostat with a conventional one-compartment three-electrode cell (10 ml of solution) at a scan rate 200 mV s^{-1}. All solutions were thoroughly deaerated by passing argon through them before the cyclic voltammetry experiments and above them during the measurements. Glassy carbon electrode (active surface area of 0.125 cm^2), platinum electrode and standard $Ag/AgCl/KCl_{aq}$. electrode were used as working, counter and reference electrodes; those were thoroughly polished and rinsed before each measurement.

2.2. Controlled-potential electrolysis: 50 mM acetonitrile solutions of methanesulfonic acid, $HBF_4 \cdot O(C_2H_5)_2$ and triethylammonium hydrochloride with 0.1 M $((n\text{-}C_4H_9)_4N)BF_4$ were electrolyzed in the presence of iron(II) clathrochelates for one hour. Molecular hydrogen production was confirmed by gas chromatography; injections (250 μL) were performed *via* a sampling loop, helium flow rate was 40 ml min^{-1}, and retention time of gaseous H_2 2.48 min.

3 Results and discussion

Electrochemical characteristics of these iron(II) clathrochelates are summarized in Table 1.

All peaks observed in their cyclic voltammograms are characteristic of diffusion-controlled current processes. In the cathodic range of these cyclic voltammograms, only one one-electron quasi-reversible wave is observed, which was assigned to redox-processes $Fe^{2+/+}$.

Table 1. Oxidation and reduction potentials (mV) and characteristics of electrochemical processes for the iron(II) clathrochelates.

Complexes	Oxidation, E_{ox}			Reduction, E_{red}			k_{obs}
	E_a	E_c	ΔE	E_c	E_a	ΔE	
$FeNx_3(B4\text{-}Py)_2$	1370	1280	90	– 1080	–870	210	953
$FeDm_3(B4\text{-}Py)_2$	1450	1360	90	– 1030	– 900	130	874
$FeBd_3(B4\text{-}Py)_2$	1480	1400	80	–1050	– 800	250	658
$Fe(Cl_2Gm)_3(B4\text{-}Py)_2$	1910	1800	110	– 450	– 380	70	1900

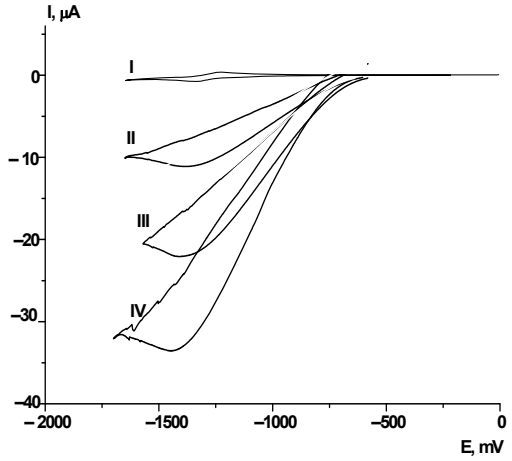

Fig. 1. Cyclic voltammogram for 0.5 mM acetonitrile solutions of $FeNx3(B4\text{-}Py)_2$ on a glassy carbon electrode in the absence and (top–bottom) in the presence of 5, 10, 15 and 25 mM of CF_3COOH.

The complexes obtained efficiently electrocatalyze hydrogen evolution (Fig. 1) from an acid solution in acetonitrile as well as from aqueous buffers with low pH (1 – 4). NMR spectroscopy data confirmed that protonation of both the pyridine moieties occurred, thus giving protonated species that were stable in these conditions. Titration of an acetonitrile solution of a clathrochelate with an acid resulted in a significant increase of the current assigned to the $Fe^{2+/+}$ pair, while the peak of the reverse process vanished. Kinetic parameters and overall efficiency of the catalytic process depended greatly on the nature of ribbed substituents in chelate fragments of these clathrochelates. Based on the dependence of the rate of the electrocatalytic process $2H^+/H_2$ on the pH value of the aqueous solution, a limiting step was identified and a catalytic mechanism elucidated experimentally. All proton reduction reactions were first order in the catalyst's concentration and second order in the acid's concentration; for all of them, rate constants and activation energies have been obtained.

4 Conclusions

Pyridinyl-functionilized iron(II) clathrochelates emerge as first homogeneous electrocatalysts of hydrogen evolution at low pH; varying their ribbed substituents allows designing electrocatalysts with better performance and stability in harsh near-industrial conditions.

Acknowledgements

This work was financially supported by RFBR (grants 13-03-00570, 14-29-04063) and Council of the President of the Russian Federation (grant SP-1292.2013.1).

III-PP34

Pt, Rh and Pt-Rh-Deposited on $MgAl_2O_4$ Spinels Catalysts for Dry and Steam Reforming of CH_4

Garcilaso V., Centeno M.A.*, Laguna O.H., Odriozola J.A.

Instituto de Ciencia de Materiales de Sevilla, Centro Mixto CSIC-Universidad de Sevilla, Sevilla, Spain

* centeno@icmse.csic.es

Keywords: steam reforming, dry reforming, platinum, rhodium, bimetallic system, $MgAl_2O_4$ spinel

1 Introduction

Among the different alternatives for the searching of renewable energy sources, the use of biogas results interesting because it is produced by the anaerobic combustion of biomass [1]. This CH_4 source may be employed for the production of heat or for the generation of syngas throughout reforming processes. However this non-conventional gas presents a high level of CO_2 that reduces its energetic density and influences adversely the yield of the process and the catalysts efficiency. Consequently, specific catalysts must be developed, adapting those used in the conventional reforming of CH_4, in order to produce active and stable solids able to work under high levels of CO_2 and H_2O.

Since thermal stability is one of the main concerns of reforming catalysts, alumina is one of the most used supports. However this solid has an acidic character that promotes deactivation by coke formation. For that reason the doping of alumina with basic species is an interesting strategy for avoiding this effect. Concerning the active phase, the use of noble metals results an expensive alternative. Nevertheless they may allow to reduce the temperature for obtaining the maximum CH_4 conversion, which would represent energy savings that justify their employment[2].

In the present work, a $MgAl_2O_4$ mixed oxide was obtained for combining the thermal stability of alumina and the basic properties of MgO [3]. This material was used as support for the synthesis of Pt, Rh and Pt-Rh catalysts those being tested under specific dry and steam reforming conditions. The principal aim of this study is to analyse, from a structural point of view, the interaction of the $MgAl_2O_4$ support with the different active phases (Pt, Rh and the bimetallic system Pt-Rh), and to evaluate the influence of such interaction in the catalytic performance of the prepared solids during both, the dry and steam reforming reactions.

2 Experimental

For the synthesis of the $MgAl_2O_4$ support, a commercial alumina (Sasol®) was grounded and then mixed with an ethanolic solution of $Mg(NO_3)_2$. The mixture was continuously stirred and heated under vacuum until the obtaining of a dried solid. This was divided in different portions that were treated under different calcination programs: MgAl12 (900ºC, 12h), MgAl24 (900ºC, 24h), MgAl36 (900ºC, 36h) and MgAl48 (900ºC, 48h). The noble metals, Pt and Rh were deposited on the prepared solids by conventional impregnation. The nominal metal loading was fixed to 2wt. %. In the case of bimetallic system, Pt was impregnated before Rh, for obtaining a 1:1 molar ratio.

Characterization of the supports and catalysts were carried out by means of XRD, N_2 physisorption, XRF, TPR-H_2, SEM and Raman Spectroscopy. The catalytic tests were performed in PID Eng&Tech Microactivity equipment using a *Hastelloy C*® tubular reactor under atmospheric pressure at 750 ºC during 6h. The products were analyzed with a micro gas chromatograph equipped with Molsieve 5A and PoraPlot Q columns, and a TCD detector. Catalyst loading of 50mg, $100<\phi<200\mu m$, diluted in quartz is activated under H_2 atmosphere before the reforming reaction sequence

(steam and dry reforming reaction).

3 Results and discussion

Concerning the obtained supports, the XRD analysis showed that higher the calcination temperature and/or time, lower the segregation of MgO and higher the degree of $MgAl_2O_4$ formation. However, under these conditions, a strong decrease of the specific area was detected. As for the catalysts, the most interesting characterization result is the easier reducibility shown by the bimetallic system, as evidenced by the lower temperature of the TPR reduction process observed in such sample compared to those of the single metal systems.

The bimetallic solid exhibited the highest catalytic activity during both dry and steam reforming reactions (Figure 1A). However, the PtMgAl24 system presented a higher efficiency of CH_4 converted per mol of noble metal (Figure 1B). This is associated to the reduction of the MgO segregation and the higher Pt dispersion evidenced in this sample. Regarding the H_2/CO molar ratio, values below 1 were obtained for all systems during the dry reforming. However, for the steam reforming, H_2/CO molar ratios above 4 were attained being especially higher for the single noble metal catalysts calcined during 12 h.

Considering that for the Fisher-Tropsch synthesis the reformate gases must present a H_2/CO ratio close to 2, our catalytic results demonstrated that, under the studied conditions and using a single reforming process (wet or dry), our solids do not fulfil such requirement. Nevertheless, by means of simulation studies using the Aspen Plus® program, it was deduced that combining dry and steam reforming conditions, such H_2/CO ratio is achievable. The searching for the adequate experimental reaction conditions is currently under realisation.

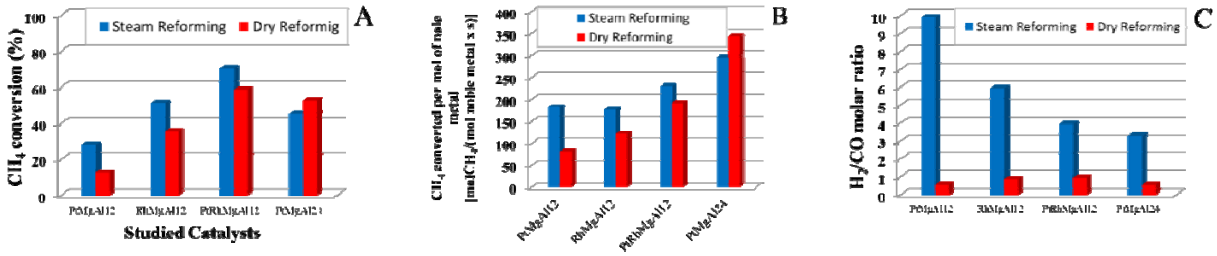

Fig. 1. Catalytic activity results during the dry and steam reforming: A) CH_4 conversion; B) Converted CH_4 per mol of noble metal; C) Obtained H_2/CO molar ratio

4 Conclusions

The time and temperature of calcination of the $MgAl_2O_4$ strongly influences the interaction of the cations and the segregation of MgO, affecting the catalytic activity and the metallic dispersion of the noble metal catalysts prepared. The systems with Pt are the most active ones, especially under steam reforming conditions. Simulation studies have demonstrated that combining steam-reforming and dry-reforming conditions allows to obtain a H_2/CO ratio of 2, and may be an adequate strategy in order to generate the required conditions for the syngas production after the reforming units.

References

[1] H.-S. Roh, K.Y. Koo, U.D. Joshi, W.L. Yoon, Catal. Letters 125 (2008) 283.
[2] S.D. Angeli, G. Monteleone, A. Giaconia, A. a. Lemonidou, Int. J. Hydrogen Energy 39 (2014) 1979.
[3] E.L. Foletto, R.W. Alves, S.L. Jahn, J. Power Sources 161 (2006) 531.

III-PP35

Hydrogen Storage System Based on the Catalytic Hydrogenation-Dehydrogenation Reactions of Aromatic Compounds

Bogdan V.I.[1,2*], Kalenchuk A.N.[2,1], Kustov L.M.[1,2]

1 - Zelinsky Institute of Organic Chemistry, Russian Academy of Sciences, Moscow, Russia
2 - Faculty of Chemistry, Moscow State University, Moscow, Russia

* vibogdan@gmail.com

Keywords: dehydrogenation, hydrogen storage, perhydro-m-terphenyl, m-terphenyl

1 Introduction

Continuous improvement of environmental standards leads to a significant increase of the interest in alternative energy sources, including hydrogen fuel cells. For their effective use, including transport, it is necessary to solve a number of technical problems associated with the rapid release and feeding of pure hydrogen to the fuel cell. On the other hand, highly explosive hydrogen requires the development of new effective and safe hydrogen storage systems. A radically new approach to this problem is based on employing organic chemical systems, i.e., organic compounds that possess a fairly high hydrogen capacity (6.0–8.0 wt %) and can operate in the reversible hydrogenation–dehydrogenation mode [1]. Hydrogen storage in the structure of chemical compounds makes such systems explosion-proof.

2 Experimental/methodology

Evaluation of the performance of catalytic composite systems was carried out by comparing the rate of hydrogen evolution from hydrogenated condensed aromatic chemical hydrides (decalin, bicyclohexyl, perhydroterphenyl) in the dehydrogenation process. Both commercial and prepared by hydrogenation substrates were used. Catalytic tests have been carried out at temperatures 280–340°C and flow rates 0,5-3 h^{-1} in a flow reactor and the optimal conditions for the dehydrogenation reaction were determined, including thermodynamic calculations.

Completeness of hydrogen saturation of the catalytic composite system for storage was evaluated by the hydrogenation reaction. Hydrogenation was carried out at a temperature of 180°C and pressure 70 atm in a laboratory high pressure autoclave PARR-300 by stirring the reaction mass. The catalytic activity was measured for commercial and prepared catalysts consisting of active components (Pt, Pd, Ni, Cr) and a support (alumina, silica gel, carbon) in varied proportions. The catalysts were prepared via an impregnation procedure based on the deposition of a metal precursor from an aqueous solution of a chloride complex followed by the reduction of the precursor with hydrogen.

3 Results and discussion (font style: Times New Roman bold 12pt)

The largest amount of hydrogen released as a result of perhydro-*m*-terphenyl dehydrogenation to *m*-terphenyl is observed with the 3%Pt/Sibunit catalyst at 320°C and 1 h^{-1}. Increasing or decreasing the amount of the active component supported on carbon leads to a decrease in the amount of hydrogen obtained in perhydro-*m*-terphenyl dehydrogenation. The maximum selectivity and conversion toward complete dehydrogenation in this case is 95%. The selectivity and conversion of *m*-terphenyl hydrogenation to perhydro-*m*-terphenyl with the 3%Pt/Sibunit catalyst reached 99%. Figures 1 and 2 show the curves of dehydrogenation of perhydro-*m*-terphenyl and hydrogenation of *m*-terphenyl on different catalysts: 1 - 10%Pt/C

(carbon BAU), 2 - 5%Pt/C (Sibunit), 3 - 3%Pt/C (Sibunit), 4 – 0.12%Pd-3.8%Ni-4.3%Cr/γ-Al_2O_3, 5 - 5%Pt/γ-Al_2O_3, 6 – 2.5%Pd/γ-Al_2O_3.

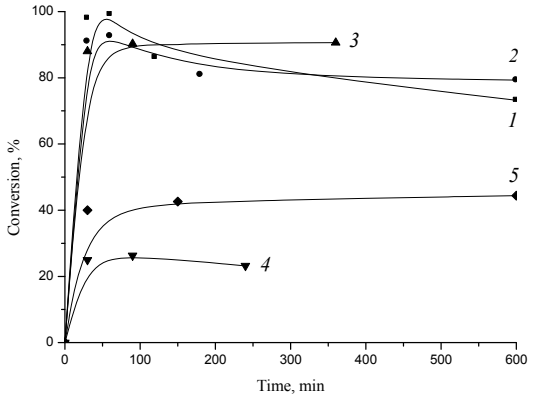

Fig. 1. Changes of the conversion on the time on stream in the dehydrogenation of perhydro-*m*-terphenyl (T = 320°C, V_L = 1 h^{-1}, P = 1 atm)

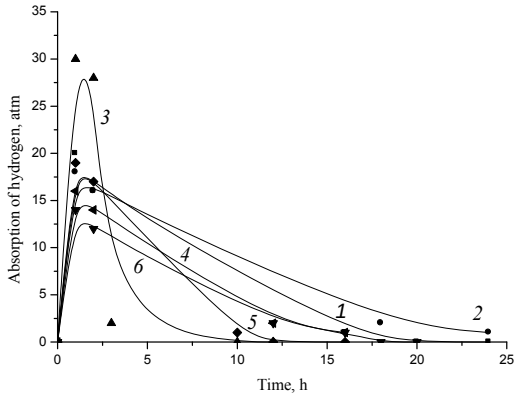

Fig. 2. Changes in the absorption of hydrogen on the time on stream in the hydrogenation of *m*-terphenyl (T = 180°C, P = 70 atm)

4 Conclusions

The experimental data shows that the use of the *m*-isomer of perhydroterphenyl as a substrate for the catalytic composite system allows us to achieve the capacity for hydrogen 6.5-7.3 wt.%. As a result of research, high conversion rates and volumes of generated hydrogen in the catalytic composite systems were obtained using some of condensed aromatic compounds in the flow reactor. The high purity of hydrogen was proved by chromatography in the dehydrogenation reaction [2].

References

[1] A. Tarasov, O. Kirichenko, N. Tolkatchev, A. Kalenchuk, V. Bogdan, L. Kustov, *Russian Journal of Physical Chemistry A*. 84 (2010) 1122.

[2] A. Kalenchuk, V. Bogdan, L. Kustov, *Russian Journal of Physical Chemistry A*. 89 (2015) 16.

III-PP36

Oxidative Coupling of Methane over Li Doped MgO on a Monolithic Structure

Nadjafi M., Yıldırım R.*

Department of Chemical Engineering, Boğaziçi University, Istanbul, Turkey

* yildirra@boun.edu.tr

Keywords: OCM, methane coupling, Li doped, MgO, monolith

1 Introduction

Abundant resources of natural gas, which is mainly methane, have motivated researchers to produce valuable products from this simple hydrocarbon. The aim of such conversion is to ease its transport and increase its value as a petrochemical feed. Oxidative coupling of methane (Eq. 1), which satisfies this aim in a single step, is a reaction of great interest [1].

$$CH_4+O_2 \longrightarrow C_2H_4 \text{ or } C_2H_6 + H_2O \quad (1)$$

However, this reaction has still not been put into practical application due to some drawbacks. Intensive researches have been done, and Li doped MgO showed higher performance than most other materials. However, all catalyst suffered from severe and drastic deactivation, especially at the beginning of the testing experiments [2]. Our aim is to investigate the effect of a monolithic structure on Li doped MgO prepared from different precursors and different preparation techniques. We also are investigating the effect of temperature and methane to oxygen ratio on both monolith and particulate catalyst. The best performing catalysts were also characterized using the methods like SEM, XRD and EDX.

2 Experimental/methodology

0.5wt% Li/MgO catalyst is used to compare the particulate and monolithic structure on OCM. Furthermore, temperature and methane to oxygen ratio effect on OCM is evaluated for both particulate and monolith. Finally, MgO is doped with different precursors of Li to see their effect on both structures. Each time, we put 200 mg of catalyst in particulate form or coated on monolith in a tubular quartz reactor with inner diameter of 10mm. In each run, after 30 minutes of reaching desired temperature, the data is taken using Shimadzu GC equipped with a thermal conductivity detector. Total flow is adjusted to 120 ml/min to have a real plug flow condition. N_2 is used as internal standard and carbon balance was always higher than 96%. Crushed and sieved quartz chips are used at top and bottom of the reactor to do preheating, mixing, and preventing undesired reactions [3].

Particulate catalyst preparation: Different precursors of Li (Li_2CO_3, Li_2O, $LiCH_3COO$, and $LiNO_3$) were doped on MgO using mixed milled and wet impregnation method. Afterward the prepared samples were calcinated at 400°C for 3hr. 0.5wt% catalyst then were crushed and sieved, only particles 0.63-0.18mm were used to reduce internal diffusion effect.

Monolith catalyst preparation: MgO is wash coated on monolith during immersing of monolith in MgO solution and drying it in a microwave furnace. When the desired amount of MgO is coated, Li is dopped. Dissolved lithium precursor (Li_2CO_3, Li_2O, $LiCH_3COO$, and $LiNO_3$) in sufficient amount of deionized water then is doped on wash-coated monolith by rolling it inside the solution or using wet impregnation technique. Afterward the prepared monoliths were calcinated at 400°C for 3hr. 0.5wt% Li/MgO catalyst is now coated on monolith and can be compared with particulate one.

3 Results and discussion

Figure 1 shows a case study of on monolith catalyst. Monolith catalyst is prepared using mixed milled method and $LiNO_3$ precursor. The methane conversion increased with increasing temperature while the C2 selectivity increased first, and then it decreased after 800 ^oC. However the C2 yield always increased within the temperature range studied because the increase in conversion was more dominant than the decrease in selectivity at higher temperatures.

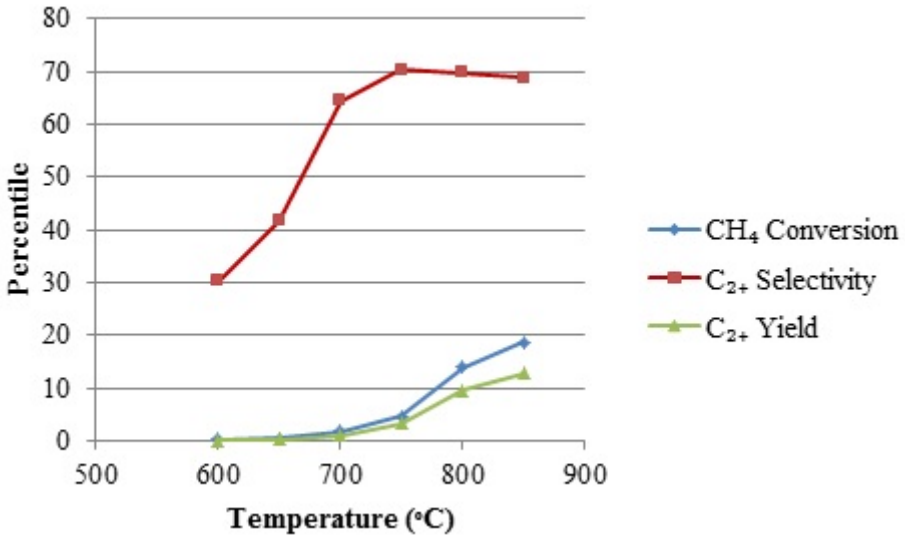

Figure 1. Case study of monolith catalyst

4 Conclusions

Our experiments show that oxidative coupling of methane can be performed over the monolithic structure, which are better for providing void volume for CH_3 combination reactions, and for better flow and heat management properties compared to particulate catalyst.

Acknowledgements

The financial support was provided by The Scientific and Technological Council of Turkey (TUBITAK) through Project 112M714.

References

[1] Arndt S, Simon U, Heitz S, Berthold A, Beck B, Görke O, et al. Li-doped MgO From Different Preparative Routes for the Oxidative Coupling of Methane. Top Catal. 2011;54(16-18):1266-85

[2] Arndt S, Laugel G, Levchenko S, Horn R, Baerns M, Scheffler M, et al. A Critical Assessment of Li/MgO-Based Catalysts for the Oxidative Coupling of Methane. Catalysis Reviews. 2011;53(4):424-514

[3] Düşova Y. an Experimental Study on Oxidative Coupling of Methane Over $Mn/Na_2WO_4/SiO_2$ Catalyst. Turkey: Boğaziçi University; 2014.

III-PP37

Ceria-Supported Cobalt Oxide Catalysts: Synthesis, Characterization and Catalytic Combustion of Producer Gas

Mungse P.[1], Saravanan G.[1], Rayalu S.[1], Dasappa S.[2], Labhasetwar N.[1*]

1 - CSIR-NEERI, Nagpur, India
2 - Indian Institute of Science Bangalore, Bangalore, India

* nk_labhsetwar@neeri.res.in

Keywords: producer gas, combustion catalyst, supported catalyst, Ce/CeO_2

1 Introduction

Producer gas is a mixture of both flammable (CO, H_2, CH_4) and non-flammable (N_2, CO_2) gases, which is formed by the gasification of carbonaceous substances including biomass. The typical stoichiometric composition of producer gas is shown in the **Fig. 1a**. This can be used as a fuel at large-scale industrial furnaces as well as gasifiers, with its relatively lower heating value than that of other gaseous fuels. Although producer gas possesses the potential as fuel, however, for certain technical reasons, it has not been explored much to meet the present energy demand. With depleting energy resources and increasing energy demand, producer gas presents a potential option to be used as a decentralized source of energy. Considering higher CO and hydrogen contents as well as presence of methane, the mixture may lead to partially incomplete combustion under the various conditions of gasifier operation. This may result in fuel slip with potential hazards from CO and hydrogen slips. We therefore, propose for the use of combustion catalyst for efficient and complete combustion of producer gas with concomitant control of CO and hydrogen slip. Only a very few studies have been explored on producer gas combustion, using heterogeneous catalysts, for instance zeolites, metal oxides and supported metal oxides [1], however, deactivation of active catalytic sites, less robustness, and poor thermal resistance were the limitations of these catalysts. Therefore, the materials with a high structural stability with improved redox properties may be alternatives to avoid these limitations. In this work, the catalytic combustion of the producer gas using conventional catalyst (e.g. Pt/Al_2O_3) and a non-noble metal catalyst (e.g. Co/CeO_2) was examined. The effect of temperature, flow rate etc. on catalytic combustion efficiency of the producer gas combustion reaction was studied.

2 Experimental/methodology

Ceria was prepared by using chitosan template method. Incipient wetness impregnation method was used to prepare the Co-incorporated catalysts. Stoichiometric amount of $Co(NO_3).6H_2O$ was impregnated on mesoporous ceria for the preparation of 10 wt. % Co/CeO_2. The synthesized catalysts were characterised using powder X-ray diffraction (*p*XRD), scanning electron microscopy (SEM). The redox properties of the synthesized catalysts were examined by hydrogen temperature programmed reduction (H_2-TPR). The catalytic combustion of producer gas was examined using fix bed laboratory evaluation assembly equipped with gas chromatograph, temperature controlled furnace and mass flow controllers as shown in **Fig. 1b**.

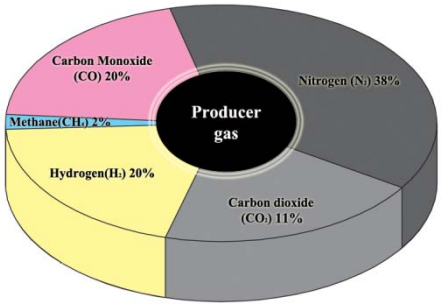

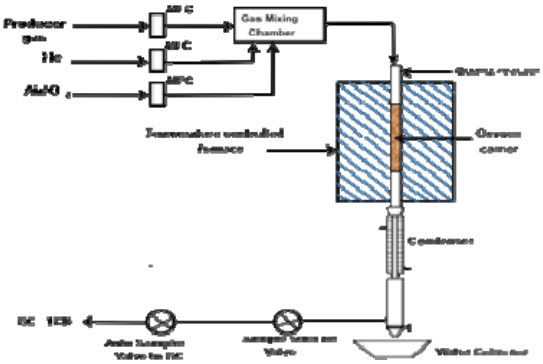

Fig.1a **Fig.1b**

Fig. 1. (a) Producer gas composition used and (b) schematic representation of experimental setup used for catalytic evaluations.

3 Results and discussion

The catalytic combustion activity of the producer gas using Co/CeO_2 is shown in **Fig. 2.** The initial concentration of CO (20%) and CH_4 (2%) of the producer gas decreases with the increase of temperature and showed 100% combustion efficiency at 300 °C and 700 °C, respectively. The combustion of CO and CH_4 produced CO_2 and H_2O and the mass balance of CO_2-formation is consistent with the stoichiometric combustion of producer gas (CO and CH_4), indicating that Co/CeO_2 can combust the producer gas completely. The TPR analysis of catalyst shows redox properties of catalyst, possibly responsible for the high catalytic activity.

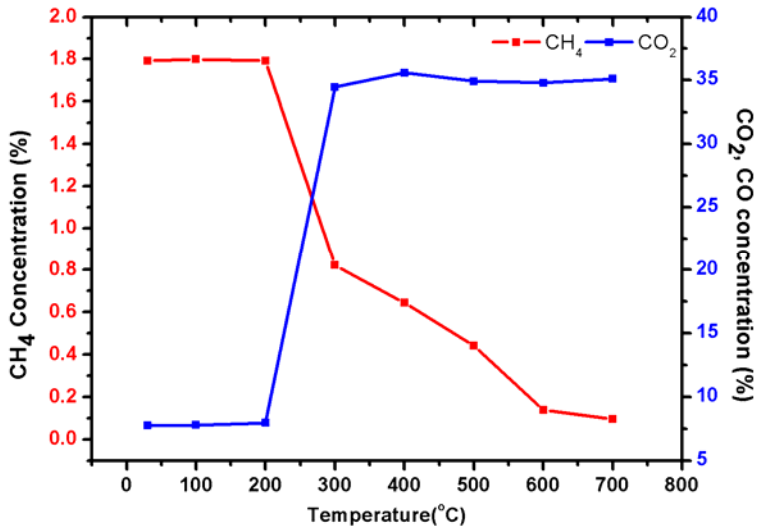

Fig. 2. Concentration of CH_4 and CO_2 on Co/CeO_2 catalyst as a function of temperature.

4 Conclusion

The catalytic combustion of producer gas has not been much explored. Since the use of producer gas as a fuel is expected to find more interest in future, it's important to study environmental and safety hazards associated with it. This study will draw the attention and need of catalytic combustion of toxic producer gas. Co/CeO_2 as producer gas combustion catalyst was synthesized through incipient wetness impregnation method and evaluated for its catalytic combustion efficiency. Our preliminary results inferred that the complete combustion of producer gas can be achieved even at moderate temperatures, commonly used for producer gas based combustion devices, thereby eliminating the risk of CO and hydrogen slip.

References

[1] P. Forzatti, Catalysis Today 83, (2003) 3-18.

III-PP39

Cyclization of Normal Alkanes to Arenes and Cycloalkanes

Kashkina E.*, Mikhailova Y., Svidersky S., Loginova A., Isaeva E., Leontyev A.

United Research and Development Centre, Moscow, Russia

* KashkinaEI@rn-rdc.ru

Keywords: cyclization, cycloalkanes, arenes catalyst

1 Introduction

The cyclization reactions are the basis of important catalytic processes for aromatic hydrocarbons production, mainly toluene, benzene and xylenes, as well as gasoline having a higher detonation resistance [1]. The practical implementation of n-alkanes cyclization process is one of the promising directions of refining processes development. Applying the cyclization process will allow efficient converting of n-alkanes of petroleum and synthetic origin into valuable components of motor fuels and oils, such as cycloalkanes and arenes.

Naphthenic hydrocarbons (cycloalkanes) are the most valuable class of chemical compounds in the composition of oils and fuels and their most high-quality part, as well as high-quality raw material for catalytic reforming process. In particular, cycloalkanes, compared with other classes of hydrocarbons contained in diesel cut, possess an optimum ratio of density and cetane index [2-3]. They provide a high viscosity index in lubricating oil formulations. Naphthenic oils (group V by API classification) produced from special oils, reserves of which are steadily decreasing, have good performance and are widely demanded in the industry.

Aromatic hydrocarbons also have good performance characteristics: their presence in petroleum products has a decisive effect such important indices as octane number (for gasoline), density and viscosity (for diesel and jet fuel) and others. Monocyclic arenes with long branched alkyl chains provide good viscosity-temperature properties for lubricating oils. However, due to limitations of ecological nature, the content of aromatic compounds in products is currently regulated.

Today, developments in n-alkanes cyclization proved to be in demand and were further developed for the cyclization of synthetic hydrocarbons. Synthetic hydrocarbons obtained in Fisher-Tropsch synthesis (FTS) are a mixture of mainly n-alkanes, which contains almost no naphthenic or aromatic compounds, and this explains the poor values of such parameters as density, chilling point and pour point of products derived from them, especially synthetic jet fuels. Cyclization process will allow production of valuable products based on synthetic hydrocarbons - components of oils with a high content of naphthenic hydrocarbons and arenes enriched components of fuels.

2 Experimental/methodology

The objective of the research was to assess the current state of scientific research and the identification of promising areas in the field of cyclization of n-alkanes.

During the work, we analyzed the data on the supposed mechanism of the cyclization process and the catalysts applied.

3 Results and discussion

Considered literature suggests that mechanism of alkanes cyclization reactions over platinum catalysts has been studied well. The literature discusses two main ways of cyclization reactions [4]:

1) bifunctional mechanism by which both metal and acid sites of the catalyst participate in reactions; applicable to systems - Pt on acidic support (alumina, silica-alumina or zeolite);

2) monofunctional mechanism involving reaction only on the metal sites; applicable to catalysts - Pt on non-acidic support (zeolite L, NaZSM-5, non-acidic alumina).

It is shown that along with alumina, zeolites in the cyclization catalyst also have activity and selectivity to the cyclization of alkanes with 6 or more carbon atoms [5]. Acidity of the zeolite support negatively affects the yield of aromatic hydrocarbons, due to parallel reactions on acidic active sites, such as isomerization and hydrocracking. Reducing the acidity of the zeolite by ion exchange with alkali is a requirement for increasing the selectivity of the zeolite catalyst to aromatic hydrocarbons. For effective reactions of cyclization zeolite cells should have a diameter of ~7Å (12-member ring), one-dimensional structure is preferred. In terms of structure, L type zeolite (LTL) if the most promising for cyclization of n-alkanes [6-7].

It is established that monofunctional catalysts containing Pt as an active component deposited on a non-acidic zeolite (type L in K-form) exhibit high activity in reactions of cyclization of n-alkanes [4]. High activity of the catalysts based on KL zeolite in cyclization of n-alkanes is explained by their low acidity contributing reduction of adverse reactions intensity - hydrocracking and received arenes hydrogenolysis, and by geometry of zeolite structure, enabling preferential target dehydrocyclization and dehydrocyclooligomerization reactions.

Promoters are added to the catalyst composition to improve efficiency of cyclization process catalysts. The use of promoter may contribute to the occurrence of the target reactions, prevent the side reactions, as well as promote involvement of the side reactions products, light alkanes, in particular, resulting from hydrocracking, into the secondary transformations, namely, dehydrocyclooligomerization. Rhenium, iridium, palladium can be used to improve activity of the catalyst in the target reactions, either directly by improving conditions of the reactions of hydrogenation and dehydrogenation, and by preventing deactivation of active sites [8-9]. Tin and indium are used to suppress excessive hydrocracking activity, particularly on acidic supports [10]. In addition, introduction of these promoters contributes to the achievement of optimal dispersion and crystallite size of the active component. Oxide promoters (WO_3, Cr_2O_3, ZnO) can help improve the overall catalytic activity of the system, and the involvement of the hydrocracking products into the dehydrocyclooligomerization reaction [1, 11].

4 Conclusions

Results of the literature review on paraffin cyclization allow to determine the main directions of research to create a highly efficient catalyst for the cyclization of normal alkanes in the arenes and cycloalkanes.

References

[1] Z. Paal, Z. Chicheri, *Catalytic reactions of hydrocarbons cyclization*. Moscow. (1988) 243.
[2] A. De Klerk, *Energy and Fuels.* 23 (2009) 4593.
[3] N. Ahmedova, S. Mamedov, R. Ahmedova, *J. Appl. Chem.* 83 (2010) 865.
[4] P. Meriaudeau, C. Naccache, *Catal. Rev.-Sci. Eng.* 39 (1997) 5.
[5] S. Ahmetov, *The technology of deep processing of oil and gas*. Ufa. (2002) 671.
[6] B. Davis, P. Venuto, *J. Catal.* 15 (1969) 363.
[7] P. Smirniotis, E. Ruckenstein, *Appl. Catal.* 123 (1995) 59.
[8] A. Cinneide, P. Gault, *J. Catal.* 37 (1975) 311.
[9] P. Weisang, P. Gault, *J. Chem. Soc. Chem. Commun*. (1979) 519.
[10] Patent 5958217 US (1995).
[11] Patent 5135898 US (1992).

III-PP40

Catalytic and Electrochemical Properties of (Cu, Ti)-YSZ for IT-SOFCs Anode

Florea M.[1*], Somacescu S.[2], Navarrete L.[3], Calderon-Moreno J.M.[2], Serra J.M.[3]

1 - University of Bucharest, Faculty of Chemistry, Bucharest, Romania
2 - "Ilie Murgulescu" Institute of Physical Chemistry, Romanian Academy, Bucharest, Romania
3 - Instituto de Tecnología Química (Universidad Politécnica de Valencia - Consejo Superior de Investigaciones Científicas), Valencia, Spain

* mihaela.florea@chimie.unibuc.ro

Keywords: surfactant, nanocrystalline, XPS, methane conversion, SOFC anode

1 Introduction

Solid oxide fuel cells (SOFC) offer a promising way of converting chemical energy into electrical energy with great efficiency. The formation of ordered ceramic nanostructures with tunable morphology and composition are required for SOFC anode. SOFC devices need to possess simultaneously a good ionic conductivity induced by the presence of oxygen vacancies and a good electronic conductivity induced by the added metal together with a high porosity allowing the fuel transport through the anodic layer [1-2]. S. Jung et al. [3] showed the anode performance depend by synthesis route. Thus, the distribution and morphology of the Cu component in $Cu/CeO_2/YSZ$ composite anodes are affected by different impregnation procedures. Our proposed synthesis method favors uniformity of the crystalline network and the active species and an improvement of the ionic and electronic conductivity as well as of the catalytic activity. Electronic conduction type will be assured by Cu^0 species resulted from strong reducing environments, but also by reduction of Ti^{4+} to Ti^{3+} giving rise to free electrons. Ionic conductivity will be ensured by incorporating species with lower valence as Y^{3+}.

2 Experimental: Synthesis and characterization

(Cu, Ti) -YSZ were synthesized by a self-assembled method, using a nonionic surfactant – Triton X100 as template. Zirconium propoxide, yttrium acetylacetonte, titanium (IV) isopropoxide, nickel acetyl acetonate and copper acetate were used as inorganic precursors. 1-Propanol was used as solvent. The gels formed were dried several days at 50 ^oC, followed by calcination in air at 700 ^oC and 900 ^oC, respectively. **X-Ray diffraction analyses** were carried out on a Schimadzu XRD-7000 diffractometer using Ni-filtered Cu Kα radiation with λ=1.5418Å. **Scanning electron microscopy (SEM)** were performed with a Philips XL-20. **X-ray photoelectron spectroscopy (XPS)** - Surface analysis performed by X-ray photoelectron spectroscopy (XPS) was carried out on PHI Quantera equipment with a base pressure in the analysis chamber of 10-9 Torr. The X-ray source was monochromatized Al Kα radiation (1486.6 eV). The spectra were calibrated using the C1s line (BE = 284.8 eV).**The catalytic activity** for partial oxidation of methane (POM) was evaluated in a continuous fixed-bed tubular reactor (length of 300 mm and i.d. of 9 mm, Hasteloy X tube), equipped with a thermo well in the center of the catalyst bed, from PID &Eng Tech.

3 Results and discussion

The XRD pattern of sample CTST700 correspond to a cubic phase of fluorite type (Fm3m), with lattice parameter c= 5.073 Å. The cubic structure is stable at room temperature with the incorporation of yttria and titania in the zirconia-based lattice and the formation of a ternary oxide solid solution. XRD detects also a secondary phase with monoclinic symmetry (C2/c), isostructural with tenorite (CuO), with slightly enlarged lattice parameters, a= 4.695, b= 3.433,

c= 5.141, a= b = 90 deg, γ = 99.470 deg. Both phases have small nanocrystallite size, around 8 nm for the zirconia-based fluorite-type phase and 12 nm for the copper oxide-based tenorite-type phase, respectively. The XRD pattern of CTST calcined at 900 ^{o}C, can be indexed to monoclinic zirconia-based phase and tenorite as secondary phase. A significant growth of crystalline sizes for both the zirconia-based main phase: 30 nm, and CuO: 25 nm, was highlighted.

After data processing the XPS results revealed that Ti2p, Zr3d and Y3d prominent XPS transitions display typically 4+ and 3+ oxidation states, respectively. A close inspection of Cu2p photoelectron spectra reveal the presence of Cu^{2+} oxidation state for all samples following the assignments of the binding energies as well as the associated shake-up satellites and their relative intensities, in agreement with XRD results.

The conversion profile recorded for the catalytic partial oxidation of methane (Fig. 1a, b) showed that CTST materials are active above 400^{o}C. At low calcination temperature 700^{o}C methane is converted ~41%, while at high calcination temperature 900^{o}C the CH_4 conversion and CO selectivity are situated in the range 80-90%. CH_4 is totally converted to CO at 800^{o}C working temperature.

Conductivity measurements showed that addition of Cu leading to a predominantly an electron conductor behaviour with a n-type conductivity. Under wet hydrogen atmosphere the DC conductivity reached values of ~ $4 \cdot 10^{-4}$ S/cm at 780 ºC. The conductivity, electrocatalytic and catalytic properties are very influenced by the presence of reduced Cu species in the structure, enhancing those properties.

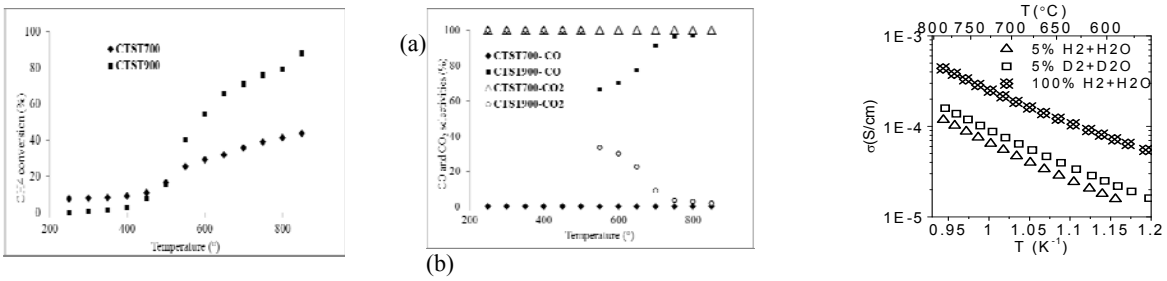

Fig. 1. Methane conversion (a), CO/CO_2 selectivity (b) and conductivity measurements at wet atmospheres (c)

4 Conclusions

The self-assembling method using Triton X100 as template was used for (Cu, Ti) –YSZ synthesis. The XRD patterns confirm formation of cubic phase of fluorite type at 700^{o}C and also a secondary phase with monoclinic symmetry, isostructural with tenorite (CuO) at 900^{o}C. The XPS results reveal that Ti2p, Zr3d, Y3d and Cu2p prominent XPS transitions display typically 4+, 3+ and 2+ oxidation states, respectively. The composite show high methane conversion and CO selectivity in the catalytic partial oxidation of methane (CPOM) at 800^{o}C. Conductivity results showed a predominately n-type behaviour, highlighting a promising IT-SOFC anode.

Acknowledgements

This work was supported by a grant of Partnerships in priority S&T domains Programm (PNII), MEN– UEFISCDI, project number 26/2012.

References

[1] Mamak, M. Metraux, G.S. Petrov, S. Coombs, N. Ozin , G.A. Green M.A. JACS 125 (2003).
[2] Rossmeis, J. Bessler, W. G. Solid State Ionics 178 (2008).
[3] Jung, S, Lu, C. He, H. Ahn,K, Gorte R.J. Vohs J.M. A. J. of Power Sources 154 (2006).

III-PP41

Photocatalytic Acetone Vapor Oxidation over TiO_2 under Controlled Periodic Illumination. Experimental and Modeling Study

Korovin E.Y.[1,2,3*], Kozlov D.V.[1,2,3], Besov A.S.[1,2,3]

1 - Boreskov Institute of Catalysis, Novosibirsk, Russia
2 - Novosibirsk State University, Novosibirsk, Russia
3 - Research and Educational Centre for Energoefficient Catalysis (NSU), Novosibirsk, Russia

* korovin@catalysis.ru

Keywords: photocatalytic oxidation, controlled periodic illumination, lifetime, active, species

1 Introduction

Heterogeneous photocatalytic oxidation of organic compounds on TiO_2 is considered as one of the most promising ways of air and water treatment. One of the approaches to increase quantum efficiency is the controlled periodic illumination (CPI), firstly suggested by Sczechowski et al. [1,2].

Working with fixed duty cycle Cornu et al. [3,4] investigated influence of t_{on} on the efficiency of methyl orange and formate oxidation. There were two sharp transitions in plots φ vs t_{on} at t_1 and t_2. Cornu et al. associated t_1 and t_2 with the lifetimes of oxidizing and reducing intermediates since they strongly depended on pH of the reaction suspension.

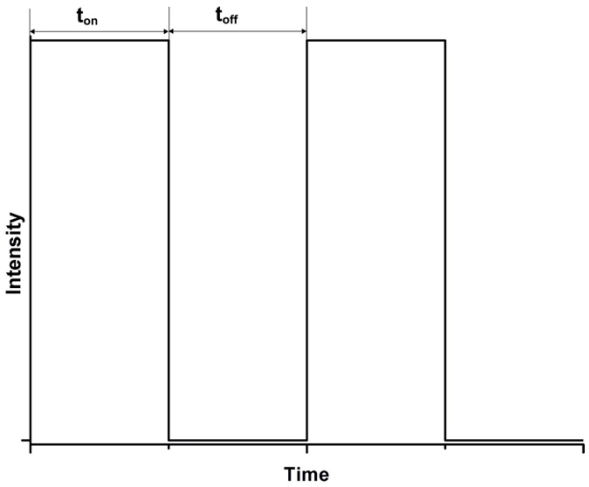

Figure 1. Schematic diagram of light pulses. Duty cycle, $\gamma=t_{on}/(t_{on}+t_{off})$. CPI period, $\tau=t_{on}+t_{off}$.

In this paper we present study of photocatalytic oxidation of acetone vapor under CPI. Equipment used in our experiment, such as extremely bright UV LED and arbitrary pulse generator, allowed us to use rectangular light pulses as short as 50 μs. Dependence of the photonic efficiency on the CPI period observed in our study is similar to the results obtained for water treatment by Cornu et al [3,4], although modelling approach and conclusions are rather different.

2 Experimental/methodology

All kinetic measurements were taken in a reactor which was installed in the automated setup. It allowed us to measure steady state values of the photocatalytic acetone oxidation in the flow-circulating mode. Standard operational parameters were the following: acetone concentration – 600 ppm, temperature – 40℃, relative humidity – 19±2%, volumetric flow rate (U) – 58 cm3/min. The CO_2 and acetone concentrations were measured using gas cell of FT-801 FTIR spectrometer (Simex, Russia)

3 Results and discussion

We investigated the effect of CPI period on photocatalytic acetone oxidation for two commercial TiO_2 samples: Degussa P25 and Hombifine N.

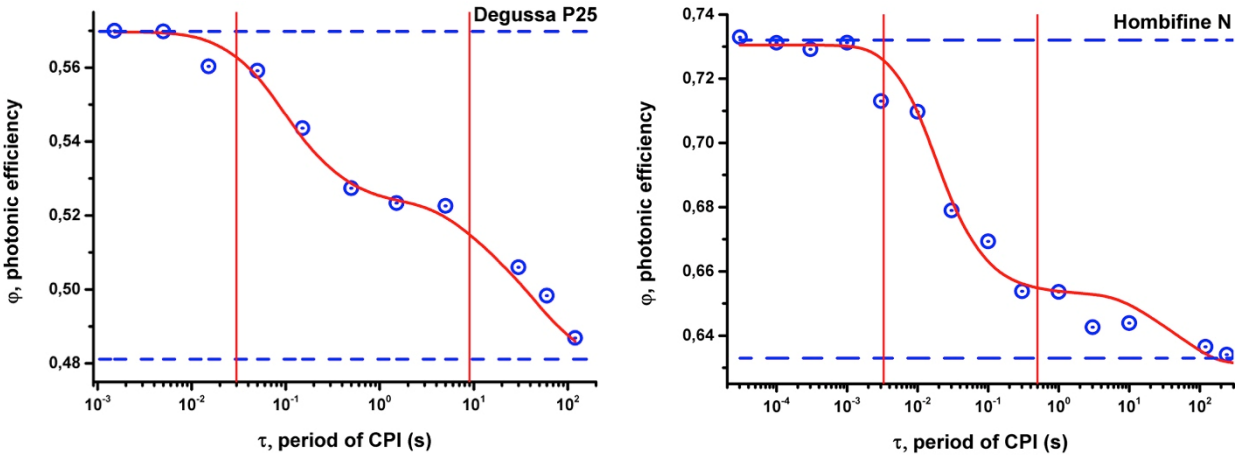

Figure 2. Photonic efficiency under CPI (duty cycle 0.5): circles – experiment, solid curve – model. Higher horizontal line – φ under constant illumination of the same average intensity, lower horizontal line – the same maximum intensity. Vertical lines indicate calculated lifetimes of active species.

The scheme for modelling experimental results in terms of active oxidative species kinetics was developed. We applied several kinetic schemes and most variants provided a good fit to the obtained data. Figure 2 shows the result of the simulation within the following system of differential equations:

$$\frac{d[Ox1]}{dt} = I - k_{Ox1} \cdot [Ox1] - k_{Rec1} \cdot [Ox1]^2; \qquad \frac{d[Ox2]}{dt} = I - k_{Ox2} \cdot [Ox2] - k_{Rec2} \cdot [Ox2]^2$$

Though various mechanisms provide a good fit, it does not affect conclusions we could make regarding mechanism of the photocatalytic oxidation. First of all lifetimes of active species are calculated and indicated on the Figure 2. Secondly our modelling shows that in terms of oxidation, at the high pulse rate the system does not distinguish how energy is provided: with the constant or intermittent illumination.

We studied the influence of intermittent illumination on photonic efficiency of acetone vapor oxidation. The general conclusion is that there are two kinetically distinguishable active species on the titania surface with lifetimes in range of 10^{-3}-10^{1} s. Since our experimental results are in good agreement with studies of Cornu et al., we can conclude that photocatalytic oxidation proceeds through the similar radical mechanism both for gas-solid and water solid interfaces.

References

[1] J. Sczechowski, C. Koval, R. Noble, Journal of Photochemistry and Photobiology A: Chemistry, 74 (1993) 273–278.
[2] J. Sczechowski, C. Koval, R. Noble, Chemical Engineering Science, 50 (1995) 3163-3173.
[3] C.J.G. Cornu, A.J. Colussi, M.R. Hoffmann, The Journal of Physical Chemistry B, 105 (2001) 1351–1354.
[4] C.J.G. Cornu, A.J. Colussi, M.R. Hoffmann, The Journal of Physical Chemistry B, 107 (2003) 3156–3160.

III-PP42

Bimetallic Catalysts Containing Palladium and Gold on Carbon Support for Hydrogen Electrooxidation: from Au Particles Coated with Submonolayers of Pd to Pd-Au Nanoalloys

Pyrjaev P.A.[1], Simonov A.N.[2], Moroz B.L.[1,3*], Zyuzin D.A.[1], Kuznetsov A.N.[1], Prosvirin I.P.[1], Bukhtiyarov V.I.[1,3]

1 - G.K. Boreskov Institute of Catalysis SB RAS, Novosibirsk, Russia
2 - School of Chemistry, Monash University, Clayton, Australia
3 - Novosibirsk State University, Novosibirsk, Russia

* moroz@catalysis.ru

Keywords: palladium-gold, electrocatalysts, carbon support, hydrogen, oxidation, reaction, CO, tolerance

1 Introduction

Bimetallic PdAu composites attract attention in view of their potential application at the anodes of polymer-electrolyte membrane fuel cells (PEMFCs) as the catalysts for the hydrogen oxidation reaction (HOR), since their resistance to CO poisoning, which is a critical issue for the low-temperature PEMFCs, may significantly exceed the CO tolerance of "conventional" anode Pt and PtRu catalysts. The aim of our work was to study the PdAu/C electrocatalysts with various surface compositions in HOR and their CO tolerance. Two different synthetic strategies were applied to prepare the PdAu/C catalysts: (*i*) electrodeposition of Pd coatings at the submonolayer level on carbon-supported Au nanoparticles (*a model approach*) and (*ii*) impregnation of the Au/C substrate with Pd(II) nitrate solution followed heat treatments for obtaining the proper Pd-Au alloying (*a pragmatic approach*). In both cases the particular attention has been paid to determination of the surface composition of PdAu nanoparticles providing the maximum catalyst activity in HOR and CO tolerance.

2 Experimental

As the catalyst supports, we used the proprietary carbon materials of the Sibunit family containing mostly 3-10 nm pores in the absence of micropores. The Au/C substrates containing Au particles of 1-5 nm in diameter were synthesized by "cationic adsorption" technique [1]. A series of PdAu/C catalysts with a variable Pd:Au molar ratio were prepared (*i*) by selective electrochemical deposition of Pd metal from the H_2PdCl_4 solution onto the carbon-supported Au particles as described in Ref. [2] and (*ii*) by incipient wetness impregnation of Au/C substrate with the $Pd(NO_3)_2$ solutions of required concentrations followed by calcination in Ar at 250°C and reduction with H_2 at the same temperature. The size, local elemental composition, electronic and structural properties of carbon-supported PdAu particles in the catalysts were studied by TEM/EDX, XRD, XPS and EXAFS using by common procedures. Electrochemical measurements were performed in a standard three-electrode cell using an Autolab PGSTAT 30 instrument. The HOR cyclic voltametry curves for the as-prepared and CO-blocked catalysts were measured at 25-60°C using a rotating disc electrode (RDE).

3 Results and discussion

By varying the time of electrodeposition of Pd on the 1.7% Au/C substrate we obtained a set of PdAu/C catalysts with a systematic variation of Pd coverage (θ_{Pd}) in the range from 0.2 to 0.8 monolayers (ML). The electrochemical data (cyclic voltammetry in a supporting electrolyte, H_{UPD} and Cu_{UPD} region analysis) confirmed that Pd is located exclusively on the surface of Au

particles through layer-by-layer growth. The RDE study demonstrates that the exchange current density (j_0) of the HOR (referred to the Pd surface area) monotonically increases with a decrease in θ_{Pd} from 0.5 to 0.2 ML. Reducing the size of the Au particles used as sites for Pd deposition from 16–19 nm to 1.5–5 nm results in *ca.* 2-fold increase in the j_0 value. The HOR current density measured after CO adsorption (j_{CO}) increases with a decrease in θ_{Pd}, passing through a maximum at θ_{Pd} = 0.30 ML, and the maximum value of j_{CO} exceeds that of the CO-blocked Pd/C catalyst at least by a factor of 10. An increase in the HOR activity observed for the CO-poisoned PdAu/C catalysts at the intermediate θ_{Pd} values is supposedly caused by an appearance of $[Pd]_{x>2}$ ensembles surrounded by $[Au]_y$ ensembles on the surface of PdAu particles, which are less favorable for CO adsorption than Pd "dimers" and "monomers".

The results of the experiments with the "electrodeposited" catalysts revealed good application prospect in the HOR for the catalysts that would contain the well-dispersed alloyPdAu particles. Implementing this idea, we have prepared a set of PdAu/C catalysts with bulk Pd:Au ratios from 0.5 to 3.9 mol/mol by the two-step procedure [3] including post-deposition heat treatments for obtaining the proper Pd-Au alloying. According to the characterization data, the catalysts comprise the alloy PdAu particles of 2-5 nm in size and with the bulk Pd:Au composition that is similar to the molar ratio of metals used in preparation. These particles are not the homogeneous alloys but have Au-enriched cores and Pd-enriched outer shells. The surface layer of PdAu particles contains more palladium at higher bulk ratio Pd:Au. However, increasing the temperature of catalyst calcination in H_2 up to 475°C leads to truly homogeneous distribution of Pd and Au in the bimetallic nanoparticles. The XPS spectra of the catalysts exhibit the negative shift increasing with the surface Pd:Au ratio that indicates a change in the electronic state of Au due to the "ligand" effect of Pd. The dependencies of j_0 and j_{CO} of the "pragmatic" PdAu/C catalysts on their surface composition generally coincide with those for the "electrodeposited" catalysts, but the absolute values of j_0 and, especially, j_{CO} were significantly higher for the alloy PdAu particles compared to Pd-electroplated Au particles with the similar surface composition.

3 Conclusions

The PdAu/C systems with controlled surface composition of the bimetallic sites prepared by selective electrodeposition of Pd on pre-immobilized finely dispersed Au particles are the valid and convenient tools for investigation of the influence of the PdAu surface composition on the catalyst HOR activity and CO tolerance. The formation of Pd-Au nanoalloys leads to a considerable increase in the HOR activity and CO tolerance of the carbon-supported bimetallic catalysts. The PdAu/C catalysts prepared by using the common procedures (ionic exchange, impregnation etc.) and containing the alloy Pd-Au particles of optimal surface composition are promising for application at the PEMFC anodes, since their CO tolerance exceeds that of the commercial available PtRu/Vulcan XC72 catalyst.

Acknowledgements

The authors thank Prof. Ya.V. Zubavichus and Drs. E.Yu. Gerasimov and T.I. Asanova for their help in carrying out this work. The financial support of the work was provided by the Russian Foundation for Basic Research (grant no. 13-03-01003) and the Grant of President of Russian Federation for government support of Leading Scientific Schools (grant SS-5340.2014.3).

References

[1] P.A. Pyrjaev, B.L. Moroz, D.A. Zyuzin, A.V. Nartova, V.I. Bukhtiyarov, *KinCat* 51 (2010) 885.

[2] P.S. Ruvinsky, S.N. Pronkin, V.I. Zaikovskii, P. Bernhardt, E.R. Savinova, *Phys. Chem. Chem. Phys.* 10 (2008) 6665.

[3] P.A. Pyrjaev, A.N. Simonov, B.L. Moroz, V.I. Bukhtiyarov, V.N. Parmon, *Russian Patent 2428769 (2011).*

III-PP43

3D Ordered Macroporous Ti-Based Catalysts: Design, Synthesis and High Catalytic Activity for the Photoreduction of CO_2 with Water to Mechane

Jiao J.Q., Wei Y.C., Zhao Z.*, Liu J., Li J.M., Jiang G.Y., Duan A.J.

State Key Laboratory of Heavy Oil Processing, China University of Petroleum, Beijing

* zhenzhao@cup.edu.cn

Keywords: photocatalytic conversion, CO_2 reduction, 3DOM catalyst

1 Introduction

Solar fuel production by CO_2 photocatalytic conversion provides a sustainable way for carbon recycling and is of significance in meeting energy demand and mitigating rising CO_2 levels. TiO_2 is by far the most common semiconductor in photocatalysis and is used in pollutant degradation, dye bleaching, and water cleaning[1]. The main drawbacks of TiO_2 are its large band gap and massive recombination of photogenerated charge carriers, which make the catalytic efficiency low. The design and synthesis of highly active photocatalyst is one of the most important scientific challenges involving light absorption, electron transfer/separation etc. for the photocatalytic reduction of CO_2. A photonic crystal is a periodic dielectric structure, which offers a unique way of light matter interaction to increase light harvesting via the slow-light effect, especially around the absorption edge of a semiconductor[2-3]. Therefores, we prepared three-dimensionally ordered macroporous materials (photonic crystals) by way of colloidal crystal-templating approach. And we designed and synthesized the novel catalyst of 3D ordered macroporous Ti-supported Au@CdS, Pt@CdS, Au@Pt core-shell NPs via the gas bubbling-assisted membrane reduction (GBMR/P) method[4-5]. These photocatalysts were characterized by scanning electron microscopy (SEM), transmission electron microscopy (TEM), X-ray diffraction (XRD), UV–Vis diffuse reflectance spectroscopy, Brunauer–Emmet–Teller (BET) analysis of nitrogen adsorption isotherm, photoluminescence spectra (PL) and the surface photovoltage (SPV) technique. Moreover, 3DOM Ti-based catalysts exhibit efficient catalytic activity for the photocatalytic reduction of CO_2 with H_2O under simulated solar irradiation.

2 Experimental/methodology

Synthesis of monodispersed polymethyl methacrylate (PMMA) microsphere was synthesized using a modified emulsifier-free emulsion polymerization technique with water-oil biphase double initiators. And 3DOM TiO_2 support was prepared by the colloidal crystal template (CCT) method using tetrabutyl titanate as precursor solution. 3DOM Ti-supported catalysts were synthesized by the process of the gas bubbling-assisted membrane reduction-precipitation (GBMR/P) method. Photocatalytic reactions were performed in a stainless-steel reactor with a quartz window on the top of the reactor. The photocatalyst was placed on a Teflon catalyst holder without being immersed in water. The light source was a 300W Xe lamp(l=320-780 nm).

3 Results and discussion

As shown in Fig. 1A, the UV-Vis diffuse reflectance spectrum of 3DOM Au@CdS/TiO_2 catalyst displays distinct and well-defined surface plasmon absorption band centered at about 550 nm, which is the plasmon absorption peak of supported Au nanoparticles. With the

increasing of CdS shell content in 3DOM Au@CdS/TiO_2 catalysts, the intensity of the absorption band at visible region is remarkably increased. And in XRD patterns (Fig. 1B), the diffraction peaks (2θ) at 25.3, 37.8, 47.9, 53.8, 55.3 and 62.8° can be indexed to the (101), (004), (200), (105), (211) and (204) crystal faces of 3DOM TiO_2 with a tetragonal anatase structure (PDF# 21-1272), respectively. And the weak diffraction peaks (2θ) at 27.4 and 36.3° can be indexed to the (110) and (101) crystal faces of 3DOM TiO_2 with a tetragonal rutile structure (PDF# 65-0191). It indicates the co-presence of anatase and rutile crystallites for 3DOM TiO_2 support, which is similar to the phase structure of P25. As shown in Fig. 2, it clearly shows the formation of the core-shell structural Au@CdS NPs. One Au nanoparticle on the surface of 3DOM TiO_2 was covered by the CdS nanoparticles and formed the core-shell structural Au@CdS nanoparticles (Fig. 2C). 3DOM Au@CdS/TiO_2 catalysts can promote the formation of CH_4 and exhibit super photocatalytic activity, which the formation rate of CH_4 are more than 15 $\mu mol \cdot g^{-1} \cdot h^{-1}$.

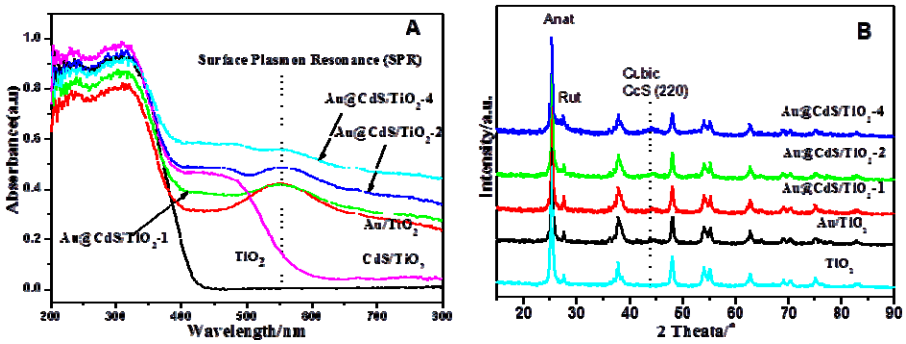

Fig. 1. The UV-Vis DRS spectra (A)and XRD patterns(B)of 3DOM Au@CdS/TiO_2 catalysts

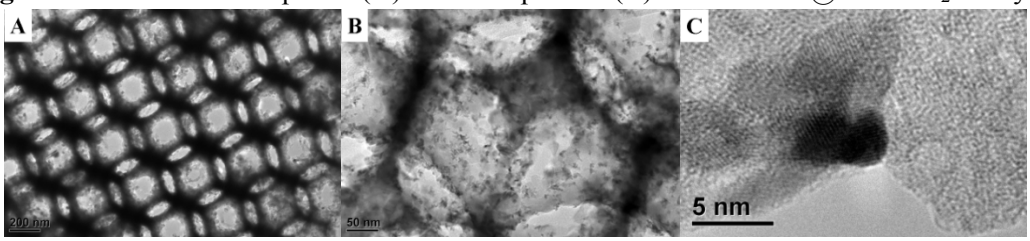

Fig. 2. TEM and HRTEM images of 3DOM Au@CdS/TiO_2 catalysts

4 Conclusions

In summary, we successfully fabricated 3DOM Ti-based catalysts by the process of GBMR/P method. The structure of catalysts is well-defined and uniformed. 3DOM Ti-based catalysts exhibit super catalytic activity for the photocatalytic reduction of CO_2 into methane. The fabrication of metal@oxides core-shell nanostructure on 3DOM oxides surface could be widely applied in various heterogeneous oxides-metals photocatalytic systems.

Acknowledgements

This work was supported in part by the NNSF of China (No. 21177160, 21303263 and 21173270), Beijing Nova Program (No. Z141109001814072), Doctoral Selective Fund (No. 20130007120011) and Science Foundation of China University of Petroleum, Beijing (No. QZDX-2011-02, 2462013YJRC13 and 2462013BJRC003).

References

[1] S. N. Habisreutinger, L. Schmidt-Mende, J. K. Stolarczyk, *Angew. Chem. Int. Ed.* 52 (2013) 7372.
[2] Q.Zhai,S.Xie,Y.Wang,et al.,*Angew. Chem. Int. Ed.* 52 (2013) 5776.
[3] R.K.Yadav,J-O.Baeg,G.H.Oh.et al.,J.Am.Chem.Soc. 134 (2012) 11455.
[4] J.Q. Jiao, Y.C.Wei, Z. Zhao, et al., *Ing. Eng. Chem. Res.* 53(2014) 17345.
[5] Y.C. Wei, J. Liu, Z. Zhao, et al., *Energy Environ. Sci.* 4 (2011) 2959.

III-PP44

Advances in Catalyst Characterization by FTIR Spectroscopy

Tsyganenko A.*

V.A.Fock Institute of Physics, St.Petersburg State University, St.Petersburg, Russia

* atsyg@photonics.phys.spbu.ru

Keywords: adsorption catalysis, FTIR spectroscopy, active sites, surface, characterization

1 Introduction

Catalyst characterization by means of IR spectroscopy has been mostly restricted to the estimation of acid site strength and concentration from the positions and intensities of the bands in the spectra of adsorbed test molecules. Low temperature adsorption of simple molecules, such as CO, H_2, N_2 and fluoroform, or symmetric highly absorbing molecules such as CF_4 or SF_6 enable us to get other information about the surface of catalysts.

2 Site Testing

Traditionaly, ammonia and pyridine were used as tests for acidity, capable to distinguish Brønsted and Lewis acid sites. Later on nitriles were suggested for the latter, while 2,5-dimethylpiridine (lutidine) was found to be a nice test for Brønsted sites [1]. Low temperature adsorption of simple gases such as N_2, H_2 or especially CO gives more detailed information about Lewis acidity, while frequency shifts of the molecules and of perturbed OH groups characterize the proton-donating ability of surface hydroxyls.

Basicity testing by adsorption of gaseous aprotonic acids, providing the data on the amount of sites, does not inform us about their relative strength. Such information can be obtained from the frequency shifts of CH proton donors: chloroform, HCN, acetylene or its derivatives. For strong basic sites fluoroform CHF_3 is the best, since it never dissociates on adsorption [2].

Ionic species, such as OH- or CN- formed as a result of dissociation of water or HCN, have certain advantage as tests, because due to their charge they interact specifically with the cations. Hydroxyl can bridge two metal atoms, testing dual cationic sites. Spectral manifestations of CO interaction with dual cationic sites were detected on basic zeolites [3]. Spectra of adsorbed cationic species, such as NH^{4+} or NO^{+} [4] are affected by the properties and local arrangement of the nearest oxygen anions.

According to the electrostatic model, frequency shifts of different test molecules can be considered as caused by linear or quadratic vibrational Stark effect [5]. More correct is the correlation of the field with the force constant, because the shift is partially due to other factors, such as the “wall effect” or the resonance interaction with other molecules. Both quantum chemical calculations and electrostatic approach predict the correlation between the electric field of the cations and integrated absorption coefficients, in a fair agreement with the experiment [6].

3 Linkage isomerism

To trap the unstable intermediates of catalytic reaction we can follow spectra evolution with temperature and observe the chain of reactant transformations, while the structure of intermediates can be clarified using isotopic substitution.

Some adsorption products, however, cannot be stabilized at low temperatures, but arise at the surface as a result of thermal excitation. So, CO forms with the cations in zeolites two kinds of complexes [7]. The energetically less favorable O-bonded species have the excess of energy and can be considered as an activated state, intermediate in catalytic reactions. Surface isomeric states were established for some other adsorbed species, such as cyanide ion CN^-[8]. The linkage isomerism can be explained by an electrostatic model, or quantum mechanical calculations. The ability for linkage isomerism depends on the local environment of the site.

4 Lateral interactions

The strength of surface sites is affected by lateral interactions between the adsorbed species. On oxides, repulsive static interaction weakens the neighbouring sites, while dynamic interaction shifts the bands of test molecules and leads to intensity redistribution between the bands [9].

Co-adsorption of acidic and basic molecules leads to mutual enhancement of adsorption. Besides the effect of induced Brønsted [10] or Lewis acidity, induced basicity in the presence of adsorbed bases has also been detected spectroscopically [11]. The concept of induced acidity is consistent with superacidity of oxides doped with SO_4^{2-} and explains the promoting action of aprotonic gaseous acids in the reactions catalyzed by Brønsted sites [12].

Due to extremely strong dynamic (resonance dipole-dipole) interaction between the molecules with very high absorbance, such as SF_6 or CF_4, which do not interact strongly with any surface sites, spectra of these molecules in adsorbed state are sensitive to the geometry of the adsorbed layer. Bandshape of these species is not the same for 2D adsorbed layers on flat crystal faces or chains of molecules in the 1D channels of zeolites [12]. This could become a new promising way for spectral characterization of catalyst surfaces.

Acknowledgement

The study was supported by a grant of the Government of Russian Federation No. 14.Z50.31.0016.

References

[1] G. Berhault et al., J. Catal. 178 (1998) 555.
[2] A.A.Tsyganenko, N.V.Zakharov, P.D.Murzin, Catal. Today. 226 (2014) 73.
[3] E. Garrone et al, J. Phys. Chem. B. 110 (2006) 22542.
[4] K. Hadjivanov, J. Saussey, J.L.Freysz, J.-C. Lavalley, Catal. Lett. 52 (1998) 103.
[5] S.M. Zverev, K.S. Smirnov, A.A. Tsyganenko, Kinetics and Catalysis. 29 (1988) 1251.
[6] E.V. Kondratieva, O.V. Manoilova, A.A. Tsyganenko, Kinetics and Catalysis. 49 (2008) 451.
[7] A.A. Tsyganenko, P.Yu. Storozhev, C. Otero Areán, Kinet. Catalysis. 45 (2004), 530.
[8] A.A.Tsyganenko, A.M.Chizhik, A.I.Chizhik, Phys. Chem. Chem. Phys. 12 (2010), 6387.
[9] A.A. Tsyganenko, L.A. Denisenko, S.M. Zverev, V.N. Filimonov V.N, J. Catal. 94 (1985) 10.
[10] A.A. Tsyganenko, E.N. Storozheva, O.V. Manoilova, T. Lesage, M. Daturi, J.-C. Lavalley, Catal. Lett. 70 (2000) 159.
[11] E.N. Storozheva, V.N. Sekushin, A.A. Tsyganenko, Catal. Letters. 107 (2006) 185.
[12] T. Hosotsubo, M. Sugioka, K. Aomura, Bull. Fac. Eng., Hokkaido Univ. 1981, N 102, 119.
[13] A. Dobrotvorskaia, T. Kolomiitsova, S. Petrov, D. Shchepkin, A. Tsyganenko. Spectrochimica Acta Part A: Molecular and Biomolecular Spectroscopy 148 (2015) 271.

.

III-PP45

New Nanodiamonds/TiO_2 Composite Materials for the Solar Energy Conversion into Hydrogen by Water Splitting

Keller V.[1], Pichot V.[2], Minetti Q.[1*]

1 - ICPEES, « Institut de Chimie et Procédés pour l'Energie, l'Environnement et la Santé », Université de Strasbourg, Strasbourg Cedex, France

2 - NS3E, « Nanomatériaux pour les Systèmes Sous Sollicitations Extrêmes», UMR 3208 (ISL/CNRS/UdS) Institut franco-allemand de recherche de Saint-Louis, Saint-Louis Cedex, France

* quentin.minetti@etu.unistra.fr

Keywords: photocatalysis, TiO_2 nanodiamonds, water splitting, hydrogen production

4 Introduction

Natural resources of energy present on Earth are decreasing year by year. That is why it is necessary to find new ways of producing energy to solve the problem of global consumption. Production of hydrogen using solar energy is one of the key solutions that are envisaged to solve this problem. The process which allows to convert the photons from the sunlight into electrons, is called photocatalysis. In our study we are using titanium dioxide (TiO_2), a cheap and common semi conductor material, as a photocatalyst in order to chemically split the H_2O molecule **[1]**. The hydrogen produced by this process could be used in the future as a source of energy more efficient that gasoline.

The production of hydrogen by titanium dioxide could be improved by chemical or electronical modifications, for example by interaction at the nanoscale with other nanomaterials. The aim of the study is to add nanodiamonds to titanium dioxide and to observe the different interactions between the two materials.

Thus, concerning photocatalytic water-splitting production, the influence of (i) the way of synthesis of the Nanodiamonds/TiO_2 composites, (ii) the composition of the composites, *i.e.* the relative amount of nanodiamonds, (iii) the nature of nanodiamonds (as synthetized or hydrogenated), (iv) the presence or absence of Pt nanoparticules and (v) the addition of methanol acting as sacrificial agent will be discussed.

5 Experimental/methodology

Titanium dioxide is synthesised by a sol-gel process **[2]** and its activity toward H_2 production by water-splitting is compared to that of the reference TiO_2 (P25). For this purpose, titanium isopropoxide ($Ti(OCH(CH_3)_2)_4$) is mixed with ethanol. After vigorous stirring for 30 min at room temperature, a mixture of distilled water, ethanol and acetic acid is added drop by drop into the solution. The resulting solution is stirred at room temperature for 1 h, and then was kept for 24 h in the dark. The obtained sol material is dried at 110 ◦C overnight and then thermally-treated for 3 h in air at 400 ◦C.

The nanodiamonds are synthesized by detonation of high explosives method **[3]**. The Nanodiamonds /TiO_2 composite are elaborated from TiO_2 (as previously described) and detonation nanodiamonds. Different strategies of synthesis have been carried out in order to obtain the composite material. (1) The first one is based on the addition of nanodiamonds during the sol gel process in order to get TiOH gel with nanodiamonds inside the gel. After a calcination step at 400°C, the Nanodiamond/TiO_2 composite is finally obtained. (2) Another way of elaboration is based on the impregnation of already synthesized and crystallized TiO_2 with a suspension of nanodiamonds by mechanical mixing in an aqueous medium under inert gas, followed by a final drying step.

Nanodiamonds with different surface chemistry were investigated, oxygenated and hydrogenated (under H_2 flow at 700°C). Nanodiamonds were also associated with the TiO_2-P25 photocatalyst in order to compare the influence of the TiO_2 nature. The synthesized materials have been characterized by TGA, XRD, UV-visible, XPS, SEM and TEM (Figure 1).

Platinum has been added (as a co-catalyst) by impregnation of H_2PtCl_6 on the composite materials; the results observed with and without platinum will be compared.

6 Results

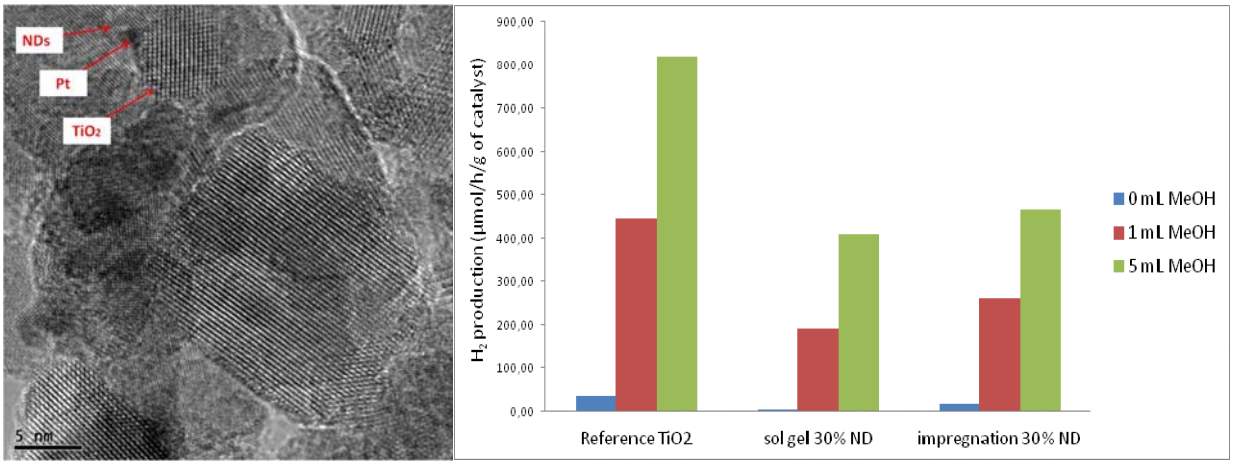

Figure 1: Left- TEM picture of a sol gel-based composite material made of 0.3 wt% Pt-ND/TiO_2; Right- Comparison of the H_2 production of 3 materials (TiO_2 sol gel, sol gel composite ND/TIO_2 with 30 wt% ND, composite ND/TIO_2 with 30 wt% ND obtained by impregnation) having 0.3 wt% Pt with different amounts of methanol added

Figure 1 shows that the sol gel synthesis incorporating nanodiamonds allows to obtain a composite material with physical contact between titania, nanodiamonds and platinum.

Water-Splitting tests were carried out into a quartz reactor containing 900mL of Ultra-pure water and 250mg of sample under flowing N_2 at 100cc/min. Methanol (from 0.1 to 1 vol. %) was used as a sacrificial agent in order to increase yields of hydrogen production. The sample activity (amount of H_2 produced) is measured by a gas phase µGC.

Figure 1 shows the amount of hydrogen obtained with the different composite materials. It allows us to compare the efficiency of the different synthesis and to say that the synthesis by impregnation of ND on TiO_2 gives a higher production of hydrogen than the sol gel synthesis.
An innovative result on the production of hydrogen from Pt-free composite Nanodiamonds/TiO_2 materials will be demonstrated.

7 Outlooks

As short-term perspectives of the project, the long time stability of the catalysts will be studied as well as the influence of the reaction temperature. The impact of the hydrogenated nanodiamonds will also be investigated.

References

[1] A. Fujishima and K. Honda, "Electrochemical Photolysis of Water at a Semiconductor Electrode," *Nature*, vol. 238, no. 5358, pp. 37–38, Jul. 1972.

[2] N.A. Kouamé et al., Preliminary study of the use of β-SiC foam as a photocatalytic support for water treatment, *Catalysis Today*, 161, 2011, 3-7.

[3] V. Pichot, M. Comet, E. Fousson, C. Baras, A. Senger, F. Le Normand, D. Spitzer, An efficient purification method for detonation nanodiamonds, *Diamond & Related Materials*, 17, 2008, 13–22.

III-PP46

Pt-Sno$_x$-Tio$_2$ Catalysts for Methanol Photocatalytic Reforming: Influence of Co-Catalysts on the Hydrogen Production

Szíjjártó G.P.*, Tálas E., Pászti Z., Mihályi J., Bálint S., Tompos A., Boráth I.

Institute of Materials and Environmental Chemistry, Research Centre for Natural Sciences, Hungarian Academy of Sciences, Budapest, Hungary

* tompos.andras@ttk.mta.hu

Keywords: TiO_2, co-catalysts, sol-gel method, methanol, H_2 production, controlled surface reactions

1 Introduction

Photocatalytic hydrogen production is a promising approach for transforming solar energy into chemical energy for storage. Methanol which can be obtained from both fossil resources and biomass is a good starting compound for H_2 generation due to its high H/C ratio. Many efforts have been made for photoinduced reforming of methanol on semiconductive oxides in the presence of water providing H_2 and CO_2. Because of its good stability and efficiency, TiO_2 is one of the most frequently used photocatalysts. In the methanol photocatalytic reforming reaction its activity can be increased by at least an order of magnitude when a proper co-catalyst is involved. In addition to decreasing the charge recombination, promoting the charge separation and the transport driven by junctions/interfaces, co-catalysts can provide reaction sites for the elementary reaction steps independent of the light absorption [1]. Pt is a very effective co-catalyst for proton reduction [1] as it shows the lowest activation energy for H_2 evolution. In our previous work we found that in the presence of a Pt co-catalyst the Sn introduction increased the activity of TiO_2 obtained by sol-gel method (SG). In these samples the Sn was not incorporated in to the lattice but the surface of TiO_2 was decorated by amorphous tin-oxide islands [2]. Recent work has reported about a vectorial electron transfer of TiO_2 -> SnO_x ->Pt as the reason of the enhanced activity of Sn grafted TiO_2 [3]. A reliable method to anchor Sn to the surface is the Controlled Surface Reactions (CSR) between tin tetraalkyls and OH groups of the oxide supports [4]. This approach leads to very small SnO_x nanoparticles uniformly distributed on the surface.

Traditionally, noble metal nanoparticles on catalyst supports are formed by high temperature H_2 treatment after impregnation with the solution of the appropriate metal precursor. However, it is believed that the high temperature treatment may destroy the surface of certain semiconductors [5]. In order to prepare co-catalyst on the surface of the photocatalysts in a more gentle way, photodeposition, reduction by $NaBH_4$ or calcination of the impregnated sample are also often used. The aim of this work is to compare the behavior of Pt-SnO_x-TiO_2 catalyst systems prepared by different methods and to find relationships between their structure and catalytic activity.

2 Experimental/methodology

The TiO_2 (Degussa Aerolyst (DA)) was modified by CSR using $Sn(C_2H_5)_4$ dissolved in decane at 150^{o}C followed by O_2 treatment up to 350 ^{o}C according to the literature [4]. SG based tin free and tin modified TiO_2 samples were prepared as described before [2]. Briefly, in the presence of citric acid and absolute ethanol titanium-isopropoxide was stirred for 180 min at room temperature and then heated at 65 ^{o}C until gel formation. In case of Sn modified samples $SnCl_4x5H_2O$ was also introduced into the mixture. The gel was dried and calcined for 5 hours at 400 ^{o}C. The Sn load was 1 w% both in samples by CSR and SG. Pt (1 w %) was introduced from aqueous solution of $Pt(NH_3)_4(NO_3)_2$. The dried samples were either reduced for 1 hour at

400 °C in H_2 atmosphere or calcined for 1 hour at 300 °C. The catalysts were characterized by means of H_2 and CO chemisorption, Raman spectroscopy, BET, EDX, XRD and XPS.
The photocatalytic reactions were carried out at room temperature in a high-throughput system with 10 quartz batch reactors equipped with magnetic stirrers. N_2 gas with 20 ml/min flow rate was continuously bubbled through all reactor units in parallel. The initial concentration of methanol was 6 w% in distilled water. Osram HQL 125W lamps were used as light sources. H_2 formation was followed by GC analysis of the outlet gas upon using argon internal standard.

3 Results and discussion

BET specific surface of DA and SG TiO_2 with or without Sn was comparable (50±10 m^2g^{-1} vs. 75 ± 10 m^2g^{-1}). According to XRD and Raman spectroscopic measurements, DA contains a certain amount of rutile beside the anatase phase while the SG samples are composed of only anatase. The EDX elemental analysis indicates a roughly uniform Sn distribution in samples from both methods but Raman spectroscopy indicates the presence of separate SnO_2 phase in SG sample as a very small shoulder at about 747 cm^{-1} which did not appear in the CSR one.

Figure 1 shows the H_2 production over SG and CSR samples in the presence of Pt co-catalyst formed by calcination (Figure 1A) and H_2 treatment (Figure 1B). In case of the SG samples calcination after Pt loading is more favorable than H_2 treatment and the Sn introduction clearly enhances the activity after both treatments. Conversely, the Sn introduction by CSR is beneficial only in the calcined case, suggesting a difference in the nature of the Sn species in the SG and CSR samples. These observations will be discussed in detail based on XPS and chemisorption results.

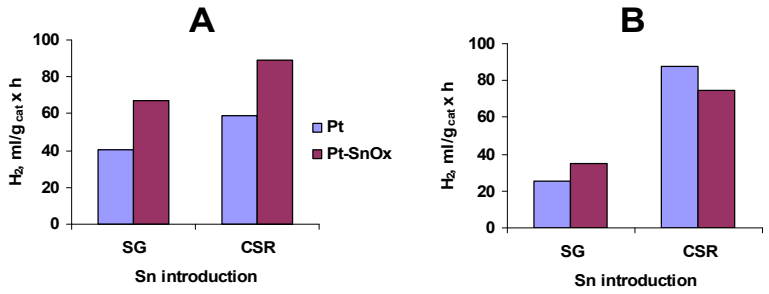

Fig. 1. H_2 formation over different TiO_2 based catalysts. SG: sol-gel prepared; CSR: Degussa Aerolyst TiO_2, Sn introduction by CSR; samples with Pt co-catalyst were calcined or H_2 treated (A and B)

4 Conclusions

Both the way of Sn introduction and the formation of the Pt co-catalyst have a decisive effect on the activity of the Pt-SnO_x-TiO_2 photocatalysts.

Acknowledgements

This project has been supported by the National Development Agency, grant No. KTIA_AIK_12-1-2012-0014. Financial support by the OTKA-project K77720 (András Tompos) and K100793 (Zoltán Pászti) is greatly acknowledged. The authors thank Dr. Ferenc Somodi for the tin modification of TiO_2 by CSR.

References

[1] J. Yang, D. Wang, H. Han, C. Li, *Acc. Chem. Res*. 46 (2013) 1900.
[2] K. Majrik, E. Tálas, Z. Pászti, I. Sajó, J. Mihály, et al, *Appl. Catal. A: General* 466 (2013) 169.
[3] Q. Gu, J. Long, H. Zhuang, C. Zhang, Y. Zhou, et al, *Phys. Chem. Chem. Phys*. 16 (2014) 12521.
[4] F. Somodi, I. Borbáth, M. Hegedűs, A. Tompos, I.E. Sajó, et al. *Appl. Surf. Sci*. 256 (2009) 726.
[5] K. Maeda, K. Teramura, D. Lu, N. Saito, Y. Inoue, et al, *Angew. Chem. Int. Ed*. 45 (2006) 7806.

III-PP47

New Approaches for Solar Fuel from Suspended Photocatalysts

Striegler K.[1*], Richter D.[1], Benndorf G.[2], Gläser R.[3]

1 - Universtät Leipzig, Faculty of Chemistry and Mineralogy, Institute of Chemical Technology, Leipzig, Germany

2 - Universtät Leipzig, Faculty of Physics and Earth Science, Institute for Experimental Physics II, Leipzig, Germany

3 - Universtät Leipzig, Faculty of Chemistry and Mineralogy, Institute of Chemical Technology, Leipzig, Germany

* karl.striegler@uni-leipzig.de

Keywords: heterogeneous, photocatalysis, hydrogen evolution, TiO_2, g-C_3N_4, Co_3O_4

1 Introduction

It was proven by Honda and Fujishima in the early 1970s that water can be split photo-electrochemically [1]. Since then, several semiconductor materials for the conversion of harvested light energy into utilizable *solar* fuels have been investigated as heterogeneous photo- or electrocatalysts [2]. However, the usage of metal nanoparticles for catalysis has been investigated thoroughly [3]. Since the reaction rate for most typical metal catalyzed reaction increases due to a larger specific surface area, other effects, like a decreased overpotential or an enhanced charge-carrier separation, play a significant role for photocatalytic water splitting [4]. Still, noble metal promoters (Au, Pt, Pd, etc.) deposited on a semiconductor and sacrificial agents are needed for a reasonable efficiency [5]. It was shown previously that the deposition of Co_3O_4 led to an increased oxygen evolution rate [6].

2 Methodology

It was the aim of this work to investigate possible quantum size effects when depositing a promoter onto a semiconductor for the hydrogen evolution. Therefore, two reference semiconductors were chosen on which Co_3O_4 with different crystal sizes were deposited [7].

I. Synthesis. $Co(OAc)_2 \cdot 4\ H_2O$ was dissolved in an a mixture of ethanol, water and ammonia in different composition. After homogenizing, the Co^{2+} solution was transferred to a 50 ml autoclave, sealed and incubated for 3 h at 150 °C. The resulting suspensions of Co_3O_4 particles were centrifuged and dried at 60 °C for 4 h. These particles were deposited onto g-C_3N_4 (graphitic carbon nitride) and TiO_2.

II. Material Characterization. The resulting materials were thoroughly characterized with N_2-sorption, elemental analysis, diffuse reflectance UV/Vis, XRD, photoluminescence and SEM. Thus, detailed information about the semidconductor material was gained for interpreting the differences in their photocatalytic activity.

III. Catalytic Testing. A 150 W Hg-medium-pressure lamp was used to irradiate a 380 ml aqueous suspension of 100 mg catalyst (incl. 0.5wt.-% Pt^0) in 10 vol-% MeOH. The resulting gases were analyzed every 2.5 min by gas chromatography to monitor the hydrogen evolution over time.

3 Results and discussion

UV/Vis spectra (Fig. 1) of Co_3O_4 suspensions show that different crystal sizes of this material result in different absorption coefficients. The larger the crystal the higher is the light absorption. These results prove that quantum size effects might play a role in the photocatalytic activity of these materials. It was shown previously that Co(II) salts or oxides have an impact on the photocatalytic activity of semiconductors towards oxygen evolution from water. This

behavior might be explained by a reduced overpotential for oxidation reactions *or* an improved electron-hole separation. In this study Co_3O_4 was deposited on TiO_2 and g-C_3N_4. The samples were tested towards their hydrogen evolution rate (HER). The presence of Co_3O_4 increases the hydrogen evolution rate of graphitic carbon nitride (Fig. 1). Thus, it was the aim of the presented work to investigate the size-dependency of cobalt oxide nanoparticles, which were deposited on the solid surface of TiO_2 and g-C_3N_4. As the results imply, such a size-dependency can be found. Although cobalt oxide accelerates the reaction, this effect is stronger for the small and large nanoparticle with a size of 6 nm and 15 nm, respectively. Generally, such an effect is explained by the alternated percentage of different surface atoms. Still, the results might be an artifact from cobalt oxide nanoparticle giving different shapes caused by the hydrothermal reaction conditions. Cyclovoltammogramms and photoluminescence measurements might clarify the role of the cobalt oxide deposited on the semiconductor materials.

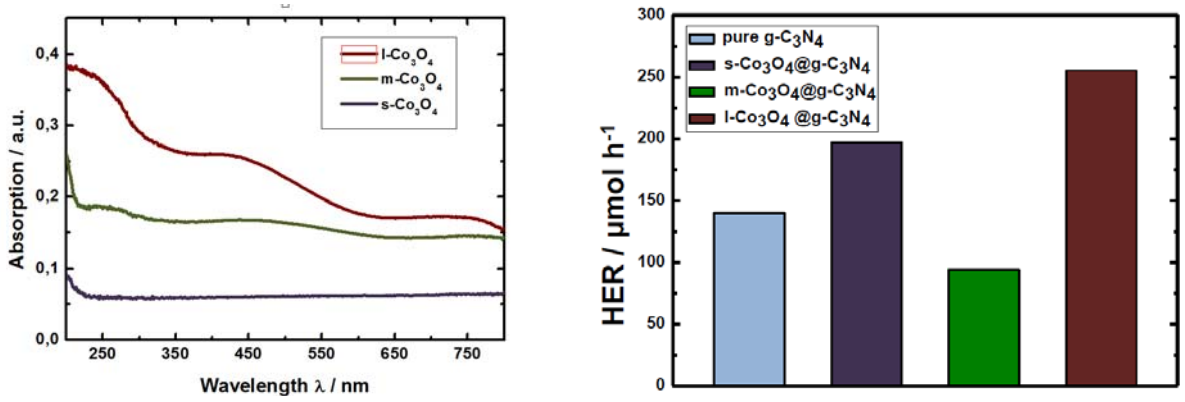

Fig. 1. Left: UV/Vis spectra of aqueous suspensions of 50 mg/l cobalt oxides. Crystallite sizes: l-Co_3O_4 15 nm, m-Co_3O_4 8 nm and s-Co_3O_4 5 nm. Right: Photocatalytic hydrogen evolution rates (HER) from modified g-C_3N_4 show that cobalt oxide acts as a promoter. The results imply a size-dependent effect.

4 Conclusions

The deposition of Co_3O_4 was investigated towards photocatalytic water splitting on two types of semiconductor. Electrostatic adsorption was used to deposit Co_3O_4 on semiconductors. While the presence of Co(II) compounds were previously shown to enhance the photocatalytic activity of semiconductors, the effect of nanoparticle size investigations have not been reported yet. In order to study the success of the particle deposition and the size of the cobalt oxide particles, the modified semiconductors were examined thoroughly. Co_3O_4 was discussed to decrease the overpotential of the water oxidation reaction and stabilize electron holes leading to a higher photocurrent. Nevertheless, a promoting effect was evident.

Acknowledgments

The authors would like to thank the ESF for financial support and research group Echem Leipzig for advices.

References

[1] A. Fujishima, K. Honda, Nature 238 (1972) 37.
[2] F.E. Osterloh, B.A. Parkinson, MRS Bull. 36 (2011) 17.
[3] X. Wang, J. Zhuang, Q. Peng, Y. Li, Nature 437 (2005) 121.
[4] R. Marschall, Adv. Funct. Mater. 24 (2014) 2421.
[5] A.A. Ismail, D.W. Bahnemann, Solar Energy Materials and Solar Cells 128 (2014) 85.
[6] J. Wang, F.E. Osterloh, J. Mater. Chem. A 2 (2014) 9405.
[7] Y. Dong, K. He, L. Yin, A. Zhang, Nanotechnology 18 (2007) 435602.

III-PP48

Synthesis of Mesoporous SnO_2 as Anode for PEMFCs

Somacescu S.[1], Petrea N.[2], Somoghi V.[3], Neatu F.[4], Neatu S.[3,5], Florea M.[4*], Sonu M.[2]

1 - "Ilie Murgulescu" Institute of Physical Chemistry, Romanian Academy, Bucharest, Romania
2 - Scientific Research Centre for CBRN Defense and Ecology, Bucharest, Romania
3 - S.C. STIMPEX S.A., Bucharest, Romania
4 - University of Bucharest, Faculty of Chemistry, Department of Organic Chemistry, Biochemistry and Catalysis, Bucharest, Romania
5 - National Institute of Materials Physics, Bucharest, Romania

* mihaela.florea@chimie.unibuc.ro

Keywords: mesoporous, SnO_2, hydrothermal, anodes for PEMFC

1 Introduction

Tin dioxide (SnO_2) is an important n-type semiconductor material, which has been widely used in many applications such as catalysis, hazardous gas sensors, heat reflecting mirrors, transparent conducting electrodes for solar cells, optoelectronic devices [1, 2]. These applications strongly depend on the structure and morphology of the SnO_2 samples, therefore special attention must be paid to the development of reproducible and cost efficient preparation methods of this material. A number of processing methods such as co-precipitation, sol-gel, chemical vapour deposition, laser ablation and thermal redox process have been developed for the preparation of SnO_2. In this study, the synthesis of mesoporous SnO_2 by a hydrothermal route, using a nonionic surfactant – Triton X100 as template, is reported.

2 Experimental

Mesoporous SnO_2 was prepared by a hydrothermal synthesis route as following: $SnCl_4$ aqueous solution was added to the micellar solution formed by a very well dispersion of template- Triton X100 in deionized water. The tetrabuthylammonium hydroxide solution was used to adjust the pH value at 11. After vigurous stirring, the obtained solution has been hydrothermaly treated at 160 ºC for 48h under autogenously pressure. The resulted precipitate was filtered and washed with distilled water, dried at 100 ºC and calcined at 600 ºC for 8h in air. **The differential thermal analysis and thermogravimetric analysis** of the dried precursors were carried out using a TG-DTA analyzer Shimadzu DTA- 60 instrument on 4-6 mg samples in N_2 atmosphere with a heating rate of 5 °C/min from room temperature to 900 °C, using alumina as reference. **X-Ray diffraction analyses** were carried out on a Schimadzu XRD-7000 diffractometer using Cu Kα radiation (λ = 1.5418 Å, 40 kV, 40 mA) at a scanning speed of 0.10 degrees min^{-1} in the 2θ range of 6 – 70 degrees with a step size of 0.02º and scan time of 2°/min. **Porosity Analysis (BET)** - Brunauer–Emmett–Teller adsorption–desorption isotherms of N_2 were investigated using a Micrometrics instrument (ASAP2010) by N_2 adsorption at the nominal temperature of liquid nitrogen (77K) and at a wide relative pressure range from 0.01 to 0.995. Prior the analysis, the samples were degassed at 150 °C for 5h using helium. **Surface analysis** performed by X-ray photoelectron spectroscopy (XPS) was carried out on **PHI Quantera** equipment with a base pressure in the analysis chamber of 10^{-9} Torr. The X-ray source was monochromatized Al Kα radiation (1486.6 eV) and the overall energy resolution is estimated at 0.65 eV by the full width at half-maximum (FWHM) of the $Au4f_{7/2}$ photoelectron line (84 eV). Although the charging effect was minimized by using a dual beam (electrons and Ar ions) as neutralizer, the spectra were calibrated using the C1s line (BE = 284.8 eV) of the adsorbed hydrocarbon on the sample surface (C–C or $(CH)_n$ bondings).

3 Results and discussion

The BET measurements confirm the mesoporosity for the calcination temperature, with high surface area - S_{BET} ~130 m^2/g. The shape of adsorption/desorption isotherm - type IV is typical for mesoporous material, with well-defined hysteresis loop according to the IUPAC classification (Figure 1). SnO_2 show a uniform pore size distribution with an average pore size diameter around 5 nm. The globular morphology of synthesized material is also characteristic for mesoporous materials with nanocrystalline framework. The XRD pattern of mesoprous material can be indexed as SnO_2 with rutile-type tetragonal symmetry, as depicted in Figure 2.

Fig. 1. Adsorption-desorption isotherms for SnO_2

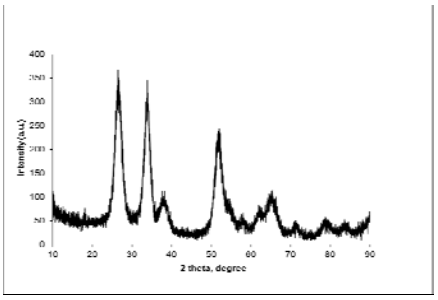

Fig. 2. X-ray diffraction pattern for SnO_2

The sample calcined at 600 ºC exhibited only the tetragonal phase with space group P42/mnm (JCDPS No. 77-0449) and the major peaks appear at 2θ = 26.8º, 33.9º, 38.6º, 51.9º, 62.1º and 65.5º. It is further observed that there is no indication of the presence of both low temperature monoclinic or high temperature cubic phases. Non-symmetrical peaks can be detected at 2θ = 62.1º and 65.8º and are indexed as (310) and (301) planes respectively. The estimated particle size of SnO_2 determined by the Scherrer equation is 9 nm. In order to determine the chemical states and to quantify the elements present on the surface and their quantification the XPS analysis was used. The characteristic BEs for Sn3d are typically assigned to +4 oxidation state. The deconvolution of the O1s photoelectron line shows a surface chemistry with the main lattice bound component (O^{2-}) as well as the OH groups and water confined on the outermost surface layer.

4 Conclusions

Mesoporous pure tetragonal SnO_2 was obtained by hydrothermal synthesis route. Surface chemistry investigations showed that oxidation state of Sn is only +4. The oxygen excess found on the surface comes from OH groups and water adsorbed from environment. The preliminary results obtained in this study show that this material is a good candidate for anode in PEMFC applications.

Acknowledgements

This work was supported by a grant of Partnerships in priority S&T domains Program (PNII), MEN– UEFISCDI, project number 56/2014.

References

[1] P.T. Wierzchowski, L.W. Zatorski, *Appl. Catal. B: Environ.* (2003) 1352.
[2] M.V. Reddy, L.Y.T. Andreea, A.Y. Ling, J.N.C. Hwee, C.A. Lin, S. Adams, *Electrochim Acta* 106 (2013) 143.

III-PP49

Ni-Based Catalysts for Methane Dry Reforming: EXAFS, TEM and DRIFT Investigation on the Au/Pt/Pd Effects

Puleo F.[1], Banerjee D.[2], Pantaleo G.[1], Longo A.[1,3], Aprile C.[4], Collard X.[4], Martinez-Arias A.[5], Liotta L.F.[1*]

1 - ISMN-CNR, Palermo, Italy
2 - DUBBLE, European Synchrotron Radiation Facility (ESRF), Grenoble, France
3 - Netherlands Organization for Scientific Research (NWO) Grenoble Cedex, France
4 - University of Namur (UNAMUR), Namur, Belgium
5 - CSIC, Madrid, Spain

* liotta@pa.ismn.cnr.it

Keywords: Ni-Au-Pt, DRM, alloy, EXAFS, CO, DRIFT, TEM

1 Introduction

Nowadays the use of CO_2 and CH_4 as chemical feedstock may contribute to reduce effectively such greenhouse gases in the atmosphere. Dry Reforming of Methane (DRM) has received considerable attention as an attractive route to produce syngas, CO + H_2, which main application is electricity generation and as intermediate in producing synthetic petroleum via Fischer–Tropsch synthesis. Nickel is the most frequently used metal in DRM because of its good catalytic activity and its cost-effectiveness as compared with Pt, Ru or Rh-based catalysts [1]. However, the formation of significant amount of carbon coke and the particle sintering at the high temperature limit its applications. The addition of second noble metals, such as Pt, Au, Pd may reduce poisoning and deactivation. Some of us have recently found for Ni-Au/$MgAl_2O_4$ catalysts that addition of gold lowered the amount of formed carbon during the DRM reaction [2]. Moreover, a trimetallic catalyst, NiAuPt/Al_2O_3, containing only 0.2wt% of Au and 0.2wt% of Pt showed improved catalytic activity and stability to carbon poisoning with respect to monometallic Ni and bimetallic Ni-Au and Ni-Pt systems [3].

Such promoting effect for the trimetallic catalyst was attributed to the formation of high active Ni-Au-Pt nanoparticles, synergistically interacting, where growth of small amount of bamboo-like carbon nanotubes occurs. Alloyed NiAuPt nanoparticles that could preferentially generate bamboo-like carbon were also postulated on the basis of XRD characterization.

In order to get more insights into the structural and surface properties of such NiAuPt/Al_2O_3 catalyst, EXAFS analyses and DRIFT investigations of CO chemisorbed species were carried out. Monometallic Ni and bimetallic NiAu, NiPt and NiPd/Al_2O_3 catalysts were studied for comparison. The DRM activity was tested in the range of temperature 400-800 °C and for the most active system, NiAuPt, a 5 days long run at 750 °C was registered.

2 Experimental

Monometallic Ni4wt%/Al_2O_3 and bi-trimetallic catalysts containing Ni4wt% and Au(0.2wt%), Pt(0.2wt%) or Pd (0.2wt%) were prepared and studied in the DRM reaction as reported elsewhere [3]. Fresh prepared and spent samples were characterized by XRD, TPR, TEM, EDX and TPO measurements. EXAFS analyses and DRIFT investigations of CO were also performed.

3 Results and discussion

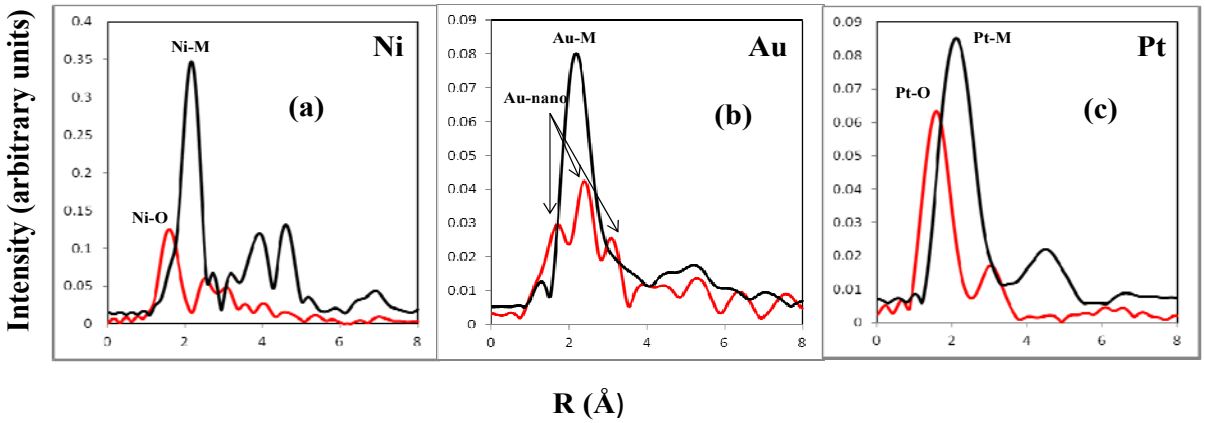

Fig. 1. Fourier transformed EXAFS spectra of (a) Ni-K edge, (b) Au-L_{III} edge and (c) Pt-L_{III} edge.

Figure 1 shows the Fourier transformed EXAFS spectra of Ni-K edge, Au-L_{III} edge and Pt-L_{III} edge in three adjacent plots. The red curves correspond to the calcined NiAuPt catalyst, while the black curve is related to the sample after reduction in H_2/Ar at 750 °C. In the Ni plot, the first peak corresponds to a Ni-O distance at □1.8 Å. After reduction, this peak is observed at a longer distance and with higher intensity suggesting Ni-metal coordination, which in turns points to nickel reduction and/or to Ni-Au/Pt alloy. In the Au plot the red curve shows three peaks at distances of 1.8, 2.5 and 3.2 Å suggesting that Au is distributed as small clusters on the surface. After reduction, a single peak with higher intensity appears suggesting local structural modification. In the Pt plot, a similar shift to that of Ni, was observed after reduction.
DRIFT spectra of adsorbed CO registered over Ni and NiAuPt catalysts evidenced for the trimetallic to a red shift of the linear carbonyl chemisorbed on nickel particles along with higher intensity of the band related to bridging carbonyls chemisorbed on the nickel particles.

4 Conclusions

EXAFS and DRIFT characterizations point out the occurrence of structural and geometrical effects induced by the addition of AuPt to Ni/Al_2O_3. The NiAuPt/Al_2O_3 catalyst demonstrated good catalytic stability during a 5 days long run at 750 °C.

Acknowledgements

The authors acknowledge the financial support provided by Italy, EFOR-CNR Project (Energies by Renewable sources) and by European Community, COST Action CM 1104. Dr. Francesco Giordano from ISMN-CNR is gratefully acknowledged for XRD measurements.

References

[1] C. Raab, J. A. Lercher, J. G. Goodwin, J. Z. Shyu, *J. Catal*. 122 (1990) 406.
[2] A. Horváth, L. Guczi, A. Kocsonya, G. Sáfrán, V. La Parola, L. F. Liotta, G. Pantaleo, A. M. Venezia, *Appl. Catal. A* 468, (2013) 250.
[3] H. Wu, G. Pantaleo, V. La Parola, A. M. Venezia, X. Collard, C. Aprile, L. F. Liotta, *Appl. Catal. B* 156–157 (2014) 350.

III-PP50

Catalysts (Nimg)Alo_x + Ceo_2 Derived of Hydrotalcite Type Structures Applied to Dry Reforming of Biogas

Mansur A.J., Vallezi Paladino L.A.*

Federal University of São Carlos, Chemical Engineering Department, São Carlos, Brazil

* anandapaladino@gmail.com

Keywords: biogas dry reforming, syngas, hydrotalcites

1 Introduction

Biogas is a product of anaerobic fermentation of organic wastes (for example vinasse) and its main constitution is 60% CH_4 and 40% CO_2 (volumetric average), both greenhouse gases. In this context, dry reforming of biogas can be used to convert it to syngas ($CO+H_2$), which assumes industrial importance once it can be applied as raw material to produce environmentally friendly liquid hydrocarbons similar to diesel and gasoline by means of Fischer-Tropsch processes [1].

In general, dry reforming of biogas is catalyzed by nickel supported in Al_2O_3, especially because of costs issues. However, nickel based catalysts are deactivated during reforming due to formation of carbon deposits over the catalyst surface. Current literature has shown catalysts whose precursors are oxides derived from hydrotalcites applied to methane and biogas dry reforming [2,3]. Rare earth oxides associated to these structures, such as CeO_2, have also been studied in recent years, due to oxygen storage and transport capacities featured by this oxide, which can improve carbon removal [4]. In this work, catalysts whose precursors are oxides derived from hydrotalcites, promoted with CeO_2, were applied to dry reforming of biogas.

2 Experimental/methodology

Hydrotalcites were synthesized by coprecipitation technique, adding a solution containing nitrates precursors of Ni, Mg, Al and Ce ((Ni+Mg)/(Al+Ce) =3) to a basic solution constituted of NaOH and Na_2CO_3. Mixed oxides were obtained by calcinations of the hydrotalcites for 5 hours at 377 K, being referenced as $NiMgAlO_x$ + CeO_2, (x= 5, 10, 15 and 25%, nominal nickel content in weight), while Ce was fixed as 5% (nominal, w/w) in all this oxides. X-ray difraction was used to characterize hydrotalcites and mixed oxides. These last ones were also characterized by CO_2 temperature programmed desorption (after reduction *in situ*) to evaluate their basicity. Catalytic tests were carried at 377 K, with a load of 100 mg of the oxides, using a total flow of 118 mL/minute with $CH_4/CO_2/N_2$ = 48/32/38 (70800 $mL.h^{-1}.g^{-1}$) and CH_4/CO_2=1,5. Before reaction, the oxides were reduced *in situ* for 1 hour, at 477 K, under flow of 10 mL/minute of H_2 and 35 mL/minute of N_2. Carbon deposited over catalyst surface during the reaction was evaluated using thermogravimetric analysis.

3 Results and discussion

Figure 1 shows hydrotalcite phase, whose characteristic peaks are next to planes (003), (006), (110) and (113). Ceria (CeO_2) is also observed in both hydrotalcite and mixed oxide.

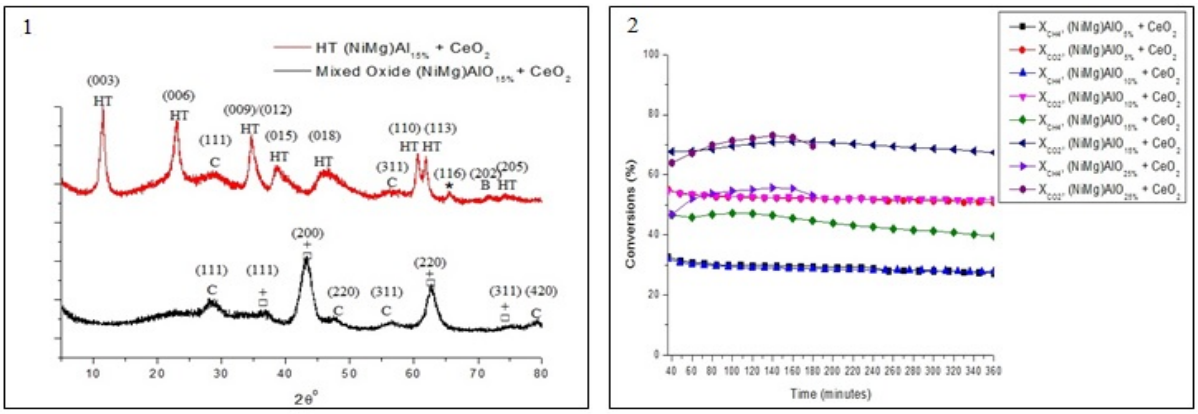

Fig. 1. Hydrotalcites and mixed oxides difratograms (HT-hydrotalcite; C-ceria; B- brucite; □- magnesium aluminium hydroxide carbonate; □- MgO; ⁺ NiO); Fig.2. Catalytic tests

Figure 2 shows that CH_4 and CO_2 conversions increased with nickel content. As detailed in Table 1, carbon deposition followed the same trend, probably because of sintering tendency of metal particles with higher nickel loads. Yet, all of them were stable, even in presence of CH_4 excess, except the one derived from $(NiMg)AlO_{25\%} + CeO_2$. Despite of this catalyst presents higher basicity (see Table 1) than $(NiMg)AlO_{5\%} + CeO_2$ and $(NiMg)AlO_{10\%} + CeO_2$ (after reduction process), this feature was not enough to ensure an extent removal of coke, most likely because of the highest active phase content. It can be said the best catalyst was the one whose precursor was $(NiMg)AlO_{15\%} + CeO_2$ mixed oxide, probably to the highest basicity presented after reduction.

Table 1. Catalysts basicity, carbon deposited after reaction H_2/CO molar ratios.

Structure	**CO_2 desorbed (μmol.g^{-1})/Carbon deposited (gC.h^{-1})/Average H_2/CO**
$(NiMg)AlO_{5\%}+CeO_2$	291/0,002/0,76
$(NiMg)AlO_{10\%}+CeO_2$	200/0,005/0,75
$(NiMg)AlO_{15\%}+CeO_2$	460/0,075/0,85
$(NiMg)AlO_{25\%}+CeO_2$	335/0,268/1,02

4 Conclusions

The catalysts presented here were all actives and stables, except the one derived from $(NiMg)AlO_{25\%} + CeO_2$ mixed oxide. H_2/CO ratios obtained make the syngas produced from biogas dry reforming able to be applied as raw material to Fischer-Tropsch processes.

Acknowledgements

The authors would like to thank CAPES, FAPESP and PRH -44/ANP the financial support.

References

[1] M.H.Rafiq, H.A.Jakobsen, R.Schmid, J.E.Hustad, *Fuel Processing Technology*. 92 (2011)
[2] A.R.González, Y.J.O.Asencios, E.M.Assaf, J.M.Assaf, *Applied Surface Science*. 280 (2013)
[3] A.F.Lucrédio, E.M.Assaf, J.M.Assaf, *Biomass and Bioenergy*. 60 (2014)
[4] C.E. Daza, S. Moreno, R. Molina, *International Journal of Hydrogen Energy*. 36 (2011)

III-PP51

Role of Rh as a Promoter on the Activity of Ni/Ceo_2-Zro_2 Catalyst for Oxidative Steam Reforming of Bio-Ethanol

Mondal T.[1], Pant K.K.[1*], Dalai A.K.[2]

1 - Indian Institute of Technology Delhi, Department of Chemical Engineering, Hauz Khas, New Delhi, India

2 - University of Saskatchewan, Department of Chemical and Biochemical Engineering, Saskatoon, Canada

* kkpant@chemical.iitd.ac.in

Keywords: oxidative steam reforming, hydrogen production, bio-ethanol, Rh promoter

1 Introduction

Hydrogen production from renewable sources such as biomass, is gaining attention due to nearly CO_2 neutral energy supply. Hydrogen production from steam reforming of ethanol has attracted great attention owing to several advantages, such as neutral CO_2 emission, low toxicity, and high hydrogen content in ethanol [1].

2 Experimental/methodology

The catalytic oxidative steam reforming of ethanol (OSRE) for hydrogen production was studied over two selected catalysts Ni/CeO_2-ZrO_2 and Rh-Ni/CeO_2-ZrO_2. The catalysts were prepared by impregnation-co-precipitation method and characterized by BET, XRD, TPR, TPD, TGA, SEM and TEM techniques.

3 Results and discussion

Characterization results revealed that addition of ZrO_2 improves the oxygen storage capacity of CeO_2 which improves catalytic activity. TPR pattern revealed that the addition of noble metals (Rh) resulted in cutback in reduction temperatures probably due to H_2 spill over phenomenon [2]. The NH_3 TPD spectra of Ni/CeO_2-ZrO_2 shows the maximum desorption is occurring at low temperatures which confirms the presence of weak acidic sites.

The effects of temperature, steam to ethanol (S/E) molar ratio, and space time on conversion and product selectivities were investigated in a tubular fixed bed reactor at atmospheric pressure at an ethanol to water molar ratio of 1:9 and oxygen to ethanol ratio of 0.5 over a temperature range of 400 to 650°C (Fig. 1). It was found that conversion increased with temperature and complete conversion achieved at 600°C on $30\%Ni/CeO_2$-ZrO_2 with maximum hydrogen yield of 3.6 mol H_2/mol ethanol reacted. With increasing temperature hydrogen selectivity increased and the same decreasing trend found in case of CH_4 selectivity. Due to the contribution of the water-gas shift reaction below 550 °C CO_2 selectivity increased, while the role of reverse water gas shift reaction is exhibited by an increase in CO selectivity above 600 °C. By changing S/E molar ratio from 9:1 to 6:1 at 600 °C in the feed, the conversion and H_2 selectivity decreased from 99 to 96% and 65 to 60 % respectively. H_2 and CO_2 selectivity was decreased while CO and CH_4 selectivity was increased with decreasing space time. This is because of ethanol decomposion favours more than that of steam reforming reaction at lower space time. After impregnation of 1wt.% Rh on $30\%Ni/CeO_2$-ZrO_2 catalyst, H_2 selectivity increased upto 72% at the same reaction conditions (Fig. 2). Also CO selectivity drops from 14% to 4% on Rh supported catalyst on above reaction conditions. This result clearly indicates that impregnation of Rh on Ni/CeO_2-ZrO_2 catalyst improves catalytic activity by enhancing water gas shift reaction. $30\%Ni$-$1\%Rh/CeO_2$-ZrO_2 catalyst was found to have better catalytic activity than that of $30\%Ni/CeO_2$-

ZrO_2 catalyst. This indicates that addition of noble metal Rh improves the catalytic activity significantly for OSRE.

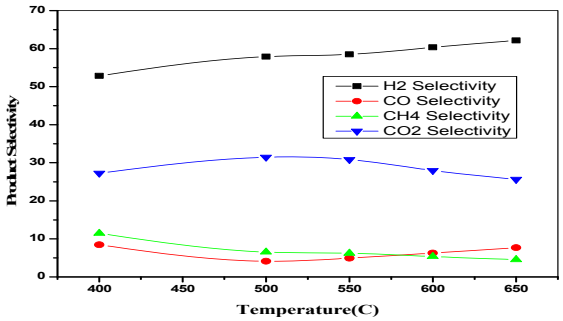

Fig. 1. Effect of temperature on product selectivity at P=1atm, T=600°C, molar ratio EtOH/H_2O/O_2 = 1:9:0.5, W/F_{AO} = 27.52Kgcat.h/Kgmol[EtOH] (Catalyst: 30%Ni-1%Rh/CeO_2-ZrO_2)

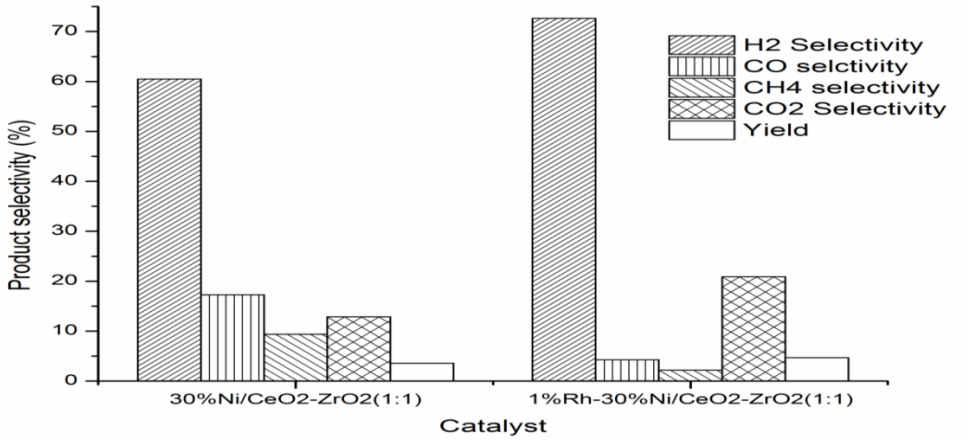

Fig. 2. Product distribution on 30%Ni/CeO_2-ZrO_2 and 30%Ni-1%Rh/CeO_2-ZrO_2 catalysts at T=600°C, P=1atm, molar ratio EtOH/H_2O/O_2 = 1:9:0.5, W/F_{AO} = 27.52Kgcat.h/Kgmol[EtOH]

4 Conclusions

Rh promoted 30%Ni/CeO_2-ZrO_2 catalyst exhibited better catalytic activity for OSRE than that of 30%Ni/CeO_2-ZrO_2 catalyst by enhancing water gas shift reaction.

References

[1] A. Bshish, Z. Yaakob, B. Narayanan, R. Ramakrishnan, A. Ebshish, *Chemical Papers* 65 (2011) 251–266.

[2] J. Kugai, V. Subramani, C. Song, M.H. Engelhard, Y.H. Chin, *J. Catalysis* 238 (2006) 430-440.

III-PP52

Ethanol Steam Reforming over $Mn_xCr_{3-X}O_4$-based Spinel-type Oxide

Smal E.A.[1,2*], Mezentseva N.V.[1,2], Sadykov V.A.[1,2], Krieger T.A.[1], Rogov V.A.[1,2], Simonov M.N.[1], Larina T.V.[1]

1 - Boreskov Institute of Catalysis, Novosibirsk, Russia
2 - Novosibirsk State University, Novosibirsk, Russia

* alageizia@mail.ru

Keywords: hydrogen production, steam reforming of ethanol, spinel-type oxide

1 Introduction

The rapid development of industry and transport in recent decades resulted in significant increase in energy consumption. According to estimates by the International Energy Agency (IEA) world energy consumption has increased by half from 1970 to 2008. IEA predicts that world energy demand will increase by 65-70% by 2030 compared to 2007 levels [1]. In order to ensure global energy and environmental security the international community is trying to reduce energy dependence on fossil fuels. Transformation of biofuels derived from the fast pyrolysis of biomass or bio-ethanol into syngas is one of the most important tasks of catalysis in the energy-related fields. [2]. Large-scale using of biofuels instead of the traditional hydrocarbon fuels can stabilize the current level of the accumulation of carbon dioxide in the atmosphere and prevent its growth. Bioethanol is the most common biofuel, accounting for 82% of all of the world's fuel from biomass. [3] Steam reforming is one of the most efficient processes for the hydrogen production from biofuels. Due to the high activity of biofuels the main problem of catalysts of steam reforming is their rapid coking that leads to deactivation. In this context it is required to design effective, inexpensive and stable catalysts for steam reforming process.

2 Experimental/methodology

Spinel-like mixed oxides $Mn_xCr_{3-x}O_4$ (x=0.3-2.7) were prepared via modified Pechini route [4]. Commercially available $Mn(NO_3)_2 \cdot 6H_2O$ and $Cr(NO_3)_2 \cdot 6H_2O$ were used as starting materials. Polymerizing agents citric acid, ethylene glycol and ethylenediamine were taken in 3.75 : 11.25 : 3.75 : 1 molar ratio to metal cations. Citric acid dissolved in ethylene glycol was added to aqueous solution of nitrate hydrates. This solution was stirred at room temperature for 2 h. After adding ethylenediamine the mixture was stirred again for 2 h and then kept at 100°C to evaporate water. The resulting gel precipitate was calcined at 500°C for 2 h in air obtaining oxide powder.

Ni or Ru (2 wt.%) were supported on oxides by the incipient wetness impregnation with $Ni(NO_3)_2$ or $RuCl_3$ solutions followed by drying and calcinations at 500°C for 2 h.

Also catalyst deposited on aluminum oxide was prepared by successive impregnation with water solutions of nitrates to obtain loading of 10 wt.% MgO, 10% $MnCr_2O_4$, 2% Ni and 2% Ru. After each coating step sample was dried in a microwave oven and calcined in air at 700°C for 2 hours.

Structural features and microstructure of the catalysts were analyzed by X-ray diffraction, TEM with EDX, UV-Vis and XPS. The reduction behavior was examined by temperature-programmed reduction (TPR H_2).

The catalytic properties of samples in ethanol steam reforming were studied by using flow reactor under atmospheric pressure in diluted (0.5% C_2H_5OH+ 2% H_2O in He, contact time 18-54 ms) and concentrated (10% C_2H_5OH+ 40% H_2O in N_2, contact time 70 ms) feeds.

To establish the route of reaction, one of the best samples was studied by in situ IR spectroscopy

during the reaction of ethanol steam reforming.

3 Results and discussion

According to XRD and UV-Vis data, as-prepared samples are comprised of several phases. Samples with a high Cr content contain cubic spinel $MnCr_2O_4$ and hexagonal Cr_2O_3. In samples with a high content of Mn phases of tetragonal Mn_3O_4 and cubic Mn_2O_3 are observed. Due to a low content of supported Ni and Ru and their strong interaction with oxides, they are not detected as separate phases. A high-resolution TEM shows nanocrystalline particles of chromium-manganese spinel with sizes up to 10 nm. In fresh sample no individual particles of RuO_2 or NiO are observed. They may be incorporated into the surface layers. In reaction conditions, Ni and Ru segregate to the surface forming metal alloy particles with sizes 2-10 nm.

According to H_2 TPR data, for all samples with supported Ru reduction of catalyst begins at lower temperatures than for unpromoted oxides. In the same time no TPR peaks of reduction of RuO_2 were observed indicating strong metal-support interaction.

All catalysts demonstrated a high efficiency and stability in the reaction of steam reforming. Sample 2%Ru+2Ni%/$MnCr_2O_4$, both bulk and supported, showed the best results. In dilute feeds evolution of hydrogen begins at 300°C and attained maximum - 2.5% - at 600°C. In concentrated feed hydrogen yield was 33% at 700°C and ethanol conversion was complete at 600°C. As by-products, methane and small (<1%) amounts of ethylene and acetaldehyde were observed at low temperatures. These results are better than previously obtained for fluorite and perovskite based catalysts earlier investigated in similar conditions in ESR [5]. Results of IR studies indicate that the rate-determining stage is transformation of ethoxy species via dehydrogenation followed by decomposition of acetaldehyde.

4 Conclusions

Highly active and stable to coking catalysts of ethanol steam reforming based on bulk/supported $MnCr_2O_4$ spinel promoted by Ni and Ru were elaborated. This is provided by a strong interaction between metal and oxide support and a high oxygen mobility and reactivity in spinel. According to *in situ* IR spectroscopy data, ESR on spinel-based catalysts proceeds via dehydrogenation route.

Acknowledgements

This work was supported by RFBR 12-03-93115 CNRS_a Project and FP7 Project "BIOGO".

References

[1] World Energy Outlook, IEA, 2009.

[2] V. Sadykov, N. Mezentseva, G. Alikina, Composite catalytic materials for steam reforming of methane and oxygenates: Combinatorial synthesis, characterization and performance, Catal. Today 145 (2009) 127–137.

[3] Аналитический отчёт «Основные тенденции развития рынка биотоплива в мире и России за период 2000-2012», ОАО «Корпорация «Развитие», 2013

[4] Patent 3 330 697 U.S. Method of preparing lead and alkaline earth titanates and niobates and coating method using the same to form a capacitor / Pechini, M.P., – 08.1963, patented 11.07.1967.

[5] V. A. Sadykov, S. N. Pavlova, G. M. Alikina, Perovskite-based catalysts for transformation of natural gas and oxygenates into syngas, Chapter 1 in a Book "Perovskite: Crystallography, Chemistry and Catalytic Performance", Nova Science Publishers, Inc, New York, 2013, pp. 1-68

III-PP53

Syngas and Hydrogen Production by Dry and Steam Reforming of Methane and Fermentation Products on Porous Ceramic Membrane-Catalytic Ni-Co-Containing Converters

Fedotov A.[1*], Antonov D.[1], Tsodikov M.[1], Uvarov V.[2]

1 - A.V.Topchiev Institute of Petrochemical Synthesis, Russian Academy of Sciences, Moscow, Russia
2 - Institute of Structural Macrokinetics and Materials Science, Russian Academy of Sciences, Chernogolovka, Russia

* alexey.fedotov@ips.ac.ru

Keywords: porous ceramic converters, reforming, hydrogen, syngas

1 Introduction

Original porous ceramic membrane-catalytic Ni-Co-containing converters highly efficient in dry and steam reforming of methane and fermentation products into syngas and hydrogen were developed. The structural peculiarities of these converters and their impact on processes character were studied.

2 Experimental/methodology

Porous ceramic membrane-catalytic converters (PCMCC) produced by self-propagating high-temperature synthesis were used for investigation. The precursors included a Ni metal powder containing 5 mass % of aluminum and a cobalt oxide (II, III) powder. The ready PCMCC contained different amounts of the Ni(Al) and Co_3O_4 active components in the ratios (mass %) 100 : 0, 95 : 5, 80 : 20, 50 : 50, and 0 : 100. The PCMCC material also contained traces of carbon of the graphite press mold in which the PCMCC sintering took place. The PCMCC were porous gas permeable tubes with one end being sealed off and the other end having a round cap of larger diameter for being mounted inside the reactor. The length of the work area (tube) of the PCMCC was 80 mm, the outer diameter was 16 mm, the wall thickness was 3 mm, the average pore diameter determined by mercury porosimetry method and the bubble point method was 1–3 μm, and the material porosity was 40–60%.

The granular catalyst experiments were performed using 2–3 mm size grains obtained by crushing the PCMCC in a jaw crusher.

The dry reforming of methane (DRM) was carried out on a PCMCC in a flow type reactor with a mounted converter (or loaded grains) under the following conditions: $CH_4 : CO_2 = 1 : 1$, T = 400–800°C, W = 20–750 L/h, P_{inlet} = 1.1 atm, P_{outlet} = 1 atm.
The dry reforming of ethanol (fermentation products) or fusel oil (DRE/FO) were conducted on the same setup under the following conditions: EtOH(FO)/CO_2=1:5, T=150-650°C, W up to 1500 l/h, P_{in}=1.1 atm., P_{out} = 1 atm. The FO composition was vol. %: propanol – 19,1; iso-butanol – 17,5; iso-pentanol – 63,4.

The compositions of the initial gas mixture and the reaction products were determined on-line by gas chromatography on a CHROM5 chromatograph with a thermal conductivity detector, high purity argon as the carrier gas (99.998 vol %, flow rate of 30 mL/min), and two chromatographic columns packed by SKT activated carbon. The gas concentrations were determined using Ecochrom software.

The morphology, structure, composition, and particle size distribution for the synthesized PCMCC structures were studied by TEM (JEM 2010, resolving power of 0.14 mm, accelerating voltage of 200 kV) and EDAX analysis. The samples were crushed, and their suspensions in ethanol were deposited on nitrocellulose film substrates, which were placed on standard copper

holder grids, which, in turn, were mounted into the electron microscope chamber.

3 Results and discussion

A non-additive increase in the catalytic activity of PCMCC based on Ni(Al) and Co_3O_4 powders taken in 1 : 1 ratio in DMR in comparison with the sum of activities of Ni- and Co-containing PCMCC was found. It was demonstrated that the specific productivity of the bimetallic sample for synthesis gas reaches 85000 L/(h dm^3) being more than twice higher than these values for PCMCC with a different nickel to cobalt ratio. It was found that the specific activity of the PCMCC in the transformation of methane into synthesis gas substantially exceeds the activity of a fixed bed of granular catalyst of the same composition in a flow type reactor.

Transformation of ethanol in the process of dry reforming differs from the reforming of methane. Ethanol is less thermodynamically stable and more reactive substrate than methane. In this regard, the conversion of ethanol in catalytic channels of a converter is practically exhaustive at temperatures above 350 °C vs. 800 °C in case of methane. According to the programmed thermogravimetry data, the main difference is the reactions of dehydrogenation to form acetaldehyde and its subsequent decarbonylation to methane. The greatest contribution to the reaction of methane formation from ethanol in the DRE processes is made by nickel, the yield of methane increasing with the increase of nickel content. On the contrary, cobalt reduces the content of CH_4 in the reaction products. In the PCMCC the processes of ethanol reforming are intensified in comparison to the implementation of the process in a flow reactor with a fixed bed of granular catalyst of the same composition. However, due to the higher reactivity of ethanol, performance increase is not so high compared to the effect observed in dry reforming of methane.

Dry and steam reforming of organic fermentation products without their preliminary separation proceed efficiently over PCMCC, yielding hydrogen containing gas. Using as feed for dry reforming process the fossil oil essentially widen recourses of feed stock for hydrogen and syngas producing base on renewable raw. It was shown that mixture of organic alcohols have not ethanol as model of fossil oil is enhance feed for producing of syngas with composition close to one obtained from ethanol.

The PCMCC structure was found to contain nanosized Ni–Co alloy particles formed on the γ-Al_2O_3, which are, apparently, responsible for the non-additive increase in the catalytic activity of the nickel–cobalt converters.

4 Conclusions

It was found that PCMCC based on Ni(Al)-Co_3O_4 (1 : 1) demonstrates a non-additive increase in catalytic activity in DRM, DRE/(FO). The reason of such peculiarity might be a presence of Ni-Co-alloy nanoparticles distributed on the surface of a segregated γ-Al_2O_3. It was also established that the specific activity of the PCMCC in the transformation of methane into synthesis gas substantially exceeds the activity of a fixed bed of granular catalyst of the same composition in a flow type reactor what might be connected with a process character in a restricted volume of converter pores.

Acknowledgements

This work was supported by the Ministry of Education and Science of the Russian Federation (agreement no. 14.607.21.0033) and RFBR 15-03-08753 A.

III-PP54

Dry Reforming of Propane over Ceo_2/Ni-Foam Catalysts

Karuppiah J., Mok Y.S.*

Jeju National University, Department of Chemical Engineering, Jeju, South Korea

* smokie@jejunu.ac.kr

Keywords: propane reforming, synthesis gas, catalysts, carbon deposition, nickel foam

1 Introduction

The catalytic C_3H_8 reforming with CO_2, in which the mixture gas being converted into synthesis gas with H_2/CO ratio of 1 has drawn great interest from the viewpoint of effective utilization of the greenhouse gases and petroleum. The synthesis gas is highly desirable for the production of value-added oxygenated chemicals and liquid fuels [1]. It is well known that the nickel metal is catalytically more active towards reforming reaction, but excess carbon deposition on the metal surface causes the deactivation catalyst. In selecting a catalyst, one needs also to consider other factors such as reactor design. Porous nickel foam (NF) templates are one of the most interesting microstructures and can be used as a catalyst support. The advantages of monolithic or foam reactors over conventional packed bed reactors includes high geometric surface area, low pressure drop when associated with high flow rates, efficient mass transfer, high thermal and mechanical stability [2]. Finally, the active site, especially novel metals can be dispersed uniformly onto the foams, and its confinement effect mainly leads to their activity and stability of supported catalysts, which is a key for the dry reforming reaction. With this background, in this work, we focused on the integration of CeO_2 on Ni-foam by single step wet impregnation method, and analyzing the catalytic activity of CeO_2 loaded Ni-foam for improving propane dry reforming reaction.

2 Experimental

Catalysts preparation

Integration of CeO_2 onto NF (2-4 wt.%) was prepared by impregnation of bare NF within cerium nitrate aqueous solutions of desired concentration. Followed by drying, the NF was calcined at 500^{o}C for 5 h in air to form the crystalline CeO_2 on NF.

Catalytic reaction and characterization

The dry reforming of propane with CO_2 was carried out in a thermo-catalytic reactor packed with 4 g of the catalyst made with cylindrical structures. The catalytic activity was studied in the temperature range of 520–600 °C for all the catalysts. The reactant gases were fed into the reactor at the proportion of 10:30:60 (C_3H_8/CO_2/N_2). The total flow rate was fixed at 300 ml min^{-1} throughout this work. During the reforming reaction, the concentrations of relevant components were analyzed by a gas chromatograph equipped with a thermal conductivity detector (TCD). Numerous techniques, such as N_2 adsorption–desorption isotherm, X-ray diffraction (XRD), field emission scanning electron microscopy (FESEM) and transmission electron microscopy (TEM), and Temperature programmed reduction (TPR) and temperature programmed oxidation (TPD) were applied for characterization of fresh and spent catalysts.

3 Results and discussion

Towards the C_3H_8 and CO_2 conversion, the 4 wt.% CeO_2/NF showed (Fig.1) an improved catalytic activity when compared to 3 wt.%, 2 wt.% CeO_2/NF and bare NF. For 4 wt.% CeO_2/NF catalyst showed desired mass loading and optimal concentration of ceria over NF which favours

for the effective nanoconfinement of CeO_2 particles and superior metal-support interaction. Thereby it was observed the enhanced catalytic reforming efficiency for C_3H_8/CO_2. Typical H_2/CO ratios obtained with the different ceria loaded NF catalysts are illustrated in Fig. 2 as a function of reaction temperature. Over the observed temperature range, the 4 wt.% of CeO_2/NF and 3 wt.% of CeO_2/NF catalysts exhibited relatively higher H_2/CO ratio than the 2 wt.% of CeO_2/NF as well as pure NF.

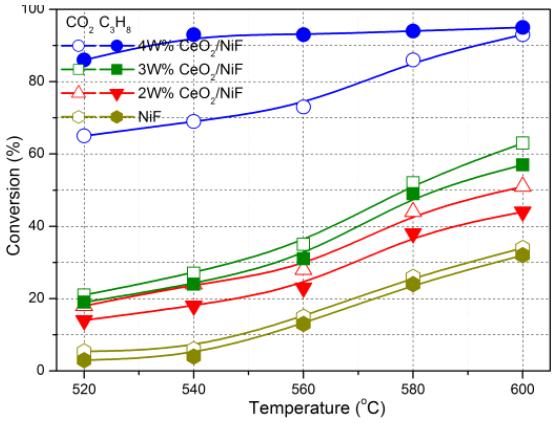

Fig. 1. Conversions efficiencies of C_3H_8 and CO_2

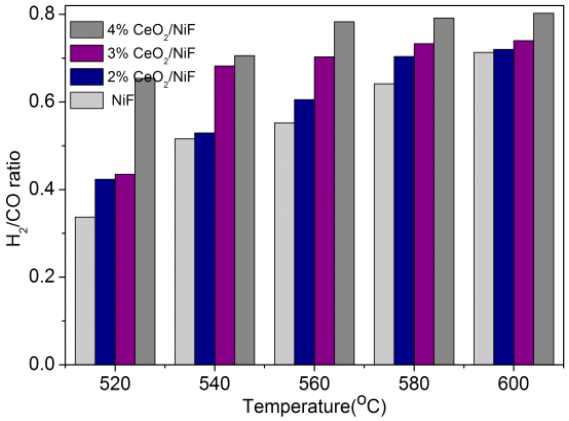

Fig. 2. H_2/CO ratios obtained with different catalysts.

The results of catalyst testing revealed that the catalysts with 4 wt.% CeO2 loading have showed the superior catalytic performance than 3 wt.% and 2 wt.% of CeO_2. After 24 h under stream at 560°C, CeO_2 catalysts showed a stable operation in presence of a deposited amorphous carbon. Carbon deposition on spent catalysts was analyzed by the temperature programmed oxidation (TPO). The structural and phase modification of the catalysts after the reforming reactions were further examined with XRD, SEM, TEM and TPO.

4 Conclusions

Nanocryatalline CeO_2 loaded NF catalysts were investigated in order to evaluate the effect of the support structure on the catalytic activity towards C_3H_8 dry reforming. It was observed the higher dry reforming activity of CeO_2-promoted NF and exhibited good stability against anti-sintering and coke resistance.

Acknowledgements

This work was supported by the research grant of Jeju National University in 2013, and by Basic Science Research Program through the National Research Foundation of Korea (NRF) funded by the Ministry of Science, ICT and future Planning (Grant No. 2013R1A2A2A01067961).

References

[1] J. Karuppiah, Y. S. Mok, *International Journal of Hydrogen Energy*. 29 (2014) 16329.
[2] P. Ciambelli, V. Palma, E. Palo, *Catalysis Today*. 155 (2010) 92.

III-PP55

A Catalytic Heater for an External Combustion Engine

Samoilov A.V.[1*], Kirillov V.A.[1], Kuzin N.A.[1], Shigarov A.B.[1], Taleb A.[2], Markides C.N.[2]

1 - Boreskov Institute of Catalysis, Novosibirsk, Russia
2 - Clean Energy Process Laboratory, Department of Chemical Engineering, Imperial College London, London, UK

* samoilov@catalysis.ru

Keywords: syngas generation, catalytic heating element, natural gas conversion, external combustion engine

1 Introduction

In many types of heat engine devices a combustible fuel is employed and its heat of combustion is transferred to a working fluid for conversion. A common type in widespread current use employs an open plasma flame as the transfer medium. Another type employs a flameless combustion process that utilizes a catalytic coating at the surface area where heat is to be applied. In practice, an increase in the flow of thermal energy being transferred to the external heat engine is the primary mechanism for improvement of its performance. At the same time, it is known that syngas (mixture of H_2 and CO), which can be prepared by the conversion of natural gas, is catalytically oxidized very easily. We hereby propose a dedicated heating element that promotes the catalytic combustion of syngas, thus generating the primary source of thermal energy input for an external heat engine device.

2 Experimental methodology

A schematic diagram of the proposed catalytic heating element (CHE) design for the one-step process of the catalytic combustion of syngas is shown in Fig. 1. A detailed presentation of the CHE device can be found in Ref. [1], nevertheless, a brief overview of the proposed design is provided here for completion.

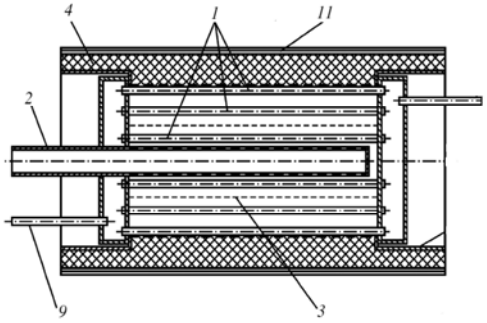

Fig. 1. Schematic diagram of the catalytic heating element (CHE).

The CHE is a cylindrical structure consisting of an annular tubular heat exchanger (1), which is located inside a gas distribution perforated tube (2) where the premixed air-fuel mixture is supplied to the element. In order to promote the uniform distribution of the fuel mixture and the extension of the mixture jets issuing from the holes around the gas distribution pipe, a perforated splitter (3) is introduced around the fuel mixture supply tube. The catalytically active layer (4) has a regular structure, and is composed of five flat and corrugated strips, wound on the tube heat exchanger (1) and sintered together. The thickness of the strips is about 1 mm with the winding pitch on the tube heat exchanger amounts to 27.5 mm. Tapes permeable to the gas form catalytically active channels with a diameter of 2.5 mm. The width of the tapes is 25 mm, and the spacing between adjacent rows of winding is 2.5 mm. The first and last rows are formed by flat ribbons, while the intermediate layers consist of alternating flat and corrugated

strips. To reduce the heat losses, the catalyst layer exceeds beyond the length of the heat exchanger. Furthermore, in order to reduce the start-up time of the heating element (11), the outer layer of the catalyst has a size larger than the critical size of ribbed channels for the penetration of flame into the porous structure.

In this work the CHE shown in Fig. 1 was tested experimentally. The concentrations of the components in the fuel mixture were measured by a GC (Crystal-2000M), and the concentrations of CO and NO_x in the exhaust gases were measured by a gas analyser (KM-900).

3 Results and discussion

The use of the aforementioned CHE device for the catalytic combustion of natural gas (here mainly methane, 86 – 98% by volume) allows the heating power and temperature to be regulated over broad ranges by suitable adjustment of the air-fuel ratio in the mixture. Table 1 shows the results of a comparison of different heat generation methods, while Table 2 shows additional analytical data for the catalytic combustion products.

This process is carried out on reinforced metal porous catalysts produced by self-propagating high-temperature synthesis. According to X-ray analysis, composite catalyst comprises the following phases: Ni, α-Cr_2O_3 and α-Al_2O_3. The specific surface area of 3.4 m^2/g; catalyst characterized by macroporous structure: a main pore volume in pores with a radius from 15 to 100 microns.

The use of such a CHE allows the generation of a high-intensity, uniform heat flux, and therefore, its employment acts to promote the intensification of the heat transfer process to the external combustion engine. In fact, it has been shown that the overall engine system efficiency can be increased to 30-35%, and by using thermochemical recuperation up to 41% [2]. Furthermore, it is evident from our current results that the syngas is generated at the desired ratio of 1:2 and that the concentration of CO and NO_x are within GOST levels.

Table 1. Comparison of different heat generation methods

Type of heating	Parameters
Flame heater 1	$T_{flame} = 1023$ °C; two propane burners: $Q_{pr} \approx 787$ W
Flame heater 2	$T_{flame} = 1847$ °C; acetylene burner: $Q_{ac} \approx 8787$ W
Catalytic heater	$T_{in} = 597$ °C; CHE: $Q_{in} = 3500$ W

Table 2. Analysis of catalytic combustion products

Inlet flow			Output data			
CH_4 (L/min)	Air_1 (L/min)	Air_2 (L/min)	CO (ppm)	NO_x (ppm)	CO_2 (vol %)	O_2 (vol %)
4	14	105	1	6	2.5	12.6

4 Conclusion

A catalytic heater was designed for external heat-engine applications. The high heat fluxes that be attained are highly beneficial for the performance of these heat engines. Tests reveal low emission levels, and a favorable ability to easily vary the output thermal power and temperature.

Acknowledgements

This work was financially supported by the Ministry of Education and Science of the Russian Federation in the framework of the Agreement on granting subsidies from 5 June 2014 № 14.577.21.0071 (unique identifier applied research (project) RFMEFI57714X0071). This research was performed under the UNIHEAT project. The authors wish to acknowledge the Skolkovo foundation and BP for the financial support.

References

[1] V. Kirillov, N. Kuzin, V. Kuzmin, *Theoretical Foundations of Chemical Technology*, 4 (2005) 407.
[2] V. Kirillov, N. Kuzin, V. Kireenkov, *Theoretical Foundations of Chemical Technology*, *in press* (2015).

III-PP56

Ethanol Steam Reforming to Hydrogen over CoNi-Based Catalysts

Braga A.H.[1], Batista J.B.O.[1], Damyanova S.[2*], Bueno J.M.C.[1]

1 - Universidade Federal de São Carlos, Departamento de Engenharia Química, São Carlos, Brazil
2 - Institute of Catalysis, Bulgarian Academy of Sciences, Sofia, Bulgaria

* sonia.damyanova@yahoo.com

Keywords: hydrogen, ethanol steam reforming, CoNi catalysts, $MgAl_2O_4$

1 Introduction

Ethanol steam reforming (ESR) is one of the possible industrial processes for hydrogen production. As a transition metal, Ni-based catalysts exhibit high activity in reforming processes and are cost-effective in comparison with noble metal-based catalysts. However, the catalyst deactivation by carbon deposition is a general problem for ESR over supported Ni catalysts. Cooking of Ni surface is an important technological problem and many experimental studies have been addressed to this process. The objective of present work was to explore the structure, surface properties and catalytic performance of Co doped Ni catalysts supported on $MgAl_2O_4$ in ESR.

2 Experimental/methodology

The $MgAl_2O_4$ support employed in this study was prepared by sol-gel method [1]. The supported Ni, Co and CoNi catalysts were prepared by incipient wetness impregnation method of carrier with aqueous solutions of $Ni(NO_3)_2.6H_2O$ and $Co(NO_3)_2.6H_2O$. The obtained solids were dried and calcined under air flow at 110^0 and 550^0 C for 12 and 6 h, respectively. The samples were labeled as 8Ni, 4Co4Ni and 8Co, where the number is the nominal metal content. The samples were characterized by XRD, XRF, XPS, EXAFS, XANES and TEM. Catalytic tests were performed in a fixed-bed quartz reactor at atmospheric pressure and temperature range of 250^0 - 700^0C. Prior to each catalytic reaction the catalyst was reduced under H_2 stream at 750^0C for 1 h. Molar ratio H_2O/C_2H_5OH of 3 was kept. The effluent gaseous products were analyzed on-line by gas chromatograph.

3 Results and discussion

Figure 1 shows the evolution of ESR reaction (outlet composition and ethanol conversion) at different reaction temperatures from 250^0 to 700^0C. Ethanol dehydrogenation to CH_3CHO is observed for all catalysts at low reaction temperatures. Increasing the Co content leads to increase of CH_3CHO formation in a broader range of temperature, which means that this product is important intermediate in the ESR. However, the catalysts show different behaviour in the C-C breaking. A correlation between the cleavage of C-C bond, producing methane and CO, and the degree of reduction and metallic area (Table 1) is well visible for N catalyst at low temperatures. In opposite to that, Co catalyst did not promote the C-C bond cleavage efficiently due to the lowest degree of reduced species. The progressive reduction of Co^{2+} on Co catalyst during ethanol activation causes a progressive C-C bond cleavage at higher temperatures, producing CO, CO_2 and H_2. The high CO_2/CO ratio for Co catalyst at 450^0C suggests a promotion of water gas shift reaction (WGSR) in a higher extension compared to that for Ni-containing catalysts. The bimetallic CoNi catalyst presents behaviours between those of Ni and

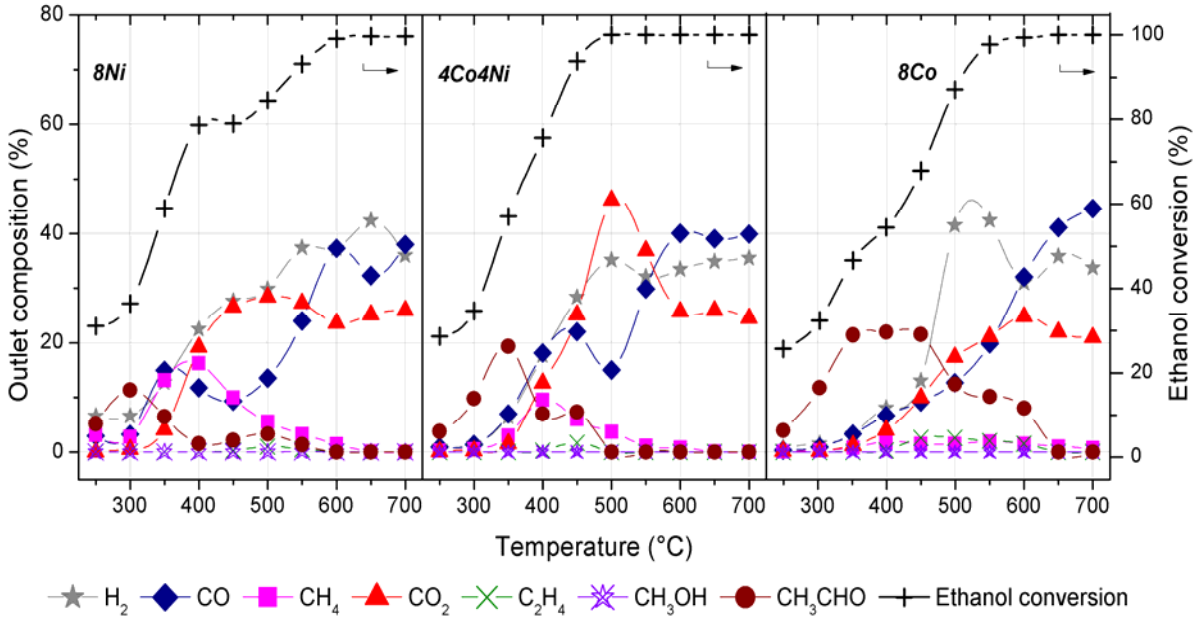

Fig. 1. Evolution of ESR as function of reaction temperature for Ni, CoNi and Co catalysts

Table 1. Physicochemical properties of catalysts

Sample	Reduction degree (%)	Metallic area ($m^2g_{cat}^{-1}$)	Carbon accum. rate ($mgCg_{cat}^{-1}h^{-1}$)
8Co	100	8.83	3.75
4Co4Ni	91	7.29	1.83
8Ni	84	0.75	2.01

Co catalyst. The lower extent of CH_3CHO formation on CoNi at low temperature compared to that of monometallic Co, due to the oxidative dehydrogenation of ethanol, suggests that CoNi catalyst is partially oxidized caused by H_2O activation. After 300^0C the lower extent of CH_4 formation for bimetallic CoNi compared to that for monometallic Ni means that the electronic modification caused by Co-Ni interaction influences the CH_x and HCO species adsorption on catalyst surface. The Co didn't promote the formation of CH_4. For all catalysts the CO_2 formation is increased at temperature > 400^0C, which means a better activation of water and promotion of WGSR, hence the H_2 is also increased. An inversion in the CO_2/CO ratio is observed after 500^0C, most probably, caused by $C + CO_2 \rightarrow 2CO$ (reverse Boudouard reaction).

4 Conclusions

It can be concluded that the different behaviours of $MgAl_2O_4$-supported Co, Ni and CoNi catalysts in ESR are related to the oxidation state of metallic components evaluated by TPR, XANES and EXAFS. Since the metallic sites are responsible for C-C bond breaking and further ethanol dehydrogenation, the Ni catalyst is the most active in ESR at low reaction temperatures (up to 350^0C). The bimetallic CoNi catalyst is more tolerant to carbon formation, showing better ability to oxidize the carbon, which is due to the alloy formation.

Acknowledgements

The authors thank FAPESP and Brazilian Synchrotron Light Laboratory for supporting this research. S.D. is gratefully acknowledged to Bulgarian National Science Fund (Project E 02/16).

References

[1] C.N. Ávila-Neto, J.W.C. Liberatori, A.M. da Silva, D. Zanchet, C.E. Hori, F.B. Noronha, J.M.C. Bueno, J. Catal. 287 (2012) 124.

III-PP57

A Study on Kinetics of Methane Oxidative Steam Reforming (OSR) over Pt-Ni/Al_2O_3 Bimetallic Catalysts

Erdinç E., Aksoylu A.E.*

Bogazici University, Department of Chemical Engineering, Istanbul, Turkey

* aksoylu@boun.edu.tr

Keywords: catalytic hydrogen production, OSR of methane reaction, kinetics, heterogeneous catalysis

1 Introduction

A fuel processor (FP) is a catalytic system that produces CO-free hydrogen from a hydrocarbon having well established distribution network, like methane [1]. Oxidative steam reforming (OSR), which is a substantially preferred reforming reaction for FPs to be used in small scale applications, is the simultaneous steam reforming and partial oxidation. In OSR, exothermic total oxidation produces energy *(almost)* enough for endothermic steam reforming, which results in energy efficiency. OSR reduces coke formation, and increases stability and hydrogen yield at relatively lower temperatures. Moreover, OSR reactors are advantageous in reformer design due to their compact size, quick response feature, and inexpensive material requirement [2].

In order to design, construct and control an efficient reactor, reliable kinetic expressions must be known for the catalytic reaction of interest. Although power-law type of rate expression does not give a detailed idea about reaction mechanism, they are beneficial for prediction of system performance, comparison of different catalysts and designing reactors. In the previous studies conducted in our laboratory, several Pt-Ni/Al_2O_3 catalysts have been designed, prepared and tested by their propane OSR performance. We also have reliable kinetic expressions for propane OSR over the Pt-Ni system [3].

In the current work, power-law type of kinetic expression for methane OSR over Pt-Ni/Al_2O_3 catalyst is obtained as a function of temperature and partial pressures of methane, oxygen and steam.

2 Experimental

0.2Pt-10Ni/Al_2O_3 catalyst was prepared by sequential impregnation method. The catalyst was reduced *in situ* prior to each experiment. In the kinetic tests, the feed compositions were designed such that the upper-lower limits of the steam-to-carbon (S/C) and carbon-to-oxygen (C/O_2) feed ratios were 3.08-2.03 and 7.34-4.00, respectively. During the tests, conversion-residence time relation was kept linear for guaranteeing that the reactions were in kinetically controlled region. Experiments were conducted at 375 °C and atmospheric pressure for different partial pressure values for each reactant (i.e. methane, oxygen, steam) at two different non-zero residence time (W/F) values (Table 1). Rate orders with respect to methane, oxygen and steam were calculated by applying multivariable non-linear optimization function of MATLAB™ to the "methane conversion versus residence time" data. For the activation energy calculations, Set 4 in Table 1 was repeated at 350 and 400 °C. A power-law type rate expression as a function of partial pressures of reactants and temperature is proposed.

3 Results and discussion

The initial methane consumption rates were listed in Table 1 with corresponding partial pressures of reactants – methane, oxygen and steam. Methane consumption rates were obtained

from intrinsic kinetic data in the initial rate region by using differential method of analysis. Reaction orders with respect to methane, oxygen and steam partial pressures were estimated as 0.81, 1.60 and 0.44, respectively by non-linear regression analysis on 17 sets of "initial rate versus partial pressures of reactants" data (Table 1). Reaction rate showed positive dependency for all reactants with a decreasing order of oxygen, methane, and steam as expected.

Table 1. Initial rates of methane OSR reaction with varying feed compositions over the 0.2Pt-10Ni catalyst at 375 °C.

Set #	P_{CH4} (kPa)	P_{O2} (kPa)	P_{H2O} (kPa)	CH_4 Consumption Rate (μmol mg^{-1} s^{-1})	R^2
1	15.21	3.80	46.28	34.25	0.98
2	16.71	3.80	46.28	45.81	0.93
3	18.36	3.80	46.28	49.17	0.93
4	19.77	3.80	46.28	43.56	0.96
5	21.27	3.80	46.28	44.06	1.00
6	22.80	3.80	46.28	57.29	0.95
7	19.77	2.69	46.28	23.72	0.99
8	19.77	2.99	46.28	37.86	0.98
9	19.77	3.37	46.28	36.36	1.00
10	19.77	4.11	46.28	55.32	0.94
11	19.77	4.49	46.28	64.70	0.93
12	19.77	4.67	46.28	61.28	1.00
13	19.77	4.11	47.64	48.08	0.99
14	19.77	4.11	50.66	55.76	0.92
15	19.77	4.11	53.70	49.78	0.93
16	19.77	4.11	56.74	61.13	0.96
17	19.77	4.11	60.80	61.15	0.99

After reaction orders were determined, Set 4 in Table 1 was repeated at 350 and 400 °C. Temperature interval was kept narrow within ±25 °C in order to eliminate any possible effect of temperature on reaction path. The apparent activation energy and the pre-exponential factor were estimated as 0.956 μmol.mgcat^{-1}.s^{-1}.kPa$^{-2.85}$ and 39.05 kJ.mol^{-1}, respectively, by using Arrhenius equation.

4 Conclusions

Kinetic study was performed for determining intrinsic reaction rates of methane OSR over 0.2Pt-10Ni catalyst at 375 °C. Multivariable non-linear optimization function of MATLAB™ was utilized to estimate reaction orders. The proposed power-law type rate expression that is reliable in the range of $2.03 < S/C < 3.08$ and $4.0 < C/O_2 < 7.34$ feed ratios has reaction orders as 0.81, 1.60 and 0.44 in methane, oxygen and steam partial pressures, respectively. The apparent activation energy for methane OSR was calculated as 39 kJ.mol^{-1} and pre-exponential factor as 0.956 μmol.mgcat^{-1}.s^{-1}.kPa$^{-2.85}$ in the 350-400 °C interval.

Acknowledgements

This work is financially supported by Boğaziçi University through project BAP 5570.

References

[1] L. Zhixiang, M. Zongqiang, X. Jingming, N. Hess-Mohr, V. M. Schmidt, *Chinese Journal of Chemical Engineering.* 14 (2006) 259-265.
[2] S. Rowshanzamir, S. M. Safdarnejad, M. H. Eikani, *Procedia Engineering.* 42 (2012) 2-24.
[3] F. Gökaliler, Z. I. Önsan, A. E. Aksoylu, *International Journal of Hydrogen Energy.* 37 (2012) 10425-10429.

III-PP58

Oxidative Steam Reforming of Logistic Fuels over a Spinel-Derived Ni(17wt.%)/Al_2O_3 Catalyst

Jiménez-González C., Gil-Calvo M., Boukha Z., De Rivas B., Gutiérrez-Ortiz J.I., González-Velasco J.R., López-Fonseca R.*

Chemical Technologies for Environmental Sustainability Group, Department of Chemical Engineering, Faculty of Science and Technology, Universidad del País Vasco UPV/EHU, Bilbao, Spain

* ruben.lopez@ehu.es

Keywords: hydrogen, methane, isooctane, n-tetradecane, nickel, aluminate, oxidative steam reforming

1 Introduction

Natural gas and liquid fuels, derived from either fossil or renewable sources, represent an attractive source of hydrogen since their distribution infrastructure is readily accessible. Among the several reforming methods available (i.e. steam reforming (SR), partial oxidation (POX), and oxidative steam reforming (OSR)), OSR is most appropriate for minimising carbon deposition in hydrocarbon reforming. OSR has several advantages of both of POX and SR, such as rapid start-up, dynamic response, and relatively rich-hydrogen yields. Moreover, it is suited for heavier hydrocarbons, such as gasoline and diesel.

Noble metal-based catalysts are more efficient because of their long-term activity and coke resistance, but their cost is high. In contrast, nickel-based catalysts appear to be a good alternative although they may undergo severe deactivation due to carbon deposition. In our previous research it was shown that $NiAl_2O_4$ spinel can be a promising catalytic precursor to develop suitable Ni/Al_2O_3 catalysts with a high reforming activity and a marked stability [1,2]. In this work, the attention has been focused on the comparison of the reforming efficiency of various hydrocarbons such as methane, isooctane and *n*-tetradecane, selected as model compounds for natural gas, gasoline and diesel, respectively, in the oxidative steam reforming over a co-precipitated $NiAl_2O_4/Al_2O_3$ catalyst.

2 Experimental/methodology

The catalyst denoted as CP(17) was prepared by co-precipitation at pH = 8 using an solution containing a mixture of $Ni(CH_3\text{-}COO)_2{\cdot}4H_2O$ and $Al(NO_3)_3{\cdot}9H_2O$ in a Ni/Al = 0.5 molar ratio with alumina (γ-Al_2O_3, 133 $m^2\ g^{-1}$) to obtain 17wt.% nickel loading [1]. The catalytic tests were performed, on 125 mg of catalyst, in a flow reactor operating at atmospheric pressure at a constant temperature (600 ºC) for 31 h. The reaction mixture consisted of the selected hydrocarbon (15.6%CH_4, 1.95%*i*-C_8H_{18} or 1.1%*n*-$C_{14}H_{30}$) and O_2 and H_2O (with a O/C=1 and H_2O/C=3) diluted in N_2 and a total flow rate equal to 800 $cm^3\ min^{-1}$. Prior to the reaction, the catalyst was activated by reduction with 5%H_2/N_2 at 850 ºC for 2 h. The catalytic results were compared on the basis of an identical carbon-based volume hourly space velocity, namely 60000 $cm^3\ C\ g^{-1}\ h^{-1}$.

3 Results and discussion

Previous studies evidenced the potential of the CP(17) catalyst for methane steam reforming at moderate volume space velocity (38400 $cm^3\ CH_4\ g^{-1}\ h^{-1}$) due to the structural homogeneity of the Ni^{2+} species present in the calcined precursor [1]. This resulted in a low crystallite size, high dispersion and metallic surface area (9.5 nm, 33% and 40 $m^2_{Ni}\ g^{-1}$, respectively) after a high temperature reduction (850 ºC).

As a general behaviour, Fig. 1 showed that the higher reforming efficiency, with respect to the corresponding thermodynamic equilibrium values (squares), was obtained for CH_4 followed by *i*-C_8H_{18} and *n*-$C_{14}H_{30}$. As for the product distribution (H_2, CO, CO_2 and CH_4 as main products), the obtained H_2 yield in oxidative steam reforming of CH_4 and *i*-C_8H_{18} was quite similar (1.2 and 1.3, respectively). Interestingly, the H_2 yield in methane OSR accounted for the 96% of the equilibrium value while it was 81% in isooctane reforming. In addition, methane OSR led to the highest H_2/CO ratio (13). On the other hand, the CP(17) sample evidenced the poorest catalytic activity in *n*-tetradecane oxidative steam reforming with a 42% initial conversion which decreased gradually during the first 5 h to reach a stationary state (38%) with time on stream. This activity loss further impacted on the resulted $Y(H_2)$ (0.3).

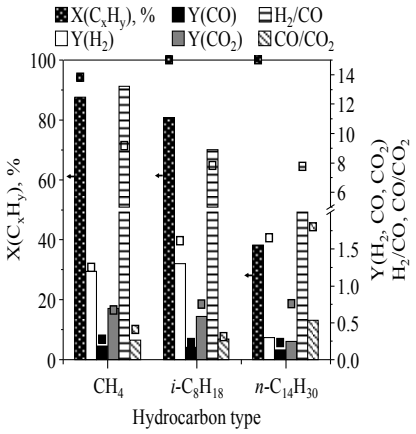

Fig. 1. Comparison of the oxidative steam reforming efficiency of various hydrocarbons.

The detected deactivation during the OSR(*n*-$C_{14}H_{30}$) could be related to several causes such as coke formation (mainly caused by catalytic decomposition of the hydrocarbon, the thermal cracking reactions or Boudouard reaction), nickel sintering and/or partial oxidation of the metallic nickel into NiO. In line of previous results [1], the OSR of CH_4 did not lead to coke deposition. In case of the heavier hydrocarbons, a notable amount of filamentous coke (24 and 37% for *i*-C_8H_{18} and *n*-$C_{14}H_{30}$, respectively) was noticed, as revealed by TPO and TEM analysis. It seems that the OSR(*n*-$C_{14}H_{30}$) is prone to form high concentration of ethylene (C_2H_4) which is a recognised coke precursor [3]. Moreover, the temperatures required for oxidation were remarkably higher than for *i*-C_8H_{18} indicating the presence of a well developed graphitic structure. Raman profiles also confirmed these results with two distinct bands D Band (amorphous coke) and G Band (graphitic coke) with clearly different I_D/I_G ratios, 1.2 and 0.8 for isooctane and *n*-tetradecane, respectively. This suggested that the nature of the deposited coke from isooctane OSR was less graphitic resulting in lower combustion temperatures.

4 Conclusions

This work confirmed the feasibility of the co-precipitated $NiAl_2O_4/Al_2O_3$ catalyst in the reforming of different hydrocarbons. It was found that the high stability of OSR of CH_4 and *i*-C_8H_{18} was related to a negligible or minor coke deposition in comparison with *n*-$C_{14}H_{30}$. In this way the effect of unavoidable filamentous coke formation on the performance of heavy hydrocarbons, with a less impact on the OSR(*i*-C_8H_{18}), could be minimised with higher reforming temperatures or higher H_2O/C ratios.

Acknowledgements

The financial support for this work provided by the Spanish Ministry of Economy and Competitiveness (CTQ2010-16752/PPQ, ENE2013-41187-R) and Gobierno Vasco (PRE_2013_2_453) are gratefully acknowledged.

References

[1] C. Jiménez-González, Z. Boukha, B. de Rivas, J.R. González-Velasco, J.I. Gutiérrez-Ortiz, R. López-Fonseca, *Energy & Fuels* 28 (2014) 7109-7121.
[2] C. Jiménez-González, Z. Boukha, B. de Rivas, J.R. González-Velasco, J.I. Gutiérrez-Ortiz, R. López-Fonseca, *Int. J. of Hydrogen Energ.* (2015), http://dx.doi.org/10.1016/j.ijhydene.2015.01.064.
[3] I. Kang, J. Bae, G. Bae, *J. Power Sources* 163 (2006) 538-546.

III-PP59

Modifying $Lanio_3$ Perovskite-Type Oxide Catalyst with Co for the Methane CO_2 and CO_2+H_2O Reforming

González-Gil R.[1], Herrera C.[1*], Larrubia M.A.[1], Alemany L.J.[1], Carvalho De Lira Lima D.[2], Resini C.[2], Teixeira Brandão S.[2]

1 - Chemical Engineering Department, University of Malaga, Malaga, Spain
2 - Instituto de Química da Universidade Federal da Bahia, Salvador, Brazil

* concepcionhd@uma.es

Keywords: LaNi1-xCoxO3, catalysts, methane, CO_2, reforming, methane, CO_2+H_2O, reforming

1 Introduction

Dry reforming of methane is a technology that allows the use of two of the major greenhouse gases: exploiting the greenhouse gas CO_2 as raw material could be more advantageous than its long-term storage. As the simulations of reforming equilibrium highlights the fact that water was always produced in the CO_2 reforming of methane and it is also present in NG or biogas composition. Therefore, CO_2 transformation conducted with water in the feed stream provokes H_2 selectivity changes at equilibrium and enable the coke gasification by catalysts with the water. The combination of CO_2+H_2O reforming of light hydrocarbons improves not only the H_2-selectivity but also modifies of carbon formation-deposition process. Nickel is mostly used for this reaction due to the availability and cost but it is rapidly deactivated by coke formation. Efforts have been made to avoid this deactivation by synthesizing Ni catalysts via introducing metal in the perovskite type oxide (ABO_3). So, in this contribution, a series of LaNi1-xCoxO3 perovskite-type oxides was well-characterized and tested in the dry and (C_2+H_2O) mixed reforming of methane with the aim to improve the H_2 selectivity and study the catalysts stability .

2 Experimental

The ternary oxides $LaNiCoO_3$ were synthesized via citrate method using metallic nitrate precursors. Catalysts were characterized before and after reaction by conventional methods. Steady state experiments were carried out at atmospheric pressure. A tubular fixed bed stainless steel reactor (i.d. 9 mm) with 100 mg of catalyst was employed. The total gas flow rate was kept constant at 0.8 Ncm^3s^{-1} with stoichiometric composition in He, $CH_4/CO_2/He$=20/20/60 for CO_2 reforming and $CH_4/CO_2/H_2O/He$=3/1/2/9 for the CO_2+H_2O reforming. The space velocity and the contact time were 6000 h^{-1} and 0.8 $ghmol^{-1}$ respectively; operating under plug flow conditions. The catalytic properties have been evaluated in terms of CH_4 and CO_2 conversions, H_2 and CO selectivity and H_2/CO ratio.

3 Results and discussion

TEM images recorded before reaction confirm the presence of Ni particles together with a phase corresponding to the lanthanum oxycarbonate in the $LaNi_{1-x}Co_xO_3$ catalysts. For $LaCoO_3$ the TEM micrographs have revealed the formation of $LaCoO_3$ particles with perovskite structure and their tendency to agglomerate. After reaction some particles appear to be aggregated, the nickel particle size being comprised between 5-15 nm and as were recorded by EDAX analysis correspond to Ni^0. Additionally, it can be observed carbon nanotubes formation, where a variable carbon content between 10-20% for the serie, were registered from the elemental analysis.

CH_4-conversion and H_2-selectivity for dry and mixed reforming for $LaNi_{1-x}Co_xO_3$ catalysts are displayed in the Figure 1. The results showed that the conversion rates of CH_4 increased in those catalysts with highest Ni content for the CO_2 reforming of methane. While the activity in terms of CH_4 conversion was similar for those Ni/Co mixed oxide catalysts by the presence of water vapor.

Hydrogen yields depend on metal and the ratio of Ni to Co. The best performance in terms of highest hydrogen yield was achieved with the $LaNiO_3$ and $LaNi_{0.8}Co_{0.2}$ catalysts for methane dry reforming. Otherwise, the positive effect of water vapor in the selective reforming of methane was also observed in the H_2-selectivity over $LaNi_{1-x}Co_xO_3$ serie, achieving similar H_2-values above 923K; as well as a significant reduction of the coke formation performed by Co incorporation in the mixed oxides.

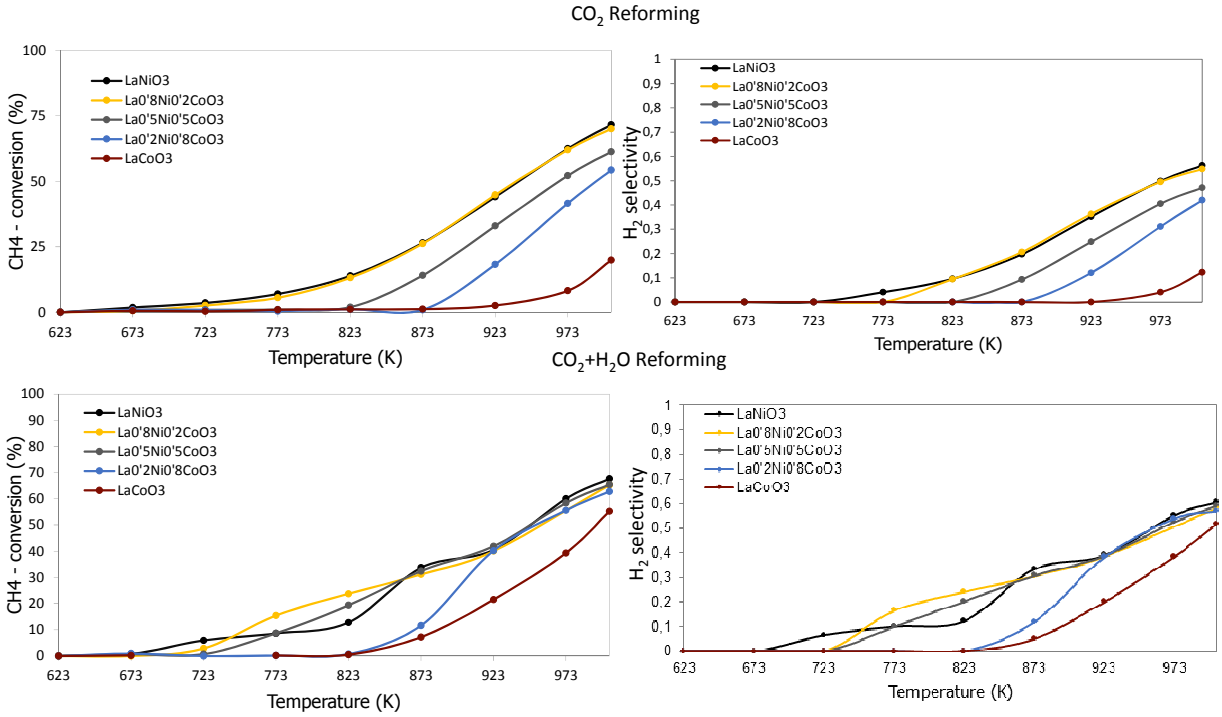

Fig. 1. Conversion/selectivity (%) vs.T (K) curves of methane CO_2 and methane CO_2+H_2O reforming over $LaNi_{1-x}Co_xO_3$

2 Conclusion

For the higher Ni content perovskite-catalysts, the Ni nanoparticles are apparently to be very sensitive to CH_4 activation in the CO_2 atmosphere; i.e., combination of CH_4 decomposition and CO_2 gasification. However, in the CO_2+H_2O reforming, methane conversions and H_2-selectivity were found to be similar at lower temperatures for this $LaNi_{1-x}Co_xO_3$ serie, because the activation of methane is mainly performed with steam while CO_2 could react eventually with H_2 and/or methane.

References

[1] C. Resini, M.C.Herrera Delgado, S. Presto, L. J. Alemany, P. Riani, R.Marazza, G. Ramis, G.Busca, International Journal of Hydrogen Energy, 33 (2008) 3728-3735

III-PP60

Development of Sulphur Tolerant Catalystsfor the Conversion of Carbon Dioxide to Methane

Kolb G.*, Neuberg S., Pecov S., Pennemann H., Zapf R., Ziogas A.

Fraunhofer ICT-IMM, Mainz, Germany

* gunther.kolb@imm.fraunhofer.de

Keywords: methanation, sulphur tolerance, microreactors, energy storage

1 Introduction

The increasing share of renewable energy generation sources in Germany creates a surplus of electric energy, when wind or sunlight is available. Therefore the storage of electric energy comes into focus to compensate the drawbacks of its irregular production by renewable sources. The chemical storage of electric energy seems to be a viable solution. One obvious solution is the electrolysis of water to hydrogen and oxygen. However, once the hydrogen is produced it needs to be stored. Alternatively it could be fed into the natural gas grid, which is well developed in Germany. The addition of hydrogen to natural gas is limited though, because the flame propagation properties of natural gas are affected by hydrogen.

The conversion of hydrogen with carbon dioxide from renewable or non-renewable sources such as biogas plants, power plants or steel fabrication to methane allows the unlimited addition of an energy carrier to the gas grid while the carbon oxides are re-utilized instead of being directly released to the atmosphere.

The methanation of carbon dioxide, also named as Sabatier process, is an exothermic reaction:

$$CO_2 + 4H_2 \Leftrightarrow CH_4 + 2H_2O \quad \Delta H = -165 \ kJ/mol \qquad (1)$$

High temperature not only reduces the maximum carbon dioxide conversion through the thermodynamic equilibrium but also favours the undesired competing reverse water-gas shift reaction (RWGS):

$$CO_2 + H_2 \Leftrightarrow CO + H_2O \quad \Delta H = +41 \ kJ/mol \qquad (2)$$

Owing to the Le Chatelier principle, the methanation reaction is favoured by elevated pressure. However, state-of-the-art electrolysers work in the pressure range above 10 bar and therefore it seems obvious to perform the reaction at similar pressure.

Carbon dioxide from biogas plants contains significant amounts of sulphur species, which tend to poison the catalysts. The focus of the current paper is on the improvement of the sulphur tolerance of ruthenium containing catalysts. Ruthenium is known to be a highly active catalyst for the methanation reaction, though its sulphur tolerance is quite low.

2 Experimental/methodology

The catalysts under investigation were introduced as coatings into microchannel reactors. The coatings were prepared by wet impregnation of a self-prepared ceria carrier with the active species prior to the wash-coating procedure which has been described previously .

The reaction was performed in small testing reactors, which have been described in detail elsewhere . The feed was provided by thermal mass flow meters and contained 80 Vol.% hydrogen and 20 Vol.% carbon dioxide apart from 1 ppm hydrogen sulphide, which was added to the hydrogen as readily prepared mixture. The feed flow rate was set in such a manner, that the Volume Hourly Space Velocity (VHSV) always amounted to 40 L/(h g_{cat}). An overpressure valve served as pressure actuator, which kept the operating pressure at 12.5 ±0.5 bar quite

reliably. The analysis was performed by an Agilent gas chromatograph, which worked on-line and with loop filling manager and separate analysis of water and permanent gases through different detectors.

3 Results and discussion

Fig.1 shows the carbon dioxide and carbon monoxide conversion and the selectivities as determined over different ruthenium containing catalysts. It is obvious from Fig. 1a, that the catalyst containing 5 wt.% Ru and 1 wt.% Rh deactivates rapidly and the deactivation is accompanied by an increasing selectivity towards carbon monoxide, which appears with a certain time shift. Addition of a higher amount of Rh (5 wt.%) slows the catalyst deactivation down (Fig.1b). The addition of 30 wt.% Ni to the catalyst formulation lead to similar initial activity as for the other samples, but further increased stability of the catalyst (see Fig.1c). The increasing selectivity towards carbon monoxide was observed after approximately 40 hours compared to 2 h and 26 h for the former samples respectively, which is attributed to the formation of nickel sulphide species, i.e. the nickel served as "sulphur trap". Ethane was found as only other by-product of the reaction system, which is formed with increasing selectivity with the course of catalyst deactivation, but only in the range of 1 %. The origin of the deactivation of the samples will be discussed applying different characterization techniques and further improved formulations will be presented.

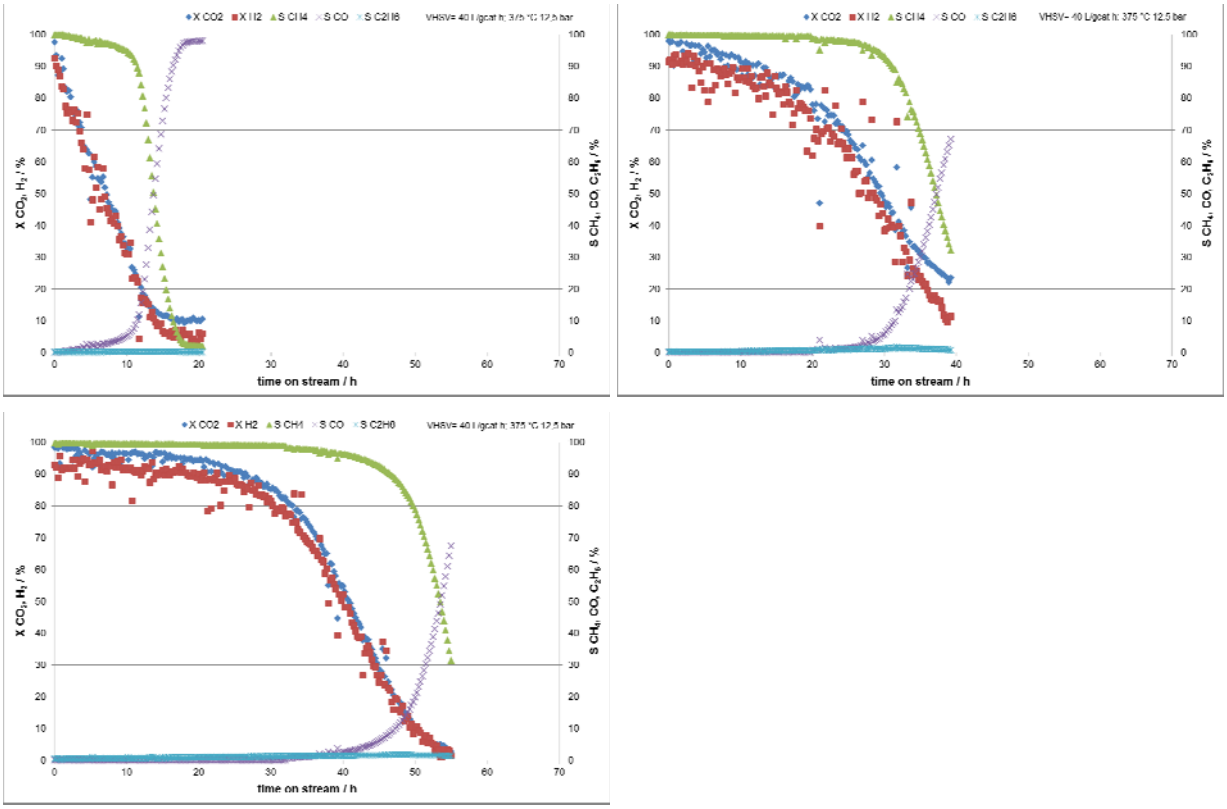

Fig. 1. Conversion of hydrogen and carbon dioxide and selectivitiy towards methane, carbon monoxide and ethane vs. time; 1a (top left): 5 wt.% Ru / 1 wt.% Rh on CeO_2; 1b (top right): 5 wt.% Ru / 5 wt.% Rh on CeO_2; 1c (bottom): 5 wt.% Ru / 30 wt.% Ni on CeO_2

References

[1] R. Zapf, C. Becker-Willinger, K. Berresheim, H. Holz, H. Gnaser, V. Hessel, G. Kolb, P. Löb, A.-K. Pannwitt, A. Ziogas, *Chem. Eng. Res. Dev.* A 81**,** (2003) 721.

[2] G. Kolb, R. Zapf, V. Hessel, H. Löwe, *Appl. Catal.* A **277,** (2004) 155.

III-PP61

Combined Aging Processes during Bio-Syngas Methanation for SNG Production

Li H.[1], Travert A.[1], Maugé F.[1], Paredes Nunez A.[2], Dreibine L.[2], Meunier F.C.[2], Mirodatos C.[2*], Schuurman Y.[2], Ordomsky V.[3], Kodakov A.[3]

1 - Laboratoire Catalyse et Spectrochimie, CNRS, EnsiCaen, University of Caen, Caen, France
2 - Institut de Recherches sur la Catalyse et l'Environnement de Lyon, Université Lyon 1, CNRS, Villeurbanne, France
3 - Unité de Catalyse et de Chimie du Solide, USTL-ENSCL-EC Lille, Villeneuve d'Ascq, France

* Claude.Mirodatos@ircelyon.univ-lyon1.fr

Keywords: bio-syngas to SNG nickel, catalysts, poisoning, operando techniques, methanation, kinetics

1 Introduction

A major barrier in the commercialization of biomass gasification into biosyngas is the presence of impurities such as ammonia, HCl, H_2S, tars and alkali in the products that are detrimental to downstream processes like the conversion of bio-syngas to substitute natural gas (SNG). The exact role and the effects of these biomass-derived impurities on methanation catalysts are poorly known. Furthermore the way that such aging (or promoting) factors can combine with structural aging processes such as metal sintering under operating conditions is not clearly documented either. In the present study, we focused on the SNG process using Ni based catalysts in order to evaluate the kinetic sensitivity of various aging/promoting factors, combining the effect of model poisons such as (i) ammonia and acetonitrile for N containing compounds, (ii) heptane, toluene and benzene as tar representatives, iii) trichloroethylene for Cl containing compounds, v) H_2S for S containing compounds, vi) Na and K for alkali containing ashes, together with metal particle sintering occurring under SNG process conditions.

2 Experimental/methodology

In parallel with conventional ageing measurements in the presence or absence of poisons typical of biosyngas, a combination of operando techniques were used under methanation conditions: (i) DRIFT spectroscopy to check the nature of the main adspecies [1], (ii) magnetic measurements to follow the changes in Ni particle size distribution on stream and (iii) steady-state isotopic transient kinetic analysis (SSITKA) for quantitatively assessing the steady-state concentration of reversibly adsorbed CO and of the methane precursors from $^{12}CO/^{13}CO$ switch at reactor entrance [2].

3 Results and discussion

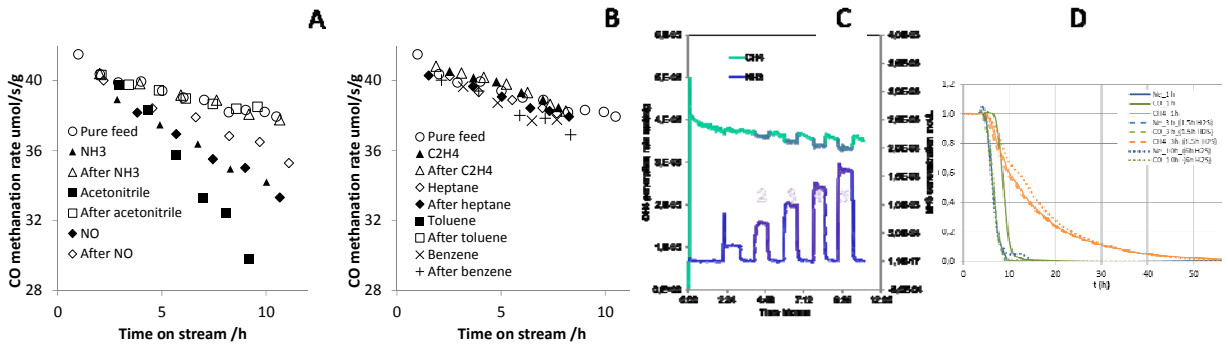

Fig. 1. A&B: Changes in methanation rate vs TOS, in the presence/absence of bio-syngas poisons; C: changes in CH_4 and NH_3 IR bands intensity; D: Changes in SSITKA curves after H_2S addition.

The main ageing effects, among which some are illustrated in Fig.1, have been analyzed by using the complementary information provided by the operando analyses:
(i) In the absence of added poisons, the CO carbonyl IR signal appeared to be correlated with the loss of activity. This irreversible ageing process is assigned, from operando analysis of Ni dispersion, to metal sintering and restructuring, as a consequence of metal carbonylation [2].
(ii) The effect of N containing poisons, superimposed with the previous irreversible Ni sintering, was totally or partially reversible. The degree of deactivation was ranked as acetonitrile> ammonia> nitric oxide, suggesting that various poisoning modes (e.g. competitive adsorption, coking, electronic effects) might be present.
(iii) Adding hydrocarbon compounds representative of tar by-products revealed that ethylene, heptane and benzene did not show obvious poisoning effects.
(iv) The addition of alkali compounds (Na^+ and K^+), present in the ashes formed during the biomass gasification, tended to decrease the inhibiting effect of CO carbonyl concentration on the methanation rate, and therefore might be classified as promoters rather than poisons.
(v) Chlorine contained in C_2HCl_3 was ranked as a strong poison but partly reversible. From its marked impact of bridged and/or multi carbonyls concentration, chlorine is assumed to act via site blocking and by decreasing electronic density at the metallic centers.
(vi) H_2S addition provoked a linear and irreversible deactivation, typical of a front catalytic bed poisoning. The carbonyl pool was decreased linearly with H_2S addition while the CH_4 transient kinetics were only weakly affected, discarding electronic effects by S deposits.
A tentative rationale of these complex aging processes is proposed on the basis of a kinetic study of the methanation reaction, based on the changes in carbonyl and CH_x active intermediates concentrations, directly measured by DRIFT and SSITKA [3]. Thus, the reversible poisoning effect of N and Cl containing species would affect essentially surface controlling steps such as hydrogenation of CH_x reacting intermediates deriving from carbonyls decomposition. It would proceed via a reversible electronic transfer from Ni to the electrophilic additives, evidenced by carbonyl bands shifts typical of electronic back-donation weakening from nickel to the CO π^* anti-bonding orbital. A reverse effect would characterize the promoting effect of alkali addition. For the added hydrocarbons, the absence of electronic effects would explain their negligible toxicity, unless surface coking might lead to diffusion limitation. S containing molecules would neutralize part of the catalytic bed without changing the reactivity of the unpoisoned active sites.

4 Conclusion

From a combination of state-of-the-art operando techniques, unique information was brought on complex surface processes under SNG reaction conditions. Strategies for improving the resistance of methanation catalysts to various types of bio-poisoning can be proposed from this mechanistic and kinetic re-investigation of one of the oldest catalytic reaction studied up to now.

Acknowledgements

This work was supported by the French National Agency for Research, project "BioSyngOp", ANR-11-BS07-026.

References

[1] H. Li, M. Rivallan, F. Thibault-Starzyk, A. Travert, F.C. Meunier, *Phys. Chem. Chem. Phys.* 15 (2013) 7321-7327.
[2] M. Agnelli, M. Kolb, and C. Mirodatos, *J. Catal.,* 148 (1994) 9-21.
[3] M. Agnelli, H.M. Swaan, C. Marquez-Alvarez, G.A. Martin, C. Mirodatos, *J. Catal.* 175 (1998) 117.

III-PP62

Highly Efficient Fischer-Tropsch Synthesis over Fe and Co Catalysts on Carbon Containing Inorganic Supports

Subramanian V[1], Khodakov A.Yu.[1], Cheng K.[2], Chernavskii P.A.[3], Paul S.[1], Ordomsky V.V.[1*]

1 - Unité de catalyse et de chimie du solide (UMR 8181 CNRS), Université Lille 1-ENSCL-EC Lille, Villeneuve d'Ascq, France

2 - State Key Laboratory of Physical Chemistry of Solid Surfaces, College of Chemistry and Chemical Engineering, Xiamen University, Xiamen, China

3 - Department of Chemistry, Lomonosov Moscow State University, Moscow, Russia

* Vitaly.Ordomsky@univ-lille1.fr

Keywords: Fischer-Tropsch, iron, cobalt, support carbon

1 Introduction

Fischer–Tropsch (FT) is an attractive route for the synthesis of non petroleum carbon sources like coal, biomass, and natural gas into wide range of hydrocarbons through intermediate synthesis of syngas (CO +H_2) through gasification or reforming. Cobalt and iron are the widely accepted catalysts for the FT synthesis. However, the efficiency of these catalysts in terms of activity, selectivity and stability is still not high enough for wide implementation in industry. Our recent studies have shown that interaction of Co and Fe with conventional inorganic supports leads to significant deactivation of the catalysts due to the formation of inactive silicates (Co-O-Si and Fe-O-Si), segregation and low contribution of the active phase (χ-Fe_5C_2) [1-2].

This work aims at developing of new catalytic systems for FT synthesis by interaction of metals with carbon on the surface of conventional silica support. It should combine the advantages of high dispersion of cobalt and iron on the surface of support with their low deactivation due to the presence of carbon.

2 Experimental/methodology

Two different approaches have been used for the synthesis of composites on the basis of Fe and Co. Iron nitrate has been mixed with fructose solution with subsequent treatment at 80°C under stirring in the presence of different amount of silica during 24 h with subsequent drying and calcination in inert atmosphere. Silica support has been preliminary impregnated by different content of fructose with subsequent calcination in inert atmosphere to deactivate the surface groups for preparation of cobalt catalysts. The final catalysts have been prepared by impregnation of cobalt nitrate with and without Pt as promoter. The materials were thoroughly characterized by elemental analysis, XPS, Mossbauer spectroscopy, magnetization, XRD, TEM, nitrogen adsorption and SSITKA analysis.

Catalytic experiments were carried out on the REALCAT platform in a Flowrence high-throughput unit (Avantium®) equipped with 16 parallel milli-fixed-bed reactors (d=2 mm) operating at a total pressure of 20 bar, 220 or 300°C , H_2/CO= 2 molar ratio. The gas and liquid products have been analyzed after the test by GC analysis for evaluation of the activity and selectivity to hydrocarbons.

3 Results and discussion

Catalysts prepared with participation of carbon present significantly higher dispersion of the metal on the surface. Fig. 1 shows that conventionally prepared cobalt catalyst over silica

contains particles with the sizes in the range 50-100 nm. At the same time, in the presence of carbon on the surface the size of cobalt nanoparticles decreases to 5-10 nm. It results in increase of the activity by up to 2 times over carbon treated catalysts in comparison with the carbon free sample. The stability of carbon containing catalyst is higher due to the suppression of metal deactivation by interaction with support.

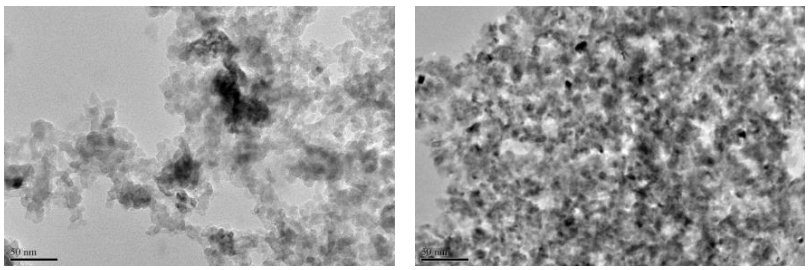

Fig. 1. TEM images of Co supported over silica and carbon-silica supports

Hydrothermal treatment during preparation of Fe based catalysts leads to condensation reaction with formation of humins stabilizing Fe species. The main effect of carbon addition during the preparation of iron catalysts for high temperature FT synthesis is in increase of the contribution of active χ-Fe_5C_2 carbide phase in the catalyst determined by analysis of magnetization (Fig. 2). At the same time, high surface area of silica support provides high dispersion and accessibility of carbide. It leads to increase of the activity by 2-3 times at the optimum composition of support (C/SiO_2 = 0.6-0.8) in comparison with silica and pure carbon supported catalysts (Fig. 2).

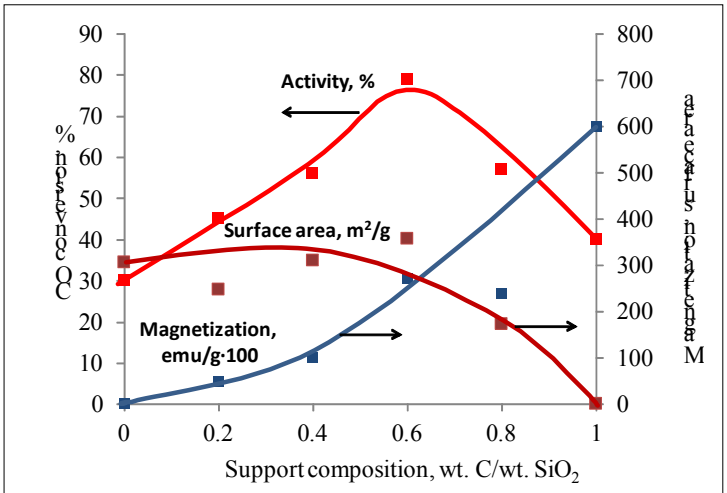

Fig. 2. Catalytic activity in FT, magnetization and surface area of the Fe catalysts with different contribution of carbon

4 Conclusions

Thus, our results show that the presence of carbon in inorganic support significantly improves the catalytic performance of the Fe and Co based catalysts in the Fischer-Tropsch synthesis. The main effect is due to the significant increase of the dispersion of metallic nanoparticles, suppression of metal deactivation by formation of silicates and increase of the contribution of the active phase by interaction with carbon.

Acknowledgements

The REALCAT platform is benefiting from a Governmental subvention administrated by the French National Research Agency (ANR) within the frame of the 'Future Investments' program (PIA), with the contractual reference 'ANR-11-EQPX-0037'.

References

[1] K. Cheng, V.V. Ordomsky, M. Virginie, B. Legras, P.A. Chernavskii, V.O. Kazak, C. Cordier, S. Paul, Ye Wang, A.Y. Khodakov, *Appl. Catal. A* 488 (2014) 66.

[2] V.V. Ordomsky, B. Legras, K. Cheng, S. Paul, A.Y. Khodakov, *Cat. Sci. Tech.* 2015, DOI: 10.1039/C4CY01631A

III-PP63

Glycerol Steam Reforming over Modified Ni/Al_2O_3 Catalysts

Kousi K.[1], Chourdakis N.[2], Matralis H.K.[1], Kondarides D. I.[2], Papadopoulou C.[1*], Verykios X.[2]

1 - Department of Chemistry, University of Patras, Patras, Greece
2 - Department of Chemical Engineering, University of Patras, Patras, Greece

* cpapado@chemistry.upatras.gr

Keywords: glycerol steam reforming, Ni/Al_2O_3, La_2O_3, B_2O_3, coke

1 Introduction

Biodiesel is by far the most common biofuel used in the EU, produced via vegetable oils transesterification [1]. About 10 wt % of the vegetal oil processed in biodiesel manufacturing is converted to crude glycerol, which cannot be absorbed by the current markets [2-4]. An interesting idea is the utilization of this crude glycerol as a raw material for the production of hydrogen or other energy carriers, with both economic and environmental advantages due to waste minimization and valorization [2-5]. In this context, steam reforming of glycerol has gained attention in recent years. As a reforming reaction, it is catalyzed by transition or noble metals and several catalytic schemes have been investigated [2, 4]. Ni-based catalysts have been proven to be active for the steam reforming of various compounds and biomass derivatives (including ethanol) and they are much more cost-effective for industrial applications than noble metals [4]. The aim of the present study is the investigation of the effects of B_2O_3 and La_2O_3 on the performance of Ni/Al_2O_3 catalysts.

2 Experimental/methodology

The catalysts were prepared by wet impregnation, using a commercial alumina. Nickel nitrate, lanthanum nitrate and boric acid were the precursor compounds. Ni content is 10 wt % in all catalysts, while La_2O_3 loading is 17 wt % and B_2O_3 is 5.6 wt %. All prepared materials and there notations are presented in Table 1. Physicochemical characterization includes N_2 adsorption-desorption (BET, BJH), XRD, DRS TPR and HR-TEM. Catalytic behavior was investigated in the temperature range 400-800 °C using a feed consisting of 20% He, 1% Ar, 75% H_2O και 4 % glycerol. In addition, catalytic tests were performed at 600, 500 and 400 °C for 3 h, with a new batch for each temperature in order to evaluate coking at each temperature. TPH, TPO, XRD and HR-TEM were applied for the assessment of the carbonaceous deposits on the spent catalysts.

3 Results and discussion

γ-Al_2O_3 is an active glycerol reforming catalyst even at 400 °C, with a 24 % conversion to liquid products (mainly acrolein, acetaldehyde and acetol). Glycerol conversion increases to 85 %, with the addition of La_2O_3, while with BAl a 100 % conversion and 39 % yield of acrolein was achieved. Conversion to gas was less than 15 % for all supports. These results show that modifiers enhance mainly dehydration reactions while for dehydrogenation and C-C bond cleavage the presence of a metal is required.

All Ni-based catalysts are more active than the corresponding supports, with an almost 100 % total conversion at 500 °C. Yet, there are differences depending on catalyst composition. Conversion to gas products and hydrogen yield are shown in Fig. 1. A 97 % conversion to gas and 83 % hydrogen yield is obtained by NiAl at 500 °C. Addition of lanthana deteriorates the textural properties but has no significant effect on Ni^0 dispersion. However, it improves the catalytic performance, increasing considerably the gas products, hydrogen yield at 400 °C and

the resistance to coking (Fig. 2, Table 1). On the contrary, B_2O_3 improves the textural properties and the dispersion of the nickel phase but decreases the yields of H_2 and other gases, while more coke is formed on this catalyst (Fig. 2, Table 1).

Table 1. Materials and their notation, S_{BET} after reduction, average nickel particle size after reduction and catalytic tests at 500 °C and 600 °C and carbonaceous deposits after testing for 3 h at 500 °C.

Catalysts	Notation	$S_{BET, R}$ (m^2/g)	$d_{Ni,R}$ (nm)	$d_{Ni,U500C}$ (nm)	$d_{Ni,U600C}$ (nm)	$C_{500°C}$ (mg C/g_{cat})
Ni/γ-Al_2O_3	NiAl	154	9.5 ± 0.5	7.6 ± 0.4	8.3 ± 1.3	121
Ni/B_2O_3-Al_2O_3	NiBAl	184	5.1 ± 0.4	4.3 ± 0.4	4.8 ±1.0	181
Ni/La_2O_3-Al_2O_3	NiLaAl	79	9.7 ± 0.6	10.7 ± 0.7	10.6 ± 0.5	39

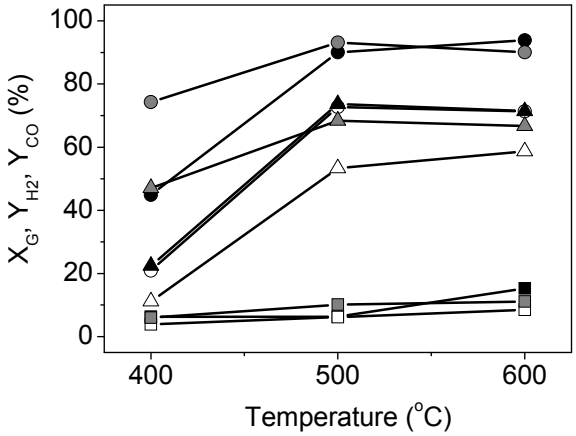

Fig. 1 Catalytic performance of NiAl (black), NiBAl(white) and NiLaAl (gray): ● conversion to gas, ▲H_2 yield, ■ CO yield.

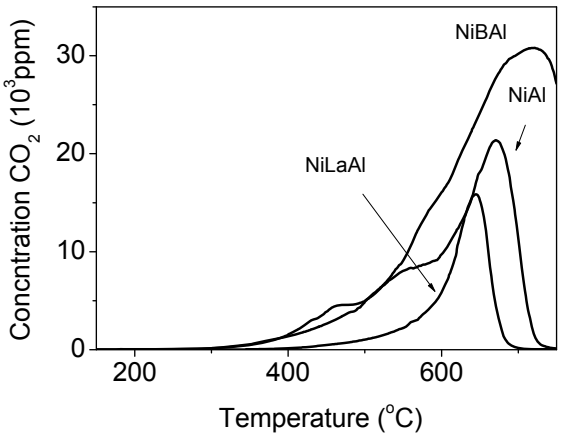

Fig. 2 Temperature programmed oxidation of carbonaceous deposits on the Ni-based catalysts.

4 Conclusions

The presence of a second oxide on Ni/Al_2O_3 catalyst has important effects on the catalytic behaviour and the resistance to coking. However, this is not due to changes in the texture and/or nickel dispersion, but must be related to the different metal-support interface and/or to a synergy effect.

Acknowledgements

This study has been co-financed by the EU (European Social Fund - ESF) and Greek national funds through the Operational Program "Education and Lifelong Learning" of NSRF - Research Funding Program: Thales. Investing in knowledge society through the European Social Fund (Glycerol2Energy project).

References

[1] Commission Staff Working Document, accompanying the document “Report from the Commission to the European Parliament and the Council: Renewable energy progress report” Brussels, 27.3.2013.
[2] P. D. Vaidya, A. E. Rodrigues, Chem. Eng. Technol., 32 (2009) 1463-1469, M. Ayoub, A.Z. Abdullah, Renew. Sust. Energy Rev.16 (2012) 2671– 2686.
[3] K. Pathak, K. M. Reddy, N.N. Bakhshi, A.K. Dalai, Appl. Catal. A 372 (2010) 224–238.
[4] P. Panagiotopoulou, C. Papadopoulou, H. Matralis, X. Verykios WIREs Energy Environ. 3 (2014) 231–253.
[5] D. Hernandez, M. Velasquez, P. Ayrault, D. Lopez, J.J. Fernandez, A. Santamaria, C. Batiot-Dupeyrat, Appl. Catal. A: Gen. 467 (2013) 315–324.

III-PP64

The Oxygen Electroreduction Reaction Performance of Pt/C Catalysts Based Onnanostructured Carbon Supports: from the RDE to the PEMFC Studies

Gribov E.N.[1,2*], Kuznetsov A.N.[1], Golovin V.A.[1,2,3], Voropaev I.N.[1], Kuznetsov V.L.[1], Okunev A.G.[1,2]

1 - Boreskov Institute of Catalysis SB RAS, Novosibirsk, Russia
2 - Novosibirsk State University, Novosibirsk, Russia
3 - Research and Educational Center for Energy Efficient Catalysis, Novosibirsk State University, Novosibirsk, Russia

* gribov@catalysis.ru

Keywords: ORR, PEMFC, RDE, carbon nanotube, carbon nanofibers, platinum

1 Introduction

One of the promising approaches to reduce the content of platinum in the Pt/C catalysts for the oxygen electroreduction reaction (ORR) in polymer electrolyte fuel cells (PEMFC) is to increase the activity and Pt utilization by optimizing the morphological properties and the structure of the porous carbon supports. In recent decades, nanostructured carbon supports - carbon nanotubes and nanofibers received much attention because of the higher electrical conductivity and the effective mass transport properties. In this work we synthesized a series of Pt/C electrocatalysts based on commercial carbon blacks and nanostructured carbon supports: the original and the modified multiwall carbon nanotubes (CNTs) and catalytic filamentous carbon (CFC). The resulting catalysts were investigated in the ORR by rotating disk electrode (RDE) method as well as in PEMC. The higher performance of the Pt/CNT catalysts is shown.

2 Experimental/methodology

Pt/C catalysts were prepared by deposition of platinum oxide on the surface of carbon support under hydrolysis of Pt (IV) chloride complexes using Na_2CO_3 as a reducing agent. The conditions of the preparation can be found in ref. [1]. The original (CNT) and a modified with carbon (CNT-gr) multiwall carbon nanotubes and catalytic filamentous carbon of “fishbone” (CFC1) and "card deck” (CNF2) types were used. Commercial 20% Pt / Vulcan XC-72 catalyst was used for comparison.

Electrochemical measurements were performed using a rotating disk electrode in a thermostated three-electrode glass cell at a temperature range of 10 - 35 ° C in 0.1 M $HClO_4$. The Pt wire and Pt foil were used as a reference and auxiliary electrodes respectively. The electrode potentials were controlled by potentiostat Autolab PGSTAT 100. All potentials are given with respect to the reversible hydrogen electrode.

Membrane-electrode assemblies (MEA) were prepared using Nafion® 212 NRE (Sigma-Aldrich Co) membrane, commercial 20 % Pt/Vulcan XC-72 (0.2 mg_{Pt}/cm^2 of Pt load) as anodic catalyst, Carbon Toray paper (TGP-H-120) and Sigracet 25BC as cathodic and anodic gas-diffusion layers, respectively. The studied sample was mixed with Black Pearls carbon black and used as cathodic catalyst with Pt load of 0.05 mg_{Pt}/cm^2. Polarization curves were obtained at 80 °C in galvanostatic mode with a scan rate of 1 mA/s (in the 0 - 0.02 A/cm^2 current density range) and of 10 mA/s (for current density higher than 0.02 A/cm^2). The hydrogen and oxygen were humidified and supplied at a fluxes of 2.4 cm^3/s and 4.8 cm^3/s, respectively. The measurements were performed using Autolab PGStat302N potentiostat equipped with a buster BSTR20A. The ohmic resistance of MEAs and hydrogen crossover currents were obtained as described in ref. [1].

3 Results and discussion

The results presented in Table 1 show that the Pt nanoparticle sizes of the Pt/CNT catalysts are in the 2.8 - 3.4 nm range. The data are in agreement with those obtained by TEM and chemisorbed CO electrooxidation. The similarity of the Pt dimension indicates the good reproducibility of the method of platinum deposition on the surface of carbon nanotubes. In order to synthesize Pt/CFC catalysts, the support was oxidized under mild conditions. This leads to a noticeable oxidation of the CFC surface and increase the average size of the platinum nanoparticles (6-12 nm). Both mass and surface activities of Pt/C catalysts in the ORR obtained by RDE method were found to be higher than those of commercial 20% Pt/Vulcan catalyst. Most likely this is due to the influence of the properties of the carbon support. Carbonization of CNT surface (20% Pt/CNT-gr) as well as higher Pt content (40% Pt/CNT) leads to higher activities of the catalysts. The performance of the catalysts in PEMFC are correlated with those obtained by RDE. The use of the nanostructured carbon supports (such as CNT) improves the efficiency of Pt/C catalysts in the ORR.

Table 1. Pt nanoparticle size (d_{Pt}) according to gas-phase CO adsorption data, mass (A_{mass}) and surface (A_{surf}) activities at 0.9 V RHE obtained in the electrochemical cell (EC) and in PEMFC.

Catalyst	d_{Pt} nm	A_{mass}^{EC}, A/g_{Pt}	A_{sur}^{EC}, $\mu A/cm^2_{Pt}$	A_{mass}^{PEMFC}, A/g_{Pt}
40%Pt/CNT	3.4	129	278	186
20%Pt/CNT-gr	3.2	81	303	
20%Pt/CFC-2	12	60	236	66
20Pt%/CFC-1	6.2	16	145	
20Pt%/CNT	2.8	18	36	
20Pt%/Vulcan	3.2	44	61	71

4 Conclusions

In this work a series of Pt/C catalysts obtained on the nanostructured carbon supports (carbon nanotubes and catalytic filamentous carbon) was studied in the ORR in the electrochemical cell as well as in the PEMFC. It was found that the use of carbon nanostructured supports such as multiwall carbon nanotubes improves the efficiency of Pt/C catalysts in the ORR.

Acknowledgements

Authors thank Dr. Kazakova M. and Dr. Krasnikov D. for the provided carbon materials. This work was supported by the RFBR grant № 13-03-01023. The work is also supported by the Ministry of Education and Science of the Russian Federation".

References

[1] E.N. Gribov, A.N. Kuznetzov, V.A. Golovin, I.N. Voropaev, A.V. Romanenko, A.G. Okunev, *Russ. J. Electrochem.*, 50 (2014) 700.

III-PP65

Mathematical Modelling Method Application for Catalytic Reforming Catalyst Operating Conditions Optimization in Industrial Reactors

Sharova E.S., Ivanchina E.D., Yakupova I.V.*

National Research Tomsk Polytechnic University, Tomsk, Russia

* yakupovaiv@tpu.ru

Keywords: catalytic reforming, Pt-catalyst, monitoring, mathematical model, optimal activity, coke, accumulation

1 Introduction

Optimization of industrial processes is one of the most important stages of mathematical modeling. The modern modifications of Pt-Re-catalysts of catalytic reforming process allow obtaining high – octane product with 96-98 octane number and selectivity can achieve 87-90 % mass. However, there is a question about their stability during the operating process, which is determined by carbon composition of raw material, technological operating condition and characteristics of reactor unit. It is only possible to solve catalyst work prediction problem by using kinetic model, which takes into consideration complex influence on deactivation of coke formation processes, poisoning and aging.

2 Experimental/methodology

The existence of formation and hydrogenation of unsaturated intermediate products of compaction is possible (Fig.1). Under certain conditions coke formation doesn't occur, because resins and asphaltenes (previous substances of coke) can hydrogenated to hydrocarbons or be in equilibrium with gas-phase reaction medium. Thus, controlling of feed temperature in reactor, it could be possible to provide process operation mode with the existence of equilibrium of formation and hydrogenation of coke structures.

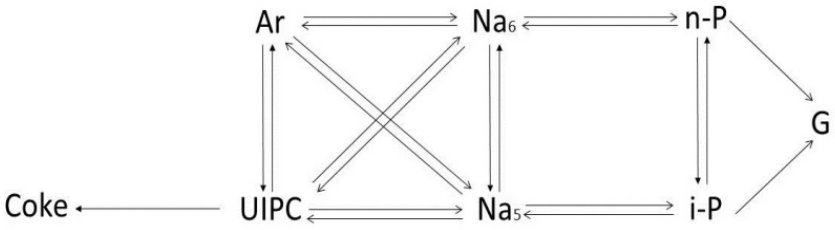

Fig. 1. Formalized scheme hydrocarbon conversions $C_8 – C_{12}$: G – gas; n-P – normal paraffins; i-P – izoparaffins; Na_6 – cyclohexanes; Na_5 – cyclopentanes; Ar – aromatic hydrocarbons; UIPC - unsaturated intermediate products of compaction

Catalyst Operating Condition Control System was designed for complete monitoring of the reforming catalyst operating condition. The system is based on the mathematical model of the naphta catalytic reforming which takes both the physical and chemical mechanisms of hydrocarbon mixture conversion reaction as well as the catalyst deactivation. The mathematical model of catalytic reforming [2] is performed as system of physical and heat balance:

$$G\left(\frac{\partial C_i}{\partial z}-\frac{\partial C_i}{\partial V}\right)=\sum_{j=1}^{n} W_j$$

$$G\left(\frac{\partial T}{\partial z}-\frac{\partial T}{\partial V}\right)=-\frac{1}{C_p^{mix}}\sum_{j=1}^{n} Q_j W_j$$

The initial conditions: Z=0, C_i=0, T=0, V=0, C_i=C_{en} (at the reactor entrance), if Z=0, T=T_{en}, where C_i - a concentration of i-th component, mol/m3; T – temperature; Z – a raw material volume, m³; W_j – j-th reaction rate, mol/(m³•h); V - a volume of the catalyst layer,m3; G - a raw material flow rate, m3/h; Q_j – j-th reaction heat, J/mol; - a heat capacity of mixture, J/mol.

Using computer modelling system the monitoring of catalytic reforming installation L-35-11/450K was done. Technological conditions: entrance temperature is 470˚C, pressure is 1.6 MPa, consumption of raw materials is 63.8 m²/hour. The catalyst used is PR-9 (Pt:Re = 0,25:0,25). The monitoring of installation was performed within the seventh work period – since 22.05.2012 to 18.03.2014. Such catalyst work indicators as “current” and “optimal” activity were determined. The chromatographic analyzes results of raw material and outlet substance compositions were used as initial data.

The monitoring of each catalytic reforming installation is concluded in determination of such catalyst work indicators as “current” and “optimal” activity. The catalyst activity [1] is defined as:

, W_k, W_0 - the chemical reaction rate, mol/sm³·s, with and without catalyst respectively; φ - the part of volume, occupied by catalyst and inaccessible for reacting mixture.

The optimal activity is defined by optimal process operation. Work at the "optimal" activity provides maximum duration of catalyst work cycle.

3 Results and discussion

The results which are presented at Fig.2 show that the amount of current activity during this work period is 0.7-1.0 points. However, a deviation from the optimal activity of 0.6 points in total can be observed. This deviation influences the accumulation of coke. For example, the total amount of coke in the catalysis is 87.73 % weight higher than the one, which could be observed during optimal operation.

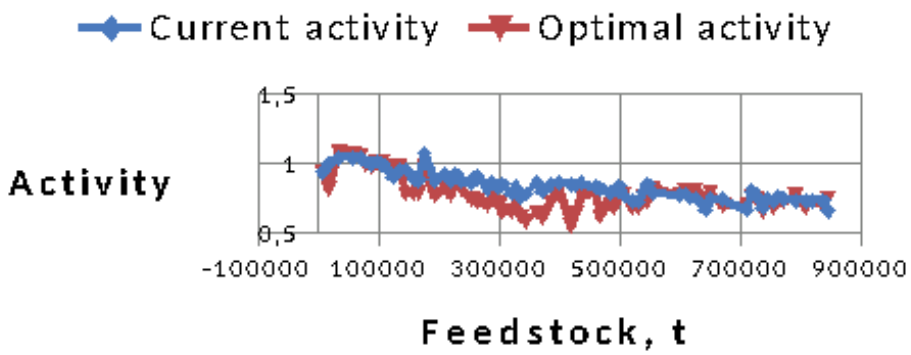

Fig. 2. The comparison of current and optimal activities of the PR-9 catalyst

Fluctuations of the catalyst’s activity during the entire work period can be associated with changes in the rate of technological regime: the feed temperature to the reactor, hydrogen gas circulation rate and the variability of the composition of the hydrocarbon feedstock.

4 Conclusions

1. The installation work is relatively close to optimal. Insignificant deviation from the optimal and current activity was observed at the end of the work period (0.6 points) which may be associated with change in the feedstock composition.

2. The amount of coke deposited at the catalyst during the current activity is 87.73 % weight higher than the optimum value.

Acknowledgements

To Komsomolsk Oil Refinery for data providing

References

[1] E.D. Ivanchina, V.V. Deriglazov, I.K. Zanin. Computer modelling system using for increasing of catalytic reforming technical economic efficiency. TPU News, Chemistry; 2011; 319: 3, p. 105-109.

[2] A.V. Kravtsov, E.D. Ivanchina, D.S. Poluboyartsev, S.A. Galushin. System analysis and efficiency increasing of oil refineries by mathematical modelling method. 2004, p.75-76

III-PP66

Methanol Synthesis from CO_2 and H_2 on Cu/ZnO Catalysts

Peroni M.[1*], Gallucci K.[1], Villa P.[1], Karelovic A.[2], Ruiz P.[2]

1 - Dipartimento di Ingegneria Industriale via Giovanni Gronchi 18, Università di L'Aquila, L'Aquila, Italy

2 - Institut de la Matière Condensée et des Nanoscience, Université Catolique de Louvain, 3 - Louvain-la-Neuve, Belgique

* marcomaddie@libero.it

Keywords: CO_2 uses, methanol synthesis, citrate route

1 Introduction

Methanol is an important commodity, which might be produced directly from CO_2 and H_2. We investigated Cu/ZnO catalysts in methanol synthesis, applying different Cu contents, calcination temperatures and two different synthesis methods: a modified citrate route [1-2] and coprecipitation [3]. Using the different synthetic methods, it was possible to vary copper crystal size in the 12-32 nm range and to investigate its effect on the catalytic performance. Mechanical mixtures of separately prepared CuO and ZnO were also studied. The catalysts were tested for methanol synthesis in mild conditions (7 bar, 140-250°C, GHSV 40 ml/min/g_{cat}).
Results provides insight to the synthetic approach of catalysts using copper and zinc oxides and in the study of the mechanistic aspects of work of catalysts containing these oxides.

2 Experimental/methodology

For the synthesis of the CuO/ZnO catalyst, a variant of the citrate method, which makes no use of nitrates as starting salts and decomposes the organic substance at mild conditions (~ 350°C 1%O_2 in N_2) was used. Coprecipitation method here utilized is performed with ammonium carbonate at 80°C and pH 6.5. This method has no necessity for a washing step to get rid of the sodium cation. Pure CuO and ZnO were synthesized separately. Mechanical mixtures of CuO and ZnO were prepared mixing both oxides in n-pentane at room temperature. Catalysts were characterized by X-ray diffraction, specific surface area, X-ray photoelectron spectroscopy and by N_2O chemisorptions.

3 Results and discussion

All synthesized Cu/ZnO catalysts are formed by CuO and ZnO phases. No mixed phase was observed. After reduction only Cu and ZnO species are present. Coprecipitation method leads to smaller CuO crystal size, higher Cu on the surface and higher Cu dispersion than citrate method. Methanol selectivity can attain 100% at temperatures lower than 180°C for catalysts prepared by coprecipitation with a small copper content, while for every catalysts prepared by citrate method, the selectivity is 100% up to 160°C. CO formation is highly favoured at high temperature and for small CuO crystal size. Large size of CuO particles favour methanol formation (Fig. 1). The apparent activation energy for methanol formation is in the range 30-52 kJ/mol, whereas that of CO formation is much higher (111-139 kJ/mol). For pure CuO, the apparent activation energy for methanol formation is about 70 kJ/mol and that of CO formation is more than 150 kJ/mol. Methanol yield, strongly depends on the amount of copper in the catalyst. The methanol formation rates and the CO formation rates depend linearly on the amount of surface exposed copper atoms. Lower the amount of surface copper atoms higher the turnover frequency (TOF) and selectivity to methanol. The reverse is observed for CO formation. TOF for methanol formation is inversely proportional to the Cu dispersion. The

turnover frequency of the CO formation is higher for small copper particles. Larger particles copper particles (20-32 nm) are much more selective to methanol than smaller ones (12-19 nm).

Pure copper is low active and ZnO is not active at all. The catalysts prepared by mechanical mixture is significantly more active than pure CuO. A synergy between CuO and ZnO is observed. These results suggest that the high activity of the CuO/ZnO catalysts prepared by cooprecipitation and citrate method is explained by the presence of CuO and ZnO, which are segregated during the calcination of the catalysts. The activity and the selectivity of CuO/ZnO catalys depends on the presence of ZnO and CuO in the mixtures and more precisely on the crystal size and the surface atoms of copper.

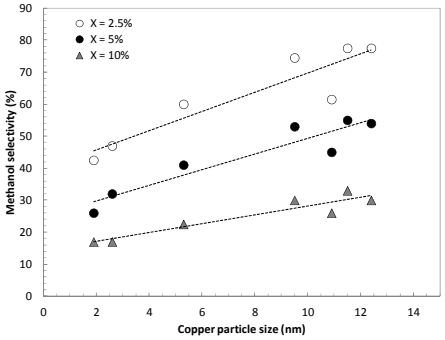

Figure 1. Correlation of Copper particle size and methanol selectivity via different synthesis methods

4 Conclusion

The optimal reaction temperature is in the range between 180°C and 200°C, because at lower temperatures there is a higher selectivity in methanol but coupled with a very low STY in methanol. At higher temperature, the STY in methanol is the highest at 225°C, but at this temperature the CO production is strongly enhanced.

The size of copper particles and the amount of surface copper atoms are crucial parameters for methanol and CO formation. Very small crystal sizes of copper boost the CO formation. On the contrary, large copper crystal sizes are highly active for the methanol synthesis. The citrate method at calcination temperatures between 400 and 500°C leads to the optimal Cu crystal size (about 20 nm). This copper crystal size, displays the lowest activation energy in the methanol synthesis and the highest selectivity to methanol. The coprecipitation method leads to smaller copper crystal size that is correlated to a low selectivity to methanol.

Catalysts synthesized by citrate and coprecipitation methods show always the phases CuO and ZnO, suggesting that the activity of the Cu/ZnO system is directly related with the presence of these two oxides. This has been demonstrated by the mechanical mixtures, which present a higher methanol formation than CuO alone. Pure ZnO is inert. These results underline the importance of the segregation of CuO and ZnO during the synthesis.

Results indicate that the best catalyst for a high formation of methanol and a low CO formation can be obtained when the catalysts present an adequate size of CuO particles, with a low copper surface atoms and an optimal interdispersion between CuO and ZnO particles.

References

[1] P.L. Villa, Solid solutions, applicable as catalysts, with a perovskite structure comprising noble metals, U.S. Patent 7,166,267, B2 (23 January 2007).

[2] P.L. Villa, Soluzioni solide a struttura perovskitica comprendenti metalli nobili, utili come catalizzatori, Italian Patent Application No. MI2001A 001519 (17 July 2001).

[3] S.I. Fujita, S. Moribe, Y. Kanamori, M. Kakudate, N. Takezawa, Applied Catalysis A: General 207 (2001)121-128

III-PP67

Active Site Analysis of Sulfided $NiMo/Al_2O_3$ Catalyst for Hydrodesulfurization of 4,6-Dimethyldibenzothiophene

Nguyene T., Adachi Y., Kobayashi K.*, Nagai M.

Tokyo University of Agriculture and Technology, Tokyo, Japan

* mnagai@cc.tuat.ac.jp

Keywords: site-type analysis, transient response, HDS, 4,6-DMDBT, P-doped, $NiMo/Al_2O_3$

1 Introduction

Recent environmental concerns require an ultra-low sulfur transportation fuel which requires an extensive investigation to develop a highly-active catalyst for the hydrodesulfurization (HDS). The two-site mechanism is well known for the HDS on Mo-containing catalysts HDS [1-4]; one site for the hydrogenation and the other site for the desulfurization. However, a simultaneous rapid desulfurization and hydrogenation reactions of the intermediates, such as the hydrogenated 4,6-dimethyldibenzothiophene (DMDBT) to 3,3-dimethylbicyclohexyl (DMBCH) and 3-methylcyclohexyl-toluene (MCHT) during the HDS of DMDBT and of octahydrodibenzothiophene to bicyclohexyl during the dibenzothiophene HDS and the denitrogenation of *o*-propylaniline to propylcyclohexene during quinoline HDN, are still debated. In this study, a new approach to the site-type analysis of the active sites of the sulfided $NiMo/Al_2O_3$ catalyst for the HDS of DMDBT was studied based on the transient response of the poisoning of carbazole, acridine and quinoline during the HDS. A stereotypically-hindered DMDBT is among the most refractory sulfur-containing molecules in gas oils and low-rank oils. A third active site on the sulfided $NiMo/Al_2O_3$ catalyst was proposed for the simultaneous desulfurization and hydrogenation of DMDBT.

2 Experimental

The phosphorus-doped $NiMo/Al_2O_3$ was prepared using aqueous solutions of $Ni(NO_3)_2 \cdot 6H_2O$, citric acid, MoO_3 and 3.5 wt% H_3PO_4 and impregnated on alumina and loaded at 5.2 wt% NiO and 9.8 wt% MoO_3 by an incipient wetness method. The precursor was dried and oxidized at 723 K for more than 12 h. One gram of the oxidized catalyst was placed in the reactor of a high-pressure flow system. After the catalyst was calcined at 723 K for 1 h, the catalyst was sulfided from 573 to 623 K at the rate of 60 Kh^{-1} in a stream of 10% H_2S/H_2 at 4 Lh^{-1} and subsequently maintained at 623 K for 3 h. The transient response study of carbazole during the HDS of DMDBT was performed at the LHSV of 10 h^{-1}, 493-553 K and a total pressure of 2.5 MPa. After the reaction had reached a steady state in about 4 h, the solution containing the mixture of the 0.2 wt% DMDBT and carbazole (or acridine and quinoline; molar ratio to DMDBT at 1:1 and 1:2) in xylene was introduced into the reactor. The reaction products were quantitatively analyzed using an FID G.C. and identified by GCMS. The catalysts were characterized by XPS, TEM and NO adsorption measurements.

3 Results and discussion

The transient response of the carbazole addition to the DMDBT HDS on the sulfided $NiMo/Al_2O_3$ catalyst for the ratio of DMDBT to carbazole at 1:1 at 493 K is shown in Fig. 1. The carbazole addition increased the concentrations of MCHT and the isomers, decreased and attained constant values, then gradually increased that of 4,6-dimethyltetrahydro-dibenzothiophene (DMthDBT) and became constant, while those of 3,3-dimethylbiphenyl

(DMBP) and DMBCH and the isomers slightly increased. The addition of acridine underwent a similar trend based on the results of the carbazole addition. These results suggested three groups of behavior of the HDS products during the competitive adsorption of the transient response. The denitrogenated compounds and the hydrogenated carbazole compounds except for tetrahydrocarbazole were not observed during the reaction at 493 K. The carbazole was competitively adsorbed on the hydrogenation site, but did not prevent the desulfurization. The competitive adsorption of the HDS products and the nitrogen compounds was considered based on the transient response of the carbazole addition for elucidation of the active sites for the HDS of DMDBT. For the adsorption and the products on the direct desulfurization site, the following equation was obtained: $(C)_{HDS}=(B)/(A)=p_{DMBP12}/p_{DMBP11}=[K_{11}/K_{12}]\ [\theta_{DMBP12}/\theta_{DMBP11}][\theta_{V11}/\theta_{V12}]$

fLayoutInCell1fAllowOverlap1fBehindDocument0fHidden0fLayoutInCell1

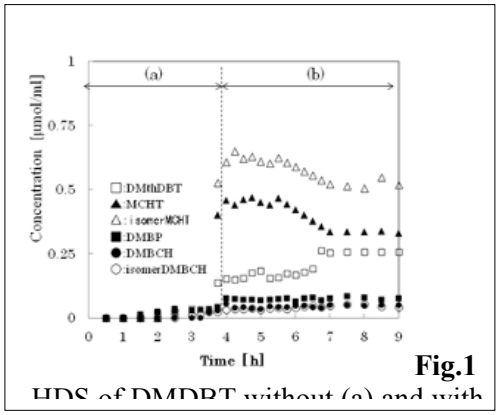

Fig.1 HDS of DMDBT without (a) and with

where θ_{DMBPi}, θ_{vi}, Ki, p_{DMBPi} are the coverage of DMBP, vacant, rate constant and i is the molar ratios of DMDBT to carbazole at (A) 1:1 and (B) 1:2. The (C) values of the other HDS products were also calculated at 493 K and are shown in Table 1. The values of (C) for the addition of carbazole to the HDS of DMDBT had similar values for the addition of acridine and qunoline. The greater increase in DMBP was observed for the addition of acridine probably due to the fact that acridine had a stronger adsorption than carbazole and quinoline. Furthermore, the inhibition order of the three nitrogen compounds underwent the same trend as the HDS products with increases in the DMBP, DMBCH and the isomers together with decreases in DMthDBT, MCHT and the isomers as listed in Table 1. As a result, three types of active sites were classified as follows: the direct desulfurization site for DMBP, the hydrogenation site for DMthDBT, MCHT and the isomers, and the simultaneous desulfurization and hydrogenation site for DMBCH and the isomers. The desorption amounts from the three active sites for the carbazole addition were calculated to be 0.077, 1.111 and 0.097 $\mu molL^{-1}g^{-1}$, respectively, for the desulfurization, hydrogenation and simultaneous desulfurization and hydrogenation sites, corresponded to the distribution of 6, 87, and 7 %, respectively. Thus, the sulfided $NiMo/Al_2O_3$ catalyst had the greater hydrogenation site than the others.

Table 1. The ratios (C) of reaction products for the molar ratios of DMDBT to the added compounds.

Product ratio for added nitrogen compound	DMBP	DMthDBT	MCHT and isomers	DMBCH and isomers
Carbazole	1.2	1.0	1.0	0.45
Acridine	1.3	0.98	0.87	0.58
Qunoline	1.4	1.1	1.0	0.45

4 Conclusions

A new approach to the site-type analysis of the active sites for the HDS of DMDBT using the transient response method proposed the presence of a third active site for the simultaneous desulfurization/hydrogenation of DMDBT to DMBCH as well as the two-sites for the hydrogenation to MCHT and the desulfurization to DMBP.

References

[1] M. Nagai, T. Kabe, J. Catal. **81** (1983) 440; M. Nagai, T. Sato, A. Aiba, *J. Catal.* **97** (1986) 52.
[2] A. Miyata, H. Tominaga, M. Nagai, *Appl. Catal. A,* **374** (2010) 150.
[3] M. Nagai, Y. Yamamoto, R. Aono, *Colloids Surf. A* **241** (2004) 257.
[4] H. Tominaga, M. Nagai, *Appl. Catal. A: Gen.* **389** (2010) 195.

III-PP68

Activity and Selectivity of Pt/Al_2O_3 and Metal Oxide Catalysts for NH_3 Combustion

Hinokuma S.[1,2,3*], Matsuki S.[1], Shimanoe H.[1], Kawano M.[1], Machida M.[1,2]

1 - Kumamoto University, Kumamoto Japan
2 - ESICB, Kyoto University, Kyoto, Japan
3 - JST PRESTO, Kawaguchi, Japan

* hinokuma@kumamoto-u.ac.jp

Keywords: Pt/Al_2O_3, metal oxide, NH_3 combustion

1 Introduction

Recently, NH_3 has been regarded as a renewable and carbon-free energy source due to the high energy density and ignorable thermal NO_x. In comparison with fossil fuel, however, NH_3 fuel has following problems: (1) the high-temperature for ignition, (2) the low combustion rate and (3) a production of fuel NO_x. In this study, the catalytic activity and selectivity of Pt/Al_2O_3 and metal oxide catalysts were evaluated to understand the catalytic behaviour and develop novel catalysts for NH_3 combustion. Our interest was also extended to a dependence of the catalytic performance on partial pressure of O_2.

2 Experimental/methodology

1.0 wt% Pt/γ-Al_2O_3 catalyst was prepared by a conventional wet-impregnation process using an aqueous solution of $[Pt(NH_3)_2(NO_2)_2]$ (Tanaka Kikinzoku Kogyo) and subsequent calcination in air at 600 °C for 3 h. As-prepared Pt/Al_2O_3 and commercial metal oxide catalysts were characterised by XRD, XRF and gas adsorption.

Catalytic NH_3 combustion was carried out in a flow reactor at atmospheric pressure (10 °C·min^{-1}, 1.0% NH_3, 0~18% O_2, He balance and W/F = 5.0×10^{-4} g·min·cm^{-3}). Dependence of NH_3 combustion activity and product selectivities on partial pressure of O_2 (λ), λ: $(pO_2/pNH_3)_{exp.}/(pO_2/pNH_3)_{stoichiom.}$, were also studied.

3 Results and discussion

Figure 1 shows NH_3 conversion, and N_2, N_2O, NO and NO_2 selectivities of as-prepared Pt/Al_2O_3 catalyst observed in the light-off curves of NH_3 combustion under excess O_2 (λ=24). The light-off of a stream of NH_3 conversion was obtained at approximately 270 °C. On the other hand, non-catalytic combustion initiated from approximately 500 °C, which is considered that NH_3 hardly ignites without catalyst. The maximum N_2O, NO and NO_2 selectivities of Pt/Al_2O_3 showed approximately 40%, 20% and 20%, respectively. In contrast to the thermodynamic expectation of NH_3-O_2 reaction to N_2 ($NH_3 + 3/4O_2 \rightarrow 1/2N_2 + 3/2H_2O$), N_2O and NO_x were kinetically-yielded from NH_3 combustion over Pt/Al_2O_3 catalyst.

To study NH_3 combustion activity of metal oxide at λ=24, the catalytic test was performed. NH_3 combustion activity (T_{10}: temperature at which NH_3 conversion reached 10%) of metal oxide showed following order: $MnO_2<Co_3O_4<Pt/Al_2O_3<Fe_2O_3\approx CuO<V_2O_5<NiO<ZnO$. Figure 2 shows the correlation between T_{10} of metal oxide and the enthalpy change ($\Delta H°$) of following reaction: $M_xO_y \rightarrow M_xO_{y-1} + 1/2O_2$, i.e., one molar oxygen desorption from metal oxide with the formation of its lower oxide phase. The plots tend to show that the high active

metal oxide has the low value of $\Delta H°$, indicating that NH_3 combustion activity of metal oxide associates with its oxygen bond energy. Therefore, the catalytic NH_3 ignition is expected to react with the oxygen of metal oxide.

NH_3 combustion activity (T_{10}), and N_2, N_2O, NO and NO_2 selectivities at 600 °C for Pt/Al_2O_3 and CuO as a function of λ were studied (Figure 3). In case of Pt/Al_2O_3 (Figure 3a), T_{10} for NH_3 combustion activity under stoichiometric to lean-burn conditions (24>λ≥1) showed low-temperature of approximately 270 °C, which dramatically increased under rich condition (1>λ). Although NO selectivity tends to decrease with an increase of partial pressure of O_2, NO_x ($NO + NO_2$) selectivity showed approximately 40% on each λ. Similar behaviour of high NO_x and N_2O selectivities could be found in MnO_2 and Co_3O_4 catalysts showing high catalytic activity for NH_3 combustion. CuO catalyst also exhibited high N_2O and NO selectivities under lean condition, but the formations of N_2O and NO were reduced in the stoichiometric reaction (λ=1) (Figure 3b).

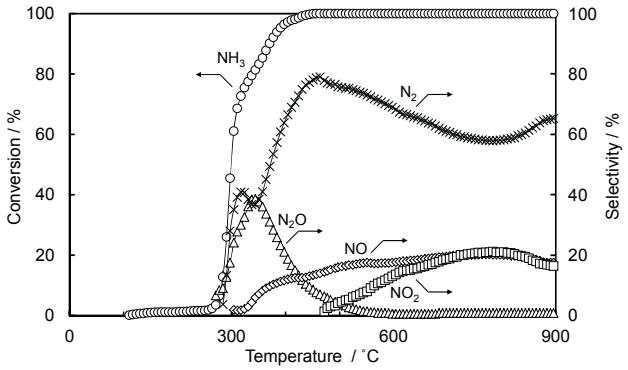

Figure 1 NH_3 conversion, and N_2, N_2O, NO and NO_2 selectivities of NH_3 combustion over Pt/Al_2O_3. Reaction conditions: 1.0% NH_3, 18% O_2, λ=24, He balance.

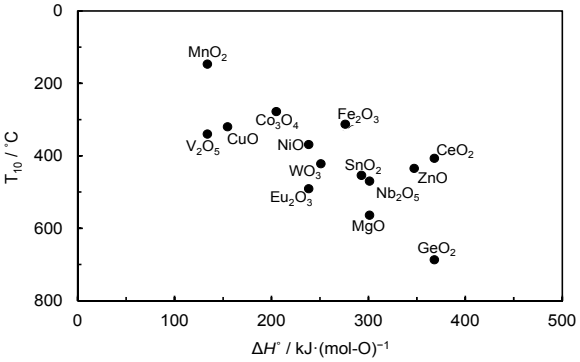

Figure 2 Correlation between NH_3 combustion activity (T_{10}) of metal oxide at λ=24 and enthalpy change ($\Delta H°$) of following reaction: $M_xO_y \rightarrow M_xO_{y-1} + 1/2O_2$.

4 Conclusions

Catalytic activity and product selectivities of Pt/Al_2O_3 and metal oxides for NH_3 combustion have been studied. Pt/Al_2O_3 showed high catalytic activity for NH_3 combustion, but N_2O and NO_x selectivities of that catalyst were high. In case of metal oxide catalysts, MnO_2 and Co_3O_4 also exhibited the higher activity than the other metal oxides, which implied that the catalytic activity of metal oxide correlates with its oxygen bond energy. On the combustion under both excess O_2 and stoichiometric condition, Pt/Al_2O_3 and metal oxide catalysts showed the high selectivities of N_2O and NO_x. However, CuO catalyst exhibited the high N_2 selectivity on the stoichiometric reaction.

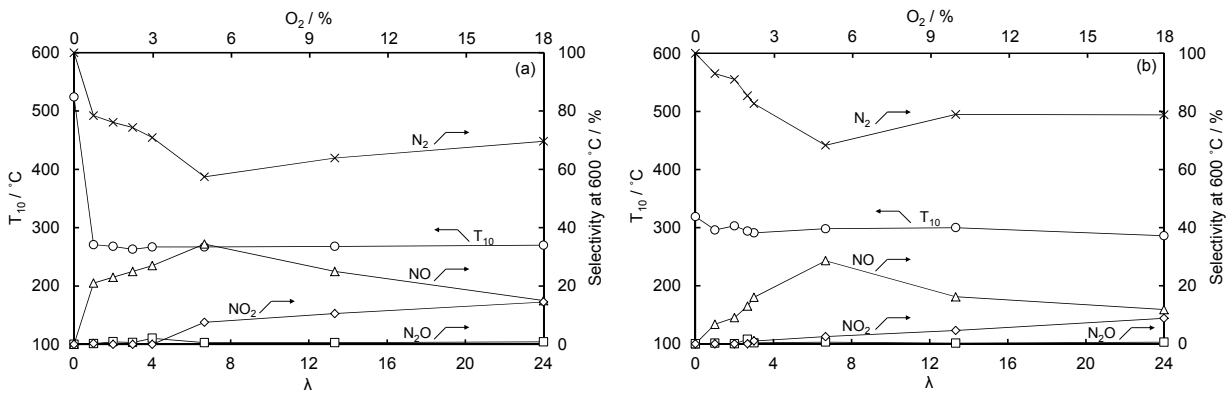

Figure 3 NH_3 combustion activity (T_{10}), and N_2, N_2O, NO and NO_2 selectivities at 600 °C for (a) Pt/Al_2O_3 and (b) CuO as a function of λ. λ: $(p_{O2}/p_{NH3})_{exp.}/(p_{O2}/p_{NH3})_{stoichiom.}$.

III-PP69

Amine Formation on Medium Temperature Water Gas Shift Catalyst. Role of Reaction Parameters

Faure R.[1], Fornasari G.[2], Gary D.[1], Malta G.[2], Molinari C.[2], Schiaroli N.[2], Vaccari A.[2*], Lucarelli C.[2]

1 - Centre de Recherche Claude-Delorme, Air Liquide, Jouy-en-Josas, France
2 - Dipartimento di Chimica Industriale "Toso Montanari", ALMA MATER STUDIORUM - Università di Bologna, Bologna, Italia

* angelo.vaccari@unibo.it

Keywords: water gas shift, Cu-catalysts, amines, methanol, reaction parameters

1 Introduction

H_2 is an important raw material in chemical and petrochemical industry [1] and one of most promising fuel option for the future. Steam Reforming (SR) of natural gas is currently the main source of H_2, feeding CH_4 and steam to produce H_2 and CO (Syngas). The CO may be further converted by means of the Water Gas Shift (WGS) reaction to increase the H_2 yield of ~ 2-5 % and decrease significantly the CO content such as required for polymeric fuel cell applications. Considering the SR-WGS integrated process, in the SR reactor small amounts of NH_3 forms from N_2 present in natural gas, that in the WGS step may give rise to amines [monomethyl (MMA), dimethyl (DMA) or trimethyl (TMA)]. These amines, due to their high solubility, fully dissolve in condensed unconverted water, recycled for economic reasons to the pre-reforming reactor, leading, to the formation of coke on the catalyst and, consequently, to its deactivation [2-3]. Aim of this work was to shed light on the role of the reaction parameters on the by-product formation in a WGS reactor operating at Medium Temperature (MTS), i.e. in just one step, allowing to decrease significantly the operational costs.

2 Experimental methodology

The Cu/Zn/Al (20 wt.% of Cu) catalyst (CAT A) was obtained by coprecipitation at 60°C and pH = 9.0 of a hydrotalcite-type (HT) precursor from the corresponding nitrates, followed by calcination at 550 °C for 6 h and reduction in programmed temperature by a H_2/N_2 gas mixture [4]. To collect data of more wide interest, the behaviour of a commercial Cu/Zn/Al catalyst (26 wt.% of Cu) was also investigated (CAT B). The tests were performed in a bench-scale plant equipped with a INCOLOY reactor, controlling the temperature by a J thermocouple sliding inside the catalytic bed. 2 mL of each catalyst were used, with 30-40 mesh particle size. A $H_2/CO/CH_4/CO_2$ gas mixture was fed, controlling the flow by mass flowmeters, while the NH_3 water solution was fed using a HPLC pump. The reaction condition used are summarize in Table 1, in which in bold are reported the values typical of industrial plants. After reaction, the gas were analysed *on-line* after H_2O condensation, using a gas chromatograph, equipped with two HWD detectors, while the by-product water solutions were analyzed *of-line* using a gas chromatograph equipped with a FID. As an internal standard, 250µL of isopropylamine were added to each 2mL sample.

Table 1. Summary of the operating conditions employed (NH_3 molar ratio calculated for the wet gas). The **bold** values are those used in the reference test

Dry Gas [v/v]	$H_2/CO/CH_4/CO_2$ = 72.0 / 18.8 / 4.6 /4.6
Pressure [bar] (P)	**15** - 20
Exit temperature [°C] (T_{out})	**320** - 340
Steam/Dry Gas [v/v] (S/DG)	**0.30** - 0.40
Contact time [s] (τ)	**3** - 6

NH_3 [molar ratio]	$\mathbf{2 \cdot 10^{-4}}$

3 Results and discussion

Both catalysts reached the equilibrium values for CO conversion regardless of the temperature; furthermore, only the thermodynamically favoured TMA was detected (>150 ppmw). The amount of by-products [methanol (MeOH) and amines] detected as a function of the reaction parameter are summarized in figure 1. CAT A gave rise always to significantly higher methanol amounts than CAT B. The increase of pressure favoured for CAT A and B the formation of methanol and amines, while increasing the temperature both catalysts showed a slight decrease in MeOH formation, while TMA content increased. It is noteworthy that Cat B in the reference test showed an amine amount lower than the detection limit, as well as in the test at 340°C.

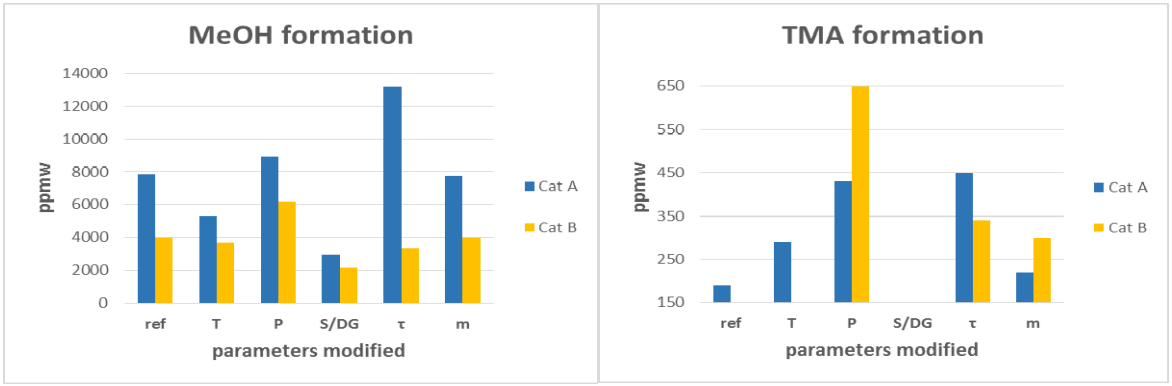

Fig. 1. Formation of MeOH and TMA for Cat A and Cat B in the reference conditions (ref) and changing the reaction parameters (see Table 1); "m" means MeOH + NH_3 co-fed.

Moving the S/DG value from 0.30 to 0.40, a relevant decrease in MeOH and TMA formation was observed for both the catalysts. Finally, increasing the contact time (τ) a significant increase of TMA production was always observed, while MeOH increased only for CAT A. On the basis of the above data, a correlations between MeOH and amine formation may be hypothesized. Thus, to shed light on the mechanism of amine formation, a further test was performed, at 15 bar, feeding a water solution containing the same amounts of NH_3 and MeOH ($4.81 \cdot 10^{-2}$ mol/L) (letter **m** in figure 1). By comparison with results obtained in the reference tests, no change in the amounts of MeOH detected was observed, showing that it partially decompose, in agreement with reaction temperature and pressure. On the other hand, TMA formation increased significantly for both catalysts, especially for the commercial one (Cat B). These results suggest that unlike the literature [5], a correlation between MeOH and amine formation may be hypothesized

4 Conclusions

In presence of NH_3 in the feed, the reaction parameters strongly affected the formation of by-products, mainly amines, on Cu-containing MTS catalysts. The increase of P and contact time favoured the formation of both MeOH and amines, while a higher S/DG value had an opposite effect. A correlation may be hypothesized between MeOH and amine formation, suggesting that amines formed by reaction of NH_3 with surface intermediates in the MeOH synthesis.

References

[1] J.N. Armor, *Appl. Catal.* **A176** (1999) 159
[2] K.S. Hayes *Appl. Catal.* **A221** (2001) 187.
[3] G. Carja, R. Nakamura, H. Niiyama, *Appl. Catal.* **A236** (2002) 91.
[4] F. Basile, G. Brenna, R. Faure, G. Fornasari, D. Gary, A. Vaccari, WO 079,323 A1 (2013) to Air Liquide.
[5] S.V. Gredig, R.A. Koeppel, A. Baiker, *Appl. Catal.* **162** (1997) 24.

III-PP70

Benefits of Hierarchization of HMFI Zeolites on the Coke Management

Pinard L.[1*], Ngoye F.[1], Gilson J.-P.[2], Fernandez C.[2], Valtchev V.[2], Quin Z.[2], Lakiss L.[2], Thomas K.[2], Vicente A.[2], Pouilloux Y.[1]

1 - IC2MP, Université de Poitiers, Poitiers, France
2 - Lab. Catalysis & Spectrochemistry, ENSICAEN, Caen, France

* ludovic.pinard@univ-poitiers.fr

Keywords: MFI, hierarchization, coke, ethanol, cracking, toxicity

1 Introduction

Many zeolite catalysts currently used commercially are already hierarchical: FCC, hydroisomerization and hydrocracking being the most important examples in oil refining. In these cases, hierarchization is brought by steam and/or acid treatments where Al is selectively removed from the framework. Recently, other methods have been rediscovered (caustic treatment where Si is removed to a greater extent than Al), studied in-depth by modern techniques and new methodologies created (fluoride treatment where Si and Al are removed at and equal rate). Moreover, the production of nanosized zeolite crystals is equivalent to hierarchization as a sizable (mesoporous) surface is developed on their external surface. This contribution focuses on the effect of hierarchization on coking and regeneration of ZSM-5 zeolite catalysts in hydrocarbon methylcyclohexane (MCH) and ethanol (EtOH) transformations. Two parent ZSM-5, one made of micron-sized crystals and the other containing nano-sized crystals were studied as well as their off springs produced by caustic and fluoride treatments.

2 Experimental

The starting material, NH_4-ZSM-5 (Si/Al=19), is a commercial micro-sized zeolite provided by Clariant. Two hierarchical ZSM-5 zeolites, A and B, were derived from P using acidic and basic post-synthesis treatments, respectively. For sample A, the fluoride treatment was performed as described by Qin et *al.*[1] For sample B, the alkaline treatment was performed as described by J.C Groen *et al.* [2]. A nano-sized commercial zeolite NH_4-ZSM-5 (noted N) with Si/Al = 41, from Clarian, was also used in this work.

3 Results and discussion

The effects of two different hierarchization procedures (alkaline and fluoride leaching) on the performances of ZSM-5 catalysts in the transformation of methylcyclohexane at 723K are highlighted and discussed in relation to their porosities. The hierarchical catalysts exhibit different porosities; namely, the fluoride treatment leads to a zeolite combining micropores and macropores while alkaline leaching adds mesopores interconnected with the native micropores.
While the initial activities and selectivities of catalysts derived from the P, A, B zeolites are very similar in the conversion of methylcyclohexane, the presence of mesopores (alkaline leaching), close to the active sites, greatly improves the stability of such a hierarchical catalyst by favoring the desorption of products. This behavior is similar to a reduction in zeolite crystal size. This increased stability is not due to a decrease of the coke toxicity, but rather to an inhibition of the growth of coke precursors, in turn related to the shorter diffusion paths of reactants and products. Two types of coke are present on the meso-/micro-porous zeolite: (*i*) a "light coke" composed of alkylbenzenes strongly adsorbed on Lewis acid sites and silanols, (*ii*)

a “heavy coke” (alkylphenanthrenes and alkylpyrenes) trapped at the intersection of the zeolite channels. While the light coke has no impact on the catalyst stability, the heavy coke poisons active sites, most probably remote from the mesopores.
During the ethanol-to-hydrocarbons (ETH) transformation at 623K and 3.0 M Pa on HZSM-5 zeolites, unwanted side reactions occur and lead also to the formation of coke. Its composition is strongly related to the dimensions and shape of the ZSM-5 pores; the structures of molecules trapped are similar than these found in MCH. The coking rate depends on the textural properties of materials and more particularly on the diffusion path length. But the catalyst lifetime is not correlated to the coking rate, it is related to the external surface, since the ethanol transformation occurs mostly by pore mouth catalysis. Additions of macropores (A) by fluorine leaching or mesopores by alkaline treatment (B) of micron-sized zeolite (P) are simple tools to increase the number of pore mouths. But, by far, the most efficient way to increase dramatically the number of pore mouth is to reduce their crystal size. The highest catalyst longevity (>100 h), is obtained in spite of a total poisoning of acid sites on hierarchical nanometer-sized zeolite (N).
The decrease in the diffusion path also offers a clear advantage in the catalysts regeneration by lowering the temperature of total coke removal.

4 Conclusion

The time on stream behavior of the various catalysts shows the advantages of hierarchization and particle size. The deactivated catalysts are extensively characterized by their residual acidity and pore volumes, nature and quantity of the carbonaceous residues and ease of decoking. One important feature is that nanosized and hierarchical zeolite crystals produce less of the very toxic coke molecules (located at channels intersections) because most coke precursors diffuse efficiently to the external surface where their deleterious effect is minimal. Nanosized ZSM-5 are systematically better than any hierarchical zeolites produced by post-synthesis treatment due, among other factors, to the much lower diffusion pathways molecules have to follow in the microporous channels.

Acknowledgements

The authors thank the French National Research Agency, ANR, (HiZeCoke Project, 2010 BLAN 723) for its financial support and Région Basse-Normandie for a post-doctoral grant for L. Al Lakiss. The authors acknowledge Clariant (Germany) for provided zeolite samples.

References

[1] Qin Z., Lakiss L., Gilson J.-P., Thomas K., Goupil J.-M., Fernandez C., Valtchev V., *Chem. Mater.,* 25 (2013) 2759.
[2] Groen J.C., Peffer L.A.A., Moulijn J.A., Pérez-Ramírez J., *Stud. Surf. Sci. Catal.*,156 (2005) 401-408

III-PP71

Biodiesel Production from Entirely Renewable Feedstocks

Mendow G.[1,2,3], Querini C.A.[1,2,3], Sanchez B.S.[1,2,3*]

1 - INCAPE, Mexico, Mexico
2 - Facultad de Ingeniería Química, Universidad Nacional del Litoral, Santa Fe, Argentina
3 - Universidad Nacional del Litoral, Santa Fe, Argentina

* bsanchez@fiq.unl.edu.ar

Keywords: ethanolysis, sodium, ethoxide, biodiesel, ethyl, ester

1 Introduction

Using bioethanol for biodiesel synthesis it is possible to obtain a 100% renewable product. Although at present ethanol is more expensive than methanol, it presents many advantages. Among the basic homogeneous catalysts used for biodiesel production, the one with best performance so far is sodium methoxide. Therefore, if the objective is obtaining biodiesel entirely composed by ethyl esters, the methoxide catalyst must be replaced. In this work, the transesterification reaction was performed using ethanol as alcohol and sodium ethoxide as catalyst.

2 Experimental/methodology

Biodiesel production process

The experiments were performed in a 500 mL flask with magnetic stirring, at 55 ºC. Refined sunflower oil and ethanol 99.5% were used as raw materials. The catalyst was sodium ethoxide solution (21 wt.%) in ethanol. The ethyl esters rich phase was purified using two consecutive washing steps. In the first one, neutral water was employed, and in the second one, a CO_2 saturated aqueous solution. Finally, the biodiesel was dried by stripping with N_2 at 80 ºC.

Figure 1. Results and discussion

Figure 1 (A) shows the monoglycerides profile, during the course of the reaction when MeONa or EtONa was used as catalysts, and methanol or ethanol was used as alcohol. As it is shown, the monoglyceride evolution during reaction was very similar for both catalysts when the alcohol used was methanol. However, the maximum concentration observed at low reaction times, was higher for the case of EtONa (%MG: 2.6 wt.%) in comparison to MeONa (%MG: 2 wt.%) which implies that the rate of disappearance of these compounds was higher when the catalyst used was sodium methoxide. Similar behavior was observed when ethanol was used as transesterification alcohol. On the other hand, when MeONa was used to catalyze the ethanolysis, the maximum monoglycerides content obtained was 4.5 wt.%, whereas the concentration measured for EtONa was 5.5 wt.%. This implies that the sodium methoxide catalyst has higher activity both for methanolysis and ethanolysis than sodium ethoxide, being this difference more pronounced when the alcohol used was ethanol. This is because the longer the carbon chain of the alcohol employed, the lower the reactivity of the alkoxide ion [1]. According to Reeve and Erikson [2], methanol is 4.4 times stronger as an acid than ethanol in an equimolar mixture. However, methoxide is less nucleofilic than ethoxide (0.82 times). The combination of these effects gives as a result that methoxide is 3.6 times more reactive than ethoxide. On the other hand, better solubility of ethanol in oil enhances mass transfer as compared to methanol [3]. Moreover, the phase distribution of the catalyst is more favorable for ethanol than methanol. As a consequence, the difference in reactivity is less pronounced than expected. In the same experiment it was observed that evolution of di- and triglycerides (not

shown) showed a similar pattern, but less marked than for the case of monoglycerides.

Catalyst consumption is shown in Fig. 1 (B). According to these results, there is a correlation between the moles of catalyst consumed due to saponification and the activity shown in Fig. 1 (A). The higher reaction rate was observed when MeONa was used as catalyst and methanol as alcohol. In this experiment, the percentage of catalyst that disappeared was only 30% of the initial concentration, this being the smallest value observed among the experiments carried out to compare different catalysts and alcohols. When EtONa and ethanol were used, the percentage of unreacted glycerides was the largest, which implies the lowest reaction rate. This correlates well with the results presented in Fig. 1 (B), which shows that 69% of the sodium ethoxide catalyst disappeared during the reaction with ethanol. This demonstrates that the reaction rate is not only affected by steric hindrance for the longer chain alcohol, but also is greatly affected by the catalyst disappearance. This is due to the less polar character of ethanol, which favors the saponification reactions during the transesterification to a greater extent than methanol. It can also be seen that using the same alcohol, either methanol or ethanol, sodium ethoxide showed greater tendency to form soaps than sodium methoxide, which is in agreement with its lower activity under identical conditions.

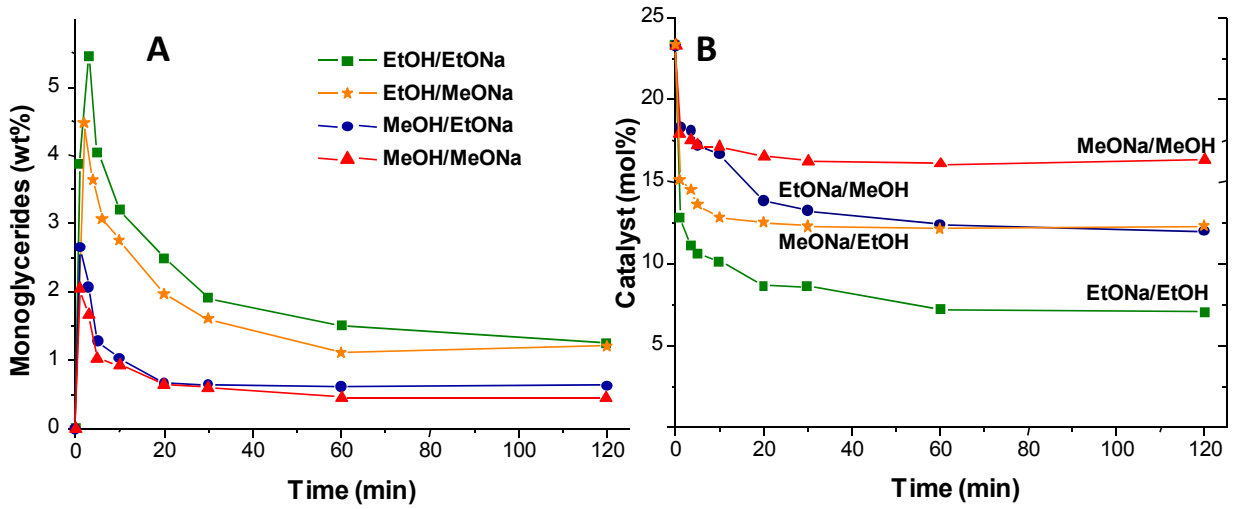

Figure 1. (A) Monoglycerides, and (B) catalyst concentration vs time using different alcohols (methanol and ethanol) and catalysts (sodium methoxide and ethoxide).

4 Conclusions

It was concluded that the methanolysis reactions are faster than the ethanolysis and sodium methoxide catalyst is more active than the corresponding ethoxide. This is due to two factors: first, the steric hindrance and secondly, that the saponification of EtONa in ethanol medium is greater than when using methanol, causing a decrease in the catalyst concentration and leading to lower conversion.

References

[1] M.G. Kulkarni, A.K. Dalai, N.N. Bakhshi, *Bioresource Technology* 98 (2007) 2027.
[2] W. Reeve, S.M. Erikson, *Canadian Journal of Chemistry* 57 (1979) 2747
[3] T. Issariyakul, M.G. Kulkarni, A.K. Dalai, N.N. Bakhshi, *Fuel Processing Technology* 88 (2007) 429.

III-PP72

Biogas Steam Reforming for Syngas Production with Structured Catalyst

Álvarez A., Martínez T. L.M., Centeno M.A.*, Odriozola J.A.

ICMSE, University of Seville-CSIC, Seville, Spain

* centeno@icmse.csic.es

Keywords: biogas steam reforming, syngas production, H_2/CO, ratio, micromonolith

1 Introduction

Fischer-Tropsch technology has become a key strategy to overcome the actual petroleum scarcity. It allows the synthesis of liquid fuels similar to the ones derived from fossil sources but much more cleaner. However, one of the main requirements is the use of syngas with a H_2/CO ratio of 2. Therefore, finding viable and cheap ways to obtain syngas with this precise ratio would increase the viability of the process at industrial scale. In this way, the use of biogas, specially the one produced by rubbishes as a syngas source, is a very attractive option since it removes two household gases, and gives an added value to wastes.

Conventional packed-bed reactors have been mostly used for the syngas production from biogas reforming. In these systems, the use of small catalyst particles could cause high-pressure drops, flow misdistribution and even, hot spots that could alter the selectivity of the process [1]. Structured catalysts overcome these drawbacks. The employ of metallic monolithic catalysts allows the use of very small parallel channels, well below 1 mm, resulting in process intensification on favoring heat and mass transfer during reaction.

The present work describes the synthesis and structuration of a modified Ni/Al_2O_3 catalyst in order to produce syngas with the desired ratio from a mixture of CH_4, H_2O, and CO_2.

2 Experimental

Powder catalyst synthesis.

The support was synthesized by impregnation of Mg(NO3)2·6H2O (Aldrich) on γ-alumina powder (Sasol) in order to obtain a 10 wt % of Mg (calculated as MgO). This support was calcined at 850ºC for 12h. The catalysts was prepared by simultaneous impregnation with a solution containing both Ni(NO3)2·6H2O (Aldrich) and Ru(NO)(NO3)3 (Johnson Matthey) in ethanol. After drying at 60ºC for 12h, the solid has a final calcination at 500ºC for 3h in order to eliminate the precursor residues. The wt% of Ni is intended to be 15%, and that of Ru wt%, 0,5%.

Slurry catalyst synthesis.

The first step for washcoating the metallic substrate is to prepare stable slurry of the previously prepared catalyst. Particle size, solid content and pH are parameters that influence the slurry stability. In this work, the as prepared powder catalyst was milled until obtaining an average particle size of 10µm. Also, since the ZPC (zero point charge) of the catalyst was 10,5, the slurry pH was adjusted to 7,1 to ensure the stabilization of the slurry through high repulsions between the particles. Finally, colloidal alumina (Nyacol, 6% Wt) and Polyvinyl alcohol (PVA, 1,14 % wt) was added to improve the catalyst adherence and the washcoating drying process. The solid content of the slurry was 18,2%. After the deposition of the catalysts, the excess of slurry was dried and calcined at 500ºC 3h.

Micromonolith preparation.

Cylindrical monoliths were prepared using 50µm thick FeCrAlloy® foils by rolling around a spindle alternate flat and corrugated foils. Prior to washcoat, the metallic monoliths were calcined in air at 900ºC for 22h in order to generate an adherent α-Al2O3 scale. The metallic monoliths were dipped into the slurry for 60s, withdrawn at constant speed and then the excess suspension eliminated by centrifugation at 600rpm for 10min. This procedure was repeated three times with intermediate drying steps at 120ºC for 30min between coatings until 167mg of the catalyst were deposited. Finally, the coated structured supports were calcined at 500ºC for 3h.

3 Results and discussion

The powder catalyst characterization showed: (A) the desired metal incorporation into the support was achieved. (B) The addition of Ni and Ru barely changes the textural properties of the modified alumina and (C) A high Ni-Ru interaction evidenced by TPR and Raman spectroscopy. The slurry and the structured monolith were also characterized. No differences were detected regarding the textural properties after structuration. However, XRD analysis showed a clear presence of RuO_2 in the slurry sample (although no Ru species were found in the powder sample) implying a modification of the catalyst structure when preparing the slurry.

The catalytic activity of the powder sample, the calcined slurry and the micromonolith were performed at 750ºC with a CH_4:H_2O:CO_2 molar ratio of 1:0,56:0,4 with a WHSV(mg/g.h)=117000 for 100h (Figure 1). All samples showed the same activity at the beginning of the reaction. Nevertheless, the slurry gets deactivated after 5 hours. This late behavior could be achieved to the presence of RuO_2, which suggests a poor metal dispersion implying a minor Ru-Ni interaction. The powder sample, which has a better Ru dispersion, presents a better stability. On the other hand, the micromonolith presented the best activity and stability, and maintained a H_2/CO ratio of 2 for 100h. This great behavior can be explained based in the advantages of the catalyst structuration, where mass and heat transport processes are improved and the carbon gasification processes are enhanced, increasing the stability.

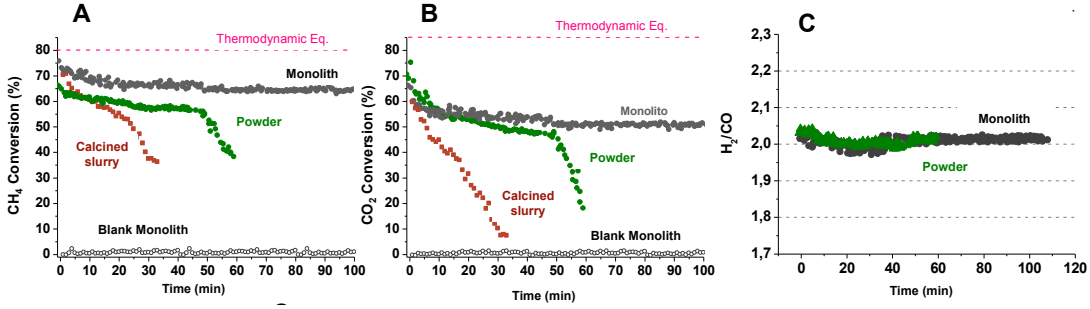

Fig. 1. (A) CH_4 Conversion. (B) CO_2 Conversion (C) H_2/CO ratio.

4 Conclusions

The catalyst structuration of a modified Ni catalyst in a metallic micromonolith allowed the syngas production with a H_2/CO ratio of 2 for at least 100h using the combined steam reforming of methane with a CH_4:H_2O:CO_2 molar ratio of 1:0,56:0,4 at 750ºC. Although the catalyst structuration generates a "less active" catalyst, the advantages of the catalyst structuration, where mass and heat transport processes are improved, increase the stability.

Acknowledgements

The authors are grateful to the support from the Spanish Ministerio de Economía y Competitividad (MINECO) (ENE2012-374301-C03-01 and ENE2013-47880-C3-2-R) and from Junta de Andalucía (TEP-8196) co-financed by FEDER funds from the European Union.

References

[1]. L.F. Bobadilla, A. Alvarez, M.I. Domínguez, F. Romero-Sarria, M.A. Centeno, M. Montes, J.A. Odriozola, *Applied Catalysis B 123-124 (2012) 379-390.*

III-PP73

Cadmium and Tin Magnetic Nanocatalysts Useful for Biodiesel Production

Alves M.B., Medeiros F.C.M., Sousa M.H., Rubim J.C., Suarez P.A.Z.*

University of Brasilia, Brasilia, Brasilia

* psuarez@unb.br

Keywords: biodiesel, hydrolysis, esterification, transesterification, Ferrites

1 Introduction

In order to address the increasing demand for energy and growing ecological awareness, biofuels have emerged in the last decades as elegant alternatives to fossil fuels, since they are obtained from renewable sources. Therefore, improvements in the technology to produce renewable fuels, such as biodiesel, are needed to gracefully meet global demand for both food and biofuels, avoiding the food, energy, and environment trilemma. However, examples that can provide large amounts of raw-materials to produce biodiesel without competing with food production, such as the palm-tree oil called Macauba (*Acrocomia sclerocarpa* M.) that produce more than 4,000 liters per hectare when associated with cattle, usually contains high FA content (we have received a sample containing about 66 % of free fatty acids in its composition), making impossible their process using traditional transesterification technologies. The aim of this work was to identify new catalytic precursors with potential application in the preparation of biodiesel both using oils with high purity, as well as using a raw material with high free-FA contents. In this sense iron/cadmium and iron/tin magnetic materials were synthesized, which were tested as catalysts in the reactions of hydrolysis, esterification and transesterification of soybean oil and soybean FA. The catalytic activity of iron/tin catalyst was further investigated in the transesterification/esterification reaction of the crude acid oil from the Macauba palm-tree (*Acrocomia sclerocarpa* M.).

2 Experimental/methodology

Two aqueous metal solutions (M^{+2} and Fe^{+3}) were mixed with a hot sodium hydroxide aqueous solution, forming two precipitates: iron/cadmium (ICdO) and iron/tin (ISnO) oxides. The analysis of this solids by ICP, FT-Raman and DRX showed ferrite like solids ($MFe^{+3}{}_2O_4$, M= Cd^{+2} or Sn^{+2}). However, all these possible steps depend on the reaction parameters and may lead to different materials. Additionally, through the Scherrer formula, the broadening of the 311 main peak allowed calculation of the mean crystalline sizes of the grains of 3.5 nm and 34.8 nm for ICdO and ISnO samples, respectively. The magnetic properties of the samples were evaluated by recording the magnetic field (H) dependence of the magnetization (M) at 27 ºC. The ISnO sample presents a loop that shows a ferromagnetic-like behavior with saturation magnetization (M_s), remnant magnetization (M_r) and coercivity (H_c) values of ca. 12.8 emu/g (at H = 13 kOe), 3.1 emu/g and 86 Oe, respectively. On the other hand, the ICdO powder displays features of superparamagnetism, with negligible remanence and coercivity in low field regime. Moreover, the data indicate that ICdO does not saturate in the magnetic field interval investigated in this work, but reaching a magnetization of 22 kOe at the maximum value of magnetic field.

The catalytic activity of ICdO and ISnO were investigated in transesterification and hydrolysis of triacylglycerides, as well as in the esterification of fatty acids, which are useful reactions for biodiesel production. In this sense the experiments were carried out using soybean oil and fatty acids (previously prepared from soybean oil) as substrate. In 5 h, the reaction yields

for esterification, hydrolysis and transesterification, respectively, were up to: 98 %, 90 % and 84 % using ICdO and 98 %, 70 % and 30 % using ISnO (Conditions: 20 g soybean oil or soybean fatty acid, 6 g methanol or 20 g water and 1 g of ICdO or ISnO, at 200 ºC, 13.6 bar in hydrolysis and 18.6 bar in others). The catalysts are apparently more active for esterification than for transesterification and hydrolysis. It is important to highlight that there is a small contribution by self-catalysis promoted by fatty acids that act as catalysts of Brönsted. To evaluate the self-catalytic behavior of fatty acids we performed an esterification reaction at 200 ºC for 2 h in the absence of catalyst that resulted in 41 % yield. Thus, these results suggest that the main catalytic activity is due to the magnetic materials. Indeed, the increasing activity during hydrolysis observed for ICdO and ISnO may also be understood as a result of the catalytic activity of the formed fatty acids.

3 Results and discussion

In sequence, crude Macauba oil containing 66 % of free fatty acid was reacted with methanol in the presence of ISnO (Conditions: 20 g oil, 6 g methanol, 1 g catalyst, at 200 ºC, 18.6 bar). Note that only the ISnO catalyst was used because its performance was superior when compared to the ICdO in the recycling experiments. It is noteworthy that both esterification and transesterification reactions take place in this experiment, given that the substrate contains, in addition to glycerides, a high content of fatty acids. During the reaction there is a decrease in acidity value, sharper at the first 2 h, reaching a low acidity, which indicates that free fatty acids were esterified producing biodiesel. On the other hand, up to 90 % of FAME was obtained after 3 h of reaction, as a result of acyl-glycerides transesterification and fatty acid esterification. After the reaction, the ISnO catalyst was recovered by magnetic separation and was reused four other times with new charges of substrate with no significant loss of activity.

Acknowledgements
We would like to thank INCT-Catalise, CAPES, CNPq and FAPDF.

III-PP74

Carbon Dioxide (CO_2) Dry Reforming of Glycerol for Hydrogen Production Using Ni/La_2O_3 and Co/La_2O_3 as Catalysts

Mohd Yunus N.[1], Mohd Arif N.N.[1], Harun N.[1], Zainal A.S.[1,2*]

1 - Faculty of Chemical & Natural Resources Engineering, Universiti Malaysia Pahang, Pahang, Malaysia

2 - Center of Excellent For Advanced Research in Fluid Flow (CARIFF), Universiti Malaysia Pahang, Pahang, Malaysia

* sumaiya@ump.edu.my

Keywords: glycerol, biodiesel, dry reforming, hydrogen, rare earth, oxide, fixed bed reactor

1 Introduction

Glycerol, a byproduct derived from transesterification of biodiesel is currently experiencing an oversupply crisis due to the higher biodiesel demand worldwide. Utilization of glycerol as feedstock helps to resolve this oversupply problem and directly rise up the price of crude glycerol and lowers the production cost of biodiesel plant [1]. Dry reforming of glycerol is aims as it offer a better pathway for the production of hydrogen and greener process as it used carbon dioxide as reactant and release water as their by-products [2]. Nickel (Ni) based catalyst has been widely used in reforming process due to its low cost as compared to noble metal catalyst. On other hand, cobalt (Co) based catalyst was selected as it provides similar activity to noble metal catalysts in the C-C bond cleavage, even at low operating temperatures. Therefore, in this study the H_2 production by glycerol dry reforming was evaluated using Ni and Co catalyst with different percent metal loading impregnated on La_2O_3 as support. The catalytic reaction was conducted in a fixed bed reactor where the reaction studies (i.e. hydrogen yield, glycerol conversion) and characterization of both catalyst was studied.

2 Experimental/methodology

Catalyst of 10 wt% Ni/La_2O_3 and 10 wt% Co/La_2O_3 were prepared via wet impregnation method. Initially, La_2O_3 support was calcined at 1073 K for 6 hours in a furnace. After that, an accurately weighted calcined La_2O_3 was mixed with $Ni(NO_3)_2.6H_20$ aqueous solution and magnetically-stirred for 3 hours. Then, the slurry was dried overnight in an oven at 383 K for 12 hours to remove excess water. The product was crushed and calcined again for 6 hours at 1073 K. It was then cooled down and sieved to a particle size of 90-200 μm for characterization and reaction studies. Catalyst characterization was performed using N_2 physisorption for Bruanaur-Emmett-Teller (BET) surface area, Scanning Elemental Analysis (SEM) and X-Ray Diffraction (XRD) analysis. For dry reforming experimental work, glycerol was flow through fixed bed reactor system via HPLC pump at a fixed temperature of 973 K. Flow of nitrogen gas to the reactor was set at 0.1 L/min flow rate at 1 bar while flow of carbon dioxide gas to the reactor was set at 9.9 ml/min at 1 bar. The composition of syngas produced was determined using online Agilent gas chromatography (GC) with TCD capillary columns and HP-Plot/Q column (30.0 m X 530 μm X 40.0 μm)

3 Results and discussion

Table 1 shows the comparison of BET surface area between 10 wt% Ni/La_2O_3 and 10 wt % Co/La_2O_3. It was found that the 10 wt% Ni/La_2O_3 exhibit large specific area and smaller metal

crystallite size as compared to 10 wt % Co/La_2O_3 which provides higher metal dispersion and larger surface area for the catalyst. These findings are co current with the results from the SEM where the morphology shows that there is presences of Ni species accumulate on the surface of La_2O_3 support.

Table 1: BET Analysis

	10 wt% Ni/La_2O_3	10 wt% Co/La_2O_3
BET specific surface area (m^2 g^{-1})	28.29	13.032
Cumulative pore volume (m^3 g^{-1})	0.0574	0.0211

FTIR analysis shows the same pattern of result for Ni and Co catalyst. Figure 1 (a) shows the XRD pattern for both Ni/La_2O_3 and Co/La_2O_3. The presence of La_2O_3 species in 10 wt% Ni/La_2O_3 was undetectable due to an increase in level of La_2O_3 dispersion that indicates formation of smaller crystallite. In contrast Co revealed additional peaks showing the formation of Co_3O_4 phase in the system resulting larger Co crystallite form. Figure 1 (b) shows yield of hydrogen for both catalyst and it shows Ni/La_2O_3 achieved 11.8 % of hydrogen which is the highest compared to Co and this can be supported by XRD and BET results.

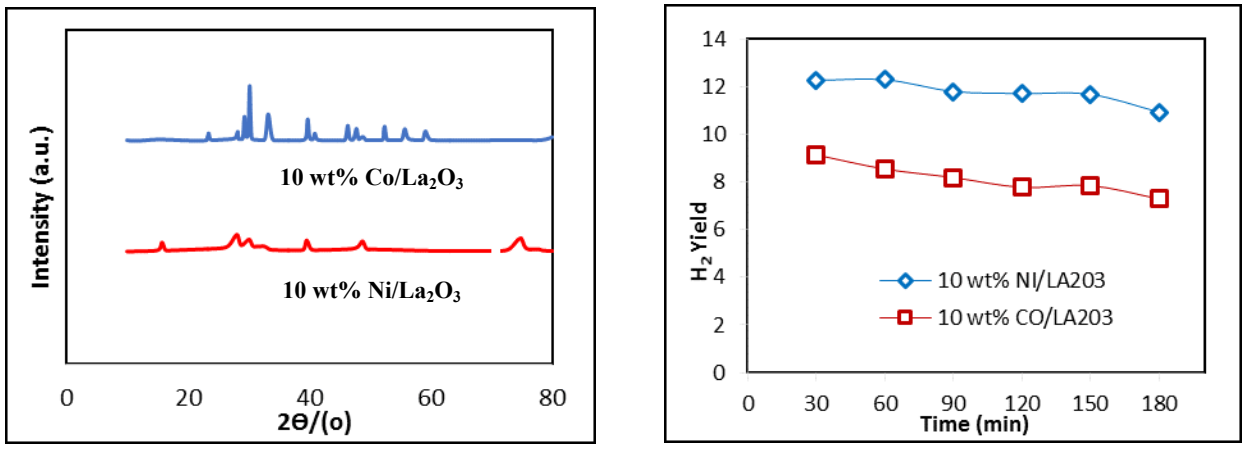

Fig. 1. (a) XRD patterns analysis of catalyst and **(b)** Yield of hydrogen of 10 wt% Ni/La_2O_3 and 10 wt% Co/La_2O_3

4 Conclusions

The Ni and Co catalyst supported by La_2O_3 have been investigated in glycerol dry reforming and both of the catalyst successfully produced hydrogen. From the results, 10 wt% Ni/La_2O_3 gives the highest H_2 yield and glycerol conversion. It is due to high activity of 10 wt% Ni/La_2O_3 towards hydrogen rich gas and great stability. Characterization analysis of XRD and BET results also revealed that 10 wt% Ni/La_2O_3 catalysts have smaller metal crystallite size which provide higher metal dispersion and larger surface area which is also proved by SEM analysis.

Acknowledgements

Authors would like to thank MOE for the research grant RDU130108, and Universiti Malaysia Pahang for financial support.

References

[1] Haas, M.J., McAloon, A.J., Yee, W.C., Foglia, T.A., (2006). A process model to estimate biodiesel production cost., *Bioresour. Technol.* 97(4):671-678.

[2] Wang, X., Li, M., Wang, M., Wang, H., Li, S., Wang, S. and Ma, X., (2009). Thermodynamic analysis of glycerol dry reforming for hydrogen and synthesis gas production., *Fuel*, 88(11): 2148-2153.

III-PP75

Catalytic Features Controlling HZSM-5 Zeolite Performance and Deactivation during the Cracking of 1-Butene to Propylene

Epelde E.[1], Santos J.I.[2], Florian P.[3], Aguayo A.T.[1], Gayubo A.G.[1], Bilbao J.[1], Castaño P.[1*]

1 - Department of Chemical Engineering, University of the Basque Country (UPV/EHU), Bilbao, Spain

2 - NMR Service, SGIKER, University of the Basque Country (UPV/EHU), "Joxe Mari Korta" Center, San Sebastian, Spain

3 - CNRS, UPR3079 CEMHTI, Orléans Cedex 2, France, and Université d'Orléans, Orléans Cedex 2, France

* pedro.castano@ehu.es

Keywords: ZSM-5, zeolite, acidity, modification, oligomerization, cracking propylene, coke, deactivation

1 Introduction

Acid MFI zeolite (HZSM-5) is used in catalytic processes linked with conventional and sustainable refining concepts. The outstanding performance of MFI zeolite is attributed to its unique acid and structural features, with very attractive shape selectivity for producing light olefins, and propylene in particular. The performance of MFI towards the production of propylene can be enhanced [1-4] by (i) selecting the proper SiO_2/Al_2O_3 ratio, (ii) calcinating with different protocols, (iii) using vapor at high temperatures, namely *steaming*, (iv) incorporating rare earth or transition metals, (v) exchanging hydroxyl groups by cations like Na^+, (iv) selecting a proper matrix of binders and fillers, and (v) by treatment with acids or bases, among others. In this work we have measured the correlations between the catalytic features (acid strength and porous structure) and its intrinsic performance (conversion, selectivity and deactivation) by a sensitivity and regression analysis, during the cracking of 1-butene to propylene using catalysts based on MFI zeolites of different SiO_2/Al_2O_3 ratio and modification degree with KOH and H_3PO_4.

2 Experimental/methodology

Catalysts were prepared based on commercial MFI zeolites (SiO_2/Al_2O_3 ratio of 30, 80 and 280), incoporating 1 and 3 wt% of K or P by incipient wetness impregnation at 70 ºC under vacuum using KOH (85 % purity) or H_3PO_4 (85 % purity) solutions, respectively. The catalysts were obtained by agglomerating 25 wt% of each zeolite with 30 wt% bentonite and alpha-alumina as catalyst inert matrix. The fresh and deactivated catalysts were characterized by elemenal analysis, XRD, ^{29}Si and ^{27}Al NMR, N_2 adsorption-desorption, adsorption-desorption of tert-butylamine (t-BA) and TG-TPO. The catalytic runs have been carried out in an isothermal fixed-bed reactor at 500 ºC; space time, 1.6 $(g_{catalyst}\ h)\ (mol_C)^{-1}$; WHSV, 8.75 h^{-1}; 1-butene (99 vol%, Air Liquide) partial pressure in the feed, 1.35 bar; time on stream, 0-5 h.

3 Results and discussion

The heat dissipated during isothermal adsorption of t-BA can be linearly correlated with the temperature of maximum t-BA desorption-cracking rate obtained in TPD of the same base. This result enables a fast characterization of the acid strength, which is a critical catalytic feature of the MFI zeolite that controls conversion and selectivity of propylene in 1-butene cracking. Thus, in accordance to previous literature [5], conversion increases and propylene selectivity decreases for zeolites with lower SiO_2/Al_2O_3 ratio, due to their higher acid strength.

On the other hand, zeolite crystal size and micropore volume are key factors controlling deactivation by coke deposition (Figure 1) and, consequently, the lifetime of the catalyst, as they favor the outward diffusion of coke precursors.

The modifications by KOH or H_3PO_4 of MFI zeolites affect their kinetic performance due to changes of these two catalytic features. On the one hand, these modifications lower acidity due to dealumination: K-modified MFI zeolites show significant drop of accessible framework Al, whereas P-modified MFI zeolites show a significant conversion of framework to extra-framework Al. On the other hand, these modifications cause desilication of the zeolites, which is greater for the MFI zeolites with the higher SiO_2/Al_2O_3 ratio, and is strongly correlated with the increase in mesoporosity and decrease in microporosity and crystal size

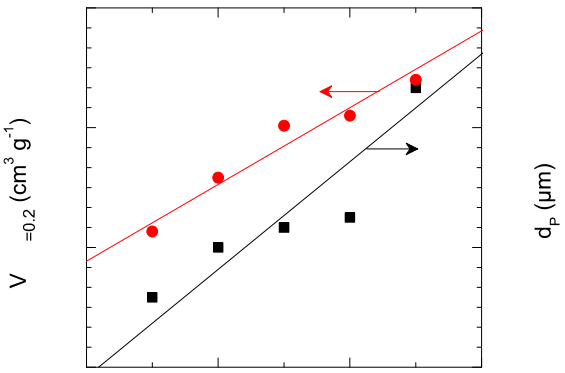

Fig. 1. Correlation between the coherent diffraction crystal size (d_P) and volume of N_2 adsorbed at $P/P_0 = 0.2$ with the amount of coke deposited after 5 h on stream.

Consequently, high propylene selectivity and slow deactivation rate by coke is obtained using high silica zeolites (SiO_2/Al_2O_3 ratio = 280) modified with of K or P, although the conversion of 1-butene is significantly decreased.

4 Conclusions

Acid strength as well as crystal size and mesoporosity are the features controlling the catalytic performance of high silica (SiO_2/Al_2O_3 = 280) MFI zeolites, which are the most promising catalysts for propylene production. Acid strength is the key factor controlling conversion of 1-butene and selectivity of propylene, whereas the diffusion length (size of the zeolite crystals and micropore volume) of the coke precursors is the key factor controlling coke deactivation and the lifetime of the catalyst. The modifications by KOH or H_3PO_4 of MFI zeolites lead to catalysts with lower activity but higher propylene selectivity and with extended lifespan due to its lower deactivation rate by coke deposition.

Acknowledgements

The financial support of this work was undertaken by the Ministry of Economy and Competitiveness (MINECO) of the Spanish Government (CTQ2013-46172-P, CTQ2010-19623 and CTQ2010-19188 projects) and by the University of the Basque Country (UFI 11/39). E. Epelde (BFI08.122) is grateful for her Ph.D. grant from the Basque Government and for the University of the Basque Country. The technical and human support provided by SGIKER (UPV/EHU) is gratefully acknowledged, particularly to Aitor Larrañaga.

References

[1] N. Rahimi, R. Karimzadeh, Appl. Catal. A: Gen. 398 (2011) 1-17.
[2] G. Elordi, M. Olazar, M. Artetxe, P. Castaño, J. Bilbao, Appl. Catal. A: Gen. 415-416 (2012) 89-95.
[3] G.L. Woolery, G.H. Kuehl, Zeolites 19 (1997) 288-296.
[4] P. Castaño, J. Ruiz-Martinez, E. Epelde, A.G. Gayubo, B.M. Weckhuysen, ChemCatChem 5 (2013) 2827–2831.
[5] L. Lin, C. Qiu, Z. Zhuo, D. Zhang, S. Zhao, H. Wu, Y. Liu, M. He, J. Catal. 309 (2014) 136-145 .

III-PP76

Catalytic Upgrading of Lignin Derived Pyrolysis Vapor via HZSM-5

Zhou G.[1], Jensen P.A.[1], Knudsen N.O.[2], Jensen A.D.[1*]

1 - Department of Chemical and Biochemical Engineering, Technical University of Denmark, Lyngby, Genmark
2 - DONG Energy, Fredericia, Genmark

* aj@kt.dtu.dk

Keywords: fast pyrolysis, lignin, HZSM-5

1 Introduction

Lignin is the second most abundant biomass component found in nature [1]. The estimated lignin production is 50 million tons/year from pulp and paper industry [2]. This number will increase with the development of new biomass utilizations, such as second generation bio-ethanol production. Hence the potential of lignin as a renewable source for chemicals and fuels should not be overlooked. By fast pyrolysis, lignin can be converted into a liquid fuel, known as bio-oil [3]. Due to its high oxygen content, a subsequent upgrading step is essential for using bio-oil as an engine fuel. In this study, lignin, obtained as a by-product from a second generation bio-ethanol plant, is pyrolyzed in a Pyrolysis Centrifuge Reactor. The pyrolysis vapor is directly upgraded catalytically using a HZSM-5 zeolite before product condensation.

2 Experimental/methodology

The lignin particles are conveyed by a screw feeder into the Pyrolysis Centrifuge Reactor that is kept at 500°C. The rotation of the blades in the reactor pushes the lignin particles onto the hot wall in order to obtain a high heating rate. The solid chars are separated from the gas by a change-in flow-direction separator (460°C), a cyclone (440°C) and a hot gas filter (300°C). The char free pyrolysis vapor is upgraded using a zeolite catalyst (HZSM-5) in a fixed bed reactor at varying temperatures from 350°C to 600°C. The liquid products are collected in a series of condensers placed in a cooling bath and a dry ice/ethanol bath. For each experiment, 30 g HZSM-5 (SiO_2/Al_2O_3=25) is used and about 30 g lignin is fed during 25 minutes.

3 Results and discussion

The product yields from fast pyrolysis and direct zeolite upgrading of the pyrolysis vapor are summarized in figure 1. Fast pyrolysis of lignin itself produces 25.8 $wt\%_{daf}$ of liquid organics. By upgrading the pyrolysis vapor over the HZSM-5 catalyst, the organic yield decreases significantly to less than 10 $wt\%_{daf}$, and a large amount of reaction water is produced. The organic yield reaches a peak at a catalyst temperature of 450°C and then decreases again at higher catalyst temperatures. At low temperature (350°C), the catalyst traps the pyrolysis vapor in the catalyst pores due to condensation and hence less organic liquid is collected. The desired organic products from the HZSM-5 upgrading are aromatics, such as benzene and toluene. The highest aromatic yield obtained is 4.0 $wt\%_{daf}$ at a catalyst temperature of 600°C.

Among the produced gases, CO and CO_2 are the major gas components. The yields of CO and CO_2 from the non-catalytic run are 4.1 $wt\%_{daf}$ and 11.4 $wt\%_{daf}$ respectively. The HZSM-5 zeolite promotes decarbonylation reactions to form CO over decarboxylation reactions to form CO_2. The yield of CO increases to 7.7 $wt\%_{daf}$ at a catalyst temperature of 600°C, while the CO_2 yield remains almost constant. The yields of valuable light olefins (including ethene and propene) increase with increasing catalyst temperature. The highest olefins yield is 4.3 $wt\%_{daf}$

obtained at a catalyst temperature of 600°C.

Via thermogravimetric analysis, the spent catalysts were heated up to 750°C under a N_2 flow. The catalyst used in the 350°C experiment, shows the highest weight loss (about 5 wt%) in thermogravimetric analysis. It verifies that the zeolite efficiently traps the pyrolysis vapor at low catalyst temperature. The trapped material does not form a graphite coke. Instead it is still reactive at elevated temperature.

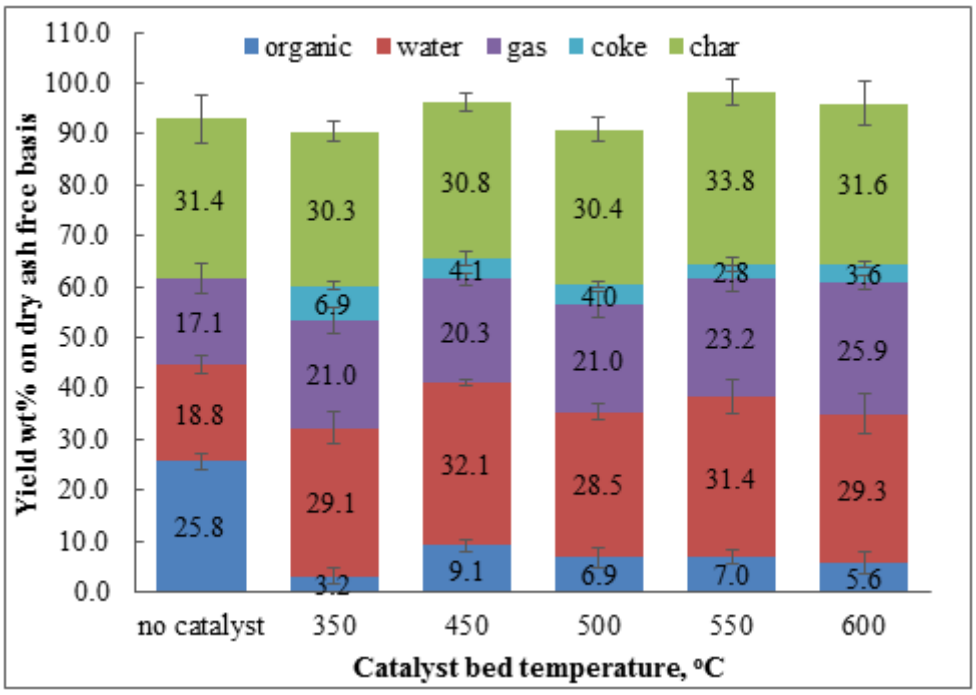

Fig. 1. Overall yields from fast pyrolysis of lignin and direct upgrading of pyrolysis vapor at catalyst temperatures from 350°C to 600°C

4 Conclusions

It is possible to convert lignin into bio-oil at an organic yield of 25.8 $wt\%_{daf}$ using a Pyrolysis Centrifuge Reactor. By direct upgrading of the pyrolysis vapor over a fixed bed of HZSM-5, the yield of organic liquid decreases significantly (<10 $wt\%_{daf}$) while the production of aromatics, such as benzene and toluene, is increased. The formation of aromatics is favored at high catalyst temperature. The highest yields of olefins and aromatics are 4.3 wt% and 4.0 wt% respectively at a catalyst temperature of 600°C. At low catalyst temperature, such as 350°C, HZSM-5 traps some of the pyrolysis vapor in the pores. However, the trapped reactant is still reactive at temperature >400°C. HZSM-5 rejects oxygen from lignin derived pyrolysis vapor mainly through the formation of H_2O and CO.

Acknowledgements

The present work is financed by DTU and Biomass for the 21st Century (B21st), funded by the Danish National Advanced Technology Foundation.

References

[1] D.J. Nowakowski, A.V. Bridgwater, D.C. Elliott, D. Meier, P. De Wild, *Journal of analytical and applied pyrolysis*, 88, 2010, 53-72.

[2] R. J. A. Gosselink, E. De Jong, B. Guran, A. Abächerli, *Industrial Crops and Products*, 20 (2), 2004, 121-129.

[3] T.N. Trinh, P.A. Jensen, K. Dam-Johansen, N.O. Knudsen, H.R. Sørensen, S. Hvilsted, *Energy & Fuel*, 27, 2013, 1399-1409.

III-PP77

Chemical Leaching of Carbon-supported PtCu Alloy Particles – Seeking for Relations between Surface Properties and Electrochemical Activity in the Oxygen Reduction Reaction

Petrova O.[1], Kulp C.[2], Pohl M.M.[3], Ter Veen R.[4], Veith L.[4], Grehl T.[5], Van Den Berg M.W.E.[6], Brongersma H.[7], Bron M.[2], Grünert W.[1*]

1 - Ruhr University Bochum, Bochum, Germany
2 - Martin-Luther-Universität Halle, Halle, Germany
3 - Leibniz-Institut für Katalyse e.V. Rostock, Rostock, Germany
4 - Tascon GmbH Münster, Germany
5 - ION-TOF GmbH Münster, Germany
6 - Huntsman Pigments, Krefeld, Germany
7 - Eindhoven University of Technology, Eindhoven, The Netherlands

* w.gruenert@techem.rub.de

Keywords: fuel cell, oxygen reduction, alloy nanoparticles, chemical leaching, core-shell particles

1 Introduction

Pt-X alloy nanoparticles (X = Cu, Co, etc.) have received much attention because of their potential as cathode catalysts for the ORR in fuel cells. They form core-shell structures with a Pt skin covering an alloy core [1], which has been related to their superior ORR activity as compared to C-supported Pt nanoparticles. P. Strasser et al. found that the Pt shell can be made on purpose by electrochemical or chemical leaching protocols (EL, CL; [2, 3]). For particles below a critical size, EL was shown to result in shells of 3-4 layers of pure Pt covering alloy cores of approximately the initial composition (often PtX_3) [2, 4]. For layers of such thickness, electronic ligand effects could not explain the strong activity gains observed. Therefore, lattice strain, which has a longer range of influence [5], was proposed to cause the beneficial effects [4].

We have studied the effect of CL of C-supported $PtCu_x$ alloy particles (x_{av} □ 3) on their structure and ORR activity. CL, which was reported to be beneficial but inferior to EL [6], might limit the release of Cu onto electrodes activated by a final EL step. Moreover, it provides unlimited sample quantities for characterization studies, in our case by XRD, electron microscopy, XAFS, XPS, and Low-energy Ion Scattering (LEIS)

2 Experimental

$PtCu_x$/C was obtained by a reductive co-deposition with ethanol, with subsequent alloying by annealing in dilute H_2 at 800 °C. Following Strasser's procedures [6], EL was performed by 200fold potential cycling between 0.5 and 1.2 V in 0.1 m $HClO_4$, CL by refluxing in 1 M H_2SO_4 for 36 h. Activities were determined with the rotating-disc electrode and will be reported for a potential of 0.9 V, related to electrochemical surface areas (ECSA) determined by CO stripping.

3 Results and Discussion

According to XRD and electron microscopy, the alloy particles exhibited a distribution of sizes around 3.5 nm, and of Cu contents around $PtCu_{2.6}$. Superstructure signals indicated order in the alloy structure. The activity of the as-made catalyst (140 μA/cm^2 Pt) was twice that of a Pt/C reference. While direct EL improved the performance by just 25 %, 265 μA/cm^2 Pt were obtained after CL, which was further increased to 315 μA/cm^2 Pt by an additional EL step.

CL resulted in an average composition of Pt_3Cu. XRD showed a wide distribution of Cu contents, including small monometallic Pt particles, and the loss of superstructure. After annealing in H_2 at 800 °C, HAADF-STEM revealed a close metal-C interaction and the coexistence of individual atoms with the particles. CL produced hollows in large particles. Smaller particles were compact and surface-enriched in Pt within 3 atomic layers. The support was sprinkled with single Pt atoms, well-crystalline alloy particles had disordered overlayers (Fig. 1). XAFS confirmed the participation of the particle bulk in dealloying: Cu was found in a more Pt-rich environment. The average Pt-Pt distance was found to be 2.67 Å before leaching and 2.70 Å after CL while the peak activity of PtCu alloy particles was related to a Pt-Pt distance of 2.72-2.74 Å in literature [7]. Coordination numbers derived suggest a shell of 3-4 Pt layers over a $PtCu_2$ alloy core, but the abundance of Pt-Pt coordinations observed might also arise from segregated Pt particles present. While XPS confirmed Pt surface enrichment, the actual thickness of the Pt skin was assessed by quantitative dynamic LEIS. It was observed that the alloy core was covered by a single Pt monolayer containing almost no Cu (Fig. 2).

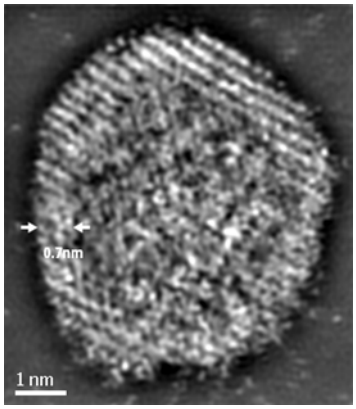

Fig. 1: HAADF-STEM image (Fourier filtered) of alloy particle after CL, with Pt enrichment in core ($Cu_{39}Pt_{61}$ vs. $Cu_{48}Pt_{53}$ in bulk), disordered surface structure, and individual Pt atoms nearby

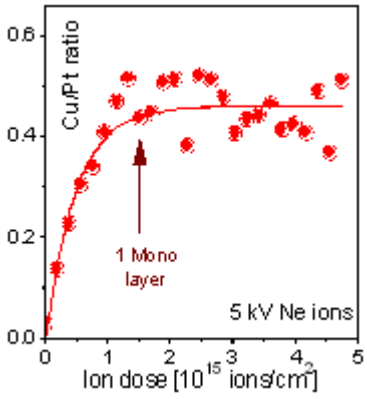

Fig. 2: Surface analysis by LEIS

This morphology is very different from that reported to result from EL (3-4 Pt layers on alloy core of original composition [2, 4]). The reason for this is unclear. The further improvement of electrochemical behavior by EL subsequent to CL may be due Pt-Cu distance further approaching the optimum value cited above.

Our observation that EL results in higher activity when starting from the CL sample with its Cu-depleted alloy core is, however, at variance with recent literature where activity after EL was described to be best for Cu-rich cores [4].

We found individual supported (Pt) atoms not only after CL but also after high-temperature alloying. This suggests that they are no intermediates of Ostwald ripening, but are strongly stabilized by the carbon support, with concomitant electronic effects. Therefore it should be examined if they can contribute to the catalytic activities observed.

4 Conclusions

Chemical leaching of carbon-supported $PtCu_3$ nanoparticles results in their significant activation for the ORR. The leached particles are covered by a monolayer of pure Pt, their cores are strongly depleted in Cu, which is different from morphologies reported in literature for alloy particles after EL. They can be further activated by electrochemical leaching.

References

[1] T. Toda, I. Igarashi, H. Uchida, M. Watanabe, *J. Electrochem. Soc.* 146 (1999) 3750.
[2] M. Oezaslan, F. Hasche, P. Strasser, *J. Phys. Chem. Lett.* 4 (2013) 3273.
[3] P. Strasser, *Rev. Chem. Eng.* 25 (2009), 255.
[4] P. Strasser, S. Koh, T. Anniyev, J. Greeley, K. More, C.F. Yu, Z.C. Liu, S. Kaya, D. Nordlund, H. Ogasawara, M.F. Toney, A. Nilsson, *Nat. Chem.* 2 (2010) 454.
[5] A. Schlapka, M. Lischka, A. Gross, U. Kasberger, P. Jakob, *Phys. Rev. Lett.* 91 (2003) 016101.
[6] P. Mani, R. Srivastava, C.F. Yu, P. Strasser, *ECS Transactions* 11 (2007), 933.
[7] S. Mukerjee, S. Srinivasan, M.P. Soriaga, J. McBreen, *J. Electrochem. Soc.* 142 (1995) 1409.

III-PP78

CO Elimination from H_2-rich Stream Processes over Hydroxyapatite Supported Palladium Catalysts

Boukha Z.*, Ayastuy J.L., Gutiérrez-Ortiz M.A., González-Velasco J.R.

Chemical Technologies for Environmental Sustainability Group, Department of Chemical Engineering, Faculty of Science and Technology, University of the Basque Country UPV/EHU, Bilbao, Spain

* zouhair.boukha@ehu.es

Keywords: Hydroxyapatite, support, Palladium, WGS, COPROX

1 Introduction

The use of hydrogen as fuel is a promising alternative to produce clean energy. However, due to the H_2 production mainly via the reforming hydrocarbons its purification is necessary to eliminate the traces of CO in the hydrogen stream, especially, when the posterior use can only tolerate very low concentration of CO (< 100 ppm). For this purpose, the water gas shift (WGS) and CO preferential oxidation (COPROX) processes are applied as post-reforming stages for removing most of the CO and producing additional H_2. Palladium-based catalysts appear to be more efficient in both reactions because of their long-term activity and selectivity and their ability to operate at low temperature [1,2]. However due to their high cost the Pd active species should be highly dispersed on the support. In this sense, current research is dedicated to the synthesis of supports less sensitive to sintering and exhibiting suitable metal-support interactions. Hydroxyapatite, $Ca_{10}(PO_4)_6(OH)_2$, crystallizes in the hexagonal system and engenders two types of zeolite-like channels that play an essential role in its properties. Moreover, the structure of apatites allows different substitutions and ion exchanges which may modulate their surface chemistry [3]. In spite of the flexibility of their properties, hydroxyapatite supported palladium catalysts have never been used as support for WGS and COPROX applications.

The present work concerns the synthesis, characterization and the activity of palladium supported on these carriers. In order to examine their catalytic efficiency the prepared catalysts were evaluated in CO preferential oxidation in H_2-rich gas mixture and water gas shift reactions. Interesting conclusions are drawn from the correlation between the distribution of Pd active species and their performance in the two investigated reactions.

2 Experimental

Hydroxyapatite support (HAp) was synthesized adding drop wise a boiled aqueous solution of calcium nitrate to a solution of $(NH_4)_2HPO_4$. The precipitate was redissolved in a nitric acid solution and neutralized with ammonia at pH 10. The resulting mixture was maintained under stirring at 80 °C for 16 h. After filtration, the recovered solid was washed well with purified water then dried at 120 °C and finally calcined at 500 ºC for 4 h. The Pdx/HAp catalysts were prepared by impregnation of the corresponding support by tetraamminepalladium (II) chloride monohydrate where x is the Pd wt.% content. The prepared catalysts were calcined at 500ºC (4 h) and finally reduced under 5%H_2/Ar at 200 ºC for 2 h. The characterization of the oxidized and reduced Pdx/HAp involved mainly XRD, FTIR, UV-Visible-NIR diffuse reflectance spectroscopy, H_2-TPR, TPO, NH_3-TPD and TEM microscopy.

The COPROX catalytic tests were performed, with flow/mass ratio of 1320 cm3 min-1 g-1, in a tubular flow reactor operating at atmospheric pressure using 150 mg of the catalyst. Prior to running the catalytic experiments, the catalysts were submitted to a pre-treatment routine consisting on their reduction at 200 ºC (1 h) in a flow 5%H_2/Ar. The reaction mixture was

composed of 1% CO, 1% O_2 and 60 % H_2 (balanced with He) and a total flow rate equal to 200 cm^3 min^{-1}, which gives an oxygen excess parameter "λ" equal to 2. In the case of the WGS reaction, the composition of feed gas (in vol.%) was $CO/H_2O/H_2/CO_2$ = 4/9.4/37.9/3 balanced to He. The temperature of the reaction was increased from room temperature up to 360 °C with a heating rate of 5 °C min^{-1}. The reaction products were continuously analysed by Gas Chromatograph equipped with a TCD detector.

3 Results and discussion

Table 1 reports characterization results of the prepared Pdx/HAp catalysts. The FTIR spectrum and XRD diffractogram corresponding to the prepared HAp support were found to be identical to the reference spectrum and patterns reported in the literature. Moreover, the absence of pyrophosphate structure confirmed that the synthesized phosphate was pure apatite. Table 1 also shows the mean Pd particle size, determined by TEM microscopy, of reduced Pdx/HAp. The results revealed the presence of small Pd particles on Pd0.5/HAp (6.4 nm), whereas on Pd2/HAp the mean particle size was larger (12.1 nm). Moreover, the deposited Pd species were, generally, highly dispersed on the support surface (36-71%).

Table 1. Properties of the prepared Pdx/HAp catalysts

	Pd, wt.%	S_{BET}, m^2 g^{-1}	Pore volume cm^3/g	Pore size, nm	Pd particle size[(a)], nm	Pd[(a)] dispersion, %	S_M[(a)], m^2 g^{-1} Pd	H_2/Pd[(b)]
HAP	0	50.3	0.45	30.3	-	-	-	-
Pd0.5/HAP	0.56	40.2/43.7[(c)]	0.37/0.37[(c)]	33.3/31.3[(c)]	6.4[(c)]	71[(c)]	240[(c)]	0.90
Pd1/HAP	0.99	40.0/44.0[(c)]	0.36/0.38[(c)]	34.2/30.8[(c)]	9.5[(c)]	49[(c)]	160[(c)]	1.05
Pd2/HAP	2.05	41.4/42.0[(c)]	0.38/0.35[(c)]	33.6/30.5[(c)]	12.1[(c)]	36[(c)]	120[(c)]	1.07

Values determined by (a) TEM and (b) H_2-TPR. (c) values corresponding to reduced catalysts.

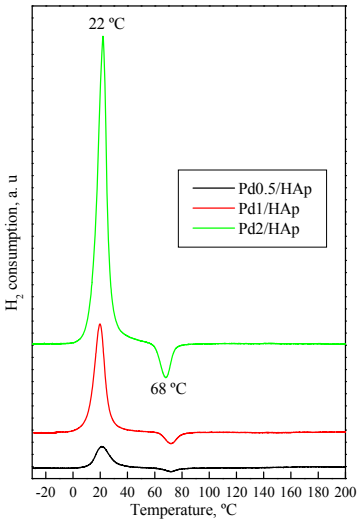

Fig. 1. H_2-TPR profiles of the Pdx/Hap catalysts

Fig.1 displays H_2-TPR profiles for the Pd(x)/CaHAp catalysts. Beside the reduction of PdO crystallites at around 22 ºC, the spectra showed a negative peak, centred at 68 ºC, which was associated with β-PdH decomposition. The determination of the Pd species, their surface chemistry and their interaction with HAp support were studied by means of UV-Visible and FTIR spectroscopy, TPO and NH_3-TPD techniques. The catalytic activity of the assayed Pdx/HAp catalysts in the COPROX and WGS reactions showed that they were active and selective (not shown). Moreover their activity was compared with classical Pd catalysts used in these types of reactions.

Interesting conclusions are drawn from the correlation between the distribution of Pd active species and their performance in the two investigated reactions.

Acknowledgements

The financial support for this work provided by Gobierno Vasco (GIC IT-657-13) and UPV/EHU (UFI11/39) is gratefully acknowledged.

References

[1] C.A. Cornaglia, S. Tosti, M. Sansovini, J. Múnera, E.A. Lombardo, Appl. Catal. A 462-463 (2013) 278.
[2] N. Iwasa, S. Arai, M. Arai, Appl. Catal. B 79 (2008) 132.
[3] Z. Boukha, M. Kacimi, M. Ziyad, A. Ensuque, F. Bozon-Verduraz, J. Mol. Catal. A 270 (2007) 205.

III-PP79

CO_2 for the Production of Methanol and Dimethyl Ether

Akarmazyan S.S.[1], Triantafyllidis K.S.[2], Kondarides D.I.[1], Papadopoulou C.[3*]

1 - Department of Chemical Engineering, University of Patras, Patras, Greece
2 - Department of Chemistry, Aristotle University of Thessaloniki, Thessaloniki, Greece
3 - Department of Chemistry, University of Patras, Patras, Greece

* cpapado@chemistry.upatras.gr

Keywords: direct, methanol-dimethyl ether synthesis, CO_2 hydrogenation, zeolites, alumina, acidity

1 Introduction

Fossil fuels depletion and environmental protection imply new routes for energy production with low carbon dioxide emissions and high-energy efficiency. Electricity generation from renewable sources (wind, solar, geothermal and hydroelectric plants) presents a very satisfactory progress. Yet, electricity demand and supply do not always coincide. On the other hand, progress in alternative fuel production for the transport sector is slow, due to various reasons, among which the availability of raw materials. An interesting idea, addressing the above problems, is to store electric energy in the form of chemical energy. Hydrogen, (coming from water electrolysis during low electricity demand) and CO_2 (from flue gas and any other CO_2-rich stream) can be used for the synthesis of a mixture of methanol and dimethyl ether, alternative fuels for heat engines or Fuel Cells [1-4]. In the present work CO_2 hydrogenation for the production of methanol/DME has been studied over bifunctional catalytic systems comprising of a methanol synthesis and a methanol dehydration catalyst.

2 Experimental/methodology

A commercial $CuO/ZnO/Al_2O_3$ (CZA1) catalyst has been selected for the methanol synthesis reaction. A variety of commercial and home-made catalysts with different acidic properties and physicochemical characteristics have been used for the methanol dehydration reaction: γ-Al_2O_3 (Al4), WO_3/Al_2O_3 (WAl4) and various zeolites, Ferrerite(10) (FER(10)), Faujasite (USY6), HZSM-5(11.5) and HZSM-5(25). The investigated materials have been characterized with respect to their textural properties (B.E.T. and B.J.H. methods) and crystallinity (XRD). Methanol dehydration catalysts have been also studied regarding their acidity by TPD-NH_3 and FT-IR with in situ pyridine sorption. Furthermore, the adsorption/desorption properties of catalysts toward methanol and water as well as the dehydration reaction mechanism have been investigated with the use of transient-MS and in situ DRIFTS techniques. Catalytic tests were performed over mechanical mixtures (1:1) of the above materials, at 3.0 MPa and temperatures 180-250 °C and a gas mixture of CO_2/H_2.

3 Results and discussion

Regardless of the catalytic configuration used, CO_2 conversion increased with temperature (180-250 °C) but it is always lower than that predicted by thermodynamics, indicating that the reaction occurs under the kinetic regime (Fig. 1A). Although there are no significant variations in the activity, there are noticeable differences regarding the yields of reaction products over the various catalysts investigated. For the catalytic configurations containing alumina the main product is methanol, indicating that methanol, produced from CO_2 hydrogenation, is not consumed for the formation of DME (Fig. 1B and C). This may be due to the poor acidity of these samples, to the nature of acid sites (Lewis and Brönsted) or to the fast deactivation of acid sites by the adsorption of water formed. Catalysts containing zeolitic materials produce mainly

DME and lower amounts of methanol, showing that these are more active for the methanol dehydration reaction and/or more resistant to deactivation than alumina (Fig. 1B and C). Differences in DME yields are observed for the various zeolites, depending on parameters such as the micropore structure, the Si/Al ratio of the zeolite and the number, strength and nature of active acid sites. Catalysts deactivate with time on stream but, in most cases, catalytic activity is almost completely restored after regeneration.

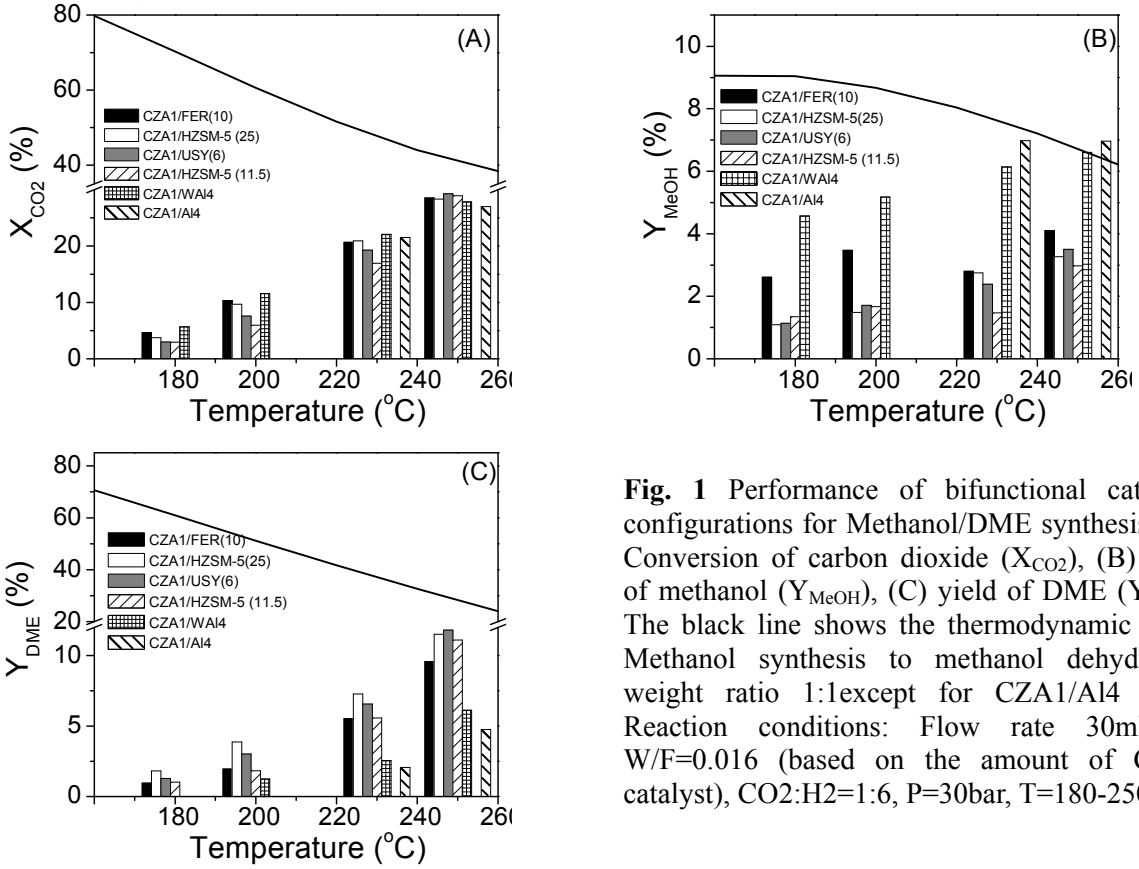

Fig. 1 Performance of bifunctional catalytic configurations for Methanol/DME synthesis: (A) Conversion of carbon dioxide (X_{CO2}), (B) yield of methanol (Y_{MeOH}), (C) yield of DME (Y_{DME}), The black line shows the thermodynamic limit. Methanol synthesis to methanol dehydration weight ratio 1:1except for CZA1/Al4 (1:2). Reaction conditions: Flow rate 30ml/min, W/F=0.016 (based on the amount of CZA1 catalyst), CO2:H2=1:6, P=30bar, T=180-250oC

4 Conclusions

The structure and the acidity (nature, number, strength, Lewis/Bronsted ratio) of the methanol dehydration component play a significant role on the selectivity of the catalytic systems for the direct hydrogenation of CO_2 to produce methanol and DME.

Acknowledgements

This study has been co-financed by the EU (European Social Fund - ESF) and Greek national funds through the Operational Program "Education and Lifelong Learning" of NSRF - Research Funding Program: Thales. Investing in knowledge society through the European Social Fund.

References

[1] Z. Azizi, M. Rezaeimanesh, T. Tohidian, M.R. Rahimpour, Chem. Eng. Proc. 82 (2014) 150-172..
[2] Y. Zhang, D. Li, Y. Zhang, Y. Cao, S. Zhang, K. Wang, F. Ding, J. Wu, Catal. Comm. 55 (2014) 49-52.
[3] F. Frusteri, M. Cordaro, C. Cannilla, G. Bonura, Appl. Catal. B: Environ. 162 (2015) 57–65.
[4] S.P. Naik, T. Ryu, V. Bui, J.D. Miller, N.B. Drinnan, W. Zmierczak, Chem. Eng. J. 167 (2011) 362–368.

III-PP80

Comparative Study of Alumina Supported Cuo-Ceo_2 and Cuo-Zno Catalysts for Steam Reforming of Dimethoxymethane

Pechenkin A.A.[1,2*], Badmaev S.D.[1,2], Belyaev V.D.[1,2], Venyaminov S.A.[1], Sobyanin V.A.[1]

1 - Boreskov Institute of Catalysis SB RAS, Novosibirsk, Russia
2 - Novosibirsk State University, Novosibirsk, Russia

* pechenkin@catalysis.ru

Keywords: dimethoxymethane, catalytic steam reforming, hydrogen, fuel cell

1 Introduction

Polymer electrolyte membrane fuel cells (PEMFC) are considered as an alternative environmentally sound source of electric power. Such fuel cells are usually fed by pure hydrogen or hydrogen-rich gas mixtures produced by catalytic conversion of hydrocarbons or oxygenated hydrocarbons.

Dimethoxymethane (DMM) is an easy to synthesize oxygenated compound of C_1 chemistry. DMM is a nontoxic and environmentally benign chemical. It is a liquid under normal conditions, and therefore can be easily stored and handled. DMM has a wide scope of applications. In particular, DMM can be used as an additive to diesel fuel to improve combustion and reduce pollutant emissions of diesel engines. These facts together with the recent data on DMM steam reforming (SR) reported in [1-4] predict increasing DMM demand that will become a promising feedstock for production of hydrogen-rich gas for PEM FC feeding.

Overall DMM SR is expressed by equation:

$CH_3OCH_2OCH_3 + 4H_2O = 8H_2 + 3CO_2$

Besides these reactions, a reverse WGSR may proceed to produce carbon monoxide:

$CO_2 + H_2 = CO + H_2O$

It is generally assumed [1-4] that DMM SR proceeds via a consecutive two-step reaction mechanism: the first step is hydration of DMM to methanol/formaldehyde over acidic catalysts (or acid sites of the catalyst); the second step is steam reforming of the produced methanol/formaldehyde over Cu-based catalysts (or Cu-based sites of the catalyst) to hydrogen-rich gas.

The present work reports the results of comparative study of alumina-supported bifunctional $CuO-CeO_2$ and CuO-ZnO catalyst in DMM SR to hydrogen-rich gas to be used for fuel cell feeding. To elucidate the role of each catalyst component in DMM SR, the data on the catalytic performance of γ-Al_2O_3, CuO/γ-Al_2O_3, ZnO/γ-Al_2O_3 and CeO_2/γ-Al_2O_3 are presented as well.

2 Experimental/methodology

$CuO-CeO_2/\gamma$-Al_2O_3 and $CuO-ZnO/\gamma$-Al_2O_3 catalyst samples were prepared by incipient wetness co-impregnating γ-Al_2O_3 (S_{BET} = 200 m^2/g, V_{pore}= 0.7 cm^3/g, granule diameter 0.25–0.5 mm) with aqueous solutions of copper (II) and cerium (III)/zinc(III) nitrates taken at the desired ratio. CuO/γ-Al_2O_3, ZnO/γ-Al_2O_3 and CeO_2/γ-Al_2O_3 were prepared by incipient wetness impregnation of γ-Al_2O_3 with aqueous solutions of copper (II), zinc (II) and cerium (III) nitrates, respectively. The samples were dried at 100°C in air and calcined at 400°C-500°C in air for 3h. The catalysts were characterized by BET, TPR, XRD, FTIR spectroscopy, HRTEM, EDX and HAADE-STEM techniques.

DMM SR experiments were performed in a fixed bed flow reactor at atmospheric pressure, GHSV=10000 h^{-1}, temperature 150-300°C and feed gas composition (vol.%): DMM/H_2O/N_2=14/70/16. Prior experiments, the catalysts were reduced in a flow of 5 vol.% H_2 + 95 vol.% N_2 at 350°C for 1h. The composition of the inlet and outlet gas mixtures was analyzed by a gas chromatograph.

3 Results and discussion

Table 1. Performance of alumina-supported CuO-ZnO and CuO-CeO_2 catalysts in DMM SR to hydrogen-rich gas

Catalyst	X (DMM), %	Outlet product concentration, vol.%					W(H_2), L H_2/g·h
		H_2	CO_2	CO	CH_3OH	CH_3OCH_3	
10%CuO-5%ZnO/γ-Al_2O_3	100	60	20	1	0.06	0.1	16.5
10%CuO-5%CeO_2/γ-Al_2O_3	100	59.5	19.5	0.5	0.7	0.6	15.5

The Table presents data on DMM conversion, outlet product concentrations and H_2 productivity at DMM SR over bifunctional catalysts at 300°C. Note that at this temperature both catalysts showed the maximum H_2 productivity (~16 L H_2/g·h) and complete DME conversion to hydrogen-rich gas with H_2 and CO contents of ~60 and ~1 vol.%, respectively. The latter fact is important as it allows using a simpler scheme for production of hydrogen-rich gas for PEM FC application that dictates strict requirements regarding the CO impurity. Indeed, the hydrogen-rich gas produced by DMM SR can be used for direct feeding of HT PEM FC without any further CO removal. For LT PEM FC feeding, the hydrogen-rich gas should be purified of CO to the level of 10 ppm, which can be achieved by selective oxidation or methanation of CO, bypassing the stage of the water-gas shift reaction.

Based on the data obtained, it is shown that the catalytic performance of CuO-CeO_2/γ-Al_2O_3 and CuO-ZnO/γ-Al_2O_3 in DMM SR is associated with the γ-Al_2O_3 acid sites and alumina-supported copper-cerium/zinc oxide species, which are responsible for, respectively, DMM hydration and methanol/formaldehyde SR.

4 Conclusions

Bifunctional CuO-CeO_2/γ-Al_2O_3 and CuO-ZnO/γ-Al_2O_3 catalysts containing on their surface both acidic and copper-based sites are active and selective for DMM SR to hydrogen-rich gas with low (1 vol.%) CO content. These catalysts provide for 100% DMM conversion with hydrogen productivity of ~16 L H_2/g_{cat}·h at GHSV = 10000 h^{-1} and T = 300°C. So, 50 g of the catalyst is sufficient to provide operation of 1 kW PEMFC-based power unit using DMM as the primary fuel.

Acknowledgements

The work was partially supported by MES (Russia).

References

[1] Q. Sun, A. Auroux, J. Shen, Journal of Catalysis. 244 (2006) 1.
[2] Y. Fu, J. Shen, Journal of Catalysis. 248 (2007) 101.
[3] S.D. Badmaev, A.A. Pechenkin, V.D. Belyaev, S.A. Venyaminov, P.V. Snytnikov, V.A. Sobyanin, V.N. Parmon, Doklady Physical Chemistry 452 (2013) 251.
[4] A.A. Pechenkin, S.D. Badmaev, V.D. Belyaev, V.A. Sobyanin, Applied Catalysis B. 166-167 (2015) 535.

III-PP81

Condensed Phase Ketonization of Propanoic Acid over CeO_2-ZrO_2 Catalysts

Jana P.[1*], Sankaranarayanan T.M.[1], Pizarro P.[1,2], Coronado J.M.[1,2], Serrano D.P.[1,2]

1 - Thermochemical Processes Unit, IMDEA Energy Institute, Madrid, Spain
2 - Chemical and Environmental Engineering Group, ESCET, Universidad Rey Juan Carlos, Madrid, Spain

* prabhas.jana@imdea.org

Keywords: ketonization, liquid phase, prapanoic acid, catalysts, CeO_2, ZrO_2

1 Introduction

Renewable liquid fuels, as well as chemicals, derived from biomass resources are gaining significant attention as alternative to the existing fossil based resources [1-2]. Among various processes, fast pyrolysis and hydrolysis are the two main conversion routes for transforming biomass into liquid fuels. In both cases, carboxylic acids are formed as one of the major intermediates, being partly responsible for undesirable properties like low pH and high oxygen content of the derived bio-oils. Thus, upgrading of these carboxylic acids is required for obtaining quality fuels. In this context, ketonization reaction, which allows coupling two carboxylic acids to form a ketone, is a very convenient route for lowering the acid content as well as oxygen concentration of the derived bio-oils through the removal of oxygen as CO_2 and H_2O [3-5].

The conversion of these carboxylic acids to ketones in a condensed phase medium at lower temperature (<300 ºC) would be preferred than the vapour phase conversion (>300 ºC), because it is more practical for upgrading intermediate liquid biofuels like bio-oil [4,5]. Thus, the present work is focused on the study of liquid phase ketonization using a model bio-oil compound, propanoic acid, in presence of CeO_2 and ZrO_2 or their mixed oxide as catalysts.

2 Experimental/methodology

CeO_2, ZrO_2 and $Ce_{0.5}Zr_{0.5}O_2$ catalysts were prepared by thermal decomposition (TD) of corresponding $Ce(NO_3)_3.6H_2O$ and $ZrO(NO_3)_2.xH_2O$ precursors at 500 ºC for 6h in air. For comparison, commercially available CeO_2 (Acros Organic) and ZrO_2 (Sigma-Aldrich) were also used for the reaction. The samples were characterized in detail using N_2 adsorption-desorption isotherms, powder X-ray diffraction pattern and FT-IR spectral analysis.

The ketonization reaction was carried out in a 100 ml stainless steel high pressure batch reactor. 0.5 g of catalyst was added to 70 ml toluene and 1 ml of propanoic acid solution. The reactor was first pressurized up to 40 bar with N_2 and subsequently heated. The reaction was carried out at 290 ºC for 6 h with stirring at 800 rpm. The products were analyzed by GC. Prior to characterization and after reaction, the catalysts were dried at room temperature in air for 12 h.

3 Results and discussion

The catalysts obtained from the TD method show significant improvement in the surface area (CeO_2-TD: 70 m^2/g and ZrO_2-TD: 53 m^2/g) than the commercially available samples (CeO_2: 12 m^2/g and ZrO_2: 5 m^2/g). This property is even higher for the 1:1 combination of Ce and Zr (83 m^2/g) than their counter oxides. Cubic crystalline phase is observed for both commercial and prepared CeO_2 samples whereas different crystalline phases, monoclinic and tetragonal, are detected for commercial and prepared ZrO_2, respectively. The XRD pattern of $Ce_{0.5}Zr_{0.5}O_2$-TD catalyst maintains the cubic geometry of the CeO_2 phase.

In comparison with the commercial catalysts, synthesized materials (CeO_2-TD and ZrO_2-TD) perform better for the ketonization of propanoic acid (PA) in liquid phase at 290 ºC. This result is attributed to the improvement of their specific surface area. Among the prepared samples, CeO_2-TD shows much higher PA conversion than ZrO_2-TD. However, the 3-pentanone selectivity from converted PA is superior for the last one. According to Figure 1A, almost all (90%) the converted PA is transformed to the desired 3-pentanone over the ZrO_2-TD catalyst. An intermediate conversion and selectivity is obtained with the mixed oxide catalyst, no synergetic effects being, therefore, detected.

FT-IR spectral analyses (Figure 1B) of all the samples reveal that Ce containing catalysts, CeO_2 and $Ce_{0.5}Zr_{0.5}O_2$, form the metal carboxylate (ν_{asym}: 1545 cm^{-1} and ν_{sym}: 1373 cm^{-1}) on reaction with PA whereas this is not the case for ZrO_2 sample. This indicates different affinities of Ce and Zr centres to PA on its transformation to ketone, which probably control their observed catalytic activities.

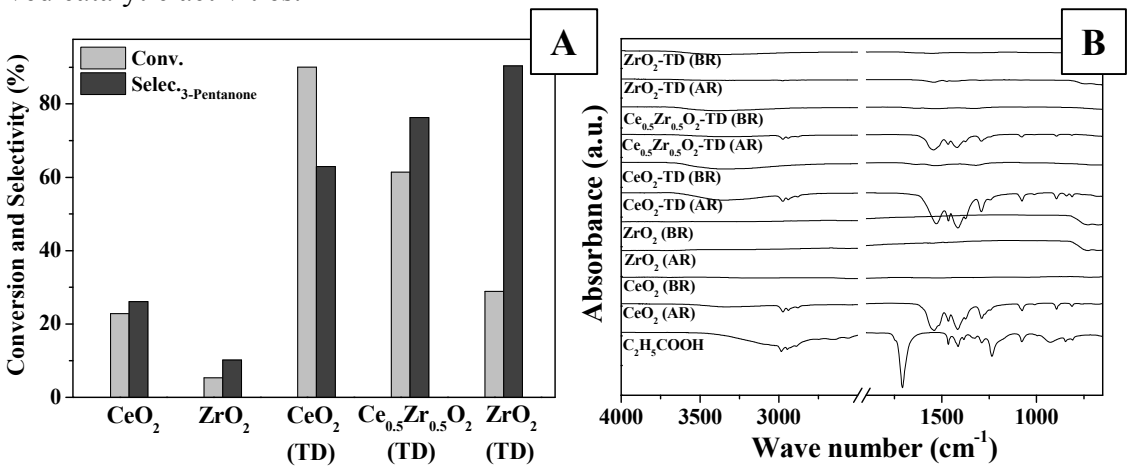

Fig. 1: A) Catalytic activity of the commercial and prepared samples in ketonization of PA and B) FT-IR spectra of the catalysts before and after the ketonization reaction.

4 Conclusions

The ketonization of propanoic acid has been studied in liquid phase and the CeO_2-ZrO_2 catalysts, active for this reaction, have been developed by thermal decomposition method. CeO_2 alone shows very good conversion, however, its modification with ZrO_2 in 1:1 ratio gives a better catalyst for this transformation in terms of 3-pentanone selectivity with high conversion rate. FTIR provides some insights on the different mechanism of ketonization on Ce and Zr sites.

Acknowledgements

The authors thank to Spanish "Ministry of Economy and Competiveness" and "Regional Government of Madrid" and the European Commision for their financial support through, respectively, the LIGCATUP (ENE2011-29643-C02-01) projects.

References

[1] J. C. Serrano-Ruiz, J. A. Dumesic, *Ener. & Environ.Sci.* 4 (2011) 83.
[2] G. W. Huber, S. Iborra, A. Corma, *Chem. Rev.* 106 (2006) 4044.
[3] E. L. Kunkes, D. A. Simonetti, R. M. West,J. C. Serrano-Ruiz, C. A. Gartner, J. A. Dumesic, *Science* 322 (2008) 417.
[4] T. N. Pham, T. Sooknoi, P. Crossley, D. E. Resasco, *ACS Catalysis* 3 (2013) 2456.
[5] R. W. Snell, B. H. Shanks, *ACS Catalysis* 3 (2013) 783.

III-PP82

Conversion of Methane into Methanol over Doped Mesoporous WO_3

Villa K.[1*], Murcia-López S.[1], Andreu T.[1], Morante J.R.[1,2]

1 - Catalonia Institute for Energy Research (IREC), Sant Adrià de Besòs, Spain
2 - University of Barcelona (UB), Department of Electronics, Barcelona, Spain

* kvilla@irec.cat

Keywords: mesoporous WO_3, photocatalysis, metal doping, CH_4, conversion, methanol

1 Introduction

In the last few years there has been a growing interest in the production of methanol to be used as an alternative fuel [1]. An inexpensive way to obtain it is by photocatalysis which is a valuable technique that allows carrying out the selective oxidation of methane to methanol at ambient temperature and pressure [2].

Prior studies indicate that WO_3 is one of the most efficient catalysts for this type of photocatalytic reaction [3]. However, the total yield remains still low. In an attempt to improve its performance, an ordered mesoporous WO_3 was tested in this photocatalytic conversion and the changes in the catalyst during the reaction was monitored by in situ DRIFTS measurements. Additionally, the influence of metal doping M/WO_3 (M=Ni, Fe, Cu) was also studied.

2 Experimental

The Ordered mesoporous WO_3 was synthetized by a replicating technique using ordered mesoporous silica KIT-6 as the template. After impregnation, the sample was dried and then calcined for 4h at 350ºC to eliminate impurities. Later, the material was sintered for 6 h at 550 ºC to obtain the WO_3 inside the silica template. The KIT-6 was removed by HF (10 % wt) solution under stirring. Finally, the catalyst was separated by centrifugation, washed sequentially with water and ethanol and dried at room temperature.

M-doped WO_3 (M=Fe, Cu and Ni) was prepared by impregnation. Solutions of respective metal nitrates in ethanol were mixed with the appropriate amount of WO_3 suspended in ethanol. The slurry was kept under stirring at room temperature for 2 h. After being dried at 100ºC for 5 h, the obtained powder was calcined at 300ºC for 5 h to eliminate the nitrates and then, sintered at 500ºC for 2 h.

The photocatalytic partial oxidation of methane was carried out in a photochemical reactor of 500 mL volume. A medium pressure mercury lamp inside the reactor was used to provide UVC-visible light irradiation. The reaction temperature was maintained at ~55˚C. A mixture of CH_4/He was sparged continuously through the photocatalytic reactor. In a typical experiment 300 mL of water containing 0.3 g of catalyst were placed in the reactor. Gas samples were periodically analyzed by gas chromatography.

3 Results and discussion

The diffraction peaks of all samples indicated the presence of the monoclinic structure of WO_3 (JCPDS 43-1035), no crystalline phases related to Cu, Ni or Fe were detected, probably due to its low concentration. Additionally, the self-reduction process of the WO_3 by the electrons generated in the photocatalytic reaction was confirmed by real time DRIFTS experiments.

On the other hand, the comparison of the performance of a commercial WO_3 (Alfa-aesar) with the as-synthesized mesoporous WO_3 evidences an improvement in the photoreactivity which would be related with a remarkable increase in the surface area of the latter from 7.8 to

151.0 m^2 g^{-1}.

As shown in Figure 1, the Ni doped WO_3 exhibits the highest rate of methanol production with a low amount of CO_2. The Ni in this configuration would be in the form of NiO (p type oxide) resulting in n-p junction that improves the charge separation and thus, a higher amount of CH_3OH is generated. Moreover, since Ni has a suitable conduction band edge (-0.5 V) for the production of hydrogen, this metal oxide can capture the photogenerated electrons and protons to generate H_2, suppressing the self-reduction of WO_3 previously described (no changes in the color of suspension were observed). Therefore, the difference in the photoactivity of the doped samples is related to the ability of electron capture of these metals.

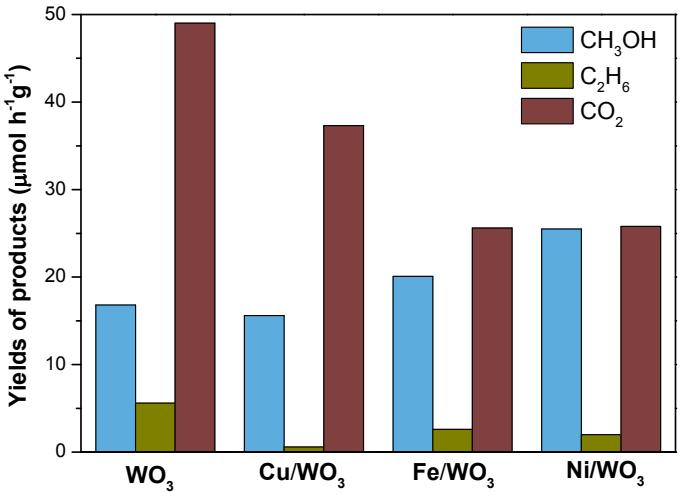

Fig. 1. Yields of products in the photocatalytic oxidation of CH_4.

4 Conclusions

The photocatalytic oxidation of methane to methanol over pure and doped WO_3 was examined. This study revealed that mesoporous catalyst can play an important role in the conversion of methane to high valuable compounds such as methanol, mainly due to its large surface area and ordered structure that increases the adsorption of the reactant molecules. On the other hand, the Ni doping markedly favoured the photocatalytic performance. For instance, selectivity toward methanol could be increased from 21.9% to 46%.

Acknowledgements

This work was supported by the European Regional Development Funds (ERDF, FEDER Programa Competitivitat de Catalunya 2007-2013) and the Framework 7 program under the project CEOPS (FP7-NMP-2012-309984).

References

[1] *Methanol synthesis tecnology*. S. Lee, Florida, CRC Press, 1990.
[2] P. Venkata, K-H. Kim, H. Song, *Renew. Sust. Energy Rev.* 24 (2013) 578.
[3] M.A. Gondal, A. Hameed, Z,H. Yamani, A. Arfaj, *Chem. Phys.Lett.* 392 (2004) 372.

III-PP83

Cs-Promoted Fer Zeolite as Ni Support in Methane Dry Reforming

Candamano S.[1*], Frontera P.[2], Macario A.[1], Crea F.[1], Barberio M.[3], Antonucci P.L.[2]

1 - Department of Environmental and Chemical Engineering, University of Calabria, Rende, Italy
2 - Department of Civil Engineering, Energy, Environment and Materials, Mediterranea University, Reggio Calabria, Italy
3 - Applied Physics Laboratory of Biology, Ecology and Earth Science Department, University of Calabria, Rende, Italy

* sebastiano.candamano@unical.it

Keywords: dry-reforming, ferrierite, ITQ-6, Cs-promoted, Ni catalysts, syngas, carbon, deposition

1 Introduction

Dry-reforming process involves the conversion of main greenhouse gases, CH_4 and CO_2, responsible of global warming. This reaction has very important environmental implications because methane and carbon dioxide can be converted into syngas (H_2-CO) which, in turn, is transformed into dimethyl ether, methanol and other valuable products in several refinery GTL (gas to liquid) and Fisher-Tropsch processes.

Nickel is catalytically active in the reforming reaction, but carbon deposition on the metal surface causes catalyst deactivation. Nature of the support, preparation method and addition of promoters [1,2] strongly affect the metal distribution and its reducibility.
Recently, zeolites were reported to be suitable supports for nickel in the dry reforming of methane [2,3].

In the present work, we have investigated a lamellar zeolite (FER), still unexplored as support, and compared the performance of Cs- promoted Ni catalysts supported on both lamellar and delaminated (ITQ-6) forms in order to understand the effect of the different textural characteristics of the support in the dry reforming of methane.

The characterization of these materials by XRD, BET area, TPR, SEM-EDX and AFM has allowed to establish interesting relationships between their catalytic performance and physico-chemical properties.

The objective was to develop a catalyst able to overcome the long-standing carbon formation and thermal sintering problems.

2 Experimental

FER (Ferrierite type zeolite) precursor was synthesized starting from a gel having the following molar composition: 1 SiO_2– 1.46 NH_4F – 0.91 HF – 1 TMPP – 9.1 H_2O (TMMP is 4-amino-2,2,6,6-tetramethylpiperidine). Pure silica ITQ-6 material was prepared according to [4]. Cation exchange was performed with 1.0 molar chloride solution of Cs^+.

Ni catalysts (5% wt/wt) were prepared by incipient wet impregnation of the supports. After impregnation, the catalysts were reduced at 500°C in H_2 with a flow rate of 20 cm^3min^{-1} for 1 hour.

The CO_2 reforming reaction of CH_4 was carried out in a continuous flow quartz tube reactor at 1 atm pressure, varying the reaction conditions in order to optimize the catalytic performance. Reaction products were analyzed by on-line gas chromatograph (GC Agilent 6590) having FID and TCD detector and appropriate columns for the detection of gas on outlet current on stream.

3 Results and discussion

Some representative results of the 10-hours catalytic tests at 700°C with an equimolar CH_4/CO_2 feed are summarized in Table 1. It is observed that the CO_2 conversion is always higher than the CH_4 conversion, because of the simultaneous occurrence of the reverse water gas shift reaction (RWGS) [5]. For all catalysts the H_2/CO molar ratio is higher than one, most probably because, under the present reaction conditions, dry-reforming is accompanied by secondary reactions, such as CO disproportionation (Boudouard reaction) and steam reforming of methane [6].

Table 1. Catalytic behavior of catalysts after 10 h reaction at 700°C.(Values at steady-state).

Sample code	CH_4 [mole%]	CO_2 [mole%]	H_2/CO	C [mole%]
Ni-FER	75	90	1.40	0.88
Ni-CsFER	73	91	1.23	0.52
Ni-ITQ-6	77	90	1.39	2.1
Ni-CsITQ-6	75	92	1.14	0.76

According to Table 1, the peculiar lamellar structure of FER allows to carry out the reaction with a lower coke formation (ca. 60%) with respect to the delaminated structure (ITQ-6).

Cesium addition to FER does not affects the reforming activity but reduces again the coke formation by decreasing the amount of nickel ensemble necessary to the occurrence of undesired carbon deposition.

According to [6] the structure, morphology and formation rate of carbon deposits depend on the formation of intermediate Ni-carbide (Ni_3C) phase which, in turn, is affected by the dimension of Ni particles deposited on the support.

The AFM image of Ni-Cs-FER catalyst shows a homogeneous distribution with no metal agglomeration.

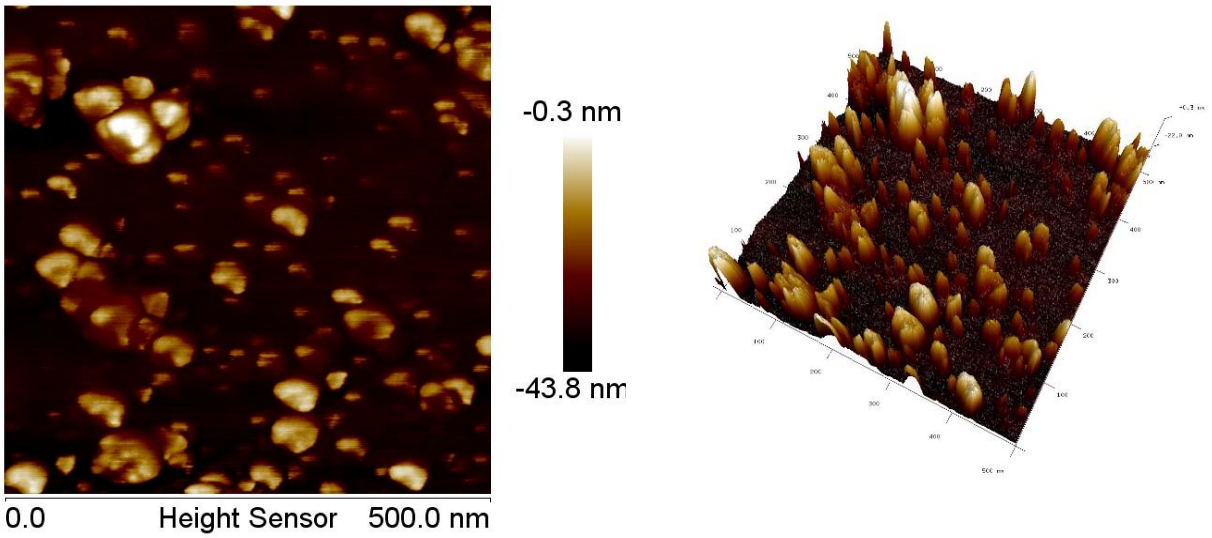

Figure 1. AFM images of Ni-Cs-FER

References

[1] O. Muraza, A. Galadima, Int. J. Energy Res. (2015),Published online in Wiley Online Library (wileyonlinelibrary.com). DOI: 10.1002/er.3295

[2] P. Frontera, A. Macario, A. Aloise, P.L. Antonucci, G. Giordano, J.B. Nagy, Catal. Today 218–219 (2013) 18–29.

[3] P. Frontera, A. Macario, A. Aloise, F. Crea, P.L. Antonucci, J.B. Nagy, F. Frusteri, G. Giordano, Catal. Today 2012;179(1):52–60.

[4] A. Corma, U. Diaz, M.Domine, V. Fornés, J. Am. Chem. Soc.,122, (2000), 2804.

[5] M.C.J. Bradford, M.A. Vannice,Catal. Reviews: Science and Engineering, 41 (1999),1–42.

[6] F. Frusteri, L. Spadaro, F. Arena, A. Chuvilin,Carbon, 40 (2002), pp. 1063–1070

III-PP84

Design of CO Tolerant Anode Electrocatalysts for PEM Fuel Cells

Gubán D.[1], Borbáth I.[1*], Pászti Z.[1], Drotár E.[1], Rojas S.[2], Tompos A.[1]

1 - Institute of Materials and Environmental Chemistry, Research Centre for Natural Sciences, Hungarian Academy of Sciences, Budapest, Hungary
2 - Instituto de Catálisis y Petroleoquímica, CSIC, Madrid, Spain

* borbath.irina@ttk.mta.hu

Keywords: anode electrocatalysts, CO-tolerance, controlled surface reactions, SnPt/C, electrocatalysts, Pt_3Sn, conducting, mixed oxides, support

1 Introduction

Reducing the amount of Pt along with increasing the metal dispersion is a key requirement for the implementation of fuel cells. CO tolerance and stability of the anode electrocatalysts also has to be improved, as the hydrogen fuel generally contains CO impurity that poisons Pt. In order to mitigate these issues, various approaches have been attempted.

In this contribution our results in development of Pt-Sn alloys supported on active carbon and novel $Ti_{0.7}W_{0.3}O_2$-C composite supports for Pt-based electrocatalysts are presented.

2 Experimental/methodology

Sn-Pt/C electrocatalysts. A 40 wt% commercial Pt/C (Quintech) catalyst was modified by tin anchoring via Controlled Surface Reactions (CSR) using $SnEt_4$ as the tin precursor [1-3].

40 wt% Pt/$Ti_{0.7}W_{0.3}O_2$-C electrocatalysts. A low temperature sol-gel-based multistep synthesis route followed by high temperature treatment (HTT) in He and reduction was applied for the composite materials preparation (Scheme 1). 40 wt% Pt loading was achieved using $NaBH_4$ and ethylene glycol [4].

All electrocatalysts were characterized by XRD, TEM, EDS and XPS techniques. The activities of the samples were compared in both methanol oxidation reaction and CO_{ad} stripping with those observed on home made 40 wt% Pt/C or PtRu/C (Quintech, Pt= 20 wt%, Ru= 10 wt%) references. Details of *in situ* EC-IRAS measurements can be found elsewhere [2,3].

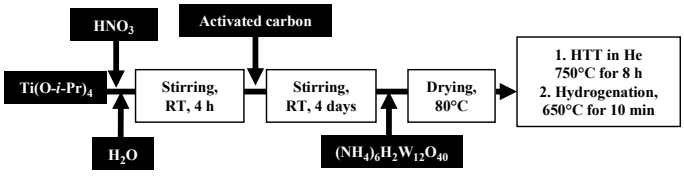

Scheme 1. Flow chart for preparing $Ti_{0.7}W_{0.3}O_2$-C composite materials.

3 Results and discussion

By means of CSR alloy-type SnPt/C electrocatalysts with wide range of the Pt/Sn ratios (Pt/Sn= 0.8-12.5) and exclusive Sn-Pt interaction were obtained. XRD demonstrated that the electrocatalysts contain a near-stoichiometric fcc Pt_3Sn alloy phase along with a certain amount of the Pt-rich $Pt_{(1-x)}Sn_x$ solid solution. The content and dispersion of the fcc Pt_3Sn phase can be controlled by tuning the reaction conditions of CSR. No evidence of the presence of SnO_2 phase was found by means of the XRD and EDS analysis. According to *in situ* XPS studies pre-treatment in hydrogen at 350°C resulted in complete reduction of the ionic tin to Sn^0. These

results demonstrate that the method of CSR is a powerful tool to create Pt-Sn bimetallic nanoparticles exclusively, without tin deposition onto the carbon support. It has been shown that the optimal balance between the Pt/Sn ratio, the amount of the fcc Pt_3Sn alloy phase and the metal particle size are responsible for the activity increase in both the CO and methanol electrooxidation. Increase of the tin content above a certain (optimal) amount gives rise to a negative effect on the catalyst performance in both reactions.

Another way for improving the CO tolerance of the electrocatalyst by the bifunctional mechanism is to create interfaces between Pt particles and an oxide-containing support which is (i) stable under the reaction conditions, (ii) electroconductive, (iii) generates OH groups as oxidants at low potential and (iv) stabilizes the small size of the Pt particles. Composites of activated carbon and $Ti_{(1-x)}W_xO_2$ mixed oxide are good candidates for this role. The challenge in the preparation of this material is that the preferable properties are linked to complete isovalent W incorporation into the rutile-TiO_2 lattice. XRD, EDS and XPS techniques confirmed the successful synthesis of the $Ti_{0.7}W_{0.3}O_2$-C composite. The uniform distribution of highly dispersed Pt particles with mean particle size of 2.3 ± 0.8 nm was verified via TEM technique.

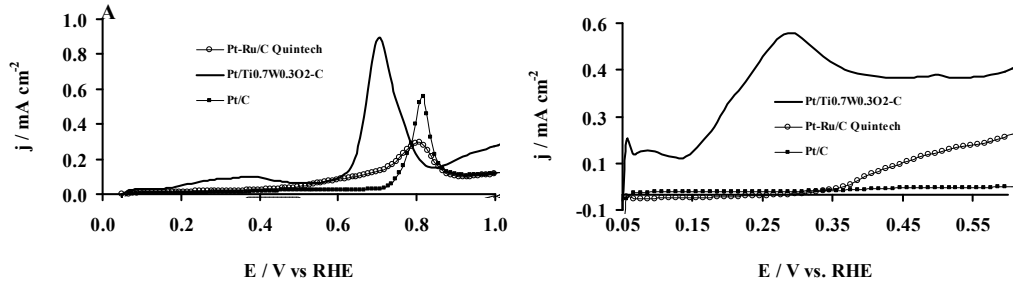

Fig. 1 CO_{ads} stripping voltammograms on home made Pt/C, PtRu/C (Quintech) and Pt/$Ti_{0.7}W_{0.3}O_2$-C catalysts (A) after Ar purging and (B) a part of the voltammograms in the "pre-peak" potential range after H_2 purging. Recorded in 0.5 M H_2SO_4 at 10 $mV \cdot s^{-1}$.

Enhanced CO tolerance of the electrocatalyst prepared using the $Ti_{0.7}W_{0.3}O_2$-C composite material is demonstrated in Fig. 1. In fact, performance exceeding that of the PtRu/C benchmark along with considerable stability during 5000 cycles for this electrocatalyst was observed.

4 Conclusions

A clear correlation between the amount of the Pt_3Sn phase and the electrocatalytic performance was established for Sn-modified Pt/C catalysts prepared by CSR. Enhanced CO tolerance along with considerable stability was achieved upon using a $Ti_{0.7}W_{0.3}O_2$-C composite material with high degree of W incorporation as a support for Pt-based electrocatalysts.

Acknowledgements

The authors are grateful to the Hungarian Scientific Research Fund (OTKA, Grant №: K100793 and K77720) and the National Development Agency (Grant №: KTIA_AIK_12-1-2012-0014) for financial support.

References

[1] S. García-Rodríguez, F. Somodi, I. Borbáth, J.L. Margitfalvi, M.A. Peña, J.L.G. Fierro, S. Rojas, *Applied Catalysis B: Environmental* 91 (2009) 83-91.

[2] T. Herranz, S. García, M.V. Martínez-Huerta, M.A. Peña, J.L.G. Fierro, F. Somodi, I. Borbáth, K. Majrik, A. Tompos, S. Rojas, *International Journal of Hydrogen Energy* 37 (2012) 7109-7118.

[3] I. Borbáth, D. Gubán, Z. Pászti, I.E. Sajó, E. Drotár, J.L. Gómez de la Fuente, T. Herranz, S. Rojas, A. Tompos, *Topics in Catalysis* 56 (2013) 1033-1046.

[4] D. Gubán, I. Borbáth, Z. Pászti, I. Sajó, E. Drotár, A. Tompos, *In: XXXVII. Kémiai Előadói Napok*, B. Bohner, B. Endrődi (Eds.) Magyar Kémikusok Egyesülete: Szeged, 2014. pp. 80-84.

III-PP86

Direct Synthesis of Dimethyl Ether from Mixture of Carbon Dioxide and Carbon Monoxide over Copper Alumina Catalysts Prepared Using the Sol-gel Method

Takeishi Kaoru*

Graduate School of Engineering, Shizuoka University, Hamamatsu-shi, Japan

* tcktake@ipc.shizuoka.ac.jp

Keywords: dimethyl ether (DME), carbon dioxide, hydrogen, direct synthesis, copper alumina, sol-gel method

1 Introduction

We have developed the excellent DME direct synthesis catalysts using by the sol-gel method. The Cu-Zn/Al_2O_3 catalysts prepared using the sol-gel method have higher activity and selectivity for DME synthesis from syngas (mixed gas of H_2 and CO) than usual DME direct synthesis catalysts, mixed catalysts of methanol synthesis catalysts and methanol dehydration catalysts [1]. This time, these catalysts are applied for DME direct synthesis from carbon dioxide and mixture of CO_2 and CO. The chemical equation of the DME direct synthesis from CO_2 will be $6H_2 + 2CO_2 \rightarrow CH_3OCH_3 + 3H_2O$. This reaction works for utilization of CO_2 and reduces of CO_2 which is one of the greenhouse effect gases. If excellent catalysts will be developed and be used widely, the problem of global warming and problem of environments such as air pollution will be solved. If hydrogen will be produced using sustainable energies such as sun light power, window power, hydropower, and so on, the produced DME works as hydrogen carrier and energy carrier.

2 Experimental

Cu-Zn/Al_2O_3 catalysts prepared using the sol-gel method were used for hydrogenation of CO_2 and/or CO. Each catalyst was used alone, not mixed with an acid catalyst such as alumina. Patented catalyst developed by Kansai Electric Power Co. (KEPCO) & Mitsubishi Heavy Industries (MHI); one of the mixed catalyst of methanol synthesis catalyst and methanol dehydration catalyst; CuO-ZnO-Al_2O_3-Ga_2O_3-MgO (100:25:15:5:1) & Al_2O_3-ZrO_2 (100:10) was prepared depending on the patent [2]. The reactions were carried out with pressurized fixed bed reactor, and the usual reaction pressure was 0.9 MPaG (absolute pressure 1.0 MPa). Reactant gas flow was H_2/(CO_2+CO)/ /Ar = 15.0/5.0/2.0 ml min^{-1}, and catalyst weight was 0.5 g. Online gas chromatographs (TCD, FID) were used for the analysis of reactants and the products, and Ar gas was used for the internal standard gas.

3 Results and discussion

First, I checked the influence on DME production activity by Cu loading percent in Cu/Al_2O_3 catalysts prepared using the sol-gel method on the DME production by CO_2 hydrogenation. The Cu(30 wt%)/Al_2O_3 catalyst produced DME fastest among the all Cu/Al_2O_3 catalysts. It is speculated that 70 wt% of Al_2O_3 in the catalyst is the best percent of Cu(active sites for methanol synthesis)/Al_2O_3(active sites for methanol dehydration). Therefore, the Al_2O_3 percent in the Cu-Zn/Al_2O_3 catalysts prepared by the sol-gel method was kept 70 wt%, and several Cu-Zn/Al_2O_3 catalysts that had different ratios of Cu/Zn were prepared using the sol-gel method. The catalysts were tested for CO_2 hydrogenation, respectively. The Cu-Zn(15-15 wt%)/Al_2O_3 catalyst produced DME fastest among the all Cu-Zn/Al_2O_3 catalysts. The maximum of DME selectivity is 14 *C*.%. However, under the reaction temperature of 160 ^oC, CO

production was reduced and DME selectivity became larger, and the biggest value was 65.8 *C*.% by the Cu-Zn(15-15 wt%) /Al_2O_3 catalyst. On the other hand, the DME production rate became slower with 15 μmol g_{-cat}^{-1} h^{-1}, and its rate was less than 1/3 of the DME production rate under 180 °C, 200 °C, and 220 °C. However, these data are much better than those by the patented catalysts developed by KEPCO & MHI [2]. For better DME selectivity, it is clarified that lower reaction temperature makes DME selectivity higher; however, the DME production rate becomes lower, so other compositions of Cu-Zn-Al_2O_3 should be developed. After many catalysts were prepared and the catalysts were tested for DME direct synthesis from CO_2, I have developed more excellent catalysts, Cu-Ga/Al_2O_3. At present, the Cu-Ga(24-6 wt%)/Al_2O_3 catalyst prepared using the consecutive sol-gel method is the best catalyst for DME direct synthesis from CO_2. The DME selectivity increased to about 30 *C*.%, and DME production rate improved to 63 μmol g_{-cat}^{-1} h^{-1}.

Then, the Cu-Zn(15-15 wt%)/Al_2O_3 catalyst and Cu-Ga(24-6 wt%)/Al_2O_3 catalyst prepared using the sol-gel method were tried for hydrogenation of various ratio mixture of CO_2 and CO for DME direct synthesis, respectively. Fig. 1 shows a part of the results of the DME production and methanol production at 220 °C, 240 °C, and 260 °C of the reaction temperature. In the case of the Cu-Zn(15-15 wt%)/Al_2O_3 catalyst (Fig. 1), the DME production rate is increased with the increasing of the ratio of CO/(CO+CO_2). On the other hand, in the case of the Cu-Ga/Al_2O_3 catalyst, there is an optimal ratio around 0.8, but the DME production rate was much slower than the rate by Cu-Zn(15-15 wt%)/Al_2O_3. Ga is one of rare-metals and very expensive, therefore Cu-Zn(15-15 wt%)/Al_2O_3 catalyst is useful as practical catalysts. From these results, CO_2 should be reformed to CO by the reverse-water gas shift reaction, and then the reformed CO should be hydrogenated to DME. Two-step DME synthesis from CO_2 would be practical for the industrial. However, I have developed the significant catalysts using the sol-gel method for DME direct synthesis from CO_2 and CO compared with the mixed catalysts such as the patent catalysts of KEPCO & MHI

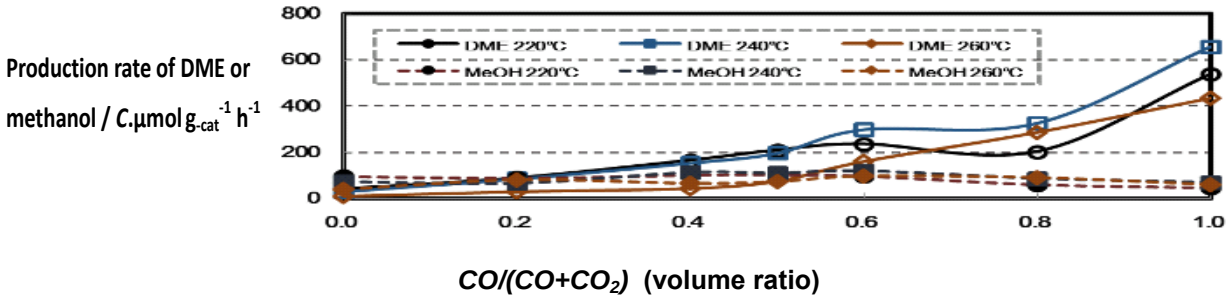

Fig. 1. Hydrogenation of CO_2 and CO mixture over Cu-Zn(15-15 wt%)/Al_2O_3 catalyst prepared using the consecutive sol-gel method. Catalyst weight: 0.5 g; reaction gas: H_2/(CO_2+CO)/Ar = 15.0/5.0/2.0 ml min^{-1}; reaction pressure: 0.9 MPaG.

4 Conclusions

I have developed the significant catalysts using the sol-gel method for DME direct synthesis from CO_2 and CO compared with the mixed catalysts.

Acknowledgements

This research was partly supported by Core Research for Evolutional Science and Technology (CREST), Japan Science and Technology Agency (JST).

References

[1] K. Takeishi, Biofuels, 1, 217-226 (2010); K. Takeishi, et. al., Japan Patent No. 41303069, and No. 4506729; etc.
[2] M. Hirano, et. al., Japan Patent No. 4467675.

III-PP87

Effect of Calcination Temperature on Stability and Activity of $Ni/MgAl_2O_4$ Catalyst for Steam Reforming of Methane

Katheria S.*, Gupta A., Deo G., Kunzru D.

Indian Institute of Technology Kanpur, Kanpur, India

* katheria@iitk.ac.in

Keywords: steam reforming of methane, nickel, catalyst, magnesium, aluminate, spinel

1 Introduction

Steam reforming of methane is a widely used conventional process for large scale production of hydrogen. Nickel as active metal and magnesium aluminate spinel ($MgAl_2O_4$) as catalyst support is widely used for this process. During preparation of $Ni/MgAl_2O_4$ catalyst, pretreatment of catalyst support and calcination temperature of nickel impregnated catalyst become important part of catalyst preparation as these can significantly influence the performance of $Ni/MgAl_2O_4$ [1]. In this work, we have demonstrated that high temperature calcination of $Ni/MgAl_2O_4$ not only enhances the activity of the catalyst but also the stability at elevated pressures.

2 Experimental

Magnesium aluminate (MG30) containing 30wt.% MgO and 70wt.% alumina, supplied by SASOL, Germany was used as the catalyst support. Three catalysts having composition of 15%$Ni/MgAl_2O_4$ were prepared for studying the effect of calcination temperature on catalyst activity and stability. First catalyst (Cat 1) was prepared by wet impregnation method in which the support (MG30) was calcined at 900°C for 4h before impregnating the required amount of $Ni(NO_3)_2.6H_2O$. The impregnated catalyst was then calcined at 500°C for 3h. For the preparation of second catalyst (Cat 2), the final calcination temperature was 850°C (instead of 500°C). The third catalyst (Cat 3) was prepared by impregnating $Ni(NO_3)_2.6H_2O$ on the as-received MG30 powder and then the impregnated support was calcined at 850°C for 3h.

Various characterization, such as BET surface area analysis, thermo-gravimetric analysis (TGA), X-ray diffraction(XRD), temperature-programmed reduction(TPR), temperature-programmed desorption(TPD), temperature-programmed oxidation(TPO) and UV-vis spectroscopy of fresh, reduced and calcined samples were done to examine the change in catalyst properties before and after use.

Steam reforming of methane was conducted in a ¼" o.d. Inconel 600 reactor which was placed in a tubular furnace. 300 mg of the catalyst (average size of 0.4 mm) was placed in the middle of the tubular reactor and the upper and lower part of catalyst tube filled with quartz chips. Prior to the activity test, the catalyst sample was reduced in H_2 flow of 60 ml/min at 850°C for 3h. All activity tests were performed at 600°C with CH_4:H_2O:N_2 molar ratio of 1:5:1 with W/F_{ao} (mass of catalyst/inlet molar flow rate of methane) of 0.95 g-h/mol. Product gases were analyzed on a gas chromatograph by a thermal conductivity detector using a 3m long Carbosphere column.

3 Results and discussion

Surface area of the as-received MG30 powder, which was 250m^2/g, reduced to 70m^2/g after

calcination at 900°C for 4h. The surface area further reduced when Ni impregnated catalysts were calcined. Formation of magnesium aluminate spinel phase was confirmed from the XRD plots of the calcined support. The diffraction patterns showed that, in all the three catalysts,the major phases were NiO and $MgAl_2O_4$. UV-vis spectroscopy analysis of the calcined catalysts confirmed the formation of $NiAl_2O_4$ after high temperature treatment of $Ni/MgAl_2O_4$ catalyst, in agreement with the earlier published results [1, 2].

Steam reforming of methane was conducted in the temperature range of 500-800°C and reactor pressure of 1-5 bar. It was observed that the activity of Cat 1 decreased with run time. At a pressure of 1 bar, the rate of deactivation was slow at 500°C but increased significantly with increasing temperature, most likely due to the carbon deposition on the catalyst.

The variation of methane conversion with run time for the three catalysts at 600°C and two different pressures (1 bar and 5 bar) is shown in Fig. 1 and 2.

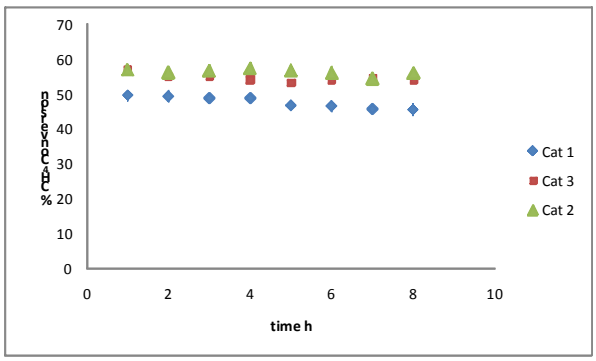

Fig. 1. Variation of methane conversion with run time for different catalyst (Temperature= 500°C and Pressure= 1bar

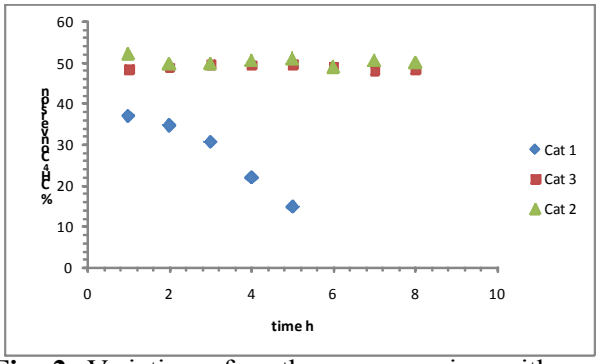

Fig. 2. Variation of methane conversion with run time for different catalyst (Temperature= 500°C and Pressure= 5bar

For Cat 1, the rate of deactivation significantly increased at higher pressure. In contrast, at identical conditions, the activity of Cat 2 and Cat 3 ,which were calcined at the higher temperature (850°C) remained stable over the duration of the run (~8h). As can be observed from Figs.1 and 2, Cat 2 and 3 were not only stable but also had a higher activity. From the activity test it was confirmed that precalcination of the catalyst support had no effect on the catalytic activity and its properties. The higher activity and stability of Cat 2 and Cat 3 catalysts can be attributed to a strong metal support interaction when the catalyst was calcined at 850°C. Stability of magnesium aluminate spinel phase and enhanced metal support interaction resulted in higher catalytic activity.

4 Conclusions

For the catalyst that was calcined at 500°C, the catalytic activity decreased significantly with increasing temperature and pressure. Calcination of the $Ni/MgAl_2O_4$ catalyst at higher temperature increases the activity and stability of the catalyst for steam reforming of methane. Precalcination of the magnesium aluminate support has no significant effect on the catalytic activity.

Acknowledgement

The financial support provided for this study by SERB, Department of Science & Technology, Govt. of India is gratefully acknowledged.

References

[1] K. O Christensen, D. Chen, R. Lødeng, & A. Holmen, *Applied Catalysis A: General* 314 (2006)9.
[2] R. J. Nielson, Catalytic Steam Reforming, *Catalyst Science and Technology*, 5 (1984) 1.

III-PP88

Effect of Nickel Complexes on the Metal Dispersion and Catalyst Activity of Ni/SBA-15 Catalyst for Methane Dry Reforming to Syngas

Hajimirzaee S.*, Iro E., Hodgson S., Olea M.

School of Science and Engineering, Teesside University, Middlesbrough, UK

* s.hajiimrzaee@tees.ac.uk

Keywords: nickel catalyst, methane, dry reforming, catalyst, life time, syngas

1 Introduction

The heavy reliance on dwindling fossil resource for fuel which generates high CO_2 emission has driving research into sustainable and environmentally friendly alternatives such as methane dry reforming reaction which has the advantage of utilizing two abundantly available green-house gases to produce syngas for fuel [1]. Nickel-based catalysts have been widely used for this reaction due to availability and low cost of nickel compared to noble metals; however, rapid coke deposition on nickel causes the catalyst to deactivate in a short time [2]. It has been shown that in addition to small nickel particles on the support, strong metal-support interaction and uniform dispersion of nickel on the support prevent the migration and coalescence of metal particles during the reaction and thus could prolong the catalyst life time and resistance against coking [3, 4]. By using the ordered mesoporous silica as support (SBA-15), which has high surface area, large pore sizes and thick pore walls for hydrothermal stability, nickel particles were confined in the channels of the mesoporous material, thus preventing metal sintering and promoting stability of the catalyst [3]. In this research, the nickel complexes $[Ni(H_2O)_6]^{2+}$, $[Ni(NH_3)_6]^{2+}$, $[Ni(en)_6]^{2+}$ where (en) is ethylenediamine, $NH_2CH_2CH_2NH_2$, and $[Ni(EDTA)]^{2-}$ EDTA is ethylenediaminetetracetic acid, $C_{10}H_{16}N_2O_8$, were synthesized and grafted onto the SBA-15 support to study how the chemical metal–support bonds affect the strength, dispersion and eventually the stability of Ni/SBA-15 catalysts in methane dry reforming in a gas mixture with three times more methane than CO_2 which only the most stable catalysts could be active for a long period of time as methane decomposition promotes faster coke deposition.

2 Experimental/methodology

SBA-15 powder was prepared through sol-gel method as described by Zhao et al.[5]. Ni/SBA-15 catalysts were prepared through incipient-wetness impregnation using different nickel complexes. Ammonium hydroxide, en and EDTA as well as deionised water were used to prepare the nickel complexes. Nickel acetate and SBA-15 were dissolved in water with weight ratio of 1/1.5/30. Then the nickel complex solution were added to SBA-15 and stirred. During filtration, two samples were prepared for each case, one without washing and another one with washing with deionised water to eliminate the counterions of the complexes. The samples were subsequently air dried at room temperature for 1 day and calcined at 550ºC for 4 h.

The catalyst activity in the dry reforming process was investigated in the Catlab system (Hiden Analytical Ltd) via temperature-programmed reaction using a fixed bed quartz reactor at atmospheric pressure. Catalyst sample was placed in a tube reactor and reduced in a 5% H_2 in argon stream at 800ºC for 1 hour prior to the reaction. Then the temperature was cooled and the reactor was flushed with pure argon. Then feed gas containing CH_4 and CO_2 with molar ratio of 2.7:1 and GHSV of 63,000 mL/(h·g_{cat}) was introduced to the reactor. The temperature of the reactor was raised linearly to 850°C at a heating rate of 10°·min^{-1}. The effluent gas was analysed on-line using a Hiden QIC-20 mass spectrometer.

Other characterisation techniques used include: Fourier Transform Infrared Spectrometry (FT-IR), Scanning Electron Microscopy (SEM)/ Energy dispersive X-ray spectroscopy (EDX), X-ray Diffraction spectroscopy (XRD), Transmission Electron Microscopy (TEM), N_2 adsorption-desorption at 77 K and Temperature Programmed Reduction (TPR).

3 Results and discussion

Methane dry reforming reactions of the six catalysts are shown in Figure 1(a) to 1(f). The Ni/SBA-15 catalysts (a), (c) and (e) which had the smallest sized nickel nano-particles as confirmed by XRD and TEM results with hydrogen reduction occurring at the higher temperature range above 500°C, had the most stable H_2 and CO yield over time and temperature up to 850°C with catalyst (e) having the earliest initial reaction at 250°C. The Ni/SBA-15 catalysts (b), (d) and (f) with bigger nickel particles, less uniform dispersion and most of the hydrogen reduction occurring at lower temperature range below 450°C had H_2 and CO yield reducing over time and temperature due to faster coke deposition.

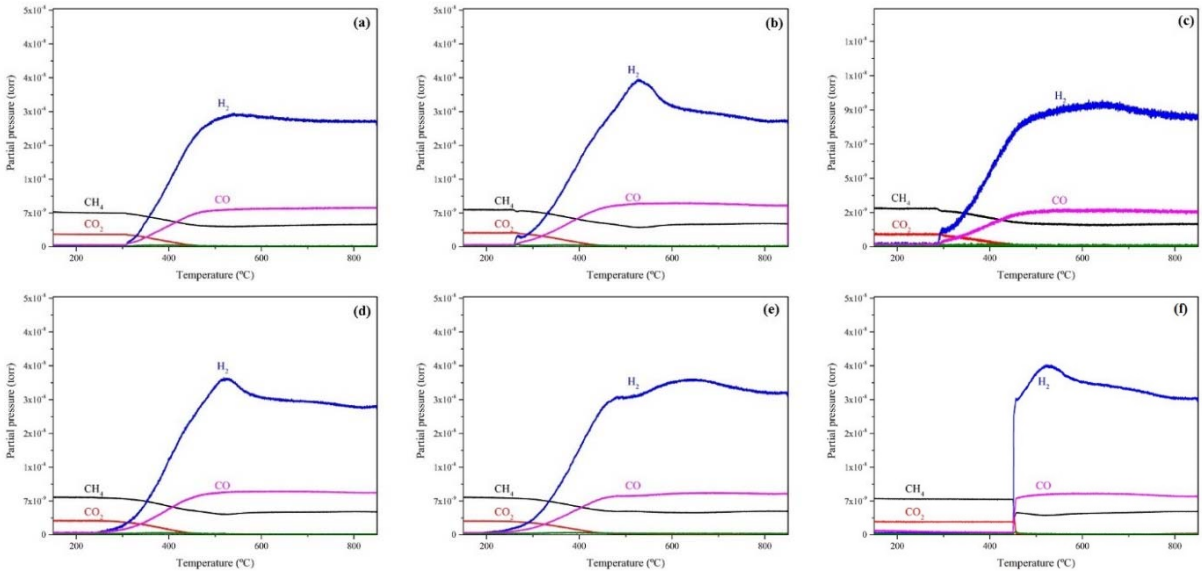

Fig. 1. TPRx of different Ni/SBA-15 samples in dry reforming of methane: (a) water -unwashed, (b)en-unwashed, (c) en-washed, (d) NH_4OH-unwashed, (e) NH_4OH-washed, (f) EDTA-unwashed

4 Conclusions

The nature of nickel complex and choosing to wash or not to wash the catalyst with deionised water after impregnation had pronounced effect on the metal-support interaction, nickel particle size, dispersion and as a result on the activity and stability of the catalyst.

References

[1] D. Pakhare, J. Spivey *Chemical Society Reviews*. **2014**, 43, 7813-7837.
[2] P. Gangadharan, K. C. Kanchi, H. H. Lou *Chemical Engineering Research and Design*. **2012**, 90, 1956-1968.
[3] N. Wang, W. Chu, T. Zhang, X. S. Zhao *International Journal of Hydrogen Energy*. **2012**, 37, 19-30.
[4] G. Valderrama, C. Urbina de Navarro, M. R. Goldwasser *Journal of Power Sources*. **2013**, 234, 31-37.
[5] D. J. Q. N. G. H. C. B. F. S. G. D. Zhao *Science*. **1998**, 279, 548-552.

III-PP89

Efficient Conversion of Organic Matters Using Ionic Liquid in Hydrogenation of Coal over Mo-Based Catalyst

Han G.B.[1*], Choi H.Y.[1], Jang J.H.[1], Lee T.J.[2], Park N.K.[2], Kang M.[2]

1 - Institute for Advanced Engineering, Yongin, Republic of Korea
2 - Yeungnam University, Gyeongsan, Republic of Korea

* gbhan@iae.re.kr

Keywords: direct coal liquefaction, Mo-based catalyst, hydrogenation, dissolution, organic matters

1 Introduction

Hydrocarbon compounds are very valuable chemicals as fuel and base materials in petrochemical industry. Direct coal liquefaction is an available technology to produce the liquefied hydrocarbon fuels with the combined cracking and hydrogenation of organic matters of coal under high temperature and pressure. The various useful hydrocarbon compounds can be produced by the cracking and recombination through the catalytic hydrogenation of the organic materials of coal. However, it was known that the organic macromolecular compounds of coal have relatively low H/C ratio as compared with oil/petroleum from which the hydrocarbon compounds can be made. Therefore, the direct coal liquefaction including the catalytic hydrogenation process with H2 is necessary for the synthesis of hydrocarbon compounds from organic materials of coal. Coal is composed of fixed carbon, volatile matters, ash and moisture and the organic materials such as fixed carbon and volatile matters are the macromolecular compounds which consist of carbon, hydrogen, oxygen, nitrogen and sulfur etc.

In this study, the hydrogenation of coal using batch-type autoclave reactor was conducted under high pressure and temperature. In the reaction test, the ionic liquid was used as an additive to improve the cracking and dissolution of organic matter of coal and the reaction efficiency of the direct coal liquefaction process with catalyst. And then the effect of the ionic liquid on the catalytic effect of the cracking and dissolution of coal was investigated for the reaction characteristics. Also, the physic-chemical properties of the solid and liquid phase of reactant and product were characterized by X-ray diffraction, proximate analyzer, elemental analysis, FT-IR spectra etc.

2 Experimental/methodology

A coal was used as a reactant for hydrogenation with H_2 in this study and then the coal was ground, collected by sieving with 200 meshes and dried overnight at 105 ^oC for the removal moisture before using in the reaction. Also, the coal after the water removal was mixed with ionic liquid before the reaction. The commercial tetralin and MoS_2 were respectively used as a solvent and catalyst without the purification.

The hydrogenation of coal was carried out using a batch reactor with a volume of 3 L. Prior to the reaction, the mixture of reagent with 50 g coal, 100 ml tetralin and 10%wt. MoS2 catalyst based on coal weight was produced using ball mill and was put into the batch reactor. The reactor was sealed, purged by gas corresponding to the desired atmosphere. After injecting the gas up to the initial pressure into the reactor, the reactor was heated up to the targeted reaction temperature and then the internal temperature and pressure were simultaneously increased. After the reaction time of 60 min based on reaching up to the targeted reaction temperature, the reactor was cooled down to room temperature and the solid, liquid, and gaseous products were selectively collected, separated and analyzed to investigate the relationship between the reaction characteristics and their physico-chemical composition.

3 Results and discussion

Fig. 1 shows the effect of ionic liquid on the direct coal liquefaction with and without using ionic liquid. As shown in Fig. 1, the conversion of coal increased with using ionic liquid as compared with the case of not using ionic liquid in direct coal liquefaction and the conversion of coal was about 67.8% based on the amount of organic matters.

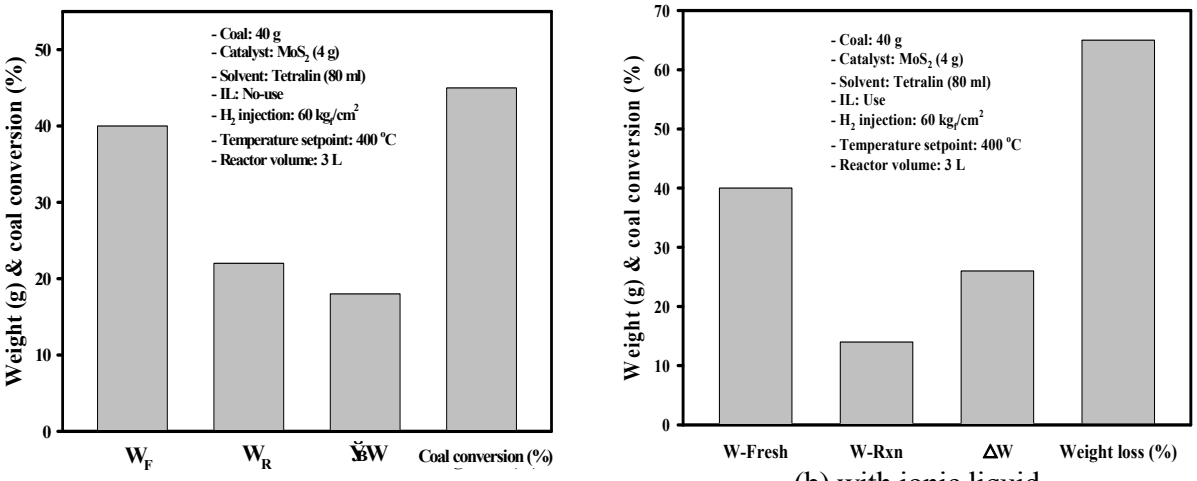

(a) without ionic liquid

(b) with ionic liquid

Fig. 1. Effect of ionic liquid on the direct coal liquefaction.

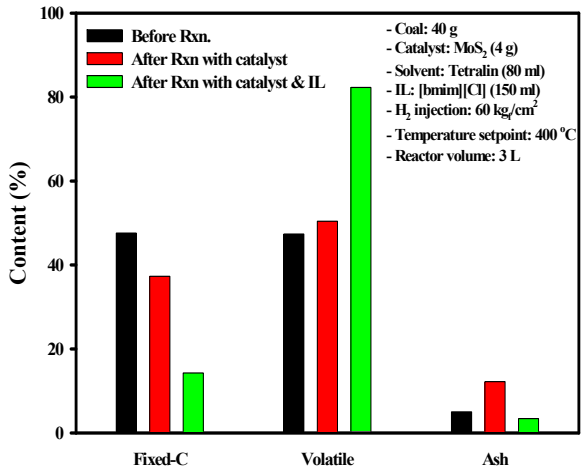

Fig. 2. Conversion of organic matters in direct coal liquefaction over Mo-based catalysts.

Fig. 2 shows the conversion of organic matters in direct coal liquefaction over Mo-based catalysts. In Fig. 2, the content of fixed carbon which was contained in the organic matters of coal decreased with using the ionic liquid as compared with the case of not using ionic liquid and then it was estimated that the conversion of the organic matters increased with using ionic liquid because the dissolution of the fixed carbon of coal was improved by the ionic liquid.

4 Conclusions

In this study, the ionic liquid was used to improve the conversion of organic matters of coal in the direct coal liquefaction and then the effect on the ionic liquid on the direct coal liquefaction was investigated. As a result, it was known that the cracking and dissolution efficiency of organic matters of coal were improved by the ionic liquid in hydrotreating process of direct coal liquefaction over Mo-based catalyst.

III-PP90

Esterification of Levulinic Acid with Butanol over Ion-Exchange Resins: a Screening Study

Tejero M.A., Ramírez E., Fité C., Tejero J., Cunill F.*

Chemical Engineering Department, Faculty of Chemistry, Universitat de Barcelona, Barcelona, Spain

* fcunill@ub.edu

Keywords: butyl, levulinate, levulinic acid, catalysis, ion-exchange, resins

1 Introduction

Alkyl levulinates are biomass derived chemicals with a large spectrum of applications. They have the potential to substitute compounds currently derived from petro-chemical routes as additives to conventional diesel or gasoline because of their physicochemical properties. Alkyl levulinates are synthesized most often from levulinic acid (LA), but also from furfuryl alcohol or directly from cellulose and sugars. LA is a platform chemical formed from hydrolysis of lignocellulose, the most readily available form of biomass, using the Biofine process.

The most widely studied alkyl levulinate is ethyl levulinate (EL), both its synthesis pathways and possible applications have been explored thoroughly. Comparatively, the potential of butyl levulinate (BL) has been left untapped. As an additive for diesel, BL is even more promising than EL: BL remains in diesel solution down to the diesel cloud point, BL blends have very small particulate matter emissions, it has a lower solubility in water than EL, good lubricity and conductivity, and a low but better cetane number.

Esterification of LA with butanol (BuOH) over several types of catalysts such as zeolites, Ru/C and heteropolyacid (HPA) supported on acid-treated clay montmorillonite (K10) has been described in literature, but the catalysis with acidic ion-exchange resins has never been attempted to the best of our knowledge. The present work studies the behaviour of different sulphonated polystyrene-divinylbenzene resins in the synthesis of BL from LA.

2 Methodology

The acidic resins used were Amberlyst™ 15 (A15), A16, A35, A36, A39, A46, A70 (Room & Haas); Purolite® CT-224 (CT-224) (Purolite), and Dowex 50Wx8, Dowex 50Wx4, Dowex 50Wx2 (Dow). The mass of dry catalyst used was 0.5 g and stirring speed was fixed at 500 rpm. Relevant resin properties are specified in Table 1.

Table 1. Properties of the acidic resin catalysts used in this study.

Catalyst	Type	Sulfonation type	Acid Capacity (meq H^+/g)*	DVB%	d_p (mm)	V_{sp}** (cm^3/g)
A15	macro	Conventionally sulphonated	4.81	20	0.40-0.63	0.622
A16	macro	Conventionally sulphonated	4.80	12	0.40-0.63	1.136
A35	macro	Oversulphonated	5.32	20	0.40-0.63	0.504
A36	macro	Oversulphonated	5.40	12	0.40-0.63	1.261
A39	macro	Conventionally sulphonated	4.82	8	0.40-0.63	1.643
A46	macro	Surface-Sulphonated	0.87	25	0.40-0.63	0.190
A70	macro	Conventionally sulphonated	2.55	8	0.40-0.63	1.149
CT-224	gel	Oversulphonated	5.34	4	0.32	1.859
Dowex 50Wx2	gel	Conventionally sulphonated	4.83	2	0.297-0.149	2.677
Dowex 50Wx4	gel	Conventionally sulphonated	4.95	4	0.297-0.149	1.920
Dowex 50Wx8	gel	Conventionally sulphonated	4.83	8	0.297-0.149	1.404

*Titration against standard base. **specific volume of swollen polymer in water, measured by ISEC technique.

The experiments were carried out in a 100ml batch reactor. System composition is as determined by means of in-line sampling to a gas chromatograph equipped with a TCD detector. Experiments last 8h at 353-393 K and 2.5 MPa in order to guarantee a system in liquid phase. Catalyst screening was done working with an excess of BuOH (molar ratio BuOH/LA = 3) in order to both minimize the possible formation of humins by polymerization of LA and avoid the formation of two liquid phases due to the formation of water during the course of the reaction.

3 Results and discussion

The conducted experiments confirm that acidic polymer catalysts can be used in order to obtain very high conversion (Fig 1) and selectivity in the esterification of LA with BuOH to BL. Selectivity toward BL remains always over 98% for all catalysts. The most relevant by-product is dibutyl ether (DBE), even though it is never more than 2% even at 393K. At operating temperature of 353K, selectivity remains over 99%.

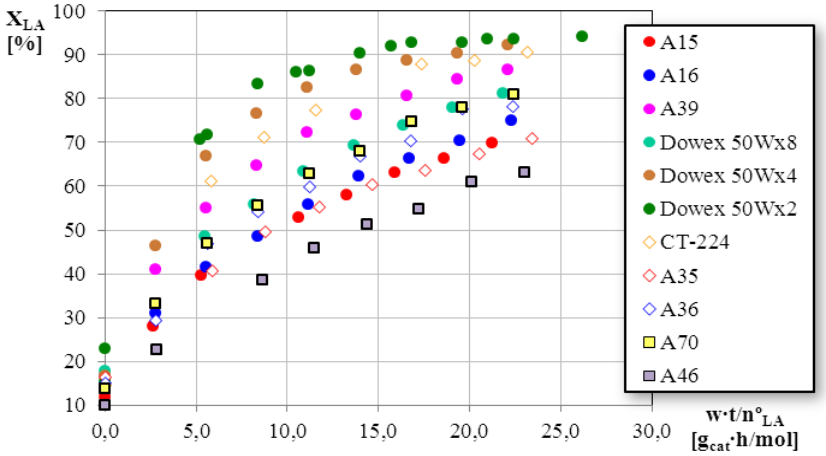

Fig. 1. Comparison of the evolution of the conversion of LA over contact time.

The catalyst with highest activity was Dowex 50Wx2. Overall gel-type resins presented better yields than macroporous ones. Because of the high polarity of LA and the formation of water, catalysts with greater capacity for swelling would favour LA esterification. Thus resins with a lesser degree of cross-linking (DVB%) present higher reaction rates. Incidentally, CT-224 was less active than Dowex 50Wx4 (both 4% DVB) despite having a higher number of active sites. This might be because oversulphonation confers greater stiffness to the polymeric structures, which impedes swelling. The lowest activity is that of A-46, which is surface-sulphonated and therefore has a very low number of active sites. BL yield was not much lower than those obtained with A15, A16 and A35. This suggests that for resins with a high degree of cross-linking (DVB>12%), swelling might be so poor that the reaction takes place mainly on active sites close to the surface. Although A70 also has a lower number of active sites, activity rates are on par with Dowex 50Wx8, yet lower than A39 (all 8% DVB). Presumably the inner structure of the active sites of A70, due to the electron donating chloride groups present in the matrix of thermostable resins confers a higher acid force to said sites, which might have a compensatory effect. Globally, higher reaction rates roughly correspond with large V_{sp}.

4 Conclusions

Esterification of LA catalysed by acidic ion exchange resins always has over 98% selectivity. Reaction rates improve as the degree of polymer cross-linking diminishes. Gel-type resins with higher swelling show better results as a whole. The reaction rates increase significantly when the swollen polymer phase is highest. Ion-exchange catalysts have been found to be more efficient than zeolites, because they have been proven to have better yields at lower temperatures and higher concentrations of LA. Compared with heteropolyacid supported on acid-treated clay montmorillonite, which have similar activity rates and selectivity, ion-exchange resins are cheap and readily commercially available.

III-PP91

Etherification of Isobutene with C_1 to C_4 Linear Primary Alcohols in Liquid-Phase: Experimental Equilibrium and Thermodynamic Analysis

Badia J.H., Fité C., Bringué R., Ramírez E., Cunill F.*

Chemical Engineering Department, Faculty of Chemistry, Universitat de Barcelona, Barcelona, Spain

* fcunill@ub.edu

Keywords: etherification, isobutene, primary alcohols, ion-exchange resins

1 Introduction

Experimental studies on equilibrium conditions and thermodynamic properties concerning innovative processes are mandatory to determine their feasibility. Recent examples in different disciplines are graphene synthesis, pharmaceutical drugs design, or novel biofuels production.

Regarding biofuels, oxygenate additives, as methyl *tert*-butyl ether (MTBE) and ethyl *tert*-butyl ether (ETBE), have been produced worldwide for decades. Increasing the ethers length, by using alcohols larger than methanol or ethanol, leads to a decrease of their vapor pressure and solubility in water, and to an increase of these ethers boiling point. As fuels, these properties are desirable because they allow a reduction of evaporative emissions and of water contamination risk, and because they provide a dilution effect of some harmful fuel components.

Larger linear alcohols, such as *n*-propanol or *n*-butanol to obtain propyl *tert*-butyl ether (PTBE) or butyl *tert*-butyl ether (BTBE), respectively, can be industrially produced through the oxo process. Alternatively, biomass-based production routes are also being studied, namely condensation of bioethanol and/or biomethanol (Guerbet Catalysis) and ABE fermentation (which produces Acetone, n-Butanol and Ethanol using microorganisms of the genus *Clostridium*). Consequently, PTBE and BTBE from *n*-propanol and *n*-butanol can be computed for the biofuel target.

Prior to scale-up studies on the feasibility of industrializing these processes, equilibrium information based on experimental data must be collected and thermodynamic properties analyses must be carried out. Actually, equilibrium and thermodynamic information of reacting systems involving alkenes and several alcohols is scarce. The present study, based on experimental work, helps to reduce this lack of information.

2 Experimental

Reactants were methanol, ethanol, 1-propanol, 1-butanol, and either 2-methylpropene (isobutene) (>99.9% G.C.) or a synthetic C4 mixture (25% wt isobutene, 40% wt isobutane and 35% wt *trans*-2-butene) as the isobutene source. All resins used as catalysts were macroreticular, strongly acidic, sulfonated polymers of styrene divinylbenzene. Most of the experiments were performed with Amberlyst™ 35 (A-35), and resins Amberlyst™ 15 (A-15), Purolite® CT275 (CT-275) and Lewatit® K 2620 (K2620) were also tested for comparative purposes.

Experiments were carried out at 313-383 K and 1.5-2.0 MPa. Assayed alcohol/isobutene molar ratios ($R^o_{OH/IB}$) were in the range 0.6-2.4. Experimental devices used were a series of catalytic fixed bed tubular microreactors (length: 15 cm, i.d.: 7 mm) disposed in line and submerged in a thermostatic bath, and a 200 cm^3 stainless-steel jacketed batch reactor equipped with a catalyst injector. Each experimental device was attached in line to an Agilent gas chromatograph equipped with a capillary column (PONA Cross-linked Methyl Silicone Gum of 50 m × 0.2 mm × 0.5 μm) to quantify the medium composition. In the fixed bed reactor, equilibrium was considered to be reached when the outlet stream composition at steady-state and at the assayed temperature did not vary with decreasing flow rate (Liquid Hourly Space Velocities ranged 1.8-20 h^{-1}). In the batch

reactor, equilibrium was reached when the composition showed no significant evolution in time (experiments lasted 5-8 h).

3 Results and discussion

MTBE experiments were conducted with A-35 and A-15 at only two temperatures, mainly to compare the results obtained in the fixed bed reactor setup with those quoted in literature, usually obtained in batch reactors. Given some lack of agreement between sources concerning ETBE equilibrium and thermodynamic data, a more extensive study was proposed: ETBE experiments were performed in both reactors systems, in a wider temperature range (313.15-383.15 K) than published to date and using A-35, CT-275 and K2620 as catalysts. MTBE and ETBE equilibrium constants, determined in separated devices with different catalysts, were in good agreement with literature data. Concerning PTBE and BTBE syntheses, available thermodynamic data are very scarce on both ethers. Thus, an extensive work has been done to estimate thermochemical data; different group-contribution methods (Joback and Modified Benson methods) were used and compared with literature data, when available. PTBE and BTBE equilibrium constants were experimentally obtained in the batch reactor device, with A-35 and using different initial compositions in the temperature range of 323 to 353 K.

Figure 1 depicts *ln* K_i, experimental equilibrium constant, versus *1/T* for the four etherification equilibria. As it can be seen, the van't Hoff equation fit well to experimental results. PTBE and BTBE equilibrium constants are between those of MTBE and ETBE, which accounts for high conversion in industrial processes.

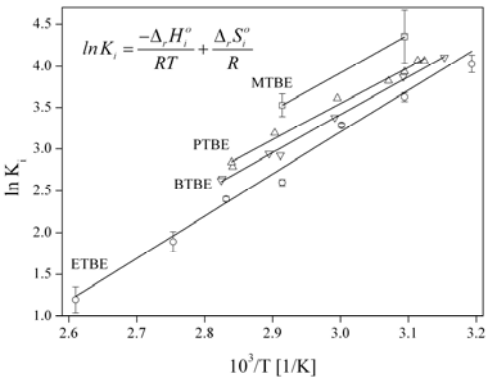

Fig. 1. Van't Hoff plot considering constant reaction enthalpy change within the temperature range

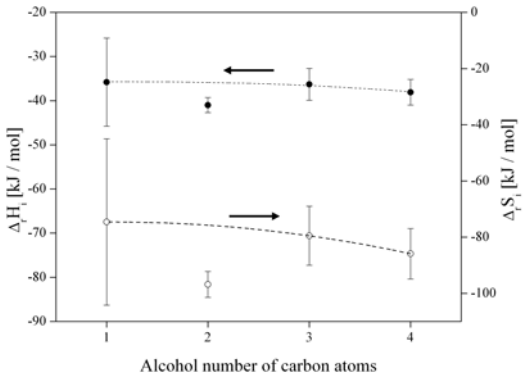

Fig. 2. Standard enthalpy and entropy changes variation with the alcohol number of carbon atoms

Estimated values for reaction enthalpy show a decreasing trend with the alcohol length with the exception of ETBE formation, which presents a lower value than expected in that trend, as shown in Figure 2. Analogous results have been obtained for the entropy variation. Estimated values agree with published data, when available.

From reaction enthalpy and entropy variations, formation enthalpies have been estimated for MTBE, ETBE, PTBE and BTBE, respectively. Values for MTBE and ETBE agree with those reported in literature, which supports the reliability of the obtained values for PTBE and BTBE, which were not published to date to the best of our knowledge.

4 Conclusions

Etherification reactions of isobutene with C_1 to C_4 linear primary alcohols have been found to be reversible and exothermic, irrespectively of the catalyst and reactor operation mode, as expected. Enthalpy and entropy variations have been estimated for each etherification reaction, and these values have been used to estimate formation enthalpies of MTBE, ETBE, PTBE, and BTBE. MTBE and ETBE results agree with published results, which support the reliability of PTBE and BTBE estimated values.

III-PP92

From Data to Knowledge: Analysis of Published Articles in Literature for Photo-Catalytic Water Splitting

Can E., Yildirim R.*

Bogazici University, Department of Chemical Engineering, Istanbul, Turkey

* yildirra@boun.edu.tr

Keywords: photo-catalytic water splitting, hydrogen production, knowledge extraction, data mining

1 Introduction

Solar energy is predicted to be a compelling solution to our increasing global energy demands in the future because it is free, renewable, and sustainable. Hydrogen has been also considered as a promising energy carrier due to its high energy density (140 MJ Kg^{-1}) which is greater than those of gasoline and coal. Besides, the energy production from hydrogen combustion does not cause carbon emission; it results in a harmless by-product of water [1]. Hence, splitting water into hydrogen and oxygen by photocatalysis has attracted considerable attention recent years

Photo-catalytic water splitting (PWS) can be investigated in 3 steps; (i) absorption of photons with energies exceeding the semiconductor band gap and leading to the generation of electron and hole pairs in the semiconductor; (ii) migration of these photo-generated particles (e^- and h^+) which resulted in charge separation; (iii) surface chemical reactions between these carriers and present compound (e.g., water, water-alcohol solution) [2].

TiO_2 is the most commonly studied and one of the most efficient alternatives among about 140 materials tested in the literature for PWS, but the energy conversion is still low. There are also some extensive works in the literature involving perovskites because of their promising activity under the visible light. Also dye sensitization of a semiconductor like TiO_2 is another method that is widely used to utilize visible light for PWS[3].

To develop an efficient photocatalyst, several parameters are needed to be optimized. Great time, labor and money are required to adjust these parameters so that the best activity is achieved. At that point, data mining, which is a method to extract knowledge from the published articles and performed experiments, can help to decide the preparation and operational variables of a new process. There are various types of data mining tools; the common ones are linear regression, logistic regression, k-nearest neighbor algorithm, decision trees, support vector machine, and artificial neural networks.

In this work, the aim is to extract knowledge from published articles about photo-catalytic water splitting in literature, then to examine whether the result of an unperformed experiment can be estimated, or not.

2 Computational Work

A great number of articles, which were published for last 10 years (between 2005 and 2014) about PWS in the literature, were studied and a comprehensive database which consists over 5000 data points from 86 different papers were constructed. The database consists of 32 variables such as semiconductor type, catalyst preparation method, promoter type and weight percent, reaction solution, light intensity and light type, and band gap, crystal structure, and particle size of catalyst material that affect quantum yield. Then models were developed using that database to predict an unperformed experiment and understand the process better. The learning algorithms that were used in this work are artificial neural network, decision tree and support vector machine. Some other supplementary tools like principal component analysis were also used to complete task.

3 Results and Discussion

TiO_2, (especially nano-sized) is the most commonly studied material due to its low cost high abundance and relatively high activity towards PWS; the 68% of TiO_2 used was in pure anatase phase, while 13% is P25 (anatase:rutile, 4:1). However, the perovskites type photo-catalysts seem to be more efficient because of their higher charge carrier mobility and charge carrier lifetime, and they result higher hydrogen production rate (μmol/g-cat/h). In all these works reported in the literature, the semiconductor materials with band gap value from 3 to 3.4 eV and particle size between 50-100 nm were examined most commonly.

Some descriptive statistics were obtained from the database first to understand the trends (number of publication, type of semiconductor, promoter, etc.) in last 10 years. As an example, Figure 1.a shows the number of scientific publications on PWS has been studied from 2005 to 2014 using a number of literature databases, including Elsevier, Wiley Online Library, and ACS Publications. The annual number of publications on PWS has increased 346% in 2014 in respect to 2005. Then more detailed analysis performed using k-nearest neighbor regression (KNNR), artificial neural networks and support vector machine. Figure 1.b shows the prediction for the results of a publication[4] by KNNR model developed from the other publications on perovskite catalysts; the model predictions are in good agreement with the experimental results reported.

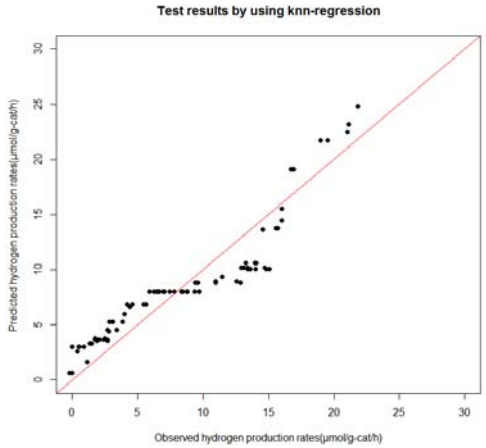

Fig 1. (a) The number of annual published articles on PWS last decade, (b) Test results of an article [4] by using k-nearest neighbor regression

3 Conclusions

The results shows that the models developed from the database indeed can generate useful knowledge to understand the process, to see trends, to make predictions for the conditions at which the experimental data are not available.

References

[1] Xie G., Zhang K., Guo B., Liu Q., Fang L., Gong J.R., *Advanced Materials*, **2013**, 25, 3820-3839.
[2] Ismail A.A., Bahnemann D.W., *Solar Energy Materials & Solar Cells*, **2014**, 128, 85-101.
[3] Meng Ni, Michael K.H. Leung, Dennis Y.C. Leung, K. Sumathy., *Renewable and Sustainable Energy Reviews*, **2007**, 11, 401-425.
[4] Kim J., Sohn Y., Kang M., *International Journal of Hydrogen Energy*, **2013**, 38, 2136-2143.

III-PP93

Further Insights into the Effect of Sulphur on the Activity and Selectivity of Cobalt–based Fischer–Tropsch Catalysts

Barrientos J.*, Boutonnet M., Järås S.

KTH - Royal Institute of Technology, Stockholm, Sweden

* javbar@kth.se

Keywords: Fischer-Tropsch, cobalt, sulphur, selectivity, deactivation

1 Introduction

The catalytic conversion of synthesis gas into hydrocarbons (Fischer-Tropsch synthesis, FTS) is receiving great attention due to its potential for converting different carbon sources (coal, natural gas and/or biomass) into liquid transportation fuels. It is generally known that sulphur compounds are severe poisons for cobalt-based Fischer-Tropsch (FT) catalysts [1]. The effect of S on the FT performance has been analysed in various literature studies [1-5]. Nevertheless, there is still no full agreement regarding its effect on the FT product distribution [4, 5].

Among different S poisoning studies it is noteworthy to mention the work from Visconti et al. [4] in which they prepared catalyst samples with different S loadings and tested these under relevant FT conditions. In this study, they observed that the selectivity to long-chain hydrocarbons decreased with increasing S content. Unfortunately, these poisoned catalysts were tested at different CO conversions and thus exposed to different water partial pressures, fact that affects both product selectivity and catalyst stability [6]. More recently, Borg et al. [5] studied the performance of cobalt-based FT catalysts with *in situ* H_2S addition. Contrariwise, they found that S has no significant effect on the primary product distribution. Pansare and Allison [7] also studied the effect of *in situ* H_2S on selectivity. Conversely, they claimed that sulphur decreased the selectivity to long-chain hydrocarbons.

In the present study, sulphur was added *ex-situ* to a cobalt-based catalyst. The resulting poisoned catalyst samples were tested under realistic FT conditions at the same operating CO conversion. The objective of this work was to elucidate this controversial effect of S and offer a better understanding of the influence of this poison on catalyst performance.

2 Experimental/methodology

A γ-Al_2O_3-supported catalyst consisting of 12 wt% Co and 0.5 wt% Pt was impregnated with different aqueous solutions of ammonium sulphide. This S impregnation was performed on previously reduced catalyst samples in order to better simulate the S-Co^0 interaction. By using this method, catalyst samples loaded with 10, 100, 250 and 1000 ppm of S were prepared. The catalyst samples were reduced in situ in a fixed-bed reactor at 350 °C for 16 h in H_2. The catalytic tests were performed at 20 bar, 210 °C and an inlet molar H2/CO ratio=2.1. The gas hourly space velocity was adjusted in order to operate at a CO conversion of 30% for all the experiments.

A fresh catalyst sample was reduced at the aforementioned conditions in a quartz tubular reactor. After reduction, the catalyst was exposed to a H_2S/H_2 flow ($H_2S/H_2=10^{-5}$) at 623 K for 2 days. The S content of the resulting catalyst was analysed in order to estimate the sulphur capacity of the catalyst, and thus, the sulphur coverage for the different poisoned samples.

3 Results and discussion

A catalyst deactivation model relating the catalyst activity to the sulphur coverage was

developed. The effect of sulphur on selectivity was successfully evaluated at the same CO conversion. The results showed that the presence of sulphur on the catalyst surface enhances the selectivity towards methane and reduces the selectivity to long chain hydrocarbons. This effect is more pronounced at high sulphur coverages. Figure 1 illustrates both the effect of sulphur on catalyst activity and on the FT product distribution.

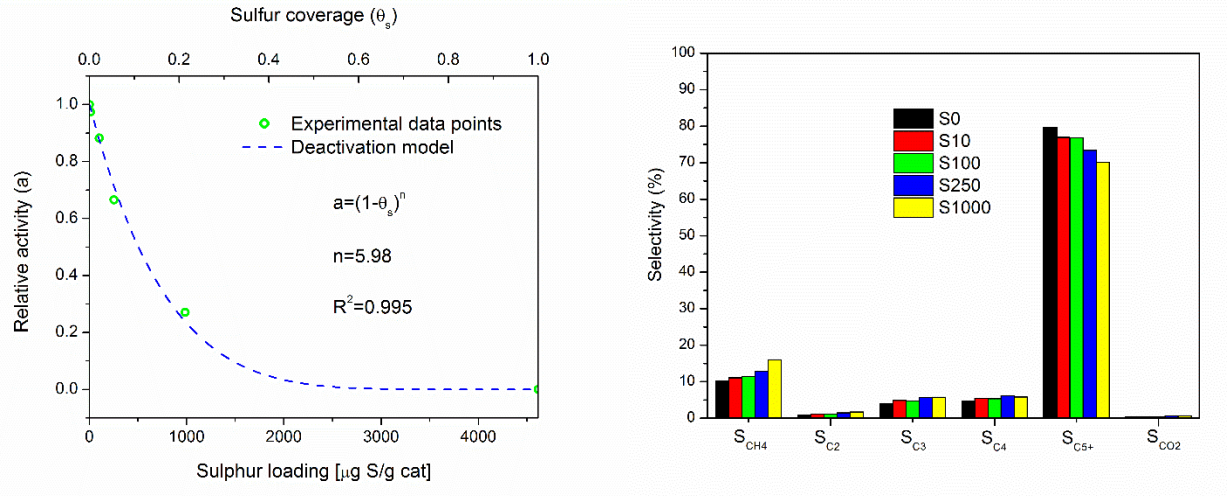

Fig. 1. Deactivation model relating the catalyst activity to the sulphur loading and the sulphur coverage (left). Carbon-based selectivities obtained for the different poisoned catalysts at 20 bar, 483 K, inlet H_2/CO=2.1 and CO Conversion=30%.

4 Conclusions

This study revealed that sulphur does have an effect on product selectivity. Further results of this work will be discussed and compared with these obtained in previous studies.

Acknowledgements

The research leading to these results has received funding from the European Union Seventh Framework Programme (FP7/2013) under grant agreement n° 308733.

References

[1] C.H. Bartholomew and R.M. Bowman, *Appl. Catal. 15 (1)* (1985)
[2] M.S. Kim, N.M. Rodriguez, and R.T.K. Baker, *J. Catal. 143 (2)* (1993)
[3] V. Curtis, et al., *Catal. Today 49 (1–3)* (1999)
[4] C.G. Visconti, et al., *Appl. Catal. A 330 (0)* (2007)
[5] Ø. Borg, et al., *J. Catal. 279 (1)* (2011)
[6] Ø. Borg, et al., *J. Catal. 248 (1)* (2007)
[7] S.S. Pansare and J.D. Allison, *Appl. Catal. A 387* (2010)

III-PP95

Hydrocracking of FT Wax over Noble Metal / SA Catalysts: Combined Experimental and Kinetic Modelling Studies

Suárez París R.[1*], L'Abbate M.E.[1], Regali F.[2], Liotta L.F.[3], Boutonnet M.[1], Järås S.[1]

1 - KTH - Royal Institute of Technology, School of Chemical Science and Engineering, Department of Chemical Engineering and Technology, Stockholm, Sweden
2 - Scania AB, Materials Technology, Engine Performance and Emissions, Södertälje, Sweden
3 - Institute for the Study of Nanostructured Materials, Palermo, Italy

* rosp@kth.se

Keywords: hydrocracking, wax, noble metal, silica-alumina, kinetic modelling

1 Introduction

Synthetic fuel production using the Fischer-Tropsch (FT) technology will play an important role in the future energy system. FT wax can be upgraded to middle distillates through a hydroprocessing step that combines cracking and isomerization. Hydroprocessing of FT wax is usually carried out on bifunctional catalysts, containing a metal and an acid function. Noble metals (Pt, Pd) supported on mesoporous silica-alumina have been previously studied and have shown high diesel selectivities [1]. However, most of the published information concerns the use of Pt-based catalysts, while Pd performance has been mainly studied on batch systems [2] or using short-chain paraffins as model compounds [3].

The aim of this work is to study and compare the catalytic behavior of Pt and Pd in paraffinic wax hydrocracking. The experimental data obtained in a lab-scale trickle-bed reactor has also been used to develop a kinetic model, based on the LHHW formalism [4].

2 Experimental / methodology

Catalysts were prepared by incipient wetness impregnation of a commercial silica-alumina support (*Siral 40*) with aqueous solutions of metal nitrates. Catalysts were characterized by means of nitrogen adsorption, H_2 chemisorption and TPD of ammonia.

Hydrocracking tests were performed in a fixed-bed tubular reactor at the following conditions: T=300 - 330 °C, P=35 bar, H_2/wax= 0.1 (wt/wt); WHSV=1-4 h^{-1}. Prior to the reaction, catalysts were reduced in situ in H_2 flow at 400°C. The wax was fed to the reactor with a high-pressure syringe pump and thermal mass flow controllers were used to feed the gases. The gaseous phase was analyzed on-line with a Perkin Elmer Clarus 500 GC. Unconverted wax and liquid products were collected in two consecutive traps and analyzed off-line with an Agilent 6890 GC.

A LHHW kinetic model has been successfully developed to predict experimental outcomes. In the model, vapor-liquid equilibrium is taken into account; liquid and gas phase reaction rates have been considered trough the evaluation of fugacities; finally, ideal probability of C-C bond breakage has been accounted when modeling the cracking reactions. The set of kinetic constants used in the model has been iteratively calculated by means of non-linear optimization.

3 Results and discussion

The physicochemical properties of two of the studied catalysts are shown in Table 1.

Table 1. Physicochemical properties.

Catalyst	Metal loading (wt%)	BET surface area (m^2/g)	avg. pore diameter (nm)	pore volume (cm^3/g)	metal dispersion (%)	avg. crystallite size (nm)
Pt06S40	0.60	447	7.9	0.94	103 [1]	1.1
Pd033S40	0.33	452	7.8	0.95	21	5.3

[1] *A dispersion higher than 100% is probably due to an adsorption stoichiometry exceeding 1*

The product distribution obtained over Pt- and Pd-based catalysts with the same metal molar loading is shown in Fig.1, for similar conversion levels (around 35%). Platinum is slightly more active than palladium, but results in higher selectivities to methane and ethane, which is attributable to a monofunctional hydrogenolysis mechanism. The selectivity to the middle distillate fraction is higher in the case of platinum. Both catalysts lead to a significant increase in the degree of isomerization of the feed.

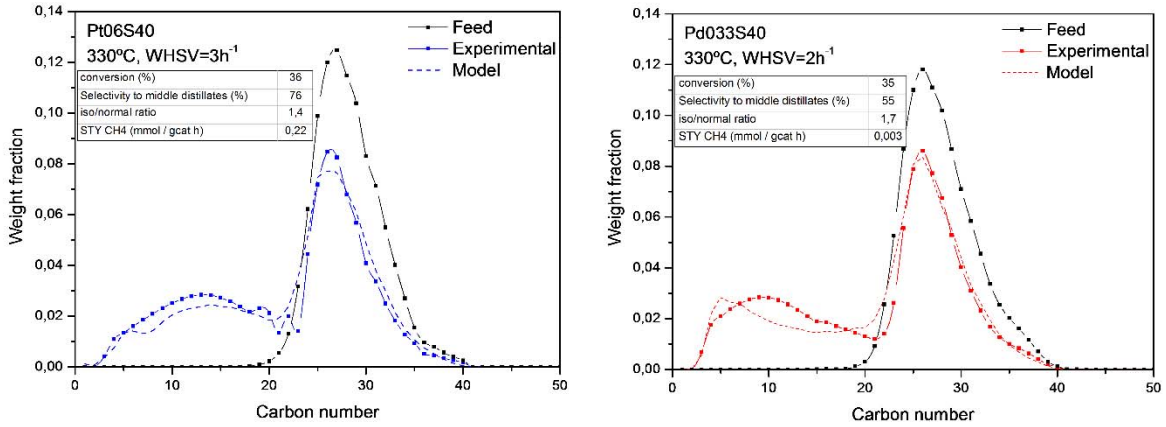

Fig. 1. Product distribution over Pt- and Pd-based catalysts at similar conversion levels.

The influence of process parameters on conversion and selectivities can be predicted with the developed kinetic model, which shows a good agreement with experimental data (Fig.1). Pt- and Pd-based catalysts will be compared considering the differences in kinetic constants (mainly activation energies, frequency factors and Langmuir adsorption constants).

4 Conclusions

Hydrocracking of paraffinic wax has been carried out over Pt/ and Pd/Siral 40 and the experimental results were used to obtain a kinetic model. Further work is ongoing to improve the model and evaluate the performance of bimetallic PtPd catalysts.

References

[1] Calemma, V. and C. Gambaro, Effect of Feed Distribution on Hydrocracking of Fischer-Tropsch Wax, in Synthetic Liquids Production and Refining (2011). American Chemical Society, p. 239-253.
[2] Lee, J., et al., Journal of Industrial and Engineering Chemistry, **17** (2011) p. 310-315.
[3] Regali, F., et al., Catalysis Today, **223** (2014) p. 87-96.
[4] Froment, G.F., Catalysis Today, **1** (1987) p. 455-473.

III-PP96

Hydrodeoxygenation of Aliphatic Esters over Nickel Phosphide Catalysts

Shamanaev I.V.[1,2*], Deliy I.V.[1,2,3], Gerasimov E.Yu.[1,2], Pakharukova V.P.[1,2], Kvon R.I.[1], Rogov V.A.[1,3], Bukhtiyarova G.A.[1]

1 - Boreskov Institute of Catalysis, Novosibirsk, Russia
2 - Research and Educational Center for Energy Efficient Catalysis, Novosibirsk National Research University, Novosibirsk, Russia
3 - Novosibirsk National Research University, Novosibirsk, Russia

* i.v.shamanaev@catalysis.ru

Keywords: hydrodeoxygenation, nickel phosphide catalysts, aliphatic esters

1 Introduction

The limited reserves of fossil fuel, increasing oil consumption, climate changes and some other reasons have recently caused an intensified search for alternative sources of energy [1,2]. Fatty acid based feedstocks such as vegetable oil, tall oil, waste-cooking oil ("yellow grease") or animal fat attract much attention. There is a commercial-available technology to convert these crudes into efficient fuel – hydrodeoxygenation (HDO). HDO leads to the mixture of hydrocarbons in the diesel fuel boiling range. This products are frequently called "green diesel", "second generation biodiesel" or "renewable diesel".

Conventional hydrotreating sulfide catalysts and precious metal catalysts are active in HDO. But sulfide catalysts suffer from deactivation in absence of sulfiding agent and precious metals are highly-priced. Transition metal phosphides are considered as promising materials for HDO of renewable feedstocks [3,4]. Supported phosphide catalysts such as Ni_2P/SiO_2, Co_2P/SiO_2, MoP/SiO_2, WP/SiO_2, Ni_2P/MCM-41 etc. are widely investigated in hydroprocessing of model compounds and real feedstocks [5].

The aims of the present work are the study of the silica-supported nickel phosphide catalysts in HDO of vegetable oil model compounds – aliphatic methyl esters (methyl heptanoate $C_6H_{13}COOCH_3$ – MH, methyl laurate $C_{11}H_{23}COOCH_3$ – ML, methyl palmitate $C_{15}H_{31}COOCH_3$ – MP), investigation of reaction conditions and carbon chain length influence on catalytic properties.

2 Experimental/methodology

The catalysts were prepared by impregnation of silica with aqueous solutions of $Ni(OAc)_2$ and $(NH_4)_2HPO_4$. At the impregnation step Ni:P molar ratio was maintained 1:2, nickel loading was about 2.5 w.%. Impregnation followed by drying at 110°C, calcination at 500°C, reduction *in situ* in hydrogen flow at 0.1 MPa, 600°C. The catalytic tests were carried out using fixed-bed continuous-flow stainless steel reactor. The HDO of the methyl esters diluted in *n*-dodecane (0.270 mol/l) were conducted at 290-310°C, 3.0 MPa, 600-1050 H_2/feed volume ratio. Catalytic activity was evaluated as the rate of the reaction at about 20% conversion of ester. Reaction mixtures were analyzed by GC-MS and GC-FID. The catalysts were characterized by elemental analysis, N_2 physisorption, H_2-TPR, XRD, HR-TEM, XPS.

3 Results and discussion

Corresponding to H_2-TPR experiments of calcinated precursors reduction of phosphates on silica surface starts at the temperatures of 600°C. XRD analysis of reduced catalysts confirmed for all catalysts the presence of Ni_2P phase on the surface of the SiO_2. Coherent-scattering region according to XRD data was 5.5 nm before reactions and almost the same after reactions.

Corresponding to HR-TEM data the mean particles sizes of nickel phosphide on the silica surface were 2.9 nm before reactions and about 3.2 nm after reactions.

XPS revealed that even passivated phosphide particles are oxidized in air. Surface atomic ratio of $Ni^{\delta+}$ to the total Ni content and $P^{\delta-}$ to the total P content are reduced during the storage in air. Therefore, *in situ* reduction is essential to carry out correct catalytic experiments.

The main HDO products of MH were *n*-hexane and *n*-heptane, of ML – *n*-undecane and *n*-dodecane, of MP – *n*-pentadecane and *n*-hexadecane. The content of acids and alcohols did not exceed 0.005 mol/l. For all of the feedstocks selectivity toward C_nH_{2n+2} hydrocarbons (where n is 7, 12 and 16 for MH, ML and MP correspondingly, Fig. 1) did not depend on ester conversion and was about 30-40%. The main gas phase products were CO and CH_4. But absence of CO_2 do not prove absence of decarboxylation route ($DeCO_2$), because methanation and water-gas shift reactions can take place during HDO. HDO activity also depends on hydrocarbon chain length and H_2/feed ratio.

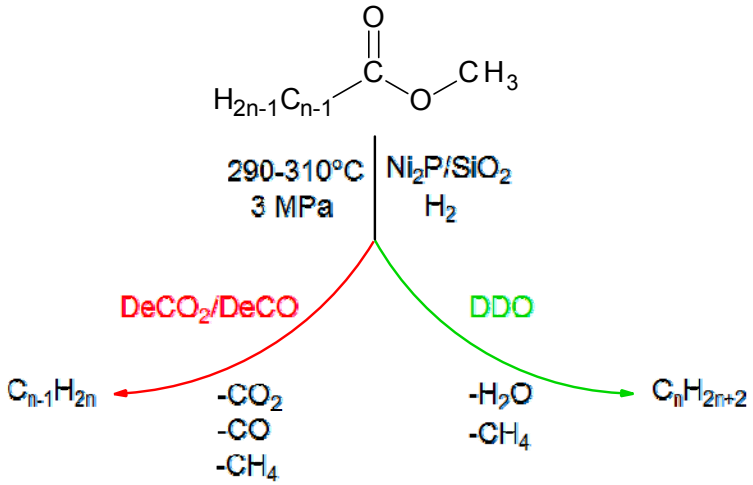

Fig. 1. HDO routes of aliphatic methyl esters: $DeCO_2$/DeCO – decarboxylation/decarbonylation, DDO – direct hydrodeoxygenation

4 Conclusions

Ni_2P/SiO_2 catalysts were synthesized by incipient wetness impregnation of SiO_2 followed by reduction *in situ* in reactor. It was found that two parallel reaction pathways occur on the Ni phosphide catalysts surface during HDO of aliphatic methyl esters: decarboxylation/decarbonylation through CO_2, CO and $C_{n-1}H_{2n}$ hydrocarbons formation and direct hydrodeoxygenation through H_2O and C_nH_{2n+2} hydrocarbons formation. Hydrocarbon chain length influence on activity but almost does not effect on selectivity.

Acknowledgements

This work was supported by the Skolkovo Foundation (Grant Agreement for Russian educational organizations no. 3 of 25.12.2014).

References

[1] I. Capellán-Pérez, M. Mediavilla, C. de Castro, Ó. Carpintero, L. Miguel, *Energy* 77 (2014) 641-666.
[2] D. Kubička, V. Tukač, *Advances in Chemical Engineering* 42 (2013) 141-194.
[3] J. Cecilia, A. Infantes-Molina, A. Rodríguez-Castellón, A. Jiménez-López, S. Oyama, *Appllied Catalysis B: Environmental* 136-137 (2013) 140-149.
[4] J. Chen, H. Shi, L. Li, K. Li, *Applied Catalysis B: Environmental* 144 (2014) 870-884.
[5] S. Oyama, T. Gott, H. Zhao, Y.-K. Lee, *Catalysis Today* 143 (2009) 94–107.

III-PP97

Hydrogen Production by Ammonia Decomposition Using Co Catalyst Supported on Mg-X(Al,Ce &La) Mixed Oxide Systems

Podila S.[1,2], Alhamed Y.A.[1,2], Alzahrani A.[1,2], Petrov L.A.[1,2*]

1 - SABIC Chair of Catalysis, Jeddah, Saudi Arabia
2 - King Abdulaziz University, Jeddah, Saudi Arabia

* lpetrov@kau.edu.sa

Keywords: hydrogen production, ammonia decomposition, mixed oxide support, cobalt catalyst

1 Introduction

Ammonia is a potential hydrogen carrier for hydrogen delivery. Because of its several desirable characteristics made it practical to store energy at much higher density against to hydrogen storage system [1]. However ammonia decomposition process for the production of CO_x free hydrogen is more attractive from an economic standpoint in comparison with other process.Much research has been devoted mainly to Group VIII metals (Ru, Ni, Ir, Fe, Co and Rh) or metal carbide/nitrides (MoNx, VCx, MoCx, VNx, etc.)[2-4]. It has been found that Ru is the most active catalyst for ammonia decomposition [4]. But high price and limited availability of Ru system is an obstacle for large scale applications. Hence developing an affordable and active catalyst for ammonia decomposition is highly desirable. Although the application of MWCNTs was found to be most active as support, there are disadvantages in the use of CNTs in this reaction, e.g. high cost, methanation, and low metal support interaction. Many literatures reported that support basicity is a necessity for efficient catalyst in ammonia decomposition reaction hence basic mixed oxides as support may enable the tailoring of a catalyst with proper strength of basicity [5]. In this respect present work, aiming the role of support composition of mixed oxide systems obtained from Mg-X (X = Al,Ce,La) hydrotalcite precursor on the activity of Co based catalyst in ammonia decomposition. To get a closer insight into the role of the support and aiming better understanding of the supported Co system on Mg-La supports with different Mg/La ratios for ammonia decomposition will also been investigated.

2 Experimental

All mixed oxide support materials were prepared by co-precipitation of Mg and X(Al,Ce,La) nitrates under super saturation conditions using a mixture of bases KOH and K_2CO_3 and calcined at 450 °C for 18 h in air. These supports were impregnated with 5wt% of Co using aqueous cobalt nitrate solution in rotary evaporator. After impregnation the catalysts were dried in oven for overnight at 100 °C and calcined the catalysts at 500 °C for 5h in nitrogen flow. These Co catalysts on MgX support (X=Al,Ce,La with Mg/X ratio 2) were denoted as 5CMAl-2, 5CMCe-2, and 5CMLa-2. Similarly Mg-La mixed oxide system with different Mg/La ratios (Mg/La = 1, 2, 3, 5, 9, 14) were prepared and impregnated with 5wt% Co which were designated as 5CMLa-1, 5CMLa-2, 5CMLa-3, 5CMLa-5, 5CMLa-9, and 5CMLa-14 respectively. Catalysts were characterized by BET, XRD, TPR, TG-DTG, CO2 TPD and CO chemisorption techniques. Catalytic activity tests were performed in a fixed bed quartz reactor under atmospheric pressure (PID system, Eng &Tech, Spain) conditions and the analysis performed by an online gas chromatograph (GC-450 Varian, USA) equipped with a thermal conductivity detector and a Poropak Q column.

3 Results and discussion

The 5wt%Co catalysts supported on MgLa, MgCe and MgAl mixed oxides(5CMLa-2, 5CMCe-2 and 5CMAl-2) were evaluated for ammonia decomposition activity at the temperature range from 300 to 550°C under atmospheric pressure. It was found that 5CMAl-2 catalyst is showing least activity compared to other catalysts though it having high surface area than others, which is due to formation of stable $COAl_2O_4$ species. Though having high surface area and high metal dispersion 5CMCe-2 catalyst is showing equal and less activity at 550°C and lower temperatures in comparison with 5CMLa-2 catalyst. These results reveal that surface area and metal dispersion are not the only parameters for ammonia decomposition activity. The high activity for 5CMLa-2 catalyst is due to high basic nature of MgLa mixed oxide which contains moderate basic sites due to Mg and strong basic sites due to La. It already reported that due to the size difference between Mg^{2+} and La^{3+} MgLa mixed oxide appears as stronger base with a smaller number of sites. To increase basic site we optimize Mg,La ratio in MgLa mixed and we found Mg/La=5:1 ratio is having more basic sites compared with other ratios. Similarly surface area, metal dispersion and metal reducibility also increased at this ratio. The XPS results also confirmed the presence of more surface cobalt species at this ratio. Consequently the 5CMLa-5 catalyst is showing highest activity among all catalysts.

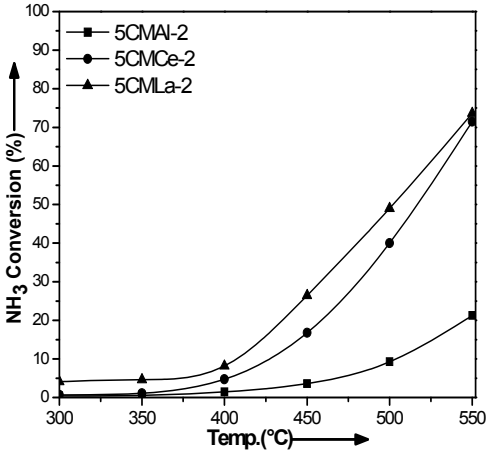

Activity study of Cobalt catalysts on MgX-2 support (Al, Ce, La) at temperature range 300-550 °C and GHSV- 6000h^{-1}

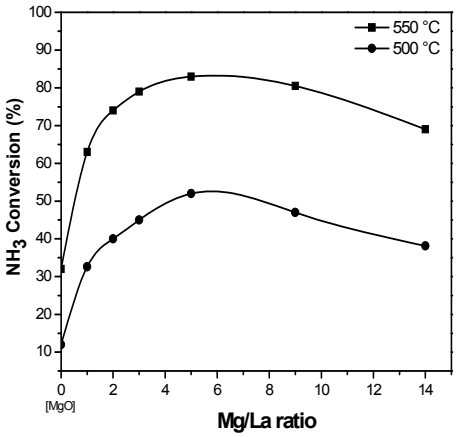

Activity study of Cobalt catalyst on Mg-La support with different Mg/La ratios at 550 & 500°C and GHSV-6000h^{-1}

4 Conclusions

Calcined Mg-La hydrotalcite precursor is the promising support for the ammonia decomposition reaction. It is highly basic, thermally stable and unveiling higher conversion values with paramount number of Co surface atoms. Co catalyst over Mg-La support is showing better activity in comparison with other supports which is due to high basic in nature. In addition cobalt catalyst on MgLa support with Mg/La=5 ratio (5CMLa-5) is found very efficient for the ammonia decomposition reaction at atmospheric pressure compared with other catalyst having different Mg,La ratios. Hence MgLa ratio 5 is seems to optimal ratio for ammonia decomposition reaction

Acknowledgements

This work was supported by SABIC Chair in Catalysis and Deanship of Scientific Research, King Abdulaziz University, Kingdom of Saudi Arabia.

References

[1] C.H.Christensen, T. Johannessen, R.Z. Sorensen, Catal. Today 111(2006)140–144.
[2] J. Zhang, H.Y. Xu, X.L. Jin, Q.J. Ge, W.Z. Li, Appl. Catal., A: General 290 (2005) 87-96.
[3] J. Zhang, H.Y. Xu, W.Z. Li, Appl. Catal., A: General 296 (2005) 257-267.
[4] S.F. Yin, B.Q. Xu, W.X. Zhu, C.F. Ng, X.P. Zhou, C.T. Au, Catal. Today, 93 (2004) 27-38.
[5] Zhang J, Xu HY, Jin XL, Ge QJ, Li WZ Appl. Catal., A: General 290 (2005) 87–96.

III-PP99

Hydrogen Production via Ethanol Steam Reforming over Supported Nikelates: from Powders to Structured Catalysts

Arapova M.[1], Pavlova S.[1*], Larina T.[1], Rogov V.[1], Krieger T.[1], Sadykov V.[1,2], Glazneva T.[1], Smorygo O.[3], Parkhomenko K.[4], Roger A.-C.[4]

1 - Boreskov Institute of Catalysis SB RAS, Novosibirsk, Russia
2 - Novosibirsk State University, Novosibirsk, Russia
3 - Institute of Powder Metallurgy, Minsk, Belarus
4 - Unversity of Strasbourg, Strasbourg, France

* pavlova@catalysis.ru

Keywords: ethanol steam reforming, nickelates, structured catalysts

1 Introduction

Oxygenates such as light alcohols derived from biomass are very perspective convenient fuel for intermediate temperature solid oxide fuel cells (IT-SOFC). Being economically sustainable, bioethanol is one of the most promising renewable fuels, its storage and transportation are easier than that of hydrogen, and internal steam reforming can be carried out directly inside the IT-SOFCs [1]. Realization of bio-ethanol steam reforming (ESR) over structured catalysts at short contact times promotes the increase of hydrogen and syngas yield. Structured supports of high thermal conductivity provide an efficient heat transfer within the reactor preventing generation of hot spots and degradation of catalysts. The main problem in ESR of all oxygenates is carbon formation and sintering of cheap Ni-containing catalysts which are the most suitable for the practical application [2]. In the previous work, catalysts based on Ln ferrites-nickelates were shown to provide a high activity, stability and selectivity in ESR. However, they have a low specific surface area (SSA) and cannot provide required performance being supported on structured substrates. The perspective approach to get over these difficulties is loading perovskites on the supports of a high SSA such as γ-Al_2O_3 with additives of alkali-earth elements to prevent formation of coke. In this study, the catalysts *m*$LnNi_{0.9}Ru_{0.1}O_3$/*n*Mg-γ-Al_2O_3 (Ln = La, Pr, *m*=10-20%wt, *n*=6-15%wt) were synthesized and tested in the ESR as granulated and structured ones.

2 Experimental

*n*Mg/Al_2O_3 supports were prepared via impregnation of aluminum hydroxide (DISPERAL) or γ-Al_2O_3 by water or organic (citric acid+ ethylene glycol) solution of $Mg(NO_3)_2$. The amount of Mg was varied from 6%wt to 15%wt. 10-20%wt of $LnNi_{0.9}Ru_{0.1}O_3$ were supported on *n*Mg/Al_2O_3 from water solution of corresponding salts followed by calcination at 500-700°C. Powdered catalysts were supported on structured substrates (platelets of corundum/Al-Si-O or metal Ni-Al foams or metallic microchannel plates) from suspension in iso-butyl alcohol, then dried and calcined at 700°C in air.

The catalysts were characterized by XRD, BET, TEM with EDX, UV-vis, XPS and TPR-H_2, FTIRS of CO test molecule. ESR was carried out in the temperature range of 500-800°C using feed 10% C_2H_5OH+40% H_2O, N_2 balance over 0.25-0.5 mm catalyst fraction or platelets with a supported active component (pre-treatment in H_2 at 500°C for 1 hour) in a plug-flow reactor at contact time 0.07s (fraction) and 0.15 s (platelets). Stability tests of structured catalysts were carried out in a pilot reactor under a realistic reaction mixture containing 30%C_2H_5OH+60%H_2O + 0÷2.5%O_2 + 7.5÷10%N_2.

3 Results and discussion

The SSA of catalysts was 50-110 m^2/g decreasing with nickelate loading. According to XRD data, the main phase in nMg/Al_2O_3 is spinel with appearance of MgO at Mg concentration of 10-15%. The increase of γ-Al_2O_3 lattice parameter evidences Mg incorporation into its structure. XPS analysis shows the enrichment of the support surface with Mg depending on the method of Mg addition. Loading of $LnNi_{0.9}Ru_{0.1}O_3$ results in further increase of the spinel lattice parameter evidencing incorporation of Ni into support with formation of $NiAl_2O_4$ being dependent on Mg concentration. This is confirmed by UV-vis data showing stabilization of Ni^{2+} mainly in tetrahedral positions of $NiAl_2O_4$ at 6%Mg while increasing Mg concentration leads to preferential stabilization of Ni^{2+}_{Oh} in NiO-MgO solid solution. The absence of perovskite reflections in XRD patterns of catalysts suggests its high dispersion that is also shown by TEM data revealing the presence of $Ln_2Ni_{1-x}Ru_xO_4$ on the catalyst surface. Thus, nickel could be distributed among different compounds as a result of its interaction with γ-Al_2O_3 and/or MgO that provides a high dispersion of Ni in the catalysts. The data of H_2-TPR and Ni2p XPS confirm the presence of different nickel states in the initial catalysts depending on Mg content. According to TEM data, reduction of initial catalysts in hydrogen or reaction media leads to formation of Ni-Ru alloy particles strongly interacting with LnO_x/MgO-Al_2O_3.

Study of the catalysts activity in ESR shows that the presence of Mg provides considerably higher values of ethanol conversion, hydrogen yield and coking stability as well. The optimal composition of the catalyst with high activity and stability has been defined. For Mg-promoted catalysts, FTIRS of adsorbed CO revealed decreased concentration of acid Lewis centers responsible for the coke formation. A low concentration of Lewis centers leads to decrease of ethylene selectivity and favours formation of intermediate hydrogen-enriched carbonaceous species which are easier oxidized that leads to effective catalyst performance.

Testing of the catalysts supported on structured foam platelets has shown that, at temperatures below 750°C, ethanol conversion and hydrogen yield are higher for the optimized active component loaded on the metallic Ni-Al foam as compared with ceramic foam. Evidently, performance of Ni-Al foam supported catalyst is better due to its high thermal conductivity that provides effective heat transfer along the catalytic bed. A long-term testing of this catalyst in ESR and oxidative ethanol steam reforming using realistic reaction mixture shows its high activity and stability in both reactions during 50 hours.

4 Conclusions

The catalysts $LnNi_{0.9}Ru_{0.1}O_3$/6-15%Mg/Al_2O_3 (Ln=La, Pr) have been characterized and studied in ethanol steam reforming as fractions and layers on structured ceramic and Ni-Al alloy substrates. The influence of Ln nature and Mg concentration on the structural and redox properties of the catalysts has been elucidated. High activity and coking stability of catalysts are provided by a high dispersion of metallic Ni and Ni-Ru alloy due to strong interaction with LnO_x/MgO-γ-Al_2O_3 support and suppressing support acidity by Mg/Ln cations. The optimal catalyst supported on Ni-Al foam substrate shows high and stable performance in a realistic reaction mixture during 50 hours.

Acknowledgements

Support by FP7 Project BIOGO, Russian Fund of Basic Research Project RFBR-CNRS 12-03-93115 and Ministry of High Education and Science of Russian Federation is gratefully acknowledged.

References

[1] H. Balat, E. Kırtay, Int. J. Hydrogen Energy, 35 (2010) 7416.
[2] M. E. Domine, E. E. Iojoiu, T. Davidian, N. Guilhaume , C. Mirodatos, Cat. Today, 133–135 (2008) 565.

III-PP100

Impact of SO_2 as Air Pollutant on Spatial PEMFC Performance

Reshetenko T.V.*, Davies K.

Hawaii Natural Energy Institute, University of Hawaii, Honolulu, USA

* tatyanar@hawaii.edu

Keywords: PEMFC, Pt cathode, airborne contaminant, sulphur dioxide, segmented cell, spatial EIS

1 Introduction

Durability, reliability and high performance of proton exchange membrane fuel cells (PEMFCs) under different environmental conditions are very important issues which must be addressed to enable the widespread adoption of these devices. Most PEMFCs use air as an oxidant which may contain pollutants such as SO_2, NO_x, CO, NH_3 and some organic compounds resulting from conventional gas and diesel powered engines and natural sources. The air contaminants are known to cause damage, significant performance loss and even cell failure in fuel cell systems where air filters cannot be employed due to weight or volume limitations. Impacts of SO_2, NO_x, CO, NH_3 on the oxygen reduction reaction and PEMFC performance were previously studied using the well-known rotating ring disk electrode technique and the convenient single cell approach [1-4]. The evaluation of fuel cell performance with a single, lumped cell does not reveal spatial behaviour. In contrast, a segmented cell system provides locally resolved voltage, current and impedance. It is a powerful tool for understanding the poisoning mechanisms and for improving the PEMFC environmental adaptability and durability. In this work, the spatial performance of a fuel cell exposed to 2 ppm SO_2 and different operating conditions was studied with a segmented cell system.

2 Experimental/methodology

A segmented cell tests were performed with commercially available 100 cm^2 membrane/electrode assemblies (MEAs) [5]. Each electrode contained a Pt/C catalyst with a loading of 0.4 $mg_{Pt}\,cm^{-2}$. A segmented 25BC gas diffusion layer (GDL, 10 segments of 7.6 cm^2) and a Teflon gasket were employed at the cathode, whereas a single GDL piece was applied at the anode. The MEA was operated under galvanostatic control of the whole cell current (0.2 and 1.0 $A\,cm^{-2}$). Other operating conditions were: 80°C, 48.3 kPa_g back pressure, 100/50% relative humidity and 2/2 stoichiometry for the anode and cathode respectively. The dry contaminant was injected into the humidified cathode air stream. The poisoning proceeded until the cell voltage reached a steady value. Subsequently, the SO_2 injection was stopped to evaluate the cell self-recovery with air. Cyclic voltammetry was applied to determine electrochemical area (ECA) and assess catalyst recovery after SO_2 impact.

3 Results and discussion

Figure 1 shows the voltage response and normalized current density for each segment vs. experiment time at an overall cell current density of 1.0 $A\,cm^{-2}$. For the first 16 h, the cell was operated with pure air resulting in a cell voltage of 0.665 V. The injection of 2 ppm SO_2 significantly decreased the voltage during a transition period that lasted ~6-7 h eventually reaching a steady state of 0.370 V. The voltage decrease was accompanied by a significant change in the current density distribution which undergoes several steps. Recovery was only partial and took ~4 h, the cell voltage reached 0.475 V instead of initial performance of 0.665 V. Chemisorption of SO_2 at intermediate potentials (0.4-0.8 V) most likely results in formation of zero-valent sulphur and leads to a decrease of the ECA, a shift of the oxygen reduction from a 4-electron to a 2-electron mechanism and an increase of H_2O_2 production, which negatively impact the PEMFC performance [3]. Moreover this sulphur species can be oxidized only at high potential (> 1.0 V) which explains the observed partial

recovery of the cell.

Figure 2 shows spatial electrochemical impedance spectroscopy (EIS) data for segments 1, 4, 7, and 10, recorded during various experiment phases. The impedance of all segments increased significantly after 1 h of SO_2 exposure. A low frequency pseudo-inductive behaviour was observed for all segments which might be associated with electrochemical transformations of adsorbed sulphur-containing species on Pt. However, further SO_2 exposure decreased the impedance of all segments. Operation with pure air after the poisoning resulted in local recovery of the cell: the inlet segments 1-6 almost restored their activity, while the outlet part did not recover. A detailed analysis of the spatial PEMFC behaviour under SO_2 exposure at low current density operation (0.2 A cm^{-2}) and recovery, possible SO_2 poisoning mechanisms and modelling results will be presented and discussed.

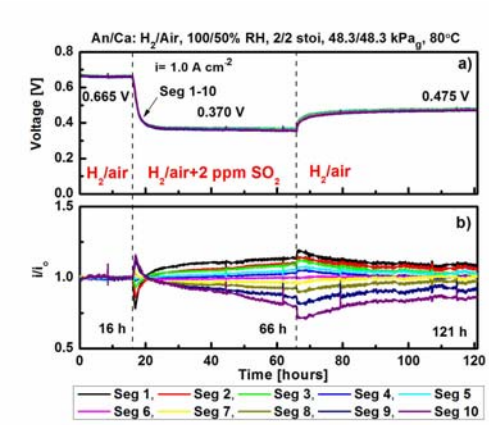

Fig. 1. Voltage (a) and normalized current density for each segment (b) vs. time.

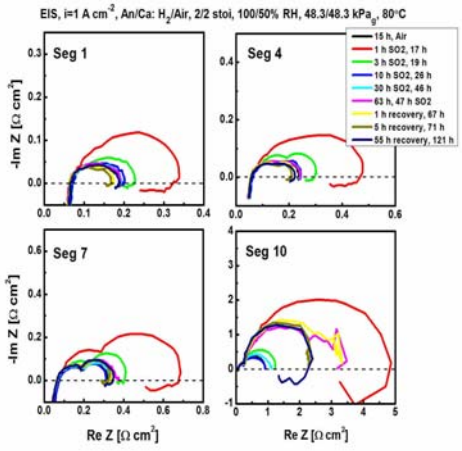

Fig. 2. EIS data for segments 1, 4, 7, 10 during the different phases of exposure to 2 ppm SO_2.

4 Conclusions

The segmented cell approach was successfully applied to study spatial PEMFC performance under SO_2 exposure as well as localized MEA properties (ECA, H_2 crossover). Moreover, the results provide the basis for a cathode poisoning model. Sulphur dioxide as an airborne pollutant was found to cause severe irreversible performance loss which is accompanied by significant current density redistribution downstream. The observed redistribution is connected with a mechanism of electrochemical SO_2 transformation and strongly depends on operating conditions. The performance can be partially recovered by reintroducing neat air and increasing potential (> 1.0 V) at which zero-valent sulphur species can be oxidized.

Acknowledgements

We gratefully acknowledge funding from Office of Naval Research (N00014-11-1-0391). Authors are also grateful to Jean St-Pierre for discussion and the Hawaiian Electric Company for their ongoing support of the Hawaii Sustainable Energy Research Facility.

References

[1] J.M. Moore, P.L. Adcock, J.B. Lakeman, G.O. Mepsted, *J. Power Sources* 85 (2000) 254.
[2] X. Cheng, Z. Shi, N. Glass, et al. *J. Power Sources* 165 (2007) 739.
[3] B.D. Gould, O.A. Baturina, K.E. Swider-Lyons, *J. Power Sources* 188 (2009) 89.
[4] Y.Zhai, G.Bender, S. Dorn, R. Rocheleau, *J. Electrochem. Soc.* 157 (2010) B20.
[5] T.V. Reshetenko, G. Bender, K. Bethune, R. Rocheleau, *Electrochim. Acta* 56 (2011) 8700.

III-PP101

Insight of 1D Γ-Al_2O_3 Nanorods Decoration by Niws Nanoslabs in Ultra-Deep Hydrodesulfurization Catalyst

Díaz De León J.N.[1*], Zepeda T.A.[1], Alonso-Nuñez G.[1], Galván D.H.[1], Pawelec B. [2], Fuentes S.[1]

1 - Universidad Nacional Autónoma de México, Centro de Nanociencias y Nanotecnología, México, Mexico

2 - Instituto de Catálisis y Petroleoquímica, CSIC, Madrid, Spain

* noejd@cnyn.unam.mx

Keywords: ultra-low sulfur diesel, alumina, nanorods, hydrodesulfurization, NiWS

1 Introduction

Nowadays, the use of diesel and gasoline fuels has increased drastically as well the quantity of pollutants emitted into the atmosphere. Thus, the production of clean fuels meeting the new environmental regulations is one of the main challenges in catalysis [1]. The conventional materials used in hydrotreating reactions consist of molybdenum sulfided promoted by cobalt or nickel, and supported over phosphated-γ-Al_2O_3 [2]. However, typical catalysts are not always able to reduce the sulfur concentrations until the required levels needed for transportation fuels, especially, in the complex petroleum fractions as Mayan-Mexican oil. In this work [3], we get insight on the use of 1D γAl_2O_3 nanorods as support for NiW ultra-deep HDS catalyst, their structure, electronic properties and morphology. Therefore, sulfided samples were tested on the 4,6´dimethyl-dibenzothiophene (4,6´DM-DBT) reaction, which is known to be more refractory to desulfurize than DBT molecule The samples also have been extensively characterized by a variety of techniques (N_2 physisorption, XRD, TPR-H_2, TPD-NH_3, FT-IR of adsorbed pyridine and HRTEM). Also, theoretical calculations have been performed by using the tight-binding method within the extended Hückel framework through the YAeHMOP computer package including f-orbitals [4].

2 Experimental/methodology

The 1D γ-Al_2O_3 nanorods linked network (Al-nR) support was prepared by soft template sol-gel method adding the triblock copolymer surfactant *pluronic* as structure directing agent. The entire synthesis procedure was reported elsewhere [2]. The obtained solids were calcined at 500°C for 4 h with a heating rate of 1°C min-1. The NiW catalyst was prepared by successive impregnation, using the pore filling method, with an aqueous solution of ammonium metatungstate (AMT) and nickel nitrate. The concentration of AMT solution was selected in order to get 20 wt. % of W (pH = 3.7) while that of nickel was adjusted to define a nominal atomic ratio r =Ni/(Ni + W) equal to 0.31 (pH = 4.4). The green final solid was calcined at 450°C for 4 h under a flow of air with a heating rate of 1°C min−1.

3 Results and discussion

Evidence of high dispersion for Ni and W species was exhibited by XRD and TPR in the oxide state for the NiW/Al-nR catalyst. This was well confirmed by HRTEM in the sulfided state; NiWS/Al-nR catalyst shown between 1-2 layers stacking and **L** values as 1.9±0.36 nm (Fig. 1A), which represents 1.7 nm lesser value than that obtained for the conventional catalyst. HRTEM and EDP rings pattern confirmed the presence of 1D γ-Al_2O_3 nanorods and a preferential plane (110), which was repeated periodically over its surface (Fig.1B). By one hand this plane is more favorable for anchoring WS_2 slabs with a tilted orientation because of the

flexibility of the hydroxyl groups, and by the other hand, the curvature of the nanorods and the excess of aluminum could allow the formation of WSAl bonds. Therefore, the NiWS type II nano-slabs in a tilted orientation was suggested as it is shown at Fig.1C. NiWS/Al-nR sample exhibited higher 4,6′DM-DBT HDS activity, same hydrogenation ability and better hydrogenolysis properties than a commercial NiWP/γ-Al_2O_3 sulfided catalyst, which probably does not lie on its weak acidity, but on the enhanced dispersed active sites. Theoretical calculations modeling the inclusion of Ni atoms on 2H-WS_2 and 1T-S-W-S (Fig.1D) cluster considering Ni in different positions were performed (Fig.1E). The computational calculations showed that Ni in the edge of the cluster exhibit a clear less metallic character than when Ni is in the corner of a 2H-WS_2 crystallite. The observed increase on the direct desulfurization pathway for 4,6′DM-DBT reaction was in agreement with these theoretical results and with a possible increase on the WS_2 nano-slabs decoration degree by Ni atoms.

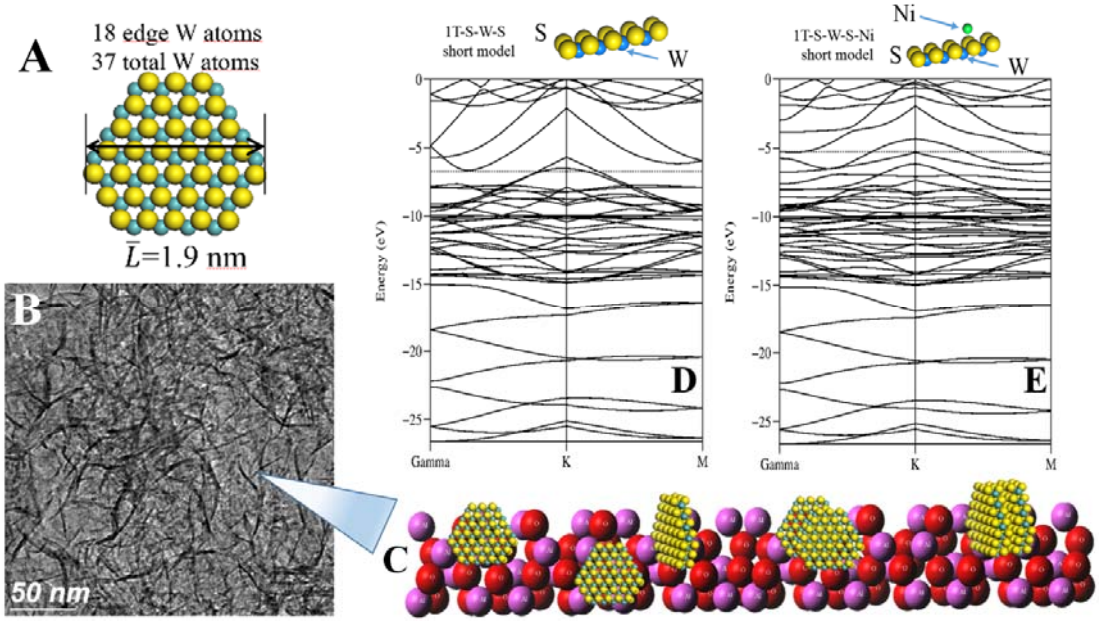

Fig. 1. Schematic representation for the WS_2 nanoslabs and its average slab length (A). Typical HRTEM micrograph of the Al-nR (B). NiWS type II nano-slabs in a tilted orientation over the Al-nR (C). The atoms are not to scale and the sizes only are illustrative. Also, Energy bands vs k points in the reciprocal space for cluster energy bands a) 1TS-W-S and b) 1T-S-W-S-Ni

4 Conclusions

The properties of the 1D γ-Al_2O_3 nanorods support play a key role on the formation, dispersion, activation and the catalytic properties of the sulfide active phase. The calculated model of slabs particles as 1T-S-W-S cluster with Ni on the top of an edge site resulted with less metallic character that when the model was a 2H-WS_2 3D crystal with Ni in a corner site, indicating that an electronic effect is occurring between the nanorods and the active sites.

Acknowledgements

The authors are grateful to E. Aparicio, F. Ruiz and I. Gradilla for their technical assistances and CONACYT project 117373 for the financial support.

References

[1] EU Fuel Regulations: http://www.dieselnet.com/standards/eu/fuel.php.
[2] T.A. Zepeda; Appl. Catal. A: Gen. 347 (2008), p. 148
[3] J.N. Díaz de León, T.A. Zepeda, G. Alonso-Nuñez, D.H. Galván, B. Pawelec, S. Fuentes; J. Catal. 321 (2015) 51–61
[4] G.A. Landrum, freely available at http://overlap.chem.cornell.edu:8080/yaehmop.html

III-PP102

Integrated Catalytic Membrane Reactor for Hydrogen Production Using Hydrocarbon-Based Fuels

Beltramini J.N.[1*], Smart S.[1], Da Costa J.D.[1], Katikaneni S.[2]

1 - NANOMAC – Chemical Engineering, Univ. of Queensland, Brisbane, Australia
2 - Research & Development Centre, Saudi Aramco Oil Company, Dhahran, Saudi Arabia

* jorgeb@uq.edu.au

Keywords: membrane reactors, hydrogen production, hydrocarbon, fuels, metal, catalysts

1 Introduction

Driven by the concern over greenhouse gas emissions, air quality and security of energy supply, hydrogen has become a contender to replace gasoline and diesel as future transportation fuel. There is an enhanced interest of discovering new ways to convert current transportation liquid fuels, such as gasoline or diesel to high content hydrogen products. Traditionally hydrogen is mostly consumed by the refining industry, 95% of which is supplied by steam reforming of natural gas[1]. Large-scale hydrogen production from natural gas by steam reforming is a well known process that uses purification methods such as pressure swing adsorption or cryogenics. However, hydrogen production at a smaller scale from fossil fuels requires further development to meet the requirements of purity, economics and versatility to fuel cell specifications. The utilization of membrane reactors for this purpose is one of the most promising options, given its advantages in energy efficiency and the ability to integrate two different processes (reaction and separation) in a single step. This paper focuses on the work currently performed for novel proof-of-concept oil to hydrogen catalytic membrane technology at the Nanomaterials Centre (NANOMAC) in partnership with Saudi Arabian Oil Company. A combination of experimental runs on autothermal reforming, water gas shift combined with hydrogen separation are conducted using functionalized silica membrane systems to purify hydrogen from a reformate stream sourced from oil based fuels. The small-scale membrane reactor will be evaluated in relation to its future economic and thermodynamic potential that could include a promising prospect of inexpensive CO_2 separation

2 Experimental/methodology

The experiments were performed using 1gram pre-reduced commercial autothermal reforming catalyst in a continuous tubular system with an interchangeable membrane tube/reactor. Two thermocouples controlled the operation temperature, one placed on the oven and the other at the centre of the catalyst bed. Air was used as source of oxygen. Two HPLC pumps fed water and hydrocarbon which were mixed and pre evaporated-evaporation before the reaction region. The total reaction pressure was maintained by using a backpressure regulator connected to a gauge. Effluent from the reactor was cooled in a double pipe condenser to liquefy the condensable vapours. The gas and liquid samples were analyzed by means of chromatography techniques. The autothermal reforming reaction was investigated at different reaction conditions as follows: T = 500 ºC, P = 3bars, WHSV = 5000 h^{-1}, O/C (molar) = 0.5, S/C (molar) = 3.

3 Results and discussion

Experimental runs were conducted on a catalytic membrane reactor (CMR) schematically shown in Figure 1. A commercial autothermal reforming catalyst in combination with a mesoporous silica membrane was operated at 500 ºC (limiting temperature of silica membrane

550 ºC) using gasoline as liquid feed.

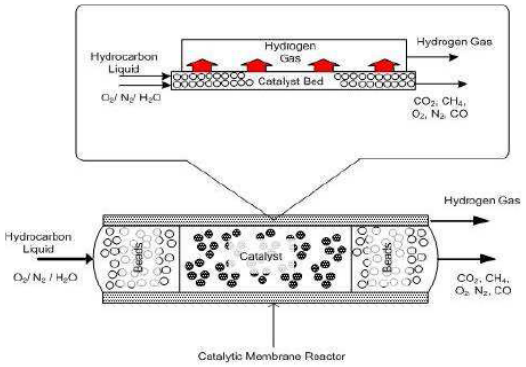

Figure 1: Schematic of the catalytic membrane reactor

As we can see in Figure 2 at the reaction temperature of 500 ºC and as the result of continuing removing hydrogen through the membrane, the hydrogen concentration not only increases with respect to fixed bed operation but also it maintain constant with time. Figure 3 compares the distribution of products gases for the CMR operation. It can be seen from Figure 3 that hydrogen is the main product of reaction (~ 75 %) with low concentration of CO, CO_2 and CH_4.

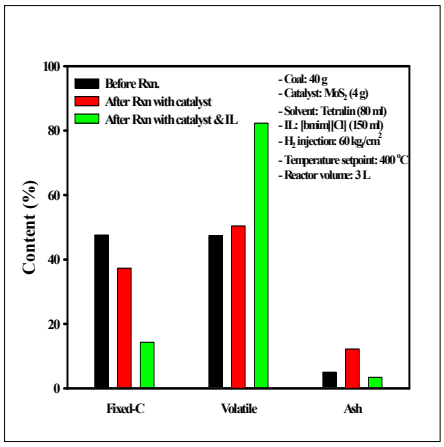

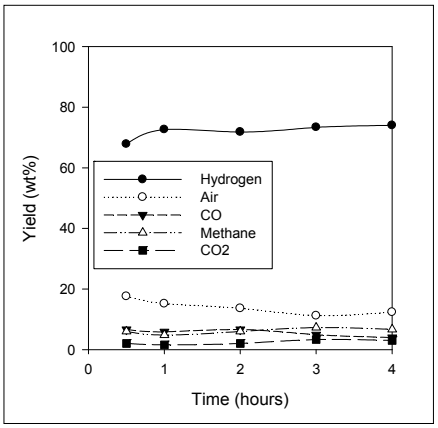

Figure 2: CMR and Fixed Bed Reactor Operation **Figure 3:** Gas Product Distribution on CMR Operation

It was found that carbon deposition is one of the problem to overcome, as if the hydrogen flux through the membrane is increased, the catalyst active sites quickly deactivate as a result of the hydrocarbon exposure. Coke formed not only deactivate the metal active sites but also block the silica membrane pores causing a sharp increase in catalyst bed pressure. If the reaction could be done at low temperature as is the case of CMR and optimum operating conditions, carbon formation could be significantly minimized.

Acknowledgment

The authors wish to acknowledge the financial support of the Saudi Aramco Oil Co. and the NANOMAC Centre

References

[1] Rostrup-Nielsen, J. R. ,*Steam Reforming of Hydrocarbons*,Danish Tech. Press, Copenhagen, (1975).

[2] Falconer, J. , Noble, R.D., Sperry, D. P. Catalytic Membrane Reactors in *Membrane SeparationsTechnology, Principles and Applications;* Noble R. D., Stern, S. A., Eds.; Elsevier Science; Amsterdam, 1995.

III-PP103

Kinetic Study of Thermoconversion of Lignocellulosic Biomass and Gasification of Charcoal in Presence of Heterogeneous Catalysts

Belyy V.A.*, Udoratina E.V.

Institute of Chemistry, Komi Science Centre, UB RAS, Syktyvkar, Russia

* skeyling@yandex.ru

Keywords: pyrolysis, gasification, biomass, catalysts, kinetics

1 Introduction

Pyrolysis is an intermediate stage of wood gasification with carbon dioxide or water vapor. The positive influence of catalysts in this process appears in decomposition of heavy pyrolysis products which represent a significant problem for the pyrolysis equipment. Therefore, in our study we have investigated the kinetics of pyrolysis and gasification of softwood in the presence of heterogeneous catalysts (Cu_2O, CuO, ZnO, NiO, MnO, Mn_2O_3, MnO_2, Fe_2O_3, Cr_2O_3, V_2O_5, La_2O_3, MoO_2, TiO_2).

2 Experimental procedure

Spruce wood was used as a substrate for the pyrolysis. The studies were carried out on TG-DSC analyzer STA 409 PC (NETZSCH, Germany), 25-1200 °C, aluminum oxide crucibles, 10 °C·min^{-1}. Finely ground spruce wood (particle size 0.1 mm) was milled with catalyst (10% by weight) and pressed into a 20 mg tablet. Pyrolysis was carried out in argon, gasification – in CO_2 and water vapor. The energy of activation was defined for assessment of catalysts influence on pyrolysis. We chose the Coats-Redfern method because there are many experimental data on wood pyrolysis, obtained by this method [1-3]. The standard deviation of the activation energy was ±1.5 kJ·mol^{-1}.

3 Results and discussion

All studied catalysts, except Cr_2O_3, increased the temperature of pyrolysis beginning (T_b), determined by TG (see the Table). The order of reaction of catalytic thermodestruction in some cases appeared above the first: second – in presence of CuO, ZnO, MnO, Mn_2O_3 and Fe_2O_3, and third with La_2O_3 and NiO. Additives of CuO, TiO_2, V_2O_5, MoO_2 and MnO_2 led to decrease E_a of pyrolysis on ~2 ÷ 5 kJ·mol^{-1}. Probably, at the initial stage of pyrolysis catalyst adsorbs products of depolymerization of lignocellulosic components on the surface. It is shown on the TG curves as a delay in beginning of mass loss and increase of the apparent reaction order. The mechanism of cleavage of liquid and gaseous products on the catalyst [4] consists in the chemisorption of a carbon atom by the catalyst (1 on Fig), which initiates cleavage of hydrocarbon molecules with release of H_2. Catalytic cleavage leads to the accumulation of carbon phase on the catalyst surface (2, 3 on Fig).

The processes of gasification are described by equations: $C + H_2O \rightarrow CO\uparrow + H_2\uparrow$ (925.9 °C) и $C + CO_2 \rightarrow 2CO\uparrow$ (849.7 °C). In the presence of the catalysts there was observed a decrease of T_b and the activation energy. The strongest changes in the kinetic parameters were observed in the course of gasification with NiO. So at the gasification of this sample with water vapor E_a value increased to 90 kJ·mol^{-1}, thus the reaction order was third. In CO_2 E_a = 145 kJ·mol^{-1}, the reaction order was second, and T_b decreased dramatically.

Table. Kinetic parameters of pyrolysis and charcoal gasification with water vapor and CO_2

Cat.	pyrolysis		water vapor gasif.		CO_2 gasif.	
	T_b, °C	E_a, kJ·mol^{-1}	T_b,°C	E_a, kJ·mol^{-1}	T_b,°C	E_a, kJ·mol^{-1}
without cat.	299.9	82.3	925.9	86.8	849.7	115.9
Cu_2O	306.7	76.9	892.7	46.4	818.7	90.7
CuO	305.3	85.0	897.1	47.3	810.3	84.6
ZnO	308.4	86.1	885.4	63.6	820.9	99.0
La_2O_3	306.2	93.5	871.4	42.1	807.4	84.9
TiO_2	308.1	78.6	910.8	53.6	822.7	95.1
V_2O_5	306.5	80.6	895.7	49.0	811.2	86.3
Cr_2O_3	296.9	82.7	915.8	55.8	831.6	118.6
MoO_2	305.3	79.1	916.3	53.2	804.2	91.6
MnO	309.4	87.3	914.8	46.7	805.9	80.6
Mn_2O_3	308.3	86.4	905.7	50.3	800.2	84.5
MnO_2	314.7	71.1	920.1	39.6	798.2	70.3
Fe_2O_3	308.4	84.7	785.7	72.6	764.4	104.5
NiO	313.2	94.0	472.5	90.1	553.2	145.3

The mechanism of gasification of carbon is the reverse mechanism of carbon precipitation on the catalyst. Both carbon dioxide and water vapor oxidize the catalyst surface atoms, thus facilitating access carbon to oxygen. Further, due to diffusion of the carbon atoms via the catalyst to its surface there is a reaction: $C + Me_mO_{n+1} \rightarrow CO\uparrow + Me_mO_n$ (4, 5 on Fig).

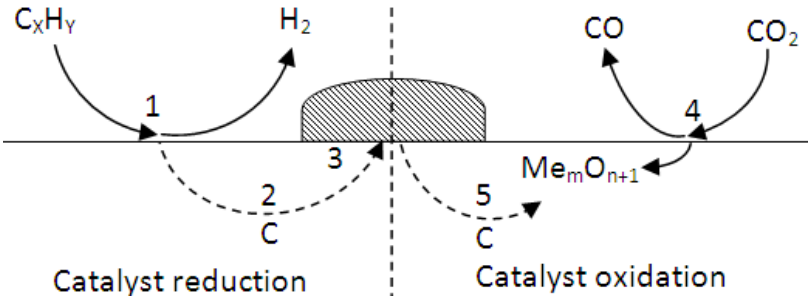

Fig. Proposed mechanism of action of oxide catalysts at pyrolysis and gasification

4 Conclusions

Summarizing experimental data, it was found out that all studied catalysts have impact on a pyrolysis stage. In this way they promote decomposition of heavy products of pyrolysis. It was defined that the catalysts reduce the temperature of beginning of gasification, both in the atmosphere of carbon dioxide, and in water vapors. On the basis of thermogravimetry data measurements and calculation of kinetic parameters it is defined that NiO has the greatest impact on the mechanism of gasification.

Acknowledgements

This work was supported by the project of the Presidium of RAS «Obtaining energy-intensive products by thermochemical conversion of renewable lignocellulosic feedstocks» (№12-P-3-1036).

References

[1] H. Yang, R. Yan, T. Chin, D.T. Liang, H. Chen, C. Zheng, *Energy and Fuels*. 18 (2004) 1814.
[2] J. Li, R. Yan, B. Xiao, D.T. Liang, D.H. Lee, *Energy and Fuels*. 22 (2008) 16.
[3] M.S. Masnadi, R. Habibi, J. Kopyscinski, J.M. Hill, X. Bi, C.J. Lim, N. Ellis, J.R. Grace, *Fuel* 117 (2014) 1204.
[4] M. Yung, W. Jablonski, K. Margini-Bair, *Energy and Fuels*. 23 (2009) 1874.

III-PP104

Kinetics of the Dehydration of 1-Butanol to Di-n-Butyl Ether: a Next Generation Biofuel

Pérez-Maciá M.A., Bringué R., Iborra M., Tejero J., Cunill F.*

Chemical Engineering Department, Faculty of Chemistry, Universitat de Barcelona, Barcelona, Spain

* fcunill@ub.edu

Keywords: biofuel, di-n-butyl ether, 1-butanol, dehydration, kinetics, ion-exchange, resin

1 Introduction

In the search of more efficient and cleaner next generation biofuels the di-n-butyl ether (DNBE) can be considered a very promising candidate [1]. DNBE has a desirable high cetane number (100); its moderate boiling temperature (142.4 ºC) reduces the volatile organic compounds emissions while permits a facile vaporization of the fuel after injection; its volumetric energy content is comparable to that of petroleum fuels (36 MJ/L) and, more important, it can be obtained from lignocellulosic biomass: 1-butanol can be produced through the ABE fermentation process [2] and subsequently DNBE could be obtained by the dehydration of 1-butanol.

In a previous work [3] we showed that di-n-butyl ether can be successfully synthesized through the bimolecular dehydration of 1-butanol over acidic ion-exchange resins. Among the tested resins, Amberlyst-70 proved to be the most suitable catalyst for industrial use due to its high selectivity to DNBE and its thermal stability, up to 473 K. In this work, a kinetic study of the dehydration of 1-butanol to DNBE over the ion exchange resin Amberlyst-70 is presented.

2 Experimental/methodology

Experiments were carried out in a 100-mL-cylindrical high pressure autoclave equipped with a stirrer and with an electrical furnace. In each experiment 70 mL of 1-butanol were charged into the reactor and, after checking for leaks, the stirring speed was set at 500 rpm and the mixture was heated up to the working temperature (413 – 463 K). When the temperature set point was reached, 1 g of sieved (particle size: 0.4-0.63mm) and dry catalyst (dried at 383 K, firstly at 0.1 MPa during 2 h and then at 1 kPa overnight) was injected into the reactor and the pressure was adjusted up to 4 MPa by means of N_2 in order to ensure liquid phase medium. The composition of the liquid mixture was analyzed in-line using a GL chromatograph equipped with a TCD detector. Samples were taken hourly during 7 hours.

3 Results and discussion

Preliminary experiment varying the mass of loaded catalyst, the stirring speed and the particle size showed that, under the selected working conditions (1g of catalyst, 500 rpm and 0.4-0.63 mm particle size), the reaction rate is not influenced by mass transfer limitations.

Three mechanistic models, with various assumptions on rate determining steps and quasi-steady state for surface species have been considered: (1) a Langmuir - Hinselwood - Hougen - Watson (LHHW) formulation; (2) an Eley-Rideal (ER) formulation in which the formed DNBE molecule remains adsorbed; (3) an ER formulation in which the formed water remains adsorbed. The elementary steps for all three mechanisms are shown in Table 1. In the three mechanisms it has been taken into account the possibility that 1 or 2 additional active sites (*) could participate in the surface reaction. Furthermore, simplified kinetic models were derived from the basic kinetic models by assuming that the amount of free active sites and/or the

adsorption of alcohol, ether and/or water are negligible. Activity coefficients calculated by the UNIFAC - DORTMUND predictive method were used to account for the non-ideal behaviour.

Table 1. Mechanistic models.

LHHW	ER-DNBE	ER-H_2O
$BuOH + * \overset{K_{BuOH}}{\longleftrightarrow} BuOH^*$	$BuOH + * \overset{K_{BuOH}}{\longleftrightarrow} BuOH^*$	$BuOH + * \overset{K_{BuOH}}{\longleftrightarrow} BuOH^*$
$2\,BuOH^* \overset{K_{sur}}{\longleftrightarrow} DNBE^* + H_2O^*$	$BuOH + BuOH^* \overset{K_{sur}}{\longleftrightarrow} DNBE^* + H_2O$	$BuOH + BuOH^* \overset{K_{sur}}{\longleftrightarrow} DNBE + H_2O^*$
$DNBE^* \overset{1/K_{DNBE}}{\longleftrightarrow} DNBE + *$	$DNBE^* \overset{1/K_{DNBE}}{\longleftrightarrow} DNBE + *$	$H_2O^* \overset{1/K_{H_2O}}{\longleftrightarrow} H_2O + *$
$H_2O^* \overset{1/K_{H_2O}}{\longleftrightarrow} H_2O + *$		

The rate expression based on water desorption as the rate limiting step in the LHHW elementary mechanism (Equation 1) has been found to be statistically the most reliable representation with physicochemical meaning of the experimental data. This equation assumes that the number of unoccupied active sites is negligible:

$$r = \frac{k\cdot\left(K_{eq}\frac{a_{BuOH}^2}{a_{DNBE}} - a_{H_2O}\right)}{\frac{K_{BuOH}}{K_{H_2O}}\cdot a_{BuOH} + \frac{K_{DNBE}}{K_{H_2O}}\cdot a_{DNBE} + \left(K_{eq}\frac{a_{BuOH}^2}{a_{DNBE}}\right)} \quad (1)$$

being Keq = exp(26.8/R+307.5/RT), in the range of 413 - 453 K.

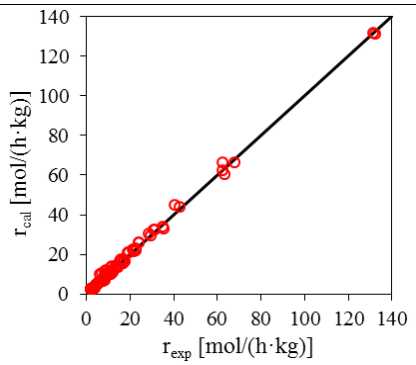

Fig. 1. Calculated with equation (1) vs. experimental reaction rates.

This model sustains the important water inhibiting effect observed. Future studies adding water in the reaction medium will be essential towards improving the kinetic model and provide more detailed information regarding the reaction mechanism.

Kinetic and adsorption equilibrium constants were grouped for mathematical fitting purposes. The optimal values of the fitted parameters are gathered in Table 2:

Table 2. Optimal values of the fitted parameters.

k [mol/(h·kg)]	K_{BuOH}/K_{H_2O}	K_{DNBE}/K_{H_2O}
$22.5 \pm 1.0\cdot\exp\left(\frac{-121421 \pm 3428}{RT}\right)$	$\exp\left(\frac{35.7 \pm 2.1}{R} - \frac{-46905 \pm 21015}{RT}\right)$	$\exp\left(\frac{49.0 \pm 2.6}{R} - \frac{6724 \pm 21414}{RT}\right)$

The dependence of the kinetic constant and the adsorption constants with the temperature follows the Arrhenius law and the Van't Hoff law, respectively. However, the high uncertainty of the adsorption enthalpy differences suggests little sensitivity to these parameters in the fit.

4 Conclusions

A classical LHHW model based on a mechanism in which de desorption of water is the rate determining step is proposed to explain the dehydration of 1-butanol to DNBE. Furthermore, both 1-butanol and DNBE participate in the adsorption term of the kinetic model. The activation energy was found to be 121±3 kJ/mol, in good line with literature data for such reaction.

References

[1] K. Melin, M. Hurme, *Cellulose Chem. Technol*. 44 (2010) 117–137.
[2] S. Nanda, A. K. Dalai, J. A. Kozinski, *Energy Science & Engineering* 2(3) (2014) 138–148
[3] M.A. Pérez, R. Bringué, M. Iborra, J. Tejero, F. Cunill, *Appl. Catal. A: General.* 482 (2014) 38.

III-PP105

Knowledge Extraction for Fischer-Tropsch Synthesis from Published Data in the Literature

Burnak B., Yildirim R.*

Bogazici University, Department of Chemical Engineering, Istanbul, Turkey

* yildirra@boun.edu.tr

Keywords: Fischer-Tropsch, CO hydrogenation, data mining, support vector machine, GTL, BTL

1 Introduction

Fischer-Tropsch Synthesis (FTS) is a clean and efficient method to produce sulfur and nitrogen-free liquid fuels and various oxygenates from syngas derived from coal, natural gas, shale gas, coal-bed gas, biogas, and biomass. FTS has been receiving renewed attraction in the literature due to depleting crude oil reserves, propagating demand in clean alternative fuels, and increasingly stringent environmental regulations [1-2].

In conventional industrial processes, the reaction temperature is maintained within 330 – 350° for high temperature Fischer-Tropsch (HTFT) conditions to increase gasoline and light olefin yield, whereas low temperature Fischer-Tropsch (LTFT) is performed within 220 – 250° range to increase wax and diesel fuel production. A typical FTS reactor operates under 25 – 45 bars [3].

Iron, nickel, cobalt, and ruthenium have been shown to enhance FTS reaction rates significantly. However, high prices and scarcity of ruthenium and high methane selectivity of nickel make them unfeasible candidates for industrial practices. Hence, most of the recent researches focus on supported iron or cobalt catalysts. Cobalt based catalysts tend to form longer hydrocarbon chains, endure longer in the reaction conditions, and show high catalytic activity, whereas iron based catalysts are preferred with low H_2:CO ratio (1:1) since it enhances WGS activity [1].

Studies demonstrate that, in addition to the type of active metal, the design of an effective catalyst requires the consideration of the support, promoter type, and applied preparation methods. Apart from the catalyst design variables, reaction conditions and feed stream composition also affects the resultant syngas conversion and product distribution [2].

Considering that FTS is invented in 1920s [3], there is a vast amount of improvement and research accumulated in the literature over decades. Abundance of the attributes related to the reaction makes the system complex and recondite. Hence, data driven models can be constructed to capture general trends and patterns by analyzing retrospective studies.

In this work, experimental data published in the literature for FTS were analyzed using support vector machine (SVM) to extract knowledge from information accumulated over years. A thorough database was constructed by using the experimental data published in the last decade. SVM was used to determine the effects and relative significances of various catalyst preparation and operating condition variables on the performance of FTS catalyst.

2 Computational Work

An extensive database containing 2404 instances for FTS catalyst performance was constructed from 223 research papers published between 2005 and 2014. The database involves 22 attributes regarding catalyst design variables such as active metal loading, support metal loading, support type, catalyst preparation method, calcination and reduction conditions (temperature, duration), as well as operating conditions such as reaction temperature, total pressure, feed composition, time on stream, gas hourly space velocity, and reactor type. All instances have three main outputs, namely CO

conversion, H_2 conversion, and selectivity to each product. The database was analyzed by constructing an SVM model in R 3.1.2 environment.

4 Results and discussion

Prior to constructing the model, the dimension of the input set was reduced by classical multidimensional scaling (MDS) to avoid the curse of dimensionality. Root mean square error (RMSE) was employed to measure the success of the models and the parameters yielding the least RMSE were chosen as the optimal set. Figure 1 shows the predictions of the model for the entire dataset. It can be observed that most of the predictions lie on the identity line with minor residuals. More detailed analyses were also performed to test the prediction power of the models for unstudied conditions, to determine the effects of individual variables, to determine the most promising experimental conditions and so on.

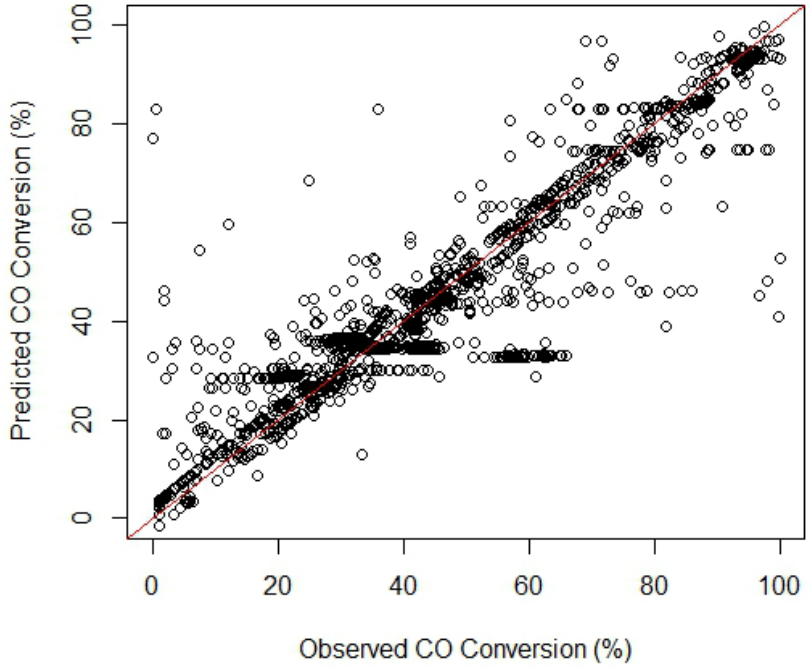

Fig.1 Predicted CO conversion vs. actual CO conversion.

4 Conclusions

A support vector machine model can be successfully implemented to model the Fischer-Tropsch synthesis data reported in the literature; the models developed can guide future experimental studies to find the optimal preparation and operation conditions.

References

[1] K. Shimura, T. Miyazawa, T. Hanaoka, S. Hirata. *Applied Catalysis A: General*, **2014**, 475, 1-9.
[2] Q. Zhang, W. Deng, Y. Wang, *Journal of Energy Chemistry*, **2013**, 22, 27-38.
[3] T. Kaneko, F. Derbyshire, E. Makino, D. Gray, M. Tamura, Ullmann's Encyclopedia of Industrial Chemistry, Electronic Release, Wiley-VCH, Weinheim.

III-PP107

Low Temperature Decomposition of Hydrogen Sulfide the Metal Catalysts under Layer of Solvent to Produce Hydrogen and Diatomic Sulfur

Startsev A.N.*, Kruglyakova O.V., Chesalov Yu.A., Paukshtis E.A., Avdeev V.I., Ruzankin S.Ph., Zhdanov A.A.

Boreskov Institute of Catalysis SB RAS, Novosibirsk, Russian Federation

* startsev@catalysis.ru

Keywords: hydrogen production, H_2S decomposition, ambient conditions, diatomic sulfur

1 Introduction

Hydrogen sulfide, H_2S, attracts attention of many researchers as an inexhaustible source of hydrogen, but numerous attempts in the development of a suitable technology for hydrogen recovery from H_2S were not crowned with success because of high cost of hydrogen produced. However, recently it was shown that the catalytic decomposition of hydrogen sulfide into hydrogen and diatomic sulfur

$$2\ H_2S \leftrightarrow 2\ H_2 + S_2^{(gas)} \qquad (1)$$

occurs on metal catalysts at ambient conditions with H_2S conversion about 15 % [1-3]. Along with hydrogen, diatomic gaseous sulfur appeared to be the reaction product. The paper demonstrates that H_2S conversion can be considerably (up to 100 %) upgraded on passing H_2S at room temperature through the metal catalyst being immersed into the solvent capable of dissolving sulfur produced [4].

2 Experimental

Experiments were carried out at room temperature in a glass absorber equipped with a magnetic stirrer. Metal catalyst, mainly a chip of stainless steel, was placed into solvent and a mixture of argon with H_2S was bubbled through the solution. At the absorber outlet, non-reacted H_2S was trapped in the aqueous zinc acetate solution for quantitative analysis. The reaction products, hydrogen and gaseous sulfur, were detected with a gas chromatograph. As a sulfur solvent, aqueous solutions of monoethanolamine (MEA), $HOC_2H_4NH_2$, and sodium carbonate, Na_2CO_3, which are widespread in industry to extract hydrogen sulfide from the exhaust gas emissions, were used. Besides, water, ethanol and aqueous hydrazine were tested as well.

3 Results and discussion

On passing H_2S through the metal catalyst at room temperature, two gaseous products are formed, hydrogen and diatomic sulfur [1-3], though H_2S conversion is relative low. When the catalyst is placed into solvent, H_2S conversion increases even in the case of water (Table). In ethanol and, especially, in aqueous hydrazine, H_2S conversion increases significantly, however gaseous sulfur formed leaves solvents on blowing-off with argon.

With MEA or soda, only hydrogen is detected in the gas phase, while sulfur is accumulated in the solvent. In 12 hours of experiment, at the steady-state level of hydrogen production (Figure) 3.6 g of sulfur was discovered in the mother solution (Table). In Infrared and Raman spectra of the solution no new bands (in comparison with the initial solvent) were found what unambiguously indicates on the dissolved diatomic gas formed in the reaction (1). An important point is that no other bands like S – S, S – H or S – O were detected with IR and Raman spectroscopy, what means high selectivity in the reaction (1) producing only hydrogen

and gaseous diatomic sulfur.

Table. H_2S decomposition on the chip of stainless steel placed into solvent. Catalyst mass is 5 g, reaction temperature is ambient. Ar flow is ~ 10 ml/min, H_2S flow is ~ 3 ml/min.

Solvent	Solvent volume, ml	Hydrogen sulfide, mmol		H_2S conversion, %	Sulfur mass in solution*, g
		fed	non-reacted		
Gas phase	-	9.23	8.81	4.6	-
Water	180	11.8	9.7	17.2	0
Ethanol	100	12.7	6.09	52.2	0.10
5% hydrazine	77	19.5	0.29	98.5	0.46
5% MEA	200	110.6	2.3	97.9	3.64
Na_2CO_3 [Na] = 0.84 %	100	53.4	10.9	79.6	1.30

* - X-ray fluorescent analysis data after non-reacted H_2S being removed with argon flow

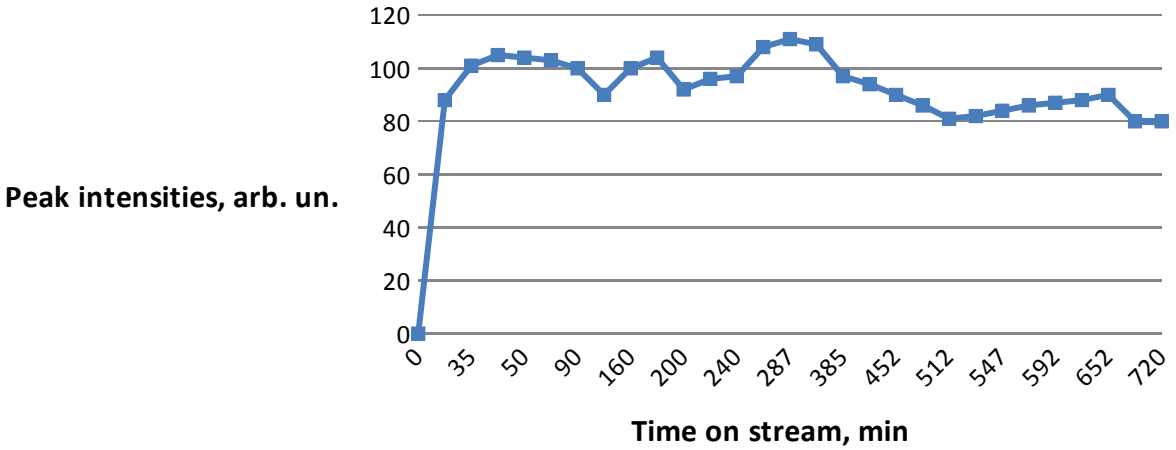

Fig. 1. Hydrogen evolution on passing H_2S through the stainless steel chip placed into 5 % MEA aqueous solution.

Main regularities of hydrogen production and sulfur recovery from the solutions are been discussed. The S_2 electronic state and the reaction (1) thermodynamics are considered. According to DFT calculations, S_2 molecule forms loosely bounded adducts with the solvent molecules. As was suggested, dissolved diatomic sulfur can be used for synthesis of new chemical substances.

4 Conclusions

Hydrogen sulfide decomposition at ambient conditions on metal catalysts under layer of solvents seems to offer new challenges and very promising opportunities to produce hydrogen from renewable inexhaustible resources, at the same time very toxic H_2S is utilized.

References

[1] A.N. Startsev, O.V. Kruglyakova, Yu.A. Chesalov, S.Ph. Ruzankin, E.A. Kravtsov, T.V. Larina, E.A. Paukshtis, *Top. Catal.* 56 (2013) 969.

[2] A.N. Startsev, O.V. Kruglyakova, *J Chem Chem Eng*. 7 (2013) 1007.

[3] A.N. Startsev, O.V. Kruglyakova, S.Ph. Ruzankin, N.N. Bulgakov, Yu.A. Chesalov, E.A. Kravtsov, V.I. Jeivot, T.V. Larina, E.A. Paukshtis, *Russ J Phys Chem*. 88 (2014) 943 (in Russian).

[4] A.N. Startsev, A.V. Pashigreva, O.V. Voroshina, I.I. Zakharov, V.N. Parmon. *Patent* Ru 2,261,838. (10.10.2005). *Patent* Uk 81,088 (26.11.2007). *Patent* Kz 57,481 (15.12.2008). *Patent* US 7,611,685 (20.12.2007).

III-PP108

Material Performance of CoO_x, CeO_2 and Co-Ce Mixed Oxide on Oxygen Storage for Solar Thermal Hydrogen Production

Calisan A., Kaya D., Uner D.*

Chemical Engineering Department, Middle East Technical University, Ankara, Turkey

* uner@metu.edu.tr

Keywords: TPR, TPO, thermal, decomposition, cobalt oxide, ceria, oxygen transport, mechanism

1 Introduction

Solar thermal hydrogen production can be briefly described as high temperature decomposition of an oxide to obtain a lower oxygen-to-metal stoichiometry. The metal can be reoxidized by steam injection, producing hydrogen. Chueh *et al.* reported that nonstoichiometric ceria can be effectively used over 500 cycles between 800 °C for water splitting and 1500 °C for thermal decomposition [1]. The main challenge is to decrease the decomposition temperatures, since it was estimated that upto 80% of the final selling price of hydrogen is coming from the contribution tracking heliostats [2]. Liu *et al.* reported that redox ability of cobalt oxide is better than ceria and this ability increases when cobalt is doped on nanometric ceria [3]. In this study, our aim is to investigate oxygen storage capacities of cobalt, cerium and their mixed oxides by testing their oxygen storage capacities over repeated cycles.

2 Experimental/methodology

Material Synthesis

CoO_x (Ege Ferro, 99%) and CeO_2 (99.9% Alfa Chem.) were used directly on pure sample experiments. The Co-Ce mixed oxide materials was prepared by the citrate based sol-gel modified pechini method. $Ce(C_2H_3O_2)\cdot 1.5H_2O$ and $CoCl_2\cdot 6H_2O$ reagents were bought from Alfa Chem (99.9%) and Matheson Coleman & Bell (99.6%). Reagents were dissolved in deionized water in separate beakers and then mixed. In a separate beaker appropriate amount of citric acid was dissolved in deionized water. Previously mixed reagents were added to citric acid solution. Solution was concentrated by evaporation at approximately 50 °C with stirring until gelation. (Ce,Co)/CA complex was put in oven at 120°C overnight. Final compound, then, calcined at 250°C (10°C/min) for 2 hours and at 600°C (10°C/min) for 4 hours. Material characterization was done by using Rigaku X-ray diffractometer (30kV, 15mA) with Cu Kα radiation (λ=1.54Å). Temperature programmed reduction (TPR), oxidation (TPO), and thermal decomposition (TPtD) experiments were done by using Micromeritics Chemisorb 2720 under the fixed flow 25ccpm. Samples were heated up to 800°C at 10 °C/min. 10% H_2-Ar, 2% O_2-He, He was used during TPR, TPO and TPtD respectively. Thermodynamic analysis were conducted by constructing Ellingham and Predominance diagrams.

3 Results and discussion

Thermodynamic analysis was performed by generating Ellingham and Predominance diagrams of the pure and mixed oxides of cobalt and ceria. The results of the analysis revealed the stability limits of the compounds and limiting temperatures. The combination of properties of cobalt and ceria is intended here: by activating the ceria sites for water splitting and the cobalt sites for decreasing the thermal decomposition temperatures.

The TPR, TPO and TPtD analysis was performed for determining the oxygen storage capacities and oxygen transfer mechanisms of cobalt, cerium and cobalt-cerium mixed oxide

structures. It was observed that oxygen capacity of the metal oxide is directly related to cobalt content in the mixed oxides. The reduction and oxidation temperatures were shifted depending on the Co/Ce ratio. As the cerium content increases the capacity of oxygen per gram material decreases as shown in Figure 1. The TPR and TPO experiments were followed by TPtD analysis. Thermal decomposition was started after 700°C for all samples except for CeO_2. The temperature range was too low to observe the thermal decomposition of this material. For $Ce_{0.75}Co_{0.25}O_x$ compound, similar oxidation peaks with reduced ceria sample were observed between 50-100 ℃. Repeated TPO, TPtD and TPO analyses revealed consistent oxygen release and storage capacities at similar temperatures each time. Data analysis by Kissinger method and redhead analysis are in progress to reveal the process orders and activation energies. The results of the thermal decomposition and regeneration is being modelled in terms of an appropriate gas solid reaction mechanism to be used for design and scale up purposes.

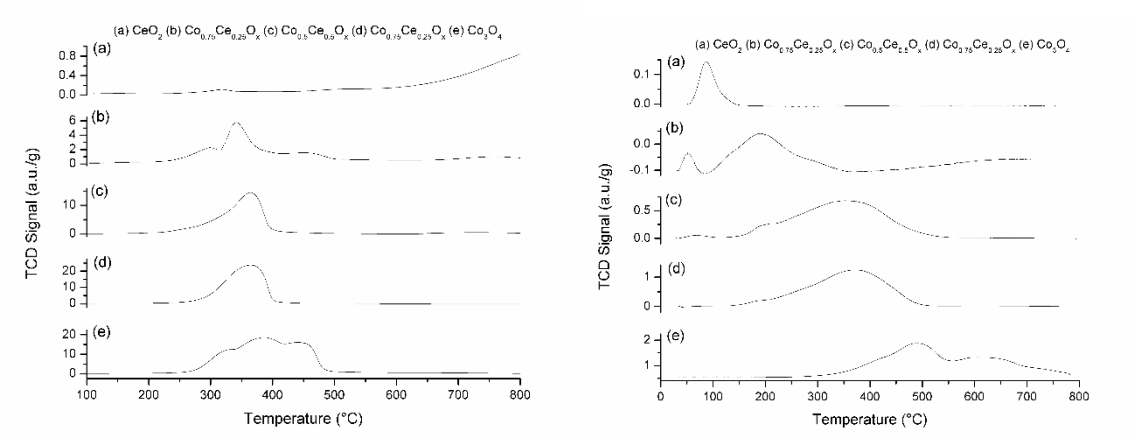

Figure 1. TPR (left) and TPO (right) profiles of the candidate materials on per gram fresh sample basis

4 Conclusions

In this study, the synergy between the unique properties of two metals with different oxide stability was investigated. Cobalt and cerium materials were selected according to thermodynamic analysis. Different molar ratio compounds were synthesized. Reduction, oxidation, and thermal decomposition experiments revealed that while ceria could not be activated by thermal decomposition up to 800 °C, cobalt content increased the oxygen storage and release capacity of the material. For $Ce_{0.75}Co_{0.25}O_x$ stoichiometry, low temperature activation by thermal decomposition was possible. The reduced from of this compound could be oxidized at temperatures between 50-100 ℃.

Acknowledgements

This project was supported by grants from Ministry of Development grants through METU YESAP program. Micromeritics chemisorption was acquired by the financial support from TUBITAK (grant no 213M006) under the project leadership of Dr. Serkan Kincal is gratefully acknowledged.

References

[1] WC. Chueh, C. Falter, M. Abbott, D. Scipio, P. Furler, SM. Haile, A. Steinfeld. *Science*. 330 (2010) 1797.
[2] C. Perkins, AW. Weimer. *AIChE*. 55 (2009) 286.
[3] J. Liu, Z. Zhao, J. Wang, C. Xu, A. Duan, G. Jiang, Q. Yang. *Applied Catalysis B: Environmental*. 84 (2008) 185

III-PP110

New Carbon Supports for Pt/C Oxygen Electroreduction Reaction Catalysts

Golovin V.A.[1,2,3*], Gribov E.N.[1,2], Maltseva N.V.[1,2], Simonov P.A.[1,2], Okunev A.G.[1,2]

1 - Boreskov Institute of Catalysis, Novosibirsk, Russia
2 - Novosibirsk State University, Novosibirsk, Russia
3 - Research and Educational Center for Energy Efficient Catalysis, Novosibirsk State University, Novosibirsk, Russia

* golovin@catalysis.ru

Keywords: carbon support, carbon corrosion

1 Introduction

Recent decades have marked by increased interest in alternative energy, in particular, in the proton exchange membrane fuel cells (PEMCF). PEMFC have several advantages, such as low temperature operation, high environmental friendliness, etc. However, these fuel cells have a significant drawback - the gradual oxidation of the carbon support during the cathodic oxygen electroreduction reaction [1], which reduces greatly the service life. Therefore, the study of corrosion resistance of carbon supports is an important task for the fuel cells commercialization. The special accelerated testing protocols - so-called "Start-stop" tests have been developed before [1] to study the carbon support corrosion in the three-electrode electrochemical cell.

2 Experimental/methodology

Commercial KetjenBlack DJ-600 sample was modified with pyrocarbon in a vertical furnace by passing ethylene in argon mixture at variable ethylene concentration (5-15 vol. %) and temperatures (650-780°C).

Modification with nitrogen was performed in the same furnace at different temperature (780-890°C) using saturated vapor of acetonitrile in argon.

Electrochemical measurements were performed in a standard three electrode cell with a hydrogen electrode as a reference electrode and a platinum foil as the counter electrode. During oxidation test the carbon support was subjected by the 1.0 - 1.5 V triangular potential with a scan rate of 0.50 V/s. The rate of potential quinone-hydroquinone (Q-HQ) peak (at ~ 0.6 V RHE [2]) change in the cyclic voltammogram (CVA) was chosen as stability criterion.

3 Conclusions

Figure 1 shows the dependence of the peak potentials in the Q-HQ region upon the cycle number for the KetjenBlack DJ-600 samples, modified with nitrogen (right) and pyrocarbon (left) and compared to the unmodified support.

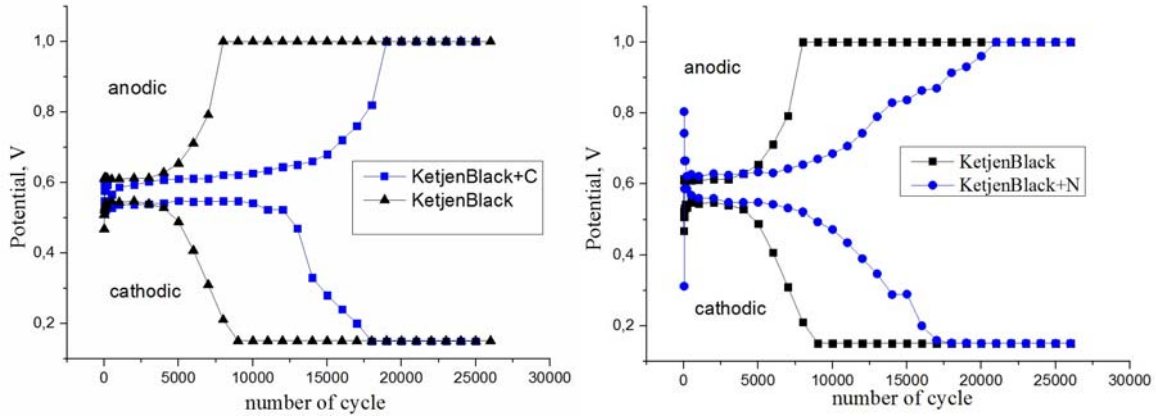

Fig. 1. The potentials of the Q-HQ peak for samples doped with nitrogen (890°C, right) and pyrocarbon (780°C, left).

Upon the cycling the shifts of the anodic and cathodic peak potentials of such groups to the higher and lower voltage values, respectively, are observed. Such a shifts can characterized the corrosion resistance of the samples: the higher the number of cycles when the shift is observed the higher is the stability of the samples. The results show that the modification of carbon black surface by both pyrocarbon and nitrogen increases the corrosion resistance of the support as it is seen from the higher number of cycles needed for the change of the Q-HQ peak potential. This behavior was explained by a partial curing of defects on the carbon black surface during the modification, leading to increasing the resistance of the support [3].

Acknowledgements

Authors thank Dr. Atsushi OHMA, Dr. Masashi ITO, Nissan Research Center, Nissan Motor Co., LTD, 1, Natsushima-cho, Yokosuka-shi, Kanagawa 237-8523, Japan. Work was supported by the RFBR grant № 13-03-01023. The work was also performed in the framework of the joint Research and Educational Center for Energy Efficient Catalysis (Novosibirsk State University, Boreskov Institute of Catalysis).

References

[1] A.P. Young, J. Stamper, E. Gyenge. *Journal of Electrochemical Society*. 156 (2009) 913 – 922
[2] Y. Shao G. Yin, J. Zhang, Y. Gao. *Electrochimica Acta.* 51 (2006) 5853–5857
[3] X. Zhao, A. Hayashi, Z. Noda, K. Kimijima, I. Yagi, K. Sasaki. *Electrochimica Acta.* 97 (2013) 33–41

III-PP111

Ni/Al_2O_3 Catalysts for Heavy Molecules Steam Reforming: Effect of Modifiers on Catalysts Structure and Activity

Garbarino G.[1*], Chitsazan S.[1], Riani P.[2], Finocchio E.[1], Busca G.[1]

1 - University of Genova, DICCA Dipartimento di Ingegneria Civile Chimica e Ambientale, Genova, Italy

2 - University of Genova, DCCI Dipartimento di Chimica e Chimica Industriale, Genova, Italy

* gabriella.garbarino@unige.it

Keywords: tar abatement, naphthalene, phenol, nickel on alumina

1 Introduction

Biomass conversion, i.e. gasification, is a highly desirable route to produce bio-hydrogen. However, at present several concerns regarding syngas quality and tars content are still to be solved. Tars are mixtures of heavy molecules that condense in cold plant points thus causing clogging and fouling of heat exchangers and pipelines. In principle, steam reforming of tars allows to purify syngas and to increase the overall efficiency since it works at temperatures compatible to those of the gasifier. The aim of our study was to characterize activity of Ni-based catalysts and to study the effect modifiers on structure and catalytic performances. Taking into account that real biomass-derived syngases contain together with heavy molecules, also lighter ones that can react each other, we used for catalytic experiments model mixtures containing phenol and/or naphthalene and alcohols such as ethanol or methanol, developing one liquid phase mixture that would be easily fed through a HPLC pump, thus reducing the line complexity.

2 Experimental/methodology

Different families of catalysts have been prepared by conventional wet impregnation and incipient wetness impregnation of Puralox 200 Sba (pure γ-Al_2O_3, 200 m^2/g) and Siralox 5/170 supports (γ-Al_2O_3 with 5% SiO_2, 170 m^2/g), both from Sasol, with Ni hexahydrate nitrate water solution, in order to obtain different nickel loadings (5%, 16%, 39% $w_{Ni}/w_{support}$). The addition of Mg, B and La was also investigated.

A complete characterization of catalysts before and after reaction with XRD, IR, UV-vis, H_2-TPR, FE-SEM was carried out to understand better the effect of modifier addition to catalyst formulation.

Catalytic activity experiments were carried out using model mixtures fed to tubular fixed bed reactor. Ethanol/phenol steam reforming experiments was carried out with the conditions described in [1]. The same catalysts were tested for steam reforming of methanol/phenol and methanol/naphthalene. In this case 88 mg catalyst were diluted in 440 mg of silica glass. For methanol/phenol mixture was used the following gas phase composition (%v/v) 0.5% phenol, 9.6% methanol, 16.5% water, 73.4% He (as carrier gas). In the case of methanol naphthalene mixture the gas composition used was 79.2% He, 10.9% H_2O, 9.9% CH_3OH and 145 ppm of $C_{10}H_8$. The reaction temperature was varied from 773 K to 1073 K waiting for each point the steady state. Products analysis in all cases was performed in the same way as described in [1].

3 Results and discussion

The addition of silica to alumina (Siralox vs Puralox) gives rise to morphologically more stable materials, retaining higher surfaces area after calcination (e.g. 142 m^2/g vs. 107 m^2/g after calcination at 1073K). The addition of Nickel to Siralox with consequent calcination at 973 K

gives rise to at least three main surface species, i.e. highly dispersed Ni^{2+} species, and, at higher coverages, two different types of NiO particles, surface and bulk-like [2]. If calcination is performed at higher temperature (1073 K) a structure similar to $NiAl_2O_4$ will be also observed. By the use of Puralox as bare support, $NiAl_2O_4$ is observed at lower coverages and lower calcination temperatures than for Siralox, showing that, in some way, the addition of silica hinders the penetration of Ni into the alumina bulk.

The addition of Lanthanum [3] (20% La_2O_3 $w/w_{alumina}$) to the formulation of 20%NiO/Al_2O_3 (Al_2O_3 Puralox calc. at 1023 K) does not prevent a huge interaction between Ni and alumina with $NiAl_2O_4$ formation, even if Lanthanum disperses on alumina in a disordered state.

Experiments of steam reforming of phenol/ethanol mixtures show that the silica-free alumina support does not produce a better catalyst than the silica-containing support, while the addition of lantana promotes the catalyst activity, although not strongly. All catalysts we studied here were deactivated by sulfur, we must invoke the poisoning of the metallic nickel sites as the main reason.

In order to have a better understanding of investigated catalysts activity in tar abatement, new mixture involving polyaromatic compounds were developed and studied. Preliminary data on methanol/naphthalene conversion shows that the highest Nickel loading (Ni39/Puralox calcined at 1073 K) catalyst is able to convert totally naphthalene at 873 K, while Ni16 achieve a maximum naphthalene conversion of 73 % only at the highest temperature (1073 K) where also methanol is completely converted. In the case of phenol/methanol Ni16 (Ni16/Puralox calcined at 1073 K) catalyst achieves the complete conversion of both reactant only at 1073 K while Ni39 converts completely the reactant at 1023 K giving a hydrogen yield of 79%.

4 Conclusions

Effect of modifiers was successfully investigated on a series of Ni/Al_2O_3 catalysts. Lanthanum addition to alumina in catalyst formulation increases catalytic activity and at the same time reduces coke deposition even if was not preventing the strong interaction of Ni on alumina. The presence of silica in catalyst formulation allows to retain a higher surface area also at high calcination temperature even if less reducible Ni species, i.e. $NiAl_2O_4$ are produced.

The two proposed model mixtures are effective to model syngas coming from biomass gasification, simplifying testing operation. Ni39/Puralox (calc. 1073 K) is effective to convert naphthalene and phenol in the tested conditions.

Acknowledgements

EF acknowledges PRA- Progetto Ricerca Ateneo 2014 – University of Genova

References

[1] G. Garbarino, A. Lagazzo, P. Riani, G. Busca, *Appl. Catal. B: Environ.*, 129 (2013) 460
[2] G. Garbarino, I. Valsamakis, P. Riani, G. Busca, *Catal. Commun.*, 51 (2014) 37
[3] G. Garbarino, C. Wang, I. Valsamakis, S. Chitsazan, P. Riani, E. Finocchio, M. Flytzani-Stephanopoulos, G. Busca, *Appl. Catal B: Environ., submitted*

III-PP112

Nickel Carbonyl Formation under Low Temperature Methanation Conditions. The Importance of Intraparticle Heat and Mass Transfer Effects

Gonzalez N., Boutonnet M., Järås S., Barrientos J.*

KTH - Royal Institute of Technology, Stockholm, Sweden

* javbar@kth.se

Keywords: nickel, carbonyl, methanation, deactivation, mass transfer

1 Introduction

Substitute natural gas (SNG) can be produced from coal, biomass or other carbonaceous sources via gasification of these materials and subsequent catalytic conversion of synthesis gas into methane (methanation) [1]. Nickel-based catalysts perform satisfactorily in regards to activity and selectivity to methane. Nevertheless, these are threatened to severe deactivation phenomena. For instance, at high CO partial pressures and low temperatures there is a high potential for nickel carbonyl formation [2].

In a previous work from Shen and Dumesic [2], a criteria based on the equilibrium partial pressure of $Ni(CO)_4$ was stablished for stable Ni particle size. For instance, nickel catalyst particles were found to sinter at temperatures slightly above 300° C and CO partial pressures as low as 85 kPa. Contrariwise, Rostrup-Nielsen et al. [3] claimed that carbonyl formation is, in practice, not a problem at temperatures above 300 °C. According to Zielinski [4], the formation of nickel aluminates can reduce the potential of carbonyl formation. Nevertheless, nickel particle sintering at similar low temperature conditions is still observed when using alumina-supported catalysts [5, 6].

More recently, Nguyen et al. [1] suggested that the use of big catalyst pellets leads to both a CO and a temperature gradient in both the gas-solid interphase and inside the catalyst pellet. Therefore, the catalyst surface may be exposed to a sufficiently high temperature and low CO partial pressure that nickel carbonyl formation is suppressed.

The objective of the present work is to elucidate the effect of catalyst pellet size on nickel carbonyl formation.

2 Experimental/methodology

The catalyst carrier used in this work was a γ-Al_2O_3 cylindrical pellet (3mm diameter and 3mm length) from Saint Gobain NorPro. A catalyst batch consisting of 30 wt% Ni was prepared by wetness impregnation of the aforementioned support. After impregnation the catalyst was calcined at 450 °C (ramp: 2.5 °C/min) for 3 h, crushed and divided into different size fractions.

The catalyst samples were reduced *in situ* in H_2 flow for 4 h at 500 °C. The different catalysts were then tested at 310 °C, 20 bar and an inlet H_2/CO ratio of 3. The spent samples were analysed by X-ray diffraction in order to estimate the average nickel particle size and therefore, evaluate nickel particle sintering.

Internal shell heat and mass transfer balances were performed for the different tested samples in order to calculate intraparticle CO concentration and temperature profiles. These calculations were performed by using COMSOL Multiphysics 5.0.

3 Results and discussion

Preliminary results point to a clear decrease in nickel carbonyl-induced particle sintering

with increasing catalyst pellet size. The observed results were supported by the models developed with COMSOL Multiphysics. Figure 1 presents a modelled spherical particle of 75 µm diameter and another cylindrical particle with the previously mentioned dimensions. As can be observed most of the large cylindrical catalyst particle is exposed to a higher temperature and lower CO partial pressure than that of the bulk gas phase, fact that reduces the potential for nickel carbonyl formation.

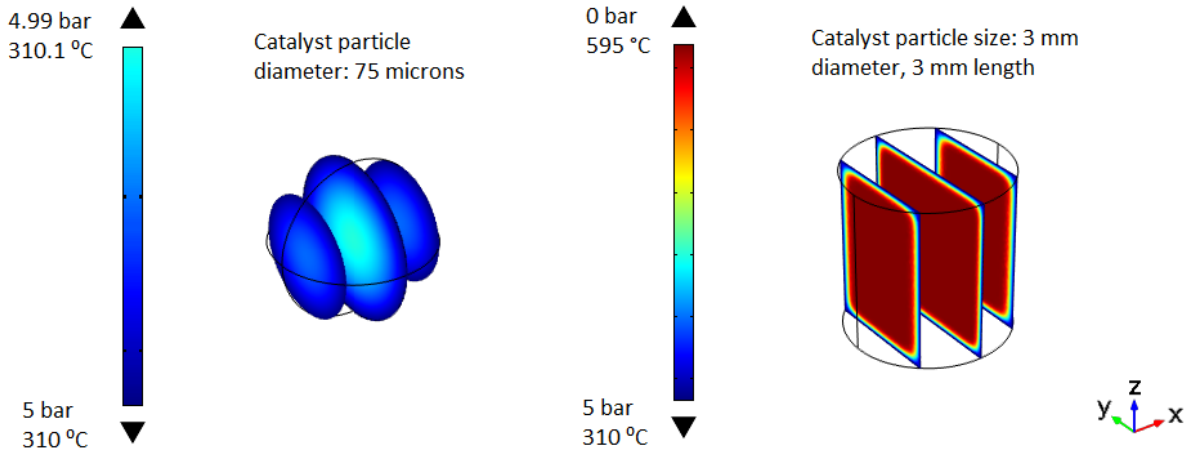

Fig. 1. Slice profiles of the internal CO partial pressure and temperature for a spherical catalyst particle of 75 µm (left) and a cylindrical particle of 3x3 mm (right). Boundary conditions: H_2/CO=3, 20 bar, 310 °C. The profiles were computed with COMSOL Multiphysics 5.0 software.

5 Conclusions

Further results of this work will be presented and the importance of the catalyst pellet size in different applications will be discussed.

Acknowledgements

The research leading to these results has received funding from the European Union Seventh Framework Programme (FP7/2013) under grant agreement n° 308733.

References

[1] T.T.M. Nguyen, L. Wissing, and M.S. Skjøth-Rasmussen *Catalysis Today* **215** (2013)
[2] W.M. Shen, J.A. Dumesic, and C.G. Hill Jr *Journal of Catalysis* **68** (1981)
[3] J.R. Rostrup-Nielsen, K. Pedersen, and J. Sehested *Applied Catalysis A: General* **330** (2007)
[4] J. Zieliński *Journal of Molecular Catalysis* **83** (1993)
[5] J. Barrientos, et al. *Applied Catalysis A: General*
[6] C. Mirodatos, H. Praliaud, and M. Primet *Journal of Catalysis* **107** (1987)

III-PP115

Praseodymium Nickelate-Cobaltite Based Functionally Graded Cathodes for Intermediate Temperature Solid Oxide Fuel Cells

Sadykov V.A.[1,2*], Eremeev N.F.[1], Fedorova Yu.E.[1,3], Amanbayeva D.G.[1,4], Lukashevich A.I.[1], Krieger T.A.[1], Muzykantov V.S.[1], Pelipenko V.V.[1], Sadovskaya E.M.[1], Bobin A.S.[1], Ishchenko A.V.[1,2]

1 - Boreskov Institute of Catalysis SB RAS, Novosibirsk, Russia
2 - Novosibirsk State University, Novosibirsk, Russia
3 - Novosibirsk State Pedagogical University, Novosibirsk, Russia
4 - Novosibirsk State Technical University, Novosibirsk, Russia

* sadykov@catalysis.ru

Keywords: perovskites, composites, oxygen, mobility, isotope, exchange

1 Introduction

State-of-the-art SOFC cathode materials based upon Sr-doped perovskites (LSFN, LSFC, LSM etc.) deteriorate in intermediate (IT) temperature range due to segregation of alkaline-earth oxides in surface, carbonization blocking surface sites and interaction at the cathode – electrolyte interface resulting in La and Sr zirconates formation blocking oxygen transport. Developing Sr-free materials with Pr completely substituting La aids in eliminating such negative effects. Perovskites like $PrNi_{1-x}Co_xO_{3-\delta}$ and their composites with doped ceria provided high overall electric conductivity, improved and stable performance as SOFC cathodes in IT range [1]. However, the oxygen mobility and reactivity in these materials controlling their performance are still not properly characterized, which is the aim of this research.

2 Experimental/methodology

Nanocrystalline oxides $PrNi_{1-x}Co_xO_{3-\delta}$ (PNC; $x = 0 \div 0.6$), $Ce_{0.9}Y_{0.1}O_{2-\delta}$ (YDC), $Pr_{0.8}Ni_{0.5}Co_{0.5}O_{3-\delta}$ and $Ce_{0.65}Pr_{0.25}Y_{0.1}O_{2-\delta}$ were synthesized by modified polymerized complex precursor (Pechini) technique. Nanocomposites PNC – YDC were prepared by using ultrasonic dispersion in isopropanol with addition of surfactants. All samples were characterized by XRD and TEM with EDX analysis. Temperature programmed desorption of oxygen (TPD O_2) was carried out at heating rate 5 °C/min and He flow rate 2.5 $l \cdot h^{-1}$. The oxygen mobility and surface reactivity were studied by the oxygen isotope exchange with $^{18}O_2$ and $C^{18}O_2$ in isothermal (IIE) and temperature programmed (TPIE) modes in static and flow (SSITKA) reactors.

3 Results and discussion

For the $PrNi_{1-x}Co_xO_{3-\delta}$ samples calcined under air at temperatures up to 1100 °C the crystal structure corresponds to orthorhombic perovskite phase with some admixture of Pr_6O_{11} phase. For $PrNi_{1-x}Co_xO_{3-\delta}$ – YDC (1:1) composites sintered under air at temperatures up to 1100 °C the structure of perovskite phase is preserved, though pronounced redistribution of cations between domains (up to $Pr_{0.8}Ni_{0.5}Co_{0.5}O_{3-\delta}$ and $Ce_{0.65}Pr_{0.25}Y_{0.1}O_{2-\delta}$ compositions) takes place.

Perovskites calcined at 1000 °C demonstrate intense oxygen desorption situated in the intermediate temperature range. Total amount of oxygen desorbed in TPD run is ~ 20 monolayers, thus demonstrating fast oxygen migration from the bulk to the surface. In $PrNi_{0.5}Co_{0.5}O_{3-\delta}$ – YDC composites much more intense desorption in the intermediate-temperature range is observed greatly exceeding that in LSFN(C) - GDC and LSM - GDC nanocomposites [2]. This suggests fast diffusion of large fraction of bulk oxygen along the PNC-YDC domains interface. In SSITKA $C^{18}O_2$ experiments all oxygen in samples was

completely exchanged for ^{18}O at the end of the run. Two types of bulk oxygen with tracer diffusion coefficients D_O differing by ~2 orders of magnitude were revealed by detailed modeling of SSITKA data. For perovskites sintered at 1000 °C $D_{fast} \sim 10^{-7}$ cm^2·s^{-1} (~ 10-15 % of all oxygen) and $D_{slow} \sim 10^{-9}$ cm^2·s^{-1} (~ 85-90 % of oxygen) at 700 °C. D_{fast} is comparable with that for LSFC and LSFN and by 4-5 orders of magnitude higher than that for LSM [2]. For composites sintered at 1000 °C $D_{fast} \sim 10^{-6}$ cm^2·s^{-1} (~ 70 % of oxygen) and $D_{slow} \sim 10^{-8}$ cm^2·s^{-1} (~ 30 % of oxygen) at 700 °C. These values of D_{fast} in composites are by 2-3 orders of magnitude higher than that for well-known LSCF-GDC composite [2]. Apparently $Ce_{0.65}Pr_{0.25}Y_{0.1}O_{2-\delta}$ domains in composite (Figure 1) are mainly responsible for their high oxygen mobility in agreement with earlier data for $Ce_{0.45}Pr_{0.55}O_{2-\delta}$ [3].

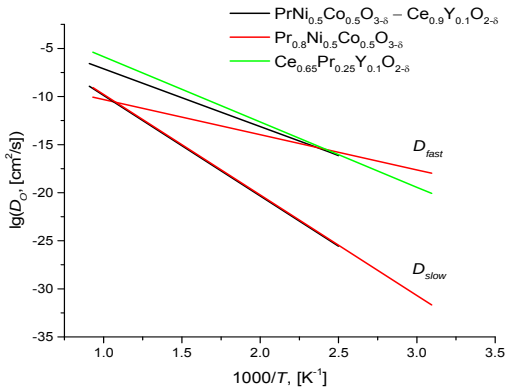

Fig. 1. Temperature dependence of oxygen tracer diffusion coefficients for to $PrNi_{0.5}Co_{0.5}O_{3-\delta}$ – $Ce_{0.9}Y_{0.1}O_{2-\delta}$, $Pr_{0.8}Ni_{0.5}Co_{0.5}O_{3-\delta}$ and $Ce_{0.65}Pr_{0.25}Y_{0.1}O_{2-\delta}$ sintered at 1100 °C

Such a high oxygen mobility in PNC-YDC composite cathodes allowed to obtain power density for anode-supported thin form solid oxide fuel cells up to 420 mW/cm^{2}at 700 ^{o}C [4] which exceeds that for traditional cathode materials.

4 Conclusions

Composites based on $PrNi_{1-x}Co_xO_{3-\delta}$ and doped ceria demonstrate very high lattice oxygen mobility and surface reactivity due to disordering caused by cations redistribution between phases. This allows them to provide promising performance as cathode materials for intermediate temperature SOFC along with a high stability to carbonization due to absence of alkaline-earth dopants.

Acknowledgements

Support by the Ministry of Education and Science of Russian Federation, German-Russian Project N_CATH, Project 2.4.50 of Presidium RAS and Zamaraev Foundation is gratefully acknowledged.

References

[1] Sh. Huang, Q. Lu, Sh. Feng, G. Li, Ch. Wang, *J. Power Sources* 199 (2012) 150.
[2] V.A. Sadykov, S.N. Pavlova, T.S. Kharlamova, et al in *Perovskites: Structure, Properties and Uses* (Eds. M. Borowski), Nova Science Publishers, New York, 2010, pp. 67–178.
[3] M.Y. Sinev, G.W. Graham, L.P. Haack, M. Shelef, *Journal of Materials Research* 11 (1996) 1960–1971.
[4] V.A. Sadykov, N.F. Eremeev, E.M. Sadovskaya, A.S. Bobin, Yu.E. Fedorova, V.S. Muzykantov, et al., *Russian J. Electrochem.* 50 (2014) 669–679.

III-PP116

Production of Hydrogen Enriched Gas by Biogas Reforming over the Multicomponent Co-containing Catalysts

Itkulova S.S.*, Nurmakanov Y.Y., Abdullin A.M., Ospanova A.Z., Imankulova S.A.

D.V. Sokolsky Institute of Organic Catalysis and Electrochemistry, Almaty, Kazakhstan

* sholpan.itkulova@gmail.com

Keywords: biogas, multicomponent catalysts, hydrogen, dry and steam reforming

1 Introduction

Nowadays, enormous attention is focused on the development of technologies involving renewable sources due to inevitable depletion of fossil fuels. Moreover, fossil fuels are the major producers of greenhouse gases, mostly carbon dioxide. Biogas is considered as a clean and environmental friendly fuel that is produced from anaerobic digestion of biomass, manure etc. Biogas contains mainly of CH_4 and CO_2 and may be associated with traces of other gases such as hydrogen sulphide, ammonia, hydrogen, carbon oxide, nitrogen, oxygen, and water vapor. Content of admixtures depends on a source from which biogas is originated. The technologies for biogas reforming reaction are the same that are used for the natural gas reforming: Steam Reforming (SRM), Dry Reforming (DRM) (eq. 1), Partial Oxidation (POX), Autothermal Reforming of methane or their combination. Reforming of biogas is an attractive way of utilization both greenhouse gases by using DRM or DRM-SRM combination. Also, its exploitation would be advantageous from financial point of view [1, 2]. By DRM syngas with a H_2/CO ratio close to unity is produced, which is useful for Fisher-Tropsch synthesis of long-chain hydrocarbons and oxygenates [3-4]. Adding steam to biogas will provide the production of the additional hydrogen.

$$CH_4 + CO_2 \leftrightarrow 2H_2 + 2CO \qquad \text{(eq. 1)}$$

However, there is still no large-scale application of CO_2 reforming of CH_4 because of absence of efficient and stable to coke deposition catalysts. Carbon dioxide reforming of biogas is endothermic reaction and it requires a high reaction temperature. The major drawback of this process, which occurs at temperatures above 640°C, is the catalyst deactivation [4]. This paper deals with the development of the new Co-containing catalysts modified with rare earth metal and performing the higher selectivity on hydrogen production and resistance to carbon deposition in dry and steam biogas conversion.

2 Experimental/methodology

The polymetallic catalysts containing Co, a noble metal (M_1), and a rare earth element and supported on alumina were prepared. The total content of Co and noble metal in the catalysts was constant and equal to 5 wt.%. The amount of rare earth metal (M_5) was varied from 0.5 to 10 wt. %.

The physicochemical properties of the catalysts were studied using TEM, BET, X-ray and TPR methods.

A model biogas with a ratio of CH_4/CO_2=1 was used. Amount of steam for providing the steam reforming of biogas was varied from 10 to 40 vol.%. The processes were carried out in a laboratory flow quarts reactor supplied with programmed heating and a controlled feeding velocity. The processes were operated under the atmospheric pressure and temperature varied within 300-800°C. The gas hourly space velocity (GHSV) was 1000 hr^{-1}. The initial and final

reaction products were analyzed on-line using the GC's.

3 Results and discussion

The catalysts activity was tested in the dry and steam reforming of biogas. Growing temperature from 300 to 700-800°C is accompanied with increase in biogas conversion from 5 to 95-100% in both processes. The effect of the amount of the rare earth metal on biogas conversion and yield of hydrogen was examined. The comparative data corresponding are presented in Fig.1 for the dry (a) and steam reforming (b) of biogas.

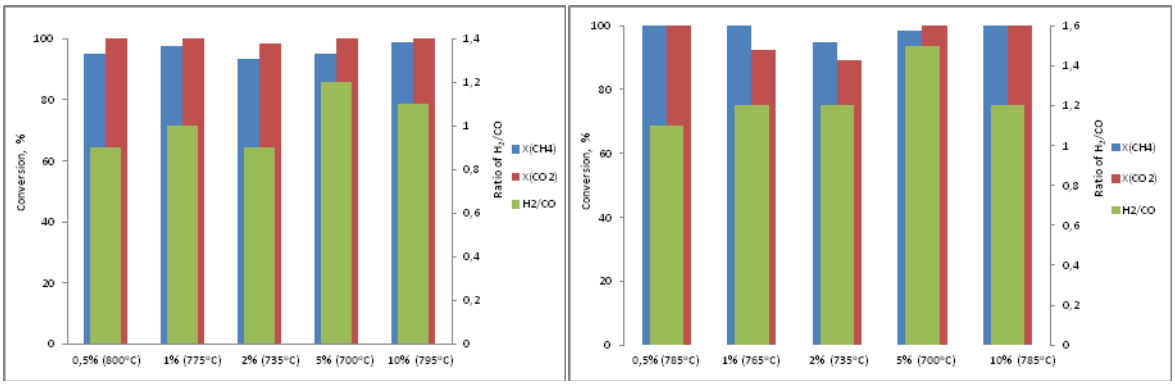

a b

Fig. 1. Comparative characteristics of the 5%(Co-M_1)M_5/Al_2O_3 catalysts in the dry (a) and steam reforming (b)

Syngas with the various ratio of H_2/CO is the only product in both processes. At steam reforming, the biogas is converted with the highest degree in comparison with dry reforming under the same conditions. Also, adding steam to biogas leads to prevailing hydrogen content in syngas formed up to 65% depending on the amount of rare earth metal and conditions.

The catalysts have shown the high stable activity in both dry and steam reforming of biogas. No loss of the 5%(Co-M_1)-5%M_5/Al_2O_3 activity was occurred during 150 hours of its continuous exploitation. No coke formation was observed by TEM.

4 Conclusions

The new multicomponent catalysts based on Co/Al_2O_3 modified with additives of noble and rare earth metals perform the high activity, stability and resistance to coke formation in production of hydrogen enriched gas by steam biogas conversion.

Acknowledgements

The authors thank the Ministry of Education and Science of the RK for sponsoring this research.

References

[1] O.A. Bereketidou, M.A. Goula. Catal. Today 195 (2012) 93-100.
[2] J. Xu, W. Zhou, Z. Li, J. Wang, J. Ma. Int. J. Hydrogen Energy 34 (2009) 6646-6654.
[3] D. San Jose-Alonso, M.J. Illan-Gomes, M.C. Roman-Martines. Int. J. Hydrogen Energy 38 (2013) 2230-2239.
[4] A. Serrano-Lotina, L. Daza. Int. J. Hydrogen Energy 39 (2014) 4089-4094.

III-PP117

Reuse of Low Value By-Products of a Biodiesel Industry. Esterification/Transesterification over Acid Catalysts

Domingues C.[1], Soares Dias A.P.[1*], Neiva Correia M.J.[1], Carvalho R.[2]

1 - LAETA, IDMEC, CERENA, IST, Universidade de Lisboa, Lisboa, Portugal
2 - IBEROL- Sociedade Ibérica de Biocombustívei e Oleaginosas S.A., Alhandra Vila Franca de Xira, Portugal

* apsoares@tecnico.ulisboa.pt

Keywords: renewable energy, biodiesel, esterification, acid oils, acid catalysts, VPO

1 Introduction

Today most of the energy is based on fossil fuels, which have a negative impact on the environment and creates a world dependence on crude producers. This dependence on fossil fuels generates worldwide socio-economics instability. The use of biomass is viewed as the most interesting alternative to produce energy with low environmental impacts. Biodiesel produced by alcoholysis of vegetable oils is pointed out as a feasible renewable fuel for diesel engines. In fact the transportation sector is major contributor to the greenhouse gases emissions and it is imperative to find a low carbon fuel for this sector.

The use of low value by-products as raw-materials for biofuels production can contribute with higher reduction of GHG, being one of the major advantages for sustainability of biofuels. However, a common drawback of this type of products for biodiesel is its high acidity that prevents the use of the commonly used alkaline catalysts. Nevertheless, acid heterogeneous catalysts allow the use of these low grade and cheaper oils and also continuous reactors, thus contributing to reduce the operating costs low grade and cheaper oils as raw-materials and continuous reactors thus contributing to reduce the operating costs [1].

2 Experimental/methodology

The esterification/transesterification of oily by-products, from a local biodiesel industry and a semi-refined rapeseed oil was carried out over acid catalysts prepared by a sol-gel like technique. Vanadyl phosphate catalysts (V/P=1 atomic ratio) were prepared using aqueous solutions of ammonium precursors and citric acid as complexation agent. After total evaporation of water at 80 ºC and vigorous stirring the xerogels were dried overnight at 120 ºC. The dried materials were crushed in a pyrex mortar and the powders were calcined for 5h in a muffle at temperatures from 500 ^{o}C to 700 ^{o}C. Details are given elsewhere [2].

The fresh and post reaction catalysts were characterized by XRD and HATR-FTIR in order to evaluates the active phases and species, and the deactivation processes.

The catalytic activity of the prepared materials was evaluated for the methanolysis reaction of semi-refined rapeseed oil and oily by-products from Iberol containing water, fatty acids and FAME. A high pressure stainless steel reactor equipped a mechanical stirrer was used for the reaction batches. For each reaction batch 100g of oil or by-product were mixed with 5g of powdered catalyst and 33 g of methanol. The reaction temperature was kept at 125ºC (6 atm) for 6h. After reaction the catalyst was separated by filtration and the FAME content of the oily liquid fraction was assessed by NIR [3].

The acidity of the raw fats and the esters phases (FAME) was assessed by KOH titration as described elsewhere [4].

3 Results and discussion

The fresh catalysts displayed orange to green shades depending on the calcination temperatures, whereas the post reaction powders showed dark orange/brown shades. These observances seem to indicate different vanadium oxidation states for fresh and post reaction catalysts.

The diffractograms, showing different crystalline phases and crystallinities, and the data on the catalytic behaviour in the Fig.1 underline the important role of calcination on the activity of the prepared catalysts. Additionally data showed that the prepared catalysts are quite active for the transesterification reaction of rapeseed oil even in mild reaction conditions (125ºC and 6 atm). In analogous reaction condition the prepared catalysts were also active for the esterification/transesterification of the acid by-products from the local biodiesel industry (Table 1). Using the same conditions oleic acid was 79% converted into methyl esters. The calcination temperature of the catalysts had a different effect on the transesterification and esterification capabilities (Fig. 2). The recalcination of the deactivated catalysts allows their reuse without significant decay of the activity.

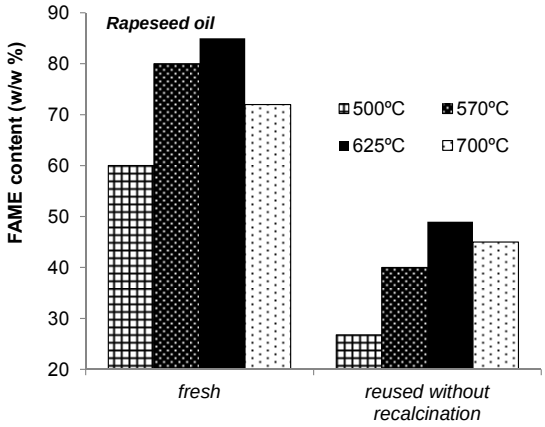

Fig. 1 Effect of the calcination temperature on the catalytic performances (rapeseed oil, 6h, 125ºC).

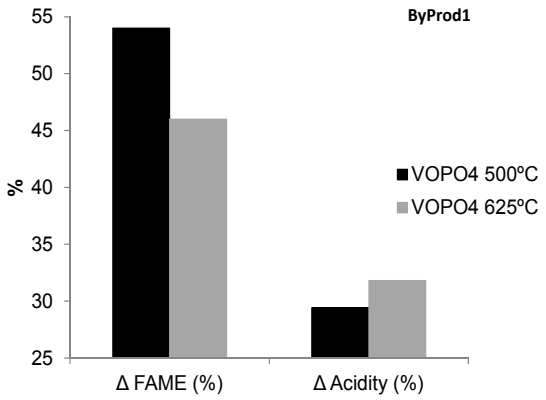

Fig. 2 Transesterification versus esterification activity of catalysts with different calcination temperatures (Byprod1; 6h, 125ºC).

Table 1. Acidity and FAME content of raw fat by-products and after reaction (calc. Temp. 625ºC).

	Raw fat (% w/w)		Esters phases (% w/w)	
	Acidity	**FAME (%)**	**Acidity**	**FAME (%)**
Byprod1	39.3	44.5	9.6	87.0
Byprod2	37.9	46.9	3.2	94.1
Byprod3	25.7	65.9	2.8	95.2

4 Conclusions

High acidity and low value by-products from a biodiesel industry were converted into biodiesel using heterogeneous acid vanadyl phosphate catalysts The non-traditional sol-gel like used technique revealed to be a simply route to synthetize such materials. The calcination temperature displays an important role on the catalytic performances of the prepared VPO materials.

References

[1] F. Su, Y. Guo, *Green Chemistry*, 2014, 16, 2934-2957.
[2] C. Domingues, M.J.N. Correia, R. Carvalho, C. Henriques, J. Bordado, A.P.S. Dias, *Journal of Biotechnology*, 2013, 164 (3), 433-440.
[3] P.Baptista, P.Felizardo, J.C.Menezes,J.N. Correia. *Analytica Chimica Acta*, 2008; 607, 153–159.
[4] A.P.S. Dias, J. Puna, M.J.N. Correia, I. Nogueira, J. Gomes, J. Bordado, *Fuel Processing Technology*, 2013, 116, 94-100.

III-PP118

Selective CO Methanation over Ceria-Supported Ni, Co and Fe Catalysts

Potemkin D.I.[1,2*], Konishcheva M.V.[1,2], Snytnikov P.V.[1,2], Sobyanin V.A.[1,2]

1 - Boreskov Institute of Catalysis SB RAS, Novosibirsk, Russia
2 - Novosibirsk State University, Novosibirsk, Russia

* potema@catalysis.ru

Keywords: carbon oxides methanation, nickel-ceria, cobalt-ceria, iron-ceria

1 Introduction

The selective CO methanation in hydrogen-rich gas mixtures in the presence of CO_2 is a promising way for deep CO removal designed for low-temperature proton-exchanged membrane fuel cell feeding applications, as well as a challenging fundamental problem of substrate-selective hydrogenation. Besides the target CO methanation reaction (1), undesirable CO_2 methanation (2) and reverse water-gas shift (3) reactions may occur, causing considerable hydrogen losses and increasing CO outlet concentration:

$CO+3H_2 = CH_4 + H_2O$; $\Delta H^o = -206$ kJ/mol (1)

$CO_2+4H_2 = CH_4 + 2H_2O$; $\Delta H^o = -165$ kJ/mol (2)

$CO_2 + H_2 = CO + H_2O$; $\Delta H^o = 41$ kJ/mol (3)

In spite of extensive research efforts Ru- and Ni-based systems remain the most active catalysts for CO and CO_2 methanation [1]. At the same time, metals such as Co and Fe are known to be active in carbon oxides hydrogenation reactions, including Fischer-Tropsch synthesis and RWGS, but the properties of Fe and Co-based systems in the selective CO methanation are not studied.

This work reports the results of comparative study of Ni-, Co- and Fe/CeO_2 catalysts, prepared from nitrate and chloride precursors, in the selective CO methanation.

2 Experimental/methodology

Catalysts with metal loading of 10 wt.% were prepared by incipient wetness impregnation of CeO_2 by the water solutions of metal's nitrate (Ni/CeO_2, Co/CeO_2, Fe/CeO_2) and chloride (Ni(Cl)/CeO_2, Co(Cl)/CeO_2, Fe(Cl)/CeO_2) salts. They were characterized by BET, XRD, TEM, EDX, XPS, FTIR and CO chemisorption techniques. Selective CO methanation was studied in a flow reactor at atmospheric pressure in the temperature interval 180 − 360 °C, at WHSV = 29 000 $cm^3g^{-1}h^{-1}$ and feed gas composition (vol.%): 1.0 CO, 20 CO_2, 10 H_2O, 65 H_2 and He-balance.

3 Results and discussion

Fig. 1 represents the temperature dependencies of the CO and CH_4 outlet concentrations in selective CO methanation for all studied catalysts. It is seen, that Fe-based and Co(Cl)/CeO_2 catalysts were inactive in CO and CO_2 methanation reactions. Ni/CeO_2 and Co/CeO_2 catalysts were active in both CO and CO_2 methanation, but showed low selectivity. Ni(Cl)/CeO_2 catalyst showed the best performance in selective CO methanation, being less active than Ni/CeO_2 and Co/CeO_2, but considerably more selective.

XRD, TEM and EDX analysis showed the presence of chlorine on the surface of Ni(Cl)/CeO_2, even the CeOCl particles (Table 1). Thus the observed differences in catalytic behavior of Ni-based catalysts could be associated with chlorine influence.

The TOFs calculated for Ni/CeO_2 and Ni(Cl)/CeO_2 catalysts at 210 °C (at this temperature

CO conversion was < 15 % and CO methatation selectivity was 100 %) were similar (Table 1). These data mean, that Ni/CeO_2 and $Ni(Cl)/CeO_2$ catalysts exhibited similar activity in CO methanation. In other words, the presence of chlorine does not significantly influence on the CO methanation activity, but it dramatically inhibits the CO_2 hydrogenation activity, thereby promoting catalyst selectivity.

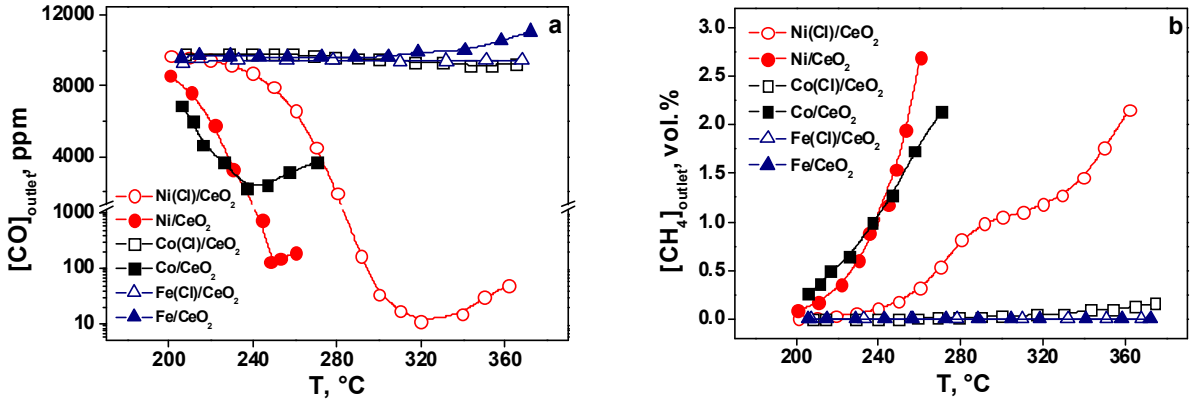

Fig. 1. The temperature dependencies of the CO (a) and CH_4 (b) outlet concentrations for the selective CO methanation over the studied catalysts. Feed gas composition (vol. %): 1.0 CO, 65 H_2, 10 H_2O, 20 CO_2 with He as balance. WHSV: 29 000 $cm^3g^{-1}h^{-1}$.

Table 1. Ni-based catalyst's characterization.

Catalyst	Phases	X[a], wt.%	D_{XRD}[b], nm	D_M[c], nm	TOF×10^3, s^{-1}
CeO_2	CeO_2	100	9	–	–
Ni/CeO_2	Ni	4	10	13	5.0
	CeO_2	96	9		
$Ni(Cl)/CeO_2$	Ni	10	>100	120	4.0
	CeOCl	48	9.5		
	CeO_2	42	19		

[a]Phase mass fraction according to the XRD analysis; [b]Average particle size determined by the XRD analysis; [c]Average size of metal particles according to the pulse CO chemisorption data.

Based on the data obtained, the nature of the active centers, origin of the observed activity order and probable mechanisms of CO and CO_2 methanation over Ni/CeO_2 and $Ni(Cl)/CeO_2$ catalysts are discussed.

4 Conclusions

Catalytic properties of Ni-, Co- and Fe/CeO_2 catalysts, prepared from nitrate and chloride precursors, in the selective CO methanation were studied. The $Ni(Cl)/CeO_2$ catalyst, prepared from $NiCl_2$ precursor, was the most efficient. This phenomenon could be explained by ceria surface blocking by chlorine species and appropriate inhibition of CO_2 hydrogenation activity.

Acknowledgements

This work was partially supported by the RFBR Grant 14-03-00457-a and MES (Russia).

References

[1] M.M. Zyryanova, P.V. Snytnikov, R.V. Gulyaev, Yu.I. Amosov, A.I. Boronin, V.A. Sobyanin, *Chem. Eng. J.* 238 (2014) 189.

III-PP119

Steady State and Dynamic Performance Analysis of OSR and Serial OSR-PROX Reactors

Başar M.S., Aksoylu A.E.*

Boğaziçi University, Department of Chemical Engineering, Istanbul, Turkey

* aksoylu@boun.edu.tr

Keywords: fuel processor, hydrogen production, oxidative steam reforming, preferential oxidation

1 Introduction

The release of large amounts of greenhouse gases through the combustion of fossil fuels has forced the researchers to develop efficient and easy-to-use decentralized power production systems in the range of 2-5 kW. By combining fuel processor (FP) and fuel cell (PEMFC) systems in small stationary units, like houses and small scale businesses, CO-free H_2 necessary for PEMFCs is produced from hydrocarbons, like CH_4, C_3H_8, LPG, etc., by FP. In the current study, a lab scale FP prototype was designed, constructed, and used in analyzing steady state and dynamic performances of individual C_3H_8 oxidative steam reforming (OSR) reactor, and serial OSR and preferential oxidation (PROX) reactors utilizing novel Pt-Ni/δ-Al_2O_3 [1] and Pt-Sn/AC [2] catalysts, respectively. The experiments have been conducted for different OSR feed compositions and reactor temperature combinations, which were determined by experimental design, and for the presence and absence of additional O_2 stream fed to the PROX reactor.

2 Experimental

The system consists of a feed section having mass flow controllers for inlet gases, an HPLC pump for water feed, a mixing zone; a reaction section having up to three vertical cylindrical ovens, which are placed inside a main oven. Temperature of each oven is controlled individually by a programmable temperature controller. The analysis section includes a Hiden Analytical HPR-20 QIC Mass Spectrometer equipped with a Faraday/SEM detector and 8-way manifold/diverter system. The bimetallic 0.2wt.%Pt-10wt.%Ni/δ-Al_2O_3 OSR and 1wt.%Pt-0.25wt.%Sn/AC PROX catalysts were prepared by sequential impregnation. 150 mg and 250 mg of fresh catalysts were placed into the OSR and PROX reactors, respectively, and were freshly reduced *in situ* prior to the tests. The experiments were conducted in the temperature range of 623-743 K in OSR unit and 380-423 K in PROX unit. After the steady state was reached for the initial OSR feed composition, step changes were applied to either C_3H_8, O_2 or H_2O flow rate, or to the O_2 flow rate at the inlet of the PROX reactor. C_3H_8, O_2 and H_2O flow rates were kept in the ranges of 5.1-7.3 ml/min, 7.3-10.3 ml/min and 44.7-59.6 ml/min, respectively. Helium was used as a balance for keeping the total feed flow fixed at 100 ml/min.

3 Results and discussion

In OSR performance tests, first, the composition of the OSR outlet was determined at steady state for the original feed; then, a positive or negative step change was given to one of the concentrations of the OSR reactants, and the transient concentration profiles for each product were determined on-line-real-time; finally, the steady state product concentrations were determined for each step change. Increasing O_2 concentration by applying a positive step (C/O_2: 2.7 → 1.9) in the feed stream resulted in increased steady state H_2, CO_2 and CO concentrations and decreased CH_4 concentration, which is an indicator of increased total oxidation and suppressed CO_2- and/or CO-methanation reactions, as given in Figure 1. Opposite trends were observed for the negative step (C/O_2: 1.9 → 2.4) applied to O_2 concentration in the feed stream.

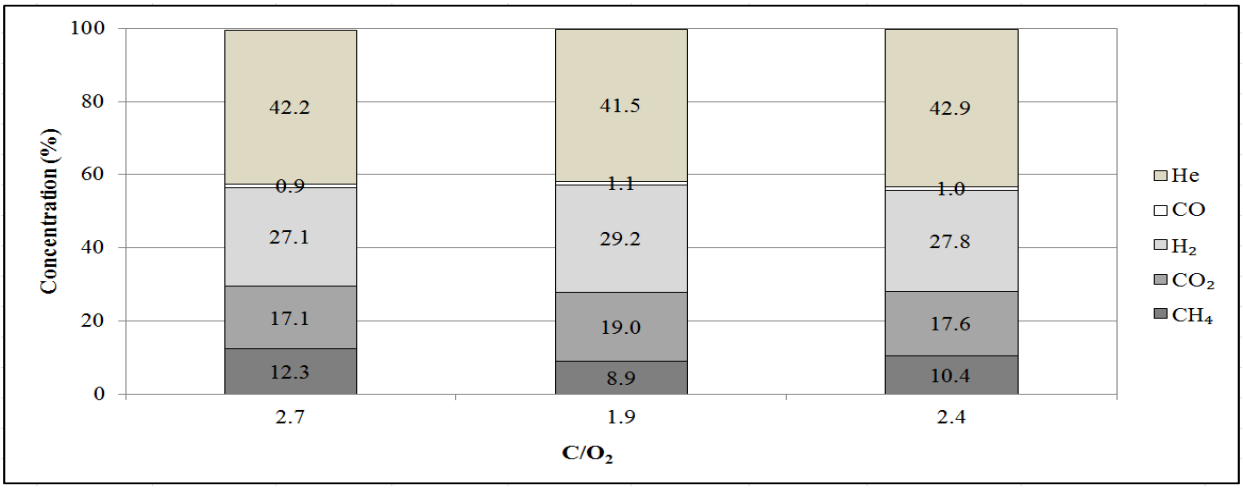

Fig. 1. Steady state concentrations of H_2, CO_2, CH_4 and CO gases at the OSR outlet at 723 K for (+) and (-) steps applied to O_2 concentration in the feed stream of OSR.

In serial OSR-PROX tests, feeding an additional O_2 stream clearly increased H_2/CO product ratio, since rate of CO oxidation reaction was greater than the rate of H_2 oxidation side reaction in the PROX reactor, as given in Figure 2. H_2/CO product ratio reached ca. 50 under the presence of 4 ml/min additional O_2 to the PROX reactor.

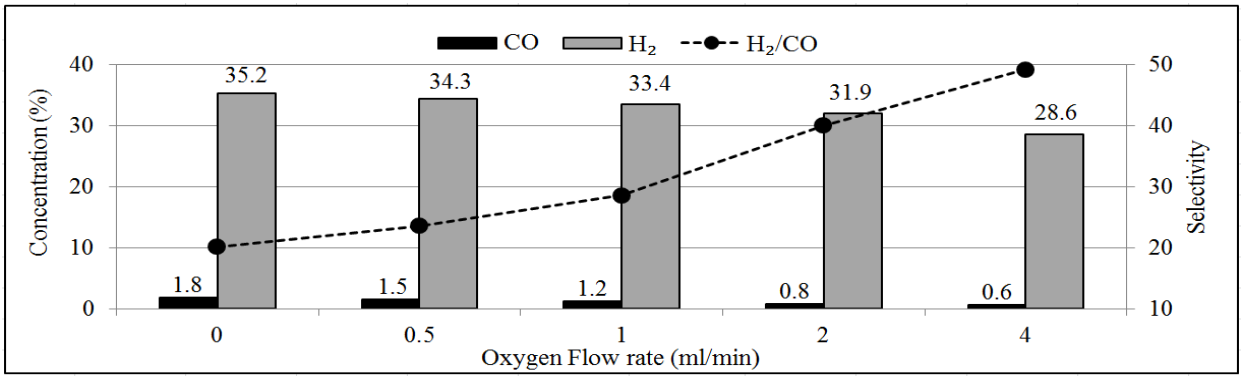

Fig. 2. Steady state concentrations of H_2 and CO, and H_2/CO ratio at the PROX outlet as a function of additional O_2 flow rates to the PROX reactor for 723 K-383 K OSR-PROX temperature combination.

4 Conclusions

Owing to the HT-WGS activity of the OSR catalyst, CO concentrations as low as 1% at the exit of OSR and 0.1% at the exit of the serial OSR-PROX system were achieved when C_3H_8 conversion in the OSR reactor was a 100%. Results confirmed the beneficial effect of O_2 addition to the PROX reactor on selectivity.

Acknowledgements

This work is financially supported by Boğaziçi University through projects BAP 5570 and 09HA505D and by State Planning Organization of Turkey through project DPT 07K120630.

References

[1] A. E. Aksoylu, A. K. Avci, B. S. Caglayan, Z. I. Onsan, *Applied Catalysis A: General*. 280 (2005) 181-188.

[2] I. I. Soykal, B. S. Caglayan, A. E. Aksoylu, *Applied Catalysis B: Environmental*. 106 (2011) 540-549.

III-PP120

Steam Reforming of Methane on Ni-Based Catalysts Characterized by Innovative Structured Carriers

Palma V., Ricca A.*, Miccio M., Martino M., Meloni E., Ciambelli P.

University of Salerno, Department of Industrial Engineering, Fisciano, Italy

* aricca@unisa.it

Keywords: hydrogen, reforming structured catalysts process, intensification

1 Introduction

The depletion of fossil fuels and the growing energy demand of the recent years shifted research attention toward alternative energy sources. Between them, hydrogen–fuel cells combination attracts the greatest interest in scientific research and technology innovation for hydrogen production intensification. Despite the amazing target to exploit renewable sources for energy, hydrogen production by fossil fuels reforming still remain the most viable solution in a transition phase toward an hydrogen based economy. Actually, the main technique to produce hydrogen is methane steam reforming (SR), a catalytic endothermic process in which the hydrocarbon reacts with steam to produce hydrogen and carbon monoxide. Due to its endothermicity, very high reaction temperature and heat flux towards the reaction system are required to achieve high methane conversion [1]. In the process intensification direction; the combination of these requirements up to now results the main limiting step of the process. Previous studies demonstrated that high thermal conductivity supports (foams, honeycomb monoliths) allow a flatter thermal profile along the catalytic bed, so resulting in a higher average temperature at the outlet section of the catalytic bed, and consequently in higher hydrocarbon conversion [2]. Furthermore, the highly conductive supports helps to flat the radial temperature profile, so reducing hot-spot phenomena, and mainly minimizing the heat transfer resistance from the heating medium to the catalytic volume. Moreover, the use of structured catalysis allows to reduce pressure drops and to minimize mass transfer limitation in the catalytic volume. In this aim, the thermal advantages achieved by using highly thermal conductive honeycomb monoliths as catalytic support may be further enhanced by forcing the flux to cross the monolithic walls. In this aim the use of Wall-Flow monoliths appear a viable solution towards the methane steam reforming intensification [3].

2 Experimental

Structured catalysts were prepared by starting from Silicon Carbide (SiC) porous walls monoliths (Pirelli Eco-technology, 150 cpsi), activated by nickel. Several aspects were investigated in this work: the nickel loading, the effect of a preliminary CeO2 based slurry deposition on the support, and the flux geometry. The Ni loaded SiC monolith was prepared by repeated impregnation phases in 1M nickel acetate solution ($C_4H_6O4Ni\text{-}4H_2O$), drying (120°C, 30min) and calcination (600°C, 2hr), in order to obtain a Ni loading of 30%wt. This procedure allows realizing a uniform and homogeneous distribution of the nickel oxide on the monolith walls and inside the porosity. For the washcoated samples, the support was preliminarily dipped in a CeO2 based slurry (2:1wt ceria : pseudo-bohemite) several times (dipping-drying-calcination cycles) up to reach a washcoat loading of 20%wt; then Ni was deposed by the impregnation steps reported above up to reach a Ni loading of 20%wt. Finally, some samples were converted in Wall-Flow configuration, by alternately plugging channels in the inlet and outlet sections, so forcing the process gas to cross the porous walls. The prepared samples were characterized by X-Ray Diffraction (XRD), Scanning Electron Microscopy (SEM) and Energy Dispersive Spectroscopy (EDAX), Surface area evaluation (BET)

and Hg penetration porosimetry.

The experimental tests were carried out in a tubular lab scale catalytic reactor in isothermal conditions. The activity tests were performed on the catalytic monoliths in the Flow-Through (FT) and Wall Flow (WF) configurations, by varying reaction temperature and GHSV (Q/V_{cat}) values.

3 Results and discussion

XRD analysis showed that the increase in the Ni load results in the increase of the characteristic NiO signals. SEM and EDAX images proved a uniform distribution of the active species and the washcoat (if present) over the SiC surface, thus confirming the effectiveness of the preparation procedure. Moreover, the porosimetric analyses confirmed that slurry was deposed inside the pores, as the mean pores diameter was reduced. The activity tests results, summarized in Figure 1, highlighted the better performances of the WF configuration than the FT, in terms of hydrogen yields and methane conversion. The WF configuration enhancement was more evident in the more extreme conditions, at the lowest operating temperatures and at highest reactants flow rate. The same behaviour was observed in the washcoated samples, since a marked improvement in catalytic performances was observed by using the WF configuration. Moreover, the comparison between hydrogen production on non-washcoated and washcoated samples confirmed the strong role of ceria on the steam reforming reaction trend: the oxygen-storage capacity, proper to the cerium oxide, accelerates the migration of oxygen from steam to the carbon [4], so resulting in a clear increasing in catalytic system performances.

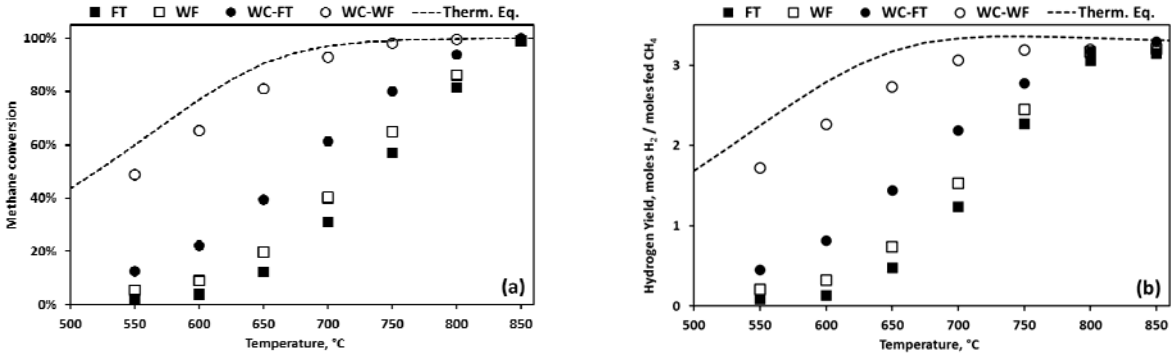

Fig. 1. Methane conversion (a) and Hydrogen yield for prepared samples tests

4 Conclusions

Specific experimental tests were carried out in order to evaluate the influence of flux geometry of Nickel based monolithic catalyst on methane SR reaction. The activity tests highlighted the improvements due to the WF configuration with respect to the FT, in terms of hydrogen yields. By forcing as to cross the monolith catalytic porous walls, heat and mass transfer mechanisms between gas and solid phases were enhanced, so resulting in faster reaction kinetics. The role of ceria as catalytic support was also investigated, highlighting that the Ni-CeO_2 interactions and the OSC properties linked to the ceria clearly improves catalyst performances.

References

[1] Y. Yan, Z. Zhang, L. Zhang, X. Wang, K. Liu, Z. Yang, *Int J Hydrogen Ener.* 40 (2015) 1886-1893.
[2] V. Palma, A. Ricca, P. Ciambelli, *Chem Eng J*. 207 (2012) 577-586.
[3] V. Palma, M. Miccio, A. Ricca, E. Meloni, P. Ciambelli, *Fuel.* 138 (2014) 80-90.
[4] K. Polychronopoulou, C.M. Kalamaras, A.M. Efstathiou. *Recent Patents on Materials Science* 4 (2011) 122-145

III-PP121

Structured Pt(2%)/CeO_2/Al_2O_3 WGS Catalyst Design: Introduction of Buffer Layer

Gonzalez Castaño M., Ivanova S., Centeno M.A., Odriozola J.A.*

Instituto de Ciencia de Materiales de Sevilla (IMCSE), Centro Mixto US/CSIC, Sevilla, España

* odrio@us.es

Keywords: water gas shift, Pt(2%)/CeO_2/Al_2O_3, micromonolith, buffer layer

1 Introduction

The WGS reaction ($CO + H_2O \rightleftharpoons CO_2 + H_2$) is moderately exothermic, equilibrium limited and characterized by high contact times needed to achieve good CO conversions [1]. The implementation of WGS units, in real and portable devices for hydrogen production and purification, involves a significant volume reactor diminution, onlybe achieved by the use of structured microreactors. In this context, the metallic micromonoliths are interesting candidates by allowing operation at higher space velocities, allowing the process intensification by a decrement of the reactor volumes, as well as, more efficient control of the reaction temperature due to improved heat and mass transport [2].

Noble metals, in particular Pt based catalysts, supported on reducible oxides have been described as very active WGS systems [3]. For these catalysts, two WGS mechanisms have been proposed: redox and associative mechanism. No matter the mechanism, water molecules should be activated prior the reaction, being a water dissociation a key step in WGS reaction [4]. The water activation is normally related the oxygen defect concentration on the surface of the catalyst, e.g. vacancies.

The aim of this study is to develop more efficient structured catalysts for the Water Gas Shift (WGS) reaction by improving the number of water activation sites. For this, a buffer layer is introduced to increase the active sites able to dissociate the water molecules. Different amounts of Pt(2%)/CeO_2/were deposited on metallic micromonoliths, characterized and tested in diverse reaction conditions. The prepared bilayer micromonoliths were constituted by: i) a CeO_2/Al_2O_3 layer as a buffer layer and ii) (Pt(2%)/CeO_2/Al_2O_3) as catalyst layer. The total amount of deposited catalyst was maintained constant meanwhile the amount of buffer was varied.

2 Experimental

The platinum was deposited on commercial CeO_2/Al_2O_3 (Sasol) by wetness impregnation using tetrammineplatinum (II) Nitrate Solution (Johnson Matthey) as precursor. The solid was calcined at 350°C during 8h with 5°C/min heating ramp. The buffer layer was composed by the same CeO_2/Al_2O_3 employed for the catalyst preparation.

The catalysts were deposited on ferritic stainless steel micromonoliths by washcoating. Two different suspensions were prepared: the buffer and the catalysts one. In order to achieve homogeneous and well-fixed catalyst layer, the rheological properties of the suspensions were adequate. The micromonoliths were calcined after each layer deposition at 450 °C and 350 °C for buffer and catalyst layer respectively. The catalytic activity was tested at 4000h^{-1} in hydrogen production conditions (4.5%CO+30%H_2O) and in clean-up conditions (7%CO+9%CO_2+30%H_2O+50%H_2) labeled respectively, model and real mixture.

3 Results and discussion

The buffer presence in the structured catalysts influences in different ways the catalyst

behavior depending on the reaction conditions probably due to the higher oxygen vacancies introduced in the buffer layer. While in model conditions the CO conversion declines, in real conditions an improved catalytic performance was observed (Fig. 1a). Moreover, the buffer layer thickness does not significant influences the catalytic performances in any reaction conditions tested. Considering the main compositional differences between the "model" and the "real" mixture, H_2 and CO_2 presence, the variation of those components was evaluated. While no significant changes are observed with the $\%CO_2$ variation, the benefit offered by the buffer incorporation in H_2 presence becomes more evident (Fig. 2a). The CO conversion decrement exhibited when H_2 is incorporated to the feed stream, expected because of the WGS equilibrium, is lowered with buffer layer presences. It should be noted that ceria based catalyst deactivation effects are related to ceria over-reduction and/or to stable carbonaceous species formation, blocking active sites. Hence, the benefit offered by the buffer layer could be related with an extra resistance achieved versus the deactivation effects happened in real mixture due to the H_2 presence.

Fig. 1. a) Catalytic activity in real mixture; b) Effect of $\%H_2$ variations on the feed stream at 310°C.

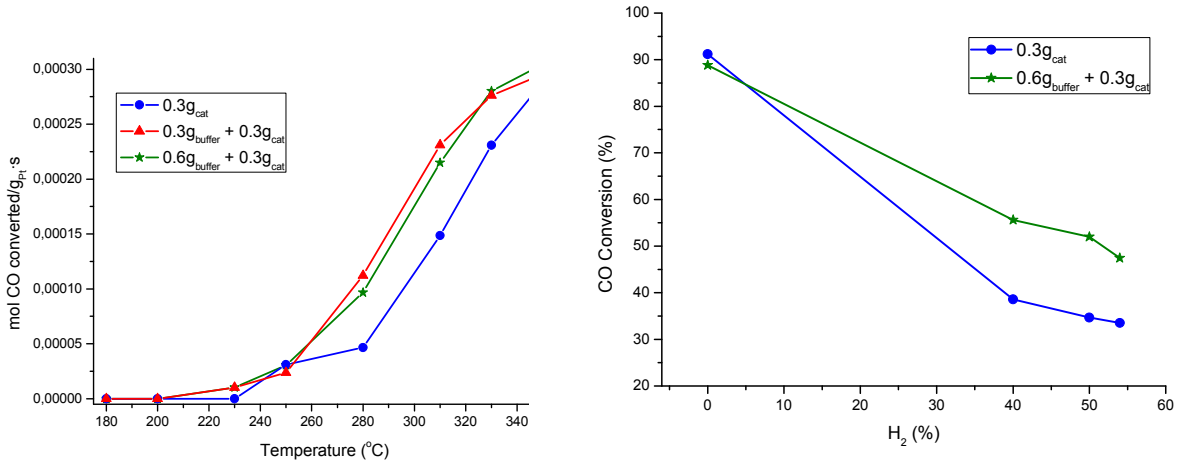

4 Conclusions

In H2 presence, the buffer layer incorporation enhances the catalytic performance probably due to the higher oxygen vacancies concentration for the water activation. The bilayer configuration is able to keep higher oxygen vacancies concentration available to activate water molecules leading to improved catalytic behaviours. It could be suggested that the buffer layer provides to the micromonolith an attenuation of the overreduction rate and hence, to carbonaceous species deactivation. In this way, the water molecules keep finding sites to be dissociated and this result on the observed increment of the catalytic performance in real conditions. Therefore, a bilayer structured catalytic system able to increase the activity and stability of the micromonolithic structures was achieved.

References

[1] C. Ratnasamy, J.P. Wagner, Catal. Rev. 51 (2009) 325.
[2] P. Avila, M. Montes, E.E. Miró, Chem. Eng. J. 109 (2005) 11.
[3] M.Gonzalez Castaño, T.R.Reina, S. Ivanova, M.A. Centeno, J.A. Odriozola, J.Catal. 314 (2014) 1.
[4] J.A. Rodriguez, P. Liu, J. Hrbek, J. Evans, M. Pérez, Angew. Chemie - Int. Ed. 46 (2007) 1329.

III-PP122

Synthesis and Characterization of CuO-ZnO-Al_2O_3 with Protonated Beta or Y-Typed Zeolite Supporter for Dimethyl Ester Production

Lin K.-S.*, Chiang C.L., Adhikari A.K., Chuang H.-W.

Department of Chemical Engineering and Materials Science/Environmental Technology Research Center, Yuan Ze University, Chung-Li City, Taiwan

* kslin@saturn.yzu.edu.tw

Keywords: dimethyl ester, carbon dioxide, CuO-ZnO-Al_2O_3, nanocatalyst, Beta/Y-type zeolites, ultrasonic treatment, XANES/EXAFS

1 Introduction

Carbon dioxide is one of the green house gases (GHGs) that have caused climate change significantly [1]. To reduce the affect of GHGs on the climate, several solutions have been proposed: improve the energy utilization efficiencies, introduce the alternative energies, capture/storage the CO_2, and convert the CO_2 to valuable chemicals [2,3]. Among the solutions, conversion of CO_2 is the most favorite method, because it can create profit by using CO_2 as a feedback to produce various valuable hydrocarbon fuels (e.g. dimethyl ester, DME). Due to the thermodynamic barriers of CO_2, it needs catalysts to decrease the activation energy and then accelerate the reaction rate during the conversion of CO_2 to other chemicals. The copper-based catalysts (e.g. CuO-ZnO-Al_2O_3, CZA) are the most popular commercial catalyst for the conversion of CO_2 to DME by reason of its cheap price and unique redox property [4]. The conversion reactions between CO_2 and DME are multistage that include methanol hydration ($CO+2H_2 \rightarrow CH_3OH$), methanol dehydration ($2CH_3OH \rightarrow CH_3OCH_3$ (DME) $+H_2O$), and water-gas shift (WGS, side-reaction, $CO+H_2O \rightarrow H_2+CO_2$). In this study, protonated beta (HBZ) and Y-Type zeolites (HYZ) were adopted as catalytic supporters to offer well-defined structure, and maximize the contact between methanol synthesis/dehydration sites in CZA catalyst.

2 Experimental

The syntheses of CZA/HBZ and CZA/HYZ were a two-stage procedure including co-precipitation and ultrasound treatment. Activated phase of CZA was prepared via co-precipitation method firstly. The aqueous solutions (1 M) of copper, zinc, aluminum nitrite hydrates ($[Cu^{2+}]$: $[Zn^{2+}]$: $[Al^{3+}]$=6:3:1), and sodium carbonate were made in advance for co-precipitation treatment. Sodium carbonate solution added into the metal nitrite solution slowly for co-precipitation of CZA until pH=7±0.2 with T=70°C for 1 h. Solid activated CZA was prepared after filtration, washing, drying (110°C, 12 h), and calcination (350°C, 5 h). Secondly, CZA slurry mixed with beta or Y-type zeolitic supporter (CZA: supporter=1:2 wt/wt) via ultrasound treatment with 90 W for 45 min. After drying and calcination, the nanocatalysts, CZA/HBZ and CZA/HYZ were synthesized successfully.

3 Results and discussion

The combination of activated CZA and zeolitic supporters provided new crystal phases of CZA/HBZ and CZA/HYZ, which were confirmed and observed by their characteristic signals in XRD patterns and FE-SEM micro-images respectively in Figure 1. Redox mechanisms of copper in nanocatalysts were investigated by H_2-TPR profile in Figure 2(a). Three reductive peaks appeared from low to high temperatures that meant the formation of CuH (α), interaction of Cu-Al (β), and reduction of bulk CuO particles (γ). Decreases of γ-reductive temperatures of CZA/HBZ and CZA/HYZ that were contributed from well-dispersion of copper in beta (-40.7°C) and Y-type (-47.0°C) zeolites were displayed in Table 1. XANES and EXAFS spectra of CZA/HBZ and CZA/HYZ nanocatalysts revealed the oxidation states of copper (Cu^{2+}) and bond distances of Cu-O (~1.95 Å) in Figure 2(b) and (c), respectively. The introduce of zeolitic supporters shrunk the bond

distances of Cu-O (R), and diminished the particle sizes of bulk CuO that caused the copper well-dispersed inside CZA/HBZ and CZA/HYZ nanocatalysts.

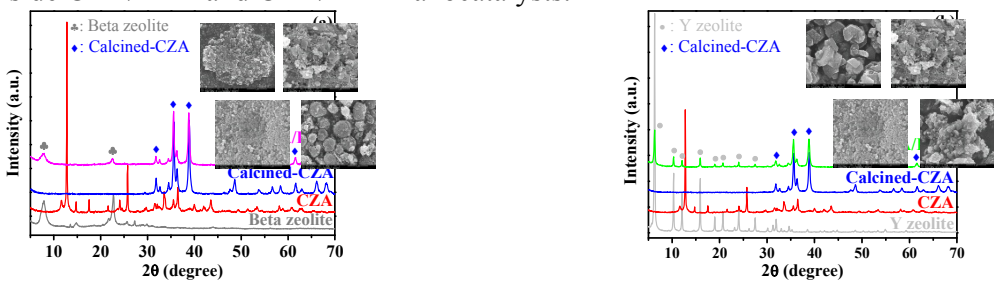

Fig. 1. XRD patterns/FE-SEM micro-images of (a) CZA/HBZ and (b) CZA/HYZ and supporters.

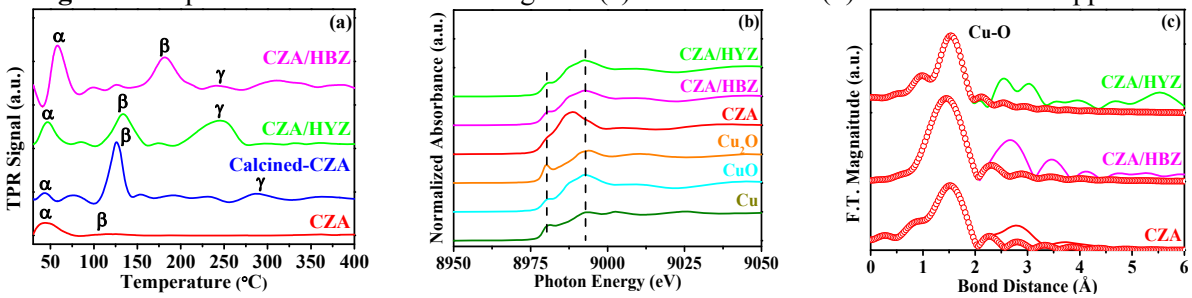

Fig. 2. (a) H_2-TPR profile, (b)XANES, and (c) EXAFS spectra of CZA/HBZ, CZA/HYZ and supporters (The best fitting curves were shown in colourful circle lines).

Table 1. H_2-TPR reductive temperature of CZA, calcined-CZA, CZA/HYZ, and CZA/HBZ.

	Reductive Temperature of Peaks (oC)		
	α	β	γ
CZA	44.2	115.5	Not available
Calcined-CZA	43.6	125.7	288.0
CZA/HYZ	46.7	134.0	247.3
CZA/HBZ	58.2	181.8	241.0

Table 2. Fine structures of CZA, CZA/HBZ and CZA/HYZ nanocatalysts.

Catalyst	Shell	CN (±0.05 Å)[a]	R (±0.02 Å)[b]	$\Delta\sigma^2$ (Å^2)[c]	R-Factor
CZA	Cu-O	2.232	1.96103	0.00175	0.00052
CZA/HBZ	Cu-O	1.470	1.91765	0.00844	0.00132
CZA/HYZ	Cu-O	2.804	1.95745	0.00401	0.00165

Notes: CNa: coordination number; Rb: bonding distance; σc: Debye-Waller factor.

4 Conclusions

Introduction of zeolitic supporters could lead copper well-dispersed in nanocatalysts that were able to overcome the barriers in DME production. Beta/Y-type zeolites as supporters were the great options for the enhancement of commercial copper-based catalysts.

Acknowledgements

The financial support of Ministry of Science and Technology of Taiwan, R.O.C. is greatly acknowledged (MOST 103-3113-E-008-003).

References

[1] R. Quadrelli and S. Peterson, *Energ. Policy*. 35 (2007) 5938.
[2] A. Dibenedetto, A. Angelini, and P. Stufano, *J. Chem. Techno. Biotechnol*. 89 (2013) 334.
[3] N.A.M. Razali, K.T. Lee, S. Bhatia, and R. Mohamed, *Renew. Sust. Energ. Rev*. 16 (2012) 4951.
[4] K. Reza and H. Mohammad, *Chem. Eng. Res. Des.* 91 (2013) 1111.

III-PP123

Tar Elimination in Pyrolysis of Sewage Sludge Using HighlyStable Ni/SBA-15 Catalyst

Iro E.*, Hajimirzaee S., Hodgson S., Olea M.

Teesside University, School of Science and Engineering, Middlesbrough, UK

* e.iro@tees.ac.uk

Keywords: tar, Ni/SBA-15 catalyst, catalytic hot gas clean-up unit, dry reforming, catalytic cracking

1 Introduction

Population growth continue to cause a surge in sewage sludge production from waste water treatment plants which is becoming more expensive to dispose and is a major contributor to uncontrolled greenhouse gases emission from landfills and incinerators which sadly, are still the major waste disposal methods in Europe [1]. Interestingly, the high organic matter (about 60 – 70% content) in sewage sludge is fast changing its global perception from an unwanted waste nuisance to a potential sustainable energy and biofuel resource via new thermochemical conversion technologies such as pyrolysis and gasification, which converts the dried sewage sludge to gas with about half the calorific value of natural gas [2], liquid (tar) and solid (char) fractions. By optimising the reactor design and operating conditions, one of the fractions could be adjusted to yield more than the other fractions. In our project, more gas fraction was desired for gas turbine to electricity applications, and so the pyrolysis reactor was operated to produce 55% gas, 16% tar and 29% char. Part of our project task was to develop a catalytic hot gas clean-up unit able to convert all or most of the tar fraction to non-condensable gas fraction to increase the gas produced and eliminate tar which has problematic consequence if present in the gas introduced to any gas turbine. Other impurities in the gas such as solid particles, hydrogen sulphide, hydrogen chloride and nitrogenous compounds removed by other processes are not discussed in this paper [3] .

The aim of this project is to develop a cheap but stable catalyst for tar elimination in the gas upgrading and clean–up process from pyrolysis of sewage sludge to gas turbine applications which could become a more attractive commercial and environmentally friendly option for sewage sludge utilisation.

2 Experimental/methodology

Synthesis of Ni/SBA-15 catalyst

SBA-15 mesoporous silica support was first synthesised by sol-gel method [4]. The complex $[Ni\ (NH_3)]^{2+}$ was then synthesised and by impregnation method at 5°C, dispersed on the prepared SBA-15 mesoporous silica.

Characterisation of Ni/SBA-15 catalyst

The synthesised Ni/SBA-15 catalyst was characterised using Fourier Transformation Infrared spectroscopy (FT-IR), Scanning Electron Microscopy (SEM)/ Energy dispersive X-ray spectroscopy (EDX), X-ray Diffraction spectroscopy (XRD), Transmission Electron Microscopy (TEM) and BET measurements. Catalytic activity, selectivity and catalyst stability was tested using the Hiden CatLab micro reactor operated at atmospheric pressure. Methane at flowrate of 27 ml/min and carbon dioxide at flowrate of 10 ml/min was flown over 35mg of catalyst in a fixed bed reactor and temperature was ramped from room temperature to 850°C. The reaction products were analysed using a quadrupole mass spectrometer. Catalyst life time was tested by passing same flow rate for methane and carbon dioxide over the same amount of catalyst at

500°C for 72 hours.

3 Results and discussion

Figure 1 shows Temperature Programmed Reduction (TPR) of catalyst under hydrogen flow. Figure 2 presents the results of methane decomposition and dry reactions simultaneously taking place. Figure 3 illustrates the results of the catalyst life time test for 72 hours.

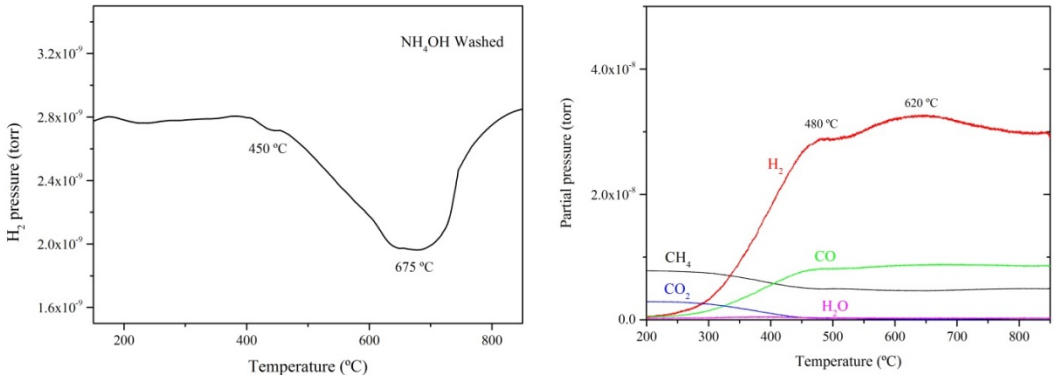

Fig.1. H_2 TPR profile (left) and methane dry reforming over Ni/SBA-15 catalyst (right)

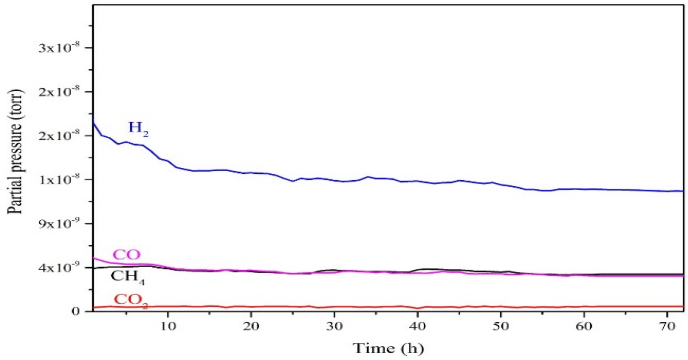

Fig.3. Catalyst life time test

4 Conclusions

Figure 1 shows that the catalyst was well reduced at the higher temperature range, in agreement with XRD and TEM results which confirms well dispersed and strongly attached NiO species on SBA-15 support which has high surface area, large pore size diameter and thick walls for hydrothermal stability which resulted in the high activity, selectivity and stability of the catalyst towards hydrocarbon cracking and reforming reactions. The Ni/SBA-15 catalyst will be scaled-up in pellets to fit into a gas clean-up unit for tar decomposition and methane reforming reactions.

References

[1] D. Fytili, A. Zabaniotou *Renewable and Sustainable Energy Reviews*. **2008**, 12, 116-140.
[2] P. Manara, A. Zabaniotou *Renewable and Sustainable Energy Reviews*. **2012**, 16, 2566-2582.
[3] D. J. M.-W. Roddy *In Comprehensive Renewable Energy*. **2012**, 5, pp 133-153.
[4] D. Zhao, J. Feng, Q. Huo, N. Melosh, G. H. Fredrickson, B. F. Chmelka, G. D. Stucky *Science*. **1998**, 279, 548-552.

III-PP124

The Chemical-Loop Bio-Alcohol Reforming for Hydrogen Production

Vozniuk O.[1,2,3*], Trevisanut C.[1], Albonetti S.[1], Cavani F.[1], Tanchoux N.[2], Quignard F.[2], Di Renzo F.[2], Millet J.M.[3]

1 - Dipartimento di Chimica Industriale "Toso Montanari",Università di Bologna, Bologna, Italy
2 - Institut Charles Gerhardt, UMR 5253 CNRS-UM2-ENSCM-UM1, ENSCM, Montpellier cedex 5, France
3 - IRCELYON, UMR5256 CNRS-Universitè Lyon 1, Villeurbanne cedex, France

* olena.vozniuk3@unibo.it

Keywords: hydrogen, water splitting, spinel, oxides, ferrites, TEM and XPS, *in-situ* DRIFTS-MS

1 Introduction

Hydrogen production is presently based on the reforming of natural gas or naphtha. Less energy intensive and more sustainable processes for H_2 production are appealing for both industry and consumer applications. A highly attractive route is steam reforming of bio-alcohols, in principle CO_2 neutral. Costly separation processes can be avoided by splitting the process into two alternated steps (chemical-loop reforming), in the aim of achieving two separate streams of H_2 and CO_x. The principle of the thermochemical-loop cycle is that an oxygen-storage material is first reduced by an ethanol stream, and then reoxidized by water, in order to produce H_2 and restore the original oxidation state of the looping-material. In this work, we report about the reactivity of various spinel ferrites in the production of H_2 from ethanol by chemical-loop reforming.[1,2]

2 Experimental part

The experiments were carried out with mixed ferrites – $CoFe_2O_4$, $MnFe_2O_4$, $Mn_{0.5}Co_{0.5}Fe_2O_4$, $Cu_{0.5}Mn_{0.5}Fe_2O_4$ and $CuFe_2O_4$, prepared by co-precipitation method[1,2]. Characterization techniques used for studying the chemical-physical properties of the materials were: BET, TEM and EDX analysis, XRD, XPS, Raman Spectroscopy and in-situ DRIFTS-MS.

3 Results and Discussion

XRD patterns of all materials showed magnetite-like spinel phases; Mn-based ferrites presented a low crystal size or were in amorphous form. The particle size, morphology and structure of the samples were investigated by TEM. The results indicate that the samples were almost uniform in both morphology and particle size distribution ~2-6 nm (fig.1-A). However, after different duration time of the chemical-loop reforming cycles the materials underwent some morphological changes and were significantly affected by sintered temperature, segregation and coke deposition (fig.1-B,C).

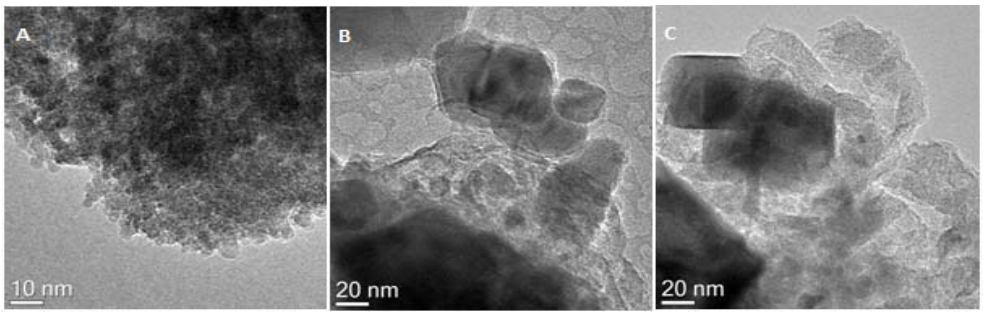

Fig.1. TEM images - $Mn_{0.5}Co_{0.5}Fe_2O_4$: (A) fresh material; (B) 6 min*10 cycles; (C) 20 min*5 cycles

Chosen ferrites were tested in a laboratory-scale plant of chemical-loop ethanol reforming. Average conversion of ethanol during the first reduction step over Mn-ferrites showed the lowest conversion compared to Co- and Cu- ferrites. This might be due to the difference in redox properties of the materials. The study of the second step, the re-oxidation of the reduced spinel with water steam, showed that high yields for hydrogen formation were obtained over chosen mixed ferrites (fig.2). However, the reduction by ethanol led to coke deposition and metal carbides formation. This turned into the generation of CO and CO_2 during the re-oxidation step, because of the gasification of carbonaceous residues. By shortening the time of each step, it was possible to reduce the coke formation during the reduction step and decrease the amount of CO_x formed during the 2nd step of the cycle. A study is in progress on the nature of coke and its mechanism of formation, related with the solid state modifications of the looping materials.

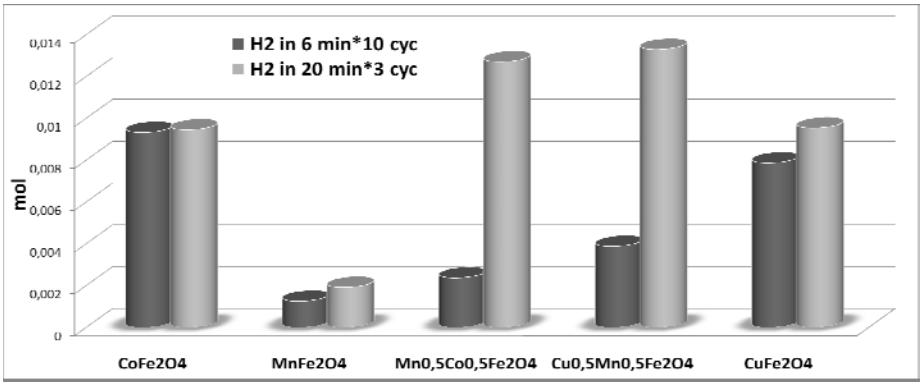

Fig.2. Moles of H_2 obtained by feeding water at 450°C during – 6 min*10 cycles; 20 min*3 cycles

4 Conclusions

The redox properties of mixed ferrites have shown promising features for hydrogen production, which make them suitable to generate hydrogen by oxidation with steam.

Acknowledgments

The project is supported by the E. U. Erasmus Mundus Sinchem program. We also gratefully acknowledge "Fondation Tuck", Rueil-Malmaison Cedex (F), project Enerbio, 2011 for PhD grant to CT.

References

[1]. Ochoa, J.V.; Trevisanut, C.; Millet, J.-M. M.; Busca, G.; Cavani, F., In Situ DRIFTS-MS Study of the Anaerobic Oxidation of Ethanol over Spinel Mixed Oxides. *J. Phys. Chem. C*. 2013, 117(45), 23908–23918.

[2] Trevisanut, C.; Bosselet, F.; Cavani F.; Millet J.M.M., A study of surface and structural changes of magnetite cycling material during chemical looping for hydrogen production from bio-ethanol. *Catal. Sci. Techn* 2015, 10.1039/C4CY01391C.

III-PP125

The Effect of Zeolite Addition into Cobalt-Based Fischer–Tropsch Catalysts

Sineva L.V.[1,2], Asalieva E.Yu.[1,3], Kulchakovskaya E.V.[1], Mordkovich V.Z.[1,2*]

1 - Department of New Chemical Technologies and Nanomaterials, Technological Institute for Superhard and Novel Carbon Materials, Moscow, Russia
2 - INFRA Technology Ltd., Moscow, Russia
3 - Department of Chemical Technology and New Materials, Lomonosov Moscow State University, Moscow, Russia

* mordkovichvz@tisnum.ru

Keywords: Fischer–Tropsch synthesis, composite catalyst, cobalt, zeolite

1 Introduction

Fischer–Tropsch synthesis (FTS) is the main stage of the technology of synthetic oil and high-quality fuel production from carbon containing feedstock (XTL), for example from natural gas or biomass. The interest to the XTL technology is increasing owing to the need to address environmental problems associated with stricter requirements for the quality of motor fuels and the practices of extraction of raw materials for the production of the fuels [1–2].

The products produced by FTS are synthetic fuel, naphtha (flammable, light oil containing various hydrocarbons that are used as feedstock for petrochemicals.), lubricants and more specialized commodities. They are clean burning, almost odorless and biodegradable – qualities that make them environmentally attractive.

Cobalt catalysts for FTS are considered as the most promising ones, because they prevent formation of undesirable aromatics and oxygenates [1–2]. At the present time the supported cobalt systems are the most common in industry and laboratory practice. However, “skeleton” cobalt catalysts represent a possible alternative for the FTS [3].

Since recently zeolite-containing catalysts are considered as promising prototypes for commercial Fischer–Tropsch catalysts due to their sorption selectivity, acidity, porosity and transport properties [4, 5]. Moreover, variations of Si/Al ratio and structural type of zeolite may allow controlling molecular mass distribution of the product, i.e. allow producing light synthetic oil or fuel fractions in the FTS, which is exactly the requirement of the “short-track” XTL. Synthetic crude oil as product of “short-track” XTL represents a mixture of hydrocarbons boiling below 400°C that does not contain sulfur, nitrogen and aromatics.

A number of experimental works are devoted to the synthesis of light synthetic oil or fuel fractions on zeolite-containing Fischer–Tropsch catalysts, using mostly ZSM-5 and Y-type zeolites [4, 6–8]. It is important to note that Beta-type zeolites combine main advantages of both Y-type and ZSM-5 in many respects, especially due to high acidity and large pore size [9]. This is the reason for choosing Beta zeolite as one of the components of the catalysts investigated in this work.

The purpose of this work was to study the effect of Beta zeolite addition into composite skeleton cobalt-based Fischer–Tropsch catalysts.

2 Experimental

The catalysts were produced by the extrusion of paste. Pastes were prepared by the techniques protected by patent [10]. All the paste samples contained 50 wt.% of highly dispersed aluminum metal powder, 30 wt.% of binder (30, 25 or 20 wt.% boehmite and correspondently 0, 5 or 10 wt.% of zeolite Beta in H-form (HB) with SiO_2/Al_2O_3 = 38). Also the paste contained 20 wt. % of highly dispersed skeleton cobalt.

The catalyst was activated in pure hydrogen (3000 h^{-1}) at 400˚C and 0.1 MPa for 1 hr. After

activation the catalyst was heated in a synthesis gas stream at 2 MPa, raising the temperature from 170 to 230˚C. Synthesis gas (molar ratio of $H_2/CO=2$ with 5 vol.% of N_2 as balance and internal reference) was supplied at gas-hour space velocity (GHSV) of 1000 h^{-1} while the temperature was raised and optimized and then GHSV was increased stepwise up to 3000 h^{-1}. Temperature was optimized for every GHSV so that the productivity was maximum possible.

3 Results and discussion

CO conversion, productivity and C_{5+} selectivity increased with zeolite introduction (Fig. 1a). Its content increase led to small but obviously reduction in these indexes.

With the introduction of 5 wt.% HB and growth of its content up to 10 wt.% methane selectivity and yield of CO_2 dropped, but yield of C_2–C_4 hydrocarbons increased (Fig. 1b).

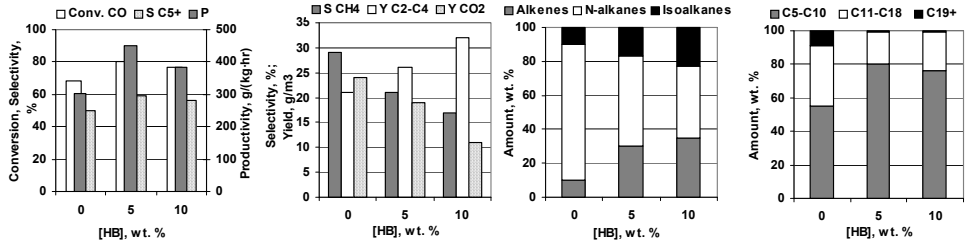

Fig. 1. The effect of the amount of HB on the basic FTS indexes (a), the byproducts formation (b), and C_5a ydrocarbons composition b ınd d). Process conditc s: 2MPa, 235°C, GHSV=d 00 h^{-1}, $H_2/CO = 2$

The composition of product obtained in the presence of the zero-zeolite sample has the highest content of n–paraffins (80%, Fig. 1c). The introduction of zeolite into catalyst and growth of its content led to decrease in content of n–paraffins to 42% at 10 wt.% HB. Content of olefins uniformly increases with stepwise introduction of zeolite from 10% was observed at HB absence to 35% at [HB] = 10 wt.%. The lowest content of iso-paraffins (10%) obtained in the presence of the zero-zeolite catalyst too. The introduction of 10 wt.% zeolite led to a significant increase up to 23%.

The fractional composition of C_{5+} hydrocarbons differed with HB introduction too; this, in the presence of zero-zeolite sample, 55% of the C_5–C_{10} fraction and 36% of the C_{11}–C_{18} fraction and C_{19+} fraction 9% were formed (Fig. 1d). The zeolite addition promoted C_5–C_{10} fraction growth to 80 % due to C_{11}–C_{18} and C_{19+} portions decreasing to 19–23 and 1% correspondently. Its amount increase has led to some decreasing of C_5–C_{10} fraction at the expense of C_{11}–C_{18} growth. This can be explained by the occurrence of bimolecular reactions on the acid sites of the zeolite.

4 Conclusions

Thus, it has been found that the introduction of H-form zeolite into a composite catalyst on skeleton Co basis has a positive effect both on the process parameters and on the composition of FTS products, namely: C_{5+} selectivity and productivity increase, and C_{19+} products are minimized. This is probably due to the processes occurring at acid sites of zeolite, where FTS products can enter various secondary reactions such as cracking, isomerization and bimolecular reactions by carbocation mechanism [4, 6–8, 11].

References

[1] Greener Fischer–Tropsch Processes, Ed. by P.M. Maitlis and A. de Klerk (Wiley–VCH, Weinheim, 2013).
[2] M. Dry and A. Steynberg, Fischer–Tropsch Technology. Studies in Surface Science and Catalysis, Elsevier, Amsterdam, 2004.
[3] F. Fischer, H. Meyer, Ber. 67 (1934) pp. 253–257.
[4] S. Sartipi, J.E. van Dijk, J. Gascon, F. Kapteijn, Appl. Cat. A: Gen., 456 (2013), pp. 11–22.
[5] A.L. Lapidus, A.Yu. Krylova, Russ. Chem. Rev., 67 (11) (1998), pp. 941–950.
[6] P. Mohanty, K.K. Pant, J. Parikh, at al, Fuel Processing Technology, 92 (2011), pp. 600–608.
[7] X. Li, K. Asami, M. Luo, K. Michiki, N. Tsubaki, K. Fujimoto, Catalysis Today, 84, Issues 1–2 (2003), pp. 59–65.
[8] J. Li, Y. Tan, Q. Zhang, Y. Han, Fuel, 89 (2010), pp. 3510–3516.
[9] S.G. Hegde, R. Kumar, R.N. Bhat, P. Ratnasamy, Zeolites, 9 (1989), pp. 231–242.
[10] RU Patent No 2405625, 2010.
[11] A.Corma, A.V.Orchilles. *Microporous Mesoporous Mater.*, **35–36**, (2000) pp. 21–40.

III-PP126

The Investigation of the ORR of the Pt/C Catalyst Produced by the Coaxial Pulsed Arc Plasma Deposition

Agawa Y.[1], Tanaka H.[1], Torisu S.[1], Endo S.[1], Tsujimoto A.[1], Gonohe N.[1*], Ilyin A.V.[2], Ivanov S.A.[2]

1 - ADVANCE-RIKO, Inc., Yokohama, Japan
2 - Interactive Corporation, Moscow, Russia

* iac@microanalysis.ru

Keywords: ORR, catalysis, coaxial, pulsed, vacuum, arc

We have developed nano-particles formation system for catalysts by a dry process. By use of a Coaxial pulsed vacuum Arc Plasma Discharge system (CAPD), highly ionized metal plasma can be generated from a target rod without any discharge gases, and deposits on flat substrates or powders to form various catalysts. Here, we investigate the electrocatalytic activity for oxygen reduction reaction (ORR) of our PtC-5% catalyst which is prepared using CAPD, For compression, commercially available PtC-20% and commercially available PtC-5% are also tested. The half-wave potential of our catalyst is higher than those of the others. The currents of four catalysts at 0.80 V, normalized by Pt mass (mass activity) and Pt electrochemically active surface area (ECSA) (specific activity), are also investigated. In both cases, the activity is much higher than those of the others, indicating that nanosized Pt particles prepared by our method can highly improve the utilization efficiency of Pt in electro-reduction of oxygen. The polarization curves are also recorded at different rotation rates. The expected increase of the limiting diffusion current density is observed as a function of the rotation rate. Thecorresponding Koutecky-Levich (K-L) plots show the first-order reaction kinetics toward the dissolved O2 on our catalyst from 0.3 V to 0.6 V. The calculated number of transferred electrons during the reduction of oxygen was between 4.03~4.18, thereby indicating that the ORR from 0.3 V to 0.6 V is dominated by a four-electron (4e-) process and O2 is reduced to OH-.

1 Introduction

This article introduces the nanoparticle formation pulse arc plasma source. This is a kind of dry catalyst manufacturing method where the target platinum is ionized through vacuum pulse arc discharge and is then caused to collide against the carrier. This method has significant advantages. First, platinum corpuscles only several nanometers across can be formed and evenly distributed across the carrier [5-9]. Also, the process is extremely easy to perform. The catalyst material can be easily changed and it is also possible to synthesize a catalyst material. This article introduces the principles of the nanoparticle formation pulse arc plasma source and reports the first attempt to create a platinum support carbon for fuel cells using this device [10, 11] and assess its characteristics. So we have investigated the experiments of oxygen reduction reaction in this paper. We could check this catalyst activity is high by ORR. We have analyzed and investigated this catalyst by using electrochemical analyzer. We report the reason why the activity of catalyst produced by CAPD is high in this paper.

2 Experimental Details

Preparation of Pt catalysts by CAPD: The vacuum chamber in the arc plasma method nanoparticle formation device contains a cylindrical container with a diameter of about 8 cm. Put about 10 to 20 cc carbon black in this container. Rotate the container to churn the powder using the two scrapers that are on the bottom of the container. Irradiate the plasma platinum over the surface of the churning carbon black powder to support platinum nanoparticles. The arc is

pulsed, the discharge time is short (100 to 200 μs) and the current value that flows through the cathode target (support material) is 2,000 to 6,000 A. Therefore, the energy density per unit hour is extremely high. This means that the cathode material condenses, vaporizes, and becomes plasma all at once, and then as atomic ions, collides with the carrier (substrate) at a high speed forming nanoparticle. Oxygen reduction reaction (ORR) measurements. Polarization curves for ORR were carried out with a conventional three-electrode cell was used, including an Ag/AgCl electrode as a reference electrode, a platinum wire as a counter electrode, and a rotation disk electrode (RDE, 2 mm in diameter) modified by catalyst as a working electrode.

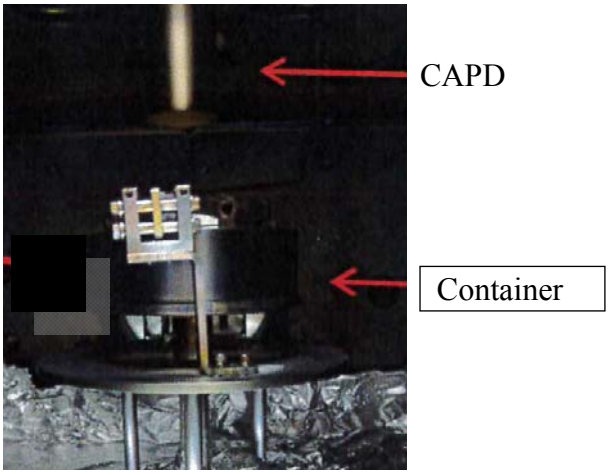

Figure 1. Experimental setup for preparation of Pt/C catalyst by CAPD.[14]

3 Experimental results

We measured a polarization test of Pt/C catalyst to investigate the performance of ORR. Measurement of Pt/C catalyst used the Pt/C-5wt% formed in CAPD,available commercially Pt/C5wt% and Pt/C20wt%. We changed the rotating speed of the rotationg disk and measured polarization characteristic to measure ORR electron-transfer pathway. A figure of (Koutecky-Levich K-L) plots was made from the above-mentioned polarization characteristic. Electron-transfer pathway of this Pt/C catalyst was 3.88 from the inclination of this figure. This result indicates hat our PtC sample catalyzes the ORR mainly through a four-electron process.

4 Conclusion

Surface area per unit of Pt/C catalyst generated by CAPD is almost same as surface area per 1g of commercially available Pt catalyst. But, the value of electron-transfer pathway of the Pt/C catalyst formed in CAPD is 3.88. In this result shows that this process is almost all four-electron reduction.

Reference

[1] Y.Yamamoto, Y. Agawa, Y.Hara, S.Amano, A.Chayayahara, Y.Horino and A.Fujii 1998 International Conference on Ion Implantation technology proceedings P1148-1150

[2] Yoshiaki Agawa, Satoshi Endou, Masamichi Matsuura and Yoshikazu Ishii: Behaviors of Metal Nano-particles Prepared by Coaxial Vacuum Arc Deposition., Advanced Material Research re Vols.123-125 (2010) pp1067-1070l

[3] Yoshiaki Agawa, Satoshi Endo, Masamichi Matsuura and Yoshikazu Ishii: Evaluation of the Pt/C catalyst for fuel cells prepared by a nano particles formation pulse arc plasma source,222nd,Electrochemical Society meeting poster 1425

[4] Yoshiaki Agawa, Satoshi Endo, Hiroyuki Tanaka, Shigemitsu Torisu, Akihiro Tsujimoto and Narishi Gonohe *:* The Seventh Tokyo Conference on Advanced Catalytic Science and Technology (TOCAT7) abstract:GP2090

Prospect of the Pt/C catalyst for fuel cells prepared by a nano particles formation pulse arc plasma source

III-PP127

The Use of Heteropolyanions and Chelating Agents for Designing TMS Catalysts for Hydroprocessing of Oil Cuts and Residues

Nikulshin P.*, Pimerzin A.

Samara State Technical University, Samara, Russia

* p.a.nikulshin@gmail.com

Keywords: hydroprocessing, heteropolyanion, CoMoS, KCoMoS, NiWS, ULSD

1 Introduction

Stricter environmental requirements for commercial oil products, as well as the need to expand the resources for their production stimulate the development of new high-effective hydrotreating (HDT) catalysts. The report presents the results of the research and development of new hydrotreating catalysts for hydroprocessing of various hydrocarbon raw feeds (FCC gasoline, diesel cuts, and vacuum gas oil (VGO).

2 Experimental

Catalysts were synthesized using the following precursors: (i) the $[Co_2Mo_{10}O_{38}H_4]^{6-}$ and cobalt complexes with chelating agents Co(*Chel*)-$Co_2Mo_{10}S/Al_2O_3$, where *Chel* were NTA, EDTA, citric acid (CA), tartaric acid with *Chel*/Co ratio equal to 1:1 [1]; (ii) the Keggin type heteropolyacid $H_3PMo_{12}O_{40}$ with cobalt citrate and potassium hydroxide; (iii) the $H_3PW_{12}O_{40}$ and nickel citrate.

Catalysts were prepared by wet impregnation of the alumina with water solutions of active components with moisture capacity control. Then the samples were dried at 120 ^{0}C (8 h) and sulfided. The prepared samples were studied by N_2 adsorption, Raman spectroscopy, XRD, HRTEM, H_2-TPR and XPS methods. Catalytic properties of the catalysts were determined in model reactions in a fixed-bed microreactor in a high-pressure flow system: (i) thiophene HDS; (ii) *n*-hexene-1 HYD, (iii) 4,6-DMDBT HDS; (iv) benzene HYD; (v) naphthalene HYD; (vi) quinoline HDN. Reaction products were identified by matching retention times with commercially available standards, as well as by GC/MS analysis using Finnigan Trace DSQ equipment. We also evaluated catalytic behavior of the prepared catalysts in a bench-scale flow reactor unit during HDT of diesel fractions (straight run gas oil, their mixture with light cycle oil, light coker gas oil), FCC gasolines and VGO.

3 Results and discussion

The CoMoS active phase was formed more selectively when using Co_2Mo_{10}HPA and Co-chelate complexes simultaneously during catalyst preparation [2]. Adding the Co-chelate significantly changed the active phase morphology due to the different interactions between the precursors and carrier surfaces in each catalyst. The catalytic activities of the Co_3[*Chel*]-Co_2Mo_{10}/Al_2O_3 samples depended strongly on the *Chel*. The CA-containing catalyst showed the highest HDS and HYD activities and the best selectivity factor.

Some structure-activity relationships were found in the HDS and HYD reactions (Figs. 1 and 2). A size effect that depended on an S-organic molecule was observed. During HDS of DBT and 4,6-DMDBT, the TOF values decreased with the grow of the particles of active phase. In HDS of DBT-derived molecules over a multi-slab CoMoS active phase, the average length of the CoMoS phase and the promoter ratio strongly affect the catalytic activity.

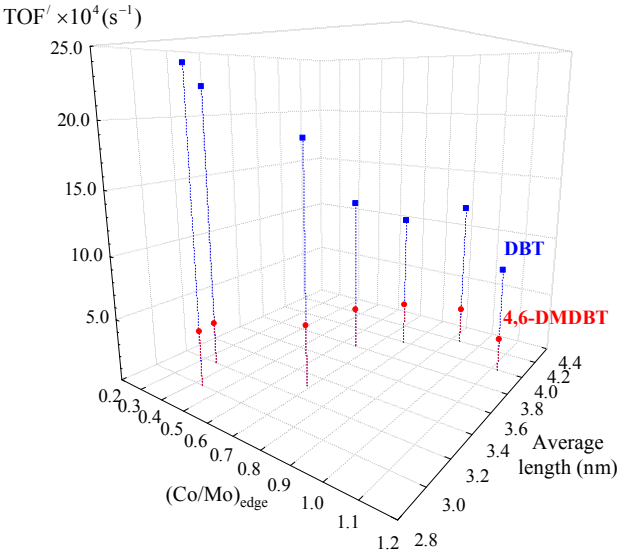

Fig. 1. 3D dependences of TOF/ number in HDS of DBT and 4,6-DMDBT over $CoMo/Al_2O_3$ catalysts on average length of CoMoS phase and $(Co/Mo)_{edge}$ ratio

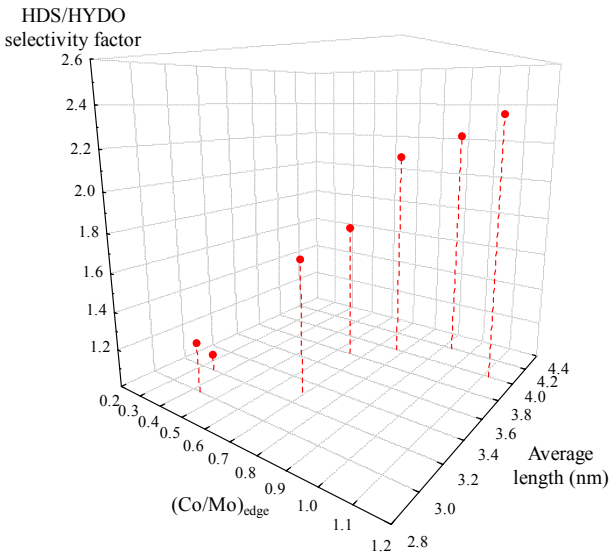

Fig. 2. 3D dependence of selectivity factor of $CoMo/Al_2O_3$ catalysts in the HDT of a mixture of thiophene and *n*-hexene-1 on average length of CoMoS phase and Co/Mo edge ratio in the CoMoS edges

The HDS/HYDO selectivities linearly depended on the number of CoMo sites on the slab edges. The selectivity increased as the average length of the active phase and the $(Co/Mo)_{edge}$ ratio increased. Further improvements in the HDS/HYDO selectivity was achieved by modifying the active CoMoS phase with the largest $(Co/Mo)_{edge}$ ratio of alkali metals. Promoting catalysts with potassium led to the partial poisoning of both types of the active sites and increased selectivity factor 4 times.

Optimization of the size and Ni/Mo(W) ratio in NiMo(W)S active phase species allowed to develop new catalysts for deep hydrotreating of VGO. NiW and NiMo catalysts supported on a mesostructured alumina provided the removing sulfur content to 500 ppm (from 2 wt .% in the feedstock) at 360 ºC, H_2 pressure of 5 MPa, LHSV 1.0 h^{-1} and H_2/feedstock 800 NL/L. The catalysts exhibited a lesser degree of deactivation and coke content after the tests.

4 Conclusions

New approaches for creating TMS catalysts were developed. Simultaneous use of Co_2Mo_{10}HPA and chelating agents allowed to change significantly the promotion ratio and morphology of CoMoS active phase type II and, thereby, catalyst properties in HDS and HYD reactions. New catalysts for (i) deep diesel hydrotreating, (ii) selective hydrotreating of FCC gasoline with saving octane number, and (ii) deep VGO hydrotreating were developed.

Acknowledgements

The work was supported by Ministry of education and science of Russian Federation (project 10.1516.2014/K) and Russian Foundation for Basic Research (project 15-03-01845).

References

[1] P.A. Nikulshin, D.I. Ishutenko, A.A. Mozhaev, K.I. Maslakov, A.A. Pimerzin, *J. Catal.* 312 (2014) 152.
[2] P.A. Nikulshin, A.V. Mozhaev, K.I. Maslakov, A.A. Pimerzin, V.M. Kogan, *Appl. Catal. B* 158–159 (2014) 161

III-PP128

Nickel-Cobalt Based Catalysts for Ethanol Steam Reforming

Moretti E.[1], Storaro L.[1], Talon A.[1], Chitsazan S.[2], Garbarino G.[2], Busca G.[2], Finocchio E[2*]

1 - Dip.to di Scienze Molecolari e Nanosistemi, Università Ca' Foscari Venezia, Venezia, Italy
2 - Dip.to di Ingegneria Civile, Chimica e Ambientale, Università di Genova, Genova, Italy

* Elisabetta.Finocchio@unige.it

Keywords: FT, IR, spectroscopy, ESR, Ni catalyst, Co catalyst, ceria, zirconia

1 Introduction

Bioethanol, i.e. ethanol from fermentation, can be a useful source of biohydrogen by catalytic ethanol steam reforming, ESR, which is a complex and widely studied reaction [1,2]. Noble metal based catalysts are reported to be needed to efficiently convert real bioethanol [3], however less expensive catalytic materials are still under investigation. Nickel based catalysts are reported to allow high hydrogen yield at high reaction temperature (>600°C), although drawbacks such as deactivation by sulphur poisoning, coking and metal particles sintering are reported [4]. Alternatively, catalysts containing Cobalt, a less reducible metal, have been proven to be effective in the same reaction mainly at low temperature [5]. In this work we report our recent results on characterization and activity in ESR of Ni and Co containing catalysts based on ceria-zirconia support with an atomic ratio Ce:Zr=9:1.

2 Experimental.

Catalysts were prepared from aqueous solution of $Ce(NO_3)_3.6H_2O$, $ZrO(NO_3)_2$, $Ni(NO_3)_2.6H_2O$ and/or $Co(NO_3)_2.6H_2O$. The resulting suspensions were left to settle overnight, then centrifuged and washed with deionized water. The samples were dried overnight at 80°C and then calcined in air flow up to 973 K for 5 h (3° min^{-1}). The catalyst samples were identified by acronyms CZ91X (X= Co and/or Ni) and have been fully characterized by ICP analysis, XRD, H_2-TPR, FT IR and UV-Vis. NIR spectroscopies (table 1). The catalytic experiments were carried out in a fixed-bed tubular quartz flow reactor, operating isothermally. ESR has been tested in the following conditions: liquid mixed feed of ethanol and water with molar ratio of 1:6 was fed to the line by a pump and heated at 500 K before feeding to the reactor (He as carrier gas). Ethanol Steam Reforming (ESR) reaction was performed from 300°C to 800°C. Analysis of reactants and products was carried out by GC equipped with TCD and FID detectors.

Table 1. Catalysts studied.

sample	Composition w/w	Surf. area $m^2\ g^{-1}$	H_2 uptake* (mmol $H_2\ g^{-1}$)	H_2 theor.* consumption (mmol $H_2\ g^{-1}$)	%red
CZ91Ni	Ni 7.6%	13	-	-	95.3
CZ91Co	Co 3.9%	12	1.23	1.29	79.5
CZ91NiCo	Ni 7.6%, Co 3.9%	12	0.70	0.88	100

* H_2 uptake for the reduction of the Ni, Co or both Ni-Co ions.

3 Results and discussion

The comparison of catalytic results of CZ91NiCo and CZ91Ni and CZ91Co shows that the bimetallic formulation significantly increases both ethanol conversion, which reaches 90% above 500°C, and hydrogen yield, which is near 80% at temperatures above 600°C K (figure 1).

These results can be explained by the synergetic effect occurring between Ni and Co in a

temperature range where the corresponding oxides are reduced by the same reaction mixture. Following previous results on bimetallic NiCo catalysts supported on stabilized zirconia we could possibly suggest that some alloying is also occurring in the bimetallic particles [5]. TPR and IR data of adsorbed probe molecules CO and methanol (namely, the easier oxidation of adsorbed methoxy species to formate species in the bimetallic formulation) also suggest the high reducibility of active phase oxides, possibly also enhanced by the availability of surface oxygen from the support [6]. Alcohols mainly adsorb dissociatively at the catalyst surfaces, pointing out the key role of the alkoxy species in reactants activation.

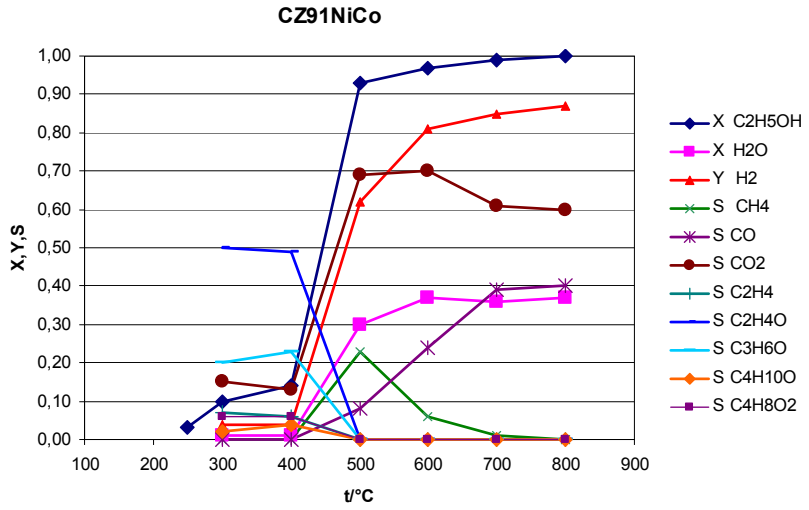

Fig. 1. Ethanol conversion (X), hydrogen yield (Y) and selectivities (S) to reaction products over CZ91NiCo, as function of temperature.

On the other side, the CZ support, mainly characterized by the ceria basic character, limits the formation of dehydration products such as ethene, in comparison to similar catalysts formulations over different supports. No deactivation phenomena were detected for the whole duration of the reactivity tests.

4 Conclusions

CZ91NiCo catalyst has proven to be very active in ESR reaction. The bimetallic formulation shows a synergic effect resulting in increased ethanol conversion and hydrogen yield (above 80% from 600°C). The basic character of Ceria-based support limits the formation of ethene, likely precursor of coke formation.

Acknowledgements

EF acknowledges the University of Genova (Progetto di Ricerca di Ateneo 2013) for partially funding this work.

References

[1] M. Ni, D.Y.C. Leung, M.K.H. Leung, *Int. J. Hydrogen Energy* 32 (2007) 3238.
[2] A.N.Fatsikostas, X.E. Verykios, *J. Catal.* 225 (2004) 439.
[3] A.Le Valant, F.Can, N.Bion, D.Duprez, F. Epron, *Int J Hydrogen Energy*. 35 (2010) 5015.
[4] G. Garbarino, A. Lagazzo, P. Riani, G. Busca, *Appl. Catal. B: Environ.* 129 (2013) 460.
[5] C. Resini, M.C. Herrera Delgado, S. Presto, L.J. Alemany, P. Riani, R. Marazza, G. Ramis, G. Busca, *Int. J. Hydrogen Energy* 33 (2008) 3728.
[6] E. Moretti, L.Storaro, A. Talon, S.Chitsazan, G.Garbarino, G.Busca, E.Finocchio, *Fuel,* submitted

III-PP129

Highly Reducible and Carburizable Precipitated Iron-Based Catalysts for Fischer-Tropsch Synthesis

Chun D.H.[1,2*], Rhim G.B.[1,3], Park J.C.[1,2], Hong S.Y.[1], Lee H.-T.[1], Yang J.-I.[1], Hong S.[1], Jung H.[1]

1 - Korea Institute of Energy Research, Clean Fuel Laboratory, Daejeon, Republic of Korea
2 - University of Science and Technology, Department of Advanced Energy Technology, Daejeon, Republic of Korea
3 - Chungnam National University, Graduate School of Energy Science and Technology, Daejeon, Republic of Korea

* cdhsl@kier.re.kr

Keywords: Fischer-Tropsch synthesis, precipitated iron-based catalysts, activation study, carburizability

1 Introduction

Fischer-Tropsch synthesis (FTS) has attracted much attention as a promising route to produce clean fuels or chemicals from syngas (H_2 + CO) derived from coal/biomass gasification or natural gas reforming. Iron-based catalysts are highly promising for the FTS due to their high activity and low cost. Furthermore, the iron-based catalysts have a great merit when they are used in the FTS using syngas with a low H_2/CO ratio (≤ 1.0), due to their potential activity for a water-gas shift (WGS) reaction. For low-temperature FTS (≤ 280 ºC), a precipitation technique is known to be the most practical preparation method of iron-based catalysts [1]. In general, iron carbides such as ε`-$Fe_{2.2}C$ and χ-$Fe_{2.5}C$ are reported to be active sites for the low-temperature FTS. Thus, the as-prepared precipitated iron-based catalysts, which are usually composed of iron oxides, need to be pre-activated into iron carbides in a CO-containing atmosphere prior to the FTS [2]. During the FTS over iron-based catalysts, considerable amounts of H_2O and CO_2 are inevitably produced as by-products, which can lead to oxidation and decarburization of active iron carbides into inactive iron oxides, respectively. Therefore, it is worth developing highly reducible and carburizable iron-based catalysts for enhanced catalytic performance in the FTS. In this study, we report highly reducible and carburizable iron-based FTS catalysts, which can be spontaneously activated in the FTS condition.

2 Experimental/methodology

The catalysts used in this study were prepared through a combination of a co-precipitation technique and a spray-drying method, in a process similar to that described previously [2,3]. In brief, a Na_2CO_3 solution was added to a solution containing both $Fe(NO_3)_3$ and $Cu(NO_3)_2$ in the desired ratio at 80 ± 1 °C until the pH reached 8.0 ± 0.1. The precipitate slurry was filtered, washed with distilled water, and subsequently re-slurried in distilled water. After completing the washing process, the required amount of K_2CO_3 solution and colloidal suspension of SiO_2 were added to the precipitate slurry, and the final mixture was spray-dried. Then, the dried sample was calcined at 400 °C for 8 h. The calcined catalysts were pressed into pellets and then crushed and sieved to obtain 300-600 μm particles for a test in a fixed-bed reactor. The chemical composition of the as-prepared catalysts was analyzed by X-ray fluorescence spectroscopy (XRF) using a Rigaku model ZSX Primus II. The Brunauer-Emmett-Teller (BET) surface area, the single point pore volume, and the average pore diameter of the as-prepared catalysts were analyzed by means of N_2 physisorption using a Micromeritics model Tristar II 3020. The FTS was carried out in a fixed-bed reactor composed of stainless steel. Using either as-prepared catalysts or pre-activated catalysts, the FTS was performed with syngas (H_2/CO=1.0, 2.8 NL/$g_{(cat)}$-h) at 275 °C and 1.5 MPa. The pre-activated

catalysts were prepared in situ with syngas (H_2/CO=1.0, 2.8 NL/$g_{(cat)}$-h) at 280 °C and 0.1 MPa for 20 h. The composition of the outlet gases was analyzed using an online gas chromatograph (GC; Agilent, 3000A Micro-GC) equipped with molecular sieve and plot Q columns. The flow rates of the gases were measured by means of a wet-gas flow meter.

3 Results and discussion

The chemical composition of the as-prepared catalysts analyzed by XRF was 100Fe/5.29Cu/4.86K/19.4SiO_2 in part per weight. The BET surface area, the single point pore volume, and the average pore diameter of the as-prepared catalysts were 203 m^2/g, 0.436 cm^3/g, and 8.60 nm, respectively. The pre-activated catalysts showed a high and stable CO conversion (83-85%) during the entire reaction time (~ 114 h), indicating that the catalysts prepared in this study are reducible and carburizable enough to maintain the active iron carbides during the FTS. Interestingly, the as-prepared catalysts also displayed a CO conversion higher than 60% at the beginning of reaction, and the CO conversion showed a slight increasing trend with increased time. This implies that the catalysts prepared in this study can be spontaneously activated during the FTS. The overall catalytic performance of pre-activated catalysts (denoted as PAC) and spontaneously activated catalysts (denoted as SAC) were comparatively evaluated during 66-114 h of reaction. While the CO conversion of SAC was lower than that of PAC (SAC: 64.1%, PAC: 84.5%), SAC showed much higher selectivity of C_{5+} hydrocarbons than PAC (SAC: 79.6 wt% in total hydrocarbons, PAC: 57.9 wt% in total hydrocarbons). Also, the CO_2 selectivity of SAC was slightly lower than that of PAC (SAC: 41.2%, PAC: 44.5%). As a result, SAC showed higher productivity of C_{5+} hydrocarbons than PAC (SAC: 0.271 g/$g_{(cat)}$-h, PAC: 0.218 g/$g_{(cat)}$-h).

4 Conclusions

The catalysts prepared in this study can be spontaneously activated during the FTS. The spontaneously activated catalysts showed high catalytic performance in terms of C_{5+} hydrocarbon productivity, which is even higher than that of pre-activated catalysts.

Acknowledgements

This work was supported by the Research and Development Program of the Korea Institute of Energy Research (GP2014-0046/B5-2440).

References

[1] R.B. Anderson, The Fischer-Tropsch Synthesis, Academic Press, Inc., New York, 1984.
[2] D.H. Chun, J.C. Park, S.Y. Hong, J.T. Lim, C.S. Kim, H.T. Lee, J.I. Yang, S.J. Hong, H. Jung, J. Catal. 317 (2014) 135.
[3] D.H. Chun, J.C. Park, H.T. Lee, J.I. Yang, S.J. Hong, H. Jung, Catal. Lett. 143 (2013) 1035.

Session IV
"Catalysis and chemicals"

IV-OP01

Selectivity in the Liquid-Phase Hydrogenation of 5-Hydroxymethyl Furfural over Ni-Al Catalysts

Perret N.*, Grigoropoulos A., Manning T., Claridge J., Rosseinsky M.J.

University of Liverpool, Liverpool, UK

* noemie.perret@liverpool.ac.uk

Keywords: 5-Hydroxymethylfurfural, Ni-Al catalysts, hydrogenation, biomass-derivatives, selectivity

1 Introduction

As the worldwide reserves of non-renewable fossil diminish, there is a growing demand on the development of sustainable feedstock. While the production of biofuels and bioenergy are still economically a challenge, the coproduction of value added chemicals could render the process cost-effective. Hemicelluloses can easily be broken down and converted to monosaccharides. The following dehydrations of sugars generate platform chemicals, such as 5-hydroxymethyl furfural (HMF) [1].The hydrogenation of HMF can produced a wide variety of valuable compounds [2]. However, selectivity in terms of targeted C=C or C=O reduction is challenging. Moreover, while most research focused on the combined hydrogenation/ hydrogenolysis of 5-HMF towards alcohols, really few studies dealt with the successive hydrogenation of 5-HMF with etherification or ring rearrangement [3].

The calcination and reduction of Ni-Al hydrotalcite-like compounds can generate catalysts with higher metal loading than Ni/Al_2O_3 synthesised by more traditional impregnation method; they can also exhibit distinct products selectivities which have yet to be fully exploited. In this study, we investigated the hydrogenation of HMF over $Ni_{1-x}Al_x$ catalysts ($0.2 \leq x \leq 0.45$) based on hydrotalcite like compounds. The effects of temperature (80-140°C), pressure (20-60bars) and solvent (water, methanol) on the catalytic response were investigated.

2 Experimental

Four hydrotalcites $Ni_{(1-x)}Al_x(OH)_2(CO_3)_{x/2}.mH_2O$, with $0.2 \leq x \leq 0.45$ and $0.3 \leq m \leq 0.7$, were prepared by precipitation of mixed aqueous solutions of $AlCl_3$ and $NiCl_2$ with solid urea. After aging for 60h at 95°C, all precipitated materials were left in suspension with NH_4HCO_3 for 5h (to remove any residual Cl), then filtered, washed and dried at 120°C for 3h. The catalysts $Ni_{1-x}Al_x$ were obtained by successive calcination (under air; 75mL min^{-1}) and reduction (under H_2, 100mL min^{-1}) at 500°C for 5h, followed by passivation at room temperature for 3h.

The crystallographic structures were confirmed by XRD. Bulk and surface Ni/Al ratios were obtained by elemental analysis (ICP) and SEM-EDX, respectively. Ni metal particles sizes were determined by TEM and XRD. Temperature-programmed reduction (TPR), H_2 chemisorption, temperature-programmed desorption (TPD), BET surface area and total pore volume were measured with a Chem-BET quantachrome and a Tristar II micromeritics.

The hydrogenation of 5-hydroxymethyl furfural was carried out in a batch stirred stainless steel reactor under constant pressure (P_{H2}= 20-60 bar) and agitation (600rpm) at temperature in the range 80-140°C. In a typical experiment 0.03g-0.09g of catalyst and a 45 mL aqueous or methanolic solution of 5-hydroxymethyl furfural reactant (C = 0.02-0.04M) were charged in the reactor. Liquid samples were analysed by GC and NMR.

3 Results and discussion

Characterisation showed that the catalysts obtained exhibit well dispersed Ni nanoparticles

(11-15nm) on the surface. The catalytic hydrogenations of HMF were conducted over $Ni_{1-x}Al_x$ ($0.2 \leq x \leq 0.45$) where an increase in Ni loading was associated with an increase in activity.

Table 1. Yields (Y) for the hydrogenation of HMF over $Ni_{0.8}Al_{0.2}$ catalysts after 20h reactions

T (°C)	P_{H2} (bars)	Solvent	X_{HMF}	Y_{FDM}	Y_{THF}	Y_{MF}	Y_{HCPN}	Y_{others}
80	60	water	1.00	0	1.00	0	0	0
140	20	water	1.00	0.04	0.10	0	0.75	0.10
140	20	Methanol	0.80	0.15	0.02	0.52	0	0.11

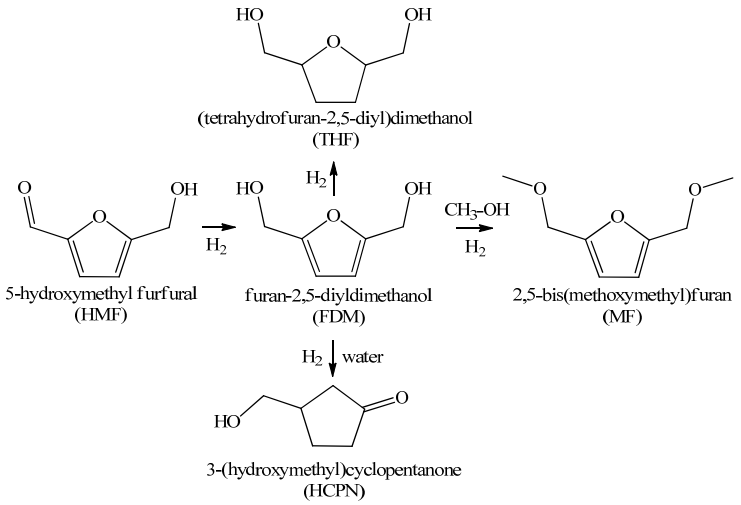

Fig. 1. Observed reaction pathway for the hydrogenation of 5-hydroxymethyl furfural

At low temperature and pressure (80°C, 20bar), successive reduction of C=O and C=C occur with formation of furan-2,5-diyldimethanol (FDM) and (tetrahydrofuran-2,5-diyl)dimethanol (THF, see Figure 1). By adjusting the reaction conditions (80°C, 60bar), 100% yields towards (tetrahydrofuran-2,5-diyl)dimethanol was obtained (Table 1). Increasing the temperature to 140°C had a drastic effect on selectivity. In water, the combined hydrogenation and ring rearrangement generated the formation of 3-(hydroxymethyl)cyclopentanone (HCPN) where 75% yield was achieved at 100% conversion (Table 1). When working in methanol, we observed the etherification of the intermediate furan-2,5-diyldimethanol with formation of 2,5-bis(methoxymethyl)furan (MF, Figure 1).

4 Conclusions

Temperature and solvent were shown to have a strong effect on the selectivity. The liquid phase hydrogenation of HMF over $Ni_{0.8}Al_{0.2}$ catalyst generated 100% yield of THF at 80°C. An increase in temperature was associated with a shift of selectivity towards HCPN and MF when working in water and methanol, respectively. We observed for the first time the formation of ether furan and cyclopentanone derivative over Ni catalysts.

Acknowledgements

We gratefully acknowledge the financial support provided by the Engineering and Physical Sciences Research Council (EP/K014749/1).

References

[1] A. A. Rosatella, S. P. Simeonov, R. F. M. Frade, C. A. M. Afonso, Green Chemistry 13 (2011) 754
[2] S. Yao, X. Wang, Y. Jiang, F. Wu, X. Chen, X. Mu, ACS Sustainable Chem. Eng. 2 (2014) 173
[3] J. Oyama, R. Kanao, A. Esaki, A. Satsuma, Chemical Communications 50 (2014) 5633

IV-OP02

Liquid-Phase Hydrogenation of Benzaldehyde and Furfural over Pd/C and Ru/C Catalysts

Mironenko R.M.[1*], Belskaya O.B.[1], Lavrenov A.V.[1], Likholobov V.A.[1,2]

1 - Institute of Hydrocarbons Processing SB RAS, Omsk, Russia
2 - Omsk Scientific Center SB RAS, Omsk, Russia

* ch-mrm@mail.ru

Keywords: furfural, benzaldehyde, hydrogenation, palladium catalysts, ruthenium catalysts, carbon supports

1 Introduction

Catalytic hydrogenation is widely used to reduce functional groups in various organic compounds. Selective hydrogenation of carbonyl compounds over supported metal catalysts is one of the methods of obtaining alcohols. Among the proposed hydrogenation catalysts, those based on noble metals have some advantages, since their high activity under mild reaction conditions and reusability. The nature of metallic component and its state in the catalyst are of key importance for hydrogenation processes. It is known that hydrogenation of aldehydes is a structure-sensitive reaction, since the particle size of supported metal affects catalyst activity. To provide the desired activity and selectivity of hydrogenation catalyst, the choice of support is also very important because features of the support affect the state of supported metal, the adsorption of reagents, and mass transfer processes. The goal of this work was to elucidate the effect exerted by the nature of carbon support on the formation of metallic sites in Pd/C and Ru/C catalysts for the liquid-phase selective hydrogenation of benzaldehyde and furfural.

2 Experimental

As the catalyst supports, we chose the carbon materials, multi-wall carbon nanotubes (CNT) and carbon black (CB), in principle differed in preparation method, structure and physicochemical characteristics such as texture and acid-base properties. The supported Ru catalysts were obtained by incipient wetness impregnation of the carbon supports with aqueous solutions of ruthenium(IV) chloride complexes. The Pd catalysts were prepared by the adsorption of palladium(II) chloride complexes from excess solution. The metal content in the catalysts was equal to 0.3, 1.0 and 1.5 wt. %. The formation of metal sites in the samples was examined by H_2-TPR. Metal dispersion in the reduced Pd/C and Ru/C samples was estimated by pulse chemisorption of CO or O_2 and directly by TEM. XPS was used to estimate the oxidation state of supported metal in the reduced catalysts. Hydrogenation of benzaldehyde in the presence of synthesized catalysts was performed in ethanol at 40 and 60 ^{o}C and a hydrogen pressure of 0.5 MPa in steel autoclave. The composition of reaction products was determined every hour by GC. Hydrogenation of furfural was carried out in aqueous solution at a temperature of 50 and 90 ^{o}C and a hydrogen pressure of 0.5 and 2.0 MPa. In this case, the reaction was controlled by measuring the volume of consumed hydrogen. The products of furfural hydrogenation were determined by GC after completion of the reaction and cooling.

3 Results and discussion

The adsorption of palladium(II) chloride complexes on CNT is less strong than their adsorption on CB. As a result, Pd complexes supported on CNT are reduced at a lower temperature with the formation of highly dispersed particles and a lower Pd^0:$Pd^{\delta+}$ atomic ratio. The adsorption capacity of CNT and CB with respect to ruthenium(IV) chloride complexes is very low. The reduction of a precursor in the Ru/CB sample led to the formation of ruthenium

particles having a higher dispersion as compared to Ru/CNT.

Hydrogenation of benzaldehyde. In the series of studied Pd/C catalysts, the highest selectivity for benzyl alcohol (98 %) with complete conversion of benzaldehyde was demonstrated by the 1 % Pd/CNT sample (40 °C, 0.5 MPa). For the Pd/C samples containing 0.3 % of palladium, the number of active sites is insufficient for accomplishing the reaction with high conversion. In this case, there is an increased fraction of products of the reaction between benzaldehyde and ethanol formed with participation of acid sites of the support. Increasing the palladium content up to 1.5 % leads to a significant increase in the toluene fraction (up to 92 %) in the reaction products.

The Ru/C catalysts are less active as compared to the palladium samples. Under the chosen reaction conditions, the presence of Ru/C samples does not provide a complete conversion of benzaldehyde. A maximum conversion of 71 % was attained in the presence of 1.5 % Ru/CNT (60 °C, 0.5 MPa). Hydrodeoxygenation into toluene is completely suppressed irrespective of the reaction conditions and ruthenium content in the catalyst; thus, high selectivity for benzyl alcohol is maintained. Among the Ru/C catalysts, most active in the formation of benzyl alcohol are the catalysts containing CNT.

Hydrogenation of furfural. The nature of carbon support was shown to affect the catalytic properties of Pd/C and Ru/C catalysts in the aqueous-phase hydrogenation of furfural (Fig. 1). The 1.5 % Pd/CB catalyst demonstrated a high selectivity (no less than 98 %) for furfuryl alcohol during hydrogenation of furfural at a temperature of 50 °C and hydrogen pressure of 0.5 and 2.0 MPa (the furfural conversion of 29 and 46 %, respectively). The 1.5 % Pd/CNT catalyst was not active under mild conditions of the reaction (50 °C, 0.5 MPa), but had a greater tendency to reduce the furan ring under severe conditions (90 °C, 0.5 or 2.0 MPa) as demonstrated by an increased yield of tetrahydrofurfuryl alcohol.

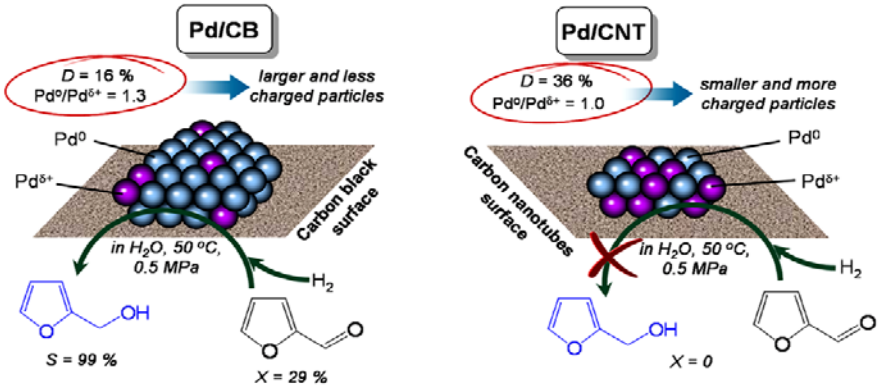

Fig. 1. Proposed effect of electronic and dispersion state of supported palladium on the catalytic properties of Pd/C in furfural hydrogenation

The ruthenium samples have a low activity in aqueous-phase hydrogenation of furfural irrespective of the support nature and reaction conditions, possibly due to irreversible adsorption of water on the active sites.

4 Conclusions

The study has revealed that the nature of carbon support affects the formation and state of supported metal in the Pd/C and Ru/C samples as well as its catalytic properties in hydrogenation of benzaldehyde and furfural.

Acknowledgements

The study was financially supported by the Russian Foundation for Basic Research (Project No. 12-03-00153a).

IV-OP03

Sustainable "Hydrogen Free" Catalytic Hydrogenation: from Concept to Reality

Li M., Cárdenas-Lizana F.*, Keane M. A.

Heriot-Watt University, Chemical Engineering, Edinburgh, UK

* f.cardenaslizana@hw.ac.uk

Keywords: gas phase, coupling reactions, alcohol, dehydrogenation-hydrogen transfer, Cu/SiO_2, supported Au catalysts

1 Introduction

Hydrogenation is a core catalytic operation in synthetic organic chemistry, accounting for 30-40% of the chemical processes in the manufacture of fine chemicals.[1] Commercial hydrogenation processes are typically operated in excess of pressurised gaseous H_2 in order to maximise product yield. Hydrogen is not a naturally occurring feedstock and production, storage and transport represent serious constraints. Over 95% of global H_2 production is fossil fuel based, notably by methane steam reforming and coal gasification and issues of sustainability now demand alternative sources with enhanced efficiencies.[2] A step change in catalytic hydrogenation must tackle H_2 utilisation and a completely new approach is called for.

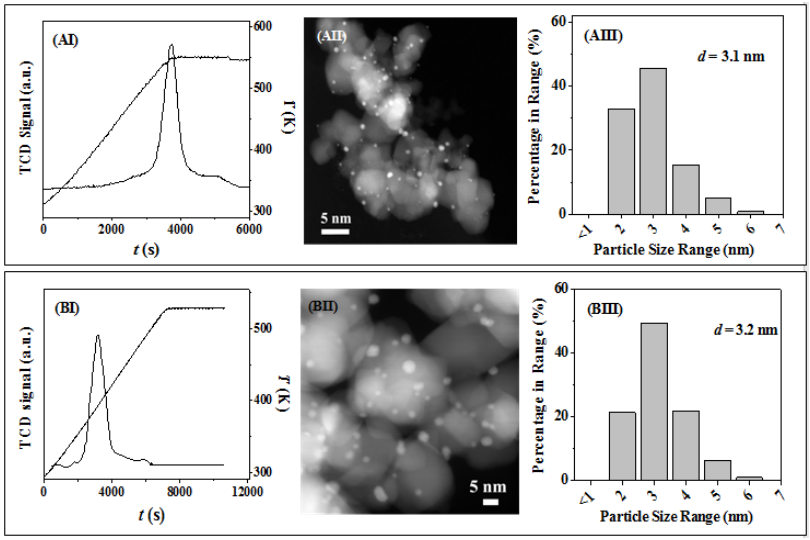

Fig. 1. (I) Temperature programmed reduction profiles, **(II)** representative STEM images and **(III)** associated metal particle size distribution histograms for **(A)** Cu/SiO_2 and **(B)** Au/TiO_2.

2 Experimental/methodology

Cu/SiO_2 and (CeO_2 and TiO_2) supported Au catalysts were prepared by deposition precipitation and/or impregnation. The catalysts were characterised in terms of elemental analysis/AAS, BET/pore volume, TPR, H_2 chemisorption/TPD, XRD, XPS, SEM, HRTEM, STEM, TGA-DSC and XPS measurements. The coupled dehydrogenation-hydrogen transfer reactions were conducted in continuous gas flow (fixed bed vertical glass reactor; P_{H2}=1 bar; T=423-593 K). The gases (H_2, N_2, Ar, O_2 and He) were of ultra high purity. The composition of the reaction/product mixtures was determined by capillary GC analysis.

3 Results and discussion

We have established the viability of continuous *in-situ* hydrogen generation (from 2-butanol dehydrogenation) and direct utilisation (in nitrobenzene hydrogenation) over (15.9% and 1.8% wt.) Cu/SiO_2 for the sustainable "hydrogen free" synthesis of commercially important products, *i.e.* 2-butanone and aniline. Dehydrogenation of 2-butanol is structure-sensitive with higher TOF over 15.9% wt. Cu/SiO_2 bearing larger (mean size=7.9 nm) Cu^0 nanoparticles. Enhanced TOF in

the hydrogenation of nitrobenzene has been demonstrated over 1.8% wt. Cu/SiO_2 that exhibited smaller Cu nanocrystals (mean = 3.1 nm) with greater H_2 uptake capacity. Exclusive production of both 2-butanone and aniline at full conversion has been achieved in the coupling of 2-butanol dehydrogenation with nitrobenzene hydrogenation over Cu/SiO_2 (conducted in N_2 as carrier). Hydrogen utilisation efficiency was appreciably greater (by a factor of up to 50) in the coupled system relative to conventional stand alone hydrogenation using pressurised H_2, a response that can be attributed to the generation of reactive hydrogen associated with the Cu sites (Cu-H) that is effectively transferred for nitro-group reduction. This circumvents the limitations associated with H_2 activation/dissociation by Cu.[3]

This approach has been further exploited with the combination of Cu/SiO_2 as a physical mixture with Au/TiO_2 (as a chemoselective hydrogenation catalyst)[4] for the gas phase coupling of benzyl alcohol dehydrogenation with nitrobenzene hydrogenation for "hydrogen-free" imine (*N*-benzylideneaniline) production. Post-activation both catalysts exhibited a narrow particle size distribution (1-6 nm) and similar nanoparticle size (3.1-3.2 nm) (see Fig. 1). Dehydrogenation of benzyl alcohol over Cu/SiO_2 delivered a ten-fold higher rate than Au/TiO_2 where the latter was appreciably more active in nitrobenzene hydrogenation . The coupled reaction generated the target imine over Cu/SiO_2, which suffered severe a severe temporal loss of activity and selectivity. Incorporation of Au/TiO_2 with Cu/SiO_2 resulted in a catalytic synergy (explained on the basis of XPS analysis combined with TGA-DSC measurements) resulting in overall enhanced imine production and full hydrogen utilisation.

The potential of this "hydrogen free" hydrogenation strategy is further demonstrated in a fully sustainable (hydrogen free, aqueous solvent, biomass reactant) process for the production of furfuryl alcohol and 2-butanone (from furfural hydrogenation using the hydrogen released from 2-butanol dehydrogenation) over Cu/SiO_2+Au/CeO_2 in continuous operation under mild reaction conditions. We demonstrate that this is the most effective among a series of strategies directed at enhancing surface availability of reactive hydrogen (see Fig. 2).

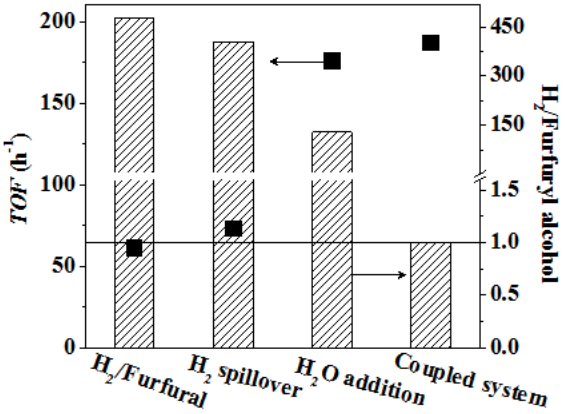

Fig. 2. Furfural turnover frequency (*TOF*;■) and H_2 utilisation with respect to furfuryl alcohol produced (H_2/Furfuryl alcohol, hatched bars) over Au/CeO_2 using different hydrogen supply strategies.

4 Conclusions

The results from this work demonstrate the feasibility of innovative coupling and cross-coupling of catalytic dehydrogenation (as a source of reactive hydrogen) with hydrogenation. Cu/SiO_2 is effective in the dehydrogenation step and we demonstrate catalytic synergy between Au and Cu in the coupled system with orders of magnitude enhanced H_2 utilisation, elevated selective hydrogenation rate and the simultaneous production of a range of high value products. Our coupled system circumvents the use of compressed H_2 from non-renewable sources with important safety and long term supply implications for large scale production.

References

[1] H. U. Blaser *et al.*, *Chimia* 64 (2010) 65.
[2] E. Cetinkaya *et al.*, *Int. J. Hydrogen Energy* 37 (2012) 2071.
[3] M. Li *et al.*, *Top. Catal.* in press.
[4] F. Cárdenas-Lizana and M. A. Keane., *J. Mat. Sci.* 48 (2013) 543.

IV-OP04

Conversion of Furfuryl Alcohol into 2-Methylfuran at Room Temperature Using Pd/TiO_2 Catalyst

Iqbal S.[1*], Liu X.[1], Aldosari O.F.[1], Miedziak P.J.[1], Edwards J.K.[1], Brett G.L.[1], Akram A.[1], Davies T.E.[2], Morgan D.J.[1], Knight D.K.[1], Hutchings G.J.[1], Nowicka E.[1]

1 - Cardiff Catalysis Institute, School of Chemistry, Cardiff, UK
2 - Stephenson Institute for Renewable Energy, Chemistry Department, The University of Liverpool, Liverpool, UK

* IQBALS13@CARDIFF.AC.UK

Keywords: furfural, 2-Methylfuran, biomass, Pd catalyst

1 Introduction

One of the most plentiful resources of renewable energy that exists in the world is biomass. The current challenge for researchers in both industry and academia is the development of efficient technologies that utilize biomass or biomass-derived chemicals to a large extent.[1] Furan derivatives are considered to be important intermediates because of their rich chemistry with carbohydrates being the most dominant source of these platform molecules.[2] Furfuryl alcohol is an important bio-derivative obtained from cellulose and hemicellulose hydrolysis. Almost all the reported work on FA hydrogenation is performed using harsh reaction conditions. In the current work we report an application of Pd-supported catalyst synthesized by wet impregnation method in selective biomass hydrogenation and we discuss the catalytic performance of Pd catalysts under different reaction conditions such as variation in pressure, solvent and amount of catalyst on the hydrogenation of FA into 2-Methylfuran (2-MF)at room temperature.

2 Experimental/methodology

Catalyst Preparation

Incipient Wetness Impregnation method

Catalysts supported on titania were prepared by a wet impregnation method. The preparation procedure is as detailed as follows. $PdCl_2$ was dissolved in water and stirred under heating and added to the support and the resulting paste formed was dried in an oven at 110°C for 16h. The powder was calcined in static air at 400°C for 3h at a ramp rate of 20°C per minute.

Characterization

XRD, TEM, and XPS have been used in order to characterize the catalysts used for current study.

Catalytic Testing

The reactor was charged with Fufuryl alcohol (1g), dichloroethane (20 ml) and catalyst (0.1g). The autoclave was sealed, pressurised with hydrogen (1-3 bar, continuously controlled or constant pressure), and stirred (1000 rpm) for 30-120 min at room temperature. The reaction mixture (after centrifuging the sample to isolate the catalyst) was analysed by GC (Varian 3800 fitted with CP wax column). Products were identified by comparison with authentic samples. For the quantification of the amounts of reactant consumed and products generated, an external calibration method was used. External standard was acetonitrile.

3 Results and discussion

Various loadings of palladium metal supported on titania have been studied and a variation in activity of catalysts is observed with respect to conversion and selectivity both. The results are

presented in table 1.

Table 1. Effect Palladium loading on catalysis for hydrogenation of furfuryl alcohol

Catalysts	Conversion (%)	Selectivity (%)	
		2-Methylfuran	Tetrahydrofurfuryl alcohol
1% Pd/TiO_2	21.4	49	51
2.5% Pd/TiO_2	46.2	92.5	7.5
5% Pd/TiO_2	65.1	85.2	13.8

Reaction conditions:- substrate (1g), catalyst (100mg), $C_2H_4Cl_2$ (20 ml), 25 °C, 3h, 1000 rpm, 1Bar H_2

A comparison among different solvents was conducted. Dichloroethane gives the best catalytic performance, and is very selective to 2-MF with very low production of tetrahydrofurfural alcohol. Very limited reduction was observed when using actonitrile and toluene as solvents. Increasing the amount of catalyst improved the overall catalytic performance. The reaction was found to be very selective to 2-MF, when we used 100 to 125 mg 5wt% Pd/TiO_2. The conversion kept increasing, but selectivity decreased when 150 mg of catalyst was used. This can be attributed to a further reduction of Pd cation, or side reactions due to the excess amount of catalyst since yield of 2-methytetrahydrolfuran and tetrahydrofurfuryl alcohol also increased associated with the higher amount of catalysts.

4 Conclusions

We have demonstrated that FA can be converted selectively into 2-MF at room temperature using very low pressure of hydrogen with Pd supported catalysts. In this work highly active Pd catalysts with an abundance of very small particles (<2nm) were prepared via a very simple impregnation method. By using these Pd catalysts, only O-H hydrogenated deoxygenation happened, C=C was very less reduced under these reaction conditions, wherein the only byproduct detected was tetrahydrofurfuryl alcohol <6%.

Acknowledgements

The authors would like to thank EPSRC (EP/K014854/1) and the Research Campus at Harwell for access to the transmission electron microscope.

References

[1] J.-P. Lange, E. van der Heide, J. van Buijtenen and R. Price, ChemSusChem, 5(2012), 150-166.
[2] G. W. Huber, S. Iborra and A. Corma, Chem. Rev.106(2006), 4044-4098.

IV-OP05

Transition Metal Oxides Nanoparticles on Activated Carbon Fibres as Efficient Catalyst for Nitroarenes Reduction under Mild Conditions

Parastaev A.[1,2], Beswick O.[1], Yuranov I.[1], Kiwi-Minsker L.[1*]

1 - Ecole Polytechnique Fédérale de Lausanne, GGRC-ISIC-EPFL, Lausanne, Switzlerand
2 - Lomonosov Moscow University of Fine Chemical Technology, Moscow, Russia

* lioubov.kiwi-minsker@epfl.ch

Keywords: MexOy, nanoparticles, functionalized, nitroarene, catalytic transfer, hydrogenation

1. Introduction

Functionalized anilines are broadly used as intermediates for the production of fine chemicals. Selective and more environmentally friendly catalytic hydrogenations have replaced their conventional production processes (Béchamp's process, reduction by sulphides) . The benchmark catalysts, consisting mainly of noble metals (Pt, Ir, Ru, etc.), are usually used under H_2 pressures up to 150 bars. Catalytic transfer hydrogenations (CTH) relying on alternative hydrogen sources (2-PrOH, HCOOH, N_2H_4, etc.) allow avoiding such high pressures . Non-precious metal (Ni, Fe, Ce, etc.) based catalysts have shown to be an alternative to noble metals when the active phase is sufficiently dispersed .

Herein, we report catalysts based on transition metal oxides supported on activated carbon fibres (ACF) developed for selective CTH of substituted nitroarenes (NAr) into corresponding anilines (An) under mild conditions using N_2H_4 as a reducing agent. Microporous ACF (SSA~2000 m^2 g^{-1}) allow stabilizing extremely dispersed metal oxide nanoparticles (NPs). Downstream separation of the catalyst is avoided with the use of structured ACF. A small diameter of elementary filaments (10 μm) prevents internal mass transfer limitations.The ACF regular macrostructure provides a low resistance to a fluid flow in continuous processes .

2. Experimental/methodology

The Me_xO_y/ACF catalysts were prepared as following. Activated carbon fibers (ACF-K-20, Kynol Europa GmbH) used in the form of woven fabric were impregnated by an ethanol solution of metal nitrates precursor and dried in air at room temperature. Prior to catalytic testing the Me_xO_y/ACF catalysts were activated in an Ar flow at 623 K (ramp – 10 K min^{-1}) during 1 h followed by a passivation at 293 K under 2% v/v air/Ar flow for 1 h.

AAS was applied to determine the metal content and possible leaching. The specific surface area and total pore volume were characterized by BET. The size, morphology and electronic properties of the NPs were investigated by SEM, STEM, XRD and XPS.

Liquid-phase CTH reactions were carried out in a commercial semi-batch stainless steel stirred reactor. The structured ACF catalyst was fixed directly on the stirrer (stirring rate ~ 2000 rpm). The composition of the reaction mixture was monitored by GC.

3. Results and discussion

Electron microscopy revealed that highly dispersed Fe_2O_3 and Co_3O_4 NPs were formed within ACF micropores (Fig. 1). The NP size is controlled by the pore size (d_{pore} <2 nm).

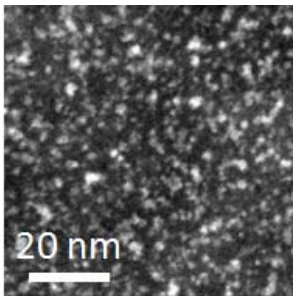

Fig. 1. STEM-HAADF image of 5%Fe_2O_3/ACF.

All catalysts were active in CTH of *para*-chloronitrobenzene (*p*CNB). Fe_2O_3/ACF and Co_3O_4/ACF exhibited an initial specific activity of one order of magnitude higher (3-6·10^{-2} $mol_{NAr}·mol_{Me}^{-1}·s^{-1}$) than CeO_2/ACF and NiO/ACF. While only *p*CAN was observed throughout the reaction over the Fe and Ce based catalysts, azoxy- and azoarene intermediates were detected over Co_3O_4/ACF and NiO/ACF. The further testing of two the most active catalysts in CTH of nitroaromatics with different substituents (-OCH_3, -CH_3, -H, -Cl, -C=C) demonstrated extremely high yields (>99 %) of corresponding anilines (Table 1). It is important to note that hydrogenation of 3-nitrostyrene containing a readily reducible vinyl-group is quantitatively selective over Co_3O_4/ACF without any additives.

Table 1. CTH of functionalized nitroarenes over 8%Fe_2O_3/ACF and 5%Co_3O_4/ACF. Reaction conditions: 333 K, substrate - 0.126 M, Fe catalyst - 2.0 mol.%, N_2H_4/*p*CNB - 3, EtOH - 100 ml.

Substrate 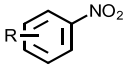	**R-**	**Fe_2O_3/ACF**		**Co_3O_4/ACF**	
		r_0, ·10^2 (mol_{NAr}· $mol_{Me}^{-1}·s^{-1}$)	**S_{An}, at X=100%(%)**	**r_0, ·10^2 (mol_{NAr}· $mol_{Me}^{-1}·s^{-1}$)**	**S_{An}, at X=100%(%)**
nitrobenzene	*p*-H-	1.6	100	4	>99
4-nitrotoluene	*p*-CH_3-	2.2	100	3.3	>99
4-chloronitrobenzene	*p*-Cl-	3.3	100	6.4	>99
4-nitroanisole	*p*-CH_3O-	1.1	100	1.2	>99
3-nitrostyrene[a]	*m*-CH_2=CH-	0.8	90*	0.4	>99*

a. Substrate - 0.016 M.

4. Conclusions

Highly dispersed Fe and Co oxide NPs (2-4 nm) deposited on ACF were demonstrated to be efficient catalysts for selective transfer hydrogenation of a variety of functionalized nitroarenes under mild conditions (T = 333 K: P = 1 bar). The challenging reduction of nitrostyrene to vinylaniline was successfully achieved over Co_3O_4/ACF with a selectivity of >99 % at full conversion.

Acknowledgements

This work was funded by the Swiss National Science Foundation (grant 200020_149869).

References

[1] H. U. Blaser, H. SteinerM. Studer, Chemcatchem. 1 (2009) 2.
[2] R. A. W. Johnstone, A. H. WilbyI. D. Entwistle, Chemical Reviews. 85 (1985) 2.
[3] H. Z. Zhu, Y. M. Lu, F. J. FanS. H. Yu, Nanoscale. 5 (2013) 16.
[4] L. Kiwi-Minsker, I. Yuranov, V. HollerA. Renken, Chemical Engineering Science. 54 (1999) 21.

IV-OP06

Oxidation, Oxidative Esterification and Ammoxidation of Acrolein over Metal Oxides: Do these Reactions Include Nucleophilic Acyl Substitution?

Koltunov K.Yu.[1,2*], Sobolev V.I.[1,3], Bondareva V.M.[1]

1 - Boreskov Institute of Catalysis SB RAS, Novosibirsk, Russia
2 - Novosibirsk State University, Novosibirsk, Russia
3 - Tomsk State University, Tomsk, Russia

* koltunov@catalysis.ru

Keywords: vanadium mixed oxide catalyst, nucleophilic acyl substitution, acrolein, acrylic acid, methyl acrylate, acrylonitrile

1 Introduction

Acrylic acid (AA), methyl acrylate (MA) and acrylonitrile (AN) are important bulk chemicals. Their production is currently based on propylene oxidative transformations, while acrolein plays a key role as an isolated or in situ intermediate in these reactions. For example, aerobic oxidation of acrolein to AA over a molybdenum-vanadium oxide catalyst is a part of the two-step propylene oxidation process (Scheme 1). Notably, this reaction proceeds normally in the presence of 2 to 40 vol% of water at 250−310°C.

MA can be synthesized directly from acrolein or even propylene as a result of oxidative esterification, on condition that methanol is added to the feed (Scheme 1).

AN is mainly produced by ammoxidation of propylene over bismuth molybdate catalysts at 400−500°C (Sohio process). There is no generally accepted opinion whether this reaction proceeds via in situ formation of acrolein or not. Nevertheless, acrolein itself undergoes oxidation in the presence of ammonia to yield AN, the rate of this reaction is at least several times as high as the rate of propylene ammoxidation (Scheme 1).

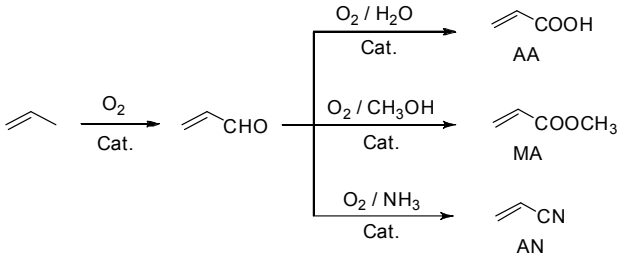

Scheme 1. Oxidative transformations of propylene and acrolein.

Taking into account a striking similarity in the acrolein conversions to AA, MA and AN, it can be surmised a common mechanism for these reactions. Obviously, a general stage should be an oxidation of acrolein into the same intermediate, which will undergo different transformations depending on the reaction conditions. The evident difference in the reactions at Scheme 1 is the presence of various reagents, such as water, methanol and ammonia.

However, no general mechanism for the reactions on Scheme 1 is suggested so far. On the other hand, it is known that nucleophilic acyl substitution in the RCOX compounds (with good leaving groups X) is a fundamental and energetically favourable route to carboxylic acid derivatives. When water, alcohols and ammonia are used as nucleophiles, carboxylic acids, esters and amides (or nitriles) are produced, respectively (Scheme 2).

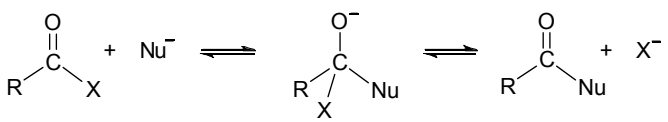

Scheme 2. Nucleophilic acyl substitution (general reaction pattern). X = halide (acid halides), acyloxy (anhydrides), alkoxy (esters), and other "good leaving" groups.

In our presentation we reasoned that catalytic oxidation of acrolein to AA, MA and AN can involve inherently nucleophilic substitution reactions with water, alcohols and ammonia. Therefore, we have shown initially that the selfsame catalyst, MoVTeNb mixed oxides, provides all three reactions, such as oxidation, oxidative esterification and ammoxidation of acrolein. The results obtained can be plausibly interpreted in terms of HAT theory and nucleophile-electrophile interactions. Recently, similar consideration was applied to catalytic oxidation of methanol over vanadia and this gave a robust explanation for predominant selectivity towards each product among formaldehyde, formic acid, dimethoxymethane and methyl formate depending on reaction conditions [1].

2 Results and discussion

The gas-phase acrolein oxidation reactions were performed using MoVTeNb oxides chosen as powerful and versatile vanadium catalyst. As expected, AA is mainly produced in the presence of water. When methanol is present in the feed, MA becomes the main product, while minor amounts of AA are also formed. When ammonia is present in the feed, AN becomes the main product. Moreover, addition of water in the feed in amount of 10 vol% practically does not influence the result of the latter reaction. Accordingly, the same catalyst provides quite efficiently oxidation, oxidative esterification and ammoxidation of acrolein (the experimental details will be disclosed in presentation). Therefore, one may propose that all these reactions are relative and, moreover, they may be happen within the same catalytic sites.

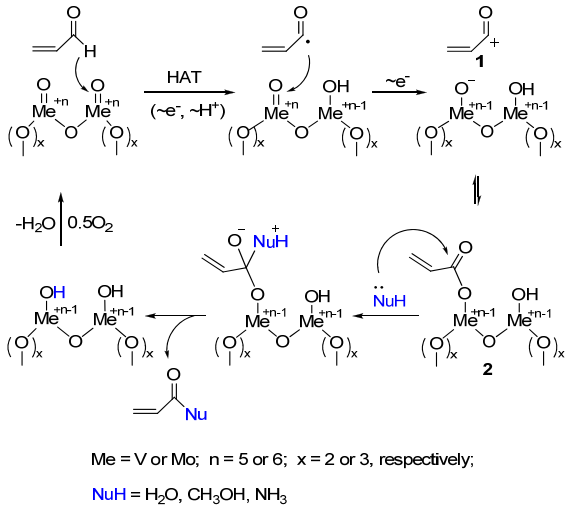

For a simplified theoretical consideration, a hypothetical sequence of the reaction steps in acrolein oxidative transformations can be outlined by the example of a monolayer dimeric metal oxide (Scheme 3). The oxidation step leads to formation of intermediates such as **1** and **2**.

Scheme 3. Proposed mechanism for oxidation of acrolein in the presence of water, methanol and ammonia over monolayer dimeric metal oxide.

Even though ion **1** does not react with a nucleophile immediately, it binds to the anion surface to form meta-stable compound **2**. Intermediate **2** is in fact a semiorganic ester, which is electrophilic enough to react with water, methanol and especially with ammonia to give AA, MA and acrylamide, respectively. Obviously, acrylamide undergoes immediate dehydration upon the reaction conditions (T > 400°C) to yield AN.

3 Conclusion

We suggest that transient acryl-vanadia/molybdenum surface complexes (formed in the oxidation stage) can react readily with typical nucleophiles, such as water, methanol and ammonia to yield the expected AA, MA and AN. The concept suggested is universal; it plausibly explains the formation of various products over the same catalyst upon oxidation conditions and is in accord with established organic and general chemistry principals.

References

[1] K.Yu. Koltunov, V.I. Sobolev, *Adv. Chem. Lett.* 1 (2013) 280.

IV-OP07

Highly Enantioselective Oxidation of Olefins and Thioethers with H_2O_2 Mediated by Chiral Titanium(IV) Complexes

Talsi E.P.[1,2], Bryliakov K.P.[1,2*]

1 - Boreskov Institute of Catalysis SB RAS, Novosibirsk, Russia
2 - Novosibirsk State University, Novosibirsk, Russia

* bryliako@catalysis.ru

Keywords: asymmetric catalysis, epoxidation, hydrogen peroxide, mechanism, sulfoxidation, titanium

1 Introduction

In the last decades, the development of catalyst systems for the asymmetric epoxidation of olefins and oxidation of thioethers to sulfoxides has been a challenging goal. While a number of biologically active chiral sulfoxides are known (including the bestseller anti-ulcer drugs esomeprazole and dexlansoprazole [1]), optically pure epoxides are valuable intermediates that can be readily involved in further asymmetric transformations via e.g. asymmetric ring-opening reactions [2].

In this contribution, we present a series of novel chiral titanium(IV) complexes of the salan and salalen families, capable of acting as highly enantioselective catalysts for the asymmetric epoxidation of olefins and oxidation of thioethers with "green" hydrogen peroxide. New insights into the mechanisms of those processes are reported.

2 Experimental/methodology

Chiral titanium(IV) salan and salalen complexes were prepared as reported [3,4]. ^{1}H and ^{13}C NMR spectra were measured on Bruker Avance 400 spectrometer at 400.13 and 100.613 MHz, respectively, or on Bruker DPX-250 at 250.13 and 62.903 MHz, respectively. Single-crystal diffraction characterization was performed at 150 K on a Bruker Apex Duo four-circle diffractometer equipped with an area detector (Mo-K_α, graphite monochromator, φ and ω scans). UV-Vis measurements were conducted on a Cary 60 spectrophotometer. The incorporation of ^{18}O into the oxidation products was determined using Agilent 7000B GC/MS with Triple Quad detector, EI - 70 eV, chromatograph Agilent 7890 equipped with a capillary column HP-5ms [30 m × 0.25 mm × 0.25μm, He carrier gas]. Enantiomeric excess values and absolute configurations were measured on a Shimadzu LC-20 HPLC chromatograph equipped with a set of Daicel chiral columns.

3 Results and discussion

A series of dinuclear chiral titanium(IV) salan and salalen complexes was synthesized, bearing different sibstituents at the chiral ligands (Figure 1).

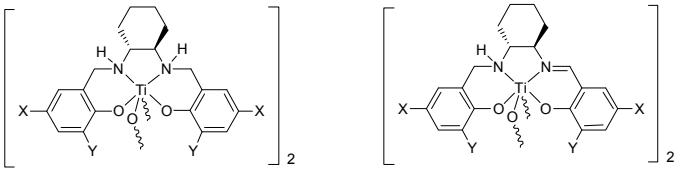

1 X= H, Y= Ph
2 X= Ac, Y= Ph
3 X= Br, Y= Ph
4 X= NO, Y= Ph
5 X= Me, Y= Ph
6 X= OMe, Y= Ph
7 X= H, Y= *o*-ClPh
8 X= H, Y= *o*-MePh
9 X= H, Y= *o*-OMePh
10 X= H, Y= *o*-PhPh
11 X= OMe, Y= *o*-OMePh
12 X= H, Y= Ph
13 X= OMe, Y= Ph
14 X= Br, Y= Ph
15 X= Ac, Y= Ph

Fig. 1. Structures of some salan (**1-11**) and salalen (**12-15**) complexes discussed in this work.

Complexes of both types appeared to be highly enantioselective catalysts for the oxidation of conjugated olefins to epoxides – precursors of biologically active complex molecules – and bulky thioethers – precursors of anti-ulcer drugs (and their steric models) – to sulfoxides with H_2O_2. Good efficiencies (TN 20 for epoxidations and TN 200-300 for sulfoxidations) were documented. A few examples are presented in Figure 2.

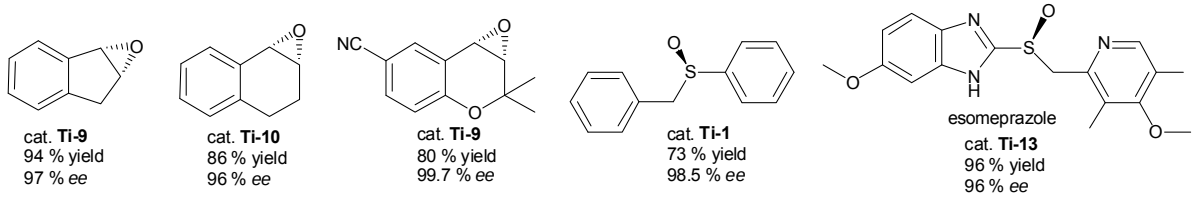

Fig. 2. Examples of asymmetric oxidations of various substrates on Ti catalysts.

Kinetic and spectroscopic studies revealed fundamental distinctions in the epoxidation and sulfoxidation mechanisms. While the active oxygen-transferring species is apparently the same for both processes ((η^2-peroxo)titanium(IV) complex), the epoxidation on Ti-salan complexes proceeds via stepwise ("Mimoun-type" [5]) mechanism, rate-limited by coordination of the olefin to the electrophilic active titanium peroxo species. In effect, variation of the olefin nucleophilicity only affects the epoxidation rate (without changing the *ee*), while the epoxidation enantioselectivity is solely determined by steric matching of the chiral ligand and the coordinated olefin.

In contrast, sulfoxidation on Ti-salalen complexes is rate-limited by generation of the titanium peroxo species upon reaction of the catalyst with H_2O_2, followed by relatively fast concerted ("Sharpless-type" [5]) oxygen transfer to the sulfide. For the asymmetric sulfoxidations, non-linear temperature dependence of the enantioselectivity has been documented, with maximum *ee*s attained at 273…283 K. This nonlinearity (*isoinversion relationship*) is indicative of the existence of two separate reaction paths, each generating two diastereomeric transition states but in varying ratios. A reaction mechanism has been proposed explaining the observed temperature dependence of enantioselectivity.

4 Conclusions

Highly enantioselective epoxidation of olefins and oxidation of thioethers with H_2O_2 on chiral titanium(IV) salan and salalen complexes is reported. The effects of steric bulk and electronic properties of chiral ligands on the enantioselectivity of oxidations have been examined. Mechanistic studies reveal distinct mechanisms operating in those processes: a stepwise mechanism for epoxidations and concerted one for sulfoxidations. For the first time, isoinversion behavior has been documented for the asymmetric sulfoxidation reactions, with T_{inv} of 273…283 K, which temperature range may be recommended for preparative reactions.

Acknowledgements

Support from the Russian Foundation for Basic Research (# 14-03-00102) is acknowledged.

References

[1] In the last 15 years, esomeprazole (marketed as Nexium™, continues to the in the top-10 worldwide best-selling drugs, with 2013 net sales of $6.135 bn in 2013), see http://www.imshealth.com/deployedfiles/imshealth/Global/Content/Corporate/Press%20Room/Global_2013/Top_20_Global_Products_2013.pdf.
[2] H. C. Kolb, M. G. Finn, K. B. Sharpless, *Angew. Chem. Int. Ed.* 40 (2001) 2004.
[3] E. P. Talsi, D. G. Samsonenko D. G., K. P. Bryliakov, *Chemistry – A European Journal* 20 (2014) 14329.
[4] E. P. Talsi, T. V. Rybalova, K. P. Bryliakov, *Submitted*.
[5] S. Huber, M. Cokoja, F. E. Kühn, *J. Organomet. Chem.* 751 (2014) 25.

IV-OP08

Catalytic Performance of Fluidizable Binder-Free Mo/HZSM-5 Catalyst in the Non-Oxidative Methane Conversion to Benzene at Severe Conditions

Zhang Z.-G.[1*], Xu Y.[1], Suzuki Y.[1], Ma H.[2], Yamamoto Y.[2]

1 - National Institute of Advanced Industrial Science and Technology (AIST), Tsukuba-shi, Japan
2 - Core Research Technology Laboratories, Meidensha Corporation, Tokyo, Japan

* z.zhang@aist.go.jp

Keywords: methane, benzene, Mo/HZSM-5 catalyst, binder-free, fluidization, fluidized-bed

1 Introduction

With a high selectivity to benzene up to 70% the non-oxidative CH_4 dehydroaromatization over Mo/HZSM-5 provides a new route of direct conversion of methane resources toward valuable chemicals. However, due to its very low equilibrium conversion (about 21% at atmospheric pressure and 1073 K), this reaction has to be performed at a temperature and a space velocity as high as possible, say, 1073 K and 10,000 mL/g/h, to gain a performance-acceptable high conversion and hourly benzene yield. Thus rapid catalyst deactivation caused by unavoidable coke formation becomes the main problem to be overcome for its practical application [1-3]. Adding a small amount of CO2 or CO into feed is helpful in improving the catalyst stability [4], but the prolonged catalyst lifetime is still short and cannot meet practical requirements. Thus, developing a practically usable, continuous catalyst-regeneration technology becomes essential, and multi-bed fluidized bed reactor systems were proposed for realization of Mo/HZSM-5's continuous regeneration [1,3]

Recently a binder-free, fluidizable Mo/HZSM-5 catalyst with a high compressive strength of 850 kgf/cm^2 was developed by Meidensha Co., Japan. In this study, this catalyst was applied to the title reaction. Its catalytic performance was evaluated in either a micro fixed-bed reactor, or a micro fluidized-bed or a two-bed type circulating fluidized bed system at the practically required severe conditions of 1073 and 10,000 mL/g/h. The results have demonstrated that this catalyst can offer a long-term stable aromatics formation activity under either periodic or continuous regeneration mode.

2 Experimental

A binder-free, spherical-shaped 6%Mo/HZSM-5(S) catalyst was used for the present study, which was manufactured by spray-drying technique and supplied by Meidensha Co. Japan. Its average particle size was measured to be about 160 μm and its minimum fluidization velocity in N2 to be 0.7 cm/s. For comparison a self-prepared 6%Mo/HZSM-5 powder catalyst was also tested in this study. All activity tests were conducted in either a micro fixed-bed reactor (10 mm i.d.) or a micro fluidized-bed one (15 mm i.d.) or a two-bed type of circulating fluidized bed reactor system (35 mm i.d.) at 1073 K and variable space velocities.

3 Results and discussion

The catalytic performance of the binder-free catalyst was first compared with the self-prepared 100% HZSM-5 based powdery catalyst in the micro fixed bed reactor at a condition of 1073 K and 10,000 mL/g/h under a periodic 5 min CH4-10 min H2 switch operation mode. The results obtained revealed that the test binder-free catalyst can exhibits the same high activity and stability as the powder catalyst does, suggesting the spray-drying shaping process brings no

negative effect to this ball-milled crystals-based, fluidizable catalyst on its performance. Comparatively, a 17% pure silica-added Mo/HZSM-5 catalyst showed a very rapid deactivation at the same condition, suggesting the necessity of developing a practically usable binder-free catalyst.

Then a three-day long test was performed in the micro fluidized bed reactor at 1073 K and 11,000 mL/g/h under a periodic 5 min CH4-20 min H2 operation mode for the binder-free catalyst to confirm its long-term activity stability. This was a daytime test without any catalyst sample removed out the reactor during three days' test, and the second and third day's test was started at heating the catalyst sample in a H2 stream up to the reaction temperature and holding it at the temperature for one hour for its full regeneration. For this operation three well-repeated performance-time dependence curves were obtained, confirming that the catalyst can maintain its long-term stability as long as it is operated in a proper regeneration mode.

To obtain a most effective regeneration mode for maintaining its high activity a six-day daytime fluidized bed test was also conducted for the binder-free catalyst at variable daily regeneration cycles. The results revealed that rather than shortening the reaction duration of reaction-regeneration cycle extending the regeneration duration is more effective for keeping the initial high activity of the catalyst and also these results suggested that the reaction duration should be shortened within 30 min and the corresponding regeneration duration extended over 60 min.

Finally, the stable performance of the catalyst was confirmed in the self-developed, two-bed type of circulating fluidized bed reactor system at 1073 K and variable space velocities under continuous regeneration mode. Typical performance-time dependences obtained are shown in Fig. 1. A stable benzene yield of about 10% was obtained in a three-day test at 1073 K and under a continuous regeneration mode.

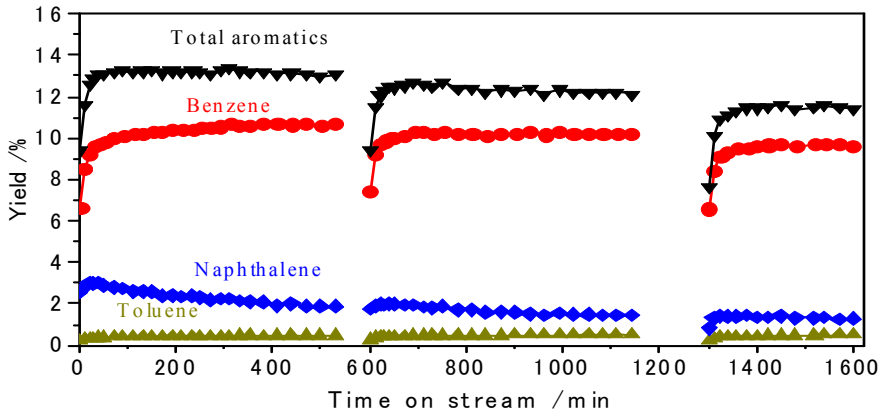

Fig. 1. Aromatics production yields reached over the fluidized binder-free catalyst in a three-day test under a continuous regeneration mode. Reactor T: 1073K and Regenerator T: 1073 K.

4 Conclusions

The fluidizable binder-free Mo/HZSM-5 catalyst enables a very high and stable aromatics production yield to be realized at 1073 K and under a continuous regeneration mode.

References

[1] Y. Xu, J. Lu, J. Wang, Y. Suzuki and Z.-G. Zhang, Chem. Eng. J., 168(2011)390-402
[2] Y. Xu, H. Ma, Y. Yamamoto, Y. Suzuki and Z.-G. Zhang, J. Natural Gas Chem., 21(2012)729-744.
[3] Y. Xu, J. Lu, Y. Suzuki and Z.-G. Zhang, H. Ma and Y. Yamamoto, Chem. Eng. Proc., 72(2013)90-102.
[4] R. Onishi, S. Liu, Q. Dong, L. Wang and M. Ichikawa, J. Catal., 182(1999)92-103

IV-OP09

Direct Dimethyl Ether Synthesis from Synthesis Gas: the Influence of Methanol Dehydration on Methanol Synthesis Reaction

Dadgar F.[1], Myrstad R.[2], Pfeifer P.[3], Holmen A.[1], Venvik H.J.[1*]

1 - Department of Chemical Engineering, Norwegian University of Science and Technology (NTNU), Trondheim, Norway

2 - SINTEF Materials and Chemistry, Trondheim, Norway

3 - Karlsruhe Institute of Technology (KIT), Institute for Micro Process Engineering (IMVT), Eggenstein-Leopoldshafen, Germany

* Hilde.J.Venvik@ntnu.no

Keywords: DME, methanol synthesis, methanol dehydration, direct synthesis

1 Introduction

Dimethyl ether (DME) can be synthesized directly from synthesis gas using a dual catalyst system that permits both methanol synthesis (Cu-based catalyst) and dehydration (acidic catalyst) in a single process unit. While syngas conversion to methanol is thermodynamically limited, further conversion of methanol to DME allows higher single-pass conversion.

The objective of this work is to study the effect that combining methanol synthesis and methanol dehydration in a single reactor, can have on the catalytic performance. In order to do so, the influence of operating conditions (space velocity, temperature, pressure, time on stream and syngas composition) on the activity, selectivity and stability of the catalyst was studied and compared for the methanol synthesis, methanol dehydration and direct DME synthesis.

2 Experimental

The experiments were conducted in a stainless steel micro packed bed reactor-heat exchanger. The reactor consists of a 6 cm long reaction slit with rectangular cross section of 8.8×1.5 mm^2, sandwiched between cross flow channels for circulation of heat transfer oil. The reactor has already been tested under similar operating conditions for methanol [1] and direct DME [2] synthesis, and is established as practically isothermal, isobaric and free from mass transfer limitations, and to have a narrow residence time distribution. Catalyst, either conventionally prepared Cu-ZnO-based methanol synthesis catalysts, a commercial H-ZSM-5 or γ-alumina methanol dehydration catalyst, or a physical mixture of these, was packed into the reactor in a particle size range of 80-125 μm. Products were analyzed online using a gas chromatograph equipped with a TCD and a FID. Experiments were conducted at temperature, pressure and space velocity ranges of 210-270°C, 10-50 bar and 150-800 Nml/(min×gr catalyst), respectively.

3 Results and discussion

Figure 1 illustrates the product yields for methanol synthesis and direct DME synthesis under identical operating conditions. The direct DME synthesis experiment was performed using a hybrid catalyst with excess amount of the dehydration component. Therefore, almost all the methanol formed was converted further to DME, i.e. the overall synthesis was controlled by methanol formation. Accordingly, the space velocity is based on the weight of the methanol synthesis catalyst for both experiments. As expected, at higher temperatures, syngas conversion and product yield are limited thermodynamically in the methanol synthesis experiment, while product yield continues to increase with temperature in the direct DME synthesis, for which the equilibrium product yield is much higher.

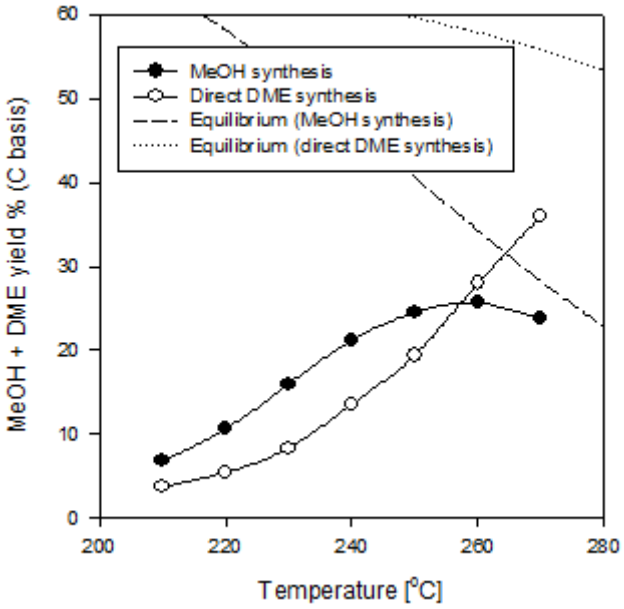

Fig. 1 Product yields against reaction temperature for methanol synthesis and direct DME synthesis, under identical SV (based on methanol synthesis catalyst weight), P=50 bar, and syngas composition $H_2/CO/CO_2/CH_4/N_2$: 56/28/5/6/5 mol%.

Apart from the apparent synergistic benefit when thermodynamics is a limiting factor, the results suggest that combining methanol synthesis and dehydration in a single reactor has a negative effect on the methanol formation kinetics. That can be observed as a lower product yield in the direct DME experiment (also lower methanol formation rates, as space velocities are identical) at lower temperatures where the effect of the reverse reaction on methanol synthesis is smaller. The apparent activation energy of methanol formation seems, however, similar for both experiments in the kinetic regime and have been estimated to 85-86 kJ/mol. Similar conclusions can be drawn using different dehydration catalyst and also under a synthesis gas with a H_2/CO molar ratio of 1.

The origin of the observed phenomena will be further discussed and investigated, including the possible inhibition by the dehydration products. Such effects are being studied by introducing DME and water to the feed of the methanol synthesis reaction.

Acknowledgements

The financial support from the Research Council of Norway (contract No 208351/E30) is gratefully acknowledged.

References

[1] H. Bakhtiary-Davijany, F. Dadgar, F. Hayer, X.K. Phan, R. Myrstad, H.J. Venvik, P. Pfeifer, A. Holmen, *Ind Eng Chem Res.* 51 (2012) 13574-13579.

[2] F. Hayer, H. Bakhtiary-Davijany, R. Myrstad, A. Holmen, P. Pfeifer, H.J. Venvik, *Chem. Eng. Process. Process Intensif.* 70 (2013) 77-85.

IV-OP10

Methanol to Hydrocarbons over ZSM-5: Diffusion and the External Particle Surface

Erickson J.K.[1], Baucherel X.[2], Gladden L.F.[1*]

1 - University of Cambridge, Department of Chemical Engineering and Biotechnology, Cambridge, United Kingdom

2 - Johnson Matthey Technology Centre, Chilton, Billingham, United Kingdom

* lfg1@cam.ac.uk

Keywords: ZSM-5, methanol-to-hydrocarbons, MTO, external surface, diffusion, zeolites

1 Introduction

The methanol to hydrocarbons process (MTH) is a valuable means by which to balance the use of fossil and renewable resources, providing a wide range of hydrocarbons from either renewable or fossil-derived methanol. MTH technology can contribute to addressing the current global propene shortage associated with shale gas growth and the expansion of coal-to-liquid in China, whilst also being an integral part of a future renewable methanol-based economy as proposed by Olah et al. [1]. ZSM-5 is the most extensively used catalyst for MTH. The reaction has been shown to proceed via the hydrocarbon pool mechanism, where polyalkylated aromatics and larger olefins form within zeolite pores and combine with acid sites to form a hybrid catalyst [2]. The mechanism consists of two catalytic cycles: one in which olefins are repeatedly methylated to form branched species, and another involving the methylation and dealkylation of aromatics to form light olefins. The selectivity towards certain products such as ethene can be used to measure the propagation of these olefin and aromatic-based cycles [3].

An established modification of ZSM-5 catalysts is the deactivation of non-shape selective acid sites on the external particle surface, commonly achieved via post-synthesis deposition of silicon alkoxides. This work describes for the first time the effect of chemical liquid deposition of tetraethyl orthosilicate (TEOS) on ZSM-5 for use as a catalyst in the MTH reaction. We have studied the roles of the external zeolite surface and diffusion in affecting the conversion, selectivity and deactivation of the MTH reaction.

2 Experimental

ZSM-5 zeolites H-Z41 and H-Z81, with similar crystallite sizes of ~70nm but different SiO_2:Al_2O_3 ratios (41 and 81, respectively) were supplied by Johnson Matthey plc. H-Z41 was silylated with TEOS in three cycles to give Sil-Z41, using the chemical liquid deposition method reported elsewhere [4]. In addition to standard techniques such as temperature-progammed desorption of ammonia and collidine, ^{29}Si and ^{27}Al MAS NMR, N_2 soprtion, and infrared spectroscopy, the effect of silylation on adsorption capacity and access of reactants to the internal pore structure was investigated using a tapered element oscillating microbalance and pulsed field gradient NMR. MTH catalyst testing was performed using a 3 mm inner-diameter quartz microreactor at 350 °C with a WHSV of 24 h^{-1} and monitored with online gas chromatography.

3 Results and discussion

Silylation of H-Z41 caused a 18 % decrease in acidity primarily due to the loss of external acid sites, while H-Z81 had a 44 % lower acidity compared to H-Z41 due to its reduced aluminium content (Table 1). In MTH catalyst testing, selectivity to ethene was the same for H-Z41 and H-Z81 but was doubled in the case of Sil-Z41, representing a shift towards the

aromatic-based mechanism. While the catalytic lifetime of H-Z81 was almost double that of H-Z41, silylation caused the lifetime of H-Z41 to decrease by approximately half (Figure 1).
In addition to reducing acidity, silylation has been shown to cause narrowing of zeolite pore mouths [5]. This will cause a shift towards smaller products by restricting the diffusion of larger molecules leaving the pores, and also a decrease in lifetime by making pores more susceptible to blockage by polyaromatics and coke deposits. Through a variety of characterisation techniques, we have found that the diffusion of larger hydrocarbons in silylated ZSM-5 is inhibited and that the MTH reaction proceeds in the absence of active sites on the external zeolite surface.

Table 1. Properties of ZSM-5 catalysts used for MTH

Zeolite	Form	Acidity (mmol/g)	Ethene selectivity
H-Z41	activated H+	0.63	9 %
Sil-Z41	silylated	0.52	18 %
H-Z81	activated H+	0.35	9 %

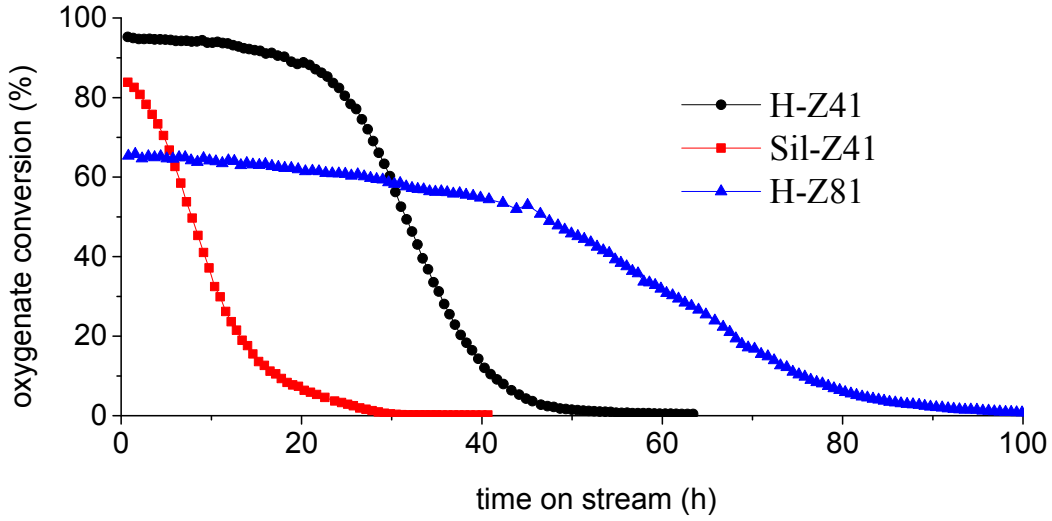

Fig. 1. Oxygenate conversion in the MTH reaction as a function of time on stream, catalysed by zeolites H-Z41, Sil-Z41 and H-Z81.

4 Conclusions

These findings suggest that catalytic activity in the MTH reaction is confined to the internal pore space of ZSM-5, while pore mouth narrowing shifts the product distribution towards smaller products and increases the rate of deactivation due to coke formation.

Acknowledgements

We thank the EPSRC and Johnson Matthey plc for supporting this work and Dr Carmine D'Agostino for his help and advice.

References

[1] G. Olah, A. Goeppert, G. Prakash, Beyond Oil and Gas: The Methanol Economy (2009) Wiley.
[2] M. Bjørgen, U. Olsbye, D. Petersen, S. Kolboe, *J. Catal*. (2004) 221, 1.
[3] S. Ilias, R. Khare, A. Malek, A. Bhan, *J. Catal*. (2013) 303, 135.
[4] S. Zheng, H.R. Heydenrych, A. Jentys, J.A. Lercher, *J. Phys. Chem. B* (2002) 106, 9552.
[5] M. Niwa, M. Kato, T. Hattori, Y. Murakami, *J. Phys. Chem*. (1986) 90, 6233.

IV-OP11

Insights in the Reaction Mechanism for HMF Oxidation to FDCA over Bimetallic Au/Pd Nanoparticles

Cavani F.[1*], Lolli A.[1], Utili L.[1], Amadori R.[1], Lucarelli C.[1,2], Albonetti S.[1]

1 - Dipartimento di Chimica Industriale "Toso Montanari", Università di Bologna, Bologna, Italy
2 - Università dell'Insubria, Como, Italy

* fabrizio.cavani@unibo.it

Keywords: HMF, 2,5-Furandicarboxylic acid, Pd–Au nanoparticles, Cannizzaro reaction

1 Introduction

Furandicarboxylic acid (FDCA) has been suggested as an important renewable building block for the synthesis of polymers, alternative to those obtained from terephthalic acid. As an example, the Avantium Company is using FDCA to produce polyethylene furandicarboxylate. The exact route for producing FDCA has not yet been disclosed but the current technology for terephthalic acid production using metal/bromide catalysts is probably being evaluated [1]. One drawback of these systems is the use of corrosive and dangerous compounds, which make the process polluting. Moreover, there are concerns regarding the purity of both the product and the final polymer. Recently Au-supported catalysts have been found to be very active for 5-hydroxymethylfurfural (HMF) oxidation to FDCA [2,3]. So far, catalyst stability and productivity on this type of catalysts are low but the possibility to obtain high product purity and process sustainability makes this approach highly interesting for the future.

2 Experimental part

Au/TiO_2, Pd/TiO_2, and $Au\text{-}Pd/TiO_2$ catalysts were prepared by the immobilization on the TiO_2 surface of the preformed monometallic and bimetallic colloids [4]. Core-shell nanoparticles were prepared from a monometallic system (Au or Pd) which had been used as seed for the nucleation of the second metal. The oxidation of 5-hydroxymethyl-2-furfural (HMF) was carried out using an autoclave. The reactor was charged with an aqueous solution containing the appropriate amount of HMF, base (NaOH), and catalyst (HMF/metal molar ratio = 100).

3 Results and Discussion

The attention has been mainly focused on the role played by the active phase in the reaction mechanism. The comparison of the activity of systems with different Pd/Au molar ratio indicated that the production of FDCA and different intermediates was strongly dependent on Pd and Au content (Figure 1). $Pd\text{-}TiO_2$ was poorly selective to FDCA because of its inability to transform the 5-hydroxymethyl-2-furancarboxylic acid (HMFCA) intermediate. Conversely, an increase in FDCA selectivity was observed increasing the gold content, especially for the sample which has Pd/Au molar ration of 1:6. Therefore, a small quantity of Pd seems to be adequate to strongly change the electronic properties of gold phase and to enhance the catalytic activity in alcohol oxidation. The catalytic activity of Pd-Au catalysts was strongly affected by thermal treatments, suggesting some modifications on the Pd-Au alloy. The segregation of Pd on the outer part of bimetallic nanoparticles might explain the modification of the path for FDCA formation, making it more similar to the one observed with the monometallic Pd. Indeed, calcined Pd/Au material was unable to transform molecules containing the –COOH functional group, such as HMFCA and 5-formyl-2-furancaboxylic acid (FFCA) intermediates. PVP-protected Pd-Au nanoparticles with different structures (alloy and core-shell) were tested in the

reaction in order to confirm the different HMF oxidation mechanisms depending on whether the active phases preferentially expose Pd or Au atoms (Figure 2A and 2B). Moreover, the Cannizzaro-type disproportionation was demonstrated to be involved in FDCA formation with some of the studied systems, indicating that this reaction must be taken in account when studying the furanic aldehydes reactivity.

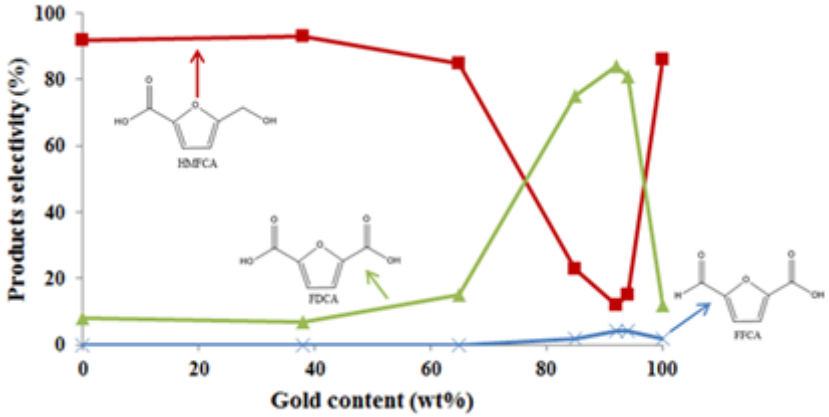

Fig. 1. Product selectivity on catalysts at different Pd:Au atomic ratios. Results are given at total conversion of HMF. Reaction conditions: temperature 70°C, O2 pressure 10 bar, reaction time 240 min, HMF:Metal:NaOH molar ratio 1:0.01:2. Legend: □ HMFCA, □ FDCA, X FFCA.

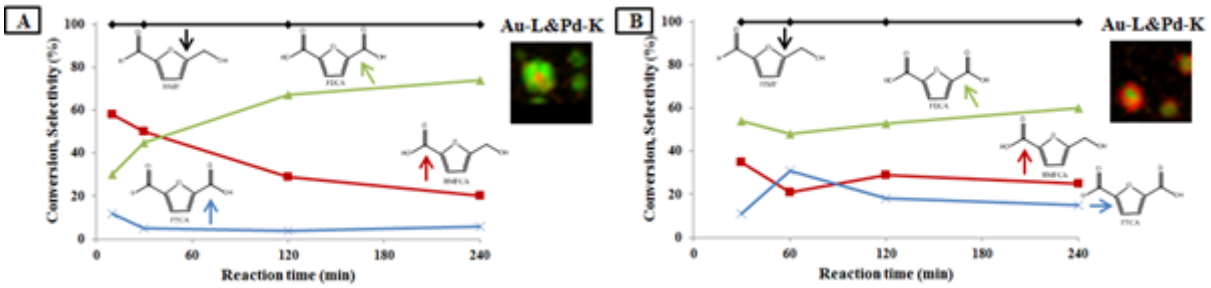

Fig. 2. HMF conversion and product selectivities as a function time on unsupported $Pd_1@Au_6$ (Fig. 1A) and $Au_6@Pd_1$ (Fig. 1B) core-shell nanoparticles. Reaction conditions: temperature 70°C, O_2 pressure 10 bar, HMF:Metal:NaOH molar ratio 1:0.01:2. Legend: ♦ HMF conversion, □ HMFCA selectivity, □ FDCA selectivity, **X** FFCA selectivity

Acknowledgments

We gratefully acknowledge INSTM for co-financing the PhD project of A.L

References

[1] C. Munoz de Diego, P. Shammel Wayne, A. Dam Matheus, J. M. Gruter Gerardus, WO Patent 2011/043660, 2011 assigned to Furanix Technologies BV.
[2] T. Pasini, M. Piccinini, M. Blosi, R. Bonelli, S.Albonetti, N. Dimitratos, J.A. Lopez-Sanchez, M. Sankar, Q.He, C. J. Kiely, G. J. Hutchings, F. Cavani Green Chem. 13 (2011) 2091.
[3] S. Albonetti, A. Lolli, V. Morandi, A. Migliori, C. Lucarelli, F. Cavani Appl. Catal. B Environmental 2015, 163, 520–530.
[4] S. Albonetti, A. Lolli, L. Utili, R. Amadori, F. Ospitali, C. Lucarelli, F. Cavani Appl. Catal. A doi:10.1016/j.apcata.2014.11.020.

IV-OP12

Noble Metal Nanoparticles Supported on Carbon-Based Materials as Catalysts for 5-HMF Oxidation to FDCA

Nese V., Schüth F.*

Max-Planck-Institut für Kohlenforschung, Mülheim an der Ruhr, Germany

* schueth@mpi-muelheim.mpg.de

Keywords: 5-HMF, FDCA, oxidation, noble metals, polyacrylate

1 Introduction

2,5-furandicarboxylic acid (FDCA) has been identified as a building block chemical for the production of bio-based polyesters and polyamides [1]. In fact, this molecule can be produced by 5-hydroxymethylfurfural (5-HMF) oxidation, which is obtained from sugars like fructose and glucose through a dehydration step.

The selective oxidation of 5-HMF to FDCA with molecular oxygen in water is a green alternative to the use of stoichiometric oxidants and processes occurring in organic solvents. The addition of a base is often necessary to achieve high FDCA yields, since the presence of hydroxide ions in the reaction mixture facilitates the oxidation of both the aldehyde and methyl-alcohol groups of 5-HMF. Additionally, it improves the solubility of the final product.

2 Experimental/methodology

In the present study, 5-HMF oxidation was performed in a 50 mL stainless-steel autoclave, in the presence of noble metal (Pt, Pd, Ru, Au) catalysts supported on porous carbon and polymeric materials. The standard reaction conditions used were 100°C, 8 bar O_2, and $NaHCO_3$ was added to the reaction mixture as the base (pH 9).

3 Results and discussion

In a first series of experiments, commercial Pt(5%)/C, Ru(5%)/C and Pd(5%)/C were used as catalysts for 5-HMF oxidation: the highest reaction rate was observed in the presence of Pt(5%)/C (full conversion was reached after 2 hours) and 91% of FDCA was obtained after 24 hours reaction time. Using Pd(5%)/C, high selectivity towards the intermediates of HMF oxidation was achieved, but the conversion and FDCA yield were 87% and 13% after 24 hours, respectively. Ru(5%)/C yielded large amounts of unidentified by-products from the early stages of the reaction.

Two Au(5%)/C catalysts were prepared with two different methods that resulted in different particle size distributions: when the carbon was impregnated with a solution of the metal precursor and subsequently reduced, very small particles were observed in the TEM images; when the metal nanoparticles were pre-formed in solution using PVA as stabilizer and deposited on the carbon support, Au particles with a diameter between 2 and 5 nm were achieved. As shown in Fig. 1, only particles with dimensions above a certain size are active for 5-HMF oxidation: only the material with bigger particles was showing a high reaction rate and yielding 95% FDCA after 8 hours.

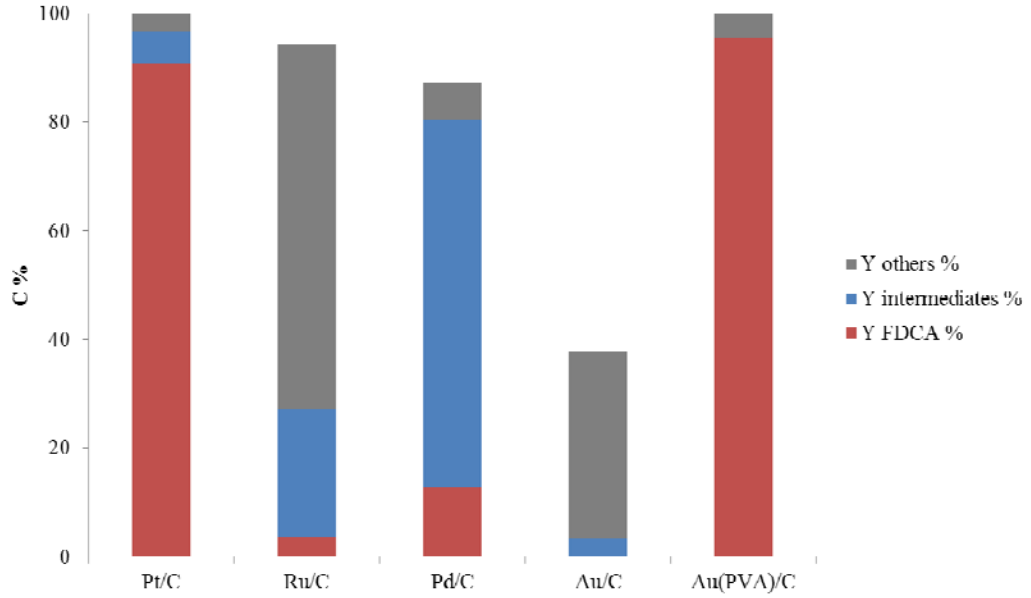

Fig. 1. Conversion of 5-HMF and yield of products after 24 hours of reaction

Two metal precursors ($Pt(NH_3)_4(NO_3)_2$ and $Ru(NH_3)_6Cl_3$) were ion-exchanged on commercial PS-DVB sulfonated polymers (Amberlyst 35 and Amberlyst 70) and the reduction of the noble metal was performed with $NaBH_4$ solution or under H_2 pressure, yielding particles with dimensions above 15-20 nm in all the materials. The low activity of these catalysts pointed out once again the importance of the metal particle size.

Since 5-HMF is an unstable product formed by the dehydration of hexoses, it would be desirable to perform FDCA synthesis in one-pot reaction starting from sugars like fructose and glucose. Unfortunately, direct oxidation of these two reactants can occur already at room temperature in the presence of noble metals like Au or Pd [2]. A study on fructose dehydration revealed that a series of highly hydrophilic sulfonated polyacrylates (DAE25) is inaccessible to the reactant, but at the same time it suppresses further degradation of 5-HMF to levulinic acid, one of the most abundant side products. As a matter of fact, no levulinic acid was formed when these polymers were present, while 44% of this by-product was obtained when Amberlyst 35 was used, the most active among a series of commercial PS-DVB sulfonated polymers. Therefore, these polyacrylates materials could be ideal supports for the preparation of catalysts suitable for the one-pot reaction from fructose to FDCA.

4 Conclusions

Pt, Pd and Au supported on carbon showed high selectivity towards the products of 5-HMF oxidation. Among them, Au(PVA)/C with particle size between 2 and 5 nm gave the best performance, yielding 95% FDCA after 8 hours of reaction. The study underlines the importance of particle dimensions in the preparation of an active catalyst. A study on fructose dehydration showed that a series of polyacrylates polymers (DAE25) could be a suitable support for the synthesis of a catalyst for the production of FDCA directly from fructose.

Acknowledgements

Funding by the ERC "POLYCAT" and the Cluster of Excellence TMFB is gratefully acknowledged.

References

[1] T. Werpy, G. Petersen, *U.S. Department of Energy, NREL/TP-510-35523,* 2004
[2] M. Besson, P. Gallezot, *Catalysis Today* 57 (2000) 127

IV-OP13

Catalytic Applications of Palladium Nanoparticles-Supported Nanocomposites in Carbonylation Reactions

Zhu Y.*

Institute of Chemical and Engineering Sciences, Singapore

* zhu_yinghuai@ices.a-star.edu.sg

Keywords: nanocatalyst, palladium nanoparticle, nanocomposite, carbonylation

1 Introduction

Supported palladium nanoparticles (Pd NPs) have been widely used as efficient catalysts in organic conversions such as Suzuki-Miyaura cross-coupling reactions due to their high activity and recyclability [1,2]. We have successfully loaded Pd-NPs on metal organic frameworks (MOF), cyclic poly(*L*-lactide)-clay, carbon nanotubes and graphene oxides to form Pd-NPs-supported nanocomposites [3-7]. The as-prepared nanocomposites have been used as catalysts for carbonylation of various aryl halides to form corresponding amides and ketones, repectively (see Eqs 1-2). These catalysts show high activity and good recyclability. Detail synthesis methods and activity will be presented.

$$Ar–X\ (X = Cl, Br, I) + CO + HNRR' \rightarrow Ar–CO–NRR' \quad \text{(Eq 1)}$$

$$Ar–I + CO + Ar'–B(OH)_2 \rightarrow Ar–CO–Ar' \quad \text{(Eq 2)}$$

2 Experimental

Pd NPs-supported catalysts were synthesized via reduction precursors of M_2PdCl_4 (M = H,K) or $PdCl_2(PhCN)_2$ by sodium borohydride, hydrazine or ethylene glycol, respectively [3-7] in the presence of corresponding supports. The supported catalysts were dried in vacuum to a constant weight before using. The resultant catalysts were fully characterized by XRD, TEM, XPS, TGA, FT-IR and ICP to identify the catalyst morphology, oxidation state and loading amount.

Aminocarbonylation reactions between aryl halides and amines were carried out at a temperature of 105°C, 120°C and 130°C, respectively. Various CO feeding pressures (1.0, 10.0, 10.3 and 12.4 bar) were examined [3-7]. K_2CO_3 (1~2eq) was used to promote the reactions.

Carbonylation reactions between arylboronic acids and aryl halides were carried out in anisole in the presence of base K_2CO_3 at a CO pressure of 6.9 bar [3].

All the products were separated either by flash chromatography or by thin layer chromatography and characterized by ^1H, ^{13}C NMR spectroscopy.

3 Results and discussion

Pd NPs-supported catalysts were easily prepared by conventional reducing processes. In general, the obtained Pd NPs were small, less than 5nm, and well dispersed according to TEM images as shown in **Figure 1**. Aminocarbonylation of aryl halides were carried out catalyzed by above supported palladium catalysts. Some results are listed in **Scheme 1 (a)** [6]. The catalysts showed high activity for aryl iodides, up to 98% yield was reached. Aryl bromides and chlorides are relatively inert. Amides products were obtained in medium to high yields under the same conditions. The carbonylation of aryl iodides lead to the formation of new carboranylaryl ketones in 51-83% isolated yields as summarized in **Scheme 1 (b)** [3].

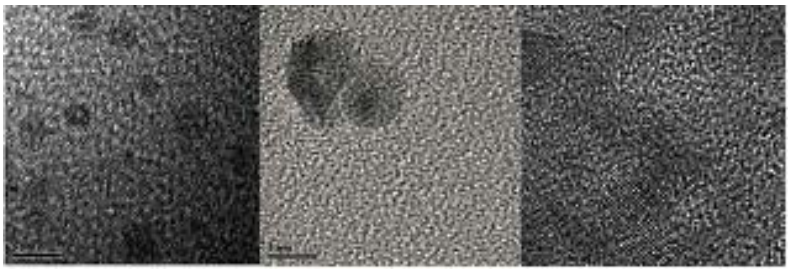

(a) (b) (c)

Fig. 1. TEM images of Pd NPs on metal organic frameworks (MOF-5) (a) [6], graphene oxide (GO) [3] and poly(L-)lactide/clay hybride (c) [5].

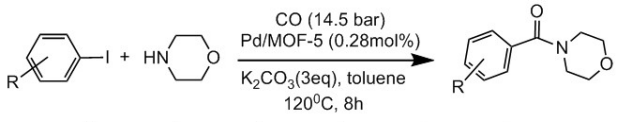

R	H	*p*-Me	*p*-OMe	*p*-NO_2
Yield (%)	98	97	75	78
R	*p*-Cl	*m*-Me	*m*-OMe	*o*-Me
Yield (%)	96	94	84	72*

(* catalyst loading Pd: 1.12mol%, 12h)

(a)

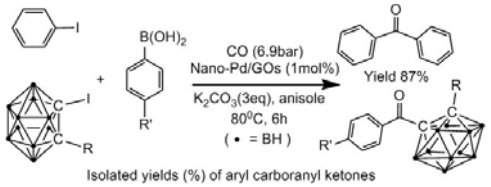

Isolated yields (%) of aryl carboranyl ketones

R	R' = H	R' = OMe	R' = F
H	51	72	66
Me	62	83	70
Ph	55	64	78

(b)

Scheme 1. Selected results for aminocarbonylation (a) [6] and carbonylation (b) [3].

4 Conclusions

Supported Pd NPs based heterogeneous catalysts are stable and recyclable with high activity for aminocarbonylation and carbonylation reactions to form corresponding amides and ketones. The catalysts are able to tolerate a wide scope of functional groups to synthesize various carbonyl compounds which are potentially important in pharmaceutical industry and fine chemistry. We are expecting their wide applications in industry.

Acknowledgements

We thank the Institute of Chemical and Engineering Sciences, GlaxoSmithKline and the Singapore Economic Development Board for funding support.

References

[1] N. Miyaura, A. Suzuki, Chem. Rev. 95 (1995) 2457-2483.
[2] Y. Zhu, N. S. Hosmane, Coord. Chem. Rev. doi:10.1016/j.ccr.2014.10.002.
[3] O. B. Algin, V. R. Vangala, S. C. Chia, L. P. Stubbs, N. S. Hosmane, Y. Zhu, Dalton Trans. 43 (2014) 5014-5020.
[4] O. B. Algin, T. Y. Karen, N. S. Hosmane, Y. Zhu, J. Organomet. Chem. 747 (2013) 184-188.
[5] A. V. Prasad, O. B. Algin, Y. L. Woo, L. P. Stubbs, Y. Zhu, J. Polym. Sci. A Polym. Chem. 51 (2013) 4167-4174.
[6] T. T. Dang, Y. Zhu, S. C. Ghosh, A. Chen, C. L.L. Chia, A. M. Seayad, Chem. Commun. 48 (2012) 1805-1807.
[7] T. T. Dang, Y. Zhu, J. S. Y. Ngiam, S. C. Ghosh, A. Chen, A. M. Seayad, ACS Catal. 3 (2013) 1406-1410.

IV-OP14

Hydrogenation Reactions in Aqueous Media Catalysed by Pd and Pt Green Nanoparticles

Di Pietrantonio K.[1,2], Tonucci L.[1,3], D'Alessandro N.[1,2*], Bressan M.[1,2]

1 - University "G.d'Annunzio" of Chieti Pescara, Chieti, Italy
2 - Department INGEO, University "G.d'Annunzio" of Chieti Pescara, Chieti, Italy
3 - Department of Philosophical, Educational and Economic Science, University "G.d'Annunzio" of Chieti Pescara, Chieti, Italy

* dalessan@unich.it

Keywords: green nanoparticles, lignin, palladium, platinum, isomerization, hydrogenation

1 Introduction

Chemoselective catalytic hydrogenation of α,β-unsaturated alcohols, aldehydes/ketones or alkenes is a demanding task for the flavour, fragrance and pharmaceutical industries. Metal nanoparticles (NPs) are good candidates as catalysts for this purpose thanks to their peculiar properties such as the high surface-to-volume ratio and the size-dependent electronic structure.

Pd and Pt NPs, synthesised in water by a simple and green way (20 °C, 1 atm), employing lignin as stabilizing/reducing agent, are able to catalyse oxidation, reduction and C-C cross coupling reactions.[1,2] Lignin is a widely available by-product of wood and paper industry.

2 Experimental

Lignin stabilized Pd and Pt nanoparticles were prepared and characterized in accordance with our previous work[1].

For the hydrogenation reactions we operated as follow: 15 mL of water was placed into an hermetically closed 20 mL vial; after a purging step with H_2, 0.3 mmol of the substrate was added and then 100 µL of Pd NPs (0.56 µmol of Pd) or Pt NPs (0.97 µmol of Pt) solution was introduced. The reaction mixture was left under static H_2 atmosphere at room pressure and temperature (20 °C) and stirred for 24 h.

3 Results and discussion

We prepared and characterized a series of twelve NPs using two metals (Pd and Pt) with different water-soluble lignins: Kraft lignin (KrLig), ammonium lignosulphonate (AmLig), calcium (CaLig) and sodium (NaLig) lignosulphonates and the corresponding low-sugar ones (CaROLig and NaROLig).

Pd NPs have spherical shape (15-25 nm) while Pt NPs are irregular and smaller (7-12 nm), as revealed in TEM images.

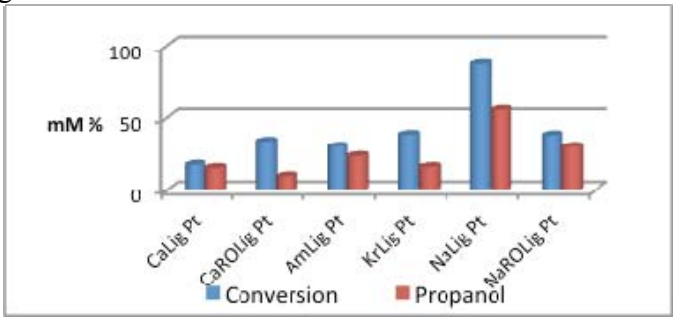

Fig. 1. Conversion of allyl alcohol and products formation in presence of Pd NPs

We investigated the different catalytic activity of Pt and Pd NPs towards the hydrogenation

of allyl alcohols in mild conditions (water media, room T and P, H_2 atmosphere).

The conversion of allyl alcohol with Pd NPs was quantitative unless with NaLig Pd (47% conversion). However, the main reaction product was propionaldehyde, the isomerization product[3] (Fig. 1).

At the contrary, when we put allyl alcohol with Pt NPs, 1-propanol was the only detectable product inside the aqueous solution (by ^{1}H NMR) (Fig. 2). However, analysing the headspace of the reaction vessels (by GC-MS) we found both hydrocarbons, namely propene and propane.

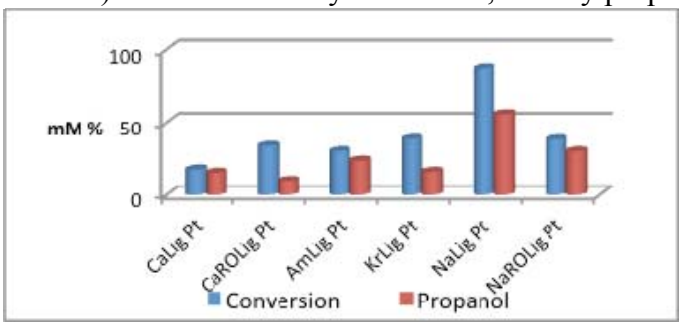

Fig. 2. Conversion of allyl alcohol and product formation in presence of PtNPs

To best understand if and how the substitutions on the sp^2 carbon of allyl alcohols address the reaction to isomerization or to the double bond hydrogenation, we tested also crotyl alcohol and 3-methyl-2-buten-1-ol. Comparing the data, with both metal NPs, we observed lower conversions when allyl alcohol is the reactant, while 3-methyl-2-buten-1-ol always showed the higher reactivity (Fig. 3).

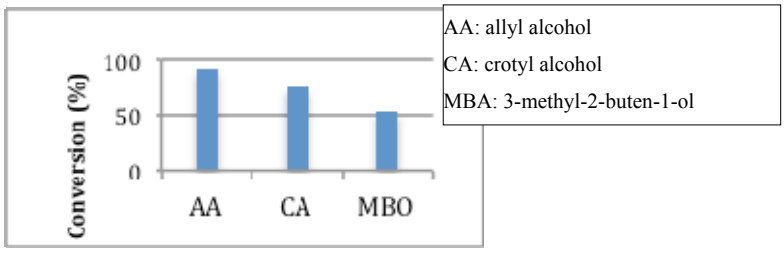

Fig. 3. Conversions of alcohols in presence of PdNPs

4 Conclusions

In presence of Pd NPs, we observed always C=C hydrogenation, isomerization and double bond migration products; in the case of Pt NPs only saturated alcohols and hydrocarbons were detected.

We are extending our work testing NPs for hydrogenation of unsaturated non-allyl alcohols, like butenol and pentenol, to obtain important saturated alcohols, useful for chemical industry as well as promising alternative fuels.

Acknowledgements

We thank the "Consorzio di Ricerca per l'Innovazione Tecnologica, la Qualità e la Sicurezza degli Alimenti S.C.R.L." (CIPE fundings 20.12.04; DM 28497) for financial support. KDP thanks the University "G.d'Annunzio" for the scholarship relative to the PhD program (cycle XXVIII).

References

[1] F. Coccia, L. Tonucci, D. Bosco, M. Bressan, N. d'Alessandro, *Green Chem.* 14 (2012) 1073.
[2] F. Coccia, L. Tonucci, N. d'Alessandro, P. D'Ambrosio, M. Bressan, *Inorg. Chim. Acta* 399 (2013) 12.
[3] E. Sadeghmoghaddam, C. Lam, D. Choi, Y.-S. Shon, *J. Mater. Chem.* 21 (2011) 307.

IV-OP15

Room Temperature Glucose Isomerization in Sn-BEA: on the Role of Diffusion under Practical Reaction Conditions

Van Der Graaff W.N.P.*, Tempelman C.H.L., Pidko E.A., Hensen E.J.M.

Inorganic Materials Chemistry Group, Eindhoven University of Technology, Eindhoven, The Netherlands

* w.n.p.v.d.graaff@tue.nl

Keywords: carbohydrate, biomass, diffusion, limitations, Sn-zeolites, sustainable chemistry

1 Introduction

Lignocellulosic biomass is expected to become an important future feedstock for sustainable production of chemicals and fuels. The isomerization of carbohydrates is a key transformation in all selective glucose conversion schemes. Such reactions can be catalyzed using Lewis acidic materials. To date, Sn-BEA zeolite has been identified as one of the most promising catalysts for aldose to ketose isomerization. The origin of the unique reactivity of this catalyst is not well understood yet. A recent theoretical study has indicated that the topology of zeolite catalyst does not influence the intrinsic activity of Sn-centers in its framework, while it may strongly influence the transport of reagents and products through the micropores to and from the active sites [1]. Here, we present the first experimental study on the role of transport phenomena on the catalytic activity of Sn-BEA in sugar isomerization by in situ solid state ^{13}C MAS NMR spectroscopy complemented by kinetic experiments. To validate the theoretical predictions and understand the role of zeolite topology, the catalytic performance of Sn-functionalized BEA, MOR, and MCM-22/ITQ-2 for isomerization of 1,3-dihydroxyacetone (DHA) and D-glucose was investigated.

2 Experimental/methodology

Hydrothermal synthesis of Sn-BEA zeolites (Sn-BEA-HF) was carried out according to the procedure reported by Corma et al. [2]. Post-synthetic modification of zeolites with framework Sn was done following a procedure recently developed in our laboratory [3]. Prior to Sn introduction, the zeolite (MOR, MCM-22/ITQ-2, BEA) was dealuminated by treatment with 65% HNO_3 at 110°C overnight. After drying (3h, 170°C), Sn-functionalization was carried out by dry impregnation with anhydrous $SnCl_4$ at 100°C for 16 h. Excess $SnCl_4$ was removed by extensive washing with methanol. The materials were calcined at 550°C for 5 h (1 K/min). In-situ NMR measurements were carried out by impregnation of the zeolite with a solution of $^{13}C_1$-labeled glucose in D_2O (Sugar:Sn ratio = 5) followed by evacuation for 15 min.

3 Results and discussion

We compared the conversion of $^{13}C_1$-labeled glucose by in-situ solid state ^{13}C NMR in a time-resolved manner directly after impregnation of the reactant in dehydrated and hydrated Sn-BEA. The NMR results are shown in Figure 1. The reaction occurs already at room temperature when the sugar was brought into contact with the dehydrated zeolite (Fig 1a). On contrary, when labelled glucose was brought into contact with a hydrated Sn-BEA zeolite, the reaction proceeded much slower (Fig. 1b). It is interesting to mention that the reaction rate was negligible, when this reaction was carried out in a batch reactor using water as the solvent. These findings strongly indicate that the exchange of the solvent molecules in the micropores with the glucose reactant molecules is slow and to some degree limits the reaction rate. Accordingly, we argue that counter-diffusion limits the catalytic reactivity of Lewis acid zeolite catalysts for glucose activation.

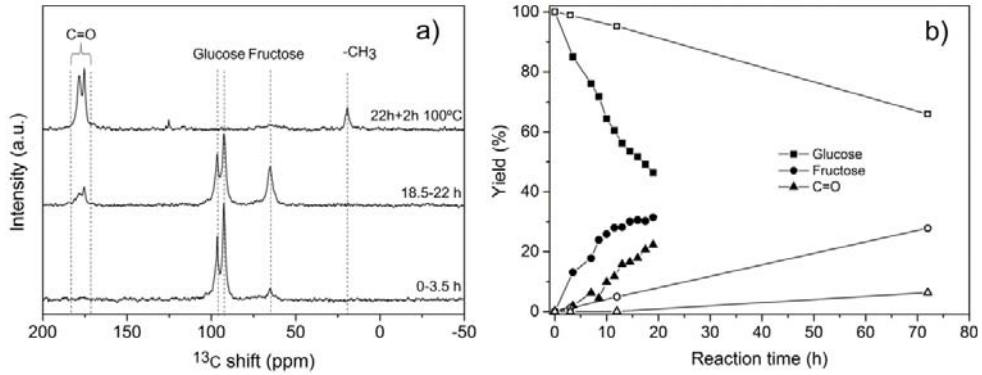

Figure 1. a) Conversion of $^{13}C_1$-glucose over Sn-BEA at room temperature; b) Conversion of $^{13}C_1$-glucose over dehydrated (closed symbols) and hydrated (open symbols) Sn-BEA.

We further investigated the importance of diffusion limitations by evaluating the catalytic reactivity of a series of Sn-modified zeolites with different topologies in the conversion of dihydroxyacetone and D-glucose. The results summarized in Table 1 show that the activities of Sn-containing 10MR zeolites (MCM-22 and ITQ-2) are lower than those of Sn-BEA and Sn-MOR. This can be correlated to the difference in pore diameter. Compared to the negligible rate of glucose conversion in the 10MR zeolites, the smaller 1,3-dihydroxyacetone is more readily converted in Sn-MCM-22 and Sn-ITQ-2, albeit at a lower rate than in Sn-BEA.

Table 1. Assessment of the catalytic performance of selected Sn-functionalized zeolites

Catalyst	d_{pore} (Å)	Si/Sn	$Yield_{ML}$ (%)[1)]		Glucose isomerization[2)]		
			70°C	90°C	Glucose (%)	Fructose (%)	Mannose (%)
Sn-MCM-22	5.5	70	25	69	>99	<1	<1
Sn-ITQ-2	5.5	36	32	71	>99	<1	<1
Sn-MOR	6.5	35	<1	14	90	10	<1
Sn-BEA-PS	6.7	80	92	98	31	29	5

[1)] Conversion of 1,3-dihydroxyacetone in methanol. 2h, 2.5 mL 0.25 M solution, 40 mg cat.
[2)] Glucose conversion at 100°C for 6h, 2.5 mL 125 mM in water, 40 mg cat.

4 Conclusions

^{13}C NMR measurements show that glucose isomerization can take place in the micropores of Sn-BEA at room temperature. Under practical conditions, the catalytic reaction rate is limited by the exchange of the solvent molecules for reactant molecules. Thus, we conclude that diffusion limitations may play a much more important role in glucose isomerization than assumed before. In keeping with this, framework Sn Lewis acid sites in 10MR zeolites such as MCM-22 convert glucose at much lower rate than in 12MR zeolites such as MOR and BEA. Compared to glucose, 1,3-dihydroxyacetone is more readily converted in the 10MR zeolites.

Acknowledgements

This work was funded by the Joint Scientific Thematic Research Programme of The Netherlands Organization for Scientific Research and the Chinese Ministry of Science and Technology.

References

[1] G. Li, E.A. Pidko, E.J.M. Hensen, *Catal. Sci. Technol*. 4 (2014) 2241.
[2] A. Corma, M. E. Domine, S. Valencia *J. Catal.* 215 (2003) 294.
[3] W.N.P. van der Graaff, G. Li, B. Mezari, E.A. Pidko, E.J.M. Hensen *ChemCatChem* (2015) accepted for publication. DOI 10.1002/cctc.201403050.

IV-OP16

A Theoretical Perspective on the Role of Cooperativity in Glucose Activation by Lewis Acid Zeolite and Oxide Catalysts

Pidko E.A.[1,2*], Hensen E.J.M.[1,2]

1 - Inorganic Materials Chemistry, Eindhoven University of Technology, Eindhoven, The Netherlands

2 - Institute for Complex Molecular Systems, Eindhoven University of Technology, Eindhoven, The Netherlands

* e.a.pidko@tue.nl

Keywords: biomass, reaction mechanism, zeolites, metal oxides, bifunctional catalysis, DFT calculations

1 Introduction

Efficient utilization of cellulosic biomass as a feedstock for future more sustainable chemical industry requires the development of new technologies for the selective conversion of carbohydrates to platform chemicals such as 5-hydroxymethylfurfural (HMF). While a number of homogeneous and heterogeneous catalysts can be used to selectively convert fructose [1], the activation of the more abundant glucose isomer is much more difficult. To achieve high HMF yields, glucose has to be selectively isomerized to fructose before the dehydration starts (Scheme 1). Recently, a number of catalytic systems capable of promoting such a reaction sequence has been introduced [1,2]. These include homogeneous ionic liquid-mediated Cr (II) and (III) chlorides [2,3] and heterogeneous Sn-BEA zeolite and WO_3 oxide catalyst [1,4]. The fundamental factors that determine the high reactivity of these very different systems have not been clarified yet. In this work we carried out a comprehensive computational study of the mechanism of glucose activation by these systems aiming at elucidation of the common features that render them efficient catalysts for the conversion of carbohydrates.

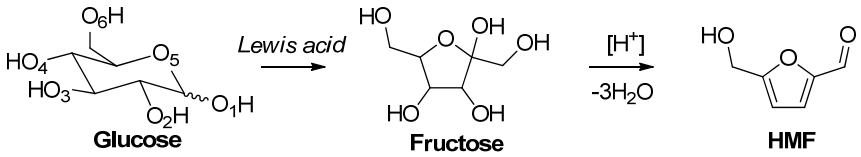

Scheme 1. Glucose conversion to HMF.

2 Experimental/methodology

Periodic DFT calculations on glucose conversion by zeolite and bulk oxide catalysts were carried out using the DFT plus damped dispersion (DFT-D3) approach with PBE exchange-correlation functional and plane-wave basis set as implemented in VASP 5.2 program. Explicit solvent (H_2O) molecules were introduced in the model to evaluate the impact of solvent-assisted reaction routes. The electron-ion interactions were described by the projected augmented wave (PAW) method. The energy cut-off was set to 400 eV. A complete unit cell of BEA zeolite and a slab model of modified WO_3 oxide surface were used as the models [5]. A detailed description of the computational methodologies used can be found in ref. [5].

3 Results and discussion

DFT calculations show that the selective sugar paths by Sn-BEA and WO_3-based catalysts are initiated by the reversible deprotonation of the O1H hydroxyl group of glucose by basic lattice oxygen centres adjacent to the catalytically active Lewis acid site. The latter binds the

activated sugar residue and directs its further transformations along the catalytic cycle. Because of only a minor energy difference between different possible glucose coordination modes, they rapidly interconvert under the reaction conditions.

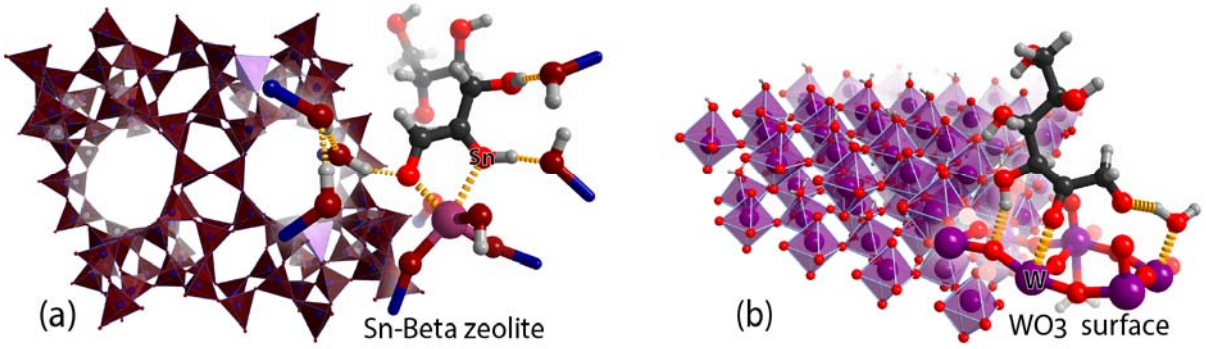

Figure 1. Representative structures of the key intermediates in glucose isomerization by (a) Sn-BEA zeolite and (b) WO_3 oxide.

The subsequent H-shift reaction upon which the aldose intermediate is transformed into the keto form is identified as the rate-determining step in the isomerization reaction. DFT calculations demonstrate that the unique reactivity of Sn-BEA zeolite and WO_3 catalyst stems from the dynamic and cooperative action of their active sites towards selective sugar transformations (Figure 1). The concerted action of lattice Sn site and neighbouring proton donors (adsorbed water or silanol groups) confined in Sn-beta micropores is essential to establish a favourable path for glucose to fructose isomerization [5]. A similar cooperative mechanism involving a synergetic action of surface hydroxyls and Lewis acid sites on WO_3 surface provides a low energy path for glucose isomerization.

4 Conclusions

A comprehensive DFT study of the mechanism of glucose isomerization by Sn-BEA zeolite and surface of WO_3 oxide reveals the crucial role of active site coopearativity for the efficient sugar transformations by these systems. The favourable reaction mechanisms involve a synergetic action of the Lewis acidic sites and neighbouring proton donors at the rate-determining H-shift step. The proposed mechanisms closely resemble the way homogeneous catalysts and enzymatic systems promote such a reaction. The activation of glucose by bio- and chemocatalysts involves the dynamic and cooperative action of their active sites towards selective glucose transformation. These fundamental insights pave the way towards a generic reactivity concept of carbohydrate activation.

Acknowledgements

This work was financially supported by the EU FP7 NMP project NOVACAM (FP7-NMP-2013-EU-Japan-604319).

References

[1] S. Van de Vyver, J. Gerboers, P.A. Jacobs, B.F. Sels, ChemCatChem 3, 82 (2013); J. Song, H. Fan, J. Ma, B. Han, Green Chem. 15 (2013) 2619.
[2] H. Zhao, J.E. Holladay, H. Brown, Z.C. Zhang, Science 316 (2007) 1597.
[3] E.A. Pidko, V. Degirmenci, R.A. van Santen, E.J.M. Hensen, Angew. Chem. Int. Ed. 49 (2010) 2530; E.A. Pidko, V. Degirmenci, E.J.M. Hensen, ChemCatChem 4 (2012) 1263.
[4] R. Bermejo-Deval, R.S. Assary, E. Nikolla, M. Moliner, Y. Román-Leshkov, S.-J. Hwang, A. Palsdottir, D. Silverman, R.F. Lobo, L.A. Curtiss, M.E. Davis, Proc. Natl. Acad. Sci. USA 109 (2012) 9727.
[5] G. Li, E.A. Pidko, E.J.M. Hensen, Catal. Sci. Technol. 4 (2014) 2241; G. Yang. E.A. Pidko, E.J.M. Hensen, ChemSusChem 9 (2013) 1688.

IV-OP17

New Insights in the Catalytic Conversion of Sugars with Sn-Beta

Tolborg S.[1,2], Sádaba I.[2], Osmundsen C.M.[2], Fristrup P.[1], Taarning E.[2*]

1 - Technical University of Denmark, Department of Chemistry, Kgs. Lyngby, Denmark
2 - Haldor Topsøe A/S, Kgs. Lyngby, Denmark

* esta@topsoe.dk

Keywords: Sn-Beta, zeolites, heterogeneous catalysis, biomass, alkali effect, mesoporous materials

1 Introduction

Tin-containing silicates have interesting catalytic properties in a variety of reactions relevant for biomass conversion such as the isomerization of glucose to fructose and the conversion of sugars to methyl lactate (ML).[1-2] Sn-Beta is often reported as being one of the most active stannosilicate catalysts; however the main challenge in the utilization of Sn-Beta is that the yield of desired products is often quite low. The presence of alkali ions is known to greatly influence the synthesis of metallosilicate materials and has been shown to change the catalytic properties of the resulting zeotype catalyst depending on the reaction system.[3-5]

2 Experimental/methodology

Conversion of carbohydrates to ML was performed in a stainless steel autoclave. Reaction conditions: 0.450 g sucrose, 0.150 g catalyst, 15 g methanol containing K_2CO_3, 170˚C, 16 hours.

3 Results and discussion

Here is reported that the presence of alkali salts during conversion of sugars with stannosilicates have a drastic impact on the resulting yields of ML.[6] Sn-Beta prepared either by hydrothermal synthesis (HT Sn-Beta) or by post-treatment of dealuminated Beta zeolite (PT Sn-Beta) in the absence of alkali metal salts, results in a poor ML yield of 20-30 % (Fig. 1). When adding small amounts of alkali salts either during synthesis or directly to the reaction media, the yield increases to 66-75%.

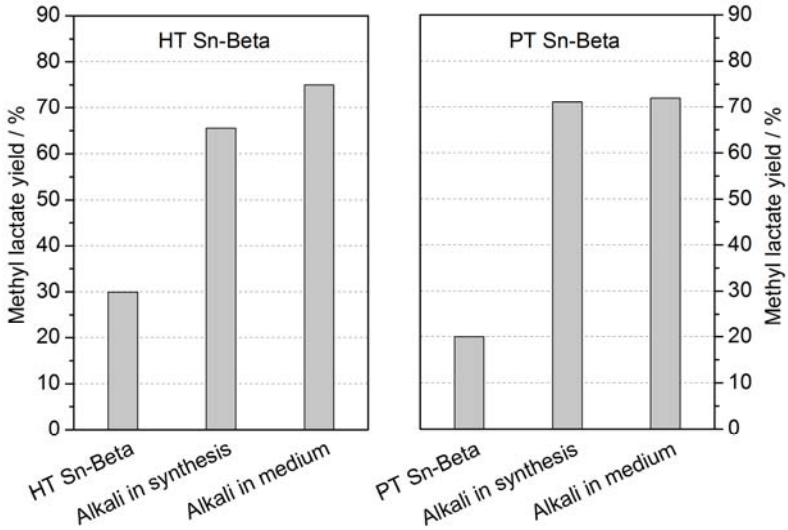

Fig. 1. Yield of methyl lactate obtained from sucrose in the presence and absence of alkali metal salts when using Sn-Beta zeolites prepared by hydrothermal synthesis (HT Sn-Beta) or by post-treatment of a dealuminated commercial zeolite (PT Sn-Beta).

It was observed that all alkali salts improve the selectivity of ML. The specific concentration of alkali salt is important, as a clear optimum is seen at distinct concentrations, varying for different samples of Sn-Beta (Fig. 2). Furthermore, it was found that the effect could be expanded to non-zeolithic stannosilicates such as Sn-MCM-41 and Sn-SBA-15.

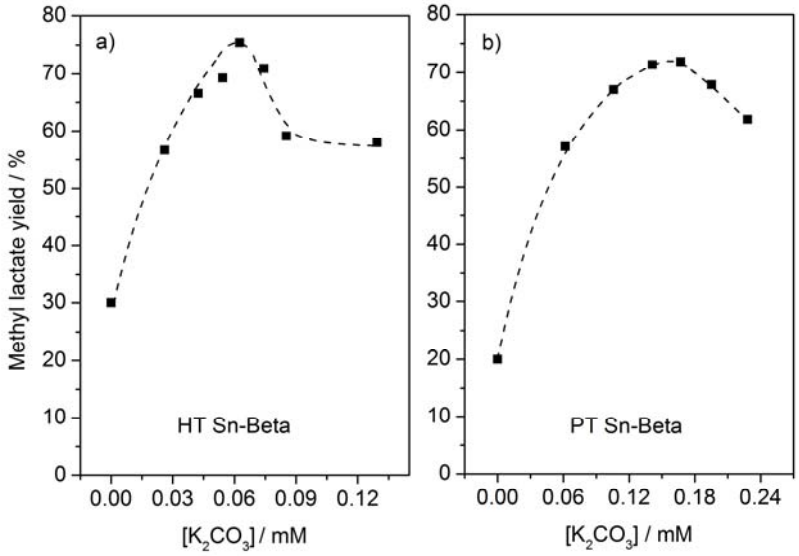

Fig. 2. The methyl lactate yield obtained from sucrose using HT Sn-Beta (a) or PT Sn-Beta (b) versus the concentrations of K_2CO_3 in methanol.

4 Conclusions

The experiments show that the total amounts of alkali metal ions present in the reaction, both in the catalyst and in solution, is essential to reach a high ML yield. The effect is not exclusive to hydrothermally prepared Sn-Beta, but can be applied to both materials prepared by post-synthesis and expanded to other non-zeolithic structures. These findings make it possible to expand on the catalyst portfolio and get a better understanding of the reaction system.

Acknowledgements

This work was funded by the Bio-Value platform (biovalue.dk) under the SPIR initiative by The Danish Council for Strategic Research and The Danish Council for Technology and Innovation, case no: 0603-00522B.

References

[1] M. S. Holm, S. Saravanamurugan, E. Taarning, *Science*, 328 (2010) 602
[2] M. Moliner, Y. Román-Leshkov, M. E. Davis, *Proc. Natl. Acad. Sci.* 107 (2010) 6164
[3] B. Notari, *Stud. Surf. Sci. Cat.* 67 (1991) 243
[4] V. N. Shetti, *J. Mol. Catal. A* 210 (2004) 171
[5] R. Bermejo-Deval, M. Orazov, R. Gounder, S. Hwang, M. E. Davis, *ACS Catalysis*, 4 (2014) 2288
[6] S. Tolborg, I. Sádaba, C. M. Osmundsen, P. Fristrup, M. S. Holm, E. Taarning, *ChemSusChem*, (2015), *in press*

IV-OP18

Mg-Al Hydrotalcites with Tailored Structure as Efficient Catalysts for Glucose Isomerization into Fructose

Delidovich I., Palkovits R.*

Chair of Heterogeneous Catalysis and Chemical Technology, RWTH Aachen University, Aachen, Germany

* palkovits@itmc.rwth-aachen.de

Keywords: hydrotalcite, glucose, fructose, solid base, isomerization

1 Introduction

Cellulosic biomass is an attractive renewable resource that can be converted into value-added products via hydrolysis giving glucose (Glu). A further efficient valorization of Glu requires its isomerization into fructose (Fru) in order to increase the reactivity of the carbohydrate feedstock [1]. Isomerization of Glu into Fru is a catalytic process with the yield of Fru in water thermodynamically limited to ca. 50%. The maximal yield attainable to date in the presence of a solid catalyst is ca. 30%. In this work we consider one of the most promising solid catalysts for isomerization, namely Mg-Al hydrotalcite (HT) in carbonate form. HTs are layered double hydroxides with the general formula $[Mg_{1-x}Al_x(OH)_2]^{x+}(CO_3)_{x/2}\cdot mH_2O$ where Mg^{2+} ions are partially substituted by Al^{3+} in the brucite-type layers; $0.17<x<0.34$. This work aims at elucidating correlations between structure and catalytic performance of HTs [2].

2 Experimental part

HTs were prepared by co-precipitation of solutions containing $Al(NO_3)_3$+$Mg(NO_3)_2$ and $NaOH$+Na_2CO_3 at constant pH. We varied: (1) the molar Al content; (2) the pH of precipitation; (3) the aging temperature and (4) H_2O or H_2O-EtOH mixtures as solvent. Catalysts were characterized by ICP-OES, N_2 sorption, sorption of acrylic acid, XRD, TG-DSC, and SEM. In a typical experiment, 100 mg catalyst were dispersed in 5 mL 10wt.% aqueous Glu solution and stirred for 1.5 h at 110 °C. Afterwards, the reaction solution was filtered and analysed by HPLC.

3 Results and discussion

Characterization of the HTs showed that the prepared materials consist of agglomerated primary platelet-like particles (40-200 nm in diameter and *ca.* 20 nm thickness) of polycrystalline nature. The size of the primary particles as well as their agglomeration depends on the preparation conditions. Interlayer carbonate anions are catalytically active sites for the isomerization of Glu, therefore, their accessibility is essential to enable high catalytic activity. These active sites are located on (i) edges of the primary HT particles and (ii) defects of the HT crystals, e.g. the places of noncoherent coalescence of the crystallites.

The best yields of Fru were obtained over catalysts with a molar content of Al $0.23<Al/(Mg+Al)<0.3$, while catalysts with $0.3<Al/(Mg+Al)<0.34$ were less active. We assign this observation to blockage of active sites with aluminium hydroxide forming in minor amounts during catalyst preparation.

Preparation conditions significantly influence the properties and catalytic activity of HTs. Aging of HTs at 150°C results in coalescence of primary particles and decrease of the defect concentrations. As a result, the basic sites of the materials aged at high temperature are hardly accessible leading to lower catalytic activity as compared to HTs aged at room temperature.

In addition, the pH of co-precipitation in aqueous solutions has a clear influence on the catalytic performance of the prepared HT materials. When precipitated at the isoelectric point

(pH 10), the primary particles of HTs are assembled into agglomerates with a "sand-rose" structure. This facilitates easy access towards the basic sites located on both basal and non-basal planes of the HTs. Preparation of HTs at pH 9.0-9.5 (i.e. below isoelectric point) gives rise to materials with less regular morphology: In this case the agglomeration takes place by stacking of the basal planes of primary particles. Consequently, catalysts prepared at pH 10 possess a greater amount of basic sites and demonstrate higher catalytic activity compared to materials synthesized at pH 9.5.

Moreover, activity of the catalysts can be improved by conducting the preparation in aqueous-ethanol solvent instead of aqueous medium. Dispersion of the primary particles of HTs increases upon addition of ethanol, enhancing basicity of the materials.

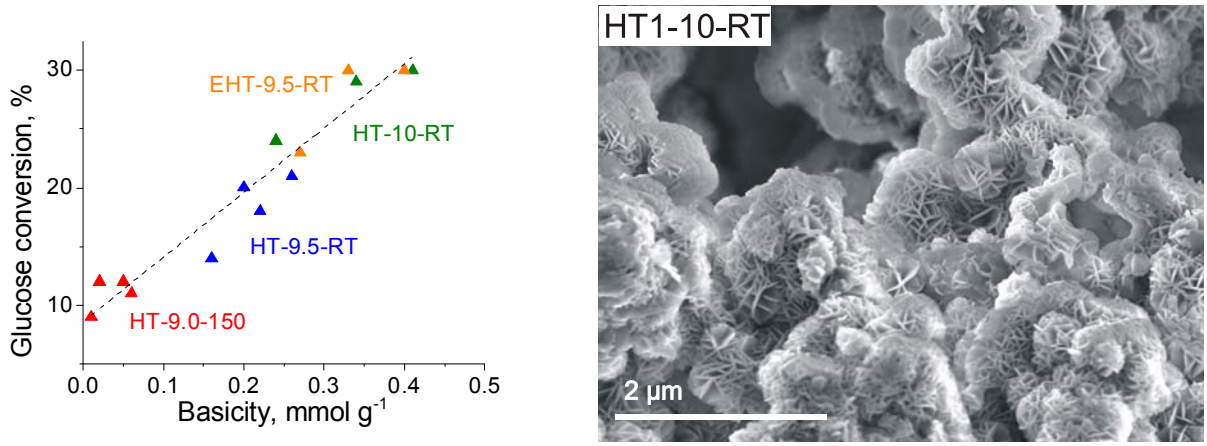

Fig.1. (Left) Glucose conversion vs. basicity of hydrotalcites. Reaction conditions: 5 mL 10wt.% aqueous glucose solution, 100 mg catalyst, 110°C, 1.5 h, 750 rpm; (right) SEM micrograph of a HT precipitated in aqueous medium at pH 10 and aged at room temperature.

In summary, basicity of the HTs correlates with the catalytic activity (Fig. 1). The best results were obtained for the most basic catalysts precipitated at pH 10 and HTs prepared in an aqueous-ethanol medium. The yield of Fru reaches up to 30% with 89% selectivity when conducting the reaction under typical conditions but for 4 hours. Although some leaching of Mg^{2+} was observed, the reaction takes place heterogeneously, as shown by a filtration test. The HT was successfully recycled 4 times without loss of activity and selectivity.

Acknowledgements

Financial support of the Alexander von Humboldt Foundation and the Bayer Foundation is acknowledged. This work was performed as part of the Cluster of Excellence "Tailor-Made Fuels from Biomass" funded by the Excellence Initiative by the German federal and state governments to promote science and research at German universities. We acknowledge funding of the Robert Bosch Foundation.

References:

[1] I. Delidovich, R. Palkovits, *Catal. Sci. Technol.* 4 (2014) 4322.
[2] I. Delidovich, R. Palkovits, *submitted.*

IV-OP19

Liquid Phase Oxidation of Glucose to Gluconic Acid over Supported Metal Catalysts

Padovani A., Schüth F.*

Max Planck Institut für Kohlenforschung, Mülheim an der Ruhr, Germany

* schueth@kofo.mpg.de

Keywords: glucose, gluconic acid, supported metals catalysts

1 Introduction

During recent years, the metal catalyzed liquid-phase oxidation of glucose to gluconic acid has received much attention, since the latter is a fine chemical used as water soluble cleansing agent and additive for food and beverages.

2 Experimental/methodology

In this study the oxidation of glucose to gluconic acid is carried out both with pure oxygen and with air as oxidizing agent under pressure, at 70°C and at room temperature, under basic or neutral conditions without pH control. Although in this study the reaction is typically run either for seven or three hours, with this system the highest values of conversion are usually reached within the first 50 minutes of reaction. The chemical oxidation of glucose to gluconic acid with nickel group metals – especially Pd and Pt, on carbon and metal oxides has been investigated for a long time [1]. As alternative to nickel group metals, Au-based supported catalysts have received much attention [2-3].

3 Results and discussion

In this work, at alkaline pH and at 70°C using pure oxygen as oxidizing agent Au(1wt%) was tested supported on metal oxides, i.e. on ZnO, Al_2O_3, TiO_2,. The conversions obtained are around 60-70%, but the selectivities to gluconic acid are low, and only a minor yield of gluconic acid is obtained (7-14%). Au was also tested on carbon as support. Instead of a microporous material, two mesoporous carbons named CA1 and SX with different surface areas were used. In general, the SX carbon supported catalyst gives better results in terms both of conversion (90-100%) and yield of gluconic acid (~90%). Au/SX carbon was also tested under alkaline conditions at room temperature: the reaction is slower with ~100% conversion and ~80% selectivity. On a micro-mesoporous carbon support, the performance is not as good, with ~90% conversion and ~60% of gluconic acid produced. Pd and Pt at 1wt% were inferior under the same conditions compared to the best gold systems. Pd/C as catalyst is the best system, with full conversion and selectivities around 70%. Pt seems to work better using the ordered structure of CMK-5 as support: the only oxidation product formed during the reaction is gluconic acid in ~68% yield and ~70% selectivity, while on the SX carbon only ~80% conversion and ~40% yield of gluconic acid are obtained.

If the noble metal content of the catalysts is increased, the performance is substantially improved: with 3% Au on SX carbon, full conversion and ~90-100% yield of gluconic acid were obtained, at 5wt% the system is not improved further (Fig.1).

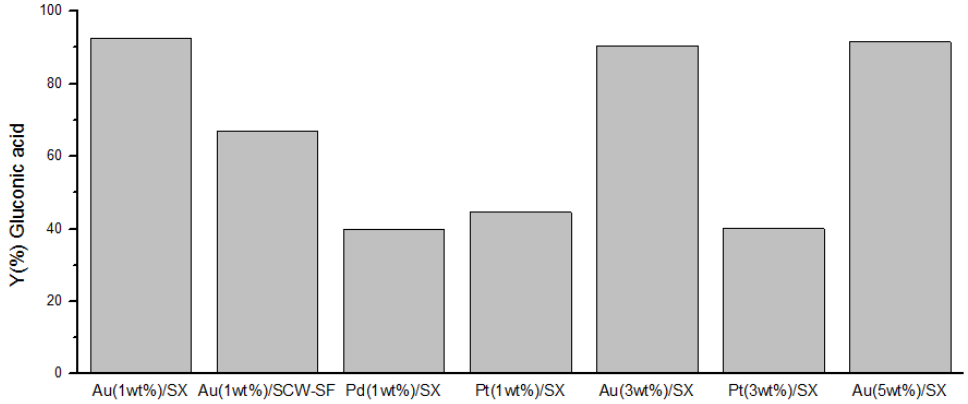

Fig. 1. Best catalysts in glucose oxidation to gluconic acid, alkaline pH, O_2, 3 bar.

The catalysts were also tested with air as oxidizing agent instead of oxygen. In this case the best results are obtained with Au(3wt%)/SX and Au(5wt%)/SX giving full conversion and ~100% and ~40% yield of gluconic acid respectively.

It would be attractive to carry out the reactions without base, and thus some catalyst systems were also tested at neutral pH, using pure oxygen as oxidizing agent. With Au(1wt%)/ZnO at 70°C the conversion is ~55% with a selectivity of ~90%, while at room temperature the values of conversion and selectivity to gluconic acid are, respectively, ~40% and ~80%, with lower amount of gluconic acid produced (~30%). Ru(1wt%)/C was also tested, but it shows no selectivity to gluconic acid.

4 Conclusions

In alkaline pH the best catalysts are Au/SX carbon, which give high conversion and yield of gluconic acid both under oxygen and air as oxidizing agent.While alkaline conditions favor the formation of gluconic acid, with the right catalyst systems reasonable yields can also be obtained at neutral pH, with Au/ZnO reaching almost 60%.

Acknowledgements

Funding by the ERC "POLYCAT" and the Cluster of Excellence TMFB is gratefully acknowledged.

References

[1] J.H. Vleeming, F.A. de Bruijn, B.F.M. Kuster, G.B. Marin, in: B. Delmon, G. Froment (Eds.), Catalyst Deactivation, Studies in Surface Science and Catalysis, Vol. 88, Elsevier, Amsterdam, 1994, p. 467.
[2] L. Jelemensky, B.F.M. Kuster, G.B. Marin, *Catal. Lett.* 30 (1995) 269.
[3] J.H. Vleeming, B.F.M. Kuster, G.B. Marin, *Catal. Lett.* 46 (1997) 187.

IV-OP20

Efficient Carbon Based Catalysts with Acid Sites and Magnetic Properties for Starch Valorization to Bio-chemicals

Anita F., Podolean I., Parvulescu V.I., Coman S.M.*

University of Bucharest, Faculty of Chemistry, Bucharest, Romania

* simona.coman@g.unibuc.ro

Keywords: carbons, magnetic nanoparticles, acid sites, starch, levulinic acid, lactic acid

1 Introduction

Along with cellulose, starch is an important raw material for the synthesis of platform molecules. However, studies conducted to date in homogeneous acid catalysis, show that the yields are relatively low (19-35%, in HCl) [1, 2]. In addition, the use of mineral acids presents a series of drawbacks related to the corrosive nature of the catalyst, the difficulty of separation at the end of reaction and hazardous waste generated. An alternative to such systems are those using solid acid catalysts, but progress is still insignificant, new active and selective solid catalyst systems waiting to be discovered and developed. An explanation for this situation is the special nature of the bio-polymer raw material and their low solubility in most of organic solvents.

Nanocatalysis represents a viable alternative to create high-performance catalysts able to convert biomass into bio-chemicals. However, the isolation and recovery of such tiny particles from the reaction mixture is not simple using conventional techniques. To overcome this problem, the use of magnetic nanoparticles (MNP) has emerged as a viable solution. Their insoluble paramagnetic nature allows an easy and efficient separation of the catalyst from the reaction mixture with an external magnet. Such a solution is very practical at the industrial level, where the separation processes represent more than half of total investments in specific equipment chemical industry.

Based on these, the main objective of this work was the design and development of carbon based catalysts (i.e., MWCNT and graphene) with acid sites and magnetic properties, suitable for the starch conversion into bio-chemicals. Commercially corn starch was used as raw material.

2 Experimental/methodology

Both graphene and MWCNT were oxidized by treating with HNO_3 at temperature. Then, the resulted graphene oxide was treated with concentrated triflic acid at 80°C for 10h resulting in GO@ SO_3CF_3, and MWCNT was modified with sulfuric acid leading to MWCNT-SO_3H. Fe_3O_4 nanoparticles were inserted into MWCNT-SO_3H using a simple protocol in which iron sulphate (II) ammonium chloride hexahydrate was dissolved in a deionized solution of hydrazine hydrate [3]. The resulted suspension of NPM@MWCNT-SO_3H particles was ultrasonicated, and the pH adjusted to 11-13. Then the catalysts were washed and dried. Their characterization was made by a number of techniques such as X-ray diffraction (XRD), Dynamic Light Scattering (DLS), Infrared Diffuse Reflectance spectroscopy with Fourier transform (DRIFT) and Elemental Analysis. Activity tests were carried out in a glass-pressure autoclave (Top 45 model, Top Industrie), at 130-180°C for 2-8h. After reaction the catalyst was recovered and the water-soluble products were separated by distillation under vacuum. The recovered products were sylilated and analysed by a GC-MS Carlo Erba Instruments QMD 1000 equipped with a Factor Four VF-5HT column.

3 Results and discussion

Compared with the oxide carriers, such as zeolite or alumina, catalysts based on carbon supports showed better performances, especially due to their higher tolerance to water and better dispersion of the catalytically active species. The functional groups of the GO/MWCNT (-OH, -COOH, etc.) works as docking centers for the active catalytic species thus providing an advanced dispersion of the active species.

This work valorizes as well this property by docking triflate and sulfate groups. The XRD patterns and DRIFT spectra of GO and MWCNT confirmed the functionalization with acid groups. On the other hand, the elemental analysis showed a higher percent of triflate grafted on the GO surface (10.32% S) by comparison with the sulfate groups grafted onto the MWCNT support (0.077% S).

Table 1 compiles the main results in the starch degradation. The GO@SO_3CF_3 catalyst is more active and selective in the process probably due to the much higher loading of acid sites. Both catalysts display Lewis/Brønsted acidity but in different proportions. Interesting enough, the selectivity to lactic or levulinic acid is not controlled by the L/B acid sites ratio but by the reaction conditions. Thus, in the presence of GO@SO_3CF_3, at 150°C, levulinic acid was preponderantly formed (60.0%) in 4h, while at 180°C lactic acid was formed in high amounts (56.6%). Differently, the MNP@MWCNT-SO_3H catalyst become active only at 180°C, and after 6h led to a small selectivity in lactic acid (49.0%). However, the advantage of using this catalyst is its simple isolation and recovery from the reaction mixture by applying an external magnetic field.

Table 1. Catalytic performances of the carbon-based materials in starch degradation

Catalyst	T (°C)	Time (h)	C (%)	Product distribution (S %)
GO@SO_3CF_3	130	4	100	Humines
GO@SO_3CF_3	130	6	100	Humines
GO@SO_3CF_3	150	2	83.8	Lactic acid (15.5), glycolic acid (7.5)
GO@SO_3CF_3	150	4	100	Lactic acid (62.9), levulinic acid (21.8)
GO@SO_3CF_3	150	6	100	Lactic acid (7.8), levulinic acid (60.0)
GO@SO_3CF_3	180	4	100	Lactic acid (56.6), glycolic acid (43.4)
MNP@MWCNT-SO_3H	150	4	0	-
MNP@MWCNT-SO_3H	180	4	0	-
MNP@MWCNT-SO_3H	180	6	100	Lactic acid (49.0), glycolic acid (28.0)

4 Conclusions

In conclusion, the synthesized carbon-based materials showed a promising behavior for catalytic applications in the recovery of municipal food wastes (rich in starch) as bio-chemicals.

Acknowledgements

Authors kindly acknowledge UEFISCDI for the financial support (project PN-II-PCCA-2011-3.2-1367, Nr. 31/2012)

References

[1] W.W. Moyer, Preparation of levulinic acid. US patent 2270328
[2] C.H.G. Hands, F. R. Whitt, *J. Soc. Chem. Ind* 66 (1947) 415.
[3] F. Peng, L. Zhang, H.J. Wang, P. Lv, H. Yu, *Carbon* 43 (2005) 2397.

IV-OP21

New Cross-Dehydrogenative Coupling Reactions with Selective C-O Bond Formation

Terent'ev A.O.*, Krylov I.B., Vil' V.A., Zdvizhkov A.T., Sharipov M.Yu.

N. D. Zelinsky Institute of Organic Chemistry, Moscow, Russia

* alterex@yandex.ru

Keywords: oxidation, peroxides, coupling, dicarbonyl, compounds, C-O bond

1 Introduction

The cross-dehydrogenative C-C coupling was studied in most detail; the C-N, C-P, and C-O cross-coupling reactions are less well developed. It is difficult to achieve high selectivity in the cross-dehydrogenative C-O coupling because the starting compounds are prone to side oxidation and fragmentation reactions giving, for example, alcohols and carbonyl compounds. This gives rise to a problem of searching for oxidizing agents and reaction conditions suitable for the cross-coupling of different types of substrates.

2 Results and discussion

In this work we found cross-dehydrogenative C–O coupling of 1,3-dicarbonyl compounds and their heteroanalogs with oximes, hydroxyamides, and peroxides (Fig. 1 and 2). The best results in coupling with peroxides were obtained with the use of the widely available copper, iron, manganese or lantanide salts as catalysts or oxidants (Fig. 1).

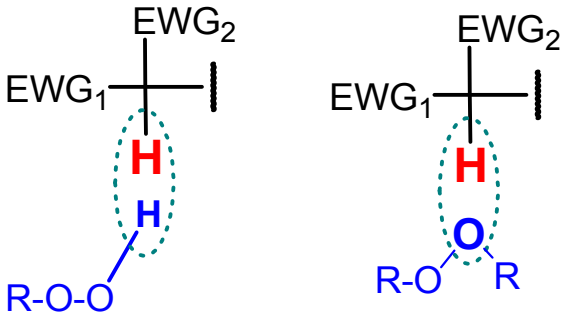

Fig. 1. Cross-dehydrogenative C–O coupling of 1,3-dicarbonyl compounds and their heteroanalogs with peroxides.

In the past decades, organic peroxides have got attention from researchers in the fields of medicinal chemistry and pharmacology because these compounds, particularly ozonides and tetraoxanes, were found to exhibit marked antimalarial, anthelmintic, and antitumor activities. Organic peroxides have been widely used for more than half a century as radical polymerization initiators in the industrial synthesis, for example, of such polymers as polystyrene, polyvinyl chloride, polyacrylates, and high-pressure polyethylene. Organic peroxides are also used for the crosslinking of silicone, acrylonitrile-butadiene, and fluorinated rubbers.

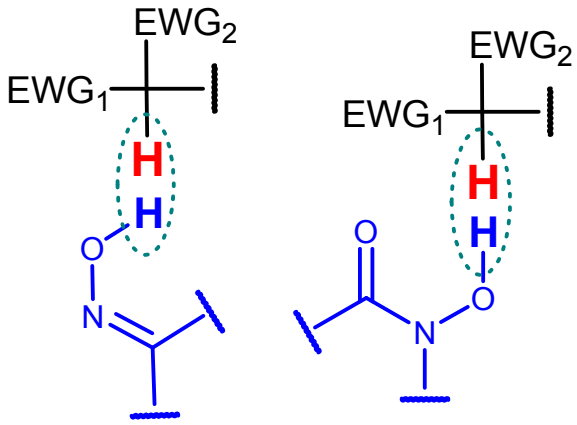

Fig. 2. Cross-dehydrogenative C–O coupling of 1,3-dicarbonyl compounds and their heteroanalogs with oximes and hyroxyamides.

In the case of Fig. 2, apparently, the reaction proceeds *via* the radical mechanism, in which the oxidizing agent serves to generate O-centred radicals from oximes and hyroxyamides. The formation of O-centred radicals was confirmed by ESR spectroscopy. The coupling described in the present study is the first example of the selective intermolecular reaction involving O-centred radicals generated in situ.

Generally speaking this work is a new approach to the solving of problem for selective oxidation of carbon atom with sp^3 hybridization.

Acknowledgements

This work was supported by the Russian Science Foundation (Grant 14-23-00150).

References

[1] A.O. Terent'ev, I.B. Krylov, M.Y. Sharipov, Z.M. Kazanskaya, G.I. Nikishin, *Tetrahedron*. 68 (2012) 10263.
[2] A.O. Terent'ev, I.B. Krylov, V.P. Timofeev, Z.A. Starikova, V.M. Merkulova, A.I. Ilovaisky, G.I. Nikishin, *Adv. Synth. Catal*. 355 (2013) 2375.
[3] A.O. Terent'ev, I.B. Krylov, V.P. Timofeev, B.N. Shelimov, R.A. Novikov, V.M. Merkulova, G.I. Nikishin, *Adv. Synth. Catal*. 356 (2014) 2266.
[4] A.O. Terent'ev, D.A. Borisov, I.A. Yaremenko, V.V. Chernyshev, G.I. Nikishin, *J. Org. Chem*. 75 (2010) 5065.
[5] A.O. Terent'ev, D.A. Borisov, V.V. Semenov, V.V. Chernyshev, V.M. Dembitsky, G.I. Nikishin, *Synthesis*. (2011) 2091.
[6] A.O. Terent'ev, V.A. Vil', G.I. Nikishin, W. Adam, *Synlett*. (2015) DOI: 10.1055/s-0034-1379982.

IV-OP22

Ketene as a Reaction Intermediate in the Carbonylation of Dimethyl Ether to Methyl Acetate on Mordenite

Rasmussen D.B.[1], Christensen J.M.[1], Temel B.[2], Studt F.[3], Moses P.G.[2], Rossmeisl J.[4], Riisager A.[5], Jensen A.D.[1*]

1 - Technical University of Denmark, Department of Chemical and Biochemical Engineering, Kgs. Lyngby, Denmark

2 - Haldor Topsøe A/S, Kgs. Lyngby, Denmark

3 - SUNCAT Center for Interface Science and Catalysis, SLAC National Accelerator Laboratory, Menlo Park, USA

4 - Technical University of Denmark, Department of Physics, Kgs. Lyngby, Denmark

5 - Technical University of Denmark, Department of Chemistry, Kgs. Lyngby, Denmark

* aj@ kt.dtu.dk

Keywords: carbonylation, dimethyl ether, methyl acetate, mordenite

1 Introduction

Recently, a novel route to ethanol (EtOH) from synthesis gas has been demonstrated, in which dimethyl ether (DME), formed from synthesis gas, reacts with CO to methyl acetate (MA), which in turn is hydrogenated to EtOH and methanol (MeOH) [1]. Mordenite has been identified to be the most active catalyst for DME carbonylation [2, 3]. The framework of Mordenite contains two types of cavities: eight-membered ring (8-MR) side pockets and 12-MR main channels. 8-MR are the active sites for MA synthesis and formation of acetyl groups as surface intermediates is the rate limiting reaction step [4]. In this study, we present unprecedented insights into formation of acetyl on Mordenite in the steady-state phase, including the DFT energies and energy barriers for all reaction steps, and present experimental evidence of the theoretical model by showing that ketene is a reaction intermediate as predicted by the DFT calculations.

2 Experimental/methodology

All calculations were performed using the GPAW [5] DFT program with the BEEF-vdW functional [6]. Ketene was detected experimentally in an experiment, in which the DME carbonylation was given 5.7 h to approach steady-state, where D_2O was introduced to the CO/DME feed. Gas-phase ketene is the only species in the system which forms a doubly deuterated acetic acid, in a reaction with D_2O. The other pathways to acetic acid: acetyl hydration, MA hydrolysis and MeOH carbonylation all result in acetic acid isotopes with, at most, a single deuterium atom. This analysis is possible because the methyl groups are not deprotonated on acidic zeolites by MeOH, DME or D_2O [3, 7].

3 Results and discussion

Our DFT calculations show that ketene is a reaction intermediate in both the 8-MR and the 12-MR (Figure 1). Additionally, formation of acetyl is significantly faster in the 8-MR than in the 12-MR, by a factor of about 5 at 438 K. Figure 2 shows the mass ratio between m/z = 62 (CH_2DCOOD) and m/z = 61 (CH_3COOD) as a function of time on stream during the experiment. Before the addition of D_2O in the system, the ratio between the signals from doubly and singly deuterated acetic acid isotopes corresponded to noise, but as D_2O was introduced, a well-defined peak emerged, showing that ketene is a reaction intermediate. Upon the introduction of D_2O the carbonylation reaction was still running and ketene intermediates were

available for conversion to CH_2DCOOD, whereby the m/z = 62 signal became prominent.

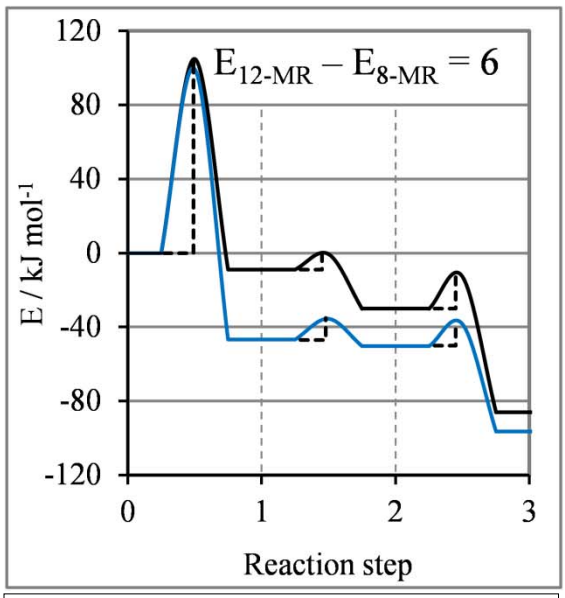

Fig.1. Reaction paths for formation of acetyl on Mordenite. Reaction steps: 0 CO in vacuum, methyl group on the zeolite; 1 Acetyl carbocation; 2 Ketene physisorbed on a Brønsted acid site; 3 Acetyl group on zeolite. Black line: reaction steps in the main channel; Blue line: reaction steps in the side pocket.

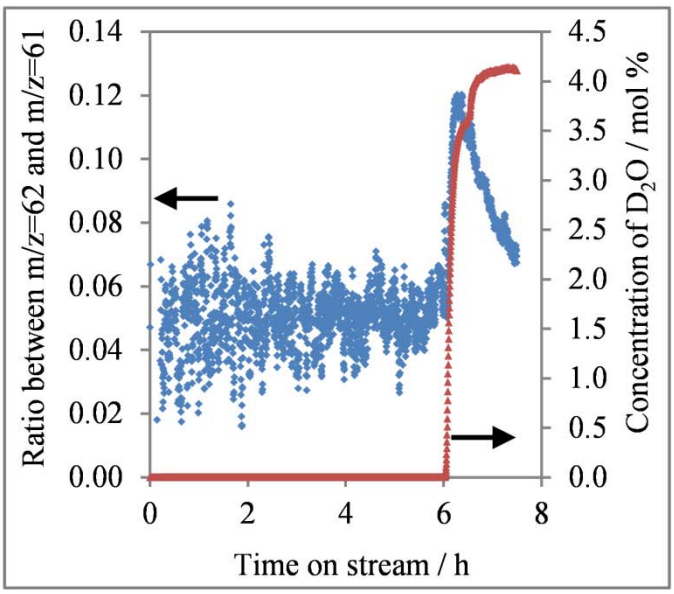

Fig.2. The ratio between the MS signal at m/z=62 (doubly deuterated acetic acid) and m/z=61 (singly deuterated acetic acid). Conditions: 9.8 bar CO, 0.2 bar DME, 300 Nml/min, 3.0 g catalyst, 438 K.

4 Conclusions

The present work shows that ketene is an intermediate in the DME carbonylation over Mordenite. Ketene undergoes base catalyzed polymerization to poly-ketones already at very low temperatures and may be involved in the build-up of the larger carbonaceous structures that lead to deactivation of the zeolite catalyst [8]. The presence of ketene is also of importance for the ongoing studies of the formation of the initial C-C bonds in acidic zeolites.

Acknowledgements

The project is financed by the Technical University of Denmark and the Catalysis for Sustainable Energy research initiative (CASE), funded by the Danish Ministry of Science, Technology and Innovation.

References

[1] X. San, Y. Zhang, W. Shen, N. Tsubaki, *Energy & Fuels* 23 (2009) 2843.
[2] P. Cheung, A. Bhan, G. J. Sunley, E. Iglesia, *Angew. Chem., Int. Ed.* 45 (2006) 1617.
[3] P. Cheung, A. Bhan, G. J. Sunley, D. J. Law, E. Iglesia, *J. Catal.* 245 (2007) 110.
[4] A. Bhan, A. D. Allian, G. J. Sunley, D. J. Law, E. Iglesia, *J. Am. Chem. Soc.* 129 (2007) 4919.
[5] J. J. Mortensen, L. B. Hansen, K. W. Jacobsen, *Phys. Rev. B* 71 (2005).
[6] J. Wellendorff, K. T. Lundgaard, A. Mogelhoj, V. Petzold, D. D. Landis, J. K. Norskov, T. Bligaard, K. W. Jacobsen, *Phys. Rev. B* 85 (2012).
[7] D. M. Marcus, K. A. McLachlan, M. A. Wildman, J. O. Ehresmann, P. W. Kletnieks, J. F. Haw, *Angew. Chem., Int. Ed.* 45 (2006) 3133.
[8] G. Natta, G. Mazzanti, G. Pregaglia, M. Binaghi, M. Peraldo, *J. Am. Chem. Soc.* 82 (1960) 4742.

IV-OP23

On the Mechanism for the First C-C Bond Formation in MTO Reaction

Liu Y.*, Müller S., Sanchez-Sanchez M., Lercher J.

Department of Chemistry and Catalysis Research Center, Technische Universität München, München, Germany

* yue.liu@tum.de

Keywords: MTO, H-ZSM-5, methanol, mechanism

1 Introduction

Catalytic conversion of methanol to hydrocarbons (MTH) on solid acids, especially on H-ZSM-5 and SAPO-34, has attracted great attention and effort in the past decades in respect of methane and syn-gas transformation as well as gasoline (MTG) and olefin (MTO) production [1]. A large amount of work has been focused on this process, but till now the full mechanism of methanol conversion is unclear. It is widely accepted that a "hydrocarbon pool" is formed which includes olefin and aromatic cycles [2]. However, how the first olefin or the first aromatic molecules are originated solely from methanol is still under debate. Diverse distinctive proposals on the first olefin or first C-C bond formation make it hard to reach a uniform consensus. These proposals can be classified by their key intemediate as oxonium ylide mechanism, carbene mechanism, carbenium ion mechanism, free radical mechanism, surface alkoxy mechansim and CO involved mechanism [3].

In this work, we study the first surface and gas products formed on acidic zeolite by reaction of methanol and some potential C_1 intermediates followed by IR spectroscopy and a mass spectrometer. We detected tens of ppm of acetic acid and methyl acetate prior to the appearance of olefin in MTO, which were assigned to the first species containing a C-C bond. A promotion of MTO reaction rate was observed as well when cofeeding CO with methanol. Based on these findings, a new reaction mechanism network is proposed involving carbonylation, aldol condensation and decarboxylation. Ethylene and propylene arise simultaneously as first olefin products but it is found that they originate from two different routes.

2 Experiments

Reactions were performed in a quarz tube reactor under ambient pressure. A commercial H-ZSM5 catalyst was pressed and sieved into 200-280 μm particles and diluted (1:20 wt.) in 355-500 μm SiC. For comparison, H-MOR catalyst was also tested. Prior to reaction, catalyst was activated in 25 mL/min He flow at 450 ^{o}C for 1h. Methanol and methylal were fed by passing 25 mL/min He through an evaporator and partial pressure was controled by modulating evaporator temperature. Reaction products were dectected on line by MS. For temperature programmed reaction, a temperature rising rate of 10 ^{o}C/min was applied.

3 Results and discussion

Steady state reaction of methylal on H-ZSM-5 was performed at 450 ^{o}C. With time on stream, the yield of olefins decreased and the DME/methanol increased correspondingly, due to deactivation of the catalyst. Between the two species, a weak peak of methyl acetate and acetic acid appeared as reaction intermediate (Figure 1). Similar trend was observed for the methanol reaction on the less stable H-MOR. Therefore, we propose that C_1 molecules including methanol, DME, methylal, formaldehyde and CO are converted to olefins via methyl acetate and

acetic acid. The latter species is formed by DME/methanol carbonylation and proposed to be the first intermediate containing a C-C bond.

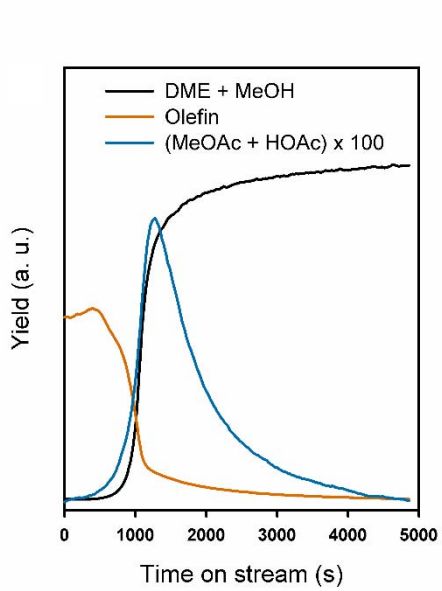

Fig. 1. Methylal to olefin conversion on H-ZSM-5 as a function of time on stream.

An obvious reaction rate increase was observed when cofeeding CO with methanol on H-ZSM-5. This promotion effect is difficult to detect under typical reaction conditions because this pathway is strongly inhibited by the presence of water, similar to the effect of water reported for DME carbonylation [4]. Even though water is generated from methanol dehydration to dimethyl ether at the initial stage, carbonylation still proceeds at a rate slow but sufficient to trigger the formation of the "hydrocarbon pool". The very low rate of this step explains the need for a certain space time, known as the induction period in MTH. A reaction mechanism is proposed based on these findings. First C-C bond is formed by carbonylation of methanol / DME, generating acetyl species as methyl acetate and acetic acid, which further transforms into ethylene and propylene.

4 Conclusions

Acetic acid and methyl acetate was for the first time observed as relevant intermediates in MTO reaction and a new mechanism for the first C-C bond and first olefin formation in MTO was proposed. The first C-C bond is generated by carbonylation of surface methoxy group, forming surface acetyl group, which further reacts into olefins.

Acknowledgements

The authors acknowledge support from Clariant Produkte (Deutschland) GmbH in the framework of MuniCat.

References

[1] C. D. Chang, *Catal. Rev.* 25 (1983) 1-118.
[2] M. Bjørgen, S. Svelle, F. Joensen, J. Nerlov, S. Kolboe, F. Bonino, L. Palumbo, S. Bordiga, U. Olsbye, *J. Catal.* 249 (2007) 195-207.
[3] M. Stöcker, *Microporous Mesoporous Mater.* 29 (1999) 3-48.
[4] P. Cheung, A. Bhan, G. J. Sunley, E. Iglesia, *Angew. Chem. Int. Ed.* 45 (2006), 1617-1620.

IV-OP24

Activity Control of Supported Catalysts with Tailored Ru Nanoparticles for Non-Oxidative Propane Dehydrogenation

Otroshchenko T., Stoyanova M., Rodemerck U., Sokolov S., Linke D., Kondratenko E.V.*

Leibniz Institute for Catalysis, Leibniz, Germany

* Evgenii.kondratenko@catalysis.de

Keywords: propane, dehydrogenation, nanoparticles, zirconia

1 Introduction

Propene is one of the most important petrochemicals mainly used as a feedstock for the production of various polymers. It is industrially produced as a by-product of steam cracking of naphtha or fluid catalytic cracking of heavy oil fractions. Therefore, it is difficult to tune its selectivity. Since demand for propene is continuously growing, non-oxidative propane dehydrogenation (PDH) was commercialized for on-purpose propene production over supported Pt- or CrO_x-based catalysts, which show high propene selectivity and long lifetime . However, Pt-based catalysts are quite expensive and CrO_x-based catalysts are toxic and lead to environmental issues. Recently, supported VO_x-based materials were demonstrated to catalyze the PDH reaction with propene selectivity similar to industrial analogs [2]. Nevertheless, they are less active than Pt-based materials.

Here, we present novel supported catalysts possessing well-defined (1 nm) Ru nanoparticles with an overall metal loading as low as 0.05 wt.%. Their PDH performance determined under industrially relevant conditions surpassed that of VO_x- and Pt-based catalysts. The high activity together with the tiny Ru content makes our materials attractive from an industrial viewpoint.

2 Experimental

Ru nanoparticles (NP) were synthesized by reduction of $RuCl_3 \cdot nH_2O$ in ethylene glycol solution [3]. SiO_2, Al_2O_3-SiO_2 with SiO_2 content of 40 and 10 wt.% (Siral 40 and Siral 10, respectively), La_2O_3-ZrO_2 ($LaZrO_x$) and Al_2O_3 were used as supports. All catalysts were synthesized by impregnation of the supports with either colloidal solutions of Ru NP in CH_3OH or with a toluene solution of vanadium acetylacetonate to attain the metal loading of 0.05 or 4 wt.%, respectively. PDH tests were carried out at 550°C in a multichannel setup consisting of 15 plug-flow fixed-bed quartz reactors. The catalysts were pre-reduced in H_2 (30 vol.% in N_2) at 550°C for 1 h, flushed with N_2 and then exposed to a feed containing 40 vol.% C_3H_8 in N_2. The feed components and the reaction products were analyzed by an on-line gas-chromatograph.

3 Results and discussion

The size and distribution of Ru NP in ethylene glycol solution and after their deposition from this solution onto grid was determined by small angle X-ray spectroscopy and transmission electron microscopy, respectively. It amounted to approximately 1 nm. As shown in our previous study [3], the size did not significantly change after deposition of NP on supports.

Propene was the main product formed over all catalysts, while CH_4, C_2H_6, C_2H_4 and C_4-olefins were minor by-products. To compare the PDH activity of prepared catalysts, we determined the rate of propene formation at a propane conversion below 10%. The values obtained are shown in Fig.1. This figure also contains the corresponding value for an industrial analogue (Pt-Sn/Al_2O_3) tested under the same reaction conditions [2].

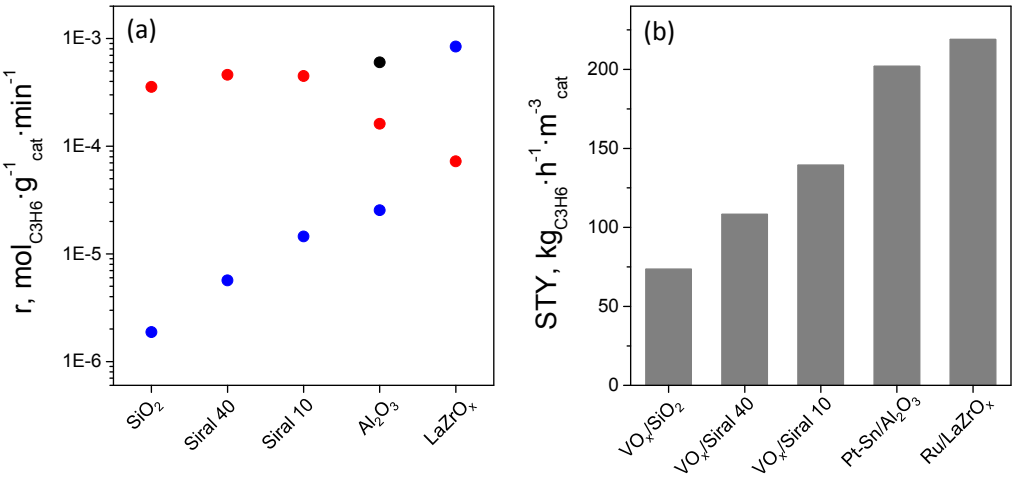

Fig. 1: Rates of propene formation (a) over Pt-Sn- (●), VO_x- (●) and Ru-based (●) supported catalysts and maximal space-time yield (STY) of propene (b) over the most active catalysts determined at 550°C.

It is obvious that the catalysts strongly differed in their activity depending on the kind (VO_x vs. Ru) of active species and support. For SiO_2-Al_2O_3-based catalysts, surface VO_x species showed significantly higher activity than Ru NP and their activity did not significantly depend on the content of SiO_2 (0-100 wt.%). Contrarily, the activity of Ru-based catalysts strongly increased with a decrease in this content. When using $LaZrO_x$ as support, VO_x species became significantly less active than those supported on SiO_2-Al_2O_3, while Ru/$LaZrO_x$ showed the highest rate of propane formation. For example, it was 450 or 2 times higher than those over Ru/SiO_2 or over the most active VO_x-based catalyst, respectively. Moreover, industrially relevant Pt-Sn/Al_2O_3 was less active than Ru/$LaZrO_x$. Since Ru loading and particle size was same for all supported catalysts, such strong difference in the activity of Ru-based catalysts can be referred to the metal-support interaction and its effect on the reaction.

It is worth mentioning that Ru/$LaZrO_x$ also performed superior to all other catalysts in terms of space-time yield (STY) of propene formation at industrially relevant propane conversion (>25%). The highest achieved value was 220 $kg_{C3H6} \cdot h^{-1} \cdot m^{-3}_{cat}$. The selectivity to propene was around 90%. This high performance was stable over 10 PDH/regeneration cycles thus proving that no structural changes occurred upon reductive/oxidative catalyst treatments.

Our contribution will discuss the trends observed during the catalytic tests together with the results of catalyst characterization by complementary methods to highlight the role of metal-support interaction and the kind of active components for propene formation. Similarities and differences in the mechanism of propane dehydrogenation over catalysts possessing VO_x species or Ru NP will be also discussed.

4 Conclusions

We have demonstrated that simple deposition of tailored Ru NP on commercial supports results in active, selective and stable catalysts for non-oxidative propane dehydrogenation even at metal loading as low as 0.05 wt.%. Such results appear promising from an applied viewpoint and provide the fundamental basis for developing active and selective PDH catalysts.

References

[1] A. Aitani, Propylene Production, in: S. Lee (Ed.), *Encyclopedia of Chemical Processing, Taylor & Francis* (2006) 2461.
[2] S. Sokolov, M. Stoyanova, U. Rodemerck, D. Linke, E.V. Kondratenko, *J. Catal.* 293 (2012) 67.
[3] C. Berger-Karin, M. Sebek, M.-M. Pohl, U. Bentrup, V.A. Kondratenko, N. Steinfeldt, E.V. Kondratenko, *ChemCatChem.* 4 (2012) 1368.

IV-OP25

Methylation Reaction of Aromatic NH-heterocycles with Using Supercritical Methanol: Competitive Homogeneous and Heterogeneous Catalysis by Si-Containing Compounds

Martyanov O.N.[1,2*], Chibiryaev A.M.[1,2], Kozhevnikov I.V.[1]

1 - Boreskov Institute of Catalysis SB RAS, Novosibirsk, Russia
2 - Novosibirsk State University, Novosibirsk, Russia

* oleg@catalysis.ru

Keywords: supercritical methanol, NH-heterocycles, methylation, Si-containing compounds, catalysis

1 Introduction

The catalytic properties of Si-containing compounds are investigated quite thoroughly for various organic reactions. But the top-level of these researches is the study of Lewis acid properties of silicas or its promotion effect (assistance) as catalyst supports. There is still a lack of reliable data on the catalytic activity of other Si-containing compounds, for example tetraalkyl orthosilicates. Recently, we have demonstrated the pronounced catalytic effect of tetramethyl orthosilicate (TMOS) on the methylation reaction of some aromatic azaheterocycles in supercritical (*sc*) methanol at 350 °C without additional methylating reagents [1,2]. The starting reagent was not commercial TMOS, but some SiO_2-containing materials (quartz, silica gel, etc.) which were reacted with *sc*-methanol to produce *in-situ* the equilibrium concentration of methyl orthosilicates by following scheme: $\mathbf{SiO_2 + CH_3OH \rightarrow Si(OCH_3)_4 + (CH_3O)_6Si_2O +}$ **(methyl oligosilicates)** $\mathbf{+ H_2O}$. It was shown that TMOS catalyzes the heterocycles methylation as homogeneous catalyst. At the same time there is indirect evidence that the solid SiO_2-surface works as heterogeneous catalyst for the methylation reaction of some aromatic azaheterocycles in *sc*-methanol. Thus, the methylation reaction in *sc*-methanol can be considered as an example of competing homogeneous and heterogeneous catalysis by Si-containing compounds.

2 Experimental

All runs were performed at 350°C and ~ 215 atm. in a batch reactor made from corrosion-resistant Hastelloy® C-276 alloy and repeated three times. The reactor was equipped with mechanical agitator MagneDrive® (Autoclave Engineers) and spinning catalytic basket Harshaw® (Autoclave Engineers), which was preliminary charged by solid SiO_2-containing material. The critical parameters of methanol are T_{cr} = 240°C, P_{cr} = 80 atm., and ρ_{cr} = 0.27 g cm^{-3}. The calculated density of the reaction mixtures were around ρ = 0.33 g cm^{-3} in supercritical phase at 350°C. The samples of the reaction mixture were collected every hour and analyzed with using the GC–MS and GC–AED.

3 Results and discussion

We have found that SiO_2 or TMOS enhance the reaction regioselectivity of heterocycle methylation in *sc*-methanol at 350 °C (**Fig. 1**), for instance up to 96–97% of 3-methylindole formation for indole reaction. The main catalytic effect is determined by the presence of TMOS that forms from the solid SiO_2-containing materials (quartz, Pyrex glass and silica gel) and methanol at these reaction conditions. Unusually, aromatic NH-heterocycles significantly accelerate the reaction of silica with methanol at 350 °C.

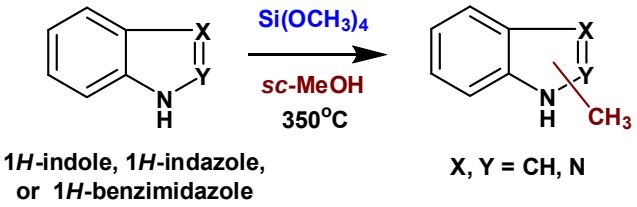

Fig. 1. Scheme of methylation reaction of some heterocycles with *sc*-methanol catalyzed by TMOS.

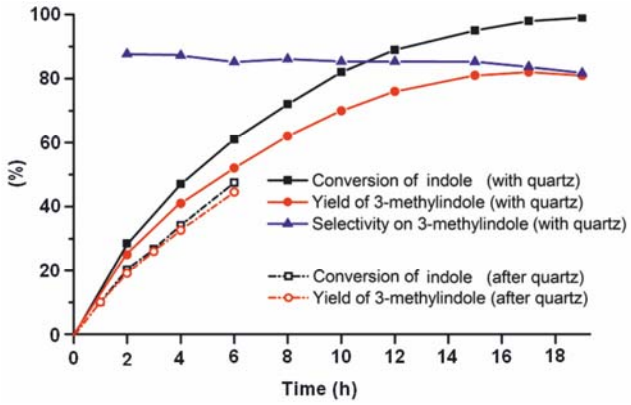

Fig. 2. Comparison of indole reaction in *sc*-methanol with using quartz sand and after its removal from the reactor.

So, we observed the cooperative concerted influence of reacting components: heterocyclic compound both provides a nucleophilic assistance to the reaction "SiO_2 + methanol" resulting in the *in-situ* formation of TMOS and is alkylated by methanol. The last reaction is catalyzed by TMOS.

But this simplified interpretation of experimental data obtained does not take into account the possible catalytic effect of the solid SiO_2-surface. In **Fig. 2** one can observe the difference in the indole conversion for the reaction in the presence of quartz (i.e. there is a solid SiO_2 in the reactor during the total reaction time) and after the removal of quartz (the last case implies the "quartz + methanol" reaction was carried out for 2 hours at 350 °C without indole, afterwards the unreacted quartz was removed out from the reactor. After the addition of the indole to the obtained solution of TMOS in methanol, the indole reaction was continued by the usual way.) It can be assumed that the difference observed is due to the extra catalytic effect of solid SiO_2-surface.

4 Conclusion

Our experimental data point to the mixed and competitive heterogeneous–homogeneous catalytic effect of Si-containing compounds (solid SiO_2 and liquid TMOS) for the methylation reaction of some aromatic NH-heterocycles with *sc*-methanol.

Acknowledgements

This work was supported by the Russian Foundation for Basic Research (No. 13-03-00595-a, 2013).

References

[1] I.V. Kozhevnikov, A.L. Nuzhdin, G.A. Bukhtiyarova, O.N. Martyanov, A.M. Chibiryaev, *J. Supercrit. Fluids* 69 (2012) 82.
[2] A.M. Chibiryaev, I.V. Kozhevnikov, O.N. Martyanov, *Appl. Catal. A: Gen.* 456 (2013) 159.

IV-OP26

Effect of Promoter Addition to SBA-15 Supported Bimetallic Co-Ni Catalysts for Dry Reforming of Methane

Atia H.[1*], Eckelt R.[1], Al-Fatesh A.S.[2], Fakeeha A.H.[2], Martin A.[1]

1 - Leibniz-Institut für Katalyse, Rostock, Germany
2 - College of Engineering, King Saud University, Riyadh, Kingdom of Saudi Arabia

* hanan.atia@catalysis.de

Keywords: bimetallic catalyst, nickel, cobalt, methane dry reforming, hydrogen production, SBA-15

1 Introduction

Dry reforming of methane (DRM) to syngas has attracted much attention in the last years for the great benefit to both environment and economy [1,2]. Nickel based materials are excellent catalysts for DRM reaction [3,4]. However, they suffer from deactivation due to Ni sintering and carbon deposition, which may also plug the reactor [5,6]. It was reported that alkali addition (Na and Mg) to the Ni based catalysts caused some decrease in carbon formation [7,8]. The type of support plays also a role, e.g., using SBA-15 as a support with its ordered mesoporous structure, narrow pore size distribution, and high surface area can anchor nanoparticles and restrain the mobility of species which otherwise might lead to metal sintering [9]. In this study, DRM was investigated over Co-Ni bimetallic supported on Sc, Mg, and La-SBA-15 catalyst with the aim to minimize carbon deposition.

2 Experimental

SBA-15 was synthesised using hydrothermal synthesis method. The prepared SBA-15 was modified by addition of the proper amount of $Sc(NO_3)_3.5H_2O$ or $Mg(NO_3)_2.6H_2O$, $La(NO_3)_3.6H_2O$ using incipient wetness impregnation. The catalysts were dried at 120 °C for 2 h and then calcined at 600 °C for 4 h. After that, they were co-impregnated with solutions of $Ni(NO_3)_2 \cdot 6H_2O$ and $Co(NO_3)_2 \cdot 6H_2O$, dried and calcined at 600 °C for 4 h. The catalysts prepared without and with modifiers were designated e.g. as Co-Ni/SBA-15 and Co-Ni/Mg-SBA-15, respectively. The total Co-Ni loading was 10 wt% (1:1) and 5 wt% for Mg, La and 2.5-10 wt% for Sc. The fresh and spent catalysts were characterized using N_2-adsorption, XRD, TGA, TEM and TPR. DRM was investigated using a stainless steel fixed bed reactor in a temperature range of 700-800 °C at atmospheric pressure. The effect of the chosen promoters on the catalytic activity and stability was studied up to 33 h time-on-stream (TOS).

3 Results and discussion

Surface areas (SA) for the bare support, fresh and spent catalysts are shown in Table 1. Upon co-impregnation of Co-Ni and subsequent loading of the promoters a loss in SA of SBA-15 in the range of 30-50% was observed with a slight change in pore volume and diameter. This indicates that active metals were embedded into the SBA-15 pore system. The results for CH_4 conversion for all catalysts showed that Sc and Mg modified SBA-15 were far more active than the rest (see Fig. 1a). The entire catalysts showed slight deactivation over 24 h TOS, but then Co-Ni/Mg-SBA-15 showed a fast deactivation compared to Sc (see Fig. 1b). CO_2 conversion is higher than CH_4 due to consecutive reactions such as reverse water gas shift reaction (r-WGS). The carbon deposition on the catalysts showed a decrease as follows: Co-Ni/Mg-SBA-15 > Co-Ni/Sc-SBA-15 > Co-Ni/SBA-15 > Co-Ni/La-SBA-15.

Table 1: Surface area measurement for fresh and spent samples and carbon deposition data.

Catalyst	Fresh			Spent (700 °C, 6 h TOS)			Carbon content[(a)] (wt.%)
	S_{BET} (m^2/g)	Pore volume (cm^3/g)	Pore diameter (nm)	S_{BET} (m^2/g)	Pore volume (cm^3/g)	Pore size (nm)	
SBA-15	819.0	0.72	5.4	-	-	-	-
Co-Ni/SBA-15	468.9	0.53	5.6	397.6	0.48	5.57	11.2
Co-Ni/La-SBA-15	584.2	0.59	5.5	504.8	0.56	5.70	7. 5
Co-Ni/Sc-SBA-15	527.8	0.55	5.4	424.3	0.51	5.96	13.7
Co-Ni/Mg-SBA-15	426.0	0.49	5.3	318.1	0.45	6.29	20.6

[(a)]Estimation of the carbon deposition by TGA analysis after 6 h reaction

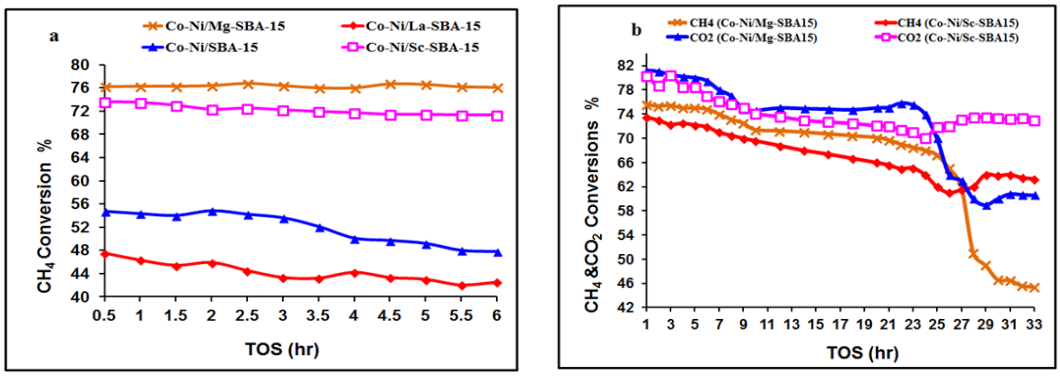

2 **Fig. 1:** CH_4 conversion vs. TOS for all catalysts under study (a) and long-term experiment over Co-Ni/Sc SBA-15 and Co-Ni/Mg-SBA-15 (b); T = 700 °C; total flow rate= 40 ml/min CH_4: CO_2: N_2 = 1: 1: 0.67.

4 Conclusions

Mg, Sc, and La promoted SBA-15 mesoporous materials were prepared and it can be seen that their addition decreases the surface area of SBA-15 but didn't block the pores. Afterwards, Co and Ni were co-impregnated on these solids; final Co-Ni/Sc- or Co-Ni/Mg-SBA-15 catalysts showed a CH_4 conversion of 73 and 76%, respectively, during the first 6 h and a slight decrease during 25 h to 66 and 73%, respectively. It seems that the stability of the Sc catalyst could be due to the generation of non-deactivating carbon deposits. The type of carbon deposition and/or location of carbon might be the reason for the deactivation of the catalysts.

References

[1] N. Wang, W. Chu, T. Zhang, X.S. Zhao, Int. J. Hydrogen energy 37 (2012) 19.
[2] A.N. Pinheiro, A. Valentini, J.M. Sasaki, A.C. Oliveira, Appl. Catal. A General, 359 (2009) 165.
[3] N. Wang, W. Chu, T. Zhang, X-S. Zhao, Chem. Eng. J 170 (2011) 457.
[4] M-S. Fan, A.Z. Abdullah, S. Bhatia, Int. J. Hydrogen Energy 36 (2011) 4875.
[5] J. Chen, C. Yao, Y. Zhao, P. Jia, Int. J. Hydrogen Energy 35 (2010) 1630.
[6] S.J. Vasconcelos, C.L. Lima, J.M. Filho, A.C. Oliveira, E.B. Barros, F.F. de Sousa, M.G.C. Rocha, P. Bargiela, A.C. Oliveira, Chem. Eng. J, 168 (2011) 656.
[7] S. Corthals, J.V. Nederkassel, J. Geboers, H.D. Winne, J.V. Noyen, B. Moens, Catal. Today 138 (2008) 28.
[8] H. Jeong, III K. Kim, D. Kim, I.K. Song, J. Mol. Catal. A 246 (2005) 43.
[9] M.T. Bore, H.N. Pham, T.L. Ward, A.K. Datye, Chem Commun. 10 (2004) 2620.

IV-OP27

New Chiral Cage Phosphines for Homogeneous Asymmetric Catalysis

Zagidullin A.A.[1*], Miluykov V.A.[1], Oshchepkova E.S.[1], Sinyashin O.G.[1], Hey-Hawkins E.[2]

1 - E. Arbuzov Institute of Organic and Physical Chemistry, RAS, Kazan, Russia
2 - Institut für Anorganische Chemie, Universität Leipzig, Leipzig, Germany

* almaz_zagidullin@mail.ru

Keywords: chiral cage phosphines, ligand, asymmetric catalysis

1 Introduction

The increasing demand to produce enantiomerically pure pharmaceuticals, agrochemicals, flavours and other fine chemicals has advanced the field of asymmetric catalytic technologies. Ligands with optically active phosphorus(III) centres have been used to some extent in transition metal-catalysed enantioselective reactions. Chiral cage phosphines are characterised by the presence of a chiral non-racemizable phosphorus atom situated at the bridgehead of a bicyclic system. The effectiveness of cage phosphines as weak, bulky ligands have been demonstrated in different asymmetric homogeneous catalysis with *ee*'s > 99% [1].

2 Experimental/methodology

From a synthetic standpoint, cycloaddition reactions of phosphacyclopentadienes (phospholes) are a convenient tool of molecular design of these chiral cage phosphine ligands [2, 3]. So, the [4+2] cycloaddition reaction of 1-neomenthyl-1,2-diphosphole with maleic acid deriatives proceeded under mild conditions with high diastereoselectivity (*d.e.* up to 88%) resulting in the corresponding enantiopure 1,7-diphosphanorbornadiene. The observed diastereoselectivity may be explained by the transition states showing one attractive and one repulsive pathway of Diels-Alder reaction and thermodynamic control of the reaction. This is the first example of a diastereoselective Diels-Alder reaction in a series of 1,2-diphospholes. The enantiopure cage phosphines show high activity and moderate enantioselectivity as ligands in Pd-catalyzed asymmetric allylic alkylation (ee = 15%) and as catalysts in [3+2] organocatalytic cycloaddition (*ee* = 68%).

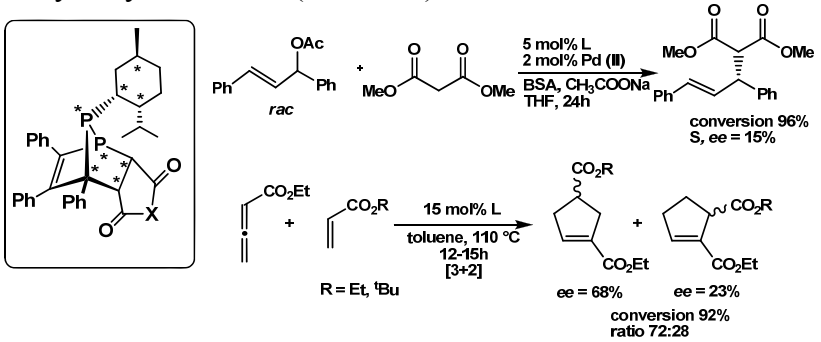

Acknowledgements

This work was supported by Council on Grants of the Russian Federation President (MK-7748.2015.3) and Russian Foundation for Basic Research (grant 14-03-31796)

References

[1] F. Mathey, *Acc. Chem. Res*., 37, (2004), 954.

[2] A. Zagidullin, I. Bezkishko, V. Miluykov, O. Sinyashin, *Mendeleev Commun*. 23 (2013), 117.

[3] A. Zagidullin, V. Miluykov, O. Sinyashin, P. Lönnecke, E. Hey-Hawkins, *Heteroat. Chem*. 25, (2014), 28.

IV-OP28

Catalytic Conversion of Cellulose to C_2-C_3 Glycols Using Heterogeneous Platinum Catalysts Supported on Cerium Oxide

Girard E.*, Delcroix D., Cabiac A.

IFP Energies Nouvelles, Rond-Point de l'Echangeur de Solaize, Solaize, France

* etienne.girard@ifpen.fr

Keywords: biomass, cellulose, glycols, dual catalysis, cerium, oxide

1 Introduction

Cellulose, the most abundant and non-food carbohydrate source on earth, has attracted considerable attention for the production of bio-sourced platform molecules. In particular, the interest for C_2-C_3 glycols has been driven by the increasing demand for ethylene glycol and bio-based polyethyleneterephtalate (PET) in the packaging industry. The conversion of cellulose to C_2-C_3 glycols is usually achieved under hydrothermal and reducing conditions -above 100°C and 1 bar of H_2- via a cascade pathway including depolymerization of cellulose to glucose, subsequent retro-aldol reactions and hydrogenation of the resulting glycolaldehyde and glyceraldehyde molecules. Multifunctional catalytic systems are thus necessary to achieve a selective formation of C_2-C_3 glycols. Depolymerization being achieved through water autoprotolysis at high temperatures, the ideal catalytic system should combine a retro-aldol active species and a hydrogenation component. In literature, most studies were dedicated to Group 6 species and particularly tungsten homogeneous catalysts associated with a hydrogenation catalyst such Ru/Ac and Raney Nickel.[1,2] In the search of replacing tungsten, original dual catalytic systems combining homogeneous and heterogeneous catalysts based on basic oxides were screened in a preliminary study. This dual approach associates the advantages of a homogeneous catalyst –selectivity and enhanced solid substrate-catalyst contact– and those of a heterogeneous one –stability and recyclability. Higher selectivities in C_2-C_3 glycols were thus obtained with a $CeCl_3.7H_2O$ homogenous salt and transition metal catalysts supported on light rare earth oxides.[3] This communication aims to illustrate the great potential of such catalytic systems to achieve high selectivities in ethylene and propylene glycols (EG and PG) from cellulose. A specific focus on a cerium oxide-based catalytic system and its role in reaction mechanisms will be presented.

2 Experimental/methodology

The heterogeneous catalysts were prepared by dry impregnation and tested as powders sieved under 150 microns. Catalysts were reduced under a H_2 flow. Catalytic tests were performed in a high throughput apparatus possessing six 100mL autoclaves working in parallel. In a typical experiment, cellulose (1.3g), cerium chloride (500 ppm) and the heterogeneous catalyst (550 mg) were dispersed in degassed water (50mL). The autoclave was sealed and thoroughly degassed. A hydrogen pressure was set at room temperature before heating and stirring at 500 rpm.

3 Results and discussion

A temperature study on the selective conversion of cellulose to C_2-C_3 glycols was first conducted with $CeCl_3.7H_2O$ and Pt(0.63wt%)/CeO_2 as catalysts (see Figure 1.a)). Temperature was varied from 190 to 250°C with an initial pressure of 25 bar H_2 at room temperature. Reaction time was 12 hours. Cellulose conversion was only 28% at 190°C but was superior to

85% from 210°C. From 190°C to 230°C, an increase in EG and PG selectivities was observed with a preferential formation of EG (see Figure 1.a)). The total C_2-C_3 glycol selectivity was 44% at 230°C. A tendency shift was observed from 240°C. Selectivity in EG+PG decreased from 44% to 22% at 250°C as a result of the enhanced formation of dehydration-hydrogenation products –mostly ethanol and 1-propanol– in this temperature range. Glycol selectivities could be finally enhanced to 52% with a reduction in reaction time from 12 to 6 hours.

Pressure effects were then studied. Hydrogen pressure was then varied from 25 to 65 bar to study the influence of pressure on the formation of C_2-C_3 glycols from cellulose (see Figure 1b)). A maximum in cellulose conversion was noted at 50 bar. While results were constant between 25 and 50 bar, a decrease in selectivity was noted since the selectivity in glycols was lowered to 37% by setting an initial pressure of 65 bar.

Considering the complex cascade reactions implied in the transformation of cellulose to glycols, a sharp balance between acidic, basic and hydrogenation catalytic sites seems required to achieve a high selectivity in glycols. The platinum content was thus varied between 0.09 and 2.4% to attempt to maximize this selectivity (see Figure 1c)). An optimum in platinum content was actually observed in the 0.35-0.63% range. In parallel, the formation of degradation products -ethanol and 1-propanol- constantly increased with metal percentages, thus limiting the selectivities in EG and PG

Figure 1. Experimental results for cellulose conversion (2.5wt% in water) with $CeCl_3.7H_2O$ (500 ppm) and Pt/CeO_2 (42.5%wt/cellulose).

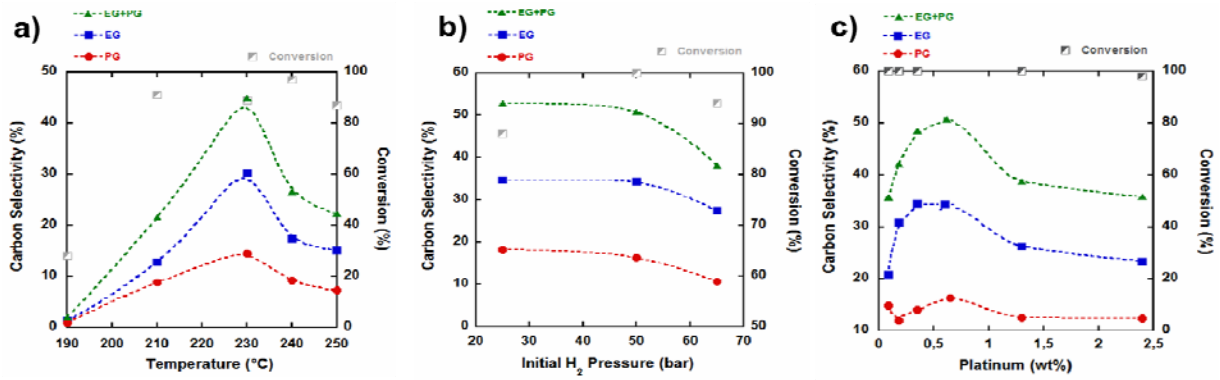

4 Conclusions

Original combinations between a $CeCl_3.7H_2O$ homogeneous catalyst and hydrogenation heterogeneous catalyst supported on cerium oxide were explored for the selective conversion of cellulose to C_2-C_3 glycols under hydrothermal conditions. The selection of a light rare earth support, *i.e.* cerium, was a key result in this study. This was actually confirmed by a recent study which evidenced the high catalytic activity of light rare earth compounds in the retro-aldol reaction and especially in the epimerization reaction.[4] Concerning the multifunctional catalytic system presented herein, temperature and platinum content were primary factors to achieve high selectivities in C_2-C_3 glycols. Thus, a total selectivity of 52% in ethylene and propylene glycols could be obtained.

References

[1] Z. Tai, J. Zhang, A. Wang, M. Zheng and T. Zhang, *Chem. Commun.* 48 (2012) 7052.
[2] Z. Tai, J. Zhang, A. Wang, J. Pang, M. Zheng and T. Zhang, *ChemSusChem* 6 (2013) 652.
[3] E. Girard, D. Delcroix and A. Cabiac, *in preparation.*
[4] R. Sun, T. Wang, M. Zheng, W. Deng, J. Pang, A. Wang, X. Wang and T. Zhang, *ACS Catal.* 5 (2014) 874.

IV-O29

Conversions of Cellulose and Its Derived Carbohydrates into Lactic Acid in Water Catalyzed by Al(III) and Sn(II) Dual Cations

Wang Y.L., Deng W.P., Zhang Q.H., Wang Y.*

State Key Laboratory of Physical Chemistry of Solid Surfaces, Collaborative Innovation Center of Chemistry for Energy Materials, National Engineering Laboratory for Green Chemical Productions of Alcohols, Ethers and Esters, Department of Chemistry, College of Chemistry and Chemical Engineering, Xiamen University, Xiamen, China

* wangye@xmu.edu.cn

Keywords: biomass, cellulose, lactic acid, homogeneous catalysis, Al(III) and Sn(II) cations

1 Introduction

The direct transformation of cellulose into high-valued chemicals is of great importance for establishing sustainable chemical processes. Although limited success has been achieved for the hydrogenation or hydrogenolysis of cellulose into polyols, the consumption of hydrogen is required in these reactions. Lactic acid, an important building-block chemical, can be obtained by the transformation of cellulose without consuming hydrogen. A few recent reports disclosed that Sn^{IV}-beta and Sn^{IV}-grafted mesoporous carbon-silica composite could catalyze the conversion of carbohydrates, such as glucose, fructose and sucrose, in an alcohol medium into alkyl lactate [1,2]. However, these Sn^{IV}-based catalysts are limited to the transformation of mono or disaccharides. Recently, we reported that lactic acid could be directly produced from cellulose with high efficiency in the presence of diluted Pb^{II} in water [3]. However, the toxicity of Pb^{II} would hinder the practical application of this system. Herein, we report an environmental benign and efficient homogeneous catalytic system for the direct conversion of cellulose into lactic acid. We demonstrate that the combination of Sn^{II} and Al^{III} cations is very efficient for lactic acid formation. The mechanism of the formation of lactic acid and the roles of the two cations in each step will also be discussed through both experimental and theoretical studies.

2 Experimental

Catalytic conversions of cellulose, hexose and triose intermediates and other biomasses were performed in a batch-type Teflon-lined stainless-steel autoclave reactor. The liquid products were analyzed by high-performance liquid chromatography (HPLC, Shimazu LC-20A) equipped with UV-vis and RI detectors and a Shodex SUGARSH-1011 column. The theoretical calculations were performed with the Gaussian 09 software package.

3 Results and discussion

We firstly examined the catalytic performances of various non-toxic metal cations including Al^{III}, Ga^{III}, Fe^{III}, In^{III}, Bi^{III}, Cu^{II}, Ni^{II}, Zn^{II}, Co^{II}, Fe^{II}, Mn^{II} and Sn^{II} for the conversion of fructose, which was demonstrated to be a key intermediate in the formation of lactic acid [3], at 463 K. Among these cations, Al^{III} exhibited the highest yield to lactic acid (41%), whereas In^{III} and Sn^{II} afforded lactic acid yields of 38% and 38%, respectively. We observed a significant enhancement on the yield of lactic acid by combining two cations with a molar ratio of 1/1. Among various combinations, the Al^{III}-Sn^{II} combination showed the highest yield of lactic acid (90%) for the conversion of fructose at 463 K. It was confirmed that the counter anions in aqueous solution did not significantly influence the catalytic behaviors, and thus the dual cations

played the true catalytic roles. We further clarified that the Al^{III}-Sn^{II} combination could catalyse the conversions of cellulose and other biomasses such as starch and inulin. The yield of lactic acid was 66% for the ball-milled cellulose in water at 463 K for 4 h. The conversion of starch and inulin provided lactic acid yields of 70-80%.

Our reaction path studies clarified that the conversion of glucose to lactic acid underwent the following three tandem reactions: (I) isomerization of glucose to fructose; (II) retro-aldol fragmentation of fructose into trioes (e.g. dihydroxyacetone and glyceraldehydes); and (III) the isomerization of trioes into lactic acid (Scheme 1).

We investigated the roles of Al^{III} and Sn^{II} in the conversion of glucose. Our studies revealed that Al^{III} alone could efficiently catalyze the isomerization of glucose into fructose (Step I) and also the isomerization of trioses into lactic acid (Step III). With increasing the the ratio of Sn^{II}/Al^{III} from 0 to 1/1, the selectivity to fructose decreased and that to lactic acid increased. This indicates that Sn^{II} is responsible for the retro-aldol fragmentation of fructose into trioses. However, a higher ratio of Sn^{II}/Al^{III} rather decreased the selectivity to lactic acid. We clarified that Sn^{II} catalyzed the conversion of trioses into polymeric by-products in the absence of Al^{III}.

Our DFT calculations for the conversion of glucose showed that the Al^{III}–OH species significantly lowered the Gibbs energy barriers for the isomerization of glucose to fructose and that of trioes to lactic acid (Scheme 1). On the other hand, Sn(II) reduced the Gibbs energy barrier for the retro-aldol fragmentation. These results further confirm that Al^{III} is responsible for the isomerization reactions (Steps I and III), while Sn^{II} plays a significant role in the selective cleavage of C-C bond in fructose into C_3 intermediates.

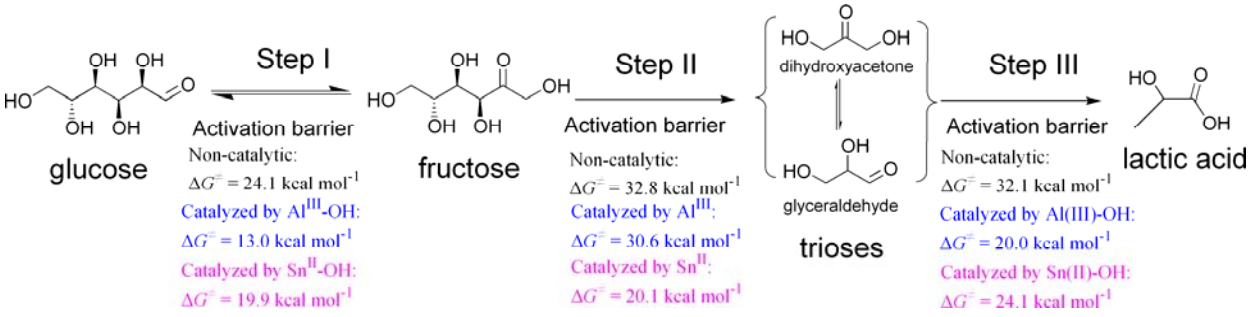

Scheme 1. Reaction pathways for conversion of glucose into lactic acid and the catalytic functions of Al^{III} and Sn^{II} in each step.

4 Conclusions

We discovered that the combination of Al^{III} and Sn^{II} dual cations worked efficiently for the direct conversion of cellulose into lactic acid in water. A lactic acid yield of 66% was attained from cellulose at 463 K. The formation of lactic acid underwent three key tandem reaction steps from glucose, i.e., the isomerization of glucose to fructose, the retro-aldol fragmentation of fructose into trioes, and the isomerization of trioes to lactic acid. We clarified that Al^{III} was responsible for the isomerization of both glucose and trioes, while Sn^{II} played a significant role in the retro-aldol fragmentation of fructose to trioes.

References

[1] M. S. Holm, S. Saravanamurugan, E. Taarning, *Science* 328 (2010) 602.

[2] F. de Clippel, M. Dusselier, R. V. Rompaey, P. Vanelderen, J. Dijkmans, E. Makshina, L. Giebeler, S. Oswald, G.V. Baron, J.F.M. Denayer, P. P. Pescarmona, P. A. Jacobs, B. F. Sels, *J. Am. Chem. Soc.* 134 (2012) 10089.

[3] Y. L. Wan, W. P. Deng, B. J. Wang, Q. Zhang, X. Wan, Z. Tang, Y. Wang, C. Zhu, Z. Cao, G. Wang, H. Wan, *Nat. Commun.* 4 (2013) 2141.

IV-OP30

OSDA-Free Beta Zeolite with High Al Content as Efficient Catalyst for Biomass Conversion

Otomo R, Yokoi T.*, Tatsumi T.

Tokyo Institute of Technology, Tokyo, Japan

* yokoi.t.ab@m.titech.ac.jp

Keywords: OSDA-free zeolite, synthesis, glucose

1 Introduction

Beta zeolite can be synthesized by a variety of methodologies typically using tetraethylammonium (TEA) cation as organic structure-directing agent (OSDA). In 2007 Xiao *et al.* reported the OSDA-free synthesis of Beta zeolite [1]. Since this pioneering work, other groups have also reported the OSDA-free synthesis of Beta zeolite [2] and its applications [3] Today, OSDA-free synthesis is one of the hottest topics in zeolite science, and it has attracted considerable attention because OSDA-free synthesis has several advantages compared to conventional ones using OSDAs. Therefore, OSDA-free synthesis of zeolites will certainly contribute to development of potential green chemical processes if thus prepared zeolites exhibit a high catalytic performance.

It has long been recognized that 5-hydroxymethylfurfural (HMF) is a bio-based "platform" material for producing useful chemicals [4]. Increasing research interest has been paid to the synthesis of HMF from sugars, particularly glucose because it is the most abundant component of woody biomass. However, this reaction is still a challenging subject because it is a multi-step reaction by way of fructose as an intermediate.

Herein, we first demonstrate an effective conversion of glucose to HMF over OSDA-free Beta zeolite whose acid properties are tuned by a simple method making the best use of its high Al content.

2 Results and discussion

First, we evaluated the catalytic performance of OSDA-free Beta zeolite (Si/Al atomic ratio = 5.5) prepared by calcination of the NH_4-form zeolite at 500 ºC, designated as Beta(OF)-Cal500 (Figure 1). The amounts of Brønsted and Lewis acids of Beta(OF)-Cal500 were 0.71 and 0.20 mmol/g, respectively, with the B/L ratio of 3.6. In the early stages of the reaction, fructose was produced through the intramolecular hydride transfer over Lewis acid sites and the yield of fructose was increased along with the glucose conversion up to the maximum (10 %) at the conversion of 44 %. Then the yield of fructose was continuously decreased and simultaneously the HMF yield was increased. This behavior confirmed that the conversion of glucose proceeded through the tandem reaction in the presence of Beta(OF) zeolites. The yield of HMF reached to the maximum of 72 % at 6 h, which is more or less the best performance that has so far been reported for a heterogeneous reaction system. At further prolonged reaction time, the

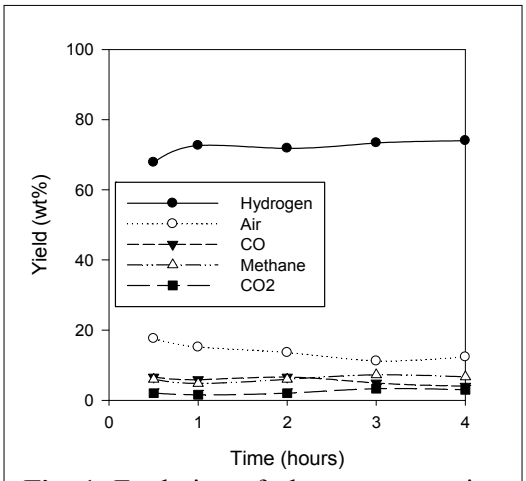

Fig. 1. Evolution of glucose conversion (○), fructose yield (■), HMF yield (◇) in the presence of Beta(OF)-Cal500.

HMF yield was gradually decreased due to its subsequent reactions.

We consider that the calcination temperature would cause the changes in acid properties of catalysts, leading to different catalytic performance. Thus, Beta(OF) catalysts with different B/L ratios were prepared by calcining the NH_4-form zeolite at different temperatures and their catalytic properties were compared (Table 1). As the calcination temperature was increased, Brønsted acid sites were decreased and consequently the B/L ratio was decreased from 3.6 to 1.1. All the catalysts showed similar glucose conversions ranging from 80 to 88 %, but different product distributions. Beta(OF)-Cal450, -Cal500, and -Cal550, which have high B/L ratios (2.9, 3.6 and 2.9, respectively), showed high selectivities to HMF (65, 66 and 67 %). On the other hand, Beta(OF)-Cal600 and -Cal700 with low B/L ratios (1.3 and 1.1, respectively) showed low selectivities to HMF (55 and 45 %) but high selectivities to fructose (12 and 15 %). These differences would be attributed to different reaction rates in the dehydration of fructose to HMF.

Table 1. Acid properties of Beta(OF) zeolites and their catalytic performance in the conversion of glucose to HMF.[a]

Entry	Catalyst	Acidity (mmol/g)[b]			Conversion[c] (%)	Selectivity (%)	
		Brønsted	Lewis	B/L ratio		Fructose	HMF
1	Beta(OF)-Cal450	0.61	0.21	2.9	81	4	65
2	Beta(OF)-Cal500	0.71	0.20	3.6	86	3	66
3	Beta(OF)-Cal550	0.62	0.22	2.9	88	4	67
4	Beta(OF)-Cal600	0.31	0.24	1.3	86	12	55
5	Beta(OF)-Cal700	0.20	0.19	1.1	80	15	45

[a] Reaction conditions: catalyst, 0.1 g; glucose, 0.67mmol; water, 4.5 ml; DMSO, 0.5ml; THF, 15 ml; temperature, 180 ºC; time, 3 h. [b] Acid properties of the samples were measured by IR observation using pyridine as probe molecule. [c] Conversion of glucose.

3 Conclusions

We first demonstrated that the high-aluminum composition of OSDA-free Beta was successfully utilized by taking advantage of the acid properties appropriate for the conversion of glucose to HMF, resulting in the yield over 70 %. The favorable features of the catalyst are proximity of Brønsted and Lewis acid sites and a high B/L ratio. The Beta(OF) zeolite showed stable activity during the consecutive runs.

Acknowledgements

We thank Dr. Ulrich Müller (BASF SE) and Feng-Shou Xiao (Zhejiang University) for helpful discussion. This work was partly performed under the framework of the INCOE (International Network of Centers of Excellence) project coordinated by BASF SE.

References

[1] B. Xie, J. Song, L. Ren, Y. Ji, J. Li, F.-S. Xiao, *Chem. Mater.* **2008**, *20*, 4533.

[2] a) G. Majano *et al*., *Chem. Mater.* 21 (2009) 4184; b) Y. Kamimura *et al*., *Chem. Asian J.* 5 (2010) 2182.

[3] B. Yilmaz *et a*l., *Catal. Sci. Technol.* 3 (2013) *3*, 2580.

[4] a) Y. Román-Leshkov *et al*., *Science* 312 (**2006)** 1933; b) J. N. Chheda *et al*., *Angew. Chem. 119* (2007) 7298; c) M. J. Climent *et al*., *Green Chem.* 13 (**2011)** 520; c) R.-J. van Putten, *et al*. *Chem. Rev.* 113 (2013) 1499.

IV-OP31

Thermooxidative Catalytic Treatment of Biomass

Kasaikina O.T.*, Pisarenko L.M., Zinoviev I.V.

N.N. Semenov Institute of Chemical Physics, Russian Academy of Sciences, Moscow, Russia

* okasai@yandex.ru

Keywords: catalytic oxidation, biomass, hydrogen, peroxide, cellulose, oligosaccharide, acids

1 Introduction

The treatment of organic wastes and biomass is very important problem, which coincides with increasing demand for natural products. Therefore, the rapid expansion of the biomass-using industry occurs in recent years the more especially as biomass is a renewable resource. It has been estimated that there is an annual worldwide production of 10–50 billion tons of dry lignocellulose, accounting for about half of the global biomass yield [1]. Lignocellulose is composed of up to 75% carbohydrates, and in the near future it will become an essential source of fermentable carbohydrates for the production of liquid biofuels as well as a large variety of commodity chemicals and biodegradable materials [2]. Lignocellulosic biomass is known to be recalcitrant to biodegradation and processing due to the rigid and compact structure of plant cell wall and catalytic technology is necessary for biomass treatment. Iron oxides are widely used in various chemical processes due to their low toxicity and relatively low cost. A new relatively simple colloid catalytic system based on iron (III) oxides combined with environmentally friendly oxidants - hydrogen peroxide and/or atmospheric oxygen was worked out [3-6] for biomass treatment.

The aim of this study is to investigate the possibilities of the colloid catalyst based on Fe(3+) oxides together with hydrogen peroxide to process lignocellulosic biomass of different origin in reaction vessels of different sizes. The main attention is brought to develop waste-free and environmentally friendly features of catalytic treatment and to reveal the optimal conditions for biomass treatment.

2 Experimental/methodology

Materials: The catalyst was produced by hydrolyzing iron (III) chloride (Merck KGaA, Germany) according to [3-6]; 30% hydrogen peroxide (analytical grade) was used for oxidative treatment of lignocellulosic materials (pine sawdust, olive pomace, oat and rice straw).

Experimental procedure: The colloidal catalyst as thin suspension is prepared in the reaction vessel; after that, biomass is placed into the vessel and in 8-10 hours H_2O_2 is added. The treatment is carried out at 60°C. Liquid micro volumes are taken periodically in the course of reaction to determine H_2O_2 and acid concentration. When all H_2O_2 had been decomposed, the solid and liquid parts of reaction mixture are separated by centrifugation. The solid residue is washed out with clean water and all the water solutions are combined. The washed solid residue is dried under the flow of warm air. We used glass and stainless steel reaction vessels of different sizes: 200 mL, 3 L, and pilot device 50 L. All vessels were equipped with stirrer, a reflux condenser and thermostatic jacket.

Analytical methods: Catalyst samples and solid oxidation products were investigated by transmission electron microscopy (TEM) on an LEO 912 AB Omega microscope (Carl Zeiss) and by micro analyst SX 100 (CAMECA, France) and AFM NT-MDT SOLVER HV.

The products obtained (both a solid product obtained after catalytic treatment and a solid residue obtained from water solution) were analyzed by FT-IR method, using Perkin-Elmer FTIR-1725 spectrometer with auxiliary device Perkin-Elmer PEDR.

3 Results and discussion

The catalytic oxidative treatment of pine sawdust, olive pomace, oat and rice straw biomass results in formation of water solution of organic acids, esters and other low molecular oxidation products derived from lignin, hemicelluloses, cellulose, lipoproteins and sugars; the solid oxidation product constitutes mainly of cellulose and its derivatives. The yield of solid residue is equal to 15-45 % [6]; it depends on biomass nature, reagents concentration ratio (biomass, catalyst, H_2O_2), and oxidation process duration.

Some special features were discovered in the processing of rice straw as compared with other biomass samples. Figure 1b shows that H_2O_2, added to the original straw rapidly decomposes (1b) without acids formation (curve 3b) and the visible destruction of rice straw. It turned out that rice straw catalyses useless H_2O_2 decay in the absence of catalyst. Sawdust and oat straw do not affect the decay of H_2O_2 (Fig.1a, curve 3a). Pre-processing of rice straw by boiling for 2 hours completely disables the straw against the decay of H_2O_2. TEM data show that boiling removes the top glossy layer and uncovers fibrillar structure. We also found that rice straw contains up to 8% of SiO_2, which forms in water phase stable finely dispersed suspension.

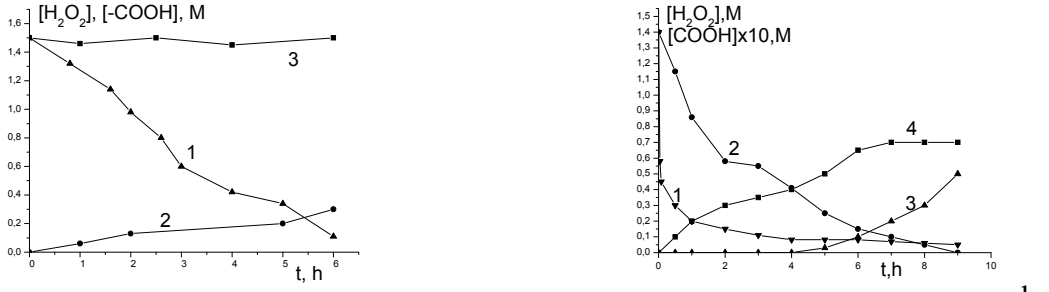

Fig.1 Kinetics of H_2O_2 consumption (1a,1b,2b) and acids accumulation (2a,3b,4b) in the catalytic processing of pine sawdust (a) and rice straw (b) at 60°C; 3a – without catalyst; 1b,3b - original straw; 2b,4b – rice straw pre-treated by boiling.

It must be noted that in a greater volume of the pilot device, the exothermic nature of oxidation reaction displays, therefore the heating is necessary only at the beginning of the treatment.

The results show that the catalytic oxidative processing of vegetable raw materials with the use of H_2O_2 and air as the oxidant and colloidal catalyst based on oxides of iron (3+) is environmentally friendly and waste-free method of recycling of plant biomass into useful products. The solid residue of biomass treatment, as a rule, represents cellulose, which is a food additive E 460 and finds application in pharmaceutical and food industries; it is also used as a component of building materials (putties, cements, composites). Water solution of organic acids and esters can be used in agriculture for fodder processing. Currently, the water phase of oxidation mixture has been successfully used for treatment of seeds and boarding seedling.

Acknowledgements

This work is partly supported by grants RSF 14-23-0018 and RFFI 14-03-00757

References

[1] Kamm B and Kamm M, *Adv. Biochem Engin/Biotechnol* (2007) 105, 175.
[2] Jørgensen H, Kristensen J.B and Felby C, *Biofuels Bioprod Bioref* (2007) 1, 119.
[3] Patent RF №2488445, (2013).
[4] Patent RF №2515319, (2014)
[5] Lesin V.I., Pisarenko L.M., Kasaikina O.T. *Colloid J.,* (2012), 74(1), 1.
[6] Kasaikina O.T., Lesin V.I., Pisarenko L.M., *Catal.Sustain.Energy*. (2014), 1, 21

IV-OP34

Heterogeneous Oligomerization of Ethylene over Highly Active and Stable Ni-Exchanged Mesoporous Materials

Hulea V.[1*], Andrei R.A.[1], Fajula F.[1], Cammarano C.[1], Popa M.I.[2]

1 - Charles Gerhardt Institut, Ecole Nationale Superieure de Chimie, Montpellier, France
2 - Techical University of Iasi, Iasi, Romania

* vasile.hulea@enscm.fr

Keywords: eyhylene oligomerization, nickel, mesoporous materials

1 Introduction

With annual worldwide capacity of 140 million tons, ethylene is among the most important basic organic chemicals. Currently ethylene is produced from crude oil derivatives (*via* steam thermal cracking), but alternative methods involving natural gas, coal and biomass proved their industrial potential. For example, methanol conversion into ethylene and propylene (*via* zeolite-catalyzed MTO process) or bio-ethanol conversion into ethylene, are very promising technologies [1]. Among the industrial applications involving ethylene, the oligomerization reaction is of considerable interest for producing starting materials for lubricants, surfactants, alcohols, amines, and acids. Ethylene oligomerization can be efficiently catalyzed by homogeneous and heterogeneous catalysts having transition metals (in particular nickel) as active sites. Usually, nickel is contained in complexes with different ligands [2], but it can also be stabilized as highly dispersed ionic species on inorganic supports [1,3,4]. Through exhaustive catalytic studies [3,4] we investigated the activity, the selectivity and the stability to deactivation of Ni-exchanged mesoporous materials for the ethylene oligomerization performed in both batch and flow mode, at low reaction temperatures. Mechanistic aspects were also discussed.

2 Experimental

AlMCM-41 (3.5 or 10 nm pore size) was prepared by direct synthesis [3]. AlSBA-15 (7.9 nm pore size) was prepared by post-synthesis alumination of a pure silica SBA-15 material using sodium aluminate as aluminium sources [4]. Calcined Na^+-mesoporous silica-alumina samples were converted into Ni^{2+}-form by cationic exchange with nickel nitrate. The catalysts were characterized by XRD, TEM, ^{27}Al-MAS NMR, ^{29}Si MAS NMR and N_2 adsorption-desorption. Ethylene oligomerization was performed in both batch and flow mode. The oligomers were analyzed by GC.

3 Results and discussion

As a general rule, under mild conditions, the catalysts were highly active and selective. Table 1 summarizes the average catalytic activity (A), the TOF values and the oligomers distributions (wt%) for representative tests. Activities (estimated by weighting the reaction mixture) were between 150 and 175 $g_{oligomers}\ g_{catalyst}^{-1}\ h^{-1}$. It is important to point that these are the highest yields ever reported in the literature with Ni-based heterogeneous catalysts. Additionally, the high TOF values exhibited by the Ni-exchanged mesoporous materials are comparable to those obtained in the ethylene oligomerization processes catalyzed by Ni^{2+}-based complexes [4]. The oligomers consisted of C4, C6, C8 and C10 olefins. Only traces of alkanes and odd carbon number alkenes were identified, indicating that the hydrogen transfer or the acid catalyzed cracking reactions are not occurring to a significant level.

Table 1. Catalytic behavior of Ni-based catalysts: batch mode, 150 °C, and 3.5 Mpa.

Catalyst	Si/Al	Ni (wt%)	A($gg^{-1}h^{-1}$)	TOF (h^{-1})	C4	C6	C8	C10
Ni-AlSBA-15 (7.9 nm)	7.0	2.6	175	14 200	40.6	37.3	14.8	7.3
Ni-AlMCM-41 (3.5 nm)	9.0	2.0	150	15 720	45.1	33.0	14.9	7.0
Ni-AlMCM-41 (10 nm)	9.0	2.0	158	16 560	40.2	33.2	15.5	11.1

In order to evaluate the deactivation rate of the catalysts, the ethylene oligomerization was carried out in flow mode, in a fixed-bed dynamic reactor, using ethylene without inert carrier gas. Table 2 compares the conversions of ethylene (%) obtained on Ni-AlSBA-15 and Ni-AlMCM-41 (pore size of 3.5 nm) with those previously obtained on representative Ni-based catalysts, such as Ni-silica-alumina (mean pore size of 3.4 nm) [5] and Ni-Y zeolite (pore diameter about 1 nm) [6]. Ni-AlSBA-15 (with shows a deactivation rate (d.r.) of 1.6 10^{-3} h^{-1}) is by far the most stable catalyst compared, for instance, to Ni-MCM-41 (d.r. 6.2 10^{-3} h^{-1}) or Ni-Y (d.r. 8.6 10^{-3} h^{-1}). Note: d.r. = $(a_0-a_t)/(a_0 \times 80)$, where a_0 is the initial conversion and a_t the conversion after 80h. The stability of the activity of the Ni-AlSBA-15 catalyst can be related to the SBA-15 topology where the large interconnected mesopores facilitate the diffusion of the products, particularly the bulkier ones, and results in a lower deactivation rate of these catalysts.

Table 2. Ethylene conversions (%) on various porous Ni-based catalysts (flow mode).

Tme-on-stream (h)	1	20	40	60	80
Ni-AlSBA-15[a]	93	90	87	84	81
Ni-AlMCM-41[a]	95	72	57	49	44
Ni-Slica-alumina[b]	70	53	36	24	15
Ni-Y zeolite[c]	58	36	24	14	7

[a] 150 °C, 3.0 MPa; [b] 0.33 wt% Ni, 300 °C, 1.1 MPa; [c] 1.13 wt% Ni, 130 °C, 3.5 MPa

The experimental results obtained on Ni-based catalysts, confirmed the existence of two types of mechanisms which contribute to the conversion of ethylene into C4-C10 olefins: one mechanism involving metallacyclic intermediates over Ni^+ active sites (to form 1-C4 and 1-C6 olefins from ethylene), and a second one based on acid catalysis (isomerization and co-oligomerization reactions), leading to the formation of octenes or higher olefins [4].

4 Conclusions

Ni-AlSBA-15 and Ni-AlMCM-41 are very active and stable catalysts for ethylene oligomerization. Productivities up to 175 g of oligomers per gram of catalyst per hour were obtained in batch mode. In a fixed-bed flow reactor, the catalysts showed very high stability of the activity with time on stream.

References

[1] A. Finiels, F. Fajula, V. Hulea, *Catal. Sci. Technol*. 4 (2014) 2412.
[2] R.H. Grubbs, A. Mihyashita, *J. Am. Chem. Soc*. 100 (1978) 7416.
[3] A. Lacarriere, J. Robin, D. Swierczynski, A. Finiels, F. Fajula, F. Luck, V. Hulea, *ChemSusChem***.** 5 (2012) 1787.
[4] R.D. Andrei, M.I. Popa, F. Fajula, V. Hulea, *J. Catal*. (2015) doi: 10.1016/j.jcat.2014.12.027
[5] R.L. Espinoza, C.P. Nicolaides, C.J. Korf, R. Snel, *Appl. Catal*. 31 (1987) 259.
[6] J. Heveling, A. Van Der Beek, M. De Pender, *Appl. Catal. A*. 42 (1988) 325

IV-OP35

Evolution of Catalytic Systems and Technologies of Production and Solid-state Processing of Ultra-high Molecular Weight Polyethylene with Ultra-durable and Ultra-modular Properties

Ruppel E.I.[1], Ivanchev S.S.[1*], Ozerin A.N.[2]

1 - Boreskov Institute of Catalysis (St.Peterburg Branch), Siberian Division, Russian Academy of Sciences, Saint-Petersburg, Russia

2 - Enikolopov Institute of Synthetic Polymer Materials, Russian Academy of Sciences, Moscow, Russia

* ivanchev@SM2270.spb.edu

Keywords: UHMWPE, morphology, technology, mechanical properties, solid-state processing

1 Introduction

In the last two decades the problem of production, processing and using of ultra-high molecular weight polyethylene (UHMWPE) - linear unbranched polyethylene with a molecular weight greater than $1\text{-}10 \cdot 10^6$ g/mol, has attracted many researchers. This engineering material, depending on the technology of production and processing, has particular molecular architecture and unprecedented mechanical properties.[1] Due to such properties as high abrasion resistance, mechanical strength and high modular characteristics, chemical resistance, low coefficient of friction, biocompatibility, the relative simplicity of the structure and thus affordability, this material has become popular. That is why it is widely used in various fields of technology and human life.

2 Results and discussion

Over the past two decades in the published literature has appeared new information that can help to revise the basic concepts of optimization technology of UHMWPE, the state of the molecular structure and morphology of the polymerization product, the possibility of management in the polymerization process and the possibility of simplifying processing of UHMWPE into products with ultra-durable and ultra-modular properties. [2 -10]

Analysis of the conditions for the formation of nanostructured components morphology of reactor powders (RP) of UHMWPE in the polymerization process allowed us to formulate the requirements for the polymerization, which would result in forming RP of UHMWPE with improved morphology and improved processability. Similar conditions were expressed in the works of Dutch researchers. [7,9,10]

These requirements are as follows:

1) During the formation of RP of UHMWPE it is appropriate to apply the single-site catalyst systems that provide live (pseudo) mechanism for the polymerization of ethylene.

2) Conditions for obtaining RP of UHMWPE (temperature, ethylene pressure, concentration of catalyst and cocatalyst, polymerization time) must correspond to that the rate of formation of the macromolecules and the rate of growing crystallites from them were comparable.

These conditions should hinder the formation of links between growing polymer chains and improve the morphology of the resulting polymer, thereby facilitating the processing RP of UHMWPE into products.

We have the examples of two types of phenoxy-imine catalyst systems, shown that compliance with these requirements provides the opportunity to get RP of UHMWPE capable of solid-state processing to produce a ultra-durable and ultra-modular threads with 2.5 -3.5 GPa and 110-130GPa,respectively.[8-10]

The processing conditions are described in [7].

The results show that modifying the technology of producing RP of UHMWPE may get UHMWPE with improved morphology, which allows realizing a solid-phase processing of RP of UHMWPE into products with ultra-durable and ultra-modular properties.

3 Conclusions

This technology is a significant step forward compared to currently available processing of UHMWPE involving solutions both in hardware design, as well as on the economy of the process. Similar technology is now also being developed by Teijin Corporation.

References

[1] S.M. Kurtz. The UHMWPE Handbook: Ultra-High Molecular Weight Polyethylene in total Joint Replacement, *El series Acad. Press*. 2004. 379 p.
[2] P.H. Geil. Polymer Single Crystals, *Chemistry*, 1968, 552
[3] P. Smith, H.D. Chanzy, B.R. Rotzinger, *Polymer Commun*. 26 (1985), 258
[4] M.B. Constantinoplskaya, S.N. Chvalun, I.V. Selihova, A.N. Ozerin, Y.A. Zubov, N.F. Bakeev. *Polymer Science, Ser. B*. №7 27 (1985), 538.
[5] I.V. Selihova, Y.A. Zubov, E.A. Sinevich, S.N. Chvalun, N.I. Ivancheva, O.V. Smoljanova, S.S. Ivanchev, N.F. Bakeev. *Polymer Science, Ser. A*. № 2 34 (1992), 92.
[6] S.S. Ivanchev, A.N.Ozerin, *Polymer Science, Ser. B*. №8 48 (2006), 1531
[7] A.N. Ozerin, S.S. Ivanchev, S.N. Chvalun, V.A. Aulov, N.I. Ivancheva, N.F. Bakeev, *Polymer Science, Ser. A*. №12 54 (2012), 1731
[8] Patent RU 2459835 (2010)
[9] S. Rastogi, Y. Yao, S. Ronca, J. Bos, J. van der Eem, *Macromolecules*. 44 (2011) 5558
[10] D. Romano, N. Tops, E. Andablo-Reyes, S. Ronca, S. Rastogi, *Macromolecules*. 47 (2014) 4750

IV-OP36

Enantiomerically Pure Zirconocene Complexes in Asymmetric Alkene Carbo- and Cycloalumination

Parfenova L.V.*, Kovyazin P.V., Zakirova I.V., Khalilov L.M., Dzhemilev U.M.

Institute of Petrochemistry and Catalysis, Russian Academy of Sciences, Ufa, Russia

* luda_parfenova@mail.ru

Keywords: zirconocenes, carboalumination, cycloalumination, asymmetric, catalysis

1 Introduction

Chiral η^5-complexes of Zr and Ti have found wide application as components of catalytic systems for highly chemo- and stereoselective construction of C-H, C-C, and metal-C bonds. Among these studies the development of catalytic enantioselective methods for alkene functionalization by organoaluminum compounds (OACs) [1-3] will give effective ways to the synthesis of important enantiomers for organic and organometallic chemistry.

2 Results and discussion

The catalytic action of enantiomerically pure conformationally rigid and non-rigid complexes Zr **1-5** in the reaction of alkenes of various structures with OACs has been studied (Scheme 1).

Scheme 1

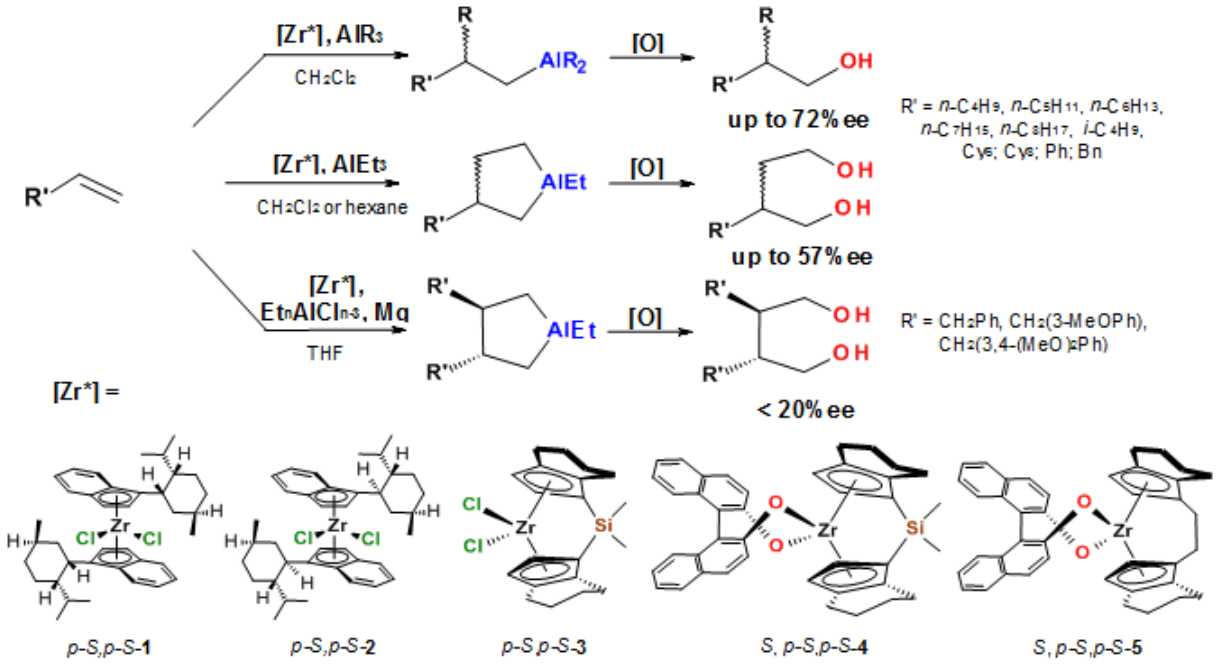

It was shown that the reaction chemo- and enantioselectivity depend on the catalyst and alkene structure, as well as solvent nature. Thus, the reaction of $AlEt_3$with linear alkenes in hydrocarbon solvents, catalyzed with complex (-)-bis-(1-neomenthylindenyl)zirconium dichloride (**1**), predominantly gives *S*-enantiomers of 3-alkyl substituted alumolanes with 23-37%*ee*. In contrast, the use of chlorinated solvent (CH_2Cl_2) provides carbometallation products in a 70-80% yield with enantiomeric purity 47-70%*ee*, *S*. In the case of vinylcycloalkanes and styrene, the process runs with the formation of roughly equal amounts of carbometallation products and substituted alumolanes with enantioselectivity of 39-69%*ee* and 40-57%*ee*, respectively.

The catalyst **2**, which contains menthyl-substituted η^5-ligands, showed the less enantioselectivity both in the carboalumination pathway (18%*ee*, *R*) and cycloalumination (24%*ee*, *R*).

The conformationally rigid complexes **3-5** exhibited lower enantioselectivity in the reaction AlR_3 (R = Me, Et) with 1-alkenes then catalyst **1**. The reaction of 1-alkenes with $AlEt_3$ in CH_2Cl_2 at room temperature in the presence of **3-5** proceeds over 24 hours with conversion of 60-90% and gives mainly acyclic OACs with yield of 20-65% and enantiomeric purity of 15-50%*ee*, *S*. Moreover, the formation of alumolanes with yield of 20-30% and 12-26%*ee*,*S* was observed. Interestingly, in these experiments we isolated enantiomerically enriched functionally substituted stereoregular alkene oligomers (up to 34%) with a number of units n=3-6.

It was found that the reaction of substituted allylbenzenes (Ar = phenyl, 4-methoxyphenyl, 3,4-dimethoxyphenyl) with $EtAlCl_2$ (Et_2AlCl) and Mg in THF in the presence of catalytic amounts of neomenthyl-substituted zirconocenes provides *trans*-3,4-dibenzylalumolanes with enantiomeric purity of 11-20%*ee*.

We showed the applicability of *R*-MTRA and (*R*)- 2- phenylselenopropanoic acid (*R*-PSPA) [4] for the estimation of enantiomeric purity and absolute configuration assignment of stereogenic centers in *β*-chiral primary alcohols and 2-substituted 1,4-butanediols resulting from oxidation and hydrolysis of organoaluminum products.

The effect of a solvent nature on the rate of intramolecular exchange between conformers of neomenthyl-substituted zirconocenes, which are formed as a result of the rotation of the indenyl fragments relative to $[ZrCl_2]$, has been shown for the first time by the means of DNMR spectroscopy. Further, we carried out a theoretical study on the possible rotamers of the conformationally non-rigid catalytically active centers. Comparison of the conformer composition and dynamics of the complexes with their activity and stereoselectivity in the reactions of OACs with alkenes led to the conclusion that the enantioselectivity of the reactions is determined by the kinetic factor, namely, by the rate of interaction in a pair: conformer of catalytically active center - substrate. Thus, in order to achieve high enantioselectivity in the studied reactions the catalyst molecule should have a specific conformational mobility for the formation of a suitable rotamer, which lifetime will be sufficient for the alkene insertion.

3 Conclusions

Thus, the rigid structure of the enantiomerically pure Zr catalysts is not the necessary condition for enantioselective transformations of terminal alkenes in the reactions with OACs. The “key-lock” relationship between catalytically active centers and substrates, i.e. the kinetics of their interaction defines the activity, chemo- and enantioselectivity of the studied catalytic systems.

Acknowledgements

The authors thank the Russian Foundation of Basic Research (Grants No. 12-03-00363a, 15-03-03227a).

References

[1] A.H. Hoveyda, J.P. Morken, *Angew. Chem. Int. Ed.* 35 (1996) 1263.
[2] U.M. Dzhemilev, A.G. Ibragimov, *Russ. Chem. Rev.* 69 (2000) 121.
[3] E.-i. Negishi, *Bull. Chem. Soc. Jpn.* 80 (2007) 233.
[4] N.V. Orlov, V.P. Ananikov, *Chem. Commun.* 46 (2010) 3212.

IV-OP37

Tuning the Selectivity of Nanocatalysts by Using the Ligand Modification Strategy: Experiment and Theory

Fu G., Chen G.X., Zhao Y., Zheng N.F.*

State Key Laboratory for Physical Chemistry of Solid Surfaces and College of Chemistry and Chemical Engineering, Xiamen University, Xiamen, China

* gfu@xmu.edu.cn

Keywords: selectivity, ligand modification, DFT, steric effect, electronic effect, atom coverage

1 Introduction

Selectivity is of paramount importance in catalysis. To realize the important structural parameters which can be tuned to achieve good selectivity are highly desirable. Recently, ligand modification strategy has been introduced to enhance the catalytic performance in selective hydrogenation reaction [1-3]. In this contribution, we combined experiments and DFT calculations to extend the scope of ligand modifation, and proposed that such a enhancement can be understood in terms of steric effect and/or electronic effect.

2 Results and discussion

The chemoselective hydrogenation of α, β-unsaturated aldehydes to the corresponding unsaturated alcohols is of fundamental interest in heterogeneous catalysis, because the formation of the saturated aldehydes favors over that of the unsaturated alcohol due to their thermodynamic nature. Previously, we have demonstrated that amine-capped Pt_3Co alloyed nanoparticles can be used as efficient catalysts for the selective hydrogenation of α, β-unsaturated aldehydes. DFT calculations showed that when the shorter-chained amines are used as capping agents, the α,β-unsaturated aldehyde still have change to sitting on the surface. On the other hand, the long carbon chains that are capped onto the Pt_3Co nanocatalysts imparted steric hindrance so that CAL molecules did not lie flat on the nanoparticle surface. Our calculations demonstrated that CAL molecules can only enter into the array of OAm molecules edge on with their aldehyde groups while the C=C bonds directed away from the catalytically active surface. This finding indicated that the presence of long-chain amines on the surface of the nanoparticles was essential to the high hydrogenation selectivity towards α, β-unsaturated alcohols [1] .

The second example would show that the coated ligand would shape the selectivity through electronic effects. The hydrogenation of nitroaromatics is a typical consecutive reaction that yields many products including nitrosoaromatics, N-hydroxyanilines, and anilines. Among them, N-hydroxyanilines are of importance in many applications. Experimentally, the high (>95%) selectivity to N-hydroxyaniline was first achieved by ethylenediamine (en) coated ultrathin Pt nanowire. DFT calculations demonstrated that the strong binding of en significantly altered the adsorption behaviors of the Pt catalysts, making the coordinated unsaturated Pt atoms only accessible by the electron deficient species, such as nitrobenzene and the nitroso intermediate. In contrast, the binding of N-hydroxyaniline with en-coated Pt nanowire becomes relative weak, which would be substituted by other stronger adsorbates (such as en, nitrobenzene or nitrosobenzene) easily once it was formed, thus switching off the deeper hydrogenation.

In fact, adsorbed H atom could also be viewed as surface modifier, which significantly affects the nature of the surface and controls the selectivity. Experimentally, we found that Pd nanosheets and Pd tetrahedra exposed by {111} facets had good catalytic activity for styrene hydrogenation but no activity for trans-stilbene hydrogenation; while Pd nanocubes enclosed by

{100} facets exhibit high activity for both of the substrates. For clean Pd{111} and Pd{100}, both substrates strongly adsorbed on the surfaces. Under typical reaction conditions, both Pd{111} and Pd{100} were covered by H atoms, and the adsorption of olefins became very weak. In this case, Rideal type hydrogenation mechanism turned out to be dominant rather than the classical Langmiur-Hinshewood type mechanism [4]. Interestingly, for the first step hydrogenation, Pd{111} was more active than Pd{100} because the Pd-H bond on Pd{111} was liable to be broken. On the other hand, the second step hydrogenation critically depended on the stability of half-hydrogenated intermediates. For trans-stilbene on Pd{111}, the half-hydrogenated intermediate was so unstable that the second step hydrogenation should overcome a barrier as high as 0.92 eV, thus inhibiting the whole hydrogenation.

3 Conclusions

The main conclusions can be summarized as follows:

(1) Ligand modification could precisely shape the selectivity through steric and/or electronic effects.

(2) Adsorbed H atom could also be viewed as a surface modifier, which would alter the stability of adsorbed molecules or intermediates as well as the hydrogenation mechanism.

Acknowledgements

We thank the financial support from Ministry of Science and Technology of China (2011CB932403), the National Nature Science Foundation of China (21131005, 20925103, 21373167, 21033006, 21133004, 21333008) and the Fundamental Research Funds for the Central Universities for financial support.

References

[1] B. H. Wu, H. Q. Huang, J. Yang, N. F. Zheng, G. Fu, *Angew. Chem. Int. Ed.* 51(2012) 3440.
[2] S. H. Pang, C. A. Schoenbaum, D. K. Schwartz, J. W. Medlin, *Nat. Commun.* 4(2013) 2448.
[3] K. R. Kahsar, D. K. Schwartz, J. W. Medlin, *J. Am. Chem. Soc.* 136(2013) 520..
[4] J. Li, P. Fleurat-Lessard, F. Zaera and F. Delbecq, *J. Catal.*,311(2014) 190.

IV-OP38

Electrochemical Fluoroalkylation and Phosphorylation Catalyzed by Transition Metal Complexes (Ni, Co Etc.) to Avoid Chemical Oxidants or Reductants

Khrizanforov M.N.*, Strekalova S.O., Khrizanforova V.V., Gryaznova T.V., Budnikova Y.H., Sinyashin O.G.

A.E. Arbuzov Institute of Organic and Physical Chemistry, Kazan Scientific Center, Russian Academy of Sciences, Kazan, Russia

* khrizanforov@gmail.com

Keywords: fluoroalkylation, phosphorylation, green chemistry, electrochemical synthesis, catalysis, transition metal complexes

1 Introduction

In recent years, a lot of therapeutic candidates or advanced materials based on of arenes with fluoroalkyl or phosphonate substituents were created, the prominent examples being anticancer, antibacterial, and anti-HIV agents. From a synthetic chemistry point of view, a wide range of methodologies for the incorporation of a phosphonic acid group or perfluoroalkyl group have been discovered and reported. However, the synthesis pathways to these compounds are very complex, often multi-step and involve high temperatures, pressures, expensive reagents and catalysts. Nevertheless, the high value for medical, agrochemical and engineering industries is the impetus that provokes and promotes exploratory research related to the simplification of the processes. That is why the aim of the work is to provide a simplified method for the catalytic fluoroalkylation products through cross-coupling reaction of organic and fluoroorganic halides, as well as phosphorylation of substrates through CH-activation of aromatic precursors excluding the use of chemical oxidants and reductants.

2 Results and discussion

The unsaturated transition metal complexes of Ni, Co with "no-innocent" ligands have been chosen as catalysts, due to several factors : Ni and Co or Pd are more accessible than Pt, wherein the nickel and cobalt compounds have a very favorable combination of properties required for organic reactions by coordination, namely a sufficiently low ionization potential (promotes oxidative addition); the tendency to form square-planar complexes and the ability to achieve pentacoordination to allow the connection; high electron affinity (promotes reductive elimination). Some properties are contradictory, but a compromise should to be reached for the successful implementation of all stages of the catalytic cycle. The successful choice of the catalytic system metal-ligand-solvent- co-catalyst ion (from sacrificial anode) in certain ratios allows to achieve the high yields of the desired products.

To achieve our goals , we tried to solve a number of interrelated tasks, namely, to study and demonstrate the possibility of electrocatalytic aromatic fluoroalkylation under mild conditions, to justify the choice of the most efficient and affordable catalysts - nickel, copper, cobalt complexes with different ligands to improve the implementation of processes in an electrochemical cell with different soluble and insoluble anodes , the process to establish patterns of cross-coupling and CH- functionalization to make assumptions about the key stages of the catalytic cycle.

As a result, a one-step catalytic method for aromatic perfluoroalkylation with metal complexes electrochemical reduction under mild conditions with decisive role of the sacrificial anode metal ion has been developed. This technique was tested with various catalysts and anode

metals. Some laws of this reaction were discovered. Some regularities of this reaction, such as the linear dependence of Ar-R_F yield vs reduction potential of the catalyst, the copper anode fundamental importance for the selective formation of the cross-coupling product, which confirms the important role of transmetallation step in the catalytic cycle, were shown.

A key role of transmetallation during the catalytic cycle has been assumed. Catalyst begins catalytic cycle for the oxidative addition reactions of M(I)L (M = Ni, Co) with R_FX, but the resulting intermediate - sigma-complex R_FMLX then either reacts with the formation R_FCuLX by transmetallation, which further reacts with PhI under conditions of electroreduction of formation of the desired cross-coupling products, or stage of the transmetallation is later, at the stage bi-organyl sigma complex $R_F(Ar)ML$. It is known that nickel complexes of the type $Ni(Ar)CF_3L$ are very stable and do not lead to cross-coupling products Ar-CF_3. Therefore transmetalation of intermediate sigma complexes with copper favors the catalytic reaction and provides a reductive elimination in the formation of cross-coupling product.

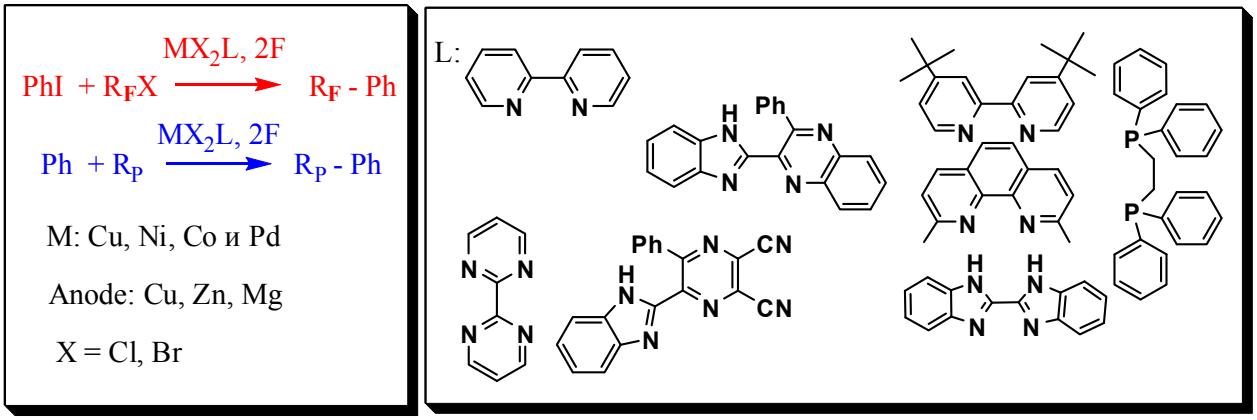

Fig. 1. Schematic representation of studied processes

3 Conclusions

New approach to C-H bonds of aromatic substrates phosphorylation, based on nickel, cobalt or manganese complex in the high oxidation states generation and regeneration on the electrode was proposed. New methods of organofluorine and organophosphorus compounds synthesis can find possible practical application for biologically active, hydrophobic or plasticizing compounds production.

Acknowledgements

The author of RFBR thanks for the financial support: grants 13-03-97025, 13-03-00139-a, 14-03-31423- mol_a and RSF for financial support grant 14-23-00016.

IV-OP39

Complexes of Rare- and Alkaline-Earth Metals for Catalytic Intermolecular Olefin Hydrophosphination and Hydroamination Reactions

Trifonov A.A.*, Basalov I.V., Kissel A.A., Yurova O.S.

Institute of organometallic chemistry of Russian Academy of Sciences, Nizhny Novgorod, Russia

* trif@iomc.ras.ru

Keywords: rare-earth metals, homogeneous catalysis, olefin, hydrophosphination, hydroamination

1 Introduction

Rare-earth complexes proved to be efficient catalysts for a wide range of transformations of unsaturated substrates (polymerization, hydroamination, hydrosilylation, hydroboration etc).

2 Results and discussion

The synthesis and characterization of heteroleptic alkyl, hydrido, amido rare-earth (+2 and +3) and alkaline-earth complexes supported by various N,N-, N,N,N,N-, N,N,O-, N_2,O_4-, N,N,P(O)-ligands as well as their catalytic activity in intermolecular olefin hydrophosphination and hydroamination will be reported. The new complexes afford highly active, chemoselective and, in the case of monoadditions, 100% *anti*-Markovnikov regiospecific catalysts (down to 0.04 mol-% loading) for the hydrophosphination of styrene with $PhPH_2$ under mild conditions. The highest TOF 330 h^{-1} at 60 °C was observed for Yb(II) amido complex. These complexes also turned out to be efficient precatalysts for the intermolecular hydroamination of styrene and pyrrolidine.

IV-OP40

Catalysts for Resource Efficiency: Organic Carbonates from CO_2 and Alkyl or Aryl Alcohols on Cs_2O/BEA Zeolite

Botavina M.*, Martra G.

Department of Chemistry and Interdepartmental Centre "Nanostructured Interfaces and Surfaces – NIS", Torino, Italy

* maria.botavina@unito.it

Keywords: CO_2, alcohol, surfaces, FTIR

1 Introduction

The relevant increase of the cost of oil and the rate of consumption of its recourse is stimulating a great efforts toward the disclosure of new routes to produce chemicals. CO_2 is a non-toxic, abundant and cheep carbon resource, so its conversion to valuable chemicals became a topic of high scientific interest. One of the perspective directions is non-reductive transformation of CO_2 to organic carbonates that can be used in the production of polycarbonate and polyurethane resins, electrolytes for lithium ion batteries, alkylating and carbonylating reagents and inert solvents. Zeolites BEA are characterized by three-dimensional 12-membered ring channel system and their large pores allow an easy diffusion of the various reactants into the zeolite structure. Modifying BEA zeolites with both Cs^+ exchanged ions and Cs-oxide like nanospecies it is possible to increase their basic properties [1] and their capacity for CO_2 activation.

2 Experimental/methodology

Cs/BEA catalyst was prepared by ion exchange of acidic BEA zeolite (RIPP, China), followed by impregnation with a solution of CsOH [2] in order to attain a final Cs/Al ratio = 1.6.

Infrared spectra were collected using a Bruker IFS 28 spectrometer (MCT detector; resolution: 4 cm-1). The samples were pressed in self supported pellets and placed in a quartz cell with CaF2 windows that allowed all thermal treatments (100 Torr O2 at 450°C for 1 h with subsequent outgassing at 450°C for 1h) and adsorption/desorption experiments to be carried out in situ.

High-resolution mass spectrometry analyses were performed using an LTQ Orbitrap mass spectrometer (Thermo Scientific).

3 Results and discussion

Introduction of Cs by wet impregnation after ion exchange significantly increase catalyst basicity. At higher Cs contents, Cs-overloading followed by the formation of Cs-oxide-like species with strong basicity dispersed within the zeolite pores takes place. FTIR analysis verifies that after ion exchange the presence of Brønsted acidic framework-bridged OH groups on the zeolite surface were not observed. The following impregnation with CsOH and subsequent Cs2O formation resulted in the almost complete disappearance also of nonacidic terminal silanols. On the surface of the impregnated samples CO2 adsorbtion with the formation of carbonates (interacting with basic centers) was observed. Methanol, ethanol, 1-and 2-propanol, butanol and catechol were adsorbed on Cs/BEA surfaces with the formation of alcolates.

Figure 1 shows methanol/CO2 co-adsorption on the surface of Cs1.6/BEA catalyst. Spectra of pure catechol registered in water (at different pH) indicated that dissociative adsorption of catechol occurred on Cs-oxide-like particles with a formation of C6H4OH- species. A strong band at 1750 cm-1 with two shoulders at 1780 and 1725 cm-1 is due to the formation of the organic carbonate species. The same band was observed after the adsorption of dimethyl carbonate on the surface of Cs1.6/BEA. The reaction is time-favoured – the first traces of the band at 1750 cm-1 can be observed after 1-2 hours of the contact and then the intensity of the band progressively increased. High-resolution mass spectrometry analyses confirmed the presence of corresponding organic carbonates in aqueous washout solutions. We also observed that the activity of the reaction between CO2 and alcohol decrease with the increase of the carbons atoms number in the alcohol chain of linear carbonates (Fig. 2).

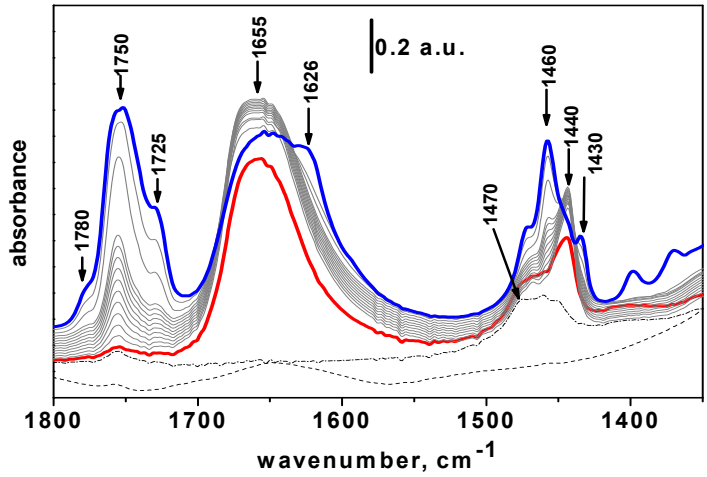

Fig. 1. Methanol/CO_2 co-adsorption on $Cs_{1.6}$/BEA. Dash line - $Cs_{1.6}$/BEAripp, dash dot line – alcohol (10 torr) adsorption, solid lines - CO_2 (100 torr) co-adsorption: red line – right away after CO_2 introduction, blue line – after 100 h of contact.

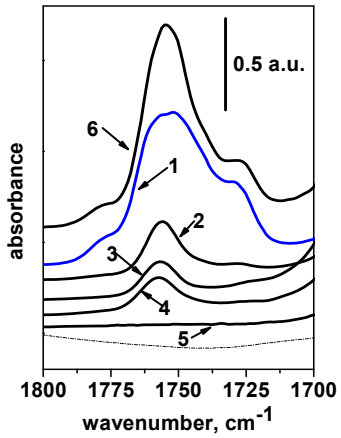

Fig. 2. Formation of organic carbonates after ca. 100 h. of alcohol/CO_2 co-adsorption on $Cs_{1.6}$/BEA: 1 – methanol, 2 – ethanol, 3 – n-propanol, 4 – iso-propanol, 5 - butanol, 6-catechol. Dash line - $Cs_{1.6}$/BEAripp before adsorption.

4 Conclusions

The efficiency of the reaction between alkyl C1-C4 alcohols and CO2 to form the corresponding organic carbonates decreased as the length of the alkyl chains increased. Conversely, an aryl alcohol (catechol) appeared as an active substance in the reaction with CO2 for the production of the carbonate. This features suggest that flexible alkyl moieties of adsorbed alcohol molecules can hinder the interaction with co-adsorbed CO2 (in the form of carbonates), whereas larger but rigid aromatic rings do not interfere with the interaction with neighbour carbonates.

Acknowledgements

The current research was supported by Italian Ministry of Education, University and Research (MIUR), project PRIN 2010-2011 "Mechanisms of CO2 activation for the design of new materials for energy and resource efficiency"

References

[1] D. Barthomeuf, Catal. Rev. *Sci. Eng*. 38 (1996) 521.
[2] C. Bisio, G. Martra, S. Coluccia, and P. Massiani, *J. Phys. Chem. C*, 112 (2008) 10520

IV-OP41

Synthesis of Monoterpenoid Dioxinols from Isopulegol and Benzaldehyde over Heterogeneous Catalysts

Stekrova M.[1], Torozova A.[1], Mäki-Arvela P.[1], Kumar N.[1], Volcho K.[2], Salakhutdonov N.[2], Murzin D.[1*]

1 - Åbo Akademi University, Turku, Finland
2 - Novosibirsk Institute of Organic Chemistry, Novosibirsk, Russia

* dmurzin@abo.fi

Keywords: addition, isopulegol, verbenol oxide, benzaldehyde, dioxinol, zeolites

1 Introduction

New biologically active substances are synthesized from a variety of compounds isolated from natural sources. It has been published recently that compounds with benzodioxin framework can possess promising analgesic activity [1]. Compounds with the mentioned structure were synthesized by the reaction between *cis*-verbenol oxide and aromatic aldehydes in the presence of an excess of montmorillonite clay [2]. Due to importance of the target compound, low selectivity towards it and a very limited amount of experimental data available, there is a need to investigate synthesis of compounds with promising biological activity.

In the current research, syntheses of compounds with the desired benzodioxin framework were investigated (Fig. 1). Besides verbenol oxide (Fig. 1, compound 1) also substrates with analogous structure, namely isopulegol (Fig. 1, compound 3) and 3-methyl-6-(prop-1-en-2-yl)cyclohex-3-ene-1,2-diol (Fig. 1, compound 2), product of verbenol oxide isomerization, were tested in the reaction with benzaldehyde.

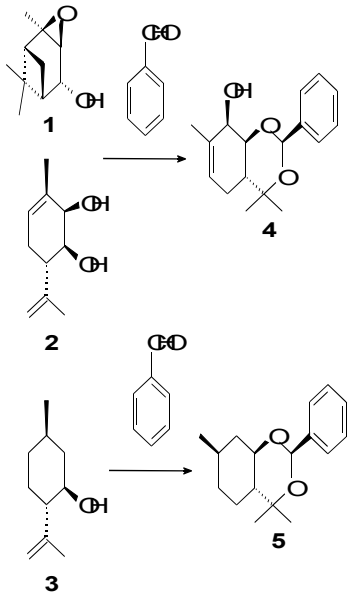

Fig. 1. Reaction schemes of addition reactions of verbenol oxide **1**, 3-methyl-6-(prop-1-en-2-yl)cyclohex-3-ene-1,2-diol **2** and isopulegol **3** with benzaldehyde

2 Experimental/methodology

Metal-modified zeolites beta were prepared, characterized and tested in the present study. As a comparison proton forms of zeolites were also evaluated for addition reactions.

The characterization of catalysts was carried out using XRD, SEM, N_2 adsorption, XPS and

FTIR spectroscopy with pyridine as a probe molecule.

Addition reactions over heterogeneous catalysts were carried out in the liquid phase using a batch-wise glass reactor. In a typical experiment the initial concentration of substrate and the catalyst mass were 0.04 mol/l and 0.3 g, respectively. The kinetic experiments were performed under the following conditions to avoid mass transfer limitation: the catalysts particle size below 90 μm and the stirring speed of 390 rpm. The catalyst was activated in the reactor at 250 °C in an inert atmosphere for 30 min before the reaction. Benzaldehyde was used in excess (V_L=50 ml) and toluene was used as a solvent or reactions were carried out without addition of any solvent. The reaction temperature was 70 °C. The samples were taken at different time intervals and analyzed by GC. The products were confirmed by GC-MS and NMR methods.

3 Results and discussion

In the present work zeolite Beta-150 (150 = SiO_2/Al_2O_3 molar ratio) was modified by iron, characterized and tested per se and in the modified form for syntheses of compounds with the desired benzodioxin framework. Three different substrates were used in addition reactions with benzaldehyde. The results obtained during the study are shown in Table 1.

Table 1. Results of addition reactions using different substrates.

Substrate	Catalyst	Conversion (%) (after 120 min)	Selectivity to desired product (%) at 75 % (* 100 %) conversion level
VO	H-Beta-150	100	* 40
	Fe-Beta-150	100	* 43
IP	H-Beta-150	100	* 16
	Fe-Beta-150	76	15
DIOL	H-Beta-150	98	8
	Fe-Beta-150	79	7

Note: VO = verbenol oxide, IP = isopulegol, DIOL = 3-methyl-6-(prop-1-en-2-yl)cyclohex-3-ene-1,2-diol

Addition reactions were observed to be influenced by the structure of the used substrate as well as by the physico-chemical properties of the catalysts. Verbenol oxide was evaluated as the most promising substrate for preparation of the compound with the desired structure.

4 Conclusions

Metal supported zeolites were prepared, characterized and tested per se and in the modified form in addition reactions of various substrates with similar structure with benzaldehyde. Activity and selectivity of tested catalysts were correlated with their physico-chemical properties. The study was mainly focused on the substrate structure and the influence of Lewis and Brønsted acid sites of catalyst on the selectivity toward desired the dioxinol product with potential analgesic activity. Detailed kinetic analyses and reaction mechanisms will be discussed in the final work.

Acknowledgements

This work is part of the activities of Åbo Akademi University Process Chemistry Centre (ÅA-PCC).

References

[1] S.Yu. Kurbakova, I.V. Il'ina, A. Pavlova, D. Korchagina, O. Yarovaya, T. Tolstikova, K.P. Volcho, N.F. Salakhutdinov, *Med. Chem. Res.* 23 (2014) 1709.

[2] I.V. Il'ina, D.V. Korchagina, K.P. Volcho, N.F. Salakhutdinov, *Russ. J. Org. Chem.* 46 (2010) 1002.

IV-OP42

Fabrication of Efficient and Stable Solid Acids via Encapsulation of PS-SO_3H within Hollow Interiors

Yang Q.*

State Key Laboratory of Catalysis, Dalian Institute of Chemical Physics, Chinese Academy of Sciences, Dalian, China

* yangqh@dicp.ac.cn

Keywords: solid acids, PS-SO_3H, hollow interior, silica, encapsulation

1 Introduction

Driven by environmental consideration and safety concerns, the replacement of hazardous and corrosive mineral acids by solid acids is one of the important tasks for green and sustainable production of chemicals. Polystyrene sulfonic acid resins are among the very important solid acids in industry and have been widely used in acid catalyzed reactions, such as esterification, olefin hydration, etherification, alkylation of phenols. They generally exhibit high concentration of acid sites but poor thermal stability and very low surface area. A straightforward strategy for improving thermal stability and increasing surface area is to prepare polymer/silica hybrid composites which could take advantages of high surface area, high thermal stability and anti-swelling properties of silica materials via either physically mixing or covalently bonding method. Though polymer/silica hybrid composites exhibit increased thermal stability, higher exposure degree of acid sites and larger BET surface area in comparison with their polymer counterparts[1], the acid strength of PS-SO_3H could not be enhanced and on the contrary it might become lower because of the reduced acid density by this approach. It has been reported that the increment of acid density and spatial proximity may increase the cooperative effect among acid sites, consequently enhancing the acid strength of PS-SO_3H[2]. Herein, we reported the synthesis of efficient and stable solid acids by encapsulation of PS-SO_3H within the hollow interiors of silica hollow nanospheres. The exposure degree of acid sites and the acid strength could be adjusted by controlling the swelling and aggregating properties of PS-SO_3H within silica hollow nanospheres.

2 Experimental/methodology

PS-SO_3H-SiO_2 yolk-shell and double-shell hollow nanospheres were prepared by sulfonation of PS-SiO_2 yolk-shell nanospheres with small and large void space using chlorosulfonic acid in CH_2Cl_2 at 273K, respectively (Scheme 1).

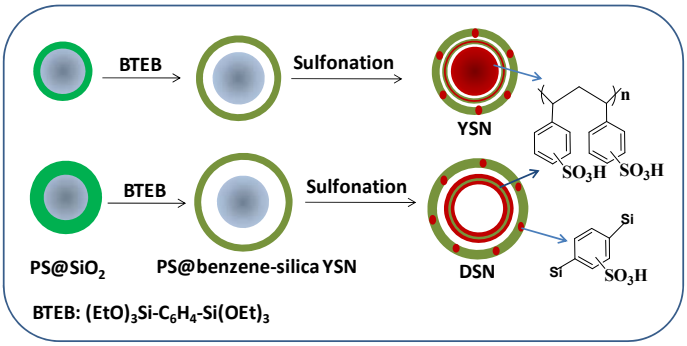

Scheme 1. Schematic illustration for the synthesis of PS-SO_3H-SiO_2 yolk-shell and PS-SO_3H-SiO_2 double-shell hollow nanospheres

3 Results and discussion

Base on the TEM image, the sulfonation of PS-SiO_2 YSNs with large and small void space results in the formation of PS-SO_3H-SiO_2 yolk-double-shell nanostructures (YDSNs) and PS-SO_3H-SiO_2 double-shell nanostructures (DSNs), respectively. Both samples have uniformly dispersed spherical morphology with particle size respectively of 367 and 387 nm, as evidenced by the HR-SEM characterizations. Notably, PS-SO_3H-SiO_2 YDSNs have double shell surrounding the core. The inner and outer shell thickness of PS-SO_3H-SiO_2 YDSNs was of around ~ 30 nm and the particle size of the inner core was about 160 nm. PS-SO_3H-SiO_2 DSNs have particle size of 387 nm with inner and outer shell thickness of 55 and 25 nm, respectively. The element mapping image of the sulfur shows that the PS-SO_3H located mostly in the core and inner shell for PS-SO_3H-SiO_2 YDSNs and mainly in the inner shell for PS-SO_3H-SiO_2 DSNs. The acid strength of PS-SO_3H-SiO_2 DSNs is higher than PS-SO_3H-SiO_2 YDSNs based on ^{31}P NMR characterization.

Table 1. The catalytic performance of solid acids in the esterification[a] of lauric acid and ethanol and Friedel-Crafts alkylation[b] of toluene with 1-hexene.

Catalysts	Esterification[a]		Friedel-Crafts alkylation[b]	
	TOF (h^{-1})	Yield (%)	TOF (h-1)	Conv. (%)
H_2SO_4	40.7	80.4	4 ± 0.1	10 ± 0.8
Amberlyst-15	3.3	42.0	23.7 ± 0.2	98.3 ± 0.5
PS-SO_3H@SiO_2 YDSNs	24.1	84.1	11.5 ± 0.2	94.9 ± 0.5
PS-SO3H@SiO_2 DSNs	20.5	83.8	7.3 ± 0.1	31.3 ± 1.0

In the esterification of lauric acid and ethanol, PS-SO_3H-SiO_2 YDSNs and DSNs with TOF of ・24.1 h^{-1} exhibit comparable activity, probably due to the similar composition and nanostructure of the two materials. In Friedel-Crafts alkylation of toluene with 1-hexene, PS-SO_3H-SiO_2 YDSNs and DSNs with TOF respectively of 11.5 and 7.3 h^{-1} is less active than Amberlyst-15 with TOF of 23.7 h^{-1}. Amberlyst-15 exhibited very fast deactivation rate during four successive cycles. The conversion of 1-hexene decreased from 97.8 % in the first cycle to 45.0 % for the fourth recycle. For PS-SO_3H-SiO_2 YDSNs, the conversion of 1-hexene was quite steady in the following seven cycles. The result suggests that PS-SO_3H-SiO_2 YDSNs is more stable than Amberlyst-15.

4 Conclusions

PS-SO_3H-SiO_2 with DSNs and YDSNs nanostructure was successfully synthesized. It was found that acid strength of solid acids is directly related with the swelling and aggregation of PS-SO_3H in a confined nanospace. PS-SO_3H-SiO_2 YDSNs are more active than PS-SO_3H-SiO_2 DSNs in the Friedel-Crafts alkylation of toluene with 1-hexene. This is due to the fact that the unique YDSNs nanostructure affords superior resistance to the swelling of PS-SO_3H during the catalytic process.

References

[1] M.A. Zolfigol, *Tetrahedron* 57 (2001) 9509.
[2] X.M. Zhang, Y.P. Zhao, S.T. Xu, Y. Yang, J. Liu, Y.X. Wei, Q.H. Yang, *Nat. Commun*. 5 (2014) 3170.

IV-OP43

Acid-Base Catalysis in the Synthesis of C-Amino-1,2,4-Triazoles from Aminoguanidine and Carboxylic Acids

Tarasova E.V.[1], Chernysheva A.V.[2], Chernyshev V.M.[1*]

1 - Platov South-Russian State Polytechnic University (NPI), Novocherkassk, Russia
2 - 25th State Research Institute of Chemmotology of the Ministry of Defence of the Russian Federation, Moscow, Russia

* chern13@yandex.ru

Keywords: amino-1,2,4-triazole, aminoguanidine, carboxylic acids, 2-guanyl hydrazides, catalytic synthesys, reaction mechanism

1 Introduction

C-amino-1,2,4-triazoles (**AT**) are employed as multifunctional reagents for the production of pesticides, medicaments, pigments, corrosion inhibitors, energetic materials, *etc*. One of the promising approaches to the synthesis of **AT** is based on the two-step reaction of aminoguanidine (**1**) with carboxylic acids which proceeds through the formation of intermediate 2-guanyl hydrazides (acylaminoguanidines, **2**):

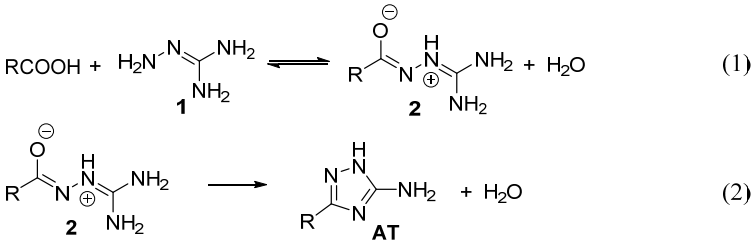

Although this method has received industrial application for the preparation of some **AT** (R = H, COOH), yields of many **AT** (R = Alkyl-, Aryl-, Heterocyclyl-, *etc*.) in the reactions of **1** with many carboxylic acids are poor, and, therefore, the method needs to be improved. The report describes the results of our studies of the mechanisms, thermodynamic and kinetic parameters of the reactions (1) and (2) under acid and base catalysis as well as new approaches to the catalytic synthesis of 3-substituted 5-amino-1,2,4-triazoles from aminoguanidine and carboxylic acids.

2 Experimental/methodology

Equilibrium constants (*K*) were determined experimentally by analysis of equilibrium reaction mixtures or calculated from the ratio of rate constants of the direct and reverse reactions, which were determined experimentally. Reaction enthalpies were calculated by the Van't Hoff equation from the temperature dependence of experimentally determined equilibrium constants.

3 Results and discussion

Formation of protonated 2-guanylhydrazides (**4**) from aminoguanidine and carboxylic acids in water solutions is a reversible acid-catalyzed reaction that proceeds with appropriate rate at pH ≤ 2 for the majority of carboxylic acids. Within the limits of experimental error equilibrium constants (*K*) do not depend from acidity of reaction mixture in the pH range 0.6-2.0 and vary from 4 to ~20 l/mol at 25 °C for simple aliphatic carboxylic acids and amino acids ($NH_2(CH_2)_nCOOH$, n = 1÷3). The *K* values for the reactions of formation of 2-guanyl hydrazides of aromatic acids are sufficiently smaller. Thus, $K = 0.23\pm0.03$ and $\sim 2\cdot10^{-2}$ l/mol for the formation of 2-guanyl hydrazides of benzoic and 3-pyridinecarboxylic acids, correspondingly. Reaction enthalpies (ΔH) are 30±2.5 kJ/mol and practically independent from the

structure of carboxylic acid.

On the basis of kinetic studies we established that mechanism of the acid-catalyzed reaction of formation of 2-guanylhydrazides in general is analogous to the mechanism of the acid-catalyzed reactions of amines with carboxylic acids in water solutions [1], however, the monoprotonated molecule of aminoguanidine (**1kat**) plays the role of nucleophile instead of a free base **1**:

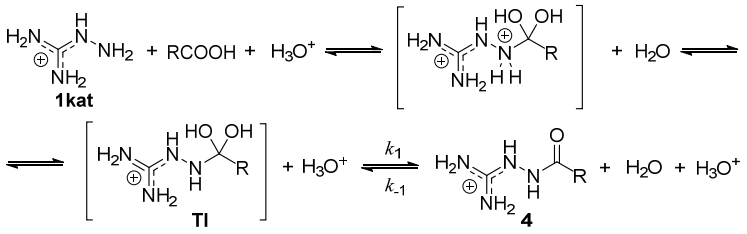

The reaction rate is described by the kinetic equation:

$$\frac{dc_{(4)}}{d\tau} = k_1 c_{(1kat)} c_{RCOOH} c_{H_3O^+} - k_{-1} c_{(4)} c_{H_2O} c_{H_3O^+}$$

At 80 °C and pH = 1.0 the apparent rate constants $k_1' = k_1 \cdot c_{H_3O^+}$ varies from 10^{-1} to 10^{-3} l/(mol·min) for simple aliphatic carboxylic acids, k_1' ~ 10^{-4} for PhCOOH and ~ 10^{-5} for pyridine-3-carboxylic acid, and k_1' ~ 10^{-4} ÷ 10^{-5} l/(mol·min) for amino acids $NH_2(CH_2)_nCOOH$ (n = 1÷3). Noteworthy, while for aliphatic carboxylic acids rate constant predictably decreases with increase of hydrocarbon chain length, for amino acids rate constant increases with increase of a number "n" of CH_2 links of $NH_2(CH_2)_nCOOH$. Apparently, it can be explained by a decrease in repulsive interactions between the protonated NH_2 group of the amino acid and aminoguanidine cation (**1kat**) during formation of transition state (**TI**). Activation energies for the reaction of formation of compounds **4** calculated from Arrhenius equation are in the range 21 ÷ 42 kJ/mol, activation energies of the reverse reaction of hydrolysis vary from 52 to 70 kJ/mol.

Kinetics and mechanisms of the thermal and base-catalyzed reactions of cyclization of 2-guanyl hyrazides into aminotriazoles (**AT**) are also considered in the report.

Taking into account kinetic and thermodynamic regularities of the reactions (1) and (2) we elaborated new one-pot methods for the preparation of 3-substituted 5-amino-1,2,4-triazoles (R = Alkyl-, Aryl-, Pyridyl-, $NH_2(CH_2)_n$-, $COOH(CH_2)_n$-, *etc*.).

4 Conclusions

Thermodynamic parameters, kinetics and mechanisms of the reactions (1) and (2) were studied and new effective approaches to the catalytic synthesis of 3-substituted 5-amino-1,2,4-triazoles from aminoguanidine and carboxylic acids were developed.

Acknowledgements

The authors are grateful to the Russian Science Foundation for the financial support of this work (grant no. 14-23-00078).

References

[1] B. Pan, M. S. Ricci, B. L. Trout, *J. Phys. Chem. B.* 114 (2010) 4389.

IV-OP44

Synthesis of Propylene Oxide with Molecular O_2 over Well Dispersed Ferrosilicate Prepared by a One-Pot Protocol

Garcia-Aguilar J.*, Miguel-García I., Berenguer-Murcia Á., Cazorla-Amorós D.

Inorganic Chemistry Department and Materials Science Institute, Alicante University, Alicante, Spain

* jaime.garcia@ua.es

Keywords: propylene epoxidation, propylene oxide, Fe-silicate

1 Introduction

Propylene oxide (PO) has a production rate by the fine chemical industries of 15 mil. Tons/year. The value of this chemical has increased dramatically over the years due to its importance as an intermediate reactant in the polymer, pharmaceuticals or textile industries [1].

The main production (around 60%) is based on the hydroperoxide process in liquid phase. As well as the liquid phase synthesis (hydroperoxide or chlorohydrin processes), the PO synthesis can be achieved in gas phase by heterogeneous catalysis. The most successful results found in the literature use Au-nanoparticles supported over titano-silicates (Au-$TiSiO_2$) and, usually the use of H_2/O_2 mixtures on the gas stream is mandatory to obtain high selectivity to PO. However, low propylene conversion and water formation are the main drawbacks [1].

On the other hand, metal oxides (Ru and/or Cu) based catalysts usually use molecular O_2 on the gas stream for propylene epoxidation. Some works have studied iron impregnated on silica for the PO synthesis in presence of N_2O as oxidizing agent. In these cases, the PO selectivity is lower than the Au-$TiSiO_2$ systems, but is possible to achieve a higher propylene conversion [2].

In this study, we have developed a one-step synthesis catalyst based on very well dispersed iron single sites on a silica structure. The catalyst has been tested in propylene epoxidation reaction, using two different atmospheres H_2/O_2 and O_2 to evaluate the behavior of the catalyst.

2 Experimental/methodology

Preparation of $Fe_{0.01}SiO_2$. The synthetic procedure has been adapted from the literature [3], using a gel composition with the following molar ratio (8738 H_2O; 410 TMOS, 237.6 Urea; 1.57 HAc; 1 Pluronic® F127), tetramethyl orthosilicate (TMOS) as silica precursor and Pluronic F127 as macroporosity formation agent. To this precursor solution, the necessary amount of $Fe(NO_3)_3 \cdot 9H_2O$ is added to obtain a Fe/Si molar ratio of 0.01. The silica solution is introduced in a Teflon autoclave to submit the sample to a thermal treatment at 40ºC (24 h) and 120ºC (6 h). Finally, the sample is calcined at 550ºC for 6 h. By this synthesis it is possible to generate µ-spheres (3-5 µm) of mesoporous silica interconnected between them with a large amount of macroporous cavities.

Propylene Epoxidation. The catalytic tests are performed in a quartz tube reactor with a feed composition O_2/C_3H_6 (10 % each) and He as carrier gas (GHSV= 10000 ml $h^{-1}g^{-1}$ in all cases). The temperature is raised up to 500ºC at 3ºC/min.

3 Results and discussion

Figure 1 shows a SEM image of the SiO_2 structures generated with and without the incorporation of Fe, where a clear difference in morphology can be observed. For the case of un-doped silica (Fig. 1 left), µ-spheres with well defined size and shape can be observed, due to the spinodal decomposition process occurring during the hydrothermal treatment. However, when Fe is incorporated (Fig. 1 right), the isolated spheres can no longer be observed and an

amorphous structure is obtained. This is due to the iron incorporated on the silica structure, that diminishes the solution/precipitation reaction during the hydrothermal treatment and hinders the formation of the spheres.

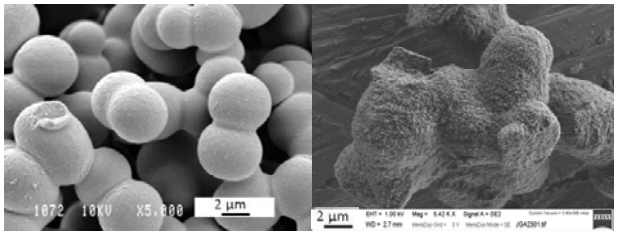

Fig. 1. Pure silica spheres (left) and $Fe_{0.01}SiO_2$ structure (right).

The catalytic tests results (Propylene conversion and propylene oxide generation and selectivity) performed with the sample $Fe_{0.01}SiO_2$ are shown in Figure 2.

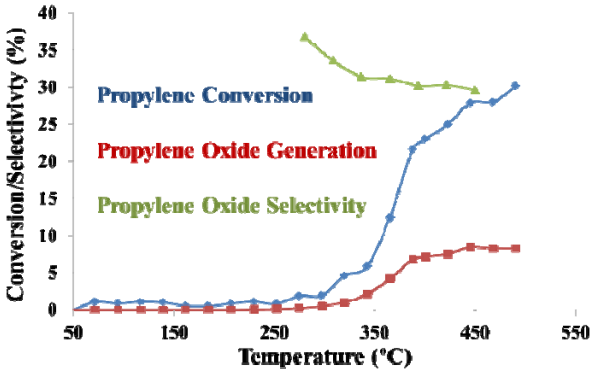

Fig. 2. Catalytic behaviour of $Fe_{0.01}SiO_2$ in O_2/C_3H_6.

The well dispersed $Fe_{0.01}SiO_2$ catalyst shows really interesting properties for the PO production with molecular O_2. The small amount of well incorporated iron (0.01% mol with respect to Si) increases considerably the catalytic properties of the material. In this sense, pure SiO_2 has not any activity in the reaction. After the reaction, carbon deposits were detected, which could be eliminated with a treatment up to 500ºC in synthetic air. Very interesting results have been achieved, with a propylene conversion around 30% with a selectivity towards PO of 30% at 450ºC with molecular O_2 using an iron-silicate based catalyst.

4 Conclusions

A novel catalyst has been synthetized for propylene epoxidation with molecular O_2 and H_2/O_2 mixtures with a good performance, due to the very well dispersed iron single-sites on the silica support. Additional characterization (FTIR and UV-VIS) is mandatory to get insights into the reaction mechanism that is taking place in the presence of the catalyst.

Acknowledgements

We thank the MINECO, GV, and FEDER (Projects CTQ2012-31762 and PROMETEOII/2014/010). A.B.M. and J.G.A. thank MINECO for their fellowships (RyC 2009-03913 and BES-2013-063678, respectively).

References

[1] T.A. Nijhuis, M. Makkee, J. A. Moulijn, B.M. Weckhuysen, Industrial & Engineering Chemistry Research. 45 (2006) 3447.
[2] Ş. Kalyoncu, D. Düzenli, I. Onal, A. Seubsai, D. Noon, S. Senkan, Catalysis Communications. 61 (2015) 16.
[3] G. Puy, C. Demesmay, J.L. Rocca, J. Iapichella, A. Galarneau, D. Brunel, Electrophoresis. 27 (2006) 3971.

IV-OP45

Synthesis of 1-Butanol and 1-Propanol from the Mixture of Methanol and Ethanol in the Presence of Hydrotalcites as Basic Catalysts

Stošić D.[1], Hosoglu F.[2], Bennici S.[1], Travert A.[3], Capron M.[2], Faye J.[2], Couturier J.-L.[4], Dubois J.-L.[5], Dumeignil F.[2,6], Auroux A.[1*]

1 - Université Lyon 1, CNRS, UMR 5256, IRCELYON, Institut de Recherches sur la Catalyse et l'Environnement de Lyon, Villeurbanne, France

2 - Université Lille 1, Sciences et Technologies, Unité de Catalyse et de Chimie du Solide, UMR CNRS 8181, Villeneuve d'Ascq, France

3 - Laboratoire Catalyse et Spectrochimie, CNRS-ENSICAEN, Université de Caen, Caen Cedex, France

4 - ARKEMA, Centre de Recherche Rhône-Alpes, Pierre-Bénite Cedex, France

5 - ARKEMA, Direction Recherche & Développement, Colombes, France

6 - Institut Universitaire de France, Maison des Universités, Paris, France

* aline.auroux@ircelyon.univ-lyon1.fr

Keywords: guerbet reaction, hydrotalcite, 1-propanol, 1-butanol, acid-base properties

1 Introduction

Nowadays, bio-ethanol is emerging as one of the key building blocks for production of renewable chemicals. This has led to identification of several conventionally produced chemicals for which production from bioethanol is an attractive alternative [1]. One such potentially interesting family of products consists of Guerbet alcohols, which are widely used in the chemical industry for applications in cosmetics, chemical intermediates, lubricants or solvents [1, 2]. For these reasons, the synthesis of Guerbet alcohols is potentially a reaction of great importance for enhancing the potential of biomass-derived chemistry. This reaction consists in the synthesis of higher alcohols from lower alcohols and involves both acidic and basic sites [3]. The reaction mechanism is most generally proposed as a four steps sequence: (1) two alcohol molecules are oxidized/dehydrogenated to aldehydes, which (2) react in an aldol condensation after proton extraction to give the aldol, which is further (3) dehydrated to vinyl aldehyde before (4) hydrogenation to the final Guerbet alcohol [4]. Basic sites are known to promote the dehydrogenation and aldol reaction, while acidic ones usually catalyze the dehydration reaction, which means that bifunctional catalysts are needed.

In this work, hydrotalcite catalysts with various Mg/Al ratios (x=2, 3, 4, 5, 6, 7), were prepared by ultrasound assisted co-precipitation method. The synthesized solids have been characterized in terms of structural, textural, and surface properties, including the acid-base and red-ox features, by a variety of techniques (BET, XRD, Raman spectroscopy, TG, and TPR). The strength, strength distribution, and number of acidic and basic sites were estimated by adsorption microcalorimetry measurements of NH_3 and SO_2, whereas their nature was evaluated by FTIR of adsorbed CO_2 and pyridine. A variation of the 'Guerbet' reaction, using a mixture of methanol and ethanol in order to produce two valuable products for the chemical industry, namely 1-propanol and 1-butanol in gas phase was performed. A special attention was devoted to the relationship between the surface acid-base features and the catalytic activity.

2 Experimental

The hydrotalcite materials were prepared by dropwise addition of $Al(NO_3)_3 \cdot 9H_2O$ and $Mg(NO_3)_2 \cdot 6H_2O$ into a solution of Na_2CO_3 in an ultrasonic bath. The pH of the solution was maintained at 9.5 by NaOH addition. The solution was kept under stirring for 1 h at room temperature and then placed in an oven at 63 °C for 24 h before washing with deionized water. The samples were further calcined at 400 °C for 4 h in an air flow. The adsorption heats were measured in a heat-flow microcalorimeter of the Tian-Calvet type (C80 from Setaram), linked to a volumetric line allowing the introduction of small doses of probe molecule. The nature of the acidic and basic sites on the surface of

the catalysts was determined by the FTIR of adsorbed pyridine and CO_2, respectively. Spectra were recorded at room temperature after desorption was carried out by evacuation for 30 min at 50, 100, 150, 200, 250 and 300 °C. The gas phase catalytic reaction was performed in a fixed bed reactor, under atmospheric pressure and at 200, 250, 300, 350 and 400 °C. The feed composition was He : methanol : ethanol = 80 % : 10 % : 10 % with a total gas flow of 50 ml/min. The tail gas out of the reactor was analyzed by an on-line GC-MS (gas-chomatography mass-spectrometry) technique.

3 Results and discussion

Figure 1 gives the total and irreversible number of acidic and basic sites present on the materials surface. The irreversible amount roughly represents the number of strong sites. The basicity of the samples increased with the Mg/Al ratio to a value of 5, after which the decrease of the number of basic sites is obvious. The acidic properties are also varying with this ratio but to a much lower extent.

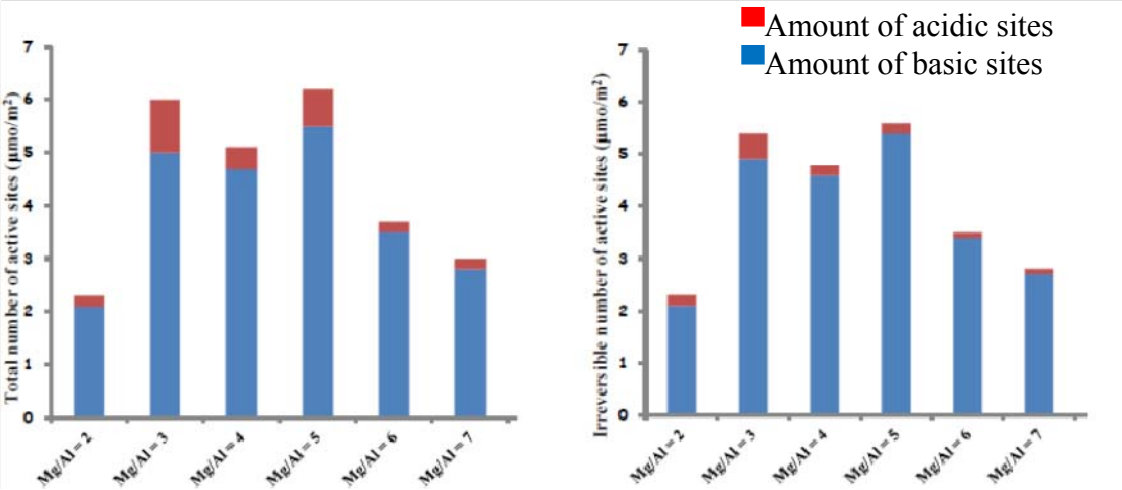

Figure 0. Histograms of amounts of acidic and basic sites for materials investigated in this work.

The results of the catalytic test showed that the conversion of ethanol and methanol is increasing with the temperature on the majority of the catalysts, except for the sample with Mg/Al=2. Furthermore, the highest conversion of both reactants was observed on the samples with Mg/Al ratio of 4 and 5, the samples with the highest amounts of active sites on their surface. Selectivity measured at 400 °C show that the main products are from Guerbet and from intra- or inter molecular dehydration reactions. The targeted products are mainly formed on the catalysts with Mg/Al ratio of 3, 4 and 5, but also the presence of many heavier products, formed by successive reactions between alcohols and reaction products, was observed.

4 Conclusions

The presented results show that it is necessary to control the amount and the strength of both acidic and basic sites in order to produce the desired products. The samples that possess high amounts of basic sites, but do not have very strong basic sites (Mg/Al= 2 and 3) are those which show the highest yields of 1-propanol and 1-butanol, without the production of heavier compounds.

Acknowledgements

French National Research Agency (ANR-09-CP2D-19) is greatly acknowledged for financial support.

References

[1] P.T. Anastas, Green Chemistry: Theory and Practice, Oxford University Press, Oxford, 1998.
[2] A.D. Patel, K. Meesters, H. den Uil, E. de Jong, K. Blok, M.K. Patel, *Energy Environ. Sci*. 5 (2012) 8430.
[3] S. Ndou, N. Plint, N.J. Coville, *Appl. Catal. A* 251 (2003) 337.
[4] A. J. O'Lenick Jr., *J. Surfactants Deterg*. 4 (2001) 311.

IV-OP46

Ni (II) Complex of Pyridyl Containing Eight-Membered Cyclic Aminomethylphosphine Basis for Design of Catalysts for Hydrogen Economy

Karasik A.A., Sharipov A.E., Shamsieva A.V., Khrizanforova V.V., Budnikova Yu.G., Musina E.I.*, Sinyashin O.G.

A.E. Arbuzov Institute of Organic and Physical Chemistry, Kazan Scientific Center, Russian Academy of Sciences, Kazan, Russia

* elli@iopc.ru

Keywords: aminomethylphosphines, nickel(II) complex, hydrogen production

1 Introduction

Cyclic aminomethylphosphine ligands cause growing interest because of their structure – combination of two donor atoms types - nitrogen and phosphorus - in sufficient proximity to each other to enhance catalytic activity of transition metal phosphine complexes.

Recently the ability of these ligands complexes to catalyze Suzuki-Miyaura reaction [1] and reactions of electrochemical oxidation and/or hydrogen production [2-4] was demonstrated. The ability of the ligands to the proton-transfer is one of the determining factors for the catalytic activity of the aminomethylphosphine nickel(II) complexes for the electrochemical hydrogen conversion [4]. The electronic and steric properties of the substituents on both nitrogen and phosphorus atoms can be used to tune the catalysts [5]. Complexes of pyridyl containing 8-membered cyclic aminomethylphosphines are examples of functionalized systems, which combined the both aminomethylphosphine and pyridylphoshpine properties [4]. Moreover the nickel (II) complexes with these ligands showed the perfect results as a catalyst for the electrochemical oxidation or production of hydrogen in the fuel cell.

Herein we report the synthesis of novel aminomethylphosphines and nickel(II) complexes with the methylpyridyl substituents on the phosphorus and the bulky α-phenylbenzyl substituents on the nitrogen atoms.

2 Results and discussion

Initial phosphine **2** was synthesized by the reduction of the corresponding phosphonate **1** [7] (Scheme 1). The condensation reaction of 6-methyl-2-phosphinopyridine **2**, formaldehyde and α-aminodiphenylmethane leads to the formation of novel 1,5-bis(α-phenylbenzyl)-3,7-bis(6-methylpyridyl)-1,5-diaza-3,7-diphosphacyclooctane **3** (Scheme 1).

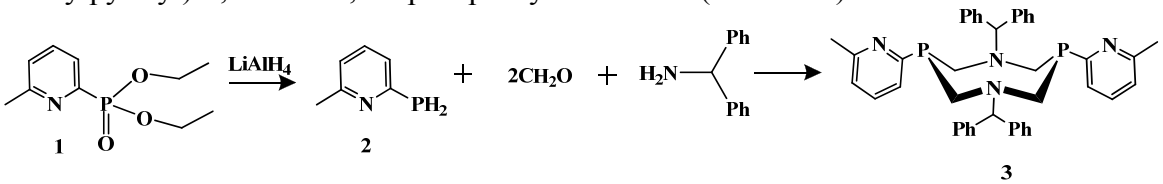

Scheme 1. Synthesis of **3**

Interaction between the ligand **3** and $Ni(BF_4)_2(CH_3CN)_6$ in a ratio of 2:1 resulted in the formation of a new bis-P,P-chelate complex **4** (Scheme 2).

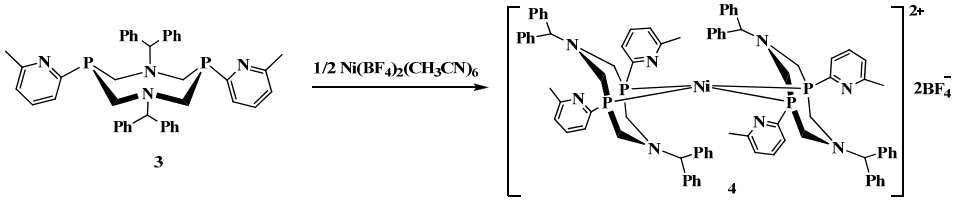

Scheme 2. Synthesis of complex **4**

Complex **4** shows catalytic activity (TOF ~13000 s^{-1}) in the electrochemical hydrogen production comparable to the most active electrocatalysts based on analogous Ni(II) complexes with unsubstituted pyridyl fragments on phosphorus atoms [4]. This fact makes it one of the most perspective catalysts for the design of the non-platinum fuel cell.

3 Conclusions

The novel 1,5-diaza-3,7-diphosphacyclooctane with methylpyridyl substituent on the phosphorus and the α-phenylbenzyl substituent on the nitrogen atom and its bis-P,P-chelate nickel(II) complex were obtained. Nickel(II) complex demonstrates high activity in the electrochemical proton reduction.

Acknowledgements

This work was financially supported by RFBR (grant 13-03-00563-a).

References

[1] Fihri A., Luart D., Len C. et.al., *Dalton Trans*., 2011, **40,** 3116
[2] Wiese S., Kilgore U.J., Dubois D.L., Bullock R.M., *ACS Catal*., 2012, **2**, 720
[3] Rakowski DuBois M., Dubois D. L., *Chem. Soc. Rev*., 2009, **38**, 62
[4] Musina E.I., Khrizanforova V.V., Strelnik I.D. et al., *Chem. Eur. J.,* 2014, **20**, 3169
[5] Kilgore U.J., Stewart M.P., Helm M.L. et al., *Inorg. Chem*., 2011, **50**, 10908
[6] Grotjahn D.B., *Chem. Eur. J*., 2005, **11**, 7146
[7] Redmore D. et al., *J. Org. Chem*., 1970, **35**, 4114

IV-OP47

Methane to Methanol – Influencing Factors for the Direct Catalytic Low Temperature Oxidation with Copper Zeolite Catalysts

Schaller B.[1,2*], Curtin T.[1], Leahy J.J.[1,2]

1 - Materials and Surface Science Institute, Department of Chemical and Environmental Sciences, University of Limerick, Limerick, Ireland

2 - Carbolea Research Group, Department of Chemical and Environmental Sciences, University of Limerick, Limerick, Ireland

* Barbara.Schaller@ul.ie

Keywords: methane oxidation, methanol, zeolite, catalyst copper

1 Introduction

A "dream" reaction of modern heterogeneous catalysis is the quantitative direct partial oxidation of methane to methanol [1]. Methanol is a flexible key component for several alternative fuels and can be obtained from renewable sources through anaerobic digestion of organic matter. Methane is very symmetric which results in extremely high C-H bond stabilities. Activating these bonds requires high activation energies. Stopping the oxidation and releasing the formed methanol from the catalyst surface are challenging problems.

Currently, methanol is synthesized via an indirect selective two-step process using syngas, which is costly and energy consuming. In nature, the C-H bond in methane can be oxidized in mild conditions using methane mono-oxygenase enzymes. One of these enzyme families contains a di-copper complex. The aim of this work is to develop a new catalytic method for this reaction and mimic this highly active di-copper complex. Indeed, from current reported literature, copper catalysts supported by zeolites seem to be relatively promising for this partial catalytic oxidation reaction [2,3].

2 Experimental/methodology

Catalyst preparation

The catalysts were prepared using two different aqueous ion exchange techniques: single exchange with pH-change and multi exchange. Copper acetate was used as a precursor salt and different zeolites as support. For the preparation of bimetallic catalysts wet impregnation using the exchanged copper-zeolites was used.

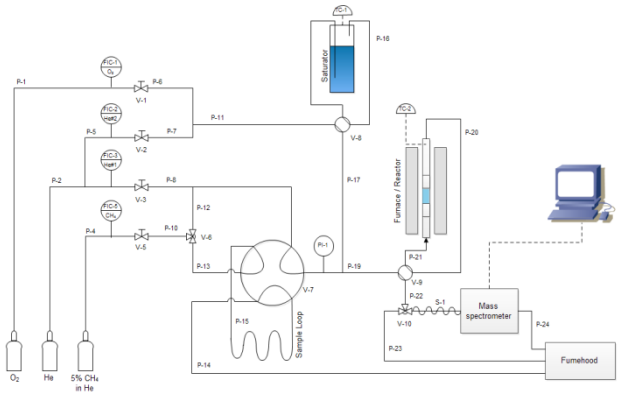

Fig. 1. Flowchart of test rig with Mass Spectrometer (MS) device for the reaction of CH_4 with O_2 to CH_3OH

Catalyst characterisation

Metal loadings were measured by Atomic Absorption Spectroscopy (AAS) using a VARIAN Spectra AA 220 instrument. For determining the oxidation state of copper and structure identification, X-ray Photoelectron Spectroscopy (XPS) was used.

Catalyst testing

The experiments were carried out on the test rig shown in Fig. 1. The catalyst was calcined and pre-treated in a high-purity oxygen stream. In order to stabilize the reactive di-copper oxygen intermediate the

catalyst was cooled to 50 °C and heated to reaction temperature [4]. Then O_2 was removed and after its disappearance, CH_4 (5 % balanced with He) was introduced at the reaction temperature. Post reaction, either dry or wet desorption was performed and the desorbing gases were continuously monitored via an online mass spectrometer (MS). Dry desorption was carried out using a dry helium stream while the catalyst bed was heated to 400 °C to desorb the total oxidised product CO_2. For the wet desorption, a wet helium stream was introduced under isothermal conditions to desorb methanol.

3 Results and discussion

As influencing factors for the direct oxidation of methane to methanol several factors were investigated: catalyst preparation, calcination and behaviour of bi-metallic catalysts.
For the aqueous ion exchange two different procedures are compared: the single exchange with pH change and multi exchange. For the single exchange with pH change an exact amount of copper salt was dissolved in water and mixed with the zeolite for 24 h. Ammonia hydroxide was used to change the pH from ~5 to 7. For the multi exchange a 0.1 molar copper acetate solution was prepared and mixed with the zeolite. After 24 h hours the catalyst was filtered and transferred into a fresh copper acetate solution. This step was repeated 3 times. A copper loading of around 4 wt.% was achieved with both techniques. From testing, the multi exchanged catalyst was found to be more active. Fig. 2. presents the Cu(I):Cu(II) ratio of the multi exchanged and pH modified catalyst before and after reaction. The most active catalyst has higher levels of Cu(I) indicating that this may be important for high activity.

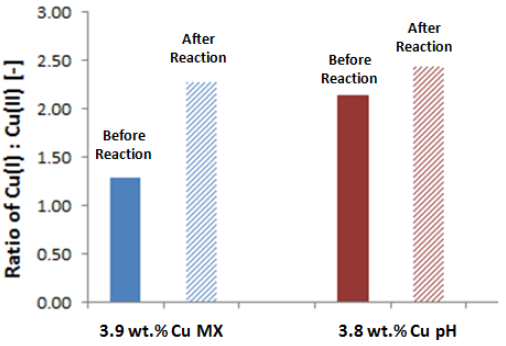

Fig. 2. Ratio of Cu(I) : Cu(II) in the multi-exchanged (MX) Cu-ZSM-5 and the exchanged pH-change (pH) Cu-ZSM-5 before and after reaction using XPS.

After preparation catalysts are calcined either in ex-situ in air or in-situ in 15 % oxygen balanced with helium or high purity oxygen. Results show that in-situ calcined catalysts show higher product amounts compared to ex-situ calcined catalyst.

Some bimetallic catalysts were prepared using the wet impregnation technique of previously prepared uncalcined copper zeolite catalysts. Some experiments show that higher methanol desorption is possible with bimetallic catalyst.

4 Conclusions

The catalytic performance of the methane to methanol oxidation is influenced by factors such as catalyst preparation and diverse pre-treatment steps.

Acknowledgements

The Earth and Natural Sciences Doctoral Studies Programme is funded under the Programme for Research in Third-Level Institutions and co-funded under the European Regional Development Fund.

References

[1] T. Sheppard, C. D. Hamill, A Goguet, D. W. Rooney, J. M. Thompson, *ChemComm*, 50 (2014), 11035.
[2] E. M. Alayon, M. Nachtegaal, M. Ranocchiari, J. A. van Bokhoven, *ChemComm*, 48 (2012), 404.
[3] E. M. Alayon, M. Nachtegaal, M. Ranocchiari, J. A. van Bokhoven, *Chimia*, 66 (2012), 668.
[4] M. H. Groothaert, P. J. Smeets, B. F. Sels, P. A. Jacobs, R. A.Schoonheydt, *JACS*, 127 (2005), 1394.

IV-OP50

Heterogeneously Catalyzed Aqueous Phase Amination and Isomerization of Biogenic Isohexides

Rose M.*, Pfützenreuter R.

Institut für Technische und Makromolekulare Chemie, RWTH Aachen University, Aachen, Germany

* rose@itmc.rwth-aachen.de

Keywords: amination, isomerization, liquid aqueous phase, heterogeneous catalysis, platform chemical, biogenic isohexide, isosorbide

1 Introduction

The replacement of conventional monomers by novel biomass-derived building blocks is of major importance for the utilization of renewable resources in polymers and plastics production. Numerous multifunctional alcohols are readily available from oxygen-rich plant biomass. Prominent examples are isohexides, a group of three rigid C6 diol isomers [1]. Isosorbide is industrially produced from starch. Recent research proved the feasibility of cellulose as raw material, thus, avoiding a competition with food production. The isomers isomannide and isoidide are accessible by isomerization via a dehydrogenation and a subsequent rehydrogenation reaction yielding an equilibrium isomer mixture [2].

2 Experimental/methodology

Further functionalization of the hydroxyl groups enables these monomers also to be used in various other polymer types. In this context the amination of alcohols is of great interest especially regarding the production of polyamides. The amination of alcohols with ammonia to primary amines is typically carried out in gas phase processes at temperatures >300°C catalyzed by Lewis acids. Due to low vapor pressures and insufficient thermal stability of biogenic substrates gas phase amination is often not possible. In recent years the homogeneously catalyzed liquid phase amination of alcohols including the isohexides has been reported [3]. It is based on the hydrogen autotransfer mechanism in analogy to the isomerization reaction but comprising three reaction steps: 1) an initial dehydrogenation of the alcohol to the ketone, 2) the formation of the imine with ammonia, and 3) the subsequent rehydrogenation to yield the primary amine (Figure 1).

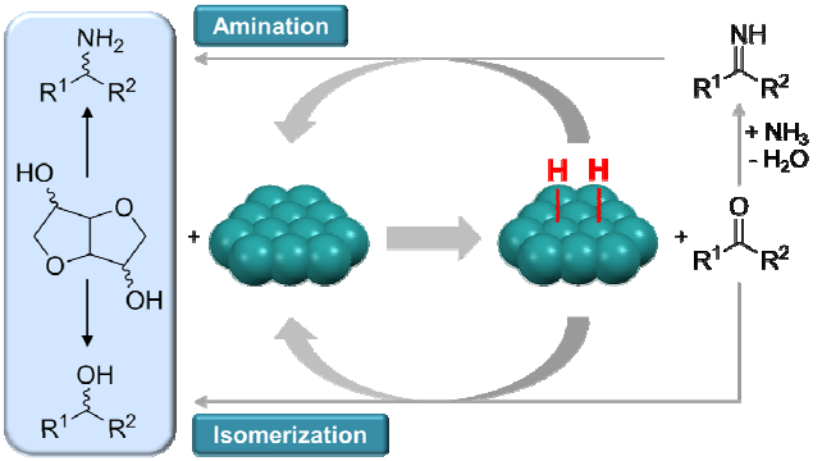

Figure 1. Reaction route for the isomerization and the amination via a dehydrogenation/rehydrogenation mechanism without overall hydrogen consumption.

3 Results and discussion

Hence, we developed a heterogeneously catalyzed process for the amination of isohexides with ammonia [4]. The reaction can be carried out in organic solvents or, much more of interest for an industrial process, even in aqueous solutions and solvent free systems of molten substrate. Catalysts were screened and reaction conditions optimized. Suitable catalysts such as Ru/C were identified that enable the reaction at temperatures of 160-200°C. By investigating the reaction conditions of the amination as well as of the isomerization in the absence of ammonia we found that a certain partial pressure of hydrogen is necessary for the reaction to occur using conventional solid catalysts. Thus, despite following the same reaction route without overall hydrogen consumption the hydrogen autotransfer mechanism can be excluded since a certain coverage of the catalysts surface with hydrogen seems to be necessary to shift the reaction towards the products.

An unusual effect of stereoselectivity of the bifunctional isohexides was observed (Figure 2). In dependence on the initial configuration of the hydroxyl groups the different mono- and diamines are obtained indicating the endo-configured hydroxyl groups to be more reactive while the exo-configured groups are the thermodynamically favored ones. Additionally, reaction kinetics of both reactions the isomerization and the amination were determined to gain insights into the reaction path and mechanism.

4 Conclusions

Overall, with this work a foundation is established for the future development of commercial processes for the production of isohexide-based amine monomers as well as of aqueous phase amination processes of biogenic alcohols in general.

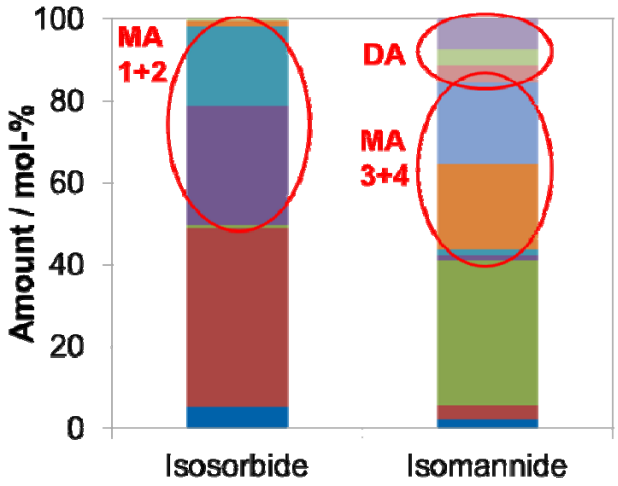

Figure 2. Varying product distribution of the differently configured monoamines (MA) and diamines (DA) upon using isosorbide and isomannide as substrate, respectively.

References:

[1] a) M. Rose, R. Palkovits, ChemSusChem 2012, 5, 167-176; b) F. Fenouillot, A. Rousseau, G. Colomines, R. Saint-Loup, J. P. Pascault, Prog. Polym. Sci. 2010, 35, 578-622.

[2] a) H. G. Fletcher Jr., R. M. Goepp Jr., J. Am. Chem. Soc. 1945, 67, 1042-1043; b) L. W. Wright, J. D. Brandner, J. Org. Chem. 1964, 29, 2979-2982; J. Le Nôtre, J. van Haveren, D. S. van Es, ChemSusChem 2013, 6, 693-700

[3] a) S. Imm, S. Bähn, M. Zhang, L. Neubert, H. Neumann, F. Klasovsky, J. Pfeffer, T. Haas, M. Beller, Angew. Chem. Int. Ed. 2011, 50, 7599-7603; b) D. Pingen, O. Diebolt, D. Vogt, ChemCatChem 2013, 5, 2905-2912.

[4] a) R. Palkovits, R. Pfützenreuter, M. Rose, „Process for the Synthesis of Primary Isohexide Amines", PCT/EP2014/065556; b) R. Pfützenreuter, M. Rose, manuscript in preparation.

IV-PP01

Production of Liquid Hydrocarbons from Syngas over the Co-Containing Supported Catalysts Modified with Rare Earth Metal

Abdullin A.M., Itkulova S.S.*, Ospanova A.Z., Nurmakanov Y.Y., Imankulova S.A.

D.V. Sokolsky Institute of Organic Catalysis and Electrochemistry, Almaty, Kazakhstan

* abdullinanuar@gmail.com

Keywords: syngas, co-catalyst, rare earth metal, Fischer-Tropsch synthesis, liquid hydrocarbons

1 Introduction

Fischer–Tropsch (FT) synthesis is an effective technology to indirectly upgrade coal, natural gas, and biomass resources to hydrocarbons that can be further upgraded to fine chemicals and fuels [1,2]. Recently, because of increased focus on energy security and the implementation of more stringent environmental legislations on liquid fuels, FT synthesis has received considerable worldwide attention in both industrial and academic domains [1-4]. Among the reported FTS catalysts, only iron and cobalt catalysts appear economically feasible on an industrial scale [5]. Cobalt-based catalysts have been widely investigated for FT synthesis due to high activity at low temperature (below 513 K), high resistance to deactivation, low water-gas shift activity and high selectivity to C_{5+} linear hydrocarbons [6]. The catalytic performance of cobalt FT catalysts can be enhanced by promotion with noble metals [7]. Two of the most important factors in determining the active cobalt surface site density that are relevant to the FTS reaction are reducibility and surface dispersion [6].

In this work the catalyst based on Co with adding noble and rare earth metals supported on alumina were synthesized and tested.

2 Experimental/methodology

The Co-containing catalyst with additives of a noble metal (M_1) and a rare earth element (M_6) and supported on alumina were prepared. The content of Co and noble metals in the catalysts was constant and equal to 5 wt.%. The amount of rare earth metal was varied within 0.5-5 wt.%.

The 5%(Co-M_1)-M_6/Al_2O_3 catalysts were tested in the Fischer-Tropsh synthesis. For hydrogenation of carbon monoxide the syngas with a ratio of $H_2/CO=2$ was used. The process was carried out in a stainless steel reactor under pressure varied from 0.5 to 1.0 MPa, temperature region of 190-235^oC, and gas hourly space velocity (GHSV) of 1000-3000 h^{-1} with using 6 mL of the catalyst.

The physico-chemical properties of the catalyst were studied by BET, TEM, X-Ray and TPR-methods.

3 Results and discussion

The effect of pressure, temperature, and space velocity on the 5%(Co-M_1)-M_6/Al_2O_3 catalysts performance in syngas conversion have been studied. The typical effect of temperature on CO conversion and selectivity over the 5%(Co-M_1)-0.5%M_6/Al_2O_3 is presented on Fig.1. It is shown that increasing temperature from 190 to 235 ^oC is accompanied with rising carbon monoxide conversion from 12.3 to 93.6%, increasing methane formation from 1.4 to 4.4%, and increasing carbon dioxide selectivity from 0.5 to 6.1% respectively. Dependence of selectivity to

formation of liquefied hydrocarbons on temperature has the extremum character. The highest yield of C_{5+} hydrocarbons is observed at 230°C. With increasing temperature from 230 to 235 °C selectivity on C_{5+} fraction is decreased from 79.7 to 62.1%.

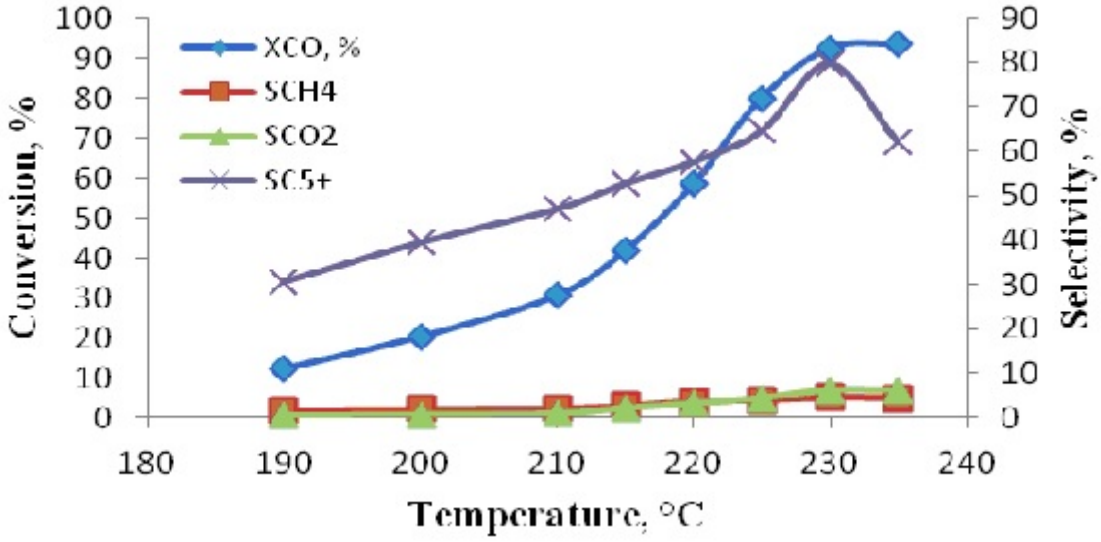

Fig. 1. Effect of temperature on hydrogenation process of CO over the 5%(Co-M_1)-0.5%M_6/Al_2O_3 at H_2/CO=2, P=1.0 MPa and GHSV=1500 h^{-1}

The 5%(Co-M_1)-0.5%M_6/Al_2O_3 catalyst was continuously tested more than 50 hours and showed no decrease in activity and selectivity in the production of gasoline-kerosene fraction of hydrocarbons. By TEM it has been observed that the addition of a noble metal leads to increase in dispersion of metal particles size. TPR analysis has shown that the noble metal also facilitates the Co reproducibility. The role of rare earth metal is in stabilisation of high dispersed state of the catalysts.

4 Conclusions

Thus, results obtained indicate that the developed multicomponent Co-containing catalysts promoted by addition of a noble metal and rare earth element are active and stable in the Fischer-Tropsch process as well as selective in producing the narrow hydrocarbon fraction.

Acknowledgements

The authors wish to thank the Ministry of Education and Science of the Republic of Kazakhstan for sponsoring this research and the Laboratory of Physicochemical studies of Catalysts of the IOCE for providing the catalyst study.

References

[1] M.E. Dry, Catal. Today. 71 (2002) 227-241.
[2] A.Y. Khodakov, W. Chu, P. Fongarland, Chem. Rev. 107 (2007) 1692-1744.
[3] J.I. Yang, J.H. Yang, H.J. Kim, H. Jung, D.H. Chun, H.T. Lee, Fuel. 89 (2010) 237–243.
[4] H. Karaca, O.V. Safonova, S. Chambrey, P. Fongarland, P. Roussel, A.G. Constant, M. Lacroix, A.Y. Khodakov, J. Catal., 277 (2011) 14–26.
[5] Y. Yao, X. Liu, D. Hildebrandt, D. Glasser, Appl. Catal. A: Gen. 433–434 (2012) 58–68.
[6] V.R.R. Pendyala, M.K.G., G. Jacobs, W. Ma, W.D. Shafer, B.H. Davis, Appl. Catal. A: Gen. 468 (2013) 38–43.
[7] F. Diehl, A.Y. Khodakov, Oil Gas Sci. Technol. 64 (2009) 11.

IV-PP02

Metalcomplex Catalysis on Oil Metalloporphyrins

Agahuseynova M.M.*, Quluyeva Z.E., Adigezalova M.B., Abdullayeva G.N.

Azerbaijan State Oil Academy, Baku, Azerbaijan Republic

* minira_baku@yahoo.com

Keywords: porphyrin, supramolecular, chemistry, oil metalporphyrine, complex, petrochemical, synthesis

1 Introduction

Metalloporphyrins connections are biocatalists that imitate properties of natural enzymes. This applies particularly to porphyrin complexes of iron (II), copper (II) and cobalt (II). The remarkable feature of these connections is absorption of molecular oxygen that in their cavity easily passes to the supraoksidny anion of Or^{2-}.

Last, because of high activity to oxidize hydrocarbons at relatively low temperatures to give the corresponding alcohols, ketones and others. Because of this, the use of metalloporphyrins as catalysts for petrochemical processes become relevant scientific and technical value. In addition, when the use of metalloporphyrins as catalysts for transformations of hydrocarbons implemented various mechanisms of enzymatic catalysis.

Over the past 25 years were obtained and studied various properties of synthetic metalloporphyrins. It is established that synthetic metalloporphyrins in catalytic properties are not inferior to natural metalloporphyrins. However, synthetic metalloporphyrins are practically insoluble in hydrocarbons. In this connection there are serious technical difficulties at using of them as catalysts or other aims.

2 Experimental/methodology

Synthesis methods of obtaining individual transition metal complexes with porphyrine consentrate have been developed. Porphyrine consentrate has been received by extraction of heavy oil and asphaltenes with asetone and ethanol. The method is based on demetalization and further metallization processes. As result of metallation reaction of porphyrine concentrate with phenylsodium it has been prepared disodium substituted derivatives, which by interaction with transition metal salts gives transition metalporphyrine complexes. Totally 16 new compaunds have been sythesized.

3 Results and discussion

The compozition and the structure of synthesized porphyrine complexes has been studies using infra-red-and electron spectroscopy methods.

It is necessary to note that synthesized transition metal-porphyrine complexes gives adducts with molecular oxygen. Transition metal-porphyrine-molecular oxygen complexes oxidize unsaturated organic compounds and alkenes. It has been shown that molecular oxygen-transition metal-porphyrine adducts oxidize alkenes giving corresponding oxiranes.

Nickel-porphyrine complex has interesting catalytic properties. This complex has been tested in hydrogenation of aromatic hydrocarbons: naphthalene and other arenes. Besides, nickel-porphyrine, prepared on the base of oil porphyrine consentrate, can be used as catalyst in hydrogenation of heavy oil resudue.

In comparison of oil metal-porphyrine complexes with corresponding complexes synthetic porphyrines it has been found that oil metal-porphyrines have good solubility in hydrocarbon condition. Thanks to this property metal-porphyrines, prepared from oil porphyrine consentrate

can be used as additives. Many of prepared transition metal-porphyrine comp- lexes have great interest as molecular oxygen carriers. On the base of expe-rimental datas it has been calculated equilibrium constants of reactions of formation of transition metal-porphyrine-molecular oxygen adducts. It has next sequence:

$$K_{Mn} >> K_{Fe} > K_{Co} > K_{Ni}$$

4 Conclusions

Thus, our studies revealed that catalytic properties of oil metalporphyrins have been studied and found that synthesized complexes fasilitate the selective reaction of olefins oxyqeneting at low temperatures. The study of complexformation influence on ligand reactionability it has been ditermined that redistribution of electron density causes the changes by reaction ability when oxygen molecules transform from free state info coordinated.

Synthesized oxygen adducts of metalporphyrine complexes are oxygen carriers and provide oxygenizating reactions in mild condition with high output.

References

[1] J.Szejtli, T.Osa, Cyclodextrin. Comprehensive Supramolecular Chemistry // Oxford: UK, 1996, v. 3, p.5-41

[2] W.Steed, J.Atwood, Supramolecular Chemistry // New York; Wiley, 2000, p.772

[3] M.M.Agahuseynova, G.N.Abdullayeva. "Refining and Petrochemicals" , 2010, №12, p. 33-35.

[4] M.M.Agahuseynova, G.N.Abdullayeva. "Refining and Petrochemicals", 2010, №1, p. 27-28.

[5]M.M.Agahuseynova, G.N.Abdullayeva., ANAS, 2009, T. LXV, №5, p.53-57

IV-PP03

Metal-Free Polymer Catalyst for Selective Semihydrogenation of Alkynes

Akhmedov V.*, Ahmadov I., Nurullayev H., Ahmadov V.

M.F.Nagiyev Institute of Catalysis and Inorganic Chemistry of the National Academy of Sciences of Azerbaijan, Baku, Azerbaijan Republic

* advesv@gmail.com

Keywords: polymeric, carbon, nitrides, metal-free catalyst, alkynes, hydrogenation

1 Introduction

Heterogeneous catalysis has a rich history of facilitating energy in the efficient selective molecular transformations and contributes to most of industrial chemical processes. Prevailing at the present time catalytic processes utilized in chemical industries use metals or metal oxides as catalysts. These systems are often high energy-consuming and not selective, wasting resources and producing greenhouse gases. Metal-free heterogeneous catalysis using carbon compounds is a potentially interesting alternative to some current industrialized chemical processes. Owing to their structural and electronic properties, polymeric nanocarbons and their nitrogen containing structural analogs provide the prerequisites required for heterogeneous catalysts. They have the correct electronic and microstructure. Their surfaces remain clean in contrast to conventional catalysts and they can provide a stable performance over a long period of time demonstrating a remarkable thermal stability. Due to the special semiconductor properties polymeric carbon nitrides (PCN) can act as a metal-free heterogeneous catalyst. PCN possessing high thermal stability can be made by condensation of different nitrogen-containing liquid precursors such as cyanamide, dicyandiamide, melamine or cyanuric acid. Depending on reaction conditions, a variety of materials such as nanoparticles or mesoporous powders can be obtained.

We have demonstrated for the first time that PCN can be successfully used as solid catalysts for the selective hydrogenation of phenylacetylene in the absence of any metal and metal oxides.

2 Experimental

High purity hydrogen (99.5%) was used. PCN was synthesized from melamine and dicyanodiamide [1]. The prepared PCN was characterized by X-ray diffraction (Bruker-D2 Phaser, Germany) and Fourier transform infrared spectroscopy (Nicolet-iS10, USA). The X-ray diffraction pattern of this compound reveals a partly crystallized (about 40%) bidimensional single phase with an interplanar distance equal to 3.24 Å, which is consistent to the theoretical values predicted by Teter and Hemley for the graphitic form of carbon nitride [2]. The infrared spectrum performed on this phase exhibits features very similar to those of carbon nitride reported in literature [3]. The group of multiple bands in the 1700–1000 cm^{-1} spectral region is characteristic of *s*-triazine ring vibrations (C=N and C–N stretching modes).

Catalyst testing was conducted at atmospheric pressure in a flow type microreactor. The following experimental conditions were used for a typical run: 0.5 g of polymeric carbon nitride was loaded into the reactor tube (inner diameter 8 mm) and a thermocouple was placed at center of the catalyst bed to monitor the reaction temperature. The temperatures used were typically between 50–250^{0}C. The catalyst was treated at room temperature for 30 min in flowing hydrogen (60 cm^3/min) and then heated to the reaction temperature. A typical experimental run consisted of passing the alkyne solutions in different solvents (acetone, cyclohexane and heptane) over the catalyst in a stream of hydrogen. All the reaction products were analyzed by chromatography equipped with FID (Agilent – 7820A) on a HP-5 capillary column 30 m long.

3 Results and discussion

Hydrogenation of carbon–carbon multiple bonds is one of the most important processes widely used in chemical industry. Currently, this type of reaction is carried out on a very large scale, using noble metals such as platinum, palladium and the first row transition metals such as nickel. We have established that PCN can replace metals for partial hydrogenation of triple bonds in acetylene compounds [4]. In the present study a highly efficient catalyst on the base of synthesized polymeric carbon nitride has been developed for partial hydrogenation of phenylacetylene providing good to excellent conversion with remarkable selectivity (up to 95-97%) without additives. Compared with known metal-containing catalysts for partial hydrogenation of multiple C-C bonds, the developed method is more advantageous: 1) this method provides a selective hydrogenation of phenylacetylene to styrene with effective catalyst recyclability and prevents the consumption of precious metals; 2) they can provide a stable performance over a long period of time demonstrating a remarkable thermal stability.

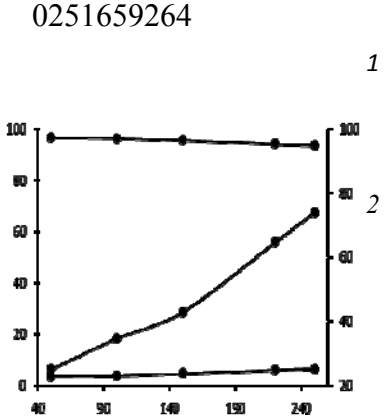

Fig. Partial hydrogenation of phenyl-acetylene in n-heptane (10-12%) vs. temperature on free-metal polymeric carbon nitride: *1*– styrene selectivity, *2*– conversion of phenylacetylene, *3* – ethylbenzene selectivity; hydrogen flow rate) = 60 cm^3/min, reactant flow rate = 0.05 cm^3/min.

Figure demonstrates the activity and selectivity of PCN in the partial hydrogenation vs. temperature for phenylacetylene molecule. PCN is so reactive that noticeable conversion of triple bonds takes place even below 50^0C. This catalyst shows significant differences in product distributions depending on the temperature: there was observed slight decreasing selectivity for the styrene by increasing the process temperature.

4 Conclusions

Since PCN possesses high thermal and chemical stability, it is a valuable and useful material for some other practical applications as well. These findings also provide potential opportunities for the advanced design of metal-free heterogeneous nanostructured catalysts.

References

[1] Kenichi Katsumata, Ryosuke Motoyoshi, Nobuhiro Matsushita, Kiyoshi Okada, J. Hazardous Materials. 260 (2013) 475–482.
[2] Teter D.M. and Hemley R.J. Science. 271 (1996). 53–55.
[3] Khabashesku V.N., Zimmerman J.L. and Margrave J.L. Chem. Mater. 12 (2000). 3264–3270.
[4]Lindlar H., Dubuis R., Org. Synth. Coll. 5. (1973) 880–893.

IV-PP04

Effect of Support on Co_x Free Hydrogen and Carbon Nanofibers Production from Methane over Fe Catalysts

Al-Fatesh A.S.*, Naeem M.A., Fakeeha A.H., Khan W.U., Ibrahim A.A., Abasaeed A.E., Raja L.A.

Chemical Engineering Department, College of Engineering, King Saud University, Riyadh, Kingdom of Saudi Arabia

* aalfatesh@ksu.edu.sa

Keywords: hydrogen production, Fe catalyst, methane decomposition, carbon nanofibers

1 Introduction

Hydrogen production has received great industrial importance and interest from the recent decade, since it is considered to be a perfect fuel for fuel cell applications [1]. In comparison to fossil fuel based energy sources, hydrogen not only have quite high heating value (141.86 MJ/kg), but also inherently cleaner fuel, since water is the only combustion product. On the other hand, the environmental study related, scientist, community has reported several serious concerns about CO_x emission and its subsequent effects on the environment [2]. Consequently, according to environmental protection view point, the quest of environment friendly energy production processes has become one of the most challenging and demanding task. Recently, catalytic decomposition/cracking of methane (CDM) has attracted massive research interest, since it offers the most promising alternative path owing to the ability of CO_x free hydrogen production [3]. In the present work, the performance of Fe based catalyst for hydrogen and nano-structured carbon production from CDM was investigated. Particularly, the effect of different supports, i.e., γ-Al_2O_3, MgO, SiO_2, La_2O_3 and TiO_2-P25 on hydrogen and carbon yield was studied, at moderate temperature of 700 °C.

2 Experimental/methodology

Supported Fe catalysts used in this study were prepared by an incipient wet-impregnation method. In all catalysts 20 wt% Fe loading was fixed. The impregnation of active metal over support was carried out under constant stirring at 80 °C for 3 h. After impregnation the catalysts were dried overnight at 120 °C and followed by calcination at a temperature of 500 °C for 3 h. CMD experiments over Fe based catalysts were performed at atmospheric pressure in a fixed-bed tubular (9.1 mm i.d. and 13 cm long) micro-reactor (PID Eng & Tech micro activity reference) at 700 ºC. Prior to activity test the catalyst was reduced under continuous flow of H_2 (40 ml/min) at 500 °C for 90 min. The In a typical test, the volume ratio of the feed gas mixture, i.e., methane/nitrogen was 10/1, whereas the total flow rate was 33 ml/min. The composition of the outlet gas was analyzed by online gas chromatography (Alpha Mos PR2100) equipped with a thermal conductivity detector.

3 Results and discussion

Figure 1(a-b) show the hydrogen yield verses time on stream (TOS) and carbon yield for Fe based catalysts supported on different carriers respectively. It is notable from results that the type of support material has a significant effect on catalytic performance. Among all catalysts the Fe-Si catalyst exhibited the least, whereas the Fe-Al catalyst presented the best performance both in terms of hydrogen and carbon yield. For instance, Fe-Al catalyst presented 52.1% initial hydrogen yield and 10.5 (gC/gFe) carbon yield as compared to initial hydrogen yield of 1.4% and carbon yield of 0.21 (gC/gFe) for Fe-Si catalyst. Since, Fe-Al catalyst performed better than

all others so this catalyst was selected to study the morphology of deposited carbon after CDM reaction. Figure 2(a-b) display the FESEM and TEM micrographs of Fe-Al spent catalysts at respectively. It is apparent from results that the Fe-Al catalyst ensured the formation of carbon nanofibers, with the typical outer diameter of 30–70 nm. Due to the interweaving of carbon nanofilaments, it remains very tough to estimate the exact length of these nanofibers form FESEM images. Nevertheless, their length varies up to micrometer range.

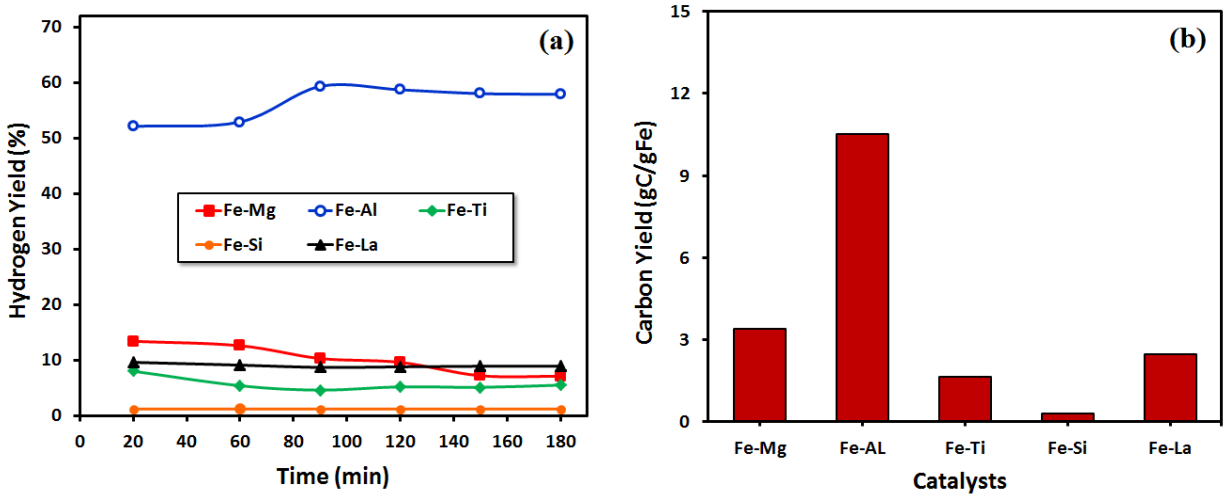

Fig. 1. Variations of H_2 and carbon yield over Fe based catalysts supported on different carriers.

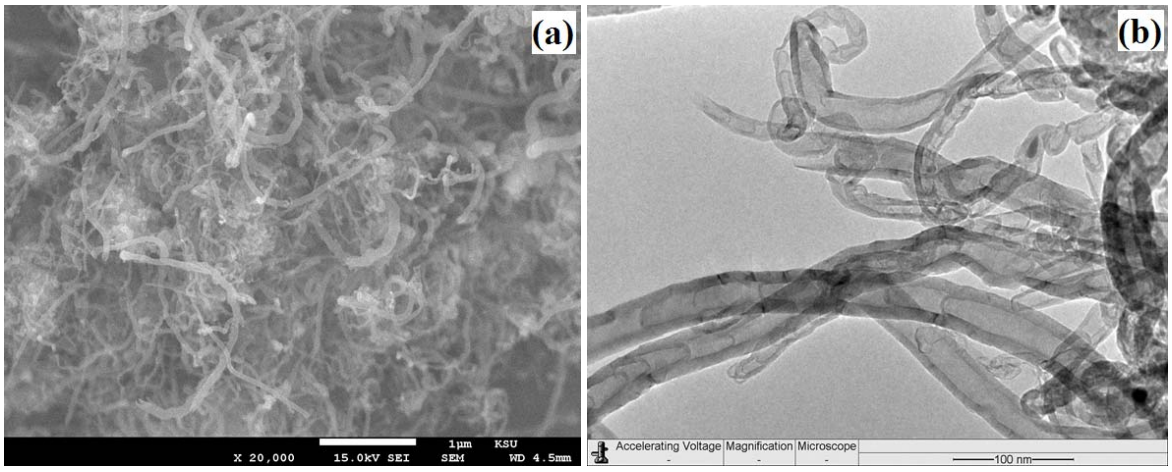

Fig. 2. FESEM (a) and TEM (b) images for Fe-Al spent catalyst.

4 Conclusions

Effect of different supports on Fe based catalysts for CDM showed that Fe-Al presented better hydrogen yield and formation of carbon nanofibers as evidenced by SEM and TEM.

Acknowledgements

The authors thankfully acknowledge their appreciation to King Abdulaziz City for Science and Technology (KACST) for funding the work through the research project # AT-34-4.

References

[1] W. Khaodee, S. Wongsakulphasatch, W. Kiatkittipong, A. Arpornwichanop, N. Laosiripojana, S. Assabumrungrat, *Int. J. Hydrogen Energy*. 36 (2011) 7696.

[2] A. Venugopal, S.N. Kumar, J. Ashok, D.H. Prasad, V.D. Kumari, K.B.S. Prasad, M. Subrahmanyam, *Int. J. Hydrogen Energy*. 32 (2007) 1782.

[3] Y. Shen, A.C. Lua, *Appl. Catal. B: Environ*. 164 (2015) 6.

IV-PP05

Novel Class of Natural Zeolite for the Catalytic Acetalization of Carbonyl Compounds and Diols

Alotaibi R.[1*], Alotaibi F.[1], Kosslick H.[2], Schulz A.[2]

1 - King Abdulaziz City for Science and Technology 1, National Center for Petrochemical Technology, Riyadh, Kingdom of Saudi Arabia

2 - Universität Rostock, Institut für Chemie Abteilung Anorganische Chemie, Rostock, Germany

* raletabi@kacst.edu.sa

Keywords: novel natural zeolites, acetalization catalysts, sustainability, green, catalysts

1 Introduction

Zeolites are an important class of catalysts expected to manage the demand of sustainability, which requires more efficient use energy and chemical resources [1]. More effective use of feedstock for production of chemicals and transportation fuels require use of heavy oil less valuable low-quality resources like oil sands or biomas decomposition products by cracking and hydrocracking in liquid phases. Under these conditions, zeolite catalyst undergo rapid deactivation and catalyst recycling is cost and process intensive. Furthermore, used synthetic zeolite catalyst are expensive. They are prepare by hydrothermal reaction from reaction gel containing expensive organic templates and cause wastewater pollution. Application of natural zeolites is very attractive. They are cheap, environmental benign and non-hazardous and can be used as spent catalyst without recycling. However, despite several thousands of literature paper consider industrial applied synthetic zeolites, only a few paper consider natural zeolite based catalysts [2]. Although a high catalytic potential of natural zeolites is expected and principally confirmed. This subject is still a "undiscovered white research landscape" of high interest and, therefore, new regarding sustainable catalysts for sustainability demands. These reasons encourage us as to start a new research topic dealing with new heterogeneous natural zeolite based catalysts. This project deals with the preliminary evaluation and improvement of Clinoptilolite and Mordenite for use as catalytic material in petrochemical process. Catalyst design will be achieved by tailoring properties taking into account key factors as structural origin, composition, stability, porosity and acidity as key parameter determining catalytic performance.

2 Experimental/methodology

Three different natural materials, probably containing natural zeolites have been obtained. Additionally, one natural zeolite sample, containing mainly clinoptilolite, called "Clinofit", has been supplied by the German partner. The materials have been worked up for further use, structural investigated by XRD and FTIR. The water capacity has been determined. Proton-exchanged samples have been catalytically tested. The aim of the preliminary investigation with provided natural materials was to determine the nature (structure) and crystallinity of provided the materials to proof that thee these materials can act as acid catalysts in order to establish a proof-of-principle that these materials can the used for the development of nature based new green catalysts .g. for cracking of heavy feedstock, and to check the usefulness of the used catalytic test reaction, namely the acetalization of benzaldehyde with 1,3-butanediol. Obtained samples will be characterized with highly sophisticated methods like solid state NMR, which have been only scarcely applied to natural zeolites. The acid property tuning will be investigated using acid catalysed model reaction. The goal is to develop the basis for the preparation of a natural zeolite based catalyst for petrochemical and petroleum refining applicationThis

acetalization has been chosen as test reaction, because it is catalyzed by acid and basic sites occurring in minerals, e.g. natural zeolites (NZ). It can be carried out in easier to handle liquid phase and it is expected to be sensitive also for the detection acid sites of lower acidic strength as well as to the number of sites (specific acid site concentration). Furthermore, the use of the diol is more space demanding because it is connected with the formation of a 6-ring beside of the phenyl ring of the benzaldehyde. It provides better information of the accessibility of site even for larger molecules as is required for the conversion of heavy feedstock. For catalytic testing the reaction solution was prepared by mixing 10g of benzaldehyde with ca.9g of 1,3-butanediol and addition of 100 mL t of toluene as solvent.. The benzaldehyde and toluene was re-distilled prior to use. The reaction was carried out in 3-necked flask connected with a condenser on the top. An oil bath was use as heating source the mixture was magnetically stirred. After heating to reflux temperature (ca. 116°C), the calcined catalyst has been added immediately. µL sized samples were used liquid ^{1}H-NMR for quantitative determination of the reaction progress. 2-dimensional ^{1}H-NMR spectra were used to confirm the assignment of NMR signals.

3 Results and discussion

The results of the catalytic tests are summarized in Table 1. All samples are catalytic active in the acetalisation of benzaldehyde with 1,3-butanediol, however, the conversions differ significantly.

Table 1: Catalytic activity (conversion) of natural zeolite sample in the acetalisation of benzaldehyde with 1.3-butanediol

Sample	Name	Catalyst amount	Conversion / %	IR /cm^{-1}
NZ 01/14	Natural Zeolite(j54)	100mg	49	988
NZ 03/14	Natural Zeolite(JNE5)	100mg	18	980
NZ 05/14	Clinofit^{R}Si materials	200mg	88	1015

These results show that the acetalisation reaction is a proper test for the evaluation of the catalytic activity of nature based green catalysts. The differences between the samples are well expressed. 100-200 mg of the material are sufficient to carry out the catalytic performance test.

4 Conclusions

The results show that the nature based zeolitic materials are catalytically active and a proper base for the development of new green catalyst for sustainable use of chemical feedstock.

References

[1] M.A. Alia-*, T. Tatsumib, T. Masudac, Appl. Catal. A: General 233 (2002) 77.
[2] S. Jeong, J.-H. Kim, G. Seo, Korean J. Chem. Eng., 18 (2001) 848.

IV-PP06

Novel Nickel(II) Complexes with 2-Iminopyridyl Ligands Containing Electron-Withdrawing Groups: Ethylene Polymerization and Oligomerization Behaviour

Antonov A.A.[1,2*], Semikolenova N.V.[1], Zakharov V.A.[1,2], Talsi E.P.[1,2], Bryliakov K.P.[1,2]

1 - Boreskov Institute of Catalysis SB RAS, Novosibirsk, Russia
2 - Novosibirsk State University, Novosibirsk, Russia

* antonov@catalysis.ru

Keywords: 2-iminopyridine, nickel, ethylene polymerization, oligomerization, methylalumoxane

1 Introduction

During the last two decades nickel(II) complexes with bidentate *N,N*-donor ligands have been attracting considerable attention as catalysts for polymerization of ethylene and linear α-olefins yielding polymeric products with various types of branching [1]. Up to date, the post-metallocene catalysts based on nickel complexes providing branched and hyperbranched polyethylene [2] are of great importance due to the unprecedented chain architectures and unique physical properties of these polymers [3].

Nickel(II) complexes with 2-[(arylimino)alkyl]pyridine ligands are of special interest due to the simplicity of ligands syntheses, rich opportunities for fine tuning of their steric and electronic properties by the introduction of different substituents into the phenyl rings, and the ability to give low-molecular-weight polyethylene with different content of branches. However, only ethylene polymerizations over 2-iminopyridine catalysts with electron-donating (alkyl) substituents at the aryl rings have been reported previously [4]. It is challenging to probe the effect of electron acceptors on the performance of nickel catalysts. Previously, introduction of electron-withdrawing groups was reported to increase the activity of analogous iron, cobalt and nickel tridentate bis(imino)pyridine catalysts for ethylene and norbornene polymerization [5].

2 Experimental/methodology

All manipulations with air- or moisture-sensitive compounds were performed under an atmosphere of argon using a glovebox, break-sealed or standard Schlenk techniques.

Syntheses of 2-iminopyridine ligands were performed in toluene by Schiff condensation of 2-formylpyridine, 2-acetylpyridine or 2-benzoylpyridine with appropriate aniline using either strong Brønsted or Lewis acids as catalysts. The ligands obtained were characterized by ^{1}H, ^{13}C and ^{19}F NMR spectroscopy.

The corresponding nickel complexes were readily prepared by the reaction of the ligand with $NiCl_2$ or $NiBr_2$*(1,2-dimethoxyethane) in dry acetonitrile, tetrahydrofuran or dichloromethane with good yields. The structure of the complexes obtained was proved by elemental analysis, X-ray diffraction studies and ^{1}H NMR spectroscopy of paramagnetic molecules.

Ethylene polymerization was performed in a 1 L steel autoclave. During the polymerization ethylene pressure, stirring speed and temperature were maintained constant. The experimental unit was equipped with an automatic computer-controlled system for ethylene feed and recording the ethylene consumption.

^{1}H and ^{13}C NMR spectra of branched polyethylenes and oligomer mixtures were recorded either on a Bruker Avance-400 MHz NMR spectrometer (at 400.130 MHz and 100.613 MHz, respectively) or on a Bruker DPX-250 MHz NMR spectrometer (at 250.130 MHz and 62.903 MHz, respectively).

3 Results and discussion

In the present work a series of 2-iminopyridine nickel(II) dichloride (or dibromide) complexes containing electron-withdrawing substituents (R_2-R_5 = F, Cl, Br, CF_3) in aryl moieties have been examined in ethylene polymerization and oligomerization using methylalumoxane as a co-catalyst.

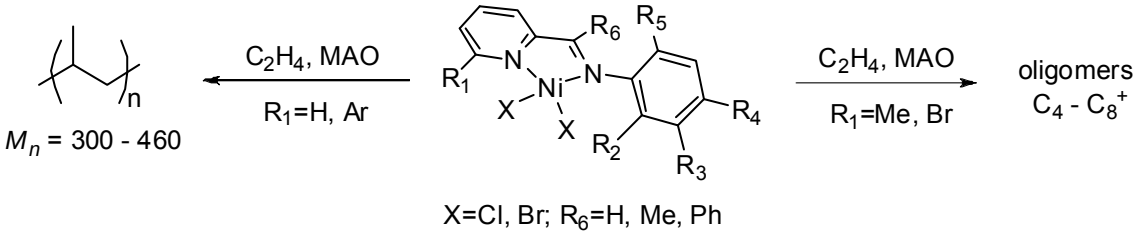

Fig. 1. 2-iminopyridine nickel(II) complexes

All complexes containing substituted 6-position of pyridine ring (R_1 = Me, Br) and fluoro-substituted phenyl ring (R_2, R_4, R_5 = F, CF_3) displayed high activities (up to $9.6 \cdot 10^6$ g·(mol Ni)$^{-1}$·h^{-1}·bar^{-1}) towards ethylene oligomerization yielding a wide variety of ethylene oligomers (1-butene, (*Z*)-2-butene, (*E*)-2-butene, 2-ethylbutene-1, 1-hexene, (*Z*)-2-hexene, (*E*)-2-hexene, (*E*)-3-hexene etc.).

Catalysts with unsubstituted or aryl-substituted 6-position of pyridine ring (R_1 = H, Ar) and *o*-trifluoromethyl group in phenyl ring turned out to be highly active towards ethylene polymerization (up to $6.6 \cdot 10^6$ g·(mol·Ni)$^{-1}$·h^{-1}·bar^{-1}) yielding low-molecular-weight branched polyethylenes (20-85 branches per 1000 determined by ^{1}H and ^{13}C NMR spectroscopy), with *sec*-butyl branches being identified. To the best of our knowledge, this is the highest reported activity for ethylene polymerizations and oligomerizations over 2-iminopyridine nickel catalysts.

4 Conclusion

New 2-iminopyridine nickel complexes have been found to be highly active catalysts of ethylene polymerization and oligomerization upon the activation with methylalumoxane. The catalytic activity as well as the product morphology has been found to correlate with the number and position of electron-withdrawing substituents.

Acknowledgements

This work was supported by the Russian Foundation for Basic Research, grant 14-03-91153.

References

[1] S. Wang, W.-H. Sun, C. Redshaw, *J. Organomet. Chem*. 751 (2014) 717.
[2] (a) T. Wiedemann, G. Voit, A. Tchernook, P. Roesle, I. Göttker-Schentmann, S. Mecking, *J. Am. Chem. Soc.* 136 (2014) 2078; (b) C. J. Stephenson, J. P. Mclnnis, C. Chen, M. P. Webersky, A. Motta, M. Delferro, T. J. Marks, *ACS Catal.* 4 (2014) 999.
[3] Z. Dong, Z. Ye, *Polym. Chem.* 3 (2012) 286.
[4] C. Bianchini, G. Giambastiani, L. Luconi, A. Meli, *Coord. Chem. Rev.* 254 (2010) 431.
[5] (a) K. P. Tellmann, V. C. Gibson, A. J. P. White, D. J. Williams *Organometallics* 24 (2005) 1; (b) A. A. Antonov, N. V. Semikolenova, V. A. Zakharov, W. Zhang, Y. Wang, W.-H. Sun, E. P. Talsi, K. P. Bryliakov, *Organometallics* 31 (2012) 1143.

IV-PP07

Thiazolium-Based Catalysts for the Etherification of Benzylic Alcohols under Solvent-Free Conditions

Bivona L.A.[1,2], Quertinmont F.[1], Beejapur H.A.[2], Giacalone F.[2], Buaki-Sogo M.[1], Gruttadauria M.[2], Aprile C.[1*]

1 - Unit of Nanomaterial Chemistry (CNano), University of Namur (UNAMUR), Department of Chemistry, Namur, Belgium

2 - Dipartimento di Scienze e Tecnologie Biologiche Chimiche e Farmaceutiche (STEBICEF), Sezione di Chimica, Università di Palermo, Palermo, Italy

* carmela.aprile@unamur.be

Keywords: organocatalysis, heterogeneous catalysis, synthetic methods

1 Introduction

Carbon-oxygen bond forming reaction is one of the most important transformations in organic synthesis and industrial processes. Ethers are largely employed as biologically active compounds, drugs, fragrances and diesel blends.[1] Several methods are reported for the preparations of ethers from alcohols, but not without limitations. A variety of Lewis acids are employed as catalysts for etherification reaction, also in presence of organosilanes. Elegant catalytic methods for etherification reactions are represented by the use of transition metals.[2] In most of the cases, the methods based on transition metal catalysts display good performances, however the homogeneous conditions used represent a major drawback for industrial applications. Ionic liquids recently emerged as a novel class of compounds with multiple possible uses from alternative "green" reaction media to active molecules in catalytic reactions. Supported ionic liquid-like phase (SILLP) are a class of materials that have interesting applications.[3]

In this work a novel class of thiazolium based supported ionic liquid phase (SBA-15-Thia, fig. 1 left) is reported.[4] The solids were tested as catalysts for the etherification of benzyl alcohols. The catalytic activity was also compared with the analogous materials based on imidazolium salts (SBA-15-Imi, fig. 1 left). The heterogeneous organocatalysts display excellent performances in the etherification of alcohols. To the best of our knowledge, this is the first time that a multilayered covalently supported imidazolium or thiazolium-based material has been reported as catalyst for the synthesis of ethers.

2 Experimental/methodology

The synthesis of the heterogeneous organocatalysts bearing either imidazolium[5] or thiazolium[4] active sites (SBA-15-Imi and SBA-15-Thia respectively) were successfully accomplished by grafting the corresponding bis-vinyl salts (bis-Imi or bis-Thia) on a thiol-functionalized SBA-15 mesoporous silica. The two materials were extensively characterized by N_2 physisorption, transmission electron microscopy, X-ray diffraction, ^{29}Si and ^{13}C MAS-NMR and elemental analysis. In order to explore their activity, 1-phenylethanol was selected as model compound. The catalytic tests were performed under solvent-free conditions at 160 °C and in different gas phase (oxygen, air, nitrogen). The etherification reaction was performed using more than 5 g of 1-phenylethanol and only 10 mg of catalysts.

3 Results and discussion

The two solids, SBA-15-Thia and SBA-15-Imi, display good specific surface area and high percentage of active sites, which are promising features for catalytic applications. It is worth to

mention that challenging conditions in terms of substrate to catalyst weight ratio (mg alcohol/ mg catalyst = 540) were employed. Both materials displayed good catalytic performances. However the SBA-15-Thia shows a better conversion and selectivity compared to the analogous imidazolium based material. This evidence highlighted that the nature of the *N*-heterocyclic ring has an important role in the reaction. In addition, the SBA-15-Thia was employed for reaction in shorter reaction time (7 h) in oxygen, air or nitrogen phase, and we observed that the selectivity increases by decreasing the percentage of oxygen in the reaction mixture. Some kinetics studies clearly evidenced an oxygen dependent behavior of the SBA-15-Thia catalyzed reaction (fig. 1 right).

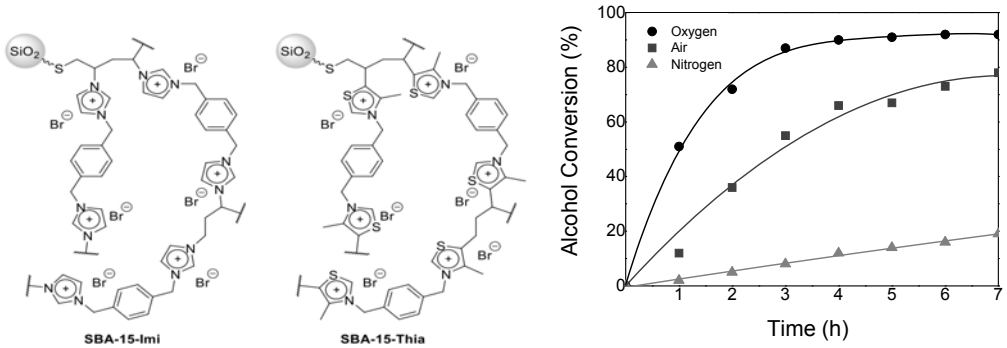

Fig. 1. SBA-15-Imi and SBA-15-Thia (left); Conversion of 1-phenylethanol with SBA-15-Thia as function of the time under oxygen, air or nitrogen atmosphere (right).

The supported thiazolium-based material was successfully used in the etherification reaction of other two benzylic alcohols and used in seven consecutive cycles without lose of catalytic activity. Further studies were carried out using unsupported thiazolium salts, with or without a methyl group at C-2 position of the thiazolium moiety (Homo-Thia-H and Homo-Thia-Me). The results of these tests show a reduced performance for the catalyst Homo-Thia-Me. This could be attributed to a negative combination of steric and electronic effects. Finally, we performed the etherification reaction of (*S*)-1-phenylethanol and the ether products indicate that the reaction follows mainly a S_N1 pathway. A mechanistic pathway was proposed.

4 Conclusions

Thiazolium and imidazolium hybrid materials were prepared and tested as catalysts for the etherification of 1-phenylethanol. The SBA-15-Thia displayed an excellent catalytic performance, also with others benzyl alcohols. These results allow proving that oxygen play an active role in the reaction probably regenerating the catalysts. This study represents the first use of thiazolium-based compounds as catalysts for the etherification reaction of alcohols.

Acknowledgements

L. A. Bivona thanks the University of Namur and the Università di Palermo for a co-founded PhD fellowship.

References

[1] A.B. Cuenca, G. Mancha, G. Asensio, M. Medio-Simon, *Chem. Eur. J.* 14 (2008) 1518-1523.
[2] K. J. Miller, M. M. Abu-Omar, *Eur. J. Org. Chem*. (2003) 1294-1299.
[3] M. Gruttadauria, F. Giacalone, P. Agrigento, R. Noto, in *Ionic Liquids in Biotransformations and Organocatalysis*, John Wiley & Sons, Inc. (2012) 361-417.
[4] L. A. Bivona, F. Quertinmont, H. A. Beejapur, F. Giacalone, M. Buaki-Sogo, M. Gruttadauria, C. Aprile, *Adv. Synth. Catal.* (2014) accepted, DOI: 10.1002/adsc.201400733.
[5] C. Pavia, E. Ballerini, L.A. Bivona, F. Giacalone, C. Aprile, L. Vaccaro, M. Gruttadauria, *Adv. Synth. Catal*. 335 (2013) 2007-2018.

IV-PP08

Propylene Oligomerization over Meso/Microporous Zeolites Modified with Chromium

Arroyave Manco J., Arboleda Echavarría J., Echavarría Isaza A.*

Universidad de Antioquia, Medelín, Colombia

* adriana.echavarria@udea.edu.co

Keywords: mesoporous-zeolites, propene, oligomerization, chromium zeolite, beta

1 Introduction

The main advantages of synthetic zeolites are that they can be engineered with a wide variety of chemical properties and pore sizes. Although the use of zeolites as catalysts are well established and there are a large increase of zeolite types and applications of theoretical approaches for prospective zeolite structures, the synthesis and modification of the commercial zeolites to avoid drawbacks associated with steric and diffusion limitations of zeolite is one of the main approaches in catalysis for zeolites [1]. Now the development of mesoporous zeolites or hierarchical zeolites has turn in the new direction to take in synthesis of zeolites [2,3,4]. Herein we evaluated the effects on the catalytic activity after incorporate mesoporosity by templating method in the conventional HBETA and loading this with Cr (loading of 1 and 3%).

2 Experimental/methodology

Meso/microporous zeolites were prepared by hydrothermal synthesis and templating method with multiwall carbon nanotubes for producing hierarchical zeolite crystals with intracrystalline mesoporosity. The composition of molar gel was 12.36 $(TEA)_2O$: 0.98 K_2O: 1.98 Na_2O: Al_2O_3: 49.71 SiO_2: 891 H_2O. The metal was incorporated through isomorphous substitution (3 and 5 wt-%). The characterization of these materials by X-ray diffraction (XRD) was used to identifying phases in a Panalytical Empyiria 2012. Surface areas were obtained in TriStar 3000 V6.08 equipment, using the BET method from the nitrogen adsorption. Additionally the materials were characterized by SEM, atomic absorption, NH_3-TPD and thermal analysis. Finally the catalytic reation were performed at 270 ºC and 26 bar in a fixed bed reactor charged with 1g of the catalyst and exposed to a feed of 5% of propylene/nitrogen with a total flow of 44 ml/min.

3 Results and discussion

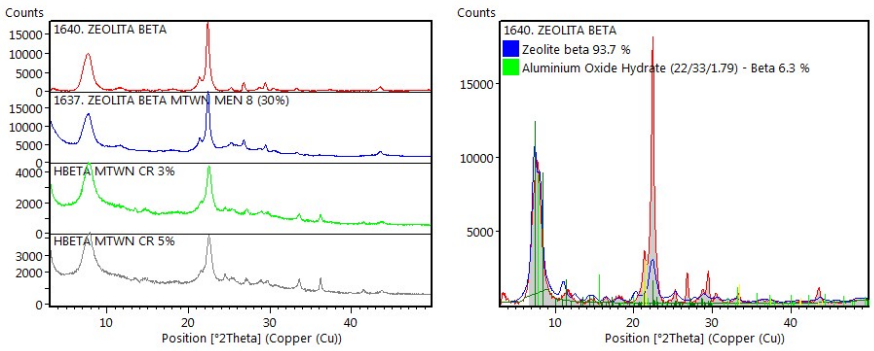

Figure 1 XRD patterns (right: as-synthesis zeolites, left: quantitative refinement of HBETA)

All samples were characterized by X-ray (figure 1) powder diffraction to identify the structure phase and determine the effect of the post-synthesis treatments on the zeolite structure. Its comparison of peak positions of XRD spectra with reference from PDF4 DATABASE indicating the presence of BEA phase. Chemical compositions of catalyst show an appreciable incorporation of Cr regarding expected. BET surface areas for hierarchical zeolite resulted in an increase of the external surface of 100 m^2/g and pore diameter of 0.58 nm.

Analysis of activity in the propylene oligomerization (figure 2), revealed that differing morphology within the zeolites has a significantly impact in the conversion. The conversion of propylene were better for the hierarchical zeolites than the parent zeolite, which agrees with the increase of pore diameter that facilitates the absorption of propylene on Bronsted acid sites and its transformations through aromatization and oligomerization reactions. The differences in the catalytic activity of Cr zeolites arises because the heteroatoms isomorphous substituted help in fine-tuning the strength of the acid sites and in introducing bifunctional features to zeolite. The selectivity to higher hydrocarbons obtained were low in all cases indicating that some hydrogen transfer may still occur. Nevertheless, the differences related to parent zeolite beta indicates the important role played by the size channel system when the reactants can diffuse into this type of pores. It is demostrated that the creation of mesopores in the zeolite has a possitive effect because improve the catalytic activity in the modified catalysts.

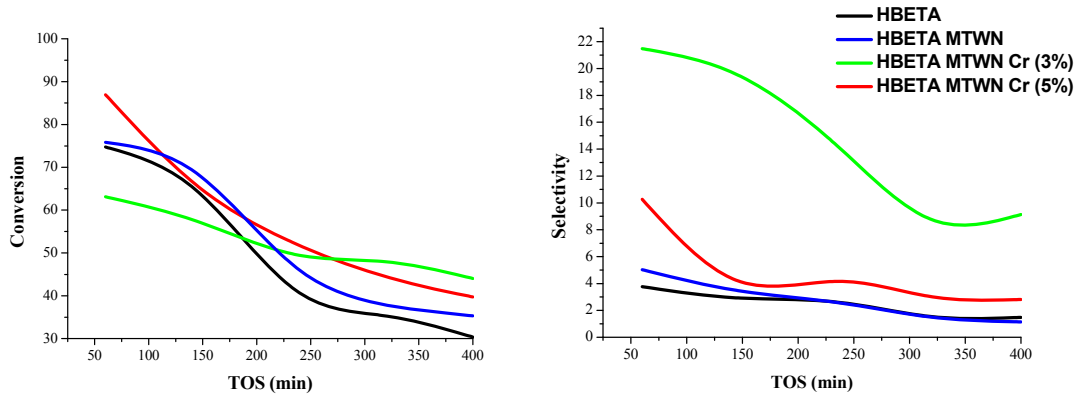

Figure 2 Conversion and selectivity meso/microporous H-BETA

4 Conclusions

An increased in accessibility of the pores of the zeolite improved the diffusional limitation of the HBETA; and the incorporation of metal created a coordinative center for propylene oligomerization.

Acknowledgements

The authors would like to thanks to UdeA and Colciencias for the financial support.

References

[1] Serrano, D. P., Escola, J. M. & Pizarro, P. Synthesis strategies in the search for hierarchical zeolites. *Chem. Soc. Rev.* **42,** 4004–35 (2013).

[2] Wang, H. & Pinnavaia, T. J. MFI zeolite with small and uniform intracrystal mesopores. *Angew. Chem. Int. Ed. Engl.* **45,** 7603–6 (2006).

[3] Tao, H. *et al.* Highly stable hierarchical ZSM-5 zeolite with intra- and inter-crystalline porous structures. *Chem. Eng. J.* **225,** 686–694 (2013).

[4] Milina, M., Mitchell, S., Crivelli, P., Cooke, D. & Pérez-Ramírez, J. Mesopore quality determines the lifetime of hierarchically structured zeolite catalysts. *Nat. Commun.* (2014). doi:10.1038/ncomms4922

IV-PP09

Factors Affecting the Activity of Oxide Catalysts in the Synthesis of N-Phenylpropionamide from Propanoic Acid and Aniline

Di Chio R.[1], Trunfio G.[1*], Deiana C.[2], Ivanchenko P.[2], Sakhno Y.[2], Martra G.[2], Arena F.[1]

1 - Dipartimento di Ingegneria Elettronica, Chimica e Ingegneria Industriale, Università degli Studi di Messina, Messina, Italy

2 - University of Torino, Torino, Italy

* gtrunfio@unime.it

Keywords: green chemistry, heterogeneous catalysis, amidation, organic chemistry, oxides

1 Introduction

Amidic group synthesis is a fundamental step for the manufacture of a variety of biological compounds and innovative materials, currently deserving a high scientific concern [1,2]. Indeed, the main current industrial processes rely on reaction between amines and activated carboxylic acids precursors or on the direct condensation between carboxylic acids and amines at high temperature [2]. All these processes suffer from serious economic and environmental drawbacks due to the use of unsafe and harmful reagents like thionyl or oxalyl chloride including *poor atom economy* and high *E-factors*, while the latter are also unfeasible for many functionalized substrates [3]. Then, the direct catalytic synthesis of amides from ammines and acids has been recently indicated as a major Green Chemistry issue [1,2].

Therefore, this work provides a comparative view of the reactivity pattern of various commercial and lab-made oxide catalysts (γ-Al_2O_3, CeO_2, ZrO_2, TiO_2) in the synthesis of N-phenylpropionamide (T, 383K) from aniline and propanoic acid, shedding lights onto the physico-chemical properties determining their catalytic functionality.

Table 1. List of catalysts used in the N-phenyl-propionamide synthesis and their catalytic performances.

Sample	Supplier	SA ($m^2 \cdot g^{-1}$)	NH_3 uptake (μmol/g)	$X_{Aniline}$	$X_{P.\ Acid}$	Amide yield[a]
γ-A_2O_3 (1.5E)	AKZO NOBEL	261	433±30	0.22	0.25	0.24
TiO_2_Merck	MERCK	10	8±1	0.05	0.04	0.04
TiO_2_P25	EVONIK	55	260±20	0.47	0.49	0.47
CeO_2_LM	Lab-made	90	65±5	0.28	0.27	0.27
ZrO_2_LM	Lab-made	21	100±10	0.08	0.10	0.09

[a] N-phenyl-propionamide yield by gravimetric analysis.

2 Experimental/methodology

The list of commercial and lab-made oxide catalysts along with their code, the main physico-chemical properties and activity data in the amidation reaction [3] are given in Table 1.

Surface Area (SA) values were determined from N_2-adsorption isotherms, elaborated by the standard B.E.T. method, while concentration and strength distribution of the surface acid sites were probed by NH_3-TPD analysis and modelling of TPD profiles according to the procedure elsewhere described [4]. IR measurements were carried out at r.t. after adsorption of propanoic acid on pre-activated samples and, subsequently, after admission of 1-pentanamine on acid saturated sample [3].

Catalyst testing in the synthesis of N-phenylpropionamide from propanoic acid and aniline was performed at 383K in a Pyrex-glass batch reactor equipped with a Dean-Stark device for azeotropic distillation operations [3]. Reagents conversion has been obtained by GC analysis, while final (24h) amide yield values (Table 1) were obtained by gravimetric analyses [3].

3 Results and discussion

Results of catalytic tests indicate that TiO_2_Merck and P25 present the lowest and highest yield, while other systems show intermediate values (Table 1). Tests at various (stoichiometric) reagents concentration show that the reaction is 0th-order, likely indicating the occurrence of a typical Langmuir-Hinshelwood (L-H) pathway kinetically controlled by adsorption-desorption phenomena, as sketched in the below reaction scheme [3,5]. In fact, in presence of (apolar) toluene as solvent, an acid-base interaction between reagents drives the formation of an adduct that, further to the adsorption on catalyst surface, undergoes an intra-molecular rearrangement with the formation of the "C-N" bond and water elimination [3].

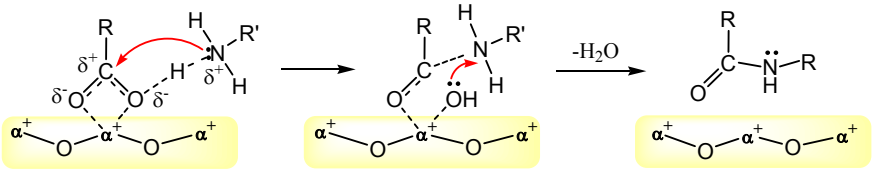

Scheme 1. *Proposed mechanism of the amidation reaction on oxide catalysts.*

IR spectroscopic measurements of adsorbed propanoic acid show the formation of *bidentate*, *bridging* and *unidentate* carboxylate species on surface Lewis acid sites, the (decreasing) reactivity roughly parallels the surface specific activity in the amidation reaction (TiO_2_P25 > ZrO_2 ≈ TiO_2_Merck ≈ CeO_2 > γ-Al_2O_3) [3]. In addition, surface acidity characterization data by NH_3-TPD analysis (Table 1) allows to obtain the TOF values of the studied systems, depicting an exponential decreasing trend on total acidity (Fig. 1), supporting the inhibiting role of the acid sites on product(s) desorption rate.

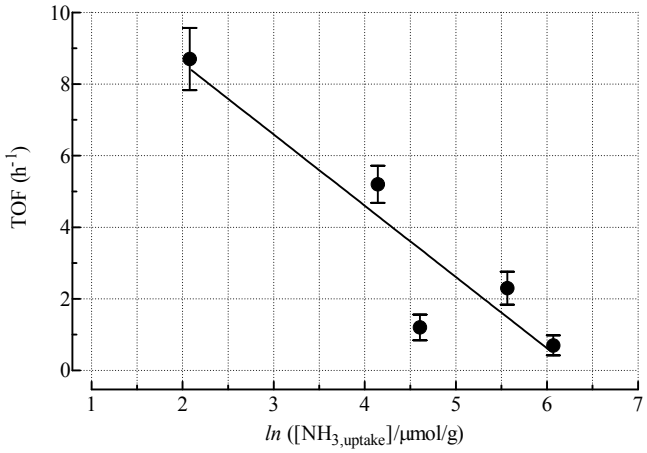

Fig 1. *Relationship between TOF and NH_3 uptake data.*

4 Conclusions

A 0th- order kinetic dependence on reagents concentration suggests that the amidation reaction proceeds via a *L-H* path kinetically controlled by desorption steps (*r.d.s.*).

The formation of *bidentate*, *bridging* and *unidentate* carboxylate intermediates account for the different amidation functionality of the studied materials.

References

[1] V. R. Pattabiraman, J. W. Bode, *Nature* 480 (2011) 471.
[2] H. Lundberg, F. Tinnis, N. Selander, H. Adolfsson, *Chem. Soc. Rev.* 43 (2014) 2714.
[3] F. Arena, C. Deiana, A. F. Lombardo, P. Ivanchenko, Y. Sakhno, G. Trunfio, G. Martra, *Catal. Sci. Technol.* xxx (2015) xxx-xxx (DOI: 10.1039/c4cy015044e).
[4] F. Arena, R. Dario, A. Parmaliana, *Appl. Catal. A* 170 (1998) 127.
[5] J. W. Comerford, T. J. Farmer, D. J. Macquarrie, S. W. Breeden, J. H. Clark, *Arkivoc* vii (2012) 282.

IV-PP10

Fischer-Tropsch Synthsis on Nanosized Metal-Polymer Composite Catalysts in Slurry Reactor

Al-Khazraji A.H.[1], Tsvetkov V.B.[2,3], Dementyeva O.S.[2*], Kulikova M.V.[2], Flid V.R.[1], Khadzhiev S.N.[2]

1 - Lomonosov Moscow State University of Fine Chemical Technologies, Moscow, Russia
2 - A.V.Topchiev Institute of Petrochemical Synthesis, RAS, Moscow, Russia
3 - Institute for Physical-Chemical Medicine, Moscow, Russia

* dementyeva@ips.ac.ru

Keywords: Fischer-Tropsch synthesis, Fe catalysts, polymers, slurry reactor

1 Introduction

Currently Fischer-Tropsch process is becoming increasingly important as the method of obtaining synthetic liquid fuels. Slurry phase synthesis technology is one of the most interesting trends in the development of this process. Addition of the polymer to nanosized metal-containing suspensions allows to prevent sedimentation and also leads to the formation of a completely new active catalyst system with unique properties. The selectivity of this catalysts can be controlled by varying the structure of polymer and its concentration.

The effect of using different polymers as active component of catalytic system was carried out and the correlation between the structure of the polymer molecules and properties of formed contacts in Fischer-Tropsch synthesis was found.

2 Experimental/methodology

Samples of catalysts were prepared by thermal decomposition of metal precursor solution in a dispersion medium of wax and polymer in an inert gas. Polyacrylonitrile (PAN), polyamide (PA), polystyrene crosslinked with divinylbenzene (PS-dVB), polyvinyl alcohol (PVA), bisphenol polyester (PE-bPh), polypropylene (PP) have been used as an additive. Fischer-Tropsch synthesis was carried out in a three-phase slurry reactor in syngas flow with CO: H_2 ratio 1: 1 (temperature range 220-300°C, P = 2 MPa). In both cases, catalysts were activated before reaction by a treatment with CO for 24 h at 300°C. The particle size of catalytic suspensions were characterized by dynamic light scattering method (DLS). The polymers flexibility was analyzed by estimating of projection orientation persistence length and orientation persistence length. The 3D-models of repeat units for analyzed polymers were built by using SYBYL 8.0. Modeling of the polymers folding into coils was carried out in implicit solvent and topological approach with application of Gasteiger–Hückel method was used to calculate partial atomic charges. The molecular dynamics (MD) simulations were performed by using a suite of programs AMBER 14. The use of implicit solvent was realized with application of the Hawkins–Cramer–Truhlar model within GB/SA formalism. The GAFF was utilized for calculating interatomic interaction energy between the polymer atoms.

3 Results and discussion

The influence of polymer structure on the catalysts properties in the Fischer-Tropsch synthesis has been fixed. It was shown that the addition of polymer into the catalyst composition generally resulted in an increase in selectivity toward target products - liquid hydrocarbons (fig. 1). At the same time reducing the formation of carbon dioxide was observed. The sample prepared with polyacrylonitrile addition (PAN) demonstrated the highest productivity on C_{5+} hydrocarbons: the yield of these products was 30% higher compared to the sample without polymer additives (WAX).

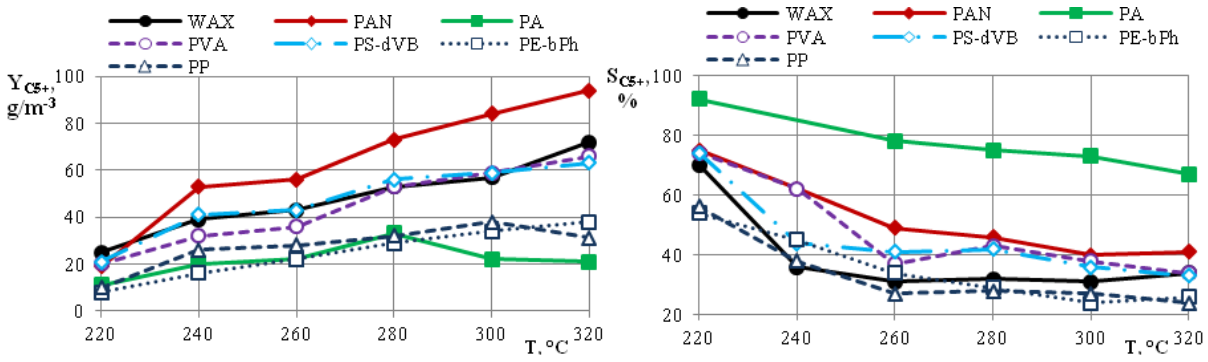

Fig. 1. Fischer-Tropsch reaction results for different temperatures (P=2 MPa, CO:H2=1:1):
a) yield of liquid hydrocarbons, g/m_{syngas}^3; б) selectivity toward liquid hydrocarbons, %.

Dispersed particles size distribution changing was fixed with dynamic light scattering measurements. Particle diameter of the formed suspensions decreased in the presence of different polymers in catalytic suspension from 450 for wax-sample to 170-220 nm, as seen by DLS-spectra.

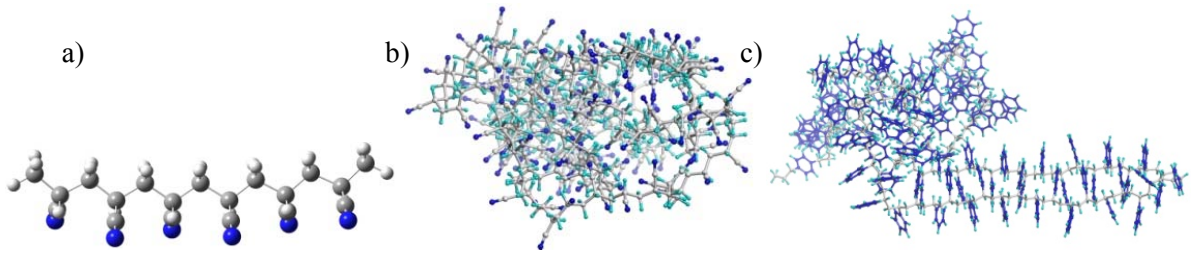

Fig. 2. Modeling of the polymers folding date. a) fragment of the original PAN-polymer chain; b) PAN-coil; c) PS-dVB -coil.

The polymers flexibility and its effect on coils formation was determined by molecular modeling method (fig. 2). Analyzing of the polymers folding into coils and comparative study of their geometry revealed significant differences of the final structure of the polymer molecules forming a complex metal-containing particle - polymer structure. View of PAN-coil allows to predict the most favorable conformation of the polymer around the metal phase particles which leads to formation the most active system for synthesis of hydrocarbons from CO and H_2.

4 Conclusions

The influence of polymer structure on the activity of catalytic system in the Fischer-Tropsch synthesis was found. Modeling techniques revealed the differences in structure conformations and flexibility of different polymers. This factor affects the properties of the resulting metal-containing particle-polymer composite structure.

Acknowledgements

This work was supported under the Program of basic scientific researches by Presidium of RAS №25 "Energy aspects of deep fossil and renewable carbon-containing raw material processing"

This work was partially carried out using of Common Use Center "New Petrochemical Processes, Polymeric Composites and Adhesives" equipment.

IV-PP11

Gas-Phase Carbonylation of Dimethoxymethane to Methylmethoxyacetate over $Cs_XH_{3-X}PW_{12}O_{40}$ Catalysts

Badmaev S.D.[1,2*], Pechenkin A.A.[1,2], Potemkin D.I.[1,2], Volkova G.G.[1], Paukshtis E.A.[1,2], Belyaev V.D.[1,2], Sobyanin V.A.[1]

1 - Boreskov Institute of Catalysis SB RAS, Novosibirsk, Russia
2 - Novosibirsk State University, Novosibirsk, Russia

* sukhe@catalysis.ru

Keywords: dimethoxymethane, carbonylation, methylmethoxyacetate, cesium, salts of $H_3PW_{12}O_{40}$

1 Introduction

In recent papers [1,2] the gas-phase carbonylation of dimethoxymethane (DMM) to methylmethoxyacetate (MMAc) over Brønsted acid sites (BAS) of zeolites was demonstrated for the first time. It was shown that under the conditions of DMM gas-phase carbonylation to MMAc, reaction (1) is accompanied by side-reaction (2) - DMM disproportionation to dimethyl ether (DME) and methyl formate (MF):

$CH_3OCH_2OCH_3 + CO = CH_3OCH_2COOCH_3$ (1)

$2CH_3OCH_2OCH_3 = 2CH_3OCH_3 + CHOOCH_3$ (2)

The mechanisms of reactions (1) and (2) were suggested, which are sililar to classic mechanisms of the Koch carbonylation reactions and Cannizzaro aldehyde disproportional reactions, respectively.

Results reported in [1-4], as well as fundamental and practical interest to carbonylation of oxygenated compounds of C_1 chemistry encouraged our studies of DMM carbonylation to MMAc over acidic cesium salts of 12-tungstophosphoric acid. The results obtained are presented in this report.

2 Experimental/methodology

Cesium salts of tungstophosphoric acid $Cs_xH_{3-x}PW_{12}O_{40}$ (x= 1.5; 2.0; 2.5) were prepared as described in [3]. They were characterized by BET, XRD, TEM, FTIR techniques [3,4]. Gas-phase carbonylation of DMM was studied in a flow reactor at pressures 1 and 10 atm in the temperature interval 80-140°C, at GHSV = 5000-6000 h^{-1} and molar ratio DMM/CO = 4/96 ÷ 4/76. The composition of the inlet and outlet gas mixtures was analyzed by gas chromatographs.

3 Results and discussion

Table 1. Performance of $Cs_xH_{3-x}PW_{12}O_{40}$ in DMM carbonylation to MMAc.

Catalyst	S_{BET} [a] m^2/g	N [b] mmol/g	X_{DMM} [c] %	S_{MMAc} [d] %	W_{MMAc} [e] mmol/(g h)	TOF [f] h^{-1}
$Cs_{1.5}H_{1.5}PW_{12}O_{40}$	57	0.128	58	11	0.2	1.56
$Cs_2H_1PW_{12}O_{40}$	103	0.118	90	12	0.5	4.2
$Cs_{2.5}H_{0.5}PW_{12}O_{40}$	216	0.048	96.5	16	0.92	19

a – BET surface area, b – concentration of BAS, c – DMM conversion, d – MMAc selectivity, e – MMAc productivity, f – rate of MMAc formation per one BAS.

Table 1 compares the catalytic properties of $Cs_xH_{3-x}PW_{12}O_{40}$ for DMM carbonylation to MMAc. The data were obtained at atmospheric pressure, T = 120 °C, molar ratio CO/DMM =

4/96 and GHSV = 5000 h^{-1}. Similarly to [1,2], MMAc, DME and MF were the main reactions products. It is seen that the activity (X_{DMM}, W_{MMAc}, TOF) and selectivity (S_{MMAc}) of $Cs_xH_{3-x}PW_{12}O_{40}$ catalysts in the DMM carbonylation reaction descended in the following order: $Cs_{2.5}H_{0.5}PW_{12}O_{48}$ > $Cs_2H_1PW_{12}O_{48}$ > $Cs_{1.5}H_{1.5}PW_{12}O_{40}$.

The most active catalyst $Cs_{2,5}H_{0,5}PW_{12}O_{40}$ provided ~100% DMM conversion and MMAc productivity ~1 mmol·g^{-1}·h^{-1} with ~16% selectivity.

The effect of pressure in the DMM carbonylation reaction was studied with the use of most active catalyst. Fig. 1 presents the effect of temperature on DMM conversion and product distribution at DMM carbonylation over $Cs_{2.5}H_{0.5}PW_{12}O_{40}$ at pressure of 10 atm.

Obviously, the DMM conversion increases with increasing temperature and exceeds 80% at 120°C. The DME concentration also increases with increasing temperature and reaches 1.7 vol.% at 120°C. The MF concentration remains constant in the temperature interval 90-120°C and amounts to ~0.7 vol.%. Concentration of the target product MMAc increases with increasing temperature and attains maximum value of 1.6 vol.% at 110°C. Under these conditions, the selectivity to MMAc was 54%, MMAc yield and productivity amounted to 40% and 2.4 mmol · g^{-1} · h^{-1}, respectively.

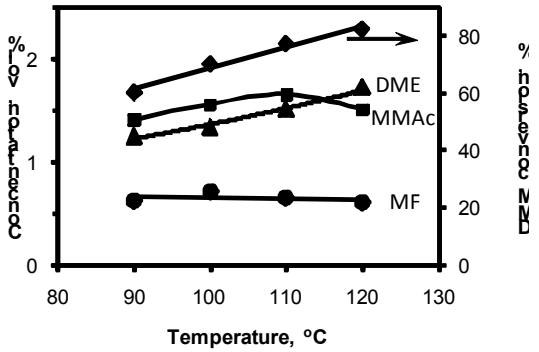

Fig. 1. Effect of temperature on DMM conversion and product distribution at DMM carbonylation over $Cs_{2.5}H_{0.5}PW_{12}O_{40}$ catalyst. Reaction conditions: P = 10 atm, GHSV = 6000 h^{-1}. Inlet composition, vol. %: DMM:CO:Ar = 4:76:20

Based on the data obtained, the nature of the active centers, origin of the observed catalytic activity order and probable mechanism of DMM carbonylation over $Cs_xH_{3-x}PW_{12}O_{40}$ are discussed. Comparative analysis of available DMM carbonylation to MMAc data is presented as well.

4 Conclusions

Catalytic properties of cesium salts of tungstophosphoric acid $Cs_xH_{3-x}PW_{12}O_{40}$ (x= 1.5; 2.0; 2.5) for the gas-phase DMM carbonylation to MMAc were studied for the first time. Among the studied catalysts, $Cs_{2.5}H_{0.5}PW_{12}O_{40}$ showed the best performance. It provided the MMAc yield ~40% at mild conditions: T = 110 °C, P = 10 atm, GHSV = 6000 h^{-1} and DMM/CO = 4/76 mol/mol.

Acknowledgements

This work was partially supported by the RFBR Grant no. 14-03-31698.

References

[1] F.E. Celik, T. Kim, A.T. Bell, *Angewandte Chemie Int. Ed.* 48 (2009) 4813.

[2] F.E. Celik, T. Kim, A.T. Bell, *Journal of Catalysis*. 270 (2010) 185.

[3] G.G. Volkova, L.M. Plyasova, A.N.Salanov, G.N. Kustova, T.M. Yurieva, V.A. Likholobov, *Catalysis Letters.* 80 (2002) 175.

[4] G.G. Volkova, L.M. Plyasova, L.N. Shkuratova, A.A. Budneva, E.A. Paukshtis, M.N. Timofeeva, V.A. Likholobov, Stud. Sur. Sci. Catal. 147 (2004) 403.

IV-PP12

Transfer Hydrogenation of Acetophenone in the Presence Bis-Imine Rhodium(I) Complexes

Nindakova L.O.[1], Badyrova N.M.[1*], Sadykov E.Kh.[2], Smirnov V.V.[1], Ushakov I.A.[1], Khatashkeev A.V.[1]

1 - Irkutsk State Technical University, Irkutsk, Russia
2 - E. Favorsky Irkutsk Institute of Chemistry, Siberian Branch of the Russian Academy of Sciences, Irkutsk, Russia

* mrk2@mail.ru

Keywords: rhodium, chiral, ligand, enantioselectivity, hydrogen transfer

1 Introduction

Transfer hydrogenation (TH) catalyzed by transition metal complexes is frequently used for reduction of multiple bonds due to availability of hydrogen donor and simplicity of experiment technique.

In particular, widely known ruthenium catalysts, containing N-(toluensulfonyl)-1,2-diphenyl-diamino-ethane, effective in asymmetric reduction arylketones in 2-propanol or a mixture of formic acid and triethylamine [1,2].

The purpose of this study was the testing of rhodium complex with three structurally similar N,N,N,N-bis-imine ligands in transfer hydrogenation of acetophenone, and establishing the composition and structure of rhodium complex with N,N'- (1R,2R)-cyclohexane-1,2-diyl)bis(1-(pyridin-2-yl)methanimine.

2 Experimental

Elemental analysis was performed on "Euro EA3000-Single", the carrier gas is argon, 120kPa, the temperature of front furnace - 980^{o}C , the chromatograph thermostat temperature - 100^{o}C.

^{1}H and ^{13}C NMR spectra was recorded on impulse spectrometer Bruker DPX250 at 298K in 5 mm ampoules using a broadband sensor BBO5mmZ3074/58.

GC analysis was carried out by Gas Chromatograph-Mass Spectrometers Shimadzu QP2010 Plus in electron impact mode at 70 eV with a subsequent scanning in range m/z 40 to 350; capillary column Equity 5. **Optical rotation** of solutions was determined by automatic digital polarimeter ADP 410 at wave length 589 nm (l = 50 mm, C = 1–5 g/100 ml). Enantiomeric excess of product was determined by Gas Chromatograph GC Agient 7890A, flame-ionization detector and chiral capillary column CYCLODEX-B (length 30 m, internal diameter 0.25 mm).

To clarify the geometry of original rhodium (I) complex with ligand **1** we used DFT B3LYP [3,4] hybrid method. The 6-31G(d) basis set was chosen to describe C, N, O, H atoms and the LanL2DZ basis set was used for Rh. All calculations were performed with Firefly version 8.1 program [5].

3 Results and discussion

Hydride transfer from 2-propanol to acetophenone in the presence system $[Rh(cod)Cl]_2$ + L], where L- bis-aldimine ligands, synthesized by condensation of (*R,R*)-1,2-cyclohexandiamine and pyridin- (**1**), quinolin- (**2**) and thiophencarboxaldehyde (**3**).

Hydrogenation of the ketone in the presence of a catalyst with ligand **1** runs with high reaction rate, for 1-4 hours achieved 100% chemical conversion of acetophenone to 1-

phenylethanol, by-products are not formed. In all cases, we observed the predominant formation of (R)-1-phenylethanol, but catalytic reaction enantioselectivity is only 28%. It is noted that at high reaction rate, leading to the rapid achievement of equilibrium ketone ↔secondary alcohol, there are low yields of predominant enantiomer. Possibly, it could be explained partial racemization of product as a result dehydrogenation reverse reaction of mixture enantiomers.

Enantioselectivity of the catalytic reaction increases in series of ligands: **2** < **3** < **1**, the activity is approximately equal for catalysts with ligands **1** and **2**.

To establish the structure of this complexes we studied interaction of a solution $[Rh(COD)Cl]_2$ in *i*-PrOH with ligand **1**using ^{1}H and ^{13}C NMR spectroscopy method. It was found that there is monodentate coordination of chiral ligand **1** to rhodium atom via nitrogen atom from one of two aldimine bonds. Cyclooctadiene molecule remains in the coordination sphere of rhodium (I) atom.

DFT calculation proves asymmetric coordination of C_2-symmetry ligand **1**.

4 Conclusions

It was found that after hydrogenation of cyclooctadien, Rh(cod)(1)Cl complex transforms into C_2-symmetry five-coordinated hydride rhodium complex, which is active in hydrogen transfer from 2-propanol to ketones.

For acetophenone coordination need to vacate a coordination site near to Rh atom, that involves changing in geometry structure of complex and breaking one or two Rh-N bonds. The last one leads to decrease of enantioface differentiation of prochiral ketone in chirality transfer step. Detailed study of reaction mechanism for optimization process will be discussed in the next researching.

Acknowledgements

Financial support: Ministry of Education and Science RF (State task from Ministry of Education and Science of Russian Federation, basic financing, project № 616)

References

[1] R. Noyori, S. Hashiguchi, *Acc. Chem. Res.* 30 (1997) 97.
[2] A. Fujii, S. Hashiguchi, N. Uematsu, T. Ikariya, R. Noyori, *J. Am. Chem. Soc.* 118 (1996) 2521.
[3] (a) A. D. Becke, *Phys. ReV.A* 38 (1988) 3098. (b) A. D. Becke, *J. Chem. Phys.* 98 (1993) 1372. (c) A. D. Becke, *J. Chem. Phys*. 98 (1993) 5648.
[4] C. Lee, W. Yang, R. G. Parr, *Phys. ReV.B* 37 (1988) 785.
[5] (a) A. A. Granovsky, Firefly version 8, http://classic.chem.msu.su/gran/firefly/index.html, (b) M.W.Schmidt, K.K.Baldridge, J.A.Boatz, S.T.Elbert, M.S.Gordon, J.H.Jensen, S.Koseki, N.Matsunaga, K.A.Nguyen, S.Su, T.L.Windus, M.Dupuis, J.A.Montgomery, *J.Comput.Chem*. 14 (1993) 1347.

IV-PP13

Kinetic of the Formation of the 5,7-Dichloro-4,6-Dinitrobenzophyroxan Complex in Hexagonal Mesophase Formed in Water by Neonol

Bakeeva R.F.*, Vahitova O.E., Sopin V.F.

Kazan National Reseach Tecnological University, Kazan, Russia

* gurf71@mail.ru

Keywords: kinetic, micelles, liquid crystal, ethoxylated, alkylphenol, 5,7-dichloro-4,6-dinitrobenzophu

1 Introduction

Investigation of the nature of the reactions in liquid crystals is an important problem, which has been poorly studied so far. Knowledge of the laws of chemical processes in the water systems constructed as liquid crystals may shed light on the transformation of the compounds in the human body, because solutions in the human cell are represented in the liquid crystal state [1]. This is especially true for biologically active compounds, such as the 5,7-dichloro-4,6-dinitrobenzophuroxan. Its antifungal activity was shown in the micellar solutions of sodium dodecyl sulfate, cetyltrimethylammonium bromide, p- (1,1,3,3-tetramethylbutyl phenoxy) polyoxyethylene glycol, Tr X-100, cetyl ether, polyoxyethylene (10), regarding *Trichophyton mentagrophyte, Candida albicans* [2]. 5,7-dichloro-4,6-dinitrobenzofuroksan is solubilized in micelles of oxyethylated nonylphenols, NPh 9-n [3]. However, behavior of this substrate in liquid crystals has not been studied so far. In this study we investigated the effect of the hexagonal mesophase formed in water by the ethoxylated alkylphenol (NPh 9-12) on the chemical behavior of substrate:

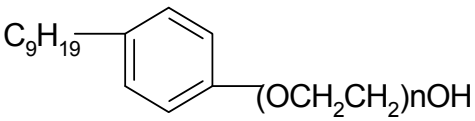

$C_9H_{19}C_6H_4O(C_2H_4O)_{12}H$,
NPh 9-12

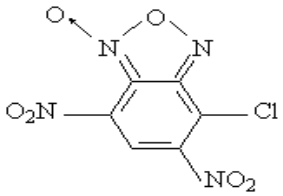

5,7-dichloro-4,6-dinitrobenzophuroxan
DChDNBPh

2 Experimental/methodology

The UV/Vis absorption spectra were measured using Agilent 8453 spectrophotometer. The type of mesophase was determined by means of polarizable microscope Biolam L 212 (LOMO).

3 Results and discussion

Micelles in system NPh 9-12 + H2O (I) were formed in the concentration of $1.24*10^{-4}$ M [2]. Fig. 1 shows the alteration of DChDNBPh spectra depending on its concentration after 24 hours after preparation. As can be seen from Fig. 1, in system (I) DHDNBFO in the micellar environment has the absorption bands at 323 nm and at 407 nm., which are close to the absorption bands in water (400 nm).

When concentration of the NPh 9-12 in system (I) reaches 30%, hexagonal mesophase is formed (texture is shown in Fig. 3). The hexagonal mesophase, or E-phase, is a hexagonally-

packed cylindrical micelles.

Injection of the DChDNBPh substrate in E-phase stimulates the reaction leading to the shift of the absorption band from 407 nm to 450 nm. This may be caused by the formation of the DChDNBPh- NPh 9-12 σ-complex (see Fig. 2). The reaction rate of the σ-complex formation was computed from the dependence A = f (τ) (Fig. 4), where A is an optical density and τ is the time in seconds. Analysis of the kinetic curve indicates a first-order reaction of DChDNBPh. First order rate constant calculated with the Guggenheim method is equal k = 0,00103 s^{-1}± 2,8967 10-5 s^{-1} , r = 0.9950

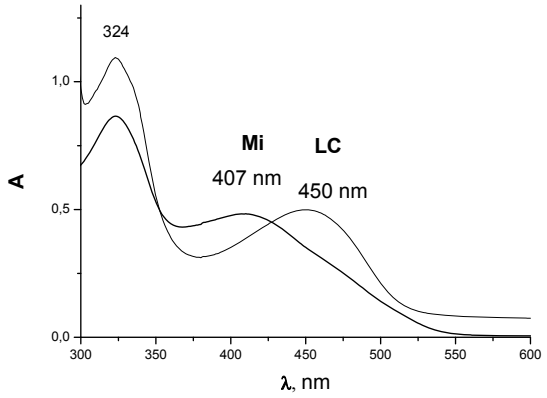

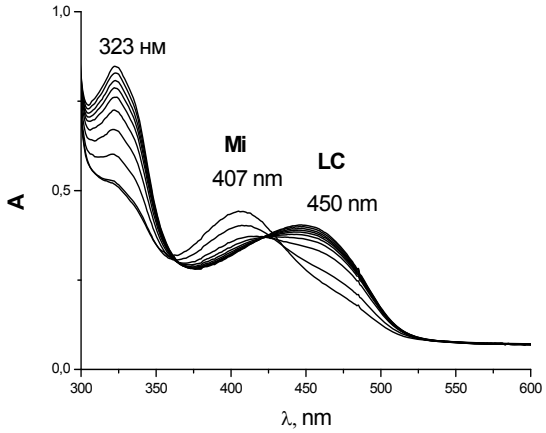

Fig.1. The alteration of UV-spectra of DChDNBPh **Fig.2.** The alteration of UV-spectra with the time in micellar and hexagonal mesophase after 24 hours. for the NPh 9-12 + H_2O + DChDNBPh system, 25 ^{0}C

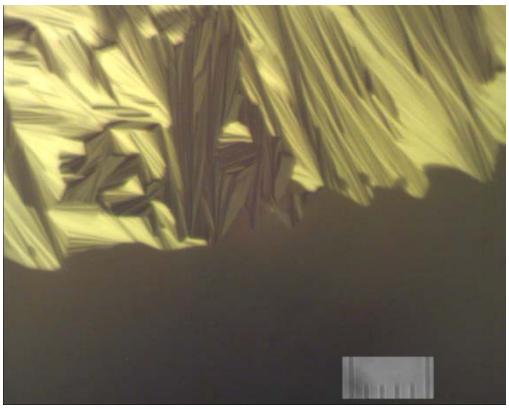

Fig.3. Fanlike texture of hexagonal mesophase NPh 9-12 + H_2O system. Crossed Nicols, x 200

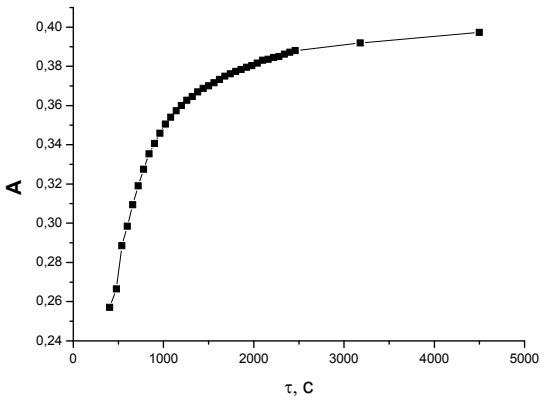

Fig.4. The alteration of optical density with time for absorbtion band at 456 nm in system NPh 9-12+ H_2O + DChDNBPh, 25 ^{0}C

4 Conclusions

Thus, this study for the first time reveals the formation of the σ-complex in the hexagonal mesophase of the NPh 9-12+ H_2O+ DChDNBPh system, whereas this complex has not been observed in the micellar pseudophase.

References

[1] G.. Braun, J. Yolken *Liquid crystals and biological structures* – M.: Mir, 1982.
[2] R.F. Bakeeva, O.E. Vakhitova, V.V .Zobov, A.D. Voloshina, T.C. Gorbunova, V.F.Sopin *Herald of Kazan Technological University* 17 (2014) 187.
[3] R.F. Bakeeva, O.E. Vakhitova, T.C. Gorbunova, L.M. Yusupova, V.F. Sopin *Herald of Kazan Technological University*. 16 (2013) 73.

IV-PP14

Oxidation of Heavy Oil in the Presence of Supercritical Water

Baybekova L.R.*, Petrov S.M., Zakieva R.R., Ibragimova D.A., Karalin E.A.

Kazan National Research Technological University, Kazan, Russia

* L_baibekova@mail.ru

Keywords: supercritical water, extra heavy crude oil, conversion, canalytic, crude oil upgrading, bitumen

1 Introduction

Supercritical fluids are now becoming more and more relevant in the processes of oil production and processing, especially in connection with development of unconventional hydrocarbon resources: heavy oil and natural bitumen. Recent academic studies have shown that supercritical solvents give high level of quality control and productivity in the reaction chemistry and the processing of materials that is difficult to provide using conventional techniques and solvents.

The transfer of material into a supercritical state occurs in a closed volume in the critical temperature and pressure, and accordingly, these values determine the critical point of each of these substances. Supercritical fluids are characterized by very low viscosity and high diffusion ability. Both characteristics are extremely important for the petroleum industry and are the basis of the practical use of the substance in the supercritical state.

2 Experimental/methodology

The aim of this work was the conversion of unconventional hydrocarbon resources in light petrochemical products. We studied heavy bituminous oil upgrading, reducing the sulfur content and increasing the yield of valuable distillate fractions.

As the object of the work was selected bituminous oil of Ashalchinskoye field with a density of 0.9715, and a viscosity of 2771 mPas at 20 ° C.

A series of experiments on the oxidation of high-viscosity oil in the presence of water in a supercritical state was performed in a laboratory catalytic reactor made of stainless steel in the temperature range with an upper limit of 380 ° C, the effect of temperature and pressure conditions was 2 hours.

Was produced by the selection of initiating agents. Components additives previously milled in a ball mill until the coarse state, and then were homogenized by a mechanochemical activation apparatus with an ultrasonic frequency of the ultrasonic waves of 22 kHz and the energy density of 5 W / cm² at the installation Ultrasonic Processor UP 400S, Hielscher. Control of nano dispersion was made on the device SORBI-M. Determination of the morphology of the surface of the carbonaceous substance carried in the raster scanning electron microscope. Initiating stabilizing additive in an aqueous medium the anionic surfactant.

3 Results and discussion

The results of experiments on the effects of water in a supercritical state on high-viscosity crude oil upgrading were impressive. The viscosity of the oil after the test decreased by 28% compared to the initial sample. In a converted oil decreased content of resin-asphaltene components and redistribution of high molecular weight paraffins from complex molecules agglomerates.

4 Conclusions

For products of conversion to perform a complex analysis, which allowed trace the

transformation of hydrocarbon components of oil. Based on these studies, we evaluated the effect of various additives in combination with thermobaric effect on the conversion of heavy hydrocarbons into lighter fractions.

IV-PP15

Bimetallic Au-Cu/Al_2O_3 Catalysts in Selective Aerobic Oxidation of Glucose and Benzyl Alcohol

Nagy G.[1], Benkó T.[1], Srankó D.F.[1], Borkó L.[1], Schay Z.[1], Sáfrán G.[2], Geszti O.[2], Beck A.[1*]

1 - Institute for Energy Security and Environmental Safety, Centre for Energy Research, Hungarian Academy of Sciences, Budapest, Hungary

2 - Institute of Technical Physics and Materials Science, Centre for Energy Research, Hungarian Academy of Sciences, Budapest, Hungary

* andrea.beck@energia.mta.hu

Keywords: catalysis, gold copper, bimetallic, selective oxidation, colloid

1 Introduction

A wide range of selective oxidative transformations of high importance in synthesis of fine chemicals and value added chemicals from biomass are promoted by gold using O_2 as oxidant at relatively low temperature and with very high selectivity. Efficiency of gold can be significantly improved or modified combining it with a second metal. We investigated earlier sol derived bimetallic AuAg nanoparticles (NPs) supported on SiO_2 in selective oxidation reactions using glucose and benzyl alcohol model substrates [1,2]. In this work alumina supported AuCu bimetallic systems were studied.

2 Experimental/methodology

Bimetallic AuCu (Au/Cu=1/1 molar ratio) and analogous monometallic aqueous sols were prepared by liquid phase reduction using $NaBH_4$ reducing and polyvinyl alcohol stabilizing agent. AuCu NPs with different structure were formed by co- (Au&Cu) and consecutive reduction of the precursor ions, Cu reduction on Au NPs (Cu→Au) and vice versa (Au→Cu). The nanoparticles were deposited on Degussa alumina support by adsorption, the total metal loadings were 1 mmol/g_{cat}. The samples were studied after calcination (400°C/air/1h) applied for removal of organic contaminations and also after consecutive reductive treatment (350°C/H_2/30min) providing metallic state of the active components. For structural characterization UV-vis spectroscopy, high resolution electron microscopy (HRTEM), X-ray photoelectron spectroscopy (XPS) and CO chemisorption followed by FTIR spectroscopy was applied. The catalyst samples were tested in selective glucose oxidation (0.1 M glucose in water, 35°C, pH: 9.5) and benzyl alcohol oxidation (1.0 M benzyl alcohol in toluene, 80°C) using O_2. The selectivity of gluconic acid formation was 100% for all the catalysts. In benzyl alcohol oxidation beside benzaldehyde only benzyl-benzoate with 4-10 % selectivity (up to around 5-10% conversion) was detected. Initial reaction rates were determined and compared.

3 Results and discussion

Table 1 presents several structural data of the catalysts in as prepared state and after calcination and reduction treatments, their catalytic activity is characterized by initial reaction rates. The particle sizes of the original nanoparticles varied between 1.8-2.8 nm in diameter. According to HRTEM studies in Au&Cu and Cu→Au samples alloyed AuCu (with around Au/Cu≈8/2 atomic ratio) and Au core with less and more Cu-oxide decoration, respectively, were formed, while in Au→Cu alloyed AuCu of less Cu-concentration than in Au&Cu was suggested with Cu-oxide decoration. The presence of some Cu-oxide separated from gold containing particles was also possible. The oxidative and reductive treatments of the supported

samples induced some restructuring of the particles diminishing the differences between them. Due to slight sintering in the bimetallic samples caused by calcination treatment the particle sizes became very similar (only in Cu→Au/Al_2O_3 was somewhat larger), that did not change during reduction. Calcination induced some segregation and oxidation of Cu as deduced from HRTEM (based on lattice parameters) and XPS (as shown by Cu/Au atomic ratios and appearance of Cu^{2+} states) results. Treatment in hydrogen reduced copper and decreased surface Cu/Au ratio that may be due to the dissolution of some copper into the alloyed phase or sintering of that. Au&Cu/Al_2O_3 was the most active among the bimetallic samples in both glucose and benzyl-alcohol oxidation. In the latter reaction all the AuCu/Al_2O_3 samples showed synergetic activity increase compared to the monometallic ones (remember that Au loading in Au/Al_2O_3 was two times higher than in bimetallic catalysts), in glucose oxidation the Cu introduction decreased the activity of Au/Al_2O_3.

Table 1. Metal particle sizes, mean lattice distances of Au(Cu) (111), Cu/Au surface atomic ratios and catalytic activity of the samples after different treatments.

Sample	pretreatment	d (*nm*)	a (Å)	Cu/Au $_{XPS}$	r_0 (*mmol/min/g_{cat}*) glucose ox.	benzyl alcohol ox.
Au/Al_2O_3	as prep.	2.7±1.1	2.34±0.03	-		
	calcined	2.8±0.9		-	7.2	2.2
	reduced	2.9±1.1		-	7.4	
Au&Cu/Al_2O_3	as prep.	1.8±0.3	2.29±0.05	3.5		
	calcined	2.7±0.5	2.32±0.03	4.2	2.3	2.9
	reduced	2.8±0.7	2.30±0.03	2.2	2.4	
Au→Cu/Al_2O_3	as prep.	1.9±0.5	2.31±0.03	3.7		
	calcined	2.6±0.6	2.32±0.03	5.3	1.3	1.8
	reduced	2.7±0.6	2.32±0.06	2.0	1.5	
Cu→Au/Al_2O_3	as prep.	2.4±2.0	2.34±0.03	5.0		
	calcined	3.5±1.2	2.33±0.03	5.8	0.9	2.2
	reduced	3.8±2.0	2.31±0.04	2.5	1.1	
Cu/Al_2O_3	as prep.	2.8±0.6	-	-		
	calcined	n.a.	-	-	0.0	0.0
	reduced	n.a.	-	-	0.0	

4 Conclusions

AuCu/Al_2O_3 (Au/Cu=1/1) catalysts derived from bimetallic colloids prepared by co- or consecutive reduction of precursor ions, presented clear synergetic activity increase in selective oxidation of benzyl alcohol as compared to the monometallic analogous, while in glucose oxidation the Cu addition decreased the activity of Au/Al_2O_3. In both reactions Au&Cu/Al_2O_3 with alloyed core (Au/Cu≈9/1 atomic ratio) and possible less Cu-oxide decoration was the most active bimetallic sample. Presumably, the size of the free extended AuCu alloy surface of increased activity was less optimal for adsorption of glucose than that of benzyl alcohol.

Acknowledgements

The research was supported by the Hungarian Science and Research Fund (OTKA K101854, OTKA K101897).

References

[1] T. Benkó, A. Beck, K. Frey, D. F. Srankó, O. Geszti, Gy. Sáfrán, B. Maróti, Z. Schay, App. Cat. A, 479 (2014) 103.

[2] G. Nagy, T. Benkó, L. Borkó, T. Csay, A. Horváth, K. Frey, A. Beck, Reac. Kinet. Mech. Cat., 2015, DOI 10.1007/s11144-015-0835-2

IV-PP16

Comparative Analysis of the Thermal Stability of Unmodified and SiO_x-Modiefed Chromia-Alumina Dehydrogenation Catalysts

Bekmukhamedov G.*, Egorova S., Shamsuvaleev B., Boretsky K., Lamberov A.

Kazan (Volga region) Federal University, Kazan, Russia

* giyjaz413@yandex.ru

Keywords: chromia-alumina catalyst, isobutane, dehydrogenation, thermal treatment

1 Introduction

Dehydrogenation of lower paraffins in the fluidized bed of a chromia-alumina catalyst is performed to obtain a C_3-C_5-olefins, which is used in production of synthetic rubber, fibers, films, plastics, high-octane additives. The temperature in the industrial dehydrogenation reactor is 530-580ºC and in the regenerator is 650-680ºC. The oxidative burning of coke on the catalyst surface in the upper region of the regenerator is carried by the combustion of the fuel gas, which results in local overheating of the catalyst. This is accompanied by an irreversible deactivation, which negatively affects the efficiency of the dehydrogenation process. Therefore, an actual task is to improve the thermal stability of chromia-alumina dehydrogenation catalyst.

The aim of this work was a comparative study of changes in the dehydrogenation activity of the unmodified and SiO_x-modified chromia-alumina catalysts under thermal treatment in the range of 900-1100°C.

2 Experimental

Catalysts were synthesized by impregnation of the alumina support with silica sol, aqueous solutions of chromic anhydride and potassium carbonate. The chemical composition of the catalysts is shown in Table 1. Catalyst activation temperature 800°C.

Table 1. Composition of the chromia-alumina catalysts.

Sample	C(Cr_2O_3), wt.%	C(K_2O), wt.%	C(SiO_2), wt.%
Cat-1	9.0	1.0	0
Cat-2	9.0	1.0	2.5
Cat-3	9.0	1.0	4.5
Cat-4	12.5	1.3	0

Catalysts were calcined in a muffle furnace; heating to 900–1100°C was performed at a rate of 4 K/min in an atmosphere of air, and the samples were kept at a specified temperature for 1 h.

The catalysts were studied by X-ray diffraction, low-temperature nitrogen adsorption, electron paramagnetic resonance, UV-Vis- and Raman spectroscopy, temperature-programmed desorption of ammonia.

Catalytic properties in the isobutane dehydrogenation reaction were determined on an automated laboratory unit in a steel flow reactor with a fixed catalyst bed.

3 Results and discussion

During thermal treatment at 900-1100°C the transformation of the catalyst support from γ-Al_2O_3 into mixture of crystalline phases of δ-, θ- and α-Al_2O_3 takes place. It is accompanied by the coalescent pore sintering and the reduction of specific surface area (S_{sp}) of catalysts. At

900°C S_{sp} decreases from 73-77 to 54-60 m^2/g, and in the range of 1000-1100°C S_{sp} decreases to 24-41 m^2/g. As a result the treatment of Cat-1 at 900-1000°C is accompanied by combination of isolated Cr(III) ions into Cr_2O_3 clusters. This leads to increase of the dehydrogenation activity - the isobutane conversion increases from 48.5% to 50.5-51.5% (Table 2).

Table 2. Conversion of isobutane in the dehydrogenation reaction.

Treatment temperature, °C	**Isobutane conversion, %**			
	Cat-1	**Cat-2**	**Cat-3**	**Cat-4**
Initial sample	48.5	53.3	54.5	50.4
900	51.4	52.3	52.1	46.8
1000	50.5	47.9	47.3	41.1
1100	36.3	42.1	43.4	32.4

At 900-1000°C in the SiO_x-modified catalysts Cat-2 and Cat-3 highly ordered Cr_2O_3 structures are formed, which leads to a decrease in the conversion of isobutane from 53.3-54.5 to 47.3-52.3%. During treatment of Cat-4 at 900-1000°C the crystallites of α-Cr_2O_3 are formed, the conversion decreases to a greater extent - from 50.5% to 41.1-46.8%.

Treatment at 1100°C is accompanied by the decrease in dehydrogenation activity of unmodified catalysts Cat-1 and Cat-4 to 32.4-36.3% due to the formation of Cr_2O_3-crystallites and solid solution α-$Al_2O_3 \cdot Cr_2O_3$.

In the modified catalysts Cat-2 and Cat-3 the active component is more stable to treatment at 1100°C compared to the unmodified catalysts due to a decrease in the amount of chromium, which incorporates to the support. In this case the dehydrogenation activity is less reduced, conversion of isobutane decreases to 42.1-43.4%.

IV-PP17

Study of Bimetallic Catalyst Pd-Ni for Styrene Hydrogenation

Betti C.[1*], Badano J.[1], Maccarrone M.J.[1], Lederhos C.[1], Carrara N.[1], Vera C.[1,2], Liprandi D.[2], Coloma Pascual F.[3], Quiroga M.[1,2]

1 - Instituto Nacional de Catalisis y Petroquimica, INCAPE, Santa Fe, Argentina
2 - Universidad Nacional del Litoral, Facultad de Ing. Quimica, Santa Fe, Argentina
3 - Servicios Técnicos de Investigación, Facultad de Ciencias, Universidad de Alicante, Alicante, Spain

* cbetti@fiq.unl.edu.ar

Keywords: bimetallic catalysts, selective hydrogenation, palladium, nickel, sulfur resistance

1 Introduction

Gasoline and BTX (Benzene, toluene and xylenes) streams coming from the cracking of petroleum must be purified in order to minimize the concentration of diolefins, responsible of gums formations. The widespread method of purification is the selective hydrogenation of vinyllic bond, keeping the aromatic rings unaltered. These streams can have up to 1000 ppm of sulfur compounds, among them thiophene is one of the most common ones [1,2], being these sulfur compounds the main cause of the loss of activity of metal catalysts in several refinery processes. The objective of this work is to evaluate the influence of the order of impregnation of Pd and Ni in bimetallic catalysts on the activity and sulfur resistance during styrene partial hydrogenation.

2 Experimental Methodology

Catalysts Preparation and Characterization: γ-Al_2O_3 Ketjen CK 300 previously calcined at 823 K (S_{BET}: 180 $m^2\ g^{-1}$) was used as support. Mono and bimetallic Pd-Ni catalysts were prepared by the incipient wetness technique using chloride salts. The bimetallic catalysts were prepared by successive impregnations. Volume and concentration of the impregnating solutions were adjusted to get 1wt % of Pd, 2.4 wt % of Ni on the final catalysts. The systems were characterized by ICP, H_2 chemisorption and XPS. *Catalytic Tests:* styrene to ethylbenzene selective hydrogenation was used as a test reaction. The reaction was performed in a stainless steel, PTFE coated stirred tank reactor, operated in batch mode at 333 K, 2 MPa H_2 pressure and 1200 rpm, using 0.3 g of catalyst and 200 mL of 5% (v/v) styrene in toluene solution. The poisoning tests were done adding 600 ppm of thiophene to the feed. Reactant and products were analyzed by GC.

3 Results and Discussion

The values of mass concentration determined by ICP technique were 1wt% of Pd and 2.4 of Ni. Table 1 shows that the dispersion of monometallic Pd/Al is 3 and 3.6 times higher than that of NiPd and PdNi, respectively. The lower H_2 adsorption on bimetallic could be due to an effect of decoration of Pd particles by Ni species, the latter being not active for H_2 adsorption.

Table 1. Catalysts naming, dispersion (D) and XPS data.

Catalyst	1st imp.	2nd imp.	D(%)	atomic superficial ratios			*Pd 3d5/2 BE (eV)*		*Ni 2p3/2 BE (eV)*	
				Cl/Al	*Pd/Al*	*Ni/Al*	*$Pd^{\delta-}$, Pd^0*	*Pd^{d+}*	*Ni^0*	*NiO*
Pd	Pd		45.1	0.0028	0.0025		334.8 (63%)	336.7 (37%)		
PdNi	Pd	Ni	12.4	0.0108	0.0016	0.015	334.5 (73%)	336.0 (27%)	851.2 (18%)	856.3 (82%)
NiPd	Ni	Pd	15.7	0.0109	0.0021	0.012	334.1 (58%)	335.5 (42%)		856.1

XPS spectra of the catalysts had a peak at 198.5 eV assigned to chloride species that were not eliminated during the thermal treatment stages [3]. On the other hand, bimetallic catalysts had a very low intensity peak for Pd $3d_{5/2}$ in the 334.1-334.5 eV range attributed to $Pd^{\delta-}$, while monometallic Pd had a band at 334.8 assigned to Pd^0 [3]; all the catalysts presented a high intensity peak at 335.5-336.7 eV

assigned to $Pd_x^{\delta+}O_yCl_z$ [4]. When analyzing the BE region of Ni $2p_{3/2}$ spectrum in the bimetallic PdNi two peaks were observed: at 852.1 eV assigned to Ni^0 and at 856.3 eV attributed to electrodeficient species of Ni^{+2}[3]. In the case of NiPd catalyst, only electrodefient Ni species are detected. Bimetallic catalysts had the highest Cl/Al atomic ratios (Table 1). The presence of $Pd^{\delta-}$ species would indicate the formation of a metallic bond or a Pd–Ni alloy.

In all the performed tests the selectivity to ethylbencene was higher than 98%. In Figure 1 are plotted the total conversion of styrene as a function of time-on-stream for all catalysts in absence or presence of poison. It can be seen that PdNi and Pd catalysts display the highest total conversion.

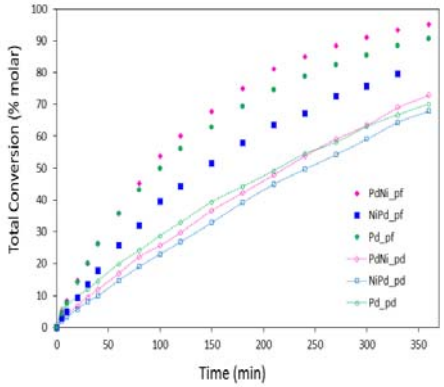

Fig. 1. Styrene total conversion as a function of time in the absence (pf) or presence of poison (pd) for all catalysts.

During the poisoning tests, a decrease in total conversions can be seen as a result of the loss of active sites, and the total conversions are quite similar for all catalysts.In order to compare the sulfur resistance of the catalysts the initial rates of reaction of styrene were determined during the tests with both sulfur-free (r^0_{sf}) and sulfur-poisoned (r^0_{sp}) feeds. From the initial reaction values and considering a simple linear deactivation model (zero order for deactivation), the fraction of poisoned sites (α) can be calculated as $\alpha = 1 - r^0_{sp}/r^0_{sf}$. Table 2 shows r^0_{sf}, r^0_{sp} and α.

Table 2. Values of fraction of poisoned sites (α)

Catalyst	Sulfur-free		Sulfur-poisoned		
	r^o_{sf} (mol mL^{-1} min^{-1})	R^2	r^o_{sp} (mol mL^{-1} min^{-1})	R^2	α
Pd	0.234	0.991	0.114	0.981	0.51
PdNi	0.240	0.992	0.102	0.993	0.57
NiPd	0.163	0.997	0.089	0.997	0.45

According to the most accepted model for sulfur poisoned of Group VIII metals, poisoning occurs by a donation of electrons from the metals to the sulfur atom.

Bimetallic PdNi catalyst turned out to be the least sulfur resistant, this is likely due to the exposed Ni^0 that promotes a strong adsorption of thiophene and thus an enhanced blocking of active sites. The higher sulfur resistance of NiPd than Pd catalyst could be related to the high surface Cl/Al ratio, indicating that $Pd^{\delta+}$oxychlorinated species prevent the adsorption of thiophene by means of steric effect (big size species) and/or an electronic effect (high electronegativity of chlorine).

4 Conclusions

The effect of the sequence of impregnation was evaluated for a series of bimetallic Pd–Ni catalysts. The properties assessed were the catalytic activity and the sulfur resistance during the selective hydrogenation of styrene. The XPS results point to the presence of different Pd^0, $Pd^{\delta-}$ and $Pd^{\delta+}O_xCl_y$ species. The presence of $Pd^{\delta-}$ species would indicate the formation of a metallic bond or a Pd–Ni alloy. The order of total conversion of styrene in the absence of sulfur was: PdNi≅Pd>NiPd. After the poisoning with thiophene the order changed to: Pd>PdNi≅NiPd. Bimetallic PdNi catalyst turned out to be the least sulfur resistant, this is likely due to the exposed Ni^0 that promotes a strong adsorption of thiophene and thus an enhanced blocking of active sites. The higher sulfur resistance of NiPd than Pd catalyst could be related to the high surface Cl/Al ratio, indicating that $Pd^{\delta+}$species prevent the adsorption of thiophene by means of steric effect and/or an electronic effect.

Acknowledgements

Authors are gratefully indebted to ANPCyT, CONICET and UNL for financing this work.

References

[1] L.F. Hatch, S. Matar, From Hydrocarbon to Petrochemicals, Gulf Publishing Co., Houston, TX, 1981.
[2] G. Chauvel, G. Lefebvre, Petrochemical Processes, Institut Francais du Petrole Publictions, Paris, 1989.
[3] NIST X-ray Photoelectron Spectroscopy NIST Standard Ref. Database 20, Version 3.5, USA, 2007.
[4] A.B. Gaspar, G. R.Dos Santos, R.De Souza Costa, M. A. P. Da Silva, Catal Today. 133 (2008) 400.

IV-PP18

Metathesis Homopolymerization of New Fullerene-Containing Norbornenes by Catalyst Grubbs 1'st Generation

Biglova Yu.N.[1*], Mikheev V.V.[1], Nuriahmetova Z.F.[1], Torosyan S.A.[2], Miftakhov M.S.[2]

1 - Bashkir State University, Department of Chemistry, Ufa, Russia
2 - Institute of Chemistry of RAS, Ufa, Russia

* bn.yulya@mail.ru

Keywords: fullerene-containing norbornenes, catalyst grubbs 1'st generation

1 Introduction

Fullerene containing thin polymer films are used as acceptor components of bulk heterojunction photovoltaic devices [1-3]. Although organic materials in solar cells are inferior to inorganic ones as far as turnaround efficiency of light (power conversion efficiency, PCE) is concerned, a number of their obvious advantages enables us to consider them as a possible alternative to traditional silicon batteries in future.

Due to low solubility of C_{60} it is difficult to obtain fullerene-based high molecular weight polymers. In this work we report the preparation and characterization of new fullerene-based monomers and a high molecular weight polymer containing C_{60}, obtained by via ring-opening metathesis polymerization.

2 Experimental

The fullerene monomers **I, II** for ROMP was prepared by cycloaddition of malonic and dichloroacetic acid derivatives to C_{60}, purified by column chromatography, and characterized by ^{1}H,^{13}C - NMR, IR, UF- spectrum, mass spectrometry (MALDI-TOF) [4].

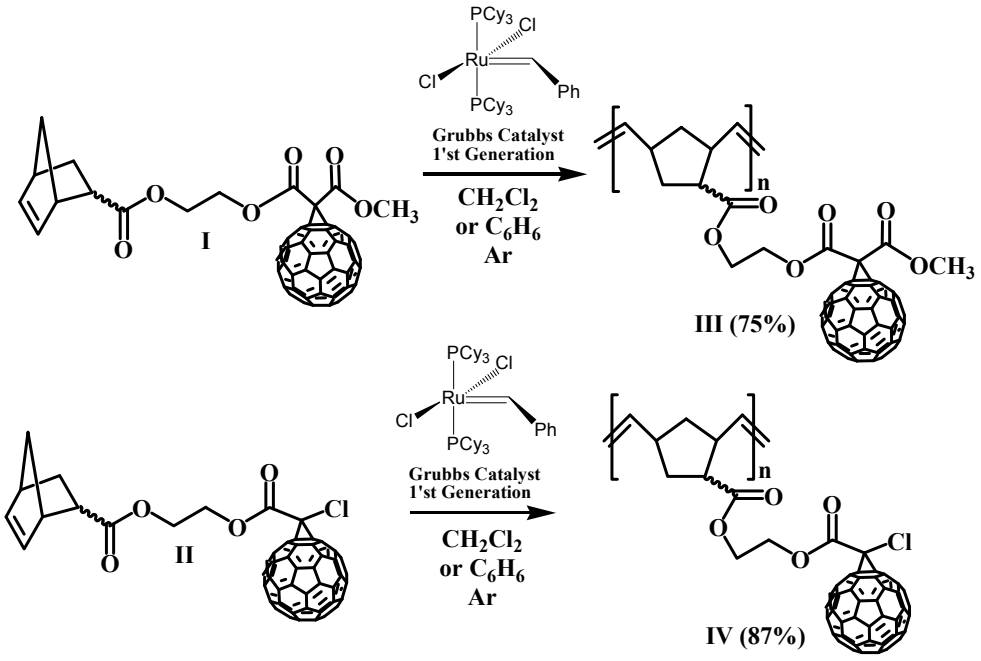

3 Results and discussion

Homopolymerization of monomers **I, II** was carried out under inert atmosphere at the presence of the Grubbs 1'st generation catalyst at room temperature in the CH_2Cl_2 solution. During the first 6 hours consumption of the initial monomers (TLC control) and precipitation were observed. The polymers **III**, **IV** are insoluble in $CHCl_3$, C_6H_6, $C_6H_5CH_3$, THF and EtOAc and is partially plumped at keeping in DMSO, so the molecular weight of polymers was impossible to estimate.

Acknowledgements

This work was supported by the Russian Foundation for Basic Research (grants № 14-03-31610 mol_a, 14-02-97008).

References

[1] Y.-J. Cheng, S.-H. Yang, C.S. Hsu, *Chem. Rev.*, 109 (2009) 5868.
[2] J.E. Conghlin, Z.B. Henson,. G.C. Welch, G.C. Bazan, *Accounts Chem. Res.* 47 (2014) 257.
[3] P. Bujak, I. Kulszewicz-Bajer, M. Zagorska, V. Maurel, I. Wielgus, A. Pron, *Chem. Soc. Rev.* 42 (2013) 8895.
[4] M.S. Miftakhov, V.V. Mikheev, S.A. Torosyan, Yu.N. Biglova, F.A. Gimalova, V.M. Menshov, A.G. Mustafin, *Tetrahedron*. 70 (2014) 8040.

IV-PP19

Catalytic Systems Based on Iron and Nickel in the Synthesis of Graft Copolymers

Blinova L.I.*, Kolyakina E.V., Grishin D.F.

Lobachevsky State University of Nizhny Novgorod, Nizhny Novgorod, Russia

* blinova.li@mail.ru

Keywords: graft copolymers, iron and nickel, catalytic systems

1 Introduction

Development of new methods for preparation of polymer materials with definite properties is the most important task in modern polymer chemistry. In recent years, the methods of controlled radical polymerization are actively developed, which allow purposefully modify the structure and properties of the polymeric material [1-4]. The effective way towards solution of this problem is realization of copolymerization, i.e. modification of polymer properties through the involvement of monomers of different nature in polymerization. This method permits to obtain statistical, gradient, block and graft copolymers. The graft copolymers are perspective materials due to the possibility of change of their structural constituents, such as the length of the grafting block, the composition and length of the fundamental block. This method opens up wide prospects to obtain materials with new properties.

2 Experimental

Vinyl monomers were washed with aqueous alkaline solution and water, dried over calcium chloride and then distilled. Solvents were purified by distillation. Reagents were placed in an ampule. After degassing the content, the ampule was sealed in vacuum. The polymerization was carried out at 25-80°C. Molecular weights were determined by SEC calibrated with polystyrene standards. The monitoring of the polymerization kinetics was made by weight method. The composition of copolymer was studied by the method of IR-spectroscopy.

3 Results and discussion

We have developed a method for producing graft copolymers on the basis of brominated polystyrene (**BPS**) in the presence of zerovalent iron and ($NiBr_2$ (PPh_3): Zn) as a catalytic system. BPS acts at the same time as the structural basis of the graft copolymer and initiator in the process of synthesis of graft copolymers (**scheme 1**). The synthesis of BPS was condiucted by bromination of polystyrene in the presence of iron powder and of iron chloride (III). It was established that the nature of catalyst and solvent affect on the yield of BPS. The highest yield of BPS was obtained in the case of the carrying out the reaction in chloroform. BPS structure was confirmed by IR spectroscopy.

It has been shown that the catalytic systems based on iron and nickel allow ones to carry out copolymerization of BPS with monomers of different nature (methyl acrylate (**MA**), methyl methacrylate (**MMA**), butyl acrylate (**BA**), tret.-butyl methacrylate (**t.-BMA**), octyl methacrylate (**OMA**), vinyl acetate (**VA**), acrylonitrile (**AN**). The process proceed in the «grafting from» mode in the temperature range 25-80°C. Exemplified by the synthesis of the graft copolymer of PS-PMMA we analyzed the influence of solvent nature and composition of the catalytic systems on the product yield. The highest yield of the graft copolymer with the lowest content of side products (cross-linking of polymer) was obtained using THF as solvent.

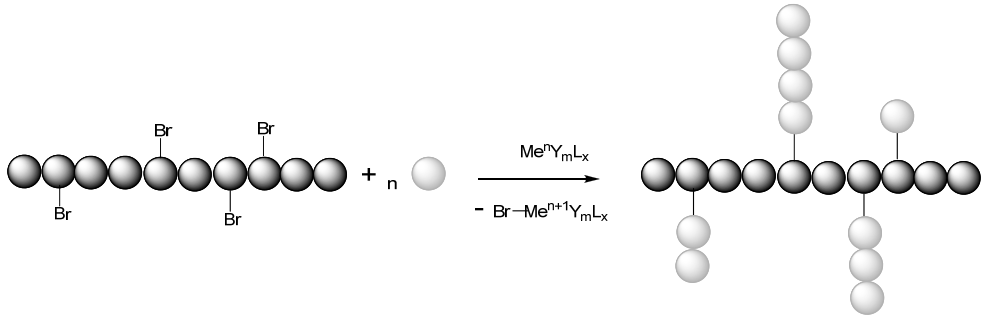

Scheme 1

It was shown that the activity of the catalytic system based on zerovalent iron increases in case of the copolymerization in the presence of PPh_3. The system based on BPS : Fe (0): PPh_3 taken in a ratio of 2: 1: 2 gives the highest yields of PST-PMMA graft copolymers. When using systems based on a nickel complex ($NiBr_2$ (PPh_3) : Zn) it was established that metallic zinc acts as a reducing agent. The note that the catalysis was realized due to zerovalent nickel complexes. The synthesis of the macrocatalyst consisting from BPS and zerovalent nickel was performed **(scheme 2)**. On the base of that macrocatalyst the graft copolymer of PS-PMMA was synthesized with the higher yield relative to the one-step method of synthesis of graft polymers in the presence of $NiBr_2$ (PPh_3): Zn system. In this case formation of crosslinked polymer was not observed at all.

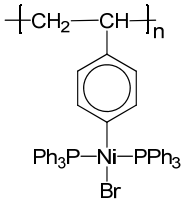

Scheme 2

Zerovalent iron systems were tested in the synthesis of graft copolymers of different natures described above. The structures of the copolymers obtained were proved with the help spectroscopic methods: IR and H^1-NMR spectroscopy. The glass transition temperature was defined for these graft polymers. It was established that in the case of synthesis of the PS-PMMA copolymers using iron and nickel catalytic systems the glass transition temperature of samples is higher than of the initial BPS and PS samples.

4 Conclusions

In such a way we have developed new approaches to the synthesis of graft copolymers of different structure. The proposed technique for obtaining graft copolymers is more effective as compared with the conventional method for producing graft copolymers based on systems polymer - monomer - radical initiator. This method gives a possibility of using zerovalent iron and catalysts based on nickel to modify the properties of the copolymers.

Acknowledgements

The work was done under the task of Ministry of Education and Science of Russian Federation (proj. 736).

References

[1] J. Nicolas, Y. Guillaneuf, C. Lefay, et al. *Prog. Polym. Sci.* 38 (2013) 63.
[2] D.F. Grishin. *Polymer Science, Series C. Selected Topics.* 53 (2011) 3.
[3] F. di Lena, K. Matyjaszewski. *Prog. Polym. Sci.* 35 (2010) 959.
[4] E.V. Kolyakina, D.F. Grishin. *Russ. Chem. Rev*. 78 (2009) 535.

IV-PP20

The First Example of Catalytic Tandem Interaction N-Allyl-N-Arylamines with Diazocompounds: Aza-Claisen Rearrangement – Carbenation

Badamshin A.G.[1*], Gafarova A.G.[2], Tomilov Yu.V.[3], Dokichev V.A.[1,4]

1 - Ufa Institute of Chemistry of the Russian Academy of Sciences, Ufa, Russia
2 - Bashkir State University, the Faculty of Chemistry, Ufa, Russia
3 - N. D. Zelinsky Institute of Organic Chemistry, Russian Academy of Sciences, Moscow, Russia
4 - Ufa State Aviation Technical University, Ufa, Russia

* alexander.badamshin@gmail.com

Keywords: Aza-Claisen rearrangement, diazocompounds, triflate, yttrium

1 Introduction.

Catalytic reactions of diazocompounds with unsaturated compounds are widely used in organic synthesis as a convenient method of obtaining practically important polyfunctional compounds of various structures [1–5].

Onto the direction of the catalytic interaction (the cyclopropanation of C=C-bond, the 1,3-dipolar cycloaddition, the introduction of the carbene into bond of C–H or C-heteroatom) and the yield of the produced reaction products are strongly influenced from the structure of both olefins and diazocompounds, as well as the catalyst nature.

Thus, for example, the diazomethane is reacted with allylamines in the presence of $(PhCN)_2PdCl_2$ to form cyclopropanes [2]. The interaction of allylamine with ethyl diazoacetate under the influence of catalysts on the basis of Co, Ni, Rh, Ru results in to the esters of unsaturated *N,N*-dialkylaminoacid by the [2, 3] – rearrangement formed *N*-ylides [3, 6].

Recently, we found triflate activating effect of rare earth elements on the reaction of 1,3-dipolar cycloaddition of diazoesters to electron deficient dipolarophiles to give the corresponding 1- or 2-pyrazolines [7].

2 Experimental/methodology.

In the present work, we studied the catalytic interaction of *N*-allyl-*N*-methylaniline (I) with diazoacetone (IIa) and ethyl diazoacetate (IIb) in the presence of $Y(OTf)_3$. The reaction was performed by 80 ^oC by addition diazocompounds into the benzene to solution of *N*-allyl-*N*-methylaniline (I) and triflate yttrium, with a molar ratio of I : N_2CHCOR : Cat = 5 : 5 : 1.

3 Results and discussion.

We have found that *N*-allyl-*N*-methylaniline (I) reacts with diazoacetone (IIa) and ethyl diazoacetate (IIb) in the presence of $Y(OTf)_3$, forming with the yields 56 and 66% *N*-(2-allylphenyl)-*N*-(acetylmethyl)-*N*-methylamine (IIIa) and ethyl *N*-(2-allylphenyl)-*N*-methylglycinate (IIIb).

This transformation is an example of a tandem reaction [8], which begins with the accession to the amino group of carbene, catalytically generated from diazocompound, and, formation of the intermediate allyl *N*-ylide which is prone to intramolecular aza-Claisen rearrangement at the *o*-position of the benzene ring [9–11].

It should be noted that at the absence of diazocompound the migration of allyl group at the *o*-position do not occurs.

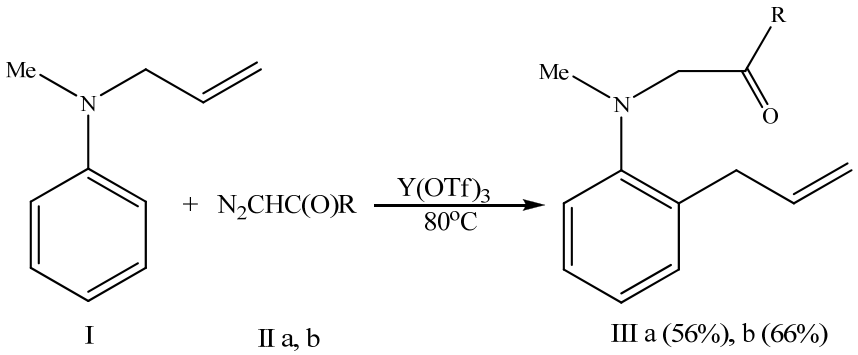

Fig. 1. The interaction of *N*-allyl-*N*-methylaniline with diazoacetone and ethyl diazoacetate.

4 Conclusions.

The possibility of catalytic reactions application of *N*-allyl-*N*-methylaniline with diazocompounds for one-pot synthesis of tertiary amines containing 2-allylphenyl substituent is shown.

Acknowledgements

Financial support provided by the Russian Science Foundation (project№ 14-33-00022) is gratefully acknowledged.

References

[1] Maas G. *Top. Curr. Chem*. 137 (1987) 75.
[2] Tomilov Yu.V., Dokichev V.A., Dzhemilev U.M., Nefedov O.M. *Russ. Chem. Rev*. 62(9) (1993) 799
[3] Shapiro E.A., Dyatkin A.B., Nefedov O.M. Diazoefiry .M. Nauka. (1992) 150.
[4] Zollinger H. *DiazoChemistry II: Aliphatic, Inorganic and Organometallic Compounds. Wein-heim: VCH.* (1995) 530.
[5] Doyle M. P., McKervey M. A., Ye T. *Modern Catalytic Methods for Organic Synthesis with Di-azo Compounds. N.- Y.: Wiley*. (1998) 652.
[6] Zhou C.-Y., Huang J.-S., Che C.-M. *Synlett*. 18 (2010) 2681.
[7] Novikov R.A., Platonov D.N., Dokichev V.A., Tomilov Yu.V., Nefedov O.M. *Russ. Chem. Bull*. 59(5) (2010) 984.
[8] Litvinov V.P. *Ros. Khim.Zh.* 49(6) (2005) 11.
[9] The Claisen Rearrangement: Methods and Applications. Ed. Hiersemann M., Nubbemeyer U. *Weinheim. Wiley-VCH Verlag GmbH & Co. KGaA*. (2007) 591.
[10] Nubbemeyer U. Top. *Curr.Chem*. 244 (2005) 149.
[11] Sharma P., Kaur N., Jain S., Kishore D. *J. Curr. Chem. Pharm. Sci.* 3(1) (2013) 80.

IV-PP21

Hydrotalcite Supported Co Catalyst with Bimodal Structure for Fischer-Tropsch Synthesis (FTS)

Jung J.-S.[1,2], Lee J.S.[1,2], Hong G.H.[1,2], Lee S.O.[1,2], Lee K.H.[1,2], Yang E.-H.[1,2], Moon D.J.[1,2*]

1 - Clean Energy Research Center, KIST, Seoul, Korea
2 - Clean Energy & Chemical Engineering, UST, Daejeon, Korea

* djmoon@kist.re.kr

Keywords: Fischer-Tropsch synthesis, GTL-FPSO, hydrotalcite, bimodal structure

1 Introduction

Recently, because of the high oil prices and limited petroleum reservoirs, stranded gas fields have received much attention as attractive resources to produce the liquid fuels by GTL-FPSO process [1]. Supported cobalt catalyst have long been used for FTS,especially when long catalyst life times and high selectivities for paraffins are required [2]. The selection of the support for a cobalt catalyst has considerable influence on FTS due to its physicochemical properties. Especailly the support with bimodal structure has taken advantages for FTS, since the pore was in the macropore to enhance mass transfer and the other was in the mesopore to maintiain higher surface area [3]. The hydrotalcite(HT)-like compound possing have bimodal structure was proposed as a new kind of support for FTS in this studies. The general from for HT is $[M_{1-x}^{II}M_x^{III}(OH)_2][A^{n-}]_{x/n}\cdot mH_2O$, where divalent ion may be Mg^{2+}, Zn^{2+} and trivalent ion may be Al^{3+}, Fe^{3+}, Cr^{3+}. The compensation anions may be NO_3^-,CO_3^{2-},SO_4^{2-},Cl^-.Generally, X can have values approximately 0.1-0.5. The HT-based catalyst have been recently reported for several process in the energy field, such as hydrogen production from the reforming process [4]. But the none study reported upto for using of HT with bimodal strucrture as support, in which the coblat is dispersed on the HT surface for FTS. The aim of this work is to examine these aspects, in the case of Co/HT with different pore size prepared to develop highly active and selective bimodal pore-stuctured catalyst for FTS.

2 Experimental/methodology

The supports were prepared by a sol-gel method with hydrotalcite (HT)-compounds $Mg_{2x}Al_2(OH)_{4x+4}CO_3\cdot nH_2O$(Sasol,MG70), Kaolin (Sigma Aldrich) and Al nitrate (Samchun). The different ratios of mentioned components were used for controlling pore size. The required amount of HT was dispersed in ethanol. The solution was mixed with the required amount of kaolin and Al nitrate. The pH of mixture slurry was adjusted by ammonia solution to the range of 9–10, then aging for 12 h at 80 ˚C. It was filtered and washed repeatedly with hot water until neutral pH. The clay was dried at 60 ◦C for 12 h and calcined at 500 ˚C for 5 h. The supports were designated as KIST 1-4. After preparing the supports, The 15 wt% of cobalt was added on the support through multiple steps using aqueous cobalt nitrate solution ($Co(NO_3)_2.6H_2O$ 98 %), following reported literature [5]. It was dried at 60 ˚C for 12 h and calcined at 400 ˚C. The catalysts were characterized by Mercury porosimetry, N_2 physisorption, TPR, XRD, SEM and TEM. Catalyst activity was studied in a fixed-bed continuous down flow reactor of 12.7 mm Id with 0.4 g of catalyst. Catalyst were reduced at 450 °C, using pure hydrogen for 12 h. Reaction was carried out at 20 bar pressure, 250 °C and GHSV of 3000 h^{-1}, with reactant mole ratio of 2 [H_2/CO]. Products were cooled in cold and hot traps and analysed through off-line GC. Non-condensable effluent gases was analysed by online GC.

3 Results and discussion

From the Mercury porosimetry analysis (Fig.1), it was found that the prepared support had bimodal structure compared to the MG70. And the different ratio of HT: Kaolin: Al nitrate made it induced different pore structure respectively. It was confirmed that the support were successfully made by the different ratio and cobalt was successfully impregnated on the prepared support as shown in Fig.2. The variation of cobalt oxide which was affected on the induced physicochemicalm proprtites was observed. The bigger size of Co_3O_4 on KIST 1 and KIST 2 was observed compared to those of KIST 3 and 4. These results were attributed to the existence of higher macro porosity, which led to formation of the lager cobalt crystallite size. And the trend was followed by the sequence of porosity of support (KIST1> KIST2> KIST3> KIST4) [6].

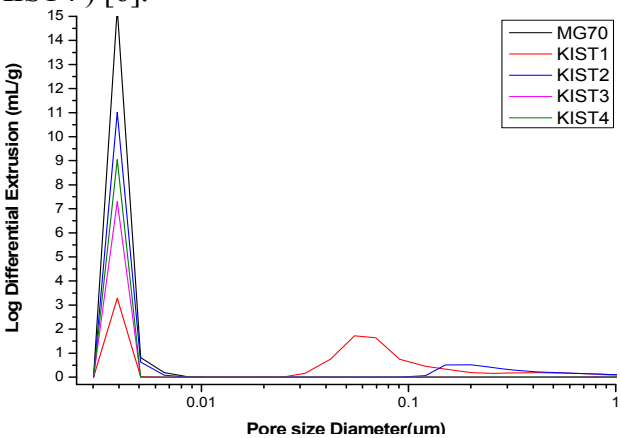

Fig. 1. Mercury extrusion as a function of pore size.

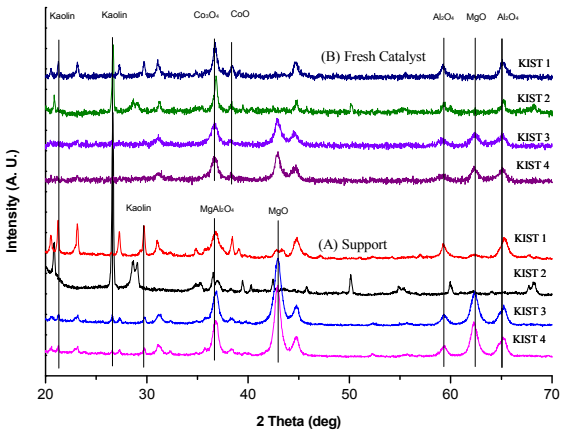

Fig. 2. XRD patterns of prepared catalysts.

4 Conclusions

The Co/MG70 catalyst had the moderate CO conversion and highest CH_4 selectivity in this work. The Co/MG70 had the higher dispersion of cobalt due to the high surface area of support supplied. But the smaller pore of MG70 caused the increase of H_2/CO. In other words, The greater diffusion rate of H_2 compared to CO firstly filled in the pore and the decreased ratio of CO to H_2 might enhance the selectivity of CH_4 and lighter hydrocarbons. And the KIST 3 and KIST 4 catalyst had the lowest CO convserison and moderate C_{8+} selectivity in this work.The Co/KIST3 and Co/KIST 4 had the low dispersion of cobalt due to the low surface area. The large pore diameter made the cobalt particles more aggregated, leading to low cobalt dispersion and low catalytic activity. On the other hands, the highest CO conversion and highest C_{8+} selectivity was observed in the KIST1 and KIST2. The Co/KIST1 and KIST2 had the moderate dispersion of cobalt and highest reducibility due to the lager cobalt crystallite size. The bimodal structure of support maintained the surface area of meso-pore and enhanced the porosity from macro-pore, which provided facile mass-transfer of heavy hydrocarbons.

Acknowledgements

This work was supported by Korea Institute of Science and Technology (Project No. 2E25404) and funded by Ministry of Trade, Industry and Energy, Korea. (Project No. 20142010102790).

References

[1] J.S. Jung, S.W. Kim, D.J. Moon, *Catalysis.Today*, 185 (2012) 168.
[2] E. Iglesia, *Applied Catal A: Gen*, 396 (2011) 91.
[3] T. Witoon, M. Chareonpanich, J. Limtrakul, *Fuel Processing Technology*, 92 (2011) 1498.
[4] A.Di Fronzo, C. Pirola, A. Comazzi, M. Nocchetti, M. Basrinini, D.C. Boffito, *Fuel*, 119 (2014) 62.
[5] J.S. Jung, J.S. Lee, G.R. Choi, S. Ramesh, D. J. Moon, *Fuel*, 149 (2015) 118.
[6] S.J. Park, J.W. Bae, J.H. Oh, K.V.R Chary, Y. W. Rhee, *J. Mol. Cat. A*, 298 (2009) 81.

IV-PP22

Deactivation Studies on Non-Oxidative Methane Conversion to Aromatics over Molybdenum Modified HZSM-5 Catalyst

Budde P.K., Upadhyayula S.*

Indian Institute of Technology Delhi, New Delhi, India

* sreedevi@chemical.iitd.ac.in

Keywords: methane, dehydro-aromatization, Bi-functional catalyst, MoO3/HZSM-5, thermo-gravimetric analysis (TGA), temperature programmed oxidation (TPO)

1 Introduction

The declining crude oil reserves have shifted focus on to natural gas as an alternative supply for fuel. Thermodynamic calculations show that methane conversion to aromatics is insignificant below 600ºC, when the formation of solid carbon is included and the formation of carbon is thermo-dynamically favourable at 300ºC. At equilibrium, formation of benzene is not significant as compared to formation of solid carbon [1]. Among the various processes, methane dehydro-aromatization to aromatics over Mo-HZSM-5/Mo-HMCM-22 catalysts seem to be most promising [2]. However, the formation of coke is inevitable. It is a great challenge to reduce the formation of the carbonaceous deposits in methane dehydro-aromatization for its potential industrial applications. This work mainly focuses on improving the catalyst activity and stability by understanding the deactivation mechanism of the catalyst.

2 Experimental/methodology

The molybdenum supported catalyst was synthesized by conventional impregnation of ammonium-heptamolybdenate (AHM) on HZSM-5, SAR-30 followed by drying at 120ºC for 12 hours, which was later calcined at 550ºC for 6 hours. The catalyst activity tests were performed in fixed bed tubular continuous flow quartz reactor at atmospheric pressure. The feed gas was passed over the catalyst at desired temperature and the outlet product mixture was heated to 200ºC to avoid in-line condensation. The standard mixture of 90% CH_4 and 10% N_2 as an internal standard used to analyse the gaseous products from the reactor. Methane conversion and selectivity to aromatics and coke was calculated by carbon balance as described in the literature [3]. Catalysts were pre-treated with 90% CH_4+H_2, H_2 and N_2 which are labelled as A, B and C, respectively. Characterization of coked catalyst was done by using XRD, TPD, TGA, TPO and HRTEM.

3 Results and discussion

The effect of pre-treatment of the laboratory prepared 2%Mo-HZSM-5 catalyst on the methane conversion and product selectivity is shown in Table-1. Catalyst pre-treated with CH_4+H_2 was found to be prone to less coking and higher aromatic selectivity than H_2 and N_2 pre-treated catalyst.

TG-DTG/DTA profiles of the spent catalyst which correspond to the different pre-treated catalyst as illustrated in Fig.-1 below. The weight loss of the catalyst between 100-300ºC is due to the desorption of moisture, latter the weight loss of the catalyst in the temperature range (450-600ºC) can be attributed to combustion of coke formed on the catalyst. DTG/DTA profiles indicate the weight loss of the catalyst and its endothermic and exothermic nature of weight loss of the catalyst. Here, the coke burning-off temperature shifted from 540ºC to 575ºC due to increase in condensation of coke.

Table 1. Methane conversion and selectivity over 2%Mo-HZSM-5 catalyst at 700ºC, GHSV=1200 $cm^3/g.h$,1atm and Time on Stream (60min).

Catalyst	$\%X_{CH4}$	Selectivity (%)					
		C_2-C_3	Benzene	T+X	Naphthalene	CO	Coke
2%Mo-HZSM-5-A	22.3	2.5	67.5	2.8	7	1.8	18.0
2%Mo-HZSM-5-B	18.0	3.5	61	5	4.4	2.6	23.5
2%Mo-HZSM-5-C	5.6	9.4	10.2	2.5	1.2	0.5	76.1

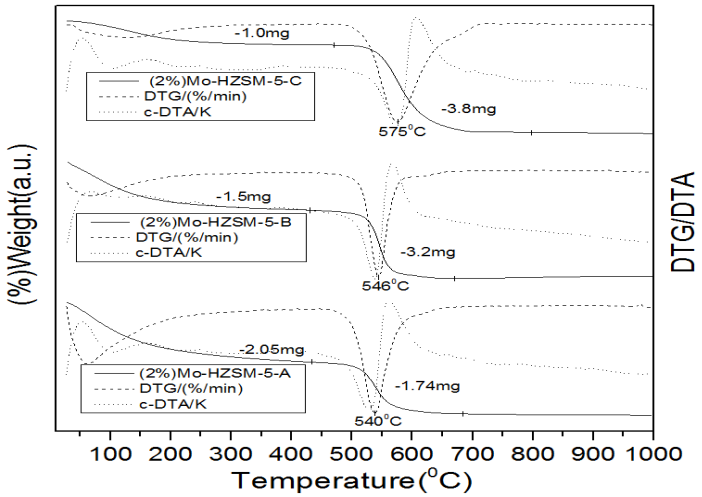

Fig.1: TG-DTG/DTA analysis of 2%Mo-HZSM-5 spent catalyst after 6h (TOS)

4 Conclusions

Molybdenum modified catalyst pre-treated with 90% CH_4+H_2 leads to formation of less coke, higher methane conversion and product selectivity. Coke deposits formed on the catalyst were characterized by TG/DTA, TPO and TEM Techniques. Performance of the catalyst decreased with molybdenum loading. Two combustion temperature regions were observed at higher (6-8%) molybdenum loading. Combustion at lower temperature (300-450ºC) was attributed to Mo_2C and molybdenum associated carbonaceous species, which are located on the external surface of the catalyst. The combustion at high temperature (450-600ºC) was due to coke deposition on the Bronsted acid sites. Kinetic analysis of the TG profiles were done by assuming that the oxidation of the coke is a first order reaction. The activation energy of the catalyst pre-treated with CH_4+H_2 is found to be lower than the N_2 and H_2 pre-treated catalyst. HRTEM images of the coked catalyst show that there is a formation of graphite layer on the Mo_2C active sites, and surrounded by the amorphous carbon on the catalyst surface. Graphite layer formation on the catalytic active site and aromatic coke formed on the Bronsted acid sites are main cause for the deactivation of the catalyst.

Acknowledgements

The authors acknowledge Dr. Sunil Maity, IIT Hyderabad for NH_3-TPD, Dr. S.Basu for TGA and Dr. B.R Mehta for HRTEM measurements.

References

[1] James J. Spivey and Graham Hutchings, *Chemical Society Reviews,* 43,792, 2014.
[2] Lunsford Jack H. *Catalysis Today*, 63, 165, 2000.
[3] Ryuichiro Ohnishi, Shetian Liu, Qun Dong, Linsheng Wang, Masaru Ichikawa, *Journal of Catalysis,* 182, 1, 92, 1999.

IV-PP23

Development of Unusual Oxidation State Metal Catalysts for C(sp2)-H Bond Functionalization Electrochemically Induced

Budnikova Y.H.

A.E. Arbuzov Institute of Organic and Physical Chemistry, Kazan ScientificCenter of Russian Academy of Sciences, Kazan, Russia

* yulia@iopc.ru

Keywords: nickel, palladium, electrochemistry, fluoroalkylation, phosphorylation, C-H bond

1 Introduction

Palladium and nickel complexes are extensively employed as efficient catalysts for a wide range of synthetically useful organic transformations such as C–H functionalization, C–C coupling, and oxidation reactions. While the most common oxidation states of palladium and nickel in its organometallic derivatives are 0 and +2, high-valent organopalladium or nickel complexes contain metal atoms in oxidation states +3 and +4. Whereas catalytic processes involving Pd and Ni complexes in oxidation states +2 and 0 have been recognized and studied for several decades, more recent studies have shown that high-valent Pd and Ni species can also act as catalytically active intermediates in various organic transformations. These processes raise the intriguing possibility that new pathways for coupling reactions might be discovered using complexes of higher nuclearity in which redox activity or substrate binding can span multiple metal centers. Electrochemical techniques can be used for the determination of the mechanism of transition metal-catalyzed reactions whatever the transition metal, provided some of the organometallic species involved in the catalytic cycle are electroactive.

Achievements of electrosynthesis mediated by nickel and palladium complexes in unusual oxidation states will be demonstrated. Important advances are associated with the development of synthetic approaches to the C = C, C-Hal, P-Cl, P-P and C-H bonds functionalization in the one-step mild conditions. The key intermediates, such as Ni(I)L, Pd (III)L(immer or monomer complexes) and others have been detected and investigated.

2 Experimental/methodology

Electrosynthesis is useful in transition metal catalysis to generate the active catalyst form without specially added reducing or oxidizing agents. Performed in mild conditions it offers more environmentally non-polluting alternatives to traditional organic synthesis. Understanding mechanistic details of catalyzed reactions may pave the way to the design of new and improved catalysts. Kinetics and thermodynamics of the electron transfer, bond cleavage, substitution, addition and other reactions can provided, as well as intermediate species can be detected characterised by various electrochemical techniques with cyclic voltammetry being the most available and favourable one. However, although electrochemical methods provide a way of mechanistic studying of reactions, they give no information on the structures of intermediates. Electrochemical methods should be used in combination with spectroscopy techniques like NMR, IR, UV–vis–NIR absorption, EPR or EXAFS to provide detailed characterization of the intermediate species.

Our group is interested in the development and mechanistic understanding of transition-metal-mediated electrocatalytic reactions, with a particular focus on fluoroalkylation and phosphorylation reactions. We also wish to gain insight into how to develop more examples of catalytic reactions at inexpensive and readily available first-row late metals such as Ni and Co which are particularly attractive for synthetic purposes, due to sufficiently low ionization

potential to favour oxidative addition, sufficiently weak metal-carbon bonds, tendency to form square-planar complexes and to reach penta-coordination to allow insertion, sufficiently high electron affinity of Ni^{II} complexes to allow reductive elimination and the ability to accept different oxidation states (0, +1, +2, +3, +4) at different stages of a catalytic cycle. Herein, we summarize the advances in electrocatalytic methods which have been shown to be applicable for functionalization of diverse substrates, such as olefins, aryl halides, white phosphorus, chlorophosphines and arenes (ligand directed C-H functionalization), consider the intermediates of catalytic cycles and prospects of this interesting and promising research area.

3 Results and discussion

Electrochemical approaches have opened up new opportunities, such as mild conditions, high rates, selectivity and convenient operation control by these parameters as current density and potential. Thus, the use of transition metal electrocatalysis to obtaine targeted derivatives from olefinic, aromatic, and phosphorus substrates in cross-coupling and ligand-directed C-H activation reactions has shown to be a high potential and powerfull method.

Acknowledgements

This research was supported by the Russian Science Foundation № 14-23-00016.

IV-PP24

Biocatalysis in Glycerol-based Biorefinery for Fine Chemicals - Conversion of Renewable Glycerol into Value-Added Products

Tudorache M.*, Ghemes G., Gheorghe A., Coman S., Parvulescu V.I.

University of Bucharest, Bucharest, Romania

* madalina.sandulescu@g.unibuc.ro

Keywords: glycerol, lipase, ionic liquid, value-added products, biocatalysis, fine chemicals

1 Introduction

Glycerol is a key aspect of the biodiesel manufacture of biomass due to huge amount of glycerol produced during the biodiesel process (*e.g.* 10 kg glycerol for each 100 kg biodiesel product). The lack of proper management for glycerol entails soon to the decrease of the industry interest in biodiesel due to its high production costs. Another possible consequence is that glycerol will become a potential environmental pollutant due to the large glycerol amount stocked in the environment. Thus, the rescue of the biodiesel market requests the implementation of new technologies involving glycerol as renewable raw material, which could be preponderantly dedicated to the biorefinery leading to value added products of fine chemical industry.

We lunched the idea of a chemo-enzymatic conversion (tandem of biocatalysis and ionic liquid catalysis) of glycerol to value-added products such as glycerol carbonate (GlyC), glycidol (GlyD) and polyglycidol (poly-GlyD) (figure 1). GlyC has numerous applications in cosmetics, pharmaceutics, detergents and adhesives industry. Additionally, GlyD and even more poly-GlyD are important precursors for polymeric industry. Therefore, we proposed green-valorisation of renewable glycerol as a promising alternative for fine chemical industry.

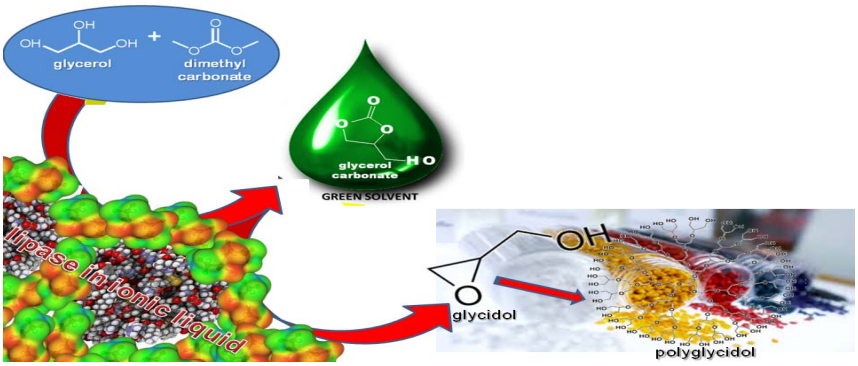

Fig. 1. Chemo-enzymatic catalysis of glycerol conversion into value-added products.

2 Experimental/methodology

Chemicals and substances used for the experiments were purchased from Sigma-Aldrich company (e.g. lipase from various sources, [emim][Cl], [bmim][Cl], [bmim][PF_6], [bmim][BF_4], glycerol, dimethyl carbonate - DMC, standards of GlyC and GlyD, etc).

Biocatalytic synthesis of GlyC/ GlyD has been performed in solvent-free system. Glycerol and DMC (dimethyl carbonate) (Gly:DMC=1:10 molar ratio) were mixed together with the biocatalyst (prepared in a previous step by simple mixing of the enzyme and ionic-liquid) in a 1.5 mL reaction vial (Eppendorf tube). The mixture was incubated for 6h under stirring at 60 ^{0}C. After the reaction, the products were analysed using gas chromatography (GC) coupled to flam ionization (FID) detector. The efficiency of the chemo-enzymatic process was evaluated based on the glycerol conversion and GlyC/GlyD selectivity. Gel permeation chromatographic (GPC)

analysis was performed for the characterization of the poly-GlyD products (average molecular weight and poly-dispersity index).

3 Results and discussion

Chemo-enzymatic process developed for glycerol conversion contains two steps: i) glycerol biotransformation to GlyC and ii) catalytic synthesis of GlyD from GlyC. GlyC synthesis was catalysed by lipase enzyme, while the GlyD production was assisted by ionic liquid catalyst. Spontaneously, GlyD can lead to poly-GlyD under basic conditions.

The biocatalytic process involved glycerol carbonylation with DMC assisted by a lipase biocatalyst [1]. The corresponding system was tested for solvent-free conditions using an excess of DMC. For this stage, the lipase biocatalyst was designed as free/ immobilized enzyme leading to different performance of the biocatalytic system for every model (*e.g.* GlyC yield of 59 and 55 % for free/ immobilized lipase) [2,3].

Further, the biocatalyst was designed as ionic liquid-coated enzyme and dedicated to the GlyD synthesis. Chemo-enzymatic model of the catalyst was prepared for different ionic liquid (e.g. [emim][Cl], [bmim][Cl], [bmim][PF_6], [bmim][BF_4]). Also, a screening of the lipase enzyme has been performed. Catalytic tests under the optimum conditions revealed the possibility to use lipase from *Candida antarctica* source combined with [bmim][BF_4]. The catalytic performance are expressed as 53 % glycerol conversion, 30 % selectivity in GlyD and 50 % selectivity in GlyC. Also, poly-GlyD product was obtained by spontaneous polymerization of GlyD under basic condition leading to a polymeric compound characterized by a molecular weight in the range of 300-500 Da with a dispersity index of n=4 and branched structure.

4 Conclusions

The proposed concept for renewable glycerol valorisation based on chemo-enzymatic process is sustained by promising experimental data, which will be presented and discussed during the presentation.

Acknowledgements

The authors kindly acknowledge to UEFISCDI for the financial support through the project PN-II-PCCA-2013, no. 273/2014.

References

[1] M. Tudorache, L. Protesescu, S. Coman ,V.I. Parvulescu, *Green Chem.,* 14 (2012) 478.
[2] M. Tudorache, A. Nae, S. Coman, V.I. Parvulescu, *RSC Advances*, 3 (2013) 4052.
[3] M. Tudorache, A. Negoi, L. Protesescu, V.I. Parvulescu, *Appl. Catal. B: Env*, 145 (2014) 120.

IV-PP25

Direct Catalytic Oxidation of Lower Alkanes

Chepaikin E.G.*, Bezruchenko A.P., Borshch V.N., Menchikova G.N.

Institute of Structural Macrokinetics and Materials Science Russian Academy of Sciences, Chernogolovka, Russia

* grig@ism.ac.ru

Keywords: homogeneous, catalysis, alkanes, dioxygen, oxidation, carbon, monoxide, DFT, calculation

1 Introduction

The direct functionalization of alkanes with dioxygen to the useful oxygenates remains a key challenge [1]. The homogeneous catalytic systems for the oxidative functionalization of alkanes C_1-C_4 were designed. These systems include complexes of rhodium and redox catalysts – iodine, copper or iron compounds. The most effective medium for the oxidation of alkanes is trifluoroacetic acid. To activate dioxygen, by analogy with the action of the biocatalysts, a reducing agent – carbon monoxide – is introduced in the gas mixture. The redox catalysts in the reduced form are converted dioxygen to the active two-electron oxidizing agents – hydrogen peroxide or its equivalents ((hypoiodic acid or metal peroxides) for the reactions:

$$2Red + O_2 + 2HX \rightarrow 2\,Ox^+ + H_2O_2 + 2X^-; \qquad 2HI + O_2 \rightarrow 2HOI;$$
$$2Cu^{I} + O_2 \rightarrow Cu^{II}\text{–O–O–}Cu^{II}; \quad Cu^{I} + Rh^{III} + O_2 \rightarrow Cu^{II}\text{–O–O–}Rh^{IV}$$

2 Experimental/methodology

The oxidized forms are reduced by carbon monoxide and alkane with catalysis by rhodium complexes. The mechanisms of methane oxidation are proposed [2]. In rhodium-iodide-chloride (Rh-I-Cl) system an active oxidant is hypoiodide, and in the rhodium-copper-chloride (Rh-Cu-Cl) – heterometallic peroxocomplex. DFT calculations to optimize the structure of the intermediates confirm the feasibility of the proposed mechanisms. Based on the experimental data there is assumed that the Rh-I-Cl and Rh-Cu-Cl catalytic systems operate according to the equations 1-4 and 5-9 respectively. The scheme represented by the equations 1-4 show methane oxidative carbonylation to acetic acid:

$$[Rh(CO)_2ClI]^- \textbf{(I)} + OI^- \rightarrow [Rh(CO)_2Cl(OI)]^- \textbf{(II)} + I^- \quad (1)$$
$$\textbf{II} + CH_4 \rightarrow [Rh(CH_3)(CO)_2Cl(OH)I]^- \textbf{(III)} \quad (2)$$
$$\textbf{III} + CO \rightarrow [Rh(CH_3CO)(CO)_2Cl(OH)I]^- \textbf{(IV)} \quad (3)$$
$$\textbf{IV} \rightarrow \textbf{I} + CH_3COOH \quad (4)$$

Methanol formation by the methane oxidation is described according to equations 5-9.

$$RhCl_3(H_2O)_3\,\textbf{(V)} + CO \rightarrow RhCl_3(H_2O)_2(CO)\,\textbf{(VI)} + H_2O \quad (5)$$
$$\textbf{VI} + CuCl \rightarrow RhCl_3(H_2O)_2(CO)CuCl\,\textbf{(VII)} \quad (6)$$
$$\textbf{VII} + O_2 \rightarrow RhCl_3(H_2O)_2(CO)(O_2)CuCl\,\textbf{(VIII)} + H_2O \quad (7)$$
$$\textbf{VIII} + CH_4 \rightarrow RhCl_3(H_2O)_2(CO)(O_2)(CH_4)CuCl\,\textbf{(IX)} \quad (8)$$
$$\textbf{IX} + 2H_2O \rightarrow \textbf{V} + CH_3OH + CO_2 + CuCl \quad (9)$$

The geometry of complexes I-IV and V-IX was optimized by DFT calculations with PBE exchange-correlation potential (program package FireFly [3]). The optimized structures are presented in Fig. 1 and 2.

3 Results and discussion

The calculated heats of reactions 1-4 are (kcal/mol): - 26.4, - 28.5, - 27.4, - 35.9, respectively. For the reactions 5-9 the following values of the heats are calculated (kcal/mol): - 6.8, - 29.4, - 16.4, - 37.6, - 32.4 respectively.

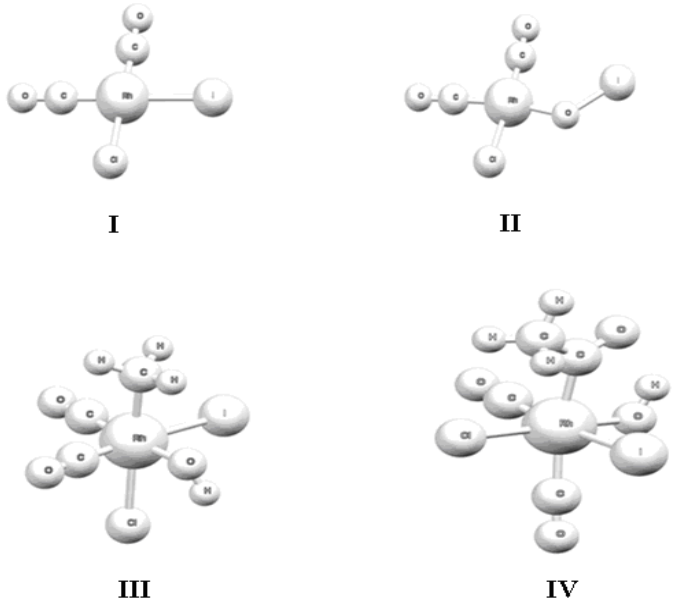

Fig. 1. Optimized structures of complexes **I-IV**

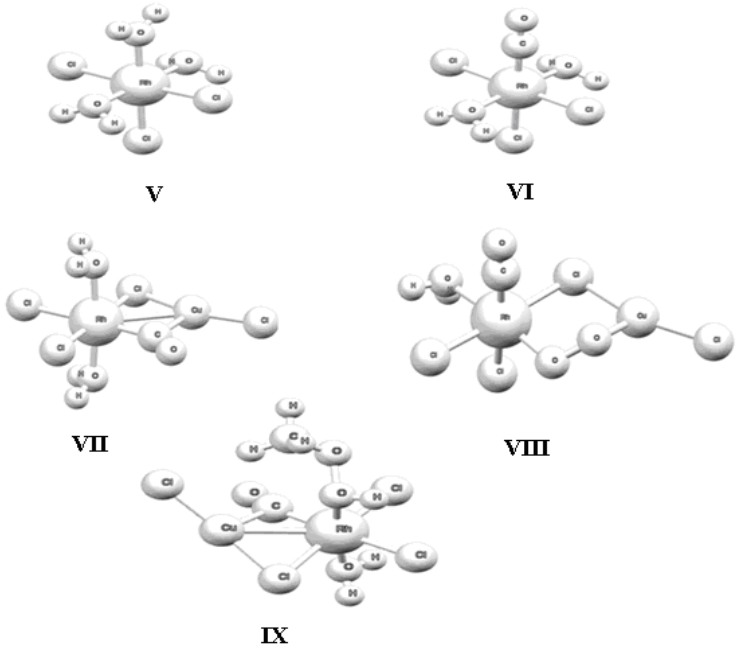

Fig. 2. Optimized structures of complexes **V-IX**

References

[1] N.J. Gunsalus, M.M. Konnick, B.G. Hashiguchi, R.A. Periana, *Isr. J. Chem.* 54 (2014) 1467–1480.

[2] E.G. Chepaikin, *J. Mol. Catal. A. Chem*. 385 (2014) 160–174.

[3] (a) A.A. Granovsky, Fire Fly v. 8, http://classic.chem.msu.su/gran/firefly/index.html (b) M.W. Schmidt, K.K. Baldridge, J.M. Boatz, S.T. Elbert, M.S. Gordon, J.H. Jensen, S. Koseki, N. Matsunaga, K.A. Nguen, S. Su, T.L. Windus, M. Dupuis, J.A. Montgomery, *J. Comput. Chem.* 14 (1993) 1347–1363.

IV-PP26

Preparation of Substituted Methylenebisphenol Using Heterogeneous Acid Catalyst

Arslanova G.G., Saigitbatalova S.Sh.*, Cherezova E.N.

Kazan National Research Technological University, Institute of Polymers, Kazan, Russia

* saygitbatalova@mail.ru

Keywords: acid catalyst, heterogeneous catalyst, methylenebisphenol, stabilizer

1 Introduction

Stabilizers are used for the protection of polymers against aging and the major group of that stabilizers relates to antioxidants. Methylenebisphenols (MBP) having at 2 and 6 position over hydroxyl group alkyl substituents [1] have high antioxidant capacity. Productional MBP preparation method is the reaction of disubstituted phenols and formaldehyde under homogeneous catalysis in the presence of strong acids. This synthesis technology has some significant drawbacks, including: a large amount of waste water and the need to neutralize the catalyst.

In this research to overcome the above drawbacks in the synthesis of the MBP stabilizers used anhydrous formaldehyde precursors which form formaldehyde under acidic catalysis.

2 Experimental/methodology

For MBP preparation based on 2,6-di-tert-butylphenol (2,6-DTBP) and 2,4-di-tert-butylphenol (2,4-DTBP) trioxane and 1,3-dioxolaneare was used as the second reagent. The reaction was conducted in the presence of formic acid. As the co-catalyst was used $HClO_4$. Also a number of heterogeneous catalysts were tested: Purolite Ct 151, Amberlist 35, 36Wet, Rezinex, Levatit a2626, KY-2. To find the optimal synthesis conditions it's conducted with reactant ratios varying: 2,4 DTBP (2,6-DTBP) to trioxane from 2:0.33 to 2:0.43 mol., 2,4 DTBP (2,6- DTBP) to 1,3-dioxolane from 2:1 to 2:3 mol., reaction time from 2 to 6 hours, the temperature from 90 to 105 ° C. After synthesis, the reaction mass was cooled, the precipitate was filtered off. The reaction products were characterized by melting point, ^{1}H NMR -, IR- spectroscopy and elemental analysis.

3 Results and discussion

During the reaction formaldehyde derivatives underwent decyclization under the acidic catalysys and formed protonated formaldehyde which is then joined the electrophilic substitution reaction with the 2,4- DTBP and 2,6- DTBP forming 2,2'-methylene-bis(4,6-di-tert-butylphenol) and 4,4'-methylene-bis(2,6-di-tert-butylphenol) as shown on scheme:

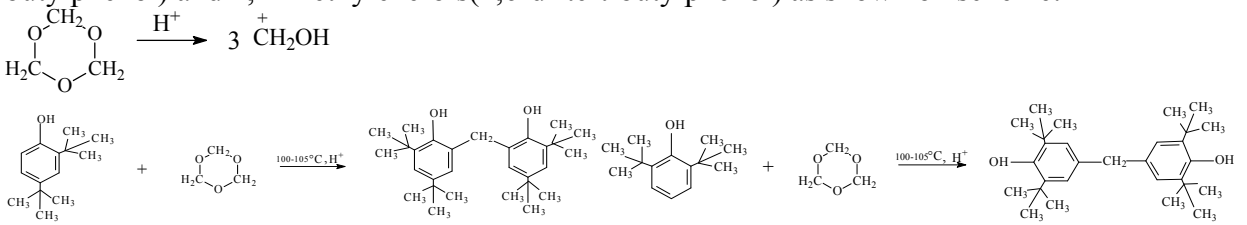

Figure 1, 2 shows the influence of the reactant ratio on the target product yeld in the reaction of 2,6- DTBP and 2,4-DTBP with trioxane in the presence of formic acid and HClO4.

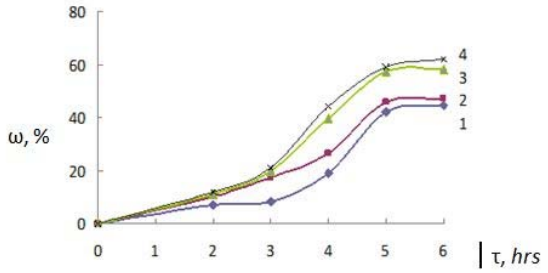

Fig.1. Influence of the reactant ratio on the yeld of 4,4'-methylene-bis(2,6-di-tert-butylphenol): 1 – 2,6- DTBP:$(CH_2O)_3$= 2:0,33; 2 - 2,6-DTBP:$(CH_2O)_3$= 2:0,363; 3 – 2,6-DTBP:$(CH_2O)_3$= 2:0,396;4 - 2,6- DTBP:$(CH_2O)_3$= 2:0,430.

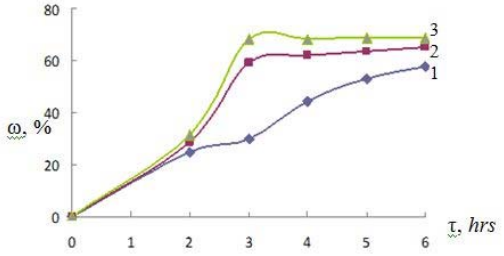

Fig.2. Influence of the reactant ratio on the yeld of 2,2'-methylene-bis(4,6-di-tert-butylphenol): 1 – 2,4- DTBP:$(CH_2O)3$= 2:0,33; - 2,4-DTBP:$(CH_2O)3$= 2:0,363; 3 – 2,4-DTBP:$(CH_2O)3$= 2:0,396.

^{1}H NMR spectrum of 2,2'-methylene-bis(4,6-di-tert-butylphenol) (acetone-d_6, 400 MHz, ppm, *J*/Hz): 1,41 s and 1,23 s (36H, CH_3); 2,08 s (2H, CH_2); 3,98 s (2H, OH); 7,08 d and 7,19 d (4H, Ar-H). Gross formula $C_{29}H_{44}O_2$: calculated C,% - 82,08, H,% - 10,38, O,% - 7,54; found C,% - 82,42, H,% - 10,524, O,% - 7,056.

^{1}H NMR spectrum of 4,4'-methylene-bis(2,6-di-tert-butylphenol) (acetone -d_6, 400 MHz, ppm, *J*/Hz): 1,4 s (36H, CH_3); 3,80 s (2H, CH_2); 5,82 s (2H, OH); 7,06 s (4H, Ar-H). Gross formula $C_{29}H_{44}O_2$: calculated C,% - 82,08, H,% - 10,38, O,% - 7,54; found C,% - 81,96, H,% - 10,439, O,% - 7,601. ^{1}H NMR spectrum data and elemental analysis corresponded to the formation of the target substances.

4 Conclusions

4,4'-methylene-bis (2,6-di-tert-butylphenol) and 2,2'-methylene-bis (4,6-di-tert-butylphenol) were obtained by the reaction of 2,4- and 2,6- disubstituted phenols with trioxane and 1,3-dioxolane. By selecting of the optimum reaction conditions and decyclization catalyst complex 62 wt % yield was achieved for the reaction of 2,6-DTBP with trioxane and for the 2,4-DTBP - 68 wt %, for the reaction with 2,6-DTBP 1,3-dioxolane highest yield was 81 wt %.

References

[1] Cherezova E.N., Balabanova F.B., Shalyminova D.P. et al. *Russian Journal of Applied Chemistry.* 2014. V. 87. N. 1. P. 42-47.

IV-PP27

Kinetics of Glyceric Acid Obtaining

Chornaja S.*, Dubencovs K., Poikane G., Zhizhkuna S., Kampars V.

Riga Technical University, Institute of Applied Chemistry, Riga, Latvia

* Svetlana@ktf.rtu.lv

Keywords: bio-diesel, glycerol, glyceric acid, oxidation catalyst

1 Introduction

In accordance to the directive 2009/28/EC of the European Parliament and of the Council of April 23, 2009 on the promotion of the use of energy from renewable sources in the European Community Member States, a mandatory 10% minimum target is to be achieved by all Member States for the share of biofuels in transport petrol and diesel consumption by 2020 in a cost-effective way [1]. Bio-diesel fuel is the most perspective kind of biofuel. Glycerol is a bio-diesel manufacturing by-product, its amount reaching up to 10% of the total mass of the products mixture, thus making it important to find a solution for the glycerol utilization problem. The glycerol water solution oxidation by oxygen in presence of supported gold catalysts demonstrates great potential in this regard. There is a wide range of valuable products that can be formed in the process of glycerol oxidation, e.g. dihydroxyacetone, hydroxypiruvic acid, glyceric aldehyde, glyceric acid, tartronic acid, ketomalonic acid, lactic acid and so on. Many authors report that reaction's conditions lead to selective formation of one of the glycerol's oxidation products [2-5], but there is a lack of publications where attention is drawn to the mathematical description of the oxidation process. These studies are necessary, as the knowledge of the process's kinetic parameters, like rate constants, rate dependencies on the process parameters, reaction activation energy value, is highly important on the stages of development of the manufacturing process technology, as well as for correct reactor design. Taking the aforementioned into account, this work is devoted to the study of the formation of glyceric acid by oxidizing glycerol with molecular oxygen in presence of commercial 1.5%Au/TiO_2 supported catalyst in the kinetic regime to find the reaction rate constants, kinetic equation parameters and the reaction activation energy value.

2 Experimental/methodology

The glycerol oxidation experiments were performed in an ROTH, Model II autoclave reactor in the kinetic region. High performance liquid chromatography (HPLC) method was used for detection of glycerol and its oxidation products. For that purpose a SHIMADZU Nexera chromatograph with ion-exchange column WATERS IC-PAC Jon-Exclusion 50 A, 7 µm (300×7.8 mm) was used. UVVIS detector SHIMADZU SPD20A with wavelength 210 nm and 40 °C was used for products identification and quantitative detection, ELSD detector ELSDLTII with 30 °C and 350 kPa was used for glycerol concentration detection in the sample. A transmission electron microscope JEOL JEM 2100 at 200 kV voltages was used to find out the size of gold particles and their distribution on the catalyst's surface.

3 Results and discussion

The following process parameters were varied during the experiments: glycerol initial concentration (0.1-0.3 mol/L), oxygen partial pressure (1-10 atm), amount of the catalyst (by varying glycerol to gold molar ratio from 1000 to 10000 mol/mol), base concentration (by varying base to glycerol molar ratio from 0.5 to 5 mol/mol) and temperature (55-70 °C). The glyceric acid was the main reaction product in the studied conditions. Glycolic, tartronic, oxalic, lactic, acetic and formic acids were detected as the reaction by-products. The experiments'

kinetic results were processed by means of MatLab software based on non-linear regression and statistical analysis (residual, R2 and F-tests).

4 Conclusions

The experimentally supported kinetic model of glycerol oxidation to glyceric acid is proposed as the result of the study. Reaction rate constants are calculated and the reaction activation energy value is found to be 145 kJ/moL. A possible glycerol oxidation reaction kinetic mechanism is proposed. The optimal parameters for selective glycerol to glyceric acid oxidation are identified for full glycerol conversion.

References

[1] DIRECTIVE 2009/28/EC OF THE EUROPEAN PARLIAMENT AND OF THE COUNCIL. *Official Journal of the European Union* L140 (2009) 16.
[2] S. Demirel-Gülen, M. Lucas, P. Claus, *Catalysis Today.* 102-103 (2005) 166.
[3] G. J. Hutchings, S. Carretin, P. Landon, J. K. Edwards, D. Enache, D. W. Knight, Y. Xu, A. F. Carley. *Topics in Catalysis*. 38 (2006) 223.
[4] E. G. Rodrigues, M. F. R. Pereira, J. J. M. Órfão. *Applied Catalysis B: Environmental.* 1-6 (2012) 115.
[5] B. N. Zope, S. E. Davis, R. J. Davis. *Topics in Catalysis.* 55 (2012) 24.

IV-PP28

MagneticaNanocomposites: Design, Synthesis and Application in Biochemicals Synthesis

Tirsoaga A., Jurca B., Parvulescu V.I., Coman S.M.*

University of Bucharest, Faculty of Chemistry, Bucharest, Romania

* simona.coman@g.unibuc.ro

Keywords: niobium, magnetic nanoparticles, glucose, lactic, acid succinic acid

1 Introduction

Last decades confirmed catalysis as a strategic field of science representing the new way to meet the challenges of sustainability. In this context, one of the big challenges is the development of cleaner catalytic processes to convert biomass to multiple platform molecules as strategic precursors for valuable products [1]. In most of the cases, to achieve such a goal, the development of new catalysts is necessary. In this context, a special attention is drawn to the solid catalysts, since the separation processes represent more than half of the total investment in equipment for the chemical and fuel industries [2]. However, these catalysts should also be highly selective to guarantee the cost-effectiveness of the process. Such a requirement can be met by nanocatalysts. Unfortunately, isolation and recovery of such tiny nanocatalysts from the reaction mixture is not easy, this limitation hampering the economics and sustainability of nanocatalytic protocols. To overcome this issue, the use of magnetic nanoparticles has emerged as a viable solution; their insoluble and paramagnetic nature enables easy and efficient separation from the reaction mixture with an external magnet [3]. Further, the stability, durability, and costs are other conditions that should be accomplished for their widespread usage in industry. In this context, the main objective of this work was the design and development of Nb-based magnetic nanocomposites suitable for the glucose conversion into biochemicals.

2 Experimental/methodology

Nb-based magnetic nanocomposites were prepared in three steps: i) the synthesis of the magnetite nanoparticles (MNP) by co-precipitation, ii) the coating of MNP with Nb_2O_5 (Nb oxalate precipitation with NaOH, in the presence of CTAB as surfactant), and iii) the surfactant decomposition through the sample calcination at 525°C. As a function of the surfactant loading, the catalysts were denoted sNb@NMP or 3sNb@MNP (denoting a loading three times higher of surfactant). The catalysts were characterized by XRD, TEM, magnetic measurements, FTIR and Raman spectroscopy. Activity tests in batch mode were carried out in a glass-pressure autoclave (Top 45 model, Top Industrie), following two different procedures: i) *glucose decomposition* in water, at 180°C, under stirring, for 4 h; ii) *glucose oxidation* in water, at 180°C and 10 bar O_2, under stirring, for 4 h. Irrespective of the route, after reaction the catalyst was magnetically recovered by placing a permanent magnet on the reactor wall and the water-soluble products were separated by distillation under vacuum. The recovered products from the liquid phase were sylilated, diluted with 1 mL of toluene and analyzed by GC-MS Carlo Erba Instruments QMD 1000 equipped with a Factor Four VF-5HT column.

3 Results and discussion

Tailoring the catalysts in the range of "nano" sizes may eliminate the important disadvantage of mass transfer limitations usually encountered on solid catalysts. Indeed, in the presence of tiny Nb@MNP particles (10 nm from TEM) the conversion of glucose was almost totally (90-100%) after only 4h (Table 1).

Table 1. Catalysts performances in the glucose decomposition and oxidation

Entry	Catalyst	P_{O2}, atm	C (%)	S (%)				
				LA	2-GlyA	1-HPA	2,3-GlyA	SA
1	sNb@MNP	-	100	51.7	45.2	-	-	-
2	sNb@MNP	10	100	30.0	7.7	20.2	-	36.1
3	3sNb@MNP	-	98.2	26.4	14.0	2.5	1.8	-
4	3sNb@MNP	10	100	12.0	12.9	11.2	-	60.0

Reaction conditions: 90 mg glucose, 50 mg catalyst, 10 ml H_2O, 180°C, 4 h. The differences in selectivity till 100% are monosaccharides. LA – lactic acid, 2-GlyA – glycolic acid, 1-HPA – 1-hydroxypropionic acid, 2,3-GlyA – glyceric acid, SA – succinic acid

Most important, in the presence of these catalysts, different platform molecules can be obtained, in different proportions, as a function of the reaction conditions. Thus, in the absence of oxygen, lactic acid is the most important product (51.7%, entry 1, Table 1); under oxygen pressure, the selectivity changed in the favor of succinic acid as the main product (60.0%, entry 4, Table 1). CTAB also exhibited a high influence upon the catalyst characteristics. While sNb@MNP is more selective to lactic acid, 3sNb@MNP displays a high selectivity to succinic acid. Another important parameter of the process is the concentration of glucose. Low working concentrations avoid competitive side reactions such as condensation and dehydration to insoluble humins [4].

As expected, the association of these catalysts with magnetic nanomaterials (MNP) allowed their simple isolation and recovery from the reaction mixture by applying an external magnetic field. Moreover, all catalysts were proven to be stable under the investigated hydrothermal reaction conditions.

4 Conclusions

The obtained catalytic results are very promising for the development of novel magnetic nanocomposites with high activity and selectivity in the synthesis of biochemicals from real biomass sources. It is the first time, in our best knowledge, where, changing the reaction conditions, the same catalyst is highly selective to different important platform molecules (lactic acid *versus* succinic acid. These important characteristics open the possibility to generate a practical process for LA or SA production in which lignin components are not always converted and humins are also formed as solid residues

However, the Nb@MNP system presented here is still under investigation with the objective to further improve its catalytic selectivities and to extend the scope of the reaction to the one-pot cellulose degradation to biochemicals.

Acknowledgements

Authors kindly acknowledge UEFISCDI for the financial support (project PN-II-PT-PCCA-2013-4-1090, Nr. 44/2014).

References

[1] C.-H. Zhou, X. Xia, C.-X. Lin, D.-S. Tong, J. Beltramini, *Chem. Soc. Rev.* 40 (2011) 5588.
[2] R. Rinaldi, F. Schüth, *Energy Environ. Sci.* 2 (2009) 610.
[3] V. Polshettiwar, R. Luque, A. Fihri, H. Zhu, M. Bouhrara, J.-M. Basset, *Chem. Rev.* 111(2011) 3036.
[4] F. de Clippel, M. Dusselier, R. Van Rompaey, P. Vanelderen, J. Dijkmans, E. Makshina, L. Giebeler, S. Oswald, G. V. Baron, J. F. M. Denayer, P. P. Pescarmona, P. A. Jacobs, B. F. Sels, *J. Am. Chem. Soc.* 134 (2012) 10089.

IV-PP29

Levulinic Acid Intercalated into LDH - a Novel Heterogeneous Organocatalyst for the Trans-Cinnamic Ester Epoxidation

Paul D., Candu N., Rizescu C., Marcu I.C., Tudorache M., Parvulescu V.I., Coman S.M.*

University of Bucharest, Faculty of Chemistry, Bucharest, Romania

* simona.coman@g.unibuc.ro

Keywords: epoxidation, organocatalysis, LDH, levulinic, acid, hydrogen, peroxide, phenyl, glycidate

1 Introduction

The epoxidation represents one of the most useful synthetic transformations in organic chemistry [1], since the epoxide ring may be opened in several ways allowing building complicated organic structures. Nevertheless, although several epoxidation methods of alkenes have been developed in the recent past, the epoxidation of cinnamic ester is not so common.
The most common procedure for the epoxidation is using hydrogen peroxide under strong alkaline conditions applying inorganic bases. However, while H_2O_2 is an ideal oxidant because it is both cheap and safe, the use of inorganic bases is undesirable, because they are hazardous and lead to the production of a large amount of wastes. One of the best ways to avoid these disadvantages is changing the stoichiometric process to a catalytic one. In this context, organocatalysis has been suggested as a possible alternative, bringing several advantages upon classical catalysis. However, in spite of the recent improvements, homogeneous organocatalysis has still the main "classical" homogeneous catalysis disadvantage, i.e., the difficulty in recovery and re-use of the organocatalytic species. Therefore, making organocatalysts insoluble and, consequently, easily recoverable and reusable may provide a "sustainable development" in this field.

The layered double hydroxides (LDH) are often preferred in chemical processes to other types of catalysts due to their versatility, simplicity, easy to modify properties and low price. Moreover, such materials represent an important basis for the development of new materials with controlled structure, controlled accessibility to the active sites, adjustable pore size and high surface areas [2]. The ability to retain and change the inorganic with organic anions makes unique these materials.

Taking into account these valuable findings we reported, not long ago, a green asymmetric epoxidation of the *trans*-methylcinnamate to (2R, 3S)-phenyl glycidate, based on the use of an efficient and recyclable organocatalyst: chiral ketone@SBILC@MWCNT@Fe_3O_4 (Y = 35%, S = 100% and e.e. = 100%) [3]. Here we report the development of a novel LA@LDH heterogeneous organocatalyst for the epoxidation of *trans*-methylcinnamate. Although the levulinic acid (LA) not generates enantiomerically pure phenyl glycidate but rather racemic mixtures several advantages like the easy catalyst preparation from cheap and renewable raw materials, the heterogeneous character of the organocatalyst, the use of H_2O_2 and the absence of any inorganic soluble base recommend it as a "green" candidate for such a reaction. All these green elements can successfully compensate any additional costs related to the separation of enantiomers from the obtained racemic mixture.

2 Experimental/methodology

Three types of hydrotalcites (Zn-Al-Cl, Mg-Al-Cl, Mg-Al-CO_3) were prepared and characterized according to procedures described in literature [4]. As intercalation method of the levulinate between the LDH layers was chosen the ionic exchange methodology. The prepared catalysts were characterized by X-ray diffraction (XRD) and infrared diffuse reflectance

spectroscopy with Fourier transform (DRIFT) and tested in the epoxidation of *trans*-methylcinnamate.

3 Results and discussion

Rapid information upon the successful organic anion intercalation between layers of hydrotalcite can be obtained from the X-ray diffraction analysis. Although the literature shows that Mg-Al-LDH is stable in the pH range = 3-10 and has a capacity exchange about 220 meq/100 g, XRD analyzes of LDH-Cl samples show that ionic exchange of levulinate not happened. DRIFT analysis confirms XRD. A possibly explanation for this failure is related to the nature of the chlorine anion, more powerful bonded than carbonate in the LDH structure and, therefore, more difficult to exchange, according to Miyata [5]. Indeed, the ion CO_3^{2-}, more loosely than Cl^-, was easily replaced from the LDH structure by organic carboxylate. Although the X-ray diffraction pattern of LDH-levulinate (LA@LDH) produced no confirmation of the Mg-Al-CO_3 exchange, the DRIFT analysis indicates the presence of the levulinate in LDH. The presence of the band assigned to the carbonyl (-C=O), located at 1750 cm^{-1} represents a firm confirmation. It is therefore possible that the organocatalyst is not entered in-between the hydrotalcite layers remaining anchored only at LDH corners, with the LDH-CO_3 layers unchanged.

Using this catalyst, the cinnamate conversion was from low to moderate (0-12%). However, the selectivities in phenyl glycidate reached very high levels (97.2%).

4 Conclusions

The LA@LDH was found to be useful as a heterogeneous organocatalyst in the epoxidation reaction of *trans*-methylcinnamate. The reaction was performed with hydrogen peroxide as epoxidation reagent and in the absence of an inorganic base (providing wastes) in the reaction medium. The obtained catalytic results display a particular importance for research in the field: in our best knowledge it is the first time when LA was used not as raw material but as organocatalyst for an organic synthesis.

The system presented here is still under investigation for further optimizations.

Acknowledgements

Authors kindly acknowledge UEFISCDI for the financial support (project PN-II-ID-PCE-2011-3-0041, Nr. 321/2011).

References

[1] A. S. Rao, In *Comprehensive Organic Synthesis: Oxidation;* Trost, B. M., Fleming, *I.,* Eds.; Pergamon Press: Oxford, 1991; Ch. 3.1
[2] L. Y. Wang, G.Q. Wu, D.G. Evans, *Mat. Chem. Phys. 104 (2007) 133.*
[3] N. Candu, C. Rizescu, I. Podolean, M. Tudorache, V. I. Parvulescu, S. M. Coman, *Catal. Sci. & Tech.*, DOI: 10.1039/C4CY00891J
[4] O. D. Pavel, R. Zăvoianu, R. Bîrjega, E. Angelescu, *Catal. Commun.* 12 (2011) 845.
[5] S. Miyata*, Clays Clay Miner*. 31 (1983) 50.

IV-PP30

Heteronuclear Coordination Compounds in the Catalysis of Low-Temperature Dissociation of Urethane Groups

Davletbaeva I.M.[1,2*], Zaripov I. I.[1], Davletbaev R.S.[3], Karimullin R.R.[1], Gumerov A.M.[1]

1 - Kazan National Research Technological University, Kazan, Russia
2 - Alexander Butlerov Institute of Chemistry, Kazan (Volga Region) Federal University, Kazan, Russia
3 - Kazan National Research Technical University n.a. A.N. Tupolev, Kazan, Russia

* davletbaeva09@mail.ru

Keywords: polyurethane, dissociation, coordination, compounds, catalysis

1 Introduction

Polyurethanes are the polymers for creating a material with a wide range of operational parameters - high hardness, high elastic modulus, high elasticity, resistance to abrasion, solvents, oils and high strength. It was shown [1] that copper coordination compounds (CCCs), produced using N,N'-diethylhydroxylamine (DEHA) and (γ-aminopropyl)triethoxysilane exhibit catalytic activity in reactions of low-temperature dissociation of urethane groups and are capable of interacting with isocyanate groups with the subsequent formation of azoaromatic derivatives. A specific feature of how these complex compounds are formed is that a larger part of copper(II) is converted to copper(I). Transition metal coordination compounds (TMCCs) based on copper and cobalt is a more effective, compared with CCC, catalyst for the reaction of dissociation of urethane groups, accompanied by the release of TDI (and, accordingly, by an increase in the concentration of NCO groups). For example, a third of urethane groups of the prepolymer undergo dissociation with CCC, whereas in the case of TMCC, nearly all urethane groups may dissociate

2 Experimental/methodology

We prepared coordination compounds from copper (II) chloride ($CuCl_2 \cdot 2H_2O$); cobalt(II) chloride ($CoCl_2 \cdot 6H_2O$); (γ-aminopropyl)triethoxysilane (AGM-9, Aldrich, 98%); and N,N'-diethylhydroxylamine (DEHA, Aldrich, 99%). Copper and cobalt chlorides were freed of crystallization water by their heating at 120°C for 48 h.

The coordination compounds were obtained at the molar ratios $[CuCl_2]:[CoCl_2]:[DEHA]:[AGM] = 1:1:1.48:0.25$ and $[CuCl_2]:[DEHA]:[AGM] = 1:1.48:0.25$. $CuCl_2$ was dissolved in DEHA under cooling to 5–10°C and permanent agitation, and then cobalt(II) chloride and AGM were added at 20–25°C.

To synthesize polyurethanes, a calculated amount of TMCCs was introduced into a polyurethane melt and the reaction system was agitated for 1 h at a residual pressure of 0.7 kPa and T = 80°C. Then, preliminarily melted and heated (to 110°C) 4,4'-methylenebis(2-chloroaniline) MOCA was introduced. After the synthesis was complete, the reaction mass was cast into molds preliminarily heated to 100°C, which were then kept in a heating box at 100°C for 24 h. Before being studied, the polyurethane samples were kept at room temperature for two weeks. The content of isocyanate groups in the reaction system was determined by titrimetry.

3 Results and discussion

Heteronuclear coordination compounds obtained based on copper and cobalt chloride. This compounds shows the ability to catalyze the low temperature dissociation of urethane groups. As the urethane oligomers were used reaction products of ether-diol oligomers with double

molar excess of 2,4-toluene diisocyanate. It was established that the dissociation is accompanied by the formation of urethane groups, carbodiimides, and the release of 2,4-toluene diisocyanate (Fig.).

(1) Dissociation of urethane groups

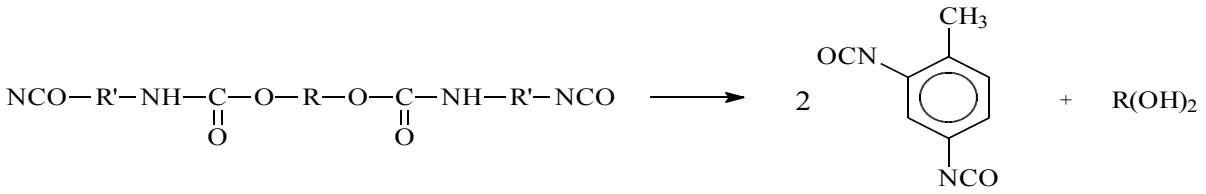

(2) Formation of an azoaromatic compound

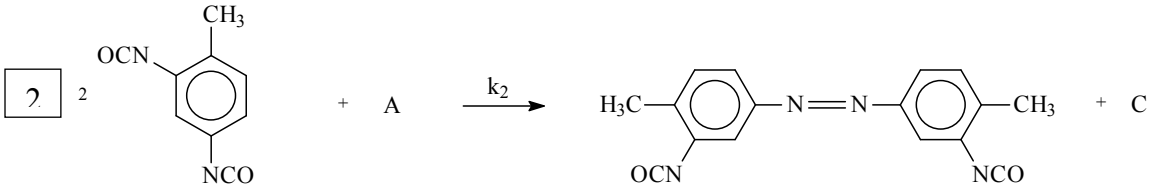

(3) Urethane formation

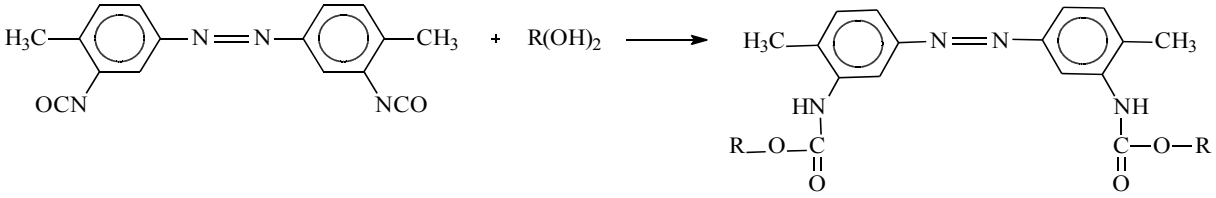

(4) Formations of carbodiimides

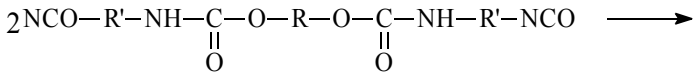

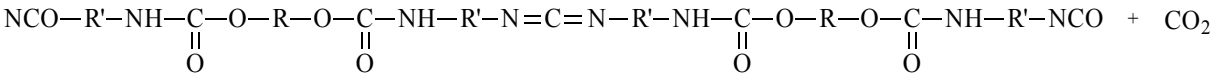

Fig. Scheme of the catalysis of low-temperature dissociation of urethane groups

The isocyanate groups of 2,4-toluene diisocyanate in para-positions and the copper ions enter to the oxidation-reduction reaction. It has been shown that cobalt ions, exhibiting a high coordinating ability in comparison with copper ions, bind formed azoaromatic fragments. Coordinating interaction has a significant impact on the supramolecular organization of polyurethanes, and the complex of physical and mechanical and electrical properties.

4 Conclusions

It was shown that transition metal coordination compounds based on copper and cobalt exhibit catalytic activity in reactions of low-temperature dissociation of urethane groups.

Acknowledgements

The authors gratefully acknowledge the financial support of the Russian foundation for basic research (Grant №15-43-02237)

References

[1] R. Davletbaev, I. Davletbaeva, O. Gumerova, Polyurethane, InTech: Rijeka, Croatia, 2012, pp. 34-52.

IV-PP31

Palladium-Catalysed Synthesis of Markovnikov Vinyl Sulphides with Aliphatic and Aromatic Thiols

Degtyareva E.S.*, Ananikov V.P.

N. D. Zellinsky Institute of Organic Chemistry, Russian Academy of Sciences, Moscow, Russia

* ed@ioc.ac.ru

Keywords: hydrothiolation, alkanethiols, stereoselective, Markovnikov, addition, palladium catalyst

1 Introduction

Formation of the C-S bond is a topic of the great interest because such molecules are used in total synthesis, in material science, and in pharmaceutical industry [1]. The simplest way of sulphides preparetion involves an addition of thiols to unsaturated hydrocarbons. Alkyne hydrothiolathion, which is carried out via radical, nucleophilic or metal catalyzed methods, can lead to the linear anti-Markovnikov products or to the branched Markovnikov vinyl sulphides.

The first example of the selective addition of aromatic thiols was published in 1992 by A. Ogawa [2], where the major product of the reaction between aromatic thiol and alkyne was Markovnikov isomer. Since then usage of number of late transition metal catalysts and f-element catalyst (Ni, Pd, Pt, Rh, Th, U, Zr) was reported as efficient method of branched vinyl sulphides synthesis. In spite of the surge of attention to such transformations main results were achieved with benzyl and aryl thiols, while insertion of the less reactive alkyl thiols is still very limited. Best results in this direction were achieved by J. Love's and T. Marks's groups [3], they mentioned reducing of the efficiency of the developed catalytic systems from primary to secondary thiols, and no products were observed with tertiary thiol [3d].

2 Results and discussion

We have examined a variety of metal complexes on the basis of Au, Cu, Ni, Pd for the catalytic reactivity in the addition reaction with aliphatic thiols and we have found that Pd complexes allow to proceed such kind of transformation with regioselective formation of Markovnikov type vinyl sulphides.

3 Conclusions

The present study is dedicated to the development of the universal catalytic system for Markovnikov-selective hydrothiolation of variety of terminal alkynes by aliphatic, benzylic, and aromatic thiols. The comparison will be made between Cu, Au, Ni, Pd complexes bearing various ligands and substituents. Detailed study of the catalytic system and optimization of the conditions for the synthetic procedure will be presented and discussed.

References

[1] I. Beletskaya, V. Ananikov, Chem. Rev. **2011**, 111, 1596-1636.

[2] H. Kuniyasu, A. Ogawa, K. Sato, I. Ryu, N. Kambe, N. Sonoda, J. Am. Chem. Soc. **1992**, 114, 5902.

[3] (a) A. Sabarre, J. Love Org. Lett. **2008**, 10, 3941-3944. (b) J. Yang, A. Sabarre, L. Fraser, B. Patrick, J. Love, J. Org. Chem. **2009**, 74, 182-187. (c) Ch. Weiss, S. Wobser, T. Marks, J. Am. Chem. Soc. **2009**, 131, 2062-2063. (d) Ch. Weiss, T. Marks, J. Am. Chem. Soc. **2010**, 132, 10533-10546. (e) Ch. Weiss, S. Wobser, T. Marks, Organometallics **2010**, 29, 6308-6320.

IV-PP32

Carbon Nanotube-Supported Pt Nanoparticles as Efficient Catalysts for Base-Free Aerobic Oxidation of 5-Hydroxymethylfurfural to 2,5-Furandicarboxylic Acid

Deng W.P.[1], Zhou C.M.[1,2], Wan X.Y.[1], Zhang Q.H.[1], Yang Y.H.[2], Wang Y.[1*]

1 - State Key Laboratory of Physical Chemistry of Solid Surfaces, Collaborative Innovation Center of Chemistry for Energy Materials, National Engineering Laboratory for Green Chemical Productions of Alcohols, Ethers and Esters, College of Chemistry and Chemical Engineering, Xiamen University, Xiamen, China

2 - School of Chemical and Biomedical Engineering, Nanyang Technological University Singapore, Singapore

* wangye@xmu.edu.cn

Keywords: 5-hydroxymethylfurfural, 2,5-furandicarboxylic acid, platinum, carbon nanotube, oxidation

1 Introduction

The selective oxidation of 5-hydroxymethylfurfural (HMF) into 2,5-furandicarboxylic acid (FDCA), a promising renewable alternative to petroleum-derived terephthalic acid, is one of the most attractive reactions for establishing the biomass-based sustainable chemical processes [1]. Several efficient catalytic systems based on noble metal catalysts (e.g. Au/CeO_2 and Pt/C), have been developed for conversion of HMF to FDCA in aqueous solution. However, these systems required the presence of equivalent strong bases (e.g. NaOH) to obtain high FDCA yields [2,3]. So far, very limited catalysts were reported to be active for the oxidation of HMF in the absence of liquid bases [4,5]. Although hydrotalcite, a solid base, supported Au catalyst exhibited superior performance for FDCA production without addition of a liquid base, the catalyst could not be used recyclably probably due to the reaction between the basic support and the acid products. Herein, we report carbon nanotube (CNT)-supported Pt (Pt/CNT) as a highly efficient and stable catalyst for the oxidation of HMF to FDCA under mild conditions in water in the absence of any bases. The mechanism of the catalytic reaction will also be discussed in detail.

2 Experimental

CNT-supported Pt catalysts were prepared by a microwave-assisted ethylene reduction method. The catalysts were characterized by N_2-physisorption, TEM, XPS and TPD. The catalytic conversion of HMF was carried out in a Teflon-lined stainless-steel autoclave. The liquid products were analyzed by a HPLC.

3 Results and discussion

We examined the catalytic behaviors of Au, Pt, Pd and Ru nanoparticles loaded on CNTs for the oxidation of HMF to FDCA in neutral water under O_2. Among all the catalysts, Pt/CNT exhibited the highest HMF conversion and FDCA selectivity. An FDCA yield of 98% was attained over the Pt/CNT catalyst at 368 K for 14 h. The Ru/CNT and Pd/CNT mainly provided 2, 5-diformylfuran (DFF) and 5-formyl-2-furancarboxylic acid (FFCA) with HMF conversions of 47% and 13%, respectively. The Au/CNT afforded a 23% HMF conversion and a 79% FFCA selectivity. Thus, Pt was a unique active component for the aerobic oxidation of HMF to FDCA without any bases.

We further investigated the catalytic performances of Pt loaded on several supports such as Al_2O_3, hydrotalcite (HT), armberlyst-15 and active carbon (AC). CNT- and HT-supported Pt catalysts showed superior performances. However, the Pt/HT catalyst could not be used

repeatedly due to the leaching of the basic HT support in the acidic solution. Pt/CNT was very stable and was recyclable without significant decreases in catalytic performance.

We found that the functional groups on CNT exerted significant effects on catalytic behaviors of the Pt/CNT catalysts. The Pt/CNT catalyst with a higher concentration of oxygen-containing groups, in particular C=O, showed higher selectivity and higher activity for the oxidation of HMF to FDCA. The influence of modification of a Pt catalyst with different model organic molecules were performed and the results confirmed that the C=O functional groups were benefit for the formation of FDCA (Table 1). We speculate that the carbonyl functional groups on CNT may facilitate the adsorption of HMF and the reaction intermediates.

Table 1. Effect of modification by model organic molecules on performances of Pt/ZrO_2.

Model molecules	HMF conv. (%)	Selectivity (%)			FDCA yield (%)
		DFF	FFCA	FDCA	
None	81	37	53	8.2	6.7
Benzoic acid	75	49	47	3.4	2.6
phenol	84	20	63	17	14
quinone	91	12	49	39	35

Reaction conditions: HMF, 0.5 mmol; HMF/Pt =100 (mol/mol); H_2O, 20 ml

The reaction mechanism for the oxidation of HMF has been investigated over the Pt/CNT catalyst. Our time-course result (Fig. 1) suggests that the first step over our Pt/CNT catalyst is the oxidation of the hydroxyl group in HMF to a carbonyl group (Fig. 1B, route a). Then, the two carbonyl groups were successively oxidized to carboxylic groups. This reaction mechanism is quite different from that proposed in other studies for the oxidation of HMF in the presence of a base, where the formation of carboxylic group is the first step (Fig. 1B, route b).

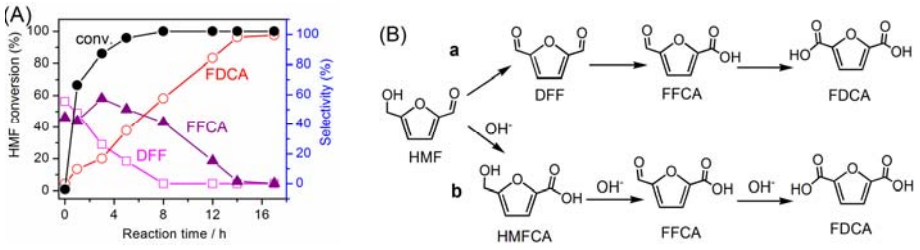

Fig. 1 (A) Time course for aerobic oxidation of HMF over Pt/CNT catalyst. (**B)** Reaction paths proposed for the conversion of HMF to FDCA.

4 Conclusions

Pt/CNT was a highly efficient catalyst for the selective oxidation of HMF to FDCA under O_2 in water without addition of any bases. An FDCA yield of 98% could be attained over this catalyst at 368 K. Pt nanoparticles and the oxygen-containing functional groups on CNTs played key roles in the selective oxidation of HMF. Pt nanoparticles were proposed to activate O_2 and HMF, while the oxygen-containing groups such as C=O enhanced the adsorption of HMF and the intermediates, i.e., DEF and FFCA onto catalyst surfaces. Our kinetic studies suggest that the reaction mechanism over the Pt/CNT is different from that proposed for the catalytic systems with a strong base additive.

References

[1] A. Corma, S. Iborra, A. Velty, *Chem. Rev.*, 107 (2007) 2411.
[2] O. Casanova, S. Iborra, A. Corma, *ChemSusChem*, 2 (2009) 1138.
[3] S. E. Davis, B. N. Zope, R. J. Davis, *Green Chem.*, 14 (2012) 143.
[4] N. K. Gupta, S. Nishimura, A. Takagaki, K. Ebitani, *Green Chem.*, 13 (2011) 824.
[5] X. Wan, C. Zhou, J. Chen, W. Deng, Q. Zhang, Y. Yang, Y. Wang, *ACS Catal.*, 4 (2014) 2175.

IV-PP33

Transformation of Glycerol to Acrolein over Isomorphously Substituted Iron Zeolites

Laforge S.L.S, Mijoin J.M.J, Pouilloux Y.P.Y, Mounguengui D.M. *

Institut des Milieux et Matériaux de Poitiers (IC2MP), UMR CNRS 7285, POITIERS Cedex 9, France

* mounguengui.diallo@univ-poitiers.fr

Keywords: zeolite, glycerol, petrochemical, iron, acrolein, isomorphous substitution

1 Introduction

Research on sustainable energy and transformation are part of alternative current challenges to the use of fossil fuels for a more sustainable future. Glycerol from biomass is becoming more abundant. It is a by-product of the transesterification of biodielsel and can turn into a variety of value-added product like acrolein. Acrolein is an important petrochemical intermediate formed by dehydration of glycerol, it serves among other things to make the acrylic acid for the manufacture of paints, adhesives or plastics [1]. Acrolein can also be produced by oxidation of propene from fossil fuel over bismuth molybdate, the yield of acrolein achieve almost 82% on this catalysts [2]. Zeolites are among the most used acid catalysts for this process with high yields. Nonetheless, the problem of these materials is the rapid deactivation by coke over time on stream. Recent studies have shown that the addition of a metal in the zeolite and the work in oxidative medium may reduce this deactivation [3]. The aim of this study is to compare two iron zeolites (Fe-MFI and Fe-BEA) prepared by post-synthetic isomorphic substitution [4] from mothers commercial zeolites MFI (Zeolyst, CBV15014) and BEA (Clariant, HCZB 150.5) with the same Si / Al ratio of 60 for the dehydration of glycerol to acrolein.

2 Experimental/methodology

The preparation consists in an NH_4F aqueous attack of the zeolite framework which involves the removal of aluminum lattice and the substitution by iron introduced as FeF_3, $3H_2O$ for 3 hours at 75 °C. After, the samples were filtered, washed and dried in the oven à 100°C for 24H. Finally, the zeolites were calcinated at 500°C on air (150 $ml.min^{-1}$) to obtain the protonic form of the iron zeolites. The isomorphous substitution stabilizes iron in the framework of zeolite in order to modulate acidity and create redox site over the materials. Reaction was carried out at 320°C in vertical furnace. The feed was a 10 mol% aqueous solution of glycerol introduced with a syringe pump (0.1$ml.min^{-1}$) at atmospheric pressure in the reactor. 300 mg of catalyst (GHSV= 2770 h^{-1}) were used in N_2 or air (15 $ml.min^{-1}$) as a carried gas. Different characterization techniques (IR, BET, MALDI-TOF, GC-MS) coupled with the method of analysis of "coke" developed at IC2MP [5] allow to shed light on the nature and type of coke formed on each catalyst to explain its influence on the catalytic properties and better understand the role of iron in zeolites.

3 Results and discussion

X-ray diffraction and nitrogen adsorption at 77K show that the physical and textural properties (table 1) of zeolites are conserved after preparation. In the first time, the reaction was carried out over H-BEA on air (15 ml/min) but the catalyst was rapidly deactivated (fig.1). The addition of 0,6wt% of iron (measured by ICP) on zeolite BEA (Fe-BEA(0,6%)) improves the catalytic performances. H-MFI is better than BEA catalysts. Fe-MFI(0,6%) is clearly the best catalyst with acrolein yield reaching 95% at the beginning of the reaction for total glycerol conversion and still 75% after 8h of the reaction (fig.1).

Table 1. Nitrogen adsorption at 77K of fresh catalysts after preparation

Zeolite	Total surface area ($m^2.g^{-1}$)	External surface area ($m^2.g^{-1}$)	Micropore volume ($cm^3.g^{-1}$)	Mesoporous volume area ($cm^3.g^{-1}$)
H-BEA	630	126	0,21	0,51
Fe-BEA (0,6%)	634	123	0,22	0,49
H-MFI	394	70	0,15	0,08
Fe-MFI (0,6%)	381	62	0,15	0,08

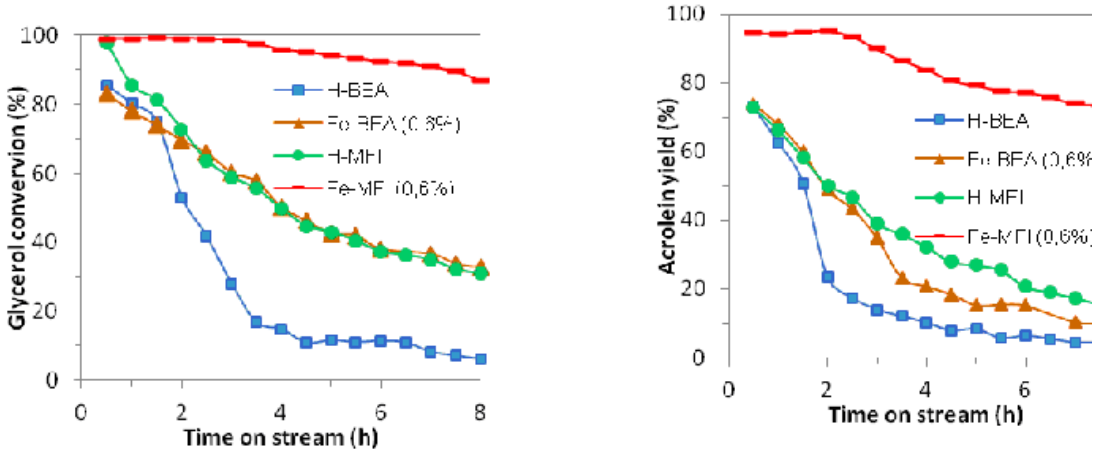

Fig. 1. Glycerol conversion and acrolein yield over MFI and BEA zeolites with and without iron at 320°C with time on stream on air (15 ml/min).

3 Conclusions

The post synthesis isomorphous substitution is easy to implement and allows the insertion of iron in the framework of zeolite with conservation of physical and textural properties. The BEA zeolite deactivates faster than MFI zeolite for the dehydration of glycerol to acrolein. Iron in BEA and MFI zeolites increases the catalytic performances with important reduction of deactivation. Fe-MFI (0,6%) give the best result for dehydration of glycerol to acrolein over zeolite.

References

[1] A. Talebian-kiakalaieh, N. A. S. Amin, H. Hezaveh, *R. and S. Energy Reviews* 40 (2014) 28-59.
[2] M. Massa, A. Andersson, E. Finocchio, G. Busca, F. Lenrick, and L. R. Wallenberg, *J. Catal.,* 297 (2013) 93–109.
[3] H. Atia, U. Armbruster, and A. Martin, *J. Catal.* 258 (2008) 71–82.
[4] S. Han, K. Schmitt, S. Schramm, D. Shihabi and C. Chang, *Inorganica Chim. Acta*, 229 (1995) 81-85.
[5] M. Guisnet and F.R. Ribeiro, Deactivation and Regeneration of Zeolite Catalysts, *Imperial College Press*, (2011).

IV-PP34

Selective Oxidation of Glycerol with H_2O_2 Catalyzed by Fe/SiO_2

Diaz E.*, De Pedro Z.M., Cobos C., Mohedano A.F., Casas J.A., Rodriguez J.J.

Chemical Engineering Section, Universidad Autonoma de Madrid, Madrid, Spain

* elena.diaz@uam.es

Keywords: glycerol selective oxidation, H_2O_2/Fe-SiO_2 system, dihydroxiacetone (DHA)

1 Introduction

In recent years, biodiesel production from transesterification of fatty acids is receiving increasing attention associated with the development of alternative energy sources. Due to glycerol is the main by-product of biodiesel and its demand cannot compensate that production, new efficient procedures for the transformation of glycerol into value-added chemicals are being studied [1]. Glycerol catalytic oxidation is one of the non-commercialized routes so far due to the commercial relevance of most of the possible reaction products [2]. The partial oxidation of glycerol has been intensively investigated using Au, Pd and Pt catalysts at different operating conditions (25-100 ºC; 1-10 atm) and, mainly, O_2 as reagent [3]. Most of the systems produce a mixture of valuable oxygenated compounds such as dihydroxyacetone (DHA), glyceric acid (GCE), glycolic acid (GCO), lactic acid (LAC), formic acid (FOR), being crucial the control of product selectivity [4].

In this work, we reported the selective oxidation of glycerol in aqueous solution to high commercial value products by means of the H_2O_2-Fe/SiO_2 system.

2 Experimental/methodology

Oxidation runs were carried out in stirred batch reactor (700 rpm) at atmospheric pressure and temperatures within the interval 50 – 90 ºC. The starting concentrations of glycerol and H_2O_2 were 50 and 64.6 $g \cdot L^{-1}$, respectively. The initial pH was adjusted to 3.0 with nitric acid. The reaction was performed using a homogeneous catalyst (aqueous solution of $Fe(NO_3)_3 \cdot 9H_2O$, Fe: 10 $mg \cdot L^{-1}$) and a solid catalyst (Fe/SiO_2, 4 $g \cdot L^{-1}$).

The 4.0 wt.% Fe/SiO_2 catalyst was prepared by wetness incipient impregnation using an $Fe(NO_3)_3 \cdot 9H_2O$ aqueous solution as precursor and SiO_2 (Merck) as support. Once impregnated, the catalyst was dried at 60 ºC for 12 h and calcinated at 300 ºC for 4 h. The catalyst was characterized by the following techniques: 77 K N_2 adsorption-desorption isotherms, total reflection X-ray fluorescence spectrometry (TXRF), elemental analysis, thermogravimetric analyses in air atmosphere (TGA), and X-ray diffraction (XRD).

The progress of the reaction was followed by periodically withdrawing, separation of the catalyst by filtration and analyzing liquid samples. Glycerol and the organic by-products were quantified by U-HPLC (Thermo Scientific) equipped with RI and UV-vis detectors and by ionic chromatography (Metrohm 790 Personal IC). A TOC Analyzer (Shimadzu TOC-VCSH) was used to measure the total organic carbon. Residual H_2O_2 concentration and iron leached were determined by colorimetric titration using a UV/vis spectrophotometer (Cary 60, Agilent). The formation of Ti(IV)-H_2O_2 complex was quantified at 410 nm while the iron concentration was measured by means of o-phenantroline method at 510 nm.

3 Results and discussion

The Fe/SiO_2 catalyst exhibited a surface area of 420 $m^2 \cdot g^{-1}$ with a mesopore volume of

0.73 $cm^3 \cdot g^{-1}$ and a mean pore size of 4.8 nm. Composition analyses via TXRF showed an iron loading of 4.4 wt.%.

The glycerol oxidation by means Fenton process resulted in a high transformation of glycerol and H_2O_2 towards a mixture of oxygenated compounds such as GCE, GCO, FOR, glyoxylic acid (GCX) and hydroxypyruvic acid (HYP) at different concentrations depending on the operating conditions. In order to improve the reaction selectivity a Fe/SiO_2 catalyst was employed. Table 1 shows the effect of the temperature (50-90 ºC) on conversion and products distribution upon oxidation of glycerol solutions by means of the H_2O_2-Fe/SiO_2 system. Increasing temperature led to a higher glycerol and hydrogen peroxide conversion, but it was also accompanied by an increase of the mineralization. Interesting yield to DHA, glyceraldehyde (GDA) and FOR were obtained at 50 ºC, while an increase of the reaction temperature was associated with a high selectivity to FOR production. The catalyst remained stable along reaction time, leaching iron only when total H_2O_2 consumption is achieved.

Table 1. Conversion, molar products distribution and CO_2/TOC_0 molar ratio obtained in the glycerol oxidation at 4 h.

System	T (ºC)	X_{H2O2} (%)	$X_{glycerol}$ (%)	Product distribution (%)					$CO_2/\mathbf{TOC}_0$ (%)
				DHA	GAD	LAC	GCO	FOR	
Fenton	70	100	99.2	-	-	-	8	90	9
Fe/SiO_2	50	23	25	38	36	-	-	26	< 2
Fe/SiO_2	70	50	72	17	5	1	1	76	12
Fe/SiO_2	90	100	97	10	-	-	1	89	21

Assuming an apparent pseudo-first kinetic order reaction rate for glycerol oxidation a fairly good fit was obtained. An apparent activation energy of 80 kJ/mol for glycerol transformation was determined.

4 Conclusions

The H_2O_2-Fe/SiO_2 system is an attractive alternative to oxidize glycerol towards value-added compounds. The reaction effluent consists of high value commercial products in variable concentrations depending on the operating conditions. Future efforts will be focused on the selective formation of DHA, a product with the highest commercial value due to its demand in the cosmetics industry.

Acknowledgements

Wish to thank the Spanish MICINN and Comunidad de Madrid for their financial support for the projects CTQ 2013-41963-R and S2013/MAE-2716, respectively.

References

[1] M. Ayoub, A.Z. Abdullah, *Renew. Sust. Energ. Rev.* 16 (2012) 2671.
[2] C. Crotti, E. Farnetti, *J. Mol. Catal. A: Chem.* 396 (2015) 353.
[3] S. Hirasawa, Y. Nakagawa, K. Tomishige, *Catal. Sci. Technol.* 2 (2012) 1150.
[4] P. Lankshman, P.P. Upare, N.T. Le et al., *Appl. Catal. A.*, 468 (2013) 260.

IV-PP35

Stages of Hydrogen Oxidation Reaction on Silver

Dokuchits E.V.[1,2*], Khasin A.V.[2], Khassin A.A.[1,2]

1 - Novosibirsk State University, Novosibirsk, Russian Federation
2 - Boreskov Institute of Catalysis, Siberian Branch of the Russian Academy of Sciences, Novosibirsk, Russian Federation

* oschtan@catalysis.ru

Keywords: hydroxyl, groups, oxidation of hydrogen

1 Introduction

The oxidation of hydrogen on silver is of interest for the theory of chemical kinetics and catalysis and can be used as a model redox catalytic reaction. This reaction makes it possible to elucidate quite clearly the nature of surface intermediates, which may assist to understand the mechanism of many important catalytic hydrogenation and oxidation reactions. The titled reaction is also of general theoretical interest for solving the problems related to reactivity of the silver surface and oxygen adsorbed on this surface. This reaction is also of practical importance for power engineering, in particular, for the development of fuel cells.

2 Experimental

The study was carried out with polycrystalline silver that was obtained via the reduction of silver oxide by hydrogen. Silver oxide was obtained by precipitation from an aqueous solution of silver nitrate with potassium hydroxide. After the precipitation, silver oxide was carefully washed with distilled water and dried. The study was performed using the volumetric static method in a glass vacuum setup equipped with McLeod gauges for pressure measurements. Hydrogen was purified by diffusion through a heated palladium capillary. Oxygen was produced by vacuum decomposition of potassium permanganate (chemical purity). The setup comprised several vessels, which made it possible to prepare the hydrogen-oxygen mixtures with specified pressure and composition. A 'stationary adsorbed layer' was obtained by consecutive transformations of three portions of a stoichiometric hydrogen-oxygen mixture, a conversion of the mixture in each portion being close to 30%.

3 Results and discussion

The earlier proposed mechanism of hydrogen oxidation over silver was considered:

$$O_2 + 2\square = 2O_{(ads)}; \quad \text{(I)}$$

$$H_2 + 2O_{(ads)} = 2OH_{(ads)}; \quad \text{(II)}$$

$$H_2 + 2OH_{(ads)} = 2H_2O. \quad \text{(III)}$$

Experiments on durable adsorption of oxygen at clean surface of silver at 298 K at initial pressure of oxygen 24.9 Pa have revealed the existence of two stages of oxygen sorption: the fast one and the slow one. Surface adsorbed oxygen forms at the first fast stage. The rate of the second stage obeys the law $\frac{N^2_{O_{(ads)}}}{t} = \text{const}$. Therefore the second stage is the diffusion of oxygen atoms into the metallic silver bulk.

The titration of adsorbed oxygen by hydrogen at 298 K and initial hydrogen pressure of 24.8 Pa showed that the only oxygen species interacting with hydrogen are those adsorbed at the surface. The quantity of surface oxygen in the experiments was 2.10×10^{-6} mol/m^2, which is close to approx. 56 % of hydrogen consumed (3.78×10^{-6} mol/m^2). The interaction of hydrogen with surface oxygen occurs in two stages: the fast one and the slow one till the reaction ends.

The quantity of hydrogen sorbed at the first (fast) stage is equal to the amount of surface adsorbed oxygen. This unambiguously indicates that hydroxyl groups form at this stage (see eq. II). At the second (slow) stage, hydrogen interacts with the surface hydroxyl groups giving water (eq. III). Reaction rate constant for the process of hydrogenation of the adsorbed hydroxyl group layer is equal to 3.15×10^{-5} $s^{-1}Pa^{-1}$ when related to the hydrogen pressure. Representing the experimental data on the slow interaction of hydrogen with the adsorbed oxygen layer in coordinates of equation:

$$\ln\left(\frac{1}{1-x}\right) = kt, \qquad (1)$$

gives the reaction rate constant k equal to 3.26×10^{-5} $s^{-1}Pa^{-1}$, which coincides to the reaction rate constant of adsorbed hydroxyl layer hydrogenation.

Therefore this is surface adsorbed oxygen species which interact with hydrogen. Oxygen which has diffused into the silver bulk (subsurface oxygen) doesn't participate in the reaction. Interaction with hydrogen occurs into two stages: fast and slow, the latter is of the first order with respect to hydroxyl groups.

Consecutive oxidation of three portions of the stoichiometric mixture $2H_2+O_2$ with total pressure of 22.8 Pa was performed over two samples: the sample, which was protractedly exposed to oxygen, and the pure silver surface. Each portion contacted the sample until the conversion extent of the mixture achieved 30 %. It was observed that the initial rates of quasi-steady state oxidation of the tree portions didn't differ for the two samples under the study. In other words, subsurface oxygen doesn't affect the rate of hydrogen oxidation.

Synthesis of water (stage III) is the central stage of the catalytic reaction. Stage (II) is fast related to the stage (III). Then the adsorbed layer at silver surface consists of hydroxyl groups and the rate hydrogen interaction with this surface is the rate of stage (III).

The reaction of hydrogen with the adsorbed layer was studied at initial hydrogen pressure of 15.7 Pa and 298 K. The adsorbed layer was prepared by subsequent conversion of 3 portions of $2H_2+O_2$ mixture. The initial rate of the interaction of hydrogen with the «stationary adsorbed layer» is 6.00×10^{-10} $mol\cdot m^{-2}s^{-1}$, while the steady state rate of the hydrogen oxidation for the stoichiometric mixture is 1.18×10^{-9} $mol\ m^{-2}\ s^{-1}$. This means that hydrogen is consumed at two stages of the process: stage II and stage III. The interaction of hydrogen with the stationary adsorbed layer is described by equation (1), i.e. the reaction rate obeys the first order kinetic law with respect to surface hydroxyl groups. The stage III can be expressed as two consecutive processes:

$$H_2 + OH_{(ads)} = H_2O + H_{(ads)}. \qquad (IV)$$

$$H_{(ads)} + OH_{(ads)} = H_2O + 2\square. \qquad (V)$$

Stage V is fast, stage IV is the elementary rate-determining stage (RDS) of the entire process of hydrogen oxidation over silver. The rate constant of stage IV is 4.87×10^{-5} s^{-1} Pa^{-1} at 298 K and hydrogen pressure of 15.6 Pa.

4 Conclusions

The proposed mechanism (I-II-IV-V) of the catalytic reaction of hydrogen oxidation over silver has one common principle feature with the mechanism of branching chain reaction of hydrogen burning: hydroxyl groups are the only species which give water by direct interaction with hydrogen molecules.

Acknowledgments

The research was performed in the frame of the project 2014/139/2211 of the Ministry of Education and Science of Russian Federation.

IV-PP36

Catalytic Carbonylation of Olefins, Alcohols and Benzyl Halides in Ionic Liquids

Eliseev O.L.*, Bondarenko T.N., Lapidus A.L., Agafonov Yu.A.

N.D. Zelinsky Institute of Organic Chemistry, Moscow, Russia

* oleg@server.ioc.ac.ru

Keywords: ionic liquids, carbon, monoxide, catalysis, palladium, carbonylation, carboxylic acids

1 Introduction

Transition metal-catalyzed carbonylation of unsaturated hydrocarbons, alcohols and halides is a direct one-step route to carboxylic acids and esters. In presented work we systematically studied application of some ionic liquids such as molten tetrabutylammonium and 1-butyl-3-methylimidazolium derivatives as a media for these reactions.

2 Experimental

This approach provides a number of unusual possibilities. The most striking result is higher activity of phosphine-free palladium catalyst than that of “traditional” Pd-phosphine complexes. Bromide-containing ionic liquids stabilize palladium in the form of nano-sized suspension, as demonstrated by TEM. For unsymmetrical olefinic substrates, regioselectivity depends on anion nature in ionic liquid. In particular, chloride improves selectivity to 2-phenylpropanoic acid in carbonylation of styrene. Due to high solubility of catalyst in molten salt, it can be used repeatedly by simple extraction of products from reaction mixture with diethyl ether. In dodecene-1 carbonylation, ten cycles were carried out without loss of activity and selectivity. Importantly, reloading procedure may be performed in air atmosphere.

3 Results and discussion

Reaction scheme for the carbonylation of 1-phenylethanol into phenylpropanoic acids is proposed. Hydroxycarbonylation of benzyl halides in ionic liquids proceeds fast in the absence of base. Therefore, formation of stoichiometric amount of halide salt may be avoided.

IV-PP37

Rhodium-Catalyzed Reductive Carbonylation of Iodobenzene

Eliseev O.L.*, Bondarenko T.N., Myshenkova T.N., Lapidus A.L., Agafonov Yu.A.

N.D. Zelinsky Institute of Organic Chemistry, Moscow, Russia

* oleg@server.ioc.ac.ru

Keywords: iodobenzene, benzaldehyde, reductive carbonylation, rhodium, synthesis gas

1 Introduction

Aromatic aldehydes are useful products because of diverse reactivity of formyl group. Usually they are synthesized by Gattermann–Koch, Reimer–Tiemann, Vielsmeier–Haag, and Duff reactions. However, these methods suffers from drawbacks like low yield, poor selectivity and generating waste and side products [1,2]. Alternatively, catalytic formylation (reductive carbonylation) of aryl halides with synthesis gas in the presence of palladium phosphine complexes was firhst reported in 1974 by Schoenberg and Heck [3] and lately by Beller [4-6] and Nagarkar [7] groups.

Somewhat surprisingly, up to now rhodium was unexplored as a catalyst for reductive carbonylation of aryl halides. This encouraged us to test rhodium salts and complexes in reductive carbonylation of iodobenzene as a model substrate.

2 Experimental

Catalytic runs were carried out in a pressurized 50 mL glass-lined steel reactor equipped with a magnetic stirrer and arrangements for automatic temperature control. The reactor was charged with reagents and catalyst, flushed with CO/H_2 (1/1) and filled with synthesis gas up to desired pressure. Then the stirrer was switched on and the reactor was heated to desired temperature. After reaction complete the reactor was cooled to ambient temperature and depressurized, the reaction mixture was extracted with ether and analyzed by GC with nonane as an internal standard. Product composition was confirmed by ^1H NMR analyses.

3 Results and discussion

Reductive carbonylation of iodobenzene gives benzaldehyde (Fig. 1)

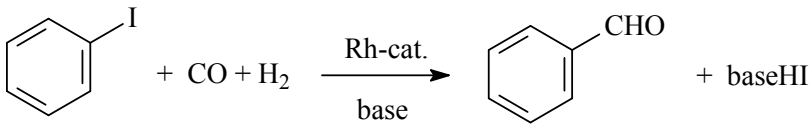

Fig. 1. Reductive carbonylation of iodobenzene

Rhodium phosphine complexes such as $HRh(CO)(PPh_3)_3$ and $RhCl(CO)(PPh_3)_2$ were found to be excellent catalysts They surpass $PdCl_2(PPh_3)_2$ in respect to activity and selectivity to benzaldehyde (Tab. 1). Aromatic solvents such as toluene and o-xylene seems to be the most suitable medium. Other solvents such as heptane, 1,4-dioxane, MEK, DMF and acetonitrile gave poor yield of benzaldehyde. In methanol solution, methyl benzoate was the main product.

Reaction is highly sensitive to the nature of the base. Replacing NEt_3 with NBu_3 resulted in almost threefold reduction in benzaldehyde yield. Somewhat higher but still low yield was achieved with Hünig's base. Inorganic bases such as potassium and cesium carbonates gave poor iodobenzene conversion and benzaldehyde yield.

Table 1. Effect of catalyst on reductive carbonylation of iodobenzene. Reaction conditions: 4.5 mmol PhI, 22 μmol catalyst, 1.5 equiv. NEt_3, 5 mL toluene. *P* 1 MPa (CO/H_2 1/1), 4 h.

Catalyst	T, °C	Conversion,%	Yield (%)		
			PhCHO	benzene	biphenyl
$PdCl_2(PPh_3)_2$	100	67.0	48	0.1	3.5
$RhCl_34H_2O$	100	18.0	2.3	10.6	2.4
$HRh(CO)(PPh_3)_3$	100	65.9	58.7	7.0	–
$RhCl(CO)(PPh_3)_2$	100	67.0	56.9	7.0	–
$RhCl(CO)(PPh_3)_2$	90	43.9	37.2	0.1	–
$RhCl(CO)(PPh_3)_2$	110	100	85.4	11.9	–
$RhCl(CO)(PPh_3)_2$	120	100	85.3	11.8	2.8

Synthesis gas pressure effects on the reaction indexes. Iodobenzene conversion reaches 100% at a total pressure of about 1–1.5 MPa and slightly decreases at higher pressure. Both selectivity and yield of benzaldehyde increase with pressure increasing while selectivity to benzene decreased. Biphenyl is a main product at atmospheric pressure but it fully disappears at a pressure 1 MPa and higher.

4 Conclusions

In conclusion, rhodium (I) triphenylphosphine complexes are good catalysts for reductive carbonylation of iodobenzene. The best catalyst formulation found: 0.5% $RhCl(CO)(PPh_3)_2$, 150% NEt_3, toluene. At 110°C and 1.5 MPa (CO/H_2 = 1/1) iodobenzene is totally converted within 2 hours giving benzaldehyde with the yield of 88%.

References

[1] F. Aldabbagh, *Compr. Org. Funct. Group Transform. II*, 3 (2005) 99.
[2] L.P. Crawford, S. K. Richardson, *Gen. Synth. Methods.* 16 (1994) 37.
[3] A. Schoenberg, R. F. Heck, *J. Am. Chem. Soc.* 96 (1974) 7761.
[4] S. Klaus, H. Neumann, A. Zapf, D. Sturbing, S. Hubner, J. Almena, T. Riermeier, P. Groß, M. Sarich, W.-R. Krahnert, K. Rossen, M. Beller, *Angew. Chem. Int. Ed.* 45 (2006) 154.
[5] A. Brennfuhrer, H. Neumann, St. Klaus, T. Riermeier, J. Almenab, M. Beller, *Tetrahedron.* 63 (2007) 6252.
[6] H. Neumann, R. Kadyrov, Xiao-Feng Wu, M. Beller, *Chem. Asian J.* 7 (2012) 2213.
[7] A. S. Singh, B. M. Bhanage, J. M. Nagarkar, *Tetrahedron Letters.* 52 (2011) 2383.

IV-PP38

Chemical and Structural Transformation of Ni(111) upon Propene Decomposition and Gold Intercalation: Monocrystalline Quasi Free-Standing Graphene Synthesis

Kovalenko S.L., Pavlova T.V., Andryushechkin B.V., Eltsov K.N.*

A.M. Prokhorov General Physics Institute RAS, Department of Technologies and Measurements on Atomic Scale, Moscow, Russia

* eltsov@kapella.gpi.ru

Keywords: monocrystalline graphene synthesis, STM, DFT, gold intercalation surface, atomic structures surface, segregation

1 Introduction

In the wake of impressive experiments performed at 'the Manchester group' on a single atomic sheet of graphite transferred on silicon oxide by means of 'Scotch Tape technology' [1,2], the academic community has struggled to create an intelligent technique for graphene layers production on a solid state surface. This issue has not been appropriately addressed so far. Both methods viewed as most promising - high-temperature annealing of hexagonal silicon carbide and cracking of hydrocarbons on surfaces of some metals (Ni, Ru, Re, etc.) – require gold intercalation under graphene to create a quasi free-standing graphene layer (the Dirac point being at the Fermi level) [3,4]. Also, the graphene electronic structure (the Dirac cone energy position, the formation of an energy band gap, etc.) varies depending on the intercalated metal (Ag, Cu, Si, Cs, etc.). The conditions under which metal intercalation under graphene is possible have been found empirically, while the intercalate atomic structure and the process explaining how alien atoms settle under a graphene layer have remained unknown.

This paper presents the results of a study of synthesis of graphene during propene adsorption at 300°C/ annealing at 500°C cycle with following gold intercalation process under the graphene monolayer on Ni(111).

2 Experimental and calculation details

The experimental study was performed in ultra-high vacuum using low-energy electron diffraction, Auger electron spectroscopy, and scanning tunneling microscopy (STM). The graphene on a Ni(111) surface was formed by a sequence of "propene adsorption at 300°C/annealing at 500°C" cycles, in which gold was first deposited on a graphene layer at 300°C, and then the entire Au/Gr/Ni(111) system was annealed at 450 °C.

The first-principles calculations were performed by using the Vienna ab-initio simulation package (VASP) based on the density functional theory. Parameters of calculations: - GGA PBE exchange-correlation functional has been used as the basis for the DFT-D2 (Grimme) correction; - PAW pseudopotentials; 5-layers Ni(111) slab with 18 A vacuum region. For calculations with molecule C_3H_6 we use LDA functional and 4-layers slab.

3 Results and discussion

Figure 1a shows energy diagram of propene molecule dehydrogenation (on terraces) and dissociation (on steps) at RT (25 °C) adsorption and following carbon atoms transformation into nickel carbide and graphene at 500 °C on Ni(111). The all energy levels and potential barriers have been calculated within DFT and with Nudged Elastic Band (NEB) approach. In Fig.1b, the

resulting graphene monolayer on Ni(111))-9.5×9.5-Au is presented. ARPES measurements show perfect Dirac cone in electron dispersion corresponding to quasi free-standing graphene.

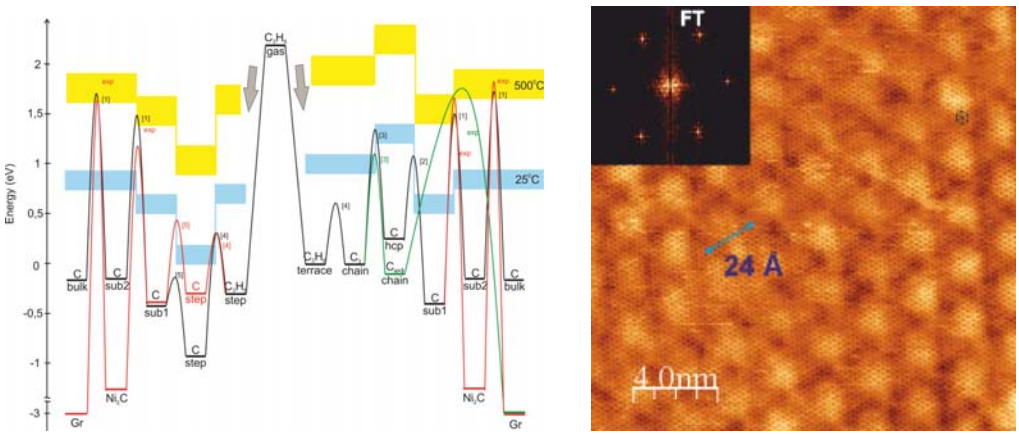

a) b)

Fig. 1 a) Energy diagram of C_3H_6 transformation and carbon structures formation on Ni(111) during propene adsorption at 300°C/annealing at 500°C cycle; b) STM image of Gr/Au/Ni(111) after gold intercalation: dislocation loop superstructure Ni(111))-9.5×9.5-Au and graphene atomic structure are clearly seen. Fourier transform image is presented as insert

4 Conclusions

1. New precise temperature programmed method for graphene synthesis on Ni(111) has been proposed and tested. As a result, monocrystalline graphene monolayer of size 6×6 mm has been grown on Ni(111).
2. Mechanism of Gr synthesis includes the following steps:

- hydrocarbon molecules dehydrogenation on terraces and complete dissociation on step edges
- carbon atomic chains formation on terraces
- carbon atoms diffusion under surface through step edges and their accumulation between nickel atomic layers in subsurface area
- at annealing, carbon atom segregation on surface with Ni_2C formation and then transformation into graphene

3. As a result of gold intercalation at 450 °C, graphene monolayer on Ni(111) is detached from nickel without any damage. Network of dislocation loops Ni(111)-9.5×9.5-Au is real indication of gold intercalation under graphene monolayer.

Acknowledgements

This work was supported in part by RFBR grant 15-02-09106-a, by RAS Presidium Program "Nanostructures: Physics, Chemistry, Biology, Basis for Nanothechnology". We are grateful to the Joint Supercomputer Center of RAS and to the Supercomputing Center of Lomonosov Moscow State University for the possibility of using their computational resources for our calculations.

References

[1] K.S. Novoselov, A.K. Geim, S.V. Morozov, et al. *Science* 306 (2004) 666.
[2] K.S. Novoselov, E. McCann, S.V. Morosov, et al. *Nat. Phys.* 2 (2006) 177.
[3] M. N. Nair, M. Cranney, F. Vonau, et al. *PHYS. REV. B* **85** (2012) 245421.
[4] A. M. Shikin, A. G. Rybkin, D. Marchenko, et al. *New Journal of Physics* 15 (2013) 013016.
[5] J. Jacobsen, L. P. Nielsen, F. Besenbacher, et al. *Phys. Rev. Lett.* **75** (1995) 489.

IV-PP39

Photooxidation of Aniline and Itsderivatives in the Presence of Heterogenized Substituted Zinc Phthalocyanines

Fedorova T.M.*, Derkacheva V.M., Luk'yanets E.A., Kaliya O.L.

Organic Intermediates and Dyes Institute, Moscow, Russia

* fedorova-tm@yandex.ru

Keywords: aromatic amines, photooxidation, phthalocyanines, heterogeneous, sensitizers

1 Introduction

Non-transition metals phthalocyanines (PcM, M = Zn, Al and others) have proved to be effective photosensitizers. Under visible light irradiation they react in triplet state with dioxygen, generating singlet oxygen ($^1O_2$) with high quantum yields. Because of such properties phthalocyanines are used in synthesis, ecology [1] and medicine (PDT) [2]. Photooxidation can be carried out both in PcM solution and with PcM supported on various carriers. The last version is more preferable due to obvious advantages of heterogeneous sensitizers (HS), such as ease of their separation from the reaction medium and possibility of a reuse.

Sulfo and carboxy substituted PcZn and PcAl immobilized on anionic exchanger Amberlite IRA 400 have been examined as HS for oxidative phenols destruction [3]. We have prepared HS by equilibrium adsorption from solutions of R_4PcZn and R_4PcAl (R=3-PhSO_2-5-*t*-Bu, 3-PhSO_2, 3-PhS, 4-*t*-Bu and others) on various carries (NH_2-SiO_2, Al_2O_3, SiO_2, Amberlite 200, Amberlite XAD7HP and others). Some of them showed high activity and selectivity in aromatic amines and phenols photooxidation [4, 5].

The purpose of the work is research of various factors influence on efficiency of selective aniline and its methyl derivatives photooxidation, sensitized by HS on the basis of the substituted PcZn, with formation of *p*-hydroxylation products.

2 Experimental/methodology

Photooxidation of aromatic amines in the water-organic mixtures (H_2O-CH_3CN, H_2O-CH_3OH) was carried out in the glass reactor (ø 35 mm) at continuous stirring and saturation with oxygen. The light-emitting diodes (λ = 664 nm) 0.2 W everyone were used as a light source. The reaction was monitored by seeding of sample aliquots at the certain intervals. Conversion of substrate and yield of product were measured by HPLC on HP 1100 Agilent series, equipped with Zorbax EclipseXDB-C8 column (4.6x150 mm, 5μm) and UV-detector (at 250 nm), the mobile phase consisted of a mixture H_2O-CH_3CN (40:60), a flow rate was 1 ml/min, internal standart – naphthalene.

Two methods were used for immobilization of R_4PcZn (R = 3-PhSO_2-5-*t*-Bu, 3-PhSO_2, 3-PhS and 4-*t*-Bu) on carriers, namely, method of equilibrium adsorption on the amino-modified silica gel (NH_2-SiO_2) or Amberlite XAD 7HP (Amb.), and also by covalent attaching of R_4PcZn sulfochlorides to NH_2-groups of carrier.

3 Results and discussion

The nature of a substituent in aniline molecule has considerable impact on its photooxidation rate. It was shown that toluidines are oxidized faster than aniline whereas introduction of Cl atom in aniline molecule slows down this reaction. Such influence of substituent properties is corresponded with the electrophilic nature of oxidizer – singlet oxygen ($^1O_2$). Its participation in aniline photooxidation is confirmed with use of standard tests: by acceleration of the process in D_2O in comparison with H_2O and delay at addition of NaN_3.

Photooxidation of aniline and its methyl derivatives in the presence of HS results in *p*-aminophenol formation.

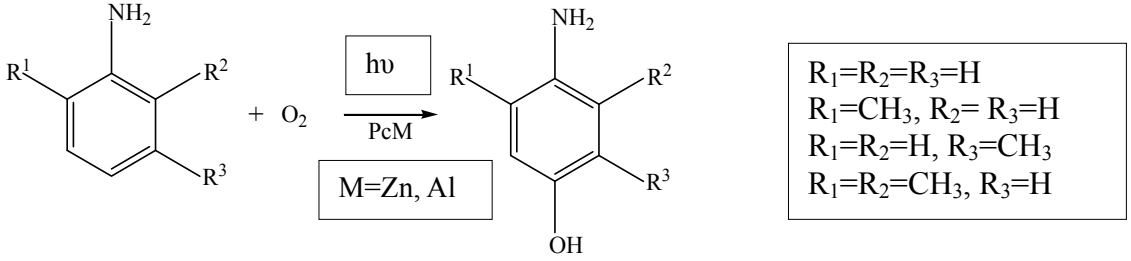

Activity and stability of sensitizers, the nature of carrier, property of solvent, concentrations of sensitizer and substrate etc. belong to effecting factors.

The HS bearing substituents R = 3-$PhSO_2$-5-*t*-Bu or 3-$PhSO_2$ in benzene rings of R_4PcZn possess highest efficiency in sensitized anilines photooxidation with dioxygen. These substituents provide at the same time monomeric state of PcZn on carrier surface and photostability. HS on the basis of PcAl were less active, than Zn-analogs.

Reaction doesn't occur in water free organic solvents, and it proceeds quicker in the CH_3CN-H_2O mixture, than in CH_3OH-H_2O that probably is connected with longer lifetime of $^1O_2$ in CH_3CN (30 micro sec) in comparison with CH_3OH (7 micro sec).

The yield of 4-amino-3,5-xylenol was 74% at almost full conversion of 2,6-xylidine in optimum conditions for irradiation time 150 min in CH_3CN-H_2O 1:1. The same conversion and yield were received with the attached HS SiO_2-NH-SO_2-(3-$PhSO_2$)$_4$-PcZn in the MeOH-H_2O 1:1 mixture.

4 Conclusions

It is shown for the first time that photooxidation of anilines leads to products of *p*-hydroxylation in the presence of the heterogenized sensitizers on the basis of the substituted zinc phthalocyanines adsorbed on Amb. or NH_2-SiO_2, or in sulfochlorid form covalent attached to NH_2-SiO_2. Selectivity of *p*-aminophenol formation is more 70%. The most effective heterogenized sensitizers, namely, adsorbed (3-$PhSO_2$-5-*t*-Bu)$_4$PcZn on Amb. and attached (3-$PhSO_2$)$_4$-(SO_2Cl)$_n$-PcZn to NH_2-SiO_2 can be used in several times. Thus the total of photocatalysts turnovers number is more than 4000.

Acknowledgements

This work was financially supported by Russian foundation of basic researches (Grants №13-03-00667, 13-03-12094).

References

[1] O. Kaliya, E. Lukyanets, G. Vorozhtsov, *J. Por. Phthal*. 3 (1999) 592-610.
[2] E.A. Lukyanets, *J. Por. Phthal.* 3 (1999) 424.
[3] D. Wöhrle, M. Kaneko, K. Nagai, R. Gerdes, O. Suvorova, *Environmental cleaning by molecular photocatalysis* (in *Molecular Catalysis for Energy Conversion*, eds. T. Okada, M. Kaneko), Springer Series in Material Science, 2008, pp. 263-298.
[4] T. Fedorova, E. Petrova, V. Derkacheva, E. Luk'yanets, O. Kaliya, Proceeding of the 11th Intern. Conf. on Environmental Science and Technology. Chania, Crete, Greece, 2009, B-263-B270.
[5] Patent RF №.2471715 (2013).

IV-PP40

A New Type of Catalyst for Hydrolytic Hydrogenation of Cellulose

Filatova A.E., Manaenkov O.V., Matveeva V.G., Sulman E.M.*, Kislitza O.V., Sidorov A.I., Doluda V.Yu., Sulman M.G., Stepacheva A.A.

Tver Technical University, Tver, Russia

* sulman@online.tver.ru

Keywords: cellulose, hypercrosslinked, polystyrene, hydrolytic, hydrogenation, sorbitol

1 Introduction

Cellulose is one of the mostly wide-spread organic materials on the earth. It has been estimated that 10^{11}–10^{12} tons of cellulose are synthesized in nature annually. It is mostly combined with hemicelluloses and lignin in the plant cell walls [1]. Cellulose is considered a likely alternative to fossil fuels as its renewable resources can provide the production of raw materials for the chemical industry and second-generation biofuels on a large scale [2 - 4].

In this paper a new type of Ru-containing catalysts based on non-functionalized and functionalized hypercrosslinked polystyrene (HPS) is proposed for cellulose hydrolytic hydrogenation. HPS is characterized by ultra-high porosity and excellent sorption properties and was successfully used as a support for nanocomposite catalysts.

2 Experimental

Low-temperature nitrogen adsorption was carried out with the surface analyzer Beckman Coulter SA 3100 to determine specific surface areas and porosity of the catalysts and the initial HPS samples. Before the analysis the samples were degassed at 120 °C in vacuum for 1 hour using the device for preliminary preparation of the samples (Coulter Corporation, USA).

Transmission electron microscopy was performed with a Techai G 30S-TWIN (FEI, USA) operated at accelerating voltage of 300 kV. Ru-containing HPS powders were embedded in epoxy resin and subsequently microtomed at ambient temperature. Images of the resulting thin sections (*ca.* 50 nm thick) were collected with the Gatan digital camera and analyzed with the Adobe Photoshop software package and the Scion Image Processing Toolkit.

3 Results and discussion

We studied the influence of the Ru content, Ru/cellulose ratio, and the type of HPS on the catalytic properties in cellulose hydrolytic hydrogenation. The highest yields of hexitol ($\eta_{hex.}$) were obtained with the catalysts containing 1 wt.% of Ru in HPS.

Table 1 show the porosity data of the initial HPS samples and the catalysts obtained from the nitrogen physisorption measurements. As shown in Table 1, MN-270 has the highest surface area as well as the specific surface area of micropores compared to the other supports

The specific surface areas of the catalysts based on MN-270 and MN-500 are lower than those of the initial supports. In the case of MN-270 where the decrease does not exceed 15%, this is easily understood as Ru nanoparticles fill the pores and the matrix can shrink because the reduction by hydrogen is carried out at 300 °C. However, for MN-500 and 1% Ru/MN-500, the surface area decreases by a factor of 5. This fact is explained by desulfurization of MN-500 which takes place at 200 - 300 °C and results in the change of the HPS structure.

The best results were obtained for 1% Ru/MN-270. This catalyst demonstrates the highest hexitol yield and the lowest yield of other products. Most likely the high efficiency of this catalyst is due to combination of the high specific surface area, narrow pore size distribution,

and small, monodisperse Ru nanoparticles.

Table 1. Porosity data for the HPS samples and the catalysts

Sample	Surface area					
	Langmuir		BET		t-plot	
	S_L,[a] m^2/g	k_L[c]	S_{BET},[b] m^2/g	k_{BET}[c]	S_t[c], m^2/g	k_t[d]
MN-270	1500	0.9995	1420	0.99962	295[e] 1140[f]	0.99667
MN-100	840	0.9998	730	0.99954	200[e] 590[f]	0.99981
MN-500	650	0.9999	540	0.99943	150[e] 450[f]	0.99996
1% Ru/MN-270	1270	0.9994	1180	0.99957	250[e] 990[f]	0.99787
1% Ru/MN-100	890	0.9999	740	0.99938	195[e] 600[f]	0.99974
1% Ru/MN-500	120	0.9985	90	0.99994	80[e] 15[f]	0.99879

[a]S_L is the specific surface area (Langmuir model); [b]S_{BET} is the specific surface area (BET model); [c]S_t is the specific surface area (t-plot); [d]k_L, k_{BET}, k_t are the correlation coefficients; [e]specific surface area according to a t-plot model; [f]specific surface area of micropores;

To evaluate stability of this catalyst, after the completion of the reaction, the catalyst was separated and used again with fresh cellulose. The results show that the repeated use of the 1%Ru/MN-270 catalyst in three consecutive reaction cycles leads to only a slight decrease of its activity which can be explained by a loss of some amount of the catalyst during filtration. The analysis of the liquid phase by atomic absorption spectroscopy showed no Ru leaching.

4 Conclusions

Ru-containing catalysts based on HPS were studied in hydrolytic hydrogenation of cellulose. We demonstrated that only the catalysts based on non-functionalized MN-270 provide high efficiency and selectivity towards hexitols due to stability of the HPS framework resulting in high surface areas of the catalysts and well-defined Ru nanoparticles. The catalysts based on functional analogues of MN-270, i.e., MN-100 and MN-500, were practically inactive in this process.

The use of the 1.0% Ru/MN-270 catalyst allows achieving the total sorbitol and mannitol yield about 50% at the ~85% conversion that is comparable with the results obtained with more complex and expensive catalytic systems. Moreover, preliminary studies show that the temperature decrease and the increase of the process duration result in the increase of the hexitol yield up to 60 – 70 %. This catalyst is also highly stable in the repeated use making it promising for cellulosic biomass conversion to feedstock for chemical synthesis and industrial production of second-generation biofuel.

Acknowledgements

This work was supported by the Russian Foundation for Basic Research (grants number 12-03-31568, 13-08-00126).

References

[1] P. Yang, H. Kobayashi, A. Fukuoka, *Chin. J. Catal*. 32 (2011) 716 - 722.
[2] G.W. Huber, S. Iborra, A. Corma, *Chem. Rev*. 106 (2006) 4044 - 4098.
[3] A. Corma, S. Iborra, A. Velty, *Chem Rev.* 107 (2007) 2411 - 2502.
[4] J.B. Binder, R.T. Raines, *J. Am. Chem. Soc.* 131 (2009) 1979 - 1985.

IV-PP41

Micro- and Mesoporous Aluminosilicates – New Efficient Catalysts for the Synthesis of Pyridines

Filippova N.A.*, Grigor'eva N.G., Agliullin M.R., Kutepov B.I.

Institute of Petrochemistry and Catalysis Russian Academy of Sciences, Ufa, Russia

* FNA1690@gmail.com

Keywords: pyridine, picolines, lutidines, zeolites, micro- and mesoporous aluminosilicates, multi-component reaction

1 Introduction

Pyridine and substituted pyridines are the important intermediates in the synthesis of pharmaceuticals, herbicides, metal corrosion inhibitors and surface-active agents. Industrially, pyridine and its derivatives are synthesized by condensation of aldehydes and ammonia over an amorphous aluminosilicate catalyst promoted by ThO_2, ZnO or CdO. The pyridine yield amounts 40-60%, and a significant amount of by-products is formed [1].

In this regard, at the Institute of Petrochemistry and Catalysis of the Russian Academy of Sciences conducted research is to develop a selective method for synthesis of pyridine over micro- and mesoporous aluminosilicates.

2 Experimental/methodology

We investigated the catalytic properties of microporous zeolites (HY, H-Beta, H-ZSM-12, H-ZSM-5), a micro-meso-macroporous zeolite HY-MMM and amorphous mesoporous aluminosilicates ASM (mesopores with a diameter of 2-7 nm) [2].

The zeolite catalysts were characterized by the X-Ray Phase (XRP) and X-Ray Diffraction (XRD) Studies, the Low Temperature Nitrogen Adsorption, and the Temperature Programmed Desorption of ammonia (TPD NH_3).

Mesoporous aluminosilicates with various chemical compositions have been prepared by sol-gel method and were characterized by nitrogen gas adsorption, transmission electron microscopy (TEM), small angle X-ray scattering (SAXS), and ^{29}Si and ^{27}Al magic angle spinning nuclear magnetic resonance (MAS NMR) [3-4]. The catalyst samples were calcined in the atmosphere of air for 3-4 hours at 540˚C.

The reaction of ethanol with formaldehyde and ammonia was conducted in a tubular, down-flow Pyrex reactor with 20 mm internal diameter at the temperature of 200-400˚C and the weight hourly space velocity (WHSV) within the range of 0.5-10 h^{-1}. The molar ratio of ethanol/formaldehyde/ammonia varies within the range of 1.0/0.4-1.1/1.5-5.0. The amount of the catalysts taken for every reaction was 0.4 g. The reaction mixture was fed from the top using a micro-pump. The product was collected at the bottom and cooled using ice-cold water.

The reaction products were analyzed by means of the gas-liquid chromatography (flame ionization detector, SE-30 column, l=25 m, the temperature of analysis 50-280˚C; the programmed heating gradient of 8˚C/min) and GC-MS (SPB-5 30 m × 0.25 mm column, the flow rate of the helium, temperature program adjustable between 40° to 300°C, the programmed heating gradient of 8˚C/min, the temperature of the ionization source is 200°C of ionization energy 70 eV).

The products were identified by comparing the mass spectra and chromatographic behavior of the separated and reference products (pyridine, picolines and lutidines).

- **Results and discussion**

We have develop a process the synthesis of pyridine and picolines by a reaction of ethanol with formaldehyde and ammonia over zeolite catalysts differed in their crystal structure, acidic properties and different porosity, and amorphous mesoporous aluminosilicates (ASM).

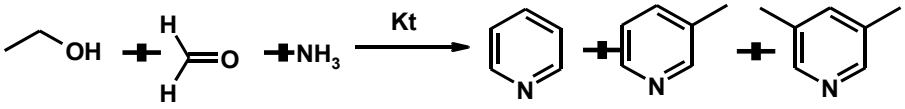

Fig. 1. Synthesis of pyridines from ethanol, formaldehyde and ammonia

We have found that the most active catalysts among microporous zeolites are H-Y and H-Beta. The conversion of ethanol are 60 and 55%, respectively (T = 400°C, w = 7 h^{-1}, mole ratio $C_2H_5OH:CH_2O:NH_3$ = 1.0:0.8:1.5).

Main reaction products in the presence of H-Beta and H-ZSM-5 zeolites are pyridine (50%) and picolines (40%), over H-Y and H-ZSM-12 zeolites - picolines (45-52%) and lutidines (19-25%).

It is shown, that the most active in the synthesis of pyridines is micro-meso-macroporous zeolite N-Y-MMM on which conversion of ethanol reaches 90%. The high activity zeolite HY-MMM due to the presence in its structure of meso- and macropores, improving diffusion reaction molecules and products reaction. In the present of zeolite H-Y-MMM as a part of reaction products predominant methylpyridine (48-54%).

Amorphous mesoporous aluminosilicates showed good catalytic activity in the reaction of ethanol, formaldehyde and ammonia is comparable to the activity of zeolite catalysts. Over sample aluminum silicate with the ratio of SiO_2/Al_2O_3 of 20 the conversion of ethanol are 50-70%. Main reaction products in the presence of ASM catalyst are 3-picolines (60%).

- **Conclusions**

Catalysts based on zeolites with a combined micro-meso-macroporous structure and mesoporous aluminosilicates showed high activity in the synthesis of pyridine and picolines (conversion of ethanol reaches 90% and 70%, respectively).

The composition of the reaction products can be controlled by changing the structural characteristics, porosity, acid properties, and varying the reaction conditions (temperature, weight hourly space velocity, the molar ratio of the reactants).

The selectivity of the pyridine formation reaches its maximum over microporous zeolites (49%) at 200-300˚C and 7 h^{-1}. The most selective formation of 3-picoline over micro-meso-macroporous zeolite H-Y-MMM and mesoporous aluminosilicate ASM (60%) at 300˚C, 7 h^{-1}.

Acknowledgements

The work was supported by Russian Foundation for Basic Research RFBR Project 14-03-97021 r_povolzhie_a

References

[1] V.V.Krishna Mohan, N. Narender, Catal.Sci.Technol. 2 (2012) 471-487.
[2] C. Baerlocher, L. B. McCusker, D. H. Olson (2007) in Atlas of Zeolite Framework Types (Amsterdam: 6th Edn. Elsevier).
[3] G. Ohlmann, H. G. Jerschkewitz, G. Lischke, B. Parlitz, M. Richter and R. Eckelt, Z. Chem. 28 (1988) 161.
[4] N. V. Kel'tsev, The Fundamentals of the Adsorption Engineering. Moscow: Chemistry. (1984) 592.

IV-PP42

Optimization of Raw Materials and Process Parameters Dehydrogenation Higher Alkanes

Frantsina E.V.[1], Ivanchina E.D.[1], Ivashkina E.N.[1], Platonov V.V.[2], Nazarova G.Y.[1*]

1 - Tomsk Polytechnic University, Tomsk, Russia
2 - LLC "KINEF", Kirishi, Russia

* silko_gy@mail.ru

Keywords: dehydrogenation, catalyst, composition of raw materials, coke formation, water feed, mathematical model

1 Introduction

The main stage of linear alkylbenzenes production (LAB) is dehydrogenation process of n-paraffins $C_{10} - C_{13}$. The formation of byproducts (diolefins, isoparaffins, cycloparaffins) occurs in this stage and it contributes to formation of coke on the dehydrogenation catalyst surface. Composition of raw materials has significant effect on the yield and quality of the LAB and accumulation rate of coke on the catalyst. It explains the importance of dehydrogenation process research in the case of processing of raw material various types whose components has different reactive capacity to the primary reaction [1–2].

The aim is to optimize the composition of raw materials and technological parameters of the process for producing olefins using experimental data from an industrial plant and computer odeling system [3–5].

2 Experimental

Influence of tridecane concentration of raw mixture on the technological parameters of dehydrogenation process of n-paraffins, duration of the catalyst operating cycle and yield of the main product were studied using the mathematical model developed dehydrogenation process. Maximum possible content of this component in the raw mixture and its optimal value in the initial mixture was determined.

The maximal production of main component is provided at the optimum content of C_{13} – components which reduces the recirculation ratio of mixture and the rate of coke deposition on the dehydrogenation catalyst. Recommendation for change of process parameters was developed.

3 Results and discussion

Using the mathematical model developed dehydrogenation process, the optimal modes of water feed to the dehydrogenation reactor at a molar ratio of reducing hydrogen / feedstock: decreasing the molar ratio of hydrogen / feedstock to 7/1 to 6/1 to compensate for the high rate of catalyst deactivation can be achieved by increasing the flow rate of water.

When the molar ratio H2 / hydrocarbon = 7 / 1rekomenduemy water flow 300 hours the catalyst is 4.5 liters / hr and 9.10 l / h on day 450-480 of the catalyst based on a predetermined concentration of 8.5% by weight of olefins. If a given concentration of olefins in the reactor product mixture is equal to 9.0-9.5 wt.%, The service life of the catalyst drop to 250-260 days at H2 / hydrocarbon = 6/1 to 350-380 days and at H2 / hydrocarbons = 7/1, it would require an adjustment mode the water supply to the reactor upwards.

4 Conclusions

It is shown that a change in the type of catalyst is necessary to adjust the recommendation

of water flow in the dehydrogenation reactor, as it is determined by the rate of coke formation reactions, which is different for different catalysts.

References

[1] Frantsina E. V. , Ivashkina E. N. , Ivanchina E. D. , Romanovsky R. V. Chemical Engineering Journal. – 2014. - Vol. 238. - p. 129-139

[2] Dolganova I. O. , Dolganov I. M. , Ivashkina E. N. , Ivanchina E. D. , Romanovsky R. V. Development of Approach to modelling and optimization of non-stationary catalytic processes in oil refining and petrochemistry //Polish Journal of Chemical Technology. - 2012 - Vol. 14 - Issue 4 - p. 22-29.

[3] Ivanchina E. D. , Ivashkina E. N. , Frantsina E. V. , Silko G. Y. , Kiselyova S. V. Determination of the Optimal Operation Mode of the Platinum Dehydrogenation Catalysts // Advanced Materials Research. - 2014 - №. 880. - p. 25-31

[4] Kravtsov A. V. , Ivanchina E. D. , Ivashkina E. N. , Frantsina E. V. , Kiselyova S. V. , Romanovsky R. V.Thermodynamic Stability of Coke-Generating Compounds Formed on the Surface of Platinum Dehydrogenation Catalysts in Their Oxidation with Water // Petroleum Chemistry. - 2013 - Vol. 53 - №. 4. - p. 267-275

[5] Ivashkina E. N. , Ivanchina E. D. , Frantsina E. V. , Platonov V. V. , Glik P. A. , Volkov M. A. , Kolmogorova V. A. Improving the Efficiency of Dehydrogenation Catalyst Resource while Reducing the H2 Gas Circulation Rate // Procedia Chemistry. - 2014 - Vol. 10. - p. 127-136

IV-PP43

Photocatalytic Conversion of Glucose in TiO_2 Aqueous Suspensions

Bellardita M., García-López E.*, Marcì G., Palmisano L.

"Schiavello-Grillone" Photocatalysis Group, Dipartimento di Energia, Ingegneria dell'informazione, e Modelli Matematici (DEIM), Università degli Studi di Palermo, Palermo, Italy

* elisaisabel.garcialopez@unipa.it

Keywords: photocatalysis, TiO_2, partial oxidation, glucose

1 Introduction

The search of alternative resources for the synthesis of chemicals currently produced from non-renewable sources has directed the activities of researchers towards the use of different raw materials such as biomass. Glucose, a major component of biomass, can be used as a model compound for the sustainable production of high value chemicals. To this aim catalytic processes at high pressure and temperature, pyrolysis, gasification or conversion under supercritical conditions have been object of intense research. In this framework heterogeneous photocatalysis can be considered as an alternative particularly because it is performed at ambient pressure and room temperature [1]. This work aims to convert glucose by a photocatalytic process in aqueous suspensions of different TiO_2 powders to obtain high added value products in soft and green conditions.

2 Experimental/methodology

Polycrystalline TiO_2 powders both commercial (Evonik P25, Merck and BDH) and home prepared have been used as photocatalysts for the glucose oxidation in aqueous suspension. Home prepared TiO_2 samples have been obtained from different Ti containing precursors. By using $TiCl_4$ three materials have been obtained, named HP, HP-R and HP-B; from $TiOSO_4$ and $Ti(OPr)_4$ the powders obtained were HPS-A and HP-IP-A, respectively. Bulk and surface characterizations were carried out in order to define the physicochemical features of the powders (See Table 1). The photoreactivity runs were carried out at room temperature and ambient pressure in a 800 mL open reactor irradiated in the UV region with an immersed 125 W medium pressure Hg lamp (Helios Italquartz, Italy). The initial aqueous glucose concentration was 1 mM. The amount of photocatalyst was enough to absorb all the photons emitted by the lamp. All of the runs lasted ca. 7 h. Samples were withdrawn at fixed intervals of time from the reacting suspension and the quantitative determination of glucose and its intermediate products were performed by HPLC analyses.

3 Results and discussion

Table 1 reports some physicochemical features of the commercial and home prepared TiO_2 powders. The home-prepared materials presented generally higher specific surface areas than the commercial ones and a lower crystallinity which did not prevent their photocatalytic activity. The degradation of glucose occurred by using all of the photocatalysts, although different conversion extent and distribution of intermediate products were observed, depending on the photocatalyst used. In Figure 1 it is reported the evolution of the substrate and the intermediate oxidation products during photocatalytic runs in the presence of TiO_2 Merck and TiO_2 HP photocatalysts. In the presence of the different powders not only the distribution of products but also the degradation rates changed.

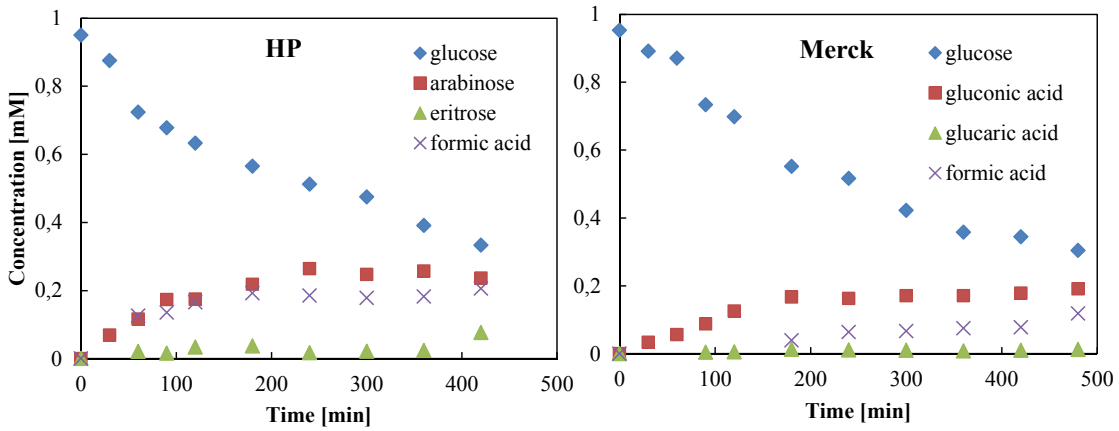

Figure 1. Evolution of glucose and their intermediate oxidation products versus irradiation time in the presence of TiO_2 HP and Merck.

The main glucose oxidation product was gluconic acid in the presence of the commercial TiO_2 Merck and BDH samples, whereas with Evonik P25 and all of the home prepared materials mainly arabinose was obtained along with eritrose, glyceraldehyde and formic acid. The isomerization of glucose into fructose was also observed. Table 2 resume some quantitative results.

Table 1. Physicochemical characterization of the TiO_2 photocatalysts

Photocatalyst	SSA (m^2/g)	Crystalline phase	Crystallinity (%)[a]	Crystallite size (nm)	Band gap (eV)
Evonik P25	50	Anatase +Rutile	72(A), 18(R)	25(A), 33(R)	3.13
Merck	10	Anatase	74	60	3.18
BDH	9	Anatase	56.3	52	3.12
HP	185	Anatase+Rutile	6.8(A)	4.6(A), 2.1(R)	3.03
HP-B	82	Brookite	*	6.6	3.25
HP-R	87	Rutile	12	3.5	3.04
HPS-A	44	Anatase	40	23.6	3.19
HPIP-A	73	Anatase	6.9(A), 4.6(R)	7.5	2.97

[a] The missing crystallinity correponds to amorphous sample; *not determined

Table 2. Photocatalytic reactivity results of glucose degradation in the presence of TiO_2 photocatalysts

		Selectivity (%)		
Photocatalyst	Glucose conversion at 7 h (%)	Fructose	Gluconic acid	Arabinose
Evonik P25	49	18	3	56
Merck	69	70	30	0
BDH	68	72	28	0
HP	68	10	0	49
HP-B	60	8	0	47
HP-R	82	0	0	60
HPS-A	44	50	0	45
HPIP-A	80	10	0	71

References

[1] J. C. Colmenares, R. Luque, *Chemical Society Reviews*, 43 (2014) 765.

IV-PP44

Study of Zeolite Ni-Al-Si-th Catalyst of Hydrocracking Vacuum Distillate by EM, DTA and Radiography

Abadzade X.I.[1], Ibragimov R.G.[2], Gasimova Z.A.[1*]

1 - Institute of Petrochemical Processes named after Academician Y.H.Mamedaliyev, Baku, Azerbaijan Republic

2 - Baku Oil Refinery named after H.Aliyev, Baku, Azerbaijan Republic

* gasimovazaira@mail.ru

Keywords: catalytic cracking, dispersibility, difractograms, pore volume, hydrocracking

1 Introduction

At the present stage the process of light hydrocracking of heavy oil fractions has increased requirements for yield and quality of the desired products along with the stable activity of the catalysts used in combination process of light hydrocracking and catalytic cracking . Economic indicators of light hydrocracking are determined by the quality of the catalyst used .

2 Experimental/methodology

Based on the previously synthesized zeolite Ni-Al-Si- th catalyst, the highly efficient wide-porous catalyst was developed for the process of heavy feed stocks light hydrocracking .
The samples of zeolite Ni-Al-Si- th catalysts have been studied using EM techniques and X-ray DTA .

The pore volume, the effective average pore size and surface area of the synthesized zeolite Ni-Al-Si- catalyst are of 0.65 cm3 / g, 85 Å and 200 m2 / g , respectively, versus 0.42 cm3 / g, and 55 Å 300 m2 / g for the basic zeolite Ni-Al-Si- th catalyst.

3 Results and discussion

It was established that the modification of the porous structure of the zeolite-containing Ni-Al-Si- catalyst increases the dispersibility of the nickel in the range of 22-70 Å versus 60-210 Å and leads to a significant reduction of coke deposition (~ 3 -less) and therefore allows to get the light hydrocracking catalyst, keeping the stable activity after prolonged use. The catalyst activity is increased.

The difractograms reflect the significant decrease of height of the peak which corresponds both to metal nickel and nickel sulfide after recovery and regeneration, comparing to the parent sample . This indicates that the metallic nickel therein is in a higher dispersed state as compared to the initial sample .

IV-PP45

Methylation and Carboxymethylation of Alcohols, Diols, Phenols and Acids with Green Reagents Dimethyl Carbonate under the Influence of Homogeneous Tungsten, Cobalt, and Manganese-Containing Catalysts

Khusnutdinov R.I.*, Shchadneva N.A., Mayakova Y.Y., Gimaletdinova L.I.

Institute of Petrochemistry and Catalysis, Russian Academy of Sciences, Ufa, Russia

* khusnutdinov@anrb.ru

Keywords: methylation, dimethyl carbonate, catalysts, tungsten, cobalt, manganese

1 Introduction

According to the literature data, the stoichiometric amounts of Al2O3, MgO, K2CO3 and KF/Al2O3 were used to promote the methylation reaction of alcohols, phenols and acids with reagent «green chemistry» dimethyl carbonate (DMC) [1−5]. The methylation required harsh conditions (200−250 oC) and proceeded non-selectively; therefore it has not been of preparative interest.

2 Experimental/methodology

Herein we report compounds and complexes of tungsten, cobalt and manganese, which are effective catalysts for the methylation and carboxymethylation of alcohols, diols, and phenols, aliphatic and aromatic carboxylic acids with dimethyl carbonate (DMC). The reaction occurred in a stainless steel micro autoclave(V=17 ml) at 180 °C for one hour. The optimal ratio of the catalyst and the reactants was defined as [cat]: [ROH, ArOH, RCOOH]: [DMC] = 1−3:100:300−500, at which the yields of esters reached 90−98%.

3 Results and discussion

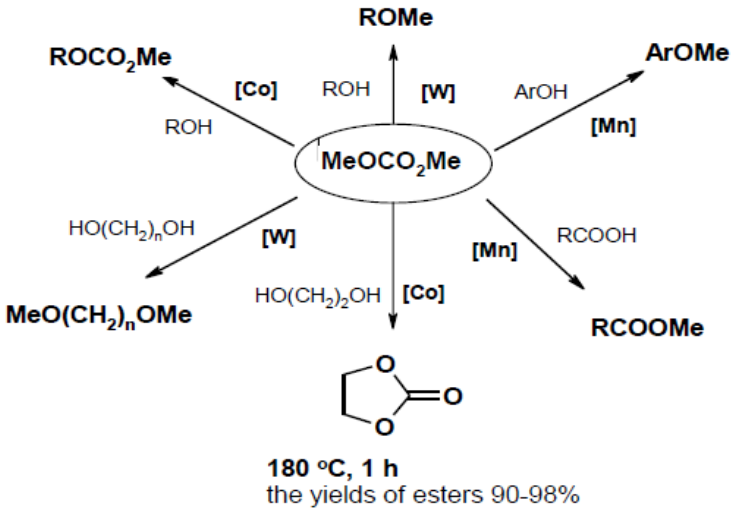

[Co] = $Co(acac)_2$, $Co(acac)_3$, $Co_2(CO)_8$; **[W]** = $W(CO)_6$;
[Mn] = $MnCl_2$, $Mn(OAc)_2$, $Mn(acac)_2$, $Mn_2(CO)_{10}$.

The best catalyst for methylation of alcohols and diols was W(CO)6. The methylation of phenols, aliphatic and aromatic carboxylic acids with DMC occurred in the presence of

compounds and complexes of manganese, namely, MnCl2, Mn(OAc)2, Mn(acac)3, and also Mn2(CO)10, which was the best. In the presence of Co2(CO)8, the carboxymethylation reaction of alcohols and diols with DMC was the major.

4 Conclusions

The advantages of homogeneous metal complex catalysts as compared to heterogeneous are the low consumption, shortening and quantitative yields.

Thus, as compared with the heterogeneous catalysts, the metal complex catalysts developed for the methylation of alcohols, diols, phenols and carboxylic acids, using DMC have a number of advantages: high reaction selectivity, shortening of the reaction, low catalyst consumption and the high yield of methyl esters.

References

[1] F. Arico, P. Tundo, Russ. Chem. *Rev. 20*10, 79 (6), 479
[2] P. Tundo, S. Memoli, D. Herault, K. Hill, *Green Chem.,* 2004, 6, 609
[3] A. J. Parrott, R. A. Bourne, P.N. Gooden, H.S. Bevinakatti, M. Poliakoff, D. J. Irvine, *Org Process Res. Dev.* 2010, 14, 411
[4] A. Bomben, M. Selva, P. Tundo, *Ind. Eng. Chem. Res.* 1999, 38, 2075
[5] W.-C. Shieh, S. Dell, O. Repic, *J. Org. Chem. 2002, 67, 2188.*

IV-PP46

Photocatalytic Oxidation of Propane: Designing Catalysts for Selectivity Tuning

Hamdy M.S.[1,2*], Berg O.[3], Mul J.[2]

1 - Photocatalytic Synthesis Group, MESA+ Nanotechnology Institute, Twente University, Enschede, The Netherlands

2 - Chemistry Department, Science College, King Khalid University, Abha, Saudi Arabia

3 - Leiden Institute of Chemistry, Leiden University, Leiden, The Netherlands

* m.s.hamdy@gmail.com

Keywords: photocatalysis, nanoparticles, TiO_2, propane oxidation, UV light, selectivity

1 Introduction

The development of a selective direct route for partial oxidation of propane is of major industrial importance, as it would allow for an efficient use of this ubiquitous feedstock in important large-scale applications such as the area of polymer synthesis. Regarding the development of catalysts to affect such reactions, many of the reported approaches rely on thermal activation at elevated temperature. Photocatalysis at ambient temperature is a smart alternative for the conventional oxidation route. TiO_2 is a large-bandgap semiconductor with high photocatalytic activity. Extensive research eff$_2$orts have been reported to modify the properties of TiO_2 for selective photocatalysis applications [1]. Significant improvements in activity have been achieved by reducing the crystallite size, for example by impregnation of TiO_2 precursors on mesoporous materials such as MCM-41 [2], and SBA-15 [3]. The current study concerns the use of TUD-1, a form of mesoporous amorphous silica in which the physical and chemical properties of which can be systematically tuned during synthesis, as a support for TiO_2 nanoparticles. TiO_2 embedded in TUD-1 are shown to be more selective for propane oxidation than commercial TiO_2. It will also be demonstrated that the size tuning of TiO_2 nano-crystals in the range of 3-8 nm has a significant effect on the performance. Moreover, the effect of the illumination wavelength is discussed, which can be used to activate either isolated titanium sites Ti^{4+}, or the nano-particles of TiO_2. Finally, it will be presented that addition of small amount of Cr^{6+} (less than 1%) to TiO_2-TUD-1 influence the photocatalytic performance and the synergy between Cr^{6+} ions and TiO_2 nanoparticles will be discussed.

2 Experimental

One batch of TiO_2-TUD-1 with a Si/Ti ratio of 2.5 (Ti-40) was synthesized by the surfactant-free procedure described earlier [4]. After drying, the solid Ti-40 sample was divided into 4 equal amounts, which were hydrothermally treated in a Teflon-lined stainless steel autoclave to 450 K (at 5 K/min.) and incubated for different times (8-24 hours). Finally the samples were calcined at 873 K (1 K/min.) for 10 hours in air. The samples were labeled as Ti-40-xh, where x = the heating time in hours. One additional sample was prepared with the same Ti loading in addition to 1wt% of Cr^{6+}. The prepared samples were characterized by means of XRD, UV-Vis, elemental analysis, HR-TEM, and N_2 physisorption. The photocatalytic performance was evaluated in a high vacuum stainless steel cell with CaF_2 windows that allowed for simultaneous ultraviolet-light irradiation and FTIR spectroscopy in transmission. Ultraviolet light was obtained from a 200 W Hg-Xe arc, the excitation frequency was selected by means of a grating monochromator (single for photochemistry, bandpass 15 nm). The samples wafers were edge-supported in a copper sample holder incorporating a resistive heater and type K thermocouples. The cell was then loaded with 2.8 mbar of propane gas and 400 mbar of molecular oxygen (1 propane: 140 oxygen) and held at 300 K. The infrared spectra

of adsorbed species were monitored in-situ by an FTIR spectrophotometer.

3 Results and discussion

The diffuse-reflectance UV-VIS spectra of all the samples were similar. Two absorption maxima were resolved, centered at 220 nm (corresponds to isolated Ti^{4+} centres) and 330 nm (associated with solid TiO_2 particles). Morphological differences between the samples were evident from the N_2 sorption isotherms. All of the isotherms are of Type IV – an indication of meso-porosity. A quantitative analysis of these isotherms yields the specific surface area, pore volume, and pore size distribution (Figure 1). It was proposed previously [5] that TiO_2 nano-particles grow within the pores of the TUD-1 matrix. Therefore, tuning the pore size should influence the size of the TiO_2 inclusions. This is confirmed by HR-TEM images of the prepared samples.

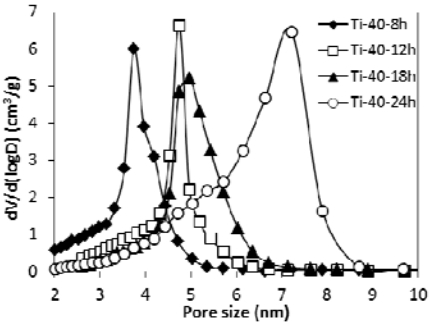

Fig.1. The pore size distrubution of the different Ti-40 samples.

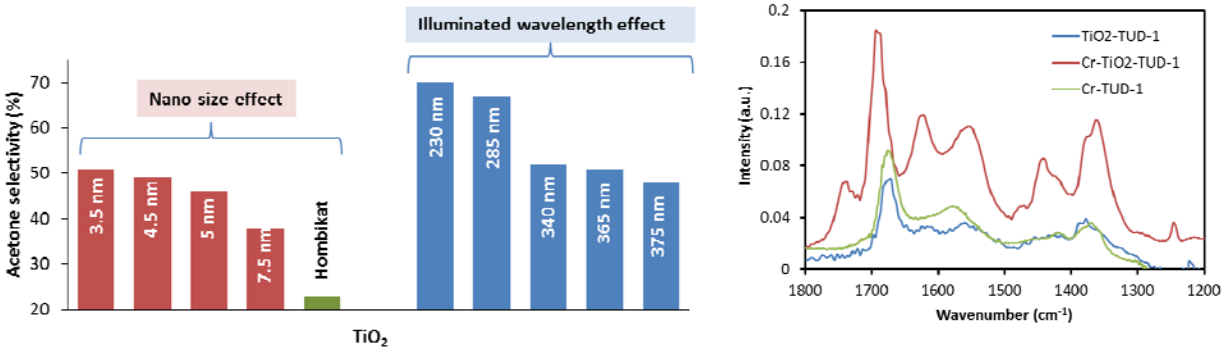

Fig. 2. Left panel: The acetone selectivity (%) obtained after 100minutes'reaction. Right Panel: The spectra of TiO_2-TUD-1 compared with Cr-TUD-1 and Cr-TiO_2-TUD-1 after 100 minutes' reaction.

A useful assay of photo-catalytic performance is the oxidation of propane to acetone (desired), carboxylates (undesired) and water. The prepared samples were evaluated under identical conditions, with 60 mW/ cm^2 of excitation at an ultraviolet wavelength of 335 nm. The total amount of products and the acetone selectivity were different. The initial reaction rates of Ti-40-12h, -18h, and -24h samples are identical and significantly greater than Ti-40-8h sample (3.5 nm). However, Ti-40-24h sample approached saturation faster than Ti-40-12h and -18h samples. For the smaller particles (i.e. Ti-40-8h) a slower rate is observed, but this rate is maintained over a prolonged period of time (i.e. up to 600 minutes). Acetone selectivity was decreased as a function of time (Figure 2) as a result of the over-oxidation reactions. The rate of the over-oxidation reaction over the Ti-40 samples is indeed different, acetone selectivity decreases slowly over a long time (600 minute) than the other samples, which decreased sharply in the first 200 minutes of the reaction in the other samples. Cr-TiO_2-TUD-1 showed a true synergy between Cr^{6+} and TiO_2 (Figure 2). The results will be dissected in details during the presentation.

References

[1] S.N.R. Inturi, T. Boningari, M. Suidan, P.G. Smirniotis, Appl. Catal. B 144 (2014) 333.
[2] A. Bhattacharyya, S. Kawi and M. Ray, Catal. Today 98 (2004) 431.
[3] A. Tual and L.G. Hubert-Pfalzgraf, J. Catal. 217 (2003) 343.
[4] M.S. Hamdy, O. Berg, J.C. Jansen, Th. Maschmeyer, J.A. Moulijn, G. Mul, Chem. Eur. J. 12 (2006) 620.
[5] M.S. Hamdy, G. Mul, Appl. Catal. B. 2015, in press.

IV-PP47

Production of Substituted Anthraquinones via Diene Synthesis in the Presence of Solution of Mo-V-P Heteropoly Acid as Bifunctional Catalyst

Gogin L.L.*, Zhizhina E.G., Pai Z.P.

Boreskov Institute of Catalysis SB RAS, Novosibirsk, Russia

* gogin@catalysis.ru

Keywords: substituted, anthraquinones, heteropoly, acid, catalyst, regeneration, multicycle, testing

1 Introduction

9,10-Anthraquinone (AQ) and its derivatives are the valuable products of organic synthesis. They are used in the production of dyes, hydrogen peroxide, and medical preparations and as catalysts for wood delignification [1].

Early [2-3] we developed one-pot processes for the preparation of substituted anthraquinones via diene synthesis in the presence of heteropoly acid $H_{17}P_3Mo_{16}V_{10}O_{89}$ (HPA-10) as a bifunctional catalyst, i.e., acidic catalyst for diene synthesis and catalyst for the oxidation of the obtained adduct. One-pot processes for the syntheses of 2-methylanthraquinone (2-MAQ) and 2,3-dimethylanthraquinone (2,3-DMAQ) are shown in schemes **A** and **B**.

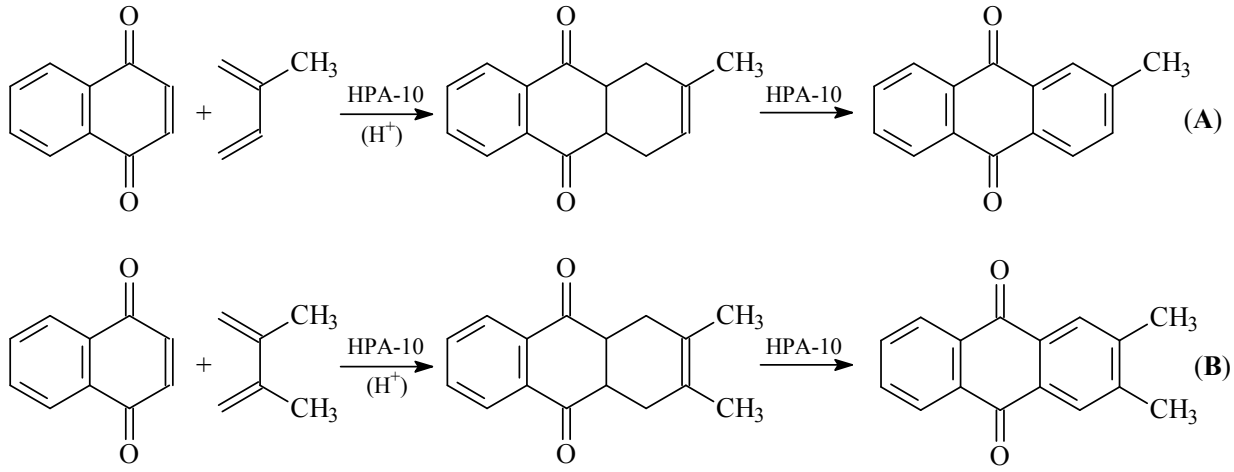

2 Experimental

In the present work, we investigated the possibility of multicycle catalyst performance. In addition to the traditional regeneration of HPA-10 solution at temperatures 160−170 °C and PO_2 = 3−4 atm [4], we tested the feasibility of substituting low concentrations of nitric acid for the same purpose. Methods for regeneration of the catalyst were alternated (see Tables below).

Experimental data were obtained for two processes:

1) 2-methylanthraquinone (2-MAQ) synthesis from NQ and isoprene; and

2) 2,3-dimethylanthraquinone (2,3-ДМАQ) synthesis from NQ and 2,3-dimethyl-butadiene.

3 Results and discussion

Experimental results are presented in Tables 1 and 2.

Table 1. Multicycle synthesis of 2-MAQ via isoprene reaction with NQ in the presence of aqueous HPA-10.

Cycle Number	*E* of aqueous HPA-10 before reaction (1), V	2-MAQ yield, %	2-MAQ purity, %	Catalyst regeneration method
1	1.098	74	97	160 °C, PO_2=4 atm, 15 min
2	1.066	70	97	150 °C, PO_2=4 atm, 20 min
3	1.064	69	97	Boiling with 0.15 ml of concentrated HNO_3, 30 min
4	1.102	73	97	Boiling with 0.15 ml of concentrated HNO_3, 30 min
5	1.099	72.5	97	160 °C, PO_2=4 atm, 15 min
6	1.068	68	97	Boiling with 0.2 ml of concentrated HNO_3, 30 min
7	1.100	74	97	160 °C, PO_2=4 atm, 15 min

Table 2. Multicycle synthesis of 2,3-dimethylanthraquinone via NQ reaction with 2,3-dimethylbutadiene catalyzed by the HPA-10 solution.

Cycle Number	*E* of aqueous HPA-10 before reaction (1), V	2,3-DMAQ yield, %	2,3-DMAQ purity, %	Catalyst regeneration method
1	1.098	81	98	150 °C, PO_2=4 atm, 20 min
2	1.063	77	98	160 °C, PO_2=4 atm, 15 min
3	1.066	77	97.5	Boiling with 0.15 ml of concentrated HNO_3, 30 min
4	1.101	80.5	98	Boiling with 0.15 ml of concentrated HNO_3, 30 min
5	1.097	80	98.5	160 °C, PO_2=4 atm, 15 min
6	1.063	77	98	Boiling with 0.2 ml of concentrated HNO_3, 30 min
7	1.104	81	98	160 °C, PO_2=4 atm, 15 min

Conditions: 80 °C, 4 ml of 0.2 M HPA-10 solution, molar ratio HPA-10:NQ 0.5:1, volume ratio HPA solution:1,4-dioxane 1:1; 7 h; NQ conversion was ≥ 99.5%. *E* value is given with respect to NHE.

Analyzing the data of Tables 1 and 2, we concluded that 0.2 M HPA-10 solution with high stability performed as a bifunctional catalyst in the MAQ and **DMAQ** synthesis over 7 cycles, resulting in a product with 68-81 % yield and 97-98 % purity. HNO_3 apparently provided a more complete oxidation of reduced HPA-10 (i.e., which resulted in a higher *E* before the next cycle) than the regeneration by O_2 in an autoclave. After the regeneration using nitric acid, the oxidative capacity of the catalyst remained essentially the same as in the first cycle because after regeneration, the *E* values were close to that of the fresh HPA-10 solution used in the first cycle.

4 Conclusions

The HPA-10 solution remained homogeneous during all cycles, retained its productivity and gave no V-containing precipitates. The target products obtained with fresh and regenerated HPA-10 solutions were shown by comparison their IR-spectra to be identical. All side products remaining in the aqueous catalyst solutions after target reactions were completely oxidized to carbon dioxide and water in the course of regeneration. The complete recovery of the properties of the bifunctional catalyst after regeneration shows its technological usefulness.

References

[1] Anthraquinone Dyes and Intermediates*, in Ullmann's Encyclopedia of Ind. Chemistry*. 2007, Vol. A.
[2] L. Gogin, E. Zhizhina, *Modern research in* Catalysis. 2 (2013) 90.
[3] L. Gogin, E. Zhizhina, *Modern research in Catalysis*. 3 (2014) 57.
[4] E.G. Zhizhina, V.F. Odyakov, *Appl. Catal. A: General*. 358 (2009) 254.

IV-PP48

Development of Bifunctional Catalysts Containing Ru and CsHPA for One-pot Conversion of Polysaccharides to Polyols

Gromov N. V.[1*], Taran O. P.[1,2], Timofeeva M. N.[1,2], Zhizhina E. G.[1], Rodikova Yu. A.[1], Parmon V. N.[1,3]

1 - Boreskov Institute of Catalysis SB RAS, Novosibirsk, Russia
2 - Novosibirsk State Technical University, Novosibirsk, Russia
3 - Novosibirsk State University, Novosibirsk, Russia

* gromov_n_v@inbox.ru

Keywords: cellulose, hemicellulose, polyoxometalate, ruthenium, cesium, bifunctional catalysis

1 Introduction

Sorbitol and xylitol are valuable chemicals used, for example, in pharmaceuticals and food industry as sweeteners, which currently are produced from starch by biotechnical or catalytic methods. One-pot hydrolytic hydrogenation methods of formation of these polyols utilizing inedible polysaccharides like cellulose and hemicelluloses which are the components of lignocellulose biomass were developed many years ago [1]. However these methods are not widely used because of soluble mineral acids (catalysts of the hydrolysis) possessing corrosive effects.

Two sequential catalytic steps (hydrolysis and reduction) must be applied to obtain polyols from polysaccharides. Acidic catalyst must be applied for hydrolysis of polysaccharides to get sugars (glucose, xylose etc.). Reduction of monosaccharides to polyols proceeds over noble metals like ruthenium. Heteropoly acids (HPAs) and cesium salts of HPA have acidic catalytic centers. Thus bifunctional catalyst Ru/CsHPA having acidic and reductive centers could be proposed for polyols production using one-pot process of hydrolytic reduction of natural polymers like cellulose and hemicelluloses under soft conditions. HPAs are also known as catalysts for “green chemistry” because they are safety for environment.

The aim of the study was the development of the bifunctional ruthenium catalysts supported on the cesium salts of the heteropoly acids for the one-pot polysaccharides conversion to valuable polyols like sorbitol and xylitol.

2 Experimental

CsHPA salts were synthesized by mixing solutions of Cs_2CO_3 and respective HPA: $Cs_XH_{3-X}PW_{12}O_{40}$, $Cs_XH_{3-X}PMo_{12}O_{40}$ (x = 1.0, 1.5, 2.0, 2.5), $H_4PMo_{11}VO_{40}$, $H_4SiW_{12}O_{40}$ (x = 2.0, 2.5, 3.0 и 3.5). Ru/C and Ru/CsHPA were prepared via impregnation the support by Ru precursor $Ru(NO)(NO_3)_3$. The catalysts was characterized investigated by IR spectroscopy, N_2 absorption, XRD, AES-ICP, TEM (for Ru-containing samples only) and tasted in one-pot hydrolytic hydration of xylan and mechanically activated crystalline cellulose. The reaction was performed in the autoclave under hydrothermal conditions of 180 °C under Ar or H_2. The concentrations of products were measured by HPLC.

3 Results and discussion

IR spectroscopy and XRD of HPAs and CsPHAs show no changes of heteropoly anion structures before and after precipitation, that indicates the stability of HPA anion during catalyst preparation. According N_2 absorption data the surface area and Cs content increase simuteneously, and CsHPAs have a microporous structure. TEM analysis of Ru/C catalysts shows that ruthenium nanoparticles have average size equal to 2 nm for all the samples.

Preliminary oxidation of the carbon support by wet air increases the dispersion of Ru.

The investigations of stability of all CsHPAs under hydrothermal conditions show that solubility of salts decreases while Cs content increases. Cs salts of P-Mo-V HPA are unstable (solubilisation is 70 w/w%). $Cs_XH_{3-X}PW_{12}O_{40}$ (X - 2, 2.5) and $Cs_XH_{4-X}SiW_{12}O_{40}$ (X - 3, 3.5) are stable sufficiently for Ru to be impregnated.

At first, the most promising CsHPAs have been tested as the acid catalysts for the hydrolysis of cellulose under Ar. $Cs_XH_{3-X}PW_{12}O_{40}$ (X - 2, 2.5) and $Cs_XH_{4-X}SiW_{12}O_{40}$ (X - 3, 3.5) are shown to be the most active in the cellulose hydrolysis. The $Cs_3HSiW_{12}O_{40}$ reveals the highest activity.

The one-pot hydrolytic hydrogenation experiments with the most perspective CsHPA salt ($Cs_3HSiW_{12}O_{40}$) and 3%Ru/C have been performed to reveal the importance of acid and metal catalytic centres in the hydrolytic hydrogenation. $Cs_3HSiW_{12}O_{40}$ and 3%Ru/C tested separately do not show activity in hydrolytic hydrogenation of cellulose. While combination of these catalysts allows producing the sorbitol with the maximum yield 14.3%. Utilization of the bifunctional catalysts containing Ru nanoparticles supported on CsHPA: 3%Ru/$Cs_2HPW_{12}O_{40}$ and 3%Ru/$Cs_3HSiW_{12}O_{40}$ gives sorbitol with high yields (60-62%**)** and selectivity up to 88% (Table 1). Beside, the low yields of glucose, 5-HMF and mannitol were detected. These products are formed via another pathway of glucose reduction.

The hydrolytic hydrogenation of xylan to xylitol over Ru/CsHPAs has also been made to show the possibility of hemicelluloses transformations to polyols over such catalysts. The yield of xylite is also very high up to 70% (Table 1).

Table 1. Yields of the products of the cellulose hydrolytic hydrogenation. Reaction conditions: cellulose (*xylan*) 450 mg, catalyst 450 mg, V 45 mL, T 180 ºC, P_{H2} 7 MPa. * - xylan has been used as a substrate.

Catalyst	Y_{Σ}, %	t, h	Sorbitol/*Xylitol*		Mannitol/ *Lixytol*		Glucose/ *Xylose*		5-HMF	
			S, %	Y,%	S, %	Y,%	S,%	Y,%	S,%	Y,%
$Cs_3HSiW_{12}O_{40}$	19.9	2	0.0	0.0	0.0	0.0	72.4	14.4	21.1	4.2
3% Ru/C	9.1	2	8.8	0.8	38.5	3.5	5.5	0.5	39.6	3.6
3%Ru/C-$Cs_3HSiW_{12}O_{40}$	25.3	2	56.5	14.3	19.4	4.9	10.7	2.7	7.9	2.0
3%Ru/$Cs_2HPW_{12}O_{40}$	58.3	3	86.6	50.5	11.0	6.4	2.4	1.4	0.0	0.0
3%Ru/$Cs_3HSiW_{12}O_{40}$	70.7	5	87.8	62.1	6.4	4.5	1.4	1.0	3.4	2.6
*3%Ru/$Cs_2HPW_{12}O_{40}$	68.1	3	90.0	60.6	9.4	6.4	3.5	2.4	0.0	0.0
*3%Ru/$Cs_3HSiW_{12}O_{40}$	96.8	2	69.6	67.4	18.0	12.5	13.1	12.7	3.8	3.7

4 Conclusions

Cs salts of HPAs with different HPA structures and Cs content as well as Ru catalysts supported on carbon and CsHPAs were prepared. All the catalysts were characterized by the different analytical methods and tested for the stability in the hydrothermal conditions. The synthesized bifunctional Ru/CsHPA catalysts (where HPA was $Cs_2HPW_{12}O_{40}$ and $Cs_3HSiW_{12}O_{40}$) showed very high stability, activity and selectivity in the one-pot hydrolitic hydrogenation of polysaccharides (cellulose and xylan). High yields of sorbitol or xylitol up to 60 and 70% respectively were archived.

Acknowledgements

The financial support of the work by the Russian Foundation for Basic Research (Grant No. 14-03-00854-a) is gratefully acknowledged.

References

[1] Sharkov V. I., *Angewandte Chemie Intern. Edit.* 2 (1963) 405-492.

IV-PP49

Conversion of Cellulose into 5-Hydroxymethylfurfural over Solid Acid Catalysts Based on Sibunit Carbon Material

Gromov N.V.[1,2,3*], Taran O.P.[1,4], Aymonier C.[2], Parmon V.N.[1,5]

1 - Boreskov Institute of Catalysis SB RAS, Novosibirsk, Russia
2 - Institut de Chimie de la Matière Condensée de Bordeaux, CNRS, ICMCB, UPR 9048, Pessac, France
3 - Universite Bordeaux, ICMCB UPR 9048, Pessac, France
4 - Novosibirsk State Technical University, Novosibirsk, Russia
5 - Novosibirsk State University, Novosibirsk, Russia

* gromov_n_v@inbox.ru

Keywords: cellulose, sibunit, oxidation, sulfonation, hydrolysis, 5-hydroximethylfurfural

1 Introduction

5-Hydroxymethylfurfural (5-HMF) is one of the most promising bio-based chemicals so-called "platform molecules". It could be used as a raw material in the production of food additives, plastics, pharmaceutics and biofuels [1]. 5-HMF is usually produced from starch and sucrose in the presence of enzymes or soluble mineral acids as a catalysts [2]. Utilization of an inedible cellulose as an alternative raw material, non-corrosive solid acid catalysts and one-pot design of the process could help to overcome the drawbacks of 5-HMF production methods. The carbon materials seem to be promising catalysts for cellulose depolymerization into valuable chemicals [3].

The aim of this work was a development of the solid acid catalysts based on graphite-like carbon Sibunit for the production of 5-HMF and glucose from cellulose and a elucidation of the mechanism of the catalytic action.

2 Experimental/methodology

The catalysts were prepared using sulfonation, oxidation and subsequent oxidation-sulfonation methods. The samples of sulfonatied Sibunit were made via treatment of carbon in fuming H_2SO_4 at 80-250 °C; the oxidized carbons were produced via oxidation by HNO_3 or wet air; oxidized-sulfonated catalysts were prepared form oxidized carbons by additional sulfonation at 200 °C. The catalysts were characterized by low-temperature N_2 absorption and titration with NaOH and tested in the one-pot hydrolysis-dehydration of a mechanically activated cellulose under hydrothermal conditions at 180 °C and 10 atm of Ar. The concentrations of products were measured by HPLC.

3 Results and discussion

Investigation of the prepared carbon catalysts by N_2 absorption shows that all the treatments lead to formation of the acidic species on the surface and simultaneous partial destroy of the carbon structure. However the sulfonation of Sibunit at the temperature above 200 °C was found to give considerable destruction of material, while the structural properties were not essentially changed at the temperatures less 200 °C. The amount of acidic groups on the surface of sulfonated carbon determined by titration increased with the increasing of the sulfonation temperature. The total amount of acidic species for the sulfonated carbons was 3-15 times higher than for the initial Sibunit. The maximal amounts were reached at the sulfonation temperatures 200 and 250 °C (1.0 and 2.7 mM/m^2). The total amount of acidic species for the oxidized samples was close and for oxidized-sulfonated ones 1.5-2 times higher than for the Sibunit sulfonated at 200 °C.

Catalytic tests of carbons showed high activity of sulfonated carbon catalysts in the cellulose hydrolysis-dehydration process. While pure carbon without sulfonate species was inactive.

HPLC analysis revealed glucose and 5-HMF as the main products. Moreover an accumulation of small amounts of cellobiose, mannose, fructose, levulinic and formic acids was detected. The maximum glucose and 5-HMF yields were reached over Sibunit sulfonated at 200 °C (46.0% and 21.5%, respectively). Oxidized and oxidized-sulfonated samples possessed the activity comparable to the activity of the catalysts sulfonated at 150 and 200 °C. The yields of 5-HMF and glucose were in the ranges of 17-20% and 28-42%, respectively. No difference in activity of oxidized and oxidized-sulfonated carbons was registered in spite of the total amount of surface species were different.

For elucidation of the mechanism of catalytic action and the role of catalysts the experiments with such intermediates as cellobiose, glucose, fructose and 5-HMF were carried out. Beside, a kinetics of substrate, intermediates and products in the presence of diluted H_2SO_4 as a catalyst and lower loading of the carbon catalyst were registered. The heterogeneous mechanism of the cellulose depolymerization was supposed base on the results of these experiments. The dissolving cellulose appeared to be a limiting step of the process while hydrolysis is the fast reaction. Rearrangement of glucose to fructose was also slow reaction. The irreversible dehydration of fructose was the most rapid step. Moreover there were different ways of glucose transformations (except glucose↔fructose→5-HMF).

Table 1. Yields of products in the cellulose hydrolysis-dehydration over carbon catalysts. Experiment conditions: cellulose 450 mg, catalyst 450 mg, volume 45 mL, stirring 1500 rpm, 180 °C, 1 MPa Ar.

Catalyst	Glucose*		5-HMF*		Yields, %**				
	Y,%	t,h	Y,%	t,h	Cellobiose	Glucose	Fructose	Mannose	5-HMF
C	0	5	0	5	0	0	0	0	0
C-S80	12.1	3	9.3	3	0	5.8	0.5	2.6	8.7
C-S150	33.5	2	17.0	5	1.2	23.5	3.6	4.0	17.0
C-S200	45.9	2	21.5	5	1.0	18.9	6.0	9.7	21.5
C-S250	35.9	2	19.0	5	1.1	26.7	7.5	9.0	19.0
C-O	40.7	3	17.8	5	3.1	27.4	1.1	8.4	17.8
C-N32	38.6	2	20.3	5	1.1	22.3	0.1	2.8	20.3
C-N23	40.0	2	18.0	5	0.6	23.7	0.4	7.7	18.0
C-O20-S200	43.7	2	17.2	5	0.0	34.5	0.5	6.6	17.2
C-N32-S200	42.8	3	17.6	5	1.1	31.9	0.0	4.8	17.6
C-N23-S200	42.6	3	15.9	5	2.9	15.3	0.0	7.6	15.9

* maxima yields and time of these yields are shown
** yields after 5 hour reaction

4 Conclusions

The availability of 5-HMF and glucose production from cellulose with quite high yields using one-pot catalytic process of hydrolysis-dehydration over sulfonated and oxidized samples of graphite-like carabon Sibunit was shown. The sample of carbon treated by fuming H_2SO_4 at 200 °C seems to be very promising one. The kinetic study allowed to evaluate rate limiting stapes and suggest reaction pathways and the mechanism of catalytic action.

Acknowledgements

The financial support of the work by the RFBR (Grant No. 12-03-93116), the Russian Ministry of Education and Science (Grant No. RFMEFI61314X0017), as well as by the Russian-French GDRI "Biomass" is gratefully acknowledged. Nikolay V. Gromov would like to thank the French Embassy in Russia for the PhD student grant.

References

[1] Taranan'ko V.E., Smirnova M.A. et.al, Pat.2363698 C1 Russia, C07D307/46, published 10.08.09.
[2] Flèche G. et.al, Pat. 4339387 USA, C07D307/46, published 13.07.82.
[3] Pang J., Wang A., Zheng M. et. al, Chem. Comm. 46 (2010) 6935-6937.

IV-PP50

Macroinitiators in the Polyaddition Reaction of 2,4-Toluene Diisocyanate

Zaripov I. I.[1], Davletbaeva I.M.[1,2], Mazilnikov A.I.[2], Davletbaev R.S.[3], Gumerov A.M.[1*]

1 - Kazan National Research Technological University, Kazan, Russia
2 - Alexander Butlerov Institute of Chemistry, Kazan (Volga Region) Federal University, Kazan, Russia
3 - Kazan National Research Technical University n.a. A.N. Tupolev, Kazan, Russia

* gumerov_am@mail.ru

Keywords: macroinitiator, polyaddition reaction, diisocyanate, polyhedral, oligosilsesquioxane

1 Introduction

The influence of reaction conditions on the mechanism of 2,4-toluene diisocyanate (TDI) polyaddition to anionic macroinitiator, which is a block copolymer of propylene oxide and ethylene (PPEG), part of the hydroxyl groups substituted on potassium alcoholate, was studied,. The relevance of this work is the fact that this reaction is the basis of obtaining polymer film nanoporous materials.

In this research was used octaglycidyl polyhedral oligosilsesquioxane (gl-POSS). The role of POSS as stabilizers of active terminal polyisocyanate units which formed during the opening N=C bond and the formation of the linear N-substituted polyisocyanates (N-polyisocyanates) was studied. This effect was specified for wide range of epoxy-POSS concentration.

3 Experimental/methodology

Block copolymers of propylene oxide with ethylene oxide of the formulas $HO[CH_2CH_2O]_n[CH_2(CH_3)CH_2O]_m[CH_2CH_2O]_nOK$ where n ≈ 14, m ≈ 48, and the potassium alcoholat group content is 10.9% of the total number of functional groups (PPEG-4202) were synthesized as macroinitiators. The monomer was 2,4-toluene diisocyanate (TDI).

To create a branch nodes and stabilization of the end of the active centers of the polymer polyaddition were used octaglycidyl polyhedral oligosilsesquioxane (EP0409 glycidyl-POSS Cage Mixture, Hybrid Plastics).

The reaction medium for the synthesis of block copolymers was toluene, acetone or ethylacetate.

The macroinitiators were preliminarily dried via vacuuming at 90–100°C and a residual pressure of 0.07 kPa for 4 h. 2,4-toluylene diisocyanate was purified via vacuum distillation under a residual pressureof 0.07 kPa. The remaining reagents were purified and dried according to conventional procedures.

The syntheses of polymers from PPEG-4202, Gl-POSS and TDI were conducted on toluene, ethyl acetate, or acetone. A calculated amount of the isocyanate was introduced into a macroinitiator solution at 25°C under stirring. The reaction was conducted at 45°C under continuous stirring for 30 min. The total amount of there actants in the solution was 25%. The resulting solution of the polymer-forming system was cast into Petri dishes. Polymer film samples were formed at room temperature.

3 Results and discussion

Based on the structure of the isocyanate group, considering the existence of two types of linear polyisocyanate homopolymers, which may occur as a result of breaking the bonds N=C or C=O. In the first case the structure of the macromolecular chain has an N-substituted polyamide (N-polyisocyanates) structure, in the second - the structure of polyacetal (O polyisocyanates). It is known that in the absence of active centers stabilizers N-polyisocyanates cyclized to

isocyanurates (hexagons).

It was shown that the nature of the solvent, the presence of acidic compounds, ambient temperature and concentration of reactants influence on reaction path between TDI and PPEG. Thus, predominant formation of O-polyisocyanate units is observed when ethyl acetate containing a catalytic amount of acetic acid used as the reaction medium. If toluene or acetone used as a solvent, is completely consumed for TDI cyclization processes. When gl-POSS used as stabilizers and crosslinking compounds reaction is accompanied by the formation of N-polyisocyanate blocks.

The effective constants of reaction and activation energies were deduced. It is shown that the activation energy of O-polyisocyanates formation reaction is more than 80 kJ / mol, the activation energy of N- polyisocyanates formation reaction is 32 kJ / mol, and cyclization activation energy is 180 kJ / mol. These findings are consistent with published data and confirm the proposed reaction mechanisms of TDI.

4 Conclusions

The mechanism of disclosure of TDI isocyanate groups exposed anionic macroinitiators by using of acidic cocatalysts and polyhedral oligomeric silsesquioxanes was studied. The preferential formation of O-polyisocyanate blocks via using catalytic amounts of acetic acid was shown. Using the gl-POSS reaction is accompanied by the formation of N-polyisocyanate blocks. The kinetic parameters of the reactions were deduced.

Acknowledgements

The authors gratefully acknowledge the financial support of the Russian foundation for basic research (Grant № 15-43-02127)

References

[1] R. Davletbaev, A. Akhmetshina, A. Gumerov, I. Davletbaeva, V. Parfenov Composite Interfaces Special Issue:The Fourth Asia Symposium on Advanced Materials (ASAM-4). 2014.21. 7.
[2] R. Davletbaev, A. Akhmetshina, A. Gumerov, I. Davletbaeva // Optical Sensors - new developments and practical applications / InTech: Rijeka, Croatia, 2014
[3] I. Davletbaeva, A. Akhmetshina, R. Davletbaev, I. Zaripov, A. M. Gumerova, and R. R. Sharifullin // Polymer Science. Series B. 2014. T. 56. №6
[4] A. Fina, D. Tabuani, A. Frache, G. Camino // Polymer.2005.46..
[5] M. Pracella, D. Chionna, A. Fina, D. Tabuani, A. Frache, G. Camino // Macromol. Symp. 2006. 234

IV-PP52

The Effect of Dealumination with HCl on MFI and FER Type Zeolites on the Dehydration of n-Butanol

Gunst D.[1,2*], Verberckmoes A.[1], Reyniers M.-F.[2]

1 - Industrial Catalysis and Adsorption Technology, Ghent University, Department of Industrial Technology and Construction, Ghent, Belgium

2 - Laboratorium for Chemical Technology, Ghent University, Department of Chemical Engineering and Technical Chemistry, Zwijnaarde, Belgium

* dieter.gunst@Ugent.be

Keywords: zeolites, butanol, dehydration, dealumination, butenes

1 Introduction

The increasing commercial production of bio-butanol makes it an interesting and emerging bio-based building block in view of the depletion and increasing costs of fossil feedstocks for the synthesis of butenes (through dehydration) that are widely used in polymers, oxygenated additives and rubbers... The dehydration of alcohols can be catalysed by acid sites, of which zeolites are the most promising. Shape selective effects of zeolites can give rise to high yields of butene isomers compared to other types of catalysts and differences in selectivity are found with the use of various zeolites. A lot of literature is available on ethanol dehydration over zeolites, whereas the research on butanol dehydration is still in its infancy[1,2].

2 Experimental/methodology

In this work, butanol dehydration was studied in a high throughput setup on the different zeolites (parent and acid treated samples) to determine the effect on the characteristics and reaction kinetics. Acid treatment is a common technique to dealuminate the zeolite lattice and remove non-framework alumina without the loss of zeolite type characteristics and to create mesopores[3,4]. Two different types of zeolites where chosen to compare the effects of zeolite topology as well.

Commercial zeolites (Zeolyst) were provided in ammonium form and were preliminary calcined at 550K for 8 hours to convert into the acid form. To investigate the effect of dealumination two different concentrations of hydrogen chloride were chosen keeping all other reaction conditions constant. 1.5 grams of zeolite were suspended in 150 ml of HCl solution of either 1M or 0.1M HCl concentration. The suspension was heated and stirred at 350 rpm until boiling point and kept under reflux during 2 hours. Afterwards the suspension was filtered and washed with deionised water until neutral pH and dried at 125°C.

The assessment of the catalysts was performed in a high throughput setup equipped with 2 tubular reactors, under typical dehydration conditions. The catalyst was diluted with inert to ensure isothermicity of the catalyst bed. The feed consisted of n-butanol (Sigma Aldrich (99,4% pure)) and nitrogen (Air Liquide) as inert carrier. The product analysis is performed with a GC equipped with an FID-detector and PONA column. As internal standard methane is used. To fully understand the effect of the treatments a broad range of site times was tested under the same ?thermal? conditions. This approach provides an accurate investigation of the effect of the mesoporosity and acid strength without being influenced by the number of acid sites.

3 Results and discussion

All used catalysts were fully characterized by means of: NH_3-TPD, XRD, ICP, SEM/EDX and N_2 adsorption. A summary of these characteristics is given in table 1.

Table 1. Characteristics of tested zeolites for n-butanol dehydration

Sample	Si/Al_{bulk}	$Si/Al_{surface}$	$Conc_{brönsted}$ (mmol/g)	S_{Int} (m^2/g)	S_{ext} (m^2/g)	V_{Micro} (cm^3/g)	V_{tot} (cm^3/g)
MFI	16.4	17.34	0.36	376.4	123.5	0.114	0.255
MFI0.1	29	39.9	0.31	361.4	127.2	0.124	0.278
MFI1.0	26.5	21.7	0.33	392.1	193.1	0.132	0.308
FER	10	15	0.41	322.5	40.5	0.132	0.245

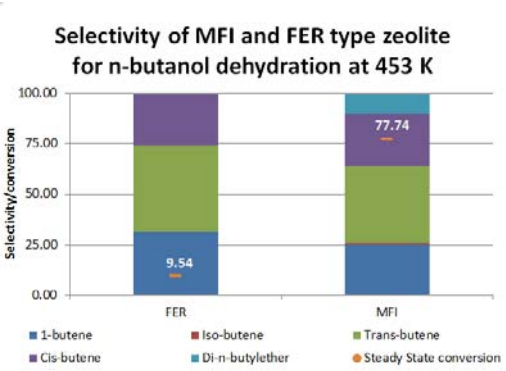

First dehydration tests on the non acid-treated commercial samples of MFI and FER show a difference in selectivities and conversion due to a difference in zeolite topology. Other characteristics were similar such as the Brönsted acid density and pore volumes. Both zeolites were tested under same site times (3.5 $mol.s/mol_{n\text{-}BuOH,o}$) at same reaction temperatures (160°C and $P_{n\text{-}BuOH,0}$: 15 kPa) and results are given in Figure 1.

4 Conclusions

In search to improve the stability, activity and selectivity of zeolite topologies for the dehydration reaction of n-butanol to butenes, the effects of dealumination of two types of zeolites were investigated. Treatment of the zeolites at two different concentrations of hydrogen chloride results in an increase in silica to alumina ratio due to the removal of framework and non-framework alumina. This also results in a slightly higher mesoporous material with higher specific area. When the acid concentrations reaches 1 M HCl we see a lower Si/Al ratio than for the treatment at lower concentrations. This could imply that not only aluminium is removed from the lattice but also silica. These improvements can result in higher resistance to deactivation caused by coke formation. Also effects in selectivity can be found due to changes in acidity strength and density.

Also noticeable differences are found with the change of zeolite topology regardless of the treatment. This supports the statement that structural differences in the zeolite lattices can be exploited to influence the activity and selectivities of n-butanol dehydration.

References

[1] D. Zhang, R. Al-Hajri, S. A. I. Barri & D. Chadwick, ChemComm 46(23) 2010.
[2] R. M. West, D. J. Braden & J. A. Dumesic, Journal of Catalysis 262 2009.
[3] M Müller, G Harvey & R Prins, Microporous and Mesoporous Materials 34(2) 2000.
[4] C. S. Triantafillidis, A.G. Vlessidis, L. Nalbandian & N.P. Evmiridis, Microporous and Mesoporous Materials 47(2-3) 2001

IV-PP53

Features of the Zeolite Containing Catalysts of Oxidative Catalytic Cracking by Thermal Analysis

Guseynova E.A.*, Mursalova L.A., Salayev M.R., Adjamov K.Yu.

«Chemistry and Geotechnological Problems of Oil and Gas» Scientific Research Institute, ASOA, Baku, Azerbaijan Republic

* elvira_huseynova@mail.ru

Keywords: oxidation, catalytic cracking, zeolite catalyst, thermal analysis

1 Introduction:

One of the most accessible directions of work intensification of catalytic cracking is to maintain a process in unconventional conditions – to existents of oxygen (Oxycracking) [1,2]. During researches [1,3] was found that the presence of an optimum amounts of oxygen increases the yield of light products from cracking products, in comparison with the traditional mode of carrying out the process, studied the effect the oxidative nature of the medium on the distribution of cracking products and the degree of conversion of raw materials. It's obviously that in evaluating the efficiency of oxidative catalytic cracking is a problem of deactivation of the catalyst.

This work is a continuation of these studies. It using thermal analysis studied the dynamics of accumulation and features of the formation of surface condensation products (CP) in condition oxidative catalytic cracking.

2 Experimental/methodology:

The proses of oxidative catalytic cracking was carried out in a flow reactor with a fixed bed industrial catalytic cracking zeolite catalyst OMNIKAT-340 at temperature 500ºC, atmospheric pressure, and volumetric velocity of feed 2 h^{-1}. The air supply to the reaction zone was 0.5% for raw materials. As a raw materials used vacuum qas oil (s.b.270 ° C – e.b.500°C).

The thermal behavior of zeolite-containing catalyst samples were studied by thermogravimetric and differential thermal analysis (TGA-DTA) installation for CD STA 429 company NETZSCH. For analysis was selected linearly linearly-polythermal heating the sample at a heating rate of 10°C /min in air´s atmosphere.

3 Results and discussion:

To determine the dynamics of coke deposits in the catalytic cracking of oxidative studies conducted derivatografic zeolite catalyst samples which differed in the length of time that the reaction medium: 15, 30, 45, 60 minutes (samples 1-4). For comparative analysis thermogram sample was removed for 15 minutes participating in the catalytic cracking process that use by traditional non oxidizing conditions (sample 5).

Discussing and analyzing the results, we can note the following:

- for all five samples in the temperature range of 25-310°C is characterized by a broad endothermic effect associated with the removal of the adsorbed pore water, accompanied by significant weight loss (5,5-15%). It should be noted that the minimum value of this index was noted for sample 5;
- on the differential curves of samples 1 to 4, after the removal of moisture, there are two exothermic peaks with maxima at 398 ... 407 ° C and 485 ... 504°C and the mass loss was 2.5-4 respectively and 10.5-12.5%. Noteworthy is that in contrast to the sample 1, the sample 5, which one the length of stay is a traditional non-oxidizing environment of

the reaction was 15 also minutes, characterized by single exothermic peak, whose maximum temperature is higher than the average of 40-125°C and reaches 525.5°C, which indicates a more condensed nature CP;

- analysis of the samples 2 and 3 indicates that part of the catalyst in the process during oxycracking within 15-45 minutes leads to a gradual increase in the degree of condensation and the number of CP. It specifies the offset of the two previously mentioned intense exothermic effects at higher temperatures pronounced total mass loss - up to 15-16.3 %. While the temperature maxima remained virtually unchanged;
- the highest number of CP contained is in the sample 4, which is explained by significantly longer cycle of his work in terms oxycracking (60 min). The degree of condensation of the CP it is very high, as evidenced by the end of their combustion temperature - 814.6°C. Despite the fact that the total weight loss of samples 2 and 4 have similar meanings, but CP formed on the surface of the former is less condensed, as evidenced by the lower end of their combustion temperature (624.7°C).

4 Conclusions:

Thus, our studies revealed distinct nature of CP, formed in the course of the traditional non-oxidative and oxidative catalytic cracking. Oxidative cracking of vacuum gas oil for 45 minutes formed two distinct phases surface CP: 1 - deposition of an amorphous type with a high hydrogen content; 2 - low coke density. Deleting the CP data observed in the temperature range 574 ... 675°C, which is lower than the regeneration temperature range of the traditional catalysts for catalytic cracking and shows promising oxycracking. It was also found that increasing the catalyst mileage oxycracking 60 minutes resulting in the formation of highly surface and graphitized structures, over which the burning temperature of 800°C, far exceeding the stability limit temperature of zeolite catalysts.

References

[1] S.I.Kolesnikov, V.O.Zvaqin, I.M.Kolesnikov // Chemistry and Technology of Fuels and Oils. 2 (1999). P.10-12.

[2] K.K.Dubrovay, A.B.Shaiman. Oxidative Cracking. 1936. 394 p.

[3] L.A.Mursalova, E.A.Guseynova, K.Yu.Adjamov // Azerbaijan chemical journal. (3) 2014, P.37-42.

IV-PP54

Effect of the Physico-Chemical Characteristics of the Various Mn-Based Oxide Catalysts on the Catalytic H_2O_2 Decomposition

Choi H.-Y., Jang J.H., Han G.B.*

Institute for Advanced Engineering, Yongin, Republic of Korea

* gbhan@iae.re.kr

Keywords: catalytic H_2O_2 decomposition, Mn-based catalyst, reaction, conditions, physic-chemical characteristics, catalytic activity

1 Introduction

Hydrogen peroxide has been utilized as an oxidizing agent in the waste water disposal facilities for the environmental remediation such as the bleaching and deodorization in the industry. The steam, oxygen and heat energy, which can be utilized in industry and other field and the reactant is a non-toxic and an environment-friendly, can be generated by the decomposition of H_2O_2. For these merits, the catalytic decomposition of H_2O_2 has been researched in view of the effect of the various oxide-based catalysts on the performance. The various metal oxide catalysts were prepared for the catalytic H_2O_2 decomposition and the effect of their characteristics on the performance was investigated in this study. The catalytic activity was compared through the variation of the temperature, pressure and reaction duration time during the catalytic H_2O_2 decomposition.

2 Experimental/methodology

The various catalysts were prepared by co-precipitation method using zirconyl nitrate ($ZrO(NO_3)_2 \cdot xH_2O$), manganese chloride ($MnCl_2 \cdot 4H_2O$), iron hydroxide ($Fe(OH)_3$), aluminium oxide (r-Al_2O_3), etc. and ammonia water (NH_4OH) as the precursors, support and precipitate, respectively. In the preparation procedure, the solid material obtained after the co-precipitation process was dried for 12 hr at 110 °C and was calcined for 4hr at 600 °C. The performance test of the various prepared catalyst was conducted using both fixed and batch type reactor.

3 Result and discussion

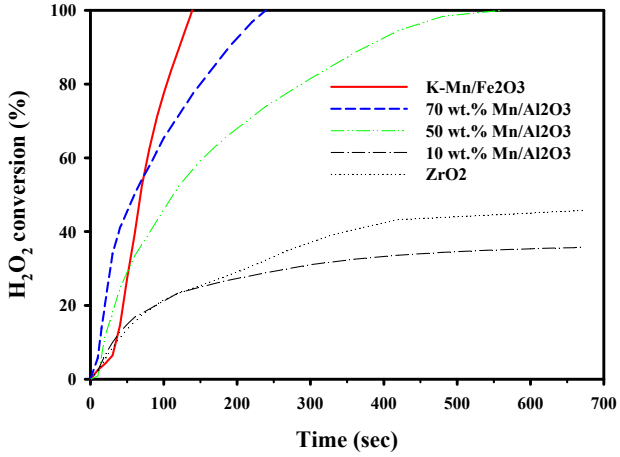

Fig. 1. H_2O_2 conversion in the catalytic H_2O_2 decomposition over Mn-based catalysts.

Fig. 1 shows the H_2O_2 conversion with the various catalysts in the catalytic H2O2 decomposition. The amount of catalyst and hydrogen peroxide were used 0.01 g and 40 ml, respectively. The conversion of H_2O_2 decomposed had a difference with the catalyst. The K-added Mn-based oxide catalyst had the highest activity with the reaction temperature and pressure among the various catalysts, simultaneously.

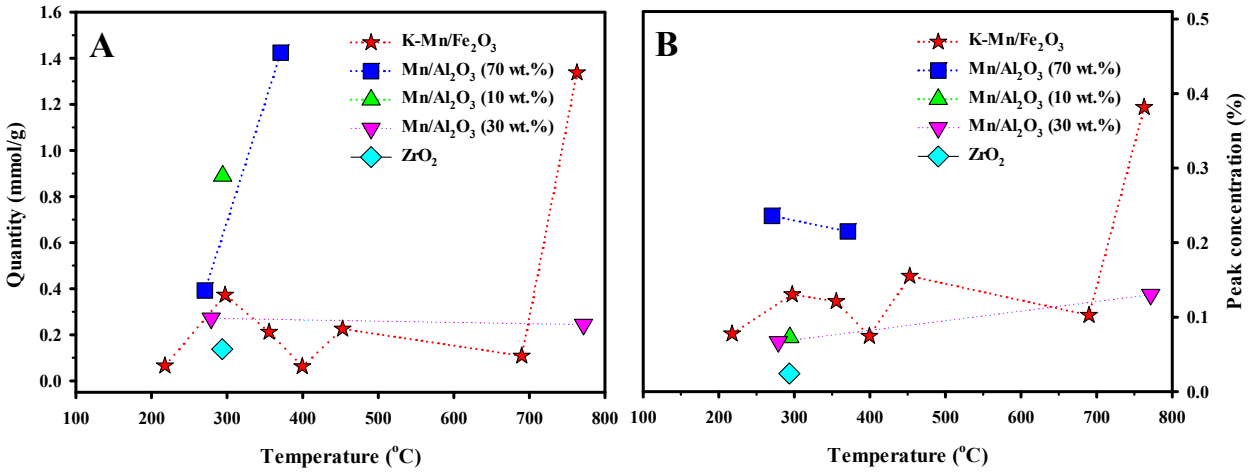

Fig. 2. Acidic properties of the various catalysts by NH_3-TPD.

Also, the physic-chemical properties of the catalysts were analyzed by SEM/EDX, XRD, XRF, NH_3-TPD. Fig. 2 shows the acidic properties with NH_3-TPD as a representative property of the various catalysts for the catalytic H_2O_2 decomposition. In this result, it was known that the strength and amount of the acidic sites of the various catalysts has an effect on the catalytic activity. Among the various catalysts, K-added Mn-based oxide catalyst had the most abundant acidic sites and strength and its activity was highest.

4 Conclusions

The relationship between the catalytic activity and the properties of the various catalysts for the catalytic H_2O_2 decomposition was investigated in this study. Consequently, it was known that the highest catalytic activity was obtained by using the K-added Mn-based oxide catalyst having the most abundant and strongest acidic sites in the catalytic H_2O_2 decomposition using the various catalysts.

Acknowledgements

This subject is supported by Korea Ministry of Environment(MOE) as "Advanced Technology Program for Environmental Industry".

IV-PP55

Investigation of the Thermocatalytic Conversion Process of Catalytic Cracking Heavy Gasoil and its Mixture with Cotton Oil by Using the Mix Catalytic System

Hasankhanova N.V.*, Mammadova T.A, Asgarova E.N., Teyubov Kh.Sh., Aliyeva S.K, Latifova T.S., Asgarli N.E., Safarova N.E.

Institute of Petrochemical Processes of Azerbaijan National Academy of Sciences, Baku, Azerbaijan Republic

* nadirexatun@mail.ru

Keywords: catalytic cracking heavy gasoil, ethylene, propylene, halloysite

1 Introduction

During the recent years the role of the catalytic cracking process assumes importance in the trend of obtaining the main feedstock to the polypropylene industry [1,2]. The investigations are carried out in most of the countries for increasing the yields of low molecular olefins, especially ethylene and propylene in the conducted deep catalytic cracking [3-6]. In the presented work has been investigated the thermocatalytic conversion process of heavy gasoil obtained from catalytic cracking process (CCHG) and its mixture with cotton oil at temperature range of 550-700°C.

2 Experimental/methodology

The catalytic conversion process of heavy gasoil and its mixture with 10% of cotton oil have been conducted in laboratory microdevice with the mass rate of 0,5-1 $hour^{-1}$ of feedstock supplying. Seokar-600 (I) and its mixture with halloysite (II) has been taken as a catalyst. The main catalyst has contained the amount of halloysite of 10% mas.

When the Seokar-600 /halloysite catalytic system is used the upper layer has been consisted of pure halloysites (approximately 5% of the height of catalyst layer), but the bottom layer of catalyst has been consisted of Seokar-600. The composition of hydrocarbon gas obtained from the catalytic cracking process of heavy gasoil and its mixture with cotton oil have been described in Table 1 and 2.

3 Results and discussion

Table 1. The hydrocrabons composition of gases obtained from the CCHG thermocatalytic conversion by using Seokar-600 (I) and its mixture with halloysite (II).

The composition of hydrocarbon gases,% wt.	**Catalysts**						
	I	**II**	**I**	**II**	**I**	**II**	**I**
	Temperature of process, °C						
	550		**600**		**650**		**700**
methane	1,4	1,8	3,2	4,0	7,6	7,2	7,8
ethane	1,0	0,9	1,2	1,4	2,0	1,4	2,1
ethylene	7,2	7,8	12,0	12,7	20,0	20,6	23,8
propane	1,9	2,1	0,95	1,1	1,4	1,2	1,6
propylene	11,8	12,4	14,6	15,3	14,7	15,2	17,1
butane	0,6	1,0	1,2	1,4	1,2	0,8	1,2
Σ butylenes	2,3	4,2	5,85	5,1	4,1	5,0	6,8
Total	26,2	30,2	39,0	41,0	51,0	51,4	60,4
Σolefin-	21,3	24,4	32,45	33,1	38,8	40,8	48,2

containing gases

The maximum yield of ethylene at 700°C in the presence of Seokar-600 and Seokar-600/halloysite mixture catalysts is accordingly of 23,8-24,4 %; but it is accordingly of 17,1-17,7 % mass in propylene. The increasing of the yield percent of olefins is observed when we add halloysite to the composition of Seokar-600 that used for all of the investigated temperatures.

The yield percent of either ethylene or propylene increases by increasing of temperature when vegetable oil of 10 % added to the composition of processed feedstock (Tabl.2).

Table 2. The composition of hydrocarbon gases obtained from the thermocatalytic conversion of CCHG fraction containing 10% vegetable oil by using Seokar-600 (I) and its mixture with halloysite (II)

The composition of hydrocarbon gases,% mass	**Catalysts**						
	I	**II**	**I**	**II**	**I**	**II**	**I**
	Temperature of process, °C						
	550		**600**		**650**		**700**
methane	1,4	2,0	3,6	4,1	7,8	8,2	8,4
ethane	1,0	1,1	1,5	1,2	2,3	1,6	2,3
ethylene	7,6	8,6	13,5	14,6	23,1	24,5	26,7
propane	2,3	2,0	2,0	1,4	1,6	1,4	1,8
propylene	12,6	13,1	15,7	16,0	16,1	16,7	18,0
butan	1,0	1,4	1,6	1,1	1,4	1,2	1,4
Σ butylenes	2,5	4,0	4,1	4,9	4,2	3,8	6,9
Total	28,4	32,2	42,0	43,3	55,1	57,4	65,5
Σolefin-containing gases	22,7	25,7	33,3	35,5	43,4	45,0	51,6

As it seen from Table 2, the maximum yield of ethylene at 700°C in the presence of Seokar-600 and Seokar-600/halloysite mixture catalysts is accordingly of 26,7-27,4, %; but it is accordingly of 18,0-18,8 % wt. for propylene.

The increase of 0,4-0,8; 1,5-0,9; 3,1-3,9; 2,9-3,0 % wt. in the yield of ethylene has been observed during the thermocatalytic conversion of CCHG at with adding 10% of cotton oil at a temperatures of 550-700°C in the presence of Seokar-600 and Seokar-600/halloysite mixture catalyst accordingly . This increase for propylene is accordingly of 0,8-0,7; 1,1-0,7; 1,4-1,5; 0,9-1,1 % wt.

References

[1] J. Fujiyam, H. Redhwi, M. Rahat Saeed, Oil and Gas Journal. 2 (2005). P. 54.
[2] T. Ren, M. Patel, Blok K. , Energy. 31 (2006). P. 425.
[3]A. Aitani, T. Yoshikawa, Ino T. , Catalyst Today.60 (2000). P. 111.
[4] A. Shaikh, E. M. Al-Mutairi, Ino T. ,Ind. Eng. Chem. Res. 47(2008). P. 9018.
[5] R. Price, B. Gaber, Y. Lvov., Journal of Microencapsulation. 18 (2001). P.713.
[6]E. Joussein, S. Petit, J. Churchman, et al. ,Clay Miner. 40 (2005). P. 383.

IV-PP56

Au-Cu^+ Synergy in $MgCuCr_2O_4$-Spinel Supported Gold Nanoparticles for Selective Oxidation of Alcohols and Olefins

Hensen E.J.M.*, Song W.

Eindhoven University of Technology, Inorganic Materials Chemistry Group, Schuit Institute of Catalysis, Eindhoven, The Netherlands

* e.j.m.hensen@tue.nl

Keywords: gold nanoparticle, spinel support, selective oxidation, reaction mechanism, DFT

1 Introduction

Supported gold nanoparticles are promising catalysts for a wide range of selective oxidation reactions. As the least reactive of all transition metals, several strategies are employed to render gold active and selective for such reactions. The nanosizing of gold and the use of supports are main approaches that help to activate dioxygen. In the present contribution, we will discuss the significant synergy between gold nanoparticles and a copper-doped $MgCr_2O_4$-spinel used as the support for the oxidation of ethanol to acetaldehyde [1] and propylene to acrolein [2].

2 Experimental/methodology

$Mg_{0.75}Cu_{0.25}Cr_2O_4$ (denoted as $MgCuCr_2O_4$) and $MgCr_2O_4$ were prepared by a coprecipitation-calcination method. Gold nanoparticles were loaded by homogeneous deposition-precipitation using urea. The gold loading was 1 wt%. The catalysts were calcined in air at 350 °C for 5 h. DFT with the PBE functional as implemented in the VASP code was employed to explore the reaction mechanism. A Hubbard *U* term was added to the PBE functional to properly treat electron localization. Spin-polarized DFT calculations were performed. The projector augmented wave method was used to describe the interaction between the ions and the electrons with the frozen-core approximation. The cut-off energy is 400 eV.

3 Results and discussion

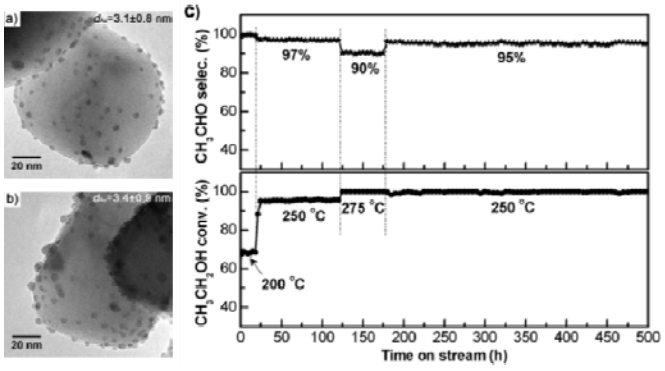

Fig. 1. TEM images of a) fresh $Au/MgCuCr_2O_4$ and b) spent $Au/MgCuCr_2O_4$ catalyst after 500 h on-stream; c) ethanol conversion and acetaldehyde selectivity (reaction conditions: catalyst 0.1 g, GHSV = 100,000 mL g_{cat}^{-1} h^{-1}, ethanol/O_2/He = 1/3/96).

The $Au/MgCuCr_2O_4$ catalyst is highly active and selective for the aerobic oxidation of ethanol to acetaldehyde (Fig. 1a and c; conversion 100%; yield ~95% at a space velocity of 100 L g_{cat}^{-1} h^{-1}). The catalyst is stable for at least 500 h and, during this time, the Au nanoparticles do not sinter (Fig. 1b). Extensive characterization by TEM, XPS and EXAFS shows that the synergy involves the close interaction between metallic and surface Cu^+ species stabilized in the support. $MgCuCr_2O_4$ is more stable than $MgCuAl_2O_4$, because in $MgCuAl_2O_4$ C Cu segregates into CuO. DFT calculations of the complete ethanol oxidation reaction mechanism explain the importance of the interface between the Au nanoparticles and the $MgCuCr_2O_4$-spinel [3].

$Au/MgCuCr_2O_4$ is also an active catalyst for the selective oxidation of propylene to acrolein

(selectivity close to 90%). The high selectivity agrees with the well-known notion that Au in interaction with Cu^{+} can selectively oxidize the allylic C-H bonds in propylene. An extensive DFT study of the reaction mechanism hints at the dynamic nature of gold atoms at the interface of the gold clusters with the support [2]. Adsorption of propylene leads to the formation of an isolated Au atom that strongly binds propylene. The reaction proceeds by activation of the allylic C-H bond by support O or adsorbed O_2 molecule (Fig.2). Detailed analysis of the electronic structures of the reaction intermediates in the catalytic cycle show that the critical role of Cu is the decrease of the desorption energy of acrolein.

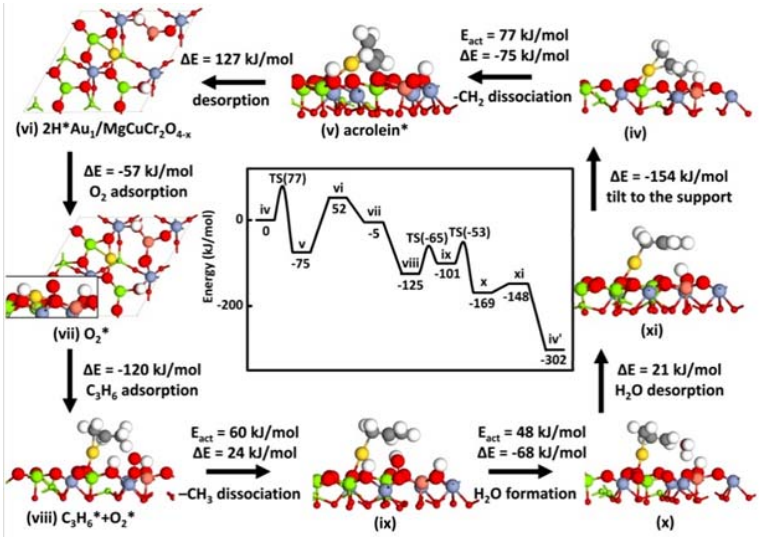

Fig. 2: Reaction energy diagram (middle) with elementary reaction steps for the oxidation of propylene to acrolein on the $Au_1/MgCuCr_2O_4$ model. Main reaction steps are: adsorbing propylene allylic C-H cleavage by support O or adsorbed O_2 species; C-O bond formation; second C-H bond cleavage to form acrolein; acrolein desorption.

4 Conclusions

Highly efficient, selective and stable oxidation of ethanol to acetaldehyde, propylene to acrolein by using $MgCuCr_2O_4$ spinel supported gold nanoparticles is reported. Density functional theory calculations provide a molecular level insight to the reaction mechanism and unravel the importance of Au-Cu synergy in both reactions.

References

[1] P. Liu, E.J.M. Hensen, *J. Am. Chem. Soc.*135 (2013) 1432.
[2] W. Song, D.M. Perez Ferrandez, L. van Haandel, P. Liu, T.A. Nijhuis, E.J.M. Hensen, *ACS Catal.* (2015) DOI: 10.1021/cs5017062.
[3] W. Song, P. Liu, E.J.M. Hensen, *Catal. Sci. Technol.* 4 (2014) 2997.

IV-PP57

Effects of Promotion Techniques on zsm-5 Activity in Conversion of Alcohols to Fuel Range Hydrocarbons

Isa Y.M.*

Durban University of Technology, Durban, South Africa

* YusufI@dut.ac.za

Keywords: zsm-5, alcohols, activity, promotion techniques, fuels, hydrocarbons

1 Introduction

Fermentation broth obtainable from organic materials is a potential source of ethanol [1]. The vision of using ethanol from fermentation as a universal feedstock for production of chemicals and fuels is surely one of the promising routes towards sustainable production. Bioethanol could be dehydrated to yield ethylene which could undergo a number of reactions that will produce priceless chemicals. The product distribution of ethanol conversion is majorly determined by the quality of ethanol, operating conditions as well as the catalyst employed in the process. While zeolites have been known to show good activity in ethanol conversion to fuel range hydrocarbons, other catalysts like cerium oxide are known to favour the production of hydrogen. The Fischer Tropsch process uses iron and cobalt catalysts for the production of different hydrocarbons [2]. The activity of these active components could also play a vital role in the transformation of ethanol to fuels and petrochemicals. This work investigates different techniques of promoting synthesized ZSM-5 zeolites with iron, cobalt and nickel as well as the efficiency of techniques with respect to catalyst activity and selectivity.

2 Experimental/methodology

A series of ZSM-5 catalysts were synthesized hydrothermally using aluminum salts and water glass as sources of alumina and silica respectively. The reagent composition was determined by the target ZSM-5 SiO_2/Al_2O_3. The pH of the batch mixture was kept below 10.8. The batches were further aged at different times (0-48 hrs.) and crystallization was done at different temperatures and times not exceeding 200°C and 96 hours respectively. The produced crystals were processed by filtration, calcination and protonation to synthesize the desired protonated form of the catalyst. A commercial zsm-5 was also purchased from Zeolyst for comparative studies with the in house catalyst.

Nitrates of cobalt and iron were used for promotion at different loadings (5%, 10% and 15%). Mechanical mixing, co-precipitation and incipient wetness impregnation were applied as promoting techniques to enhance catalyst performance. The synthesized catalysts were characterized using XRD, BET, XRF and SEM.

The catalyst activity was tested using a fixed bed reactor at different space velocities and temperatures in the range of 200-450°C. The feed used include ethanol and water mixtures of various composition, isopropanol and butanol. Other alcohols were investigated so as to have a better understanding of the most probable reaction path during ethanol conversion.

3 Results and discussion

Powder XRD patterns of the catalyst synthesized confirmed the presence of 2 theta values for the target ZSM-5 catalysts. Figure 1 shows the diffractogram of the synthesized zsm-5 catalyst. The presence of the zsm-5 characteristic peaks at 2 theta = 7-9° and 23-25° further confirm the successful synthesis of zsm-5. All the synthesized material had relative crystallinities of not less than 90% when compared to the commercial zsm-5 catalyst. The BET surface area and particle sizes are all seen to be a function of aging. The SEM analyses further confirmed that the zeolites formed were crystalline and had different morphologies depending on the technique used in incorporating the promoter and synthesis conditions. Figure 2 shows the micrograph of un-promoted zsm-5 with average particle size of 0.2μm. The incorporation of metals altered both the particle morphology as well as size.

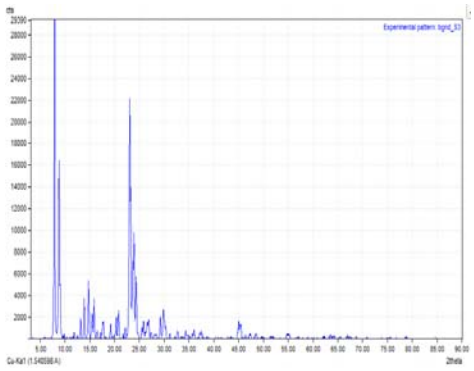

Figure 1. Diffractogram of synthesized zsm-5

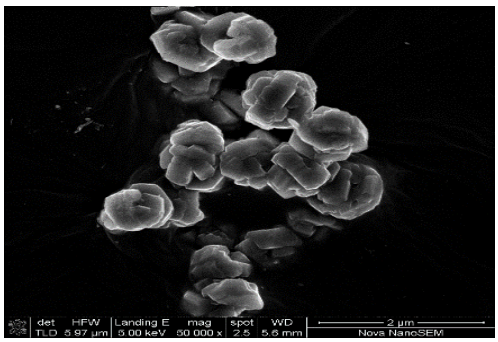

Figure 2: Micrograph of synthesized ZSM-5

All the catalysts showed 100% activity for ethanol and isopropanol conversion with liquid hydrocarbons forming a significant amount of the products. Loading of 5% iron oxide on the commercial catalyst by incipient wetness impregnation showed selectivity to gasoline range hydrocarbons of 72% in the liquid products whereas the in house catalyst showed a better selectivity of 98% during ethanol conversion. Co crystallization of both commercial and in house ZSM-5 showed different selectivity when compared to the unpromoted zsm-5. However, 5% loading of nickel showed the highest selectivity towards gasoline range hydrocarbons (99%) when ethanol was used as a feedstock. Conversion of isopropanol shows that promoting the ZSM-5 with both iron had more significant changes to hydrocarbon selectivity when compared to promotion with cobalt oxide. Promoting the in house zsm-5 with 5% Co did resulted in a selectivity towards gasoline of 63% which was slightly less than that obtained from the unpromoted commercial zsm-5.promoting with Iron under the same conditions shows 78% selectivity towards gasoline range hydrocarbons. In all three cases, the selectivity for diesel range hydrocarbons was less than 30%

4 Conclusions

ZSM-5 catalyst have been successfully synthesized and characterised, various promotion techniques and promoters used on zsm-5 catalysts showed that both the promotion techniques as well as promoting agents had a significant impact on the product distribution. It has been observed that ethanol as well as isopropanol could serve as potential sources of hydrocarbons in the fuel range. Finally the operating parameters greatly influence the product distribution of alcohols over zsm-5 catalysts.

References

[1] G Dragone, S. Mussatto, J. Amleida e Silva and J.Teixeira , *Biomass and Bioenergy (2011)*
[2] S. Ali , N. Asmawati M. Zabidi and D. Subbarao, *Chemistry central Journal*. (2011)

IV-PP58

Fischer-Tropsch Synthesis in Presence of Composite Materials Based on Pyrolyzed Polymers of Different Structure

Ivantsov M.I.[1,2], Kulikova M.V.[2], Chernavskii P.A.[1], Karpacheva G.P.[2*]

1 - Lomonosov Moscow State University, Faculty of Chemistry, Moscow, Russia
2 - A.V.Topchiev Institute of Petrochemical Synthesis, RAS, Moscow, Russia

* ivantsov@ips.ac.ru

Keywords: Fischer-Tropsch synthesis, cobalt, catalysts, nanocomposites, magnetism

1 Introduction

Innovative method of producing composite materials based on polymeric matrix IR-pyrolysis is offered in TIPS RAS. These materials are catalysts of Fischer-Tropsch synthesis which is second stage of refining processes of petroleum feedstocks in environmentally friendly components of motor fuels [1].

2 Experimental/methodology

For catalysts preparation following polymers: polyacrylonitrile (PAN), polybiphenyl amine (PDFA), polystyrene (PS), polyvinyl alcohol (PVA) and cellulose (CL) were used.

Catalysts were prepared in two stages: at first stage joint solution of polymer and salt was received, at second stage IR –pyrolysis of synthesized system was carried out.

Fischer-Tropsch synthesis was carried out in fixed bed reactor without pre-reduction stage. Magnetic characteristics of composites were measured on vibration magnetometer *in situ* [2].

Samples were also analyzed by X-ray «Geiger Flex» diffractometer («Rigaku»).

3 Results and discussion

All synthesized samples are active in synthesis of hydrocarbons from CO and H_2. Samples prepared by using PVA and PAN demonstrated maximum activity. CO conversion for these samples reach the value of 100%.

Liquid hydrocarbon productivity of contacts Co-PAN, Co-PDFA, Co-PVA is much than productivity of industrial analogs (to 2700 g/kgMe/hour).

Samples with greatest productivity value (Co-PDFA, Co-PAN, Co-PVA) were studied by magnetometric *in situ* method. Presence of Co ferromagnetic particles was shown by field dependences of nanocomposite materials. Also, according to magnetic characteristics metal's degree of reduction for sample before catalysis was determined.

It was determined by XRD method, that dominant phases for Co-PDFA, Co-PAN and Co-PVA samples are metal, metal along with oxide and oxide respectively.

These results correlate with magnetometric data.

4 Conclusions

It was established that composition (structure or nature) of a polymeric matrix has impact on nature of active centers, and, as a result, influences on Fischer-Tropsch synthesis indicators.

It was assumed that higher activity related with polyconjugated cyclic structure which formed during polymer pyrolysis.

The presence of cobalt and cobalt oxide phases which are responsible for active centers of different nature activities for Co-PDFA and Co-PAN samples was proved.

It was assumed that high catalytic activity of Co-PVA sample results from activation in syngas medium during Fischer-Tropsch synthesis.

Acknowledgements

This work was supported under the Program of basic scientific researches by Presidium of RAS №25 «Energy aspects of deep fossil and renewable carbon-containing raw material processing».

This work was partially carried out using of Common Use Center "New Petrochemical Processes, Polymeric Composites and Adhesives" equipment.

References

[1] Khadzhiev S.N., Krylova A.J., Karpacheva G.P., Kulikova M.V., Ljadov A.S., Sagitov S.A., Zemtsov L.M., Muratov D.G., Efimov M.N.// CATALYST AND METHOD OF OBTAINING ALIPHATIC HYDROCARBONS FROM CARBON OXIDE AND HYDROGEN IN ITS PRESENCE // Patent RU 2 492 923 C1

[2] Chernavskij P.A., Pankina G.V., Chebotarev B.P., Kiselev V.V., Lunin V.V.// VIBRATION MAGNETOMETER// Patent RU 2 444 743 C2

IV-PP59

Conceptual Design of the Catalytic H_2O_2 Decomposition Process for the Production of Dry Oxidizing Agent Used in the NO Oxidation

Jang J.H., Choi H.Y., Han G.B.*

Institute for Advanced Engineering, Yongin, Republic of Korea

* gbhan@iae.re.kr

Keywords: H_2O_2 catalytic decomposition, dry oxidizing agent, NO oxidation, conceptual design

1 Introduction

NOx is a major air pollutant produced by the combustion of fossil fuel. The many efforts have been conducted to improve the removal efficiency of NOx. The selective catalytic reduction (SCR) process has been known as a general and usual NOx treatment process[1-5]. However, SCR process has the disadvantage of the difficult installation, operation/maintenance cost to increase due to high operation temperature for the activity of used catalyst. Therefore, to develop the NOx treatment process having the low cost and high efficiency is necessary. Many technologies of the NOx treatment have been conducted and the NO oxidation using the various wet and dry oxidants was investigated to improve the NOx removal efficiency. The dry oxidant can be produced by the H_2O_2 decomposition and then iron, zirconium and some other transition metal-based oxide were used for the catalytic H_2O_2 decomposition. In this study, the catalytic process for H_2O_2 decomposition was investigated for the production of the dry oxidizing agent to use for the NO oxidation. The catalytic H_2O_2 decomposition over the various catalysts for the dry oxidant production and the combination with NO oxidation process using dry oxidant produced was investigated under the various reaction conditions (e.g., temperature, amount of catalysts, gas composition and space velocity).

2 Experimental/methodology

The experimental H2O2 decomposition system combined with NO oxidation was constructed to conduct for the production of the dry oxidizing agent and the NO conversion. In experimental set-up, the outside diameter and length of the reactor for the H_2O_2 decomposition was 1/2 inch and 50 cm, respectively, and the outlet of the H_2O_2 decomposition process was combined with the inlet of NO oxidation process. The outside diameter of reactor for the NO oxidation process was 1/2 inch. The amount of the catalyst packed was about 0.5 g and the operation temperature was about 150 ℃. The basic reaction conditions were shown in the table 1.

Table 1. Basic reaction conditions.

Factor	Value
Catalysts	
Temperature	70 - 200 ℃
Space Velocity	5,000 - 30,000 ㎤/g-cat.·h
[H2O2]/[NO]	1.0 - 3.5
NO concentration	1,000 – 5,000 ppm

3 Results and discussion

Fig. 1 shows the H2O2 decomposition efficiency depending on the different catalysts for the dry oxidant production by H2O2 decomposition. The reaction temperature for the catalytic H2O2 decomposition was 150 ℃. The catalysts having the highest activity for H_2O_2 decomposition were K-Mn/Fe2O3 and Na-Mn/Fe_2O_3 catalysts.

Fig. 2 shows the NO conversion with the dry oxidant in the NO oxidation process combined with the catalytic H_2O_2 decomposition over the various catalysts. It was known that the NO conversion reached about 100% when the catalyst used in the H_2O_2 decomposition process were K-Mn/Fe_2O_3, Na-Mn/Fe_2O_3.

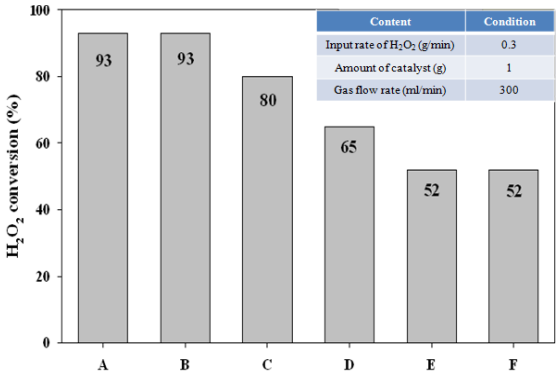

Fig. 1. H2O2 decomposition efficiency depending on the catalyst type for the dry oxidant production (A: K-Mn/Fe2O3 (70%), B: Na-Mn/Fe2O3 (70%), C: Mn/Al2O3 (30%), D: Mn/Al2O3 (10%), E: Fe2O3, F: S-ZrO2).

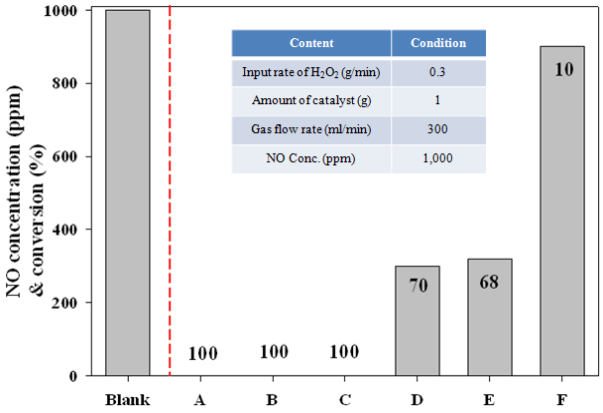

Fig. 2. NO conversion using the dry oxidant produce by H2O2 decomposition according to the catalyst type.(A: K-Mn/Fe2O3 (70%), B: Na-Mn/Fe2O3 (70%), C: Mn/Al2O3 (30%), D: Mn/Al2O3 (10%), E: Fe2O3, F: ZrO2, value: NO conversion).

4 Conclusions

In this study, H_2O_2 decomposition and NO oxidation processes were combined and operated for the dry oxidant production and NO oxidation to improve the NOx treatment efficiency. Under the optimized operation conditions, the H_2O_2 decomposition efficiency was about 93% in the H2O2 decomposition process over KMnO4-based catalyst and then, simultaneously, the NO conversion reached about 100% in the NO oxidation process.

Acknowledgements

This subject is supported by Korea Ministry of Environment(MOE) as "Advanced Technology Program for Environmental Industry

References

[1] R. Qi and R. T. Yang, Appl. Catal., B, (2003), 44, 217–225.
[2] Y. Liu, J. Zhang, C. Sheng, Y. Zhang and L. Zhao, Chem. Eng.J., (2010), 162, 1006–1011.
[3] M. Bai, Z. Zhang and M. D. Bai, Environ. Sci. Technol., (2012), 46, 10161–10168.
[4] R. P. Dahiya, S. K. Mishra and A. Vee□ind, IEEE Trans. Plasma Sci., (1993), 21, 346–348.
[5] S. S. Lin and M. D. Gurol, Environ. Sci. Technol., (1998), 32, 1417–1423.

IV-PP60

Gas Phase Glycerol Acetylation to Fuel Additive over Solid Acid Catalysts

Kale S.[1*], Armbruster U.[1], Umbarkar S.[2], Dongare M.[2,3], Eckelt R.[1], Martin A.[1]

1 - Leibniz Institute for Catalysis, Rostock, Germany
2 - National Chemical Laboratory, Pune, India
3 - Mojj Eng. Syst. Ltd, Pune, India

* sumeet.kale@catalysis.de

Keywords: glycerol, acetylation, triacetin, catalyst

1 Introduction

In the recent years, biodiesel has gained significant attention as renewable and sustainable transportation fuel. Glycerol is inevitably produced by 10 wt% in total biodiesel production which resulted in a large surplus of low value glycerol in the market. Glycerol esterification with acetic acid (acetylation) is one of the processes to valorize glycerol to useful chemicals such as monoacetin (MAG) and diacetin (DAG) that have applications in cryogenics and polymers. Triacetin (TAG) can act as cold flow improver and viscosity reducer for biodiesel [1]. Glycerol acetylation is usually performed in batch operation using homogeneous catalysts like H_2SO_4, p-toluenesulfonic acid or heterogeneous acidic catalysts such as heteropolyacids [2], ion exchange resins like Amberlysts [3], etc. However, the solid catalysts get deactivated due to leaching of active species. On the other side, it would be attractive to transform liquid phase batch processes to continuous flow processes, as this has several advantages, especially in the view of their implementation in industry. Surprisingly, very few reports are currently available on continuous flow glycerol acetylation [4]. In the present work, several silica-based catalysts (SiO_2-MO_x in molar ratio of 30:1) were prepared, characterized and evaluated in the gas phase acetylation of glycerol for their catalytic activity.

2 Experimental

The SiO_2-MO_x catalysts (MO_x = TiO_2, MgO, ZrO_2, SrO and Sc_2O_3 using precursor ammonium titanyl oxalate (ATO), magnesium acetate, zirconium oxychloride, strontium nitrate, and scandium nitrate, respectively, were prepared by the sol-gel method. In a typical procedure, SiO_2-TiO_2 catalyst was synthesized by dissolving 5.7 g of ATO in 30 g of distilled water. This solution was added to the aqueous solution of 120 g of TEOS (tetraethyl orthosilicate precursor for SiO_2) and conc. HCl (0.4 ml). Under stirring, aqueous ammonium acetate (buffer) solution was added to the above solution to form transparent yellow coloured gel, which was further aged for 12 h at 70 °C. To this gel, 110 g of aqueous ammonia solution (3wt%) were added and the sample was again aged for 12 h at 70 °C, further dried and calcined at 500 °C. Similarly, catalysts with MgO, ZrO_2, SrO and Sc_2O_3 were prepared.

3 Results and discussion

The prepared catalysts were studied with physico-chemical methods to evaluate the specific amount of acid sites as well as textural and structural properties (BET, Pyridine IR, XRD and others). XRD-patterns didn't show any peaks, i.e. all the catalysts were found to be X-ray amorphous. BET surface areas, pore volumes and pore diameters of SiT30 and SiMg30 are close to SiO_2. Other samples showed an increase in BET surface area. SiZr30 catalyst with highest surface area showed strongly intense Lewis acid sites, whereas all other catalysts

showed significantly less intense Lewis acid sites.

Table 1. Physico-chemical and acidic properties of the catalysts

Catalysts	BET surface area (m^2/g)	Pore Volume (cm^3/g)	Pore diameter (nm)	Band Intensity (L-Py) at 250 °C (a.u.)
SiO_2	395	0.92	9.8	0
SiTi30	404	0.81	8.7	0.46
SiMg30	375	0.85	9.1	0.42
SiZr30	572	0.60	3.7	1.64
SiSc30	451	0.75	6.3	0.45
SiSr30	275	0.86	11.3	0.06

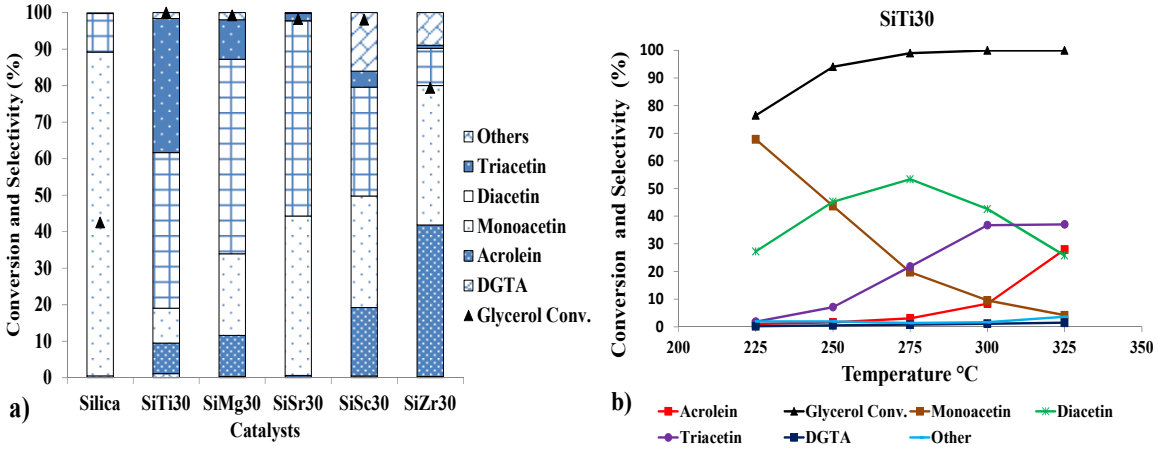

Fig. 1 a) Screening of catalysts (acetic acid/glycerol = 6, 0.6 g of catalyst, T = 300 °C, GHSV = 1707 h^{-1}). b) Effect of temperature on catalytic performance of SiTi30 (acetic acid/glycerol = 6, 0.6 g of catalyst, GHSV = 1707 h^{-1}) (DGTA = diglycerol tetraacetate).

All catalysts except the pure support showed high activity (almost 100% glycerol conversion) at 300 °C. Interestingly, SiTi30 showed high selectivity for triacetin (36.8%), whereas SiZr30 showed comparatively high selectivity for acrolein (41.5%), possibly due to its outstanding acidity (*c.f.* Fig. 1a). The curve for SiTi30 shows that acrolein selectivity rises with temperature (28% at 325 °C, Fig. 1b). The formation of diglycerol tetraacetate (DGTA) oligomer as by-product was observed, as previously also reported for batch runs [3].

4 Conclusions

Among the prepared catalysts, SiTi30 showed the best catalytic performance with complete conversion of glycerol and 37% selectivity for triacetin. SiZr30 is selective towards acrolein (41.5%). It seems that an optimum amount of Lewis acid sites is responsible for high activity and selectivity for acetins.

Acknowledgements

The authors like to thank Dr. U. Bentrup for pyridine IR data and Dr. M. Schneider for XRD studies.

References

[1] N. Rahmat, A. Z. Abdullah, A. R. Mohamed, *Renew. Sustain. Energy Rev.* 14 (2010) 987-1000.
[2] S. Zhu, Y. Zhu, X. Gao, T. Mo, Y. Li, *Bioresour. Technol.* 130 (2010) 45-51.
[3] S. Kale, S. B. Umbarkar, M. K. Dongare, R. Eckelt, U. Armbruster, A. Martin, *Appl. Catal. A: Gen.* 490 (2015) 10-16.
[4] M. Rezayat, H. S. Ghaziaskar, *Green Chem.* 11 (2009) 710-715.

IV-PP61

A Novel Coupling of Cyclohexanol Dehydrogenation and Cinnamaldehyde Hydrogenation Using In-Situ Liberated H_2 in One Reactor under Identical Conditions

Marella R.K.[1,2], Kalevaru V.N.[2*], Rama Rao K.S.[1], Burri D.R.[1], Martin A.[2]

1 - Catalysis Laboratory, Indian Institute of Chemical Technology, Hyderabad, India
2 - Leibniz-Institut für Katalyse an der Universität Rostock e.V., Rostock, Germany

* narayana.kalevaru@catalysis.de

Keywords: cyclohexanol, cyclohexanone, cinnamaldehyde, hydrocinnamaldehyde, coupling reaction

1 Introduction

Coupling of industrially important dehydrogenation and hydrogenation reactions in gas phase over a single catalyst bed have several advantages such as operational simplicity, good energy efficiency, enhanced conversion and eco-friendly process [1]. Interestingly, the in-situ released hydrogen from the dehydrogenation step can be effectively utilized in the hydrogenation of second reactant in such a way that this approach not only completely eliminates the supply of external hydrogen in the reactant feed mixture for hydrogenation but also provides an opportunity to combine and perform two reactions simultaneously in one step under one set of reaction conditions. Only a few reports are available on this type of coupling process which involves a catalytic hydrogen transfer [e.g. 2-3]. The present study is the first attempt of combining dehydrogenation of cyclohexanol (CHOL) and hydrogenation of cinnamaldehyde (CAL) in one step to produce cyclohexanone (CHONE) and hydrocinnamaldehyde (HCA) using a single reactor over Cu/Al_2O_3 catalysts (Scheme 1). The target products have high commercial significance; cyclohexanone is used for the manufacture of caprolactam in nylon-textiles and hydrocinnamaldehyde is an intermediate in the synthesis of anti-viral pharmaceuticals, particularly HIV protease inhibitors. However, cyclohexene (CHENE) and hydrocinnamyl alcohol (HCAL) are the by-products of this combined reaction.

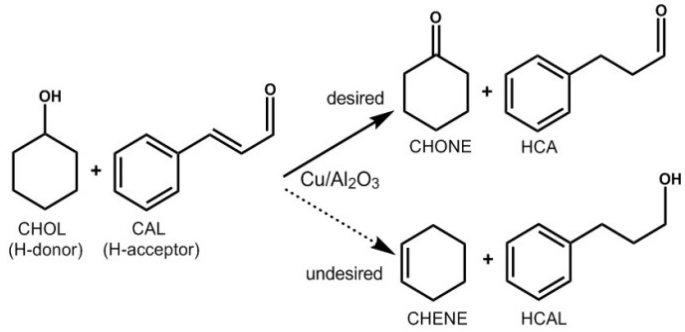

Scheme 1. Coupling of cyclohexanol dehydrogenation and cinnamaldehyde hydrogenation in one-step.

2 Experimental

Commercial γ-Al_2O_3 (Sudchemie, BET surface area 223 m^2/g) was used as a support for preparing the present Cu/γ-Al_2O_3 catalysts with varying Cu loadings (2.5 to 10 wt%) by impregnation method. These catalysts were characterized by XRD, TPR, XPS, ICP, TEM etc. The catalytic tests were carried out in a fixed bed reactor at atmospheric pressure under N_2 flow in the temperature range of 250 to 325 °C. About 2 g of the catalyst was used for catalytic tests. Prior to testing, the catalyst was reduced under H_2 flow at 280 °C for 3 h. The products were collected in an ice-cold trap for every 30 min and analysed by off-line GC equipped with FID using AT-5 capillary column.

3 Results and discussion

The BET surface area values decrease gradually from 221 to 185 m^2/g, as the copper loading increases from 2.5 to 10 wt%. XRD showed that the reflections corresponding to CuO phase could only be seen in the catalysts with higher Cu loading (>5 wt% Cu). Similarly, the XRD patterns of reduced catalysts revealed the presence of metallic Cu^0 phase in the catalysts having >5 wt% Cu content. From XPS analysis it was observed that the chemical state of copper was Cu^{2+} for calcined catalysts and for reduced catalysts it is in between Cu^+ or Cu^0. TPR patterns of Cu/Al_2O_3 catalysts exhibited two types of reduction peaks in the temperature range of 150 to 300 °C. The peaks corresponding to lower temperature are due to the reduction of highly dispersed CuO species and high temperature peaks may be due to the reduction of bulk CuO particles. TEM analysis of reduced catalysts shows high dispersion of smaller copper particles. Fig. 1 depicts the influence of Cu loading on the catalytic activity and selectivity for coupling process. With increase in the copper loading from 2.5 to 7.5 wt%, the cyclohexanol conversion increased from 36 to 70% and then decreased to 51% while the conversion of cinnamaldehyde increased from 19 to 64% and then decreased to 50%. Similarly, selectivity of cyclohexanone and hydrocinnmaldehyde also increased in a similar fashion with Cu loading (i.e. from 75 to 93% and then levelled off). Besides, various important reaction parameters such as temperature, space velocity (GHSV), mole ratio and flow rate of reactants were also optimized. For instance, with increase in the mole ratio of cyclohexanol and cinnamaldehyde to 2 : 1, nearly 100% conversion of cinnamaldehyde and 80% cyclohexanol conversion with 90% selectivity of cyclohexanone and 80% selectivity of hydrocinnamaldehyde could be obtained. However, the catalyst displays gradual deactivation due to coking. As a result, after 8 hours-on-stream over 7.5wt% Cu catalyst, the conversion of cyclohexanol decreased from 80 to 67% while conversion of cinnamaldehyde decreased from ~100 to 88%. However, the selectivity of cyclohexanone was decreased from 92 to 80% while the hydrocinnamaldehyde selectivity remains more or less constant at 85%.

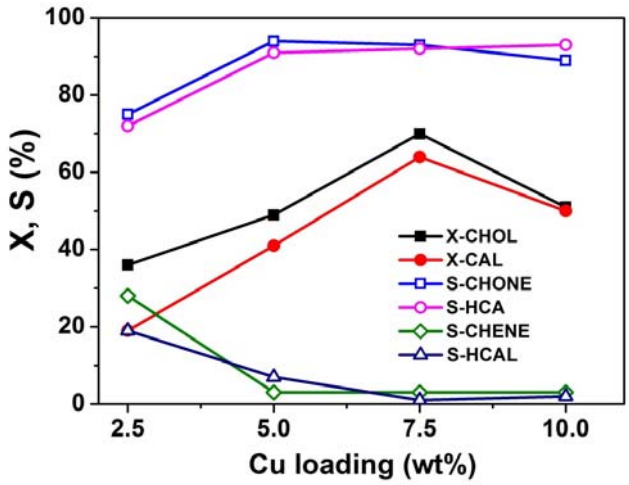

Fig. 1. Influence of Cu loading on coupling of cyclohexanol and cinnamaldehyde over $Cu/\gamma\text{-}Al_2O_3$ catalysts (T=275 °C, V_{cat}=1.4 ml, Total flow=3.7 l/h, GHSV=2690 h^{-1}, CHOL : CAL : N_2=1 : 1 : 40)

4 Conclusions

Cu/Al_2O_3 catalysts demonstrate overwhelming performance towards novel coupling of cyclohexanol dehydrogenation and cinnamaldehyde hydrogenation reaction. Results revealed that the Cu loading has strong influence on the catalytic performance. Among all, 7.5wt% Cu/Al_2O_3 exhibited the best performance plus significantly high yields of cyclohexanone (70%) and hydrocinnamaldehyde (80%) could be successfully achieved for the first time.

Acknowledgements

The authors thank DST, India and DAAD, Germany for financial support (Project No. 57036665).

References

[1] H. Y. Zheng, Y. L. Zhu, Z. Q. Bai, L. Huang, H. W. Xiang, Y. W. Li, *Green Chem*. 8 (2006) 107.
[2] K. S. Rama Rao, B. David Raju, S. Narayanan, B. M. Nagaraja, A. H. Padmasri, V. Siva Kumar, US 7015359B1 (2008).
[3] A. Javaid, C. S. Bildea, *Chem. Eng. Technol*. 9 (2014) 1515.

IV-PP62

Black Oil Macromolecular Structuring Technology in the Process of its Oxidation for Obtaining the Bituminous Isolation Materials

Kemalov A.F., Kemalov R.A.*, Abdrafikova I.M., Abaas M.A.A., Maltseva A.G.

Kazan (Volga region) Federal University, Institute of Geology and Petroleum Technologies, Kazan, Russia

* kemalov@mail.ru

Keywords: residual, oil, stock, paraffin-asphaltene associates, physical-chemical modification

1 Introduction

One of the effective ways to improve the properties of special bitumen is their chemical and physical modification. When selecting the source raw material, the results of the earlier studies were taken into consideration [1], proving that the oxypolymerization ends at the stage of bitumen obtaining. Therefore, the raw material for special bitumen production is the flux oil of naphthene-aromatic sub-structure - Karabashsky NBZ (KNBZ) and paraffin-naphthene substructure - Elkhovsky NPU (ENPU) OJSC "Tatneft" (Table 1).

Table 1. Physical-chemical properties of flux oil

Indices	Flux oil		
	Karabashsky NBZ	Elkhovsky NPU	Mordovo-Karmalsky NB
Density, kg/m^3	0,9686	0,9878	0,9985
Relative viscosity, RV_{80},	22,96	51,76	80,0
Content, %mass.:			
- CAB	18,25	28,23	55,8
- sulphur	0,492	0,887	5,2
- paraffins	< 2,0	15,0	15,0
Asphaltenes/resin	0,64	0,45	0,47

2 Experimental

The investigations of structural-dynamical properties of flux oil by impulse NMR show high inhomogeneity of chemical group composition of resinous-asphalthene materials (RAM) in the flux oil of ENPU (Fig.1) due to high content of paraffin HC (Table 1), corresponding to high content of phase A – 75%mass. and low frequency of core precessions of the phases under study. Formerly it was found out, that the structural dynamical analysis (SDA) of oil disperse systems has the phases A, B and C, which are conventionally classified as oil, resins and asphaltenes respectively, due to their different content and molecular mobility.

3 Results and discussion

In the course of investigations of BIM, based on special bitumens of ENPU (both with MBM and without it - bitumens 1 and 2), it was determined an inverse proportion of covering strength on rheological characteristics of BIM. Therefore, MBM usage in oxidation of ENPU flux oil significantly increases the hardness (Fig. 3), and it is characterized by multiply less values of dynamic viscosity and shearing stress of BIM, what proves the existence of BIM structural net, formed by their micelle structure. It was revealed, that the dissolution rate of bitumen-1 in aromatic solvent is higher than the one of bitumen-2.

The studied samples shall be divided into two groups in the content and composition of paraffin structures. So, the bitumens with Tsoft equal to 85 and 1000C the total content of methylene and methyl groups is lower, and the branching of paraffin structures is higher, than in the bitumens with Tsoft equal to 103 (bitumen-2) and 1240C. Alongside with that, bitumen-1 has low content of aromatic structures; its asphaltenes are more condensed and less oxidized, than the ones of bitumen-2.

The change of asphaltene structure in special bitumens promotes their high chemical homogeneity with resin components due to the mutual diffusion of phases B and C (Fig. 1).

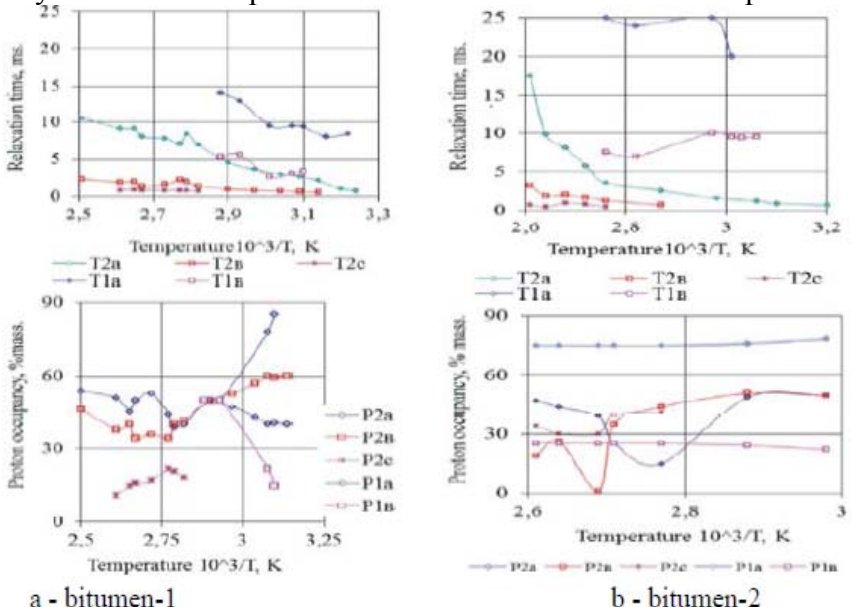

Fig. 1. The results of the analysis of structural-dynamical states of special bitumens of Elkhovsky NPU

4 Conclusions

The results of the investigations, taking into consideration the data, obtained by impulse NMR, infrared spectroscopy and physical-mechanical analysis show that the BIM are plastified due to the asphaltenes, which have the properties of "heavy" resins, because of oxidative polymerization of MBM and flux oil components of ENPU.

Acknowledgements

The work is performed according to the Russian Government Program of Competitive Growth of Kazan Federal University

References

[1] Kemalov, A.F., R.A. Kemalov. Development of the Technology of Macromolecular Structuring of Naphtha Crude Residues During Their Oxidation to Produce Bitumen Insulation Materials. World Applied Sciences Journal (Special Issue on Techniques and Technologies), 22 (2013) 91-95.

IV-PP63

Intensification of Chemical-Technological Oil Refining Processes by the Use of Wave Technologies

Kemalov A.F., Kemalov R.A.*, Gainullin V.I., Valiev D.Z.

Kazan (Volga region) Federal University, Institute of Geology and Petroleum Technologies, Kazan, Russia

* kemalov@mail.ru

Keywords: wave technology, microwave radiation, the wave non-linear mechanics

1 Introduction

Traditional methods of intensification of chemical and technological processes of oil refining are energy intensive and often reached effect's value does not cover the costs. In this regard, there is the task to use modern high technologies, ensuring the achievement of the required effect without the high material and energy costs, among which most promising and effective are the wave technologies. The aim of this study was to investigate the effect of wave impacts on the speed and depth of chemical processes. We would like to draw attention on the technologies which use wave methods of impacting oil refining chemical-technological processes are applied for enhancement of physical-chemical properties and fractional composition of oil and oil products. The increase in the light hydrocarbon fraction molecules oscillation amplitude during oil fraction distillation, contributes to weakening of intermolecular interactions, separation of these molecules from supermolecular structure solvation shells and transfer to a vapor phase, which results in increase in the yield of light fractions. The decrease in such amplitude may be used in crystallization of various solutions or melts in order to obtain optimal system properties. The use of wave exposure methods is an efficient means for intensification of oil refining chemical and technological processes [1].

2 Experimental

The main effect of acoustical treatment of oil stocks and its products is connected with the action of audible and ultrasonic frequency band elastic oscillations on the substance and progress of various reactions and processes due to cavitation, acoustic pressure and acoustic wind.

The action of a 2450 MHz electromagnetic field on the substance makes polar or polarizable molecules or ions orient in accordance with the field pulsation. Due to phase discordance between the field fluctuations and dipole rotation, the radiation energy turns into molecular motion energy and the entire volume of the substance is heated from the inside as opposed to conventional heating of surface by heat transmission.

A particular rise of exploratory activity in the use of microwaves in organic chemistry was in 1989 after publication of two articles written by French authors who used household microwave ovens for heating reaction mixtures and despite some technical difficulties observed a significant reduction in the period of Diels-Alder reactions, Claisen reactions, etherificafion, oxidation etc. at equal target product outputs.

3 Results and discussion

The use of microwave irradiation (MIR) contributes to a considerable acceleration of petrochemical processes, increases selectivity and yield of products and improves ecological characteristics of industrial processes.

The essence of wave methods of oil stock and products treatment lies in molecule energizing (molecule activation) aimed at inducing their transformation in a positive direction by exposure to various physical fields on intramolecular, molecular and intermolecular bonds. The molecule energizing (molecule activation) means energizing by an electromagnetic radiator, which radiated frequencies are resonant with frequencies of oil stock and products molecule.

Oil is an extremely complex mixture of various classes of carbons and heteroatom compounds in complex intermolecular bonds, which form a disperse system with a complicated internal structure; therefore a wide oil vibrational spectrum range is expected. In means that in order to ensure target influence on oil components it is necessary to choose the object of such influence. In this regard, a quantum-chemical analysis of the Carbon-Carbon bond (C-C) and Carbon-Hydrogen bond (C-H), implemented at atomic level (not at molecular), is of a significant interest (Syunyaev, et al., 1990).This analysis is all the more important as thermodeconstructive, thermocatalytic and many other means of influence on oil stock are based on stimulating, breaking and formation of such bonds.

4 Conclusions

The use of wave exposure methods is an efficient means for intensification of oil refining chemical and technological processes.

Acknowledgements

The work is performed according to the Russian Government Program of Competitive Growth of Kazan Federal University

References

[1] R.A. Kemalov, A.F. Kemalov, D.Z. Valiev. Viscous Flow Activation Thermodynamics and Structural-group analysis of High-Viscosity oil under ultrasonic exposure. *Oil industry*, 11 (2011) 21

IV-PP64

Bitumen Isolation Materials Producing Technology Based on Macromolecular Structuring of Naphtha Crude Residues during their Oxidation

Kemalov A.F., Kemalov R.A.*, Abdrafikova I.M., Abaas M.A.A., Maltseva A.G.

Kazan (Volga region) Federal University, Institute of Geology and Petroleum Technologies, Kazan, Russia

* kemalov@mail.ru

Keywords: paraffin-asphalt associates, physical-chemical modification, oxidative polymerization

1 Introduction

The results of our previous studies [1] evidencing that oxidative polymerization is accomplished at the stage of construction bitumen synthesis were taken into account during selection of raw material sources. As the result, tars of naphthene-aromatic (Karabash Oil-Bitumen Plant (KOBP)) and paraffin-naphthene bases (Elkhovskiy Petroleum Refining Plant (EPRP) OAO "Tatneft") served as the raw material for production of special bitumen.

2 Experimental

A choice of a co-product of wood processing (CWP) as a modifying agent of bitumen is related with high convergence mechanism of reciprocal transformations of their components in high-temperature oxidation. CWP contains unsaturated acids, which reduce the release of asphaltenes in oxidative polymerization together with petroleum acids. The choice of the multicomponent bifunctional modifier (MBM)-a component of polymer oils production (CPOP) as the main raw material is stipulated by its high capacity to chemical structuring due to the formation of esters better film-forming ability. Oil dispersed systems according to the structural-dynamic analysis (SDA) contain the phases A, B and C, which due to their different concentration and molecular mobility are conventionally referred to oils, resins and asphaltenes, respectively.

3 Results and discussion

Based on the naphthene-aromatic composition and small content of paraffinic hydrocarbons, KOBP tar is the most convenient raw material for the production of BIM, what is confirmed by studies of structural-dynamic (Fig. 1) and physical-mechanical properties of the final products.

It was found that manganese dioxide (MD) at 240°C and above forms salts with the organic acid which are soluble in bitumen medium and as a result catalyzing the oxidation. It was identified that the maximum reduction in the time of material presence in the reaction zone reveals at the introduction of the three-component modifier with simultaneous increase of bitumen-1 output (special bitumen EPRP, modified MBM, T = 100°C) by 17% m and the formation of degradation products reduces by 15-17%. It is known that the inhibitors capable to slowing of polymerization are destroyed at 250°C and the presence of MD and CPOP. Low physical and mechanical properties of BIM based on bitumen-3 (special bitumen KOBP, modified MBM) can be explained by the high content of carbenes and carboids 0.81% and structural features of phases A (90%) and B, in which phase A has a negative impact on the film-forming ability of BIM.

Our studies of BIM based on special bitumen EPRP (both with MBM and without-bitumen-1 and -2) have identified inverse proportional dependence between hardness of C and the

rheological characteristics of BIM. Thus, the implementation of MBM in the oxidation of tar EPRP promotes a significant increase in the hardness (Fig. 3) and characterizes by lower dynamic viscosity and shear tension of BIM, what is an evidence of a spatial lattice structure in BIM formed by their micelle structure. It was found that the resolution rate of bitumen-1 in an aromatic solvent is higher than for bitumen-2.

Abnormally of high physical-mechanical (Fig. 2) and low rheological properties of BIM obtained from bitumen-1 containing up to 41% of asphaltenes (Table 2) compared with GOST 5631-79 with asphaltene content up to 39% can be explained by the chemical structure of the disperse system components (Fig. 3a), high chemical homogeneity of phases B and C, the frequency of precession of the nuclei and the content of phase B. This phenomenon according to IR spectroscopy is confirmed by a comparative analysis of the structural-group composition of bitumens and separated asphaltenes (Tables 3 and 4). In this case, bitumen with Tm equal to 85, 100 and 124°C belong to the same type of oxidizing material, i.e. tar EPRP together with additives of different oxidation.

Changes of the structure of asphaltenes in special bitumens promote their high chemical homogeneity with the components of resins due to reciprocal diffusion of phases B and C.

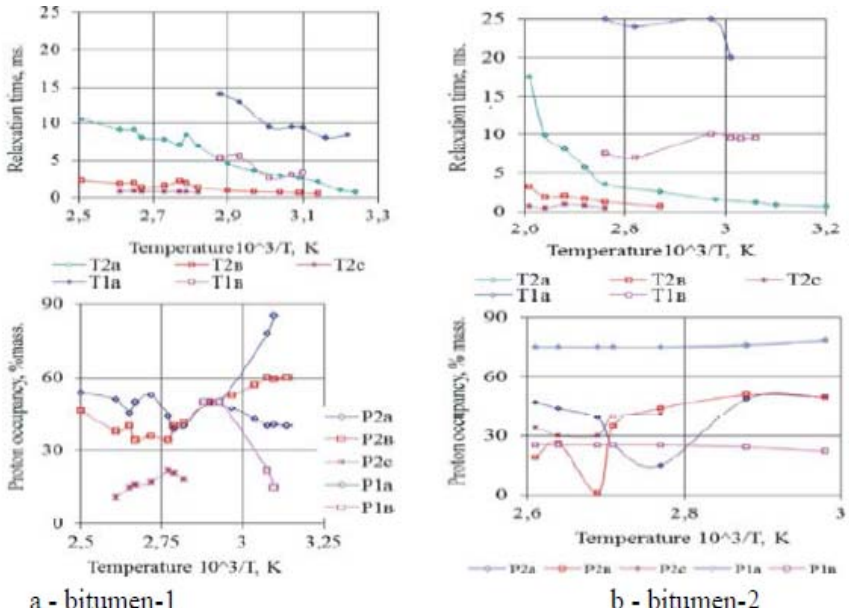

Fig. 1. Dependences of the spin-spin relaxation time and hydrogen proton occupancies in phases a, b and c on temperature.

4 Conclusions

In our studies, we have determined using impulse NMR, IR spectroscopy and physical-mechanical analysis that BIM are plasticized due to asphaltenes possess the properties of the "heavy" resins as a result of oxidative polymerization of MBM components and tar EPRP that BIM the fact that.

Acknowledgements

The work is performed according to the Russian Government Program of Competitive Growth of Kazan Federal University

References

[1] Kemalov, A.F., R.A. Kemalov. Development of the Technology of Macromolecular Structuring of Naphtha Crude Residues During Their Oxidation to Produce Bitumen Insulation Materials. *World Applied Sciences Journal* (Special Issue on Techniques and Technologies), 22 (2013) 91-95.

IV-PP65

Ways of Regeneration of Highly Effective Catalysts Based on Mo-V-P Heteropoly Acid Solutions

Zhizhina E.G.*, Gogin L.L., Pai Z.P.

Boreskov Institute of Catalysis, SB RAS, Novosibirsk, Russia

* zhizh@catalysis.ru

Keywords: heteropoly, acid catalyst, regeneration, multicycle, testing

1 Introduction

Mo-V-phosphates are polyoxometalates, which are widely used nowadays. Free Mo-V-P heteropoly acids (HPA) and their salts belong to the same class of compounds. Most of these acids have Keggin composition $H_{3+x}PMo_{12-x}V_xO_{40}$ (HPA-x). They contain easily reducible V^V, and by its expense such compounds have rather high redox potential *E* and are quite strong oxidizers. This allows their use in homogeneous and heterogeneous catalysis. In particular, in homogeneous catalytic oxidation processes involving O_2 HPA-x are used as *reversible oxidizers*. Oxidation reactions of substrates (Su) in the presence of the HPA-x solutions are usually performed in two stages, (1) and (2), in different reactors. The sum of these stages is a catalytic reaction (3), the oxidation of substrate by O_2. Stages (1) and (2) constitute the catalytic cycle of reaction (3) [1].

$$^m/_2\ Su + {}^m/_2\ H_2O + HPA\text{-}x \longrightarrow {}^m/_2\ SuO + H_mHPA\text{-}x \quad (1)$$

$$H_mHPA\text{-}x + {}^m/_4\ O_2 \longrightarrow HPA\text{-}x + {}^m/_2\ H_2O \quad (2)$$

$$Su + {}^1/_2\ O_2 \longrightarrow SuO \quad (3)$$

The individual performance of stages (1) and (2) shows the high selectivity (to 99 %) of target reaction (1). Because the reduced catalyst solutions (H_mHPA-x, where m is the number of electrons accepted by HPA-x) are complex equilibrium mixtures of HP anions with various integers **m** (including m = 0) and cations VO^{2+} and VO_2^+, the average reduction degree of such solutions **m** is equal to $[V^{IV}]$ / $[H_mHPA\text{-}x]$. Here $[V^{IV}]$ is the total concentration of V^{IV}, and $[H_mHPA\text{-}x]$ is the total concentration of HP anions. The latter is equal to the initial [HPA-x].
In the catalyst regeneration, according to reaction (2), V^{IV} in HP anions is oxidized to V^V, and the reduction degree of HPA-x decreases. Therefore, in the catalytic process (3) HPA-x is a *reversible* acting oxidizer (i.e., a catalyst), in which vanadium atoms undergo redox transformations: $V^V \rightarrow V^{IV} \rightarrow V^V$. The catalyst productivity, or its oxidative capacity (the amount of Su oxidized in the single cycle by 1 L of the catalyst solution), depends on $[V^V]$ before reaction (1). Therefore, in many testing catalyst cycles according to schemes (1) + (2), a maximum catalyst regeneration is required to provide the highest $[V^V]$ in the HPA-x solution and, thus, the maximum possible amount of substrate that is oxidized in the following cycle. Stage (2) is a *common* and *key* step of the catalytic processes (3).

2 Experimental

The HPA-x catalyst solution regeneration is usually performed at temperatures 150−170 °C and P_{O_2} =3−4 atm [2]. Note that not only oxygen may be used for regeneration. In principle, it is possible to reoxidize strongly reduced HPA-x solution by the 30 % H_2O_2 solution. We have used this method in the development of process of vitamin K_3 synthesis [3]. This oxidizer is really good, since it environmentally harmless. However, H_mHPA-x oxidation in this case is not complete, since vanadium ions appear to catalyze H_2O_2 decomposition into oxygen and water.

Therefore, the oxidative capacity of the HPA-x solution after regeneration by H_2O_2 will be essentially reduced starting from the second cycle. Moreover, organic admixtures present in the catalyst solution after reaction (1) are not completely oxidized during such regeneration, and, thus, will accumulate from cycle to cycle, reducing *E* before target reaction (1) and catalyst productivity in whole.

We have also tried to use the concentrated HNO_3 for the HPA-x solution regeneration [4]. Though this oxidizer is not good regarding environment, it may be used in small amounts under certain conditions as assistant during the oxidation by air oxygen. In the case of HNO_3 assistance catalyst regeneration may be performed under atmospheric pressure. In case if there is organic residue from the previous cycle, it is completely oxidized to carbon dioxide and water by the nitric acid admixture during catalyst regeneration before the next cycle.

3 Results and discussion

In our studies [1-4] we have shown that catalysts based on the HPA-x solutions completely restore their properties during regeneration which can be carried out in various ways.

For example, recently we investigated the possibility of multicycle HPA-10 ($H_{17}P_3Mo_{16}V_{10}O_{89}$) performance as a bifunctional (acidic and oxidation) catalyst in the synthesis of 2,3-dimethylanthraquinone (7 cycles). In addition to the regeneration of the HPA solution by O_2 at 150−160 °C, we tested the feasibility of its substitution by low concentrations of nitric acid for the same purpose. Methods for regeneration of the catalyst were alternated.

Table 1. Multicycle synthesis of 2,3-dimethylanthraquinone (2,3-DMAQ) via NQ reaction with 2,3-dimethylbutadiene catalyzed by the HPA-10 solution.

Cycle number	E_{cat} before reaction (1), V	2,3-DMAQ yield, %	2,3-DMAQ purity, %	Catalyst regeneration method
1	1.098	81	98	150 °C, P_{O_2}= 4 atm, 20 min
2	1.063	77	98	160 °C, P_{O_2}= 4 atm, 15 min
3	1.066	77	97.5	Boiling, HNO_3 (0.15 ml), 30 min
4	1.101	80.5	98	Boiling, HNO_3 (0.15 ml), 30 min
5	1.097	80	98.5	160 °C, P_{O_2}= 4 atm, 15 min
6	1.063	77	98	Boiling, HNO_3 (0.2 ml), 30 min
7	1.104	81	98	160 °C, P_{O_2}= 4 atm, 15 min

Conditions: 80 °C, 4 ml of 0.2 M HPA-10 solution, molar ratio HPA-10:NQ 0.5:1, volume ratio HPA solution:1,4-dioxane 1:1; 7 h; NQ conversion ≥ 99.5%. E_{cat} values are given with respect to NHE.

HNO_3 apparently provided a more complete oxidation of reduced HPA-10 (i.e., higher E_{cat} before the next cycle) than the regeneration by O_2 in an autoclave. After the regeneration using HNO_3, the oxidative capacity of the catalyst remained essentially the same as in the first cycle because after regeneration the E_{cat} values were close to that of the fresh HPA-10 solution used in the first cycle.

4 Conclusions

The HPA solution remained homogeneous during many cycles, retained its productivity and gave no V-containing precipitates. The complete recovery of the properties of the HPA-x catalyst after regeneration shows its technological usefulness in various oxidation processes.

References

[1] E.G. Zhizhina, V.F. Odyakov, M.V. Siminova, *Kinetics and Catalysis*, 49 (6) (2008) 814.
[2] E.G. Zhizhina, V.F. Odyakov, *Int. J of Chemical Kinetics*, 46 (9) (2014) 567.
[3] K.I. Matveev, E.G. Zhizhina, V.F. Odyakov, I.G. Kolesnik, *RU Pat*., 2142935, 1999.
[4] K.I. Matveev, E.G. Zhizhina, V.F. Odyakov, *RU Pat*., 2165406, 2001.

IV-PP66

Synthesis of a Novel Anthracene Based Schiff Base-Copper(II) Complex as a Potential Catalyst

Kocak A.[1*], Malkondu S.[1], Turhan D.[1], Kocak N.[2]

1 - Selcuk University, Science Faculty, Department of Chemistry, Konya, Turkey
2 - Necmettin Erbakan University, Deparment of Science Education, Faculty of Education, Konya, Turkey

* akocak@selcuk.edu.tr

Keywords: schiff base-copper(II), antracene, synthesis, excimer

1 Introduction

Schiff base metal complexes have been studied widely due to their several chemical and physical properties and their wide range of applications in numerous scientific areas [1]. These types of complexes have been prudently explored in recent years and such studies have been the subject of many papers and reviews. Schiff base ligands are easily synthesized and form complexes with almost all metal ions. Many Schiff base complexes show excellent catalytic activity in various reactions at high temperature and in the presence of moisture. Many of them are centered on the catalytic activity of Schiff base metal complexes in a large number of homogeneous and heterogeneous reactions such as oxidation, epoxidation, hydroxylation, aldol condensation, polymerization and hydrogenation reactions [2-4].

Considering wide catalytic properties of Schiff base complexes, we have designed a simple methyl anthracenylimine benzoate (**MAB**) derivative, which has the ability to form self-assembled anthracenyl excimer species with a specific metal ion.

2 Experimental/methodology

NMR spectra were recorded at room temperature on a Varian 400 MHz spectrometer in DMSO-d6 or CDCl3. Chemical shifts are expressed in δ units. IR spectra were obtained on a Perkin Elmer Spectrum 100 FTIR spectrometer. UV-vis spectra were measured with a Perkin Elmer Lambda 25 spectrometer. The fluorescence spectra were measured on a Perkin Elmer LS 55 spectrometer in 1 cm quartz cells with slit 6 nm. Excitation wavelength of MAB is of 388 nm. High resolution mass spectra were recorded on a Bruker Daltonics MicroToF II mass spectrometer. All starting materials and reagents used were of standard analytical grade from Aldrich and Merck used without further purification. The stock solutions of metal ions in MeCN were prepared from their perchlorate salts.

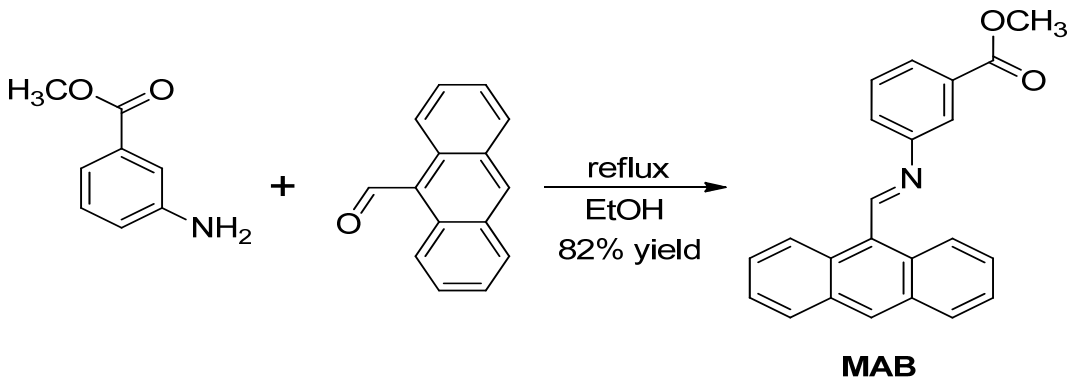

Scheme 1. Synthetic route to **MAB**

MAB was readily synthesized by the route outlined in Scheme 1. Methyl 3-aminobenzoate

was prepared starting from benzoic acid. Fischer esterification of benzoic acid afforded methyl benzoate in quantitative yield. The nitration of methyl benzoate with a mixture of HNO_3/H_2SO_4 provided methyl 3-nitrobenzoate in good yield. Reduction of methyl 3-nitrobenzoate with Fe powder/AcOH gave methyl 3-aminobenzoate, the condensation reaction of which with 9-anthracene carboxaldehyde provided **MAB** in 82% yield. The structures of the intermediates and final product were verified by ^{1}H NMR, ^{13}C NMR and FT-IR spectroscopy and HRMS.

3 Results and discussion

The complexing ability of **MAB** toward a wide range of metal ions (Li^+, Na^+, Cs^+, Mg^{2+}, Ca^{2+}, Sr^{2+}, Ba^{2+}, Ag^+, Mn^{2+}, Fe^{2+}, Co^{2+}, Ni^{2+}, Cu^{2+}, Zn^{2+}, Cd^{2+}, Hg^{2+}, Pb^{2+}, Al^{3+} and Fe^{3+}) has been investigated by fluorescence spectroscopy (λ_{ex} = 388 nm) in MeCN at 20 ^oC (Figure 1). In the absence of any metal ion, **MAB** shows a very weak emission at 439 nm in MeCN due to the highly efficient PET (photoinduced electron transfer) process between the methyl 3-aminobenzoate receptor moiety and the anthracene fluorophore. Among the nineteen metal ions, only Cu^{2+} was found to give a distinct spectral change. The addition of Cu^{2+} (5.0 equiv) induces two new emission bands, a weak monomer emission band centred at 471 nm and a strong excimer emission band centred at 594 nm, indicating strong complex formation with Cu^{2+} ions. Under similar conditions, the other tested metal ions had very little effect on the emission. The value of the sensing index (I_{594}/I_{439}) for **MAB** to Cu^{2+} is 14.8 whereas it is less than 0.4 for the other metal ions. Therefore, **MAB** shows high selectivity toward Cu^{2+} over other competing metal ions.

4 Conclusions

In conlusion, a novel anthracene-based, highly selective fluorescent receptor has been synthesized through simple synthetic route, and its sensing ability for a wide range of metal ions (Li^+, Na^+, Cs^+, Mg^{2+}, Ca^{2+}, Sr^{2+}, Ba^{2+}, Mn^{2+}, Fe^{2+}, Fe^{3+}, Co^{2+}, Ni^{2+}, Cu^{2+}, Ag^+, Zn^{2+}, Cd^{2+}, Hg^{2+}, Al^{3+} and Pb^{2+}) has been explored. **MAB** exhibits high selectivity and sensitivity for Cu^{2+} in the presence of various metal ions with a significant emission enhancement via unique copper(II)-directed static excimer formation. The basis of the excimer formation has been investigated and found to be a static in nature from a survey of the excitation and absorption spectra. The results demonstrate that disassociation of the excimer species to monomers is caused by the temperature and solvent fraction. This dissociation process enables **MAB** to be used as a temperature and solvent sensor. The Job's plot and mole-ratio curves reveal a 1:2 (M:L) stoichiometry. **MAB** exhibits a high sensing index value of 14.8 for Cu^{2+} ions. The detection limit is sufficiently low to determine micromolar levels of Cu^{2+} ions. The present study is a good example of a receptor in which the rational conversion of excimer species to monomers can be monitored distinctly. The copper complex of **MAB** will be further explored as catalyst in some organic reactions.

Acknowledgements

We thank SUBAP (Grant Number 14401027) for financial support.

References

[1] K.C. Gupta, A. K. Sutar, *Coordination Chemistry Reviews*, 252 (2008) 1420.
[2] P. Roy, M. Manasserob, *Dalton Transaction*, 39 (2010) 1539.
[3] J. Tong, Y. Zhang, Z. Li, C. Xia, *Journal of Molecular Catalysis A: Chemical,* 249 (2006) 47.
[4] H. Sharghi, M. A. Nasseri, *Bulletin of the Chemical Society of Japan*, 76 (2003) 137.

IV-PP67

Determination of Pt-Catalyst Efficiency of Reforming Process for Different Industrial Plants

Koksharov A.G.*, Ivanchina E.D.

Tomsk Polytechnic University, Tomsk, Russia

* antonkg@tpu.ru

Keywords: catalytic reforming, Pt-catalyst, rate, constant mathematical model, non-stationary kinetic model

1 Introduction

One of the main goals of the reforming process is to increase the aromatics concentration. In addition to the target reactions dehydrocyclization of paraffins and dehydrogenation of cyclohexanes also some undesirable reactions that decrease the liquid yield (light hydrocarbon gas formation by hydrocracking) always occur to some extent. Rates of the individual reactions depend on the catalyst selectivity and process conditions. Using the obtained values of the rate constants of chemical reactions and non-stationary kinetic model we calculated the main indicators of the catalytic process in industrial units L-35-11/600 and LCh-35-11/1000, under different operating conditions of the catalyst RG-682.

2 Experimental/methodology

We use non-stationary mathematical model is a system of differential equations to the extent that the use of the inner surface of the catalyst pellet (η) and coke formation.
The mathematical model of catalytic reforming:

$$\begin{cases} G_c \dfrac{\partial C_i}{\partial Z} + G_c \dfrac{\partial C_i}{\partial V} = \sum_j k_j \cdot C_i \cdot \eta_j, \\ G_c \dfrac{\partial T}{\partial Z} + G_c \dfrac{\partial T}{\partial V} = \dfrac{1}{\rho \cdot C_p^{mix}} \sum_j \Delta H \cdot k_j \cdot C_i \cdot \eta_j. \end{cases}$$

The initial conditions:

$$Z = 0 \quad T = T_{en} \quad C_i = C_i^{en};$$
$$V = 0 \quad T = T_{en} \quad C_i = C_i^{en}.$$

Where Ci - a concentration of i-th component, mol/m3; T – temperature; Z – a raw material volume, m³; i - number of components in the mixture; j - number of reactions; kj - rate constant j-th reaction; ΔH - the thermal effect of the j-th reaction J/mol; ρ - density, kg/m3; V - a volume of the catalyst layer,m3; G - a raw material flow rate, m3/h.

Accounting for non-stationary model made it possible to calculate the values of the rate constants of reactions (Table. 1).

Table 1- rate constants of chemical reaction for the catalyst (in relative units, one adopted for the hydrocracking reaction rate)

Reaction	RG-682	
	L-35-11/600	LCh-35-11/1000
hydrocracking of n-P	0,53	0,28
n-P → izo-P	0,23	0,14
izo-P → n-P	0,08	0,16
n-P → N-6	0,31	0,31

hydrocracking of izo-P	1,00	0,48
izo-P → N-6	0,27	0,38
N-5 → izo-P	0,23	0,16

3 Results and discussion

The catalyst has different rate constants for the reactions dehydrocyclization, isomerization, and hydrocracking of paraffins, thus affecting the performance of the catalysts and the resulting yield.

The results of the calculation of the yield in industrial units L-35-11/600 and LCh-35-11/1000 using a catalyst of the brand RG-682 are shown in Figure 1.

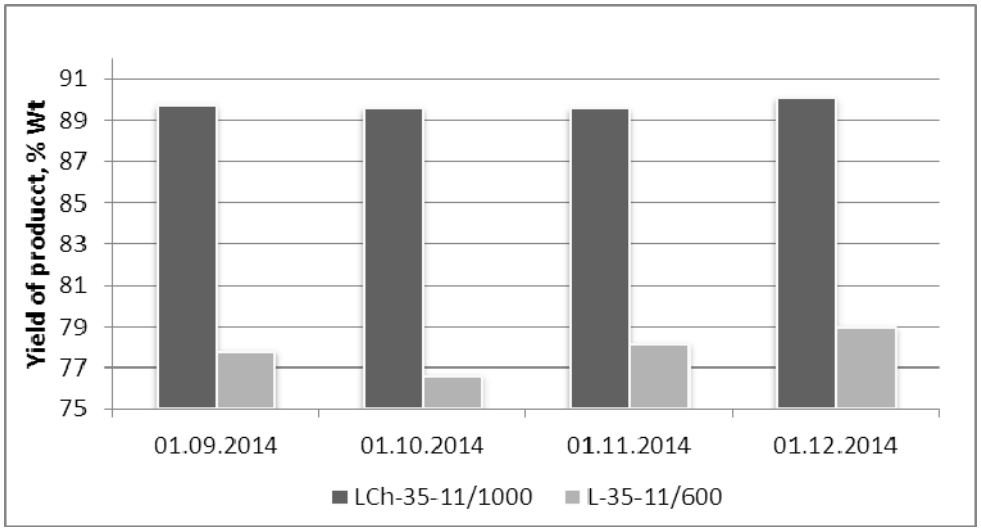

Fig.1. Calculation of yield on units L-35-11/600 and LCh-35-11/1000.

Technological parameters of the unit LCh-35-11/1000 provided low activity of the catalyst in spite of this, it possible to obtain the yield in the range of 89-90% by weight.

5 Conclusions

1. Using non-stationary mathematical model derived rate constants of chemical reactions on the catalyst RG-682 at its operation in various the reforming units.
2. Calculations yield of the objective product at the L-35-11/600 and LCh-35-11/1000.

References

[1] E.D. Ivanchina, V.V. Deriglazov, I.K. Zanin. Computer modelling system using for increasing of catalytic reforming technical economic efficiency. TPU News, Chemistry; 2011; 319: 3, p. 105-109.
[2] A.V. Kravtsov, E.D. Ivanchina, D.S. Poluboyartsev, S.A. Galushin. System analysis and efficiency increasing of oil refineries by mathematical modelling method. 2004, p.75-76

IV-PP68

New Chiral Catalysts of Nitroaldol Condensation

Konev V.N.*, Khlebnikova T.B., Malysheva L.V., Pai Z.P.

Boreskov Institute of Catalysis, Department of Catalytic Processes of Fine Chemical Synthesis, Novosibirsk, Russia

* Konevv@catalysis.ru

Keywords: chiral, catalysts, diterpenes, levopimaric, acid

1 Introduction

Nitroaldol condensation (the Henry reaction) is an efficient method of carbon-carbon bond formation between the nucleophilic part of the nitroalkane and the electrophilic center of the aldehyde or ketone. Thus, the Henry reaction can be considered as a convenient way for 1,2-amino alcohols and α-hydroxy acids producing. Asymmetric version of the nitroaldol condensation is carried out with the use of metal complexes containing chiral ligand.

Complexes of copper (I) and (II) with nitrogen-containing ligands are efficient catalysts of Henry reaction used for preparation of nitroalcohols from nitroalkanes and aldehydes. The work presented in the paper is devoted to the development ofthe synthesis of the new chiral copper catalysts for nitroaldol condensation containing tetradentate ligands derived from natural terpenes.

2 Results and discussion

Synthesis of chiral nitrogen-containing compounds is based on the transformations of natural optically pure levopimaric acid contained in rosin produced by coniferous trees. In our earlier work we developed procedures of the P-, N-containing ligands synthesis starting from tricyclic diterpenes, levopimaric and dehydroabietic acid[1].

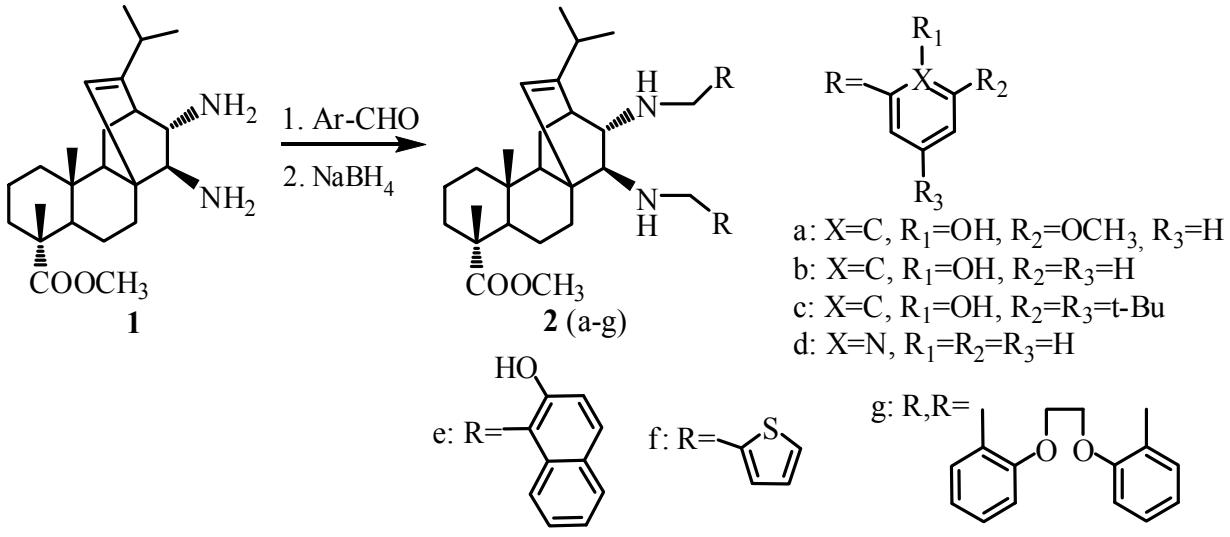

Fig. 1. The structure of the synthesized ligands

The key step in the synthesis of diterpene nitrogen-containing derivatives is the productionof trans-1,2-diamine (**1**) from fumaropimaric acid methyl ester [2]. This transformation is based on a synthetic possibilities of Curtius reaction. The new optically pure

Schiff bases were synthesized by the interaction of trans-1,2-diamine (**1)** with various aldehydes. Diastereomerically pure diamines (**2 a-g**) were synthesized by the sodium borohydride reduction of the corresponding Schiff bases. The structures of the obtained compounds is confirmed by IR, NMR, mass-spectrometry analysis.

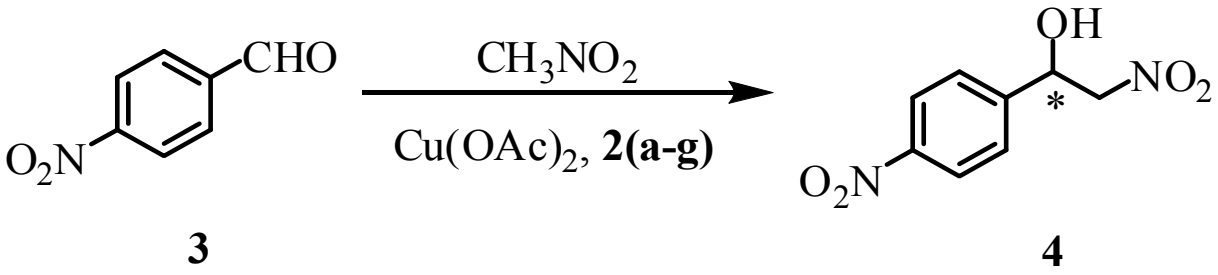

Fig. 2. Asymmetric nitroaldol condensation

Study of asymmetric induction of obtained chiral copper catalysts with tetradentate ligands **2 (a-g)** was carried out in the reaction of 4-nitrobenzaldehyde with nitromethane. Racemic mixtures of nitroalcohols were formed in the nitroaldol reaction carried out in the presence of complexes with ligands (**2 c, d, f, g**). Copper complex with ligand **2b** showed the highest activity, at that nitroalcohol **4** was formed in 98% yield and the 60% ee optical purity. The study of other derivatives of benzaldehyde showed that the aldehydes containing acceptor groups in the benzene ring are more reactive. Yields of chiral alcohols for various nitro benzaldehyde derivatives are 45 - 99%, with an enantiomeric purity of the products being from 30 to 60% ee.

3 Conclusions

Thus, we have developed and synthesized the novel chiral copper complexes with nitrogen-containing ligands, which catalyze the reaction of nitromethane with aldehydes to give nitroalcohol in yields of 45-99% and optical purity of 60% ee.

Acknowledgements

The work is supported by RAS Program of basic researches, project N 5.7.3

References

[1] T.B. Khlebnikova, N.N. Karpyshev, O.V. Tolstikova, A.G. Tolstikov, *Chirality*. 16 (2004) 40-50.
[2] V.N. Konev, T.B. Khlebnikova, Z.P. Pai, *Chem. for Sustainable Development.* 19 *(*2011) 165-168.

IV-PP69

Green n-Octanol Oxidation on Promoted Silver Catalysts

Kotolevich Y.[1*], Kolobova E.[2], Cabrera Ortega J.E.[3], Tiznado Vazquez H. J.[1], Bogdanchikova N.[1], Cortés Corberán V.[4], Zanella R.[5], Pestryakov A.[2]

1 - Centro de Nanociencias y Nanotecnología, UNAM, Ensenada, México
2 - Tomsk Polytechnic University, Tomsk, Russia
3 - Universidad Autónoma de Baja California, Ensenada, México
4 - Institute of Catalysis and Petroleumchemistry (ICP), CSIC, Madrid, Spain
5 - Centro de Ciencias Aplicadas y Desarrollo Tecnológico (UNAM), México, México

* Julia.Kotolevich@gmail.com

Keywords: n-octanol oxidation, silver catalysts, support, modification

1 Introduction

Selective alcohol oxidation is one of the key transformations in organic synthesis and in industrial practice. Conventional methods were based in the use of stoichiometric oxidants, which produce great amounts of undesirable subproducts. This drives the efforts made to adapt it to green chemistry principles [1], by implementing processes based on catalysis and non-toxic oxidants. Platinum group metals (PGM) have been used for this reaction, but they are costly (and possibly short supply in the future), which is a major barrier to worldwide spread of green chemical processes. Au nanoparticles (NPs) show similar or higher catalytic activity giving a new strategy to design PGM-free catalysts. One may expect that silver, as a group IB metal but less expensive than gold, could be a good alternative for designing of PGM-free catalysts for this reaction. Ag catalysts are industrially used for gas phase selective oxidation processes (ethylene epoxidation) but are much less studied for liquid-phase process.

Among all types of alcohols, unbranched primary alkanols show the lowest reactivity for selective oxidation, and very often *n*-octanol is tested as a model molecule for these [2]. Few works report catalytic oxidation of *n*-octanol on Ag-based catalysts, but in vapour phase [3]. For this reason, we selected this reaction to assess the feasibility of new "green" processes of alcohol selective oxidation using silver catalysts under very mild conditions and with clean oxidants.

This work is aimed to development of Ag-based heterogeneous catalysts for liquid phase selective oxidation of *n*-octanol. Modification of the support with transition metal additives with electron donor (La, Mg) and electron acceptor (Fe, Ce) properties was used as a tool for transforming and stabilizing silver species. Thus, the effect of support modification on the catalytic performance the active species of silver has been investigated.

2 Experimental

Titania Degussa P25 was used as base support. Support modifiers (M = Ce, La, Fe or Mg) were deposited on titania by impregnation with aqueous nitrate solution (molar ratio Ti/M = 40). Ag (nominal loading 2.3 wt. %) was deposited from $AgNO_3$ solution by deposition-precipitation with NaOH. Catalysts precursors were centrifuged and washed twice, and dried under vacuum at 80°C for 2 h, and the resulting samples were used with no further calcination treatment. Catalysts were characterized with S_{BET}, FTIR CO, XPS and HRTEM.

Catalytic tests for *n*-octanol oxidation were conducted at 80 ºC and atmospheric pressure for 6 h, using 0.1 M *n*-octanol in *n*-heptane with no base added, a molar ratio *n*-octanol/metal =100, and 30 mL/min O_2. Reactants and products were periodically analyzed by GC.

3 Results and discussion

The BET area of the support TiO_2 was reduced by modification with all modifiers: some 20% with La, Ce and Fe and 50% with Mg. However, further Ag deposition did not modified it, excepting for the unmodified TiO_2, giving similar values for all catalysts (ca. 45 m^2/g) but that with Mg (ca. 30 m^2/g). Analytical Ag content was ca. 2 wt. % for all catalysts. However the modification of the support had a strong effect on catalytic performance.

Under the conditions tested, Ag/TiO_2 catalyst showed relatively low activity (2.5% conversion with 90% octanal selectivity after 6 h). Support modification with La had no effect but that with Ce, Mg and Fe increased conversion by a factor or 5, 3 and 2.5 times, respectively. This allows grouping roughly the catalysts into two groups: A) active (Ag on Ce, Mg and Fe modified titania) and LA) little active (Ag on TiO_2 or $LaTiO_2$).

By analogy with Au catalysts [4], it was hypothesized that the active sites of silver catalysts in the selective alcohol oxidation are partly charged metal clusters $Ag_n^{\delta+}$. In fact, FTIR of CO adsorption, showed one peak at 2162 cm^{-1}, that can be assigned to $Ag_n^{\delta+}$ charged clusters, for all the active catalysts samples, in good agreement with catalytic properties. HRTEM data of active samples showed that average Ag particle sizes (7, 3 and 1 nm for Ce, Mg and Fe containing supports, respectively) parallels the order of their catalytic activity. XPS data of the most active Ce modified sample showed binding energies E_b (Ag $3d_{5/2}$) = 366.0 eV and E_b (Ce $3d_{5/2}$) = 882.0 eV, due to decoration of Ag particles with CeO_2, and E_b (O 1s) = 529.4 eV and E_b (C 1s) = 283.3 eV, respectively. Thus, XPS data demonstrate that carbonaceous deposits contain not only carbon, but consist of oxygenated carbon structures. Fe and Mg modified samples showed E_b (Ag $3d_{5/2}$) = 368.3 eV, which corresponds to Ag^0, while E_b (Fe 2p) = 711.7 eV and E_b (Mg 2p) = 51.2 eV are characteristic for oxides with reduced content of oxygen. Main carbon species for samples modified by Fe and Mg oxides are related with elementary amorphous carbon or small graphite particles (E_b (C1s) are from 284.9 to 285.1 eV).

At a variance, HRTEM and FTIR CO data of the less active catalysts did not show any Ag species formed neither $Ag_n^{\delta+}$. Their XPS characterization showed E_b (Ag $3d_{5/2}$) = 367.8 eV and E_b (O1s) = 530.0 eV both corresponding to Ag_2O, which explains the low activity of these samples. Main carbon species for these samples are also related to elementary amorphous carbon or small graphite particles.

Comparison of catalytic and spectroscopic data showed that partly charged metal clusters $Ag_n^{\delta+}$ are probable active sites of silver catalysts in the studied process. Additions of support modifying Ce, Fe and Mg oxides influence structural and electronic properties of Ag-based catalysts and stabilize these active species.

4 Conclusions

Titania supported silver catalysts shows little activity for liquid phase oxidation of octanol under the mild (and demanding) conditions tested. However, Ag catalysts activity can be increased markedly through the appropriate support modification. Partly charged metal clusters and $Ag_n^{\delta+}$ are the most probable active sites for this reaction. As a consequence, Ag catalysts supported on modified with Ce, Fe and Mg oxides titania can be a promising alternative system for *n*-octanol oxidation. Further studies are being conducted to further promoting their activity and compare it to gold based catalysts [5].

References

[1] P.T. Anastas, J.C. Warner, Green Chemistry: Theory and Practice, Oxford University Press, New York, 1998.
[2] V. Cortés Corberán et al., Applied Catal. A: General. 474 (2014) 211.
[3] G. D. Yadov, R. K. Mewada Chemical Engineering Research and Design. 90 (2012) 86.
[4] S. Martínez-González et al., Catalysis Today 227 (2014) 65.
[5] Y. Kotolevich et al., Submitted to Europacat XII

IV-PP70

Highly Active and Recyclable Metal Oxide Catalysts for Prins Condensation of Bio-Renewable Feedstocks

Costa V.[1], Bayahia H.[2], Kozhevnikova E.[2], Gusevskaya E.[1], Kozhevnikov I.[2*]

1 - Universidade Federal de Minas Gerais, Belo Horizonte, Brazil
2 - University of Liverpool, Liverpool, UK

* kozhev@liverpool.ac.uk

Keywords: Prins condensation, formaldehyde, beta-pinene, metal oxides, renewable feedstock

1 Introduction

Terpenes are important renewable feedstock for the perfumery, food and pharmaceutical industries. The development of sustainable chemical processes utilizing renewable raw materials with the use of environmentally benign heterogeneous catalysis is a major challenge for academia and industry [1].

Nopol is an optically active bicyclic primary alcohol used in the agrochemical industry to produce pesticides and also in soap fragrances, detergents and other household products due to its balsamic odor [2]. Nopol is generally produced by Prins condensation of β-pinene and paraformaldehyde (eq. 1) using homogeneous acid catalysts. These methods, however, suffer from severe reaction conditions, low yields and unwanted side products.

We now report that certain metal oxides such as Nb_2O_5, Cr_2O_3 and especially Zn(II)-Cr(III) mixed oxide are highly efficient and recyclable heterogeneous catalysts for Prins condensation (1). To our knowledge, little research on the use of metal oxides as the catalysts for Prins reaction has been reported so far.

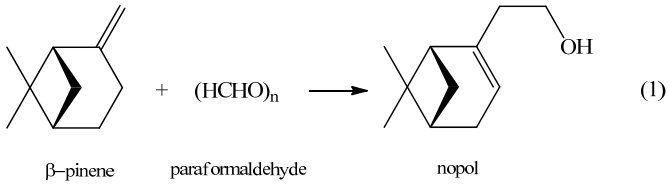

(1)

2 Experimental

Experimental details on catalyst preparation and characterization (BET, XRD, Py-FTIR and NH_3 adsorption microcalorimetry) are given elsewhere [3]. Prins condensation was carried out in a glass reactor equipped with a magnetic stirrer and a reflux condenser. In a typical run, the reactor was charged with β-pinene (5 mmol), paraformaldehyde (10–30 mmol HCHO), acetonitrile solvent (5–10 mL) and a catalyst (0.1–0.5 g) and placed in an oil bath heated to 80 ^oC. The reaction was followed by gas chromatography (GC) by taking aliquots of the reaction mixture at appropriate time intervals and using dodecane as a GC standard [3].

3 Results and discussion

Fig. 1 shows the time course for reaction (1) in the presence of supported 20%Zn-Cr(1:6)/SiO_2 catalyst and bulk Nb_2O_5, Cr_2O_3 and Zn-Cr (1:6) oxides. It can be seen that the reaction is almost complete in 2 h, followed by a rather slow increase in conversion afterwards. Nb_2O_5 is the most active amongst these catalysts giving 100% β-pinene conversion in 4 h. However, it is less selective than Cr_2O_3 and Zn-Cr. In terms of the nopol yield, Zn-Cr (1:6) is the best (97%), followed by 20%Zn-Cr(1:6)/SiO_2 (94%), Cr_2O_3 (92%) and Nb_2O_5 (88%) in 10 h reaction time. After reaction, the oxide catalysts were easy to recover by filtration and reused. The Zn-Cr oxide is on a par with the best heterogeneous catalysts reported so far ([3] and

references therein). On top of that, it has the advantage of being a robust material which is easy to prepare and handle.

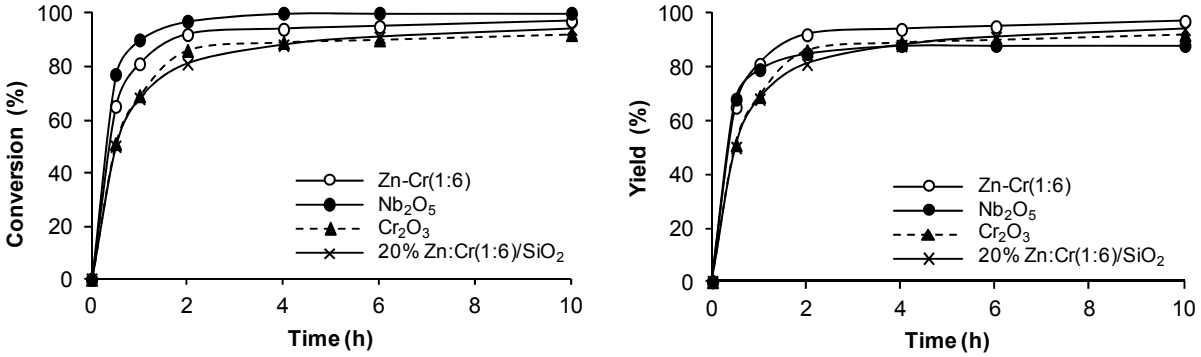

Fig.1. Conversion of β-pinene (left) and nopol yield (right) vs. time (80 ºC, 0.50 g catalyst, 5.0 mmol β-pinene, 30 mmol paraformaldehyde, 5.0 mL acetonitrile). Catalyst pre-treatment: Cr_2O_3 and Zn-Cr (1:6) were calcined at 300 ºC in N_2 for 5 h, 20%Zn-Cr(1:6)/SiO_2 at 400 ºC/N_2/5 h and Nb_2O_5 at 110 ºC/air/3 h.

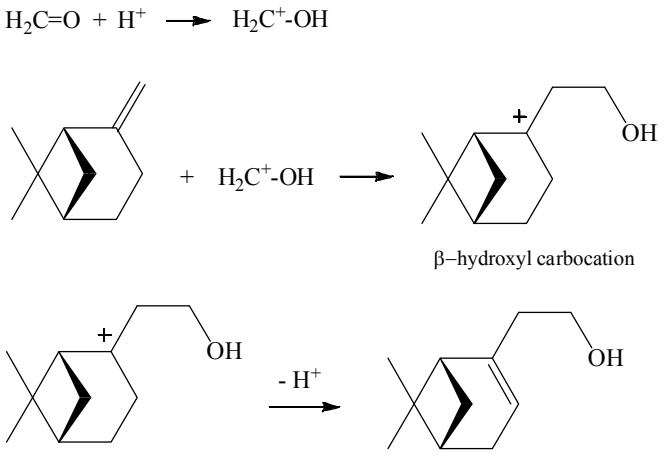

A plausible mechanism of nopol synthesis by Prins condensation (1) involves protonation of the aldehyde followed by attack on the methylene group of β-pinene to form β-hydroxyl carbocation intermediate, which undergoes proton elimination to yield nopol. The reaction therefore involves both protonation and deprotonation and is thus subject to acid and base catalysis. The acid properties of Nb_2O_5 and Zn-Cr mixed oxide were characterised by FTIR spectroscopy of adsorbed pyridine and ammonia adsorption microcalorimetry. An appropriate combination of acid-base properties of the Zn-Cr oxide is thought to be responsible for its high efficiency.

4 Conclusions

We have demonstrated that the metal oxides such as Nb_2O_5, Cr_2O_3 and especially Zn-Cr (1:6) mixed oxide are highly active and recyclable heterogeneous catalysts for Prins condensation providing a clean, high-yielding route for the synthesis of nopol by the condensation of β-pinene with paraformaldehyde. The results obtained show that metal oxides are promising environmentally benign catalysts for Prins condensation of bio-renewable feedstocks.

References

[1] A. Corma, S. Iborra, A. Velty, *Chem. Rev*. 107 (2007) 2411.
[2] K. Bauer, D. Garbe, H. Surburg, *Common Fragrance and Flavour Materials. Preparation, Properties and Uses*, VCH Verlagsgesellschaft, 1990.
[3] V. Costa, H. Bayahia, E. Kozhevnikova, E. Gusevskaya, I. Kozhevnikov, *ChemCatChem* 6 (2014) 2134.

IV-PP71

A One-Step Technique for *in situ* Synthesis of the Aerogels of the Multi-Walled Carbon Nanotubes

Kuznetsov V.L.[1,2,3], Krasnikov D.V.[1,2*], Kazakova M.A.[1,2], Moseenkov S.I.[1], Smirnova T.E.[3], Suslyaev V.I.[3], Dorofeev I.O.[3]

1 - Boreskov Institute of Catalysis, Novosibirsk, Russia
2 - Novosibirsk State University, Novosibirsk, Russia
3 - National Tomsk State University, Tomsk, Russia

* krasnikovdmitry@gmail.com

Keywords: multi-walled carbon nanotubes, aerogels, bimetallic catalysts

1 Introduction

Aerogels of multi-walled carbon nanotubes (MWCNTs) combine unique mechanical, thermal and electrical properties of nanotubes with specific characteristics of aerogels [1]. This material as well as MWCNT forests [2] can be more promising than conventional MWCNT powder for such applications as EMI and acoustic shielding, gas sensors and substrates for biological objects. Usually MWCNT aerogel synthesis includes MWCNT-based gel formation supplied by specific cross-linking agents and following supercritical drying [3-4]. However, One-step MWCNT aerogel production during the synthesis of nanotubes is to be more cost-efficient. Catalyst sputtering during MWCNT growth [5] and additional reactive ion etching of catalyst during synthesis of MWCNT forest [6] led to aerogel formation. In the present work, we report one-step MWCNT aerogel production via catalytic CVD technique under conditions close to industrial nanotube synthesis (T~1000 K, P~ 1 atm).

2 Experimental/methodology

The catalysts used consist of nanosized mixed metal oxides of Fe,Co Ca or Mg. Fe-Co alloy is an active component of this catalysts [7]. An activation of preformed [8] catalyst was carried out in the same conditions as following MWCNT growth (i.e. *in situ*; 670^{o}C, C_2H_4/Ar , 1:1, 400 sccm). Ethylene decomposition on the catalyst surface led to Fe, Co species reduction followed by alloy formation with subsequent nanotube nucleation and growth [9]. Catalyst structural changes and MWCNT aerogel morphology were observed with HRTEM (JEM-2010) and SEM (JSM6460LV). N_2 adsorption isotherms (77 K) were determined with ASAP-2400 (Micromeritics). Electric and magnetic polarizabilities of MWCNT aerogels were measured by open microwave resonator with a measuring hole in one of the mirrors (8-12 GHz).

3 Results and discussion

In situ activation of the preformed catalyst results in the formation of multiple nanosized active centers on the surface support particle (fig. 1B). This self-assembling system provides multi-center growth of MWCNTs. Following tangling of the MWCNTs results in the formation sponge-like and rigid structure of aerogel (fig. 1 C,D). Due to intensive MWCNT growth, a volume of resulting material significantly increases in comparison with the initial catalysts. This leads to the formation of aerogels with density of 0.03-0.08 g/cm^3. Any shape of MWCNT aerogels is possible to obtain by using different geometry of preformed catalyst (balls, cylinders etc.) (fig.2A). Pores of size >120 nm occupy >95% of MWCNT aerogel volume whereas smaller pores take up <2%. MWCNT aerogels showed polarizability intermediate to that of metal conductors and dielectrics with values close to metals while having a substantially lower weight (fig.2B).

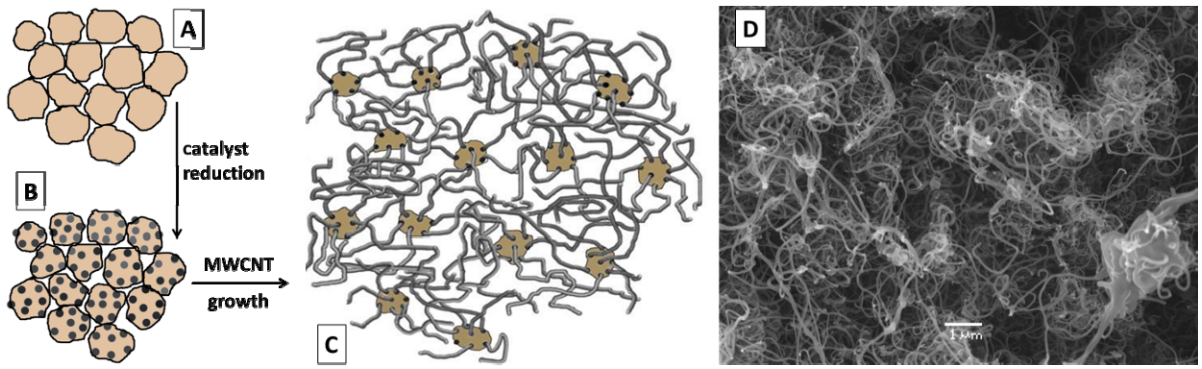

Fig. 1. A-C: A scheme for the formation of the MWCNT aerogel structure; **D:** Typical SEM microphotography of the internal structure of the MWCNT aerogel.

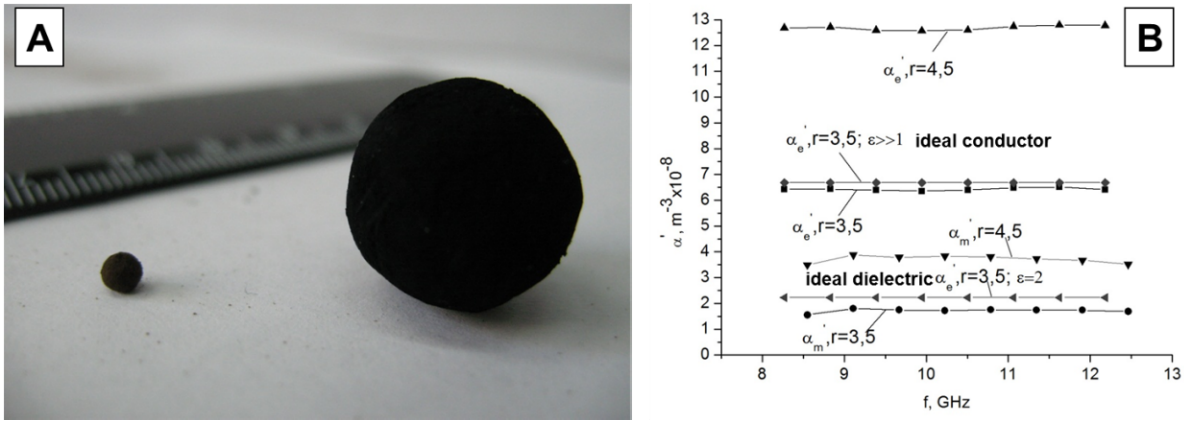

Fig. 2. A: Preformed catalyst (brown sphere on the left) and the MWCNT aerogel produced from it; **B:** Frequency dependence of real part of electrical (a'_e) and magnetic polarizabilities (a'_m) in comparison with a'_e of ideal conductor (r=3.5; ε>>1) and ideal dielectric (r=3.5; ε=2).

4 Conclusions

A new cost-efficient technique for one-step *in situ* MWCNT aerogel production under conditions close to industrial nanotube synthesis was developed. Such properties of the aerogels as S_{BET}, pore size distribution, density, conductivity and shape can be varied in a wide range. *In situ* produced MWCNT aerogels demonstrate high electrical conductivity (several S/cm), remain stable in different solvents and hold more than 2500 their weight. Due to high polarizability, MWCNT can be employed as low weight reflecting coatings. Macroporous and rigid structure combined with high surface area allow MWCNT aerogel to be promising support material for a different compounds including biological and supramolecular species.

Acknowledgements

This research was partially supported by grant of Ministry of Science and Education of Russia RFMEFI60714X0046.

References

[1] J. Zou, J. Liu, A.S. Karakoti et al. *ACS Nano* 12 (2010) 7293
[2] D.N. Futaba, K. Hata, T. Namai et al. *The Journal of Physical Chemistry B*. 15 (2006) 8035
[3] M.B. Bryning, D.E. Milkie, M.F. Islam et al., *Advanced Materials* 5 (2007) 661
[4] S. Nardecchia, D Carriazo, ML Ferrer et al., *Chem. Soc. Rev*. 2 (2013) 794
[5] X. Gui, H. Li, K. Wang et al. *Advanced materials* 5 (2010) 617
[6] M. Xu, D.N. Futaba, T. Yamada et al. Science 330 (2010) 1364
[7] V.L. Kuznetsov, D.V. Krasnikov, A.N.Shmakov et al. *PSS (b)* 12 (2012) 2390
[8] V.L. Kuznetsov et al. *Russian patent application* No 2014146924 (2014)
[9] V.L. Kuznetsov, A.N. Usoltseva, A.L. Chuvilin et al. *Physical Review B* 23 (2001) 235401

IV-PP72

Carbon Nanomaterials in 1,2-Dichloroethane Dechlorination and Aliphatic Alcohols Conversion. The Role of Surface Chemistry and Carbon Matrix Structure

Tveritinova E.A., Zhitnev Yu.N., Kulakova I.I..*, Savilov S.V., Maslakov K.I., Lunin V.V.

Lomonosov Moscow State University, Moscow, Russia

* inna-kulakova@yandex.ru

Keywords: carbon nanomaterials, dechlorination, 1,2-dichloroethane, conversion of alcohols

1 Introduction

The problems of environmental protection require the creation of new environmentally friendly catalysts, what must be thermally persistent, easily recycled and resistant to aggressive media. These requirements are met by carbon nanomaterials, which have a regular porous structure with a low content of micropores, the developed surface with a large number of functional groups which are important for the catalysis. They exhibit catalytic activity in processes such as oxidative dehydrogenation of ethylbenzene and light alkane [1], dehydration and dehydrogenation of aliphatic alcohols [2]. The aim of this work was to identify the catalytic activity of carbon nanomaterials with the different structure of their carbon matrix in conversion of 1,2-dichloroethane and C2-C4 alcohols.

2 Experimental

The following carbon nanomaterials we used as catalysts: detonation nanodiamond (ND), carbon nanoflakes (UNFs), including doped with nitrogen (UNFs-N), carbon nanotubes (CNTs), These materials are formed by carbon atoms in state sp^3-, sp^2 -, and curved sp^2 - hybridization, respectively. The composition of the surface functional groups of these materials was due to the conditions of cleaning after synthesis.

The surface and structure of the carbon materials were characterized using different methods: BET, DTA, SEM, TEM, XPS, XRD, TPR, diffuse reflectance IR spectroscopy.

The catalytic properties of the materials are studied using the pulsed microcatalytic method. We have studied the dichloroethane dechlorination and the conversion of all alcohols C2-C4: ethanol, 1- propanol, 2-propanol, 1- butanol, 2-butanol and t-butanol in the presence of selected nanocarbon catalysts.

3 Results and discussion

Catalytic activity in 1.2-dichloroethane conversion was exhibited only by ND, and the selectivity to ethylene was almost 100%. Regeneration of the deactivated ND-catalysts with hydrogen not only restored their activity, but also increased it. Because other carbon nanomaterials did not showed catalytic properties in the process of 1,2-dichloroethane dechlorination, we concluded that the key role in catalysis plays a "diamond" structure of ND and hydrogen groups on its surface.

In the conversion of aliphatic C2-C4 alcohols CNTs and ND showed catalytic activity in various degrees, while UNFs were inactived. The conversion of secondary alcohols (2-propanol and 2- butanol) on CNTs occurs with predominant formation of the dehydration products (propene,1- butene and 2- butene) with a selectivity of ~90%, whereas the main products of conversion on ND are dehydrogenation products (acetone and butanone). This allowed us to

conclude that the Lewis acid centers play a key role in the catalysis on the surface of the CNTs, while the basic oxygen-containing centers on the ND surface responsible for the catalysis on it.

The conversion of t-butanol on CNTs starts almost at room temperature, reaches 100% at 160^0C and proceeds with 100% selectivity to isobutene. In the case of ND the conversion of t-butanol in isobuten reaches 75% only at 300^0 C. These experimental data confirm participation in the conversion of aliphatic alcohols on the CNTs surface oxygen-containing Lewis sites and unsaturated surface C=C bonds. Catalytic centers in the conversion of aliphatic alcohols on ND are only oxygen-containing surface groups (e.g., carbonyl, carboxyl, etc.) UNFs-N, containing 10% nitrogen, exhibit catalytic activity only in the conversion of primary alcohols, and products dehydrogenization are mainly formed. This nanocarbon material was inert in the conversion of 2-propanol and 2-butanol, that allows to judge about the participation only of nucleophilic nitrogen-containing groups in the conversion of alcohols.

4 Conclusion

Metal-free carbon nanomaterials due to their unique structure and composition of surface functional groups, thermal stability and resistance to aggressive environments, as well as relatively low cost can compete with traditional metal containing and oxide catalysts. These catalysts one can consider as novel class of catalysts with large potential for industrial application.

References

[1] D.S.Su, N.Maximova, J.J.Delgado, N.Keller et.al. Catal.Today 102-103 (2009) p.110-114
[2] E.A.Tveritinova, I.I.Kulakova, Yu.N.Zhitnev, A.V.Fionov, A.Lund et al.
Rus.J.Phys.Chem. A 86, 26 (2012) p.26-31

IV-PP73

Synthesis of CO and H_2 Conversion Nanoheterogeneous Catalysts in Disperse Systems

Kulikova M.V., Karpacheva G.P., Khadzhiev S.N.*

A.V.Topchiev Institute of Petrochemical Synthesis, RAS, Moscow, Russia

* m_krylova@ips.ac.ru

Keywords: nanoheterogeneous catalysts, Fischer-Tropsch synthesis, methanol synthesis

1 Introduction

Development of a heterogeneous catalysis is directed on creation of catalysts with most regular structure, on the directed formation on support surface of special clusters or nanodsized particles of active component now.

Along with it catalysis in disperse phase providing synthesis of catalyst nanosized particles in liquid or solid dispersion medium intensively develops.

Results of last period researches on synthesis of ultrafine and nanosized particles of CO and H2 conversion catalysts suspended in liquid hydrocarbon medium or distributed in solid organic matrix are given in report.

2 Experimental/methodology

Synthesis of nanoheterogeneous contacts were carried out by various methods in disperses media, including using organic matrix method.

Catalytic tests were carried out in fixed bed and slurry phase reactors.

3 Results and discussion

At synthesis of nanoheterogeneous contacts in liquid hydrocarbon medium nanosize stable suspensions with a size of particles no more than 50 nm were obtained. The disperse phase in such disperse systems isn't inclined to sedimentation that does them perspective for industrial realization in liquid-phase slurry -reactors.

Nanosized Fe and Co contacts prepared by method of precursor decomposition in dispersive medium are highly effective in Fischer-Tropsch synthesis. Their activity in CO conversion and liquid products specific productivity in two and more times exceeds this indicator for the catalysts which are traditionally used in slurry-reactors.

Ultrafine Cu-Zn catalysts prepared similarly allow carrying out synthesis of methanol with activity on CO conversion, equal 37% per pass, and selectivity to 98%. And change of the direction of reaction towards formation of dimethyl ether by introduction to catalyst of dehydrating component is possible.

At synthesis of nanoheterogeneous contacts distributed in solid organic matrix methods for obtaining of polymercontaining composite materials are used. Initial organic matrixes represent polyconjugated systems decomposing to carbon during formation of the catalyst. Thus particles of 10-20 nm in size metal are formed from salts immobilized on polymers.

4 Conclusions

Synthesized nanosized particles show high activity and selectivity in CO and H_2 conversion which is carried out in fixed bed or liquid-phase reactors. So, Fe and Co catalysts of this type have demonstrated extremely high activity in Fischer-Tropsch synthesis. In fixed bed reactor at

CO conversion close to 100% specific productivity by liquid products next larger than at traditional catalysts is observed.

Acknowledgements

This work was supported under the Program of basic scientific researches by Presidium of RAS №25 «Energy aspects of deep fossil and renewable carbon-containing raw material processing».

This work was partially carried out using of Common Use Center "New Petrochemical Processes, Polymeric Composites and Adhesives" equipment.

IV-PP74

Titanium (+4) Complexes Containing 2-(Hydroxymethyl) Phenol Derivatives as Pre-Catalysts for the Polymerization of Ethylene

Kurmaev D.A.[1], Mukharinova A.I.[1], Gagieva S.Ch.[1], Tuskaev V.A.[1,2], Bulychev B.M.[1*]

1 - Moscow State University, Chemical Department, Moscow, Russia
2 - Nesmeyanov Institute of Organoelement Compounds, Russian Academy of Sciences, Moscow, Russia

* dmitrykurmaev@mail.ru

Keywords: titanium, coordination compounds, ethylene, polymerization

1 Introduction

The polymerization of olefins by single-site catalysts has experienced a phenomenal growth in the last decades. Numerous highly active single-site homogeneous catalysts based on metals across the transition series have been reported. Among them metal complexes with OO-type ligands (especially where ligand structure contain both phenol and alcohol hydroxyls) are indeed unique. In recent studies, we have found the ability of lithium and magnesium compounds to promote the catalytic process due to the products of secondary coordination.

Herein, we report the synthesis of tetranuclear titanium complexes, stabilized by saligenin-type ligand – 4-bromo-2-(hydroxymethyl)-6-methoxy-phenol and their utility as polymerization catalysts.

1 Experimental/methodology

All manipulations of air-sensitive materials were performed with rigorous exclusion of oxygen and moisture in oven-dried Schlenk glassware on a dual manifold Schlenk line, interfaced to a high-vacuum line. X-ray diffraction data for the single crystals of **3** were collected using a "Bruker SMART APEX DUO" CCD diffractometer, for the single crystals of **4** – using "Bruker SMART APEX II" diffractometer. Polymerization of ethylene was performed in a 100 mL reactor (Parr Instrument Co.) equipped with a magnetic stirrer and inlets for loading components of catalytic systems and ethylene at a total ethylene and toluene vapors pressure of 0.7 atm.

3 Results and discussion

Ligand **1** was synthesised by bromination of o-vanillin with subsequent reduction with $NaBH_4$. The ligand was treated with $TiCl_2(OiPr)_2$, but the formation of the desired product **2** wasn't occur. NMR indicated the formation of a set of complexes.

Carrying out the reaction under more severe conditions was accompanied by chemical modification of the ligand - alcoholic hydroxyl was substituted by chlorine, and compound **3** was obtained (scheme 1).

By the reaction of the ligand **1** with titanium tetraisopropoxide compound **4** has been obtained. The molecular structures of the complexes **3**, **4** are shown in Figure 1.

Pre-catalysts **3-4** were completely inactive in presence of MAO, Me_3Al or Et_2AlCl, but been activated by binary co-catalyst Et_2AlCl-Bu_2Mg, exhibited moderate to high activities toward ethylene polymerization, giving high molecular weight polymers with broad molecular weight distributions. Catalytic activity of compounds **3-4** is 2570-3000 kg of PE (mol of Ti atm)$^{-1}$ h^{-1}. The molecular mass of the polymers is 4.2 10^5-5.8 10^5; PDI – 2.4-2.8, respectively.

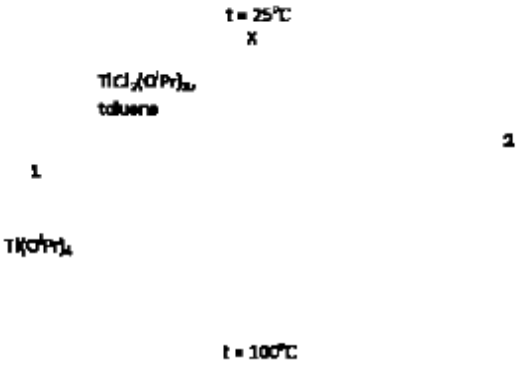

Scheme 1. Synthesis of titanium (+4) complexes based on ligand **1**.

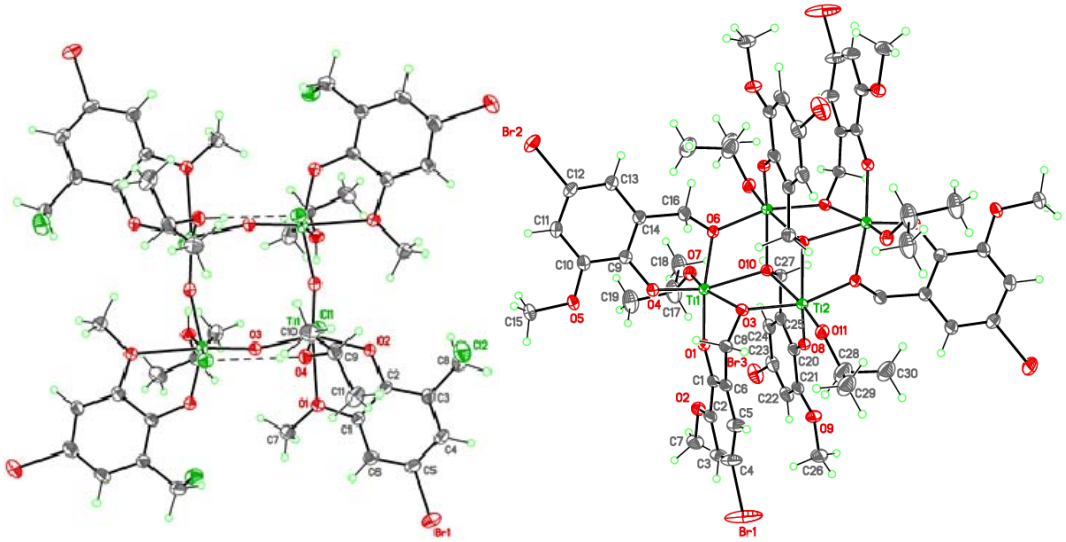

Fig. 1. The molecular structure of the complexes **3**, **4**. Atoms are represented as thermal ellipsoids (P = 50%). The hydrogen atoms are not shown.

4 Conclusions

A series of novel tetranuclear titanium complexes (**3-4**) bearing $[O,O,O]^{2-}$-type ligand (**1**) were synthesized in high yields.

We speculate that observed ability of magnesium chloride (which appears in the catalytic system as the result of the interaction of $MgBu_2$ with $2AlEt_2Cl$) to promote the catalytic process is due to the products of secondary coordination.

Further modification of these systems to enhance their catalytic performance is underway and will be reported in due course.

Acknowledgements

This work was supported by the Russian Foundation for Basic Research (14-03-00904, 13-03-12181, 14-03-31260).

IV-PP75

Catalytic Conversion of Mechanically Activated Aspen Wood in Supercritical Ethanol in the Presence of Zeolites with Different Si/Al Ratio

Sharypov V.I.[1], Baryshnikov S.V.[1], Beregovtsova N.G.[1], Vos'merikov A.V.[2], Kuznetsov B.N.[1*]

1 - Institute of Chemistry and Chemical Technology SB RAS, Krasnoyarsk, Russia
2 - Institute of Petroleum Chemistry SB RAS, Tomsk, Russia

* bnk@icct.ru

Keywords: aspen-wood, catalytic conversion, ethanol, zeolites

1 Introduction

In recent decades, much attention has been focused on the production of chemicals from renewable lignocellulosic biomass as an alternative to fossil fuels. Thermal conversion of biomass in supercritical aliphatic alcohols is a perspective method for obtaining low-boiling hydrocarbons. Supercritical fluids are finding an increasing application in chemical processing of plant biopolymers because they have a high diffusing capacity and low viscosity. The use of solid acid catalysts including zeolite allows to intensify the transformations of various types of lignocellulosic biomass, as well as its major components – cellulose, hemicelluloses and lignin to low molecular mass organic products.

We have previously demonstrated that the intensive pre-treatment in a activator mill AGO-2 reduces the degree of polymerization and crystallinity of aspen wood and increases its reactivity in acid hydrolysis.

The aim of this work was to study the transformations of mechanically activated aspen wood in sub- and supercritical ethanol in the presence of zeolites with different silicate module.

2 Experimental

The sample of aspen wood, which was used in this study contained (in % wt. on dry wood): 46.3 – cellulose; 20.4 – lignin; 24.1 – hemicellulose; 3.6 – soluble substances; 5.2 – extractives; 0.5 – ash. The dried wood was mechanically activated by treatment in a tensile energy planetary activator mill (AGO-2) at the acceleration of grinding bodies 600 $m \cdot s^{-2}$ during 30 min. The high silica zeolites in H-form (H-HSZ) with a molar ratio SiO_2/Al_2O_3 = 30–100 were used.

Thermal conversion of wood in ethanol was carried out in a rotary autoclave at 270 and 350 °C. These temperatures were chosen based on the results of the preliminary study of wood thermal conversion by thermogravimetric method. They correspond to two maxima of the mass loss on the DTG curve. Operating pressure in the autoclave was varied in the range of 4.0–20.0 MPa. The soluble in ethanol products was analyzed by GC-MS. The content of sugars in the water-soluble products was determined by GC. Samples of mechanically activated aspen wood and solid residues of its thermal dissolution in ethanol were investigated by IR, XRD and chemical analysis methods.

3 Results and discussion

It was established that during the conversion of mechanically activated aspen wood in ethanol medium the increase of pressure in an autoclave from 4.0 to 20.8 MPa leads to the increase of the degree of wood conversion into liquid and gaseous products from 56 and

67 wt.% to 95.5 and 76.0 wt.% at a process temperatures of 270 °C and 350 °C, respectively.

At the process temperature 270 °C in subcritical conditions, the yield of products extracted with ethanol reached to 55.2 wt.%. They mainly consist of fraction boiling up to 180 °C (60 wt. %). The growth of pressure increased the yield of products extracted by ethanol to 76.2 wt.%. Simultaneously the yield of fraction boiling above 180 °C was substantially increased. Our studies have shown that all the basic components of wood: cellulose, hemicelluloses and lignin are transformed under these conditions. Hemicelluloses was the most reactive component, while cellulose was the most stable. The growth of the pressure increases the conversion of all wood components. The degree of hemicelluloses conversion reached 100 wt.% at pressure of 15.2 MPa. At a higher pressure (20.0 Mpa) the conversion of lignin was more than 70 wt.% and cellulose – 67 wt.%.

Solid residue of aspen wood thermal conversion at 350 °C consists of coke and ash. Possibly, at this temperature, the two competing processes are occurred: the decomposition of wood components with formation of products soluble in ethanol and their secondary conversions into coke. The growth of the pressure increases the density of ethanol vapor, preventing the interaction of obtained products with the formation of coke.

The use of zeolite catalysts increases the yield of light fraction of liquid products and reduces the yield of the fraction boiling above 180 °C. The highest yield of light fraction (59.9 wt.%) was obtained in the presence of catalyst H-HSZ – 30 with Si/Al ratio 30 at the process temperature 350 °C (Fig).

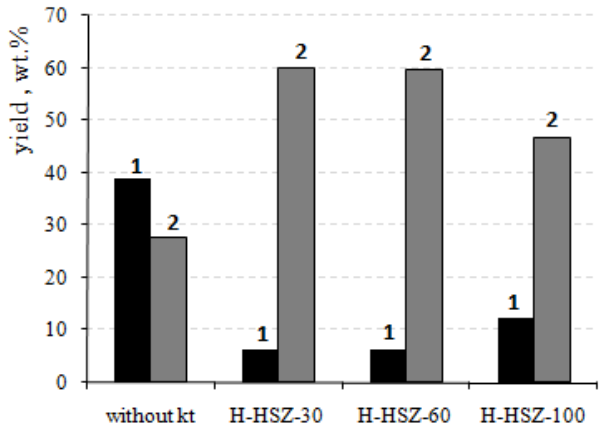

Fig. Influence of catalysts on the yield of liquid products of aspen wood thermal conversion in ethanol at 350 °C, 18 MPa: 1 – fraction b.p. > 180 °C, 2 – fraction b.p. < 180 °C

According to GC-MS data the obtained liquid products consist of several groups of substances. They are formed from ethanol, from wood components and by interaction of products of wood and ethanol conversions. Zeolite catalysts decreased the content of phenol and furfural derivatives in liquid products. While the content of the ethyl esters, especially ethyl levulinate was increased significantly in the presence of catalysts.

4 Conclusions

It was shown that the increase of pressure of mechanically activated aspen wood conversion in ethanol from 4.0 to 20.8 MPa significantly increases its conversion degree (up to 95.5 and 76.0 wt.% at a temperatures of 350 °C and 270 °C, respectively).

The use of zeolites as catalysts in this process increased the yield of liquid fraction boiling up to 180 °C by 1.7–2.2 times and reduced the yield of the fraction boiling above 180 °C by 3.2–6.3 times at a process temperature of 350 °C and pressure of 18.0 MPa.

IV-PP76

Bio-Inspired "Buckyball-Shaped" Photocatalytic Architectures

Altunoz Erdogan D.[1], Solouki T.[2], Ozensoy E.[1*]

1 - Bilkent University, Department of Chemistry, Ankara, Turkey
2 - Baylor University, Department of Chemistry & Biochemistry, Waco, USA

* ozensoy@fen.bilkent.edu.tr

Keywords: TiO_2 template, bio-inspired, photocatalyst

1 Introduction

Naturally occurring biological systems with complex structures, textures, and geometries can serve as efficient templates for the design and production of novel catalytic materials with extraordinary surface morphologies, shapes, and compositions [1-3]. These sacrificial biotemplates allow the synthesis of unique catalysts with complex and unprecedented hierarchical pore structures. In this contribution, we used a *Lycopodium clavatum* (LC) spore as a bio-template to synthesise a buckyball-shaped TiO_2 photocatalytic architecture with an unusual surface morphology which is not feasible to be attained by conventional bottom-up synthetic strategies. Photocatalytic degradation of Rhodamine B by UVA illumination was utilized to demonstrate the photocatalytic functionality of these bio-inspired buckyball-shaped TiO_2 structures, whose catalytic performance can be optimized by varying the relative precursor concentrations and calcination temperature.

2 Experimental

A template-assisted synthetic strategy was employed to obtain micron-sized buckyball-like TiO_2 architectures. Bio-template was coated with an inorganic TiO_2 thin film *via* sol-gel technique [3] to replicate the fine-structural details of the underlying biomaterial. Successful TiO_2 coating was performed by mixing the precursor (*i.e.*, titanium (IV) isopropoxide or TIP) with ethanol using different TIP:ethanol volume ratios (3:2, 2:1, 3:1; v/v; respectively). Calcination process was performed to remove the original biotemplate and to control the crystallinity of the TiO_2 overlayer. The photocatalytic activity of the obtained micron-sized buckyball-like TiO_2 architectures under UVA irradiation was evaluated by using the discoloration rate of Rhodamine B (RhB) dye solutions [4].

3 Results and discussion

A typical SEM image of the LC biotemplate after titanium (IV) isopropoxide deposition at 25 ^oC is presented in Figures 1a and 1b demonstrating the presence of the TiO_2-coated overlayer on the biotemplate which is also verified *via* EDX measurements. Even after calcination at elevated temperatures (*e.g.* > 800 ^oC) buckyball-shaped TiO_2 structures preserve their structural details (Figure 1c). Photocatalytic RhB degradation performance of the micron-sized buckyball-like TiO_2 architectures was examined under UVA irradiation by obtaining the apparent first-order rate constants (k′) as a function of calcination temperature and TIP loading in the precursor solution which in turn, allow the fine-tuning of the grain size and crystal structure of the TiO_2 overlayer. Bio-inspired buckyball-shaped TiO_2 structure with a TIP:EtOH loading of 2:1, v/v and calcined at 800 ^oC yielded the highest k′ value among all of the investigated micron-sized buckyball-like TiO_2 architectures. The crystallographic structure of the outermost layer for this highly efficient catalyst was composed of ~ 50 wt.% anatase and 50 wt.% rutile.

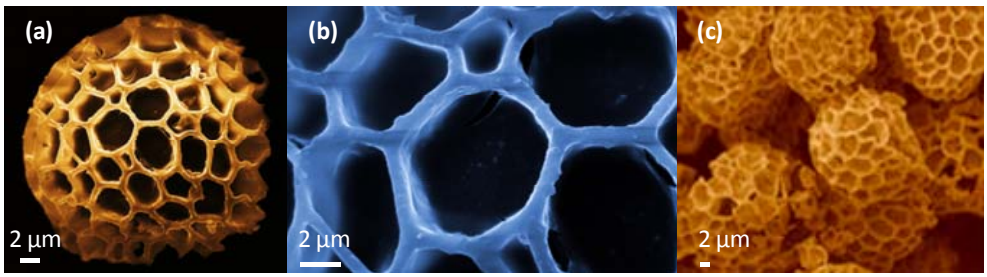

Fig. 1. SEM images of the buckyball-shaped TiO_2 photocatalytic structures.

4 Conclusions

In the current study, bio-inspired buckball-shaped TiO_2 structures were synthesized using a sacrificial template-assisted sol-gel method. We showed that by simply altering the titanium (IV) isopropoxide:ethanol volume ratio in the synthesis mixture, as well as the calcination temperature, one could fine-tune the crystal structure and the surface composition of the buckyball-like TiO_2 overlayer. It was also illustrated that the unique surface morphology and the pore structures of the LC biotemplates could be successfully transferred to the inorganic TiO_2 overlayer by effective removal of the biological scaffold. Moreover, we demonstrated the catalytic functionality of these micron-sized buckyball-like TiO_2 architectures in the photocatalytic degradation of Rhodamine B dye.

Acknowledgements

The authors acknowledge the financial support from the Scientific and Technological Research Council of Turkey (TUBITAK) (Project Code: 113Z543) and the USA National Science Foundation (NSF EAGER Award 1346596).

References

[1] M. R. Jones, K. D. Osberg, R. J. Macfarlane, M. R. Langille, C. A. Mirkin, *Chem. Rev.* 111 (2011) 3736.
[2] H. Zhou, T. Fan, D. Zhang, *ChemSusChem* 4 (2011) 1344.
[3] S. Sotiropoulou, Y. Sierra-sastre, S.S. Mark, C. A. Batt, *Chem. Mater.* 20 (2008) 821.
[4] D. A. Erdogan, M. Polat, R. Garifullin, M. O. Guler, E. Ozensoy, *Appl. Surf.* Sci. 308 (2014) 50.

IV-PP77

KMo Alumina Supported Catalysts for the Synthesis of Methylmercaptan from Syngas and H_2S: New Insight into the Nature of the Active Phase

Cordova A.[1], Lamonier C.[1*], Blanchard P.[1], Lancelot C.[1], Frémy G.[2]

1 - University of Lille UCCS France, Villeneuve d'Ascq, France
2 - Arkéma Groupement de Recherches de Lacq, Lacq, France

* carole.lamonier@univ-lille1.fr

Keywords: potassium, molybdenum catalysts, sulfide catalyst, methylmercaptan, XPS

1 Introduction

Nowadays methylmercaptan (CH_3SH) is an industrially chemical of major importance used as raw material mainly for the production of valuable organosulfur compounds such as methionine, an amino acid used as poultry feed supplement [1]. Methylmercaptan is currently manufactured at industrial scale by the reaction of methanol with hydrogen sulfide [2]. This route needs a multiple-step pathway for the synthesis of methanol, which results in raised costs of production. The development of a new route using a simple feedstock (syngas/hydrogen sulfide) is then increasingly attractive for industrial application. The production of methylmercaptan from the one-step reaction of syngas and hydrogen sulfide has been studied since 1980s. Its production at laboratory scale is usually carried out using K-Mo based catalysts with alumina [3] or silica as carriers [4]. Looking at the earlier works concerning the synthesis of methylmercaptan, most of the researches have been focused in the development of efficient catalytic systems and the determination of the reaction mechanisms starting from $CO/H_2/H_2S$ or $COS(CS_2)/H_2$ reactants [5]. Concerning active phase determination, a Mo^{6+}-S_x-K^+ phase was first proposed as active phase using $CO/H_2/H_2S$ mixture [6] but the exact nature remains unclear. In this work, the nature of the active phase has been studied as well as the improvement of catalytic performances.

2 Experimental/methodology

Mo and various K(Na)Mo catalysts with fixed metal amounts (8.1 Mo wt%, 6.6 K wt.%) were prepared by incipient wetness impregnation method using ammonium heptamolydate, (AHM), potassium nitrate, $K(Na)_2MoO_4$ and K_2MoS_4 solutions impregnated on alumina support. The catalysts performance was evaluated in a fixed-bed flow reactor under reaction conditions of 10 bars, temperature range 280-300-320 °C, feed gas composition $CO/H_2/H_2S$ = 1/2/1 (v/v) and GHSV = 1333 h^{-1}. Reactants and products were analyzed by on-line GC. Prior to testing, the catalysts were activated in-situ by sulfidation. Before activation, catalysts were characterized by elemental analysis (ICP), BET, XRD, Raman spectroscopy and XPS. An extensive study of Mo sulfided catalysts was performed by XPS and TEM.

3 Results and discussion

In K_2MoO_4 and K_2MoS_4-based catalysts, the preservation of the impregnated species was observed by Raman and XPS. These species precipitate inside the porosity during their incorporation, leading to crystallized species whereas a good dispersion of Mo species was observed using AHM based solutions. The catalytic results showed that the simultaneous presence of Mo and K in the catalytic system allowed to achieve higher CO conversion and

CH_3SH selectivity and a decrease in CO_2 selectivity, highlighting the favorable influence of the coexistence of both metals in the catalytic system. The incorporation of K and Mo coming from a unique precursor was beneficial when considering catalysts time and costs preparation.

A careful XPS analysis of potassium containing sulfide catalysts (fig 1.) brings out the presence of a new molybdenum sulfide phase with an unusual Mo3d (K-Mo^{4+}(S)) binding energy coexisting with classical 2H-MoS_2 (Mo^{4+}(S)). Taking into account literature data on intercalated Li_xMoS_2 material, this phase is assumed to be a potassium intercalated phase K_xMoS_2 in which potassium can stabilize the unusual 1T-MoS_2 phase with octahedral coordination of Mo. It is proposed for the first time for supported catalysts.

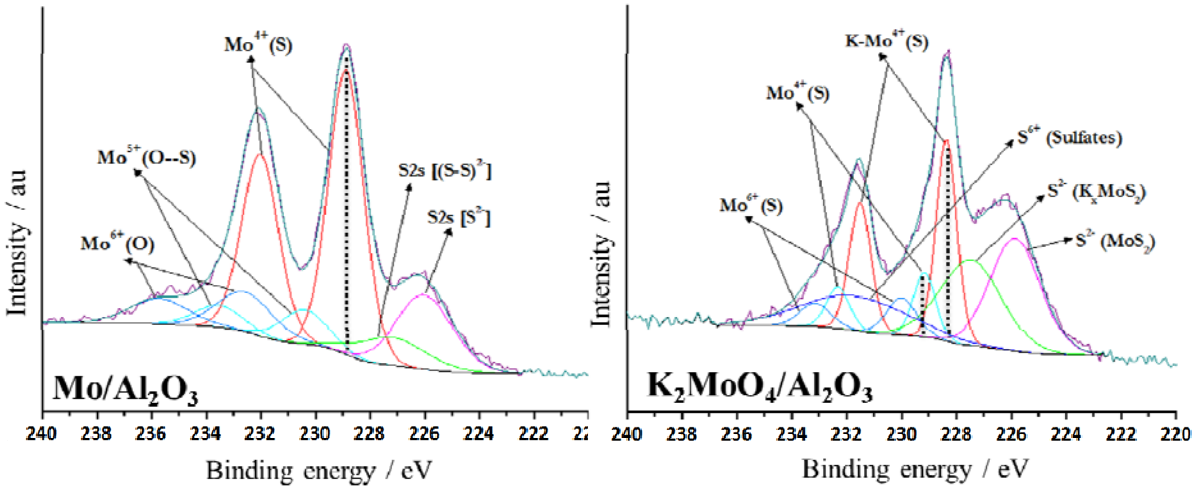

Fig 1. Mo3d XPS spectra for Mo/Al_2O_3 and K_2MoO_4/Al_2O_3 sulfide catalysts

Moreover a good correlation has been obtained between the relative amount of intercalated K_xMoS_2 and CO conversion as well as CH_3SH productivity taking into account the quantity of molybdenum detected by XPS. The study by HRTEM of these samples suggested that intercalation of K on MoS_2 phase has an effect over the slab length and stacking degree of MoS_2 layers.

4 Conclusions

The presence of an intercalated K_xMoS_2 has been shown for the first time in supported KMo sulfide catalysts. By correlating the amount of this phase with the catalytic performances, we observed that the higher the amount of K_xMoS_2 in the catalyst, the higher the CO conversion and CH_3SH productivity in the reaction of syngas with hydrogen sulfide. Based on these statements intercalated K_xMoS_2 is proposed as the active phase in the reaction of thiolation of syngas. Catalytic performances can be improved by changing the support and increasing the Mo loading.

Acknowledgements

The research leading to these results has received funding from the European Union Seventh Framework Programme (FP7/2007-2013) under grant agreement n° 241718 EuroBioRef.

References

[1] W. Leuchtenberger, K. Huthmacher, and K. Drauz, *Appl. Microbio. Biotechno.* 69 (2005) 1.
[2] H. O. Folkins, *"Production of organic thiols*," U.S. Patent N° 27860791957.
[3] B. Zhang, S. H. Taylor, and G. J. Hutchings, *Catal. Let.* 91 3–4 (2003) 181.
[4] A. P. Chen, Q. Wang, Y. J. Hao, W. P. Fang, and Y.-Q. Yang, *Catal. Let*, 121, 3–4 (2008) 60.
[5] O. Y. Gutiérrez, C. Kaufmann, A. Hrabar, Y. Zhu, and J. a. Lercher, *J. Catal.* 280 (2011) .264.
[6] Y.-Q. Yang, S. Dai, Y. Yuan, R. Lin, D. Tang, and H. Zhang, *Appl.Catal.* A: Gen. 192 (2000) 175.

IV-PP78

Investigation of Palladium Catalysts Supported on Highly Porous Cellular Metal Carriers

Laskin A.*, Kirgizov A., Ilyasov I., Lamberov A.

Kazan (Volga region) Federal University, Kazan, Russia

* artemka166@mail.ru

Keywords: selective hydrogenation, highly porous cellular metal support

1 Introduction

Industrial purification of ethylene and propylene processes for further polymerization carried out by selective hydrogenation in the gas phase in the reactors with irregular granular catalyst bed. Catalyst is a palladium, dispersed on the alumina surface, in the form of spheres, cylinders or other geometries, which characterized by insufficient heat- and mass transfer in the catalyst bed. Poor thermal conductivity of the inorganic carrier causes the formation of local overheating in the granular bed, which leads to a change in physical properties (density, viscosity) of the hydrocarbon stream with an increase its uneven distribution over the cross section of the reactor and the subsequent deterioration in the running of the catalyst. Formation of local overheating with increasing temperature of the recommended technological regime also cause reactions of deep hydrogenation of acetylene and diene hydrocarbons to alkanes and oligomerization processes, leading to a decrease in the selectivity of the main components and the rapid deactivation of the catalyst, respectively. Large grain diameter of catalyst, usually more than 3 - 2 mm, is not provide good mass transfer of the starting components and reaction products resulting from diffusion limitations associated with the location of the active component in a depth granules. This leads to inefficient use of the active component and the deep side reactions hydrogenation of acetylene and diene to the alkane hydrocarbons with decreased catalyst activity and selectivity. Reducing the size of the grains of the catalyst to reduce the adverse effects of diffusion limitations with the increasing availability of the active component to the reacting molecules causes the growth of hydraulic resistance with disabilities improve productivity of industrial reactors.

2 Experimental/methodology

Traditional alumina carrier was obtained by calcining boehmite extrudates in air at 550 ° C (2 h). On nickel HPCM obtained elktrochemically deposition metal coated with aluminum hydroxide by reacting with nitric acid. Calcining the resultant composite is further led to the formation of secondary aluminum oxide layer. Catalysts were prepared by impregnating the respective adsorption of carriers benzene solution of palladium acetylacetonate, followed by drying at 100 ° C and calcination at 300 ° C for 2 hours. The concentration of active component in the finished catalyst was 0.5 weight%.

The surface area (BET), volume, pore size and pore size distribution (BJH) of carriers was determined by nitrogen sorption (Autosorb iQ, Quantachrome, USA) -195,7 ° C. X-ray diffraction of carriers (XRD) was carried out on diffractometer XRD 7000S (Shimadzu) using a long-wave radiation CuK_α (λ = 1,54187Å). Image scanning electron microscopy (SEM) were recorded on MERLIN by Carl Zeiss Microscopy. IR spectra were obtained at a temperature of - 83 ° C in the Fourier spectrometer Bruker Vertex 70. Temperature program reduction (TPV) samples and dispersion of palladium measured by CO chemisorption was performed on an automated chemisorption analyzer AutoChem 2950 HP (Micromeritics, USA).

3 Results and discussion

A highly porous cellular composite material based on nickel (HPCM) is a reticulate structure with a honeycomb cell size of 2 mm, a width of the webs formed by nickel of 200 micron, which is fixed γ-Al_2O_3 layer thickness of 20 microns (Fig.1).

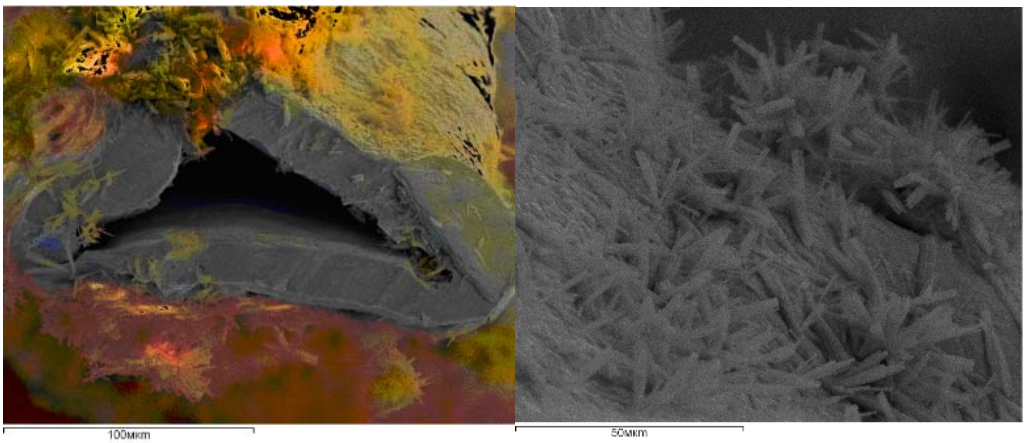

a b

Fig. 1. SEM picture: a - jumper HPCM, b - the surface of the composite HPCM

Alumina produced on the surface of Ni-HPCM is different in morphology and texture characteristics of γ-Al_2O_3, synthesized without the substrate, which is associated with a variety of textural and morphological properties of their precursors - aluminum hydroxides. Specific surface area for γ-Al_2O_3/Ni-HPCM is 319 m^2/g, total pore volume is 0.135 cm^3/g, and for γ-Al_2O_3 is S = 108 m^2/g, pore volume is 0.29 cm^3/g.

Various methods for the synthesis of oxide structures are responsible for the differences in the characteristics of the acid sites of the two carriers, that confirmed by data TPD of ammonia. Subsequent application of a palladium salt on γ-Al_2O_3/Ni-HPCM and conventional γ-Al_2O_3 according to IR spectroscopy of adsorbed carbon monoxide lead to the formation of palladium particles, varying in diameter and charge state. For palladium particles supported on γ-Al_2O_3/Ni-HPCM characterised more uniform particle size distribution and the electronic states (d_{av} = 4.6 nm, D = 24,5 %), than for the conventional alumina (d_{av} = 2.8 nm, D = 39,5 %). Greater interaction force inflicted Pd precursor to the surface acid sites of conventional alumina support γ-modification compared to γ-Al_2O_3/Ni-HPCM systems, determine the high dispersion of the active component and a wide range of charge state confirm TPR results in hydrogen.

Smaller values of selectivity conversion of acetylene hydrocarbons for catalysts based on conventional γ-Al_2O_3 compared with samples of γ-Al_2O_3/ Ni-HPCM due to the presence of large crystallites of palladium and the metal particles are characterized by the presence of surface atoms of the active component with low electron density on the valent orbitals.

4 Conclusions

In order to assess the possibility of use as a highly porous medium permeable to the cellular material coated on its surface alumina hydrogenation catalyst investigated the effect of the texture, and morphologic characteristics to its acidic properties and catalytic properties of palladium particles deposited by the reaction of hydrogenation of acetylene hydrocarbons. The formation of a narrow range of charge states of palladium particles deposited by surface atoms that are characterized by a high electron density on the valent orbitals catalysts Ni-based HPCM, determines a higher selectivity of the conversion of acetylene hydrocarbons (S = 78,3%) as compared with the conventional catalyst (S = 42,6%), was synthesized using γ-Al_2O_3.

IV-PP79

Aqueous Phase Hydro-deoxygenation of Glycerol towards One-step Production of "Green" Propene

Lemonidou A.A.[1,2*], Zacharopoulou V.[1], Vasiliadou E.S.[1]

1 - Department of Chemical Engineering, Aristotle University of Thessaloniki, Thessaloniki, Greece
2 - Chemical Process & Energy Resources Institute, CERTH, Thessaloniki, Greece

* alemonidou@cheng.auth.gr

Keywords: green propene, biomass conversion, molybdenum, oxides, glycerol, hydro-deoxygenation

1 Introduction

The demand for propene, a valuable olefin, has increased significantly over the past years, especially for the production of plastics (polypropylene). The majority of olefins are produced via steam cracking, one of the most energy-consuming industrial processes, resulting in particularly high CO_2 emissions. In addition to the arising environmental concerns, the finite natural resources address the significance of innovative procedures, utilizing renewable and sustainable resources, as raw materials. [1] Over the past decade, biomass has received considerable attention, as technological advances enable the development of inventive processes for the production of valuable bio-chemicals and bio-fuels, substituting the finite natural resources. Glycerol, one of the 12 top building block chemicals derived from biomass, is a readily available, low-cost molecule that can be upgraded to high added-value products; the production of lower hydrocarbons from glycerol has recently been explored, promising catalytic glycerol conversion to alkanes and alkenes, such as ethane and propane. [2] Complete glycerol de-oxygenation, along with the formation of a C=C bond in a one-step process, is a challenging path; complete oxygen removal could lead to propene formation, linked with a succeeding notable increase in product value. Within this context, a novel "green" propene production method has been developed using biomass-derived feedstock: propene can be selectively formed via one-step glycerol hydro-deoxygenation reaction (HDO), over Mo-based catalysts. [3]

2 Experimental/methodology

Mo (20.8% wt) and Fe-Mo catalysts (Mo: 19.3 & Fe: 2.7 % wt), supported on commercial carbons, were synthesized by combining wet impregnation and co-precipitation methods [2]. Samples were characterized using BET, XRD and TPD NH_3 techniques. Prior to their evaluation, catalysts were pre-reduced at 500ºC, under H_2 flow. Glycerol HDO experiments were conducted in a batch reactor; the typical reaction conditions were: 300°C temperature, 8.0 MPa H_2 pressure, 2.0 w/w % aq. glycerol solution and 2h reaction time. Products of both gas and liquid phase were analyzed offline, using Gas Chromatography (GC).

3 Results and discussion

This research subject focuses on the investigation of the various parameters affecting the catalytic performance of glycerol conversion to propene via HDO reactions; this novel research subject has not yet been thoroughly explored in the open literature. Hence, the present work is an initial attempt to cope with the above-mentioned issues and comprehend the intricate reaction pathways. Propene can be effectively produced through glycerol HDO; reaction product distribution confirms that propene is the main reaction product (100% selectivity in the gas phase), with overall selectivity values up to 75.0%, after a six-hour reaction (88.8% glycerol conversion). [3]

The partially reduced MoO_2 is considered the active phase of the reaction providing bi-

functional properties (metallic-acidic function) and thus, enhancing consecutive dehydration-hydrogenation stages. In order to investigate the various HDO reaction steps, experiments were performed using all the major liquid products of the reaction as a feed: 2-propenol, 2-propanol, 1-propanol, propanal, propylene glycol and 1,3-propanediol. 2-Propenol, as well as 2-propanol, reacts selectively towards propene formation. Propylene glycol is primarily converted to propanal, as well as to propanols, while 1,3-propanediol and propanal to 1-propanol. The reactant activity order, based on propylene formation rate, is the following: 2-propenol>>2-propanol>propylene glycol>>1-propanol>1,3-propanediol>propanal. According to product distribution of the above-mentioned experiments, successive dehydration-hydrogenation stages are proposed; following the key reaction path, glycerol can be initially dehydrated to acrolein and then the latter can be hydrogenated to 2-propenol (reduction of the carbonyl group), which is finally converted to propene (loss of oxygen while preserving the C=C double bond) through a dehydration/ hydrogenation stage (Figure 1). Alcohol dehydration is a parallel, secondary step towards the formation of the desired product, substantiated by the significant 2-propanol conversion to propene.

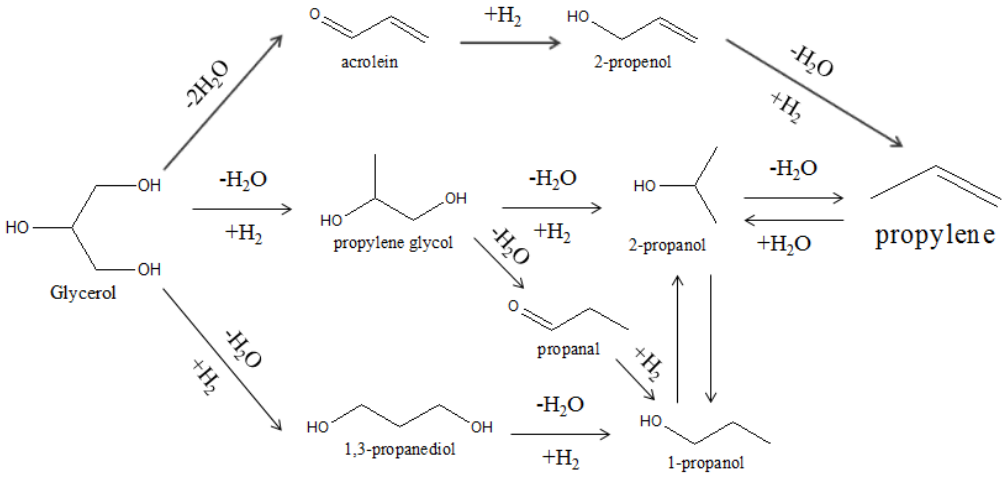

Fig. 1. Glycerol Hydro-deoxygenation Reaction Pathways

4 Conclusions

Glycerol HDO towards propene formation is a novel, alternative and environmentally-friendly chemical process, promising substantial contribution into meeting the increasing demand for propene, worldwide. Catalytic results of this study validate that this innovative method can lead to propylene production via HDO reactions, using biomass-derived feedstock. Propene is primarily produced via the acrolein-2-propenol route via sequential dehydration/ hydrogenation steps.

Acknowledgements

This research has been co-financed by the European Union (European Social Fund – ESF) and Greek national funds through the Operational Program "Education and Lifelong Learning" of the National Strategic Reference Framework (NSRF) - Research Funding Program: THALIS. Investing in knowledge society through the European Social Fund.

References

[1] A.M. Ruppert, K. Weinberg, R. Palkovits, *Angew. Chem. Int. Ed.* 51 (2012) 2564.
[2] J.C. Souza Fadigas, R. Gambetta, C.J. de Araujo Mota, V.L. da Conceicao Goncalves, *US pat.* 8841497 B2 (2014).
[3] V. Zacharopoulou, E. Vasiliadou, A.A. Lemonidou, Green Chem. (2015) DOI:10.1039/C4GC01307G.

IV-PP81

Development of Chemical Conversion for Methanol/Carbon Dioxide to Dimethyl Carbonate by V_2O_5 Catalysts

Lin K.-S.*, Yu S.H., Chuang H.-W., Adhikari A.K., Chiang C.L.

Department of Chemical Engineering and Materials Science/Environmental Technology Research Center, Yuan Ze University, Taiwan

* kslin@saturn.yzu.edu.tw

Keywords: dimethyl carbonate, carbon dioxide, methanol, V_2O_5 catalyst, resource recovery, XANES/EXAFS

1 Introduction

CO_2 is the main global warming potential (GWP) greenhouse gas with 50~60%. Direct influence on environmental and green-house effects has become an important issue for environmental protection all over the world [1]. The direct synthesis of dimethyl carbonate (DMC) from CH_3OH and CO_2 has attracted considerable attention. DMC has been used as a green chemical and an alternative to corrosive and toxic reagent. Therefore, the direct synthesis of DMC is an effective way to solve environmental pollution [2]. Due to its high mixing octane number (105), excellent compatibility with hydro-carbonates and high amount of O_2 in the molecule (3 times than methyl-tert-butyl ether) can reduce the emission of off-gas after adding it to gasoline/petroleum. DMC becomes an important additive of gasoline/fuel oil due to its many advantages nowadays [3].

2 Experimental

In order to eliminate the mineral impurities, the commercial activated carbon (AC) was first treated with H_2SO_4 aqueous solution. Cu–Ni/AC catalyst with the metal loading were prepared by an incipient wetness impregnation in which $Cu(NO_3)_2 \cdot 3H_2O$ and $Ni(NO_3)_2 \cdot 6H_2O$ were impregnated on supports. The V-Cu-Ni/AC catalyst was prepared by co-impregnation using aqueous solutions containing NH_4VO_3. After the co-impregnation, the mixtures were stirred at ambient temperature, ultrasonicated, and aged, followed by drying at 90°C. The fully dried product was crushed carefully in an agate mortar to give the catalyst precursors, which were then calcined at 500°C in a N_2 flow, and further reduced in a H_2 flow at 500°C.

3 Results and discussion

Figure 1 shows the XRD patterns of Cu–Ni/AC and V-Cu-Ni/AC catalysts with different V contents. For all catalysts, the broad and weak peaks at around 2h = 23° were attributed to the characteristic diffraction of AC. The intensity and the width of C dispersion characteristic peak varied versus different contents of V. Two peaks at around 2h = 43° and 50° were assigned to be the diffraction of Cu-Ni alloy, while a peak located at 2h = 75 degree was believed to be due to the Ni species. New diffraction peaks were detected at 2h = 24.2°, 26.6°, 32.9°, 53.7° due to the increase of V content. The dispersion of active metal particles on the surface of the support is crucial to enhance the catalytic activity. As further disclosed in FE-SEM of Fig. 1 for the V-Cu-Ni/AC catalyst, the brighter gray portions corresponded to AC support, whereas the darker dots were the catalyst particles. It was evident that the active metal particles were well dispersed on the surface of the catalyst support. The primary particle size estimated from the FE-SEM micrographs were observed in the range of 10-40 nm.

Figure 2 shows the NH_3-TPD profiles of Cu-Ni/AC catalysts with V contents. It was found that desorption peak area of the Cu-Ni/AC catalyst was higher than those of V-Cu-Ni/AC

catalysts. Moreover, desorption peak areas of V-Cu-Ni/AC catalysts decreased obviously. These results indicated that V addition resulted in a decrease of surface acidity of catalyst.

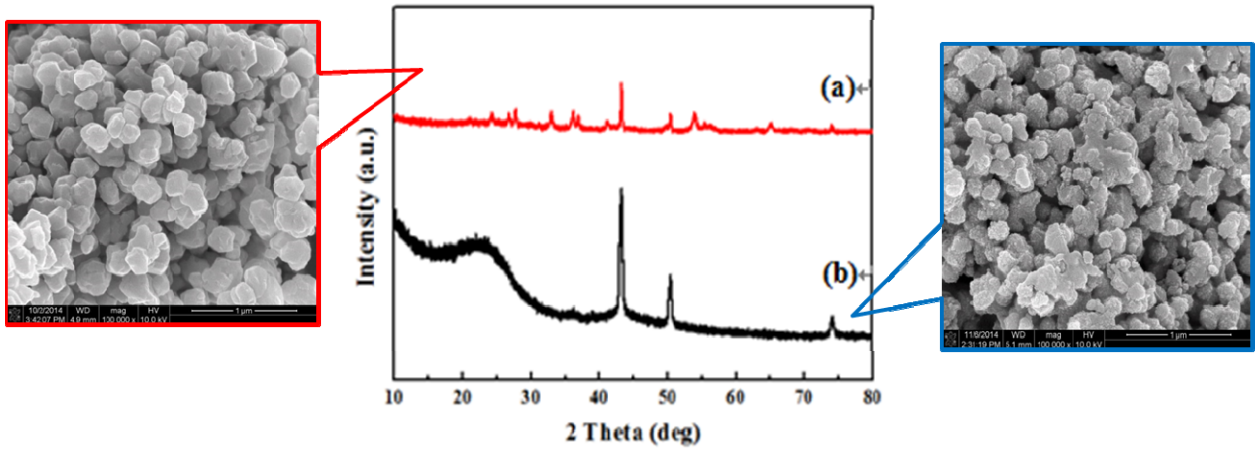

Fig. 1. XRD patterns of (a) V-Cu-Ni/AC and (b) Cu-Ni/AC.

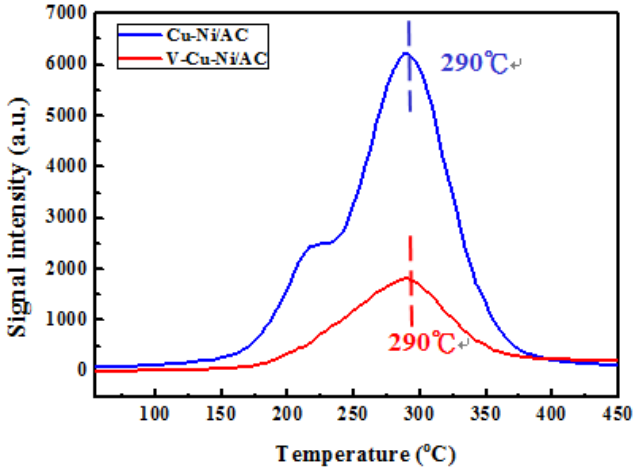

catalyst	reaction results	
	methanol conversion (%)	DMC yield (%)/mmol
Cu-Ni/AC	6.44	5.62
V-Cu-Ni/AC	7.76	6.98

Fig. 2. NH_3-TPD curves of Cu-Ni/AC and V-Cu-Ni/AC.

4 Conclusions

The particle sizes and aggregation effect increased and appeared after adding V_2O_5. The particle size of Cu-Ni/AC and V-Cu-Ni/AC catalysts were about 10~40 nm. The compositions and d-spacing of Cu-Ni/AC and V-Cu-Ni/AC were confirmed by XRD patterns and TEM micro-images successfully. The NH_3-TPD indicated that V addition resulted in a decrease of surface acidity of catalyst. A good correlation between catalytic activity and acidity (acid amount) was found in NH_3-TPD. V-Cu-Ni/AC catalyst could be readily prepared and applied in the direct synthesis of DMC from CH_3OH and CO_2. The experimental results showed that V could effectively improve the catalytic activity and the selectivity of catalysts.

References

[1] Bian J., Xiao M., Wang S., Lu Y., and Meng Y., Carbon nanotubes supported Cu–Ni bimetallic catalysts and their properties for the direct synthesis of dimethyl carbonate from methanol and carbon dioxide, *Applied Surface Science*, 255, 7188-7196 (2009).

[2] Li C., Zhang X. and Zhang S., Environmental benign design of DMC production process, *Chemical Engineering Research and Design*, 84, 1-8 (2006).

[3] Bian J., Xiao M., Wang S., Lu Y., and Meng Y., Direct synthesis of DMC from CH_3OH and CO_2 over V-drop Cu-Ni/AC catalysts, *Catalysis Communications*, 10, 1142-1145 (2009).

IV-PP82

Effect of Microemulsion-Synthesized Support in the Aqueous Phase Reforming Reaction of Glycerol

Lombardi E.*, Basile F., Fornasari G., Mafessanti R., Vaccari A.

University of Bologna, Dep. of Industrial Chemistry, Bologna, Italy

* erica.lombardi@unibo.it

Keywords: microemulsion, aqueous phase reforming, glycerol

1 Introduction

Glycerol has been studied intensely in the last years due to its high potential availability both to produce fuels and to transform it into high valuable platform molecules. Within different approaches the Aqueous Phase Reforming reaction (APR) represents a valuable pathway to obtain liquid products and hydrogen, with the main products depending on the reaction conditions and catalyst [1]. The most used catalysts for this type of reaction are VIII group metals supported on oxides. Several studies have analyzed the effect of alloying of different metals or modifying the acid/basic sites of the support, whereas little attention has been devoted to the control of the support morphology and the metal dispersion and accessibility.

The present study is focused on the analysis and enhancement of the APR reaction modifying the reaction parameters and studying a Pt based catalyst supported on TiO_2 synthetized by water in oil microemulsion technique [2]. Microemulsion synthesis of oxides, compared to other traditional pathways (i.e. precipitation and co-precipitation), allows a better control of the parameters of reaction, so the obtainment of nanocrystals with controlled porosity and morphology and, in case of particular mixed oxides, a peculiar crystalline phase.

2 Experimental

TiO_2 was synthesized optimizing a method reported in literature [3] by mixing an acid-containing water-in-oil microemulsion with a solution of organics containing the titanium precursor. The obtained microemulsion under stirring allowed the slow hydrolysis to form the oxide. The reaction was completed and the solid extracted from the micelles by heating at reflux temperature. The oxide was than calcined and impregnated with different metal loadings of Pt.

APR reactions were carried out in a 300ml stainless steel Parr autoclave loaded with 17,1% wt. glycerol in water solution and 0,45g of catalyst. Temperature and time were set in the range 200-250°C from 30minutes to 7h and under autogenous pressure. Liquid products were analyzed by HPLC with RID detector and gas products by GC equipped with TCD detector.

3 Results and discussion

Characterization data of TiO_2 obtained by microemulsion (TiO_2-m) were compared with a commercial sample. The former method shows a higher surface area ($200 m^2/g$) and progressive size and shape pores (type H2 hysteresis) with narrow distribution of the pore diameter. In contrast, the commercial sample presented slit shaped pores (type H3) and wider distribution of pore diameter confirming that microemulsion synthesis allows a more homogeneous support preparation and a better control of pore dimension. The TEM image (Fig.1) shows as a result a very small and narrow distribution of the Pt particles supported on TiO_2-m.

The synthesized catalysts were tested in the APR reaction of glycerol. TiO_2-m showed

higher yields (2,5% H_2 yield) than the commercial (1,5%) at 1% wt. Pt loading after 3h of reaction at 250°C, evidencing the importance of the support preparation in the APR reaction.

The Pt/TiO_2-m catalyst was applied for a wide study of APR reaction with extended liquid and gas product analysis and modifying the reaction parameters. Temperature effect on the reaction indicates after 3h a small glycerol conversion (9%) and hydrogen productivity (0,24mol/h*g^{Pt}) at 200°C with Pt/TiO2-m 1% wt. catalyst. Increasing the temperature at 225°C and 250°C leads to conversions up to 12% and 51%, but in both cases H_2 productivity was respectively 0,7 and 1,3mol/h*g^{Pt} with increasing selectivity towards liquids: propylene glycol lactic acid, hydroxyacetone, and 1-propanol accounting for the 90% of the products in solution.

A change on Pt/TiO_2 metal loading from 1% to 3% wt. produced at 225°C an increase in conversion from 12 to 31% with a rate proportional to the amount of metal. The same trend was not observed on the 3% wt. Pt on commercial TiO_2, which shows lower performances. These data indicate that the TiO_2 prepared by microemulsion allows high dispersion and accessibility of the Pt even at high metal loading. The observation is confirmed by TEM analyses showing the metal particles between 1-2nm for both the 1% and 3% wt. Pt catalysts. At 250°C the increase in metal loading leads to a conversion of 73% with a hydrogen productivity of 0,68mol/h*g^{Pt} with a significant enhancement of yields in the four main liquid products.

A study on the mechanism of reaction and liquid products was performed at 225°C using different times of reaction and solutions containing to 5,7% wt. of glycerol to enlighten the trend of the primary and secondary products in a wide range of glycerol conversion. Primarily, the conversion increases constantly up to 7h of reaction. In the gas phase H_2 selectivity decreases slightly during reaction while CO_2 and CH_4 remain constant; on the other hand, the production of light hydrocarbons as ethane and propane increases with the time of reaction. Liquid phase primary product from dehydration reaction is hydroxyacetone (in accordance with [4]) that leads to secondary products with high yields as propylene glycol and 1-propanol. Moreover, the dehydrogenation of the primary hydroxyl group of glycerol through an aldehydic intermediate gives ethylene glycol by C-C cleavage and lactic acid by rearrangement as primary products; the latter further decarboxylated to ethanol. No products were observed for the possible dehydration of the secondary hydroxyl group of glycerol, probably due to the adsorption mechanism favoured by small dimension of Pt particles.

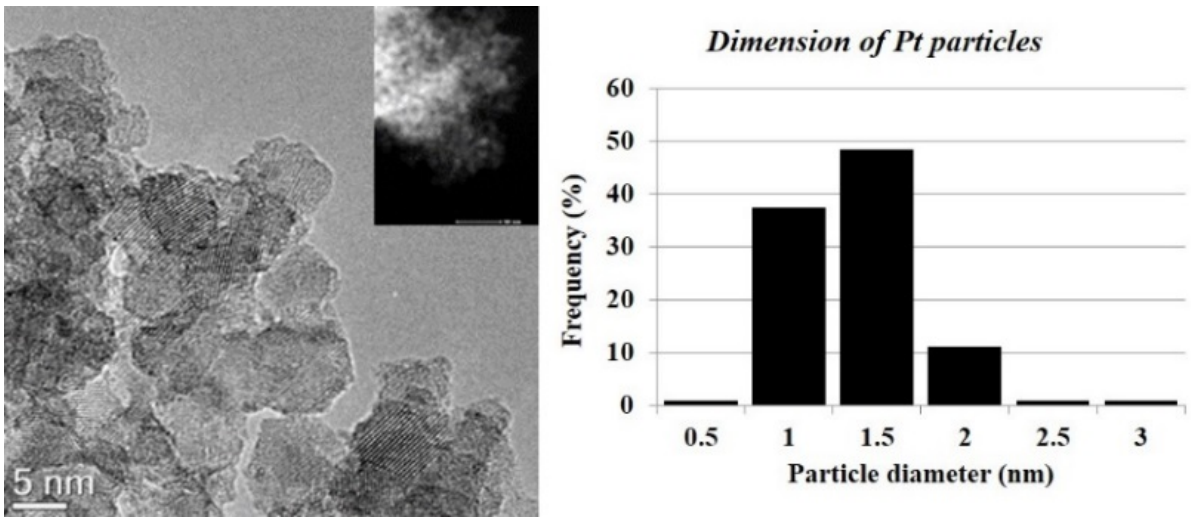

Fig. 1: TEM images of Pt dispersion on TiO_2-m and STEM-HAADF image of the porous structure of the support (left); Pt particles dispersion on the surface (right)

4 Conclusions

The application of microemulsion synthesis of TiO_2 in APR is beneficial to conversion of glycerol, H_2 productivity and selectivity in liquid products. The study on the reaction conditions

and the complete identification of liquid and gas products allow to indicate two main pathways (dehydrogenation and dehydration) leading to different products. This is the base to address the APR reaction towards platform molecules in the liquid phase.

References

[1] R. R. Davda, J. W. Shabaker, G.W. Huber, R. D. Cortright, J. A. Dumesic, *Appl. Catal. B: Env.* 56 (2005) 171
[2] M.J. Schwuger, K. Stickdornt, *Chem. Rev*. 95 (1995), 849
[3] M. Andersson, A. Kiselev, L. Osterlund and A. E. C. Palmqvist, *J. Phys. Chem. C* 111 (2007) 6789
[4] A. Wawrzetz, B. Peng, A. Hrabar, A. Jentys, A.A. Lemonidou, J.A. Lercher, *J. Catal.* 269 (2010) 411

IV-PP83

Obtaining (Z)-3-Hexene with Ni Catalysts Supported on Alumina Modified with Magnesium Precursor

Maccarrone M.J.[1], Lederhos C.[1], Betti C.[1], Coloma-Pascual F.[2], Vera C.[1*], Quiroga M.E.[1]

1 - Instituto de Investigaciones en Catálisis y Petroquímica, INCAPE, Santa Fe, Argentina
2 - Facultad de Ciencias, Universidad de Alicante, Alicante, Spain

* jmaccarrone@fiq.unl.edu.ar

Keywords: hydrogenation, (Z)-3-hexene, nickel, modified alumina, 3-hexyne

1 Introduction

The selective hydrogenation of internal alkynes for Z-alkene stereoisomers is applicable in the petrochemical and pharmaceutical industry. Nickel catalysts are still an interesting alternative low-cost compared with Lindlar or Pd catalysts [1]. This paper evaluates the activity and selectivity of a Ni 1% catalyst in the selective hydrogenation of 3-hexyne modifying the alumina support with a 5 and 10% magnesium precursor with excellent results in conversion values (ca.100%) for the reaction time considered.

2 Experimental

Due to the low values of solubility of Mg salt in water the preparation of the catalysts was performed by successive impregnations of the alumina support with a magnesium salt solution ($MgS0_4.7H_2O$) for obtaining 5 or 10 % of MgO. After each impregnation, the sample was dried in an oven approximately 18h , cooled in the desiccator 30 minutes, and calcined 3 h at 823K. These modified supports were impregnated with a 1% wt nickel nitrate precursor salt solution of $[Ni(NO_3)_2.\ 6H_20]$, dried in oven at 1273K, cooled down in a desiccator for 24 h and calcined 3h at 823K. Previously to each catalytic test, the samples were reduced 1h at 673 K.
The concentration of Ni and Mg were checked by ICP in OPTIMA 21200 Perkin Elmer equipment. The electronic state of the metals, and the atomic ratios was studied by X-ray photoelectron spectroscopy (XPS) on a VG-Microtech Multilab Equipment. C 1s signal was used as a reference.

The catalyst evaluations were carried out in a semicontinuous stainless steel stirred tank reactor equipped with a double helix stirrer, using 75 mL of a 2% (v / v) 3-hexyne in toluene solution. The tests were conducted using the following conditions: 1.5 bar of hydrogen pressure, reaction temperatures 303 and 323 K; 800rpm, catalyst mass 0.3 g, particle size 60-100 mesh during 200 min. The reactants and products were analyzed by gas chromatography using a flame ionization detector and a capillary column PRO GS-GAS.

3 Results and discussion

Table 1. shows the Ni $2p_{3/2}$ binding energies (BE) for the monometallic nickel catalysts reduced at 673 K, and the Ni/Al and Mg/Al atomic ratios. Accordingly to the bibliography these BE can be assigned to electro-deficient nickel species (Ni^{n+}, with n close to 2), probably interacting with alumina [2]. The BEs of Mg modified monometallic catalysts are slightly higher than the unmodified catalyst, attributed to an electronic effect due to the higher electronegativity of Ni.

In Figure 1 shows the total conversion of 3-hexyne vs. time for the monometallic Ni catalysts supported on γ -alumina unmodified and modified with Mg at 303 and 323 K. As expected in the Figure it can be seen the higher values of conversions are obtained at higher reaction temperature. At 303 K, Ni1 % catalyst modified with 5% MgO on alumina presented

the highest 3-hexyne total conversions. This result could be explained by a synergistic effect of Mg on Ni , which promotes increased generation of actives sites as mentioned by other authors [3] . On the other hand, at 323K there is very slight difference of total conversion between the unmodified and Mg modified catalysts.

Table 1. Binding energies (BE) for Ni $2p_{3/2}$ and atomic ratios obtained by XPS.

Catalysts	XPS			Selectivity to (Z)-3-hexene	
	BE (eV)	Atomic ratios			
	Ni $2p_{3/2}$	Ni/Al	Mg/Al	303K	323K
NiN1%	857,34	0,013	-	63	70
NiN1% +5%MgO	856,92	0,005	0,048	69	59
NiN1% +10%MgO	856,97	0,015	0,086	63	63

On Table 1 are presented the selectivities to (Z)-3-hexene at 303 and 323K. It can be seen that moderate selectivities are obtained for the nickel unmodified or modified catalysts. Lower selectivities are obtained at 323K for the modified Mg catalysts.

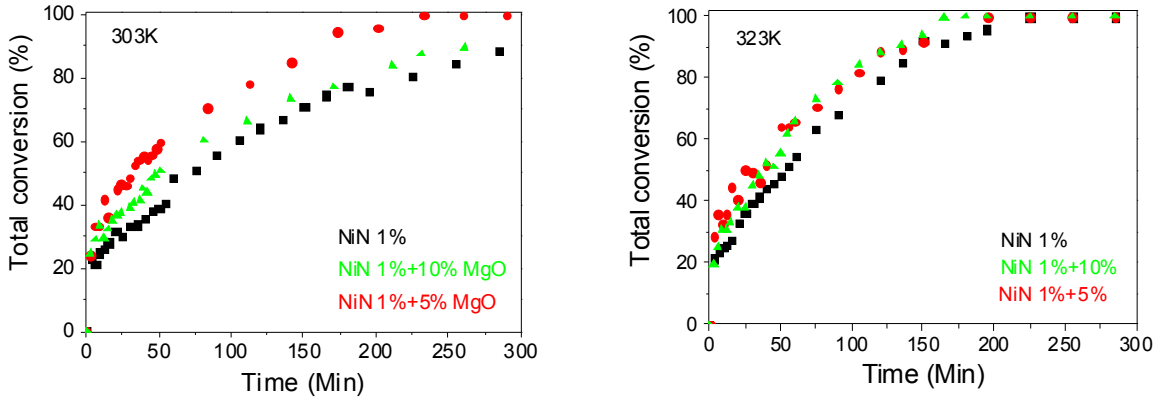

Fig. 1. Total conversion of 3 - hexyne vs reaction time for the Ni/Al_2O_3 modified and unmodified at 303 and 323K

4 Conclusions

Low-cost monometallic nickel (1wt % of Ni) catalysts unmodified or modified with Mg were prepared. The Ni1 % catalyst modified with 5% of MgO presented higher values of 3-hexyne total conversion (ca. 100%) and moderate selectivity (□70%) at 303K. Besides this prepared catalyst is inexpensive compared to the Lindlar catalyst (5 wt % of Pd) or others mentioned in the literature.

Acknowledgements

The financial support of UNL, CONICET and ANPCyT is greatly acknowledged.

References

[1] Maccarrone M. J., Torres G., Lederhos C., Betti C., Badano J. M., Quiroga M. and Yori J. In Hydrogenation, I. Karamé (Ed.), InTech, Rijeka, Croatia. (2012) Chapter 7, pp 159-184

[2] NIST X-ray Photoelectron Spectroscopy Database NIST Standard Reference Database 20, Version 3.5. National Institute of Standards and Technology, USA, 2007. http://srdata.nist.gov/xps/

[3] A. Romero, J. Ramirez, L. Cedeño. Revista Mexicana de Ingeniería Química 2(2) (2003) 75

IV-PP84

Catalytic Carbonylation as a Component of Alternative Route for GTL Processes

Makaryan I.[1*], Sedov I.[1,2], Arutyunov V.[1], Savchenko V.[1,2]

1 - Institute of Problems of Chemical Physics of the Russian Academy of Sciences, Chernogolovka, pRussia

2 - Faculty of Fundamental Physical and Chemical Engineering, Lomonosov Moscow State University, Moscow, Russia

* irenmak@icp.ac.ru

Keywords: natural gas, GTL, syngas, partial oxidation, catalytic carbonylation

1 Introduction

Gas-to-liquids (GTL) processes intended for production of synthetic liquid fuels as well as other chemical and petrochemical products (methanol, lubricants, waxes et.) from hydrocarbon gases have been of interest for the past three decades. At the same time manufacturing GTL products is extremely expensive. The technology of their production traditionally consists of three steps, and each of these steps is costly itself, especially the step of syngas production.

2 Main Principles of Alternative GTL Processes. New GTL Products

We have suggested an alternative "without syngas" route for GTL. It consists of two stages: direct partial oxidation of natural or associated petroleum gases into methanol and CO and/or olefins and CO with subsequent catalytic carbonylation of oxidation products [1] (Fig. 1).

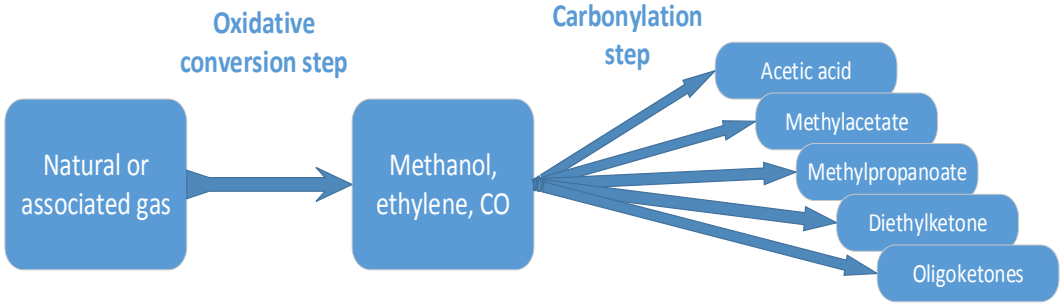

Fig. 1. Suggested scheme of alternative GTL processes

At present many carbonylation reactions operate industrially in large-scale production. Platinum group metals based catalysts (PGM catalysts) are the most effective catalysts for carbonylation processes [2]. PGM catalysts represent metal complexes with organic heteroatom ligands of different structure that is responsible for catalyst activity and selectivity to definite product. Of especial interst are processes which use all three main oxidation products – ethylene, methanol and carbon monooxide, e.g.:

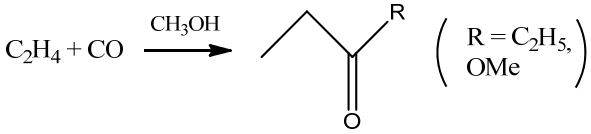

This reaction is catalyzed by palladium complexes with phosphine ligands under relatively

low pressures.

The process with participation of all above mentioned oxidation products (ethylene, methanol, CO) forming the most value-added product – MMA, represent combination of methoxycarbonylation of ethylene into methyl propanoate and condensation of the latter with formaldehyde yielding methyl methacrylate. The route of these consecutive reactions was firstly commercialized in the *Lucite Alpha process:*

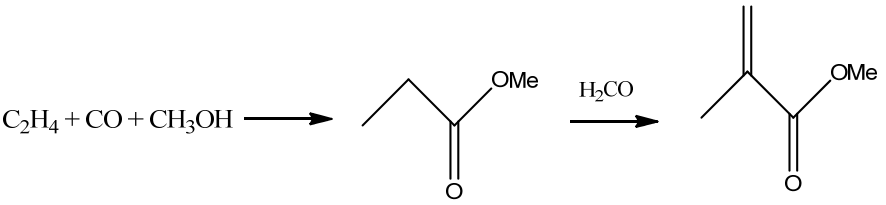

Such approach to gas conversion is particullarry attractive because CO unconditionally forms along with the methanol and ethene during the partial oxidation of natural gas in quantities suffucient for a further carbonylation step. Therefore, there is no need for energy consuming steam conversion or oxidation of methane into syngas. PGM catalysts are active under milder conditions and show much higher selectivity compared to other catalysts.

This approach allows developing an integrated two-stage conversion (an alternative GTL). Methanol and olefins produced according to this method can form such valuable marketable chemicals and petrochemicals as diethylketone, methylacetate, dimethylcarbonate, methylpropanoate, ethylidenediacetate, oligoketones, polyketones etc., avoiding energy consuming steps for separation of intermediate products. High efficiency of new GTL processes is determined by not only production of chemicals with high added value, but also by simultaneous production of purified dry fuel methane gas with high methane index.

3 Conclusions

Combination of gas phase partial oxidation and subsequent catalytic carbonylation makes possible to develop alternative GTL processes without complicated and costly stage of syngas formation. Such new type GTL processes can be successfully used for the monetization of stranded natural and associated petroleum gases by converting them into high value-added marketable products in demand.

Acknowledgements

This work was supported by the Department of General Chemistry and Material Sciences of the Russian Academy of Sciences (Program No.7)

References

[1] V.I. Savchenko, I.A. Makaryan, I.G. Fokin, I.V. Sedov, R.N. Magomedov, M.G. Lipilin and V.S. Arutyunov, *Neftepererabotka i Neftechimiya*, **8** (2013) 21

[2] I.A. Makaryan, I.V. Sedov, V.I. Savchenko, *Johnson Matthey Technol. Rev.*, **59** (2015) 14

[3] B. Harris, 'Acrylics for the Future', *Ingenia*, **45** (2010) 19

IV-PP85

Isomerization of Verbenol Oxide to a Diol with Paramenthenic Structure Exhibiting Anti-Parkinson Activity

Mäki-Arvela P.[1*], Torozova A.[1], Stekrova M.[1], Kumar N.[1], Aho A.[1], Heinmaa I.[2], Volcho K.P.[3], Salakhutdinov N.F.[3], Murzin D.Yu.[1]

1 - Process Chemistry Centre, Åbo Akademi University, Turku/Åbo, Finland
2 - Institute of Chemical Physics and Biophysics, Tallinn, Estonia
3 - N. N. Vorozhtsov Institute of Organic Chemistry, Russian Academy of Sciences, Novosibirsk, Russia

* pmakiarv@abo.fi

Keywords: zeolite, isomerization, pharmaceutical, terpenoid

1 Introduction

Development of new pharmaceuticals, especially from natural compounds is currently of high interest. Some of the commonly used drugs have also severe side effects, for example Levodopa, which is the main drug for the Parkinson desease. It is a chiral amino acid, (*S*)-2-amino-3-(3,4-dihydroxyphenyl)propanoic acid, which is known to cause several side effects, such as nausea, hallucinations, paranoia [1]. In verbenol oxide isomerization the desired product is diol (2) (Fig. 1), which has been previously synthesized in the presense of a large amount of K10 clay [1].

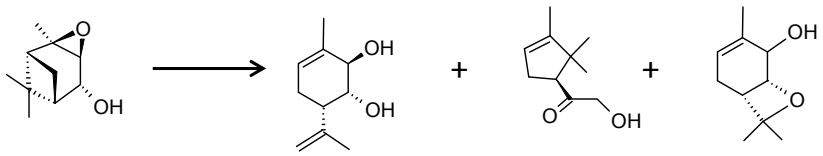

1 2 3 4

Fig. 1. The reaction scheme for production of diol (2) starting from verbenol oxide (1). The other main products were cyclopentyl hydroxyl ketone (3) and oxetane (4).

The aim of this work is to systematically study for the first time catalytic isomerization of verbenol oxide (VO) (1) to diol (2) over different zeolites by varying the SiO_2/Al_2O_3 ratio and structure of zeolites. This diol is a potential alternative to L-Dopa.

2 Experimental

Several commercial NH_4-USY and NH_4-ZSM-5 zeolites with different Si/Al ratio were used as catalysts. They were transformed to corresponding proton forms via step calcination at 500°C. The isomerization of verbenol oxide was performed typically in dimethylacetamide as a solvent at 140°C using the initial concentration of VO 0.016 mol/l and 75 mg catalyst. In addition, high stirring speed (390 rpm) and small catalyst particles (<90 Φm) were used in order to avoid the mass transfer limitations. The samples were withdrawn from the reactor and analyzed by GC. The reaction products were identified with GC-MS and NMR. The catalysts were characterized by XRD, nitrogen adsorption, SEM, TEM, solid state MAS NMR and pyridine adsorption desorption with FTIR.

3 Results and Discussion

The structures of H-Y and ZSM-5 zeolites were confirmed by XRD. The specific surface areas of H-Y zeolites were about 800 m^2/g, whereas those for ZSM-5-23 and ZSM-5-80 were 443 and 570 m^2/g, respectively. The number in zeolite name denotes different SiO_2 to Al_2O_3 ratio. The amount of Brønsted acid sites determined by ^{27}Al MAS NMR at 55.2 ppm for H-Y-12 was 8.9 fold that of H-Y-80 (Fig. 2a). Furthermore the pyridine adsorption showed that the amount of Brønsted acid sites was inversely proportional to SiO_2 to Al_2O_3 ratio. The amount of Lewis acid sites was also higher with the zeolites possessing low SiO_2/Al_2O_3 ratio.

a) **b)**

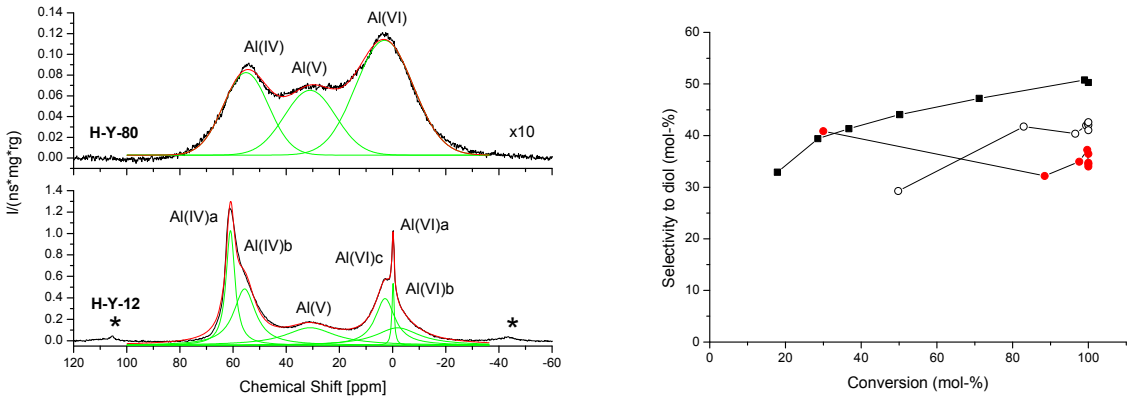

Fig. 2. a) ^{27}Al MAS NMR spectra of H-Y-80 (above) and H-Y-12 (below), b) selectivity to the desired diol (2) as a function of verbenol oxide conversion at 140°C in dimethyl-acetamide. Symbols: H-USY-80 (■), H-USY-15 (o) and H-USY-12 (●).

The most active catalysts were the large pore H-Y zeolites with a low Si/Al ratio, whereas medium pore ZSM-5 zeolites exhibited lower initial rates. The large pore zeolites facilitated the total conversion of verbenol oxide within 120 min, whereas over medium pore zeolites ZSM-5-23 and ZSM-5-80 only 51 % and 58 % conversion, respectively, was achieved.

Selectivity towards the desired diol (2) decreased as a function of verbenol oxide conversion over the most acidic H-Y-12 zeolite, whereas it increased over the mildly acidic H-Y-80 zeolite being 48 % at complete conversion of verbenol oxide (Fig. 2b). The second most abundant product was a cyclo pentyl ketone (3), which was formed parallelly with a diol. These results showed that a large pore zeolite H-Y-80 with relatively mild acidity was the most efficient in diol formation.

4 Conclusions

Catalytic isomerization of verbenol oxide to the diol exhibiting anti-Parkinson activity was for the first time systematically investigated for the first time. The results showed that a large pore zeolite H-Y with a mild acidity was active and selective for the studied reaction. In the final work the catalyst physic-chemical properties will be related to the catalytic performance and the reaction mechanism will be proposed.

References

[1] Ardashov, O. V., Pavlova, A.V., Il'ina, I.V., Morozova, E.A., Korchagina, D.V., Karpova, E.V., Volcho, K.P., Tolstikova, T.G., Salakhutdinov, N.F., *J. Medic. Chem.* 54 (11), (2011), 3866.

IV-PP86

Exploring New Synthetic Ways for Cyanopyridines

Mari M.[1*], Cavani F.[1], Kuenzle N.[2], Hanselmann P.[2], Janssen M.[2]

1 - Università di Bologna, Dipartimento di Chimica Industriale Toso Montanari, Bologna, Italy
2 - Lonza Ltd, Visp, Switzerland

* massimiliano.mari@unibo.it

Keywords: 3-cyanopyridine, 2-methylglutaronitrile, cyclodehydrogenation, niacin

1 Introduction

Niacin (nicotinic acid) is a compound with a yearly market growth of around 5-6%, total consumption of 40.000-50.000 tons, 75% of which is used as additive for feed, the rest in food industries and pharmaceuticals. Commercial production of niacin is conducted either by means of the direct liquid phase oxidation of alkylpyridines with nitric and chromic acid or by the catalytic gas-phase ammoxidation of 3-methylpyridine (β-picoline) and hydrolysis of 3-cyanopyridine [1]. With the aim of finding new routes for the synthesis of β-picoline and cyanopyridines, we investigated the feasibility of two alternative routes, i.e., the direct cyclodehydrogenation of 2-methylglutaronitrile (2MGN), an inexpensive raw material obtained as a by-product from the DuPont Adiponitrile process, and the condensation of acetaldehyde and acetonitrile.

2 Experimental/methodology

Magnesium oxide-based catalysts (Mg/Fe/O, Mg/Cr/O, Mg/Al/O) were prepared by coprecipitation in the form of mixed hydroxycarbonate; the resulting precipitate was dried at 120°C and calcined at 450°C. In bifunctional systems, the metals (Pd, Pt) were deposited over the basic support by means of incipient wet impregnation, starting from the organic salt of the metal. Catalytic tests were carried out in a continuous-flow lab reactor. In the first set of experiments 2MGN was vaporised and mixed with nitrogen as carrier gas. The mixture was passed through the catalytic bed (prereduced with hydrogen at 350°C for bifunctional catalysts) and products were accumulated in an acetone trap. Contact times were 0.35-0.40s, feed composition was 5% 2MGN in nitrogen with a total flow of 40ml/min. The solution containing the products and the unconverted reagent was analyzed by means of GC. In the second set of experiments a mixture of acetonitrile and acetaldehyde (in form of paraldehyde) was vaporized and mixed with nitrogen as carrier gas. The reagents were passed through the catalytic bed and products were accumulated in an acetone trap.

3 Results and discussion

As reported in the literature [2], 2MGN can be hydrogenated to produce the di-amino derivative, which is then cyclised in the presence of a bifunctional catalyst to produce 5-methyl-2,3,4,5-tetrahydropyridine after release of ammonia; the latter is then dehydrogenated to β-picoline and finally ammoxidised to 3-cyanopyridine. We investigated if it was possible to cyclise 2MGN directly, while avoiding the loss of the ammonia molecule (which finally has to be reintroduced to produce the cyanopyridine). We used bifunctional catalysts containing a metal active species (Pt, Pd or Ru, 1% wt) supported over basic (MgO) or acidic/basic ($MgFe_2O_4$, $MgCr_2O_4$ $MgAl_2O_4$, ZrO_2) supports.

Catalysts showed different reactivity as a function of composition (nature of the active element, nature of the support), but in general the predominant products were short-chain nitriles with negligible formation of cyanopyridines or methylpyridines. This is shown, for example, in Figure 1, reporting the distribution of products obtained with the catalyst based on

Pd1%/$MgAl_2O_4$. Besides the formation of propionitrile, crotylonitrile, acrylonitrile and methacrylonitrile, also relevant amounts of C deposits accumulated on the catalyst surface. Some experiments were also carried out in the presence of air, with the aim of both achieving a more favourable equilibrium conversion at moderate temperature and limit the accumulation of carbonaceous deposits, however, only limited improvements were achieved. Results demonstrate that under the conditions examined radical-like fragmentation of 2MGN is highly favoured compared to cyclisation.

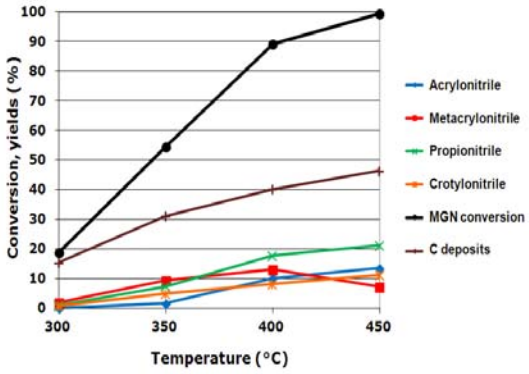

Fig. 1. 2MGN conversion and selectivity to products as a function of temperature with Pd1%/$MgAl_2O_4$ catalyst.

Another set of experiments was carried out by co-feeding acetaldehyde and acetonitrile (with a large excess of the latter compound), using either acidic (HY zeolite), basic (MgO), or bifunctional systems (Mg/Fe/O, Mg/Al/O). In this case, it was expected that the condensation of two acetaldehyde and one acetonitrile molecules would generate picoline. The reaction, carried out in the gas-phase between 350 and 450°C, led to the formation of several products with low yield to picolines, mainly due to the lower reactivity of acetonitrile compared to acetaldehyde.

4 Conclusions

We explored alternative synthetic pathways for the production of picolines and cyanopyridines by means of gas-phase transformations using basic or bifunctional catalysts, starting from either 2-methylglutaronitrile or acetonitrile/acetaldehyde mixtures. The reactions showed low selectivities due to strong fragmentation of the reactant 2MGN into smaller nitriles or to scarce reactivity of acetonitrile leading to a preferred transformation of acetaldehyde into several by-products.

References

[1] T. V. Andrushkevich, E. V. Ovchinnikova, *Catalysis Reviews: Science and Engineering. 54(2012) 399-436.*

[2] S. Lanini, R. Prins, *Applied Catalysis A: General.137(1996) 287-306.*

IV-PP87

Highly Selective Pd-Cu Supported Catalyst for Liquid-Phase Semihydrogenation of Substituted Alkynes

Mashkovsky I.S.[1], Markov P.V.[1], Bragina G.O.[1], Baeva G.N.[1], Tkachenko O.P.[1], Kozitsyna N.Yu.[2], Vargaftik M.N.[2], Stakheev A.Yu.[1*]

1 - Zelinsky Institute of Organic Chemistry RAS, Moscow, Russia
2 - Kurnakov Institute of General and Inorganic Chemistry RAS, Moscow, Russia

* st@ioc.ac.ru

Keywords: stereoselective, hydrogenation, alkyne, heterobimetallic, complex, Pd-Cu catalyst

1 Introduction

The semihydrogenation of carbon-carbon triple bond is of fundamental importance for both fine chemicals production and laboratory practice. Pd-supported catalysts are proved to be the best for hydrogenation of alkynes to alkenes in terms of selectivity. However Pd can catalyze undesirable C=C double bond hydrogenation, which results in the loss of selectivity. Improved selectivity of Pd catalyst in semihydrogenation can be achieved using bimetallic compositions (Pd-Ni, Pd-Zn, Pd-Ag, Pd-Cu) and the main problem is to avoid or minimize formation of monometallic Pd^0 species. A possible solution of this problem is the use of Pd-M heterobimetallic acetate complexes for the catalyst preparation as a precursor of active component. Pd and second metal atom in this complex are linked together by strong acetate bridges thus remaining in contact during all stages of catalyst preparation. The precursor structure enables formation of highly homogeneous bimetallic nanoparticles in a final catalyst [1].

2 Experimental/methodology

Selective semihydrogenation of diphenylacetylene (DPA) was studied as a model reaction. The catalysts were prepared by impregnation of Al_2O_3, (Sasol, S_{sp}=150 m^2/g) with acetic acid solutions of $PdCu(CH_3COO)_4$, $Pd_2Cu(CH_3COO)_6$ $PdCu_2(CH_3COO)_6$ complexes (pH = 2.6-2.8). The catalysts were dried overnight at room temperature, calcined (550°C, 4 h) and reduced in 5%H_2/Ar (550°C, 1 h) before catalytic measurements. A commercial Lindlar catalyst («Aldrich») was taken for comparison. Reaction was carried out in autoclave at 10 atm H_2 and room temperature in methanol. The reaction kinetics was monitored by the rate of H_2 uptake, and the reaction products were analyzed using H-NMR.

3 Results and discussion

The Pd-Cu/Al_2O_3 catalysts demonstrate extremely high selectivity in the hydrogenation of DPA to olefin. It was found that increase of the Cu content from Pd:Cu = 2:1 to Pd:Cu = 1:2 leads to a nearly complete suppression of the hydrogenation of stylbene to diphenylethane (Fig. 1).

A detailed kinetic study revealed substantial change of the reaction kinetics due to Cu addition. Introduction of Cu increases the reaction order in DPA from 0 to ~ 0.5-0.8, indicating a significant decrease in the strength of the alkyne adsorption on the surface of the bimetallic nanoparticles. The reaction rate of the second hydrogenation stage is reduced by 10-15 times (Fig. 1) thus increasing turnover frequency ratio TOF_{DPA}/TOF_{ST} from 4.9 to 30, which enables effective kinetic control of alkyne hydrogenation over Pd-Cu bimetallic catalyst.

The change in the reaction kinetics significantly improves selectivity of Pd-Cu catalyst in stylbene formation and *Z-/E*-olefin ratio (Table 1).

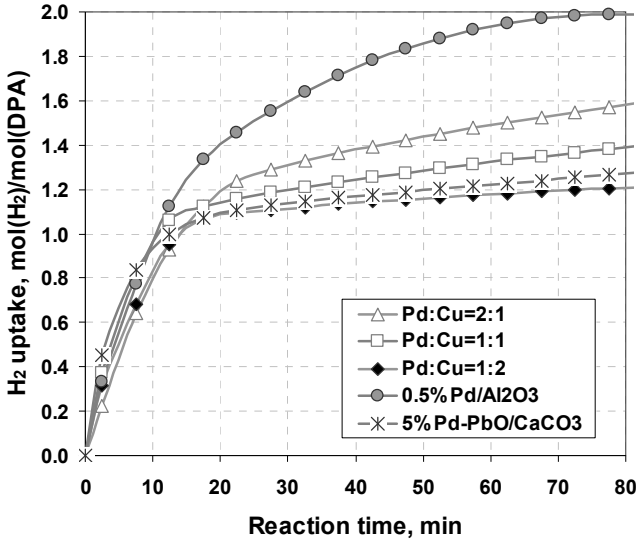

Fig. 1. Effect of Pd:Cu ratio on the performance of Pd-Cu/Al_2O_3 in DPA hydrogenation in methanol. Conditions: P=10 atm, t = 25°C, $m_{Pd:Cu}$ = 2.5 mg, $m_{Lindlar}$ = 7.5 mg

Thorough study of Pd-Cu catalysts by IR spectroscopy of adsorbed CO revealed formation of highly homogeneous bimetallic particles as evidenced by the almost complete disappearance of bridged bonded CO. On the other hand, Pd electronic state does not significantly changed, as indicated by the coincidence of the absorption band of the linear bonded CO for mono- and bimetallic catalysts.

Remarkably, comparison of characteristics for Pd-Cu and Lindlar catalysts demonstrate that the bimetallic Pd-Cu system is superior to Lindlar catalyst in terms of selectivity, being more active.

Table 1. Kinetic characteristics of DPA hydrogenation over Pd-Cu/Al_2O_3 catalyst with various Pd:Cu ratio.

Catalyst	TOF_{DPA}, s^{-1}	TOF_{ST}, s^{-1}	TOF_{DPA}/TOF_{ST}	S_{ST}, %	Z/(E + Z), %
Pd:Cu = 2:1	2.65	0.22	12.0	-	-
Pd:Cu = 1:1	3.05	0.15	20.0	90.6	96.1
Pd:Cu = 1:2	2.45	0.08	30.1	95.7	99.3
5%Pd-PbO/$CaCO_3$	0.16	0.01	29.0	94.1	97.5
0.5%Pd/Al_2O_3	5.77	1.17	4.9	73.2	90.3

4 Conclusions

Pd-Cu catalysts synthesized via acetate heterobimetallic complexes demonstrate excellent selectivity to stilbene and high stereoselectivity in terms of *Z-/E*-olefin formation. From the practical viewpoint this result is of great interest, since it was found that the Pd-Cu catalyst demonstrates superior activity and selectivity in comparison with commercial Lindlar catalyst (Pd/PbO/$CaCO_3$). It should be noted that this performance is achieved at a substantially lower content of noble metal (1% instead of 5% Pd). Furthermore, the absence of toxic Pb components makes Pd-Cu catalyst promising for usage in pharmaceutical and food industries.

Acknowledgements

This work was supported by the Russian Foundation for Basic Research (grant 13-03-12176).

References

[1] I.S. Mashkovsky et al., Mendeleev Commun. 24 (2014) 355.

IV-PP88

Catalytic Conversion of Cellulose to C_2-C_3 Glycols by a Dual Combination of a Homogeneous Metallic Salt and a Perovskite-Based Heterogeneous Catalyst

Girard E.*, Delcroix D., Cabiac A.

IFP Energies Nouvelles, Rond-Point de l'Echangeur de Solaize, Solaize, France

* etienne.girard@ifpen.fr

Keywords: biomass, cellulose, glycols, dual catalysis, cerium salts, perovskites

1 Introduction

The conversion of cellulose to C_2-C_3 glycols is usually achieved under hydrothermal - above 100°C and 1 bar- and reducing conditions via a cascade pathway including depolymerization of cellulose to glucose, subsequent retro-aldol reactions and hydrogenation of the resulting glycolaldehyde and glyceraldehyde molecules.[1] Multifunctional catalytic systems are thus necessary to achieve a selective formation of C_2-C_3 glycols. Depolymerization being achieved through water autoprotolysis at high temperatures, the ideal catalytic system should combine a retro-aldol active species and a hydrogenation component. A fine balance between acidic, basic and hydrogenation catalytic sites associated with an excellent hydrothermal stability of the heterogeneous support is thus necessary to achieve a high selectivity in glycols. Original dual catalytic systems combining a homogeneous metallic salt and a platinum-supporting heterogeneous catalyst for the conversion of cellulose into C_2-C_3 glycols are presented. The results obtained for the conversion of glucose with the different catalytic systems were discriminated as a function of the selectivity of key transformation products of cellulose, namely ethylene glycol (EG), ethanol (EtOH), 1,2-butanediol (1,2-BDO), propylene glycol (PG), 1-propanol (1-PrOH), lactic acid (LA), sorbitol and 1,2-hexanediol (1,2-HDO). These products were regrouped in C_2-C_4, C_3 and C_6 molecule pools depending on the main reactions implied in their formation. Thus, this methodological approach allowed us to identify original and efficient dual catalytic systems for the conversion of cellulose to C_2-C_3 glycols.[2] This communication aims to illustrate the great potential of such catalytic systems to achieve enhanced selectivities in ethylene and propylene glycols (EG and PG) from cellulose.

2 Experimental/methodology

The heterogeneous catalysts were prepared by dry impregnation and tested as powders sieved under 150 microns. Catalysts were reduced under a H_2 flow. Catalytic tests were performed in a high throughput apparatus possessing six 100mL autoclaves working in parallel. In a typical experiment, cellulose (1.3g), cerium chloride (500 ppm) and the heterogeneous catalyst (550 mg) were dispersed in degassed water (50mL). The autoclave was sealed and thoroughly degassed. A hydrogen pressure was set at room temperature before heating and stirring at 500 rpm.

3 Results and discussion

To explore this dual concept, an initial screening of heterogeneous catalysts with varying acid base properties was first performed with a $CeCl_3.7H_2O$ homogeneous catalyst (see Entries 1 to 4). The Lewis acid nature of Pt/ZrO_2 yielded a high selectivity in LA. Being reported as basic oxides, mixed oxides of earth alkaline elements and zirconium and perovskites in particular were then considered as promising candidates.[3] Among the different solids tested – $Pt/CaZrO_3$,

$Pt/SrZrO_3$ and $Pt/BaZrO_3$– the $Pt/BaZrO_3$ catalyst achieved the highest selectivities in glycols with 21.7% and 19.2% for EG and PG, respectively. C_2-C_4 molecules were preferentially formed using $Pt/BaZrO_3$ while $Pt/CaZrO_3$ produced enhanced yields of C_3 molecules. No particular selectivity was noted using $Pt/SrZrO_3$. Remarkably, the $Pt/BaZrO_3$ could be additionally shown to exhibit enhanced hydrothermal stability.

The influence of the homogeneous catalyst was then investigated using Pt/BaZrO as the reference heterogeneous catalyst. A blank experiment confirmed the strong impact of the homogeneous catalysts on selectivity (see Entry 5). Three other rare earth chlorides with various sizes and electronegativities –$NdCl_3.7H_2O$, $GdCl_3.7H_2O$, $ErCl_3.7H_2O$– were then tested to study cation effects (see Entry 6 to 8). The overall glycol selectivity was lower than those obtained for $CeCl_3$. Unlike $CeCl_3$, the preferential formation of C_3 molecules was observed. This illustrated the specific results obtained with a light rare earth chloride salt.

The impact of the counter-anion on the selectivity of the reaction appeared significant too (see Entries 9 and 10). Using a cerium triflate salt allowed to achieve high selectivities to glycols (>30%). Selectivities with cerium sulfate were comparatively slightly lower. In both cases, the preferential formation of C_3 molecules was determined. Thus, it was evidenced a strong versatility of this system with a balance between C_2-C_4 and C_3 molecules strongly dependent on the type of counter-anion.

Table 1. Experimental results for the conversion of cellulose at 230°C with an initial H_2 pressure of 25 bar for 12 hours.

Entry	Homogeneous Catalyst	Heterogeneous Catalyst	Conversion[a] (%)	Carbon identification (%)	Apparent carbon selectivity (%)							
					C_2-C_4 molecule pool			C_3 molecule pool			C_6 molecule pool	
					EG[b]	EtOH[b]	1,2-BDO[b]	PG[b]	1-PrOH[b]	LA[c]	Sorbitol[c]	1,2-HDO[b]
1	$CeCl_3.7H_2O$	$Pt(0.7wt\%)/ZrO_2$	56	38	1.5	1.0	3.9	1.2	2.4	13.2	n.d.[d]	0.2
2	$CeCl_3.7H_2O$	$Pt(0.7wt\%)/CaZrO_3$	86	52	11.1	3.0	2.0	15.8	11.9	4.7	n.d.[d]	1.4
3	$CeCl_3.7H_2O$	$Pt(0.7wt\%)/SrZrO_3$	96	26	8.2	1.7	1.1	9.2	0.2	0.8	n.d.[d]	1.8
4	$CeCl_3.7H_2O$	$Pt(0.7wt\%)/BaZrO_3$	97	58	21.7	2.5	2.3	19.2	0.3	2.3	2.4	2.5
5	-	$Pt(0.7wt\%)/BaZrO_3$	82	50	9.8	1.9	0.8	8.4	0.4	0.4	n.d.[d]	1.0
6	$NdCl_3.7H_2O$	$Pt(0.7wt\%)/BaZrO_3$	>99	35	11.3	2.9	1.7	13.0	0.9	2.3	n.d.[d]	1.7
7	$GdCl_3.7H_2O$	$Pt(0.7wt\%)/BaZrO_3$	>99	35	11.9	1.9	0.4	13.4	0.9	2.4	n.d.[d]	2.4
8	$ErCl_3.7H_2O$	$Pt(0.7wt\%)/BaZrO_3$	88	57	9.6	2.7	2.8	14.2	1.5	4.8	n.d.[d]	3.1
9	$Ce(OTf)_3$	$Pt(0.7wt\%)/BaZrO_3$	88	57	7.2	6.0	2.8	24.9	7.7	4.8	n.d.[d]	1.6
10	$Ce_2(SO_4)_3.8H_2O$	$Pt(0.7wt\%)/BaZrO_3$	90	46	3.2	2.7	1.5	21.6	1.0	3.8	0.4	4.3

[a] Determined by TOC measurements. [b] Determined by gas chromatography. [c] Determined by HPLC. [d] Not detectable.
EG: ethylene glycol, EtOH: ethanol, 1,2-BDO : 1,2-butanediol, PG: propylene glycol, 1-PrOH: 1-propanol, LA: lactic acid, 1,2-HDO: 1,2-hexanediol.

4 Conclusions

Original and efficient combinations between a metallic salt homogeneous catalyst and hydrogenation heterogeneous catalyst were explored for the selective conversion of cellulose to C_2-C_3 glycols under hydrothermal conditions. The appropriate choice of the support through its acid-base balance was particularly critical to access high yields of glycols. Perovskites and particularly barium zirconate exhibited a promising potential to do so. Its association with $CeCl_3.7H_2O$ achieved the highest selectivity in ethylene glycol and propylene glycol, leading to a global value of 40.1%. The selection of a light rare earth homogeneous catalyst, *i.e.* cerium chloride, was a key result in this study. A strong versatility between C_2-C_4 and C_3 molecules was also demonstrated using chloride, sulfate or triflate counter-anions in cerium salts.

References

[1] A. Wang, T. Zhang, *Acc. Chem. Res.* (2013) 1377.
[2] E. Girard, D. Delcroix, A. Cabiac, *submitted*.
[3] G. Zhang, H. Hattori and K. Tanabe, *Appl. Catal.* 36 (1988) 189.

IV-PP89

MoCrGa Catalysts Supported on Natural Clays for the Process of Oxidative Conversion of Propane-Butane Mixture

Massalimova B.

Arkalyk State Pedagocical Institute after named I.Altynsarin, Arkalyk, Kazakhstan

* massalimova15@mail.ru

Keywords: propane-butane, oxidation, clays

1 Introduction

Due to the depletion of natural hydrocarbon resources, the need of implementation of the intensive technologies and solutions of environmental problems increases urgency with a more efficient chemical processing of components such as oil and gas. According to forecasts for the near future, saturated C_1-C_4 hydrocarbons not only will retain but also will strengthen their position as a raw material for the production of unsaturated hydrocarbons. Therefore, the problem of searching for the ways of their effective conversion into different oxygen-containing compounds is also urgent. Only the optimal choice of catalysts can ensure targeted synthesis with the predominant formation of a desired compound selected from these products [1].

2 Experimental/methodology

The experiments were carried out at atmospheric pressure in a continuous-flow unit with a fixed-bed quartz-tube reactor. Oxidative conversion of propane-butane mixture by air to oxygen-containing compounds at T=573-873K and space velocity 330-15000ч$^{-1}$ on polyoxide catalysts containing 1-10% Mo, Ga, Cr of different composition and ratio supported on natural Torgai clays (TC), Sary-Ozek, Chankanai, IK-30 and IR-301 zeolites. Analysis for the reactants and products was carried out chromatographically with an "Agilent Technologies" instrument. The catalysts were characterized by XRD analysis, and their surface area, porosity, and elemental composition were determined [1].

3 Results and discussion

It was found that the partial oxidation of propane and the propane-butane mixture at 350-750^{o}C with varying the catalytic mixture composition and the contact time (τ) yielded acetone, methyl ethyl ketone, methanol, acetaldehyde, crotonic aldehyde, butanol, and acetic acid, as well as C_2-C_3 unsaturated hydrocarbons. The main products are oxygen-containing compounds (mainly acetone and acetaldehyde), propylene, ethylene, and CO.

The tests on natural clays (white clay, the base phase is kaolin $Al_2[OH]_4Si_2O_5$ (ASTM-29-1488) and α-quartz SiO_2, as well as red clay, which differs from the white clay by the presence of haematite Fe_2O_3 and the absence of α-quartz (less than 1%) showed that investigation in this direction is also of certain interest. The treatment of clay specimens with hydrochloric acid slightly changed their phase composition. The specific surface area and porosity of the sorbent specimens examined were determined by the Brunauer-Emmett-Teller low-temperature nitrogen adsorption technique. It was found that the clay surface area is 10-16 m^2/g and the optimum pore radius of ranges from 20 to 50 Å. The treatment of sorbents with 10% HCl facilitated the development of pores and an increase in the pore radius. The elemental analysis of the initial sorbent specimens and those treated with 10% HCl showed that the clay specimens predominantly contained oxide compounds of Si and Al, as well as Ca, Mg, Fe, and Na. The SiO_2/Al_2O_3 ratio (silica modulus) was 5-0.4. The silica modulus increases after acid treatment.

Supported polyoxide catalysts on the basis of Mo, Cr, Ga, Bi, and Ce as well as natural clays of Kazakhstan, were tested in the process of oxidative conversion of propane-butane mixture. The influence of reaction temperature, contact time, composition and content of active component of catalyst were determined. The gas mixture used for oxidation contained from 6,6 to 80,0% C_3H_8-C_4H_{10} mixture and from 7,0 to 20,0% oxygen in different ratios at 523-873K and W=300-15000h^{-1}.

It was found that the partial oxidation of propane-butane mixture with varying the catalytic mixture composition and the contact time yielded acetone, methyl ethyl ketone, methanol, acetaldehyde, crotonic aldehyde, butanol, and acetic acid, as well as C_2-C_3 unsaturated hydrocarbons. It was shown that conversion proceeds with the formation of gaseous and liquid products. Important petrochemicals, such as acetone (773-823K) and acetaldehyde (623-673K) are main liquid products. Ethylene is the main product of gas phase. Yield of ethylene increases beginning from 723K.

The investigation on influence of the nature of carrier on yield of acetone from reaction temperature was carried out. It was shown that more high yields of acetone were produced over Torgai white clay (TWC).

Ternary catalyst is more active than two-component samples. Optimal space velocities for catalysts with different content of active phase over carriers were determined. Up to 50,9% of acetone and 38,0% of methyl ethyl ketone on 5%MoCrGa/TC were produced at W=450h^{-1}. Increase of content of methyl ethyl ketone in catalysate was observed at reduction of propane-butane in reaction mixture. The determination of the product composition showed that the process follows a complex mechanism including oxidation, oxidative dehydrogenation, and cracking [1-2].

The optimal conditions for synthesis of products were detected:

- 50,9% of acetone was produced on 5%MoCrGa/TWC catalyst at 823K and W=450h^{-1} in reaction mixture C_3-C_4:O_2:N_2:Ar=5:1:4:5;
- 41,0% of acetaldehyde was produced on 10%MoCrGa/TWC catalyst at 723K and W=450h^{-1} in reaction mixture C_3-C_4:O_2:N_2:Ar=5:1:4:5;
- 80,0% of methyl ethyl ketone was produced on 5%MoCrGa/TWC+ZSM-5+$Al_n(OH)_{3n-1}NO_3$ catalyst at 723K and W=3150h^{-1} in reaction mixture C_3-C_4:O_2:N_2:Ar=1:1:4:1;
- 71,4% of ethylene was produced on 1%MoCrGa/TWC catalyst at 723K and W=450h^{-1} in reaction mixture C_3-C_4:O_2:N_2:Ar=5:1:4:5;
- 83,0% of benzene was produced on 1%MoCrGa/TWC catalyst at 823K and W=750h^{-1} in reaction mixture C_3-C_4:O_2:N_2=7:1:4.

4 Conclusions

Suggested in this research work catalytic reactions can be base for creation of industrial C_3-C_4 mixture utilization process and for production of valuable oxygen-containing compounds.

References

[1] B.K.Massalimova. XXI International Conference on Chemical Reactors Materials. Delft, The Netherlands, 2014. P.396-397.

[2] S.A.Tungatarova, B.K.Massalimova, K.Dossumov. Partial oxidation of propane-butane to acetone and acetaldehyde//9th Novel Gas Conversion Symposium. May 30th-June 3rd 2010. Lyon, France. P.194.

IV-PP90

Magnetically Recoverable Biocatalyst for 2,3,6-Trimethylphenol Oxidation

Matveeva O.V.*, Lakina N.V., Doluda V.Yu., Sulman E.M., Shimanskaya E.I.

Tver Technical University, Tver, Russia

* omatveevatstu@mail.ru

Keywords: oxidation, horseradish, peroxidase, magnetic nanoparticles, immobilization

1 Introduction

Currently the new applications of enzymes are developed, among them are fine organic synthesis, pharmaceuticals, biosensors, biofuels and many others. The improvement of the stability of enzymes allows the reducing of its required amount in the reaction, the extension of the life of enzyme reactors, the increasing of the potential for enzyme reuse or maintaining of good biosensors signal [1]. Therefore, the immobilization of enzymes on various organic and inorganic supports is one of the most promising fields of biotechnology. It is obviously that the immobilization of enzymes can directly affect the cost of the process and the quality of the target products.

The recent years, the magnetic nanoparticles are an alternative support for immobilized enzymes, which have a number of advantages in comparison with conventional matrixes. Among them are the large surface area, which leads to the increase in contact between the reactants and the catalyst, good catalyst activity and availability, simplicity and efficiency of the magnetic separation of the catalyst from the reaction mixture. These advantages can optimize operating costs and improve the purity of the product [2,3].

In this paper the activity of the enzyme peroxidase (EC 1.11.07, HRP) immobilized on magnetic nanoparticles Fe_3O_4 was studied. The syntesized biocatalyst was studied in the oxidation reaction of 2,3,6-trimethylphenol (TMP) with hydrogen peroxide to 2,3,5-trimethylhydroquinone (TMHQ), the precursor of vitamin E (Figure 1).

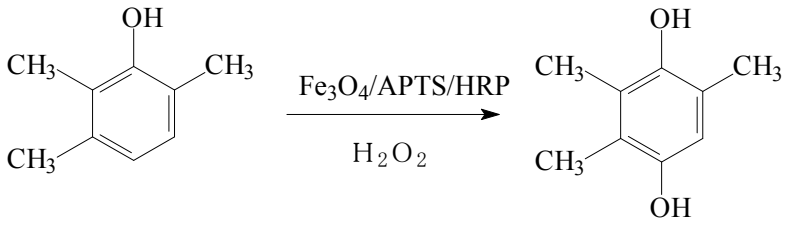

2,3,6-trimethylphenol 2,3,5-trimethylhydroquinol

Fig. 1. Trimethylphenol oxidation reaction.

2 Experimental

$FeCl_3 \cdot 6H_2O$ (3 mmol), succinic acid (1 mmol) and urea (30 mmol) were completely dissolved in ethyleneglycol (30 ml). The solution obtained was inputted in a teflon beaker (50 ml) in the stainless steel autoclave (Parr Instr.) and was soaked at 200°C for 4 hours. After cooling to the room temperature, the black precipitate was separated with magnet and washed with ethanol several times until a clear solution. Then the obtained nanoparticles were treated with the solution of 150 ml of ethanol, 1 ml of water and 35 µl of 3-aminopropyltriethoxysilane (APTS). The solution was stirred for 5 hours on a magnetic stirrer and then washed with distilled water and ethanol. Then APTS-coated nanoparticles were treated HRP. As the result the biocatalyst Fe_3O_4/APTS/HRP was obtained.

3 Results and discussion

In this work the effect of pH and temperature on the rate of formation of TMHQ was studied. The biocatalyst has the higher activity at pH = 7.2. The 50°C was the optimum of the temperature. The biocatalyst had the activity decrease only by 29% during 8 cycles.

To compare the activity of native and immobilized peroxidase the dependence of activity on the concentration of trimethylhydroquinone in time at the temperature 40°C was plotted (Figure 2).

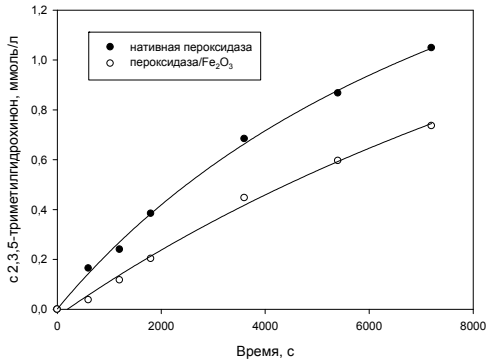

Fig.2 – Kinetic curves of the TMHQ yield dependence on time (c_{TMP} = 0.0015 mol/l, T = 40 ^{0}C, pH = 6.5)

From Figure 2 it can be concluded that the activity of peroxidase immobilized on the magnetic nanoparticles was slightly reduced compared to the activity of the native enzyme. It can be explained by the fact that peroxidase immobilized on magnetic nanoparticles is stabilized by the formation of stable complexes with iron.

4 Conclusions

The results indicate the prospects for further researches to improve the method of catalytic oxidation of TMP to TMHQ and improving the effectiveness of the biocatalyst based on HRP, immobilized on magnetic nanoparticles.

References

[1] J. Kim, J. W.Grate, P. Wang, *Chemical Engineering Science* 61 (2006) 1017-1026

[2] V. Polshettiwar, R. Luque, A. Fihri, H. Zhu, M. Bouhrara, J.-M. Basset, *Chem. Rev.* (2011) 111, 3036–3075

[3] Y. Jiang, C. Guo, H. Xia, I. Mahmood, C. Liu, H. Liu *Journal of Molecular Catalysis B: Enzymatic* 58 (2009) 103-109

IV-PP91

Catalytic Oxidation of Veratryl Alcohol – a β-O-4 Lignin Model Compound - to Veratraldehyde

Melián R.M.[1,2*], Saravanamurugan S.[1,2], Kegnæs S.[1,2], Riisager A.[1,2]

1 - Technical University of Denmark, Lyngby, Denmark
2 - Centre for Catalysis and Sustainable Chemistry, Lyngby, Denmark

* mayro@kemi.dtu.dk

Keywords: heterogeneous catalysis, oxidation veratryl, alcohol, lignin, veratraldehyde, ruthenium

1 Introduction

Lignin is the second most abundant natural polymer and represents 40% of the energy content in lignocellulosic biomass. It is viewed as the obvious candidate to serve as a renewable feedstock of basic aromatic chemicals. In lignocellulosic material the composition as well as the molecular weight and structure of the lignin differ from plant to plant (hardwood, softwood, grass etc.), impeding the developments on lignin valorization processes. However, three monolignol monomers p-coumaryl, coniferyl and sinapyl alcohol are common building blocks. They are connected with various linkages with the most common one being the β-O-4 linkage. Due to lignin complexity and variability, several simpler, low molecular weight lignin model compounds have been prompted in the study of lignin valorization [1-3]. The oxidation of veratryl alcohol to veratraldehyde is a benzylic oxidation representing the valorization of one of the β-O-4 model compounds of lignin. Since the product veratraldehyde is a useful flavorant and odorant the transformation has been comprehensively studied by both enzymatic and homogeneous catalyst systems [4-5].

2 Experimental/methodology

In the present work we have prepared, characterized and examined the performance of heterogeneous catalysts with ruthenium or other transitions metals supported on γ-alumina for the conversion of veratryl alcohol to veratraldehyde by aerobic oxidation in water (Fig. 1). Ru/Al_2O_3 showed superior catalytic activity yielding up to 89% veratraldehyde at 160 ^oC with 5 bar air pressure. Under prolonged reaction time the decarbonylated product veratrol formed but no increase in formation of veratric acid was observed. The Ru/Al_2O_3 catalyst could be reused in three consecutive reaction but with gradually lower yield [6].

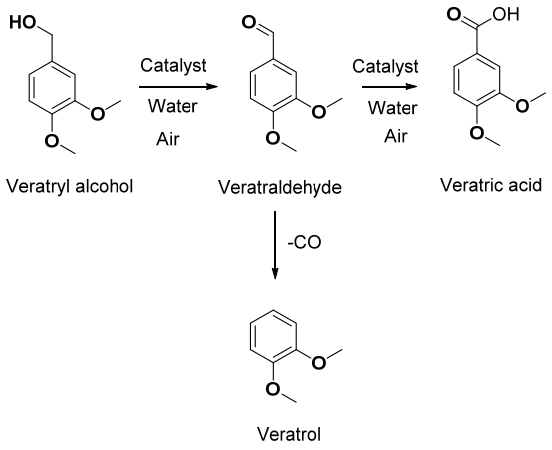

Fig. 1. Aqueous catalytic aerobic oxidation of veratryl alcohol.

Acknowledgements

The authors appreciate financial support to the work from The Danish Agency for Science, Technology and Innovation (International Network Programme, 12-132649), Haldor Topsøe A/S and the Technical University of Denmark.

References

[1] J. Zakzeski, PCA Bruijnincs, AL Jongerius, BM Weckhuysen, *Chem. Rev.* 110 (2010) 3552
[2] PT Patil, U Armbruster, M Richter, A Martin, *Energy & Fuels* 311 (2006) 4713
[3] C Zhao, JA Lercher, *ChemCatChem* 4 (2012) 64
[4] TM Larson, M Anderson, JO Rich, *Biotechnol. Lett.* 35 (2013) 225
[5] P Zucca, G Mocci, A Rescingo, E Sajust, *J. Mol. Catal. A: Chem* 278 (2997) 220
[6] M Melián-Rodríguez, S Saravanamurugan, S Kegnæs, A Riisager, (2015) Submitted

IV-PP92

Pd-Ce Nanoparticles on Functional Fe-MIL-101: An Efficient Catalyst for Glycerol Oxidation

Zhu Y.[1*], Li X.[2], Adrian K.T.[2], Ding J.[2], Xue J.M.[2]

1 - Institute of Chemical and Engineering Sciences, Singapore
2 - Department of Materials Sciences & Engineering, National University of Singapore, Singapore

* zhu_yinghuai@ices.a-star.edu.sg

Keywords: metal organic frameworks, nanocatalyst, biomass conversion, selective oxidation

1 Introduction

Glycerol is a by-product of biodiesel. Due to the increased demand of biodisel, glycerol production is continually increased [1]. Therefore, selective oxidations of glycerol into more value added chemicals are of great interest in current biomass research. Dihydroxyacetone (DHA), a simple oxidation product of glycerol, is currently the most popularly used sunless tanners, which is the only active ingredient approved by the US Food and Drug Administration (FDA) for sunless tanning [2]. Currently, DHA is mainly produced from an atom-inefficient fermentation process [2]. Transition-metal nanoclusters with particle size around 5nm own big surface area, and demonstrate physical and chemical properties which are significantly different from their bulk counterparts. In addition, the type catalysts own the advantage of both homogeneous and heterogeneous catalysts, well dispersion in reaction mixture and easily separation from product mixtures [3,4]. We have studied the potential applications of the metal organic frameworks supported metal nanoparticles-based catalysts for the oxidation of biomass-based glycerol to DHA. In the presentation, we report the synthetic methods and catalytic performances the Pd-Ce NPs/functional Fe-MIL-101 for the selective oxidations of biomass-based alcohols of glycerol, ethanol, etc. to corresponding aldehyde and ketone products.

2 Experimental/methodology

All reagents were purchased from Sigma. Neocuproine functionalized MOF was synthesized by reacting MOF Fe-MIL 101-NH_2 with great excess of 1,10-phenanthroline-2,9-dicarbonyl dichloride, which was in situ generated from 2,9-dicarboxylic acid-1,10-phenanthroline and thionyl chloride, in dichloromethane. Catalyst Pd-Ce NPs/functional Fe-MIL 101 was prepared by co-precipitation methods from precursors of $PdAc_2$ and $Ce(acac)_3$ reducing by $NaBH_4$ in DMF. The catalyst was characterized by TEM, XPS, FT-IR and ICP. Oxidation was conducted in a mixed solvent of acetonitrile/Deion water. Oxygen (3bar) was used as oxidant in the presence of co-oxidant benzoquinone at 60°C. The products were analyzed by GC and HPLC.

3 Results and discussion

Figure 1 (a,b) shows the TEM images of the supported catalyst. It can be seen that the Pd-Ce NPs are small, ~5nm, and well dispersed on the functionalized Fe-MIL 101. The catalytic oxidation results are detailed in Scheme 1. No significant difference was observed for Pd-Ce NPs supported and pristine functional Fe-MIL 101 as demonstrated in Figure 1 (c). The catalyst shows reasonable activity for glycerol oxidation to DHA, which is comparable with other supported metal nanoparticles such as Pt-Bi/C (DHA yield 44.8%)[5]. Ethanol and other alcohols also have been converted to corresponding aldehydes with medium yields. Further, the catalyst can be easily recovered by conventional filter or centrifugation with sustained activity.

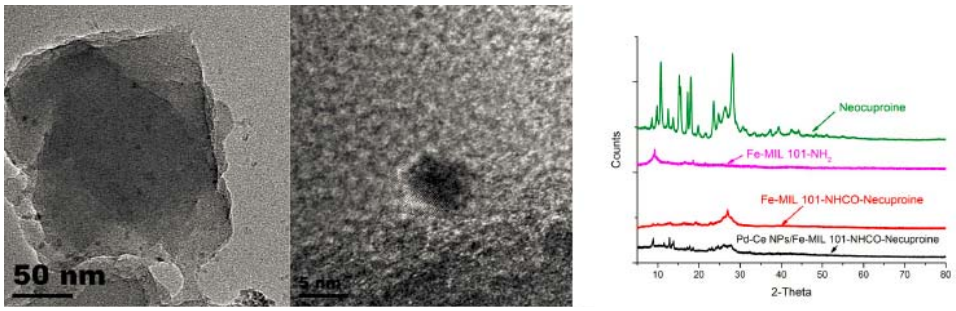

(a) (b) (c)

Fig. 1. TEM images (a,b) of and XRD spectra (c) of the catalyst composites.

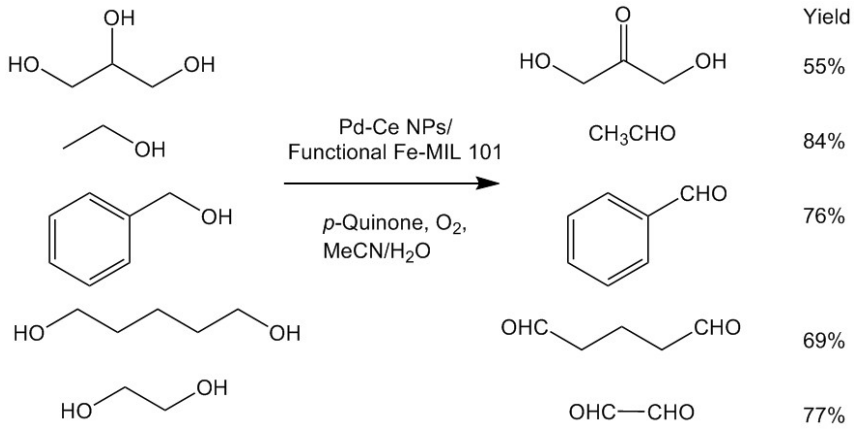

Scheme 1. Pd-Ce NPs/functional Fe-MIL 101 catalyzed alcohol oxidation.

4 Conclusions

Neocuproine-functionalized Fe-MIL 101 supported Pd-Ce NPs-based catalyst, Pd-Ce/Fe-MIL 101-N=$CH_{Neocuproine}$, has been synthesized. The catalyst shows medium to good activity for selective oxidation of glycerol to DHA and other alcohols to produce corresponding aldehydes.

Acknowledgements

We thank SMART *(Singapore-MIT Alliance for Research and Technology)* Innovation grant and ICES, A*STAR for financial support.

References

[1] R. Christoph, et al., *Glycerol*, in *Ullmann's Encyclopedia of Industrial Chemistry*. 2000, Wiley-VCH Verlag GmbH & Co. KGaA.
[2] Dihydroxyacetone, *Market Research Report* 2012, http://marketpublishers.com.
[3] R. Ferrando, J. Jellinek, R. L. Johnston, *Chem. Rev*. 108 (2008) 845-910.
[4] Y. Zhu, N. S. Hosmane, *Coord. Chem. Rev.* doi:10.1016/j.ccr.2014.10.002.
[5] D. Liand, S. Cui, J. Gao, J. Wang, P. Chen, Z. Hou, *Chinese. J. Cat*. 32 (2011) 1831-1837.

IV-PP93

Oxidative Dehydrogenation of Ethane on MoVTeNbO Catalysts

Mishanin I.I.[1*], Lunin V.V.[1,2], Bogdan V.I.[1,2]

1 - Lomonosov Moscow State University, Moscow, Russia
2 - Zelinsky Institute of Organic Chemistry, Moscow, Russia

* arnochem@yandex.ru

Keywords: selective oxidation, ethane, ethylene, Mo-V-Te-Nb mixed metal oxide catalyst

1 Introduction

The oxidative dehydrogenation (ODH) of light paraffins is one feasible alternative to the current industrial productions of olefins. This method has several important advantages. Firstly, ODH – is an exothermic process which should serve as an incentive to implement it in a production of olefins. Secondly, the oxygen, entered with the feedstock, reacts with the carbon and prevents the formation of coke on the catalyst surface.

MoVTeNbO catalysts, prepared by hydrothermal synthesis, were found to be extremely active and highly selective in the ODH of ethane [1].

2 Experimental

Mo/V/Te/Nb mixed metal oxide catalyst was prepared by hydrothermal synthesis as reported [2]. Ammonium heptamolybdate, telluric acid, vanadyl sulfate and niobium oxalate were used to prepare the catalyst. Mo/V/Nb mixed metal oxide catalyst was prepared similarly as the Mo/V/Te/Nb catalyst. The prepared catalyst was characterized by XRD, SEM and XPS analysis.

The catalytic tests were carried out under steady-state conditions at atmospheric pressure, using a fixed-bed titanium reactor (an inner diameter of 1 cm and a length of 54 cm), in two modes: cyclic (separate feeding of reagents) and flow-type (continuous feed gas mixture). In the flow-type mode the feed (60 ml min^{-1}) consisted of a mixture of ethane/oxygen with molar ration of 75/25. Experiments were carried out in the 340 to 400 temperature range. The catalyst volume was 1.8 cm^3 (2 g), and the remaining volume of the reactor was filled with quartz particles. In the cyclic mode the feed consisted of ethane. Reactants and reaction products were analyzed by gas chromatography, using two columns: Porapak Q and Zeolite A.

3 Results and discussion

The catalytic results for the oxidative dehydrogenation of ethane on MoVTeNbO and MoVNbO catalysts are presented in Table 1. Ethylene, carbon oxides and water were the main reaction products. Acetic acid was found in trace quantities.

Table 1. ODH of ethane on MoVTeNbO and MoVNbO catalysts (the flow-type mode)

Sample	Temperature, °C	Conversion, %	Selectivity, %		
			C_2H_4	CO_2	CO
MoVTeNbO	340	6	98	2	0
	360	18	92	3	5
	380	34	88	3	9
	400	37	85	3	12
MoVNbO	360	9	68	16	16
	400	21	70	9	21

According to the presented data on MoVTeNbO catalysts high selectivity to ethylene is reached at 340 °C. Conversion achieves 37% at temperature 400 °C; however selectivity to

ethylene decreases to 85%. Some growth inhibition of conversion upon transition from 380 to 400 °C is connected with that about 95% of the oxygen are consumed at 380 °C. At 400 °C the full consumption of gaseous oxygen takes place.

The lack of an oxidizer of reactionary mix leads to irreversible changes of the catalyst, decrease of the activity and selectivity (fig. 1). Rise in temperature to 400 °C facilitates tellurium reduction by ethane from Te^{+6} oxidation level to Te^{0}-state with the subsequent its sublimation and destruction of an active and selective phase.

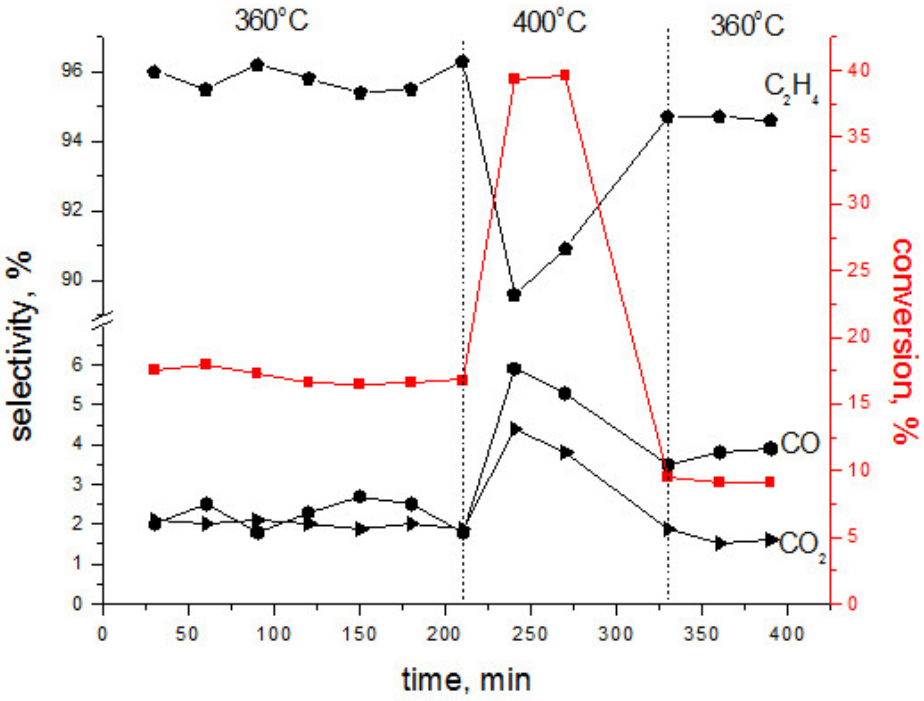

Fig. 1. Change of ethane conversion and selectivity to products over MoVTeNbO catalysts as the function of reaction time. (Reaction conditions for ethane oxidation: C_2H_6/O_2 molar ratio of 3/1, m_{cat} = 2.0 g, the flow rate 60 ml/min)

At research of the oxidative dehydrogenation of ethane in the cyclic mode it was established that the molar fraction of the active oxygen, participating in reaction, compounds 3%.

4 Conclusions

Low values of exchange oxygen of solid and gas phases may be cause high selectivity to ethylene. In the most optimum process parameters conversion of ethane reaches 18%, oxygen - 50%, selectivity to ethylene - 92% at 360 °C. Rise in temperature to 400 °C increases conversion of ethane; however selectivity to ethylene decreases to 85%. Under such conditions the catalyst is irreversible deactivated in connection with tellurium reduction. Thus, the catalyst deactivated in reaction of the ODH of ethane shows lower conversion and selectivity to ethylene which are similar to the data received for Mo-V-Nb catalysts which aren't containing tellurium.

Acknowledgements

Financial support was provided by RFBR (grant № 13-03-12266-ofi_m) and the company Ltd. “Envirocat”.

References

[1] J. López-Nieto, P. Botella, P. Concepción, A. Dejoz, M. Vázquez, *Catal. Today*. 91-92 (2004) 241-245.

[2] P. Botella, E. García-González, A. Dejoz, J.M. López Nieto, M.I. Vázquez, and J. González-Calbet, *Journal of Catalysis*. 225 (2004) 428-438.

IV-PP94

Oxidative Catalytic Upgrading of Biomass-Derived Glycolaldehyde to Glycolics

Modvig A.E.[1,2*], Fristrup P.[1], Riisager A.[1,2]

1 - Technical University of Denmark, Lyngby, Denmark
2 - Centre for Catalysis and Sustainable Chemistry, Lyngby, Denmark

* ammod@kemi.dtu.dk

Keywords: catalysis oxidation, biomass, glycolaldehyde

1 Introduction

Lignocellulosic biomass is a potential renewable carbon-source for industrial production of important chemical compounds, e.g. polymers, fuel components etc. The most studied catalytic strategy for conversion of polymeric carbohydrates into chemicals and fuels includes acid catalyzed depolymerization of cellulose or hemicellulose to glucose or xylose, followed by dehydration to produce C6 and C5 chemicals such as 5-hydroxymethylfurfural (HMF) and furfural. Both of these chemicals can be transformed into a range of de- or re-functionalized "furanic" compounds, with varied carbon content, by reduction, oxidation, esterification, retro Diels-Alder, etc. thus serving as valuable platform chemicals.

2 Experimental/methodology

Lignocellulose can also be transformed into smaller liquid chemical building blocks by partial thermal degradation (i.e. by pyrolysis). A major byproduct obtained from pyrolysis is the C2 chemical, glycolaldehyde (GAD). Noticeably, glycolaldehyde contains, like HMF, both an aldehyde and an alcohol moiety which potentially makes glycolaldehyde prone for re-functionalization into value-added and useful "glycolic" chemicals in an analogous manner as demonstrated for HMF. However, since glycolaldehyde has received significant less attention, only limited chemo-catalytic technology have been developed for efficient and selective transformation of glycolaldehyde. An overview of the breakdown of cellulose to glycolics is presented in Fig. 1.

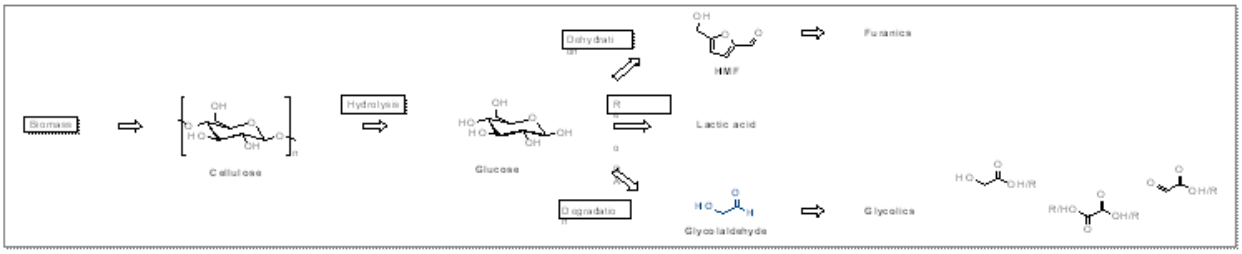

Fig. 1. Breakdown of cellulose into glycolics

In this work, oxidative functionalization of GAD are explored using heterogeneous metal-catalyst with air as oxidant under relative mild reaction conditions. Generally, catalyst activity and selectivity were found to depend significantly on the nature of catalyst as well as the applied reaction conditions thus making an *a priori* selection difficult. However, a few very promising catalyst candidates have been identified.

Acknowledgements

The project is conducted in the framework of the BIO-VALUE platform funded under the SPIR initiative by The Danish Council for Strategic Research and The Danish Council for Technology and Innovation in corporation with Haldor Topsøe A/S and Aarhus University.

IV-PP95

Mathematical Analysis Options to Upgrade Plants of Dehydrogenation Isoamylenes to Isoprene and Conduct Pilot Tests

Nazarov M.V.*, Lamberov A.A., Urtyakov P.V.

Kazan (Volga region) Federal University, Kazan, Russia

* humic-acid@mail.ru

Keywords: dehydrogenation of isoamylenes to isoprene, pilot tests

- Introduction

As a result, the flow of the endothermic dehydrogenation reaction in the adiabatic regime, there is a decrease in reactor temperature, the value of which depends on the amount of steam fed is an inert coolant. Reducing the temperature drop in the range of 20 °C can be achieved only by diluting feed steam in the ratio 1:40 mol/mol (or 1:10 kg/kg). An amount of steam consumption increases the cost of the product and reduces the efficiency of the process. Thus, the use of an adiabatic reactor capacitive contact type in this case is uneconomical.

The intensification of the dehydrogenation reaction can be obtained by increasing the gas temperature by heating it or by introducing additional superheated steam, in a catalyst layer. It is also possible to implement the systems consisting of two reactors in series, where the gas is passed through the first reactor is heated again, and then passes through the second reactor. In this paper, we consider three possible options for the implementation of the dehydrogenation process with an additional intensification of the process:

- a reactor with an additional introduction of superheated steam into the catalyst bed;
- two consecutive heated reactor with intermediate gas;
- two consecutive reactor by adding additional superheated steam into the gas before it is fed into the second reactor.

The aim of this work is the mathematical modeling of the various areas of technological process optimization in the dehydrogenation of isoamylenes to isoprene, analysis of the results and selects the best in terms of energy efficiency optimization method, and conducting pilot tests.

2 Experimental/methodology

The object of research is the process of dehydrogenation of isoamylenes to isoprene (Figure 1) in the presence of a potassium and cerium promoted iron oxide catalyst. The chemical composition of the catalyst is presented in Table 1.

Table 1. Chemical composition of a potassium and cerium promoted iron oxide catalyst

Composition	Fe_3O_4	K_2O	CeO_2	CaO	MgO	MoO_3
ω, % wt.	72,51	3,60	14,90	2,60	3,10	3,29

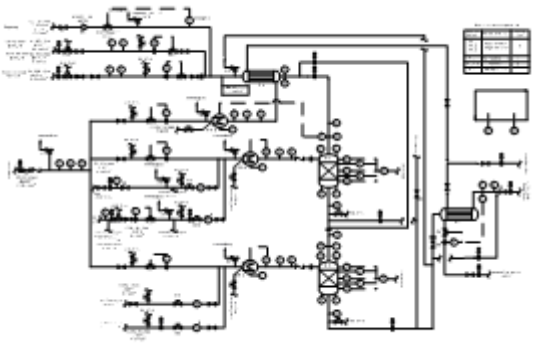

Fig. 1. Block diagram of a pilot plant test a potassium and cerium promoted iron oxide catalyst during the dehydrogenation of isoamylene to isoprene

3 Results and discussion

Carrying out the process for the dehydrogenation of isoamylenes to a two-reactor circuit further supplying steam into the second reactor in comparison with traditional allows to increase the absolute yield of isoprene 13-15 %, while maintaining selectivity at a level of 86-90 %. Thus, the total dilution steam to feedstock weight ratio of 1:10 at a volumetric feed rate of 0.8 h^{-1} to activity allowed to increase to 52 %.

Thus, the operation of the plant with an additional supply of steam to the second reactor indicated on the existing scheme in the second dehydrogenation step technical limitations to exploit the potential of iron oxide catalysts in full. The main limitation on the degree of conversion of the existing scheme is insufficient thermal energy necessary for the occurrence of endothermic dehydrogenation reaction. In this connection the modernization of reactors to ensure the supply of steam into the middle catalyst layer.

4 Conclusions

In order to improve the effectiveness of existing factory circuits dehydrogenation of isoamylenes explored to increase the yield of isoprene. To compensate for heat losses occurring in the reactor by the endothermic reactions, necessary heat input to the reaction zone.

Optimal in terms of energy efficiency was selected (two consecutive reactor by adding additional superheated steam into the gas before it is fed into the second reactor) optimization method. Implementation of this scheme is expected to increase the activity on 10-12 % while maintaining selectivity.

For practical realization of the goal to increase the yield of isoprene were conducted pilot tests in the dehydrogenation isoamylenes to isoprene process using a pilot plant with two reactors connected in series with additional steam to the second reactor. Thus, sampling and analysis was carried out of the contact gas, after the first and after the second reactor, enabling a comparative analysis of the results using the conventional scheme, and an intermediate circuit with a two-reactor steam supply.

Based on the results conducted by pilot test shows that carrying out the process for the dehydrogenation of isoamylenes to isoprene a two-reactor circuit further supplying steam into the second reactor in comparison with traditional allows to increase the absolute yield of isoprene activity 13-15 %, while maintaining selectivity at a level of 86-90 %. Thus, carrying out the dehydrogenation process with an intermediate supply steam to the reactor is promising, and may be used in the present dehydrogenation process cycle plant. On the basis of pilot tests, it was proposed to test the scheme in terms of operating the dehydrogenation reactors.

IV-PP96

Hypercrosslinked Polystyrene-Supported Palladium Catalysts for Suzuki Cross-Coupling Reaction

Lyubimova N., Nikoshvili L.*, Matveeva V., Sulman M., Sulman E.

Tver Technical University, Tver, Russia

* nlinda@science.tver.ru

Keywords: Suzuki cross-coupling, palladium, hypercrosslinked, polystyrene

1 Introduction

Palladium-catalyzed reactions of C-C bond formation are a versatile tool in organic synthesis. Among the existing coupling reactions the Suzuki coupling is of particular importance. It involves the reaction between aryl halides and arylboronic acids to yield unsymmetrical biaryls with high selectivity. Suzuki coupling requires mild reaction conditions and is tolerant to the presence of different functional groups [1].

Catalysts used in the Suzuki reaction have been traditionally based on homogeneous palladium phosphine complexes, which are rarely recoverable without elaborate and wasteful procedures, and therefore commercially unfavorable. Moreover, phosphine ligands are expensive, toxic; and in large-scale applications the phosphines may be more costly than the metal itself. In recent years there has been an increasing interest in developing greener processes. In this context, heterogeneous catalysis is emerging as an alternative to homogeneous processes since the catalysts can be recovered and reused. Catalyst recovery also decreases contamination of products with residual metal species [2].

In the last decade the development of new ligand-free catalytic systems, which allows for the Suzuki reaction under mild conditions in aqueous media, attracted increased attention of scientific community. The most well known ligand-free catalyst is Pd/C [3]. In comparison with the expensive and unstable homogeneous palladium complexes, Pd/C is easy to manufacture and can be separated from the reaction mixture by conventional filtration or centrifugation. However, the main disadvantage of the use of ligand-free catalysts is irreversible leaching of palladium. Therefore, the problem of searching of new ligand-free catalysts is still of great importance. Despite the diversity of methods of synthesis of ligand-free catalysts (using inorganic carriers (oxides and metal salts, zeolites, magnetic nanoparticles), carbon supports (activated carbon, carbon nanotubes, graphene)), nanostructured polymers can be considered as the most promising supports [3, 4] in order to govern nanoparticle growth and prevent their aggregation. The variety of properties (presence of functional groups, degree of crosslinking, hydrophilicity or hydrophobicity, etc.) of polymers provide the opportunity to influence the process of formation of nanoparticles [5].

In this work we investigated the hypercrosslinked polystyrene (HPS)-supported palladium catalysts in Suzuki cross-coupling of 4-bromoanisole and phenylboronic acid (Fig. 1).

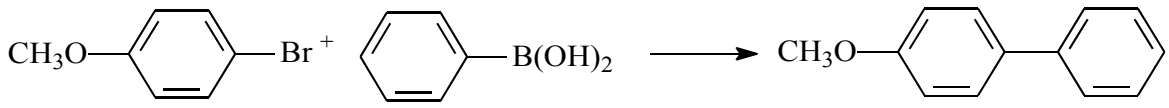

Fig. 1. Suzuki cross-coupling reaction of 4-bromoanisole and phenylboronic acid

2 Experimental

Pd/MN100 catalysts with different metal loadings were synthesized via conventional wet-impregnation method according to the procedure described elsewhere [6] using the following

metal precursors: $PdCl_2(CH_3CN)_2$, $Pd(OAc)_2$, $PdCl_2$. In a typical experiment, 3 g of pretreated, dried and crushed (<60 m) granules of MN100 were impregnated with 9 mL of precursor (e.g. $(CH_3CN)_2PdCl_2$) solution in THF of a certain concentration. The Pd-containing polymer was dried at 70°C, treated with Na_2CO_3, washed with distilled water till neutral pH, and dried again at 70°C.

The Suzuki cross-coupling reaction was carried out in a 60 mL isothermal glass batch reactor installed in a shaker and connected to a gasometrical burette. The total volume of liquid phase was 30 mL. Reaction was carried out at ambient pressure at variation of solvent nature and composition, temperature, nature and concentration of base, substrate-to-catalyst ratio and stirring rate.

Samples were periodically taken and analyzed via GC-MS (Shimadzu GCMS-QP2010S) equipped with a capillary column HP-1MS (30 m × 0.25 mm i.d., 0.25 μm film thickness). Helium was used as a carrier gas at flow rate 1 mL/min. Analysis conditions: oven temperature 60 C (isothermal), injector and interface temperature 280 C, ion source temperature 260 C, range from 10 up to 200 m/z.

3 Results and discussion

During the variation of solvent nature it was found that the use of mixture of low-molecular weight alcohols (e.g. EtOH, *i*-PrOH) with water allows relatively high activity at mild temperatures (60-70°C) along with the absence of the necessity to use phase transfer agents. Besides, the mixture of EtOH with water is favorable from the environmental point of view. Best results were obtained for the catalyst synthesized while using $PdCl_2(CH_3CN)_2$ as the precursor, e.g. in EtOH/water mixture of 5:1 at 70 ºC, conversion of 4-bromoanisole for 1 h was more than 93%.

The possibility of catalyst separation and multiple reuses was also investigated. After first run the catalyst was separated by filtration, successively washed with ethanol, hexane and acetonitrile and allowed to dry at 80 ºC. The separated catalyst was reused under the chosen reaction conditions. It was revealed that synthesized Pd/HPS catalysts can be reused four times without essential loss in activity.

4 Conclusions

HPS-supported palladium catalysts were found to be promising (active, selective and stable during four runs) for the Suzuki cross-coupling reaction of 4-bromoanisole and phenylboronic acid in order to produce the corresponding biaryl with high yield at mild reaction conditions in environmentally favourable solvents.

Acknowledgements

Financial support was provided by the Ministry of Education and Science of the Russian Federation (grant no. RFMEFI57414X0121).

References

[1] K. Köhler, R.G. Heidenreich, S.S. Soomro, S.S. Pröckl, *Adv. Synth. Catal.*, 350 (2008) 2930.
[2] N.T.S. Phan, D.H. Brown, P. Styring, *Tetrahedron Letters*, 45 (2004) 7915.
[3] J. Sołoducho, *Advances in Chemical Engineering and Science*, 3 (2013) 19.
[4] D. Astruć, *Inorg. Chem.*,46 (2007) 1884.
[5] L. Durán Pachón, *Appl. Organomet. Chem.*, 22 (2008) 288.
[6] E.M. Sulman, L.Zh. Nikoshvili, V.G. Matveeva, I.Yu. Tyamina, A.I. Sidorov, A.V. Bykov, G.N. Demidenko, B.D. Stein, L.M. Bronstein, *Top. Catal.*, 55 (2012) 492.
[7] L. Nikoshvili, E. Shimanskaya, A. Bykov, I. Yuranov, L. Kiwi-Minsker, E. Sulman, *Catal. Today*, 241 (2015) 179.

IV-PP97

Enantioselective Hydrogenation of Prochiral Arylketones and Keto Acid ethers Catalyzed by $Pd(acac)_2$- Chiral Base

Nindakova L.O.*, Strakhov V.O., Chvanova K.A.

Irkutsk State Technical University, Irkutsk, Russia

* nindakova@istu.edu

Keywords: palladium, chiral, modifier, enantioselectivity, hydrogenation

1 Introduction

Enantioselective hydrogenation of organic carbonyl compounds with prochiral C=O bond now use for synthesis of optical active secondary alcohols, which have be employed for production drugs, perfume components and agrochemicals.

Metal nanoparticles application for catalytic hydrogenation of unsaturated bonds is very exciting and becoming popular research area [1, 2], since they could be effective and selective catalysts in such cases.

Enantioselective hydrogenation of prochiral ketones (acetophenone) and keto acid ethers by molecular hydrogen over colloidal palladium, which have been formed in system $Pd(acac)_2$ - chiral base - H_2 was studied.

2 Experimental

Hydrogenation experiments carried out in autoclave Büchiglasuster cyclone 075 at pressure 5 bar). Reaction monitoring was studied by Gas Chromatograph-Mass Spectrometers Shimadzu QP2010 Plus in electron impact mode at 70 eV; capillary column Equity 5 (30мх0.25 мм, 95% dimethylpolysyloxane, 5% diphenylpolysyloxane, carrier gas - hellium). Enantiomeer product excess was determined by Gas Chromatograph GC Agient 7890A, flame-ionization detector and chiral capillary column CYCLODEX-B (length 30 m, internal diameter 0.25 mm). Optical rotation of pure compounds and solutions was determined by automatic digital ADP 410 at wave length 589 nm (l = 50 mm, C = 1–5 g/100 ml).

Microstructure and morphology of Palladium nanoparticles was studied by high-resolution **TEM** method. Images were obtained in FEI Tecnai G^2 c with accelerating voltage 200 kV, equipped energy dispersion detector (EDAX) for carrying out elemental analysis.

In situ drop of catalyst solution (C_{Pd} = 1-5 mmol/l) was applied on supporting grid, which coved by carbon film, and dried in Argon atmosphere. Coverage conditions eliminate melting and decomposition of researching compounds under the influence of electron beam.

3 Results and discussion

In system $Pd(Acac)_2$-chiral base-H_2 the formation of colloid Palladium is taking place during 1 hour. As a chiral bases we used natural alkaloid (-)cinchonidine (Cin) and its N- and N,N'-protonated derivatives: Cin*HCl and Cin*2HCl, they were preliminary synthesized and characterized by physical and chemical methods.

We found that reaction rate of hydrogenation of acetophenone at p_{H_2} = 5 bar decreases with increasing ratio of Cin/Pd in ratio range 0.5 - 1.0 – 1.5 (2.31; 1.17; 0.73 mmol/l*h) and increases in modifiers series Cin < Cin*HCl < Cin*2HCl.

The highest hydrogenation rate is observing in hydrogenation of ethylbenzoylformate (up to 180 mol Sub/g-atom Pd*h).

In hydrogenation of methylpyruvate we found abrupt decreasing of reaction

enantioselectivity (from 86% to 55%) during the reaction time. It needs optimizing reaction conditions to prevent this phenomenon.

Palladium nanoparticles, formed in catalytic system $Pd(acac)_2$- chiral base –MeOH after 1 hour, were studied by high-resolution TEM method. Measured the average size of nanoparticles is 6,0±0,9 *nm* for chiral base = (-)-cin; 4,4±0,9 *nm* and 4,3±0,6 *nm* for Cin*HCl and Cin*2HCl, respectively. At the atomic resolution we can see crystal structure of nanoparticles. Figure shows microphotographies of colloidal dispersions, formed in systems.

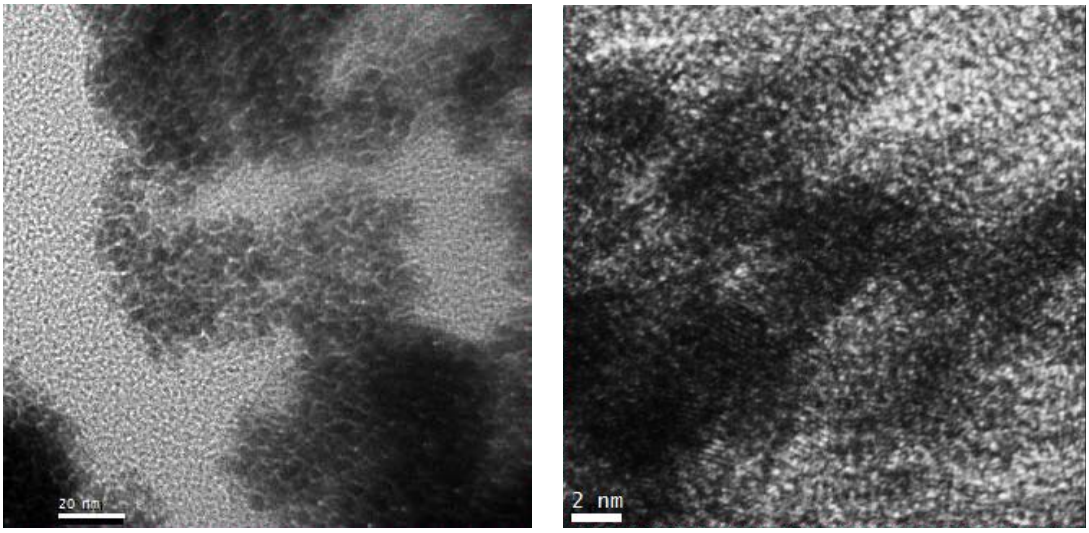

Figure. TEM microphotographies of dispersion from catalytic system $Pd[acac]_2$ - chiral base – H_2,: a) chiral base – (-)-Cin, (scale bar 20 nm); b) chiral base – Cin*HCl (scale bar 2 nm)

4 Conclusions

Ultradispersed (nanoscaled) catalysts based on $Pd(Acac)_2$ compounds were obtained and characterized by high-resolution TEM, X-ray analysis, scanning electron microscopy methods. As a modifiers was used nature alkaloid (-)-cinchonidine and its protonated derivatives. Catalysts were tested in hydrogenation of acetophenone and keto acid ethers. In hydrogenation of methylpyruvate enantiomeric excess reaches to 86% of predominant enantiomer methyl lactate.

Acknowledgements

Financial support: Ministry of Education and Science RF (State task from Ministry of Education and Science of Russian Federation, basic financing, project № 616)

References

[1] S. Jansat, M. Gómez, K. Philippot, G. Muller, E. Guiu, C. Claver, S. Castillón, B. Chaudret, J. *Am. Chem. Soc.* 126 (2004) 1592

[2] P. J. Collier, J. A. Iggo, R. Whyman, *J. Mol. Cat. A: Chemical* 146 (1999) 157

IV-PP98

Cumene Hydroperoxide Decomposition in the Presence of Organic Group II Metal Salts

Nurullina N.*, Batyrshin N., Kharlampidi Kh.

Kazan National Research Technological University, Department of General Chemical Technology, Kazan, Russia

* nyryllina@mail.ru

Keywords: 2-ethylhexanoates, cumene hydroperoxide decomposition, catalytic activity

1 Introduction

Advances in the oxidation of aromatic hydrocarbons are largely determined by the efficiency of the catalyst employed, specifically by its activity, selectivity, and ease of preparation. Among the known catalysts for "soft" initiation of activation processes, non-transition metal 2-ethylhexanoates are very active ones [1].

In order to understand why the decomposition of organic hydroperoxides depends on the nature of the metal, we studied the catalytic action of Subgroup IIA and IIB metal 2-ethylhexanoates ($M(EH)_2$) in the decomposition of cumene hydroperoxide (CHP).

2 Experimental/methodology

The catalytic activity of the ethylhexanoates was estimated in terms of CHP decomposition rate. CHP was decomposed using an ampule technique. CHP concentration was determined by iodometric.

3 Results and discussion

All of the ethylhexanoates catalyze CHP decomposition. The activity of $M(EH)_2$ decreases in the following order:

$$Mg(EH)_2>Ca(EH)_2>Cd(EH)_2>Zn(EH)_2>Hg(EH)_2.$$

The main products of CHP decomposition in the presence of any catalyst are dimethylphenylcarbinol (DMPC), acetophenone (AP), α-methylstyrene (α-MS), methanol, phenol, and acids.

The formal kinetic scheme of the process is

$$ROOH + M(EH)_2 \leftrightarrow [ROOH \cdot M(EH)_2], \quad (I)$$

$$[ROOH \cdot M(EH)_2] \rightarrow M(EH)_2 + \text{products}. \quad (II)$$

Using the Lineweaver–Burk method [2] we determined kinetic parameters of the overall decomposition process. The thermodynamic characteristics of complexation were calculated via the van't Hoff equation.

We discovered a correlation between the ionization potential of the metal and the rate of peroxide decomposition in the presence of $M(EH)_2$ (Table). Higher CHP decomposition rates are observed in the presence of the 2-ethylhexanoates of metals with lower ionization potentials (Mg, Ca and Cd). All parameters of the catalytic decomposition take their minimum values in the case of $Cd(EH)_2$, and it is cadmium that has the lowest ionization potential in the subgroup consisting of Zn, Cd, and Hg.

Magnesium and calcium, which differs noticeably in atomic and ionic sizes from the Subgroup IIB metals, has more pronounced metallic properties. Covalent bonds are less typical for magnesium and calcium than for zinc or mercury; like cadmium, magnesium and calcium more readily forms ionic bonds.

There is a large contribution from covalent bonding in the Zn and Hg complexes, and these

complexes are less active than the Cd, Ca and Mg complexes, in which the coordination bond is more ionic. This finding suggests that the higher the ionicity of the bond, the higher the activity of the catalyst. Accordingly, the purely ionic magnesium complexes should be much more active than the zinc-subgroup metal complexes. However, the zinc subgroup metal complexes also display high catalytic activity, which is obviously due to the additional polarization effect. This effect is favorable for the formation of covalent bonds in the mercury and zinc complexes and, to a lesser extent, in the cadmium complex.

Table. Overview of the properties of elements II Group of the Periodic System

Element	**Atomic weight**	**Electronic configuration**	**Ion radius M^{2+}, нм**	**Standard electrode potential $E^0_{Э^{2+}/Э^0}$, V**	**Ionization potential, eV**	
					IP_1 $M^0 \rightarrow M^+$	**IP_2 $M^+ \rightarrow M^{2+}$**
Mg	24.30	$3s^2$	0.066	-2.37	7.64	14.51
Ca	40.08	$4s^2$	0.104	-2.87	6.11	11.87
Zn	65.38	$3d^{10}4s^2$	0.083	-0.763	9.39	17.89
Cd	112.40	$4d^{10}5s^2$	0.103	-0.403	8.99	16.84
Hg	200.59	$4f^{14}5d^{10}6s^2$	0.112	+0.850	10.43	18.65

4 Conclusions

Therefore, the catalytic properties of the Subgroup IIB carboxylates depend mainly on the nature of the interaction force in the formation of the ROOH–$M(EH)_2$ intermediate. For the compounds of cadmium, calcium and magnesium, which belong to the main subgroup, the bond in the intermediate is primarily determined by electrostatic factors. In the case of zinc and mercury a significant role in the intermediate is played by covalent bonding.

Acknowledgements

This research was supported by the Ministry of Education and Science of Russian Federation as part of the state contract (“PNIL 02.14”, base part).

References

[1] N. Nurullina, N. Batyrshin, Kh. Kharlampidi, *Kinetics and Calal*ysis. V. 48, № *5* (2007). P. 695–700.
[2]. I. Berezin, K. Martinec. *Basic physical chemistry of enzymatic catalysis.* M.: High School, 1977. 280 p.

IV-PP99

Selective Hydrogenation of Furfural Using SiO_2 Based Catalysts: Impact of Reaction Conditions and Metals Employed

O'Driscoll Á[1,2,3*], Leahy J.J.[1,2,3], Curtin T[1,2,3]

1 - University of Limerick, Limerick, Ireland
2 - Materials and Surface Science Institute, University of Limerick, Limerick, Ireland
3 - Carbolea Research Group, University of Limerick, Limerick, Ireland

* aine.odriscoll@ul.ie

Keywords: biomass, hydrogenation, liquid phase, furfural, furfuryl, alcohol, silica

1 Introduction

Over the past decade there has been an increase in research utilising biomass as a start material due to the high demand and depleting stocks of fossil fuels. The production of fine chemicals is one of the many research areas to stem from this broad topic. Furfural is a functional by-product produced naturally from biomass in the biofuel industry. It has an extensive number of derivatives including furfuryl alcohol which is used extensively in the polymer and chemical manufacturing industry. Furfuryl alcohol is produced by the catalytic hydrogenation of furfural in liquid or vapour phase. Copper chromite catalysts are used for this process despite posing severe environmental threats as chromium is toxic to many aquatic organisms. The challenges associated with the disposal of this catalyst have created a significant research emphasis on attaining a suitable alternative. Literature has shown the use of chromium free catalysts can be used to produce furfuryl alcohol however they have proved unsuitable for industrial application due to high production costs and catalyst deactivation. The aim of this research is to produce an inexpensive catalyst suitable for industrial use.

2 Experimental/methodology

Eight precious metal catalysts were produced by wet impregnation techniques to make 1 and 2 wt% of copper, nickel, platinum or palladium supported on SiO_2. The catalysts were hydrogenated in the liquid phase under the following conditions: 100°C, 20 bar hydrogen, 1 g of catalyst, 25 ml of furfural and 175 ml solvent. A comparison was conducted between each catalyst for the conversion of furfural and the selectivity to furfuryl alcohol. Two solvents, ethanol and toluene were employed to establish the influence of solvent on the reaction. The superior catalyst was further exposed to five additional temperatures ranging from 50–170°C to investigate the influence of temperature on selectivity to furfuryl alcohol.

3 Results and discussion

From the selection of catalysts analysed 2%Pt/SiO_2 revealed the highest selectivity to furfuryl alcohol with ethanol employed as the solvent. Literature states that use of an alcohol as solvent has a positive influence on the reaction as the alcohol group acts as a hydrogen donor contributing to the conversion of furfural. The polarity of the alcohol influences the product selectivity and selection should oppose that of the reactant. Solvent testing showed the use of an alcohol as solvent had a significant influence of the production of undesirable products including difurfuryl ether and 2-furaldehyde diethyl acetal due to interactions between the alcohol and both the reactant and desired product furfuryl alcohol. Neither product was formed when toluene was employed however furfural conversion was lower. Temperature studies were conducted to establish an optimum reaction temperature in a low range with these results displayed in figure 1(a) and (b).

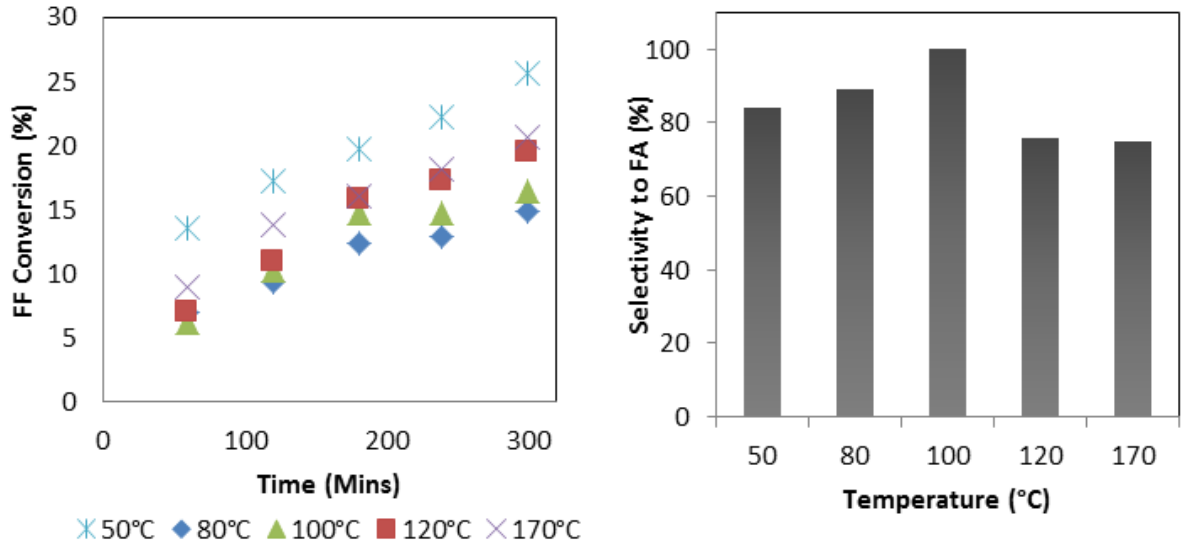

Fig. 1. shows the influence of temperature for (a) conversion of furfural using 2%Pt/SiO_2 with toluene as solvent and (b) selectivity to furfuryl alcohol at 15% conversion.

The percentage conversion of furfural increased over time for each temperature examined as seen in figure 1 (a). The selectivity to furfuryl alcohol was seen to follow a similar pattern indicating that the catalyst was still active at 300 minutes. This also indicates that there is no interaction between the solvent and the desired product which is confirmed as derived products are not formed. Figure 1 (b) shows the selectivity to furfuryl alcohol at 15% conversion where it was observed that the highest selectivity was at 100°C with higher temperatures giving lower selectivity. However, the difference observed between all temperatures is minor with a wide time range observed for the corresponding 15% conversion. This indicates that selectivity is independent of temperature and for this reaction it is dependent on conversion. The superior conversions are seen from 50°C and 170°C indicating that temperature is not a significant influence on conversion which is strongly dependent on solvent and catalyst selection.

4 Conclusions

The use of an alcohol as solvent results in interactions between the reactant and the desired product affecting the overall production of furfuryl alcohol. It was found that 2%Pt/SiO_2 hydrogenated at 100°C in toluene gave the best results for this segment of the research as there was no formation of undesired products. Further analyses of these results deemed selectivity and conversion to be independent of temperature and dependent only on solvent and catalyst selection with further work focused on the impact of bimetallic platinum based catalysts on the hydrogenation reaction.

Acknowledgements

The Earth and Natural Sciences Doctoral Studies Programme is funded by the Higher Education Authority (HEA) through the Programme for Research at Third Level Institutions, Cycle 5 (PRTLI-5) and is co-funded by the European Regional Development Fund (ERDF).

References

[1] W. Rojas, J.J. Martínez, P. Reyes, *Dyna-Colombia*, 77(163), (2010), 151-159.
[2] A. B. Merlo, V. Vetere, J.F. Ruggera, and M.L. Casella, *Catalysis Communications*, 10(13), (2009), 1665-1669.
[3] P. Panagiotopoulou, N. Martin, and D.G Vlachos, *Journal of Molecular Catalysis A: Chemical*, 392(0), (2014), 223-228.

IV-PP100

Selective Hydrogenation of 2-Methyl-3-Butyne-2-Ol Catalyzed by Embedded Polymer-Protected PdZn Nanoparticles

Okhlopkova L.B.[1*], Matus E.V.[1], Prosvirin I.P.[1], Kerzhentsev M.A.[1], Ismagilov Z.R.[1,2]

1 - Boreskov Institute of Catalysis, Novosibirsk, Russia
2 - Institute of Coal Chemistry and Material Science, Kemerovo, Russia

* mila65@catalysis.ru

Keywords: titania, polyvinylpyrrolidone, PdZn nanoparticles, selective hydrogenation, 3-methyl butynol

1 Introduction

Semi-hydrogenation of the triple bond in long-chain alcohols is of particular interest because hydrogenation products are intermediates in the synthesis of vitamins and fragrant substances. Wall coated capillary microreactors possessed distinct advantages such as improved temperature control, selectivity, and both environmental and safety issues resulting from the use of small quantities of reagents and solvents. Crystalline TiO_2 mesoporous thin films with embedded nanoparticles supported on the channel walls can be readily obtained via a template sol-gel process [1]. Bimetallic PdZn catalysts are widely used for selective hydrogenation of acetylene alcohols. In this paper we report the structure and catalytic studies of the incorporated into titania monometallic Pd and bimetallic PdZn colloid nanoparticles stabilized by PVPone (polyvinylpyrrolidone) and PVPine (polyvinylpyridine). The hydrogenation of 2-methyl-3-butyn-2-ol (MBY) was used as a probe reaction to evaluate the activity and selectivity of the samples in hydrogenation of acetylene alcohols. The results have been compared with the catalysts prepared by conventional impregnation.

2 Experimental

The PdZn bimetallic nanoparticles were synthesized by a polyol method. The amount of PdZn nanoparticles was chosen to obtain 1 wt.% Pd metal loading in TiO_2. The molar composition of the final solution was $1Ti(O\text{-}iPr)_4 : 0.009$ Pluronic F127 : $32C_2H_5OH:8C_4H_9OH : 1.3H_2O : 0.18HNO_3$. The solvent was evaporated at 293 K and relative humidity (RH) of 80%, followed by two activation procedures. The low-temperature activation included calcination at 573 K for 2 h under a residual pressure of 13 mbar with a heating rate of 1 K/min. The high-temperature activation comprised calcination in air at 673 K for 2 hours with stepwise equalizing every 100 K for 1 hour and a heating rate of 1K/min, and subsequent reduction in a 30 vol.% H_2/Ar flow at 673 K for 2 hours. The samples are noted according to their synthesis procedure: the letter denotes activation conditions. ‘‘L’’ and ‘‘H’’ stands for low-temperature and high temperature activation, respectively. For comparison we prepared samples by combined impregnation with inorganic $PdCl_2$ and $ZnCl_2$ precursors. The samples are marked in accordance with the synthesis procedure: “C” and “I” correspond to the samples obtained by embedding colloid nanoparticles and impregnation, respectively. The number at the end means the molar ratio PVP/Me. The symbol “-one” stands for polyvinylpyrrolidone and “–ine” means polyvinylpyridine. Catalysts were investigated by a few physical and chemical methods: HRTEM, XPS, AES-ICP, XRF, thermogravimetric analyses and differential thermal analyses.
Hydrogenation of 2-methyl-3-butyn-2-ol (MBY) was carried out in autoclave reactor with a total volume 130 ml at 333K and 5 bar H_2 pressure under intensive stirring at 2000 rpm. A substrate-to-palladium molar ratio was 2100. Prior to activity measurements, the samples were reduced at 523 K at a H_2 pressure of 10 bar for 2 h. Analysis of the reaction mixture was performed off-line with gas chromatograph Agilent 7890A equipped with a SKTFT-50X

capillary column (diameter: 0.22 mm, length: 30 m) and a FID detector

3 Results and discussion

Data in table 1 clearly show important differences between the impregnated and nanoparticle-based catalyst. An effect of stabilizer, PVP/Me ratio and activation conditions on catalytic properties was also given. The impregnated catalyst is less active and selective to MBE. Thus, the selectivity is about 68.3% for the impregnated $PdZn/TiO_2$ and reaches 88.9% for the nanoparticle-based catalyst. Increasing the concentration of PVPone when synthesizing the nanoparticles results in an improvement of the selectivity reaching 88.9% at a conversion of 95% at a molar ratio of PVP/PdZn 10, while activity varies slightly in the range 1.1 до 1.8 molPd/s. The activity and selectivity of the samples prepared from PdZn- PVPine is lower than those of the samples containing PdZn nanoparticles stabilized with polyvinylpyrrolidone. The samples subjected to low-temperature activation at 573 K and 13 mbar for 2 hours exhibit higher selectivity compared with the samples calcined in air at 673 K and reduced at 673 K in 30 vol.% H_2/Ar. These results can be explained by the electronic effect of the stabilizer and by the different average size and composition of the nanoparticles.

Table 1. Effect of stabilizer, PVP/Me ratio, activation conditions and preparation method on the activity at 50% conversion and selectivity at 95% conversion of the Pd/TiO_2 and $PdZn/TiO_2$ samples in hydrogenation of 2-methyl-3-butyn-2-ol.

Sample	PVP/Me, mol/mol	dn, nm	Activity, molMBY/molPd/s	Selectivity, %
Pd/TiO_2.C-5one	0	8.6	2.1	74.2
$PdZn/TiO_2$.C-L-10one	10	4.4	1.6	88.9
$PdZn/TiO_2$.C-L-5one	5	6.5	1.1	86.5
$PdZn/TiO_2$.C-L-2.5one	2.5	6.0	1.3	81.3
$PdZn/TiO_2$.C-H-2.5one	2.5	7-20	1.9	73.6
$PdZn/TiO_2$.C-L-0one	0	2.9-38	1.8	81.5
$PdZn/TiO_2$.C-L-10ine	10	2	1.0	70.2
$PdZn/TiO_2$.C-H-10ine	10	-	0.5	58.0
Pd/TiO_2.I-H	0	-	0.53	66.5
$PdZn/TiO_2$.I-H	0	2.5-56	0.41	68.3

4 Conclusions

Pd/TiO_2 and $PdZn/TiO_2$ on titania catalyst have been prepared following two methods: a traditional impregnation with inorganic salt followed by calcination and reduction and a colloidal approach in which mono- and bimetallic nanoparticles were first synthesized and subsequently embedded in support sol, dried and annealed in vacuum at 573 K. Nanoparticle-based bimetallic catalysts have shown higher activity and selectivity compared to impregnated PdZn catalysts when applied in selective hydrogenation of 2-methyl-3-butyn-2-ol. The main factor determining the high selectivity of samples is the use of polyvinylpyrrolidone as a stabilizer. In this respect, the kind and amount of the stabilizer, conditions of catalyst activation are key factors in the synthesis of the catalysts. Other important parameters are average size and composition of the particles. Bimetallic catalysts with average particle size of 4.4 nm and narrow particle size distribution was the most active and selective.

Acknowledgements

Authors are grateful to the Dr. Yu. V. Patrushev for a gas-chromatographic analysis, Dr. E.Yu. Gerasimov for investigation of the catalysts by TEM

References

[1] L. Protasova, E. Rebrov, T. Glazneva, A. Berenguer-Murcia, Z. Ismagilov, J. Schouten, *J. Catal.* 271 (2010) 161

IV-PP101

Capillary Microreactor with PdZn(Ti,Ce)O_2 Coating for Selective Hydrogenation of 2-Methyl-3-Butyne-2-Ol

Okhlopkova L.B.[1*], Kerzhentsev M.A.[1], Ismagilov Z.R.[1,2]

1 - Boreskov Institute of Catalysis SB RAS, Novosibirsk, Russia
2 - Institute of Coal Chemistry and Material Science, Kemerovo, Russia

* mila65@catalysis.ru

Keywords: capillary microreactor, Ce-doped titania, PdZn nanoparticles, selective hydrogenation

1 Introduction

Fused silica capillary to act as a microreactor for multiphase reactions has been recognized for the last decade. The application of this system in fine chemical synthesis is aimed to avoid mass- and heat-transport limitations and improve selectivity for a series of sequential reactions. The synthesis of fragrance and vitamins involves semi-hydrogentaion of alkyne alcohol as a crucial step. Thin films with embedded nanoparticles obtained via a sol-gel process using a template-based precursor solution have been developed as catalysts for selective hydrogenation. Recently the use of Ce-doped catalytic coatings has been highlighted to improve the stability of the mesoporous titania matrix [1]. Here we present the use of microcapillary reactor with Ce-doped titania films holding Pd or $Pd_{80}Zn_{20}$ nanoparticles for 2-methyl-3-butyne-2-ol(MBY) hydrogenation. The results are compared with the hydrogenation over Pd/(Ti, Ce)O_2 powder catalyst in a batch reactor at a hydrogen pressure 5 bar.

2 Experimental

The coatings and powders were prepared using a template sol–gel method. The molar ratio between the reagents in the resulting sol was 1 $Ti(O–iPr)_4$:0.05 $Ce(NO_3)_3{\cdot}6H_2O$: 0.009 Pluronic F 127 : 40 C_2H_5OH : 1.3 H_2O : 0.13HNO_3. The ethanol suspension of colloidal nanoparticles was added to the sol. The resulting sol was dip coated on the internal surface of fused silica capillary with an internal diameter of 250 μm and a length of 10 m. The gas (H_2/He) and liquid (0.05-0.3 M solution of 2-methyl-3-butene-2-ol in methanol) were mixed in a T-mixer. The capillary was annealed at 573 K for 2 h under a residual pressure of 13 mbar and in situ reduced at 573 K at hydrogen flow for 1 hour.

Pd/(Ti,Ce)O_2 powder was first annealed at 573 K for 2 h and placed in an autoclave reactor with a total volume 130 ml, then reduced in situ at 523 K at a H_2 pressure of 13 bar for 2 h. Hydrogenation of 2-methyl-3-butyn-2-ol (MBY) was carried out at 333 K and 5 bar H_2 pressure under intensive stirring at 2000 rpm. Analysis of the reaction mixture was performed off-line with gas chromatograph Agilent 7890A equipped with a SKTFT-50X capillary column (diameter: 0.22 mm, length: 30 m) and a FID detector.

3 Results and discussion

Figure 1 shows the selectivity to 2-methyl-3-butene-2-ol (MBE) at different conversion of 2-methyl-3-butyne-2-ol (MBY) on Pd/(Ti,Ce)O_2 powder in batch reactor and Pd/(Ti,Ce)O_2 coating on inner surface of capillary microreactor. The selectivity to alkene alcohol is higher than that observed in the batch reactor, where there is no need for a catalyst separation step.

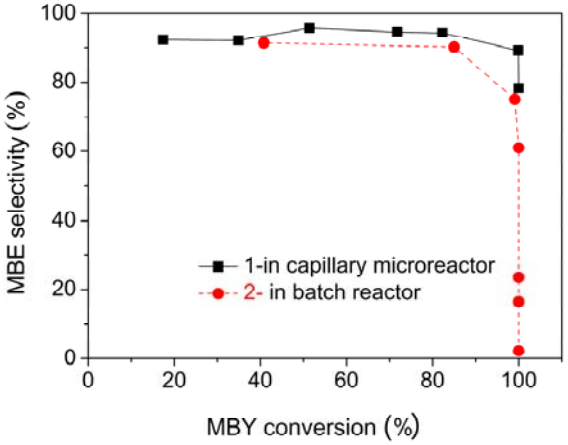

Fig. 1. Selectivity to MBE as a function of MBY conversion over Pd/(Ti, Ce)O_2 in capillary microreactor (1) and (2) batch reactor.

The effect of the liquid residence time, the presence of Zn and the hydrogen partial pressure was studied by comparing the Pd/(Ti, Ce)O_2 and $Pd_{80}Zn_{20}$/(Ti,Ce)O_2 coatings. An addition of Zn improves the selectivity to 2-methyl-3-butene-2-ol at high conversion of 2-methyl-3-butyne-2-ol (Figure 2). The selectivity was further improved towards 94 % at 99.8% over $Pd_{80}Zn_{20}$/(Ti,Ce)O_2 coating by decreasing hydrogen partial pressure to 0.5.

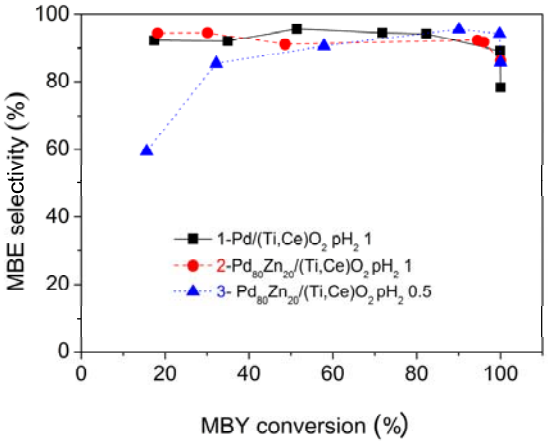

Fig. 2. Selectivity to MBE as a function of MBY conversion in capillary microreactor over (1) Pd/(Ti, Ce)O_2 H_2 partial pressure 1, (2) $Pd_{80}Zn_{20}$/(Ti,Ce)O_2 H_2 partial pressure 1 and (2) $Pd_{80}Zn_{20}$/(Ti,Ce)O_2 pH_2 0.5. Hydrogen flow rate 2 ml/min (STP). Temperature: 323 K

4 Conclusions

Capillary microreactors coated with Ce-doped titania containing embedded Pd or $Pd_{80}Zn_{20}$ nanoparticles were tested in the 2-methyl-3-butyne-2-ol hydrogenation. The Pd/(Ti,Ce)O_2 catalyst showed an order of magnitude higher activity compared to commercial catalyst and demonstrated an increased selectivity to 2-methyl-3-buten-2-ol of 89% at 99.9% conversion compared with batch reactor. The highest selectivity to semihydrogenated product of 94 % at 99.8% was obtained over $Pd_{80}Zn_{20}$/(Ti,Ce)O_2 coating at 323K and hydrogen partial pressure of 0.5.

References

[1] L.B. Okhlopkova, M.A. Kerzhentsev, Z.R. Ismagilov, *Surf. Eng.* 31 (2015) 78

IV-PP102

New Catalysts for Lignin Depolymerisation

Opris C.M.*, Tudorache M., Parvulescu V.I.

University of Bucharest, Faculty of Chemistry, Department of Organic Chemistry, Biochemistry and Catalysis, Bucharest, Romania

* cristina_opris88@yahoo.com

Keywords: lignin depolymerisation, catalyst, niobia, cobalt, magnetite

1 Introduction

The depletion of the oil resources and the increase of the demand of oxygenated chemicals require new strategies for development. The use of renewable materials is one of alternatives. Despite their complex structure, lignin is usually seen as a waste product of the pulping process and a low value material [1]. By using an adapted conversion technology [2] it can be converted providing an important source for the production of phenolic compounds [3]. However, the variety of linkages between units and trends to forming condensed structures induces difficulties in catalytic processing of lignin [4]. The scope of this study is to present a catalytic alternative depolymerisation for the lignin by using bifunctional catalysts. It describes prepared stable catalysts stable under depolymerisation reaction conditions, able to improve the accessibility and activity of the metal sites as well as the minimisation of repolymerisation and related side reactions [5].

2 Experimental/methodology

Multicomponent separable magnetic heterogeneous catalysts were prepared by successive covery of magnetite by niobia and cobalt-nanoparticles. Magnetite core nanoparticles were prepared by co-precipitation method, using $Fe(NO_3)_3.xH_2O$ and $FeCl_2.4H_2O$ as as Fe^{3+} and Fe^{2+} sources. Niobia prepared by microemulsion method using an ammonium oxalate complex of niobium as precursor and hexadecyltrimethylammonium bromide as surfactant were deposed on these nanoparticles. Finally cobalt, in varied concentrations, was supported onto the Nb_2O_5/magnetite composite using the precipitation-deposition method by using cobalt acetate as cobalt source. Before catalytic tests the sample were calcinated and reduced in presence of hydrogen.

Synthesized catalysts (Nb_2O_5, Nb_2O_5-Fe_3O_4, x%Co-Nb_2O_5-Fe_3O_4 (x=1,2,3,4,5,10,20) were characterized by thermal analysis, powder X-ray diffraction, Raman spectroscopy, XPS, FTIR and DRIFT spectroscopy, BET analysis. Lignin depolymerization was carried out in autoclave, starting from lignin as a raw material in water or ethanol as solvents.

The identification and quantification of the fragments resulted from the lignin depolymerization were performed in both liquid and solid phase. The two phases obtained after reaction were separed by centrifugation and liquid phase was analised by HPLC. The fragment of lignin from solid phase was extracted with tetrahydrofurane and analysed by GPC. The solid reziduu remained after extraction was acetylated with pyridine and acetic anhydride and then analysed by GPC.

Table 600. **Results and discussion**

The immer erization techniques it offered a picture of the catalysts synthesized. Fig.1 depicts comparative XRD patterns of Co-Nb_2O_5-Fe_3O_4 catalysts and of their intermediates. These demonstrate that: i) the magnetic core remained unaffected by the next deposition steps, ii) niobia exists on amorphous layer, iii) cobalt, after reduction with hydrogen is present in cubic phase.

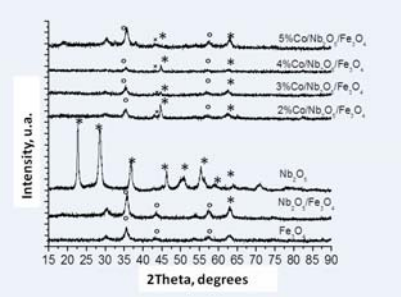

Fig.1. XRD pattern for synthesized catalysts (×=Cubic cobalt, card 00-042-1467, °=niobia, card 00-028-0317, *= magnetite, card 00-019-0629)

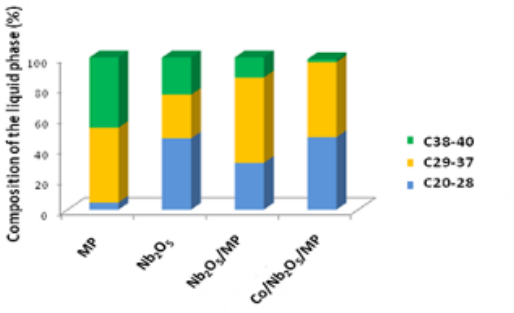

Fig.2. Composition of the liquid phase after lignin depolymerisation

The other immer erization techniques provided additional information about the oxidation state of the elements, size of the particles and dispersion. The performances of the catalytic tests were evaluated taking into account the lignin fragment distribution between liquid and solid phase of the reacted mixture. Fig.2. shows the composition of the liquid phase building block entities resulted after lignin depolymerisation. Lignin fragments found in the liquid phase (HPLC-DAD/MS analysis) were distributed in three different groups according to the fragments molecular weight, as it is shown in Table 1. These average molecular mass fragments correspond to immer, trimer and tetramer.

Table 1. Molecular fragments identified using the HPLC-MS/MS analysis of the lignin defragmentation products

Fragment group	MW range	Dominant MW
C_{20-28}	200-400	388; 361
C_{29-C37}	400-600	558
C_{38-40}	600-850	737; 744

The conversion of lignin on prepared catalysts varied from 15% for Fe_3O_4 to 53% for $Co/Nb_2O_5/Fe_3O_4$. The capability of niobia to catalyze the acidic hydrolysis of the β-O-4' bounds coupled to the affinity of the Co for assisting the breaking of the C-C bonds *via* hydrogenolysis lead to different dominant molecular fragment.

4 Conclusions

This study demonstrates that is possible to depolymerise lignin and to produce a cocktail of oxygenated compounds corresponding to dimer, trimer and tetramer building block entities of lignin.

Acknowledgements

This work was supported by the strategic grant POSDRU/159/1.5/S/137750.

References

[1] S. H. Ghaffar, M. Fan, *Biomass and Bioenergy*, 57 (2013) 264-279.
[2] Y.C. Lin, G.W. Huber, *Energy Environmental Science*, 2 (2009) 68-80.
[3] Wahyudiono, M.Sasaki, M. Goto, *Fuel*, 88 (2009) 1656–1664.
[4] P. Azadi, O. R. Indewildi R. Farnood, D.A. King, *Renewable and Sustainable Energy Reviews*, 21 (2013) 506-523.
[5] A. Toledano, L. Serrano, A. Pineda, A. A. Romero, R, Luque, J. Labidi, *Applied Catalysis B: Environmental*, 145 (2014) 43-55.

IV-PP103

Deactivation of Mixed Oxides as Catalysts for Ethanol Condensation: *in situ* DRIFT Spectroscopy Studies

Quesada J., Faba L., Diaz E., Ordonez S.*

University of Oviedo, Oviedo, Spain

* sordonez@uniovi.es

Keywords: catalyst deactivation, bioethanol, Guerbet reaction, basic mixed oxides, DRIFT spectroscopy

1 Introduction

Ethanol is nowadays considered as one of the most promising bio-platform molecules, being obtained by fermentation of different biomass feedstock [1]. Its high value is due not only to its good properties as biofuel but also to its potential as building block for the added-value chemical productions. The bioethanol upgrading implies the increase of its carbon chain length, usually by the Guerbet reaction of two short-chain alcohols coupling. This reaction is a key of interest in the last years, with several studies about catalytic activity and reaction mechanisms. The most accepted reaction pathway includes different steps catalyzed by different active sites, so catalytic properties have an important role in tuning the reaction to one of other products, in such a way that highest selectivities of 1-butanol are obtained with a good basicity/acidity equilibrium [2] whereas 1,3-butadiene is favored by strong basic materials [3].

Despite of the efforts devoted to identify the optimum catalyst, there are not deep studies about the stability of these materials, being these studies needed for scaling-up this process. A deep deactivation study implies the analysis not only of the evolution of reactant conversion and intermediates and products selectivities in gas phase, but also a study of possible changes in the morphological and structural catalytic properties by analyzing of the catalytic surface (with techniques as DRIFT spectroscopy). A complete study of Mg-Zr and Mg-Al stability in the ethanol condensation is presented in this work, justifying the conversion and selectivities evolutions by surface changes observed by DRIFT spectroscopy and different characterization techniques.

2 Experimental/methodology

Reactions were carried out in a 0.4 cm i.d. U-shaped fixed bed quartz reactor in which 0.02L/min (s.t.p.) of helium-ethanol mixture (1.5mL/min of ethanol) was fed. 150 mg of catalyst were used in each run. Reactor outgoing gases were on-line analysed by gas chromatography using a HP6890 GC with a FID detector. Spent catalysts were collected at 1, 2, 4, 6 and 8 h time on stream and characterized by different techniques, such as nitrogen physisorption and TPD.
Reactions at similar conditions were performed in a DRIFTS chamber (in a Nicolet Magma IRTF Spectrometer, using a ZnS window) in order to follow the evolution of the characteristic peaks of adsorbed reactants and products during the reaction. Kubelka-Munk method was used to analyse these results.

3 Results and discussion

Activity studies confirm the key role of catalytic properties in the ethanol gas-phase condensation. **Table 1** summarizes the main results obtained at different temperatures with Mg-Zr and Mg-Al catalysts. At medium temperatures, higher conversions are obtained with MgAl, whereas the conversion at 723 K is 40 % higher with MgZr (increase directly relate to a high ethylene production). MgAl is much more selective to the main route. The highest selectivity to 1-butanol is reached with MgAl at low temperatures, whereas the maximum of 1,3-butadiene is obtained with MgZr at 723 K. These results show the high influence of basicity to enhance the

condensation, since MgZr is more basic (1.71 μmol CO_2/m^2) than MgAl (1.01 μmol CO_2/m^2) and the selectivity to 1,3-butadiene is higher with this material, and the role of acidity in the other steps of the process (the acidity of MgAl is stronger than the acidity of MgZr, justifying the higher selectivity of 1-butanol).

Table 1: Summary of the results of catalytic activity at 523 / 623 / 723 K

	Conv. (%)	Ethylene (%)	Acetaldehyde (%)	1,3-butadiene (%)	1-butanol (%)
Mg-Zr	7.5 / 9.1 / 53.7	0 / 28.1 / 57.8	91.7 / 62.2 / 16.2	0 / 0 / 18.7	8.3 / 5.0 / 6.2
Mg-Al	15.1 / 17.4 / 38.3	1.3 / 7.1 / 16.5	81.3 / 80.8 / 65.8	0 / 0 / 0.5	15.5 / 7.0 / 11.1

Deactivation studies demonstrate a high influence of reaction temperature in the catalytic stability of both materials. Thus, there is not a relevant decrease neither in the ethanol conversion not in the product selectivities at temperatures lower than 700 K (decreases lower than 5% in 8 h), whereas an important decrease in the ethanol conversion is observed at 723 K, from 54 to 23% in 8 h time-on-stream in the case of MgZr and from 40 to 25% with MgAl. DRIFT spectroscopic studies demonstrate the existence of two different deactivation causes. In the case of MgZr, (**Fig. 1** shows the spectra evolution at 723 K, as example), bands related to ethoxide adsorption (deprotonated ethanol coordinated with a Mg surface atom) keep almost constant with time, so active sites that promote the first step do not suffer any modification, whereas signals of butoxide adsorption disappears after 6 hours. Bands of acetaldehyde and butanal adsorptions increase their intensity, as consequence of a stronger adsorption, but the loss of activity is proportional to the intensity of a new signal at 1536 cm^{-1}, related to the strong adsorption of molecules containing C=C. Considering the high selectivity of this side-product obtained with MgZr and the possible oligomerization of this compound, this fact is proposed as the main cause of deactivation. On the other hand, spectra of MgAl samples indicate a higher influence of other products adsorbed on stronger acid sites. These hypothesis were corroborated by results obtained in the characterization of spent catalysts.

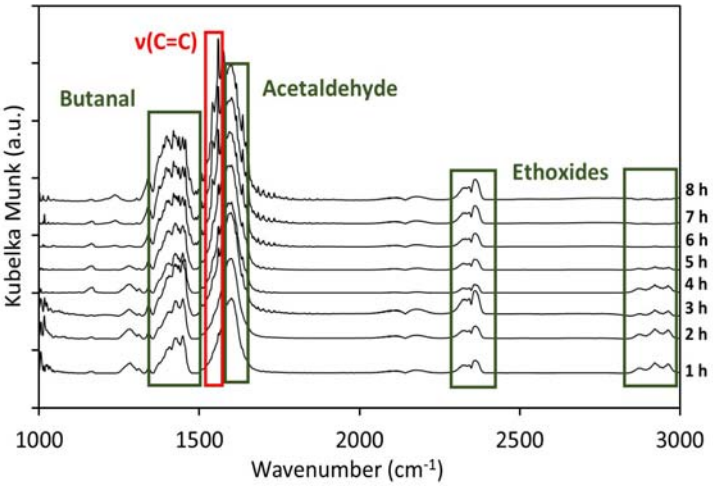

Fig. 1. Evolution of DRIFT results in the ethanol condensation at 723 K with MgZr

4 Conclusions

The higher acidity/basicity ratio was identified as the key catalytic property that justifies the activity of mixed oxides in ethanol condensation. According to DRIFT studies, olefin polymerization and adsorption of side-products were proposed as main deactivation causes.

Acknowledgements

This work was supported by the Spanish Government (contract CTQ2011-29272-C04-02). J. Quesada thanks the Government of the Principality of Asturias for a Ph. D. fellowship (Severo Ochoa Program).

References

[1] C. Angelici, B. Weckhuysen, P. C. A. Bruijnincx, *ChemSusChem* 6 (2013) 1595
[2] M. León, E. Díaz, S. Ordóñez, *Catal. Today* 164 (2011) 436
[3] J. T. Kozlowski, R. J. Davis, *ACS Catal.* 3 (2013) 1588

IV-PP104

Modification of Skeletal Nickel Surface on Effects of Hydrogenation for Adsorption Behavior of p–Nitrotoluene

Osadchaya T.*, Afineevskiy A., Prozorov D., Lukin M.

Ivanovo State University of Chemistry and Technology, Research Institute for Thermodynamics and Kinetics of Chemical Processes, Dep. of Physical and Colloid Chemistry, Ivanovo, Russia

* osadchayatyu@gmail.com

Keywords: liquid-phase hydrogenation, p-nitrotoluene, modifying skeletal nickel, catalyst, FTIR

1 Introduction

High-performance eco-friendly liquid phase hydrogenation technologies provide a high yield and quality of final products, raw materials and energy savings, can eliminate or substantially reduce the anthropogenic influence of existing production at the regional ecological environment due to a sharp decline in toxic gas emissions, waste water and solid waste. Hence, the problem of expanding the applications of catalytic technologies formulated industrial section of the European Association of Societies of catalytic EFCATS is a priority [1].

Skeletal nickel and supported palladium catalysts are the most widely used in laboratory practices and technologies, the liquid-phase hydrogenation of various classes of organic compounds [2].

Hydrogenation reaction of 4-nitrotoluene was selected as the most simple example of a large number of processes reduction of compounds containing nitro group and various substituents. 4-aminotoluene - complete hydrogenation product of 4-nitrotoluene - is a raw material for production of various fine chemicals, in particular, various grades of disperse dyes [3].

The purpose of this work is to investigation of the effect of surface modifiers of skeletal nickel on its activity in the liquid-phase hydrogenation of *p*-nitrotoluene.

The sodium sulfide was chosen as a modifier because due to the ability to block the active sites of skeletal Nickel catalyst [4, 5]. This property of modifying agents will affect the specific binding energy distribution.

2 Experimental/methodology

Skeletal Nickel catalyst was obtained by sodium hydroxide treatment of the Nickel-aluminum alloy according to the standard method [6]. Catalyst particle size was 4.8 μm. Active catalyst had a specific surface area: 90±2 m^2/g, porosity: 0.5±0.05.

The hydrogenation was carried out by static method in the closed system with intensive stirring liquid phase. All the experiments were carried out in a batch laboratory scale stirred tank reactor with stirring frequency of the reaction mixture about 3600 rpm, atmospheric pressure of hydrogen and temperature of the liquid phase being 303K. The aqueous solutions of 2-propanol with molar fractions of alcohol x_2= 0.073; 0.191; 0.68 were used.

Modification of the surface was carried out according to [4] by sodium sulfide.

Physicochemical analysis of quantitative and qualitative composition of reaction samples was performed by liquid chromatography (“Shimadzu LC-6A”). *p*-nitrotoluene adsorption behavior have been examined by means of in-situ FTIR spectroscopy (Avatar 360 FT-IR ESP, USA).

3 Results and discussion

Figure 1 shows the kinetic curves of *p*-nitrotoluene hydrogenation on sodium sulfide pretreatment catalyst. Sodium sulfide pretreatment generally leads to decreasing catalytic

activity [4]. However, the activity of the catalyst was increased almost in 1.5 times at low concentrations of sodium sulfide and reaches the maximum in 52 cm^3 (H_2)/ (s ·kg (Ni)) for 0.05 mmol Na_2S/g (Ni). This fact is possible to explain by the formation of new active centers of surface or by shifting the surface balance between individual adsorption forms of hydrogen toward the most active one in the investigated process [5]. In this case, the hydrogen and 4-nitrotoluene are adsorbed on the different active centers, "metallic" and "organometallic" respectively. α-form molecular hydrogen, H_2 or $H_2^{\delta+}$ associated with one or two surface atoms, γ-form - unionized form atomic hydrogen H or $H^{\delta+}$ with binding energy less than β-form but higher than the α-form are associated with the nickel surface [7].

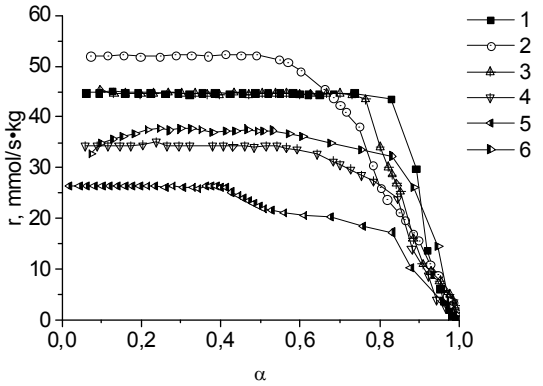

Fig. 1. Kinetic curves of *p*-nitrotoluene hydrogenation in the solvent 2-propanol-water (x_2=0.073): T=303K, $n_{p\text{-nt}}$=4.4·10-mol/gNi, m_{kat}=0.5 g, modified with sodium sulfide; 1 – 0.025 mmol Na_2S/g Ni; 2 – 0.05 mmol Na_2S/g Ni; 3 – 0.2 mmol Na_2S/g Ni; 4 – 0.6 mmol Na_2S/g Ni; 5 – 1 mmol Na_2S/g Ni; 6 - without sodium sulfide additive

4 Conclusions

We studied the kinetics of *p*-nitrotoluene hydrogenation on skeletal and modified skeletal Nickel catalyst in aqueous solutions of 2-propanol and find out that some condition can turn the effect of poison catalyst into promoter. This fact is possible to explain by the formation of new active centers of surface or by shifting the surface balance between individual adsorption forms of hydrogen toward the most active one in the investigated process. This enhance of the catalyst stability is explained by elimination of the most unstable-working surface active centers of the reaction space and by the stabilization of the remaining ones.

Acknowledgements

We thank Department of Safeguards, Vienna International Centre for funding.

The work carried out as part of the Ministry of Education and Science of the Russian Federation state task (project № 1800)

References

[1] 22nd North American Meeting of the Catalysis Society: Detroit, June 2011.
[2] K. Min, J. Choi, Y.Chung, W. Ahn, R. Ryoo, P. Lim, Appl. Catal. A: Gen. 337 (2008) 97.
[3] R. Bruckner, Organic Mechanisms. (2010) 883.
[4] M. Lukin, D. Prozorov, M. Ulitin, U. Wdovin, Kinet. Catal. 54 4 (2013) 434 (in Russian).
[5] M. Lukin, A. Afineevskiy, J. Physicochem. 49 4 (2013) 451(in Russian).
[6] M. Ulitin, A. Barbov, V. Shalyuhin, V. Gostikin, J. Appl. Chem. 66 3 (1993) 497 (in Russian).
[7] M. Susik, I. Arsent'eva, M. Ristic, J. Serb. Chem. Soc. 54 9-10 (1989) 473.

IV-PP105

Fischer-Tropsch Synthesis over the Multicomponent Fe-Based Catalysts Modified with Additives of Rare Earth Metals

Ospanova A.Z.[1], Yemelyanova V.S.[2], Itkulova S.S.[1*], Abdullin A.M.[1], Nurmakanov Y.Y.[1], Imankulova S.A.[1]

1 - D.V. Sokolsky Institute of Organic Catalysis and Electrochemistry, Almaty, Kazakhstan
2 - Research Institute of New Chemical Technologies and Materials, Almaty, Kazakhstan

- altynai_17_91@mail.ru

Keywords: Fischer-Tropsch synthesis, Fe-based catalyst, syngas, rare earth metal

1 Introduction

The case for investing in alternative fuel-production technology to reduce dependence on crude oil has become increasingly compelling due to the uncertainty in oil prices combined with diminishing oil reserves. The Fischer–Tropsch synthesis (FTS) is an area that is receiving revived interest worldwide as an alternative technology to produce transportation fuels as well as chemicals from syngas [1].

Several group VIII metals such as iron, cobalt, nickel, and ruthenium are known to be active components of the FTS catalysts. Among the catalysts containing such active metals, iron-based catalysts have considerable merits, particularly when the FTS is performed with hydrogen-deficient syngas (H2/CO), due to their potential activity for a water–gas shift (WGS) reaction as well as their high activity and low cost [2–4]. Compared to other metal catalysts for FTS, an iron-based catalyst is distinguished by higher conversion, selectivity to the lower olefins, and flexibility to the process parameters. However, the use of iron catalyst does not solve the problem of insufficient selectivity, which represents a general limitation of FTS [5-7].

We have studied the Fe-containing catalysis promoted by the transition metals (M1 and M2), modified by additives of the rare earth metals VIII Group metals and supported on alumina in the Fischer-Tropsch synthesis. The FTS performance of catalysts was tested in a fixed-bed reactor and correlated with the characterization results.

2 Experimental/methodology

The Fe-containing catalysts were prepared by the impregnating alumina with appropriate compounds. Total metal content was 19 wt.%. The content of Ce or La was equal to 5 wt.%.

The Fe-based catalysts were tested in the Fischer-Tropsh synthesis. For hydrogenation of carbon monoxide the syngas with a ratio of H2/CO=2 was used. The process was carried out in a stainless steel reactor under pressure varied from 0.5 to 1.5 MPa, temperature region of 250-340ºC, and gas hourly space velocity (GHSV) of 1000-4000 h-1 with using 6 mL of the catalyst.

The physico-chemical properties of the catalyst were studied by BET, TEM, X-Ray and TPR-methods.

The initial and final reaction gaseous products were on-line analysed. The liquid hydrocarbons and aqueous fractions were analysed after their collection and separation.

3 Results and discussion

The effect of temperature on the process of hydrogenation of carbon monoxide over the 14% (Fe-M1-M2)-5% La/Al2O3 and 14% (Fe-M1-M2)-5%Ce/Al2O3 catalysts at H2/CO=2, P=1.0 MPa, and GHSV=1500 h-1 is presented in Fig.1a and Fig.1b respectively. With an increase in temperature from 270 to 340ºC, the CO conversion increases from 54.0 to 72.7% and

34.8 to 73.8 % respectively.

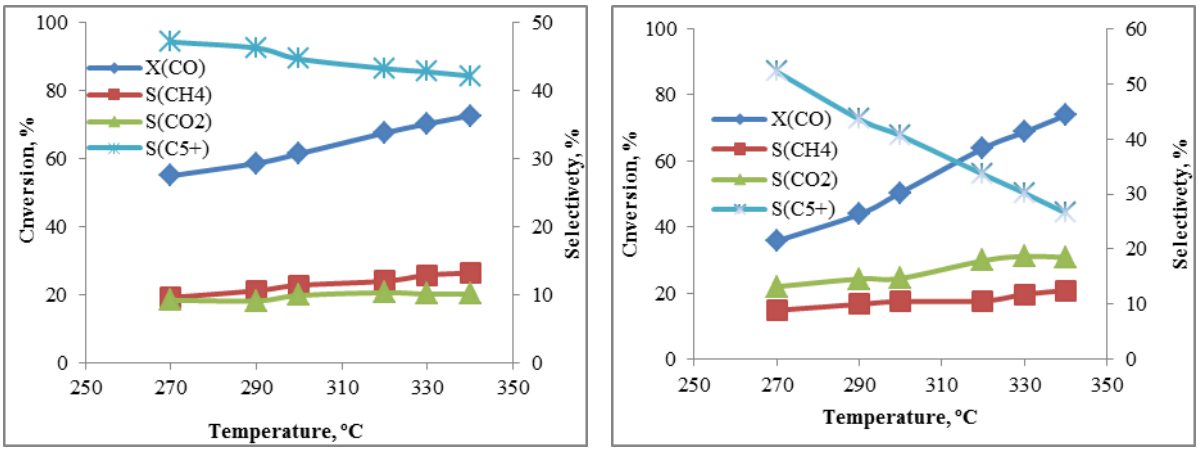

Fig. 1. Effect of temperature on the conversion of CO and selectivity by products over (a) 14% (Fe-M1-M2) -5% La/Al2O3, and (b) 14% (Fe-M1-M2)-5%Ce/ Al2O3 catalysts at H2 /CO = 2.0, P = 1.0 MPa, and GHSV = 1500 h-1

The liquefied hydrocarbons (C5+) are the main reaction products over both catalysts. The nature of rare earth metal has an effect on selectivity of Fe-based catalysts. Higher production of C5+ and methane is produced over the catalyst modified with La, while Ce additive causes the decrease in yield of C5+ fraction and length of hydrocarbon chain and promotes the carbon dioxide formation.

By TEM it has been shown that the catalysts are very dispersive. The particle size is less than 2 nm.

4 Conclusions

The results obtained show that the synthesized nano-sized iron-based catalysts have the high activity and selectivity on C5+ fraction in the FTS. They are active in the formation of narrow hydrocarbon fractions. Lanthanum -containing catalyst is an effective catalyst for the production of gasoline and kerosene fraction.

Acknowledgements

The authors wish to thank the Research Institute of New Chemical Technologies and Materials, Almaty, Kazakhstan for sponsoring this research and the Laboratory of Physicochemical Studies of Catalysts of the IOCE for providing the catalyst characteristics studies.

References

[1] M. Masukua, W. Ma, D. Hildebrandt, D. Glasser, B. Davis, Fluid Phase Equilibria. 314(2012) 38.
[2] D. H. Chun, J. C. Park, S.Y. Hong, J. T. Lim, C. S. Kim, H. Lee, J. Yang, S. Hong, H. Jung, Journal of Catalysis. 317 (2014) 135-143.
[3] M. Dry, Catal. Today 6. (1990) 183-210
[4] M. Dry, Encyclopedia of Catalysis. 3(2003) 347-403.
[5] M. Feyzi, M. Irandoust, A. A. Mirzaei, Fuel Processing Technology. 90 (2011) 1136-1143.
[6] S. Itkulova, G. Zakumbaeva, R. Arzumanova, V. Ovchinnikov, Studies In Surface Science And Catalysis. (2207) 75-85.
[7] M. Qing, Y. Yang, B. Wu, J. Xu, C. Zhang, P. Gao, Y. Li, Journal of Catalysis. 279 (2011) 111-122.

IV-PP106

Selective Oxidation of Toluene Using Noble Metals under Mild Condition

Peneau V.[1*], He Q.[2], Shaw G.[1], Kiely Ch. J.[2], Hutchings Gr. J.[1], Nowicka E.[1]

1 - Cardiff Catalysis Institute, School of Chemistry, Cardiff, UK
2 - Department of Material Science and Engineering, Lehigh University, Lehigh, US

* peneauv@cardiff.ac.uk

Keywords: Toluene, C-H bond activation, noble metals, benzoic acid

1 Introduction

The selective oxidation of hydrocarbons under mild conditions remains a challenging topic in the field of catalysis. Various studies have been reported concerning the oxidation of hydrocarbons, such as linear alkanes and aromatic compounds, using noble metals nanoparticles. The aim of this study is to investigate the selective oxidation of toluene using tertiary butyl hydroperoxide at 80 °C with supported noble metal nanoparticle catalysts prepared by sol-immobilisation techniques.

2 Experimental/methodology

Catalysts were prepared by Sol-immobilisation which involves the preparation of colloidal nanoparticles stabilised by PVA and reduced by NaBH4. Noble metal (Gold, Platinum and Palladium) colloids were used to form monometallic, bimetallic and trimetallic nanoparticles which were supported on activated carbon and TiO_2 with the catalysts having a total metal loading of 1wt%.

These catalysts have been tested for toluene oxidation with TBHP at 80 ºC, under atmospheric pressure in a first set of experiments followed by experiments using 10 bar pressure. Gas and liquid phase products were analysed and quantified by GC.

3 Results and discussion

Characterisation of the catalysts was carried out by STEM and XPS to confirm the core-shell and alloy structures of the particles. STEM analysis showed that the catalyst had a particle size distribution between 1 and 6 nm with a mean value of 2.3 nm (Figure 1), as well as the particle morphology. XPS confirmed the formation of the core shell. The order of addition of the metals into the preparation determined the morphology of the nanoparticles with sequential addition forming core shell structures and co-addition forming homogeneous alloy nanoparticles. [1]

All catalysts are selective to benzoic acid however for low conversion we observe benzaldehyde-dimethylacetal and methyl benzoate as reaction products. The highest activities were observed for catalyst containing Au. Time online reactions show that the addition of Pd and Pt has a promoting effect and the trimetallic alloy AuPdPt/ C catalyst shows the best activity.

Further experiments have been run using AuPdPt/ C catalyst; reuse tests and catalyst

characterisation after reaction reveal the contamination of the catalyst.

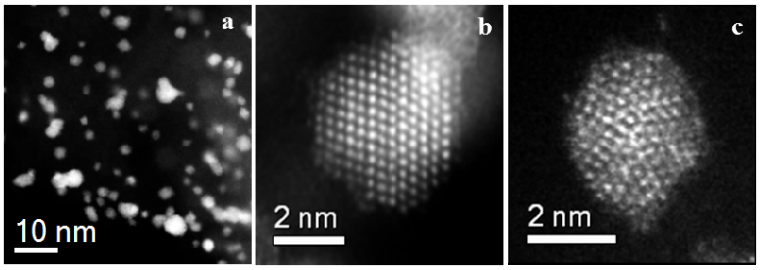

Fig. 1. Scanning transmission electron microscopy Electron microscopy analysis of the Au–Pt/C catalyst made by simultaneous sol-immobilisation. (a) A low magnification STEM-HAADF image; (b, c) higher magnification STEM-HAADF images.

4 Conclusions

Set of Au, Pd and Pt catalyst have shown their activity to oxidise toluene in presence of TBHP as initiator. Trimetallic catalyst supported on carbon shows promising results towards benzoic acid. Further experiments using O_2 as oxidant will be run in order to investigate to possibility of activated O_2.

Acknowledgements

We thank the EPSRC and Cardiff University for financial support.

References

[1] V. Peneau, Q. He, G. Shaw, S. A. Kondrat, T. E. Davies, P. Miedziak, M. Forde, N. Dimitratos, C. J. Kiely and G. J. Hutchings, Phys. Chem. Chem. Phys., 2013,15, 10636-10644

IV-PP107

Mechanistic Understanding on MoO_3 Catalyzed Transesterification between Phenol and Dimethyl Carbonate

Peng B.*, Ember E.E., Lercher J.A.

Lehrstuhl II für Technische Chemie and Catalysis Research Center, Department of Chemistry, Technische Universität München, Garching, Germany

* bo.peng@mytum.de

Keywords: transesterification, phenol, dimethyl, carbonate, MoO_3

1 Introduction

Polycarbonates (PC) are high-performance engineering materials with unique physicochemical properties that make them suitable for many applications. [1] However, the conventional synthesis routes toward PC often involve the use of highly toxic reagents, *e.g.*, phosgene. Therefore, in the last decades, considerable efforts have been made for the development of phosgene-free routes for sustainable PC synthesis. The two-step synthesis of diphenyl carbonate (DPC), a key monomer for phosgene-free PC synthesis, has been achieved by transesterification between phenol and dimethyl carbonate (DMC). In present investigation, supported MoO_3 catalysts have been explored as highly selective and active catalyst for the transesterification of DMC and phenol under mild reaction conditions. Combined spectroscopy and reactivity data showed that orthorhombic microcrystalline MoO_3 is the important phase for the selective transesterification between DMC and phenol.

2 Experimental /methodology

MoO_3-SiO_2 catalysts were synthesized by impregnation method. [2] The catalysts were characterized by XRD, Raman and IR. The catalytic transesterification was performed in a batch reactor between 433 and 473 K under inert conditions and the products were analyzed by GC. *In-situ* IR spectroscopic measurements were performed with Bruker ISF88 IR spectrometer.

3 Results and discussion

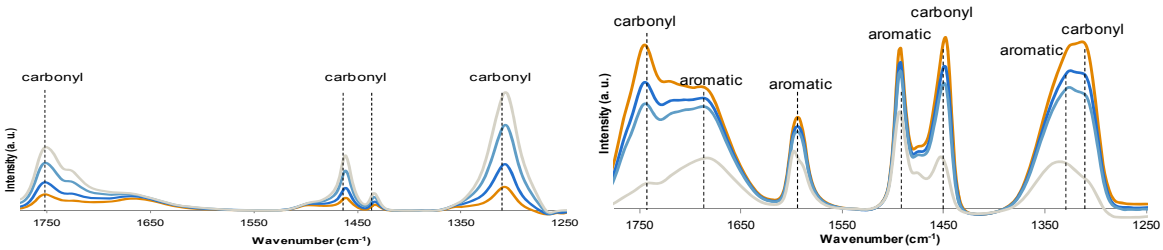

Figure 1. Comparison of the IR spectra of adsorbed DMC (left) and MPC (right) on MoO_3-SiO_2 followed by high temperature desorption.

The catalytic activity and selectivity in DPC synthesis strongly depend on the surface morphology. Using an optimized synthesis procedure enabled the synthesis of a MoO_3 catalyst with high content of microcrystalline orthorhombic MoO_3. Detailed spectroscopic study on the complex composition of MoO_3 further showed the existence of a larger fraction of coordinatively unsaturated Mo-O. To understand the elementary activation processes better, temperature dependent IR measurements were performed using DMC and methyl phenyl

carbonate (MPC), a key intermediate formed during transesterification, as probe molecules. The comparative IR spectra of adsorbed DMC and MPC shown in Figure 1 indicated the formation of a symmetric surface adsorbed carbonate, when DMC is used as probe molecule while the formation of stable asymmetric carbonate species was only observed when phenol was present as well.

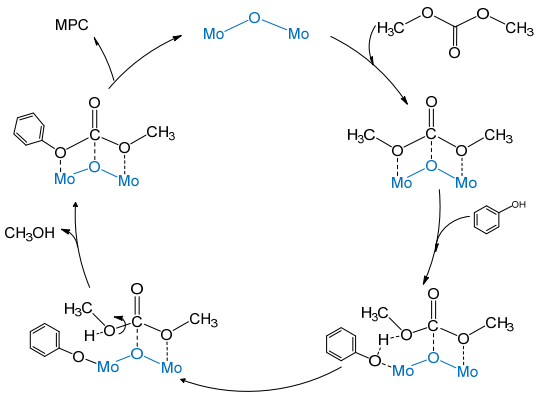

Scheme 1. Proposed catalytic cycle for the MoO_3 catalyzed MPC synthesis.

Summarizing all the experimental data on the interaction of the reactants enabled to propose a catalytic cycle for the most critical step in the transient DPC formation, shown in Scheme 1. The adsorption of DMC on the coordinatively unsaturated sites at microcrystalline MoO_3 results, thus, in the transient formation of symmetric carbonate species on the surface. In the presence of phenol, the concomitant formation of asymmetric carbonate takes place. This may occur by the more favored adsorption of phenol on the same catalytically active sites of the molybdena. Following the surface reconstruction and the release of a MeOH molecule, the formation of MPC takes place. The proposed reaction sequence is in line with the observed negative reaction order for phenol as well as the zero order for DMC at high DMC concentrations and first order at low DMC concentrations.

4 Conclusions

Active orthorhombic microcrystalline MoO_3 supported on SiO_2 was synthesized. Detailed spectroscopic analysis of the surface enabled reactions showed that the competitive adsorption of DMC and phenol on the coordinative unsaturated active sites of MoO_3 results in the formation of stable asymmetric surface carbonate species, from which target molecule is formed.

Acknowledgements

The authors acknowledge the support from EU's 7th Framework Program (FP7/2007~2013) under grant agreement NMP-LA-2010-245988 (INCAS).

References

[1] V. Serini, "Polycarbonates" in *Ullmann's Encyclopedia of Industrial Chemistry*, Wiley-VCH, Weinheim, 2000.
[2] Z.-h. Fu, Y. Ono, *J. Mol. Catal. A: Chem.* 118 (1997) 293-299.

IV-PP108

MP/C (M: Ni, Mo, W) Catalysts Hydrodenitrogenation of Aminocaprolactam: Effect of the H_2 Pressure

Abba M.O., Pereñiguez R.*, Caballero A.

Instituto de Ciencia de Materiales de Sevilla and Dpto Química Inorgánica (CSIC-Universidad de Sevilla), Seville, Spain

* rosa@icmse.csic.es

Keywords: hydrodenitrogenation, aminocaprolactam, caprolactam, high pressure

1 Introduction:

Catalytic hydrodenitrogenation (HDN) is an industrial process for the removal of organonitrogen compounds from hydrocarbons of crude oil to obtain stable and environmentally acceptable products. The HDN is performed for avoiding the burning of N containing fuels which generates NO_x emissions, known as pollutant gases that react to form smog and acid rain. The organonitrogen compounds removed are mainly quinolines and porphyrins and their derivatives, which can be grouped as heterocyclic nitrogen compounds, being also applied for aliphatic amines. HDN of petroleum has generally catalysed by cobalt and nickel as well as molybdenum disulphide or less often tungsten disulphide, supported on Al_2O_3 [1]. However, the HDN could be also applied in other routes, starting from heterocycle amines as alpha-aminocaprolactam (ACL) for producing high value compounds [2]. A previous work [3] studied the synthesis of alpha-amino-epsilon-caprolactam starting from L-lysine, which derived from biomass. This reaction involved the first step of the process (Fig. 1A) which final aim is the obtaining of epsilon-caprolactam (CL), by deamination of alpha-amino-epsilon-caprolactam (ACL). CL is a high value compound due to its implication as a precursor in the nylon 6 production. The aim of the present study is to perform a preliminary evaluation of the effect of pressure in HDN reaction of ACL to CL (Fig. 1B) using 10% monometallic phosphide (Ni, Mo and W) supported on carbon as catalysts.

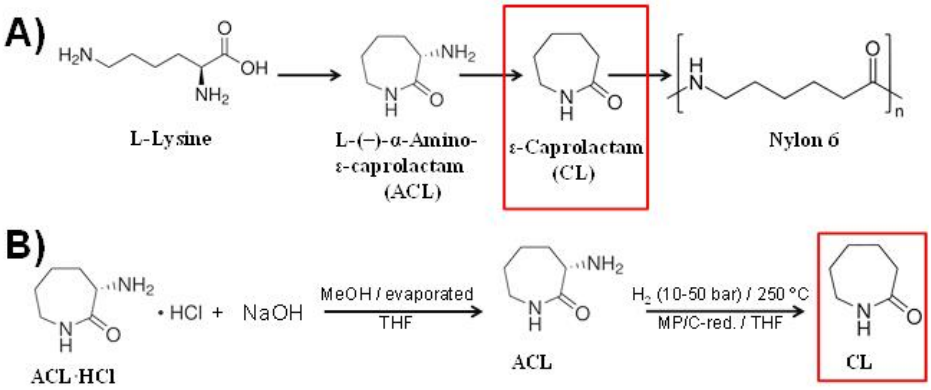

Fig. 1. Scheme of the reactions involved.

2 Experimental:

The catalysts were prepared by co-impregnation in a rotary of an aqueous solution containing the phosphorous and metal (Ni, Mo or W) precursors. This solution in contact with the carbonaceous support (Cabot Vulcan) was stirring at room temperature for 3 hours and then at 50 ºC under vacuum. The systems obtained were reduced in H_2 5% vol. in Ar at 900 ºC for 3h and then it was passivated in an atmosphere of O_2 0.5% vol. in He at room temperature for 4 h.

The catalysts are labelled as MP/C-red, being M: Ni, Mo or W at 10 wt. %. The physicochemical properties of the catalysts prepared were studied by the characterization techniques of XRD, BET, SEM, TPR and XPS. For the catalytic performance, the ACL·HCl precursor was firstly neutralized by adding NaOH in a methanol solution (0.1 M of ACL·HCl). After that, the solvent was removed and redissolved in tetrahydrofuran (THF), with the consequent precipitation of NaCl. For the HDN of ACL, the solution of 10 ml obtained (ACL/THF) was placed in a 70 ml stainless steel autoclave *Sentinel* with 20 mg of catalyst. The reactor was flushed with nitrogen, and hydrogen sequentially at room temperature. Then the system was pressurized in H_2 until the desired pressure, and heated at 250 ºC under stirring. After 15 hours, the conversion and selectivity were determined by GC analysis, using an HP 5890 gas chromatograph equipped with a capillary column (Elite 1).

3 Results and discussion:

The XRD data show two wide peaks ascribed to carbon phases that were also detected in the XRD of the support without metal impregnation. This fact makes difficult the ascription of phases resulting in a mixture of oxides, phosphates and phosphides of the metals. In the case of NiP/C-red., the Ni_2P phase was clearly identified. The micrographs obtained by SEM (Fig. 2), recording secondary electrons (SE) and backscattered electrons (BSE, to obtain better contrast for heavier elements like metals in contrast with C or P) show the formation of well dispersed nanoparticles (around 10 nm), mainly in MoP/C-red. system.

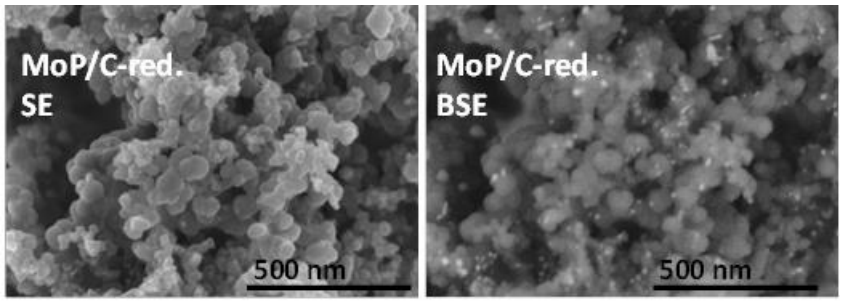

Fig. 2. SEM images of secondary electrons (SE) and backscattered electrons (BSE).

Table 1 presents the results of catalytic HDN of ACL for the systems MP/C-red. In general the conversion obtained was close to 100% in most of the cases, independently of the pressure applied even the catalyst tested. The main difference observed was the selectivity to the desired product CL, that was calculated as the percentage of the CL versus the total of products registered. In general, low and moderate pressures (10-30 bar) result in better selectivity, being the MoP/C-red. the most promising for HDN of ACL. These results would improve the costs for industrial application, compared with the previous one published [2], where the authors used noble metals as catalysts and a mixture of H_2/H_2S instead of pure H_2.

Table 1. Catalytic performance of the systems.

Catalyst	Pressure	S_{CL} (%)	Catalyst	Pressure	S_{CL} (%)	Catalyst	Pressure	S_{CL} (%)
	10	43		10	45		**10**	**75**
	20	**51**		**20**	**62**		20	29
NiP/C-red.	30	27	**MoP/C-red.**	**30**	**71**	**WP/C-red.**	30	32
	40	30		40	36		40	22
	50	24		50	32		50	54

References

[1] T.C. Ho, Catal. Rev. Sci. Eng. 30 (1) (1988) 117
[2] J.W. Frost, US 2010/0145003 A1
[3] J.W. Frost, WO 2005/123669 A1

IV-PP109

Conversion of Heavy Hydrocarbons into Light Oils Using Nanoparticles and Complexes of Transition Elements

Petrov S.M.[1*], Gussamov I.I.[1], Abdelsalam Y.I.[1], Ibragimova D.A.[1], Baybekova L.R.[1], Kayukova G.P.[2]

1 - Kazan National Research Technological University, Kazan, Russia
2 - A.E. Arbuzov Institute Of Organic And Physical Chemistry, Kazan, Russia

* psergeim@rambler.ru

Keywords: catalyst, heavy oil, bituminous oil, conversion, viscosity reduction

1 Introduction

Development of human civilization and economically developed countries pursuit to resource independence inevitably leads to redistribution of world commodity markets. Hydrocarbon resources will remain the main energy generator for transport and power industry, and will be the basis of the most synthetic materials and chemical products over the next 50-100 years. All over the world there is a growing interest in the development of alternative types of reserves of hydrocarbon resources: gas hydrates, shale oil and gas, heavy oil and natural bitumen. Global reserves of natural bitumen are about 260 billion tons according to United Nations estimation. Russian reserves of the commercially available crude oil is about 1.8 billion tons and the volume of heavy crude oil is about 4.5 billion tons in the bituminous sands according to the major oil operator – British Petroleum (BP). That's why scientific researches, industrial experiment works and pilot projects on the new types of hydrocarbon resources development and on searching effective methods of their production and cost-effective technologies of processing are becoming relevant.

2 Experimental/methodology

Samples of bituminous oil from Ashalchinskoye field, that located on the territory of the Republic of Tatarstan, were selected as objects of the study. There are almost no n-alkanes in oil, and the light hydrocarbons yield is at least 20%. Metal compounds Fe2O3, ZnO, NiO, salt Co [acac] 2, NiSO4, NiCO3, CuSO4 were selected as additives for catalytic conversion of resine-asphaltene components in the light hydrocarbon oil, and the following components were selected as excipients: Al2O3, ethane, 2 -hydroxy-1,2,3-propanetricarboxylic acid and water. Fe2O3 magnetite was used in coarsely dispersed condition of 250 to 800 microns, in a finely dispersed state to 250 nm and nano-dimensional state to 25 nm. The advantage of nanoparticles is in their accessibility to organic molecules of oil stock practically of any shape and size, which is especially important in the processing of heavy types of hydrocarbons. Particles of silicon and aluminum oxides, Al2O3, and SiO2 were used in a coarsely dispersed state through to 25 microns and nano-dimensioned state 40 nm stabilized by 4-methyl-2-pentanone. Experiments on catalytic conversion of bituminous oil were held in a high pressure reactor at temperatures from 250 to 380 ° C, and pressures from 1 to 21MPa, with a different ratio of vapor to the crude oil from 1: 1 to 1: 4.

3 Results and discussion

Hydrocarbon yield is reduced by increasing the amount of tars during all experiments where the process temperature is below 300°C. The asphaltenes content is reduced by 28% in the conversion products in the presence of SiO2 and Al2O3, at a temperature of 290°C. Reduction of the content of alcohol-benzene resins up to 22% occurs after increasing temperature up to

375°C and using a catalyst of iron-oxide. The experiment in the presence of zinc oxide nanoparticles reduces the content of n-alkanes in the final product and the content therein of branched structures, also reduces the viscosity by more than 2 times, while the component composition is not changed practically. In conversion products is a noticeable reduction in the concentration of asphaltenes by 29%, with increasing content of alcohol-benzene resins after introducing into the reaction mixture Al2O3, Ni in the nano state and poly-α-olefins. Comparison of the results of component analysis of a bituminous oil and its thermocatalytic treatment indicates conversion of the resins into light hydrocarbons. Yield of the gasoline fraction increased from 9.8 to 15% with this slightly reduced yield of fractions 200-350°C in the conversion products after the experiment with Fe2O3 and NiCO3. Experiment held at 350 ° C and under pressure of 7.8 MPa in the presence of Al2O3 and nano sized Ni particles in a poly-α-olefins markedly increases the yield of light fractions up to 39% in conversion products. The amount of gasoline and diesel fraction increases to 42% in the transformed oil in a reducing atmosphere in the presence the reaction mixture of SiO2 and Al2O3.

4 Conclusions

Based on these studies, we evaluated the effect of various additives in combination with thermobaric effect on the conversion of heavy hydrocarbons into lighter fractions. The obtained results promote the evolutiont of this important area of refining, as a development of unconventional hydrocarbon resources.

IV-PP110

Ethanol Conversion to Useful Products: Ethylene, Diethyl ether, Higher Hydrocarbons, Acetaldehyde and Acetone

Phung T.K., Garbarino G., Busca G.*

University of Genova, Department of Civil, Chemical and Environmental Engineering, Genova, Italy

* guido.busca@unige.it

Keywords: ethanol, ethylene, diethyl ether, hydrocarbons, acetaldehyde, acetone

1 Introduction

Ethanol produced by fermentation of lignocellulosics, denoted as "second generation bioethanol", could become a primary intermediate in the frame of a new industrial organic chemistry based on renewables.

Among the secondary intermediates potentially obtainable by converting (bio)ethanol, ethylene and diethyl ether can be obtained by catalytic dehydration

$C_2H_5OH \rightarrow C_2H_4 + H_2O$ (1)

$2\ C_2H_5OH \rightarrow C_2H_5OC_2H_5 + H_2O$ (2)

Also acetaldehyde can be obtained by ethanol, through dehydrogenation:

$C_2H_5OH \rightarrow C_2H_4O + H_2$ (3)

and it possibly condensates to acetone through aldol condensation reaction.

Moreover, a number of studies report on the possibility to produce other hydrocarbons, in particular aromatics and higher olefins, from ethanol.

The aim of this work is to investigate the feasibility of ethanol conversion to useful products over different acido-basic oxide catalysts and study the ethanol conversion mechanisms as well as the nature of the basicity/acidity of catalytically active solids.

2 Experimental/methodology

2.1 Characterization

Catalyst characterization was performed by TEM, XRD, UV-vis, TG-DTA, XRD, NH_3-TPD, Raman spectroscopy and IR spectroscopy.

2.2 Catalytic experiments

Catalytic experiments were performed at atmospheric pressure in a tubular flow reactor using oxide catalyst (60-70 mesh sieved) or the mixture of catalyst and quartz (60-70 mesh sieved) and feeding 7.9% v/v ethanol in nitrogen. The carrier gas was passed through a bubbler containing ethanol maintained at constant temperature (298 K) in order to obtain the desired partial pressures. The temperature in the experiment was varied stepwise from 373 K to 873 K.

The outlet gases were analyzed by a gas chromatograph (GC) Agilent 4890 equipped with a Varian capillary column "Molsieve 5A/Porabond A Tandem" and TCD and FID detectors in series. In order to identify the compounds of the outlet gases, a gas chromatography coupled with mass spectroscopy (GC-MS) Thermo Scientific with TG-SQC column (15 m x 0.25 mm x 0.25 μm) was used.

3 Results and discussion

Several catalysts allow essentially stable 99.9 % yield to ethylene. This can be obtained on H-FER on H-FAU zeolite at 523-573 K until > 400 min time on stream [1]. On very pure γ-Al_2O_3 at yield approaches 99 % at 573 K for 400 min [1-2]. Also with slightly sulphated zirconia yield to ethylene approaches 100 % at 573 K.

Maximum yields to DEE are obtained on H-MFI (50) zeolite at 453-473 K and on H-BEA zeolite and on a WO_3/TiO_2 catalyst [1] at 473 K (> 73 %) (Fig. 1, left). The reaction path in ethylene and diethyl ether synthesis has also been investigated by flow reactor measurements, TPSR as well as IR studies. The investigated catalysts were characterized by different techniques such as IR spectroscopy of adsorbed pyridine (Fig. 1, right).

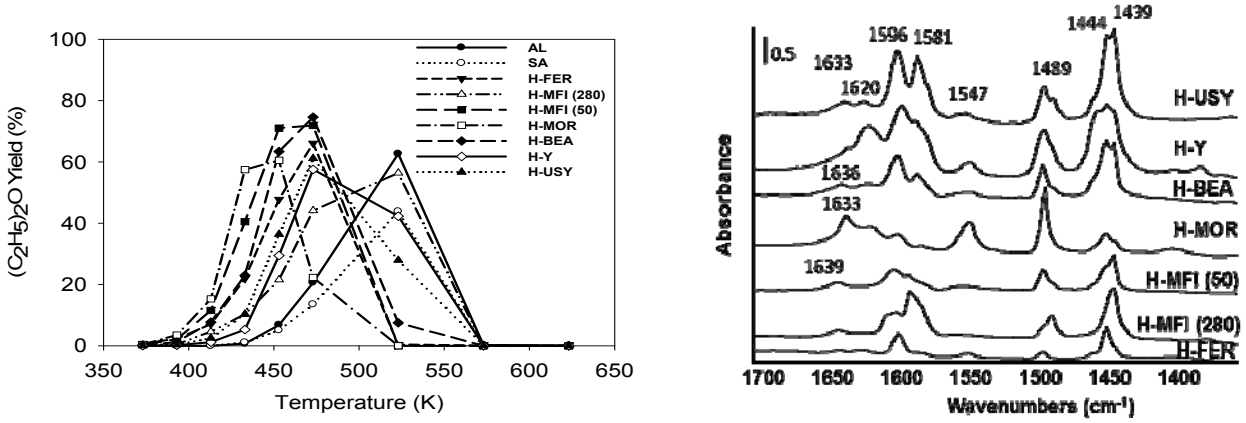

Fig. 1. (left) Diethyl ether yield as a function of temperature. Reaction condition: at atmospheric pressure in a fixed-bed tubular quartz reactor using 0.5 g of catalysts with 1.43 h^{-1} WHSV in nitrogen from 373 K to 623 K; (right) FT-IR subtraction spectra of surface species arising from pyridine adsorbed on pure zeolites at room temperature.

Using H-ZSM-5 zeolite depending on Si/Al ratio and modifiers (such as P, Fe and Ni), as well as reaction conditions, higher yields can be obtained in higher hydrocarbons such as propene, butenes and BTX aromatics.

Over catalysts displaying basicity (calcined hydrothalcite [4], La_2O_3-Al_2O_3) and semiconductor behaviour (ZnO, ZrO_2, TiO_2) a number of other products can be obtained, including carbonyl compounds and high hydrocarbons. On ZnO catalyst 50 % yield in acetone has been obtained at 773 K while selectivity of 64 % in acetaldehyde is found at 623 K (conversion 48%). Attempts to improve selectivity and yields into acetaldehyde, acetone, butenes, butadiene and aromatic have been undertaken.

4 Conclusions

Ethanol is a very versatile intermediate that can be converted with high selectivity/yield in a number of useful products over heterogeneous catalysts. The catalytic activity is correlated with acido-basic and electronic character of the catalyst.

Acknowledgements

TKP acknowledges funding by EMMA (Erasmus Mundus Mobility with Asia) in the framework of the EU Erasmus Mundus Action 2.

References

[1] T.K. Phung, L. Proietti Hernandez, A. Lagazzo, G. Busca, *Appl. Catal. A* 493 (2015) 77.
[2] T.K. Phung, A. Lagazzo, M.A. Rivero Crespo, V. Sanchez Escribano, G. Busca, *J. Catal.* 311 (2014) 102.
[3] T.K. Phung, C. Herrera, M.Á. Larrubia, M. García-Diéguez, E. Finocchio, L.J. Alemany, G. Busca, *Appl. Catal. A* 483 (2014) 41.
[4] T.K. Phung, L. Proietti Hernandez, G. Busca, *Appl. Catal. A* 489 (2015) 180.

IV-PP111

Synthesis of Platform Molecules from Cellulose over Bifunctional Magnetic Nanocatalysts

Podolean I.*, Coman S.M., Parvulescu V.I.

University of Bucharest, Faculty of Chemistry, Department of Organic Chemistry, Biochemistry and Catalysis, Bucharest, Romania

* iunia.podolean@chimie.unibuc.ro

Keywords: biomass, valorization, ruthenium, niobium, magnetic, one-pot

1 Introduction

Research into the biomass valorization as a renewable raw material, received an unprecedented interest. A great variety of catalysts have already been tested for a such purpose. Among these, ruthenium based catalysts have proved to be very active and selective in transformations like hydrogenations (levulinic acid to γ -valerolactone, glucose to sorbitol, butyric acid to n-butanol), pyrolysis of lignocellulosic biomass, etc. [1]. Recently our group discovered that ruthenium supported magnetic nanoparticles are also very efficient in oxidation of levulinic to succinic acid [2]. On the other hand, niobium oxide gain increased interest as catalyst and catalytic support in hydrothermal biomass conversion in subcritical water, due to its high stability and acidity [3]. Based on these considerations, our purpose was to prepare bifunctional Ru/Nb_2O_5-based catalysts, using magnetic carbon nanotubes as support. Designed catalysts were testes in one-pot conversion of cellulose to platform molecules.

2 Experimental/methodology

Different techniques and precursors were used to prepare niobic acid ($Nb_2O_5 \cdot nH_2O$). Niobium ammonium oxalate was precipitated in the presence of NH_4OH or KOH while niobium ethoxide was mixed and heated with dodecylamine and precipitated with HCl. For comparison a commercial niobic acid purchased from Sigma-Aldrich was used as well. Commercial carbon nanotubes (CNTs) were functionalized with carboxylic groups before introduction of magnetic nanoparticles and deposition of niobic acid by treating with a 1:1 (v/v) mixture of concentrated H_2SO_4/HNO_3 at 70°C for 12hours. To introduce the magnetic nanoparticles into CNTs, Mohr salt was used as precursor and ammonium hydroxide as precipitating agent. Carbon nanotubes were functionalized subsequently by coprecipitation of niobic acid. To this material ruthenium was deposed by wet impregnation. The obtained catalysts were denoted as $MCNT@Nb_2O_5$_A_B_C@Ru, where A B and C are the niobium precursor, precipitation agent and calcination temperature. Rutenium was impregnated onto niobium modified MCNTs using a Ru(III)chloride solution in water. Overall, the catalyst synthesis is represented in Figure 1. The obtained catalytis were characterized by XRD, ICP-OES, TG-GTA, DRIFT etc. The catalytic tests were performed in high-pressure HEL reactor, using 50 mg of catalyst and 50 mg of cellulose in 10 mL of water at different temperatures (150°C, 180°C, 200°C).

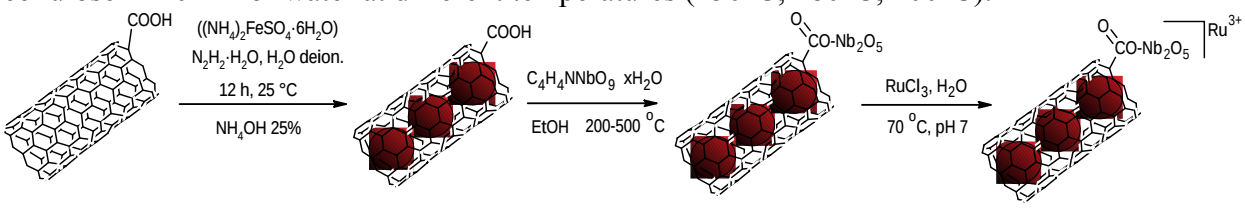

Fig. 1. Preparation of bifunctional $MCNT@Nb_2O_5@Ru$ catalysts

3 Results and discussion

The characterization techniques demonstrated the successful deposition of niobium and ruthenium onto magnetic carbon nanotubes. The hydrothermal conversion, and oxidation of cellulose led to very promising results. The cellulose conversion was between 60-90% at reaction times higher than 8 hours even at 150°C. Hydrothermal conversion of cellulose in the presence of niobium led to lactic acid (cca. 15%), glycolic acid (cca. 15%) and γ-hydroxybutyric acid (cca. 30%) as main products. There was no significant effect of the niobium precursor or precipitation agent, instead the calcination temperature of the catalysts influence the product distribution. Catalysts calcinated at lower temperature (200°C) led to the formation of levulinic acid (cca. 10%) at the reaction temperature of 200°C. All studies, regardless of the used technique (infrared spectroscopy in the presence of pyridine, butylamine titration, NH_3 volumetric and gravimetric analysis, NMR) showed the presence of Lewis and Brønsted acid sites on the surface of niobium pentoxide. Niobic acid treated at temperatures between 100°C and 300°C, contains more acid sites than those calcined at temperatures between 500°C and 600°C, which are practically inactive [4]. To obtain levulinic acid from cellulose the catalyst must possess both Lewis and Bronsted acidity, the optimum ratio being about 1:1 [5]. Commercial (crystalline) niobia was almost inactive. At lower reaction temperature of 150°C instead of levulinic acid the succinic acid was formed. Adding ruthenium to the catalytic system resulted in an important increase of the selectivity in levulinic acid (for hydrothermal conversion of cellulose) and succinic acid (for cellulose oxidation). Besides, the catalysts maintained their magnetic properties after recycles. Using glucose instead of cellulose as reaction substrate resulted in very different distribution of products. Lactic and glycolic acids were obtained in smaller quantities compared to cellulose. At the same time, hydroxymethylfurfural was the main product (around 70%) followed by xylose (around 15%) and ribose (around 10%).

4 Conclusions

A series of new magnetic bifunctional catalysts were obtained using carbon nanotubes as stable catalytic support, niobic acid for the acidic function and ruthenium as active species. Additionally, magnetic nanoparticles were inserted inside the carbon nanotubes offering more functionality for the catalyst recovery, especially in the case of microcrystalline cellulose conversion. A synergic effect of niobia and ruthenium led to a high cellulose conversion resulting in different platform molecules as lactic, glycolic and levulinic acids. Introducing oxygen in the system gave a good selectivity to succinic acid.

Acknowledgements

This work was supported by the strategic grant POSDRU/159/1.5/S/137750, ”Project Doctoral and Postdoctoral programs support for increased competitiveness in Exact Sciences research” cofinanced by the European Social Found within the Sectorial Operational Program Human Resources Development 2007 – 2013

References

[1] M. Besson, P. Gallezot, C. Pinel, *Chem. Rev.* 114 (2014) 1827.
[2] I. Podolean, V. Kuncser, N. Gheorghe, D. Macovei, V.I. Parvulescu, S.M. Coman, *Green Chem* 15 (2013) 3077.
[3] I. Nowak, M. Ziolek, *Chem. Rev*. 99 (1999) 3603.
[4] P. Batamack, R.Vincent, J. Fraissard, *Catalysis Letters* 36 (1996) 81.
[5] R. Weingarten, Y.T. Kim, G.A. Tompsett, A. Fernández, K.S. Han, E.W. Hagaman, W.C. Conner, J.A. Dumesic, G.W. Huber, *J. Catal.*, 304 (2013) 123.

IV-PP112

"Green" Propylene Glycol: Kinetic Determination for the Valorization of Biodiesel Side Stream

Rajkhowa T.*, Thybaut J.W., Marin G.B.

Laboratory for Chemical Technology, Ghent University, Gent, Belgium

* tapas.rajkhowa@ugent.be

Keywords: glycerol, propylene, glycol, intrinsic, kinetics, copper, biodiesel

1 Introduction

In triglyceride transesterification to fatty acid methyl esters, 10 wt% of glycerol byproduct is formed. Upgrading the latter into a more valuable chemical will increase the sustainability and commercial viability of the biodiesel production process. Moreover, it will allow the synthesis of 'green' chemicals instead of petroleum-based ones. Among other alternatives, glycerol hydrogenolysis towards 1,2 propanediol or propylene glycol is a relevant and attractive valorisation route.

It has been widely accepted that glycerol hydrogenolysis on a Cu catalyst proceeds through a dehydration-hydrogenation with an acetol intermediate [1]. Although many researchers have investigated glycerol hydrogenolysis, very few have focused on investigating and modelling the kinetics [2]. In this work, the reaction kinetics were studied over an industrial copper catalyst supported on alumina. The objective of the work is to develop an intrinsic kinetic model for the hydrogenolysis reaction of glycerol to propylene glycol, aiming at a better understanding of the catalytic chemistry and opening up perspectives for rational catalyst design.

2 Intrinsic kinetic experimentation and modelling

The experimental glycerol hydrogenolysis investigation has been performed using a high throughput kinetics setup [3]. The experiments were performed using a trickle bed reactor in which pure glycerol was co-currently fed with hydrogen over a fixed catalyst bed. Intrinsic kinetic experiments were then performed by varying the space time, the hydrogen to glycerol molar ratio, hydrogen pressure and temperature.

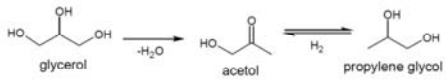

$$r_1 = \frac{k_1 K_G C_G}{1 + \sqrt{K_H C_{H2}} + K_G C_G + K_A C_A + K_P C_P + K'_2 K_A C_A \sqrt{K_H C_{H2}}}$$

$$r_2 = \frac{k_2 K_A C_A K'_2 K_H C_{H2}}{\left(1 + \sqrt{K_H C_{H2}} + K_G C_G + K_A C_A + K_P C_P + K'_2 K_A C_A \sqrt{K_H C_{H2}}\right)^2}$$

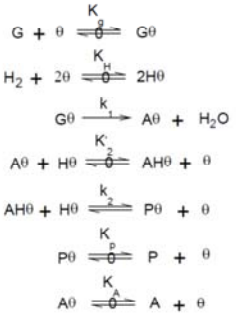

Figure 1: Reaction scheme for glycerol hydrogenolysis along with the proposed reaction mechanism and the corresponding rate equations.

The glycerol hydrogenolysis reaction mechanism has been proposed based on the one reported by Gandarias [4]. It was assumed that glycerol, acetol and propylene glycol competitively adsorb on identical active sites along with dissociative hydrogen adsorption. The surface reactions were considered to be rate determining with the adsorption steps being quasi-equilibrated.

3 Results and discussion

From a) it can be observed that at iso conversion and pressure, the selectivity towards the reaction intermediate, i.e., acetol, increases with temperature. b) illustrates how the glycerol conversion increases with the space time and how this increase is faster at elevated temperature.

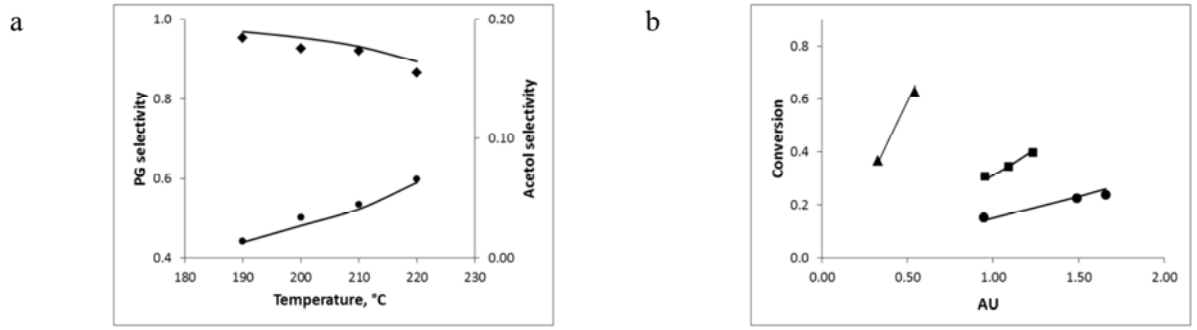

Figure 2: Temperature effect on selectivity and conversion. a) Propylene glycol(♦) and acetol(●) selectivity vs temperature b) Glycerol conversion at 200 °C(●), 210 °C(■) and 230 °C(▲) as a function of the space time. Symbols: experimental, solid lines: model simulations.

Model parameter values have been obtained by regression and are reported in Table 1, together with the corresponding confidence intervals, apart from the adsorption entropies which were fixed a priori based on statistical thermodynamics considerations. All parameter values were statistically and physically significant, e.g., the activation energy for acetol formation, $Ea_1 = 169 kJ\ mol^{-1}$, significantly exceeds the one for its further conversion into propylene glycol, $Ea_2 = 70 kJ\ mol^{-1}$, reflecting the above discussed temperature effect on the selectivity.

Parameter	Pre-exponential factor/ ΔS^0	$\Delta E_a / -\Delta H^0$
k_1^{comp} ($m^3\ kg^{-1}\ s^{-1}$)	$(76.9 \pm 2.2)*10^{-6}$	57.0 ± 4.2
k_2^{comp} ($m^6\ mol^{-1}\ kg^{-1}\ s^{-1}$)	$(25.6 \pm 0.74)*10^{-8}$	-38.2 ± 1.8
K_{H2} ($m^3\ mol^{-1}$)	$-30*10^3$	52.0 ± 0.8
K_G ($m^3\ mol^{-1}$)	-26.6	112.9 ± 4.3
K_A ($m^3\ mol^{-1}$)	-90	26.9 ± 1.05
K_P ($m^3\ mol^{-1}$)	-100	19.1 ± 1.4

Table 2 : Parameters estimates from the model simulation. $\mathbf{k_1^{comp} = k_1.K_G}$ and $\mathbf{k_2^{comp} = k_2.K_A.K_{H2}.K_2'}$

4 Conclusions and future work

Mechanistic insights into liquid phase glycerol hydrogenolysis has been gained. Temperature and space time effects on hydrogenolysis activity and product selectivity have been investigated and could be rationalized in terms of statistically significant model parameters. The methodology will be extended towards alternative catalysts, aiming at a rational catalyst design.

Acknowledgements

This work was supported by the Institute for the Promotion of Innovation through Science and Technology in Flanders (IWT Vlaanderen)

References

[1] M.A. Dasari, P.-P. Kiatsimkul, W.R. Sutterlin, G.J. Suppes, Appl. Catal. Gen. 281 (2005) 225.
[2] Z. Zhou, X. Li, T. Zeng, W. Hong, Z. Cheng, W. Yuan, Chin. J. Chem. Eng. 18 (2010) 384.
[3] N. Navidi, J.W. Thybaut, G.B. Marin, Appl. Catal. Gen. 469 (2014) 357.
[4] I. Gandarias, P.L. Arias, J. Requies, M.B. Güemez, J.L.G. Fierro, Appl. Catal. B Environ. 97 (2010) 248.

IV-PP113

Research of Hydrogenation of the Nitrobenzene in Supercritical Carbon Dioxide with Use Ru/HPS Catalysts

Sulman E.*, Rakitin M., Petrova A., Doluda V., Matveeva V., Sulman M.

Tver Technical University, Tver, Russia

* sulman@online.tver.ru

Keywords: aniline, nitrobenzene, supercritical carbon dioxide

1 Introduction

Catalytic hydrogenation of a nitrobenzene is important chemical and technological process of receiving aniline which is in turn used as intermediate in synthesis of polyurethanes, rubbers, pharmaceuticals, pesticides and herbicides. Process of gas-phase hydrogenation of a nitrobenzene is usually carried out with use of Ni-or Cu-containing catalysts, fractional pressure of hydrogen of 1-5 atm. and temperature 250-300 ^{0}C, while liquid-phase hydrogenation - with use of Pt-, Pd-, Ni-containing catalysts at a temperature of 50-220 ^{0}C and pressure of 10-50 atm. both in the environment of various solvents, and in their absence, thus selectivity on a main product makes 75-95% [1].

Application of supercritical carbon dioxide ($CO_{2(sc)}$) in selective hydrogenation of a nitrobenzene has the considerable interest of researchers that is caused by advantages supercritical fluids application: high heat and mass transfer, formation of new molecular complexes and decrease of processes flammability.

2 Experimental/methodology

Catalytic hydrogenation of a nitrobenzene was carried out on the Parr Series 5000 Multiple Reactor System installation. It consists from six steel the thermostated reactors, the having unions for a purge, supply for gas and sample valve. Mixing was provided by the magnetic stirrer with electric motor (the maximal range of speeds in a minute – 1600). Control of pressure was made by means of pressure units. The thermostatting of the reactor is carried out by a programmable heating element. Accuracy of maintaining of temperature makes 0.1 °C.

Reference experiment in isopropanol was made as follows. A flask with shots of the catalyst, a nitrobenzene and isopropanol 3 times of 100 ml of nitrogen under pressure blew 2 MPa, then heated to necessary temperature in a nitrogen atmosphere and gave gaseous hydrogen.

Reference experiment in supercritical carbon dioxide was made as follows. A flask with catalyst and a nitrobenzene was purged 3 times of 300 ml of carbon dioxide under pressure blew 20 atm., then contents were heated to the necessary temperature then carbonic acid before achievement of the predetermined pressure (1-20 MPas) was pumped. On reaching equilibrium of $CO_{2(sc)}$ through a burette gave gaseous Hydrogenium to the reactor and began reaction timing. Hashing of a reaction mixture was made by the rotor four-blade mixer set in motion by the electric motor (the maximal range of speeds in a minute – 700). Monitoring of pressure was made by means of the manometer. The thermostatting of the reactor was carried out by the heating block with the programmable controller. Accuracy of maintaining of temperature makes 0.1 °C.

High-quality and quantitative identification of intermediates of synthesis was carried out by a gas-liquid chromatography method with mass and spectrometer detecting of substances. For this purpose used a gas chromatograph of GS-2010 (Shimadzu, Japan) with the capillary column HP-1MS which effectiveness made 4300 theoretical plates on pentadecane, and determined a gas one-quadrupole mass spectrometer of GSMS-QP2010S (Shimadzu, Japan) of Concentration of a nitrobenzene and aniline by reference substances and the corresponding gage dependences with use

of diphenylamine as the external standard.

3 Results and discussion

Data on activity of catalysts are presented in table 1. Temperature is specified for a maximum yield of aniline at maximum conversion of a nitrobenzene.

Table 1. Activity of the studied catalysts

Catalyst	Solvent	Temperature, ° C	Selectivity, %	Nitrobenzene conversion, %	Aniline yield, %
1% Ru/HPS	isopropanol	170	81.8	99.6	79.2
3% Ru/HPS	isopropanol	190	100.0	99.8	95.3
5% Ru/HPS	isopropanol	140	88.2	96.2	84.9
3% Ru/HPS	$CO_{2(sc)}$	100	100.0	99.8	96.2

From table 1 it is visible that use of supercritical carbon dioxide allows to reduce considerably temperature of carrying out process without decrease of aniline yields and conversion of nitrobenzene.

4 Conclusions

Carbon dioxide is perspective solvent for carrying out organic synthesis, including hydrogenation of organic nitrocompounds. On the example of process of catalytic hydrogenation of a nitrobenzene with use of the Ru-containing catalysts positive influence of $CO_{2(sc)}$ is shown. Decrease of influence of a matrix by activity of heterogeneous catalysts that testifies to increase in availability of the fissile Ru-centers to the reacting substratum in the environment of supercritical carbon dioxide is established.

Acknowledgements

Authors thanks Ministry education and science of Russian Federation for financial support (grant RFFR № 13-08-00403 A).

References

[1] M. Kantam, R. Chakravati, U. Pal, B. Sreedhar, *Advanced Synthesis and catalysis*, 2008, vol. 350, pp. 822-827.

IV-PP114

Catalytic Transformation of Glycerol to Lactic Acid over Au-Pt Supported Catalysts Prepared by Redox-Method

Redina E.[1*], Kirichenko O.[1], Greish A.[1], Shesterkina A.[1], Vikanova K.[2], Tkachenko O.[1], Kapustin G.[1], Kustov L.[1,3]

1 - N.D. Zelinsky Institute of Organic Chemistry, Russian Academy of Sciences, Moscow, Russia
2 - Lomonosov Moscow State University of Fine Chemical Technologies, Moscow, Russia
3 - Chemistry Department of Moscow State University, Moscow, Russia

* redinalena@yandex.ru

Keywords: glycerol, gold catalysts, lactic acid

1 Introduction

In the recent years, renewable bio-based feedstock sources have become increasingly important in the chemical industry. Glycerol (Gly), as a large-scale by-product in biodiesel production, is a versatile feedstock for the synthesis of a wide range of different chemicals [1]. Among them lactic acid (LA) is an important platform molecule for the fine organic synthesis. In addition, poly-lactic acid is a well-known biodegradable polymer, which has a great number of applications in medicine and as a packing material [2]. The most prominent way to obtain LA from Gly is a catalytic oxidative route. Anyway, it is still a challenging task, and there are only a few works concerned with the aerobic catalytic Gly oxidation to LA with high to moderate yields [3-5]. The most beneficial results were obtained with supported bimetallic Au-Pt catalysts. In this work we aimed at evaluation of the activity of low-loaded Au-Pt catalysts supported on active oxides (TiO_2, CeO_2, $CeZrO_x$) in the Gly aerobic oxidation to LA. The catalysts were prepared by facile redox-method ensuring the formation of close contact between the two metal components (Au-Pt) responsible for the synergetic effect in the catalysts activity.

2 Experimental/methodology

The catalysts were prepared by the redox-method in a two-step mode described in our works [6-7]. The first step was the preparation of the parent monometallic Pt catalysts (Pt/MO_x, where MO_x = TiO_2, S_{BET} = 61 m^2/g; CeO_2, S_{BET} = 37 m^2/g, $CeZrO_x$, S_{BET} =73 m^2/g) by a deposition-precipitation method from an H_2PtCl_6 aqueous solution followed by the reduction of the catalyst with H_2. To deposit the Au species, the prepared parent monometallic Pt sample was saturated with H_2, and the required amount of an Au precursor solution ($HAuCl_4$) with a definite concentration was added to the monometallic sample. The obtained catalysts were characterized by TPR-H_2, STEM, XPS, DRIFTS-CO and CO adsorption techniques.

The liquid-phase oxidation of Gly was performed in the batch-mode in alkali media with a molar ratio NaOH:Gly =2-4 at 40-100^oC under the O_2/N_2 pressure of 5 bar or just in air under atmospheric pressure. The analysis of the products obtained in the liquid phase was performed by NMR spectroscopy (Bruker Avance II, 300 MHz) with an external standard (sodium benzoate). The experimental error was within 3%.

3 Results and discussion

The strong Au-Pt interaction in the bimetallic catalysts proved by XPS and TPR-H_2 methods drastically changed their activity compared to the monometallic Au and Pt samples in Gly to LA oxidative transformation. Moreover, it was observed that both the particle size of Au/Pt NPs and the support characteristics greatly influenced the catalyst activity and selectivity.

When performing the reaction with TiO_2 supported Au/Pt catalysts, the highest activity and selectivity to LA were obtained for the catalyst with the lowest Au content and the atomic ratio Au:Pt=0.025:1. Although the same was observed for the catalysts supported on either CeO_2 or $CeZrO_x$, among the low-loaded Au/Pt catalysts the highest conversion of Gly and selectivity to LA were characteristic of 0.025%Au/1%Pt/TiO_2 (Fig. 1 A). The use of this catalyst provided a 80% Gly conversion and a 50% LA selectivity in air at 60°C with a lowered ratio NaOH:Gly=2. The scheme of Gly oxidation to LA is presented in Fig. 1 B.

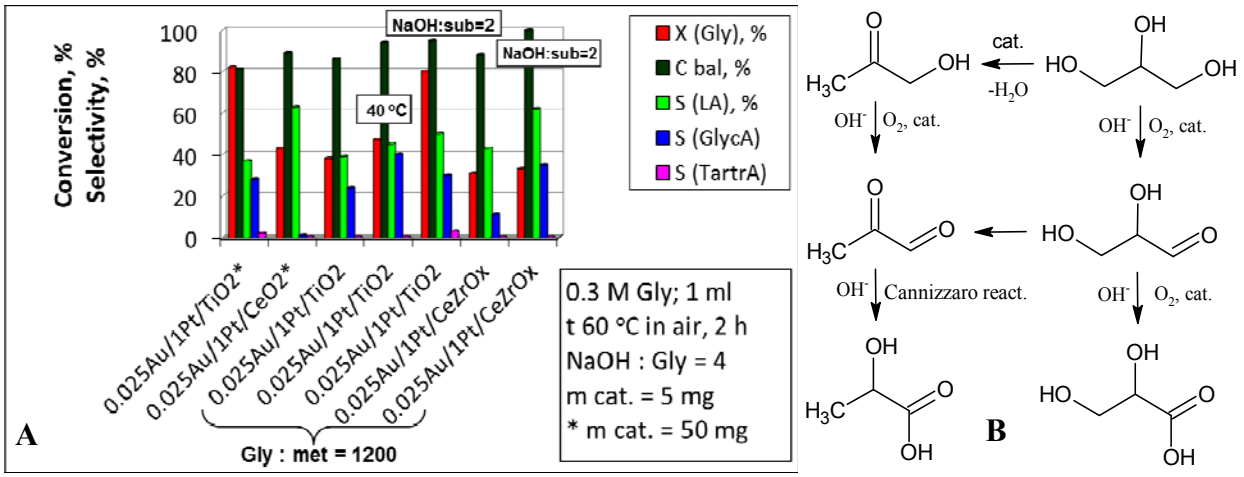

Fig. 1. The activity and selectivity of the low-loaded Au/Pt catalysts supported on TiO_2, CeO_2, $CeZrO_x$ in Gly to LA oxidative transformation. LA-lactic acid; GlycA-glyceric acid; TartrA-tartronic acid; C bal-carbon balance (**A**); the scheme of Gly oxidation to LA and GlycA (**B**).

It was noticed that the activity of the catalysts correlated with the degree of the "Au/Pt NPs-support" interaction, which changed according to the following order: Au/Pt/TiO_2 > Au/Pt/$CeZrO_x$ > Au/Pt/CeO_2. Furthermore, the lower was the size of Au/Pt NPs, the higher was the degree of the "Au/Pt NPs-support" interaction.

4 Conclusions

The low-loaded Au/Pt catalysts showed the high activity in Gly to LA oxidation even under very mild conditions not used before. The most efficient catalyst appeared to be 0.025%Au/1%Pt/TiO_2.

References

[1] P.S. Shuttleworth, M. De Bruyn, H.L. Parker, A.J. Hunt, V.L. Budarin, A.S. Matharu,J.H. Clark, *Green Chem.* 16 (2014) 573–584.
[2] Michiel Dusselier, Pieter Van Wouwe, Annelies Dewaele, Ekaterina Makshina, Bert F. Sels, *Energy Environ. Sci.*, 6 (2013)1415-1442. (font style: Times New Roman 11pt)
[3] Y. Shen, S. Zhang, H. Li, Y. Ren, H. Liu, *Chem. Eur. J.* 16 (2010) 7368–7371.
[4] R. Kumar, P. Purushothaman, J. van Haveren, D.S. van Es, I. Melián-Cabrera, J.D.Meeldijk, H.J. Heeres, *Appl. Catal. B: Environ*. 147 (2014) 92–100.
[5] H.J. Cho, C.-C. Changa, Wei Fan, Green Chem. 16 (2014) 3428–3433.
[6] E. Redina, A. Greish, R. Novikov, A. Strelkova,O. Kirichenko, O. Tkachenko, G. Kapustin, I. Sinev, L. Kustov, *Applied Catalysis A: General* 491 (2015) 170–183
[7] E. Redina, O. Kirichenko, A. Greish, A. Kucherov, O. Tkachenko, G. Kapustin, I. Mishin, L. Kustov, *Catal. Today* (2015), http://dx.doi.org/10.1016/j.cattod.2014.12.018

IV-PP115

Peculiarities of Obtaining Alkyl-Substituted 1,4-Benzoquinones in Two-Phase Systems in the Presence of Mo-V-P Heteropoly Acid Solutions

Rodikova Y.A.*, Zhizhina E.G., Pai Z.P.

Boreskov Institute of Catalysis, SB RAS, Department of Catalytic Processes of Fine Organic and Bioorganic Synthesis, Novosibirsk, Russia

* rodikova@catalysis.ru

Keywords: alkylphenols, benzoquinones, catalytic oxidation, heteropoly acid, homogeneous, catalysis

1 Introduction

Alkyl-1,4-benzoquinones (ABQ) such as 2,6-dimethyl-1,4-benzoquinone (DMBQ) and 2,3,5-trimethyl-1,4-benzoquinone (TMBQ) are reactive synthesis precursors and have many applications known for this type of compounds. Nowadays the demands towards environment safety bring necessity to revise existing preparation methods of such compounds and to search for alternative synthesis ways. There are a lot of papers describing ABQ preparation by using various approaches to obtain green processes. However, most of the reported procedures require long reaction times, utilize strong oxidants in large excess, afford products with only modest yields, and use non-reusable catalysts. For this reason, the development of synthetic methods which enable a facile access to these quinones is desirable.

The benzoquinone preparation studies presented are entirely based on the use of heteropoly acids with formula $H_{3+x}PMo_{12-x}V_xO_{40}$ (Mo-V-P HPAs) that enter into the most widely used class of Keggin-type polyoxometalates (POMs). These POMs are characterized by strong Brønsted acidity, high proton mobility, fast electron transfer, high oxidation potential, and excellent resistance against hydrolysis and oxidative degradation in solution. These properties make them very attractive catalysts for oxidation of different organic substrates.

2 Experimental/methodology

2,6-Dimethylphenol (DMP) and 2,3,6-trimethylphenol (TMP) were purchased from Aldrich Chemical Company (99% purity) and used without additional purification. Organic solvents with purity of 98% were purchased from Sibreakhim (Novosibirsk) and applied without preliminary distillation.

A series of Keggin-type $H_{3+x}PMo_{12-x}V_xO_{40}$ aqueous solutions with different content of vanadium atoms (x = 2-6) as well as high-vanadium solutions of formula $H_aP_zMo_yV_xO_b$ ($2 \le z \le 3$, $9 \le y \le 16$, $7 \le x \le 12$, $50 \le b \le 89$) were synthesized from the stoichiometric amounts of V_2O_5, MoO_3, H_2O_2, and H_3PO_4 according to the methods described in [1-2].

The composition of catalysts before and after reaction was investigated by ^{51}V and ^{31}P NMR on a Bruker AVANCE 400 spectrometer at 105.24 MHz and 162.0 MHz, respectively, with $VOCl_3$ and 85 % H_3PO_4 as external standards. Redox potential *E* and pH of the HPA solutions were measured at room temperature by the pH-meter "inoLab pH 730" from Wissenschaftlich-Technische Werkstatten GmbH (WTW).

The oxidation reactions were carried out in a thermostatic glass reactor (volume 100 mL) under atmospheric pressure in a two-phase system: aqueous HPA solution/solution of substrate in a definite organic solvent. The reactor was equipped with a reflux condenser to avoid loss of water and organic solvent. After reaction completion the phases were separated by a funnel. The reduced catalyst was reoxidized in a separate step with O_2 at the temperature of 140-170 °C and partial oxygen pressure of 4 atm. The regeneration was performed in a thermostatic stainless

steel autoclave equipped with a backflow condenser.

Substrate conversion and product amount were determined by the GC-FID (gas chromatography with flame ionization detector) method using a HROMOS GH-1000 chromatograph with a capillary column St-WAX. Tetramethyl-1,4-benzoquinone (DQ) purchased from Merck-Schuchardt (99.9 % purity) was used as an internal standard.

3 Results and discussion

The different reaction parameters which determine relationship between reaction time and selectivity was investigated in order to get the best reaction conditions.

Firstly, the influence of a number of organic solvents (OS) on the selectivities of DMBQ and TMBQ was studied. The amount of quinones appears to be strongly dependent on the type of OS. It was found that the use of appropriate OS allows one to increase the product selectivity from ~7 to 41 % for DMBQ and from 20 to 58 % for TMBQ in the presence of trichloroethylene and octanol-1, respectively.

Encouraged by this result, we tried to improve catalyst activity and desired product yields based on the assumption that a higher reaction temperature and a presence of water-soluble organic component such as HOAc would be beneficial. The results obtained showed that increased reaction temperature as well as content of HOAc in the range of 30-45 vol. % (for oxidation of DMP) accelerate the reaction and improve the quinones selectivity.

The Mo-V-P HPAs are reduced easily and reversibly to form mixed-valence species, heteropoly blues, which retain the structure of the parent oxidized anions (as was confirmed by NMR). The total number of accepted electrons during the reduction of HP-anions in the course of substrate oxidation can be quite high and depends on the vanadium content in HPA solution. As a result, the high vanadium content is preferred to increase the catalyst productivity and makes it possible to carry out the catalytic oxidation processes at a lower catalyst concentration (catalyst to substrate molar ratio). Furthermore, the vanadium content has an influence on the oxidation potential of catalyst *E* that is one of the important factors affecting the oxidation rate and product selectivity. Since the anion structure retains upon reduction, the additional negative charge is compensated for by protonation of the anion from solvent. Therefore, the observed pH value after reaction is higher. The optimized reaction conditions are presented in Table 1.

Table 1. Optimized conditions of DMP and TMP oxidations to the corresponding quinones.

Substrate	Catalyst	OS	T [°C]	HOAc [vol.%]	[Cat]/[Su]	E_0 [V]	Time [min]	Selectivity [%]
DMP	0.25 M	trichloroethylene	60	30	5	≥ 0.91	20	85
TMP	$H_{17}P_3Mo_{16}V_{10}O_{89}$	octanol-1	60	-	3.3	≥ 0.98	45	99

4 Conclusions

The influence of various parameters such as concentration of substrate, solvent, temperature, catalyst composition et al. on the catalytic process was examined in details regarding the selectivity of 2,6-dimethyl- and 2,3,5-trimethyl-1,4-benzoquinones. At the temperature of 60 °C under optimized conditions, DMBQ was produced with selectivity of 85 % whereas the selectivity of TMBQ was 99 %. Actually no polymerization of substrate occurred under the optimized conditions. The catalyst can be separated and reused. Mo-V-P HPA solutions are remarkable catalysts because they possess not only a fairly high oxidation potential, but also their reduced forms are very easily reoxidized by oxygen (air).

References

[1] V. Odyakov, E. Zhizhina, R. Maksimovskaya, *Appl. Catal. A: Gen*. 342 (2008) 126

[2] V. Odyakov, E. Zhizhina, *Rus. J. Inorg. Chem.* 54 (2009) 409

IV-PP116

Efficient Metal-Free Pathway to Vinyl Thioesters with Calcium Carbide as the Acetylene Source

Rodygin K.S.[1*], Ananikov V.P.[2]

1 - Institute of Chemistry, Saint Petersburg State University, Saint Petersburg, Russia
2 - N. D. Zelinsky Institute of Organic Chemistry of the Russian Academy of Sciences, Moscow, Russia

* konstantinrs@rambler.ru

Keywords: calcium, carbide, vinyl, sulphides, thiovinylation

1 Introduction

Catalytic organic reactions showed great potential in development of cost-efficient and environmentally benign synthetic procedures. A variety of techniques aimed for generation of new C–C, C–Hal, C–O, C–P, C–S bonds via catalytic processes, were successfully employed in the search for new pharmacological substances, materials, and synthetic building blocks. However, there are not many catalytic reactions, where inexpensive, ton-scale substance is used to produce useful building blocks in synthetic chemistry [1].

Calcium carbide is an industry-scale product, traditionally synthesizing from coal, hydrocarbons and biomass. The low production costs put calcium carbide in a better position to serve as a sustainable resource for organic chemistry.

2 Experimental

We developed an alternative straightforward protocol for the preparation of vinyl thioesters via reaction of calcium carbide with thiols. This elegant and cost-efficient procedure can be widely employed in laboratory practice towards preparation of useful building blocks. Mechanistic studies have demonstrated that the thiovinylation involves the initial *in situ* formation of acetylene, thus, clearly demonstrating the potential of calcium carbide as an acetylene replacement in organic synthesis.

Acknowledgements

K. S. Rodygin gratefully acknowledges Saint Petersburg State University for a postdoctoral fellowship (№ 12.50.1560.2013). The authors also express their gratitude to Centre for Magnetic Resonance, and Centre for Chemical Analysis and Materials Research (Saint Petersburg State University) for physicochemical measurements.

References

[1] Ananikov V.P., Khemchyan L.L., Ivanova Yu.V., Bukhtiyarov V.I., Sorokin A.M., Prosvirin I.P., Vatsadze S.Z., Medved'ko A.V., Nuriev V.N., Dilman A.D., Levin V.V., Koptyug I.V., Kovtunov K.V., Zhivonitko V.V., Likholobov V.A., Romanenko A.V., Simonov P.A., Nenajdenko V.G., Shmatova O.I., Muzalevskiy V.M., Nechaev M.S., Asachenko A.F., Morozov O.S, Dzhevakov P.B., Osipov S.N., Vorobyeva D.V., Topchiy M.A., Zotova M.A., Ponomarenko S.A., Borshchev O.V., Luponosov Y.N., Rempel A.A., Valeeva A.A., Stakheev A.Yu., Turova O.V., Mashkovsky I.S., Sysolyatin S.V., Malykhin V.V., Bukhtiyarova G.A., Terent'ev A.O., Krylov I.B., "Development of new methods in modern selective organic synthesis: preparation of functionalized molecules with atomic precision", *Russ. Chem. Rev.*, **2014**, 83, 885 – 985.

IV-PP117

Liquid-Phase Methanol Synthesis Using Polymerstabilized Catalysts Based on Zinc

Rubin M.A.[1], Sulman E.M.[1*], Smelkova V.V.[1], Murzin D.Yu.[2], Sidorov A.I.[1], Warna J.[2]

1 - Tver Technical University, Tver, Russia
2 - Åbo Akademi University, Turku, Finland

* sulman@online.tver.ru

Keywords: liquid-phase methanol synthesis, heterogeneous catalysis, polymer, carrier

1 Introduction

Modern chemical industry consume considerable amount of methanol for the obtaining of formaldehyde, for the synthesis of alcohol esters of organic and inorganic acids, methyl tertiary butyl ether [1]. Novel prospective ways of methanol application such as waste water purification, synthetic protein, fuel cells, conversion into hydrocarbons for the fuel obtaining have recently appeared. It was practically revealed that the gas for methanol synthesis must contain the components in a ratio close to stoichiometric. To obtain such a ratio it is necessary in most cases to change gas composition.

Now there exist gas-phase (two-phase) and liquid-phase (three-phase) catalytic methods of methanol synthesis. The simplicity of the reactor design, rather uniform distribution of liquid and gas over the reactor cross section, the possibility of the catalyst input and output without the system stoppage, rather low gas axial diffusion and effective use of the reaction heat as well as relatively low temperature of the process are the advantages of liquid-phase synthesis [2, 3].

In this paper the results of the study of the kinetics and modeling of methanol synthesis process on polymer-stabilized catalysts – Zn on hypercrosslinked polystyrene are presented.

2 Experimental

Synthesis of ZnO-containing catalyst based on MN-100. The catalyst was prepared by impregnation of MN-100 (Hypercrosslinked polystyrene, Purolite Int.) with $Zn(CH_3COO)_2$ in a solution containing THF, methanol and distilled water. In a typical procedure, 0.845 g of $Zn(CH_3COO)_2$ was dissolved under nitrogen in 7 mL of the solvent mixture consisting of 5 mL of THF, 1 mL of water and 1 mL of methanol, to which 3 g of MN 100 were added. The suspension was continuously stirred for 10 min to allow absorption of the solution by the polymer granules. Then the sample was treated with the Na_2CO_3 solution, and after 10 min stirring, it was dried. After that the catalyst was washed with water at pH=6.4-7.0 and dried. The ZnO content was calculated according to loading. The samples were designated as MN100-Zn-3%, MN100-Zn-5%, MN100-Zn-7.5%, and MN100-Zn-10%, respectively.

The above method was used for the synthesis of ZnO/Cu-containing catalysts.

Experimental technique

The experiments were conducted in a flow-type laboratory steel reactor (Parr Instruments), volume 25mL. The reaction mixture was analyzed by the method of gas chromatography on KRISTALLUX 4000M chromatograph.

3 Results and discussion

Some ZnO-containing catalysts based on MN100 were characterized by the low-temperature nitrogen physisorption:

ID cat.	BET specific surface area (SSA), m^2/g

MN-100	723
MN100-Zn-3%	834
MN100-Zn-5%	770
MN100-Zn-7.5%	665
MN100-Zn-10%	446

By liquid nitrogen physisorption it was shown that all the catalysts have micro-mesoporous structure with the SSA varied from 446 m^2/g to 834 m^2/g depending on Zn loading. It is noteworthy that the decrease of the SSA at higher zinc concentrations is mainly due to the decrease of microporosity. The existence of mesopores as well as high values of the SSA makes HPS based catalytic systems promising candidates for methanol synthesis from the viewpoint of catalytic NP stabilization inside the HPS mesopores.

The results of XPS study revealed the presence of zinc in the form of Zn^{+2} in the catalysts.

It was found out during the preliminary experiments that methanol is most actively synthesized on MN100-Zn-3% catalyst which has the best results according to the data of nitrogen low-temperature adsorption. Methanol synthesis on this catalyst was performed at varying the pressure (1.5 – 5 MPa), the rate of the initial gas mixture feed and the temperature. Isopropyl alcohol was used as the reaction medium. Industrial MEGAMAX700 was tested for the comparison of the results obtained.

Methanol maximal yield was achieved at a temperature of 170˚C and a gaseous flow rate 270 mL/min. The data obtained were used for the calculation of the apparent activation energy (E_{act}) of methanol synthesis which made 6 - 10 кJ/mol. E_{act} low value is probably explained by relatively high temperatures of the process which provide prevailing of the kinetic stages rates over the diffusion ones.

In the case of bimetallic Zn-Cu catalysts, it was revealed that the method of the catalyst synthesis (consecutive impregnation of metal-containing salts or co-precipitation) does not play any significant role in the methanol accumulation rate. Moreover, the addition of Cu to ZnO seems to have no positive impact on methanol formation rate.

Aknowlegments

Authours sincerely thank FP7-NMP-2013-LARGE-7 (Grant Agreement Number 604296) project for financial support.

References

[1] B. Hu, K. Fujimoto, ApplCatalA-Gen. 346 (2008) 74–178.

[2]S. Schimpf, A. Rittermeier, X. Zhang, A. Li, M. Spasova, W. Mauritz, E. van den Berg, M. Farle, Y. Wang, R. Fischer, M. Muhler, Chemcatchem. 2 (2010) 214 – 222.

[3]X. Zhang, Fuel. 89 (2010) 1348–1352.

IV-PP118

High Catalytic Activity of Nanoheterogeneous Systems Based on Aqueous Solutions of Cationic Surfactants of Low Concentrations in Hydrolysis of Phosphorus Acid Esters

Ryzhkina I.S.*, Kiseleva Yu.V., Konovalov A.I.

A.E. Arbuzov Institute of Organic and Physical Chemistry, Kazan Scientific Center, RAS, Kazan, Russia

* ryzhkina@iopc.ru

Keywords: hydrolysis, catalytic activity, nanoreactors, surfactants, solutions of low concentrations

1 Introduction

We have recently found that nanoassociates are formed in the highly dilute aqueous solutions of bioactive compounds (10^{-6}-10^{-20} M) with the participation of external physical (geomagnetic and low-frequency electromagnetic) fields [1]. These nanoassociates are responsible for their unusual physicochemical properties. In the present work we have study a catalytic activity of the highly diluted aqueous solutions (10^{-2}-10^{-16} M) of cationic surfactants **1**, **2** in the hydrolysis of phosphorus acid esters **3**, **4** by a complex of physicochemical methods (DLS, NTA, UV, ^{31}P NMR).

2 Experimental/methodology

Solutions prepared by successive serial dilutions were kept under ambient conditions and under conditions of reduced external physical fields (in a permalloy container) for 24 hours at 25°C. Using this approach allows to determine the threshold concentration (c_{th}) below and above which nanoassociates [1] and domains [2] are formed in diluted solutions.

3 Results and discussion

The solutions of surfactant **1** are dispersed systems in which micelles, domains and nanoassociates are formed in various concentration ranges (10^{-2}-10^{-3}, 10^{-2}-10^{-5}, 10^{-6}-10^{-12} M respectively) (fig. 1, curve 1) [3]. By NTA method it has shown that in the solutions **1** at $1\cdot10^{-5}$ M and $1\cdot10^{-7}$ M concentration of domains and nanoassociates equals approximately 10^{8} particles/mL. The formation of domains (D~300 nm) was also observed in water-ethanol (10 %vol. ethanol) solution **3** at $1\cdot10^{-4}$ M. Adding the water-ethanol solution **3** to diluted aqueous solution **1** leads to the formation of mixed domains **1+3**. Concentration dependences of size (D, effective hydrodynamic diameter) of nanoassociates **1** and domains **1+3** are comparable, but D of domains **1+3** (fig. 1, curve 2) is more then D of nanoassociates in solution **1** (fig. 1, curve 1) and D of domains in solution **3**. ^{31}P NMR signal of substrate **3** (δ = -17,4 ppm) and products of the hydrolysis **6, 8** (δ = -8,4; -9,4 ppm) (Scheme 1) disappears in case of the forming mixed domains **1+3**.

Scheme 1. Catalysis of hydrolysis of substrate **3** in nanoheterogeneous systems based on aqueous solutions of cationic surfactants of low concentrations

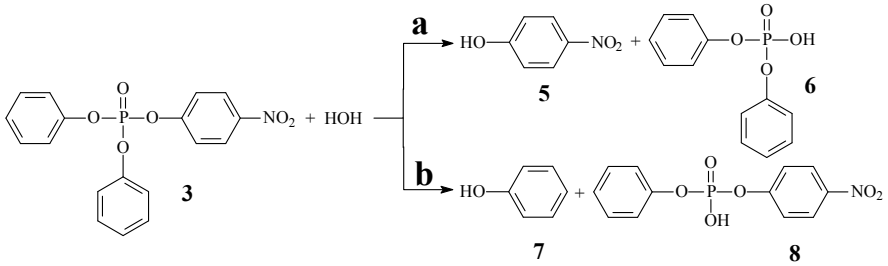

The kinetics of hydrolysis **3** and **4** in aqueous solutions of surfactants **1**, **2** was studied by spectrophotometry from the increase in optical density due to the formation of *p*-nitrophenolate (λ 400 nm) at pH 8.0. The correlation between self-organization of **1** and **1+3** solutions (fig. 1) and the observed rate constant (k_{obs}) of the reaction (fig. 2, curve 1) was established. In solutions **1+3** ($c_1=1\cdot10^{-9}$ M, $c_3=1\cdot10^{-4}$ M) where mixed domains with extreme size are formed (fig. 1, curve 2), k_{obs} is higher than k_{obs} in the micellar solution (10^{-2} M) and k_{obs} of alkaline hydrolysis **3** at pH 8.0 on approximately two and five orders respectively (fig 2, curve 1).

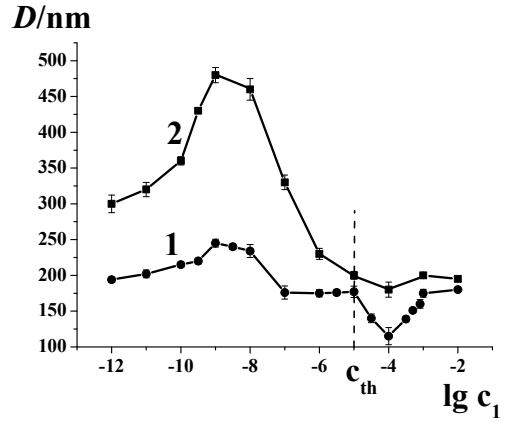

Fig. 1. Concentration dependences of the particle size (D) in solutions of **1** (*1*) and **1+3** (*2*); $c_3 = 1\cdot10^{-4}$ M, 25°C.

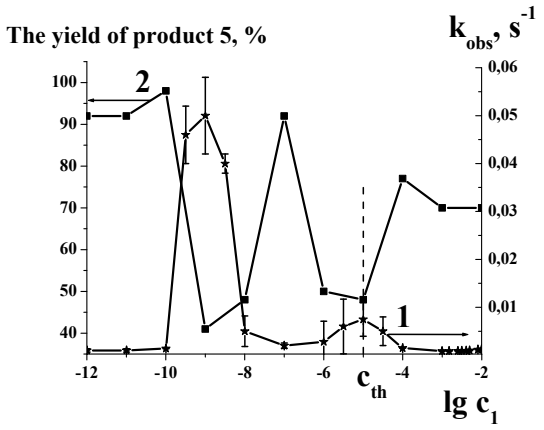

Fig. 2. Concentration dependences of k_{obs} (*1*) and the yield of the hydrolysis product **5** (UV method) (*2*) in solutions of surfactant **1**, pH 8.0, 25°C.

From ^{31}P NMR and UV experiments the yields of the hydrolysis products **5-8** (fig. 2, curve 2) are found. The results show that hydrolysis **3** occurs in two ways (scheme 1, **a** and **b**) in ranges of low concentrations of solutions **1** with maximum at $1\cdot10^{-9}$ and $1\cdot10^{-5}$ M, where nanoassociates and domains with extremely sizes are formed (fig. 1, curve 1). Analogical scheme was shown for hydrolysis of phosphorus acid esters in micellar systems [4, 5]. An important point is that the catalytic activity of nanoheterogeneous system formed at $1\cdot10^{-9}$ M is considerably higher than the catalytic activity of systems at $1\cdot10^{-5}$ M and $1\cdot10^{-2}$ M. Hydrolysis **3** occurs by one way (scheme 1, **a**) with maximum yield of product **5** by analogy with alkaline hydrolysis at $1\cdot10^{-4}$, $1\cdot10^{-7}$ M and 10^{-10}-10^{-12} M, where domains and nanoassociates are rearranged (fig. 1). The rate of hydrolysis at these concentrations is considerably lower (fig. 2, curve 2) then at $1\cdot10^{-9}$ and $1\cdot10^{-5}$ M. Nanoassociates are not formed at 10^{-6}-10^{-12} M in hypoelectromagnetic conditions, and catalytic activity disappears.

4 Conclusions

The obtained results demonstrate that a highly reactivity nanoreactors (mixed domains) are formed in systems based on aqueous solutions of cationic surfactants of low concentrations and solutions of phosphorus acid esters. The nanoreactors are capable to cleave phosphorus acid esters with high rate at low concentrations of surfactants in mild conditions mimicking hydrolytic enzyme reactions.

Acknowledgements

This work was financially supported by the RFBR (Project No. 13-03-00002).

References

[1] A.I. Konovalov, I.S. Ryzhkina, *Russ. Chem. Bull., Int. Ed.* 63 (2014) 1.
[2] M. Sedlák, D. Rak, *J. Phys. Chem. B*. 117 (2013) 2495.
[3] I.S. Ryzhkina, O.A. Mishina, et al. *Doklady Physical Chemistry*. 459 (2014) 166.
[4] S.H. Gellman, R. Petter, R. Breslow. *J. Am. Chem.Soc*. 108 (1986) 2388.
[5] B.A. Burnside, I.Y. Szafraniec, et al. *J. Org. Chem.* 53 (1988) 2009.

IV-PP119

Differential Selectivity Measurements as Effective Means for Mechanistic Studies of Catalytic Reactions

Schmidt A.F.*, Kurokhtina A.A., Larina E.V.

Irkutsk State University, Chemistry Department, Irkutsk, Russia

* aschmidt@chem.isu.ru

Keywords: differential selectivity, mechanistic studies

1 Introduction

The differential selectivity of a catalyst is rarely considered in kinetic investigation. However, differential selectivity measurements have a number of advantages in comparison with catalytic activity measurements. When complex catalytic processes accompanied by intensive catalyst transformations occur outside the catalytic cycle (formation, deactivation and/or poisoning of the active species) the differential selectivity can be the sole tool to clarify the nature of the active species and kinetics of the elementary steps in the catalytic cycle. We attempted to briefly review the basic principles and practices of mechanistic studies based on differential selectivity measurements, including the use of artificially created competitive reactions.

2 Conclusions

The comparison with traditional kinetic investigations based on the activity measurements highlights that the approach has many advantages [1]:

1. Differential selectivity does not depend on the amount of true active species when the reaction products form on the same active catalysts. It makes the interpretation of experimental data much simpler.

2. Artificial multi-route reactions arising upon addition of several substrates with similar properties (competing reaction method) are completely sufficient to assume that the reaction products form on the same active catalyst.

3. The independence of differential selectivity on the total amount of active catalyst allows for the derivation of mechanistic information about catalytic cycle intermediates in reactions with numerous catalyst transformations occurring outside the catalytic cycle (formation and deactivation of active species), i.e. when the concentration of the active species is non-stationary.

4. The visualization of kinetic data by plotting the phase trajectories of the reaction products allows one to estimate the changes in the differential selectivity without using a mathematical description based on definitive mechanistic hypotheses.

5. The practice of studying differential selectivity in complex catalytic processes demonstrates that differential selectivity measurements provide information about the nature of the active species, the catalyst resting state, rate-limiting step within the catalytic cycle, and degree of reversibility of its stages.

6. The differential selectivity equations are much simpler in comparison with activity (rate) equations. This is only possible with differential selectivity measurements of a catalyst but not with activity measurement.

The greatest advantage of the study of differential selectivity is the possibility of studying the reactions carried out with high ratios of substrate/catalyst, i.e. real catalytic conditions, because model reaction studies may lead to incorrect conclusions.

Acknowledgements

This work was supported by a grant from the Russian Scientific Found (no. 14-13-00062)

References

[1] A. Schmidt, A. Kurokhtina, E. Larina, Catal. Sci. Technol. 4 (2014) 3439.

IV-PP120

Some Aspects of Kinetics and Mechanism of the Heterogeneous Iso-Butane/Butene Alkylation over Solid ZrO_2-Al_2O_3/HY Catalyst

Semikin K.[1*], Smirnova D.[2], Sladkovskiy D.[2], Postnov A.[3], Malt'zeva N.[3], Murzin D.[1]

1 - St. Petersburg State Technological Institute (Technical University), Laboratory of Catalytic Technologies, St.Petersburg, Russia

2 - St. Petersburg State Technological Institute (Technical University), Resource-Saving Department, St.Petersburg, Russia

3 - St. Petersburg State Technological Institute (Technical University), General Chemical Technology and Catalist Department, St.Petersburg, Russia

* kirse@mail.ru

Keywords: alkylation, zirconium-zeolit catalysts, high-octane component, resource-saving technology

1 Introduction

Nowdays, there is a constant tendency to improve not only operating characteristic but also environmental properties of motor gasoline. In order to reduce the total content of aromatic hydrocarbons manufacturers produce a high-octane reformate by dilution with non-aromatic components. One way of producing such components is the alkylation of isobutane with butylenes to produce isooctane and its isomers (trimethylpentanes). The desired product of this process named as alkylate. The alkylate complies with the technical, operational and environmental requirements of modern European and American standards. The alkylate has a low vapor pressure, it does not contain sulfur, oxygen, nitrogen and aromatics. The present work is focused on the development of efficient catalysts for producing of alkylate and new energy-saving technology of production gasoline based on the use of alkylate. The purpose of this research is to analyze the mechanism of heterophase alkylation reactions on ZrO_2-Al_2O_3/HY catalyst based on experimental results.

2 Experimental/methodology

The alkylation of iso-butane with 2-butene was performed in a plug-flow reactor operated in continuous mode. Operating parameters of the process: temperature range (50-125) °C; pressure 7 atm; paraffins / olefins ratio 19/1, space velocity 3 h^{-1}).

The calculation of the rate constants of reactions was carried out by Box complex method. The determination of the kinetic parameters (activation energy E_a and pre-exponential factors k_0) was carried out by least squares.

3 Results and discussion

The aim of this work was to examine the rates of different alkylation reaction. The main reactions occurring during the alkylation of isobutane and the rates equations for each reaction step are given in Table 1.

Table 1. Reactions and rates equations of the alkylation on ZrO_2-Al_2O_3/HY

Step	Reactions	Rate equations
1	$iC_4H_{10} + C_4H_8 \rightarrow C_8H_{18}$ (TMP)	$r_1 = k_1 \cdot P_{c4} \cdot P_{ic4}$
2	$iC_4H_{10} + C_4H_8 \rightarrow C_8H_{18}$ (DMH)	$r_2 = k_2 \cdot P_{c4} \cdot P_{ic4}$
3	$2C_8H_{18} \rightarrow C_{10}H_{22} + C_6H_{14}$	$r_3 = k_3 \cdot P^2_{c8}$
4	$C_{10}H_{22} \rightarrow C_4H_{10} + C_6H_{12}$	$r_4 = k_4 \cdot P_{c10}$

The rate constants of these reactions were determined by minimizing of function $\min_{k_{1}...k_{n}} \sum_{i=1}^{N}(C_i^{calc}(k_1...k_2) - C_i^{exp})^2$, where i – component index, N – component number, $k_{1}...k_{2}$ – rate constants, n – reaction number, C_i^{calc}– calculated concentrations of component i, C_i^{exp}– experimental results concentrations. Arrhenius equation was used for the temperature dependence of reactions rates.
Table 1 describes the determined activation energy and pre-exponential factors for reactions steps listed above.

Table 2. Kinetic parameters of the iso-butane/butene alkylation on ZrO_2-Al_2O_3/HY

Step No	E_a, kJ/mol	k_0, mol/(s·g)
1	7.3	54
2	21.0	356
3	26.1	3013
4	34.6	21998

The validation of the model was checked by comparison of the experimental and calculated values of the concentrations obtained using the kinetic parameters. The values of the concentrations of the reaction products at different temperatures are listed in Table 3.

Table 3. Experimental data and calculated results at different temperatures

Temperature, ^{0}C	Concentration, % mol.							
	50		75		100		125	
	experiment	model	experiment	model	experiment	model	experiment	model
$C_{8(TMP)}$	**78.0**	78.3	71.2	68.2	57.7	57.2	47.0	46.7
$C_{8(DMH)}$	**3.2**	3.1	3.8	3.9	4.4	4.5	5.0	4.8
$\sum C_6$	**10.0**	9.7	15.0	15.2	23.5	21.9	30.0	29.0
C_{10}	**8.0**	7.9	8.2	10.2	9.2	11.0	9.5	10.0
nC_4	**1.0**	0.9	2.0	2.5	5.0	5.4	8.0	9.5

4 Conclusions

Kinetics of heterogeneous iso-butane/butene alkylation over solid ZrO_2-Al_2O_3/HY catalyst was modelled using experimental data of a plug-flow reactor. The validation of the model was checked using all experimental data and the predicted results.

The results obtained is used for development of technology with fast and close contact of the catalyst and hydrocarbon at a high yield while minimizing trimethylpentane undesirable secondary reactions.

Acknowledgements

Work carried out in accordance with the grant №381 of the Russian Government to support research conducted under the guidance of leading research scientists at Russian institutions of higher education on the topic: "The process of alkylation of isobutane with light olefins on solid catalysts using reactive distillation technology" contract №14.Z.50.31.0013, on 03/19/2014.

References

[1] P. Zernov, D. Murzin, O. Parputs, N. Kuzichkin, *Izv. Vyssh. Uchebn. Zaved. Khim. Khim. Tekhnol.* 9 (2014) P.100-104.

IV-PP121

Alkylation of Phenol Using Ionic Liquid Catalyst: A Mechanistic Study

Shaurya M., Elavarasaran P., Parveen F., Upadhyayula S.*

IIT Delhi, New Delhi, India

* sreedevi@chemical.iitd.ac.in

Keywords: alkylation, tert-butylation, phenol, p-cresol, ionic liquid (IL), semi-empirical

1 Introduction

The Alkylation of Phenols using Ionic Liquid (IL) catalyst (N- butyl (1, 4-sulfonic acid) triethylammonium hydrogen sulphate) has been investigated by performing Quantum chemistry calculations to understand the *tert*-butylation reaction mechanism qualitatively at molecular level and obtain relative rates, reaction barriers, and product selectivity. All gas phase of reactants, products, intermediates and transition states were fully optimized using a semi-empirical PM3 method, in MOPAC'09. In order to identify transition state (TS), SADDLE calculations in MOPAC package were successfully applied, to generate trial geometries for unknown transition state complexes[1]. All ground states were positively identified for local minima (zero imaginary frequency, i.e. without –ve force constant) and for TS (one single imaginary frequency)[2] . Vibrational frequencies were also checked to confirm ground states and TS which are necessary for calculating thermodynamic parameters. In all experiments equimolar ratios of reactants were used along with ionic liquid.

2 Methodology

Saddle Calculation and Activation Energy calculations

SADDLE method automatically locates a transition state between the reactant and product geometries. It is particularly useful for finding complex transition states, when more than two bonds are involved (breaking or making). The input data consists of the geometries of the reactants and products, specified with same numbering and connectivity. The keywords SADDLE AND XYZ were used for finding the approximate geometry for TS. In these calculations, reactant and product geometries were optimized and compared in a progressive and systematic manner with reference to one another to converge or attain maximum heat of formation, by invoking the SADDLE keyword. Finally, we approach the approximate transition state region and this can be refined by gradient minimization procedure by invoking TS. The apparent activation was obtained for each set of reactant and products through force calculations on both ground state and transition state geometries by subtracting free energy of reactants from free energy of the TS

3 Results & Discussion:

Alkylation of p-cresol with tert-butyl alcohol is an acid catalysed reaction and product selectivity largely depend on acidity, solvent and temperature of the system. Major products of the reaction are C-alkylated and O-alkylated products. O-alkylated product is a result of t-butyl attack on oxygen in p-cresol (O-alkylation) that leads to the formation of ether besides the C-alkylated products.

According to this mechanism, the ionic liquid ester formed, also proceeds by two pathways, one via the formation of transition state GTS1, GINT and GTS2 to yield TBC and another via the formation of GTS3 followed by O-alkylated product, cresyl tert-butyl ether (CTBE) .The formation of ether is consistent with the observation of Liu et al[3] in the same reaction, using

pyridine based ionic liquid catalysts conducted, in a non-polar solvent. They explained that the ether product is thermodynamically unstable and continuously consumed to yield TBC via an intermediate. The formation of O-alkylated product is also explained by figure 1 which shows the corrected electronic energies (*E*) for *tert*-butylation of *p*-cresol excluding the effect of solvent

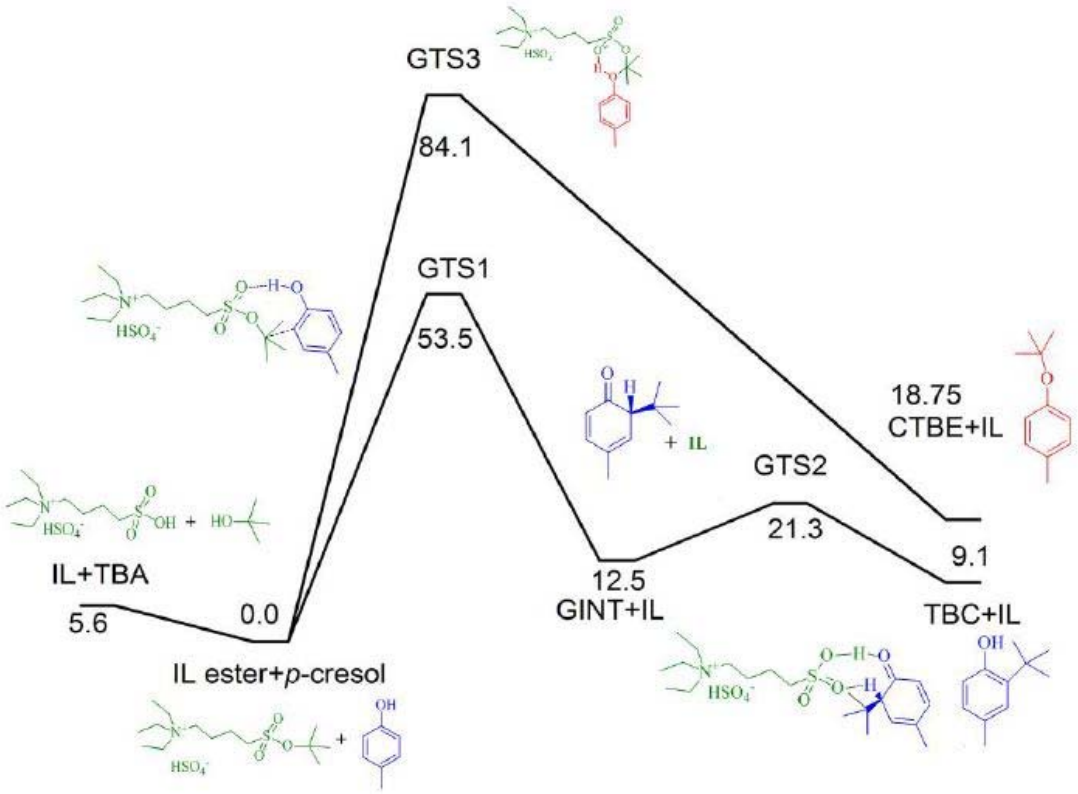

Fig. 1. Schematic view of corrected electronic energies (*E*) for *tert*-butylation of *p*-cresol excluding solvent effect as given in figure in cal/mol.

4 Conclusion

The *tert*-butylation of phenols in ionic liquids is modelled using semi empirical computational techniques considering the p-cresol alkylation. The mechanism involved and reactivity have been studied at the molecular level both in the presence and absence of solvent. In the presence of polar solvent C-alkylation pathway is favoured. In the absence of solvent or in the presence of non-polar solvent both C and O-alkylation pathways lead to the desired product formation.

References

[1] Tasi, G.; Mizukami, F.; Toba, M.; Niwa, S.-i.; Palinko, I., Molecular Electrostatics, Energetics, and Dynamics of the Alkylation of Naphthalene: Positional Isomerization of Monoalkylnaphthalenes at Hartree−Fock and Correlated Levels with BSSE Corrections, *The Journal of Physical Chemistry A* **2000**, *104*, 1337.

[2] *James J. P.Stewart.MOPAC Manual, (Seventh Edition) PUBLIC DOMAINCOPY, FUJITSU LIMITED,1993*

[3] Liu, X.; Zhou, J.; Guo, X.; Liu, M.; Ma, X.; Song, C.; Wang, C., SO3HFunctionalized Ionic Liquids for Selective Alkylation of p-Cresol with tert- Butanol, *Industrial & Engineering Chemistry Research* **2008**, *47*, 5298

IV-PP122

Preferential Hydrogenation of Carbon Monoxide to Olefins over Catalysts of Perovskite-Type Ferrites

Sheshko T.F.[1*], Serov Y.M.[1], Dementieva M.V.[1], Shulga A.[1], Chislova I.V.[2], Zvereva I.A.[2]

1 - Peoples Friendship University of Russia, Faculty of Science, Physical and Colloidal Chemistry Department, Moscow, Russia

2 - Saint-Petersburg State University, Saint-Petersburg, Russia

* sheshko@bk.ru

Keywords: hydrogenation, carbon monoxide, olefins, ferrites, perovskite

1 Introduction

Hydrocarbon synthesis from CO and H_2 on heterogeneous catalysts (Fischer-Tropsch synthesis) is now regarded as a real alternative to their production of oil. Known and proven in industry processes provide a relatively wide range of products with different content of olefins in the individual hydrocarbons fractions. Therefore, an essential object of research is to increase the selectivity of the hydrocarbons synthesized by limiting the number of atoms C, as well as development of catalytic systems allowing to convert carbon oxides into olefins at atmospheric pressure, and having high performance in the processes described. In connection with the development of highly efficient catalysts based on nanostructured perovskite systems, study of the role of various factors affecting their adsorption, catalytic activity, selectivity and stability is promising.

2 Experimental/methodology

Studied in this paper layered oxides $GdFeO_3$, $SrFeO_{3+x}$, $GdSrFeO_4$, $Gd_2SrFe_2O_7$ and solid solutions $Gd_{2-x}Sr_{1+x}Fe_2O_7$ (x = 0,1 - 0,6) were synthesized by the high temperature solid state reactions and by sol-gel technology.

Characterization by powder X-ray diffraction (XRD) and scanning electron microscopy (SEM), has been performed for the determination of the structure and morphology of synthesized samples. XRD was performed on a Thermo ARL X'TRA diffractometer using CuKα radiation. The SEM images of synthesized samples were obtained on Carl Zeiss EVO 40EP and Zeiss Supra 40VP scanning electron microscopes. Mössbauer spectra have been recorded at room temperature by using spectrometer Wissel (57Co in a rhodium matrix with activity 10 mKu), the isomeric shifts were calculated with respect to α-Fe. In order to evaluate the part of paramagnetic species the intensity of the signals was determined precisely up to the factor of resonance absorption.

The hydrogenation of carbon oxide was studied in a flow catalytic unit at atmospheric pressure in a unit temperature range of 573 to 823 K, ratios of the components [$CO:H_2$] = 1:1, 1:2 and 1:4 and space velocities 1.5 - 3.0 l / h. Analysis of the products was performed by chromatography (Crystal 5000) using a column of stainless steel filled with Poropac Q at 393 K.

3 Results and discussion

Among synthesized ferrites there are three-dimensional perovskites $GdFeO_3$, $SrFeO_{3+x}$, and two-dimensional perovskite-type layered structures $GdSrFeO_4$, $Gd_2SrFe_2O_7$, $Gd_{2-x}Sr_{1+x}Fe_2O_7$, belonging to Ruddlesden-Popper phases $A_{n+1}B_nO_{3n+1}$ (n=1,2) and built up on the block principle from perovskite layers with different thickness. X-ray powder diffraction confirmed the presence of single phase for samples obtained both by high temperature solid state reactions and by sol-gel technology as well.

Scanning electron microscopy demonstrated decreasing of size of particles of complex ferrite from 10 μm, obtained by ceramic technology, up to 200 nm, obtained by the sol-gel technology. Mössbauer spectroscopy showed the difference of electronic state of complex ferrite, prepared by ceramic technology (Fe^{+3}) and oxides obtained by sol-gel technology (Fe^{+3} in the three different surrounding and Fe^{+4}).

Reaction products of hydrogenation of carbon monoxide are hydrocarbons C_1 - C_5, the main ones are methane, ethylene, propylene. The greatest amount of olefins formed in the reaction was observed in the stoichiometric ratio of CO and H_2. The catalytic activity (rate of product formation) increases in the series: $SrFeO_{3-x}$ < $GdSrFeO_4$ < $Gd_{1,6}Sr1_{,4}Fe_2O_7$ < $Gd_{1,8}Sr_{1,2}Fe_2O_7$ < $Gd_2SrFe_2O_7$ < $GdFeO_3$, that is a correlation with the number of alternating perovskite layers in the ferrites structure – 1, 2, ∞ . However, samples with n = 2 showed the highest selectivity for ethylene and propylene (Figure 1).

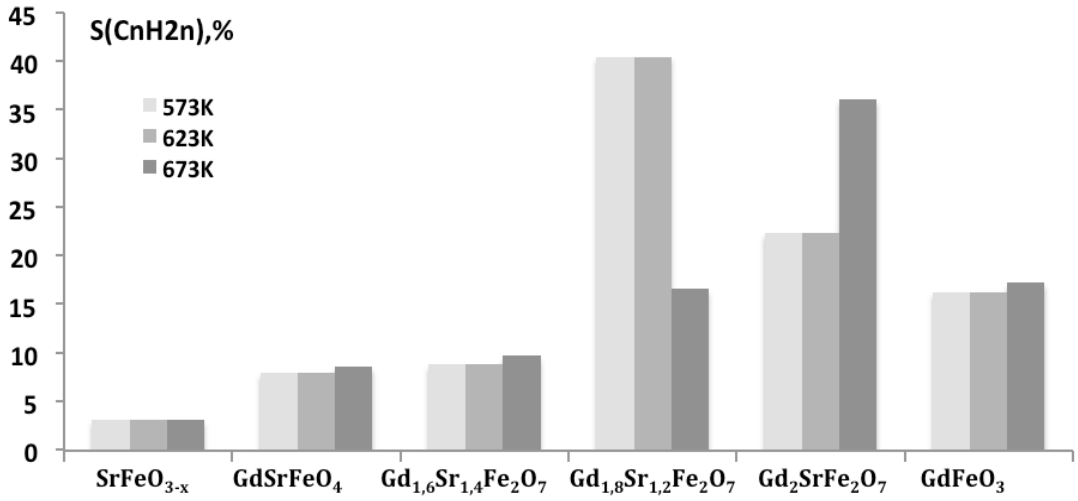

Fig. 1. Total olefin selectivity during the reaction in a ratio of $CO:H_2$=1:2.

The increase in strontium content in layered oxides $Gd_{2-x}Sr_{1+x}Fe_2O_7$ to x = 0.6 lowers the symmetry of atoms Fe^{+3} and increases the number of oxygen vacancies, which affect the selectivity (the maximum value of its observed at x = 0.3). Suggested that heterovalent state of iron (Fe^{3+}, Fe^{4+}) is favorable for the CO activation, which leads to the formation of C * and CH_x radicals. It is shown that under the influence of the reaction medium and the temperature there is changing the state of the active centers: probably a partial iron reduction.

Higher catalytic performance of perovskite-like ferrites synthesized by sol-gel method, may be related to their nanocrystalline state with a porous structure, as well as iron heterovalent state.

4 Conclusions

Catalytic properties of advanced materials - perovskite-type ferrites $A_{n+1}Fe_nO_{3n+1}$ (A=Gd, Sr; n=1, 2, ∞) were investigated in the carbon monoxide hydrogenation at atmospheric pressure. It was found correlation between the catalytic activity, selectivity to olefins and methods synthesis of complex oxides, the number of perovskite layers, crystallite size, cationic composition and iron valence state.

Acknowledgements

This work was supported by the Russian Foundation for Basic Research (№ 14-03-00940).

IV-PP123

Hydrodearomatization Processes in Dispersion Systems: Unsupported Ni-W-S Catalysts Synthesized In Situ

Sizova I.A.[1*], Serdyukov S.I.[1,2], Shaydullina G.[3], Maximov A.L.[1,2]

1 - A.V. Topchiev Institute of Petrochemical Synthesis RAS, Moscow, Russia
2 - Moscow State University, Dep. of Chemistry, Moscow, Russia
3 - LECO, Russia

* isizova@mail.ru

Keywords: hydrodearomatization, unsupported, catalysts, nickel-tungsten, sulfides, LCO

1 Introduction

In recent years the interest in studying of nanoscale particles as catalysts in dispersion systems significantly increased. It is connected to the fact that new promising possibilities of using nanomaterials in many areas of science and technology in particular to obtain of efficient and selective catalysts has been discovered [1-2]. The such dispersed-phase catalytic approach was used for hydroconversion of heavy oil residue, in Fischer-Tropcsh process [3]. In this research *in situ* synthesis and catalytic activity in hydrogenation of aromatic hydrocarbons in the presence of nanosized tungsten/nickel sulfides are described. The three different approaches for catalysts synthesis (from emulsion of ionic liquids in hydrocarbons, from emulsion of water in hydrocarbons and by thermolysis of precursor in hydrocarbon solutions) have been studied.

2 Experimental

To obtain the catalysts *in situ* in the ionic liquid, thermostable ionic liquid [BMPip][CF_3SO_3] as the solvent for the precursor has been selected. The complex of nickel-thiotungstate $[BMPip]_2Ni(WS_4)_2$ was used as a precursor. It was obtained by the new method of precipitation from the solution of ammonium thiotungstate $(NH_4)_2WS_4$.

Two types of precursors for the sulfide catalysts obtained *in situ* in hydrocarbon solution of substrate have been studied:

1) Complex of nickel-tiotungstate $[BMPip]_2Ni(WS_4)_2$,
2) Synthesis of catalysts through reverse microemultion (aqueous solution of precursors)/(hydrocarbon solution of substrate). Ammonium thiotungstate $(NH_4)_2WS_4$ and nickel nitrate were used as the precursors.

As a substrate the naphthalene, methylnaphthalenes and dimethylnaphthalenes in various solvents, such as hexadecane and benzene, have been selected. Using obtained catalysts the possibility of light cycle oil (LCO) hydrotreating has been investigated.

The hydrogenation of aromatic compound has been conducted under hydrogen pressure of 5 MPa and the temperature 350°C, with the hydrogen/feed about 60.

The catalysts were characterized by high resolution transmission electron microscopy (HRTEM), fourier transform infrared spectroscopy (FTIR) and X-ray photoelectron spectroscopy (XPS).

Analysis of hydrogenation products of model systems was performed on gas chromatograph. The quantitative content of aromatic hydrocarbons in the LCO hydrogenation products determined by high-performance liquid chromatography (HPLC). Component composition was determined by two-dimensional gas chromatography mass spectrometry (Pegasus® 4D GCxGC-TOFMS).

3 Results and discussion

Nickel-tungsten catalysts obtained *in situ* in a ionic liquid showed high activity in the hydrogenation of aromatic compounds. For example, when the ratio of naphthalene/tungsten was 7/1 and reaction time 10 hours naphthalene conversion was 100%. The main product was tetralin. When 1-octene used as a solvent conversion of naphthalene was 80%, whereas the 1-octene practically no hydrogenated, conversion in this case was only 5%. This is related to the fact that the aromatic hydrocarbons are well solved in ionic liquids, and the solubility of olefins in ionic liquids is limited. From the results we can conclude the following: ionic liquid can be used for the selective hydrogenation of aromatics in the mixture with olefins.

Nickel-tungsten catalysts obtained by *in situ* decomposition of the precursor $[BMPip]_2Ni(WS_4)_2$ in hydrocarbon solution of substrate showed high activity in the hydrogenation of aromatic compounds. For example, when the ratio of naphthalene/tungsten was 105/1 and reaction time 5 hours, naphthalene conversion was 100%. The catalysts gave high selectivity to decalins, at ratio of naphthalene/tungsten 7/1 and reaction time 10 hours decalins selectivity was 100%.

The possibility of *in situ* preparation of nanosized catalysts in hydrocarbon solution of substrate through reverse microemultion has been demonstrated. In this case a nonionic surfactant SPAN-80 has been used. The catalytic activity of obtained emulsions in hydrogenation reactions of aromatic hydrocarbons was studied for model systems as 10% solutions of naphthalene, 1-methylnaphthalene and 2-methylnaphthalene in n-hexadecane and benzene. The effect of surfactant concentration on the catalytic activity has been studied under optimal atomic ratio W/Ni = 1/1. Naphthalene conversion was 98% in optimal conditions. The main product was tetralin, decalins selectivity was 20%.

Also, the possibility of LCO hydrotreating using obtained catalysts has been investigated. It was shown that the total sulfur content decrease up to 0.02wt.%, and a significant reduction in the content of polyaromatic hydrocarbons was demonstrated.

4 Conclusions

In this research sulfide nickel-tungsten catalysts obtained *in situ* in ionic liquids and *in situ* in the hydrocarbon solution of substrate has been studied. Unsupported nickel-tungsten sulfide systems are the promising catalysts for the aromatic hydrocarbons hydrogenation processes in dispersion system. Also, the possibility of LCO hydrodearomatisation using obtained catalysts has been shown.

Acknowledgement

This research was supported by the Russian Ministry of Education and Science (№ 14.607.21.0074, the Federal Target Program «The studies and development in the priority areas for Russian scientific and technological complex in 2014-2020», Project Unique Number RFMEFI60714X0074).

References

[1] Edited by Franklin (Feng) Tao. Metal Nanoparticles for Catalysis: Advances and Application. RSC Catalysis Series. 2014
[2] S. Khadzhiev, Kh. Kadiev, M. Kadieva. *Petroleum Chemistry*. 2013 (53) 374
[3] S. Khadzhiev, *Petroleum Chemistry*. 2011 (51) 1

IV-PP124

In Situ Synthesis of Unsupported Transition Metal Sulfide Catalysts for Hydrodearomatization Processes

Sizova I.A.[1*], Serdyukov S.I.[1,2], Maximov A.L.[1,2]

1 - A.V. Topchiev Institute of Petrochemical Synthesis RAS, Moscow, Russia
2 - Moscow State University, Dep. of Chemistry, Moscow, Russia

* isizova@mail.ru

Keywords: hydrodearomatization, unsupported, catalysts, transition, metal, sulfides

1 Introduction

Traditionally, transition metal sulfides are used as hydrotreating catalysts for petroleum fractions. Alumina-supported Mo or W promoted by Co or Ni are often used as industrial catalysts [1]. These compositions have optimal combination of such properties as activity, stability, cost, etc. However, recently extensive studies have been conducted in the field of transition metal sulfides such as Nb, Os, Ru, Rh, Re. Ruthenium sulfide showed the highest hydrogenation and hydrodesulphurization catalytic activity [2-4]. For example, Lacroix et al. [4] presented that the ruthenium sulfide hydrogenating activity exceed in 6 times the activity of MoS_2.

Usually metal sulfides are supported on porous materials such as silica-alumina, Al_2O_3, silica oxide, to increase the surface area of the catalyst and decrease amount of the active component. A new approach to the synthesis of catalysts is renunciation of the use of supports in its synthesis, i.e. to use of nanoparticles of catalysts dispersed in the hydrocarbon feedstock.

In this research the possibility of obtaining sulfide catalysts *in situ* in hydrocarbon solution of substrate for hydrogenation of aromatic hydrocarbons has been investigated.

2 Experimental

The preparation method of sulfide catalysts *in situ* in the hydrocarbon solution of substrate for the hydrogenation of polyaromatic hydrocarbons was developed. Used precursors were oil-soluble salts: tungsten carbonyl $W(CO)_6$, ruthenium carbonyl $Ru_3(CO)_{12}$ and molybdenum carbonyl $Mo(CO)_6$.

Synthesized catalysts were characterized by HRTEM, FTIR-spectroscopy and XPS.

Catalytic activity in hydrodearomatization reaction was studied. As a substrate the solution of naphthalene in benzene have been selected. It was shown that the addition of 2.5 wt.% elemental sulfur to hydrocarbon solution is necessary for the formation active phase of sulfide catalysts. The hydrogenation of naphthalene has been conducted under a hydrogen pressure of 5-7 MPa and the temperature 350°C, with the hydrogen/feed about 60.

3 Results and discussion

The influence of metal carbonyl concentration on naphthalene conversion was studied and kinetic parameters of naphthalene hydrogenation were obtained. It was shown that ruthenium sulfide prepared from ruthenium carbonyl $Ru_3(CO)_{12}$ has the highest catalytic activity. When the ratio of naphthalene/ruthenium was 56/1 and reaction time 5 hours naphthalene conversion was 96% and decalin selectivity was 25%.

Also the influence of nickel addition on catalytic activity was studied. Added nickel was in oil-soluble salts form (nickel(II) 2-ethylhexanoate $Ni(C_7H_{15}COO)_2$). Catalytic activity obtained catalysts increases in the case of nickel addition and optimal M/Ni ratio was found (M = Ru, W, Mo), for tungsten W/Ni ratio was 1/2, for molybdenum Mo/Ni ratio was 1/2 and for ruthenium Ru/Ni ratio was 1/3.

Also effect of hydrogen pressure in process were investigated. It was shown that the catalytic system W/Ni (ratio was 1/2) has the the highest catalytic activity. When the ratio of naphthalene/tungsten was 210/1 and reaction time 5 hours naphthalene conversion was 100% and decalin selectivity was 64%.

4 Conclusions

In this research sulfide catalysts have been obtained *in situ* in the hydrocarbon solution of substrate using oil-soluble precursors such as metal carbonyl for the first time. Obtained unsupported transition metal sulfide catalysts are the promising catalysts for the aromatic hydrocarbons hydrogenation processes.

Acknowledgement

Current research was supported by the Russian Academy of Science (Program 8, Reg. № 01201352582).

References

[1] A.N. Startsev, Sulfide hydrotreating catalysts: synthesis, structure and properties, Novosibirsk Academic. Publishing House "Geo" 2007.
[2] N. Hermann, M. Brorson, H. Topsøe, *Catalysis Letters*. 65 (2000) 169
[3] C. Jacobsen, E. Tornqvist, H. Topsøe, *Catalysis Letters.* 63 (1999) 179
[4] M. Lacroix, N. Boutarfa, C. Guillard, M. Vrinat, M. Breysse, *Journal of Catalysis.* 120 (1989) 473

IV-PP125

Selective Oxidation of Alkylarenes with H_2O_2 Catalyzed by γ-Keggin Divanadium-Substituted Polyoxometalate

Skobelev I.Y.[1*], Zalomaeva O.V.[1], Evtushok V.Yu.[1,2], Maksimov G.M.[1], Kholdeeva O.A.[1,2], Carbó J.J.[3], Poblet J.M.[3]

1 - Boreskov Institute of Catalysis, Novosibirsk, Russia
2 - Novosibirsk State University, Novosibirsk, Russia
3 - Universitat Rovira i Vigili Marcel lí Domingo, Tarragona, Spain

* skobelev@catalysis.ru

Keywords: selective oxidation, pseudocumene, polyoxometalate, hydrogen, peroxide

1 Introduction

The selective oxidation of aromatic rings of alkylsubstituted arenes with atom efficient and green oxidants, e.g., aqueous H_2O_2, is a challenging goal of organic synthesis. A demanding task is the aromatic oxidation of 1,2,4-trimethylbenzene (pseudocumene, PC) and 2-methylnaphthalene (2-MN) leading to 2,3,5-trimethyl-1,4-benzoquinone (TMBQ, vitamin E key intermediate) and 2-methyl-1,4-naphthoquinone (2-MNQ, Vitamin K_3), respectively. Recently, Mizuno and co-workers reported H_2O_2-based aromatic hydroxylation of some alkylbenzenes catalyzed by a divanadium-substituted polyoxometalate (POM), $[\gamma\text{-}PW_{10}V_2O_{40}]^{5-}$, in the presence of a mineral acid [1]. In this work, we explored the catalytic properties of this POM in the selective oxidation of PC and 2-MN and studied the reaction mechanism by experimental and theoretical methods.

2 Experimental/methodology

$(Bu_4N)_4H[\gamma\text{-}PW_{10}V_2O_{40}]$ (shortly, $\gamma\text{-}PW_{10}V_2$) was prepared according to the literature [2] with some modifications [3] and characterized by ^{31}P and ^{51}V NMR and IR spectroscopy. Other reactants were obtained commercially and used as received. Catalytic oxidations were carried out in temperature-controlled glass vessels at 30–80ºC under vigorous stirring. Reactions were initiated by the addition of H_2O_2 (30% in water) either in one portion or stepwise to a mixture containing aromatic substrate (PC or 2-MN), $\gamma\text{-}PW_{10}V_2$ catalyst and $HClO_4$ in 1 mL of MeCN/*t*-BuOH (1:1 v/v). Samples of the reaction mixture were taken periodically and analyzed. The oxidation products were identified by GC–MS and ^1H NMR and quantified by GC and HPLC.

DFT calculations were carried out with Gaussian 09 C01 release with B3LYP functional using IEF-PCM (MeCN as a solvent) implicit solvation model. For V and W atoms LANL2DZ pseudopotential was used. The 6-31G(d,p) basis set was used to C and H atoms as well as for O atoms of water and hydrogen peroxide molecules and directly bonded to V. For remaining atoms 6-31G basis set was used.

3 Results and discussion

Under conditions of H_2O_2 deficiency, PC oxidation with H_2O_2 in the presence of $\gamma\text{-}PW_{10}V_2$ proceeded with high selectivity of aromatic ring hydroxylation (>95%) and unusual regioselectivity toward 2,4,5-trimethylphenol (2,4,5-TMP). The ratio of 2,4,5-, 2,3,5- and 2,3,6-TMP isomers was 7 : 1 : <0.15. Optimization of the reaction conditions has led to TMP yield of 73% based on the oxidant. The presence of a mineral acid ($HClO_4$) and *t*-BuOH was crucial for the catalytic activity. With an 8-fold excess of H_2O_2, TMBQ formed along with other overoxidation products; TMBQ selectivity reached 41% at PC conversion of 41%. Atypical

regioselectivity was also found in the oxidation of 2-MN where 6-MNQ predominated over 2-MNQ. The ratio of the 6-MNQ/2-MNQ isomers depended on the concentration of acid, catalyst and oxidant.

The lack of products derived from the oxidation of methyl groups indicates electrophilic hydroxylation mechanism and argues against electron transfer or hydrogen atom transfer mechanisms. Studies on PC oxidation by DFT revealed that the formation of 2,4,5- and 2,3,5-TMP is, most likely, due to peroxo complex $[\gamma\text{-}PW_{10}O_{38}V_2(O_2)]^{3-}$ (**I**), which may arise from dehydration of hydroperoxo complex $[\gamma\text{-}PW_{10}O_{38}V_2(OH)(OOH)]^{3-}$ (**II**) formed upon interaction of the diprotonated POM, $H_2[\gamma\text{-}PW_{10}V_2O_{40}]^{3-}$ (**III**), with H_2O_2. If **II** were the main oxidizing species, 2,3,6-TMP isomer would predominate. The oxygen transfer from peroxo complex **I** to the aromatic ring of PC presumably occurs through the formation of an arene oxide intermediate. The role of acid is, therefore, to favor the formation of **III** which then leads to **II.** In turn, *t*-BuOH may facilitate the formation of **I** through stabilization of the released water by hydrogen bonding. In contrast to PC oxidation, the presence of neither acid nor *t*-BuOH is required for H_2O_2-based oxidation of 2,3,6- and 2,3,5-TMP to TMBQ [4]. Hydroperoxo complex **II** is supposed to be the active species responsible for the formation of TMBQ.

The kinetic regularities and estimated rate constants acquired from the kinetic study on PC oxidation with H_2O_2 are in good agreement with the theoretically predicted reaction mechanism where peroxo complex **I** is the main species responsible for the aromatic ring hydroxylation.

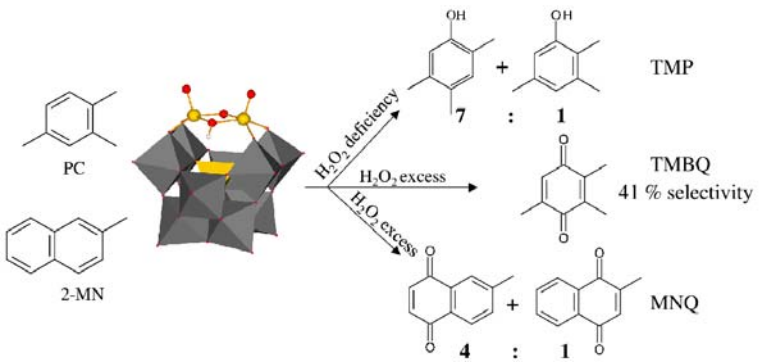

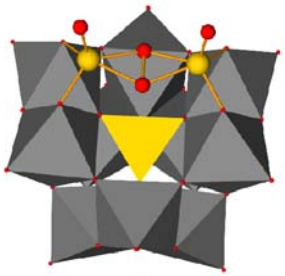

DFT structure of peroxo complex $[\gamma\text{-}PW_{10}O_{38}V_2(O_2)]^{3-}$.

4 Conclusions

Polyoxometalate $(Bu_4N)_4H[\gamma\text{-}PW_{10}V_2O_{40}]$ catalyzes the selective oxidation of PC with aqueous H_2O_2 to produce either 2,4,5-/2,3,5-TMP (ca. 7:1) or TMBQ, depending on the substrate to oxidant ratio. The oxidation of 2-MN proceeds with unusual regioselectivity toward 6-MNQ. Both kinetic and DFT studies on the PC oxidation implicate peroxo complex $[\gamma\text{-}PW_{10}O_{38}V_2(O_2)]^{3-}$ as the key intermediate leading to 2,4,5-/2,3,5-TMP.

Acknowledgements

The help of Dr. R.I. Maksimovskaya and N.V. Maksimchuk in POM characterization by ^{31}P and ^{51}V NMR is greatly appreciated. The research was partially supported by the Russian Foundation for Basic Research (grants 13-03-12042 and 14-03-31431). I.Y.S. acknowledges Polyoxometalate Chemistry for Molecular Nanoscience (PoCheMoN) action in the framework of European Cooperation in Science and Technology (COST) program and Universitat Rovira i Vigili (Tarragona, Spain) for financial support.

References

[1] K. Kamata, T. Yamaura, N. Mizuno, *Angew. Chem. Int Ed.* 51 (2012) 7275.
[2] K. Kamata, K. Yonehara, Y. Nakagawa, K. Uehara, N. Mizuno, *Nature Chem.* 2 (2010) 478.
[3] O.V. Zalomaeva, V.Yu. Evtushok, G.M. Maksimov, O.A. Kholdeeva, *J. Organomet. Chem., submitted.*
[4] I.D. Ivanchikova, N.V. Maksimchuk, R.I. Maksimovskaya, G.M. Maksimov, O.A. Kholdeeva, ACS Catal. 4 (2014) 2706.

IV-PP126

Strong Synergetic Effect of Ceria and Alumina in Aerobic Oxidative Esterification of Benzyl Alcohol and Benzaldehyde over Gold Nanoparticles Supported on Nanostructured Ce-Al-O Mixed Oxides

Smolentseva E.[1*], Costa V.V.[2], Cotta R.F.[2], Beloshapkin S.[3], Simakova O.[4], Gusevskaya E.V.[2], Simakov A.[1]

1 - Universidad Nacional Autónoma de México, Centro de Nanociencias y Nanotecnología, Ensenada, México

2 - Departamento de Química, Universidade Federal de Minas Gerais, Belo Horizonte, Brazil

3 - Materials & Surface Science Institute, University of Limerick, Limerick, Ireland

4 - Laboratory of Industrial Chemistry and Reaction Engineering, Process Chemistry Centre, ÅboAcademi University, Åbo/Turku, Finland

* elena@cnyn.unam.mx

Keywords: nanostructured oxides, sol-gel, gold nanoparticles, benzyl alcohol, oxidative esterification

1 Introduction

The oxidation of alcohols is one of the most challenging reactions in synthetic organic chemistry. The resulting carbonyl compounds are widely used in various fields of the chemical industry. For example, methyl esters find a commercial use as solvents, diluents, extractants and flavoring agents [1-4]. Gold nanoparticles (NPs) are considered to be promising catalysts for the aerobic oxidation of alcohols, which involve O_2 as an oxidant, due to their high activity and stability. However, most of the gold systems reported for the oxidative esterification of alcohols require the presence of base (usually NaOH or K_2CO_3) and only a few catalysts based on AuNPs were found capable to promote a direct transformation of alcohols to esters using molecular oxygen as an oxidant in the absence of any base additive.

In the present work, the performance of AuNPs supported on nanostructured unitary Al_2O_3 and CeO_2 and binary Ce-Al-O oxides was studied in the liquid-phase aerobic oxidation of benzyl alcohol and benzaldehyde in methanol solutions under neutral conditions, for the first time as far as we know.

2 Experimental/methodology

Nanostructured Ce-Al-O mixed oxides with different content of ceria (10 and 30 wt. %) were prepared by sol-gel method using organometallic precursors as described previously [5]. Commercial CeO_2 (Alfa-Aesar) was used as a support as well. Gold catalysts (3 wt. % Au) were synthesized by deposition-precipitation route using urea as precipitation agent as in [5]. The structural and electronic properties of gold samples were studied by N_2 adsorption, XRD, TEM, XPS and UV-Visible spectroscopy under temperature-programmed reduction or oxidation. Obtained materials were catalytically studied in the oxidative esterification of benzyl alcohol and benzaldehyde. The reactions were carried out in a homemade stainless steel reactor equipped with a magnetic stirrer. In a typical run, a mixture of the substrate (2.5 mmol), solvent (3 mL), and the catalyst (10 mg; 0.9 – 2.0 μmol of Au) were transferred into reactor. The reactor was pressurized with oxygen to the total pressure of 10 atm and placed in an oil bath; then the solution was intensively stirred at 110 °C for the reported time. The reactions were followed by gas chromatography (GC) (Shimadzu 17 instrument fitted with a Carbowax 20 M capillary column and a flame ionization detector). At appropriate time intervals, stirring was stopped and

after catalyst settling aliquots were taken and analyzed by GC.

3 Results and discussion

Gold catalysts supported on Ce-Al-O mixed oxides showed better performance in the liquid-phase oxidative esterification of benzyl alcohol and benzaldehyde without usage of any base promoter than gold supported on individual oxides. The strong synergetic effect of ceria and alumina can be explained by the enhanced oxygen storage capacity of the materials prepared from mixed oxides as compared to pure alumina and ceria. Thus, the introduction of ceria nanospecies into alumina facilitates the oxygen activation by AuNPs and strongly improves their performance in the oxidation processes.

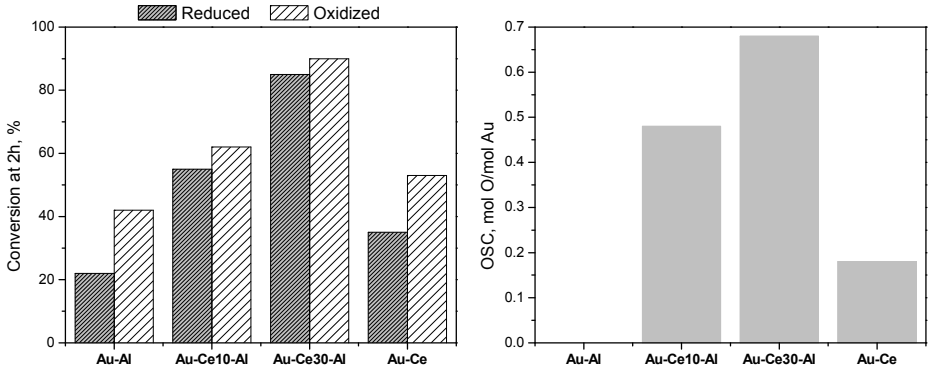

Fig. 1. Conversion of benzyl alcohol at 2 h of reaction over Au catalysts supported on various nanostructured oxides after different pre-treatments (left). Oxygen storage capacity (OSC) measured via oxygen adsorption at room temperature over the same reduced gold catalysts (right) [5].

4 Conclusions

Gold nanoparticles supported on Ce-Al-O mixed oxides prepared by sol-gel route demonstrates higher activity in the liquid-phase aerobic oxidative esterification of benzyl alcohol and benzaldehyde than gold supported on unitary ceria and alumina. The thermal pre-treatment in oxygen resulted in more active catalysts than pre-treatment in hydrogen. The order of the catalytic activity is as following: $Au/Al_2O_3 < Au/CeO_2 < Au/Ce(10)\text{-}Al < Au/Ce(30)\text{-}Al$. The data obtained in this work may be applied for the development of new effective catalysts for industrial application in the oxidative esterification of a wide variety of alcohols using environmentally benign molecular oxygen in the absence of any co-catalysts or additives.

Acknowledgements

The authors thank to E. Flores, P. Casillas, F. Ruiz, E. Aparicio and J. Peralta for their kind technical support in this work and the financial support from CNPq, FAPEMIG and INCT-Catálise (Brazil) and CONACyT and DGAPA (Mexico) through grants 179619 and 203813.

References

[1] A. S. K. Hashmi, G. J. Hutchings, Angew. Chem. Int. Ed. 2006, 45, 7896-7936.
[2] G. J. Hutchings, Chem. Commun. 2008, 1148-1164.
[3] A. Corma, H. Garcia, Chem. Soc. Rev. 2008, 37, 2096-2126.
[4] C. Della Pina, E. Falletta, L. Prati, M. Rossi, Chem. Soc. Rev. 2008, 37, 2077-2095.
[5] E. Smolentseva, A. Simakov, S. Beloshapkin, M. Estrada, E. Vargas, V. Sobolev, R. Kenzhin, S. Fuentes Appl. Catal. B: Environ. 115-116 (2012) 117-128.

IV-PP127

Synthesis, Characterisation and Activity Testing of Titanium-Containing Zeolite Systems of the MFI-type

Sofianos A.*, Kolesnikov A.V., Maanaso M.F.

Tshwane University of Technology, Department of Chemical, Metallurgical and Materials Engineering, Pretoria, Republic of South Africa

* sofianosa@tut.ac.za

Keywords: titanium silicalite, phenol hydroxylation, hydrogen peroxide

1 Introduction

Selective oxidation in the liquid phase is currently applied in the chemical industry for manufacturing a wide variety of chemicals ranging from commodities to high-value-added fine chemicals. Heterogeneous catalysts only started to play a significant role in this area at the beginning of the 1980s with the synthesis and the industrial applications of titanium silicalite-1 (TS-1). The successful design of TS-1 by Enichem (1) as an oxidation catalyst for environmentally benign industrial oxidation reactions with hydrogen peroxide comprises one of the most important innovations in heterogeneous catalysis over the last thirty years. This zeolitic-type material of the MFI-type incorporates titanium in the framework and displays unique catalytic properties for oxidation reactions of alkanes, alkenes and aromatic hydrocarbons, with the hydrogen peroxide system replacing oxygen as the oxidation agent, at moderate reaction conditions and with water as the main by- product of the oxidation.

The unique performance of this MFI-type zeolite catalyst, which is isomorphous with the ZSM-5 zeolite and silicalite-1, is attributable to the specific features of isolated Ti4+ active sites incorporated in the silica structure of the zeolite framework. These were shown to be able to efficiently promote activity and selectivity in oxidation reactions with hydrogen peroxide. In contrast, non-isolated titanium, such as segregated titanium dioxide, TiO2, forms an "Anatase-like" phase, which not only is inactive for these reactions but also imposes severe diffusion limitations to oxidation over TS-1 zeolites by filling the pores of with inactive material. Further, depending on the conditions of preparation, some extra-framework titanium exists which forms an amorphous TiO2 phase in the pores. This may be partially removed by a diluted acetic acid wash or by other means prior to the use of the zeolite for the catalytic reaction.

This paper, describes the synthesis, characterization and activity- testing of a series of Ti-silicalite catalysts (TS-1) using the hydroxylation of phenol as the test reaction. In addition, high-silica ZSM-5 zeolites and silicalite-1, comprising isomorphous zeolite systems of the MFI-type were also produced and characterized and their textural and structural properties were compared with those of the TS-1 zeolite.

2 Experimental section

For the synthesis of TS-1 titanium-silicalite nanocrystals standard methods based on the hydrothermal synthesis of zeolites as described in the literature (1 - 3) were used. These comprise the use of organic precursors such as tetraethyl orthosilicate (TEOS) and tetra butyl ortho titanate (TBOT). In our case, we have predominantly used colloidal silica (Ludox® HS 30%) as the silica source and tetrapropyl ammonium hydroxide (TPAOH) as the template. Experiments with the use of tetrapropyl ammonium bromide (TPABr) were successful in the synthesis of ZSM-5 zeolites; however, the TS-1 produced with this combination (using ammonia as the base) did not crystallize very well. For the hydrothermal synthesis of a series of ZSM-5 zeolites, silicalite-1 and titanium silicalite (TS-1), 1–litre, stirred, high-pressure SS 316 autoclaves and other smaller, high pressure, teflon-lined SS vessels (50 ml, 100ml and 200 ml) without stirring were used.

For characterization, the zeolite nano catalysts were tested with XRD, SEM, TEM, FTIR, and

UV-VIS. Results from Raman spectroscopy are still outstanding. The spatial distribution of the titanium and silicon in the TS-1 micro particles was studied with EDS. Finally, N2-adsorption isotherms were obtained, in order to determine the textural properties of the nano catalysts.

For the preparation of theTS-1 zeolite precursor gel [2] Solution A, comprising 45g TEOS in a flask was placed in an iced bath under argon atmosphere, and 2.4g Ti (OBu)4 was added under intensive stirring. A clear solution was formed. Thereafter, Solution B, consisting of 100 g of aqueous solution of 20% TPAOH was added to Solution A in a drop wise process under stirring, with the aim to maintain a clear solution; the temperature was allowed to rise to 60^0C. The final pH was adjusted to 12. Thereafter, the mixture was placed in a teflon-lined, one-litre autoclave and was allowed to crystallize at 175^0C, under stirring. After crystallization was completed (96 hours), calcination followed using a procedure similar to that for the ZSM-5 zeolite. The molar composition of the precursor gel was nSiO2: nTiO2: nTPAOH: nH2O = SiO2: 0.027 TiO2: 0.36TPAOH: 35H2O. The ratio of Si:Ti was 24.

To evaluate the catalytic performance of the synthesized TS-1, the hydroxylation of phenol with hydrogen peroxide was carried out as the test reaction. The batch oxidation procedure was as follows: 18.g g of phenol was dissolved in 64 ml methanol or acetone solvent inside a round-bottomed, 250 ml flask, equipped with a thermometer, dropping funnel and a stirrer. 1.88g TS-1 catalyst (10% to phenol) was added. Finally, 20g of 30% H2O2 was slowly added when the temperature had reached 70oC. Overall reaction time was 6 hours. Samples of the reaction mixture were regularly withdrawn and analyzed using gas chromatography with a capillary column.

3 Results and discussion

Fully crystalline TS-1 zeolite nano crystals were obtained at a temperature of 175^0C and a time period of 96 hours, and above, in both autoclave systems. The XRD pattern was identical with that of the isomorphous MFI zeolites, namely ZSM-5 and silicalite-1. The patterns at 2Θ = 7.96, 8.91, 14.00, 14.87, 20.92, 23.28, 23.97, 24.52, 26.66 are typical for the ZSM-5 zeolite and its isomorphous zeolites. TS-1 catalyst crystallizes in the orthorhombic system; the crystallites were calculated to be in the range of 20 – 40 nm, whereas the pore size amounts 0.53 x 0.56nm as in the case of ZSM-5 zeolites.

SEM, XRD, FTIR, EDS and UV-vis techniques were used to illustrate the effects of the preparation procedure on the structure and the morphology of each of the three series of zeolites obtained (TS-1, silicalite and ZSM-5). The existence of isolated Ti4+ active sites incorporated in the silica structure was clearly demonstrated with the strong band appearing in the FTIR spectra at 960 cm-1with the stretching vibration of [SiO4] units influenced by the presence of adjacent Ti-atoms incorporated in the framework. Neither pure silicalite-1, nor the ZSM-5 zeolites show a band at around this frequency and thus this band at 960 cm -1 is considered a “fingerprint” for the existence of titanium in the zeolite matrix.

The catalytic results obtained, showed that using the TS-1 with methanol as solvent, considerable conversion of the phenol substrate was achieved within only a few hours (2 h, conversion of phenol> 40%) and the selectivity results towards the catechol and hydroquinone were above 60%. These results were dependent on the solvent; when acetone was used, the conversion was lower (residence time: 2h; conversion only 25% ; selectivity:40%).

4 Conclusions

It was demonstrated that the TS-1 catalysts prepared at our laboratories have textural and structural properties similar to those described in the literature [1-3] and that they display significant catalytic activity in the hydroxylation of phenol. The product selectivities obtained were also high, however they were dependent on the solvent used.

References

[1] Notari, B. in Grobet, P. J., Mortier, E. P., Vansant, E. F. and Schulz-Ekloff, G. (Eds.), *Innovation In Zeolite Materials Science.* Elsevier, Amsterdam, 37 (1988) 413.
[2] Taramasso, M. P. G and Notari, B., *US Patent*, 4410501 (1983)
[3] Huan g, D. G., Zhang, X., Chen, B. H. and Chao, Z. S., *Catalysis Today*, 158 (2010) 510

IV-PP128

Ch-Phosphorylation of Aromatic Substrates Involving Redox-Activated Co, Ag, Mn, Fe, Ni and their Complexes

Strekalova S.O.*, Khrizanforov M.N., Gryaznova T.V., Budnikova Y.H.

A.E. Arbuzov Institute of Organic and Physical Chemistry, Kazan Scientific Center, Russian Academy of Sciences, Kazan, Russia

* So4nar36@yahoo.com

Keywords: phosphorylation, catalysis, transition metal complexes

1 Introduction

Relevance of the methods of C-H phosphorylation of aromatic compounds with metals and their complexes is an important research direction that is little studied to date. The review published in recent years devoted to developments in the field of formation CP bonds in various catalytic reactions, almost without considering the examples of aromatic C-H phosphorylation bonds [1-3].

2 Results and discussion

Therefore, the development of catalytic methods especially with regard to the requirements of "green chemistry" is fundamentally important today.

The aim of this work is to find new reactions capable to activate and transform catalytically inert C-H bonds in organic molecules to carbon-phosphorus functional groups using redox -activated metals Co, Mn, Fe, Ni and their complexes.

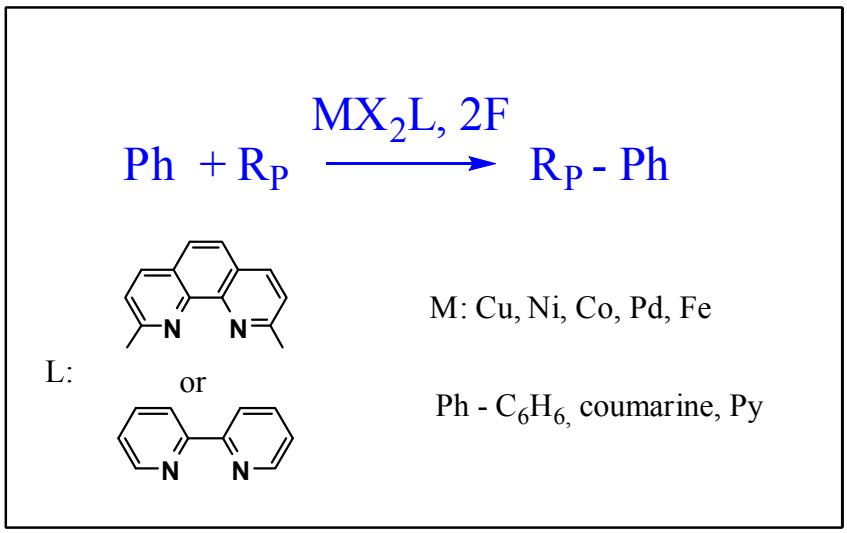

Fig. 1. Schematic representation of studied processes

3 Conclusions

Within this work it was shown that the electrochemical activation of metal complex to M (III) oxidation state (apart from Ag) allows to add the dialkylphosphite to the aromatic substrates (benzene, pyridine, coumarine) successfully. Silver nitrate yields to monoalkylphosphonate in th same electrochemical conditions.

Acknowledgements

The author of RFBR thanks for the financial support: grants 13-03-97025, 13-03-00139-a, 14-03-31423- mol_a and RSF for financial support grant 14-23-00016.

References

[1] C. S. Demmer, N. Krogsgaard-Larsen, L. Bunch. *Chem. Rev*. 111 (2011) 7981
[2] D. S. Glueck, Top. *Organomet Chem*. 31 (2010) 65
[3]G. Evano, A.-C. Gaumont, C. Alayrac, I. E. Wrona, J. R. Giguere, O. Delacroix, A. Bayle, K. Jouvin, C. Theunissen, J. Gatignol, A. C. Silvanus. *Tetrahedron* 70 (2014) 1529

IV-PP129

Metalcomplex Catalysis in Synthesis of Biological Active Esters of the Isovaleric Acid

Suerbaev Kh.A.*, Zhaksylikova G.Zh., Appazov N.O., Kudaibergenov N.Zh.

Al-Faraby Kazakh National University, Almaty, Republic of Kazakhstan

* khsuerbaev@mail.ru

Keywords: isobutylene, hydroalcoxycarbonylation, metalcomplex catalysis, biological active esters

1 Introduction

Hydroalkoxycarbonylation of olefins with carbon monoxide and alcohols under condition of homogeneous catalysis with transition metal complexes allows facile one-step synthesis of practically useful carbon acid esters. Many of them have biological activity and are constituents of drugs or valuable intermediate products in drug synthesis. Hydroalkoxycarbonylation of isobutylene with carbon monoxide and alcohols in the presence of catalytic systems based on Palladium Phosphin Complexes ($Pd(PPh_3)_4$-PPh_3-TsOH, $Pd(Acac)_2$-PPh_3-TsOH) was applied for preparing of biological active isovaleric acid esters: l-menthylisovalerate (main active component of the spasmolytic medicine “Novovalidolum”), ethylisovalerate (intermediate product for obtaining sedative and spasmolytic medicines “Ethyl ether of α-bromisoveleric acid” (EEBIA) and “Corvololum-K”), cyclohexylisovalerate (bactericide activity against Staphylococcus aureus, Escherichia coli, Pseudomonas aeruginosa; antifungus activity against Candida albicans), benzylisovalerate (bactericide activity against Escherichia coli, Staphylococcus aureus) and monoglyceryde of isovaleric acid (bactericide activity against Escherichia coli, Pseudomonas aeruginosa; and antifungus activity against Candida albicans).

2 Experimental/methodology

The reaction were performed in a stainless-stell autoclave. The reaction was performed without solvent. The [alcohol]:[isobutylene]:[Pd]:[PPh_3]:[p-TsOH] ratio was 435:565:1:7:12. The autoclave at room temperature was charged with the catalytic system and alcohol. The autoclave was hermetized, purged in duplicate with carbon monoxide for deaeration, and charged with olefine, after which required carbon monoxide pressure was effected, and stirring and heating were started. The reaction products were isolated by fractional distillation.

3 Results and discussion

Hydroalkoxycarbonylation reaction of isobutulene with carbon monoxide and alcohols (ethanol, cyclohexanol, l-menthol, benzyl alcohol, glycerol) in the presence Palladium Phosphin Complexes carried out at conditions: temperature 100^0C; CO pressure 2,0 MPa; reaction time 4 h. [1-3]. The yields of the products were 57,0-96,0%. The selectivity in linear reaction products was 100%. Such a high regioselectivity is apparently provided both by the structure of the starting alkene (isobutylene) and by the reaction mechanism. The most probable is a hydride mechanism.

New efficient technologies for preparation of drugs (Novovalidolium, EEBIA and Corvalolum-K) are based on isovaleric acid esters were worked out. Novavalidolum – is a spasmolytic (sedative) medicine; it has a sedative effect on the nervous system and a moderate reflex vaso-dilating effect. EEBIA possesses sedative and spasmolytic properties; it is included in Corvalolum-K composition and may be used for producing other medicines. Corvalolum-K is

a combined medicine and consists of EEBIA, phenobarbital, sodium hydroxide, peppermint oil, ethyl alcohol and water. Corvalolum-K possesses anetic and spasmolytic properties.

Due to the more advanced technology of production the Medicines will have better qualitative characteristics. The cost of production of the Medicines with the use of new technologies is 2-3 times lower as compared to the medicines produced by existing at the present traditional technologies.

4 Conclusions

Biological active isovaleric acid esters were synthesized by isobutylene hydroalkoxycarbonylation in the presence of catalytic systems based on Palladium Phosphin Complexes.

New, efficient technologies for preparation of drugs are based on the isovaleric acid esters – "Novovalidolum", "Ethyl ether of α-bromisovaleric acid" and "Corvalolum-K" – were worked out.

Acknowledgements

The financial support of this work was provided by the Ministry of Education and Science of the Republic of Kazakhstan.

References

[1] Kh. Suerbaev, G. Abyzbekova, K. Shalmagambetov, K. Zhubanov, *Russian Journal of General Chemistry*. 70 (2000) 516.

[2] Kh. Suerbaev, E. Chepaikin, B. Dzhiembaev, N. Appazov, G. Abyzbekova, *Petroleum Chemistry.* 47 (2007) 345.

[3] Kh. Suerbaev, G. Zhaksylykova, N. Appazov, *J. Pet. Environ. Boitechnol* (2013) 4:164 DOI:10.4172/2157-7463.1000164.

IV-PP130

Selective Hydrogenation of Hexanoic Acid to Hexanol under Mild Conditions over Titania-Based Pt-Re Catalyst

Suknev A.P.[1], Zaikovskii V.I.[1,2], Kaichev V.V.[1,2], Paukshtis E.A.[1,2], Sadovskaya E.M.[1,2], Bal'zhinimaev B.S.[1*]

1 - Boreskov Institute of Catalysis SB RAS, Novosibirsk, Russia
2 - Novosibirsk State University, Novosibirsk, Russia

* balzh@catalysis.ru

Keywords: selective hydrogenation, hexanoic acid, hexanol, platinum, rhenium, atomic dispersion

1 Introduction

Liquid-phase hydrogenation of carboxylic acids is a crucial component of a number of strategies for the conversion of biomass into fuels and chemicals. The reaction products, alcohols, are widely used in industry as nonionic surfactants, running resins, plasticizers, cosmetics, etc. This process is catalyzed by bimetallic Pt-Sn and Ru-Sn catalysts occurred under severe reaction conditions ($T \leq 300°C$ and $P \leq 300$ bar) with an alcohol selectivity of only 40-75% [1]. Recently, the novel Pt and Pd catalysts promoted with rhenium showed a higher selectivity (*ca*. 90%) in hydrogenation of acids to alcohols under milder conditions [2,3]. A more pronounced performance was shown by the metal-organic pincer-type complexes demonstrating at $T \leq 100°C$ and $P \leq 50$ bar the 100% alcohol selectivity due to heterolytic activation of the molecular hydrogen to form metal hydride [4]. Here, we tried to stabilize on the titania surface the Pt-ReO_x species of atomic dispersion and to test in hydrogenation of hexanoic acid under reaction conditions similar to that of the highly selective homogeneous catalyst. Moreover, the kinetics assisted reaction mechanism was proposed.

2 Experimental/methodology

Commercial anatase titania (Hombifine N) was used as a support. The catalyst preparation profile included consecutive deposition of rhenium and platinum via incipient wetness impregnation from their water solution of ammonium perrhenate and platinum amine complexes with further thermal decomposition and reduction under controlled gas media. The chemical composition of the catalysts, order of metal deposition, and temperature of redox treatments were optimized. The size, metal charge and chemical composition of the Pt-ReO_x species were characterized by means of HRTEM, STEM-HAADF with line EDX analysis, XPS and FTIR. The hydrogenation process in dodecane or dioxane as a solvent was performed in a Parr reactor with GC analysis at P_{H2} = 25-75 bar and T = 110-150°C.

3 Results and discussion

The key approaches for stabilizing the highly dispersed Pt-ReO_X species on the TiO_2 surface were 1) the formation of low-valence and low-coordinated ReO_X clusters ($x \leq 1$) due to strong interaction of the Re precursor with the support under inert gas media and 2) a further formation of Pt-O-Re centers due to strong interaction of the Pt precursor with the formed ReO_X species, which are able to dissociate heterolytically the molecular hydrogen similar to that of the homogeneous metal-organic catalyst. Indeed, the highly dispersed particles of *ca*. 0.5 nm in size were observed on the titania surface, where the Re:Pt ratio followed from line EDX analysis of rhenium and platinum was close to 2:1 (Fig. 1A). In addition, according to XPS and FTIR data, Pt is metallic, while Re is in the partially oxidized (Re^{1+} or Re^{2+}) states. The kinetic study confirmed that the reaction rate constant linearly increases with number of Pt-ReO_X centers, and

the highest activity was achieved at Re:Pt = 2 (Fig. 1B, see the cross-point) which is in agreement with EDX data. A further adding of superstoichiometric platinum did not increase the reaction rate because of large low-active Pt particles were formed only. We believe that, as for the *Ru-NPy* pair in pincer complexes, the neighboring *Pt–O* atoms are able to activate molecular hydrogen with generation of Pt hydride for efficient hydrogenation of the carbonyl group of acid.

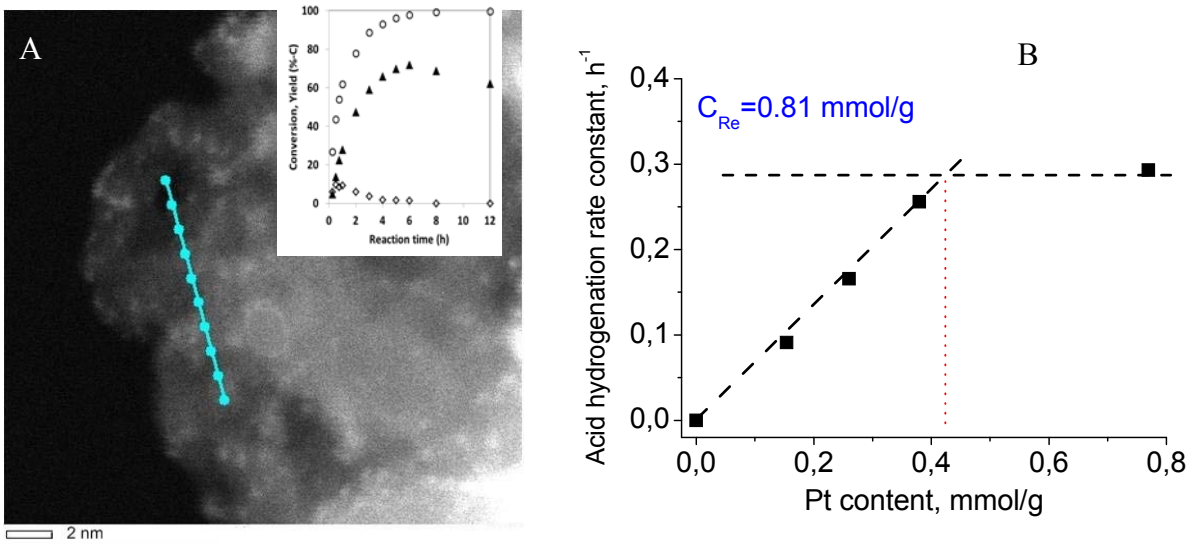

Fig. 1. (A) STEM-HAADF image of the 5% Pt-15% Re/TiO_2 sample with line EDX analysis of Pt and Re (the inset); (B) the hydrogenation rate constant *vs* the Pt content in catalysts with monolayer coverage by renium (0.81 mmol/g).

It was shown that the side reaction of acid esterification with hexanol catalyzed by acid itself is homogeneous and decreases noticeably the hexanol selectivity. The use of dioxane as a solvent allowed us to significantly suppress esterification, so that the selectivity reached 99% which is close to that of the homogeneous catalyst. The TOF value of 40 h^{-1} is one order higher than those known from the literature. The first order kinetics towards target and side reactions described well the kinetic data obtained in a wide range of reaction conditions. Finally, the Pt-ReO_X/TiO_2 catalyst revealed high stability during at least 5 recycles for 20 hours.

4 Conclusions

The Pt-ReO_X species ($x \leq 1$) of atomic dispersion were stabilized on the titania surface. It was shown that these centers with the atomic ratio Re/Pt = 2 are highly active and selective in hydrogenation of hexanoic acid to hexanol. The first order kinetic model of the hydrogenation process described well the kinetic data obtained in a wide range of reaction conditions. High TOFs (up to 40 h^{-1}) and selectivities (up to 99%) and stability were demonstrated under mild reaction conditions.

References

[1] R. Srinivasan and B.H. Davis, *Appl. Catal. A: Gen.* 87 (1992) 45-67.
[2] H.G. Manyar, C. Paun, R. Pilus, D.W. Rooney, J.M. Thompson and C. Hardacre, *Chem. Commun.* 46 (2010) 6279-6281.
[3] Y. Takeda, Y. Nakagawa and K. Tomishige, *Catal. Sci. Technol.* 2 (2012) 2221-2223.
[4] P.A. Dub and T. Ikariya, *ACS Catal.* 2 (2012) 1718-1741.

IV-PP131

Effect of Technological Parameters on the Process of Epichlorohydrin Synthesis

Flid V.R.[1], Sulimov A.V.[2*], Danov S.M.[2], Ovcharova A.V.[2], Trushechkina M.A.[3]

1 - Moscow State University of Fine Chemical Technologies, Moscow, Russia
2 - Nizhni Novgorod State Technical University, Nizhni Novgorod, Russia
3 - R&D Engineering Centre "Syntez", Moscow, Russia

* asulimov@mail.ru

Keywords: epichlorohydrin, epoxidation, titanium-containing zeolite, hydrogen peroxide, epoxy, resins

1 Introduction

Epichlorohydrin is an important product of basic organic synthesis. The main method for production of epichlorohydrin is dehydrochlorination of glycerol α,β-dichlorohydrins in an alkaline medium. However, this method has low efficiency, poorly utilizes the starting reagents, and is ecologically unsafe.

At present, one of promising techniques for production of epichlorohydrin is the liquid-phase oxidation of allyl chloride with hydrogen peroxide in an organic solvent on a heterogeneous catalyst, titanium-containing zeolite. However, evidence about physicochemical aspects of this process can hardly be found in the literature.

The goal of our study was to examine the influence exerted by various factors on the process of liquid-phase oxidation of allyl chloride with an aqueous solution of hydrogen peroxide on a titanium-containing zeolite. In particular, the effect of the amount of the solvent, temperature, and reagents ratio was analyzed.

2 Experimental

The epoxidation of allyl chloride was studied in a laboratory batch reactor equipped with an electromagnetic rabble and a system maintaining a constant temperature. To maintain the components in the liquid state, an excess pressure of 0.5–1.5 atm was used.

3 Results and discussion

Allyl chloride was epoxidized with an aqueous solution of hydrogen peroxide on a titanium-containing zeolite in the presence of an organic solvent. Alcohols, ketones, and ethers can be used as solvents. Our studies have shown that methanol provides the highest epoxidation rates and high yield of epichlorohydrin. In this process, the solvent serves as a homogenizer of allyl chloride and hydrogen peroxide, thereby providing their interaction at the surface of the solid catalyst. It should be noted that the amount of the solvent strongly affects the basic aspects of the process. Because the ternary system constituted by allyl chloride, methanol, and water has a limited solubility region, the choice of the solvent concentration is limited by the possibility of obtaining a homogeneous reaction mixture, on the one hand, and by the inadvisability of its strong dilution complicating the subsequent isolation of epichlorohydrin, on the other.

To study the effect of the solvent concentration on the process of allyl chloride epoxidation, we carried out a set of experiments at various methanol : allyl chloride molar ratios. The solvent concentration was varied in the range 50–80 wt %, which lies within the mutual solubility region of the allyl chloride–methanol–water ternary system.

It was found that, as the content of the solvent in the reaction mass is lowered, the initial rate of epichlorohydrin formation grows, with this relationship being linear. Variation of the methanol content within the range 50–80 wt % only slightly affects the yield of epichlorohydrin,

which remains constant: 94–96% at a hydrogen peroxide conversion of 96–98%. Thus, it is advisable to perform the epoxidation process at a solvent content close to 55–65 wt %, which corresponds to a methanol : allyl chloride molar ratio of (4–6) : 1. Lower solvent concentrations are undesirable because of the possible transition of the system from a homophase to a heterophase state, despite the possible increase in the initial rate of the process. Solvent contents exceeding 65 wt % fails to provide a desired increase in the process selectivity, and only diminishes the epoxidation rate and largely complicates the subsequent stage of epichlorohydrin isolation because of the strong dilution of the reaction mass. At a solvent content of 55–65 wt %, the epoxidation rate is sufficiently high and an effective heat removal is provided, which rules out reaction mass overheating leading to undesirable consequences.

To evaluate the effect of the initial allyl chloride : hydrogen peroxide ratio on the basic aspects of the process, we carried out a set of experiments at various initial ratios between these reagents. The allyl chloride : hydrogen peroxide molar ratio was varied within the range (1–6) : 1. An increase the concentration of hydrogen peroxide (decrease in the initial allyl chloride : hydrogen peroxide ratio) results in that the initial rate of epichlorohydrin formation grows.

It should be noted that variation of the initial allyl chloride : hydrogen peroxide ratio also strongly affects the yield of epichlorohydrin. For example, an increase in the initial ratio from 1 : 1 to 3 : 1 at a constant conversion of 95% makes the yield of epichlorohydrin higher. Further increase in the concentration of allyl chloride fails to raise the yield of the target product. The reason is that the rate of the target process decreases with increasing initial allyl chloride : hydrogen peroxide ratio, and, as a consequence, a longer residence time is necessary for reaching high conversions of hydrogen peroxide. This leads to an additional development of undesirable processes of successive transformations of epichlorohydrin. Thus, the optimal initial allyl chloride : hydrogenperoxide molar ratio for synthesis of epichlorohydrin is 3 : 1.

To evaluate the effect of temperature, we carried out a set of experiments in the temperature range 30–60°C. Raising the temperature within this range results in that the initial rate of the process becomes 3.5 time higher. It should be noted that raising the temperature at which epichlorohydrin is synthesized intensifies not only the target reaction, but also a number of side transformations, which is confirmed by the decrease in the yield of epichlorohydrin. Thus, the final choice of the optimal temperature for synthesis of epichlorohydrin will be determined by the formation rate of the target product and the process selectivity, as well as by the demand for the by-product formed. In the authors' opinion, the range of optimal temperatures for the process of allyl chloride epoxidation is 40–50°C.

To evaluate the influence exerted by the amount of the catalyst, we performed a set of experiments with the catalyst content in the range 0–32 g/l. It was found that this amount strongly affects the process rate. The initial rate of the epoxidation process linearly depends on the amount of the catalyst, which confirms that the reaction occurs under kinetic control. Variation of the catalyst content has no effect on the yield of epichlorohydrin, which remains nearly constant. Thus, the amount of the catalyst used in epoxidation in a batch reactor will primarily affect the process rate, and, therefore, its content should be determined by the design of the reactor unit, and for the most part by its ability to remove the released heat.

4 Conclusions

The following process conditions are suggested for epoxidation of allyl chloride with aqueous solutions of hydrogen peroxide in an organic solvent in a batch reactor: solvent methanol, temperature 40–50°C, allyl chloride : hydrogen peroxide molar ratio 3 : 1, solvent concentration 55–65 wt %. Experiments performed under nearly optimal conditions can produce epichlorohydrin in 96–97% yield at a quantitative conversion of hydrogen peroxide.

Acknowledgements

This work was supported by the Ministry of Education and Science of the Russian Federation (grant agreement no. 14.577.21.0093 from August 25, 2014); a unique identifier for applied scientific research (project) RFMEFI57714X0001).

IV-PP132

Lactulose Isomerisation over Magnetic Nanoparticles Incorporated with Borate Ions

Sulman A.M., Sulman M.G., Sulman E.M.*, Doluda V.Yu., Lakina N.V.

Tver Technical University, Tver, Russia

* sulman@online.tver.ru

Keywords: lactulose, lactose, isomerization

1 Introduction

Selective synthesis of lactulose from lactose is one of the important reactions for pharmaceutical and food applications due to lactulose prebiotics properties [1]. Moreover lactose is a large-scale, low cost substrate of dairy industry: annually, million tons of lactose are produced worldwide and its isomerization to lactulose can be a possible way to obtain valuable products [1, 2]. There are several catalytic methods for lactulose syntheses including homogeneous catalytic isomerization by strong acids [1, 3], strong bases, amphoteric catalysts (hydroxyls, sulphites, borates); heterogeneous catalytic isomerization (ion exchange resins, alumosilicates) [4, 5]; biocatalytic isomerization by galactosidases and isomerase enzymes [6-8] and electrocatalytic isomerization. Lactose isomerization is a complex chemical process characterized by the formation of numerous side products such as epilactose, galactose, glucose, fructose and isosacharinic acid along with lactulose.

2 Experimental

Catalyst synthesis.

7.2 g of iron chloride (III) was dissolved in 100 ml of water. The solution prepared was added to 150 ml of 1M sodium hydroxide solution. Precipitated iron hydroxide (III) was separated by centrifugation and washed with distillated water. After that the precipitate was calcined at 300 °C for 3 hours and stored under air. 0.1M solutions of boric acid in water were prepared under nitrogen, 5 ml of boric acid solution was added to iron oxide suspension and the suspension was shaken for 2 hours under nitrogen. After this catalyst was filtrated from solution, washed by methanol and water and dried at 60^0C. The filtrate was analyzed on borate ions absence by adding Alizarin Red solution in sulfuric acid.

Lactose isomerization methodology

The isomerization was conducted batchwise in a Parr 4561 autoclave. The reactor was equipped with a heating jacket, a cooling coil, a filter in a sampling line and a substrate chamber (for placing lactose solution without mixing with the catalysts), hollow shaft concave blade impeller to ensure efficient mixing. The effective liquid volume was 50 ml (total volume 150 ml). The reactor was operated at ambient pressure under nitrogen and temperature between 70 and 90 °C. Samples of the reaction mixture were periodically removed for the analysis. The reaction in the samples was stopped by placing the sample in an ice-bath and adding a few drops of HCl to neutralize pH.

HPLC analysis

The analysis of the reaction solution was performed using ULTIMATE-3000 HPLC chromatograph. Ion exchange 250*4 mm tungsten column characterized by a theoretical plate number of 82000 was chosen for sample analysis. Reprogel H (7 mkm) served as a stationary phase, whereas a 0.1 $mmol.L^{-1}$ sulfuric acid solution in deionized water was used as the mobile phase. The flow rate was held constant as 0.5 $mL.min^{-1}$ at 80 bar and 30 °C. The refractometer detector was used for components detection. The concentrations of lactose, lactulose, glucose, fructose, galactose, epilactose and isosacharinic acid were determined using external standards.

NMR analysis

NMR spectra were recorded on a Bruker AM300 500 MHz NMR spectrometer (Moscow, A.

N. Nesmeyanov Institute of Organoelement Compounds of Russian Academy of Sciences). 1H chemical shifts were referenced to the residual solvent signal at δ 4.70 (D_2O) The spectra were recorded once with 30 mg of lactulose, lactose and dried reaction mixture dissolved in 700 μL of D_2O.

3 Results and discussion

The performance of synthesized and traditional catalysts was evaluated under the following reaction conditions: lactose initial concentration 0.3 mol/l, reaction temperature 70°C and catalyst concentration 0.1 mol/l and pH=11.

Table 1. Catalysts activity characteristics in lactose isomerization process

Catalyst	TOF*, $s^{-1}*10^2$	Conversion, %	Selectivity, %
NaOH	0.51	48	55
$Na_2B_4O_7$	1.25	95	88
$NaAlO_2$	0.84	72	78
Fe_3O_4-2-BO_3	0.82	75	80
Fe_3O_4-4-BO_3	0.84	77	82
Fe_3O_4-6-BO_3	0.90	82	85

The HPLC and NMR analyses showed formation of lactulose and the main side products – glucose, fructose, galactose which were detected for all catalyst, and isosacharinic acid, epilactose were detected in traces. The highest TOF (Table 1) was found to be 0.0125 s^{-1} for conventional $Na_2B_4O_7$ catalysts, while for the most active Fe_3O_4 based catalyst the TOF was 0.0093 s^{-1} and for the most active iron oxide Fe_2O_3-6-BO_3 based catalyst the TOF was 0.9 s^{-1}. The highest lactose conversion and the process selectivity for the most active HPS based catalyst was found to be 82% and 85% respectively, however it is lower compared to commonly used $Na_2B_4O_7$ catalyst.

4 Conclusions

A series of borate modified catalysts based on magnetic nanoparticles (III) were synthesized. The catalysts activity strongly depends on surface concentration of borate ions. The catalytic properties of the synthesized catalysts have been examined under a wide variety of reaction conditions in lactose isomerization process. The most active catalyst providing the highest lactulose yield was found to be Fe_3O_4-6-BO_3, however the catalytic activity of the synthesized catalyst is lower compared to the most active sodium tetraborate homogeneous catalyst and higher compared to conventional heterogeneous catalysts. Nevertheless the possibility of heterogeneous catalysts easy magnetic separation from the reaction mass has a lot of advantages for the industrial implementation.

Aknowlegments

This work has been supported by the Ministry of Education and Science of the Russian Federation.

References

[1]M. Aider, D.d. Halleux, *Trends in Food Science & Technology*. 18 (2007) 356-364.
[2]A.I. Ruiz-Matute, M.L. Sanz, N. Corzo, P.J. Martin-Alvarez, E. Ibanez, I. Martinez-Castro, A. Olano, *Journal of Agricultural and Food Chemistry*. 55 (2007) 3346-3350.
[3]H. Hohno, S. Adachi, *Journal of Dairy Science*. 65 (1982) 1421-1427.
[4]M. Angel de la Fuente, M. Juarez, D. de Rafael, M. Villamiel, A.M. Olano, *Food Chemistry*. 66 (1999) 301-306.
[5]R. Gounder, M.E. Davis, *Journal of Catalysis* (2013).
[6]Y.-S. Kim, J.-E. Kim, D.-K. Oh, *Bioresource Technology*. 128 (2013) 809-812.
[7]Y.-S. Kim, D.-K. Oh, *Bioresource Technology.* 104 (2012) 668-672.
[8]Y.-S. Song, H.-U. Lee, C. Park, S.-W. Kim, *Carbohydrate Research*. 369 (2013) 1-5.

IV-PP133

Selective Synthesis of Butadiene from Ethanol over ZrBEA Catalysts

Sushkevich V.L.*, Ivanova I.I.

Lomonosov Moscow State University, Moscow, Russia

* vitaly.sushkevich@gmail.com

Keywords: butadiene, ethanol, Zr beta, infrared spectroscopy, DFT

1 Introduction

The recent developments render the ZrBEA zeolite as a material with very high potential as catalyst in such processes as Lewis acid-catalyzed transformation of levulinic acid to γ-valerolactone, etherification of alcohols, the Meerwein–Ponndorf–Verley–Oppenauer (MPVO) oxidation-reduction reactions, and butadiene synthesis from ethanol. The latter reaction is very important for the diversification of the industrial routes of synthesis of butadiene, which is an important monomer for the rubbers and elastomers production. Recent assessment of the economic, environmental, health, safety and operation aspects of naphtha-based and ethanol-based routes suggested the alternative ethanol to butadiene conversion process as a promising sustainable substitute for the dominant naphtha-based method, which can contribute to decreased use of fossil fuel reserves.

However, the nature of its active sites, which is a necessary prerequisite for understanding mechanisms of reactions and design of new catalysts, has not been fully investigated. Experimental and theoretical data suggests that ZrBEA should possess two distinctive types of Lewis sites, designated herein as “closed” and “open” Zr(IV) sites. However, the real configuration of the present sites, and which of those sites are catalytically active, remains unknown. Another open question is how the Zr loading and distribution affects the ratio between closed and open Zr(IV) sites, and their respective activity.

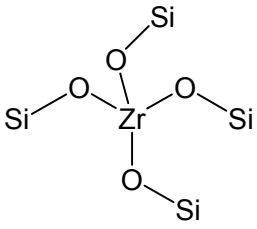

"Closed" site

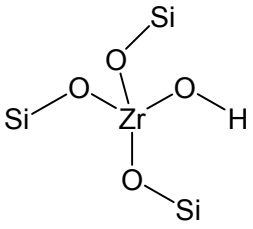

"Open" site

All these open questions motivated the present study on the determination of the structure of active sites for selective ethanol transformation into butadiene over ZrBEA by combination of infrared spectroscopy and DFT calculations.

2 Experimental

ZrBEA catalysts with Si/Zr ratio within 100-800 were synthesized using the procedure described elsevere [1]. For catalytic tests in the reaction of ethanol transformation into butadiene all the catalysts were modified with 1 wt% of silver.

The catalysts were characterized by N_2 adsorption, FTIR spectroscopy of adsorbed probe molecules, TEM, XPS, XRD. The catalytic tests were performed under atmospheric pressure in flow-type fixed-bed reactor. The weight hourly space velocity (WHSV) was varied within 0,1-0,6 h^{-1}, reaction temperature was 593K.

For quantum chemical calculations the geometries of the structures obtained by adsorption of CO on the cluster models were optimized within the DFT framework with the hybrid functional B3LYP using a LANL2DZ effective core potential basis set for Zr and the standard 6-31G(d, p) basis set for C, O, Si, and H atoms. Vibrational spectra have been calculated within the

harmonic approximation.

3 Results and discussion

Ethanol conversion into butadiene is a complex process involving at least four consequitive reaction steps: (1) ethanol dehydrogenation into acetaldehyde; (2) aldol condensation of acetaldehyde into crotonaldehyde; (3) Meerwein–Ponndorf–Verley-Oppenauer (MPVO) reaction between crotonaldehyde and ethanol leading to crotyl alcohol and acetaldehyde and (4) dehydration of crotyl alcohol into butadiene. On metal containing oxide catalysts steps (2) and (3) were demonstrated to be rate determing steps [2].

The increase of Zr content in ZrBEA up to 2 wt% leads to the significant enhancement of the butadiene formation rate from 36 to 132 μmol/g·s due to the increase of the amount of Zr Lewis sites responsible for steps (2) and (3). However, the catalytic activity does not show direct correlation with the total amount of Zr sites. FTIR data of adsorbed CO shows coexistence of two Lewis sites, which basing on the results of DFT calculations were attributed to "open" (2185 cm^{-1}) and "closed" (2176 cm^{-1}) sites (see Figure below). Whereas the amount of closed sites does not show any relationship with the catalytic activity of difference ZrBEA samples in the ethanol conversion into butadiene, the "open" sites demonstrated linear correlation with the initial rate of butadiene formation. Such selective activity of open sites could be attributed to the higher acid strength of open sites, as well as their better steric accessibility compared to the closed sites.

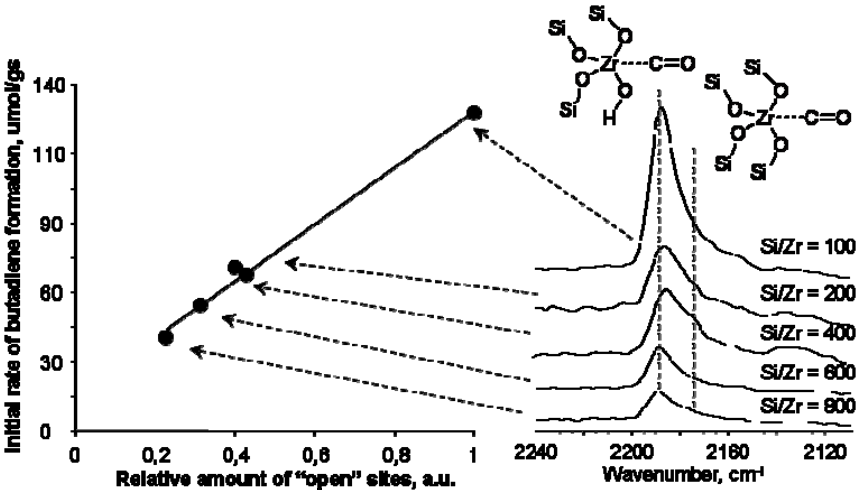

4 Conclusions

Combination of the results of the FTIR and the DFT calculations suggests that the Zr(IV) Lewis acid sites in ZrBEA catalysts are represented by isolated Zr atoms in tetrahedral positions of the zeolite crystalline structure linked with four ("closed" site) and three ("open" site) silicon atoms. The catalytic activity in butadiene synthesis form ethanol isshown to correlate with the amount of "open" sites. High efficiency of the "open" sites can be rationalized in terms of higher acid strength and better steric accessibility of such sites.

Acknowledgements

Authors thank the Russian Science Foundation for the financial support (№14-23-00094).

References

[1] Y. Zhu, G. Chuah, S. Jaenicke, J. Catal., 227 (2004) 1-10
[2] V. Sushkevich, I. Ivanova, E. Taarning, Green Chem., submitted

IV-PP134

Gamogen-Catalytic Vinylation of Aromatic Acetylene Alcohols

Ziyadullaev O.E.*, Turabdjanov S.M., Ikramov A.I., Irgashev Yo.T.

Tashkent Chemical Technological Institute, Tashkent, Uzbekistan

* bulak2000@yandex.ru

Keywords: gamogeneous catalysis, aromatic acetylenic, alcohols, acetylene, a solvent product outlet, intermediate and auxiliary connections

1 Introduction

Vinyl ethers in the industry, as initial products they are used to obtain acetals, corotinoida, oligonucleotides, citrals, herbal preparations, polymers, heteropolymers, glue, lacquer, emulsion, paint, alkyd resins, artificial leather, plasticizers, oil additives [1, 2].

2 Experimental

Vinylation reaction with aromatic acetylenic alcohol (AAA) gamogeneous methods. The influence of the nature and amount of catalyst, the molar ratio of the starting materials during the reaction temperature on the yield of the product. Definitely purity, structure, elemental composition and physical constants and quantum chemical calculations of the synthesized compounds. The optimal conditions for the synthesis of a product with a high yield.

Vinylation reaction of aromatic acetylene alcohols (AAA) containing phenyl group in its molecule in the presence of acetylene has been investigated and properly vinyl ethers (VE) have been synthesized [3].

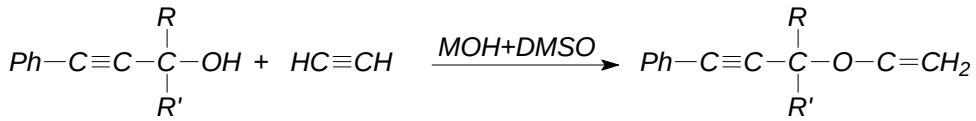

$R = -CH_3$, $R^I = -C_2H_5$; $R = -CH_3$, $R^I =$ izo $-C_3H_7$, $R = -CH_3$, $R^I = -C(CH_3)_3$; $R = -CH_3$, $R^I = -C_6H_3$, $Ph = -C_6H_5$.

The influence of temperature, catalyst and solutions nature on the yield of AAA VE has been studied systematically and analyzed. On the basis of received results DMSO solution in the presence of catalyst KOH, when acetylene influences on AAA at temperature 120^{0}C, for 6 hours it has been determined that VE comes out with highest yield.

Theoretically, when the temperature rises, it can be explained the decrease of AAA VE yield as follows. Orientation polarity of hydrogen positive charged in AAA hydroxyl group towards triple bond of acetylene depends on the exchanging of catalysts metal cations with active hydrogen of acetylene and acetylenes forming. It is known, it is determined the fall down in the product yield on account of the orientation polarity, having decreased alongside with rising of temperature, intensifying of acetylene molecule motion, as a result, on account of the damage of its special regulated arrangement. It has been determined the decrease of solubilization of alcoholates alongside with the increase of their molecular weight, and this opposes acetylene joining and it has been observed the decrease in the formation of VE. Acetylene and solution are sent into the system with extra amount for the purpose of increasing product yield it will bring to rise in price of the cost of the product synthesizing. Extra expenditure of acetylene and solution causes lasting of reaction duration and recycling demands to implement complicated technological processes.

3 Conclusions

To sum up, it has been observed the decrease in vinyl ethers productivity owing to the

formation of acetylenes reacting with metals and their hydrolysis, the increase of alcoholates stability formed by joining AAA containing ethyl, isopropyl and triple radicals with metals.

References

[1] Temkin O.N. Sorosovskiy educational journal. 1998. №6. p. 32-41.
[2] Favoriskiy A.E. Seleccted works. M.: Pub. House Asc. USSR, 1961. p. 790.
[3] Ziyadullaev O.E., Mirkhamitova D.Kh., Nurmanov S.E. Journal of talks of academicians of science of the Republic of Uzbekistan. 2012. №3. p. 167-176.

IV-PP135

The Gold Particle Catalysed Mechanism for the Oxidation of Hydroxymethylfurfural to 2,5-Furandicarboxylic Acid: a DFT Study

Thomas L.M.[1], Lee A.F.[2], Wilson K.[2], Willock D.J.[1*]

1 - Cardiff University, Cardiff, UK
2 - Aston University, Birmingham, UK

* thomasl63@cardiff.ac.uk

Keywords: biomass, DFT, gold nanoparticle, oxidation, HMF

1 Introduction

Hydroxymethylfurfural (HMF), (figure 1) is obtained from dehydration of sugars such as glucose, fructose and xylose[1]. This biomass derived molecule is the subject of great interest as it can be used as a platform to replace traditional chemical feedstocks used within industrial processes. This versatility has seen HMF labelled a "top 10" molecule by the United States department of energy[2]. One such molecule obtained from HMF is 2,5-furandicarboxlyic acid (FDCA), (figure 1), which is obtained via an oxidation reaction. FDCA being a dicarboxylic acid can undergo polymerization to form polymers suitable for usage within the packaging industry, therefore replacing crude oil derived terephthalic acid. It is reported this oxidation to FDCA can be performed using heterogeneous gold nanoparticles as catalysts under mild reaction conditions[3]. There is some debate within the literature regarding the oxidation route and therefore computational modelling is required to shed light on this reaction.

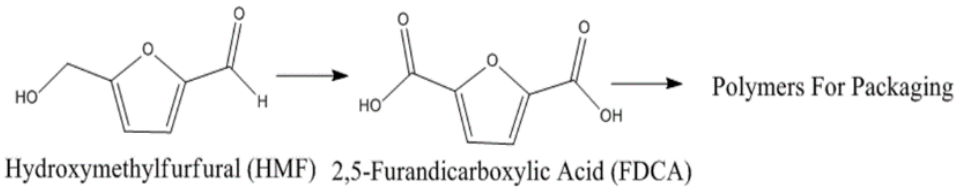

Figure 1. Pathway for conversion of HMF to polymers for packaging materials.

2 Experimental/methodology

Here a detailed computational (DFT) study is presented discussing the interaction of HMF with gold clusters various sizes (Figure 2). The effect of alloying gold particles with palladium is presented along with the influence of the following particle supports: Fe_2O_3, and TiO_2. Dispersion interactions have been included within calculations and the importance of accounting for dispersion within mechanistic studies will be presented.

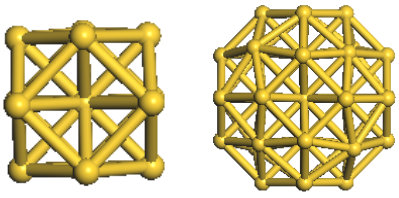

Figure 2. Au_{13} and Au_{38} clusters studied.

Acknowledgements

The authors of this work would like to thank Fujitsu and HPC Wales for computing facilities used to perform calculations along with Nextek.

References

[1] Chheda, J. N., Roman-Leshkov, Y. & Dumesic, J. A. Production of 5-hydroxymethylfurfural and furfural by dehydration of biomass-derived mono-and poly-saccharides. *Green Chem.* **9,** 342–350 (2007).

[2] Bozell, J. J. & Petersen, G. R. Technology development for the production of biobased products from biorefinery carbohydrates—the US Department of Energy's "Top 10" revisited. *Green Chem.* **12,** 539 (2010).

[3] Casanova, O., Iborra, S. & Corma, A. Biomass into chemicals: aerobic oxidation of 5-hydroxymethyl-2-furfural into 2,5-furandicarboxylic acid with gold nanoparticle catalysts. *ChemSusChem* **2,** 1138–44 (2009).

IV-PP136

REALCAT: A New High-Throughput Platform Dedicated to the R&D in Catalysis for Biorefineries

Paul S.[1,2*], Heyte S.[1,3], Thuriot Roukos J.[1], Araque Marin M.[1,2], Dumeignil F.[1,3,4]

1 - Unité de Catalyse et de Chimie du Solide, UCCS, UMR CNRS 8181, Villeneuve d'Ascq, France
2 - Ecole Centrale de Lille, ECLille, Villeneuve d'Ascq, France
3 - Université de Lille, Villeneuve d'Ascq, France
4 - Institut Universitaire de France, IUF, Maison des Universités, Paris, France

* sebastien.paul@ec-lille.fr

Keywords: high-throughput, biorefineries, chemocatalysis, biocatalysis, hybrid catalysis

1 Introduction

Catalysis under all of its forms (heterogeneous, homogeneous or biocatalysis) is of upmost interest in crucial domains such as Environment, Food, Health, Energy, which are at the inner core of the current societal demands. The development of new catalysts with improved performances is therefore a highly strategic issue.

Innovation in catalysis is based, on the one hand, on forefront fundamental research to develop new catalytic concepts and, on the other hand, on an experimental phase devoted to the synthesis, characterization of the catalytic formulations and on the measurement of their properties/performances. The experimental part of the development of a new catalyst is time- and money-consuming, as traditional "trial and error" methods for synthesizing and testing catalysts are still needed. "*A priori*" theoretical prediction of optimal catalyst composition, structure and conditions of preparation for a given reaction is actually not yet possible. Therefore, there is a strong need for rapid preparation, characterization and screening of catalytic systems.

2 Description of the REALCAT platform

The main objective of the REALCAT project (French acronym standing for 'Advanced High-Throughput Technologies Platform for Biorefineries Catalysts Design') (Fig.1), which will be presented in details in this communication, is to set up a highly integrated platform devoted to the acceleration of innovation in all the fields of industrial catalysis with an emphasis on emergent biorefinery catalytic processes. In this extremely competitive field, REALCAT consists in a versatile High-Throughput Technologies (HTT) platform (Fig. 2) devoted to innovation in heterogeneous, homogeneous or biocatalysts and their combinations under the ultra-efficient very novel concept of hybrid catalysis.

Fig. 1. The REALCAT logo

The REALCAT platform, representing a 10 M€ funding from the French government, is a complete, unique, and top-level HTT workflow including (i) robots for the automated synthesis of

catalysts and novel biocatalysts, (ii) rapid characterization tools and (iii) a series of versatile parallel continuous and batch reactors - for gas phase, liquid phase or three phases reactions - combined with ultra-fast analytical tools at the top of the state-of-the-art for the analysis of the products in the reactors effluents. Moreover, within the frame of the REALCAT project, methodological developments will also be carried out in partnership with private companies in order to develop innovative HTT tools for catalysis not yet available on the market. This will ensure that the REALCAT platform remains the most advanced level of HT equipment for catalysis in the world in the future.

Fig. 2. The REALCAT platform

Three laboratories, all located on Lille University's campus (North of France) have gathered their forces to design such a challenging project: UCCS, specialized in homogeneous and heterogeneous catalysis; Institut Charles Viollette (ProBioGEM team), specialized in biocatalysis and CRIStAL, specialized in computer engineering, data treatment, bio-informatics, modelling and analysis of biologic systems. This integrated combination of skills is of outstanding importance for the optimization of the different operations of the platform. This will make REALCAT a major actor of high-level R&D catalysis programs on hot topics such as biorefinery, energy, environmental, food and health applications.

3 Conclusions

In this lecture the REALCAT platform will be described in details and the first results issued from it will be presented. A focus will be put on the potential of the platform and on the possibilities for external users to get an access to REALCAT.

Acknowledgements

The REALCAT platform is benefiting from a governmental subvention administrated by the French National Research Agency (ANR) within the frame of the 'Future Investments' program (PIA), with the contractual reference 'ANR-11-EQPX-0037'. The Nord-Pas-de-Calais Region and the FEDER as well as the Centrale Initiatives Foundation are thanked for their financial contribution to the acquisition of the equipment of the platform.

IV-PP137

Pd-Catalyzed Selective Hydrogenolysis of γ-Ketoamides as a New Approach to the Synthesis of 5-Alkylpyrrolidin-2-Ones or Linear Carboxylic Acid Amides

Turova O.V.*, Berezhnaya V.G., Starodubtseva E.V., Vinogradov M.G.

N. D. Zelinsky Institute of Organic Chemistry of the Russian Academy of Sciences, Moscow, Russia

* turova@ioc.ac.ru

Keywords: Pd-catalyzed hydrogenolysis, γ-ketoamides, pyrrolidin-2-ones, linear carboxylic acid amides

1 Introduction

Synthesis of 5-alkyl- and 5-arylpyrrolidin-2-ones based on the Pd-catalyzed C-O bond hydrogenolysis of hydroxy lactams has been recently elaborated by us [1]. At the same time, difficulties can be occurred to prepare individual hydroxy lactams from the effect of ring-chain tautomerism. In the present work, possibility of using available γ-ketoamides in the open form as convenient starting substrates is first demonstrated.

2 Experimental/methodology

Under conditions of the Pd-catalyzed C-O-hydrogenolysis in the presence (if needed) acid cocatalyst (see Table 1), the model open amides **1** are converted *in situ* to form **2**, a precursor of the target heterocycles **3** (Scheme 1).

Scheme 1

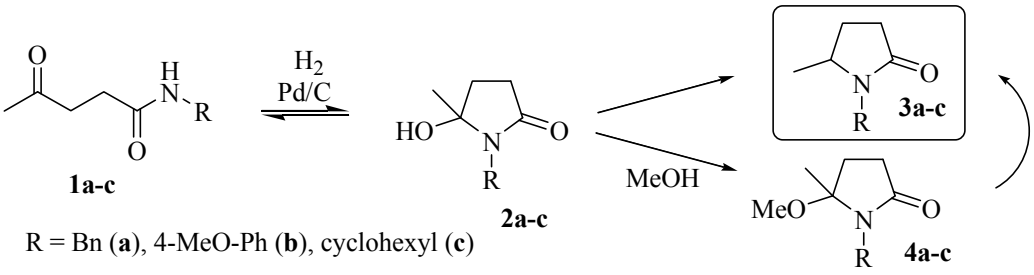

R = Bn (**a**), 4-MeO-Ph (**b**), cyclohexyl (**c**)

Table 1. Hydrogenolysis of levulinic acid amides **1a-c** in MeOH[a]

Entry	Ketoamide	**1**/HCl	Conversion, %	Products, %	
				3	**4**
1[b]	**1a**	-	90	80	20
2	**1a**	-	80	100	0
3	**1a**	100/1	83	100	traces
4	**1a**	100/10	94	100	0
5	**1b**	100/10	100	100	0
6	**1c**	100/10	60	70	30

[a] **1**/Pd = 100, 60 °C, 6 h. [b] 50 °C, 24 h.

3 Results and discussion

In MeOH, which is preferable solvent, the methoxy derivative **4** may be also formed as the by-product (see table 1, entry 1). However, increasing the temperature to 60 °C and the use of HCl as co-catalyst allowed to achieve 100% selectivity at the almost complete conversion of substrates **1a**,**b** (entries 2-5). The third substrate **1c** showed the lesser reactivity and

hydrogenolysis selectivity (entry 6).
In contrast to levulinic acid amides **1**, Pd-catalyzed hydrogenolysis of 3-benzoylpropionic amides **5** proceeds exclusively with participation of ketogroup via the intermediate hydroxy amide **6** (scheme 2).

Scheme 2

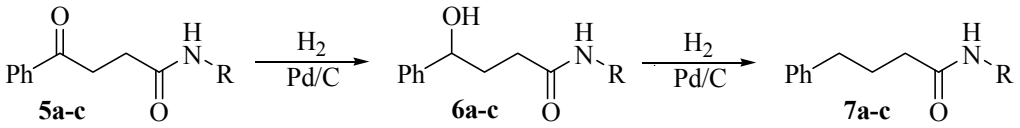

R = Bn (**a**), Bu (**b**), *tert*-Bu (**c**)

4 Conclusions

The Pd-catalyzed hydrogenolysis of N-alkyl(aryl)substituted γ-ketoamides has been first realized using levulinic and 3-benzoylpropionic amides as model substrates. In most cases, the process takes place selectively with participation of cyclic (hydroxylactam) or the open tautomeric form of substrate to yield, correspondingly, substituted pyrrolidin-2-ones or linear amides.

Acknowledgements

The reported study was partially supported by RFBR, research project No. 13-03-00423.

References

[1] O. V. Turova, V. G. Berezhnaya, E. V. Starodubtseva, V. A. Ferapontov M. G. Vinogradov, *Russ.Chem. Bull.* (*Int. Ed*.), 64 (2015), in press.

IV-PP138

Insights on the Mechanism for the Transformation of Ethanol on Basic Oxides (Lebedev and Guerbet Reactions)

Velasquez Ochoa J.[1*], Chieregato A.[1], Bandinelli C.[1], Fornasari G.[1], Cavani F.[1], Mella M.[2]

1 - Dipartimento di Chimica Industriale "Toso Montanari", Università di Bologna, Bologna, Italy
2 - Dipartimento di Scienze ed Alta Tecnologia, Università degli Studi dell'Insubria, Como, Italy

* juliana.velasquez2@unibo.it

Keywords: surface, intermediates, DRIFTS, Guerbet mechanism, Lebedev theoretical modelling

1 Introduction

In line with the increasing interest in generating higher value chemicals from bio-alcohols such as ethanol, we felt necessary to review the mechanism of upgrading of these compounds. In particular, it is of great importance to understand the surface reactions occurring when ethanol interacts with oxides having basic properties, which are ubiquitous ingredients in catalysts to produce higher alcohols (Guerbet reaction), olefins (Lebedev process), or ethyl acetate (Tishchenko reaction) [1]. Our review highlighted that the accepted mechanism of ethanol transformation still contained several aspects lacking a robust support; these are discussed in this work and alternatives are proposed based on reactivity tests, spectroscopy (in-situ diffuse reflectance infrared) and computational calculations. Interestingly, it was possible to exclude the role of the acetaldol as the key intermediate in the formation of both butanol and butadiene. As a consequence, a novel mechanistic theory was proposed to explain not only the present results, but also most of the scientific literature on the Lebedev and Guerbet chemistry. This new approach provides a rational description of the intermediates shared by the two reaction pathways as well as a different perspective on the catalysts properties that are necessary to direct the reaction pathway toward the higher alcohol or the olefin [2]. A reference catalyst made of MgO was used for experiments.

2 Experimental

MgO catalyst was prepared by precipitation from an aqueous solution of $Mg(NO_3)_2 \cdot 6H_2O$. The solid was calcined at 450°C for 8 h in air. The surface area was 86 m^2/g. Reactivity experiments were carried out using a continuous flow glass reactor. Inlet feed molar ratio was constant (2 mol% of Ethanol in N_2). Downstream products were monitored by on-line gas-chromatography analysis.

DRIFTS-MS: The sample was pre-treated at 450°C in a He flow and then cooled down to room temperature. Ethanol was fed at 0.6 $\mu l.min^{-1}$ until saturation. After the evacuation of physically adsorbed ethanol, the temperature program was run (until 450°C at 10°C min^{-1}). Selected mass spectrometry signals (m/z) were monitored continuously in time and temperature.

DFT-calculations: The modelling was carried out employing gas phase electronic structure calculations by means of the Gaussian09 suite at the Density Functional Theory (DFT) level. Specifically, the B3LYP DFT functional together with the 6-31++G(d,p) basis set were used to optimize relevant stationary points along the reaction paths.

3 Results and discussion

Ethanol reactivity tests performed at 250 and 400°C over MgO varying residence time showed that 1-butanol was a primary product, as well as acetaldehyde and ethylene; also crotyl alcohol was among the main products. C_4 aldehydes (3-hydroxybutanal, crotonaldehyde and butyraldehyde) and C_4 olefins (butenes and butadiene) were only detected as secondary products at high temperature.

In situ DRIFT spectroscopy showed the evolution of the surfaces species with the temperature (see Figure 1). In this way, it was possible to detect the intermediates of the ethanol transformation; these included an activated form of the ethanol (a carbanion) and an adsorbed form of crotyl alcohol.

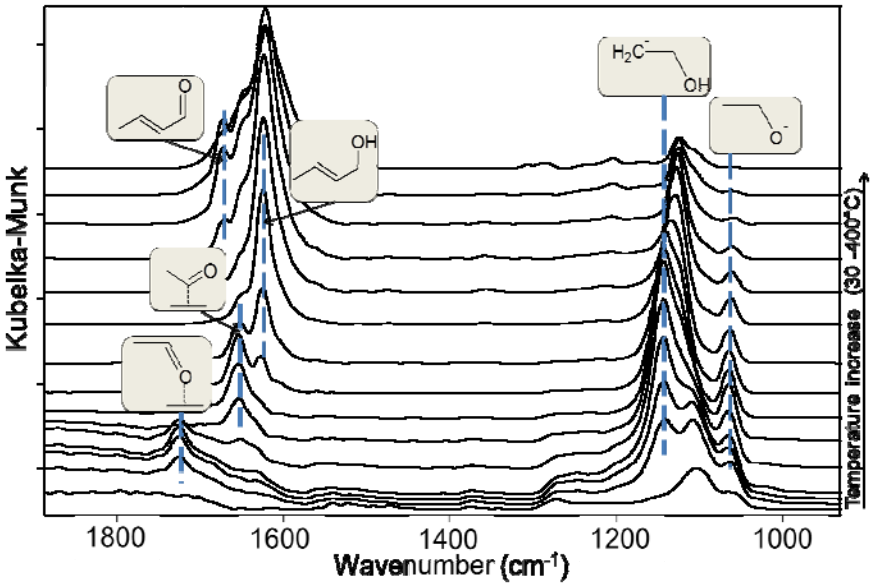

Figure 1. DRIFT spectra of ethanol adsorption on MgO and its transformation with temperature.

DFT calculations confirmed that the formation of carbanion species was less energetically demanding than ethanol dehydrogenation, the latter leading to acetaldehyde (on Mg3C sites). Further calculations on the reactivity of this carbanion specie showed that it could easily form ethylene, which formed in large amounts even over this basic catalyst. Moreover, it could either attack acetaldehyde to form a precursor of the crotyl alcohol - which then dehydrated to form butadiene - or another ethanol molecule to form 1-butanol. These results made clear that the formation of crotonaldehyde by aldolic condensation, supposedly favoured by the basicity properties of the catalysts, was not the key reaction to explain the products distribution as it has been stated in the literature [3]. Instead, we proposed that crotonaldehyde is formed after crotyl alcohol; In fact, the tests carried out by feeding some of the possible intermediates showed that the alkenol produces a similar product distribution to that one obtained with the ethanol.

4 Conclusion

The proposed new mechanism for the transformation of ethanol into C_4 compounds over MgO made it possible to draw a unifying picture of the different routes leading to either 1-butanol (Guerbet reaction), butadiene (Lebedev process), or ethylene. The suggested mechanism discards the key role of both acetaldol and crotonaldehyde as the reaction intermediates, usually accepted as being shared between the two pathways leading either to the alcohol or the diolefin.

Acknowledgements

Consorzio INSTM (Firenze) is acknowledged for the PhD grant to C.B.

References

[1] C. Angelici, B. M. Weckhuysen, P. C. Bruijnincx, ChemSusChem. 6 (2013) 1595.
[2] A. Chieregato, J. Velasquez Ochoa, C. Bandinelli, G. Fornasari, F. Cavani, M. Mella, ChemSusChem. 8 (2015) 377.
[3] E. V. Makshina, W. Janssens, B. F. Sels, P. a. Jacobs, Catal. Today. 198 (2012) 338.

IV-PP139

Catalysis by the Noble Metals in the Process of Obtaining New Biologically Active Compounds

Vereshchagina N.V.*, Antonova T.N., Kopushkina G.Yu., Shelekhova A.I.

Yaroslavl State Technical University, Chemical Engineering Department, Yaroslavl, Russia

* nadezhda.vereshagina@bk.ru

Keywords: dicyclopentadiene, dicyclopentene, catalysts of hydrogenation

1 Introduction

The synthetic medication, which include biologically active compounds of aromatic and/or a cyclic structure with functional groups have a large share among the medication in the pharmaceutical industry.

As a potential source of biologically active compounds oxygen-containing derivatives of dicyclopentadiene, having the structure close to the frame, can be used, for example, mono- and diketones: 3-oxotricyclo[5.2.1.$0^{2.6}$]decane, 3,4-dioxotricyclo[5.2.1.$0^{2.6}$]decane.

We proposed to use dicyclopentene, as hydrogenated analogue dicyclopentadiene, for preparation this compounds with a high degree of purity.

2 Experimental/methodology

The hydrogenation reaction of dicyclopentadiene with hydrogen in the liquid phase in the presence of catalysts on the bases of noble metals used for obtaining of dicyclopentene.

3 Results and discussion

It is established that the most activity showing finely dispersed catalyst (1 % Pd/C). It allows selective formation of dicyclopentene under mild conditions (atmospheric pressure, temperature of 40 to 80 °C) at full conversion of the original dicyclopentadiene. The high activity of this catalyst is determined by its structure. The catalytic activity in the structure of palladium deposited on charcoal give its clusters small size (2-3 nuclear). Carbon matrix prevents to formation clusters of large size.

Selective obtaining of dicyclopentene in the process of hydrogenation of dicyclopentadiene in the presence of 1 % Pd/C is possible in result the sequence of saturation of double bonds dicyclopentadiene (tricyclo[5.2.1.$0^{2.6}$]decadiene-3,8). Double bond of bicycloheptene fragment its molecule saturated as the first and obtained dicyclopentene have a structure as tricyclo[5.2.1.$0^{2.6}$]decene-3.

The use of finely dispersed catalyst under conditions of intense mixing converts three-phase system in a state of pseudohomogeneous. As a result, the hydrogenation process can be realized in the reactor, simulating the ideal mixing reactor. The catalyst is easily separated from the reaction products and can be reused without prior activation.

3 Conclusions

A new way of obtaining oxygen containing products based on dicyclopentadiene (for example, 3-oxotricyclo[5.2.1.$0^{2.6}$]decane and 3,4-dioxotricyclo[5.2.1.$0^{2.6}$]decane) for pharmaceutical synthesis are proposed and studied.

IV-PP140

The Conversion of Propane into Aromatic Hydrocarbons over Ga-Containing Zeolite Catalysts

Vosmerikova L.[1*], Volynkina A.[1], Zaikovskii V.[2], Vosmerikov A.[1], Fedushchak T.[1]

1 - Institute of Petroleum Chemistry, Siberian Branch of RAS, Tomsk, Russia
2 - Institute of Catalysis, Siberian Branch of RAS, Novosibirsk, Russia

* lkplu@ipc.tsc.ru

Keywords: aromatization, propane, H-Ga-Al-catalysts

1 Introduction

The use of the components of natural and associated petroleum gas as a feedstock for production of valuable chemical products acquires an ever-increasing importance, which is particularly critical due to a gradual depletion of oil reserves. In this case, production of aromatic hydrocarbons from light alkanes attracts not only manufacturers, but also researchers solving the fundamental problems of catalysis [1]. The efficiency of aromatization of light alkanes strongly depends on the catalyst and the conditions of its application. Typical aromatization catalysts are systems consisting of the supporter – H-form of pentasil and the modifying components, mainly zinc, gallium, platinum, or palladium [2-4]. To increase the yield of aromatic hydrocarbons, a thermal or chemical modification of zeolites is used. The main methods of their chemical modification are ion exchange, impregnation with solutions of salts and isomorphous substitution of framework aluminum atoms.

The aim of this work is to establish the relationship between the localization of gallium introduced into a zeolite by different methods and the catalytic activity of the resulted contacts in the course of propane aromatization.

2 Experimental/methodology

We have investigated the Ga-containing zeolite catalysts prepared by different methods. Modification of the zeolite with gallium was carried out by impregnation, ion exchange, mechanical mixing, and isomorphous substitution. The concentration of gallium oxide in the sample was 1.85 wt%. The acidic properties of Ga-containing catalysts were tested by the method of temperature programmed desorption of ammonia (TPD). The specific surface area and the pore size distributions were determined using a Micromeritics ASAP 2020 instrument (USA). HR TEM images were obtained in a Jeol JEM-2010 electron microscope (Japan).

The catalysts under study were tested in the course of propane conversion in a flow-type reactor at atmospheric pressure, the reaction temperature 400-600 ^{o}C, and the feed space velocity 500 h^{-1}. The reaction products were analyzed by GLC using a Chromatek-Kristall 5000.2 chromatograph. In order to estimate the catalytic activity of the samples, the degree of propane conversion was estimated. The yield and formation selectivity of the gaseous and liquid products were also calculated.

3 Results and discussion

The studies have shown that the Ga-containing zeolite catalysts prepared by different methods are characterized by virtually the same total catalyst activity (estimated from the degree of propane conversion) but different aromatization activities. The highest activity and selectivity towards formation of aromatic hydrocarbons from propane was exhibited by the catalyst produced by impregnation of zeolite. For this sample, the propane conversion and the yield in aromatic hydrocarbons at 550 °C are 95 and 44.5 %, respectively (Table 1).

The zeolite manufactured by the method of hydrothermal synthesis differs only slightly in its selectivity towards formation of aromatic hydrocarbons from the sample prepared by impregnation. This indicates that both methods result in the formation of an approximately equal number of active sites in the zeolite structure. These centers, having nearly similar structure activate the propane molecules and promote their subsequent conversion into aromatic hydrocarbons. The lowest activity of propane aromatization is exhibited by zeolites modified with gallium by the methods of ion exchange and mechanical mixing. For example, the yield in aromatic hydrocarbons over the Ga-containing zeolite manufactured by ion exchange at 550 °C is 37.8% for a propane conversion 95%.

Table 1. Characteristics of the process of propane conversion over Ga-containing catalysts (T = 550 °C)

Method of gallium introduction	X, %	S_1, %	S_2, %	S_3, %	S_4, %	Y, %
isomorphous substitution	95	5.7	47.0	2.7	43.8	41.7
impregnation	95	5.2	45.4	2.4	46.9	44.5
ion exchange	95	5.3	51.3	3.3	40.0	37.8
mechanical mixing	93	5.4	51.1	3.1	40.1	37.3

Note. X is the conversion of propane; S_1, S_2, S_3 and S_4 is the selectivity towards a formation of hydrogen, C_1-C_2 alkanes, C_2-C_4 alkenes and aromatics, respectively; Y is the yield of aromatic hydrocarbons.

Using TEM data, it was found out that gallium in a zeolite catalyst produced by isomorphous substitution is in a cation- dispersed state. Under high magnification, the zeolite impregnated with gallium was observed to contain particles measuring 2-4 nm on the on the surface of the zeolite crystals, which provided a higher contrast. For the Ga-containing zeolite prepared by ion exchange no GaL signal was present in the EDX spectrum from a large number of particles, which may be due to the low Ga content in this sample and an insufficient sensitivity for the spectrometer to detect any signals from Ga. On the other hand, there still were some particles (very few) measuring about 3 nm on the surface of certain crystals. These particles are similar to those detected in the sample prepared by the impregnation method. The method of ion exchange appears to be unsuitable for fixation of gallium on the zeolite surface. Large GaOx aggregates with disordered structure were observed in the sample, containing gallium introduced by mechanical mixing, which were localized on the surface of the sample. Moreover, the surface contained pores and asperities due to mechanical processing.

4 Conclusions

Thus, the investigations have shown that the Ga-containing ZSM-5 zeolite catalysts, prepared in different ways, differ in their physical, chemical and acid properties due to local inhomogeneities in the distribution of aluminum and gallium in the crystalline aluminosilicate framework. The Ga-containing zeolite catalyst prepared by impregnation has been observed to demonstrate the highest catalytic activity and selectivity for formation of aromatic hydrocarbons from propane.

References

[1] Kh. Minachev, A. Dergachev, *Russ. Chem. Rev.* 59 (1990) 885.
[2] V. Parmon, A. Noskov, *Katal. Prom-sti.* 4 (2007) 3.
[3] A. Dergachev, A. Lapidus, *Ross. Khim. Zh.* 52 (2008) 15.
[4] V. Zaikovskii, L. Vosmerikova, A. Vosmerikov, *Kinet. Catal.* 53 (2012) 731.

IV-PP141

Dehydration of Biodiesel-Derived Crude Glycerol into Acrolein over HPW Supported on Cs-Modified SBA-15

Liu R., Wang T.*, Jin Y.

Beijing Key Laboratory of Green Reaction Engineering and Technology, Department of Chemical Engineering, Tsinghua University, Beijing, China

* wangtf@tsinghua.edu.cn

Keywords: crude, glycerol, dehydration, acrolein, alkaline, metal, ions, SBA-15, tungstophosphoric, acid

1 Introduction

Acrolein has broad industrial and agricultural applications, and is used in the production of acrylic acid and its esters. The current technology for producing acrolein is based on the selective oxidation of propylene over the complex multi-component $BiMoO_x$-based catalysts [1]. However, this technology will become less competitive as the crude oil price increases. The development of selective dehydration of pure glycerol provides a route to the sustainable production of acrolein. Nowadays, the price of refined glycerol is 900−1000 US$/ton, while crude glycerol is available at only ~150 US$/ton [2]. This makes the sustainable production of acrolein from crude glycerol much more competitive compared with that from pure glycerol reported in our previous work.

2 Experimental

The HPW/Cs-SBA catalyst was prepared using the two-step vacuum impregnation method reported in our previous work [3]. In the first step, an aqueous solution of Cs_2CO_3 (Alfa Aesar) was introduced under vacuum. Then HPW was impregnated using $H_3PW_{12}O_{40}{\cdot}nH_2O$ (Alfa Aesar) aqueous solution in a similar way to form $Cs_{2.5}H_{0.5}PW_{12}O_{40}$ with a 50 wt% loading of HPW. The final catalyst samples were denoted as HPW/Cs-SBA.

Glycerol solution with different feed composition was used to study the effect of impurities. The aqueous solutions were prepared with pure glycerol ($C_3H_8O_3$, ultrapure, HPLC Grade, Alfa Aesar) or crude glycerol. The synthetic crude glycerol contained one of the following impurities: methanol, FFA (linoleic acid), FAME (methyl oleate), glycerides (glycerol monostearate), Na^+ (NaCl) and K^+ (KCl). The weight percent of impurity in each synthetic crude glycerol was 5wt%. Desalted plant crude glycerol was also used as feedstock. Ion exchangers was used in the desalination process [4]. A commercial ion-exchange resin D001-CC provided by Tianjin Bohong Resin Technology Co. Ltd was used to remove the alkli metal ions.

The experiments of glycerol dehydration were carried out at 300 ^oC under atmospheric pressure in a fixed bed reactor (10 mm i.d.) using 0.5 g catalyst.

3 Results and discussion

Several kinds of synthetic crude glycerol with methanol, methyl stearate or alkli metal ions were prepared and used to study the influence of different impurities on the product distribution. Among the impurities commonly contained in crude glycerol, only the alkli metal ions caused catalyst deactivation and decrease in acrolein selectivity. The reason was that alkli metal ions deposited on the HPW/Cs-SBA catalyst surface to form alkaline salts of HPW by neutrilization and decreased the effective medium Brønsted acid sites.

In order to increase the stability of HPW/Cs-SBA during the catalytic conversion of plant crude glycerol, the alkli metal ions were removed by glycerol desalination with ion-exchange resin. Figure 1 shows the glycerol conversion and product selectivity as a function of the

reaction time with 20 wt% aqueous solution of plant crude glycerol and desalted crude glycerol at 300 °C. It can be seen that the glycerol conversion decreased from 100% to 90% and the acrolein selectivity decreased from 86% to 79% after 40 h of reaction with plant crude glycerol. In comparison, the acrolein yield kept stable at 86% when desalted crude glycerol was used, which was similar to that with pure glycerol. To investigate the thermal stability of the catalyst for desalted glycerol dehydration, the reaction was carried out after 3 h regeneration of the catalyst at 500 °C in the air. The HPW/Cs-SBA catalyst showed good thermal stability and gave the same activity and selectivity as before regeneration. These results showed that it was feasible to use desalted crude glycerol to efficiently produce acrolein. Because the desalination process was much cheaper than the whole purification process for refined glycerol production, this approach significantly enhanced the competitiveness of acrolein production from glycerol.

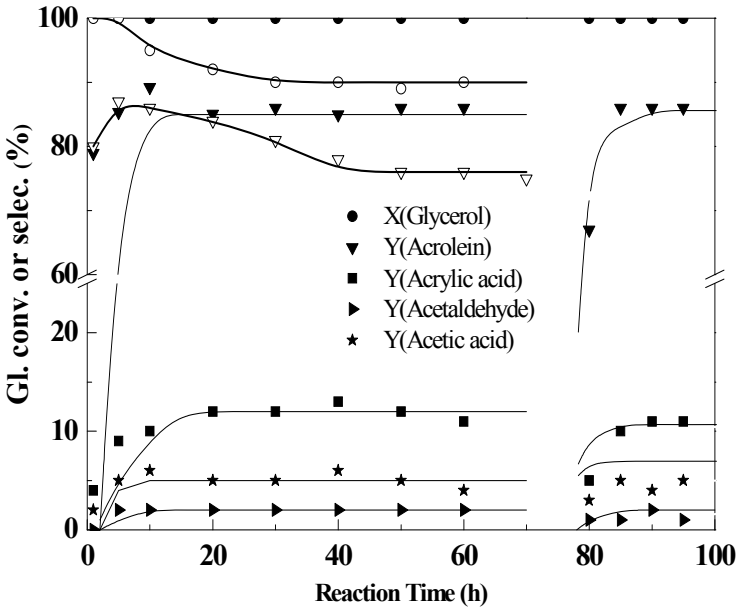

Fig. 1. Glycerol conversion and product selectivity with 20 wt% plant crude glycerol (open symbol) and desalted crude glycerol (closed symbol) at 300 °C before and after in situ regeneration at 500 °C for 3 h.

4 Conclusions

The feasibility of using crude glycerol as feedback for the acrolein production by dehydration reaction was explored in this work. When using crude glycerol for dehydration to acrolein, the HPW/Cs-SBA catalyst showed good resistance to organic impurities such as methanol and fatty acid. But the alkaline metal ions such as Na^+ and K^+ converted the medium acid sites to weak acid sites and significantly decreased the yield of acrolein. Among all the impurities, only the alkaline metal ions need to be removed before the dehydration reaction. After desalination of the plant crude glycerol with ion-exchange resin, the catalyst gave 86% acrolein yield, which was as high as that with pure glycerol. The catalyst showed good stability after coke-burning regeneration process. Our work provides a green and efficient route to produce acrolein from crude glycerol, which is a promising alternative and complement to the petroleum-based production of acolein due to its economic and environmental benefits.

References

[1] Katryniok, B.; Paul, S.; Dumeignil, F.,ACS Catal.(2013) 1819-1834.

[2] Tudorache, M.; Negoi, A.; Tudora, B.; Parvulescu, V. I.; Konaka, A.; Tago, T.; Yoshikawa, T.; Nakamura, A.; Masuda, T. Appl. Catal. B. 146 (2014) 274-278.

[3] Liu, R.; Wang, T.; Jin, Y. Catal. Today. 233 (2014) 127-132.

[4] Xiao, Y.; Xiao, G.; Varma, A. Ind. Eng. Chem. Res. 52 (2013) 14291-14296.

IV-PP142

Modified Nickel Catalysts for Oxidation of Methane

Dossumov K.[1], Yergaziyeva G.Y.[2*], Myltykbayeva L.K.[2], Mironenko A.V.[2]

1 - Centre of Physic-Chemical Analysis and Investigation Methods, Almaty, Kazakhstan
2 - The Institute of Combustion Problems, Almaty, Kazakhstan

* ergazieva_g@mail.ru

Keywords: methane, oxidation, nickel-based, catalys, synthesis, gas

1 Introduction

The partial oxidation of methane into synthesis gas has created significant interest for researchers in the field of petrochemistry, because we will be able to use natural gas for at least 100-150 years as one of basic resources of the petrochemical industry. Synthesis gas is also known to be an important material connecting methane with petrochemistry and can be directly converted to methanol which is a useful raw material for various chemicals; i.e., ethanol, formaldehyde, acetic acid, and methyl esters and at.al [1]. In order to achieve a practical application of the oxidative conversion of methane, the development of highly active, stable, selective, and cost-effective catalysts are desired [2].

The most effective and economic catalysts for steam reforming and autothermal reforming have been known to be Ni based catalysts, especially Ni/ γ-Al_2O_3 catalysts, because novel metals are expensive even though their high activity [3]. However, as well known, Ni based catalysts suffer from fast deactivation and poor process ability due to high coke deposition. In order to solve this problem, many attempts have been tried by researchers. Introduction promoting additives in the Ni catalyst is one of the effective ways to reduce the formation of the coke [4].

In this study, we investigated the effects of promoting additives (Co_2O_3, CeO_2, La_2O_3) on the performance and the physicochemical characteristics of the nickel catalysts.

2 Experimental/methodology

Experiments to test the efficiency of the catalysts were carried out using an automated flow catalytic device (FCI-1 LLC). The device consists of three main parts; the preparation of the initial gas mixture, a quartz flow-type reactor, and a gas chromatograph for the product analysis. The reaction was performed at atmospheric pressure and the temperature was studied in the range of 600-900 ^oC. The amounts of the reaction products were determined by an absolute calibration method using a gas chromatograph equipped with a thermal conductivity detector (GC-1000 LLC "Chromos"). The catalysts were prepared by the impregnation of γ-Al_2O_3 (S_{BET} = 190 m^2/g) with a solution of $Ni(NO_3)_2 \cdot 6H_2O$, drying at 350 ^oC (for 2 hours), and then calcination at 500 ^oC for three hours. Morphology of the catalysts was observed by a scanning electron microscope (SEM) using S-4100 (Hitachi High-Technologies Corporation) and a transmission electron microscope (TEM) using Technai G220 (FEI Company).

3 Results and discussion

The Ni/γ-Al_2O_3 catalyst was modified with oxides of cobalt, cerium, and lanthanum. The catalysts were evaluated during the reaction at the W = 4500 h^{-1} and the ratio of the reaction mixture was CH_4: O_2: Ar = 2:1:3.6. The modification of the Ni/γ-Al_2O_3 catalyst reduced the yield of CO_2 in the reaction products with the increasing CO yield. Among the tested catalysts, the NiLa/ γ -Al_2O_3 catalyst was the most effective one for the formation of synthesis gas because of the decreasing CO_2 content from 2.5 to 0.1%. For the reaction using the La-modified catalyst,

the H_2 yield also increased from 81% to 83%.

The SEM photographs of the Ni-M/γ-Al_2O_3 (M = La, Ce, and Co) catalysts used for 30 h indicated a different situation for the coke formation (Figure 1). The Ni/γ-Al_2O_3 and NiCo/γ-Al_2O_3 catalysts formed a significant amount of the tube- or yarn-like cokes, whereas no significant amount of coke was observed on the surface of the NiCe and NiLa/γ-Al_2O_3 catalysts. The addition of cerium and lanthanum in nickel-based catalyst enhances the catalytic activity via increase of the active component. Also having the high ability for oxygen storage allows regulating the oxygen concentration on the surface of the catalysis.

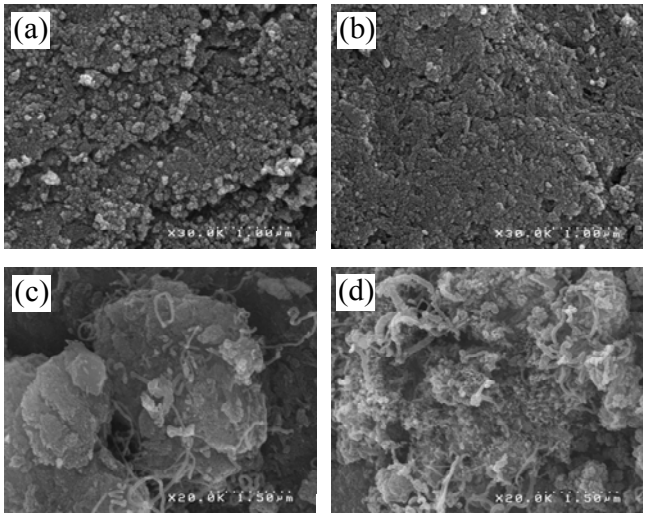

(a) NiLa/γ-Al_2O_3, (b) NiCe/γ-Al_2O_3,
(c) NiCo/γ-Al_2O_3, (d) Ni/γ-Al_2O_3

Fig. 1 SEM photographs of M-Ni/γ-Al_2O_3 catalysts after reaction at 750 ºC for 30 h

These results suggested that the addition of La and Ce improved the surface properties of the Ni/γ-Al_2O_3 catalyst. We tried to determine the amount of coke on the Ni/ γ -Al_2O_3 (after the reaction for 30 h at 750 ^oC) by TG-DTA measurement, however, no significant amount of coke was detected.

4 Conclusions

The addition of modifiers (Co, Ce, and La) to the Ni/γ-Al_2O_3 catalyst increased the yields of H_2 and CO with the decreasing CO_2 content in the reaction products. We successfully developed the most effective NiLa/ γ -Al_2O_3 catalyst, which showed a high stability for 30 hours with excellent selectivities such as 83% to hydrogen and 99% to carbon monoxide at the 95% methane conversion. Determined, that the introduction of additives of cerium and lanthanum in Ni/γ-Al_2O_3 catalyst increases its stability to coke formation.

Reference

[1] K. Dossumov, D.Kh. Churina, L.K. Myltykbaeva, S.A.Tungatarova, European Applied Sciences 7 (2013) 92-94.
[2] L. Vella, J. Villoria, S. Specchia, N. Mota, J. Fierro, V. Specchai. Catal Today 171 (2011) 84-96.
[3] Hu Jiubiao, Yu Changlin, Bi Yadong, Wei Longfu, Chen Jianchai, Chen Xirong. Chinese Journal of Catalysis 35(2014) 8–20.
[4] Tae Yong Kim, Sung Min Kim, Won Su Lee, Seong Ihl Woo. Int J Hydrogen Energy 38 (2013) 6027-6032.

IV-PP143

Catalytic Hydrogenation of Dienone for Getting Vitamins and Odorous Substances

Suyunbayev U., Yergaziyeva G.*, Zhumagazin A.

Institute of Combustion Problems, Almaty, Kazakhstan

* ergazieva_g@mail.ru

Keywords: hydrogenation β-ionone, dehydro β-ionone, citral, citronellal

1 Introduction

Catalytic hydrogenation in a liquid phase is one of significant methods of receiving various organic compounds. Feature of liquid-phase processes is possibility receiving the composite connection under comparatively mild conditions of temperature.

Carrying out processes of catalytic hydrogenation of organic compounds is of great importance for production of products in the pharmaceutical, food and perfumery industry. The modern industrial production of odorous substances is based mainly on chemical and timber-chemical raw materials, some odorous substances receive from essential oils. World release of odorous substances is 100 thousand tons. In everyday use odorous substances play a very important role, since it is difficult to present modern life without toilet soap, cologne, perfume, cosmetic products, detergents, medicines, etc. In industry, many odoriferous substances (citronellal, etc.) receive a batch process, the replacement of this method to a new environmentally friendly and economically effective way flow will allow increasing productivity of the process.

It should be noted that in literature and also on production almost completely there are no data about hydrogenation of organic substances with the conjugated olefinic linkage on stationary catalysts in a liquid phase [1-3]. Thus, systematic research of influence of different parameters on selectivity of hydrogenation of odorous substances in a periodic duty is of interest in two aspects. On the one hand, these data provide new information that expand ideas about general regularities of this process, complementing and clarifying the existing theoretical views on this question. On the other hand - allow to pick up optimum stationary catalysts and conditions for a periodic and continuous way of the hydrogenation of organic substances.

In this paper, the aim is studying of reaction of a hydrogenation β-ionone and citral in the presence of metals VIII of group in a wide variation of experimental conditions in a periodic duty and further development of the continuous way of hydrogenation β-ionone in dihydro - β-ionone and citral in citronellal.

2 Results and discussion

The following reactions are taken as a basis of process:

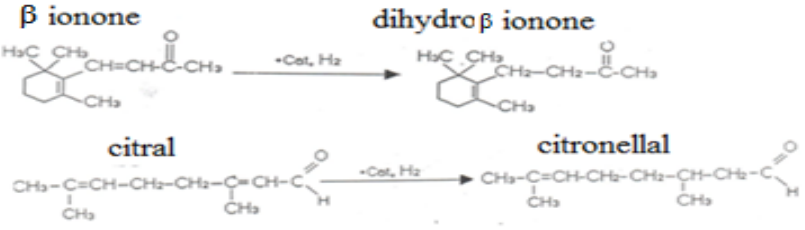

Experiments were made on kinetic installation of high pressure at a variation a process

condition: Tr=373-773 K, P=0,1 - 9,8 MPa, $T_{red.}$ catalyst = 393-893 K. The results are presented in figure 1. Figure 1 shows a change of composition of getting products of reaction hydrogenation β-ionone over metals VIII of group in 96% ethanol at 2,0 MPa and temperature 303 K. Determined, that the nature of metal has essential effect on row saturation of unsaturated bonds in the molecule β-ionone.

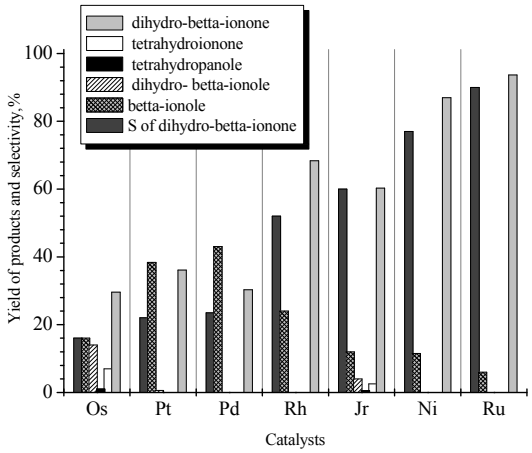

Figure 1. Effect of the metals nature on products yield

On selectivity of hydrogenation β-ionone in dihydro-β-ionone the studied catalysts settle down in the following row: Ru>Ni>Pd>Rh>Jr>Pt>Os. The nickel, ruthenium and palladium can be used as selective catalysts for hydrogenation β-ionone in dihydro-β- ionone by the continuous process.

Considering a number of indexes of profitability and availability in our next researches, nickel supported catalysts were used for hydrogenation β-ionone and citral. Studying of hydrogenation of citral into citronellal over nickel containing catalyst showed that the selectivity for citronellal of 86-87%.

References

[1] L. Ruixia, Y. Yancun Yu [et.all], *Journal of Catalysis.* 269 (2010) 191.
[2] J.C. Serrano-Ruiz, A. Sepúlveda-Escribano , F. Rodríguez-Reinoso, D. Duprez, *Journal of Molecular Catalysis A: Chemical*. 268 (2007) 227.
[3] H. Rojas, G. Díaz , J. J. Martínez, C. Castañeda, A. Gómez-Cortés, J.Arenas-Alatorre**,** *Journal of Molecular Catalysis A: Chemical*. 363 (2012) 122.

IV-PP144

The Spectral Analysis of Hydrocarbons in the Oil from the Well1311 of Surakhani Field

Yolchuyeva U.C.*, Jafarova R.A., Rzayeva N.A., Abbasova N.A.

Institute of Petrochemical Processes named after Y.G.Mammadaliyev, Baku, Azerbaijan

* ulviyya.yolcuyeva@gmail.com

Keywords: oil, Surakhani field, polycyclic, aromatic, hydrocarbons, the method of IR spectroscopy, UV spectroscopy

1 Introduction

It is known that the study of the properties of the oil , its various branches of the national economy, including its efficient use in petrochemical industry, as well as allows the study of its genetics.

2 Experimental

In various kinds of oils the amount of aromatic hydrocarbons (AH) varies from 15% to 50%. AH in petrochemical industry is a very important raw material.Thus,using the reactions of the alkylation,oxidation,dehydrogenation,isomerization and other of aromatic hydrocarbons,there are obtained substances for different purposes on basis which are manufactured important products to the national economy.

The oils which producedin the oilfields of Azerbaijan have the unique properties.With their low low sulfur,low resin,light-coloured,rich with fractions are being light oils ,they have a high biological activity.Surakhani oil can be attributed to such oils.Sorakhani oil is being white oil (kerosene) is rich in saturated paraffin-naphthene hydrocarbons and it has been using in folk medicine for a long time.Studies have shown that there are considerable amount of the rasig the biological activity relic hydrocarbons in Surakhani oils.

The composition and properties of Surakhani oil fractions have been studied in previous researches.The crude oil (Surakhani oil well № 1311)in comparision due to another numbers of the wells in the same fields has a relateviely high density(r=842.5 kq/m3) .

Silicosis gel (AEC) a solvent hexane, hexane-benzene (1: 1), benzene, ethyl-benzene (1: 1) are used as adsorbents in the shown process. The results are presented in the table:

№	Components group	The amount, weight of percent	Beam refraction coefficien, n_d^{20}	Density 20^0 S, kq/m^3
1	Methane-naphthene	75.42	1.4550	0.8250
2	I Aromatic	5.87	1.5108	0.8368
3	II Aromatic	3.68	1.5357	0.8695
4	III Aromatic	6.23	1.5768	0.9026
5	IV Aromatic	4.7	1.5990	0.9848
6	Resin	4.1	–	1.0031

As shown in the table the component of oil well number 1311 includes paraffin-naphthene, I, II, III, IV group of aromatic hydrocarbons,resinous compounds.The separate group of hydrocarbons has been studied by the method of the IR and UV spectroscopy.

In IR spectra the absorption bands were observed in the following:
724, 1459, 2924, 1375, 2856 sm^{-1} spectral field of the CH2 group C-H mathematical relation in accordance with deformation of valence vibrations and absorption lines are arranged. 960, 1032 sm^{-1} in spectral field is arranged naphthene, and in 3011 sm^{-1} is arranged the benzene ring C-H bonds at, 1604 sm^{-} C=C, and in 702, 779, 812, 879 sm^{-1} field is located the replaced absorption lines in accordance with aromatic hydrocarbons.

UV- spectrum analysis shows that , I, II, III, IV groups The composition of the aromatic fractions, especially 1, 2 və 3 are are multilink aromatic hydrocarbons. In the fractions composition is found 4 and 5 multilink aromatic hydrocarbons in small quantities.

IV-PP145

Oligopeptide Modified Mesoporous Silica Catalyts for Direct Aldor Reaction

Yoshida A.*, Takasaka T., Ebi Y., Sato R., Naito S., Ueda W.

Kanagawa University, Yokohama, Japan

* ayoshida@kanagawa-u.ac.jp

Keywords: mesoporous silica, peptide catalyst, direct aldol reaction

1 Introduction

Mesoporous silicas have been regarded as potential support materials for catalysts and adsorbents. However, its applicability is still limited because their inner surfaces are covered with silanol groups, which are rather inert to promote reactions while it can act as effective hydrogen boding donors/acceptors. The vast number of researches has been reported to introduce catalytically active components, such as metal nanoparticles, enzymes and organic functionalities inside porous structure [1]. Oligopeptide is also nice candidate for investing with asymmetric catalytic activity to mesoporous silicas, because immobilization of oligopeptide on solid surfaces is an established technique as the solid phase peptide synthesis. In this work, the Pro-Pro-Asp tripeptide molecules, which are reportedly effective homogeneous catalyst for direct aldol reaction [2], were immobilized on the surfaces of various mesoporous silica supports and investigated the cooperative characteristics of peptide molecules and silanol groups.

2 Experimental

Mesoporous silicas of SBA-15, MCM-41 and KIT-6 were prepared according to the standard methods. Prior to the peptide introduction, NH_2 functionalities were introduced on mesoporous silica surfaces by using the silane coupling agent of 3-aminopropyltriethoxysilane derivative which has the bulky protecting group on the nitrogen atom for providing high dispersion of NH_2 groups on silica surfaces [3]. Pro-Pro-Asp tripeptide molecules were immobilized on NH_2 groups on silica surface by sequential introduction of the corresponding amino acids applying a solid phase peptide synthesis technique (Fig. 1). Microporous silica and aminomethyl polystyrene resin were also modified with the tripeptide using the same procedure. The obtained Pro-Pro-Asp tripeptide-modified catalysts are denoted as PPA-catalysts. The direct aldol reaction was carried out under the following conditions. To dispersions of PPA modified catalysts (containing 25 μmol of peptide) in 3 mL of acetone, *p*-nitrobenzaldehyde (151 mg, 1 mmol) and the internal standard material of *o*-dichlorobenzene (20 mg) were added. The suspensions were stirred at ambient temperature for 48 h with periodical sampling for determining the yield of the aldol product by HPLC analyses.

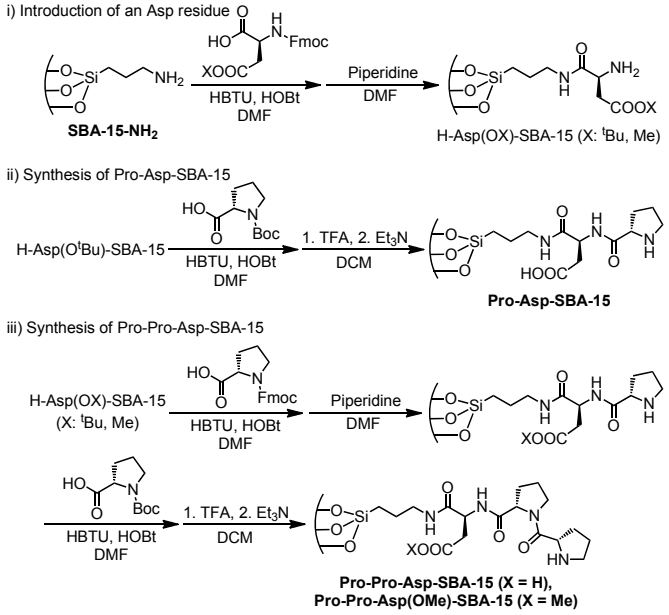

Fig. 1. Synthetic procedure for tripeptide-modified SBA-15.

3 Results and discussion

The results of the aldol reaction, N_2 physisorption analyses and loading amount of peptide are summarized in Table 1. N_2 physisorption analyses revealed that the PPA-mesoporous catalysts maintained its quite large surface area and pore volume even after immobilization of the tripeptide. Mesoporous structure and large pore volume may provide those catalysts for accessibility of substrate molecules to the catalytically active PPA peptide molecule. The loading amount of PPA peptide on mesoporous silicas are in the range of 0.11~0.15 mmol/g, suggesting that averagely 6 ~ 10 nm^2 of the surfaces are allowed for each PPA peptide molecules. Those values indicate that each peptide molecules are well dispersed on the mesoporous silica surface. The direct aldol reaction of 4-nitrobenzaldehyde and acetone was conducted using various PPA tripeptide modified catalysts. PPA-MCM-41 exhibited the highest catalytic activity among the prepared catalysts. 68% of the aldol product was yielded for 8 h with 18 % of *e.e.* The maximum yield of 81% was achieved at 24 h. The other peptide modified mesoporous silica catalysts of PPA-SBA-15 and PPA-KIT-6 also showed higher catalytic activity than the PPA-silica and PPA-resin catalysts. Those results show that mesoporous silica supports with wide surface area and large pore volume facilitate diffusion of reactants and products to/from catalytically active peptide molecules immobilized on the supports. Interestingly, the enantioselectivity of PPA-mesoporous and microporous silica catalysts are inverted comparing to those of PPA-resin and reported result at homogeneous conditions [2]. The silica based supports afforded *R* enantiomer predominantly whereas the resin support and free peptide molecules in homogeneous conditions afforded *S* enantiomer. The PPA-resin catalyst with selective protection of the carboxylic group on the side chain of the Asp residue exhibited inverted enantioselectivity to afford *R* enantiomer with 16% of e.e., suggesting that the carboxylic group dominates enantioselectivity. The observation of almost identical enantioselectivity to the silica based supports indicates that the carboxylic group was inactivated when the PPA molecule is immobilized on the silica surfaces. This inactivation of carboxylic group is probably caused by formation of hydrogen bonding with surface silanol groups.

Table 1. Direct aldol reaction of 4-nitrobenzaldehyde and acetone catalysed by tripeptide-modified mesoporous silica catalysts

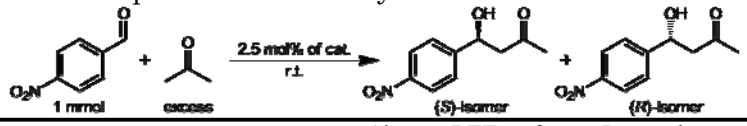

Catalysts	Time / h	Yield / %	*ee* / %	Abs. Conf.[b]	BET surface area / $m^2 \cdot g^{-1}$	Pore volume / $cm^3 \cdot g^{-1}$	Loading amount of PPA / $mmol \cdot g^{-1}$
PPA-MCM-41	8	68	18	*R*	833	0.73	0.13
PPA-SBA-15	8	35	17	*R*	545	0.90	0.15
PPA-KIT-6	8	26	15	*R*	642	0.44	0.11
PPA-silica	8	17	17	*R*	276	1.20	0.08
PPA-Resin	9	2	26	*S*	<5	-	0.55

[a]All values and the absolute configuration were determined using HPLC analyses. [b]Absolute configuration of the predominatly formed enantiomer.

4 Conclusions

The catalytically active PPA peptide was successfully heterogenized by using solid phase peptide synthesis technique. The mesoporous silica supported catalysts exhibited superior catalytic activity to the microporous silica and resin supported catalysts. Wide surface area and mesoporous structure may facilitate diffusion of reactants and products to/from catalytically active peptide molecules immobilized on the support surfaces.

References

[1] A. P. Wight, M. E. Davis, Chem. Rev. 102 (2002) 3589.
[2] P. Krattiger, R. Kovasy, J. D. Revell, S. Ivan, H. Wennemers, Org. Lett. 7 (2005) 1101.
[3] J. C. Hicks, C. W. Jones, Langmuir 22 (2006) 2676.

IV-PP146

The Method of Dealumination of Zeolite Ferrierite with Ammonium Hexafluorosilicate

Zalyaliev R.F.*, Mukhambetov I.N., Lamberov A.A.

The Kazan (Volga) Federal University, Kazan, Russia

* zalyaliev.r@gmail.com

Keywords: dealumination, zeolite, ferrierite, skeletal isomerizationn, isobutene

1 Introduction

Interest in the zeolite ferrierite is caused mainly due to the relevance of obtaining isobutene skeletal isomerization of n-butenes. Ferrierite exhibits high activity in the isomerization reaction at relatively low temperatures (400-450 ºC), but has weak initial selectivity (< 50 %). For him known methods of modifying based on different techniques of dealumination that lead to an increase in selectivity. Removing the aluminum cations may be carried out acid treatment, the influence of chelators, hydrothermal dealumination, as well as interaction with ammonium hexafluorosilicate (AHFS).

2 Results and discussion

Effective dealumination of ferrierite succeeded spend only by hydrothermal treatment. Herewith during the hydrothermal treatment, the aluminum cations deposited in the zeolite channels and are the cause the low stability of catalysts. Therefore development of zeolite with high module remains actual problem.

This paper investigates the interaction AHFS with zeolite ferrierite at the temperature higher than 200 ºC and considering the possibility dealuminating of the zeolite by replacement of aluminum on silicon in order to obtain high-silicon zeolites with SiO_2/Al_2O_3 more than 55.

3 Conclusions

The obtained samples (SiO_2/Al_2O_3 = 64, 74) were investigated by TPD of ammonia, low temperature nitrogen adsorption, ^{29}Si, ^{27}Al NMR, X-ray analysis, IR spectroscopy. Optimal samples of has the following catalytic performance: conversion – 40 %, selectivity – 87 % (at the temperature 450 ºC).

IV-PP147

Paramagnetic Nickel Complexes in the Catalytic Carbon-Carbon Bond Formation Reactions

Flid V.R., Shamsiev R.S., Zamalyutin V.V.*

Moscow State Academy of Fine Chemical Technology (MITHT), Moscow, Russia

* zamalyutin@mail.ru

Keywords: Paramagnetic, Nickel, Complexes, Norbornadiene, Cross-coupling, Aryl, Halides

1 Introduction

The interest in transition metal complexes, including nickel, with uncharacteristic degree of oxidation is largely due to their ability to participate in catalytic processes. Paramagnetic complexes Ni(I) and Ni(III) are present in a homo- reactions and cross-coupling of aryl halides [1], the oligomerization of ethylene and propylene [2], dimerization of norbornadiene (NBD) [3]. However, their role in catalysis still remains unclear.

2 Results and discussion

When interacting $NiAll_2$ (all-C_3H_5, 1-$CH_3C_3H_4$, 2-$CH_3C_3H_4$, 1-$C_6H_5C_3H_4$) NBD with fixed paramagnetic nickel(I) complex was discovered, which was with triaxial anisotropy of the g-factor at 77 K characterized. Such complexes are observed in the system containing no conventional stabilizing ligands for the first time. On the contrary, their presence leads to the disappearance of paramagnetic particles. The formation of Ni(I) is provided to reduce the positive charge of nickel in $NiAll_2$. When interacting with NBD $NiAll_2$ stationary relative concentration of Ni(I) differ significantly, assuming at 298 K the value range of 10^{-3} - 10^{-6} of the total nickel concentration.

Obviously, the nickel(I) complex includes a NBD molecule as a stabilizing ligand. Dependence of the concentration of paramagnetic particles from the structure $NiAll_2$ indicates possible involvement of allyl ligand in the formation of Ni(I). The mechanism of formation of Ni(I) is based on the reaction of stoichiometric allylation NBD, and $NiAll_2$ and $Ni(NBD)_2$. counterdisproportionation. The main stages was gained both experimental and theoretical confirmation of the use of model systems.

Probably, an important role in the formation of the Ni(I) complex plays nickel hydride. Experimentally proved its presence in the reaction system. At the same time, compounds observed in ESR spectra could not be related to hydride compounds. Probably, paramagnetic nickel hydride posesses very labile and easily implement NBD to the Ni-H bond. π, σ- nickel NBD complexes formed in this case significantly more stable and dominate among the compounds Ni(I).

Through the use of DFT/PBE method, the "hydride" route in the catalytic dimerization of NBD theoretically was sounded. However, its contribution to the overall process is probably unsignificant.

Our results do not allow definitely to establish the role of the paramagnetic nickel complexes in catalysis. Nevertheless, there is no doubt in that Ni(I) forms due to the extraordinary ability of the NBD to stabilize unstable compounds in the valence states which are not specific for them.
A series of highly effective and available catalysts for homocoupling of aryl halides based on nickel complexes with diazabutadiene ligands. New catalysts being used in low concentrations allow to obtain high yields of biaryls various types, including sterically hindered, as well as compounds containing various substituents in the aryl fragments. For the first time through the method of ESR spectroscopy discovered and investigated paramagnetic nickel(I) complex, the

most likely intermediate compound in the catalytic reaction. Based on the spectral, kinetic and calculated quantum-chemical data the mechanism of aryl halides homocoupling based on nickel complexes was proposed. The process is based on the traditional for metal complex catalysis stages.

The initiation of the process begins with initial nickel(II) salt reduction by zinc in the presence of diazabutadiene derivative. A formed nickel(0) complex starts the catalytic cycle and at the first stage molecule coordinates ArX as π-ligand, and then carries out its oxidative addition. The process then continued with one-electron reduction of the complex Ni(II). The resulting compound is involved in the process of oxidative addition of a new ArX molecule to form an active intermediate diaryl $L_2XNi(III)Ar_2$. Its decay is accompanied by reductive elimination and biaryl formation of a new Ni(I) intermediate. Regeneration of the catalyst may occur by the one-electron reduction with zinc to the initial Ni(0). Since the method of forming fixed ESR nickel(I) intermediate with a high concentration, apparently, the rate-limiting step is one-electron reduction of the complex Ni(I) with DAB, under the action of metallic zinc.

3 Conclusions

The results obtained in this work did not conclusively establish the role of paramagnetic complexes of Ni-catalyzed processes of norbornadien dimerization and homocoupling of aryl halides. However, on the basis of kinetic, spectroscopic and calculated quantum-chemical data corresponding mechanisms was suggested. Through the usage of the DFT/PBE method theoretically was proved "hydride" route in the catalytic dimerization of NBD. The second process is based on the traditional metal complex catalysis stages.

Acknowledgements

This work was supported by the Russian Foundation for Basic Research, grant nos. 14-03-00419.

References

[1] V.N. Valaeva, A.F. Asachenko, P.S. Kulyabin, V.R. Flid, A.Z. Voskoboinikov. *Russ. J. Org. Chem.* 47 (2011) 1774. (font style: Times New Roman 11pt)
[2] V.V. Saraev, P.B. Kraikivskii, D.A. Matveev, A.I. Vilms, M.D. Gotsko, V.V. Bocharova, S.N. Zelinskii. *Current Catalysis.* 1 (2012) 149.
[3] Y.Y. Otman, O.S. Manulik, V.R. Flid. *Kinetics and Catalysis.* 49 (2008) 419.

IV-PP148

Microwave Assisted Heterogeneous Vapor-Phase Oxidation of 3-Picoline to Nicotinic Acid over Vanadium–Titanium Oxide Catalytic System

Alkayeva Y.[1], Shutilov A.[2,3,4], Zenkovets G.[2,3*]

1 - Fordham University, New York, United States
2 - Boreskov Institute of Catalysis, SB RAS, Novosibirsk, Russia
3 - Novosibirsk State University, Novosibirsk, Russia
4 - Novosibirsk State Technical University, Novosibirsk, Russia

* zenk@catalysis.ru

Keywords: 3-picoline, oxidation, heterogeneous, vapor-phase catalysis, microwave heating, vanadium–titanium oxide system

1 Introduction

One-step heterogeneous gas-phase oxidation of 3-picoline over vanadium-titanium oxide catalysts using air as an oxidizing agent is a better and cleaner way to obtain nicotinic acid (vitamin B_3) [1]. In this investigation to heat a catalyst to 250-270°C, conventional energy was applied. Due to high energy consumption some alternative energy sources can be considered. One of the promising substituents is microwave (MW) irradiation that is becoming increasingly popular as a clean, cheap, convenient method of heating, increasing yields, and decreasing reaction times while using less power input [2]. Microwave irradiation is a way of applying energy directly to the reaction system rather than through other media. The conversion of electromagnetic energy in heat occurs simultaneously and evenly by heating a solid catalyst while microwave transparent materials (insulation, reactor wall and gas phase) are penetrated without energy consumption. The aim of this work is to investigate the influence of microwave energy on heterogeneous vapor-phase oxidation of 3-picoline over V-Ti-O system.

2 Experimental

Binary V-Ti-O catalysts and vanadia were prepared by spray drying of a mixture of titanium dioxide (anatase form) and vanadyl oxalate solution followed by calcination at 450°C for 4 h [1,3]. Microwave "Discover" system with "Open vessel" option (CEM Corporation) was used to heat the catalyst. A sample of the catalyst (0.25-0.50 mm) mixed with quartz was placed on a frit support in a tubular quartz reactor (diameter 15 mm, length 50 mm) with a coaxial thermocouple pocket. A non-metallic Fiber Optic Thermocouple was used to control and measure the temperature in a catalyst layer. The set parameter ranges were: microwave power 18-160 W, temperature 170-220°C. For comparison, some experiments were performed in a conventional oven. The initial components and reaction products were analyzed by Gas Chromatography (Shimadzu GC-8A) equipped with Porapak-Q, Carbowax, Molecular Sieves, and Equity Columns.

3 Results and discussion

By using both sources of energy, conventional and MW, vanadia-titania catalysts produce the same products: nicotinic acid, 3-pyridinecarbaldehyde, 3-cyanopyridine, and CO_2.
Fig. 1 represents the rate of 3-picoline transformation calculated per square meter and the selectivity for nicotinic acid as a function of a catalyst composition in conventional and MW systems. All experiments in conventional oven shown in this figure were performed at 250 °C, and conversion (X) of about 40%. Experiments in MW heated reactor were performed at the

measured temperature of about 180 °C, and at a conversion range of 30–50%.

It can be seen (Fig. 1a) that by conventional heating, the binary catalysts are noticeably more active than individual oxides. The highest activity was observed over the binary catalysts containing 20–75% of vanadium oxide. By microwave heating, the dependence is entirely different: vanadium oxide reveals the highest activity. The higher is the percentage of vanadium oxide in the binary catalyst, the higher is the rate of the 3-picoline transformation. Titanium oxide as the less active catalyst was observed in microwave oven as well.

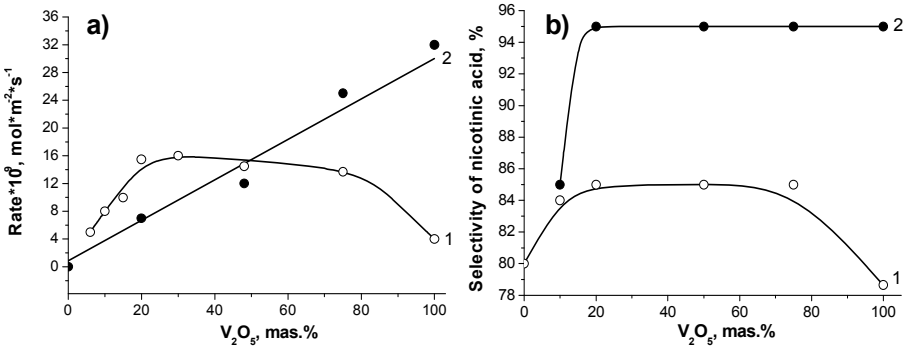

Fig. 1. a) - Rate of 3-picoline transformation as a function of catalyst composition.

b) - Selectivity for nicotinic acid as a function of catalyst composition.

1–conventional heating: 250°C, X ~ 40%; 2–microwave heating: 180°C, X = 30-50%.

Selectivity for the nicotinic acid versus catalysts composition is given in Fig.1b. As can be seen, microwave assisted 3-picoline oxidation is more selective toward nicotinic acid than a traditional conventional method. Selectivity for nicotinic acid is 95% for the binary catalyst samples containing 20–75% of V_2O_5. This is 10% higher than selectivity for nicotinic acid obtained in conventional heated reactor. Individual V_2O_5 is much more selective when heated in microwave oven. Selectivity for 3-pyridinecarbaldehydeis is lower in MW system than in conventional oven on all catalysts. Selectivity for CO_2 is lower in MW system as well. For binary catalysts containing 20–75% of V_2O_5, selectivity for CO_2 ranges between 2 and 3%. Different behavior of individual vanadium oxide in two systems, MW and CH, can be explained by considering a sufficient distinction between MW and CH. Temperature profiles in the particle of a catalyst heated by each individual source are entirely different. Due to specific temperature distribution, the lattice oxygen in the microwave effective dielectric vanadium oxide becomes more mobile inducing the rate of 3-picoline oxidation to nicotinic acid.

4 Conclusions

Application of microwave energy as a remote heating source to the heterogeneous vapor-phase oxidation of 3-picoline has several new advantages. This method consumes less energy and creates an optimal temperature profile in vanadium-containing catalyst particles making a positive contribution to the selectivity and capacity of the green method of nicotinic acid synthesis.

References

[1] E.M. Alkaeva, T.V. Andrushkevich, G.A. Zenkovets, G.N. Kryukova, S.V. Tzybulya, *Catal. Today* 61 (2000) 249.

[2] Y. Alkayeva, R. Gibadullin, M. Merakhovich, A. Abdurakhmanov, A. Holubyeva, A. Shutilov, G. Zenkovets, *Appl. Catal. A: General* 491 (2015) 1.

[3] G.A. Zenkovets, G.N. Kryukova, S.V. Tsybulya, E.M. Alkaeva, T.V. Andrushkevich,O.V. Lapina, E.B. Burgina, L.S. Dovlitova, V.V. Malakhov, G.S. Litvak, *Kinet. Catal.*41 (2000) 572.

IV-PP149

Pt Based Bimetallic Catalysts Prepared by Conventional Impregnation and Deposition and Reduction in Liquid Phase Methods for Selective Hydrogenation of Citral

De Miguel S., Rodriguez V., Scelza O., Stassi J., Vilella I., Zgolicz P.*

Instituto de Catálisis y Petroquímica, UNL-CONICET, Santa Fe, Argentina.

* pzgolicz@fiq.unl.edu.ar

Keywords: Pt-based, bimetallic catalysts, carbon nanotubes, selective hydrogenation of citral

1 Introduction

In the fine chemical industry, supported bimetallic catalysts are frequently used, because such systems exhibit interesting yields with regard to their applications. An important example of application is the selective hydrogenation of the carbonyl group (C=O) of α,β-unsaturated aldehydes into α,β-unsaturated alcohols (UA) [1]. However, the challenge in the development of bimetallic catalysts for this type of reaction is to achieve the hydrogenation of the C=O without affecting the C=C olefinic bond, since, the hydrogenation of the C=C is thermodynamically more favorable than the hydrogenation of the C=O, and usually, low yields are obtained with typical monometallic catalysts of hydrogenation [1,2]. In this sense, bimetallic nanoparticles allow a better tailoring of the electronic and catalytic properties. The final selectivity of these bimetallic nanoparticles depends both on the second metal/noble metal ratio and the interaction between the active metal and the reduced or ionic species of the second metal, which act as Lewis acid sites to promote the hydrogenation of the carbonyl group [1]. However, both the interaction between the metals and the type of promoter species formed strongly depend on the nature of the support and the preparation method. In this work, Pt-based bimetallic catalysts multi-walled carbon nanotubes-supported were prepared by two methods (conventional impregnation followed of a reduction step in H_2 flow (CI) and deposition-reduction in liquid phase (RLP)) in order to study and compare their performances in the citral hydrogenation.

2 Experimental/methodology l

Commercial carbon nanotubes (MWNT, 211m^2/g, purity>95%) were purificated by successive treatments with aqueous solutions with inorganic acids. The purificated support (CNP) were used to prepare Pt based bimetallic catalysts (5wt%) using an aqueous solution of H_2PtCl_6/promoter (promoter: $FeCl_3$, $SnCl_2$, $GaNO_3$, or $InNO_3$). Two types of reduction were carried out: under H_2 flow at 350 ºC and reduction in liquid phase using $NaBH_4$ at low temperature. Additionally a thermal treatment with N_2 at high temperature (700ºC) were carried out on the reduced samples. The metallic phase of the catalysts was characterized by temperature programmed reduction (RTP), test reactions (cyclohexane dehydrogenation-CHD, cyclopentane hydrogenolisis-CPH and benzene hydrogenation-BH), XPS, and TEM. The hydrogenation of citral (3,7-dimethyl-2,6-octadienal) was carried out in a discontinuous volumetric reaction equipment with a device for sampling the reaction products using 2-propanol as a solvent, P atm, 70ºC and 1400 rpm.

3 Results and discussion

Characterization results. From TPR results for catalysts prepared by CI, it is was observed that the Pt reduction peaks of PtSn, PtIn, PtGa samples, showed a shift to higher or lower temperature and a higher area than that corresponding to the TPR profile of the monometallic one. This fact together with the lower H_2 consumption observed at the temperatures where the

promoter are reduced, would be indicating that a co-reduction between Pt and promoter metals occurs. On the contrary, the higher H_2 consumption observed at high temperatures in catalysts prepared by RLP, evidence a poorer interaction between metals in these catalysts. XPS results evidenced the presence of a high P^o/P^{ionic} ratio (P: Sn, Ga, In) in bimetallic catalysts prepared by CI while for catalysts prepared by RLP this ratio is inverted. PtFe catalysts prepared on both methods showed only the presence of ionic species. Besides, the results from test reactions (CHD and CPH) for catalysts prepared by CI treated and untreated with nitrogen evidenced the presence of mainly electronic effects in PtSn, PtGa, and PtIn catalysts and geometric ones in the PtFe catalyst. However, since the change in the activation energy with respect to the monometallic catalysts is opposite for PtSn (higher) and PtGa and PtIn (lower) catalysts, a different electronic modification is suggested. For catalysts prepared by RLP the change in the initial reaction rate depend on the nature of promoter, but any case, the Ea_{BH} value does not change significantly. Thus, these characterization results show that the addition of a second metal modifies the structure of Pt particles, but different effects, such as dilution, blocking or decorating of particles would prevail according to the electronic state (ionic, reduced or alloyed) and the nature of the promoter and the preparation method. The characteristics of the metallic phase were correlated with the catalytic behavior in the citral hydrogenation. Table 1 shows the results of activity and selectivity. The addition of a second metal significantly improves the selectivity to UA in all the bimetallic catalysts prepared by CI due to both the activation of the C=O and the poisoning of acid sites of the support. Except for PtFe catalyst, the catalysts prepared by RLP do not show a significant change in the selectivity to UA with respect to the monometallic one. These results can be related to the higher and ordered modification of the Pt metallic phase in catalysts prepared by CI than those prepared by RLP. Besides, the lower activities in the last catalysts, also evidence a higher blocking effect in these samples. The results found with PtFe catalysts prepared by both methods would be related to the formation of PtFe complexes which help to explain the high interaction of the metals in the final catalyst. Besides, the N_2-thermal treatment do not increase the particle size as it was expected in catalysts prepared by CI, but improve the selectivity in PtSn and PtGa catalysts probably due to the formation of a more adequate bimetallic phase. Only the PtSn-RLP catalyst treated with N_2 showed a better selectivity to UA. For the other catalysts prepared by RLP neither the activity or selectivity to UA were improved after the thermal treatment probably due to an even higher blocking effect in these catalysts with respect to those untreated.

Tabla 1. Hydrogenation Results: S_{UA}: selectivity UA, T: reaction time at 95 % of citral conversion

Catalyst (CI)	**S_{AI} (%)**	**T (h)**
Pt	7.0	7.2
PtFe(2.5%wt)	93 **(95)**	7.5 **(20)**
PtSn(1.0%wt)	89 **(97)**	3.0 **(7.0)**
PtGa(1.8%wt)	91 **(98)**	0.8 **(>20)**
PtIn(2.5%wt)	97 **(95)**	0.5 **(0.13)**
Catalyst (RLP)	**S_{AI} (%)**	**T (h)**
Pt	16.0	3.5
PtFe(2.5%wt)	92 **(89)**	20 **(>24)**
PtSn(1.0%wt)	4 **(79)**	2 **(12)**
PtGa(1.8%wt)	28 **(26)**	6 **(>24)**
PtIn(2.5%wt)	46 **(-)**	6.5 **(-)**

*values in bold and brackets correspond to results obtained for the catalysts submitted to the N_2-thermal treatment

4 Conclusions

Pt metallic phase is more strongly modified in bimetallic catalysts prepared by CI than in those prepared by RLP. Besides, phases more adequated for selective hydrogenation were obtained in catalysts prepared by CI or PtFe catalysts probably due to the presence of more highly ordered metallic phases. In consequence, the hydrogenation results highly depended on the catalyst preparation method, the thermal treatment and the nature of the second metal.

References

[1] J. P. Stassi, PhD Thesis, Universidad Nacional del Litoral, Santa Fe-Argentina (2008).
[2] P. Mäki-Arvela; J.G. Hájek; T.Salmi; D.Yu. Murzin, *Appl. Catal. A: General*, 292 (2005) 1.

IV-PP150

Study of the Reaction Network of Fischer-Tropsch Synthesis by Multicomponent Steady-State Isotopic Transient Kinetic Analysis

Ledesma C.[1*], Yang J.[2], Blekkan E.A.[1], Holmen A.[1], Venvik H.J.[1], Chen D.[1]

1 - Norwegian University of Science and Technology, Trondheim, Norway
2 - SINTEF Materials and Chemistry, Trondheim, Norway

* cristian.l.rodriguez@ntnu.no

Keywords: Fischer-Tropsch synthesis, isotopic labeling, kinetics, reaction, mechanism

1 Introduction

Fischer-Tropsch synthesis (F-T) is one of the most important processes to transform a mixture of carbon monoxide and hydrogen (also called synthesis gas) into hydrocarbons and liquid fuels by using catalytic systems. The wide variety of products that can be obtained points out the complexity of the reaction mechanism, which is known to be a polymerization like mechanism, but the nature of the main intermediates corresponding to paraffin and olefin formation as well as in chain growth are still in debate. Steady-State Isotopic Transient Analysis (SSITKA) is considered a powerful technique to investigate reaction mechanisms by labelling isotopically at least one of the reactants [1]. This technique has been employed with other methods (i.e. DFT, transient methods) in order to create a model to describe the transient curves of the main intermediates of Fischer-Tropsch synthesis [2]. However, these methods are not capable to determine the rate constants involved or describe the effect of reaction conditions or catalyst composition in the reaction step to explain the performance of the catalyst. In this work, a new method based on multicomponent SSITKA measurements allowed mapping the kinetic parameters of the Fischer-Tropsch synthesis over a Co-Re/CNT catalyst under methanation conditions at 210°C and 1,85 bar.

2 Experimental/methodology

CO hydrogenation reaction has been performed using a fixed-bed quartz reactor (4 mm i.d.). The 20% wt. Co and 0.5% wt. Re over carbon nanotubes (CNT) catalyst has been diluted inert silicon carbide to improve the isothermal conditions along the catalyst bed. Prior to reaction, the catalyst was reduced in 10 NmL/min H_2 at 623 K. After 16 h of reduction, the catalyst was cooled down to 483 K, H_2/CO/Ar (15/1,5/33,5 NmL/min) mixture was introduced and the pressure was adjusted to 1,85 bar. Once the steady state was achieved after 6 hours on stream, SSITKA experiments were carried out by switching between $H_2/^{12}CO$/Ar and $H_2/^{13}CO$/Kr. The reaction order of the reactants has been determined by varying their partial pressure. The transient responses of Ar, Kr, ^{12}CO, ^{13}CO, $^{12}CH_4$ and $^{13}CH_4$ were monitored with a Balzers QMG 422 quadrupole mass spectrometer (MS). The concentrations of H_2, CO, Ar and C_1-C_6 hydrocarbons were analysed with a GC-MS (Agilent GC7890B – MSD5977A) equipped with multiloop, TCD, FID and MSD detectors. The isotopic distribution of C_2, C_3 and C_4 hydrocarbons were calculated as a linear combination of the fragmentation patterns of the corresponding isotopic products [3].

3 Results and discussion

The measured site coverage of the various intermediates on the catalyst surface obtained under F-T synthesis allows the elucidation of their nature by testing kinetic dependences of the

intermediate concentration with the different carbon numbers on the corresponding olefin and paraffin formation rate. The paraffin ($r_{t,n}$) and olefin formation ($r_{o,n}$) reactions have been evaluated as a function of the H_2 partial pressure, in order to investigate the reaction order towards this reactant (Figures 1a and 1b). Chain propagation reaction ($r_{p,n}$) has been evaluated as a function of the carbon number, as depicted in Figure 1c.

$r_{t,n}=k_{t,n}\theta_{Cn}(\theta_{H2})^2$ $r_{o,n}=k_{o,n}\theta_{Cn}\theta_{H2}$ $r_{p,n}=k_{p,n}\theta_{Cn}\theta_{C*}$

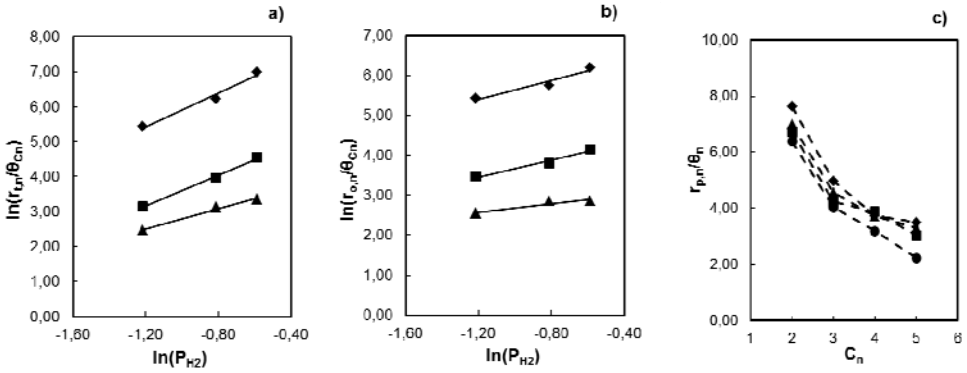

Fig. 1. Hydrogen reaction order in paraffin formation (a) and olefin formation (b) reactions at different carbon number: ■: C_2; ♦: C_3, ▲: C_4; c) Chain growth rate and site coverage as a function of the carbon number at different P_{CO} and P_{H2} (in bar): ♦: P_{CO}=0,06, P_{H2}=0,56; ■: P_{CO}=0,11, P_{H2}=0,56; ▲: P_{CO}=0,06, P_{H2}=0,44; ●: P_{CO}=0,06, P_{H2}=0,30.

Figures 1a and 1b show a H_2 reaction order towards paraffin and olefin formation of 2 and 1, respectively for C_2 and C_3 intermediates. This reaction order can only be explained by the presence of hydroxycarbene like intermediates. However, the lower reaction order in C_4 compound indicates that alkylene like intermediates may also be present. Chain propagation reaction rate (figure 1c) decreases with the carbon number, as expected. The similar trends obtained at different conditions demonstrate that the nature of the growing monomer is the same for all the conditions tested. Besides, the different values obtained at each carbon number indicate that the growing monomer depends on CO and H_2 partial pressures.

4 Conclusions

This work shows a powerful method to identify the kinetic mapping of the FT reaction network over a Co-Re-based catalyst by analysing the site coverage of the main intermediates obtained by multicomponent SSITKA. This methodology can be an effective tool to study the effect of catalytic properties, such as promotion, particle size or support characteristics in the reaction mechanism.

Acknowledgements

The authors are very grateful for financial support from the Research Council of Norway.

References

[1] C. Ledesma, J. Yang, D. Chen, A. Holmen, *ACS Catal.* 4 (2014) 4527.
[2] J. Yang, Y. Qi, J. Zhu, Y. Zhu, D. Chen, A. Holmen, *J. Catal.* 308 (2013) 37.
[3] N. S. Govender, F. G. Botes, M. H. J. M. de Croon, J. C. Schouten, *J. Catal.* 312 (2014) 98.

IV-PP151

The Characteristics of Phosphoric Acid Modified Niobia Catalysts in the Gas Phase Glycerol Dehydration

Lee Kyu Am[1], Moon Dong Ju[2], Park Nam Cook[3], Kim Young Chul[3*]

1 - Department of Chemicals Engineering, Chonnam National University, Gwangiu, Republic of Korea

2 - Korea Institute Science and Technology, Seoul, Republic of Korea

3 - Faculty of Applied Chemical Engineering and the Research Institute For Catalysis, Chonnam National University, Gwangju, Republic of Korea

* youngck@chonnam.ac.kr

Keywords: acrolein, glycerol dehydration, niobium, oxide, phosphoric acid

1 Introduction

The depletion of fossil fuels along with other environmental concerns has led to increased interest in new avenues for renewable energy. Biodiesel, which is produced via trans-esterification reactions with the oils of plants, animals, algae, etc., is emerging as an alternative energy resource. The amount of glycerol is about 10 wt% of total biodiesel yield [1]. The techniques for utilizing surplus glycerol are interesting and many research groups have been studying the transformation of glycerol to valuable chemical products [2]. Acrolein, which is produced by the dehydration of glycerol, is used for not only producing acrylic acid but also various other chemicals [3]. Various solid acid catalysts, such as zeolites, niobium, zirconium, titanium, silica-alumina, are used in the production of acrolein. In this study, we conducted gas phase glycerol dehydration reactions using phosphoric acid-loaded niobium oxide catalysts.

2 Experimental/methodology

We synthesized PO_4/Nb_2O_5 catalysts by simple impregnation method, wherein we mixed the required amount of H_3PO_4 with powdered niobium oxide and stirred the solution at 70 °C for 1 h. Subsequently, the water was evaporated, under low vacuum conditions, using a rotary evaporator. After evaporation, the PO_4/Nb_2O_5 samples were dried at 100 °C for 24 h. Finally, the dried samples were calcined at 400 °C for 4 h. The catalysts were denoted as x-PO_4/Nb_2O_5(x = Phosphoric acid wt%).

A gas phase glycerol dehydration reaction was carried out, under atmospheric pressure, using a PO_4/Nb_2O_5 catalyst. 10 wt% of glycerol solution was fed using an HPLC Pump. Ar was used as the carrier gas. The liquid phase was evaporated by passing through an evaporator maintained at 310 °C. The vapor was then fed into a quartz reactor tube (length 350 mm, i.d. 8.8 mm) maintained at 300 °C using an electric split furnac; 0.4 g of the catalyst was supported on the quartz wool. The gaseous product was condensed using an ice trap maintained at –5 °C and collected on an hourly basis for analysis using GC17A and GCMS-QP5000 equipped with a Petrocol capillary column. The condensed product was analyzed after 2 h.

3 Results and discussion

Above 40 wt% of phosphoric acid in PO_4/Nb_2O_5, the crystalline pattern of $NbPO_5$ was confirmed at 20.542°, 28.985°, 35.846°, and 56.027°. This pattern indicates an orthorhombic $NbPO_5$ diffraction pattern (JCPDS PDF-1 #40-0124). It was reported that the $NbPO_5$ crystal was synthesized on loading niobium oxide with phosphoric acid by the impregnation method given in the reference [4].

The elemental binding energy and metal concentration on the catalyst surface were

investigated by XPS analysis. In our results, increasing the phosphoric acid loading led to a relative reduction in niobium concentration. This could imply that phosphate covers the niobium surface. In the used catalyst, the concentration of phosphorous and niobium decreased. This could be explained by a loss of elements and carbon deposition that occurs during the reaction. For binding energy, we propose that an increase in phosphoric acid loading leads to a decrease in the niobium binding energy. In the fresh 50 wt% PO_4/Nb_2O_5 catalyst, the binding energy of Nb $3d_{5/2}$ was 206.21 eV. This binding energy indicates the presence of NbO_2. Therefore, the $NbPO_5$ crystal could be synthesized by adding phosphoric acid.

The crystallinity of the catalysts was observed using transmission electron microscopy. We confirmed that fresh Nb_2O_5 and 20 wt% PO_4/Nb_2O_5 catalysts were amorphous. In the fresh 50 wt% PO_4/Nb_2O_5 catalyst, the $NbPO_5$ crystal was observed; however, its crystallinity was not very high. The used Nb_2O_5 and 20 wt% PO_4/Nb_2O_5 catalyst were amorphous. Moreover, deposited carbon, in the form of crystalline graphite, was also not observed. In the used 50 wt% PO_4/Nb_2O_5 catalyst, we observed that the $NbPO_5$ crystal grew well.

We carried out gas phase glycerol dehydration using a PO_4/Nb_2O_5 catalyst. In our experiment, the best catalytic performance was obtained using 20 wt% PO_4/Nb_2O_5. We believe that 20 wt% PO_4/Nb_2O_5 has the appropriate BET surface area and acidity, resulting from its amorphous state, for gas phase glycerol dehydration.

Table. 1. Binding energies of the fresh catalyst determined by XPS

Catalyst	Binding energy (eV)		
	Nb $3d_{5/2}$	Nb $3d_{3/2}$	P 2p
20 wt% PO_4/Nb_2O_5	207.63	210.36	132.26
50 wt% PO_4/Nb_2O_5	206.21[a]	208.99	132.61

a. NbO_2 binding energy

4 Conclusions

In this work, we synthesized PO_4/Nb_2O_5 catalysts using a simple impregnation method and produced acrolein through gas phase glycerol dehydration. Above 40 wt% of phosphoric acid in PO_4/Nb_2O_5, nanosized $NbPO_5$ crystals were formed. We confirmed the presence of this crystal through XRD, XPS, and TEM analysis. The $NbPO_5$ crystal is formed because an increase in phosphoric acid loading decreases the niobium binding energy. The best performing catalyst was 20 wt% PO_4/Nb_2O_5. From our results, it is evident that the appropriate BET surface area and acidity are important, which differs from our previous work on liquid phase dehydration [2].

Acknowledgements

This study was supported by the Priority Research Centers Program through the National Research Foundation of Korea (NRF), funded by the Ministry of Education, Science, and Technology (2009-0094055), Republic of Korea, and supported partly by the Ministry of Knowledge Economy of Korea and the Korea Institute of Science and Technology (KIST Grant No. 2E24834 & 2MR2190)

References

[1] N.Lili, D. Yunjie, C. Weimiao, G. Leifeng, L. Ronghe, L. Yuan,X. Qin, *Chin. J. Catal.*29 (2008) 212.
[2] Young Yi Lee, Kyu am Lee, Nam Cook Park, Young Chul Kim, *Catal. Today.* 232 (2014) 114.
[3] Kaori Omata, Shoko Izumi, Toru Murayama, Wataru Ueda, *Catal. Today.* 201 (2013) 7.
[4] Zhen-Chen Tang, Ding-Hua Yu, Peng Sun, Heng Li, He Huang, Bull. *Korean Chem. Soc.*31 (2010) 3679.

IV-PP152

Fischer-Tropsch Synthesis (FTS) Reaction over Co-based Catalyst Supported on Al-SBA-15

Kim N.Y.[1,2], Jung J.-S.[1,3], Park J.I.[1], Ramesh S.[1], Kim S.W.[1,3], Ahn B.S.[1,3], Lee K.Y.[2], Moon D.J.[1,3*]

1 - Clean Energy Research Center, KIST, Seoul, Korea
2 - Department of Biological & Chemical Engineering, Korea University, Seoul, Korea
3 - Clean Energy & Chemical Engineering, UST, Daejeon, Korea

* djmoon@kist.re.kr

Keywords: Fischer-Tropsch synthesis, Co-based catalyst, Al-SBA-15, mesoporous, materials

1 Introduction

Fischer-Tropsch Synthesis (FTS) is regarded as a key technology in GTL-FPSO process which produces liquid fuels such as gasoline, diesel and wax from the synthesis gas [1-3]. The use of mesoporous silica as supports for FTS catalyst has been explored. Mesoporous molecular sieves not only allow for higher active metal dispersion but also make uniform pore size distribution. Zeolite materials are also used in FTS reaction and because of the acid site which improves isomerization during the reaction under way, it was preferred to use in upgrading and FTS reaction. However there are some reports about silanol groups in zeolite which lead to retard the reduction of metallic cobalt [4]. Furthermore by the Anderson–Schulz–Flory (ASF) distribution of FTS reaction, it is inherently found to have a wide-range of hydrocarbon distribution from methanol to heavy waxy product. Moreover, the hydrocarbon selectivity towards gasoline range products is generally known to be limited to a maximum of 48 mol% [5]. In this work, we synthesized Co-based catalyst supported on the modified SBA-15 to obtain the mild reduction condition and selective products with certain carbon number distribution.

2 Experimental/methodology

For the comparison of the acid site on the catalyst support, modified SBA-15 was prepared with the molar ratio of Si/Al= 0, 5, 7 and 10 and ZSM-5 was also measured against SBA-15. Supports were prepared by conventional method with the use of tetraethyl orthosilicate (TEOS) and aluminum isopropoxide as a silica and aluminum precursors, respectively [6]. Nonionic triblock copolymer $EO_{20}PO_{70}EO_{20}$ (P123, Aldrich) was used as surfactant. Catalysts were prepared by impregnation method using cobalt nitrate as an active metal precursor, and were characterized by N_2 physisorption, NH_3-TPD, TPR, XRD, TGA, SEM and TEM. During the reaction, product gases (C_1-C_9) were analyzed by online GC, and higher hydrocarbons (C_5-C_{44}) were analyzed by offline GC and GC-MS.

Table 1. Physical Properties of Prepared Catalysts

Catalysts	BET S.A. (m^2/g)	Total Pore Volume (cm^3/g)	Average Pore Diameter (nm)	Micro/MesoPorous
SBA-15	857	1.02	5.8	Mesoporous
10-Al-SBA-15	690	1.14	6.6	Mesoporous
7-Al-SBA-15	403	1.03	10.9	Mesoporous
5-Al-SBA-15	371	1.08	11.6	Mesoporous
Co-ZSM-5	174	0.24	5.55	Microporous

3 Results and discussion

The physical properties of prepared supports were obtained by the N_2 physisorption analysis. With increase in the ratio of the amount of alumina to SBA-15 materials, the BET surface area was decreased and the average pore diameter was increased. Interestingly, the total pore volume of catalysts was almost the same throughout the SBA-15 series catalysts despite the change in alumina ratio. Reducibility of prepared catalysts was measured by using the H_2-TPR method. It was found that the Co-SBA-15 and Co-ZSM-5 catalysts have similar reduction profiles. However, in case of the alumina added SBA-15 catalyst, much broader and blunt reduction peaks were shown due to the formation of segregated cobalt and alumina support. By controlling the amount of alumina, we can obtain the catalyst which has the prop-er reducibility and appropriate interaction between the cobalt and support materials.

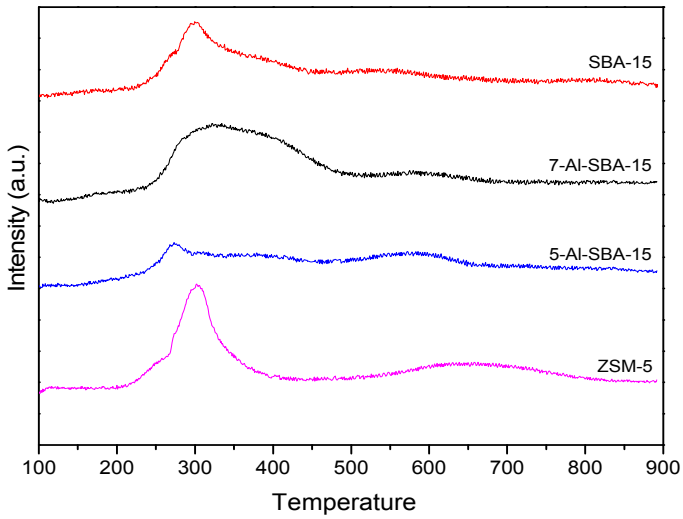

Fig. 1. H_2-TPR of prepared catalysts.

4 Conclusions

It was found that with the increase of the Si/Al ratio, the interaction between cobalt metal and support was increased. It was considered that the strong interaction between the active metal and support makes the catalysts hardly reducible materials. Indeed, by adding the alumina to SBA-15, the weak acid site was also increased and the isomerization during the reaction was activated. Therefore it showed relatively middle range hydrocarbon distribution compared with the catalyst which uses SBA-15 as a support.

Acknowledgements

This work was supported by Korea Institute of Science and Technology (Project No. 2E25404) and funded by Ministry of Trade, Industry and Energy, Korea. (Project No. 20142010102790).

References

[1] J.S. Kang, S.V. Awate, Y.J. Lee, S.J. Kim, M.J. Park, S.D. Lee, S.I. Hong, Dong Ju Moon, *J. of Nanosci. & Nanotech*., 10 (2010) 3700.
[2] J.S. Jung, S.W. Kim, D.J. Moon, *Catalysis.Today*, 185 (2012) 168.
[3] J.S. Jung, J.S. Lee, G.R. Choi, S. Ramesh, D. J. Moon, *Fuel*, 149 (2015) 118.
[4] J. He, Z. Liu, Y. Yoneyama, N. Nishiyama, N. Tsubake, *Chem. Eur*. J., 12 (2006) 8296.
[5] A. Vinu, V. Murugesan, W. Bohlmann, M. Hartmann, *J. Phys. Chem. B*, 108 (2004) 11496.
[6] Y. Li, W. Zhang, L. Zhang, Q. Yang, Z. Wei, Z. Feng, C. Li, *J. Phys. Chem. B*, 108 (2004) 9739.

IV-PP153

Kinetics for Hydrogen Production from Glycerol Steam Reforming Reaction Using Ni-Fe-Ce/Al_2O_3

Sub G.G.[1], Moon D.J.[2*], Park N.C.[3], Kim Y.C.[3]

1 - Department of Chemicals Engineering, Chonnam National University, Gwangiu, Republic of Korea

2 - Korea Institute Science and Technology, Seoul, Republic of Korea

3 - Faculty of Applied Chemical Engineering and the Research Institute For Catalysis, Chonnam National University, Gwangju, Republic of Korea

* djmoon@kist.re.kr

Keywords: glycerol steam reforming, hydrogen catalyst, nickel, kinetics

1 Introduction

In recent years, hydrogen energy has received much attention as an alternative energy. Therefore, extensive research has been conducted to find sustainable sources for hydrogen. Biomass is a promising candidate for hydrogen production because it has relatively high hydrogen content, and nontoxic. During the production of biodiesel, glycerol by-product is formed approximately 10% [1-2]. Some studies have been carried out on glycerol steam reforming by the different metal and nobel metal catalysts [3]. Previous studies have shown that Cerium and iron increased the reducibility of the Ni-based catalysts [4-5]. In this paper, we examined the kinetics of glycerol steam reforming and investigated the glycerol reaction order and activation energy using Ni-Fe-Ce/Al_2O_3 catalyst.

2 Experimental/methodology

The Ni-Fe-Ce/Al_2O_3 catalyst was prepared by impregnation method and as follows. First, Al_2O_3 was impregnated with ferric nitrate and cerium nitrate solutions, dried at 100 °C for 24 h, and calcined at 500 °C for 5 h in air. Secondly, the Fe-Ce/Al_2O_3 catalysts were further impregnated with a Ni nitrate solution, dried, and then calcined again using the method described above.

This experiment, the glycerol steam reforming, was conducted in a 6-mm ID fixed-bed quart reactor containing 0.03g Ni-Fe-Ce/Al_2O_3 catalyst at atmospheric pressure and temperature of 723-823K.

Ar gas was used as carrier gas. 12-30 wt.% glycerol solution (corresponding to $\frac{W}{F_{A0}}$ of 0.65-2.03) was used as feed to ensure stoichiometrically excess steam. The glycerol solution was fed into the reactor by an HPLC pump, vaporized in a preheater (563K) and passed over the catalyst inside the reactor. Reactor outlet gases were separated into a liquid phase and a gas phase in a condenser. The gaseous products were analyzed on-line by gas chromatography.

3 Results and discussion

The experimental data is obtained in kinetically controlled reaction regime of negligible mass transport limitations. In this paper, internal transport in the reaction system was ignored, because commercial 1-mm ball-type was employed. External transport as minimized by selecting suitable total flow rate, and there was no significant change in glycerol conversion when the total flow rate exceeded over 300ml/min.

The values of activation energy and reaction order based on the power-law model calculated with experiment data. Fig. 1 shows the relation between glycerol conversion rate and glycerol

solution concentration. Fig. 2 is Arrhenius plot. Thought these plots, the activation energy and reaction order were found to be 40.81 kJ/mol and 0.349, respectively.

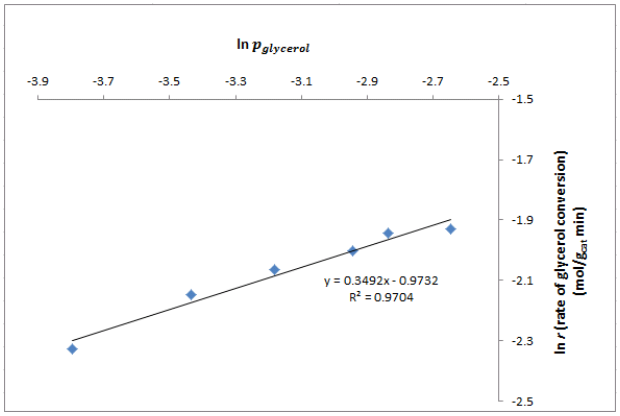

Fig. 1. A plot of ln *r* vs. ln$P_{glycerol}$ at 723K

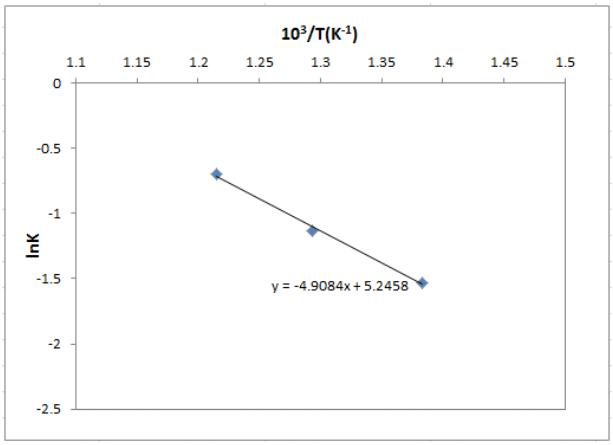

Fig. 2. A plot of 1000/T vs. *ln K* at atmospheric pressure

4 Conclusions

The experimental data is obtained in kinetically controlled reaction regime. The activation energy and the reaction order for the glycerol steam reforming reaction using Ni-Fe-Ce/Al_2O_3 catalyst were found to be 40.81 kJ/mol and 0.349, respectively, based on a power-law model.

Acknowledgements

This study was supported by the Priority Research Centers Program through the National Research Foundation of Korea (NRF), funded by the Ministry of Education, Science, and Technology (2009-0094055), Republic of Korea, and supported partly by the Ministry of Knowledge Economy of Korea and the Korea Institute of Science and Technology (KIST Grant No. 2E24834 & 2MR2190)

References

[1] Chirag D. Dave, K.K. pant, *Renew. Energy*. 36 (2011) 3195.
[2] Binlin Dou, Chao Wang, Youngche Song, Haisheng Chen, Yujie Xu, *Energy Convers. Manage*. 78 (2014) 253.
[3] Seung-hoon Kim, Jae-sun Jung, Eun-hyeok Yang, Kwan-Young Lee, Dong Ju Moon, Catalysis Today. 228 (2014) 145.
[4] A. Iriondo, V.L. Barrio, J.F. Cambra, P.L. Arias, M.B. Guemez, M.C. Sanchez-Sanchez, R.M Navarro, J.L.G. Fierro, *Int. J. Hydrogen Energy*.35 (2010) 11622.
[5] SHI Qiujie, PENG Ziqing, CHEN Weiqing, ZHZNG Ning, *J. Rare Earth*. 29 (2011) 861.

IV-PP154

Heterogeneous Lipase-Active Biocatalysts for Oil Triglycerides' Hydrolysis and Interesterification

Kovalenko G.A.[1,2*], Perminova L.V.[1], Beklemishev A.B.[1,3], Kuznetsov V.L.[1,2]

1 - Boreskov Institute of Catalysis SB RAS, Novosibirsk, Russia
2 - Novosibirsk State University, Novosibirsk, Russia
3 - Institute of Biochemistry, Novosibirsk, Russia

* galina@catalysis.ru

Keywords: biocatalysts lipase' activity, nanocarbon-in-silica, matrix, interesterification, biodiesel

1 Introduction

Nowadays, considerable attention has been given to the lipase-active biocatalysts for industrial scale implementation because these enzymes are powerful tools for catalyzing not only hydrolytic breakdown of fats and oils with subsequent release of free fatty acids, diglycerides, monoglycerides, and glycerol, but various reverse reactions of synthesis – triglycerides' esterification, interesterification, as well as acidolysis, alcoholysis, aminolysis. Therefore, R&D of commercially attractive heterogeneous biocatalysts, as well as proper selection of strategy to improve their properties (enzyme activity and stability) by appropriate procedure of lipase' immobilization is still an exciting goal. It has been argued that the using the whole or partially destroyed microbial cells as active components for biocatalysts and preparation of the whole-cell biocatalysts are more profitable for industry.

This research was devoted to the preparation of heterogeneous biocatalysts by entrapment of lipase-active components, such as whole cells or cells' lysates of an *Escherichia coli* recombinant strain (r*E.coli*/lip), inside silica xerogel, as well as inside {nanocarbon-in-silica} composites. Nanocarbons such as multiwalled carbon nanotubes and carbon nanospheres were included inside SiO_2-matrix together with lipase-active components. The properties (enzyme activity and stability) of the biocatalysts were studied in dependence of physical-chemical characterictics of the nanocarbons included. The prepared lipase-active biocatalysts were examined for oil triglycerides' hydrolysis and interesterification.

2 Experimental

Heterogeneous lipase-active biocatalysts were prepared by entrapment of lipase-active components r*E.coli*/lip inside silica xerogel and {nanocarbon-in-silica} composites as described in [1–3]. Multiwalled carbon nanotubes (CNT) with different tubes' diameters (Ø9–11 nm, S_{sp}=320 m^2/g, "thin" and Ø20–22 nm, S_{sp}=140 m^2/g, "thick") and carbon nanospheres with bulbous structure (Ø5–6 nm, S_{sp}=485 m^2/g, "nano-onion") were included as functional additives. CNTs were included both as aggregates larger than 150 nm obtained in a pyrolytic installation and as suspension after dispersion using ultrasonic disintegrator. The prepared biocatalysts had the following optimal compositions, in wt% of dry substances: r*E.coli*/lip cells or cells' lysates – 20–40, nanocarbons – 0–10, maltodextrin – 0–20, SiO_2 – balance to 100. The moisture of dried granules of biocatalysts (0.1 to 2 mm in size) averaged between 7–10 wt%.

The activity of prepared biocatalysts was determined in a periodic batch reactor or in a continuous packed-bed reactor. The emulsified tributyrine was used as substrate for hydrolysis at 20°C. Oil-fat blends of vegetable oils (⅔) and of fully hydrogenated one (⅓) were used as substrates for interesterification at 60–75°C. The triglycerides' esterification for the methyl- or ethyl fatty acids' esters (biodiesel) was carried out with participation of methyl- or ethyl-acetate at 40–50°C, hexane being used as solvent.

3 Results and discussion

Triglycerides' hydrolysis by the silica- and {nanocarbon-in-silica} biocatalysts was studied. It was found that the activities of the prepared biocatalysts depended strongly on the characteristics of nanocarbons included inside SiO_2-xerogel, in particular their specific area and dispersity. The biocatalysts with included aggregates of "thick" CNT were the 1.3–2 folds more active in comparison with the reference {no carbon-in-silica} biocatalysts; whereas the biocatalysts prepared with dispersed "thin" CNT possessed the lowest activity.

Silica- and {nanocarbon-in-silica} biocatalysts prepared by entrapment of r*E.coli*/lip lysates were studied in the process of interesterification in oil-fat blends. In this case, basing on the effect on conversion (*x*,*%*) in the 1st reaction cycle the included nanocarbons can be arranged in the following order: no nanocarbon (*50%*) > aggregated "thick" CNTs (*35%*) ≈ aggregated "thin" CNTs (*35%*) > dispersed "thin" CNTs (*25%*) > "nano-onion" (*20%*). After 4th reaction cycle, the {"nano-onion"-in-silica} biocatalyst deactivated completely, as well as the {CNTs-in-silica} biocatalysts retained up to ~30% of initial activity.

It was found that the prepared biocatalysts exhibited high operational stability in the process of biodiesel production by interesterification of sun flower oil and methyl- or ethyl-acetate and operated for more than 1000 h, the half-life time being equal to 720 h at 40°C (Fig.).

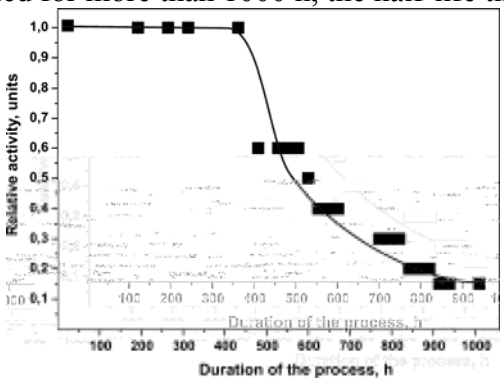

Fig. Interesterification' activity of the lipase-active biocatalyst during the process of biodiesel production

Conditions: 40°C, 0.1 M vegetable oil and 2.3 M ethyl-acetate in hexane, a batch reactor, 150 rpm

4 Conclusions

Lipase-active heterogeneous biocatalysts were prepared by entrapment of recombinant r*E.coli*/lip whole cells or their cells' lysates inside silica xerogel, as well as inside {nanocarbon-in-silica} composites. The study on the effect of the included nanocarbons, in particular multiwalled carbon nanotubes (CNTs) with different diameters and dispersity, as well as nanospheres on the initial activity of the prepared biocatalysts was carried out in the processes of triglycerides' hydrolysis and interesterification. It was shown that the use of aggregated "thick" CNTs yielded the biocatalysts with the highest initial activity in the tributyrine' hydrolysis; 250 U/g and 1000 U/g for entrapped whole cell and cell' lysates respectively. The lowest activities of the biocatalysts were determined using dispersed "thin" CNTs and "nano-onion" uniformly distributed inside biocatalysts; 50 U/g and 400 U/g for entrapped whole cell and cell' lysates respectively. In the case of triglycerides' interesterification, the {no carbon-in-silica} biocatalysts prepared by entrapping r*E.coli*/lip lysates and maltodextrin inside pure SiO_2-xerogel (no carbon) possessed the highest triglycerides' interesterification activity, half-life time being more than 70 h and 720 h at 75°C and 40°C respectively.

References

[1] G.A. Kovalenko, L.V. Perminova, T.V.Chuenko, L.I. Sapunova, E.A. Shlyakhotko, A.G. Lobanok, Appl. Biochem. Microbiol. 47 (2011) 151.

[2] G.A. Kovalenko, L.V. Perminova, N.A. Rudina, I.N. Mazov, S.I. Moseenkov, V.L. Kuznetsov, J. Mol. Catal. B: Enzym. 76 (2012) 116.

[3] G.A. Kovalenko, A.B. Beklemishev, L.B. Perminova, T.V. Chuenko, A.L. Mamaev,I.D. Ivanov, S.I. Moseenkov, V.L. Kuznetsov, Appl. Biochem. Microbiol. 49 (2013) 296.

IV-PP155

Highly Selective Catalysts for Synthesis of Alkylaromatic Hydroperoxides and Prospects of their Industrial Application

Dahnavi E.M.[1*], Kurganova E.A.[2], Frolov A.S.[2], Koshel G.N.[2], Kharlampidi Kh.E.[3]

1 - Tomsk State University, Tomsk, Russia
2 - Yaroslavl State Technical University, Yaroslavl, Russia
3 - Kazan State Technological University, Kazan, Russia

* dahnavi@rambler.ru

Keywords: selective oxidation, liquid-phase oxidation, ethylbenzene, i-propylbenzene, cymene, N-hydroxyphtalimides, mathematical models

1 Introduction

During oxidation of some alkylaromatic hydrocarbons, in particular, ethylbenzene, i-propylbenzene, cymene, the corresponding hydroperoxides are formed and widely used in industry as a basis for initiation additives or intermediates in synthesis of valuable products of chemical engineering. To accelerate the liquid-phase oxidation of hydrocarbons to hydroperoxides various catalytic systems have been proposed. However, these processes are still carried out in industry without catalysts. The problem of catalytic oxidation of the corresponding hydrocarbons is connected with the fact that known catalytic systems indeed increase the rate of their oxidation, however, they do not provide adequate selectivity towards hydroperoxides. This can result in uncontrollable decomposition of hydroperoxides at the strengthening stage followed by thermal explosion.

The research carried out both in Russia and abroad has demonstrated that some derivatives of N-hydroxyphtalimides are highly active and selective catalysts of hydroperoxide formation in oxidation of alkylaromatic hydrocarbons, including i-propylbenzene, ethylbenzene and cymene. They provide new opportunities for intensification of existing processes in industry.

2 Experimental

In the present work the results of model tests of the process of hydrocarbons oxidation in conditions close to industrial process are shown. Technical hydrocarbons, which were not additionally purified, were used as a feed. Basic experiments were carried out in the presence of hydroperoxides, which were specially released from industrial oxidate of the corresponding hydrocarbon via sodium salt. N-hydroxyphtalimides were synthesized using hydroxylamine and corresponding phthalic anhydride according to our method. The purity of obtained catalysts was determined using spectral methods. Analysis of oxidation reaction mass was carried out iodometry and chromatography methods. The off-gases containing O_2, CO, CO_2, H_2, CH_4 and heavier hydrocarbons were analyzed chromatographically. Catalytic oxidation of i-propylbenzene has been widely studied, and the results obtained give the ground to apply them in industry.

3 Discussion

High selectivity of hydroxyperoxide formation in the presence of phtalimide systems even at high conversions of i-propylbenzene (30-40%) demonstrate that phtalimides do not practically participate in hydroperoxide decomposition, i.e. strengthening of oxidate under these conditions is technologically reasonable. A number of researchers consider that high rate and selectivity of hydroperoxide formation are connected with proceeding of the main reactions (1) – (2) – (3) according to the following scheme:

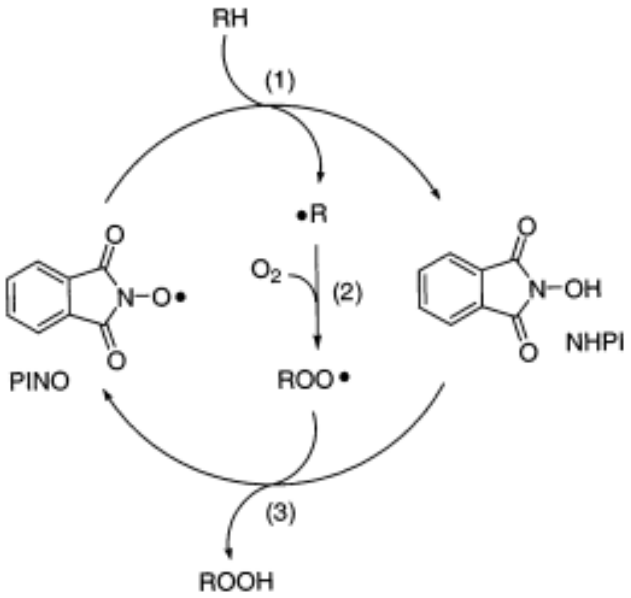

Another important aspect of intensification of i-propylbenzene industrial oxidation process in the presence of phtalimide systems, in particular, N-hydroxyphtalimide, is high conversion of the feed per single run. 40% i-propylbenzene conversion was achieved at 130 ^{o}C per 1 h, which is two times higher compared to industrial process. It is noteworthy that selectivity towards i-propylbenzene remains above 90 %. If i-propylbenzene oxidation is carried out with 17-20 % conversion (typical for industrial process), selectivity reaches 94-96 %. If applied industrially, the obtained results may provide significant economic impact, in particular, in co-production of phenol and acetone, styrene and propylene oxide due to increase in reactor productivity, significant off-loading in oxidate fractionation node as well as reduction of production wastes.

In the present work a comparative results of kinetic studies of catalytic oxidation of ethylbenzene and i-propylbenzene are shown. Mathematical models of the processes have been developed taking into account the parameters of instrumentation of industrial processes. Technical-and-economic indices of corresponding processes in the case of oxidation catalysts based on hydroxyphtalimides have been determined. The only limitation for application of new method in existing industry is connected with possible difficulties to provide heat removal in oxidation reactors. To overcome the problem one should increase the heat-exchange surface of built-in coils and use fractional air supply to different levels of reactor. The calculation results demonstrate that process performance in accordance with proposed method, in particular, production of hydroxyperoxide, would allow using only one fractioning step instead of two in the currently used method, reduce energy intensity of production by 40±5 %, increase the productivity of reactor section by 60-70 %. This may result in significant economic effect. Higher economic effect could be reached, if one develops new oxidation reactors operating in different hydrodynamic modes taking into account kinetics of i-propylbenzene oxidation in the presence of phtalimide catalysts.

4 Conclusions

The fundamentals of industrial oxidation of ethylbenzene, i-propylbenzene, cymene and other hydrocarbons are quite similar, thus, one can expect high economic effect for these processes. However, to make final decision on their application in industry it is necessary to carry out pilot tests and develop all technological steps of production and separation of corresponding products taking into account the backflow recycle and catalysts. Results of pilot tests can support the propositions on high effectiveness of application of new catalytic systems and provide required information to prepare initial data for design basis.

Session V
"Catalysis and environmental protection"

V-OP01

Highly Accessible TiO_2 Nanoparticles Embedded at the Surface of SiO_2 for the Photocatalytic Degradation of Pollutants under Visible and UV Radiation

Cani D.[1], Pescarmona P.P.[1,2*]

1 - COK, University of Leuven, Leuven, Belgium
2 - Chemical Engineering Department, University of Groningen, Groningen, The Netherlands

* p.p.pescarmona@rug.nl

Keywords: photocatalysis, TiO_2/SiO_2, composite, pollutants degradation, supported nanoparticles, UV radiation, visible light

1 Introduction

Industrial growth causes increasing problems connected to pollution of water streams but common purification techniques such as biochemical oxidation and physical treatment processes have several disadvantages. Since the discovery of the photocatalytic properties of TiO_2 by Fujishima and Honda in 1972 [1], relevant research efforts focussed on photocatalysis as an efficient alternative for the degradation of pollutants. The decrease of the size of the active phase to the nanoscale is a powerful approach to enhance photocatalytic activity [2]. However, nanoparticles suffer from agglomeration during the reaction, which leads to loss of surface area and of accessibility of the active phase. Here, we present an original strategy to stabilise TiO_2 nanoparticles by embedding them in a porous silica matrix while fully preserving their accessibility by ensuring their location at the surface of the material.

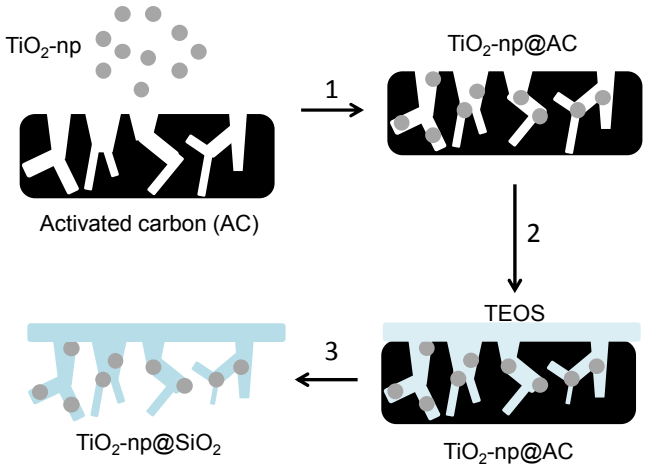

Fig. 1. The multi-step synthesis method used to produce a photocatalyst with highly accessible TiO_2 nanoparticles.

2 Experimental section

TiO_2 nanoparticles were embedded at the surface of SiO_2 through a multistep synthesis procedure (Fig. 1). First, the desired amount of TiO_2 nanoparticles was deposited on activated carbon (1). Then, the TiO_2-carbon composite was impregnated with TEOS (2). Finally, the material was calcined to burn off the carbon support and to produce TiO_2-SiO_2 photocatalysts with fully accessible nanoparticles and high surface area (3). A series of materials with different ratios between TiO_2 and SiO_2 was prepared following this method. The photocatalytic activity

was tested in the degradation of phenol and rhodamine B (1 mg/ml of photocatalyst, 200 ppm aqueous solution of pollutant). The mixture was stirred for 1 h in the dark to achieve adsorption/desorption equilibrium before irradiation for the selected time (typically 3 h).

3 Results and discussion

Characterisation by means of TEM (Fig. 2), N_2-physisorption and XRD indicated that the composite TiO_2-SiO_2 materials display high surface area and discrete TiO_2 nanoparticles dispersed on the SiO_2 support. Both these properties are fundamental for the photocatalytic performance. Indeed, the composite materials showed higher photocatalytic activity compared the TiO_2 P25 benchmark in the degradation of different types of probe molecules (phenol and rhodamine B) under UV radiation. The highest degree of photocatalytic degradation of the pollutants was obtained with the composite with a 60% loading of TiO_2, which reached 72% degradation of rhodamine B compared to 45% obtained with TiO_2 P25 under the same conditions (Fig. 2). Remarkably, these photocatalysts are also active under visible light due to the presence in the structure of residual C atoms from the carbon template. The TiO_2-SiO_2 photocatalysts could be efficiently recycled in consecutive tests.

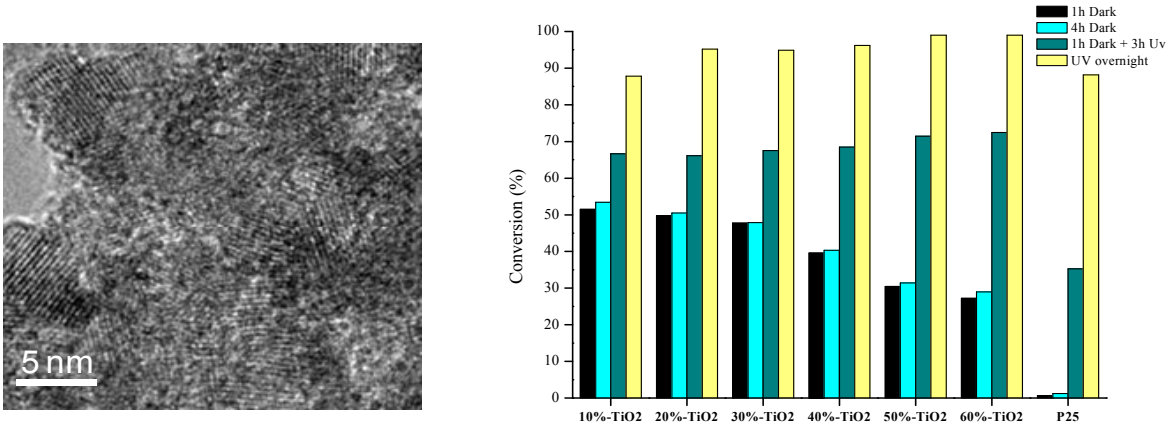

Fig. 2. TEM image of the composite material showing individual and crystalline TiO_2 nanoparticles embedded on a SiO_2 support (left). Photocatalytic degradation of Rh.B under UV radiation (right).

4 Conclusions

A new synthesis method was developed to prepare a series of TiO_2/SiO_2 composites in which TiO_2 nanoparticles are embedded at the surface of SiO_2. The obtained materials display high surface area and well-dispersed, highly accessible TiO_2 domains. These features led to an excellent photocatalytic activity in the degradation of pollutants. This synthesis method is of general applicability and can be promising for preparing supported nanoparticles with different composition.

Acknowledgements

The authors acknowledge sponsoring in the frame of START1 research program of KU Leuven.

References

[1] A. Fujishima, K. Honda, *Nature* 238 (1972) 37.

[2] M. Addamo, V. Augugliaro, A. Di Paola, E. Garcia-Lopez, V. Loddo, G. Marci, R. Molinari, L.Palmisano, M. Schiavello, *J. Phys. Chem. B* 108 (2004) 3303.

V-OP02

Photocatalytic Activity of the Uranyl Modified Titania, Silica and Alumina under Visible Light Irradiation

Filippov T.[1,2], Kolinko P.[1], Glebov E.[3], Kozlov D.[1,2*]

1 - Boreskov Institute of Catalysis, Novosibirsk, Russia
2 - Research and Educational Centre for Energoefficient Catalysis (Novosibirsk State University), Novosibirsk, Russia
3 - Voevodsky Institute of Chemical Kinetics and Combustion, Novosibirsk, Russia

* kdv@catalysis.ru

Keywords: photocatalysis, titanium dioxide, uranyl, nitrate, visible light, volatile organic compounds

1 Introduction

Photocatalysis is known as a promising method for destruction of various toxic pollutants. TiO_2 was selected as the most active metal oxide semiconductor among heterogeneous photocatalysts and today it plays an important role in many industrial and technological processes, environmental and biomedical applications. However pure TiO_2 photocatalysts are active only under the mild UV irradiation with photon energy equal or higher than its band gap (3.2 eV). On the other hand, ultraviolet or near-ultraviolet radiation (λ<400 nm) occupies only about 4% of the solar light spectrum [1]. In order to utilize solar light efficiently in the visible region (λ>420 nm) which covers large range of the solar spectrum, the development of visible-light-driven photocatalysts has started over last decades [2].

It is well known that uranyl ions in water could be synthesized by visible light and after excitation the oxidizing potential of uranyl ions becomes as high as 2,6-2,7 V [3]. At the same time the gas phase photocatalytic oxidation of organic species with uranyl-modified photocatalysts was weakly investigated. The influence of spectral characteristics, uranyl quantity and nature of the support were not investigated. These questions were the subject of current research.

2 Experimental/methodology

In the current work photocatalyst samples were synthesized by incipient wetness impregnation method with the use of TiO_2, γ-Al_2O_3 and SiO_2 as support. The $UO_2(NO_3)_2$ content was varied from 0.2 to 10 wt.%.

The activity of catalysts was measured in the reaction of acetone and ethanol vapor photooxidation in the static reactor at room temperature. The high pressure Xe-lamp and the 450 nm LED were used as the light sources. The visible regions of the spectrum was cutoff with the Optical glass filter ZhS-11 were used to cutoff the visible region (λ > 420 nm) from the Xe-lamp irradiation. Ethanol, acetaldehyde and CO_2 gas concentration were measured with the gas chromatograph equipped with FID and with the FTIR spectrometer equipped with gas cell.

UV-VIS spectroscopy with the diffuse reflectance attachment, XPS spectroscopy and fluorescence methods were used for additional photocatalysts characterization.

3 Results and discussion

Results of investigation demonstrated that:

All the synthesized photocatalysts oxidize ethanol and acetone even under the visible light with wavelength higher than 470 nm. Acetaldehyde was registered as the intermediate of C_2H_5OH photocatalytic oxidation whereas CO_2 was registered as the final products of both ethanol and acetone vapor PCO (Figure 1, **a**).

Although pure unmodified TiO_2 was not active under visible light (λ>420 nm) it was found to be the best support for uranyl nitrate and the $UO_2(NO_3)_2/TiO_2$ sample demonstrated highest photooxidation rate up to 470 nm incident light wavelength (Figure 1, **b**) [4].

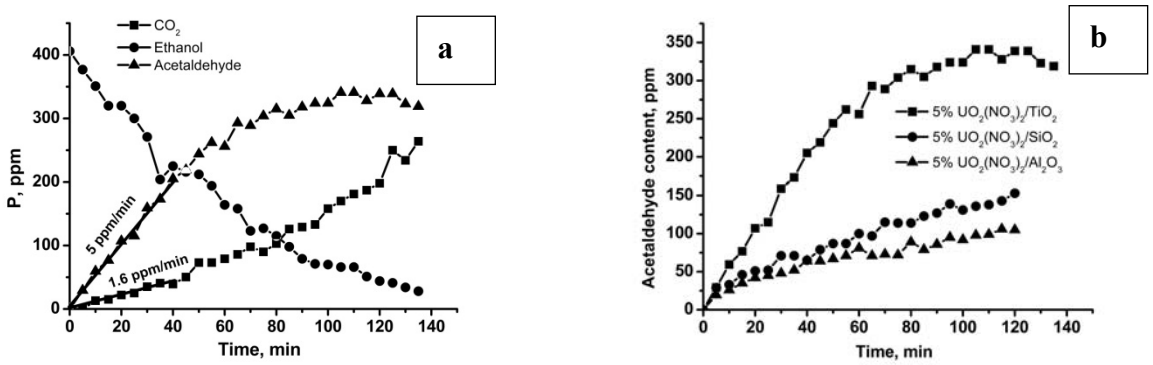

Fig. 1. (**a**) Kinetic curves of the ethanol vapor removal and CO_2 and acetaldehyde accumulation during the PCO of ethanol vapor in the static reactor under visible light; (**b**) Kinetic curves of the acetaldehyde accumulation during the ethanol PCO on the $UO_2(NO_3)_2/TiO_2$, $UO_2(NO_3)_2/SiO_2$ and $UO_2(NO_3)_2/Al_2O_3$ samples under visible light (λ > 420 nm)

Photocatalytic activity of all uranyl modified photocatalysts depended on the uranyl content and the type of support (Table 1).

Table 1. Photocatalytic activity of the uranyl modified catalysts with different $UO_2(NO_3)_2$ content under visible light (λ>420 nm) in the ethanol vapour PCO.

Sample	U content, wt. %	Rate of acetaldehyde formation, ppm/min	Rate of CO_2 formation, ppm/min
0.5% $UO_2(NO_3)_2/TiO_2$	0.41	1.6	0.25
2% $UO_2(NO_3)_2/TiO_2$	1.7	3.0	0.63
5% $UO_2(NO_3)_2/TiO_2$	3.9	5.0	1.6
5% $UO_2(NO_3)_2/SiO_2$	-	0.91	0.01
5% $UO_2(NO_3)_2/Al_2O_3$	-	0.73	0.23

Additional experiments were conducted to investigated the optical properties of the uranyl modified TiO_2. UV-VIS diffuse reflectance spectra revealed that the most active $UO_2(NO_3)_2/TiO_2$ sample absorbs even lower amount of visible light than uranyl modified silica and alumina. Also the luminescence intensity of the $UO_2(NO_3)_2/TiO_2$ is much lower than of the uranyl modified silica and alumina samples.

4 Conclusions

The possible explanation of the increase of uranyl photocatalytic activity when it is deposited onto the TiO_2 surface is its photophysical interaction with the TiO_2 energy states.

Acknowledgements

Authors would like to thank the Russian President Grant for Leading Scientific Schools (NSh-1183.2014.3).

References

[1] C. Gueymard, *Solar Energy*. 76(4) (2004) 423.
[2] M. Pelaez, N. T. Nolan, et al., *Appl. Catal. B*. 125 (2012) 331.
[3] V. Balzani, F. Bolletta, M. T. Gandolfi, M. Maestry, *Topics in Current Chem*. 75 (1978) 1.
[4] P. A. Kolinko, T. N. Filippov, D. V. Kozlov, V. N. Parmon, *J. Photochem. Photobiol. A*. 250 (2012) 72.

V-OP03

Combining the Photocatalyst Pt/TiO_2 and the Non-photocatalyst $SnPd/Al_2O_3$ for Effective Photocatalytic Purification of Groundwater Polluted with Nitrate

Hirayama J.[1*], Kamiya Y.[2]

1 - Graduate School of Environmental Science, Hokkaido University, Sapporo, Japan
2 - Research Faculty of Environmental Earth Science, Hokkaido University, Sapporo, Japan

* hirayama@ees.hokudai.ac.jp

Keywords: photocatalysis, nitrate reduction, groundwater purification, tin-palladium bimetal

1 Introduction

Pollution of groundwater with nitrate (NO_3^-) is serious problem in the world. Since NO_3^- is toxic in human body, the World Heath Organization recommends the concentration of NO_3^- in drinking water below 0.8 mmol dm^{-3}. In the present study, we propose a photocatalytic reaction system combining a semiconductor photocatalyst (Pt/TiO_2) and a supported bimetallic non-photocatalyst ($SnPd/Al_2O_3$) dispersed in water. In this photocatalytic system (Pt/TiO_2-$SnPd/Al_2O_3$ system), H_2 is formed by a photocatalytic reaction over Pt/TiO_2 with the aid of a sacrificial compound, and the formed H_2 is consumed as a reductant for non-photocatalytic reduction of NO_3^- in water over $SnPd/Al_2O_3$ [1]. Here we applied the photocatalytic system for the purification of real groundwater and investigated the effects of compounds in the groundwater on the photocatalytic and non-photocatalytic performances [2].

2 Experimental

Pt/TiO_2 with 0.5 wt% Pt was prepared by photodeposition method using TiO_2 (Evonik P25), and $H_2PtCl_6 \cdot 6H_2O$ in aqueous methanol solution. $SnPd/Al_2O_3$ was prepared by incipient wetness method using Al_2O_3 (Aerosil Alu C), aqueous $PdCl_2$ solution, and aqueous $SnCl_2$ solution. Loading amount of Sn and Pd were fixed to 2.3 wt% and 4.2 wt%, respectivety. Photocatalytic reduction of NO_3^- in water was carried out in a Pyrex reaction vessel connected to a closed gas circulation system. The catalyst powder of Pt/TiO_2 (500 mg) and $SnPd/Al_2O_3$ (100 mg) were dispersed in the reaction solution (250 cm^3, $[NO_3^-]$ = 1.0 mmol dm^{-3}) with 1.0 mmol dm^{-3} glucose and then the suspension was irradiation with a 300 W Xe lamp ($\lambda > 300$ nm). The products in liquid and gas phases were analyzed by using two ion-chromatographs and a gas-chromatograph, respectively. Groundwater polluted with NO_3^- was obtained from a well in Kitami, Hokkaido, Japan (GW).

3 Results and discussion

The Pt/TiO_2-$SnPd/Al_2O_3$ system effectively and selectively promoted the photocatalytic reduction of NO_3^- to N_2 in aqueous NO_3^- solution (KNO_3-aq), whereas Pt/TiO_2 or $SnPd/Al_2O_3$ alone showed little or no activity under the reaction conditions (Table 1). The photocatalytic activity and selectivity to N_2 for the system were higher than those for the $SnPd/TiO_2$.

Table 1 Photocatalytic reduction of nitrate in water in the presence of various catalyst [1]

Entry	Catalyst	Conversion [%]	Selectivity [%]		
			NO_2^-	NH_4^+	gas[f]
1	Pt/TiO_2	0	---	---	---
2	$SnPd/Al_2O_3$	2	0	31	69

3	Pt/TiO_2 + $SnPd/TiO_2$	39	0	10	90
4	$SnPd/TiO_2$	19	0	23	77

Fig. 1 shows time courses for the photocatalytic reduction of NO_3^- over the Pt/TiO_2-$SnPd/Al_2O_3$ system. In case of KNO_3-aq, complete decomposition of NO_3^- was obtained after 36 h. On the other hand, elevation of the NO_3^-conversion was almost stopped after 12 h in the real groundwater (GW), indicating that the catalysts were deactivated during the reaction in GW. This was due to the negative effect of the compounds in GW on the activities over Pt/TiO_2, $SnPd/Al_2O_3$, or both.

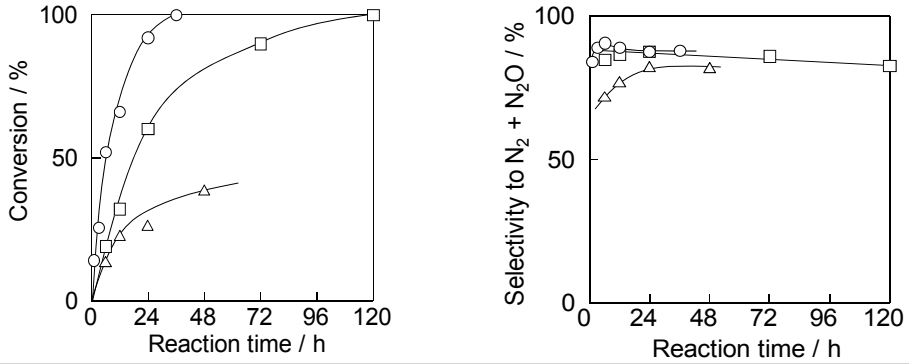

Fig. 1 Time courses for photocatalytic reduction of NO_3^- in (△) GW, (□) GW-Ox, and (○) KNO_3-aq in the Pt/TiO_2-$SnPd/Al_2O_3$ system.

To investigate the effects of the organic compounds in GW on the photocatalytic performance of the Pt/TiO_2-$SnPd/Al_2O_3$ system, we treated GW with photocatalytic oxidation in the presence of Pt/TiO_2 to decompose the organic compounds and conducted the photocatalytic reduction of NO_3^- in the treated solution (GW-Ox) over the Pt/TiO_2-$SnPd/Al_2O_3$ system. The decomposition rate of NO_3^- in GW-Ox was nearly twice that in GW, and NO_3^- was completely decomposed at 120 h. At 100% conversion, the selectivity to N_2 + N_2O was 83%, which was almost the same as that in KNO_3-aq. Thus, removing the organic compounds from GW makes it possible to decompose NO_3^- selectively to N_2 and N_2O. However, the reaction rate for NO_3^- decomposition in GW-Ox was slower than that in KNO_3-aq, indicating that compounds other than the organic ones in GW negatively affected the catalytic performance of the Pt/TiO_2-$SnPd/Al_2O_3$ system.

Thus we further investigated the influence of ionic compounds in GW on the Pt/TiO_2-$SnPd/Al_2O_3$ system. Chloride ion in KNO_3-aq did not affect the conversion of NO_3^- and selectivity. When SO_4^{2-} or SiO_3^{2-} was present in KNO_3-aq, the conversion of NO_3^- significantly decreased. This was because poisoning of Pt/TiO_2 with SO_4^{2-} and SiO_3^{2-}, and that of $SnPd/Al_2O_3$ with polymerized silicate ions. In contrast to anionic compounds, cationic ones in GW did not affect both photocatalytic and non-photocatalytic performances at all.

4 Conclusions

Combining the photocatalyst Pt/TiO_2 and the non-photocatalyst $SnPd/Al_2O_3$ in water produced the effective photocatalytic reaction system for photocatalytic purification of groundwater polluted with NO_3^-, though pretreatment of the groundwater to remove the organic compounds from it was necessary because they poisoned both Pt/TiO_2 and $SnPd/Al_2O_3$. Anionic compounds including SO_4^{2-} and SiO_3^{2-} also lowered the photocatalytic performance of the Pt/TiO_2-$SnPd/Al_2O_3$ system in the groundwater, while there was no influence of cationic compounds on the system.

References

[1] J. Hirayama, H. Kondo, Y. Miura, R. Abe, Y. Kamiya, *Catal. Commun.* 20 (2012) 99.
[2] J. Hirayama, Y. Kamiya, *ACS Catal*. 4 (2014) 2207.

V-OP04

Hierarchically Porous Fe-Silicalites for Total Oxidation of Organic Molecules

Sashkina K.A.[1,2,3*], Labko V.S.[4], Parkhomchuk E.V.[1,3,2]

1 - Boreskov Institute of Catalysis SB RAS, Novosibirsk, Russia
2 - Novosibirsk State University, Novosibirsk, Russia
3 - Research and Education Centre, NSU, Novosibirsk, Russia
4 - State Scientific Institution "The Joint Institute for Power and Nuclear Research – Sosny", Minsk, Belarus

* sashkina@catalysis.ru

Keywords: hierarchical, zeolite, nanozeolite, Fe-silicalite-1, heterogeneous, Fenton system, advanced, oxidation, processes, (AOPs)

Design of zeolite materials containing transition metal compounds is of great importance for the development of catalysts for green liquid phase oxidation [1]. Zeolite matrices stabilizes active iron-containing species in the highly dispersed state and protects them against the deactivation [2]. Iron-containing zeolites are effective catalysts both for partial and total oxidation of organic compounds by nontoxic reagents (O_2, H_2O_2) under mild conditions [3]. Total oxidation by means of heterogeneous Fenton-like systems including Fe-zeolite/H_2O_2 is a topical process for water decontamination [4].

The key problem of zeolite catalysts is intracrystalline diffusion constraints resulting in low utilization of zeolite active surface especially in adsorption and catalytic processes involving large molecules [5]. The effective approach for enhancing zeolite surface accessibility is to produce hierarchically porous zeolites, having besides micropores an additional system of meso- and macropores [6].

The present study describes the synthesis of hierarchically porous Fe-silicalite materials with desired texture. Catalytic performance of hierarchically porous Fe-silicalites was studied in total peroxide oxidation of different organic molecules – phenol, EDTA, lignin and clarithromycin lactobionate, belonging to the group of macrolide antibiotics.

1 Results and discussion

To create hierarchically porous Fe-silicalites with desired texture, two main approaches were applied: template synthesis [7] and patterning Fe-silicalite nanocrystals [8]. Template approach was to fill arrays composed of closely packed monodisperse polymer microspheres with Fe-silicalite precursor followed by the hydrothermal synthesis and the calcination of obtained composites, resulting in the formation of 3D ordered macroporous Fe-silicalite materials (Fig. 1a).

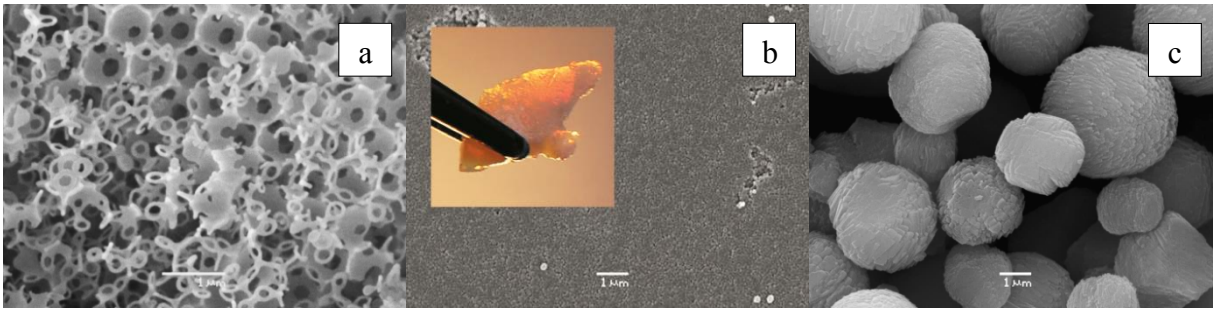

Fig. 1. SEM images of 3D macroporous Fe-silicalite material (a), pellets built of Fe-silicalite nanocrystals (b) and Fe-silicalite microbeads (c). The inset shows a photograph of Fe–silicalite pellets.

The assembling of Fe-silicalite nanocrystals into random and close packing was carried out *via* drying or centrifugation of nanozeolite suspensions, respectively. Fig. 1b shows SEM image and a photograph of Fe-silicalite pellets consisting of closely packed nanobeads. Fe-silicalite pellets built of closely packed nanobeads show good mechanical stability in benzene and water. Large FeZSM-5 microbeads with the average size of 5 μm have been also designed for comparing structural features of nanozeolite materials (Fig. 1c).

The synthesized samples were characterized by a number of methods: laser diffraction analysis, X-ray diffraction, scanning and transmission electron microscopy, energy-dispersive X-ray spectroscopy, argon and nitrogen adsorption measurements, inductively coupled plasma optical emission spectrometry, UV visible diffuse reflectance spectroscopy and temperature-programmed desorption of ammonia.

All hierarchical Fe-silicalites exhibited high crystallinity, high BET surface area (369-550 m^2/g), external surface area (84-277 m^2/g) and total pore volume (0.50-0.75 cm^3/g). Calcined Fe-silicalite-1 materials contained highly dispersed ferric clusters no more than 3 nm in size according to TEM, UV-visible DR spectroscopy and EDS mapping.

Hierarchically porous Fe-silicalites were tested in total liquid phase catalytic oxidation of different organic molecules, including phenol, the natural polymer – lignin, macrolide antibiotic – clarithromycin lactobionate and metal ion complexing agent – EDTA by H_2O_2 at low temperatures (298-323 K) compared with Fe-silicalite microspheres and homogeneous Fenton reagent. The use of heterogeneous Fenton system Fe-silicalite/H_2O_2 allowed increasing the efficiency of hydrogen peroxide utilization for phenol oxidation compared with the homogeneous Fenton system due to the adsorption of phenol on the zeolite surface. Performances of hierarchical Fe-silicalites in oxidation of large organic molecules by hydrogen peroxide were significantly improved *vs.* the reference Fe-silicalite microbeads, resulted from increasing catalytic sites accessibility. Heterogeneous Fenton system based on Fe-silicalites is promising for post-treatment of sewage and liquid nuclear wastes by the destruction of radionuclide–organic acid complexes with the following radionuclides sedimentation. Another direction of heterogeneous Fenton-system practical use is preparation of biomedical samples, containg macromolecules such as DNA and proteins, for radiocarbon analyses by accelerating mass spectrometer.

Acknowledgements

The authors thank N.A. Rudina, A.B. Ayupov, S.V. Bogdanov, E.Yu. Gerasimov, A.I. Lysikov, T.V. Larina, L.A. Akimova, A.V. Poluhin for their help in the samples characterization. The work was performed with partial support of the Skolkovo Foundation (Grant Agreement for Russian educational organization №1 on 28.11.2013) and RSFC grant 14-13-01155.

References

[1] I.W.C E. Arends and R. A. Sheldon, Appl. Catal., A, 2001, 212, 175.
[2] Sashkina K.A., Parkhomchuk E.V., Rudina N.A., Parmon V.N. Microporous & Mesoporous Materials, 2014, 189, 181.
[3] Kuznetsova E.V., Savinov E.N., Vostrikova L.A., Parmon V.N. Applied Catalysis B, Environmental, 2004, 51/3, 165.
[4] S. Navalon, M. Alvaro and H. Garcia, Appl. Catal., B, 2010, 99, 1.
[5] J. Pérez-Ramírez, C. H. Christensen, K. Egeblad, C. H. Christensen and J. C. Groen, Chem. Soc. Rev., 2008, 37, 2530.
[6] V. Valtchev and L. Tosheva, Chem. Rev., 2013, 113, 6734.
[7] K.A. Sashkina, V.S. Labko, N.A. Rudina, V.N. Parmon, E.V. Parkhomchuk, Journal of Catalysis, 2013, 299, 44.
[8] K.A. Sashkina, N.A. Rudina, A.I. Lysikov, A.B. Ayupov, E.V. Parkhomchuk, J. Mater. Chem. A, 2014, 2, 16061.

V-OP05

CO_2 Methanation on Commercial Ni/Al_2O_3 and Ru/Al_2O_3 Catalysts

Garbarino G.[1*], Bellotti D.[2], Riani P.[3], Magistri L.[2], Busca G.[1]

1 - University of Genova, DICCA Dipartimento di Ingegneria Civile Chimica e Ambientale, Genova, Italy

2 - University of Genova, DIME Dipartimento di Ingegneria Meccanica, Energetica, Gestionale e dei Trasporti, Genova, Italy

3 - University of Genova, DCCI Dipartimento di Chimica e Chimica Industriale, Genova, Italy

* gabriella.garbarino@unige.it

Keywords: hydrogen, carbon, dioxide, methanation, ruthenium on alumina, catalyst, activation, stability

1 Introduction

CO_2 hydrogenation with renewable hydrogen is an interesting option as a CO_2 Capture and Storage technology (CCS) allowing to reduce the emissions of greenhouse gases and at the same time to produce useful compounds, i.e. hydrocarbons, alcohols, formic acid.

Methanation reaction was widely studied in last decades and applied in industry to convert COx (mainly CO) present in hydrogen prior to ammonia synthesis. Thus the developed catalysts are mainly optimised for CO and not for CO_2 conversion. To date, commercial catalysts optimized for methanation feeds primarily composed of carbon dioxide are apparently lacking. A number of studies are currently undertaken to characterize CO_2 hydrogenation processes and to develop and optimize catalysts [1,2]. Ni/Al_2O_3 are confirmed to be very active in CO_2 methanation [3,4], the coproduction of CO depends on catalyst loading and pretreatment. The aim of the present study was to investigate activation, catalytic activity and stability of Ni/Al_2O_3 and Ru/Al_2O_3 commercial catalysts.

2 Experimental/methodology

Ni/Al_2O_3 and Ru/Al_2O_3 were purchased from ACTA (Pisa, Italy) and were characterised with XRD, IR, UV-vis, H_2-TPR, FE-SEM before and after reaction.

Catalytic experiments were carried out in a fixed-bed tubular silica glass flow reactor, operating isothermally, loaded with 700 mg of silica glass particles (60-70 mesh sieved) and variable amounts of catalyst. Gaseous mixtures of CO_2 and H_2 (with excess H_2) diluted with nitrogen were fed, 75 ml_{NTP}/min. Temperature was varied step by step in-between 523 K and 773 K and then descending back to 523 K. GHSV was varied in between 15000 and 55000 h^{-1}. Experiments have been performed without any pretreatment ("as received sample") or after a prereduction.

Moreover a series of experiment was done in order to determine the kinetic orders of reactant partial pressures and the possible use of the best catalyst in intermittent conditions.

Products analysis was performed on line using a Nicolet 6700 FT-IR instrument with previous calibration using gas mixtures with known concentrations, in order to have quantitative results. Produced water was partially condensed before the IR cell.

3 Results and discussion

With both catalysts the thermodynamic equilibrium was approached at 723K and 773 K while at lower temperature, where methanation reaction is largely favoured the best catalyst result to be Ru-based one in the descending temperature experiment, where the catalyst appears

to be definitively activated. A simple pre-reduction of this catalysts did not improve low temperature conversion, but the activation was observed on stream. In figure 1 the obtained results at 648 K are reported for the two catalysts under investigation. It is possible to observe that ruthenium takes approximately 100 minutes to reach the steady state value, while Nickel takes only few minutes; even though Ru based catalyst demonstrate better performance after activation procedure without coproducing CO as by-product that was instead present with nickel.

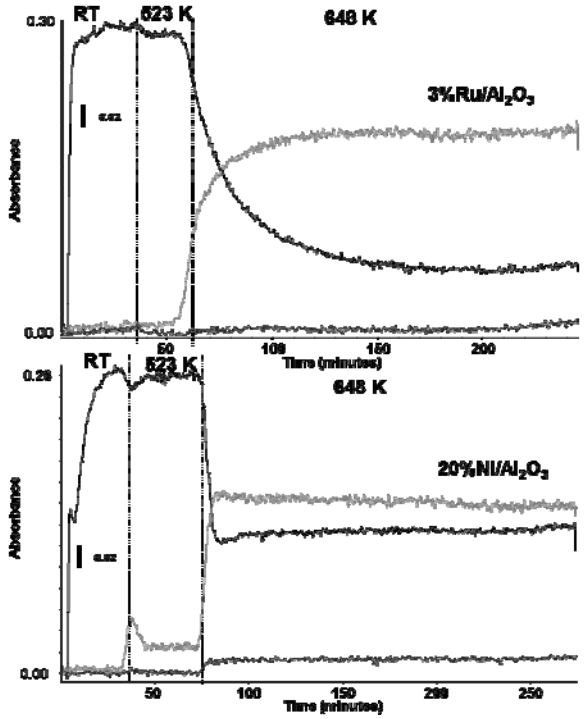

Fig. 1. CO_2, CO and CH_4 absorbances in function of time at RT, at 523 K and 648 K for 3%Ru/Al_2O_3 catalyst (top) and 20%Ni/Al_2O_3 catalyst (bottom) in the following conditions: 6%CO_2, 30% H_2, 64% N_2, 75 Nml/min with a GHSV= 55000 h^{-1}.

4 Conclusions

Both investigated catalysts results to be active for CO_2 methanation in the reported conditions arriving at the displacement of thermodynamic equilibrium at 773 K. Ruthenium based catalysts results to be more active and at 648 K completely selective to methane without any coproduction of CO that was instead evidenced on Ni-based catalyst. 3% Ru/Al_2O_3 is an excellent catalyst for CO_2 methanation, arriving at 96% methane yield with no CO coproduction at 573 K at 30000 h^{-1} GHSV in excess hydrogen. Kinetic orders of reactant partial pressure were successfully determined for both catalysts. To provide optimal activity, Ru/Al_2O_3 catalyst must be conditioned on stream, simple reduction in hydrogen not giving rise to a fully active catalyst. This behaviour suggests that activation implies not only reduction but also other chemical conversion. Ru/Al_2O_3 catalyst was not deactivated after nine cycles thus may be adopted in intermittent condition operations.

References

[1] W. Wang, J. Gong, *Front. Chem. Sci. Eng*. 5 (2011) 2

[2] C. Janke, M.S. Duyar, M. Hoskins, R. Farrauto, *Appl. Catal. B: Eviron*. 152-153 (2014) 184

[3] S. Abelló, C. Berrueco, D. Montané, *Fuel* 113 (2013) 598

[4] G. Garbarino, P. Riani, L. Magistri, G. Busca, *Int. J. Hydr. En.* 39 (2014) 11557

V-OP06

CO_X Hydrogenation on Promoted Iron Based Catalysts: the Key Role of the Potassium on the Process Selectivity

Martinelli M.[1], Falbo L.[1], Visconti C.G.[1*], Lietti L.[1], Forzatti P.[1], Bassano C.[2], Deiana P.[2]

1 - Politecnico di Milano, Dipartimento di Energia, Milan, Italy
2 - ENEA- Italian Agency for New Technologies, Energy and Environment, Rome, Italy

* carlo.visconti@polimi.it

Keywords: carbon, capture, utilization, CO_2 hydrogenation, Fischer-Tropsch, iron catalysts, potassium

1 Introduction

The one-pot catalytic hydrogenation of CO_2 to liquid hydrocarbons is a very attractive process to convert a primary green-house-molecule into added value products. A Fischer-Tropsch like chemistry would be desirable, but only a few information is available in the open literature on the reactivity of CO_2 at high temperature and pressure in the presence of H_2 and of catalysts based on VIII group metals [1-3]. The hydrogenation of CO_2 containing streams over Co-based catalyst has been recently studied by some of us [1]. It has been shown that in absence of co-fed CO, CO_2 is easily hydrogenated to methane and light hydrocarbons, while, in presence of CO, CO_2 behaves as inert specie. On the contrary, we have shown that heavy hydrocarbons can be produced on Fe-based catalysts even starting from CO_2 containing feed-gases [2].

Potassium is well known to improve the long-chain hydrocarbons in CO hydrogenation on Fe-based catalysts. Lee et al. [3] reported a positive effect of potassium also in CO_2 hydrogenation, but they examined catalysts containing K loading as low as 3 at.%. Such loadings are appropriate for converting CO/H_2 mixtures, but no information are available for CO_2 rich feed-gases. In this work, the performances of Fe-based catalysts with different K-loadings were comparatively investigated in presence of $H_2/CO_2/N_2$, $H_2/CO/N_2$ and $H_2/CO/CO_2$ mixtures. A particular attention was devoted to the quantification of paraffins and olefins in the products, because their relative content can give informative indications on the nature of the catalytic surface and on the nature of the ad-species.

2 Experimental/methodology

Following the procedure reported in [4], 100Fe/10Zn catalysts (atomic ratio) were prepared by co-precipitation of ferric and zinc nitrates. The obtained precursor was promoted with Cu and K by adopted the incipient wetness impregnation techniques with copper nitrate and potassium carbonate aqueous solutions. Samples with K/Fe atomic ratios of 0.02, 0.04 and 0.1, named with sample tags "Fe2K" (100Fe/10Zn/1Cu/2K), "Fe4K" (100Fe/10Zn/1Cu/4K) and "Fe10K" (100Fe/10Zn/1Cu/10K) were prepared, characterized and tested.

Activity tests were carried out in a lab-scale fixed-bed reactor operating 24/7. Before starting the activity tests, the catalysts were activated at 270°C for 1h, feeding syngas (H_2/CO = 2). Then, the catalysts were tested for few hundreds hours at the following process conditions: 220°C, 30 barg, 6000 $Ncm^3/h/g_{cat}$, H_2/CO_x inlet molar ratio = 1-3.

3 Results and discussion

As shown in Table 1, for K/Fe atomic ratios between 0.02 and 0.10, potassium has only a slight effect on the CO_2 hydrogenation rate. Also, potassium has minor effect on the selectivity to CO, which shows a weak local minimum for the sample Fe4K, in correspondence to which a local maximum in the CO_2 conversion is observed. On the contrary, as shown in Fig. 1,

potassium shows a strong effect on the distribution of the hydrocarbon products. Upon increasing the K-loading, the chain growth probability (α) grows (from 0.56 to 0.64), as well as the fraction of unsaturated species in the products (from 53.6% to 88.6%).

Table 1. CO, CO_2 and H_2 conversions and CO selectivity during CO_2 and CO/CO_2 hydrogenations.

Sample Tag	Fe2K		Fe4K		Fe10K	
Conditions	$H_2/CO_2/N_2$	$H_2/CO/CO_2$	$H_2/CO_2/N_2$	$H_2/CO/CO_2$	$H_2/CO_2/N_2$	$H_2/CO/CO_2$
χ_{CO} [%]	-	10.3	-	11.2	-	12.7
χ_{CO2} [%]	8.9	2.4	9.3	2.6	7.1	2.5
χ_{H2} [%]	16.1	24.9	19.9	30.3	18.4	33.0
sCO [%]	19.5	-	17.3	-	23.7	-

These results can be explained by attributing to potassium a role in stabilizing/promoting the formation the carbides species on the catalyst surface. Upon increasing the K-loading, more carbides and less metal/oxide sites are available: as a consequence, the chain growth process is more effective, and the fraction of olefins undergoing secondary hydrogenations decreases. In addition to this effect, the presence of higher K-contents weakens H_2 chemisorption, thus making the catalyst less hydrogenating.

On the contrary, in the case of the hydrogenation of CO/CO_2 mixtures, K slightly promotes the CO conversion, while both the CO_2 conversion and the product distribution are substantially unaffected. In this case, indeed, the H* concentration on the surface is intrinsically low because of the strong CO adsorption and carbides are stabilized by the presence of high concentrations of CO in the gas phase. Similar effects were also observed during pure CO hydrogenation tests.

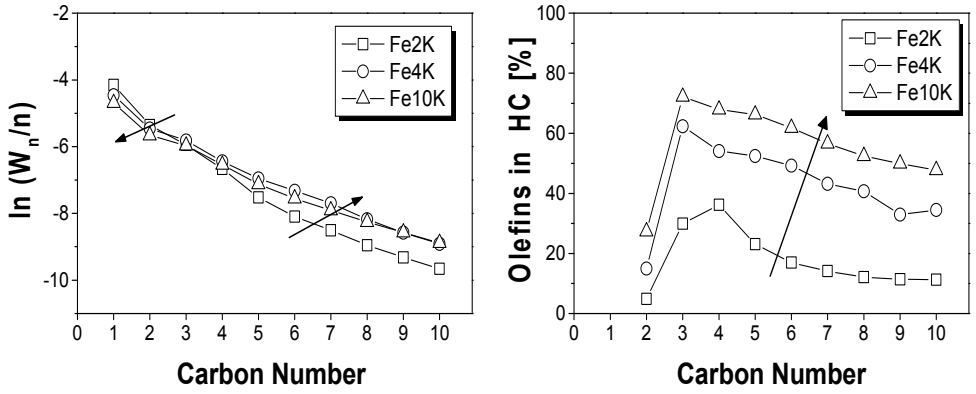

Fig. 1. ASF distribution (left) and fraction of olefins in the products (right) during CO_2 hydrogenation on iron catalysts with different K-loadings (220°C, 30 barg, $H_2/CO_2 = 3$, GHSV = 6000 $Ncm^3/h/g_{cat}$).

4 Conclusions

The presence of potassium dramatically changes the product distribution during CO_2 hydrogenation on Fe-based catalysts. High K-loadings promote the chain growth process and inhibit the secondary reactions of primary olefins. Observed results can be explained in terms of K-effects (i) on the nature of the surface species, (ii) in inhibiting the double-bond shift, and (iii) as electron donor, able to modify the relative adsorption strengths of H_2, CO and CO_2.

Acknowledgements

ENEA (Italy) is gratefully acknowledged for the financial support.

References

[1] C.G. Visconti, L. Lietti, E. Tronconi, P. Forzatti, R. Zennaro, E. Finocchio, *Appl. Catal. A: Gen*. 355 (2009) 61.
[2] T. Riedel, H. Schulz, G. Schaub, K.-W. Jun, J.S. Hwang, K-W. Lee, *Top. in Catal*. 26 (2003) 41.
[3] M.-D. Lee, J-F. Lee, C.-S. Chang, *Bull. Chem Soc. Jpn*. 62 (1989) 2756.
[4] M. Martinelli, C.G. Visconti, L. Lietti, P. Forzatti, C. Bassano, P. Deiana, *Catal. Today* 228 (2014) 77.

V-OP07

Conversion of CO and H_2 to Liquid Hydrocarbons via Dimethyl Ether on Zeolit Catalysts

Ionin I., Bukina Z., Kolesnichenko N.*, Khadzhiev S.

Topchiev Institute of Petrochemical Synthesis RAS (TIPS RAS), Moscow, Russia

- nvk@ips.ac.ru

Keywords: dimethyl ether, liquid hydrocarbons, modified zeolites

1 Introduction

Russia takes a special place with regard to the natural gas stocks (NG) and volumes of its extraction. Chemical processing of natural gas offers the prospects of a step-by-step transition from raw materials export to the export of products of deeper processing that will provide powerful start to the development of domestic innovative economy. The synthesis of hydrocarbons via intermediate conversion of methane in synthesis gas (syngas) is more attractive. The syngas can be converted into hydrocarbons via methanol and/or dimethyl ether (DME) on zeolites (Fig. 1). Zeolites have structure and space-regular cannel system and cavities with severely defined diameters and represent ideal matrix for stabilization of catalytically active sites. High termic and chemical stability of zeolites allow obtaining functional materials which can efficiently work under unfavorable conditions such as higher temperature and corrosive medium.

2 Experimental/methodology

The dates, obtaining in the field of creation of new processes of liquid hydrocarbons production with use zeolite catalysts (ZSM-5 with $SiO_2/Al_2O_3 \geq 30$) generalized in the present work. Catalysts were modified by metals II and VIII groups of periodic system [1,2]. Experiments of catalytic transformation DME to gasoline (DTG) were carried out in the fix bed reactor flow-circulation type at pressure range 5-10 MPa and temperature 340-370 °C, weight velocity for DME ≥2 h-1.

n- Results and discussion

The liquid hydrocarbons are the major products of DME conversion on catalyst modified by metals VIII group of periodic system at pressure 5-10 MPa. Composition of liquid products represents a wide range of hydrocarbons from C_4 to C_{12} (table 1). With comparison Mobil process the liquid hydrocarbons contain small quantity of aromatics.

Depending on the process conditions can be obtained as high-octane gasoline (octane number ≥90, benzene is not present, the durene ≤1 wt.%), and the mixture of hydrocarbons with a low aromatic content (in wt.%: iso-paraffins ≥69, aromatic hydrocarbons ≤7,5, including durene <1), which is essentially analogous to a light synthetic oil, which can be used as a product of processing of associated petroleum gas (APG) for injection into the pipeline. Selectivity is more than 75%.

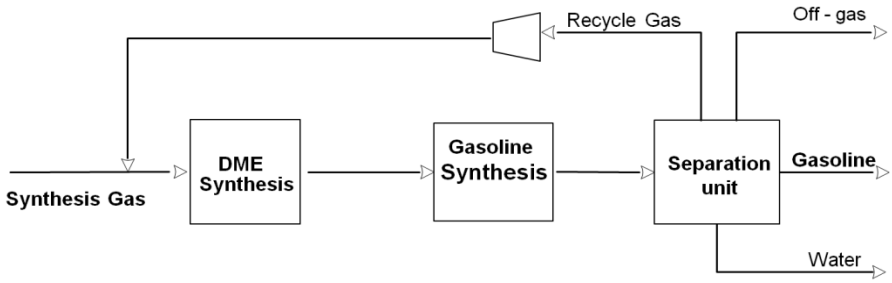

Fig. 1. Conversion of CO and H_2 via dimethyl ether to liquid hydrocarbons

For this process the composition of the catalyst was optimized with further modification of the zeolite matrix by lanthanum. Modification of the zeolite with a high content of lanthanum cations was carried out in an autoclave at a temperature of 220°C and pressure of water vapor (2Mpa). Under these conditions, ion exchange in zeolites undergo in the whole volume of zeolite crystals [3,4].

A study of stable run of catalyst showes, that catalyst activity after 100 hours does not change. Run time of DTG catalyst more than 700 hours.

Table 1. Composition of gasoline produced by Mobil and TIPS RAS

Composition, wt.%	Mobil	TIPS RAS	
		type I	type II
i- paraffin's	51	60	73
n- paraffin's		7	6
naphthenes	7	8	11
aromatics	38	25	≤ 8

4 Conclusions

TIPS RAS has developed the technology of highly selective preparation of the gasoline range hydrocarbons from CO and H_2 via oxygenates (DME and methanol) which is an analog process to the one of TIGAS by Haldor Topsoe company, which uses synthesis gas with the ratio of $H_2/CO = 1$. Advantage of the method developed in TIPS RAS is ability to use the synthesis gas of practically any composition with achievement of high conversion of synthesis gas for pass, thereby reducing the flow of the recycle gas, thus reducing capital costs.

The benefits of this technology can also be attributed to flexibility in orientation to the final product with respect to the characteristics and needs of a particular oil field in certain processed products based on their consumption on the premises and transport possibilities.

References

[1] RU Patent 2442650. 2010.
[2] RU Patent 2442767. 2010.
[3] RU Patent 2070829. 1996
[4] L.Kitaev, Z. Bukina, V. Yushchenko, D. Ionin, N. Kolesnichenko, S. Khadzhiev. *Russian Journal of Physical Chemistry A.* Vol. 88. 3 (2014). 381.

V-OP08

Performing Industrial Scale Steam Reforming of CO_2-Rich Gas

Mortensen P.M.*, Dybkjær I.

Haldor Topsoe A/S, Kgs. Lyngby, Denmark

* pmor@topsoe.dk

Keywords: carbon formation, CO_2-reforming, dry reforming, industrial scale

1 Introduction

Synthesis gas production is one of the largest industries in the world with its development stemming back from 1930 [1]. Important bulk chemicals as hydrogen, ammonia, and methanol are produced on the basis of this. Reforming of methane with mixtures of steam and carbon dioxide (in the following referred to as CO_2-reforming) or with carbon dioxide alone ("dry methane reforming", DMR) is receiving much attention as it in theory offers a way of using CO_2, which in many industries is considered as a waste product and environmentally is considered as a polluting greenhouse gas. CO_2-reforming also offers a direct route to production of synthesis gas with a relatively low H_2/CO ratio (in the order of 1 or lower), which is suitable for production of CO rich gas required for, e.g., higher alcohol synthesis or acetic acid [2].

One of the primary tasks in the development of CO_2-reforming or DMR is to find operating conditions in combination with a suitable catalyst to avoid carbon formation. Nickel, cobalt, and noble metal catalysts have been tested as catalyst for CO_2-reforming, with nickel being the most investigated system, as this is the conventional choice in steam methane reforming (SMR) and a relatively cheap catalyst in comparison to noble metals [2].

Haldor Topsoe A/S has many years of experience in reforming. The first startup of a steam reformer designed by Haldor Topsoe A/S dates back to 1956. In the current work, our experience within the field of CO_2-reforming and DMR is summarized, giving the scientific background for the development and explaining how this has been bridged to industrial scale plants [3].

2 CO_2-reforming: from laboratory development to industrial scale

CO_2-reforming and DMR are closely related to steam methane reforming (SMR), and reaction mechanism and kinetics are comparable in the two reactions [3]. This implies that much of the knowledge developed in the field of SMR can be applied on CO_2-reforming as well. Thus, catalysts for CO_2-reforming can be found from already developed SMR catalysts. The primary challenge of CO_2-reforming is carbon formation, as the low H/C ratio of the feed implies that a high potential for carbon formation exists. The primary focus in the development of CO_2-reforming and DMR has therefore also been on the development of catalysts resistant to carbon formation.

A typical industrial scale reforming process will operate at around 30 barg. A mixture of CH_4, CO_2, and H_2O will be fed to a tubular-like reactor at a temperature of ca. 400°C and then heated to an exit temperature of ca. 900°C in order to achieve sufficient conversion of the endothermic reforming reactions. A general tool in designing a SMR, DMR, or CO_2-reforming process, is evaluating the thermodynamics and in this way develop the limits for carbon formation. This will be dependent on operating conditions, but also the catalyst. The limits for carbon formation can be illustrated in a Tøttrup diagram as shown in Figure 1. This shows the severity of operation for a specific gas composition evaluated on the basis of the O/C and H/C ratios of the gas (or the inlet H_2O/CH_4 and CO_2/CH_4 ratios).

Nickel based catalysts, as the general choice for reforming, is prone to carbon formation, which gives some restrictions on the application of this type of catalyst. Industrial scale references of CO_2 reforming with nickel catalysts are illustrated in Figure 1 as the green points.

High fractions of CO_2 have been processed, but this has been accompanied by a high fraction of H_2O in the feed as well as to decrease the severity for carbon formation.

As alternative to the traditional nickel catalyst, the SPARG (Sulphur PAssivated ReforminG) process has been used to perform CO_2 reforming at much more severe conditions with high content of CO_2 and low co-feed of water (see orange points in Figure 1). In this concept, a small co-feed of sulphur is used to partly passivate a nickel catalyst which markedly reduces the potential for carbon formation.

The last process demonstrated in industrial scale is use of a noble metal catalyst. This lowers the affinity for carbon formation significantly compared to Ni and therefore makes reforming possible on much more severe conditions, illustrated by the blue points in Figure 1.

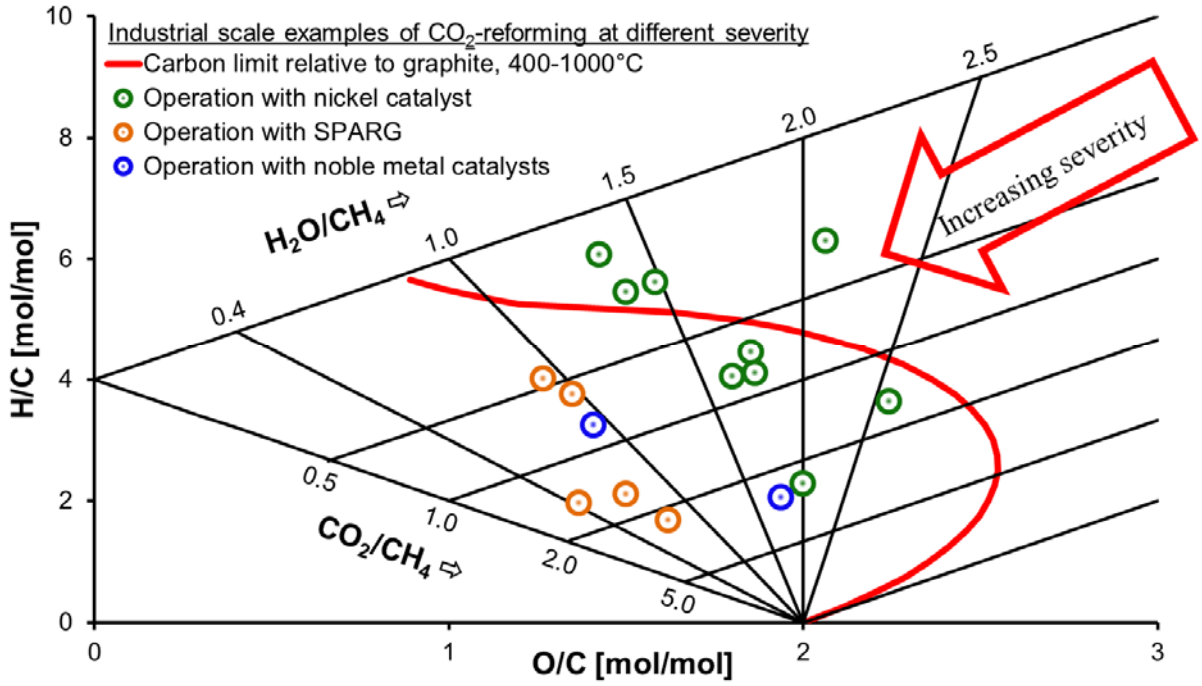

Fig. 1. Tøttrup diagram illustrating the carbon limit with respect to graphitic carbon relative to the O/C and H/C ratio of the gas at 400-1000°C and 25 bar. The O/C and H/C ratio can be translated to inlet conditions of H_2O/CH_4 and CO_2/CH_4 as also shown. Points represent industrial scale references. Green: Nickel catalyst references, Orange: SPARG references, Blue: Noble metal catalyst references.

3 Conclusions

Much work has been done to understand the limits for carbon formation during reforming. These limits are especially challenged when performing CO_2-reforming or DMR. A nickel based catalyst is the industrially preferred catalyst and this has been successfully used for CO_2 reforming as long as a sufficient co-feed of H_2O is present to balance the severity of the gas. Pushing the boundaries further has been done by using the SPARG process approach or noble metal catalysts. This is a clear example of how laboratory work performed to understand the reactions has been bridged to industrial scale.

References

[1] J.R. Rostrup-Nielsen, *Stud. Surf. Sci. Catal.* 147 (2004) 121.
[2] J.R. Rostrup-Nielsen, L.J. Christiansen, Concepts in syngas manufacture, Imperial College Press, (2011)
[3] P.M. Mortensen, I. Dybkjær, *Submitted to Appl. Catal. A. Gen.* (2015)

V-OP09

Methanol Synthesis from Steel Mill Gases

Bukhtiyarova M.[1*], Schlögl R.[1,2]

1 - MPI for Chemical Energy Conversion, Mülheim a.d. Ruhr, Germany
2 - Fritz Haber Institute of MPG, Berlin, Germany

* Marina.Bukhtiyarova@cec.mpg.de

Keywords: methanol synthesis, benzene, catalyst, stability

1 Introduction

The green-house effect is caused by the release of carbon dioxide into the atmosphere from different power and chemical plants [2]. Conversion of CO_2 to methanol by catalytic hydrogenation is recognized as one of the most promising processes to stabilize the atmospheric CO_2 level because of a potentially large demand for methanol as both a fuel and a basic chemical. The methanol synthesis is the way to store electrocatalytically produced hydrogen using fluctuatingly appearing renewable energy [1].

The emitted gases from steel mill can be used for methanol synthesis. As main components the gases contain CO, CO_2, H_2 and N_2 which are gas feed mixture for methanol synthesis. However, the steel mill gases are contaminated by different impurities: N- and S-compounds, polycyclic aromatic hydrocarbons, BTEXs and metals. To understand which impurities should be removed from gas mixture it is necessary to measure their influence on catalytic performance. There is practically no information about influence of BTEX and PAHs in literature. At the first set of experiment we studied the catalytic properties using the gas feed containing benzene as impurity.

2 Catalytic test

Methanol synthesis is performed over a Clariant industrial catalyst. The setup is equipped with liquid storage vessel to collect methanol-water mixture. The temperature of vessel was kept at 5°C to condense the liquid products. The concentration of methanol is measured by gas chromatography-mass spectrometry.

The methanol synthesis is carried out using different gas compositions such as synthesis gas (H_2/CO/CO_2), H_2:CO_2 = 3:1, H_2/CO_2/(500 ppm C_6H_6 in N_2), . This is done to understand how feed gas mixture influence on catalytic behaviour of the industrial catalyst. Catalyst testing is performed at the temperature range of 190 – 260°C and pressure of 15 – 30 bars.

3 Results and discussion

There is discussion about the origin of the carbon atom in methanol in literature: carbon monoxide or carbon dioxide. The early works report that the main source of carbon in methanol molecule is carbon monoxide [3]. However, later on researchers found by different experiments (isotopic labelling of CO_2 [4] or varying the concentration of CO and CO_2 in the feed [5]) that the origin of the carbon atom is CO_2 when the methanol synthesis is performed over Zn-containing catalyst.

The first set of measurement was carried out with H_2/CO_2 = 3:1 molar ratio at different temperatures, pressure of 30 bar and space velocity of 4800 h^{-1}. It was shown that CO_2 conversion and methanol yield increase with temperature since the reaction rate is higher at higher temperature. However, selectivity to methanol decreases (Fig.1), that can be explained by two competitive reactions: methanol synthesis ($CO_2 + 3H_2 = CH_3OH + H_2O$, ΔH = -49,7 kJ/mol) and reverse water gas shift reaction ($CO_2 + H_2 = CO + H_2O$, ΔH = 41,2 kJ/mol). These

two reactions have different thermal effects, high temperature results in higher contribution of reverse water gas shift reaction and production higher CO amount.

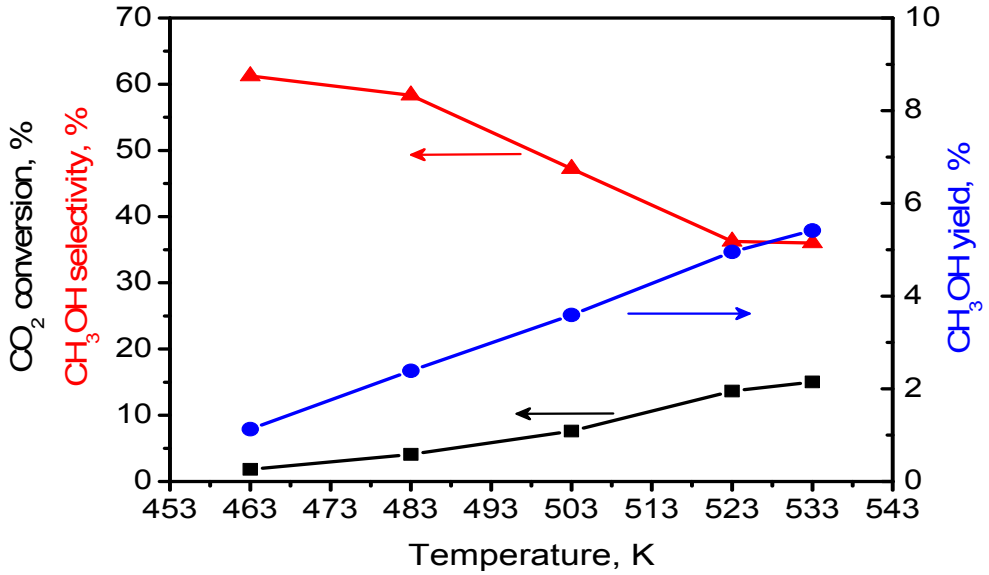

Figure 1. Catalytic performance of industrial catalyst at 30 bars and 4800 h^{-1}

The stability test with benzene in the feed gas was done at 250°C, 15 bars and 4800 h^{-1} for 250 hours. The methanol rate of ~0.27 – 0.30 kg/(kg_{cat}*h) practically does not change during the experiment, that confirms stability of the catalyst at the chosen reaction conditions. The TEM images showed the formation of carbon layer on the copper particles. It is worth to note that toluene also was detected as by-product of reaction. It can be caused by reaction of benzene with carbon-containing molecule following by toluene formation. The methanol synthesis with benzene impurities is done at temperature range of 190 – 260°C to understand which reaction conditions can be critical for using gas containing aromatic compounds.

4 Conclusions

The methanol synthesis performance depends on reaction conditions such as gas feed, temperature, space velocity and pressure. The low temperature and high pressure are preferable for high methanol selectivity and methanol yield. The presence of benzene impurities in the gas mixture does not change catalytic activity with time-on-stream; the catalyst is stable under the reaction conditions.

References

[1] S. Chunshan, Catal. Today 115 (2006) 2;
[2] M. Turco, G. Bagnasco, C. Cammarano, P. Senese, U. Constantino, M. Sisani, Appl. Catal. B 77 (d2007) 146;
[3] K. Klier, J. Catal. 56 (1979) 407;
[4] G.C. Chinchen, P.J. Denny, D.G. Parker, M.S. Spencer, D.A. Whan, Appl. Catal. 30 (1987) 333.
[5] N. Thomas, E. Kunkes, S. Zander, R. Schlögl, M. Behrens, 2nd International Symposium on Chemistry for Energy Conversion and Storage, 2013

V-OP10

Molybdenum-Based Catalysts for the Biogas Dry Reforming

Gaillard M., Virginie M.*, Khodakov A.

UCCS - Unité de Catalyse et de Chimie du solide - UMR 8181, Villeneuve d'Ascq, France

* Mirella.Virginie@univ-lille1.fr

Keywords: biogas dry reforming, sulfur, molybdenum, promoters, stability

1 Introduction

In the worldwide current energy situation, it is crucial to develop new pathways for renewable energy production. In Europe, methanisation is an alternate way widely implemented because it produces biogas from organic waste digestion. This gas contains CH_4 and CO_2 and the major advantage for the utilization of biogas is the consumption of the two main greenhouse gases for the production of syngas (H_2, CO), which could be industrially attractive for the Fischer-Tropsch process, eventually setting up a promising waste-to-liquids fuel substitute.The major technological challenge for CO_2 reforming of biogas is to develop catalysts, which can tolerate contaminants such as hydrogen sulphide, present as impurity in the above-mentioned biogas.

The nature of the work herein introduced lies in the development and optimization of catalysts enabling the dry reforming of methane (DRM), paying particular attention to the stability of the studied systems in the presence of sulphur. Some attempts have aimed at developing DRM catalysts in order to improve their performance in terms of cocking suppression. To the best of our knowledge, few researchers have reported sulphur resistant catalysts for CO_2 reforming of biogas [1].

In this context, it is of great interest to design a catalyst with the potential to maintain its activity in the presence of sulphur and/or in a sulphided state.It is widely known that molybdenum (Mo) based catalysts exhibit sulphur tolerance, whereas Ni based catalysts are very sensitive to carbon deposition and S-poisoning [2]. This Ni sensitivity leads to an increasing need for Mo-based catalysts in industry.

The goal of this study was to investigate the effects of the sulphidation on the catalytic performance of Mo-based catalysts. Metallic promoters were used to enhance the catalyst thermal stability and help suppressing carbon deposition. The catalysts were characterized by BET, TPR, XRD, Raman spectroscopy and XPS. An attempt was made to elucidate the relation between the catalysts structure and catalytic activity.

2 Experimental/methodology

A set of Mo supported on γ-Al_2O_3 catalysts, promoted with Ni, Ce, Mg, Pb and W has been synthesized (promoter/Mo ratio = 1/10) by an incipient wetness co-impregnation method. The catalysts were calcined at 600°C for 4h.

The catalytic tests of methane dry reforming (DRM) were performed on the catalysts previously reduced overnight under a H_2 flow.The quartz fixed bed reactor (i.d. 1 cm) wasfed with a CH_4:CO_2:N_2=1:1:1.6 mixture with a total flow of 90ml/min (GHSV = 6800 h^{-1}), at a temperature range of 650°C-800°C. To study the influence of sulphur, the Mo catalysts werepreviously exposed to a H_2S/H_2 flow, and then tested in the DRM conditions.

3 Results and discussion

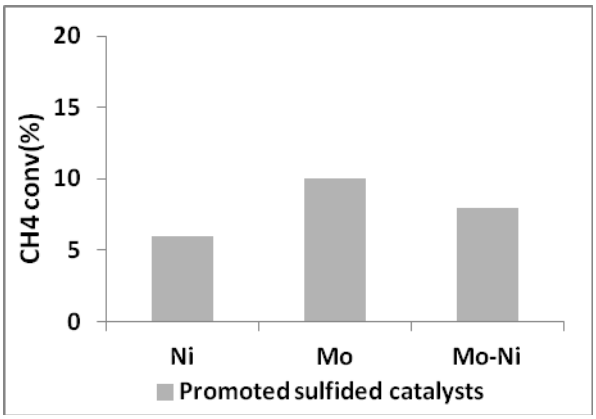

Fig. 1. Methane conversion on nickel and molybdenum sulphite catalysts at 750°C in the presence of sulphur

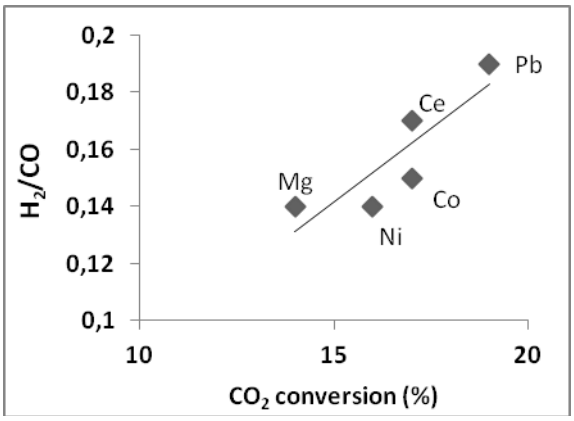

Fig. 2. Influence of the promoter on the RWGS reaction (750°C)

The synthesized then sulphurized catalysts have been tested in DRM in the presence of sulphur (>1%).The results obtained at 750°C, for the Ni reference catalyst, the Mo catalysts alone or promoted with Ni are shown in fig. 1. The sulphided Mo catalyst exhibits twice activity of the Ni catalyst.The Ni, as a promoter of Mo catalyst, does not contribute to increase the catalyst activity. Additionally, TGA was performed on this catalysts and no trace of carbon deposit has been found. Hence, the Mo catalyst presents the benefit of being stable and active without and with presence of sulphur, while the Ni catalyst activity drops drastically.

The fig. 2 displays the H_2/CO ratio obtained in DRM as a function of the CO_2 conversion. The promoters impact on the Reverse Water Gas Shift (RWGS) reaction rate. The Ni favours the hydrogenation reaction and the smallest side reaction ratio is being obtained with Pb promotion, leading to an increase in H_2/CO ratio with the increase in CO_2 conversion.

Moreover, the electronegativity difference between the used promoters and Mo can control the interaction set in the catalyst and therefore the conversions. Yet the catalytic performance is also affected by the Mo dispersion and catalyst reducibility.

4 Conclusions

The Mo catalysts have shown some very promising features for the DRM in the presence of sulphur. They also exhibited higher stability to carbon deposition. The reaction rate and H_2/CO in syngas can be further optimized by efficient use of promoters.Our characterisation results are indicative of strong interaction between the molybdenum and promoters, occurring during catalysts preparation, activation and reaction. .

Acknowledgements

We are grateful to the University of Lille 1 and the Région Nord Pas-de Calais for the funding of this scholarship.

References

[1] T. Osaki, T. Horiuchi, K. Suzuji*, Applied Catalysis A: General*, 155 (1997) 229-238
[2] J. Gao, Z.Hou, H. Lou, « Fuel Cells : Technologies for the Fuel Processing », Dushyant Shekhawat, J. K. Spivey and David A. Berry (Eds) 2011 (Chapter 7)

V-OP11

Stepwise Tuning of Multi-Sites CuZnZr-HZSM5 Catalysts for Direct DME Synthesis from CO_2-H_2 Mixtures

Frusteri F.[1], Bonura G.[1*], Cannilla C.[1], Drago Ferrante G.[1], Aloise A.[2], Catizzone E.[2], Migliori M.[2], Giordano G.[2]

1 - CNR-ITAE, Istituto di Tecnologie Avanzate per l'Energia "Nicola Giordano" , Messina, Italy
2 - Università della Calabria, Dip. Ingegneria per l'Ambiente e il Territorio ed Ingegneria Chimica, Arcavacata di Rende, Italy

* giuseppe.bonura@itae.cnr.it

Keywords: CO_2 hydrogenation, dimethyl ether, Cu-ZnO-ZrO_2 catalysts, zeolites

1 Introduction

In the last years CO_2 hydrogenation into alternative clean fuels, like dimethyl ether (DME), has attracted great interest. DME is characterized by a good profile of combustion (i.e., near-zero smoke, low NOx emissions, …) and a full compatibility with existing infrastructures (transportation and storage facilities as for LPG) or end-users (no modification of the engine required) [1]. Differently from the conventional process in which the DME synthesis by dehydration of methanol (MeOH) represents the second step, the one step production of DME by CO_2 hydrogenation could help to overcome the thermodynamic restriction existing for methanol synthesis, enhancing so the CO_2 conversion [2-4].

In this work the optimization of multifunctional systems, based on the combination of CuZnZr methanol catalysts and HZSM-5 zeolites of different acidity [5,6], is studied. Factors affecting activity, selectivity and productivity of multi-site CuZnZr-zeolite catalysts are discussed. The feasibility of the direct hydrogenation of CO2 to DME, by an integrated catalytic process, is also addressed.

2 Experimental

Three methanol CuZnZr catalysts at different composition were prepared by gel-oxalate coprecipitation method [4] (see Table 1). Their activity was evaluated in the CO_2-to-methanol hydrogenation reaction at 3.0 MPa in the T_R range 180-240°C, using a fixed bed reactor.

Four home-made HZSM-5 zeolites, characterized by different acidity, were prepared by tuning the Si/Al ratio (see Table 2). Catalytic behavior and stability in the presence of water (side-product of reaction) were investigated at atmospheric pressure in the MeOH-to-DME dehydration reaction.

CuZnZr catalysts and HZSM-5 zeolites were combined in different ways: conventional physical mixing or coprecipitation of the methanol precursors in a solution containing zeolite particles finely dispersed. These multifunctional catalysts were tested under the same conditions adopted for methanol synthesis.

3 Results and discussion

Preliminary tests were carried out in CO_2-to-MeOH hydrogenation reaction to find out the best CuZnZr composition suitable to maximize the methanol yield. At 3.0 MPa and 240°C (Tab. 1), all the catalysts exhibited a good activity-selectivity pattern with a similar methanol yield (7-8%). However, a thorough normalization of such data in terms of copper loading pointed out a superior surface functionality of the IT-OX/1 catalyst in CO_2 activation (877 $mol_{CO2}/m^2/h$).

With regard to the catalytic data in the MeOH dehydration reaction, the zeolite with a Si/Al_{bulk} of 38 (UNI-25) showed the best compromise between activity and resistance to the

deactivation of acid sites by water presence (Tab. 2).

At last, a comparison of the performance of multifunctional systems prepared by simple mixing evidenced that there is no need for a great number of acid sites (like in UNIT-25/1-PM) to run the direct CO_2-to-DME hydrogenation reaction with high productivity: a metal-oxide/acid site ratio of 9:1 was enough (see Tab. 3). Furthermore, the generation of a hybrid system by coprecipitation accounts for a superior productivity of DME (*STY*, 0.250 $kg_{DME}/kg_{cat}/h$), as the result of a long-range "homogeneity", both in terms of morphology and sites distribution, due to a better contact among metal-oxide and acid sites.

Table 1. Physico-chemical properties and performances of the CuO–ZnO–ZrO_2 methanol catalysts (T_R, 240°C; P_R, 3.0 MPA, GHSV, 10,000 *N*L kg_{cat}^{-1} h^{-1}; $CO_2/H_2/N_2$, 9/3/1).

Catalyst	Composition [wt.%]			S_{BET}	X_{CO2}	S_{MeOH}	Y_{MeOH}	Surface rate × 10^6
	CuO	ZnO	ZrO_2	[m^2 g^{-1}]	[%]	[%]	[%]	[mol_{CO2} m_{Cu}^{-2} h^{-1}]
IT-OX/1	28.0	28.6	43.4	158	14.7	51.1	7.5	877
IT-OX/3	40.0	13.1	46.9	154	16.3	45.6	7.4	716
IT-OX/6	56.8	27.7	15.5	145	17.9	44.3	7.9	674

Table 2. Physico-chemical properties and performances of the HZSM-5 zeolites (T_R, 200°C; P_R, 0.1 MPA, WHSV, 2 g_{MeOH} g_{cat}^{-1} h^{-1}; MeOH/N_2, 1/21).

Catalyst	Si/Al_{bulk}	S_{BET}	NH_3 uptake	MeOH conversion [%]		Net change of conv.
		[m^2 g^{-1}]	[%]	no water	water 15 vol.%	[%]
UNI-15	27	360	602	60.5	55.1	-8.8
UNI-25	38	365	515	51.1	54.0	+5.5
UNI-50	68	316	354	42.2	40.8	-3.3
UNI-100	127	382	147	22.2	22.3	+0.8

Table 3. Catalytic multifunctional systems CuZnZr-HZSM5 used in direct CO_2-to DME hydrogenation reaction. (Experimental: T_R, 240°C; P_R, 3.0 MPA, GHSV, 10,000 *N*L kg_{cat}^{-1} h^{-1}; $CO_2/H_2/N_2$, 9/3/1).

Catalyst	Preparation method	MeOH cat/zeolite [wt/wt]	X_{CO2} [%]	*STY* (kg_{DME} kg_{cat}^{-1} h^{-1})
UNIT-25/1-PM	physical mixing	1:1	12.8	0.201
UNIT-25/9-PM	physical mixing	9:1	16.4	0.247
UNIT-25/9-OX	coprecipitation	9:1	16.9	0.250

4 Conclusions

Multifunctional CuZnZr-HZSM5 systems resulted to be effective to produce DME by CO_2 hydrogenation in one step. With respect to the conventional physical mixing between methanol catalyst and zeolite, the incorporation of metal-oxide and acid sites in a single system can enhance the CO_2 conversion, also allowing a higher rate of MeOH formation/dehydration on neighbour surface sites.

Acknowledgements

This work was financially supported by Italian Research Fund (PON R&C 2007-2013, PON02_00451_3362376) through the "BIO4BIO" project, Biomolecular and Energy valorization of residual biomass from Agroindustry and Fishing Industry.

References

[1] R. Ahmad, D. Schrempp, S. Behrens, J. Sauer, M. Döring, U. Arnold, *Fuel Process. Technol.* 121 (2014) 38.
[2] G. Bonura, M. Cordaro, L. Spadaro, C. Cannilla, F. Arena, F. Frusteri, *Appl. Catal. B: Environ.* 140–141 (2013) 16.
[3] G. Bonura, M. Cordaro, C. Cannilla, A. Mezzapica, L. Spadaro, F. Arena, F. Frusteri, *Catal. Today* 228 (2014) 51.
[4] F. Frusteri, M. Cordaro, C. Cannilla, G. Bonura, *Appl. Catalysis B: Environ.* 162 (2015) 57.
[5] M. Migliori, E. Catizzone, A. Aloise, G. Giordano, *Ind. Eng. Chem. Res.* 53 (2014) 14885.
[6] M. Migliori, A. Aloise, G. Giordano, *Catal. Today* 227 (2014) 138.

V-OP12

New Fiberglass Based Pt Catalyst for VOC and CVOC Removal

Kovalyov E.V.[1], Suknev A.P.[1], Gulyaeva Yu.K.[1], Zaikovskii V.I.[1,2], Kaichev V.V.[1,2], Bal'zhinimaev B.S.[1*]

1 - Boreskov Institute of Catalysis, Novosibirsk, Russia
2 - Novosibirsk State University, Novosibirsk, Russia

* balzh@catalysis.ru

Keywords: deep, oxidation, VOC, platinum, fiberglass, clusters, SSITKA

1 Introduction

Catalytic abatement of volatile organic compounds (VOCs) is an efficient and environmentally good way to treat these harmful emissions. The catalysts for this process contain a variety of different noble metals, metal oxides and mixtures of those to fulfill the high abatement requirements such as high purification degree, the absence of toxic byproducts (CO, chlorine, phosgene, dioxins) and poison resistance. In spite of a high content of noble metal, Pt/Al_2O_3 is the most active and widely used catalyst. Catalytic performance is known to be determined by the size of Pt nanoparticles. However, the dispersed metal particles tend to beaggregated at high temperatures, thus reducing the catalytic activity. So, the development of active and stable catalyst with a low content of noble metal is a real challenge.

Here, we present the new data on the fiberglass (FG) based Pt catalysts, their preparation and characterization by means of XPS, HRTEM/STEM, UV-Vis DRS, etc., as well as on their high performance in VOC and CVOC (chlorinated VOC) abatement.

2 Experimental/methodology

Commercial leached fiberglass textile modified with 10% Zr was used for catalyst preparation. Platinum was confined in the bulk of glass via ion exchange of protons with a Pt(II) tetramine complex solution. The highly dispersed metal clusters were stabilized in the upper layers of glass fibers by redox treatments at elevated temperatures. Meanwhile, the ratio of metal species located on the external fiber surface to the bulk one was controlled by the heating rate of platinum complexes decomposition, so that in the best catalysts Pt was confined mostly in the bulk. The Pt/FG catalyst where metal is deposited on the external surface of the fiber was prepared using the anionic platinum precursor (H_2PtCl_6). The prepared catalysts were tested in deep oxidation of hydrocarbons (methane, propane, butane, ethylbenzene, etc.) and oxidative destruction of different chlorinated hydrocarbons, including dioxins. The kinetic studies on deep propane oxidation were performed in a flow reactor at wide range of reaction conditions. The SSITKA study using $^{18}O_2$ was carried out in deep oxidation of propane.

3 Results and discussion

Optimization of parameters of the ion exchange process and further redox treatments allowed us to confine a very small 1-1.5 *nm* Pt clusters (Fig. 1A) in the bulk of glass at a depth of 10-20 *nm*. Nevertheless, the reaction rate is not limited by diffusion of the reactants at such a depth. It was shown clearly that the highly dispersed Pt clusters are responsible for activity because the contribution of surface particles to the observed reaction rate at the same platinum content is negligible. Although the Pt content (0.01-0.02% wt.) is 30-60 times lower, the fiberglass catalysts reveal a higher activity in deep oxidation of C_1-C_4 paraffins than traditional/commercial ones. Similar data were obtained in deep oxidation of aromatic

hydrocarbons (Fig. 1B). Basing on the kinetic data for deep oxidation of propane as well as on the dispersion of Pt nanoparticles, we calculated turnover frequencies (TOFs) for fiberglass catalysts and compared with those for Pt supported on alumina and silica. It appeared that TOF of 0.01%Pt/FG is 5-10 times higher in comparison with conventional catalysts. This catalyst revealed high performance in CVOC abatement and did not produce more harmful compounds

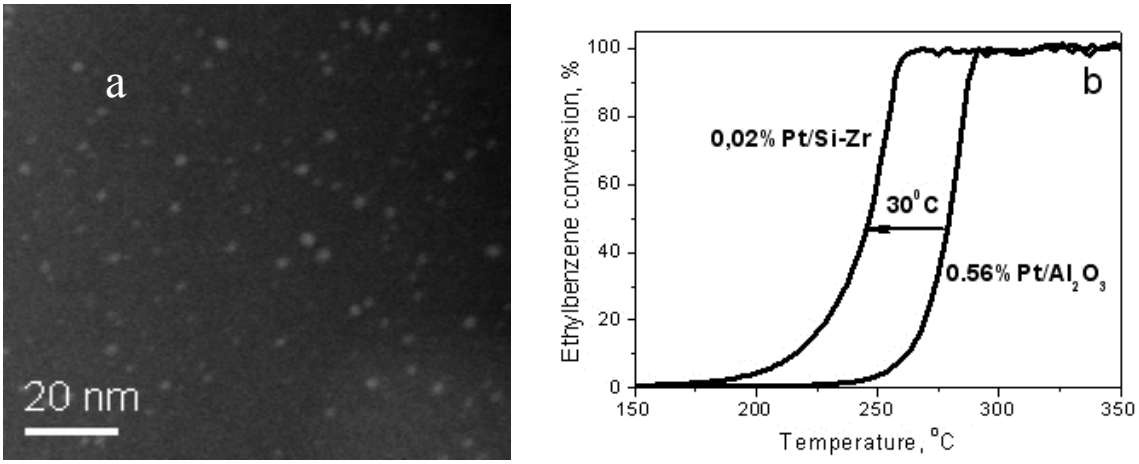

Fig.1.(a) STEM-HAADF image of the 0.01%Pt/FG catalyst; (**b**) deep oxidation of ethylbenzene on the 0.02%Pt/FG-Zr catalyst compared with commercial one. Feed gas: 1.2% C_8H_{10} + 16% O_2 + He, GHSV = 4000 h^{-1}.

like phosgene and dioxines. Moreover, the Pt/FG catalyst demonstrated high efficiency in the destruction of 1,2,3,4-TeCDD (95%), so that the residual concentration did not exceed 0.4 ppb.

To elucidate the reasons of so high specific activity of the 0.01%Pt/FG sample, the SSITKA study with labeled molecular oxygen was performed. The 0.12%Pt/FG catalyst where platinum was located only on the surface of the fiber was used as a reference one because the activity of a similar sample with 0.01%Pt was negligible. Surprisingly, unlike 0.12%Pt/FG, in the case of 0.01%Pt/FG sample the stepwise replacement of $^{16}O_2$ by $^{18}O_2$ in the feed gas did not lead to the formation of mixed $^{16}O^{18}O$ oxygen, while in the reaction product CO_2 the equilibrium distribution between different oxygen isotopic fractions took place. This means that the molecular oxygen species are active in deep oxidation of propane on highly dispersed Pt species located in fiberglass bulk.

High performance of fiberglass based catalysts was successfully demonstrated in the VOC removal from synthetic rubber plant (JSC Nizhnekamskneftekhim, Russia) when the catalyst showed a purification efficiency of 99.9% for more than 4 years of its operation.

4 Conclusions

The highly dispersed 1 *nm* Pt species were stabilized in the bulk of Zr-silicate glass at a depth of 10-20 *nm*. These small Pt clusters showed high performance in both VOC and CVOC abatement. In spite of a very low noble metal content (0.01-0.02%), the Pt/FG catalysts showed a higher activity in comparison with conventional ones containing 30-60 times more platinum. The TOF was 5-10 times higher as compared with the alumina-, or silica-supported Pt catalysts. The SSITKA study showed that molecular oxygen species are active in deep oxidation of hydrocarbons. The high performance of the fiberglass catalyst was successfully confirmed at industrial level.

V-OP13

Synergetic Effect of Pd Addition on Catalytic Behaviour of Monolithic Catalysts for Diesel Vehicle Emission Control

Yashnik S.A.[1*], Danchenko N.M.[2], Ismagilov Z.R.[1,3]

1 - Boreskov Institute of Catalysis, Novosibirsk, Russia
2 - Ural Electrochemical Integrated Plant, Novosibirsk, Russia
3 - Institute of Coal Chemistry and Material Science, Kemerovo, Russia

* yashnik@catalysis.ru

Keywords: diesel, emission control, monolithic catalyst, noble metal, manganese, synergetic effect

1 Introduction

The TWC catalysts for catalytic converter of diesel engines usually contain noble metals – Pt and Pd, which have high catalytic activity in CO and hydrocarbon oxidation. In the last decade there has been a trend of progressive alteration of the preferred loadings of Pt or Pd, depending mostly on dynamics of market-value of these metals. The catalytic systems with a low noble metal (Pt, Pd, Rh) content and their combination with transition metal oxides are shown to be attractive option for TWC perfecting, especially for close-coupled converters operated at high temperatures [1,2]. There is a great number of data on non-additive increase of catalytic activity of noble metals combination with transition metal oxides in the oxidation of carbon monoxide and hydrocarbons [2-7].

We early demonstrated synergetic effect of Pt and manganese oxides which allows decreasing the Pt loading to 0.7-1.05 g/L in the catalytic system for diesel engine exhaust treatment [7], but such Pt loading is enough high. Here, we are reporting our systematic study of the effect of Pd addition into Pt-MnO_x-Al_2O_3 monolithic catalysts on their catalytic activity and stability in hydrocarbon and CO oxidation. We are discussing also Redox properties, particles size and morphology, and interaction of nanoscale Pt/Pd particles with Mn-modified alumina in order to explain a positive effect of Pd on catalytic behaviour of Pt-Mn-alumina catalyst.

2 Experimental

The PdPt/MnO_x-Al_2O_3 catalysts have been prepared by wetness impregnation of cordierite monolithic substrate (400 cpsi) preliminarily washcoated by MnO_x-Al_2O_3 with solutions of Pt and Pd precursors, and subsequent treatment at 600°C. The catalyst preparation approach emphasized variation of a Pd precursor (H_2PdCl_4, $Pd(CH_3COO)_2$, $Pd(NO_3)_2$ and $Pd(NH_3)_4(NO_3)_2$), total Pd-Pt loading (0-0.70 g/L or 0-0.11 wt.%) and Pd/Pt ratio.

Catalytic activity of the initial and aged samples was tested in DIESEL test runs with a mixture of propane/propene (100/200 ppm), CO (1900 ppm), NO (300 ppm), O_2 (14.6 vol.%), CO_2 (2.5 vol%), H_2O (3.9 vol%), and N_2 (balance) at 67000 h^{-1}, in two heating/cooling cycle. The catalyst aging was carried out at 750°C in flow of dry or wet air.

Redox properties of the initial and aged Pt-MnO_x/Al_2O_3 and PdPt-MnO_x/Al_2O_3 catalysts were studied by TPR-H_2, size and nanostructure of active particles – by HRTEM and CO-chemosorption, the interaction of Pt/Pd with MnO_x and Al_2O_3 – by the chemical differentiating dissolution.

3 Results and discussion

In the DIESEL test the activity of washcoated Pt-MnOx-Al_2O_3 monoliths with Pt loading 0.17 g/L greatly increases by addition of Pd. The catalytic activity of the PdPt-MnOx-Al_2O_3 increases with Pd loading, which is characterized by a decrease of the temperature of 50%

conversion of HC and CO (Fig.). The light-off temperature for the PtPd-MnO_x-Al_2O_3 monolith with total noble metal loading 0.52g/l is lower when the atomic Pt/Pd ratio is higher. The sample containing 0.17gPt/L – 0.35gPd/L prepared using $Pt(NH_3)_2(NO_2)_2$ and $Pd(NO_3)_2$ is more active in the reaction of HC and CO oxidation than the samples prepared using H_2PtCl_6 and H_2PdCl_4.

Important to note that the bimetallic PdPt-Mn-Al_2O_3 catalysts are characterized by synergetic effect in catalytic activity. For example, catalytic activity of Pd(0.35)Pt(0.17)-Mn-Al_2O_3 is higher than the sum of the activities of 0.17 g/L of Pt and 0.35 g/L of Pd catalysts. At the same loading of noble metals the bimetallic PdPt-MnO_x-Al_2O_3 catalysts are more thermostable than the monometallic Pt-MnO_x-Al_2O_3 and Pd-MnO_x-Al_2O_3 monoliths.

The catalytic activity in light hydrocarbon oxidation is shown to correlate with RedOx properties of PdPt-MnO_x/Al_2O_3 catalysts and Pt-Pd particles size. The non-additive increase of catalytic activity of bimetallic catalyst is suggested to connect with a formation of nanoscale PdO-PtO_x particles on surface of Mn_3O_4 and a modification of alumina structure by Mn^{3+} and Pt(Pd)-cations.

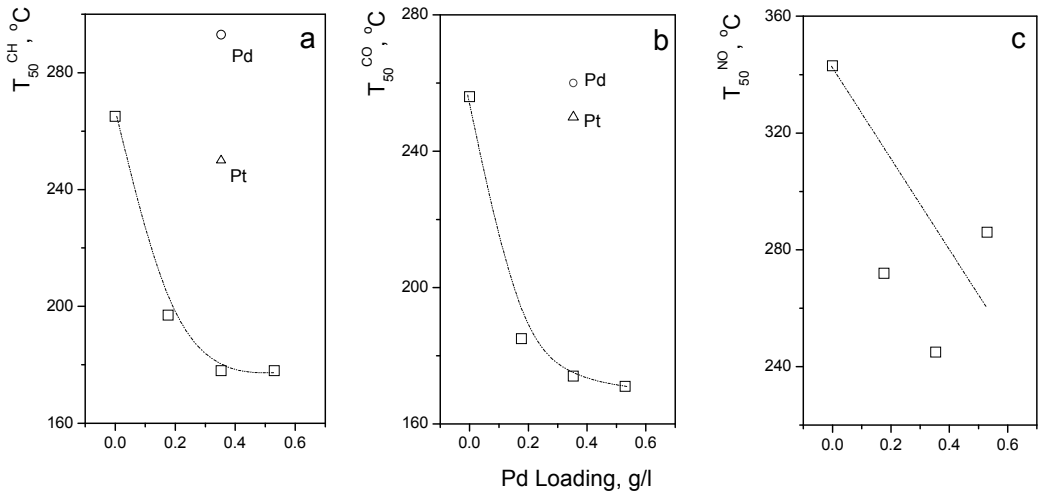

Figure. Temperature of 50% conversion of CH (T_{50CH}, °C) and CO (T_{50CO}, °C) and NO conversion at 400°C (X_{NO}, %) for monolithic catalysts prepared using $Pt(NH_3)_2(NO_2)_2$ (0.17 g/L) and $Pd(NO_3)_2$ vs Pd loading. The catalysts have been aged at 750°C in dry air.

4 Conclusions

Advantages of the synergetic effects of Pt, Pd and manganese oxides observed in the light hydrocarbon oxidation resulted in the development of the new diesel exhaust catalyst with a Pt loading as low as 0.17 g/L instead of traditional amount of 1.0-1.2g/L at the Pd loading of 0.35 g/L. The PtPd-MnO_x-Al_2O_3 catalyst has high activity in low temperature oxidation of light hydrocarbons and high thermal stability.

Acknowledgements

The work is supported by Federal Agency of Scientific Organizations (V46.5.6.).

References

[1] R.M.Heck, R.J.Farrauto. Catalytic air pollution control. Commercial Technology. New York, VNR, 1995, P.206.
[2] S.A. Yashnik, V.V. Kuznetsov, Z.R. Ismagilov, *Topics in Catal.*, 30/31 (2004) 293.
[3] J. Carno, M. Ferrandon, E.Bjornbom, S. Jaras, *Appl. Catal., A* 155 (1997) 265.
[4] M. Ferrandon, J. Carno, S. Jaras, E. Bjornbom, *Appl.Catal., A* 180 (1999) 141.
[5] Y.J. Mergler, J. Hoebink, B.E. Nieuwenhuys, *J.Catal.*, 167 (1997) 305.
[6] B.E. Nieuwenhuys, *Adv.Catal*. 44 (1999) 259.
[7] S.A. Yashnik, Z.R. Ismagilov, A.V. Porsin, et. al., *Topics in Catal*. 42-43 (2007) 465.

V-OP14

Propane Oxidation over Pd/Al_2O_3: Selectivity, Activity and Size Effect

Khudorozhkov A.K.[1,2*], Prosvirin I.P.[1,2], Chetyrin I.A.[1,2], Bukhtiyarov V.I.[1,2]

1 - Boreskov Institute of Catalysis SB RAS, Novosibirsk, Russia
2 - Novosibirsk State University, Novosibirsk, Russia

* hak@catalysis.ru

Keywords: propane oxidation, size effect, selectivity, selective oxidation

1 Introduction

Precious metal supported catalysts are widely used as catalytic converters of automotive engines exhaust. The efficiency of catalytic converter is strongly depends on the activity, stability and selectivity of supported metal in CH_x and CO oxidation reactions. The reaction conditions, such as the temperature and concentrations of exhaust components, also can change the catalyst behavior. Identification of factors changing the catalytic properties of the active component can help one to create the most efficient catalytic converter, which would provide total hydrocarbons and carbon monoxide oxidation at various exhaust composition and temperature.

The aim of this work was to reveal the correlations between the palladium particles dispersion in $Pd/\gamma\text{-}Al_2O_3$ catalysts and its activity, stability and selectivity towards propane oxidation at different temperatures and C_3H_8:O_2 ratios

2 Experimental/methodology

Three $Pd/\gamma\text{-}Al_2O_3$ catalysts with different palladium particles sizes (2, 5 and 11 nm, next denoted as Pd2, Pd5 and Pd11, respectively) were prepared via wet impregnation and subsequent calcination of support ($\gamma\text{-}Al_2O_3$, Sasol, S_{BET}=215 m^2/g). $Pd(NO_3)_2$ aqueous solution was used as the precursor. Catalyst samples than were tested in propane oxidation reaction at different temperatures (350, 400, 450 °C) and C_3H_8:O_2 ratios (1:1, 1:5, 1:15) in continuous stirred-tank flow reactor. TOF values were used as the measure of catalytic activity. Palladium dispersion was determined by XRD, TEM and CO chemisorption methods, whereas Pd charge state and the catalyst surface composition were determined by XPS technique.

3 Results and discussion

It was shown that TOF values increased with palladium particles size in total propane oxidation reaction. Moreover, the difference between the activities of high and low dispersed catalysts increases with temperature (see Fig. 1). It was also shown that at higher temperatures the increase of C_3H_8:O_2 ratio lead to the change of reaction path from total oxidation to steam conversion of propane. The selectivity towards CO formation in the steam conversion reaction decreased with palladium particles dispersion.

XPS in-situ studies revealed that Pd^{2+}/Pd^0 ratios increase with particles size. Thus, it is believed that the Pd/Al_2O_3 catalyst activity, stability and selectivity in propane oxidation reaction strongly depends on the relative concentrations of Pd^{2+} and Pd^0, which, in turn, can be controlled by the catalyst preparation technique, reaction temperature and CH_x:O_2 ratio in inlet gaseous mixture.

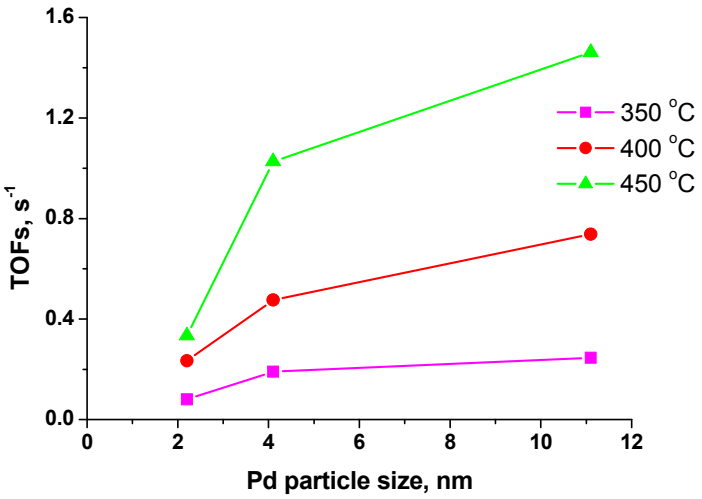

Fig. 1. Size effect for Pd/Al_2O_3 catalysts in total propane oxidation (C_3H_8:O_2=1:15) reaction at different temperatures

4 Conclusions

A series of Pd/Al_2O_3 catalysts with different palladium particles size were studied in propane oxidation reaction with varying the C_3H_8:O_2 ratios and the temperature of inlet gaseous mixture. It was shown that in propane-rich mixtures the change of reaction path from total oxidation to steam conversion occurred. Negative size effect was revealed for total propane oxidation reaction. Catalytic properties of supported palladium are strongly depend on Pd^{2+} and Pd^0 relative concentrations, which in turn can be the function of reaction temperature and CH_x:O_2 ratio in the inlet gaseous mixture.

Acknowledgements

Financial support of this work was provided by the Russian Science Foundation (grant 14-23-00146).

V-OP15

Methane Oxidation over Palladium: on the Mechanism in Rich Methane-Oxygen Mixtures at High Temperatures

Stotz H.[1], Maier L.[2], Deutschmann O.[1,2*]

1 - Institute for Chemical Technology and Polymer Chemistry, Karlsruhe Institute of Technology (KIT), Karlsruhe, Germany

2 - Institute for Catalysis Research and Technology, Karlsruhe Institute of Technology (KIT), Karlsruhe, Germany

* deutschmann@kit.edu

Keywords: methane oxidation, palladium, detailed kinetics, *in-situ* sampling, catalytic partial oxidation

1 Introduction

Palladium-based catalysts are widely used in emission control systems for gas-engines to avoid methane slip. Methane oxidation can proceed over oxidized and reduced palladium, making it difficult to separate both the kinetic processes occurring on the active phases.

As first steps towards a detailed kinetic scheme of the methane oxidation over palladium this work focus on the development of the surface reaction kinetics for the catalytic partial and total oxidation under conditions where reduced palladium is the only active phase present. We present a surface reaction mechanism evaluated by comparison of simulated species profiles in a catalyst channel with experimentally obtained axially resolved species concentration profiles by in-situ sampling within a commercial Pd/Al_2O_3 coated cordierite honeycomb monolith.

2 Kinetic Model and Numerical Simulation

Numerical simulations of the steady-state species concentrations profiles in a catalyst channel were performed using DETCHEM^{CHANNEL} [1]. Axial wall-temperature profiles of the center channel from in-situ measurements were provided for the calculation. The model assumes cylindrical symmetry and solves the two-dimensional steady-state flow field using the boundary-layer approximation. Chemical source terms in the washcoat are calculated via the effectiveness factor model in order to account for internal pore transport limitations. Detailed heterogeneous reaction kinetics were developed using the mean-field approximation, including 6 gas-phase species (CH_4, O_2, CO, CO_2, H_2, H_2O) and 11 surface intermediates (CH_4*, CH_3*, CH_2*, CH*, C*, O*, OH*, CO*, CO_2*, H*, H_2O*). Kinetic parameters of 20 reversible elementary steps were derived from transition-state theory and semi-empirical methods for a Pd(111) surface in the limit of zero coverage. Selected steps were corrected for coverage dependent activation energies. The newly formulated surface reaction kinetics obeys thermodynamic consistency.

Since the reaction mechanism is based on elementary molecular steps, it presents all the global processes in the CH_4/O_2 mixture over palladium catalyst, including (i) partial oxidation and/or (ii) steam reforming of methane to syngas; (iii) methane combustion; (iv) water-gas-shift reaction; (v) surface carbon formation. The mechanism includes a pyrolytic and an oxygen-assisted path to activate methane on the Pd surface. Although atomic adsorbed oxygen O* is the key species of the mechanism, it does not consider a bulk-phase oxidation of Pd.

3 Experiments

Experimental profiles for different carbon-to-oxygen ratios between 0.9 and 1.0 were measured using in-situ sampling technique within a Pd/Al_2O_3 coated monolithic honeycomb catalyst. The gas composition at various axial positions inside a center channel of the monolith was analyzed using FT-IR, MS, and GC/MS, respectively [2].

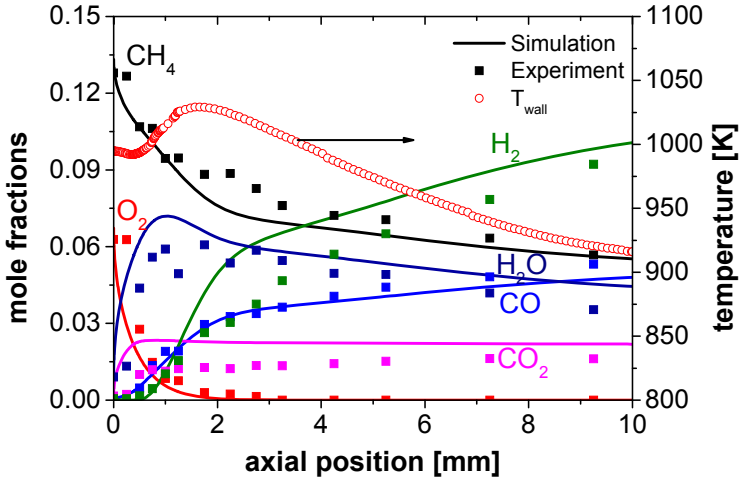

Fig. 1 Comparison of simulated and experimental species [2]and wall-temperature profiles within the catalytic section at 4 slpm and a measured catalyst inlet C/O-ratio of 0.94.

4 Results and Discussion

Figure 1 shows measured wall-temperature and species concentration profiles compared with the simulated profiles. Methane first undergoes total oxidation within a small 0.5 mm zone, right at the entrance of the catalyst, the partial oxidation products, H_2 and CO, are not observed. At the end of the total oxidation zone at 0.5 mm, most of the oxygen is converted. Further downstream (0.5-3.3 mm) an extended oxy-reforming zone is found, where CH_4 is consumed by combined total and partial oxidation as well as steam reforming. After consumption of all oxygen at axial positions > 3.3 mm, steam reforming of CH_4 is the preferred conversion path, leading to a prolonged consumption of CH_4 and a simultaneous decrease in H_2O concentrations. This observation is supported by the fact that CO and H_2 show a further increase in concentration, while the CO_2 signal remains constant.

5 Conclusion

The indirect formation of synthesis gas is the preferred route for partial oxidation of methane. The developed multi-step surface reaction kinetics on reduced palladium, predicts all features of the experimental spatially-resolved species profiles. Additional experiments are recommended to clarify the oxidation state of Pd in operando, in particular in the entrance zone of the catalyst.

Acknowledgements

Financial support by the Helmholtz Research School Energy-Related Catalysis is gratefully acknowledged.

References

[1] O. Deutschmann, S. Tischer, S. Kleditzsch, V. M. Janardhanan, C. Correa, D. Chatterjee, N. Mladenov, H. D. Minh, H. Karadeniz, M. Hettel, DETCHEM Software package, Karlsruhe, Germany, 2014.

[2] C. Diehm, O. Deutschmann, International Journal of Hydrogen Energy 39 (2014) 17998–18004.

V-OP16

Hierarchical Pd/ZSM-5 Catalysts for Methane Oxidation in the Presence of Steam

Petrov A.W.[1,2*], Ferri D.[1], Van Bokhoven J.A.[1,2], Kröcher O.[1,3]

1 - Paul Scherrer Institut, Villigen, Switzerland
2 - ETH Zürich, Department of Chemistry and Applied Biosciences, Zürich, Switzerland
3 - EPF Lausanne, Institute of Chemical Sciences and Engineering, Lausanne, Switzerland

* andrey.petrov@psi.ch

Keywords: catalytic methane oxidation, hierarchical ZSM-5, palladium

1 Introduction

Catalytic methane oxidation is applied in exhaust gas treatment to reduce unburnt methane emissions in stationary combustion processes as well as in natural gas vehicles to mitigate the severe greenhouse effect of methane [1]. Pd is the precious metal of choice for methane oxidation. Several supports for Pd-based catalysts are reported to provide higher activity than the commonly used Al_2O_3, e.g. CeO_2, SnO_2, ZrO_2 or zeolites [2,3,4]. The latter material is advantageous because of many adjustable parameters (lattice type, Si/Al ratio, acidity, pore size and shape), which allow to tailor the support for the requirements of catalyzed reaction. However, Pd/zeolite catalysts suffer from rapid deactivation under reaction conditions, especially in the presence of steam. It is considered that poor performance of Pd-based catalysts is due to extensive sintering of Pd nanoparticles and formation of inactive $Pd(OH)_2$ species [5].

In this work a novel approach is proposed with the aim to inhibit sintering of Pd particles dispersed on zeolite support. Small Pd clusters are stabilized within constricted mesopores of ZSM-5 obtained by desilication with NaOH in the presence of tetrapropylammonium bromide.

2 Experimental/methodology

Commercial Na-ZSM-5 (Zeochem PZ-2/40, Si/Al=20) was used as a starting material. A series of desilicated supports was obtained by leaching the parent zeolite with a solution containing 0.2M NaOH and 0.2M TPABr at 65°C for 10, 30, 60 and 300 min. The corresponding samples were denoted as D0 (parent), D10, D30, D60 and D300. The parent zeolite and the leached samples were then ion-exchanged with a $Pd(NH_3)_4(NO_3)_2$ solution at room temperature for 24h to obtain 1 wt.% Pd loading. After drying at 120°C for 24h, the samples were calcined in air at 500°C for 2h and then pressed, crushed and sieved to obtain 150-200μm fraction.

Catalytic activity was evaluated in a quartz glass plug-flow reactor (ID = 6 mm) with a feed of 1 vol.% CH_4 and 4 vol.% O_2 (bal. N_2) at GHSV=30,000 h^{-1} and with a heating ramp of 10°C/min. To simulate wet conditions 5 vol.% of water vapour was added to the flow.

The outlet gas flow composition was analyzed by mass-spectrometry. Structural properties were evaluated by nitrogen physisorption, X-Ray diffraction and electron microscopy.

3 Results and discussion

Table 1. BET surface area and total pore volume of parent and desilicated ZSM-5 from N_2 adsorption

Sample	S_{BET}, m^2	V_{total}, cm^3/g
D0	539	0.393
D10	504	0.432
D30	492	0.480
D60	497	0.474

D300	469	0.490

Table 1 shows that the total pore volume increased with leaching time. Figure 1 illustrates that the catalytic activity of all samples was very similar under dry conditions. A slight decrease of the light-off temperature was observed for the samples leached for 30 and 60 min. The addition of 5 vol.% water vapour in the stream increased the light-off temperature of the D0 sample by 100°C, whereas for the leached samples the shift is only 50-60°C, with the lowest temperatures achieved by the D30 catalyst.

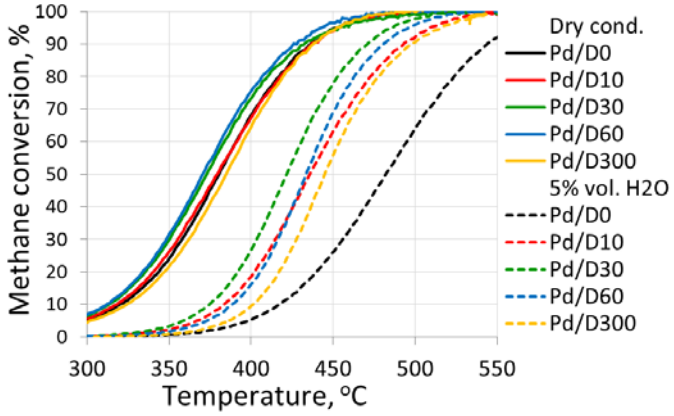

Fig. 1. Methane conversion curves in dry and humid conditions for D0-D300 samples

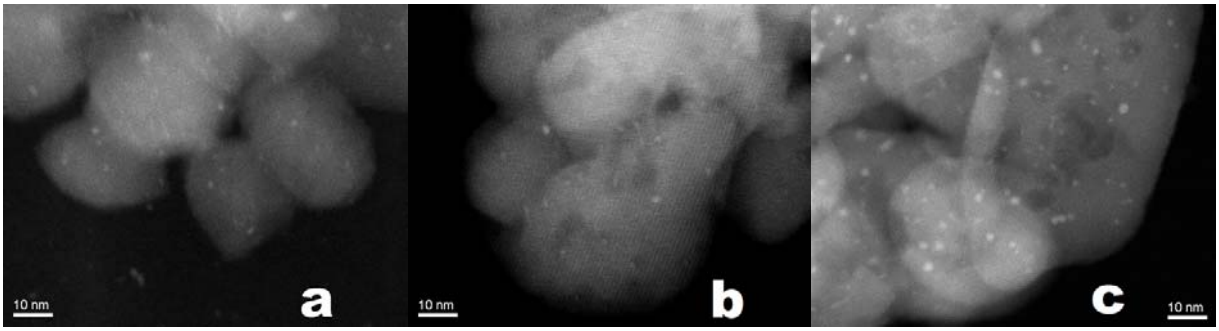

Fig. 2. STEM images of calcined samples (a) Pd/D0, (b) Pd/D30 and (c) Pd/D300.

STEM images (Fig. 2) of calcined D0, D30 and D300 catalysts reveal constricted mesopores in samples D30 and D300 (dark areas in the ZSM-5 crystallite). Some Pd nanoparticles in D30 and D300 samples were located within these constricted mesopores. Increased activity in the presence of water vapour could be explained through these isolated from each other Pd nanoparticles.

4 Conclusions

Palladium nanoparticles stabilized on desilicated ZSM-5 support with constrained mesopores showed promising results in methane combustion in the presence of water vapour.

References

[1] P. Gelin, M. Primet, Appl Catal B. 39(1) (2002) 1-37.
[2] T. Takeguchi et. al., Appl. Catal A. 252 (2003) 205-214.
[3] R. Ramírez-López, I. Elizalde-Martinez, L. Balderas-Tapia, Catal. Today. 150(3-4) (2010) 358-362.
[4] Y. Li, J.N. Armor, Appl. Catal B Environmental. 3 (1994) 275-282.
[5] C.F. Cullis, T.G.Nevell, D.L. Trimm, J. Chem. Soc., Faraday Trans. 1(1) (1972) 1406.

V-OP17

Mixed Ionic-Electronic Conducting Catalysts for Catalysed Gasoline Particulate Filter

Lopez-Gonzalez D.[1*], Jimènez-Cadena G.[2], Tsampas M.[1], Boréave A.[1], Klotz M.[2], Tardivat C.[2], Cartoixa B.[3], Pajot K.[4], Vernoux P.[1]

1 - CNRS, UMR 5256, IRCELYON, Institut de Recherches sur la Catalyse et l'Environnement de Lyon, Villeurbanne, France

2 - Laboratoire de Synthèse et Fonctionnalisation des Céramiques, UMR3080, CNRS/Saint-Gobain, Cavaillon Cedex, France

3 - CTI, Céramiques Techniques Industrielles, Salindres, France

4 - PSA PEUGEOT CITROËN, Centre technique de Vélizy, Vélizy-Villacoublay, France

* diego.lopez-gonzalez@ircelyon.univ-lyon1.fr

Keywords: GPF, nano-cell catalyst, gadolinia-doped ceria, gasoline direct injection, soot

1 Introduction

Future changes in Europe regulation (Euro 6c in 2017) concerning particle matter (PM) abatement will probably lead to the implementation of filter devices in direct injection gasoline (GDI) engines. Catalyzed-Gasoline Particulate Filter (cGPF) can be combined with conventional three way converter (TWC) to meet pollutants standards. Recently, electro-promoted nano-dispersed catalysts for vehicles exhaust after-treatment is getting growing attention [1] since they can combine electrochemical promotion of catalysis [2] and high metallic active site availability. Nano-cell catalysts are composed of nano-electrodes (two different natures of metallic nanoparticles) supported on a mixed ionic-electronic conductor (MIEC). This study reports the preparation and catalytic performances of MIEC based-cGPFs for GDI exhaust treatment. Catalysts were composed of Pd and Rh nanoparticles dispersed on gadolinia-doped ceria (CGO), a mixed oxygen-electronic conductor. These materials have been washcoated in SiC mini-GPFs equipped or not with a filtration membrane. Catalytic activity measurements have been performed independently in lean and rich feed conditions for different catalyst loadings and locations inside mini-cGPFs. Finally, the impact of PM on catalytic performances has been explored.

2 Experimental/methodology

Pd and Rh nanoparticles were dispersed on CGO ($Ce_{0.8}Gd_{0.2}O_2$, Nextech, 34 m²/g) using incipient wetness method. The Pd/Rh ratio was 5 for an overall PGM loading of 1.3 wt%. Powdered catalysts were washcoated into SiC mini-GPFs (1x2 inch) either in the walls porosity or on the surface of a SiC filtration membrane deposited by CTI on the surface of the inlet channels (Table 1). Catalytic tests were carried out in a pilot plant scale which simulates the exhaust line of a GDI engine. Particulate Matter (PM) was generated using a mini Combustion Aerosol Standard (mini-CAST). The total flow rate was 20 Nl/min using N_2 as carrier gas. Tests were carried out under two different conditions: rich (O_2 /CO/CO_2 /NO/C_3H_6/C_3H_8/H_2O: 4000 ppmv/ 1.4 vol.%/ 14 vol.%/ 740 ppmv/ 1125 ppmv/ 375 ppmv/1%) and lean (O_2 /CO/CO_2 /NO/C_3H_6/C_3H_8/H_2O : 1 vol.%/ 6000 ppmv/ 14 vol.%/ 740 ppmv/ 1125 ppmv/ 375 ppmv/1%). Mini cGPFs were placed downstream a mini commercial three-way converter (1x0.8 inch) to mimic a real GDI exhaust after-treatment. Exhausts were sampled with an on-line IR analyzer, a microGas Chromatograph and a chemiluminescence analyzer. Soot particle number and size distribution were measured using an Engine Exhaust Particulate Sizer.

Table 1. Characteristic of the tested GPFs

cGPF	Catalyst loading in porous walls / g/L	SiC Filtration Membrane	Catalyst loading onto the membrane/g/L
Config 0	86	No	-
Config 1	-	Yes	12
Config 2	80	Yes	12
Config 3	80	Yes	12 (only CGO)
Config 4	80	Yes	-

3 Results and discussion

Figure 1 displays catalytic results (NO reduction and CO oxidation) together with the filtering efficiency in lean operating conditions. Differences between samples are only significant at high conversions since the commercial mini-TWC placed upstream cGPFs is very active. The maximum CO conversion was reached in a short temperature interval (250-280 ºC). All the samples showed high performances for NOx conversion, especially those equipped with a catalytic layer on the filtration membrane such as Config 2. This can be attributed to a higher availability of catalytic sites. The filtration membrane has a strong impact on the filtering efficiency (Fig. 1C). Furthermore, in a lesser extent, the presence of catalyst in the porosity of the membrane also improves the soot filtration. On the other hand, the higher the catalyst loading, the higher the pressure drop.

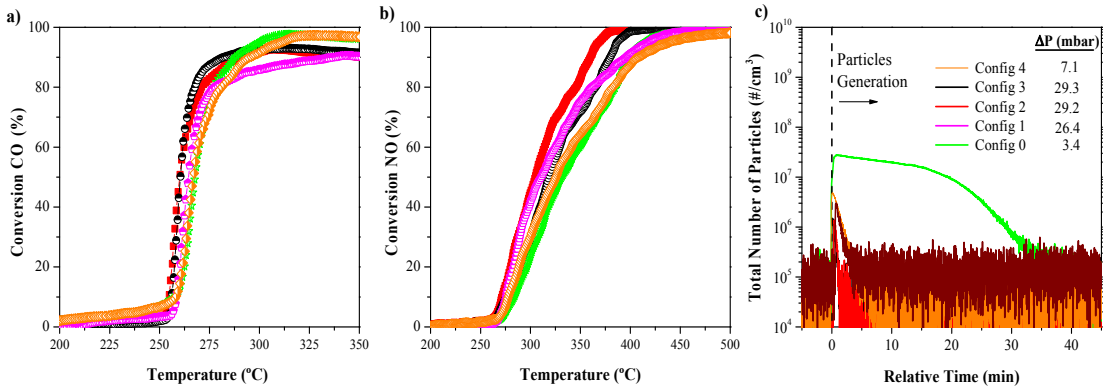

Fig. 1. Catalytic results of the different c-GPFs: a) CO conversion, b) NO conversion and c) Particles number

4 Conclusions

Washcoated MIEC-based catalysts inside mini-GPFs have been tested for GDI exhaust aftertreatment using a bench scale plant. The presence of a membrane in GPFs modifies both, their catalytic and filtering performance. The impact of the membrane, the catalyst loading and location as well as the presence of soot particles on the catalytic properties will be discussed.

Acknowledgements

This study was performed in the "Triptic-H" project, partially funded by the French National Research Agency (ANR), ANR-2011-VPTT-003.

References

[1] W. Y. Hernandez, A. Hadjar, A. Giroir-Fendler, P. Andy, A. Princivalle, M. Klotz, A. Maroub, C. Guizard, C. Tardivat, C. Viazzi, P. Vernoux, *Catal. Today*. 241 (2015) 143.

[2] P. Vernoux, L. Lizarraga, M.N. Tsampas, F.M. Sapountzi, A. De Lucas-Consuegra, J.L. Valverde, S. Souentie, C.G. Vayenas, D. Tsiplakides, S. Balomenou, E.A. Baranova, *Chem. Rev.*, 113 (2013) 8192.

V-OP18

Surface Chemistry of Glycerol on Metals and Metal-Oxides as Model Catalysts for Biomass Conversion

Calaza F.[1*], Sterrer M.[1,2], Freund H.-J.[1]

1 - Department of Chemical Physics, Fritz-Haber-Institut der Max-Planck-Gesellschaft, Berlin, Germany

2 - Institute of Physics, Karl-Franzens-Universität Graz, Graz, Austria

* calaza@fhi-berlin.mpg.de

Keywords: glycerol, bio-fuels, biomass usage, surface chemistry, renewable energies, model catalysts

1 Introduction

Employing renewable sources from vegetal oil to produce chemicals and energy appears to be one of the most important technological approaches to solve the need for replacement of oil. In this way, the new concept of bio-refineries to produce energy and derivatives from biomass comes into the picture. When obtaining biodiesel from biomass conversion, about 10 % of the reaction by-product is glycerol [1]. Thus, it is accepted that glycerol will play a very important role in bio-refineries future and it is, therefore, mandatory to search for new processes to upgrade this by-product into more valuable chemicals.

Glycerol is a highly functionalized compound which could be used as a starting material for a great variety of chemical products of industrial interest [2]. One of the interesting upgrades for glycerol is to produce propylene glycol by dehydration followed by hydrogenation [3]. In another aspect, glycerol can be selectively oxidized, in acid or basic conditions, to different products of interest depending if the targeted hydroxyl is in primary or secondary position [4, 5]. Furthermore, glycerol can be reacted with metal catalysts to obtain H_2 and CO (reforming reactions) [6]. Another interesting upgrade is to obtain dihydroxyacetone or acrolein using reducible metal oxides as catalysts which present a variety of acid-base sites [7].

2 Experimental

All experiments were performed in an ultra-high vacuum chamber with capabilities for infrared absorption and x-ray photoemission spectroscopies (IRAS and XPS), temperature programmed desorption (TPD) and low energy electron diffraction (LEED). The model catalysts used were either metal single crystals (Pd(111) and Au(111)) and their corresponding chemisorbed oxygen structures or oxides or cerium oxide (CeO_2(111)) films grown on top of a Ru(0001) single crystal. Using this battery of surface science techniques we studied the adsorption and further decomposition of the polyol and are able to distinguish adsorbed intermediates in-situ.

2 Results and discussion

When the polyalcohol is adsorbed on the metallic Pd surface it primarily decomposes into H_2 and CO, with traces amount of formaldehyde and methane. On the other hand, on the Au(111) surface, it interacts very weakly showing no decomposition. Preliminary results regarding influence on the chemistry observed in the presence of chemisorbed oxygen or surface oxide thin films show that the interaction with both surfaces can be tuned towards different products (Pd) or boost up its reactivity on the coinage metal (Au). These later results are of interest to understand the mechanistic processes of selective catalytic oxidation of glycerol. Results from IR spectroscopy upon adsorption of the molecule onto the surface at low temperatures, show its adsorption geometry and the cleavage of specific intra/intermolecular

hydrogen bonds are key parameters dictating the decomposition pathways observed for the polyalcohol at higher temperatures.

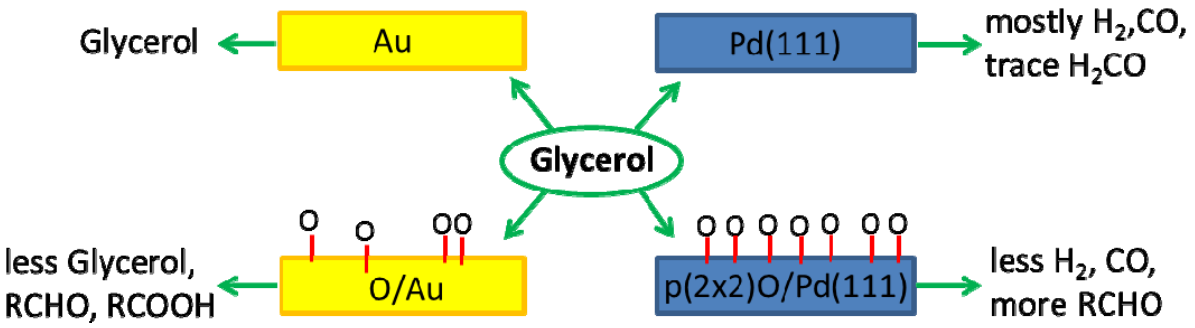

Scheme 1. Different reactivity of glycerol molecules depending on metal substrate and the presence of oxygen species.

Some preliminary results of the interaction of glycerol with cerium oxide films will be shown and compared with the single crystal metals. CeO_2 is a very versatile reducible oxide with high oxygen storage capabilities, thus being a good candidate for selective oxidation or oxidative dehydration reactions. In the past years, several studies have shown that its role as a catalyst, especially in the presence of oxygen vacancies, is of great importance.

4 Conclusions

The adsorption and reactivity of glycerol with metal single crystals and metal oxide model catalysts have shown that this polyalcohol promptly reacts on Pd surfaces producing mostly CO and H_2, thus presenting promising results for using this metal for reforming reactions. The presence of oxygen on Pd opens up other decomposition pathways where more aldehyde is observed. For the case of Au surface, the interaction is very weak on the clean surface, but it can be boosted up with chemisorbed oxygen, and formation of carboxylates as intermediates towards total combustion were observed. The present results show the importance of studying adsorption and reactivity of polyalcohols as model compounds from biomass conversion catalysis at the atomistic level. Great understanding can be reached from these surface science studies which can be then applied for the development of new catalytic materials.

Acknowledgements

F.C. is grateful to the Alexander-von-Humboldt foundation for a Georg Forster fellowship.

References

[1] N. Dimitratos, J.A. Lopez-Sanchez, G.J. Hutchings, *Top. Catal.* 52 (2009) 258.
[2] J.W. Medlin, *ACS Catalysis*. 1 (2011) 1284.
[3] M.A. Dasari, P-P. Kiatsimkul, W.R. Sutterlin, G.J. Suppes, *App. Cat. A: General.* 281 (2005) 225.
[4] L. Prati, P. Spontoni, A. Gaiassi, *Topics in Catalysis.* 52 (2009) 288.
[5] G.J. Hutchings, *Angew. Chem. Int. Ed.* 50 (2011) 10136.
[6] O. Skoplyak, M.A. Barteau, J.G. Chen, *ChemSusChem.* 1 (2008) 273.
[7] G.M. Lari, C. Mondelli, J. Perez-Ramırez, *ACS Catalysis*. 5 (2015) 1453.

V-OP19

Ionic Liquids Based Silica Microreactors for the Efficient Conversion of Carbon Dioxide

Buaki-Sogo M.[1], Garcia H.[2], Aprile C.[1*]

1 - Unit of Nanomaterial Chemistry (CNano), University of Namur (UNAMUR), Department of Chemistry, Namur, Belgium

2 - Technical University of Valencia, Chemical Technology Institute (ITQ-CSIC), Valencia, Spain

* carmela.aprile@unamur.be

Keywords: CO_2 conversion, imidazolium, ionic liquid cyclic, carbonates, silica, microreactors

1 Introduction

Research involving carbon dioxide conversion attracts the interest of the scientific community since carbon dioxide is a non-toxic, renewable and easily available source of carbon. Its reaction with epoxides to produce high added value products like carbonates and polycarbonates is one of the most important topics in green chemistry [1]. To carry out this transformation, is necessary a catalyst able to activate either the carbon dioxide molecule, either the epoxide or both species [2]. In the last years, ionic liquids have demonstrated a good catalytic activity in the CO_2 transformation under both homogeneous [3] and heterogeneous conditions [4, 5, 6]. There are different strategies for the heterogeneization of ionic liquids involved in the transformation of carbon dioxide including adsorption and grafting of the ionic liquid moiety onto a solid support [4], [7].

Herein, we present a novel heterogeneization strategy in which a double alkyl chain imidazolium ionic liquid has been polymerized as liposome-like structure and used as template for the synthesis of mesoporous silica [8]. The organic-inorganic hybrid silica microreactors, synthesized in one-pot procedure, present porous shell and accessible imidazolium core. The novel catalysts displayed excellent performances in the synthesis of cyclic carbonates via chemical fixation of carbon dioxide into various epoxides [8].

2 Experimental/methodology

The N,N'-bis(10-undecenyl)-2-methylimidazolium ionic liquid was synthetized starting from 2-methylimidazolium and 11-bromo-1-undecene in toluene, as previously reported [9]. The silica microreactors were synthetized via the sol-gel method [10, 11], and using the double alkyl chain imidazolium ionic liquid (Figure 1) as structure directing agent. The final material, appeared as a hollow silica sphere with a porous inorganic shell and active imidazolium core, was characterized by TEM, ^{29}Si-MAS-NMR spectroscopy, elemental analysis and N_2 adsorption. The catalytic tests were carried out in a batch reactor with individual temperature control and mechanical stirring, designed to operate at high pressures.

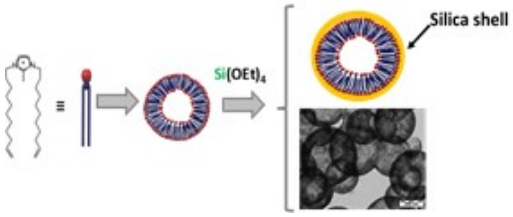

Fig.1. Synthesis of the silica microreactors and TEM image of the as-prepared materials.

3 Results and discussion

The novel imidazolium based silica microreactors were synthesized following a straightforward one-pot procedure and used as catalysts for the synthesis of cyclic carbonates. The operation pressures of CO_2 ranged between 50 and 90 bar and other parameters like temperature, presence of solvent and relative epoxide to catalyst ratio were also tested.

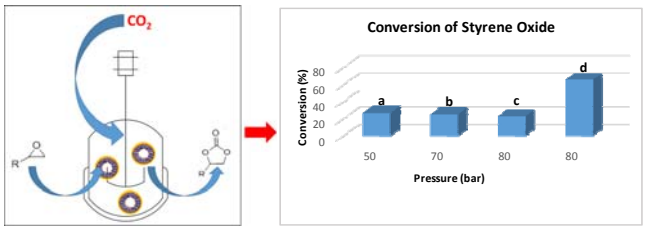

Fig.2. Reaction scheme (left) and tests performed within the silica microreactors (right); tests *a*, *b* and *c* were performed in the presence of solvent (DCM) at 50, 70 and 80 bar, respectively; test *d* was performed without solvent at 80 bar.

The materials showed good performance for the reaction of CO_2 with different epoxides; for the transformation of styrene oxide into styrene carbonate the best conversion (53 %, figure 1 right, test d) was obtained in the absence of solvent. Under the selected conditions the turnover number (TON =300) was one of the higher reported in the literature [7]. The excellent catalytic activity was justified by the presence of a confined space within the microreactors with the consequent increases of local concentration of the regents. Moreover, these materials were used in consecutive catalytic cycles with no substantial decrease of the catalytic performances.

4 Conclusions

An imidazolium ionic liquid bearing two undecenyl chains was polymerized leading to a liposome-like structure. This polymeric matrix acted as template for the preparation of porous silica architecture. The solid behaves as an organic/inorganic hybrid microreactor with enhanced catalytic activity for the synthesis of cyclic carbonates starting from carbon dioxide and epoxides. The good performances were confirmed by the high TON and selectivity obtained. Moreover, the catalytic activity was maintained in multiple catalytic cycles although a small decrease in the carbonate yield was observed after the first run.

Acknowledgements

The authors acknowledge the FRS-FNRS funding. M.B-S is gratefully acknowledged for an Incomming Post-Doctoral Fellowship of the *Academie Universitaire de Louvain* co-funded by the Marie Curie Actions of the European Commision.

References

[1].P. Pescarmona.; M. Taherimehr. *Catal. Sci. Technol*., 2012, 2, 2169-2187
[2].T. Sakakura; J. Choi; H. Yasuda. *Chem. Rev*. 2007, 107, 2365-2387
[3].M. North; R. Pascuale.; C. Young. *Green. Chem*. 2010, 12, 1514-1539
[4]. L. Han; H. Choi; S. Choi.;B. Liu; D. Park. *Green Chem.* 2012, 13, 1023
[5]. Y. Gu.; G. Li. *Adv. Synth. Catal*. 2009, 351, 817-847
[6]. F. Jutz; J-M. Andanson; A. Baiker. *Chem. Rev.* 2011, 111, 322-353
[7]. C. Aprile; F. Giacalone; P. Agrigento; L. Liotta; J-A. Martens; P. Pescarmona; M. Gruttadauria. *ChemSusChem*. 2011, 4, 1830-1837
[8]. M. Buaki-Sogo; H. Garcia ; C. Aprile;. *Catal. Sci. Technol*., 2015, 5, 1222-1230
[9]. M. Buaki; C. Aprile; A. Dhaksinamoorthy; M. Alvaro; H. Garcia. *Chem. Eur. J.* 2009, 15, 13082-13089
[10]. C.T. Kresge.; M.E. Leonowizc; W.J. Roth; J.C. Vartuli; J.S. Beck. *Nature.* 1992, 359, 710
[11]. J.S. Beck. *J. Am. Chem. Soc*. 1992, 114, 10834

V-OP20

One-Pot Natural Alcohol Amination Catalyzed by Gold-Containing Catalysts

Demidova Yu.S.[1,2*], Simakova I.L.[1,2], Beloshapkin S.[3], Wärnå J.[4], Suslov E.V.[5], Volcho K.P.[5], Salakhutdinov N.F.[5], Simakov A.V.[6], Murzin D.Yu.[4]

1 - Boreskov Institute of Catalysis, Novosibirsk, Russia
2 - Novosibirsk State University, Novosibirsk, Russia
3 - Materials & Surface Science Institute, University of Limerick, Limerick, Ireland
4 - Åbo Akademi University, Turku/Åbo, Finland
5 - Novosibirsk Institute of Organic Chemistry, Novosibirsk, Russia
6 - Centro de Nanociencias y Nanotecnología, UNAM, Ensenada, México

* yulia.s.demidova@gmail.com

Keywords: natural monoterpene alcohol, amination, gold nanoparticles, one-pot

1 Introduction

Complicated amines are important chemicals *per se* or as intermediates for fine organic synthesis. In particular complicated terpene amines, synthesized from renewable raw materials, were recently shown to exhibit specific physiological properties and can be used as intermediates of potential drugs for neurological diseases [1]. A perspective approach to control synthesis of complicated amines is the one-pot alcohol amination over heterogeneous catalysts, consisting of three consecutive steps: dehydrogenation of alcohol to aldehyde, which interacts with an amine to form imine and finally hydrogen transfer to produce the secondary amine. The one-pot multistep reaction holds a high potential for increasing the efficiency for chemical synthesis of medicinally and biologically important compounds. At the same time, the complexity of this process is reflected by a large number of parameters which can influence each step. Thus, the purpose of the current work is to study general regularities of one-pot alcohol amination in the presence of gold-containing catalysts and to obtain systematic knowledge about the key parameters determining the catalyst performance including the investigation of the support nature and the catalyst redox activation effect. Myrtenol, which represents a natural terpene alcohol with a primary OH-group and C=C double bond, and aniline were selected as model substrates (Fig. 1).

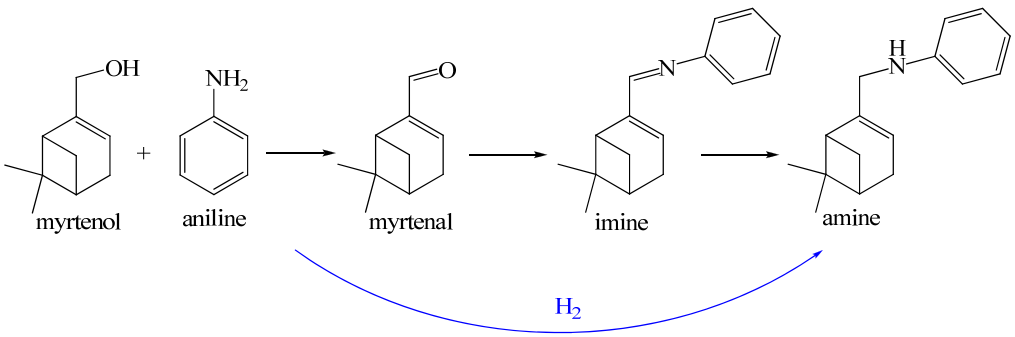

Fig. 1. General reaction network of one-pot myrtenol amination with aniline over gold catalysts.

2 Experimental

Liquid-phase myrtenol amination was carried out in a stainless steel reactor, equipped with an electromagnetic stirrer (1100 ppm) and a sampling system. In a typical experiment, a mixture of myrtenol (1 mmol), aniline (1 mmol) and Au catalysts (92 mg) in toluene (10 ml) was intensively stirred at 413-453 K under N_2 atmosphere. The reaction components were analyzed

by GC using a SLB-5ms column, GC-MS as well as ^{1}H- and ^{13}C-NMR. A series of gold catalysts including Au and AuPd samples over different metal oxides (ZrO_2, MgO, Al_2O_3, CeO_2, La_2O_3) were prepared by deposition-precipitation method using urea as a precipitating agent, pre-treated under oxidizing or reducing atmospheres and characterized by TEM, XPS and TPR/TPO-MS.

3 Results and discussion

To study the effect of the catalyst support and redox thermal pre-treatment a series of nanosized gold catalysts over ZrO_2, Al_2O_3, CeO_2 and La_2O_3 pre-treated under oxidizing or reducing atmosphere were tested. First, the catalytic performance in each step was found to be strongly dependent on acid-base properties of the support requiring a certain balance between different sites for efficient alcohol amination [2]. Among the catalysts tested in the reaction zirconia-supported gold catalyst with both acidic and basic surface sites afforded optimum consecutive myrtenol transformations resulting in the myrtenol total conversion and selectivity to the target amine of about 53%. The basic sites on metal oxides surface were suggested to be required for the initial alcohol activation, while the availability of protonic groups was important for the target amine formation. At the same time it was found that the catalytic activity and selectivity can be also regulated by the catalyst redox pre-treatment. Differences in activity and selectivity between pre-reduced and pre-oxidized catalysts were demonstrated to be related to an extent of ammonia removal from the catalyst surface rather than to the electronic state of gold species depending on the type of catalysts redox pretreatment. The amount of ammonia species remained on the catalyst surface influenced surface acidity determining catalytic behavior in different amination steps.

A special attention was given to kinetic investigations with a further development of the kinetic model. The reaction kinetics was modelled based on the mechanistic considerations with the catalyst deactivation step introduced into the mechanism [3]. The kinetic model was compared with experimental data through numerical data fitting showing a good correspondence (degree of explanation equal to 95%), which confirms its applicability. In fact, the developed model is a very generic one and can be used for a number of other hydrogen borrowing reactions.

4 Conclusions

One-pot myrtenol amination was studied in the presence of nanosized gold catalysts supported on different metal oxides with equimolar amounts of the substrates in the temperature range 413-453 K under nitrogen pressure. It was shown that catalytic activity and product distribution in one-pot alcohol amination can be regulated by the metal oxide support properties, namely acidity and basicity, interactions of Au with other metals and conditions of catalyst pre-treatment. A mechanistic model for hydrogen borrowing reaction taking into account catalyst deactivation was developed from the proposed reaction mechanism resulting in a kinetic model, which was able to describe experimental data with sufficient accuracy.

References

[1] I.G. Kapica, E.V. Suslov, G.V. Teplov, D. V. Korchagina, N.I. Komarova, K. P. Volcho, T.A. Voronina, A.I. Shevela, N. F. Salakhutdinov, *Pharm. Chem. J.* 2012, 46, 3.

[2] Yu.S. Demidova, I.L. Simakova, M. Estrada, S. Beloshapkin, E.V. Suslov, D.V. Korchagina, K.P. Volcho, N.F. Salakhutdinov, A.V. Simakov, D.Yu. Murzin, *Appl. Catal. A: Gen.* 464-465 (2013) 348-356.

[3] Yu.S. Demidova, I.L. Simakova, J. J. Wärnå, A.V. Simakov, D.Yu. Murzin, *Chem. Eng. J.* 238 (2014) 164-171.

V-OP21

Utilization of CO_2 in the Process of Olefins Production

Nowicka E.*, Reece C., Willock D., Golunski S., Hutchings G.J.

Cardiff Catalysis Institute, Cardiff University, Cardiff, United Kingdom

* nowickae@cf.ac.uk

Keywords: dehydrogenation, CO_2, TAP, reactor, propane

1 Introduction

The oxidative dehydrogenation (ODH) of alkanes to alkenes by molecular oxygen is a relatively new and a promising technology. The presence of O_2 may however, lead to process flammability, production of carbon oxides and over-oxidation, resulting in poor process selectivity. This can be overcome by using a safer, milder and readily available oxidant: CO_2.[1] As the issue of CO_2 emissions has become one of the main subjects in environmental chemistry, this reaction seems to serve also a great example for CO_2 utilization.[2] The route of this reaction may follow Mars van Krevelen mechanism, where CO_2 will dissociate on the surface of catalyst, facilitating further dehydrogenation. Catalysts with high oxygen storage capacity (OSC) and ability to dissociate CO_2 in low temperatures would be ideal for this process. One of the active metal oxides, which possess these properties, is CeO_2. Addition of ZrO_2 to CeO2, however, increase OSC and additional presence of another metal oxide-Al_2O_3 has a positive influence on the surface area and catalyst thermal stability.[3] Here, we report the oxidative dehydrogenation of propane (ODP) with the use of CO_2 and Pd/ Ce-Zr-Al-O_x based catalyst. The use of temporary analysis programme (TAP) reactor for CO_2 dissociation over Pd/Ce-Zr-Al-O_x catalyst was also investigated.

2 Experimental/methodology

Catalysts were prepared by physical grinding method to give support composition Ce: Zr: Al: 1:1:2. Further Pd was wet impregnated onto calcined support following the protocol: to the aqueous solutions of Pd precursor, requisite amount of support was added under vigorous stirring at room temperature. The solution was agitated in this way until it formed a paste, which was dried at 120°C for 12h and further calcined. Catalytic measurements were performed using a fixed bed laboratory micro reactor at atmospheric pressure, keeping GHSV at 6385 h^{-1} and total flow rate of 15 mL min^{-1}. Reaction mixture consisted of He, CO_2 and C_3H_8, keeping He on the level of 26% volume and using different ratio between CO_2 and C_3H_8. The reactants and products were analysed by a Varian 3800 online gas chromatograph using Porapak Q and Molsieve columns with TCD and FID detector.

3 Results and discussion

Pd supported catalyst were highly active for the oxidative dehydrogenation of propane. Studies with different CO_2: C_3H_8 ratio over 5%Pd/Ce $_{0.25}$Zr $_{0.25}$Al $_{0.5}$O $_{1.75}$ catalyst showed that changing the ratio between CO_2: C_3H_8 lead to increase in CO_2 and C_3H_8 conversion This may be attributed to the fact, that CO_2 is changing the equilibrium in the reverse water-gas shift reaction, as well as faster CO_2 dissociation over Pd supported catalyst. When investigating the metal loading on Ce-Zr-Al-O_x support for activity in ODP reaction, it was found that catalyst with 7% Pd loading increased the conversion of propane to more than 35% during 0.5 h reaction, as it is shown in **Figure 1**.

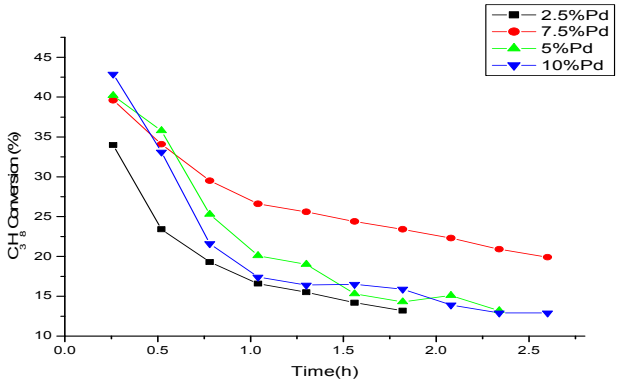

Fig. 1. Conversion of C_3H_8 in ODP with $Ce_{0.25}Zr_{0.25}Al_{0.5}O_{1.75}$: different Pd loading

Studies involving TAP measurements over $5\%Pd/Ce_{0.25}Zr_{0.25}Al_{0.5}O_{1.75}$ clearly showed CO production from CO_2 at temperature higher than 300°C. These findings indicate that CO_2 dissociate on the surface of the catalyst yielding highly oxidative O species, maintaining Ce in a highly oxidized state, therefore helping to facilitate the dehydrogenation process.[4]

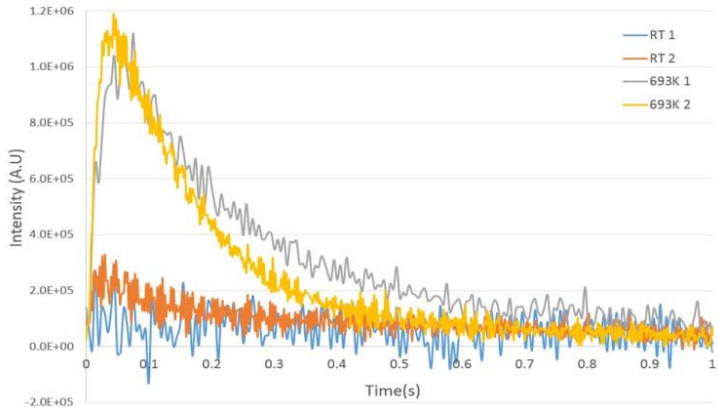

Fig. 2. TAP reactor analysis: Mass 28 at RT and 420°C pulsing CO_2

The most active catalyst has been fully characterized using several techniques, e.g.: TEM, EXAFS and TPRDO. Also DRIFT analysis with CO_2 and CO will be presented.

4 Conclusions

Pd based catalysts have been found very active for propane dehydrogenation process with the use of CO_2. The role of CO_2 in reverse water gas shift reaction as well as in oxidative dehydrogenation via Mars van Krevelen mechanism will be fully presented.

References

[1] M. B. Ansari and S.-E. Park, *Energy & Environmental Science*, 2012, **5**, 9419-9437.
[2] K. M. K. Yu, I. Curcic, J. Gabriel and S. C. E. Tsang, *Chemsuschem*, 2008, **1**, 893-899
[3] M. Chen, J. Xu, Y. Cao, H.-Y. He, K.-N. Fan and J.-H. Zhuang, *Journal of Catalysis*, 2010, **272**, 101-108.
[4] O. Demoulin, M. Navez, J. L. Mugabo and P. Ruiz, *Applied Catalysis B: Environmental* (2007) 70, 284-293

V-OP22

Selective 1,2-Propanediol Formation via Tandem Reaction Cycle of Methanol Reforming-Glycerol Hydrodeoxygenation

Lemonidou A.A.[1,2*], Yfanti V.-L.[1], Vasiliadou E.S.[1]

1 - Department of Chemical Engineering, Aristotle University of Thessaloniki, Thessaloniki, Greece
2 - Chemical Process and Energy Resources Institute (CERTH/CPERI), Thessaloniki, Greece

* alemonidou@cheng.auth.gr

Keywords: glycerol hydrodeoxygenation, methanol reforming, Cu-catalyst, reaction, pathways

1 Introduction

Glycerol (GLY), being a by-product of various biomass conversion processes is a high available, low-cost and renewable feedstock for the production of chemicals which are at present produced using oil derivatives. Catalytic hydrodeoxygenation (HDO) of glycerol to 1,2-propanediol (1,2-PDO) is a process of commercial and environmental significance. However, the need of external H_2 supply may render the process unprofitable. This work presents an innovative method according to which, glycerol is subjected to HDO conditions and selectively converts to 1,2-PDO under inert atmosphere. Aqueous methanol (MeOH) reforming generates H_2 required for GLY HDO in a tandem reaction cycle under identical conditions [1,2]. A $Cu_{0.6}Zn_{0.3}Al_{0.1}$ catalyst, was proved to be the most efficient material for the above reaction cycle [3]. In this study, efforts are directed towards optimizing the performance of the promising catalyst by tuning the operating conditions and testing its stability. In addition, emphasis was placed on the elucidation of the reaction pathways.

2 Experimental/methodology

The $Cu_{0.6}Zn_{0.3}Al_{0.1}$ catalyst was prepared using the oxalate gel co-precipitation method [3]. The standard catalytic tests were conducted in an autoclave 100ml reactor (Parr Instruments) at 250°C and 3.5MPa initial N_2 for 1h employing a reactant mixture 82v/v% H_2O, 9v/v% MeOH and 9v/v% GLY. The stability of the catalyst was tested for five reaction cycles. The effect of operating conditions was investigated by varying the parameters at ranges of C_{MeOH}: 4.5-36v/v%, T:200-250°C, P:1.0-3.5 MPa N_2, 1.0-8.0MPa H_2, w_{cat}:0.1-1.4g. The method of intermediate addition to the reactant mixture was applied so as to elucidate the reaction pathways. Small amounts of hydroxyacetone (HA) and glyceraldehyde (GLA) were separately added in the aqueous feed solution of GLY and MeOH and the reaction rates were calculated. In addition, experiments using intermediate (HA) and final (1,2-PDO) products as reactants were also performed.

3 Results and discussion

Under the optimum operating conditions (t=1h, T=250°C, P_{N2}=1.8MPa, 36v/v% C_{MeOH} +9v/v% C_{GLY}), GLY was almost fully converted (96.4%), while 1,2-PDO was the major product formed with 77.0% selectivity and a site time yield equal to 14.1h^{-1}. Higher C_{MeOH} resulted in increased H_2 formation rates and as a consequence a significant increase in 1,2-PDO selectivity was obtained. It was found that temperature increment positively affects the activity, but its combination with longer reaction times disfavors 1,2-PDO selectivity, due to consecutive HDO of 1,2-PDO to 1-propanol. When H_2 is externally supplied, increment of P_{H2} favored both activity and 1,2-PDO selectivity. The latter is due to increased H_2 solubility in liquid phase. On the other hand, when H_2 is in-situ formed, variation of P_{N2} did not have a significant effect on catalyst performance. In this case, H_2 is generated nearby the catalytic active sites and readily consumed by absorbed glycerol. This provides the ability of operating at lower system

pressures. Upon catalyst reuse, an activity loss of 33.0% was observed, due to Cu agglomeration. However, the performance was stabilized after the 3rd run, because of Cu redispersion, as evidenced by the measurement of the active Cu area. Worthy to note that TOF did not vary, revealing the structural integrity of the nature of the active sites.

For GLY HDO three different mechanisms were considered: a) dehydration-hydrogenation (HA route), b) dehydrogenation-dehydration-hydrogenation (GLA route) and c) direct GLY hydrogenolysis [3]. **Table 1** shows the reactant consumption and product formation rates for each test. In both tests with intermediate addition, HA and GLA added were fully converted and 1,2-PDO was the main product formed. The latter excludes a direct mechanism. HA addition in the feed negatively affects methanol APR rate and consequently H_2 availability. This was not observed when GLA was added, while in both cases glycerol rate was unaffected. It could be inferred that HA and MeOH compete for the same catalytic active sites. On the other hand, there is no competitive adsorption between reactants and GLA, as GLA reaction rate is much faster than MeOH and GLY rates. 1,2-PDO formation rate decrease upon intermediate addition (by 60% and 30% with HA and GLA addition, respectively). Decreased 1,2-PDO rate in the case of HA is a result of low H_2 availability (low MeOH APR rate), while the addition of GLA seems to have an inhibition effect on GLY HDO to 1,2-PDO. Taking the aforementioned into account as well as the identification of HA in all tests, it can be inferred that GLY HDO under the present reaction conditions primarily proceeds via the dehydration-hydrogenation mechanism. However, contribution of the GLA route to 1,2-PDO formation cannot be excluded. When 1,2-PDO and methanol were used as reactants, 1,2-PDO presented low reactivity pointing out that it is a rather stable component and 1-propanol was the main product formed via sequential HDO of the target diol. Hydrogenation of HA intermediate to 1,2-PDO is a reversible equilibrium-limited reaction, however under our experimental conditions 1,2-PDO dehydrogenation is not favoured.

Table 1. Reaction rates

Feed (mmol)	Consumption rate · 10^{-3} [mol/g_{cat}·hr]				Formation rate · 10^{-3} [mol/g_{cat}·hr]	
	MeOH	**GLY**	**1,2-PDO**	**HA**	**1,2-PDO**	**HA**
MeOH (66.8)+GLY(36.9)	3.42	21.74	-	-	14.17	3.34
MeOH (66.8)+GLY(36.9)+HA(3.9)	1.77	16.92	-	-	5.68	-
MeOH (66.8)+GLY(36.9)+GLA(3.9)	3.79	21.28	-	-	10.06	2.98
MeOH (66.8)+1,2-PDO(36.9)	1.29	-	5.81	-	-	2.01
MeOH (66.8)+HA(3.9)	1.26	-	-	2.67	0.9	-

4 Conclusions

The present innovative method validates the potentiality of glycerol HDO to 1,2-PDO under inert atmosphere. High 1,2-PDO yield (74.3%) was achieved over the $Cu_{0.6}Zn_{0.3}Al_{0.1}$ catalyst and under the optimum operating conditions. Finally, the elucidation of reaction pathways showed that GLY HDO primarily proceeds via the dehydration-hydrogenation mechanism.

Acknowledgements

The project "Novel integrated process for the hydrogenolysis of bio-glycerol to 1,2-propanediol without hydrogen addition" is implemented under the "ARISTEIA", project number 37. Action of the OPERATIONAL PROGRAMME "EDUCATION AND LIFELONG LEARNING" and is co-funded by the European Social Fund (ESF) and National Resources.

References

[1] A.A. Lemonidou and E.S. Vasiliadou, *Eur. Pat. Off. Appl. No EP11179515.9 2011*
[2] E.S.Vasiliadou, V.-L.Yfanti, A.A.Lemonidou, *Appl. Catal. B: Environ. 136, (2015), 258.*
[3] A.Martin, U.Armbruster, I.Gandarias, P.Arias, *Eur.J.Lipid Sci.Technol. 115, (2013), 9.*

V-OP23

Gold Catalysts for CO-Free Hydrogen Production from Formic Acid Derived from Biomass

Zacharska M.[1,2*], Bulushev D.A.[1,3], Estrada M.[4], Guo Y.[2], Beloshapkin S.[2], Kriventsov V.V.[3], Leahy J.J.[1,2], Simakov A.V.[4]

1 - Chemical & Environmental Sciences Department, University of Limerick, Limerick, Ireland
2 - Materials & Surface Science Institute, University of Limerick, Limerick, Ireland
3 - Boreskov Institute of Catalysis, SB RAS, Novosibirsk, Russia
4 - Centro de Nanociencias y Nanotecnologia, UNAM, Ensenada, Mexico

* Monika.Zacharska@ul.ie

Keywords: hydrogen production, formic acid decomposition, K-doping, Au Catalysts

1 Introduction

Formic acid (FA) is a non-toxic by-product of biomass cellulose hydrolysis used for production of levulinic acid. Catalytic FA decomposition has a great potential to produce hydrogen for fuel cells. Furthermore, FA can be used as a hydrogen donor in catalytic hydrogenation reactions.

Gold has an ability to perform highly selective and efficient catalysis at low temperature to achieve targets of green chemistry. Au can catalyze all kinds of reactions considered as the domain of Pt and Pd catalysts. Thus, Ojeda and Iglesia showed that well dispersed Au supported on Al_2O_3 gave higher turnover frequencies (TOFs) in FA decomposition than those for supported Pt [1]. Doping with alkali metals have been reported to increase considerably the catalytic performance of a Pd/C catalyst in FA decomposition [2]. In this paper, we report for the first time that doping of a Au/Al_2O_3 catalyst with potassium carbonate improves the catalytic activity by a factor of 4.5 and leads to about 100% selectivity to H_2 at low temperatures (<360 K).

2 Experimental/methodology

All catalysts were prepared by deposition-precipitation technique to get 3 wt.% of Au [3]. Potassium carbonate was deposited by impregnation on the most active catalyst. The catalysts were characterized by TEM, EXAFS and XPS. Vapour-phase FA (1.9 vol.%) decomposition reaction was carried out in a fixed bed quartz reactor. Activity tests were performed at atmospheric pressure with 23.5 mg of catalyst reduced in a 1 vol.% H_2/Ar mixture for 1 h at 573 K and cooled in He to the reaction temperature. A total flow rate equal to 51 cm^3 min^{-1} was used in all experiments. In the first step, a number of calcined Au catalysts supported on a different metals oxide and pre-treated in oxygen at 623 K were tested. In the second step, the catalytic properties of the pre-calcined Au sample with the highest activity and selectivity (Au/Al_2O_{3calc}) was compared to those for noncalcined sample (Au/Al_2O_3) doped with 3 and 6 wt.% of K.

3 Results and discussion

Figure 1a) compares the temperature for 50% conversion and selectivity for pre-calcined Au catalysts on different supports in FA decomposition. The activity trend for Au on the supports was the following: $MgO \leq CeO_2 << ZrO_2 \sim La_2O_3 < Al_2O_3$. The Au/Al_2O_{3calc} catalyst showed the highest activity and selectivity for H_2 production. It is important that the mean Au particle sizes were close for all catalysts (2.4-3.0 nm). The XPS analysis indicated the presence of mainly metallic state (93.4% Au^0) in the Au/Al_2O_{3calc} catalyst. Figure 1b) demonstrates the activity of the Au/Al_2O_{3calc} catalyst as compared to the noncalcined Au/Al_2O_3 sample with smaller mean Au particle size of 1.9 nm (after the reaction). At 373 K, the noncalcined Au/Al_2O_3 catalyst was

3 times more active than the Au/Al_2O_{3calc} catalyst. The obtained results can be explained by the presence of atomically dispersed Au species or clusters with a few atoms, which could be active sites of the reaction in accordance with the data of refs.[1,4]. Among the used supports alumina may provide better stabilization of such sites. Calcination might cause sintering of Au which decreases the amount of the Au active sites.

To further improve the catalytic properties the noncalcined Au/Al_2O_3 catalyst was doped with K carbonate. The $3K\text{-}Au/Al_2O_3$ sample was 4.5 times more active than the undoped Au/Al_2O_3 catalyst in spite of the activation energies increased considerably with doping from 53-54 to 94 kJ mol^{-1}.The selectivity to hydrogen was about 100% for all K-doped Au/Al_2O_3 catalysts. Additionally, the catalyst doped with 3 wt.% of K was also the most stable in the reaction for at least 25 h in this series of the catalysts. As the behaviour of the Au catalysts after doping with K carbonate is similar to that of the Pd/C catalyst discussed earlier [3], we use the same explanation of the K doping effect. At the used conditions, FA is condensed in the pores of the catalyst and transforms K carbonate to K formate, thus increasing considerably the concentration of formate ions in the solution. These ions become active intermediates of the reaction decomposing on the Au active sites with the formation of only H_2 and CO_2.

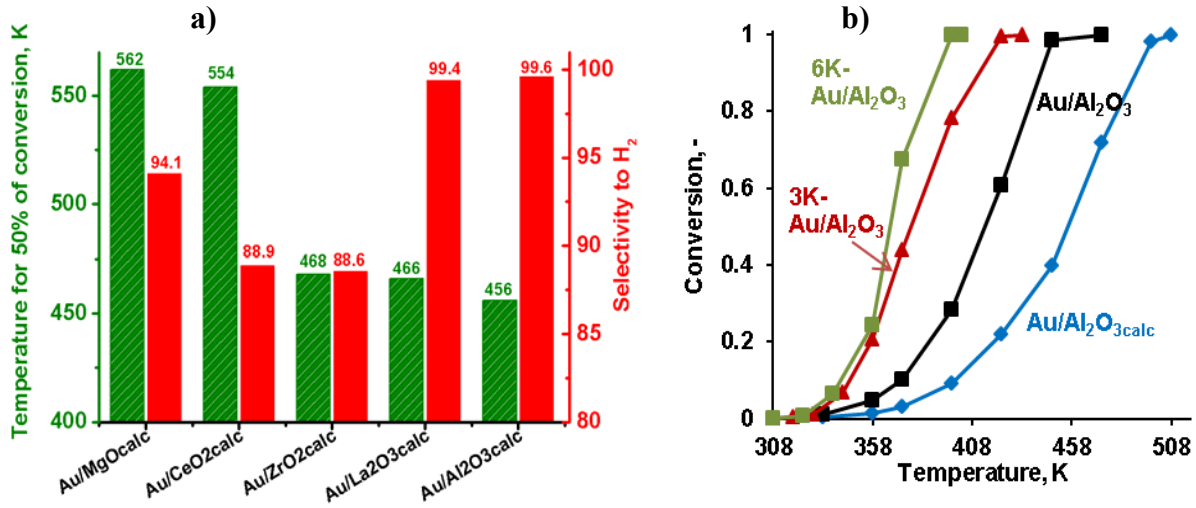

Fig. 1. a) Temperature for 50% of conversion and H_2 selectivity for calcined 3 wt.% Au catalysts on different metal oxides and b) temperature dependence of conversion in the decomposition of FA over pre-calcined and doped with K and undoped noncalcined 3 wt.% Au/Al_2O_3 catalysts.

4 Conclusions

We showed that alumina is the best support to stabilize active Au species for FA decomposition. The 3 wt.% Au/Al_2O_3 catalyst with 3 wt.% of K is an effective and stable catalyst in FA decomposition reaction at relatively low temperature (<360 K). It provides CO free hydrogen production from FA decomposition. The K-doping effect could be explained by the presence of K^+ ions in FA condensed in the catalyst's pores, which stabilize formate ions in the solution providing a different mechanism of FA conversion through these ions as compared to the undoped catalyst.

References

[1] M. Ojeda, E. Iglesia, *Angewandte Chemie*. 121 (2009) 4894.
[2] L. Jia, D.A. Bulushev, S. Beloshapkin, J.R.H. Ross, *Applied Catalysis*. 160 (2014) 35.
[3] Y.S. Demidova, I.L. Simakova, M. Estrada, S. Beloshapkin, E.V. Suslov, D.V. Korchagina, K.P. Volcho, N.F. Salakhdniov, A.V. Simakov, D.Yu. Murzin, *Applied Catalysis*. 464 (2013) 348.
[4] N. Yi, H. Saltsburg, M. Flytzani-Stephnopoulos, *ChemSusChem*. 6 (2013) 816.

V-OP24

Bimetallic Catalysts Promising in Bio-Fuel Production

Tsodikov M.V.[1*], Chistyakov A.V.[1], Gekhman A.E.[2], Moiseev I.I.[3]

1 - A.V.Topchiev Institute of Petrochemical Synthesis RAS, Moscow, Russia
2 - N.S.Kurnakov Institute of General and Inorganic Chemistry RAS, Moscow, Russia
3 - I.M. Gubkin Russian State University of Petroleum and Gases, Moscow, Russia

* tsodikov@ips.ac.ru

Keywords: products, alcohols, rapeseed oil, catalysts, structure, hydrocarbon fuel, catalytic activity

1 Introduction

Ethanol, 2-methylpropanol-1, 3-methylbutanol-1, mixture of fermentation organic products, glycerol and rapeseed oil are known to give rise bio-fuel components under hydro-deoxygenation conditions. In this paper, new catalysts based on alumina and zeolite supports containing nanosized bimetallic active components of I, II, VI, VIII groups have been tested in the reactions. Selective conversions of bio-substrates into alkanes, olefins, aromatics and naphthenic hydrocarbons components of gasoline and diesel fractions were observed.

2 Experimental/methodology

Industrial and laboratory elaborated catalyst samples were used in catalytic experiments. Both gaseous and liquid organic products in aqueous and organic phases were identified by GC-MS technique. The catalysts were tested in a PID Eng & Tech microcatalytic fixed-bed flow reactor unit, equipped with relevant instrumentation and control devices, under 350 °C, 5 atm of Ar, and substrates space velocity in the range of 0.6 h^{-1}. The local structure and charge state of active components were studied by XAS, XPS, XRD and TEM EDX. Relationships between structure of active components and catalytic activity of catalysts are discussed.

3 Results and discussion

Ethanol conversion to fraction of alkanes C_5-C_{10+}[1] at 300-350^{0}C in inert atmosphere was found to be catalyzed with industrial Pt/Al_2O_3 catalyst after special pre-activation:

$$mC_nH_{2n+1}OH + H_2 \rightarrow C_{mn}H_{2mn+2} + mH_2O,$$
were $n \geq 1$; $m \geq 2$

2-methylpropanol-1 and 3-methylbutanol-1 were converted into 2,5-dimethylhexane and 2,7-dimethyloctane, respectively:

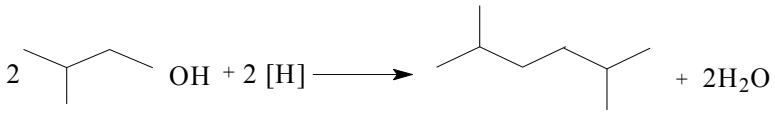

Cross-condensation of ethanol with acetone, bio alcohols, and glycerol in the presence of Pt/Al_2O_3 и [W(Ta)-Re]-catalytic systems leading toward the formation of new hydrocarbon with

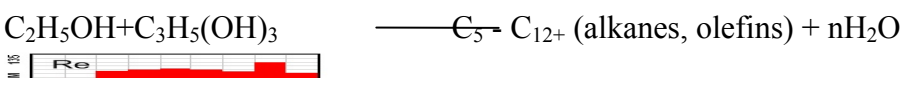

enlarged and branched carbon skeleton was observed[1]:

Ethanol/bio-alcohol transformation is multivariate reaction and mainly depends on feed-stock composition, reagent structure, and catalyst composition:

1. in the presence of modified platinum-contained catalyst reaction involves oligomerization of ethylene as intermediate;
2. aldol condensation is the main stage of hydrocarbons forming in the presence of W(Ta)-Re/Al_2O_3 and Pd-Zn/ Al_2O_3 catalysts;
3. alkane-aromatic hydrocarbons forming according to well-known "hydrocarbon pool" mechanism[2] in the presence of Pd-Zn/ZSM-5 catalyst.

Hydrogen consumed in product forming reactions originated from in-situ in reaction zone via parallel reaction dehydrogenation and aromatization of initial alcohol.

In the presence of original $Pt\text{-}Sn/Al_2O_3$ catalyst at 400-420^{0}C and 30 am H_2 rapeseed oil was unexpectedly found to yield dominantly narrow alkane-olefins C3, C18 and H_2O[3]:

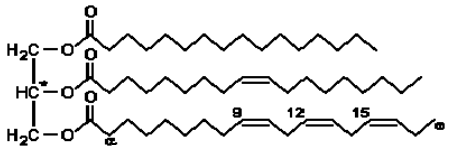

$\longrightarrow C_3 + C_{18} + H_2O$

The selectivity of direct deoxygenation reaches up to 99%. The acid rest of the starting reagent converts quantitatively into C3 and C18 hydrocarbons (~ 92%). The total yield of C1 and C2 hydrocarbons as well as carbon oxides does not exceed 0,5-0,7 % that provides minimization of the carbon loss in the process of rapeseed oil deoxigenation.

Conversion of products fermentation and rapeseed oil into alkane-aromatic components of gasoline and kerosene without loading of molecular hydrogen was found. Hydrogen consumed for rapeseed oil hydrogenative deoxygenation was formed in the reaction zone via coupled reaction carrying out of ethanol aromatization.

Structure and evolution of the catalyst active sites were studied using TP-desorption of molecules-probes, XAFS, XPS, X-Ray and TEM HR.

Acknowledgements

RFBR (grants 13-03-12034, 15-03-06479), Council on Grants at the President of the Russian Federation for the Support of Young Scientists MK-5328.2014.3 are appreciated for financial support.

References

[1] A.Chistyakov, M. Chudakova, M.Tsodikov, A. Gekhman, I. Moiseev Chemical Eng. Trans., V.24, 2011, 175-180

[2] Andrey V. Chistyakov, Vadim Yu. Murzin, Mikhail A. Gubanov, Mark V. Tsodikov CHEMICAL ENGINEERING TRANSACTIONS, 2013, VOL. 32, 2013, 619-624

[3] A.V. Chistyakov, P.A. Zharova, M.V. Tsodikov, S.S. Shapovalov, A.A. Pasinskiy, V.Yu. Murzin, A.E. Gekhman, I.I. Moiseev, 2015, published in Doklady Akademii Nauk, 2015, Vol. 460, No. 1, pp. 57–59.

V-OP25

NO Oxidation and Standard SCR over Fe-ZSM-5 Catalysts. Combining Moessbauer Spectroscopy and Reactivity Studies on the Search for the Active Sites

Ellmers I.[1], Huang H.[2], Perez Velez R.[3], Brückner A.[3], Schünemann V.[2], Grünert W.[1*]

1 - Ruhr University Bochum, Bochum, Germany
2 - Universität Kaiserslautern, Kaiserslautern, Germany
3 - Leibniz-Institut für Katalyse e.V. Rostock, Rostock, Germany

* w.gruenert@techem.rub.de

Keywords: Standard SCR, NO oxidation, Fe zeolites, Mössbauer spectroscopy, active sites

1 Introduction

Fe zeolites have attracted major interest in catalysis because of their potential for a variety of reactions important for NOx abatement and for oxidations with N_2O and with H_2O_2. The identification of their active sites has been complicated by the abundance of different site structures formed by Fe species in zeolites. Apart from isolated Fe oxo cations located at three cation sites, oligomeric Fe oxo structures have been postulated. There can be irregular Fe oxo clusters of different sizes as revealed by EPR spectroscopy [1] and detected near the crystal boundaries by STEM [2], and well-crystalline particles on the external surfaces. In earlier papers, the role of binuclear Fe oxo clusters was emphasized [3]. They were considered as a majority species, e.g. derived from EXAFS measurements [4]. Meanwhile such sites have been lumped into the category "oligomers" because evidence offered for them has been considered inconclusive.

Work on Fe-containing catalysts may benefit from Mössbauer spectroscopy which differentiates Fe sites according both to oxidation state and coordination. However, due to the competition between thermal and spin coupling energies in very small clusters, measurements at very low temperatures, including examination of external field influence, are mandatory when the iron speciation in Fe zeolites is explored. We present here a study on active sites for standard SCR (sSCR) and NO oxidation, where catalytic rate data have been combined with state-of-the-art Moessbauer measurements on isotopically enriched samples.

2 Experimental

Fe-ZSM-5 (Si/Al ≈ 14, ≤ 0.7 wt-% Fe) was prepared via Solid-State Ion Exchange. In some cases, cation sites were partially blocked by inert cations (Na, Ca) prior to introduction of Fe. Activities were measured in flow regime with 1000 ppm NH_3, 1000 ppm NO, 2 % O_2 in He for sSCR, and 1000 ppm NO, 2 % O_2 in He for NO oxidation, both at a GHSV of 750,000 h^{-1}. For Moessbauer spectroscopy, samples were used for the corresponding reaction at 673 K for 45 min, cooled to room temperature in He and filled into capillaries. Mössbauer spectra have been measured at temperatures down to 5K and external fields up to 5 T in a setup equipped with a superconducting magnet. Analysis with a combination of Lorentzian doublets and sextets and paramagnetic subspectra has been made with a spin-Hamiltonian formalism as described in [5].

3 Results and Discussion

The catalytic behavior of the isotopically enriched samples is in agreement with that of conventional samples reported recently [6]. Specifically, Fe-ZSM-5 calcined at 873 K after preparation is drastically activated for NO oxidation by contacting the catalyst with sSCR feed at the same temperature (Fig. 1a). From experiments with variation of the Fe content, it will be

demonstrated that the active site of NO oxidation is a minority of the Fe present even at <0.7 wt-% Fe. In sSCR, the iron introduced into a ZSM-5 with 50 % of exchange sites blocked by Na is most active, while it is least active in the zeolite with 25 % of exchange sited blocked by Ca (Fig. 1b). Experiments with variation of the Fe content show the existence of two different active sites, where the one with the larger intrinsic activity is populated at the higher Fe contents, most likely a clustered species.

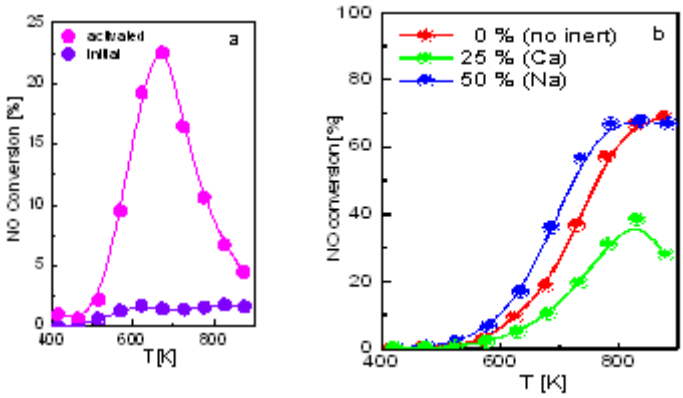

Fig. 1. NO conversions in NO oxidation (a) and sSCR (b); exchange capacity blocked: a - 25 % (by Ca), b – see legend. Activation by contact with sSCR feed at the same temperature (a). Fe contents - 0.39 … 0.43 wt-%.

Fig. 2 shows typical Moessbauer spectra, where the sample with the highest sSCR activity has been selected as an example. The spectra have been analyzed by five components. K1 arises from Fe(III)oxide nanoparticles, K2 indicates high-spin Fe(II) ions. K4 and K5 are attributed to isolated paramagnetic Fe(III) oxo ions appearing in EPR at g' ≈ 4. (K4) and g'≈ 6 and 2 (K5). K2 arises from two species because its intensity varies with the field: some of its intensity at low field appears in K1 at high field, where the shape of the residual signal indicates a diamagnetic structure. While the former may indicate very small Fe oxo aggregates (oligomers), the latter should arise from paired Fe oxo structures with an even number of Fe(III) ions, most likely from bridged Fe(III)-O-Fe(III) dimers. To our best knowledge, this is the first hard proof for an existence of this structure, which is, however, a minority site (ca. 20 % of Fe in Fig. 2). Measurements at higher temperatures (e.g. 77K) do not resolve signals K2, K4, and K5 and underestimate K2.

The comparison of Mössbauer spectra before and after activation for NO oxidation shows that clusters are destroyed and the intensity of signal K5 increases significantly, however, without direct correlation between activity and signal intensity. Possible reasons for this will be discussed. Regarding sSCR, high activities have been observed with samples offering large intensities of the K2 state. The chances to identify of the clustered site for sSCR in more detail will be discussed.

Fig. 2. Mössbauer spectra of Fe-ZSM-5 catalyst (sample "50 % (Na)" in Fig. 1b). T = 5 K, at low and high magnetic fields.

4 Conclusions

Moessbauer spectrosopy at low temperatures, comparing spectra at low and high fields, is a powerful tool for the identification of active sites in Fe zeolites. The method was successfully employed to identify active sites of NO oxidation and standard SCR in Fe-ZSM-5 or narrow down candidates for them.

References

[1] M. Santhosh Kumar, M. Schwidder, W. Grünert, A. Brückner, J. Catal. *227 (2004) 384.*
[2] A.A. Battiston, J.H. Bitter, F.M.F. de Groot, A.R. Overweg, et al. J. Catal. *213 (2003) 251.*
[3] H.-Y. Chen, W.M.H. Sachtler, Catal. Today 42 (1998) 73.
[4] A.A. Battiston, J.H. Bitter, D.C. Koningsberger, J. Catal. 218 (2003) 163.
[5] V. Schünemann, H. Winkler, *Rep. Progr. Phys. 63 (2000) 263.*
[6] I. Ellmers, R.P. Vélez, U. Bentrup, A. Brückner, W. Grünert, J. Catal. 311 (2014) 199.

V-OP26

The Rate Determining Step for the Selective Catalytic Reduction of NO by Ammonia

Moses P.G.[1*], Janssens T.V.W[1], Falsig H.[1], Lundegaard L.F.[1], Vennestrøm P.N.R.[1], Giordanino F.[2], Borfecchia E.[2], Lamberti C.[2,3], Bordiga S.[2], Godiksen A.[4], Mossin S.[4], Beato P.[1]

1 - Haldor Topsoe A/S, Lyngby, Denmark
2 - Dept. of Chemistry, NIS Centre of Excellence and INSTM Reference Center, University of Turin, Torino, Italy
3 - Southern Federal University, Rostov-on-Don, Russia
4 - Dept. of Chemistry, Centre of Catalysis and Sustainable Chemistry, Technical University of Denmark, Lyngby, Denmark

* pogm@topsoe.dk

Keywords: selective catalytic Rreduction, zeolites, Cu-CHA, mechanism, density, functional theory, spectroscopy

1 Introduction

The current technology of choice to reduce NOx emissions from power plants and exhausts from diesel-driven vehicles is based on the selective catalytic reduction of nitrogen oxides by ammonia (NH_3-SCR). The best known catalysts for this reaction are V_2O_5 supported on TiO_2, and Cu- or Fe- exchanged zeolites. In NH_3-SCR, NO is reduced by ammonia to N_2 and H_2O, according to the equation $4\ NO + 4\ NH_3 + O_2 \rightarrow 4\ N_2 + 6\ H_2O$. Despite the fact that this reaction has been known for many years, the precise mechanism and the rate determining step of this reaction are still under discussion. Since adding NO_2 to the reactant gas mixture enhances the rate of the SCR reaction, it has been argued that the activation of NO by O_2 is the rate determining step of the SCR reaction[1–4]. This conclusion is questioned, based on an observation that the rate of NO oxidation over a Cu-zeolite is much slower than the SCR reaction, which suggests that the activation of NO to NO_2 cannot be part of the SCR reaction.[5] Based on a new reaction scheme for the SCR reaction, the contradiction about NO activation by O_2 being the rate determining step can be resolved.

2 Experimental/methodology

A reaction scheme for the SCR reaction is constructed, in which only stable molecules are adsorbed and desorbed from the catalyst, and which describes the overall stoichiometry of the NH_3-SCR reaction correctly. By example of a Cu-CHA catalyst, the stability of the intermediates appearing in the reaction scheme and the transition state energies of relevant reaction steps have been verified by density functional theory (DFT). These calculations were performed using a real space grid-based projector augmented wave method (GPAW-package),[6] and the BEEF-vdW functional to account for Van der Waals interactions.[7]

3 Results and discussion

From the reaction scheme, it can be determined that the rate determining step for NH3-SCR over a Cu-CHA catalyst is the activation of NO by O_2 on a Cu^+ site. The two possibilities that follow from the reaction scheme are 1) the formation of a nitrate from O2 and NO adsorbed on a Cu-ion in the zeolite or 2) the formation of a nitrite by reaction with a nitrate and NO.[8,9] Figure 1 shows the calculated activation barriers for these steps. The calculated activation barrier for the formation of the nitrate is about 1.0 eV; that of the transformation to nitrite is

about 0.7 eV, indicating that the formation of the nitrate intermediate is the rate determining step.

To reconcile the activation of NO by O_2 as the rate determining step in NH_3-SCR with a low activity for NO oxidation to NO_2 in the absence of NH_3, it is realized that the rate of this reaction is the result of a catalytic cycle that is different from that of the NH3-SCR reaction. The NO activation in the SCR reaction is not a complete catalytic cycle, since the Cu^+ is oxidized to a Cu^{2+}. Since no NH_3 is present in the oxidation of NO to NO_2, the reduction of the Cu site to complete the catalytic cycle must be different from the corresponding reduction in the SCR cycle. If this reduction is much slower, compared to SCR, then this step becomes rate determining in the NO oxidation to NO_2.

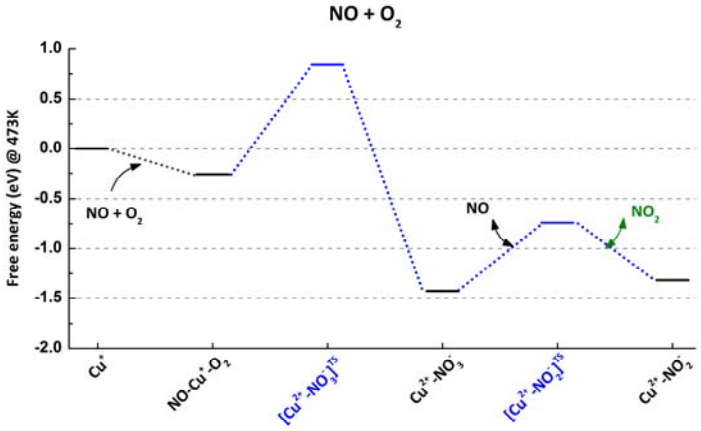

Figure 1. Calculated energies and activation barriers for NO activation by O_2 in NH_3 –SCR over a Cu-CHA catalyst

4 Conclusions

We have shown, based on a new reaction scheme for NH_3-SCR, that the rate determining step of the NH_3-SCR reaction is the activation of NO by oxygen to a nitrate species, and that this is not in contradiction to a very low rate for NO oxidation to NO_2 in the absence of ammonia. The reaction scheme further provides new insights in the role of several reaction intermediates, resulting in a deeper understanding of the NH_3-SCR reaction.

Acknowledgements

CL and KAL thank the support from the Mega-grant of the Russian Federation Government to support scientific research at Southern Federal University, No.14.Y26.31.0001. SM acknowledges financial support by the Danish Independent Research Council DFF 1335-00175 and DFF 09-070250, and Carlsbergfondet for supporting the upgrade of the EPR instrument at DTU. Sachem is acknowledged for making TMAdaOH available.

References

[1] Devadas, M. et al. *Catal. Today* **2007**, *119*, 137.
[2] Long, R. Q.; Yang, R. T. *J. Catal* **2002**, *207*, 274.
[3] Metkar, P. S.; Balakotaiah, V.; Harold, M. P. *Catal. Today* **2012**, *184*, 115.
[4] Wallin, M. *J. Catal.* **2003**, *218*, 354.
[5] Ruggeri, M. P.; Nova, I.; Tronconi, E. *Top. Catal.* **2013**, *56*, 109.
[6] Enkovaara, J. et al. *J. Phys. Condens. Matter* **2010**, *22*, 253202.
[7] Wellendorff, J. et al. *Phys. Rev. B* **2012**, *85*, 235149.
[8] Wang, D.; Zhang, L.; Kamasamudram, K.; Epling, W. *ACS Catal.* **2013**, *3*, 871.
[9] Ciardelli, C.; Nova, I.; Tronconi, E.; Bandl-konrad, B. *Chem. Commun.* **2004**, *20133*, 2718.

V-OP27

Structure-Activity Relationship for Cu-Zeolite NH_3-SCR Catalysts

Ruggeri M.P.[1], Nova I.[1], Tronconi E.[1*], York A.P.E.[2]

1 - Dip.Energia, Politecnico di Milano, Milano, Italy
2 - Johnson Matthey Technology Centre, Sonning Common, UK

* enrico.tronconi@polimi.it

Keywords: zeolite, structure, Cu-CHA, Cu-BETA, Cu-SAPO-34, *in-situ* DRIFTS

1 Introductio

Metal exchanged zeolites are excellent materials for the abatement of NO_x emissions from lean burn engines and are largely employed as wash-coated monolith for the NH_3-SCR technology. A demand for excellent performance of SCR systems is essential to comply with the current NO_x emission limits, as the exhaust gas temperature decreases for improvements in the combustion process. Due to their very good low temperature activity, Cu zeolites are the preferred catalysts; however, different zeolite structures could, in principle, result in different catalytic behaviour and selectivity towards undesired products, such as ammonium nitrate or N_2O [1]. The aim of this study is the elucidation of the structure-activity relations for three different Cu exchanged zeolites, namely a Cu-BETA, a Cu-SSZ-13 and a Cu-SAPO-34.

Steady state experiments were aimed at the comparison of the catalyst in terms of performance and selectivity towards by-products, whereas transient runs and in-situ DRIFT experiments were dedicated to the mechanistic investigation of SCR reactions and byproduct formation mechanisms.

2 Experimental/methodology

Three Cu zeolite catalysts, characterized by different zeolite structures (BETA, SSZ-13 and SAPO-34) but by the same Cu loading (2 % w/w) have been tested in the form of powders, in order to rule out any role of mass transfer phenomena. Steady state data have been collected varying NO_X feed concentration, temperature and gas flow under typical NH_3-SCR conditions (NO_2/NO_X = 0-1, T = 150-550 °C, 266'250/937'500 Ncc/h*$g_{a.p.}$, He used as carrier gas). Transient experiments included NH_3 and NO_2 adsorption + TPD, NO TPSR after nitrates adsorption, NO_2 adsorption after NH_3 adsorption. Transient experiments results were also analyzed by in-situ spectroscopic techniques, in order to collect information regarding surface species formation and stability.

3 Results and discussion

Results of NH_3 adsorption/desorption experiments revealed comparable NH_3 storage capacities for the three catalysts, with only small differences depending on the catalyst structure: the Cu-BETA had the lowest NH_3 storage capacity, the Cu-CHA the highest. Interestingly, the behaviour in the TPD was found different for the three catalysts: in particular, the Cu-BETA and the Cu-SAPO catalysts showed only one NH_3 desorption peak at 330/340 °C whereas the Cu-CHA showed two desorption peaks, at 300 and at 430 °C; this is in accordance with various literature reports on similar catalysts [2, 3].

In addition, Figure 1A shows results obtained during a TPD performed after NO_2 adsorption: the Cu-BETA showed lower nitrates storage capacity and nitrates stability with peaks at 250 and 370 °C; on the other hand, small pore zeolites (Cu-CHA and Cu-SAPO) exhibited similarly higher nitrates stability, with desorption peaks at 330 and 400 °C. As regards

NH_3 oxidation activity, the Cu-BETA showed the lowest activity while the Cu-CHA had the best performance. Related to the SCR activity, namely in the cases of Standard SCR (NO_X conversion reported in Figure 1B) , NO_2 SCR and Fast SCR activity, the Cu-SAPO-34 was the worst catalyst. However, as reported in Figure 1B, the same Cu-zeolite, tested after an ageing process carried out for 2 hours at 750°C, exhibited enhanced Standard SCR performance. A general improvement of SCR activity of the aged Cu-SAPO compared to the fresh sample was evident also for NH_3 oxidation, NO_2 SCR and Fast SCR. Such an improvement can be ascribed to an improved Cu dispersion.

Lower nitrates stability on Cu-BETA possibly explains higher $deNO_x$ activity observed in presence of NO_2, confirmed by greater nitrates reducibility by NO in NO TPSR experiments. On the other hand, this catalyst showed also greater NH_4NO_3 formation and greater N_2O selectivity on Cu-BETA when NO_2 is present, in particular under NO_2 SCR conditions as noticeable by inspection of Figure 1C. In particular, as regards N_2O selectivity, the Cu-SAPO showed the lowest selectivity towards this undesired product.

The systematic in-situ DRIFT study aimed at clarifying the mechanisms of SCR reactions and N_2O formation, confirmed different stability of nitrites/nitrates species, in line with the experimental evidence collected during steady state and transient runs experiments.

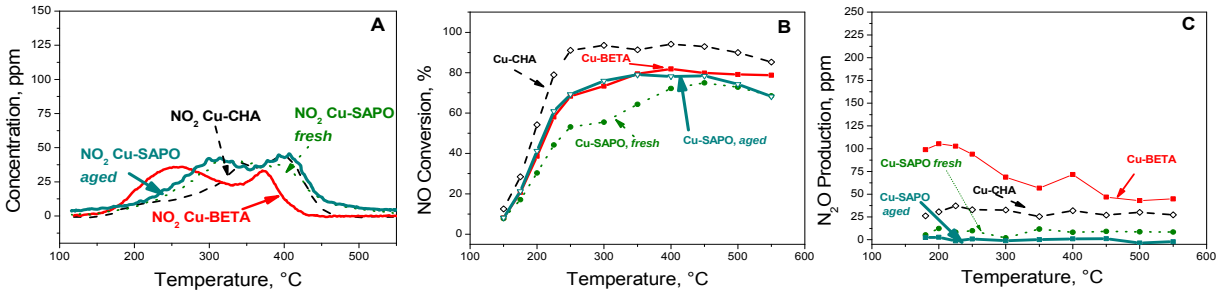

Fig. 1. Comparison of Cu-BETA, Cu-CHA, Cu-SAPO fresh and Cu-SAPO aged: A) TPD results after NO_2 adsorption at 120°C; B) NO_X Conversion in Standard SCR; C) N_2O production in NO_2 SCR.

4 Conclusions

Comparison of the activity of Cu-BETA, Cu-SAPO and Cu-CHA catalysts characterized by the same Cu loading suggests an important role of the zeolite structure in determining not only the $deNO_X$ activity, but also the product distribution (NH_4NO_3 formation and selectivity towards N_2O). In particular, from the results obtained by in-situ DRIFTS and transient runs experiments, zeolite structure and Cu distribution seem to strongly affect the formation of nitrites/nitrates surface species, which play a key role in the mechanism of SCR reactions.

References

[1] J. H. Kwak, R. G. Tonkyn, D. H. Kim, J. Szanyi, C. H.F. Peden, *J. Catal* 275 (2010)
[2] I. Lezcano-Gonzalez, U. Deka, B. Arstad, A. Van Yperen-De Deyne, K.Hemelsoet, M. Waroquier, V. Van SpeyBroeck, B. M. Weckhuysen and A. M. Beale, *Phys. Chem. Chem. Phys*. 16 (2014) 1639.
[3] D. Wang, L. Zhang, K. Kamasamudram and W. S. Epling, *ACS Catalysis* 3 (2013) 871.

V-OP28

Influence of the Preparation Method and Used Support on the Activity of Fe-Loaded Zeolites Catalysts for the NH_3-SCR of NO_x

Gil S.*, Garcia-Vargas J.M., Retailleau L., Giroir-Fendler A.

Université Lyon 1, CNRS, UMR 5256, IRCELYON, Institut de Recherches sur la Catalyse et l'environnement de Lyon, Villeurbanne, France.

* sonia.gil@ircelyon.univ-lyon1.fr

Keywords: selective catalytic reduction (SCR), NOx removing, NH_3-SCR, Fe-zeolite

1 Introduction

Environmental protection standards with respect to air pollutants such as nitrogen oxides (NO_x) are becoming increasingly stringent [1]. Selective catalytic reduction of NO_x by NH_3 (NH_3-SCR) is one the most efficient technologies used for removing NO_x, where the vanadia catalyst is the first commercialized catalytic system. However, several problems still remain, e.g. toxicity of vanadia, formation of N_2O at high temperatures and instability when these catalysts are applied for diesel vehicles [2,3]. Therefore, there are continuous efforts in developing new catalysts. Fe-loaded zeolites received much attention due to its high activity, thermal stability and sulfur and water resistance than the vanadia catalyst, under SCR reaction conditions [4,5]. It is well recognized that the activity of Fe-loaded zeolites for SCR depended strongly on the preparation method [4,5]. The aim of the present work was to investigate the influence of the preparation method and the support used (ZSM-5, Beta and LTL) on the SCR-NH_3 activity of the different Fe-loaded zeolites catalysts.

2 Experimental/methodology

ZSM-5, Beta and LTL supports were hydrothermally synthesized, as described in detail elsewhere [6]. The active phase (Fe) was introduced by impregnation (IMP) and in-situ hydrothermal (HT) methods and, these catalysts after aged were characterized by N_2 adsorption, ICP, RMN, XRD, XPS and TEM. Catalytic tests were carried out using 25 mg of catalyst and a reactant mixture containing [NO] ≈ [NH_3] ≈ 1000 ppm, [O_2] ≈ 8 vol.%, [H_2O] ≈ 3 vol.% and He as carrier gas (GHSV = 142.000 h^{-1}). Temperature was increased by a ramp of 2°C min^{-1} up to 500°C. After this treatment, all catalysts were tested during the cooling ramp.

3 Results and discussion

XRD spectra of the zeolites and the Fe-loaded zeolites catalysts are quite similar, which means that the crystalline nature of the zeolites was not modified after the Fe incorporation. No peaks could be assigned to the presence of metallic iron or iron oxide, evidencing high Fe dispersion. XPS results showed that, Fe cations were presented mainly as Fe^{3+} ions (Fe_2O_3, 711 eV), along with a small amount of Fe^{2+} (FeO, 709 eV) in the case of the hydrothermal catalysts, whereas the impregnated catalysts presented the formation of aggregated Fe^{3+} ions (Fe_3O_4, 710.76 eV). Moreover, for a given preparation method, the Fe particles size follows this trend Fe/ZSM-5 > Fe/Beta > Fe/LTL. This could be attributed to the zeolite structure, where the iron solution is expected to enter more easily into the Beta or LTL than on the ZSM-5 porosity [5], Table 1, favoring the higher dispersion.

The preparation method used affects the SCR activity of Fe-loaded zeolites catalysts. The hydrothermal catalysts presented higher activity and N_2 selectivity than the impregnated one. This could be a consequence of the partial pores blockage of the zeolite, with the impregnated

catalysts, then some of the active Fe sites could not participate in the reaction and also, the Fe_3O_4 oxides formation due to the Fe particles agglomeration [5,7]. Moreover, the N_2O formation was lower for the hydrothermal catalysts than for the impregnation ones, which could be also attributed to the absence or lower amount of Fe_3O_4 oxides presented in these catalysts [8]. Moreover, for a given preparation method (hydrothermally synthesis) and same Fe amount (1%wt. Fe) the NH_3-SCR activity at low temperature follows this trend Fe/LTL ≈ Fe/Beta > Fe/ZSM-5. However, the N_2-selectivity of Fe/LTL decreases dramatically at higher temperatures, Fig. 1. This indicates that the framework structure and/or pore geometry are crucial for determining the SCR activity [5,9].

Table 1. Physicochemical properties of hydrothermal catalysts.

Catalysts	Si/Al $_{RMN}$	Fe loading (wt.%)$_{ICP}$	BET surface area (m^2g^{-1})	Total pore volume (cm^3g^{-1})	Average pore size (nm)
HT-Fe/ZSM-5	27,3	1	376	0.14	5.1
HT-Fe/Beta	8,4	1	670	0.29	9
HT-Fe/LTL	2,9	1	401	0.31	8.6

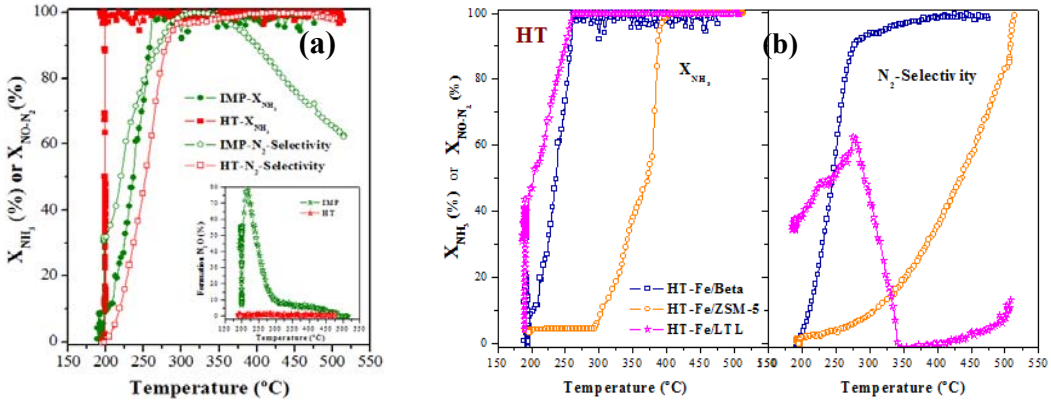

Fig. 1. (a) Comparison impregnated and hydrothermal **Fe-Beta** catalysts activity and **(b)** NH_3-SCR activity of **Fe-loaded zeolites** catalysts hydrothermally synthesized.

4 Conclusions

The particular NH_3-SCR behavior of the catalysts depends on the preparation method and the zeolite nature. Thus, the hydrothermally synthesis allowed a more active catalyst, maintaining the selectivity to N_2 with low N_2O formation and, the framework structure and/or pore geometry was crucial for determining the SCR activity.

Acknowledgements

The authors gratefully acknowledge to the French Government for the UREENOx project (ANR11-VPTT-002-03).

References

[1] D2008/50/CE European Council (May 21, 2008).
[2] M. Yates, J.A. Martín, M.A. Martín-Luengo, S. Suáreza, J. Blanco, *Catal. Today* 120 (2005) 107.
[3] P.L.T. Gabrielsson, *Top Catal*. 28 (2004)177.
[4] G. Qi, R.T. Yang, *Appl. Catal. B: Environmental* 60 (2005) 13.
[5] B. Pereda-Ayo, U. De La Torre, M.J. Illán-Gómez, A. Bueno-López, J.R. González-Velasco, *Appl. Catal. B: Environmental* 147 (2014) 420.
[6] D. Uzio, J. Peureux, A. Giroir-Fendler, J.A. Dalmon, J.D.F. Ramsay, *Stud. Surf .Sci. Catal.* 87 (1994) 411.
[7] S. Xiaoyan, L. Fudong, S. Wenpo, H. Honget, *Chinese J. of Catal. 33 (2012) 454.*
[8] R.Q. Long, R.T. Yang, *J. Catal.* 194 (2000) 80.
[9] M. Santhosh Kumar, J. Pérez-Ramírez, M.N. Debbagh, B. Smarsly, A. Brückner, *Appl. Catal. B: Environmental* 62 (2005) 244.

V-OP29

$CeVO_4$-Based as Efficient and Stable Catalyst for NH_3 Selective Catalytic Reduction of NO_x – Application to Diesel Exhaust Gas

Gillot S.[1,2,3], Dujardin C.[1,3,4], Dacquin J.-Ph.[1,2,3], Granger P.[1,2,3*]

1 - UCCS, France
2 - University of Lille, Villeneuve d'Ascq, France
3 - Cité Scientifique, Villeneuve d'Ascq, France
4 - ENSCL, France

* pascal.granger@univ-lille1.fr

Keywords: SCR, DeNOx, ammonia, vanadium, diesel exhaust gas

1 Introduction

Reduction of NO_x by NH_3 is recognized as the most efficient technology for practical application for both stationary and mobile sources. However commercial V_2O_5–WO_3/TiO_2 or V_2O_5–MoO_3/TiO_2 can suffer from vanadium toxicity due to the presence of V_2O_5. By contrast, cerium orthovanadate material ($CeVO_4$) has interesting properties related to the stabilization of Ce^{3+} and V^{5+} cations in tetragonal zircon-type structure. This compound is also active in oxidation reaction thanks to its reducibility. In the present study we investigated the catalytic behaviour of $CeVO_4$ in the Selective Catalytic Reduction of NO_x by ammonia. Particular attention was focused on the impact of synthesis procedure and thermal ageing treatments on the catalytic activity in standard SCR, fast SCR and NO_2 SCR conditions.

2 Experimental/methodology

$CeVO_4$ was prepared according to Xie's method [1] using Na_3VO_4 and $Ce(NO_3)_3{,}6H_2O$ precursors. The precursors were dissolved in water at different pH adjusted by dropwise addition of NaOH solution. Then, the mixture was treated in hydrothermal conditions at 180°C for 24h. The solid thus obtained was washed in water and ethanol. BET, SEM, Raman spectroscopy, XRD and XPS analyses were achieved before and after thermal ageing treatment. NO, NO_2, NH_3, N_2 and N_2O concentrations were measured during temperature-programmed reactions in a fixed bed reactor at GHSV=150,000 $mL.g^{-1}.h^{-1}$ from 200°C to 550°C under standard, fast and NO_2 conditions. Realistic gas mixture consisted of 400 ppm NO_x+400 ppm NH_3+8 vol.% O_2+10 vol.% CO_2 +10 vol.% H_2O in Helium with NO/NO_x ratio equal to 0.9, 0.5 and 0.3 for standard, fast and NO_2 SCR respectively. The thermal ageing treatment consisted of ageing the catalyst in 10 vol.% H_2O in air between 500°C to 850°C.

3 Results and discussion

XRD patterns evidenced the formation of the tetragonal zircon-type structure for $CeVO_4$ and also the presence of bulk CeO_2 impurity in small extent when the final pH of the solution was higher than 2. Subsequent, thermal ageing at 500°C, 600°C and 850°C led to a progressive sintering and a correlative decrease of the specific surface area from 46 m^2/g to 0.5 m^2/g. It should be noticed that the characterization by Raman spectroscopy and XRD confirmed the absence of V_2O_5 segregation independently the synthesis or thermal ageing procedure.

The catalytic performances were evaluated in presence of steam, CO_2 and an excess of O_2 on aged samples at different temperature. $CeVO_4$ synthesized at final pH=3.3 and further aged at 500°C in 10 vol.% H_2O/air exhibited interesting NO_x conversion with a complete selectivity to

N_2 formation in the wide range of temperature whatever the NO/NO_x ratio. In Fast SCR conditions, the conversion of NO_x to N_2 remains stable around 90-95% between 200°C and 400°C at 150,000h^{-1}. In standard conditions with NO/NO_x=0.9, the NO conversion progressively increased from 34% at 200°C to 79% at 450°C. NO_x conversion also progressively increased until 99% at 450°C for NO_2 SCR.

Table 1. Specific surface area and crystalline size of $CeVO_4$ (pH=3.3) according to the ageing temperature

	After drying at 80°C	Ageing temperature 500°C	600°C	850°C
BET surface area (m^2/g)	46	17.7	5.8	0.5
$CeVO_4$ crystalline size (nm)*	27	46	85	96

* estimated from XRD using Scherrer method

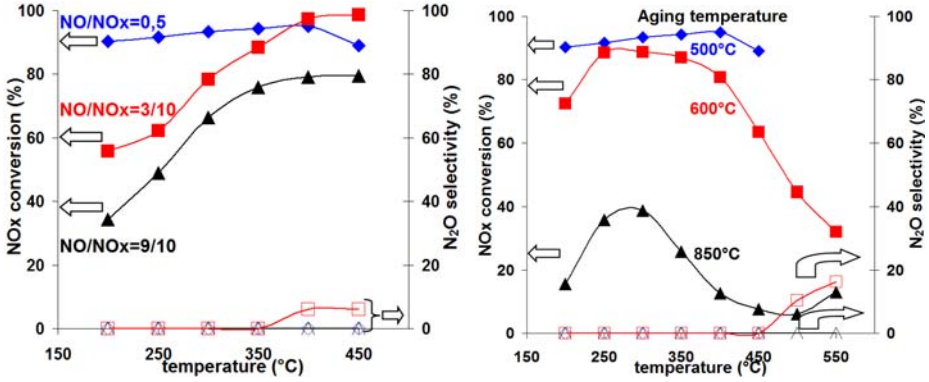

Fig. 1. Comparison of NO_x conversion and N_2O selectivity of $CeVO_4$ (pH=3.3) in standard, fast and NO_2 SCR after thermal ageing at 500°C (A) and in fast SCR after thermal ageing under 10%H_2O/air at 500°C, 600°C and 850°C (B)

The NO_x conversion in fast SCR conditions was slightly decreased between 250 and 350°C after ageing at 600°C whereas ammonia oxidation led to NO and N_2O above 500°C. Clearly, the sintering of active phase strongly influences the catalytic performances at high temperature. The final thermal ageing at 850°C which was accompanied by very low specific surface area also led to a significant decrease of NO_x conversion at the expense of NH_3 oxidation above 500°C. The conversion reached 39% at 300°C which is quite high if we take into account its low specific surface area. This point suggested that the stabilization of specific surface area for $CeVO_4$ is a key point for further application of $CeVO_4$ in mobile sources. Subsequent incorporation was found to improve the catalytic performances limiting the impact of deactivation. XPS analysis and adsorption of probe molecules provided important information related to the resistance to deactivation of acidic and redox functions.

4 Conclusions

This study reports the first application of CeVO4 in deNOx catalysis for stationary and mobile sources. The CeVO4 catalyst is promising for stationary sources applications. The catalyst exhibited NOx conversion to N2 around 93% at 150,000 mL.g-1.h-1 between 200 and 400°C after thermal ageing at 500°C in 10%H2O/air. In the case of mobile sources, the stabilization of specific surface area will be discussed.

Acknowledgements

The authors gratefully acknowledge financial support from the French National Agency for Research (UreeNOx Project, Ref. ANR-11-VPTT-002).

References

[1] B. Xie et al., *J. Clust. Sci.* 22 (2011) 555.

V-OP30

Base-Promotion of Selective Decomposition of Ammonium Formate and Formic Acid over Au/TiO_2 under SCR-Relevant Conditions

Sridhar M.[1,2*], Ferri D.[1], Van Bokhoven J.A.[1,2], Kröcher O.[1,3]

1 - Paul Scherrer Institut, General Energy Department, Villigen, Switzerland
2 - ETH Zurich, Institute for Chemical and Bioengineering, Zurich, Switzerland
3 - École Polytechnique Fédérale de Lausanne (EPFL), Institute of Chemical Sciences and Engineering, Lausanne, Switzerland

* manasa.sridhar@psi.ch

Keywords: ammonium, formate, gold catalysis, effect of base, formic acid, decomposition, SCR

1 Introduction

Urea has been one of the most widely used ammonia storage compounds for selective catalytic reduction (SCR) of NO_x in automobiles. However, the observable problems with urea solution initiated research efforts to replace this compound with alternative ammonia precursors, such as concentrated guanidinium formate, ammonium formate (AmFo) and methanamide solutions, that are more thermally stable, freeze at lower temperature, have higher ammonia storage capacity, and decompose more selectively [1,2]. AmFo is experimentally the simplest choice to study the activity and behaviour of catalysts for the decomposition of the aforementioned precursors under realistic conditions [3]. We have recently identified Au/TiO_2 as a uniquely selective catalyst to convert AmFo into CO_2 without oxidizing the co-evolved ammonia even under highly oxidizing conditions prevalent in the exhaust gases [4]. Since, AmFo thermolyzes into ammonia and formic acid in the gas-phase, it is important to understand the effect of ammonia on formic acid decomposition as a step towards catalyst optimization. A promotional effect of ammonia was observed on the decomposition rate which also entailed an enhanced selectivity for CO_2 formation [5]. Such a promotional effect of the basic gas-phase reactant was also realized as a catalytic effect by introducing a base metal oxide (La_2O_3) into the catalyst. Additionally, by corollary, it is shown that acid-modification (WO_3) of the catalysts results in suppressed activity.

2 Experimental

The catalysts were prepared by incipient wetness impregnation of $HAuCl_4$ on commercial anatase, 10 wt% La_2O_3-TiO_2 and 10 wt% WO_3-TiO_2 (Cristal Global). The gold composition was fixed at 0.5 wt%. The catalysts were washcoated on cordierite monoliths and tested on a laboratory-scale reactor setup in a feed containing 650 ppm AmFo or formic acid, 0-7800 ppm ammonia, 10 vol% O_2, 5 vol% H_2O and balance N_2 at 750 $L \cdot h^{-1}$ in order to realize very high GHSVs in the range 50,000 h^{-1} to 300,000 h^{-1}. Full experimental details are given elsewhere [4,5].

3 Results and discussion

A systematic investigation of the effect of ammonia on formic acid decomposition revealed a highly beneficial influence on the reaction rate and the CO_2 yield in the temperature range 160–300 °C (Fig. 1a). Ammonia oxidation did not occur at any of the studied temperatures and space velocities which is remarkable considering the high concentrations of O_2 (10%) and H_2O (5%) in the feed. Analogously, it was found that La_2O_3-modification results in significant promotion, while modification by WO_3 causes an opposite effect leading to suppressed activities

(Fig. 1b). At 300 °C, using the lowest contact time, formic acid decomposition rate increased 3.5-fold over Au/La_2O_3-TiO_2 and decreased 0.7-fold over Au/WO_3-TiO_2. Under the same conditions, CO_2/CO ratio underwent an increase by a factor of 10 in the case of Au/La_2O_3-TiO_2 compared to the unmodified Au/TiO_2, while WO_3-modification halved the CO_2/CO ratio. Determination of kinetic orders with respect to formic acid strongly suggested surface-poisoning of all the catalysts, with Au/La_2O_3-TiO_2 exhibiting the most negative order. CO_2 adsorption on the three catalytic systems analyzed using FTIR spectroscopy confirmed the high basicity of Au/La_2O_3-TiO_2 in the form of high CO_2-uptake. The presence of La_2O_3 favored the formation of smaller gold particles as indicated by HAADF-STEM analysis. Thermal aging of Au/La_2O_3-TiO_2, leading to gold particle growth to the gold size range of Au/TiO_2, did not alter the base-induced trends in activity and CO_2 selectivity. The activity tests of the modified supports in the absence of gold confirmed the crucial role of gold for the realization of such a base-induced promotional effect.

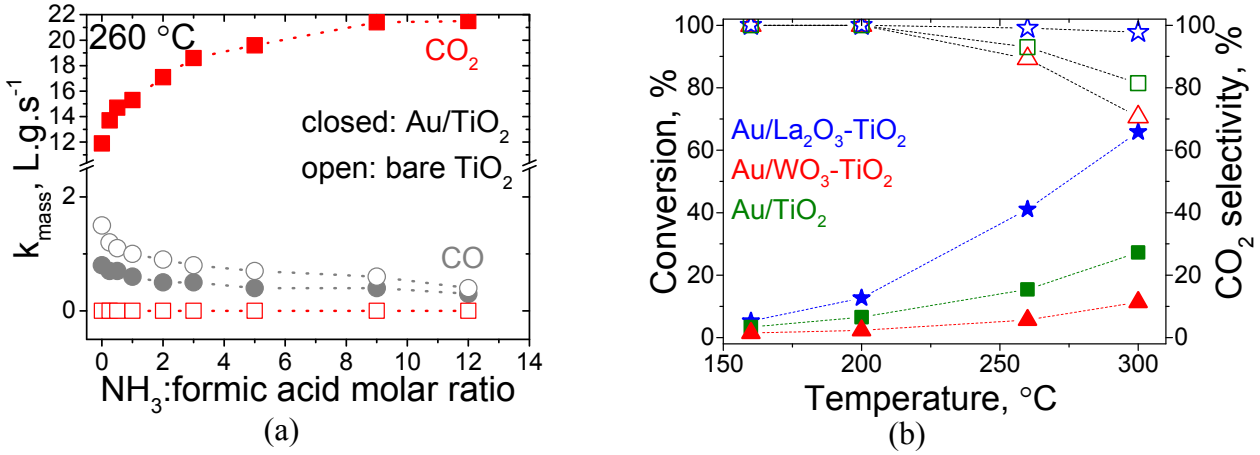

Fig. 1. (a) Effect of ammonia on rate constants for CO_2 and CO production from formic acid decomposition at 260 °C, (b) effect of La_2O_3- and WO_3-modification on formic acid decomposition (closed symbols: conversion, open symbols: CO_2 selectivity).

4 Conclusions

Fast decomposition of the formate part of alternative ammonia precursor compounds presents two advantages: (1) the cationic part is destabilized and (2) formic acid is no longer available to form side products like methanamide or HCN [3]. Au/TiO_2 apart from being a highly active and selective catalyst for AmFo decomposition also showed an enhanced decomposition activity in the presence of excess gas-phase ammonia. As a rational step towards further catalyst optimization, the observed promotional effect of the basic gas-phase reactant was transformed into a catalytic effect by support-modification with a basic additive.

Acknowledgements

Financial support from the Swiss National Science Foundation (SNF, project number 200021_143430/1) is gratefully acknowledged. Sincere thanks to Martin Elsener for his technical support and guidance.

References

[1] T. V Johnson, Int. J. Engine Res. 10 (2009) 275.
[2] C. Gerhart, H.-P. Krimmer, B. Hammer, B. Schulz, O. Kröcher, D. Peitz, T. Sattelmayer, P. Toshev, G. Wachtmeister, A. Heubuch, E. Jacob, SAE Int. J. Engines 5 (2012) 938.
[3] O. Kröcher, M. Elsener, E. Jacob, Appl. Catal. B Environ. 88 (2009) 66.
[4] M. Sridhar, D. Peitz, J. van Bokhoven, O. Kröcher, Chem. Commun. 50, (2014) 6998.
[5] M. Sridhar, J.A. van Bokhoven, O. Kröcher, Appl. Catal. A Gen. 486 (2014) 219.

V-OP31

Sulfur-Tolerant $BaO/ZrO_2/TiO_2/Al_2O_3$ Quaternary Mixed Oxides for $DeNO_X$ Catalysis

Say Z.R.[1], Mihai O.A.[2], Tohumeken M.E.[1], Ercan K.E.[1], Olsson L.E.[2], Ozensoy E.[1*]

1 - Department of Chemistry, Bilkent University, Ankara, Turkey
2 - Chemical Reaction Engineering and Competence Centre for Catalysis, Chalmers University of Technology, Göteborg, Sweden

* ozensoy@fen.bilkent.edu.tr

Keywords: NSR/LNT, $Al_2O_3/ZrO_2/TiO_2$, Pt, DeNOx, FTIR, TPD

1 Introduction

Some of the major challenges of NO_x Storage Reduction (NSR) or Lean NOx Trap (LNT) catalysts are associated with sulfur poisoning and thermal/structural stability [1-6]. On the other hand, improvement of sulfur tolerance of an NSR/LNT system need to be accomplished without comprising the NO_x storage capacity. TiO_2 which has a moderately high surface acidity is known as a promising oxide support/promoter against sulfur poisoning, providing much lower temperature for sulfur elimination, but leading to a relatively limited NOx storage capacity [7]. In the current contribution, we focus on the surface chemistry of $Al_2O_3/ZrO_2/TiO_2$-based NSR/LNT catalysts. In particular, we elucidate the NO_x and SO_x adsorption and thermal regeneration performances under reducing conditions at the molecular level by means of in-situ FTIR and TPD techniques. Moreover, NO_x uptake capacities aforementioned materials are quantitatively investigated in the presence and absence of sulfur poisoning via flow mode performance analysis tests.

2 Experimental/methodology

Detailed description of synthesis of ZrO_2/TiO_2 (ZT) binary and $Al_2O_3/ZrO_2/TiO_2$ (AZT) ternary oxide systems via co-precipitation technique has been explained in detail in one of our former reports [3]. The synthesis of the support materials is followed by BaO and Pt addition via incipient wetness impregnation method, forming catalytic materials in the form of $Pt/Al_2O_3/ZrO_2/TiO_2$, $Pt/BaO/Al_2O_3/ZrO_2/TiO_2$, and $Pt/BaO/Al_2O_3$ (Pt/Ba/Al). Structural properties of the synthesized catalysts were investigated via XPS, ex-situ Raman spectroscopy, TEM, EDX, XRD and BET while their NOx uptake and release behavior was investigated by employing the flow mode catalytic performance experiments as well as in-situ FTIR and TPD measurements.

3 Results and Discussion

As illustrated in Figure 1, sulfur regeneration capability of $Al_2O_3/ZrO_2/TiO_2$–supported materials are noticeably higher in the presence of a reducing agent (i.e. $H_2(g)$). While complete SO_x regeneration is achieved around 773 K on Pt/AZT, this temperature (c.a. 973 K) is much higher for Pt/Ba/Al. However, NO_x sorption ability of Pt/AZT without the basic oxide storage domains (i.e. BaO and K_2O) is too low to be considered for LNT applications at the relevant operational temperatures (e.g. 573 K) due to the high surface acidity/low basicity of this surface. Therefore, Pt/AZT material are enriched and modified by incorporation of a basic storage domain, namely BaO. While addition of 8wt % BaO has a minor influence on sulfur regeneration temperature, 20wt % BaO loading drastically change the materials characteristics as shown in the in-situ FTIR results. These findings are also supported by the TPD data as

illustrated in Figure 2. SO_x uptake capacities of investigated BaO-containing catalysts can be ranked in a decreasing order as Pt/20Ba/Al > Pt/20Ba/AZT > Pt/8Ba/AZT. Finally, all materials were tested in quantitative flow reactor measurements performed under realistic catalytic conditions (data not shown) and Pt/8BaO/AZT catalyst revealed a superior NSC at 573 K upon sulfur poisoning and subsequent regeneration, surpassing the catalytic performances of all of the currently investigated materials including the conventional Pt/20BaO/Al benchmark catalyst [8].

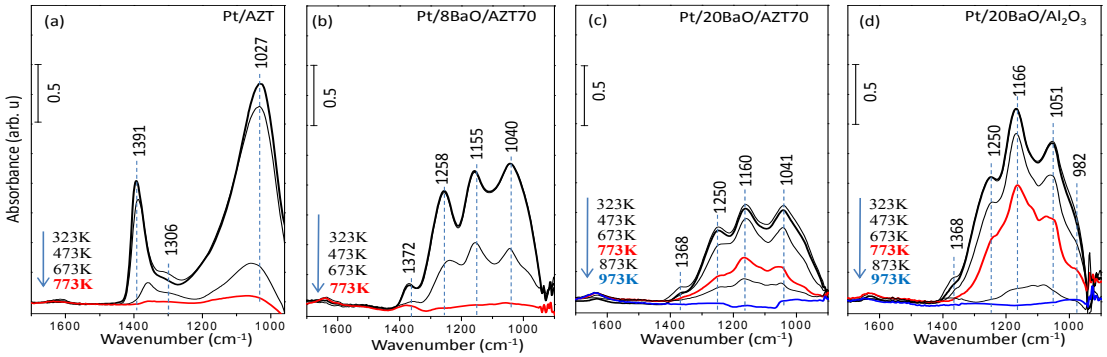

Figure 1. FTIR spectra related to SO_x release properties of sulfur-poisoned (a) Pt/AZT, (b) Pt/8Ba/AZT, (c) Pt/20Ba/AZT and (d) Pt/20Ba/Al in the presence of H_2(g).

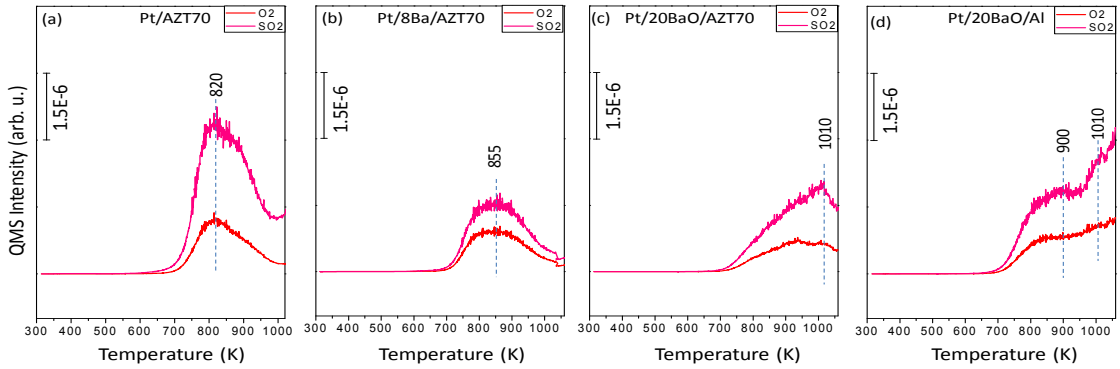

Figure 2. TPD profiles related to SO_x desorption from sulfur-poisoned (a) Pt/AZT, (b) Pt/8Ba/AZT, (c) Pt/20Ba/AZT and (d) Pt/20Ba/Al surfaces.

4 Conclusions

It is a great challenge to synthesize catalytic materials revealing superior sulfur tolerance and high NO_x uptake capacity. In this study, we provide fundamental insights regarding the molecular-level understanding of the adsorption characteristics of acidic adsorbates such as NO_x and SO_x on a novel ternary oxide catalytic support material, whose surface properties can be fine-tuned to optimize NSR/LNT performance.

Acknowledgements

We acknowledge the financial support from the Scientific and Technological Research Council of Turkey (TUBITAK) (Project Code: 111M780).

References

[1] Z. Say, E.I. Vovk, V.I. Bukhtiyarov, E. Ozensoy, Topics in Catalysis 56, 950 (2013).
[2] Z. Say, E.I. Vovk, V.I. Bukhtiyarov, E. Ozensoy, Applied Catalysis B: Environmental 142-143, 89 (2013).
[3] Z. Say, M. Tohumeken, E. Ozensoy, Catalysis Today 231, 135 (2014).
[4] Z. Say, M. Dogac, E.I. Vovk, Y.E. Kalay, C.H. Kim, W. Li, E. Ozensoy, Applied Catalysis B: Environmental 154-155, 51 (2014)
[5] M. Dogac, Z. Say, E.I. Vovk, C.H. Kim, E. Ozensoy, ChemCatChem (2015) submitted.
[6] G.S. Senturk, E.I. Vovk, V.I. Zaikovskii, Z. Say, A.M. Soylu, V.I. Bukhtiyarov, E. Ozensoy, Catalysis Today 184, 54 (2012).
[7] S. Matsumoto, Y. Ikeda, H. Suzuki, M. Ogai, N. Miyoshi, Applied Catalysis B: Environmental 25, 115 (2000).
[8] Z. Say, O. Mihai, M. Tohumeken, K.E. Ercan, L. Olsson, E. Ozensoy, Applied Catalysis B: Environmental (2015) submitted

V-OP32

Opportunities for Ceria-based Catalysts versus Platinum Catalysts in Diesel Soot Combustion

Giménez-Mañogil J., García-García A.*

MCMA Group, Dept. of Inorganic Chemistry, Faculty of Sciences, University of Alicante, Alicante, Spain

* a.garcia@ua.es

Keywords: ceria-zirconia, copper, platinum catalyst, soot combustion, NO_2 production

1 Introduction

Noble metal-based catalysts, such as platinum, have been developed to promote the oxidation of NO to NO_2, which is more oxidant than O_2, and decrease the combustion onset temperature of soot under realistic diesel conditions. However, their high cost has led to the consideration of other lower-priced materials that can be competitive in terms of catalytic activity. These include, besides cerium-based catalysts, those using transition metals.

Copper-doped ceria (and ceria-zirconia) mixed oxides have managed to overcome activity and selectivity of undoped oxides in reactions such as soot combustion [1]. The Cu-ceria interface interactions confer a synergistic effect, which enhances the redox properties of the catalyst due to the stabilization of highly reactive copper species [2].

Even though a large number of catalytic formulations have been tested for catalytic combustion of diesel soot, a lot of work is still needed in order to advance towards a rational catalyst design. Therefore, the overall aim of this research is to conduct a systematic study of the ceria-based catalysts' activities for soot combustion, comparing to a commercial Pt/alumina catalyst in a set of experiments (under isothermal/ramp modes and under different gas atmospheres) to explore the opportunities of ceria-based catalysts versus noble metal supported catalysts for this application. The results obtained from the NO_2 and "active-oxygen"-assisted soot combustion, as well as the NO ↔ NO_2 recycling efficiencies, were discussed.

2 Experimental

The $Ce_{0.8}Zr_{0.2}O_2$ support (CZ) was prepared by the co-precipitation method, and the solid obtained after filtration was dried and calcined at 500°C for 1 hour in air. The $Ce_{0.8}Zr_{0.2}O_2$-supported catalyst with 2% Cu (Cu2/CZ) was prepared by incipient wetness impregnation with an aqueous solution of $Cu(NO_3)_2 \cdot 3H_2O$ and subsequent drying and calcination at 500°C for 1 h. This amount of Cu was chosen from a previous optimization study [3]. The commercial $1\%Pt/Al_2O_3$ was supplied by Sigma-Aldrich (Pt1/AL).

The catalysts were characterized by N_2 adsorption-desorption isotherms at -196°C, XRD, Raman spectroscopy, XPS and H_2-TPR. They were tested for NO oxidation to NO_2 in TPR conditions (from room temperature up to 700ºC at 10ºC/min), and for soot combustion (TPR and isothermal reactions at 400, 425 and 450ºC). The gas mixture used comprised 500 ppm NOx, 5% O_2 and N_2 balance (or $5\%O_2$ and N_2 balance); the gas flow was fixed at 500 ml/min (GHSV = 30,000 h^{-1}).

3 Results and Discussion

According to the whole characterization results, copper remains well-dispersed (absence of segregated phases corresponding to CuO) onto the ceria-zirconia's surface and evidences of copper incorporation into the lattice were not revealed. The procedure of incipient wetness impregnation led to a dramatic improvement of the copper entities' reducibility (with regard to bulk CuO) and a concomitant ceria reduction at low temperatures was also quantified. This

synergistic effect explains the relevant improvement in the NO oxidation capacity to NO_2 that this very low copper doping provides to the ceria zirconia support. In spite of these satisfactory results, Cu2/CZ sample is still far from the NO_2 production capacities of the platinum catalyst (47% versus 75%, expressed as maximum NO_2 production in a TPR experiment).

In spite of the very high NO_2 production capacity and excellent efficiency towards the NO ↔ NO_2 recycling activities exhibited by the platinum catalyst, the superior production and transfer of "active oxygen" towards the soot surface (even in the loose-contact mode) combined to a moderate activity for NO_2 production in a convenient temperature range lead to a more and more positive performance of the 2% Cu catalyst, thus emulating the noble-metal catalyst's behavior for the complex solid-solid-gas reaction involved in the diesel soot combustion. In this sense, Figures 1 and 2 reflect the different trends in activity obtained for the selected catalysts as a consequence of the relevance of the "active oxygen"-assisted soot combustion as the temperature becomes higher and higher.

At 400°C, Pt-catalyst is the most active one (the three experiments are conducted with the same amount of catalyst) and only if the soot combustion reaction rate is expressed in terms of price, the most efficient catalyst becomes Cu2/CZ (Figure 1). More interestingly, at 450°C, the copper-containing catalyst outperforms the catalytic response given by the noble metal-catalyst, expressed as combustion rate (Figure 2).

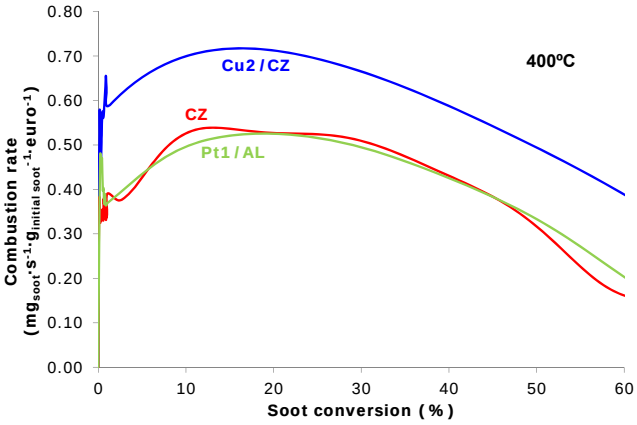

Figure 1. Soot combustion rates, expressed per euro of catalyst cost, versus soot conversion under isothermal conditions (400ºC).

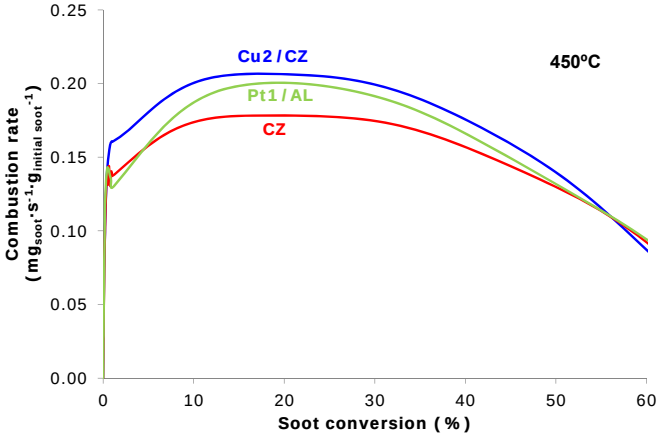

Figure 2. Soot combustion rates versus soot conversion under isothermal conditions (450ºC).

4 Conclusions

A catalyst prepared by incipient wetness impregnation of $Ce_{0.8}Zr_{0.2}O_2$ with a 2% of copper allows outperforming the catalytic performance exhibited by a commercial platinum catalyst under NOx/O_2 at 450°C, thus revealing the opportunities of ceria-based catalysts in the context of soot combustion application.

Acknowledgements

The authors gratefully acknowledge the financial support of Generalitat Valenciana (PROMETEOII/2014/010 project) and the Spanish Ministry of Economy and Competitiveness (CTQ2012-30703 project) and the UE (FEDER funding).

References

[1] Q. Liang, X. Wu, D. Weng, Z. Lu, *Catal. Commun.* 9 (2008) 202.
[2] A. Martínez-Arias, M. Fernández-García, J. Soria, J.C. Conesa, *J. Catal.* 182 (1999) 367
[3] J. Giménez-Mañogil, A. Bueno-López, A. García-García, *Appl. Catal., B* 152-153 (2014) 99.

V-OP33

Low Temperature Method for Measuring Oxygen Storage Capacity of Ceria-Containing Oxides

Porsin A.[1*], Alikin E.[2], Bukhtiyarov V.[1,3]

1 - Boreskov Institute of Catalysis SB RAS, Novosibirsk, Russia
2 - Ecoalliance, Ltd., Novouralsk, Russia
3 - Novosibirsk State University, Novosibirsk, Russia

* avp@catalysis.ru

Keywords: three-way catalyst, ceria, ceria-containing oxide, oxygen storage capacity

1 Introduction

Ceria-containing oxides ($Ce_xM_{1-x}O_2$) are an intrinsic part of three-way catalysts (TWC): they increase the activity of TWC while reduce the load of precious metals and the cost of TWC. Ceria damps fluctuations of oxygen in exhaust gases, keeping its content at the catalyst surface equal to the stoichiometric ratio. These conditions provide the effective oxidation of CO and hydrocarbons to CO_2 and H_2O simultaneously with the reduction of NO_x to N_2 [1].

Dynamic oxygen storage capacity (OSC) of $Ce_xM_{1-x}O_2$, which refers to oxygen kinetically available for chemical reactions, allows one to predict the performance of TWC. OSC can be measured under cycling flow conditions when a gas with O_2 alternates a gas with CO [2]. In this method, oxygen is accumulated in the oxide lattice while the gas with O_2 passes through the sample. A release of oxygen and catalytic oxidation of CO to CO_2 proceed during the next alternative step, when the gas with CO passes through the sample. The OSC in this method is calculated from the amount of CO transformed to CO_2. $Ce_xM_{1-x}O_2$ acts as a catalyst. However, $Ce_xM_{1-x}O_2$ is almost inactive in the oxidation of CO at temperatures below 300 ^{O}C [2], which makes the OSC measurement impossible. Therefore, OSC is usually studied at sufficiently high temperatures (e.g. 400 ^{O}C).

Addition to $Ce_xM_{1-x}O_2$ of a more active catalyst allows one to decrease the temperature of the CO oxidation stage and thus to expand the boundaries of OSC research. For instance, CO oxidation on a Pt/Al_2O_3 catalyst is possible at temperatures from 150 ^{O}C [3]. Expanding the boundaries of OSC research toward lower temperatures is of great interest because it enhances the understanding of TWC properties.

2 Experimental/methodology

Mixtures comprising 56% Pt/Al_2O_3 and 44% $Ce_xM_{1-x}O_2$ were used to measure OSC. The content of Pt on Al_2O_3 was 0.8%. The mixtures were deposited on a cordierite honeycomb support from a suspension. The supported catalysts were subjected to the flow of a mixture of O_2, CO, and CO_2 in N_2. The flows of CO and CO_2 were constant and equaled 0.6 and 9.3 vol %, respectively, while the flow of oxygen was changed every 100 s from 0 to 1 vol % and backwards (Fig. 1). OSC of the samples was studied at heating of the gas flow with the constant rate (5°C/min). The temperature change within each 100-s cycle did not exceed 8 °C. During the experiment, the content of CO was measured at the outlet of the reactor.

In the presence of oxygen, CO was completely oxidized to CO_2. After switching off the O_2 supply (between t_1 and t_2 in Fig. 1), CO was oxidized with oxygen accumulated in the catalyst Pt/Al_2O_3+$Ce_xM_{1-x}O_2$. The amount of oxygen reacted with CO was calculated from the equation $CO+O = CO_2$. The oxygen capacity was determined for each cycle of changing the oxygen flow rate and then recalculated per unit mass of the ceria-containing oxide. The amount of oxygen accumulated in Pt/Al_2O_3, which was measured in separate experiments, was taken into account.

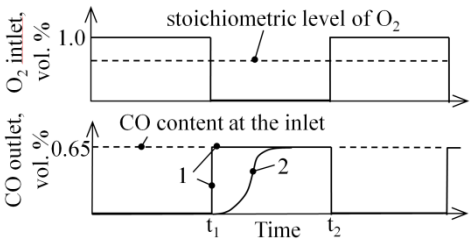

Fig. 1. Scheme of changes in CO and O_2 content within one measurement cycle. Interval t_1–t_2 corresponds to a period when CO is oxidized with lattice oxygen. Lines 1 and 2 are CO contents for a hypothetical sample with zero OSC and for $Ce_xM_{1-x}O_2$, respectively. The area between lines 1 and 2 corresponds to the amount of CO that is oxidized with lattice oxygen.

3 Results and discussion

Results of the OSC study of two oxides $Ce_xPr_{1-x}O_2$ are compared in Fig. 2, 3 with those of the two most studied oxides (CeO_2 and $Ce_{0.75}Zr_{0.25}O_2$). The original data clearly show the large differences between the capabilities of oxides in CO oxidation with the lattice oxygen (Fig. 2). There is the well-known result that the OSC of $Ce_{0.75}Zr_{0.25}O_2$ is greater than that of CeO_2 at the traditional temperature (about 400^OC). However, at low temperatures, the temperature dependence of OSC indicates that the situation changes to the contrary (Fig. 3). The same result was obtained for the other pair of oxides ($Ce_xPr_{1-x}O_2$). For example, the OSC of $Ce_{0.5}Pr_{0.5}O_2$ is two times larger at 480^OC, but three times smaller at 250^OC, than the OSC of $Ce_{0.85}Pr_{0.15}O_2$.

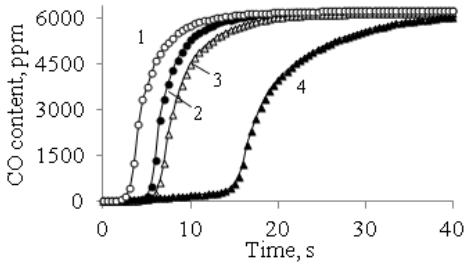

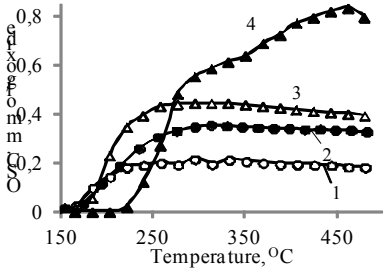

Fig. 2 (left). Change in the outlet content of CO measured at 480 ^OC between moments t_1 and t_2 (see Fig. 1). **Fig. 3 (right)** Temperature dependence of OSC. Numerals in both figures are the same: 1 – CeO_2, 2 – $Ce_{0.75}Zr_{0.25}O_2$, 3 – $Ce_{0.85}Pr_{0.15}O_2$, 4 – $Ce_{0.5}Pr_{0.5}O_2$

The larger OSC of $Ce_{0.85}Pr_{0.15}O_2$ at low temperatures explains the lower T_{50} (about 200^OC) of the catalyst $Pt/Al_2O_3+Ce_{0.85}Pr_{0.15}O_2$ compared with T_{50} (about 260^OC) of the catalyst $Pt/Al_2O_3+Ce_{0.5}Pr_{0.5}O_2$, which were obtained under conditions equivalent to the TWC test. The study represents also how the particle morphology of Ce-containing oxides correlates with OSC, with the activity of TWC, and with the content of CO, HC, and NO_x in automotive exhausts.

4 Conclusions

The suggested method allows studying the OSC of ceria-containing oxides at lower temperatures. This information is utterly essential for understanding the behavior of TWC and thus for their development.

Acknowledgements

The authors are grateful to M. Schneider, S. Bochkarev for the calculation program design.

References

[1] M. Funabiki, T. Yamada, K. Kayano, Catal. Today 10 (1991) 33.
[2] M. Boaro, C. Leitenburg, G. Dolcetti, A. Trovarelli, J. Catal. 193, 338–347 (2000).
[3] M. Haneda, T. Watanabe, N. Kamiuchi1, M. Ozawa, Appl. Catal. B 142–143 (2013) 8.

V-OP34

Soot Oxidation with Ceria-Zirconia Catalysts Prepared by Different Precipitant

Deng X., Hu X., Zheng J., Chen B.*

National Engineering Laboratory for Green Chemical Production of Alcohols-Ethers-Esters, State Key Laboratory for Physical Chemistry of the solid surfaces, College of Chemistry and Chemical Engineering, Xiamen University, Xiamen, China

* jbzheng@xmu.edu.cn,chenbh@xmu.edu.cn

Keywords: ceria-zirconia, mixed oxide, diesel, soot, combustion, catalyst precipitant

1 Introduction

The reduction of soot particulate emitted from diesel engines has attracted more attention due to its harm to environment and human health [1]. Currently, the most commonly used method for removing soot from engine exhaust is the use of diesel particulate filter with catalyst to oxidize soot at certain temperature or by burning oil in the filter at certain period. Clearly, filter with catalytic oxidation is favorite in application, but the issue is how to prepare effective catalysts with more favorable structure for transferring or activating oxygen species thus better catalytic oxidation activity at lower temperature. The partial substitution of Ce^{4+} ions with Zr^{4+} ions was reported to be beneficial for generating oxygen vacancies and ceria-zirconia (Ce-Zr) catalysts have been extensively applied in soot oxidation. However, the studies often focused on the effect of cerium precursor [2], cerium loading [3], calcination temperature [4], etc. Herein, we reported that active Ce-Zr catalysts can be successfully synthesized using different precipitants, and corresponding characterizations were also carried out to illustrate the structure-activity relationship.

2 Experimental/methodology

$Ce_{0.75}Zr_{0.25}O_2$ catalysts were prepared based on co-precipitation method using KOH, $NH_3.H_2O$, and their mixture as precipitant. The precipitates were dried at 120 °C and calcined at 500 °C for 5 h. The obtained catalysts were labelled as K-CZ, K-CZ and KN-CZ, respectively.

N_2 adsorption-desorption isotherms were measured volumetrically using a Micromeritics ASAP 2020 instrument. XRD characterization was carried out on an X' Pert Pro automatic powder diffractometer operated at 40 kV and 30 mA, using Cu Kα (λ=0.15406 nm) monochromatized radiation. XPS patterns were collected using a VG MiltiLab 2000 spectrometer with Mg Kα radiation and a multichannel detector.

The oxidation of soot (10 mg printex-U carbon), contacted loosely with 190 mg catalyst, was evaluated on a tubular quartz reactor, and temperature-programmed oxidation reaction (TPO) run from 25 to 700 °C at a rate of 2 °C min^{-1} in a stream 5% O_2 balanced with N_2 at a flow rate of 50 ml min^{-1}. The catalytic activity was evaluated by the values of T_{10}, T_{50}, T_{90}, represented as the temperatures at 10%, 50%, and 90% of soot conversion, respectively.

3 Results and discussion

First, XRD characterization was used to determine the effect of precipitant on particle size of the catalysts. As shown in Fig. 1a, all the CeO_2-based catalysts is characteristic of a typical crystalline fluorite structure with four sharp diffraction peaks corresponding to (111), (200), (220) and (311) plane, respectively. It is noted that these peaks arising from Zr insertion shift to high 2θ and become wider as compared to that of pure CeO_2. This suggested zirconium is partially loaded into the ceria lattice and some appears to be segregated as a separated phase.

According to Scherrer's formula, the particle size of KN-CZ (4.7 nm) is smaller than that of K-CZ, N-CZ (Table 1). It indicates that precipitant plays a vital role in particle size of catalysts.

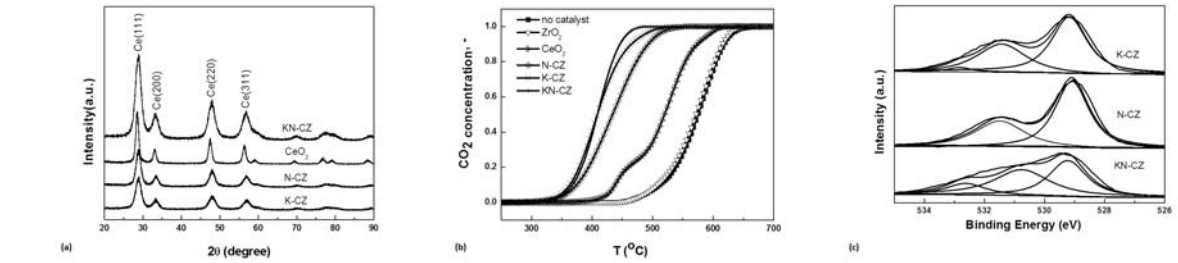

Figure 1 XRD patterns (a), TPO profiles (b), and O 1s XPS spectra of Ce-based catalysts

Then, the TPO profiles for soot oxidation over CeO_2-based catalyst were carried out for exploring the effect of particle size on catalytic performance. And the tested results (Fig. 1b and Table 1) indicates that the soot oxidation takes place around 438 ^oC (T_{10}) and the corresponding T_{90} for CeO_2 catalyst is near 574 ^oC. However, the TPO profiles for all Ce-Zr catalyst were shifted to lower temperature compared with that of CeO_2 catalyst. The order of oxidation activity is KN-CZ>K-CZ>N-CZ.

Table 1 Soot oxidation activities and physicochemical properties of various Ce-based catalysts

Catalyst	T10 (oC)	T50 (oC)	T90 (oC)	SBET (m2/g)	Dp (nm)	O2- (%)	O22- (%)	O2- (%)	Ce3+/Ce 4+
K-CZ	367	413	469	54.3	6.8	2.3	41.4	56.3	1.1
N-CZ	375	434	493	91.3	7.1	0.2	35.9	63.9	0.96
KN-CZ	367	409	446	78.5	4.7	14.0	43.6	42.3	0.89
CeO2	438	520	574	41.3	9.2	-	-	-	-
ZrO2	507	572	616	22.3	24	-	-	-	-

The precipitant can affect the particle size, and this will affect the chemical state of ceria due to interaction of Ce with Zr. Therefore, XPS characterization was performed for the Ce-based catalysts. The results showed that the KN-CZ catalyst possesses almost the lowest superficial ratio of Ce^{3+}/Ce^{4+} to that of other Ce-Zr samples, but it provides the highest quantity of absorbed oxygen species (O_2^- and O_2^{2-}) on the surface (Fig. 1c and Table 1). Therefore, it can be concluded that the Ce^{3+} and Ce^{4+} species significantly affect the capacity for activating oxygen. Combined with the activity of soot oxidation, it is concluded the quantity of adsorbed oxygen species, affected by precipitant, plays a vital role in soot oxidation.

4 Conclusions

The Ce-Zr catalysts with different oxidation activity were synthesized using precipitants. And the precipitant affects the particle size of catalyst, and modify the interaction of Ce with Zr. The suitable interaction results in increasing the quantity of absorbed oxygen species, which is closely linked with the performance for soot oxidation.

Acknowledgements

The authors would like to thank the National Natural Science Foundation of China (21303140) for financial support.

References

[1] B.A.A.L van Setten, M. Makkee, J.A. Moulijn, *Catal. Rev. Sci. Eng.* 43 (2001) 489.
[2] N. Guillén-Hurtado, A. Bueno-López, A. García-García, *Appl. Catal. A: Gen.* 437-438 (2012) 166.
[3] L. Zhu, J. Yu, X. Wang, J. Hazard. Mat. 140 (2007) 205.
[4] E. Aneggi, C. de Leitenburg, A. Trovarelli, *Catal. Today* 181 (2012) 108.

V-OP35

Mechanistic Investigations of Soot Combustion by Ag Supported Catalysts

Serve A.[1], Epicier T.[2], Aouine M.[3], Cadete Santos Aires F.J.[1], Tsampas M.[1], Cartoixa B.[4], Pajot K.[5], Vernoux P.[1*]

1 - Université de Lyon, Institut de Recherches sur la Catalyse et l'Environnement de Lyon, UMR 5256, CNRS, Université C. Bernard Lyon 1, Villeurbanne, France

2 - Université de Lyon, MATEIS, UMR 5510, CNRS, INSA de Lyon, Villeurbanne Cedex, France

3 - Université de Lyon, Institut de Recherches sur la Catalyse et l'Environnement de Lyon, UMR 5256, CNRS, Université C. Bernard Lyon 1, Villeurbanne, France

4 - CTI, Céramiques Techniques Industrielles, Salindres, France

5 - PSA PEUGEOT CITROËN, Centre technique de Vélizy, Vélizy-Villacoublay, France

* philippe.vernoux@ircelyon.univ-lyon1.fr

Keywords: soot oxidation, diesel particle filter, silver, yttria-stabilized zirconia, E-TEM

1. Introduction

Since Particulate Matter emissions have been regulated by US/EU standards for Diesel vehicles, Diesel Particle Filter (DPF) has become mandatory to satisfy the required levels. To assist the regeneration of the DPF, oxidation catalysts combining good activity and stability under exhaust conditions are used. Ag-supported catalysts have been already reported as active materials for soot combustion, related to the high mobility of Ag to get in contact with the soot [1]. This study investigates the soot oxidation mechanism on Ag nanoparticles supported on Yttria-Supported Zirconia (YSZ), an oxygen ionic conductor. YSZ is a thermally stable support, active for soot oxidation thanks to its bulk oxygen mobility [2]. This study aims to investigate the synergy for soot combustion between Ag nanoparticles and YSZ. Different characterizations techniques, such as temperature programmed oxidation (TPO) and reduction (TPR), isotopic $^{18}O_2$ exchange, XPS and Environmental Transmission Electron Microscopy (E-TEM) have been implemented. Various kinds of oxide supports: inert (SiO_2), non-conductive (ZrO_2), reducible (ceria-zirconia) and O^{2-} conductor (YSZ) have been used to understand the mechanism.

2. Experimental

Various Ag-supported samples were prepared by aqueous impregnation of silver nitrate (Alfa Aesar, 99.9%) over YSZ (Tosoh), ZrO_2 (Tosoh), $Ce_{0.7}Zr_{0.3}O_2$ (Solvay), SiO_2 (Sigma-Aldrich), and followed by a calcination at 700°C for 4 hours. Samples displayed Ag loadings of 1%wt. Catalysts were characterized by XRD, SEM, TEM, BET and particle size distribution by Laser diffraction.

Soot oxidation was studied using a mixture of carbon black (Printex U) and catalyst in tight and loose contact conditions. In addition, experiments were conducted in intimate carbon/catalyst contact which was achieved by propene cracking as detailed in [2]. Temperature-programmed oxidation (TPO) experiments were performed by heating the mixture under different oxygen partial pressures: 1, 5 and 10% O_2 in He at 10°C/min up to 700°C. TPR (Temperature-Programmed Reduction) analysis, using 1% H_2 in He, and XPS were also performed to quantify the level of Ag oxide as well as its interaction with the support. $^{18}O_2$ TPO and isothermal $^{18}O_2$ exchanges were performed to detect the nature of the active oxygen species involved in soot oxidation. Cycled TPO experiments were realized to determine the stability of the catalyst. Finally, a last generation ETEM (TITAN 80-300 kV from FEI™) equipped with an aberration corrector was used to in-situ observe the soot oxidation on Ag/YSZ catalyst.

3. Results and discussion

TPO experiments under loose contact (fig. 1) show that 1%Ag/YSZ displays far better performance than YSZ with a CO_2 selectivity higher than 95%. Catalytic performances of Ag/YSZ catalyst was found to increase with the oxygen partial pressure. $TP^{18}O$ experiments demonstrate that the presence of Ag promotes the fuel-cell-type electrochemical mechanism of YSZ which takes place during soot combustion. Similar experiments have been performed with SiO_2, ceria-zirconia and ZrO_2 supported catalysts to highlight the synergy between the Ag nanoparticles and YSZ.

E-TEM allowed in-situ observations of soot oxidation by Ag/YSZ, in conditions similar to those of a DPF. Recorded movies show silver nanoparticles tunneling through the soot and consuming it (figs. 2 a, b, c). They appear to adopt the shape of the soot and deform themselves to cover the particle surface. This demonstrates, for the first time, the high mobility of Ag nanoparticles in contact with soot. However, when all PM is burned, some Ag particles, no more in interaction with the YSZ support, can sinter and, even worse, evaporate (figs. 2 d, e, f). Therefore, the thermal and cycling stability of Ag/YSZ catalyst have been investigated under DPF exhaust conditions.

4. Conclusions

Ag/YSZ catalysts display remarkable performances for high oxygen partial pressures. Isotopic exchanges confirm the crucial role of YSZ bulk oxygen species while in-situ E-TEM observations have underlined the fast mobility of Ag nanoparticles. A mechanism will be discussed according to all the characterizations techniques.

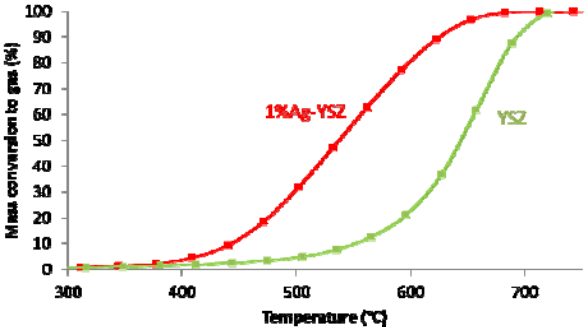

Fig.1: Soot to gas conversion with respect to temperature during TPO, 5%O_2/He, loose contact

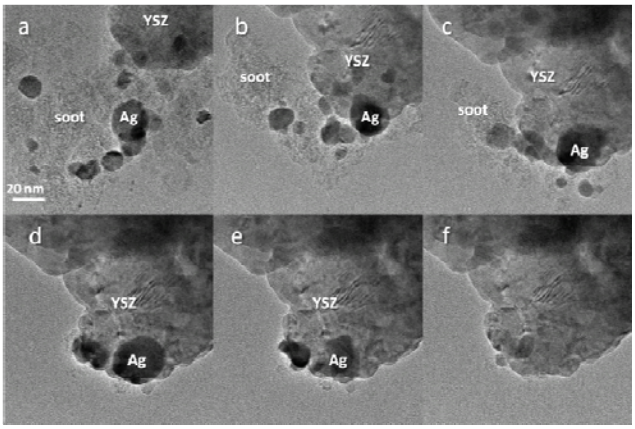

Fig.2: E-TEM observations of 1%Ag-YSZ+soot mixture under 450°C, 0,6mbar, 80keV, every 30s

Acknowledgements

The authors are grateful to ADEME (Agence de l'Environnement et de la Maîtrise de l'Energie) for the PhD grant of A. Serve.

References

[1] E. Aneggi, J. Llorca, C. de Leitenburg, G. Dolcetti, A. Trovarelli, Appl. Catal. B, 91 (2009) 489.
[2] E. Obeid, L. Lizarraga, M.N. Tsampas, A. Cordier, A. Boréave, M.C. Steil, G. Blanchard, K. Pajot, P. Vernoux, J. Catal. 309 (2014) 87.

V-OP36

Strong Enhancement of deSoot Activity of Transition Metal Oxides by Alkali Doping – Surface Promotion versus Intercalation

Jakubek T., Kaspera W., Legutko P., Zasada F., Piskorz W., Stelmachowski P., Indyka P., Grybos J., Sojka Z., Kotarba A.*

Jagiellonian University, Faculty of Chemistry, Krakow, Poland

* kotarba@chemia.uj.edu.pl

Keywords: soot combustion, manganese, iron, cobalt oxides, alkali, promotion, nanostructurization, work function, DFT

1 Introduction

The aim of this study is to develop an innovative robust catalytic material for soot combustion in the low temperature regime. The proposed materials are comprised of model 3*d*-metal (manganese, iron, cobalt) oxides, surface decorated or intercalated by alkali ions, which act as promoters. The guiding hypothesis consists in exploration on how the catalytic reactivity can be associated with the work function and surface/bulk status of alkali. The effect of the alkali promoters location on the surface vs. bulk (intercalation) was elucidated. The study focuses on the exploration of the key parameters governing the catalytic process: surface alkali dispersion, formation of new phases (nanostructurization), soot-catalyst interaction, topology of the soot molecular framework and the influence on the Fermi level caused by alkali doping of Mn, Fe and Co oxides. The methodology combining the experimental investigations and DFT molecular modeling allows for the establishment of rational principles for designing the optimal soot oxidation catalyst based on manganese (layered birnessite KMn_4O_8 and cryptomelane KMn_8O_{16}), iron (layered $K_2Fe_{22}O_{34}$, tunneled $KFeO_2$) and cobalt (layered $KcoO_2$) oxides.

2 Experimental/methodology

A series of potassium nanostructured manganese, iron and cobalt oxides were prepared by the reaction of stoichiometric amounts of K_2CO_3 with α-Fe_2O_3 or $KMnO_4$ and $Mn(CH_3COO)_2$ (for cryptomelane) or glucose (for birnessite) as well as KOH with Co_3O_4. The samples were thoroughly characterized by several methods including XRD, SEM-EDX, HR-TEM/FIB, XPS, RS, BET. The electronic properties and alkali dynamics were probed by the surface work function (Kelvin Probe) and ionic conductivity measurements. The stability and surface state of alkali dopants was investigated by the Species Resolved Thermal Alkali Desorption. Catalytic activity in soot combustion (loose and tight contact) was determined by TPRS and isothermal oxidation (TG/DTA – QMS) for various catalyst/soot ratios. The cluster DFT modeling of coronene as a robust molecular epitome of soot particles was performed using the $Dmol^3$ program package with a rPBE functional and a DNP basis with polarization functions. Transition states were located using a LST/QST with BFGS refinement. The postulated reaction intermediates were confirmed experimentally by the SIMS-TOF and XPS measurements.

3 Results and discussion

Structural and morphological XRD, SEM/TEM, RS investigations revealed that the addition of alkali led to the nanostructuration of Mn, Fe and Co oxides by the formation of tunneled ($KFeO_2$) and layered ($K_2Fe_{22}O_{34}$, KMn_4O_8, KMn_8O_{16}, $KcoO_2$) structures. It was found by SR-TAD studies that such structures are beneficial for the high mobility of the potassium promoter

(bulk diffusion, surface segregation and desorption), allowing for the remote activation of soot by alkali transfer from the surface to the soot particles. The comparison of the soot combustion activity of the investigated catalysts shows a strong promotional effect (dramatic lowering of the reaction temperature window) of alkali additions (Fig. 1). The transformation of iron oxide into ferrites by potassium addition lowers the light off temperature by about 70°C and 100°C for $K_2Fe_{22}O_{34}$ and $KfeO_2$, respectively, whereas for the transformation from manganese spinel to nanostructured potassium oxides leads to the temperature decrease of 130°C and 150°C for KMn_4O_8 and KMn_8O_{16}. The nanostructuration of the cobalt oxide has a similar effect, lowering the light of temperature by 80°C.
The observed correlations reveal that the unique, concise parameter – the catalyst work function – plays the key role in the soot combustion process.

For the most combustion reluctant graphitic soot, epitomized by coronene, the role of the termination topology and strain induced by local carbon rehybridization on oxygen attack mechanism was discussed based on the quantum chemical modeling. Quantum chemical modeling was used to discuss the role of the termination topology and strain induced by local carbon rehybridization during an oxygen-attack mechanism for the most combustion reluctant graphitic soot, which was epitomized by coronene. It was found that the reactivity sequence increases as armchair, zig-zag, free-edge, as gauged by the activation energies: E_{act} = 30.5/76.5, 43.5/90.5, 116.1 kcal/mol for singlet/triplet pathways, respectively.

The energetic profiles of the oxidation cascade revealed that the reaction occurs by the sequence of oxidation, thermal fragmentation steps. The most demanding is the primary dioxygen attack and the preferred focus on the free-edge sites of the graphitic soot. The key intermediates appearing during the reaction progress are featured by C=O, C-OH, and COOH functionalities, redistribution of the carbon rings and the formation of new carbon-oxygen rings, as revealed additionally by XPS and SIMS. The computational and experimental results show that the rate determining the first attack of a O_2 molecule can be facilitated by the alkali transferred from the catalyst surface to the soot particle.

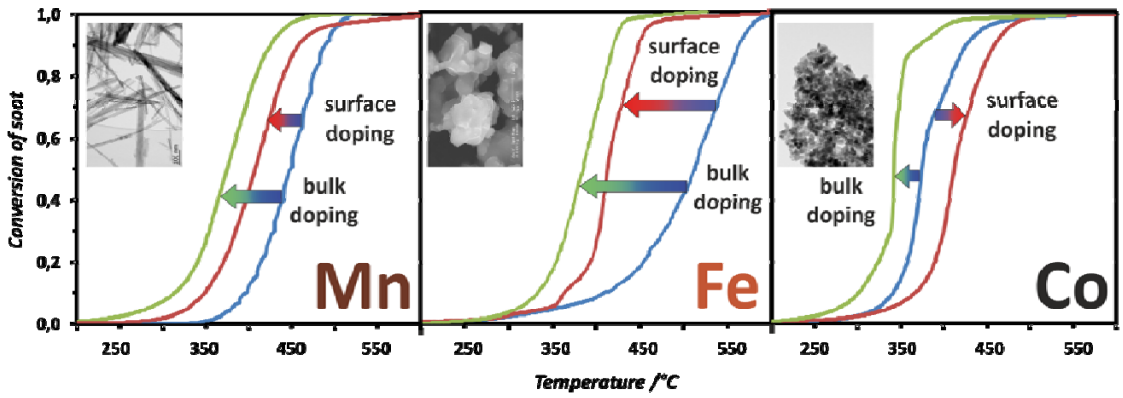

Fig. 1. The results of soot combustion for Mn, Fe and Co oxides bulk (intercalated) and surface (decorated) by potassium and the SEM/TEM images of the most active phases.

4 Conclusions

Based on the experimental and molecular modeling results an integral picture of the soot combustion process over alkali promoted catalyst was advanced and the crucial multifaceted role of alkali promotion was elucidated in detail. It allows for establishment of rational guidelines for designing robust materials for DPF applications based on ternary metal oxides.

Acknowledgements

Financial support by the National Science Centre (NCN) of Poland, Grant No. 2011/01/B/ST4/00574 is acknowledged.

V-OP37

Structure-Activity Relation of Iron Oxide Catalysts in Soot Oxidation

Wagloehner S., Kureti S.*

Technical University of Freiberg, Institute of Energy Process Engineering and Chemical Engineering, Chair of Reaction Engineering, Freiberg, Germany

* kureti@iec.tu-freiberg.de

Keywords: soot oxidation, iron oxide, diesel exhaust

1 Introduction

Diesel particulate filters (DPF) represent a state-of-the-art technology for the removal of soot from diesel exhaust. However, the continuous regeneration of these filters remains a considerable challenge, as the trapped soot causes backpressure effects potentially decreasing the engine efficiency. While the DPF regeneration with NO_2 is already established for heavy duty vehicles, the catalytic soot oxidation by O_2 is considered to be a promising procedure for passenger cars, ships and working machines. Since iron based catalysts are known to reveal high potential for soot oxidation [1], the present paper addresses the targeted design of efficient iron oxide samples implying the evaluation of physical-chemical characteristics driving the catalytic activity.

2 Experimental

Seven bare iron oxide catalysts were evaluated towards their soot oxidation activity under oxygen-rich conditions. The catalytic studies were performed by temperature programmed oxidation (TPO) using tight contact mixtures of catalyst and soot. A home-made carbon black originated from propene combustion was taken as model soot. The catalysts were thoroughly characterised by employing powder X-ray diffraction (PXRD), N_2 physisorption, high resolution transmission electron microscopy (HRTEM), temperature programmed reduction by H_2 (HTPR), temperature programmed desorption of NH_3 (NH_3-TPD), temperature programmed desorption of O_2 (O_2-TPD) and thermogravimetry coupled with difference thermal analysis (TG/DTA). Special notice was put on the NH_3-TPD data, which were used for the modelling of the NH_3 adsorption and desorption. This model included elementary reactions and implied the specific number of Bronsted and Lewis acid sites.

3 Results and discussion

For the assessment of the catalytic performance, the temperature of maximum CO_2 production (T_{max}) was taken. T_{max} of the catalysts appeared between 330 and 415°C, whereas the Fe_2O_3 sample prepared by flame spray pyrolysis (FSP) indicated highest activity (T_{max} = 330°C). For reference, $T_{CO2,max}$ of bare soot was found at 570°C clearly demonstrating the effect of the catalysts.

In the correlation of the soot oxidation efficiency and determining physical-chemical characteristics, a connection between proportion of Lewis acid sites as well as relative crystallinity of the catalysts was deduced as shown in Figure 1. This contour diagram demonstrates highest activity for moderate crystallinity (ca. 0.5) and a high amount of specific Lewis acid sites, whereas a moderate quantity of specific Lewis bond NH_3 and high (1.0) or low (ca. 0) crystallinity reveal poor activity. The importance of Lewis acid surface sites is ascribed to their capability of transferring oxygen, whereas the constructed NH_3 adsorption/desorption model points to very similar nature of these surface sites for the iron oxides investigated.

Moreover, our mechanistic studies with $^{18}O_2$ reported lately [2] suggest that oxygen is pumped from the iron oxide to the soot by physical contact points thus leaving oxygen vacancies on the catalyst surface, i.e. Lewis acid sites. These vacancies are refilled by diffusion of surface and bulk oxygen. In surface diffusion, oxygen migrates from neighbouring Lewis acid sites, whereas diffusion of bulk oxygen occurs along lattice vacancies. The present structure-activity study confirms the importance of the transport of crystalline oxygen, as the amorphous iron oxide sample shows rather low catalytic activity, although it exhibits a medium surface concentration of Lewis acid sites. This finding is associated with faster oxygen diffusion in crystalline structures as referred to amorphous domains.

Hence, the derived correlation of Lewis acid sites, crystallinity and catalytic activity coincides with the mechanistic suggestions thus accounting for the highest efficiency of the Fe_2O_3 sample originated from FSP. This catalyst implies the largest number of surface defect sites as well as moderate crystallinity both evoking fast diffusion of oxygen to contact points. This knowledge on determining characteristics identified in this paper is considered to be an important tool for the rational development of advanced iron oxide catalysts for soot oxidation.

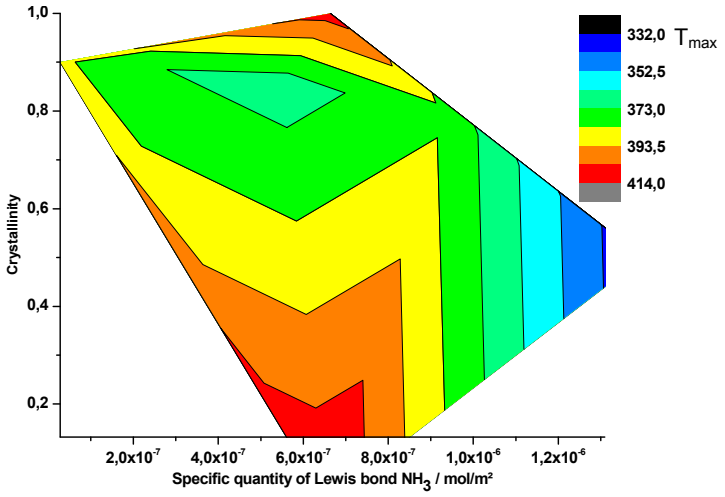

Figure 1: Correlation of T_{max}, quantity of specific Lewis bond NH_3 and crystallinity of the iron oxide catalysts [3].

4 Conclusions

The correlation of structure and activity of iron oxides for soot oxidation shows Lewis acid sites and moderate crystallinity of the catalysts to be crucial. These results coincide with mechanistic studies thus representing the base for the targeted design of advanced catalysts.

References

[1] Z. Zhang, D. Han, S. Wie, Y. Zhang. *J. Catal.* 276 (2010) 16.
[2] S. Wagloehner, S. Kureti, S. *Appl. Catal. B* 125 (2012) 158.
[3] S. Waglöhner, J.N. Baer, S. Kureti, *Appl. Catal. B* 147 (2014) 1000.

V-OP38

Pd-Doped LaFeCo Perovskites for Three-Way Catalysis. Studies on Active Sites and Response to Thermal Stress

Heikens S.[1], Mondragon Rodriguez G.[2], Saruhan-Brings B.[2], Grünert W.[1*]

1 - Ruhr University Bochum, Bochum, Germany
2 - DLR Cologne, Köln, Germany

* w.gruenert@techem.rub.de

Keywords: three-way catalysis, perovskites, active sites, stability, redox cycling

1 Introduction

Noble-metal doped perovskites have been recently studied as catalysts for redox reactions, e.g. N_2O decomposition [1], selective reduction of NO [2, 3], and methane oxidation [4]. Particular attention has been paid to their application as three-way catalysts [5], which has already found commercial application [6]. The catalysts were described as intelligent materials because of their presumed capability to accommodate the state of Pd on the timescale of the λ fluctuations, with segregation into nanoparticles in lean regime and re-sorption of Pd^{2+} into the perovskite under rich conditions [7].

We present here a study of the active sites of Pd-substituted $LaFe_yCo_{1-y}O_3$ perovskites and of their response to thermal stress. It will be shown that activity in the oxidation reactions is largely contributed by the perovskite surface while NO reduction is most effectively catalyzed by Pd-X (X = Co and/or Fe) alloy particles, which are also highly active in N_2O decomposition.

2 Experimental

$LaFe_{0.65}Co_{0.35-x}Pd_xO_3$ perovskites were prepared with the dry citrate method, with final calcination at 700°C for 3 h. Pt and Rh containing catalysts (x = 0.025) were made for comparison. The samples were tested in a flow reactor under stationary conditions at temperatures between 50 and 500°C under stoichiometric, lean, and rich conditions (1,1 % CO, 1000 ppm NO, 1000 ppm propene, with 9500 ppm O_2 (stoichiometric), 8500 ppm O_2 (rich), 10500 ppm O_2 (lean), balance He, GHSV – 60,000 h^{-1}). In addition, experiments were made with oscillating feed compositions (0.4 and 2 Hz). The catalyst was conditioned with a redox cycling treatment (15 min O_2 (2 %/He) alternating with CO (2 %/He), 5 cycles) at 400°C, 650°C, or 900°C. Reference measurements were made with a commercial Pd-rich three-way catalyst. The catalysts were characterized by XRD, N_2 physisorption, TPR, and XAFS: in-situ XANES for monitoring of reduction/reoxidation processes, ex-situ fluorescence EXAFS of characteristic states.

3 Results and Discussion

Conditioning at 400°C resulted in a drastic increase of activity for all reactions when studied in stationary regime. This was accompanied by a significant increase of the BET surface area. Comparison with Rh and Pt containing samples, but also with Pd-substituted perovskite after more severe treatments suggests that activity in CO and propene oxidation is dominated by the contribution of the perovskite surface while NO reduction proceeds exclusively on the metal. The activated Pd perovskite outperformed the commercial TWC in CO oxidation but was somewhat less active in propene oxidation and NO reduction.

In TPR, the first reduction event related to the formation of Pd metal occurred at ≈140 °C, but with a H_2 consumption largely exceeding the quantity required to reduce all Pd^{2+}. XAFS and XRD of reduced perovskites indicated the formation of an alloy phase containing Pd and

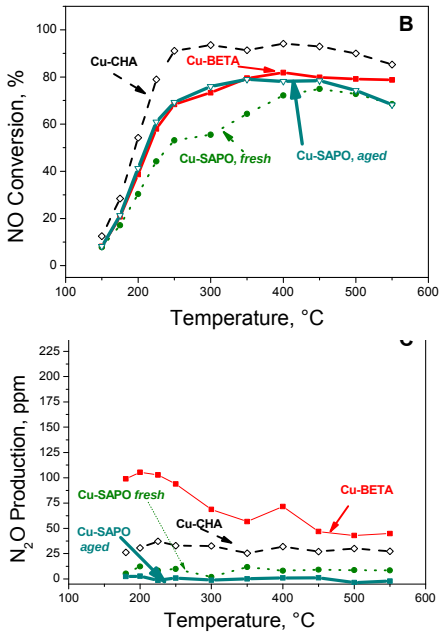

Fig. 1. EXAFS of Pd substituted perovskite after different treatments

either of the reducible perovskite components (for XAFS see Fig. 1a). The formation of this alloy phase may explain the drastic activation of the initial perovskite for NO reduction: While NO conversion in stoichiometric feed remained below 50 % in the initial state (Fig. 2), light-off temperatures (T_{50}) around 330 °C were found after conditioning at 400 °C. The alloy was also highly active in N_2O decomposition. Upon reoxidation at 400 °C, the alloy was destroyed, but Pd returned to the +2 state only partially while Pd metal particles remained on the surface as well (Fig. 1b).

Redox cycling at 650 °C resulted in moderate deactivation, in particular regarding CO oxidation and NO reduction while the same treatment at 900 °C affected the oxidation of propene rather than that of CO, but shifted T_{50} of NO reduction propene conversion beyond 500 °C for Pd-containing perovskites. The degree of reoxidation decreased with increasing temperature of treatment, and after reoxidation at 650 °C and 900 °C even the alloy phase could be still be detected (Fig. 1b). The low activity in presence of a stable alloy phase suggests that the latter is not accessible for the feed. Notably, upon reduction at 900 °C, about two thirds of Fe and Co were reduced, but the perovskite lattice was still detected in XRD.

While periodic variation of the feed composition had no strong influence on the conventional TWC, it changed the catalytic behavior of the initial Pd-doped perovskite completely (Fig. 2): complete NO conversion was achieved without redox conditioning. Such effect of the dynamic regime was not observed when the catalyst was activated previously, which suggests that the active Pd-X alloy may be formed from the initial catalyst in the phases of rich feed composition or with CO, which is abundantly stored on the perovskite surface.

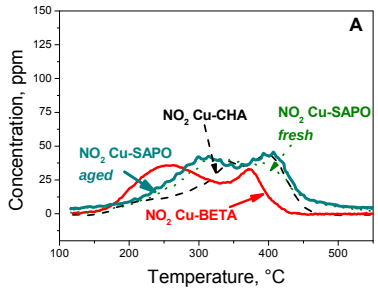

Fig. 2. Conversions over initial Pd-substituted perovskite in stationary and dynamic (0.4 Hz) regimes

4 Conclusions

The noble-metal doped perovskites were somewhat inferior to the reference TWC with respect to activity and, in particular, to stability, but exhibited high activity for all reactions of three-way catalysis. Upon reduction, Pd formed alloy nanoparticles with reducible elements of the perovskite matrix, which are highly active in NO reduction and in N_2O decomposition. Redox cycling of Pd was not completely reversible at 400°C, and irreversibility was enhanced with increasing temperature.

References

[1] J.P. Dacquin, C. Dujardin, P. Granger, *J. Catal*. 253 (2008) 37.
[2] G.C. Mondragón-Rodríguez, B. Saruhan, O. Petrova, W. Grünert, *Top. Catal.* 52 (2009) 1723.
[3] P. Miquel, Y. Yamin, K. Lombaert, C. Dujardin, P. Granger, *Top. Catal.* 52 (2009) 1791.
[4] Y. Lu, A. Eyssler, E.H. Otal, S.K. Matam, O. Brunko, A. Weidenkaff, D. Ferri, *Catal.Today* 208 (2013) 42.
[5] S. Keav, S.K. Matam, D. Ferri, A. Weidenkaff, *Catalysts* 4 (2014) 226.
[6] H. Tanaka, *Catal. Surv. Asia* 9 (2005) 63.
[7] H. Tanaka, M. Uenishi, M. Taniguchi, I. Tan, K. Narita, M. Kimura, K. Kaneko, Y. Nishihata, J. Mizuki, Catal. Today 117 (2006) 321.

V-OP39

Three-Dimensionally Ordered Macroporous Perovskite Catalysts: Controllable Alignments and Approach for Catalytic Applications

Arandiyan H.*, Scott J., Amal R.

Particles and Catalysis Research Group, School of Chemical Engineering, The University of New South Wales, Sydney, Australia

* h.arandiyan@unsw.edu.au

Keywords: three-dimensionally ordered macropore, perovskite, supported noble metals, self-assembly

1 Introduction

Noble metal nanoparticle (NPs) is one of good choices for enhancing the intrinsic catalytic activity of 3DOM metal oxides [1]. Compared to the bulk La-based perovskite-type oxides, the Pt NPs embedded in three-dimensionally ordered macroporous-mesoporous (3DOM-m) counterparts display unique physicochemical properties due to their porous structures, high surface areas, and strong redox ability that are favourable for the improvement in catalytic performance. Previously, we observed that 3D macroporous La-Sr-Mn-O derived with PMMA as hard template and DMOTEG, EG, P123, L-lysine, and PEG400 as surfactant and stabilizer showed exceptional catalytic activity for the CH_4 combustion. Recently, we have extended our attention to the fabrication and catalytic properties of noble metal NPs embedded in 3DOM-m perovskite-type oxides with mesoporous walls. In this work, we demonstrate, for the first time, the facile dual-template preparation of 3DOM-m $La_xCe_{1-x}CoO_3$ (LCCO) with formation of highly crystalline mesoporous walls by employing polymethyl methacrylate (PMMA) microspheres as hard template and of its supported Pt nanoparticles (NPs) by adopting the gas-bubbling cetyltrimethyl ammonium bromide (CTAB)-assisted reduction route.

2 Experimental/methodology

The well-arrayed monodispersed PMMA microspheres with an average diameter of ca. 260 nm were synthesized according to the procedure described elsewhere [2]. The rhombohedral *x* wt% Pt/3DOM-m $La_xCe_{1-x}CoO_3$ (*x* wt% Pt/3DOM-m LCCO; *x* = 0-6 wt%) with crystalline mesoporous walls were fabricated using by the gas-bubbling cetyltrimethyl ammonium bromide (CTAB)-assisted reduction route described previously [3]. The dried sample was calcined to remove the impurities after calcination in furnace according to two steps: heated in a N_2 flow of 50 mL/min at a ramp of 1 °C/min from RT to 300 °C and calcined at this temperature for 3 h; and then the solid was heated in an air flow of 50 mL/min at a ramp of 1 °C/min from RT to 800 °C and kept at this temperature for 4 h. For comparison purpose, we also prepared a bulk-LCCO catalyst using the sol-gel method and after calcination at 850 °C for 5 h. Physicochemical properties of the materials were characterized by a number of analytical techniques.

3 Results and discussion

It is found that the CTAB acted as the stabilizing surfactant of Pt NPs and the promoting agent for mesopore formation. Hence, this work provides a facile synthesis of thermally stable Pt NPs supported on high-surface-area 3DOM LCCO, as illustrated in Figure 1. By controlling the synthesis conditions (CTAB added amounts and $H_2PtCl_6/NaBH_4$ mass ratio), high-density Pt NPs could be successfully loaded on the surface of hierarchically ordered macro/mesoporous LCCO, thus obtaining the *x* wt% Pt/3DOM-m $La_xCe_{1-x}CoO_3$ nanocatalysts (Figure 1). More

than 98% of the particles identified in the HRSEM images displayed a high-quality 3DOM structure with high degree of alignment perpendicular to the first layer (Figure 1). The introduction of an excessive amount (6 wt%) of Pt had no significant effects on the quality of 3DOM structure. It was found that the obtained *x* wt% Pt/3DOM-m $La_xCe_{1-x}CoO_3$ catalysts have attracted much attention because of their unique properties, such as high surface areas, controllable compositions, crystallinity, thermal and chemical stability, high porosities, narrow pore size distributions as well as their excellent catalytic performance for oxidation of hydrocarbons .

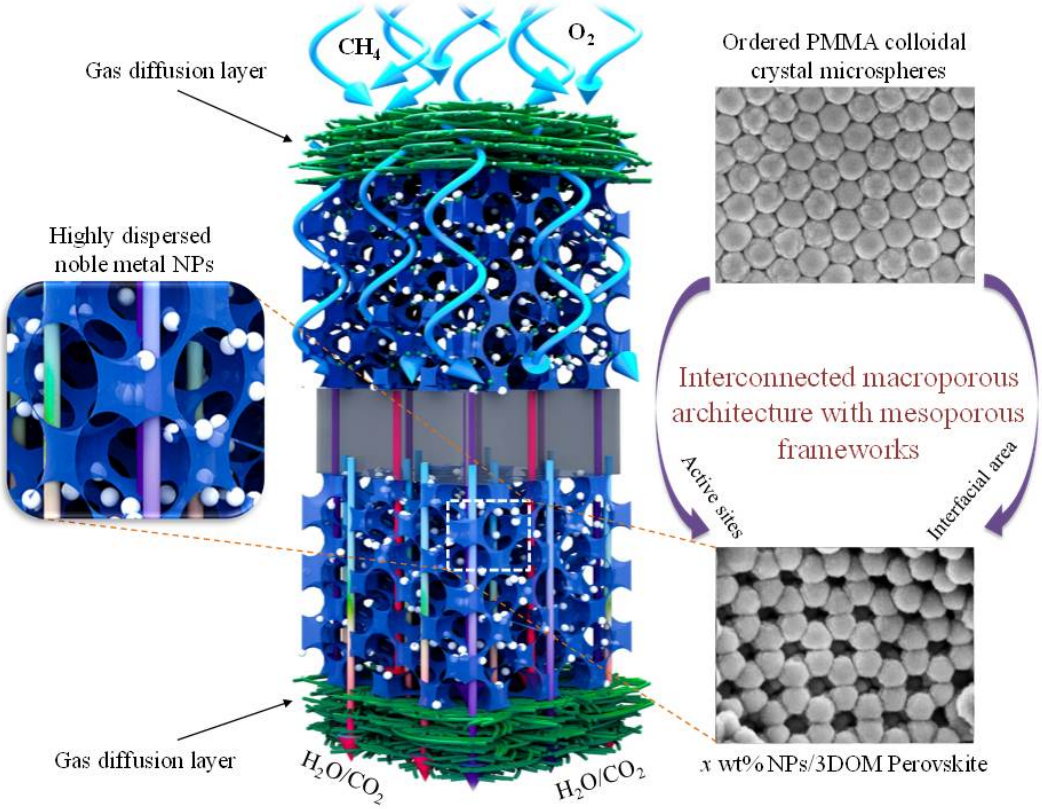

Fig. 1. Schematic illustration of loading noble metal NPs on 3DOM perovskite catalysts.

To the best of our knowledge, besides CH_4 oxidation [1-3], there even have been no reports on combining all of the above features into a single promising NPs/3DOM-m perovskite for other reactions such as oxidative coupling of methane (OCM), methane partial oxidation (MPO), methane dry reforming (MDR), the methane combustion reaction (MCR), steam methane reforming (SMR), and autothermal methane reforming (ATR). Simple substitution of a foreign cation into the nanohybrid make-up at either the A- or B-sites, and/or metal NPs can be employed to tune the catalyst to the specific reaction.

4 Conclusions

In summary, we have demonstrated a facile synthesis of 3DOM LCCO with mesoporous walls and a high surface area and *x* wt% Pt/3DOM-m $La_xCe_{1-x}CoO_3$ with high dispersion of ultrafine Pt NPs by the gas-bubbling CTAB/P123-assisted reduction method.

References

[1] Arandiyan, H.; Dai, H.; Li, J., et al. *Journal of Physical Chemistry C* 118 (2014) 118, 14913-14928.
[2] Arandiyan, H.; Dai, H.; Li, J., et al. *Chemical Communications* 49 (2013) 10748-10750.
[3] Arandiyan, H.; Dai, H.; Li, J., et al. *Journal of Catalysis* 307 (2013) 327-339.

V-OP40

Highly Active $LaKCoO_3$ Perovskite-type Complex Oxide Catalysts over Alumina Washcoated Monolith for the Simultaneous Removal of Diesel Soot and Nitrogen Oxides

Tang L., Zhao Z.*, Wei Y., Liu J., Li K.

China University of Petroleum, Beijing, China

* zhenzhao@cup.edu.cn

Keywords: perovskite-type oxides, washcoat monolithic, cordierite, diesel soot, catalysts, simultaneous removal of diesel soot and nitrogen oxides

1 Introduction

In recent years, it is known that diesel particulate emissions cause serious problems for human health. Many automobile companies and research institutes have tried to develop various methods to solve this problem. At present, the widely accepted solution is the diesel particulate filter (DPF), which is one of the most effective systems to reduce particulate matter. The preferred material is called cordierite, Honeycomb cordierite is the substrate in common use because of high mechanical strength, stability at high temperatures and temperature shocks and low thermal expansion coefficient. Various methods, e.g. dip-coating, direct synthesis chemical vapor deposition, have been applied to deposit catalytic coatings on cordierite substrate. the slurry coating is the most popular one. Typically, the slurry consists of small particles (dp<5 m) in order to penetrate into the macropores of cordierite, so that a good anchoring of the layer is obtained. In fact, in our previous works we reported high activity and selectivity towards N_2 and CO_2 for several catalytic systems containing the nanometric $La_{1-x}K_xCoO_3$ and $La_{1-x}K_xMnO_3$[1] perovskite oxides are good candidate catalysts for the simultaneous removal of diesel soot particle and NOx reaction under loose contact conditions. For the purpose of practical application, we investigated the catalytic performance of $LaKCoO_3$ perovskite oxide surported on cordierite monoliths.

2 Experimental/methodology

The monolithic catalysts were prepared by impregnating the as prepared monolith with aqueous solution of metal salt ($La(NO_3)_2.6H_2O$, $Co(NO_3)_2.6H_2O$, KNO_3, citric acid) in an evaporator at the constant temperature. The aqueous solution of metal salt was stirred at 25 ^oC for 2-4h.The impregnated sample was mixed well and then evaporated in a rotary evaporator at constant temperature of 120 ^oC overnight and calcined at 650 ^oC with the heating and cooling rate of 1 ^oC /min in flowing air for 4h. Finally, a typical preparation process of $LaCoO_3$/ɤ-Al_2O_3/cordierite or $LaKCoO_3$/ɤ-Al_2O_3/cordierite was proceeded to form the monolithic catalyst.

3 Results and discussion

As shown in Fig. 1, compared with the DPF coated with perovskite $LaKCoO_3$ catalyst, the blank DPF obviously has excessive accumulation of carbon smoke particles, it will reduce the service life of the DPF and the combustion efficiency of engine. The combined system shows high catalytic performance, the emmitions of PM, CO, hydrocarbon can meet the need for the Chinese National V standard under different conditions, NOx emissions decreased, and can reach the Chinese National IV standard. The results are shown in Table 1.

The cordierite substrate has irregular flat surface, as seen in Fig.1, and such structure is good for dip-coating. After dip-coating, the crystal grains with different regular shapes

completely and compactly cover the irregular surface of cordierites so that the irregular surface of cordierite substrate could not be observed any more (Fig. 2a). The layer thickness is quite uniform with a minimum value of about 8μm on the walls (Fig. 2b), SEM analysis confirmed an adequate and quite homogeneous coating of the cordierite surface.

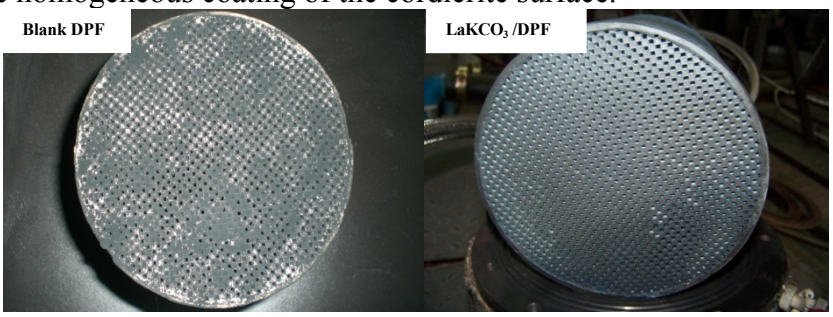

Fig.1. Photographs of the blank DPF compared with the one coated with perovskite $LaKCoO_3$ catalyst after the bench testing.

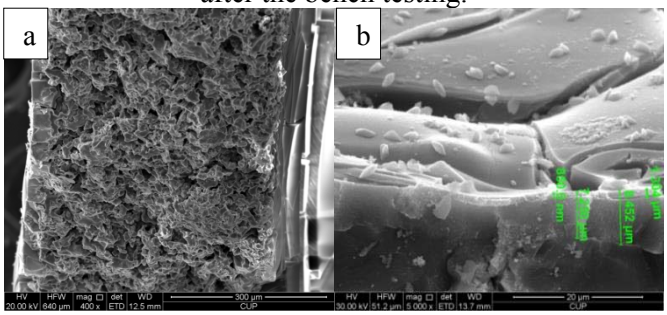

Fig.2. SEM images of different samples: longitudinal section of the channel (a); details of the longitudinal view of the channels (b).

Table 1 Activity results for the bench testing

	PM $gkw^{-1}h^{-1}$	NO_X $gkw^{-1}h^{-1}$	CO $gkw^{-1}h^{-1}$	THC $gkw^{-1}h^{-1}$
Before the exhaust gas purification	0.48	4.85	4.08	0.34
After the exhaust gas purification	0.03	3.28	0.32	0.13

4 Conclusions

Cordierite-monolith-supported $LaKCoO_3/\gamma$-Al_2O_3 catalysts were prepared using the alumina precursor. Their activity was assayed in the simultaneous removal of soot (carbon black) and NOx. The precursor result in good layer adherence and in lower tendency towards the formation of cracks. On the other hand, the alumina catalysts presented a less uniform and less stable coating of the cordierite surface. Therefore, it demonstrated that the monolithic catalysts prepared in this work will be promising for many catalytic reactions including VOCS oxidization and automobile exhaust treatment, and it also offered a new route for more efficient utilization of the quick-developing nano-catalysts.

Acknowledgements

This work was supported by the National Natural Science Foundation of China (No. 21477164, 21177160), the 863 Program of China (No.2009AA06Z346) and the Scientific Research Key Foundation for the Returned Overseas Chinese Scholars of State Education Ministry.

References

[1] Hong Wang, Zhen Zhao, Peng Liang, Chun-ming Xu. Catalysis Letters (2008)124:91-99.

V-OP41

Identification of Low-T Standard SCR Reaction Intermediates on Fe-, Cu-Zeolite Catalysts by Chemical Trapping Techniques

Ruggeri M.P., Selleri T., Nova I., Tronconi E.*

Dip.Energia, Politecnico di Milano, Milano, Italy

* enrico.tronconi@polimi.it

Keywords: NO oxidation, standard SCR, zeolite catalysts, chemical trapping, nitrites, nitrates

1 Introduction

Metal promoted zeolites are efficient SCR (Selective Catalytic Reduction) catalysts, exhibiting peculiar behaviours depending on the exchanged metal, Fe- or Cu- [1]. Low temperature activity of these systems is essential in order to comply with the current NO_x emission limits for Diesel vehicles. The catalytic mechanism governing the low-T SCR performance of the Standard SCR reaction on Fe-, Cu- promoted zeolites is however still debated. Despite a general agreement that the Standard SCR reaction is initiated at low T by the oxidative activation of NO, diverging proposals about the nature of the related reaction intermediates have been recently published, including NO^+/nitrites (formal N oxidation state = +3) [2, 3] and nitrates (N = +5) [4]. Chemical trapping techniques, combined with both transient response methods and ex-situ IR spectroscopy, have been already applied successfully to identify the primary products formed in the oxidative activation of NO over a Fe-zeolite catalysts [5]. In this work the same techniques are applied to a Cu-zeolite catalyst and the results compared to the Fe-zeolite, in order to rationalize differences in the catalytic chemistries.

2 Experimental/methodology

Transient $NO+O_2$ and NO_2 adsorption runs were performed at 120°C on mechanical mixtures of Fe-ZSM-5 (22 mg) or Cu-CHA (16 mg) + BaO/Al_2O_3 (44 mg) powders, as well as on their individual components. The use of the mechanical mixture was designed to capture onto BaO, a well-known NO_x trap, unstable reaction intermediates resulting from NO activation over Fe or Cu and from NO_2 adsorption. The trapped intermediates were then identified by i) analyzing their thermal decomposition products by TPD runs; ii) probing their reactivity with NH_3; iii) ex-situ FTIR analysis of the BaO/Al_2O_3 phase unloaded and separated from the test reactor mixture.

3 Results and discussion

Figure 1A shows TPD profiles collected on the Fe- and Cu-zeolite containing mixtures after isothermal adsorption of $NO+O_2$ at 120 °C. The catalysts exhibited similar behaviours. Notably, NO and NO_2 were desorbed in equimolar amounts with a maximum at 200°C, and with a greater NO_2 evolution above 200 °C. These results are in line with the thermal decomposition of Ba nitrites/HONO [5]. The same experiments were carried out also on the individual components of the mixtures, where no appreciable storage of NO_x was observed: this suggests that nitrites are initially formed on the metal active sites, and then trapped and stabilized on the barium phase. The interaction between the two phases may proceed via gaseous HONO (in equilibrium with nitrites) or via direct solid phase interaction. Presence of nitrites is also confirmed by ex-situ FTIR analyses of the BaO/Al_2O_3 phases separated from the physical mixtures after exposure to $NO+O_2$. For the Fe- and Cu-based mechanical mixture, respectively, Figures 1B and 1C show FTIR spectra collected over the BaO/Al_2O_3 phase: in both cases, several bands are evident (1100, 1220, 1270, 1350 cm^{-1}) which can be assigned to different nitrite species or to free nitrite ions [4], with a greater presence of nitrates species (1380-1410 cm^{-1}) on the BaO/Al_2O_3 phase

coming from the Cu-CHA containing mixture. Chemical trapping techniques thus enable direct observation of unstable reactive nitrites intermediates, which are particularly hard to detect over metal exchanged zeolites due to the overlapping of their IR bands with the zeolite features.

Nitrites storage on the BaO phases was eventually confirmed by their reactivity with NH_3 at 120 - 140 °C (temperatures at which nitrates are not reactive) to give Standard SCR products (N_2 and H_2O). Differences between the reactivity of stored nitrates with NH_3 over the two catalysts are ascribed to a greater stability of nitrates species formed on Cu-CHA.

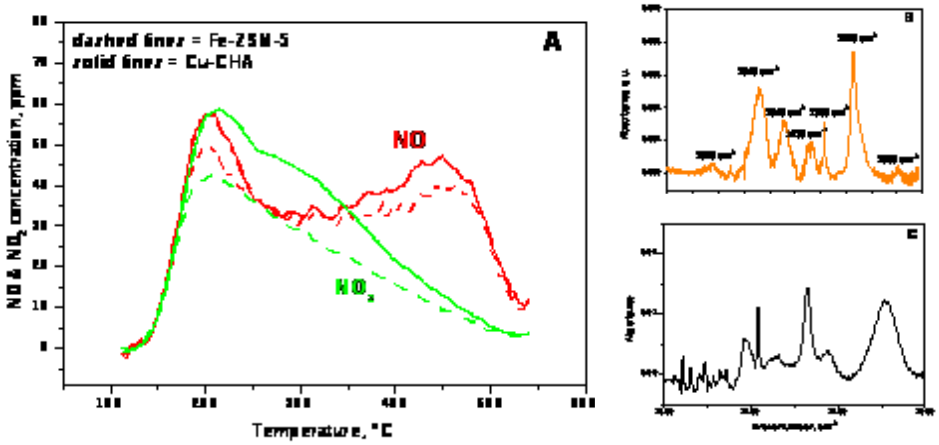

Fig. 1. TPD run in He (T=120-550°C; heating rate=15°C/min) following NO+O_2 adsorption at 120°C (NO=500 ppm; O2=8%) A) gas phase results on Fe-ZSM-5+BaO/Al_2O_3 and on Cu-CHA+BaO/Al_2O_3; Ex situ IR analysis of B) BaO/Al_2O_3 component from the Cu-CHA containing mixture; D) BaO/Al_2O_3 component from the Fe-ZSM-5 containing mixture.

The collected data: i) provide direct evidence of nitrites formation in the oxidative activation of NO over both Fe- and Cu-zeolites; ii) rule out nitrates as potential reaction intermediates in the low-T Standard SCR reaction; iii) suggest a possible equilibrium between nitrites and HONO in the gas phase. On such a basis, low-T redox mechanisms for NO oxidation and Standard SCR over Fe- and Cu- zeolite catalysts, consistent with the new experimental observations, are proposed and discussed, iv) evidenced differences in the relative abundance of nitrites/nitrates species on Fe- and Cu zeolites, in line with the greater stability of NOx adspecies already reported for Cu zeolites [1].

4 Conclusions

Nitrites have been identified as the primary products of the NO oxidative activation over Fe- and Cu-zeolites. The improved understanding of the Standard SCR chemistry at low temperature will play a key role in the development of more effective metal exchanged zeolite catalysts and of more detailed and realistic simulation models.

References

[1] M. Colombo, I. Nova, E. Tronconi, *Catalysis Today* 151 (2010) 223.
[2] J.H. Kwak, J.H. Lee, S.D. Burton, A.S. Lipton, C.H.F. Peden, and J. Szanyi, *Angewandte Chemie - International Edition* 52 (2013) 9985
[3] M.P. Ruggeri, I. Nova, and E. Tronconi, *Topics in Catalysis* 109 (2013) 56
[4] C. Paolucci, A.A. Verma, S.A. Bates, V.F. Kispersky, J.T. Miller, R. Gounder, W.N. Delgass, F.H. Ribeiro, and W.F. Schneider, *Angewandte Chemie* 1 (2014) 126
[5] M.P. Ruggeri, T. Selleri, M. Colombo, I. Nova, and E. Tronconi, *Journal of Catalysis* 266 (2014) 311
[6] E. Kaiser, and C. Wu, *Journal of Physical Chemistry* 1701 (1977) 81

V-OP42

Improved Low- and High-temperature NH_3-SCR Activity Over Cu-CHA Prepared by Solid-State Ion-Exchange Facilitated by NH_3 and NO

Shishkin A.*, Shwan S., Härelind H., Carlsson P.-A., Skoglundh M.

Competence Centre for Catalysis, Chalmers University of Technology, Gothenburg, Sweden

* shishkin@chalmers.se

Keywords: low-temperature activity, high-temperature activity, NOX, reduction, solid-state ion-exchange, SSZ-13 copper

3 Introduction

Copper-exchanged zeolites offer promising perspectives to many technological applications. An example is the reduction of nitrogen oxides in the exhaust from diesel engines through selective catalytic reduction using ammonia as a reducing agent (NH_3-SCR) [1]. The conventional way to introduce copper into zeolites is by aqueous ion exchange or by high-temperature solid-state ion exchange (SSIE). However, there are several drawbacks using these methods [2]. Shwan et al. [2] showed in a recent publication that highly active copper-exchanged zeolites can be prepared by exposing a physical mixture of copper oxide and zeolite to NO and NH_3 at 250°C, so called [NO+NH_3]-SSIE. The method is new and not yet fully developed.

This presentation will focus on optimizing the copper oxide concentration used in the physical mixture before treatment. Furthermore, we are showing that Cu-CHA prepared by [NO+NH_3]-SSIE can possess high low- and high-temperature NH_3-SCR activity compared to Cu-CHA prepared by conventional aqueous-based ion-exchange, even by using lower copper content [3].

2 Experimental

The zeolite CHA was prepared in F^- media using the molar composition of the synthesis gel as follows: 1.0 SiO_2 : 0.05 Al : 0.5 OSDA : 0.5 HF. The gel was transferred to a Teflon lined autoclave and heated to 150 °C for 3 days without agitation, whereafter the product was recovered by centrifugation and washed excessively with milli-Q water. To perform Cu-SSIE, dry mixtures of the CHA and either 0.5%, 1.0% or 2.0% CuO were grinded, whereafter placed in a quartz tube and exposed to a gas mixture of NH_3 and NO (850 ppm each) in Ar, at 250 °C for 5 hours. For the comparison, one sample with 3.0% Cu content was additionally prepared by conventional aqueous-based ion-exchange as described in ref [3]. All prepared samples were tested for NH_3-SCR, NO oxidation and NH_3 oxidation, and characterized extensively with NH_3-TPD, NO-TPD, NO_2-TPD, H_2-TPR, BET, XRD, UV-Vis, SEM, TEM and ICP.

Figure 1 Results and discussion

Figure 1 shows the NO conversion for the different Cu-CHA samples during NH_3-SCR together with the XRD pattern of the 2.0% Cu-CHA sample before and after the [NH_3+NO]-SSIE. For the [NO+NH_3]-SSIE-prepared catalysts the activity for NO reduction increases with increasing copper content. Moreover, it is clearly seen that using the [NO+NH_3]-SSIE method allows us to prepare a catalyst (2.0% Cu-CHA) which shows higher NH_3-SCR activity both at low and high temperatures compared to the conventionally prepared one. Moreover, the XRD study shows strongly pronounced decrease of the reflections intensities related to presence of CuO (2theta 36.2 and 39.6°) in the mixture after the [NH_3+NO] treatment. That means that CuO

is consumed during the treatment likely forming mobile copper species which migrate to ion-exchange sites in the zeolite forming copper species active for NH_3-SCR. It is remarkable that the 2.0% Cu-CHA sample prepared by the [NO+NH_3]-SSIE method does not only show higher low-temperature NH_3-SCR activity compared to the sample prepared by conventional aqueous-based ion-exchange but it is also more active and stable at high temperatures reaching full NO conversion at the broad temperature range of 255-500 °C, unlike the 3.0 % Cu-CHA sample. The usage of less amount of Cu in this case makes it even more remarkable and allows to reduce the cost for the catalyst synthesis.

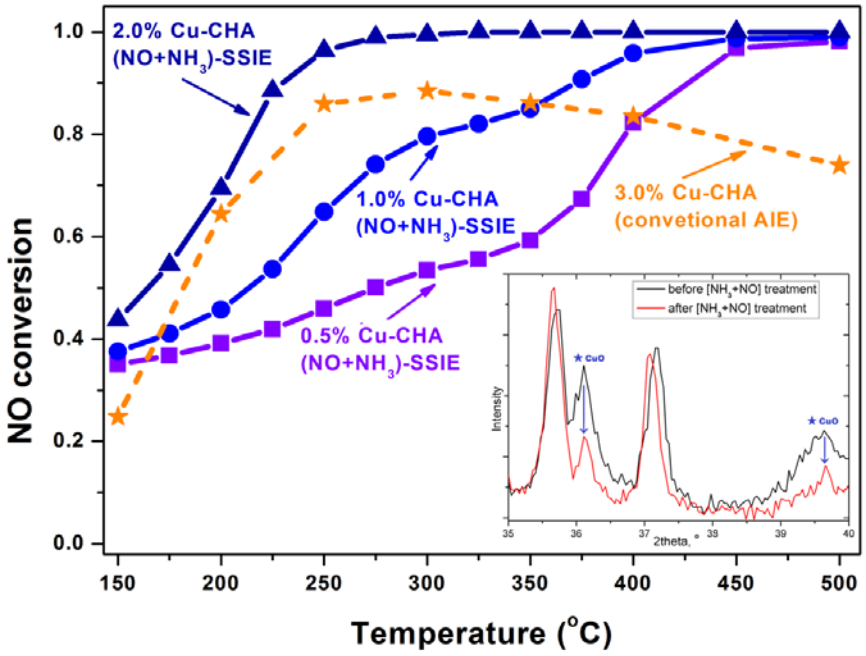

Fig. 1. NO conversion for Cu-CHA samples with 0.5 – 3% copper loading prepared using conventional aqueous ion-exchange and by solid-state ion-exchange in presence of NO and NH_3. The insert shows the X-ray diffraction patterns for the 2.0% Cu-CHA sample prepared by solid-state ion-exchange with decreased intensities of the CuO reflections after the [NH_3+NO] treatment.

4 Conclusions

We have shown that Cu-CHA prepared by [NO+NH_3]-SSIE can possess relatively high activity both for low- and high-temperature NH_3-SCR compared to Cu-CHA prepared by conventional aqueous-based ion-exchange, even by using lower copper content [3]. The study shows that the 2.0% Cu-CHA sample prepared by the [NO+NH_3]-SSIE method possesses the highest NH_3-SCR activity among the studied catalysts.

Acknowledgements

This work has been performed at the Competence Centre for Catalysis (KCK) which is hosted by Chalmers University of Technology and financially supported by the Swedish Energy Agency and the member companies: AB Volvo, ECAPS AB, Haldor Topsøe A/S, Scania CV AB, Volvo Car Corporation AB and Wärtsilä Finland Oy.

References

[1] S. Brandenberger, O. Krocher, A. Tissler, R. Althoff, Catal Rev 50 (2008) 492-531.
[2] S. Shwan, M. Skoglundh, L.F. Lundegaard, R.R. Tiruvalam, T.V.W. Janssens, A. Carlsson, P.N.R. Vennestrøm, ACS Catalysis 5 (2014) 16-19.
[3] A. Shishkin, H. Kannisto, P.-A. Carlsson, H. Harelind, M. Skoglundh, Catalysis Science & Technology 4 (2014) 3917-3926.

V-OP43

Thermal Aging Resistance of Cu-Zeolite Based Catalysts on NH_3-SCR for Lean Burn Engines Exhaust Control

De La Torre U.[1], Pereda-Ayo B.[1], González-Velasco J.R.[1*], Moliner M.[2], Corma A.[2]

1 - Department of Chemical Engineering, Faculty of Science and Technology, University of the Basque Country, Bilbao, Spain

2 - Instituto de Tecnología Química, Universidad Politécnica de Valencia, Valencia, Spain

* juanra.gonzalezvelasco@ehu.es

Keywords: NH_3-SCR, Cu-Zeolite, chabazite, aging, NOx conversion, N_2 selectivity

1 Introduction

Diesel engines have the highest thermal efficiency, and consequently release less CO_2 into the atmosphere as main gas contributing to global warming. The engine operates in excess of oxygen, making conventional three-way catalysts ineffective [1]. Among different alternatives, engine manufacturers and catalyst suppliers are considering the use of SCR with NH_3 as reductant for NO_x removal in end-of-pipe technologies. Non-noble metals like copper or iron supported on ZSM5 and BETA zeolites are among the most active catalysts for NH_3-SCR process, although most recently Cu-Chabazite are appearing as very promising catalysts [2].

2 Experimental/methodology

SCR catalysts consisted of copper-supported zeolites. Cu-BETA and Cu-ZSM5 catalysts were prepared by ion exchange [3] on commercial zeolites supplied by Zeolyst International, namely CP414E (BETA, Si/Al=12.5) and CBV5524G (ZSM5, Si/Al=25), and the optimal copper contents were determined. Cu-CHA catalyst was prepared by ion exchange on a synthesized CHA with a Si/Al ratio of 10.5 [4]. The prepared powdered catalysts were then pelletized, crushed and sieved to 0.3-0.5 mm. The prepared catalysts were submitted to accelerated aging under 5% H_2O in Ar during 16 h at 750 ºC. Physical and chemical properties of the catalysts before and after aging process were determined by N_2 physisorption, NH_3-temperature programmed desorption, H_2-temperature programmed reduction, XRD and ICP/AES.

The SCR experiments were performed in a down flow stainless steel reactor with 1.0 g of pelletized catalyst. The composition of the feed gas mixture was 750 ppm NO, 750 ppm NH_3 and 6 % O_2 using Ar as balance gas. Total flow rate was set at 3000 ml min^{-1}, which corresponded to a space velocity (GHSV) of 90,000 h^{-1}. The NO, NO_2, NH_3 and N_2O concentrations at the reactor exit were monitored every 40 ºC, once the gas composition had been stabilized for at least 10 min, by an online FTIR multigas analyzer (MKS 2030).

Table 1. Copper content, surface area, acidity and reducibility of fresh and aged catalysts.

Catalyst	Cu content, wt%	Surface area, m^2/g		Acidity, ml NH_3		Reduced area, ml H_2	
		Fresh	Aged	Fresh	Aged	Fresh	Aged
Cu-BETA	2.1	501	362	2.44	1.13	6.56	7.11
Cu-ZSM5	1.4	381	274	1.68	1.22	19.35	17.21
Cu-CHA	3.9	579	481	3.31	2.95	25.95	24.26

3 Results and discussion

Figure 1 shows NO_x conversion for the three prepared catalysts before and after aging. All fresh catalysts achieve very high NO_x conversion, but Cu-CHA resulting in the best catalytic performance due to the wider temperature windows (140-380 ºC) even with high N_2 selectivity

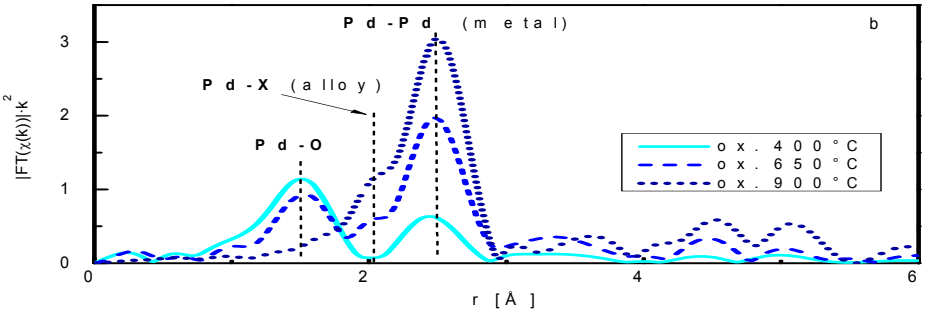

Fig. 1. NO_x conversion for a) Cu-CHA, b) Cu-BETA and c) Cu-ZSM5 before (black line) and after hydrothermal aging (red line).

(not shown). Moreover, NO_x conversion profile is practically maintained the same up to 380 ºC, with a drastic reduction above that temperature, achieving only 10% conversion at 500 ºC. This effect is related with the moderate loss in the BET surface (17%) or acidity (11%) of this catalyst after aging. This fact is also suggested to be responsible of some reduction in N_2 selectivity (around 10%), due to promote formation of N_2O and NO_2 at intermediate and higher temperatures, respectively.

On the contrary, hydrothermal aging of Cu-BETA and Cu-ZSM5 provokes a savage decrease in their catalytic performance. The aged BETA supported catalyst never achieves more than 50% NO_x conversion while the aged Cu-ZSM5 can achieve 60% conversion at 380 ºC, but produces NO at intermediate temperature, emitting even more than the amount introduced. Concerning selectivity, same tendency as with Cu-CHA catalyst were observed, with formation of N_2O at intermediate temperature and NO_2 at high temperature, e.g. 12% NO_2 selectivity with Cu-ZSM5 above 420 ºC. This trend is related to the loss of specific surface, acidity and reducibility of the catalysts as observed in Table 1.

4 Conclusions

The superior performance both in NO_x conversion and selectivity to N_2, especially after accelerated hydrothermal aging, for NH_3-SCR reaction is demonstrated. The main advantage corresponds with practically total NO_x conversion in a wider temperature window, from 220 to 380ºC, which is practically maintained after severe aging treatment. On the contrary, the aging process provokes a savage decrease in the catalytic activity of Cu-ZSM5 and Cu-BETA in the whole range of temperature. The activity loss is suggested to be related with the loss in BET surface, acidity and surface reducibility provoked by the thermal aging of each catalyst.

Acknowledgements

Authors wish to acknowledge the financial support provided by the Spanish Economy and Competitivity Ministry (CTQ2012-32899) and the Basque Government (IT657-013). One of the authors (UDLT) wants to acknowledge to the Basque Government for the PhD Research Grant (BFI-2010-330).

References

[1] J.R. González-Velasco, M.A. Gutiérrez-Ortiz, J.L. Marc, M.P. González-Marcos, G. Blanchard. *Appl. Catal. B: Environmental* 33 (2001) 314.
[2] (a) S.J. Schmieg, S.H. Oha, C.H. Kima, D.B. Brown, J.H. Lee, C.H.F. Peden, D.H. Kim, *Catal. Today* 184 (2012) 252, (b) M. Moliner, C. Martínez, A. Corma, *Chem. Mater.* 26 (2014) 246.
[3] B. Pereda-Ayo, U. De La Torre, M.J. Illán-Gómez, A. Bueno-López, J.R. González-Velasco. *Appl. Catal. B: Environmental* 147 (2014) 420.
[4] S. I. Zones, *U. S. Patent 4 544 538* (1985).

V-OP44

Dual Function Catalyst for SCR and CO-Oxidation

Pedersen K.H.*, Castellino F., Jensen-Holm H., Thøgersen J.R.

Haldor Topsoe A/S, Lyngby, Denmark

* kihp@topsoe.dk

Keywords: dual funcion catalyst, DeNOx, CO oxidation, combined cycle, power plants, HRSG

1 Introduction

Combining SCR and CO-oxidation functionality into one catalyst allows combined cycle power plants to meet their CO and NOx emission regulations with the lowest possible pressure drop. The classic layout is to equip the heat recovery steam generator (HRSG) with two different catalysts, i.e. an SCR catalyst and an oxidation catalyst with the latter usually located before the ammonia injection grid. Combining these two catalysts into one will lead to a reduction in total catalyst volume, thus decreasing the pressure drop as well as the SO_2 oxidation and this in turn will be beneficial for both the overall plant efficiency and maintenance. Moreover, retrofitting plants with SCR-only can in certain cases be simplified, i.e. the existing SCR catalyst can simply be replaced with the dual function catalyst to achieve CO oxidation as well. Haldor Topsøe A/S has developed such catalyst, the DNX® GTC-802, which is specially designed for combined cycle gas turbines. Its performance in terms of high activity and low pressure drop is recognized as state-of-the-art technology for removal of CO and NOx.

2 Experimental and results

Selective catalytic NOx reduction (SCR) in flue gas is mostly carried out by vanadium pentoxide (V_2O_5) catalyst on a titanium dioxide (TiO_2) carrier. In this process, NH_3 mixed into the flue gas reacts with the NO and NO_2 on the catalyst, forming nitrogen and water. Typical operation temperatures are around 300-400°C and the catalyst is shaped as a monolith, i.e. long straight parallel channels to ensure high surface area and low pressure drop. To achieve CO oxidation activity, it is common to apply noble metals from the Pt group which shows high activity at temperatures above 200°C. The CO oxidation catalyst is also shaped as a monolith.
Obviously, combining SCR and CO oxidation activity in one catalyst will be highly beneficial. This has also been attempted in the industry where commercial SCR catalysts have been "doped" with noble metals, e.g. Pt and Pd, and thus functionalized with CO oxidation activity. However, impregnation by simple dipping in noble metal solutions gives rise to an uneven distribution through the monolith and thus in an ineffective and thereby costly use of the noble metals. The reason is that e.g. Pd adsorbs very fast on the vanadia-sites of the SCR catalyst and therefore excess amounts of noble metals must be applied to reach a sufficiently high concentration in the part of the catalyst element that has the shortest contact time with the impregnation liquid. Moreover, Pd will be depleted from the impregnation liquid depending on the contact time between catalyst and liquid. The consequences of the strong affinity of Pd for vanadia-sites are shown in Fig. 1a. where SCR catalyst has been submerged into a Pd solution for different times. The Pd load obtained on the catalyst is much higher than that estimated from the liquid conc. and the porosity of the catalyst (in this case 110 ppm wt), e.g. after 5 minutes the Pd load is 4 times higher. Therefore, simply dipping a monolith with a length of for instance 50 cm in a Pd solution would result in longitudinal gradients caused by the difference in contact time between the first part submerged in the liquid and the last part. The difference in Pd load may be up to 5 times. However, at the temperatures relevant for the dual function operation, the CO oxidation rate is controlled by external mass transfer. This implies that high concentrations of Pd in regions of the monolith would not enhance the oxidation activity but would instead

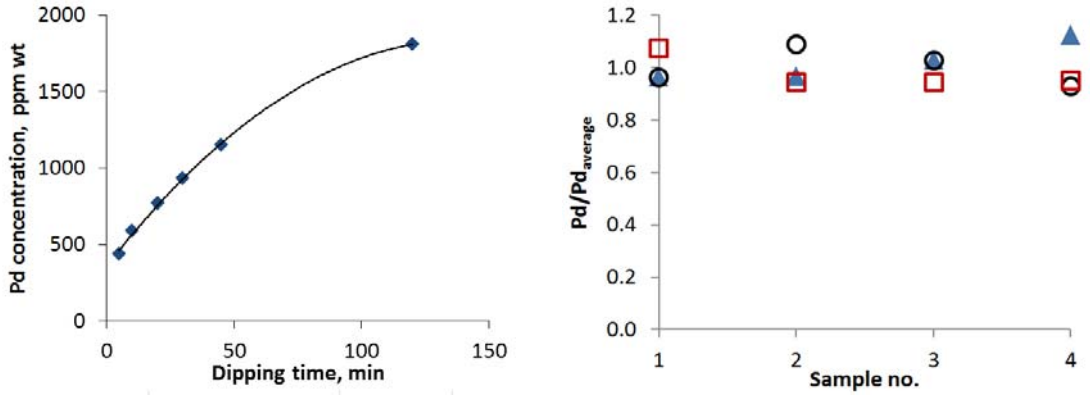

Figure 1: (a) Effect of dipping time in a $PdNO_3$ solution on the Pd bulk concentration of a vanadia-based SCR catalyst. **(b)** Pd concentration on 4 different DNX® GTC-802 monoliths relative to the average concentration of the same four monoliths. The monoliths were all 50 cm long and the three concentrations correspond to top, middle and bottom of the monoliths, respectively.

compromise the DeNOx activity because the catalyst will be more prone to convert the NH_3 into N_2 or even to NOx as a result of the enhanced oxidation activity (NH_3 oxidation rate is not controlled by external mass transfer alone). This is, of course, an unwanted scenario since the reduced SCR activity has to be compensated by using an increased catalyst volume.

The GTC-802 has been designed to provide the same high SCR activity as an SCR-only catalyst by keeping the noble metal contents at a low level throughout the catalyst (Pd for this catalyst). On the other hand, this level is still high enough to provide the same oxidation activity as an oxidation-only catalyst. A new proprietary method for adding the active sites for the SCR and CO oxidation reactions to a titania support has been developed. With this method both the distribution and level of noble metals are controlled. Fig. 1b. illustrates the normalized Pd concentrations on four different monoliths being 50 cm long and prepared by this method. The deviation in Pd concentration from monolith average is maximum 12% which is negligible compared to what can be obtained by simple dipping of the monolith into a Pd solution.

Table. Test conditions. Gas inlet composition: 50 ppmv NO_x, 55 ppmv NH_3, 100 ppmv CO, 15 %vol O_2, 10 %vol H_2O, N_2 balance. Temperature: 350 °C.

	Catalyst	DeNOx, %	DeCO, %	NH_3 slip, ppmv
SCR only	GT-201	93.5	0	5.7
Dual function	GTC-802	92.9	97.8	4.4

The dual function catalyst has been compared with an SCR-only catalyst (Table 1). High NOx removal efficiencies have been obtained in both cases but the dual function catalyst additionally combines the SCR activity with a high CO oxidation. Thus, with this catalyst the required catalyst volume and thereby the resulting pressure drop will be reduced compared to using single catalysts dedicated for NOx removal and CO oxidation.

3 Conclusions

Haldor Topsoe has developed GTC-802, a dual function catalyst with the same SCR activity as an SCR-only catalyst but with CO oxidation functionality as well. In this way the total required catalyst volume to achieve a desired NOx and CO removal efficiency can be significantly reduced, thereby reducing pressure drop and in turn improving plant efficiency. With respect to plants that have to comply with CO emission limits but today has an SCR catalyst only, the dual function catalyst may simply replace the existing SCR catalyst in the HRSG. Finally, it can be added that the dual function catalyst provides an option for VOC removal as well.

V-OP45

A Kinetic Study of Hg Oxidation over Vanadia Based Catalyst

Usberti N.[1], Beretta A.[1*], Nash M.[2], Alcove S.[2]

1 - Dipartimento di Energia, Politecnico di Milano, Milano, Italy
2 - Johnson Matthey, Technology Center, Sonning Common, United Kingdom

* alessandra.beretta@polimi.it

Keywords: mercury, oxidation, NOX effect, HCl effect, temperature effect, V_2O_5 catalyst

1 Introduction

Among the various air pollutants emitted from coal-fired power plants, elemental mercury is a major environmental issue that has attracted considerable attention in recent years. It is now well known in literature that the presence of a SCR-DeNO_X unit affects mercury speciation, since the SCR catalyst favors the highly desired conversion of Hg^0 to the ionic species Hg^{2+} in the presence of HCl according to the stoichiometry: $Hg+2HCl+1/2O_2 \rightarrow HgCl_2+H_2O$. Several studies have investigated Hg oxidation over V-based catalysts; a number of macroscopic kinetic effects have been unanimously recognized, but the mechanism and kinetics behind them are still under study. For instance, the temperature dependence of Hg^0 conversion is typically reported as moderate or even negative [1]; this phenomenon, though broadly observed, has been little addressed and understood. It is known that external mass transfer limitations and the thermodynamics of the oxy-chlorination of Hg^0 play a role at high temperatures (> 400°C) [2, 3]. Also, the surface interaction of the chemical species typically present in the SCR reactor can modify the availability and strength of the active sites and thus affect the kinetics of Hg^0 oxidation. For example, it is well known that NH_3 adsorption inhibits the Hg oxidation.

This work aims at deepening the comprehension of the complex surface interactions that occur on the SCR catalyst in the presence of NO (whose effect has been reported by other studies to be either positive or negative [4]) and HCl under different operating temperatures as the initial step toward a systematic kinetic investigation of this complex reacting system.

2 Experimental/methodology

Experiments were performed over a $V_2O_5/MoO_3/TiO_2$ catalyst in a plug-flow plate-type reactor. This consisted of a rectangular quartz tube (section 32x22 mm), wherein a sample holder allowed for the placement of four plates of catalyst (400x25x1 mm) in a parallel configuration. The feed mixture consisted of 3.5% O_2, 10.5% H_2O, 0-10 ppm HCl, 0-300 ppm NO, 10 μg/Nm^3 of Hg^0 in N_2 with AV = 21 Nm/h; the temperature was varied in the range 170 – 400°C. Mercury balance and speciation were analyzed by an on-line Tekran instrument.

3 Results and discussion

Hg^0 oxidation reference tests were performed in the absence of the DeNOx reactants; Figure 1, panel A shows the results in black symbols. In the whole temperature range, Hg^0 conversion progressively increased with temperature, contrarily to what is commonly reported in the literature (where tests are usually performed in the presence of NO and NH_3); here, we estimated an apparent activation energy of 4.8 Kcal/mol. Since this weak temperature dependence was observed even at temperatures as low as 175°C, it seems informative of the surface kinetics, rather than being the result of full external mass-transfer control (which may be expected at higher temperatures [2]); in other words, it could be associated with the relevance of adsorption-desorption steps of the reacting species.

Experiments were then performed with NO co-feed (Figure 1, panel A, red symbols). A

promotion of Hg^0 conversion (about 5-10%) was observed up to 325°C; at increasing temperature, though, conversion declined. Thus, above 350°C, a progressively important loss of conversion was observed in comparison with the reference tests and a negative T-dependence appeared.

To better comprehend the surface interactions behind this evidence, we performed experiments at varying HCl inlet concentration, with and without NO. Tests were first performed at 300 and 400°C without NO (Figure 1, panel B). At both temperatures, no Hg^{2+} was formed in the absence of HCl, but Hg^0 conversion grew with increasing HCl content with asymptotic trends. Notably, below 3 ppm HCl, the conversion curves were almost coincident, thus insensitive to temperature; this suggests that, at very low HCl concentration, HCl adsorption was not equilibrated and was the kinetically controlling step. Above 5 ppm HCl, surface saturation was apparently reached and the weak positive T-dependence was confirmed.

Similar experiments were performed in the presence of 300 ppm NO (Figure 1, panel C). At 300°C, NO co-feed enhanced Hg^0 conversion over the whole range of HCl concentration studied. Surprisingly, a net conversion of Hg^0 to Hg^{2+} was observed in the absence of HCl and it amounted to about 43%; thus, an additional route of oxidation to HgO was active in the presence of NO. This demonstrates that at 300°C NO or, more likely, NO-related surface or gas phase species (e.g. nitrites, nitrates and NO_2) promoted the oxidation of Hg^0 to ionic Hg. Indeed the formation of NO_2 and surface nitrates is expected to pass through a maximum at 300-350° due to the kinetics and thermodynamics of NO oxidation.

At 400°C, instead, the co-feed of NO strongly inhibited Hg^0 conversion. The effect was dramatic at low HCl concentration and such that the conversion curve lost the typical asymptotic trend, while it assumed an increasing trend. This suggests that the formation of NO-related surface species competed with and hindered HCl adsorption.

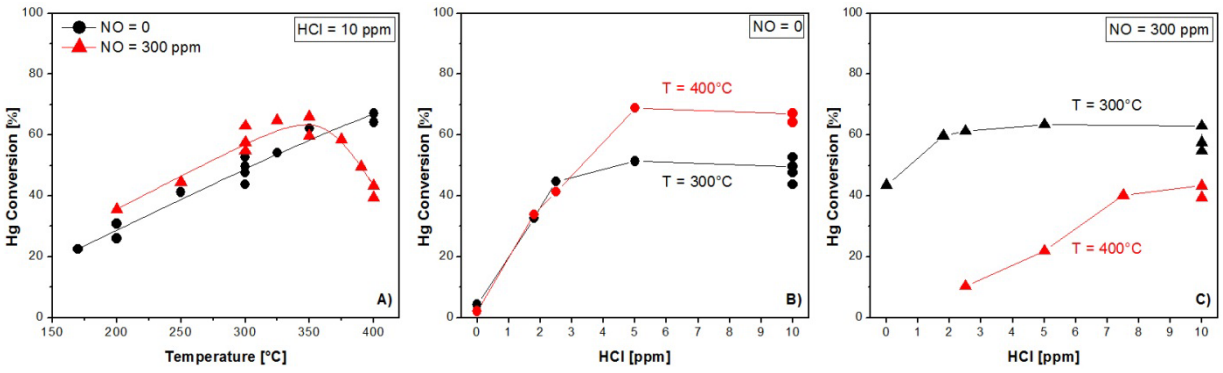

Fig. 1. Panel A: Hg^0 conversion over temperature; panels B and C: Hg^0 conversion over HCl inlet concentration with or without co-feeding 300 ppm NO at 300°C and 400°C.

4 Conclusions

The rate of Hg oxy-chlorination is strongly affected by surface coverage effects, thus the apparent activation energy is highly sensitive to the feed composition. The adsorption of HCl plays a key kinetic role and seems the RDS at low HCl concentration. NO (directly or indirectly) promoted Hg conversion up to 325°C but it had a negative effect at higher temperatures.

References

[1] S. Niksa, N. Fujiwara, Journal of the Air and Waste Manag. Ass., 55 (2005) 1866-1875;
[2] A. Beretta, N. Usberti, L. Lietti, P. Forzatti, M. Di Blasi, A. Morandi, C. La Marca, Chem. Eng. J., 257 (2014) 170-183;
[3] Madsen K., Thogersen J.R., Frandsen F., ICC 2012, Munich, 2012;
[4] F. Wang, G. Li, B. Shen, Y. Wanga, C. He, Chem. Eng. J., 263 (2015) 356–363.

V-OP46

Absorption and Oxidation of NO_x from Flue Gasses to Nitric Acid – An Atom Efficient NO_x Abatement Strategy Using Ionic Liquids

Thomassen P.L.*, Fehrmann R., Mossin S.L.

Center for Catalysis and Sustainable Chemistry, Department of Chemistry, Technical University of Denmark, Lyngby, Denmark

* pett@kemi.dtu.dk

Keywords: NOx abatement, alternative, DeNOx, Ionic, liquids, nitric acid

1 Introduction

Formation of NO_x during high temperature combustion with air is inevitable and of increasing environmental concern. NO_x participates in detrimental photochemical reactions in both the stratosphere and the troposphere, depleting the ozone layer and contributing to the greenhouse effect [1]. Furthermore, higher NO_x concentrations cause severe health conditions, such as cancer and several respiratory diseases. The main constituent of NO_x in flue gas is nitric oxide (NO).

In larger installations, NO_x is removed by selective catalytic reduction (SCR) using a transition metal catalyst to facilitate reduction of NO_x with ammonia. SCR exhibits excellent conversions and selectivity, when run at temperatures around 300ºC.

In order to reduce their carbon footprint, several countries have begun experimenting with, and implementing, biomass firing in power plants. The catalytic activity of the traditional high dust SCR setup decreases significantly within the first few hundred operating hours, when firing biomass. The poisoning of the catalyst is mostly due to alkaline aerosols. The deactivation can be overcome by placing the SCR reactor at the tail end of the flue gas treatment system, the low dust position. At this point however, the temperature of the flue gas has decreased significantly and a costly heat exchange becomes necessary. The deactivation is also a problem for the maritime industry, in waste incineration plants etc.

As described above, there is a demand for alternative deNO_x solutions. Several alternatives exist; fast SCR, low temperature SCR catalysts and absorption and oxidation with ionic liquids (ILs). This work revolves around the latter possibility.

Previous studies have shown that several ILs can absorb and oxidise NO_x species to nitric acid, at room temperature [2]. This oxidation can be done using only the excess oxygen and generated water present in the flue gas. This work presents a detailed spectroscopic study into the mechanism and kinetics of the reaction, mainly carried out by attenuated total reflectance Fourrier-transform infrared (ATR-FTIR) spectroscopy

2 Short experimental section

The *in-situ* ATR-FTIR experiments were conducted by placing a thin IL film on top of a temperature controlled ATR plate (Specac Golden Gate, High Temperature Diamond ATR). A specially designed gas cap was placed on top of the IL film, allowing a pre mixed simulated flue gas to be passed over the IL film. The reaction was monitored using a Nicolet iS5 FTIR spectrophotometer, with a resolution of 2-4 cm^{-1}, in the range 600-4000 cm^{-1}, and with a scan rate of 4-32 scans per spectrum, depending on the rate of reaction. The specific peaks for nitric acid were deconvoluted using Peakfit 5.0, giving a time resolution of the total rate of the reaction. Furthermore, the spectra were analysed to identify possible reaction intermediates. In all cases, the IL was regenerated under air flow at 125ºC [3].

3 Results and discussion

The overall reaction for the oxidation of NO to nitric acid in ILs follows the reaction scheme shown in (1) [2]:

$$4\ NO + 3\ O_2 + 2\ H_2O <--> 4\ HNO_3 \quad (1)$$

The kinetics of the reaction were determined by monitoring the rate of formation of nitric acid, when exposing the IL to a constant gas flow of varying concentrations. The IL is insignificant in size compared to the gas flow, thus the gas composition is considered constant. The reaction order in NO was determined to be 2, which is consistent with the proposed rate equations for autoxidation NO in different reaction media [4].

Spectroscopic investigations revealed several likely reaction intermediates. Three different N_2O_4 species, two with N-O-N bonds (both a cis- and a trans- conformation) and one species with a N-N bond. The presence of these three species suggests that NO associates with the nitrate of the IL, giving an NO-NO_3 adduct with an N-O-N bond, which can exist in both a cis and a trans conformation. The N-N is consistent with dimerisation of gaseous NO_2 being dissolved in the IL as N_2O_4. NO_2 can likely undergo dimerisation both as a dissolved species in the IL or by being released to the gas phase and subsequently dissolved as N_2O_4.

We believe that the oxidant in the reaction is molecular oxygen, since the reaction is highly reversible. The observed reversibility strongly suggests that no atomic oxygen radicals are present during reaction, as these would likely oxidise the IL. In order to utilise all 4 oxidation equivalents either a dimeric species of N^{III} or a singular N^{I} species would be expected as intermediates in the oxidation step. The first of the two seems as the most likely and spectroscopic evidence of HONO, a N^{III} species formed from reaction between NO_2 and water, was found in the spectra. All in all, the above findings have led to the proposed catalytic cycle presented in Figure 1 below.

4 Conclusions

Different techniques have shown that a variety of ILs can absorb and oxidise NO from a simulated flue gas, utilising the excess oxygen and water already present. This reaction is highly reversible. A rate law has been experimentally determined, and was found to be in accordance with the ones proposed in literature. *In-situ* spectra were examined and several reaction intermediates have been proposed. The findings have been collected and presented as a catalytic cycle with reaction coefficients amounting to that of the total reaction known from the literature.

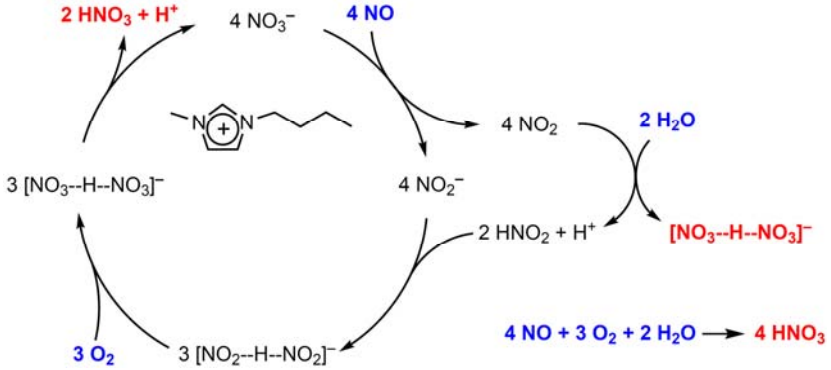

Figure 1: Catalytic cycle for the oxidation of NO in ionic liquids. In this case the 1-butyl-3-methylimidazolium cation is depicted, but research has shown other cations to also be active in this reaction.

References

[1] Finlayson-Pitts et. al, The Formation of Gaseous Nitrous Acid (HONO): A Key Determinant in Tropospheric Ozone and Fine Particles. (2001) p. 166.
[2] Thomassen, P. L. et. al, *ECS Trans*. (2012) 50, 433
[3] Kunov-Kruse, A. J. et. al, *Green Chem.* (2013) 15, 2843
[4] Goldstein, S. Czapski, G. *J. Am. Chem. Soc.* (1995) 49, 12078

V-OP47

N_2O Decomposition over Spinel Nanocatalysts - Experimental and DFT Theoretical Approaches to Catalyst Tuning

Zasada F., Kaczmarczyk J., Grzybek G., Janas J., Indyka P., Grybos J., Piskorz W., Kotarba A., Sojka Z.*

Jagiellonian University, Faculty of Chemistry, Krakow, Poland

* sojka@chemia.uj.edu.pl

Keywords: reaction mechanism, DFT, modelling, redox sites, isotopic labelling, surface reactive oxygen species, kinetics

1 Introduction

Spinels are excellent redox model catalytic materials of wide fundamental and practical interest due to their well-defined structure, ability to facile morphological variations and high flexibility in modifying their electronic properties via non/off-stoichiometry and site selective doping. Depending on the synthesis method, faceted nanocrystals of spinels expose well-defined planes, allowing for sensible investigations into structure-reactivity relationships at both model and practical conditions. This fact assists in designing of redox-tunable active sites of high performance and preferential development of surface terminations of high site density and optimal structure. The central points of our study consist in synthesis of the Mn, Fe, and Co nanospinel catalysts of controlled grain morphology and size, identification and in-depth characterization of the active sites, their redox tuning for optimal performance and catalytic kinetic studies of N_2O decomposition. The experiments are interpreted by means of DFT molecular modeling.

2 Experimental/methodology

Nanostructured Mn_3O_4, Fe_3O_4 and Co_3O_4 catalysts of controlled morphology were obtained via microwave assisted. The samples were characterized with XRD, XPS, RS, UV-Vis, EPR, SQUID, BET, FE-SEM/HR-TEM/EDX/EELS, and TPR/TPO as well as $^{16}O/^{18}O2$ isotopic exchange techniques. The catalytic measurements of N_2O decomposition were performed in a quartz flow reactor with GHSV of 5000-7000 h^{-1} in the range of 300 – 1000 K and in pulse mode using isotopically labeled reactants. The work function was measured by contact potential difference (Kelvin probe). For all computations (VASP package) a spin resolved DFT and DFT+U level of theory with B3LYP and PBE correlation-exchange potentials and PAW were used. For inclusion of pressure and temperature effects the interaction of the spinel surface with the reactants was modeled within the atomistic thermodynamics approach.

3 Results and discussion

The synthesized spinel samples regardless their morphology (retrieved by inversed Wulff construction) were monophasic and exhibit the (100), (111) and (110) facets only, as revealed by XRD and HR-TEM and Raman investigations. TPSR measurements showed that all samples exhibited large differences in N_2O decomposition activity, reaching full conversion below 450 ^oC, 700 ^oC, and 850 ^oC for Co_3O_4, Fe_3O_4, Mn_3O_4, respectively. Selective substitution of tetrahedral and octahedral parent cations, constituting the spinel (verified by XRD, RS, SQUID and EPR) revealed that octahedral ions, play the role of prime active sites in deN_2O reaction. The catalytic performance of the nanospinel was analyzed in terms of the redox properties of the catalyst probed by TPR/TPO and pulsed CO/O_2 surface titration and work function

measurements and the catalysts stoichiometry. In the case of the most active stoichiometric cobalt spinel, the well-balanced redox properties of the octahedral Co^{3+} sites account well for the high sustainable N_2O turnover. For the inverse spinel Fe_3O_4 the octahedral sites are occupied by mixed valence Fe^{2+}/Fe^{3+} cations, resulting in enhanced susceptibility for deep oxidation leading to transformation of the magnetite phase to maghemite at the surface region. As a result the observed steady state deN_2O catalytic activity is characteristic for the surface maghemite stable at the reaction conditions. Similar transformation was observed for Mn_3O_4 catalyst, but its lower activity is additionally constrained by the strong Jahn-Teller effect of octahedral Mn^{3+} cations. As a result, the change of the Mn^{3+} redox state during the catalytic cycle is accompanied by strong structural relaxation which enhances the activation barrier. Isotopic experiments revealed complex interfacial mechanism of recombination of oxygen adspecies produced by N_2O decomposition into final O_2, which involve the surface O^{2-} anions.

Detailed structure of the exposed (100), (110) and (111) facets, surface composition and specific coordination of all exposed metal and oxygen ions were established, with special emphasis on the electronic structure of the surface active sites. The projected electronic density of states where analyzed in terms of the electronic and magnetic structure of the investigated spinels, with emphasis on the edge-sharing octahedra, forming regular strips responsible for redox properties, crucial for their catalytic behavior. The redox properties of the spinels were discussed in terms of the spin and charge transfer polaron dynamics for M^{2+}/M^{3+} and M^{3+}/M^{4+} redox couples. The obtained results allowed for an in-depth rational account of the catalytic behavior of the manganese, iron, and cobalt spinel catalysts for decomposition of nitrous oxide.

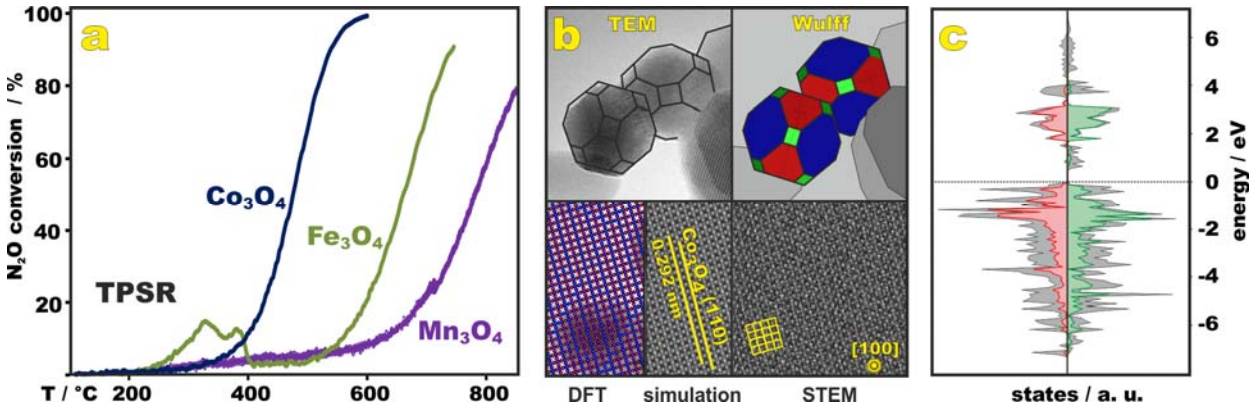

Fig. 1. deN_2O conversion profiles for Co, Fe, and Mn nanospinel catalysts (a), morphology of the Co_3O_4 grain and structure of the active (100) plane (b), DOS structure of cobalt spinel (grey) showing the contribution of the active octahedral Co sites shown in green and red (c).

4 Conclusions

A comprehensive multi-techniques experimental and theoretical DFT approach allowed for identification and quantification of the manganese, iron and cobalt spinel active sites, explaining their nature and redox properties, to provide an integral account of the observed large differences in the N_2O decomposition activity and the reaction mechanism.

Acknowledgements

Financial support by the National Science Centre (NCN) of Poland, Grant No. 2011/03/B/ST5/01564 is acknowledged.

V-OP48

K-$Cu_xCo_{3-x}O_4$ as Highly Efficient Catalysts for N_2O Decomposition from HNO_3-Exhaust Streams

Franken T., Palkovits R.*

RWTH Aachen University, Institut für Technische und Makromolekulare Chemie, Aachen, Germany

* palkovits@itmc.rwth-aachen.de

Keywords: environmental catalysis, mixed spinels, N_2O decomposition

1 Introduction

For a worldwide decrease of greenhouse gas emissions not only CO_2 but also other strong greenhouse gases such as e.g. CH_4, N_2O and SF_6 have to be considered. Especially by decreasing N_2O emissions, a high number of CO_2 equivalents can be reduced, as N_2O has a 310 times higher global warming potential compared to CO_2[1]. Main sources of N_2O are emissions from agriculture due to the use of fertilizer. Also industrial processes such as HNO_3 production and combustion processes contribute significantly to the overall N_2O emissions. For complete removal of N_2O emissions, current strategies rely on additional heating of the gas streams for a complete decomposition of N_2O into N_2 and O_2 out of tail gases from HNO_3 production. To avoid such energy inputs, suitable catalysts should enable high N_2O decomposition activity below 500°C in the presence of O_2, NO and H_2O. An industrially applied catalyst is Fe-ZSM-5. This catalyst achieves 50 % conversion at a temperature ($T_{50\%}$) of 430 °C in ideal reaction conditions [2]. Compared to the average temperatures of the tail gases (T = 250 – 500 °C) the activity is still too low for quantitative conversions without additional energy input. Herein, we present a promising catalyst with high activities below 500°C in realistic reaction conditions.

2 Results and discussion

Co_3O_4 shows already high activities for N_2O decomposition into N_2 and O_2.[3] In order to enhance the catalytic activities varying amounts of Co were exchanged by several metals (Mg, Cu, Co, Cr, and Zn) in the spinel phase. Using these materials as catalysts shows that the integration of Cu highly increases the catalytic activity compared to Co_3O_4. Furthermore, a strong dependency of the catalytic activity on the degree of metal exchange in $Cu_xCo_{3-x}O_4$ was found (Figure 1a)).[4] For lower Cu amounts higher catalytic activity is achieved. Reducing the amount to x = 0.25 results in highly active catalysts which show higher activities than pure Co_3O_4. For $Cu_{0.25}Co_{2.75}O_4$ full conversion was already achieved at 410°C in ideal reaction conditions ($c(N_2O)$ = 1000 ppm, GHSV = 54000 h^{-1}). These findings point to a strong synergetic effect between Cu and Co if Cu is applied in the proper ratio.

To increase the catalytic activity even more a series of doping metals (Ba, K, Sr, Na) was tested. Using various amounts of dopants shows that the strongest promotional effect was achieved with a molar ratio of n(K) to n(Cu)+n(Co) of 0.01. In ideal reaction conditions 0.01K-$Cu_{0.25}Co_{2.75}O_4$ shows full conversion at 330 °C. This is 80 °C lower than for the undoped catalyst. To investigate the performance of this catalyst in industrial conditions, additional gases (O_2 (c = 2 %) , NO (c = 200 ppm) and H_2O (c = 0.5 %); GHSV = 54000 h^{-1}) were first added single wise and later all together to reconstruct real reaction conditions (Figure 1b).

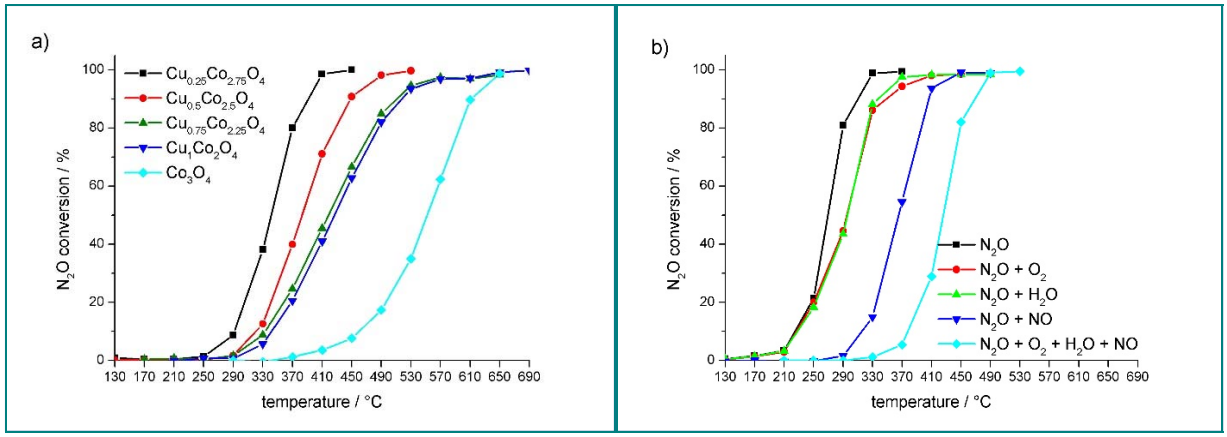

Fig. 1. a) Influence of the amount of Cu in $Cu_xCo_{3-x}O_4$ on the N_2O decomposition activity in ideal reaction conditions ($c(N_2O)$ = 1000 ppm in N_2, GHSV = 54000 h^{-1}). b) Performance of 0.01K -$Cu_{0.25}Co_{2.75}O_4$ in real reaction conditions ($c(N_2O)$ = 1000 ppm, $c(O_2)$ = 2 %, c(NO) = 200 ppm, $c(H_2O)$ = 0.5 % in N_2; GHSV = 54000 h^{-1}) and in the presence of the single gases.

In the presence of H_2O and O_2 the necessary decomposition temperatures increases only slightly, while the presence of NO has a strong influence. But still, at a high GHSV of 54000 h^{-1} and in the presence of all inhibitory gases (NO, O_2, H_2O) present under realistic reaction conditions, the catalyst K-$Cu_{0.25}Co_{2.75}O_4$ shows full conversions at temperatures as low as 490 °C. In the case of the not doped catalyst a much stronger inhibition by O_2 and H_2O was observed. This emphasises that desorption of oxygen is facilitated due to doping with K.

In long term experiments under stable reaction conditions and high GHSV (54000 h^{-1}) 0.01K-$Cu_{0.25}Co_{2.75}O_4$ shows no deactivation and a stable N_2O conversion of at least 72 % at 400 °C in realistic exhaust stream conditions. Even an increase of the gas flow rates leads only to minor changes of the conversions. First results on supported catalysts emphasise that the amount of active species can be highly reduced by the use of proper supports without significant loss of activity.

3 Conclusions

The introduced 0.01K-$Cu_{0.25}Co_{2.75}O_4$ catalyst shows high activities in the conditions of exhaust gases of HNO_3 production. Introducing this catalyst after the $DeNO_x$ unit in the reaction plant could enable operating temperatures of the DeN_2O stage as low as 330 °C. Overall, this development facilitates a more environmentally benign production of HNO_3 with minimum energy requirement for treatment of the exhaust gases.

Acknowledgement

We like to acknowledge the financial support by the Max Buchner foundation.

References

[1] United Nations Framework Convention on Climate Change UNFCCC, Conference of the Parties 8 (2003) 28.3. (fccc/cp/2002/8 p. 15).
[2] J. Pérez-Ramírez, F. Kapteijn, K. Schöffel, J. A. Moulijn, *Appl. Catal. B* 44 (2003) 117.
[3] C. Ohnishi, K. Asano, S. Iwamoto, M. Inoue, *Stud. Surf. Sci. Catal.* 162 (2006), 737.
[4] T. Franken, R. Palkovits, *manuscript under preparation.*

V-OP49

N_2O Decomposition over $CuO\text{-}CeO_2$ Mixed Oxides: Effect of Preparation Procedure

Konsolakis M.[1*], Carabineiro S.A.C.[2], Papista E.[3], Marnellos G.E.[3,4], Tavares P.B.[5], Figueiredo J.L.[2]

1 - School of Production Engineering and Management, Technical University of Crete, Crete, Greece

2 - Laboratório de Catálise e Materials (LCM), Laboratório Associado LSRE/LCM, Faculdade de Engenharia, Universidade do Porto, Porto, Portugal

3 - Department of Mechanical Engineering, University of Western Macedonia, Kozani, Greece

4 - Chemical Process & Energy Resources Institute, CERTH, Thessaloniki, Greece

5 - CQVR Centro de Química–Vila Real, Departamento de Química, Universidade de Trás-os-Montes e Alto Douro, Vila Real, Portugal

* mkonsol@science.tuc.gr

Keywords: N_2O decomposition, $CuO\text{-}CeO_2$ mixed oxides, impregnation, precipitation, exotemplating

1 Introduction

Nitrous oxide (N_2O) is one of the most significant greenhouse gases, due to its high global warming potential (~300 times higher as compared to CO_2). Moreover, it has a very long lifetime in the atmosphere (about 150 years), severely contributing to the depletion of the stratospheric ozone layer [1]. Hence, considerable efforts have been devoted on the N_2O emissions control from anthropogenic sources, with the catalytic decomposition to be considered as one of the most efficient and cost-effective technologies [1].

In spite of the excellent catalytic performance of noble metals (NMs)-based catalysts, their high cost and sensitivity to off gases constituents (i.e. O_2, NO, SO_2, H_2O) limits their widespread industrial application. Therefore, the development of NMs-free catalysts of low cost and adequate de-N_2O performance is of paramount importance. Recently, it has been reported that mixed oxides could possibly act as candidates for N_2O degradation, with CeO_2 to be a key component due to its unique redox properties. Furthermore, Cu-based catalysts have received considerable attention in heterogeneous catalysis due to their adequate performance and low cost. Thus, it has been shown that $CuO\text{-}CeO_2$ mixed oxides confer a synergistic interaction effect toward enhanced reducibility and catalytic performance [2].

In the present work, the effect of preparation procedure on the N_2O decomposition is investigated by employing three different catalysts types, *i.e.*, i) bare CeO_2, ii) Cu supported on CeO_2 and iii) Cu-Ce mixed oxides. In all three cases, impregnation, precipitation and exotemplating methods were employed, whereas commercial samples were also used for comparison. All materials were characterized by BET, XRD, H_2-TPR, SEM and XPS in order to correlate the de-N_2O performance with the morphological, structure and surface properties.

2 Experimental/methodology

Three different types of materials were synthesized: i) bare CeO_2 prepared by precipitation (Ce-pp) and exotemplating (Ce-exo) in comparison to commercial CeO_2 (Ce-com), ii) Cu/CeO_2 oxides synthesized by impregnation of the above materials with CuO (Ce-pp+Cu, Ce-exo+Cu, Ce-com+Cu), iii) Ce-Cu mixed oxides prepared in one stage by precipitation (Ce-Cu-pp) and exotemplating (Ce-Cu-exo) using cerium and copper nitrates as precursors. For comparison, a material prepared by mechanical mixing of commercial CeO_2 and CuO (Ce-Cu-com) was also

examined. The as prepared materials were characterized by N_2 adsorption at 196 ºC, temperature programmed reduction (TPR), X-ray photoelectron spectroscopy (XPS), scanning electron microscopy/energy-dispersive X-ray spectroscopy (SEM/EDS) and X-ray diffraction (XRD).

3 Results and discussion

Figure 1 depicts the de-N_2O performance, in the absence of O_2, over the single CeO_2 and Ce-Cu mixed oxides prepared by different routes.

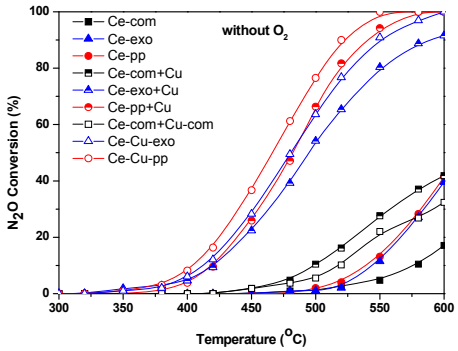

Fig. 1. N_2O conversion in the absence of O_2. Reaction conditions: 1000 ppm N_2O, GHSV=40000 h^{-1}.

The results clearly show the inferior N_2O conversion performance of single oxides, never exceeding 40% at 600°C. On the contrary, a superior de-N_2O performance was obtained by mixed oxides. The optimum performance was observed for Cu-Ce mixed oxides prepared by co-precipitation, which achieves complete N_2O conversion at 550ºC. The remarkable activity of Cu-Ce-pp samples can be ascribed to their superior reducibility at low temperatures in conjunction with the high concentration of Ce^{3+} sites. These factors are crucial for N_2O decomposition, since they contribute to the facilitation of oxygen desorption from the catalyst surface as well as to the regeneration of active sites.

4 Conclusions

The N_2O decomposition over bare or mixed CeO_2 and CuO oxides was investigated, with particular emphasis on the impact of synthesis procedure (impregnation, precipitation, exo-templating) on the surface and redox properties. The obtained results revealed that the superiority of Cu-Ce mixed oxides prepared by precipitation compared to all other composites, can be ascribed to its excellent redox properties linked to Ce^{4+}/Ce^{3+} and Cu^{2+}/Cu^{+} redox couples.

Acknowledgements

The authors thank Fundação para a Ciência e Tecnologia (FCT) for financial support. SACC acknowledges Investigador FCT program (IF/01381/2013/CP1160/CT0007), with financing from the European Social Fund and the Human Potential Operational Program. The Associate Laboratory LSRE/ LCM is supported by FCT and FEDER through project PEst-C/EQB/LA0020/2013. MK is thankful for Greece–Portugal Bilateral Educational Programme (MK). Authors are thankful to Dr. Carlos M. Sá (CEMUP) for assistance with XPS and SEM analyses. Financial support by the program "THALIS" implemented within the framework of Education and Lifelong Learning Operational Programme, co-financed by the Hellenic Ministry of Education, Lifelong Learning and Religious Affairs and the European Social Fund is gratefully acknowledged.

References

[1] M. Konsolakis, A. Alygizou, G. Goula, I.V. Yentekakis, *Chem. Eng. J.* 230 (2013) 286-295.
[2] M. Konsolakis, Z. Ioakeimidis, *Appl. Sur.Sci.* 320 (2014) 244–255.

V-OP50

Catalytic Degradation of N_2O Emissions by Nanoshaped CuO/CeO_2 Materials

Zabilskiy M.[1*], Djinović P.[1], Tchernychova E.[2], Erjavec B.[1], Pintar A.[1]

1 - National Institute of Chemistry, Laboratory for Environmental Sciences and Engineering, Ljubljana, Slovenia

2 - National Institute of Chemistry, Laboratory for Materials Chemistry, Ljubljana, Slovenia

* maxim.zabilskiy@ki.si

Keywords: CuO/CeO_2, nanoshaped catalyst, N_2O decomposition, CeO_2 nanocubes, CeO_2 nanorods

1 Introduction

Considerable industrial emissions of N_2O into the atmosphere (about 400 million tons of CO_2 equivalent annually), its high global warming potential (310 times higher as compared to carbon dioxide), long atmospheric lifetime (approx. 120 years) and contribution in ozone layer depletion stimulate scientist to develop new, low-temperature technologies for N_2O degradation in exhaust gases [1,2]. Among efficient catalysts for N_2O decomposition, CuO/CeO_2 materials show very promising results [3,4]. It was reported, that nanoshaped ceria (nanocubes and nanorods) with well-defined [100] and [110] reactive planes possess higher catalytic activity than conventional polycrystalline ceria nanoparticles [5]. Therefore, the main purpose of this work was to investigate in detail the influence of nanoparticle shape and exposed crystal planes of CeO_2 supports on catalytic property of CuO/CeO_2 solids in low temperature N_2O degradation.

2 Experimental and methodology

Nanoshaped CeO_2 supports were synthesized by hydrothermal method. Briefly, 0.15 M $Ce(NO_3)_3 \cdot 6H_2O$ (99 % purity, Sigma-Aldrich) solution was added to 6M NaOH (99 % purity, Merck) for synthesis of ceria nanocubes (CeO_2-C) and nanorods (CeO_2-R), or to 1M NaOH solution for preparation of polycrystalline CeO_2 (CeO_2-P). Suspensions were aged at 180 °C (CeO_2-C) or 100 °C (CeO_2-R and CeO_2-P) for 24 hours, centrifuged, dried at cryogenic temperature and finally calcined at 400 °C for 4 h. In order to prepare CuO/CeO_2 catalysts, 2-8 wt. % of Cu was deposited by precipitation from $Cu(NO_3)_2 \cdot 3H_2O$ (99.5 % purity, Sigma-Aldrich) by Na_2CO_3 (99.999 % purity, Merck), followed by freeze-drying and calcination at 400 °C for 4 h. Synthesized solids were marked as X-Cu/CeO_2-M (where X represents nominal Cu content in wt. %, M represents morphology of utilized CeO_2 supports – cubes (C), rods (R) or polycrystalline (P)). Prepared materials were thoroughly characterized by N_2-sorption, SEM, HR-TEM, XRD, H_2-TPR, *in-situ* DRIFTS and *operando* DR UV-Vis techniques. Catalytic activity was investigated in a fixed-bed reactor operating in the temperature range from 300 to 550 °C with N_2O feed concentration of 2500 ppmv (WHSV = 120 L/(g_{cat} h)).

3 Results and discussion

Prepared CeO_2 supports significantly differ in BET specific surface area. The highest S_{BET} was measured for CeO_2-P sample – 115 m^2/g, while increasing NaOH concentration to 6M and hydrothermal temperature to 180 °C result in lower surface areas: 87 m^2/g for CeO_2-R and 29 m^2/g for CeO_2-C, correspondingly. Cu loading as well as utilized support greatly influence the physical-chemical, redox and catalytic properties of investigated catalysts. Accordingly to the results of H_2-TPR, TEM and DR UV-Vis analyses, several copper species are present on the

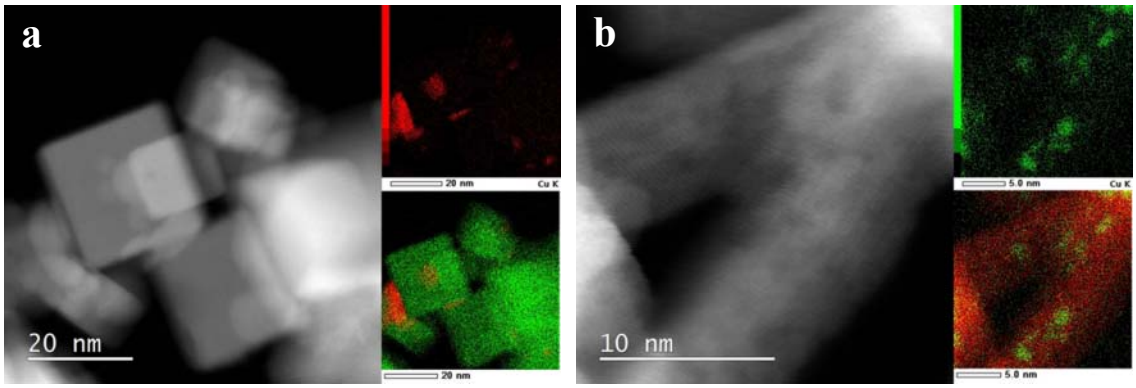

Fig. 1. BF-STEM image and EDX mapping of Cu, as well as overlay of Ce and Cu distribution observed for 4-Cu/CeO_2-C (a) and 4-Cu/CeO_2-R (b) samples

surface of CuO/CeO_2 oxides. By increasing copper loading from 2 to 8 wt. %, the growth of CuO particles from highly dispersed Cu species, through small CuO clusters and finally to bulk CuO phase takes place. Utilizing high surface area CeO_2-R and CeO_2-P supports resulted in higher Cu dispersion and smaller CuO clusters (less than 5 nm for 4-Cu/CeO_2-R, see Fig. 1b). Existence of both Cu^{+1}/Cu^{+2} and Ce^{+3}/Ce^{+4} ionic pairs in all studied samples was proved by means of DR UV-Vis examination. *In-situ* DRIFT spectroscopy with adsorbed CO also confirmed presence of Cu^{+1} and Cu^0 species, which are believed to be active sites for catalytic N_2O decomposition.

The highest N_2O conversions were achieved by catalysts based on CeO_2-R (exposed [100] and [110] facets are less stable and more reactive, S_{BET} = 87 m^2/g). Among them, 4-Cu/CeO_2-R resulted in highest activity per copper loading (3.8 mol $N_2O/(mol_{Cu}$ h) at 375 °C). At the same time 4-Cu/CeO_2-C (exposed [100] planes, S_{BET} = 27 m^2/g) and 4-Cu/CeO_2-P (exposed least reactive [111] planes, S_{BET}=110 m^2/g) resulted in lower activity as compared to 4-Cu/CeO_2-R (3.5 and 1.7 mol $N_2O/(mol_{Cu}$ h) at 375 °C, respectively). Long-term tests (100 h) with 4-Cu/CeO_2-R catalyst at 400 °C confirmed exceptional catalytic stability of the investigated catalysts even in the inhibiting atmospheres (presence water vapor/NO/O_2), which can be attributed to its ability to regenerate active sites by desorption of molecular oxygen from the catalyst's surface. Finally, mechanism of N_2O degradation over Cu/CeO_2 catalyst was proposed based on results of *operando* DR UV-Vis, DRIFTS and alternating N_2O/N_2 thermogravimetric examinations.

4 Conclusions

We have shown that activity of CuO/CeO_2 materials in catalytic N_2O degradation depends on both shape induced activity of CeO_2 ([100] and [110] facets are more reactive) and its BET surface area. Developed catalysts are stable for 100 h even in the presence of NO, O_2 and H_2O, which makes them appealing for potential industrial application. By using surface-sensitive *operando* techniques, the mechanism of studied reaction over CuO/CeO_2 catalyst was proposed.

Acknowledgements

The authors gratefully acknowledge the financial support of the Ministry of Education, Science and Sport of the Republic of Slovenia through Research program P2-0150.

References

[1] A.R. Ravishankara, J.S. Daniel, R.W. Portmann, *Science* 326 (2009) 123.
[2] J. Pérez-Ramírez, F. Kapteijn, K. Schöffel, J.A. Moulijn, *Appl. Catal. B Environ.* 44 (2003) 117.
[3] M. Zabilskiy, P. Djinović, B. Erjavec, G. Dražić, A. Pintar, *Appl. Catal. B Environ.* 163 (2015) 113.
[4] M. Zabilskiy, B. Erjavec, P. Djinović, A. Pintar, *Chem. Eng. J.* 254 (2014) 153.
[5] E. Aneggi, D. Wiater, C. de Leitenburg, J. Llorca, A. Trovarelli, *ACS Catal.* 4 (2014) 172.

V-OP51

Pd-Cu Catalysts Supported on Anion Exchange Resins for the Simultaneous Catalytic Reduction of Nitrate and Reductive Dehalogenation of 4-Chlorophenol from Water

Olaru A. E.[1], Capat C.[1], Frunza L[2], Papa F.[3], Munteanu C.[3], Udrea I.[1], Bradu C.[1*]

1 - University of Bucharest, Research Center for Environmental Protection and Waste Management, Bucharest, Romania

2 - National Institute of Materials Physics, Magurele, Romania

3 - Institute of Physical Chemistry of the Romanian Academy, Bucharest, Romania

* corina.bradu@g.unibuc.ro

Keywords: Pd-Cu bimetallic catalyst, water-phase, nitrate reduction, dehalogenation of chlorophenols

1 Introduction

The increasing of food demanding as a natural result of world population growth determined a large use of fertilizers and phytosanitary products in agricultural practices Nitrates and adjacent pesticides, especially organochlorine pesticides and their degradation by-products, are the main concerned pollutants found in natural waters originating from agricultural areas [1]. A series of physico-chemical and biological methods were developed for nitrate removal from water. Among these, liquid-phase catalytic reduction of the nitrates seems to be a convenient technique applied in this situation [2]. For organochlorine pesticides, characterized by high toxicity and persistence, several approaches like adsorption or advanced oxidation processes has been proposed [3]. An alternative approach for the reduction of the ecotoxicity of water polluted with organochlorine compounds could be the catalytic hydrodechlorination. Usually, the research studies are dedicated to a single or a class of pollutant (e.g. nitrates or organochlorine pesticides). This work is focused on the simultaneous removal of nitrate and organochlorine compounds from aqueous media through a catalytic reduction process, which could contribute to the protection and remediation of natural water resources.

2 Experimental

In this purpose, a bimetallic Pd-Cu catalyst supported on an anion exchange resin (*A-520E Purolite*) was prepared by successive deposition of the metals (2%Pd and 0.5%Cu). In the first step, palladium was introduced by ion exchange with the functional groups $-N(CH_3)_3^+Cl^-$ present onto the styrene–divinylbenzene polymeric matrix of the resins, using as precursor the $[PdCl_4]^{2-}$ complex. In order to enhance the interaction Pd-Cu, the second component was deposited by a controlled surface reaction, in which Cu^{2+} was reduced by the hydrogen adsorbed on the pre-reduced Pd surface [4]. The morphological and structural characterisation of the catalyst was achieved by means of: Scanning Electron Microscopy with Energy Dispersive X-ray spectroscopy (SEM-EDX), X-Ray Diffraction analysis (XRD), X-Ray Photoelectron Spectroscopy (XPS), microphotography and Atomic Absorption Spectrophotometry (AAS). The catalytic tests were carried out in a continuous flow system with a fixed bed reactor (0.4 g catalyst) in which the aqueous solution (0.25-1.0 $mL.min^{-1}$) circulates concurrently with the hydrogen flow (10-100 $mL.min^{-1}$). The initial concentrations of nitrate and 4-chlorophenol (4-CP) were 100 $mg.L^{-1}$ and 50 $mg.L^{-1}$ respectively.

3 Results and discussion

The successive deposition of the palladium and copper on the anionic resin, as described

previously, resulted in peripheral distribution of the both active phase components (Fig. 1). The similar distribution of copper and palladium revealed by the SEM-EDX analysis, confirm the deposition of the second metal by a controlled surface reaction.

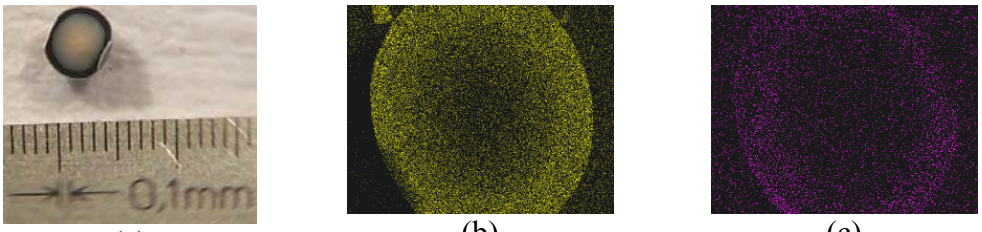

(a) (b) (c)

Figure 1. Micro-photos of Pd-Cu/A-520E (a) and SEM EDX images of Pd (b) and Cu (c) distribution on support

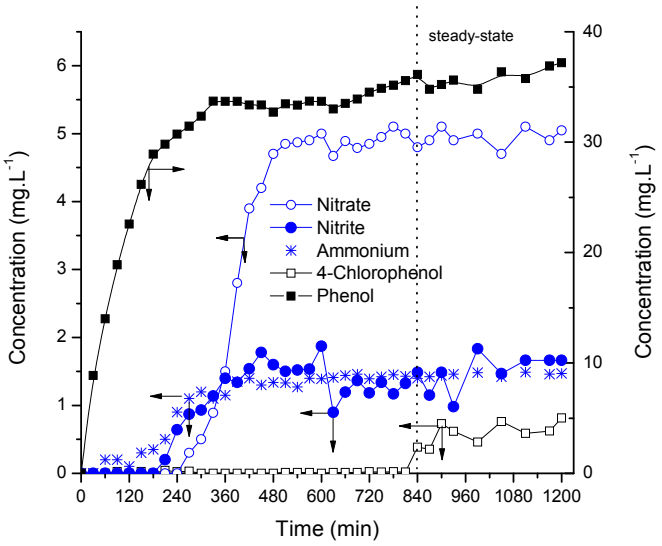

Figure 2. Catalytic performance of Pd-Cu/A-520E for simultaneous removal of nitrate and 4-CF

Firstly, the catalysts were tested in the reduction of NO_3^-. At the beginning the nitrate was eliminated by ion exchange and catalytic reduction. When the steady-state was attained, depending on operational parameters, the conversion of nitrate could reaches 95%, with 93% selectivity on N_2. The hydrodechlorination of 4-CP in the presence of nitrate was almost complete (conversion higher than 98%) while removal of nitrate was maintained at the same level of conversion with only a very small decrease in selectivity (Fig. 2).

The stability of the catalyst was assessed by determining the amount of palladium and copper in the used catalyst (100 h test) compared to the fresh one. The Pd load decreased insignificant (less than 0.015%). The cooper leaching was higher but not exceeding 0.50% of the initial amount.

4 Conclusions

A Pd-Cu catalyst supported on strong base anion resin was prepared by successive deposition of the metals (ion exchange for Pd and controlled surface reaction for Cu). The as-synthesized catalyst exhibited high catalytic activity in the simultaneous selective reduction of nitrate to nitrogen and hydrochlorination of 4-CP to phenol, attended by a good stability.

Acknowledgements

The authors thank the Romanian Authority ANCSI for the financial support under the project INTEGRATREAT 100/2012.

References

[1] C. Ravier, L. Prost, M.H. Jeuffroy, A. Wezel ,L. Paravano, R .Reau, *Land Use Policy*,. 42(2015) 131.
[2] T. J. Strathmann, C. J. Werth, J. R. Shapley, Nanotechnology Applications for Clean Water, 2nd Edition, Elsevier, (2014) 339.
[3] A. R. Ribeiro, O. C. Nunes, M. F.R. Pereira, A. M.T. Silva, Environ. Int. 75 (2015) 33.
[4] F. Epron, F. Gauthard, J. Barbier, *Appl. Catal. A*, 237 (2002) 253.

V-PP01

Structured Cartridges with Glass-fiber Catalysts: New Trend in the Design of Catalytic Reactors for Pollution Control

Lopatin S.A.[1,2], Zazhigalov S.V.[1,2], Mikenin P.E.[1,2], Pisarev D.A.[1,2], Baranov D.V.[1,2,3], Zagoruiko A.N.[1,2,4*]

1 - Boreskov Institute of Catalysis SB RAS, Novosibirsk, Russia
2 - Research and Educational Center for Energy Efficient Catalysis, Novosibirsk State University, Novosibirsk, Russia
3 - Novosibirsk Technical State University, Novosibirsk, Russia
4 - Tomsk Polytechnic University, Tomsk, Russia

* zagor@catalysis.ru

Keywords: glass-fiber catalyst, pressure, drop, mass transfer, reactor design

1 Introduction

Development of the new and improvement of existing heterogeneous catalytic processes for pollution control is an actual task of great practical importance. One of the possible paths for the progress in this area is development and application of new geometrical forms of catalysts, characterized with low pressure drop and, simultaneously, with high heat and mass transfer efficiency, thus providing the maximum use of the catalytic potential of its active components. Many various new forms of catalysts, e.g. wire mesh catalysts, foam catalysts, micro-fibrous catalysts are currently discussed [1].

One of the promising directions of development in this area includes application of the catalysts on the base of the flexible micro-fibrous supports, e.g., glass fibers. Glass-fiber catalyst (GFC) is a new type of catalytic systems, where the support represents itself the glass microfibers, structured in form of threads in the woven or knitted fabrics. The possible active components may include noble metals and/or oxides of transient metals, depending upon the requirements of the target catalytic process [2,3].

2 Design of catalytic reactors for glass-fiber catalysts

From engineering point of view, the GFCs are specific due to their original geometry and flexibility, opening the unique possibilities for creation of new types of structured catalytic beds [4,5]. In turn, this makes possible the creation of principally new designs of catalytic reactors.

The numerous methods of GFC layers arrangement were proposed during last two decades [4]. They include flat multi-layer [6], radial [7] and axial [8] structured packings. The most efficient among them are the prismatic structured cartridges, which may be used for creation of the catalyst beds of any size and geometry (Fig.1).

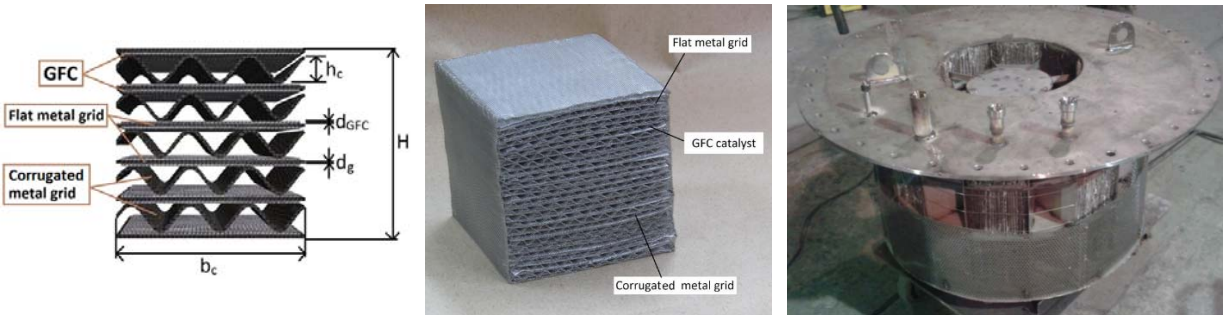

Fig.1. Different designs of axial GFC cartridges: prismatic GFC cartridge (left and center), radial block from prismatic axial cartridges (right).

3 Pressure drop and mass transfer properties of the structured GFC cartridges

Prismatic axial GFC cartridges are characterized with the very low pressure drop [5], slightly exceeding that for the monolith catalyst. At the same time, GFC cartridges are more efficient in terms of mass transfer due to more intensive turbulization of the flow in the cartridge. The mass transfer in packed bed of granulated catalysts is even more intensive, but such beds are characterized with much higher pressure drop. Obviously, the pressure drop and mass transfer are in contradiction and in this case the objective comparison may be based on the relationship between value of the mass transfer coefficient and unit pressure drop. Such relationships for different types of catalysts are plotted in Fig.2 [9].

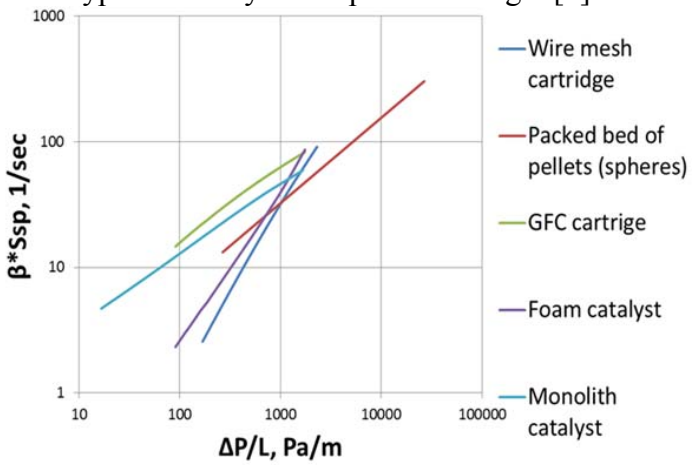

Fig.2. The relationship between mass transfer coefficient and unit pressure drop for different types of catalyst beds under variation equivalent diameter of the gas passage [9].

As seen from Fig.2, GFC cartridges provide the best compromise between high mass exchange and low pressure drop than all other forms of existing catalysts in the wide range of flow velocities and passage sizes, thus highlighting the superb engineering potential of structured fiber-glass catalytic systems.

Such cartridges may find the wide application in the pollution control processes, where the intensive mass transfer is important for the overall process efficiency.

Acknowledgements

The work was performed in the framework of the joint Research and Educational Center for Energy Efficient Catalysis (Novosibirsk State University, Boreskov Institute of Catalysis). The Skolkovo Foundation (Grant Agreement for Russian educational organizations no. 3 of 25.12.2014) supported this work.

References

[1] E.Reichelt, M.P.Heddrich, M.Jahn, A.Michaelis. *App. Catal. A: Gen.* 476 (2014) 78.
[2] B.Balzhinimaev, E.Paukshtis, S.Vanag, A.Suknev, A.Zagoruiko. *Catal. Today,* 151(2010), 195.
[3] P.Mikenin, P.Tsyrulnikov, Y.Kotolevich, A.Zagoruiko. *Catalysis in Industry*, 1(2015), 65.
[4] A.Zagoruiko, B.Balzhinimaev. *Chemical Industry Today* (in Russian), 2 (2011) 11.
[5] S.Lopatin, A.Zagoruiko. *Chem. Eng. J.* 238 (2014) 31.
[6] A.Zagoruiko, S.Vanag, B.Balzhinimaev, E.Paukshtis, L.Simonova, A.Zykov, S.Anichkov, N.Hutson. *Chem. Eng. J.* 154 (2009) 325.
[7] Russian Patent No. 2200622 (2002).
[8] Russian Patents Nos. 66975 (2007), 101652 (2010), 124888 (2012), 124924 (2012), 124925 (2012), 125094 (2012), 145037 (2014).
[9] S.Lopatin, P.Mikenin, D.Pisarev, D.Baranov, S.Zazhigalov, A.Zagoruiko. *Chem. Eng. J.* (2015), accepted to publication (doi: 10.1016/j.cej.2015.02.026).

V-PP02

Catalysts on the Base of Ceramic Highly-Porous Block-Cellular Carriers

Gasparyan M.D., Liberman E.Yu., Grunsky V.N.*, Obukhov E.O.

Russian Mendeleev University of Chemical Technology, Moscow, Russia

* migas56@yandex.ru

Keywords: ceramic highly-porous cellular, materials, active layer, catalytic activity

1 Introduction

At the last 20-30 years, a ceramic highly-porous cellular materials (HPCM) or foam ceramics obtained by different technologies of pore formation are widely used as filters for refining metal melts, heat insulation materials, carriers of catalysts and sorbents in metallurgy, chemistry and petrochemistry, transport and nuclear industry.

Small volume catalytic systems based on ceramic HPCM developed in Russian Mendeleev University of Chemical Technology are used in various liquid-phase catalytic processes: nitration of aromatic and reduction of nitrocompounds, hydrorefinement of petroleum products, waste water from nonionic surfactants, as well as in gas-phase environmental catalysis for the conversion of toxic products of burnout of motor fuels and localization of volatile radionuclides in exhaust of special manufactures.

2 Experimental/methodology

Ceramic HPCM with different composition are produced using the slip technology by the method of replication structure of the polymer matrix of polyurethane foam (PUF). The essence of the method is thermodestruction of the polymer matrix impregnated with a ceramic slurry, and subsequent sintering of the components of the slip at high temperature to produce a solid framework that duplicate the original shape of the PUF with the porosity of 10÷80 ppi. Electrocorundum, aluminomagnesium spinel, zirconia, silicium carbide, etc. are used in the slurry as a dispersed phase; as the main binder - fine ground alumina or porcelain mass; sintering and hardening additives are: MgO, TiO_2 and SiC.

Next, to develop surface, improve the strength characteristics and to make future catalysts specified properties the active substrate is applied on the ceramic frame by the method of successive impregnation and heat treatment. It may contain the following components or their combinations: γ-Al_2O_3, SiO_2, SO_4^{2-}/ZrO_2 (super acid), hydrophilic or hydrophobic zeolites.

The final stage of preparation of catalysts is the application by different methods (impregnation from solutions and suspensions, chemical precipitation) a wide range of catalytically active compositions: from monometallic layers of Ni, Co, Pd, Pt, Cu, Ag etc., or oxides of these metals to compositions of a complex structure of type $Au/Ce_{0,72}Zr_{0.18}Pr_{0.1}O_2$ or $Me_{0,1}Zr_{0,18}Ce_{0,72}O_2$, where Me - rare earth metals.

Thus obtained catalysts have the extremely high available external surface (up to 2700 m^2/m^3), low hydro- or gas-dynamic resistance, high specific surface of the active layer (up to 450 m^2/g), high coefficient of external diffusion, a high degree of mixing and dispergation. These characteristics in combination with traditional for ceramics characteristics: high mechanical strength and durability, chemical and thermal stability, the possibility of forming products of any configuration allow to activate mass transfer processes with the high efficiency and load on the catalyst and with high speeds at low concentrations of reacting substances, and also to eliminate abrasion and fly ash of catalyst in the reaction zone.

3 Results and discussion

As an example, characteristics of highly-porous block-cellular catalyst for the oxidation of hydrogen with the palladium active layer applied by chemical precipitation [1] are presented. Figure 1 shows electron micrographs of the sample of catalyst, indicating the formation of the compact palladium coating on the surface of the ceramic frame (Fig.1b), consisting of coarse aggregates with well-developed external surface and a significant amount of micropores. The cellular structure of HPCM after application of palladium remains stable (Fig.1a).

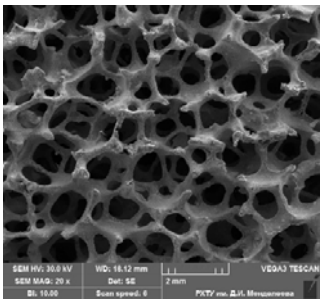
a

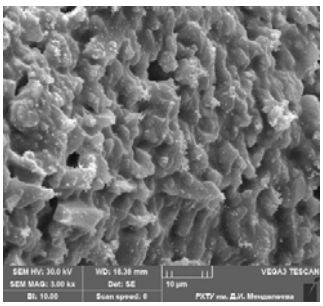
b

Fig. 1. SEM micrographs of the sample of ceramic catalyst with applied palladium active layer: a - the frame structure, b - the surface of partition cell

This block catalyst shows the ultra-high catalytic activity in the process of hydrogen oxidation, passing in the kinetic area. The rate constant of the oxidation reaction of hydrogen with the concentration of 600-1500 ppm in the air with a volume flow rate of 0.5-10 m^3/h in the temperature range of 70-150°C reaches the value 130 s^{-1}, and the stable operation of the catalyst starts at a temperature 110°C.

Catalytically active compositions on the base of rare-earth metals, containing, for example, nano-dispersed multi-component solid solution $Pr_{0,1}Zr_{0,18}Ce_{0,72}O_2$ with crystallite size 8-15 nm (Fig.2) have been designed for oxidation of hydrocarbons and carbon monoxide in the exhaust gases of vehicles. Their use allows to achieve 100% conversion of CO and CH at temperatures of 280-300 °C and to minimize the content of precious metals in the catalysts [2].

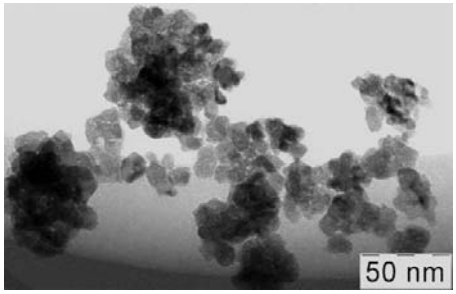

Fig. 2. TEM micrographs of the crystallites $Pr_{0,1}Zr_{0.18}Ce_{0.72}O_2$ in catalyst active layer

4 Conclusions

Applied highly-porous block-cellular catalysts demonstrated the high catalytic activity and specific productivity in a number of processes of catalytic oxidation, reduction, and hydrogenation, exceeding the similar parameters of the bulk and honeycomb catalysts.

References

[1] Gasparyan M.D., Grunsky V.N., et al. The use of ceramic high-porous block-cellular palladium catalysts in the process of hydrogen isotopes oxidation. Glass and Ceramics, 2014, no.11, pp. 22-25 (in Russian).

[2] Liberman E.YU., Mikhaylichenko A.I., et al. Features of the synthesis of the solid solution $Zr_{0,2}Ce_{0,8}O_2$ - component of trifunctional catalysts. Chemical technology, 2003, no. 11, pp. 5-7. (in Russian)

V-PP03

The Synthesis Charcterization and Catalytic Performances of Three-Dimensionally Ordered Macroporous x-CeO_2/Al_2O_3 Catalysts for Diesel Soot Combustion

Jin B.F., Wei Y.C., Zhao Z.*, Liu J., Duan A.J.

State Key Laboratory of Heavy Oil Processing, China University of Petroleum, Beijing, China

* zhenzhao@cup.edu.cn

Keywords: three-dimensionally ordered macroporous, materials, x-CeO_2/Al_2O_3, catalysts soot combustion

1 Introduction

Diesel engine vehicles are a promising power source for light vehicles owing to good power performance and high fuel efficiency[1]. However, the emission of soot particle matter (PM) can cause human carcinogen[2]. Thus, it is crucial to reduce emissions of particulate matter before the wide utilization. The combination of traps and oxidation catalysts in the continuously regenerating particulate trap (CRT) appears to be one of the most efficient and economic after-treatment techniques for diesel engines. This key challenge is to find effective catalysts for soot combustion that operates at low temperature. In our work, a series of three-dimensionally ordered macroporous (3DOM) x-CeO_2/Al_2O_3 catalysts were prepared by the method of micropores-diffused precipitation (MDP) using ammonia solution as the precipitation. These catalysts were estimated for catalytic oxidation of soot. They were characterized by the techniques of SEM, XRD, H2-TPR, and TEM.

2 Experimental

3DOM Al_2O_3 support was prepared via a precursor thermal decomposition-assisted colloidal crystal templating method. The synthesis of 3DOM x-CeO_2/Al_2O_3 catalysts was carried out by the method of micropores-diffused precipitation (MDP) in our lab[3]. Typically, $Ce(NO_3)_3 \cdot 6H_2O$ and distilled water were mixed in a precursor tank (Beaker I). The solution containing ammonia was stored in another tank (Beaker II) as precipitation agent. The precursor solution (Beaker II) was diffused into the membrane reactor via the holes distributed on the wall of the ceramic membrane tubes by a constant flow pump, and the precipitation of Ce^{3+} occurred while meeting precipitation agent in membrane reactor, yielding $Ce(OH)_3$. The slurry mixture was deposited, filtered, dried and calcined. Finally, 3DOM x-CeO_2/Al_2O_3 were obtained.

3 Results and discussion

From XRD patterns (Fig. 1), four main characteristic diffraction peaks of 3DOM x-CeO_2/Al_2O_3 catalyst (x=10-40%) shifted to high angle in comparsion with pure CeO_2 catalyst. The result demonstrates the formation of Al-Ce-O solid solutions. The H_2-TPR profiles (Fig. 2) indicates that the enhancement of the reducibility of supporting ceria prepared by MDP method. SEM (Fig. 3) and TEM (Fig. 4) images exhibit a well-defined three-dimensional ordered macroporous structures. The long-range order of the inverse opals remain. The structure is favorable for the mass tranfer because of their connectivity.The values of T_{10}, T_{50} and T_{90} for soot combustion over catalysts under conditions of loose contact between soot and catalyst are listed in Tables 1. Compared with pure Al_2O_3, the catalytic activity for soot oxidation is remarkably enhanced after supporting CeO_2 on the surface of 3DOM Al_2O_3 catalysts.

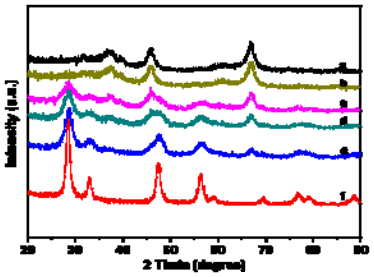

Fig. 1. XRD patterns of the prepared catalysts: (a) Al_2O_3; (b)2%CeO_2/Al_2O_3;(c) 10%CeO_2/Al_2O_3; (d) 20%CeO_2/Al_2O_3 ; (e)40% CeO_2/ Al_2O_3;(f) CeO_2

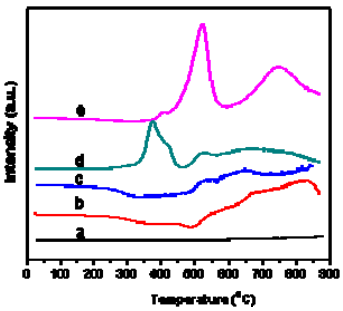

Fig. 2. H_2-TPR profiles of 3DOM catalysts: (a) Al_2O_3; (b)10%CeO_2/Al_2O_3;(c)20%CeO_2/Al_2O_3; (d)

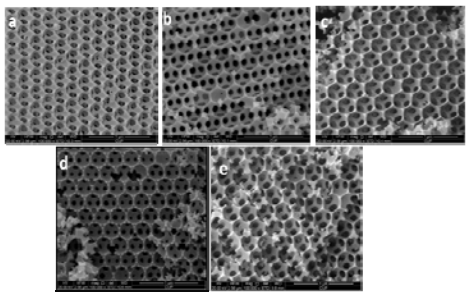

Fig. 3. SEM images of the catalyst samples (a)Al_2O_3; (b)2%CeO_2/Al_2O_3; (c)10%CeO_2/Al_2O_3; (d) 20%CeO_2/Al_2O_3; (e) 40%CeO_2/Al_2O_3;

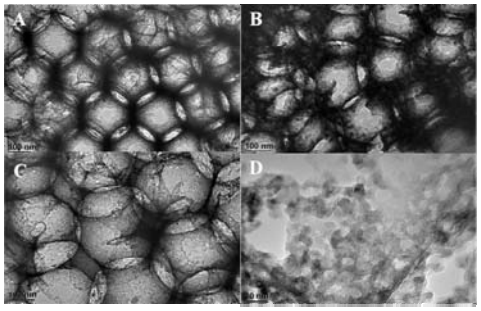

Fig. 4. TEM images of the catalyst samples (A) Al_2O_3; (B) CeO_2; (C)-(D) 40%CeO_2/Al_2O_3;

Table 1. The catalytic performances of 3DOM catalysts for soot combustion.

Catalyst	T_{10}/℃	T_{50}/℃	T_{90}/℃	S_{CO_2}
CeO_2	305	384	425	85.1
40%CeO_2/Al_2O_3	293	379	425	79.6
20%CeO_2/Al_2O_3	291	384	430	73.7
10%CeO_2/Al_2O_3	283	386	436	80.9
2%CeO_2/Al_2O_3	283	408	478	73.5
Al_2O_3	362	530	586	57.5

4 Conclusions

We successfully fabricated 3DOM CeO_2/Al_2O_3 catalysts by micropores-diffused precipitation (MDP) method using ammonia solution as the precipitation agent There exists a synergistic effect between CeO_2 and Al_2O_3, leading to the formation of Al-Ce-O solid solutions. The synergistic effect is crucial to enhancing the catalytic performance.

Acknowledgements

This work was financially supported by NSFC (Grant Nos.21177160, 21477146, and 21303263), Beijing Nova Program (Grant No. Z141109001814072), Specialized Research Fund for the Doctoral Program of Higher Education of China (No. 20130007120011) and the Science Foundation of China University of Petroleum-Beijing (Grant Nos. YJRC-2013-13 and 2462013BJRC003).

References

[1] M. E. Gálvez, S. Ascaso et al., Appl. Catal. B., 152-153(2014)88.
[2] N. E. Olong, K. Stowe et al., Appl. Catal. B., 74(2007)19.
[3] Y. Wei, J. Liu, Z. Zhao et al., Angew. Chem. Int. Ed., 50 (2011) 2326.

V-PP04

Are Perovskite Materials Efficient for Tree Way Catalysis? A Theoretical Study of $LaFeO_3$

Paul J.-F., Berrier E.*, Blanck D.

Unité de Catalyse et de Chimie du Solide, Université Lille 1, Villeneuve d'Ascq, France

* dimitri.blanck@ed.univ-lille1.fr

Keywords: de-NOx, $LaFeO_3$, reactivity, DFT, particle, morphology

1 Introduction

Automotive exhaust gas depollution is performed through Tree Way Catalysis (TWC) using supported nanoparticles of platinum-group metals (PGM) metal as catalysts. Because of their price and their availability issues, the reduction of PGM content in catalysts is a key economic and environmental requirement.. While perovskites are used from mid-70 [1] in catalysis as support, this class has attracted a recent interest [2] in the design of active phases with reduced noble metal content. Particularly in TWC, the intrinsic redox capacity of iron makes $LaFeO_3$ (LFO) a good candidate for NO_x reduction and CO oxidation. However, the mechanism of TWC reaction on this noble-metal free catalyst is still lacking. A better understanding of this catalyst is needed to access an improved activity.

2 Methodology

First-principle calculations were performed within the framework of DFT+U[4] using the Vienna Ab-initio Sofware Package VASP[4]-[7]. Pseudopotentials Projected Augmented Wave (PAW)[4] were used. The spin-polarized generalized gradient approximation functional parameterized by Perdew, Burke, and Ernzerhof (GGA-PBE) is used to describe exchange and correlation energies of electrons[8].

3 Results and discussion

The formation energies of several surfaces were first calculated for identifying the relevant LFO surfaces. Accordingly, the LFO (100) and (121) surfaces were found to be the most stable ones, which is in good agreement with experimental data. The particle morphology was thus computed as is shown in Figure 1.

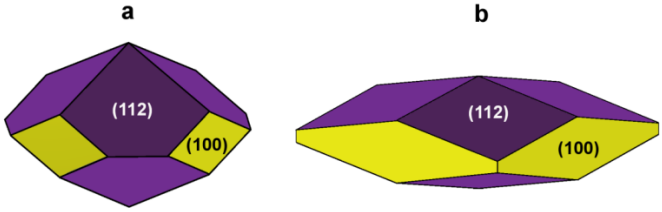

Figure 1. Wulff reconstruction of a LFO crystal in contact (a) with a partial pressure of 0.15bar of H_2O at 300K and (b) in vacuum

The influence of water, which is present in the feed, on the relative stability of LFO surfaces was also investigated. We found that the two most stable surfaces found in vacuum were still the most stable under a partial pressure of water. To be more precise, water adsorption was found to slightly change the shape of the particles but not the nature of the exposed surfaces.
Eventually, we have considered the adsorption and reactivity of target molecules of high relevance for TWC, namely CO and NO on the two most stable surfaces the (100) and (112). The most probable mechanism involves the formation of an oxygen vacancy in a first step

followed by the dissociation of NO on this site. The computed activation energy of the rate-determining step was found to reach 135 kJ.mol^{-1}, as shown in Figure 2.

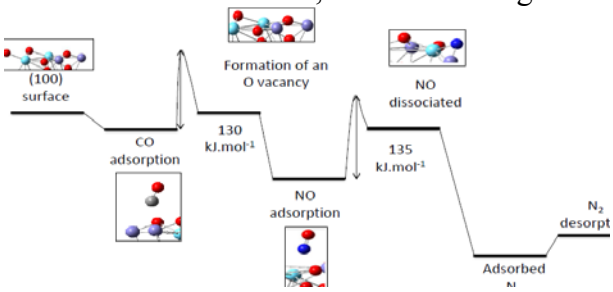

Figure 2. Reactional mechanism proposed for NO dissociation

4 Conclusions

The most stable surfaces of LaFeO3 perovskite are proposed in the present work to be the (112) and the (100) ones. This trend is plausibly generalizable for other III-III perovskite materials. A reactional mechanism for NO reduction has been proposed over these surfaces, featuring a low activation energy (135 kJ.mol-1). NO dissociation is mediated by the formation of an oxygen vacancy. In a second step this vacancy is regenerated by NO. This mechanism is similar to a Mars Van Krevelen mechanism typical for oxide materials.

Acknowledgements

We thank the European Commission for funding this work within the NEXTGENCAT project under the grant agreement #280890

References

[1] P. K. Gallagher, D. W. Johnson Jr., E. M. Vogel, F. Schrey, Mater. Res. Bull., 1975, 10(7), 623-627
[2] H. J. Zhang, G. Chen, Z. H. Li, J. Catal. 2012, 295, 45-58.
[3] W. Yang, R. Zhang, B. Chen, N. Bion, D. Duprez, S. Royer, Appl. Surf. Sci., 2007, 253(20), 8345-8351.
[4] G. Kresse, J. Joubert Phys. Rev. B, 59 (1999), p. 1758
[5] G. Kresse and J. Hafner, Phys. Rev. B, 1993, 48, 13115-13118.
[6] G. Kresse and J. Furthmüller, Phys. Rev. B, 1996, 54, 11169-11186.
[7] VASP 5.3. Available at http://cms.mpi.univie.ac.at/vasp/.
[8] J. P. Perdew, K. Burke, M. Ernzerhof, Phys. Rev. Lett., 1996, 77(18), 3865-3868.
[9] T. Peterlin-Neumaier, E. Steichele, J. Magn. Magn. Mater. 1986, 59(3-4), 351-356.

V-PP06

Soot Oxidation on Manganese Oxide Catalysts in Diesel and Gasoline Exhaust

Wagloehner S., Nitzer-Noski M., Kureti S.*

Technical University of Freiberg, Institute of Energy Process Engineering and Chemical Engineering, Chair of Reaction Engineering, Freiberg, Germany

* kureti@iec.tu-freiberg.de

Keywords: soot oxidation, manganese, oxide, diesel exhaust, gasoline exhaust

1 Introduction

Diesel engines and gasoline engines with direct fuel injection represent very effective combustion motors. However, a critical issue is the output of harmful soot particles, which are carcinogenic and contribute to the greenhouse effect. For the abatement of soot, particulate filters are widely employed, particularly for diesel engines. Particulate filters operate in the wall flow mode including the mechanical deposition of soot onto the porous filter walls. But, as a result of soot filtration, the loaded filter can cause backpressure potentially decreasing the engine efficiency. Hence, a regeneration step is mandatory to remove the soot deposits from the filter. Catalytically coated particulate filters aiming the activation of the soot/O_2 reaction are developed since many years. However, their efficiency is related to tight proximity of soot and catalyst, whereas under practical conditions loose contact mostly predominates. Thus, the soot oxidation catalysts known so far exhibit rather limited benefit in real driving scenarios [1, 2]. To overcome this issue our paper addresses the development of novel highly active manganese oxide catalysts for the regeneration of diesel as well as gasoline particulate filters.

2 Experimental

A series of bare manganese oxide samples was evaluated towards their soot oxidation activity in synthetic diesel and gasoline model exhaust. The catalysts were thoroughly haracterized by powder X-ray diffraction (XRD), N_2 physisorption, scanning electron microscopy, temperature programmed reduction by H_2 and temperature programmed desorption of NH_3. For the catalytic tests performed by temperature programmed oxidation (TPO) tight contact catalyst/soot powder mixtures were taken, while a home-made soot originated from C_3H_6 combustion was employed. Additionally, for practical assessment, the best catalyst was coated onto a laboratory-scaled particulate filter followed by soot deposition and catalytic testing.

Furthermore, the transfer of oxygen from the gas-phase to soot was investigated by TPO with $^{18}O_2$. After this isotopic TPO, a HTPR was performed to quantify the accumulation of ^{18}O in the catalyst.

3 Results and discussion

As a result of the TPO tests, Mn_3O_4 prepared by flame spray pyrolysis (FSP) was identified as the best catalyst tested providing soot combustion already at 300°C under diesel and gasoline exhaust conditions (Fig. 1). The correlation of physical-chemical characteristics of the catalysts with their soot oxidation kinetics showed that the number of surface oxygen vacancies and particle size determine the catalytic performance by affecting the supply of oxygen. These results substantiate the high efficiency of the Mn_3O_4 obtained from FSP.

Additionally, clear enhancement of soot oxidation was observed when performing tests with the laboratory-scaled particulate filter coated by the FSP-Mn_3O_4 catalyst. Moreover, the FSP-

Mn_3O_4 catalyst revealed high thermal stability. After hydrothermal exposure at 750°C and thermal treatment at 1050°C its activity did not alter significantly in the TPO tests carried out with the catalyst/soot powder blends [3].

The isotopic TPO studies of FSP-Mn_3O_4/soot suggested that oxygen was transferred from the surface and bulk of the catalyst to the soot by physical contact points. A strong contribution of bulk oxygen (ca. 60%) occurred for tight as well as loose contact. The role of gas-phase O_2 was found to refill the oxygen vacancies of the catalyst [3].

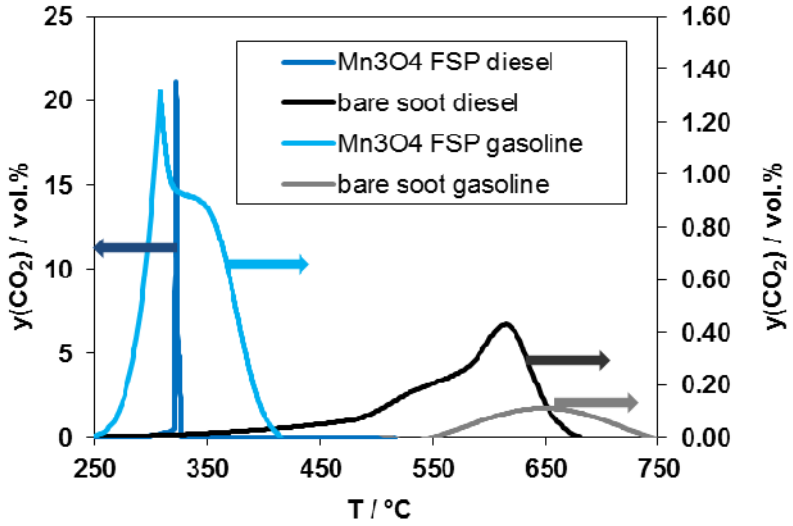

Figure 1: TPO study with bare soot as well as tight contact mixtures of soot with FSP-Mn_3O_4 under diesel and gasoline exhaust conditions. m(soot) = 0.12 g, m(cat.) = 0.96 g; gasoline conditions: $y(O_2)$ = 1%, $y(H_2O)$ = 2%, N_2 balance; diesel conditions: $y(O_2)$ = 10%, N_2 balance [3].

4 Conclusions

We evaluated bare manganese oxide catalysts for the oxidation of soot. The best catalyst was the FSP-Mn_3O_4 sample implying high activity in diesel as well as gasoline model exhaust. Additionally, FSP-Mn_3O_4 only slightly changed its performance after hydrothermal and thermal exposure.

The correlation of the physical-chemical properties and the soot oxidation activity of the catalysts showed that high amount of surface oxygen vacancies and small particle sizes are crucial for the oxidation of soot. These findings coincide with the mechanistic studies of FSP-Mn_3O_4/soot suggesting that the supply of oxygen occurs from the gas-phase and catalyst bulk via the surface of the catalyst to the contact points of the soot. The contribution of the bulk is very pronounced indicating strong mobility of inner oxygen, particularly when comparing with other catalysts, e.g. iron oxides.

Moreover, the test of a laboratory-scaled DPF coated with FSP-Mn_3O_4 indicates soot oxidation activity below 350°C indicating the potential for continuous soot conversion in real exhaust.

References

[1] B.W.L. Southward, S. Basso, *SAE Technical Paper Series* 2008-01-0481.
[2] S. Waglöhner, S. Kureti, *Appl. Catal. B* 125 (2012) 158.
[3] S. Waglöhner, M. Nitzer-Noski, S. Kureti, *Chem. Eng. J.* 259 (2015) 492.

V-PP07

Development of MnO_x-based Catalysts for the Catalytic Wet Air Oxidation (CWAO) of Organic Pollutants

Trunfio G.[1], Di Chio R.[1], Rahim S.H.A.[1], Espro C.[1], Milone C.[1], Galvagno S.[1], Spadaro L.[2], Arena F.[1,2*]

1 - Dipartimento di Ingegneria Elettronica, Chimica e Ingegneria Industriale, Università degli Studi di Messina, Messina, Italy
2 - Istituto CNR-ITAE "Nicola Giordano", Messina, Italy

* Francesco.Arena@unime.it

Keywords: CWO, mineralization, purification, MnOx catalyst, heterogeneous catalysts

1 Introduction

The increasing alarm on environmental issues is drawing worldwide a great scientific and technological concern on the development of new purification technologies. In the specific case of water, this would enable extensive reclaim and/or recycle of civil and industrial wastewaters to reduce the overall water consumption [1-9]. In fact, the disposal of wastewater streams containing toxic and/or recalcitrant pollutants requires proper decontamination treatments to accomplish the even stricter regulations. Among the various technologies, involving the exploitation of biological, physical or chemical treatments, proposed during last decades, Catalytic Wet Air Oxidation (CWAO) processes is the most versatile one, ensuring very large operative ranges both in terms of rate and organic load [1,3]. Metal leaching, active radical generation, catalyst deactivation, pollutants chemistry, and reaction conditions still representing the main obstacle of the process scale-up, the discovery/improvement of cheap, robust and active catalyst would represent the main challenge of heterogeneous CWAO technology [1-11].

Co-precipitated catalysts, employed in previous works, allowed us to determine the mechanism and main requirements for a CWAO catalyst; notably, structural, morphological and redox properties of the active phase altogether determine the CWAO efficiency of the system [2,10-13]. Improving surface exposure and redox pattern, by a proper tuning of the structure and dispersion of the active phase, is a benchmark for enhancing the performance of the $MnCeO_x$ system. Then, we developed a new class of MnO_x catalysts dispersed on CeO_2 by a new preparation method to better control the oxidation state of manganese and the "oxide-support" interaction, enhancing the synergistic effect of ceria on the MnO_x redox features [12-15].

2 Experimental

$MnCeO_x$ catalysts with Mn/Ce atomic ratio between 0.3 and 3.0 were synthesized *via* the novel *redox-precipitation* method [12], while a reference sample was prepared *via* the classic co-precipitation route [2,10-12]. Solids were dried at 373K (16h) and further calcined in air at 673K (6h). The list of the catalysts used in this work is reported in Table 1.

Samples were characterized by XRF, XPS, N_2-physical adsorption, XRD and TPR techniques, while the "used" catalysts were probed by TGA measurements. The testing in the CWAO of various model polluting substrates has been performed at 423K in a batch reactor fed by a continuous O_2 flow. Substrate and total organic carbon (TOC) conversion, and CO_2 formation were monitored by HPLC, TOC, and gravimetric analyses, respectively.

3 Results and discussion

Surface area values of redox catalysts sensibly higher than co-precipitated one evidence at

once strong improvement of the main requirements of CWAO catalyst (Table 1). XRD data evidence two very broad peaks spanned in the ranges of 20-38° and 40-60°, respectively, for all the "redox-precipitated" systems, indicating a prevalently amorphous arrangement [12-15], while the co-precipitated sample shows some resolved peaks of the cerianite and pirolusite phases [12-15]. CO-TPR measurements show that the peculiar structure of redox-precipitated systems reflects in significantly lower temperature of onset reduction and peak maximum than co-precipitated one [12-15].

Catalytic tests in the CWAO of phenol show that a Mn/Ce atomic ratio of 1 is the optimal catalyst composition, ensuring at 150°C and 1.5 MPa a complete phenol removal in ca. 10 min and a CO_2 production corresponding to a mineralization extent of 80% (6h) [4-7]. Acetic acid is the most refractory substrate, attaining total removal only after 2 hours, according to the fact that this is the most stable by-product formed during the CWAO of heavy organic compounds [1-7].

TGA analyses of the used samples well match with CO_2 selectivity for a satisfactory C-mass balance, and confirm that the pollutants are firstly removed by adsorption on the catalyst surface and, then, slowly (*r.d.s.*) oxidized to CO_2 [2,4-7].

Table 1. List of the studied catalysts and their main performances in the CWAO of phenol.

Catalyst	$(Mn/Ce)_{at}$[a]	SA_{BET} ($m^2 \cdot g^{-1}$)	t_{Conv}[b] min	S_{CO2} %
M1C3	0.34	168	60	45
M1C2	0.47	161	30	62
M1C1	0.98	154	10	80
M2C1	2.12	140	18	74
M3C1	2.76	114	30	68
M1C1-P	1.00	101	60	35

[a] From XRF analyses
[b] Time of 100% phenol conversion at 150°C

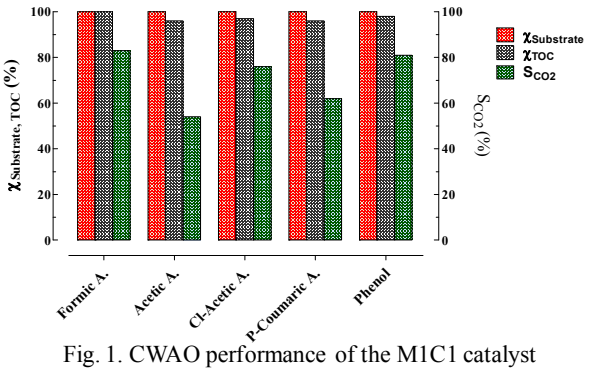

Fig. 1. CWAO performance of the M1C1 catalyst on different substrates.

4 Conclusions

CWAO tests confirm the high activity of $MnCeO_x$ catalysts for the liquid-phase mineralization of different organic recalcitrant compounds. The "redox-precipitated" catalysts show better performances than co-precipitated ones at any Mn/Ce atomic ratio, worthy of potential industrial exploitation.

References

[1] F. Larachi, *Top. Catal.* 33 (2005) 109.
[2] F. Arena, J. Negro, A. Parmaliana, L. Spadaro, G. Trunfio, *Ind. Eng. Chem. Res.* 46 (2007) 6724.
[3] A. Cybulski, *Ind. Eng. Chem. Res.* 46 (2007) 4007.
[4] F. Arena, G. Trunfio, J. Negro, L. Spadaro, *Appl. Catal. B* 85 (2008) 40.
[5] F. Arena, C. Italiano, A. Raneri, C. Saja, *Appl. Catal. B* 99 (2010) 321.
[6] F. Arena, C. Italiano, L. Spadaro, *Appl. Catal. B* 115-116 (2012) 336.
[7] F. Arena, C. Italiano, G. Drago Ferrante, G. Trunfio, L. Spadaro, *Appl. Catal. B* 144 (2014) 292.
[8] F. Arena, *Catal. Sci. Technol.* 4 (2014) 1890.
[9] F. Arena, D. Lombardo, G. Drago Ferrante, C. Italiano, L. Spadaro, G. Trunfio, *Desalin. Water Treat.* (2013) DOI: 10.1080/19443994.2013.867412.
[10] F. Arena, A. Parmaliana, G. Trunfio. *Stud. Surf. Sci. Catal.* 172 (2007) 489.
[11] F. Arena, G. Trunfio, J. Negro, C. Saia, A. Raneri, L. Spadaro, *Stud. Surf. Sci. Catal.* 175 (2010) 493.
[12] F. Arena, G. Trunfio, J. Negro, B. Fazio, L. Spadaro, *Chem. Mater.* 19 (2007) 2269.
[13] F. Arena, G. Trunfio, J. Negro, L. Spadaro, *Mater. Res. Bull.* 43 (2008) 539.
[14] F. Arena, L. Spadaro, Patent WO2012168957A1, December 2012.
[15] F. Arena, G. Trunfio, J. Negro, B. Fazio, L. Spadaro, *J. Phys. Chem. C* 113 (2009) 2822.

V-PP08

Attractive Route for New Hydroxyapatite Supported Calcium-Manganese Oxides for Total Oxidation of Toluene

Chlala D.[1], Giraudon J.-M.[1*], Nuns N.[2], Labaki M.[3], Lamonier J.-F.[1]

1 - Université Lille1, UMR 8181 CNRS, UCCS, Villeneuve d'Ascq, France
2 - IMMCL Chevreul, Institut des Molécules et de la Matière Condensée, Lille, France
3 - Lebanese University, Laboratory of Physical Chemistry of Materials (LCPM)/PR2N, Faculty of Sciences, Fanar, Jdeidet El Metn, Lebanon

* jean-marc.giraudon@univ-lille1.fr

Keywords: manganese, calcium, oxide, hydroxyapatite, catalytic oxidation, VOC

1 Introduction

The research of new catalytic materials requires available cheap and non-toxic components. Phyllomanganates such as birnessite, buserite and related phases are amongst the strongest known natural oxidants and Mn is an easily reducible/oxidable element. Hence such materials represent an efficient class of catalysts for total oxidation of volatile organic compounds. Among them well dispersed Ca manganese oxides have not been studied so far. A new and original synthetic pathway may involve hydroxyapatite, $Ca_{10}(PO_4)_6(OH)_2$ (HAP) which is a safe and non-toxic material [1]. HAP can play both the role of a catalyst support and a Ca supplier agent to get Ca manganese oxide phases. Indeed HAP is recognized for its ability to easily exchange calcium ions exposed on the surface at site I (coordinated by 9 oxygen ions) and site II (coordinated by five oxygen ions and one hydroxyl group). A previous work reported on efficient Mn-HAP catalysts for direct imine formation by oxidative coupling of alcohols and amines but mainly focused on the acido-basic properties of the catalyst [2]. Pioneering work in this field aiming to dope HAP with a Cu active phase has been very recently reported [3]. The hypothesis of 5 possible sites for Cu location has been proposed on the features of HAP structure and experimental results. Additionally it was found that the Cu location and species can be adjusted owing to the method of preparation.

In the present work, the wet impregnation has been adopted to disperse 10 Mn wt% species on HAP. The main challenging task is to be able to determine the location and nature of Mn species taking into account that HAP flexible structure offers a wide range of possible cationic as well as anionic substitutions.

2 Experimental/methodology

The reference Al support supplied by Alfa Aesar (gamma-Al_2O_3, purity: 99.97%; S_{BET} = 72 m^2/g) was used as received. The HAP was synthesized from a previous experimental procedure [1]; the Ca/P was found to be 1.60 (elementary analysis) and the S_{BET} was 94 m^2/g. Mn was added to the supports by wet impregnation using $Mn(NO_3)_2.4H_2O$ from Sigma Aldrich. The resulting powders were calcined at 400°C for 4h to get Mn-Al and Mn-HAP samples.

Numerous techniques of characterization such as XRD, Raman spectroscopy, BET, SEM, H_2-TPR, O_2-TPD experiments, XPS and ToF-SIMS have been used to identify the Mn species and its location in Mn-HAP. Catalytic total oxidation of toluene in air was studied and the catalytic performance of Mn-HAP was compared with those of Mn-Al.

3 Results and discussion

XRD analyses only show the characteristic peaks of HAP for Mn-HAP while it is found the presence of the pyrolusite phase beta-MnO_2 (PDF n°24-0735) along with phases of gamma-

Al_2O_3 (PDF n°10-0425) and AlO(OH) (PDF n°83-1505) in the Mn-Al sample. The non-observance of related Mn oxide phases over the surface indicates amorphous or/and well dispersed Mn oxides. Laser Raman spectra are characterized by 3 weak peaks at 505, 550 and 630 cm^{-1}. These features are very similar to those reported for related Mn layered oxides such as birnessite-pristine type materials [4].

Investigation by XPS of the Mn $2p_{3/2}$ core level having an apparent maximum at a binding energy of 642.4 eV well agrees with a Mn^{4+} oxidation state. ToF-SIMS measurements performed in static conditions clearly identify $Ca_xMn_yO_z^+$ ions of significant intensity such as $CaMnO_2^+$, $Ca_2MnO_3^+$ and $Ca_2MnO_2^+$ ions (Fig.1). The detection of such ions supports the existence of some Ca-Mn oxides at the outermost layers of the catalyst in agreement with layered oxide structures (birnessite-pristine) suggested by Raman study.

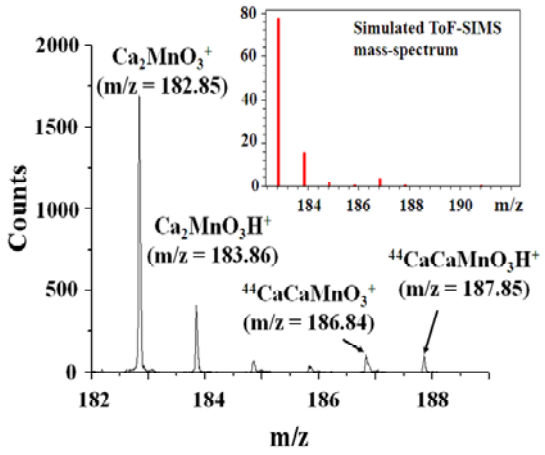

Fig. 1. ToF-SIMS mass spectrum of Mn-HAP m/z: 182-189 range.

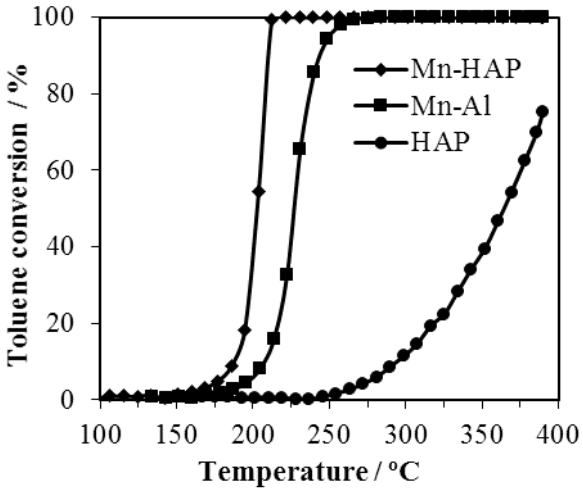

Fig. 2. Toluene conversion over the catalysts (800 ppmv toluene in air)

Hence the lower Mn average oxidation state values obtained from H_2-TPR and O_2-TPD experiments, of 3.3 and 3.5 respectively, suggests the substitution of some Ca^{2+} from surface and bulk sites of HAP by Mn^{2+} ions. The toluene conversion in function of temperature is given over the different catalysts (Fig.2). The specific activity based on T_{50} (°C) decreases as follows: HAP (365) < Mn-Al (227) < Mn-HAP (203). The best activity achieved on Mn-HAP can be rationalized by the formation of well dispersed/amorphous high valence Mn phases partially in interaction with Ca^{2+} expelled from the HAP channels on the support.

4 Conclusions

HAP has been shown to be a Ca^{2+} supplier agent to get partially well dispersed/amorphous Ca-Mn oxide phases on HAP. This catalyst is an efficient catalyst for toluene total oxidation.

Acknowledgements

Authors would like to thank the Agence Universitaire de la Francophonie (AUF) – Région du Moyen-Orient and IRENI project for financial supports.

References

[1] L. Silvester, J.-F. Lamonier, R.-N. Vannier, C. Lamonier, M. Capron, A.-S. Mamede, F. Pourpoint, A. Gervasini and F. Dumeignil, J. Mater. Chem. A. 2 (2014) 11073.
[2] B. Chen, J. Li, W.Dai, L. W. and S. Gao, Green Chem. 16 (2014) 3328.
[3] Z. Qu, Y. Sun, D. Chen, and Y. Wang, J. Mol. Catal. A: Chem. 393 (2014) 182.
[4] R. Baddour-Hadjean and J.-P. Pereira-Ramos, Chem. Rev. 110 (2010) 1278.

V-PP09

Unravelling the Complexity of CO Oxidation Catalysis on Au Nanoclusters

Nikbin N.[1], Austin N.[2], Christiansen M.[1], Vlachos D. G.[1], Stamatakis M.[3*], Mpourmpakis G.[2]

1 - University of Delaware, Department of Chemical Engineering, Newark, USA
2 - University of Pittsburgh, Department of Chemical Engineering, Pittsburgh, USA
3 - University College London, Department of Chemical Engineering, London, UK

* m.stamatakis@ucl.ac.u

Keywords: DFT, kinetic Monte Carlo, charge transfer, metal-oxide, support effects, poisoning

1 Introduction

The CO oxidation reaction is of key importance in the development of catalytic converters for emissions control. Gold has attracted significant attention in this context since the late 80's, after experimental evidence by Haruta and co-workers suggested that Au, while inert in bulk, exhibits high activity at the nanoscale [1]. Despite the intense research on Au-catalysed CO oxidation during the past 30 years, the underlying reaction mechanisms are still debated [2], and it is difficult to decouple the effects of support versus particle size/morphology. An emerging consensus is that under-coordinated Au sites are active towards CO oxidation. Yet, the experimentally observed magic number activity of Au nanoclusters supported on defective MgO contradicts this consensus [3]. For instance, Au_6 appears as almost inert towards CO oxidation, Au_8 is highly active and Au_{10} exhibits lower activity than Au_8. Motivated by this complexity, we employ first-principles-based kinetic modelling to elucidate the physico-chemical phenomena that give rise to the magic number activity. We discover that various factors determine the CO oxidation activity of sub-nanometer Au, in particular: charge transfer, size and shape effects, reconstruction, adsorbate binding configurations, and cluster poisoning by carbonate.

2 Methodology

We first investigated the electronic and structural properties of MgO-supported Au_6, Au_8 and Au_{10}, using the Becke-Perdew86 (BP86) functional, the resolution of the identity approximation and the sv(p) basis set implemented in Turbomole 6.5. For each cluster, we considered three different cases for the support: defect-free, with an O-vacancy, and with a Mg-vacancy. We then isolated the cluster from the MgO support maintaining its structure and charge state, and investigated the CO oxidation pathways on the different sites at the B3LYP/LANL2DZ level, using Gaussian 09. The data from these calculations served as input to *Zacros* (http://zacros.org), our graph-theoretical kinetic Monte Carlo (KMC) simulation package [4, 5]. This input consists of a lattice structure, an energetics model, a reaction mechanism, and the conditions of the simulation along with controls such as the frequency of sampling and reporting. We explicitly modelled the top and bridge sites of the clusters, and the binding of multi-dentate species, such as carbonate. Strong repulsive interactions between O_2 adsorbates were accounted for, since the first-principles calculations showed that at most one oxygen molecule can bind to any of these clusters. More details are presented in [6] and [7].

3 Results and discussion

Au nanoclusters of up to 13 atoms in size exhibit planar geometries. When supported on MgO with O vacancies, they exhibit negative charges close to one electron. Clusters supported on a perfect MgO appear as almost neutral (slightly negatively charged). Mg-vacancies result in

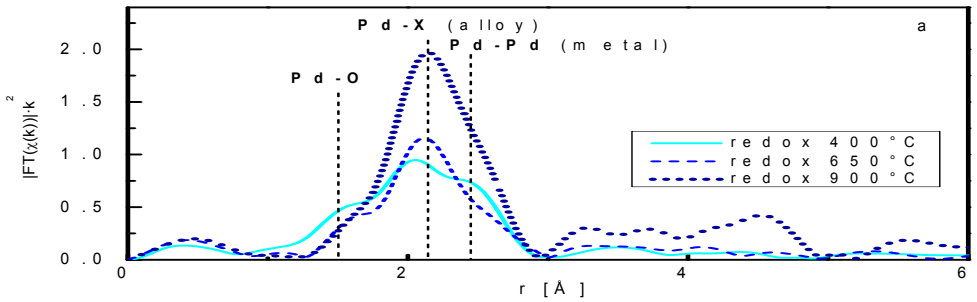

Fig. 1. Average number of CO_2 molecules produced per site in an ensemble of 100 Au_6^- clusters (a). After exhibiting some transient activity Au_6^- is poisoned. The turnover frequencies (TOF) are noted. Ensembles of 10 clusters for Au_8^- (b) and Au_{10}^- (c) exhibit stable activity, with Au_8^- having higher TOF.

positively charged clusters. It was found that only the negatively charged clusters could bind O_2, so we studied the CO oxidation steps ($CO^* + O_2^* \rightarrow CO_2 + O^*$, $CO^* + O^* \rightarrow CO_2$) on Au_6^-, Au_8^- and Au_{10}^-, considering every possible adsorption configuration of CO and O_2. Consequently, our KMC models incorporate approximately 160 elementary steps (adsorption, reaction, diffusion, and desorption). By simulating ensembles of Au nanoclusters for each of the three structures, we obtained estimates of the turnover frequency and provided possible explanations for the experimentally observed magic number activity. Au_6^- was found to exhibit transient activity, followed by carbonate formation which leads to the eventual poisoning of the nanocluster (Fig. 1a). A cluster "breathing" mode was critical in carbonate formation, highlighting the importance of accounting for such reconstruction mechanisms. Both Au_8^- and Au_{10}^- are catalytically active, with Au_8^- exhibiting noticeably higher activity than Au_{10}^- (Fig. 1b, c). The rate determining step (RDS) on Au_{10}^- is the tilting of bidentate O_2 to an active monodentate binding configuration. On Au_8^-, the reaction proceeds via a 4-centre intermediate, whose decomposition is the RDS.

4 Conclusions

Using first-principles kinetic modelling we investigated the CO oxidation behaviour of sub-nanometre Au catalysts consisting of a few metal atoms, unravelling a high degree of complexity in the catalytic behaviour thereof, and elucidating competing physicochemical phenomena that result in the experimentally observed "magic number" activity. Catalysis at the sub-nanoscale, despite being attractive due to the atomic-level precision of the catalysts and its often unprecedented performance, remains an empirical field. Simulations, such as ours, can significantly advance our understanding and lead to better catalysts and processes.

Acknowledgements

Computational resources and support from the Center for Simulation and Modeling (University of Pittsburgh) and the Legion High Performance Computing Facility (UCL) were instrumental in this work. Financial support from a start-up grant from the University of Pittsburgh, a Marie Curie International Outgoing Fellowship within the European Commission's FP7, and the US Department of Energy (Grant № DE-SC0010549) are gratefully acknowledged.

References

[1] M. Haruta, T. Kobayashi, H. Sano, N. Yamada, *Chem Lett*. 2 (1987) 405.
[2] M. C. Kung, R. J. Davis, H. H. Kung, *J Phys Chem C*. 111 (2007) 11767.
[3] M. Arenz, U. Landman, U. Heiz, *ChemPhysChem*. 7 (2006) 1871.
[4] M. Stamatakis, D. G. Vlachos, *J Chem Phys*. 134 (2011) 214115.
[5] J. Nielsen, M. d'Avezac, J. Hetherington, M. Stamatakis, *J Chem Phys*. 139 (2013) 224706.
[6] M. Stamatakis, M. Christiansen, D. G. Vlachos, G. Mpourmpakis, *Nano Lett*. 12 (2012) 3621.
[7] N. Nikbin, N. Austin, D. G. Vlachos, M. Stamatakis, G. Mpourmpakis, *Catal Sci Technol*. 5 (2015) 134.

V-PP10

Effect of Au and Ag on the Performance in CO and VOCs Oxidation of Alumina Supported Cu-Mn Catalysts

Tabakova T.[1*], Kolentsova E.[2], Dimitrov D.[2], Petrova P.[1], Karakirova Y.[1], Avdeev G.[3], Nihtianova D.[4], Ivanov K.[2]

1 - Institute of Catalysis, Bulgarian Academy of Sciences, Sofia, Bulgaria
2 - Department of Chemistry, Agricultural University, Plovdiv, Bulgaria
3 - Institute of Physical Chemistry, Bulgarian Academy of Sciences, Sofia, Bulgaria
4 - Institute of Mineralogy and Crystallography, Bulgarian Academy of Sciences, Sofia, Bulgaria

* tabakova@ic.bas.bg

Keywords: design of Cu-Mn/alumina catalysts, gold catalysts, Ag, CO and VOCs oxidation

1 Introduction

The catalytic oxidation of CO and volatile organic compounds (VOCs) has high importance in the field of environmental protection and sustainable chemistry. These catalytic processes have been considered as some of the most efficient ways to reduce harmful emissions from various chemical industries. The design of new catalytic formulations with improved efficiency in the removal of air pollutants is an attractive topic because of the great variety of VOC molecules. Various systems based on transition metal oxides have been reported as efficient catalysts in the oxidation of VOCs. Among the transition metal oxides catalysts, copper and manganese oxides have been considered as some of the most active and promising catalysts for the combustion of VOCs. During the past two decades gold-based catalysts have been proven to be effective for many reactions of environmental significance [1]. The results of our recent study of Au/CeO_2 catalysts for catalytic abatement of VOCs and CO in waste gases motivated present work. The aim was to develop cost-effective and catalytically efficient formulations by promotion of alumina supported Cu-Mn mixed oxides with Au or Ag. The role of Au or Ag on the structural and catalytic properties of $Cu\text{-}Mn/Al_2O_3$ catalysts for simultaneous elimination of different type air pollutants – CH_3OH, $(CH_3)_2O$ and CO in waste gases from formaldehyde production, as well benzene as representative of aromatic hydrocarbons, was examine in detail.

2 Experimental/methodology

A series of mixed oxides of Cu and Mn with different Cu/Mn ratio were prepared by wet impregnation of γ-alumina (0.6-1.0 mm grain size). Prior to the impregnation, the carrier was calcined for 2 hours at 500 ^oC in a ceramic furnace. The impregnated samples were calcined at 450 ^oC. The total amount of transition metal oxides phase was 20 wt. %. Gold and silver-containing (2wt. %) catalysts were synthesized by deposition-precipitation at 60 ^oC and pH 7.0 and 9.0, respectively. After filtering and careful washing, the precursors were dried at 80 °C and calcined in air at 400 °C for 2 h. Catalysts were characterized by means of BET, XRD, HRTEM, TG/DTA, TPR and EPR spectroscopy. The catalytic activity of the samples was measured using continuous flow equipment with fixed bed stainless steel reactor at atmospheric pressure.

3 Results and discussion

The results of the catalytic activity measurements over alumina supported Cu-Mn catalysts showed that the sample with ratio Cu:Mn = 2:1 demonstrated the best performance in the oxidation of CO and MeOH, whiles the sample with ratio Cu:Mn = 1:5 was more active in the combustion of $(CH_3)_2O$. The sample Cu:Mn = 2:1 exhibited also slightly higher activity than Cu:Mn = 1:5 for complete benzene oxidation (CBO) in the whole temperature range. The

highest difference (91 and 82 % conversion, respectively) was registered at 300 °C.

The promotion of Cu:Mn = 2:1 by Au caused improvement of catalytic activity toward oxidation of CO and MeOH. The strongest effect was observed on the CO oxidation activity (Fig. 1A). The addition of gold influenced also MeOH oxidation activity, especially in the low temperature range (Fig. 1 B). In contrast, Au promotion did not affect $(CH_3)_2O$ oxidation (Fig. 1 C). The deposition of Ag affected beneficially MeOH oxidation activity of Cu-Mn mixed oxides (Fig. 1 B), slightly CO oxidation (Fig. 1 A) and negatively $(CH_3)_2O$ oxidation (Fig. 1 C). A slight improvement of CBO over Au/Cu-Mn and Ag/Cu-Mn samples was achieved.

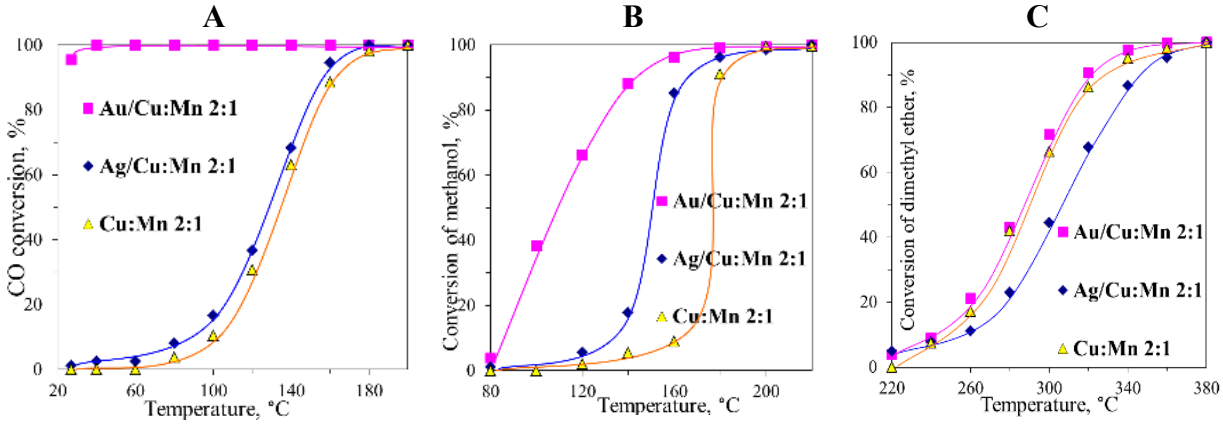

Fig. 1. Catalytic activity in oxidation of CO (A), MeOH (B) and DME (C) over studied samples.

The diffraction lines of γ-Al_2O_3 were clearly identified in the XRD patterns of all samples. Additionally, the lines of CuO were registered. However, the presence of a highly dispersed Cu-Mn spinel phase with a relatively small crystallite size could be suggested. There were no diffraction peaks assignable to Au or Ag. Detailed TEM investigations (SAED, HRTEM and XEDS) revealed that all components are homogeneously distributed on the support crystals. Crystallographic phase's identification will be carried out by measuring the distances among the diffraction fringes in order to extend XRD observations. The comparison of TPR profiles indicated that deposition of Au altered the complex shape of the peak, registered for Cu-Mn support and improves its reducibility. The addition of Ag caused only slight effect on the reduction behaviour. EPR spectroscopic measurement indicated that the spectrum of alumina supported Cu-Mn sample consisted of a signal with g_{II} = 2.3572 и $g_{\perp}$= 2.1025 due to distorted octahedral coordinated Cu^{2+} ions. The presence of resolved hyperfine splitting in parallel region suggested the existence of isolated Cu^{2+} ions on the support. The shape of the EPR spectrum remained the same after Au and Ag deposition, but the intensity of EPR signal decreased due to the trapping of electrons in Cu^{2+} sites, indicating formation of EPR silent Cu^{+} sites.

4 Conclusions

Deposition of nanosized Au particles on alumina supported Cu-Mn oxides enhances significantly CO and MeOH oxidation activity. Promotion by Ag improves only performance in MeOH oxidation. In-depth analysis of XRD, TEM, H_2-TPR and EPR data will be performed in order to clarify the relationship between improved catalytic behaviour and structural features.

Acknowledgements

The authors from Institute of Catalysis and Agricultural University gratefully acknowledge the financial support by the Bulgarian National Science Fund (Project DFNI T 02/4).

References

[1] S. Scirè, L. Liotta, *Appl. Catal. B: Envir.* 125 (2012) 222.
[2] T. Tabakova, D. Dimitrov, M. Manzoli, F. Vindigni, P. Petrova, L. Ilieva, R. Zanella, K. Ivanov, *Catal. Commun*. 35 (2013) 51.

V-PP11

Change in the Chemical Composition of an LNT as a Result of its Ageing in Diesel Exhaust Gases: Physical and Chemical Analysis

Dubkov A.A.[1,2*], Carberry B.[2], Schneider M.[2], Linzen F.[2], Smirnov M.Yu.[1], Kalinkin A.V.[1], Salanov A.N.[1], Shmakov A.N.[1], Gerasimov E.U.[1], Bukhtiyarov V.I.[1,3]

1 - Boreskov Institute of Catalysis SB RAS, Novosibirsk Russia
2 - Ford Forschungszentrum Aachen GmbH, Aachen, Germany
3 - Novosibirsk State University, Novosibirsk, Russia

* adubkov@catalysis.ru

Keywords: LNT, deactivation, characterization, XPS, SI-XRD, poisoning

1 Introduction

Use of NOx storage/reduction catalysts (NSR, LNT) is recognized to be one of the efficient methods of removal of nitrogen oxides (NO_x) from diesel exhaust gases. On these catalysts, absorption and subsequent reduction of NOx is taking place. Under lean (normal for diesel engines operation) conditions, nitrogen oxides are absorbed by Ba-components (BaO, $Ba(OH)_2$, $BaCO_3$) of the NSR catalyst, as Ba nitrite and/or nitrate. Then, under rich conditions (artificially created by using special regimes of diesel fuel combustion), these nitrites/nitrates are being reduced to elemental nitrogen. Besides legislative components of the diesel exhaust gases that have to be neutralized (carbon monoxide, hydrocarbons, nitrogen oxides and soot), diesel exhaust gases, in particular, also contain S- and P-compounds, that cause LNT poisoning. Present work is focused on investigation of a nature of the compounds formed in NSR catalyst during its ageing in exhaust of the diesel engine operating under realistic NOx aftertreatment protocol.

2 Experimental

To prepare samples of fresh and aged LNT catalyst, pieces of the same size were cut from the same locations (~ 1.5 cm from the catalyst inlet) of fresh and aged LNT bricks. In the initial (fresh) state, main wash-coat components were Pt, γ-Al_2O_3, $BaCO_3$ and Ce-Zr mixed oxide. Characterization of the samples was performed using XPS (SPECS (Germany) working on MgKα 1253.6 eV irradiation), SEM, XRD with synchrotronic irradiation (SI station in Nuclear Physics Institute, Novosibirsk, Russia), TEM using JEM-2010 machine (Japan), with cell resolution of 0.14 nm, acceleration voltage of 200 kV. XPS spectra were obtained from 2 types of samples: (1) Plates of the monolith catalyst that were carefully cut along the catalyst channels, to represent untouched washcoat in the catalyst channels, and (2) Wash-coat that was carefully scrubbed from the brick substrate and mechanically powdered. Samples for SEM investigation represented a cube of 1×1×1 cm^3. In these samples, channels were filled with epoxy resin, and the plane, which is perpendicular to the channels, was polished. XRD investigations were carried out with plate samples, while TEM studies were performed using powdered samples.

3 Results and discussion

It was found using XPS method, that with progressing into aging of the NSR catalyst, it is accumulating the following impurities: sulfur in form of sulfates, phosphorus in form of phosphates, and Ca and Zn in oxidation state (2+). Moreover, S was found both in plated and in powdered samples, while P, Ca and Zn were found only in plated samples (Fig. 1).

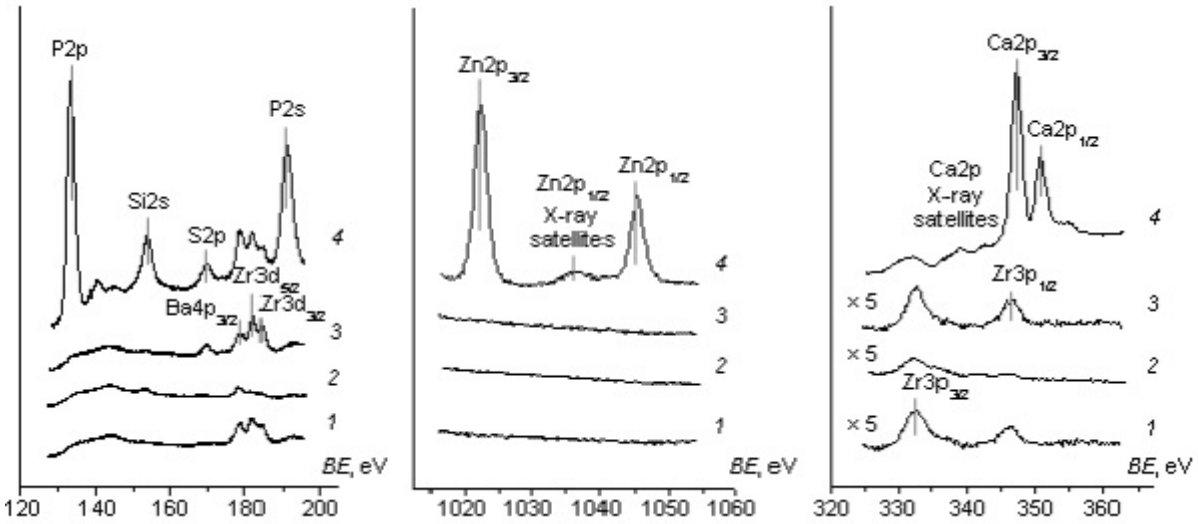

Fig.1. XP spectra of powdered (*1*, *3*) and plated (*2*, *4*) specimens of fresh (*1*, *2*) and aged (*3*, *4*) catalyst, showing accumulation of the impurities (S, P, Ca, Zn) in aged sample.

This means that S is distributed over the whole thickness of the wash-coat layer, while P, Ca и Zn are concentrated only in the very surface layer that is in contact with the exhaust gas flow. Distribution maps of the elements in the cross-section of the wash-coat layer (elemental maps) built based on the SEM measurements, confirm that in aged samples sulfur is distributed over the whole wash-coat layer.

New surface phases appearing in the NSR catalyst during and as a result of ageing and associated with S and P were identified using SI-XRD method. These phases were found to be barium sulfate ($BaSO_4$) and cerium phosphate ($CePO_4$). In aged sample, crystallites of barium sulfate were detected also using TEM method.

4 Conclusions

Using a number of physical and chemical methods, it was found that during the LNT catalyst ageing under real diesel exhaust conditions, accumulating of the impurities such as S, P, Ca and Zn is taking place. Sulfur is being distributed over the whole thickness of the wash-coat layer, while phosphorus, calcium and zinc are being concentrated in the thin sub-surface layer of the wash-coat. Sulfur was found to be bonded into barium sulfate, while phosphorus – into cerium phosphate.

Acknowledgements

The authors (MYS, AVK, VIB) thank the Russian Science Foundation (Grant 14-23-00146) for financial support.

V-PP12

The Process of H_2S Selective Catalytic Oxidation for on-site Purification of Hydrocarbon Gaseous Feedstock. Technology Demonstration at Bavly Oil Field in Republic of Tatarstan

Ismagilov Z.[1,2], Parmon V.[1], Yarullin R.[3], Mazgarov A.[4], Khairulin S.[1*], Kerzhentsev M.[1], Golovanov A.[5], Vildanov A.[4], Garifullin R.[5]

1 - Boreskov Institute of Catalysis SB RAS, Novosibirsk, Russia
2 - Institute of Coal Chemistry and Material Science SB RAS, Kemerovo, Russia
3 - OJSC "Tatneftekhiminvestholding", Kazan, Russia
4 - OJSC "Volga research institute of hydrocarbon feed", Kazan, Russia
5 - OJSC "Tatneft", Al`metyevsk, Russia

* sergk@catalysis.ru

Keywords: hydrogen sulphide, catalyst, oil-associated gas

1 Introduction

More than 40 % or > $70*10^{12}$ nm^3 of the world's hydrocarbon gas reserves are hydrogen sulphide containing natural and oil-associated gases [1]. This feedstock is a significant potential resource for energetics and chemical synthesis. However, high content of hydrogen sulphide (1-30 vol.%) excludes direct application of these gases as fuels or raw materials for downstream production. The currently used flame combustion of such gases leads to air pollution with toxic sulfur di- and trioxides, sulfuric acid, products of incomplete combustion of hydrocarbons, and carcinogenic soot, amount of which attains one million tons a year. Thus, the development of the technical solutions for reliable on-site purification of these gases is a problem of the highest priority for the Russian Federation and the whole world.

2 Experimental/methodology

Technology of direct selective oxidation of hydrogen sulphide

In the Laboratory of Environmental Catalysis of the Boreskov Institute of Catalysis, new processes based on direct catalytic oxidation of hydrogen sulphide were developed [2-3]. The technology is schematically depicted in Fig. 1.

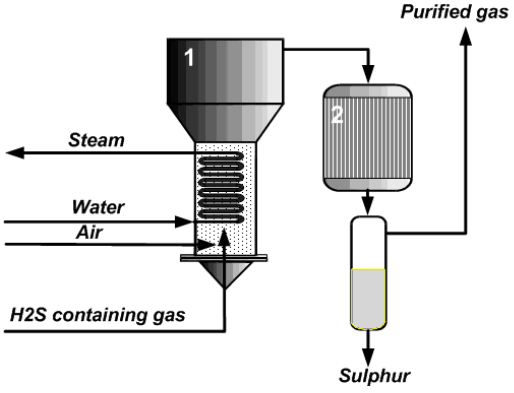

Figure 1: The technology of direct selective oxidation of hydrogen sulphide

A raw hydrogen sulphide containing gas is supplied to the reactor with a fluidized bed of catalyst, simultaneously oxygen (or air) is fed into the catalyst bed as a separate flow. The excessive heat of the exothermic reaction of H_2S oxidation is efficiently removed by a heat-

exchanger immersed into the fluidized bed. The bed temperature is controlled by the regulation of the amount of heat removed from the bed with a heat-exchange agent.

The technology was successfully tested in pilot scale on the largest sour gas fields, refineries and gas processing plants in Russia [3-4]. In 2011 full scale industrial installation was set into continuous operation at the Bavly oil-field (OJSC "Tatneft" – company-operator) [4-6].

Industrial installation of direct selective oxidation of hydrogen sulphide

The general view of the industrial installation is presented in Fig. 2.

Figure 2: Industrial installation for direct selective oxidation of hydrogen sulphide

3 Results and discussion

The efficiency of hydrogen sulphide removal was proved to exceed 99%.

During two years of continuous operation:

- 120 10^6 m^3 of commercial gas were produced;
- 1200 tons of hydrogen sulphide were recovered as elemental sulfur;
- emission of more than 2300 tons of sulfur dioxide and sulfuric acid to the atmosphere was prevented;
- pollution damage for the amount of $ 10 million was averted.

Characteristics of the produced sulfur surpass those specified by Russian National Standard #127.1-93 (commercial grade sulfur 9990).

4 Conclusions

The technology for purification hydrocarbon feedstock based on direct selective oxidation of hydrogen sulphide has been developed. The efficiency of the technology has been proved upon field testing of an industrial installation.

References

[1] S. Santo , M. Rameshni. Journal of Natural Gas Science and Engineering 18 (2014)
[2] Z.R. Ismagilov, V.N. Parmon, S.R. Khairulin, et al., US Patent No 4,886,649 (1989)
[2] Z.R. Ismagilov, S.R. Khairulin et al., Oil & Gas Journal April (1994)
[3] Z.R. Ismagilov, S.R. Khairulin, M.A. Kerzhetsev et.al., Hydrocarbon Technology International. Winter Issue (1994-1995)
[4] Z.R. Ismagilov, S.R. Khairulin, M.A. Kerzhentsev et al, Catalysis in Industry (2004)
[5] Z.R. Ismagilov, V.N. Parmon, S.R. Khairulin et al. Gas Chemistry (2011).
[6] Z.R. Ismagilov, S.R. Khairulin M.A. Kerzhentsev et al. Utility model patent. № RF 149826 (2014)

V-PP13

Pd Catalysts Supported on Metal Organic Coordinated Structures in Chlorobenzene Hydrodechlorination and CO Oxidation

Agafonov A.A.[1,2*], Lokteva E.S.[1,2], Maslakov K.I.[1,2], Strokova N.E.[1], Voronova L.V.[1]

1 - Lomonosov Moscow State University, Chemistry Department, Moscow, Russia
2 - Institute of Hydrocarbons Processing of the Siberian Branch of the RAS, Omsk, Russia

* agafonov1994andrey@gmail.com

Keywords: hydrodechlorination, MOF-5 palladium catalyst, chlorobenzene, CO oxidation

1 Introduction

Disposal of chlorinated organic compounds, one of the most widespread types of industrial wastes, is between urgent problems for ecological chemistry nowadays. Hydrodechlorination (HDC) provides useful dioxins-free method of chlorobenzenes-containing wastes processing. Pd catalysts supported on different supports are active in HDC. It was found that the presence of Pd both in metal and in oxidized state is profitable for the catalytic performance, and such composition could be provided using appropriate support. It was demonstrated early, that Pd/MOF catalysts are active in some reactions, such as CO oxidation [1]. In this work the attempt was made to prepare Pd/MOF-5 catalysts using two methods, one was aimed on inclusion of Pd to the framework of the support, the other comprised application of Pd by impregnation. Both samples were tested in CO oxidation in pulse microcatalytic system and in chlorobenzene HDC in packed-bed continuous flow gas-phase system.

2 Experimental

Two methods were used to produce Pd/MOF-5: the first one included preparation of MOF-5 (terephtalic acid, $Zn(NO_3)_2.6H_2O$ and $Pd(NO_3)_2$ were used as parent substances, DMF as a solvent, hydrazine hydrate as reducing agent) [2] with further reductive supporting of Pd from palladium nitrate (sample 1); the second way consisted of direct co-precipitation of Pd/MOF-5 from the solution containing Pd^{2+} ions with further reduction under vacuum (10^{-5} atm) at 190ºC according to [3] (sample 2). Pd/MOF-5 were characterized by TGA (449PC Jupiter Netzsch, Netzsch GmbH), XRD (Rigaku MiniFlex 600), AAS (Thermo Fisher Scientific, iCE 3000), SEM (JSM 6490 LV, JEOL), low-temperature N_2 adsorption-desorption (Micometrics ASAP 2000), XPS (Kratos Axis Ultra DLD). Catalytic tests were performed in gas-phase hydrodechlorination of chlorobenzene at 100-250°C (flow-type fixed bad tubular reactor, 51 mg of catalyst, H_2:chlorobenzene = 30 (mol.)), and in CO oxidation by pulse microcatalytic method using the mixture of 2 vol.% CO and 1 vol.% O_2, balance He, pulse value 1 ml; the products were analyzed by GC.

3 Results and discussion

Two preparation methods of Pd/MOF-5 were used to provide Pd sites supported on MOF structure (sample 1) and involved into the framework of MOF (sample 2).

The results of TGA analysis of Pd/MOF-5 (1) and (2) are similar to those reported in literature and confirm the MOF-5 structure, but TG curve of sample 1 includes 3 discrete peaks of mass loss at the temperatures below 300ºC, associated with DMF removal, as it was shown by online MS analysis; whereas for the sample 2 this interval contains no peaks due to vacuum activation as the last synthesis step. The sample 1, according to SEM results includes faceted

particles of cubic structure as well as less crystalline ones; sample 2 consists mainly of needle-shaped particles. All particles have dimensions less than 1 μm.

XRD diffraction pattern for sample 2 is similar to those of MOF-5 described in literature [1]. Diffraction pattern of sample 1, in addition to MOF-5 peaks, contains many additional peaks, some of them could be attributed to the presence of ZnO, NaCl and other admixtures. NaCl presence was confirmed by XPS.

To characterize oxidation state of Zn by XPS a modified Auger parameter (the sum of E_B of $Zn2p_{3/2}$ electrons and kinetic energy of Auger spectrum of ZnLMM) was used. The values of 2009.5 and 2009.4 eV were found for the samples 1 and 2 correspondingly, that is similar to the value of 2010 eV for ZnO [4], but could be attributed also to Zn^{2+} in the other compounds such as carbonic acid salts.

S_{BET} of the samples 1 (87 m^2/g) and 2 (38 m^2/g) was much lower the values characteristic for MOF-5 structure. Taking into account the results of other methods, confirming the formation of MOF structure, it can be connected with the storage of the samples taken for nitrogen adsorption in non-appropriate wet conditions, that lead to partial decomposition before analysis.

The content of Pd found by AAS is very low: $2*10^{-5}$ wt. % of Pd in sample 1, and $4*10^{-6}$ wt. % of Pd in sample 2, which is much less than in similar catalysis described in [2]. As it is shown by XPS-method, both obtained samples contain Pd^0 (E_B of Pd3d electrons of about 335.0 eV, 69 and 63% for the samples 1 and 2) as well as Pd^{2+} in PdO and $PdCl_2$.

Only sample 2 demonstrated catalytic activity in CO oxidation (CO conversion 8% at 100 ºC; 34% at 150 ºC; 79% at 200 ºC; 98% at 250 ºC), in spite of 5 times less Pd content than in the sample 1. It is known that both Pd/MOF [1] and Pd/ZnO_2 [5] are active in CO oxidation, the second due to PdZn alloy formation. So the catalytic performance of the sample 2 could be attributed to the presence of both mentioned systems.

Both samples demonstrated also good performance in chlorobenzene HDC to benzene and cyclohexane in continuous flow system. Stable state chlorobenzene conversion values were 7% at 150ºC, 10% at 200ºC and 13% at 250ºC on sample 2; on sample 1 about 10% both at 150 and 200ºC. Taking into account very low Pd loading the TOF values are very high. In view of contradictory data about the composition of the samples 1 and 2 additional data are desired to describe the nature of the active sites of the samples tested.

4 Conclusions

Two samples were prepared using two methods of Pd/MOF-5 production, with Pd included in framework or supported on it. Characterization by SEM, DSC-TG, and XRD confirms the presence of MOF sructure in both samples, together with other crystalline phases for sample 1, but S_{BET} values are much lower than that for MOF-5 structure. Both samples demonstrate high activity in HDC of chlorobenzene at very low Pd content; sample 2 was active in CO oxidation as well.

Acknowledgements

This work was maintained by Russian Foundation for Basic Researches (13-03-00613). This work was supported in part by M.V. Lomonosov Moscow State University Program of Development.

References

[1] W. Kleist, et al., *Thermochimica Acta,* 499 (2010) 71–78.
[2] S. Gao et al., *Applied Catalysis A: General,* 388 (2010) 196–201.
[3] S. Opelt et al., *Catalysis Communications,* 9 (2008) 1286–1290.
[4] M. Biesinger et al., *Applied Surface Science,* 257 (2010) 887-898.
[5] N. Iwasa et al., *Appl.Catal. B: Environmental,* 79 (2008) 132.

V-PP14

A New, Active Iron-complex Catalyst for Converting CO_2 into Cyclic Carbonates and Cross-Linked Polycarbonates with Enhanced Properties

Taherimehr M.[1], Cardoso Costa Sertã J.P.[1], Kleij A.W.[2,3], Whiteoak C.J.[2], Pescarmona P.P.[1,4*]

1 - COK, University of Leuven, Leuven, Belgium
2 - ICIQ, Tarragona, Spain.
3 - ICREA, Barcelona, Spain
4 - Chemical Engineering Department, University of Groningen, Groningen, The Netherlands

* p.p.pescarmona@rug.nl

Keywords: CO_2 fixation, iron, pyridylamino-bis(phenolate) complex, green polycarbonates, cross linking, cyclic carbonates

1 Introduction

The finite availability of fossil resources is stimulating the production of chemicals from alternative and sustainable carbon resources, among which CO_2 is an attractive (being non-toxic, inexpensive and renewable) yet challenging C_1-feedstock (being thermodynamically very stable).[1] The atom-efficient reaction of CO_2 with epoxides can generate two valuable products: cyclic carbonates and polycarbonates. Cyclic carbonates find application as green solvents, as electrolytes in Li-ion batteries and as intermediates for the synthesis of polymers and fine chemicals, whereas the biodegradable polycarbonates can be used in the synthesis of polyurethanes, thermoplastics and polymer resins.[2] Here, we present a study of iron(III) pyridylamino-bis(phenolate) complexes, FeX[O_2NN'] (**A:** X = Cl; **B:** X = Br), as novel homogeneous catalysts for the coupling reaction between CO_2 and a range of epoxides.[3]

2 Experimental

The synthesis of the iron pyridylamino-bis(phenolate) complexes was performed following a previously reported procedure.[4] The catalytic tests were performed in a high-throughput unit consisting of 24 batch reactors which can operate simultaneously at the chosen temperature and CO_2 pressure. Information on the analysis of the reaction products is provided in Table 1.

3 Results and discussion

Iron(III) pyridylamino-bis(phenolate) complexes are highly active homogeneous catalysts for the reaction of different epoxide substrates and oxetane with CO_2 (Table 1). The addition of a Lewis base co-catalyst allowed significant reduction in the catalyst loading needed to reach high product yields (Table 1, entries 1 and 3-5). The catalysts are remarkably robust, and unpurified substrates can be used without concerns for the presence of water impurities in the reaction set-up. With terminal epoxides, the reaction was fully selective towards the cyclic carbonate product (Table 1, entries 9-11). With cyclic epoxides, the selectivity could be switched between cyclic and polymeric carbonate by tuning the reaction conditions and the catalyst to co-catalyst ratio (Table 1, entries 3&5, and 6&8). Among the studied epoxide substrates, 1,2-epoxy-4-vinylcyclohexane could be converted with nearly complete selectivity to the polycarbonate (Table 1, entry 8). The obtained polymer presents pending vinyl groups, which allow post-synthetic cross-linking with 1,3-propanedithiol (Fig. 1). The cross-linked polycarbonate displayed an increase of 55 °C in the glass transition temperature compared to the as-synthesised polymer (Fig. 1). The improved T_g

value and the enhanced chemical resistance of this cross-linked polycarbonate open new opportunities for the application of these green polymers as thermosetting plastics.[3]

Table 1. Catalytic screening of complexes **A** and **B** in the reaction of CO_2 with different epoxides. Reaction conditions: 60°C, 80 bar, 18 h. 15 mmol epoxide, 3 mmol mesitylene (as internal standard).

Entry	Epoxide	Catalyst/ co-catalyst	Cat:co-cat loading (mol%)[a]	Metal: nucleoph.	Epoxide Conv.[b] (%)	Sel.$_{polycarb.}$[c] (%)	Sel.$_{cyclic\ carb.}$[c] (%)	Carbonate linkages (%)[d]	TON[e]	M_n[f] (gmol^{-1})	PDI[g]
1		**A** / -	5:0	1:1	79	88	12	-	16	-	-
2		**B** / -	5:0	1:1	67	79	21	-	13	-	-
3		**A** / Bu_4NCl	0.5:0.5	1:2	60	82	18	96	120	1418	1.1
4		**A** / Bu_4NBr	0.5:0.5	1:2	63	60	40	-	126	-	-
5		"	0.5:5	1:10.5	95	0	>99	-	200	-	-
6	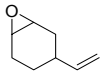	**A** / Bu_4NCl	0.5:0.5	1:2	48	98	2	86	96	1995	1.2
7		**A** / Bu_4NBr	0.5:0.5	1:2	27	78	22	-	54	-	-
8		"	0.5:5	1:10.5	92	0	>99	-	184	-	-
9	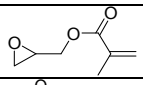	**A** / Bu_4NBr	0.5:0.5	1:2	>99 [h]	0	>99	-	200	-	-
10	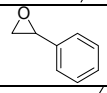	**A** / Bu_4NBr	0.5:0.5	1:2	96 [h]	0	>99	-	192	-	-
11	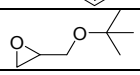	**A** / Bu_4NBr	0.5:0.5	1:2	88 [h]	0	>99	-	176	-	-

[a] Relative to the epoxide. [b] Based on ^{1}H NMR of the reaction mixture. [c] Based on ^{1}H NMR and FT-IR. [d] Based on ^{1}H NMR of the purified copolymer. [e] Turnover number, defined as $mol_{converted\ epoxide}/mol_{Fe}$. [f] Determined by GPC in THF at 30°C against polystyrene standards. [g] Polydispersity index defined as PDI = M_w/M_n.[h] Reaction conditions: 85 °C, 80 bar, 3 h.

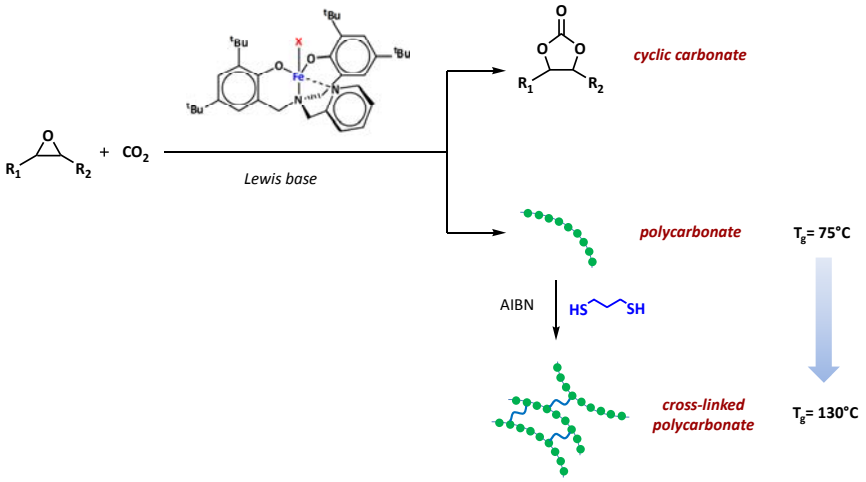

Fig. 1. Reaction of CO_2 with epoxides catalysed by iron(III) pyridylamino-bis(phenolate) complexes and post-synthetic cross-linking of the polycarbonate.

4 Conclusions

Fe[pyridylamino-bis(phenolate)] complexes, alone or in combination with ionic Lewis bases, are highly active and versatile homogeneous catalysts for the coupling reaction of CO_2 and epoxides. The parameters governing the selectivity of the reaction towards cyclic or polymeric carbonates were studied and optimised to control and maximise the selectivity towards each of the two valuable products. The physicochemical properties of the polycarbonate obtained from 1,2-epoxy-4-vinylcyclohexane could be significantly improved by post-synthetic cross linking.

References

[1] M. Peters, B. Köhler, W. Kuckshinrichs, W. Leitner, P. Markewitz, T. E. Müller, *ChemSusChem* 4 (2011) 1216.
[2] P. P. Pescarmona, M. Taherimehr, *Catal. Sci. Technol*. 2 (2012) 2169.
[3] M. Taherimehr, J. P. Cardoso Costa Sertã, A. W. Kleij, C. J. Whiteoak, P.P. Pescarmona, *ChemSusChe,* (2015) DOI 10.1002/cssc.201403323.
[4] K. Hasan, C. Fowler, P. Kwong, A. K. Crane, J. L. Collins, C. M. Kozak, *Dalton Trans*. (2008) 2991.

V-PP15

Design of Catalysts of Carbon Dioxide Conversion of Methane

Mironenko A.*, Kazieva A., Mansurov Z., Kudyarova Z.

The Institute of Combustion Problems, Almaty, Kazakhstan

* anamir.48@mail.ru

Keywords: methane, carbon dioxide, syngas, fiberglass, nanostructured catalyst

1 Introduction

The reaction of carbon dioxide conversion of methane (DR) is one way that allowing to convert natural gas – methane into valuable end products, representing the gas mixture of hydrogen and carbon monoxide in different ratios [1]. From this viewpoint, it is the most secure method, in contrast to the partial oxidation of methane by atmospheric oxygen and steam-oxygen conversion.

In this reaction, the contacts on the basis of nickel oxide have maximum spreading, however, in spite of high activity of these catalysts, their use is limited by significant carbonization processes [2, 3]. In this regard, at the present time a search of new catalytically-active compounds is occurred, these compounds can became as an alternative to nickel contacts. From this viewpoint, the catalysts consisting of cobalt oxides and its compounds are modified with other oxides are of interest.

In recent years, the high-temperature fiberglass is used as a basis in the various processes, in spite of the low surface area, its hydraulic, technological characteristics as well as flexibility in application is vastly superior to traditionally used contacts, including block system of catalysts.

2 Experimental/methodology

The synthesis "solution combustion" is carried out according to the equation:

$$Me(NO_3)_2{*}6H_2O + 2NH_2CH_2COOH + 4.5O_2 \rightarrow MeO + 4CO_2 + 11H_2O + 2NO_2$$

Investigations on catalytic activity in reaction of RD of polyoxide catalysts system on the basis of fiberglass consisting of magnesium oxides, nickel and cobalt were carried out. The activity of catalysts was tested on-line with using of gas chromatographic analysis method on device «ХРОМОС ГХ-1000», is equipped with software (SW), and data recording to the computer.

Synthesized samples are examined by XRF, SEM, TEM methods as well as thermo-programmed reduction by hydrogen.

3 Results and discussion

X-ray analysis showed that after passing of synthesis by "solution combustion" method, on the surface of samples, depending on the initial composition of the charge (nitrate salts), there is phase formation of nanostructured systems is occurred: Co3O4, MgO, NiCo2O4, 3CoO • 5NiO, MgNiO2.

The obtained TEM-images have shown that linear dimension of surface structures on the fiberglass is in interval 5-17 nm. The data of TIS indicates on step process for recovery of active components.

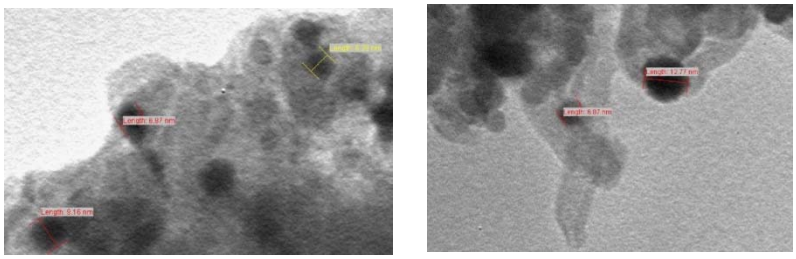

Fig. 1- TEM images from different locations of sample №9

The temperature effect and composition of (MgO, NiO, CoO) polyoxide catalysts on their catalytic activity in the reaction of DR is studied. It was found that the temperature in the interval of 850-900 0C is the optimal temperature of the process.

Variation of sample composition at the temperature 850 ^{0}C has shown that samples containing magnesium oxide – 2 %, nickel – 1,4% and cobalt – 1,6 % have optimal characteristics.

Also, the influence of volume velocity on activity of synthesized samples was investigated. It was found that in the interval of 3200-9600 h-1 the activity of catalyst is almost on the same level: the conversion of initial products is 98-99%, the yield of hydrogen is - 42-43%, and carbon monoxide is - 52-53%.

The analysis of experimental data, is based on the ratio H_2O/CO, shows that most complete conversion of methane and carbon dioxide into reaction products is occurred on the catalyst at temperatures of 850-900 °C: H_2O/CO = 0,092 and 0,072 respectively. The material balance calculations on carbon have shown that the unbalance on carbon average 0.45% and during the tests was almost on a level with a defection of ± 1%.

4 Conclusions

From obtained experimental data it was found that nanostructured catalysts on the basis of high-temperature fiberglass are exhibit the high catalytic activity during the process of carbon dioxide processing of methane (DR) into the synthesis gas, the ratio H_2/CO is close to 1. It is shown that DR process the conversion of methane and carbon dioxide reaches 98-99% and the yields of hydrogen and carbon monoxide comprises 42 and 52%, respectively. Also it was found that the content of magnesium oxide is introduced into catalyst system has a major influence on the basic characteristics of DR process. It was shown that catalytic activity remains almost constant during 30 hours of catalyzator work at 850 ° C.

Thus, inference should be drawn that catalysts on the basis of fiberglass have fairly good perspectives at processing of natural gas - methane into valuable synthesis gas for chemical industry

References

[1]. O.V. Krylov, Catalytic processing of natural gas / O.V. Krylov // Kinetics and catalysis. – 1999. - T.40, №1. - P. 151-157.

[2]. The formation of condensation products in the process of carbon dioxide conversion of methane on Ni-contain catalyst / L.V.Galaktionova , L.A. Arkatova, T.S. Kharlamova, L.N. Kurina, Yu.S. Naiborodenko, N.G. Kasatsky, N.N. Golobokov // Physical chemistry journal. – 2007. – T.81, № 10. - P.1917-1920.

[3]. Carbon dioxide reforming of methane to synthesis gas over Ni-MCM-41 catalysts / Liu D., Raymond Lau, Armando Borgna, Yanhui Yang // Appl. Catal. A: General.- 1 May 2009. - Vol. 358, Issue 2. – P. 110-118.

V-PP16

Modified Ni-Al Layered Double Hydroxides as Catalyst Precursors for Utilization of Carbon Dioxide

Gabrovska M.[1*], Shopska M.[1], Edreva-Kardjieva R.[1], Nikolova D.[1], Bilyarska L.[1], Crişan D.[2]

1 - Institute of Catalysis, Bulgarian Academy of Sciences, Sofia, Bulgaria
2 - "Ilie Murgulescu" Institute of Physical Chemistry, Romanian Academy, Bucharest, Romania

* margo@ic.bas.bg

Keywords: Ni-Al layered double hydroxides, Mg and Cr modifiers, CO_2 removal by methanation

1 Introduction

Utilization of carbon dioxide (CO_2) has become an important global issue due to the significant and continuous rise in atmospheric CO_2 concentrations. Carbon dioxide is a major greenhouse gas and makes a significant contribution to global warming and climate change. Hence, there is an urgent need to reduce its accumulation in the atmosphere. It was specified in our recent study [1], that the co-precipitated Ni-Al layered double hydroxide (Ni^{2+}/Al^{3+}= 3.0/1) is a precursor of effective catalyst for fine CO_2 removal from H_2-rich gas stream through the methanation reaction (hydrogenation of CO_2 to methane).

Ni-Al layered double hydroxides represent a class of layered materials with a chemical composition expressed by the general formula $[Ni^{2+}_{1-x}\ Al^{3+}_{x}\ (OH)_2]^{x+}\ [A^{n-}_{x/n}]\cdot mH_2O$, where Ni^{2+} and Al^{3+} ions are located in the brucite-like hydroxide layers, while the charge compensating exchangeable anions (A^{n-}) and water molecules are situated in the interlayer space of the layered structure. Withal, *x* represents the Al^{3+} fraction and *m* is the number of the water molecules. A wide variety of M^{2+} or M^{3+} cations may be accommodated or substituted in the octahedral sites of the brucite-type sheets by other ones having similar ionic radius, forming different layered compounds [2]. In this study we report on our attempts to further improve the catalytic activity of the Ni-Al catalyst. A modification of the brucite-like layer by partial isomorphous substitution of Ni^{2+} ions with Mg^{2+} as well as of Al^{3+} with Cr^{3+} ones was done. The aim of this study is to elucidate the role of the modifier on the activity in CO_2 removal through methanation by variation of the reduction and reaction temperature as well as the space velocity.

2 Experimental/methodology

NiAl, NiMgAl and NiCrAl layered precursors with molar ratios of M^{2+}/M^{3+} = 3.0, where M^{2+} = Ni or Ni+Mg and M^{3+} = Al or Cr+Al, were synthesized by co-precipitation at constant pH and temperature. The total amount of the adsorbed hydrogen (H_2-chemisorption) was used to determine the specific Ni^0 surface area (Ssp_{Ni}) and the Ni^0 particle size (d_{Ni}) of the reduced precursors (400, 450, 530 and 600°C for 3 h with hydrogen). The metanation activity were performed by means of gaseous mixture of $CO_2/H_2/Ar$=0.65/34.35/65.0 vol. % in the temperature interval 220−400°C and GHSV=3000−22000 h^{-1} after 'in situ' reduction of the precursors by hydrogen at 400, 450, 530, and 600°C for 3 h. A variation of the GHSV was applied at each reaction temperature until registration of 0−50 ppm CO_2 levels.

3 Results and discussion

The catalytic activity is evaluated by the GHSV at which the residual concentration of CO_2 at the reactor outlet was 10 ppm, the latter being an admissible limit in the industrial ammonia production. The catalytic runs show that all catalysts hydrogenate CO_2 successfully to CO_2 levels of 0–10 ppm at reaction temperatures between 400 and 280°C and GHSV within 3000–

22000 h^{-1}. Bearing in mind that the lower temperatures are thermodynamically favorable for the reaction under study, the activity of the catalysts is represented at the reaction temperatures of 260, 240 and 220°C (Fig. 1).

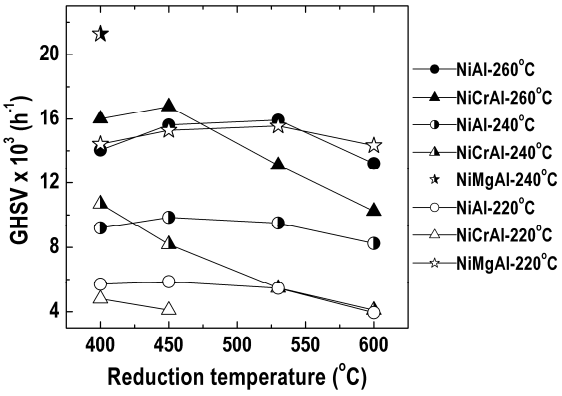

Fig. 1. Catalytic activity

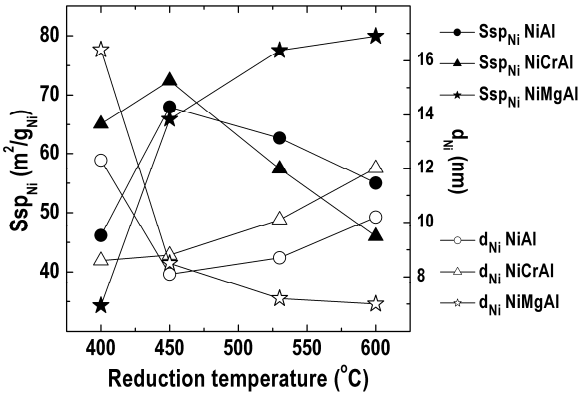

Fig. 2. Ssp_{Ni} and d_{Ni} of metal Ni

NiMgAl catalyst hydrogenates CO_2 completely at 0 ppm level at a reaction temperature of 260°C, raising GHSV to 22000 h^{-1}, irrespective of reduction temperature (Fig. 1). The catalyst purifies the reaction mixture from CO_2 at 10 ppm level at a reaction temperature of 240°C and GHSV = 22000 h^{-1}, only after reduction at 400°C. Further increase of the reduction temperature up to 530 and 600°C brings about a successful purification at 0 ppm level. NiMgAl catalyst dominates in the activity at a reaction temperature of 220°C, also. A possible explanation of the observed catalytic activity may be found in the results obtained from H_2-chemisorption experiments. An increase of the Ssp_{Ni} and decrease of d_{Ni} is observed after reduction above 500°C (Fig. 2) because of the retarding the effect of the Mg on the Ni^0 sintering. It is well-known that Mg acts as spacer/barrier thus minimizing sintering via Ni^0 particle migration. As the Ni^0 particle size becomes smaller, numerous Ni^0 atoms will be exposed to the surface (active sites where the reaction can take place) thus provoking higher catalytic activity.

The differences in the activity of NiCrAl and NiAl catalysts is related to the role of Cr^{3+} ions to stabilize the gamma-Al_2O_3 phase at low temperatures (reduction at 400 and 450°C), thus preventing the formation of hardly reducible $NiAl_2O_4$ spinel-like phase. As a result, the number of the easily reducible Ni^{2+} ions rises and the Ssp_{Ni} increases. At higher reduction temperatures, Cr^{3+} and Ni^{2+} ions form hardly reducible $NiCr_2O_4$ spinel, so Ssp_{Ni} decreases causing the activity loss. The methanation activity of NiAl catalyst after reduction at 400 and 450°C can be ascribed to the presence of readily reducible Ni^{2+}-O species, because the formation of $NiAl_2O_4$ spinel-like phases is realized at temperatures higher than 520°C. Further treatment above 530°C induces aggregation or sintering of the Ni^0 particles, causing diminution of both Ssp_{Ni} and number of Ni^0 atoms on the catalyst surface (Ni^0 dispersion) thus leading to a decrease of the methanation activity.

4 Conclusions

The studied catalytic compositions are found to be promising catalyst precursors for deep CO_2 removal from hydrogen-rich gas streams through the methanation reaction, depending on the technological regime of the catalyst activation: (i) NiCrAl and NiAl catalysts – at low and medium reduction temperatures and (ii) NiMgAl catalyst – at higher reduction temperatures.

References

[1] M. Gabrovska, R. Edreva-Kardjieva, D. Crişan, P. Tzvetkov, M. Shopska, I. Shtereva, *React. Kinet. Mech. Cat*. 105 (2012) 79.

[2] F. Cavani, F. Trifirò, A. Vaccari, *Catal. Today* 11 (1991) 173.

V-PP17

Two-Dimensional $SrNb_2O_6$ as an Efficient Photocatalyst for the Preferential Reduction of Carbon Dioxide in the Presence of Water

Xie S., Zhang Q., Wang Y.*

State Key Laboratory of Physical Chemistry of Solid Surfaces, Collaborative Innovation Center of Chemistry for Energy Materials, National Engineering Laboratory for Green Chemical Productions of Alcohols, Ethers and Esters, College of Chemistry and Chemical Engineering, Xiamen University, Xiamen, China

* wangye@xmu.edu.cn

Keywords: $SrNb_2O_6$, nanoplate, photocatalysis, carbon dioxide reduction

1 Introduction

The gradual depletion of fossil resources and the growing emission of CO_2 have stimulated the research activities toward the utilization of CO_2 for the production of fuels and chemicals. Among various transformations of CO_2, the photocatalytic reduction of CO_2 with H_2O is one of most attractive but highly difficult routes. The rapid recombination of photogenerated electron-hole pairs and the low adsorption ability and reactivity of CO_2 on catalyst surfaces may cause the lower efficiency [1]. We have demonstrated that the addition of basic oxides or Pt@Cu_2O cocatalyst onto TiO_2 and the using of solid-gas reaction mode can enhance the activity and selectivity for CO_2 photoreduction [2-4]. Here, we report our recent finding that the synthesis of a novel two-dimensional (2D) $SrNb_2O_6$ with high CO_2 chemisorption and enhanced electron-hole separation abilities can accelerate the preferential reduction of CO_2 in the presence of H_2O.

2 Experimental

$SrNb_2O_6$ nanocrystals with different morphologies were mainly synthesized by hydrothermal method, and were denoted as $SrNb_2O_6$−*X*−*Y*, where *X* is the morphology and *Y* is the value of surface area ($m^2\ g^{-1}$). Photocatalytic reduction of CO_2 in the presence of H_2O was carried out in a stainless-steel reactor with a quartz window on the top of the reactor using solid−gas interface reaction mode. Reaction conditions were as follows: catalyst, 0.010 g; CO_2 pressure, 0.2 MPa; H_2O, 4.0 mL; light source, Xe lamp (λ = 300-780 nm); irradiation time, 10 h.

3 Results and discussion

The conditions used for the hydrothermal synthesis determined the product morphology. A higher pH value (pH = 13), higher temperature (≥ 493 K) and a longer hydrothermal time (≥ 24 h) were required for the formation of 2D nanoplate morphology. The $SrNb_2O_6$−plate−105 sample exhibited a lateral size of 50-300 nm and the thickness of nanoplates was ~12 nm, the HRTEM image and the SAED pattern revealed the single crystal nature of this sample (Fig. 1A).

To gain insights into the feature of the $SrNb_2O_6$ nanoplate, we chose 6 representative samples with different morphologies (Table 1) for further studies. These samples were all monoclinic $SrNb_2O_6$ in crystalline structure. The band gap energy evaluated from UV-vis did not change significantly with the morphologies and were 3.7-3.8 eV.

The photocatalytic results displayed in Table 1 suggest that the morphology plays a key role in determining the catalytic activity. For example, the $SrNb_2O_6$−plate−50, which had a similar surface area or CO_2 adsorption amount to the $SrNb_2O_6$−particle−46, produced a significantly larger amount of (CO + CH_4). On the other hand, the comparison of the catalysts with the same

morphology but different surface areas showed that the larger surface area favoured the activity. Thus, the $SrNb_2O_6$−plate−105 exhibited excellent activity for the photocatalytic reduction of CO_2 without any promotes or cocatalysts, which was even better than the Pt−TiO_2. It should be mentioned that the selectivity of consumed electrons for CO_2 reduction was higher for the $SrNb_2O_6$ nanocrystals than that for TiO_2 and Pt−TiO_2.

To understand the effect of morphology deeply, we performed transient photocurrent response measurements. The photocurrent density increased in the following sequence: $SrNb_2O_6$−SSR−2.2 < $SrNb_2O_6$−particle−3.7 < $SrNb_2O_6$−particle−46 < $SrNb_2O_6$−rod−8.5 < $SrNb_2O_6$−plate−50 < $SrNb_2O_6$−plate−105 (Fig. 1B). These results demonstrate that the $SrNb_2O_6$ nanoplate favours the separation of photoexcited charge carriers. The correlation of these results with the catalytic activity (Table 1) suggests that the separation of photogenerated electron-hole pairs is the activity-determining process in our system.

Photocatalyst	Amount (μmol)			Select. for CO_2 reduction (%)	CO_2 chemisorption (μmol g^{-1})
	CO	CH_4	H_2		
$SrNb_2O_6$−SSR−2.2	0.41	0.026	0.098	84	0.45
$SrNb_2O_6$−particle−3.7	0.51	0.054	0.24	75	0.75
$SrNb_2O_6$−rod−8.5	0.76	0.092	0.45	71	1.7
$SrNb_2O_6$−particle−46	0.65	0.062	0.21	81	8.7
$SrNb_2O_6$−plate−50	1.05	0.20	0.38	83	9.2
$SrNb_2O_6$−plate−105	1.66	0.33	0.65	82	21
TiO_2 (P25)	0.14	0.042	0.24	56	-
0.5 wt% Pt−TiO_2	0.12	0.57	3.63	40	-

Table 1. Photocatalytic behaviours of the $SrNb_2O_6$ catalysts for the reduction of CO_2.

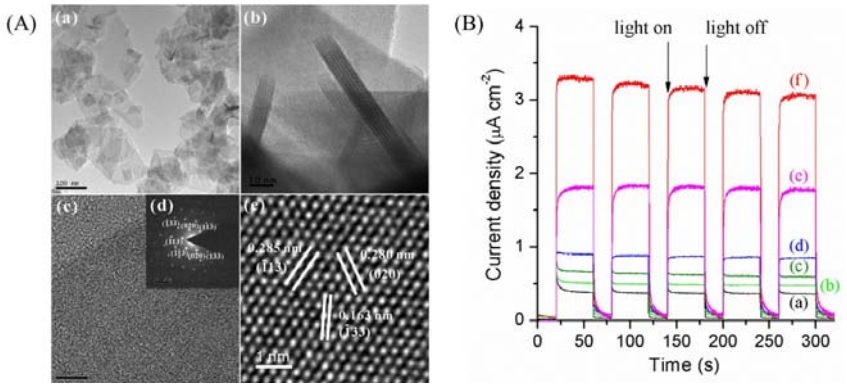

Fig. 1. (A) TEM images of $SrNb_2O_6$ nanoplates. (a) Top view, (b) side view, (c, d) HRTEM image and SAED pattern, (e) HRTEM image. (B) Transient photocurrent responses for (a) $SrNb_2O_6$−SSR−2.2, (b) $SrNb_2O_6$−particle−3.7, (c) $SrNb_2O_6$−particle−46, (d) $SrNb_2O_6$−rod−8.5, (e) $SrNb_2O_6$−plate−50, (f) $SrNb_2O_6$−plate−105.

4 Conclusions

We have succeeded in synthesizing $SrNb_2O_6$ nanoplates by a simple hydrothermal method and demonstrated that the $SrNb_2O_6$ nanoplate is a promising photocatalyst for the preferential reduction of CO_2 to CO and CH_4 in the presence of H_2O vapour. The open 2D structure and high surface area contribute to the photocatalytic CO_2 reduction by enhancing the separation of photogenerated electron-hole pairs. The larger surface area could also enhance CO_2 chemisorption, favouring its subsequent reduction.

References

[1] W. Fan, Q. Zhang, Y. Wang, *Phys. Chem. Chem. Phys.* 15 (2013) 2632.
[2] S. Xie, Y. Wang, Q. Zhang, W. Fan, W. Deng, Y. Wang, *Chem. Commun.* 49 (2013) 2451.
[3] Q. Zhai, S. Xie, W. Fan, Q. Zhang, Y. Wang, W. Deng, Y. Wang, *Angew. Chem. Int. Ed.* 52 (2013) 5776.
[4] S. Xie, Y. Wang, Q. Zhang, W. Deng, Y. Wang, *ACS Catal.* 4 (2014) 3644.

V-PP18

Design and Development of Efficient AC-Based Adsorbents for CO_2 Removal

Eropak B.M.[1], Aksoylu A.E.[1*], Çağlayan B.S.[2]

1 - Boğaziçi University, Department of Chemical Engineering, Istanbul, Turkey
2 - Advanced Technologies R&D Center, Boğaziçi University, Istanbul, Turkey

* aksoylu@boun.edu.tr

Keywords: AC adsorbents, CO_2 removal, CO_2 adsorption, selective CO_2 adsorption

1 Introduction

Thermal power plants fed by fossil fuels, including coal, oil and gas generate CO_2 as a by-product, which accounts for 40% of total CO_2 emissions. Since reducing CO_2 emissions is crucial for environmental concerns, there is a growing interest on CO_2 capture (CC) technologies. CC technologies also provide an advantageous way for many issues, such as selective separation of CO_2 from the natural gas reserves, selective separation of CO_2 from flue gas mixtures, and selective separation of CO_2 from the shifted-syngas ($CO+ H_2$) prior to the generation of electricity. CC is a demanding technology considering the fact that CO_2 concentrations may be lower than 10-15%, like in the effluent stream of WGS units, meaning a limited thermodynamic driving force for the operation. Adsorption seems to be the most promising technology due to its reasonable removal efficiency, especially by using solid sorbents that offers potential energy savings with lower capital and operating costs [1, 2]. In order to be used in pre-combustion and post-combustion technology applications, selective adsorption has attracted great interest.

In this study, activated carbon (AC) based adsorbents, which have large surface area and suitable porosity, were investigated for their CO_2 capturing ability. Structural modification of AC is an important parameter for CO_2 adsorption properties. Different oxidation procedures and alkali impregnation, such as NaOH and KOH impregnation, were applied. Selective adsorption of CO_2 from CO_2-CH_4 mixtures was studied on AC-based adsorbents and the effects of temperature, pressure, and adsorbate gas composition were investigated.

2 Experimental

The AC-based adsorbents used in this study were prepared via different oxidative, alkali and thermal treatments. HNO_3 or air oxidation procedures were applied over AC samples followed by washing with HCl. 10% NaOH or KOH were added to the oxidized samples through using solution impregnation in order to introduce basic groups on the adsorbent surface. Air oxidized-alkali impregnated samples were calcined at 200 ºC, 250 ºC and 300 ºC, whereas HNO_3 oxidized-alkali impregnated samples were calcined at 175 ºC, 200 ºC and 250 ºC. CO_2 adsorption and/or selective CO_2 adsorption performance of the samples were analyzed by using a gravimetric analyzer system integrated to a mass spectrometer. Adsorption and desorption isotherms were obtained in the pressure range of 0-1000 mbar, and the experiments were conducted at room temperature, 120 ºC and 200 ºC. 4 different feed streams were used in order to observe the effect of adsorbate composition: (i) 100% CO_2, (ii) 100% CH_4, (iii) 50% CO_2-50% CH_4 mixture, (iv) 10% CO_2-90% CH_4 mixture.

3 Results and discussion

A comparative analysis of the results of the adsorption experiments conducted under pure

CO_2 and pure CH_4 flow revealed that CO_2 adsorption is more favorable than that of CH_4 on NaOH and KOH impregnated AC-based adsorbents. Studies on selective adsorption of CO_2 from CO_2-CH_4 mixtures were also performed on AC-based adsorbents with high CO_2 adsorption capacity and stability. The amounts of CO_2 and CH_4 adsorbed at room temperature were 4 times higher than those measured at 120 ºC and 200 ºC, and surface saturation was reached at lower pressure values when the experiments were conducted at high temperatures**.** The effect of CO_2 partial pressure, in other words adsorbate gas composition, was investigated. Figure 1 shows that mass uptake on the adsorbent surface increases with increasing CO_2 concentration in the feed stream.

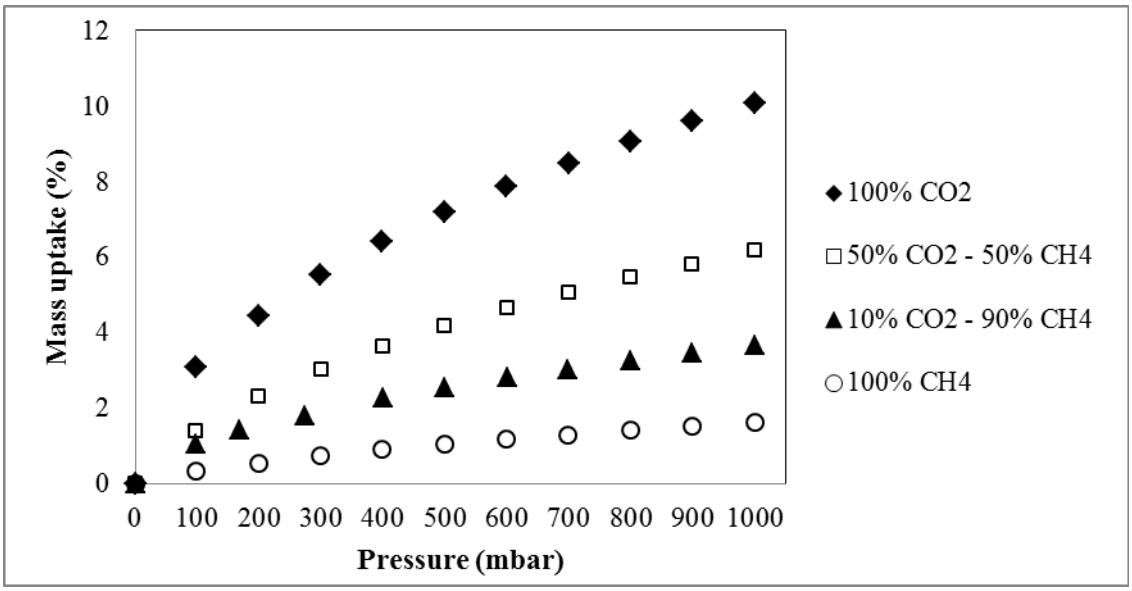

Fig. 1. Mass uptake on an AC-based adsorbent (air oxidized, NaOH impregnated, calcined at 200 ºC) for different feed stream compositions.

4 Conclusions

In preparation of AC-based CO_2 adsorbents, different oxidation procedures, followed by alkali, NaOH or KOH, impregnation, were applied to a commercial AC. The results showed that alkali impregnation enhances CO_2 adsorption capacity, and CO_2 adsorption is more favorable than CH_4 adsorption. However, variations in post-calcination temperature have not showed any significant effect. Alkali impregnated ACs were found to be promising adsorbents as they have both high adsorption capacity and selectivity towards CO_2 adsorption.

Acknowledgements

This work is financially supported by TUBITAK through project 113M263.

References

[1] S. García, M. V. Gil, C. F. Martín, J. J. Pis, F. Rubiera, C. Pevida, *Chemical Engineering Journal.* 171 (2011) 549-556.

[2] C. Shen, C. A. Grande, P. Li, J. Yu, A. E. Rodrigues, *Chemical Engineering Journal.* 160 (2010), 398-407.

V-PP19

Preperation and Characterization of Ni-Based Catalysts for Oxy-CO_2 Reforming of Methane by Using Wet Impregnation Method

Hacioglu M., Gürkaynak A.T.*, Özdemir H., Öksüzömer M.A.F.

Department of Chemical Engineering, Istanbul University, Istanbul, Turkey

* tubag@istanbul.edu.tr

Keywords: combined partial oxidation and CO_2 reforming of methane, synthesis gas, Ni catalyst

1 Introduction

The study aims at exploring a concept which can convert coal-bed methane (containing methane, air and carbon dioxide) to synthesis gas. CO_2 reforming of methane (DRM) to produce synthesis gas has attracted interest by the means of environmental and industrial perspectives. The environmental viewpoint stem from the fact that both CO_2 and methane are viewed as harmful greenhouse gases. CO_2 reforming of methane convert the two greenhouse gases into a valuable feedstock: CO and H_2 [1]. The synthesis gas (a mixture of H_2 and CO) is a versatile feedstock for methanol and Fischer-Tropsch synthesis and several other carbonylation, hydrogenation and reduction reactions [2]. Even though the coke deposition rate in CO_2 reforming of methane can be minimized by modification of catalyst, high energy requirement prevents commercialization of the process. On the other hand although partial oxidation of methane (POM) is a highly energy efficient reaction due to its exothermic nature, it is hard to control the temperature of the reaction if the heat transfer from the catalyst surface to the gas phase is poor. Moreover, POM requires pure oxygen which is also costly. An interesting approach is to combine the advantages of DRM and POM results in a reaction called oxy-CO_2 reforming of methane [3]. By coupling the exothermic partial oxidation reaction with the endothermic reforming reaction, the methane-to-syngas conversion can be operated in a safer manner than partial oxidation and more energy efficient manner than CO_2 reforming. Additionally, by changing the feed composition, one can control the product ratio of H_2/CO and thus the selectivity for various Fischer–Tropsch synthesis products. Finally, one can use those natural gas reserves containing substantial amounts of CO_2 [4].

2 Experimental/methodology

10% and 15% (wt.%) Ni loaded on Al_2O_3, MgO, ZrO_2, $MgAl_2O_4$, SiO_2, TiO_2 and CeO_2 catalysts were prepared by impregnating the support with an aqueous solution of $Ni(NO_3)_2.6H_2O$. An appropriate amount of $Ni(NO_3)_2.6H_2O$ that was solved in 25 ml deionized water was impregnated to supports under mixing at 60°C. Slurry was dried at 120°C for 15 h and calcined 800°C for 5h.

Nickel crystallite sizes were calculated by Scherrer's equation and both these results and the surface areas can be seen in Table 1. The catalytic reaction tests were carried out in a conventional micro quartz reactor (Id ¼ 6 mm) under atmospheric pressure at 800°C. The reactant stream consisting of $CH_4/CO_2/O_2/N_2$= 3/1.3/1/3.7 (by volume) was fed in at a gas hourly space velocity (GHSV) of 30000 ml g^{-1} h^{-1}. Prior to reaction, each catalyst was reduced in situ in 10% H_2/N_2 flow at 800ºC for 2 h. Effluent gases were analyzed by on-line gas chromatograph (GC) .

3 Results and discussion

Figure 1 shows the XRD pattern of the fresh Ni/Al_2O_3 catalyst. Ni/Al_2O_3 catalysts shows the characteristic peaks of NiO at $2\theta=43.3^\circ$, 37.2°, 62.9° and $NiAl_2O_4$ at $2\theta=19.1^\circ$, 31.4°, 37°, 45°, 59.7°, 65.5°.

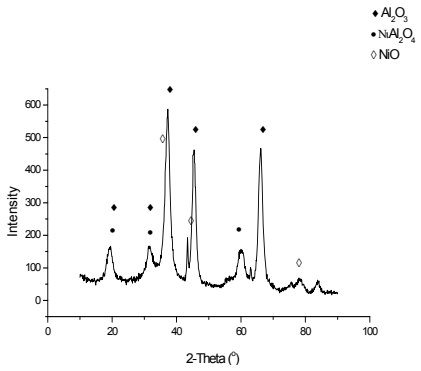

Fig. 1. XRD patterns of the Ni/ Al2O3

Catalyst	Surface Area(m^2/g)	Crystallite Size(nm)
Ni/Al_2O_3	138.5	7
Ni/ZrO_2	24.1	25.8
Ni/TiO_2	8.7	38.5
Ni/SiO_2	100.4	12.7
Ni/CeO_2	5.5	37
$Ni/MgAl_2O_4$	33.5	28.6
Ni/MgO	21.7	29.2

Table 1. BET analysis and crystallite sizes of catalys

Catalyst	GHSV (l/kg h)	Conversion of CH_4	Conversion of CO_2	Selectivity of H_2	Selectivity of CO	H_2/CO
Ni/Al_2O_3	30000	92	89.6	95,8	99,2	1,48
Ni/MgO	30000	22.4	0	6.7	28.5	1.50

Table 2. Results and activity for Ni/Al_2O_3 and Ni/MgO

4 Conclusions

The combined air partial oxidation and CO_2 reforming of coal bed methane reaction results over impregnated Ni/Al_2O_3, Ni/MgO, Ni/ZrO_2, $Ni/MgAl_2O_4$, Ni/SiO_2, Ni/TiO_2 and Ni/CeO_2 catalysts. Ni/Al_2O_3 and Ni/MgO are presented in Table 2 for 10% Ni loading. The Ni/Al_2O_3 catalyst shows the conversions of CH_4 and CO_2 %92 and 89,6 respectively during the reaction. In the case of Ni/MgO catalyst, the initial conversions of CH_4 and CO_2 are %76 lower than those of Ni/Al_2O_3 catalyst. And the conversions of CH_4 and CO_2 decrease markedly in the reaction. The activity tests of different Ni loadings are still in progress.

Acknowledgements

This study was supported by The Scientific and Technological Research Council of Turkey, Engineering Research Grant Committee (MAG) through project No: 213M381

References

[1] C.Y. Lu, H.H. Tseng, M.Y. Wey, L.Y. Liu, K.H. Materials Science and Engineering B 157 (2009) 105–112.

[2] E. Bayrakdar, T. Gürkaynak Altınçekiç, M.A.F Öksüzömer, Fuel Processing Technology 110 (2013) 167–175

[3] U. Oemar, Catalytic Oxidative CO_2 Reforming of Methane Over Bimetallic Pd-Ni Catalyst (2011)

[4] E. Ruckenstein, H.Y. Wang, Combined Catalytic Partial Oxidation and CO_2 Reforming of Methane Over Supported Cobalt Catalysts, (2001).

V-PP20

A Honeycomb-Type Ni/CeO_2 Catalyst for CO_2 Methanation to Transform Greenhouse Gas into Useful Resources

Fukuhara C.[1*], Hayakawa K.[1], Murabayashi K.[2], Khono Y.[1], Watanabe R.[1]

1 - Shizuoka University, Department of Applied Chemistry and Biochemical Engineering, Graduate School of Engineering, Hamamatsu, Japan
2 - Cataler Corporation, Kakegawa, Japan

* tcfukuh@ipc.shizuoka.ac.jp

Keywords: honeycomb-type catalyst, CO_2 methanation, wash-coat, CO_2 utilization

1 Introduction

The CO_2 methanation is a famous reaction that calls a familiar Sabatier reaction for the hydrogenation of CO_2. Recently, the CO_2 methanation has also come to be paid to attention as a reaction that converts the greenhouse gas into a useful resource gas and is one of the promising hydrogen careers, produced by renewable energy. Such attention has thus accelerated the research of the catalyst and system development for methanation more than before.

The important point in constructing the CO_2 methanation system is to develop the catalyst having a rapidly transforming ability of CO_2 and to eliminate the reactive exothermic energy to the reactive zone efficiently. Additionally, the processing of a large amount of raw material gas is requested from an industrial viewpoint. The structured reaction system that integrates a reactive zone and a heat-transferring zone is an effective reaction system to solve the problem of efficient elimination of thermal energy and the problem of the mass processing of CO_2.

For constructing the structured methanation system in this study, first, we investigated the performance of methanation of some nickel-based catalyst loaded on various support. Secondly, a structured catalyst with Ni/CeO_2 component having the highest methanation ability was prepared by wash-coating method on an aluminum honeycomb-fin and was measured its catalytic property and durability performances.

2 Experimental

The 10 wt% Ni-loaded granular catalyst was prepared by a wet impregnation method. The Al_2O_3 (ALO-8), TiO_2 (TIO-4), ZrO_2 (ZRO-3) and CeO_2 (CEO-2), which were provided by Catalysis Society of Japan, were used as the support materials. The support and $Ni(NO_3)_2 \cdot 6H_2O$ were added into a distilled water and well-stirred for 14 h at room temperature. After drying, the obtained powder was calcined at 500°C for 3 h so as to be a Ni-based granular-type catalyst.

Fig.1 Overview of the prepared honeycomb-type Ni-based catalyst.

The structured catalyst was prepared by a wash-coat method using an aluminium substrate with a honeycomb-fin configuration (18mmφ x 45mm-length, cell density 100cpsi, apparent surface area 183 cm^2). The granular Ni-based catalyst was first dispersed in distilled water to prepare the slurry. Then, the honeycomb-fin substrate was immersed in this slurry. By drying at 27°C for 24 h, the honeycomb-type catalyst as shown in Figure 1 was obtained.

The prepared catalyst was placed in the center of the reactor tube. The catalyst was reduced by H_2 at 500°C for 2 h before the reaction. After the reduction, reactants (CO_2/H_2/He =1/4/5 molar ratio, total gas volume=70 ml·min^{-1}) were supplied to the catalyst. The catalyst of 300 mg was loaded and GHSV based on the net volume of the catalyst layer was 14,000 h^{-1}. The reaction temperature range was from 200 to 500°C. Outlet gases were analysed by GC-TCD.

3 Results and discussion

Figure 2 shows the effect of reaction temperature on CO_2 conversion over the Ni/Al_2O_3, Ni/TiO_2, Ni/ZrO_2 and Ni/CeO_2 catalysts. Over 350°C, all catalysts showed high CO_2 conversion which is almost equilibrium value. In contrast, the significant difference in activity was observed below 350°C. The Ni/CeO_2 and Ni/ZrO_2 catalysts displayed a high activity of 84.7 % and 70.0 % conversion at 250°C, while the Ni/Al_2O_3 and Ni/TiO_2 catalysts showed a low CO_2 conversion. These results satisfied with the previous report [1]. The higher basic supports such as the CeO_2 and ZrO_2 would enhance the partial electron transfer from the supports to Ni element [2]. The increased basicity of the support might improve the ability of CO_2 activation on Ni-site, and in turn produced a higher activity.

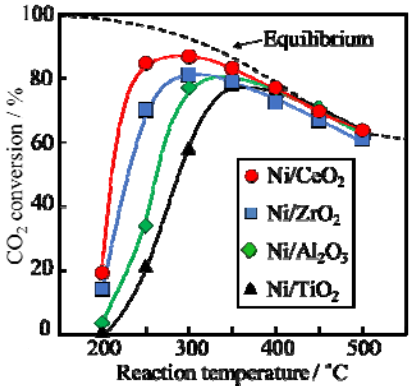

Fig.2 Methanation performance of various Ni-loaded catalysts.

By wash-coating Ni/CeO_2 component on the honeycomb-fin, the two types of the fin catalyst were prepared. One was the honeycomb-fin with straight flow channels (abbreviated as plain-type). Another was that with random flow channels, which was composed by connecting the plain-type fin with 1/4 length in series (abbreviated as stack-type). Figure 3 shows CO_2 conversion of the two types of the structured catalysts comparing with the granular-type catalyst. The prepared fin catalysts showed a high activity at 300°C or more. Then, the activity of the stack-type catalyst was higher than that of the plain-type catalyst. Such tendency might be caused from improving the mass transfer diffusion by stacking the substrate in series. A lower activity at 250°C or less compared with the granular catalyst might be mass transfer limitation. It was thought that the optimum temperature of methanation over the honeycomb-fin catalyst is 300°C as a result.

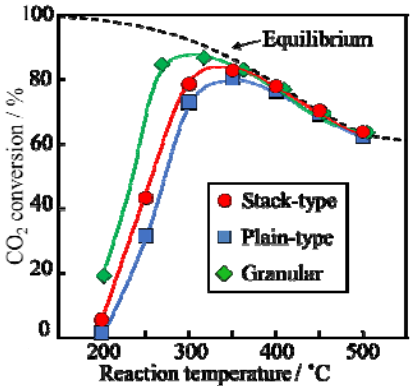

Fig.3 Methanation performance of the structured and granular catalysts.

Figure 4 shows the durability performance and the selectivity to CH_4 over the stack-type structured catalyst for about 120 h at 350°C. The catalytic performance did not deactivate at all. Additionally, the selectivity to CH_4 did not also decrease during the reaction. The developed catalyst has a high and practical potential to be used as a catalyst for the production of energy resource from CO_2.

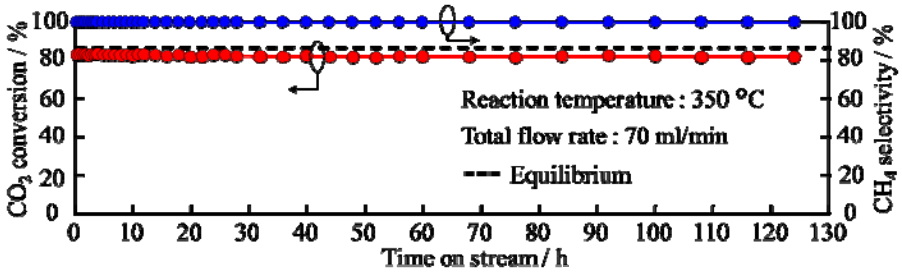

Fig.4 Durability performance of the stack-type structured catalyst.

4 Conclusions

The Ni/CeO_2 was selected as the suitable component of CO_2 methanation, comparing to the Ni/Al_2O_3, Ni/TiO_2 and Ni/ZrO_2. The honeycomb-fin type catalyst with Ni/CeO_2 prepared by the wash-coating showed a relatively high activity. The durability performance of the honeycomb-fin catalyst showed a high and stable performance for methanation.

References

[1] S. Tada, T. Shimizu, H. Kameyama, R. Kikuchi, Int. J. Hydrogen Energy 37 (2012) 5527.
[2] T. Iizuka, Y. Tanaka, K. Tanabe, J. Catal. 76 (1982) 1.

V-PP21

CO_2 Capture by Hierarchical Mesoporous Chabazite Type Zeolites

Hillen L.*, Degirmenci V.

CenTACat, Department of Chemistry and Chemical Engineering, Queen's University, Belfast, Northern Ireland

* lhillen02@qub.ac.uk

Keywords: zeolite, SSZ-13, mesoporous, CO_2 capture

1 Introduction

Zeolites have numerous advantageous properties as an adsorbent for CO_2 capture when compared with their alternatives such as their high thermal stability and tuneable pore sizes [1]. In industrial gas separations, low silica zeolites such as faujasite (FAU) and LTA type zeolites (A, Y, 13X) are used extensively. On the other hand SSZ-13 with the chabazite (CHA) framework is a highly siliceous zeolite which has a less hydrophilic surface due to reduced Al content. Moreover, SSZ-13 differs from FAU and LTA type materials in that all of its cation sites are free to interact with adsorbed molecules. Many cation sites in FAU or LTA are located within hardly accessible sodalite cages [2]. While studies have been carried out to investigate SSZ-13 as a sorbent for CO_2 capture, these studies have been limited to microporous SSZ-13. The well-defined conventional microporous SSZ-13 zeolite crystal has pore size of 3.8 Angstrom which induces diffusion limitations. Introducing mesoporosity; i.e. pores larger than 2 nm, could provide fast adsorption/desorption kinetics alongside the desirable properties of zeolites such as the ability to work well at flue gas temperatures. In this study, we investigated the CO_2 adsorption efficiency of mesoporous SSZ-13 type zeolites.

2 Experimental/methodology

SSZ-13 was synthesised with the use of structure directing agent (SDA) trimethyl adamantyl ammonium hydroxide (TMAdOH). Mesoporous SSZ-13 type zeolites with different aluminium to silica ratios (20, 40) were synthesised by dual templating methods employing SDA and a mesopore generating template (octadecyl-(3-trimethoxysilylpropyl)-ammonium chloride - TPOAc) together [3]. Different template ratios were used to achieve varying degrees of mesoporosity throughout the material (mesoporogen/SDA: 4/20, 8/20 and 12/20). In addition, exchange of Na was performed to obtain Cu, Ca and K analogues along with the proton (H) form of the meso-SSZ-13 (TPOAc/TMAdOH: 8/20) zeolite. Materials were characterised for their structural and textural properties by XRD, N_2 physisorption, SEM and elemental compositions were determined by ICP-AES. CO_2 adsorption was carried out at ambient temperature and pressure by flowing CO_2 (4%) and N_2 (96%) through the adsorbent packed within a quartz tube. The inlet and the effluent CO_2 concentration were determined by a GC equipped with TCD. Adsorption/desorption cycles were carried out to investigate the regenerability of the sorbent.

3 Results and discussion

CO_2 adsorption experiments showed that the ratio of mesoporogen/SDA (TPOAC/TMAdOH) has a substantial effect on the CO_2 adsorption capacity. Na-meso-SSZ-13 prepared with 8/20 template ratio has 1.01 $mmol \cdot g^{-1}$ of adsorption capacity which is higher than that of meso-SSZ-13 (0.94 $mmol \cdot g^{-1}$) synthesized with 4/20 template ratio. Further increase in

mesopore generating template resulted in a higher still adsorption capacity (1.16 mmol·g^{-1} for 12/20 material). The trend in CO_2 adsorption capacity is in agreement with their mesoporous pore volumes and further increase in mesopore generating template results in more amorphous phase observed by XRD analysis suggests optimum synthesis conditions. Adsorption/desorption cycles have been carried out to investigate rate of sorption.

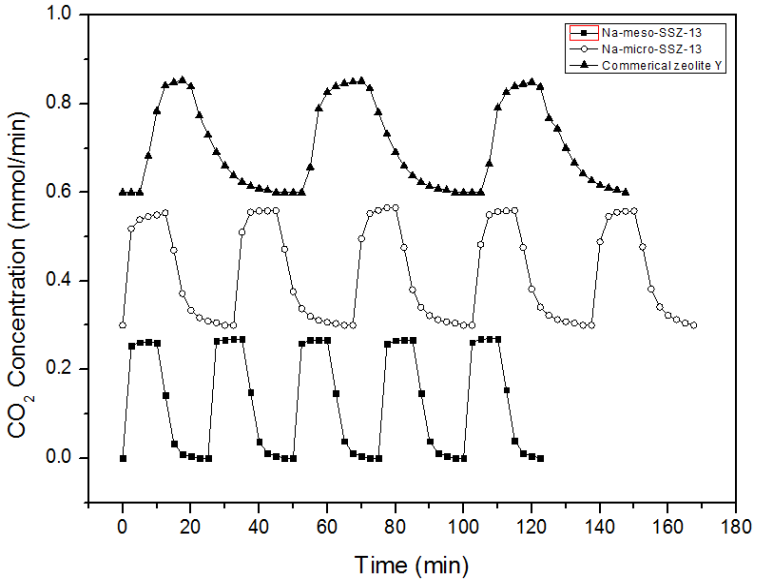

Figure 1. CO_2 breakthrough curves of microporous and mesoporous SSZ-13 compared with that of commercial zeolite Y

It has been observed that commercial zeolite Y has the highest CO_2 adsorption capacity which is 2.85 mmol·g^{-1}. This is substantially higher than the mesoporous SSZ-13 zeolites. However the benefit of introducing mesoporosity can be observed when the rate of adsorption is considered. Zeolite Y has a capture rate of 0.062 mmol·min^{-1}, on the other hand meso-SSZ-13 has 0.070 mmol·min^{-1}. CO_2 breakthrough curves of Na-micro-SSZ-13, Na-meso-SSZ-13 and zeolite Y are depicted in Figure 1. There was no loss of capacity or decrease in adsorption/desorption rate over longer period of time indicating the stability of the mesoporous materials. The faster adsorption/desorption is clearly the result of the introduction of mesopores, which allows fast diffusion of adsorbed gases. In the case of a large scale industrial operation, faster kinetics of mesoporous zeolites provide prospects of substantial savings by easing the requirements of high temperature (pressure) differences in TSA (PSA) cycles and thus decreasing the heating (pumping) costs for the same amount of CO_2 to be captured.

4 Conclusions

In this study we have successfully synthesized hierarchical mesoporous chabazite type zeolites and demonstrated their high potential as an adsorbent for CO_2 capture. The effect of degree of mesoporosity, Si/Al ratio, and the cation on the CO_2 adsorption will be presented.

References

[1] Yang J., Zhao Q., Xu H., Li L., Dong J., Li J., J. Chem. Eng. Data., 57 (2012) 3701-3709
[2] Pham T.D., Liu Q., Lobo R.F., Langmuir, 29 (2013) 832-839
[3] a) Wu L., Degirmenci V., Magusin P.C.M.M., Lousberg N.J.H.G.M., Hensen E.J.M., J. Catal., 298 (2013) 27– 40. b) Wu L., Degirmenci V., Magusin P.C.M.M., Szyja B.M., Hensen E.J.M., Chem. Commun., 48 (2012) 9492-9494.

V-PP22

Autocatalytic Fixation of Carbon Dioxide

Marakushev S.A.*, Belonogova O.V.

Institute of Problem of Chemical Physics, Russian Academy of Sciences, Chernogolovka, Russia

* marak@cat.icp.ac.ru

Keywords: autocatalytic cycles, CO_2 fixation, organocatalysis, bifurcation points, reversibility

1 Introduction

Carbon dioxide conversion to organic chemical compounds is of great importance both in the chemical industry, and in carbon storage in ecosystems. This conversion requires activation of thermodynamically stable CO_2 by metal complexes in various redox states or by metalloenzymes. Recently, organocatalysts (containing no metals) have been intensely studied as coordination substrates for binding and activating CO_2. However, too little attention is paid to investigating chemical autocatalytic CO_2 fixation, a process occurring universally in chemosynthetic microorganisms. It is in autocatalytic cycles of CO_2 fixation that organocatalysis occurring really in nature can be observed.

2 Results and discussion

This paper deals with the origin and development of primitive ancient autocatalytic cycles of CO_2 fixation based on biomimetic combinatorial (modular) bicycles containing the general sequence of reactions intermediates (malate↔fumarate↔succinate) [1]. These three intermediate bicycle reactions are bifurcation points in the direction of specific cycles. The following reactions have succinate as a bifurcation point: (*a*) succinate → fumarate + H_2 ($f(\sigma_1)$ – 3-hydroxypropionate (3-HP) cycle) or (*b*) succinate + CO_2 + H_2 → 2-oxoglutarate + H_2O ($f(\sigma_1, \sigma_2)$ – reductive citrate (RC cycle), where σ_i are the homeostatic parameters of those transformations that may serve as a general characteristic for feedback systems, and $f(\sigma_i)$ is a homeostatic function that defines the reaction route. Here, the H_2 and CO_2 chemical potentials are homeostatic parameters σ_1 and σ_2, respectively. The decrease in H_2 chemical potential (reaction *a*) results in the formation of fumarate, which occurs independently of the CO_2 chemical potential, and the initiation of the 3-HP cycle ($f(\sigma_1)$). The increase in both H_2 and CO_2 chemical potentials (reaction *b*) forms 2-oxogutarate ($f(\sigma_1, \sigma_2)$) and initiates the RC cycle. This well-pronounced negative feedback of the autocatalytic bicycle causes its divergence into these two directions depending on the chemical potentials of the hydrothermal environment. These potentials are the driving forces for natural selection in autocatalytic proto-metabolic systems.

The kinetic irreversibility conditions (i.e., a large deviation from thermodynamic equilibrium used in self-reproduced chemical systems) cannot provide natural selection among autocatalysts [2, 3]. Natural selection only occurs if reaction reversibility and the autocatalyst A_i termination reaction are considered (Fig. 1):

$S + A_i \rightleftarrows 2A_i$ (k_i, k_{-i}) (1)

$A_i \rightarrow W$ (k_w) (2),

where S is a substrate, W is a waste product formed when autocatalyst A_i is irreversibly withdrawn from the autocatalytic cycle, and k_i, k_{-i} and k_w are the forward, reverse, and waste production rate constants, respectively, at the stages of autocatalyst amplification and autocatalyst termination.

A stationary state with positive A_i values is only possible if the reverse reaction (k_{-i}) is involved [4]. At the same time, kinetic irreversibility is necessary for autocatalyst termination (the formation of waste products). Several populations of autocatalysts can coexist at high stationary rate of substrate inflow, but a single population exists at a low rate and does not

disappear at any positive substrate flow [2]. It is considered that carbon fixation of CO_2 using the reducing power of hydrogen or that of less efficient reducing agents is not sufficient to bring about irreversibility [5], that clearly defines the need for the development of reversibility conditions (leading to competitiveness of different reactions of CO_2 fixation cycles).

The activation of thermodynamically stable CO_2 by organocatalysts (dicarboxylic, keto- and hydoxy acids, including phosphorylates compounds) and also metal organocomplexes in various redox states and the simultaneous development of theoretical concepts of autocatalytic coupled cycles of CO_2 fixation will make it possible to perform experimental chemical realization of such systems.

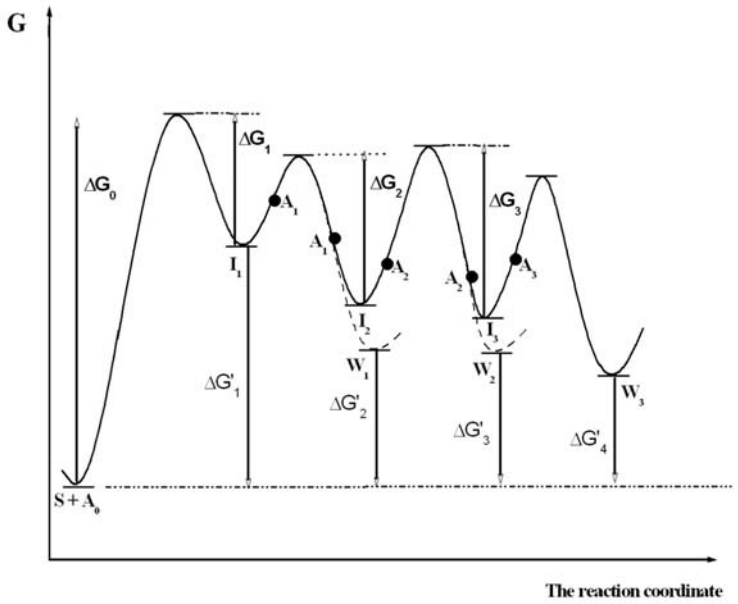

Fig. 1. The scheme of distribution of energy in the autocatalytic cycles. ΔG_0 - activation energy of the "initially" reaction; S – substrate, I_i – reactions intermediate, A_i – cycles autocatalyst, ΔG_1, ΔG_2, ΔG_3 – cost of reaction reversibility, $\Delta G'_1$, $\Delta G'_2$, $\Delta G'_3$, $\Delta G'_3$, $\Delta G'_4$ – cost of reaction irreversibility, W – waste product.

Acknowledgements

This study was supported by the Presidium of the Russian Academy of Sciences (Basic Research Program no. 28, subprogram 1 "The evolution of the organic world and planetary processes")

References

[1] S. Marakushev A., O. Belonogova V. J. Theoret. Biol. 257 (2009) 588.
[2] V. Parmon, Russ J Phys Chem. 76 (2002) 126.
[3] S. Marakushev, O. Belonogova, Orig Life Evol Biosph. 43 (2013) 263.
[4] E. Arslan, I. Laurenzi, J Chem Phys. 128 (2008) 015101.
[5] R. Pascal, A. Pross, J. Sutherland, Open Biol. 3 (2013) 130156.

V-PP23

Surface Oxidation Mechanism of Pb-Based Materials by Utilization of CO_2 as an Oxidant

Calisan A., Uner D.*

Chemical Engineering Department, Middle East Technical University, Ankara, Turkey

* uner@metu.edu.tr

Keywords: Mars-Van Krevelen mechanism, shrinking core model, CO_2 reduction

1 Introduction

CO_2 sequestration is the key challenge of the 21st century chemical and energy production. Processes where CO_2 is used as a raw material for further chemical manufacture will probably be the ultimate goal of the carbon neutral technologies. The potential of CO as a syngas component increases the attention to chemical looping technologies where metal oxide is used as oxygen carrier. Mars and Van Krevelen (1954) described the principle of this mechanism as the vacancy created by the reaction is filled by a reactant atom from the bulk, rather than the gas phase [1]. Ceria fits Mars-Van Krevelen mechanism during dry reforming reactions since a series of surface reactions occur in the active sites. Ceria can supply oxygen from its lattice due to its high oxygen storage and transport capacity. The transported oxygen can be replaced by dissociation of CO_2. It is known that Ce^{3+} surface sites is active during the adsorption and activation of CO_2. [2]

2 Experimental/methodology

Technical grade metallic lead rods were used for the reaction tests. 495.9 gr metallic lead rods were put into reactor. The reactor and its oven was specially designed for the metal oxidation reactions. Oxidative gas was selected as CO_2 with a flow rated of 50ccpm. Reactor was heated with a rate of 8 ^oC/min. Product gas stream was sent to FT-IR's gas cell for continuous spectral measurement. A gas cell apparatus was installed to Perkin Elmer Spectrum 100 FT-IR Spectrometer for detection of change in product gas of the reactor output. CO formation rate was observed from change in molecular vibrational energy of product gas.

3 Results and discussion

The CO_2 was successfully reduced over Pb according to the reaction $Pb + CO_2 \rightleftharpoons PbO + CO$ as shown in Figure 1. The change in the wavelength 2000-2200cm^{-1} shows the evolved CO in the gas phase. The magnitude of the CO peaks increases as temperature increases. The first signals was observed after 100 ^oC. The magnitude of this signal is small and stays stable up to 400 ^oC. The CO formation increases between 400 and 800 ^oC. Reactor was kept isothermal when 800 ^oC was reached since previous experiments showed that the temperatures higher than 800 ^oC increases the possibility of thermal decomposition of formed lead oxide. After the experiment, samples were collected from the surface of oxidized lead. It was found that carbon deposits at the surface was detected from SEM/EDX analysis. The coke formation was believed to be the clue of Boudard reaction.

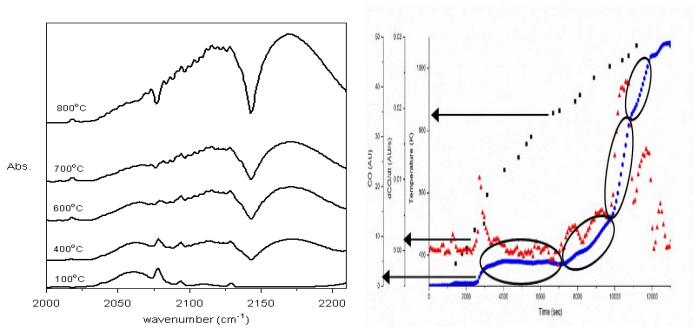

Figure 1: CO evolution band (left), CO formation as temperature increases (right)

Rate of the CO evolution was calculated in order to observe steps of CO_2 reduction steps. Mainly four periods were observed. 1st period was the longest stable period of the experiment. It was found that CO evolution rate was stable between 200 °C and 550°C. The periods 2nd to 4th shows the change in the rate of CO evolution period. Firstly, slow increase in the CO evolution was observed between 550 °C and 650°C. Then, CO formation increases rapidly up to 720 °C. The rate was getting slower up to 800 °C and became stable during the isothermal period.

It is assumed that shrinking core model fits the mechanism of Pb-based material oxidation. As the CO_2 is reduced by metallic lead, the thickness of the lead oxide layer increases. The thickness of the PbOx layer determines the magnitude of the diffusion resistance. In the mass transfer region, activation energy was estimated as $E_a = 120.9 kJ/mole$ as shown in Figure 2.

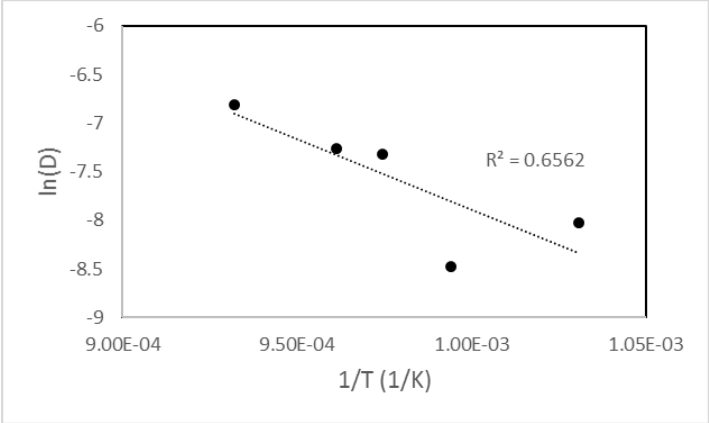

Figure 2: Activation energy estimation in mass transfer region

4 Conclusions

CO_2 reduction is increases considerably after 400°C. Formed CO was monitored by FTIR. Shrinking core model was applied to the FTIR data to find activation energy. By the assumption of mass transfer region, it is found that $E_a = 120.9 kJ/mole$ between 700 °C and 800 °C. Formed lead oxide was regenerated via thermal decomposition around 880°C. Mars and van Krevelen mechanism was proposed for the surface reaction between CO_2 and Pb. These studies encouraged that Mars and van Krevelen reaction rate can be applied for CO oxidation on PbO**.**

References

[1] P. Mars, DW. Van Krevelen, *Spec. Suppl. te Chem. Eng. Sci*. 3 (1954) 41.
[2] C. DE Leitenburg, A. Trovarelli. J. Kaspar. *J Catal.* 166 (1997) 98

V-PP24

Catalytic Activity of Supramolecular Systems Based on Mono- and Dicationic Surfactants with Aromatic or Heterocyclic Moieties

Gaynanova G.A.*, Yackevich E.I., Lukashenko S.S., Mirgorodskaya A.B., Zakharova L.Ya.

A.E. Arbuzov Institute of Organic and Physical Chemistry, Kazan Scientific Center, Russian Academy of Sciences, Kazan, Russia

* ggulnara@bk.ru

Keywords: supramolecular, catalysis, cationic, surfactant, micelle, microemulsion

1 Introduction

The catalysis of reactions in supramolecular systems based on surfactants is of current interest. The compartmentalization of reagents within nanosized micelles or microdrops results in a sharp increase in their local concentrations and affects their microenvironment thereby influencing their reactivity. This provides wide possibility for the control of the rate of ion-molecular reactions, namely hydrolytic cleavage of esters. These processes generally proceed in Stern layer of aggregates and dramatically depend on surfactant structure and charge, magnitude of the micellar surface potential.

In this work a comparative study of the aggregation behavior and catalytic effect on the rate of transfer of the phosphoryl and acyl group in different organized media based on cationic surfactant was carried out. To optimize the relationship between a structure and catalytic activity, it was investigated amphiphiles of varying nature, particularly mono- and dicationic surfactants with aromatic or heterocyclic moieties and different length of alkyl chain and spacer.

2 Experimental

The surface properties of the surfactants were studied on a K6 tensiometer (Kruss, Germany) using the Du Nouy ring detachment method at 25 ^{o}C. The bromide ion concentration in surfactant solution was determined using I-160MI ion meter equipped with a bromide-selective electrode. Average aggregate size and zeta potential were measured by dynamic and electrophoretic light scattering techniques (Malvern ZetaSizer Nano, Malvern Instruments, UK).

The surface potential was defined by the method of spectral probes. *p*-Nitrophenol was used as a probe. Acid-base properties of *p*-nitrophenol were studied by measuring the absorption of its ionized form at different pH values. The spectra were recorded on a Specord 250 Plus UV-VIS spectrophotometer in quartz cells

The reaction kinetics was studied spectrophotometrically on a Specord 250 Plus UV-VIS spectrophotometer in thermostated cuvettes. The reactions were monitored through changes of optical density of the solutions at the wavelength of 400 nm (formation of *p*-nitrophenolate anion).

3 Results and discussion

Aqueous micellar systems and oil-in-water microemulsions based on convenient and gemini cationic surfactants has been formed. Surfactant series with trialkylammonium, dimethylbenzilammonium and morpholinium head groups are involved in the study. Concentration boundaries of their existence and structural transitions of aggregates have been established. Quantitative parameters characterizing the aggregation behavior of the systems

(critical micelle concentrations, degree of counterion binding, aggregation numbers, the size and surface potentials) were obtained.

An important property of supramolecular systems determining their use in catalytic compositions is the ability to solubilize hydrophobic compounds. In this work, we studied the solubilization of nonpolar esters, dyes and spectral probes in the micellar solutions and microemulsions based on the cationic surfactants. Then we investigated their catalytic effect in the reaction of nucleophilic substitution. Micelles and microemulsions rate effect was studied toward to alkaline hydrolysis of *p*-nitrophenylic esters of carbonic acids (acetate, caprylate, caprinate, laurate, and myristate) and phosphorus acid esters. Changing the values of the observed rate constant of the esters hydrolysis were analyzed as a function of surfactants concentration, their structure and morphology of aggregates formed in the tested systems. Correlations between aggregation characteristics and reaction rate have been found. The most pronounced catalytic effect was observed for dicationic surfactants: maximal acceleration of *p*-nitrophenyl esters hydrolysis (up to 250 times) was observed at low concentration of surfactant within the area of existence of spheroid micelles. It was shown that surface potentials of the normal microemulsions are lower than those for the micellar solutions based on the same surfactant by ca. 100 mV. This is the main reason of the fact that rate constants of hydrolysis of esters are higher (by factor of 3–10) in micellar solutions as compared to microemulsions.

4 Conclusions

Supramolecular systems based on mono- and dicationic surfactants provide large opportunities for targeted design of systems with a high solubilizing capacity and controlling catalytic effect in ester bond cleavage. This makes it possible to recommend them for the wide application in chemical catalysis.

Acknowledgements

This work is supported by the Russian Science Foundation (grant **№ 14-50-00014)**

V-PP25

Supramolecular Catalytic System Based on Amphiphilic Triphenylphosphonium Bromide for the Hydrolysis of Phosphorus Acid Esters

Gaynanova G.A.[1*], Vagapova G.I.[1], Valeeva F.G.[1], Galkina I.V.[2], Zakharova L.Ya.[1], Sinyashin O.G.[1]

1 - A.E. Arbuzov Institute of Organic and Physical Chemistry, Kazan Scientific Center, Russian Academy of Sciences, Kazan, Russia
2 - Kazan Federal University, Kazan, Russia

* ggulnara@bk.ru

Keywords: triphenylphosphonium bromide, hydrolysis, phosphorus acid esters

1 Introduction

The biomimetic nature of micellar catalysis permits to achieve significant enhancement of reaction rate under mild conditions. The main factors determining the catalytic effect is a factor of the microenvironment change and increase the local concentration of reagents. The quantitative assessment of these parameters will shed light on the mechanism of the reaction. The most studied cationic surfactants in this context are alkyltrimethylammonium and alkylpyridinium halides. However, the change of the atom of the charged center and transition to surfactant with highly hindered head groups might have a significant impact on the catalytic effect. The aim of this work is the investigation of alkyltriphenylphosphonium bromides (TPPB) properties such as the solubilizing activity to the hydrophobic substrates and catalytic effect on the alkaline hydrolysis of phosphorus acid esters.

2 Experimental/methodology

The rate of substrate hydrolysis was monitored through changes in absorbance at 400 nm (the formation of p-nitrophenol anion) using the spectrophotometer Specord 250 Plus (Germany) in thermostated cuvettes with a pathway of 1.0 or 0.5 cm. The kinetic dependences processing was carried out using the Berezin equation and original computer programs. Aggregation numbers were calculated using pyrene (98%, Acros Organics) as a probe.

3 Results and discussion

It is well known that the transfer of a phosphoryl group is important in the processes taking part in an organism; therefore investigated phosphonium salts were tested as catalysts in the nucleophilic substitution reaction of p-nitrophenyl esters of alkylchloromethylphosphonic acid when the hydrophobicity of amphiphilic compound and substrate vary. A series of trimethylammonium bromides (TMAB) was studied under the same conditions for determining of head group role.

The kinetic curves of substrate hydrolysis have maximum that can be explained by the strong binding of the substrate with the micelles, which leads to transition of the substrate into aggregates at low concentrations of surfactant. Further increasing the concentration of the amphiphilic compound causes a growth in the number of micelles, and therefore the dilution of the reagents (decrease of the rate constant). The processing of kinetic dependence by Berezin equation allows to obtain rate constants in the micellar phase and the binding constants of the reactants.

4 Conclusions

The comparison of the results obtained for TPPB-series with the ammonium analogues was carried out. It was found that the higher the value of rate enhancement for TPPB achieved through concentration factor can be explained by the high aggregation activity.

Acknowledgements

This work is supported by Russian Scientific Foundation, grant no. 14-50-00014

V-PP26

Modified by Lanthanum Cerium - Containing Catalysts for Converting Bio-Ethanol into Ethylene

Dossumov K.[1], Yergazieva G.Y.[2*], Telbayeva M.M.[2], Tayrabekova S.[3], Kalihanov K.[3], Suyunbayev U.[2]

1 - Centre of Physic Chemical Methods of Investigation and Analysis, Almaty, Kazakhstan
2 - The Institute of Combustion Problems, Almaty, Kazakhstan
3 - Kazakh National University named Al-Farabi, Almaty, Kazakhstan

* ergazieva_g@mail.ru

Keywords: cerium, catalyst, bio-ethanol, ethylene

1 Introduction

Recently the attention of researchers is concentrated on bio-ethanol use, as the raw materials alternative to oil. From ethanol it is possible to receive by a catalytic method important chemical products as a divinyl, aromatic hydrocarbons, ethylene, hydrogen, etc. Large environmental friendliness, and also profitability of similar productions on condition of saturation of the industry products of biomass are caused by undoubted advantages in comparison with using as raw materials of an oil fraction, natural and casing-head gases.

Ethylene represents the considerable interest as raw materials for the production organic synthesis, from it receive more than 200 valuable connections the most important of which are ethyl chloride, ethylene dichloride-1,2, ethylene oxide, ethylene glycol and others.

Ethylene is received generally by a pyrolysis method as raw materials use the ethane, propane, butane containing in casing-head gases of oil production, gases of thermal and catalytic cracking, and also fluid hydrocarbons: natural gasoline and low-octane gasoline - naphthas fractions of straight distillation of oil. However this process endothermic also demands high temperatures of carrying out reaction. For ecological, and also economic reasons to use as a feed stock for receiving olefins of C_1-C_4 alcohols more actually [1,2].

Earlier the metal oxides (Cr, Cu and Ce) supported on various carriers (Al_2O_3, Al_2O_3HZS-5 and CaA) were investigated in the conversion of bio-ethanol to ethylene. The highest activity was exhibited by the catalyst Ce/γ-Al_2O_3. In this paper the influence of lanthanum oxide as modifying additives to structure Ce/γ-Al_2O_3 catalyst was investigated.

2 Experimental/methodology

The catalytic activity of the catalysts was studied in the flow regime using an inert gas medium in the 250–450°C range of temperatures with hourly space velocities (HSVs) of 1500–13000 h–1. The raw materials and the reaction products were determined using a gas chromatograph (GC-1000 LLC "Chromos"). The catalysts were prepared via incipient wetness impregnation of the support, followed by drying at room temperature and 300°C, with subsequent calcination at 500°C for 3 h. Before each experiment, the catalysts were reduced in a hydrogen flow for 1 h at 500°C and atmospheric pressure.

3 Results and discussion

The effect of lanthanum oxide on the catalyst activity Ce / γ-Al_2O_3 was investigated in the dehydration reaction of ethanol in the temperature range of 300 - 400C, at HSV = 6000 hr^{-1}. The results showed that at a reaction temperature of 350 °C a conversion of ethanol was 100%. The catalysts by activity in the dehydration of ethanol are located in a row: 3%Ce+1%La/γ-Al_2O_3 (C_{C2H4}= 96 vol.%) > 3%Ce+2%La/γ-Al_2O_3 > (C_{C2H4}= 93 vol.%) > 3%Ce+3%La/ɣAl_2O_3 (C_{C2H4}=

86 vol.%). The range activity of catalysts changes with increase of reaction temperature to 400°C: 3%Ce+3%La/γAl_2O_3 (C_{C2H4}= 98 vol.%) > 3%Ce+2%La/γ-Al_2O_3 (C_{C2H4}= 92 vol.%) > 3%Ce+1%La/γ-Al_2O_3 > (C_{C2H4}= 89 vol.%).

Textural characteristics of the developed catalysts were revealed by BET method. The results are presented in Table 1. The modifying of cerium catalyst by lanthanum (1 mass. % up to 3 mass. %) leads to increase of a specific surface area of the catalyst from 162 to 174 m^2/g. The phase composition of the catalysts was determined via electron microscopy. The results of electron microscopy showed that Ce/γ -Al_2O_3 catalyst characterized by formation a particles with 10 nm in size. Doping Ce/γ-Al_2O_3 with lanthanum increases the dispersion of the catalyst, but some aggregates of fine (2 nm) particles are observed in the aggregates, along with particles 10 nm in size.

Table 1. Textural characteristics of catalysts

Catalyst	Temperature of treatment	Surface Area /(m^2/g)	Pore volume /(cm^3/g)	Average pore size /nm
3% Ce/ Al_2O_3	500	133	0,079	2,36
3%Ce + 1%La /Al_2O_3	500	162	0,069	1,71
3%Ce+2%La /Al_2O_3	500	173	0,074	1,72
3%Ce+3%La /Al_2O_3	500	174	0,075	1,72

4 Conclusions

Thus doping Ce/γ-Al_2O_3 with lanthanum leads to formation of nanoparticles (2 nm) and to increase its surface area, thereby increasing the catalyst efficiency in the getting ethylene from bio-ethanol.

References

[1] R. Kanaparthi, Mei Hui L., Yi-Fan H., A. Borgna, Catalysis Communications. 10 (2009) 567.
[2] M. Ryan Westa, L. Edward, A. Dante, *Catalysis Today*. 147 (2009)115.

V-PP27

An *in-situ* FTIR-DRIFTS Study on Carbon Dioxide Reforming of Methane on Pt-Ni/Al_2O_3

Demirel S.E., Aksoylu A.E.*

Department of Chemical Engineering, Bogazici University, Istanbul, Turkey

* aksoylu@boun.edu.tr

Keywords: *in-situ* FTIR-DRIFTS, catalytic hydrogen production, dry reforming, heterogeneous catalysis

1 Introduction

Carbon dioxide reforming of methane (CDRM) is an important reaction for the utilization of the two major greenhouse gasses, namely methane and carbon dioxide [1].The aim of this work is to understand the routes and mechanistic steps of the CDRM reaction on the active sites of the Pt-Ni/Al_2O_3 bimetallic catalysts with different Ni:Pt ratios, which had been designed by our group and shown to have high activity and selectivity in CDRM reaction. The freshly reduced bimetallic catalysts with different Ni:Pt ratios, i.e. 0.2Pt-15Ni/Al_2O_3 and 0.3Pt-10Ni/Al_2O_3,were characterized by a detailed Fourier Transformed/Diffuse Reflectance Infrared (FTIR-DRIFT) analysis via using CO as a probe molecule in order to define the planes of the active phases present on the catalysts. In addition, FTIR-DRIFT analysis was performed under the flow of individual reactants (CO_2 and CH_4) and reactant mixtures, both at room temperature and at the highest possible temperatures which allow reliable operation of the FTIR-DRIFT cell, aiming to understand the adsorption properties of the reactants and to determine the species formed on the active sites during the CDRM reaction.

2 Experimental

The catalyst samples were firstly reduced *ex situ* at 773 K for 2 h under H_2 flow. The FTIR absorbance spectra were collected on a Bruker Vertex 70V equipped with a Mercury-Cadmium-Telluride (MCT) detector. The spectra were collected at a 4 cm^{-1} resolution in the 4000-600 cm^{-1} range. Ex situ reduced catalyst samples in a very fine powder form were diluted with dry KBr for improved S/N ratio. Prior to the tests, an *in-situ* catalyst pre-treatment was performed. First, sample was heated to 573 K under He flow. An *in-situ* reduction under a flow of %10 H_2/He at 573 K was performed for 1 hour followed by a He flush at 593 K for 1 h. The spectrum of the solid catalyst taken after the pre-treatment was subtracted from the spectrum of the catalyst obtained after exposure to the adsorption mixture. Individual adsorption and reaction experiments were conducted both at room temperature and at 573 K under 1% CO/He, 10% CH_4/He, 10% CO_2/He and 40%CO_2-40%CH_4-20%He mixtures.

3 Results and discussion

Investigation of the metal surface of both of the catalysts by CO adsorption at room temperature revealed that three bands, associated with CO interaction with alumina support, were observed over both catalysts (Fig.1 a-b). Those bands can be identified at around 2150, 1630 and 1360 cm^{-1}. Last two of those bands can be assigned to the carbonate species produced upon contact of CO with alumina support while the first one shows H-bonding of CO with surface hydroxyl groups of alumina on Al-ions [2-4]. As the Ni:Pt ratio decreased, bands around 2050 cm^{-1} became more prevalent, indicating that although it may be superimposed by the band of linear CO on Ni particles, there is also a band around 2050 cm^{-1} associated with the linear adsorption of CO on Pt sites. Peaks at 1850 cm^{-1} and 1929 cm^{-1} can be assigned to bridged CO

on Ni (111) and Ni (100) planes [4-5]. Those apparent peaks obtained at room temperature were diminished as the CO adsorption experiments were conducted at 573 K. The band around 2050 cm^{-1} was still observed on 0.3Pt-10Ni/Al_2O_3 indicating a significant interaction between CO and the catalytic surface, which is most probably strengthened by Pt via surface alloy formation.

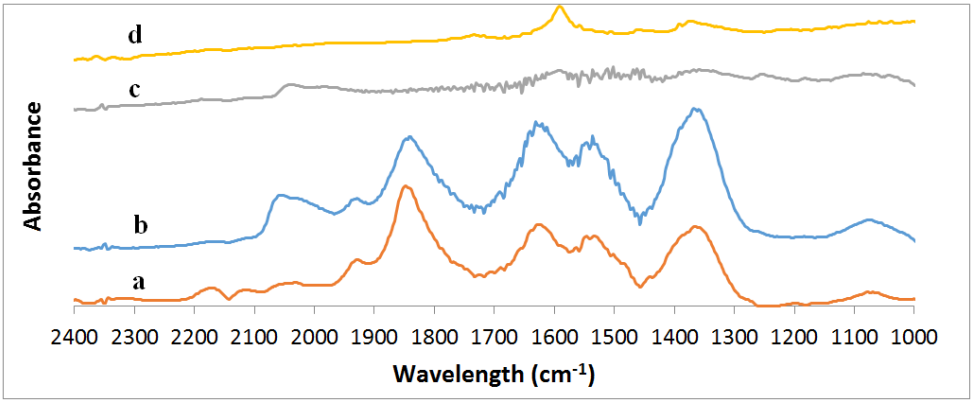

Fig. 1. Spectra obtained upon He flush following %1CO adsorption on: a) 0.2Pt15Ni at room temperature, b) 0.3Pt10Ni at room temperature, c) 0.3Pt10Ni at 573 K, d) 0.2Pt15Ni at 573 K.

In CO_2 and CH_4 adsorption experiments, bands around 1630, 1540 and 1360 cm^{-1} were still observed indicating that alumina support is an active support in dissociation of these reactants and in forming carbonate species (figures not shown). As the CO_2 adsorption test temperature was increased to 573 K, peak at 1540 cm^{-1}, associated with monodentate carbonate species, was strengthened. In CH_4 adsorption tests, C-H stretching band was observed at 3016 cm^{-1} both at room temperature and at 573 K. Although the bands related with carbonate species were weakened as the adsorption temperature was increased, bands were still significantly larger on the 0.3Pt-10Ni/Al_2O_3.

4 Conclusions

The results obtained from the in-situ FTIR-DRIFTS analysis revealed that Pt has a significant role on the structure of the active sites as well as on course of the reaction by both affecting the surface carbonate formation and CO adsorption mechanisms. FTIR-DRIFT results indicate that CO_2 activation/utilization is directly affected by the Ni:Pt ratio of the bimetallic catalysts.

Acknowledgements

This work is financially supported by TUBITAK through project 111M144, and Boğaziçi University through project BAP-M6755.

References

[1] S. Ozkara-Aydınoğlu, E. Özensoy, A. E. Aksoylu, *Int. J. Hydrogen Energy*. 34 (2009) 9711-9722.

[2] F. Di Gregorio, L. Bisson, T. Armaroli, C. Verdon, L. Lemaitre, C. Thomazeau, *App. Cat. A: General*. 352 (2009) 50-60.

[3] T. Montanari, L. Castoldi, L. Lietti, G. Busca, *App. Cat. A: General*. 400 (2011) 61-69.

[4] F. Gökaliler, *'Characterization and Performance Analysis of Fuel Flexible OSR-WGS catalysts'*, Ph. D. Dissertation, Bogazici University (2012).

[5] J. A. C. Dias, J. M. Assaf, *J. Power Sources*. 130 (2004) 106-110.

V-PP28

An Experimental Study on Characterization and Mixed Reforming Performance of Co-Based Bimetallic Catalysts

Erşahin S.[1], Çağlayan B.S.[1,2], Aksoylu A.E.[1*]

1 - Boğaziçi University, Department of Chemical Engineering, Istanbul, Turkey
2 - Advanced Technologies R&D Center, Boğaziçi University, Istanbul, Turkey

* aksoylu@boun.edu.tr

Keywords: mixed reforming, catalytic syngas production, heterogeneous catalysis, CO_2 utilization

1 Introduction

Catalytic dry reforming of methane (CDRM) utilizes two major greenhouse gases (CO_2 and CH_4) in the process and produces syngas with more suitable H_2/CO ratio for further applications like Fischer-Tropsch synthesis, both of which have great importance for environmental and industrial aspects. There are two major drawbacks of CDRM process. CDRM is a highly endothermic reaction (800-900°C), which causes catalyst sintering. Additionally, methane cracking and Boudouard reactions creates carbon deposition which leads to catalyst deactivation. The drastic operating conditions impose the investigation on the development of new catalysts with improved stability and activity through preventing metal sintering and reducing coke formation. Stable CDRM activity is achieved when carbon formed at the methane dehydrogenation sites are cleaned by the surface oxygen formed from CO_2 disproportionation. Previous studies in our group have shown that Co-Ce/ZrO_2 has high activity with some activity loss due to coke formation [1, 2].CDRM catalysts that suffer from severe coke deposition may sustain stable and high activity when additional oxygen source other than CO_2 is present in the process [3].

The aim of this study was to investigate the mixed reforming performance of Co-Ce supported on ZrO_2 in a detailed fashion. In this context, CH_4:CO_2 ratio in the feed, the presence and amount of H_2O or O_2 in the feed stream and reaction temperature were considered as the experimental parameters. The effects of type and amount of additional oxygen source in mixed reforming on the oxidation states of the active phases, Co and Ce, were studied by XPS.

2 Experimental

Co-Ce catalyst was prepared by sequential impregnation. Co-Ce/ZrO_2 catalyst was calcined *in situ* in dry air (30 mL/min) for 4h at 773K and subsequently reduced *in situ* under H_2 flow (50 mL/min) for 2 h at 773 K as pre-treatment. CDRM + SR (Steam Reforming) mixed reforming performance tests were performed in a quartz down-flow micro-reactor at 873K, 923K and 973K with CH_4/CO_2 feed ratios of 2 and 1 and S/C ratios of 1 and 0.5. Feed and product streams were analysed by using an Agilent Technologies 6850 gas chromatograph (GC) equipped with a Thermal Conductivity Detector (TCD) and HayeSep D column. CDRM + POX (Partial Oxidation) mixed reforming performance tests were performed at 873K, 923K and 973K with CH_4/CO_2 feed ratios of 2 and 1, and for 4%, 7% and 10% O_2 concentrations in the feed. Feed and product streams were analysed by using an Agilent Technologies 6850 GC equipped with a TCD and Carboxen 1000 column. Freshly reduced and spent Co-Ce/ZrO_2 samples were characterized using X-Ray Photoelectron Spectroscopy (XPS), and the oxidation states of the metallic species present on the catalysts were analysed.

3 Results and discussion

The effects of temperature, CH_4/CO_2 feed ratio, additional oxygen source type and its

concentration in the feed were investigated; as an example, the effects of steam/carbon feed ratio and temperature on methane conversion in CDRM+SR is presented in Figure 1.

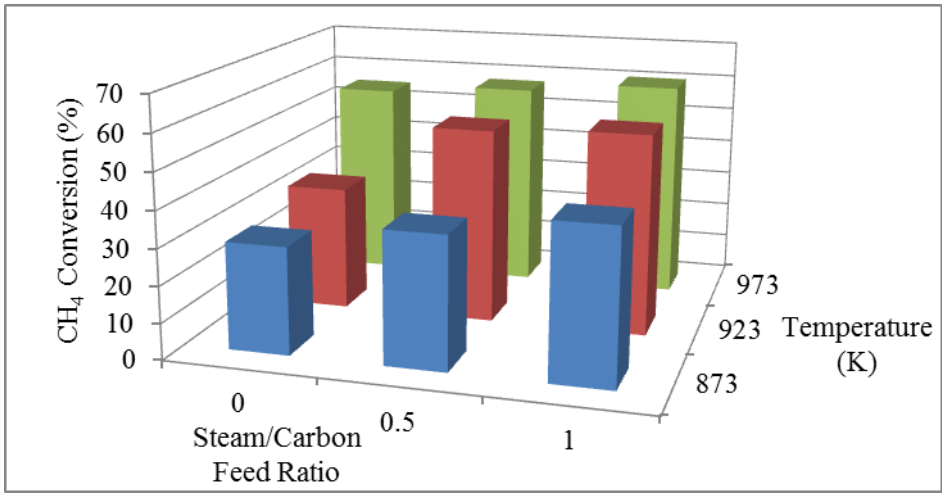

Fig. 1. CH_4 at the end of 6 h TOS conversion values obtained for CH_4/CO_2 feed ratio of 2.

As CDRM is favored at higher temperatures due to its extreme endothermicity, mixed reforming activity was increased with increasing temperature. Co-Ce catalyst has improved stability in mixed reforming compared to those in individual CDRM. The possibility of controlling the H_2/CO product ratio and reaching the same activity, i.e. methane conversion, at lower temperatures are the other advantages of mixed reforming over CDRM. The results showed that methane conversion increased with decreasing CH_4/CO_2 feed ratio indicating the additional methane was not fully utilized by the catalyst. Another advantage of using low CH_4/CO_2 ratio in mixed reforming was suppressing H_2/CO ratio close to unity. In CDRM + POX, the H_2/CO product ratio was constant and close to unity for the whole temperature range, whereas in CDRM+SR, the H_2/CO product ratio was pushed close to unity at high temperatures. The additional oxygen source, steam or oxygen, did not have a significant effect on activity, i.e. CH_4 and CO_2 conversion values. XPS analyses on spent samples showed that the presence and type of the additional oxygen source has a non-negligible effect on the oxidation states of the active phases.

4 Conclusions

The results showed that H_2/CO product ratio can be controlled, and the addition of steam or oxygen improved overall performance and stability in mixed reforming compared to those in individual CDRM. In CDRM + POX mixed reforming, the H_2/CO product selectivity was much closer to unity than that in CDRM + SR mixed reforming.

Acknowledgement

Financial support provided by TUBITAK through Project 111M144 and by Boğaziçi University through project BAP M6755 is greatly acknowledged. Financial support provided by Prof. Mahir Arıkol scholarship fund is greatly appreciated.

References

[1] S. Ozkara-Aydınoglu, A. E. Aksoylu, *Catalysis Communications*.11 (2010) 1165-1170.
[2] S. Ozkara-Aydınoglu, A. E. Aksoylu, *International Journal of Hydrogen Energy*.11 (2010) 1165-1170.
[3] V. R. Choudhary, Kartick C. Mondal, *Applied Energy*. 83 (2006) 1024-1032.

V-PP29

DR UV-Vis Study of Copper(II) Oxo/Peroxocomplexes in Cu-Substituted ZSM-5

Yashnik S.A.[1*], Taran O.P.[1,2], Ismagilov Z.R.[1,3], Parmon V.N.[1,4]

1 - Boreskov Institute of Catalysis SB RAS, Novosibirsk, Russia
2 - Novosibirsk State Technical University, Novosibirsk, Russia
3 - Institute of Coal Chemistry and Material Science, Kemerovo, Russia
4 - Novosibirsk State University, Novosibirsk, Russia

* yashnik@catalysis.ru, oxanap@catalysis.ru

Keywords: Cu-ZSM-5 copper, peroxocomplex copper, oxocomplex, UV-Vis spectroscopy

1 Introduction

All methanotrops produce a copper-containing monooxygenase. There is a binuclear copper complex that is able to reversible oxidation/reduction cycle from Cu(I) to Cu(II) as well as to a oxygen activation. So, elucidation of the oxygen activation pathways are very important for the understanding the mechanism of oxidative action of monooxygenase type enzymes. The Cu-containing zeolites [1] are of interest for biomimetic approach due to the square-plain coordination of Cu(II) ions in copper oxide/hydroxide clusters and nanoparticles [2], easy transformation Cu(I) – Cu(II) [3], and formation of α–like site [1,4].

Here the DR UV-Vis spectroscopy was used to reveal condition where a peroxo/oxo complexes copper (II) are formed in CuZSM-5 catalysts.

2 Experimental

Two samples of Cu-ZSM-5 were prepared by ion-exchange of H-ZSM-5 with aqueous and ammonia solution of copper acetate, at room temperature. After 48 hours, the zeolite samples were filtered and washed with distilled water. The samples were dried and calcined in air at 500°C. The copper content was 1 and 2.8 wt.%, respectively.

Capacity of Cu-ZSM-5 to stabilize the oxo/peroxocomplexes was studied using activation in hydrogen peroxide (solid/solution) and in O_2 atmosphere (solid/gas).

For activation in H_2O_2, the Cu-ZSM-5 sample (pellets of 0.1-0.25 mm) was placed into the quartz cell and treated by 1M solution of H_2O_2 or solution containing 1M H_2O_2 with 0.01 or 0.02 M NaOH. The weight ratio of zeolite to solution was 1/3.

For activation in O_2, the Cu-ZSM-5 sample (pellets of 0.1-0.25 mm) was placed into the home-made UV-Vis DR quartz cell, evacuated into vacuum at 25°C and treated in 250 mbar of O_2 at 400°C.

For alternative pathway, the sample was evacuated into the UV-Vis DR cell at 400°C, after that 130 mbar of oxygen was added.

UV-Vis DR spectra of Cu-ZSM-5 were obtained at room temperature using a Shimadzu UV-2501 PC spectrophotometer equipped with a diffuse reflectance accessory (ISR-240 A).

3 Results and discussion

The square-plain copper-oxide structure is found to form peroxocomplexes at adding of hydrogen peroxide. This reaction takes place mainly in alkaline solution with pH 10 and above. The square-plain copper-oxide structure are present in the over-exchanged Cu-ZSM-5 and formed from isolated Cu(II) ions at treatment of the under-exchanged Cu-ZSM-5 by sodium hydroxide solution. Peroxocomplexes dicopper(II) over external surface and inside channels of Cu-ZSM-5 contain two Cu(II) ions bonding through terminal OOH-group and bridged OO-

group. They observed as ligand to metal charge transfer band (CTB L-M) at 21500 and 26500 cm^{-1} of DR UV-Vis spectra, respectively (Fig.1, C.3). They are similar to peroxocomplexes copper(II) in homogeneous copper nitrate solution and colloid solution of $Cu(OH)_2$ [2]. Over Cu-ZSM-5, they are gradual destroyed, and more stable terminal complex CuOOH (35500 cm^{-1}) is formed. The latter was observed by UV-Vis DR even after a drying of Cu-ZSM-5.

Unlike previously observed in [3], UV-Vis DR bands at 22000 and 28000 cm^{-1} attributed to Cu-dimers [3] were not observed in the our CuZSM-5 activated under 1st oxidizing conditions (Fig. 2, C.2). However, weakly intensive a.b. at 22500 and 27900 cm^{-1} appeared in UV-Vis DR spectra after activation of CuZSM-5 in vacuum at 400°C (Fig.2, C.3). The absorbance at 22500 cm^{-1} became stronger under subsequent high-temperature calcination of vacuum-dehydrated Cu-ZSM-5 in oxidizing atmosphere (2^d mode, Fig.2, C.4). Similar changes in the UV-Vis DR spectra of Cu-MFI were observed previously by Praliaud [5] and Teraoka [6]. They connected UV-Vis DR band at 22500 cm^{-1} with reoxidation of Cu^+ ions of nearby Cu^{2+}-Cu^+ or Cu^+-Cu^+ and attributed its to CTB L→M in copper dimer bridged by extra-lattice oxygen [5,6]. Such copper pairs have to be formed due to reduction by vacuum of Cu^{2+}-ions in structures with extra-lattice oxygen, for example in dimer, chain-like and square-planar copper-oxide structures.

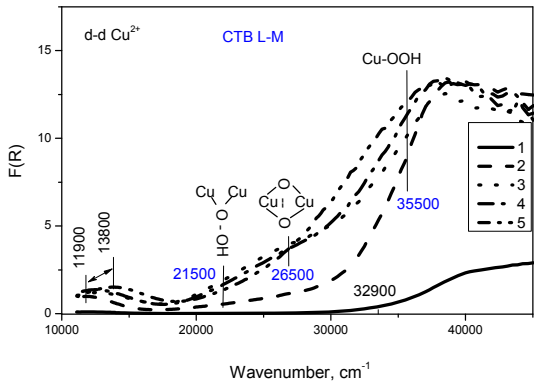

Fig. 1. UV-Vis DR spectra of 1%Cu-ZSM-5-30 before (1) and after adding 1M solution of H_2O_2 (2), 1M solution of H_2O_2 with 0.01 or 0.02 M NaOH (3 and 4) in 10 min and in 5 hrs (5).

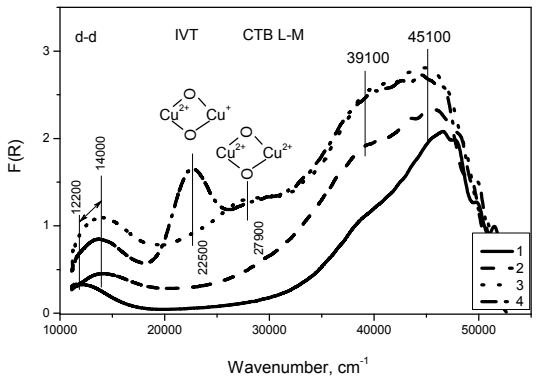

Fig. 2. UV-Vis DR spectra of 2.8%Cu-ZSM-5 before (1) and after dehydration at 400°C in O_2 (static condition, 2), in vacuum (3), and the latter after subsequent oxidizing treatment (4).

4 Conclusions

Cu-ZSM-5 possess the capability to stabilize copper(II) pero/oxocomplexes at treatment by hydrogen peroxide in alkaline solution as well as high-temperature calcination in O_2-containing atmosphere. Peroxocomplexes copper(II) characterized by CTB L-M 21500 and 35500 cm^{-1} could be considered as structural model of active site of hemocyanine and dopamine monooxygenase containing two copper ions located near and long distance, respectively.

Acknowledgements

The study was supported by the RSF grant 14-13-01155.

References

[1] P.J.Smeets, M.H.Groothaert, R.A.Schoonheydt, *Catalysis Today*. 110 (2005) 303.
[2] G.L.Elizarova, D.I.Kochubey, V.V.Kriventsov, et.el, *J. Colloid Interface Science*. 213 (1999) 126.
[3] S.A.Yashnik, V.F.Anufrienko, V.A.Sazonov, Z.R.Ismagilov, V.N.Parmon, *Kin. Cat.* 53 (2012) 377.
[4] S.A.Yashnik, V.F.Anufrienko, Z.R.Ismagilov, *Catalysis Today*. 110 (2005) 310.
[5] H. Praliaud, S. Mikhailenko, Z. Chajar, M. Primet. *Appl. Catal. B: Environ.,* 16 (1998) 359.
[6] Y. Teraoka, C. Tai, H. Ogawa1, H. Furukawa, S. Kagawa. *Appl. Catal. A: Gen.* 200 (2000) 167.

V-PP30

Structured Glass-Fiber Catalysts for Selective Oxidation of H_2S

Mikenin P.E.[1,2], Lopatin S.A.[1,2], Zazhigalov S.V.[1,2], Pisarev D.A.[1,2], Baranov D.V.[1,2,3], Zagoruiko A.N.[1,2,4*]

1 - Boreskov Institute of Catalysis, Novosibirsk, Russia
2 - Research and Educational Center for Energy Efficient Catalysis, Novosibirsk State University, Novosibirsk, Russia
3 - Novosibirsk Technical State University, Novosibirsk, Russia
4 - Tomsk Polytechnic University, Tomsk, Russia

* zagor@catalysis.ru

Keywords: glass-fiber catalyst, hydrogen sulphide, selective oxidation, vanadia, iron, oxide

1 Introduction

Improvement of the sulfur recovery degree in Claus plants is a traditionally important environmental protection task in the processing of natural gas and oil. The optimization potential of existing Claus units in this respect is practically exhausted. Hence, the main tool for efficiency increase of sulfur recovery over the last few decades is the application of Claus tail gas clean-up processes [1]. Among these processes, the technologies based on selective catalytic oxidation of hydrogen sulfide into sulfur by oxygen are worthy mentioning [1,2] These processes use the catalysts on the base of iron oxides, which are characterized with high H_2S oxidation selectivity into sulfur. However, these catalysts have rather low activity, especially, at temperatures below 200ºC. Another important challenge in this area is development of the catalyst with enhanced mass transfer properties.

One of the promising directions of development in this area includes application of the catalysts on the base of the flexible micro-fibrous supports, e.g., glass fibers. Glass-fiber catalyst (GFC) is a relatively new type of catalytic systems, where the support represents itself the glass microfibers, structured in form of threads in the woven or knitted fabrics. The possible active components may include noble metals and/or oxides of transient metals, depending upon the requirements of the target catalytic process [3,4]. The glass-fiber catalysts (GFCs) may be structured in a form of cartridges, characterized with a low pressure drop [5] and extremely low mass transfer limitations [6]. In our recent study [3] we have demonstrated that GFCs, containing vanadia supported at glass-fiber fabric covered by an external layer of porous silica provide high activity in the low-temperature area and acceptable selectivity in H_2S oxidation reaction.

This study was dedicated to more wide screening of glass-fiber catalysts for this reaction.

2 GFC preparation and testing

The samples of glass-fiber catalysts were prepared by means of impulse surface thermo-synthesis IST method [7]. The preparation included the supporting of the thin layer of porous SiO_2 at the external surface of glass micro-fibers with following impregnation of this layer with solution of the active component precursor and fuel additive [4]. The list of active components included vanadia (4 and 8% mass V) and iron oxide (1 and 2% Fe), as the most active (V_2O_5) and most selective (Fe_2O_3) oxides in the target reaction, as well as copper chromite (2.5% Cu, 4.4% Cr), which was also considered earlier as an efficient catalyst for H_2S oxidation [8]. The value of the unit surface area in these samples varied in the range of 10-30 m^2/g. Commercial $FeOx/Al_2O_3$ (10% mass Fe, 110 m^2/g) catalyst was taken as the reference.

The samples were tested in H_2S oxidation reaction in the gas mixture, containing 1% vol. of

H_2S, 1% O_2 and helium as balance. Gas flow rate was equal to 1.5 ml/sec per g of catalyst. The temperature was varied in the range 175-250ºC. The results are given in the Fig.1

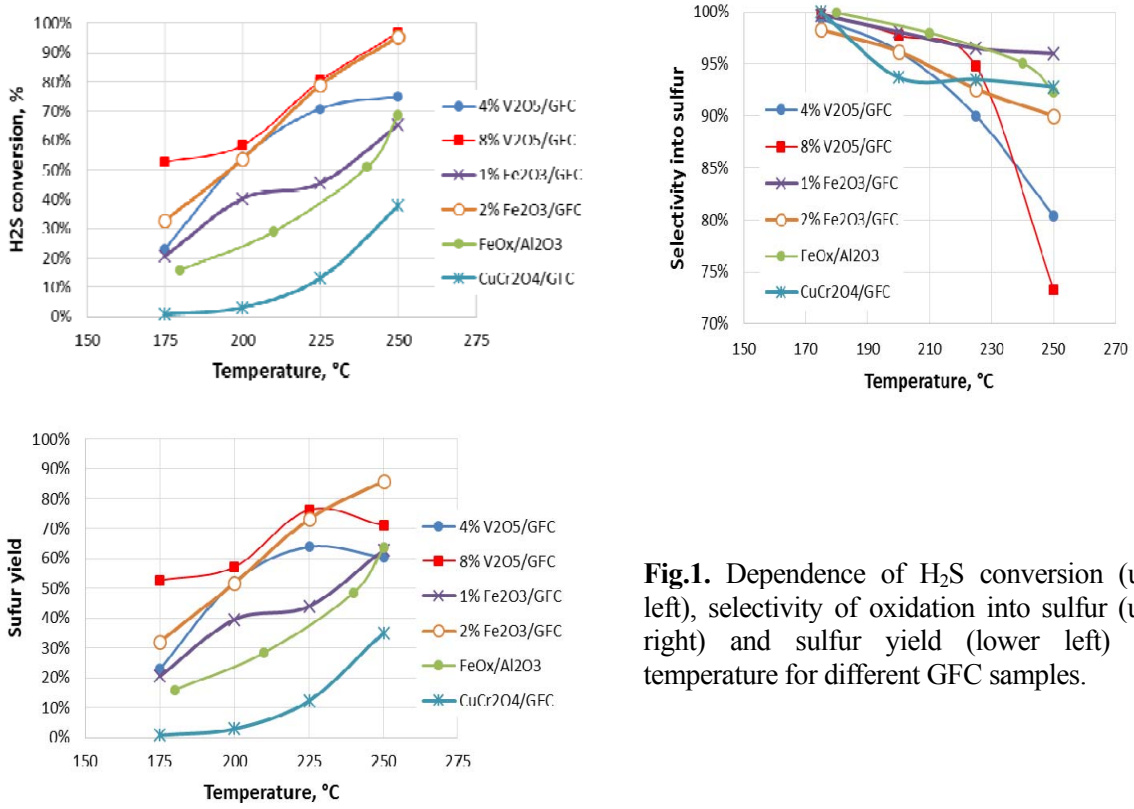

Fig.1. Dependence of H_2S conversion (upper left), selectivity of oxidation into sulfur (upper right) and sulfur yield (lower left) upon temperature for different GFC samples.

All vanadia and iron samples showed rather high oxidation activity, significantly exceeding that for conventional catalyst. Notably, Fe/GFC is much more active than conventional Fe/Al_2O_3 despite the much lower content of iron oxide. Cu-Cr catalyst has demonstrated much lower activity. The vanadia catalysts appeared to be more active, than iron ones, but less selective, especially at high temperatures. According to sulphur yield data (yield = H_2S conversion x selectivity) the most promising are the GFC containing V_2O_5 and Fe_2O_3. Vanadia provides better performance at lower temperatures while the iron oxide GFC is advantageous at higher temperatures. These catalysts may be recommended for practical application both separately and in combination.

Acknowledgements

The work was performed in the framework of the joint Research and Educational Center for Energy Efficient Catalysis (Novosibirsk State University, Boreskov Institute of Catalysis). The Skolkovo Foundation (Grant Agreement for Russian educational organizations no. 3 of 25.12.2014) supported this work.

References

[1] A.Zagoruiko, V.Shinkarev, S.Vanag, G.Bukhtiyarova. *Catalysis in Industry,* 4 (2010), 343.
[2] P.F.M.T. van Nisselrooy, J.A. Lagas, *Catal. Today* 16 (1993), 263.
[3] B.Balzhinimaev, E.Paukshtis, S.Vanag, A.Suknev, A.Zagoruiko, *Catal. Today* 151(2010), 195.
[4] P.Mikenin, P.Tsyrulnikov, Y.Kotolevich, A.Zagoruiko. *Catalysis in Industry*, 1(2015), 65.
[5] S.Lopatin, A.Zagoruiko. *Chem. Eng. J.* 238 (2014) 31.
[6] S.Lopatin, P.Mikenin, D.Pisarev, D.Baranov, S.Zazhigalov, A.Zagoruiko. *Chem. Eng. J.* (2015), accepted to publication (doi: 10.1016/j.cej.2015.02.026).
[7] Y.Kotolevich, E.Suprun, M.Sharafutdinov, P.Tsyrulnikov, A.Salanov, V.Goncharov, *Russ. Phys. J.* 12 (2011), 48.
[8] N.Kundo. *Chem. Sust. Dev.* 7(1999), 259.

V-PP31

Photocatalytic Oxidation of CO over TiO_2 Modified by Noble Metals

Kolobov N.S.[1,2,3], Selishchev D.S.[1,2,3*], Kozlov D.V.[1,2,3]

1 - Boreskov Institute of Catalysis, Novosibirsk, Russia
2 - Novosibirsk State University, Novosibirsk, Russia
3 - Research and Educational Centre for Energoefficient Catalysis (NSU), Novosibirsk, Russia

* selishev@catalysis.ru

Keywords: photocatalysis, titania, CO oxidation, Pt, Pd, Au nanoparticles

1 Introduction

Photocatalytic oxidation (PCO) processes have being intensively studied for the treatment of polluted water and air in recent decades. In particular, many types of volatile organic compounds (VOCs) could be completely decomposed over TiO_2-based photocatalysts under ambient conditions [1-3]. In addition to VOCs, carbon monoxide is one of the major air pollutants [4]. Also, CO can be produced as a final oxidation product together with CO_2 and water in the PCO of organic compounds.

The main drawback of unmodified TiO_2 photocatalyst is very low activity in the photocatalytic oxidation of carbon monoxide due to the low adsorption of CO on the TiO_2 surface. It is known that deposition of noble metals, such as Pt, Pd, Au, on the TiO_2 surface increases the CO chemisorption and thus can lead to increased activity of TiO_2 in the reaction of CO photocatalytic oxidation. Therefore, this work aims to synthesize TiO_2 photocatalysts modified by noble metals and to investigate their photocatalytic activity in the reaction of CO oxidation under UV irradiation.

2 Experimental/methodology

M/TiO_2 photocatalysts were prepared by deposition precipitation method. Typically, 2 g TiO_2 Hombifine N (100% anatase, S_{BET} ~ 350 m^2/g) were suspended in 30 ml distilled water and certain aliquot of aqueous solutions of metal precursor (H_2PtCl_6 or $HAuCl_4$ or $PdCl_2$) was added. To reduce metal precursor to metal, threefold excess of $NaBH_4$ was added into solution. The content of noble metal in M/TiO_2 samples was measured the X-ray fluorescence analysis using the ARL spectrometer with rhodium anode.

Kinetic experiments were carried out in a static reactor installed in the cell compartment of FT-IR spectrometer Vector 22 (Bruker, Germany). Typically, the samples were uniformly deposited onto the glass support to obtain layer with surface density equaled 1 mg/cm^2 and irradiated by high performance UV LED (Nichia, Japan) with λ_{max} ~373 nm. Concentrations of CO and CO_2 in the gas phase during the reaction were determined by FT-IR analysis using the Beer-Lambert law. Photocatalytic activity of samples synthesized was estimated as initial rate of CO_2 formation calculated by linearization of initial part of CO_2 accumulation kinetic curve.

3 Results and discussion

Three series of M/TiO_2 with M content varied from 0.01 to 4.0 wt. % were synthesized. The results of X-ray fluorescence analysis showed that the amount of M (Pt, Pd or Au) in the synthesized catalysts were close to calculated values.

Modified TiO_2 samples were tested in the reaction of CO oxidation at ambient conditions with or without UV irradiation. The rate of CO oxidation under UV irradiation was 1.5-5 times greater than the rate of oxidation without lighting if we compare the different metals used for

modification. It indicates that light energy can be used instead of thermal energy to increase the rate of CO oxidation over such type of catalyst.

Kinetic curves of CO removal in the case of TiO_2 samples modified by Pt, Pd or Au with 0.5 wt.% content are presented in the Fig. 1. The Pt/TiO_2 sample showed the best activity and fast conversion of 850 ppm CO to CO_2.

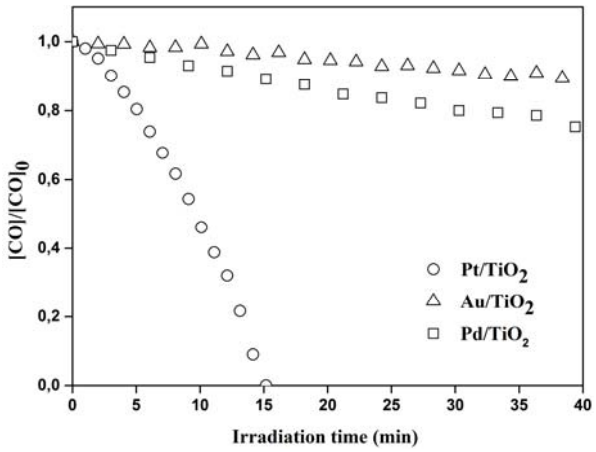

Fig. 1. Kinetic curves of CO removal during the PCO over TiO_2 catalyst modified by 0.5 wt.% Pt, Pd or Au.

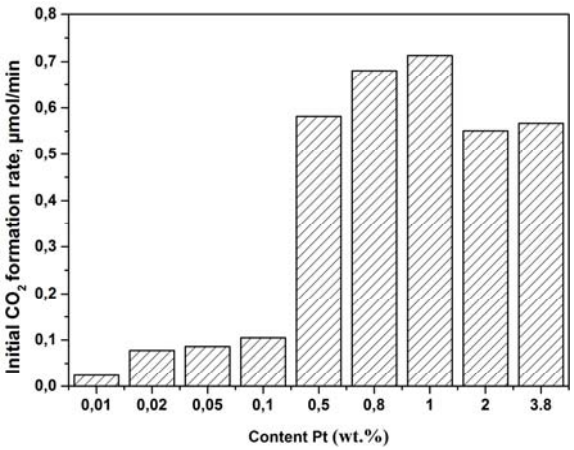

Fig. 2. Dependence of the initial rate of CO_2 formation during the PCO on the Pt content in Pt/TiO_2 photocatalysts.

The dependence of the CO oxidation rate on noble metal content in the catalysts was investigated. In the case of Pt/TiO_2 and Pd/TiO_2 samples activity increased with increase in the metal content up to an optimum level: 1 wt.% for Pt/TiO_2 and 0.05 wt.% for Pd/TiO_2 (Fig. 2). In contrast, Au/TiO_2 samples revealed lower activity and there was no clear dependency on the Au content. This seems to be due to the fact that the activity of Au-containing catalyst is highly dependent on the preparation technique.

4 Conclusions

The deposition of noble metals (Pt, Pd or Au) on TiO_2 by impregnation and subsequent chemical reduction of precursor compounds allows us to synthesize catalysts active in CO photooxidation.

The kinetics of the CO oxidation in the static reactor over synthesized catalysts with or without UV irradiation was investigated by IR spectroscopy. The rate of CO oxidation under UV irradiation 1.5-5 times greater than the rate of oxidation without irradiation depending on the metal used.

The optimum metal content in Pt/TiO_2 and Pd/TiO_2 samples corresponded to the highest photocatalytic activity in the CO oxidation was observed. In the case of Au/TiO_2 samples CO oxidation rate had no clearly defined by the Au content. The rate of CO oxidation for the most active sample in each series increases in the following sequence: $Au/TiO_2<Pd/TiO_2<Pt/TiO_2$, wherein Pt-containing sample in 6-fold more active compared to other samples.

Acknowledgements

This work was supported by the Skolkovo Foundation (Grant Agreement for Russian educational organization №1 on 28.11.2013) and Russian President Grant № MK-3141.2015.3.

References

[1] J. Zhao, X. Yang, *Build. Environ*. 38 (2003) 645
[2] H. Eianga, S. Futamura, T. Ibusuki, *Appl. Catal. B. Environ.* 38 (2002) 215
[3] D.S. Selishchev, P.A. Kolinko, D.V. Kozlov, *J. Photochem. Photobiol. A. Chem* 229 (2012) 11
[4] Environmental protection in Russia, *Federal Statistics Service*, Moscow (2012)

V-PP32

Characterization Of The Automotive Exhaust Gas Aftertreatment Catalysts With Flow Chemisorption Methods

Carberry B.[1], Schneider M.[1], Ukropec R.[1], Boerensen C.[1], Dubkov A.A.[2,1*]

1 - Ford Forschungszentrum Aachen GmbH, Aachen, Germany
2 - Boreskov Institute of Catalysis SB RAS, Novosibirsk, Russia

* adubkov@catalysis.ru

Keywords: automotive catalyst, thermal stability, pulse, chemisorption, TPD, TPR, TPO

1 Introduction

Automotive exhaust catalysis is one of the most socially important technologies contributing on a global level to environmental protection. With tighter emissions standards, exhaust gas aftertreatment catalysts have to provide improved efficiency and robustness, including high resistance to thermal deactivation. It is important for engineers to be able to analyse catalysts failures etc. very efficiently in terms of time and resources spent. In this work, thermal stability of selected automotive exhaust catalysts (TWC, LNT, SCR) was characterized using laboratory flow reactor chemisorption methods. The work was performed at Ford Research Centre in Aachen (Germany).

2 Experimental

To prepare samples of the catalysts, pieces cut from the full-size catalysts were crashed and sieved; fraction of 0.25-0.50 mm (in some cases - > 0.5 mm) was used for experiments.

Experiments were performed with Autochem II 2920 machine (Micromeritics), using methods:

1. Pulse chemisorption of CO
2. Temperature-Programmed Reduction (H_2-TPR)
3. Temperature-Programmed Oxidation (O_2-TPO)
4. Temperature-Programmed Desorption of ammonia (NH_3 TPD)

Data were processed with standard routines, and using Matlab scripts developed by the authors.

To investigate thermal stability, samples of LNT or SCR catalysts were calcined at selected temperature, and then characterized with above mentioned methods. Then, the same procedure was repeated, but each time with increased calcination temperature. Calcination temperatures in a range of 600 to 900 (1000°C) were applied for LNT (SCR) catalysts characterization, correspondingly.

Pulse chemisorption was performed at 35°C using pulses of 10% CO in He for pre-reduced sample. Temperature-Programmed Reduction (TPR) was performed in 10% H_2-Ar, starting from 40°C and as a rule - up to calcination temperature. Temperature-Programmed Oxidation (TPO) was performed in 2% O_2-He for the sample that was reduced in the TPR run, after cooling it down to 40°C in He. To prepare samples for NH_3 TPD experiments, after calcination, they were cooled down to 120°C in He and treated 30 min in 15% NH_3-He flow. TPD run itself was then performed with rate of 10°C/min started from 120°C up to calcination temperature used on a given step.

In all experiments described above, response of the system was measured with TCD, and all following calculations were made based on the detector calibrations to corresponding components.

3 Results and discussion

Thermal aging of the LNT studied with CO pulse chemisorption and TPR/O. Evolution of the LNT (diesel prototype catalyst was used) properties after consecutive calcinations at 600, 700, 800 and 900°C displayed the following main TPR features:

- In the low-temperature region (<~250°C), H_2 consumption was very sensitive to the

calcination temperature, and correlated with the amount of chemisorbed CO at 35°C.

- In the mid-temperature region (~250-~600°C), H_2 consumption was also quite sensitive to the pretreatment temperature, being lower with increasing aging temperature.
- In the High-temperature region (above ca. 600°C), H_2 consumption in TPR run is nearly insensitive to calcination temperature (i.e., to aging/sintering).

Several surface and bulk species and corresponding processes for their reduction/oxidation were proposed while interpreting the results measured with pulse chemisorption, TPR and TPO. Tentative mechanism of thermal deactivation of the LNT was suggested.

Measured results clearly show that temperature limit for absolutely safe LNT operation is 700°C; excursions to 800°C result in slow deactivation; above 800°C sintering/active sites lost become faster; above 900°C deactivation is very fast. Corresponding recommendations for temperature regimes of the LNT were given.

Thermal Aging of the SCR catalyst studied with ammonia TPD. Efficiency of the SCR catalyst in NH_3-NO_x reaction measured in the laboratory flow reactor, as a function of the pretreatment temperature showed decrease after pretreatment of the catalyst at 900°C.

Catalytic activity of the Me-zeolite SCR catalysts is known to be strongly related to its adsorption capacity towards ammonia, and to its temperature dependence.

Investigating thermal deactivation of SCR catalyst consisted in pre-treatments of the SCR catalyst at 600…1000°C and recording of the NH_3 TPD profile after each pre-treatment.

It was found that critical temperature for keeping initial level of ammonia adsorption is ca. 900°C. Above 900°C, amount of the NH_3 adsorbed by the catalyst at 120°C decreased sharply. After 1000°C, NH_3 adsorption capacity dropped 10-fold versus fresh SCR catalyst.

The results of the TPD set were in reasonable agreement with catalytic performance results. Interpretation to the features observed in NH_3 TPD profiles were made, including discussing different adsorbed ammonia species.

Based on the results of the current study, corresponding recommendations for temperature regimes of the SCR catalyst were developed.

Analysis of the In-Field failed (IFF) Three-Way Catalyst (TWC). In-field failed three-way catalyst was investigated using pulse chemisorption and H_2 TPR technique. Fresh catalyst and oven-aged catalyst were also investigated in parallel.

Pulse chemisorption showed that IFF and oven-aged TWC have 2 orders of magnitude lower PGM dispersion compared to fresh sample.

At least 5 features were distinguished in measured TPR profiles. These features in H_2 TPR profiles were interpreted using results available in literature.

With ageing, PGM and support oxides were sintering thus drastically changing TPR profile, with appearance or disappearance of some TPR peaks. Key features in the TPR profile were distinguished that can be used as indicators for evaluating degree of ageing TWC.

4 Conclusions

In the presented work, applications of the chemisorption methods (pulse chemisorption, Temperature-programmed desorption (TPD), reduction (TPR) and oxidation (TPO)) to characterization of the thermal aging of the automotive exhaust catalysts, was described.

Pulse chemisorption and TPR were applied to study deactivation of the LNT catalyst. Relatively safe rich operation temperature for LNT was found to be ca. 800°C. Above this temperature, rapid irreversible deactivation due to PGM and support sintering were taking place.

For evaluated NH_3 SCR catalyst, ammonia TPD study helped to determine not-to-exceed temperature of ca. 900°C. Above this temperature, there is a high probability that zeolite will undergo destruction, so all NH_3 SCR reaction related properties will be irreversibly lost.

For the sample of the in-field failed three-way catalyst, temperature of the exposure was deducted based on the characterization of the catalyst with CO pulse chemisorption and TPR.

V-PP33

Kinetic and Mechanistic Studies of Dehydrogenation of Propane and Isobutane Assisted by High-Throughput Tools

Sokolov S.[1], Bychkov V.Yu.[2], Rodemerck U.[1], Stoyanova M.[1], Linke D.[1], Kondratenko E.V.[1*]

1 - Leibniz Institute for Catalysis, Rostock, Germany
2 - Semenov Institute of Chemical Physics, Moscow, Russia

* Evgenii.Kondratenko@catalysis.de

Keywords: mechanistics studies of dehydrogenation, propane, isobutane

1 Introduction

Non-oxidative dehydrogenation (DH) of propane and isobutane are established commercial processes for on-demand production of the corresponding olefins employing supported CrO_x or Pt-Sn catalysts. The active components have disadvantages of being toxic and expensive respectively. We have recently demonstrated that supported VO_x constitute a suitable alternative for propene DH catalysts . In the current study, we investigated their potential for isobutane DH and compare their performance to that in propane DH. In particularly, we focused on finding correlations between structural characteristics of VO_x species, acidic properties of supports and coke formation.

2 Experimental

The catalysts were prepared by grafting $VO(acac)_2$ onto silica (MCM-41), Siral® (Sasol) aluminosilicates with various SiO_2 content and alumina . They are further abbreviated as V/Si for VO_x/MCM-41, V/S1 for VO_x/Siral 1 with 1 wt.% SiO_2 and by analogy for other Sirals, V/Al-LS and V/Al-HS for VO_x/Al_2O_3-NorPro (low surface) and VO_x/Al_2O_3-Chempur (high surface) respectively. The index before the abbreviation stands for V content in wt.%.

For operando catalysts characterization, we used an in-house designed setup containing 5 continuous-flow fixed-bed reactors equipped with temperature-resistant UV-vis probes. Brønsted and Lewis acidity of the catalysts was determined by in situ IR pyridine adsorption. All catalytic tests were carried out at 550 °C in an in-house developed setup containing 15 continuous-flow fixed-bed reactors operating in parallel. The amount of coke on spent catalysts was determined in the temperature-programmed oxidation experiments performed in a setup containing 8 individually heated continuous-flow fixed-bed reactors . In situ thermogravimetric (TG) experiments were performed in SETSYS Evolution (Setaram) thermobalance. Rate constants of coke formation and catalyst deactivation were derived from evaluation of TG and catalytic tests with in-house developed software respectively.

3 Results and Discussion

The VO_x/SiO_2-Al_2O_3 catalysts showed different initial activity, propene selectivity and on-stream stability depending on SiO_2 content: 5V/Si was the most stable and selective while 3V/Al-LS was the fastest to deactivate . We also found that these catalyst characteristics are influenced by degree of polymerization of VO_x species. To understand the origins of different on-stream stability of the catalysts, the rate constants of catalyst deactivation (k_{deac}) and carbon deposition (k_{coke}) were obtained from kinetic evaluation of catalytic and in situ TG experiments . Unexpectedly, we did not observe any relation between catalysts acidity and k_{coke} or k_{deac}. Instead, these constants were found to correlate with VO_x polymerization degree. The latter was estimated from edge energy (E_{Edge}) of VO_x species derived from

UV-vis spectra: higher polymerized species have lower E_{Edge}. When k_{coke} and k_{deac} are plotted vs. E_{Edge} (Fig.1), it becomes evident that coke formation, and likewise catalyst deactivation, soars with rising degree of VO_x polymerization. This relation was verified in separate tests where conversion of propene (coke precursor) over 3V/Al-LS, 4V/S10 and 5V/Si was studied. The catalysts were selected as carrying large, medium and small VO_x species respectively and gave the initial rates of carbon formation [mg(C)g(V)$^{-1}$min^{-1}] of 1150, 800 and 650. Presumably, adsorbed C_3H_6 molecules have higher chances to react with each other and form surface carbonaceous species on larger VO_x particles.

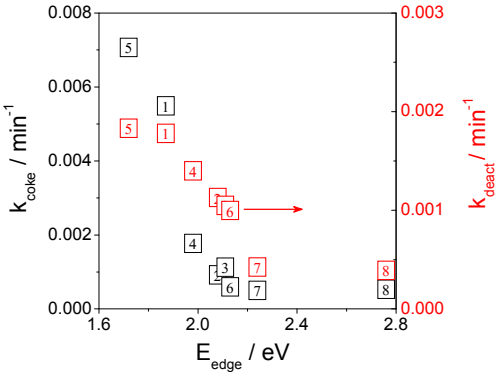

Fig. 1. Catalyst deactivation (k_{deact}) and coke deposition (k_{coke}) rate constants vs. edge energy. 1 - 3V/Al-LS, 2 - 4V/S1, 3 - 4V/S10, 4 - 6V/S10, 5 - 13V/S10, 6 - 5V/S40, 7 - 5V/S70, 8 - 5V/Si

Similarly to propane DH, 5V/Si was the most stable in isobutane DH, while 2V/Al-HS and 4V/S10 deactivated faster. However, 2V/Al-HS showed the lowest selectivity to carbon (S_C). Also, the selectivity to isobutene ($S_{isobutene}$) on 2V/Al-HS was always higher than on 4V/S10 and 4V/Si and was less sensitive to isobutane conversion ($X_{isobutane}$) than on 4V/S10 and 4V/Si (Fig. 2). Lower $S_{isobutene}$ on the two latter catalysts stems from their high activity for isobutene isomerization to n-butenes. To study pathways of coke formation, the coke precursors, isobutene and n-butene, were converted over the catalysts. 2V/Al-HS exhibited by far the highest selectivity to coke in these reactions. These results suggest that large VO_x species on Al_2O_3 are still very active in coke formation, but isobutene conversion to coke is suppressed under isobutane DH conditions, because the olefin and the alkane compete for the same sites. Conversion of n-butene into coke apparently proceeds faster than of isobutene. It involves DH of n-butene into butadiene and its further conversion into coke, possibly through Diels-Alder cyclization, on sites other than active in DH. Isomerization of isobutene into n-butene over 2V/Al-HS is slow compared to 4V/S10 and 4V/Si, thus carbon deposition through a faster route is suppressed over 2V/Al-HS for a shortage of coke precursor.

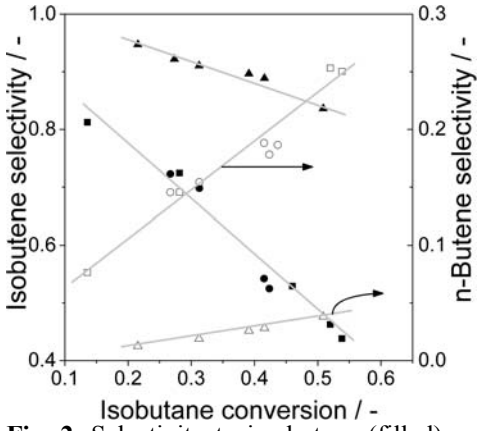

Fig. 2. Selectivity to iso-butene (filled) and to n-butenes (plain) vs. conversion of isobutane. ▲ - 2V/Al-HS, ● - 4V/S10, ■ - 4V/Si.

In summary, the results obtained so far indicate that higher degree of polymerization of supported VO_x species promotes consecutive reactions of C_3-C_4 olefins resulting in carbon deposits. Yet, ability of isobutene to transform into n-butenes opens new and swift path to higher byproducts and eventually coke. Hence, optimization of VO_x-based DH catalysts should encompass higher dispersion of VO_x phase and suppression of isomerization activity.

References

[1] S. Sokolov, M. Stoyanova, U. Rodemerck, D. Linke, E.V. Kondratenko, J. Catal. 293 (2012) 67-75.
[2] S. Sokolov, M. Stoyanova, U. Rodemerck, D. Linke, E.V. Kondratenko, Catalysis Science & Technology 4 (2014) 1323-1332.
[3] U. Rodemerck, E.V. Kondratenko, M.J.G. Fait, S. Sokolov, D. Linke, in: A. Hagemeyer, A.F. Volpe (Eds.), Modern Applications of High Throughput R&D in Heterogeneous Catalysis, Bentham Science Publishers, 2014, pp. 254-283
[4] S. Sokolov, V.Y. Bychkov, M. Stoyanova, U. Rodemerck, U. Bentrup, D. Linke, Y.P. Tyulenin, V.N. Korchak, E.V. Kondratenko, ChemCatChem 7 (2015) 1691-1700.

V-PP35

Catalytic Neutralization of Toxic Emissions of Furnaces of Oil Heating

Gil'mundinov Sh.A., Sassykova L.R., Massenova A.T.*, Bunin V.N., Rakhmetova K.S.

D.V.Sokolskii Institute of Organic Catalysis and Electrochemistry, Laboratory of Catalytic Synthesis, Almaty, Kazakhstan

* almasenova@mail.ru

Keywords: block, catalysts, emission, motor, transport

1 Introduction

Problem of cleaning of exhaust gases of motor transport and departing gases of the industry - one of essential problems of the mankind, drawing attention of the public and the scientific leading countries of the world. Preservation of the environment from industrial and transport pollution constantly makes increasing demands to improvement of ways of preparation of catalysts of neutralization and cleaning of gas emissions of harmful impurity. Modern environmental problems of the Republic of Kazakhstan are difficult, diverse and territorially differentiated. On emissions of harmful substances from stationary sources in atmosphere the country is in the lead three, conceding to Russia and Ukraine.

In Kazakhstan daily throw out about 3 million tons of harmful substances, such as carbon oxide, nitrogen oxides, hydrocarbons, etc. Level of air pollution of many industrial cities of Kazakhstan exceeds more than 6-10 times existing standard limits because of emissions of motor transport, boiler-houses and plants. In Kazakhstan, in country scales, the share total emissions of polluting substances in atmosphere all technogenic sources reaches on the average 60 %. In the industry traditionally degree of recycling of toxic substances on an average level and, as consequence, regions of its disposition are a source of emissions of the most toxic substances. Among known ways of recycling and neutralization of harmful emissions of the industry and motor transport the most effective is deep catalytic oxidation of organic substances to carbon dioxide and water.

2 Experimental/methodology

The block catalysts on the metal carrier with the honey comb structure of channels were developed and prepared for 8 furnaces of heating of oil and carried out the skilled - industrial tests of catalysts with the joint-stock company "Embamunai-gas" on real waste gases of furnaces of heating of oil for the purpose of decrease in toxic emissions. 17 samples of block catalysts for 8 furnaces of heating of oil have been prepared. Catalysts were made from a heat resisting foil by winding of the smooth and goffered foil in the metal block of the cylindrical form, with the subsequent drawing of active components. Diameter of the block filter for furnace PTB-10/64 is equal 410 mm, height 400 mm. For furnace PT-16/150 diameter of catalytic filter - 500mm, height 400мм, catalyst dimensions on the furnace PT-3,5 were 900 mm on 400 mm. Catalytic filters were established directly on pipes of departing gases of furnaces of heating of oil after samplers to the catalyst. For the purpose of decrease heat emission the catalyst was wrapped by heat-insulating mineral cotton wool with a reflecting foil. In the course of work of the furnace temperature of gases was defined before and after the catalyst by means of the mercury thermometer and a gas analyzer temperature-sensitive element. Concentration of toxic gases before and after catalytic filters measured by means of gas analyzer MCI-150 (firm "Bosh").

3 Results and discussion

Block catalysts have the cylindrical form and are convenient in placing directly at a source of toxic emissions. The developed catalysts possess high degree of cleaning of departing gases of the industry from carbon oxide - 90-100 %, at temperatures from 90°C and above, from various hydrocarbons on 80-100 %. In a complex with carbon oxide, or with hydrocarbons catalysts will neutralize nitrogen oxide on 40-100 %, depending on their ratio. For example, at use of the block catalysts containing a mix of cobalt and manganese oxides the greatest degree of transformation CO in CO_2 (to 100 %) it is reached for one pass at volume speeds of a gas mix from 10 000 h^{-1} to 100 000 h^{-1} and temperature 110°C.

The developed effective catalysts of cleaning of exhaust gases of motor transport and waste gases of the industrial enterprises from toxic impurity on the metal carrier correspond under characteristics to standard EURO-3.

The party of catalytic filters - 4 samples has been established on the furnace with compulsory giving of air PTB-10/64 on "S.Balgimbaevo's" deposit. The temperature of departing gases to the catalyst was equal to 350°C, concentration of toxic gases to the catalyst by carbon oxide (CO) - 1280 ppм, on nitrogen oxide (NO) – 49 ppм, on sum by nitrogen oxides (NO_x) - 51ppм. After catalyst the indication was equal on CO – 5 ppм, on NO-39 ppm, on (NO_x) - 41ppм. Efficiency of neutralization of toxic emissions was equal on CO - 99.6 %, on NO - 20.4 %, on NO_x 19,6 %.

Other party of the catalytic filters has been established on 5 furnaces of heating of oil and water on a deposit "Southwest Camyshitovoye". On the furnace PT-3,5 with compulsory giving of air and on 4 furnaces PT-16/150 with the own draught of air. Efficiency of decrease in toxic emissions on furnace PT-3,5 with the catalytic filter was equal on CO - 66.8 %, on NO - 20.6 %, NO_x - 20 %, and on SO_2-100 %. Decrease in toxic emissions on furnace PT-16/150 after the catalyst was on CO - 100 %, on NO - 7,7 %, NO_x - 7.7 %, on SO_2 - 57.1 %.

During carrying out of trial tests it is revealed, that catalytic filters work effectively and decreased contents of the toxic gases from 7.7 % on nitrogen oxides to 100 % on carbon oxide.

4 Conclusions

Catalytic filters on metal blocks are developed for furnaces for heating of oil which work effectively and reduce the content of poisonous gases: CO - 100 %, NO - 7,7 %, NO_x - 7.7 %, on SO_2 - 57.1 %.

V-PP36

Study of the Interaction of Chloroform and Hydrogen with the Metallic Species in Precious Metals Supported Catalysts for the Hydrodechlorination of Chloroform

Arevalo-Bastante A.*, Omar S., Palomar J., Gómez-Sainero L.M., Alvarez-Montero M.A., Rodriguez J.J.

Departamento de Química-Física Aplicada, Sección de Ingeniería Química, Universidad Autónoma de Madrid, Madrid, Spain

* alejandra.arevalo@uam.es

Keywords: chloroform, hydrodechlorination, palladium, platinum, rhodium, ruthenium

1 Introduction

Chloroform (TCM) plays an important role in the chemical and pharmaceutical industry, where it is used as solvent and reactant. However, because of its high toxicity and carcinogenic character, TCM is classified nowadays among the most hazardous gas pollutants. Catalytic hydrodechlorination (HDC) becomes one of the most promising emerging technologies for removing this compound. Noble metals supported on activated carbon (Pd/C, Pt/C, Rh/C and Ru/C) were shown to be fairly active in the HDC of TCM (1), with notable differences in stability and products distribution depending on the predominant metal species.

For a better knowledge of reaction mechanisms, catalysts of Pd, Pt, Rh and Ru were prepared using CeO_2-Sm_2O_3 as support in order to obtain high proportions of zero-valent metallic species, and those catalysts were tested in the HDC of TCM. The catalysts were characterized by XPS, and a density functional theory (DFT) analysis was conducted to study the activation of hydrogen and TCM by metal clusters (2).

2 Experimental/methodology

The catalysts, based on noble metals (palladium, platinum, rhodium and ruthenium) supported on ceria-samaria (CeO_2=80% w/w; Sm_2O_3=20% w/w) with metal contents of 1 wt%, were prepared by incipient wetness impregnation (Pd/CS, Pt/CS, Rh/CS and Ru/CS). The support was previously calcined at 300 ºC in airstream for 2 hours (flow rate = 100 ºC·hour^{-1}). The HDC experiments were conducted in a continuous flow reaction system, consisting of a quartz fixed bed reactor coupled to a gas-chromatograph with a FID detector to analyze the reaction products. The catalysts were reduced previously at 300 ºC using 50 Ncm^3·min^{-1} of hydrogen for 2 hours. The operating conditions used were: Atmospheric pressure, total flow rate of 100 Ncm^3·min^{-1}, an initial concentration of TCM of 1000 ppm, a space-time of 0.4-1.73 kg·h·mol^{-1}, H_2/TCM molar ratio of 100 and a reaction temperature of 250 ºC. All computational studies were performed with the Gaussian 09 program with density functional methods, as implemented in the computational package.

3 Results and discussion

The proportion of zero-valent species (Me^0) in the catalysts was measured by XPS was 78.8 %, 80.4 % and 86.8 % for Pd/CS, Pt/CS and Rh/CS respectively. Figure 1 shows the TCM conversion obtained with all the catalysts along 15 hours. Pt/CS and Pd/CS are more active than Rh/CS and Ru/CS as similar conversions values were obtained at lower space-time values. This can be attributed to their higher hydrogenation capability as suggested by the selectivity patterns (higher hydrocarbons and DCM were favoured for the latter in detriment of methane) and the dissociative adsorption energies of H_2 on the different metals (Table 1). A pronounced decrease

of activity with Rh/CS and Ru/CS is observed, and also for Pt/CS though in a lower extent, while Pd/CS showed very stable activity. The extent of deactivation followed a similar trend that the increase of the dissociative adsorption energy (Table 1) were Ru ≈ Rh > Pt > Pd. DFT results showed that total dissociation of TCM is favoured in the zero-valent species of Pt, Rh and Ru. This implies a higher amount of chloromethanes derived radicals for the available H_2, leading to the formation of a higher amount of hydrocarbons of more than one carbon atom, that can be adsorbed on the catalyst surface.

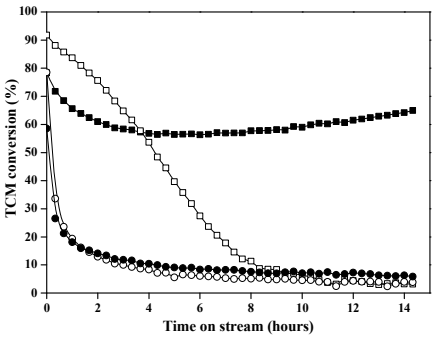

Fig. 1. Evolution of TCM conversion with time on stream at a H_2/TCM molar ratio of 100 and a reaction temperature of 250 ºC using:

(■) Pd/CS (τ = 0.4 kg·h·mol^{-1});
(□) Pt/CS (τ = 0.4 kg·h·mol^{-1});
(○) Rh/CS (τ = 0.8 kg·h·mol^{-1});
(●) Ru/CS (τ = 1.73 kg·h·mol^{-1})

Furthermore, the higher stability of Pd/CS catalyst compared to that supported on activated carbon (1) is ascribed to its significant lower amount of Pd^{2+}, species which promotes the associative adsorption of the chloromethane and therefore the poisoning of the active sites of the catalyst.

Table 1. Calculated enthalpy of dissociative adsorption of TCM and hydrogen on metal clusters.

Atomic species	ΔH_d TCM (kcal/mol)	ΔH_d H_2 (kcal/mol)
Pd^0	-64.3	-14.5
Pd^{2+}	-67.8	-37.1
Pt^0	-109.0	-17.2
Pt^{2+}	-53.8	-19.3
Rh^0	-134.1	-12.9
Rh^{2+}	-58.5	-12.2
Ru^0	-161.0	-13.7
Ru^{2+}	-75.5	-2.5

4 Conclusions

Pd/CS catalyst shows the best performance in the HDC of TCM, showing a high activity and good stability. The latter can be related to the lower strength of adsorption of chloroform on zero-valent Pd clusters, which prevent coke formation and the low amount of electro-deficient species which avoids the non-dissociative adsorption of the chloromethane.

Acknowledgements

The authors gratefully acknowledge financial support from the Spanish *Ministerio de Economía y Competitividad* (MINECO) through the project CTM2011-28352.

References

[1] M. Martin-Martinez, L.M. Gómez-Sainero, M.A. Alvarez-Montero, J. Bedia, J.J. Rodriguez, *Appl. Cat. B: Environ*. 132-133 (2013) 256.

[2] S. Omar, J. Palomar, L.M. Gómez-Sainero, M.A. Alvarez-Montero, M. Martin-Martinez, J.J. Rodriguez, *J. Phys. Chem*. C. 115 (2011) 14180.

V-PP37

Mineralization of Aniline and Reactive Dye Blue 5 Solutions by Photocatalytic Ozonation

Orge C.A., Pereira M.F.R., Faria J.L.*

LSRE-LCM, Departamento de Engenharia Química, Faculdade de Engenharia, Universidade do Porto, Porto, Portugal

* jlfaria@fe.up.pt

Keywords: aniline, reactive dye, TiO_2, photocatalytic ozonation, mineralization, water

1 Introduction

Photocatalysis has shown to be adequate for the degradation of a wide range of pollutants, but in some cases the complete mineralization is slowly attained; therefore, it is mainly economically advantageous for diluted streams . In addition to photocatalysis, ozonation is able to selectively convert recalcitrant organic compounds and can be used with superior performances in some high strength waste waters . Molecular ozone can oxidise water impurities via direct selective reactions between ozone (O_3) and other chemical species, or via indirect O_3 reactions, which involve the formation of hydroxyl radicals (HO•) . The disadvantage of this process is the limited mineralization of the organic compounds. Therefore, it is necessary to modify the method when the definite removal of the pollutant and its degradation intermediates is required . Generally, a combination of several methods improves the removal of pollutants from the wastewater compared with the individual treatments . Irradiation of O_3 in aqueous solutions by UV light produces additional $HO^{\bullet}$ radicals, and consequently, the efficiency of contaminants removal should increase. The present targets at the photocatalytic ozonation of aniline (ANL) and C. I. Reactive Dye Blue 5 (RDB) in the presence of P25. In order to verify the presence of synergetic effects, photocatalysis (Light/P25) and catalytic ozonation (O_3/P25) were also carried out, as well as, photo-ozonation (O_3/Light).

2 Experimental

The removal of pollutants was carried out in a glass immersion photochemical reactor loaded with 250 mL of ANL (C_0 = 1 mM) or RDB (C_0 = 200 ppm) and 125 mg of photocatalyst. The reactor was equipped with a Heraeus TQ 150 medium-pressure mercury vapour lamp located axially and a DURAN 50® glass cooling jacket was placed around the lamp (main resulting emission lines at λ_{exc} = 365, 405, 436, 546 and 578 nm). The experiments were performed at 150 cm^3 min^{-1} and with an inlet ozone concentration of 50 g m^{-3}. The catalyst selected was commercial TiO_2 from Evonik Degussa Corporation, sample P25. ANL concentration was analysed by HPLC with Lichrocart Purospher Star column. For RDB, solution decolourisation was followed by UV/Vis spectrophotometry at the maximum absorption wavelength, previously determined (λ = 603 nm) with a JASCO V-560 UV/Vis spectrophotometer. The degree of mineralisation was followed by TOC analysis in a Shimadzu TOC-5000A Analyzer.

3 Results and discussion

The conversion of ANL and RDB as function of time under the selected experimental conditions is described in Figure 1. Except for photocatalysis (Light/P25), ANL was completely removed in all tested oxidative processes at early times with no significant differences observed for the remaining systems. Similar performance was observed during RDB degradation. These results were expected since O_3 by itself is an extremely powerful oxidant

capable of reacting with a vast range of compounds, and it attacks selectively aromatic moieties and unsaturated bonds, such as ANL and RDB.

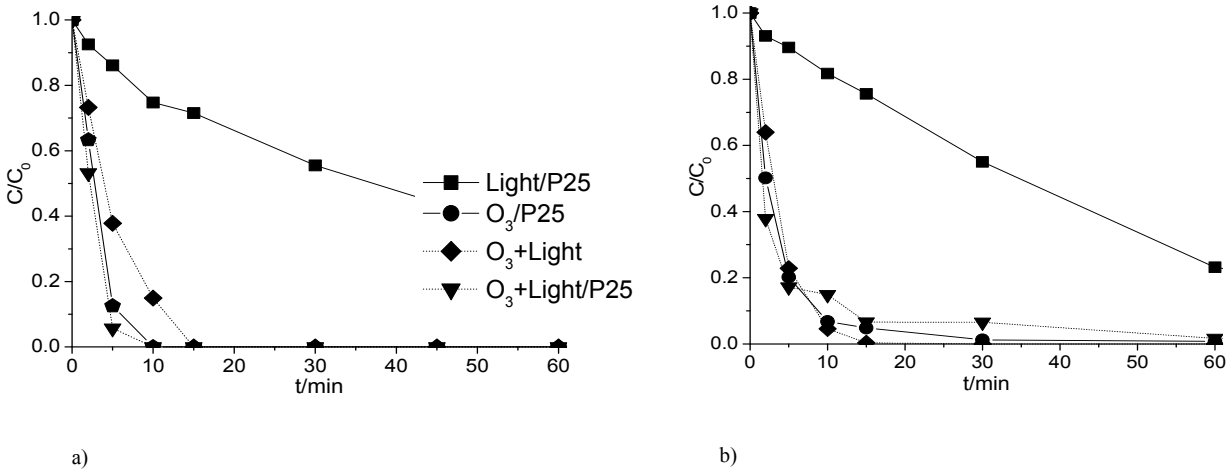

Fig. 1. Degradation of ANL a) and RDB b) by tested oxidation processes.

The degradation of these molecules resulted in the formation of several intermediates further transformed into saturated compounds, which are not significantly mineralized by O_3 alone. Therefore, it is expected that the advantage of combining O_3 with light and/or catalyst will be noticed in terms of TOC removal (Fig. 2). The best TOC removal was achieved by photocatalytic ozonation, which means that in addition to parent compounds, a considerable amount of oxidation by-products were also degraded. Photo-ozonation also presented a good performance during RDB degradation, leading to mineralization level of 65%. Although photocatalysis presented worse performance than catalytic ozonation in degradation of ANL and RDB, in terms of TOC removal this did not happen.

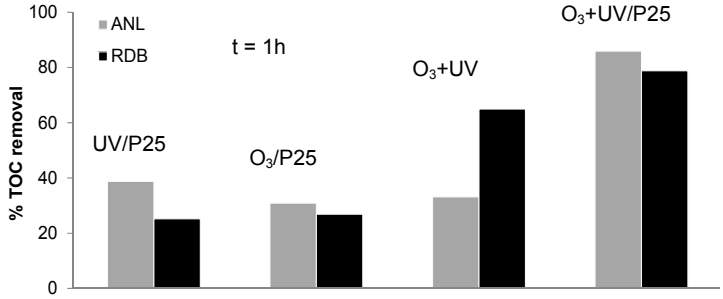

Fig. 2. Percentage of TOC removal during ANL and RDB degradation.

4 Conclusions

All tested oxidation processes completely removed ANL and RDB in a short reaction time, with the exception of photocatalysis. The combination of ozone, light and P25 lead to maximum mineralization.

Acknowledgements

This work was co-financed by FCT and FEDER under Program COMPETE (Project UID/EQU/50020/2013) and the research fellowship BPD/ 90309 / 2012 (CAO).

References

[1] V. Augugliaro, M. Litter, L. Palmisano, J. Soria, *Journal of Photochemistry and Photobiology C: Photochemistry Reviews* 7 (2006) 127.
[2] B. Kasprzyk-Hordern, M. Ziólek, J. Nawrocki, *Applied Catalysis B: Environmental* 46 (2003) 639.
[3] S. Wang, F. Shiraishi, K. Nakano, *Chemical Engineering Journal* 87 (2002) 261.

V-PP38

Mixed MoTi-Pillared Clay as a Catalyst for Selective Catalytic Reduction of NO by NH_3

Rejeb R.[1*], Kalfallah B.L.[1], Delahay G.[2]

1 - Laboratoire de Chimie des Matériaux et Catalyse, Département de Chimie, Faculté des Sciences de Tunis, Tunis, Tunisie

2 - Institut Charles Gerhardt Montpellier, UMR 5253, CNRS-UM2-ENSCM-UM1, Equipe MACS, Ecole Nationale Supérieure de Chimie, Montpellier Cedex 5, France

* rejebranda@gmail.com

Keywords: molybdenum, titanium, sulphate, pillared clay, SCR, nitrogen oxides

1 Introduction

Selective catalytic reduction (SCR) of nitrogen oxide (NO) by ammonia is the most universal method used for the removal of this pollutant from industrial flue gases. The SCR-NO process is currently performed with TiO_2 carrier that supports the active components, i.e., V_2O_5 and WO_3 or MoO_3 [1]. It is well known that V_2O_5-MoO_3 supported on TiO_2 is one of the industrial SCR-NO catalysts. However, the use of TiO_2 as a catalyst support is limited by its low specific surface area, porosity and resistance to sintering compared to Ti-pillared clay (Ti-PILC) that offer a better surface area, porosity, thermal stability and sufficient acidic functions.

In order to develop efficient catalyst for SCR-NO, considerable efforts have been made to investigate Ti-pillared clay (Ti-PILC) and their SCR behaviour to substitute the conventional TiO_2 [2-5]. So far, there has not been any published work describing a method for the preparation of molybdenum supported on Ti-PILC or studying the effect of molybdenum amounts on the physico-chemical properties of Ti-PILC nor discussing the catalytic activity of the mixed MoTi-pillared clays. For this reason, it has been interesting to investigate SCR-NO by ammonia over mixed MoTi-Pillared clay prepared in presence and absence of sulfate.

2 Experimental/methodology

The starting material was commercial clay mineral provided by Sigma Aldrich. The intercalating Ti-solution was prepared by slowly adding $TiCl_4$ into HCl (6M) or H_2SO_4 (3M) under vigorous stirring. The Mo-solution was also prepared at room temperature by dissolving ammonium heptamolybdate ($(NH_4)_6Mo_7O_{24}$, $4H_2O$) in distilled water. For mixed intercalation, both intercalating Ti-solution and Mo-solution were simultaneously added to the suspension of the initial clay under vigorous stirring. After 24h, the solid fraction was separated by centrifugation, dried at room temperature and finally calcined at 400 °C.

3 Results and discussion

The SCR activities of the investigated samples are shown in Fig. 1. The Ti-PILC exhibits smaller activity in SCR-NO reaction. After molybdenum addition to Ti-pillared clay (MoTi-PILC), the total acidity and the NO conversion increased significantly. This result indicates that molybdenum contribute to the improvement of the surface acidity and the SCR-activity.

The NO conversion over sulphated Ti-pillared clay (STi-PILC) is mainly related to the surface acidity and especially to Bronsted acid sites enhanced after sulphate addition [3, 4]. The catalytic behaviour of the sulphated MoTi-pillared clay (SMoTi-PILC) is largely related to total acidity of the catalyst. The addition of molybdenum onto sulfated Ti-PILC increased slightly the Bronsted acidity and considerably the Lewis acidity. These results demonstrate the beneficial role of molybdenum in the mixed MoTi-PILC catalyst. Furthermore, the best efficiency was

obtained with mixed MoTi-PILC having the highest acidity.

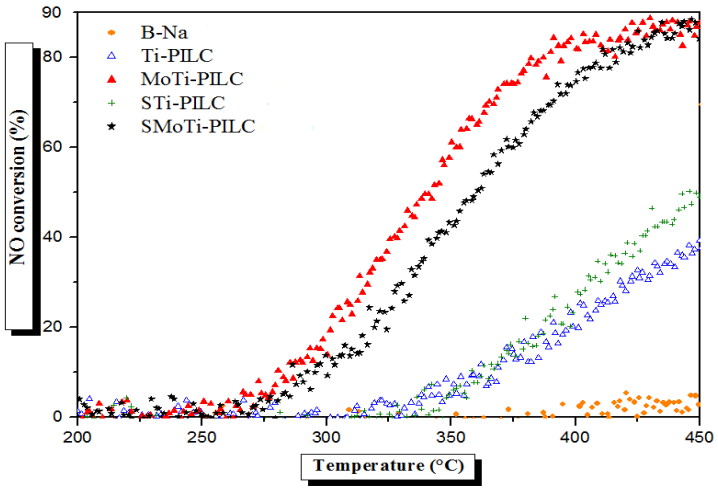

Fig.1: NO conversion as a function of temperature.

4 Conclusions

The addition of molybdenum to Ti-pillared clay, prepared in absence or in presence of sulphate, enhanced the total acidity and the NO removal activity. Furthermore, the promoting effect of sulfate was not found in presence of molybdenum. The best catalyst for SCR-NO reaction is mixed MoTi-PILC, having the highest acidity. It could be envisaged as a support for transition metals, such as vanadium, for the catalysis of SCR-NO or other chemical reactions.

References

[1] P. Grange, V. I. Parvulescu, Chem. Rev. 111 (2011) 3155.
[2] T. Grzybek, Catal. Today. 119 (2007)125-132.
[3] L. Khalfallah Boudali, A. Ghorbel, P. Grange, Catal. Lett. 86/4 (2003) 251.
[4] L. Khalfallah Boudali, A. Ghorbel, P. Grange, F. Figueras, Appl. Catal. B. 59 (2005) 105.
[5] J. Arfaoui, L. Khalfallah Boudali, A. Ghorbel, G. Delahay, Catal. Today. 142 (2009) 234.

V-PP39

Preferential Oxidation of Carbon Monoxide over NiO/CeO_2 and $NiO\text{-}CuO/CeO_2$ in Hydrogen-Rich Streams: Effect of Copper

Chagas C.A.*, Schmal M.

Federal University of Rio de Janeiro, Rio de Janeiro, Brazil

* chagas@peq.coppe.ufrj.br

Keywords: hydrogen, preferential oxidation, carbon monoxide, copper nickel, selectivity to CO_2

1 Introduction

Preferential oxidation of CO (CO-PROX) with an appropriate catalyst is one of the most economically and technologically promising methods for remove CO from H_2-rich gas streams, as compared to other processes [1]. The crucial requirements for the PROX reaction are high CO oxidation rate and high selectivity to CO_2. Selectivity is crucial considering the competing H_2 oxidation that may lead to a decrease in the overall fuel cell efficiency. Besides oxidation of both CO and H_2, methanation and WGS reactions can also take place simultaneously [2]. Several catalyst formulations have been reported in open literature and tested for this purpose. Particularly, copper-containing catalysts have been the object of numerous publications in the environmental catalysis field, due to their catalytic properties for CO oxidation applications [3]. Some works reported in literature suggesting that copper oxide catalysts are actives and selective as the platinum-group catalysts when operating at a lower reaction temperature [4]. However, the debate about what copper species are most beneficial in the preferential oxidation of CO is still open in literature and not well understood. In the present study, we investigated the effect of addition of CuO oxides species on supported NiO. We have prepared and characterized monometallic (NiO/CeO_2) and bimetallic ($NiO\text{-}CuO/CeO_2$) system and tested for CO-PROX reaction.

2 Experimental/methodology

NiO/CeO_2 and $NiO\text{-}CuO/CeO_2$ supports were prepared by incipient wet impregnation method [5]. The nominal loading amount of NiO and CuO were 20 and 5 wt. %, respectively. The catalysts were characterized by X-ray diffraction measurements and fluorescence (XDR, XFR), reduction in thermal programmed reduction (TPR), high-resolution transmission electron microscopy (HRTEM) and textural analysis. The catalytic tests were carried out in a continuous-flow and fixe-bed microreactor, using 150 mg of catalyst and operating at atmospheric pressure. The reaction was performed at different temperatures from 50 to 200 °C, in steps of 25 °C and kept for 30 minutes at each temperature. The feed composition consisted in 1 vol.% CO, 1 vol.% O_2, 60 vol.% H_2 and He balance at a flow rate of 150 $cm^3\ min^{-1}$.

3 Results and discussion

The physicochemical properties of the catalysts are listed in Table 1. It shows that the chemical analysis for all the samples closer to the nominal values.

Table 1. Physical and Chemical properties of the samples.

Catalyst	Chemical composition (wt%)			S_{BET}	Vp	R_m
	NiO	CuO	CeO_2	($m^2\ g^{-1}$)	($m^2\ g^{-1}$)	(nm)
CeO_2 (support)	-	-	100	48	0.205	11.2
$20NiO/CeO_2$	18.9	-	81.1	33	0.154	11.05

20NiO-5CuO/CeO_2	22.2	6.2	71.6	39	0.116	8.76

As expected, the insertion of NiO led to a decrease in the specific surface area (from 48 to 33 m^2 g^{-1}) and pore volume (from 0.205 to 0.154 cm^3 g^{-1}) of ceria. On the other hand, the addition of CuO on NiO/CeO_2 increased the specific surface area (from 33 to 39 m^2 g^{-1}) and a decreased the pore volumes (from 0.154 to 0.116 cm^3 g^{-1}), as shown in Table 1. The CO and O_2 conversion and selectivity to CO_2 for the samples are shown in Fig. 1. Note that all samples exhibited CO conversion increases with temperature, with a maximum at 125 °C for the promoted Cu sample and at 170 °C for the unpromoted sample. For higher temperature, the conversion decreases competing with the oxidation of H_2 affecting the CO_2 selectivity. The CO_2 selectivity of the NiO-CuO/CeO_2 catalyst was 100% up to 150 °C. Then, the CO_2 selectivity decreased significantly (T = 200 °C, S_{CO2} = 53%).

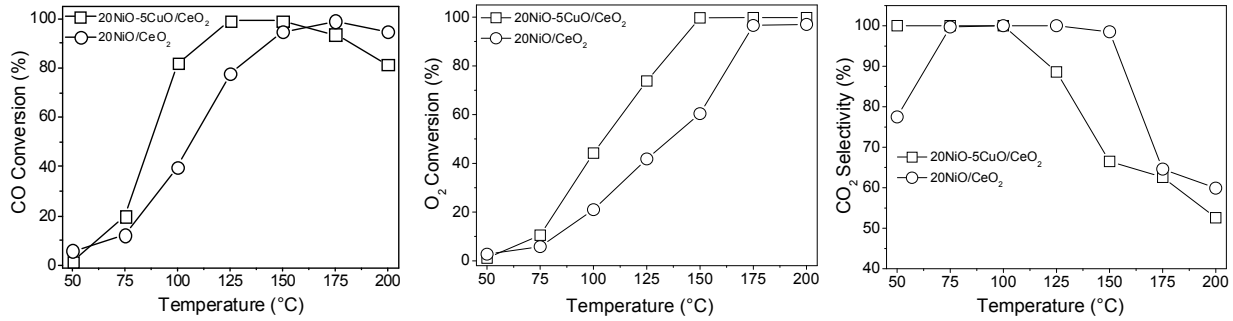

Fig. 1. CO and O_2 conversion and selectivity to CO_2 as a function of reaction temperature.

The stability of the catalysts for CO-PROX were tested with time on stream at 200 °C for 30 h and the results are shown in Fig. 2.

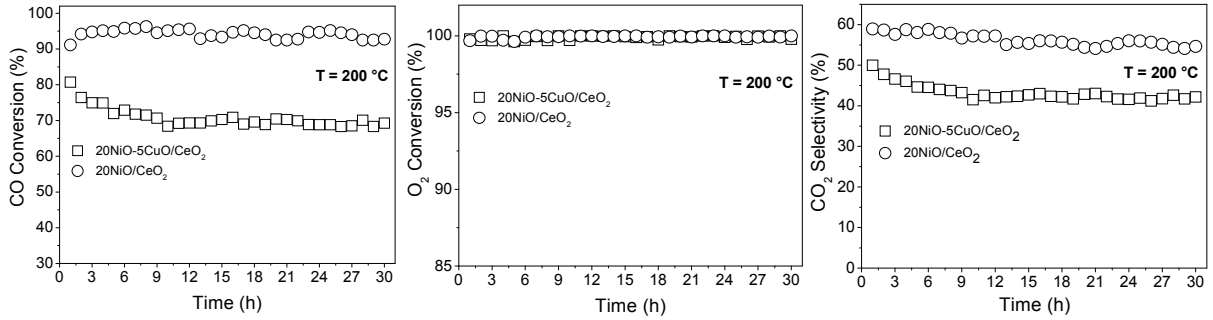

Fig. 2. CO and O_2 conversion and CO_2 selectivity under isothermal conditions at 200 °C.

4 Conclusions

The NiO/CeO_2 and NiO-CuO/CeO_2 were active and selective to CO-PROX reaction until 200 °C and also showed good stability during time on stream. These materials are promising catalysts for CO-PROX reaction presenting more resistant to methanation than platinum-group catalysts reported in the literature.

Acknowledgements

The authors acknowledge financial support by CAPES (Coordenação de Aperfeiçoamento de Pessoal de Nível Superior).

References

[1] S. H. Oh, R.M. Sinkevitch, J. Catal. (1993) 142.
[2] M. Priscila, N. F. P. Ribeiro, M. M. V. M. Souza, J. Power Sources (2006) 158.
[3] W. Liu, M.F. Stephanopoulos, J. Catal. (1995) 153.
[4] T. S. Mozer, F. B. Passos, Int. J. Hydrogen Energy (2011) 36.
[5] S. Lin, H. Daimon, S. Ha, Appl. Catal. A (2009) 366.

V-PP40

Photocatalytic Reduction of Nitrate to Nitrogen in Water under Visible Light Irradiation in the Presence of $Pt/SrTiO_3$: Rh Photocatalyst and $SnPd/Al_2O_3$ Non-Photocatalyst

Hirayama J.[1], Kamiya Y.[2*]

1 - Graduate School of Environmental Science, Hokkaido University, Sapporo, Japan
2 - Research Faculty of Environmental Earth Science, Hokkaido University, Sapporo, Japan

* kamiya@ees.hokudai.ac.jp

Keywords: nitrate reduction, photocatalysis, visible light, groundwater purification, Tin-palladium

1 Introduction

Pollution of groundwater with nitrate (NO_3^-) is a serious problem in the world. Drinking water with high NO_3^- concentrations causes various diseases, including blue baby syndrome. Thus, NO_3^- in groundwater must be decomposed for drinking water. Photocatalytic reduction of NO_3^- has attracted much attention as a method for the decomposition of NO_3^-. We have proposed a photocatalytic reaction system combining a semiconductor photocatalyst (Pt/TiO_2) and a supported bimetallic non-photocatalyst ($SnPd/Al_2O_3$) dispersed in water [1], but this system can work only under UV irradiation because Pt/TiO_2 is a UV light active photocatalyst. In the present study, we expand the photocatalytic system to NO_3^- reduction driven by visible light by using $Pt/SrTiO_3$:Rh instead of Pt/TiO_2 [2].

2 Experimental

$SrTiO_3$:Rh was prepared by calcining a mixture of $SrCO_3$, TiO_2, and Rh_2O_3 at 1373 K. Modification of $SrTiO_3$:Rh with Pt was conducted by a photodeposition method with $H_2PtCl_6 \cdot 6H_2O$ in aqueous methanol solution. Loading amount of Pt was fixed to 0.1 wt%. $SnPd/Al_2O_3$ was prepared by an incipient wetness method using Al_2O_3 (Aerosil Alu C), aqueous $PdCl_2$ solution, and aqueous $SnCl_2$ solution. Loading amount of Sn and Pd were fixed to 2.3 wt% and 4.2 wt%, respectively. Just before the reaction, $SnPd/Al_2O_3$ was reduced with $NaBH_4$.

Photocatalytic reduction of NO_3^- in water was carried out in a Pyrex reaction vessel connected to a closed gas circulation system at 298 K. The catalyst powder of $Pt/SrTiO_3$:Rh (500 mg) and $SnPd/Al_2O_3$ (150 mg) were dispersed in 250 mL KNO_3 solution (0.8 mM) with 10 vol% CH_3OH and then the suspension was irradiated with a 300 W Xe lamp with cutoff filter ($\lambda > 420$ nm). The products were analyzed by using two ion chromatographs and a gas chromatograph, and by the iodometric titration.

3 Results and discussion

Table 1 summarizes the data of the photocatalytic reduction of NO_3^- in water under visible light irradiation for 6 h. $Pt/SrTiO_3$:Rh alone (Entry 1) showed negligible activity, while is a visible light-active photocatalyst. This is because $SrTiO_3$:Rh itself and Pt metal are incapable of activating NO_3^-. $SnPd/Al_2O_3$ also showed only low catalytic activity (Entry 2). The conversion (3%) in Entry 2 was due to non-photocatalytic reduction of NO_3^- with methanol over SnPd bimetal. In contrast to these, the high conversion was obtained, if both $Pt/SrTiO_3$:Rh and $SnPd/Al_2O_3$ were present in the reaction solution (Entry 3). In addition, formation of undesirable NH_4^+ was suppressed with low level (6% selectivity). When the reaction was conducted under dark conditions, the conversion was low even in the co-presence of both catalysts (Entry 4). Thus, the enhanced activity show in Entry 3 was strongly related to the photocatalytic reaction.

The catalyst that $SrTiO_3$:Rh modified directly with SnPd bimetal was much less active than Pt/$SrTiO_3$:Rh–SnPd/Al_2O_3 system (Entry 5). SnPd/$SrTiO_3$:Rh did not produce H_2 at all in the absence of NO_3^- in water even though visible light was irradiated, indicating that this did not act as a photocatalyst probably due to shielding effect of incident light by, and formation of a number of recombination sites on the SnPd bimetal.

Next, we investigated a reaction mechanism over the Pt/$SrTiO_3$:Rh–SnPd/Al_2O_3 reaction system. The amount of H_2 needed to the reduction of NO_3^- was calculated from the converted NO_3^-, and producted NH_4^+ and N_2, and it was found that this was three times larger than the amount of H_2 evolved by the photocatalytic reaction over Pt/$SrTiO_3$:Rh in the absence of NO_3^-. This result suggested that methanol as well as the products includingH_2CO and HCO_2H, which were formed by photo-oxidation of methanol, other than H_2 must act as reductants for NO_3^- over$SnPd/Al_2O_3$ (Fig. 1).

Thus we further investigated non-photocatalytic reduction of NO_3^- with CH_3OH, H_2CO, and HCO_2H in the presence of SnPd/Al_2O_3 under the dark conditions. In the reaction where CH_3OH, H_2CO, and HCO_2H was added simultaneously, the conversion was 17% at 6 h, which was almost the same as the conversion for the photocatalytic reduction of NO_3^- in the Pt/$SrTiO_3$:Rh–SnPd/Al_2O_3 system. By comparison of the decomposition rate of NO_3^- with each compound, it was found that mainly H_2CO and HCO_2H, in addition to H_2, acted as reductants for NO_3^- reduction, but CH_3OH was almost completely ineffective although it was abundantly present in the reaction solution.

Table 1 Photocatalytic reduction of nitrate in water under visible light irradiation.

Entry	Catalyst	Conversion	Selectivity/%	
		/%	NH_4^+	N_2
1	Pt/$SrTiO_3$:Rh	< 1	---	---
2	SnPd/Al_2O_3	3	35	65
3	Pt/$SrTiO_3$:Rh+ SnPd/Al_2O_3	16	6	94
4[a]	Pt/$SrTiO_3$:Rh+ SnPd/Al_2O_3	5	9	91
5	SnPd/$SrTiO_3$:Rh	8	16	84

[a]Under dark conditions.

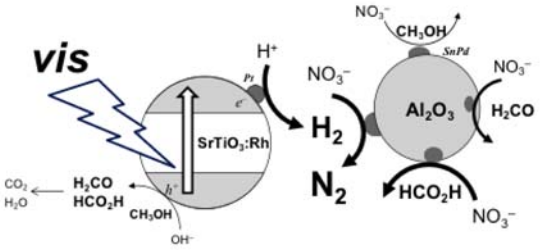

Fig. 1 Schematic illustrations of the reaction mechanism of photocatalytic reduction of NO_3^- in water in the co-presence of Pt/$SrTiO_3$:Rh and SnPd/Al_2O_3 under visible light irradiation.

4 Conclusions

The photocatalytic reaction system comprising Pt/$SrTiO_3$:Rh and SnPd/Al_2O_3, which were dispersed in water, efficiently and selectively promoted the photocatalytic reduction of NO_3^- in the presence of methanol under visible light irradiation. Products including H_2CO and HCO_2H, which were formed by photo-oxidation of methanol over Pt/$SrTiO_3$:Rh, other than H_2 acted as reductants for NO_3^- over SnPd/Al_2O_3.

References

[1] J. Hirayama, H. Kondo, Y. Miura, R. Abe, Y. Kamiya, Catal. Commun. 20 (2012) 99.
[2] J. Hirayama, R. Abe, Y. Kamiya, Applied Catalysis B: Environmental. 144 (2014) 721.

V-PP41

Co, La and Ce Modified Pd-Al_2O_3 - Catalysts for Methane Combustion

Todorova S.[1*], Stefanov P.[2], Naydenov A.[2], Tzaneva B.[3], Stoyanova D.[2]

1 - Institute of Catalysis, Bulgarian Acad. Of Sciences, Sofia, Bulgaria
2 - Institute of General and Inorganic Chemistry , Bulgarian Acad. Of Sciences, Sofia, Bulgaria
3 - Technical University of Sofia, Bulgaria

* todorova@ic.bas.bg

Keywords: methane combustion, Pd-Co/Al_2O_3 catalysts, Pd-Co-La/Al_2O_3 catalysts, Pd-Co-La-Ce/Al_2O_3 catalysts

1 Introduction

Methane, being a greenhouse gas, plays a significant role in the global warming. Most of the catalysts, designed for methane combustion, are based on palladium – separately or in combination with different metals or metal oxides, supported on alumina. The main problem in the practice is the deactivation of the Pd-based catalysts. An alternative for the stabilization of the support and the catalytic active phase could be found in the introduction of rare earth oxides into the existing catalytic systems. La_2O_3 is an excellent stabilizer of the specific surface area of supports like Al_2O_3 and ZrO_2. CeO_2 is also well known as an alternative for stabilization of PdO since it hinders the PdO reduction and promotes Pd re-oxidation when PdO–CeOx contact is available.

2 Experimental

The single-component (Pd/Al_2O_3 and Co/Al_2O_3) and multi-component (Pd+Co/Al_2O_3, Pd+Co/$LaAl_2O_3$, Pd+Co/$LaCeAl_2O_3$) samples were prepared by impregnation of γ-Al_2O_3 with aqueous solutions of $Co(NO_3)_2.6H_2O$, $Pd(NO_3)_2.2H_2O$, $Ce(NO_3)_2.4H_2O$ and $La(NO_3)_3.2H_2O$. The palladium and cobalt contents in each one of the prepared samples were approximately 0.03 wt % and 0.3 wt%, respectively. The catalysts were characterized by X-ray diffraction (XRD), X-ray photoelectron spectroscopy (XPS), electron paramagnetic resonance (EPR), transmission electron microscopy (TEM) and reaction kinetics measurements.

4 Results and discussion

Finely dispersed palladium particles were formed on the surface of all samples. According to the XPS data Pd^{2+} and Pd^{4+} present on the surface of the fresh catalysts modified with Co only, while the major part of the surface palladium in the La and Ce containing samples is in the form of Pd^0.

The following order of activity is observed: Pd+Co/Al_2O_3>Pd+CoLaCe/Al_2O_3>Pd+CoLa/ Al_2O_3>Pd/ Al_2O_3. The modification of Pd/Al_2O_3 with Co significantly improves its catalytical activity. This effect is explained by the stabilization of palladium as PdO on the support due to strong interaction between Pd particles and the surface cobalt oxide phase. It is very likely that, when La and Ce are deposited before the Co deposition, the formation of cobalt surface phase is hindered as well as the further stabilization of PdO phase. The Pd+Co/Al_2O_3 sample demonstrates remarkable stability after ageing. However, the activities of the catalysts, modified with La and Ce drop after ageing, most probably due to sintering of palladium.

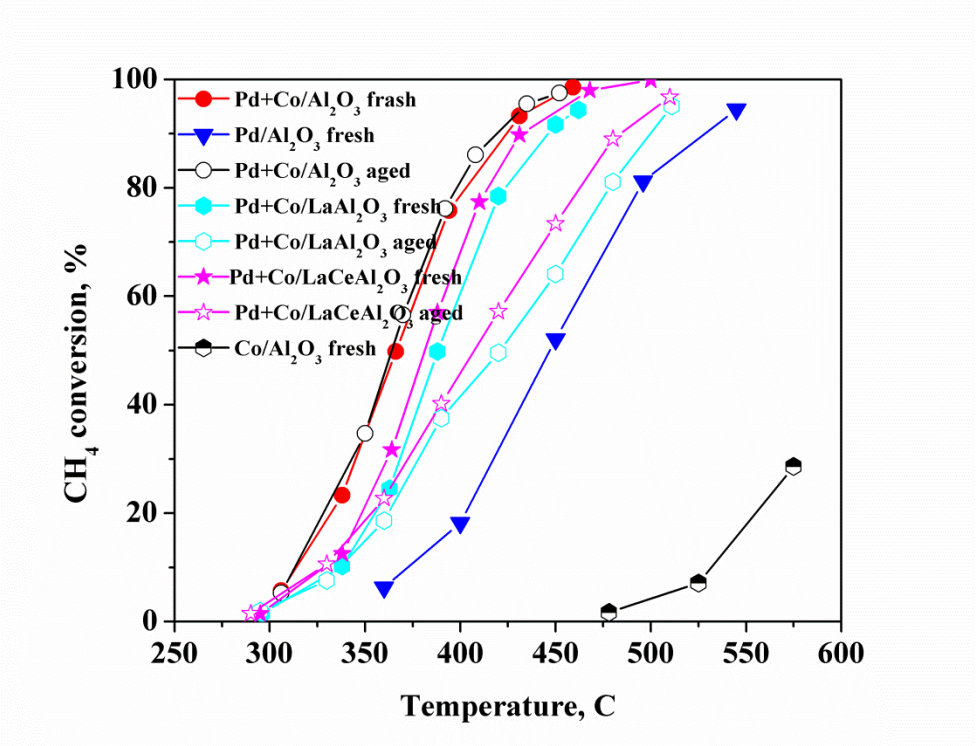

Fig. 1. Temperature dependencies of the methane conversion

4 Conclusions

The alumina-supported palladium catalysts, modified with cobalt demonstrate high activity and stability in the reaction of complete methane oxidation. The active species in the methane oxidation over Co-modified palladium catalyst are PdO clusters. The role of the surface cobalt oxide phase is to stabilize the palladium in its oxidized state and to serve as reservoir of the oxygen species. The modification with La and Ce prevent Co-Al phase formation and as result the stabilization of palladium in form of PdO.

Acknowledgements

The authors are gratefully acknowledged to the National Science Fund of Bulgaria (Grant No TO1/6) for the financial support

V-PP42

Deep Ethanol Oxidation over Nanosized Co-Mn-Al Mixed Oxides Supported on Pelletized Magnesia-Alumina

Jirátová K.[1*], Balabánová J.[1], Kovanda F.[2], Obalová L.[3]

1 - Institute of Chemical Process Fundamentals of the Czech Academy of Sciences, Praha, Czech Republic

2 - University of Chemistry and Technology, Praha, Czech Republic

3 - Institute of Environmental Technology, VŠB - Technical University of Ostrava, Ostrava, Czech Republic

* jiratova@icpf.cas.cz

Keywords: ethanol, deep oxidation, catalysts, cobalt-manganese, mixed oxides, magnesia-alumina

1 Introduction

Volatile organic compounds (VOC) emitted in industrial gases can be eliminated applying the catalytic total oxidation. We found high catalytic activity of the Co-Mn-Al mixed oxides, obtained by heating of the coprecipitated layered double hydroxide (LDH) precursor, in the ethanol total oxidation [1]. Activity of this catalyst was remarkably increased by addition of small amount of the potassium promoter. The catalysts prepared by pelletizing the powdered material contained high amounts of expensive cobalt, which was not fully utilized in the catalytic reaction. Therefore, we focused on preparation of supported catalysts with lower concentration of active components placed exclusively in the outer shell of the support pellets. In the present study, we applied the method of impregnation using acidic solution of metal salts in combination with a support having basic properties that could limit penetration of active components into the support pellets.

2 Experimental

The catalysts were prepared by impregnation of magnesia-alumina pellets (5x5 mm, Sasol) with aqueous solutions containing Co, Mn and Al nitrates (molar ratio of Co:Mn:Al=4:1:1) and subsequent heating at 500 °C in air. The prepared samples were characterized by chemical analysis, powder XRD, measurement of nitrogen adsorption at -196°C, TPD of CO_2, and TPR. Distribution of active metals in the catalyst pellets was determined by SEM. Catalytic activity in the total oxidation of ethanol, which was chosen as a model VOC, was measured under unsteady-state conditions with heating rate of 2.27 °C min^{-1} (100–400 °C), at ethanol concentration in air of 1.5 g m^{-3} and GHSV 20 000 ml g_{cat}^{-1} h^{-1}. Temperatures T_{50}, at which 50% conversion of ethanol was observed, were chosen as a measure of the catalysts activity. For comparison, the pellets (5x5 mm) of commercial Co-Mn-Al mixed oxide catalyst (ASTIN 2-100) were also examined.

3 Results and discussion

Results of chemical analysis, amounts of reducible components, and amounts of CO_2 desorbed from the catalysts are summarized in Table 1.The sum of Co and Mn in the supported catalysts varied from 4 to 15 wt. % (commercial catalyst with about 55 wt. % of Co+Mn exhibited uniform distribution). The magnesia-alumina support contained, apart from 30 wt. % of Al_2O_3, about 1 wt. % of Na. Basic properties of the support as well as surface area of the samples were decreasing with gradual adding the active metal oxides. The SEM imaging confirmed limited penetration of active metals into support pellets (Fig. 1a). Powder XRD patterns of all samples showed diffraction lines corresponding to spinel-like phases.

Table 1. Chemical analysis, redox and basic properties of the catalysts, depth of Co, Mn penetration in the pellets, and temperatures T_{50} of ethanol oxidation

Sample	Cat-0	Cat-5	Cat-10	Cat-10[a]	Cat-15[a]	Cat-20[a]	ASTIN 2-100
Co, wt. %	0	3.33	4.75	6.55	9.35	11.82	45
Mn, wt. %	0	0.82	1.22	1.62	2.31	2.94	9.8
Na, wt. %	0.8	0.59	0.67	-	0.67	0.64	2.6[b]
Surface area, m^2/g	130	105	59	87	68	55	87
H_2-TPR, mmol/g[c]	0	0.46	0.70	0.67	1.28	1.63	5.74
CO_2-TPD, mmol/g[c]	1.50	1.11	0.92	0.86	0.87	0.67	0.18
L[d], %	0	47	45	40	34	47	100
T_{50}, °C	-	234	209	193	172	200	183

[a]twofold impregnation, [b] potassium,[c] temperature range 25-500 °C, [d]depth of (Co+Mn) penetration L=layer/pellet radius

Ethanol conversion over the examined catalysts is demonstrated in Fig. 1b. The most active sample, even more active than the commercial Co-Mn-Al mixed oxide catalyst with almost 55 wt.% of (Co+Mn), was the catalyst with much lower content (only about 12 wt.%) and non-uniform distribution of Co and Mn in the pellets. The main reaction byproduct, acetaldehyde, was completely transformed into CO_2 at temperatures lower than 300 °C (Fig. 1c). Formation of the other reaction byproduct, CO, was not detected.

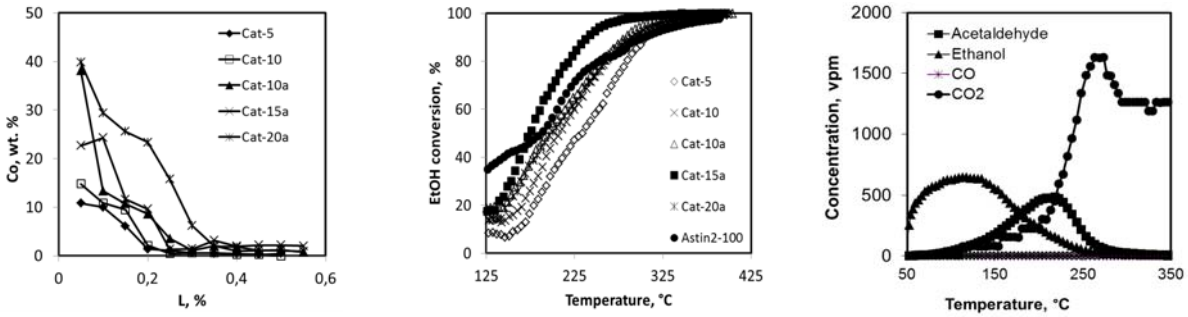

Fig. 1.a) Distribution of cobalt in the supported Co-Mn-Alcatalysts, b) conversion curves of ethanol, c) reaction components as a function of reaction temperature for the most active catalyst Cat-15[a]

4 Conclusions

Impregnation of the magnesia-alumina pellets having basic properties with acidic solution of Co, Mn and Al nitrates led to limited penetration of metal cations into the support and formation of catalysts with non-uniform distribution and reduced content of active components. The formed active layer in the support resisted to attrition during the catalytic reaction. The activity of the supported catalysts slightly differed from that of the commercial catalyst with uniform distribution of Co and Mn and (Co+Mn) about 55 %. Supported catalyst with optimum concentration (ca. 12 wt. %) showed better catalytic properties than the commercial one.

Acknowledgements

The authors thank the Czech Science Foundation for the financial support (project P106/14-13750S).

References

[1] K. Jirátová, J. Mikulová, J. Klempa, T. Grygar, Z. Bastl, F. Kovanda, *Appl. Catal. A* 361 (2009) 106.

V-PP43

Synthesis of Macro-Porous Cu-Sn-Zr Catalyst for SO_2 Reduction

Lee T.H.[1], Seong Y.B.[1], Lee J.W.[1], Kim M.J.[1], Park C.J.[1], Choi W.Y.[1], Lee T.J.[1*], Park N.-K.[2], Baek J.-I.[3], Lee J.B.[3]

1 - Yeungnam University, Chemical Engineering, Gyeongsan, Republic of Korea
2 - Yeungnam University, Institute of Clean Technology, Gyeongsan, Republic of Korea
3 - Korea Electric Power Research Institute, Daejeon, Republic of Korea

* tjlee@ynu.ac.kr

Keywords: macro-porous, PMMA, coal gasification process

1 Introduction

In coal gasification process, sulfur compounds such as H_2S and COS can be contained in synthetic gas, due to the sulfur component in coal, and the sulfur compounds contained in synthetic gas can be selectively removed with a desulfurization sorbents on the hot gas desulfurization process. SO_2 is produced in the regeneration process of the sulfide sorbent. SO_2 can be conversed to elemental sulfur by catalytic reduction process using a reducing agent.

2 Experimental/methodology

In this study, the macro-porous Cu-Sn-Zr catalyst was prepared in order to SO_2 decomposition. The catalytic activity of Cu-Sn-Zr catalyst for SO_2 reduction was confirmed in our previous study. Thus, the porous materials were synthesized in order to enhance the catalytic activity. The template was used for the formation of macro-pores and the nano-spherical beads of poly-methyl-methacrylate (PMMA) were used as a template. Therefore, PMMA colloidal nano-beads were synthesized with MMA by the suspension polymerization method in this study. Tin chloride, copper nitrate, zirconium oxy nitrate were used as a precursor for a synthesis of Cu-Sn-Zr Catalyst, and was impregnated over PMMA beads by rotary vacuum evaporator. The solid material of Cu-Sn-Zr/PMMA was thermal treated for 4 h at 600 ^oC.

3 Results and discussion

The porous morphology of Cu-Sn-Zr catalyst prepared in this study was observed by SEM analysis, as shown in Fig.1. The surface area of this material measured by nitrogen adsorption method was approximately 80 m^2/g and non-porous Cu-Sn-Zr catalyst surface area was 40 m^2/g. In reaction test, the activity macro-porous Cu-Sn-Zr catalyst was tested under regenerator-off gas contained with steam(20 mol%), oxygen(4 vol%). Reaction temperatures(300~500 ^oC) was regulated by a temperature controller. In activity test, the conversion of SO_2 was approximately 95 %, sulfur yield was 93 % at 400 ^oC. On the other hand, the SO2 conversion of non-porous Cu-Sn-Zr catalyst was 78 %, sulfur yield was 75 % at 400 ^oC.

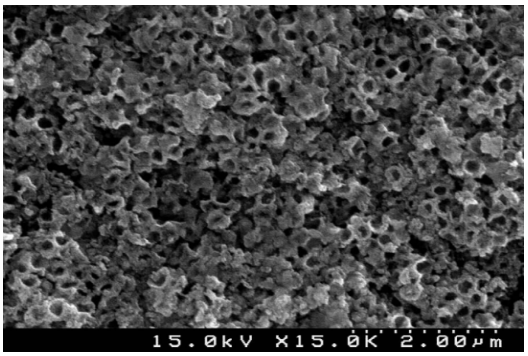

Fig. 1. SEM image of macro-porous Cu-Sn-Zr catalyst

4 Conclusions

Macro-porous Cu-Sn-Zr catalyst has a larger surface area than non-porous Cu-Sn-Zr catalyst. So, macro-porous Cu-Sn-Zr catalyst has a higher catalytic activity than the non-porous Cu-Sn-Zr catalyst. Thus, the use of a macro-porous Cu-Sn-Zr catalyst can be obtained a high catalytic reactivity.

Acknowledgements

This work was supported by Energy Efficiency and Resources R&D program of the Korea Institute of Energy Technology Evaluation and Planning (KETEP) grant funded by the Korea government Ministry of Knowledge Economy (2011201020004A), Korea Electric Power Corporation (KEPCO) and Korea Western Power co., Ltd.

References

[1] N.-K. Park, J. Y. Park, T. J. Lee, J.-I. Baek, C. K. Ryu, *Catalysis Today*, 174 (2011) 46

V-PP44

Degradation of Paracetamol by Homogeneous Catalytic Photo-Fenton Process in an Open Channel Reactor

Jáuregui Haza U. J.[1*], Abreu Zamora M. A.[1], González Labrada K.[2], Robaina León Y.[1], Valdés Callado M.[1]

1 - Instituto Superior de Tecnologías y Ciencias Aplicadas, La Habana, Cuba
2 - Instituto Superior Politécnico José Antonio Echeverría, La Habana, Cuba

* ulises.jauregui@infomed.sld.cu

Keywords: homogeneous catalysis, photo-fenton, open channel reactor, paracetamol

1 Introduction

The conventional wastewater treatment plants do not warranty the degradation of emergent persistent organic pollutants (POPs), among them the pharmaceuticals. Advanced Oxidation Processes, like photodegradation using artificial ultraviolet radiation or solar radiation, are proposed as an alternative for the treatment of contaminated water with POPs. These processes were defined as those that involve the in situ formation of highly reactive radicals, especially hydroxyl radicals, in sufficient quantities to produce the water purification [1]. In the present work, the hydrodynamic characterization and evaluation of an open channel reactor for ultraviolet degradation of paracetamol by homogeneous catalytic photo-Fenton are presented.

2 Results & discussion

Hydrodynamic characterization of the open channel reactor

The hydrodynamic characterization of the reactor (Fig. 1) was performed through the analysis of the residence time distribution (RTD) using a radioactive ^{99m}Tc tracer. This process was done in two steps. First, the open channel reactor was evaluated in continuous mode operation. To evaluate the influence of the volume of fluid in the reactor and the diameter of the flow distributor's orifices on the flow pattern, an experimental 3^2 design was used. The dependent variables were the mean residence time (Trm), the number of perfectly mixed tanks and the mean residence time of the model in the main flow. Several hydrodynamic models, using the software DTSPro v.4.2, were evaluated. The best hydrodynamic model was the model of perfectly mixed tanks in series exchanging with stagnant zones. The average relative error of estimation was 8.7 %. Then, the mixing time in the overall reacting system operating in close loop mode was determined, been of 34 minutes.

Photodegradation of paracetamol

In all experiments, the volume in the reactor was 5 L and the initial concentration of paracetamol was 100 mg/L, taking into account the results of previous studies [2]. All experiments were carried out with pH control, using technical water. The samples (10 mL) for analysis were taken at regular time intervals (30 min, 1h, 2h, 4h and 6h in photolysis and photolysis with H_2O_2 experiments and 15 min, 30 min, 1h, 2h, 4h and 6h in photo-Fenton experiments). The monitoring of the paracetamol concentration was done by HPLC.

In photolysis experiments, the pH was equal to 7. The intensification of photolysis with H_2O_2 was studied at two values of pH (3 and 7) and different concentrations of oxidant (6.9, 13.9, 27.8, 41.7, 55.6, and 69.5 mmol/L) were employed corresponding to the half, one, two, three, four and five times the stoichiometry of the oxidation reaction. In the photo-Fenton experiments various concentrations of Fe^{2+} ($FeSO_4 \cdot 7H_2O$) (0.48 and 1.39 mmol/L) and H_2O_2

(13.90 and 55.56 mmol/L) at pH = 3 were used according to a factorial design 2^2.

Figure 2 shows the results of the degradation of paracetamol by photolysis and photolysis with H_2O_2 at different values of pH and different concentration of H_2O_2. The best results were obtained for photo-Fenton process, when the pharmaceutical was completed destroyed at 15 minutes with mineralization of 85 % at 6 hours.

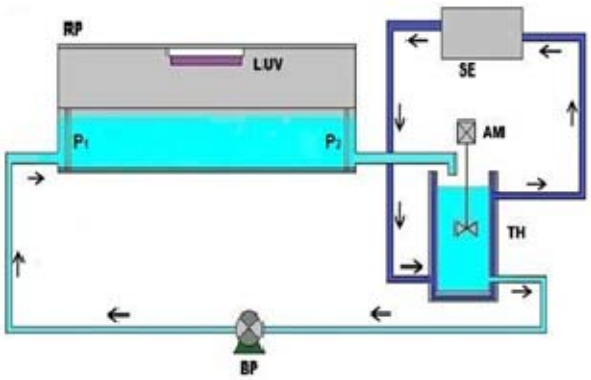

Figure 1: Experimental setup: RP: open channel reactor, LUV: UV lamp, TH: stirred tank, SE: thermostat, BP: peristaltic pump

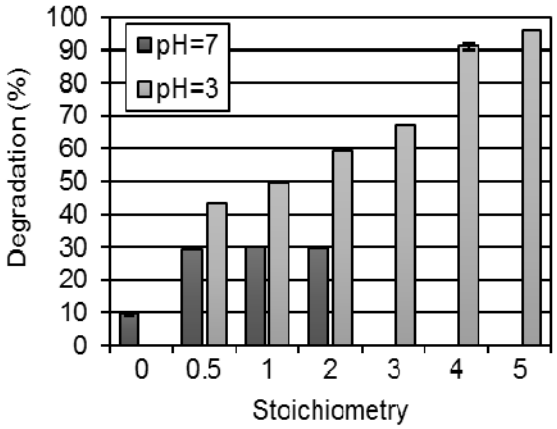

Figure 2: Degradation of paracetamol by photolysis and photolysis with H_2O_2

References

[1] W. H. Glaze, J. W. Kang. The chemistry of water treatment involving ozone, hydrogen peroxide and ultraviolet radiation. Ozone-Science & Engineering 9 (1987) 335-352.

[2] I. Quesada, C. Julcour. Sonolysis of levodopa and paracetamol in aqueous solutions, Ultrasonics Sonochemistry 16 (2009 a) 610-616.

V-PP45

Catalytic Oxidation of Polycyclic Aromatic Hydrocarbons (PAH) over Zeolite Type Catalysts: Effect of Si/Al Ratio, Structure and Acidity

Pitault I.S.[1], Gelin P.A.[2], Fiani E.M.[3], Meille V.A.[4], Bornette F.R.[4], Vanoye L.A.[4], Soufi J.I.[4,2*]

1 - Université Lyon1, CNRS, UMR 5007, Laboratoire d'Automatique et de Génie des Procédés, Villeurbanne Cedex, France

2 - Université Lyon1,CNRS, UMR 5256, Institut de Recherches sur la Catalyse et l'Environnement de Lyon, Villeurbanne Cedex, France

3 - ADEME Agence de l'Environnement de la Maîtrise de l'Energie, Angers Cedex01, France

4 - Ecole de Chimie Physique Éléctronique de Lyon, CNRS, UMR 5285, Laboratoire de Génie des Procédés Catalytique, Villeurbanne Cedex, France

* jso@lgpc.cpe.fr

Keywords: catalytic oxidation, 1-methylnaphtalene, 1-methylnaphtalene, conversion, carbon dioxide, selectivity zeolite, acidity

1 Introduction

PAHs show adverse health effects. For instance, benzo(a)pyrene is classified as carcinogenic by IARC. Therefore, at the international level, many countries have committed themselves to minimizing air emissions through the Aarhus Protocol on POPs which was signed in 1998 under the Geneva Long Range Transboundary Air Pollution Convention. At the French level, emission limit values for PAHs have been introduced in a recent regulation on combustion plants with a thermal input higher than 20 MWth (Ministerial Decree of 26 August 2013).

Catalytic oxidation is one of the most promising technologies to reduce the emissions of air pollutants [1]. Metal oxides or supported noble metals methods are the most investigated catalysts for the destruction of organic pollutants.

Acid zeolites (protonic forms) have been considered as effective cheap alternative catalysts to metal oxides for hydrocarbons oxidation [2]. Catalytic performances of these zeolites were associated with the presence of Bronsted acide sites.

In this work, the removal of 1-methylnaphtalene (1-MN), a model compound representative of PAH, by catalytic combustion in the presence of steam is investigated.

The behavior of various acidic zeolites towards the gas-phase catalytic oxidation of 1-MN is investigated. The effect of some parameters on 1-MN oxidation is studied: the structure of the zeolite, Lewis and Bronsted acidity and Si/Al ratio. The performance of these zeolites is compared to 0.97 wt% Pt/Al2O3 which is one of the most active catalysts in complete oxidation of naphthalene [3].

2 Experimental/methodology

Catalytic activity experiments were carried out in a vertical stainless steel tube reactor, which in turn is placed in a tube furnace. Catalytic activity is measured over the temperature range 150°C-400°C and the temperature is measured by thermocouple axially placed in the catalyst bed. Catalysts are packed to a constant volume to give a gas hourly space velocity of 20000 h-1 for all studies. The two liquids (1-MN and water) are injected with syringe pumps. Prior to the catalytic tests, the samples (100mg) are treated in air (10 L/h/g) at 500°C for one hour. The reaction feed is 9% of oxygen, 10% of water and 500 ppm of 1-MN in nitrogen. The gases (1-MN, CO, CO2) at the reactor outlet are analysed on-line by a gas chromatograph.

In this work, we study the oxidation activity which is expressed as 1-MN conversion (X) and carbon dioxide selectivity (Y). There are determined as follows:

$$X = \frac{A_{blank} - A_{out}}{A_{blank}}$$

With Ablank: Area of 1-MN peak before the reaction; Aout : Area of 1-MN peak at the reactor outlet during the reaction.

$$Y = \frac{Ac_{out}}{A_{max}}$$

With Acout: Area of carbon dioxide peak during the reaction; Amax: Theoretical area of carbon dioxide peak when the 1-MN is totally converted to CO2.

3 Results and discussion

The zeolite catalysts (HFAU, HZSM-5, BETA, mordenite) are compared to the 0.97 wt% Pt/Al2O3 catalyst. One of the methods to compare catalysts is to plot light-off curves with 1°C/min decreased oven program temperature from 350°C to 150°C. Figure 1 shows the 1-MN conversion as a function of the reaction temperature under 0.97 wt% Pt/Al2O3 catalyst. 100% conversion of 1-MN is obtained around 320°C. With the same catalyst, second method consists in measuring the conversion during one hour and a half of temperature steps. No difference between conversions measured with the two methods is observed. Thus, no deactivation on this catalyst is occurred.

Regarding zeolite catalysts, conversion measurement with step program temperature is required due to the deactivation induced by the formation of coke under acid sites[2].The acidity of the zeolite is characterized, after and before catalytic test, with pyridine/CO adsorption followed by FTIR. The correlation between acid properties, structure and Si/Al ratio and catalytic activity is discussed.

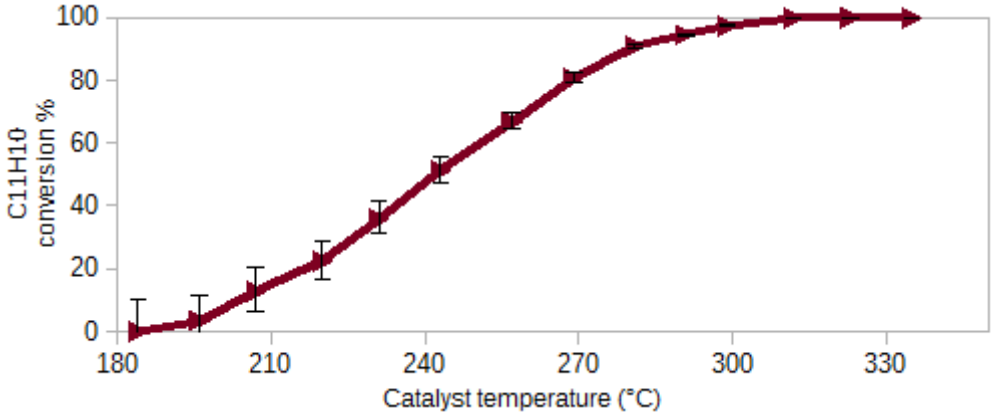

Fig. 1. Light-off curve over 0.97 wt %Pt/Al_2O_3. Feed composition: 460 ppm 1-MN, 9% O_2 in N_2 VVH=20000h^{-1}

Acknowledgements

The authors gratefully acknowledge the Agence de l'Environnement et de la Maîtrise de l'Energie (ADEME) and ATOLL ENERGY.

References

[1] M. Taralunga, J. Mijoin, P. Magnoux, Applied Catalysis B: Environmental 60 (2005) 163-171.

[2] S. C. Marie-Rose, T. Belin, J. Mijoin, E. Fiani, M. Taralunga, F. Nicol, X. Chaucherie, P. Magnoux, Applied Catalysis B: Environmental 90 (2009) 489-496.

[3] Xiao-Wen., Shen, Shou-Cang., Yu, L. E., Kawi, S., Hidajat, K., Simon Ng, K. Y. Zhang, Applied Catalysis A: General 250 (2003) 341-352.

V-PP46

Synthesis and Catalytic Performances of Nanostructured Lanthanum Cobaltite Catalytic Thin Films Prepared by Physical Vapour Deposition

Vilasi P.[1,2], Vernoux P.[1], Briois P.[2], Billard A.[2], Arab Pour Yazdi M.[2*]

1 - CNRS, UMR 5256, IRCELYON, Institut de Recherches sur la Catalyse et l'Environnement de Lyon, Villeurbanne, France
2 - IRTES-LERMPS, UTBM, Belfort, France

* pauline.vilasi@utbm.fr

Keywords: perovskite films, nanowires catalysts, thin films, sputtering, Diesel oxidation catalyst

1 Introduction

Reduction of pollutants emissions contained in vehicles exhaust gas are among the main priorities of future European standards. A way to meet those standards requirements is to equip vehicles with a catalytic post-treatment able to minimise the rejection of pollutants in the atmosphere. Nowadays, noble metals, such as platinum and palladium, are used because of their high catalytic performances. However, those metals are quite expensive and their sintering at rather low temperature decreases their catalytic performances. These observations had encouraged the development of new free noble metal catalysts. In that case, perovskite ceramics seem promising since these compounds are cheaper than noble metals and could be implemented as Diesel oxidation catalysts. However, the main drawback of perovskites are their rather low specific surface areas. In this present study, we propose to use the reactive magnetron sputtering technique to produce nanostructured thin films of perovskites. Coatings of silver and strontium double substituted lanthanum cobaltite perovskite have been deposited on dense alumina and YSZ (Yttria-Stabilized Zirconia) substrates by reactive magnetron sputtering. Deposition parameters such as the current applied to the metallic targets and the oxygen partial pressure have been optimized to generate nanowires. Catalytic performances of the perovskite layers have been carried out for CO oxidation.

2 Experimental/methodology

Thin films of $La_{1-x-y}Sr_xAg_yCoO_3$ (x=0,1, y=0,48 for LSACO-8; x=0,2, y=0,48 for LSACO-7; and x=0,23, y=0,21 for LSACO-5) perovskites have been prepared by using reactive magnetron sputtering at room temperature from a La (thickness : 3 mm, diameter : 200 mm, purity : 99,9 %), Ag, Sr and Co targets (thickness : 6 mm, diameter : 200 mm, purity : 99,9 %). The applied current on targets was in the range 0.35-0.4 A, 1.1-1.2 A, 8-12 mA and 0.6-1.2 A for Co, Sr, Ag and La, respectively. The pressure inside the sputtering chamber was 1.5 Pa. Depositions were performed in reactive conditions with a flow of oxygen and argon of 20 and 50 sccm, respectively. The draw distance between targets and substrates was 50 mm. Films were deposited on commercial dense disks (diameter: 16 mm, thickness: 0.6 mm) of alumina (KERAFOL 95) and Yttria-Stabilized Zirconia (YSZ, LEPMI). All of as-deposited coatings were found to be amorphous. After a calcination at 773K for 2 hours, XRD have shown that they have crystallized into the required perovskite structure. SEM, EDX and XPS analysis have been performed to determine the chemical composition of the films after calcination as well as their microstructure.

A continuous flow quartz reactor was used for the catalytic performance measurements. The overall flow rate, 4.5 L h^{-1}, was monitored with mass flow controllers (Brooks). The CO

concentration (CCO) was 3000 ppmv (Air Liquide, CO 1 ± 0.002 % in He); oxygen concentration (Air Liquide, O_2 99.95 %) was 3%, helium was used as carrier gas. CO, CO_2 and O_2 were analyzed by using an on-line micro gas-chromatograph (R3000 SRA Instruments). CO_2 was detected with a CO_2 IR analyzer (Horiba VA 3000).

3 Results and discussion

The microstructure of lanthanum cobaltite thin films after calcination at 773K strongly depends on the silver loading in the perovskite (Fig. 1). For low Ag level, such as LSCO-5, films are rather dense with cracks whereas for high loadings, such as LSACO-7 and LSACO-8, layers presents a nanowire type morphology. The thickness of the perovskites films is around 1.5 µm.

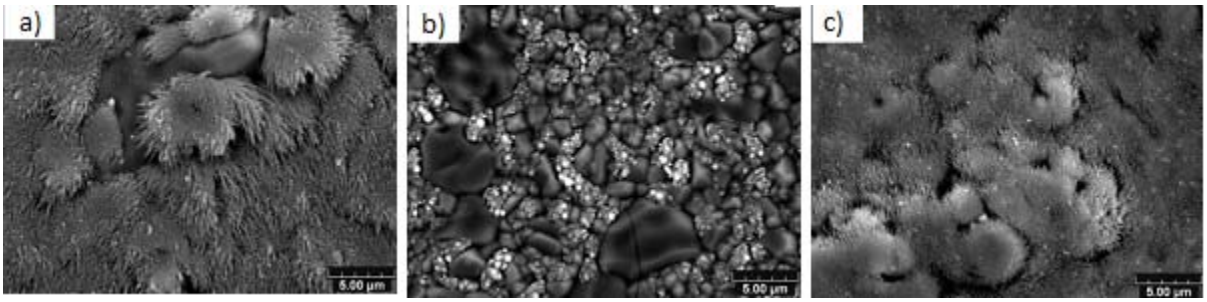

Fig.1: SEM images of perovskite films surfaces: LSACO-8 a), LSACO-5 b), LSACO-7 c).

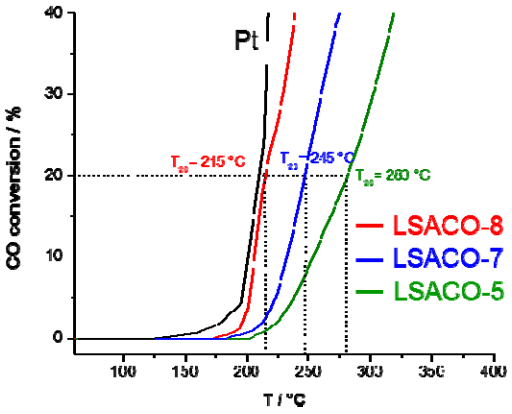

Fig.2: CO conversion as a function of temperature of lanthanum cobaltite thin films interfaced on YSZ. Comparison with a Pt film prepared by PVD (thickness = 80 nm).

Catalytic performances for CO oxidation (Fig. 2) increase with the Ag loading inside the perovskite and therefore with the film porosity induced by nanowires. Values of T20, temperature at 20% of CO conversion, decreases from 280°C down to 215°C between LSACO-5 and LSACO-8. In addition, catalytic properties of LSACO-8 are similar to those a Pt thin film interfaced on the same substrate. XPS analysis have evidenced a surface segregation of Ag as well as the presence of Ag oxide. Thermal stability of these catalytic perovskites films have also been tested.

4 Conclusions

Nanostructured silver and strontium double substituted lanthanum cobaltite perovskite thin films have been synthetized by reactive magnetron sputtering. A nanowire type morphology has been achieved for high Ag loadings. These nanowires, thermally stable at 500°C, increase the porosity of the catalytic films and then their catalytic properties.

V-PP47

Photocatalytic and Ozone Combined UV Treatment for VOCs Abatement at Trace Concentrations

Montecchio F.[1*], Delin J.[2], Kaijser P.[2], Mills J.[3], Engvall K.[1], Lanza R.[1]

1 - Dept. Of Chemical Engineering, Division of Chemical Technology, KTH, Royal Institute of Technology, Stockholm, Sweden
2 - Scandinavian Centriair AB, Sävedalen, Sweden
3 - Techniair Ltd, Tudor Cottage Calleywell Lane, Ashford, United Kingdom

* fmon@kth.se

Keywords: photocatalyst, VOCs, UV, air, ozone

1 Introduction

The use of UV light in combination of other oxidation agents (ozone, hydrogen peroxide, photocatalyst) for water purification has proved a high efficacy for both water purification and disinfection [1], [2].

Many air emissions also need a purification stage to abate toxic VOCs and a similar system may be a valid alternative to the current incineration technologies because it saves a high amount of fuel and it reduces dramatically the CO_2 emissions. This research area is quite innovative and it requires a further investigation to match the performances of an incinerator.

The aim of this work is the study of the efficiency of a treatment with UV and photocatalyst to degrade trace concentrations of VOCs with a low UV power. The catalysts will be both commercial and specifically prepared and the UV-catalyst system will be combined with ozone to study the synergic effect of all the possible oxidants.

2 Experimental/methodology

The experimental set up is composed by a reactor with a cylindrical body, a length of 320 mm and a diameter of 180 mm. At the center of the reactor, different UV-C lamps can be placed axially. The lamps investigated in this work are low-pressure Hg lamps and the power varies between 14 and 42W. The walls of the reactor can be coated by the photocatalyst and this study investigates commercial catalysts as. Aeroxide P-25, Aeroxide P-90, and Cristal PC-105 as well as catalysts specifically synthesized.

The liquid pollutant is fed in an evaporator with a syringe pump and the vapor is then mixed with the main air stream. The air flow rate is adjusted by flow meters and external ozone may be added to the stream. The external ozone is generated by the *A2Z Ozone Systems S-3G Lab* generator and the ozone output can be adjusted up to 3 g/hr.

After the reactor, the organic products are analyzed with a GC Agilent 7890B coupled with a MS 5977A. The ozone concentration is monitored with an ozone analyzer, *2B Technologies UV-106L*, and the temperature and humidity are also monitored and controlled.

The aim of the first tests is the investigation of the VOC degradation due to the UV + ozone only. The main investigated variables are temperature, humidity and flow rate. The study is going to be extended by including the catalysts coated on the reactor inner walls and by study the performances of a UV+catalyst system and of a combined UV+ozone+catalyst system.

3 Results and discussion

Figure 1 shows the results of the first tests with the UV+ozone system. The VOC degradation is studied at different inlet concentrations and residence times inside the reactor.

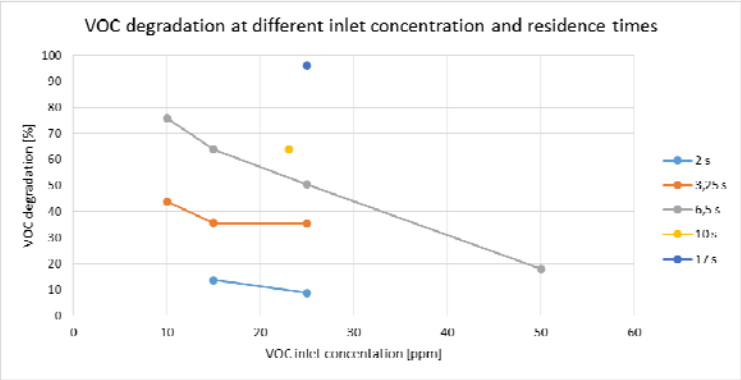

Fig. 1. VOC degradation at different inlet concentrations and reaction residence time.

First, the Figure shows that this system has a great potential for the VOC abatement because high values of conversion can be achieved with a very high residence time. However, such a high residence time is not affordable in many applications, therefore the maximization of the degradation will be sought with other media. Another result is the linear decrease of the VOC degradation with the inlet concentration suggesting a simple first-order correlation.

This study will be completed by testing the whole range of inlet concentrations, residence times and ozone concentrations. Then, the catalyst will be implemented in the system to investigate its potential application.

Among commercial catalysts, Aeroxide P-25, Aeroxide P-90, and Cristal PC-105, other catalysts will be synthesized with different techniques (e.g. sol-gel [3] or microemulsion) and different dopants. The use of dopants is mainly aimed to increase the affinity towards organic compounds or prolong the reactive time [4].

After the screening of the catalyst, the most promising ones will be combined with ozone to study the synergic potential of both the oxidants.

4 Conclusions

This work investigates the use of a combined system made by UV-C lamps, ozone and photocatalysts to abate the VOCs present in air emissions. The study is focused on trace concentration and the current investigation involves the influence of VOC, ozone concentration and residence time in the final conversion.

The results show a good potential of the current system for the designed application and they suggest a correlation between the VOC initial concentration and the conversion.

This preliminary study will be extended and different photocatalysts will be implemented to improve the global conversion and evaluate the efficiency of the catalysts compared to ozone as oxidation agent.

References

[1] W.A.M. Hijnen *et al.*, Water research 40 (2006) 3-22
[2] W. Yang *et al.*, Critical Reviews in Environmental Science and Technology 44, 13, 2014
[3] C. Su *et al.*, Catalysis Today 96 (2004) 119–126
[4] J. Zhu *et al.*, Journal of Molecular Catalysis A: Chemical 216, 35–43 (2004)

V-PP48

Direct Synthesis of Cyclic Carbonates by Oxidative Carboxylation of Styrenes over Ti-Containing Catalysts

Maksimchuk N.V.*, Ivanchikova I.D., Ayupov A.B., Kholdeeva O.A.

Boreskov Institute of Catalysis SB RAS, Novosibirsk, Russia

* nvmax@catalysis.ru

Keywords: carbon dioxide, cyclic carbonates, heterogeneous catalysis, mesoporous, titanium-silicates, MIL-125, oxidative carboxylation

1 Introduction

Utilization of CO_2 and its transformation into useful organic chemicals has become an increasingly popular research topic. In particular, the synthesis of cyclic carbonates via cycloaddition of CO_2 to epoxides is one of the promising technologies for chemical fixation of carbon dioxide. On the other hand, the direct synthesis of cyclic carbonates from olefins, an environmentally benign oxidant and CO_2 might become a more economically viable process due to the use of low-cost and easily available raw materials, viz., olefins, and avoidance of the separation of epoxides after their synthesis. In this work, we explored the catalytic performance of a mesoporous mesophase titanium-silicate, Ti-MMM-E, prepared by a simple and versatile evaporation-induced self-assembly (EISA) technique [1] in the oxidative carboxylation of styrenes using two environmentally friendly oxidants, H_2O_2 and *tert*-butylhydroperoxide (TBHP). For the sake of comparison, other types of Ti-containing catalysts, specifically, mesoporous titanium-silicate Ti-MMM-2 and metal-organic framework MIL-125, were also examined. The effects of reaction conditions on the olefin conversion and carbonate yield have been studied. Special attention was drawn to the crucial issues of the catalyst stability and recyclability as well as employment of solvent-free conditions.

2 Experimental/methodology

The Ti-MMM-E catalyst was prepared through EISA in ethanol/H_2O/HCl solution using tetraethoxy titanium (IV) modified with acetylacetone (1:1 mol/mol) as titanium precursor, tetraethylorthosilicate as silica precursor, and cetyltrimethylammonium bromide as template as described previously [1]. Ti-MMM-2 [2] and Ti-MIL-125 [3] were prepared by hydrothermal synthesis according to the literature protocols.

Catalytic experiments were carried out in thermostated stainless steel Parr-4792 reactor with PTFE insert under 8 bar CO_2. Typical reaction conditions were as follows: styrene/TBHP(H_2O_2)/TBABr/Ti molar ratio = 1/1.5/0.1/0.06, MeCN (if any), biphenyl (internal standard for GC). The mixture was stirred continuously while the pressure (8 bar) and temperature (30-90 °C) were kept constant during the reaction. After specified reaction time (24 or 48 h), the reactor was cooled down by ice water and depressed before opening The reaction products were identified by GC-MS and quantified by GC. After the catalytic run, catalyst was separated by filtration, washed with solvent, dried in air at room temperature overnight, calcined in air at 350 ^oC for 2 h and at 550 ^oC for 4 h, and then reused. The catalyst was characterized by DR UV–vis spectroscopy, N_2 adsorption measurements, and elemental analysis before and after reuse.

3 Results and discussion

Among the catalysts studied, the mesoporous titanium-silicate Ti-MMM-E prepared by the simple and affordable EISA methodology demonstrated superior catalytic performance in terms

of substrate conversion and carbonate selectivity in the oxidative carboxylation of styrenes using TBHP as oxidant and tetrabutylammonium bromide (TBABr) as cocatalyst at mild reaction conditions (Figure 1). We evaluated the impact of the reaction conditions (solvent nature, temperature and reactant concentrations) on the styrene conversion and carbonate selectivity using Ti-MMM-E as the most prospective catalyst. Rise of the temperature from 30 to 70 ^{o}C increased both substrate conversion and carbonate selectivity. A multiplication of the reactant loading in the reactor revealed that increase in the initial concentration of styrene while keeping constant the molar ratio of all the reactants improved carbonate selectivity and conversion. Under green solvent-free conditions, the selectivity towards styrene carbonates reached 69-70 % at 92-98.5 % substrate conversion at 70 ^{o}C and 8 bar CO_2 (Fig. 1). Thus the volume yield of styrene carbonates as high as 0.3 kg per L of the reaction mixture could be achieved.

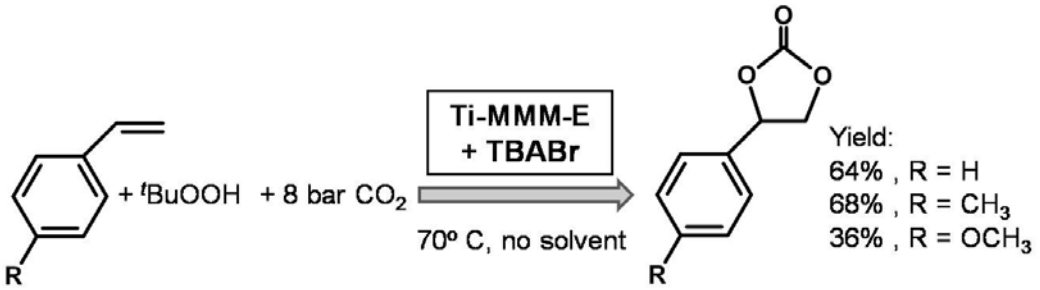

Fig. 1. Oxidative carboxylation of styrenes by Ti-MMM-E/TBABr/TBHP/CO_2 system.

Importantly, no titanium leaching into solution occurred and the Ti-MMM-E catalyst could be easily recovered by simple filtration and used repeatedly without a significant deterioration of the catalytic performance. Studies by DRS-UV, and N_2 adsorption confirmed the retention of the catalyst structure.

4 Conclusions

The mesoporous titanium-silicate Ti-MMM-E prepared by evaporation-induced self-assembly is an efficient heterogeneous catalyst for the oxidative carboxylation of styrenes with *tert*-butyl hydroperoxide and carbon dioxide in the presence of tetrabutylammonium bromide as cocatalyst under mild solvent-free conditions (50-70 ^{o}C, 8 bar CO_2).

Acknowledgements

The research was partially supported by RFBR (grants N 13-03-92699 and 13-03-00413). Authors thank Dr. J.-S. Chang and the Research Group for Nanocatalyst of Korea Research Institute of Chemical Technology for the synthesis of Ti-MIL-125.

References

[1] I.D. Ivanchikova, M.K. Kovalev, M.S. Mel'gunov, A.N. Shmakov, O.A. Kholdeeva, *Catal. Sci. Technol*. 4 (2014) 200.
[2] O. A. Kholdeeva, M. S. Melgunov, A. N. Shmakov, N. N. Trukhan, V. V. Kriventsov, V. I. Zaikovskii, M. E. Malyshev and V. N. Romannikov, *Catal. Today* 91-92 (2004) 205.
[3] M. Dan-Hardi, C. Serre, T. Frot, L. Rozes, G. Maurin, C. Sanchez and G. Férey, *J. Am. Chem. Soc*. 131 (2009) 10857.

V-PP49

Hydrogenation of Terpineol to Dihydroterpineol over Various Catalysts

Ilichev I.S.[1], Radbil A.B.[1], Kozlov I.A.[2], Ignatov A.V.[2], Semyonycheva L.L.[3], Novoselov A.S.[3*]

1 - JSC Managing company "Biochemical Holding "Orgkhim", Nizhniy Novgorod, Russia
2 - CJSC "Russkiy katalizator", Nizhniy Novgorod, Russia
3 - Lobachevskiy State University of Nizhniy Novgorod, Research Institute of Chemistry, Nizhniy Novgorod, Russia

* snova1983@yandex.ru

Keywords: terpineol hydrogenation, Raney, nickel, palladium catalysts

1 Introduction

Natural or synthetic α-terpineol is one of the most important and demanded substances, utilized in perfumery and cosmetics to give to remedies the smell of lilac. Dihydro-α-terpineol is also actively used as component of fragrances, perfume compositions and odorants. However, there were discovered only *trans*-form in nature (in American turpentine and pine oil), while *cis*-modification is just obtained synthetically. Dihydro-α-terpineol is commercially demanded in the world. The direct way to produce it is hydrogenation of synthetic terpineol. Synthetic α-terpineol represents a liquid mixture of terpineol isomers: α-terpineol (90-94%), β-terpineol (3-5%), γ-terpineol (2-4%) and terpinene-1-ol (1-2%).

2 Experimental

In presented work the technique of dihydro-α-terpineol obtaining was enclosed in heterogeneous catalytic hydrogenation of terpineol by the reaction below:

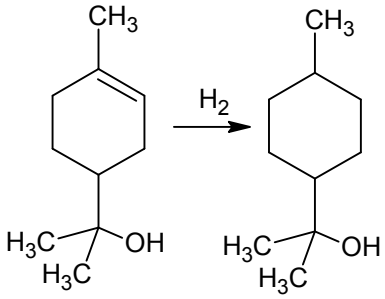

Experiments of terpineol hydrogenation to dihydroterpineol were carried out in laboratory reactor over powder and cellular catalysts in ethylacetate solution under pressure of hydrogen 0.7-1.1 MPa and temperature 70°C.

Powdered Raney nickel and palladium-covered γ-Al_2O_3, as well as block-structured α-Al_2O_3 catalysts, covered by γ-Al_2O_3 and pyrocarbon as substrates for palladium coatings, were investigated.

The hydrogenation process was controlled by decrease of hydrogen pressure. All products were analyzed by gas chromatography method.

3 Results and discussions

As shown in Table 1, conversion of α-terpineol significantly depends on the catalyst structure. Thus, the hydrogenation process over skeletal Raney nickel and powdered palladium catalyst lasts for 3 hours, while the same yield of dihydro-α-terpineol over block-structured palladium catalyst is achieved for 1 hour. In addition, the process is suspended with decreasing of hydrogen pressure in the system.

Hydrogenation over catalyst with pyrocarbon substrate requires separate words. The 90% yield of dihydro-α-terpineol reaches under lower pressure and for shorter time. This can be explained by more developed surface area of carbon.

Table 1. α-Terpineol hydrogenation with various catalysts of various structure

№	Structure	Substrate	Active metal and its content, % wg	Pressure of H_2, MPa	Time, hour	Yield, %
1	Skeletal	-	Raney Ni	1.1	3	94
2	Powder	γ-Al_2O_3	0.6% Pd	1.1	3	94
3	Block	γ-Al_2O_3	0.5% Pd	1.1	1	93
4	Block	γ-Al_2O_3	0.5% Pd	0.9	2	89
5	Block	γ-Al_2O_3	0.5% Pd	0.7	2	84
6	Block	Pyrocarbon	0.5% Pd	0.7	1	90

4 Conclusions

As a result of terpineol hydrogenation data analysis in all of the investigated reactions dihydro-α-terpineol was obtained with high yield (84-94%) for 1-3 hours at 70°C. There were shown that the most active catalysts are block-structured palladium catalysts.

V-PP50

Catalyst for Complete Oxidation of Nitrogen Containing Samples

Sevinç A.[1,2*], Karakaş G.[1], Atamer İ.B.[2]

1 - Middle East Technical Univeristy, Ankara, Turkey
2 - Terralab A.S., Ankara, Turkey

* alpersvnc@gmail.com

Keywords: catalyst nitrogen oxidation, catalytic combustion, Al_2O_3, CuO, CeO_2

1 Introduction

High temperature catalytic oxidation of nitrogen contaiining compounds has great importance for the analysis of environmental and industrial samples and the control of emissions of waste incineration facilities. The complete oxidation of nitrogen in different functional groups, ammonia and nitrates to NO and NO_2 is a crucial step for the determination of nitrogen in samples and NO_x abatement [1,2]. Altough platinum group metals have excellent oxidation activity, they are expensive and easily poisoned by the presence of S, Cl and P containing organic substances. Therefore, there is a great interest to develop new active, selective and resistant catalyst to treat waste oxidation gases. In this study, the catalytic activities of CuO and CuO-CeO catalysts for the complete oxidation of various nitrogen containing functional group are investigated at different temperatures and the results are compared with platinum catalyst.

2 Experimental Method

The catalyst samples were prepared to obtain a loading of 10% Cu, 3%Cu-7%Ce, 1% Pt over the Al_2O_3 as a suppport by incipient wetness method. After impregnation, the catalyst samples dried at 110 ^oC for 24 hours and calcined at 500 ^oC for 5 h in a furnace. Characterization of the catalyst samples was performed by X-ray powder diffraction (XRD) and BET. EDTA, urea, potassium nitrate, ammonium chloride, thiourea, pyridine, glycine, yeast extract, and metylamine were selected as model components representing various nitrogen containing functional groups. The experiments were performed in a quartz tubular reactor in two zone furnace and the sample first oxidized at 700-850 ^oC under air flow of 50 ml/min and the waste gases treated in second zone at 500^oC over catalyst bed. The catalytic activities of the samples were investigated by mass spectrometry by analyzing combustion products.

3 Results and Discussion

BET surface area values of the catalysts samples are given in Table 1. It is seen that the surface area changes significantly when impregnating cerium and copper on Al_2O_3.

Table 1. BET Surface area of the catalyst

Sample	BET Surface Area (m^2/g)
Al_2O_3	314.8
1%Pt/Al_2O_3	309.6
10%Cu/Al_2O_3	244.3
3%Cu- 7%Ce/Al_2O_3	261.0

In Figure 1, the diffraction peaks of Cu/Al2O3, Cu-Ce/Al_2O_3 and Pt/Al_2O_3 samples are shown. Results show that CuO is highly dispersed over the Al_2O_3 support in all the catalysts.

The low amount of CuO over the Al_2O_3 support does not allow to form bulk CuO so this XRD result is expected[3]. In the samples containing cerium oxide, characteristic peaks of crystalline CeO_2 are clearly seen which is in agreement with literature [3].

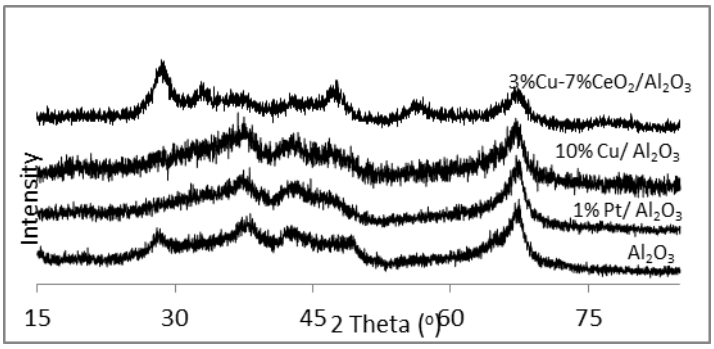

Figure 1. XRD patterns of catalyst samples and support

NO (m/z=30) signals observed in mass spectrometry for urea and EDTA samples having equivalent mass of nitrogen (7.52 mg), over 10%Cu/Al_2O_3 catalyst sample are shown in figure 2. As it is seen from the figure, EDTA oxidation follows at least two step mechanism compared with the simple structure of urea.

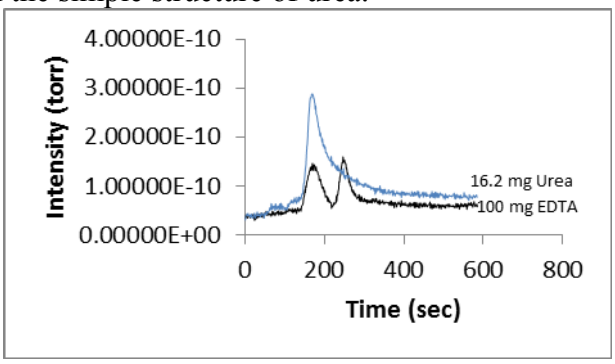

Figure 2. Change in amount of NO in the combustion gases

4 Conclusions

In this study Cu/Al_2O_3, Cu-Ce/ Al_2O_3 and Pt/Al_2O_3 catalyst samples are tested for the complete oxidation of various nitrogen containing functional groups at different temperatures. The characterization of physical properties of catalyst samples was performed by XRD and BET. The catalytic activities of the samples were investigated by analysing of combustion products of model components with mass spectrometry.

Acknowledgement

We would like to thank KOSGEB due to their support and founding this research.

References

[1] Merriam, J., Mcdowell, W., & Currie, W. (n.d.). A High-Temperature Catalytic Oxidation Technique for Determining Total Dissolved Nitrogen. Soil Science Society of America Journal, 1050-1050.

[2] Chen, C., Xu, Z., Keay, P., & Zhang, S. (n.d.). Total soluble nitrogen in forest soils as determined by persulfate oxidation and by high temperature catalytic oxidation. Australian Journal of Soil Research, 515-515.

[3] Águila, G., Gracia, F., & Araya, P. (n.d.). CuO and CeO_2 catalysts supported on Al_2O_3, ZrO_2, and SiO2 in the oxidation of CO at low temperature. Applied Catalysis A: General, 16-24.

V-PP51

Oxidative Desulfurization of Light Oil Distillates Using Ozone

Akopian A.V.*, Rakhmanov E.V., Grigoriev D.A., Anisimov A.V.

Chemistry Faculty of Lomonosov Moscow State University, Moscow, Russia

* arvchem@yandex.ru

Keywords: oxidation, ozone, sulfur, desulfurization

1 Introduction

Tightening environmental regulations on sulfur content in motor fuels requires improvement of existing and development of new technologies for the removal of sulfur compounds. Existing large-hydrotreating process requires high financial and energy costs, which makes it's introduction on mini-refineries unprofitable. Among the alternative methods with low cost the most promising process is oxidative desulfurization [1]. The aim of our work is developing new oxidative desulfurization technology using ozone as an oxidant.

2 Results and discussion

In this work the oxidant was used with catalytic system, which contains a transition metal salt with an organic ligand capable of forming under the influence of ozone oxidative active complex and further oxidize the fuel present in the sulfur-containing compounds, followed by adsorption of oxidation products on silica gel. In this method, the ozone is prevented from direct contact with the fuel, making the process not only cheap and accessible, but also safer. The results are shown in the table.

Fuel type	Salt/ligand	Initial sulfur content, ppm	Residual sulfur content, ppm
Gasoline	$CuSO_4$/ sodium gluconate	700	180
Gasoline	$CuSO_4$/ EDTA	700	330
Gasoline	$VOSO_4$/ sodium gluconate	700	195
Diesel	$CuSO_4$/ sodium gluconate	3500	2090
Diesel	$CuSO_4$/ EDTA	3500	2355

3 Conclusions

This process allows to achieve the degree of desulfurization of gasoline and diesel fractions 74 and 60%, respectively.

Acknowledgements

The work was carried out in the framework of the Federal Target Program "Research and development on priority directions of scientific-technological complex of Russia" for 2014-2020 with the financial support of the Ministry of Education and Science of the Russian Federation in 2014 - 2015 (grant agreement № 14.607.21.0051 on "Development of a framework of complex technology catalytic processing of unconventional oil kerogen containing rock into liquid hydrocarbons")

References

[1] K. Yazu, M. Makino, K. Ukegawa Chemistry Letters. 1 (2004) 1306.

V-PP52

Investigation of Commercial Catalyst for Methane Oxidation after Real Operation Condition

Alikin E.A.*

Ecoaliance Ltd, Novouralsk, Russia

* alikin@eco-nu.ru

Keywords: methane oxidation, palladium, sulphur, carbon, layer, catalyst reduction

1 Introduction

CNG transport is actively developed throughout the world. In spite of essential increase of ecological parameters of such vehicles, the problem of neutralization of unburned methane, which is greenhouse gas, arises. Palladium catalysts with high metal surface concentration (3-6%) are still irreplaceable for methane oxidation in commercial application. However such catalysts are quickly deactivated during operation in lean fuel-air mixtures. The target of this study is a search of causes of palladium catalysts deactivation under life tests.

2 Experimental

The object of research is an active layer of monolith catalyst after 13000 km run (3 months of operation) within a bus. The active layer Pd(2.5%)-Pt(0.6%)/(Al_2O_3+$Ce_{0.5}Zr_{0.5}O_2$) was separated from ceramic carrier. Physical-chemical characteristics of the powder was investigated by BET, XRD, TEM-EDX and other methods. Desulfatation test of catalyst powder was performed by TGA equipped with MS. Catalytic activity tests of monoliths was performed in flow reactor system (MEXA-9500 HORIBA).

3 Results and discussion

The catalyst layer researched by TEM-EDX shows that there is an accumulation of essential amount of sulfur in the alumina structure (Figure 1a). Sulfur concentration are vary 1,5-4% against areas of oxide carrier. Besides, essential part of carbonic deposits that covers palladium particles (Figure 1b), they are also present separately in the form of filamentous particles.

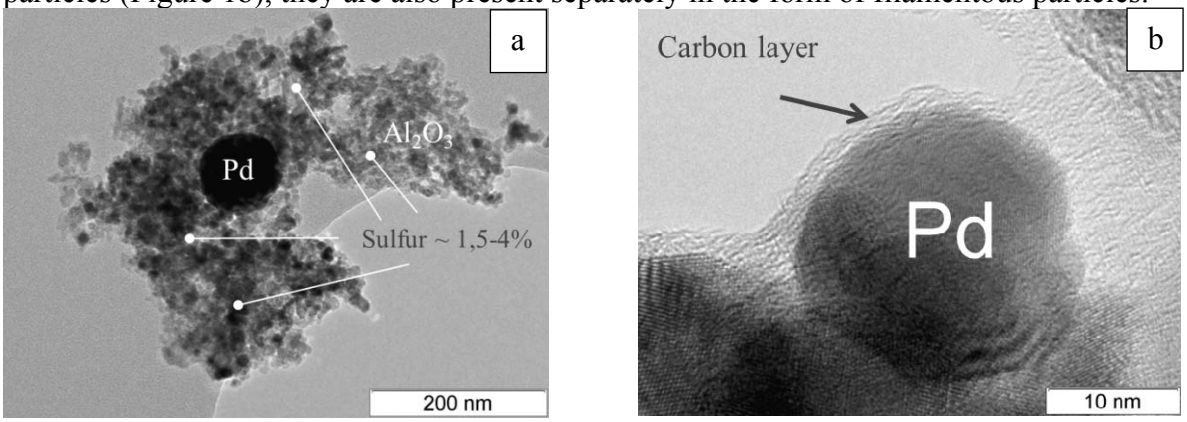

Fig. 1. Microstructure of catalyst layer after 13000 km run

As a result of sulfur poisoning this catalyst sample loses its activity, methane oxidation temperature rises more than 100 °C, oxidation efficiency reduces for 50% (Figure 2b). Low efficiency was unchangeable during prolonged holding in lean reaction gas mixture.

Next step we tried to select the conditions (temperature, gas media) for desorbing of sulfur compounds using TGA with MS. During heating in air desorbing of sulfur takes place in the wide temperature range 550-1030 °C with maximum of 780 °C. Catalyst activity after this

procedure rises insignificantly (Figure 2c). However rich methane media passes through the catalyst during a few minutes the sulfur desorption is more intensive even at 580-600°C temperature. After this procedure methane conversion in 550 ^{O}C almost completely recovers to the previous level (Figure 2d).

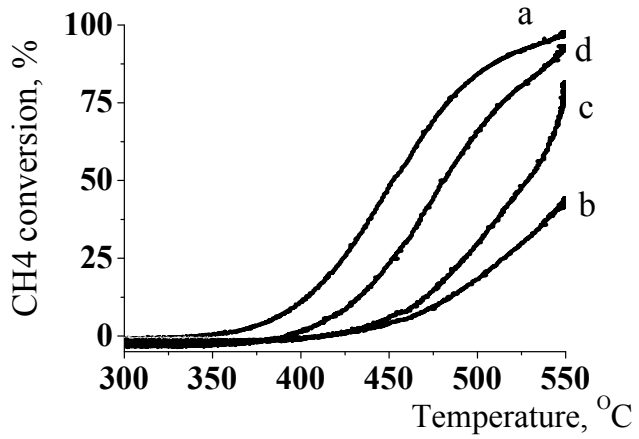

a – fresh sample

b – sample after run 13000 km

c – sample «b» after annealing 1000 ^{O}C/1h in muffle

c – sample «b» after treatment in CH_4-rich media in 570 °C/5 min

Fig. 2. – Methane oxidation light-off curves

4 Conclusions

Commercial catalyst loses its activity due to sulfur poisoning of Al_2O_3 with subsequent covering of palladium particles with carbonic deposits. Catalyst activity may be partially recovered by treatment in the medium enriched by methane. During the process sulfur compounds desorbing takes place.

Acknowledgements
The author are grateful to E. Gerasimov and M. Smirnov for interpret of TEM results.

V-PP53

EPR Spectroscopic Study of the Active Species of Iron-catalyzed Enantioselective Epoxidation

Lyakin O.Y.[1,2], Zima A.M.[1,2], Bryliakov K.P.[1,2], Talsi E.P.[1,2*]

1 - Boreskov Institute of Catalysis SB RAS, Novosibirsk, Russia
2 - Novosibirsk State University, Novosibirsk, Russia

* talsi@catalysis.ru

Keywords: biomimetic, enantioselective, epoxidation, EPR, iron, mechanism

1 Introduction

In Nature, metalloenzyme-catalyzed oxidations often exhibit exquisite substrate specificity as well as regioselectivity and/or stereoselectivity. This stimulates chemists to develop synthetic bioinspired systems that may have broader substrate scope and tunable selectivity, which makes them challenging protagonists of environmentally friendly catalytic chemistry of the near future.[1a] Catalyst systems based on iron complexes with tetradentate N_4-donor, mainly, aminopyridine ligands, H_2O_2, and carboxylic acid as an additive have attracted particular attention in the last decade due to high efficiency and selectivity in the preparative oxidations of C–H and C=C groups of various organic molecules.[1b] Although the mechanistic landscape of aminopyridine iron catalysts has been discussed in a series of elegant experimental works, the problem of direct experimental detection and identification of the elusive oxygen-transferring species in these catalysts is far from being solved.[1c]

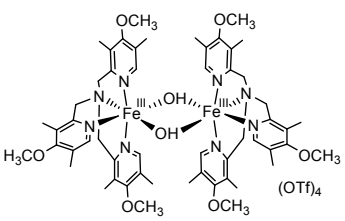

1

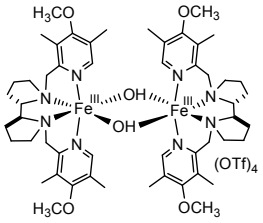

2

In the present study we have undertaken an EPR spectroscopic study of the active species of the highly effective and enantioselective catalyst systems (epoxidizing olefins with up to 99% *ee*)[2] based on aminopyridine iron complexes **1** and **2** with electron-donating substituents at the pyridine rings.

2 Experimental/methodology

Complexes **1** and **2** were synthesized by mixing appropriate amounts of the corresponding ligand (1 equiv), iron(II) triflate (1.05 equiv) and H_2O_2 solution (0.5 equiv) in CH_3CN followed by slow diethyl ether diffusion into the resultant solution at 5 °C. For complex **2**, the X-ray structure was obtained. EPR spectra (−196 °C) were measured on a Bruker ER-200D spectrometer at 9.3–9.4 GHz, modulation frequency 100 kHz, modulation amplitude 5 G. Measurements were conducted in a quartz finger Dewar filled with liquid nitrogen. Samples were prepared by mixing the reagents directly in a quartz EPR tube (d = 3 mm) in a 1.8:1 CH_2Cl_2/CH_3CN mixture at −90…−75 °C. To measure the reactivity of intermediates **1b** and **2b** towards alkene oxidation, the appropriate amount of a frozen alkene solution was rapidly placed into the EPR tube containing frozen solution of preliminary generated intermediates **1b** or **2b**. After the solution melting at −85 °C, the decay rates of **1b** and **2b** were monitored at this temperature.

3 Results and discussion

The starting dinuclear complexes **1** and **2** were EPR silent. The addition of the excess of CH_3COOH (10-50 equiv) to these complexes at room temperature resulted in the formation of the low-spin (S = 1/2) acetoxo-iron(III) complexes $[(L)Fe^{III}(OC(O)CH_3)]^{2+}$ **1a** (g_1 = 2.58, g_2 =

2.38, g_3 = 1.72) and **2a** (g_1 = 2.54, g_2 = 2.41, g_3 = 1.79) displaying different stability at room temperature ($\tau_{1/2}$(**1a**) = 2 min, $\tau_{1/2}$(**2a**) = 1 h). The addition of 3 equiv of H_2O_2 to just prepared samples **1**(**2**)/CH_3COOH at −80…−75 °C led to the formation of new low-spin (S = 1/2) iron-oxygen intermediates **1b** (g_1 = 2.070, g_2 = 2.005, g_3 = 1.956) and **2b** (g_1 = 2.071, g_2 = 2.008, g_3 = 1.960) extremely unstable even at −85 °C ($\tau_{1/2}$(**1b**) = 5 min, $\tau_{1/2}$(**2b**) = 4 min). The evaluated maximum concentration of **1b** and **2b** did not exceed 1-2% of the total iron concentration. It should be noted that the samples **1**(**2**)/H_2O_2 containing no acetic acid displayed no EPR signals in the range g = 1.5–3.

To directly assess the reactivity of **1b** and **2b** towards alkene epoxidation, the rates of decay of **1b** and **2b** in the absence and in the presence of various alkenes were compared. It was found that the addition of relatively small amounts of cyclohexene or *cis*-*β*-methylstyrene ([alkene]/[Fe] = 0.5) to the samples containing **1b** or **2b** results in the decrease of the half-life time of **1b** and **2b** from $\tau_{1/2}$ = 4-5 min to $\tau_{1/2}$ < 0.5 min at −85 °C, whereas electron-deficient alkenes (1-acetyl-1-cyclohexene and cyclohexene-1-carbonitrile with an [alkene]/[Fe] ratio up to 10) do not visibly affect the decay rates of **1b** and **2b**. Hence, **1b** and **2b** are highly reactive towards electron-rich alkenes even at −85 °C. To quantify the products of interaction of **1b** and **2b** with cyclohexene, catalytic oxidation experiments at −85 °C were performed. 4.5 and 5.3 TN cyclohexene oxide were obtained 15 min after the reaction onset with catalysts **1** and **2**, respectively (TN = moles of product per mole of Fe, [Fe]:[H_2O_2]:[CH_3COOH]:[C_6H_{10}] = 1:10:20:30, [Fe] = 0.02 M). The total amount of other cyclohexene oxidation products was <1% with respect to the epoxide. Thus, the active species **1b** and **2b** oxidize cyclohexene at −85 °C with >99% selectivity towards the epoxide.

The g-values and line widths of intermediates **1b** and **2b** are very similar to those of spectroscopically well characterized model oxoiron complex $[(TMC)Fe^{V}{=}O(NC(O)CH_3)]^{+}$ (TMC = tetramethylcyclam).[3] On the basis of this similarity and reactivity data, we have assigned intermediates **1b** and **2b** to the oxoiron(V) $[(L)Fe^{V}{=}O(OC(O)CH_3)]^{2+}$ active species of selective alkene epoxidation by the catalyst systems studied herein.

4 Conclusions

In summary, the extremely unstable iron-oxygen intermediates formed in bioinspired catalyst systems based on dinuclear ferric complexes with aminopyridine ligands containing electron-donating substituents, H_2O_2 and acetic acid have been detected by EPR spectroscopy for the first time. The detected intermediates **1b** and **2b** are highly reactive and selective towards electron-rich alkene epoxidation even at −85 °C. They exhibit rhombic EPR spectra with the main values of g-tensor close to those of known oxoiron(V) complexes. Presumably, the observed small g-tensor anisotropy is due to the delocalization of unpaired electron over the organic ligand.

Acknowledgements

The authors thank the Russian Foundation for Basic Research for the financial support of this work, grant 14-03-00102.

References

[1] (a) L. Que, Jr., W. B. Tolman, *Nature* 455 (2008) 333. (b) E. P. Talsi, K. P. Bryliakov, *Coord. Chem. Rev.* 256 (2012) 1418. (c) K. P. Bryliakov, E. P. Talsi, *Coord. Chem. Rev.* 276 (2014) 73.

[2] O. Cussó, I. Garcia-Bosch, X. Ribas, J. Lloret-Fillol, M. Costas, *J. Am. Chem. Soc.* 135 (2013) 14871.

[3] K. M. Van Heuvelen, A. T. Fiedler, X. Shan, R. F. De Hont, K. K. Meier, E. L. Bominaar, E. Münck, L. Que, Jr., *Proc. Natl. Acad. Sci. U.S.A.* 109 (2012) 11933.

V-PP54

Analysis of Performance of a Bimodal Cu-CHA as SCR Catalyst Coupled in a NSR-SCR Dual System

Cortés-Reyes M.[1], De La Torre U.[2], Pereda-Ayo B.[2], Herrera M.C.[1], Larrubia M.A.[1], González-Velasco J.R.[2], Alemany L.J.[1*]

1 - Departamento de Ingeniería Química, Facultad de Ciencias, Campus de Teatinos, Universidad de Málaga, Málaga, Spain

2 - Departamento de Ingeniería Química, Facultad de Ciencia y Tecnología, Universidad del País Vasco, Bilbao, Spain

* luijo@uma.es

Keywords: Cu-CHA, NSR-SCR, double, bed, zero emission

1 Introduction

The reduction of NO_x emission in diesel vehicles and new biofueled engines below the limits imposed by regulations is an important environmental problem. In recent times, the combination of after-treatment systems (NSR-SCR) emerges as a promising solution [1,2]. NSR (NO_x Storage and Reduction) technology operates alternatively under lean and rich conditions and conventional Lean NO_x Traps (LNTs) are formulated with a high surface area support (Al_2O_3), incorporating platinum and alkaline/alkaline earth spread as monolayer oxides. However, a drawback of these catalysts is the NH_3 slip produced during the regeneration step [1-3]. SCR (Selective Catalytic Reduction) process is based on the reaction between the ammonia and NO_x and it is developed for stationary emission sources or heavy-duty vehicles with NH_3 as supplied reducer (urea tank).To achieve zero emission in light diesel vehicles, hybrid systems NSR-SCR have been proposed [1,2]. The most studied catalysts for SCR catalyst are exchanged zeolites, such as ZSM5, or BETA, with iron or copper as metals, despite of presenting low hydrothermal stability. Actually, small pores zeolites as chabazite have proposed. Nevertheless, some studies indicate that a bimodal distribution could be more adequate. This contribution is focused on the DeNOx of a combined system NSR-SCR, over Pt-Ba-K/Al_2O_3 and Cu-chabazite catalysts, with a bimodal porous distribution and synthesized in one step; and the decoupling of the performance of individually catalytic bed.

2 Experimental

NSR (Pt-Ba-K/Al_2O_3) and SCR (Cu-CHA) homemade catalysts have been prepared and well-characterized by DRX, XPS, N_2 adsorption-desorption, TEM, SEM and Raman. The experiments were performed in a down flow stainless steel reactor, with 1 g of 0.03-0.05 mm pelletized sample. SCR feed conditions consist of 750 ppm NO, 750 ppm NH_3 and 6% O_2 in Ar for different GSHV and the presence of water was also studied. LNT catalyst and double configuration (NSR-SCR dual system) were run under NSR conditions between long lean (150s) and short rich (20s) periods. The composition of the lean gas mixture was 750 ppm NO and 6% O_2 using Ar as balance gas; this oxygen was replaced by 4% H_2 during the rich period. All the experiments were carried out in the temperature range between 150-450 ºC, analyzing the outlet gases concentration by online FTIR multigas analyzer (MKS 2030).

3 Results and discussion

The Pt-Ba-K/Al_2O_3 formulation presents a high adsorbed NO_x conversion and almost complete N_2 selectivity values [3] and the Ba/K combination hinder practically the NH_3 slip even at lower temperatures. However, it has been subjected to extreme conditions, such as a high hydrogen concentration in short periods to increase undesirable products to value the

performance of dual system. In the Cu-CHA with a bimodal porous distribution synthesized in one step, the Cu is incorporated as Cu +1/Cu +2 oxide forms. In Figure 1 are represented the NO conversion values as a function of temperature in the standard SCR conditions. Complete NO-conversion values are registered in the SCR whole range, being mainly Cu^{2+} species that are involved in the DeNOx-SCR process. It was checked the NO conversion increase at lower space velocity, otherwise, N_2O production is higher due to ammonia nitrates decomposition. Nevertheless, in all cases the selectivity to nitrogen is almost 100%. The presence of water in the feed stream improves SCR efficiency, showing lower N_2O values and a higher N_2-selectivity.

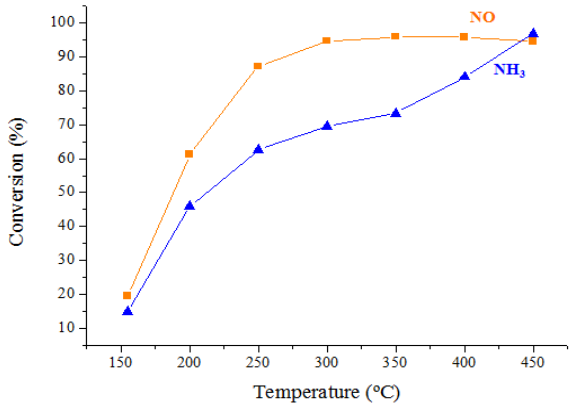

Fig. 1. NO (■) and NH_3 (▲) conversion profiles over Cu-CHA for standard SCR conditions

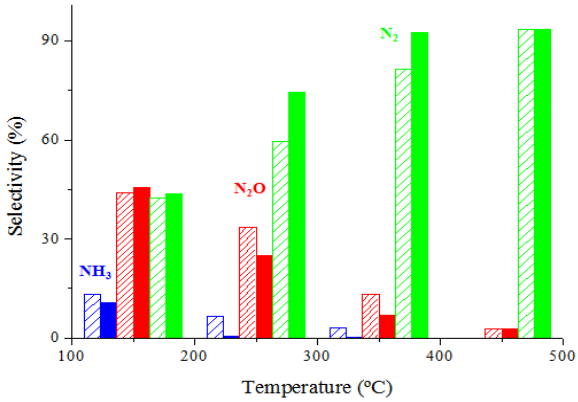

Fig. 2. NH_3, N_2O and N_2 selectivity in NSR conditions for Pt-Ba-K/Al_2O_3 catalyst (striped) and NSR-SCR coupled system (plain)

Decoupled fixed-bed catalysts have been studied individually to confirm that exist an improvement in the NOx elimination with these catalyst formulations. In fact, the combination of double-bed of NSR-SCR catalysts provokes a sensible increase of the nitrogen production and a reduction of N_2O and NH_3; that it can be observed from data represented in Figure 2. Cu-CHA as SCR coupled system is acting as a NH_3 trap and even in extreme conditions during the short rich-periods. It is possible to couple with others LNT_catalysts that produce more ammonia and during much longer in rich periods with low H_2 concentration supplied.

4 Conclusions

This combination of after-treatment systems consisting of a LNT catalyst with minimum NH_3 emission and a copper-chabazite, highly selective to N_2, acts as an effective NO_x removal process.

Acknowledgements

MCR acknowledges the Spanish Ministry of Education, Culture and Sport for a FPU grant.

References

[1] U. De La Torre, B. Pereda-Ayo, J.R. González-Velasco, *Chem. Eng. Journal*. 207-208 (2012) 10.
[2] R. Bonzi, L. Lietti, L. Castoldi, P. Forzatti, *Catalysis Today.* 151 (2010) 376.
[3] M. Cortés-Reyes, I.S. Pieta, M.C. Herrera, M.A. Larrubia, L.J. Alemany (submitted).

V-PP55

$(Gd,Sr)_{n+1}Fe_nO_{3n+1}$ Catalysts Applied in Dry (Carbon Dioxide) Methane Reforming

Kryuchkova T.A.[1*], Khairullina I.A.[1], Sheshko T.F.[1], Serov Y.M.[1], Chislova I.V.[2], Zvereva I.A.[2]

1 - Peoples Friendship University of Russia, Faculty of Science, Physical and Colloidal Chemistry Department, Moscow, Russia
2 - Saint-Petersburg State University, Saint-Petersburg, Russia

* tatyanakruychkova@mail.ru

Keywords: carbon dioxide, methane reforming, ferrites, perovskite

1 Introduction

Catalysts based on perovskite-type layered structures are alternative catalysts based on noble metals in a variety of high temperature catalytic processes of the industrial synthesis and gas purification as they are able to maintain their catalytic and mechanical properties under the severe reaction medium.

Synthesis gas (a mixture of H_2 and CO) is an input material for many chemical and petrochemical products. Carbon dioxide (dry) reforming of methane is a perspective way to produce synthesis gas to existing. Derived synthesis gas has a low H_2/CO ratio close to unity, it can be used in the Fischer-Tropsch process, two greenhouse gases (CO_2 and CH_4) are utilized in this process and natural gas can be used as a feedstock.

2 Experimental/methodology

The perovskite-type ferrites $GdSrFeO_4$, $Gd_2SrFe_2O_7$, $GdFeO_3$ and solid solutions $Gd_{2-x}Sr_{1+x}Fe_2O_7$ (x = 0,1 - 0,6) were synthesized by the high temperature solid state reactions and by sol-gel technology.

Characterization by powder X-ray diffraction (XRD) and scanning electron microscopy (SEM), has been performed for the determination of the structure and morphology of synthesized samples. XRD was performed on a Thermo ARL X'TRA diffractometer using CuKα radiation. The SEM images of synthesized samples were obtained on Carl Zeiss EVO 40EP and Zeiss Supra 40VP scanning electron microscopes.

Mössbauer spectra have been recorded at room temperature by using spectrometer Wissel (^{57}Co in a rhodium matrix with activity 10 mKu), the isomeric shifts were calculated with respect to α-Fe. In order to evaluate the part of paramagnetic species the intensity of the signals was determined precisely up to the factor of resonance absorption.

Analysis of acid-base properties of the samples surface was performed by adsorption of pyridine (Py). Their concentration in solutions were determined by UV - spectroscopy on single-beam scanning spectrophotometer SF-103.

The catalytic activity were studied in a flow apparatus at atmospheric pressure in the temperature range of 773-1223 K and flow rates of 0.5-1.0 l/h. Experiments were carried out with feeding a mixture of gases in a ratio of components CH_4:CO_2 = 1: 1,1: 2 and 2:1. Analyses of the products were performed by chromatography (Crystal 2000M) in a column of stainless steel filled with Porapack Q at 393K.

3 Results and discussion

The complex physico-chemical methods of investigation showed that synthesized catalysts

are well-crystalline homogenous perovskite-type ferrites with different number of perovskite layers $GdSrFeO_4$ (n=1), $Gd_2SrFe_2O_7$ (n=2), $GdFeO_3$ (n=∞) and solid solutions $Gd_{2-x}Sr_{1+x}Fe_2O_7$. Samples obtained by ceramic technology are in microcrystalline state and the iron atoms are found in one state - Fe^{3+}, which is magnetically ordered; oxides prepared by sol-gel technology are in nanocrystalline state and iron atom is in a heterovalent state (Fe^{3+} coexists with Fe^{+4}) in three different symmetry fields. A lowering of the symmetry of the surrounding of Fe^{+3} atoms is attributable to the presence of oxygen vacancies. Found that the adsorption of CH_4 and CO_2 occurs at different centers. Suggested that the Fe^{3+} ions are responsible for the formation of atomic hydrogen and carbonate complexes occur at ions Gd^{3+} and Sr^{2+}.

The maximum conversion (α_{CH4} = 37%, α_{CO2} = 57%) and products formation rate (W_{H2} = 0,07 mol/(h∗g), W_{CO}= 0,16 mol/(h∗g)) were achieved by performing the reaction at an equimolar ratio of CH_4 and CO_2.

On almost all investigated ferrites among the reaction products was detected water, the quantity of generated carbon monoxide was 2-4 times greater than the quantity of hydrogen and carbon dioxide conversion was almost two times higher methane conversion. Activation energies of CO formation and the corresponding values of lnk_0 were less than the similar values of E_a and lnk_0 for hydrogen. Based on these data suggested that the DRM reaction is complicated by the reverse steam reforming of CO.

It is shown that an increase in the number of perovskite layers (n) in the complex oxides structure leads to an increase in the catalytic activity. And a partial substituted or complete replacement of ions Gd^{3+} by ions Sr^{2+} leads to some reduction of activity. Among the systems of variable composition $Gd_{2-x}Sr_{1+x}Fe_2O_7$ obtained by the sol-gel technology samples with x = 0.3 had the highest activity. Increase of strontium content led to lowering of the symmetry of the surrounding of Fe^{+3} atoms, occurrence of heterovalent state of iron atoms (Fe^{3+}, Fe^{4+}) with oxygen vacancies. It influenced increase in the total surface acidity and catalytic activity in terms of CO_2 conversion. The catalytic activity was increased in the row $SrFeO_{3-x}$ (n=∞) ≈ $GdSrFeO_4$ (n=1) ≈ $Gd_{2-x}Sr_{1+x}Fe_2O_7$ (n=2) < *$GdFeO_3$ (ceramic)* (n=∞) < *$GdFeO_3$ (sol-gel)* (n=∞). Higher catalytic properties of perovskite-type ferrites synthesized by sol-gel technology can be associated with their nanocrystalline state, a porous structure, as well as with heterovalent iron state and oxygen vacancies, which probably are favorable for the surface oxidation-reduction reactions and the process of CO_2 activation.

4 Conclusions

The perovskite-type ferrites $(Gd,Sr)_{n+1}Fe_nO_{3n+1}$ (n=1, 2, ∞) were studied. Obtained catalytic properties in carbon dioxide methane reforming. It is shown that samples synthesized by ceramic technology are present in microcrystalline state and oxides prepared by sol-gel technology are in nanodispersed state. Heterovalent state of iron atoms (Fe^{3+}, Fe^{4+}) with oxygen vacancies has been found in perovskite-type ferrites prepared using sol-gel technology. It is reflected in the increase in the total number of electron-seeking surface centers and activity of CH_4 and CO_2 conversion.

Was shown the role of the structure of perovskite-type ferrites in the catalytic methane conversion.

Acknowledgements

The reported study was supported by RFBR grant 14-03-00940.

V-PP56

Mechanistic Kinetic Modeling of NO Oxidation over a Commercial Cu-Zeolite Catalyst for Diesel Exhaust Aftertreatment

Fahami A.R., Nova I., Tronconi E.*

Dip.Energia, Politecnico di Milano, Milano, Italy

* enrico.tronconi@polimi.it

Keywords: Cu-zeolite, NO oxidation, reaction, modeling, Redox mechanism

1 Introduction

The Standard SCR reaction has been recently studied over Cu and Fe–zeolites by many research groups in order to establish a mechanism consistent with kinetic evidence [1]. A detailed understanding of NO oxidation to NO_2 over SCR catalysts is believed to be crucial to describe the mechanism of Standard NH_3-SCR [2]. A key point in fact is to clarify whether formation of NO_2 generates an active intermediate on the surface of SCR catalysts [3], or just leads to a terminal product in the gas phase [4].

In this work we aim at developing and validating a mechanistic kinetic model for NO oxidation to NO_2 over Cu–zeolite catalysts. Firstly, a Redox mechanism is proposed in line with previous research [4,5], and consequently a rate equation is derived from the steps of the mechanism. Then, a systematic set of steady state kinetic runs is carried out over a commercial state-of-the-art Cu-zeolite SCR catalyst to cover the effects of several operating variables. The results of such experiments are eventually used to estimate the intrinsic rate parameters of the proposed kinetic mechanism.

2 Experimental/methodology

A commercial Cu-zeolite originally in the form of wash-coated cordierite honeycomb monolith (400 cpsi–5 mils) was crushed to particles and sieved (140–200 mesh) in order to prevent mass transfer limitations. A quartz tubular microreactor (ID = 6 mm) was loaded with 60 mg of the catalyst powder. The species concentrations at the reactor outlet were continuously measured by a quadrupole mass spectrometer and a UV analyzer in parallel.

3 Results and discussion

In the assumed mechanism, copper dimers $(Cu\text{-}O\text{-}Cu)^{+2}$ are regarded as the active sites for the NO oxidation reaction, consistently with recent literature [6]. The first step is the oxidative activation of NO on the Cu sites, forming nitrites as surface intermediates (Cu^{+2}-ONO). In the next step, nitrites decompose and result in the evolution of gaseous NO_2, leaving reduced Cu sites (Cu^{+1}). This step is believed to be the Rate Determining Step (RDS) of the NO oxidation mechanism at low temperature. Finally, the reduced sites are reoxidized by oxygen to form copper dimers again. Blockage of the active sites by water as well as by nitrate buildup via the reaction between nitrites and NO_2 are taken also into account as inhibitory steps.

The effect of several operating variables on NO oxidation was investigated in the kinetic runs, including temperature, NO, O_2, H_2O and NO_2 concentrations (Figure 1), and space velocity. Since at higher temperatures NO oxidation approached thermodynamic equilibrium, only the results in the 150 to 350°C T-range are shown. The rate parameters of the individual steps in the kinetic mechanism were estimated by multi-response non-linear regression based on the least squares method, using the temporal evolutions of the relevant gaseous species

concentrations (NO, NO_2) as experimental responses. The model responses were generated by integrating in time a transient isothermal pseudo-homogeneous plug-flow model of the test microreactor. The experimental (symbols) and fitted (solid lines) NO conversions are compared in Figure 1. According to both the experimental and the fit results, NO has a kinetic order close to one (Fig.1A), oxygen has a positive fractional reaction order (Fig.1B), while H_2O is associated with a strong inhibition effect on NO oxidation (Fig.1C), which is well predicted by the model thanks to the assumption of water blocking the active sites. NO_2 also exhibits a strong negative effect on the rate of NO oxidation (Fig.1D), in line with other reports [1,3]. Again, the coverage of the Cu-sites by nitrates invoked in the proposed mechanism does a good job in describing such an inhibitory effect.

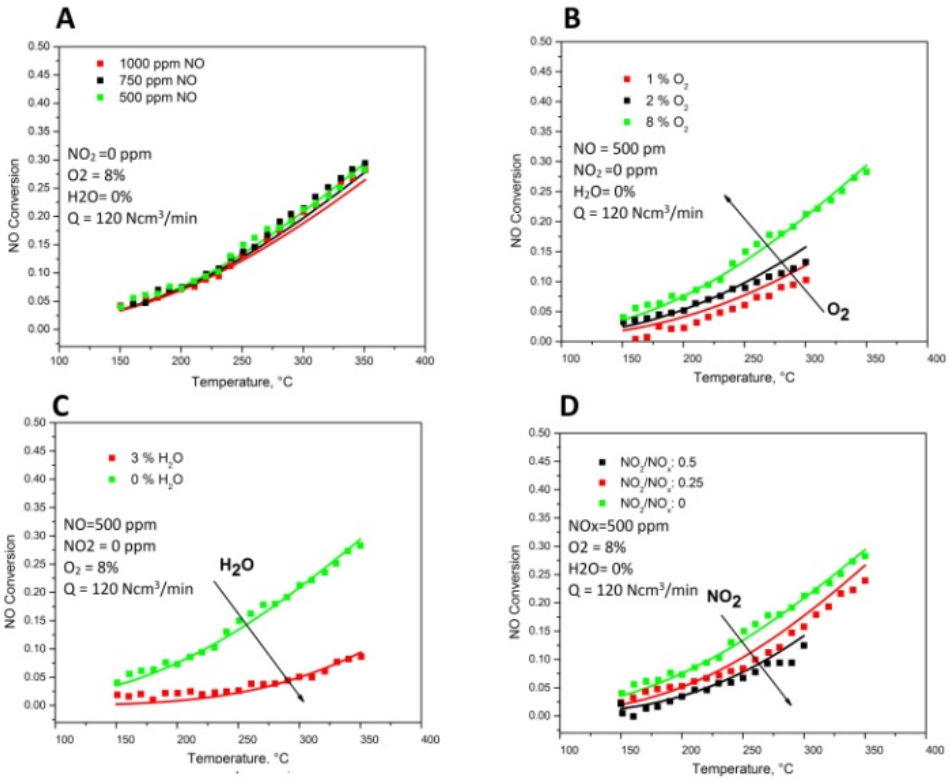

Fig. 1. NO oxidation over Cu-zeolite, GHSV= 120,000 [Ncc/h/$g_{catalyst}$] A) NO effect, B) Oxygen effect, C) H_2O effect, D) N_2O effect. Helium is used as the carrier gas.

4 Conclusions

We show that the predictions of a kinetic model based on our proposed redox mechanism for NO oxidation to NO_2 are quantitatively in accordance with the experimental data for a variety of conditions. This mechanistic model seems therefore a step forward towards a better understanding of the SCR-deNO_x activity of Cu-zeolites.

References

[1] I. Ellmers, et al. *Journal of Catalysis.* 311 (2014) 199.
[2] H. Sjövall, R.J. Blint, and L. Olsson, *Appl. Catal. B: Environmental.* 92 (2009) 138.
[3] P.S. Metkar, V. Balakotaiah, and M.P. Harold, *Catalysis Today.* 184 (2012) 115.
[4] M.P. Ruggeri, et al. *Journal of Catalysis.* 311 (2014) 266.
[5] M.P. Ruggeri, I. Nova, and E. Tronconi, *Topics in Catalysis.* 56 (2013) 109.
[6] A.A. Verma, et al. *Journal of Catalysis*. 312 (2014) 179.

V-PP57

Modelling Hydrocarbon Deactivation of SCR Zeolite Catalysts

Selleri T.[1], Nova I.[1], Tronconi E.[1*], Weibel M.[2], Schmeißer V.[2]

1 - Dip.Energia, Politecnico di Milano, Milano, Italy
2 - Daimler AG, Germany

* enrico.tronconi@polimi.it

Keywords: NH3-SCR, Cu, zeolites, poisoning, hydrocarbons modelling

1 Introduction

NH_3-SCR currently represents the leading technology for the NOx abatement from lean burn Diesel engines. However, in the upcoming years, due to the enforcement of stricter emissions regulations, demanding challenges awaits. In particular, the low temperature and cold start performances of the deNOx systems are of major concern. In these conditions, the catalytic devices upstream of the SCR converter in the after-treatment train (such as the Diesel Oxidation Catalyst) are not operative, leading to a significant hydrocarbon (HC) slip that impacts negatively on the activity of the SCR catalyst. Furthermore, medium- and long-term performances are decreased by coking and by strong T-gradients occurring during catalyst regeneration.

The aim of this contribution is to develop a reliable numerical simulation tool of the HC poisoning process, useful for the design of effective SCR systems.

2 Experimental/methodology

In the present work, an extension of the 1D+1D model of SCR monolith converters developed by Tronconi et al. [1] is proposed. In particular, a kinetic scheme accounting for different HC poisoning effects has been implemented and validated. Experimental data for model calibration were collected at Daimler labs over a commercial Cu zeolite monolith sample exposed to different types of HCs such as C_2H_2, C_3H_6 and $C_{10}H_{22}$. Fitting procedure of kinetics parameters was performed through a genetic algorithm optimization routine written in MATLAB.

3 Results and discussion

According to previous literature indications [2], a preliminary kinetic model of the HC deactivation process was developed according to a dual site approach, which includes: i) a redox site (S1), where NO is oxidatively activated and HC poisoning occurs due to partial oxidation, intermediate adsorption and coke formation; ii) an acid site (S2), responsible for ammonia and HC adsorption. In order to keep the model complexity as low as possible, only two lumped HC molecules were considered as representative of broad classes of compounds: light HC (C_2H_2, C_3H_6 …) and heavy HC ($C_{10}H_{22}$, $C_{12}H_{24}$, …).

Hydrocarbon poisoning is a complex phenomenon that involves different processes, depending on the nature of the HC considered as well as the type of zeolite structure. Light HC compounds are known not to compete significantly with NH_3 for adsorption on acid sites. It has been reported [3] that oxygenated compounds generated during partial oxidation of small hydrocarbons are responsible for catalyst deactivation due to active site blocking. On the contrary, heavy HC are adsorbed unconverted on the catalyst surface, leading to pore blocking and to a strong decrease in performances [4].

In order to reproduce as many as possible of such effects, both lumped light and heavy HC molecules were adsorbed on S2 sites. Then, for light HCs, a spillover mechanism from acid to redox metal sites, similar to the one reported in [2], was introduced in the kinetic scheme. Here,

the HC compound undergoes an oxidative activation step on the catalyst leading to the formation of oxygenated intermediates and poisoning of redox metal sites. Increasing the temperature, complete oxidation may occur and activity is recovered. In this way, effects on the ammonia storage and desorption dynamics, normally limited, but also effects on the catalytic activity were described correctly. Moreover HC oxidation by NO_2 was accounted for in the model, a crucial step to accurately describe the HC effects in SCR reactions with NO_2 such as the Fast SCR. Figure 1A shows e.g. the HC promoting effect on NO_2 conversion for NO_2 SCR.

The model was initially validated against experimental and literature data, showing good agreement. In particular lab scale transient and stationary tests on monolith samples of a commercial Cu zeolite catalyst, addressing the combined effects of propene poisoning and temperature increase [4], were correctly predicted. Moreover the model was able to properly represent the NO conversion dynamics when propylene pulses were fed to the SCR reactor in isothermal experiments [5] over both Fe and Cu zeolite catalysts.

The model has been then fitted to dedicated experimental data collected at DAIMLER on a commercial Cu zeolite. For this purpose, a specific routine written in MATLAB, based on the genetic algorithm toolbox, was developed. Figure 1A shows the fit of the promoting effect of HC on NO_2 conversion in a NO_2 SCR run. In Figure 1B, the fit of NH_3 oxidation in presence of acetylene is presented: the model is able to correctly account for both NH_3 and C_2H_2 concentration profiles as well as for the outlet CO production. In all the considered cases, model simulations were found to be in good agreement with the experimental results.

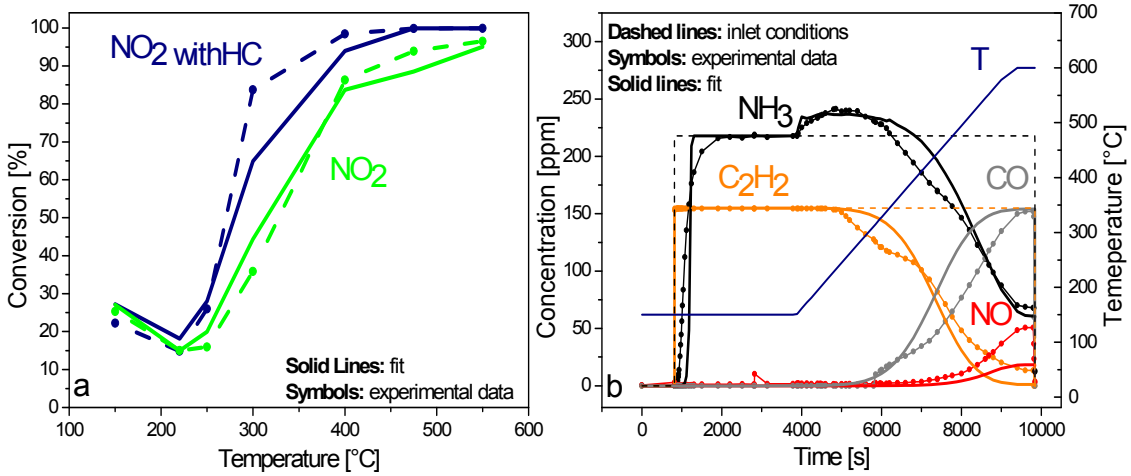

Fig. 1. Fit results. A) NO_2 SCR with and without C_2H_2: SV=66000 h^{-1}; NH_3 = 223 ppm; C_2H_2=170 ppm; NO_2=165 ppm O_2=10%; H_2O=10%. B) NH_3 oxidation with C_2H_2: SV=66000 h^{-1}; NH_3=218 ppm; C_2H_2=155 ppm; O_2=10%; H_2O=10%; T=150 °C-550 °C; heating rate=5°C/min.

4 Conclusions

HC poisoning is one of the most relevant issues for the operation of NH_3-SCR converters at low temperature. Its inclusion in numerical simulation tools is crucial for time and cost effective development and optimization of advanced catalysts and systems.

References

[1] D. Chatterjee, T. Burkhardt, M. Weibel, I. Nova, A. Grossale, E. Tronconi, *SAE Technical Paper* 2007-01-1136 (2007).
[2] I. Nova, C. Ciardelli, E. Tronconi, D. Chatterjee, B. Bandl-Konrad, *AIChE Journal* 52 (2006) 3222.
[3] J. Luo, H. Oh, C. Henry, W. Epling, *Appl. Catal. B: Environm.,* 123 (2012) 296.
[4] I. Malpartida, O. Marie, P. Bazin, M. Daturi, X. Jeandel, *Appl. Catal. B: Environm.* 102 (2011) 190.
[5] J. Li, R. Zhu, Y. Cheng, C. Lambert, R. Yang, *Environmental Science and Technology*, 44 (2010) 1799.

V-PP58

Green Synthesis of Ruthenium Nanoparticles on Magnetic Carbon Nanostructures and their Use for the Selective Hydrogenation of Nitroaromatics

Bertolucci E.[1*], Raspolli Galletti A.M.[2], Axet M.R.[3], Serp P.[3]

1 - Scuola Normale Superiore of Pisa, Pisa, Italy
2 - University of Pisa, Department of Chemistry and Industrial Chemistry, Pisa, Italy
3 - University of Toulouse, Laboratoire de Chimie de Coordination composante ENSIACET, Toulouse, France

* bertolucci.elisa@gmail.com

Keywords: magnetic carbon nanostructure, nanocatalysts, green chemistry, ruthenium nanoparticles, hydrogenation

1 Introduction

Carbon nanostructures finds a wide range of applications in different industrial and technological fields. In particular their promising electrical, chemical and physical properties could improve the catalytic activity of metal nanoparticles attached on their surface. [1] However an essential aspect for practical application of these nanomaterials in catalytic industrial processes is their recoverability and recycling. For this reason anchoring magnetic nanoparticles on the surface of carbon nanosupports could be a strategic choice able to guarantee their efficient magnetic separation from the reaction media. [2]

There are several protocols to support metal species over carbon nanostructures: deposition from solution; self-assembly methods; electro- and electrophoretic deposition and deposition from gas phase. The aim of this work is to propose a new sustainable and eco-friendly procedure to anchor ruthenium or/and magnetite nanoparticles on the surface of multiwalled carbon nanotube (CNT) and graphene oxide (GO). This green method is based on the use of: an alcohol as a solvent and reducing agent, monomode microwave as heating source, short reaction time, in the absence of hazardous reducing and stabilizing agents.

Finally the new monometallic and bimetallic catalysts are employed in the selective hydrogenation of p-chloronitrobenzene (p-CNB) to p-chloroaniline (p-CAN) under mild reaction conditions.

2 Experimental/methodology

The microwave syntheses of monometallic and bimetallic nanocatalysts were performed in a CEM Discover S-class system. The instrument consisted of a single-mode cavity. It works with a continuous power generation and control of power supply and it is capable of supplying power with 1W increments from 0 to 300 W. The system is equipped with a vertically focused IR temperature sensor.

For the preparation of monometallic systems (ruthenium or magnetite nanoparticles over carbon nanostructures) 1g of support (CNT, GO) and the iron or ruthenium precursors ($[Fe(OAc)_2]$ or $[Ru(acac)_3]$) were suspended in isopropanol, and MW-irradiated. At the end of the treatment the catalysts were recovered, washed and dried. The bimetallic systems (ruthenium over magnetic carbon nanostructures) were prepared following a “one-pot” technique, where first magnetic carbon nanosupports were synthetized as described above, then the $[Ru(acac)_3]$was added inside the microwave reactor and reduced. The final product was magnetically recovered, washed and dried.

The hydrogenation reactions were carried out in an autoclave reactor equipped with

mechanical stirring. Typically, 100 mg of catalyst were dispersed in 25 ml of solvent under sonication, then pre-treated at 110°C under 30 bar of hydrogen for 1h. 0,4 g (2,54 mmol) of the nitroaromatic compound was dissolved in 25 ml of solvent and the solution was added to the autoclave. The reactor was pressurized at 30 bar of hydrogen and heated at 60°C for 2h.

3 Results and discussion

The nanocatalysts were characterized by Transmission electron microscopy (TEM) micrograph, Inductively Coupled Plasma-atomic emission spectroscopy (ICP-AES), Auger Electron Spectroscopy (AES), X-Ray diffraction (XRD) and superconducting Quantum Interference Device analysis (SQUID). The characteristics of these new systems are summarized in Table 1.

Table 1. Characteristics of the synthetized nanocatalysts

Catalysts	Ru(%)	Fe(%)	H(%)	C(%)	Dm (nm) $_{Ru}$	Dm_{Fe3O4} (nm)
Ru@CNT	1,4	---	0	91,61	1,6	---
Ru@GO	0,77	---	0	94,46	2,6	---
Fe_3O_4@CNT[a]	---	15,8	0,88	62,97	---	4,9 (6,9)
Fe_3O_4@GO[a]	---	16,36	1,32	62,26	---	3,1 (5,8)
Ru@(Fe_3O_4-CNT)	1,13	13,54	0,6	70,34	1,4	5,4
Ru@(Fe_3O_4-GO)	0,58	18,09	0,12	79,96	2,5	5

The Fe_3O_4@CNT, Fe_3O_4@GO, Ru@(Fe_3O_4-CNT) and Ru@(Fe_3O_4-GO) nanocatalysts show a remarkable magnetic behaviour able to guarantee an easy and efficient magnetic separation from the reaction medium. Their promising magnetic properties were also confirmed by SQUID analysis. Furthermore all the nanocatalysts were employed in the selective hydrogenation of 4-chloronitrobenezene (p-CNB) to 4-chloroaniline (p-CAN) under mild reaction conditions. Ru@CNT, Ru@GO, Ru@(Fe_3O_4-CNT) and Ru@(Fe_3O_4-GO) show 100% of selectivity and a remarkable conversion in the first reaction hour. In particular the Ru@(Fe_3O_4-GO) has the best Turnover frequency 328 h^{-1}, followed by the Ru@GO nanocatalyst with 286 h^{-1}.

4 Conclusions

Several magnetic nanocatalysts were prepared following a new sustainable and eco-friendly procedure and they were characterized by TEM, XRD, ICP-AES and SQUID analysis. The new catalytic systems were employed in the selective hydrogenation of pCNB to pCAN showing high selectivity. The ruthenium on magnetic graphene oxide Ru@(Fe_3O_4-GO) shows the highest catalytic activity and thanks to its magnetic properties it is easily recoverable and recyclable. This study opens the way for industrial employ of magnetic recoverable nanostructures.

Acknowledgements

The authors thank Scuola Normale Superiore for E.B PhD. Fellowship.

References

[1] A. A. Balandin, *Nat Mater* 10 (2011) 569 .

[2] a) N. J. S. C. L. M. Rossi, F. P. Silva, R. V. Goncalves, *Nanotechnology Reviews* 2 (2013) 597; b) B. Baruwati, V. Polshettiwar, R. S. Varma, *Tetrahedron Letters* 50 (2009) 1215; c) S. Shylesh, V. Schünemanm, W. R. Thiel, *Angewandte Chemie International Edition* 49 (2010) 3428 d) V. Polshettiwar, R. Luque, A. Fihri, H. Zhu, M. Bouhrara, J.-M. Basset, *Chemical Reviews* 111 (2011) 3036.

V-PP59

Catalytic Wet Oxidation of Organic Wastewater over TiO_2 Supported Ru-Pt Bimetallic Catalysts

Gu S.Y., Wu L.H., Chen H.N.*

Sinopec Shanghai Research Institute of Petrochemical Technology, Shanghai, China

* chenhn.sshy@sinopec.com

Keywords: catalytic wet oxidation, Ru-Pt TiO_2 bimetallic catalyst, wastewater

1 Introduction

Organic wastewater from chemical industries containing hazardous pollutants can cause severe environmental problems [1]. It must be treated to satisfy the industrial process water demands or the stringent water quality regulations. Catalytic wet air oxidation (CWAO) is one of the most efficient, economical and environmental-friendly advanced oxidation process in treating wastewater. The process usually performed under high O_2 pressure (0.5–20 MPa) at elevated temperature (125–320 °C) and in the presence of catalyst [2]. In this study, bimetallic Ru-Pt/TiO_2 catalysts with total metal loading of 1wt% were prepared by impregnation method. These catalysts were characterized by XRD, N_2 physical adsorption, H_2-TPR and TEM, and applied to catalytic wet oxidation (CWO) of organic wastewater.

2 Experimental/methodology

I. Preparation and characterization of catalysts

Ru-Pt/TiO_2 catalysts with total metal loading of 1wt% were prepared by impregnation method. Briefly, 5g of TiO_2 was mixed with the appropriate amount of the $RuCl_3$ and H_2PtCl_6 precursor. After impregnation, the mixture was dried at 80 °C for 24h, and then introduced in a tubular quartz reactor and reduced under flowing hydrogen at 300°C for 2 h. The prepared catalysts were characterized by XRD, N_2 physical adsorption, H_2-TPR and TEM.

II. Catalytic oxidation reactions

Experiments were carried out in a 1 L autoclave reactor loaded with 4g catalyst and 600 mL aqueous solution (containing acrylic acid, succinic acid and PEG-1000, respectively). The reactor was then charged with N_2 twice. After heated to certain temperature, the reactor was pressurized with 5 MPa O_2, and then the stirrer was switched on. Liquid samples were periodically withdrawn from the reactor and analyzed the COD value with Hach DR2800.

3 Results and discussion

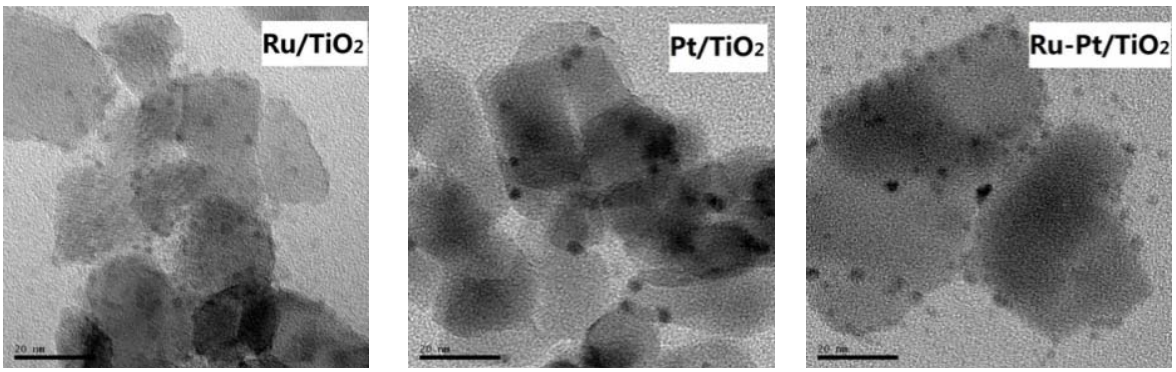

Fig. 1. TEM image of Ru/TiO_2, Pt/TiO_2 and Ru-Pt/TiO_2 catalysts

Figure 1 shows the TEM image of Ru/TiO_2, Pt/TiO_2 and $Ru\text{-}Pt/TiO_2$ catalysts. The results indicates that Ru, Pt and Ru-Pt are highly dispersed on TiO_2 support with particles less than 5 nm.

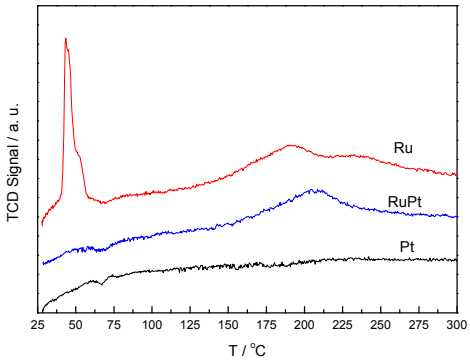

Fig. 2. H_2-TPR profiles of Ru/TiO_2, Pt/TiO_2 and $Ru\text{-}Pt/TiO_2$ catalysts

Figure 2 shows the H_2-TPR profiles of Ru/TiO_2, Pt/TiO_2 and $Ru\text{-}Pt/TiO_2$ catalysts. Different from monometallic Ru/TiO_2 or Pt/TiO_2 catalyst, bimetallic $Ru\text{-}Pt/TiO_2$ shows a wide peak at 207 °C.

Table 1. The comparison of TiO_2, $1\%Ru/TiO_2$, $1\%Pt/TiO_2$ and $0.4\%Ru\text{-}0.6\%Pt/TiO_2$ catalysts on CWO of acrylic acid, succinic acid and PEG-1000 aqueous solution

Organic substrate	Catalyst	*T* (°C)	Initial COD (mg/L)	COD removal (%)
acrylic acid	TiO_2	130	7380	18.5
	1%Pt			92.6
	1%Ru			32.1
	0.4%Ru-0.6%Pt			93.7
succinic acid	TiO_2	200	6290	8.2
	1%Pt			26.1
	1%Ru			89.7
	0.4%Ru-0.6%Pt			91.9
PEG-1000	TiO_2	170	9300	55.5
	1%Pt			95.9
	1%Ru			95.4
	0.4%Ru-0.6%Pt			96.6

Table 1 shows the reaction data of CWO of acrylic acid, succinic acid and PEG-1000. The results clearly show that bimetallic $0.4\%Ru\text{-}0.6\%Pt/TiO_2$ catalyst has higher oxidation activity than monometallic Ru/TiO_2 or Pt/TiO_2 catalyst.

4 Conclusions

The bimetallic $Ru\text{-}Pt/TiO_2$ catalyst was synthesized by impregnation method. In CWO of acrylic acid, succinic acid and PEG-1000 aqueous solution, it shows higher reaction activity than that for monometallic Ru/TiO_2 or Pt/TiO_2 catalyst. The synergic effect between Ru and Pt is the main reason that high CWO efficiency was achieved.

References

[1] J. Levec, A. Pintar, *Catalysis Today*, 124 (2007) 172–184.
[2] F. Luck, *Catalysis Today*, 53 (1999) 81–91

V-PP60

Decomposition of N_2O by Ruthenium Catalysts: Influence of the Support

Zheng J., Meyer S., Köhler K.*

Catalysis Research Center, Department of Chemistry, Technische Universität München, Garching, Germany

* klaus.koehler@tum.de

Keywords: nitrous oxide decomposition, support influence, ruthenium catalysts

1 Introduction

Nitrous oxide is one of the most harmful greenhouse gases, an important source of stratospheric nitrogen oxides as well as a by-product during the SCR of NO_x. Noble metal catalysts such as Ru or Rh are known to be highly active for the decomposition of N_2O, whereby ruthenium represents the better choice from an economic point of view. The properties of the catalysts can be significantly influenced by the nature of the support, leading to substantial variation of the catalytic performance [1]. Studies on the influence of the support on the properties and the activity of supported Ru catalysts for N_2O decomposition are rare and, as often found in heterogeneous catalysis, there is no conclusive picture on the role of the support up to now. The present work focuses on the impact of the support on the electronic and structural properties of Ru catalysts and their activity in N_2O decomposition.

2 Experimental/methodology

Ru particles supported on various oxides (MgO, SiO_2, CeO_2, Al_2O_3, TiO_2), activated carbon (AC) and silicon carbide (SiC) were prepared by impregnation followed by thermal treatment. Catalytic tests were performed in a fixed bed reactor using an equal catalyst volume and equal amounts of Ru for each run. The conversion of N_2O and the gaseous products formed were analyzed by FTIR and mass spectrometry. The catalysts were characterized by temperature programmed reduction (TPR), N_2 adsorption (Brunauer–Emmett–Teller, BET), transmission electron microscopy (TEM), and X-Ray diffraction analysis (XRD).

3 Results and discussion

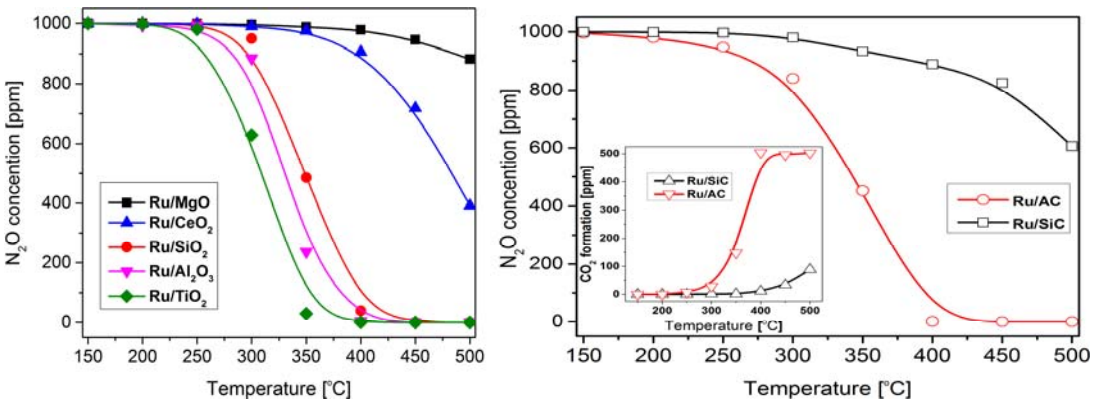

Fig. 1. Decomposition of N_2O over different Ru catalysts. The data were recorded at steady state conditions at different temperatures.

The catalytic performances are given in Figure 1. Ru/TiO_2 is found to be the most efficient catalyst and decomposes N_2O almost completely at 350 °C. The conversion of N_2O over Ru/MgO is only 10% even at temperatures up to 500 °C. For comparison, the activity of Ru catalysts supported on carbon-based materials was studied. Ru/AC possesses a high activity, which is comparable to Ru/SiO_2. Ru/SiC is less active. In both cases, CO_2 was detected in the exhaust stream during N_2O decomposition. The amount of CO_2 formation was proportional to the consumption of N_2O, indicating that AC and SiC act as stoichiometric reducing agents rather than as "inert" supports.

TEM and XRD investigations show that the particle sizes of Ru differ only slightly for the various supports. The substantial variation of the catalytic performance of the different catalysts therefore implies that the decomposition of N_2O is not preferably controlled by geometrical phenomena. H_2-TPR shows that the Ru species could be completely reduced at 250 °C for most of the catalysts except for Ru/MgO. Ru/TiO_2 possesses the lowest temperature of reduction to metallic Ru (151 °C with a shoulder at 111 °C). Based on the activity on N_2O decomposition, it can be assumed that the performance of Ru catalysts is linked to the redox properties (reducibility) of Ru.

4 Conclusions

The catalytic performance of Ru catalysts in the decomposition of N_2O is significantly affected by the support with Ru/TiO_2 exhibiting the best performance. Carbon or carbon-containing materials do not act only as support but also as stoichiometric reducing agents. The redox properties of the Ru catalyst, which are closely related to the support, must be taken into account as the key parameter for the explanation of the catalytic activity.

Acknowledgements

China Scholarship Council (CSC) and TUM Graduate School (TUM-GS) are acknowledged for the financial support.

References

[1] H. Beyer, J. Emmerich, K. Chatziapostolou, K. Koehler, *Applied Catalysis a-General*. 391 (2011) 411.

V-PP61

Catalytic Effect of Carbon Nanotubes in the Electrochemical Reduction of Nalidixic Acid

Patino Y.[1], Pilevar S.[2], De Wael K.[2], Diaz E.[1], Ordonez S.[1*]

1 - University of Oviedo, Oviedo, Spain
2 - University of Antwerpen, Antwerpen, Belgium

* sordonez@uniovi.es

Keywords: nalidixic acid, carbon nanotubes, electrocatalyst, differential pulse voltammetry

1 Introduction

In recent years pharmaceutical and personal care products (PPCPs), considered as emerging pollutants, are produced in large quantities. They enter into the environment from personal, veterinary and aquaculture uses, being able to persist in the environment and cause deleterious in organisms [1]. This kind of pollutants has been detected in surface, ground and drinking water in different countries around the world [2]. For this reason, the development of effective techniques for removing these pollutants is of key interest.

A representative antibiotic, nalidixic acid (NAL), has been selected as model compound for studying the degradation of this kind of compounds by electrochemical methods. The reduction depends on the catalytic activity of the anode which can be modified in order to increase the removal rate. In this way, carbon nanotubes (CNTs) are presented as promising catalysts since they have the ability to mediate electron transfer reactions when are used as an electrode [3].
In this study, the electrochemical reduction of NAL on bare glassy carbon electrode (GCE) and CNT-modified GCE was investigated using differential pulse voltammetry (DPV). Three different CNTs have been used -MWCNTs, MWCNT-NH_2, MWCNT-COOH- with the aim to investigate the effect of functionalization in the NAL reduction.

2 Experimental/methodology

Modified GCE were prepared by drop of MWCNTs (manufactured by DropSense) disperse into dimethylformamide (DMF) by ultrasonication until obtaining a well-dispersed suspension. The suspension was deposited on the GCE area, and then dried under room temperature before electrochemical measurements.

Differential pulse voltammetry was performed using a μ- Autolab Potentiostac/Galvanostat PGSTAT from Methrom. The used electrodes were bare GCE and MWCNTs-modified GCE as working electrode-, saturated calomel electrode (SCE) as reference electrode and platinum as auxiliary electrode. Before DPV, a constant potential was applied to enable the deposition of NAL on the working electrode surface producing an increase of nalidixic reduced.

3 Results and discussion

The effect of pH, stirring rate, scan rate (SR) and deposition time (DT) on DPV was studied obtaining the best results at the following conditions: pH=5.0, stirring rate (150 rpm), SC=50mV/s and DT=30 s.

With the optimized operation parameters, the NAL response was studied under different working electrodes (Figure 1). Modified GCE has a significant catalytic effect on NAL reduction, significantly increasing the signal intensity. The peak current follows the same order than the electrode area (determined by CV), MWCNT (0.076cm^2) > functionalized MWCNT (0.069 cm^2 –NH_2 and 0.070 cm^2 –COOH) > Bare (0.064 cm^2).

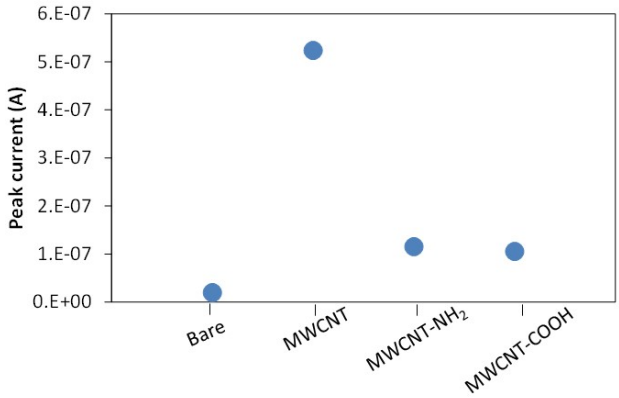

Fig.1. Electrocatalytic effect of MWCNTs for NAL degradation (1 10^{-5}M) in PBS buffer

Different cycles of DPV were carried out for NAL removal using MWCNT-modified GCE. As shows in Figure 2, NAL removal continue constant after 10 DPV cycles for a total sample volume of 5 mL. The electrode surface is blocked after several cycles such a way that the degradation cannot increase. The sample volume was reduced in order to improve the removal. A complete elimination was obtained for a total volume of 1.5 mL after 15 DPVs.

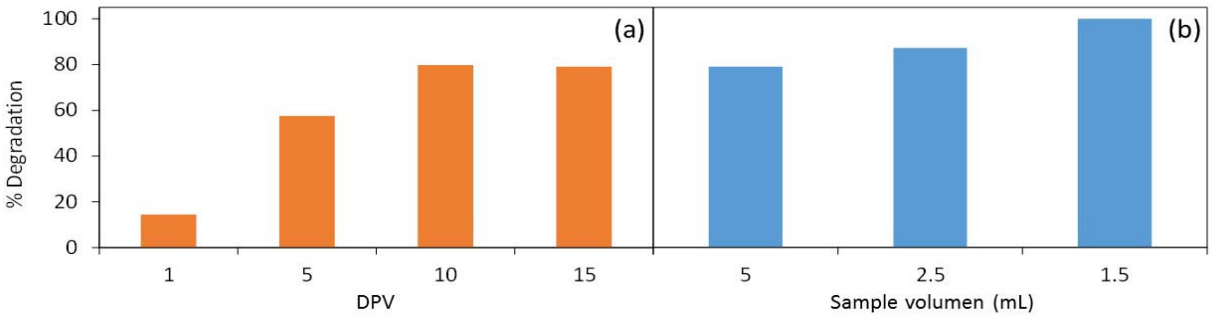

Fig. 2. Electrochemical reduction of NAL (1 10^{-5}M) by DPV using MWCNT modified GCE as working electrode in PBS buffer. (a) Different DPV at total volume of 5mL and (b) different total volume at 15 DPVs.

4 Conclusions

The MWCNT modified electrodes act as efficient catalysts for electrochemical reduction of NAL, especially the MWCNT without functional groups. The removal of NAL with MWCNT modified GCE was around 80 % after 10 DPV cycles for 5mL of total volume, increasing to 100 % when the total volume is 1.5 mL.

Acknowledgements

This work was supported by the Spanish Government (contract CTQ2011-29272-C04-01, -02 and -03). Y. Patiño thanks the Government of the Principality of Asturias for a Ph.D. fellowship (Severo Ochoa Program).

References

[1] D. W. Kolpin, E. T. Furlong, M. T. Meyer, E. M. Thurman, S. D. Zaugg, L. B. Barber, H. T. Buxton, *Environmental Science & Technology* 36 (2002) 1202.
[2] M.Carballa, F. Omil, J.M. Lema, M. Llompart, C. García-Jares, I. Rodríguez, M. Gómez, T. Ternes, *Water Research* 38 (2004) 2918.
[3] Y-P. Li, H-B. Cao, C-M. Liu, Y. Zhang, *Journal of Hazardous Materials* 148 (2007) 158.

V-PP62

Perturbing the Surface Polarity of Cellulose to Improve its Catalytic Conversion to Glucose

Diaz M., Lima E.*

Instituto de Investigaciones en Materiales, UNAM, Mexico, Mexico

* lima@iim.unam.mx

Keywords: cellulose, amino, acids, catalytic conversion, glucose

1 Introduction

Cellulose (MC) conversion into useful chemicals has become a major research goal, but its highly ordered molecular structure inhibits its depolymerisation and hence reduces its reactivity.

In order to take advantage of this raw material, efforts have been made to convert cellulosic materials into valuable chemicals and renewable fuels.

Recent research showed that a small change on the surface polarity of MC significantly improves its catalytic conversion to glucose

This work intends to perturb the hydrogen bond network of MC grafting different combinations of amino acids onto its surface and then, depolymerise the material in the presence of acid catalysts. As a model of MC, cellobiose (Cb) was also perturbed and catalytically hydrolyzed.

2 Experimental/methodology

To perturb the MC and Cb surfaces and increase their reactivity, different amino acids were grafted onto the materials surface, weakening the hydrogen bond network.

Both MC and Cb were hydrothermally treated with alanina (Ala), Phe (Phe) and proline (Pro) and with three different combinations of two amino acids: Ala-Phe, Ala-Pro and Pro-Phe. This treatment leads to surface-modified materials.

The structural and textural properties of the resulting materials were analysed by XRD, SEM, and ^{13}C CP MAS NMR and IR spectroscopies

For the evaluation of the modification in the reactivity of the modified materials, an acid hydrolysis was performed. The conversion of cellulosic materials was carried out in a 50 mL stainless steel at 150 ºC under magnetic stirring, using water as solvent. Hydrolysis reactions were performed in the presence of two different acids: hydrochloric acid (HCl) or tungstophosphoric acid ($H_3PW_{12}O_{40}$). The products were anaylsed by HPLC, using water as mobile phase.

3 Results and discussion

^{13}C CP MAS NMR and SEM characterization showed remarkable differences as a consequence of treatment with amino acids for both MC and cellobiose.

When compared the grafted-celluloses ^{13}C CP MAS NMR spectra to that of MC, it can be seen some important changes in the chemical shifts on the carbonyl region (170-180 ppm), suggesting an interaction between the carbonyl group of the amino acid and the MC surface. In addition, the samples containing Phe showed peak broadening in the region of the aromatics (120-140 ppm) indicating the interaction between the planar ring and the MC chain, this interaction caused a very noticeable change in morphology, as it can be observed on Figure 1. In the samples containing Phe this is more evident, inducing the formation of porous surfaces.

In the case of modified cellobioses, from the modified samples with a single amino acid the more damaged morphologically is the one with phenylalanine, as already reported for MC [1].

Similarly, samples of modified with two amino acids, those with larger change in its

surface are those containing Phe (Cb Phe and Cb Ala-Phe, Cb Pro-Phe).

The characterization and reactivity results suggest that the surface of the MC can be modified to increase their conversion to glucose. Amino acids on the surface are likely to modify the network of hydrogen bonds, some of which can break due to the interaction between the amino acids with the MC chains, thus opening reactive sites.

The hydrolysis reaction with best results is the one conducted with $H_3PW_{12}O_{40}$ and modified materials with Ala and Phe, reaching a MC conversion of 68% and glucose selectivity of 20%.

In the case of acid hydrolysis of Cb, the amino acid modification has not a clear and significant effect on the total amount of converted Cb, the maximum difference is 12% between the hydrolysis of ungrafted Cb catalysed by HCl and the hydrolysis of modified Cb with Pro-Phe catalysed by HCl.

Moreover, where it does is clear an influence of the grafting is in the change in selectivity towards glucose: lower selectivities are obtained when Cb is not modified with amino acids. In addition, higher selectivities towards glucose are obtained with the heteropolyacid as catalyst.

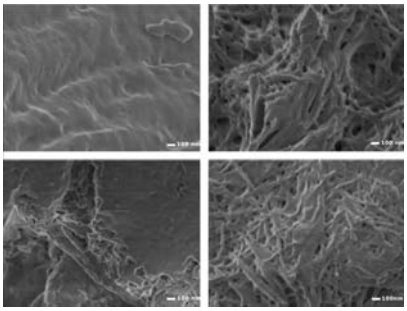

Fig. 1. Micrographs of a) MC, b) MC Ala-Phe, c) MC Ala-Pro, d) MC Pro-Phe

4 Conclusions

Amino acid grafting is insufficient to damage the primary structure of the cellulosic materials, but it does causes significant modifications at superficial level on Cb and MC.

The grafted celluloses that showed considerable textural changes were those modified with a combination of amino acids, specifically using phenylalanine. In the case of the different grafted cellobioses, their surfaces were more damaged when they were modified with Ala.

Surface modification experienced by Cb and MC, as a result of the grafting of amino acids, is sufficient to increase their reactivity. In the case of cellulose, the increase in reactivity is directly reflected in its higher conversion when hydrolyzed in the presence of HCl or $H_3PW_{12}O_{40}$. Catalytic degradation of the MC to glucose is easier and more selective when MC is simultaneously modified with Ala and Phe and the catalyst is $H_3PW_{12}O_{40}$. On the other hand, the catalytic hydrolysis of Cb is practically independent of the modification with amino acids and used catalyst. However, the change has a significant effect on glucose production. If it is desired to achieve a high conversion of Cb and high glucose production, Cb should be modified with Pro and Phe and conducting the reaction in the presence of $H_3PW_{12}O_{40}$.

Acknowledgements

Thanks are due to CONACYT and PAPIIT-UNAM for Grants 220436 and IN101214.

References

[1] M. Hernández, E. Lima, A. Guzmán, M. Vera, O. Novelo, and V. Lara, *Appl. Catal. B Environ.*, 144, (2014), 528.

V-PP63

Co Catalysts for the Dry Reforming of Biogas

San Jose-Alonso D., Illan-Gomez M.J., Roman-Martinez M.C.*

Department of Inorganic Chemistry, University of Alicante, Alicante, Spain

* mcroman@ua.es

Keywords: dry reforming, biogas, cobalt, alumina, spinel

1 Introduction

The dry reforming of methane (DRM) is an interesting process because it produces synthesis gas with a desirable H_2/CO ratio, contributes to the removal of two greenhouse gases and offers a solution for the valorization of biogas [1-3]. Previous results have shown that cobalt catalysts supported on $Al_2O_3$are very suitable for DRM [4], but the activity for biogas reforming was not addressed. Thus, this work is focused in the study of the catalytic behavior of Co catalysts in the DRM reaction using a oxygen containing gas mixture resembling the composition of biogas. Catalysts with a 9 wt.% nominal Co content have been prepared considering two variables: support (Al_2O_3 and $MgAl_2O_4$) and presence of K as promoter.

2 Experimental/methodology

The catalysts have been prepared by excess solution impregnation using aqueous solutions of KNO_3 and $Co(NO_3)_2.6H_2O$ (10 ml/g) of the appropriate concentration to achieve the nominal metal contents: 9 wt. % Co and 1wt.% K. The K containing catalyst was prepared by co-impregnation. The mixture was kept at 333 K until solvent evaporation. Finally the catalysts were dried in an oven at 373 K for 24 h.

Catalytic activity experiments were carried out in a fixed bed quartz reactor coupled to a gas chromatograph (HP5890 series II) with a thermal conductivity detector. The reaction conditions were: 973 K, 0.18 g of catalyst, a gas mixture $CH_4/CO_2/O_2$= 37.5/37.5/25.0, 60 ml/min, a space velocity of 22,000 h^{-1} and 6 h time on stream. Prior to the catalytic activity tests, the catalysts were reduced in situ (H_2, 40 ml/min) at 773 K for 90 min.

To determine the amount of deposited carbon, the used catalysts were submitted to Temperature Programmed Oxidation (TPO) experiments, using a thermobalance (TAInstruments SDT-2960) coupled to a mass spectrometer (BalzersThermostar), under the following conditions: 20 mg of catalyst was heated, at 20 K/min, up to 1223 K, in a gas mixture of 16 vol.% O_2 in He (100 ml/min). The amount of deposited carbon was determined from the weight loss and from the amount of evolved CO_2 (m/z = 44).

3 Results and discussion

Table 1 collects the most relevant parameters regarding the catalytic behaviour of the three catalysts studied in this work. Data corresponding to the DRM of methane with a CH_4:CO_2 = 50:50 mixture have been also included as a reference.

It can be observed that methane conversion increases and CO_2 conversion decreases when the feed contains oxygen and that these two changes show a similar magnitude. This means that CH_4 is consumed to produce CO_2, revealing that the total oxidation of methane is taking place, consuming about 10% of the fed methane.

Table 1. Catalytic activity parameters determined in the dry reforming of biogas.

Catalyst	Air (%)	Conversion CH_4(6h)	Conversion CO_2(6h)	CO (ml/min) (6h)	CO Yield [a] (6h)	Deactivation [b] (%)	Deposited carbon (6h) % molar [c]	Deposited carbon (6h) mg/g [d]
Co/Al_2O_3	0	72	83	46.4	77.3	1	0.57	290
	25	80	68	33.6	74.7	1	0.02	10
$Co/MgAl_2O_4$	0	65	74	41.7	70.0	-1	0.25	125
	25	77	65	32.1	71.3	0	0.02	10
KCo/Al_2O_3	0	58	70	38.4	64.0	2	0.08	40
	25	68	57	28.5	63.3	2	0.05	25

[a] CO yield: moles of CO produced divided by moles of CH_4 and CO_2 introduced in the feed

[b] Deactivation, calculated as the difference between conversion at 30 minutes and 6h divided by conversion at 30 minutes and multiplied by 100.

[c] (mol of deposited carbon/mol of converted carbon)*100 (at t=6h)

[d] mg of carbon deposited per gram of catalyst

Thus, it seems that three reactions occur simultaneously: CO_2 methane reforming, methane decomposition and total oxidation of methane. Note that the amount of CO produced is lower when the feed contains O_2, however the CO yield (CO moles/(CH_4+CO_2 moles)) is almost not affected. The catalysts stability is neither affected by the presence of oxygen. Regarding the carbon deposition, it is, as expected, much lower in oxygen rich conditions.

Thus, in the presence of oxygen, the Co/Al_2O_3catalyst is the most active followed by $Co/MgAl_2O_4$. For these two catalysts the carbon deposition is quite low. Finally, the KCo/Al_2O_3 catalyst is the less active and presents the largest amount of deposited carbon.

4 Conclusions

Catalysts Co/Al_2O_3 and $Co/MgAl_2O_4$ are very active for biogas reforming, with high CO yield and low carbon deposits, while the addition of K as a promoter does not bring any advantage.

Acknowledgements

The authors thank the financial support to Generalitat Valenciana (Project PROMETEOII/2014/010).

References

[1] D. Deublein, "Biogas from waste and renewable resources: an introduction", Ed. Wiley-VCH, 2008

[2] J. Xu, W. Zhou, Z. Li, J. Wang, J. Ma, Int. *J. Hydrogen Energy* 34 (2009) 6646

[3] M. Harasimowicz, P. Orluk, G. Zakrzewska Trznadel, A.G. Chmielewski, *J. Hazard. Mater*. 144 (2007) 698

[4] D. San José-Alonso, J.Juan-Juan, M.J. Illán-Gómez, M.C. Román-Martínez, *Appl. Catal. A* 371 (2009) 54

V-PP64

Pd Nanoparticles via Water in Oil Microemulsion as Catalyst for Nitrite Reduction

Perez-Coronado A.M.*, Calvo L., Alonso N., Heras F., Rodriguez J.J., Gilarranz M.A.

Sección de Ingeniería Química, Facultad de Ciencias, Universidad Autónoma de Madrid, Madrid, Spain

* anamaria.perez@uam.es

Keywords: Pd nanoparticles, nitrite reduction

1 Introduction

Metal nanoparticles (NPs) research has recently become the focus of intense work due to their unusual properties compared to bulk metal. Among these metallic NPs, Pd NPs have been widely used as catalysts in hydrogenation and dehydrogenation, as well as cracking and carbon-carbon bond forming reactions such as Suzuki or Heck couplings. Some of these reactions have been often reported as structure-sensitive, being necessary the development of methods that are able to control the NPs size. The reverse microemulsion (water in oil, w/o) technique is of special interest since the NPs size can be controlled using different water-to-surfactant molar ratio (w_0) and/or different reductor-to-metal molar ratio [1]. In this work, catalytic reduction of nitrite in aqueous phase has been studied as an intermediate and critical step in the reduction of nitrate. One of the major limitations in the catalytic reduction of nitrate is the production of ammonium (*versus* N_2), being considered the nitrite hydrogenation as the key step. Therefore, the aim of this work is to study size effect in nitrite reduction in aqueous phase, using non supported Pd NPs. pH effect is also considered.

2 Experimental/methodology

The preparation of Pd NPs was carried out through the reduction of $Pd(NH_3)_4Cl_2 \cdot H_2O$ with hydrazine in AOT/isooctane reverse micellar solution. The synthesis of Pd NPs was achieved by mixing equal volumes of two reverse micellar solutions with a w_0 in a range 3-12 and AOT concentration of 0,35 M in isooctane. After a 10 min of reduction, isooctane was evapored in a rotary evaporator at 368 K and the NPs were purified from excess of surfactant by addition of methanol followed by centrifugation (this washing was carried out three times). The Pd NPs synthesized were characterized by transmission electron microscopy (TEM) at 400 kV (JEOL, mod. JEM-4000 EX).

Nitrite hydrogenation runs were carried out during 4 hours in a jacketed glass reactor where H_2 was continuously fed at 50 $N \cdot mL \cdot min^{-1}$ flow rate under vigorous stirring (500-700 rpm) in order to facilitate hydrogen distribution through the nitrite solution (150 mL and 50 mg /L). The reaction temperature, 303 K, was controlled by a thermostatic bath connected to the reactor jacket. In some experiments, CO_2 was introduced to the reaction media for buffering the solution at a pH value around 6. Nitrite and ammonium concentrations were analyzed by ion chromatography (Metrohm 790 Compact IC Plus).

3 Results and discussion

Pd NPs were prepared under different values of w0 (3, 7 and 12) in order to study the influence of Pd NPs size on the nitrite reduction. Pd NPs size increase with increasing w0, achieving values of 6.2, 7.7 and 11.6 nm. It has been reported that the role of AOT is to act as a protecting agent, allowing to control NPs growth in microemulsion. An increase of this ratio at constant concentration of surfactant will increase the average diameter of the droplets and consequently the size of the NPs [2].

Figure 1 shows the conversion results obtained with non supported Pd NPs using 2.45 mg Pd/L in all experiments. Significant differences were found in nitrite conversion depending on the Pd NPs size. Higher sizes always led to higher conversions. This behaviour contrasts with the reported in most of the works in literature, indicating the nitrite hydrogenation as a size-independent reaction [3]. The pH was found as a key parameter in nitrite reduction, since relatively higher nitrite conversion values (50–80 %) were achieved when reaction was buffered with CO_2.The reduction of nitrite led to the formation of hydroxide ion, increasing the pH of the reaction medium up to 8-9.5 and decreasing the activity.

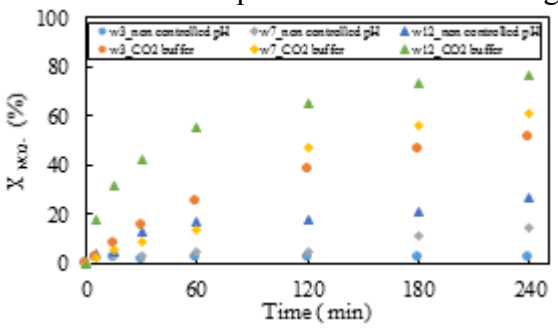

Figure 1. Influence of nitrite conversion on Pd NPs size.

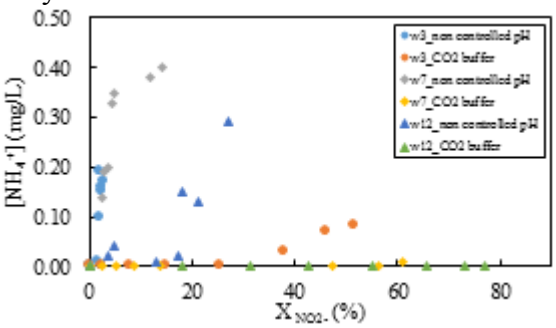

Figure 2. Influence of ammonium concentration on Pd NPs size.

Significant differences in selectivity were observed, depending on the pH (Figure 2). Ammonium selectivity increased with lower Pd NPs size in the runs developed under non-controlled pH. Moreover in the reactions with lower conversion, selectivity towards ammonium also increased with similar conversion values. Lower ammonium selectivity values were always found when the pH of the nitrite reduction was controlled, below 0,08 mg/L. It can be also seen null ammonium concentration when higher size Pd NPs were tested. Some works in literature reported that large Pd particles are favourable for selectivity to N_2 in nitrite hydrogenation, proposing that N_2 formation proceeds on terraces, whereas ammonium formation is supposed to proceed on low coordination Pd sites on edges, corners and defects.

4 Conclusions

Pd NPs with different particle sizes (6.2, 7.7 and 11.6 nm) have been prepared using water/AOT/isooctane microemulsions. Particle size has a significant role in the nitrite reduction, large particles led to a higher catalytic activity. Control of pH through CO_2 bubbling was beneficial to both nitrite conversion and N_2 selectivity.

Acknowledgements

The authors greatly appreciate financial support from the Spanish MICINN (CTQ2012-32821). The SusFuelCat project has received funding from the European Union's Seventh Framework Programme for research, technological development and demonstration under grant agreement N° 310490 (www.susfuelcat.eu).

References

[1] N. Semagina, A. Renken, D. Laub, L. Kiwi – Minsker, *Journal of Catalysis* 246 (2007) 308-314.
[2] I. Mikami, Y. Sakamoto, Y. Yoshinaga, T. Okuhara, *Applied Catalysis B*, 44 (2003) 79-86.
[3] Y. Zhao, J.A. Baeza, N. Koteswara Rao, L. Calvo, M.A. Gilarranz, Y.D. Li, L. Lefferts, *Journal of Catalysis*, 318 (2014) 162.

V-PP65

$CaO/CoFe_2O_4$ Synthesized by Citrate Precursor Method for Transesterification Reaction

Borges D.G.[1*], Moores A.[2], Assaf J.M.[1]

1 - Laboratory of Catalysis, Department of Chemical Engineering, São Carlos Federal University, São Carlos, Brazil

2 - Center for Green Chemistry and Catalysis, Department of Chemistry, McGill University, Montreal, Canada

* diogonbor@yahoo.com.br

Keywords: biodiesel, transesterification, cobalt ferrite, citrate precursor

1 Introduction

Biodiesel is one of popular alternative energy in the world due to characteristics like be biodegradable and renewable, non-toxic and low CO emission [1]. Heterogeneous catalysts had been widely investigated for offer many advantages such as simple separation in reaction medium, less consumption of energy and cost, as well as easier glycerol recovery [2]. One of the most used catalysts is CaO, due to low price, long catalyst life, high activity and requirement of moderate reaction conditions, although some disadvantages like low surface area and leaching [1]. In last years has increased the research of the use of magnetic nanoparticles as an alternative to reduce the environmental problems, due to the high surface compared to the volume of crystals, expecting that result in a excellent magnetic material [3]. Cobalt ferrite had been widely studied due to its high electromagnetic performance, excellent chemical stability, mechanical hardness, high coercivity, and moderate saturation magnetization, which makes it a good candidate for the electronic components used in computers, recording devices, and magnetic cards [4].

2 Experimental

Cobalt ferrite ($CoFe_2O_4$) was prepared by citrate precursor method. Stoichiometric quantities of $Co(NO_3)_2.6H_2O$, $Fe(NO_3)_3.9H_2O$ and $C_6H_8O_7.H_2O$ were dissolved in distilled water and this mixed (citrate-nitrate solution) was heated at 90°C with continuous stirring. After the evaporation of excess of water, first a highly viscous gel was obtained and finally a powder. It was sintered at 300°C, to acid decomposition. The ferrite synthesized was used as a support for impregnation of the calcium oxide at mass concentrations of 30, 40 and 50%. CaO supported on $CoFe_2O_4$ were obtained by calcination at 650°C for 1 hour. These materials were characterized by XRD, BET, SEM, EDS, TDP-CO_2 and SQUID.

The catalytic activity was evaluated through of transesterification between methyl acetate/ethanol and soybean oil/ethanol. The tests with methyl acetate/ethanol were performed with molar ratio = 6 /1, 4% wt/wt and temperature of 70°C. In the tests using soybean oil was varied the ratio ethanol/oil (6:1, 12:1, 24:1) at the same temperature (70°C). After the reaction, the catalyst was separated and the supernatant was recovered for composition analysis by gas chromatography (GC). The method used to evaluate the stability of the materials was the reuse of the catalysts in subsequent runs in the same reaction conditions to evaluate the catalytic activity during 1 hour for each reaction cycle.

3 Results and discussion

The hysteresis curves of the $CoFe_2O_4$ in SQUID tests showed ferromagnetic characteristic at

room temperature with a saturation magnetization of 56 emu/g. The XRD showed diffraction patterns of $CoFe_2O_4$, CaO, $Ca(OH)_2$ and $CaCO_3$, its was expected due to the rapid hydration and carbonation of CaO in presence of water vapor and atmospheric CO_2. Strong basic sites on $CaO/CoFe_2O_4$ were confirmed by TPD-CO_2, with basic sites density of 14 μmol/m^2.

The catalytic performance of the 50-$CaO/CoFe_2O_4$ catalyst in the methyl acetate transesterification showed conversion level above 85%, reaching the equilibrium after 120 minutes. The run tests of the catalysts containing 30, 40 and 50% of CaO showed that the conversion depends of the calcium content incorporated on support. The ester yield in tests with soybean oil/ethanol with the 50-$CaO/CoFe_2O_4$ catalyst represented in Figure 1 shows that varying the reaction time and the ethanol/oil ratio resulted in a gradual increase in the esters conversion. This is justified by the fact that the transesterification of vegetable oils is a kinetically favored reaction when an excess of alcohol is used relative to the triglyceride. The Figure 2 shows the recycle tests using the 50-$CaO/CoFe_2O_4$ catalyst in the methyl acetate transesterification reaction. The gradual loss of catalytic activity may be due to loss of catalyst during the reaction, which is impregnated in the wall of the reactor or had been removed of the supernatant in extraction process. To verify that the leached of the Ca^{2+} ions which were not active in the reaction, tests were made by removing the solid catalyst of reaction medium and results showed that after this removal the reaction stopped.

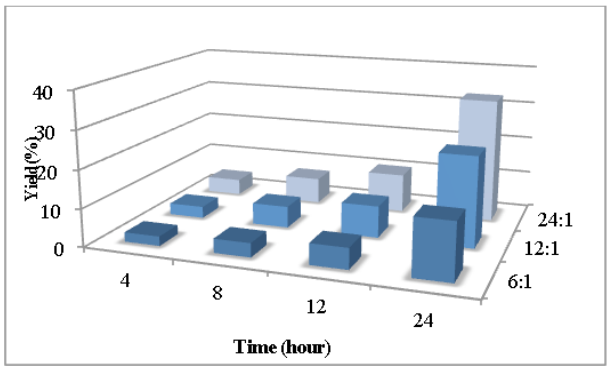

Fig. 1. Catalytic evaluation of 50-$CaO/CoFe_2O_4$ catalyst in transesterification between soybean oil and ethanol.

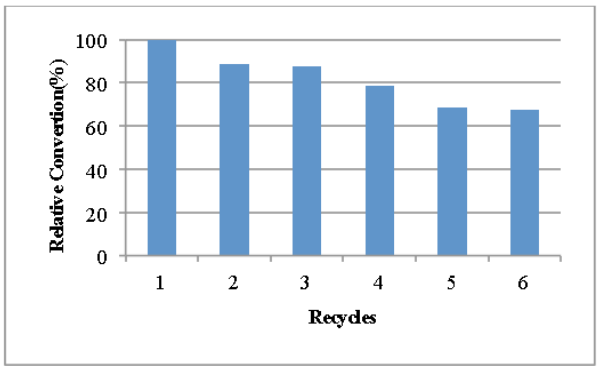

Fig. 2. Recycles of 50-$CaO/CoFe_2O_4$ catalyst.

4 Conclusions

The results confirmed that the $CaO/CoFe_2O_4$ can be considered a promising heterogeneous catalyst. It can be easily separated from reaction due to the magnetic characteristic of cobalt ferrite and be reused for successive batches, showing no contribution of homogeneous activity.

Acknowledgements

Thanks for the financial support to CNPQ and CAPES.

References

[1] I. I., Sebastianus; A., Prasetyo;T.S., Nugroho.Procedia. *Environmental Sciences* 23 (2015) 394 – 399.
[2] S.L., Lee; Y.C., Wong; Y.P., Tan; S.Y., Yew. *Energy Conversion and Management* 93 (2015) 282–288.
[3] Huixia, F.; Baiyi, C.; Deyi, Z and Jianqiang, Z; Lin, T. *Journal of Magnetism and Magnetic Materials* 356 (2014) 68–72 .
[4] Naseri, M.A.; Saion, E. B.; Ahangar, H. A.; Hashim, M.; Shaari, A. H. *Journal of Nanomaterials* 210(2010) 80-88.

V-PP66

EXAFS Study in Operando Conditions of Au/Co-Doped CeO_2 Catalysts for Methanol Oxidation Reaction

Manzoli M.[1*], Agostini G.[2], Vindigni F.[1], Lamberti C.[1], Dimitrov D.[3], Ivanov K.[3], Tabakova T.[4]

1 - Department of Chemistry and NIS Interdepartmental Centre, University of Torino, Torino, Italy
2 - European Syncrotron Radiation Facility, Grenoble , France
3 - Departmemt of Chemistry, Agricultural University, Plovdiv, Bulgaria
4 - Institute of Catalysis, Bulgarian Academy of Sciences, Sofia, Bulgaria

* maela.manzoli@unito.it

Keywords: EXAFS, gold catalysts, Co-doped ceria, CH_3OH, oxidation

1 Introduction

Supported gold nanoparticles attracted significant attention due to their high catalytic activity in various oxidation reactions at low temperatures. The catalytic oxidation of Volatile Organic Compounds (VOCs), such as methanol, is a subject of considerable interest due to their relevance in many industrial applications.

The oxidation activity of gold catalysts is closely related to the size of the Au particles and to the ability of the support to provide active oxygen species. For this reason, the selection of the proper support is a critical factor. Ceria is very attractive, due to its ability to maintain high metal dispersion and to change Ce oxidation state depending on the redox conditions, which results in rapid formation and elimination of oxygen vacancy defects. The doping of ceria can increase the concentration of oxygen vacancies. Recently, we observed a strong influence of the nature of the added oxide on the activity of ceria-based gold catalysts for catalytic abatement of VOCs and CO in waste gases [1]. Gold catalyst supported on ceria modified by Co_3O_4 exhibited the best performance. Ceria supports with different amount of Co_3O_4 were prepared in order to optimize the content of dopant.

The aim of this work was an accurate EXAFS study on the nature of the active sites exposed at the surface of highly dispersed gold catalysts supported on ceria modified by Co_3O_4. Research efforts were focused to achieve information on the local structure of the active sites in terms of position of cobalt atoms in respect to the gold metallic phase.

2 Experimental/methodology

The gold samples were prepared in two steps:
(i) mixed CeO_2–Co_3O_4 supports were prepared by a simple mechano-chemical mixing procedure: a mixture of cerium hydroxide and (5, 10, 15 wt%) Co_3O_4 was subjected to mechano-chemical milling for 30 min in a mortar and calcination at 400 °C for 2 h;
(ii) gold (3 wt.%) was introduced by the deposition–precipitation method at pH 7, temperature 60 ^oC, and full control of stirring speed, reactant feed flow rates.

After filtering and careful washing, the precursors were dried under vacuum at 80 °C and calcined in air at 400 °C for 2 h. Moreover, unmodified Au/CeO_2 and Au/Co_3O_4, used as blank samples, were also prepared.

EXAFS measurements were done in transmission mode at both Au L3 and Co K edges. All samples were measured as prepared and after an oxidation pre-treatment in O_2 at 400 °C to mimic the activation before the catalytic tests and to follow the effect of such activation on the nature of the exposed active sites. Then, a mixture of methanol vapor/O_2/He mixture (20% O_2-He) was fluxed at r.t. and the samples have been heated up to 100°C in the same mixture.

3 Results and discussion

Catalytic tests demonstrated that the addition of 5, 10 and 15 wt% Co_3O_4 significantly affected the activity of Au/CeO_2. The best performance was observed in the case of the catalyst doped by 10 wt% Co_3O_4, over which 100% CH_3OH conversion degree at 40 ^oC was obtained. The characterization data indicated that the high defectivity of ceria exposed faces, along with the presence of gold nanoparticles with the smallest size and the highest hydrogen consumption (e.g. highest oxygen mobility) were found over this gold sample.

The methanol oxidation reaction was investigated in-operando conditions. The first set of spectra was collected at room temperature. Then, starting from the catalysts previously oxidized, another set of spectra were recorded in operando conditions starting from room up to 120 °C. Au/CeO_2 as well as the bare support (ceria modified by 10 wt.% Co_3O_4) were measured as reference samples, too.

Three spectra were measured at each temperature, to evaluate the experimental uncertainty. The data analysis was performed by means of simulations and non-linear fitting procedures, paralleled by the ratio method for the first shell.

The analysis of the data at the Au L3 edge revealed that the active sites present on the most active sample (with 10 wt% Co_3O_4) are those where cationic gold sites are strongly interacting with Co.

4 Conclusions

The correlation of the catalytic activity with the findings, provided by EXAFS study about the nature and structure of the active sites allows to bridge the gap of experimental data previously obtained by HRTEM, XRD FTIR, TPR and to clarify the precise nature of the synergy between the gold phase and the Co-doped ceria support, which resulted in an excellent CH_3OH oxidation activity.

Acknowledgements

Bulgarian authors gratefully acknowledge the financial support by the Bulgarian National Science Fund (Project DFNI T 02/4).

References

[1] T. Tabakova, D. Dimitrov, M. Manzoli, F. Vindigni, P. Petrova, L. Ilieva, R. Zanella, K. Ivanov, *Catal. Commun*. 35 (2013) 51.

V-PP67

Effect Promoter of Cobalt on the Catalyst Ni-Mg-Al Obtained via Hydrotalcites for the Dry Reforming of the Methane

Zazi A.[1,2*], Gonzalez-Delacruz V.M[3,2], Halliche D.[1], Holgado J.P.[3], Caballero A.[3], Bachari K.[4], Saadi A.[1], Tezkratt S.[2], Cherifi O.[1]

1 - Laboratoire de Chimie du Gaz Naturel, Faculté de Chimie, USTHB, Algerie
2 - Departement de Chimie, Faculté des Sciences,UMMTO,Tizi Ouzou, Algerie
3 - Instituto de Ciencia de Materiales de Sevilla (CSIC-University of Seville) and Departamento de Quimica Inorganica, University of Seville, Seville, Spain
4 - Centre de Recherches Scientifiques (CRAPC), Alger, Algeria

* aliz6dz@yahoo.fr

Keywords: dry reforming, HDL, cobalt, nickel, methane, synthesis, gas

1 Introduction.

The production of the synthesis gas and the hydrogen represents one stakes major in the chemical industry in the world. These two gases are obtained via the reforming of the methane by one of the three proceeded:-Dry reforming of methane: $CH_4 + CO_2$ --------- $2CO + 2H_2$

-Steam reforming of methane: $CH_4 + H_2O$ --------- $CO + 3H_2$

-Partial oxidation of methane: $CH4 + ½ O_2$ ---------- $CO + 2H_2$

The reaction of the dry reforming drew a big attention by a wide public of researchers thanks to its contribution on the decrease of the atmospheric concentration of both greenhouse gases CO_2 and CH_4.

The majority of all works had for objective to improve the yield on this reaction and to increase the life cycle of catalysts which is poisoned by the deposit of coke which is until this day the major problem of this process.

Synthetic Mg–Al layered double hydroxide materials have found many applications due to their unique physicochemical properties; Catalysis is one of these applications(5).

This work consists in the preparation of materials catalysts which can bring better performance.

2 Experimental:

Catalysts synthesis:

The Catalysts materials were synthetized by classical method of coprecipeation at basic pH (pH=11), as reported by Miyata [3]. An aqueous solution containing an appropriate amounts of nitrate salts of divalent metals and trivalent metal (Mg, Al, Ni and Co), with molar ratio of $M^{2+} / M^{3+} = 2$.

The obtained slurry was hydrothermally treated for 24 h at 60°C, centrifuged, washed several times with bidistilled water til neutral pH. The obtained solids were dried at 70°C during a night and calcined under air in 800°C during 6 hours with ramp of 4 °C / min.

Catalyst characterization:

X-ray powder diffraction patterns are recorded in a Siemens D-501 equipment, with a Bragg-Brentano configuration using Cu Kα (λ=1,5418Å) and varying of 2θ values from 5 to 80°. FTIR spectra in the region of 4000 to 400 $cm^{-1}$are obtained using Perkin Elmer spectrometer by the KBr pellet technique. The surface areas of the solids are measured by employing the BET method where a micromeritics ASAP on system 2010 apparatus is used. Elemental analyses of metals of the samples was carried out by ICP Horiba Jobin Yvon Ultima 2 type apparatus .

SEM images where obtained by Hitachi S-5200 microscopy, with a field emission filament, using accelerating voltage of 5kV.

(TPR) experiments were done according to the experimental conditions described else-where [4]. A H_2/Ar mixture (5% H_2, 50 ml/min flow) was used as the reducing atmosphere from room temperature up to 900°C, with a heating rate of 10 C°/min. A thermal conductivity detector previously calibrated using CuO and mass spectrometer in line with the TCD, calibrated with references mixtures were used to detected variations of reducing agent concentration, and possible sub-products formation.

Catalytic activity tests:

The catalytic experiments were carried out at atmospheric pressure in tubular quartz reaction. Wool is used as support for the catalytic bed. The CH_4 and CO_2 reactants were mixed at ratio of 1 diluted in He (10:10:80 in vol); The catalysts are heated from room temperature until 700°C at 1°C/min rate ; The simple stays at 700°C during 11h; Gas hourly space velocity (GHSV) :300000 L/kgh; Analysis is given by gas chromatograph (Varian CP-3800) with column Porapak Q.

Before reaction, samples were reduced under hydrogen (5%H_2/Ar) at 700°C during 1hour. (2)

3 Results and discussion:

The result of the ICP shows that the experimental composition is coherent with the nominal composition for each sample and the $M2^+/M^{3+}$ ratio is around 2.

X-ray diffraction patterns of the samples before calcination shows that training hydrotalcites structures. X-ray diffraction patterns after calcination shows oxides mixtures of NiO and MgO.

The results of BET surface areas shows that BET areas increases after calcination for all samples except in the case of Mg Al solid.

The results of H_2-TPR measurements of the calcined samples showed a single reduction peak in the case of NiMgAl at higher temperature reduction (around 800°C), indicating the existence of species of NiO with strong interaction resulting from the formation of the NiO–MgO solid solution, characterized by its high stability. The NiMgAl catalyst shows a significant CH_4 conversions such as 87,0%, 92,0 %, respectively for NiMgAl and NiMgCoAl versus 86,0% and 90,0%, for CO_2 conversions respectively.

4 Conclusions:

The present study showed that the catalysts based on nickel and which is prepared by the Local hydrotalcite way gives a good activity for CH_4 / CO_2 reaction and that the addition of cobalt also improves the activity. A good stability is also observed for the catalysts of this study.

Acknowledgements

I find this opportunity to express my deep gratitude to Mister Juan P.Holgado, Victor Gonzalez - DelaCruz and all the staff of Ciencia de Materiales Instituto de Sevilla (CSIC-University of Seville).

References

[1] Victor M. Gonzalez-DelaCruz, Juan P. Holgado, Rosa Pereniguez, Alfonso Caballero, Journal of Catalysis 257 (2008) 307-314.

[2] C.E. Daza , C.R. Cabrera ,S. Moreno , R. Molina , Applied Catalysis A: General 378 (2010) 125–133

[3] Miyata, Clays and Clay Miner.23 (1975) 369

[4] Umberto Costantino, Massimo Curini, Francesca Montanari, Morena Nocchetti, Ornelio Rosati, Journal of Molecular Catalysis195 (2003) 245-252.

[5] Andrey I. Tsyganok, Tatsuo Tsunoda, Satoshi Hamakawa, Kunio Suzuki, Katsuomi Takehira, and Takashi Hayakawa, Journal of Catalysis 213 (2003) 191–20

V-PP68

On the Correlations between Redox Properties and Catalytic Performances of $Ce_xPr_{1-x}O_{2-\delta}$ Catalysts towards Environmentally Relevant Oxidation Reactions

Giménez-Mañogil J.[1], Guillén-Hurtado N.[1], Fernández-García S.[2], Calvino-Gámez J.J.[2], García-García A.[1*]

1 - MCMA Group, Department of Inorganic Chemistry, Faculty of Sciences, University of Alicante, Alicante, Spain

2 - Faculty of Sciences, University of Cádiz, Cádiz, Spain

* a.garcia@ua.es

Keywords: Ceria-praseodimia, NO oxidation, CO-PROX, redox properties

1 Introduction

Mixed oxides having a high oxygen storage capacity and reactivity of lattice oxygen are used in several applications, such as automotive catalysis, selective oxidations, oxidative dehydrogenation of organic compounds, and some other reactions [1]. Among these materials, mixed oxides containing rare earth cations with variable oxidation states deserve particular attention. Praseodymium has multiple oxidation states and it is one of the cations lastly investigated for ceria doping [2]. The corresponding mixed oxides can undergo more oxygen exchange at a lower temperature than pure ceria and it is also known that the Ce-Pr-O compositions are more promising than the trivalent rare-earth substituted ceria formulations. It could be assumed that Pr-containing mixed oxides should exhibit intermediate and close to optimal combination of capacity, stability and reactivity with respect to reversible oxygen evolution/uptake, but in catalytic oxidation reactions with practical application not all the reactive oxygen can be available and the establishment of redox-catalytic performances relationships in different environmental reactions could be of special interest [3].

The present work is devoted to prepare and characterize a series of $Ce_xPr_{1-x}O_{2-\delta}$ mixed oxides and to analyze the trends in the order of catalytic activities towards the NO oxidation to NO_2 and the preferential oxidation of CO in H_2 rich stream (CO-PROX). The correlations between catalytic performances obtained and redox properties are explored.

2 Experimental

A series of oxides with the general formula $Ce_xPr_{1-x}O_{2-\delta}$ (x=0, 0.2, 0.5, 0.8, 1.0) was prepared by a co-precipitation method in alkali media. The corresponding solids obtained after filtration were dried and calcined at 500°C for 1 hour. The catalysts were characterized by N_2 adsorption-desorption isotherms at -196°C, XRD, Raman spectroscopy, XPS, H_2-TPR and CO-TPR. They were tested for NO oxidation to NO_2 (from room temperature up to 750ºC at 10ºC/min). The gas mixture used comprised 500 ppm NOx, 5% O_2 and N_2 as balance; the gas flow was fixed at 500 ml/min (GHSV = 30,000 h^{-1}). Catalytic activity in PROX reaction was performed in the 150-500°C temperature range. The inlet total gas flow was 100 mL/min, containing 50% H_2, 1% CO, 1% O_2 and He as balance (GHSV= 12,000 h^{-1}).

3 Results and Discussion

Figure 1 shows the NO_2 production profiles for the series of catalysts investigated along

with the uncatalyzed reaction. It can be seen that a low loading of praseodymium increases significantly the activity for the NO oxidation to NO_2 with regard to pure ceria. In general terms, increasing the Pr content yields to higher activities and decreases the temperature to achieve the maximum NO_2 production. This trend is in good agreement with the redox properties of the catalysts if analyzed by H_2-TPR experiments, where the availability of oxygen under reducing atmosphere increases with the praseodymium content.

Interestingly, the trends in activity order obtained from PROX reaction are very different from those obtained in the NO oxidation reaction. Figure 2 represents the CO conversion percentages obtained on the basis of the CO_2 produced. The highest activity (86.8% of CO) is exhibited by the $Ce_{0.8}Pr_{0.2}O_{2-\delta}$ composition at 450 °C, and consequently, the order of activity cannot be correlated to the H_2-TPR results. However, CO-TPR curves, (not shown for the sake of brevity) revealed some interesting features, since the main peak of reduction is slightly and progressively moved towards higher temperatures from 330°C for $Ce_{0.8}Pr_{0.2}O_{2-\delta}$ to 423°C for $PrO_{2-\delta}$. Moreover, the samples containing Ce and Pr, show a certain relationship between the CO-TPR profiles and the catalytic behavior. Thus, at 450°C, when the reduction temperature is lower, the conversion of CO becomes higher.

Reasonable hypothesis to account for these diverse experimental trends are: the different temperature range where both catalytic reactions (NO oxidation and PROX) take place and/or the different acid character of the NO and CO molecules which interact differently with the ceria-praseodimia mixed oxides' surfaces.

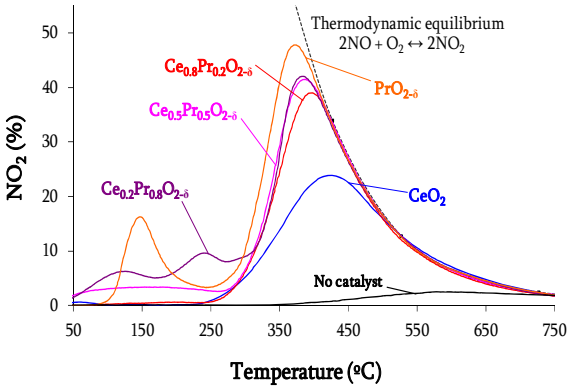

Figure 1. NO_2 production profiles versus temperature for the series of catalysts studied.

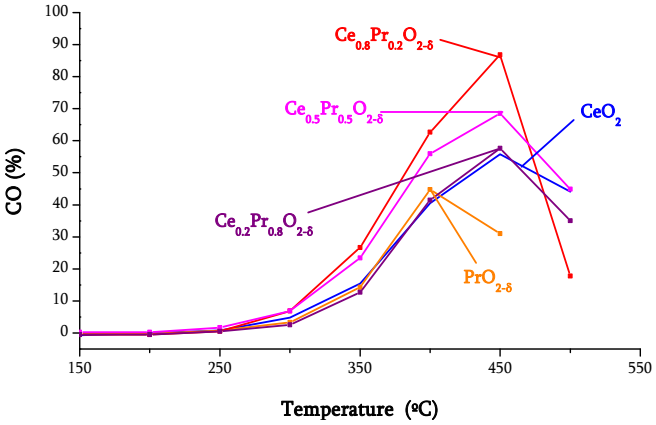

Figure 2. CO conversion in the PROX reaction for the series of catalysts studied.

4 Conclusions

The trend in activity order for a series of $Ce_xPr_{1-x}O_{2-\delta}$ mixed oxides towards the NO oxidation to NO_2 and towards CO-PROX reaction are completely different, despite both are oxidation reactions of relevant interest from an environmental viewpoint. The understanding of the features that govern the activity towards different catalytic oxidation reactions can be of key importance in the designing of effective catalysts.

Acknowledgements

The authors gratefully acknowledge the financial support of Generalitat Valenciana (PROMETEOII/2014/010) and MINECO (CTQ2012-30703 project) and UE (FEDER funding).

References

[1] M.Y. Sinev, G.W. Graham, L.P. Haack, M. Shelef, *Journal of Materials Research* 11 (1996) 1960.
[2] M.-F. Luo, Z.L. Yan, L.-Y. Jin, *Journal of Molecular Catalysis A: Chemical* 260 (2006) 157.
[3] L. Ilieva, G. Pantaleo, I. Ivanov, A. Maximova, R. Zanella, Z. Kaszkur, A.M. Venezia, D. Andreeva, *Catalysis Today* 158 (2010) 44.

V-PP69

Identifying the Nature of the Copper Entities over Ceria-Based Supports to Promote Diesel Soot Combustion: Synergistic Effects

Giménez-Mañogil J., García-García A.*

MCMA Group, Dept. of Inorganic Chemistry, Faculty of Sciences, University of Alicante, Alicante, Spain

* a.garcia@ua.es

Keywords: copper, entities, ceria-zirconia, soot, combustion, synergy

1 Introduction

Noble metal-based catalysts have been developed to promote the oxidation of NO to NO_2 and decrease the combustion onset temperature of soot under realistic diesel conditions. However, their high cost has led to the consideration of other lower-priced materials that can be competitive in terms of catalytic activity.

Catalysts combining copper and active ceria-based materials have demonstrated promising behavior towards CO-PROX reaction [1], among others. However, these findings cannot be directly extrapolated to other oxidation reactions less studied from a fundamental point of view, such as diesel soot combustion and NO oxidation to NO_2.

Main properties of the dual system copper-ceria appear related to the synergetic interactions between the two constituents which are determined by their interfacial features [1, 2]. Therefore, by tuning the interfacial properties and generating active sites of different nature, one could explain the observed ceria promoting catalytic activity.

The aim of this research is to synthesize catalysts exhibiting a wide range of degrees of copper incorporation/distribution/contact on a ceria-zirconia mixed oxide by preparing catalysts with a high degree of copper incorporation (copper insertion), well-dispersed copper on the porosity and different degrees of physical interaction. Their catalytic activities towards diesel soot combustion and NO oxidation were studied. A different support allowing a high degree of copper dispersion (alumina) and CuO bulk were also chosen for comparative purposes.

2 Experimental

The $Ce_{0.8}Zr_{0.2}O_2$ support (CZ) was prepared by the co-precipitation method, and the solid obtained after filtration was dried and calcined at 500°C for 1 hour in air. CZ and a commercial γ-Al_2O_3 support were doped with 2 wt% of copper (Cu2/CZ and Cu2/AL, respectively) by incipient wetness impregnation (IWI). This amount of Cu was optimized in a previous study [3].

On the other hand, physically-mixed samples of CuO (obtained by calcination of $Cu(NO_3)_2 \cdot 3H_2O$ in air, at 500ºC, for 1 hour) and CZ under loose (LO) and tight (TI) contact modes, with 2 wt% of Cu, were prepared. Another catalyst was obtained by subsequent calcination of the tight contact-sample at 500ºC in air, for 1 hour (Cu2CZ-TI-500). In addition, $Ce_{0.76}Zr_{0.19}Cu_{0.05}O_2$ (CZCu-CP) was synthesized by co-precipitation, with 2 wt% of copper.

These catalysts were characterized by N_2 adsorption-desorption isotherms at -196ºC, XRD, Raman spectroscopy, XPS and H_2-TPR. They were tested for NO oxidation to NO_2 in TPR conditions (from 25ºC to 700ºC at 10ºC/min), and for soot combustion: under TPR (from 25ºC to 700ºC) and isothermal conditions (450°C). The gas mixture used comprised 500 ppm NOx, 5% O_2 and N_2 balance; the gas flow was fixed at 500 ml/min (GHSV = 30,000 h^{-1}).

3 Results and Discussion

According to XRD and Raman spectroscopy results (not shown for sake of brevity), bulk CuO entities were detected in the physically-mixed samples; but were not observed in those catalysts

prepared by IWI and co-precipitation, which means that a high copper dispersion was achieved. Regarding XPS, Cu^{2+} is mainly present in all the samples. However, Cu^{+} species were identified for CZCu-CP, allowing us to deduce that copper was inserted into the ceria lattice.

Figure 1 depicts the H_2-TPR profiles. Physically-mixed samples show two different reduction regions, the first one is invariant and corresponds to copper reduction only; the second one is related to the ceria reduction and mainly depends on the type of contact achieved. In contrast, an important decrease in the copper and cerium reduction temperatures is achieved when copper is added by IWI or co-precipitation, due to the close interfacial interactions Cu-Ce. CZCu-CP shows higher reduction temperatures than Cu2/CZ, due to the presence of Cu^{+} (as seen in XPS) and the required diffusion of H_2 into the lattice (there is no surface copper enrichment on this catalyst as detected for the IWI sample -Cu2/CZ-).

Soot combustion experiments under TPR conditions (Figure 2) reveal different trends in activity depending on the temperature range, which can be associated to interfacial interactions (as seen on Figure 1). At low temperatures, the trends in activity are similar to those observed for the NO oxidation reaction. Cu2/CZ shows the highest activity due to the synergistic effect observed between Cu-Ce and to the surface copper enrichment (as seen in XPS). However, at higher temperatures, the Cu-Ce contact in Cu2CZ-TI is enough to promote the catalytic activity, in agreement with the profile observed in the region 2 of H_2-TPR results (not achieved by LO procedure). Conversely, Cu2/AL presents a very low catalytic activity. Although copper is well dispersed onto the support, no synergistic effects between Cu and Al_2O_3 support are established.

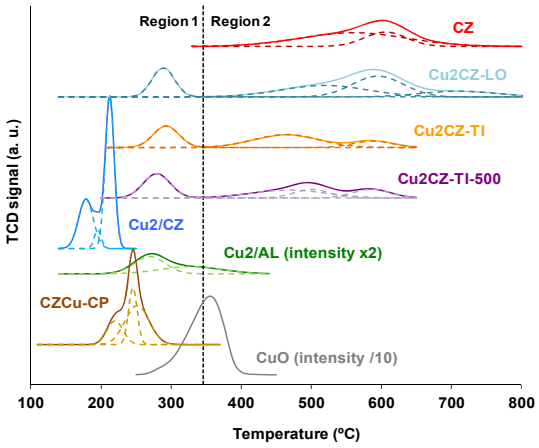

Figure 1. H_2-TPR deconvoluted profiles for the studied catalysts.

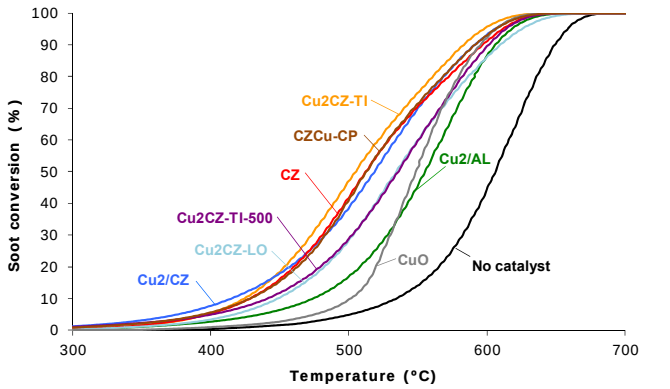

Figure 2. Soot conversion versus temperature under TPR conditions (NO_x/O_2).

4 Conclusions

The interfacial interactions between copper and ceria were found to be of key importance on the catalysts' reducibility and the catalytic activity for NO oxidation to NO_2 and diesel soot combustion reactions. These interfacial interactions can be tuned by conducting different procedures of copper incorporation onto ceria-zirconia.

Acknowledgements

The authors gratefully acknowledge the financial support of Generalitat Valenciana (PROMETEOII/2014/010) and MINECO (CTQ2012-30703) and the UE (FEDER funding).

References

[1] A. Martínez-Arias, D. Gamarra, M. Fernández-García, A. Hornés, P. Bera, Zs. Koppány, Z. Schay, *Catal. Today* 143 (2009) 211.
[2] A.P. Jia, G.S. Hu, L. Meng, Y.L. Xie, J.Q. Lu, M.F. Luo, *J. Catal.* 289 (2012) 199.
[3] J. Giménez-Mañogil, A. Bueno-López, A. García-García, *Appl. Catal., B* 152-153 (2014) 99.

V-PP70

Catalytic Performance of 2%CuO/$Ce_{0.8}Zr_{0.2}O_2$ Loaded over SiC-DPF in NOx-Assisted Combustion of Diesel Soot

Quiles-Díaz S., Giménez-Mañogil J., García-García A.*

MCMA Group, Department of Inorganic Chemistry, Faculty of Sciences, University of Alicante, Alicante, Spain

* a.garcia@ua.es

Keywords: DPF, copper/ceria-zirconia, soot, combustion, NOx

1 Introduction

The CRT (Continuously Regenerating Trap) system is efficient for soot removal under determined conditions in diesel exhaust. This system is a combination of filter and an oxidation catalyst, where a DPF (Diesel Particulate Filter) is located downstream a Pt-containing DOC (Diesel Oxidation Catalyst) supported on a cordierite monolith. Both CO and unburned hydrocarbons are oxidized to CO_2 and H_2O in the DOC, where NO is also oxidized to NO_2. Particulate matter is filtered in the DPF, where the NO_2-assisted combustion takes places. Since NO_2 is more oxidant than O_2, the combustion onset temperature of soot is significantly decreased [1, 2]. During the last decade, topics of interest have been focused on: i) deposition of the catalytic coating directly onto the filter and ii) replacing Pt by cheaper active phases, being copper-doped ceria-zirconia mixed oxides one of the most promising options.

The catalytic performances of a 2%CuO/$Ce_{0.8}Zr_{0.2}O_2$ powder sample towards the soot combustion and the NO oxidation reaction have been recently reported in the literature by our group [3]. However, as far as we are concerned, the copper-doped ceria-zirconia-catalyzed regeneration of DPFs has not yet been reported, being this the main goal of the current study.

2 Experimental

The ceria-zirconia catalyst (CeZr) was prepared by the co-precipitation method and 2 wt% copper was incorporated by the incipient wetness impregnation method (2%Cu/CeZr).

A reduced scale SiC diesel particulate filter (SiC-DPF) was used as structured support, with 2.5 cm of diameter and 7.5 cm of length. The as-received DPFs were washed with water and acetone, dried at 110ºC and calcined at 700ºC for 2h. The 2%Cu/CeZr catalyst was incorporated onto the ceramic support by a single dipping of the DPFs in an aqueous solution of 2%Cu/CeZr, which were placed in an ultrasonic bath. Then, they were dried at 110ºC and calcined at 600ºC for 2h. Finally, the soot particles were loaded onto the active phase containing-DPFs by immersion into a soot/methanol suspension under vigorous stirring [1].

2%Cu/CeZr/SiC-DPF and 2%Cu/CeZr (powder) were tested for NO oxidation to NO_2 under TPR conditions and successive cycles (from room temperature up to 800ºC at 10ºC/min), and for soot combustion (TPR from room temperature up to 800ºC at 10ºC/min). The gas mixture used comprised 500 ppm NOx, 5% O_2 and N_2 balance; the gas flow was fixed at 500 ml/min. Different reactor configurations (horizontal reactor; inner diameter 3 cm and tubular reactor; inner diameter 1 cm) were needed for DPFs and powders, respectively.

3 Results and Discussion

As shown in Figure 1, a very high activity is reached by the active phase-loaded DPF towards the NO oxidation reaction, pointing out the satisfactory catalytic performance of the catalytic-coated filter. Furthermore, the catalytic profile of NO_2 production is not seen significantly modified after four successive cycles with the same DPF, allowing us to conclude that the catalytic coating

(achieved with the simple and solvent-free coating procedure consisting of immersion) is stable and the corresponding coated-DPF can be reused in several cycles without a significant decrease in its activity.

Soot combustion experiments revealed high activity shown by the loaded-filter (green line) if compared with the unloaded-DPF (blue line), as depicted in Figure 2. As can be seen the soot combustion profile obtained with the mixture of catalyst and soot under loose contact mode (very gentle mixture of soot and catalyst with a spatula) is quite similar to that obtained with the loaded-filter, verifying the good choice of conducting catalytic experiments under this procedure (loose-contact) to simulate the performance of this type of catalysts in a real filter. It should be remarked that with the purpose of conducting a proper comparison between the soot combustion profiles, an identical soot-catalyst ratio was employed in all the experiments. On the contrary, the soot conversion profile obtained under tight contact conditions (intimate mixture of soot and catalyst in an agate mortar) is very far from those mentioned above, and, consequently, does not simulate the real physical contact achieved in a diesel particulate filter.

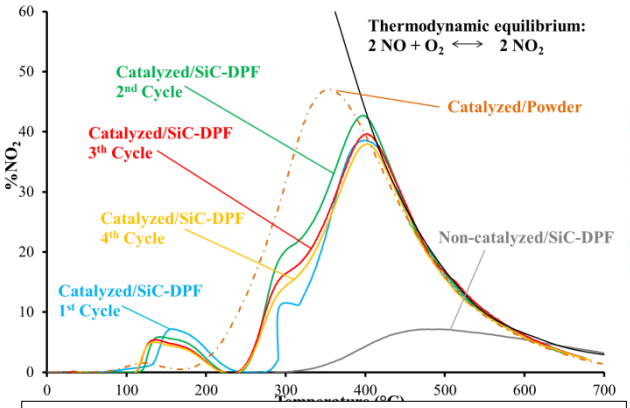

Figure 1. NO_2 production profiles under TPR conditions. Solid lines: successive cycles with the same loaded-DPF (1^{st}-4^{th}).

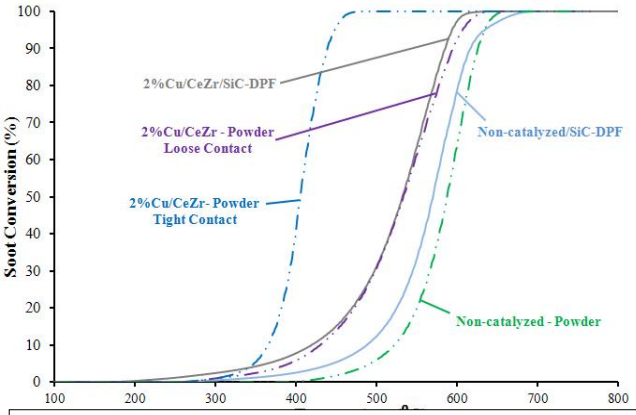

Figure 2. Soot conversion profiles under TPR conditions for different soot/catalyst configurations.

4 Conclusions

Incorporation of very active copper/ceria-zirconia active phase onto a SiC-DPF has been successfully achieved by a proper coating procedure consisting of immersion in an aqueous suspension. Very similar catalytic performances towards NO oxidation to NO_2 were obtained (when compared with the catalyst in powder form) under repeatable measurements. It was verified that the loose-contact mode is a good choice to simulate the catalytic performance of this type of active phase in a real Diesel Particulate Filter.

Acknowledgements

The authors gratefully acknowledge the financial support of Generalitat Valenciana (PROMETEOII/2014/010 project) and the Spanish Ministry of Economy and Competitiveness (CTQ2012-30703 project, UE-FEDER funding).

References

[1] C.A. Neyert, E.E. Miró, C.A. Querini, *Chemical Engineering Journal* 181 (2012) 93.
[2] M. Valencia, E. López, S. Andrade, M.L. Iris, N. Guillén-Hurtado, V. Rico-Pérez, A. García-García, C. Salinas-Martínez de Lecea, A. Bueno-López, *Topics in Catalysis* 56 (2013) 452.
[3] J. Giménez-Mañogil, A. Bueno-López, A. García-García, *Applied Catalysis B: Environmental* 152-153 (2014) 99.

V-PP71

Pd-Cu Nanostructured Catalysts for Water Phase Reduction of Nitrates. Influence of the Support and of the pH

Papa F.[1], Balint I.[1], Negrila C[2], Olaru E.A.[3], Munteanu C.[1], Zgura I.[2], Bradu C.[3*]

1 - Institute of Physical Chemistry of the Romanian Academy, Bucharest, Romania
2 - National Institute of Materials Physics, Magurele, Romania
3 - University of Bucharest, Research Center for Environmental Protection and Waste Management, Bucharest, Romania

* corina.bradu@g.unibuc.ro

Keywords: Pd-Cu bimetallic catalyst, Pd-Cu nanoparticles, water-phase nitrate reduction

1 Introduction

Liquid-phase catalytic reduction of the nitrates seems to be an adequate technique for the removal of nitrate from natural water. In order to obtain greater activity and selectivity to nitrogen, different catalysts have been designed. The proposed catalysts are in majority supported bimetallic systems based on noble metals, such as Pd, Pt, Rh and Ru (1–5 weight %) promoted especially with Cu, Sn and In (0.2–1 weight %) [1].The main goal of this study was to evaluate the performance of supported bimetallic Pd-Cu nanoparticles prepared by alkaline polyol method in the selective reduction of nitrates from water to nitrogen. In this respect, the supported nanoparticles catalysts (Pd-Cu/Al_2O_3 and Pd-Cu/TiO_2) were tested in the reduction of nitrate ions in aqueous solution in comparison with bimetallic Pd-Cu catalyst obtained by impregnation method. The results were analysed in correlation with the morphological and structural characteristics of the catalytic systems obtained through X-ray diffraction (XRD), transmission electron microscopy (TEM), X-ray photoelectron spectroscopy (XPS), atomic absorption spectrometry (AAS) and by CO chemisorption technique. Also, the influence of the pH conditions on the activity and selectivity of the NO_3^- reduction process was emphasized.

2 Experimental

In this study, a series of supported bimetallic Pd-Cu (with molar ratio Pd:Cu of 4:1 and total metal loading of 2%.) catalysts were prepared. The active components were introduced by impregnation or by deposition of nanoparticles previously synthesized (Table 1). The polyvinylpyrrolidone (PVP)-protected bimetallic nanoparticles were prepared following a modified protocol of alkaline polyol method [2]

Table 1. The prepared catalysts

Catalyst	Notation	Preparation method
Pd-Cu/Al_2O_3	PCA-np	nanoparticles by alkaline polyol method
Pd-Cu/ TiO_2	PCT-np	nanoparticles by alkaline polyol method
Pd-Cu/Al_2O_3	PCA-imp	successive impregnation
Pd-Cu/ TiO_2	PCT-imp	successive impregnation

The catalysts performance in the reduction of the nitrate ions was evaluated in a series of semi-batch experiments. The tests were carried out in a thermostated reactor (20.0 ± 0.1^{0}C) with a capacity of 250 mL, equipped with a magnetic stirrer. In a typical run, H_2 with a flowrate of 100 mL·min^{-1} at a pressure of 1 atm was bubbled in 200 mL of NO_3^- solution (100 mg.L^{-1}) in the presence of 0.10 g catalyst. Three cyclic runs were carried out for selected catalyst in order to assess his stability.

3 Results and discussion

For the nanostructured catalysts, the TEM images show good dispersion of nanoparticles on the support with a particle size in the range from 3 to 9 nm. The measured crystallographic orientation parameter of 2.25-2.27 Å, corresponds to Pd(111). Corroborating the TEM, XRD, XPS and CO chemisorption data it can be suggested that the Pd-Cu nanoparticles obtained by the modified protocol of the alkaline polyol method have a crystalline Pd core and a shell reach in amorphous cooper as metallic Cu or CuO. Compared to the catalyst obtained by successive impregnation method, the supported nanoparticles catalysts have a smaller Pd crystallite size and more important coverage of the palladium surface with copper.

The prepared catalysts were firstly tested in the reduction of nitrate anions from aqueous solutions without pH control. The Pd-Cu supported on titania show an increased activity compared to those supported on alumina. In particular, for PCT-np the conversion of nitrate overcomes 90% in the first 60 min. These differences on the catalytic activity might be explained by the type and intensity of the interactions between the active phase components and the support. The higher activity of the Pd-Cu catalysts supported on TiO_2 might be attributed to the more reduced state of the copper (due to electron transfer from the support to the metals). Also, it was observed that irrespective of the support used, higher conversions of nitrate were reached for the nanostructured catalysts.A better performance for PCT-np was obtained when the CO_2, used for the pH control, was introduced after the nearly complete removal of NO_3^-.

The stability of the PCT-np catalyst was assessed by determining the amount of Pd and Cu leached from catalyst. Furthermore, three cyclic runs were carried out for the PCT-np catalyst. As can be seen from figure 1, the catalyst performance is less affected in terms of nitrate conversion between the three cycles.

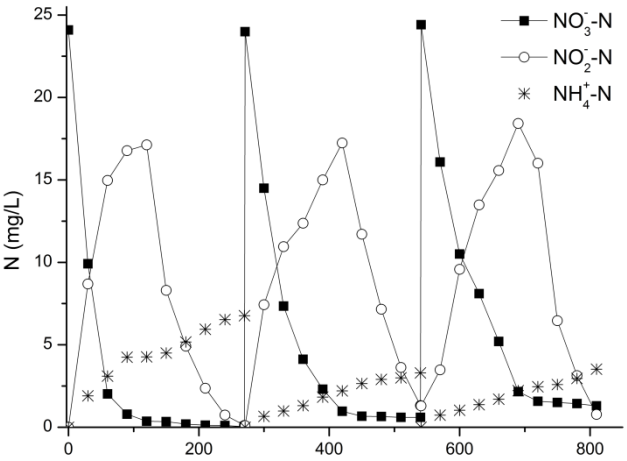

Figure 1. Nitrate reduction on PCT-np in three consecutive reaction cycles

4 Conclusions

A modified protocol of alkaline polyol method was successfully used to obtain well dispersed Pd-Cu nanoparticles for of alumina and titania supported catalysts. The supported nanoparticles catalysts have a smaller Pd crystallite size and more important coverage of the palladium surface with copper in comparison with the catalyst obtained by impregnation method. It was assumed that these specific characteristics of the nanostructured catalysts led to their superior activity in the reduction of nitrate. Nevertheless, the choice of the support appeared to be an important aspect. For the selected PCT-np catalyst, better activity and selectivity toward nitrogen were achieved within a combined uncontrolled-controlled pH process. The PCT-np catalyst was relatively stable for three consecutive cyclic runs.

Acknowledgements

The authors thank the Romanian Authority ANCSI for the financial support under the project INTEGRATREAT 100/2012.

References

[1] J. Hirayama, R. Abe, Y. Kamiya, *Appl. Catal. B*, 144 (2014)721.
[2] F.Papa, C. Negrila, A. Miyazaki, I. Balint., *J. Nanopart. Res.*,13 (2011) 5057.

V-PP72

Red Mud Catalysts for Sulphide Oxidation in Wastewater

Cruceanu A.[1*], Zavoianu R.[1], Pavel O.D.[1], Florea M.[1], Bradu C.[2], Olaru E.[2]

1 - Department of Organic Chemistry, Biochemistry and Catalysis, Faculty of Chemistry, University of Bucharest, Bucharest, Romania

2 - PROTMED Research Centre, University of Bucharest, Bucharest, Romania

* anca.cruceanu@chimie.unibuc.ro

Keywords: red mud, sulphide wastewater oxidation, catalysis

1 Introduction

This contribution investigates an alternative route for the valorisation of red mud (RM) industrial waste generated worldwide from the Bayer process applied in alumina refineries by utilizing it as raw material in the manufacture of oxidation catalysts. Such catalysts may be utilized for the oxidation of sulphide ions from wastewaters to elementary sulphur using air as oxidation agent. Sulphide ions often occur in industrial waste waters from oil refineries, fossil fuel gasification plants, paper and pulp mills, or after the anaerobic oxidation of sewage water. They may also be encountered in certain well waters. The sulphide ions from water have to be removed due to their toxicity and obnoxious odour [1-5]. The preparation method proposed for the obtaining of the catalysts involves the functionalization of trivalent iron sites from RM waste by treatment with polycarboxylic acids. The functionalization plays an important role in stabilizing the Fe(III) active species which otherwise could become inactive either following their conversion to Fe(II)S during the redox process or their precipitation as $Fe(OH)_3$ at high pH values reached due to the RM composition (during preparation). Two functionalization agents (e.g. disodium ethylenediamminotetraacetic acid Na_2H_2EDTA and trisodium citrate Na_3CIT) were selected bearing in mind that the coordination of Fe(III) in the ligands field should be strong enough to avoid its precipitation as sulphide or hydroxide while maintaining its ability to change the oxidation state during its involvement in the redox cycle.

2 Experimental/methodology

Red mud deposit from Tulcea alumina plant in Romania has been utilized for the obtaining of iron containing catalysts: RMN (red mud neutralized with 35% NaCl solution), RM-E and RMN-E (RM and RMN modified with Na_2H_2EDTA solution), RM-C and RMN-C (RM and RMN modified with Na_3CIT solution) and RM-E-C and RMN-E-C (RM and RMN modified with both Na_2H_2EDTA and Na_3CIT solutions). The concentration of polycarboxylic acid salt solution was calculated based on the amount of Fe in the solid undergoing treatment so that the Na_2H_2EDTA/Fe and Na_3CIT/Fe molar ratio to be 1-1,5 and respectively, 1-2. The raw red mud was submitted to contact with the corresponding sodium salts solutions (weight ratio L/S=10:1) at room temperature during 6 days with 30 min agitation (300rpm)/day. The solid was separated by filtration, washed with distilled water until the conductivity of the water decreased below 100microS/cm and dried at 60°C during 24 h.

The catalysts were characterized by DRIFT, DR-UV-Vis, XRD, surface area and porous structure determinations. The preliminary catalytic tests for the oxidation of sulphide by oxygen from air were performed using a two-necked glass flask reactor equipped with a teflon-coated stirrer bar, a gas-inlet tubing connected to a dry air supplier and a reflux condenser, at ambient temperature and pressure, under 4L/h air flow using 1 g of catalyst and 75 mL of synthetic waste water (freshly prepared by dissolving an adequate amount of Na_2Sx9H_7O in deoxygenated distilled water) containing 1 g sulphide/L, under continuous stirring (350 rpm) during 2 hours. Another set of experiments aimed to investigate their stability under operating conditions and the possibility of using it in 4 repeated reaction cycles (2 h each) has been performed. The catalyst used in one reaction cycle was separated from the reaction mixture, before being

introduced in the next cycle.

3 Results and discussion

The spectroscopic analyses of the catalysts by XRD, DRIFTS and DR-UV-Vis-NIR indicated the presence of the organic ligands in all the functionalized samples. The most significant modifications were noticed in the DRIFTS spectra. The spectra of citrate modified samples RM-C and RMN-C show a shift to lower wavenumbers of un-split bands characteristic for $\nu_{as}(COO^-)$ and $\nu_s(COO^-)$ vibrations at ~1640 cm^{-1} and 1400 cm^{-1} indicating their deprotonation following the coordination to Fe(III). A weak intensity band at ~800 cm^{-1} attributed to Fe-O-Fe vibrations may be a consequence of the citrate excess utilized in the preparation. In the spectra of Na_2H_2EDTA functionalized samples, RM-E and RMN-E, the coordination of the ligand to Fe(III) is proved by the shift to lower wavenumbers of the bands characteristic to $\nu_{as}(COO-)$ and $\nu_s(COO-)$ vibrations as well as a similar shift of the bands characteristic to C-N bonds compared to the spectrum of the free ligand. In the spectra of the samples functionalized with the mixture of ligands, RM-E-C and RMN-E-C the bands at 1626 cm^{-1}, ~1400 cm^{-1}, 1120 cm^{-1} characteristic for the coordination of EDTA and citrate anions have lower intensity and are also shifted to lower wavenumbers. Besides that, there are some spectral modifications that indicate either the perturbation of Fe(III)EDTA by the concomitant presence of the citrate anion, or the complexation of the citrate anion with Fe(III)-EDTA chelate which would mean that the iron would be coordinated by two oxygen atoms belonging to different sources. These modifications are: the shifting of the weak band around 800 cm^{-1}, related to Fe-O-Fe bonds vibrations in the iron citrate to 850 cm^{-1}, and an intense split band at 615 cm^{-1}, which is shifted compared to the band at 625 cm^{-1} characteristic to iron citrate [5-7].

The results of the catalytic tests performed with the functionalized RM and RMN samples showed an increase by 40% of the sulfide ion removal from wastewaters as well as the absence of FeS in the treated wastewaters compared to un-functionalized iron containing catalysts. The relatively low conversion values may be due both to the high concentration of sulfide ions in the synthetic wastewaters and the factors affecting the mass transfer (air flow, air dispersing system, etc). Another advantage of the functionalization is the enhanced stability of the solids towards deactivation. The most stable are RM-E-C and RMN-E-C for which the decrease of activity after 4 reaction cycles is only about 15%.

4 Conclusions

The preparation method for iron containing solids prepared using RM is simple and does not need expensive apparatus and technology. Besides the formation of Fe(III) complexes on the surface of the RM and RMN solids, this method allows also the re-adsorption of the complexes formed in the solution following the dissolution of iron by the complexation agents. The catalysts obtained by functionalization present catalytic activity for sulfide oxidation under mild reaction conditions even at room temperature and avoid the formation of Fe(II)S in treated wastewater. Even if the activity of these solids is lower, taking into account the low price of the RM the subject deserves further investigation.

Acknowledgements

Authors acknowledge the financial support of this work by UEFISCDI through PCCA2 project 78/2014.

References

[1] Shaobin Wang, H.M. Ang, M.O. Tadé, *Chemosphere* 72 (2008) 1621.
[2] H. Genç-Fuhrman, J. C.Tjell, D. McConchie, *J. Colloid Interface Sci.* 271 (2004) 313.
[3] A. Haaning Nielsen, P. Lens, J. Vollertsen,T. Hvitved-Jacobsen, *Water Res.* 39 (2005) 274.
[4] S. J. Palmer, R. L. Frost, *J. Mater. Sci.* 44 (2009) 55.
[5] M. Johnston, M.W. Clark, P. McMahon, N. Ward, *J. Hazard. Mater.* 182 (2010) 710.
[6] C. C. Wagner, E. J. Baran, *Spectrochim. Acta Mol. Biomol. Spectros.* 75 (2010) 807.
[7] A.Cruceanu, R. Zăvoianu, E. Angelescu, *Prog. Catal.* 10 (1-2) (2001) 27.

V-PP73

Photocatalytic Activity in the Degradation of Phenol over Zn^{2+}:Al^{3+}:W^{6+} Layered Double Hydroxide Prepared by Coprecipitation

Barrera A.[1*], Padilla F.[1], Tzompantzi F.[2], López-Gaona A.[2], Castellanos S.G.[1]

1 - Universidad de Guadalajara, CUCI, Laboratorio de Nanomateriales Catalíticos, Ocotlán, México

2 - Universidad Autónoma Metropolitana-Iztapalapa, Depto. de Química, México, México

* arturobr2003@yahoo.com.mx

Keywords: ZnAlW, LDH, photocatalyst, phenol, degradation, structure

1 Introduction

Contaminant organic compounds in aqueous effluents have exceeded permitted levels, causing pollution of rivers, lakes and drinking fountains [1]. The main problem deals with the discharges from industries: pesticides, fertilizers, drugs and other recalcitrant chemicals [2]. One of these pollutants is phenol and its derivatives, whose use is quite extensive and present high toxicity [2]. To destroy these chemicals, it has been proposed several approaches, being catalytic photoconversion one of the most promissory methods. Among others, TiO_2, Fe_2O_3 and ZnO, have been used to degrade persistent organic pollutants [3]. However, it is necessary to explore the development of new materials that have new and improved adsorption and photocatalytic properties in order to obtain higher degradation efficiency. On this regard, in the present work is reported the synthesis of layered double hydroxides (LDHs) of Zn^{2+}:Al^{3+} and Zn^{2+}:Al^{3+}:W^{6+}, their structure properties as well as their photocatalytic activities in the degradation of phenol in aqueous medium.

2 Experimental/methodology

LDHs were prepared by the co-precipitation method, using $Zn(NO_3)_2.6H_2O$ and $Al(NO_3)_3.9H_2O$ with a molar ratio Zn/Al = 3/1 as precursors; H_2O_4W was added to the mixture to obtain a concentration of 5wt% of W^{6+}. Urea was added (molar ratio H_2O/urea 2/1) as precipitating. The resulting solution was heated at 363 K with vigorous stirring for 48 h. The obtained solids were washed with distilled water at 363 K, followed by drying at 373 K for 12 h and calcination at 573 K for 12 h. The samples were denominated ZnAlW-X where X indicates de treatment temperature. The solids were characterized by N_2 physisorption, XRD and UV-Vis spectroscopy. Photocatalytic activity of the materials was carried out in a batch-type photo-reactor under UV radiation (λ= 254 nm) containing an aqueous solution of 80 ppm of phenol.

3 Results and discussion

Table 1 shows the textural properties of ZnAl and ZnAlW LDH treated at 373 and 573 K. It can be seen that the S_{BET} and VP_T of ZnAl-373 were low (13.0 m^2g^{-1} and 0.1 cm^3g^{-1}), but when it was calcined at 573 K, its S_{BET} and VP_T increased to 62.0 m^2g^{-1} and 0.17 cm^3g^{-1} respectively. The presence of W^{6+} produced a significant increment of S_{BET} and VP_T even at 373 K, i.e., 85.0 m^2g^{-1} and 0.42 cm^3 for ZnAlW-373. The N_2 adsorption isotherms of ZnAl and ZnAlW are of type IV and their hysteresis loop is of the H3-type indicating the presence of aggregates of plate-like particles or slit-shape pores (Fig.1). XDR patterns showed loss of crystallinity and structural changes in both, the ZnAl-573 and ZnAlW-573 (Fig.2). Fig.3 shows the photocatalytic activity

for the ZnAl and ZnAlW LDH. The photoconversion of phenol over ZnAl-373 was rather low (~10%). In contrast, ZnAl-573 reached 66%. Whereas, improved phenol photoconversion was obtained in ZnAlW-373 (~75%) and ZnAlW-573 (~92%).

Table 1. Textural properties of ZnAl and ZnAlW LDH.

Material	S_{BET} ($m^2.g^{-1}$)	APS (nm)	VP_T ($cm^3.g^{-1}$)
ZnAl-373	13.0	3.0	0.1
ZnAl-573	62.0	1.1	0.17
ZnAlW-373	85.0	2.0	0.42
ZnAlW-573	84.0	2.7	0.57

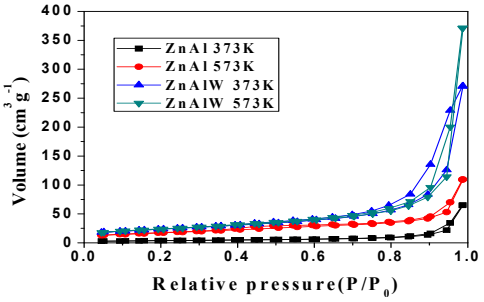

Figure 1. N_2 adsorcion - desorption isotherms

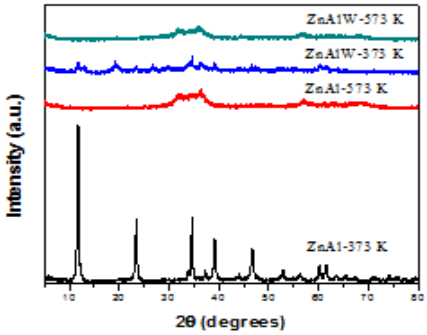

Figure 2. XRD patterns of ZnAl and ZnAlW

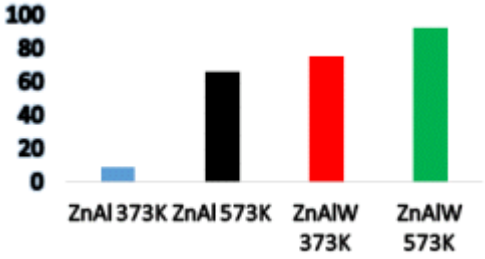

Figure 3. Photocatalytic degradation of phenol on ZnAl and ZnAlW after 4 h of UV irradiation

4 Conclusions

ZnAl and ZnAlW LDH were prepared by the co-precipitation method. ZnAl contain slit-shape pores which are enlarged with doping with W^{6+}.The photocatalytic activity of ZnAl is improved both with treatment temperature and doping with W^{6+}. In the last case the photoconversion is significantly increased obtaining 75% for ZnAlW-373 and 92% for ZnAlW-573 at 4h of UV irradiation.

Acknowledgements

F. J. Padilla thanks to CONACYT-México for the scholarship granted.

References

[1] M. Arias Estévez, E. López Periago, E. Martínez Carballo, J. Simal-Gándara, J.C. Mejuto. L. García Río, *Agr. Ecosyst & Environ.*, 123, (2008) 247.

[2] A. Roos, A. Blair, J. Rusiecki, J. Hoppin, M. Svec, M. Dosemic, D. Sandler, M. Alavanja, *Environ.Health Persp.*, **113** (2005) 49.

[3] J. S. Valente, F. Tzompantzi, J. Prince, J. G. H. Cortez, and R. Gomez, *Appl. Catal. B-Environ*, **90**, (2009) 330.

V-PP74

Photodegradation of Phenol over Al_2O_3-Nd_2O_3 Nanomaterials Doped with Fe, Mg, and Zn Oxide

Barrera A.[1*], Salazar K.G.[1], Tzompantzi F.[2], Padilla F.J.[1], Castellanos S.G.[1], López-Gaona A.[2]

1 - Laboratorio de Nanomateriales Catalíticos, CUCI, Universidad de Guadalajara, Ocotlán, México

2 - Depto. de Química, UAM-Iztapalapa, México, México

* arturobr2003@yahoo.com.mx

Keywords: phenol photodegradation, Al_2O_3-Nd_2O_3 nanomaterials, structure

1 Introduction

In recent years, great efforts have been devoted to the development of alumina nano-structured materials due to their interesting scientific and technological applications [1]. A special case deals with alumina nanomaterials containing rare earths oxides because they can be used in several catalytic applications. The use of the alumina-lanthanide oxide nanomaterials is attractive especially in the photodegradation of contaminant organic compounds in aqueous medium since rare earths oxides modify the characteristics of alumina. Previously, it has been reported that Al_2O_3-Nd_2O_3 binary oxides show a high capability to photodegrade phenol in aqueous medium [2]. However, it is necessary to improve the photocatalytic performance of Al_2O_3-Nd_2O_3 nanomaterials. For this purpose, the photodegradation of phenol over Al_2O_3-Nd_2O_3 nanomaterials doped with 1.0 wt% of Fe, Mg or Zn oxide is reported in the present work. These nanomaterials were characterized N_2 physisorption, X-ray diffraction, UV-Vis and Raman spectrocopy.

2 Experimental/methodology

The nanomaterials were synthesized by a combined method of dissolution of organic precursors at high temperature [3] and the conventional sol-gel route. Al_2O_3-Nd_2O_3-M_xO_y (M = Fe, Mg, Zn) nanomaterials (Al-Nd-M) with 5 wt% of Nd_2O_3 and 1 wt% of metal oxide were prepared by dissolving 0.011 moles of hexadecyltrimethyl-ammonium bromide (CTAB) and 0.18 mol of aluminium tri-sec-butoxide in 0.22 mol of butanol and 0.078 mol of 2-methyl-2,4-pentanedione at 70°C for 1h with continuous stirring. Separately required amounts of Nd acetylacetonate and Fe, Mg, or Zn acetylacetonate were dissolved in a solution containing 0.009 mol of oleic acid, 0.012 mol of oleylamine and 0.004 mol of octadecene at 330ºC for 1h with continuous stirring. After that, the acetylacetonate dissolution was cooling down to 70ºC. Afterwards, both dissolutions were mixed at 70°C for 1h with continuous stirring. Then, a required volume of deionized H_2O was added. The obtained gels were aged at 70ºC for 12h and washed with ethanol for several times. The gels were dried at 100ºC for 12h and calcined at 500ºC for 2h. Then nanomaterials were characterized by N_2 physisorption, X-ray diffraction, UV-Vis and Raman spectroscopy. The photocatalytic activity experiments in the degradation of phenol were carried out by using a Pen-Ray UV lamp (λ=254 nm), 200 mL of aqueous phenol dissolution and 200 mg of Al-Nd-M photocatalyst. Aliquots of the irradiated phenol dissolution were collected each hour for a period of 6h.

3 Results and discussion

Textural properties of the Al-Nd-M nanomaterials are shown in Table 1. The S_{BET} of Al_2O_3

(306.0 m^2g^{-1}) was improved by addition of 5 wt% of Nd_2O_3 (322.0 m^2g^{-1}), however the S_{BET} of Al-Nd-M decrease to a values close to 300 m^2g^{-1} being the nanomaterial with 1 wt% of MgO that with the highest S_{BET} (312 m^2g^{-1}). The specific pore volume is constant for all the nanomaterials (~1.1 cm^3g^{-1}). Conventional XRD patterns (Fig. not shown) of Al-Nd-M nanomaterials show crystalline planes corresponding to the γ-Al_2O_3 phase and the appearance of a small diffraction feature at about 2θ = 32º is attributed to the (110) plane of Nd_2O_3. Small angle XRD patterns of Al-Nd-M show a small diffraction peak at about 1° indicating the presence of metal oxide nanoparticles.

Table 1. Textural properties of Al_2O_3-Nd_2O_3-MO (M: Fe,Mg and Zn).

Sample	S_{BET} (m^2g^{-1})	VP_T (cm^3g^{-1})	Degradation % after 5h of UV irradiation
Al_2O_3	306.0	1.0	69
Al-Nd	322.0	1.2	79
Al-Nd-Fe	294.0	1.2	55
Al-Nd-Mg	312.0	1.1	91
Al-Nd-Zn	307.0	1.1	84

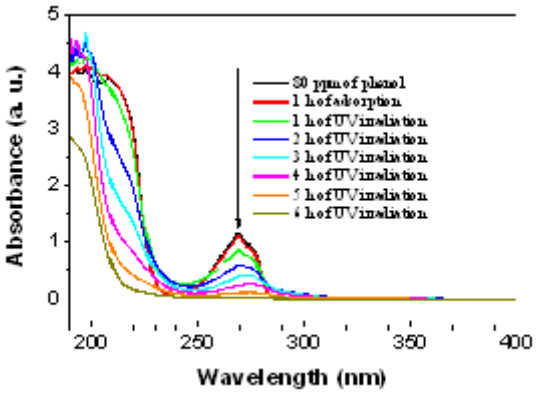

Fig. 1. UV photodegradation of phenol over Al-Nd-Mg nanomaterial.

The presence of metal oxide nanoparticles is corroborated by the appearance of a small absorption band at 205 nm in their UV-Vis spectra. Photocatalytic activity data (Table 1), shows that pure γ-Al_2O_3 exhibit high photoconversion of phenol (~ 60%) at 5h of UV irradiation. However, addition of 5wt% of Nd_2O_3 improved the phenol photoconversion for about 14%. With exception of Al-Nd doped with 1 wt% of Fe oxide showing a lower phenol photoconversion (~ 55%), Al-Nd doped with 1 wt% of Zn or Mg oxide (Fig. 1) enhanced their phenol photoconversion to 84 and 91% respectively after 5h of UV irradiation.

4 Conclusions

Al_2O_3-Nd_2O_3 nanomaterials doped with 1.0 wt% of Mg or Zn oxide exhibited high specific surface area (> 300.0 m^2g^{-1}) and high specific pore volume (□1.1 cm^3g^{-1}). The photodegradation of phenol over Al-Nd was improved by doping with 1 wt% of Zn or Mg oxide obtaining phenol photoconversions near to 90% after 5h of UV irradiation. In contrast, doping with 1 wt% of Fe oxide was in detriment of the specific surface area and phenol photoconversion.

Acknowledgements

K. G. Salazar thanks to CONACYT-México for the scholarship granted.

References

[1] K. J. Klabunde, *Introduction to the Nanoworld*, *Wiley-Interscience, Hoboken, New Jersey,*(2004).
[2] A. Barrera, F. Tzompantzi, J. M. Padilla, J. E. Casillas, G. Jácome-Acatitla, M. E. Cano, R. Gómez, *Appl. Catal. B: Environ*, 144, (2014) 362-368.
[3] R. Si, Y.-W. Zhang, H.-P. Zhou, L.-D. Sun, C.-H. Yan, Chem. Mater. 19 (2007) 18-27.

V-PP75

Polyisobutylene Oligomer-Bound Polyoxometalates as Efficient and Recyclable Catalysts for Biphasic Oxidations with Hydrogen Peroxide

Yahya R.[1], Craven M.[1], Kozhevnikova E.[1], Steiner A.[1], Kozhevnikov I.[1*], Samunual P.[2], Bergbreiter D.[2]

1 - University of Liverpool, Liverpool, UK
2 - Texas A&M University, College Station, USA

* kozhev@liverpool.ac.uk

Keywords: desulfurization, epoxidation, polyoxometalates, hydrogen, peroxide, functional, polymers

1 Introduction

Polyoxometalates (POMs) have found applications in various disciplines, of which catalysis is by far the most important [1]. POMs, especially those comprising Keggin polyanions, serve as precursors of efficient catalysts for environmentally benign biphasic oxidations with hydrogen peroxide. These reactions typically involve phase-transfer catalysis with peroxo polyanion transport through the water-organic interface and require an efficient agent to move the peroxo polyanions from the aqueous phase into the organic phase. Commonly, quaternary ammonium cations with C_8–C_{18} alkyl groups are used as phase-transfer agents to facilitate organic phase solubility of the POM. However, more efficient biphasic oxidation processes using the POM/H_2O_2 system could address specific challenges which include improving catalyst activity and recyclability in alkane-water two-phase systems. This is particularly important for reactions such as the POM-catalyzed oxidative desulfurization with aqueous H_2O_2 as the "green" oxidant. Here we report on the use of amine terminated polyisobutylene (PIB) oligomer as a highly efficient phase-transfer agent for Keggin POM catalysts in oxidative desulfurization and alkene epoxidation with H_2O_2 in a heptane-water two-phase system [2]. Both reactions are the subject of much current interest.

2 Experimental

The oxidation of dibenzothiophene (DBT) and epoxidation of cyclooctene were carried out in a two-phase system containing heptane as an organic solvent and aqueous H_2O_2 at 25-60 ^oC in a 50-mL glass reactor equipped with a magnetic stirrer, a reflux condenser and a heat circulator. The reactions were monitored by GC. The amount of unreacted H_2O_2 was determined by titration with $KMnO_4$ for the efficiency of hydrogen peroxide use to be estimated [2].

3 Results and discussion

We found that PIB oligomer-bound Keggin POMs are highly active and easily recyclable catalysts for DBT oxidation with H_2O_2 in a heptane-water biphasic system, yielding DBT sulfone as the sole product (Table 1). The two catalyst components can simply be added separately to the reaction mixture to form the active catalyst *in situ*. The PIB amine was introduced as a 0.5 M heptane solution of diethylamine terminated PIB (PIB_{1000}-$CH_2N(CH_2CH_3)_2$) synthesized from commercially available PIB oligomer with a molecular mass of 1000 Da [2]. The POM was a heteropoly acid hydrate $H_3PW_{12}O_{40}$, $H_3PMo_{12}O_{40}$ or $H_4SiW_{12}O_{40}$, hereafter abbreviated as PW, PMo and SiW. The catalyst activity increased with the PIB/POM molar ratio, levelling off at a ratio of 4:1 – 6:1. PW exhibited the highest activity followed by PMo. With PW, the conversion of DBT reached 100% in 0.5 h at 60 ^oC and a

PIB/PW molar ratio of 6:1. In contrast, SiW predictably showed no activity in agreement with its well-known resistance to form peroxo species. Importantly, practically no decomposition of H_2O_2 took place in the PIB-POM reaction system, giving >99% efficiency of H_2O_2 utilization. Excellent recyclability of the PIB-PW catalyst was observed – 5 times without loss of activity.

Table 1. Oxidation of DBT by H_2O_2 catalyzed by PIB-POM in heptane-H_2O two-phase system.[a]

POM	PIB/POM (mol/mol)	Temp. (°C)	Conv. (%)	H_2O_2 efficiency (%)
PW	1:1	60	70	> 99
PW	4:1	60	97	>99
PW	6:1	60	100	>99
PW	4:1	40	49	>99
PW	4:1	25	30	>99
PMo	4:1	60	73	>99
SiW	4:1	60	0	>99

[a] Heptane (10 mL), DBT (0.50 mmol, 1 wt%), aqueous 30% H_2O_2 (0.15 mL); molar ratios: DBT/POM = 90:1, DBT/H_2O_2 = 1:3; 0.5 h reaction time. DBT sulfone was the only reaction product observed.

The PIB-POM catalyst was also found efficient for cyclooctene epoxidation (Table 2). This reaction is the standard test for epoxidation catalysts and was used here for proof of concept. The PW catalyst was more active than PMo, as in the case of DBT oxidation, yielding 100% at 60 °C in 0.5 h reaction time. Again, the decomposition of H_2O_2 was negligible (>99% efficiency of H_2O_2 utilization), and the catalyst could be reused.

Table 2. Epoxidation of cyclooctene by H_2O_2 catalyzed by PIB–POM in heptane-H_2O two-phase system.[a]

POM	Temp. (°C)	PIB/POM (mol/mol)	Time (h)	Yield[b] (%)	Initial rate[c] (mmol/min)
PMo	60	6:1	0.5	99	0.059
PW	60	6:1	0.5	100	0.083
PW	60	4:1	0.5	92	0.075
PW	60	3:1	0.5	96	0.080
PW	30	3:1	2.5	94	0.031
PW	60	1:1	0.5	88	0.056

[a]Heptane (10 mL), cyclooctene (9.71 mmol, 1.0 mL), aqueous 10% H_2O_2 (1 mmol, 0.3 mL), $H_3PW_{12}O_{40}\cdot 20H_2O$ or $H_3PMo_{12}O_{40}\cdot 28H_2O$ (6.48 μmol). [b]Yield based on the initial amount of H_2O_2. [c]Initial rate calculated over the first 10 min of the reaction.

4 Conclusions

We have demonstrated that the PIB oligomer-bound Keggin POMs are efficient and recyclable catalysts for environmentally benign biphasic oxidations with H_2O_2, including the oxidation of DBT to DBT sulfone and cyclooctene epoxidation, in a heptane-water system. These catalysts self-assemble in situ by mixing commercial Keggin POMs and amine terminated PIB oligomer. The activity of PIB-POM compares well with the results reported so far.

Acknowledgements

We thank EPSRC (IK), the Welch Foundation (DB, Grant A-0639), and the National Science Foundation (DB, Grant CHE-1362735) for financial support.

References

[1] I.V. Kozhevnikov, *Catalysis by Polyoxometalates*, Wiley, Chichester, 2002.
[2] R. Yahya, M. Craven, E. F. Kozhevnikova, A. Steiner, P. Samunual, I. V. Kozhevnikov, D. E. Bergbreiter, *Catal. Sci. Technol.*, 2015, DOI: 10.1039/C4CY01394H.

V-PP76

Catalytic Combustion of Toluene over MnO_x-CeO_2 Mixed Oxides

Benadda A.[1*], Rahou S.[1], Barama A.[1], Djadoun A.[2]

1 - LMCCCO, Faculté de Chimie, USTHB, Algiers, Algeria
2 - Laboratoire de Géophysique, FSTGAT, USTHB, Algiers, Algeria

* abenadda@usthb.dz

Keywords: MnOx-CeO_2 mixed oxides, solid solution, catalytic combustion, toluene

1 Introduction

Volatile organic compounds (VOCs), are a major class of atmospheric pollutants, that are released in the atmosphere by different manufacturing processes, motor vehicles and domestic activities [1,2]. The VOC's generated by industrial processes are generally eliminated by thermal combustion, however, the catalytic combustion is more advantageous as it enables to operate at lower temperatures which leads to the limitation of the formation of by-products, such as dioxins and nitrogen oxides and carbon monoxide [2]. In the present work, two MnO_x-CeO_2 solids were prepared using co-precipitation and redox methods and then the catalytic performance of these systems was probed in the toluene combustion reaction.

2 Experimental

2.1. Catalysts Preparation

The solids, MnO_x-CeO_2 with a molar ratio Mn/Ce=1, were prepared by two methods, carbonate route (MnCe-CPC) and redox route (MnCe-RED), the solids were dried at 100°C and calcined at 500°C for 5 hours (heating rate 5°C/min). The Pure oxides were also prepared using the carbonate route and were labeled MnO_x and CeO_2.

2.2. Catalysts characterization

The prepared solids were calcined at 500°C, and characterized by XRD, H_2 temperature-programmed reduction (H_2-TPR) , nitrogen adsorption-desorption technique and SEM.

3 Results

The XRD analysis of the solids showed that the only crystalline phase detected is cerium oxide.

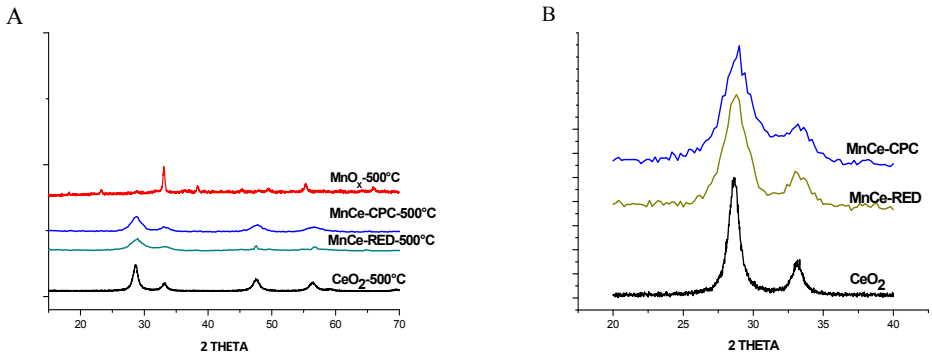

Fig 1. XRD patterns of solids : the vertical lines correspond to the position of diffraction lines of CeO_2 JCPDF#34-0394 B :shift XRD lines.

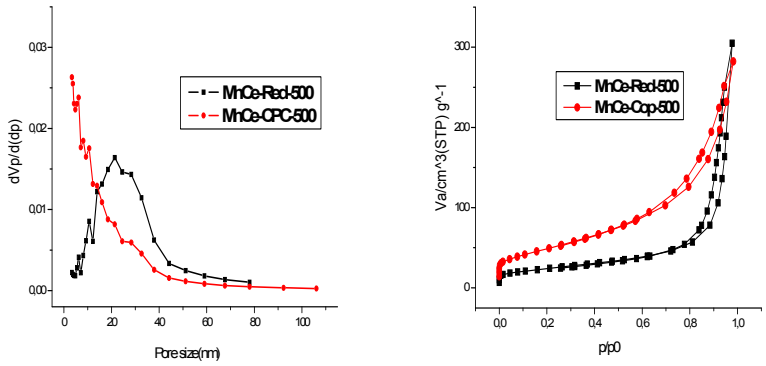

Fig 2: The nitrogen adsorption/desorption isotherms and pore distribution.

The N_2 adsorption/desorption isotherms of all catalysts belong to type II according to the IUPAC classification and have a pore distribution in the mesopores region.

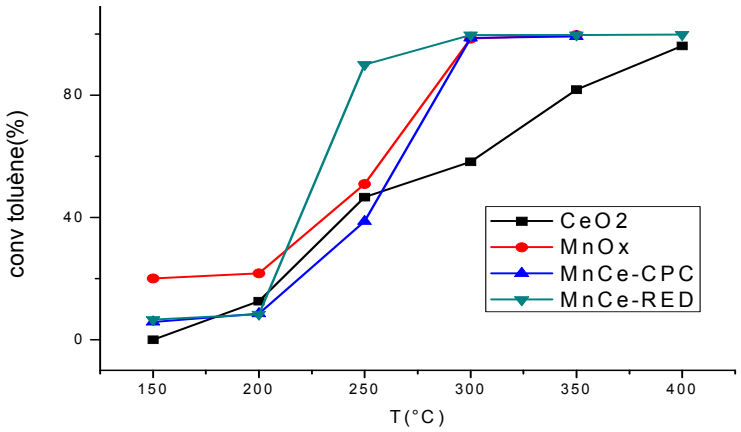

Fig 3: Toluene conversion on pure and mixed oxides.

The solids showed good performances in the toluene combustion reaction which seemed to depend strongly on the preparation method. The catalyst prepared by the redox method exhibited the best catalytic activity, over which the conversion of toluene could achieve 90% at 250°C and 100% at 300°C.

4 Conclusion

MnO_x-CeO_2 mixed oxides prepared by the co-precipitation and redox methods lead to a good catalytic activity in the total oxidation of toluene. The textural properties and catalytic behavior depend on the preparation method. The XRD analysis suggested the formation of a solid solution between manganese and cerium oxide.

References

[1] R.J. Heinsohn, R.L. Kabel, Sources and Control of Air Pollution, Prentice Hall, Upper Saddle River, NJ (1999).

[2] R.E. Hester, R.M. Harrison Volatile Organic Compounds in the Atmosphere, Royal Society of Chemistry (1995).

V-PP77

Effect of Preparation Method on Catalytic Properties of Co-Mn-Al Mixed Oxide for N_2O Decomposition

Klyushina A.[1], Obalová L.[1*], Karásková K.[2], Jirátová K.[3]

1 - Faculty of Metallurgy and Materials Engineering, Institute of Environmental Technology, VŠB – Technical University of Ostrava, Ostrava, Czech Republic

2 - Faculty of Metallurgy and Materials Engineering, VŠB – Technical University of Ostrava, Ostrava, Czech Republic

3 - Institute of Chemical Process Fundamentals CAS, Prague, Czech Republic

* lucie.obalova@vsb.cz

Keywords: nitrous oxide, catalytic decomposition, cobalt oxides, IR spectroscopy, XRD, Raman

1 Introduction

Nitrous oxide (N_2O) has a high global warming potential (310 times higher than CO_2) and contributes to the destruction of stratospheric ozone. The low-temperature catalytic decomposition of N_2O (up to 450°C) to nitrogen and oxygen offers attractive solution for decreasing N_2O emissions in tail gas from nitric acid production plants.

Cobalt spinel catalysts are supposed as ones of the most active catalysts for N_2O decomposition [1-6]. The catalytic activity of spinels depends essentially on the degree of substitution and the occupation of the tetrahedral and octahedral sites. The preparation method of the spinel precursors determines final oxide texture, surface composition and plays a crucial role in ultimate performance of these materials [4].

The present article is dealing with comprehensive analysis of the effect of preparation method on the N_2O decomposition performance of Co-Mn-Al mixed oxide catalyst prepared by three different methods to obtain new information about key parameters influencing catalytic activity for N_2O decomposition.

2 Experimental

Co-Mn-Al mixed oxides were prepared by three different methods while the Co:Mn:Al molar ratio of 4:1:1 was kept constant in all catalysts. At first, Co-Mn-Al layered double hydroxide with the Co:Mn:Al molar ratio of 4:1:1 was prepared by co-precipitation of the corresponding nitrate solution in an alkaline Na_2CO_3/NaOH solution at 25 °C and pH 10 (Co-Mn-Al-ht-ex). The washed and dried product was calcinated for four hours at 500 °C in air. The second method of catalyst preparation was the mechanochemical reaction of Co, Mn, Al nitrates with NH_4HCO_3 (Co-Mn-Al-carb). The third method of catalyst synthesis was calcination of corresponding nitrates for four hours at 500 °C in air (Co-Mn-Al-nitr).

The catalysts were characterized by AAS, XRD, Raman, FTIR, H_2-TPR, TPD-CO_2 and NH_3 and tested for N_2O decomposition in inert gas and simulated waste gas from HNO_3 production.

3 Results and discussion

The chemical analysis data, textural data and redox properties of calcined samples are listed in the Table 1. The highest specific surface area was observed for Co-Mn-Al mixed oxide prepared for carbonate precursor. From XRD patterns (not show) one can see that the diffraction lines are attributed to the Co-Mn-Al spinel-like phase for all samples. FTIR and Raman spectra of measured samples (not shown) showed characteristic bands of Co-, Mn- and Al-O vibrations but they are not identical for all samples. Differences were observed also in reducibility of samples. Results of N_2O catalytic decomposition in inert and simulated industrial conditions are

presented in Fig. 1. The highest catalytic activity was achieved on the calcined precursors having carbonates in their molecules, Co–Mn–Al-carb and Co–Mn–Al-HT-ex, the lowest one on the calcined Co–Mn–Al nitrates, probably due to the lowest surface area, less advantageous porous structure and worse reducibility. Simulating industrial conditions by adding oxygen, water and NO to the inert, the N_2O conversions decreased for all samples, the least affected conversion being that for the Co-MnAl-carb.

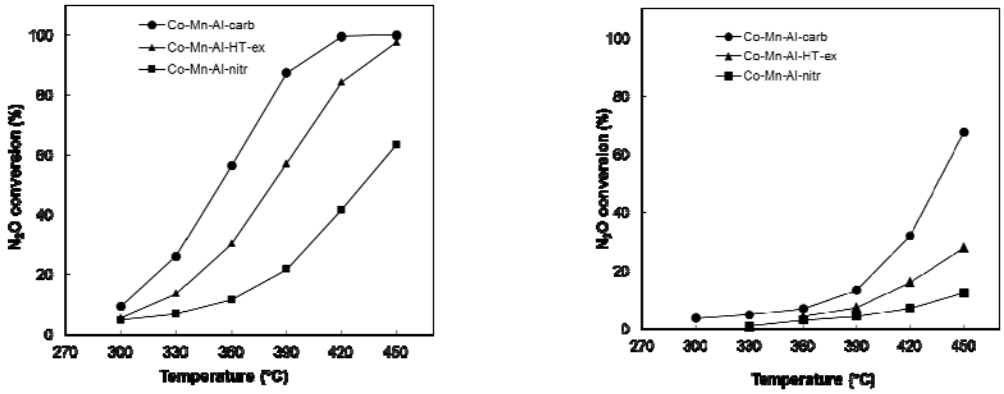

Fig. 1. Temperature dependence of N_2O conversions over Co-Mn-Al mixed oxide. Conditions: 1000 ppm N_2O in He (a) and 1000 ppm N_2O + 5%O_2 + 3%H_2O + 200ppm NO/He (b) atmospheric pressure, GHSV=20 l $g^{-1}h^{-1}$

Table 1. Chemical composition, textural data and redox properties of Co-Mn-Al mixed oxide

Sample	Co	Mn	S_{BET}	V_{meso}	V_{micro}	r_{meso} [a]	TPR-H_2	T_{max} °C
	wt %	wt %	$m^2.g^{-1}$	$cm^3\ g^{-1}$	$cm^3\ g^{-1}$	nm	25-1000 °C	
Co-Mn-Al-carb	45.7	11.7	134	0.78	0.058	12.4	13.12	352, 731
Co-Mn-Al-HT-ex	49.6	13.3	93	0.48	0.046	10.8	12.50	337, 637, 789
Co-Mn-Al-nitr	48.4	12.9	35	0.15	0.015	21.7	13.48	418, 595, 697

4 Conclusions

Co-Mn-Al mixed oxides with the molar ratio of Co:Mn:Al = 4:1:1 were prepared by three different methods, characterized and tested in N_2O catalytic decomposition. The preparation method influenced the physical-chemical properties of the catalysts and their catalytic activities. The highest activity showed Co-Mn-Al-carb prepared mechanochemically due to the highest surface area and pore volume.

Acknowledgements

This work was supported by the Czech Science Foundation (project 14-13750S) and by Ministry of Education, Youth and Sports of the Czech Republic in National Feasibility Program I (project "TEWEP" LO1208) and project SP2014/48.

References

[1] K. Asano, C. Ohnishi, S. Iwamoto, Y. Shioya, M. Inoue, Appl. Catal. B 78 (2008) 242-249.
[2] K. Karásková, L. Obalová, K. Jirátová, F. Kovanda, Chem. Eng. J. 160 (2010) 480-487.
[3] L. Obalová, K. Karásková, K. Jirátová, F. Kovanda, Appl. Catal. B 90 (2009) 132-140.
[4] W. Piskorz, F. Zasada, P. Stelmachowski, A. Kotarba, Z. Sojka, Catal. Today 137 (2008) 418-422.
[5] B.M. Abu-Zied, Chin. J. Catal. 32 (2011) 264-272.
[6] P. Stelmachowski, G. Maniak, A. Kotarba, Z. Sojka, Catal. Commun. 10 (2009) 1062-1065.

V-PP78

K/Co_4MnAlO_x Catalyst for N_2O Abatement from Nitric Acid Plant Waste Gases – Results of Pilot Plant-Scale Testing

Obalová L.[1], Karásková K.[1], Kovanda F.[2], Jirátová K.[3], Šrámek J.[4], Kustrowski P.[5], Chromčáková Ž.[1], Pacultová K.[1*], Kočí K.[1], Borovec K.[1], Dej M.[1]

1 - VŠB-Technical University of Ostrava, Ostrava, Czech Republic
2 - University of Chemistry and Technology, Prague, Czech Republic
3 - Institute of Chemical Process Fundamentals of the ASCR, Prague, Czech Republic
4 - CHEMOPROJEKT CHEMICALS, Praha, Czech Republic
5 - Jagiellonian University, Krakow, Poland

* katerina.pacultova@vsb.cz

Keywords: mixed oxide, catalysts, nitrous oxide, decomposition, pilot plant, kinetic modelling

1 Introduction

Catalytic decomposition of N_2O, strong greenhouse gas, which is typically present in the tail gases from nitric acid plant, is well known from the scientific literature. However, only small number of catalysts has been commercialized and only few studies devoted to the catalysts tested in pilot plants were reported [1-4]. Depending on the location in the process, the approaches of lowering of N_2O from nitric acid plants can be classified into three groups: (i) preventing of N_2O formation in the ammonia burner, (ii) N_2O removal from NO_x gases between the ammonia burner and the absorption column, and (iii) N_2O removal from the tail gas downstream (low temperature deN_2O). The choice of suitable deN_2O technology depends on the current arrangement of the nitric acid plant, which can be radically different, which means that each approach is necessary to be developed. The offer of commercial catalysts suitable for low temperature N_2O decomposition available nowadays at the market is very limited [4].

Our recent research activities have been focused on development of a catalyst for the low temperature N_2O decomposition, covering the catalysts development and preparation, their laboratory and pilot plant-scale testing in N_2O decomposition including the long term activity and stability tests and assessment of usage of such a catalyst in the full scale plant based on the mathematical model of pilot plant reactor.

2 Experimental/methodology

The K-doped Co-Mn-Al mixed oxide deN_2O catalyst was prepared by heating the coprecipitated Co-Mn-Al layered double hydroxide with Co:Mn:Al molar ratio of 4:1:1, subsequent impregnation with KNO_3, pelletizing into 5x5 mm tablets and heating at 500 °C. Testing of catalytic N_2O decomposition was performed in a pilot-plant fixed bed stainless steel reactor (310 mm i.d, temperature range from 300 to 450 °C, inlet pressure 0.6 MPa); reactor inlet was connected to the bypassed tail gas from the nitric acid production plant downstream the SCR NO_x/NH_3 catalyst. Feed to the reactor varied between 300 and 600 kg h^{-1} and contained typically 400-700 ppm N_2O together with oxygen, water vapor and low concentration of NO, NO_2 and NH_3. The infrared (N_2O, NO, NH_3) and chemiluminescence (NO, NO_2) on-line analyzers were used for analysis of the gas at the catalyst bed inlet and outlet. Reactor was equipped with on-line monitoring concentrations of all measured gas components, temperature in catalyst bed and pressure drop. Fresh and used catalysts were characterized by AAS, XRD, XPS, N_2 physisorption, He pycnometry, Hg porosimetry, thermal alkali desorption and H_2-TPR.

3 Results and discussion

The catalyst prepared in the pilot plant-scale contained slightly lower amount of Mn and Al than intended (Table 1); however, its activity in N_2O decomposition was comparable with that of samples prepared in laboratory. Performance of the catalyst tested in the pilot plant-scale conditions was very good and stable (Fig. 1).

Table 1 Physicochemical characterization of the fresh and used K/Co_4MnAlO_x catalyst

Catalyst	Co:Mn:Al:K[1)]		S_{BET}	V_{meso}	TPR[3)]
	AAS	XPS	($m^2\ g^{-1}$)	($cm^3\ g^{-1}$)	(mmol H_2/g)
Fresh	4:0.66:0.74:0.17	4:0.7:1.9:0.38	93.0	0.213	5.61
Used [2)]	4:0.73:0.91:0.15	4:1.1:2.5:0.52	86.8	0.205	5.73

[1)] Molar ratio [2)] For 112 days [3)] (25-500°C)

The long term testing showed slight increase in N_2O conversion; average N_2O conversion of 90 % at 450 °C, GHSV=8 620 $m^3\ m_{bed}^{-3}\ h^{-1}$ and p=0.6 MPa was determined. This increase could be connected with changes of surface composition observed by XPS, which confirmed slight reduction of Co^{3+} to Co^{2+} and enrichment of the surface with K; observed changes in pore structure could also contribute to this finding.

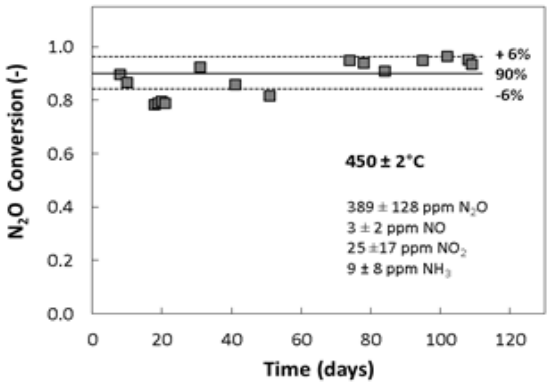

Fig. 1. Stability over K/Co_4MnAlO_x in the pilot plant test (GHSV=8 620 $m^3\ m_{bed}^{-3}\ h^{-1}$, p=0.6 MPa)

The kinetic parameters of N_2O decomposition evaluated from experiments performed over the catalyst tablets in the pilot plant reactor describe the reaction rate including internal diffusion hindering effect and can be fitted by the 1st order rate law. At the assumption that these data are not influenced by macrokinetic phenomena of the pilot plant reactor, they were directly used for the reactor scale-up calculations.

4 Conclusions

The K/Co_4MnAlO_x catalyst designed on the basis of laboratory tests was successfully prepared in the pilot plant-scale. The catalysts showed the same catalytic activity in laboratory and pilot plant-scale testing of N_2O decomposition, when high and stable output in N_2O removal was reached. The slight changes in surface composition observed after 112 days catalyst testing in the pilot plant reactor did not negatively affect the catalytic performance. The developed deN_2O K/Co_4MnAlO_x catalyst can be considered as very promising for commercial application.

Acknowledgements

Financial supports of the Technology Agency of the Czech Republic (project no. TA 01020336), Czech Science Foundation (project no. P106/14-13750S) and Ministry of Education, Youth and Sports of the Czech Republic in the "National Feasibility Program I", project LO1208 "TEWEP" are gratefully acknowledged.

References

[1] M. Inger, M. Wilk, M. Saramok , G. Grzybek , A. Grodzka, P. Stelmachowski , W. Makowski, A. Kotarba , Z. Sojka, Ind. Eng. Chem. Res. 53 (2014) 10335
[2] M Inger, P Kowalik, M Saramok, M Wilk, P Stelmachowski, G Maniak, P. Granger, A. Kotarba, Z. Sojka, Catal. Today 176 (2011) 365
[3] M C. E. Groves, A. Sasonov J. Integr. Eviron. Sci. 1 (2010) 211
[4] M. Hoang, A. J. Hill. Industrial Emission Treatment Technologies, Municipal and Industrial Waste Disposal, ISBN: 978-953-51-0501-5, Available from: http://www.intechopen.com/

V-PP79

DFT Studies on the Mechanisms of Nickel-Catalyzed Reductive Carboxylation of Styrenes Using CO_2 as the Building Block

Yuan R.M.[1*], Lin Z.[2]

1 - Department of Chemistry, Xiamen University, Xiamen, People's Republic of China
2 - Department of Chemistry, The Hong Kong University of Science and Technology, Hong Kong, People's Republic of China

* yuanrm@xmu.edu.cn

Keywords: carbon, dioxide, reductive carboxylation, DFT studies, nickel catalyst

1 Introduction

Greenhouse effect has been recognized as one of the important environmental issues, and CO_2 makes up a significant percent of total greenhouse gas (GHG) emissions.[1] On the other hand, CO_2 is an attractive C1 building block for organic synthesis because of its low cost and abundance. However, its high stability and low reactivity are the biggest challenge to development of useful chemical reactions involving carbon dioxide. Recently, significant efforts have been devoted to convert CO_2 into carboxylic acids and derivatives.[2] Among those reported reactions, carboxylation of unsaturated organic compounds catalyzed by low-valent nickel complexes is well investigated. Here, we studied the detailed mechanisms of the nickel-catalyzed reductive carboxylation of ester-substituted styrenes H_2C=CHAr using CO_2 as the building block to form α-carboxylated products (eq 1) by DFT calculations. [3] With the aid of the DFT calculations, we obtained important insights regarding the substrate scope, ligands and reaction conditions used.

2 Experimental/methodology

Two possible mechanisms, the oxidative-coupling mechanism and the nickel-hydride mechanism, were calculated and compared.

Scheme 1 gives the detailed aspects of the oxidative-coupling and the nickel-hydride mechanisms calculated.

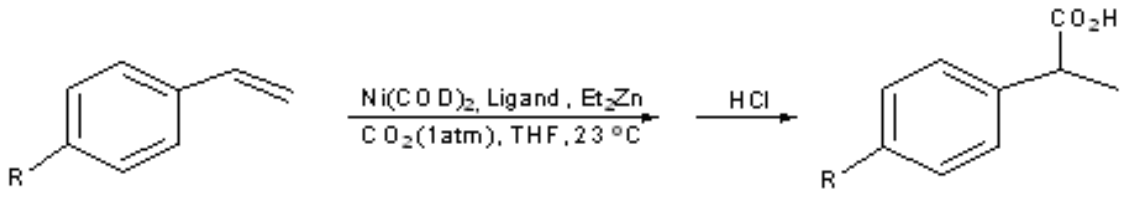

(1)

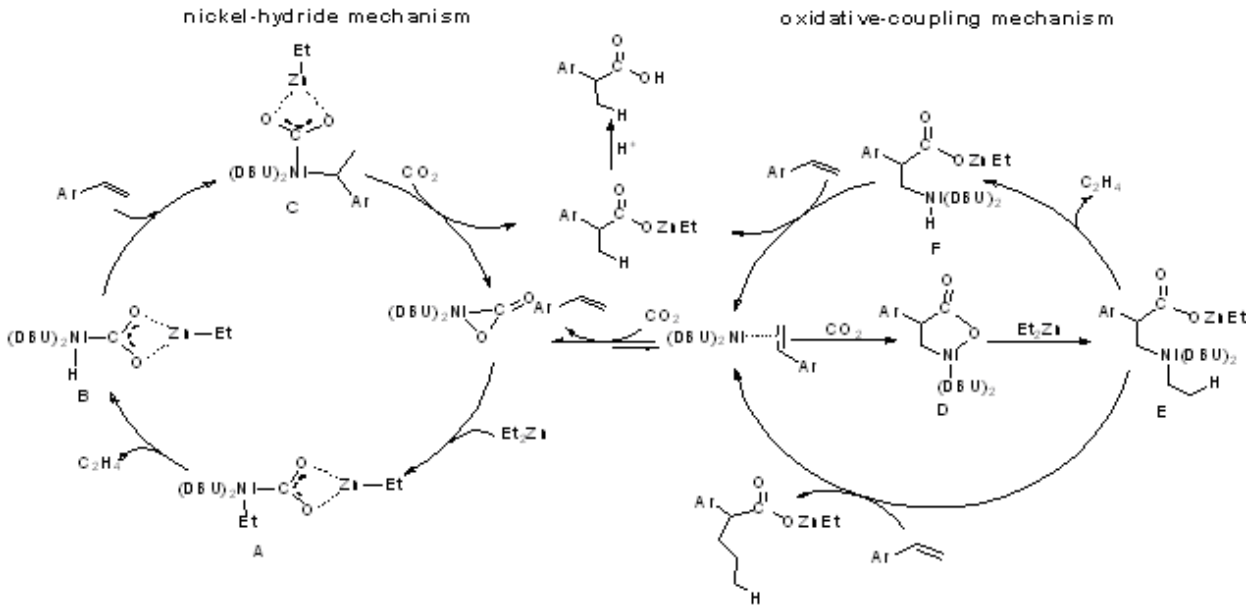

3 Results and discussion

Our calculation results show that in the oxidative-coupling mechanism, the metallacycle intermediates (**D**) (Scheme 1) generated from oxidative coupling between CO_2 and a styrene substrate molecule on the nickel(0) metal center corresponds to a thermodynamic sink. i.e., both the barriers for the reverse and forward steps from the intermediates are particularly high (30.3 and 33.4 kcal/mol). In other words, CO_2-styrene oxidative coupling should be avoided in order for smooth reductive carboxylation of styrenes.

In the nickel-hydride mechanism, the nickel-hydride species **B** (Scheme 1) is the active species, from which styrene insertion into the Ni-H bond followed by reductive elimination to produce α-carboxylated product. Calculations show that when the ester-substituted styrene H_2C=CHAr (Ar = C_6H_4-*p*-COOMe) is used as the substrate either of these two steps (insertion and reductive elimination) can be the rate-determining step, and both the transition states $\mathbf{TS_{6\text{-}8}}$ and $\mathbf{TS_{8\text{-}1}}$ (Figure 1) are only slightly more stable than the oxidative coupling transition state (19.8 vs 21.0 kcal/mol) leading to the thermodynamic sink. The very limited preference for the nickel hydride pathway over the oxidative coupling pathway suggests that the reaction outcome can be easily manipulated/affected by substituents on the aryl ring of a styrene substrate as well as other factor such as the pressure used in the reactions.

Consistent with the experimental observation, the calculation results show that electron-withdrawing substituents such as NO_2, CN and COOMe, promote the nickel hydride mechanism and facilitate the reductive carboxylation reactions. It was also found that high CO_2 pressure promotes the formation of the thermodynamic sink, explaining why 1 atm of CO_2 was used in the experimentally reported reactions.

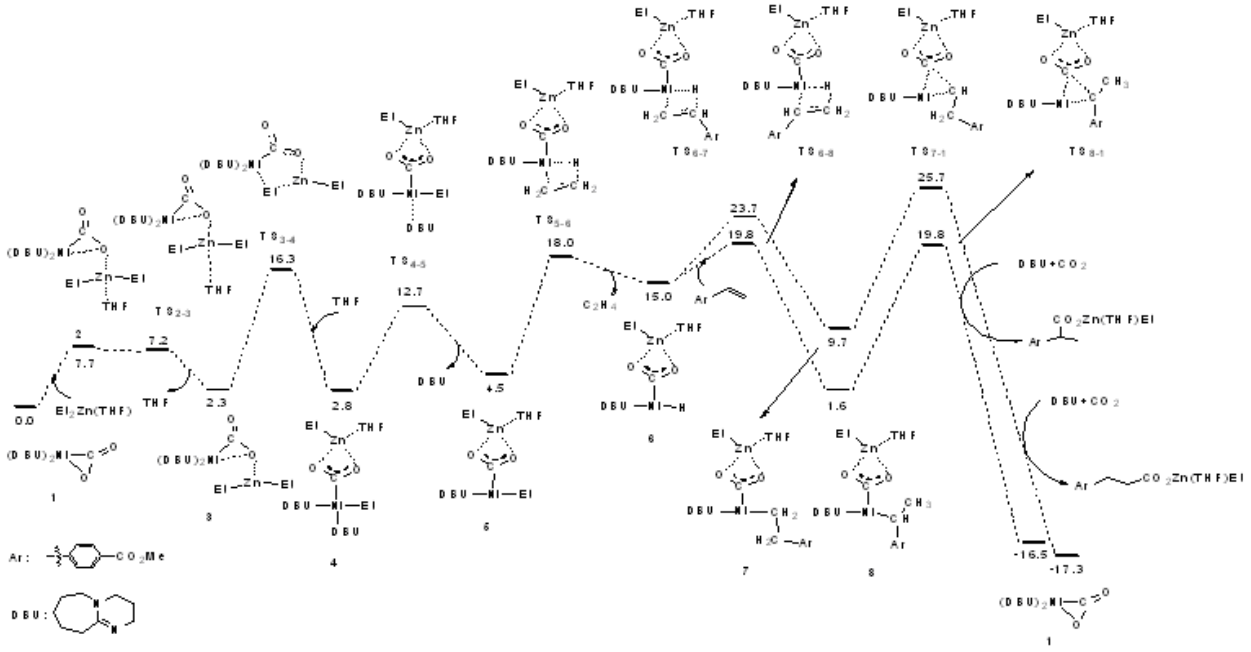

Figure 1. Free energy profiles calculated for the nickel-hydride mechanism based on the catalytic cycle shown on the left-hand side of Scheme 1. The free energies are given in kcal/mol.

4 Conclusions

In the most favorable pathway of the nickel hydride mechanism, it was also found that ligand (here DBU) dissociation and association are often involved, explaining why bidentate ligands such as COD and bipyridine are ineffective for the catalytic reactions. When Cs_2CO_3 and KHMDS were used as ligands, it was found that the oxidative coupling between alkyne and CO_2 can be effectively suppressed. However, both the Cs_2CO_3 and KHMDS ligands are not very effective ligands to promote the reductive carboxylation. All these results are consistent to the experimental observations.

References

[1] (a) Hileman, B. Chem. Eng. News. **1995**, 27, 18-23; (b) Hileman, B. Chem. Eng. News. **1997**, 17, 9-10.

[2] (a) Huang, K.; Sun, C. L.; Shi, Z. J. Chem. Soc. Rev. **2011**, 40, 2435-2452. (b) Maeda, C.; Miyazaki, Y.; Ema, T. Catal. Sci. Technol. **2014**, 4 1482-1497. (c) Cokoja, M.; Bruckmeier, C.; Rieger, B.; Herrmann, W. A.; Kühn, F. E. Angew. Chem. Int. Ed. **2011**, 50, 8510-8537.

[3] Williams, C. M.; Johnson, J. B.; Rovis, T. J. Am. Chem. Soc. **2008**, 130, 14936-14937.

V-PP80

Catalytic Decomposition of NF_3 Exhausted in Semiconductor Manufacturing Process over γ-Al_2O_3 Catalyst with H_2O or without H_2O

Lee J.W.[1], Lee T.H.[1], Seong Y.B.[1], Kim M.J.[1], Park C.J.[1], Choi W.Y.[1], Park N.-K.[2], Lee T.J.[1*], Chang W.C.[3], Choi H.-Y.[4]

1 - Yeungnam University, Chemical Engineering, Gyung San, Republic of Korea
2 - Yeungnam University, Institute of Clean Technology, Gyung San, Republic of Korea
3 - KOCAT Incorporated, Republic of Korea
4 - Institute for Advanced Engineering, Yongin, Republic of Korea

* tjlee@ynu.ac.kr

Keywords: NF3, γ-Al2O3, hydrolysis

1 Introduction

Nitrogen fluoride (NF_3) has been widely used as plasma etching and cleaning gas in semiconductor production. NF_3 has an enormously large global warming potential of 17,000 times than that of CO_2 and long lifetime for the decomposition in atmospheric condition. Therefore, it is required to remove the wasted NF_3 by safe and low cost method. The energy consumption required for the decomposition of NF_3 by the hydrolysis or oxidation reactions with the catalytic process is relatively lower than that of the direct decomposition. Therefore, the catalytic reaction of NF_3 decomposition can be very useful for commercialization of NF_3 decomposition process.

Table 1. Experimental/methodology

It is known that solid acid catalysts have been mostly used for NF_3 decomposition. In this study, γ-Al_2O_3 catalyst was prepared in order to decompose NF_3. NF_3 and H_2O were used for reactant. This study was progressed two ways. One way is hydrolysis and other is reaction without H_2O. These catalytic activity tests were carried out at 400℃, space velocity of 15000ml/g cat·h for 35 h, respectively.

In hydrolysis of NF_3, hydrogen fluoride (HF) is produced as presented in reaction (1). HF produced by hydrolysis of PFCs over Pt/Al_2O_3[1] leads a rapid deactivation of the catalyst due to the formation of AlF_3 by interaction of Al_2O_3 with HF as presented in reaction (2). Γ-Al_2O_3 is also conversed into AlF_3 by the gas-solid reaction of NF_3 and Al_2O_3 in the absence of water according to reported paper[2].

(1) $2NF_3 + 3H_2O \rightarrow 6HF + NO + NO_2$
(2) $Al_2O_3 + 6HF \rightarrow 3H_2O + 2AlF_3$
(3) $2NF_3 + Al_2O_3 \rightarrow 2AlF_3 + NO + NO_2$

Table 1. Results and discussion

Fig. 1 shows NF_3 conversion by the catalytic hydrolysis and gas-solid reaction without H_2O. In case of reaction without H_2O, reactivity was highly maintained for 1 h of initial time, but the conversion of NF_3 gradually decreased during reaction of decomposition. After the activity test of 15 h, the conversion of NF_3 was indicated less than 20%. On the other hand, in case of hydrolysis, catalytic activity was rapidly reduced in initial time. After that the conversion of NF_3 was maintained at about 40% for 35 hours.

Fig. 2 shows XRD patterns of fresh and reacted catalysts. AlF_3 was observed in XRD pattern of reacted catalysts and the different crystal structures, which is hexagonal and orthorhombic AlF_3 structures, were confirmed by hydrolysis and gas-solid reaction.

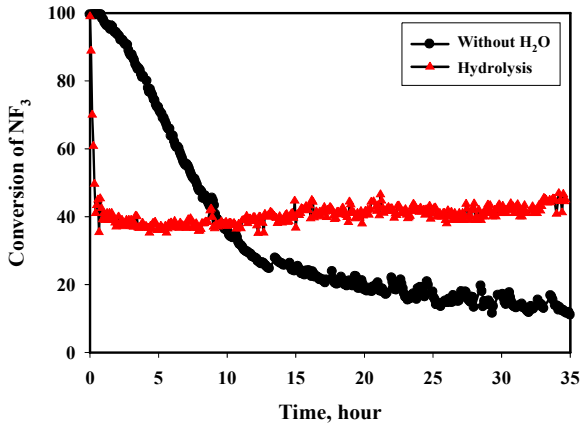

Fig. 1. Conversion of NF_3 by hydrolysis and without H_2O.

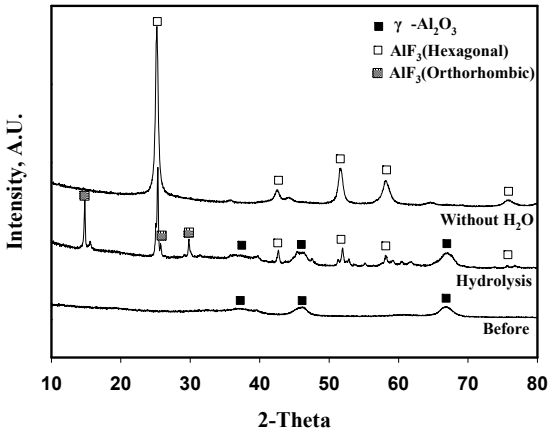

Fig. 2. XRD patterns of fresh and reacted γ-Al_2O_3 catalysts.

Catalyst	Fresh	Reacted	
		Hydrolysis	Without H_2O
Surface area(m^2/g)	205	139	21

Table 1. BET surface area of fresh and reacted catalysts

Meanwhile, the surface area of γ-Al_2O_3 catalysts decreased after hydrolysis and reaction without H_2O. The different surface area of catalyst was exhibited with hydrolysis and gas-solid reaction, as shown in Table 1.

4 Conclusions

In hydrolysis, the conversion of NF_3 rapidly decreased from 100% to 40% in 30 min after reaction start due to formation of AlF_3. The conversion of NF_3 was also kept at about 40% for 35 h after 30 min. In case of reaction without H_2O, the conversion of NF_3 was significantly reduced for 35 hours without H_2O condition because of the gas-solid reaction of NF_3 and Al_2O_3. It was confirmed by XRD analysis of fresh and reacted catalyst that Al_2O_3 was conversed into AlF_3. However, the catalytic decomposition was occurred by hydrolysis over γ-Al_2O_3. Therefore, it was concluded that catalytic hydrolysis was more effective NF_3 decomposition process than gas-solid (NF_3-Al_2O_3) reaction without H_2O in long term test.

Acknowledgements

This work was supported by the Global Excellent Technology Innovation of the Korea Institute of Energy Technology Evaluation and Planning (KETEP), granted financial resource from the Ministry of Trade, Industry & Energy, Republic of Korea. (No. 20135010100750)

References

[1] M.M Farris, A.A Klinghoffer, J.A. Rossin, and D.E. Tevault, ""Deactivation of a Pt/Al_2O_3 catalyst during the oxidation of hexafluoropropylene," Catalysis Today, Vol. 11, No. 2, 11, 501-516 (1992)

[2] S.H. Lee, N.-K. Park, S.H. Yoon, W.C. Chang, T.J. Lee, Clean Technol., 15 (4), 273 (2009).

V-PP81

"Bifunctional" [Mn-Ce/Fe-Zeolite] Catalysts for Selective Catalytic Reduction of NO_x by NH_3 at Low Temperature

Krivoruchenko D.S.[1], Stakheev A.Yu.[1*], Bokarev D.A.[1], Telegina N.S.[1], Kustov A.L.[2], Thøgersen J.R.[2]

1 - N. D. Zelinsky Institute of Organic Chemistry, Moscow, Russia
2 - Haldor Topsøe A/S, Lyngby, Denmark

* st@ioc.ac.ru

Keywords: zeolite, fast-SCR, beta, manganese, iron, cerium

1 Introduction

Iron-containing zeolites (mostly FeZSM-5 and FeBeta) are widely used as the catalysts for selective catalytic reduction of NO_x by ammonia. Our preliminary results indicated that a favorable low-temperature performance in NH_3-SCR can be attained by additional impregnation of Fe-Beta with 8-16% Mn [1]. In this study we focused on two issues: 1) to improve additionally the performance of Mn/Fe-Beta by modification with Ce; 2) to discriminate a contribution of the zeolite component (FeBeta) to the SCR activity of Mn-Ce/zeolite catalyst.

2 Experimental/methodology

The catalytic systems based on FeBeta and HBeta zeolites were prepared by co-impregnation with $Mn(NO_3)_3$ and $Ce(NO_3)_3$ followed by drying and calcination. Catalytic activities of Mn-Ce-Fe/Beta were evaluated using gas mixture composed of 550 ppm NH_3, 520 ppm NO, 10% O_2, 6% H_2O balanced by N_2 at GHSW = 270 000 h^{-1}. Mn-Ce-Fe/Beta catalyst was characterized by H_2-TPR and XRD.

3 Results and discussion

1) Improvement of low-temperature performance by the modification with Ce

SCR activities of Mn-Ce-Fe/Beta are compared in Fig. 1(A). One can clearly see that the introduction of Ce improves low-temperature activity at 150-250°C. Introduction Ce also

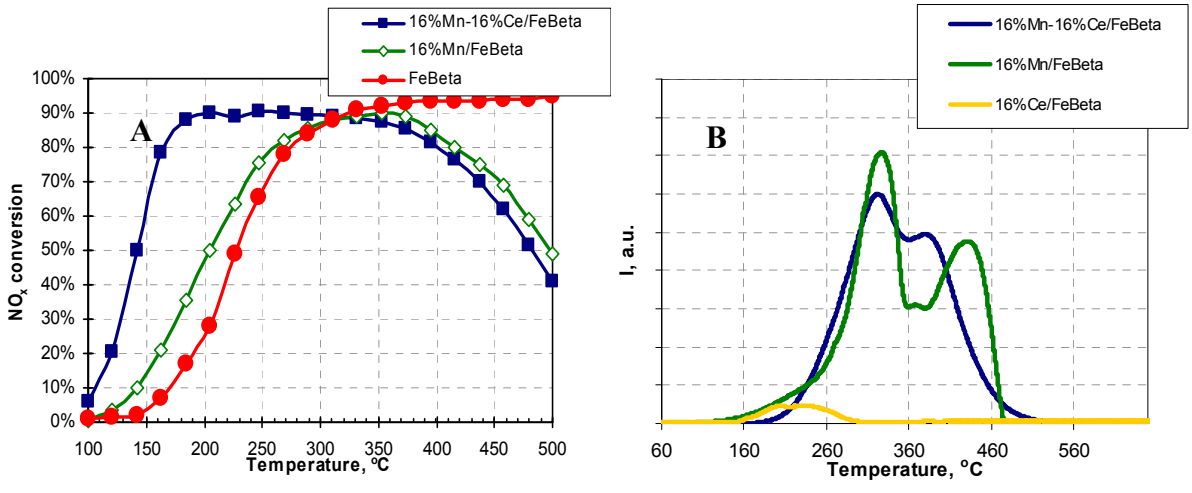

Fig 1. A) SCR activities of Mn-Ce-Fe/Beta; **B)** H_2-TPR profiles

increases oxidative activity at temperatures above 400°C, which leads to NH_3 depletion and

formation of additional NO_x.

Figure 1(B) shows Ce effect on H_2-TPR profiles of Mn-Ce-Fe/Beta catalysts. Introduction of Ce evidently decreases of the temperature of $Mn_3O_4 \rightarrow MnO$ transition. The decrease of the reduction temperature indicates that the reducibility of manganese oxides and ceria were enhanced, possibly due to the formation of solid solution, in which the mobility of the oxygen species was increased significantly. In turn, this results in the increased activity of Mn-Ce-Fe/Beta in NO oxidation (not shown).

2) Discrimination of the zeolite component contribution to the SCR activity of Mn-Ce/zeolite

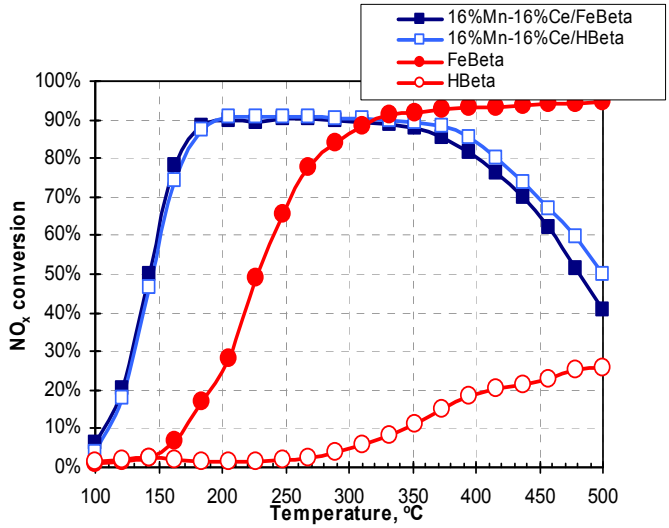

Fig.2. NO_x conversions over MnO_x-CeO_2/FeBeta and MnO_x/FeBeta

It is important to discriminate a contribution of the Standard SCR activity of FeBeta "carrier" to the overall activity of MnO_x-CeO_2/FeBeta. In order to minimize this contribution, MnO_x-CeO_2/HBeta and MnO_x/HBeta were prepared by loading Mn-Ce and Mn species over HBeta, which is essentially inactive in Standard SCR.

NO_x conversions over MnO_x-CeO_2/FeBeta and MnO_x-CeO_2/HBeta are compared in Fig. 2. It is clear, that the contribution of the Standard SCR activity of FeBeta to the overall activity of MnO_x-CeO_2/Beta catalyst is marginal. The data indicate that the bifunctional pathway evidently predominates.

All these results suggest that the observed improvement of low-temperature $DeNO_x$ over Mn-Ce-Fe/Beta stems from the SCR "bi-functional" pathway comprising two steps: (1) oxidation of NO to NO_2 over Mn-Ce oxide species followed by (**2**) fast-SCR over zeolite component [2]

$$\mathbf{2NO + O_2 \rightarrow 2NO_2} \qquad \mathbf{(1)}$$

$$\mathbf{4NH_3 + 2NO + 2NO_2 \rightarrow 4N_2 + 6H_2O} \qquad \mathbf{(2)}$$

4 Conclusions

NH_3-$DeNO_x$ activity of the Mn/Beta at 150-300°C can be significantly enhanced by additional modification with and Ce. Modification with Ce leads to enhanced oxidation activity of Mn-Ce species thus promoting "bi-functional" SCR mechanism.

Our data indicated that the "bi-functional" pathway predominates over MnO_x-CeO_2/Beta, and a contribution of the standard-SCR activity of zeolite component is negligible.

Acknowledgements

The support of Russian Foundation for Basic Research (Grant: 15-03-07802 A) is gratefully acknowledged. D. Krivoruchenko is grateful to Haldor Topsøe A/S for financial support in the framework of Ph.D. student support programme.

References

[1] D.S. Kivoruchenko, A.V. Kucherov, N.S. Telegina, D.A. Bokarev, P. Selvam, A.Yu. Stakheev, *Rus. Chem. Bull*, 63(2) (2014) 389

[2] A.Yu. Stakheev, G.N. Baeva, G.O. Bragina, N.S. Teleguina, A.L. Kustov, M. Grill, J.R. Thøgersen, *Top. Catal.* 56(1-8) (2013) 427

V-PP82

Increase of CO Photocatalytic Oxidation Rate on Titania under Moderate H_2O Coverages

Barsukov D.V.*, Subbotina I.R.

Zelinsky Institute of Organic Chemistry RAS, Moscow, Russia

* barsukovdenis@mail.ru

Keywords: photocatalysis, adsorbed water, TiO_2, carbon, monoxide, oxidation, oxygen, species

1 Introduction

Photocatalytic oxidation method is commonly used for removing volatile organic compounds from air, but for CO this method is usually considered as ineffective mainly due to competition for adsorption sites between H_2O and CO. This work demonstrates that the role of water is more complex than just a competitive adsorbent, and the positive influence of adsorbed water on CO oxidation rate occurs at moderate H_2O coverages.

2 Experimental/methodology

Catalytic measurements were carried out in closed glass reactor (V = 91.7 cm^3) with quartz (S_{ill} = 4.2 cm^2) and CaF_2 windows for UV-illumination and DRIFT measurements, respectively. Gas mixture of CO and O_2 (1:1, 10 torr total pressure, typically) was used for photocatalytic oxidation reactions. DRL-400 lamp was utilized as UV-light source, with 5-cm length water filter to prevent overheating. Electron impact ionization mass-spectrometer was used for gas phase measurements. TiO_2 undoped samples: Hombifine N (~300 m^2/g) and Degussa P25 (~50 m^2/g), 0.2% wt Pt-doped TiO_2 – Hombifine N and 2.5% Mo^{6+}/SiO_2 single site photocatalyst were inspected in activity tests under varied water coverages. The latter were determined by integration of broad IR band (4710-5400 cm^{-1}) with calibration by thermogravimetry.

3 Results and discussion

Conducted experiments revealed the dependence "CO photocatalytic oxidation rate — water coverage" is not monotonous for titania. Figure 1 demonstrates the effect of adsorbed water coverages on CO photocatalytic oxidation (**PCO**) rate over TiO_2. This result is in opposition of anticipations.

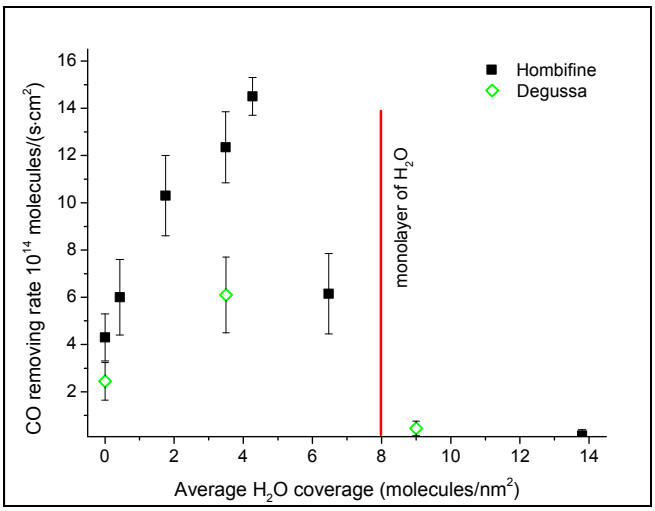

Fig. 1. Influence of water coverage on CO photocatalytic oxidation rate over TiO_2.

Vacuum treatment with strong heating (>150°C) doesn't increase oxidation activity of TiO_2, but only decreases, so the maximal activity of TiO_2 is about moderate water coverages (~4 molecule/nm^2) for both examined undoped TiO_2 samples.

It is well known that high temperature pretreatment greatly improve TiO_2 photocatalytic oxidation activity with regard to CO by generation of oxygen vacancy sites [1]. On the other hand, carbon monoxide PCO rate just decreasing in a wide range of water concentration from 0% RH at ambient temperature [2]. Thus, if H_2O acted as just competitive adsorbent then TiO_2 activity would reduce in Mo^{6+}/SiO_2 activity manner (see Table 1). The table indicates that even at relatively low surface concentration water poisons the active $2.5Mo^{6+}/SiO_2$, while TiO_2 oxidation activity significantly rises and even exceeds 0.2% Pt/TiO_2 activity.

Table 1. Catalyst activities of photocatalytic CO oxidation under degassed and partially H_2O covered surfaces.

Sample	CO removing rate, 10^{14} molecules/(s·cm^2)	
	Degassed surface	**0,5 monolayer of H_2O**
TiO_2 Hombifine N	4.3	14.5
TiO_2 Degussa P25	2.4	6.1
2.5% Mo^{6+}/SiO_2	25.4	1.4
0.2% Pt/TiO_2	6.2	6.8

In contrast of CO, many organic substances have an extremal dependence of their PCO rates on water pressure with optimal H_2O concentration at ambient temperature usually lying in 5-50% room humidity, according to a substance [3] with corresponding water coverages from 1 to 3 monolayers and more. For organic substances the positive role of water is usually assigned to preventing deactivation of active sites by generated organic intermediates. This explanation seems to be less suitable for CO because it is hardly to propose generation of stable intermediates in CO oxidation process. The more likely cause is that adsorbed water contribute to formation of active oxygen forms (O_2^{2-}, $O_2^{-}\cdot$, $HO_2\cdot$, H_2O_2 and other) from gaseous oxygen since that amount of photosorbed oxygen is enhanced in presence of adsorbed water [4].

From these materials it is easy to suggest that on TiO_2 the process of carbon monoxide photocatalytic oxidation is greatly influenced by adsorbed water and active oxygen species generated from gaseous oxygen play key role in the increase of CO photocatalytic oxidation rate.

4 Conclusions

It was found that under moderate coverages adsorbed water unexpectedly increase the rate of photocatalytic CO oxidation on TiO_2.

These results allow to suggest that for TiO_2 in presence of adsorbed water, CO oxidation mechanism is distinct from that one for fully degassed TiO_2 surface and forms of photosorbed oxygen play key role in oxidation rate enhancement.

References

[1] N.G. Petrik, G.A. Kimmel, *J. Phys. Chem. Lett.* 2013. V. 4, P. 344−349.
[2] H. Einaga, M. Harada, S. Futamura, T. Ibusukiet, *J. Phys. Chem. B.* 107 (2003) 9290.
[3] J. Zhao, X. Yang, *Building and Environment.* 38 (2003) 645,
T.N. Obee, R.T. Brown, *Environ. Sci. Technol.* 29 (1995) 1223.
[4] G. Munuera, V. Rives-Arnau, A. Saucedo, *J.C.S. Faraday I.* 75 (1979). 736.

V-PP83

Supported Polymer-Metal Comlexes for n-Octane Oxidation by Hydrogen Peroxide under Mild Conditions

Zharmagambetova A.K., Auyezkhanova A.S.*, Altynbekova K.A.

1 D.Sokolskii Institute of Organic Catalysis & Electrochemistry, Almaty, Kazakhstan

* a.assemgul@mail.ru

Keywords: bimetallic catalysts, polymer-modifier catalysts, n-octane, hydrogen peroxide oxidation

1 Introduction

Recently the development of new highly efficient and selective catalysts for hydrocarbon oxidation under mild conditions is of theoretical and practical interest. Biomimetic approach to the preparation of catalysts for the above mentioned process is one of the promising directions of research [1-3]. Organic compounds, surfactants and polymers can be used as ligands in the design of metal complex catalysts.

In this paper we present the results of the development of bimetallic nickel-iron polymer-containing catalysts supported on sorbents and their use as catalysts for oxidation of n-octane by hydrogen peroxide under mild conditions.

2 Experimental/methodology

The catalysts were prepared by adsorption of $NiCl_2$ and $K_4[Fe(CN)_6]$ from water solution on inorganic sorbents such as alumina, silica-alumina, silica, zinc oxide modified with the polymer. The total percentage content of the active phase was 1% at a ratio of Ni:Fe = 1:3. Water-soluble polyhexamethylene guanidine (PHMG) was used as polymer modifier.

Oxidation of n-octane was carried out in a thermostated glass reactor in acetonitrile at 40ºC and atmospheric pressure [4]. The duration of the process was 240 minutes. The oxidant was 30% aqueous solution of hydrogen peroxide. Analysis of the reaction products was carried out by chromatography ("Crystal-2000", Russia).

The catalysts were studied by electron microscopy.

3 Results and discussion

In the beginning the developed catalysts were tested in the process of hydrogen peroxide decomposition. The maximum rate of the reaction ($6.5 \cdot 10^{-4}$ mol/s) was achieved on the 1% Co-Ni-PHMG/Al_2O_3 catalyst. Low reaction rate was observed on the catalyst supported on zinc oxide.

Chromatographic analysis of the reaction products indicates the formation of alcohols and ketones. The highest degree of conversion of the substrate is observed in the presence of 1% Co-Fe (1:3)-PHMG/Al_2O_3 catalyst. The lowest activity showed 1%Co-Fe(1:3)-PHMG /ZnO (Table 1).

Table 1. Oxidation of n-octane on 1% Co-Fe(1:3)-PHMG/support catalysts.
Reaction conditions: $[H_2O_2] = 0.31 \cdot 10^2$ mole/l, CH_3CN - 5 ml, T = 40ºC, P = 1 atm, duration - 360 min.

Catalyst	Products of reaction		Conversion, %	Selectivity,%
	ol %	one %		
1% Co-Fe(1:3)-PHMG/Al_2O_3	10.0	2.2	12.2	$S_{\Sigma ol}$ – 82.0
1% Co-Fe(1:3)-PHMG/AlSi	6.1	3.2	9.3	$S_{\Sigma ol}$ – 65.6
1% Co-Fe(1:3)-PHMG/SiO_2	4.0	2.4	6.4	$S_{\Sigma ol}$ – 62.5
1% Co-Fe(1:3)-PHMG/Al_2O_3	1.3	0.5	1.8	$S_{\Sigma ol}$ – 72.2

The developed cobalt-iron catalyst was studied by TEM. According to TEM images, the metal particles of 10 nm are evenly spread in the polymers which are fixed on the surface of Al_2O_3 (Figure 1).

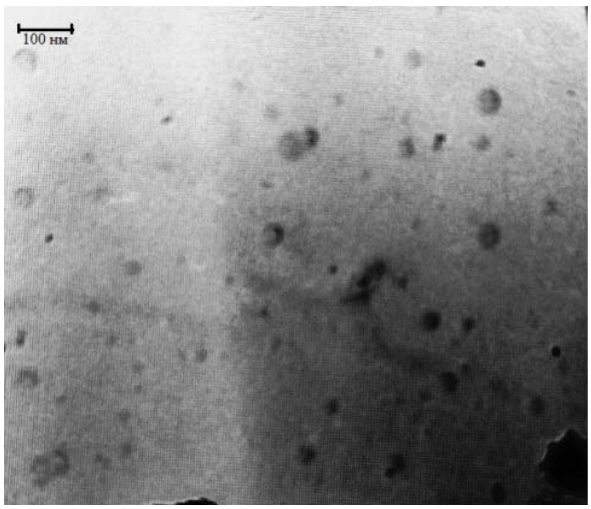

Fig. 1. TEM images of 1% Co-Fe(1:3)-PHMG/Al_2O_3

4 Conclusions

Thus, the developed heterogenized catalysts based on polymer-metal complexes fixed on inorganic sorbents are active in both decomposition of H_2O_2, and the reaction of n-octane oxidation under mild conditions. The optimum catalyst for n-octane oxidation is PHMG-containing cobalt-iron complexes supported on alumina. n-Octane conversion was 12.2%.

References

[1] E. A. Karakhanov, A. L. Maksimov, E. A. Ivanova, *Russian Chemical Bulletin.* 4 (2007) 621-630.
[2] E.I. Karasevich. *Oxidation Communications.* 33 (2010) 741-781.
[3] J.T. Groves. *Nature Chemistry*. 6 (2014) 89-91.
[4] P.Z. Safarov, O.I. Kartonozhkina, A.K. Zharmagambetova, *Izvestia NAS RK, ser. Chem. (Proceedings of Kazakh National Academy of Sciences, in Russian)* 3 (2005) 3-10.

V-PP84

Sorption of Sulfur-Containing Molecules on CuZnAl-O Catalysts from Model and Straight-Run Diesel Fuel

Yashnik S.A.[1], Salnikov A.V.[1*], Kerzhentsev M.A.[1], Ismagilov Z.R.[1,2], Jin Y.[3], Koseoglu O.R.[3]

1 - Boreskov Institute of Catalysis SB RAS, Novosibirsk, Russia
2 - Institute of Coal Chemistry and Material Science SB RAS, Kemerovo, Russia
3 - Saudi Aramco, Research and Development Center, Dhahran, Kingdom of Saudi Arabia

* salnikov@catalysis.ru

Keywords: oxidative desulfurization, diesel fuel, CuZnAl-O catalyst, dibenzothiophene, adsorption

1 Introduction

During the last decade the requirements to the limits of sulfur content in motor fuels have been constantly toughened. In accordance with the current emission standard EURO-V, the content of sulfur in diesel fuel should not exceed 10 ppmw [1]. The sulfur compounds become more resistant to hydrodesulfurization with increasing boiling point, as the dominant compound class changes from thiols, sulfides and thiophene in the naphtha to substituted benzothiophenic derivatives in the distillate [2]. In the vacuum gas oil and vacuum residue, the sulfur is contained mainly in compounds of the dibenzothiophene family. One of perspective methods for diesel fuels desulfurization is selective oxidation of their sulfur-containing compounds over catalysts with oxygen (ODS). During this process sulfide and heterocyclic sulfur-compound transform to sulfur dioxide, and hydrocarbon fragments are oxidized to carbon dioxide and water [1]. According to [3] CuZnAl-O catalysts can be promising for ODS. Their catalytic properties in oxidation of sulfur-containing compounds may be connected also with high affinity of some of their components – namely Cu and Zn to sulfur. The goal of this work is to study sulfur adsorption capacity of CuZnAl-O in a model (DBT-Toluene) and a straight-run diesel fuel. Catalyst textural properties, XRD and chemical composition as well as conditions of sulfur removal from spent catalyst have been studied with the aim to elucidate main correlations between stages of adsorption and oxidation of sulfur compounds of diesel fuel.

2 Experimental

CuZnAl-O catalysts were prepared by the precipitation [5]. The chemical composition of the catalysts was studied by AAS-ICP. Cu content was 45 wt.%, Zn 25 wt.%. Textural properties of the spent catalysts were studied by N_2 adsorption at 77 K, using an adsorption unit ASAP-2400. The XRD composition of catalysts was studied in HZG-4C diffractometer. Temperature-programmed reduction with hydrogen (TPR-H_2) was carried out in a flow reactor equipped with a thermal conductivity detector at 25-800^{o}C, with heating rate 10^o/min. DTA-TG-MS was studied using PG NETZSCH STA 409. Analysis of gas products was carried out in a mass spectrometer NETZSCH QMS 403C. CHNS analysis was performed by Vario MicroCube.

The catalysts were tested in the sorption process in model hydrocarbon fuel containing 0.1wt.% S as dibenzothiophene (DBT) in toluene and 1.0 wt.% S in straight-run diesel fuel. Samples were studied in a flow reactor placed in a furnace with a fluidized bed of quartz sand. A loading of the catalyst granules (0.5-1.0 mm) was 2 g. Adsorption was studied at GHSW = 3000 h^{-1}, WHSV = 6 h^{-1}, temperature was 380oC for model fuel and 470^{o}C for diesel fuel. These conditions were found optimal for ODS [6]. Liquid product was collected in the reflux condenser cooled to 5°C. Analysis of total sulfur was performed using a sulfur analyzer ASE-2. GC analysis was performed in a GC Crystal-2000M equipped with TCD and flame photometric detector.

3 Results and discussion

XRD study has shown that the fresh CuZnAl-O catalyst contains CuO and ZnO phases as well as highly dispersed spinel phase. According to TPR-H_2 results the catalyst is reduced by hydrogen in a single step at a temperature of 200-300°C, and are characterized by the fact that the H_2 uptake is slightly less than that of stoichiometric reduction of Cu(II) of the catalyst composition. Comparison with [4] allows us to conclude that Cu is in the Cu(II) state and likely located in CuO and $CuAl_2O_4$. The sorption time of sulfur compounds was about 1 and 3 hours for the model fuel and the diesel fuel, respectively. The total amount of sulfur adsorbed during this time is presented in Table (M_s^{sum}, g/g). At identical experimental conditions, the sorption capacity of the catalyst with respect to sulfur depended on the nature of sulfur compound. Taking into consideration the composition of sulfur compounds of diesel fuel, we concluded that the sorption capacity decreased with the change of sulfur-compound family from thiophene to DBT.

XRD composition of CuZnAl-O catalyst changes during experiments on sulfur sorption, the only changes observed in XRD are reduction of Cu (II) to Cu_2O and CuO. The CHNS analysis showed that the spent catalysts have sulfur and carbon accumulated on the catalyst surface (Table). According to DTA-TG-MS analysis, thiophene and its derivatives (prevailing in straight-run diesel fuel) adsorb on the catalyst surface via the mechanism of the chemical adsorption. Hence, the sulfur in spent catalysts is represented mainly by metal sulfates, which are decomposed at 700-850°C with the evolution of SO_2. At the same time, DBT and its derivatives are adsorbed via the physical adsorption mechanism. In this case, sulfur and carbon are removed from the surface simultaneously at temperature ca. 200°C as a mixture of CO_2, SO_3 and H_2O. Carbon deposits are products of the hydrocarbon condensation, they are oxidized into CO_2 and H_2O at 200-500°C.

Table. Physico-chemical properties of spent catalysts.

#	Fuel	M_s^{sum}, g/g	CHNS data, wt.%			Textural properties		
			C	H	S	S_{BET}, m^2/g	$V_\Sigma(N_2)$, cm^3/g	D_{BJH}, nm
1	DBT(0.1wt.% S)-Toluene	$0.35 \cdot 10^{-2}$	1.75	0.49	0.45	79.5	0.20	10.3
2	Diesel Fuel (1.0 wt.% S)	$1.6 \cdot 10^{-2}$	8.39	0.47	2.71	57	0.20	14.2

4 Conclusions

It has been shown that CuZnAl-O catalysts actually possess sorption capacity. The trend of an increase of the sorption capacity of sulfur at the transition from DBT derivatives to simpler sulfur containing molecules has been observed. DTA-TG-MS analysis has shown that sulfur on the catalyst surface is represented by adsorbed sulfur compounds or sulfides/polysulfides and sulfates of metals. Carbon deposits on the surface are products of the hydrocarbon condensation

Acknowledgements

This work was studied by financially supported ARAMCO under contract No.6600022642. The authors thank L. M. Khitsova and V.Y. Malysheva for the DTA-TG-MS analysis.

References

[1] Z. Ismagilov, S. Yashnik, M. Kerzhentsev, V. Parmon, A.Bourane, F.M. Al-Shahrani, A.A. Hajji, and O.R. Koseoglu. *Catalysis Reviews: Science and Engineering* 53 (2011).
[2] A. Stanislaus, A. Marafi, Mohan S. Rana. *Catalysis Today* 153 (2010).
[3] L. Gao, Y. Tang, Q. Xue, Ye Liu and Y. Lu. *Energy and Fuels* 23 (2009).
[4] J.A. Rodriguez, J.Y. Kim, J.C. Hanson, M. Perez, A.I. Frenkel *Catalysis Letters* 85 (2003).
[5] US Patent Application 20130026072, A.Bourane, O.R. Koseoglu, Z.R. Ismagilov, S.A. Yashnik, M.A. Kerzhentsev, V.N. Parmon, 2013-01-31
[6] US Patent Application 20130028822, A.Bourane, O.R. Koseoglu, Z.R. Ismagilov, S.A. Yashnik, M.A. Kerzhentsev, V.N. Parmon, 2013-01-31.

V-PP85

Role of Electron-Acceptor Sites during Destructive Sorption of CF_2Cl_2 over MgO and VO_x/MgO Aerogels

Shuvarakova E.I.[1,2*], Bedilo A.F.[1,2], Mishakov I.V.[1,3], Vedyagin A.A.[1,3]

1 - Boreskov Institute of Catalysis SB RAS, Novosibirsk, Russia
2 - Novosibirsk Institute of Technology, Moscow State University of Design and Technology, Novosibirsk, Russia
3 - Novosibirsk State Technical University, Novosibirsk, Russia

* Katerina.shuv@gmail.com

Keywords: destructive sorption, EPR, MgO, aerogels, halocarbons

1 Introduction

Halocarbons, especially the ones containing no hydrogen atoms, are extremely stable and are believed to destroy the Earth ozone layer. Therefore, development of active destructive sorbents capable of their decomposition without harming the environment is of substantial practical interest. Particular interesting nanocrystalline mesoporous materials with high reactivity are aerogel-prepared alkaline-earth metal oxides prepared by sol–gel method followed by drying in an autoclave. This method yields samples with high specific surface areas and developed mesoporous structure due to the release of organic solvents under supercritical conditions avoiding the detrimental effect of the surface tension on the texture of the materials [1].

Small amounts of vanadium added to nanocrystalline MgO aerogels were shown to promote their activity in destructive sorption of halocarbons. This reaction is characterized by a prolonged induction period, which is considerably shortened after the vanadium addition [1, 2]. However, the origin of this induction period remained mysterious. In this study we characterized electron-donor and electron-acceptor sites [3] during the destructive sorption reaction of dichlorodifluoromethane on the surface of MgO and VO_x/MgO aerogels.

2 Experimental/methodology

VOx·MgO aerogels were prepared using an earlier reported method [1]. Mg ribbon was dissolved in methanol, diluted with toluene and slowly hydrolyzed with added dropwise distilled water. When a clear gel was prepared, vanadium (V) triisopropoxide oxide was added to the gel and mixed. The obtained mixed gel was dried in an autoclave to remove the solvents under supercritical conditions followed by calcination in air at 500°C.

In the reaction with CF_2Cl_2, the samples of nanocrystalline MgO aerogels with vanadium concentrations 0, 1, 5, 10 and 26 wt. % were studied. The sample was loaded into an ampoule used for EPR measurements and activated in 30 ml/min nitrogen flow for 1 hour. Then the reaction with CF_2Cl_2 was carried out with the following spin probe adsorption. Perylene and anthracene dissolved in toluene ($2*10^{-2}$ M) were used as spin probes for characterization of weak electron-acceptor sites. 1,3,5-Trinitrobenzene was used as the spin probe for characterization of electron-donor sites. The concentration of active sites was measured by EPR immediately after adsorption and after heating for 18 hours at 80°C.

3 Results and discussion

It was found that addition of vanadium had a catalytic effect on the interaction of nanocrystalline MgO aerogels with halocarbons, accelerating the formation of the active sites on the surface of the nanoparticles. The electron-acceptor sites on the surface of initial samples of MgO and VOx/MgO were not observed. Their concentration gradually increased during the

induction period, reaching a clearly defined maximum in the active state when the rapid topochemical destructive sorption reaction occurred. As the vanadium concentration was increased, the time for reaching the active state decreased. It was shown that even small amounts of vanadia added homogeneously as a mixed aerogel or as a separate phase had a catalytic effect on the MgO reaction with CF_2Cl_2.

A good correlation was observed between the rate of the halocarbon destructive sorption and the concentration of weak electron-acceptor sites characterized using anthracene or perylene as spin probes (Fig. 1). The concentration of electron-donor sites decreased during reaction with CF_2Cl_2 and did not correlate with reactivity. These results clearly demonstrate that weak electron-acceptor sites are accumulated on the MgO surface during the induction period of its reaction with CF_2Cl_2. Apparently such sites are somehow related to fluorine and/or chlorine atoms accumulated on the MgO surface during the induction period.

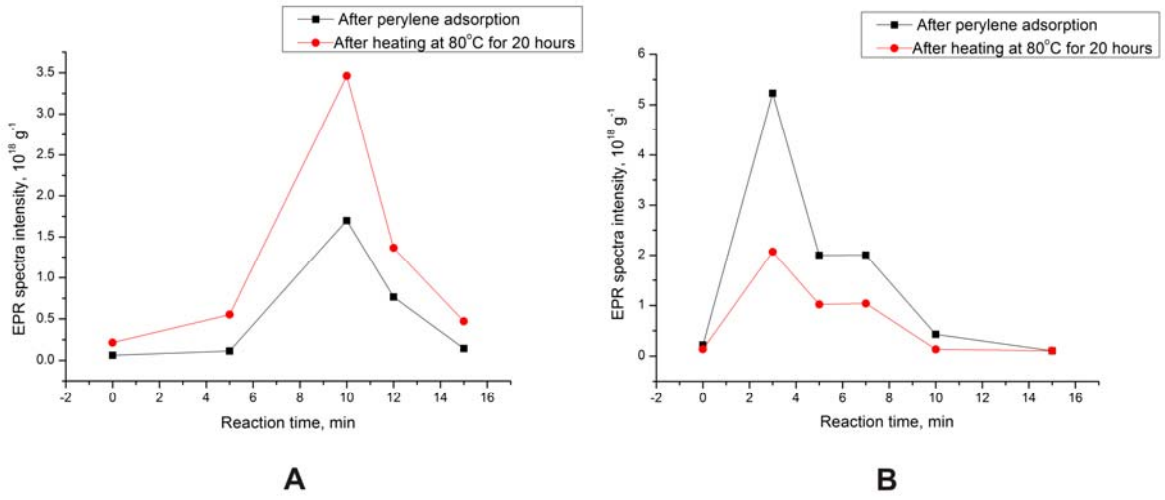

Fig. 1. Dependence of the intensities of EPR spectra observed after perylene adsorption from toluene solution on AP-MgO (A) and AP-MgO modified with 5% of vanadium (B) on time on their reaction with CF_2Cl_2.

4 Conclusions

The obtained results clearly demonstrate that surface electron-acceptor sites are formed during the induction period of reaction between nanocrystalline pure or modified MgO samples and halocarbons and account for the beginning of the fast bulk reaction. This process seems to be one of rare examples when surface active sites are shown to be responsible for a bulk solid-state reaction.

Acknowledgements

This study was supported in part by Russian Foundation for Basic Research (Grants 13-03-12227-ofi_m and 15-03-08070-a).

References

[1] E.V. Ilyina, I.V. Mishakov, A.A. Vedyagin, A.F. Bedilo, K.J. Klabunde *Microporous Mesoporous Mater.* 175 (2013) 76.

[2] A.F. Bedilo, E.I. Shuvarakova, A.M. Volodin, E.V. Ilyina, I.V. Mishakov, A.A. Vedyagin, V.V. Chesnokov, D.S. Heroux and K.J. Klabunde.: *J. Phys. Chem. C,* 118 (2014) 13715.

[3] A.F. Bedilo, E.I. Shuvarakova, A.A. Rybinskaya, D.A. Medvedev, *J. Phys. Chem. C* 118 (2014) 15779.

V-PP86

The Synergistic Effect for [RedOx + Zeolite] CombiCat in NH_3-SCR: Contributions of Different Pathways to the Overall Mechanism

Mytareva A.I.[1*], Stakheev A.Yu.[1], Bokarev D.A.[1], Kustov A.L.[2], Thøgersen J.R.[2]

1 - Zelinsky Institute of Organic Chemistry, Moscow, Russia
2 - Research & Development, Haldor Topsøe A/S, Lyngby, Denmark

* aimytareva@gmail.com

Keywords: synergistic effect, Fast SCR, Standard SCR, ceria–zirconia, zeolite

1 Introduction

Recently we have shown that combined catalysts (CombiCats) with high performance in selective catalytic reduction of NO_x (SCR NO_x) can be obtained by mixing RedOx component and zeolite [1]. For [CeO_2-ZrO_2 + FeBeta] and [Mn/CeO_2-ZrO_2 + FeBeta] compositions a pronounced synergistic effect was observed and the catalytic activity of the CombiCats significantly exceeds activity of the individual components. It was suggested that the synergistic effect over CombiCats stems from the "bifunctional pathway" comprising NO oxidation over RedOx component followed by Fast SCR on FeBeta.

$$2\ NO + O_2 \leftrightarrow 2\ NO_2$$

$$NO + NO_2 + 2\ NH_3 \rightarrow 2\ N_2 + 3\ H_2O$$

The "bifunctional pathway" operates in parallel with the Standard SCR pathways over Mn/CeO_2-ZrO_2 and FeBeta.

$$2\ NO + 2\ NH_3 + ½\ O_2 \rightarrow 2\ N_2 + 3\ H_2O$$

Thus, the SCR activity of the [Mn/CeO_2-ZrO_2 + FeBeta] CombiCat is the summation of three pathways. In this study we attempted to discriminate semi-quantitatively their contributions. For this purpose NH_3-SCR activities of individual components and CombiCats were measured. CombiCats were prepared by mixing Mn-Ce/CeO_2-ZrO_2 with FeBeta (high Standard and Fast SCR activity), H-Beta (only Fast SCR activity), USY and SiO_2-Al_2O_3 (no activity in Standard and Fast SCR) in order to easily distinguish Standard SCR and "bifunctional pathway" contributions.

2 Experimental/methodology

SCR activities of composite catalysts prepared by mixing zeolites (H-Beta, FeBeta, USY, SiO_2-Al_2O_3) with Mn-Ce/$Ce_{0.75}Zr_{0.25}O_2$ (loaded with 8 wt% Mn and 8 wt% Ce by incipient wetness co-impregnation) at 1/3 volumetric ratio were measured. Feed gas composition: 500 ppm NO, 600 ppm NH_3, 10 vol% O_2 and 6 vol% H_2O balanced with N_2.

3 Results and discussion

NH_3-SCR performances of the individual components and CombiCats based on Mn-Ce/$Ce_{0.75}Zr_{0.25}O_2$ are compared in Fig. 1. Individual Mn-Ce/$Ce_{0.75}Zr_{0.25}O_2$ demonstrates a reasonable NH_3-SCR activity at 100–180°C, however at T_{react}>180°C NO_x conversion passes through a maximum and rapidly decreases. Standard SCR activities of H-Beta, USY and SiO_2-Al_2O_3 are negligible in whole temperature region, while NO_x conversion over FeBeta exceeds 60% at 500°C.

Mixing Mn-Ce/$Ce_{0.75}Zr_{0.25}O_2$ with FeBeta results in a significant change of the overall reaction pattern. Firstly, NO_x conversion is improved within 100–200°C, though at T_{react}>250°C

steep decrease in NO_x conversion is observed. Presumably, this is the result of competitive NH_3 oxidation over Mn-Ce/Ce-Zr component.

Remarkably, [Mn-Ce/Ce-Zr + FeBeta] and [Mn-Ce/Ce-Zr + H-Beta] demonstrate essentially identical performance despite very different Standard SCR activities of FeBeta and H-Beta. This observation suggests primary importance of Fast SCR activities of zeolite components which are similar [2].

When we used components inactive in Fast SCR (USY and SiO_2-Al_2O_3) performance of CombiCat is essentially identical to that of individual Mn-Ce/CeO_2-ZrO_2 and no synergistic effect is observed. A minor improvement of NO_x conversion can be attributed to marginal Fast SCR activity of USY and SiO_2-Al_2O_3, however the overall effect is incomparable with that observed for [Mn-Ce/Ce-Zr + H-Beta] composition.

Quantitative analysis of NO_x conversion data allowed us to distinguish contributions of three main pathways. At 100 – 180ºC SCR proceeds through Standard SCR on Mn-Ce/Ce-Zr and "bifunctional pathway" on [Mn-Ce/Ce-Zr + zeolite]. In the temperature range of 210 – 410ºC "bifunctional pathway" predominates. Contribution of Standard SCR activity of FeBeta is minor and becomes apparent at T_{react}>250ºC as indicated by somewhat better NO_x conversion over [Mn-Ce/Ce-Zr + FeBeta] as compared to [Mn-Ce/Ce-Zr + H-Beta].

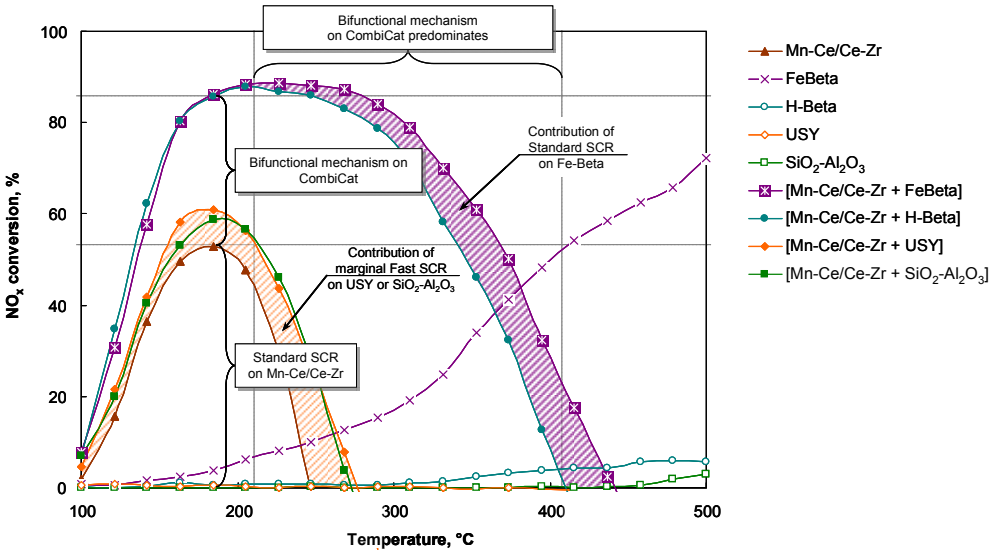

Fig. 1. NH_3-SCR activities of individual components and CombiCats.

4 Conclusions

Three different pathways in NH_3-SCR on CombiCats were discriminated. It was shown, that Fast SCR activity of zeolite component is a prerequisite of synergistic effect, while Standard SCR activity plays a minor role in the overall performance of CombiCats.

Acknowledgements

The support of Russian Foundation for Basic Research (Grant: 15-03-07802 A) is gratefully acknowledged. A. Mytareva is grateful to Haldor Topsøe A/S for financial support in the framework of Ph.D. student support programme.

References

[1] A.Yu. Stakheev, G.N. Baeva, G.O. Bragina, N.S. Teleguina, A.L. Kustov, M. Grill, J.R. Thøgersen, *Top. Catal.* 56(1-8) (2013) 427

[2] R. Pérez Vélez, I. Ellmers, H. Huang, U. Bentrup, V. Schünemann, W. Grünert, A. Brückner, *J. Catal.* 316 (2014) 103

V-PP87

Conversion of Lignin Catalyzed with Sub- and Supercritical Water

Bogdan V.I.[1,2*], Koklin A.E.[1], Kustov A.L.[2,1], Lunin V.V.[2,1]

1 - Zelinsky Institute of Organic Chemistry, Russian Academy of Sciences, Moscow, Russia
2 - Moscow State University, Chemical Department, Moscow, Russia

* vibogdan@gmail.com

Keywords: lignin, lignosulphonate, depolymerisation, sub- and supercritical water

1 Introduction

Research in the field of processing of plant biomass is of considerable interest for developing technologies based on renewable raw materials. The main components of biomass are polysaccharides, such as cellulose, hemicellulose, and lignin. Lignin is a framework biopolymer consisting of guaiacylpropane, syringylpropane, and p-hydroxyphenylpropane structural units linked by C–O and C–C bonds. Lignocellulose materials are wastes of industry, agriculture, forestry, and household. Currently there are no technologies of complete processing of lignin-containing waste to produce useful products; instead, in some cases, extremely environmentally unfriendly processes, involving mineral acids and alkalis, are used. From this point of view, studies of the conversion of lignin in sub- and supercritical water, which could form the basis for developing energy effective and environmentally friendly processes of recycling of anthropogenic waste, in particular from the pulp and paper and hydrolysis industries, is of paramount importance.

2 Experimental

Conversion of sodium lignosulphonate (LS) is studied in sub- and supercritical water (SCW) in the temperature range 200-430°C at 220 atm and the residence times 2.5-10 min. Soluble products of the LS depolymerization are analyzed using HPLC and GC-MS. Thermogravimetric, elemental, IR and NMR spectral analyses of insoluble products of LS conversion are carried out [1] .

3 Results and discussions

The interaction of SLS with sub- and supercritical water produced a dark brown precipitate and water soluble phenolic compounds. It is shown that methoxyaril ether bonds and aromatic structures do not undergo any destruction in SCW. The formation of insoluble precipitate is related to decarboxylation and desulfonation of lignin polymeric fragments. The soluble part the conversion products of LS in SCW consists of the unreacted fragments of the LS macromolecule that retained hydrophilic S- and O-containing groups. It also includes soluble products of the depolymerization of lignin having phenylpropane fragments in their structure, such as vanillin, guaiacol, etc., and the products of secondary transformations: low molecular weight acids and aldehydes. The products of the depolymerization of LS predominantly consist of compounds containing guaiacyl aromatic structure. The chemical diversity of the products is due to transformations of only the propyl fragment of the structural unit of lignin under hydrothermal conditions.

Hydrogenolysis of C–C bonds, dehydrogenation, and oxidation provide the formation of alkyl, olefin, alcohol, aldehyde, and ketone substituents of the guaiacyl structure in the products of conversion of lignin in SCW. In addition, the depolymerization products contain phenol and 4-(propene-3)phenol. As shown above, the hydrolysis of aryl–alkyl ether bonds in the lignin

model compounds under the influence of supercritical water takes a long time (5 min). This suggests that, during treatment of LS with SCW, phenol is formed from p-hydroxyphenylpropane structural fragments. The absence of branched alkyl substituents at the aromatic nucleus in the conversion products of LS indicates that the process of depolymerization is associated with the rupture of ether bonds between structural fragments of lignosulfonate. In [2, 3], the conversion of lignin from cedar and beech wood in SCW is discussed. The authors believe that the β-O-4 (alkyl–aryl) ether bond is easily cleaved in supercritical water.

To establish how the parameters of the process (temperature, reaction time) influence the yield of monomeric products, we determined the content of vanillin, guaiacol, and phenol in the products of the conversion of LS by HPLC. During treatment of SLS in subcritical water (200–373°C), guaiacol and phenol are virtually not formed. The yield of vanillin decreases as the temperature increases from 200 to 320°C. It is known that ether bonds are hydrolyzed when catalyzed with acids. However, despite the low value of pKw, 11.0–11.5, no depolymerization of LS is observed. This is because the hydrolysis of ether bonds of lignin competes with condensation reactions. With increasing temperature and acidity of the medium, the hydrolysis speeds up, as does the condensation reactions, with the latter becoming predominant under certain conditions. Therefore, when wood is treated with concentrated mineral acids, only polysaccharides pass into a soluble state, whereas lignin is produced in the form of an insoluble residue, because the condensation reaction dominate the hydrolytic cleavage [4]. With a further increase in temperature above the critical point of water, the yield of conversion products increases by an order of magnitude. The increase in the depolymerization rate may be associated with a change in the depolymerization mechanism. In supercritical water, free radical reactions dominate over ionic reactions [5]. Another factor affecting the product yield is the reaction time. It increases from 2.5 to 10 min (410°C, 220 atm), the concentration of vanillin and guaiacol increase from 4.5 · 10–4 to 7.6 · 10–4 mol/l and from 7.4 · 10–4 to 1.8 · 10–3 mol/l, respectively. However, the yield of phenol decreases from 9.5 · 10–4 mol/l to 0, which can be attributed to the participation of phenol in the formation of new bonds between the aromatic structures.

Thus, varying the temperature and reaction time makes it possible to adjust the rate and extent of LS depolymerization. In the subcritical region, the conversion proceeds through hydrolysis. In the supercritical region, it is dominated by free radical processes.

Acknowledgements

This work was supported by the Russian Foundation for Basic Research (grant # 11-03-12190-ofi_m and 13-03-12266-ofi_m) and by EnviroCat Ltd. (Russia).

References

[1] A.G. Khudoshin, V.V. Lunin, V.I. Bogdan, *Russian J. Physical Chemistry B.* 5 (2011) 1069.
[2] K. Ehara, S. Saka, H. Kawamoto, *J. Wood Sci.* 48 (2002) 320.
[3] K. Ehara, D. Takada, Sh. Saka, *J. Wood Sci.* 51 (2005) 256.
[4] V.I. Azarov, A.V. Burov, A.V. Obolenskaya, Chemistry of Wood and Synthetic Polymers: A Textbook (St. Petersburg State Forest Technical Academy, St. Petersburg, 1999) [in Russian].
[5] N. Akiya, Ph.E. Savage, *Chem. Rev.* 102 (2002) 2725.

V-PP88

Aqueous Phase Hydrodeoxygenation of Phenol on Bifunctional Catalyst Systems: Ru/C and Acids

Koklin A.E.[1*], Kondratyuk A.V.[1,2], Lunin V.V.[1,2], Bogdan V.I.[1,2]

1 - Zelinsky Institute of Organic Chemistry, Russian Academy of Sciences, Moscow, Russia
2 - Lomonosov Moscow State University, Moscow, Russia

* akoklin@gmail.com

Keywords: hydrodeoxygenation, hydrogenation, phenol, aqueous phase, catalysis, ruthenium, nafion

1 Introduction

Biomass is considered as a perspective feedstock for production of fuels and chemicals through the depletion of fossil fuels and the increasing concern over environmental protection. Biomass is exposed to pyrolysis and liquefaction with formation of bio-oil. It contains a lot of phenolic compounds together with high water concentration. Bio-oil hydrodeoxygenation is one of available process for removal of oxygenates and increasing of its value. Highly selective hydrodeoxygenation of phenolic compounds to cycloalkanes in aqueous phase has been reported using bifunctional catalysts in batch reactor [1]. For enhancing efficiency and for more convenient operation of process, it is reasonable to use flow reactors.

2 Experimental

The hydrodeoxygenation of phenol was carried out in a fixed-bed vertical flow high-pressure reactor (an inner diameter of 0.4 cm and a length of 25 cm). Phenol conversion was performed at 150–250°C and 7.5 MPa. A ruthenium catalyst supported on active carbon (Ru/C, 5 wt % Ru) was prepared by the wetness impregnation method. The catalyst volume was 0.5 cm^3 (0.21 g), and the remaining volume of the reactor was filled with quartz particles. As the acid function phosphoric acid (0.5 wt %) in an initial solution of phenol or DuPont Nafion SAC-13 (0.5 $см^3$) in the form of a mechanical mixture with Ru/C were used. Phenol conversion was studied in aqueous solution with a concentration of 1 wt % (0.106 M). A scheme of the laboratory setup and experimental details were presented in [2]. The phenol solution was supplied at a rate of 0.2 or 1.0 ml/min, keeping the ratio of phenol-to-hydrogen at 1:15 or 1:30 respectively. Liquid and gaseous products were analyzed by gas chromatography (using capillary column Thermo TR-5MS 30 m × 0.25 mm) and were identified with chromatograph–mass spectrometer system (Focus GC/DSQII, Thermo Fisher Scientific, the same column). Internal standard butanol-1 was used to determine the product concentration in aqueous phase. C_2-C_6 hydrocarbons including cyclohexane were detected only in gas phase.

3 Results and discussions

Phenol was selected as the model compound of bio-oil to investigate the hydrodeoxygenation process in aqueous solutions. The major products obtained when the aqueous phenol solution and hydrogen were passed over supported ruthenium catalyst were cyclohexanol and cyclohexane. C_2-C_6 hydrocarbons were also formed in small amount as a result of hydrocracking of cyclohexane. The formation of benzene was not detected under studied conditions. Some results of the phenol transformation on catalysts Ru/C + acid are presented in Table 1. After shift of solution acidity from neutral to acidic using H_3PO_4 (pH 2.5) the complete conversion of phenol was obtained. This was accompanied by changing in the composition of products: cyclohexanone disappeared and a yield of cyclohexane increased. The same trend was observed using a solid acid as Nafion. The reaction pathway for conversion of phenol to hydrocarbons in aqueous phase is shown in Fig. 1. The following sequence of

reactions takes place. Initially hydrogenation of phenol leads to cyclohexanone and cyclohexanol. Further the alcohol undergoes dehydration to form cyclohexene which quickly hydrogenates to cyclohexane. Also ring opening was observed with the formation of light hydrocarbons C_2-C_6.

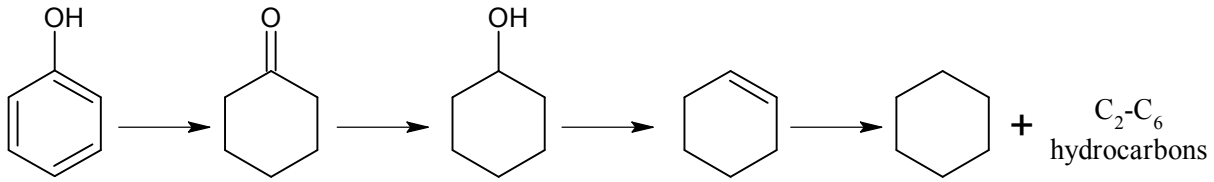

Fig. 1. Schema of aqueous phase hydrodeoxygenation of phenol on Ru/C + acid

Table 1. Aqueous phase hydrodeoxygenation of phenol

Catalyst	Feed flow-rate, g $g_{Ru/C}^{-1}$ h^{-1}	*T*, °C	Conv., %	Selectivity, %			
				Cyclo-hexanol	Cyclo-hexanone	Cyclo-hexane	C_2-C_6
Ru/C	2.9	200	93	83	5	9	3
Ru/C - H_3PO_4	2.9	200	100	76	0	19	5
Ru/C - H_3PO_4	0.6	150	100	51	0	46	3
Ru/C - H_3PO_4	0.6	250	100	0	0	34	66
Ru/C - Nafion	0.6	150	100	81	0	16	3

4 Conclusions

Phenol, a lignin monomer model compound, was converted to cyclohexane and fully hydrogenated hydrocarbons using bifunctional catalyst systems (Ru/C and acid) in a fixed-bed flow reactor. Addition acid function as mineral acid (H_3PO_4) or solid acid (Nafion) to the ruthenium catalyst leads to increasing of cyclohexane selectivity at a complete conversion of phenol. It indicates the acidity of the catalyst system is the determinative factor for cyclohexane formation from phenol in an aqueous medium.

Acknowledgements

This work was supported by the Russian Foundation for Basic Research (grant # 11-03-12190-ofi_m and 13-03-12266-ofi_m) and by EnviroCat Ltd. (Russia).

References

[1] C. Zhao, J. He, A.A. Lemonidou, X.Li, J.A. Lercher, *J. Catal.* 280 (2011) 8.
[2] A.E. Koklin, T.A. Klimenko, A.V. Kondratyuk, V.V. Lunin, V.I. Bogdan, *Kinetics and Catalysis*. 56 (2015) 84.

V-PP89

Kinetics and Mechanism of the Total Oxidation of CO and p-Xylene and their Mixtures on Supported Copper Catalysts

Gaidai N.A.[1*], Luu C.L.[2], Nguyen T.[3], Hoang T.C.[2], Ha C.A.[3], Ho S.T.[2], Agafonov Yu.A.[1], Lapidus A.L.[1]

1 - JSC Managing company "Biochemical Holding "Orgkhim", Nizhniy Novgorod, Russia
2 - Institute of Chemical Technology, Vietnam Academy of Science and Technology, Ho Chi Minh, Vietnam
3 - HoChiMinhCity University of Technology, Ho Chi Minh, Vietnam

* gaidai@server.ioc.ac.ru

Keywords: carbon, monoxide, xylene, spported, copper, catalysts, platinum, total, oxidation

1 Introduction

One of effective and economic ways for the removal of toxic impurities of chemical plants is their total catalytic oxidation. Supported copper catalysts are active ones in total oxidation of CO and aromatic hydrocarbons. Their activity can be increased at addition of small amounts of noble metals. Such catalysts can be more active than ones containing only noble metal [1, 2]. Kinetics of CO oxidation over Cu-catalysts can be corresponded to Langmuir-Hinshelwood [3] (when adsorbed CO and O_2 (in molecular or atom forms) interact on the surface in the slow step), or Eley-Rideal [4] (the interaction proceeds between an adsorbed molecule/particle and a molecule from gas), or Mars-van Krevelen [5, 6] (adsorbed on copper CO interacts with lattice oxygen) mechanisms. It was proposed an adsorption [7] or Mars-van Krevelen [8] mechanisms for total oxidation of xylene on oxide catalysts. This work is devoted to the study of kinetics and mechanism of separate and mutual CO and p-xylene oxidation on Cu/CeO_2 catalysts without and with Pt.

2 Experimental

Catalysts were prepared by the urea nitrates combustion method. $Ce(NO_3)_3.6H_2O$, $Cu(NO_3)_2.3H_2O$, (H_2PtCl_6 complex for Pt-catalysts) and urea $CO(NH_2)_2$ were mixed in a minimum volume of distilled water in order to obtain a transparent solution. The catalysts were investigated by TPR, XRD, TEM, BET, EDS-methods. The kinetic experiments were carried out in a gradientless flow circulating system at atmospheric pressure, the temperature range was 125-250°C. The values of initial partial pressure of carbon monoxide (P^o_{CO}), p-xylene (P^o_{xyl}), oxygen ($P^o_{O_2}$), and specially added carbon dioxide ($P^o_{CO_2}$) and vapor water ($P^o_{H_2O}$) were varied in the range: 2.5÷20; 2.1÷11.3, 35÷210, 0-25 and 0÷ 32 hPa, respectively. Transient response method was applied to study the process mechanism. Relaxation curves, describing a transition of the system to a new steady state, were obtained by a jump change of the corresponding concentrations. The installation contained 3 independent lines and was connected with mass-spectrometer. The residence time was 5 s. For all the experiments the relaxation time was lower than the turnover time. This allowed characterizing the observed relaxations as own ones.

3 Results and Discussion

A change of Cu and Pt concentrations in the limit of 5.0-10.0 and 0.05-0.3 % (wt.), respectively, showed that the optimal contents of Cu and Pt were 7.5 and 0.1%, respectively, for

CO and xylene oxidation. These catalysts are denoted as Cu/Ce and PtCu/Ce. The data of TPR showed that the presence of Pt resulted in the increase of the dispersity of Cu and its reduction degree. The rate of CO oxidation (r_{CO}) was considerably more than the rate of xylene oxidation ($r_{xyl.}$) on both catalysts. The form of kinetic equation for CO oxidation was equal on Cu/Ce and PtCu/Ce, but the values of the constants were different. Too most can tell about xylene oxidation. The following equations were obtained for separate oxidation of CO and p-xylene:

$$r_{CO} = \frac{k_{CO} P_{CO} P_{O_2}^{0.5}}{P_{O_2}^{0,5} + k_1 P_{CO_2}}, \qquad r_{xyl.} = \frac{k_{xyl.} P_{xyl.} P_{O_2}^{0.5}}{P_{O_2}^{0.5} + k_2 P_{xyl.} + k_3 P_{H_2O} + k_4 P_{CO_2}}.$$

These equations are corresponded to the proceeding the reactions in the middle surface coverage. The presence of Pt increased the values of all constants but the constants in the numerators were increased in more extent than in denominators, that's why the rates of CO and xylene oxidation were higher on PtCu/Ce. Xylene had a big influence on CO oxidation at mutual oxidation but CO little affected on xylene oxidation. The presence of small amounts of xylene (2.1 hPa) considerably decreased the rate of CO oxidation, the further increase of xylene (till 11.3 hPa) had a little influence on CO oxidation. Complex mutual influence exerted at oxidation of such different in nature substances. New intermediate compounds, which are oxidized with low rate in comparison with separate oxidation, are formed at mutual oxidation of CO and xylene. This resulted in a change of process kinetics.

Data of unstationary investigations showed that the introduction of Pt resulted in the increase of bond strength of all reaction components. Data showed that carbon monoxide and xylene as well as oxygen participated in the reaction as adsorbed species and the steps of their adsorption were quick. It was shown that at CO oxidation the amount of adsorbed O_2 was more than CO and at xylene oxidation the amount of adsorbed xylene exceeded adsorbed O_2, what agreed with stationary kinetic data. The lattice oxygen made a little contribution in the reactions. The step-schemes of CO and xylene oxidation were proposed.

Thus, obtained data showed that oxidation of CO and xylene and their mixtures proceeded on adsorption mechanism.

4 Conclusions

Active supported copper catalysts were proposed for CO and xylene oxidation, their properties, kinetics and mechanism of total oxidation of CO and xylene were studied.

Acknowledgements

The work is supported by grant of Russian Fund of Fundamental Investigations (№13-03-93001 Viet_a) and Vietnam National Foundation for Science and Technology Development (NAFOSTED) under grant No.104.03-2012.60.

References

[1] T.S.Mozer, F.B.Passos, *Intern. J.Hydrogen Energy*. 36 (2011) 13369.
[2] J.Kugai, T.Moriya, S.Seino, T.Nakagawa, Y.Ohkubo, H.Nitani, H.Daimon, T.A.Yamamoto, *Intern. J.Hydrogen Energy.* 37 (2012) 4787.
[3] J-Q.Lu, C-X.Sun, N.Li, A-P.Jia., M-F.Luo, *Appl. Surf. Sci.* 287 (2013) 124.
[4] S.Ordóñez, L.Bello, H.Sastre, *Appl. Catal. B*. 38 (2002) 139.
[5] A.D Benedetto, G.Landy, L.Lisi, G.Russo, *Appl.Catal. B.* 142-143 (2013) 169.
[6] X.Xi, S.Ma, J-F.Chen, Y.Zhang, *J Environ. Chem. Eng.* 2 (2012) 1011.
[7] I.A.Kulesh, M.S.Kharson, E.A.Kastzman, S.L.Kiperman, *Kinetika i Kataliz*. 36 (1995) 691.
[8] J.A.Juusola, R.F.Mann, L.Dowine, *J.Catal.* 17 (1970) 106.

V-PP90

Catalytic Flow Syntheses of Oligopeptides in the Glycine – Trimetaphosphate – Imidazole System

Serov N.Yu.*, Shtyrlin V.G.

Kazan Federal University, A.M. Butlerov Chemistry Institute, Kazan, Russia

* Serov.Nikita@gmail.com

Keywords: flow, chemistry, glycine, trimetaphosphate, imidazole, oligopeptides, kinetics

1 Introduction

One of the most important and unsolved problems of modern science is prebiotic peptide synthesis. Despite of numerous research efforts, the optimal conditions, kinetic parameters and mechanisms of peptide synthesis in early stages of biochemical evolution are still not established. To develop the prebiotic peptide synthesis problem the oligopeptides formation kinetics in the glycine – sodium trimetaphosphate – imidazole system in water has been investigated in flow conditions at different temperatures and pH values. It should be mentioned that trimetaphosphate has been firstly used for the peptide synthesis by Rabinowitz et al. [1] and imidazole was introduced only for the solid state oligoglycines production [2].

2 Experimental

The syntheses have been performed using Syrris ASIA-330 flow chemistry system in the following cyclic regime: after passing through the heated tube reactor reaction mixture returned to the stirred vessel where the desired pH value has been maintained with automatic titrator Metrohm Basic Titrino 794 by adding sodium hydroxide solution. Then the reaction mixture was pumped to the tube reactor again. The flow rate and temperature of the tube reactor have been strictly controlled. The kinetics of the processes has been monitored by the HPLC and NMR methods. Probes from the flow system have been automatically taken, diluted with eluent, injected into the Knauer Smartline HPLC system, and analyzed by the ion-pairing reversed-phase chromatography. For several experimental runs probes have been manually taken and diluted with D_2O. The ^{1}H and ^{31}P NMR spectra of these probes have been recorded on a Bruker Avance III 400 NMR spectrometer.

3 Results and discussion

The formation of significant amounts of glycylglycine and diglycylglycine has been established. Kinetic dependences for the oligopeptides concentrations approach plateau through 10-30 hours. Glycylglycine yields after 20 hours are 10-50 % (depends on conditions), diglycylglycine yields reach 2 %. Oligopeptides yields increase with temperature increasing from 45 to 75 °C. Final dipeptide yields at pH 9.5 and 10.5 are the same and at pH 11.5 nearly two times smaller. At the same time tripeptide yields at pH 9.5 are more than two times higher than that at pH 10.5 and at pH 11.5 only minor amounts of the tripeptide are observed. Figure 1 shows the examples of kinetic dependences for the glycylglycine and diglycylglycine concentrations at different pH values. Some dependency of the oligopeptides yields from the tube reactor residence time has been established.

The formation of the glycine N-triphosphate, cyclic glycylphosphate, and imidazole N-phosphates as intermediates in the oligopepides synthesis has been observed by the ^{1}H and ^{31}P NMR method.

Several experimental runs have been performed without imidazole for comparison. The small catalytic effect of imidazole on the dipeptide formation has been revealed. At the same

time imidazole addition has great influence on the diglycylglycine yield.

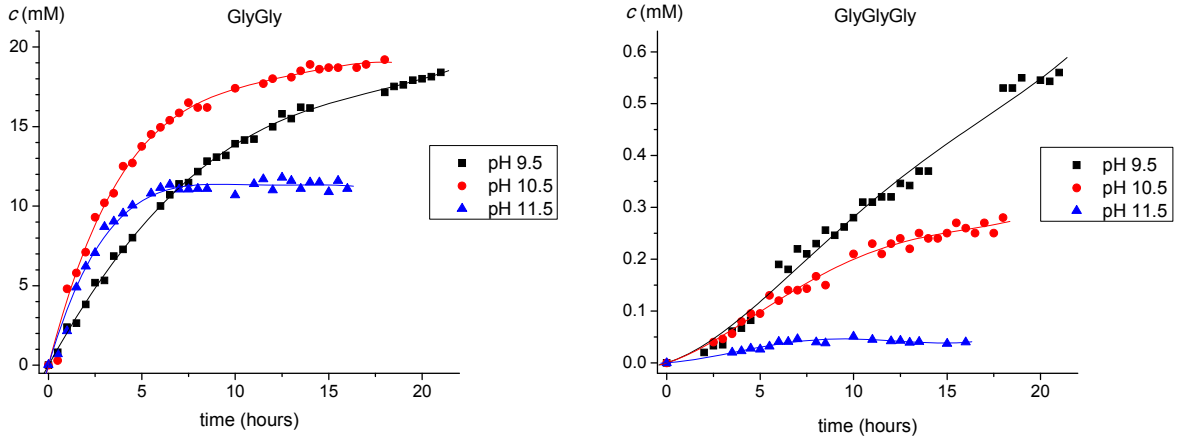

Fig. 1. Time dependences of glycylglycine and diglycylglycine concentrations for the glycine – trimetaphosphate – imidazole (1:1:1) system; all initial concentrations are equal 0.1 M; the tube reactor residence time is 1 hour; $T = 60$ °C.

Kinetic dependences obtained have been modelled with the MAT DS computer program from V.N. Govorukhin [3]. The kinetic parameters of oligopeptides formation reactions have been calculated. On the basis of the literature, experimental data, and mathematical modelling the oligoglycines formation mechanism has been proposed. For validation of this mechanism the structures of reagents, products, intermediates, and some transition states have been optimized by the GAMESS program [4] on different computation levels. The polarisable continuum model (C-PCM) [5] was used to account for solvent effects.

4 Conclusions

The oligopeptides synthesis kinetics in the glycine – sodium trimethaphosphate – imidazole system has been investigated in flow regime at different temperatures and pH values. The synthesis conditions were optimized. The reaction mechanism was proposed and grounded on the basis of quantum-chemical computation results. The system investigated may be used as a good model for peptide synthesis in prebiotic conditions.

Acknowledgements

The authors thank Dr. Kh.R. Khayarov for the registration of the ^{1}H and ^{31}P NMR spectra and helpful discussion.

References

[1] J. Rabinowitz, J. Flores, R. Kresbach, G. Rogers, *Nature.* 224 (1969) 795.
[2] H. Sawai, L.E. Orgel, *J. Mol. Evol.* 6 (1975) 185.
[3] http://kvm.math.rsu.ru/matds/index.htm
[4] M.W. Schmidt, K.K. Baldridge, J.A. Boatz, S.T. Elbert, M.S. Gordon, J.H. Jensen, S. Koseki, N. Matsunaga, K.A. Nguyen, S. Su, T.L. Windus, M. Dupuis, J.A. Montgomery, *J. Comput. Chem.* 14 (1993) 1347.
[5] M. Cossi, N. Rega, G. Scalmani, V. Barone, *J. Comput. Chem.* 24 (2003) 669.

V-PP91

A Study of Glycolysis of Polyethylene Terephthalate Waste in the Presence of Catalyst for the Production of Bis(2-Hydroxyethyl)Terephthalate

Rakhmatullina A.P.[1], Bogachyova T.M.[2], Satbaeva N.S.[1*]

1 - Kazan National Research Technological University, Department of Synthetic Rubber, Kazan, Russia

2 - Kazan National Research Technological University, Department of General Chemical Engineering, Kazan, Russia

* nazgul-satbaeva@mail.ru

Keywords: waste polyethylene terephthalate, glycolysis, ethylene, glycol, zinc, acetate

1 Introduction

Chemical recycling of plastic waste is mainly focused on the use of polyethylene terephthalate (PET) waste. This type of recycling is economical and environmentally safe way – depolimerization (glycolysis) of PET bis(2-hydroxyethyl)terephthalate, which can be used in resynthesis of PET. Another common method of chemical recycling of PET is directed on producing an inexpensive unsaturated polyester resin used in other areas of the chemical industry.

2 The experimental

The investigation of recycling of PET wastes by glycolysis in the presence of a catalyst - zinc acetate was carried out. Glycolysis of PET was conducted in two ways: in the temperature range of 140-180°C and with using microwave irradiation (MW). Catalyst concentration ranged from 0.125 to 1.0 wt%. The reaction was carried out until the complete decomposition of polymer. The resulting product was identified by IR spectroscopy and titrimetric by determination of hydroxyl number.

3 Results and discussion

Investigating the degradation of PET in the presence of zinc acetate (1 wt%) in the temperature range of 140-180°C showed that the increased temperature results in an increase in the conversion of PET (fig. 1).

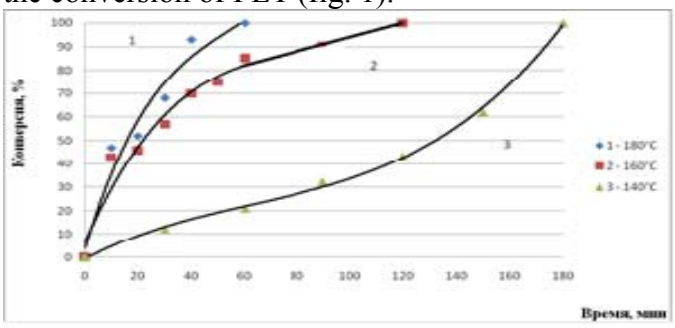

Figure 1. Conversion of PET in the presence of zinc acetate (1 wt%) in function of time for different temperatures, °C: 1 - 180; 2 - 160; 3 - 140

Investigation of dosage of catalyst (fig. 2) showed that increasing the concentration of the catalyst leads to decrease in time of destruction of polymer.

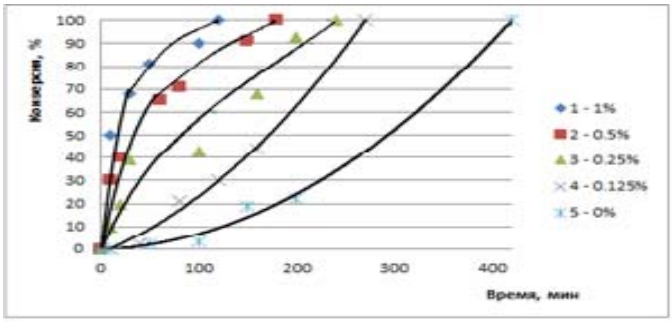

Figure 2. Conversion of PET in function of time for different catalyst concentration (at 160°C), %: 1 - 1; 2 -0.5; 3 - 0.25; 4 - 0.125; 5 - 0

A significant improvement in the quality of occurring chemical recycling of PET and the shortening of the required thermal effects can be achieved by using the energy of the electromagnetic field of MW range.

According to our results the same time of reaction (60 min.) leads to the same yield of the monomer at a different concentration of catalyst - 1.0; 0.5 and 0.25 wt% (power of MW - 450W). Therefore, an optimal concentration of catalyst is 0.25 wt%.

The resulting product was studied by IR spectroscopy (fig. 3); key functional groups are identified. The infrared spectrum of product was compared with the spectrum of bis-2-hydroxyethyl terephthalate: they are almost identical.

Figure 3. IR spectrum of product of PET degradation – bis-2-hydroxyethyl terephthalate

4 Conclusion

1. The optimum conditions of degradation of PET: temperature degradation, concentration of catalyst, the ratio of initial components were estimated.

2. It was identified by IR spectroscopy that the resulting product is a bis-2-hydroxyethyl terephthalate and it can be used as a valuable raw material for synthesis of biodegradable polymers for medical purposes.

Acknowledgements

The study was financially supported by the Russian Ministry of Education within the basic part of the state task.

V-PP92

The Aluminum Oxide Active Catalyst's Regeneration Using Supercritical Carbon Dioxide

Sagdeev A.[1], Galimova A.[1*], Gumerov F.[2]

1 - Nizhnekamsk Chemical Technological Institute (Branch Institute) of the Kazan National Research Technological University, Nizhnekamsk, Russia

2 - Federal State Budgetary Educational Institution of Higher Professional Education "Kazan National Research Technological University", Kazan, Russia

* tukhvatova-albinka@mail.ru

Keywords: catalyst regeneration, supercritical, fluid extraction, cosolvent

1 Introduction

Activated aluminum oxide is used as a catalyst for the dehydration of methyl phenyl carbinol. During the dehydration reaction of methyl phenyl carbinol the carbon deposition occurs on the catalyst surface which reduces the catalyst activity [1].

2 Results and discussion

Activated aluminum oxide catalyst was regenerated at temperature of 423 K and within the pressure range 10÷30 MPa [2].

As it was mentioned above if modifiers 0.1 - 20 wt % such as methanol, ethanol etc. are added the dissolution ability of SC CO_2 is increased On this basis the impact of various co-solvents on the catalyst mass during the regeneration was studied. Chloroform, methanol, acetone and dimethylsulfoxide (DMSO) were chosen as co-solvents. Co-solvents concentration varied from 1 to 9 wt. %. The optimum value of co-solvent concentration falls within the range of 1.5–2.5%.

The analysis of catalyst mass change in the course of its regeneration using the modified SC carbon dioxide with the optimum co-solvent concentration was made at the temperature of T= 423 K and pressure P = 20 MPa (Fig. 1). . It is seen from the diagram that the regeneration efficiency with the DMSO adding has increased by 140% due to polar compounds removal.

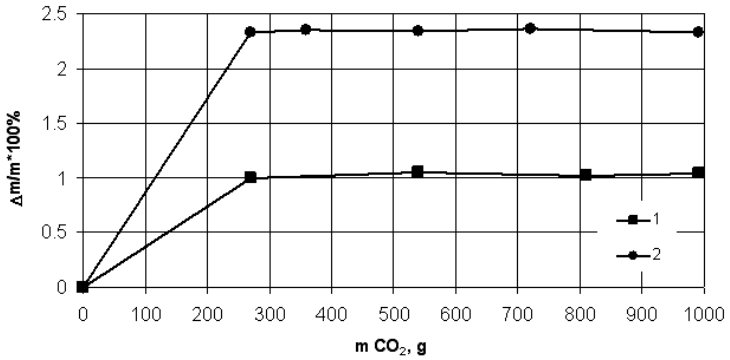

Fig. 1. Change in the mass of the catalyst in the course of its regeneration versus the mass of extractant used (modified CO_2) : 1 – SC CO_2; 2 – SC CO_2 + 2% DMSO

This data is supported by the IR spectra of the deactivating compounds for catalysts samples regenerated with pure and modified SC CO_2 (Fig. 2).

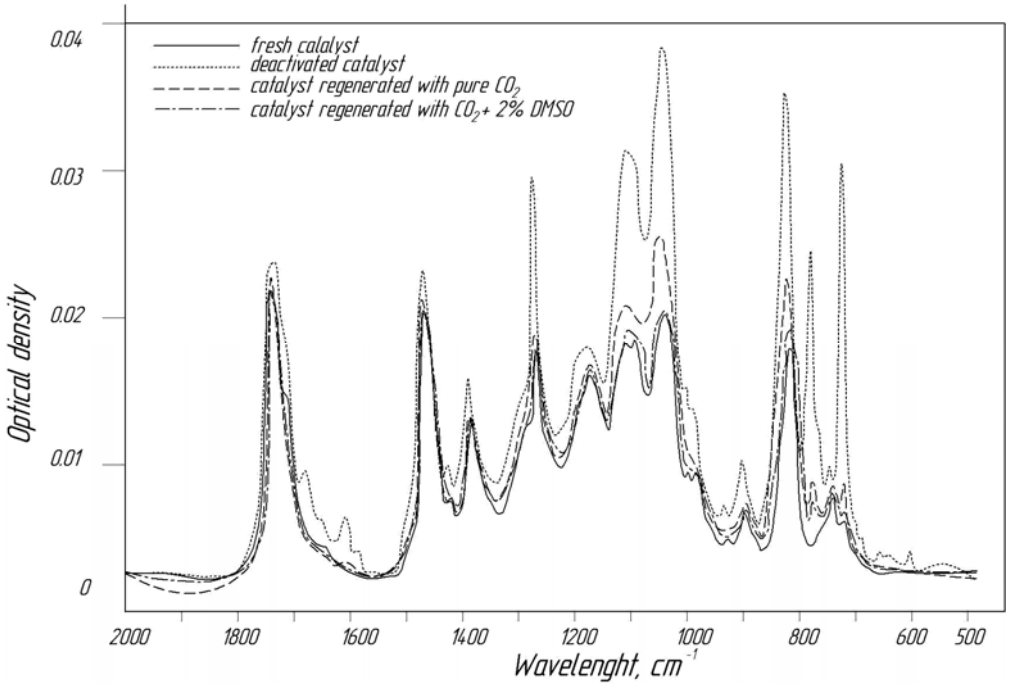

Fig. 2. The IR spectra of the deactivating compounds for catalysts samples regenerated with pure and modified SC CO_2

In this case the conversion rate of methyl phenyl carbinol (methyl phenyl carbinol conversion) and selectivity to styrene were the criteria for activated aluminum oxide catalyst activity evaluation. The results of methyl phenyl carbinol conversion and activated aluminum oxide catalyst selectivity analysis are in the Table

	Fresh catalyst	**Catalyst regenerated by air-steam mixture**	**Catalyst regenerated by pure supercritical CO_2**
MPC Conversion, %	99.80	99.69	99.77
Styrene Formation Selectivity (towards decomposed MPC), % mol.	100	86.99	93.97

4 Conclusions

Regenerated catalyst MPC conversion value, i.e. the catalyst regenerated activity, proves the SCFE method efficiency for removal of contaminants from the surface of activated alumina.

References

[1] P.Kirpichnikov, L.Averko-Antonovich, Yu. Averko-Antonovich. Chemistry and technology of synthetic rubber. L.: Himiya, 1975. 480 pages.

[2] Gumerov, F.M. Regeneration of the Catalysts by Supercritical Fluid Extraction / F.M. Gumerov, A.A. Sagdeev, A.T. Galimova, K.A. Sagdeev // International Journal of Analytical Mass Spectrometry and Chromatography. – 2014. – V. 2, P. 1-14.

V-PP93

The Composite Rubberized Material with Coated Photocatalytic Layer

Salyakhova M.A.*, Pukhacheva E.N., Zaripova V.M., Uvaev V.V.

Open Joint Stock Company "Kazan Chemical Research Institute", Kazan, Russia

* milya_salyah@mail.ru

Keywords: titanium, dioxide, self-decontamination, photocatalytically, active antibacterial properties, the composite rubberized material

1 Introduction

Protective clothing made from rubberized material provides protection from toxic, corrosive chemicals and flame. Materials are used for the manufacture of protective clothing for workers in the chemical, oil and gas, metallurgical industry, working in conditions of flame action and carrying out various rescue operations. After infection by toxic chemicals protective clothing requires decontamination by special solutions, which makes certain load on the environment - pollution from wastewater.

A photocatalytic decomposition of these substances adsorbed on the surface of rubberized material is an alternative to this method of decontamination of chemical clothing.

2 Experimental

The composite rubberized protective material is developed. It comprises a fabric basis, a polymeric rubber coating and a thin film layer which contains the photocatalytically active titanium dioxide with a particle size of 10-15 nm. The photocatalytically active titanium dioxide obtained at the laboratory of the Boreskov Institute of Catalysis was used for produce the rubberized composite material. The coating of photocatalytic layer does not reduce protective properties of the rubberized material.

Figure 1 shows the micrograph of the composite rubberized material obtained by the universal digital high definition video microscope HIROX KN-7700, Japan (an increase of 140 times).

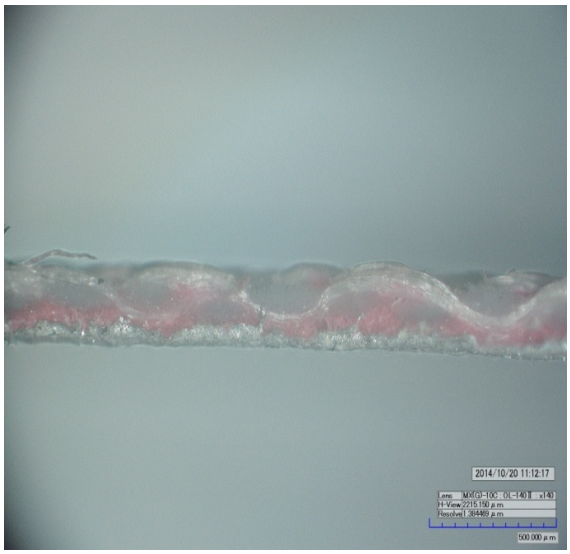

Fig. 1 The micrograph of the composite rubberized material

We have determined the photocatalytic activity of the composite rubberized material by

the oxidation reaction of methyl orange indicator at UV irradiation with falling radiation power of 10 mW/cm^2. The results of determining the degree of methyl orange indicator decomposition at UV irradiation are shown in Table 1.

Table 1 - The degree of methyl orange indicator decomposition at UV irradiation of the composite rubberized material

Specimen	Ratio Rubber: TiO2	The degree of methyl orange indicator decomposition,%
TiO_2	------	45
Material 1	1:1	27
Material 2	1:2	40
Material 3	1:3	53

3 Results and discussion

We have evaluated antibacterial properties of the material coated with titanium dioxide by the standard method, which has concluded at the study of the sensitivity of microorganisms, placed on a solid nutrient medium - agar, to the action of the photocatalyst at UV irradiation. Test culture: gram of positive spore forming bacterium Bacillus subtilis and gram of negative non spore forming bacterium Escherichia coli. The method is based on the formation of so-called zones of inhibition around the test specimen material. Tests have shown that the bacteria do not grow at UV irradiation for 3-4 hours, the growth delay zone of Bacillus subtilis culture is 3.5 cm and the growth delay zone of Escherichia coli culture is 3,5 cm (Figure 2).

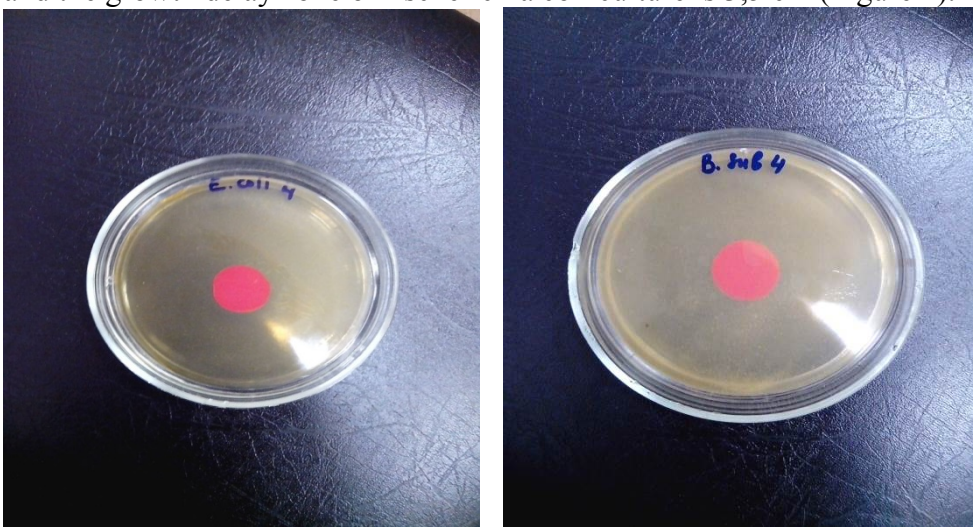

Fig. 2 - The growth delay zone of Escherichia coli culture and the growth delay zone of Bacillus subtilis culture

3 Conclusions

Using of materials with photocatalyst will allow to decontaminate the outer surface of clothing after exposure to toxic chemicals and bacteria without special decontaminating solutions by UV or sunlight irradiation, i.e. as a result of self-decontamination.

V-PP94

Electromagnetic Catalytic Reactor of Water Treating from Oils and Hydrocarbons

Bachurikhin A.L.[1,2*], Efendiev M.S.[1,2]

1 - Zelinsky N.D. Institute of Organic Chemistry of the Russian Academy of Science, Moscow, Russia

2 - OJSC DagNefteProduct, Makhachkala, Russia

* mesckalin@yandex.ru

Keywords: clearing of water from oil pollution, hydrocarbons, electromagnetic processing

1 Introduction

The problem of clearing of water resources from oil pollution is rather actual now. Annual total emission of mineral oil in the seas and oceans as a result of consequences of extraction and emergencies is estimated on different sources, including the National academy of sciences the USA on the average from 6 up to 8 million tons. Nevertheless, the problem of operative and effective liquidation of consequences of similar emissions is far from the decision in view of low efficiency of existing technological decisions, and including, absence high-efficiency the reactor equipment. The majority of known processes of clearing of water environments from oil pollution is based on use the methods of oxidation **[1]**, flotation **[2]**, absorbtion **[3]**, and also methods of biological clearing **[4]**. Under the total characteristics, including productivity, a degree of clearing, simplicity of technological decisions, the economic and power efficiency, the mentioned ways are conditionally suitable for the decision of similar problems.

3 Experimental

The clearing process of water environments from oil pollution and dangerous hydrocarbons aromatic and olefinic the lines, based on use is developed and tested in industrial scale as basic reactionary unit of the device of electromagnetic processing water environments. The principle of work is based on the phenomenon of acceleration microparticles association of mineral oil in conditions of interaction of an external variable magnetic field with ferromagnetic sorbent which particles have own constant magnetic field. As a result of such interaction there are intensive association processes the hydrocarbonic components being consequence of concentration in places of impacts of ferromagnetic particles of electromagnetic, thermal and mechanical energies. Further, passing through the polysorbtional layers, the integrated particles of hydrocarbons are absorbed much faster, than similar particles of smaller diameter.

Working parameters of a reactor electromagnetic association:

Initial concentration of mineral oil	—	100 ÷ 1 mg/L
Final concentration of mineral oil	—	0,5 ÷ 0,05 mg/L
Working volume of a reactor	—	30 L
Productivity on initial water	—	Up to 100 m3/h
Operating mode	—	Continuous
Working temperature	—	0 ÷ 50ºC
Working pressure	—	0 ÷ 1,0 MPa

Besides direct use of the specified installation during water treating, there are variants of her modification, allowing her use in a number of adjacent tasks of oil extracting and processing. In particular, her use is planned during preliminary processing, tars, bitumen sand, in manufacture of dyes, etc. spheres.

3 Conclusions

The general distinctive characteristics of installation:

1) High efficiency
2) Stability to a high level of pollution of communications (a rust, sand, fine stones)
3) Standardization of a design with an opportunity of fast replacement of elements (a grid, a pipe, nozzles and so forth)
4) Absence of a problem of deterioration in case of use the plastic case of a reactor

Installation has passed industrial tests in a zone of the Caspian pool: Russia, Republic Dagestan.

References

[1] JP 2005246354. Water purification device to remove oil component from kitchen wastewater by ozone. Auth. Koyashiki, Kazuo
[2] RU Pat. 2075452. The method of sewage treatment of slaughterhouses and meat-packing plants. Auth. Zhuravlyov S.G., etc.
[3] RU Pat. 2077493. Method of clearing of potable water. Gajdadymov V.B., etc.
[4] RU Pat. 2076150, Clan bacteria acinetobacter species (bicoccum), used for weeding and water from mineral oil, clan bacteria arthrobacter species, used for weeding and water from mineral oil, clan bacteria rhodococcus species, used for weeding and water from mineral oil, the method of biological clearing of oil pollution (variants), Auth. Murzakov Boris Gerasimovich, etc.

V-PP95

Optimization of Catalytic Gas-To-Liquid Technology for Better Carbon Efficiency

Ermolaev I.S.[1,2*], Ermolaev V.S.[1,2], Mordkovich V.Z.[1,2]

1 - Technological Institute for Superhard and Novel Carbon Materials, Moscow, Russia
2 - INFRA Technology, Moscow, Russia

* ermolaevis@tisnum.ru

Keywords: GTL, Fischer–Tropsch synthesis, synthesis gas, reformer, carbon efficiency

1 Introduction

The prospects of industrial application of Gas-to-Liquid technologies (GTL) depend strongly on the overall carbon efficiency of this complex combination of catalytic processes.

The gas-to-liquids (GTL) technology for liquid hydrocarbons (LHs) production on the basis of Fischer-Tropsch (FT) process includes two main catalytic stages[1]: 1. Conversion of methane into syngas (mixture of CO and H_2); and 2. Fischer-Tropsch synthesis to produce liquid hydrocarbons from the syngas.

The syngas production technology is the most capital-intensive stage, the cost of which is up to 60% of the construction costs of a GTL plant. Selection of technological solutions for the production of syngas is usually determined by the required H_2/CO molar ratio. For FT synthesis, the optimum molar ratio of H_2/CO is 2.0–2.2[2]. This ratio can be obtained using various methods of conversion of hydrocarbon gases.

A combined steam and dry reforming (SDR) as a version of steam reforming is the most common method for syngas production. The injection of carbon dioxide into the steam reformer allows controlling the H_2/CO ratio. It was shown elsewhere[3,4,5] that the efficiency of SDR-including GTL can be controlled by re-circulation technique of FT tail gases, which allows to reach high energy efficiency of GTL process. The alternative methods are represented by more recently developed autothermal reforming (ATR)[2,6,7] and partial oxidation (POX)[2,8], which are used by the most recent industrial GTL plants ORYX GTL by Sasol-Chevron and Pearl GTL by Shell, respectively.

2 Experimental

The purpose of this work is to study the effect of different methods of natural gas-to-syngas conversion with different circulation loops of FT tail gas on the GTL efficiency.

Overall process flow diagram for the GTL process is shown in figure 1, where SC – small circulation loop of tail gas; BC – big circulation loop of tail gas; SBC – stabilized blowdown circulation loop. Simulation of this flow diagram was done by using mathematical models, which allow considering all main steps of this technology.

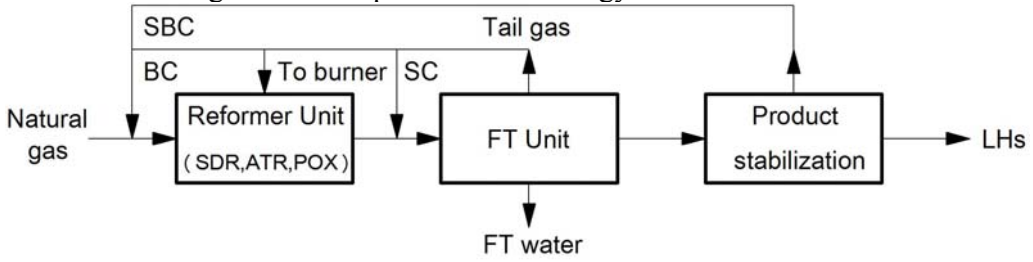

Fig. 1. Overall GTL process flow diagram for the GTL process.

3 Results and discussion

The results of simulation (Fig.2a) show that the best carbon efficiency for no-recirculation flowsheets is achieved in the case of SDR and reaches 52.15%, which is 5.25% higher than the

efficiency of ATR-based flowsheet and 6.05% higher than that of the POX-based flowsheet. However, the carbon efficiency of these processes can be significantly increased by introduction of circulation loops. As a result, the highest carbon efficiency of appr. 63% was demonstrated by the ATR-based flowsheet with combined SBC-SC loop.

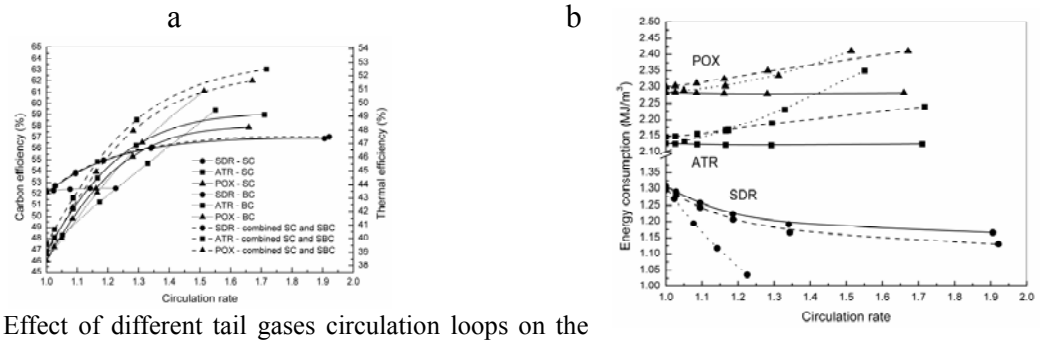

Figure 2. Effect of different tail gases circulation loops on the efficiency (a) and on the energy consumption of GTL process (b) using SDR, ATR and POX.

Application of the most obvious SC loop allows increasing efficiency of technology for all methods of syngas production. The optimum value of the SC re-circulation rate is around 1.3 for all three methods of syngas production and provides the flowsheet carbon efficiency of appr. 56 %. A further increase of the re-circulation rates beyond the optimum value does not lead to significant increase in process efficiency. The efficiency jump provided by the introduction of SC loop is more significant for ATR and POX cases. The reason is related with the main effect of the SC loop, i.e. with the decrease of circulation purge directed to burners. In the case of SDR-based flowsheet it means that the tubular furnace requires more fresh natural gas, which leads to suppression of efficiency growth.

Although the best carbon efficiency is achieved in the case of the ATR with combined SC-SBC loops, the technology choice is burdened by much higher energy expense of ATR- and POX-based processes in comparison with the SDR-based process, which consumes almost two times less energy (Fig.2b). Moreover, the introduction of circulation loops leads to even lower energy consumption values for SDR case. The ATR- and POX-based processes, in contrast, increase their energy consumption with introduction of circulation loops. So high energy consumption is determined by the use of ASU, which consumes almost half of necessary power. The POX-including GTL requires more energy than the ATR-including one just because of higher oxygen consumption and hence more powerful ASU.

4 Conclusions

The results of simulation suggest that the highest carbon efficiency can be reached with ATR- or POX-based GTL. However, it is reasonable to suggest that a better way of producing syngas in GTL technology is combined steam and dry reforming (SDR) due to much lower power consumption. The practical choice of syngas production method can be different due to factors, which lie outside the process energy efficiency, such as cost of reformers, or operating costs, or access to electricity and water, etc.

References

[1] Mordkovich, V.Z. Higher One-Pass Conversion and Productivity in a Scaled-up Pilot GTL Unit. The 10th Natural Gas Conversion Symposium, Doha, Qatar, March 2-7, 2013. Abstracts. #687, 1-2.
[2] Steynberg, A.P.; Dry, M.E. Fischer–Tropsch Technology; Elsevier: Amsterdam, The Netherlands, 2004, Vol. 152.
[3] Maitlis, P.M.; Arno de Klerk. Greener Fischer–Tropsch Processes for Fuels and Feedstocks; Wiley: Weinheim, Germany, 2013.
[4] Ermolaev, I.S.; Ermolaev, V.S.; Mordkovich, V.Z. Substantiating the Selection of Recirculation Circuits in Technology for Synthesizing Liquid Hydrocarbons from Natural Gas. Theoretical Foundations of Chemical Engineering, 2013, Vol. 47, No. 2, 153–158.
[5] Lange, J.-P. Economics of Alkane Conversion. Sustainable Strategies for the Upgrading of Natural Gas. NATO Science Series II: Mathematics, Physics and Chemistry, 2005, 191, 51-83.
[6] Panahi, M.; Rafiee, A.; Skogestad, S.; Hillestad, M. A natural gas to liquid process model for optimal operation. Ind.Eng.Chem. Res. 2012, 51, 425-433.
[7] L.Iandoli, C.; Kjelstrup, S. Exergy analysys of a GTL process based on low-temperature slurry F-T reactor technology with cobalt catalyst. Energy & Fuels, 2007, 21, 2317-2324.
[8] Rostrup-Nielsen, J.; Christiansen, L.J. Concepts in Syngas Manufacture. Catalytic science series, vol. 10; Imperial college press: London, England, 2011.

V-PP96

Catalytic Performance of Ni-Based Catalysts Supported on λ-Al_2O_3-ZrO_2-TiO_2-CeO_2 Composite Oxide for CO_2 Methanation

Abate S.*, Mebrahtu C., Perathoner S, Gentiluomo S., Giorgianni G., Centi G.

University of Messina, Messina, Italy

* abates@unime.it

Keywords: CO_2 methanation, Ni-based catalysts, composite oxides support, metal-support, interaction

1 Introduction

Increasing emissions of carbon dioxide arising from the widespread production of energy from fossil fuels is a critical matter regarding the global warming. The hydrogenation of CO_2 into oxygenates and/or hydrocarbons have been the most investigated reactions to obtain fuels [1]. Among several hydrogenation reactions, methanation of carbon dioxide following the Sabatier reaction is the most advantageous one regarding thermodynamics. Nickel based catalysts are the most studied materials for the latter reaction, because of their high activity and low price, but metal sintering at reaction conditions diminishes their industrial viability [2]. The type of support used for heterogeneous catalysts is an important factor to consider on solving such problems. Metal-support interactions play a role on catalyst performance in terms of the active site dispersion, activity and stability of the catalysts [3]. In this work, we focused our attention on the selection of different supports for Ni-based catalysts with constant Ni content. A series of composite oxide supported Ni-based catalysts were prepared using an impregnation-precipitation method for synthesis of the composite supports and wet impregnation technique to load Ni metal. The as-synthesized catalysts were characterized using X-ray diffraction (XRD), transmission electron microscopy (TEM), N_2-adsorption-desorption isotherms, temperature programmed reduction by H_2 (H_2-TPR) and CO chemisorption.

2 Experimental

I.Commercial γ-Al_2O_3 (Sasol-Puralox SCCa-20/200) was impregnated with aqueous solutions of Zirconyl nitrate, Titanium (IV) isopropoxide and Cerium (III) nitrate hexahydrate salts in different ratios to get the desired percentages. 3 g of each composite support were taken and impregnated with an aqueous solution of Ni $(NO_3)_2.6H_2O$ with a predetermined amount of nickel to obtain a final loading of 20%Ni on the composite supports. The impregnated samples were dried in an oven at 120°C for 16 hrs and calcined at 450°C for 5 hrs. For comparison 3 g of commercial γ-Al_2O_3 was taken and impregnated with 20%Ni and treated equally with the newly synthesized supports.

II.Methanation reaction was performed at atmospheric pressure on pre-reduced catalysts in a pilot reactor with a fixed catalytic bed , 1 cm length and at space velocity of 25000 h^{-1}. 10 mg (i.e. pre mixed with an inert) of catalyst were exposed to a CO_2/H_2 (1:4 ratio) mixture in a temperature range of 300-400°C. Products were analyzed by on-line GC equipped with a TCD detector.

Catalysts were designed as 20%Ni/100% γ-Al_2O_3 = Ni/A; 20%Ni/85% γ-Al_2O_3-5% ZrO_2-5%TiO_2-5%CeO_2 = Ni/C11; 20%Ni/70% γ-Al_2O_3-10% ZrO_2-10%TiO_2-10%CeO_2 = Ni/C12 and

20%Ni/55% γ-Al_2O_3-15% ZrO_2-15%TiO_2-15%CeO_2= Ni/C13.

3 Results and discussion

The significant difference in XRD patterns (fig 1a) of the γ-Al_2O_3 support and the composite oxides confirm the successful loading of the mixed oxides (ZrO_2-TiO_2-CeO_2) in the different percentage range 5-15% for each one. It is also found that the average crystallite size of NiO, calculated from measured values using the Scherrer formula (d= kλ/Bcosθ), is increasing as the percentage of the loaded oxides increased (12 nm-16 nm).

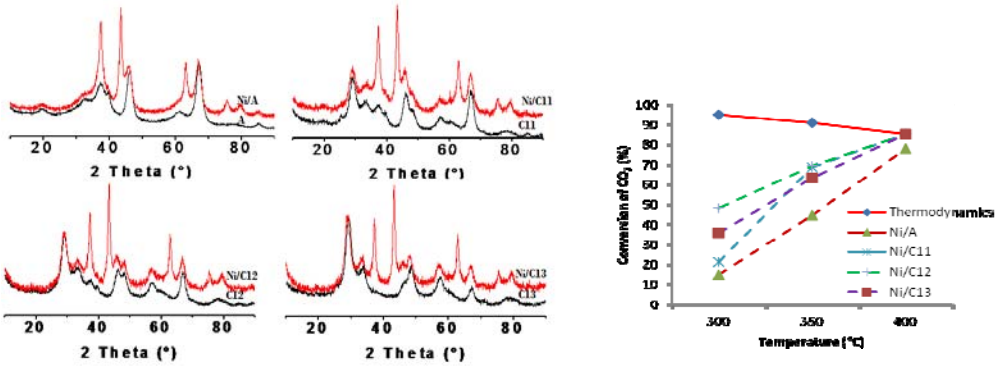

Fig. 1 (a) XRD Pattern of supports compared with the Ni/composite supported catalysts

(b) Effect of composition of the different supports on CO_2 conversion

Fig. 1b shows CO_2 conversion over supported Ni catalysts as a function of reaction temperature. CO_2 conversions gradually increased as the temperature was raised, and at 400°C reached the equilibrium represented by the continuous line in Fig. 1b calculated by taking CO_2 methanation and RWGS reactions into account. Apparently among the catalysts investigated the Ni/C12 catalyst which has 10% of each loading oxide shows better activity (69.36% conversion of CO_2 to CH_4 at 350°C). This might be mainly attributed to the fact that it is the optimum loading of the composite oxides to the conventional support (γ-Al_2O_3) which influence the metal-support interaction inhibiting the incorporation of nickel species into the lattice of γ-Al_2O_3, as confirmed by TPR profile. Furthermore, except for Ni/A and Ni/C13 catalysts no CO was detected at the reactor outlet in all temperature ranges.

4 Conclusions

Methanation of CO_2 has been studied over Ni-based quaternary system composite supported catalysts. Loading of composite oxides to γ-Al_2O_3 was found to be beneficial for the high conversion and stability of the catalysts at relatively low temperatures.

Acknowledgements

The authors would like to thank The HELMETH EU project " Integrated High-Temperature ELectrolysis and Methanation for Effective Power to Gas Conversion" and SINCHEM grant i.e. a Joint Doctorate program selected under the Erasmus Mundus Action 1 Program (FPA 2013-0037).

References

[1] G. Centi, S. Perathoner, *Catal. Today* 148 (2009) 191–205
[2] X. Duan, G. Qian, X. Zhou, Z. Sui, D. Chen, W. Yuan. *Appl Catal B Environ*, 2011, 101, 189-196.

V-PP98

Preparation of Cobalt Titanate Nanoparticles and the Study of their Photocatalytic Behaviors

Fodil Cherif N.[1,2*], Fares A.[1,2], Barama A.[1]

1 - Laboratoire de Matériaux Catalytiques et Catalyse en Chimie Organique, Faculté de Chimie, USTHB, Alger, Algérie

2 - Centre de Recherche Scientifique et Technique en Analyses Physico-Chimiques CRAPC, Tipasa, Algérie

* li162007@yahoo.fr

Keywords: cobalt, titanate, coprecipitation, spinel type structure, water treatement, photocatalysis

1 Introduction

Cobalt titanates are known as useful materials because of the possibility of their technical application as green pigments, catalysts or in electric devices. Three cobalt titanates are known. They are the following: cobalt methatitanate, $CoTiO_3$, having the ilmenite structure, cobalt orthotitanate, Co_2TiO_4, with inverse spinel structure, and pseudobrookite-type cobalt dititanate, $CoTi_2O_5$ [1]. Several methods were used for the preparation of cobalt titanates. The most popular is a solid-state reaction between titanium dioxide and cobalt oxide [2]. Although, this method needs high temperature, long time and small amounts of unreacted initial compounds can be expected. Therefore, the methods based on the synthesis in the solution phase, like precipitation [3], sol-gel [4], or Pechini process [5], providing suitable mixing of the reagents, have recently been studied intensively. Photocatalytic degradation processes have been widely applied as techniques of destruction of organic pollutants in waste water [6]. With an appropriate light irradiation, the photocatalyst generates electron/hole pairs with free electrons produced in the empty conduction band and leaving positive holes in the valence band. These electron/hole pairs are capable of initiating a series of chemical reactions that eventually mineralize the pollutants [7].

2 Experimental/methodology

5 ml of titanium chloride was transferred a beaker, mixed with 100 ml of distilled water (DW). 2.2 g of Cobalt chloride was transferred into a 100 ml beaker and 20 ml of DW was added to it and the contents were stirred for 5 minutes till the solution was clear. These as prepared solutions were stirred together for 30 minutes at 40°C. Then, required quantity of KOH was transferred dropwise by means of burette into the beaker containing the mixed solutions. The contents were continuously stirred after addition of KOH. After 2 hours, the content was filtered, washed with hot DW for 10 to 15 times in order to eliminate chloride ion. After sufficient washing, the precipitate was dried in air oven for 8 hours at 90°C. The dried powder was annealed at 600°C and 900°C for 2 hours in a furnace. Nitrogen adsorption isotherms allow determining the specific surface area by means of the BET method, was recorded on a Quantachrome Novawin 2. XRD patterns of the powders were recorded on Xpert-pro diffractometer, with Cu K_α radiation in the 2θ range from 5 to 90° at 3° min^{-1}. Raman spectroscopy was performed on Horiba Labram HR Evolution. Microstructural characterization was performed by scanning electron microscopy (SEM) in a Zeiss Supra mke apparatus. XPS spectra were recorded with a Thermo VG Scientific ESCALAB 250 spectrometer equipped with a monochromatic Al Kα X-ray source (1486.6 eV and 500 µm spot size). The photocatalytic activity of as prepared catalysts was evaluated by degradation of aqueous solution of methylene blue (MB) under UV light irradiation. 50 mg of catalyst was added to 50 ml of 10 mg/L aqueous

solution of MB. Before illumination, the mixture was stirred in dark for 30 min to achieve adsorption desorption equilibrium between catalyst and dye solution. The solution was exposed to UV light under stirring. At given time intervals, 5 ml of aliquots was withdrawn and centrifuged to remove catalyst. The concentration of methylene blue in aqueous solution was determined with the help of UV-Vis spectrophotometer.

3 Results and discussion

The XRD patterns of the powders calcined at different temperatures (Fig.1 (a)); showed a clear difference in the peak position between the XRD patterns of powders calcined at 600 °C and 900 °C. Pure cobalt titanate phase (Co_2TiO_4) with inverse spinel structure was obtained at 900 °C. The main lines of Co_2TiO_4 (JCPDS PDF 39-1410) were clearly identified. The patterns also indicate that higher calcinations temperatures promote an increase in crystallite size. The values of crystallite size are listed in table 1. The XPS samples surveys (Fig.1 (b)) indicate that cobalt, titanium and oxygen are the major components on the surface of theses powders.

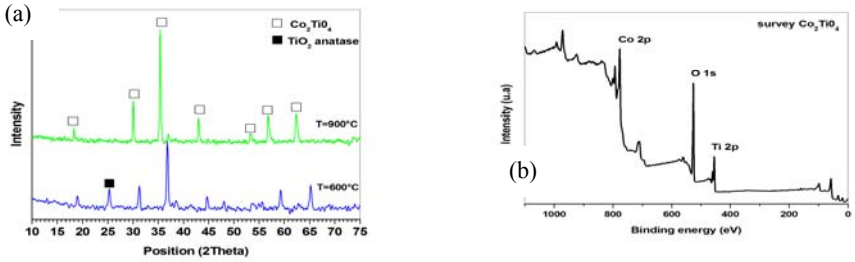

Fig.1. (a) XRD patterns of powder obtained at 600 °C and 900 °C. (b) XPS survey of powder calcined at 900°C.

Table 1. The phase, crystallites grain sizes and surface BET of coprecipited samples.

Catalysts	Phase	Phase (%)	Cs (nm) XRD	S_{BET} (m^2/g)	Lattice parameter (Å)
600°C	TiO_2 Co_3O_4	10 90	29 36	67	a=b= 4.975; c= 2.95 a=b=c= 8.088
900°C	Co_2TiO_4	100	42	10	a=b=c= 8.412

Laser Raman spectroscopy results showed five Raman active modes for the catalyst calcined at 900°C, which is an indication of the formation of an inverse spinel structure. FTIR results showed for the catalyst calcined at 600°C, two strong absorption bands located at 661 and 564 cm^{-1} which is an indication of the formation of Co_3O_4 with a spinel structure. Photocatalytic experiments showed that the concentration of MB did not obviously decrease in the presence of catalyst calcined at 900°C when the suspension was irradiated with UV radiation at wavelength λ = 365 nm. We reach 15 % of degradation after 3 hours of irradiation. But 40 % of degradation was obtained with catalyst calcined at 600°C after 4 hours of irradiation.

4 Conclusion

In this work, a study has been carried out on photocatalytic behavior of cobalt titanate nanoparticles toward a cationic dye such as methylene blue. The obtained results showed a better activity of a mixed phase obtained at 600°C during a period of 3 hours under UV exposure.

References

[1] K.T. Jacobs, G. Rajitah, *Journal of Chemical Thermodynamics*. 42 (2010) 879.
[2] A.M Yankin, V.F. Balakirev, *Inorganic Materials*. 38 (4) (2002) 309.
[3] G. Busca, V. Lorenzelli, V.S. Escribano, R. Guidetti, *Journal of Catalysis*. 131 (1991) 167.
[4] D.J. Taylor, P.F. Fleig, R.A. Page, *Thin Solid Films*. 408 (2002) 104.
[5] K. Eguchi, N. Shimoda, K. Faungnawakij, T. Matsui, R. Kikuchi, S. Kawashima, *Applied Catalysis B: Environmental*. 80 (2008) 156.
[6] Erik Casbeer, Virender K. Sharma, Xiang-Zhong Li, *Separation and Purification Technology*. 87 (2012) 1.
[7] P.K. Dutta, S.O. Pehkonen, V.K. Sharma, A.K. Ray, *Environmental Science and Technology*. 39 (2005) 1827.

V-PP99

CO_2 Hydrogenation to Light Olefins on a High Surface Area K-Promoted Iron Catalyst

Visconti C.G.[1], Martinelli M.[1], Falbo L.[1], Infantes-Molina A.[1], Gaeta M.[1], Lietti L.[1*], Forzatti P.[1], Palo E.[2], Picutti B.[3]

1 - Politecnico di Milano, Dipartimento di Energia, Milan, Italy
2 - KT-Kinetics Technologies SpA, Rome, Italy
3 - Maire Tecnimont Group SpA, Milan, Italy

* luca.lietti@polimi.it

Keywords: CO_2 hydrogenation, C_2-C_4 olefins, iron, glycolate, complexes, Fe_3O_4, α-Fe_2O_3

1 Introduction

Lower olefins (C_2-C_4) are the key building blocks of the chemical industry with the largest production volume. These hydrocarbons are traditionally produced by steam cracking of naphtha. However, the strategic determination of several countries to decrease their dependence on imported crude oil, the progressive depletion of known oil sources, and the pressing necessity to minimize the carbon footprint have directed the research efforts into the identification of alternative feedstocks and processes to produce these species. The synthesis of lower olefins from synthesis gas (either directly or via methanol) or via dehydrogenation of lower paraffins have been largely investigated in the last decades. An alternative and sustainable option gaining interests in the latter years is the synthesis of lower olefins through the catalytic hydrogenation of CO_2. To date, however, only a little is known on this process. Potassium promoted iron based catalysts have been reported to be promising for the CO_2 hydrogenation to light hydrocarbons [1]. In fact, even at temperatures higher than 300°C, required to drive the product selectivity towards shorter hydrocarbons chains, iron catalysts have a methanation activity and a secondary olefins hydrogenation activity lower than cobalt [1,2]. It has been shown that the conversion of iron oxide precursor to iron carbide is crucial to achieve high olefins selectivity [3].

In this work, a Fe-based catalyst with high surface area and a spinel structure, easy to be carburized, has been prepared. The catalyst has been tested in the CO_2 hydrogenation and its performance have been compared to those of K-promoted reference model catalysts.

2 Experimental/methodology

Fe-catalysts were prepared by taking the cue from the procedure reported in [3]. Briefly, a $Fe(NO_3)_3$ aqueous solution was mixed at RT with an glycolic acid solution by using a molar ratio glycolic acid/Fe of 1.073. The resulting solution was dried in a rotary evaporator at 60°C for 3 h and then in static air at 45°C overnight. The obtained precursor was calcined at 350°C. Different calcination times (15, 30 and 60 min) were explored in order to identify the best conditions to obtain an iron oxide with a spinel structure and a high surface area. The calcined precursor was subsequently promoted with potassium (K/Fe = 0.02 molar ratio).

Other two catalysts were prepared for comparison purposes by K-IWI of reference model samples of commercial α-Fe_2O_3 (4.6 m^2/g) and Fe_3O_4 (5.2 m^2/g) powders. The obtained samples were named "K-Fe_2O_3" and "K-Fe_3O_4", respectively. All the catalysts were characterized by N_2 adsorption-desorption, X-ray diffraction and H_2 temperature programmed reduction.

Activity tests were carried out in a lab-scale fixed bed reactor operating 24/7. The catalysts were activated in syngas (H_2/CO = 1) at 0 barg for 1h at 300°C. Then the catalysts were tested at 300°C, 5 barg, H_2/CO_2 inlet molar ratio of 3.41 L(STP)/h/m_{cat}^2.

3 Results and discussion

We found that the thermal treatment has a dramatic effect on the morphological proprieties and on the crystal structure of the catalyst. Indeed, the surface area decreases from 66 to 23 m^2/g by increasing the calcination time from 15 min to 60 min, and at the same time the spinel structure (isostructural to Fe_3O_4) is progressively transformed to a corundum-type (isostructural to α-Fe_2O_3). According to our understanding, during the thermal decomposition of the iron glycolate complexes formed from the interaction of the iron salt and the glycolic acid, CO is released so that some Fe(III) is reduced to Fe(II) and the spinel Fe_3O_4 is formed. When the phenomena is complete, the presence of atmospheric O_2 results in the re-oxidation of lower metal valence Fe(II) to the high valences states Fe (III) so that only α-Fe_2O_3 structure is obtained at calcination of 30 or 60 minutes.

The obtained catalyst with the highest surface area and the greatest content of Fe_3O_4 (namely K-Fe15) was tested in CO_2 hydrogenation. In the first 20 h on stream the activity and the selectivity of the catalyst changed from a dominant RWGS regime to a system where both RWGS and the synthesis of hydrocarbons from CO take place. This transient is due to a catalyst reconstruction which involves the transition from Fe_3O_4 to α-Fe and FeC_x. At steady state conditions, measure CO_2 conversion was 45%, while the C_2-C_4 olefins carbon selectivity achieved 40% (Fig. 1). On the opposite, the reference materials, tested at the same flow rate per unit of catalytic surface (41 L(STP)/h/m^2_{cat}), were both characterized by lower activity and light olefins selectivity. We explain this result by considering that the smallest crystallites size and the spinel structure of the home-made sample improve the reducibility and the formation of well dispersed active iron carbide centres.

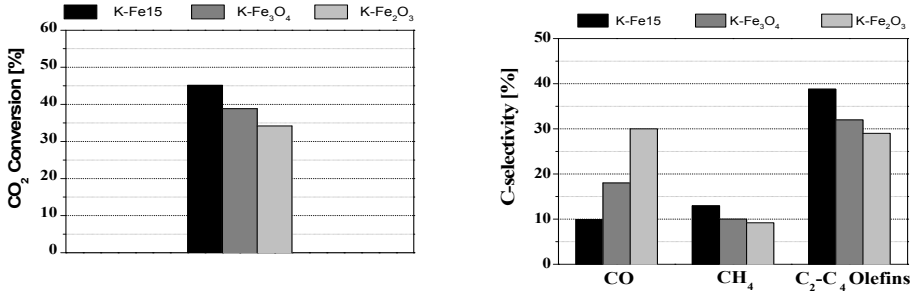

Fig. 1. (left) CO_2 conversion and (right) C-selectivity for K-Fe15, K-Fe_3O_4 and K-Fe_2O_3 (T = 300°C, P = 5 barg, H_2/CO_2 = 3 and GHSV = 41 L(STP)/h/m^2_{cat})

The effect of the process conditions on the CO_2 conversion and on the process selectivity has been also investigated, and the results will be shown during the presentation.

4 Conclusions

A K-promoted bulk iron catalyst with high surface area (66 m^2/g) was prepared by thermal decomposition of iron glycolate complexes. The catalyst was found to be active in the CO_2 hydrogenation, with the C_2-C_4 olefins being the most abundant species in the products pool.

Acknowledgements

Stamicarbon B.V. is gratefully acknowledge for the financial support.

References

[1] T. Riedel, M. Claeys, H. Schulz, G. Schaub, S.-S. Nam, K.-W. Jun, M.-J. Choi, G. Kishan, K.-W-Lee, *Appl. Catal. A: Gen*. 186 (1999) 201.
[2] C.G. Visconti, L. Lietti, E. Tronconi, P. Forzatti, R. Zennaro, E. Finocchio, *Appl. Catal. A: Gen*. 355 (2009) 61.
[3] Patent US 5,140,049 assigned to Exxon Research and Engineering Co., 1992.

V-PP100

The Analysis of Carbon Dioxide Reforming of Methane (CDRM) Performance of Co-Ce/ZrO_2 System

Paksoy A.I., Aksoylu A.E.*

Bogazici University, Department of Chemical Engineering, Istanbul, Turkey

* aksoylu@boun.edu.tr

Keywords: methane dry reforming, carbon dioxide, utilization, catalytic hydrogen, production

1 Introduction

Carbon dioxide reforming of methane (CDRM), a catalytic process where CO_2 and CH_4 are utilized to produce synthesis gas, has received considerable attention lately. Compared to other routes of indirect utilization of CH_4, such as steam reforming and partial oxidation, the most important advantage of CDRM is the consumption of thermodynamically stable greenhouse gas CO_2. Moreover, the low H_2/CO ratio obtained in CDRM is preferable for further processes like Fischer-Tropsch synthesis. However, due to the endothermic nature of the reaction, high temperatures are required which results in coking and/or metal sintering. Co is an adequate choice as a primary metal with its stable performance, abundance and relatively low cost. A suitable metal(s)-support combination in CDRM can provide resistance to both coke deposition and sintering. Carbon accumulation in CDRM can be controlled by using a support like ZrO_2 which enhances the dissociative adsorption of CO_2 producing CO and surface O, where the latter being responsible for the cleaning of carbon formed from the H_2 producing sites. Additionally, the anti-coking property of the CDRM catalysts can be improved by introducing a second metal, like Ce, that can increase the oxygen storage capacity owing to its redox ability. [1]

The aim of this study is to establish a link between Co:Ce loading ratio and CDRM performance of the catalyst, and to confirm the roles of Co, Ce and ZrO_2 in Co-Ce/ZrO_2 system. The favorable combination(s) of catalyst and reaction condition for stable performance were investigated through following an experimental design involving the Co and Ce loadings, reaction temperature and CH_4/CO_2 feed ratio as parameters. The activity, stability and selectivity profiles of Co-Ce/ZrO_2 catalysts with different Co and Ce loadings were obtained and analyzed. XPS, SEM-EDX and HRTEM-EDX techniques were utilized for further discussion.

2 Experimental

Catalysts with 4 different Co:Ce ratios, 5%Co-2%Ce/ZrO_2, 5%Co-3%Ce/ZrO_2, 10%Co-2%Ce/ZrO_2 and 10%Co-3%Ce/ZrO_2, were prepared by sequential impregnation method. Calcination *in situ* in dry air for 4 h at 773 K and a subsequent reduction *in situ* in H_2 for 2 h at the same temperature were conducted as a pretreatment. The CDRM performance tests were conducted in a quartz microreactor at the space velocity of 20000 mL/h.g catalyst for the temperature interval of 873-973 K and CH_4/CO_2 feed ratios of 1/1, 2/1 and 1/2. All freshly reduced and selected spent samples were characterized by XPS, SEM-EDX and HRTEM-EDX.

3 Results and discussion

The performance of the catalysts is discussed in terms of CH_4 and CO_2 conversion and activity, and H_2 yield. H_2/CO product ratio is used as the measure of selectivity. For all tested catalysts, higher reaction temperatures were found beneficial for both activity and selectivity (Figure 1). However, the activity order of catalysts changes with temperature, which most probably results from the different dynamics of carbon and oxygen forming reactions. The

Co:Ce loading ratio of the samples affects the mechanisms of both processes and changes their relative extent.

For the catalysts with 10% Co loading, high activity losses and more tendency towards H_2 formation were observed indicating the dominant role of Co in CH_4 dehydrogenation. Coke accumulation observed over the catalysts that have high Co:Ce loading ratios indirectly showed that Ce and ZrO_2 are responsible for surface oxygen production and/or transfer; relatively low amount of Ce, ZrO_2 or the combination of both leads to limited surface oxygen and consequently, insufficient carbon removal. This relation was also confirmed by the comparative evaluation of electromicroscopic analysis of freshly reduced and spent samples. It was also noticed that CO_2 conversion profile is more stable than that of CH_4, highlighting the difference between the rates of CO_2 dissociation and CH_4 dehydrogenation. At all tested temperatures, increasing CH_4 source in the feed caused all catalysts to suffer from coke deposition most probably due to higher carbon accumulation rate compared to rate of surface oxygen production. The performance test results indicated that decreasing the CH_4/CO_2 ratio in the feed enhanced the stabilizing effect of Ce in CDRM activity (Figure 1). The changes in Ce^{+3}/Ce^{+4} ratio on freshly reduced and spent catalysts with different Co:Ce loading ratio, measured by XPS, confirmed this effect.

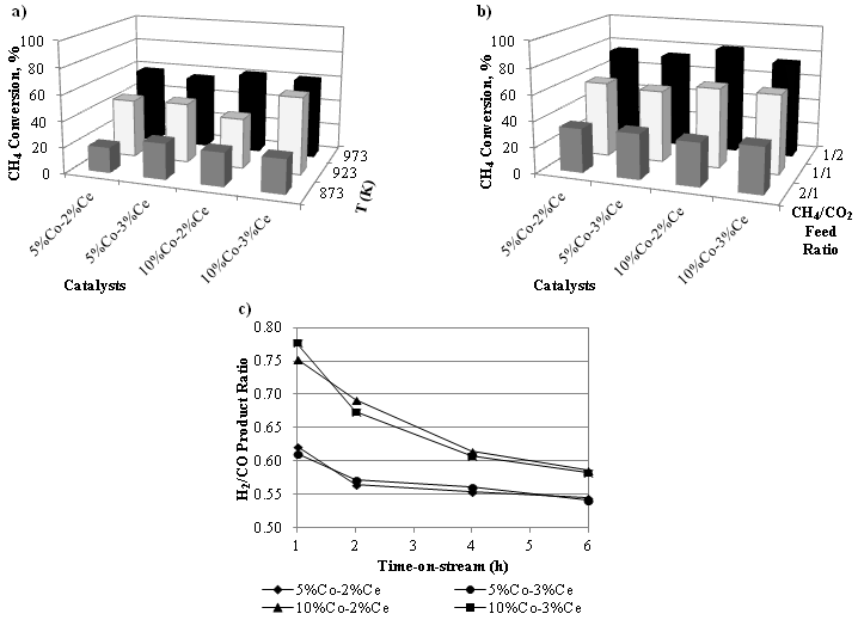

Fig. 1. Activity and selectivity trends of tested catalysts (a) CH_4 conversion (CH_4/CO_2=1/1); (b) CH_4 conversion (T=973 K); (c) H_2/CO product ratio (T=873 K; CH_4/CO_2=2/1).

4 Conclusions

This parametric study concluded that cobalt is dominantly responsible for CH_4 dehydrogenation, which is mostly favored at high temperatures, and both Co loading and Co:Ce loading ratio change product distribution. Ceria limits coke deposition by enhancing surface oxygen transfer, and its activity is limited by the CO_2 concentration in the feed.

Acknowledgements

This work is financially supported by TUBITAK through project 111M144 and Boğaziçi University through project BAP M 6755.

References

[1] A. I. Paksoy, B. Selen Caglayan, A. E. Aksoylu, *Applied Catalysis B: Environmental*. 168 (2015) 164-174.

V-PP101

Novel Imidazolium Based Catalyst for the Chemical Fixation of Carbon Dioxide

Bivona L.A.[1,2], Fichera O.[1], Buaki-Sogo M.[1], Fusaro L.[1], Gruttadauria M.[2], Aprile C.[1*]

1 - Unit of Nanomaterial Chemistry (CNano), University of Namur (UNAMUR), Department of Chemistry, Namur, Belgium

2 - Dipartimento di Scienze e Tecnologie Biologiche Chimiche e Farmaceutiche (STEBICEF), Sezione di Chimica, Università di Palermo, Palermo, Italy

* carmela.aprile@unamur.be

Keywords: chemical fixation of carbon dioxide, polyhedral oligomeric silsesquioxane (POSS), ionic liquids, catalysis

1 Introduction

Development of green processes based on chemical fixation of carbon dioxide has attracted the attention in industrial chemistry due to the possibility to transform a waste, such as CO2, into useful products.1 CO2 gas is produced in large amounts from fuel combustion and represents an easy available, inexpensive and abundant carbon source. However, due to its thermodynamic and kinetic stability, its conversion is difficult to achieve and an efficient catalyst is required.2 Cyclic carbonates, synthetized through the reaction between CO2 and epoxides, are interesting compounds that can be used for several applications, such as electrolytes for lithium batteries, polar aprotic solvents, intermediates for organic synthesis and precursor for pharmaceuticals. Various homogeneous and heterogeneous processes have been proposed for this reaction. Recently, ionic liquids have emerged as a novel class of organocatalysts. In particular, imidazolium-based ionic liquids have become very attractive because they are one of the most efficient catalysts for CO2 fixation to produce cyclic carbonate from epoxydes.3

Here the synthesis and applications of a novel class of imidazolium catalyst based on the functionalization of polyhedral oligomeric silsesquioxane (POSS) is presented. The POSS have been functionalized with imidazolium units to obtain an imidazolium-based POSS (POSS-mim-Cl, fig. 1 left). This new material was employed for the reaction of CO2 and epoxides in homogeneous conditions with excellent results. In addition, it was easily recovered from the reaction mixture. To the best of our knowledge, the application of these materials for the fixation of CO2 is a domain still unexplored.

2 Experimental/methodology

The synthesis of POSS-mim-Cl was carried out by means of a synthetic strategy divided in two steps: the first step employed a commercially available octa-vinyl POSS which was reacted with chloropropanethiol, through a thiol-ene reaction. Once the product (POSS-Cl) was obtained, the following step was its functionalization with an excess of 1-methylimidazole to obtain POSS-mim-Cl. The material was extensively characterized by ^{1}H, ^{13}C and ^{29}Si-NMR, and elemental analysis. In order to explore its catalytic activity, styrene oxide was selected as model compound for the chemical fixation of CO_2. In addition, different parameters (solvent, temperature, pressure of CO_2, and mass of the catalyst) were modified to find the best condition for CO_2 fixation.

3 Results and discussion

The POSS-mim-Cl was obtained with high yield. ^{1}H and ^{13}C NMR spectra confirm the

structure of the catalyst and elemental analysis shows a high degree of functionalization. ^{29}Si NMR spectrum displays different signals suggesting the presence of the hepta imidazolium-based POSS. The chemical fixation of CO_2 was performed using styrene oxide as starting material and varying different parameters such of pressure of CO_2, temperature, amount of catalyst and solvent. The catalytic tests were carried out in a batch reactor for 3 h, in homogeneous conditions. The POSS-mim-Cl displayed good catalytic performances. When using water as co-solvent, the material showed good conversion (70 %) and TON (410) with a CO_2 of 40 bar, at 150°C and using 110 mg of catalyst. However, the presence of water decreased the selectivity due to the formation of the styrene glycol as by-product. In order to increase the selectivity, other solvents were also tested. The best results were obtained when using isopropanol. Under these conditions almost quantitative conversion and selectivity > 90% were obtained (TON of 553, fig. 1 right).

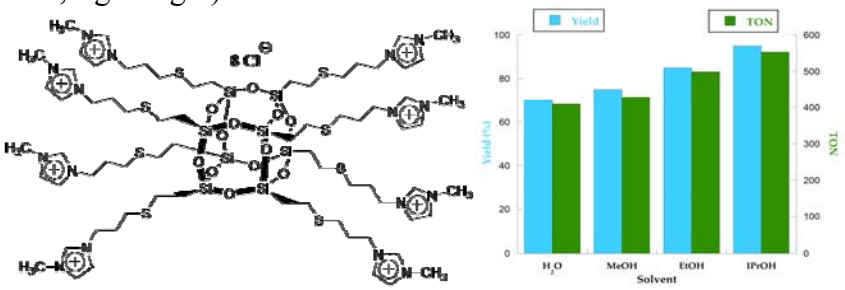

Fig. 1. Structure of the catalyst POSS-mim-Cl (left); Yield and TON of the fixation of CO_2, varying co-solvent at 40 bar, 150°C, using 110 mg of catalyst for 3 h (right).

Additional tests were performed in anhydrous solvents and excellent results in term of both yield and selectivity (> 99 %) were obtained. In order to study the influence of the nano-cage, 1-butyl-3-methyl imidazolium chloride (bmimCl) was also tested as catalyst in the same conditions than POSS-mim-Cl. It is worth to mention that POSS-mim-Cl displayed better performance (TON = 429) than the bmim-Cl (TON = 328). POSS-mim-Cl was also recovered by extraction from the reaction mixture, and its structure was confirmed by ^{1}H and ^{29}Si NMR spectroscopy.

4 Conclusions

A novel class of imidazolium based catalyst was prepared and tested for the reaction of CO_2 with epoxides. The POSS-mim-Cl displayed excellent catalytic performance, especially if anhydrous ethanol was used as co-solvent. The results were compared with those obtained with bmimCl, proving that the nano-cage (POSS) plays a positive role in the reaction probably due to the proximity effect.[4] As far as we know this is the first use of imidazolium-based POSS as catalysts for the chemical fixation of CO_2.

Acknowledgements

L. A. Bivona thanks the University of Namur and the Università di Palermo for a co-founded PhD fellowship.

References

[1] a) W.-L. Dai, S.-L. Luo, S.-F. Yin, C.-T. Au, *Applied Cat. A: General* 366 (2009) 2-12; b) J. H. Clements, *Ind. Eng. Chem. Res.* 42 (2003) 663-674.

[2] T. Sakakura, J.-C. Choi, H. Yasuda, *Chemical Reviews* 107 (2007) 2365-2387.

[3] C. Aprile, F. Giacalone, P. Agrigento, L.F. Liotta, J. A. Martens, P. P. Pescarmona, M. Gruttadauria, *ChemSusChem* 4 (2011) 1830-1837.

[4] a) M. Buaki-Sogo, H. Garcia, C. Aprile, *Catal. Sci. Technol.* (2015) DOI: 10.1039/C4CY01258E. b) M. Taherimehr, A. Decortes, S. M. Al-Amsyhar, W. Lueangchaichaweng, C. Whiteoak, E. C. Escudero-Adán, A. W. Kleij, P. P. Pescarmona, *Catal. Sci. Technol.* 2 (2012), 2231-2237.

V-PP102

Real-Time *in situ* Atomic-Scale Study of the Surface Termination of Ceria Nanoparticles under Vacuum, O_2 and CO_2 Pressures by Environmental Transmission Electron Microscopy

Cadete Santos Aires F.J.[1*], Aouine M.[1], Daniel C.[1], Meunier F.C.[1], Farrusseng D.[1], Epicier T.[1,2]

1 - Institut de Recherches sur la Catalyse et l'Environnement de Lyon, UMR 5256 CNRS/UCB Lyon 1, Villeurbanne, France

2 - Laboratoire MATEIS, UMR 5510, CNRS/INSA de Lyon, Villeurbanne Cedex, France

* francisco.aires@ircelyon.univ-lyon1.fr

Keywords: environmental TEM, high resolution TEM, ceria, CO_2/O_2, adsorption, surface termination

1 Introduction

Studying functional materials under (quasi) realistic conditions (variable P and T, liquid environment) within the microscope has been a constant concern for scientists since the early days of electron microscopy [1,2]. The advent of Cs-corrected transmission electron microscopes has brought a new impulse to environmental transmission electron microscopy (ETEM) studies [3]. This is particularly true in the field of catalysis in which high resolution imaging of the catalyst surface is required to assess structural/chemical evolutions in presence of controlled gaseous environments. Here we present a study on the adsorption of both O_2 and CO_2 on ceria nanoparticles (NPs) at room temperature. These preliminary steps are part of a global approach aimed at gaining fundamental insights at reactions used for the valorization of CO_2 and the related global warming issues.

2 Experimental/methodology

The studies were performed in the Ly-EtTEM (Lyon Environmental and tomographic Transmission Electron Microscope), a 80-300 kV TITAN objective lens C_s-corrected Environmental TEM from FEI equipped with a GATAN high resolution Imaging Filter (GIF) recently installed in Lyon. The analysis was carried out at room temperature varying the gas pressures from 10^{-6} mbar (vacuum) up to 2 mbar.

3 Results and discussion

It is well-known that under vacuum conditions the incident electron beam induces a partial reduction of ceria [4]. As a consequence cerium surface atoms become highly mobile as it can be readily observed on {100} facets and electron energy-loss spectroscopy (EELS) shows that the characteristic features related with Ce^{4+} species rapidly decrease in intensity both on the O-K and Ce-$M_{4,5}$ edges.

In the presence of dioxygen (O_2 pressure in the mbar range) this beam-induced reduction is "healed" and the surface of ceria NPs is stabilized as it can be confirmed by the absence of mobility of surface cerium atoms on {100} facets as well as by the *in situ* real-time dynamic monitoring of the O-K and C-$M_{4,5}$ edges by EELS that now remain unaltered under irradiation.
Finally, under CO_2 pressure (10^{-2} - 1 mbar), the {100} facets become more stable from both structural and chemical points of view. We notice that the surface terminations of the ceria nanoparticles under vacuum are different from those observed under CO_2. Under vacuum the terminal contrasts observed are strong and clearly correspond to the formation of a terminal cerium plane (Fig.1 left). A different contrast can be noted in the case of the sample exposed to

CO_2 (Fig.1 right) hinting at the presence of stabilized species at the position of oxygen atoms at the surface termination. The stabilization of surface oxygen atoms is likely related to CO_2 adsorption and the formation of carbonate species, as observed by FT-IR spectroscopy under similar temperature and pressure conditions.

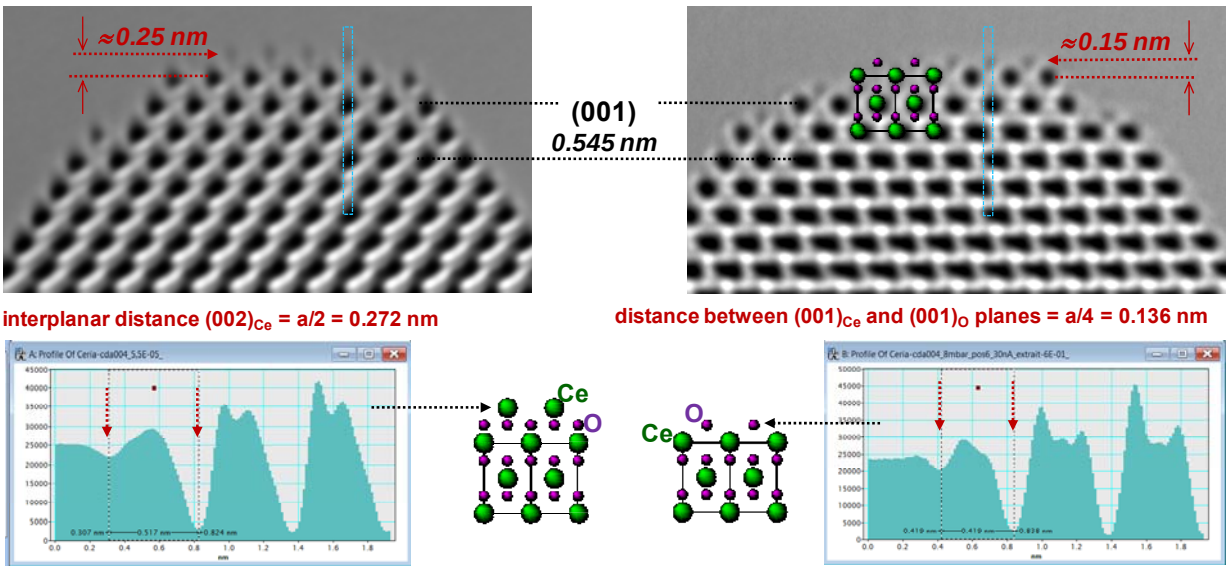

Fig. 1. HRTEM images (top, video frames averaged) and cross-sections of surface contrasts with proposed models (bottom) of CeO_2[110] under vacuum (left) and under 0.8 mbar of CO_2 (right).

4 Conclusions

This high spatial resolution study (structural/chemical) of ceria nanoparticles by environmental TEM not only clearly shows the capability of observing/measuring real-time atom mobility at the surface of nanoparticles and chemical evolution (reduction) but also enables the indirect detection of surface adsorbates (here carbonates due to CO_2 adsorption) by monitoring the surface termination structural evolution.

Acknowledgements

The authors would like to thank the CLYM (Consortium Lyon-St-Etienne de Microscopie) for the access to the Ly-EtTEM.

References

[1] L. Marton, *Bull. Acad. Roy. Belg. Cl. Sci.* 21 (1935) 553.
[2] R.T.K. Baker *et al*, *J. Catal.* 26 (1972) 51.
[3] J.B. Wagner *et al*, *Micron* 43 (2012) 1169.
[4] L.A.G. Garvie and P.R. Buseck, *J. Phys. Chem. Solids* 60 (1999) 1943.

V-PP103

Au/MgO-Type Catalysts for the Carbonylation of Glycerol with Urea. Effect of the Morphology and Macro/Meso-Porous Structure of the Support

Hernández W.Y.[1*], Van Oudenhove M.[2], Verberckmoes A.[2], Van Der Voort P.[1]

1 - Center for Ordered Materials, Organometallics & Catalysis (COMOC), Department of Inorganic and Physical Chemistry, Ghent University, Ghent, Belgium

2 - Industrial Catalysis and Adsorption Technology (INCAT), Department of Industrial Technology and Construction, Faculty of Engineering & Architecture, Ghent University, Ghent, Belgium

* yesid.hernandez@ugent.be

Keywords: glycerol conversion, gold-supported catalysts, magnesium oxide, macro-mesoporous structure

1 Introduction

The reaction of glycerol with urea to form glycerol carbonate has become a relevant research topic during the last few years. This process utilizes two inexpensive and readily available compounds and additionally provides a route to upgrade the surplus production of glycerol formed in large quantities as byproduct during the production of biodiesel [1]. Although the reaction of glycerol with urea can proceed by increasing the temperature of the system, several heterogeneous catalysts (mostly Zn-based ones) have been found to improve its rate and selectivity to glycerol carbonate [2]. It is accepted that the existence of well-balanced acid-base properties of the catalyst are responsible of the activity and selectivity during the reaction. Hutchings et al. [3] presented a gold supported on magnesia catalyst as a high active and selective system for the glycerolysis of urea. These authors suggest that the combination of the basic properties of the support with the Lewis acidity of the gold-supported nanoparticles results in the improvement of the yield and selectivity. Moreover, the support can also play an additional role concerning to the stabilization of the gold nanoparticles and/or the occurrence of different metal-support interaction effects (e.g. charge withdrawing effects). Thus, the rational design of MgO-type supports (considering parameters such as morphology and porous structure) and the study of the gold-support interactions originated in these types of materials represent a feasible way to improve the catalytic efficiency and stability of Au/MgO-type catalysts.

This work describes the synthesis of MgO-type supports by a hydrothermal synthesis route, employing Pluronic P123 block copolymer surfactant or cetyltrimethylammonium bromide (CTAB) as soft-templates. Gold nanoparticles were deposited on the most relevant supports (in terms of surface and morphology) and used as catalysts for the synthesis of glycerol carbonate.

2 Experimental/methodology

In a typical synthesis, P123 or CTAB were dissolved in water at 60 ºC and under vigorous stirring to form a transparent solution. After that, the $Mg(NO_3)_2.6H_2O$ was added to the clear solution (surfactant/Mg molar ratio equal to 0.03). An aqueous ammonia solution (25 wt%) was added dropwise at room temperature to the resulting liquid mixture under stirring until having a final pH close to 10. After precipitation, the slurry was transferred to a 50-mL Teflon-lined stainless steel autoclave for hydrothermal treatment at the selected temperature (120 ºC) for 12 or 24 h. The obtained solid was filtered out and washed three or four times with distilled water and ethanol (for the removal of the majority of the surfactant) and then dried overnight at 100 ºC. MgO was formed by calcination at 500 ºC, 3h, using a very slow calcination program.

3 Results and discussion

Figure 1 shows the XRD patterns of the samples calcined at 500 ºC. All the materials present the reflections characteristic of a pure MgO periclase-phase. Nevertheless, depending on the surfactant used, the MgO particles exhibit a different morphology. The SEM micrographs of the samples prepared with P123, CTAB and without addition of surfactant (denoted as samples P-, C- and W-) are shown in figure 2-a, 2-b and 2-c, respectively. In the absence of surfactant or using CTAB, a similar morphology of hexagonal nanoplates is observed. Higher agglomeration is seen without using surfactant. On the other hand, the presence of P123 provokes the formation of randomly piled aggregates of sheets. Those types of structures allow the formation of flower-like agglomerates with an open macroporous structure. In all the samples, the textural analysis reveals the formation of mesoporous structures (IV-type isotherms). However, the material synthesized in presence of P123 is the one with the highest surface area and pore volume (table 1).

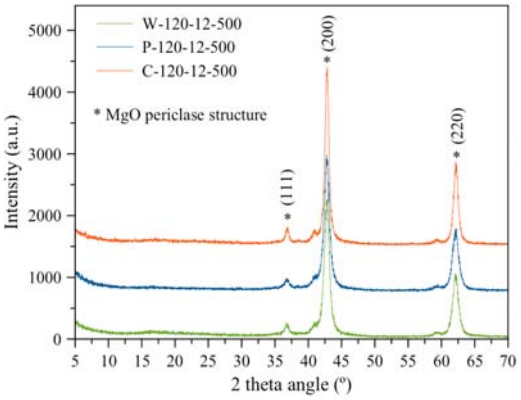

Fig, 1. XRD patterns

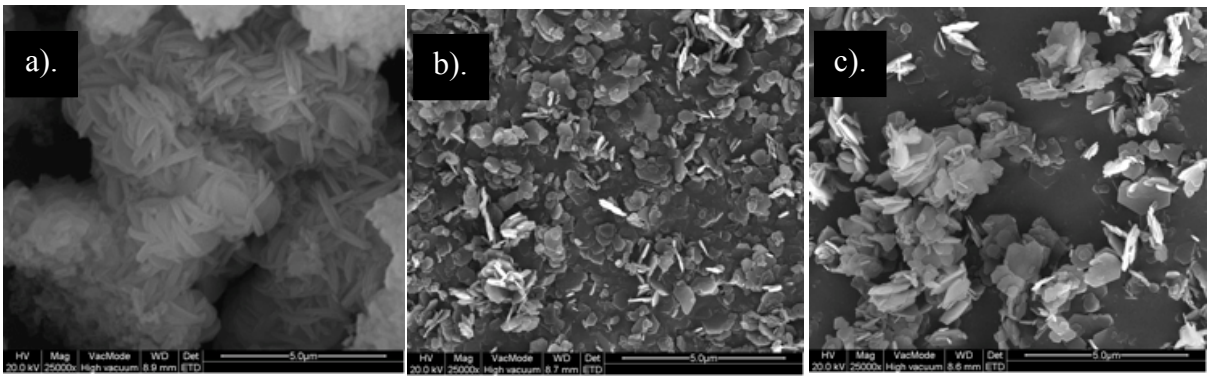

Fig. 2. SEM images of a). P-120-12-500, b). C-120-12-500 and c). W-120-12-500 materials

Table 1. Textural properties of the synthesized materials

Code	S_{BET} (m^2/g)	Pore Vol. (cm^3/g)	Av. Pore size (Å)
W-120-12-500	136	0.22	64
C-120-12-500	97	0.23	96
P-120-12-500	163	0.31	76

4 Conclusions

The combination of an open macro and mesoporous structure and a relevant surface area make the P-120-12-500 solid an interesting material to support gold-nanoparticles. Such textural and morphological properties are expected to influence the stabilization and dispersion of the deposited metallic phase and the diffusional processes involved during the catalytic reaction.

References

[1] M.O. Sonnati, S. Amigoni, E.P.T de Givenchy, T. Darmanin, O. Choulet, F. Guittard, *Green Chem.* 15 (2013) 283.
[2] M. Aresta, A. Dibenedetto, F. Nocito, C. Ferragina, *J. Catal*. 268 (2009) 106.
[3] C. Hammon, J.A. Lopez-Sanchez, M.H. Ab Rahim, N. Dimitratos, R.L. Jenkins, A.F. Carley, Q. He, C.J. Kiely, D.W. Knight, G.J. Hutchings, *Dalton Trans.* 40 (2011) 3927.

V-PP104

Synthesis of Organic Carbonates Using Catalyst Containing K Metal from Waste Source

Ab. Rahim M.H.*, Paroo I.V., Maniam G.P.

Faculty of Industrial Sciences & Technology, Universiti Malaysia Pahang, Kuantan, Malaysia

* mohdhasbi@ump.edu.my

Keywords: glycerol, boiler, ash, glycerol, carbonate, organic, carbonates, catalyst

1 Introduction

Over the years production of glycerol as a crude waste from biodiesel making industries has been largely increasing. For every 100 kg of biodiesel produced, 10 kg of glycerol is produced as a by-product which corresponds to 10 weight percentage of biodiesel. It is estimated that by the year 2016, the production of crude glycerol will reach 4 billion gallons.[1] Thus, in order to make this waste a useful substance for future use, the conversion of glycerol to other value added product is suggested.[2] Glycerol carbonate is one of the value added product of glycerol which is important to many industries. Glycerol carbonate has low toxicity, noble biodegradability and high boiling point.[3] There are various methods to produce glycerol carbonate using different sources of starting material. However the method used in this study is the most prominent method of near to a green synthesis approach whereby it uses bio-renewable feedstock. Besides, glycerol and urea are relatively cheaper and readily available.[3,4] On the other hand introducing waste material from local palm oil industry in Malaysia which is boiler ash has certainly raised the benchmark to the synthesis of organic carbonate to another level. This does not only propose a cheaper and economical route of transforming polyols into carbonates but also support proper disposal of waste for the betterment of our environment.

2 Experimental/methodology

Catalyst preparation

Raw boiler ash obtained from palm oil mill in Lepar Hilir, Pahang, Malaysia was dried at 110 ˚C overnight and then powdered using mortar and pestle (denoted as BA 110) and sieved using 200µm sized sieve. Later, 2g of the sieved ash were loaded on the combustion boat and calcined under static air at temperature (500 ^{o}C, 700 ^{o}C, 900 ^{o}C and 1100 ^{o}C respectively) for 4 h. The catalysts were later denoted as BA 500, BA 700, BA 900 and BA 1100, respectively.

Catalytic Testing

The reaction was carried out using a three-neck round bottom flask. Typically, glycerol was allowed to heat up to 150 ^{o}C for under the flow of nitrogen gas. When the temperature reached 150 ^{o}C, urea and 0.25g catalyst was added to the reaction and stirred using magnetic stirrer. The molar ratio of glycerol to urea used was (1:1.5). Sampling was done from 0 h to 4 h. The results were analysed using Gas Chromatography-Flame Ionised Detector (GC-FID) Agilent Technologies 7890A equipped with Varian Capillary Column, CP-ParaBOND Q (25m, 0.53mm, 10µm). Similar method was used to synthesis other organic carbonates (i.e ethylene carbonate and propylene carbonate) using the most effective boiler ash from the study.

3 Results and discussion

Table 1 show that boiler ash calcined at 900 ^{o}C is the most effective catalyst which has significant yield, conversion and selectivity. The yield of glycerol carbonate obtained follows the order of BA 900 > BA 700 > BA 1100 > BA 110 > BA 500. This could have resulted from the influence of basic metal oxides present in the catalyst with almost similar strength even after

different heat pre-treatment was carried out. It is also justified that potassium (K) as the most major metal in the catalyst could have been the target metal that has actively played the role in the catalytic activity of boiler ash.

Table 1: Effect of boiler ash calcination temperature on glycerol conversion, glycerol carbonate selectivity and yield

No.	Catalyst	Temp. heat treatment (°C)	Gly. conv. %	Selectivity %				GC Yield %	TOF (mmol/g cat. h^{-1})
				GC	Comp. (3)	Comp. (5)	Comp. (6)		
1	Blank	-	78.7	32.8	24.0	43.1	-	25.8	-
2	BA 110	110	91.1	83.5	1.9	11.1	3.5	76.2	136.7
3	BA 500	500	91.1	82.7	4.3	10.0	2.9	75.3	136.7
4	BA 700	700	94.1	88.6	3.5	4.8	2.9	83.4	141.2
5	BA 900	900	93.6	90.1	4.1	3.9	1.9	84.3	140.4
6	BA 1100	1100	89.8	85.6	5.5	6.4	2.4	77.0	134.7

Reaction conditions: Temperature, 150 ˚C; Gas, N_2; Glycerol: Urea, 1: 1.5 (Molar ratio); Catalyst mass, 0.25 g; Time, 4 h; Standard stirring rate, 340 rpm. TOF: calculated based on the mmol of glycerol converted per gram catalyst per total reaction time (h). Relative Standard Deviation (RSD): < 5%. Note: Gly. is Glycerol; GC is Glycerol carbonate; Comp. (3) is 2, 3-dihydroxypropyl carbamate; Comp. (5) is 4-(hydroxymethyl) oxazolin-2-one; Comp. (6) is (2-oxo-1,3-dioxolan-4-yl)methyl carbamate.

Figure 1 illustrates the product validation of propylene carbonate and ethylene carbonate using ^{13}C NMR. From the figure it is evident that using similar synthesis approach other organic carbonates can be produced.

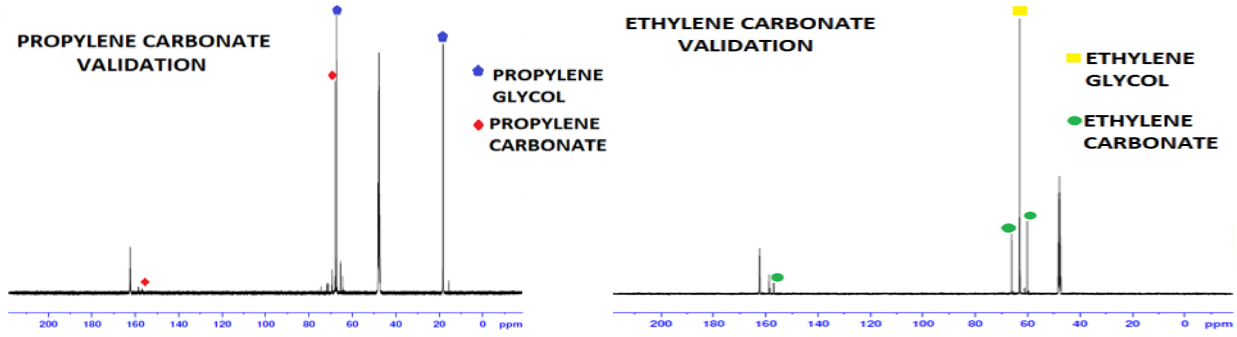

Fig. 1: Validation of Propylene Carbonate and Ethylene Carbonate uisng ^{13}C NMR.

4 Conclusions

In conclusion, this near to green synthesis approach of organic carbonates will be beneficial to both industry and environment fundamentally.

Acknowledgements

The authors thank Universiti Malaysia Pahang and the Ministry of Education for Research Acculturation Collaborative Effort (RACE, RDU121301) and Fundamental Research Grant Scheme (FRGS, RDU140135).

References

[1] N. Rahmat, A. Z. Abdullah, and A. R. Mohamed, *Renew. Sustain. Energy Rev.* 14 (2010) 987.
[2] D. T. Johnson and K. A. Taconi, *Environ. Prog.* 26 (2007) 338.
[3] M. Aresta, A. Dibenedetto, F. Nocito, and C. Ferragina, *J. Catal.* 268 (2009) 106.
[4] S. Fujita, Y. Yamanishi, and M. Arai, *J. Catal.* 297 (2013) 137.

V-PP105

Simultaneous Removal of O-Dichlorobenzene and NO_x over TiO_2-Al_2O_3 Supported Vanadium Catalysts

Boukha Z.*, Gallastegi-Villa M., Aranzabal A., González-Velasco J.R.

Chemical Technologies for Environmental Sustainability Group, Department of Chemical Engineering, Faculty of Science and Technology, University of the Basque Country, Bilbao, Spain

* zouhair.boukha@ehu.es

Keywords: NO and o-DCB, removal, TiO_2-Al_2O_3, support, vanadium

1 Introduction

Titania, typically used as support for the active metals, is known to improve the catalytic activity and to stabilize the structure of active centres [1]. However, its catalytic uses as a bulk material are strongly limited by its poor chemical, mechanical, textural, structural stability and high cost. A way of circumventing some of these limitations might be the dispersion of titania on high surface area oxide supports presenting advantageous properties. Alumina is a good candidate as titania support. In fact, numerous studies are presently available on TiO_2/Al_2O_3 catalytic system. Most of them, however, are devoted to the investigation of the influence of TiO_2 on the catalytic properties of the transition aluminas in various catalytic processes [2].

On the other hand, the simultaneous removal of NO_x and Polychlorodibenzo-*p*-dioxins (PCDD) compounds, produced during Municipal Waste Incineration (MWI), is a process with high environmental interest [3]. Because of their structural similarity to PCDDs, 1,2-Dichlorobenzene (o-DCB) has been frequently used as model compound. VO_x/TiO_2 appears as the most promising catalyst where the redox behavior of V appears to be strongly affected by vanadium-support interactions and additives.

To gain some further insight on the discussed topics, the major objective of this work is the investigation of the textural, structural, surface chemistry, and catalytic behavior, in simultaneous removal of o-DCB and NO, of a series of high surface area V/TiO_2-Al_2O_3 samples.

2 Experimental

The TiO_2-Al_2O_3 support (Ti-Al), with TiO_2 composition equal to 10.6 wt.%, was prepared by impregnation of alumina (saint Gobain SA 63158) with a solution of titanium butoxide (dissolved in butanol-1). The obtained suspension was maintained under stirring at 40 ºC for 3 h. After complete evaporation of the organic solvents under reduced pressure, through a rotary evaporator, the catalysts were dried overnight at 120 ºC and calcined at 600 ºC for 4 h. The Vx/Ti-Al and Vx/Al catalysts (where x indicates the weight percentage of V) were prepared by impregnation where NH_4VO_3 was used as vanadia precursor (diluted in oxalic acid). Their characterization involved mainly N_2 physisorption, XRD, FTIR, UV-Visible, NH_3-TPD, CO_2-TPD and TEM techniques. The catalytic tests were performed, on 1.5 g of catalyst, in a fixed bed reactor operating at atmospheric pressure. The gas mixture corresponding to simulated MWI feed consisted of O_2 (10%), CO_2 (10%), NO (300 ppm), NH_3 (300 ppm), o-DCB (100 ppm) and balanced Ar (total flow of 2 L min^{-1}).

3 Results and discussion

The composition and textural characterization of supports and vanadium catalysts are presented in Table 1. Concerning the Ti-Al support, the incorporation of TiO_2 causes a small decrease in the surface area of the alumina (10%), and in the pore volume, indicating a good distribution of

Ti on the surface. This result was confirmed by TEM.

Table 1. Characterization and activity results of the prepared catalysts

Samples	V, wt.%	S_{BET}, $m^2 g^{-1}$	Pore volume, $cm3\ g^{-1}$	Pore size, nm	H_2/V molar ratio (H_2-TPR)	Activity at 350ºC	
						X_{NO}	$X_{o\text{-}DCB}$
Alumina	-	224	0.58	7.5	-	-	-
V1/Al	0.96	201	0.53	7.5	1.22	0	7
V2/Al	2.10	207	0.53	7.5	0.99	24	4
V4/Al	3.67	196	0.49	7.5	1.07	46	22
Ti-Al	-	201	0.50	7.5	-	-	-
V1/Ti-Al	1.36	202	0.52	7.6	1.08	17	3
V2/Ti-Al	2.35	201	0.50	7.6	1.00	46	20
V4/Ti-Al	3.99	192	0.48	7.6	1.12	70	44

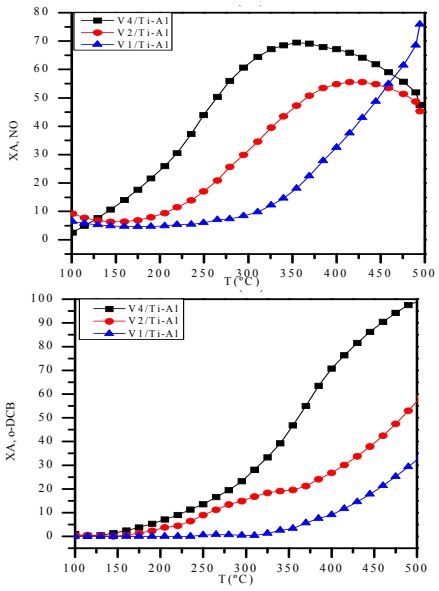

Fig. 1. o-DCB and NO conversions vs. temperature on the Vx/Ti-Al catalysts

The catalytic performances, in term of NO and o-DCB conversions, of the Vx/Ti-Al catalysts are shown in Fig. 1. The results reported in Table 1 also showed that the progressive addition of V improves the activity of the assayed catalysts in both reactions. Moreover, the presence of TiO_2 in the catalysts formulation increases markedly their catalytic activity and selectivity to produce N_2O and CO (not shown). On the most active catalyst (V4/Ti-Al) the NO activation starts around 100 °C. Its conversion increased rapidly to reach about 70% at 350 ºC, and then it decreases with the reaction temperature. Over the same catalyst, the o-DCB conversion presents different trend. The activity increases with the reaction temperature up to 500 ºC when it is close to 100 ºC.

4 Conclusion

Titania was successfully dispersed on the alumina surface. The modification of alumina support by TiO_2 seems to improve the catalytic activity of the Vx/Al catalysts in the simultaneous removal of NO and o-DCB process. In order to explain this effect, a correlation between the catalysts activity and the VO_x species properties was made.

Acknowledgements

The financial support for this work provided by Gobierno Vasco (GIC IT-657-13) and UPV/EHU (UFI11/39) is gratefully acknowledged.

References

[1]S. Bagheri, N.M. Julkapli, and S.B.A. Hamid, Sci. World J. 2014 (2014) 1
[2] G.M. Dhar, B.N. Srinivas, M.S. Rana, Manoj Kumar, S.K. Maity, Catal. Today 86 (2003) 45–60
[3] E. Finocchio, G. Busca, M. Notaro, Appl. Catal. B 62 (2006) 12

V-PP106

Effect of the Nature and Location of Cu Species in Cu-BETA Catalysts for NH_3-SCR of NO_x

Urrutxua M., Pereda-Ayo B., De La Torre U., González-Velasco J.R.*

Department of Chemical Engineering, Faculty of Science and Technology, University of the Basque Country, Bilbao, Spain

* juanra.gonzalezvelasco@ehu.es

Keywords: Cu species, BETA, FT-IR, NH_3-SCR

1 Introduction

The use of diesel and lean burn gasoline engines in vehicles application is increasing due to their higher fuel efficiency and lower CO_2 emissions compared to stoichiometric gasoline engines. However, the excess of oxygen in the environment makes NO_x reduction a challenging endeavor. SCR technology runs the engine under continuous lean mode and needs an external source of reductant for NO_x elimination, e.g. NH_3 obtained from urea hydrolysis. Cu exchanged ZSM-5 was first reported to be an effective catalyst for NO_x reduction on lean exhaust [1].

This work aims to elucidate the nature and location of Cu species in BETA zeolite catalysts, to be related with NH_3-SCR activity. Thus, a series of prepared catalysts is extensively characterized and the activity for NO_x reduction is tested in reactor experiments.

2 Experimental

Four Cu/BETA catalysts were synthesized by wet-ion exchange using copper acetate as precursor. The as-received BETA zeolite was used in its ammonic or protonic form, resulting in NH_4^+/Cu and H^+/Cu catalysts. Alternatively, an intermediate ion exchange with Na^+ ions was performed over NH_4^+/BETA and H^+/BETA zeolites, afterwards being submitted to copper ion exchange, resulting in NH_4^+/Na/Cu and H^+/Na/Cu catalysts. After ion exchange, catalysts were calcined at 500 ºC during 4 hours. The prepared catalysts were characterized in terms of XRF, N_2 adsorption-desorption, EPR, H_2-TPR, TEM and FT-IR adsorption of NO and CO.

The SCR experiments were performed in a downflow stainless steel reactor with 0.8 g of 0.3-0.5 mm pelletized Cu/BETA catalyst. The composition of the feed gas mixture was 660 ppm NO, 660 ppm NH_3 and 6% O_2 using Ar as balance gas. Total flow rate was set at 2880 ml/min, which corresponded to a space velocity (GHSV) of 86,500 h^{-1}. NO, NO_2, NH_3 and N_2O concentrations at the reactor exit were continuously monitored by online FT-IR multigas analyzer (MKS 2030).

3 Results and discussion

The prepared catalysts presented a Cu loading of 3.3% ± 0.2%. The adsorption of NO and NO_2 over the catalysts was followed by FT-IR, revealing three common IR features for all prepared catalysts: 1575 cm^{-1} which is due to the formation of superficial nitrates, 1622 cm^{-1} ascribed to NO_2 adsorbed on Cu^{2+} and 1908 cm^{-1} which is due to the interaction between NO and Cu^{2+} [2]. Interestingly, only the catalysts prepared by intermediate Na^+ exchange, i.e. NH_4^+/Na/Cu and H^+/Na/Cu, presented an IR feature centered at 1814 cm^{-1}, which is attributed to Cu^+–NO species. Besides, the Cu^+–NO interaction was composed of 3 contributions (1803, 1814 and 1823 cm^{-1}) which suggests the presence of different types of exchanged Cu species.

Figure 1 shows the evolution of H_2 consumption during temperature programmed reduction experiments, presenting two separated peaks representative of CuO aggregates reduction (low temperature) and Cu ions reduction (high temperature) [3]. The H_2 consumption profile was

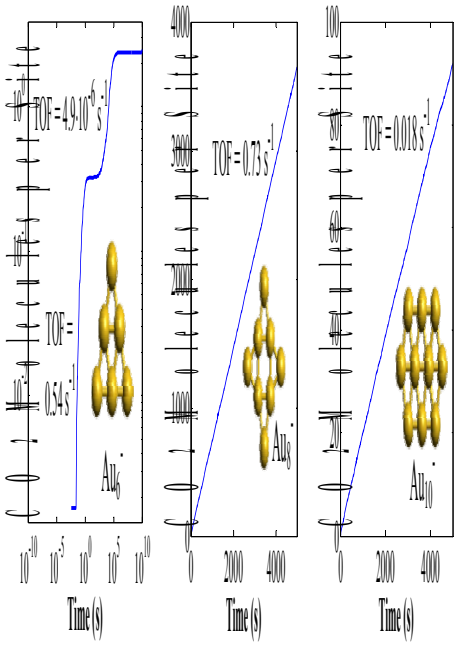

Figure 1. H_2 consumption of prepared catalysts during TPR.

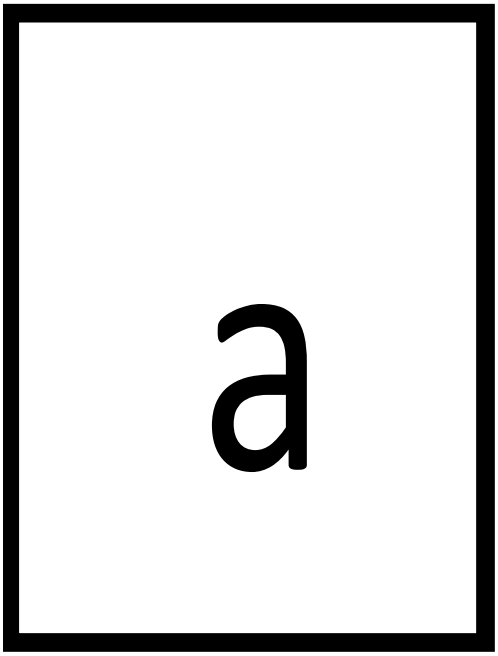

Figure 2. Conversion of NO_x and selectivity to N_2, N_2O and NO_2 for prepared Cu/BETA catalysts.

deconvoluted in five different contributions located at 280, 365, 450, 495 and 545 ºC and assigned to reduction of external CuO clusters, CuO clusters located in the zeolite channels and three different types of copper ions, respectively, related to the contributions observed by FT-IR. The integration of deconvoluted H_2 consumption peaks allows quantifying the nature and location of species. The amount of CuO aggregates, which comprises CuO external clusters and intrachannel nanosized CuO particles with peaks located at 280 and 365 ºC, respectively, accounted for around 45% of the total H_2 consumption disregarded of the catalyst. The reduction temperature of Cu ions increased in the order NH_4^+/Na/Cu < H^+/Na/Cu < NH_4^+/Cu < H^+/Cu, suggesting that the NH_4^+/Na/Cu catalyst contains the easiest reducible ions, located at accessible position of the zeolite framework. Accessibility to Cu ions decreases with temperature.

Figure 2 illustrates the SCR activity of the prepared catalysts. The NO_x conversion followed the trend NH_4^+/Na/Cu > H^+/Na/Cu > NH_4^+/Cu > H^+/Cu in accordance with the accessibility to copper ions determined by H_2-TPR. NH_4^+/Na/Cu resulted in the most active catalyst with maximum NO_x conversion of 87% and 92% of selectivity to N_2 achieved around 350 ºC.

4 Conclusions

The most active catalyst for NH_3-SCR of NO_x was NH_4^+/Na/Cu. The coexistence of Cu^{2+} and Cu^+, and easily reducible copper ions located at accessible exchangeable sites, lead to a highly active and selective NH_3-SCR catalyst for NO_x removal to N_2.

Acknowledgements

The authors wish to thank to the Spanish MICINN (CTQ2012-32899, BES-2013-065349) and the Basque Government (IT657-13, BFI-2010-330) for their financial support.

References

[1] M. Iwamoto, H. Furukawa, Y. Mine, F. Uemura, S.I. Mikuriya, S. Kagawa, *J. Chem. Soc., Chem. Commun.* (1986) 1272.
[2] K.I. Hadjiivanov, *Catal. Rev.-Sci. Eng.* 42 (2000) 71.
[3] B. Pereda-Ayo, U. De La Torre, M.J. Illán-Gómez, A. Bueno-López, J.R. González-Velasco, *Appl. Catal. B: Environ.* 147 (2014) 420.

V-PP107

Separation and Recycling of $NiFe_2O_4$ Nanocatalyst for CO_2 Decomposition with CH_4 Recovery from Steel Industrial Flyash

Lin K.-S.*, Chiang C.L., Adhikari A.K.

Department of Chemical Engineering and Materials Science/Environmental Technology Research Center, Yuan Ze University, Chung-Li City, Taiwan

* kslin@saturn.yzu.edu.tw

Keywords: Flyash, CO_2 decomposition, spinel structure, Zinc/nickel/manganese, ferrite, nanocatalyst, steel industry wastes, resource recovery

1 Introduction

Recently, over 0.2 million tons per year of flyash hazardous wastes are produced from steel industries in Taiwan and they cause potential environment pollution. The flyashes are ultrafine particles with toxic metals that can be leached out, bioaccumulated, and intaked into body having high risk for human beings or environment [1]. In stainless steel/carbon steel manufacturing plants, the $ZnFe_2O_4$ is major components and can be easily separated/purified using magnetic separation method after ball mill process. The $NiFe_2O_4/ZnFe_2O_4/MnFe_2O_4$ nanocatalysts are used for CO_2 reductive decomposition [2,3]. Carbon dioxide is the main greenhouse gas and play important role in the global warming, Hence its emission from steel companies, powder generation plants, and petrochemical industries has attracted the global attention. Therefore, the structural characterization and CO_2 decomposition efficiencies of $NiFe_2O_4/ZnFe_2O_4$ separated from flyash were studied and compared with as-synthesized ferrites in the present study.

2 Experimental

The metallic ferrite nanocatalysts were obtained by two methods including hydrothermal synthesis from commercial chemicals and magnetic separation from steel industrial flyash. Nickel sulfur and iron nitrite hydrates were stirred for well-dissolved with 1,000 rpm for 30 min. The pH value of solution was adjusted to 8-10 by adding ammonium with stirring for 2 h. Base solution putted into Teflon-lined steel autoclave, and then heated to 180°C for 6 h. After cooling, filtering, washing, and drying, the nickel ferrite nanocatalyst ($NiFe_2O_4$) was synthesized from hydrothermal synthesis. The next method was magnetic separation. The fine-particle flyash was obtained via ball-milling the well-dried flyash. Afterward the magnetic ferrite nanocatalysts were selected by magnetic separation in machine.

3 Results and discussion

The XRD patterns indicated the spinel structures of magnetic flyash after separation shown in Figure 1(a-i). FE-SEM micrographs showed that the flyash were mostly ball-like shape whereas XPS spectra showed that $ZnFe_2O_4$ is main component of the flyash surface. However, the main structures of flyash with weak magnetic or non-magnetic were both spinel and ZnO

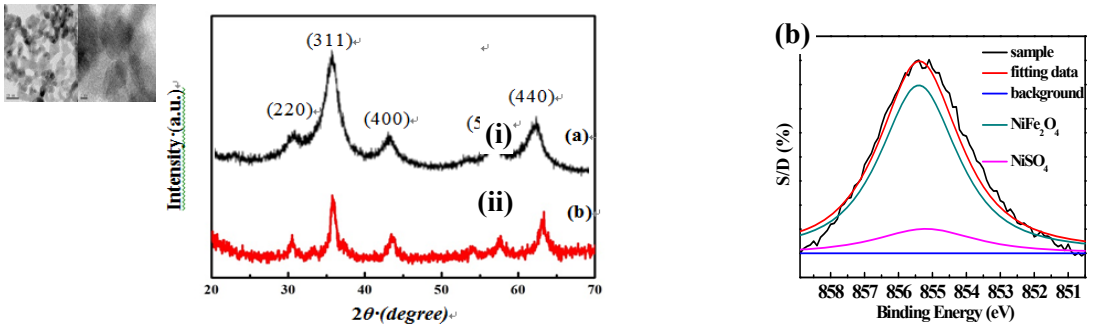

Fig. 1. (a) XRD patterns/HR-TEM micro-images and (b) XPS spectra of $NiFe_2O_4$.

structures. They have ball and bar shapes like morphology. The XPS spectra showed the most of

these flysah possessing ZnO structure. The N_2 adsorption/desorption isotherms of flyash were determined as a Type IV. On the other hand, the XRD patterns of $NiFe_2O_4$/$ZnFe_2O_4$/$MnFe_2O_4$ nanocatalysts prepared from hydrothermal method also have spinel structure shown in Figure 1(a-ii). Based on FE-SEM and HR-TEM micrographs, the particle sizes were ranged from 5-20 nm and uniform nanocatalysts were found. The XPS spectra showed central metals of $NiFe_2O_4$, $ZnFe_2O_4$, and $MnFe_2O_4$ are Ni(II), Zn(II), and Mn(II), respectively (Figure 1b). In addition, N_2 adsorption/desorption isotherms of $NiFe_2O_4$, $ZnFe_2O_4$, and $MnFe_2O_4$ were all Type V. The efficiencies of CO_2 decomposition and methanation processes were measured in response to the different temperatures (Figure 2). Once the reaction temperature increased, more CH_4 was produced. After methanation of CO_2, the surface of flyash was characterized using XPS and Fe_3C structure was observed on the surface. From the GC/TCD analyses, the yields of CH_4 production of as-synthesized $NiFe_2O_4$, $MnFe_2O_4$, and $ZnFe_2O_4$ were 99.8, 89.6 and 22.3%, respectively. In addition, the yield of CH_4 production of flyash was only 6.2%.

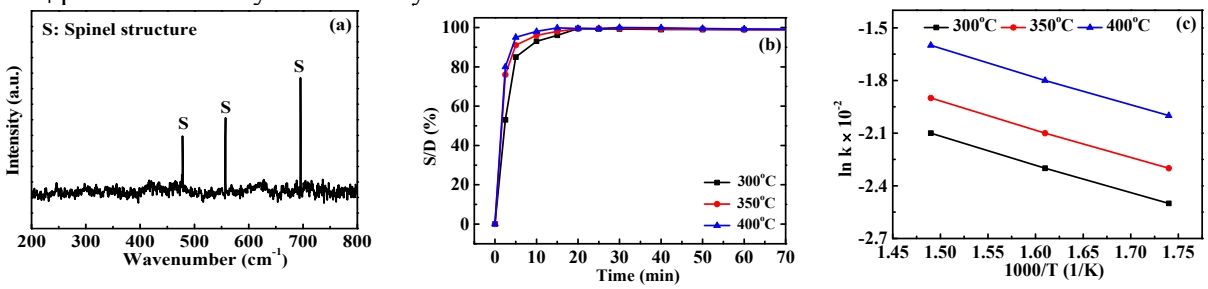

Fig. 2. (a) Raman spectra of $NiFe_2O_4$, (b) S/D values for CO_2 decomposition onto $NiFe_2O_4$ within 70 min, and (c) Arrhenius plot of $NiFe_2O_4$ at various temperatures.

Table 1. r^2 and K_{SA} Value of flyash from steel industry , $ZnFe_2O_4$, $NiFe_2O_4$ and $MnFe_2O_4$.

		Flyash	$ZnFe_2O_4$	$NiFe_2O_4$	$MnFe_2O_4$
First order $-\ln\left[\frac{C}{C_0}\right] = K_{SA}\rho_a t$	R-squared (r^2)	0.9896	0.9716	0.999	0.9990
	Rate constant (l/time·m^2)	0.00377	0.00038	0.00049	0.00053

Table 2. Activation energy (E_a) of flyash, $ZnFe_2O_4$, $NiFe_2O_4$ and $MnFe_2O_4$

Sample	E_a (kJ/mol)
Flyash	279
$ZnFe_2O_4$	272
$NiFe_2O_4$	117
$MnFe_2O_4$	139

4 Conclusions

The catalysts prepared from hydrothermal method showed better CO_2 decomposition performance compared to the catalysts separated from the steel industries flyash. Moreover, the yields of CH_4 from synthesized catalysts were more than 90% while only 6% for flyash catalyst.

Acknowledgements

The financial support of Ministry of Science and Technology of Taiwan, R.O.C. is greatly acknowledged (MOST 103-3113-E-008-003).

References

[1] R.M. Sherrard, N.E. Carriker, M.S. Greeley, *Integr. Enviro. Assess. Manage*. 11 (2015) 5.
[2] L. Ma, R. Wu, H. Liu, W. Xu, L. Chen, S. Chen, *Solid State Sci.* 13 (2011) 2172.
[3] L. Ma, L. Chen, S. Chen, *Mater. Chem. Phys*. 114 (2009) 692.

V-PP108

Regeneration of the Hydrogenation Catalysts by Supercritical Fliud Extraction

Sagdeev A.A.[1], Gallyamov R.F.[1], Sagdeev K.A.[1], Gumerov F.M.[2*]

1 - Nizhnekamsk Chemical Technological Institute, Nizhnekamsk, Russia
2 - Kazan National Research Technological University, Kazan, Russia

* gallyamovrf@gmail.com

Keywords: catalyst regeneration, supercritical fluid extraction, co-solvent

1 Introduction

Catalyst regeneration is one of the main problems in providing technical and economic efficiency of the vast majority of oil refining and petrochemical processes. One of the promising method for catalysts' regenerating is the supercritical fluid extraction (SCFE) process [1].

The aim of the present work is to explore the possibility of regeneration of spent catalyst from the enterprise of "Nizhnekamskneftekhim" (nickel-on-kieselguhr, palladium catalyst LD-265) in a supercritical carbon dioxide (SC-CO_2) medium [2].

2 Results and discussion

In the first series of experiments, the regeneration of the catalyst was performed by using pure SC-CO_2. For the purpose of the greater effect there was investigated the influence of concentration of different nature co-solvents of (chloroform, dimethylsulfoxide (DMSO), methanol and acetone) on the change in mass of the catalysts in the process of regeneration [3]. The extraction kinetics of catalyst regeneration at T=423 K using modified by various additives SC-CO_2 with an optimal concentration of co-solvents is presented in Fig.1.

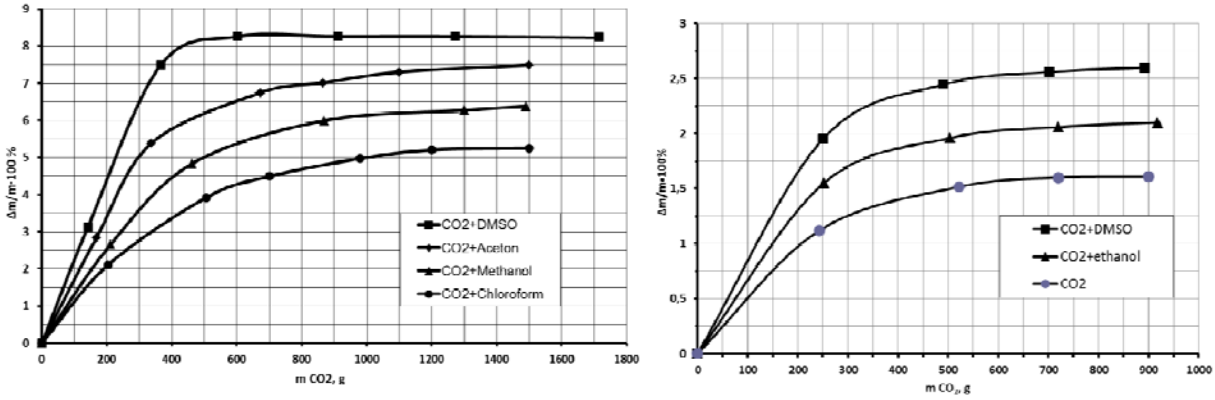

a

b

Fig. 1. Change of catalyst's mass in the course of its regeneration
a – nickel-on-kieselguhr *P*=30 MPa,
b – palladium catalyst LD- 265 *P*=20 MPa

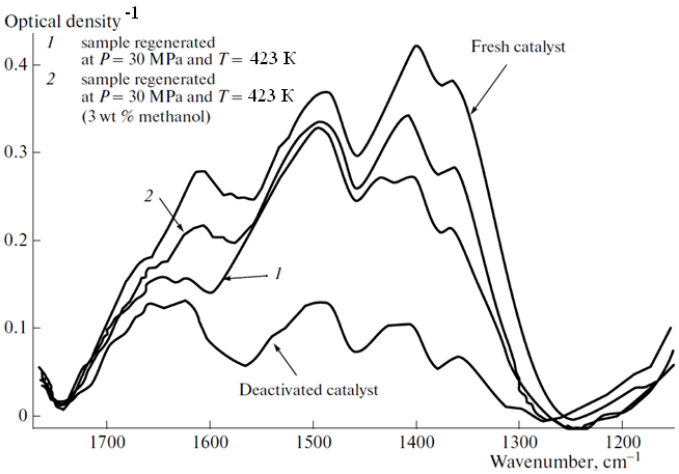

The greatest degree of extraction decontamination compounds is provided when used as co-solvent DMSO, which has a high polarity, and allows the most complete extraction of polar compounds.

The IR spectra of the regenerated catalyst samples (Fig. 2) confirm the occurrence of changes, primarily a decrease in the amount of deactivating compounds. The activity of the nickel-on-kieselguhr catalyst was estimated from the extent of hydrogenation of ethylene to ethane (table 1).

Evaluation of the activity of samples of the aluminum-palladium catalyst was carried out on the residual value of diene and bromine numbers in the hydrogenation product (table. 2).

Fig. 2. The IR spectra of the samples of nickel-on-kieselguhr catalyst, regenerated using pure and modified SC CO_2

Table 1. Activity of the samples of nickel-on-kieselguhr catalyst subjected to various treatments in the hydrogenation of ethylene

Product	Samples			
	initial catalyst	spent catalyst	regenerated (SC CO_2+ 3%wt methanol)	regenerated (SC CO_2)
Ethane, vol %	91,5	87,7	92,9	92,3
Ethylene, vol %	8,5	12,3	7,7	7,1

Table 2. Comparative analysis of hydrogenation results of the benzene-toluene-xylene-fractions, obtained on samples of the palladium catalyst LD-265

Activity index	Samples			
	steam-air treatment	regenerated (SC CO_2)	regenerated (SC CO_2+6%wt DMSO)	regenerated (SC CO_2+6%wt ethanol)
Diene number, gJ_2/100g	2,85	2,4	1,5	2,0
Bromine number, gBr_2/100g	20,5	19,0	16,2	17,0

3 Conclusions

Thus, the obtained values of the catalytic activity of the hydrogenation catalyst samples demonstrate the effectiveness of the extraction process, at the level of requirements imposed on the catalysts.

References

[1] F.M. Gumerov, A.N. Sabirzyanov, G.I. Gumerova. Sub- and Supercritical Fluids in Polymer Pub. FEN Processing 2000, 328 p.

[2] Catalysts: Regeneration using supercritical fluid CO2 extraction process: thesis by publication / F.M. Gumerov, A.A. Sagdeev, T.R. Bilalov, R.F Gallyamov, K.A. Sagdeev et al.; under the general editorship of Professor F. M. Gumerov. – Kazan: Pub «Otechestvo», 2015. – 264 c.

[3] Gumerov, F.M. Regeneration of the Catalysts by Supercritical Fluid Extraction / F.M. Gumerov, A.A. Sagdeev, A.T. Galimova, K.A. Sagdeev // International Journal of Analytical Mass Spectrometry and Chromatography. – 2014. – V. 2, P. 1-14.

V-PP109

CO_2 Adsorption Kinetics on Chemically Modified Activated Carbon

Selen Çağlayan B.[1,2*], Aksoylu A.E.[1]

1 - Department of Chemical Engineering, Bogazici University, Istanbul, Turkey
2 - Advanced Technologies R&D Center, Bogazici University, Istanbul, Turkey

* selenbur@boun.edu.tr

Keywords: activated carbon, adsorbents, CO_2 adsorption, isotherms, CO_2 adsorption kinetics

1 Introduction

CO_2 adsorption capacity of activated carbons at a given temperature and pressure depends the pore structure and the properties of functional groups introduced to the surface by certain pretreatments. CO_2 adsorption capacities of a commercial activated carbon subjected to different treatments such as HNO_3 oxidation, air oxidation, alkali impregnation and heat treatment under helium gas atmosphere were determined by gravimetric analyses for 298-473 K temperature and 0-20 bar pressure range. The experimental details can be found elsewhere [1]. It is possible to fit the kinetic data to both pseudo-first and pseudo-second order models aiming to determine the appropriate reaction order for the adsorption processes based on R^2 correlation coefficient values. Pseudo-first and pseudo-second order kinetic models as well as the intra-particle diffusion model were applied to the experimental kinetic data on the CO_2 adsorbent samples studied for the 1 bar CO_2 pressure.

2 Experimental

The chemically modified activated carbon based adsorbents used in this study are given in Table 1.

Table 1. List of activated carbon based adsorbents.

Name	Treatment
AC1	HCl washed NORIT ROX
AC2	HCl washed and air oxidized NORIT ROX
AC3	HCl washed and HNO_3 oxidized NORIT ROX
AC4-200	Na_2CO_3 impregnated and calcined (200°C) AC2
AC4-250	Na_2CO_3 impregnated and calcined (250°C) AC2
AC4-300	Na_2CO_3 impregnated and calcined (300°C) AC2
AC5-175	Na_2CO_3 impregnated and calcined (175°C) AC3
AC5-200	Na_2CO_3 impregnated and calcined (200°C) AC3
AC5-250	Na_2CO_3 impregnated and calcined (250°C) AC3
AC5-250-400He	Na_2CO_3 impregnated and calcined (250°C) AC3 subjected to He treatment at 400°C
AC4-300-600He	Na_2CO_3 impregnated and calcined (300°C) AC2 subjected to He treatment at 600°C

The adsorption and desorption isotherms of all samples were obtained at 25, 120/180 and 200°C in the 0-20 bar pressure range. Pseudo-first and pseudo-second order kinetic models as well as the intra-particle diffusion model were used to describe the kinetic behavior of the adsorbents.

3 Results and discussion

The CO_2 adsorption kinetic plots revealed a two-step adsorption process for all the adsorbents (Figure 1); a relatively fast kinetic region phase followed by a slow one till reaching the equilibrium. Pseudo-first and pseudo-second order kinetics explain adsorption for the kinetic region for most of the samples. When the whole adsorption data range is considered, the adsorption cannot be explained by any model due to complex nature of the adsorbents, but the adsorption behavior fits rather well to pseudo-first order kinetics at 120°C for the alkali impregnated samples, and at 25°C for non-impregnated samples and the adsorbents subjected to high temperature helium treatment as well.

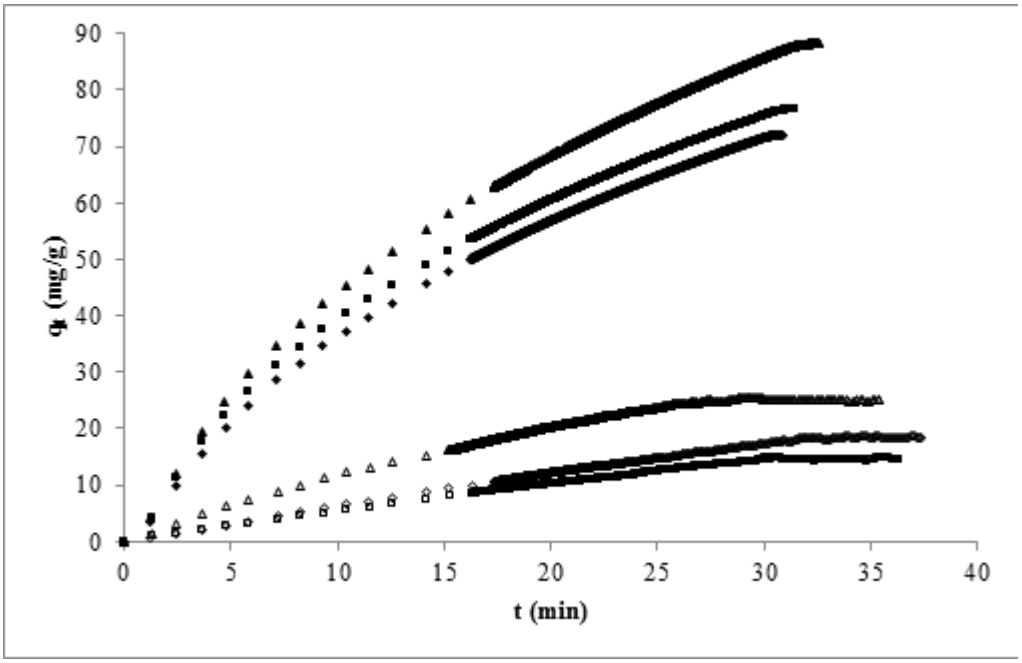

Figure 1. The kinetic plots of AC4 samples: (■) AC4-200, (▲) AC4-250 and (♦) AC4-300 at 25ºC (filled data points) and 120ºC (hollow data points).

Acknowledgements

This work is financially supported by TUBITAK through project 113M263 and by Boğaziçi University Research Fund through project BAP-M6755.

References

[1] B.S. Caglayan, A.E. Aksoylu, *J. Hazard. Mater*. 252–253 (2013) 19–28.

V-PP110

Epoxidation of Fatty Acid Methyl Esters of Vegetable Oils by Air

Kulazhskaya A.D., Sapunov V.N., Udaev S.A., Voronov M.S.*

Mendeleev University of Chemical Technology of Russia, Moscow, Russia

* kulazhskaya_92@inbox.ru

Keywords: fatty acid methyl esters, vegetable oils epoxidation, atmospheric, oxygen, hydroperoxide

1 Introduction

The epoxidation of vegetable oils and fatty acid methyl esters of vegetable oils are widely used to produce plasticizers and lubricants now. A number of methods of epoxidation is characterized by using different epoxidizing agents: epoxidation with peroxyacids [1], the epoxidation of organic hydroperoxides [2], epoxidation with hydrogen peroxide [3]. These methods have significant disadvantages. For example, the use of peracid produced *in situ* from the corresponding organic acid and hydrogen peroxide, is always associated with the use of expensive corrosion resistant equipment. Organic hydroperoxides are highly toxic and explosive compounds. A concentrated solution of hydrogen peroxide is also very expensive.

In this paper, it is shown the possibility of obtaining a mixture of epoxy compounds of fatty acid methyl esters of vegetable oils by reacting unsaturated compounds with air oxygen. The purpose of research is definition of the mechanism and kinetics of the process.

2 Experimental/methodology

The process was carried out in a glass column reactor. The mixture of methyl esters of fatty acids of sunflower oil was charged into the reactor, bubble feeding air was started and then mixture was heated up to the target temperature. During the study of the epoxidation the homogeneous metal complex catalyst based on molybdenum was added to the reaction mixture. The course of study of the oxidation reaction was carried out without catalyst. Synthesis was performed for 5 hours. Hydroperoxide content was determined by iodometrically titration, accumulation of epoxides fixed by gas-liquid chromatography.

3 Results and discussion

When the oxidation of mixture of fatty acid methyl esters of sunflower oil with no catalyst was carried out, accumulation of hydroperoxides, epoxides, and weak organic acids was observed. Based on this fact probable mechanism of formation epoxy compounds was supposed [4]: non-catalytic interaction of peroxide radicals with unsaturated compounds (Fig.1.) and classical hydroperoxide epoxidation with metal complex catalyst (Fig.2.).

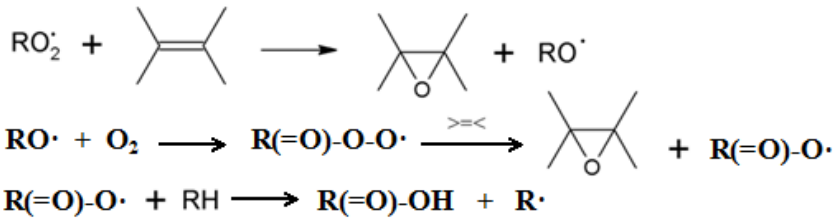

Fig. 1. Non-catalytic route of process of epoxidation.

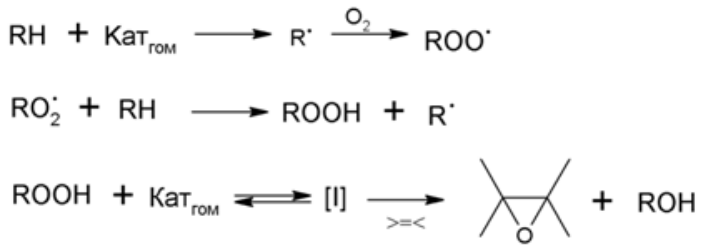

Fig. 2. Catalytic route of process of epoxidation.

4 Conclusions

Kinetic regularities of oxidation and epoxidation of fatty acid methyl esters was studied. Mathematical model based on the proposed mechanisms was composed, it describes the experimental data adequately.

References

[1] Venu Babu Borugadda, Vaibhav V Goud, EnergyProcedia 2014. V. 54. P. 75 - 84.
[2] M. Guidotti, N. Ravasio, R. Psaro, E. Gianotti, L. Marchesec, S. Coluccia, Applied Catalysis A: General 2011. V. 401. P. 189 – 198.
[3] A. Campanella, M. A. Baltanás, M. C. Capel-Sánchez, J. M. Campos-Martín, J. L.G. Fierro, Green Chem 2004. V. 6. P. 330 - 334.
[4] I.A. Krylov, I.U. Litvintsev, V.N. Sapunov, Kinetic and Catalysis 1982.

V-PP111

Perovskite-Based Catalysts as Alternative to Commercial Three-Way-Catalysts? – Impact of Cu and Ca Doping and Optimisation of Surface Properties

Shoen A.[1,2,3], Dacquin J.-Ph.[1,2,3], Dujardin C.[1,3,4], Granger P.[1,2,3*]

1 - UCCS, Villeneuve d'Ascq, France
2 - University of Lille, Villeneuve d'Ascq, France
3 - Cité Scientifique, Villeneuve d'Ascq, France
4 - ENSCL, France

* pascal.granger@univ-lille1.fr

Keywords: TWC, perovskite, postcombustion catalysis, iron copper

1 Introduction

Three-way catalysis (TWC) is an expensive technology due to extensive use of precious metals (Platinum group metal PGM). Previously, perovskite-type materials were developed for three-way applications especially to stabilize PGM from thermal sintering. This strategy led to interesting outcomes with lower PGM contents. In this study, low cost Fe-based perovskites being non-toxic and thermally stable were investigated. However, the main drawback lies in the surface reconstruction and a usual lanthanum enrichment which affects their catalytic properties [2]. A better optimisation of the surface proprieties can be obtained through partial substitution of A- and B-site ($LaFe_{1-x}Cu_xO_3$ and $La_{1-x}Ca_xFe_{1-x}Cu_xO_3$). It was also found that none stoichiometric perovskite especially lanthanum-deficient perovskites leads to significant enhancement of the catalytic performances.

2 Experimental/methodology

The perovskite catalysts were prepared by a conventional citrate method and finally calcined in air at 600 °C. BET, H_2-TPR, Raman spectroscopy, XRD and XPS characterisations were performed before and after catalytic measurements. NO_x and reductants concentrations were measured during temperature-programmed reactions in a fixed bed continuous-flow reactor with WHSV=60,000 $mL.g^{-1}.h^{-1}$ from 110°C to 500°C under stoichiometric, lean, and rich conditions. Realistic feed gas compositions consisted of 0.1% NO, 15 % CO_2, 10 % H_2O, CO (0.5 %; 0.7 %; 0.9 %), CH_4 (150 ppm; 225 ppm; 300 ppm), C_3H_6 (300 ppm; 450 ppm; 600 ppm), C_3H_8 (150 ppm; 225 ppm; 300 ppm), O_2 (0.935 %; 0.777 %; 0.609 %), and H_2 (0.167 %; 0.233 %; 0.3 %).

3 Results and Discussion

Partially substituted $LaFeO_3$ with Cu and Ca were characterized from XRD highlighting an orthorhombic perovskite structure. Surface compositions as well as the reducibility of the solids are strongly influenced by Cu substitution whereas Fe prevents the degradation of the structure in reducing atmosphere.

The conversion profiles of CO, NO and propene vs. T during temperature-programmed reactions are presented in Fig. 1. Temperatures corresponding to 50 % conversion of CO under stoichiometric conditions and NO under rich conditions as well as their surface properties are reported in Table 1. The reference $LaFeO_3$ catalyst exhibits poor catalytic performances. By contrast, a significant enhancement of CO and NO conversion is observed for the La-deficient sample, $La_{0.7}FeO_3$. This enhancement is related to higher Fe surface concentration evidenced by

XPS analysis.

Table 1. Temperatures of 50 % conversion of CO (stoichiometric) and NO (rich) and surface properties of the low-cost Fe-based perovskite catalysts.

Catalyst	T_{50} CO	T_{50} NO	Fe/La	S. S. A. (m^2/g)
$LaFeO_3$	492 °C	*460 °C* (T_{25})	0.41	9.5
$La_{0.7}FeO_3$	382 °C	494 °C	1.47	31.9
$LaFe_{0.9}Cu_{0.1}O_3$	305 °C	489 °C	0.42	18.4
$LaFe_{0.8}Cu_{0.2}O_3$	294 °C	*501 °C* (T_{25})	0.40	13.8
$La_{0.9}Ca_{0.1}Fe_{0.9}Cu_{0.1}O_3$	288 °C	478 °C	-	21.4
$La_{0.8}Ca_{0.2}Fe_{0.8}Cu_{0.2}O_3$	279 °C	469 °C	-	24.0

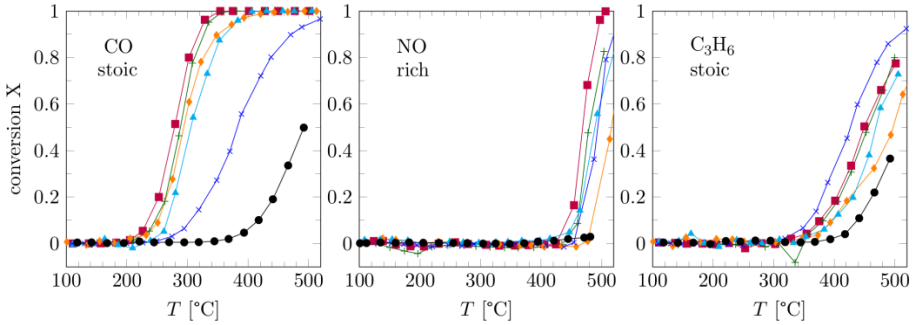

Fig. 1. CO, NO, and C_3H_6 conversions on Fe-based perovskite catalysts: $LaFeO_3$ (●), $La_{0.7}FeO_3$ (x), $LaFe_{0.9}Cu_{0.1}O_3$ (▲), $LaFe_{0.8}Cu_{0.2}O_3$ (♦), $La_{0.9}Ca_{0.1}Fe_{0.9}Cu_{0.1}O_3$ (+), $La_{0.8}Ca_{0.2}Fe_{0.8}Cu_{0.2}O_3$ (■).

The partial substitution of La and Fe by Ca and Cu enhances the catalytic performances (Fig. 1). Copper addition led to a CO activation at much lower temperature ~300 °C whereas NO and propene were converted above 400-450 °C. Replacing part of La by Ca leads to higher activities, with light-off conversion curves shifting more than 200 °C for CO oxidation as compared to $LaFeO_3$. Propene oxidation is enhanced for $La_{1-x}Ca_xFe_{1-x}Cu_xO_3$ perovskites (x = 0.1, 0.2) and $La_{0.7}FeO_3$ catalysts. XRD analysis of used catalysts confirms the stability of the perovskite structure in the presence of steam assigned to the presence of Fe. Low temperature CO conversion is very interesting since CO is known to strongly adsorb on Pt which inhibit NO reduction to N_2 at low temperature. The combination of Cu and Ca doping and surface composition optimisation will also be investigated.

4 Conclusions

Fe-based perovskites are low-cost alternatives to partly replace noble metals in conventional 3-way catalysts. Surface composition optimisation strongly enhances the catalytic activity of the perovskite by increasing the accessibility of the active sites. Cu and Ca doping further increases the catalytic activity especially CO oxidation which can avoid CO inhibition on noble metals. Combination of partial substitution, non-stoichiometric formulation is a first step for further optimisation. Anyway, the presence of low content of noble metals seems to be inevitable for the conversion of NO.

Acknowledgements

The research leading to these results has received funding from the European Union's 7th Framework Programme under grant agreement no 280890-NEXT-GEN-CAT.

References

[1] G. Kremenic et al. *J Chem Soc. Faraday Transactions 1(8*) (1985) 939.
[2] Y. Wu et al. *Applied Catalysis B* 125 (2012) 149.

V-PP112

Effect of Desilication of HY Zeolite in Pt/HY Catalysts for Polystyrene Hydrocracking

Salbidegoitia J.A., Fuentes E.G., Gonzalez-Marcos M.P.*, Gonzalez-Velasco J.R.

Group of Chemical Technologies for Environmental Sustainability, Department of Chemical Engineering, Faculty of Science and Technology, The University of the Basque Country, Bilbao, Spain

* mp.gonzalezmarcos@ehu.es

Keywords: desilication, zeolite, polystyrene hydrocracking

1 Introduction

Polystyrene (PS) hydrocracking to fuels is studied as an alternative in plastic recycling, with bifunctional Pt/HY catalysts. Big polymer molecules cannot enter the internal pores of the catalysts[1]. Hierarchical supports with high external surface area have been found suitable for this kind of processes[2]. In this work, a desilication treatment was carried out to increase external surface area of the support, thus improving polymers accessibility to the active sites.

2 Experimental

Bifunctional catalysts: Four supports were prepared from NH_4Y zeolite (Zeolyst Corp., Si:Al = 6). HY was obtained by direct calcination of NH_4Y (1 K min^{-1}, 823 K). The other three supports were obtained by desilication with NaOH: 10 g of NH_4Y zeolite were mixed with 1 L of NaOH solutions of different concentrations (0.1 M: hHY1, 0.2 M: hHY2 and 0.3 M: hHY3) plus 10 g of tetrapropilammonium hydroxide (TPAOH) as pore directing agent to protect the zeolite structure[3].

Four catalysts with nominal 0.5 wt.% Pt were prepared on the supports by ionic exchange[4], using tetraammineplatinum(II) nitrate (Alfa Aesar, 99.99%). 10 g of the support in powder form were slurred in deionised water (1 L) and then heated to 353 K under continuous stirring and reflux at pH=7 for 24 h. Afterwards, the solid was separated, washed, dried (393 K, 12 h), calcined (823 K, 2 h) and reduced in hydrogen flow (800 K, 3 h).

Catalysts were characterized by: XRD, SEM, N_2 physisorption (BET and external surface, 77 K), NH_3-TPD (acid strength), FTIR of adsorbed pyridine (Py) (Brønsted and Lewis acidity[5], 423 K), FTIR of absorbed 2,6-di-*tert*-butylpyridine (DTBPy), (external acidity[6], 423 K), XRF (actual Pt content), TEM and H_2 chemisorption (Pt dispersion, 308 K).

Catalytic activity: PS hydrocracking in the liquid phase was carried out at kinetic regime[1]: 5% PS (M_W = 192,000 g·mol^{-1}, M_n = 120,000 g·mol^{-1}) solved in decahydronapthalene, 623 K, 180 bar of H_2, 1800 rpm, 2.36 $g_{Cat.}·L^{-1}$ in slurry, with an stirred autoclave reactor. PS conversion was evaluated by GPC. Selectivity was analyzed by GC-FID.

3 Results and discussion

Table 1 shows measured catalyst properties. XRD showed no significant change of support relative crystallinity with desilication, although desilicated supports were less crystalline than the original support. Desilication improved external surface area up to 40%. Despite the loss of total acidity and acid strength, Brønsted acid sites, essential for cracking reactions, remain nearly constant with desilication in the studied range. These facts mean that most of silicon removed came from extraframework species related to structural defects, and the accessibility of the acid sites increased slightly, in good agreement with $S_{Ext.}/S_{BET}$. Pt dispersion significantly increased with desilication, as local big Pt particles were found with TEM in untreated Pt/HY.

Table 1. Properties of the catalysts.

Catal.	Crystal.	$S_{Ext.}$	NH_3, μmol·g^{-1}				Py, μmol·g^{-1}		Acces.	Pt[a]	Disp.[b]	d_{Pt}[b]
	%	m^2·g^{-1}	T	W	M	S	B	L	%	%	%	nm
Pt/HY	100	117	497	272	149	76	180	160	26.4	0.5	*35*	*3.1*
Pt/hHY1	91	146	479	385	64	30	216	123	27.2	0.5	57	1.9
Pt/hHY2	93	156	472	378	61	33	179	118	29.8	0.5	60	1.8
Pt/hHY3	90	161	448	373	48	27	176	113	30.1	0.5	83	1.3

Key to acidity: T, total; W, weak; M, medium; S, strong; B, Brønsted; L, Lewis; Acces., accessible.
[a]Nominal; [b]Estimated by TEM.

Desilicated hierarchical catalysts showed higher PS hydrocracking rates, which improved with desilication, as shown in Figure 1(a). This fact can be attributed to the higher accessibility of PS to the active sites. Apparent activation energy is not significantly affected by desilication. Small differences were found with desilication on the chemical nature of PS hydrocracking products, although products in the diesel range significantly increased at the expense of products in the gasoline range and gases, particularly at low temperature, what is probably related to the lower acid strength of the desilicated catalysts. Figure 1(b) shows TOF values for all the studied catalysts.

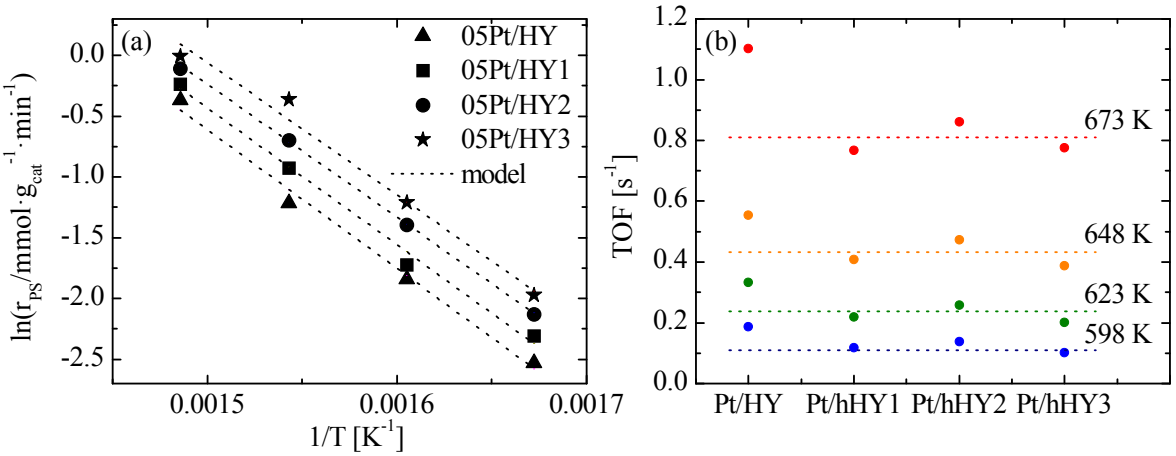

Fig. 1. Experimental rates (a) and TOF values (b) with temperature for the prepared catalysts.

4 Conclusions

Desilication of HY increases mesoporosity with small loss of crystallinity or Brønsted acid sites, decreases acid strength and improves Pt dispersion in the catalysts, thus increasing PS hydrocracking rate and selectivity to diesel range. TOF values of untreated Pt/HY are higher than those of the desilicated catalysts, which could be related to its higher acid strength.

Acknowledgements

Authors thank Spanish Ministry for Science and Innovation (CTQ2010-17277), Basque Government (GIC-IT-657-13, BFI-2010-150) and UPV/EHU (UFI11/39) for economic support.

References

[1] E.G. Fuentes-Ordóñez, J.A. Salbidegoitia, J.L. Ayastuy, M.A. Gutiérrez-Ortiz, M.P. González-Marcos, J.R. González-Velasco, *Catal. Today* 227 (2014) 163–170.
[3] D.P. Serrano, J.M. Escola, P. Pizarro, *Chem. Soc. Rev.* 42 (2014) 4004–4035.
[3] D. Verboekend, J. Pérez-Ramírez, *ChemSusChem* 7 (2014) 753–764.
[4] J. De Graaf, J. van Dillen, K.P. de Jong, D.C. Koningberger, *J. Catal.* 203 (2001) 307–321.
[5] C.A Emeis, *J. Catal.* 141 (1993) 347–354.
[6] A. Corma, V. Fornés, L. Forni, F. Márquez, J. Martínez-Triguero, D. Moscotti, *J. Catal.* 179 (1998) 451–458.

V-PP113

Study of Supported Pt/TiO_2 Catalysts with Enhanced Activity in CO Oxidation

Shutilov A.[1,2,3*], Pakharukov I.[1,2], Oleynik A.[1,3], Zenkovets G.[1,2]

1 - Boreskov Institute of Catalysis, SB RAS, Novosibirsk, Russia
2 - Novosibirsk State University, Novosibirsk, Russia
3 - Novosibirsk State Technical University, Novosibirsk, Russia

* alshut@catalysis.ru

Keywords: CO oxidation, heterogeneous, nanostructured catalysis, noble metal, TiO_2, temperature, hysteresis

1 Introduction

Supported Pt/TiO_2 catalysts are active in the low-temperature CO oxidation, used for the environmental protection. It is known that modifying of this catalyst by the additives of transition metal results in a substantial increase in their activity [1, 2]. The aim of this work is to develop Pt/TiO_2 catalysts, doped by Fe, with enhanced activity in low-temperature CO oxidation.

2 Experimental

Catalysts 1 wt.% Pt/TiO_2 and 1 wt.% Pt, (0.03-0.55) wt. % Fe/TiO_2 were prepared by impregnating of the TiO_2 with iron and platinum nitrate solution followed by drying and heat treatment in air at 500°C. Catalysts were investigated by XRD, HREM, XPS and adsorption methods. Catalytic activity in oxidation of CO was conducted at a flow-circulation installation BI-CATr (oxy) (Russia) with circulation rate of the reaction mixture 1000 liters per hour and increasing and then decreasing the temperature in the range from 25 to 150°C. Composition of the reaction mixtures were analyzed by a chromatograph equipped with a thermocatalytic detector on a column filled with carbon SKT mark. Measurements were carried out on the fraction of catalyst 0.25-0.5 mm at the following reaction mixture: 1 vol. % CO, 10 vol. % O_2, N_2 balance, feed rate was 4.46×10^{-3} mol/min.

3 Results and discussion

According to XRD catalysts 1 wt.% Pt/TiO_2 and 1 wt.% Pt, (0.03-0.55) wt. % Fe/TiO_2, represent the anatase phase for all concentrations of iron. Oxide or metallic platinum reflexes are not detected. It indicates on highly dispersed platinum species.

Investigation of $Pt,Fe/TiO_2$ catalysts with HREM method showed that the real structure of the support is a nanocrystalline, on the surface of the support well crystalline platinum particles with the size of 1.5 - 3.5 nm are observed. At the same time the dimensions of Pt in Pt/TiO_2 catalyst are 1.5 - 6.0 nm. Note that the interplanar distances of the crystal lattice of platinum obtained by HREM showed no apparent changes in compare to standard values of metal platinum. Based on this, it can be assumed that there is no introduction of iron into platinum particles. Probably, Fe^{3+}, Fe^{2+} ions are stabilized either in the lattice of anatase to form a substitution solid solution or in interblock boundaries of nanocrystalline anatase structure.

According to XPS data, both Pt/TiO_2 and $Pt,Fe/TiO_2$ catalysts contain two types of Pt states in different atomic ratios – Pt^0 ($E_b(Pt4f_{7/2})$ = 71.1 eV) and $Pt^{\delta+}$($E_b(Pt4f_{7/2})$ = 72.1 eV) (Tabl. 1). At the similar platinum content the ratio of $Pt^{\delta+}/Pt^0$ grows with an increasing of the iron concentration to 0.28 wt.%, and then it decreases at 0.55 wt% of Fe.

The temperature dependences of CO oxidative conversion in the course of catalyst heating or

cooling in the reaction mixture are compared in Tabl 1. The heating and cooling curves do not coincide. The hysteresis recurred persistently for all studied catalysts (Fig.1). Activity of Pt/TiO_2 catalyst is much lower than that of $Pt,Fe/TiO_2$. The activity of $Pt,Fe/TiO_2$ catalysts increases with an increasing of iron content from 0.03 to 0.28 wt. %: the 50% CO conversion temperature decreases from 127 to 62^{0}C, and the reaction rate rises. But the further increase of iron content to 0.55 wt. % leads to decrease the catalytic activity. The optimum amount of Fe for the most effective CO oxidation was estimated to be 0.28 wt.%.

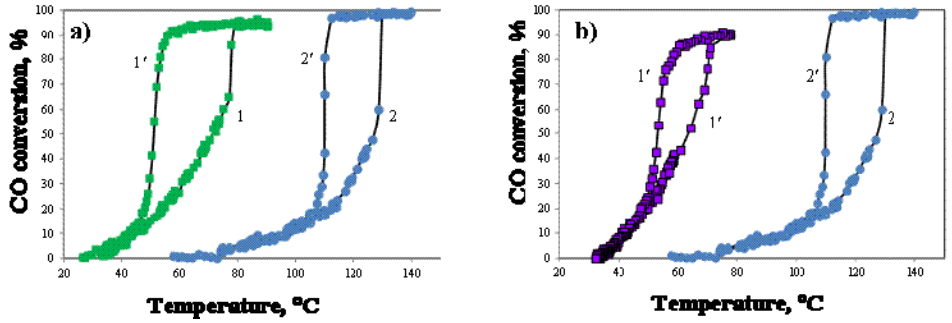

Fig. 1. Temperature dependence of CO oxidative conversion when the reaction system is (1, 2) heated and (1', 2') cooled over different catalysts: **a)** 1 wt.% Pt, 0.03 wt.% Fe/TiO_2 (1', 1'), 1 wt.% Pt/TiO_2 (2, 2'), **b)** 1 wt.% Pt, 0.55 wt.% Fe/TiO_2 (1', 1'), 1 wt.% Pt/TiO_2 (2, 2').

Table 1. Influence of the Fe content on the ratio of $Pt^{\delta+}/Pt^0$ in $Pt,Fe/TiO_2$ catalysts and their catalytic properties when the reaction mixture is heated or cooled.

Composition, wt.%	$T^{heat}_{50\%}$, °C	$T^{cool}_{50\%}$, °C	$W\times10^5$, mol CO g^{-1} min^{-1} at 60^{0}C	$Pt^{\delta+}/Pt^0$
1% Pt/TiO_2	127	109	0	0.44
1% Pt, 0.03 % Fe/TiO_2	71	51	3.2	0.80
1 % Pt, 0.14 % Fe/TiO_2	70	51	3.3	1.34
1% Pt, 0.28 % Fe/TiO_2	62	53	5.1	1.55
1% Pt, 0.55 %Fe/TiO_2	69	62	3.4	1.0

4 Conclusions

Thus, the improvement of the catalytic activity of Pt/TiO_2 catalyst in low-temperature CO oxidation could be achieved by modification of a small amount of iron. The relationship between Pt/TiO_2 and $Pt,Fe/TiO_2$ behaviours depends on the chemical composition and real structure. The introduction of iron additives in Pt/TiO_2 catalyst results in the formation of nanocrystaline structure of support. It leads to increase in platinum dispersion and change in the electronic state. For the optimum amount of Fe in the catalyst 1 wt.% Pt, 0.28 wt.% Fe/TiO_2 the $Pt^{\delta+}/Pt^0$ ratio arises to maximum value of 1.55. It is due to the changes in the interaction of platinum with support because the iron stabilized in nanocrystalline structure of TiO_2. This provide the high catalytic activity $Pt,Fe/TiO_2$ catalysts in low-temperature CO oxidation.

Acknowledgements

This work was supported by RSCF grant № 14-23-00037

References

[1] A.A. Shutilov, G.A. Zenkovets, G.N. Kryukova, V.Yu. Gavrilov, E.A. Paukshtis, A.I. Boronin, S.V. Tsybulya, *Kinet. Catal.* 49 (2008) 271.

[2] O.S. Alexeev, S.Y. Chin, M.H. Engelhard, L. Ortiz-Soto, M.D. Amiridis, *J. Phys. Chem. B.* 109 (2005) 23430.

V-PP114

Composite Carbon /Zeolite Adsorbent-Catalysts for Organic Containing Wastewater Purification Using Wet Peroxide Oxidation

Taran O.[1,2], Yashnik S.[1], Ayusheev A.[1*], Prihod'ko R.[3], Ismagilov Z.[1], Goncharuk V.[3], Parmon V.[1,4]

1 - Boreskov Institute of Catalysis SB RAS, Novosibirsk, Russia
2 - Novosibirsk State Technical University, Novosibirsk, Russia
3 - Dumansky Institute of Colloid and Water Chemistry NASU, Kiev, Ukraine
4 - Novosibirsk State University, Novosibirsk, Russia

* a.ayusheev@gmail.com

Keywords: composite, carbon, nanomaterials, zeolite, CWPO, phenol

1 Introduction

Catalytic wet peroxide oxidation (CWPO) is one of the most economical and environment-friendly advanced oxidation processes. Previously we have shown that Fe and Cu-containing zeolites with MFI structure possess a high catalytic activity in the CWPO of refractory organic pollutants [1]. A promoting effect of graphite-like carbon in Fenton-like process was also revealed [2]. Hence composite carbon nanostructures/zeolites(porous matrix) materials can be very effective adsorbent-catalysts for organic containing wastewater purification due to high adsorption capacity of carbon nanomaterials, high catalytic activity of Fe and Cu-containing zeolites, and porous structure of composite providing mass transport and filtration.

The aim of this study was the development of preparation mode of the composite adsorbent-catalysts and the testing of the prepared adsorbent-catalysts in a purification of solutions of model organic substrates: formic acid and phenol. Formic acid is an intermediate in deep oxidation of most organic compounds and the main reason for leaching of the active components of the catalysts into the reaction solution. Phenol is a typical wastewater pollutant.

2 Experimental

Two preparation mode were used for the synthesis of composite adsorbent-catalysts.

Method 1 is mechanical mixing of the zeolite H-ZSM-5 with Si/Al= 30 and the content of Fe^{3+} framework ions equal to 0.65 wt.%, with the mesoporous graphite carbon Sibunit. The composites were formed by the pressing. The weight ratio of carbon/zeolite was varied from 75/25 to 0/100.

Method 2 is pyrolysis of carbon compounds supported on the zeolite. Polyvinyl alcohol (PVA) was used as a carbon source. PVA was supported on surface of the zeolites H-ZSM-5 (Si/Al=30, Fe-0.65 wt%) and Cu-ZSM-5 (Si/Al=30, Fe-0.65 wt%, Cu-1 wt%) by impregnation. Composites were heated in inert (N_2) or reducing (H_2) conditions. The carbon content was 12 wt.%.

The catalysts were characterized by ICP-AES, EPR, XRD, DR UV-Vis and tested in CWPO of formic acid and phenol at pH 3 using a batch and a flow reactors. Reaction conditions: 0.1M HCOOH, 7mM PhOH, 1M H_2O_2, 3 gL^{-1} catalyst, 30-50ºC. The concentration of formic acid and phenol in solutions was determined by HPLC in a Phemomenex Synergi 4u Hydro-RP 80A column using a Shimadzu LC-20A chromatograph with a diode array detector.

3 Results and discussion

Composites prepared by method 1 showed the catalytic performance in phenol oxidation;

it increased proportional to the amount of Fe^{3+} ions in them. Their adsorption capacity appeared to be on the proportional rise with the content of the carbon material.

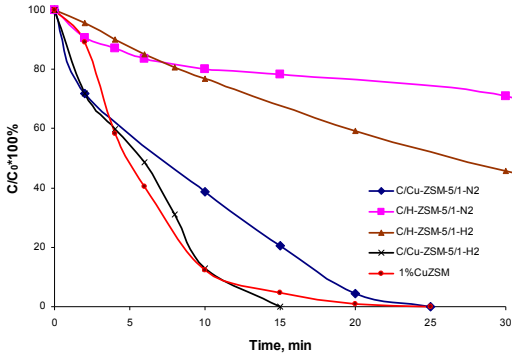

Figure. Kinetics of phenol peroxide oxidation over the zeolite 1% Cu-ZSM-5-30 and the composite catalysts prepared by the method 2 (7 mM PhOH, 1 M H_2O_2, 3 g·L^{-1} catalyst, 50 ºC).

The carbon composites prepared by method 2 and contained Cu-zeolite exhibited higher catalytic activity in the oxidation of phenol compared to composites based on copper-free zeolite H-ZSM-5 (Figure) and composites prepared by method 1. The phenol oxidation rate over the reduced composites was higher than that over the zeolites treated in inert atmosphere. Reduction treatment allows removal of O-containing surface species which inhibit peroxide oxidation [3].

Moreover, initial catalytic activity was higher for carbon-containing composites than one of zeolite catalysts. The last observation can not be explained by phenol adsorption, such as the reaction was started after the achievement of the adsorption equilibrium. One possible reason for increase of phenol oxidation rate is a change of reaction mechanism in the presence of carbon materials. Probably, oxidation proceeds on the surface of the graphite-like carbon, and electronic and conductive properties of carbon are particularly important. We believed the heterogeneous reaction steps involve the electrons transfer through the graphite π-π system from adsorbed substrate to the oxidant. Such relationships have been described for other reactions [3-5].

In the case of the formic acid oxidation, on the contrary the composite was less active on the initial step of reaction than zeolites. This result can be attributed to the hydrophobicity of the carbon surface and a peculiarity to the nature of the substrate.

4 Conclusions

The carbon/zeolites composite absorbent-catalysts were prepared by two preparation modes and tested in CWPO of phenol and formic acid. The obtained results testify that the combination of carbon and the zeolite can improve the adsorption capacity as well as the catalytic activity in the CWPO of organic substrates. However, the catalytic activity depends on the substrate nature and the mechanism of its interaction with the surface of the solid catalyst.

Acknowledgements

The study was supported by the RFBR-NANU grant 14-03-90417.

References

[1] O.P. Taran, S.A. Yashnik, A.B. Ayusheev, A.S. Piskun, R.V. Prihod'ko, Z.R. Ismagilov, V.V. Goncharuk, V.N. Parmon, *Appl. Catal. B* 140-141 (2013) 506-515.
[2] O. Taran, E. Polyanskaya, O. Ogorodnikova, V. Kuznetsov, V. Parmon, M. Besson, C. Descorme, Appl. Catal. A 387 (2010) 55-66.
[3] O. P.Taran, E. M.Polyanskaya, O.L. Ogorodnikova, C. Descorme, M. Besson, V.N. Parmon, Catalysis in Industry, 3(2) (2011) 161–169.
[4] J.M Austin, T. Groenewald, M. Spiro, *J. Chem. Soc., Dalton Trans.* 6 (1980) 854-859.
[5] L.Okhlopkova, A.Lisitsyn, V.Likholobov, M.Gurrant, H.Boehm Appl. Catal. A. 204 (2000) 229-240.

V-PP115

Effect of SO_2 on N_2O Decomposition over Ir Catalysts Supported on CeO_2-Modified Al_2O_3

Pachatouridou E.[1,2*], Iliopoulou E.[1], Konsolakis M.[2], Yentekakis I.V.[3]

1 - Chemical Process and Energy Resources Institute (CPERI)-Centre for Research and Technology Hellas (CERTH), Thessaloniki, Greece

2 - School of Production Engineering and Management, Technical University of Crete, Crete, Greece

3 - School of Environmental Engineering, Technical University of Crete, Crete, Greece

* e_pahat@cperi.certh.gr

Keywords: N_2O decomposition, iridium, alumina, ceria, SO_2

1 Introduction

Nitrous oxide (N_2O) has recently attracted great attention, due to its deleterious environmental impact. N_2O is a powerful greenhouse gas with a global warming potential (GWP) about 300 times higher than that of CO_2, while at the same time it notably contributes to stratospheric ozone depletion [1]. Therefore, the abatement of N_2O emissions from combustion and chemical processes is of significant importance. Among the different remediation methods, the catalytic decomposition of N_2O to N_2 seems to represent the most promising approach. Up to date several catalytic systems have been evaluated for N_2O decomposition. Among them, noble metal-based catalysts exhibit satisfactory performance at low temperatures. Additionally, the use of structural and/or surface modifiers seems to enhance further their intrinsic activity [2]. Except N_2O, other components that typically exist in flue gas are O_2, SO_2, H_2O, etc. The effect of SO_2 and/or O_2 on the activity of Ir catalysts for the N_2O decomposition is investigated in the present study.

2 Experimental/methodology

A series of Ir catalysts supported either on bare alumina (Al_2O_3) or CeO_2-modified alumina (AlCe: 80 wt. % Al_2O_3 and 20 wt. % CeO_2) were investigated for N_2O decomposition, in the presence of SO_2 and/or O_2. Supporting materials were synthesized *via* the co-precipitation method, while incorporation of the active phase (0.5 wt. % Ir) was carried out through the impregnation method, using $IrCl_3 \cdot H_2O$ as precursor salt. The catalysts were characterized by means of N_2 physisorption (BET), H_2-TPR, XRD and TEM techniques and evaluated for N_2O decomposition in a bench-scale, fixed bed reactor unit, in the temperature range of 200°C to 600°C. Selected catalytic samples were also characterized in "used" state to explore the impact of reaction conditions on catalyst's characteristics.

3 Results and discussion

N_2O conversion values as high as 99.0% and 96.9% were obtained over Ir/AlCe sample, during the N_2O decomposition in the absence and in the presence of O_2, respectively, compared to 98.0% and 66.4% achieved over the Ir/Al_2O_3 sample (Table 1). In the presence of SO_2 under oxygen deficient conditions (N_2O+SO_2 reaction) the N_2O conversion is decreased to 82.2% over Ir/Al_2O_3 catalyst, whereas the de-N_2O performance of Ir/AlCe sample remained almost unaffected (93.6%). However, in the co-presence of SO_2 and O_2 ($N_2O+O_2+SO_2$), the N_2O conversion over Ir/Al_2O_3 and Ir/AlCe catalysts is notably decreased to 61.6 and 39.2% respectively. Most interestingly, the N_2O conversion increases from 66.4% over the fresh

Ir/Al_2O_3 sample to 78.2% over the sulphated catalyst (i.e. catalyst after the corresponding reaction, in which 50 ppm SO_2 was co-present), implying the beneficial effect of sulfidation (Table 1).

Table 1. N_2O conversion (%) of Ir-based catalysts under various feed composition. Reaction conditions: 1000ppm N_2O, 50ppm SO_2, (2 % O_2), Ft=900 cm^3/min, W_{cat}=0.6 g, GHSV=40000 h^{-1}.

Feed	% N_2O Conversion	
	0.5 wt.% Ir/Al_2O_3	0.5 wt. % Ir/AlCe
N_2O	98.0	99.0
N_2O+SO_2	82.2	93.6
N_2O (Sulphated Catalyst)	74.4	58.4
N_2O+O_2	66.4	96.9
$N_2O+O_2+SO_2$	61.6	39.2
N_2O+O_2 (Sulphated Catalyst)	78.2	45.7

4 Conclusions

The effect of SO_2 and/or O_2 on the decomposition of N_2O over Ir catalysts supported either on bare Al_2O_3 or CeO_2-promoted Al_2O_3 was investigated. The superior performance of CeO_2-promoted catalysts under oxygen excess conditions was clearly revealed. However, the co-presence of O_2 and SO_2 in the feed stream resulted in a decrease of N_2O conversion, being more intense over Ir/AlCe catalyst. Interestingly, the de-N_2O performance of Ir/Al_2O_3 catalyst was notably enhanced upon sulfidation, which is not the case for Ir/AlCe catalyst. The obtained results are interpreted on the basis of characterization studies, which reveal the impact of CeO_2 modification in conjunction with the reaction conditions on the physicochemical characteristics and de-N_2O performance.

Acknowledgements

This research has been co-financed by European Union (European Social Fund) and Greek national funds through Operational Program "Education and Lifelong Learning" of the National Strategic Reference Framework (NSRF)-Research Funding Program: THALES-Investing in knowledge society through the European Social Fund (MIS 375643).

References

[1] D.J. Wuebbles, *Science*, 326 (2009) 56-57.
[2] M. Konsolakis, F. Aligizou, G. Goula, I.V. Yentekakis, *Chemical Engineering Journal,* 230 (2013)286-295.

V-PP116

Highly Active Nanocatalysts by Ion Beam Surface Modification

Artioli N.[1], Solt H.[1], Bazin P.[1], Aureau D.[2], Etcheberry A.[2], Rousseau S.[3], Blanchard G.[3], Moral N.[4], Busardo D.[5], Bruma A.[6], Malo S.[6], Daturi M.[1*]

1 - Laboratoire Catalyse et Spectrochimie, ENSICAEN, Université de Caen, Caen, France
2 - IREM-Institut Lavoisier, Versailles Cedex, France
3 - PSA Peugeot Citroën Centre Technique de Vélizy A, Cedex, France
4 - Renault Automobiles, Centre Technique de Lardy, 1 Lardy, France
5 - Quertech, Caen, France
6 - CRISMAT, UMR CNRS ENSICAEN 6508, Caen Cedex 4, France

* marco.daturi@ensicaen.fr

Keywords: ion, bombardment, surface, treatment, nanocatalyst, cerium, oxide, Pt, nanoparticles

1 Introduction

Interface science is at the forefront in the development of new materials for advanced technological applications [1]. In particular, surface properties strongly influence catalysis which is essentially a surface phenomenon. One of the novel applications of ion beam irradiation includes the modification of the catalytic activity of solid catalysts [2]. In this study we evaluated the effect of ion irradiation on the catalytic properties of $Ce_{0.7}Zr_{0.3}O_2$ and the supported noble metal catalyst Pt/ $Ce_{0.7}Zr_{0.3}O_2$, which plays an important role in automotive exhaust control applications, among others.

2 Experimental/methodology

Industrial catalysts $Ce_{0.7}Zr_{0.3}O_2$ and Pt (1%w/w) /$Ce_{0.7}Zr_{0.3}O_2$ were bombarded with N^+ ions with a current density of 3.75 μA/cm^2. The effect on the catalytic properties is analyzed by Temperature Programmed Oxidation (TPO) and Reduction (TPR) experiments which were carried out on catalyst wafers (50-60 m3 $kg^{-1}h^{-1}$) in a flow infrared cell (293-823 K, 2000 ppm CO, CH_4, C_3H_6, C_6H_{14}, H_2 and 10% v/v O_2) connected to a quadrupole mass spectrometer (Omnistar, Pfeiffer) to detect both the adsorbed and gas species. High Resolution Transmission Electron Microscopy (HRTEM, TECNAI 30G^2) and X-Ray Photoelectron Spectroscopy (XPS, k-alpha ThermoScientific) were used for microstructural analyses.

3 Results and discussion

The differences in the catalytic activity of $Ce_{0.7}Zr_{0.3}O_2$ and Pt/ $Ce_{0.7}Zr_{0.3}O_2$ before and after the ion irradiation were evaluated performing TPO experiments of 2000 ppm CO, CH_4, C_3H_6, C_6H_{14} in 10 % O_2 in the range 293-823 K. It was noticed that $Ce_{0.7}Zr_{0.3}O_2$ bombarded catalyst achieved the 50% of conversion of the different species at temperatures (T50) which were roughly 20 K lower than the correspondent T50 values measured before ion bombardment. The Pt/ $Ce_{0.7}Zr_{0.3}O_2$ catalytic system showed as expected higher activity respect to the unmodified $Ce_{0.7}Zr_{0.3}O_2$ with significantly lower T_{50} values (70-90 K) due to the presence of the noble metal. The ion bombardment induced a further decrement of the T50 values of about 40 K. The T_{50} values of the representative pollutants are reported in details in Table 1 for both catalysts.

The higher catalytic activity of $Ce_{0.7}Zr_{0.3}O_2$ and Pt/$Ce_{0.7}Zr_{0.3}O_2$ catalysts after ion bombardment is strictly related to their enhanced reducibility, as shown by TPR experiments carried out using H_2 as a reductant. It was observed that $Ce_{0.7}Zr_{0.3}O_2$ catalyst treated with ion irradiation presents a remarkably higher reducibility respect to the unmodified catalyst. As a result, the peak of H_2 consumption was measured at 585 K, a temperature roughly 100 K lower than that reported for the corresponding non bombarded catalyst. In the presence of Pt, the

reduction was achieved at lower temperature (520 K) than on the bare support and the ion bombardment lead to a further decrement of the temperature linked with the maximum of the reduction peak to 340 K.

Table1 T_{50} values of representative pollutants combustion measurements

	$Ce_{0.7}Zr_{0.3}O_2$		$Pt/Ce_{0.7}Zr_{0.3}O_2$	
	non treated	bombarded	non treated	bombarded
T_{50} CO (K)	739	696	640	579
T_{50} C_3H_6 (K)	756	738	682	645
T_{50} C_6H_{14} (K)	764	754	693	660

The higher reducibility of both $Ce_{0.7}Zr_{0.3}O_2$ and Pt/ $Ce_{0.7}Zr_{0.3}O_2$ bombarded catalysts was also confirmed by FTIR study of H_2 reduction between 373 and 773 K. The evolution of surface hydroxyl species vibrational modes ν(OH) was used as probe of the surface oxidation state [3]. In particular, the band assigned to the hydroxyl group coordinated to two cations in close proximity with an oxygen vacancy (~3630 cm^{-1}) was observed to increase in intensity with the reduction temperature until 673 K and to be always more intense for the bombarded catalysts respect to the corresponding untreated ones. The results are in line with HRTEM analysis (Fig. 1) which revealed that the sample, after ion bombardment, is characterized by a uniform distribution of nanoparticles on the catalytic surface, as well as by the formation of atom vacancies and incomplete terraces. XPS clearly shows that the spectra, thus the associated microstructures, are modified after the bombardment. Local charges seem to be created, in line with the enhanced catalytic properties.

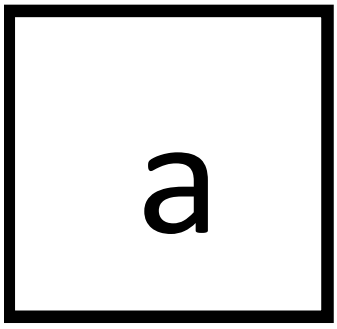

Fig.1 HRTEM characterization of Pt nanoparticles supported on $Ce_{0.7}Zr_{0.3}O_2$

Analogous results have been obtained from the study of alternative catalytic systems such as Pd/Al_2O_3 treated with the same ion bombardment protocol, which provokes a remarkable change in the particle morphology, as highlighted by both XPS and IR studies.

4 Conclusions

The present study revealed that ion irradiation significantly enhanced the catalytic activity and the stability of both $Ce_{0.7}Zr_{0.3}O_2$ and the $Pt/Ce_{0.7}Zr_{0.32}O_2$ catalysts and it suggests the feasibility of this method for the effective and controlled surface modification of several catalytic materials.

Acknowledgements

This material is based upon work supported by the French National Research Agency ANR (Agence Nationale de la Recherche) under the project ANR-10-VPTT-003

References

1 Jain I.P., Agarwal G., *Surf. Sci. Rep.*66, 77 (2011).

2 Busardo D., Guernalec F., Method for the ion beam treatment of a metal layer deposited on a substrate WO 2010092297 A1(2010)

3 Daturi M, Finocchio E., Binet C., Lavalley J.C., Fally F. and Perrichon V., *J. Phys. Chem. B* 103(23), 4884 (1999)

V-PP117

Effect of Metal Loading in Pt/Hβ Catalysts for PS Hydrocracking

Salbidegoitia J.A., Fuentes E.G., Gonzalez-Marcos M.P.*, Gonzalez-Velasco J.R.

Group of Chemical Technologies for Environmental Sustainability, Department of Chemical Engineering, Faculty of Science and Technology, The University of the Basque Country, Bilbao, Spain

* mp.gonzalezmarcos@ehu.es

Keywords: platinum zeolite catalyst, polystyrene hydrocracking

1 Introduction

Diffusion limitations are common when working with polymers. In particular, we have shown that external mass-transfer can be controlled in catalytic polystyrene (PS) hydrocracking in the liquid phase to fuels, but the big size of polymer molecules limits their accessibility to the external catalytic surface[1]. Optimizing catalysts for this process, besides maximizing external surface[2], involves minimizing platinum content while maintaining enough hydrogenation activity. Thus, we studied in this work the effect of platinum content in Pt/Hβ catalysts on the catalytic performance in the process.

2 Experimental

Bifunctional catalysts: Five catalysts with nominal platinum content of: 0.1, 0.3, 0.5, 0.7 and 1 wt.% were prepared by ionic exchange[3] of tetraammineplatinum (II) nitrate (Alfa Aesar, 99.99%) on a Hβ zeolite (Zeolyst Corp. SiO_2:Al_2O_3 ratio of 25). 10 g of the powdered support were slurred in deionised water (1 L) and then heated to 353 K under continuous stirring and reflux, at pH=7, for 24 h. Afterwards, the solid was filtered, washed, dried (393 K, 12 h), calcined (823 K, 2 h) and reduced in hydrogen flow (800 K, 3 h). Characteristics of the catalysts such as: BET and external surface (N_2 physisorption, 77 K), acid strength (NH_3-TPD), Brønsted and Lewis acidity[4] (FTIR of absorbed pyridine (Py), 423 K), external acidity[5] (FTIR of adsorbed 2,6-di-*tert*-butylpyridine (DTBPy), 423 K), metallic content (ICP) and Pt dispersion (H_2 chemisorption and TEM), were measured.

Catalytic activity: PS hydrocracking in the liquid phase was studied, and the optimized operational conditions for a kinetic regime[1] were: 5% PS (M_W = 192,000 g·mol^{-1}, M_n = 120,000 g·mol^{-1}) solved in decahydronapthalene, 623 K, 180 bar of H_2, 1800 rpm, 2.36 g·L^{-1} of catalyst (average particle size 230 μm) in slurry, with an stirred autoclave reactor. PS conversion was evaluated by gel permeation chromatography (GPC) and the evolution was followed by assuming continuous distribution kinetics. Liquid and gas product selectivity was analyzed by gas chromatography with flame ionization detector (GC-FID)[2].

3 Results and discussion

The main properties of the catalysts are shown in Table 1. External surface area is around 200 m^2·g^{-1}, relatively independent of metallic content, as expected. Total acidity (NH_3-TPD) is nearly constant up to 0.7 wt.% Pt, acid strength slightly increasing with Pt loading. Higher Pt content produces a moderate decrease in total acidity and acid strength. Brønsted sites are majority up to 0.5 wt.% Pt, Brønsted to Lewis ratio increasing with Pt loading. Above 0.7 wt.% Pt, however, Lewis sites are majority and independent of Pt content. Probably, for high Pt loading, metal particles partially block pyridine access to micropores.

DTBPy molecule cannot enter small pores, and was used to estimate external acidity of the

catalysts. Hβ support with no metal was used as a reference with 100% accessibility[5]. Table 1 shows a significant decrease of accessible acidity with metal loading. Regarding metal dispersion, values around 60% were obtained, with relatively small values of Pt particle size in all the range (around 2 nm).

Table 1. Properties of the catalysts.

Catalyst	S, $m^2 \cdot g^{-1}$		NH_3, $\mu mol \cdot g^{-1}$				Py, $\mu mol \cdot g^{-1}$		Acces.	Pt	Disp.	d_{Pt}
	BET	Ext.	T	W	M	S	B	L	%	%	%	nm
01PtHB	425	172	463	183	224	56	284	204	67	0.1	58	1.9
03PtHB	468	198	461	182	229	50	249	172	41	0.23	36	3.0
05PtHB	406	187	453	185	216	52	225	84	29	0.58	60	1.8
07PtHB	530	201	453	151	240	62	96	145	26	0.6	76	1.4
1PtHB	486	176	400	154	197	50	109	142	21	0.8	61	1.8

Key to acidity: T, total; W, weak; M, medium; S, strong; B, Brønsted; L, Lewis; Acces., accessible.

Figure 1(a) shows initial reaction rate for PS hydrocracking with temperature for the different catalysts. Although higher metal loading produces higher rates, Figure 1(b) shows that TOF decreases with Pt loading, what is probably related to the higher accessibility of the acidic sites. Selectivity was checked to be hardly affected by Pt loading in the studied range.

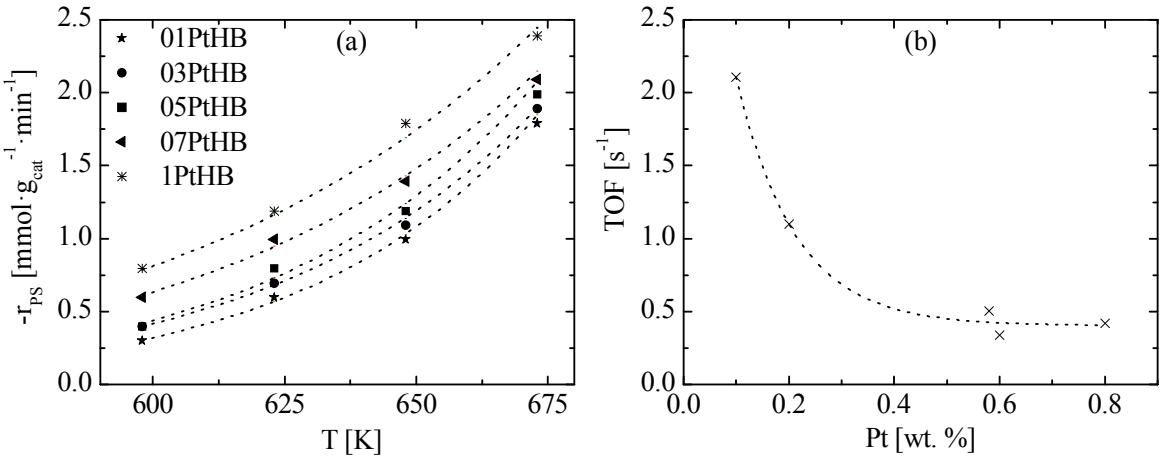

Fig. 1. Initial PS hydrocracking rate with temperature (a) and TOF values at 598 K (b).

4 Conclusions

PS hydrocracking to liquid fuels has been studied as a model reaction for plastic recycling, in the kinetic regime. A bifunctional 0.1 wt.% Pt/Hβ catalyst prepared by ionic exchange has proven to be adequate for this process: it produces good yields, with higher TOF and no relevant variation on the selectivity to the desired products.

Acknowledgements

The authors thank Spanish Ministry for Science and Innovation (CTQ2010-17277), Basque Government (GIC-IT-657-13; BFI-2010-150) and UPV/EHU (UFI11/39) for economic support.

References

[1] E.G. Fuentes-Ordóñez, J.A. Salbidegoitia, M.P. González-Marcos, J.R. González-Velasco, *Ind. Eng. Chem. Res.* 52 (2013) 14798-14807.

[2] E.G. Fuentes-Ordóñez, J.A. Salbidegoitia, J.L. Ayastuy, M.A. Gutiérrez-Ortiz, M.P. González-Marcos, J.R. González-Velasco, *Catal. Today.* 227 (2014) 163-170.

[3] J. De Graaf, J. van Dillen, K.P. de Jong, D.C. Koningberger, *J. Catal.* 203 (2001) 307-321.

[4] C.A Emeis, *J. Catal.* 141 (1993) 347-354.

[5] A. Corma, V. Fornés, L. Forni, F. Márquez, J. Martínez-Triguero, D. Moscotti, *J. Catal.* 179 (1998) 451-458.

V-PP118

Insights into the Elementary Kinetics of the Low-Temperature NO_x Reduction by H_2 on $Pt/WO_3/ZrO_2$ under Lean Conditions

Hahn C.*, Endisch M., Kureti S.

Technical University of Freiberg, Institute of Energy Process Engineering and Chemical Engineering, Chair of Reaction Engineering, Freiberg, Germany

* Christoph.Hahn@iec.tu-freiberg.de

Keywords: NO_x reduction by H_2, Pt catalyst, kinetic modelling, thermodynamic consistency

1 Introduction

For the removal of NO_x from the oxygen-rich exhaust of diesel engines, catalytic abatement technologies are applied since a couple of years implying the selective catalytic reduction by NH_3 and NO_x storage reduction catalysts. However, a constraint of these techniques is their limited efficiency below 175°C. For the NO_x reduction at low temperatures, the H_2-deNO_x reaction has been shown to reveal promising potential. But, classical Pt/Al_2O_3 catalysts perform in a narrow range from 50 to 150 °C only and they include considerable N_2O selectivity of about 80% [1]. Contrary, we recently reported on an advanced $Pt/WO_3/ZrO_2$ catalyst exhibiting high practical relevance. This catalyst showed marked efficiency between 50 and 450 °C and very low N_2O selectivity of about 10% [2].

2 Modelling

To unravel the improved performance of $Pt/WO_3/ZrO_2$ in the lean H_2-deNO_x this work addresses the elementary kinetic modelling. The model was developed based on a detailed reaction mechanism [2] as well as kinetic examinations conducted in a gradient-free loop reactor and implied a network of 48 elementary reaction described by Arrhenius-based rate expressions. Kinetic parameters were taken from literature [3] and were determined by fitting calculations and thermodynamic constraints. Pre-exponential factors of adsorption were estimated from the kinetic gas theory. Also, the kinetic parameters for adsorption and desorption of O_2 were deduced from independent TPD study [4].

3 Results and discussion

Selected fits of NO traces and calculated H_2O proportions are demonstrated in Figure 1 (left) showing satisfactory agreement with the experimental data. The kinetic model also provided simulation of the coverage of the Pt surface (Figure 1, right) showing that the active sites are predominantly covered by NO in the temperature range from 80 to 200°C. These results are in line with in situ DRIFTS studies previously reported [2]. The simulations additionally evidenced that the rate determining step of NO reduction is the dissociation of chemisorbed NO forming N and O surface species. The improved N_2 selectivity of $Pt/WO_3/ZrO_2$ was found to be associated with the relatively high surface coverage by N, which combines to yield N_2. As another consequence, the production of N_2O originated from the reaction of chemisorbed N and NO is suppressed. Furthermore, above 200°C, chemisorbed oxygen becomes the dominating surface species thus strongly inhibiting the NO dissociation resulting in drastic decrease in catalytic H_2-deNO_x performance.

The developed kinetic model was validated by simulating experiments with various feed contents. Additionally, the thermodynamic consistency of the model and the implemented kinetic parameters was proven by checking Gibbs free enthalpy of the surface reactions (Figure

2) [4].

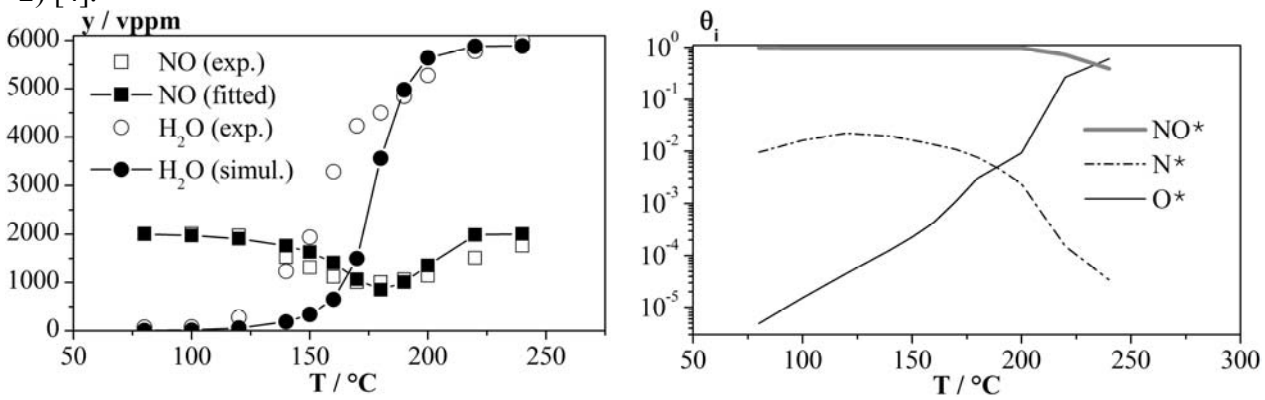

Fig. 1. Left: Fractions of NO and H_2O in H_2-O_2-NO_x reaction on $Pt/WO_3/ZrO_2$; right: simulated surface coverages. Conditions: $y(NO_x)$ = 2000 vpm, $y(H_2)$ = 6000 vpm, $y(O_2)$ = 6%, N_2 balance, SV = 77000/h.

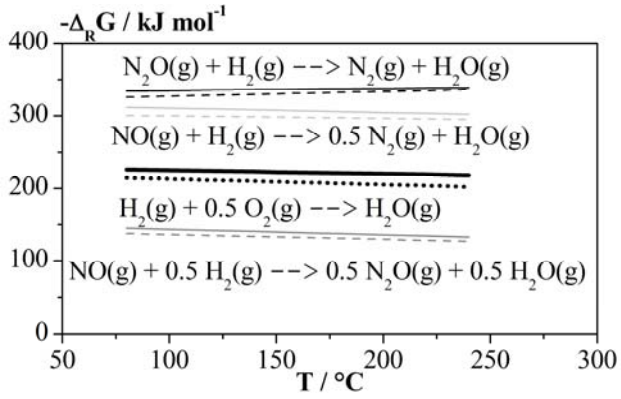

Fig. 2. Gibbs free enthalpy calculated with thermo-chemical data (solid lines) and kinetic parameters of the surface reaction on $Pt/WO_3/ZrO_2$ (dashed lines).

4 Conclusions

As a result of the elementary kinetic model, we conclude that the marked H_2-deNO_x performance and high N_2 selectivity of $Pt/WO_3/ZrO_2$ is related to the significantly lower energy barrier of the dissociation of chemisorbed NO as compared to Pt/Al_2O_3 [3]. This results in increased Pt coverage by N predominately evoking N_2 instead of N_2O [4]. These findings are in line with our recent in situ DRIFT spectroscopic studies [2] and allow the rational catalyst design in future work.

Acknowledgements

The authors gratefully acknowledge the financial support from German Research Foundation (KU 1459/3-2) and European Social Fund (DynMo).

References

[1] H. Hamada, M. Haneda, Appl. Catal. A 421 (2012) 1.
[2] F.J.P. Schott, P. Balle, J. Adler, S. Kureti, Appl. Catal. B 87 (2009) 18.
[3] J. Koop, O. Deutschmann Appl. Catal. B 91 (2009) 47.
[4] C. Hahn, M. Endisch, F.J.P. Schott, S. Kureti, Appl. Catal. B (2015), DOI: 10.1016/j.apcatb.2014.12.033

V-PP119

$VO_x/TiO_2/ZSM5$ Catalysts Activity for the Simultaneous Abatement of NO_x and PCDDs for MWI Plants

Gallastegi-Villa M.*, Aranzabal A., González Marcos J.A., González-Velasco J.R.

Department of Chemical Engineering, Faculty of Science and Technology, University of Basque Country, Bilbao, Spain

* miren.gallastegui@ehu.es

Keywords: NO_x, PCDDs, catalytic removal, VO_x, species, titania, zeolites

1 Introduction

VO_x/TiO_2 catalysts, specially ungraded with W or Mo oxides, have been developed for the NO_x selective catalytic reduction (SCR) with ammonia. They have also been reported to be efficient in the total oxidation abatement of dioxins (PCDDs).Therefore, the simultaneous removal of NO_x and PCDDs in the municipal solid waste incineration plants (MSW) by the catalytic technology is a highly interesting alternative to current non destructive methods.

The TiO_2 is reported to be the most active support due to the best dispersion of VO_x monolayer [1]. However TiO_2 shows low surface area, low resistance to sintering and high cost. Therefore, other supports are widely analyzed in the literature. Metal exchanged zeolites show high SCR activity and has recently gained interest as potential catalyst for the oxidation of chlorinated volatile organic compounds, due to their high selectivity towards total oxidation products [2]. Therefore, zeolites may be a suitable catalyst for the simultaneous removal of NO_x and PCDDs. Then, the present work is essentially devoted to the determination of $VO_x/TiO_2/ZSM5$ catalysts activity in the simultaneous removal of NO and 1,2-dichlorobenzene (o-DCB, taken as a model molecule for PCDDs). Moreover, the TiO_2 effect was analyzed by varying from 0 to 100%.

2 Experimental/methodology

$VO_x/TiO_2/ZSM5$ (V/xTi/Z, being x the TiO_2 mass fraction) catalysts were prepared by the wet impregnation method in two steps. Firstly, the desired quantity of Ti(V)butoxy dissolved on butanol was added to H-ZSM5. Them, after dried overnight at 110 ºC and calcined at 520 ºC for 3 h the desired amount of NH_4VO_3 to obtained 3% of V complexed with 2 moles of oxalic acid for 1 mole of V was impregnated. Finally, the samples were dried and calcined at 500 °C for 3 h (1 ºC·min-1). The catalysts were characterized by ICP, N_2 physisorption, XRD, UV-vis-NIR, NH_3-TPD and H_2-TPR. Catalytic tests were performed as light-off curve on fixed bed reactor (1.5 g) by feeding constant total flow of 2 $L_N \cdot min^{-1}$of simulated gas mixture representative of a MSW incinerator flue gas (100 ppm o-DCB, 300 ppm NO, 300 ppm NH_3, 10 % O_2, 10 % CO_2 and balance Ar).

3 Results and discussion

Fig. 1. shows o-DCB and NO conversions as a function of reaction temperature. V/Ti shows the highest conversion at lower temperature on both reactions, being T_{50} values 260 ºC and 150

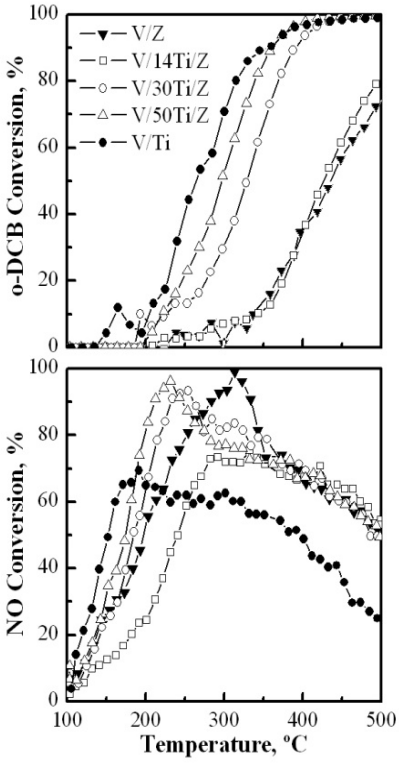

Fig. 1. Catalytic activity

ºC for o-DCB oxidation and NO reduction, respectively. The performance of V/Z catalyst is improved by the addition of more than 14 wt. % of TiO_2, by shifting the light-off curves to lower temperatures, and reaching higher NO conversion (>90%) in the range of temperature between 200 and 300 ºC, in comparison to the 70% conversion obtained by the V/Ti catalyst.

The better SCR performance of zeolites is due to their high surface acidity [3]. NH_3-TPD results show that the addition of TiO_2 to V/Z catalyst, reduce its surface acidity (0.79 mmol NH_3/g) about 21% (V/14Ti/Z), 30% (V/30Ti/Z) and 42% (V/50Ti/Z). Thus, the maximum NO conversion is also reduced as TiO_2 concentration increases.

Catalysts characterisation results suggest that the catalytic activity is related to the VO_x species. Fig. 2. shows UV-Vis spectra and their corresponding first-derivative curves to identify more easily the UV-Vis bands. The anatase (330 nm) and isolated VO_x species (370-410 nm) bands are observed over all the catalysts. However, V/14Ti/Z and V/Z catalysts also show a little band at 470 nm associated to d-d transition of V^{+5} ions in distorted octahedral symmetry. Moreover, V/T, V/50T/Z and V/30T/Z show a band centered at 668 nm related to the d-d transitions of V^{+4} in square pyramidal coordination.

H_2-TPR profiles confirm the formation of crystalline V_2O_5 over V/Z and V/14Ti/Z catalysts. Both show two reduction peaks whereas a unique reduction peak related to isolated VO_x species is obtained with V/T, V/50Ti/Z and V/30Ti/Z catalysts. However, XRD patterns show no diffraction peaks assigned to V_2O_5 species, evidencing its high dispersion and small particle size. XRD analyses confirm the addition of TiO_2 as anatase crystalline structure and the intensity of its diffraction peaks increase while the intensity of H-ZSM5 peaks decrease drastically as TiO_2 content increases. On the other hand, the reducibility of the V/Z is slightly improved by the TiO_2 addition and may be therefore is improve the catalytic performance [1]. Finally, the increase of the TiO_2 loading leads to a gradual decrease in BET surface area.

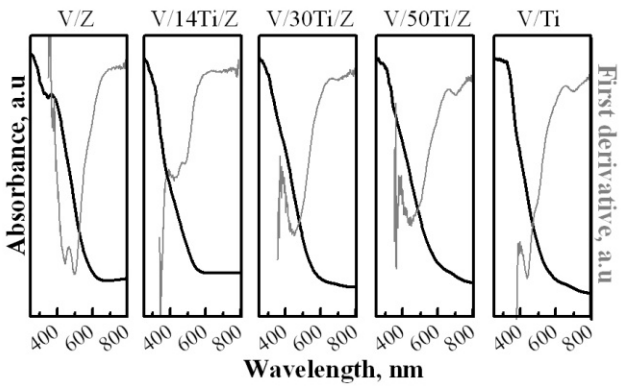

Fig.2. UV-vis spectra and the first derivative

4 Conclusions

It has been found that V/Ti/Z catalyst is valid for the simultaneous removal of NO and o-DCB. More than 14% of TiO_2 is necessary to avoid the formation of small V_2O_5 crystallites and thus obtain similar catalytic activity to V/Ti catalyst. Furthermore, the use of zeolite improves the SCR performance at high temperature.

Acknowledgements

The authors thank for the financial support to Spanish Ministry of Economy and Competitiveness (CTM2012-31576), Basque Government (S-PE11UN074) and University of the Basque Country (INF12/37 and UFI 12/37). M.G.V. acknowledges also to the Basque Government for the Grant BFI-2011-238.

References

[1] F. Bertinchamps, C. Grégoire, E.M. Gaigneaux, Applied Catalysis B: Environmental. 66 (2006) 10.
[2] J.R. González-Velasco, R. López-Fonseca, A. Aranzabal, J.I. Gutiérrez-Ortiz, P. Steltenpohl, Applied Catalysis B: Environmental. 24 (2000) 233.
[3] S.S.R. Putluru, A. Riisager, R. Fehrmann, Vanadia supported on zeolites for SCR of NO by ammonia, Applied Catalysis B: Environmental. 97 (2010) 333-339.

V-PP120

Selective Oxidation and Hydrogenation of CO over Precious Metal Catalysts for Fuel Cell Applications

Mohamed Z.*, Singh S., Friedrich H.

School of Chemistry and Physics, University of KwaZulu-Natal, Durban, South Africa

* chemcatm@gmail.com

Keywords: PEMFC, WGS, PROX and SMET

1 Introduction

Increased attention has now turned to the development of fuel cell powered systems, because of their expectedly low environmental impact. Proton-exchange membrane fuel cells (PEMFCs) are, at this moment, the most studied type of hydrogen-based electrical power sources, both for static and mobile power applications [1]. PEMFCs use either hydrocarbons or hydrogen, which offers maximum power density, as the fuel.

The production of H_2 is usually accomplished by a series of catalytic reactions such as; steam reforming, partial oxidation and auto-thermal reforming which is followed by the water-gas shift (WGS) reaction [2]. Following the WGS reaction, however, the amount of CO generated is still too high, and it can be removed by the preferential oxidation (PROX) and/or by selective methanation (SMET) of CO to sub-ppm levels [3]. Catalysts for these reactions are usually noble based metals (Au, Pt, Pd, Ru, Rh and Ir). South Africa on the other hand possesses rich amounts of some of these noble metals including Pt, which will be focused on in this study.

2 Experimental/methodology

Pt supported on TiO_2 and ZrO_2 catalysts were synthesized using the wet-impregnation and deposition precipitation methods. These catalysts were characterized by; BET surface area and pore volume, inductively-coupled plasma optical emission spectroscopy (ICP-OES), powder X-ray diffraction (XRD), scanning electron microscopy (SEM), energy dispersive X-ray spectroscopy (EDX), HR transmission electron microscopy (TEM), temperature programmed techniques (TPR,TPO and TPD), and chemisorption analysis (CO, H_2 and O_2).The synthesized catalysts were tested using a custom built reactor for both PROX and SMET activity, within the stipulated PROX and SMET temperature ranges, with varying GHSVs. The effect of CO_2 and stability of the catalyst for these reactions were also investigated.

3 Results and discussion

Table 1. shows the surface characteristics of the supports and the deposited Pt catalysts. Following the deposition of Pt on both the supports a decrease in surface area and pore volume is observed. This suggests that the Pt particles are situated on the surface of these supports, but due to the low metal loadings these cannot be seen in XRD. This result is also evident that the Pt particles are well dispersed over the supports, which is usually a characteristic for materials prepared by this method of synthesis. SEM-EDS shown in Figure 1. confirms the uniform dispersion of these Pt particles over the supports and are confirmed by line scans . HRTEM results indicated particle sizes ranging from 10-15nm. Temperature programmed studies conducted showed that the materials are reduced at temperatures below 100 °C, and can be readily oxidized following their reductions.

Table 1. Surface characterization of Pt samples

Catalyst	BET surface area (m2/g)	Pore Volume(cm3/g)	Nominal wt% (%)	ICP wt% (%)
TiO_2	156	0.63	-	-
Pt-TiO_2	84	0.26	1	1
ZrO_2	97	0.32	-	-
Pt-ZrO_2	51	0.24	1	0.7

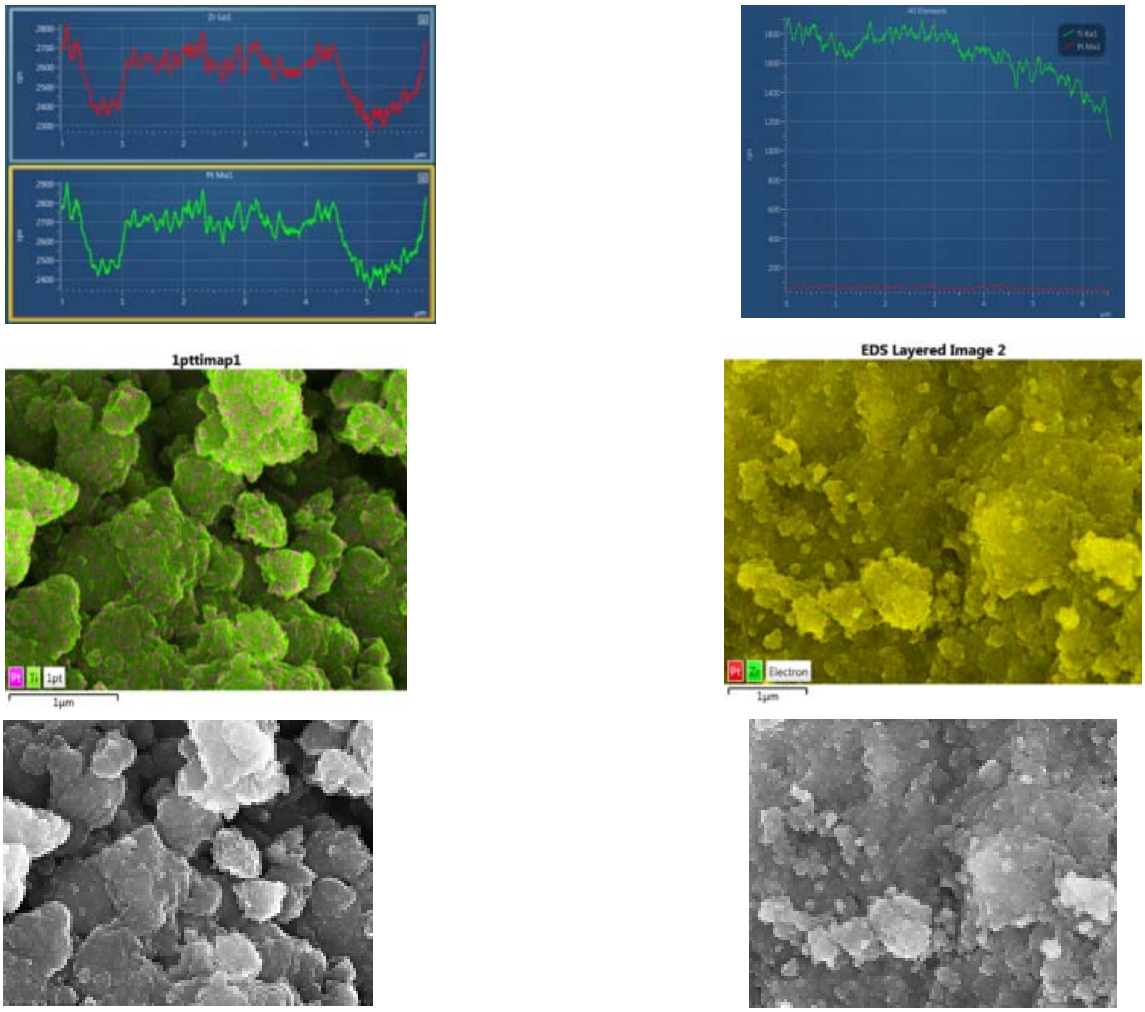

Fig. 1. SEM images of (A) Pt-TiO_2 and (B) Pt-ZrO_2 showing the metal dispersions using EDS mapping and line scans

4 Conclusions

Synthesis of these materials using different preparation methods gives rise to catalysts with varying metal dispersions and particles sizes. These could either enhance or retard their activity during the catalytic reactions.

Acknowledgements

We would like to thank the NRF and HySA for funding of the project and the University of Kwa-Zulu Natal.

References

[1] E. Moretti, L. Storaro, A. Talon, P. Patrono, F. Pinzari, T. Montanari, G. Ramis and M. Lenarda. *Appl. Catal. A: Gen.* 344, (2008)165.
[2] O. Pozdnyakova, D. Teschner, A. Wootsch, J. Kröhnert, B. Steinhauer, H. Sauer, L. Toth, F.C. Jentoft, A. Knop-Gericke , Z. Paál , R. Schlögl. *J. Catal.* 237, (2006)1.
[3] Y. Hasegawa, R. Maki, M.Sano and T. Miyake. *Appl. Catal. A: Gen.* 371, (2009)67.

V-PP121

Enhanced-SCR Reaction over a Commercial Fe-Zeolite Catalyst: Activity and Mechanism

Marchitti F., Nova I., Tronconi E.*

Dip.Energia, Politecnico di Milano, Milan, Italy

* enrico.tronconi@polimi.it

Keywords: ammonium, nitrate, DeNOx, Urea/NH_3-SCR, Fe-zeolite catalyst

1 Introduction

The new generation of Diesel engines, optimized for reduced fuel consumption, release exhaust gases at lower temperatures. In addition to the tightening emissions regulations, this demands for more effective aftertreatment systems in the 180-250°C T-window. Typically, a certain amount of NO is oxidized to NO_2 upstream of the SCR converter in order to enable the Fast-SCR reaction, i.e. the most effective NOx + NH_3 reaction. It is well known however that NO oxidation calls for a noble metal catalyst (DOC), which is costly and also prone to deactivation [1]. In order to overcome the DOC issues, an alternative solution is represented by the Enhanced-SCR (E-SCR) reaction, which involves spraying a NH_4NO_3 (AN) aqueous solution into the feed stream to the SCR converter. Promising results have been reported over commercial V_2O_5–WO_3/TiO_2 and Fe-zeolite catalysts [2-4]. The aim of this work is to elucidate the Enhanced-SCR mechanism, with a particular focus on the key steps responsible for the improvement of the DeNOx activity.

2 Experimental/methodology

Both the NH_3-SCR and E-SCR reactions were investigated over core samples (about 6 cm^3) drilled from a commercial Fe-Zeolite washcoated monolith catalyst supplied by Umicore. Isothermal steady-state and transient runs were carried out in the T=150–500°C and GHSV = 35000-100000 h^{-1} ranges. Typical feed concentrations of NOx (NO_2/NOx = 0-0.5) and NH_3 were 500 ppm, with 8 % O_2, 5 % H_2O v/v and N_2 as balance gas. In E-SCR runs an aqueous solution of AN was also dosed upstream of the SCR catalyst. The solution concentrations and the pump flow rates were selected to result in AN feed concentrations of 100-350 ppm. The concentrations of NO, NH_3, NO_2, and of N_2O in the outlet gases were continuously monitored by a UV-analyzer (ABB Limas 11HV) and a ND-IR-analyzer (ABB Uras 26).

3 Results and discussion

The potential of AN to improve the low temperature SCR activity was first investigated in steady state runs. Over the tested Fe-Zeolite the NO conversion at Standard SCR conditions (NO_2/NOx = 0) was definitely boosted by AN injection in the low-T range, with a maximum 80% improvement at 180°C upon addition of 250 ppm of AN, which resulted in a DeNOx activity very close to the Fast-SCR activity. A set of transient response (TRM) runs was then performed to address the mechanistic aspects of E-SCR. Figure 1A shows a transient run at 190°C: initially 500ppm of NO were fed to the reactor, and a steady state was reached after 500s. After 1175s from the NO feed, the pump was switched on to feed 5% H_2O + about 200ppm AN: the NO outlet concentration dropped suddenly to roughly 320ppm and, at the same time, NO_2 was formed, its outlet concentration increasing up to an average value of 180ppm. This clearly indicates that AN was able to oxidize NO to NO_2 quantitatively according to reaction (1). In a subsequent step the NH_3 feed was started and correspondingly all the NO_2 was consumed according to the Fast-SCR reaction (2). Figure 1A clarifies therefore that the

Enhanced-SCR reaction (3) results from the combination of reactions (1) and (2):

$$NO + NH_4NO_3 \rightarrow NO_2 + N_2 + 2H_2O \quad (1)$$
$$2NH_3 + NO + NO_2 \rightarrow 2N_2 + 3H_2O \quad (2)$$
$$2NH_3 + 2NO + NH_4NO_3 \rightarrow 3N_2 + 5H_2O \quad (3)$$

Accordingly, the AN promoting effect of E-SCR derives from the in situ generation of a stoichiometric amount of NO_2 via the very fast, direct oxidation of NO by AN, reaction (1). Figure 1B shows another transient run in which AN and ammonia were co-fed to the Fe-zeolite catalyst. In stage (1) the feed composition (AN + NO + NH_3) enabled the occurrence of the Enhanced-SCR reaction; at a given point (t = 9270s) NO was removed from the feed (stage (2)). In the absence of NO, after a transient, NH_3 recovered its feed level and was no longer consumed. Stage (2) in Figure 1B indicates that, at least under the tested conditions, there is no direct reaction between AN and NH_3. These results were confirmed at other operating conditions.

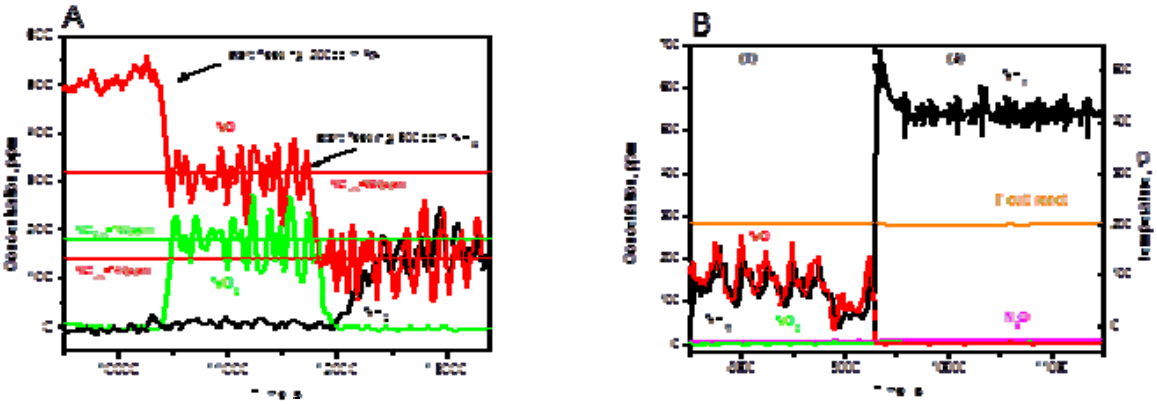

Fig. 1 A-B. Transient runs: A) T = 190°C, GHSV = 75,000 h^{-1}. Feed: AN = 0-200ppm, NH_3 = 0-500ppm, NO = 500ppm, H_2O = 5%(v/v), O_2 = 0%(v/v). B) T = 200°C, GHSV = 100,000 h^{-1}. Feed: AN = 200ppm NH_3 = 500ppm, NO = 0-500ppm, H_2O = 5%(v/v), O_2 = 8%(v/v).

4 Conclusions

Both transient and steady state runs confirm that AN injection can greatly improve the low-T deNOx activity of a Fe-Zeolite catalyst via the E-SCR reaction. Essentially, the promoting role of ammonium nitrate consists in generating NO_2 *in situ* via reaction (1). In presence of NH_3 such NO_2 can further react according to the very effective Fast-SCR reaction (2): this explains the greatly enhanced SCR activity. We show also that at low temperatures AN is preferably reduced by NO rather than by NH_3, and that N_2O formation is not incremented by AN injection.

Acknowledgements

The financial support of EU Project CO_2RE – CO_2 REduction for long distance transport (SCP1-GA-2012-284909) is gratefully acknowledged.

References

[1] A. Winkler, D. Ferri, R. Hauert, *Catalysis Today* 155 (2010) 140.
[2] P. Forzatti, I. Nova, E. Tronconi, *Angewandte Chemie* 121 (2009) 8516.
[3] P. Forzatti, I. Nova, E. Tronconi, *SAE Technical Paper* 2010-01-1181 (2010)
[4] P. Forzatti, I. Nova, E. Tronconi, A. Kustov, J.R. Thøgersen, *Catalysis Today* 184 (2012) 153.

V-PP122

Magnetic Carbon Xerogels for the Catalytic Wet Peroxide Oxidation of 4-Nitrophenol Solutions

Ribeiro R.S.[1], Silva A.M.T.[2], Faria J.L.[2*], Gomes H.T.[1]

1 - LCM – Laboratory of Catalysis and Materials – Associate Laboratory LSRE-LCM, Department of Chemical and Biological Technology, School of Technology and Management, Polytechnic Institute of Bragança, Bragança, Portugal

2 - LCM – Laboratory of Catalysis and Materials – Associate Laboratory LSRE-LCM, Departamento de Engenharia Química, Faculdade de Engenharia, Universidade do Porto, Porto, Portugal

* jlfaria@fe.up.pt

Keywords: hybrid magnetic nanocomposites, catalytic wet peroxide oxidation (CWPO), 4-Nitrophenol

1 Introduction

Catalytic wet peroxide oxidation (CWPO) is a well-known advanced oxidation process for the removal of organic pollutants from industrial process waters and wastewater. Specifically, CWPO employs hydrogen peroxide (H_2O_2) as oxidation source and a suitable catalyst to promote its decomposition via formation of hydroxyl radicals ($HO^{\bullet}$), which exhibit high oxidizing potential and serve as effective species in the destruction of a huge range of organic pollutants . When an iron salt is used in CWPO, through the so-called Fenton process , high degradation rates of organic pollutants are obtained. However, the Fenton process usually requires a final separation step for Fe ions present in the treated water, increasing the treatment costs. More recently, carbon materials have been shown as active metal-free catalysts for the CWPO of organic pollutants in aqueous solutions; nevertheless carbon materials still show low catalytic activity in comparison with metal-based catalysts .

In the present work, nanostructured hybrid composites containing iron magnetic species and carbon xerogels materials are synthesized and tested as catalysts in the CPWO of highly concentrated 4-nitrophenol solutions (5 g L^{-1}). In this way, the synergistic effects that can arise from the combination of the high catalytic activity of iron oxide species with the flexibility for tuning the textural properties of carbon-based materials are explored. In addition, *in-situ* magnetic separation of the catalysts at the end of the treatment process is a further advantage.

2 Materials and methods

A carbon xerogel (CX) was prepared by polycondensation of resorcinol with formaldehyde (with a molar ratio of 1:2), following the procedure described elsewhere : 9.91 g of resorcinol were dissolved in 18.8 mL of deionised water, 13.5 mL of formaldehyde solution being then added and the pH adjusted to 6.1. The gelation step was allowed to proceed at 85 ^{o}C during 3 days, the recovered gel being afterwards grounded (particle sizes in the range 0.106-0.250 mm), dried in an oven (from 60 ^{o}C to 150 ^{o}C, defining a heating ramp of 20 ^{o}C day^{-1}) and pyrolyzed at 800 ^{o}C under a N_2 flow (100 mL min^{-1}) in a tubular vertical oven, resulting in CX materials. $CX/Fe_{0.05}$ was synthesized using the same procedure, except that iron (III) chloride hexahydrate was added to the resorcinol solution (considering a Fe/resorcinol molar ratio of 0.05) prior to formaldehyde. The solids recovered from pyrolysis were then washed with 1 L of an HCl solution (pH = 3) at 50 ^{o}C and dried overnight at 60 ^{o}C, resulting in the $CX/Fe_{0.05}$ materials.

CWPO experiments were conducted in a 250 mL well-stirred (600 rpm) glass reactor loaded with 50 mL of a 4-NP aqueous solution (5.0 g L^{-1}), during 24 h at T = 50 ^{o}C, considering a catalyst load = 2.5 g L^{-1}, and using the stoichiometric amount of H_2O_2 needed to completely

mineralize 4-NP (17.8 g L^{-1}). Pure adsorption runs and blank experiments, without catalyst, were also performed in order to discriminate the adsorption and non-catalytic components of 4-NP removal by CWPO, respectively.

3 Results and discussion

The ability of the magnetic composites to act as catalysts in the CWPO of 4-NP was evaluated. Comparisons between the removal of 4-NP by CWPO in the presence of CX and in a series of three consecutive runs using $CX/Fe_{0.05}$ are shown in Figure 1a. Non-catalytic removal of 4-NP is also shown for comparison. As observed, a marked increase in the removal of 4-NP is observed when using $CX/Fe_{0.05}$ as catalyst, even in its third consecutive reuse. In addition, adsorption of 4-NP on $CX/Fe_{0.05}$ was found negligible (ca. 9%). Therefore, $CX/Fe_{0.05}$ is univocally an active catalyst for CWPO of highly concentrated 4-NP solutions. Nevertheless, some Fe leaching was observed even at the end of the third run (4.8 mg L^{-1}). Bearing this in mind, the effect of the initial pH on the 4-NP removals and Fe leaching was assessed through an additional CWPO run performed without any pH adjustment. As observed in Figure 1b, the 4-NP removal decreased from 77% to 45% when the initial pH was not adjusted, whereas the Fe leaching dropped from 10.4 mg L^{-1} (at pH = 3) to 2.5 mg L^{-1}. In this way, further studies are now being conducted in order to maximize catalyst activity and minimize Fe leaching levels, through the synthesis of magnetic carbon xerogels with improved Fe dispersion and stability.

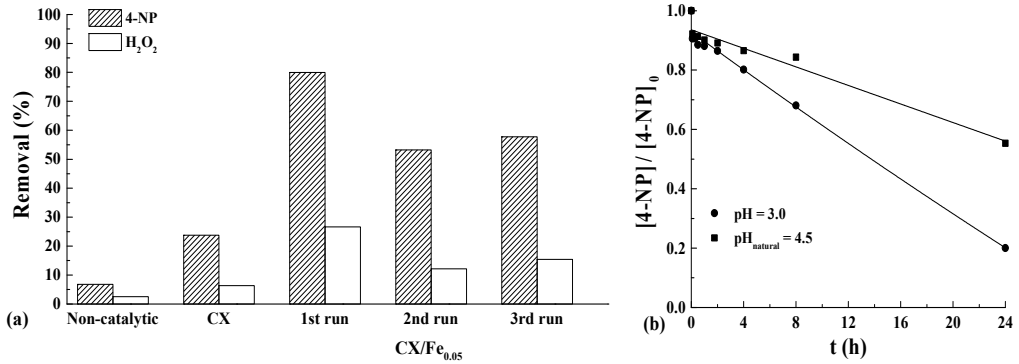

Fig. 1. (a) 4-NP and H_2O_2 removals obtained after 24 h in CWPO runs performed at pH = 3; (b) effect of the initial pH on the 4-NP removal by CWPO when using $CX/Fe_{0.05}$ as catalyst.

4 Conclusions

High catalytic activity is obtained when magnetic carbon xerogels are used in the CWPO of highly concentrated 4-NP solutions. Nevertheless, further studies are required in order to increase the catalytic stability of these materials.

Acknowledgements

Work supported by project UID/EQU/50020/2013, co-financed by FEDER through COMPETE, QREN and ON2, and by FCT – Fundação para a Ciência e a Tecnologia. Rui S. Ribeiro acknowledges financial support from the FCT individual Ph.D. grant SFRH/BD/94177/2013. Adrián M.T. Silva acknowledges the FCT Investigator 2013 Programme (IF/01501/2013), with financing from the European Social Fund and the Human Potential Operational Programme.

References

[1] P.R. Gogate, A.B. Pandit, Advances in Environmental Research. 8 (2004) 501.
[2] H.J.H. Fenton, Journal of the Chemical Society, Transactions. 65 (1894) 899.
[3] A. Rey, A. Bahamonde, J.A. Casas, J.J. Rodríguez, Water Science and Technology. 61 (2010) 2769.
[4] H.T. Gomes, B.F. Machado, A. Ribeiro, I. Moreira, M. Rosário, A.M.T. Silva, J.L. Figueiredo, J.L. Faria, Journal of Hazardous Materials. 159 (2008) 420.

V-PP123

Acceleration of Catalytic Ozonation of Ammonium Ion in Water over Cobalt Oxide Catalyst by Repeated Use

Mahardiani L.[1], Kamiya Y.[2*]

1 - Graduate School of Environmental Science, Hokkaido University, Sapporo, Japan
2 - Research Faculty of Environmental Earth Science, Hokkaido University, Sapporo, Japan

* kamiya@ees.hokudai.ac.jp

Keywords: ammonium ion, cobalt oxide, catalytic ozonation, wastewater treatment, repeated use

1 Introduction

Ammonium nitrogen (NH_3 and NH_4^+) in industrial effluent and household sewage and generated by intensive agricultural activities can cause eutrophication for aquatic ecosystem with serious consequences for drinking water sources and fisheries. Therefore, it is necessary to remove the ammonium nitrogen from water and preferably to decompose it into harmless compounds like di-nitrogen (N_2). Catalytic ozonation is an attractive method, in which ozone is utilized as an oxidant to decompose the ammonium nitrogen, because the reaction proceeds at ordinary temperature and pressure.

We have previously reported that Co_3O_4 was highly active and selective catalyst with low solubility for the catalytic ozonation of NH_4^+ in water [1]. Here we report on acceleration of the catalytic ozonation of NH_4^+ in water over Co_3O_4 catalyst by repeated use.

2 Experimental

Co_3O_4 was prepared from $Co(NO_3)_2$ by a precipitation method and calcined at 450°C for 3 h. Catalytic ozonation of NH_4^+ in water (NH_4Cl, 10 mmol L^{-1}) was carried out in a batch reactor at 60°C with vigorous stirring in a stream of O_2/O_3. For some experiments, an aqueous solution with high NH_4^+concentration (30 mmol L^{-1}) was used as a reaction solution. Concentration of NH_4^+ and NO_3^- were determined by using ion chromatographs. After the reaction, the catalyst was separated by filtration, washed with distilled water and dried overnight at 100°C. The spent catalyst was then reused for the catalytic ozonation of NH_4^+ under the reaction conditions similar to those for the first run. The reactions were repeated for several times.

3 Results and discussion

The conversion and selectivity to gaseous compounds for the catalytic ozonation of NH_4^+ over Co_3O_4 at 6 h for its repeated use are shown in Fig. 1. For comparison, the reaction over Al_2O_3, Mn_5O_8 and SnO_2, which also have low solubility for the reaction [1], were also carried out. The conversion of NH_4^+ for Co_3O_4 was increased by the repeated use with slight change in the high selectivity to gaseous compounds. Ammonium ion was completely decomposed after the second reuse of Co_3O_4. Meanwhile, for Al_2O_3 and Mn_5O_8, the acceleration was not observed by their repeated uses. As for SnO_2, the acceleration was observed for the repeated use but only little. Namely, enhancement of the catalytic activity by the repeated use was specific for Co_3O_4.

To investigate how far the catalytic activity of Co_3O_4 was enhanced by repeated use, the reaction over Co_3O_4 with high NH_4^+ concentration was repeatedly conducted. The conversion was increased from 31% for fresh catalyst to 81% for 9 time-reused catalyst. The selectivity was basically unchanged by the repeated use.

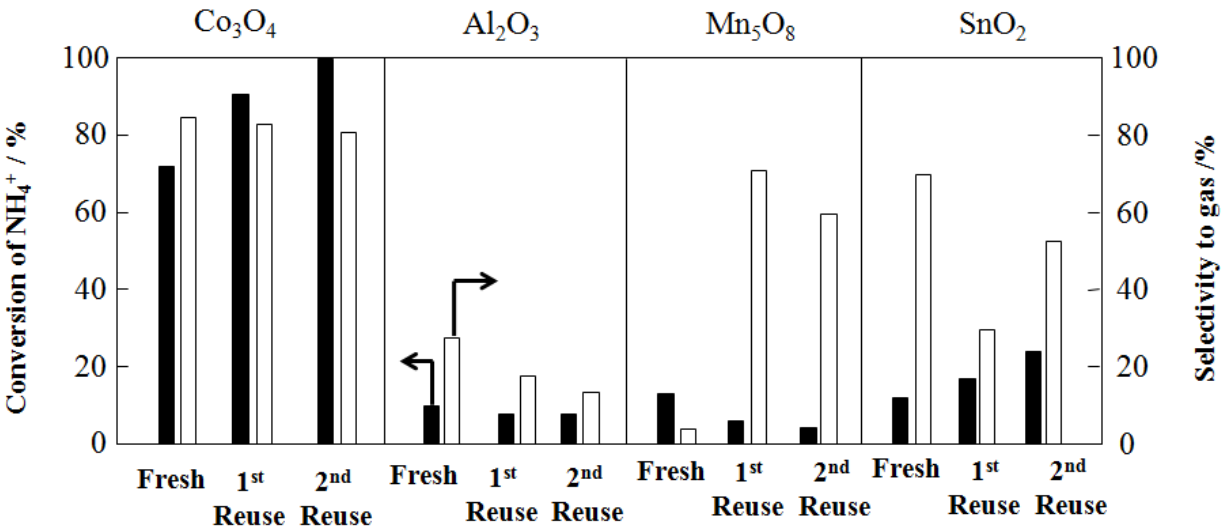

Fig. 1 Repeated uses of oxide catalysts for catalytic ozonation of NH_4^+ in water.

Characterization of physical and chemical properties for the fresh and spent Co_3O_4 catalyst was conducted to investigate what caused the acceleration effect. Surface area of catalyst was decreased by repeated use, and there was no difference in the crystalline structure between fresh and spent catalyst. However, there was a significant difference in NH_3-TPD profiles for the fresh and spent catalyst, where large peak was observed for the spent catalyst while fresh one gave only a small one. The formation of acid sites on the spent catalyst may be caused by the oxidation of catalyst surface with O_3 under the reaction conditions. Thus, we speculated that the formation of the acid sites, maybe Lewis acid site, lead to the acceleration of the reaction over Co_3O_4 by the repeated use due to effective activation of O_3 and/or NH_4^+ on them.

4 Conclusions

Catalytic activity of Co_3O_4 for catalytic ozonation of NH_4^+ was significantly enhanced by the repeated use of the catalyst even after 9 times-reuses. Crystalline structure and degradation of surface area of spent catalyst were not the reason for acceleration. The formation of acid sites by oxidation of catalyst with O_3 may lead to the enhancement activity of Co_3O_4.

Acknowledgements

We acknowledge Dr. Toru Murayama (Hokkaido University) for his help on XRD measurement.

References

[1] S. Ichikawa, L. Mahardiani, Y. Kamiya, *Catal. Today* 232 (2014) 192 – 197.

V-PP124

Novel Hybrid Perovskite Catalysts For DeNOx Applications

Ercan K.E.[1], Say Z.[1], Vovk E.I.[1,2], Pantaleo G.[3], Liotta L.[3], Venezia A.[3], Ozensoy E.[1*]

1 - Department of Chemistry, Bilkent University, Ankara, Turkey
2 - Boreskov Institute of Catalysis, Novosibirsk, Russian Federation
3 - CNR-Institute for the Study of Nanostructured Materials (ISMN), Palermo, Italy

* ozensoy@fen.bilkent.edu.tr

Keywords: $DeNO_x$, $LaCoO_3$, $LaMnO_3$, $LaCo_xMn_{1-x}O_3$, perovskite

1 Introduction

Air pollution due to the emission of toxic gases has serious adverse effects on human health. Recent studies point out that perovskite-based $DeNO_x$ catalysts can be considered as potential candidates that can create alternatives for high-cost Pt-based conventional NO oxidation catalysts [1]. In one of our recent studies, we reported that $LaMnO_3$ has much higher NOx adsorption capacity and higher structural stability as compared to $LaCoO_3$ [2]. La-based simple perovskites such as $LaMnO_3$ and $LaCoO_3$ can reveal either high thermal stability or high NO oxidation capability but do not possess both of these merits at the same time [1,2]. Along these lines, catalytic activity and thermal stability of La-based perovskites can be fine-tuned via designing hybrid $LaCo_xMn_{1-x}O_3$ perovskite structures (Figure 1). In the current work, hybrid perovskite structures were synthesized by varying Co and Mn loadings (x=0.1-0.9) and the structural characterization of these catalysts were carried out via XPS, XRD, ex-situ FTIR, BET and TEM techniques. In addition, the interaction of NO_x and SO_x species with the surface of the hybrid perovskite structures was also comprehensively elucidated at the molecular level by means of in-situ FTIR and TPD techniques.

2 Experimental/methodology

Detailed description of the synthesis protocol of the conventional $LaCoO_3$, $LaMnO_3$ catalysts has been reported in a former report of GM company [1]. The synthesis of the hybrid perovskites in the current work was carried out by co-precipitation of La, Mn and Co-based nitrate precursors via citrate method in the form of $LaCo_xMn_{1-x}O_3$ (x=0.1-0.9).

3 Results and Discussion

Figure 1 represents the schematic illustration of the synthesis protocol. Greater oxidation capability of $LaCoO_3$ perovskites are synergistically combined with the thermally stable $LaMnO_3$ perovskites through the formation of hybrid perovskites in the form of $LaCo_xMn_{1-x}O_3$. NOx adsorption and release properties of hybrid perovskites were analyzed via TPD. NO(g) desorption channels of the investigated materials during nitrate decomposition is shown in Figure 2. These TPD results indicate that NO desorption characteristics are strongly influenced by Mn/Co ratio in the catalytic formulation. Figure 2 suggest that Co-rich hybrid perovskites can store and release a significantly higher amount of NOx species where $LaCo_{0.8}Mn_{0.2}O_3$ catalyst seems to store the greatest amount of NOx as compared to all of the other hybrid and simple perovskites. The superior NOx oxidation and storage capability of the $LaCo_{0.8}Mn_{0.2}O_3$ system can be associated with the particular relative populations of mixed-valence Co and Mn sites (i.e. Co^{2+}/ Co^{3+} and Mn^{2+}/ Mn^{3+}) in the hybrid perovskite unit cell, presence of substitutional and/or interstitial defects as well as relative density of oxygen vacancies on the hybrid perovskite surface.

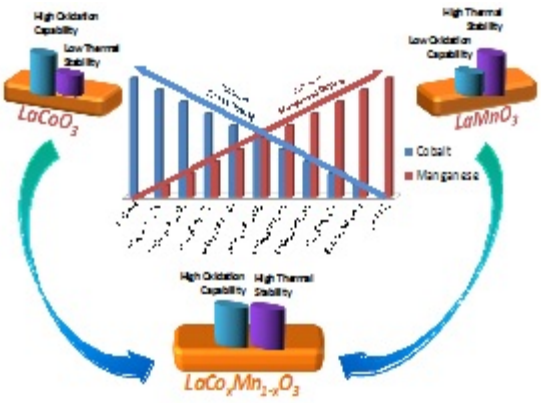

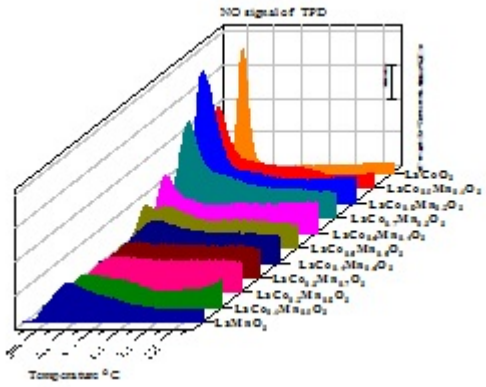

Figure 1: Material design strategy for the synthesis of hybrid perovskites.
Figure 2: NO(g) TPD profiles of H_2 pre-treated perovskites.

Furthermore, nature of the NOx (i.e. nitrite, nitrate) or SOx (sulfite, sulfate) species formed during the adsorption of NO_2 or SO_2+O_2 on the hybrid perovskites were investigated via in-situ FTIR in comparison to the conventional perovskites (i.e. $LaCoO_3$ and $LaMnO_3$). The interaction of the adsorbed NOx and SOx species with H_2 and their corresponding resistances against reduction was also studied via in-situ FTIR. Thermal sulfur regeneration of the hybrid perovskites after sulfur-poisoning was also investigated via TPD experiments.

4 Conclusions

In the current work, a novel synthesis strategy has been utilized in order to design novel hybrid perovskite structures that can combine unique functional characteristics of different conventional perovskite structures within a single catalytic architecture. Our results indicate that through this novel approach, NOx/SOx oxidation, adsorption, storage and release properties of hybrid perovskite architectures can be fine-tuned in an attempt to obtain next generation Pt-free DeNOx catalysts not only revealing superior activity but also possessing enhanced stability.

Acknowledgements

Authors acknowledge the financial support from the Scientific and Technological Research Council of Turkey (TUBITAK) (Project Code: 213M585).

References

[1] C. Kim, G. Qi, K. Dahlberg, W. Li, Science (2010) 1624–1627,327 (2010)
[2] Z. Say, M. Dogac, E.I. Vovk, Y.E. Kalay, C.H. Kim, W. Li, E. Ozensoy, Applied Catalysis B: Environmental 154-155, 51 (2014)

V-PP125

NH_3-SCR and NH_3 Oxidation over V-Based Catalysts: Design of "High-Efficiency" NH_3-SCR Reactor for Stationary Applications

Beretta A.[1*], Usberti N.[1], Lietti L.[1], Forzatti P.[1], Di Blasi M.[2], Morandi A.[2]

1 - Dipartimento di Energia, Politecnico di Milano, Milano, Italy
2 - ENEL Ingegneria e Ricerca SpA, Pisa, Italy

* alessandra.beretta@polimi.it

Keywords: V_2O_5-WO_3/TiO_2 catalyst, NH_3-SCR, NH_3-oxidation, indirect kinetic scheme, kinetic analysis

1 Introduction

NH_3-SCR is the state of art technology for NO_X abatement from power plant flue gases. The reaction (NH_3+NO+1/4 O_2→N_2+3/2H_2O) involves a 1 to 1 consumption ratio, but full-scale reactors typically operate at NH_3/NO inlet ratios of 0.8, in order to keep NH_3 slip below 2 ppm. Increasing the NH_3/NO inlet ratio (High Efficiency SCR process) and adding an extra catalyst layer able to efficiently convert the unreacted NH_3 to N_2 could be a strategy to enhance the NO_X abatement while maintaining NH_3 slip under this limit. This configuration is successfully applied in automotive SCR after-treatment systems [1]. In this work, the kinetics of the NH_3/NO/O_2 reacting system over V_2O_5-WO_3/TiO_2 catalysts was studied under conditions of NH_3/NO ratio ≥ 1 and temperature up to 400°C, where some ammonia oxidation is expected.

2 Experimental/methodology

A high vanadia load (3% w/w) catalyst was prepared and tested in fine powders in a quartz-diluted fixed-bed microreactor. NH_3-SCR tests were carried out on a catalyst bed of 30 mg, a total flow rate of 650 cm^3/min (NTP), a gas mixture consisting of 30 ppm NO, 2% H_2O, 3.5% O_2, in He; NH_3 concentration was set at 33 or 150 ppm. NH_3 oxidation was also tested under the same operating conditions, but in the absence of NO, at varying NH_3 concentration. Data were quantitatively analyzed by a pseudo-homogeneous 1D reactor model accounting for the possible impact of intraporous mass transfer limitations within the catalyst particles

3 Results and discussion

Figure 1 shows in symbols the experimental NO (panel a) and NH_3 conversion (panel b) obtained in NH_3-SCR tests performed over the home-made catalyst. In the low temperature window, where the process was uniquely controlled by the kinetics of the SCR reaction, NO conversion increased with increasing NH_3 inlet concentration. Despite the excess of NH_3, the low concentration of reactants exalted the kinetic dependence on NH_3 surface coverage. The data collected at temperatures below 300°C were used to fit the parameters of an Eley-Rideal rate expression ($r_{SCR} = k_{SCR}C_{NO}\theta_{NH3}$), wherein ammonia adsorption was described by adopting the same coverage dependent heat of adsorption of ammonia, independently estimated by Lietti et al. [2] in previous studies. Above 325°C, NO conversion passed through a maximum at increasing temperature (also observed in [3]), as commonly observed in SCR tests at the onset of ammonia oxidation; however, since the experiments were performed under excess ammonia, the high temperature decrease of NO conversion could not be attributed to a lack of surface NH_3. The experiments were thus interpreted as the evidence of an unselective NH_3-oxidation route, giving rise to some NO production (NH_3+5/4O_2→NO+3/2H_2O).

NH_3 oxidation was then studied by dedicated tests; Figure 2 reports in symbols the

measured conversion of NH_3 (panel a) and the corresponding outlet concentration of NO (panel b). NH_3 conversion decreased with increasing inlet concentration: data were in fact well described by a simple rate expression of the form: $r_{Ox\text{-}NH3} = k_{Ox}\theta_{NH3}$, which again incorporated the same coverage-dependent heat of adsorption derived in [2].

However, by assuming an indirect reaction scheme, wherein NH_3 oxidation leads to the formation of NO which in turn prompts the NH_3-SCR reaction, a very nice description of the results (conversion and product distribution) was obtained, as shown by the solid lines in Figure 2). The scheme proposed was validated by simulating the SCR tests over the entire temperature range. As shown in Figure 1 by the solid lines, a very satisfactory match was found; notably, the calculated treads in Figure 1 are pure predictions at temperatures above 300°C.

The kinetic investigation was extended to commercial catalysts with low and medium V-loads. On these catalysts the NH_3-SCR tests did not show provide clear evidence for NH_3-oxidation and NH_3-oxidation tests showed above 95% selectivity to N_2. However, a quantitative analysis based on the independent estimate of the intrinsic rate of NH_3-SCR, showed that the two-step kinetic scheme is fully in line with the observation of only few ppm NO slip in the NH_3-oxidation tests.

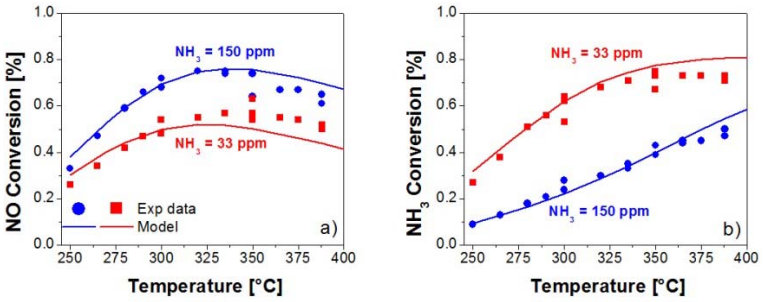

Fig. 1. Measured and calculated NO conversion (panel a) and NH_3 conversion (panel b) in SCR tests

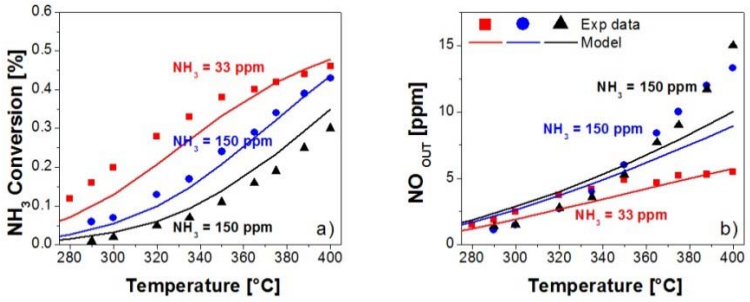

Fig. 2. Measured and calculated NH_3 conversion (panel a) and outlet NO concentration (panel b) in NH_3-ox tests.

4 Conclusions

The results of this study give new perspectives to the design of High Efficiency SCR reactors, operating at NH_3/NO close to 1. The impact of the rate and stoichiometry of NH_3 oxidation herein developed could be crucial on the final performance of the reactor (NO conversion and NH_3 slip); its accurate description is a pre-requisite for correctly estimating the final composition of the gas stream, and thus addressing on a truthful basis the design of an additional NH_3-SCO (Selective Catalytic Oxidation) bed layer.

References

[1] M. Colombo, I. Nova, E. Tronconi, V. Schmeiβer, B. Bandl-Konrad, L. Zimmermann, Appl. Catal. B: Environ. 2013, 142, 861.
[2] L. Lietti, I. Nova, S. Camurri, E. Tronconi, P. Forzatti, AIChE, 1997, 43, 2559.
[3] R. Nedyalkova, K. Kamasamudram, N.W.Currier, J.Li, A. Yezerets, L. Olsson, J.Cat. 2013,299,101.

V-PP126

Synthesis and Properties of Silver-Containing Photocatalytic Systems on the Base of Titania

Vodyankin A.A.*, Nikitich M.P., Pasalskaya K.O., Vodyankina O.V.

Tomsk State University, Tomsk, Russia

* orzie@mail.ru

Keywords: photocatalysis, titania, silica, photoreduction, silver

1 Introduction

Photocatalytic processes have become quite actual in the recent time due to the increased interest in energy-saving technologies and effective oxidation of organic pollutants. Titania is generally considered the most popular material for photocatalysts due to its high stability, relatively cheap price and noticeably higher photoactivity [1]. Besides, the addition of small-sized silver particles to titania surface has been found to improve the photocatalytic properties of samples due to the formation of Schottky barrier responsible for lowering the rate of exciton recombination, influence on the band gap characteristics and general affinity of silver to oxidation processes [2, 3]. Moreover, the addition of silver particles to small clusters of anatase can induct a notable sensitizing effect, increasing the radiation absorbance in the visible spectrum. The purpose of the present work is to create silica-supported catalysts with anatase clusters and silver nanoparticles and to investigate the influence of the Schottky barrier on the photocatalytic properties of the prepared samples due to the electron-hole separation on the border between the metal particle and semiconductor.

2 Experimental

In the following study the samples used represent pure titania (Degussa P25), modified titania/silica and titania/alumina, with all of them also promoted with silver nanoparticles. The supported TiO_2 silica-based samples were prepared by grafting technique using tetraisopropylorthotitanate (TTIP) as a precursor, while the addition of silver was made by photoreduction [4] and impregnation methods. The amount of titania was varied approximately from 1 to 6% for the supported samples. The SiO_2 support prepared by sol-gel method was used according to [5]. All of the prepared catalysts were examined by XRD, FTIR, UV-Vis spectroscopy, TEM, AES, and Brunauer–Emmett–Teller method, also being tested in a model photocatalytic reaction, namely the degradation of methylene blue.

3 Results and discussion

The supported TiO_2/SiO_2 samples prepared by grafting have shown the presence of both anatase and amorphous titania as it is demonstrated by the results of XRD analysis. According to the FTIR data, the titanium atoms are chemically bound to the silica surface via Si-O-Ti groups. UV-Vis spectroscopy has also demonstrated a peak of plasmon resonance at ~535 nm in the silver-containing catalysts prepared by photoreduction method and a notable absorbance shift towards the UV region most probably due to the increase of the titania band gap length after the addition of silver.

The relative photocatalytic constants of the model photocatalytic reaction of methylene blue decomposition for all samples are shown in Fig. The highest photoactivity is demonstrated by the sample containing 6% wt. titania and 0.5% wt. silver added via photoreduction, most likely due to the expected effects of silver influencing on the properties of titania being an active component in the reaction. It should be also noted that unlike the $Ag/TiO_2/SiO_2$ series, the

titania-silica samples without Ag don't show the same correlation of the amount of active component and photocatalytic activity. This indicates the specific behaviour of the support (silica) depending on the properties of the loaded titania and photodeposited silver particles as well. Besides, a considerably high activity is shown by one of supported silver-titania samples with the lowest amount of silver. This can be due to the specific properties of dispersed silver, like both the particle size and their shape.

It should be noted that the activity increase is observed both for unsupported and supported TiO_2 catalysts with addition of Ag. One of the reasons of this is the O^- anion radical formation on the Ag particle – TiO_2 interface border. Further work is in progress to clarify this matter.

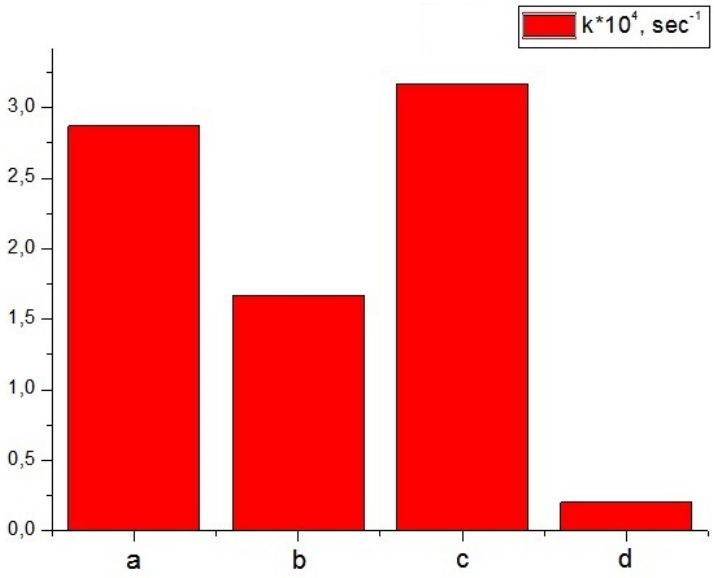

Fig. Relative constants of photocatalytic degradation of methylene blue for the tested samples: a) 0,5% Ag/TiO_2, b) 6% TiO_2/SiO_2, c) 0,5% Ag / 6% TiO_2 / SiO_2, d) TiO_2 Degussa P25.

4 Conclusions

The silver particles dispersed on the surface of both pure titania and titania/silica grafted systems do increase the photocatalytic activity of the samples, not influencing on the relative surface area.

The grafting technique responsible for the preparation of titania/silica systems also seem to increase the photocatalytic activity of the samples in the model reaction. The best photoactivity in the testing reaction is shown by **0.5 % Ag / 6% TiO_2 / SiO_2** catalyst.

Acknowledgements

The work was financially supported by the Russian Federal Fund for Assistance to Small Innovative Enterprises (FASIE).

References

[1] O. Carp, C. L. Huisman, A. Reller, *Progress in Solid State Chemistry*. 32 (2004) 33-177
[2] V. Vamathevan, R. Amal, D. Beydoun, G. Low, S. McEvoy, *Journal of Photochemistry and Photobiology A: Chemistry*. 148 (2002) 233-245
[3] Y. F. Wang, J. H. Zeng, Y. Li, *Electrochimica Acta*. 87 (2013) 256-260
[4] A.A. Evstratov, C. Chis, A.A. Malygin, J.-M. Taulemesse, P. Gaudon, T. Vincent, *Rossiiskii Khimicheskii Zhurnal*. 51 (2007) 52-60
[5] Mamontov G.V., Izaak T.I., Magaev O.V., Knyazev A.S., Vodyankina O.V. // Russ. J. Phys. Chem. A. 2011. V. 85. № 9. P. 1540.

V-PP127

Epoxidation of Fatty Acid Methyl Esters of Plant Oils with Hydrogen Peroxide

Voronov M.S., Sapunov V.N., Alexandrova J.V., Kulazhskaya A.D.*

Mendeleev University of Chemical Technology of Russia, Moscow, Russia

* vms90@rambler.ru

Keywords: epoxidation, ion exchange resin, fatty acid methyl esters, peracetic acid, hydrogen peroxide

1 Introduction

Currently epoxidation of vegetable oils and their derivatives is carried out with solutions of peracetic acid generated *in situ* from an aqueous solution of acetic acid and hydrogen peroxide in the presence of acidic catalysts such as ion exchange resins [1, 2, 3, 4]. However, the presence of the three-phase system complicates the mathematical description of the epoxidation process, and reduces the lifetime of the catalyst due to mechanical damage.

The aim of this study was to simplify the epoxidation process by separate production a solution of peracetic acid flowing solutions of acetic acid and hydrogen peroxide through a fixed bed of catalyst (*ex situ*), and following epoxidation of fatty acid methyl esters. A further object is to compare the efficiency of two processes epoxidation.

2 Experimental procedure

Epoxidation *in situ* is carried out in a glass reactor in the presence of cation exchange resins Amberlyst 15 Dry. The reactor is charged fatty acid methyl esters, the catalyst and acetic acid, and then with stirring is added dropwise an aqueous solution of 37 wt% hydrogen peroxide during 2 minutes. The reaction time was 3 hours.

In a two-stage process, at first, the solutions of hydrogen peroxide and acetic acid is passed through a fixed bed of the catalyst at 50 ° C and then prepared solution is added into a glass reactor with previously loaded fatty acid methyl esters, equipped with a jacket and a reflux condenser. Epoxidation process carried out in thermostatically controlled conditions (50 ° C). Further, separation of layers was carried out, and the aqueous phase was again passed through a fixed catalyst bed. There were four such cycles with different times of reaction epoxidation.

The concentration of peracetic acid and hydrogen peroxide was determined by the method described in [5]. The content of epoxides was determined by gas-liquid chromatography.

3 Results and discussion

Comparative characteristics of the two methods is shown in the example of the epoxidation reaction of methyl esters of fatty acids of rapeseed oil at molar ratio double bonds: acetic acid: hydrogen peroxide = 1 : 4.7 : 1.7, with 10 % by weight of aqueous phase ion-exchange resin Amberlyst 15 Dry.

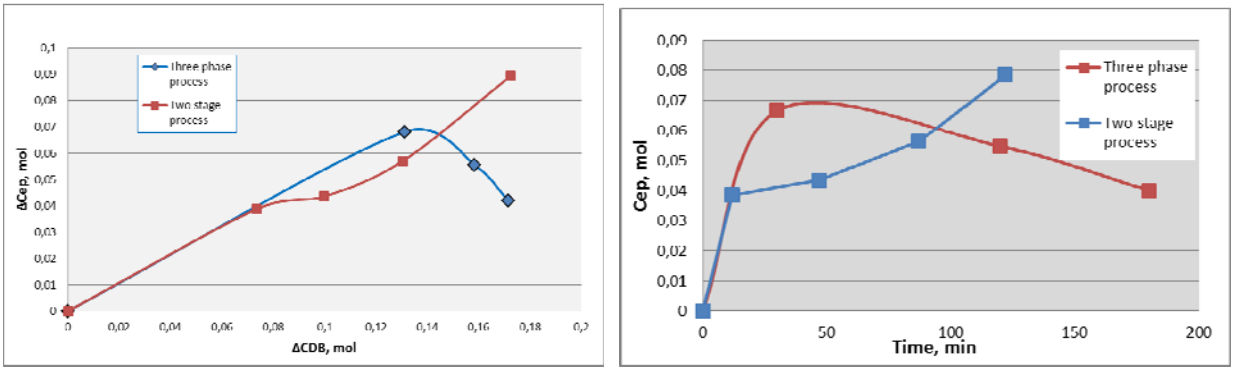

(a) (b)

Fig. 1. The dependence of selectivity of epoxides (a) and time dependence of the yield of epoxides (b) in comparison of two methods of epoxidation.

Two stage process shows greater selectivity of epoxides compared with a batch process. Reuse of the aqueous phase in the process reduces the actual time the epoxidation, catalyst does not reduce its activity and does not wear out.

4 Conclusions

Thus, comparison of the two methods of epoxidation of the fatty acid methyl esters of vegetable oils with peracetic acid showed the greatest selectivity for the process related to reusing the aqueous phase. The method of separate preparation of epoxidizing agent can significantly reduce the overall process time and simplify its modeling.

References

[1] S. Sinadinovic-Fiser, M. Jankovic, Z.S. Petrovic, JAOCS 2001.V. 78.P. 725 – 731.
[2] R. Mungroo, N. C. Pradhan, V. V. Goud, A. K. Dalai, J Am Oil Chem Soc 2008. V. 85. P. 887 – 896.
[3] V.V. Goud, A.V. Patwardhan, N. C. Pradhan, Ind. Eng. Chem. Res. 2007. V. 46. P. 3078 – 3085.
[4] M. Janković, S.Sinadinović-Fišer, O. Govedarica, Ind. Eng. Chem. Res. 2014. V. 53. P. 9357 − 9364.
[5] Dudley Sully B., Williams P. L., *Analyst.* 1962. V. 87. P. 653-657.

V-PP128

Mesoporous Nanomaterials Based on Ceria: Synthesis and Catalytic Application

Zagaynov I.V.[1*], Liberman E.Yu.[2]

1 - A.A. Baikov Institute of Metallurgy and Materials Science, Moscow, Russia
2 - D. Mendeleev University of Chemical Technology of Russia, Moscow, Russia

* igorscience@gmail.com

Keywords: ceria, mesopores, solid solution, CO oxidation

1 Introduction

Nanoscale ceria is very attractive for TWC, SOFC, etc. Doped CeO_2-materials are considered as more promising solid solutions for use in these goals. The introduction of smaller isovalent non-reducible cations like Zr^{4+} and Ti^{4+} into the ceria lattice enhances OSC by creating intrinsic oxygen vacancies thereby increasing the oxygen mobility by facilitating the Ce^{3+}/Ce^{4+} redox process. Whereas doping of aliovalent non-reducible cations (Gd^{3+}) into the ceria lattice enhances oxygen storage capacity (OSC) mainly through the extrinsic oxygen vacancies. Recently, the use of variable valence dopants into ceria lattice has attracted much attention. It is known that the properties of ceria materials are dependent on the initial powder properties such as homogeneity, particle size, porous structure, and phase purity. It is clear that the quality of the synthesized powder changes with the preparation method. However, the simplest method for production of nanoscale ceria, especially for catalytic applications, is necessary to be used for obtaining a large quantity of intermediates. Among them, the most suitable and simplest method is co-precipitation with ultrasonic treatment (sonochemical method). Ultrasound irradiation can induce the formation of particles with a much smaller size and higher surface area than those reported by other methods and this technique has good reproducibility.

2 Experimental/methodology

Cerium (III) nitrate, zyrconyl nitrate, gadolinium nitrate, and titanium (IV) chloride were used as metal precursors. Appropriate amounts of salts were dissolved into 500 mL distilled water containing of nitric acid (pH=2) to give final concentrations of 0.04 M. Then, deposition was carried out by addition of aqueous ammonia at 30°C under stirring to reach pH 10. Sonication was used during dissolution of salts in distilled water (10 min), and after receiving the sediment (10 min). The resulting precipitate was filtered, washed with distilled water, dried at 150°C for 12 h, and calcined in static air at 500°C for 1 h in a muffle furnace. To study the composition, structure, and morphology of the samples a range of modern instrumental techniques was used [1].

3 Results and discussion

Single-phase material having the fluorite structure solid solution of CeO_2 ($Gd_xZr_yTi_zCe_{1-x-y-z}O_2$), wherein the cation-dopants (Gd^{3+}, Zr^{4+}, Ti^{4+}) is distributed throughout ceria, was obtained. Zr enters deep into the crystal lattice of ceria, Gd and Ti largely located in the surface planes of the crystal lattice. Thus, a substitutional solid solution with selective cation-dopants position was synthesized.

It has been found that the crystallite size was not dependent on the type and quantity of dopant and was 9-10 nm, and specific surface was about 85 m^2/g.

Obtained catalysts were investigated in CO oxidation reaction, using modeling mixture consisted of a) $CO-O_2-N_2$, b) $CH_4-CO-O_2-N_2$. It was shown that these composites are highly efficient catalysts for the oxidation of CO and preferential oxidation of CO [2].

4 Conclusions

Therefore, using such mesoporous system in the oxidation processes, would eliminate a number of problems: 1) The high temperature conversion; 2) Low stability and short lifetime of the catalyst; 3) Low amount of active surface oxygen and oxygen storage capacity (OSC).

Acknowledgements

This work was supported by RFBR grants: 13-08-01007-a, 14-03-31022-mol-a.

References

[1] I.V. Zagaynov, A.V. Vorobiev, S.V.Kutsev, *Materials Letters* 139 (2015) 237.
[2] I.V. Zagaynov, *ISACS13, Abstract book* (2014) P04.

V-PP129

Catalysts for Selective Hydrogenation of Benzene in the Presence of Other Aromatic Compounds

Konuspayev S.R.*, Auyezov A.B., Shaimardan M., Konuspayeva Z.S., Bizhanov Zh.A.

al-Faraby Kazakh National University, Almaty, Kazakhstan

* srkonuspayev@mail.ru

Keywords: benzene, ruthenium, hydrogenation selectivity, benzoperene, hydrogen

1 Introduction

Creation of new catalysts for selective hydrogenation of benzene stood before us with the problem of complete removal of benzene from gasoline. It is known that the incomplete burn of gasoline containing benzene form a strong carcinogen benzopyrene in the exhaust gases, therefore, on the Euro standard, its content should not exceed 1%. For the adoption of the new requirements to reduce the benzene content of 0.1% is no technology to achieve them. Creating the selective hydrogenation catalysts of small amounts of benzene conversion can fully open towards this condition. Despite numerous studies of the hydrogenation of benzene, is still not established a selective hydrogenation catalyst in the presence of other aromatic compounds. We have previously [1] have been developed rhodium catalysts on carbon (sibunite, CAU, BAU) which spend small amounts of selective hydrogenation of benzene with full conversion. In [2] were obtained bimetallic Rh-Au catalysts siral synthetic aluminosilicate-40. As carriers there were tested activated carbons were prepared from apricot kernels and rice husk [3].

In the present report are available ruthenium catalysts on birch charcoal (BAU), which has a large surface area and high mechanical strength.

2 Experimental/methodology

Experiments were carried out in an autoclave, which allows maintaining a constant temperature and hydrogen pressure of 5 to 100 bar, equipped with a turbine agitator and sampler inlet of the reaction, and also allows to measure the amount of hydrogen absorbed. Catalysts were prepared by tank water metal carrier after necessary processing reduced in a stream of hydrogen in the temperature range 250-300^{0}C. The reaction products and starting compounds were analyzed by GLC. Catalysts have been verified by complexes of physico-chemical methods.

3 Results and discussion

Ruthenium has been applied to the activated carbon BAU (birch activated carbon), with a surface area up to 1000 m^2/g. Figure 1 shows the kinetic curves of Comparative hydrogenation of benzene, toluene, and cumene. If the hydrogenation of benzene is at 8-0 ml/min and the absorbed hydrogen amount, calculated on the H_2 uptake 1200 ml, when introducing the hydrogenation of toluene and cumene practically do not react. Absorbed no more than 50 ml of hydrogen 3% Ru / BAU is exceptional hydrogenation of benzene and toluene and cumene are not hydrogenated. At 1% Ru / BAU observed several different picture hydrogenation of toluene at speeds three times lower than that of benzene, and cumene in these conditions, virtually no hydrogenated. The selectivity of the hydrogenation of benzene to 3% Ru / RAU is 98%, 1% Ru / RAU does not exceed 70%. Determined by the order of the reaction by reacting components and other kinetic parameters.

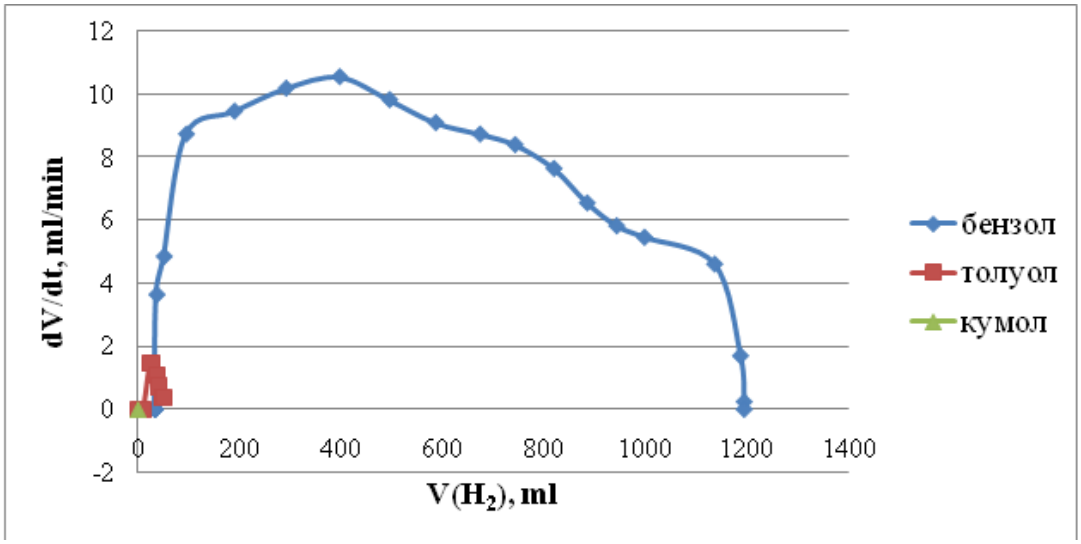

Fig. 1. Hydrogenation of aromatic compounds of 3% Ru / RAU in ethanol at 80° C and 4.0 MPa.

The selective effect of the catalyst is an unknown function, as different content ruthenium catalyst has a strong influence on the selectivity. We have previously shown [1-4] that the selectivity of the hydrogenation of benzene on a rhodium catalyst has an exceptional impact on the presence of the surface of the charged form of rhodium metal that was shown by XPS. Effect of ruthenium on the surface of BAU gives grounds to assert that there is a more subtle and unidentified law.

References

[1] Konuspayev S.R., Shaimardan M., Nurbayeva D.R., Auyezov A.B., Boronin A.I. Development of catalysts hydrogenation of benzene in creating environmentally friendly gasoline // Neftechimia. 2010, №1, P.48-51.

[2] Konuspayeva Z.S., Auezov A.B., Konuspayev S.R. et. Bimetallic Catalists for Selective Benzene Hydrogenation for Environmental Gasoline Production.- IX Int. Conf. Mech. of Catal. Reac., 2012, St.Petersburg, Russia. P.100.

[3] J.M. Jandosov, Z.A. Mansurov, M.A. Biisenbayev, Z.R. Ismagilov, N.V. Shikina, I.Z. Ismagilov, S.R. Konuspayev, M. Shaymardan， Mesoporous Carbon-Based Rhodium Catalysts for Benzene Hydrogenation.//Eurasian Chem.-Techn. 2012, V.14, P.37-40.

[4] Konuspayev S.R., Auyezov A.B., Shaimardan M. et al. Catalysts for selective hydrogenation in the presence of other aromatic compounds. // Roscatalysis-2, Novosibirsk 2014, V. 2. P.111.

V-PP130

Utilizing Water as the Oxygen Atom Source: Catalytic Formation of Lactams From Amines

Khusnutdinova J.R.[1], Gellrich U.[2], Milstein D.[2*]

1 - Okinawa Institute of Science and Technology Graduate University, Okinawa, Japan
2 - Department of Organic Chemistry, Weizmann Institute of Science, Rehovot, Israel

* david.milstein@weizmann.ac.il

Keywords: pincer, ruthenium, water, lactams, amines, dehydrogenation

1 Introduction

Utilizing water as an inexpensive and "green" reagent and solvent is of high practical importance for developing new environmentally friendly transformations in organic synthesis. This work will focus on developing a new atom-economical approach to dehydrogenative transformations in water catalyzed by the Ru pincer complex. In particular, we were able to develop a novel method for the synthesis of lactams directly from amines in the absence of oxidants, using water as the only reagent and a source of oxygen atom in the amide group [1]. This transformations is accompanied by the formation of H_2 gas as the only by-product, thus providing an ultimately atom economical and "wasteless" way for lactam synthesis. This is advantageous compared to other existing methods for lactam formation that typically involve the use of strong oxidants such as PhIO [2], ^{t}BuOOH [3], $RuO_2/NaIO_4$ [4] that also lead to the formation of stoichiometric waste products. In this report, we will focus on the mechanistic studies of the catalytic system through a combined experimental and DFT study.

2 Experimental

All operations were performed in a nitrogen-filled glove box or using Schlenk technique. The complex **1** was prepared as described previously [5]. General procedure for catalytic reactions: a 50 mL pressure tube was charged with pyrrolidine (1 mmol), **1** (10 μmol) in combination with NaOH (15 μmol) or catalyst **2** (10 μmol), 1.5 mL of dioxane and 1.5 mL of water. The reaction mixture was heated at 135-150 ^{o}C for 48h. After 48h, the reaction mixtures were cooled down in ice bath, H_2 pressure was released. Pyridine (20 μL) was added as an internal standard, and the reaction samples were analyzed by NMR in D_2O solution. The yields of products and conversion were determined by NMR integration vs. pyridine as an internal standard. The products were identified by GC-MS and by comparison with authentic samples.

3 Results and discussion

Complex **1** in combination with NaOH shows catalytic activity in the conversion of pyrrolidine to 2-pyrrolidone in dioxane-water mixture at 150 ^{o}C (Figure 1). Similar reactivity was observed with other cyclic amines [1]. In this work, we established that **1** acts as a pre-catalyst for the formation of catalytically active "dearomatized" species **2** under the reaction conditions. The species **2** is responsible for the observed catalytic activity and shows superior activity at lower temperatures as compared to our previously reported results. We will discuss possible pathways for the formation of a catalytically active dearomatized species under the reaction conditions.

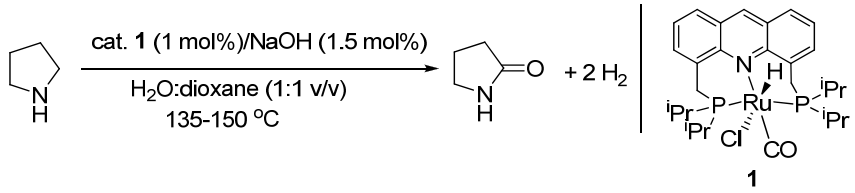

Fig. 1. Ru-catalyzed cyclic amine-to-lactam conversion with water.

The combined experimental study of the reaction intermediates and isotopic exchange experiments are consistent with the proposed pathway of this transformation shown in Figure 2 that involves imine and hemiaminal intermediates. The DFT study shed light on the mechanism of each of these steps. The possibility of the reverse reaction, hydrogenation of lactams to amines, was also considered and tested experimentally.

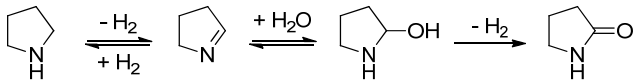

Fig. 2. Proposed pathway for cyclic amine-to-lactam conversion.

4 Conclusions

We have developed an atom ecomonical way of lactam synthesis by reaction of amines with water with liberation of H_2 gas, in the absence of added oxidants. This transformation is a rare example of a reaction in which water is used directly for oxygenation of a CH_2 group of organic substrates [6-7]. The mechanistic studies of this reaction suggest that water plays an important role in this transformation as the oxygen atom source and also facilitates other steps in the proposed mechanism. The acridine-based pincer ligand provides a unique scaffold that allows for facile dehydrogenation steps in this system.

Acknowledgements

This research was supported by the European Research Council under the FP7 framework (ERC No 246837), the Israel Science Foundation and the Kimmel Center for Molecular Design. We thank Gregory Leitus (Department of Research Support) for X-ray diffraction analysis.

References

[1] J. R. Khusnutdinova, Y. Ben-David, D. Milstein, D. *J. Am. Chem. Soc.* 136 (2014) 2998.
[2] R. M. Moriarty, R. K. Vaid, M. P. Duncan, M. Ochiai, M. Inenaga, Y. Nagao, *Tetrahedron Lett.* 29 (1988) 6913.
[3] X.-F. Wu, M. Sharif, A. Pews-Davtyan, P. Langer, K. Ayub, M. Beller, *Eur. J. Org. Chem.* 2013 (2013) 2783.
[4] K. Tanaka, S. Yoshifuji, Y. Nitta, *Chem. Pharm. Bull.* 36 (1988) 3125.
[5] C. Gunanathan, D. Milstein, *Angew. Chem. Int. Ed.* 47 (2008) 8661.
[6] E. Balaraman, E. Khaskin, G. Leitus, D. Milstein, D. *Nat. Chem.* 5 (2013) 122..
[7] R. E. Rodríguez-Lugo, M. Trincado, M. Vogt, F. Tewes, G. Santiso-Quinones, H. Grützmacher, *Nat. Chem.* 5 (2013) 342.

V-PP131

Effects of La and Ce Promotion on CDRM Performance of Co-Ni/ZrO_2 Catalysts

Bal H., Demirhan C.D., Aksoylu A.E.*

Department of Chemical Engineering, Boğaziçi University, Istanbul, Turkey

* aksoylu@boun.edu.tr

Keywords: catalytic hydrogen production, dry reforming, heterogeneous catalysis, carbondioxide, utilization

1 Introduction

Carbon dioxide reforming of methane (CDRM) is a catalytic process where CH_4 and CO_2 are utilized to produce valuable synthesis gas. Compared to other methods, such as steam reforming and partial oxidation, the most important advantage of CDRM is the consumption of CO_2 which is one of the most abundant greenhouse gases whose concentration rise in the atmosphere has been considered as the most common reason for the abrupt climatic changes. The low H_2/CO ratio obtained in CDRM is preferable to be used both in Fischer-Tropsch synthesis and in the production of formaldehyde, polycarbonates or methanol. The main drawbacks of this process are coking and metal sintering, which are the results of the need for high reaction temperatures due to endothermicity of the reaction. ZrO_2 is an appropriate support for reducing carbon accumulation during CDRM, since it enhances dissociative adsorption of CO_2 and migration of the produced O on the catalyst surface to oxidize and gasify the coke formed on catalytic sites. Introducing a promoter (e.g. Ce and La) to form a bimetallic catalyst system also improves the anti-coking property. Preliminary studies of our group have shown that Ce-doped Co/ZrO_2 displays high activity and has a very limited activity loss [1,2]. Additionally, presence of Ni proved to increase CDRM activity [3].

The aim of this study was to design and develop effective Co-La bimetallic, and Co-Ni-La and Co-Ni-Ce trimetallic CDRM catalysts supported on ZrO_2. The favorable reaction conditions for stable performance were investigated through following an experimental design involving the reaction temperature, CH_4/CO_2 feed ratio and space velocity as the parameters. The activity, selectivity and stability of the catalyst as well as the type of carbon deposited on it during reactions performed under various reaction conditions were observed.

2 Experimental

Co-La catalyst was prepared by sequential impregnation, whereas Co-Ni-La and Co-Ni-Ce catalysts were prepared by co-impregnation. The catalysts were calcined *in situ* in dry air for 4 h at 773 K and subsequently reduced *in situ* in H_2 for 2 h at the same temperature. The performance tests were conducted in a quartz micro reactor for the temperature interval of 873-973 K with CH_4/CO_2 feed ratios of 1/1, 2/1, 1/2, and space velocities of 20000 and 60000 mL/h g-catalyst. Agilent Technologies 6850 gas chromatograph (GC) equipped with a Thermal Conductivity Detector (TCD) and a HayeSep D column was used to analyze feed and product compositions. SEM and Energy Dispersive X-Ray (EDX) tests were performed on freshly reduced and spent Co-Ni-Ce/ZrO_2 catalyst samples in order to elucidate their micro-structural properties, and to observe the morphology and localization of the deposited carbon.

3 Results and discussion

The results of the metal mapping studies confirmed well dispersion of Co, Ni and, Ce over

ZrO_2, and SEM results indicated that deposited carbon has both filamentous and graphitic structures. It was observed in performance tests that higher reaction temperatures were beneficial for both increased activity and selectivity, i.e. obtaining H_2/CO product ratio values close to 1. The decrease in space velocity resulted in an increase in CH_4 and CO_2 conversions and H_2/CO ratio in product stream. The effect of CH_4/CO_2 feed ratio on CH_4 conversion at 923 K for all catalysts tested are presented in Figure 1 as an example. 5Co5Ni2La catalyst experienced more activity loss compared to 5Co3Ni2La when CH_4/CO_2 feed ratio is 2/1. Addition of Ni to Co-based catalysts improved activity. However, on La promoted catalysts, increasing Ni-loading caused increased coke formation for CH_4-rich feeds; whereas coke formation was suppressed when Ce was used as the promoter. It was also seen that increasing space velocity led to a decrease in the conversion values and selectivity towards CO without affecting the stability profile.

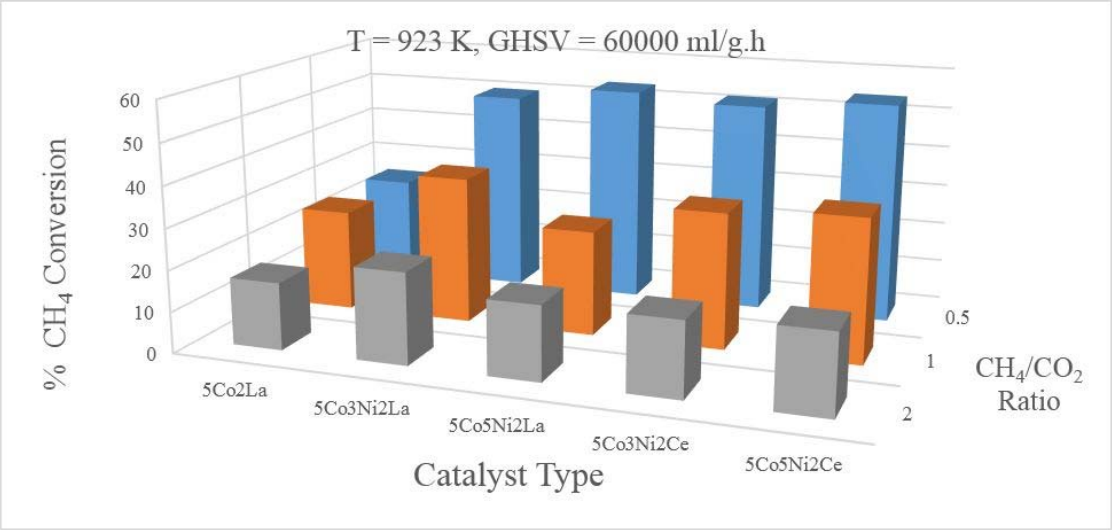

Fig. 1. The effect of CH_4/CO_2 feed ratio on CH_4 conversion at 923 K.

4 Conclusions

La and, more successfully, Ce were proven to be suitable promoters for enhancing the stability of Co- and Ni-based CDRM catalysts. Ce dominantly participated in carbon removal process through forming an additional oxygen storage capacity and regulating surface oxygen transfer. For optimum activity and stability, small amount of Ni addition was found sufficient. Co-Ni-Ce trimetallic system was shown to be the most active and stable catalyst at all reaction conditions. 5Co5Ni2Ce configuration was found to give the optimum performance.

Acknowledgements

This work is financially supported by TUBITAK through project 111M144, and Boğaziçi University through project BAP-M6755.

References

[1] S. Ozkara-Aydınoglu, A. E. Aksoylu, *Int. J. Hydrogen Energy*.11 (2010) 1165–1170.
[2] A. I. Paksoy, B. S. Caglayan, A. E. Aksoylu, *Appl. Catal. B: Environ.* 168 (2015) 164–174.
[3] S. Ozkara-Aydınoglu, A. E. Aksoylu, *Int. J. Hydrogen Energy*.11 (2010) 1165–1170.

V-PP132

Photocatalytic Oxidation of Diethyl Sulfide Vapor over TiO_2 Deposited on Porous Supports

Selishchev D.S.[1,2,3*], Kozlov D.V.[1,2,3]

1 - Boreskov Institute of Catalysis SB RAS, Novosibirsk, Russia
2 - Novosibirsk State University, Novosibirsk, Russia
3 - Research and Educational Centre for Energoefficient Catalysis (NSU), Novosibirsk, Russia

* selishev@catalysis.ru

Keywords: photocatalysis, titania, activated carbon, silica, composite photocatalyst, diethyl sulfide

1 Introduction

Volatile organic compounds containing N, S, P or Cl heteroatoms are often highly toxic and very dangerous for human health [1], and some of them could be used as chemical warfare agents (CWA) [2]. One of the best known CWAs is bis(2-chloroethyl) sulfide or mustard gas (HD). This species is a highly toxic vesicant which causes destruction of cell membranes and nucleic acids. In this way the development of effective methods for HD neutralization is an important task to ensure human safety.

The method of photocatalytic oxidation (PCO) using TiO_2-based photocatalysts is regarded as one of the promising methods of CWA disposal due to the high oxidative ability of TiO_2 under UV irradiation. The main objective of the current study was to investigate the PCO of diethyl sulfide (DES) as one of the HD simulants in the gas-phase over composite photocatalysts in which TiO_2 was deposited onto activated carbon (AC) or SiO_2 surfaces [3].

2 Experimental/methodology

Composite photocatalysts were synthesized by thermal hydrolysis of $TiOSO_4$. Typically, a certain amount of activated carbon or silica powder was suspended in a titanyl sulfate water solution (300 mL) and boiled for 5 hours under constant mixing. The calculated TiO_2 content in the sample was varied in the range of 65-80 wt. % for AC-containing samples and 10-80 wt. % for SiO_2-containing samples. The reference TiO_2 sample was synthesized by the same procedure without addition of support (AC or silica). The photocatalysts synthesized were characterized by atomic emission spectroscopy, nitrogen adsorption at 77 K, X-ray diffraction, FT-IR analysis.

Oxidation of the DES vapor was investigated in a 0.3 L static reactor installed in the cell compartment of a Nicolet 380 FT-IR spectrometer (Thermo Fisher Scientific Inc., USA) under UV irradiation produced by a UV LED (Nichia, Japan) with λ_{max} ~373 nm. Concentrations of DES and other oxidation products in the gas phase were calculated using the Beer-Lambert law.

3 Results and discussion

Composite TiO_2/activated carbon (TiO_2/AC) and TiO_2/SiO_2 photocatalysts with TiO_2 contents in the 10 to 80 wt. % range were synthesized. All TiO_2-based samples were in the anatase form, with a primary crystallite size of about 11 nm. It was demonstrated that the specific surface area and pore volume of the composite photocatalyst are slightly lower than the algebraic sum of the corresponding values of TiO_2 and adsorbent (AC or SiO_2). This means that a partial blocking of the support surface by TiO_2 nanoparticles occurs.

The main purpose of our work was to study the PCO of diethyl sulfide with the composite photocatalysts and to investigate their stability in long-term experiments. In this connection in the beginning we optimized the quantity of the photocatalyst in the reactor. It was demonstrated that studies of long-term photocatalyst use should be done using a relatively low TiO_2 quantity

(0.5 mg/cm^2) because in this case we can assume that the entire photocatalyst surface is irradiated and is involved in the reaction process. Then we chose the photocatalyst with good proportions of adsorptivity and photocatalytic activity in each series. There were 70%TiO_2/AC, 40%TiO_2/SiO_2 and reference TiO_2 sample.

Finally, we investigated DES PCO over chosen photocatalysts. Acetaldehyde, formic acid, ethylene and SO_2 were registered as the intermediate products of DES PCO which were completely oxidized to the final oxidation products – H_2O, CO_2, CO and SO_4^{2-} ions.

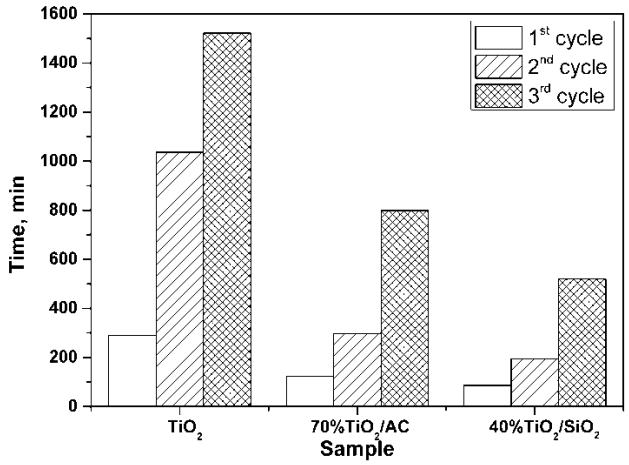

Fig. 1. Time values of 90% DES conversion into CO_2 in three oxidation cycles for pure TiO_2 and TiO_2/adsorbent composite photocatalysts

The influence of the support on the kinetics of DES PCO and on the TiO_2/AC and TiO_2/SiO_2 samples' stability during three long-term DES PCO cycles was investigated. In each subsequent oxidation cycle over the same sample a decrease of DES PCO rate was observed. This means that a strong deactivation of the samples occurs. To estimate the extent of photocatalyst deactivation the time of 90% DES mineralization was calculated in each cycle. Calculated times for all samples in each oxidation cycle are presented in Figure 1. The highest PCO rate was observed for TiO_2/SiO_2 photocatalyst for all three cycles.

To evaluate the activity of photocatalysts the turnover frequency values (TOF) were calculated for three photocatalysts (TiO_2, TiO_2/AC and TiO_2/SiO_2) for the same amount of mineralized DES. It was demonstrated that the TOF value for composite TiO_2/SiO_2 photocatalysts was 3.5 times higher than for pure TiO_2.

4 Conclusions

The usage of composite photocatalyst results in up to an 8-fold decrease of DES removal time if compared with pure unmodified TiO_2. This could be explained by an increase of the available surface area in the case of composite photocatalyst and reversible transfer of non-volatile intermediates from TiO_2 surface to the support surface thus keeping the photocatalyst surface available for further interaction with substrate. Additionally the removal of intermediates – acetaldehyde and formic acid – occurs faster over composite photocatalyst.

The long-term oxidation of DES leads to a strong deactivation of the photocatalyst. The deactivation decreases in the following sequence: TiO_2>TiO_2/AC>TiO_2/SiO_2. The most active and stable catalyst is the TiO_2/SiO_2 one which contains 40 wt. % of TiO_2. The calculated TOF number for this sample is 3.5 times higher than for pure TiO_2.

Acknowledgements

The work was supported by the Skolkovo Foundation (Grant Agreement for Russian educational organization №1 on 28.11.2013)

References

[1] A. Watson, G. Griffin, *Environ. Health Perspect*. 98 (1992) 259
[2] P. Robinson, Ed. *Public Health Response to Biological and Chemical Weapons: WHO Guidance*, 2nd ed. (2004) 340
[3] D. Selishchev, D. Kozlov, *Molecules* 19 (2014) 21424

V-PP133

High Temperature N_2O Decomposition over Massive and Supported Mixed Oxides: Principles of Activity Regulation

Pinaeva L.G.[1*], Ivanov D.V.[1], Sadovskaya E.M.[1,2], Isupova L.A.[1]

Boreskov Institute of Catalysis SB RAS, Novosibirsk, Russia
Novosibirsk State University, Novosibirsk, Russia

* pinaeva@catalysis.ru

Keywords: N_2O decomposition, oxygen, exchange, perovskite, fluorite

1 Introduction

Possibility to abate N_2O formed during nitric acid production immediately downstream of the ammonia combustion Pt-Rh gauzes aroused interest in the reaction of its catalytic decomposition at high temperatures. Numerous systems including both bulk and supported oxides of transition metals and lanthanides were tested in this reaction. Our studies of La-Sr-Mn-O composites showed that their catalytic activity of N_2O decomposition at T>600^{0}C correlated with the coefficient of lattice oxygen self-diffusion [1]. We checked in this study whether following increase of activity was possible by using the materials with *a fortiori* higher lattice oxygen mobility—La-Sr-Fe-O and CeO_2.

2 Experimental/methodology

Several types of catalytic systems were prepared: 1) La-(Sr-)Fe mixed oxides, 2) their composites with CeO_2 – by mechanochemical method, 3) supported $MeOx/Al_2O_3(CeO_2)$ (Me = Fe, Co, Ni, Cu) – by impregnation through Pechini route, and characterized by means of XRD, XPS, HRTEM, EDX, UV–Vis DRS, TPD O_2. The kinetics of $^{18}O/^{16}O$ oxygen exchange have been analyzed both in the isothermal (SSITKA, 800^{0}C) and temperature programmed (TPIE, 100^{0}C÷900^{0}C) modes at 0.005 atm oxygen partial pressure, and the rates of surface oxygen exchange (R_s) and lattice oxygen diffusion (R_{bulk}) have been evaluated. Activity in the reaction of N_2O decomposition was tested in the temperature interval 700-900^{0}C and characterized by R_{N2O} value.

3 Results and discussion

Replacement of Fe for Mn in perovskite lattice resulted in increase of the rates of both bulk oxygen exchange and N_2O decomposition. However, following rise of R_{bulk} at partial Sr replacement for La ($La_{0.4}Sr_{0.6}FeO_3$) from $6\cdot10^{-3}$ s^{-1} to $2.5\cdot10^{-2}$ s^{-1} as calculated for 800^{0}C was accompanied by decrease of R_s value from 8 s^{-1} to 3 s^{-1}, thus hindering following rise of activity. Non-additively high R_{N2O} was measured for $LaSrFeO_4$(surface)–$La_{0.4}Sr_{0.6}FeO_3$ composite that exhibited increased rate of surface oxygen exchange compared with that for the individual $LaSrFeO_4$ phase (R_s = 13 s^{-1} and 8 s^{-1}, respectively), on retention of high lattice oxygen mobility characterizing $La_{0.4}Sr_{0.6}FeO_3$ sample. Such synergetic effect was attributed to heterostructured interfaces formed at intergrowing of perovskite lattices.

The same principle of activity regulation was checked for CeO_2 based samples prepared by different manners. CeO_2 itself revealed the highest bulk oxygen mobility (R_{bulk} >0.1 s^{-1}), but negligible activity due to extremely low R_s value around 1 s^{-1}. First, it was shown that at the same surface concentration of supported Me, substantially higher R_{N2O} and general rates of oxygen exchange values characterized $MeOx/CeO_2$ samples compared with corresponding $MeOx/Al_2O_3$ ones (Fig.1A) that undoubtedly pointed to importance of bulk oxygen mobility.

TPIE and SSITKA measurements revealed possible effect of CeO_2 lattice modification by Me^{n+} on the rate of oxygen transfer both in the bulk and in the near subsurface layers correlating well with samples activity.

For $LaFeO_3$(surface)–CeO_2 composites both the rate of oxygen exchange in the subsurface layer and R_{N2O} increased non-additively in a comparison to $LaFeO_3$ and CeO_2 used for their preparation (Fig.1B). It was proved that decoration of ceria surface by finely dispersed LaOx, FeOx and $LaFeO_3$ species was accompanied by accumulation of oxygen vacancies or extended defects arisen after modification of near subsurface layers of fluorite lattice by inserted Fe^{3+} ions.

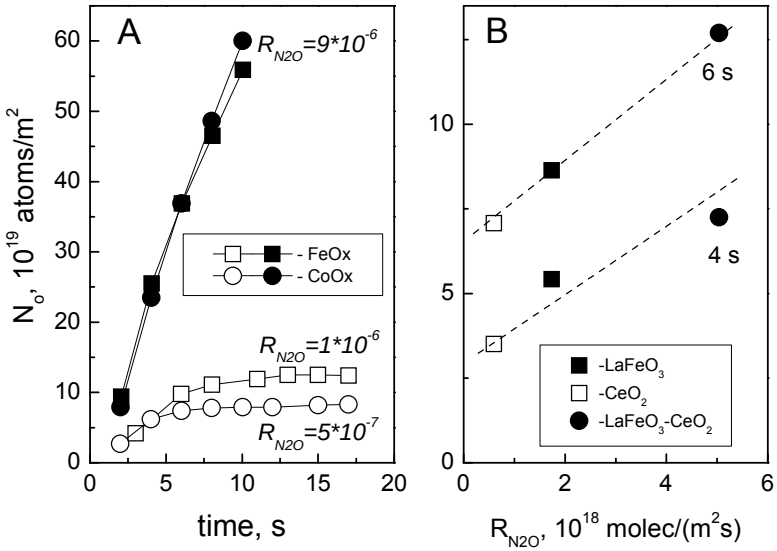

Fig. 1. A) Time dependencies of exchanged oxygen N_0 for Fe(Co)Ox/Al_2O_3 (□,○) and Fe(Co)Ox/CeO_2 (■,●) samples characterized by different R_{N2O} (mole/(m^{2}s)) values. B) R_{N2O} *versus* N_o as calculated for different periods of time (4 and 6 s) for $LaFeO_3$-CeO_2 based samples.

4 Conclusions

For all types of studied oxide systems high bulk oxygen mobility opens additional pathway of oxygen supply from the near subsurface layers to adsorbed species formed after N_2O decomposition on the active surface sites. Formation of heterostructured interfaces on the surface of intergrown composites or mixed solutions enriched by oxygen vacancies promotes oxygen exchange in the surface and near subsurface layers thus hastening O_2 desorption.

References

[1] D.V. Ivanov, E.M. Sadovskaya, L.G. Pinaeva, L.A. Isupova, J. Catal., 267 (2009) 5; D.V. Ivanov,
[2] L.G. Pinaeva, E.M. Sadovskaya, L.A. Isupova, Kinet. Catal., 52 (2011) 401; D. V. Ivanov, L. G.
[3] Pinaeva, L. A. Isupova, A. N. Nadeev, I. P. Prosvirin, L. S. Dovlitova, *Catal. Lett.*, 141 (2011) 322.

V-PP134

Development of the Methods for Fast Catalytic Air Purification from CWAs

Kolinko P.[1,2*], Lyulyukin M.[1], Besov A.[1,2], Parkhomchuk E.[1,2,3], Kozlov D.[1,2,3]

1 - Boreskov Institute of Catalysis SB RAS, Novosibirsk, Russia
2 - Novosibirsk State University, Novosibirsk, Russia
3 - Research and Educational Centre for Energoefficient Catalysis (Novosibirsk State University), Novosibirsk, Russia

* kolinko@catalysis.ru

Keywords: air purification, CWA, adsorption, oxidation, metal oxides, Fe-ZSM-5

1 Introduction

In today's world there is a high probability of terrorist attacks and technological disasters. The result is a deadly emission of volatile organic compounds or its aerosols. If this happens indoors a lot of victims could occur. Sad examples are the attack in the Tokyo subway in March 20, 1995 and the accident at a chemical factory Union Carbide, which occurred in December 3, 1984 in Bhopal (India). In this way the fast air purification method from the dangerous contaminants is of interest.

Common method of man's protection against CWA is the using of special isolating cloths which is preventing the contact of CWAs vapors and aerosols with the human body. At the same time, many of the CWAs can be absorbed on the surfaces and the risk of danger will remain. In this regard, the development of the method for the fast air and surface purification becomes important. In addition, this method will allow rapid degassing in the places where it is impossible to use personal protective clothes, such as in the subway and other crowded places [1].

The indoor air and surfaces purification can be achieved by adsorption of contaminants on the surface of various sorbents, as has been shown previously by J. Romano et al. [2]. Most CWAs are compounds with branched structure and high molecular weight, and therefore can be easily adsorbed on a solid surface [3]. CWAs adsorption on the adsorbents requires further neutralization. Suitable method for CWAs degradation is photocatalytic oxidation when used the titanium dioxide as an adsorbent. But the complete oxidation is achieved within about ten hours or more [4].

The army decontamination solutions (DS2 or 'MAKS') could not purify the air from CWAs vapors. In this way we need the universal technique for fast air and surfaces purification from CWAs vapors and aerosols. Fast means less than 5 minutes.

In our study, we propose the method which includes fast adsorption step and subsequent degradation of adsorbed CWA by the Fenton system.

2 Experimental/methodology

Since the CWA are highly toxic compounds it is safe tu use less toxic simulants in the research of new decontamination methods. Such substances were butyl-β-chloroethylsulfide (BCES), dimethyl methylphosphonate (DMMP) and O,O-diethyl-O-3,4,5-trichlorophenylphosphate (DETCPP), which are conventional imitators of mustard and organophosphorus CWAs. In the current work were used nanosized samples of TiO_2, AlOOH, SiO_2, MgO, Fe_2O_3 as the adsorbent.

Adsorption experiments were conducted in the isolated 11 l glass cylinder or in the 3.6 m^3 cubic plastic chamber.

The concentration of gaseous organic compounds and CO_2 in the chamber's air was measured by means of the FT-IR spectrometer Vector-22 (Bruker) equipped with a long path gas cell G-3-8-H (Infrared Analysis Inc.).

3 Results and discussion

All volatile CWA's simulants could be removed from the gas phase by TiO_2, AlOOH, SiO_2, MgO, Fe_2O_3 aerosols with different efficiencies. SiO_2 and AlOOH aerosols demonstrated the highest rates of CWA's simulant removal. Fig. 1 (**a**) demonstrates the BCES concentration profile during its adsorption with the SiO_2 aerosol.

The dependence of the characteristic removal time on the specific surface area of adsorbent materials was studied. Optimum sorbent surface area should be higher than 200 m^2/g (Fig. 1. **b**).

Purification of the surfaces from the non-volatile simulants also takes less than 5 minutes due to its absorption by nanosized oxide aerosols.

The subsequent decontamination of oxide aerosols could be provided by the heterogeneous Fenton system.

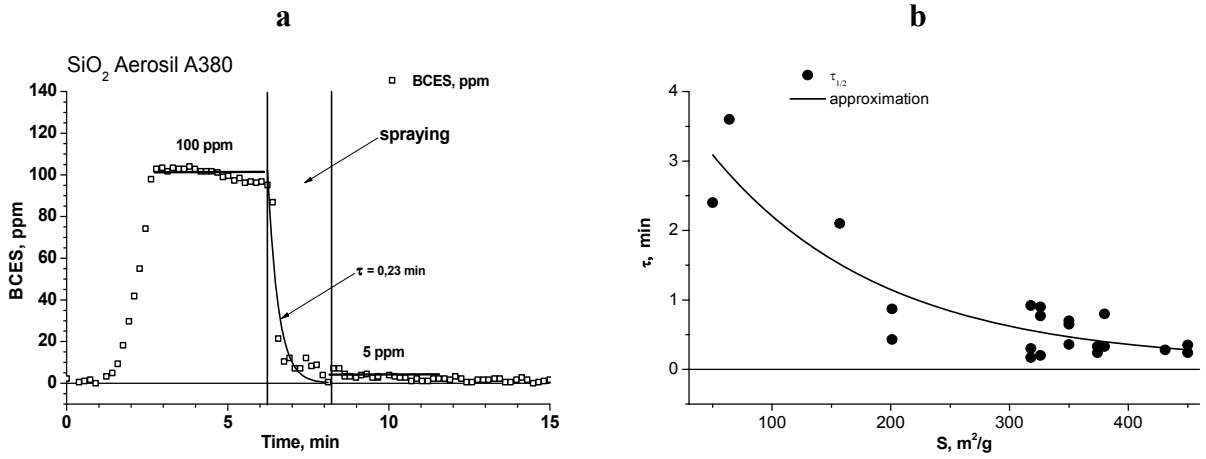

Fig. 1. (**a**) Kinetic curves of air purification from BCES in the static reactor (V = 11 l); (**b**) The dependence of the characteristic time (τ) of vapors removal from the specific surface area of adsorbent being aerosolized.

4 Conclusions

Vapours of simulant CWA can be fast removed from air and surface via adsorption and catalytic oxidation over metal oxide nanosized aerosol particles. It is possible to perform the air and surface purification in practically any place.

Acknowledgements

Authors would like to thank the Russian President Grant for Leading Scientific Schools (NSh-1183.2014.3).

References

[1] N. Zander, E. Kowalski, A. Rawlett, J. Orlicki, Decontamination of Chemical Agent Simulant by Nanometal Oxides, Army Research Laboratory, Aberdeen Proving Ground, MD 21005-5069, 2007.
[2] J. Romano, B. Lukey, H. Salem, Chemical Warfare Agents: Pharmacology, Toxicology, and Therapeutics, Second Edition, CRC Press, 2011.
[3] G. Wagner, P. Bartram, O. Koper, K. Klabunde, *J. Phys. Chem. B* 103 (1999) 3225.
[4] A. Vorontsov, A. Besov, V. Parmon, *Appl. Catal. B* 129 (2013) 318.

V-PP135

Stabilization Effect of Pd–Rh Alloyed Nanoparticles in Three-Way Catalysts

Vedyagin A.A.[1,2*], Volodin A.M.[1], Stoyanovskii V.O.[1], Kenzhin R.M.[1], Mishakov I.V.[1,2], Plyusnin P.E.[3], Shubin Yu.V.[3]

1 - Boreskov Institute of Catalysis SB RAS, Novosibirsk, Russia
2 - Novosibirsk State Technical University, Novosibirsk, Russia
3 - Nikolaev Institute of Inorganic Chemistry SB RAS, Novosibirsk, Russia

* vedyagin@catalysis.ru

Keywords: alloyed Pd–Rh catalysts stabilization, donor sites, exhaust gas neutralization

1 Introduction

Three-way catalysts are well known systems used for neutralization of gasoline automotive emissions. As a rule they contain palladium and rhodium as active components providing the conversion of pollutants via a number of oxidation and reduction reactions. The catalysts with atomically dispersed or sub-nanometer sized ionic clusters of precious metals have been recently shown to have the highest activity in these reactions. In our previous study [1], we have observed that alumina donor sites play defining role in stabilization of atomically dispersed forms of supported Pd. Original catalytic and spectroscopic methods were developed for characterization of active sites responsible for high activity of these catalysts in the CO oxidation reaction. The present study is focused on the activity and stability of bimetallic Pd–Rh catalysts obtained from heterometallic complexes and supported on γ-Al_2O_3. The total precious metal loading in the synthesized samples was as low as 0.2 wt. % that complicated the use of the most of conventional physical and chemical methods of characterization.

2 Experimental/methodology

γ-Al_2O_3 was used as a support for all prepared catalysts. The support was obtained by calcination of commercial $Al(OH)_3$ hydroxide (Condea) at 700°C for 12 h. Incipient wetness impregnation of the support with double complex salt $[Pd(NH_3)_4]_3[Rh(NO_2)_6]_2$ was applied to synthesize the bimetallic Pd–Rh catalysts. The atomic Pd/Rh ratio in the impregnation solution was 3/2. The concentrations of the complexes were selected to obtain the total metals loading of 0.2 wt. %. Mechanical mixture of monometallic Pd- and Rh-containing catalysts with similar metals loading was used as a reference sample. Electron paramagnetic resonance (spin probe method), luminescence spectroscopy, UV-Vis spectroscopy, and testing reaction of ethane hydrogenolysis used for characterization of active sites of the catalysts are described elsewhere [1-2]. Catalytic testing conditions as well as so-called prompt thermal aging (PTA) procedure are reported in [3, 4].

3 Results and discussion

It was found by the spin probe method that both mono- and bimetallic Pd-containing complexes are stabilized on the same donor sites of the alumina surface. Bimetallic-alloyed state of prepared Pd-Rh catalysts was also confirmed by results of ethane hydrogenolysis reaction (Fig.1). As it could be clearly seen from the graph, the state of rhodium in mechanical mixture is equal to that of monometallic Rh sample. In this case, one can conclude that there is no Pd-Rh interaction. At the same time, the light-off curve for bimetallic Pd-Rh sample is shifted into the high temperature region thus indicating the formation of alloyed nanoparticles. The presented data are of great agreement with the catalyst behavior in CO oxidation and NO_x reduction reactions.

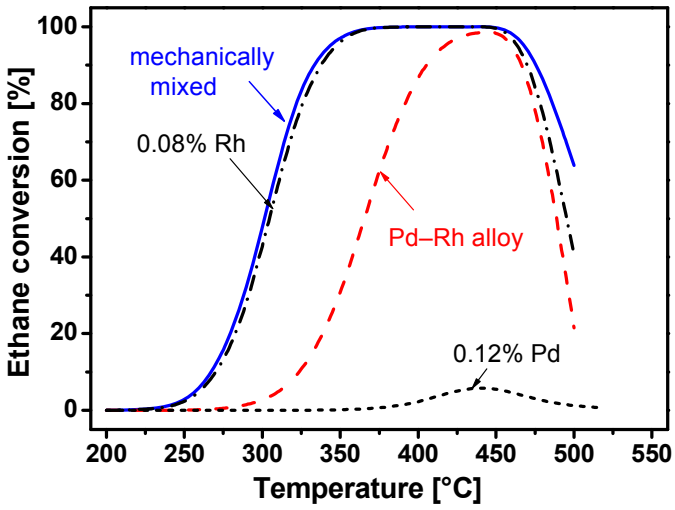

Fig.1. Experimental light-off curves of ethane hydrogenolysis testing reaction for bimetallic (0.12% Pd – 0.08% Rh)/alumina, mechanically mixed (0.12% Pd/alumina + 0.08% Rh/alumina), monometallic 0.12% Pd/alumina, and 0.08% Rh/alumina samples.

Using the UV-Vis and luminescence spectroscopies it was shown that bimetallic Pd-Rh system is characterized by the highest stability in oxidative conditions at temperatures as high as 1000°C. The stabilization effect of alloyed Pd-Rh particles related to both bulk diffusion of rhodium ions into support and surface diffusion of palladium followed by its sintering will be discussed.

4 Conclusions

The main problem of monometallic Pd and Rh catalysts application consists in their rapid deactivation at elevated temperatures. In case of Pd/alumina catalysts, the mentioned loss in catalytic activity is stipulated by the palladium surface diffusion, sintering, and partial covering by support. Bulk diffusion of Rh^{3+} into support followed by its irreversible encapsulation in corundum phase seems to be the predominant reason for deactivation of Rh-containing systems. The experimental data observed in present work indicated the reciprocal stabilization effect of these metals being in alloyed state. It should be also noted that low precious metals loading used in this study allowed us to synthesize the catalysts with active sites in the form of isolated ionic clusters.

Acknowledgements

This study was supported by Russian Foundation for Basic Research (Grant No. 13-03-00988-a) and Russian Academy of Sciences (project No. V.45.3.2).

References

[1] A.A. Vedyagin, A.M. Volodin, V.O. Stoyanovskii, I.V. Mishakov, D.A. Medvedev and A.S. Noskov // *Appl Catal B* 103 (2011) 397.
[2] V.O. Stoyanovskii, A.A. Vedyagin, G.I. Aleshina, A.M. Volodin, A.S. Noskov // *Appl Catal B* 90 (2009) 141.
[3] A.A. Vedyagin, M.S. Gavrilov, A.M. Volodin, V.O. Stoyanovskii, E.M. Slavinskaya, I.V. Mishakov, Y.V. Shubin // *Top Catal* 56 (2013) 1008.
[4] A.A. Vedyagin, A.M. Volodin, V.O. Stoyanovskii, R.M. Kenzhin, E.M. Slavinskaya, I.V. Mishakov, P.E. Plyusnin, Yu.V. Shubin // *Catal Today* 238 (2014) 80.

V-PP136

Synthesis Effect on CH_4 Partial Oxidation over Ni-CeO_2 Catalysts

Venezia A.M.[1*], Pantaleo G.[1], La Parola V.[1], Deganello F.[1], Singha R.K.[2], Bal R.[2]

1 - Institute of Nanostructured Materials, CNR, Palermo, Italy
2 - Indian Institute of Petroleum, Dehradun, India

* venezia@pa.ismn.cnr.it

Keywords: methane, catalytic, partial oxidation, Ni catalysts, CeO_2

1 Introduction

The production of synthesis gas from natural gas is an important step in the gas to liquid (GTL) technology. The syngas is actually produced by methane reforming processes which are highly energetic and capital intensive and are based on the endothermic steam and dry reforming reactions. A promising alternative to these processes is the partial oxidation of methane (POM) represented by the following reaction

$2\ CH_4 + 1/2\ O_2 \rightarrow CO + 2H_2 \qquad \Delta H°\ 298\ K = -35.5 kJmol\text{-}1$

The products H_2 and CO are in a ratio of 2, appropriate for methanol or Fischer-Tropsch synthesis [1]. The Ni based catalysts are the most suitable for the process, however they generally suffer from deactivation by Ni sintering and by coke formation [2]. The aim of the present study is to investigate the effect of different synthesis procedures of Ni-CeO_2 catalysts on their performance in the methane partial oxidation reaction, aiming to achieve an active and stable catalytic material.

2 Experimental/methodology

Ni-CeO_2 catalysts were prepared by conventional co-precipitation (CP), by wet impregnation (WI), by microwave assisted CP and WI (mw-CP) and (mw-WI) and by hydrothermal (HT) procedures. The effect of the different syntheses on the catalyst structural properties was investigated by XRD, TPR, TGA, TEM and XPS. The catalytic behavior of the catalysts was tested in the methane partial oxidation reaction carried out at 1 atm in a temperature range of 400 °C – 800 °C using He diluted feed gas mixture with $CH_4/O_2 = 2$, WHSV=60000 $mLg^{-1}h^{-1}$. On stream stability tests were also performed.

3 Results and discussion

As shown in Fig.1a and Fig. 1b, total methane combustion occurred within the 450 °C < T< 650 °C temperature range. At around 650 °C partial oxidation of methane started, reaching total methane conversion at 700°C - 800 °C with CO selectivity close to thermodynamic limit. Differences were observed in the POM light off temperatures. The catalyst prepared by hydrothermal treatment was the most active and stable followed by the catalyst prepared by microwave assisted co-precipitation. During the stability test at high temperature, as shown in Fig. 2 the catalysts exhibited different behavior.

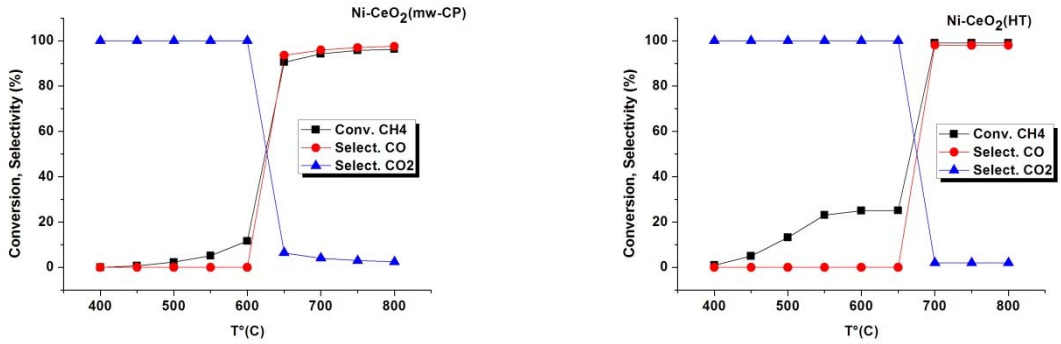

Fig.1a. CH_4 conversion and CO and CO_2 selectivity as a function of temperature in partial oxidation of methane.

Fig.1b CH_4 conversion and CO and CO_2 selectivity as a function of temperature in partial oxidation of methane.

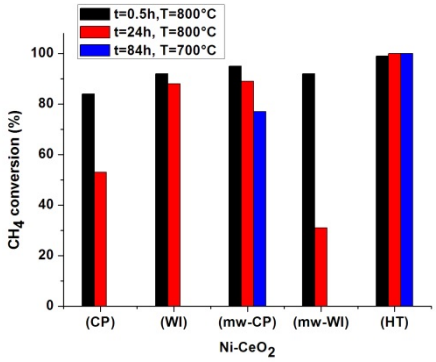

Fig. 2 Methane conversion, after different time on stream at the indicated temperatures, for the differently prepared catalysts.

As derived from the TGA results no significant amount of carbon formed during the reaction. According to the XRD analyses, nickel particle sintering occurred to an extent depending on the preparation procedure.

4 Conclusions

The catalyst preparation procedure affected the catalytic performance of the Ni-CeO_2 catalysts. The main differences were observed in the on stream stability. As arisen from the structural results, the deactivation was largely due to the nickel particle sintering related to the Ni-support interaction modulated by the synthesis.

Acknowledgements

The Bilateral Collaboration Program supported by Italian CNR and Indian CSIR is kindly acknowledged.

References

[1] Saleh A. Al-Sayari, The Open Catalysis Journal, 6 (2013) 17-28.
[2] G. Pantaleo, V. la Parola, F. Deganello, P. Calatozzo, R. Bal, A M. Venezia, Appl. Catal. B 164 (2015)135-143

V-PP137

Improved Diesel Soot Oxidation Performance of Manganese-Substituted Strontium Ferrite

Khobragade R.[1], Saravanan G.[1], Rayalu S.[1], Bakardjieva S.[2], Subrt J.[2], Labhasetwar N.[1*]

1 - CSIR-NEERI, Nagpur, India
2 - IIC, ASCR, Prague, Czech Republic

* nk_labhsetwar@neeri.res.in

Keywords: diesel soot, perovskites, oxidation, catalyst, $SrFeO_{2.83}$, Mn-substitution

1 Introduction

Diesel engines are superior to the gasoline engines in terms of fuel consumption with lesser CO_2-emission, higher energy efficiency etc. [1]. Although, diesel engines have several advantages than that of gasoline engines, however, it emits particulate matter (PM), commonly known as soot due to the incomplete combustion of diesel fuel. The size of PM varies in the range between 1 and1000 nm that can be easily inhaled by human and attributed for several respiratory diseases. Diesel particulate matter consists of both organic (benzene, xylene, toluene etc.) and inorganic moieties (ash, trace amounts of phosphorous, chromium, zinc, silicon, iron and calcium) [2]. Recently, diesel engine emission norms were tightened further due to the severe adverse effects not only on health but also on environment. It has been proved that after-treatment technologies, for instance diesel oxidation catalysts (DOC) and diesel particulate filters (DPF) are efficient to reduce the emissions of CO, HC and PM. However, most of the diesel oxidation catalysts require platinum group metals (PGM) (Pt, Pd, Rh, etc.)[3]. Therefore, there is an essential need to search the alternatives to PGM due to their not only high cost but also their localized availability. Perovskites among the various mixed oxide type materials may be anticipated to partly replace the current PGM catalysts due to their thermal stability at elevated temperatures, flexibility in tailoring of structures as well as physiochemical properties, and comparable catalytic activity [4]. In this study, we successfully prepared the pure phase of strontium ferrite ($SrFeO_{2.83}$) and manganese (Mn) substituted strontium ferrite $SrFe_{1-x}Mn_xO_{2.83}$ (x = 5, 10) through co-precipitation method, followed by step-wise calcination at 900 ºC for various duration. Our results inferred that Mn-substitution enhances significantly the catalytic activity for soot oxidation by about 125 ºC.

2 Experimental

The pure perovskite phase of $SrFeO_{2.83}$ [5] and Mn-substitutes $SrFe_{1-x}Mn_xO_{2.83}$ (x = 5, 10) were prepared by co-precipitation method followed by calcination at 900 °C. The aqueous solution of nitrate precursors ($Sr(NO_3)_2$, $Fe(NO_3)_3.9H_2O$) and $Mn(NO_3)_2.4H_2O$)with intended stoichiometry were co-precipitated using the aqueous solution of NaOH. The co-precipitate mass was then calcined step-wise at 900 °C for 8, 24 and 8 h, respectively. $SrFeO_{2.83}$ and $SrFe_{1-x}Mn_xO_{2.83}$ (x = 5, 10) were characterized by powder X-ray diffraction (pXRD), scanning electron microscopy (SEM) and transmission electron microscopy (TEM). The redox properties of $SrFeO_{2.83}$ and $SrFe_{1-x}Mn_xO_{2.83}$ (x = 5, 10) were examined by temperature programmed desorption (TPD) and temperature programmed reduction (TPR). Thermal stability of $SrFeO_{2.83}$ and $SrFe_{1-x}Mn_xO_{2.83}$ (x = 5, 10) was examined under harsh oxidation conditions at 700 ºC for 2 h. The catalytic activity of $SrFeO_{2.83}$ and $SrFe_{1-x}Mn_xO_{2.83}$ (x = 5, 10) was evaluated using state-of-the-art fixed-bed flow reactor.

3 Results and discussion

Figure 1*a* shows the pXRD profiles of $SrFeO_{2.83}$ and $SrFe_{1-x}Mn_xO_{2.83}$(x = 5, 10), confirming the formation of pure perovskite phase of both $SrFeO_{2.83}$ and $SrFe_{1-x}Mn_xO_{2.83}$ (x = 5, 10). The 2θ values of $SrFeO_{2.83}$ shifted to lower 2θ values with increasing of Mn-substitution, indicating that the lattice of $SrFeO_{2.83}$ is most likely altered upon Mn-substitution. The particles of both $SrFeO_{2.83}$ and $SrFe_{1-x}Mn_xO_{2.83}$ (x = 5, 10) were agglomerated due to the alcinations temperature of 900 ºC, as shown in the Figures 1b and 1c. The pure phase of $SrFeO_{2.83}$ showed the catalytic activity for the oxidation of soot, which is further increased significantly with increasing of Mn-substitution, as shown in Figure 2. The maximum soot oxidation temperature observed for $SrFe_{1-x}Mn_xO_{2.83}$ (x = 5, 10) is 425 ºC, which is significantly lower (125 ºC) than that for the oxidation temperature bare soot (550 ºC).

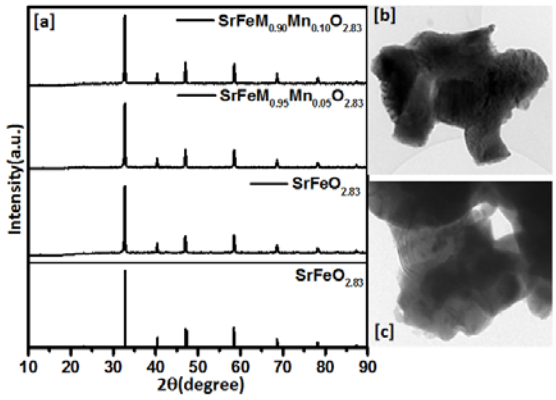

Fig. 1.a. pXRD patterns of $SrFeO_{2.83}$ and $SrFe_{1-x}Mn_xO_{2.83}$ **b.** HR-TEM image for $SrFeO_{2.83}$ and **c.** $SrFe_{0.95}Mn_{0.05}O_{2.83}$

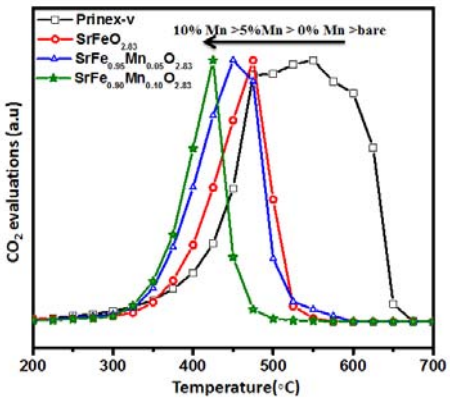

Fig. 2. Oxidation of soot on $SrFeO_{2.83}$ and $SrFe_{1-x}Mn_xO_{2.83}$ using fixed-bed flow reactor

4 Conclusions

The pure perovskite phase of $SrFeO_{2.83}$ and $SrFe_{1-x}Mn_xO_{2.83}$ (x = 5, 10) was synthesized through co-precipitation method followed by step-wise calcination at 900 ºC. Both $SrFeO_{2.83}$ and $SrFe_{1-x}Mn_xO_{2.83}$ showed the catalytic activity for the oxidation of soot and Mn-substitution enhances the catalytic activity significantly. The maximum catalytic oxidation temperature of soot decreased for 10 % of Mn-substitution in $SrFeO_{2.83}$ by 125 ºC. Present strontium ferrite type diesel soot oxidation catalysts are of significance considering commonly available abundant precursors of Fe and Mn and their relative environmental safety.

References

[1] G. Corro, React. Kinet. Catal.Lett. 75, 1 (2002) 89
[2] Jun Xi, Bei-Jing Zhong, Chem. Eng. Technol. 29 (2006) 6
[3] B.A.A.L. van Setten, M. Makkee, J.A. Moulijin, Catal.Rev.43 (2001) 489
[4] N. K. Labhsetwar, M. Dhakad, S. S. Rayalu, R. Kumar, J. Subrt, H. Haneda, S. Devotta, T. Mitsuhashi, Topics in catalysis. 42-43, 1-4, (2007) 299
[5] S. Diodati, L. Nodari, M. M. Natile, U. Russo, E. Tondello, L. Lutterotti and S. Gross,Dalton Trans., 41(2012) 5517.

V-PP138

Selective Elecrochemical Reduction of NOx

Hansen K.K.*

Technical University of Denmark, Lyngby, Denmark

* kkha@dtu.dk

Keywords: NO, O_2, Ba, LSMC, CGO, deNOx

1 Introduction

Removal of NOx from diesel trucks and cars are of major importance. Traditionally the removal of Nox is done using the selective catalytic reduction (SCR) of Nox. Here a reducing agent is needed. An alternative solution is to use an all solid state electrochemical reactor based on an oxide ionic conducting electrolyte, as suggested by Pancharatnam et al. [1]. The major obstacle of this approach is high power consumption, due to the competing reduction of O_2 at the cathode [2]. One way to solve the selectivity problem is to add a Nox storage compound, in the form of potassium or barium nitrate. This can be done in two ways; either by adding the nitrates in a separate layer on the top of the electrode or by getting the nitrates into the structure, by wet infiltration. The latter approach will be described in this text. A concept useful for removal of Nox is a porous cell stack as shown in the figure below. The porous cell stack consists of alternating layers of electrode and electrolyte. By making the cell porous gas can be forced through the cell, thereby getting in close contact with the electrodes.

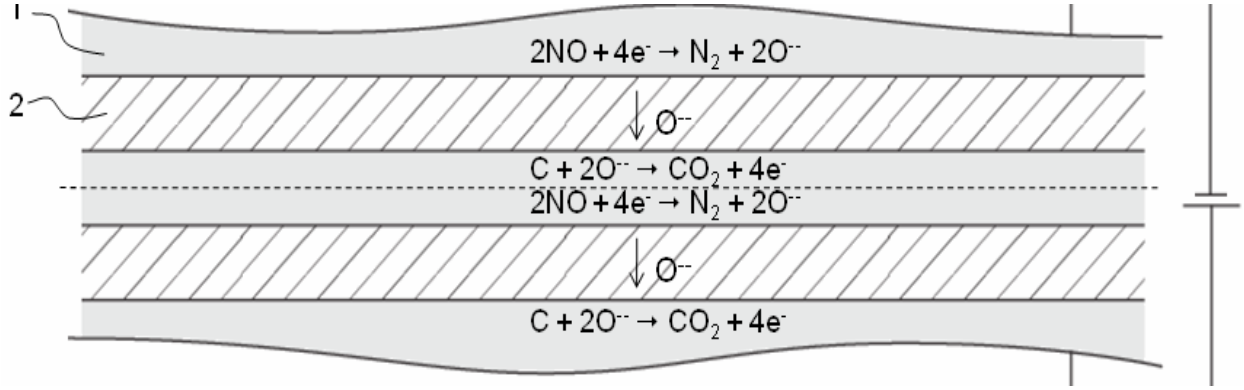

Fig. 1. A porous cell stack useful for removal of Nox from exhaust gasses. The porous cell stack is seen to be constructed from alternating layers of electrode and electrolyte. A potential is applied between top and bottom electrodes in order to reduce the Nox. 1 electrode, 2 electrolyte.

2 Experimental/methodology

Porous cell stacks of LSMC/CGO composite electrodes and CGO electrolytes were made by tape casting followed by lamination and sintering. Pore formers were added to the suspension used for the tape casting in order to produce the porous cell stacks. The cells were then coated with porous gold layers on the top and bottom electrodes. After this the cells were infiltrated with $Ba(NO_3)_2$. The cell was mounted in an one atmosphere setup with possibility of controlling the gas composition and flow rates. Electrical connection was done using two thermocouples mounted at the top and bottom electrodes respectively. A Gamry Ref 600 potentiostat was used for the electrochemical measurements. Gas conversion was measured using a Thermo scientific CLD and an Agilent μ-GC.

4 Results and discussion

Selected results are shown in Figure 2. As it can be seen the NOx can be reduced at temperatures down to 300 °C with a current efficiency of up to 32% (as the cell is a 11 layer stack, the current efficiency is actual 6.4%).

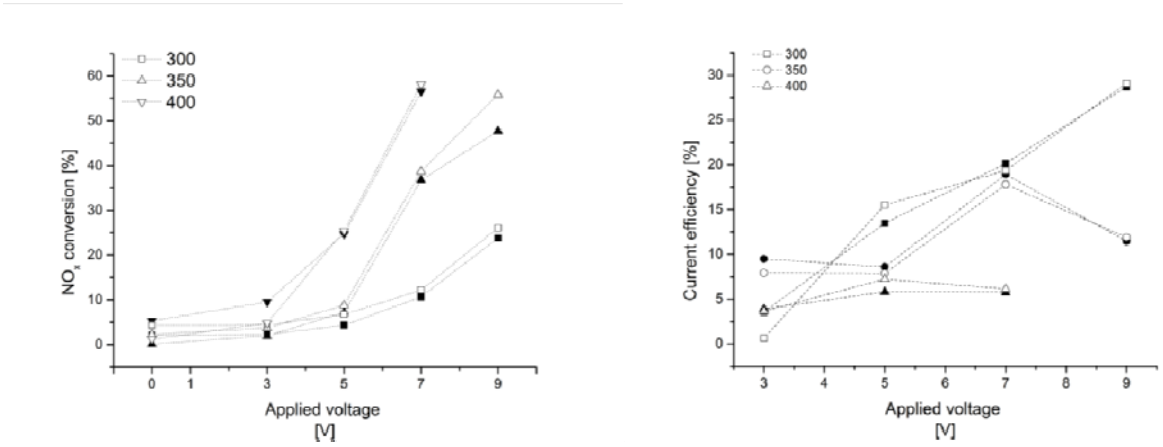

Fig. 2. Conversion of Nox to nitrogen shown to the left as a function of temperature and voltage. To the right current efficiencies as a function of applied voltage. Measured on an 11 layers porous cell stack with LSMC/CGO electrodes. 1000 NO ppm and 10% oxygen in Ar.

4 Conclusions

It has been shown that a full ceramic cell can be used to remove NOx from synthetic gasses containing large amounts of oxygen. Current efficiencies of up to 6.4% have been obtained. Removal of NOx at temperatures down to 300 °C has been shown possible.

Acknowledgements

Anja Friedberg is thanked for help with the experimental work.

References

[1] S. Pancharatnam, R.A. Huggins, D.M. Mason, *J. Electrochem. Soc.,* 122 (1975) 869
[2] K. Kammer Hansen, *Appl. Catal. B: Environmental*, 100 (2010) 427

V-PP139

Hydrogenation of 2,4,6-Trinitrobenzoic Acid on Pd/Sibunit Catalysts

Belskaya O.B.[1,2*], Mironenko R.M.[1], Rodionov V.A.[1], Talsi V.P.[1], Sysolyatin S.V.[3], Likholobov V.A.[1,2]

1 - Institute of Hydrocarbons Processing SB RAS, Omsk, Russia
2 - Omsk State Technical University, Omsk, Russia
3 - Institute for Problems of Chemical and Energetic Technologies SB RAS, Biysk, Russia

* obelska@ihcp.ru

Keywords: 2,4,6-trinitrobenzoic acid, 2,4,6-triaminobenzene, hydrogenation, carbon-supported, palladium catalyst

1 Introduction

The catalytic hydrogenation of trinitroaromatic compounds is of interest as a model reaction in the development of theoretical basis for the liquid-phase hydrogenation of organic compounds; in addition, it is of practical importance for utilization of explosives. The use of catalytic hydrogenation for safe deactivation of one of the most common explosives, trinitrotoluene (TNT), has substantial environmental advantages over its utilization by explosion, oxidation or chemical reduction. 2,4,6-Trinitrobenzoic acid (TNBA) is among the most accessible and promising products of trinitrotoluene transformation. The reduction of all nitro groups may lead to 2,4,6-triaminobenzene (TAB) – the essential component for the synthesis of various commercial products, in particular, phloroglucinol, which is used to produce azo dyes, as components of heat-resistant thermosetting resins and insulation for conductors, as well as in the synthesis of antibacterial and antiviral preparations [1].

Some features of trinitroaromatic compounds – high oxidation potential, strong adsorption on the surface of metal catalysts, high exothermic effect of the reduction to triamine, and side-reactions between the intermediates to polymers at hydrogenation – initiate studies that aim both to reveal the effect of reaction conditions on the rate and conversion and to obtain new stable catalytic systems. Our study examined the effect of TNBA hydrogenation parameters (temperature, pressure, concentration of reactant, and nature of solvent) as well as conditions of the catalyst synthesis and pretreatment on the process rate and selectivity. The mesoporous carbon material Sibunit, which has a high mechanical strength, chemical stability and a developed surface area [2], was chosen as a support for the palladium catalysts.

2 Experimental/methodology

The 5%Pd/C catalysts were synthesized by the hydrolytic precipitation of palladium polyhydroxo complexes (PHC) on the surface of the carbon material followed by palladium reduction with sodium formate. The texture properties of Sibunit were found by analyzing the nitrogen adsorption-desorption isotherms at 77 K (ASAP-2020, Micromeritics). Palladium content in the catalysts was determined by atomic absorption spectroscopy (AA-6300, Shimadzu). CO pulse chemisorption at room temperature (AutoChem II 2920, Micromeritics) and transmission electron microscopy (JEM-2100, JEOL) were used to estimate the particle size of palladium. The catalytic hydrogenation was performed in an autoclave with controlling the volume of absorbed hydrogen. The conversion products were examined by ^{1}H and ^{13}C NMR spectroscopy (Avance-400, Bruker), IR spectroscopy (IRPrestige-21, Shimadzu), and elemental analysis (Vario EL cube, Elementar Analysensysteme GmbH).

3 Results and discussion

Variation of the reaction conditions has demonstrated that hydrogenation of TNBA in the presence of Pd/C catalyst leads to the target TAB only at a high hydrogen pressure (0.5 MPa); however, a further increase in the pressure to 0.8 MPa (at a temperature of 50 °C) initiates undesirable reactions leading to the formation of by-products. Temperature elevation from 50 to 70 and 90 °C (at a pressure of 0.5 MPa) increases hydrogen conversion and results in a selective formation of TAB. The hydrogenation of TNBA was studied in different media: acetone, ethyl and isopropyl alcohols, water, and ethyl acetate. Water with the addition of $NaHCO_3$ was found to be the most efficient solvent. When the reaction is carried out at a temperature of 50 °C and pressure of 0.5 MPa, a complete hydrogenation of TNBA to TAB occurs at a 170 g TNBA / 1 g Pd ratio. An increase in the substrate concentration in a solution (420-1670 g TNBA / 1 g Pd) at the same catalyst weight and reaction conditions decreases the hydrogen conversion and reaction rate but increases the yield of by-products.

The role of H_2PdCl_4 hydrolysis conditions in the formation of palladium PHC to provide a necessary dispersion of the supported metal and activity in hydrogenation of TNBA was studied. The hydrolysis was performed with aqueous solutions of precipitants containing the K^+, Na^+ and Li^+ cations and the CO_3^{2-}, HCO_3^- and OH^- anions; the pH of precipitation was varied in the existence region of palladium PHC in the impregnating solution. Higher dispersions of the supported palladium were observed at pH below 5, with a potassium-containing precipitant, and in the presence of carbonate or hydrocarbonate anions.

4 Conclusions

The catalyst having the highest dispersion of palladium particles and synthesized with the use of $KHCO_3$ precipitant showed the maximum activity in the target reaction of TNBA hydrogenation to TAB (with a selectivity above 90%) under the specified conditions (a temperature of 50 °C and a pressure of 0.5 MPa). The NMR analysis of the products that formed upon variation of TNBA hydrogenation conditions was used to suggest a scheme of the transformations occurring in the presence of Pd/C catalysts:

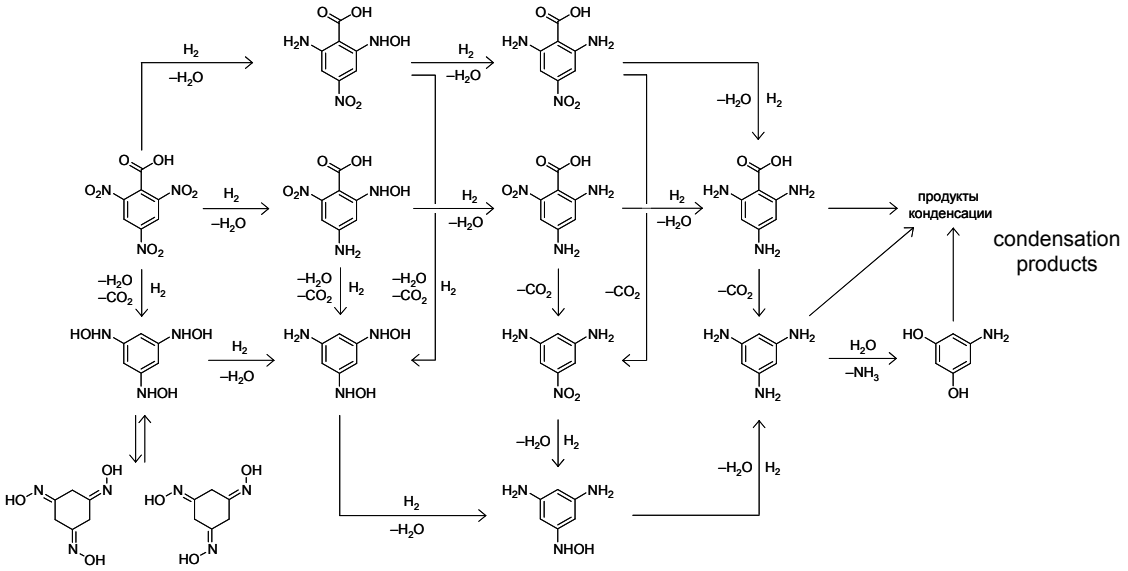

References

[1] V.A. Tartakovsky, S.A. Shevelev, M.D. Dutov et al. Problems of trotyl (TNT) processing into condensation monomers, polymers and dyes. In: Conversion Concepts for Commercial Applications and Disposal Technologies of Energetic Systems, Ed. H. Krause, Kluwer Acad. Publ., Dordrecht, 1997, pp. 137–145.

[2] US Patent 4978649, Russian Patent 2008969

V-PP140

Biocatalytic Generation of Oil-Displacing Systems in Low-Temperature Reservoirs of Viscosity Oil

Altunina L.K., Svarovskaya L.I.*, Guseva Yu.Z.

Institute of Petroleum Chemistry Siberian Branch of the Russian Academy of Sciences, Tomsk, Russia

* sli@ipc.tsc.ru

Keywords: carbamide, urease enzymatic, hydrolysis, viscosity oil, oil-displacement

1 Introduction

In some industrialized countries, viscosity oil is regarded as the main reserve of oil production in the coming years. In Russia there are two major fields of abnormally viscosity oil are under commercial development, the Yaregskoye oilfield and the Permocarbonic oil pool in Usinskoye oilfield (Komi Republic) with total geological reserves of 870 million tons [1].

To enhance oil recovery from low-temperature reservoirs, complex technologies have been developed. They are based on the injection of steam, which reduces oil viscosity, followed by the injection of surfactant-based oil-displacing systems [2, 3]. These oil-displacing systems, along with surfactants, contain nitrogen compounds, including ammonium nitrate and carbamide. The carbamide in the reservoir is hydrolyzed due to steam temperature to yield CO_2 and NH_3. Ammonia at dissolution in water forms an alkaline buffer solution, the maximum capacity of which ranges pH 9.0–10.0, which improves the washing properties of the system, stimulates oil desorption from the porous reservoir rock and thereby enhances oil recovery. Carbon dioxide, in contrast to ammonia, is much more soluble in oil than in water.

2 Experimental/methodology

To hydrolyze carbamide we used soybean meal containing the urease enzyme and crystalline urease at different concentrations. The hydrolysis rate was assessed by monitoring changes in pH with time, the carbamide concentration, and accumulation of CO_2 and ammonia in the solution. The 5–500 times diluted solutions of the oil-displacing system with carbamide concentrations ranging from 0.65 to 320 g/L were the objects under study. The initial 50% solution of the surfactant-based oil-displacing system consisted of (in g/L) Neonol AF9-12 (20), ammonium nitrate (160.0), carbamide (320.0), and water (500); pH 6.5.

The effect of the products of carbamide hydrolysis on the displacement of viscosity oil was examined using a linear oil-saturated reservoir model, which was represented by three thermostated columns packed with disintegrated carbonate rock (fraction 0.16–0.50 mm). The reservoir model was saturated with an iso-viscous degassed oil from Permocarbonic oil pool in Usinskoye oilfield. Oil displacement and after washing of the residual oil with water were simulated after the columns treating with a 10% solution of the system (control column) and solutions of the system added with 0.1% carbamide and 1% soybean meal (test columns). The after washing of the residual oil was performed with water until the complete water cut of the product at the outlet. The volume of the liquid phase, the pH, and the concentration of components of the buffer solution the system – ammonium nitrate and carbamide were determined at the outlet. Using the results of measurements we calculated oil displacement factor, the change in oil saturation, and the completeness of carbamide and ammonium nitrate yields.

3 Results and discussion

The maximum values of pH 9.3 were obtained in different modes of carbamide hydrolysis

by crystalline urease. The enzyme/substrate ratio of 0.1:32 was considered as optimal.

The catalytic activity of urease contained in soy-bean meal was investigated at concentrations of 0.1–10 g/dm^3. The optimal soybean meal : carbamide ratio was 5:32; at this ratio, the pH reached a value of 9.3 within 2 h.

The investigation of the influence of the surfactant-based oil-displacing system containing the products of enzymatic hydrolysis of carbamide on the viscosity of high-viscosity oil showed that after thermostatting, the viscosity of the oil from Usinskoye oilfield decreased at 20–40 °C minimally by 10–30 % and maximally by a factor of 2–4. However, the character of rheological behaviour of the oil (pseudoplastic) remained substantially unchanged.

The effect of the hydrolysis products on the viscosity oil displacement from the reservoir model was studied at a constant temperature of 30 °C, which was identical to the reservoir temperature in Usinskoye oilfield. The efficiency of oil displacement with water was 45.5–59.6 %. After the treatment of the model and thermostatting, to accumulate the hydrolysis products the ultimate displacement of the residual oil was carried out with water. The increment in the oil displacement efficiency for the control column treated with the enzyme-free solution of the system was 9.8, and that for the test columns it was 19.3 and 15.1 %. The absolute oil displacement efficiency, using crystalline urease hydrolyzing carbamide in the composition of the oil-displacing system, was 64.6 % and using soy-bean meal it was 74.7 %, against that of 55.3 % for the control column.

4 Conclusions

Therefore in the reservoir conditions to hydrolyze carbamide in oil-displacing system at pH increase to 9.0–9.3 one can use urease of vegetable origin, the activity of which depends on the substrate : enzyme ratio.

Carbon dioxide, formed during the carbamide hydrolysis at a low temperature, reduces the viscosity of the oil from Usinskoye oilfield minimally by 10–30% and maximally by a factor of 2–4.

When the enzymatic hydrolysis of carbamide by urease or soybean meal is employed in the process of oil displacement from the reservoir model, the absolute oil displacement efficiency increases from 55.3 (control) to 64.6 or 74.7 %, respectively.

Thus, simultaneous injection of an oil-displacing solution containing carbamide and a hydrolyzing enzyme into a reservoir generates *in situ* an effective oil-displacing system that is capable of increasing the displacement of viscosity oil from the low-temperature oil pool. The data obtained forms the scientific basis for biotechnology of enhanced oil recovery.

Acknowledgements

The work was supported by the grant agreement № 14.607.21.0022, performed under the Federal Target Program "Research and development on priority directions of scientific-technological complex of Russia in 2014-2020".

References

[1] L. M. Ruzin and I. F. Chuprov, Engineering Principles of Developing Deposits of Abnormally Viscous Oils and Bitumens, Ed. by N. D. Tskhadaya. (UGTU, Ukhta 2007). - 244 c.

[2] L.K. Altunina, L.I. Svarovskaya and T. Gerelmaa An integrated physicochemical and microbiological method for enhanced recovery of viscosity oils from low temperature reservoirs in Mongolia. Petroleum Chemistry. - V. 53. - No. 2 (2013). - P. 87–91.

[3] L. K. Altunina and V. A. Kuvshinov, Enhancement of Oil Recovery with Surfactant Compositions (Nauka, Novosibirsk, 1995). - 198 c.

V-PP141

The Rehydration of Centrifugal Thermal Activation Products of Gibbsite – the Industrial Waste of Catalyst KDM

Matveyeva A.N.*, Pakhomov N.A.

St. Petersburg State Institute of Technology (Technical University), Department of General Chemical Technology and Catalysis, Saint-Petersburg, Russia

* ann.matveeva1@gmail.com

Keywords: catalyst KDM, gibbsite, CTA product rehydration, pseudoboehmite, bayerite

1 Introduction

A low-waste and reagent-free production arouses much interest. A carrier of manufacturing microspherical chromium oxide/alumina catalyst KDM for fluidized-bed isobutane dehydrogenation is the product of centrifugal thermal activation (CTA) of gibbsite (GB) [1]. The method of CTA based on a transformation of the nonporous crystalline gibbsite – $Al(OH)_3$, into an amorphous product (AM) by dint of fast heating up to the dehydration temperature and cooling. The CTA product is the pseudomorphosis over gibbsite, but unlike it has the developed volume of pore, specific surface area and high reactivity. A fractional structure of microparticles the catalyst KDM needs is from 50 to 140 microns for providing the stable mode in fluid bed in use. However all Russian works make the gibbsite with a large quantity of the small fraction. Therefore after the CTA process a classification is performed to separate the target fraction and the particles less then 50 microns are the industrial waste.

The purpose of present research is the development of ways for recycling the waste of carrier of KDM catalyst production. Among them was considered the most perspective way – the method of rehydration of CTA product into a pseudoboehmite (PB) or a bayerite (BA) of which is possible to get γ- and η-Al2O3 respectively.

2 Experimental/methodology

The conditions of synthesis of the PB and BA adjustment was performed on the samples of thermoactivated products, which were made on an experimental TSEFLAR™ installation in Boreskov Institute of Catalysis from Achinsk[1] (A-CTA) and Bogoslovsk[2] gibbsite (B-CTA).

In Table 1 the fractional structure of the original samples is shown, where d stands for the equivalent diameter of particles. For the rehydration the A-CTA product was used in the original form, and the B-CTA product was crushed in an agate mortar and only fraction ≤ 40 microns was selected.

Table 1. The fractional structure of the original samples

Sample	Mass content, %		
	d ≤ 40 μm	40 < d ≤ 100 μm	d > 100 μm
A-CTA	55	41	4
B-CTA	6	88	6

The rehydration of samples was carried out in the water environment (the ratio S/L=1:2-1:3) at various pH, achievable by adding in suspension of ammonia solution, azotic or acetic acid solution. After the rehydration the sediments were filtered, washed, dried at 110°C and investigated by the thermal (TA) and X-rays analyzes.

1 Product of Achinsk Alumina Refinery, Achinsk, Russia
2 Product of Bogoslovsk Aluminium Smelter, Krasnoturyinsk, Russia

3 Results and discussion

The formation of bayerite is shown in the alkaline environment and pseudoboehmite in the acidic one (Table 2). The degree of rehydration depends on the pH of suspension, the nature of the starting gibbsite, the morphology and the phase composition of CTA products.

Table 2. The characteristics of the CTA products rehydration in different conditions

Sample	Conditions of rehydration				TA, mass %					LOI[3] (800°C), mass %
	Electrolyte	pH	T_r, °C	t_r, h	$Al(OH)_3$		BE[1]	AM	PB[2]	
					GB	BA				
A-CTA	-	-	-	-	9	-	18	73	-	18,8
A-CTA-1a	$NH_3 \cdot H_2O$	10-11	30-35	24	9	44	4	43	-	30,9
A-CTA-2b	HNO_3	5-5,5	70-90	4	9	13	79			27,2
A-CTA-2d	CH_3COOH	5-5,5	70-90	4	9	4	16	71		28,0
B-CTA	-	-	-	-	-	-	-	+ χ-Al_2O_3	-	10,4
B-CTA-1a	$NH_3 \cdot H_2O$	10-11	30-35	24	-	21	+ χ-Al_2O_3		-	17,4
B-CTA-2a	HNO_3	5-5,5	70-90	4	-	-	+ χ-Al_2O_3			16,2

[1] Boehmite. [2] Borders of thermoeffect of PB are not distinctly detectable. [3] LOI – the loss on ignition.

The yield of BA from the B-CTA is almost twice as low as from the A-CTA, although the latter contains a large number of coarse particles. The starting B-CTA product, according to the data of scanning electron microscopy (SEM), consists of solid particles and contains besides the amorphous phase – the crystalline phase χ-Al2O3 with low reactivity. The A-CTA product, according to the data of TA and X-rays analyses, consists predominantly of the reactive amorphous phase and, according to SEM data, has more friable and easily peptizable structure.

4 Conclusions

The highest yields of product rehydration in the comparable conditions were achieved from the A-CTA gibbsite from nepheline raw material, lower – from the B-CTA gibbsite, which was obtained by the method of Bayer.

Acknowledgements

Work is performed within the State contract №14.Z50.31.0013 from March 19, 2014.

References

[1] Microspherical chromium oxide/alumina catalyst KDM for fluidized-bed isobutane dehydrogenation: Development and industrial application experience / Pakhomov N.A. [et al.] // Catalysis in Industry. 2012. 4(4). P. 298-307.

V-PP142

Iron-containing Catalysts from By-Products of Underground Water Ozonation

Tkachenko I.S.[1,2*], Tkachenko S. N.[1,3], Egorova G.V.[1], Lunin V. V.[1], Golosman E.Z.[4], Lokteva E.S.[1,2], Likholobov V.A.[2]

1 - Lomonosov Moscow State University, Chemistry Department, Moscow, Russia
2 - Institute of Hydrocarbons Processing of the Siberian Branch of the RAS, Omsk, Russia
3 - LLC NVF 'TIMIS', Moscow, Russia
4 - LLC "NIAP –CATALYZATOR", Novomoskovsk, Russia

* i-t@timis.ru

Keywords: Fe, catalyst, ozone, decomposition, water, treatment, green, chemistry

1 Introduction

In this research, we present the ecologically safe way of processing of ferriferous slimes, produced as by-products of underground water ozonation, as raw materials in the synthesis of the catalysts suitable for cleaning of dry air-gas streams from residual amounts of ozone. The technology of underground water purification by ozonation in combination with the sorption on the granulated activated absorbent carbon (GAC) and activated coal fiber sorbents (AF) provides full deodorization, disinfection, and decrease of concentration of ions of the total iron [1] from 0,57-0,94 mg/l to the maximum permissible concentration (MPC) for underground water of 0.03 mg/l or even lower amounts (Fig. 1).

About 4 tons of ferriferous slimes are annually formed at the water treatment station in Lianozovsky dairy plant (Moscow) as the result of the return washing of the pressure filters containing granular hydroanthracite. It is very desirable to find ways of utilization of this by-product, containing iron oxides. The synthesis of ozone and its application in water purification is a good example of implementation of green chemistry principles [2] in the industry. Ozone as a non-polluting oxidant is widely used in a number of modern technologies. However, due to its toxity, the problem of decreasing the concentration of residual ozone to maximum permissible concentration (MPC) is very important. The best way to destroy residual ozone is its catalytic decomposition.

2 Experimental

To prepare the catalysts, wet wastes were mixed in different proportions with cement- talume binder, granulated, subjected to hydrothermal synthesis at 90°C, and calcinated at 400°C. Catalysts were tested on porosity, specific surface, average mechanical durability of a granule and efficiency in ozone decomposition.

The activity of catalysts in ozone decomposition was estimated using γ value [3] that can be calculated according to the formula given below (i). The value of γ shows the number of ozone molecules that decomposed during collisions with the surface of the catalyst.

$$\gamma = 4\boldsymbol{\omega} \cdot ln[C_0/C]/\boldsymbol{u} \cdot \boldsymbol{S} \quad \text{(i)}$$

where C_0 and C (mg/l) are concentrations of ozone in the feed stream and in effluent from catalytic reactor respectively; $\boldsymbol{w}$ is space velocity of a gas stream, cm^3/s; $\boldsymbol{u}$ is thermal velocity of molecules, cm/s (u = 360 m/s for air at 20 °C); and $\boldsymbol{S}$ is external geometrical surface of all granules of the catalyst in the reactor, cm^2.

XRD analyses were conducted on powder diffractometer DRON-3M in filtered CoK_α-radiation. The porosity was measured using Quantachrome AUTOSORB-1 instrument. Mossbauer spectra of ^{57}Fe nuclei were measured on the spectrometer MS-1104Em using the "constant acceleration" mode.

3 Results and discussion

As was demonstrated by XRD analysis, the main components of the ferriferous wastes (slime after water treatment) are goethite α-FeO(OH), lepidocrocite γ-FeO(OH) and α-Fe_2O_3. During calcination at

400°C lepidocrocite converts to iron oxides: α-Fe_2O_3 (hematite) and γ-Fe_2O_3 (maghemite).

Using Mossbauer spectroscopy at 20°C, it was proved the presence of Fe^{3+} hydroxides and oxides (doublet designated as (1) in Fig. 2). The essential broadening of this doublet (1) confirms a nanodisperse state of the most part of the iron hydroxides and oxides in the calcinated ferriferous precipitate, with a size of particles of about 5 - 10 nm. The line (2) in Fig.2 confirms the data of XRD analysis about the presence of hematite in ferriferous raw materials. The line (3) corresponds to the presence of the phase comprising Fe^{2+} cations.

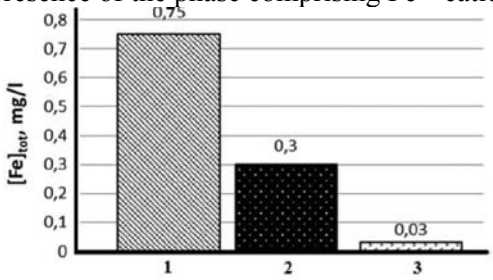

Figure 1 [1]. The total content of iron ions in initial water (1); in water purified by ozonation with GAC sorption (3); MPC of iron oxides in tap water (2).

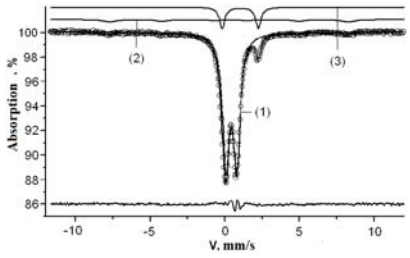

Figure 2. Mossbauer spectra of ferriferous raw materials obtained.

The optimal catalyst comprises 60 wt.% of the ferriferous raw material and 35 wt.% of cement binder (line 3 in Table 1). Such mixture provides mechanical strength and a high catalytic activity in dry ozone decomposition (Table 1), and can be used in industrial processes. After calcination the crushing strength is 1,8±0,1 kg/mm (based on diameter of granule) which is comparable with the characteristics of other industrial catalysts e.g. «Goptalum» GTT. Catalyst porosity is 53 ±5%. Specific surface area of this catalyst is 145 ±12 m^2/g. For comparison, «Goptalum» has specific surface area 125 m^2/g. Kinetic studies showed that the decomposition of ozone proceeds in internal diffusion region with activation energy about 15.5 ± 0.7 kJ/mol. This iron-containing catalyst contain no metal oxides from 1st substance hazard category.

Table 1. Activity of iron catalysts in the reaction of ozone decomposition in a dry gas flow

№	Ferriferous raw material, wt.%	Cement-talum, wt.%	Clay G-1, wt.%	S of all granules of the catalyst in reactor, см^2	Activity in the reaction of ozone decomposition $\gamma_{ср}\cdot10^4$
1	33	60	7	33	1,0±0,1
2	43	50	7	36	1,2±0,1
3	60	35	5	40	1,7±0,1
4	65	30	5	destruction of the catalyst granules	
5	80	15	5		
6	«Goptalum» GTT				2,4±0,2

4 Conclusions

Thus, the new iron-containing catalyst was synthesized using ferriferous wastes produced during ozonation of underground water coupled with sorption by carbonaseous absorbent. Production of the effective iron-containing catalysts from the wastes formed during purification of artesian water with subsequent use of the catalysts for residual ozone decomposition to ecologically safe concentrations agrees completely with the principles of green chemistry. Instead of landfilling iron-containing wastes are used in the downstream process of ozone decomposition to produce oxygen. Mechanical properties and catalytic efficiency in ozone decomposition of the optimized catalyst comprising : 60 wt.% of the ferriferous raw material and 35 wt.% of cement talume binder are comparable with those of industrial catalyst Goptalum GTT.

Acknowledgements

This work was maintained by russian scientific foundation (14-33-00018).

References

[1] Tkachenko, I., Tkachenko, S., Lunin, V., Sverdlikov, A. , Puzenkov, E. 2012. Pure Water Problems and Decisions Moscow. Russia.v.3–4, p. 116–120.

[2] Anastas, P., Warner, J., Eds. 1998."Green Chemistry: Theory and Practice".Oxford University Press. Oxford. GB.

[3] Lunin, V., Popovich, M., Tkachenko, S. 1998. Physical Chemistry of Ozone. MSU Publishing House. Moscow. Russia.

V-PP143

Sol-Gel Synthesis of Robust Silica Monoliths by Interfacial Solution/Precipitation Reactions: Application in the Preferential Oxidation of Carbon Monoxide

Garcia-Aguilar J.*, Miguel-García I., Berenguer-Murcia Á., Cazorla-Amorós D.

Inorganic Chemistry Department and Materials Science Institute, Alicante University, Alicante, Spain

* jaime.garcia@ua.es

Keywords: silica monolith, silica thin film, capillary, microreactor, PrOxCO

1 Introduction

The Preferential Oxidation of carbon monoxide (PrOxCO) in H_2-rich gas streams is one of the most important challenges for H_2 purification in fuel cell industry. The development of devices and micro-devices for small scale PEM fuel cells applications has considerably grown during the last decades and, in this context, the development of adapted PrOxCO catalytic systems for these low power devices would be mandatory for their implementation.

A very interesting alternative to already existing microreactor configuration for PrOxCO is the use of fused silica capillaries. In this sense, it is possible to synthetise the inorganic phase as a filling inside the capillary [1]. However, one problem of synthesizing a SiO_2 matrix in the capillary is the intrinsic shrinkage of the structure occurring during the synthetic protocol (hydrolysis, gelation and/or calcinations) [2]. This shrinkage may produce the detachment of the silica filling from the capillary walls and generate preferential gas paths, impoverishing the catalytic properties of the microreactor.

In this study, we report a new synthetic route to completely avoid the silica shrinkage during the formation of the structure, by incorporating a mesoporous silica thin film over the inner walls of the capillary prior to the SiO_2 filling synthesis. These novel materials have been loaded with Pt nanoparticles and tested as microreactors in PrOxCO reaction.

2 Experimental/methodology

Preparation of Silica Thin Film. A mesoporous silica thin film has been synthetized by a very well established sol-gel procedure, using CTAB as structure directing agent [3].

Preparation of Silica Filling. The silica filling has been synthetized inside de pre-coated capillary adapting an existing procedure (8738 H_2O; 410 TMOS, 237.6 Urea; 1.57 HAc; 1 F127, molar ratio) [2]. The silica gel inside the capillary is treated at 40ºC for (24 h) and 120ºC (6 h), the two steps are very important to produce the well-anchored silica network.

Preparation of Pt nanoparticles. Pt nanoparticles were synthesized by solvent reduction using ethylene glycol and PVP as reduction and capping agent, respectively. The necessary volume of the colloidal suspension (with a perfectly known concentration) was flowed with a syringe pump through the filled capillary. Three microreactors have been prepared to evaluate the catalytic behavior of the samples with different length (20 and 27 cm) and metal loading (1 and 2 wt % Pt, with respect to silica weight). Experimental conditions of the catalytic tests are; $CO/O_2/H_2$/He 2/2/30/66 % vol. GHSV= 120000 ml $h^{-1}g^{-1}$.

3 Results and discussion

In Figure 1, an enhanced adherence of the SiO_2 filling to the capillary walls can be observed for the sample where a thin film has been coated prior to the synthesis (Fig.1 right). On the contrary, in the absence of this coating (Fig.1 left), the SiO_2 structure suffers a non-negligible

shrinkage that reflects in an important detachment from the capillary support and poorer mechanical properties of the microreactor. FE-SEM analysis of a treated mesoporous silica thin-film confirmed that the aforementioned synthesis protocol results in the partial dissolution of the silica thin film, giving rise to an enhanced adherence of the catalyst to the support.

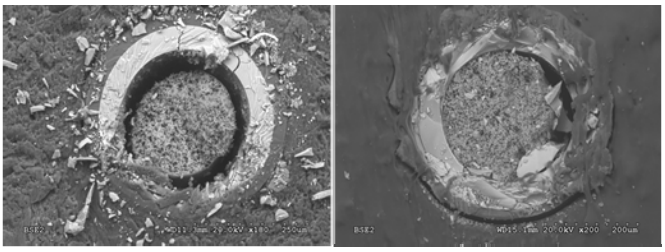

Fig. 1. Silica filled capillary, without and with mesoporous silica thin film (left and right, respectively).

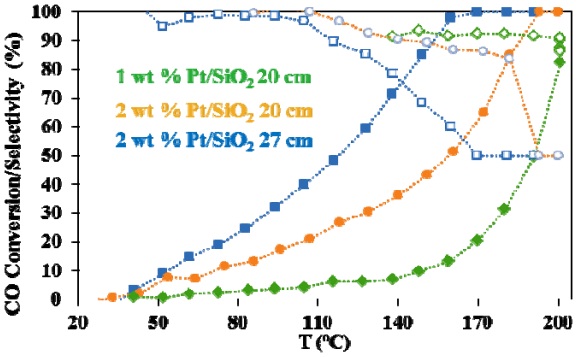

Fig. 2. Performance of the microreactors in the PrOxCO reaction. Solid symbols correspond to CO conversion and hollow symbols to the selectivity.

The catalytic results of the microreactors prepared in this work are shown in Figure 2. All the samples present a very good catalytic performance up to 200ºC. For the samples with the same length and different metal loading, a higher CO conversion is observed for the microreactor with 2 wt % of Pt, and a similar selectivity is obtained for the two samples. On the other hand, for the longest microreactor (blue) a higher CO conversion is observed, although at the expense of lower selectivity at high reaction temperature.

4 Conclusions

A novel methodology has been developed to anchor silica monoliths inside capillary tubes, depositing a mesoporous silica thin-film prior to the synthesis of the monolith. This technique has been successfully used to prepare Pt-loaded microreactors with a very good performance in the PrOxCO reaction.

Acknowledgements

We thank the MINECO, GV, and FEDER (Projects CTQ2012-31762 and PROMETEOII/2014/010). A.B.M. and J.G.A. thanks MINECO for their fellowships (RyC 2009-03913 and BES-2013-063678, respectively).

References

[1] K. Liu, A. Wang, T. Zhang, *ACS Catalysis*. 2 (2012) 1165.
[2] A. Galarneau, J. Iapichella, D. Brunel, F. Fajula, Z. Bayram-Hahn, K. Unger, *Journal of Separation Science*. 29 (2006) 844.
[3] D. Zhao, P. Yang, *Chemical Communications*. 1 (1998) 2499.

V-PP144

Photocatalytic Removal of NO Under Visible Light Irradiation over Sol-Gel Synthesized $PbTiO_3$ Nanoparticles

Tabari T., Uner D.*

Chemical Engineering Department, Middle East Technical University, Ankara, Turkey

* uner@metu.edu.tr

Keywords: photocatalysis, $PbTiO_3$ perovskite tyor oxide, visible light, NO oxidation, sol-gel method

1 Introduction

TiO_2 has attracted intensive attention with the advantages of low-cost, high activity, photochemical stability and environmental friendliness [1]. However, TiO_2 only can absorb the ultraviolet (UV) light occupying a small fraction (<6%) of the solar energy due to its large band gap of 3.0 eV above, which limits its practical applications [2]. Many efforts have been made to extend the optical response of TiO_2 into the visible-light region (400-750 nm), including nonmetal (e.g. N, C, F, S) or transition metal doping (e.g. Cr, Cu, Fe), organic dye-sensitizing and compositing with a semiconductor of a narrow bandgap [3]. Nevertheless, the photocatalytic activity is still low, and there are problems in stability or applicability. Among the vast majority of metal oxide photocatalysts, perovskite-type oxides are prominent in their broad diversity of properties. As a typical $A^{2+}B^{4+}O_3^{2-}$ type perovskite structure photocatalyst, $SrTiO_3$ was found active in purification target decomposition without applying any external potential [4]. However, it requires ultraviolet (UV) radiation whose energy exceeds the bandgap of 3.2 eV of the perovskite crystalline phase, practically ruling out the use of sunlight as an energy source for photooxidation. $PbTiO_3$ perovskite type oxide material is important because of its piezoelectricity, ferroelectricity, and colossal magneto-resistivity which make it highly attractive for fundamental research and various technical applications [5]. Also, the catalytic and photocatalytic property of $PbTiO_3$ is studied against different type of pollutants [6-8]. In this work, for the first time photocatalytic oxidation of $PbTiO_3$ against NO is investigated under ambient light irradiation.

2 Experimental/methodology

The synthesis developed here to prepare $PbTiO_3$ is based on the sol-gel process involving polymeric glass network, which can be seen as deriving from ‘‘in situ polymerizable method’’. For the preparation of the photocatalyst, titaniumisopropoxide (TIP) and lead acetate was dissolved in ethyl alcohol at room temperature. Then, citric acid (Aldrich, purity> 99.5%) was added to the solution and the gel formed immediately. The obtained gel was placed in an oven and kept there for 24h at 120 °C, then calcined for 5h at 650 °C till obtaining a yellow powder. The photocatalytic oxidation of NO on $PbTiO_3$ surface was studied according to a modified methodology based on ISO-22197:2007(E) standard method. The optimal condition of reaction obtained at different concentrations of NO, different flow rates and different relative humidity. Further details of experimental methodology was reported in our previous work (I. Bayar, T. Tabari, D. Uner, Appl. Surf. Sci. under review).

3 Results and discussion

Physico-chemical properties of $PbTiO_3$ studied systematically by: XRD, DT-TGA, BET, UV-DRS, TPR, TEM and SEM. XRD showed pure crystalline structure of $PbTiO_3$, TG-DTA showed the crystallization temperature is around 650 ˚C, based on BET the surface area is

around 10.28 m^2/g. UV-DRS revealed $PbTiO_3$ bandgap (2.7 eV) is lower than that of TiO_2 (3.2 eV). TPR showed that $PbTiO_3$ release oxygen at lower temperatures and the activity of the catalyst is higher than TiO_2. SEM results revealed a porous structure of the perovskite and agglomeration of the particles that is also supported by XRD and BET results. The agglomeration of the nano-scale particles were revealed by TEM.

In order to investigate photocatalytic efficiency of the prepared material, the performance of $PbTiO_3$ (0.1 g) was compared to TiO_2 (Degussa P25, 0.19 g) as photocatalyst under ambient light irradiation. First the reactor was shielded with an aluminium foil. NO flow was started until the NO concentration was found to be stable for a 10 minutes. Then the reactor was exposed to the visible light by removing the aluminium foil and switching on the light source. An immediate decrease in the NO concentration was observed upon exposure to light. As shown in Figure. 1, a high conversion of NO is occurred over $PbTiO_3$ (46%), the NO conversion in the presence of TiO_2 under visible light is very low (10%). A sharp decrease of NO concentration over $PbTiO_3$ were recorded in the initial minutes of illumination. This enhanced activity at the beginning of illumination can be related to the light absorption by the catalyst because of additional short term activation. However, since the amount of $PbTiO_3$ is almost half of TiO_2, the photocatalytic activity of Perovskite is higher than TiO_2. In the presence of humidity and NO, structure of active surface of catalyst is changed to $PbTi_3O_7$ which leads to higher bandgap energy and lower tendency for oxygen releasing. So, the catalytic activity decreased in this case.

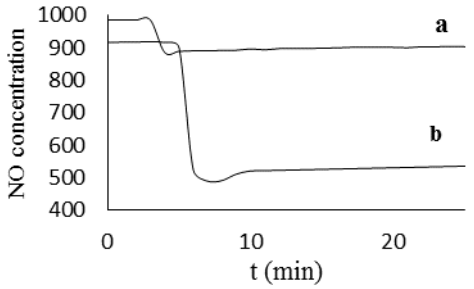

Fig. 1. Nitric oxide concentration against irradiation time: (a) TiO_2 (0.19 g) and (b) $PbTiO_3$ (0.1 g).

4 Conclusions

The results showed high photocatalytic activity of prepared $PbTiO_3$ against NO ambient visible irradiation. However, it should be emphasized that catalytic performance under solar light leads to better results than visible light irradiation.

Acknowledgements

This work was financially supported by 2216-Research fellowship for international researchers, TUBITAK. Financial support from TUBITAK (grant no 213M006) under the project leadership of Dr. Serkan Kincal is gratefully acknowledged..

References

[1] M. Li, P. Tang, Z. Hong, M. Wang, Colloids Surf. *A Physicochem. Eng. Asp.* 318 (2008) 285.
[2] M. Li, Z. Hong, Y. Fang, F. Huang, *Mater. Res. Bull*. 43 (2008) 2179.
[3] Y. Cong, J. Zhang, F. Chen, M. Anpo, D. He, J. Phys. Chem. C. 111 (2007) 10618.
[4] D. Wang, J. Ye, T. Kako, T. Kimura, *J. Phys. Chem. B.* 110 (2006) 15824.
[5] M. Yashima, K. Omoto, J. Chen, H. Kato, X. Xing, *Chem. Mater.* 23 (2011) 3135.
[6] C. Zhen, J. C. Yu, G. Liu, H. M. Cheng, *Chem. Commun*. 50 (2014) 10416.
[7] S. Yin, Y. Zhu, Z. Ren, C. Chao, X. Li, X. Wei, G. Shen, Y. Han, G. Han, *J. Mat. Chem. A.* 2 (2014) 9035.
[8] W. Li, Y. Zhong, *Adv. Mat. Res*. 568 (2012) 356.

V-PP146

Coherent Synchronized Monooxidation of Ethylene by Hydrogen Peroxide on a Biomimetic Catalyst

Nagieva I.T.[1,2], Gasanova L.M.[2], Nasirova U.V.[2*], Nagiev T.M.[1,2]

1 - Baku State University, Baku, Azerbaijan Republic
2 - Nagiev Institute of Catalysis and Inorganic Chemistry, National Academy of Sciences of Azerbaijan, Baku, Azerbaijan Republic

* tnagiev@azeurotel.com

Keywords: biomimetic, kinetics, ethylene, hydrogen peroxide, monooxigenase, heterogenous

1 Introduction

Heterogeneous biomimetic catalysts synthesized on the basis of iron porphyrin complexes been the analogs of a ferment of cytochrome P-450, carry out efficiently the processes of gas-phase monooxidation, epoxidation and hydrooxilation of hydrocarbons [1]. Biomimetic catalyst- iron(III) perfluorotetraphenylporphyrin, drawn on aluminium oxide (per-FTPhPFe(III)/Al_2O_3) displayed high activity and selectivity in the processes of oxidizing a great series of hydrocarbons. Using of immobilized biomimetic catalyst, per-FTPhPFe(III)/Al_2O_3 and ecologically pure hydrogen peroxide as oxidizer ("green oxidizer") the high selective process of ethylene oxidation was realized [2].

2 Experimental/methodology

Experimental studies have demonstrated the possibility of flexible control over ethylene monooxidation by hydrogen peroxide for the production of both ethyl alcohol and acetaldehyde (temperature, 120°C; H_2O_2 concentration, 30%; molar ratio, C_2H_4:H_2O_2=1:1,7; rate of supply, C_2H_4 0,22 l/h, H_2O_2 1,72 ml/h) to obtain the best output of ethyl alcohol, 15.4 wt.% (acetaldehyde 12 wt. %) and, in contrast (temperature, 200°C; concentration of a solution of hydrogen peroxide in water, 30%; molar ratio C_2H_4:H_2O_2=1:1.7), an acetaldehyde yield of 34.6wt. % (ethanol 4.6 wt. %). The selectivity of the process under the conditions of maximum ethyl alcohol yield and minimum acetaldehydeyield was virtually 100 wt. %, recalculated for monooxigenase products. Selectivity in obtaining maximum acetaldehyde yield was somewhat lower (87 wt. %) due to the production of CO_2 as a by-product.

3 Results and discussion

The kinetic regularities obtained as a result of experimental studies provide an idea (albeit incomplete) of the mechanism of ethylene monooxidation by hydrogen peroxide.

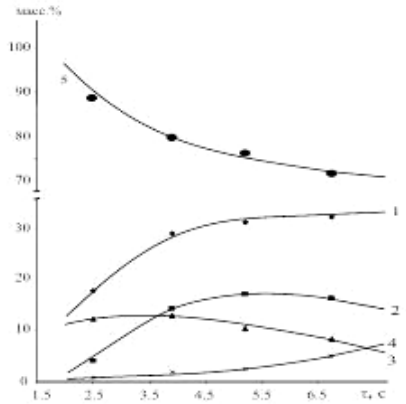

Fig.1. Product yields of ethylene monooxidation reaction as function of (a) the contact time τ under the following conditions: T =140 °C, (a) W_{C2H4}=0.22 l/h,(b) W $_{H2O2}$=1.72m l/h, C_{H2O2}=25% ;
1-C_2H_4conversion, 2-CH_3CHO yield, 3-C_2H_5OHyield, 4 - CO_2yield,5 - O_2 yield.

It can be seen from the kinetic data shown in Fig.1 that kinetic curves 1 and 5 (which

correspond to the yields of monooxigenase products and molecular oxygen) are coherently synchronized; i.e., the highest O_2 yield corresponds to the lowest yield of monooxigenase products, while the lowest yield of molecular oxygen corresponds to the highest yield of monoxide compounds. Both curves (1 and 5) in Fig.1 approach one another asymptotically with a negligible phase shift.

The coherent synchronized character of the catalase and monooxigenase reactions is nicely illustrated by the scheme.

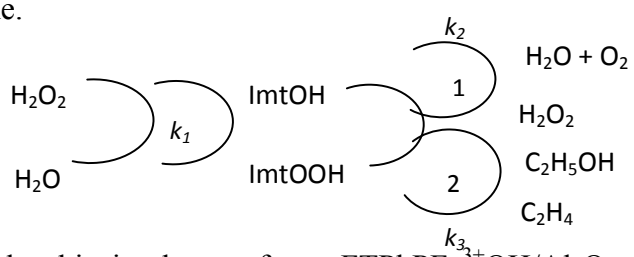

Where ImtOH is the biosimulator of per-FTPhPFe^{3+}OH/Al_2O_3, ImtOOH is the per-FTPhPFe^{3+}OOH/Al_2O_3intermediate, 1 is the catalase (primary) reaction, 2 is the monooxigenase (secondary) reaction, k_1 is the intermediate production rate, k_2 is the catalase reaction rate, and k_3 is the monooxigenase reaction rate.

Kinetic simulation of ethylene oxidation above a biomimetic catalyst by different methods:

1)UsingMichaelis-Menten equation in terms of the Lineweaver-Burk coordinates:

$1/V = 1/V_{\max} + k_m/V_{\max} \cdot 1/[C_2H_4]$ whichallowed to determine the effective reaction rate and effective activation energy for the ethylene oxidation reaction (E_{eff} =42.0 kJ/mol); this value agrees with the activation energy for enzymatic reactions.

2) Using the method of stationary concentration: $r_{C_2H_4} = k_{\text{eff}}[C_2H_4]$, $k_{эфф} = \frac{k_1 k_3}{k_2}[\text{Im } tOH]$

3)Applyingequation

Determinant $D = \nu\left(r_{2,H_2O_2}/r_{C_2H_4} + r_{1,H_2O_2} - r_{2,H_2O_2}/r_{C_2H_4}\right)^{-1}$ [3],whichdetermined quantitative characteristic of coherent-synchronized oxidation reactions - catalase and monooxigenase : $k_{эфф}^{мон} = \frac{r_{1,H_2O_2} D}{[C_2H_4]}$

4 Conclusions

By comparing the kinetic parameters obtained using the three different methods, we conclude that in kinetic descriptions of complex chemical reactions(includingcoherent-synchronized reactions) the determinant equation yields a more complete description than other methods.

Reference

[1] T.M. Nagiev. Coherent Synchronized Oxidation Reactions by Hydrogen Peroxide. Elsevier, Amsterdam, 2007. p.325

[2] U.Nasirova, I.Nagieva, L.Gasanova, T.Nagiev, Journal of Materials Science and Engineering B 2(4)(2012), p.306-312

[3] T.M.Nagiev. Chemical conjugation.M.Nauka, 1989.216 p.

V-PP147

Hydrogen Production from Olive Mill Wastewater through Steam Reforming. Catalyst Development

Casanovas G.A.*, Llorca P.J.

Institute of Energy Technologies. Technical University of Catalonia, Barcelona, Spain

* albert.casanovas.grau@upc.edu

Keywords: hydrogen, olive mill wastewater, cerium, lanthanum, oxide, steam reforming

1 Introduction

Olive mill wastewater (OMW) contains phenolic compounds, fatty acids, lipids and sugars among other organic molecules that transform this waste into a serious environmental problem affecting soils and aquatic ecosystems [1]. Currently this waste is mainly deposited into artificial ponds and its transformation and valorization is a key point in transforming the olive oil industry into an environmentally friendly one.

Hydrogen production from catalytic steam reforming of the liquid phase of OMW provides a reduction of organic content in this waste, and thus, a reduction of the environmental contamination, while producing a valuable product [2,3]. The catalyst must be capable to reform light and heavy molecules, cyclic and aromatic compounds, acidic and alcoholic compounds, among others. The different nature of organic compounds present in the liquid to be reformed forces a different approach of the catalyst development, looking for a stable multi-compound steam reforming catalyst.

In this work, catalytic honeycombs functionalized with several lanthanum-stabilized ceria as catalytic support and impregnated with platinum were tested for OMW steam reforming. Catalysts were also tested for steam reforming of model compounds such as acetic acid and 2-phenylethanol. Catalytic results were related to physical surface properties of support.

2 Experimental/methodology

A series of $Ce_{(1-x)}La_xO_{(2-\ x/2)}$ (x : 0-0.5) were prepared by precipitation of $CeCl_3 \cdot 7H_2O$ and $La(NO_3)_3 \cdot 6H_2O$ using NH_4OH as a precipitating agent and used as catalytic supports. Ceramic monoliths (Corning 400cpsi) were functionalized with approximately 500 mg (25% w/w) of catalytic support using a gel of polyvinylalcohol (PVA). The resulting monoliths were impregnated with a $PtCl_2$ aqueous-acetone solution to keep Pt load between 0,5-2% (w/w based on catalytic support weight).

Monolithic catalysts were tested under distillated OMW, acetic acid, and 2-phenylethanol steam reforming at atmospheric pressure, temperature between 873-1023K, and weight-to-flow (W/F) values ranging from 0.4 to 1.6 $g \cdot min \cdot mL_{OMW}^{-1}$. Results were evaluated by means of chromatographic analyses of effluent dry gas and post-reaction condensate liquid. Total Organic Carbon (TOC) and Chemical Oxygen Demand (COD) of reactants and post-reaction condensate were also used to evaluate the reaction extension. Characterization of supports was conducted by means of X-Ray photoelectron spectroscopy (XPS) analyses, X-Ray diffraction (XRD), Temperature Programmed Reduction (TPR), and Temperature Programmed Desorption of NH_3 (TPD-NH_3).

3 Results and discussion

Distillated OMW present values of 5.41 g $C \cdot L^{-1}$ and 4.05 g $O_2 \cdot L^{-1}$ in TOC and QOD analyses respectively. More than 90% of organic matter is removed after steam reforming conducted at 973K and W/F=0.83 $g \cdot min \cdot mL^{-1}$. The selectivity of the process, based on the effluent dry gas composition, mainly corresponds to H_2 (>72%) and CO_2 (>26%).

Samples were exposed to steam reforming of acetic acid and 2-phenyletanol at 1023K, atmospheric pressure, and W/F ranging from 0.4 to 1.6 $g \cdot min \cdot mL_{OMW}^{-1}$. Steam to carbon (S/C) was set at a value of 6 which represents a more severe condition than OMW steam reforming with TOC values 15 times higher. Under these conditions selectivity of H_2, CO, and CO_2, are close to 63, 9, and 26% respectively.

Figure 1 shows XPS results of $Ce_{(1-x)}La_xO_{(2--x/2)}$ powders. A slight enrichment of La on the surface at high Ce/La ratios is observed while $Ce_{0.5}La_{0.5}O_{1.75}$ presents a high enrichment of Ce on the surface, this result is in accordance with the literature [4]. A maximum in surface Ce^{4+}/Ce^{3+} concentration is found for $Ce_{0.75}La_{0.25}O_{1.875}$ support composition. This has been related to the catalytic behavior.

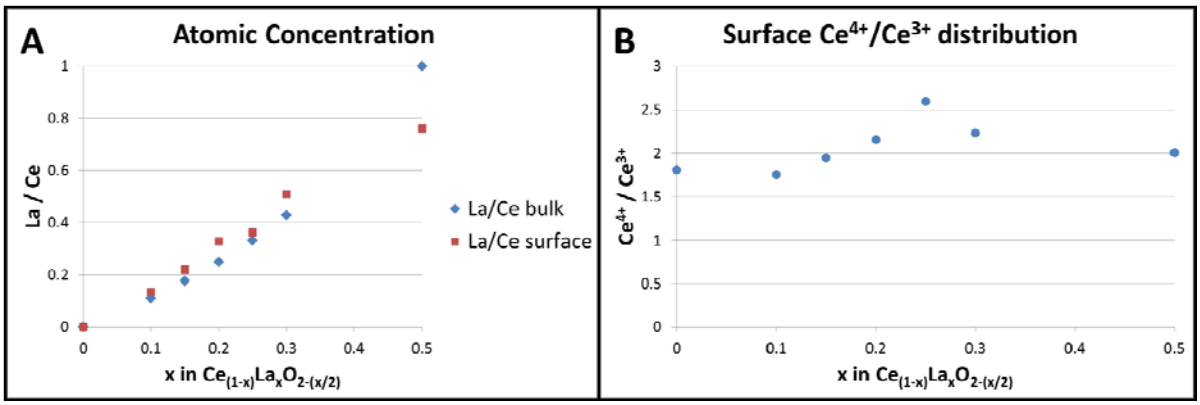

Fig. 1. XPS results of synthetized supports. A) Bulk and surface atomic concentration comparison. B) Ce^{4+} and Ce^{3+} surface distribution

4 Conclusions

Ceramic monoliths functionalized with Pt-based catalysts supported on various $Ce_{(1-x)}La_xO_{(2--x/2)}$ catalytic supports present good catalytic performance under steam reforming of distillated OMW, acetic acid, and 2-phenylethanol. Catalytic results have been related to surface properties of catalytic support.

Acknowledgements

This work has been funded through grant MINECO ENE2012-36368. J.L. is grateful to ICREA Academia program. OMW samples were gently provided by "Agrícola Sant Isidre la Fatarella" (Tarragona, Spain).

References

[1] A. Roig, M.L. Cayuela, M.A. Sánchez-Monedero, *Waste Manag*. 26 (2006) 960.
[2] S. Tosti, C. Accetta, M. Fabbricino, M. Sansovini, L. Pontoni, *Int. J. Hydrogen Energy* 38 (2013) 10252.
[3] A. Casanovas, A. Galvis, J. Llorca, *Int. J. Hydrogen Energy* In Press.
[4] V. Belliere, G. Joorst, O. Stephan, F. De Groot, B.M. Weckhuysen, J. Phys. Chem. B 110 (2006) 9984.

V-PP148

Bulk Mixed Al-Transition Metal Oxide Catalysts for Enhanced Oxidation of 1,2-Dichloroethane

Khaleel A.*, Nawaz M.

UAEU, Al-Ain, UAE

* abbask@uaeu.ac.ae

Keywords: mixed, oxides, oxidation, chlorinated, organic, compounds, sol-gel

1 Introduction

Several catalytic systems based on metal particles or metal oxides can promote the oxidation of chlorinated organic compounds (COC) [1-2]. The decomposition of 1,2-dichloroethane (DCE) usually starts with dehydrochlorination resulting in vinyl chloride (C_2H_3Cl) and HCl. Further oxidation may take place yielding carbon oxides, CO and CO_2. However, deep catalytic oxidation of DCE and many other COC usually takes place at relatively high temperatures, ≥ 400 °C. In previous studies we found that catalysts based on bulk mixed oxides of transition metals and γ-alumina or titania exhibit significant catalytic activity in the oxidation of COC [3]. In the present study, mixed oxides of γ-alumina and different transition metals were prepared and studied for the oxidation of DCE. Catalytic activity and selectivity vs. composition and selected preparative conditions were investigated.

2 Experimental/methodology

Template-free sol-gel method was employed to prepare highly porous aerogel and xerogel metal-doped γ-Al_2O_3. Aluminum sec-butoxide and transition metal nitrates, or chlorides were used as precursors. Composites containing Cu (II), V(III), Cr(III), and other transition metal ions were prepared. The general formula Al-M-x will be used to represent the composites where "M" refers to the dopant metal ion and "x" refers to its molar fraction, 100 x M/M+Al.

The catalytic activity of composites containing different concentrations of Cu(II), V(III), and Cr(III) was studied in the oxidation of DCE. The reactions were investigated using a fixed-bed flow reactor under atmospheric pressure. The reactor was coupled with an FTIR spectrometer equipped with a continuous flow gas cell, from Pikes Technology, for continuous monitoring of the reaction products. DCE adsorption and subsequent decomposition on the surface of the catalysts was studied in-situ using DRIFTS.

3 Results and discussion

Mesoporous powders with relatively high surface areas, 300-500 m^2/g, and large total pore volumes, 1.4-2.0 cc/g, were prepared. Besides different other preparative conditions, the gel formation was dependent on the type of metal ion dopant and its concentration. As an example, the presence of Fe(III) or V(III) at a molar concentration of 10% significantly enhanced the gel formation process. The particle size, surface area, and porosity were also dependent on the preparative conditions and the composition. Surface areas of xerogel and aerogel powders were around 300 and 700 m^2/g, respectively. The type of precursor also played a role in the textural properties of the final product. Metal acetylacetonate (acac) as a precursor was compared with metal nitrates and chlorides. The presence of transition metal ions resulted also in noticeable enhancement of the surface acidic and redox properties as indicated by pyridine adsorption, NH_3-TPD, and H_2-TPR studies.

The catalytic activity study showed that Al-Cu and Al-Cr oxide composites possessed a promising catalytic activity for the oxidation of DCE as shown in Figure 1. Reactions over

undoped γ-alumina produced vinyl chloride (VC) and HCl as major products and relatively small amounts of CO_2. On the other hand, reactions over Cu- and Cr-doped catalysts showed enhanced capability for deep oxidation resulting in CO_2 as the major product. On the contrary, V(III)-containing catalysts showed a considerably lower catalytic activity. The nature of the products was also dependent on the transition metal present. While VC was the major Cl-containing hydrocarbon product from reactions over Al-V-3 and Al-Cr-3, it formed only in negligible amounts over Al-Cu-3 catalyst where the deep oxidation product, CO_2, was the major product. The catalytic activity of the Cu-containing catalysts decreased as the Cu ions concentration increased. The results of the catalytic activity and adsorption studies indicate that the tendency of γ-alumina towards adsorption and dehydrochlorination combined with redox properties of transition metal ions can be tailored to enhance the oxidation of DCE and possibly other COC.

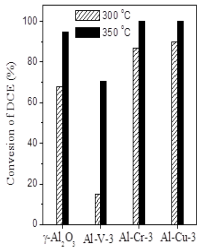

Fig. 1. Conversion of DCE over undoped and doped γ-alumina containing 3% metal ions at 300 and 350 °C

4 Conclusions

The employed sol-gel method resulted in mesoporous powders of undoped and metal-doped γ-alumina with high surface areas, large pore volumes, and significant acidity. The doped catalysts showed promising activity in the deep oxidation of 1,2-dichloroethane at relatively low temperatures compared with pure γ-alumina. The nature of the products was strongly dependent on the presence as well as on the type of dopant ion. Cu- and Cr-doped catalysts showed significantly higher catalytic activity in the deep oxidation of DCE. Retaining the γ-alumina acidity after doping combined with the redox properties of the transition metal ions promoted dehydrodechlorination and further oxidation of the reaction intermediates.

Acknowledgements

The financial support from United Arab Emirates University through NRF grant, 2011, is acknowledged with gratitude.

References

[1] C. Zhang, C. Wang, W. Zhan, Y. Guo, G. Lu, A. Baylet, A. Giroir-Fendler, *Appl Catal B: Environ.* 129 (2013) 509.
[2] S. Scire, S. Minico, C. Crisafulli, *App. Catal B: Environ.* 45 (2003) 117.
[3] A. Khaleel, A. Al-Nayli, *Appl Catal B: Environ.* 80 (2008) 176.

V-PP149

Green Alternative for Guideline Monoterpenoids to Value-Added Products – Tailored the Biocatalytic Transformation of α-Pinene

Tudorache M.*, Gheorghe A., Parvulescu V.I.

University of Bucharest, Bucharest, Romania

* madalina.sandulescu@g.unibuc.ro

Keywords: immobilised enzyme, alpha-pinene, alpha-pinene oxide, verbenol, biocatalytic oxidation, green process

1 Introduction

In the era of renewable carbon sources as a key element in biorefinery, we know of only biomass alternative for the replacement of fossil resources. Recently investigations demonstrated both terrestrial and marine environments contain important renewable carbon sources represented often by monoterpenoid compounds (monoterpenes).

Monoterpenes are important and abundant natural resources, well-known as the starting materials for industries of flavors, pharmaceuticals, perfumery and food as well as the precursors applied in the pesticides and polymeric industries. In this context, α-pinene is known as a platform molecule due to its high reactivity and potential to be transformed in various derivatives (e.g. α-terpinyl, bornyl acetates, ρ-cymene, α-pinene oxide, myrtenol, verbenol, verbenone, ρ-methyl-acetophenone, thymol, carvacrol, among others).

At present however, classical chemical procedures are still the primary approaches to obtain monoterpenes. Although some unique oxidants or catalysts are available, the conventional chemical procedures have generally been proved to be of low stereo-, regio-, and chemo-selectivity and as a consequence give rise to undesirable mixtures of products. Recently, there has been a significant progress in the field of monoterpene biotransformation which offers many advantages, such as: i) simple manipulation, ii) use of mild reaction conditions, iii) high efficiency, iv) appreciable reaction-, region- and stereo-selectivity, and v) it's more environmental friendly nature. Therefore, the biotransformation represents a powerful tool for the utilization of monoterpenes.

In this study, biocatalytic oxidation of α-pinene designed in varied configurations has been investigated for the production of value-added products (e.g. α-pinene oxide, verbenol, pinanediol, camphene, campholenal).

2 Experimental/methodology

Biocatalysts were constructed as lipase enzyme absorbed/entrapped/cross-linked leading to the specific configurations. The immobilization approaches are detailed in the previous papers [1,2]. Biocatalytic oxidation of α-pinene was performed in the mixture of substrate and oxidation agent (1:1= α-pinene:H_2O_2/UHP) catalysed by lipase enzyme (50 mg/mL). The reaction was developed in ethyl acetate for 24 h under room temperature. Then, the reaction phases were separated by centrifugation. The supernatant was further frozen and extracted with pentane. The evolution of the biocatalytic process was followed based on GC-MS/FID analysis of the reaction products.

3 Results and discussion

We developed a biocatalytic system for α-pinene oxidation based on lipase catalysis. Screening of the lipase enzyme from different sources (e.g. *Aspergillus niger*, *Candida antarctica*, *Candida cylindracea*, *Pseudomonas cepacia*, *Rhizopus niveus*, Porcine Pancrease) allowed to set up the most performing lipase on the proposed configuration. Therefore, *Aspergillus niger* lipase was chosen as biocatalyst for α-pinene derivatisation. Also, the biocatalytic system was tested for two different oxidation agents (e.g. H_2O_2 and UHP) demonstrating the influence of this reagents on the selectivity of the process.

Lipase enzyme was immobilized leading to varied configurations (e.g. absorption, entrapment, covalent and cross-linking). The biocatalysts were tested; the results are presented in table 1. Enzyme immobilization using the entrapment approach allowed to improve the α-pinene conversion and moreover to concentrate the selectivity onto verbenol production. The other biocatalyst configurations behaved similar between them in term of selectivity leading to α-pinene oxide as dominant product next to verbenol, camphene, campholenal.

Table 1. The effect of biocatalyst design on biochemical route of the α-pinene oxidation process.(CLEA-cross-linked enzyme aggregates and CLEMPA–cross-linked enzyme aggregates onto magnetic particles).

biocatalyst	**Conversion (%)**	**Selectivity (%)**			
		α-pinene oxide	camphene	verbenol	campholenic aldehyde
Free lipase	15.30	57.61	2.09	1.04	3.12
Adsorbed lipase	13.25	43.21	3.20	2.21	4.35
Covalent attachment of lipase	10.50	47.90	2.34	10.75	3.21
Entrapped lipase	22.58	26.34	1.36	21.00	1.67
CLEA	27.06	35.31	0.38	3.06	6.53
CLEMPA	9.61	42.37	0.89	3.06	8.20

4 Conclusions

Biocatalytic system for α-pinene valorization had been developed for production of value-added products, especially α-pinene oxide and verbenol.

Acknowledgements

The authors kindly acknowledge to UEFISCDI for the financial support through the project PN-II-PCCA-2013, no. 105/2014.

References

[1] M. Tudorache, A. Nae, S. Coman, V.I. Parvulescu, *RSC Advances*, 3 (2013) 4052.

[2] M. Tudorache, A. Negoi, L. Protesescu, V.I. Parvulescu, *Appl. Catal. B: Env*, 145 (2014) 120.

V-PP150

Characterization and Application in Catalytic Reduction of MB of $Fe_3O_4SiO_2Ni$ Nanoparticles

Kurtoglu K., Gubbuk I.H., Akgemci E.G.*

Necmettin Erbakan University, Faculty of Ahmet Kelesoglu Education Chemistry, Department of Chemistry, Konya, Turkey

* eakgemci@konya.edu.tr

Keywords: dye degradation, magnetic, nanoparticle

1 Introduction

Design of nanocomposites consisting of functional metals and different matrices is a promising research area for the fabrication of a variety of catalysts, adsorbents, and optical and electrical devices. In this study, nickel ions intercalated into $Fe_3O_4SiO_2$ interlayer forming a nanocomposite of magnetic and nickel nanoparticles ($Fe_3O_4SiO_2Ni$). The magnetic nickel nanocomposites were characterized by scanning electron microscopy (SEM), X-ray powder diffraction (XRD) and measurements. $Fe_3O_4SiO_2Ni$ was used as a catalyst for reduction of organic dye with $NaBH_4$.

2 Experimental/methodology

All chemicals were analytical reagent grade: copper nitrate (Merck), sodiumborohydride and azo dyes (all from Sigma Aldrich). Water used for the preparation of all solutions was deionised by reverse osmosis. $FeCl_3$ and $FeCl_2$ were purchased from Sigma Aldrich.

The magnetic nanoparticle, Fe_3O_4, was prepared by a precipitation method. Briefly, 60mL of $FeCl_2$ and $FeCl_3$ aqueous ethanol solution with a concentration ratio of 5:1 was prepared, 1.0 mol/L ammonia solution was added drop by drop with vigorous stirring until pH 10, and a black product was obtained. Then, the black product was crystallized under 50 ◦C water bath for 3 h. Subsequently, separated with magnet, the obtained black magnetite particles were washed with ethanol for 3 times, dried at 50 ◦C for 12 h [1]. Fe_3O_4 spheres were coated by SiO_2 films, by using TEOS as a precursor. The resulting $Fe_3O_4SiO_2$ particles were loaded with *Ni* nanoparticles. The material showed better performance than a conventional Fe_3O_4 catalyst in catalytic reduction of methylene blue (MB) with $NaBH_4$. It can be separated from the reaction mixture by a magnet and be recycled without obvious loss of catalytic activity [2].

Catalytic activity of $Fe_3O_4SiO_2Ni$ was investigated by means of degradation of MB by sodium borohydride in aqueous solutions. Typically, 300 mL of the $1x10^{-4}$ mol L^{-1} MB solution was mixed with 0.010 g of $Fe_3O_4SiO_2Ni$. Thereafter, 5 mL of the sodium borohydride solution was added to the dispersion and the reaction was monitored by UV-VIS spectrometry. Study of the catalytic activity of $Fe_3O_4SiO_2Ni$ was conducted at the laboratory temperature.

3 Conclusions

In this study, $Fe_3O_4SiO_2Ni$ composites have been synthesized by a chemical method, with Fe3O4 as a substrat, nickel nitrate as a metal precursor and TEOS as a stabilizator. These composites accessible and highly dispersed Ni nanoparticles, thus resulting in high catalytic activities in the degradation of MB.

The chemical reaction between the MB and $Fe_3O_4SiO_2Ni$ in solution leads to the bleaching of MB diluted solution. The bleaching mechanism in acidic media is attributed to a pair of electrons belonging to nitrogen (N) atoms which would receive H^+ (proton). This leads to a

resonance with the benzene rings inside the MB molecule that is then itself reduced, forming a leucomethylene blue molecule (MB colorless solution) (Figure 1) [3].

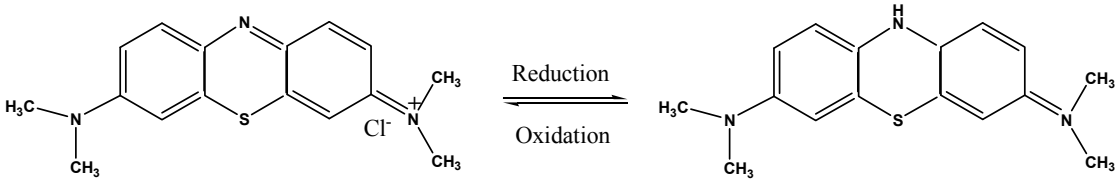

Methylene Blue (MB) Leucomethylene Blue (LMB)

Fig.1. Catalytic reduction of MB with $NaBH_4$.

Acknowledgements

This research was supported under Necmettin Erbakan University BAP Projects funding. Authors gratefully acknowledge the financial support of the Necmettin Erbakan University.

References

[1] Q. Chang, K. Deng, L. Zhu,G. Jiang, C. Yu, H. Tang, *Microchim Acta* (2009) 165:299–305
[2] Y. Chi, J. Tu, M. Wang, X. Li, Z. Zhao, *J Colloid and Interf. Sci.* 423 (2014) 54–59.
[3] A. Mignani, S. Fazzini, B. Ballarin, E. Boanini, M. C. Cassani, C. Maccato, D. Barreca, D. Nanni, *RSC Adv*., 5 (2015), 9600–9606.

XI European Workshop on Innovation in Selective Oxidation (ISO `15) "Selectivity in Oxidation: Key to new resources valorization"

ISO-KN1

Liquid-Phase Selective Oxidation Catalysis with Metal-Organic Frameworks

Kholdeeva O. A.[1,2*]

1 - Boreskov Institute of Catalysis SB RAS, Novosibirsk, Russia
2 - Novosibirsk State University, Novosibirsk, Russia

* khold@catalysis.ru

Keywords: selective oxidation heterogeneous catalysis, metal-organic frameworks, liquid phase

Porous coordination polymers or metal-organic frameworks (MOFs) have attracted much recent attention due to a unique ensemble of properties, such as crystalline open structures, extremely high surface areas, tunable pore size and functionality, as well as high contents of uniform and accessible metal sites [1]. In the past decade, a number of MOFs with good thermal and solvolytic stability have been designed and implemented [2, 3]. A considerable scientific effort was directed to evaluation of their potential as heterogeneous catalysts for organic synthesis, in particular, for the production of oxygenated compounds [3].

In this presentation, we give an overview of catalytic applications of MOFs of the MIL family (MIL stands for **M**aterials of **I**nstitute **L**avoisier) in liquid-phase selective oxidations [4-9]. Bearing in mind the growing environmental concern, we focus on the catalytic systems that employ environmentally benign oxidants, such as molecular oxygen, aqueous hydrogen peroxide and *tert*-butyl hydroperoxide (TBHP). Our aim is to demonstrate the possibilities of MOFs in the selective oxidation of a wide range of organic compounds, with special attention to

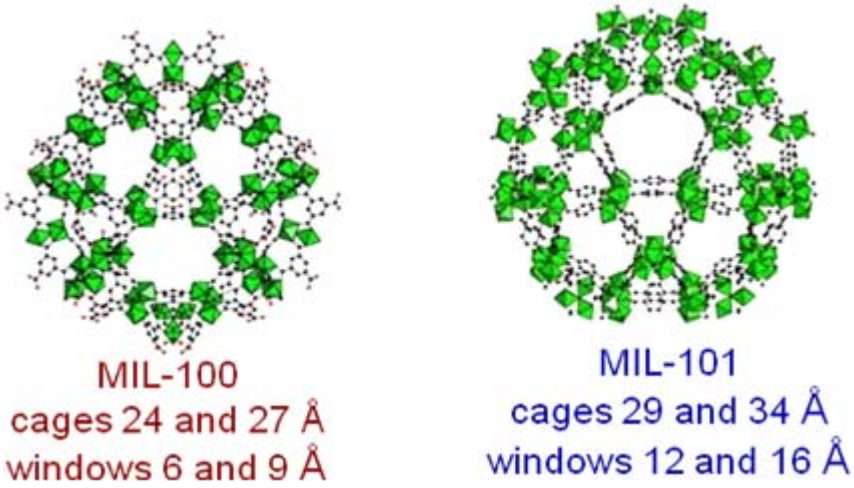

the critical issues of the catalysts stability and reusability and the nature of catalysis.

We will start with evaluation of the catalytic properties of the mesoporous chromium- and iron-based carboxylates MIL-100 and MIL-101 in the liquid-phase oxidation of hydrocarbons (alkanes, alkenes, aromatics) under mild conditions [4-6]. The impact of the transition metal nature on the reaction selectivity and the role of diffusion and adsorption will be discussed in the light of recent results acquired for solvent-free selective oxidation of cyclohexane and cyclohexene with molecular oxygen and/or TBHP and oxidation of anthracene with TBHP in chlorobenzene. Mechanistic features of the oxidation catalysis by MOFs will be addressed, and

a particular case of a biomimetic behavior of Fe-MIL-100(101) will be highlighted. Peculiarities of adsorption of various organic compounds on MIL-100 and MIL-101 and their consequences for catalysis are discussed.

In the second part of the lecture, we will provide examples of the application of MIL-101 as a mesoporous support for transition-metal complexes, such as polyoxometalates (POM) and phthalocyanines (Pc). The elaborated POM/MIL-101 hybrid materials demonstrate superior catalytic performance in epoxidation of a broad range of alkenes with H_2O_2 [7], while FePc/MIL-101 enables efficient oxidation of phenolic compounds using TBHP [8]. Effects of the MOF support on the catalyst activity and selectivity will be analyzed, and the reasons for the improved catalytic behavior will be suggested.

Stability of MOFs under turnover conditions and factors leading to catalyst deactivation were thoroughly investigated. Based on these studies, recommendations on the choice of proper reaction conditions for exploitation of MOFs in the liquid-phase oxidation processes can be given. Finally, we will show an example how a MOF, the structure of which is destroyed by the reaction medium, can act as a precursor for a highly active, selective, truly heterogeneous and recyclable catalyst. The case study is H_2O_2-based oxidation of alkylphenols over Ti-MIL-125 that affords corresponding *p*-bezoquinones with ca. 100% selectivity [9].

A comparison of the selected MOFs with conventional single-site catalysts (transition-metal-substituted zeolites, aluminophosphates and mesoporous silicates) will be provided in terms of catalyst activity (TOF), productivity (TON), selectivity, and stability toward metal leaching. The scope and limitations of the MOF-based catalyst systems will be discussed.

Acknowledgements

The author is grateful to all co-authors of the joint papers published in the field of oxidation catalysis by MOFs. The financial support of the Russian Foundation for Basic Research (grant N 13-03-00413) is greatly appreciated.

References

[1] Thematic Issue on Metal-Organic Frameworks, *Chem. Rev*. 112 (2012).
[2] G. Férey, C. Mellot-Draznieks, C. Serre, F. Millange, J. Dutour, S. Surblé, I. Margiolaki, Science 309 (2005) 2040.
[3] Y.K. Hwang, G. Férey, U-H.Lee, J.-S. Chang in *Liquid Phase Oxidation via Heterogeneous Catalysis,* Eds: M.G. Clerici and O.A. Kholdeeva, Wiley, New Jersey, 2013, Ch. 8.
[4] N.V. Maksimchuk, K.A. Kovalenko, M.S. Melgunov, V.P. Fedin, O.A. Kholdeeva, *Adv. Synth. Catal.* 352 (2010) 2943.
[5] N.V. Maksimchuk, K.A. Kovalenko, V.P. Fedin, O.A. Kholdeeva, *Chem. Commun.* 48 (2012) 6812.
[6] (a) I.Y. Skobelev, A.B. Sorokin, K.A. Kovalenko, V.P. Fedin, O.A. Kholdeeva, *J. Catal*. 298 (2013) 61; (b) O.A. Kholdeeva, I.Y. Skobelev, I.D. Ivanchikova, K.A. Kovalenko, V.P. Fedin, A.B. Sorokin, *Catal. Today*, 238 (2014) 54.
[7] (a) N.V. Maksimchuk, M.N. Timofeeva, M.S. Melgunov, A.N. Shmakov, Yu.A. Chesalov, D.N. Dybtsev, V.P. Fedin, O.A. Kholdeeva, *J. Catal.* 257 (2008) 315; (b) N.V. Maksimchuk, K.A. Kovalenko, S.S. Arzumanov, Yu.A. Chesalov, A.G. Stepanov, V.P. Fedin, O.A. Kholdeeva, *Inorg. Chem.* 49 (2010) 2920.
[8] O.V. Zalomaeva, K.A. Kovalenko, Yu.A. Chesalov, M.S. Mel'gunov, V.I. Zaikovskii, V.V. Kaichev, A.B. Sorokin, O.A. Kholdeeva, V.P. Fedin, *Dalton Trans.* 40 (2011) 1441.
[9] I.D. Ivanchikova, J.S. Lee, N.V. Maksimchuk, A.N. Shmakov, Yu.A. Chesalov, A.B. Ayupov, Y. K. Hwang, C.-H. Jun, J.-S. Chang, O.A. Kholdeeva, *Eur. J. Inorg. Chem*. (2014) 132.

ISO-KN2

Microstructured Reactors as Efficient Toolfor the Operation of Selective Oxidation Reactions

Kolb G.*, Pennemann H.

Fraunhofer ICT-IMM, Mainz, Germany

* gunther.kolb@imm.fraunhofer.de

Keywords: selective oxidation, plate heat-exchangers, microreactors

1 Introduction

Selective oxidation reactions are re-considered currently to improve the efficiency and ultimately the sustainability of the processes under operation. The performance of the catalysts applied for these reactions highly depends on the operating conditions which are in turn determined by the reactor technology.

The exothermic character of selective oxidation reactions creates a challenging task for the heat management of the chemical reactor hosting them. Microchannel plate heat-exchanger technology offers unique opportunities of integrated heat removal by the introduction of energy consuming processes into the reactor, such as endothermic reactions or, closer to conventional solutions, evaporation of liquids. The plate heat-exchanger reactor, which is coated with thin layers of catalyst allows improved heat and mass transfer in the catalyst and therefore avoids hot-spot formation and related problems. Owing to the high rate of oxidation reactions, which creates most of the heat of reaction at the reactor inlet, it gets obvious that co-current cooling is the preferred solution for selective oxidation reactions. The current contribution provides an overview of the research activities in the field of selective, partial and preferential oxidation reactions.

2 Production of chemicals

The selective or better partial oxidation of ethylene to ethylene oxide is a prominent reaction which has attracted extensive efforts owing to its hazardous character and difficult heat management. While early work still focused on laboratory applications , microchannel reactors were designed and built in pilot scale to demonstrate the feasibility of the process. However, practical problems and system costs prevented the industrialization of the process to date.

Other reactions such as ammonia oxidation to nitrogen oxides , the oxidation of alcohols to aldehydes and of toluene to benzaldehyde and benzoic acid have been investigated, however, these early applications were still limited to laboratory scale. The production of hazardous chemicals such as hydrogen peroxide was investigated for the industrial scale through laboratory tests and scale-up calculations, however, the on-site production of hydrogen peroxide for sterilization purposes in de-centralised plants remains an interesting option. Further and mostly more recent publications deal with selective or preferential oxidation over zeolites also by photo-catalytic reactions .

3 Hydrogen supply for fuel cells

The partial oxidation of fuels is an alternative to steam reforming and autothermal reforming, which does not require complicated water management. However, the heat management of the reaction is a critical issue in adiabatic reactors which leads to degradation of the catalysts by severe hot spot formation. Operation without steam in the reactor feed leads easily to coke formation, which is dealt with by (a) specific catalyst design , (b) introduction of

coatings at the reactor walls resistant against carbon formation, (c) re-cycling of steam containing fuel cell off-gas into the reactor feed.

The selective or better preferential oxidation of carbon monoxide in a hydrogen rich product stream of a reformer is required, in case the reformate is fed to a PEM fuel cell ultimately, because the carbon monoxide poisons this fuel cell type. While larger amounts of carbon monoxide are removed by water-gas shift, the last portion (0.3-1%) is removed by selective oxidation over noble metal (platinum) containing catalysts. The practical application of the reaction suffers from two main issues, which are (a) the high degree of conversion required and (b) the high reaction enthalpy of carbon monoxide oxidation. Low temperature PEM fuel cells can tolerate only 10-100 ppm of carbon monoxide, depending on their specific design.

The application of ceramic or metallic monoliths as reactors for de-centralised applications, which is obvious at a first glance when considering aspects of system cost and future mass-production, creates problems of system control and complexity. The adiabatic monolithic reactor generates too much heat, which has led to the introduction of multiple (up to four) reactors switched in series . Fixed bed reactors with integrated cooling suffer from local over-heating of the catalyst, which impairs their performance dramatically. The group of the author has designed and operated single stage reactors of kW-scale for the selective oxidation of carbon monoxide with integrated cooling by water evaporation and two-staged oxygen addition, which allowed stable and dynamic operation of the system at the required low carbon monoxide concentration .

References

[1] Kestenbaum, H., Lange de Olivera, A., Schmidt, W., Schüth, H., Ehrfeld, W., Gebauer, K., Löwe, H., Richter, T.; *"Synthesis of ethylene oxide in a catalytic microreactor system"*, Stud. Surf. Sci. Catal. **130,** (2000) pp. 2741-2746.

[2] Kestenbaum, H., Lange de Olivera, A., Schmidt, W., Schüth, F., Ehrfeld, W., Gebauer, K., Löwe, H., Richter, T.; *"Silver-catalyzed oxidation of ethylene to ethylene oxide in a microreaction system"*, Ind. Eng. Chem. Res. **41,** 4 (2000) pp. 710-719.

[3] Rebrov, E. V., de Croon, M. H. J. M., Schouten, J. C.; *"Design of a microstructured reactor with integrated heat-exchanger for optimum performance of highly exothermic reaction"*, Catal. Today **69,** (2001) pp. 183-192.

[4] Jensen, K. F.; *"Microchemical systems: Status, challenges, and oportunities"*, AIChE J. **45,** 10 (1999) pp. 2051-2054.

[5] Quiram, D. J., Hsing, I.-M., Franz, A. J., Jensen, K. F., Schmidt, M. A.; *"Design issues for membrane-based, gas phase microchemical systems"*, Chem. Eng. Sci. **55,** (2000) pp. 3065-3075.

[6] Wörz, O., Jäckel, K.-P., Richter, T., Wolf, A.; *"Microreactors - a new efficient tool for reactor development"*, Chem. Eng. Technol. **24,** 2 (2001) pp. 138-143.

[7] Cao, E., Gavriilidis, A., Motherwell, W. B.; *"Oxidative dehydrogenation of 3-methyl-2-buten-1-ol in microreactors"*, Chem. Eng. Sci. **59,** (2004) pp. 4803-4808.

[8] Ge, H., Chen, G., Yuan, Q., Li, H.; *"Gas phase catalytic partial oxidation of toluene in a microchannel reactor"*, Catal. Today **110,** 1-2 (2005) pp. 171-178.

[9] Pennemann, H., Hessel, V., Löwe, H.; *"Chemical Micro Process Technology - from laboratory scale to production"*, Chem. Eng. Sci. **59,** 22-23 (2004) pp. 4789-4794.

[10] Sebastian, V., Irusta, S., Mallada, R., Santamaria, J.; *"Microreactors with Pt/zeolite catalytic films for the selective oxidation of CO in simulated reformer systems"*, Catal. Today **147S,** (2009) pp. S10-S16.

[11] Yuan, R., Fan, S., Zhou, H., Xu, Z., Lin, C., Fei, E., Wu, L., Wang, X.; *"Photocatalytic degradation and seective oxidation of typical gas phase molecules with TS-1 and HZSM-5 zeolites"*, Acta Chim. Sin. **71,** 10 (2013) pp. 1404-1410.

[12] Pennemann, H., Hessel, V., Kolb, G., Löwe, H., Zapf, R.; *"Partial oxidation of propane using a micro structured reactor"*, Chem. Eng. J. **135,** 1 (2008) pp. S66-S73.

[13] Kolb, G.; *Fuel Processing for Fuel Cells,* 1 Ed.; Wiley-VCH, Weinheim (2008).

[14] O'Connell, M., , Kolb, G., , Schelhaas, K.-P., , Schuerer, J., Tiemann, D., , Keller, S., , Reinhard, D., , Hessel, V., ; *"An investigation into an integrated water gas shift and preferential oxidation reactor system on the kW scale"*, Ind. Eng. Chem. Res. **10917-10923,** (2010).

[15] O'Connell, M., Kolb, G., Schelhaas, K. P., Schuerer, J., Tiemann, D., Ziogas, A., Hessel, V.; *"The development and evaluation of microstructured reactors for the water-gas shift and preferential oxidation reactions in the 5 kW range"*, Int. J. Hydrogen Energy **35,** (2010) pp. 2317-2327.

ISO-OP01

V-, Nb, and Ti-Promoted Hexagonal Tungsten Bronzes as Selective Catalysts in the Transformation of Glycerol and Methanol in Aerobic Conditions

Soriano M.D.[1], Chieregato A.[1], Zamora S.[1], Bandinelli C.[2], Cavani F.[2], Lopez Nieto J.M.[1*]

1 - Instituto Tecnologia Quimica, UPV-CSIC, Valencia, Spain
2 - Dipartimento Chimica Industriale e di Materiali, Universitá di Bologna, Bologna, Italy

* jmlopez@itq.upv.es

Keywords: metal oxides bronze, glycerol to acrylic acid, methanol oxidation, tungsten, vanadium, niobium

1 Introduction

Promoted mixed metal oxides bronzes have attracted considerable attention in the last years in the field of material science [1], although at the moment, they have been less studied in catalysis. Recently, they have been reported as selective catalysts in the one-pot oxidative transformation of glycerol to acrylic acid [2], when both redox and acid sites are present [2].
The catalytic transformation of methanol could be used for determining both redox and acid sites under reaction conditions [3]. In this paper we present the synthesis, characterization and catalytic performance for the aerobic conversion of glycerol and methanol of Nb-, Ti- and V-promoted tungsten oxide with hexagonal tungsten bronze (HTB) structures.

2 Experimental

The catalysts were prepared hydrothermally at 175°C for 48 h from gels with a X/(W+X) molar ratio in gel of 0.17 (X= Nb, Ti or V). Finally, they were heat-treated at 450-600ºC (in N_2 atmosphere) depending on precursor. The heat-treated materials were characterized with various techniques (XRD, N_2-adsorption, RAMAN, SEM/TEM, XPS, NH_3-TPD and TPR analysis).

Reactivity experiments for glycerol or methanol (in the 250-450ºC range) were carried out in continuous flow quartz reactor, operating at atmospheric pressure [2].

3 Results and discussion

Table 1 shows some characteristics of the catalysts. X-ray diffraction patterns of as-synthesized and samples heat-treated at 450 ºC can be assigned to hexagonal a tungsten bronze (HTB) structure (JCPDS: 85-2460).

Table 1. Characteristics of unpromoted and promoted hexagonal tungsten bronze (*h*-WOx) catalysts

Sample	Heat-treatment (ºC)	S_{BET} [a] $m^2\ g^{-1}$	M/(W+M) ratio [a]	TPD-NH_3 $\mu mol_{NH3}\ g^{-1}$
h-WO_X	450	31	0	135.0
Nb-WO_X	600	21	0.20	121.0
Ti-WO_x	500	17	0.12	72.3
V-WO_X	600	19	0.19	87.5
V,Nb-WO_X	600	57	0.28 (V/Nb=0 .75)	192

However, the thermal stability of this crystalline structure strongly depends on the promoter: up to 600ºC in Nb- or V-containing samples; up to 500ºC for Ti-containing sample

and 450ºC for unpromoted sample. The surface area of the solids synthesized decreased as follows: V,Nb-WOx > h-WOx > Nb-WOx > V-WOx > Ti-WOx (Table 1), although the higher surface area of h-WOx can be related to the lower heat-treatment temperature [4]). On the other hand, the chemical composition of these materials (determined by EDS microanalysis), revealed a homogeneous distribution of the elements.

Figure 1 shows the selectivity to the main reaction products during the aerobic transformation of methanol or glycerol. Dimethylether (DME), formaldehyde (FMA) and COx were mainly formed from methanol, whereas acrolein, acrylic acid and COx (in addition to heavy compounds) were formed from glycerol. In addition, V-free catalysts are active and selective to reaction products formed by acid catalysis (i.e. DME or acrolein) while the presence of V-sites favours, by redox mechanism, the direct formation of formaldehyde from methanol [2b, 3] or the consecutive reaction of acrolein to acrylic acid [5].

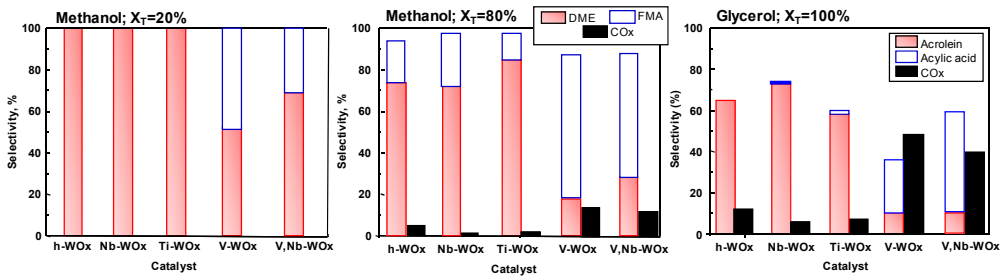

Fig.1. Selectivity to main reaction products during the aerobic transformation of methanol (at 20 and 80% conversion) and glycerol (at 100% conversion) over hexagonal tungsten bronzes.

However, the formation of carbon oxides is also favoured at high alcohol conversions, probably as a consequence of the minority presence of extra-framework V-species [2a]. In fact, it has been recently proposed how tailoring redox and acid sites makes possible to optimize formation of acrylic acid from glycerol [5].

4 Conclusions

Redox and/or acid sites can be incorporated in tungsten hexagonal bronzes by isomorphous substitution of W^{5+} and W^{6+} by M^{4+} and/or Me^{5+} such as Nb, Ti or V improving their catalytic performances in aerobic transformation of alcohols.

Acknowledgements

JMLN thanks the MINECO-Spain (CTQ2012-37925-C03-1) for financial support. CIRI and ISTM are acknowledged for the grant to AC.

References

[1] M. Greenblatt, Chem. Rev. 88 (1988) 31.
[2] a) M.D. Soriano, P. Concepción, J.M. López Nieto, F. Cavani, S. Guidetti, C. Trevisanut, Green Chem. 13 (2011) 2954; b) A. Chieregato, M.D. Soriano, F. Basile, G. Liosi, S. Zamora, P. Concepción, F. Cavani, J.M. López Nieto, Appl. Catalysis B 150–151 (2014) 37.
[3] a) J.M. Tatibouët, Appl. Catal. A: Gen 148 (1997) 213; b) M. Badlani, I.E. Wachs, Catal. Lett. 75(2001) 137.
[4] E. García-González, M.D. Soriano, E. Urones-Garrote, J.M. López Nieto, Dalton Trans. 43 (2014) 14644–14652.
[5] A. Chieregato, M. D. Soriano, E. García-González, G. Puglia, F. Basile, P. Concepción, C. Bandinelli, J.M. López Nieto, F. Cavani, ChemSusChem 8 (2015) 398-406.

ISO-OP02

Metal-Free Heterogeneous Catalysts for the Epoxidation of Alkenes with H_2O_2

Lueangchaichaweng W.[1], Sheng X.[1], Vankelecom I.F.[1], Pescarmona P.P.[2,1*]

1 - COK, University of Leuven, Leuven, Belgium

2 - Chemical Engineering Department, University of Groningen, Groningen, The Netherlands

* p.p.pescarmona@rug.nl

Keywords: metal-free catalysts, functionalised carbon, epoxidation, hydrogen peroxide, heterogeneous catalysis

1 Introduction

The epoxidation of alkenes with H_2O_2 is an industrially relevant route to produce epoxides, which are valuable and versatile compounds. Many heterogeneous catalysts in which the active site is a metal centre have been developed for this reaction (*e.g.* TS-1, Ti-MCM-41, Ga_2O_3).[1] Here, we show for the first time that epoxidation reactions can be catalysed also by metal-free heterogeneous catalysts obtained by straightforward functionalisation of carbon materials.

2 Experimental

Activated carbon (AC, from Norit, surface area = 863 m^2/g) was refluxed in a concentrated HNO_3 aqueous solution (2, 6, 8 or 12 M) for a chosen time (t = 2, 6, 24 or 48 h). Next, the solid was washed with distilled and dried at 80°C. The obtained samples were characterised by TPD, XPS, ATR-FTIR, N_2-physisorption and SEM. The epoxidation tests were performed at 80°C using 2 mmol alkene, 4 mmol 50 wt.% H_2O_2, 40 mg of catalyst, 2.0 g of solvent.

3 Results and discussion

We present the design and synthesis of a novel class of metal-free epoxidation catalysts containing phenol and carboxylic acid groups as active sites (Fig. 1). The idea behind this original class of heterogeneous catalysts stems from the reported ability of phenol and carboxylic acids to activate hydrogen peroxide towards the epoxidation of alkenes.[2] The switch from a homogeneous to a heterogeneous system was achieved by functionalising the surface of activated carbon with the desired oxygenated groups by means of an acid treatment. Activated carbon is an attractive starting material, because it has high surface area, is inexpensive and sustainable, as it can be prepared from agricultural wastes.

A series of functionalised activated carbons was prepared by varying the concentration of HNO_3 and the time of the acid treatment. The obtained functional groups at the surface of the carbon material include carboxyl groups, lactones, anhydrides, phenol and carbonyl groups, as evidenced by TPD analysis.[3] The desired phenol and carboxyl groups are the major species (Fig. 2). All the functionalised carbon materials are active in the epoxidation of alkenes with hydrogen peroxide, with the activity being correlated to the amount of phenol and carboxylic acid groups present at the surface of the material. The most active catalyst could achieve high epoxide yields (Fig. 1). The selectivity varied according to the type of alkene employed: complete selectivity towards the epoxide was observed with cyclooctene, whereas both epoxide and diol products were obtained from limonene. The catalysts are truly heterogeneous (no leaching) and they retain their activity upon recycling.

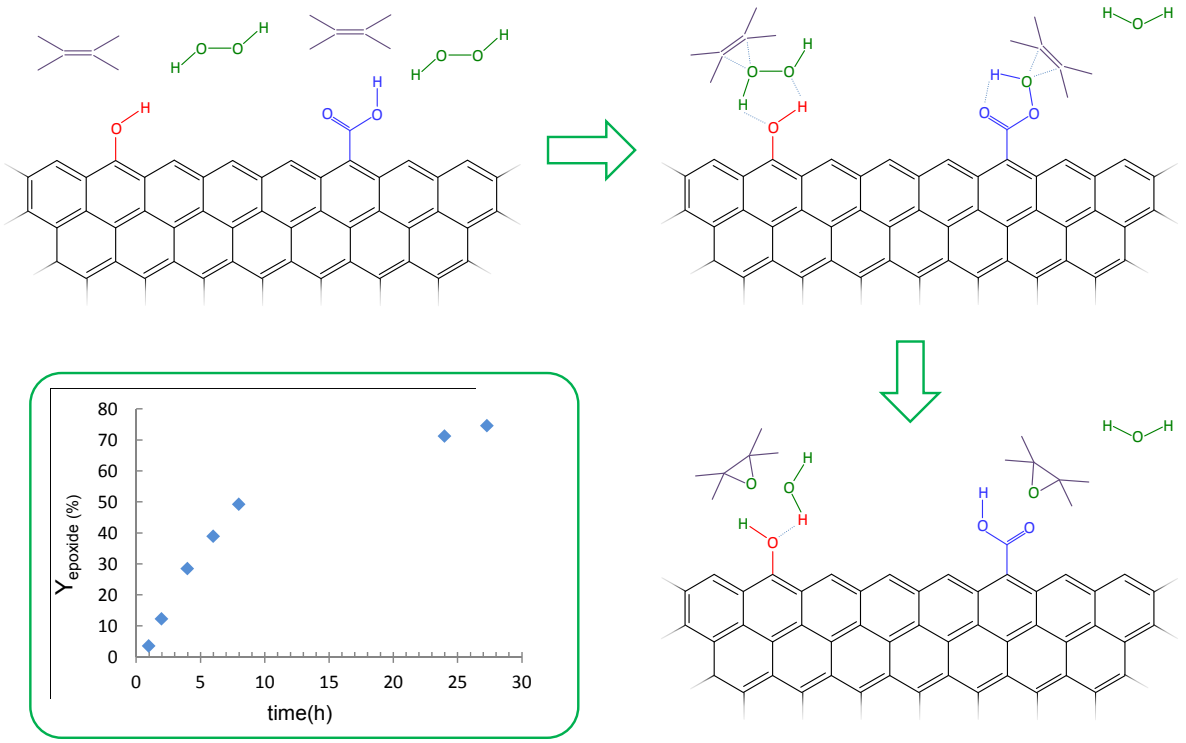

Fig. 1. Functionalised activated carbon as heterogeneous catalyst for the epoxidation of alkenes with H_2O_2.

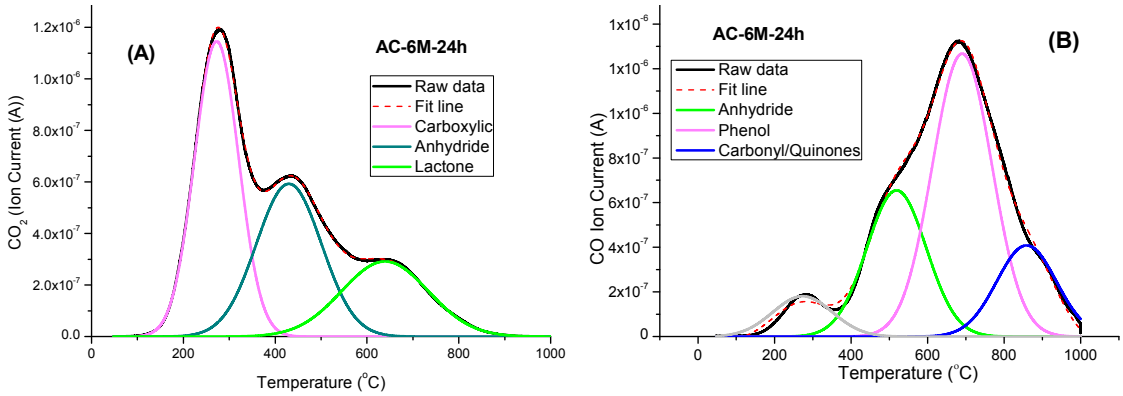

Fig. 2. Deconvolution of (A) CO_2 signal (m/z = 44) and (B) CO signal (m/z = 28) in the TPD profile of activated carbon treated with 6M HNO_3 for 24h (AC-6M-24h).

4 Conclusions

An innovative class of metal-free catalysts for the epoxidation of alkenes with the environmentally friendly oxidant hydrogen peroxide was introduced. These catalysts show promising epoxidation activity, thus opening new perspectives as a green alternative to conventional metal-based heterogeneous catalysts.

References

[1] W. Lueangchaichaweng, N.R. Brooks, S. Fiorilli, E. Gobechiya, K. Lin, L. Li, S. Parres-Esclapez, E. Javon, S. Bals, G. Van Tendeloo, J.A. Martens, C.E.A. Kirschhock, P.A. Jacobs and P.P. Pescarmona, *Angew. Chem., Int. Ed.*, 53 (2014) 1585.

[2] (a) J. Wahlen, D.E. De Vos, P. A. Jacobs, *Org. Lett.,* 5 (2003) 1777; (b) H. Shi, Z. Zhang and Y. Wang, *J. Mol. Catal. A: Chem.*, 238 (2005) 13.

[3] J.L. Figueiredo, M.F.R. Pereira, M.M.A. Freitas and J.J.M. Órfão, *Carbon*, 37, (1999) 1379.

ISO-OP03

Tuning the Selectivity in Pd Catalyzed Liquid-Phase Oxidation of Benzyl Alcohol: an *in situ* ATR-IR Study

Campisi S.[1], Villa A.[1], Chan Thaw C.E.[1], Ferri D.[2], Prati L.[1*]

1 - Università degli Studi di MIlano, Dipartimento di Chimica, Milano, Italy
2 - Paul Scherrer Institute, Villigen, Switzerland

* laura.prati@unimi.it

Keywords: selective oxidation, ATR-IR, support, bimetallic, alcohol oxidation, surface

1 Introduction

The liquid-phase oxidation of alcohols to the corresponding carbonyl and carboxylic compounds represents a relevant class of industrial catalytic process for fine chemicals production [1]. Employing heterogeneous catalysts in combination with molecular oxygen or hydrogen peroxide as oxidants can confer to these processes great benefits in terms of safety and sustainability. Supported noble metal nanoparticles (Pt, Pd and Au NPs) have been extensively investigated as catalysts in alcohol oxidation [1]. However tuning the selectivity in heterogeneously catalyzed reactions requires a fine design of catalysts with specific active sites. Indeed several parameters, such as the nature of the metal, particle sizes and morphology, support properties and metal-support interactions play a crucial role in determining the structure of active sites.

Selective oxidation of benzyl alcohol is a widely used model reaction but it is also an important industrial process for benzaldehyde production. In benzyl alcohol oxidation the main byproduct is toluene, which is reported to be formed by disproportionation of benzyl alcohol or by reaction of the intermediate metal-hydride with the alcohol instead of O_2 [2, 3, 4]. The addition of Au to Pd catalyst has been reported to limit the formation of toluene hindering the disproportionation pathway [5].

In order to clarify the role of the metal and the support in determining the selectivity of the benzyl alcohol oxidation, Au, Pd and AuPd catalysts were prepared by immobilizing polyvinyl alcohol (PVA) protected metal nanoparticles on different supports (TiO_2, NiO, Al_2O_3). Catalytic tests have been followed from both point of views, the substrate (by measuring product evolution), and the support (by using *operando* attenuated total reflection infrared (ATR-IR) spectroscopy) [6]. ATR-IR spectroscopy recently emerged as an ideal tool for this kind of study, allowing to probe the solid-liquid interface between the catalyst surface and the solution. Indeed by monitoring the evolution of surface species during the reaction it is possible to unravel mechanistic aspects and to obtain indirect information about the structure of active sites.

2 Experimental/methodology

Monometallic (Au, Pd) catalysts were prepared by sol immobilisation: a metal sol, formed by using PVA as protective and agent $NaBH_4$ as reducing agent, was immobilized on the support. Bimetallic catalysts were prepared following a procedure previously reported [7] which ensured the production of alloyed nanoparticles. The Au-Pd molar ratio was in all the cases 6-4 mol/mol. An exhaustive characterization of the as prepared catalysts was carried out with various complementary techniques (DRIFTS, TEM/SEM) which confirmed the alloy presence and the high metal dispersion on all the supports.

Catalytic tests were performed in a glass batch reactor at 60°C (0.3 $molL^{-1}$ benzyl alcohol solution in cyclohexane, alcohol/metal molar ratio 500, pO_2 2 bar).

A thin layer of catalysts deposited on an internal reflection element (ZnSe IRE) was used to

investigate the liquid-phase oxidation of benzyl alcohol by ATR-IR spectroscopy. For the measurement a home-built stainless steel flow-through cell serving as a continuous-flow reactor was mounted onto the ATR attachment (Optispec) within the FT-IR spectrometer. The cell was kept at 60°C throughout the measurements by a thermostat. Cyclohexane solvent and benzyl alcohol in cyclohexane (0.02 M) were flown over the catalyst layer at a rate of 10 mL min^{-1} by a peristaltic pump located after the cell.

3 Results and discussion

Pd and AuPd supported on Al_2O_3, TiO_2 and NiO were prepared by the sol immobilization technique. TEM experiments evidenced that Au and Pd show similar particle diameters and that the addition of Pd to Au clusters results in bimetallic particles even some differences in Au/Pd ratio were revealed considering different particles.
Catalysts were tested in liquid-phase benzyl alcohol oxidation. Au/TiO_2 (Table 1) was not very active, whereas Pd/TiO_2 showed higher activity than $AuPd/TiO_2$. Benzaldehyde was the main product in both cases (84-88%) but the nature of by-product differs in the two cases. Interestingly the Au addition prolonged significantly the catalyst life.

Table 1. Comparison of TiO_2-supported catalysts activities in benzyl alcohol oxidation

Catalyst [a]	Activity [b]	Selectivity (%) [c]			
		Toluene	Benzaldehyde	Benzoic acid	Benzyl Benzoate
Pd/TiO_2	532	10	84	1	3
$AuPd/TiO_2$	124	1	88	8	2

[a] Reaction conditions: alcohol/metal = 500/1 mol/mol, 60 °C, *p*O2 = 2 bar, 1250 rpm. [b] Mol of Benzyl alcohol converted per hour per mol of metal calculated after 15 min of reaction. [c] Selectivity at 90% conversion.

ATR experiments allowed us to highlight that the presence of Au facilitates the desorption of products thus possibly reducing deactivation due to irreversible adsorption. The correlation between higher catalyst-life and easier desorption of products was confirmed by testing the different catalysts prepared. Moreover this study took into account the influence of the preparation technique on the reaction pathway particularly studying the role of the protective agent used for generating the metal nanoparticles.

4 Conclusions

Monometallic Au and Pd and bimetallic AuPd nanoparticles were synthesized using sol immobilization technique and used in liquid phase oxidation of benzyl alcohol. The *operando* ATR-IR spectroscopy evidenced that the addition of Au to Pd drastically limited irreversible adsorption thus decreasing the deactivation and partially modifying the selectivity of the reaction. Not only the metal participates in determining this beneficial effect but also the support and the protective agent can be used to tune the reaction pathway .

References

[1] T. Mallat, A. Baiker, Chem. Rev. (2004) 104, 3037-3058.
[2] M. Sankar, E. Nowicka, P.J. Miedziak, G.L. Brett, R.L. Jenkins, N. Dimitratos, S.H. Taylor, D.W. Knight, D. Bethell, G.J. Hutchings, Faraday Discuss. (2010), 145, 341-356.
[3] C. Keresszegi, D. Ferri, T. Mallat, A. Baiker, J. Phys. Chem. B (2005) 109, 958-967.
[4] A.Savara, C.E.Chan-Thaw, I.Rossetti, A.Villa, L.Prati ChemCatChem DOI: 10.1002/cctc.201402552
[5] A.Villa, D. Wang, P. Spontoni, R. Arrigo, D. Su, L. Prati, Catal. Today (2010) 157, 89-93.
[6] D. Ferri, A. Baiker, Top. Catal. (2009) 52, 1323-1333.
[7] D. Wang, A. Villa, F. Porta, D. Su, L. Prati, Chem. Commun. (2006), 1956-1958.

ISO-OP04

Ethanol Selective Oxidation into Syngas over Pt-Promoted Fluorite-Like Oxide: SSITKA and Pulse Microcalorimetry Study

Simonov M.N.[1,2*], Sadykov V.A.[1,2], Rogov V.A.[1,2], Bobin A.S.[1,2], Sadovskaya E.M.[1,2], Mezentseva N.V.[1,2], Roger A.-C.[3], Van Veen A.C.[4]

1 - Boreskov Institute of Catalysis SB RAS, Novosibirsk, Russia
2 - Novosibirsk State University, Novosibirsk, Russia
3 - University of Strasbourg, Strasbourg, France
4 - University of Warwick, Warwick, UK

* smike@catalysis.ru

Keywords: ethanol, partial oxidation, syngas, mechanism, SSITKA, microcalorimetry

1 Introduction

Biofuel derived from renewable feedstocks can be used as a source of hydrogen for fuel cells as well as syngas for chemical industry. Ethanol is the most widespread biofuel with the annual production rate of 84.5 billion L in 2011 [1]. Syngas production by ethanol steam reforming on traditional catalysts is hampered by their rapid deactivation due to coking. This problem can be solved by using catalysts based on oxides with a high lattice oxygen mobility and reactivity able to transform ethanol into syngas by selective oxidation (Pt/CeZrO etc) [2]. Their tailor-made design requires elucidation of the mechanism of ethanol selective oxidation on such catalysts, which is the aim of this work.

2 Experimental/methodology

$Pr_{0.15}Sm_{0.15}Ce_{0.35}Zr_{0.35}O_2$ fluorite-like oxide was prepared by polymerized complex precursor (Pechini) route and calcined in air at 900°C for 2 h [3]. Pt (1.4wt.%) was supported via incipient wetness impregnation with H_2PtCl_6 solution. Isotope transient experiments at steady state conditions in a flow reactor (SSITKA) were carried out as earlier described [4]. After achieving the steady state, a flow of 1% C_2H_5OH + 0.5% O_2 in He was switched to that of 1% C_2D_5OH + 0.5% O_2 in He (or 1% C_2H_5OH + 0.5% $^{18}O_2$), and concentrations of reagents and products were monitored by a mass-spectrometer UGA 200 (Stanford Research Systems, USA) and GC (Chromos GH-1000, Russia). Rates and heats of the catalysts reduction/reoxidation by pulses of ethanol/O_2 in He for catalyst in the steady state were estimated using a Setaram Sensys DSC TG calorimeter and a pulse kinetic installation equipped with GC, MS and gas sensors.

3 Results and discussion

At a low (350 °C) temperature, conversions of ethanol and O_2 were 45 and 90%, respectively, and CO to CO_2 ratio in products was ~ 1. ^{18}O in CO and CO_2 appears right after the switch to C_2H_5OH + $^{18}O_2$ feed, and its concentration slowly grows in time due to fast exchange with the surface and bulk of catalyst. At the steady state ^{18}O fraction in CO_2 and CO is equal to ~ 0.3 and 0.01, respectively. Hence, unlabeled CO is produced by ethanol/acetaldehyde decomposition on Pt, while CO_2 is formed with participation of the oxide support oxygen. A small fraction of $C^{18}O$ appears due to reverse water gas shift (RWGS) reaction. These conclusions agree with SSITKA results obtained at high temperatures. Two-fold increase in CO to CO_2 ratio was observed at 700°C while atomic isotope fractions of ^{18}O in CO_2 and CO became almost equal. This is explained by the increase of the reaction rate of RWGS leading to

CO formation and intense isotopic exchange between CO and CO_2.

In SSITKA experiments with switching the stream of $C_2H_5OH + O_2$ to that of $C_2D_5OH + O_2$ the value of the kinetic isotope effect is equal to 1. This proves that the rate of ethanol selective oxidation is determined by C-C bond rupture in ethanol or acetaldehyde molecules, while C-H bond rupture in the ethanol dehydrogenation step proceeds easily.

Typical results of pulse microcalorimetric studies are shown in Figure 1. In all pulses conversion of ethanol and O_2 was ~ 90-95%. The heat effects of the steady-state catalyst reduction by EtOH pulses correspond to ethanol oxidation by bridging surface oxygen species of support with the heat of adsorption ~ 550 kJ/mol O_2. The amount of oxygen removed by each pulse is in range of 5-7% of monolayer (up to 30% of monolayer after 4 pulses), thus exceeding greatly the amount which can be adsorbed on Pt particles. So, a high reaction rate and coking stability could only be provided by fast surface/lattice oxygen diffusion to Pt particles. Analysis of the data of oxygen isotope exchange between $C^{18}O_2$ and steady-state catalyst gives values for coefficient of fast oxygen diffusion along the surface/domains interfaces ~10^{-12} cm^2/s at 700 °C which is sufficient to provide required oxygen transfer [5]. Concentrations of products in the 1st pulse of ethanol are equal to those in the reaction mixture pulse (Fig. 1a). This result clearly demonstrates step-wise redox mechanism with independent activation of ethanol and O_2. Heats of the steady state surface reoxidation by O_2 pulses are in the range of 435-546 kJ/mol corresponding to replenishment of bridging M_2O species of the oxide support [5].

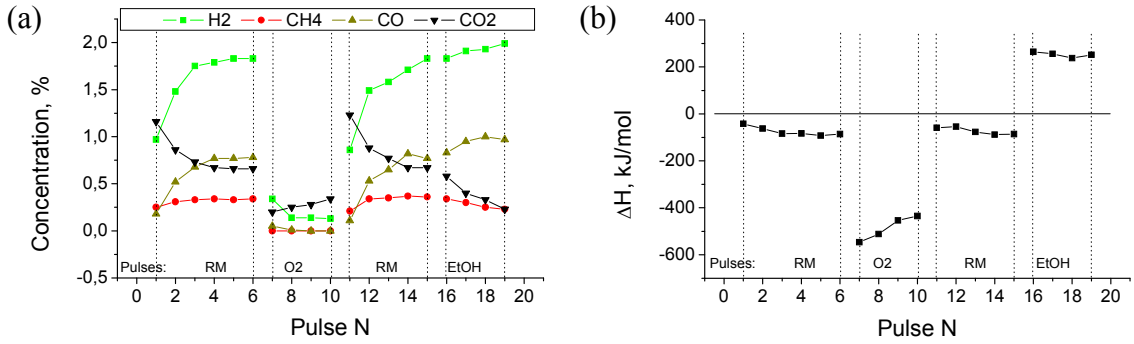

Fig. 1. Products concentrations (a) and heat effects (b) in consecutive pulses of reaction mixture (RM, 1% C_2H_5OH + 0.5% O_2), 0.5% O_2, 1% C_2H_5OH supplied at 450°C on the steady-state catalyst.

4 Conclusions

For Pt/ $Pr_{0.15}Sm_{0.15}Ce_{0.35}Zr_{0.35}O_2$ catalyst the mechanism of ethanol selective oxidation into syngas can be described by step-wise red–ox scheme including ethanol oxidative decomposition on Pt sites (the rate determining step is C-C bond breaking) and fast reoxidation of reduced support sites by O_2. Rapid oxygen migration from oxide support to Pt provides conjugation between these steps.

Acknowledgements

Support by Russian Fund of Basic Research Project RFBR-CNRS 12-03-93115, FP7 Project BIOGO (NMP-LA-2009-604296) and the Ministry of Education and Science of the Russian Federation is gratefully acknowledged.

References

[1] J. Sun, Y. Wang. *ACS Catal*. 4 (2014) 1078-1090.
[2] S. M. de Lima, I. O. da Cruz, G. Jacobs, et al. *J. Catal.* 257 (2008) 356–368.
[3] V.A. Sadykov, T.G. Kuznetsova, G.M. Alikina, et al. Chapter 5. In: McReynolds DK (ed) *New topics in catalysis research*. Nova Science Publishers, New York, (2007) pp 97–196.
[4] E. Sadovskaya, Y. Ivanova, L. Pinaeva, et al. *J Phys Chem A.* 111 (2007) 4498–4505.
[5] A.S. Bobin, V.A. Sadykov, V.A. Rogov, et al. *Top Catal.* 56 (2013) 958–968.

ISO-OP05

Selectivity Control in Oxidation of 1-Tetradecanol on Supported Nano Au Catalysts

Martínez-González S.[1], Ivanova S.[2], Domínguez M.I.[2], Cortés Corberán V.[1*]

1 - Institute of Catalysis and Petroleumchemistry (ICP), CSIC, Madrid, Spain
2 - Institute of Materials Science of Seville (ICMS), University of Seville - CSIC, Seville, Spain

* vcortes@icp.csic.es

Keywords: tetradecanol, alcohol selective oxidation, gold catalysts, fatty alcohols, myristaldehyde

1 Introduction

Selective oxidation of fatty alcohols, i.e., linear long-chain alkanols, has been scarcely investigated to date, probably due to their very low oxidation reactivity as non-activated, primary aliphatic alcohols, and to the challenges that their physical properties (hydrophobicity, high melting and boiling points) impose for its oxidation via green chemistry processes [1]. However, its use for high value chemicals production is of great interest, inasmuch their corresponding aldehydes and esters are commercially important for pharma, agrochemical and fragrance industries, among others. For instance, myristaldehyde (tetradecanal), used as flavor additive for human food, and myristyl myristate (tetradecyl tetradecanate), broadly used in cosmetics as skin conditioning agent and emulsifier, can be produced by selective oxidation of tetradecanol, a representative higher fatty alcohol.

Recently, we reported for the first time that the selective oxidation of tetradecanol is feasible in the liquid phase in accordance with green chemistry principles using nano sized gold catalyst, air as oxidant at near atmospheric pressure, and an alkane solvent without base addition [2]. The results showed that selectivity depended not only on the catalyst nature but also on the reaction conditions. Selectivity to the ester was better when decane was used as solvent instead of heptane. Under the conditions tested, i.e., using a constant alcohol/metal (A/M) ratio, a sharp selectivity trend change (increase of acid formation) was observed when conversion reached a critical value, regardless the temperature. It was hypothesized it was due to a change in the reaction mechanism caused by the water produced, once it saturated the hydrophilic support surface.

The aim of this work is to investigate the operation parameters that allow control the selectivity of the reaction to the desired product (aldehyde or ester), as well as to verify that hypothesis on the role of the support surface. To reach those goals we studied the effect of reaction temperature, A/M ratio and run time on the product distribution and its evolution with conversion.

2 Experimental

Catalyst was prepared by depositing Au by the direct anionic exchange method, assisted by NH_3, on a commercial CeO_2-Al_2O_3 support (Puralox® 20, Sasol), as detailed in [2]. Then it was dried at 100 ºC overnight and calcined at 300 ºC for 4h in air. Catalyst composition determined by X-ray microfluorescence spectrometry (XRMF) in wt.% was 2.0 Au, 77.7 Al_2O_3, 20.3 CeO_2. Samples were characterized by textural analysis, XRD and HRTEM. Gold particle size distribution was determined from HRTEM images.

Catalytic activity for *n*-tetradecanol oxidation was studied in a semicontinuous reactor. Tests were conducted at 80-120 ºC and atmospheric pressure for 6 h, using 0.1 M *n*-tetradecanol in *n*-decane with no base added, molar ratios A/M = 50-200, and 30 mL/min O_2 flow. Reactants and products were periodically analyzed by GC using a FID detector.

3 Results and discussion

In the conditions tested, the main product was tetradecanal (with selectivity up to 90%), with smaller amounts of the ester (octanyl octanoate) and, for some tests and at high conversions, tetradecanoic acid. As expected, final conversion increased by increasing the reaction temperature and decreasing the A/M ratio, reaching conversions as high as 60 % in 6 h (Fig.1). It is noteworthy that ester formation was detected in all analyses; even when acid was not detected. This implies that it is generated via formation of the hemiacetal, which consecutive oxidation produces directly the ester [3]. Its selectivity was higher (20-25%) at 80 ºC and slightly increased (10 to 15 %) with increasing conversion at higher temperatures, but was not affected but the sharp change in selectivity to acid (and aldehyde) observed 110-120 ºC (Fig. 1, down). As previously found [2], acid formation started when a certain value of conversion is reached. Interestingly, this critical value varied with A/M ratio, being roughly inversely proportional to it. Thus, it is proportional to catalyst load, and hence to the total bare support surface available. This agrees with our hypothesis: the higher the catalyst amount, the higher is the amount of water that can be absorbed by the catalyst bare support surface and, consequently, the higher is the conversion needed to produce the amount of water that may adsorb that surface before starting to react with the aldehyde to produce the acid.

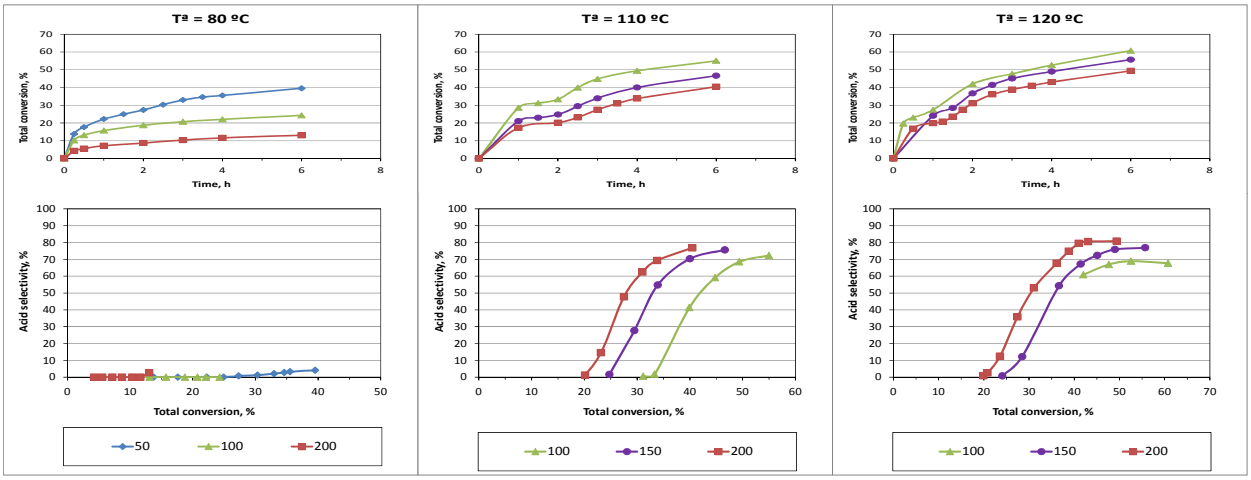

Fig. 1. Influence of A/M ratio on tetradecanol oxidation on Au/CeO_2-Al_2O_3: conversion *vs*. run time (upper row) and selectivity to acid as a function of conversion (lower row). T^a = Reaction temperature.

4 Conclusions

Product distribution in tetradecanol oxidation on Au/CeO_2-Al_2O_3 catalyst depends strongly on operation conditions. Formation of the acid requires the availability of free water reactant in the apolar solvent. This involves that water produced by the very reaction saturates previously the hydrophilic bare support surface. As a consequence, the alcohol/metal ratio is the critical factor to keep high selectivity to the aldehyde at high conversions. This could be a limitation for a continuous process. Nevertheless, by proper selection of conditions, aldehyde yields up to 30 % with 90% selectivity, and acid yields up to 40% with 90% selectivity can be reached.

References

[1] V. Cortés Corberán et al., *Applied Catal. A: General.* 474 (2014) 211.
[2] V. Cortés Corberán et al., *Catalysis Today*. 238 (2014) 49.
[3] T. Ishida et al., *ChemSusChem* 5 (2012) 2243

ISO-OP06

Promoted Au and Ag Catalysts for Liquid Phase Selective Oxidation of Octanol

Kotolevich Y.[1], Kolobova E.[2], Cabrera Ortega J.E.[3], Tiznado Vazquez H. J.[1], Bogdanchikova N.[1], Cortés Corberán V.[4*], Zanella R.[5], Pestryakov A.[2]

1 - Centro de Nanociencias y Nanotecnología, UNAM, Ensenada, México
2 - Tomsk Polytechnic University, Tomsk, Russia
3 - Universidad Autónoma de Baja California, Ensenada, México
4 - Institute of Catalysis and Petroleumchemistry (ICP), CSIC, Madrid
5 - Centro de Ciencias Aplicadas y Desarrollo Tecnológico (UNAM), México, México

* vcortes@icp.csic.es

Keywords: n-octanol oxidation, gold catalysts, silver catalysts, red-ox treatment, support modification

1 Introduction

The transformation of fatty alcohols (i.e., alkanols C_{8+}) as a source of fine chemicals is commercially attractive for pharmaceutical, agrochemical and fragrance industries, among others [1]. However, non-activated, primary aliphatic alcohols are the most difficult type of alcohols to oxidize selectively, as compared with the oxidation of more reactive benzyl or C_1-C_4 aliphatic alcohols. Thus, selective oxidation of *n*-octanol (one of the lower fatty alcohols) has attracted much less attention though 1-octanol is often used as the alkanols model molecule in comparative studies of alcohols reactivity on different catalysts, including very active Au nanoparticles (NPs). Some parameters that regulate the catalytic properties of Au NPs for the *n*-octanol selective oxidation (reaction conditions, support nature and its modification) have been systematically investigated [2, 3] as tools for improving their catalytic performance.

On the contrary few works report catalytic oxidation of *n*-octanol based on silver catalysts, but in vapor phase [4]. The main interest to replace Au for Ag in biomass transformation deals with the metals' price (Ag is 72 times cheaper than Au), although their catalytic properties differ. Therefore the investigation of the parameters that enhance the catalytic performance of Ag NPs without compromising the cost is of paramount importance.

In this work we compare the catalytic activity of Au and Ag supported on titania for liquid phase *n*-octanol selective oxidation to investigate the effect of: a) support modification with metal oxides (La, Ce, Fe or Mg); and b) catalyst pretreatment with H_2 and O_2 atmospheres.

2 Experimental

Titania Degussa P25 was used as base support. Oxide modifiers (of Ce, La, Fe or Mg) were deposited on support (molar ratio Ti/M = 40) by impregnation with aqueous solutions of nitrates, followed by drying at 110ºC for 4 h, and calcination at 550°C for 4 h. The nominal loadings were 4 wt. % Au and 2.3 wt. Ag, respectively. Au dispositive were made from $HAuCl_4 \times 3H_2O$ by deposition-precipitation (DP) with urea, Ag dispositive were prepared from $AgNO_3$ by DP with NaOH followed by vacuum drying with at 80°C for 2 h. Samples were characterized by FTIR of adsorbed CO, XPS, HRTEM, and textural analysis.

Catalytic properties for *n*-octanol oxidation were studied either without or with catalyst sample pretreatment at 300°C in H_2 or O_2 atmosphere. Tests were conducted at 80 ºC and atmospheric pressure for 6 h, using 0.1 M *n*-octanol in *n*-heptane with no base added, a molar ratio *n*-octanol/metal =100, and 30 mL/min O_2. Reactants and products were analyzed by GC.

3 Results and discussion

In the mild conditions tested, as prepared catalysts with Au showed higher activity, but those with Ag were also active for liquid phase oxidation. The main product was octanal, with smaller amounts of the ester (octanyl octanoate) and, for some catalysts, traces of the octanoic acid. Both, the titania modifiers (Ce, La, Fe or Mg) and the pretreatment in H_2 or O_2, showed a significant influence on the octanal selectivity and yield.

Support modification by the tested modifiers did not influence octanol conversion on Au catalysts, but the ester selectivity increased by La addition and decreased by Fe addition. On the contrary, support modification did not affect the higher octanal selectivity (90-100%) of Ag catalysts, but increased markedly (three to fivefold) their octanol conversion with Ce (Fig. 1a), Mg or Fe. Interestingly also red-ox pre-treatments had a different effect on the activity of Au and Ag catalysts: while activity of Au catalysts was increased by H_2 treatment from 4 to 40 mol. % (Fig. 1b), that of Ag catalysts was decreased by both treatments. They also increased the selectivity to ester for gold catalysts between two (with Ce, La, Mg) and fourfold (with Fe), but did not alter the product distribution for Ag catalysts. According to FTIR CO, HRTEM, XPS, H_2 TPR data, support modifiers influenced the structural and electronic properties of Au and Ag species through a metal-support and metal-modifier interaction.

Comparison of catalytic and spectroscopic data showed that partly charged metal clusters $Au_n^{\delta+}$ and $Ag_n^{\delta+}$ are probable active sites of their respective catalysts in the studied process. Therefore, additions of support modifying metal oxides influence structural and electronic properties of Ag species and stabilize the active species, while both redox pretreatments reduce their number.

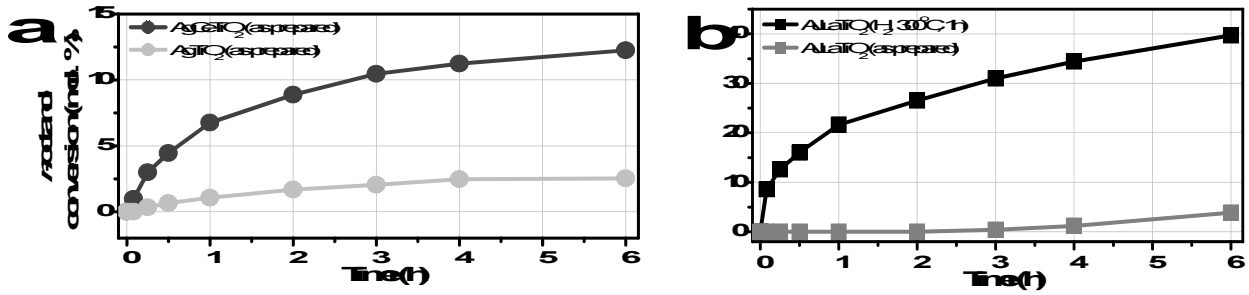

Fig. 1. Activity in *n*-octanol oxidation on the best catalysts: a) $AgCeTiO_2$ b) $AuLaTiO_2$

4 Conclusions

Both Au and Ag on titania are active for liquid phase *n*-octanol oxidation, and partly charged metal clusters $Au_n^{\delta+}$ and $Ag_n^{\delta+}$ are probable active sites of the catalysts for this. Ag catalysts are less active (but more selective to octanal). However, through the appropriate support modification Ag catalysts activity can be increased markedly. As a consequence, Ag catalysts supported on modified titania supports can be a promising alternative system for *n*-octanol oxidation. Reducing or oxidizing pretreatments are deleterious of these catalysts, but modify the product distribution on Au catalysts.

References

[1] V. Cortés Corberán et al., Applied Catal. A: General. 474 (2014) 211.
[2] V. Cortés Corberán et al., Catalysis Today. 238 (2014) 45.
[3] T. Ishida et al, ChemSusChem. 5 (2012) 2243.
[4] G. D. Yadov et al. Chemical Engineering Research and Design. 90 (2012) 86.

ISO-OP07

Selective Epoxidation of Propylene to Propylene Oxide on Gold-Based Catalysts: a Theoretical Study

Moskaleva L.V.*

Institute of Applied and Physical Chemistry and Center for Environmental Research and Sustainable Technology, Universität Bremen, Bremen, Germany

* lyudmila.moskaleva@gmail.com

Keywords: density functional theory, Au(321) surface, propylene oxidation, propylene oxide selectivity

1 Introduction

Epoxidation of propylene is crucial for the production of propylene oxide (PO), a valuable raw material for polyurethane foams and resins, and propylene glycol. [1]. At present, the two major methods used for the commercial PO production suffer from complexity and utilize hazardous or costly reagents [2]. Therefore, efforts have been made to develop a "green" process that could directly and selectively epoxidize propylene to PO.

The coinage metals (Au, Ag, and Cu) have been investigated as catalysts for propylene epoxidation [1]. The common challenge identified for all of them is the need to suppress undesirable reaction pathways leading to either total oxidation or the formation of other partially oxidized products, e.g., acrolein, acetone, propanal. The selectivity was shown to sensitively depend on temperature, particle size, and support as well as on the presence of co-reactants such as H_2 or H_2O in the reactants mixture [1]. Addition of hydrogen or water vapor facilitates the activation of O_2 and greatly increases the selectivity to PO. Thus far, the best performance was achieved on Au-based catalysts: C_3H_6 conversion of 5.0–9.8% [3], PO selectivity of 90–96% [3], and H_2 efficiency 30–47% [4].

In this work a detailed transformation network of competitive reaction pathways following the initial steps of propylene oxidation on the model Au(321) surface has been studied.

2 Computational methodology

The slab-model calculations were performed with a plane-wave DFT-based method using the gradient-corrected PBE exchange-correlation functional. The projector augmented wave (PAW) method was used to describe the interaction between atomic cores and electrons. The stepped and kinked Au(321) surface was selected to model defect-rich Au nanoparticles and Au surfaces with rough morphology in general. Transition states of the reactions were determined by applying the dimer method [5].

3 Results and discussion

The epoxidation of propylene on Au is believed to proceed in analogy to the accepted mechanism of ethylene epoxidation, via a primary or secondary oxametallacycle (OMMP1 or OMMP2) formed from addition of O to the C=C bond of propylene [6]. A competing H abstraction from the CH_3 group forming allyl is thought to be leading to total combustion [7]. In the present work several new interesting insights into the reaction mechanism have been identified:

(i) **A new direct pathway to epoxide**, not passing via an oxametallacylcle. This pathway of Eley-Rideal type, where propylene reacts directly from the gas phase with adsorbed O involves activation barriers (0.33-0.65 eV) of comparable height to those leading to the formation of a secondary metallacycle, OMMP2 (0.37-0.51 eV), a commonly assumed PO precursor. However, both metallacycle intermediates easily undergo an intramolecular H-transfer reaction to propanal

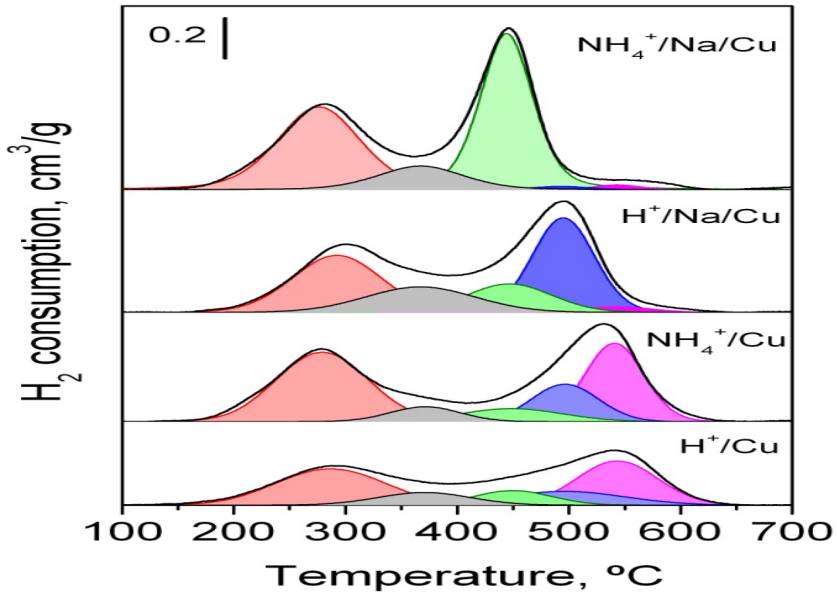

Fig. 1. Comparison of the energetics for the two epoxide formation routes: the O route (pink) and the OOH path (blue). Dotted lines indicate undesirable side reactions. Energies relative to gas-phase O_2, H_2, and clean Au(321). Stars indicate adsorbed species.

and acetone, respectively. The activation energy of the intramolecular H-transfer is always notably lower than that for the isomerization to PO. Therefore, a direct epoxide formation seems to be a more plausible route than the oxametallacycle path. Nevertheless, an abstraction of a hydrogen atom from the methyl group by adsorbed atomic O was found to have the lowest activation barrier of all primary pathways (0.11-0.47 eV).

(ii) It has been commonly assumed that the allyl species formed after the abstraction of a hydrogen atom from the CH_3 group of propylene is a precursor to total combustion. In contrast, this work shows that **allyl should easily react with O or OH forming acrolein or allyl alcohol, respectively**. More likely **precursors to total combustion are oxametallacycle intermediates**.

(iii) **Co-feeding of H_2 or water to the reactants mixture not only makes the activation of O_2 easier but also drastically improves the selectivity to PO due to the formation of HOO species** which further acts as an oxidizing agent as illustrated in Fig. 1. In the OOH pathway the formation of epoxide has a significantly lower activation barrier than the acetone formation. The peroxide pathway to PO lies overall lower in energy than the O-pathway.

4 Conclusions

The present work questions some of the earlier assumptions regarding the mechanism of PO formation. Peroxo species formed *in situ* are found to be responsible for the high selectivity of epoxidation on gold-based catalysts in the presence of H_2 or H_2O.

Acknowledgements

The author acknowledges the financial support from the German Research Foundation (DFG) within the Project No. MO 1863/2-2.

References

[1] D. L. Trent, in *Kirk-Othmer Encyclopedia of Chemical Technology*, *Vol. 20*, Wiley, New York, 1996.
[2] J. Huang, M. Haruta, *Res. Chem. Intermed.* 38 (2012) 1.
[3] A. K. Sinha, S. Seelan, S. Tsubota, M. Haruta, *Angew. Chem. Int. Ed.* 43 (2004) 1546.
[4] J. Huang, T. Takei, T. Akita, H. Ohashi, M. Haruta, *Appl. Catal. B* 95 (2010) 430.
[5] G. Henkelman, H. Jónsson, *J. Chem. Phys. 111 (*1999) 7010.
[6] S. Linic and M. A. Barteau, *J. Am. Chem. Soc.* 124 (2002) 310.
[7] D. Torres, N. Lopez, F. Illas, R. M. Lambert, *Angew. Chem. Int. Ed.* 46 (2007), 2055.

ISO-OP08

Oxidant-Free Formal Oxidation of Alcohol Substrates towards Higher Value Added Products

Khaskin E.[1,2], Milstein D.[2*]

1 - Okinawa Institute of Science and Technology Graduate School, Onna-son, Japan
2 - Weizmann Institute of Science, Rehovot, Israel

* david.milstein@weizmann.ac.il

Keywords: oxidation, ruthenium, alcohols, carboxylic acid, deuteration, dehydrogenation

1 Introduction

Recently, a novel ruthenium catalyzed reaction discovered in 2005 in the Milstein group, has been used to transform alcohols into esters and amides without an oxidant, with the concurrent evolution of hydrogen gas [1]. This transformation and other like it that utilize the same basic mechanism, involving synthesis of amides, may have profound implications for chemical feedstocks as a number of new products becomes available at a cheaper price, since expensive oxidants do not need to be used, and the only byproduct is hydrogen. I will discuss previous work on the transformation of alcohols to carboxylic acid salts without the use of an oxidant with water as the only reagent [2] and selective deuteration of alcohols in the α carbon position [3]. In addition, current work focused on intercepting the putative intermediate aldehyde with a view to creating value added products, will also be discussed.

2 Experimental/methodology

The catalytic reaction for the modification of alcohols is typically carried out on a ~0.3 mmol scale (of the alcohol substrate) with 0.01 to 1 mol% of the organometallic Ru precatalyst that is activated by the presence of base. For the production of carboxylic acid salts (carboxylate), the solvent used was water and the reaction was carried out with a constant argon flow at rapid reflux to remove hydrogen gas produced. A slight excess of base is necessary in order to drive the reaction forward by deprotonating the catalyst-deactivating carboxylic acid, thus forming the carboxylate anion, and for activating the catalyst. For production of other organic substrates, dioxane solvent was used at reflux. The amount of base required depends on whether the base is necessary to just activate the catalyst, or whether it is needed to activate the alcohol coupling partner.

For the selective deuteration reaction, a similar procedure was used, but the reaction was carried out in a closed system in D_2O in order to prevent hydrogen gas escape and enable reversible hydrogenation of the carbonyl intermediate.

After a typical reaction time of 16-24 hours depending on the reaction, the product was isolated via extraction in an organic solvent and quantifying the amount produced by NMR and/or GC/FID against an internal standard. Isolation of the product via column chromatography, or acid/base extraction technique was performed in a few cases to confirm the yields obtained by other analytical methods.

3 Results and discussion

Benzylic and aliphatic substrates could be efficiently transformed to carboxylic acid salts utilizing water as solvent. The reaction proceeded more rapidly for benzylic substrates, but the yields of both types of products were high, generally more than 70/80% (Figure 1).

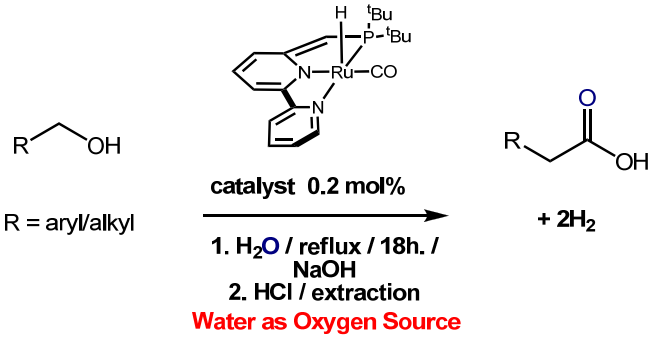

Fig. 1. General scheme for the production of carboxylic acids from alcohols without the use of an oxidant [2]

The same reaction, but carried out in a closed system in order to trap hydrogen gas, and utilizing D_2O as a solvent, was able to show selective deuteration of alcohols in the α carbon position when a catalytic amount of base was used. With the use of large amounts of base, deuteration in the β carbon position could also be observed. In this way, complete deuteration of ethanol, an important deuterated solvent, was achieved directly from deuterated water under relatively mild conditions. Secondary alcohols required milder conditions than primary ones and the transformation proved remarkably facile for benzylic substrates (Figure 2).

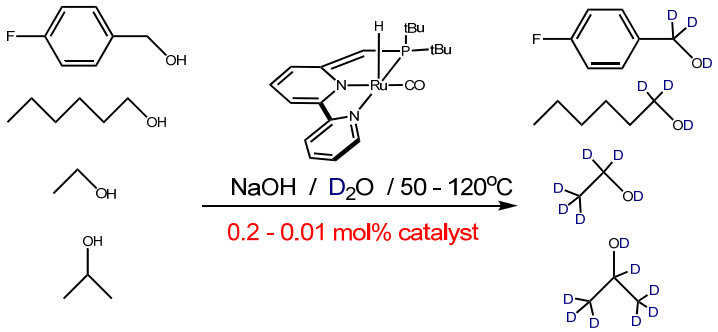

Fig. 2. General scheme for the selective deuteration of alcohols [3]

In addition to the above two examples, where an oxygen or H_2 unit was introduced into the substrate, it proved possible to introduce other additives that give higher value added products when organic solvents were utilized. These recent results will also be presented at EuropaCat.

4 Conclusions

Significant progress has been achieved in oxidation of alcohols by completely eliminating the oxidant. Transformation to the ester [1] can be avoided by introducing a suitable trapping agent for the aldehyde and/or ketone, enhancing the scope of the original ester forming reaction. These transformations are carried out in water or dioxane at refluxing temperature and may provide significant cost savings in the fine and bulk chemical industries.

Acknowledgements

E.K. would like to acknowledge the Okinawa Institute of Science and Technology for partial financial support for the period of 2014-2015 when part of this work was carried out at the Weizmann Institute.

References

[1] J. Zhang, G. Leitus, Y. Ben-David, D. Milstein, *J. Am. Chem. Soc.* 127 (2005) 10840.
[2] E. Balaraman, E. Khaskin, G. Leitus, D. Milstein, *Nat. Chem.* 5 (2013) 122.
[3] E. Khaskin, D. Milstein, *ACS Catal.* 3 (2013) 448.

ISO-OP09

Metal-Support Interaction – a Key Reason for Ag Catalyst Activity in Low-Temperature Oxidation

Mamontov G.V.[1*], Dutov V.V.[1], Grabchenko M.V.[1], Zaikovskii V.I.[2,3], Sobolev V.I.[1,2], Vodyankina O.V.[1]

1 - Tomsk State University, Laboratory of Catalytic Research, Tomsk, Russia
2 - Boreskov Institute of Catalysis SB RAS, Novosibirsk, Russia
3 - Novosibirsk State University, Novosibirsk, Russia

* GrigoriyMamontov@mail.ru

Keywords: metal-support interaction, ultrasmall Ag particles, interface, low-temperature oxidation

1 Introduction

The metal-support interaction in supported catalysts is very important for understanding of both nature of catalytic action and mechanisms of oxidative reactions [1]. Catalytic properties of small (less than 5 nm) particles of active component depend significantly on chemical properties of support. Features of "metal/support" interface for Pd, Pt and Au catalysts are under close attention of investigators in recent years [2]. However, interest to supported Ag catalysts constantly increases due to unique catalytic activity of silver in oxidative reaction [3]. The aim of the present work is to reveal the role of silver-oxide support interaction in low-temperature oxidation. The Ag-"inert" support (Ag/SiO_2 catalysts) and Ag-"active" support (Ag/CeO_2 catalysts) interfaces were studied in details.

2 Experimental/methodology

The interfacial interaction between "inert" silica support and supported ultrasmall silver particles was studied by variation of ratio between Ag loading and concentration of SiOH groups on silica surface. First series of Ag/SiO_2 catalysts was prepared by wetness impregnation method using $AgNO_3$ as precursor of active component and silica with various surface concentrations of silanols.

To study the metal-support interaction in Ag/CeO_2 catalysts the co-deposition and wetness impregnation methods were used to prepare the catalysts. The samples prepared were studied using a complex of physicochemical techniques and tested in reactions of CO oxidation, deep oxidation of formaldehyde, aerobic and anaerobic dehydrogenation of ethanol to acetaldehyde. The features of metal-support interfaces were studied using a complex of TPx methods and HR TEM.

Series of $Ag/CeO_2/SiO_2$ catalysts were prepared by impregnation method with different order of ceria and silver precursors introduction to reveal the role of Ag-CeO_2 and Ag-SiO_2 interactions in different low-temperature oxidation reactions.

3 Results and discussion

According to IR spectroscopy data, stabilization of silver with formation of Si-O-Ag bonds took place on Ag-SiO_2 interface. High temperature pre-treatment of silica support (700-900 ^oC) led to decrease of silanols concentration from 5-7 to 0.5-1.0 OH group/nm^2 (measured by TPD H_2O). Weak interaction of silver with silica support and high re-dispersing ability of silver particles under red-ox treatments were observed for samples prepared on the basis of high-temperature pre-treated silica. High activity in low-temperature CO oxidation (from -40 ^oC) was observed for those catalysts.

High concentration of silanols on silica surface provided strong interaction between silver and silica with formation of small silver particles (Fig. 1a). Lower activity in CO oxidation was observed for Ag/SiO_2 catalysts prepared on the basis of hydrophilic silica.

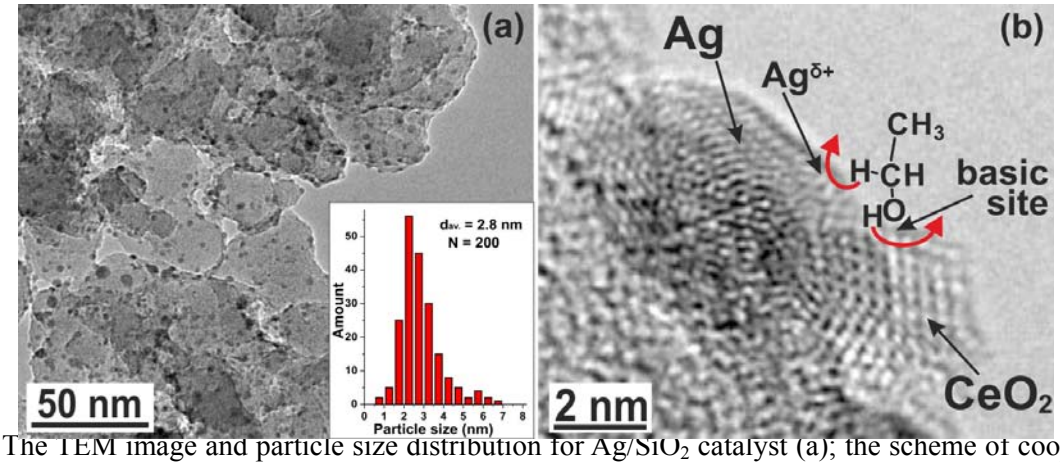

Fig. 1. The TEM image and particle size distribution for Ag/SiO_2 catalyst (a); the scheme of cooperation of active sites in ethanol dehydrogenation on Ag-CeO_2 interface in $Ag/CeO_2/SiO_2$ catalyst (b)

Strong interaction between Ag and CeO_2 was observed for Ag/CeO_2 catalyst prepared by co-deposition method. Formation of small clusters (less than 2 nm) weakly bonded with ceria surface were observed in case of Ag/CeO_2 catalyst prepared by impregnation method. The activity of Ag/CeO_2 catalysts prepared by impregnation method in CO oxidation was higher in comparison with one prepared by co-deposition method.

Impregnation of silica with ceria and Ag precursors was used to prepare $Ag/CeO_2/SiO_2$ catalysts. It was shown that silver particles were located on the surfaces of both ceria and silica particles. Introduction of ceria on silica surface did not significantly influence on its activity in low-temperature CO oxidation in comparison with Ag/SiO_2 catalyst. It is noteworthy that the influence of ceria addition on Ag/SiO_2 activity became significant at 80-150 ^oC in formaldehyde oxidation.

Significant activity increase in reaction of ethanol dehydrogenation to acetaldehyde over $Ag/CeO_2/SiO_2$ catalysts was observed compared to the one over Ag/SiO_2 catalyst. The mechanism of cooperation of CeO_2 and Ag active sites on the enhanced Ag-CeO_2 interface was proposed (Fig. 1b).

4 Conclusions

Thus, it was shown that silver-oxide support interaction plays the key role in oxidation of organic compounds. The weak interaction of ultrasmall silver particles with both "inert" (silica) and "active" (ceria) supports is a compulsory condition for high activity in low-temperature CO oxidation. The oxidation of CO even at temperatures below 0 ^oC takes place only in the presence of Ag-SiO_2 interaction, while the enhanced Ag-CeO_2 interface is a reason for elevated activity in deep oxidation of formaldehyde and dehydrogenation of ethanol to acetaldehyde. The cooperation of active site of silver and ceria takes place only at temperatures above 50 ^oC and depends on its interaction force.

Acknowledgements

This research was supported by "The Tomsk State University Academic D.I. Mendeleev Fund Program" grant.

References

[1] N. Acerbi, S.C.E. Tsang, G. Jones, S. Golunski, P. Collier, *Angew. Chem. Int. Ed.* 52 (2013) 7737.
[2] N. Mizuno, *Modern Heterogeneous Oxidation Catalysis: Design, Reactions and Characterization*, Wiley-VCH, Weinheim, (2009) 341 p.
[3] T. Mitsudome et al., *Angew. Chem*. 122 (2010) 5677.

ISO-OP10

Study of a New Process for the Synthesis of Adipic Acid: the Oxidative Cleavage of Trans-1,2-Cyclohexanediol

Solmi S.*, Rozhko E., Malmusi A., Lolli A., Albonetti S., Cavani F.

Alma Mater Studiorum – Università di Bologna, Dipartimento di Chimica Industriale "Toso Montanari", Bologna, Italy

* stefania.solmi2@unibo.it

Keywords: adipic acid, oxidative cleavage, supported, Ru, polyoxometalate, Au nanoparticles

1 Introduction

Adipic acid (AA) is an important chemical intermediate mainly used for the production of Nylon-6,6. All current industrial processes employ the final oxidation of either the KA Oil or of cyclohexanol with an excess of nitric acid and a homogeneous Cu/V based catalyst [1]. This procedure shows some drawbacks that imply relatively high costs in terms of energy consumption, materials and environmental protection.

This communication reports about the results of a study aimed at the development of a more sustainable catalytic process for AA synthesis, by means of a two-step transformation, in which cyclohexene is first transformed into *trans*-1,2-cyclohexanediol (CHD) with hydrogen peroxide [2], and the glycol is then oxidized with oxygen to AA [3]; more specifically, here we report about the second step, carried out using various heterogeneous and homogeneous catalysts.

2 Experimental

Catalytic tests were carried out in a semi-continuous glass autoclave reactor (100 ml) equipped with a vapor condenser. The substrate (0.5 g of CHD), the solvent (25 ml of H_2O), the catalyst and eventually a base or an acid, were loaded in the reactor. When the desired temperature was reached, the feed of oxygen was started (flow rate of 100 Nml/min, pressure 4 bar). At the end of the reaction, the catalyst was separated from reaction mixture and the pH was adjusted between 2 and 3. Quantitative analysis was done by means of HPLC.

3 Results and discussion

First we studied the reactivity of a $Ru(OH)_3/Al_2O_3$ (4.9 % wt) catalyst. Tests carried out at different pH showed that a strong basic pH is necessary in order to activate the hydroxyl groups of CHD; despite this, under these conditions support dissolution and metal leaching were negligible. After 5 hours, best results achieved were: CHD conversion 77 %, AA yield 3 %, Glutaric Acid (GA) yield 10 %, Succinic Acid (SA) yield 24 %, and 1-hydroxycyclopentanecarboxylic acid (HCPA) yield 19 %. The very low yield to AA was due to the concomitant occurrence of several side-reactions, as shown in Figure 1; the reaction scheme was determined by carrying out experiments at different reaction time and starting from the various possible intermediates, such as 1,2-cyclohexanedione (CHDO) and 2-hydroxycyclohexanone (HCHN). CHDO was found to be the key intermediate of the reaction, precursor for the formation of several by-products; this was due to the fact that CHD is oxidized directly to CHDO because the Ru^{n+} species coordinates both hydroxyl groups of CHD.

Tests with homogeneous $H_5PMo_{10}V_2O_{40}$ catalyst were conducted at pH 2; under these conditions, the reaction was very selective to AA, but the latter then reacted with the unconverted CHD generating the corresponding esters; therefore, we had to carry out an additional transesterification of the esters with methanol or hydrolysis to obtain the pure acid. Another drawback of the POM is that it is an homogeneous system difficult to recover from the

reaction mixture. In this case, the key intermediate compound was HCHN, and the reaction turned out to be very selective, because there was no formation of any of the by-products (HCPA, GA and SA) which formed under basic conditions with the Ru-based catalyst; however, after 6 hours, the yield of AA was 9.5 % only.

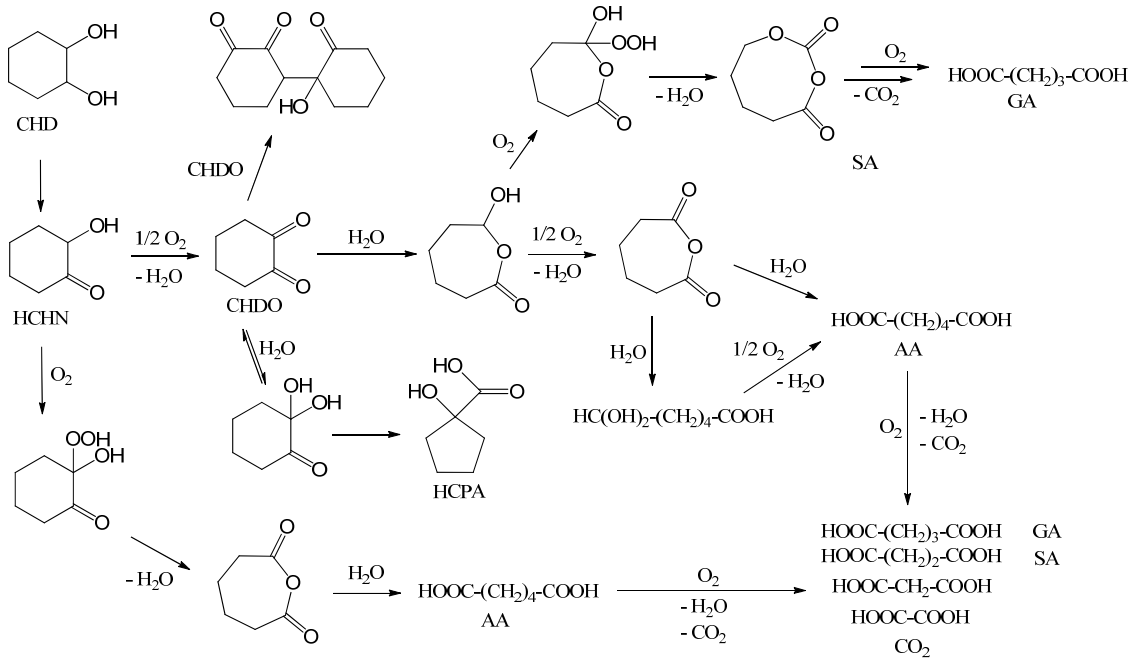

Fig. 1. Overall reaction scheme in CHD oxidation with Ru-based catalyst.

Finally, we studied the reactivity of Au nanoparticles supported on two different oxides: TiO_2 and MgO (in both cases containing 1.5 % wt Au). We tested the reactivity at different pH values, but with both catalysts a basic pH was anyway necessary in order to allow CHD oxidation; therefore, the basicity of MgO was not strong enough to activate the reactant. However, we obtained better AA yield (24 % with Au/TiO_2, 22 % with Au/MgO) and selectivity compared to Ru-based catalysts, while working with a less basic pH. In this case also, the key intermediate compound was HCHN and not CHDO, because of the ability of Au nanoparticles to coordinate only one hydroxyl group in CHD; this allowed to obtain better yield to AA than with the Ru-based catalyst.

4 Conclusions

With $Ru(OH)_3/Al_2O_3$ under the strongly basic conditions at which the catalyst was active, the reaction showed poor selectivity. Au-based catalysts were more selective to produce AA because the oxidation of CHD took place in less basic conditions than in the case of the supported Ru catalyst, and gave rise to the formation of HCHN as the key intermediate, which is oxidized into AA with good selectivity. P/Mo/V polyoxometalate catalyst was very selective in CHD oxidation, because there were no side reactions occurring under the acid pH at which the POM is active. However, an additional step of hydrolysis was necessary to obtain the pure product AA, and a precipitation was necessary to separate the catalyst.

References

[1] F. Cavani, S. Alini, in "Sustainable Industrial Chemistry", Wiley VCH, Wilheim, (2009) 367
[2] C. Antonetti, A.M. Raspolli Galletti, P. Accorinti, S. Alini, P. Babini, K. Raabova, E. Rozhko, A. Caldarelli, P. Righi, F. Cavani, P. Concepcion, Appl. Catal. A 466 (2013) 21.
[3] E. Rozhko, K. Raabova, F. Macchia, A. Malmusi, P. Righi, P. Accorinti, S. Alini, P. Babini, G. Cerrato, M. Manzoli, F. Cavani, ChemCatChem 5 (2013) 1998.

ISO-OP11

Influence of the Ionic Liquid Presence on the Selective Oxidation of Glucose over Molybdenum Based Catalysts

Sayago C.M.[1,2], Carrasco C.J.[1,2], Ivanova S.[1,2], Montilla Ramos F.J.[1,2], Galindo Del Pozo A.[1,2], Odriozola Gordón J.A.[1,2*]

1 - Instituto de Ciencia de Materiales de Sevilla, Universidad de Sevilla-CSIC, Seville, Spain
2 - Departamento de Química Inorgánica, Universidad de Sevilla, Sevilla, Spain

* odrio@us.es

Keywords: selective oxidation, glucose, molybdenum based catalysts, ionic liquids

1 Introduction

The biomass is an abundant carbon source and it is the only sustainable carbon source nowadays. Carbohydrates constitute 75% of the annual renewable biomass [1] with glucose as cellulose´s monomer the most abundant monosaccharide. Efficient conversion of cellulose and glucose to valuable compounds, as called platform chemicals, is of great importance and it is current topic of interest in Chemistry [2, 3].

Within the glucose platform chemicals, D-Gluconic acid is an important intermediate, which can be obtained by oxidation of glucose. It is widely used in food and pharmaceutical industries and it is usually produced by enzymatic oxidation of D-glucose with an annual market of about 100.000 tons per year [2]. However, the biochemical method has several drawbacks such as low space-time, slow reaction rate and difficulty in the separation of enzyme from product [4]. Replacing the enzymatic catalyst with efficient heterogeneous one seems the perfect solution and becomes a serious challenge in the recent years.

Generally, the selective oxidation of carbohydrates is difficult due to the multi-functionality of the molecules. In this way, glucose can be oxidized at anomeric position (C_1), at primary alcohol (C_6) or secondary alcohol (C_2-C_4) functions, resulting in distinct products. Therefore, the used catalysts have to be active and especially selective.

Recently, a group of compounds, the as called ionic liquids (ILs), shown a great potential in carbohydrate chemistry either as a catalyst or solvent. Many studies have reported the conversion of glucose into valuable compounds in ILs [4], however, the use of the ionic liquid as an integral part of the catalyst is scarcely studied.

In this context, the aim of this work is to study the influence of the IL on the catalytic performance of Mo based compounds, when used as solvent or as integral part of the catalyst in the selective liquid-phase oxidation of glucose by H_2O_2 under mild conditions.

2 Experimental

The catalysts used in this study are the oxodiperoxomolybdenum complex $[MoO(O_2)_2(H_2O)_n]$ dissolved in 1-butyl 3-methyl imidazolium hexafluorophosphate, [Bmim][PF_6], and 3 hybrids based on IL's cations (Emim, Bmim or Hexmim) and Keggin anion $PMo_{12}O_{40}^{3-}$.

Selective glucose oxidation was carried out in presence of catalyst in batch reactor in glucose:oxidant ratio 1:3 using as solvents distilled water and [Bmim][PF_6], respectively. When in aqueous solution appropriate amount of the heterogeneous hybrids (2.5 mol% of glucose) were added and, in the same way, the $[MoO(O_2)_2(H_2O)_n]$ complex was added to [Bmim][PF_6] solution. Both mixtures were heated under vigorous stirring till 60 °C during 18 hours. The samples were analysed by HPLC.

3 Results and discussion

The obtained results in terms of glucose conversion are presented in Fig. 1. The oxodiperoxomolybdenum complex exhibits higher conversion (53 %) in comparison to the heterogeneous [Bmim]-Mo catalyst (26 %) (Fig. 1. (a)), however, higher selectivity to gluconic acid is observed with the later catalyst (Table 1). When the IL part of the hybrid is modified the most active IL-Mo catalyst appears to be the [Emim]-Mo (Fig. 1. (b)) with 36 % of conversion followed by [Bmim]-Mo (26 %) and [Hexmim]-Mo (15 %). It seems that the activity of these catalysts strongly depends on IL component, with a smaller cation resulting in higher activity. The selectivity to gluconic acid follows the same trend, being [Emim]-Mo the most selective catalyst (79 %) followed by [Bmim]-Mo (28 %) and [Hexmim]-Mo (14 %).

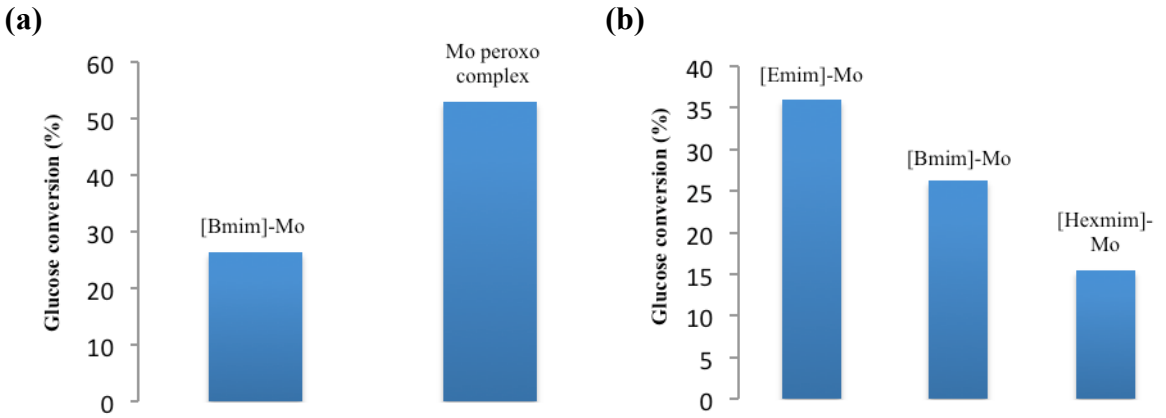

Fig. 1. Glucose conversion (%): (a) IL as part of the catalyst vs. IL as solvent, (b) Influence of different ILs as part of the same Mo based catalyst

Table 1. Product distribution (mol%) obtained for glucose conversion over molybdenum based catalysts.

Catalyst	Product distribution (mol%)				
	Glucaric acid	Glucuronic acid	Gluconic acid	Lactic acid	Formic acid
[Emim]-Mo	3	0	79	18	0
[Bmim]-Mo	6	46	28	20	0
[Hexmim]-Mo	0	17	14	22	47
Mo peroxo complex	1	37	9	15	38

4 Conclusions

The influence of ionic liquid presence on the selective oxidation of glucose over molybdenum based catalysts is studied. The ionic liquid is used either as solvent or as a part of hybrid material. Higher selectivity to gluconic acid is obtained when IL takes part of the molybdenum catalyst. The use of different ILs change the catalysts behaviour, smaller the IL component higher the activity and selectivity.

Acknowledgements

The authors acknowledge the Junta de Andalucía (Proyecto de Excelencia FQM-7079).

References

[1] A. Corma, S. Iborra, A. Velty, *Chem. Rev.* 107 (2007) 2411
[2] M. J. Climent, A. Corma, S. Iborra, *Green Chem.* 13 (2011) 520
[3] J. Song, H. Fan, J. Ma, B. Han, *Green Chem.* 15 (2013) 2619
[4] M. Chidambaram, A. T. Bell**,** *Green Chem.* 12 (2010) 1253

ISO-OP12

Morphology-Dependent Nanocatalysts: Rod-Shaped Metal Oxides

Li Y., Shen W.*

Dalian Institute of Physcial Chemistry, Chinese Academy of Sciences, Dalian, China

* shen98@dicp.ac.cn

Keywords: morphology-dependent nanocatalysis, metal oxides, nanorods, crystal facet, metal-oxide interface, metal-support interaction

1 Introduction

Nanostructured metal oxides are widely used in heterogeneous catalysis where their catalytic properties are closely associated with their size, morphology, and crystal phase at nanometer level [1]. The effect of particle size has been documented in the past two decades, but the morphology of the oxide nanoparticles has rarely been concerned. We illustrate that the redox and acidic-basic properties of metal oxides largely depend on their morphologies by taking Co_3O_4, Fe_2O_3, CeO_2, TiO_2 and La_2O_3 nanorods as typical examples. The catalytic activities of these rod-shaped oxides are mainly governed by the nature of the exposed crystal planes. Moreover, the exposed planes of these rod-shaped oxides mediated the manner and strength of metal-support interaction in the integrated metal-oxide catalysts.

2 Experimental

All the rod-shaped oxides were prepared by a hydrothermal method with the aid of proper surfactants. Loading of metal (copper and gold) particles on the oxides was done using a deposition-precipitation method. Structural analysis was conducted by Raman spectroscopy, XPS, NMR, XRD and TEM techniques. Catalytic reaction was conducted with a continuous-flow fixed-bed quartz reactor.

3 Results and discussion

Spherical Co_3O_4 nanoparticles have a size of ~10 nm and are mainly constructed by truncated octahedron, which are surrounded by the {111} and {001} planes. Co_3O_4 nanorods have a diameter of 5-10 nm and a length of 100-300 nm, and preferentially exposes the (110) planes [2]. When being used to catalyze CO oxidation, the Co_3O_4 nanoparticles showed marginal CO conversion and rapidly deactivated. But the Co_3O_4 nanorods showed 100% CO conversion during the initial 6 h, and the CO conversion only slowly decreased to 80% after reaction for 12 h at -77 °C. The reaction rate of CO oxidation over the Co_3O_4 nanorods was 3.91×10^{-6} mol CO/g.s, which was one order of magnitude larger than that over the nanoparticles. Kinetic studies confirmed that the preexponential factor of the nanorods is almost one order larger than that on the nanoparticles, suggesting the large presence of active sites. The {110} planes on the Co_3O_4 nanorods are rich in active Co^{3+} species that are responsible for the much higher activity in CO oxidation.

The crystal–phase effect of Fe_2O_3 nanorods in selective reduction of NO with CO or NH_3 was further examined [3]. For the reduction of NO by CO, the reaction readily started at 175 °C on the γ–Fe_2O_3 nanorods whereas it occurred at 325 °C over the α–Fe_2O_3 nanorods. At 500 °C, the conversion of NO approached 95% on the γ–Fe_2O_3 nanorods but it was only 40% on the α–Fe_2O_3 nanorods. In ammonia SCR, the γ–Fe_2O_3 nanorods showed 80% NO conversion in a temperature range of 200–400 °C with N_2 selectivity of about 98%. On the α–Fe_2O_3 nanorods, however, the temperature window for 80% NO conversion has shifted to 330–450 °C. These

outstanding properties of the γ–Fe_2O_3 nanorods are intimately associated with the exposed (110) and (001) planes. The simultaneous exposure of iron and oxygen ions on these facets have significantly enhanced the adsorption and activation of NO and NH_3 and thereby promoted the overall reaction efficiency.

The exposed surface planes of the rod-shaped oxides also mediated the manner and strength of metal-support interaction. Supported Au nanoparticles often show distinctively high activity at the initial stage of the reaction but suffer from a rapid deactivation caused by the easy sintering of gold nanoparticles. Rod-shaped ceria has the potential to stabilize gold nanoparticles of about 3nm at elevated temperatures and under reactive atmosphere [4]. The Au/ceria-rod catalyst was highly active and stable for CO oxidation at room temperature and the conversion of CO maintained at 75-90% for 100 hours. Kinetic studies revealed that the turnover frequency (2.7×10^{-2} s^{-1}) of surface gold atoms in the Au/ceria-rod catalyst was 1.5 times greater than the gold particles supported on conventional ceria (1.8×10^{-2} s^{-1}). That is, ceria nanorods not only enhanced the activity but also stabilized the Au particles during CO oxidation through the strong chemical bonding of gold onto the rod-shaped ceria. In addition, La_2O_3 nanorods greatly promoted the activity of copper nanoparticles in alcohol dehydrogenation [5]. The La_2O_3 nanorods exposed about 40% (110) plane that was terminated by La^{3+}-O^{2-} pairs acting as the basic sites. Cu particles of about 4.5 nm were preferentially anchored on the (110) surface, showing a crystal-facet selective deposition pattern. The basic sites on the (110) facet of the La_2O_3 nanorods activated alcohol while the neighboring Cu nanoparticles efficiently transferred hydrogen atoms.[4] Moreover, the shape effect of other metal oxides in the activation and conversion of small molecules like CO, CH_3OH, H_2, and O_2 are also discussed in the presentation.

4 Conclusions

The correlation between the catalytic properties and the exposed facets verified the chemical nature of the morphology effect. Moreover, the interaction between the rod-shaped oxides and the metal nanoparticles in metal-oxide catalyst systems showed a crystal facet-selective deposition pattern and the interaction on different crystal facets of the oxide supports varied significantly.

References

[1] Y. Li, W.Shen, Chem. Soc. Rev. **2014**, *43*, 1543-1574.
[2] X. Xie, Y. Li, Z.-Q. Liu, M. Haruta, W. Shen, Nature **2009**, *458*, 746-749.
[3] X. L. Mou, B. S. Zhang, Y. Li, L. D. Yao, X. J. Wei, D. S. Su, W. Shen, Angew. Chem. Int. Ed. **2012**, *51*, 2989-2903.
[4] N. Ta, J. Y. Liu, S. Chenna, P. A. Crozier, Y. Li, A. Chen, W. Shen, J. Am. Chem. Soc. **2012**, *134*, 20585-20588.
[5] F. Wang, R. Shi, Z.-Q.Liu, P. J. Shang, X. Pang, S. Shen, Z. Feng, C. Li, W. Shen, ACS Catal. **2013**, *3*, 890-894.

ISO-OP13

On the Mechanisms of Selective Bioinspired Oxidations Catalyzed by Aminopyridine Manganese Complexes

Talsi E.P.[1,2], Ottenbacher R.V.[1,2*], Bryliakov K.P.[1,2]

1 - Novosibirsk State University, Novosibirsk, Russia
2 - Boreskov Institute of Catalysis SB RAS, Novosibirsk, Russia

* ottenbacher@catalysis.ru

Keywords: C-H hydroxylation, asymmetric epoxidation, manganese, hydrogen peroxide, biomimetic

1 Introduction

The catalytic systems for selective and sustainable oxidative functionalization of hydrocarbons are of great demand, albeit natural oxygenases mediate such processes smoothly at mild conditions. In recent decades there have been huge efforts put on creating the synthetic biomimetic catalysts that could model the structures and functions of natural metalloenzymes, mainly focusing on iron-based systems. Manganese(II) complexes with chiral aminopyridine ligands turned out to be competitive counterparts of those iron catalysts in terms of activity and (stereo)-selectivity. However, the mechanisms of manganese-catalyzed selective oxidations, such as C-H hydroxylation and asymmetric epoxidation, still lack experimental evidence. Herein, we report the experimental insight into the mechanisms of regioselective and stereospecific C-H hydroxylations and enantioselective epoxidations with H_2O_2, catalyzed by aminopyridine manganese complexes.

2 Experimental/methodology

Chiral aminopyridine ligands and corresponding manganese complexes were synthesized as described [1]. ^{1}H NMR spectra were recorded on a Bruker AVANCE 400 or DPX-250 NMR spectrometer at 400.13 or 250.13 MHz. Enantiomeric excesses (*ee*) were measured on a Shimadzu LC-20 chromatograph equipped with a set of chiral columns. The incorporation of ^{18}O into the products of oxidation and the corresponding yields were determined using Agilent 7000B GC/MS with Triple Quad detector, chromatograph Agilent 7890 equipped with a capillary column "HP-5ms". $H_2{}^{18}O$ (97 atom % ^{18}O) was purchased form Sigma-Aldrich.

3 Results and discussion

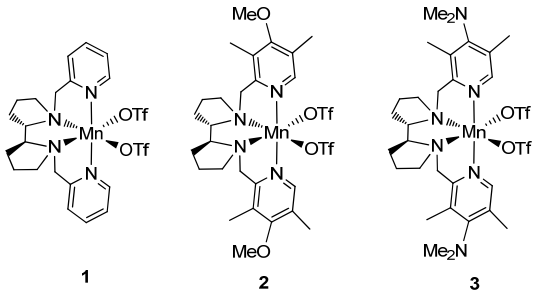

Fig. 1. Aminopyridine manganese complexes

Recently we proposed (on the basis of asymmetric epoxidations in the presence of different sterically hindered carboxylic acids) that the active oxidizing agent in the systems **1**/H_2O_2/RCOOH are complexes $[(\mathbf{L})Mn^{V}{=}O(OC(O)R)]^{2+}$ [2]. Additional evidence in favour of involvement of manganese-oxo species could be obtained in isotopic (^{18}O) labelling studies using $H_2{}^{18}O$. However, epoxidation of styrene by the system **Mn**/H_2O_2/AcOH in the presence of

large excess of $H_2{}^{18}O$ (1000 eq. *vs.* **Mn**) showed zero incorporation of labelled oxygen into the product. On the other hand, in the absence of carboxylic acid, the same system yielded a 35 % ^{18}O-enriched styrene epoxide, with mono-labelled styrene diol as by-product (87 % of ^{18}O), indicating a so-called "water-assisted" oxidation pathway (fig. 2). Active oxidizing species implied by this mechanism are *cis*-HO-Mn^V=O complexes. Adding large excess of carboxylic acid suppresses binding labeled water to Mn centre, thus accounting for the absence of ^{18}O-labeled epoxide. To disclose the nature of active Mn^V=O species, Hammett analysis was attempted (using *p*-substituted chalcones and **1** as catalyst). The active species was found to be electrophilic; good linear correlation between the log (k_X/k_H) and σ^+_p (ρ^+= -1.5, indicates an electron-demanding transition state) was obsereved. Furthermore, the log ((100+*ee*)/(100-*ee*)) was also highly linear versus σ^+_p of the substituents, the epoxides of more easily oxidizing substrates displaying lower *ee*s. Thus, the overall epoxidation rate is limited by an electron transfer to the oxometal species, to form an acyclic carbocationic intermediate [1].

Selective C-H hydroxylations of adamantane and *cis*-1,2-dimethylcyclohexane (DMCH) by the systems **2(3)**/H_2O_2/$H_2{}^{18}O$ also resulted in incorporation of ^{18}O into the corresponding tertiary alcohols (27 % and 18 % for adamantane and 18 % and 7 % for DMCH respectively), providing evidence in favour of "water-assisted" mechanism involving manganese(V)-oxo species (fig. 2). Competitive benzylic oxidations of *p*-substituted cumenes revealed a highly linear Hammett correlation vs. σ_p^+ (ρ^+= -1.0, indicates an electron-demanding transition state). The ρ^+ value is typical for a hydrogen-atom transfer mechanism, with formation of an electron-deficient radical intermediate. Primary *KIE* in the oxidation of cumene/α-D-cumene for complexes **1**-**3** was 3.8-3.9, the *KIE* values for the oxidation of cyclohexane/d_{12}-cyclohexane falling in the range 3.8-4.1 that, which is evidence for an H-atom abstraction mechanism. The H-abstraction results in formation of carbon-centered radicals (which was confirmed by partial erosion of *cis*-configuration in the oxidation of DMCH catalyzed by **3**: *RC* > 99 % at 0°C, = 97.1 % at +20°C and = 94.3 % at +30°C).

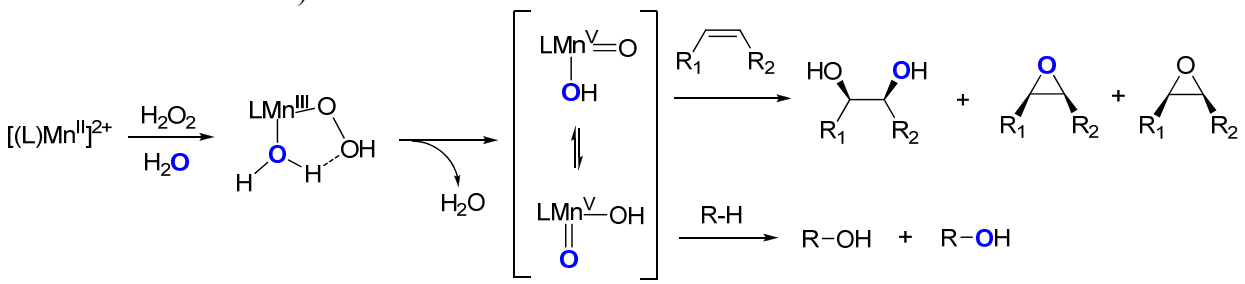

Fig. 2. Proposed 'water-assisted' oxidation mechanism for Mn catalyzed oxidations with H_2O_2. ^{18}O represented in blue.

4 Conclusions

In conclusion, insights into the mechanisms of (1) selective epoxidations and (2) C-H oxidations mediated by aminopyridine manganese complexes have been achieved on the basis of kinetic and isotopic labelling studies. The data obtained bear evidence in favour of the key role of Mn^V-oxo species, the most likely catalytically active sites of both processes.

Acknowledgements

Financial support from the Russian Foundation for Basic Research (grant 14-03-00102) is gratefully acknowledged.

References

[1] R. Ottenbacher, D. Samsonenko, E. Talsi, K. Bryliakov, *ACS Catalysis*. 4 (2014) 1599-1606.
[2] O. Lyakin, R. Ottenbacher, K. Bryliakov, E. Talsi, *ACS Catalysis*. 2 (2012) 1196-1202.

ISO-OP14

Catalytic Upgrading of Furfural by Oxidative Methylation over Au NPs-Based Catalysts

Papanikolaou G.*, Ampelli C., Genovese C., Perathoner S., Centi G.

University of Messina, Dep. of Electronic Engineering, Industrial Chemistry and Engineering, Messina, Italy

* gpapanikolaou@unime.it

Keywords: furfural, selective oxidation, Au nanoparticles (NPs)

1 Introduction

In the last years, the climate changes, the negative effects of the oil prices on the global economy and the depletion of the oil resources, have focused the attention to the development of new methodologies for biomass conversion into compounds with higher added value, to be used in the industry of fuels and fine chemicals. In this context, upgrading and valorization of C5 fraction coming from lignocellulosic wastes for the synthesis of important platform molecules, is of key relevance to diminish the dependence on fossil fuel sources [1]. By the oxidative esterification reaction of furfural, it is possible to produce methyl 2-furoate (2-MF), a compound that may widely be used in the field of flavourings and fragrances. The exceptional catalytic properties of Au nanoparticles (NPs) dispersed on metal-oxide based supports, has allowed to find a new and eco-friendly synthetic route for the oxidative esterification [2].

In this contribution, we report on a sustainable approach to produce 2-MF from furfural, by selective oxidative esterification with methanol using size-controlled Au NPs-based catalysts. Cerium dioxide (CeO_2) and zirconium dioxide (ZrO_2) were used as metal oxide supports and synthesized via chemical precipitation method. Gold nanoparticles were deposited onto the metal oxide support by two different techniques: i) deposition-precipitation and ii) photo-deposition. All the catalysts with Au deposited by precipitation were finally treated in air at different temperatures (200 and 400 °C). The main purpose was to optimize the methodology of synthesis of the Au NPs-based catalysts and identify a method to modulate size and dispersion of the Au NPs, in order to obtain high catalytic performances.

2 Experimental

CeO_2 and ZrO_2 were prepared by *chemical precipitation method*. Briefly, $Ce(NO_3)_3 \cdot 6H_2O$ (or $ZrOCl_2 \cdot 8H_2O$) was dissolved in distilled water and the pH was adjusted to about 8-9. Then, the precipitate was collected from the solution by centrifugation, dried and finally calcined at 300 °C (650 °C for ZrO_2). On each support, 1 wt. % Au was added by deposition-precipitation or photo-deposition techniques.

The as-prepared catalysts were fully characterized by AAS, UV-Visible Diffuse Reflectance Spectroscopy, XRD, and TEM analyses. Finally, they were tested in the process of oxidative methylation of furfural by using a modified lab-scale commercial autoclave reactor (Parr Instrument Company) at 120 °C and 6 bar O_2. The detection of the reaction products was performed by GC-FID and GC-MS analysis.

3 Results and discussion

The reaction mechanism for the furfural oxidative esterification with methanol can follow different schemes, passing through the formation of a hemiacetal intermediate. Subsequently, the hemiacetal can be oxidized directly into 2-MF, or can be converted into the corresponding 2-furaldehyde-dimethyl-acetal and then to 2-MF.

Analysis by TEM of the Au NPs-based catalysts was carried out in order to determine a correlation between structural properties and catalytic activity. Figure 1 shows some HRTEM images referred to Au/ZrO_2 with Au deposited by deposition-precipitation and treated at 400 °C. It can be observed that well dispersed and small Au NPs are present over the ZrO_2 surface (particle diameter below 5 nm).

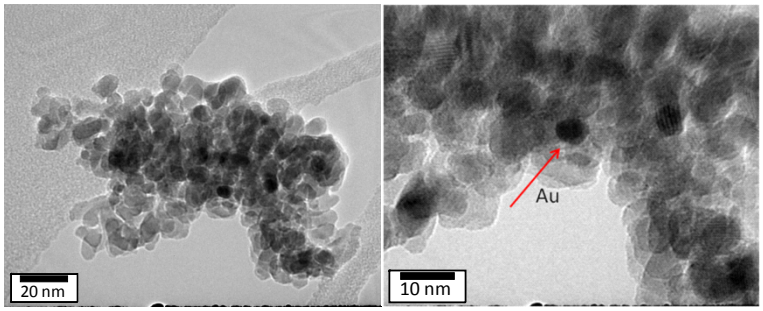

Fig. 1. HRTEM images of Au/ZrO_2 (Au reduced at 400 °C)

Table 1 reports the conversion and 2-MF selectivity values (after 6 h of reaction) for the most representative tested Au-NPs-based catalysts. Results obtained with Au/CeO_2 showed high conversion but low selectivity to 2-MF, except for the catalyst with Au deposited by photo-deposition which gave also high selectivity. On the contrary, Au/ZrO_2 catalyst with Au deposited by deposition-precipitation method and treated at 400 °C, allowed to obtain very high conversion (99%) and 2-MF selectivity (100%). Morphological characterization data of the most active catalysts suggest that having small and well dispersed Au NPs onto the metal oxide support is the key to enhance the catalytic performances, favouring the oxidation of the hemiacetal into ester, rather than the reoxidation of the acetal into the ester.

Table 1. Catalytic performances in the furfural oxidative esterification reaction.

Sample	T (°C)	Conversion (%)	2-MF selectivity (%)
Au/CeO_2[a]	200	88	8
Au/CeO_2[a]	400	81	10
Au/CeO_2[b]	-	84	82
Au/ZrO_2[a]	200	63	10
Au/ZrO_2[a]	400	99	100
Au/ZrO_2[b]	-	57	90

[a] Au loading by deposition-precipitation
[b] Au loading by photo-deposition

Conclusions

Gold NPs-CeO_2(ZrO_2)-based catalysts resulted very active in the catalytic oxidative esterification of furfural with methanol, opening new perspectives in the sustainable production of fine chemicals (perfumes and flavouring agents).

Acknowledgements

This work was realized in the frame of the European Project ECO^2CO_2 (Eco-friendly biorefinery fine chemicals from CO_2 photo-catalytic reduction).

References

[1] E.Taarning, I.S. Nielsen, K. Egeblad, R. Madsen, C.H. Christensen, *ChemSusChem.* 1 (2008) 75.
[2] A. Stephen, K. Hashmi, G.J. Hutchings, *Angew. Chem. Int. Ed.* 45 (2006) 7896.

ISO-OP15

Selective Oxidation of 5-HMF to 2,3-Diformylfuran on Intercalated VPO Catalysts

Grasset F.[1], Katryniok B.[1,2], Paul S.[1,2*], Pera-Titus M.[3], Clacens J-M.[3], Decampo F.[3], Dumeignil F.[1,4,5]

1 - Unité de Catalyse et de Chimie du Solide, UCCS, UMR CNRS 8181, Villeneuve d'Ascq, France
2 - Ecole Centrale de Lille, ECLille, Villeneuve d'Ascq, France
3 - Eco-Efficient Products and Processes Laboratory, Shanghai, China
4 - Institut Universitaire de France, IUF, Maison des Universités, Paris, France
5 - Université de Lille, Villeneuve d'Ascq, France

* sebastien.paul@ec-lille.fr

Keywords: intercalated VPOs, selective oxidation, 5-HMF

1 Introduction

5-Hydroxymethylfurfural (5-HMF) is one of the key bio-based platform chemicals identified by the U.S. Department of Energy. [1] Its structure contains a hydroxyl and an aldehyde moieties together with a furan ring, allowing many chemical reaction variations. However, this rich chemistry also makes 5-HMF suffer from poor stability. [2,3] In contrast, 2,5-diformylfuran (DFF) produced by oxidation of the hydroxymethyl group of 5-HMF (Fig. 1) proved to be stable under its crystalline form. [3] Interestingly, DFF can be used either as a monomer, or as a starting material for the synthesis of ligands, drugs, and antifungal agents. Vanadium-based catalysts have been proposed for the oxidation of 5-HMF into DFF. The use of V_2O_5 supported on TiO_2 increases the yield to DFF up to 97% at 110 °C in toluene after 1.5 h of reaction under air (P = 16 bar) [4]. Carlini et al. [5] found that $VOPO_4{\cdot}2H_2O$ could oxidize 5-HMF in MIBK, giving 50% selectivity at 98% of 5-HMF conversion under oxygen (P = 1 bar) at 80 °C after 6 h. Here, we report encouraging results on long alkyl chain trimethylammonium intercalated vanadium phosphorus oxides (I-VPO) for the efficient selective oxidation of 5-HMF to DFF under relatively mild conditions using conventional and green solvents. Mechanistic aspects of the reaction are also explored.

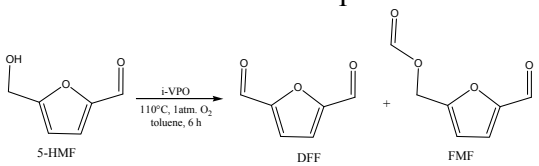

Fig. 1. Oxidation of 5-HMF to DFF

2 Experimental

$VOPO_4{\cdot}2H_2O$ was prepared by refluxing V_2O_5 (11.8 g) and H_3PO_4 (85%, 104.6 g) in water (275 mL) for 16 h. The resulting solid was isolated by filtration, washed with acetone, and dried under static air at room temperature (RT) for 2 days. $VOHPO_4{\cdot}0.5H_2O$ was prepared by refluxing V_2O_5 (11.8 g) and H_3PO_4 (85%, 16.5 g) in 2-butanol (250 mL) for 16 h. The resulting solid was recovered by filtration, washed with acetone, and dried under static air at RT for 2 days. The intercalated compounds (I-VPOs) were synthesized by adding $VOPO_4{\cdot}2H_2O$ or $VOHPO_4{\cdot}0.5H_2O$ (1 eq.) to an aqueous solution (30 mL) of CnTAB (1 eq.) at RT. The pH was adjusted to 7.5 using concentrated NH_4OH before the mixture was heated to 75 °C for 48 h. The resulting solids were recovered by filtration, washed with water, and dried under static air (50 °C, 2 days). The intercalated samples were labeled $C_nVO(H)PO_4$, where n indicates the length of the alkyl chain. The 5-HMF oxidation tests were performed in 30 mL glass tubes

equipped with a reflux condenser. The catalyst (30 mg) was introduced into the reaction tube and 3 consecutive vacuum/O_2 cycles were performed. A solution of 5-HMF (0.1 M, 3 mL) was added and the mixture was heated to the desired temperature under oxygen at 800 rpm stirring. After the test, the tube was cooled down to RT and the clear solution was recovered by syringe filtration. The analysis of the recovered solution was performed on a Varian CP 3800 – Saturn 2000 GC-MS equipped with a CP Wax 58 (FFAP) CB capillary column.

3 Results and discussion

Oxidation of 5-HMF over $VOPO_4 \cdot 2H_2O$ and $VOHPO_4 \cdot 0.5H_2O$ gave a high conversion of 5-HMF but yielded many by-products resulting in a poor selectivity to DFF (< 10%). Only aromatic solvents offered good DFF selectivity (> 63%) at full conversion. In contrast, the use of oxygenated solvents resulted in the formation of large amounts of degradation products originating either from 5-HMF or from the solvent itself. In contrast, the use of I-VPOs in toluene resulted in an increase of 5-HMF conversion as well as in the selectivity to DFF (82-83%) with a weak impact of the alkyl chain length (Table 1). The results were found independent of the initial vanadium oxidation state (V^{5+} for $VOPO_4 \cdot 2H_2O$ and $C_{14}VOPO_4$; V^{4+} for $VOHPO_4 \cdot 0.5H_2O$ and $C_{14}VOHPO_4$), which evidences that both oxidation states are involved during the catalysis supposedly via a Mars-Van Krevelen mechanism.

The only observed by-product in these cases was FMF (Fig. 1), which presumably forms via a homogeneous reaction pathway of 5-HMF involving radical intermediates (most likely on the hydroxymethyl group of 5-HMF) generated from the interaction of 5-HMF and C_nVOPO_4. In addition, this radical intermediate might also react with toluene to generate benzyl free radicals leading to benzyl alcohol and benzaldehyde upon reaction with oxygen. The fact that oxidation of 5-HMF performed in an oxygenated solvent such as MIBK gave poor selectivity to DFF can be then attributed to the weak stability of the solvent toward oxidative conditions and presence of free radicals.

Table 1. Performances of the intercalated VPOs in the catalytic oxidation of 5-HMF

Entry	Catalyst	5-HMF Conversion (%)	DFF Selectivity (%)
1	$C_{10}VOPO_4$	85	76
2	$C_{12}VOPO_4$	90	82
3	$C_{14}VOPO_4$	91	87
4	$C_{14}OHVOPO_4$	90	82
5	$C_{16}VOPO_4$	90	84
[HMF] = 0.1 M, toluene = 3mL, catalyst = 15 mg, time = 6 h, oxygen = 1 atm.			

4 Conclusions

Intercalation of alkyl trimethylammonium chains in $VOPO_4 \cdot 2H_2O$ generated heterogeneous catalysts that selectively oxidize 5-HMF to DFF with high yields using molecular oxygen at 110°C in toluene. In contrast, oxygenated or polar solvents favor 5-HMF degradation pathways. The formation of FMF was ascribed to a radical mechanism involving 5-HMF decomposition in solution, whereas the formation of DFF proceeded at the surface of the catalyst.

References

[1] A. Corma, S. Iborra, A. Velty, Chem. Rev. 107 (2007) 2411.
[2] T. Welpy, G. Petersen, http://www1.eere.energy.gov/biomass/pdfs/35523.pdf.
[3] A. Gandini, M.N. Belgacem, Prog. Polym. Sci. 22 (1997) 1203.
[4] G. Durand, P. Faugeras, F. Laporte, C. Moreau, M-C. Neau, G. Roux et al., WO9617836, 1995.
[5] C. Carlini, P. Patrono, A/M.R. Galletti, G. Sbrana, V. Zima, Appl. Catal. A: Gen. 289 (2005) 197.

ISO-OP16

Oxidation of 5-Hydroxymethyl Furfural to 2,5-Diformylfuran in Aqueous Media over Heterogeneous Manganese Based Materials

Neatu F.[1], Petrea N.[2], Petre R.[2], Sonu M.[2], Somoghi V.[3], Florea M.[1], Parvulescu V.I.[1*]

1 - University of Bucharest, Department of Organic Chemistry, Biochemistry and Catalysis, Bucharest, Romania

2 - Scientific Research Centre for CBRN Defense and Ecology, Bucharest, Romania

3 - SC Stimpex SA, Bucharest, Romania

* vasile.parvulescu@g.unibuc.ro

Keywords: HMF, DFF, heterogeneous catalysis, oxidation

1 Introduction

5-Hydroxymethyl-2-furfural (HMF) represents an important, versatile and available primary renewable platform molecule that is structurally found into numerous pharmaceuticals, antifungal agents, as well as polymers. 2,5-Diformylfuran (DFF) is one of the oxidation products of HMF which can be used as monomer for the production of fluorescent materials[1] or as a starting compound for the synthesis of drugs, antifungal agents or ligands[2]. Oxidation of HMF can lead to various other products (Scheme 1) and thus the selectivity to DFF remains an issue to be overcome under mild conditions. Recent reports revealed the use of stoichiometric oxidants generating toxic wastes[3], while the reported heterogeneous catalytic systems are active only in harsh reaction conditions[4]. Considerable efforts have been made to find versatile heterogeneous catalysts for the synthesis of DFF, but without a real progress. Herein, we report a manganese-copper catalyst able to perform the oxidation of HMF to DFF under mild aqueous conditions.

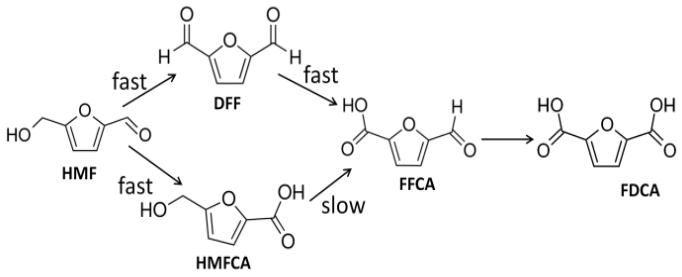

Scheme 1. Reaction pathways in oxidation of HMF (DFF : 2-diformyl furan; FFCA: 5-formyl-2-furancarboxylic acid; HMFCA: 5-hydroxymethyl-2-furancarboxylic acid).

2 Experimental/methodology

Catalysts synthesis

The Cu-/Mn-based catalysts were prepared by simultaneously adding dropwise two aqueous solutions into a flask under vigorous stirring at room temperature, while maintaining pH of 10: one containing copper nitrate (0.015 M), manganese nitrate (1.1 M) and aluminum nitrate (0.3 M) in deionized water (180 mL) and the second containing sodium hydroxide (2.5 M) and sodium carbonate (1 M) in deionized water (180 mL). The slurry was aged for 18 h at 75 °C. The final precipitate was filtered, thoroughly washed until pH 7 and dried overnight at 100 °C in an oven. The same procedure was used for the synthesis of catalysts containing only the

individual metals (Cu or Mn). For a better comparison, all the catalysts were used (i) as prepared, (ii) calcinated, and (iii) in the rehydrated form. In the last case, the samples were first calcined and then hydrated with bidistillated water at room temperature for 24h. The slurry was then dried overnight at 100 °C in air atmosphere.

Catalysts characterization

The prepared catalysts have been investigated using different characterization techniques like powder X-ray diffraction, DRIFT, and textural analysis. The XRD patterns were collected in the range 2θ from 5 to 80° in steps of 0.02° 2θ/s (Shimadzu 7000). DRIFT spectroscopy was used for the characterization of the heterogeneous catalysts and for the evaluation of their stability (Thermo Electron Corporation Nicolet 4700, with in-situ capabilities). The textural measurements using isothermal adsorbtion-desorbtion at N_2 liquid temperature and multi-point method were performed on a Micromeritic ASAP 2010 sorption analyzer.

Catalytic reactions

Catalytic experiments were performed under vigorous stirring in a stainless steel autoclave at temperature of 90 °C, 1 mmol of substrate (HMF), 10 mL of MiliQ water, 0.05 g of catalyst. The products were analyzed by high-performance liquid chromatography (HPLC).

3 Results and discussions

Synthesis of DFF from HMF was performed under various conditions. The effect of amount of catalyst, pressure of oxygen, reaction temperature and reaction time were studied. Also, materials containing only Mn or Cu have been tested for comparison. The best results are presented in Table 1. Higher amount of catalysts and oxygen pressures resulted in a higher conversion and selectivity to DFF, due to an increase in the availability and number of catalytic active sites and higher oxygen concentration in the reaction mixture, respectively. Contrarily, increasing the reaction temperature over 90 °C and the reaction time resulted in a decrease of selectivity in DFF. A higher temperature or reaction time favoured the formation of an advanced oxidation product like 5-formyl-2-furandicarboxilic acid (FFCA).

Table 1. Oxidation of HMF in different conditions.

No.	Catalyst	P_{O_2} (bar)	Temp (°C)	Conversion (%)	S_{DFF} (%)
1.	Mn-Cu dried	8	90	80	74
2.	Mn-Cu calcinated	8	90	90	87
3.	Mn-Cu calcinated	8	60	68	80
4.	Mn-Cu calcinated	4	90	54	60

Reaction conditions: 1 mmol 5-HMF, 10 mL water, 50 mg catalyst, Teflon-lined autoclave, 4- 8 bar, 60-90 °C, 24h.

4 Conclusions

In conclusion, this study proved that mixed manganese-copper oxide is a highly effective heterogeneous catalyst for the selective oxidation of HMF to DFF in the presence of molecular oxygen in water.

Acknowledgements

This work was supported by a grant of the Romanian National Authority for Scientific Research, CNDI–UEFISCDI, project number PCCA-II-166/2012.

References

[1] J. Ma, Z. Du, J. Xu, Q. Chu, Y. Pang, *Chemsuschem*. 4 (2011) 51-54.
[2] A. Gandini, *Green Chemistry*. 13 (2011) 1061-1083.
[3] M.O. Kornpanets, O.V. Kushch, Y.E. Litvinov, O.L. Pliekhov, K.V. Novikova, A.O. Novokhatko, A.N. Shendrik, A.V. Vasilyev, I.O. Opeida, *Catalysis Communications*. 57 (2014) 60-63.
[4] G.D. Yadav, R.V. Sharma, *Applied Catalysis B-Environmental*. 147 (2014) 293-301.

ISO-OP17

Key Parameters Controlling Selectivity and Conversion in OCM: from Experiments and Modelling, towards an Optimised Reactor Design

Serres T.[1], Alexiadis V.[2], Schuurman Y.[1], Thybaut J.W.[2], Mirodatos C.[1*]

1 - Institut de Recherches sur la Catalyse et l'Environnement de Lyon, Université Lyon 1, CNRS, Villeurbanne, France

2 - Ghent University, Laboratory for Chemical Technology, Ghent, Belgium

* Claude.Mirodatos@ircelyon.univ-lyon1.fr

Keywords: OCM, V/S, micro-kinetic, modeling, reactor design

1 Introduction

Despite decades of intense research on oxidative coupling of methane (OCM) catalysts, the yields in ethane and ethylene remain below ca 25%, which drives the research towards innovative engineering solutions. Thus, an integrated reactor-heat exchanger was proposed to combine the exothermic OCM with the endothermic reforming, where the unreacted methane and the non-selective coupling products (water and carbon dioxide) collected at the OCM compartment outlet are recycled and reformed into syngas through the reforming compartment [1]. These strategies imply a careful control of the catalytic/kinetic descriptors such as the ratio active catalyst surface to reactor volume. The latter was shown from micro kinetic modeling to monitor the distribution of radicals in the catalytic zone (inside and outside porous volume) as a strategic parameter for favoring the gas phase coupling rather than the surface full oxidation [2]. The present work focuses on the effect of this Volume-to-Surface (V/S) ratio on the catalytic performance (activity, C_2 selectivity and ethylene-to-ethane ratio) of two Sr-La/CaO (LSC) and Mn/Na/$WSiO_2$ (MNW) OCM catalysts.

2 Experimental/methodology

Figure 1 reports a scheme of the volume-to-surface ratio considered in this work.

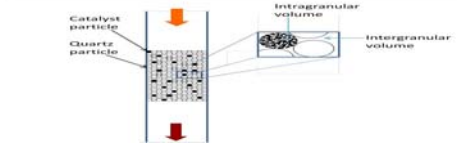

Fig. 1: Scheme of the volume-on-surface measurement for the fixed-bed reactor

All the experimental data obtained by varying the V/S ratio in a wide range are compared with model calculated ones. The latter are based on a comprehensive OCM microkinetic that specifically accounts for the V/S ratio via the corresponding catalyst and reactor descriptors.

3 Results and discussion

Figure 2 illustrates the similar trends observed for the changes in activity and C_2 selectivity vs V/S in the experimental as well as in the calculated data.

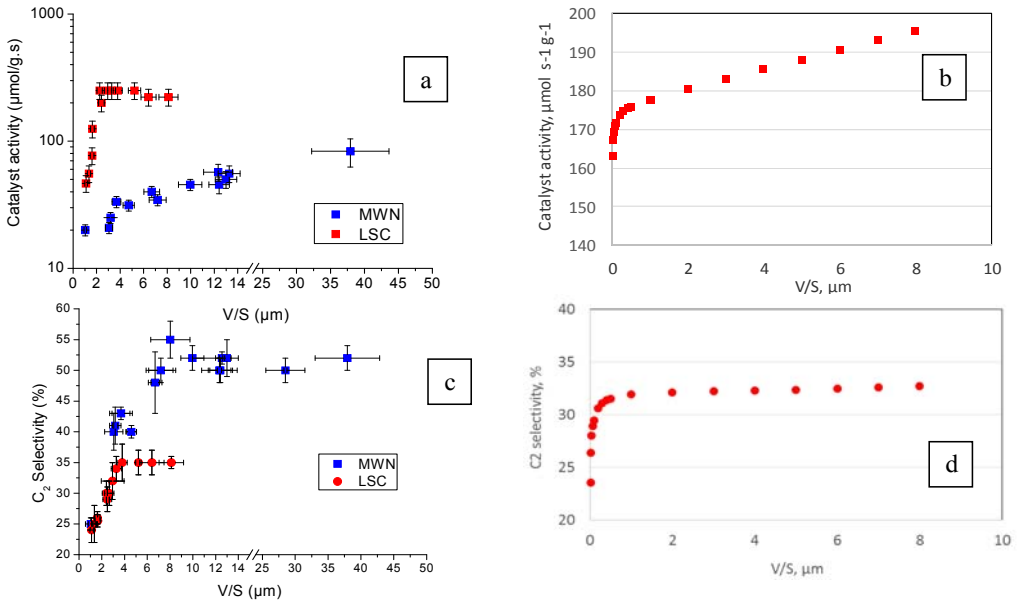

Fig. 2. *OCM activity (a,b) and selectivity (c, d) (in µmol of converted methane/s.g of catalyst) versus the V/S ratio. 10% methane conversion, 800°C, 16/4/1 vol/vol $CH_4/O_2/N_2$. (a, c) Experimental data and (b,d) Calculated results.*

The increasing C2 selectivity with increasing V/S is assigned to the increasing probability of coupling of methyl radicals in the gas phase to form ethane and the decreasing probability of their collision with the catalyst surface to form carbon oxides. According to the model simulations the CH_3 radical concentration is much higher in the catalyst pores as compared to the interstitial gas phase, since they are surface produced intermediates. A similar analysis was performed for the changes in the ethylene/ethane ratio vs V/S, indicating that ethane dehydrogenation is mainly a thermally induced, gas phase, phenomenon controlled by the gas phase reaction C_2H6 <-> C_2H_5·+H· with negligible contribution from the catalytic surface, since C_2H_5 radicals formed on the surface are quenched rapidly. It can be noted however that the nature of the catalyst plays also a major role, as expected from surface reactivity and selectivity depending strongly on surface composition.

4 Conclusions

A comprehensive OCM microkinetic model using catalyst descriptors was used to assess experimental data while fundamentally accounting for the observed dependence of the catalytic performance on the operating V/S ratio. The simulation results were found in line with the experimental observations. These results are deemed to provide strong guide-lines for further reactor design and optimisation.

Acknowledgements

This work was supported by the OCMOL project, 7th EU FP, Grant 228953 (www.ocmol.eu).

References

[1] J.W. Thybaut, G.B. Marin, C. Mirodatos, Y. Schuurman, A.C. van Veen, V.A. Sadykov, H. Pennemann, R. Bellinghausen, L. Mleczko, Chem. Ing. Tech. 86 (2014) 1855–1870.

[2] J.W. Thybaut, J. Sun, L. Olivier, A. C. Van Veen, C. Mirodatos, G. B. Marin, Catal. Today 159, (2011) 29-36.

ISO-OP18

Oxygen Availability and Catalytic Performance of $NaWMn/SiO_2$ Mixed Oxide and its Components in Oxidative Coupling of Methane

Gordienko Yu., Usmanov T., Bychkov V., Lomonosov V., Fattakhova Z., Tulenin Yu., Shashkin D., Sinev M.*

Semenov Institute of Chemical Physics, R.A.S., Department of Kinetics and Catalysis, Moscow, Russia

* sinev@chph.ras.ru

Keywords: oxidative coupling of methane, catalyst, lattice, oxygen

1 Introduction

Supported mixed $NaWMn/SiO_2$ oxide is a promising catalyst for ethylene production from methane via its oxidative coupling [1,2]. Its structural features and catalytic performance have been extensively studied (see, e.g., [3]). In spite of that, some important issues are still not well understood, including the nature of its catalytic activity. Recently it was demonstrated that water has a strong positive effect on activity and selectivity of this catalytic system and the rates of methane and ethane oxidation tend to increase at increasing conversion [4,5]. On the other hand, it was shown that the rates of light alkane oxidation over this catalyst can be described in the framework of the classical Mars-van Krevelen (redox) kinetic scheme [6]. The latter agrees with the idea that the $NaWMn/SiO_2$ oxide lattice oxygen participates in the C-H bond activation [7]. In this work we attempted to shed more light onto the properties of reactive lattice oxygen, on the role of components in this mixed oxide system, and on the relationships between its composition, structure, oxygen availability and catalytic performance.

2 Experimental

Mixed $NaWMn/SiO_2$ oxide and samples containing its components (Na, W, Mn) and their combinations (Na-W, Na-Mn, W-Mn) supported on silica were obtained using two techniques: incipient wetness impregnation and sol-gel (S-G) synthesis. Correspondingly, Aldrich Davisil grade 646 and tetraethoxysilane were taken as silica sources. After gelation (in the case of S-G synthesis) and drying, all samples were finally calcined at 850-900°C. Their phase composition was studied using powder X-ray diffraction (DRON-2 diffractometer, Cu K_α radiation). Oxygen TPD and redox experiments were performed using differential scanning calorimeter (Setaram DSC-111) and thermobalance (Setaram Setsys TG) equipped with on-line GC and MS analytic systems, respectively. Catalytic performance in methane oxidation was studied using a conventional quartz microreactor with on-line GC analysis of the reaction mixture.

3 Results and discussion

The samples of the same composition obtained by impregnation and S-G synthesis have similar phase composition: all Na-free samples are amorphous, whereas in the presence of Na the formation of α-cristobalite as the main phase (in agreement with literature data) is observed.

Also in agreement with literature, the samples containing all three dopants (Na, W, Mn) demonstrate high selectivity (above 70%) to C_2-hydrocarbons at methane conversions exceeding 15%. Selectivity of one- and two-component systems is substantially lower. Such samples are also much less active compared to the three-component ones.

Catalytic performance correlates with the amount of oxygen that can be reversibly released from the samples during their heating in inert gas (He). Also, only three-component system

demonstrates a stable oxygen release-uptake behaviour in repeated cycles of heating in He and oxidizing O_2-He gas flows. One may conclude that the presence of all three doping components is critical for both catalytic performance and oxygen availability in such conditions. It is likely that Na is responsible for the formation of crystalline structure in which W and Mn interact in an optimal way to form the sites capable of providing such exchangable oxygen. If pulses of oxygen are supplied at 700-800°C onto the sample after heating in He at 800°C, a complex DSC signal that consists of fast exothermal and slow endothermal parts is observed indicating that the sample first consumes oxygen and then slowly releases it with a characteristic time about 150-200 s. The latter is much more than the characteristic time of OCM reaction at the same temperatures (< 1 s.). This allows one to consider this form of oxygen as a relatively weakly-bonded lattice oxygen that may participate in a catalytic reaction of redox type.

At heating between ~700 and 800°C the three-component sample can reversibly release ~16.5 μmole/g O_2, which is substantially less than the amount of transition metals present (170 and 72 μmole/g of W and Mn, respectively). On the other hand, the same sample can provide much more oxygen while reduced in methane and/or hydrogen (~300 μmole/g), which is nearly equivalent to the total content of transition metals (if the reduction of W^{6+} to W^0 and Mn^{3+} or Mn^{4+} to Mn^{2+} is considered). Although according to the data of MS analysis during the reduction with methane all gaseous products typical for OCM reaction (C_2-hydrocarbons, carbon oxides) form, it is very doubtful that such high degrees of reduction may take place during the steady-state catalytic reaction in the presence of even small concentrations of gaseous oxygen. After such deep reduction the sample starts to consume oxygen at temperatures as low as 350°C, and at typical OCM temperatures this process becomes almost instantaneous. But according to the data of kinetic measurements in steady-state regime [6], the rates of the catalyst reduction with methane and its re-oxidation with O_2 are comparable.

4 Conclusions

The alkali component (Na) in the mixed oxide system NaWMn/SiO_2 is required for the formation of appropriate crystalline phase (mainly α-cristobalite) in which W and Mn interact in an optimal way to form the structures containing exchangable oxygen that is responsible for light alkane activation in the conditions of steady-state OCM reaction. Almost total reversible reduction of transition metals (W and Mn) accompanied with the formation of gaseous products typical for OCM (C_2-hydrocarbons, carbon oxides) may occur if this system interacts with methane in the absence of gaseous oxygen.

Acknowledgements

Authors acknowledge the financial support from the Russian Foundation for Basic Research (Project No. 13-03-00668 A).

References

[1] X.P. Fang, S.B. Li, J.Z. Lin, Y.L. Chu. *Journal of Molecular Catalysis (China)*. 6 (1992) 255.
[2] D.J. Wang, M.P. Rosynek, J.H. Lunsford. *Journal of Catalysis*. 155 (1995) 390.
[3] S. Arndt, T. Otremba, U. Simon, M. Yildiz, H. Schubert, R. Schomäcker. *Applied Catalysis A: General*. 425-426 (2012) 53.
[4] K. Takanabe, E. Iglesia. *Angewante Chemie International Eddition*. 47 (2008) 7689.
[5] V. Lomonosov, Yu. Gordienko, M. Sinev. *Topics in Catalysis*. 56 (2013) 1858.
[6] V.I. Lomonosov, Yu.A. Gordienko, M.Yu. Sinev. *Kinetics and Catalysis (Russ.)*. 54 (2013) 474.
[7] V. Salehoun, A. Khodadadi, Y. Mortazavi, A. Talebizadeh. *Chemical Engineering Science*. 63 (2008) 4910.

ISO-OP19

Alkaline-Earth Promoted $SrTiO_3$ and Sr_2TiO_4 in Oxidative Methane Coupling: Role of Microstructure and Surface Composition on Activity, Kinetics and Oxygen Exchange

Ivanov D.V.[1*], Isupova L.A.[1], Gerasimov E.Yu.[1,2], Dovlitova L.S.[1], Glazneva T.S.[1,2], Prosvirin I.P.[1,2]

1 - Boreskov Institute of Catalysis SB RAS, Novosibirsk, Russia
2 - Novosibirsk State University, Novosibirsk, Russia

* ivanov@catalysis.ru

Keywords: oxidative methane coupling, strontium, titanate, layered perovskites, oxygen exchange, kinetics

1 Introduction

Natural gas is an abundant resource for chemical industry. However, only 7% of the total amount produced natural gas is involved in chemical processing, mainly in production of methanol, ammonia and oxyaldehydes [1]. Therefore, direct conversion of methane, main component of natural gas, to the useful chemicals has been recognized as one of the most technologically important and challenging problems.

For about three decades the advantageous process of the direct methane conversation to C_2 hydrocarbons via oxidative methane coupling reaction (OCM) has been extensively studied, but never commercialized. The reasons are low selectivity and C_2 yield of the known catalysts, high exothermicity and technological restrictions. Perhaps the C_2 yield and selectivity limitations can be improved if we can understand what kind of surface oxygen species, being the active sites for methane activation, governs both the OCM reaction and the secondary total oxidation reaction, how its concentration depends on the catalyst composition.

In this work we attempted to take a close look in catalytic performance of alkaline-earth promoted strontium titanates $SrTi_{0.9}A_{0.1}O_3$ and $Sr_2Ti_{0.9}A_{0.1}O_4$ (A = Mg, Ca, Ba), being the active catalysts of OCM [2], and to find the correspondence between the microstructure, catalytic activity, kinetics of OCM and oxygen exchange properties.

2 Experimental/methodology

All the samples were prepared by mechanochemical method: activation in a planetary ball mill followed by calcination in air at 1100 °C. The samples were studied by XRD, XPS, HREM, IR, Differential Dissolution Method. Catalytic activity was measured in a fixed-bed quartz tube reactor (5 mm i.d.) at 850 – 900 °C and ambient pressure in the reaction mixtures varied from $40\%CH_4 + 5\%O_2$ in He to $10\%CH_4 + 5\%O_2$ with the flow rate varied from 2 to 8.3 cm^3/s, corresponding to the contact time $\tau = 0.05 – 0.012$ s. Oxygen exchange was studied by Steady State Transient Kinetic Analysis $^{16}O_2/^{18}O_2$ at 850 °C and contact time $6.5 \cdot 10^{-3}$ s.

3 Results and discussion

In this work we demonstrated high activity (Y C_2 > 20%) and selectivity (S C_2 > 60%) of Mg and Al-substituted Sr_2TiO_4 in OCM reaction. Detailed kinetic analysis, together with electron microscopy, XPS, XRD and IR methods, allowed us to establish the quantitative relationships between methane conversion, selectivity, temperature and reactant ratio and to reveal the influence of surface composition and microstructure on activity. As follows from microscopic data under reaction conditions the layered perovskite phase $Sr_{2-x}Mg_xTiO_4$ is

destroyed and nanoparticles of (Sr, Mg)O oxide are segregated on the surface (Fig. 1). It strongly increases the activity and selectivity of strontium titanates. The level of (Sr, Mg)O segregation correlates with the rate of methane conversion. It means that active oxygen ion-radicals under reaction conditions are formed in (Sr, Mg)O oxide.

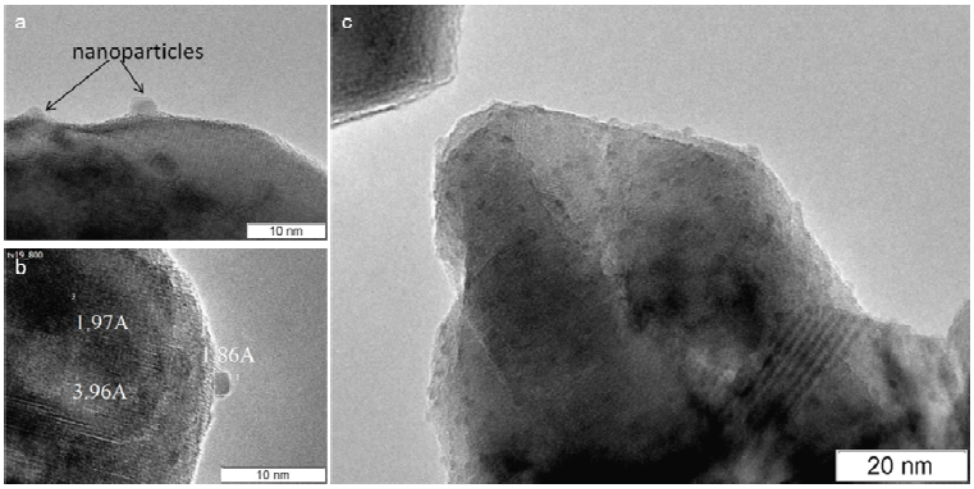

Fig. 1. HREM images of SrTiO3(a) and SrTi0.9Mg0.1O3(b and c) after catalytic tests [2].

To anticipate what kind of oxygen ion-radicals are formed (Sr, Mg)O oxide, we studied the CO_2 adsorption by IR spectroscopy and determine the type and concentration of the surface carbonate species, which decomposition under reaction conditions may result in active oxygen formation. It was found that most active catalysts contains mainly monodentate carbonate, characterized by IR bands at 1455–1460 cm^{-1}and1480–1500 cm^{-1}(asymmetric stretching vibrations of C-O).

Oxygen exchange experiments demonstrated that the most active catalysts are characterised by the highest rate of oxygen exchange at 850 °C. Moreover, the correlation was found between the yield of C_2 hydrocarbons and the ratio R_s/D_{bulk}, where R_s is the rate of the surface hetero-exchange and D_{bulk} is the coefficient of the bulk oxygen diffusion. It indicates that under the OCM conditions high oxygen exchange between surface and bulk takes place, which probably influence the surface concentration of the active oxygen species. The questions concerning the relationship between oxygen exchange properties and activity in OCM are discussed.

4. Conclusions

In this work we have demonstrated that under OCM conditions surface composition and microstructure of alkaline-earth promoted $(Sr,A)TiO_3$ and $(Sr,A)_2TiO_4$ may undergone a change revealing (Sr,A)O mixed oxide on the surface of the particles, which strongly increases both catalytic properties of titanates and the rate of the oxygen hetero exchange between surface and bulk. The correlation was found between the rate constant of methane conversion and the amount of (Sr, A)O oxide. It means that active oxygen ion-radicals under reaction conditions are formed in (Sr, Mg)O oxide and surface/bulk oxygen exchange may regulate its concentration.

Acknowledgements

The reported study was supported by RFBR, research project No.12-03-31608 mol a.

References

[1] Jasimuz Zaman, *Fuel Processing Technology* 58 (2-3) (1999) 61-81.
[2] D.V. Ivanov, L.A. Isupova, E. Yu. Gerasimov, L.S. Dovlitova, T.S. Glazneva, I.P. Prosvirin, *Appl Catal a-Gen* 485 (2014) 10-19.

ISO-OP20

Redox Treatment of Orthorhombic $Mo_{29}V_{11}O_{112}$ and Relationships between the Crystal Structure, Microporosity and Catalytic Performance for the Selective Oxidation of Ethane

Ishikawa S.I[1], Kobayashi D.K[1], Konya T.K[1], Ohmura S.O[1], Murayama T.M[1], Yasuda N.Y[2], Sadakane M.S[3], Ueda W.U[1*]

1 - Catalysis Research Center, Hokkaido University, Sapporo, Japan
2 - JASRI/SPring-8, Sayo, Japan
3 - Graduate School of Engineering, Hiroshima University, Hiroshima, Japan

* s.ishikawa@cat.hokudai.ac.jp

Keywords: structural change, microporosity, selective oxidation of ethane

1 Introduction

Orthorhombic $Mo_{29}V_{11}O_{112}$ oxide (MoVO) has attracted much attention because of their outstanding catalytic performance for the selective oxidation of ethane [1]. MoVO is a layered structure comprised of pentagonal $[Mo_6O_{21}]^{6-}$ unit and $\{MO_6\}$ (M = Mo, V) octahedral. The arrangement of the pentagonal $[Mo_6O_{21}]^{6-}$ unit and the $\{MO_6\}$ octahedral forms framework unit. Voids in the framework are filled with pentamer units comprised of five octahedra, resulting in the formation of hexagonal and heptagonal channels. The heptagonal channel in MoVO structure acts as a micropore with 0.40 nm in diameter which can adsorb small molecules like as light alkanes. The size of the channel is tuneable by redox treatment [2]. Recently, we have reported that the heptagonal channel converts ethane to ethene inside the channel, resulting in significantly high catalytic activity [1]. This time, the relationship between the microporosity and the catalytic activity for the selective oxidation of ethane is discussed.

2 Experimental

An aqueous solution of $VOSO_4$ was added to the aqueous solution of $(NH_4)_6Mo_7O_{24}$ (Mo/V=4) and poured into an autoclave for hydrothermal reaction at 175 ºC for 48 h. Dried samples were treated with oxalic acid, then calcined at 400 ºC for 2 h under static air (MoVO (0)). MoVO (0) was heat-treated under 70 ml min^{-1} of 5% H_2/Ar at 400 ºC for a given length of time. Obtained samples are abbreviated as MoVO (δ) (δ: 0.8, 2.9, 4.2, 5.4, 6.1, 6.8) where δ corresponds to the number of oxygen evolved from the unit cell ($Mo_{29}V_{11}O_{112-\delta}$). MoVO (2.9) and MoVO (6.8) were again calcined under static air at 400 ºC for 2 h (MoVO (2.9)-AC and MoVO (6.8)-AC, respectively). The selective oxidation of ethane was carried out in gas phase at atmospheric pressure in a conventional flow system with a fixed bed reactor at 300 ºC under $C_2H_6/O_2/N_2$ = 5/5/40 ml min^{-1} gas flow.

3 Results and discussion

By the redox treatments, no impurities are observed by XRD, IR, Raman. In addition, the redox treatments caused no change in their bulk composition and external surface area. Figure 1 shows the micropore volume measured by propane adsorption (V_{C3H8}) and ethane conversions at 10 min from starting the reaction of MoVO catalysts. The ethane conversion were increased with increasing δ until MoVO (4.2) (from 13.7% to 33.0%) and then decreased drastically for the further δ increase (from 33.0% to 0.5%). For the catalysts after the air calcination, the ethane conversion of MoVO (2.9)-AC was 10.0%. Surprisingly, the ethane conversion of MoVO (6.8)-AC was 31.2%, three times higher than that of MoVO (2.9)-AC while both of them were calcined in the same condition. Adsorption behaviour of V_{C3H8} upon the reduction was well

matched with that of the ethane conversion. The molecular size of propane (0.43 nm) is a little larger than the size of the heptagonal channel (0.40 nm), indicating that the increase of V_{C3H8} between MoVO (0) ~ MoVO (4.2) corresponds to an expansion of the heptagonal channel. TPR shows that there are two kinds of lattice oxygen in the $Mo_{29}V_{11}O_{112}$ structure, one is evolved in the early stage of the reduction and hardly comes back by reoxidation. The other is continuously evolved during the reduction and reversibly comes back by reoxidation. We abbreviated the former oxygen as α-oxygen and the latter oxygen as β-oxygen. From TPR, it was found that the evolution of α-oxygen is finished by the reduction up to MoVO (4.2). XRD, IR, Raman showed that α-oxygen is placed in the pentamer unit and β-oxygen is placed in the framework unit. From the propane adsorption, an expansion of the heptagonal channel was implied by the reduction up to MoVO (4.2). Therefore, the α-oxygen should be the oxygen in the pentamer unit which faced to the heptagonal channel (O_{29} in Figure 2 (A)) and the evolution of the α-oxygen should be related to an expansion of the heptagonal channel. For the reoxidized catalysts, MoVO (2.9)-AC had the α-oxygen, while almost no α-oxygen in MoVO (6.8)-AC was observed. Actually, V_{C3H8} of MoVO (6.8)-AC was twice higher than that of MoVO (2.9)-AC. Since another catalytically affective factors of these catalysts were almost the same, we concluded that the evolution of α-oxygen increased the catalytic activity. The increase of the catalytic activity between MoVO (0) ~ MoVO (4.2) should be due to the evolution of the α-oxygen. The void generated by the evolution of the α-oxygen may moderately activate gaseous oxygen, resulting in the increase of the catalytic activity. The crystal structure of MoVO catalysts at each reduction state is simulated by Rietveld refinement. Figure 2 (B) illustrates the diameters of the heptagonal channel. The diameter in the short axis (D_2) increased with increasing δ in the range of MoVO (0) ~ MoVO (4.2), however, was drastically decreased for the further reduction by the expansion of pentagonal $[Mo_6O_{21}]^{6-}$ unit. The drastic decrease of V_{C3H8} (as well as V_{C2H6} (data not shown)) of the catalysts above MoVO (5.4) should be due to the decrease of D_2. Since ethane is converted inside the heptagonal channel, the loss of the catalytic activity by the reduction above MoVO (5.4) should be due to an inaccessibility of ethane to the heptagonal channel.

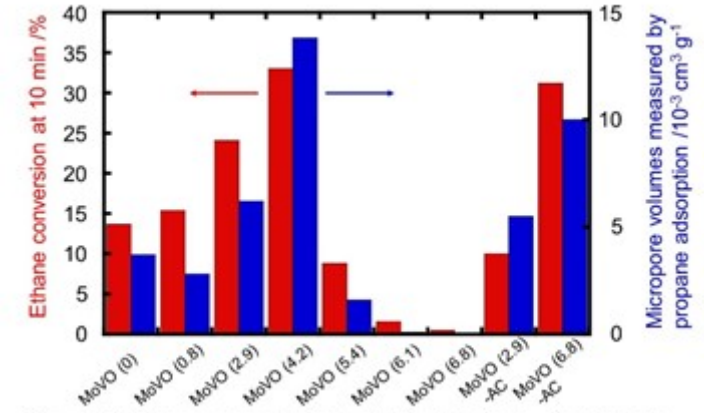

Figure 1 Ethane conversion at 10 min from starting the reaction (Red) and micropore volumes measured by propane (blue) adsorption of MoVO catalysts.

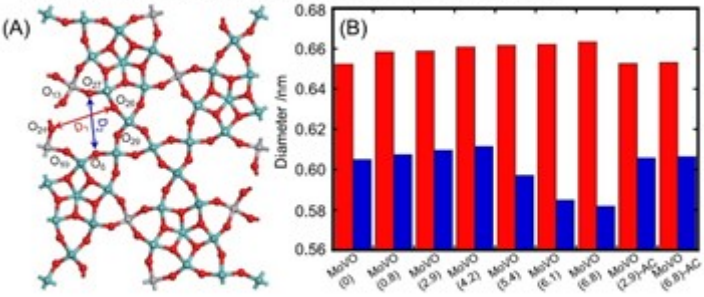

Figure 2 (A) Structural model of MoVO. (B) Diameters of heptagonal channel (Red bar, D_1, Blue bar, D_2).

4 Conclusion

Relationships between the crystal structure, microporosity, and catalytic activity was found.

References

[1] Ishikawa, S.; Yi, X.; Murayama, T.; Ueda, W. *Appl. Catal. A: Gen*. **2014**, *474*, 10-17.
[2] Sadakane, M.; Ohmura, S.; Kodato, K.; Fujisawa, T.; Kato, K.; Shimidzu, K.; Murayama, T.; Ueda, *Chem. Commun*. **2011**, *47*, 10812-10814.

ISO-OP21

The Selective Oxidation of Polysaccharides to Formic Acid at the Presence of P-Mo-V Heteropoly Acid Catalysts. The Mechanism of Reaction

Taran O.P.[1,2*], Gromov N.V.[1], Zhizhina E.G.[1], Rodikova Yu.A.[1], Parmon V.N.[1,3]

1 - Boreskov Institute of Catalysis SB RAS, Novosibirsk, Russia
2 - Novosibirsk State Technical University, Novosibirsk, Russia
3 - Novosibirsk State University, Novosibirsk, Russia

* oxanap@catalysis.ru

Keywords: heteropoly acid, cellulose, hemicellulose, formic acid, formaldehyde mechanism

1 Introduction

Cellulose and hemicelluloses - the main components of plant biomass (40 – 60 % of biomass) are promising raw materials for production fuels and valuable chemicals. [1]. However polysaccharides derivatives reduction demands a lot of reducing agent. Molecular hydrogen produced from fossile hydrocarbons is usually proposed as a reducing agent. However formic acid produced from polysaccharides can be used as reducing agent or resource of hydrogen for fuels production [2].

P-Mo-V heteropoly acids having acidic and oxidative catalytic centers were suggested as bifunctional acidic-oxidative catalysts for formic acid production using one-pot processes of hydrolytic oxidation of natural polymers like cellulose and hemicelluloses under soft conditions [2 – 4]. Many researchers believe that one-pot process consists of two sequential catalytic steps (hydrolysis and oxidation). Acidic catalyst should be used for hydrolysis. Oxidation of monosaccharide to formic acid proceeds over oxidative catalyst via several steps. However high yields (more than 60%) of formic acid and absence of such intermediates as gluconic and glucuronic acids makes this hypothesis implausible.

The aim of this work was the study of kinetics and elucidation the mechanism of the process of one-pot oxidative hydrolysis of polysaccharides in the presence of HPAs providing the formation of formic acid with high selectivity.

2 Experimental

HPAs ($Co_{0.6}H_{3.8}PMo_{10}V_2O_{40}$, $H_5PMo_{10}V_2O_{40}$, $Co_{0.6}H_{3.8}PMo_{10}V_2O_{40}$, $Li_{2.4}H_{4.6}PMo_8V_4O_{40}$, $H_{11}P_3Mo_{16}V_6O_{76}$ and $H_{17}P_3Mo_{16}V_{10}O_{89}$) were synthesized, characterized by NMR and tested in ball-milled cellulose hydrolitic oxidation. All experiments were carried out in high-pressure autoclave (Autoclave Engineers, USA) under intensive stirring (1500 rpm). The concentration of cellulose or hemicelluloses was 10 g L^{-1} and heteropoly acid concentration calculated on amount of vanadium varied from 0.5 mM to 20 mM. The experiments were performed at various temperatures (130, 140, 150 and 180 °C) and different pressures (1, 2, 5 MPa) of gas mixture containing 20% of O_2 and 80% of N_2. Samples to analyze were periodically drawn from the autoclave. The aliquots of the reaction mixture were thoroughly filtered and the concentrations of products were measured by HPLC using a Shimadzu Prominence LC-20 system equipped with diode array and refractive index detectors and a Rezex Organic Acids H+ column (Phenomenex, 300 mm * 5.0 mm) thermostated at 40 °C. The eluent (1.25 mM H_2SO_4 aqueous solution) was supplied at the 0.6 mL min^{-1} flow rate. Formaldehyde concentration was measured after derivatization with chromotropic acid on λ 570 nm.

3 Results and discussion

The HPLC analysis of components dissolved in reaction solution showed that under all conditions the main product of the one-pot process is formic acid. Only low amounts of glucose and acetic acid were also detected at some cases. Besides the formation of the formaldehyde was registered after derivatization with the chromotropic acid.

The optimization of the process parameters was performed at the presence of $Co_{0.6}H_{3.8}PMo_{10}V_2O_{40}$ as the catalyst. The variation of temperature (130, 140, 150 and 180 °C) showed that the temperature 150 °C is the optimal for the cellulose and arabino-galactan hydrolytic oxidation, but 120 °C for xylan. Note, the optimal temperatures for hydrolysis of the tested polysaccharides with sulfuric acid are about 30 °C higher. The highest yield of formic acid were 66% for cellulose, 45% for arabino-galactan, 42% for xylan. The yields for formaldehyde were 2, 1,7, 2.2%, respectively. Activation energy for polysaccharide hydrolytic oxidation was measured using the dependence of reaction rates from the temperatures. The kinetics of the oxidation of the glucose, formic acid and formaldehyde were also studied.

The screening of the different catalysts was performed in cellulose hydrolysis under the optimal conditions (the temperature 150 ºC and pressure of gas mixture 5 MPa). $H_5PMo_{10}V_2O_{40}$, $Co_{0.6}H_{3.8}PMo_{10}V_2O_{40}$, $Li_{2.4}H_{4.6}PMo_8V_4O_{40}$, $H_{11}P_3Mo_{16}V_6O_{76}$ and $H_{17}P_3Mo_{16}V_{10}O_{89}$ were tested. The highest reaction rate is observed in presence of HPA which has higher oxidative potential and gives the lowest pH.

The influence of vanadium content on reaction rate was studied using $Co_{0.6}H_{3.8}PMo_{10}V_2O_{40}$. All experiments were made at pH of reaction solution equal to 1.50 for prevention the influence of acidic properties of HPA. The results obtained showed that the formic acid yield does not change when concentration of vanadium atoms decrease from 20 to 10 mM and sharply fall at content of vanadium less then 10 mM.

4 Conclusions

The observed results allowed us to suppose that one-pot oxidative-hydrolysis in the presence of P-Mo-V heteropoly acids proceeded by a mechanism similar to the periodate oxidation. Vanadium species can connect to hydroxide groups of sugars and broke C-C bond to give formic acid and shorted sugar. Finally such oxidation of C6-aldose leads to formation of 5 molecules of formic acid a 1 formaldehyde molecule (Figure 1). Moreover connection of vanadium to polysaccharides molecules facilitating hydrolysis is also possible.

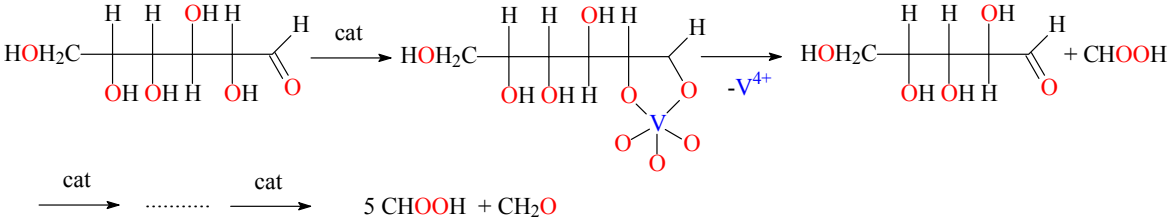

Fig. 1. Proposed mechanism of formic acid formation from C6 aldose in the presence V-containing heteropolyacyd catalysts.

Acknowledgements

The financial support of the work by the Russian Foundation for Basic Research (Grant 14-03-00854-a), and Russian Ministry of Education and Science (Project V.46.4.4) is gratefully acknowledged.

References

[1] A.M. Ruppert, K. Weinberg, R. Palkovits, *Angew. Chem. Int. Ed.* 51 (2012) 2564 – 2601.
[2] J. Li, D.-J. Ding, L. Deng et. al., *ChemSusChem* 5 (2012) 1313-1318.
[3] R. Wölfel, N. Taccardi, A. Bösmann, P. Wasserscheid, *Green Chem.* 13 (2011) 2759
[4] J. Albert, R. Wölfel, A. Bösmann, P. Wasserscheid, *Energy Environ. Sci.* 5 (2012) 7956.

ISO-OP22

Study of M-Doped NiO (M = Li, Mg, Al, Ga, Ti, Nb) Catalysts by *in situ* Electrical Conductivity Measurements in Correlation with their Catalytic Performances in Ethane Oxydehydrogenation

Popescu I.[1], Skoufa Z.[2], Heracleous E.[3,4], Lemonidou A.A.[2,3], Marcu I.C.[1,5*]

1 - University of Bucharest, Research Center for Catalysts and Catalytic Processes, Bucharest, Romania

2 - Aristotle University of Thessaloniki, Department of Chemical Engineering, Thessaloniki, Greece

3 - Chemical Process Engineering Research Institute (CPERI), Centre for Research and Technology Hellas (CERTH), Thessaloniki, Greece

4 - International Hellenic University, School of Science and Technology, Thermi, Greece

5 - University of Bucharest, Department of Organic Chemistry, Biochemistry and Catalysis, Bucharest, Romania

* ioancezar.marcu@chimie.unibuc.ro

Keywords: doped nickel oxide, electrical conductivity, ethane oxydehydrogenation, reaction mechanism

1 Introduction

Doped NiO has been reported [1] as efficient catalyst for the low temperature ethane oxy-dehydrogenation (ODH), which is an attractive alternative to the conventional steam cracking route for ethylene production. The electronic and redox properties of oxide catalysts strongly influence their catalytic performance in oxidation reactions [2]. *In situ* electrical conductivity measurements constitute a powerful technique for the investigation of electronic and redox properties of oxidation catalysts and can help understanding their catalytic behavior [3].

In this work, electrical conductivity of two series of doped NiO catalysts, i.e. M-NiO (M = Li, Mg, Al, Ga, Ti, Nb) and Nb(x)NiO (x = Nb at. %), was studied as a function of temperature and oxygen partial pressure and temporal responses during sequential exposures to air, ethane – air mixture (reaction mixture) and pure ethane in conditions similar to those of catalysis were analyzed. Comparisons between the different catalysts and correlations between their redox and semiconductive properties and their catalytic performance in ethane ODH have been established.

2 Experimental

Both M-NiO oxides with a M/(Ni+M) atomic ratio of 0.15 and Nb(x)NiO oxides with Nb/(Ni+Nb) atomic ratios of 0.01, 0.05, 0.10, 0.15 and 0.20 were prepared by the evaporation method, characterized with several techniques and tested in ethane ODH as described elsewhere [1, 4, 5]. The catalytic test was performed in a fixed bed quartz reactor operating at atmospheric pressure, in the temperature range from 300 to 425 °C. The electrical conductivity measurements were performed in the reaction temperature range under different flowing gases in a quartz tube cell containing the catalyst pellet between two platinum electrodes connected to a megaohmmeter.

3 Results and discussion

The intrinsic activity in ethane ODH roughly decreased while the ethylene selectivity at isoconversion continuously increased with increasing valence of the dopant cation and niobium content for both M-NiO and Nb(x)NiO series, respectively. Nb(15)NiO catalyst gave the lowest intrinsic activity but the highest ethylene selectivity suggesting that this material contains the lowest surface density of unselective (but also active) catalytic sites.

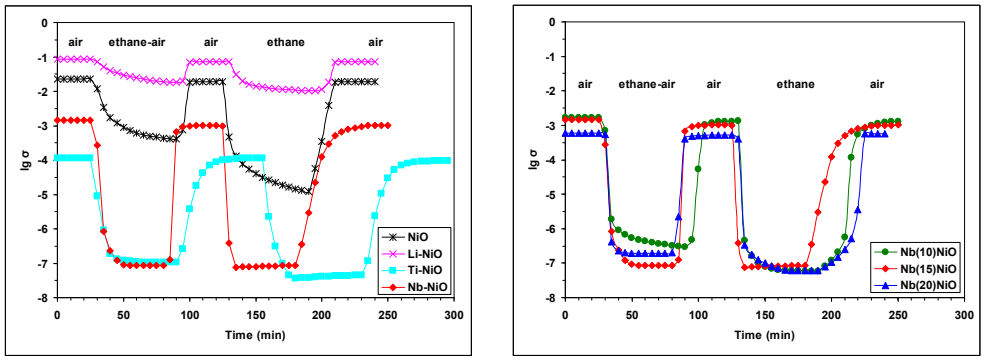

Fig. 1. Variation of σ during sequential exposures to different gas flows for selected catalysts at 400 °C.

The electrical conductivity measurements showed that pure NiO as well as all the doped NiO catalysts behaved as p-type semiconductors in the reaction temperature range both under air and under the ethane-air reaction mixture. The temporal responses of electrical conductivity of selected catalysts during sequential exposures to different gaseous atmospheres in conditions similar to those of catalysis are presented in Fig. 1.

Except for Nb-NiO, the electrical conductivity of the M-NiO catalysts in air decreased with increasing the valence of doping cation, indicating the consumption of charge carriers (positive holes) due to the doping effect. The different behavior of Nb-NiO can be explained by a reduction of the niobium doping cation valence. In the Nb(x)NiO series, the electrical conductivity in air decreased continuously with increasing the niobium content. The intrinsic activity in ethane ODH roughly followed the p-type semiconductivity under air for both M-NiO and Nb(x)NiO catalysts. All the catalysts were partially reduced under the reaction mixture at 400 °C (Fig. 1), an inverse correlation between their p-type conductivity in these conditions and the ODH selectivity being observed for both M-NiO and Nb(x)NiO series studied. The observed decrease of the electrical conductivity of the M-NiO catalysts in the presence of ethane suggests that ethane is transformed by consuming the positive holes existing in the p-type oxide catalyst. The observed correlations between the results of the *in situ* electrical conductivity measurements and the catalytic results indicate that O^- species, the chemical equivalent of the positive holes - charge carriers, are the active sites for ethane activation; however conversion to the targeted product, ethylene, occurs only when their concentration is low and the attack to the activated ethane is milder.

4 Conclusions

The *in situ* electrical conductivity studies performed in the present work and the important correlations of both activity and selectivity with electrical conductivity that were obtained highlight the role of non-stoichiometric oxygen species for ethane ODH over doped NiO based catalysts and provide a clear and direct evidence for a heterogeneous redox mechanism involving surface lattice O^- species.

Acknowledgements

This work was partially financed by the University of Bucharest, project UB 256/2014.

References

[1] E. Heracleous, A.A. Lemonidou, *J. Catal*. 270 (2010) 67.
[2] J.M. Herrmann, *Catal. Today*. 112 (2006) 73.
[3] J.M. Herrmann, in: *Catalyst Characterization, Physical Techniques for Solid Materials*, B. Imelik and J. C. Védrine (eds.), Plenum Press, New York, 1994, ch. 20.
[4] E. Heracleous, A.A. Lemonidou, *J. Catal*. 237 (2006) 162.
[5] Z. Skoufa, E. Heracleous, A.A. Lemonidou, *Catal. Today*. 192 (2012) 169.

ISO-OP23

In-situ XPS and XAS Studies of a New Phenomenon of Kinetic Hysteresis in Selective Methane Oxidation over Platinum

Pakharukov I.Yu[1,2*], Bukhtiyarov V.I.[1,2], Chetyrin I.A.[1,2], Prosvirin I.P.[1,2], Parmon V.N.[1,2], Murzin Y.V.[3], Zubavichus Y.V.[3]

1 - Boreskov Institute of Catalysis SB RAS, Novosibirsk, Russia
2 - Novosibirsk State University, Novosibirsk, Russia
3 - National Research Center "Kurchatov Institute", Moscow, Russia

* ilyapakharukov@yandex.ru

Keywords: methane oxidation concentration, hysteresis, NAP-XPS, Pt catalyst

1 Introduction

Recently, we discovered a new phenomenon of kinetic hysteresis in selective oxidation of methane over platinum catalysts [1]. We found that the activity and selectivity of the platinum catalysts in a steady state depends greatly on a way of achieving the steady state. Using this hysteresis one can directly control the selectivity and activity of the platinum catalyst even with low initial activity (e.g., at low temperature), improve the conversion from 10 to 90%. For this purpose, oxygen concentration in the reaction mixture is decreased to a level less than O_2:CH_4=1.5 at the atmospheric pressure. It leads to certain increase in the methane conversion and selectivity. To achieve the maximum methane conversion (80-90%) the oxygen concentration in the initial reaction mixture is then increased up to a ratio of O_2:CH_4≤2.

Since this is undescribed phenomenon, we have no literature data to understand its nature. To establish the reasons of this phenomenon, we studied changes in oxidation state of the active component in real platinum catalysts by *in-situ* X-ray photoelectron spectroscopy (XPS) and X-ray absorption spectroscopy methods (XANES and EXAFS).

2 Experimental/methodology

In-situ XPS experiments were carried out on a photoelectron spectrometer VGESCALAB "High Pressure" [2] equipped with a special high-pressure cell and a quadrupole mass spectrometer with two-stage differential pumping and high-precision mass flow-controllers. Experiments were conducted at constant methane concentration (partial pressure of about 0.008 mbar) with varying the O_2:CH_4 ratio in the range from 0.2:1 to 2:1. *In-situ* XAS experiments were carried out at STM-station of Kurchatov Synchrotron Center (at the atmospheric pressure).

The catalyst (1 wt.%Pt/γ-Al_2O_3) under study was prepared via a wet impregnation of γ-Al_2O_3 with a platinum nitrate solution followed by air-drying and calcinations in air. The grain size of the catalyst is 0.25-0.5 mm. The average size of supported platinum particles was about 1.5 nm.

3 Results and discussion

Previous studies of the hysteresis were conducted in reactors at the atmospheric pressure. Therefore, there was no certainty that the experiment can be repeated at low pressures of about 0.01 mbar. However, our *in-situ* XPS experiments showed the presence of similar kinetic hysteresis (Fig. 1). Study included testing possible catalytic activity of the alumina support and *in-situ* cell. It was shown that the pure support and *in-situ* cell were not active in the reaction.

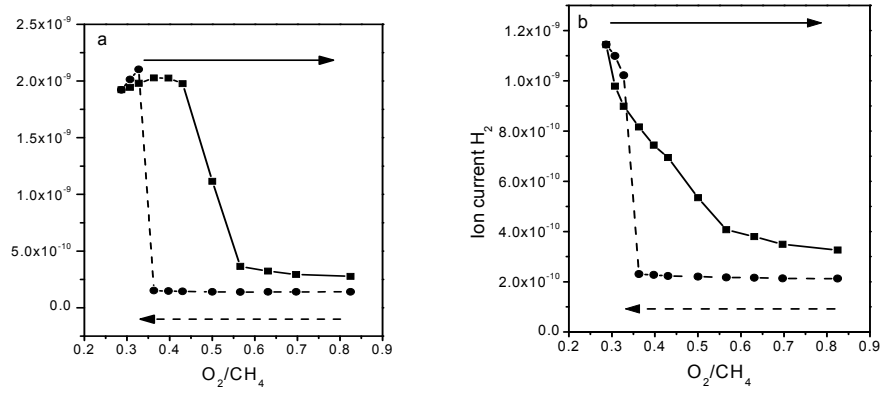

Fig.1. The kinetic hysteresis in the methane oxidation over 1 wt.%Pt/γ-Al_2O_3 catalyst detected by *in-situ* mass spectrometry at pressures of about 0.01 mbar, T=460°C

To identify the platinum oxidation state under the reaction conditions a number of reference compounds with different oxidation states of platinum (0, 2+, 4+) were investigated (Fig. 2a). The *in-situ* XPS spectra were recorded simultaneously with measurement of components concentrations. Analysis of XPS spectra showed that a transition of the catalyst to the active state was accompanied by shifting Pt4f line towards lower values of binding energy (Fig. 2b). Thus, activation of the platinum was associated with its partial reduction.

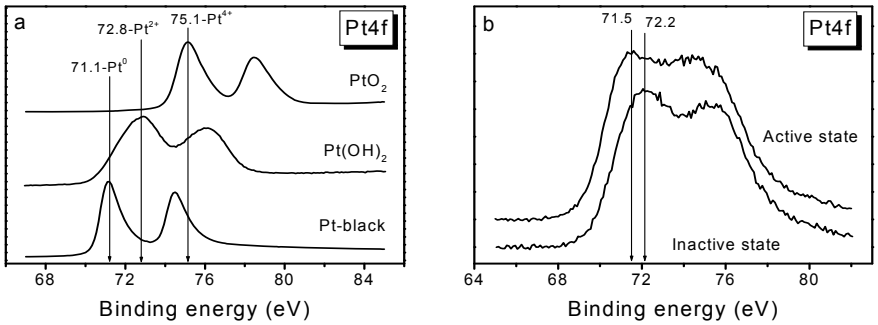

Fig.2. Changes in the platinum oxidation state: a - reference samples; b – Pt in the reaction

The XAS data obtained at the atmospheric pressure also implied that the activation was associated with predominant formation of the metallic platinum, whereas oxidation of platinum surface was responsible for less active state. The reaction mechanisms for explanation of these data are discussed.

4 Conclusions

The *in-situ* experiments allowed us to find out the cause of the kinetic hysteresis phenomenon in the selective methane oxidation over platinum catalysts.

Acknowledgements

This work was supported by the President Grant for Government Support of the Leading Scientific Schools of the Russian Federation (grant SS-5340.2014.3).

References

[1] I. Pakharukov, I. Bekk, M. Matrosova, V. Bukhtiyarov, V. Parmon, *Dokl. Phys. Chem.* 439 (2011) 131.

[2] Aiqin Wang, Xiao Yan Liu, Chung-Yuan Mou, Tao Zhang, *Journal of Catalysis* 308 (2013) 258.

ISO-OP24

Quasicatalytic and Catalytic Oxidation of Methane to Methanol by Nitrous Oxide over FeZSM-5 Zeolite

Starokon E.V.*, Parfenov M.V., Pirutko L.V., Panov G.

Boreskov Institute of Catalysis SB RAS, Novosibirsk, Russia

* starokon@catalysis.ru

Keywords: methane to methanol, nitrous oxide, FeZSM-5, zeolite, Alpha-oxygen, quasicatalytic reaction

1 Introduction

Huge natural resources of methane and the ability of Fe-containing enzymes methane monooxygenases (MMO) to perform its oxidation to methanol inspire new and repeated attempts of chemists to run this reaction in a catalytic way. However, for many decades this problem remains unsolved. In this connection, of great interest are FeZSM-5 zeolites containing special Fe^{II} complexes (α-sites) that are capable of stoichiometric decomposition of nitrous oxide with deposition of the oxygen anion-radical (the α-oxygen, O_α) [1]:

$$(Fe^{II})_\alpha + N_2O \rightarrow (Fe^{III}\text{-}O^{\bullet-})_\alpha + N_2 \quad (1)$$

Similar to the active oxygen of MMO, O_α exhibits a very high reactivity at 25°C. The present work is devoted to the α-oxygen oxidation of CH_4, including both the surface formation of methanol and a catalytic cycle of the reaction with the products desorption into the gas phase.

2 Experimental/methodology

The study was carried out with a sample of FeZSM-5 zeolite containing 2.0 wt% Fe, similar to the one that has been used in our previous studies [2, 3]. The sample had $C_\alpha = 5.7\times10^{19}$ site/g (95 μmol/g). Experiments on methane oxidation were performed with a conventional flow setup with chromatographic analysis of the gas phase. In quasicatalytic experiments, surface products were extracted with an aqueous solution of acetonitrile and analyzed using GC, ^{1}H NMR, and gas chromatography-mass spectrometry [3, 4].

3 Results and discussion

This work is a continuation of our studies [2-4] on the mechanism of methane oxidation by α-oxygen over FeZSM-5. Previously, using a vacuum setup, it was shown that at 160°C methane is oxidized to methanol. Spillover of methanol from α-sites liberates them for further oxidation cycles. Such a surface reaction with TON greater than 1, but without product desorption into the gas phase, we have named quasicatalytic. Based on this result one can assume that this quasicatalytic mode of reaction can be conducted also in a conventional flow-type setup, which is well supported by the data presented in Table 1.

Table 1. Quasicatalytic oxidation of methane in a flow-type setup. Reaction conditions: 0.36 g catalyst; feed mixture: 20% CH_4 + 2% N_2O with He balance; flow rate 30 cm^3/min.

Exp. no.	T, °C	Time, h	TON per α-site			Composition of products extracted, mol. %				
			Total products	Products extracted	Coke	CH_3OH	DME	C_2H_4	AA	Others (heavy)
1.	160	4	4.4	2.6	1.8	87	13	0.0	0.0	0.0
2.	175	4	5.2	3.3	1.9	77	23	0.0	0.0	0.0
3.	200	4	6.9	4.1	2.8	68	32	0.0	0.0	0.0

The main products produced by the quasicatalytic reaction and extracted from the surface

are methanol and DME. In addition, coke is formed, the amount of which was determined in situ by burning it in an air flow. The total amount of methane oxidation products increases with the temperature rise. The fraction of methanol in the products decreases due to its conversion into coke and DME.

In the temperature range 275-300°C the reaction proceeds in a catalytic way with desorption of methanol, CO, CO_2 acetaldehyde (AA) and ethylene into the gas phase (Table 2). The addition of water vapor in the feed mixture substantially reduces the formation of coke and strongly increases the selectivity for methanol. At 275°C and a 30% H_2O, the major product of the reaction is methanol, which selectivity is 62%. The yield of methanol is rather small. But variety of approaches available for modifying the catalytic properties of zeolites can certainly improve the result.

It is interesting to note that the selectivity for CO strongly increases with increasing the selectivity for methanol. Experiments have shown that this is due to the Cannizzaro reaction: $HCHO \rightarrow CH_3OH + CO$. The occurrence of this reaction explains the absence of formaldehyde in the products of methane oxidation. It is noteworthy that DME was not detected among the products although, as shown above, it was one of the main products in the quasicatalytic oxidation of methane. This is because at catalytic conditions DME acts as an intermediate and is fully consumed by the process of coke formation on the FeZSM-5 surface.

The reaction of methane with O_2 (instead of N_2O) is very slow and totally unselective, producing only small amounts of CO and CO_2 (no. 9).

Table 2. Reaction parameters of 2-h catalytic experiments. Reaction conditions: 0.36 g FeZSM-5; feed mixture: 20% CH_4 + 2% N_2O + (0÷30%) H_2O with He balance; flow rate 30 cm^3/min.

Exp. no.	T, °C	H_2O in the feed, %	Average conversion, %		Average selectivity, %						Coke amount, μmol C/g
			N_2O	CH_4	CH_3OH	CO	CO_2	C_2H_4	AA	Coke	
1	275	0.0	37	2.2	2.7	9.3	4.0	2.8	0.2	81	1800
2	275	10	15	0.65	31	33	6.0	5.0	0.0	25	160
3	275	20	6.2	0.27	57	32	5.0	0.0	0.0	6.0	17
4	275	30	3.2	0.19	62	32	3.0	0.0	0.0	3.0	~7
5	300	0.0	58	3.6	1.9	12	6.0	3.3	0.8	76	2800
6	300	10	37	1.9	9.3	29	7.5	5.7	0.5	48	970
7	300	20	31	1.3	19	32	7.5	5.7	0.8	35	460
8	300	30	21	0.75	42	45	4.5	1.0	0.0	7.5	58
9[a)]	300	20	0.4[a)]	0.02	0.0	70	30	0.0	0.0	n/d	n/d

[a)] The feed mixture contains 2% O_2 instead of 2% N_2O.

4 Conclusions

The present study was conducted over a wide temperature range covering both the quasicatalytic and catalytic modes. An important result of the work is that a comparison of quasicatalytic and catalytic data can provide new information on the reaction mechanism, including a possibility of identifying potential intermediates that are invisible under conventional catalytic conditions. A mechanistic scheme presenting main steps of both reaction modes was suggested.

Acknowledgements

The work was supported in part by RFBR: project no. 15-03-03218_a.

References

[1] K. Dubkov, N. Ovanesyan, A. Shteinman, E. Starokon, G. Panov, *J. Catal.* 207 (2002) 341.
[2] E. Starokon, M. Parfenov, L. Pirutko, S. Abornev, G. Panov, *J. Phys. Chem. C* 115 (2011) 2155.
[3] E. Starokon, M.Parfenov, S.Arzumanov, L. Pirutko, A. Stepanov, G. Panov, *J. Catal.* 300 (2013) 47.
[4] M. Parfenov, E. Starokon, L. Pirutko, G. Panov, *J. Catal.* 318 (2014) 14–21.

ISO-PP01

Trinuclear Copper Oxo-Clusters in ZSM-5 Zeolite for Selective Methane Oxidation to Methanol

Li G., Hensen E.J.M., Pidko E.A.*

Inorganic Materials Chemistry group, Eindhoven University of Technology, Eindhoven, The Netherlands

* e.a.pidko@tue.nl

Keywords: methane, methanol, trinuclear, Cu/ZSM-5

1 Introduction

The unique ability of over-exchanged Cu/ZSM-5 zeolite to oxidize CH_4 to CH_3OH at low temperature of 100 °C has been related to extra-framework binuclear $[Cu(\mu\text{-}O)Cu]^{2+}$ complexes [1]. However, an inherent limitation of this catalyst system is the difficulty of extracting the methanol product mainly caused by the strong binding of the extra-framework oxygen (O_{EF}) bridging between the two Cu^{2+} ions and the high Lewis acid strength of the cuprous sites formed upon methanol formation. In this work, we report the results of a computational study on the nature of active Cu complexes in Cu/ZSM-5 zeolite and their reactivity towards methane oxidation. We address the feasibility of the formation of larger trinuclear Cu complexes in the zeolite micropores. This is followed by a computational analysis of the reactivity of the most stable bi- and trinuclear Cu complexes towards methane oxidation.

2 Methodology

DFT calculations were performed using the VASP software. The exchange-correlation energy was described by generalized gradient approximation PBE functional. Plane-wave basis set with a cutoff of 400 eV in combination with the projected augmented wave (PAW) method was used. Brillouin zone-sampling was restricted to the Γ point. The nudged-elastic band method was used to determine the minimum energy path and to locate the transition state structure for methane oxidation to methanol reaction.

To account for the effect of temperature as well as presence of H_2O and O_2 upon the catalysts activation on the stability of different extra-framework Cu complexes in Cu/ZSM-5 *ab initio* thermodynamic analysis was employed. The following reversible reactions were considered to compare equilibria among species with different chemical compositions:

$$\frac{2m-n-2x+2}{4}O_2 + \frac{n-2}{2}H_2O + x(CuO) + 2H\text{-}ZSM\text{-}5 \leftrightharpoons Cu_xO_mH_n/ZSM\text{-}5$$

The reaction free energy $\Delta\Gamma$ was calculated per zeolite unit cell according to:

$$\Delta\Gamma(T,P) = \Delta E - \frac{2m-n-2x+2}{2}\Delta\mu_O - \frac{n-2}{2}\Delta\mu_{H_2O}$$

ΔE is the total electronic energy and $\Delta\mu_i$ are the chemical potential differences of water and oxygen.

3 Results and discussion

The stabilities of different potential cationic Cu complexes in ZSM-5 zeolite were investigated by periodic DFT calculations. We assume that multinuclear Cu cations are formed in ZSM-5 zeolite via self-organization of cationic Cu species [2] such as Cu^+, CuO^+ and $[CuOH]^+$, previously considered as extra-framework species in Cu/ZSM-5, and their protolysis with zeolitic Brønsted acid sites. The DFT-computed energies predict binuclear Cu complexes to be the preferred species in Cu/ZSM-5 at 0 K. However, a finite temperature analysis of the Cu speciation including the effect of the gas atmosphere by the *ab initio* thermodynamic approach demonstrates that oxygenated $[Cu_3(\mu\text{-}O)_3]^{2+}$ and hydroxylated $[Cu_3(\mu\text{-}OH)_2(\mu\text{-}O)]^{2+}$ trinuclear

complexes (Figure 1a) are preferred over mono- and binuclear species at conditions typically employed for the activation of Cu/ZSM-5 catalysts, i.e. high-temperature treatment (800 K) in an O_2-rich atmosphere or in the presence of water vapor, respectively.

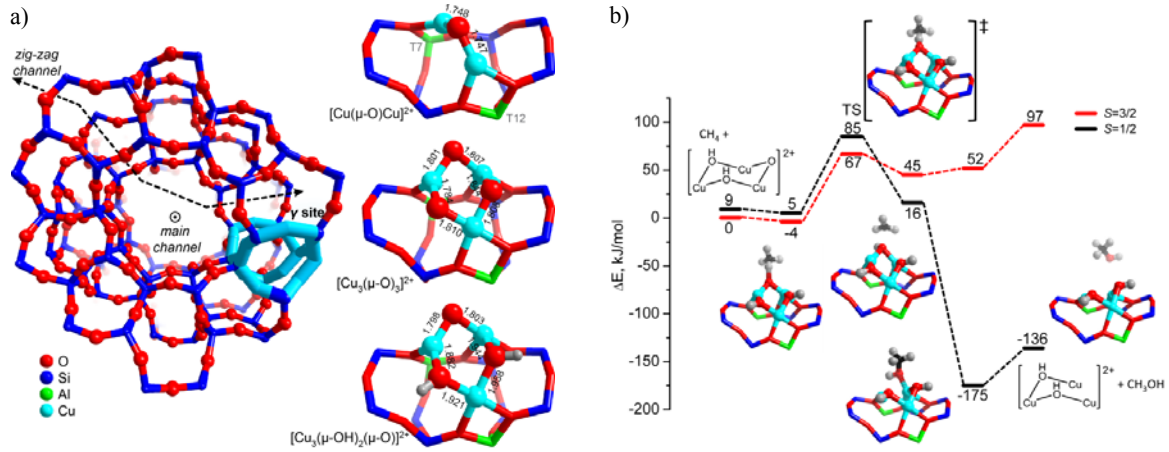

Figure 1. a) Schematic representation of ZSM-5 framework and selected location for accommodation extra-framework Cu-containing species. b) Reaction paths for methane oxidation to methanol over trinuclear hydroxylated $[Cu_3(\mu\text{-}OH)_2(\mu\text{-}O)]^{2+}$ complex in the high (S = 3/2) and low-spin (S = 1/2) electronic configurations.

The reaction energy diagrams for methane oxidation over trinuclear $[Cu_3(\mu\text{-}OH)_2(\mu\text{-}O)]^{2+}$ complex are shown in Figures 1b. Methane is activated in a similar manner as on binuclear Cu site via homolytic C–H bond cleavage The reaction product is a $CH_3^{\bullet}$ radical and a biradical $[Cu_3(\mu\text{-}OH)_3]^{2+}$ extra-framework ion. Accordingly, direct formation of CH_3OH via a rebound mechanism is thermodynamically unfavorable over the high-spin PES. Thus, C–H activation over $[Cu_3(\mu\text{-}OH)_2(\mu\text{-}O)]^{2+}$ will most likely involve a spin-crossing transition (S = 3/2 → S = 1/2). The resulting radical pair in the S = 1/2 electronic configuration recombines readily, resulting in CH_3OH coordinated to a single Cu ion in the partially reduced $[Cu_3(\mu\text{-}OH)_2]^{2+}$ complex. Methanol desorption from this cluster is much more favorable than from the Cu^+ dimer. The regeneration of the initial active complex can be accomplished by oxidation in O_2.

4 Conclusions

Using the combined approach of periodic DFT calculations and *ab inito* thermodynamic analysis, the reaction mechanism of methane oxo-functionalization over extra-framework Cu complexes in Cu/ZSM-5 zeolite has been explored. It is demonstrated that trinuclear Cu-oxo cationic complexes correspond to the most thermodynamically stable species in Cu exchanged zeolite activated in O_2-rich atmosphere. The reactivity comparison predicted that the trinuclear complexes provide a more energetically facile reaction pathway towards methanol than the binuclear sites. Besides the facilitated initial C–H bond activation, the specific electronic configurations of such sites favor the direct radical rebound resulting in methanol formation.

Acknowledgements

This work was financially supported by the EU NEXT-GTL project.

References

[1] J. S. Woertink, B. F. Sels, R. A. Schoonheydt et al., *Proc. Natl. Acad. Sci. U.S.A.* 106 (2009) 18908.
[2] E. A. Pidko, E. J. M. Hensen, R. A. van Santen, *Proc. R. Soc. A* 468 (2012) 2070.

ISO-PP02

Remarkable Enhancement of O_2 Activation on YSZ Surface in a Dual-Bed for Catalytic Partial Oxidation of CH_4

Richard M.[1], Can F.[1], Duprez D.[1], Gil S.[2], Giroir-Fendler A.[2], Bion N.[1*]

1 - University of Poitiers, CNRS UMR 7285, Institut des Milieux et Matériaux de Poitiers (IC2MP), Poitiers Cedex9, France

2 - University of Lyon 1, CNRS UMR 5256, IRCELYON, Villeurbanne, France

* nicolas.bion@univ-poitiers.fr

Keywords: heterogeneous catalysis, YSZ, perovskite, isotopic exchange, partial oxidation of methane

1 Introduction

To find an alternative to polluting energies, the demand for natural gas to produce synthetic fuels has drastically increased in recent decades. Methane conversion to synthesis gas (CO/H_2) is a promising way to yield more easily transportable liquid fuels such as Fischer–Tropsch products or chemicals like methanol [1]. Catalytic partial oxidation of methane (CPOM) was suggested first by Liander for producing syngas [2]. In recent works, yttria-stabilized zirconia (YSZ) has appeared as a promising catalyst for this reaction in which lattice oxygen ions are incorporated into the products via a *Mars-van Krevelen (MvK)* mechanism at 1173 K [3]. Some perovskite solids also demonstrate catalytic efficiency in CPOM [4]. In this work, we used oxygen isotopic exchange technique to demonstrate a remarkable oxygen activation and mobility on YSZ surface at moderate temperature (698 K) when perovskite materials is placed upstream in a dual catalyst bed. Then this system is investigated in CPOM to check whether its behaviour resulted in an improvement in catalytic activity.

2 Experimental/methodology

$LaMnO_3$ perovskite (35 $m^2.g^{-1}$) was prepared by the citrate route and the 8mol% YSZ material (13 $m^2.g^{-1}$) was supplied by TOSOH. For the Pd/YSZ material, 0.2 wt% of Pd was added by wet impregnation. We have undertaken heterolytic temperature programmed oxygen isotopic exchange (TPOIE) and CPOM experiments in a set-up already described elsewhere [5]. A U-form reactor was placed in a closed recycle system connected to a mass spectrometer for the monitoring of the gas phase composition. Experiments were undertaken on 13.3mg of $LaMnO_3$ and 20mg of YSZ or Pd/YSZ. The samples were subjected to an activation step (flow $^{16}O_2$ at 973 K), a purge (using vacuum), then reactants were charged: 55mbar of $^{18}O_2$ at 473 K for TPOIE and 60 mbar of $2CH_4$:$^{18}O_2$ at 698K for CPOM experiments. The m/z values of $^{16}O_2$, $^{16}O^{18}O$ and $^{18}O_2$ were monitored to follow the exchange and H_2, CH_4, $H_2{}^{16}O$, $H_2{}^{18}O$, $C^{16}O$, $C^{18}O$, $C^{16}O_2$, $C^{16}O^{18}O$, $C^{18}O_2$ were also recorded during CPOM experiments.

3 Results and discussion

The fraction of 18O16O and 16O2 formed during the TPOIE experiments is shown in Figure 1. The exchange started respectively at 533 K and 773 K on LaMnO3 and YSZ isolated samples via a simple mechanism (18O2(g)+16O2(s) ⇔ 18O16O(g)+18O(s)) involving a single lattice oxygen atom to form in gas phase $^{16}O^{18}O$ isotope. For the dual-bed $LaMnO_3$-YSZ, the exchange activity started at 533 K with a considerable enhancement of the exchanged atom fraction contrasting with the expected cumulative number of atoms exchanged. This surprising activity is characterized by the modification of the isotopic distribution since isotope $^{16}O_2$ is first observed in the gas phase (Fig. 1 red curves). Additional experiments revealed that

$LaMnO_3$/YSZ contact is not necessary to observe the phenomenon in contrast to the presence of oxygen vacancies in the YSZ solid since it is not observed with pure ZrO_2 or Y_2O_3 materials. Furthermore, the improvement of the exchange was also detected with other perovskite materials such as $LaCoO_3$. This considerable activity is suspected to be due to the formation of an active singlet oxygen species (E=+94.7kJ/mol) on perovskite bed able to activate the exchange at moderate temperature on YSZ placed downstream [6].

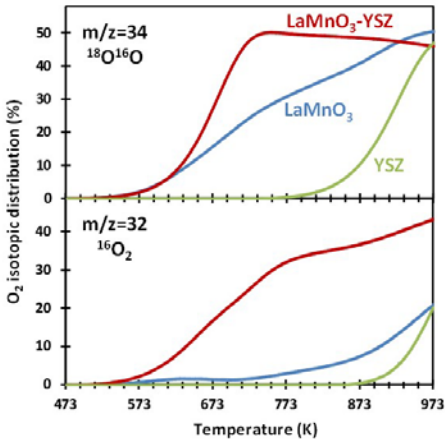

Fig. 1. Evolution of $^{16}O^{18}O$ and $^{16}O_2$ distributions during the TPOIE experiments.

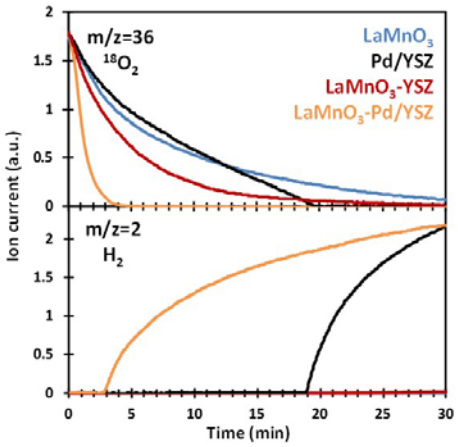

Fig. 2. Evolution of $^{18}O_2$ and H_2 intensities as a function of time during the CPOM reaction at 698 K.

In a second part, the behaviour of the dual-bed system was investigated in CPOM and to prevent the limiting step of methane activation, 0.2 wt% of Pd was added on YSZ what does not affect the oxygen exchange properties. Two steps are identifiable during the reaction: 1/ a consumption of the CH_4 and $^{18}O_2$ was observed while there was an increase in CO_2 signals. This is clearly due to the complete oxidation of CH_4, which is confirmed to occur through a *MvK* mechanism for dual catalyst bed. 2/ the appearance of H_2 slightly before the total consumption of O_2 occurred with the simultaneous production of CO. Direct CPOM is proposed to explain the formation of H_2. Different formulations are compared in Figure 2 for $^{18}O_2$ conversion and H_2 production. Complete oxidation is enhanced in the dual-bed systems (only 3 min against 19 min for Pd/YSZ alone), thus indicating that the beneficial effect observed in terms of oxygen exchange positively influences the oxidation activity. Finally, *MvK* mechanism is not observed for $LaMnO_3$ alone and Pd particles are crucial at this temperature to activate CH_4.

4 Conclusions

The perovskite bed, placed upstream YSZ, enables the formation of an active singlet oxygen species able to activate the exchange process from 533 K with O atoms of the YSZ structure. This behaviour positively influences the catalytic oxidation activity at 698 K. This discovery opens avenues to explore new combinations to produce efficient and industry-compatible catalytic systems for syngas production.

References

[1] B.C. Enger, R. Lødeng, A. Holmen, *Appl. Catal. A: General* 346 (2008) 1.
[2] H. Liander, *Trans. Faraday Soc*. 25 (1929) 462.
[3] J. Zhu, J.G. van Ommen, H.J.M. Bouwmeester, L. Lefferts, *J. Catal* 233 (2005) 434.
[4] F. Mudu, B. Arstad, E. Bakken, H. Fjellvåg, U. Olsbye, *J. Catal*. 275 (2010) 25.
[5] D. Martin, D. Duprez, *J. Phys. Chem.* 100 (1996) 9429.
[6] M. Richard, F. Can, D. Duprez, S. Gil, A. Giroir-Fendler, N. Bion, *Angew. Chem. Int. Ed.* 53 (2014)

ISO-PP03

A Qualitative Kinetic Analysis of Steady-State Selective Oxidation Process: Role of Water and Oxygen

Sprung C.[1*], Yablonsky G. S.[2], Schlögl R.[1], Trunschke A.[1]

1 - Fritz Haber Institute of the Max Planck Society, Dept. of Inorganic Chemistry, Berlin, Germany
2 - Department of Chemistry, Parks College, Saint Louis University, Saint Louis, USA

* sprung@fhi-berlin.mpg.de

Keywords: selective oxidation, kinetics, role of water and oxygen, two-route mechanism on two different sites, apparent kinetic orders

1 Introduction

Acrylic acid is a valuable large-scale product in the chemical industry. The currently applied two-step process starts with propene as reactant, forming acrolein as major intermediate, which is then further oxidised. A one-step process, starting from propane, has been the subject of intensive research for more than two decades, however not yet transferred into production.[1] The underlying sequence of consecutive and perhaps parallel reaction steps reveals great diversity from a chemical point of view; the rather inert C-H bonds have to be activated under the same conditions as a more reactive intermediate shall be oxidised selectively. The first hydrogen abstraction may be considered rate determining, however, more valuable is the mechanistic understanding beyond this step, which is the key for the formation of selective oxidation products. In this contribution, the focus was put on the role of water and oxygen on possible active sites and the oxidation and reduction, respectively, of those sites.

2 Approach

There were analysed trends in steady-state kinetic dependences obtained in experimental studies of selective oxidation of propane over a MoVTeNb M1 oxide catalyst.[2] Based on these experimental results, various reaction networks and corresponding steady-state kinetic models have been studied systematically using graph theory methods.[3] The conceptual investigation was based on a reaction network containing two independent cycles: (i) propane dehydrogenation and (ii) selective oxidation of propene (considered as the only product of cycle 1). Propane, oxygen, water, propene, and acrylic acid were considered as components in this reaction network. Non-selective oxidation products were left out preliminary for reasons of simplification. The dynamically changing active sites at the surface of the catalyst were included in the catalytic cycles.

In analysis of kinetic trends, a special attention was paid to detailed analysis of apparent kinetic orders, $n_{app} = \partial \ln R / \partial \ln C_i$, where R is a steady-state rate of substance change, and C_i is a concentration of gaseous substance. In a number of typical situations, apparent kinetic orders (n_{app}) provide information on the mechanistic framework and moreover present an estimate of some surface intermediates.[3]

3 Results and discussion

The kinetic trends observed in experiments did show a positive apparent kinetic order for both propane and water. The conversion rates of propane and oxygen were, however, independent and inverse proportional on the oxygen partial pressure, respectively. Different functions of water were analysed systematically: (1) activation and (2) deactivation in the corresponding "buffer" steps, (3) participation in the catalytic cycle, and (4) a function as spectator. An impact of water on the kinetic apparent orders of all reactants was characterized.

The mechanism presented in Figure 1 is in agreement with the experimental trends. Propane

reduces an oxidised centre ZO to Z while oxidized to propene (first cycle). Z is subsequently re-oxidised to ZO by gas-phase oxygen. Water activates this cycle through a buffer step, without participating in the reaction. The selective oxidation of propene takes place on a second, independent, centre X. Propene reduces the hydrated centre XH2O to X, which is subsequently oxidised and re-hydrated. An oxygen buffer step causes the negative apparent kinetic order of $R(O_2)$ regarding the oxygen concentration. Table 1 summarises the apparent kinetic orders of all reactants with respect to the rate of propane consumption, $R(C_3H_8)$(1. cycle), rate of propene consumption, $R(C_3H_6)$(2. cycle), and rate of oxygen consumption, $R(O_2)$ (both cycles). In our analysis, two balances on two independent centres, Z and X, were considered. It was found that apparent kinetic orders can be presented as a concentration of one centre or a sum of several centres (see Table 1). The re-oxidation steps to XO and ZO could be assumed fast compared to the other reaction steps, hence, the concentrations of centres X or at least Z can be considered low. Under these assumptions, the propane conversion rate is independent on $p(O_2)$. The oxygen conversion rate is of negative kinetic order with respect to $p(O_2)$. It can be explained by the role of oxygen in propene consumption (Table 1): oxygen participates in the buffer step reducing the abundance of XH2O centres. This phenomenon was more pronounced for high partial pressures of water supporting the presence of such a buffer step.

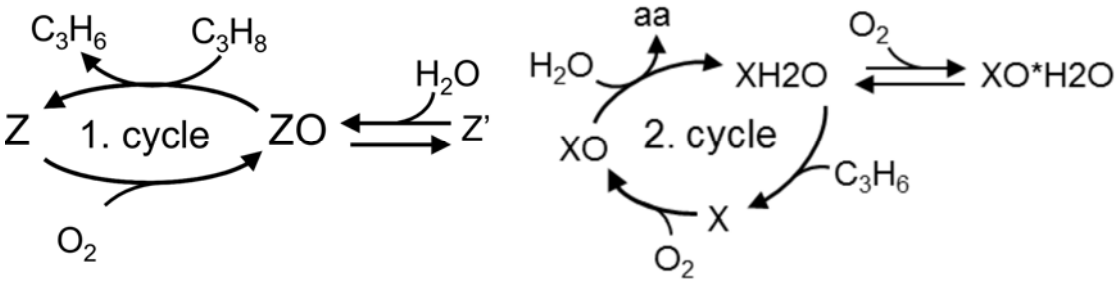

Fig. 1. Two-route mechanism: propane dehydrogenation (1. cycle) and selective oxidation (2. cycle).

Table 1. Representation of apparent kinetic orders of C_3H_8, H_2O, O_2, and C_3H_6 with respect to the rates of C_3H_8, O_2, and C_3H_6 by surface coverages θ. $R(C_3H_6)$ represents the rate of the second cycle.

n_{app}	$R(C_3H_8)$	$R(O_2)$	$R(C_3H_6)$
C_3H_8	$\theta_{ZO} + \theta_{Z'}$	$\theta_{ZO} + \theta_{Z'}$	no influence
H_2O	$\theta_{Z'}$	$\theta_{Z'} + \theta_{XO}$	θ_{XO}
O_2	θ_Z	$\theta_Z + \theta_X - \theta_{XOH2O}$	$\theta_X - \theta_{XOH2O}$
C_3H_6	no influence	$\theta_{XH2O} + \theta_{OXH2O}$	$\theta_{XH2O} + \theta_{OXH2O}$

4 Conclusions

The mechanism in Fig. 1 represents a two-route mechanism on two sites of different nature for understanding kinetic features of selective oxidation of propane to acrylic acid over a MoVTeNb M1 oxide catalyst, potentially carrying multiple active centres.[2] Water activates as a buffer the catalytic centre for propane consumption. In the propene consumption route, oxygen is both a participant and a 'poison', which reduces the number of active centres probably in combination with water.

References

[1] M. M. Lin, Appl. Catal. A: Gen. 207 (2001) 1.
[2] R. Naumann d'Alnoncourt, L.-I. Csepei, M. Hävecker, F. Girgsdies, M. E. Schuster, R. Schlögl, A. Trunschke J. Catal. 311 (2014) 369.
[3] G. M. Marin, G. S. Yablonsky: Kinetics of Chemical Reactions, Decoding Complexity; 2011, Wiley-VCH, Weinheim.

ISO-PP04

Nanomaterial Based Catalysts for Low-Temperature Oxidation of Carbon Monoxide

Bakaev V.A.[1], Vershinin N.N.[1*], Berestenko V.I.[1], Efimov O.N.[1], Kabachkov E.N.[1,2], Kurkin E.N.[1,2]

1 - Institute of Problems of Chemical Physics of the Russian Academy of Sciences, Chernogolovka, Russia

2 - Scientific Center in Chernogolovka of the Russian Academy of Sciences, Chernogolovka, Russia

* vernik@icp.ac.ru

Keywords: carbon monoxide, low-temperature oxidation, SiC, nanodiamond, TiC, TiN

1 Introduction

Catalytic systems working efficiently at low concentration of CO at room temperature are to be used in devices for air purification from carbon monoxide (CO) in homes and offices. It was found [1-4] that , the use of nanodiamond (ND) and nanosized silicon carbide (SiC) supports for platinum metals allows the development of catalysts for oxidation of CO, which can operate efficiently at low concentration of carbon monoxide at room temperature.

2 Experimental/methodology

We synthesized CO catalysts based on nanosized supports (titanium nitride, titanium carbide, titanium carbonitride and titanium dioxide) including platinum and/or palladium clusters. Catalytic oxidation of CO was studied at room temperature at low concentration (less than 200 ppm) characteristic of homes and offices. TiN, TiC and TiC_xN_y particles of 10 ÷ 60 nm size prepared by us by plasma chemical method and industrial titanium dioxide crystallites of 5-9 nm size were used as supports. The CO catalyst was synthesized using the procedure described in [1-3].

3 Results and discussion

The clusters (Pt, Pd) are specified by high quantity of surface atoms and, hence, high catalytic activity in the reaction of CO oxidation at low concentration. The catalysts showed high catalytic activity in the reaction of oxidation of CO at room temperature.

4 Conclusions

New nanomaterial based CO catalysts can possibly be used in catalytic and photocatalytic systems for air purification from toxic gases in homes and offices.

References

[1] Catalyst and method of its preparation/ N.N.Vershinin, O.N.Efimov, // Russian patent N 2348090 of February 27, 2009.

[2] Nanocatalyst and method of its preparation/ N.N.Vershinin, O.N.Efimov, V.A.Bakaev, I.I.Korobov// Russian patent N2411994 of February 20, 2011.

[3] Detonation nanodiamonds as catalyst supports/N.N. Vershinin, O.N. Efimov, V.A. Bakaev, A.E. Aleksenskii, M.V. Baidakova, A.A. Sitnikova, A.Ya. Vul//Fullerenes, *Nanotubes and Carbon Nanostructures,* 19: 1, 63-68, 2011.

[4] N.N.Vershinin, V.A.Bakaev, I.L.Balikhin, O.N.Efimov, E.N.Kabachkov, B.V.Torbov, E.N.Kurkin «Nanocatalysts for catalytic and photocatalytic air purification from toxic gases in homes» C. 166-167 in Proceedings of the II Russian Congress on catalysis(Volume 1), Samara, 2-5 October, 2014.

ISO-PP05

Gold Supported on Fe-Doped Ceria Supports Prepared through the Microemulsion Method for the PROX Reaction

Laguna O.H.[1*], Centeno M.A.[1], Boutonnet M.[2], Odriozola J.A.[1]

1 - Instituto de Ciencia de Materiales de Sevilla, Seville, Spain
2 - Royal Institute of Technology (KTH), Department of Chemical Technology, Div. of Chemical Technology, Stockholm, Sweden

* ohlaguna@icmse.csic.es

Keywords: water-in-oil microemulsion, Fe-doped ceria, oxygen vacancies, gold catalyst, PROX, CO oxidation

1 Introduction

The purification of H_2 produced by reforming of organic molecules is required for the feed of PEMFC that present a low tolerance to CO (< 50 ppm). Such purification is carried out in different steps but the final levels are achieved in units of CO selective oxidation under the presence of H_2. In this sense, active and selective catalysts able to oxidize CO without H_2 consumption are required. Gold-based catalysts have been widely employed in oxidation reactions [1]. Similarly, reducible oxides such as CeO_2 have demonstrated an acceptable performance in the CO oxidation reaction due to their oxygen mobility and oxygen storage capacity. The modification of the CeO_2 framework with heteroatoms like Fe significantly improves the oxygen mobility of the ceria through the creation of oxygen vacancies [1].

Considering the described scenario, the present work proposes the synthesis of gold catalysts combining the ability of adsorbing and dissociating CO of this noble metal, and the oxygen mobility of the Fe-doped ceria systems for supplying structural oxygen. The gold nanoparticles may cooperate with the modified supports for the enhancement of the activation of the O_2 and CO molecules during the oxidation reaction.

2 Experimental/methodology.

Fe-doped ceria systems (10, 25 and 50 Fe At.%) previously studied by us [2], were employed as supports. These solids were synthesized through the microemulsion method (N-octane 53 wt.%; cetyl trimethyl ammonium bromide 13 wt.%; 1-butanol 13 wt.%; aqueous phase 21 wt.%). For every system, two microemulsions were prepared. The first one containing the required amounts of cerium and iron nitrates dissolved in the aqueous phase, and the other microemulsion containing an excess of NH_3. After the mixture of both microemulsions, a precipitate was obtained and kept under stirring during 24 h. The precipitate was washed with a 50/50 vol.% methanol/chloroform mixture, then dried at 60 ºC for 24 h and finally calcined at 500 ºC for 2h. The gold catalysts were prepared by the deposition-precipitation method employing $HAuCl_4 \cdot 3H_2O$ as precursor for obtaining a 1 wt.% loading of gold . After gold deposition, the catalysts were calcined at 300 ºC for 2h. The obtained solids were characterized by means of XRF, N_2 adsorption/desorption isotherms, XRD, H_2-TPR, UV-Vis, Raman spectroscopy and XPS. The catalytic activity measurements were carried out in a fixed-bed reactor. Prior to the catalytic tests the solids (100 mg, particle size ϕ =100–200 μm) were activated with 30 ml/min of air for 1 h at 300 ºC. Then, the materials were submitted to a 100 ml/min of the mixture of reaction (CO = 2 vol.%; O_2 = 1 vol.%; H_2 = 50 vol.% and N_2 for balance). The products of reaction were followed by on-line gas chromatography in a Varian® CP-4900 instrument equipped with two modules (a Porapak® Q column in the first one and a Molecular Sieve 5A in the second one, and TCD detectors in both cases).

3 Results and discussion

The XRF results demonstrated that the obtained loadings of gold were similar to the intended values for the systems doped with 10 and 25 Fe At.%. Nevertheless, the AuCeFe50 solid exhibited a lower amount of loaded gold. No modification of the XRD diffraction lines of the supports was detected in the patterns of the gold samples.. In the case of the catalysts with 10 and 25 Fe At.%, no signals associated to the presence of gold phases were observed either. However the AuCeFe50 not only presented the segregation of crystalline α-Fe_2O_3, but also the (111) crystallographic plane of metallic gold was detected. The Raman signal associated to oxygen vacancies of the supports was vanished after the deposition of gold in all cases, demonstrating the capital role of these defects on the nucleation of gold deposits.

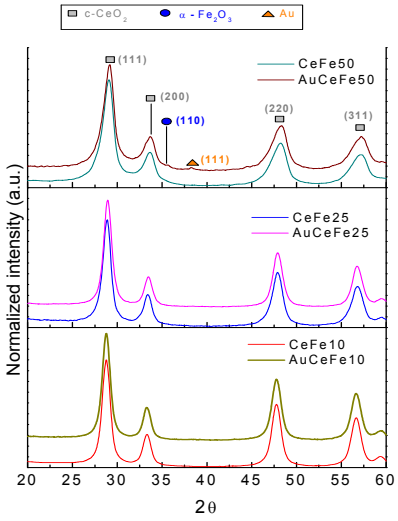

Figure 1. XRD patterns of the supports and the gold catalysts

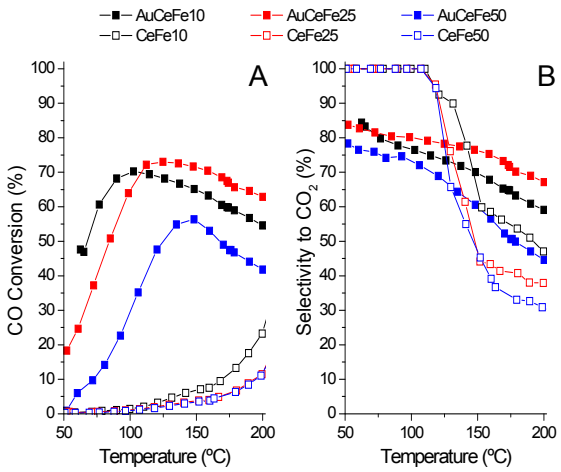

Figure 2. Catalytic activity of the supports and the gold catalysts: A) CO conversion; B) Selectivity to CO_2

The catalytic activity measurements showed a huge increment of the CO conversion at lower temperatures after the deposition of gold. This suggests the enhancement of the oxidation abilities of the catalysts. Considering that as higher the population of oxygen vacancies in the support is, higher the catalytic activity (at lower temperatures) of the corresponding catalyst, these punctual defects must be responsible of the easier activation of the O_2 and CO molecules for the oxidation reaction.

4 Conclusions

The oxygen vacancies population of the Fe-doped support strongly influences their interaction with gold. Higher the amount of oxygen vacancies higher the amount of gold deposited. Concerning the catalytic activity, the presence of noble metal greatly increases the CO conversion at lower temperatures of the Fe-doped supports in all cases. However, a superior catalytic activity is showed by the gold catalyst whose support presented the highest oxygen vacancies population.

References

[1] O.H. Laguna, F. Romero-Sarria, M.A. Centeno, J.A. Odriozola, Journal of Catalysis, 276 (2010) 360-370.

[2] O.H. Laguna, M.A. Centeno, M. Boutonnet, J.A. Odriozola, Applied Catalysis B: Environmental, 106 (2011) 621-629

ISO-PP06

Silica-Supported Silver-Containing OMS-2 Catalysts for Ethanol Oxidative Dehydrogenation

Dutov V.[1*], Mamontov G.[1], Sobolev V.[1,2], Vodyankina O.[1]

1 - Tomsk State University, Tomsk, Russia
2 - Boreskov Institute of Catalysis SB RAS, Novosibirsk, Russia

* dutov_valeriy@mail.ru

Keywords: selective oxidation, ethanol, manganese, octahedral, molecular, sieve, silver, silica

1 Introduction

High activity of supported silver catalysts in selective oxidation of alcohols was shown in many studies [1, 2]. Catalytic activity of Ag-containing catalysts, in particular, Ag/SiO_2, may be increased by addition of transition metal oxides [3]. Manganese oxides are expected to be suitable modifiers for Ag/SiO_2 catalyst due to reversible Mn^{4+}/Mn^{3+} redox cycle. It is known that silver-containing cryptomelane-type manganese dioxide catalysts (Ag/OMS-2) have high activity and selectivity in oxidation of alcohols, in particular, octanol-1 and ethanol [4, 5]. However, oxidation of ethanol over OMS-2 catalysts is carried out using gas mixture containing low concentration of oxygen, generally 1-10 vol. % [5, 6] because of high activity of these catalysts in deep oxidation. One of the ways to control the redox, catalytic and acid-base properties of metal oxides is the use of different supports. The purpose of present research work is to design the method to prepare highly effective $Ag/OMS\text{-}2/SiO_2$ catalysts and investigate their catalytic properties in oxidative dehydrogenation of ethanol.

2 Experimental

To prepare Ag/OMS-2 catalysts two different methods were used. At first, OMS-2 sample was prepared by procedure described in [7], and then it was impregnated with water solution of $AgNO_3$ followed by calcination in air flow at 500 ^oC (Ag/OMS-2-I). In the co-precipitation method (CP) $AgNO_3$ was added in course of preparation of OMS-2. Nominal amount of Ag was 5 % wt. The $Ag/OMS\text{-}2/SiO_2$ catalysts were prepared by the sequential impregnation (SI) and co-precipitation (CP) methods. In the first method silica was impregnated with appropriate quantity of $KMnO_4$ solution and then dried at 60 ^oC. The obtained $KMnO_4/SiO_2$ sample was added into the acidified water solution of $Mn(NO_3)_2$ under stirring. After that the obtained mixture was heated in autoclave for 24 h, then the precipitate was filtered, washed and dried. The obtained $OMS\text{-}2/SiO_2$ sample was impregnated with water solution of $AgNO_3$ followed by calcination in air flow at 500 ^oC. According to the second method, $KMnO_4/SiO_2$ was added into the mixed solution of $Mn(NO_3)_2$ and $AgNO_3$. The catalysts were characterized by TPR-H_2, TPO, TPSR-C_2H_5OH, XRD, TEM, AES and N_2 adsorption at -196 ^oC. Catalytic activity of the samples in ethanol oxidation was tested in a flow fixed-bed reactor at atmospheric pressure using 0.5 g of catalyst. Gas mixture containing 2 %vol. C_2H_5OH and 18 vol. % O_2 in He was passed through reactor at total flow rate of 60 cm^3/min. The effluents from the reactor were analyzed by on-line gas chromatography. Prior to catalytic experiment the catalysts were treated in 8 % O_2/He at 500 ^oC for 1 h.

3 Results and discussion

Investigation of chemical composition of the prepared catalysts revealed that using of co-precipitation method (CP) resulted in partial loss of Ag due to leaching of silver in course of hydrothermal treatment.

The OMS-2, Ag/OMS-2-I and Ag/OMS-2-CP catalysts were used as model systems for detailed characterization of supported catalysts. To investigate the effect of silver addition on the active sites of OMS-2 TPSR of adsorbed ethyl alcohol were carried out. Formation of water was observed for all catalysts at 80 °C in course of ethanol adsorption in pulse mode, therefore adsorption and dehydration of ethanol occurred on the acid sites. The quantity of adsorbed alcohol was 221, 172 and 142 μmol/g for OMS-2, Ag/OMS-2-CP and Ag/OMS-2-I catalysts, respectively. Carbon dioxide was the main product of TPSR and released at 170 and 230 °C.
Investigation of catalytic activity of prepared OMS-2/SiO_2, Ag/OMS-2/SiO_2-SI and Ag/OMS-2/SiO_2-CP catalysts in oxidative dehydrogenation revealed that addition of silver results in increasing of the ethanol conversion. This may be explained by increasing of reaction ability of surface oxygen in the presence of silver, which was confirmed by TPR-H_2. The effect of silver content and Mn/Ag molar ratio on the catalytic properties was investigated. It was stated that silver content insignificantly effect on the ethanol conversion. However, selectivity towards acetaldehyde depends on silver content. For Ag/OMS-2/SiO_2-CP catalyst the selectivity towards acetaldehyde at temperatures above 200 °C is lower in comparison with the one for Ag/OMS-2/SiO_2-SI due to low silver content (higher molar ratio Mn/Ag) or formation of mixed Ag-Mn phase in course of synthesis via co-precipitation.

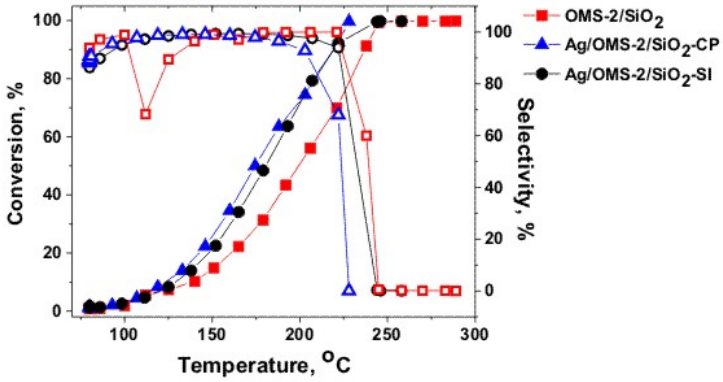

Fig. 1. Catalytic properties of OMS-2/SiO_2, Ag/OMS-2/SiO_2-SI and Ag/OMS-2/SiO_2-CP

Generally, deep oxidation activity of Ag-containing supported catalysts is higher than the one for OMS-2/SiO_2, which may be associated with increasing of reoxidation ability in presence of silver (according to TPO data).

4 Conclusions

The Ag/OMS-2/SiO_2 and OMS-2/SiO_2 catalysts were synthesized and tested in ethanol oxidation. It was stated that silver addition increases the reducibility and reoxidation ability of OMS-2, as a consequence catalytic activity increases. Catalytic properties of Ag/OMS-2/SiO_2 catalysts may be controlled by variation of Mn/Ag molar ratio and preparation method.

Acknowledgements

This work was supported by the RFBR (project mol_NR 14-33-50483)

References

[1] L. Ma, L. Jia, X. Guo, L. Xiang, *Chinese Journal of Catalysis*. 35 (2013) 108.
[2] O. Vodyankina, A. Blokhina, I. Kurzina, V. Sobolev, K. Koltunov, *Catalysis Today*. 203 (2013) 137.
[3] T. Kharlamova, G. Mamontov et al., *Appl. Catal. A: General*. 467 (2013) 519.
[4] G. D. Yadav, R. K. Mewada, *Chemical Engeneering Research and Design*. 90 (2012) 86.
[5] J. Chen, J. Li et al., *Chinese Journal of Catalysis*. 28 (2007) 1034.
[6] H. Zhou, J. Y. Wang et al., *Microporous and mesoporous materials*. 21 (1998) 315.
[7] R. N. DeGuzman, Y-F. Shen, E. J. Neth, S. L. Suib et al., *Chem. Mater. 6* (1994) 815.

ISO-PP07

A Heterogeneous Single-Site Organocatalyst for Alkene Epoxidation

Tyablikov I.A., Romanovsky B.V.*

Department of Chemistry, Lomonosov Moscow State University, Moscow, Russia

* igortabl3@gmail.com

Keywords: heterogeneous organocatalyst, SBA-15, mesoporous, silica, alkene epoxidation

1 Introduction

Organocatalysis is one of the most challenging goals in modern catalytic chemistry. Many key organic reactions such as aldol condensation, Mannich reaction, numerous cycloadditions, and other were shown to be carried out in homogeneous metal-free conditions using organocatalysts [1]. On the other hand, in the literature there are some excellent examples of solid catalysts with immobilized organocatalytic centers [2], which show the activity quite analog to homogeneous ones, so as to realize the well-known concept of single-site catalytic materials. These catalysts are evident to be of both academic and industrial interest. 2.2.2-trifluoroacetophenone (TFAP) [3] is proven to be an effective organocatalyst for selective epoxidation of alkenes with hydrogen peroxide under room temperature conditions.

Given that, in this work we aimed to develop catalyst with immobilized TFAP organocatalyst for the epoxidation of alkenes.

2 Experimental/methodology

Heterogeneous epoxidation catalyst based on TFAP was synthesized by three-step assembling procedure. First step was a synthesis of the SBA-15 support according to the method reported in [4]. Second step was the modification of SBA-15 via interaction of silanol groups with trimethoxyphenylsilane in toluene under refluxe using hydrochloric acid as a catalyst. Finally, the acylation of surface anchored phenyl groups with trifluoroacetic anhydride in the presence of aluminum chloride was performed.

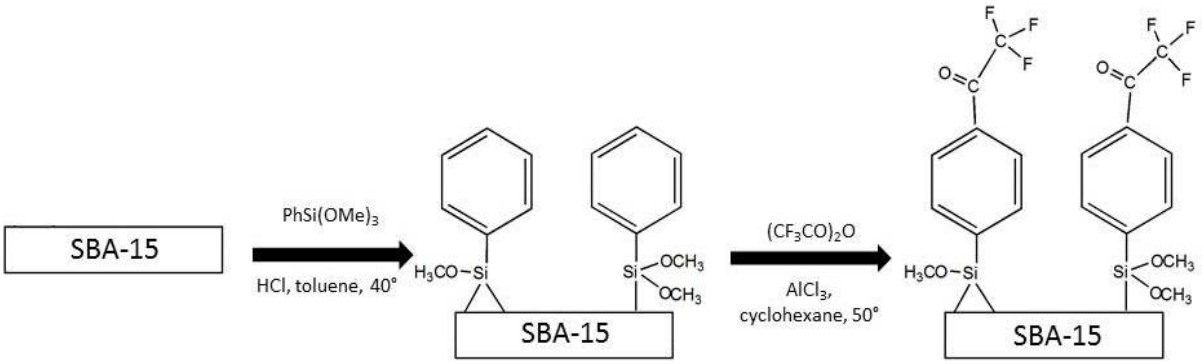

Fig. 1. Synthetic route to produce heterogeneous TFAP catalyst

Obtained samples were characterized by nitrogen adsorption-desorption measurements, UV-Vis and NMR spectroscopy. Liquid-phase epoxidation of propene substrate was performed in a batch reactor at 25 °C and 9 MPa using 28% hydrogene peroxide as an oxidant, acetonitrile as a sacrificing agent and *tert*-butanol as a solvent.

3 Results and discussion

Nitrogen adsorption measurements for both as-synthesized SBA-15 support and material modified by phenylation and then acylation showed the noticeable decrease of surface area and mean pore size which suggests the anchoring of TFAP catalytic species to the pore walls. The TFAP surface centers were successfully quantified by using ^{19}F NMR technique. The catalytic tests showed that the heterogeneous organocatalyst exhibits selectivity of propene conversion into propylene oxide of 100% with peroxide efficiency of 20%. What is the most important, this hybrid catalyst prepared by such a way could be easily separated from the reaction media by filtration and reused without any loss in activity.

4 Conclusions

The hybrid catalyst prepared by surface assembling of 2.2.2-trifluoroacetophenone molecules from their constituents using SBA-15 mesoporous silica as a support allows, for propene epoxidation with H_2O_2 at ambient temperature, to produce propylene oxide with selectivity of 100% and peroxide efficiency of 20%.

Acknowledgements

The authors thank the Russian Science Foundation for the financial support (grant No. 14-23-00094).

References

[1] P.I. Dalko, L. Moisan, *Angew. Chem. Int. Ed.* 43 (2004) 5138 – 5175.
[2] R.A. Shiels, C.W. Jones, *J. Mol. Catal.A:Chem*. 261 (2007) 160.
[3] D. Limnios, C.G. Kokotos, *J. Org. Chem.* 79 (2014) 4270–4276.
[4] V. Meynen, P. Cool, E.F. Vansant, *Micropor. Mesopor. Mater.* 125 (2009) 170-223

ISO-PP08

Selective Photo-Oxidation of α-pinene with Dioxo-Mo(VI) Complex /TiO_2 with Different Textural Properties

Martínez H.*, Páez E.A., Martínez F.

Cicat, Escuela de Química, UIS, Bucaramanga, Colombia

* hmartinezquinonez@gmail.com

Keywords: dioxoMo complex titania, nanotubes, surface, functionalization, selective photo-oxidation

1 Introduction

Dioxomolybdenum complexes anchored on TiO_2 are active on the selective photo-oxidation of hydrocarbons with O_2, but the concentration of the Mo complex tend to be low, affecting its activity [1,2]. Anchoring is carried out through on the surface hydroxyl groups. The amount of Mo complex depends on the concentration and accessibility of the OH groups. The concentration, distribution and accessibility of OH groups influence the chemical reactivity of the support [1] which depends on the preparation method. In the present work the photo-assisted oxygen transfer to α-pinene with O_2 with dioxo-dichloro-(4,4'-dicarboxylic acid-2,2'-bipyridine) Mo (IV) anchored on TiO_2: a- commercial Degussa P-25, b- Aldrich nanopowder and c- synthetized TiO_2 nanotubes (with different textural properties and different amounts of hydroxyl groups on the surface) was evaluated.

2 Experimental/methodology

TiO_2 nanotubes were synthesized by the hydrothermal method [3]. A solution of hexamethyldisilazane (HMDS) (Aldrich) in toluene (40 mL) was added to TiO_2 (1g), previously dehydrated. The mixture was stirred under N_2 flow for 24 hours. The amount of functionalized OH groups was determined collecting the released NH_3 on a solution of 2% H_3BO_3 and titrated (0.1N HCl). The nature of the OH groups (bridge, isolated and germinal) was observed by IR-PAS: the TiO_2 samples were heated (100 °C for 48 h) and stored under vacuum before taking the spectra. The amount of OH groups was determined by TGA: the TiO_2 samples were heated under N_2 from 25 °C to 120 °C at 10 °C/min, maintaining 120º during 10 min (adsorbed H_2O elimination), and then heated at 20 °C/min, from 120 º to 500 °C (OH elimination).
Silylated TiO_2 samples were suspended in toluene then a solution of 2,2'-bipyridine-4,4'-dicarboxylic acid was added. A toluene solution MoO_2Cl_2 was added to a toluene suspension of the previously obtained solid. α-pinene epoxidation was carried out in a 15-mL batch microreactor (Hg lamp, λ= 360 nm) at 19 °C in oxygen. α-pinene (10^{-2} M) in CH_3CN was thoroughly deoxygenated by bubbling N_2 before the addition of the catalyst (15 mg).

3 Results and discussion

TiO_2 textural properties were determined by N_2 adsorption-desorption and the surface OH density on TiO_2 was evaluated by HMDS titulation, IR and TGA (see Table 1).

Table 1. Textural properties and density of surface OH groups of the TiO_2 supports

TiO_2 Support	S BET (m^2g^{-1})	Total OH's/nm^2 [a*]	Reactive OH's/nm^2 [b*]	DioxoMo (mmol g^{-1})[a]
Degussa P-25	50	5,4	4,8	0,15
nanopowder	200	27,5	22,8	0,72
Nanotubular	330	31,6	26,3	0,81

[a] Calculated by TGA [b] Calculated by NH_3 titulation in HMDS sililation. [*] Average value of three measurements (+ 0,1)

Functionalization degree of the OH groups was followed by IR-spectroscopy PAS. The intensity of signals at 3555, 3745 and 3750 cm^{-1} are associated with the Ti-OH groups with a hydrogen type interactions, -OH isolated and geminal groups $Ti(OH)_2$ respectively [4] (see fig. 1-a,b), and confirm that the increase in surface area, like as it observed in the nanopowder and nanotubes samples leads to an increase in the number of hydroxyl groups prone to functionalize. This same intensity ratio is maintained in the subsequent steps of silylation and functionalization (fig. 1-c, d), that confirming that nanotubular TiO_2 (with a greater number of -OH susceptible to functionalize) has the highest amount of complex anchored.

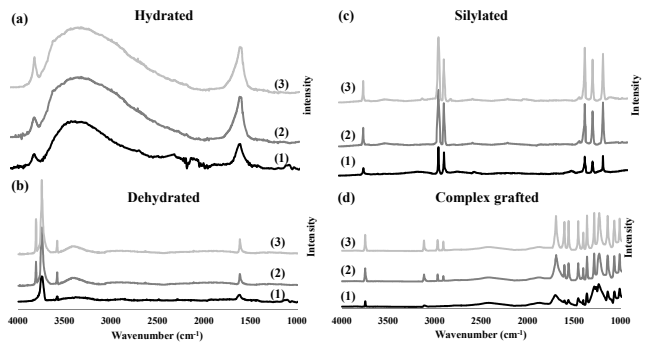

Fig. 1. IR-PAS TiO_2 monitoring (1)- P25, (2)-Aldrich nanopowder, (3)-nanotubes.

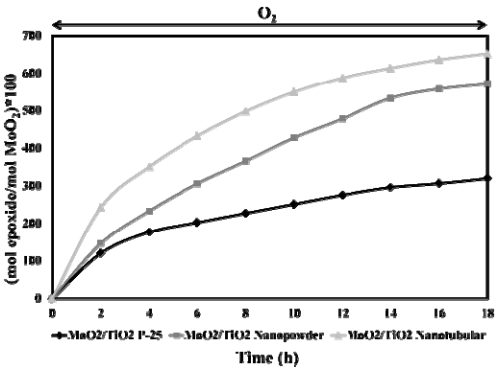

Fig. 2. Oxide α-pinene formation under molecular oxygen with various MoO_2/TiO_2

Figure 2 shows oxide α-pinene formation in the presence of the different dioxo-molybdenum(VI)/TiO_2 catalysts. It appears that there is a strong influence of hybrid MoO_2/TiO_2 catalysts on the α-pinene conversion. The MoO_2/TiO_2 nanotubes system is the most active with respect to the other catalysts based on the commercial TiO_2 (P-25) and Aldrich nanopowder supports. Such behavior could be related to an increased amount of dioxo-Mo(VI) species grafted over the surface of the nanotubular TiO_2 (see Table 1). MoO_2/TiO_2 (nanotubular) shows the highest surface density of hydroxyl groups required for the anchoring of the Mo(VI) complex, and hence the highest content of dioxo-Mo(VI) complex covalently anchored.

4 Conclusions

Dioxo-Mo(VI)-dichloro[4,4'-dicarboxylate-2,2'-bipyridine] complex anchored on various TiO_2 is active, selective and stable for the photo-assisted epoxidation of α-pinene. The textural properties of the TiO_2 support and the density of surface hydroxyl groups have a strong impact on the amount of the Mo complex grafted on the surface and hence on the catalytic properties.

Acknowledgements

The authors gratefully acknowledge the Universidad Industrial de Santander (project DIEF 9313) for financial support.

References

[1] F. Martínez, H. Martínez, M.F. Caceres, E.A. Páez, S. Valange, J. Barrault, *11th European Congress on Catalysis – EuropaCat XII*, Lyon, France, septembre 6th – 13th, 2013.
[2] H. Arzoumanian, , N.J. Castellanos, F. Martínez O., E.A. Páez-Mozo, F. Ziarelli, *Eur. J. Inorg. Chem*. (2010) 1633.
[3] L. Bey Fen, T. K. Han, N. M. Nee, B. C. Ang, M. R. Johan, *Appl. Surf. Sci*. 258 (2011) 431.
[4] M. Ramakrishna, M. S. Hamdy, G. Mul, E. Bouwman, E. Drent, *J. of Catal*. 260 (2008) 288.

ISO-PP09

Study on Kinetics of Liquid Phase Photocatalytic Oxidation of Dibutyl Sulfide over Fullerenes

Arsentyev A.V.[1,2*], Vorontsov A.V.[1,2]

1 - Novosibirsk State University, Novosibirsk, Russia,
2 - Boreskov Institute of Catalysis SB RAS, Novosibirsk, Russia

* alexars.92@mail.ru

Keywords: photocatalysis, C70, C60, visible light, selectivity

1 Introduction

Fullerenes represent a relatively new allotropic modification of carbon that was discovered in 1985 by Kroto et al. after vaporization of carbon species from the surface of a solid disk of graphite using a focused pulsed laser [1]. The discovery made a revolution in molecular design and it leads to obtaining other novel structures such as graphene and carbon nanotubes. Afterwards photochemical reactivity of fullerene was proved: quantum yield of singlet oxygen production in toluene solution of fullerene C_{60} is almost 100% [2]. Photoexcited fullerene transfers electron leading to generation reduced oxygen species ($O_2^{-\bullet}$ and $^{\bullet}OH$) [3]. Information on photocatalytic activity of fullerenes is available in the literature. However, kinetic studies were never undertaken. In the present work, the influence of several parameters on the rate and selectivity of dibutyl sulfide (DBS) photooxidation on C_{70} is investigated.

2 Experimental/methodology

Fullerene C_{70} (99%, Aldrich), dibutil sulfide (96%, Aldrich), toluene (99.5%, Reachim) were used in the experiments. Solution of fullerene C_{70} in toluene was prepared with necessary concentration and after addition of DBS was irradiated with visible LED lamp (10 W) in a batch reactor under continuous stirring and air bubbling. Naphthalene was used as internal standard. Spectral effects of light were studied using cut-off filters. Spectrum of light was measured with spectroradiometer ILT950. Products were identified with GC-MS (CP-3800 + Saturn 2000). Quantitative analyses of reaction mixture were carried on with gas chromatography (Hewlett Packard 5890, capillary column CP-Sil 8 CB and flame ionization detector).

3 Results and discussion

With the help of GC-MS we found that the major products of photooxidation of DBS (Bu_2S) are dibutil sulfoxide Bu_2SO, dibutil sulfone Bu_2SO_2, and dibutil disulfide Bu_2S_2.

The influence of spectral composition of irradiating light is illustrated in Fig. 1 and 2. Filters were selected to study the influence of wavelength on activity of fullerene C_{70}. Linear dependence of DBS consumption rate on photon flux with various wavelengths indicates that fullerene C_{70} has an equal activity in whole visible light range (Fig. 2). However, selectivity to products changed and dibutyl sulfone Bu_2SO_2 appears to form in larger quantities in reaction at lower irradiance (Fig. 1). Generation of dibutyl sulphide Bu_2S_2 is accelerated at higher irradiance.

In another experiment irradiation intensity was varied. It was shown that selectivity of oxidation depends on irradiation intensity. The ratio Bu_2SO:Bu_2SO_2 decreases when the intensity decreases. So it is possible to control selectivity for this reaction by changing light intensity. The influence of reagent Bu_2S and fullerene C_{70} concentration was also studied. Both experiments showed quite weak dependence of rate and selectivity of reaction in a wide range of parameters varied.

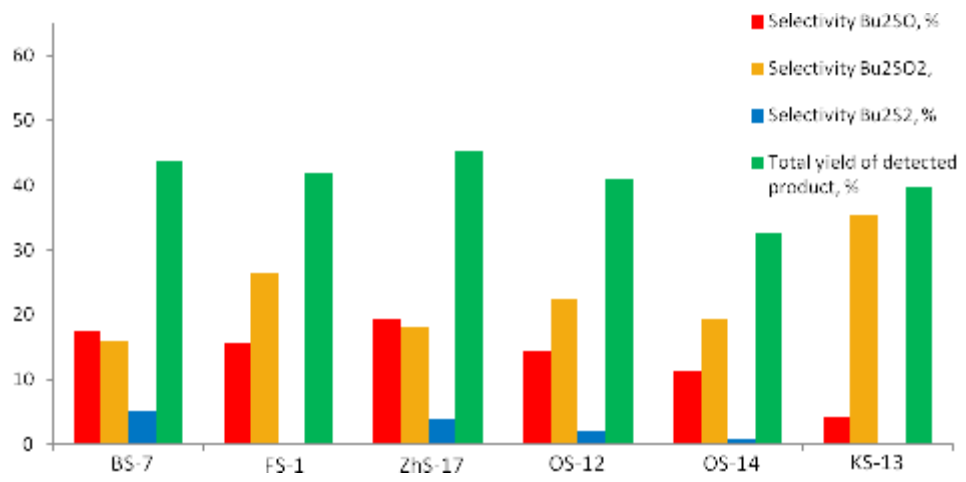

Fig. 1. Comparison of Bu_2S oxidation selectivity on fullerene C_{70} after 18 min of irradiation.

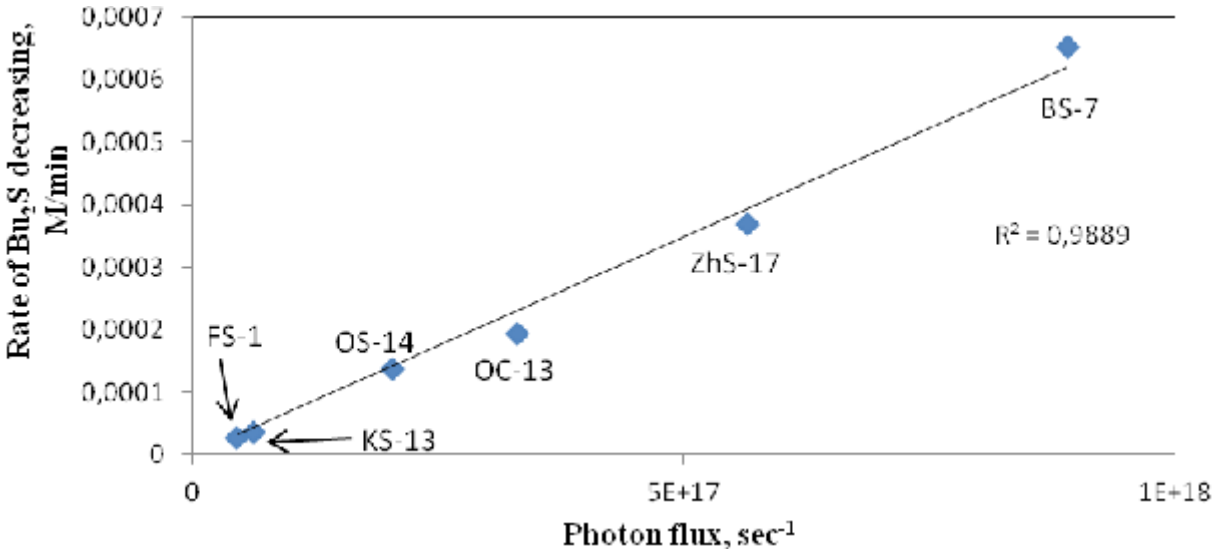

Fig. 2. Correlation between rate of reaction and photon flux; different filters were used as marked.

3 Conclusions

The kinetics of organic sulphide Bu_2S photooxidation with fullerene C_{70} as catalyst was studied under visible light. Intensity of irradiation affects on the rate and selectivity. Fullerene C_{70} has equal activity in whole visible light range.

Acknowledgements

The support of the base budget project V.45.3.7 as well as RFBR project 15-08-01936 is gratefully acknowledged.

References

[1] H. Kroto, J. Heath, S. O'Brien, R. Curl, R. Smalley, *Nature.* 318, (1985) 162.
[2] F. Prat, R. Stackow, R. Bernstein, W. Qian, Y. Rubin, C. Foote, *J. Phys. Chem. A.* 103 (1999), 7230-7235
[3] Y. Yamakoshi, N. Umezawa, A. Ryu, K. Arakane, N. Miyata, Y. Goda, T. Masumizu, T. Nagano, *J. Am. Chem. Soc.* 125, (2003) 12803-12809

ISO-PP10

Liquid Phase Oxidation of L-Sorbose over Metallic and Bimetallic Particles Stabilized in Polymer Matrix

Torozova A.S.[1,2*], Doluda V.Yu.[1], Sulman E.M.[1], Murzin D.Yu.[2]

1 - Tver State Technical University, Dep. Biotechnology and Chemistry, Tver, Russia
2 - Abo Akademi University, Turku, Finland

* torozova@gmail.com

Keywords: oxidation, L-sorbose, ascorbic, acid nanoparticles, hypercross-linked polystyrene

1 Introduction

The oxidation of monosaccharides is of great scientific and practical importance because compounds containing carboxyl groups are intermediates for several valuable fine chemicals such as pharmaceuticals and biologically active substances.

The oxidation reactions are often carried out with expensive and toxic stoichiometric oxidants. This way offers a direct route to the target products; however, the reaction frequently affords non negligible amounts of the side-products and requires additional purification as well as neutralization of the waste. The principles of "green" chemistry are based on the respect for the environment, therefore the task is to develop catalysts which should be easily removed from the reaction medium and reused with high efficiency. It is known that supported transition metal nanoparticles are highly active as heterogeneous catalysts in alcohols and monosaccharides oxidation with molecular oxygen or air [1-3]. Hypercross-linked polystyrene was chosen for the present study. Such structure combines both micropores and macropores and can be considered for regulated nanoparticle growth. This research focuses on the oxidation process of L-sorbose with synthesis of commercially interesting target product 2-keto-L-gulonic acid (ascorbic acid production).

2 Experimental/methodology

The monometallic and bimetallic nanosized catalysts were synthesized by the sorption of the precursors ($H_2PtCl_6 \cdot 6H_2O$, $Pd(CH_3COO)_2$, $HAuCl_4 \cdot 2H_2O$) from THF in the hypercross-linked polystyrene (HPS) matrix. In case of Pt-Au catalyst it was followed by sodium bicarbonate treatment for the precipitation of metal oxides.

The experimental set-up for oxidation at atmospheric pressure was a four necked glass flask (total volume 100 ml) for feeding the catalyst, the solvent, the reactant and cooling with a condenser. The constant heating was organized with a thermostat. Stirring speed during the reaction was 1000 rpm and furthermore, the catalyst particle size below 0.71 μm was used in order to perform the processes under kinetic regime. Evaluation of catalytic properties in L-sorbose oxidation was done with mass of 1 g of the reactant and the catalyst in 10 ml of water with adding NaOH as alkaline agent at 70°C.

The identification of the reaction mixture composition was performed with a mass spectrometer – gas chromatograph. The column used was Reprogel-H, Dr. Maicsh Gmbh, Germany, 500 mm × 8 mm.

3 Results and discussion

The next nanostructured catalytic systems (as the carrier and stabilizer HPS was used) were synthesized: 1%Pd/ HPS, 1%Pd-0.3%Pt/ HPS, 1%Pd-1%Pt/ HPS, 3%Pt/ HPS, 3%Pt –2%Au/ HPS. Selectivity to 2-keto-L-gulonic acid and conversion of L-sorbose after 6 h for tested

catalysts are given in Table 1.

Table 1. Selectivity to 2-keto-L-gulonic acid and conversion after 6 h.

Catalyst	Selectivity	Conversion
1%Pd/ HPS	8	21
1%Pd-0.3%Pt/ HPS	11	38
1%Pd-1%Pt/ HPS	10	44
3%Pt/ HPS	46	31
3%Pt –2%Au/ HPS	41	88

The most active catalyst was 3%Pt –2%Au/ HPS, showing the selectivity of 41% at conversion of 88% after 6 hours of the reaction. It is seen from the graph (Fig.1) that the selectivity to the target product 2-keto-L-gulonic acid increases with increasing conversion, and the selectivity to the side-product 5-keto-D-glukonic acid goes through the maximum and after it gives new products of overoxidation.

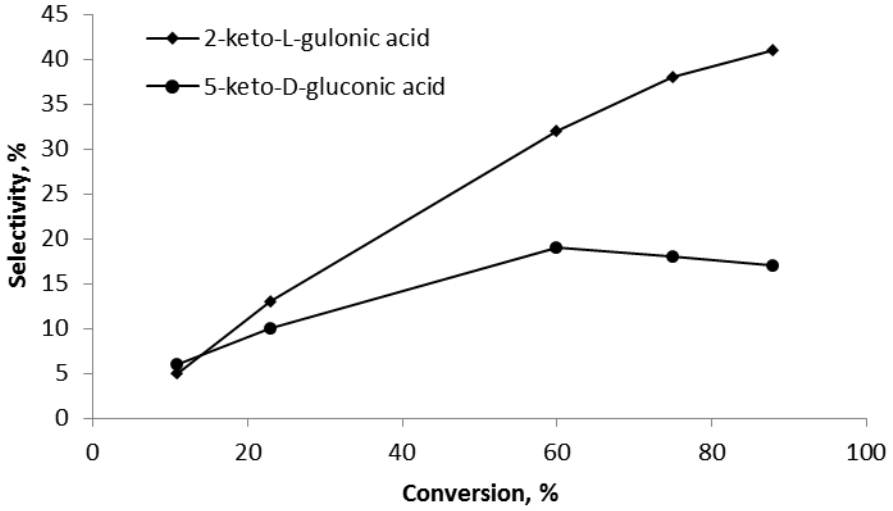

Fig. 1. Selectivity to 2-keto-L-gulonic acid (target product) and 5-keto-D-glukonic acid (side-product) as a function of conversion

Increasing the experiment time to 8 hours selectivity decreases as the target product is overoxidized and gives new side-products.

4 Conclusions

The unique features of HPS facilitate incorporation of various compounds into the nanostructured HPS matrix and, thus, nanoparticle formation. Such hybrid materials give the opportunity to prevent the agglomeration of nanoparticles and do not require ligands for stabilizing, that makes nanoparticles more active in catalytic processes. It can be stated that in this limited experimental series the highest selectivity achieved for the target compound, 2-keto-L-gulonic acid was 41 % at 88 % of L-sorbose conversion over 3%Pt –2%Au/ HPS in water with NaOH as alkaline agent at 70°C. The reaction network is complex and further studies are required to optimize the formation of the target product.

References

[1] Haijun Zhanga, Naoki Toshima, *Applied Catalysis A: General* 400 (2011) 9–13

[2] Sari Rautiainen, Olga Simakova, Hongfan Guo, Anne-Riikka Leino, Krisztián Kordás, Dmitry Murzin, Markku Leskelä, Timo Repo, *Applied Catalysis A: General.* 485 (2014) 202–206

[3] Putla Sudarsanam, Baithy Mallesham, D. Naga Durgasri, Benjaram M. Reddy, *Journal of Industrial and Engineering Chemistry.* 20 (2014) 3115–3121

ISO-PP11

Propylene Glycol Oxidation over Cr-MIL-101 with Tert-butyl Hydroperoxide

Torbina V.[1], Ivanchikova I.[1,2], Kholdeeva O.[1,2], Vodyankina O.[1*]

1 - Tomsk State University, Tomsk, Russia
2 - Boreskov Institute of Catalysis SB RAS, Novosibirsk, Russia

* vodyankina_o@mail.ru

Keywords: propylene glycol, metal-organic framework, selective oxidation, hydroxyacetone

1 Introduction

Oxidation of alcohols to corresponding carbonyl compounds plays a key role in organic synthesis. In particular, the selective oxidation of vicinal diols is a challenging goal because these compounds are prone to C-C fission. Traditional methods for such transformations are based on the use of inorganic oxidants, e.g., chromium (VI) reagents. However, from both economic and environmental viewpoints, there is a growing demand for atom efficient catalytic methods employing environmentally benign oxidants [1].

Conversion of biomass-derived feedstocks to valuable products remains a formidable challenge. Propylene glycol (PG) can be produced from glycerol, which is a low-cost by-product in transesterification of triglycerides for biodiesel production [2]. A number of valuable products that find application in the production of fine chemicals and pharmaceutics can be obtained through oxidation of PG. Generally, PG is oxidized to methyl glyoxal in the gas phase [3]. However, thus far, publications in the field of catalytic liquid phase oxidation of propylene glycol are scarce.

Metal-organic frameworks (MOFs) have attracted great attention as heterogeneous catalysts thanks to a unique combination of properties, such as crystalline open structures, extremely high surface areas, tunable pore size and functionality, and large fraction of accessible metal centers [4]. In this work, we explored the potential of the chromium terephthalate Cr-MIL-101 in the selective oxidation of PG using *tert*-butyl hydroperoxide (TBHP) as oxidant. The effects of reaction conditions (temperature, concentrations, solvent nature) on this reaction were evaluated.

2 Experimental/methodology

Cr-MIL-101 was prepared according to the literature [5] and activated in vacuum prior to use. Catalytic oxidations were carried out in thermostated glass vessels at 40-70 °C under vigorous stirring (500 rpm). Typically, the reaction was initiated by the addition of TBHP (0.125 or 0.25 mmol) to a mixture containing PG (0.5 mmol), 1 ml of solvent (methanol, ethyl acetate or acetonitrile) and 3 mg of the catalyst. Aliquots of the reaction mixture were withdrawn periodically by a syringe through a septum and analyzed by GC (30 m ZB-WAX capillary column) using chlorobenzene as internal standard. Methyl glyoxal and formaldehyde were determined as ortho-phenylenediamine derivatives.

3 Results and discussion

The oxidation of PG over MIL-101 with TBHP leads to hydroxyacetone (HA) as the main product (Figure 1). Products derived from the oxidative cleavage of C-C bond (acetic acid and formaldehyde) were not detected. Moreover, HA overoxidation products, methyl glyoxal (MGO) and pyruvic acid, were not found. However, an experiment with MGO as substrate

demonstrated an unexpectedly high conversion (75 % versus 25 % theoretically predicted), which allowed us to suggest that MGO could undergo non-oxidative transformations under the reaction conditions. The increase in temperature accelerated the PG oxidation process. At 40 °C, substrate conversion did not exceed 4 % after 8.5 h while at 50 and 70 °C it attained 18 % ([TBHP]/[PG] = 0.25). HA selectivity was practically unaffected by the reaction temperature in the range of 50-70 °C and remained at the level of 60 %. Thus the efficiency of the oxidant utilization was ca. 70 %. Similar results were obtained using acetonitrile and ethyl acetate as solvents whereas in methanol the reaction stopped in 2 h and produced only 5% conversion. In ethyl acetate, increasing TBHP/PG molar ratio from 0.25 to 0.5 allowed enlargement of PG conversion up to 30 % but reduced HA selectivity from 60 to 30%. Nevertheless, no acetic acid and formaldehyde were detected. The mass balance between the reactants converted and products detected, especially for enhanced TBHP/PG molar ratio, was not complete. One of possible reasons for that could be non-oxidative transformations of the oxidation products (for example, MGO). Further work is in progress to clarify this matter.

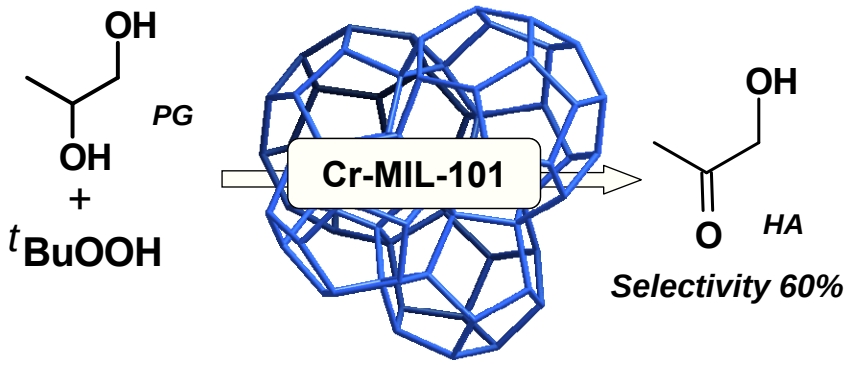

Figure 1. PG oxidation with TBHP over MIL-101

4 Conclusion

Hydroxyacetone was shown to be the predominant product of PG oxidation with TBHP over Cr-MIL-101 under mild conditions (50-70 °C). C-C cleavage, which is typical of PG oxidation [2], did not take place in the catalytic system studied.

Acknowledgements

Authors thank Dr. K. Kovalenko for the synthesis of MIL-101. The research was supported by "The Tomsk State University Academic D.I. Mendeleev Fund Program" grant.

References

[1] Sustainable Industrial Processes, F. Cavani, G. Centi, S. Perathoner and F. Trifiro (Eds.), Wiley-VCH, Weinheim, 2009.
[2] E. Diaz, M.E. Sad, E. Iglesia, *ChemSusChem.* 3 (2010) 1063.
[3] M. Ai, A. Motohashi, S. Abe, *Applied Catalysis A: General* 246 (2003) 97.
[4] A. Corma, H. García, F.X. Llabrés i Xamena, *Chem. Rev.* 110 (2010) 4606.
[5] G. Ferey, C. Mellot-Draznieks, C. Serre, F. Millange, J. Dutour, S. Surble, I. Margiolaki, *Science.* 309 (2005) 2040.

ISO-PP12

Influence of Pre-Treatment on the Oxidative Coupling of Methane over MgO Catalysts

Schwach P., Tarasov A., Willinger M., Schlögl R., Trunschke A.*

Fritz-Haber-Institut der Max-Planck-Gesellschaft, Berlin, Germany

* trunschke@fhi-berlin.mpg.de

Keywords: OCM, MgO, methane activation

1 Introduction

The functionalization of methane remains a challenging target from an academic as well as an industrial point of view. New concepts for the catalytic activation of C-H bonds in oxidation reactions are needed to overcome the current limitations in selectivity, which hamper broad utilization of, for example, the oxidative coupling of methane (OCM) for production of olefins from natural gas.

In a previous work on OCM over model MgO catalysts [1, 2], we found that the initial performance of freshly calcined MgO is governed by a surface-mediated coupling mechanism involving direct electron transfer between methane and oxygen. The abundance of structural defects, in particular mono-atomic steps and Lewis acid/base pairs, correlate with the initial rates of both methane consumption and C_{2+} hydrocarbon formation. During time on stream MgO sinters and loses activity in the steam-containing atmosphere at the high reaction temperatures of OCM. The deactivation process involves the depletion of mono-atomic steps and the reconstruction of the MgO termination under formation of polar and faceted surfaces.

In this work, the impact of pre-treatment of MgO with N_2, CO_2, O_2, H_2 and H_2O on the reactivity of the resulting catalysts in OCM is studied. CO_2, O_2, H_2 or H_2O are either reactive gases or formed during the OCM reaction. Analysis of their influence on the catalyst is of main importance to understand the deactivation mechanism in OCM over alkaline earth oxides and to develop alternative strategies and stabilization concepts.

2 Experimental/methodology

Magnesium oxide (Puratronic®, 99.998 % m. b., Alfa Aesar) served as model catalyst in this work. Prior to catalytic testing, the catalyst was treated in the reactor in 20 % O_2, CO_2, H_2 or H_2O in N_2 or in pure N_2 feed for 1 hour at reaction temperature (1023 K) before switching to the feed (90 mL·min^{-1}, $CH_4/O_2/N_2$=3/1/1). The first GC measurement was taken less than 2 minutes after switching.

Changes of the MgO surfaces due to pre-treatment were characterized by IR spectroscopy of adsorbed probe molecules (CO and CH_4), electron microscopy, UV-vis spectroscopy, and thermal gravimetric (TG) analysis. Paramagnetic defects were studied by EPR spectroscopy.

Figure 1 **Results and discussion**

Figure 1 shows the influence of the pre-treatment of MgO with N_2, CO_2, O_2, H_2 or H_2O on the yield of C_{2+} hydrocarbons and on the C_2H_4/C_2H_6 ratio in the product mixture. The catalysts pre-treated in N_2, CO_2, and O_2 show almost no difference. Treatment in N_2 or vacuum is used as reference in this work. Comparison between O_2 and N_2 treatment indicates that the partial pressure of oxygen has no significant effect in the range of the chosen conditions. CO_2 has been considered as a poison in the OCM reaction over Li/MgO [3], however, over pure MgO, CO_2 has no effect. This is in agreement with the fact that $Mg(CO_3)_2$ decomposes at a temperature below the reaction temperature.

Pre-treatment with H_2O considerably lowers the C_{2+} yield as well as the C_2H_4/C_2H_6 ratio. In the presence of steam, the MgO primary particle sinter and the active sites responsible for high methane conversion and high selectivity (i.e. mono-atomic steps), vanish at the same time. These results directly proof the detrimental effect of steam on OCM activity over MgO and explain self-poisening of MgO in OCM by the unavoidable reaction product water. Pre-treatment of MgO with steam at 1023 K can be used as accelerated procedure in deactivation studies, since few hours pre-treatment results in a similar low activity as 300 hours time on stream in OCM. After 48 hours treatment in steam at 1023 K, bulk paramagnetic defects have been observed by EPR spectroscopy. The defects are most-likely V^{-}like centers formed due to the incorporation of OH-groups in the MgO matrix [4].

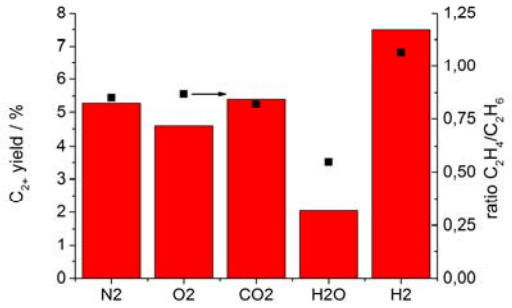

Fig. 1 Influence of pre-treatment in the OCM at T=1023 K, $CH_4/O_2/N_2$=3/1/1, W/F= 0.033 g·s·ml^{-1}

Surprisingly, pre-treatment in H_2 improves the performance in the OCM reaction in terms of C_{2+} yield. The C_2H_4/C_2H_6 and CO_2/CO ratios are also affected. IR spectroscopy of adsorbed CH_4 provides an explanation. The amount of adsorbed CH_4 increases on MgO treated by H_2 by a factor of 3 in comparison to MgO treated in vacuum. This indicates that H_2 treatment considerably increases the amount of active sites. To understand the effect of hydrogen better, H_2 pulsed TG experiments have been performed. Since MgO is an irreducible oxide, mass losses observed upon H_2-pulses at 1023 K indicate a restructuration of the MgO surface.

4 Conclusions

The pre-treatment of a nanostructured MgO catalyst with N_2, CO_2, O_2, H_2 and H_2O and the analysis of the changes in reactivity helped to interpret the deactivation mechanism of MgO in OCM [1, 2]. CO_2 and O_2, have no (or minor) effects on the OCM reactivity. H_2O has a detrimental influence due to sintering of the primary particles, while H_2 pre-treatment increases the concentration of active sites for CH_4 adsorption and activation.

Acknowledgements

This work was conducted in the framework of the COE “UniCat” (www. unicat.tu-berlin.de) of the German Science Foundation.

References

[1] P. Schwach, W. Frandsen, M. G. Willinger, R. Schlögl, A. Trunschke, *J. Catal.*, (2014) submitted.
[2] P. Schwach, N. Hamilton, M. Eichelbaum, L. Thum T. Lunkenbein, R. Schlögl, A. Trunschke, *J. Catal.*, (2014) submitted.
[3] E. V. Kondratenko, M. Baerns, Handbook of Heterogeneous Catalysis. (2008) 13:13.17:3010–3023.
[4] H. Kathrein, F. Freund, J. Nagy, *J. Phys. Chem. Solids*, 45 (1984), 1155-1163.

ISO-PP13

New Insights in the Catalytic Oxidation of Levulinic Acid to Succinic Acid

Podolean I., Papuc B., Parvulescu V.I., Coman S.M.*

University of Bucharest, Faculty of Chemistry, Bucharest, Romania

* simona.coman@g.unibuc.ro

Keywords: ruthenium, magnetic nanoparticles, oxidation, levulinic acid, glucose, succinic acid

1 Introduction

Nowadays, due to the increasing environmental concerns, many efforts have been made to develop oxidation systems using environmentally-benign molecular oxygen as a sole oxidant. In this respect, Ru-based oxidation catalysis was rapidly developed being envisaged to play a major role in the renewable sources capitalization [1]. On the other hand, magnetic materials have attracted special attention because the magnetic properties make possible the complete recovery of the catalyst by means of an external magnetic field [2].

Based on the present state-of-the art and our interest in biomass capitalization to value-added chemicals, not long ago we developed a Ru(III)/functionalized silica-coated magnetic nanoparticles catalyst which was proven to be highly active, selective and easily recoverable catalyst for the oxidation of levulinic acid (LA) to succinic acid (SA) under green conditions [3]. Encouraged by these initially promising results, here we report the optimization of the former MNP-NH_2/Ru^{III} catalyst in order to further improve its catalytic performances in the LA oxidation to SA. In this scope the loading of the ruthenium species was varied (1-5wt.%) keeping constant the content of $–NH_2$ linker moieties. To extent the catalyst utility, LA was replaced with glucose as raw material.

2 Experimental/methodology

The catalysts were prepared in several steps, involving: a) the magnetite synthesis; b) its coating with silica, c) APTES functionalisation by silanisation, and d) ruthenium deposition by wet impregnation. The obtained catalysts were characterized by XRD, Mossbauer spectroscopy, magnetic measurements, EXAFS, DLS and DRIFT spectroscopy and tested in the LA oxidation using molecular oxygen as oxidation agent.

3 Results and discussion

The characterization of the former MNP-NH_2/Ru^{III} catalyst and correlation with catalytic performances indicated a certain cooperation of the acid/base sites as responsible for the LA oxidation to SA. For the new synthesised catalytic systems the base co-catalyst seem to be successfully supplied by the free $–NH_2$ moieties, while the acidity was ensured by the existing $Ru(OH)_xCl_{3-x}$ and $[Ru(H_2O)_5OH]^{2+}$ species [3] docked through hydrochloride -C-$NH_3^+Cl^-$ species on the surface of the magnetic nanoparticles. An additional variation of the NH_2/Ru atomic ratio can be made when the content in -NH_2 moieties is kept at the same level but the loading of ruthenium is varied. Therefore, catalysts with 1, 3 and 5% Ru were prepared and tested in the LA oxidation to SA (Figure 1). As Figure 1 shows, the concentration of ruthenium influences not only the catalytic activity but also the selectivity to SA. The optimum of ruthenium loading seems to be 4wt.%, a higher amount leading to a strong degrease not only of the LA conversion but also of the SA selectivity. However, when we express the catalytic activity by TOF (moles of transformed LA/[moles of catalytic active phase x time]) or by TON (moles of transformed LA/moles of catalytic active phase) the most performing catalytic sample

seems to be, in fact the MNP-NH_2-Ru(1wt.%) sample (Figure 2). The obtained catalytic results suggest that an important feature of the highly active and selective catalysts is the high dispersion of catalytic active sites.

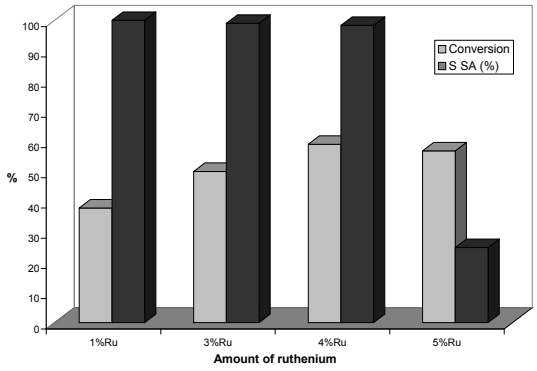

Fig. 1. The LA oxidation in the presence of MNP-NH_2/Ru^{III} with different amounts of ruthenium (180°C, 6h)

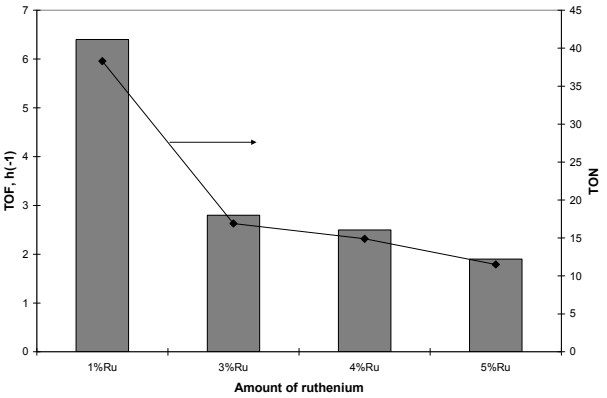

Fig. 2. The TOF and TON variation as a function of the ruthenium amount

As expected, the absence of intraparticle mass-transfer limitations and the improved Ru dispersion on silica-coated magnetite nanoparticles (MNP-NH_2/Ru^{III}) compared to the micrometer-sized commercial silica powder (SiO_2-NH_2/Ru^{III}) led to significant differences in the catalytic behaviour of the samples. In the presence of ruthenium based silica (SiO_2-NH_2/Ru^{III}) the conversion of LA was lower than 5% with a selectivity to SA of 92%. In the presence of MNP-NH_2/Ru^{III} (4 wt.%Ru) the efficient synthesis of SA from glucose by one-pot hydrogenolysis/oxidation concept was also possible at 150°C and 10 atm O_2. The gluconic acid was not detected in the reaction products, the main product of the oxidation reaction being SA. The selectivity was of 76.7% for a total conversion, after 11 h. Many other products as glycolic acid, glyceric acid, 3-hydroxybutanoic acid, ethylene glycol or lactones were also detected but in low amounts. Increasing the temperature at 180°C, glucose was totally converted with a yield to SA of 86.7%, in only 6 h.

4 Conclusions

The oxidation of LA and glucose to SA requires catalysts with both acid-base properties. The optimization of the MNP-NH_2/Ru^{III} showed that the optimum composition to achieve the highest catalytic performances comprises an excess of basic sites, ie a ratio NH_2/Ru >1 and 1wt.% Ru. These catalysts exhibit activity not only in the oxidation of LA but also of glucose. In this case the best results corresponded to C_{LA} = 59%, S_{SA} = 98.3%; $C_{glucose}$ = 100%, and S_{SA} = 62.7%.

Acknowledgements

Authors kindly acknowledge UEFISCDI for the financial support (project PN-II-PT-PCCA-2013-4-1090, Nr. 44/2014).

References

[1] M. Pagliaro, S. Campestrini, R. Ciriminna, *Chem. Soc. Rev*. 34 (2005) 837.
[2] V. Polshettiwar, R. Luque, A. Fihri, H. Zhu, M. Bouhrara, J.-M. Basset, *Chem. Rev*. 111 (2011) 3036.
[3] I. Podolean, V. Kuncser, N. Gheorghe, D. Macovei, V. I. Parvulescu, S. M. Coman, *Green Chem* 15 (2013) 3077.

ISO-PP14

Vanadium-based Catalyst for Ethanol Transformation: Relation Between Structure and Catalytic Activity

Malmusi A.*, Dellapasqua M., Velasquez Ochoa J., Cavani F.

Dipartimento di Chimica Industriale "Toso Montanari" - Alma Mater Studiorum - Università di Bologna, Bologna, Italy

* andrea.malmusi3@unibo.it

Keywords: vanadates, ethanol, acidity, dehydrogenation, catalysts

1 Introduction

Transition metal Vanadates are widely studied as catalysts for methanol oxidation to formaldehyde[1,2]. Conversely, there are few information in literature regarding the catalytic properties of these materials in the transformation of ethanol, which is of interest nowadays in the context of the production of high added value chemicals starting from bio-alcohols. The aim of this work was to investigate ethanol transformation over V/Fe and V/Cu mixed oxides, under both aerobic and anaerobic conditions, and correlate catalyst behaviour with chemical-physical characteristics.

2 Experimental/methodology

The catalysts were synthesized adding either $Fe(NO_3)_3 \cdot 9H_2O$ or $CuCl_2 \cdot 2H_2O$ aqueous solution to a solution containing NH_4VO_3 and $H_2C_2O_4$, at controlled pH; the obtained precipitates were dried and then calcined at 650°C for 3 hours. Catalysts were tested in a fixed-bed gas-phase glass rector. Catalytic activity experiments were carried out feeding either ethanol or ethanol and oxygen. The reaction products were analysed by means of on-line GC and the catalysts were characterized both before and after reaction by means of SEM, XRD, Raman and FT-IR spectroscopy. Operando DRIFT experiments were carried out with ethanol continuous feeding at 573 K.

3 Results and discussion

Figure 1 and 2 show the trend of ethanol conversion and products yields plotted in function of time-on-stream at 573 K, with Fe/V/O and Cu/V/O catalysts, respectively, under anaerobic conditions.

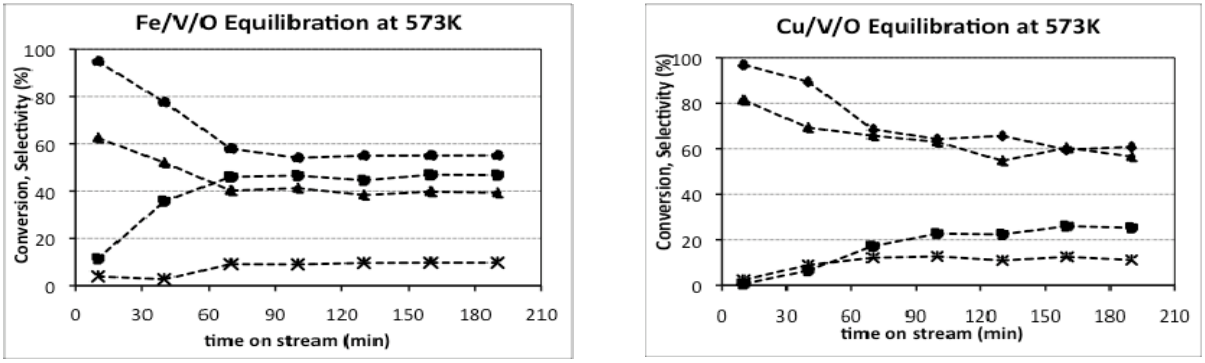

Fig. 1: Ethanol conversion and products selectivity as function of time-on-stream with Fe/V/O (left) and Cu/V/O (right) catalysts: ●: Ethanol conversion; ■: Ethylene selectivity; ▲: Acetaldehyde selectivity; ×: C3/C4 selectivity.

Both catalysts showed an "equilibration time" during which the behaviour was not stable, and metal oxides were progressively reduced. Besides acetaldehyde and ethylene, also C_3/C_4 compounds, such as ethylacetate, crotonaldehyde, crotyl alcohol, and acetone, were formed. The C_4 compounds are formed by consecutive reactions on acetaldehyde, via either Tishchenko dimerization to ethylacetate or aldol condensation and dehydration [3,4]. The relative contribution of the acid-catalysed dehydration to ethylene and the dehydrogenative/condensation pathway leading to acetaldehyde and C_3/C_4 compounds changed in function of catalyst structure and composition, as highlighted by characterisation of both fresh and equilibrated (reduced) catalysts. XRD and SEM characterization showed that in the case of Fe/V/O catalyst, the iron vanadate compound was progressively reduced into a spinel mixed oxide, which showed relevant acid properties. The latter were confirmed by means of operando DRIFT/MS experiments. Therefore, a high ethylene/(acetaldehyde + C_4) selectivity ratio was finally observed. In the case of the Cu/V/O system, instead, metallic Cu formed during catalytic test with ethanol feeding; the catalyst finally showed a much lower ethylene/(acetaldehyde + C_4) selectivity ratio, because of its lower catalyst acidity and because of the presence of Cu^0, which enhanced the dehydrogenative properties.

Co-feeding of oxygen at 573 K hindered catalyst reduction and led to higher activity in oxidative dehydrogenation. For example, Fe/V/O was stable in its oxidized form under aerobic conditions, and showed the preferred formation of acetaldehyde and CO_x to the detriment of ethylene. Conversely, Cu/V/O showed less Cu^0 formation than without oxygen in feed, and acetaldehyde and CO_x were the main products.

4 Conclusions

Fe/V and Cu/V mixed oxides were tested as catalysts for ethanol transformation under both aerobic and anaerobic conditions and were characterized before and after catalytic tests. Results showed that product distributions changed depending on the grade of catalysts reduction, highlighting the relationship between products distribution and the characteristics of the mixed oxides. For both catalysts, the presence of reduced phases contributed to increase catalyst acidity, shifting the products distribution from acetaldehyde to ethylene. However, this phenomenon was less evident in the case of Cu/V/O, because of the segregation of metallic Cu.

References

[1] L.E. Briand, J.M. Jehng, L. Cornaglia, A.M. Hirt, I.E. Wachs, *Catal. Today,* **78** 257-268 (2003)
[2] M. Massa, R. Haggblad, A. Andersson, *Top Catal,* **54** 685-697 (2011)
[3] J. Velasquez Ochoa, C. Trevisanut, J.-M.M. Millet, G. Busca, F. Cavani, *J. Phys. Chem. C,* **117** 23908-23918 (2013)

ISO-PP15

Structure and Reactivity of Nanostructured MnO_x Catalysts in the Liquid Phase Selective Oxidation of Benzyl Alcohol with Oxygen

Gumina B.[1], Cannilla C.[2], Spadaro L.[2], Di Chio R.[1], Trunfio G.[1], Arena F.[1*]

1 - Dipartimento di Ingegneria Elettronica, Chimica e Ingegneria Industriale, Università degli Studi di Messina, Messina, Italy

2 - Istituto CNR-ITAE "Nicola Giordano", Messina, Italy

* Francesco.Arena@unime.it

Keywords: MnO_x catalysts, promoters, selective oxidation, benzyl alcohol, mechanism kinetics

1 Introduction

The selective oxidation of alcohols is a very important class of industrial synthesis reactions to obtain a variety of chemicals used for manufacturing high added-value products like drugs, vitamins, fragrances and innovative materials [1]. However, the use of special and expensive precursors and reagents raises significant environmental and economic concerns due to poor *atom economy* and high *E-factor* [2]. Then, the discovery of eco-friendly catalytic technologies for the selective oxidation of alcohols with oxygen has been recently designated as a major *Green Chemistry* topic. Although noble-metal catalysts drive the oxidation of many alcoholic substrates under mild conditions, high cost, deactivation phenomena and safety issues hinder their industrial applications [1,3]. Despite a lower activity, bare and promoted MnO_x catalysts exhibit a highly selective activity pattern in the liquid phase aerobic oxidation of alcohols, rendering them a viable alternative to noble-metal catalysts [3]. However, decay phenomena and the need for regeneration-rejuvenation steps have also been documented [4,5].

Therefore, this work is aimed at highlighting the mechanistic issues of the reactivity pattern of bare and promoted (Ce, Fe) MnO_x catalysts in the aerobic liquid phase oxidation of benzyl alcohol to benzaldehyde. A systematic analysis of activity data sheds lights onto the factors controlling the functionality of MnO_x catalysts, while a simple kinetic model allows predicting their activity-stability pattern over a wide range of experimental conditions.

2 Experimental/methodology

Cerium and iron promoted MnO_x catalysts with different atomic ratios were prepared via the redox-precipitation route and characterized by XRF, N_2-physical adsorption, XRD, CO-TPR and DRIFT analyses [4,5]. Catalytic tests in the aerobic liquid phase oxidation of benzyl alcohol with O_2 were carried out into a 3-necked pyrex glass flask reactor containing a solution (50 mL) of benzyl alcohol (0.1 mol/L), toluene (solvent) and ethyl benzoate (int. std). The solution was heated at 343K under stirring and O_2 flow, adding, then, 0.45 g of powdered catalyst (t_0).

3 Results and discussion

Table 1 shows a good agreement between design and experimental Mn/Ce/Fe atomic ratios along with the presence of significant amounts of potassium, resulting in an asymptotic growth of the K/Mn ratio with MnO_x loading [4]. Promoters addition has a positive impact on surface texture, indicated by systematically larger surface area values of the composite catalysts than bare oxides. This has been ascribed to the fact that the redox-precipitation route promotes a *quasi-molecular* dispersion of the oxide phases, hindering any long-range ordered structure [4].

Both C and F systems are not active under std reaction conditions, while the MnO_x material exhibits a remarkable performance leading to a complete conversion of alcohol to benzaldehyde (S>99%) in 3h.

Table 1. Physico-chemical properties of the studied catalysts.

Catalyst	Chemical Composition (wt%)[a]				atomic ratio			SA (m^2/g)	PV (cm^3/g)	APD (nm)
	MnO_x	CeO_x	FeO_x	KO_x	(Ce/Mn)	(Fe/Mn)	(K/Mn)			
M1C1	34.4	65.3	0.0	0.2	0.98	0.0	0.01	190	0.46	25
M3C1	59.9	36.9	0.0	3.3	0.31	0.0	0.10	184	0.57	27
M5C1	66.9	28.4	0.0	4.8	0.21	0.0	0.13	159	0.56	30
M9C1	77.0	17.6	0.0	5.4	0.11	0.0	0.13	136	0.49	31
M	93.5	0.0	0.0	6.5	0.0	0.0	0.13	94	0.34	31
C	0.0	100	0.0	0.0	0.0	0.0	0.0	128	0.10	3
F	0.0	0.0	100	0.0	0.0	0.0	0.0	33	0.10	15
M6C1F1	65.0	21.6	9.7	4.5	0.16	0.16	0.13	135	0.26	27
M3F1	74.6	0.0	20.9	4.7	0.0	0.31	0.12	136	0.38	27

A direct relationship between activity and reducibility suggests that MnO_x plays the role of active phase, while minor is the contribution of promoters to the functionality of composite catalysts [6]. Despite no effects on selectivity (S>99%), promoters influence the reactivity of the MnO_x phase (Fig. 1A). Among Ce-based catalysts, M1C1 shows the poorest activity with a final conversion of 50%, while a complete alcohol conversion signals that the reactivity of M3C1, M5C1 and M9C1 samples compares to the bare M system. Replacement of Ce with Fe enhances the activity as M6C1F1 and M3F1 catalysts show conversion rates higher than M3C1 (Fig. 1B).

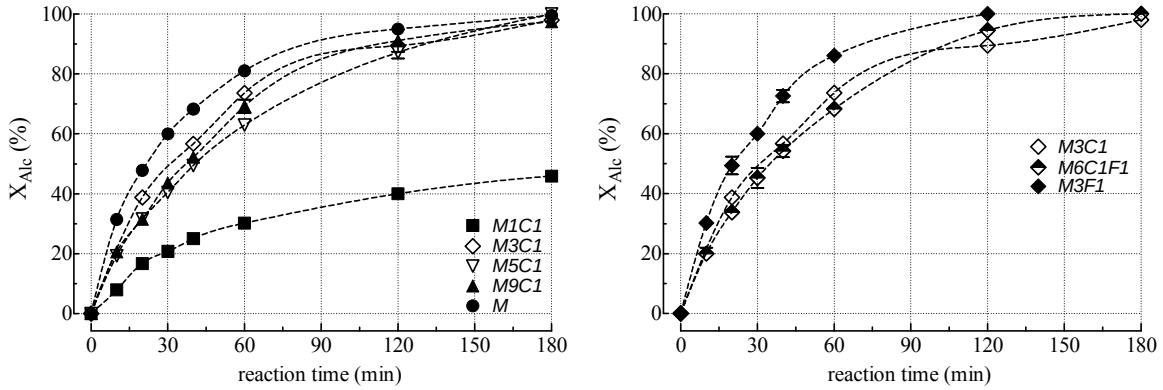

Fig. 1. Activity of catalysts in the selective oxidation of benzyl alcohol with O_2 at 343K.

The initial reaction rate values signal that the reactivity of Ce-promoted systems lowers with the Mn/Ce ratio, despite a fairly constant MnO_x rate rules out significant *electronic effects* [4]. The substitution of Ce with Fe has a positive influence on activity, while a constant MnO_x rate indicates the absence of significant chemical effects also in Fe-promoted catalysts [4].

4 Conclusions

The reactivity of bare and promoted (Ce, Fe) MnO_x catalysts is assessed [4].
Remarkable deactivation phenomena disguise 0^{th}-order reaction kinetics [4,5].
The activity-stability pattern is determined by strong adsorption phenomena [5].

References

[1] T. Mallat, A. Baiker, *Chem. Rev.* 104 (2004) 3037.
[2] R.A. Sheldon, I. Arends, U. Hanefeld, "Green Chemistry and Catalysis", WILEY-VCH Verlag GmbH & Co. KGaA, Weinheim, Germany (2007).
[3] C. Parmeggiani, F. Cardona, *Green Chem.* 14 (2012) 547.
[4] F. Arena, B. Gumina, A.F. Lombardo, C. Espro, A. Patti, L. Spadaro, L. Spiccia, *Appl. Catal. B* 162 (2015) 260.
[5] F. Arena, B. Gumina, C. Cannilla, L. Spadaro, A. Patti, L. Spiccia, *Appl. Catal. B* 170-171 (2015) 233.

ISO-PP16

Structural Peculiarities and Catalytic Properties of Supported Vanadium Oxide Catalysts for Oxidative Dehydrogenation

Sushchenko E.*, Kharlamova T.

Tomsk State University, Chemistry Faculty, Tomsk, Russia

* konfetty13@mail.ru

Keywords: vanadium oxide, oxidative dehydrogenation

1 Introduction

Propylene and styrene are important monomers for polymeric industry. Propane and ethylbenzene dehydrogenation (DH) over Cr_2O_3/Al_2O_3 and Fe_2O_3 catalysts, respectively, are conventional ways to produce the said compounds. However, DH of saturated hydrocarbons has many disadvantages. Therefore, the oxidative dehydrogenation (ODH) was suggested as an alternative way to produce propylene and styrene. Catalysts based on supported vanadium oxide demonstrated promising results in ODH of hydrocarbons [1]. Activity and selectivity of supported vanadium oxide catalysts depend on support nature and vanadium content, determining oxidation state, coordination number, aggregation state, and structure of vanadium oxide species on the support surface [1]. This work is devoted to the study of the structural peculiarities and catalytic properties in ODH reactions of vanadium species at the surface of different supports.

2 Experimental

VO_x/SiO_2, VO_x/TiO_2, VO_x/Al_2O_3, VO_x/AlC catalysts (Table 1) were synthesized by wetness impregnation using aqueous solution of NH_4VO_3. SiO_2, TiO_2, γ-Al_2O_3 and carbon-modified γ-Al_2O_3 (AlC) were used as catalyst supports. The nominal V_2O_5 content was 12 or 3.5 %wt. to ensure 0.2-0.25 monolayer coverage. The catalysts were characterized by low temperature N_2 adsorption, XRD, IR and Raman spectroscopy, UV-Vis DRS and H_2-TPR. Catalytic activity of the samples in ODH reactions was determined using flow catalytic unit with online chromatographic analysis of the products.

Table 1. Sample characteristics.

Sample	V_2O_5, wt.%	V_2O_5, monolayer	SSA, m^2/g	D_{XRD}, nm
VO_x/Al_2O_3	12	0.25	183	8
VO_x/AlC	12	0.21	211	41
VO_x/SiO_2	12	0.2	289	19
VO_x/TiO_2(12)	12	>>1	10	38
VO_x/TiO_2(3.5)	3.5	0.24	59	-

3 Results and discussion

According to XRD data, VO_x/Al_2O_3, VO_x/SiO_2, VO_x/TiO_2(12) samples are composed of phases of the support (γ-Al_2O_3, amorphous SiO_2 or anatase) and V_2O_5. The VO_x/AlC contains graphite phase along with γ-Al_2O_3 and V_2O_5. Only anatase phase was detected in VO_x/TiO_2(3.5). V_2O_5 was well crystallized in both VO_x/TiO_2 and VO_x/AlC with the mean crystallite size of ~40 nm. VO_x/SiO_2 and VO_x/Al_2O_3 samples contained V_2O_5 phase in dispersed state.

According to Raman spectroscopy data, VO_x/AlC, VO_x/SiO_2, VO_x/TiO_2(12) catalysts contained crystalline V_2O_5, whereas VO_x/TiO_2(3) did not contain one according to XRD data. The absence of V-O bands in the spectrum of VO_x/TiO_2(3) indicated the presence of vanadium

oxide mainly in the form of polymerized surface vanadium oxide species. However, in contrast to XRD data, there were no bands typical for crystalline V_2O_5 at 145, 196, 284, 404, 481, 550, 701, 994 cm^{-1} in the spectrum of VO_x/Al_2O_3, but only shifted peaks at 124, 187, 266, 379, 457, 538, 680, 978 cm^{-1} and new ones at 497, 620 cm^{-1}. This indicated the possible interaction of vanadium oxide with Al_2O_3 to form some surface vanadium oxide species.

According to UV-vis DRS, ligand-to-metal charge transfer bands of V^{5+} are present in the spectra of all samples, which are overlapped with those of support in the case of VO_x/TiO_2 and VO_x/Al_2O_3. The spectra of initial VO_x/SiO_2, $VO_x/TiO_2(12)$ and VO_x/AlC indicates the presence of V^{5+} in dispersed V_2O_5, with the spectra of VO_x/SiO_2, $VO_x/TiO_2(12\%)$ remaining practically unchanged before and after the catalyst testing. The spectra of VO_x/Al_2O_3 and $VO_x/TiO_2(3.5)$, in their turn, indicates the presence of V^{5+} in the form of polymerized surface vanadium oxide species. However, the presence of amorphous V_2O_5 phase is possible in VO_x/Al_2O_3 as well. The spectrum of VO_x/AlC was similar to that of VO_x/Al_2O_3 after the catalyst testing, indicating the interaction of VO_x with the support.

According to H_2-TPR data, $VO_x/TiO_2(12)$ reduction is characterized by two peaks of H_2 consumption, namely, weak peak at 360-530ºC corresponding to reduction of polymerized vanadium oxide species as well as intense peak above 550ºC corresponding to reduction of bulk V_2O_5. The TPR profile of $VO_x/TiO_2(3.5)$ is characterized by the H_2 consumption from 400 to up to 700ºC with maxima at 516 and 580ºC, which seems to be caused by the reduction of polymerized surface vanadium oxide species. The VO_x/SiO_2 profile contains weak peak at 200-450ºC attributed to amorphous vanadium oxide species, and intense peak above 450ºC attributed to dispersed V_2O_5 crystalline particles. The TPR profiles of VO_x/AlC and VO_x/Al_2O_3 are characterized by only one peak of H_2 consumption with maximum at 595ºC and 536ºC, respectively. The narrow instansive peak in the VO_x/AlC profile is caused by the reduction of V_2O_5 crystalline particles, while wide peak in the VO_x/A_2O_3 profile is caused by the reduction of polymerized surface vanadium oxide species as well as dispersed V_2O_5 particles of low crystallinity. Interestingly, the TPR profiles of VO_x/AlC and VO_x/Al_2O_3 after the catalyst testing are similar and characterized by a wide peak with maximum at 590ºC. This, in accordance with Raman and UV-vis DRS data, also indicates the interaction of VO_x with Al_2O_3 to form polymerized surface vanadium oxide species.

According to the catalytic data, $VO_x/TiO_2(3.5)$ showed the highest catalytic activity, but the main product of the propane conversion was CO_x. VO_x/Al_2O_3 showed propane conversion comparable to that of $VO_x/TiO_2(3.5)$, but the highest selectivity towards propene among samples studied. The VO_x/AlC and $VO_x/TiO_2(12)$ showed lower activity, with the selectivity towards propene being, respectively, comparable and lower to that of VO_x/Al_2O_3. The VO_x/SiO_2 showed low activity and selectivity towards pronene. Therefore, the interaction of VO_x with the support to form polymerized surface vanadium oxide species in VO_x/Al_2O_3 and $VO_x/TiO_2(3.5)$ results in the increase of catalyst activity, while selectivity depends on the strength and electron density change of V-O-support bond in the formed surface vanadium oxide species.

4 Conclusions

The interaction of vanadium oxide with the support to form polymerized surface vanadium oxide species was shown to result in increase of catalyst activity, while selectivity depends on the strength and electron density change of V-O-support bond in the formed surface vanadium oxide species.

Acknowledgements

This research was supported by “The Tomsk State University Academic D.I. Mendeleev Fund Program” grant.

References

[1] O.V. Buyevskaya, M. Baerns, *Catal.*, 16 (2002) 155.

ISO-PP17

Silica Supported Vanadia Catalysts for Selective Methane Oxidation: Impact of Morphology and Heteroatom Doping on Catalyst Performance

Wallis P.*, Schönborn E., Wohlrab S., Kalevaru N., Martin A.

Leibniz Institute for Catalysis, Rostock, Germany

* philipp.wallis@catalysis.de

Keywords: mesoporous, silica, vanadia, methane oxidation, formaldehyde

1 Introduction

At present, methane valorization is clearly dominated by energy production. Intense research efforts are directed towards broadening the scope of methane as feedstock. Areas of interest are dry reforming, selective oxidation of methane and oxidative coupling of methane [1]. Selective oxidation of methane to formaldehyde is investigated over supported vanadia catalysts [2]. Several approaches to improve the selectivity to formaldehyde (S_{HCHO}) are reported in literature: First, homogenous gas phase admixture like of carbon dioxide can be used to improve S_{HCHO} [3]. Second, textural properties of the support as pore diameter and surface fractality have been probed for reactivity tuning [4,5]. As Ti-doping of siliceous supports has also been observed to improve selectivity (V/Ti-MCM-41 [6]) but may alter pore size distribution in some cases, it is the aim of this study to put the effects of pore size distribution and heteroatom doping in perspective. This will be done by comparing Ti-doped and Ti-free silica supports of various pore size distributions and evaluate the effect on selectivity.

2 Experimental

SBA-15 synthesis was done according to a procedure by Zhao et al. [7] in a variant, where the batch was stirred at 35 °C for 12 h after addition of $Si(OEt)_4$; variation of pore size distribution was achieved by mesophase ageing at 80 °C (V/SBA-15-T1) and 90 °C (V/SBA-15-T2) [8]. Ti-SBA-15 was synthesized by dissolving 4.00 g Pluronic P123 in 125 mL 2M HCl at 40 °C. 0.51 g Cp_2TiCl_2 (Strem) were added and the resulting mixture stirred at 40 °C for 3 h. 9 mL $Si(OEt)_4$ was added and stirred together for 20 h at 40 °C. The obtained slurry was then kept at 100 °C for 24 h, filtered, washed and dried overnight to give a white powder. Template was removed via calcination. 2.27 g Ti-SBA-15 were obtained. During calcination, all supports were heated from RT with 1 K/min to 650 °C, kept at 650 °C for 16 h and then cooled to RT with 1 K/min. VO_x was grafted onto support by incipient wetness impregnation of aqueous NH_4VO_3 solution and subsequent calcination, nominal V content 2.8 wt% [9]. Catalytic tests in selective oxidation of methane to formaldehyde were carried out at T=550-690 °C; GHSV=94,000–360,000 L/kg_{cat}h; admixture: CH_4: O_2 = 7: 2: 1 where admixture was CO_2, N_2, Ar, CH_4. Product gas was kept at 180 °C for analysis and composition was determined using an infrared gas detector (Gasmet CX1000).

3 Results and discussion

Maximum achieved space-time-yield was 3.6 kg/kg_{cat}h (686 °C, 360,000 L/kg_{cat}h) over V/Ti-SBA-15 compared to 3.2 kg/kg_{cat}h over V/SBA-15-T1 (665 °C 360,000 L/kg_{cat}h). Catalytic tests showed S_{HCHO} = 50% at 1% methane conversion (X_{CH4}) over 0.2 wt% Ti containing V/Ti-SBA-15 (d_{pore} 6 nm), while S_{HCHO} of V/SBA-15-T1 and V/SBA-15-T2 (d_{pore} < 5 nm) was between 40 and 50% at comparable conversion (Fig. 1A). Over the range of conversion

observed, samples containing larger pores (see PSD in Fig. 1B) exhibit higher selectivity of formaldehyde formation.

If diffusion limitation and contribution of inner-pore gas phase reaction can be excluded, this trend may be due to altered equilibrium surface structure distribution of vanadia due to a change in support morphology [4]. As was shown by general support variation [10], V-O-Support bonds are important for methane activation. Surface density of V-O-Support moieties may decrease for identical V-loading as the ratio of monomeric $O=V(\text{-}O\text{-}Support)_3$ to polymeric $O=V(\text{-}OV)_n(\text{-}O\text{-}Support)_{3\text{-}n}$) decreases. For identical support morphology and extended time-on-stream, initially different distributions of V between monomeric and polymeric species are expected to equalize due to reaching thermodynamic equilibrium; hence exhibiting identical catalytic activity at this stage. However for support variation e.g. surface roughness, pore curvature or heteroatom doping, thermodynamic equilibrium distribution may differ yielding different catalytic activity.

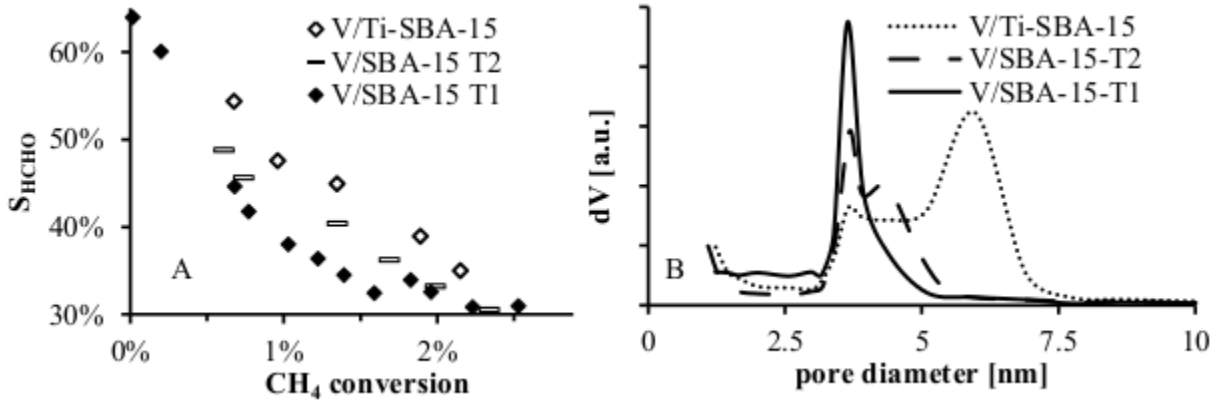

Fig. 1. X_{CH4} vs. S_{HCHO} plot (A) of supported VO_x catalysts and their different pore size distributions (B).

4 Conclusions

The results clearly show improved selectivity towards formaldehyde for Ti-modified samples. Further investigations will clarify the role of titanium as structural or electronic promoter by testing if a similar effect can also be achieved by application of Ti-free silica support of similar pore size distribution.

Acknowledgements

The authors acknowledge experimental assistance by M. Heyken and financial support by BMBF Germany (FKZ: 031A168C)

References

[1] S. T. Oyama, *ACS Symposium Series*. 638 (1996) 2.
[2] N. Ohler, A. Bell, *J. Catal.* 231 (2005) 115.
[3] O. Demoulin, I. Seunier, F. Dury, M. Navez, R. Rachwalik, B. Sulikowski, S.R. Gonzalez-Carrazan, E.M. Gaigneaux, P. Ruiz, *Catal. Today.* 99 (2005) 217.
[4] M.A. Smith, A. Zoelle, Y. Yang, R.M. Rioux, N.G. Hamilton, K. Amakawa, P.K. Nielsen, A. Trunschke, *J. Catal.* 312 (2014) 170.
[5] Y. Yang, G. Du, S. Lim, G. Haller, *J. Catal.* 234 (2005) 318.
[6] O. Ovsitser, M. Cherian, A. Brückner, E.V. Kondratenko, *J. Catal.* 265 (2009) 8.
[7] D. Zhao, Q. Huo, J. Feng, B.F. Chmelka, G.D. Stucky, *J. Am. Chem. Soc.* 120 (1998) 6024.
[8] D. Zhao, J. Feng, H. Qisheng, N. Melosh, G.H. Fredrickson, B.F. Chmelka, G.D. Stucky, *Science.* 279 (1998) 548.
[9] C. Pirovano, E. Schönborn, S. Wohlrab, V. Kalevaru, A. Martin, *Catal. Today.* 192 (2012) 20.
[10] I. Wachs, *Spec. Period. Rep.: Catal.* 13 (1997) 37.

ISO-PP18

Selective Oxidation of Cyclic-Alkane, Catalyzed by Nano Size SWNTs Supported Pt and Pd Complexes Catalysts

Machado K., Mishra G.*

Universidade de Trás-os-Montes e Alto Douro (UTAD), Vila Real, Portugal

- mishrags@utad.pt

Keywords: heterogeneous catalysis, carbon nano-tubes, metal complexes, alkane, oxygen

1 Introduction

Single wall carbon nano-tubes (SWNTs) have used much broader applications such as catalysis, gas storage and separation, nanoprobes, chemical sensors and high strength composites [1]. Magnetic SWNTs have been used, either only Fe or Fe/Co, Co/Ni/Fe, Ni/Co in catalysis [2]. An application of supported metal complex over nano-size materials have combined advantages of homogeneous over heterogeneous in catalysis, such as tremendous catching power liquid wastes, easy magmatic separation, large surface area, less toxic and economical. Functionalized SWNTs have much attention, which allow covalent anchoring with a targeted metal complex. Particularly, pincer complexes, they are well known form long time but their appropriate application in heterogeneous catalysis is still untouched field of research.

Oxidation of cyclohexane (*Cy-hx*) is a key process because it's oxidized products which are use for the production of polyamide-6, nylon-6 and additives etc.. Earlier, precursors of Co have been used for *Cy-hx* oxidation with Air/O_2 mixture at above 150 ºC (*ca.* 4 % conv. With *ca.* 85 % selectivity) [3]. The prospect of operate with molecular O_2 as "*greener oxidant*" and cheaper oxidant with nanoparticles catalysts is constitute the selective product formation, reducing by-products and energy saving. Recently, di(ethylthio)alkanes Pd complexes over silica have also developed for the same reaction with O_2 and achieved 16 % conv. [4]. Hence, the main purpose of this work is to use *NH_2*-functionalized supramagnetic SWNTs as novel support Pd and Pt complexes as recyclable catalysts for the oxidation of *Cy-hx* with O_2 to achieve high turnover numbers (TONs) and selective product under solvent free condition.

2 Methodology

2.1 *Synthesis of Nano-Catalysts and Oxidation Technique:* The SWNTs have been prepared by the method [5]. Surface was modified by $[NH_2(CH_2)_3Si(OCH_3)_3$ in toluene, refluxed for 12 h and carefully washed with H_2O in order to obtained NH_2-functionalized magnetic SWNTs. Both $Pd^{(II)}$ and $Pt^{(II)}$ pincer complexes have been prepared [6] and bonded with *functionalized* SWNTs in presence of K_2CO_3 in dry toluene, refluxed overnight.

Teflon line reactor having a 22 mL capacity was used for the conducting all oxidation reactions. It was initially charged with substrate and catalyst and removed air and introduced O_2. After reaction, liquid mixture was injected in GC with pentanone as internal standard. The characterization TEM, FTIR, TGA, AAS and GC/MS have been performed at CQ-VR centre.

3 Results and discussion

The amino-functionalized magnetic SWNTs support have been used for anchoring of active species of $Pd^{(II)}$ and $Pt^{(II)}$ (pincer -*NNN* and –*SNS* ligands) complexes as selective catalysts for *Cy-hx* oxidation with cheaper and greener oxidant (molecular oxygen). Due to changing the electronic properties, these hetero-atoms in the side-arms complexes could be useful for the fine-tuning of high catalytic activity. Typical fiber like texture of SWNTs/Pd catalyst is seen in

TEM image *Fig.1* at 240 nm magnification. In *Fig.2*, the testimony of Pd complex over support was distinguished by the different peak positions by TEM-EDS *i.e.* Co at 0.9, 6.4 and Ni at 1.1, 6.6 of functionalized SWNTs and one additional Pd peak, after the anchoring at 2.4.

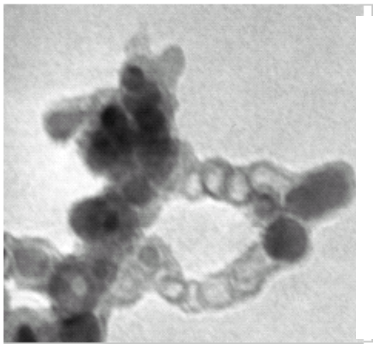

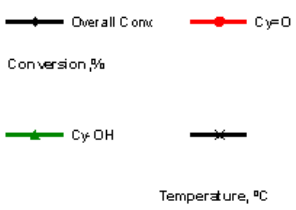

Fig.1 **Fig.2**

Novel magnetic SWNTs supported SWNTs/Pd and SWNTs/Pt catalysts have been applied for the oxidation reaction of *Cy-hx* hydrocarbon using molecular O_2 as oxidant in batch reactor. Notably high TONs 1946 were achieved with SWNTs/Pd and 1678 with SWNTs/Pt catalyst.

We have also run additional oxidation reaction with only SWNTs, to check the effect of support *i.e.* non-functionalized SWNTs (6 h at 150 ºC and $p(O_2)$ 10 bar). It was obtained not very low overall yield *i.e.* 11.6 % with *K/A* ratio1.5. It's reflects that SWNT is also taking part to improve the catalytic activity.

For ideal reaction condition of *Cy-hx* oxidation in respect of temperature was investigated between 100 to 225 ºC with SWNTs/Pd catalyst (*Fig.2*). Best Pd catalyst results have been obtained overall conversion 22.9 % (*Cy=O*, 12.01 % and *Cy-OH*, 9.35 %) with selectivity 93.3 %, under above condition. Other catalytic system SWNTs/Pt has also exhibits good catalytic activity, overall conversion 20.7 % but better *K+A* selectivity 95.2 % was obtained, in compression to Pd catalyst. Trash amount of some by-products were also observed. At 225 ºC, black unidentified oil material was observed. Free radicals *CyOOH* was also detected in the reaction solution with PPh_3 treatment. It is confirming the radical type mechanism.

4 Conclusion

Magnetic nano-catalysts give mainly *Cy=O* and *Cy-OH* products of the corresponding *Cy-hx* were obtained with very high TONs 1946 for Pd catalyst and 1678 for Pt catalyst. Highest 22.9 % conv. (93.3 selectivity %) is achieved by Pd catalyst. This magnetic nano-catalytic study is opening the gateway for the development of more sustainable catalyst for future easy magnetic separation process.

Acknowledgements

The authors express gratitude to FCT, Portugal, for the financial support through Indo-Portuguese Cooperation project: *FCT/9701/25/10/2013/S*.

References

[1] D.S. Bethune at al., *Nature*, 1993, **363**, 605-607.
[2] C.E. Snyder at al., *Int. Pat.* 1989, WO 9/07163.
[3] A.M. Thayer, *Chem. Eng. News*., 1992, **70**, 27-49.
[4] G.S. Mishra, S. Sinha, *Catal. Lett*., 2008, **125**,139 –144.
[5] Y. Makita, S. Suzuki, H. Kataura, Y. Achiba, *Eur. Phys. J. : D*, 2005, **34**, 287–289.
[6] Q.Q. Wang, R.A. Begum, V.W. Day, K.B. James, *Inorg. Chem*., 2012, **51**, 760−762.

ISO-PP19

Catalytic Synthesis of 2-Methyl-1,4-Naphthoquinone in 1%Au/HPS Presence

Shimanskaya E.I.*, Doluda V.Yu., Sulman E.M.

Tver Technical University, Tver, Russia

* shimanskaya-tstu@yandex.ru

Keywords: 2-methyl-1,4-naphthoquinone, 2-methylnaphthalene, catalytic oxidation, gold

1 Introduction

Selective oxidation of aromatic compounds opens access to a great number of useful products. Quinones with various functional groups are important intermediate in fine organic synthesis as quinone fragments are part of difficult molecules of the substances used in manufacture of vitamins and medical products. An example of such compounds is 2-methylnaphthalene. The 2-methylnaphthalene oxidation stage has a low selectivity, and consequently a small target product yield. At oxidation 2-methylnaphthalene such products, as 2-methyl-1,4-naphthquinone, isomerous 6-methyl-1,4-naphthquinone, methyl groups oxidation products, dinaphthquinone, epoxiquinone and other products of deep oxidation are formed. It necessary to find the way of selective synthesis of menadione. There are a lot of catalysts described in literature which are applied in the menadione synthesis, however the majority of them gives low selectivity (<40%), is toxic, pollutes the prime product and gives a considerable quantity of by-products [1]. We decided to use the based on HPS catalyst, because of its properties. Hypercrosslinked polystyrene (HPS) is rigid polymeric network of polystyrene linked by methylene bridges [2].

2 Experimental

Synthesis of 1%Au/ HPS

The 5%Au/ HPS catalyst was prepared as follows: 3 g of polymer was impregnated with 0.086 g of Ph_3PAuCl in 8.5 mL of THF under stirring and dried at 70°C. Next the catalyst was treated with 0.5 g of Na_2CO_3 in 12 mL of H_2O. Then it was dried again and washed to a pH of 7.

Oxidation methodology

The oxidation reaction was conducted batchwise in a glass apparatus that permits independent control over parameters such as the substrate concentrations, temperature and the stirring rate. A solution of the substrate in the appropriate solvent (20 mL) prepared at a predetermined concentration was placed in the reactor. The high stirring rates employed here ensured good mixing without diffusion limitations. Samples of the reaction mixture were periodically removed for analysis. The oxidation process was carried out at the following reaction conditions: reaction temperature 80°C, substrate initial concentration 0.035 mol/L.

3 Results and discussion

At first industrial non-catalytic reaction of 2-methylnaphthalene oxidation by a H_2O_2 has been in vitro researched. Oxidation was conducted in the glass reactor within 2 hours at the temperature 80°C. Concentration of a 2-methylnaphthalene solution in acetic acid is 0.035 M. Samples were taken every 15 minutes during the reaction and analyzed using GC-MS. The yield of the process attained 43%.

2-methylnaphthalene catalytic oxidation was carried out with use of HPS-based Au-catalyst in H_2O_2 presence. Synthesis of such system was carried out by introduction of metal in a carrier

by impregnation on a moisture capacity of Wilkinson complex salt. The yield of the process attained 72%.

4 Conclusions

The yield of the non-catalytic process attained 43%. The yield of the catalytic process attained 72%.

Acknowledgements

This work has been supported by Russian Ministry of Education and Science.

References

[1] Miyashita K., Imanishi T. *Chem. Rev*., v. 105, p. 4515 (2005)
[2] Doluda V.Yu, E.M. Sulman, V.G. Matveeva, M.G. Sulman, N.V. Lakina, A.I. Sidorov, P.M. Valetsky, L.M. Bronstein *Chem. Eng. Journal*, Vol. 134, 256 (2007)

ISO-PP20

Mo-Incorporated KIT-6 Mesoporous Silica Catalysts with High Performance for the Selective Oxidation of Propane to Acrolein

Liu Q.L., Li J.M., Zhao Z.*, Gao M.L., Liu J.

State Key Laboratory of Heavy Oil, College of Science, China University of Petroleum, Beijing, China

* zhenzhao@cup.edu.cn

Keywords: Mo-KIT-6 catalyst, framework-incorporation, highly dispersed active sites, propane selective oxidation, acrolein

1 Introduction

The selective oxidation of alkanes is of fundamental and industrial significance because it provides a potential route to effectively transform alkanes instead of olefins to value-added chemicals for effective utilization of abundant natural gas and shale gas resources. The 3D interconnected mesoporous silica KIT-6 with large pores and thick pore walls, high hydrothermal stability, high specific surface area and large pore volume has attracted much attention for potential applications in catalysis[1-3]. Molybdenum-based catalysts are one of the most efficient catalysts employed in the selective oxidation of alkanes[4-6]. The performance of these catalysts is strongly related to the nature of the active species. This kind of framework-incorporated catalysts is different from supported catalysts. The framework-incorporation contributes to achieving high concentrations of highly dispersed active sites and high stability of catalysts which may have high activity for selective oxidation[7,8]. In this work, we synthesized the Mo-KIT-6 catalyst that gave good catalytic performance for the selective oxidation of propane to acrolein.

2 Experimental

Mo-incorporated mesoporous molecular sieves (Mo-KIT-6) were synthesized by one-pot co-assembly method using nonionic triblock copolymer surfactant Pluronic P123 ($EO_{20}PO_{70}EO_{20}$, MW=5800, Aldrich) and n-butanol (BuOH) as a structure-directing mixture, tetraethyl orthosilicate (TEOS) as silica source and ammonium heptamolybdate (AHM) as a molybdenum source in hydrochloric acid. A typical procedure was as follow: 2.0 g of Pluronic P123 was added into 4.0 g 35 wt % HCl with stirring at 308 K for 4h and the acquired amount of AHM was dissolved in 72 g water. Then, the two solutions were mixed. 2.0 g of BuOH was added and the stirring was continued for 1 h. Subsequently, 4.3 g of TEOS was added to the homogeneously clear solution. The subsequent step was similar to the literature[9]. In the filtration and washing processes, the Mo species that is not incorporated into the catalysts would be washed away. The samples were labeled as xMo-KIT-6, x denotes Mo content in recipe (Mo:Si=X:100, molar ratio). The final Mo contents in Mo-KIT-6 samples were determined by inductively coupled plasma (ICP) measurement.

3 Results and discussion

Figure 1 exhibits the several characterization results of Mo-KIT-6 catalysts. It can be seen that the materials are well ordered mesostructure similar to that of KIT-6. However, it is notable that the diffraction peak shifts to low angle and peak intensity decreases with the increase of Mo contents. This can be attributed to the incorporation of Mo species into framework of molecular sieves. The wide-angle XRD pattern and Raman spectra indicate that the catalysts mainly contain highly dispersed MoO_x species. The results of catalytic activity show 8Mo-KIT-6 sample is the best catalyst and its catalytic activity results are illustrated in Table 1.

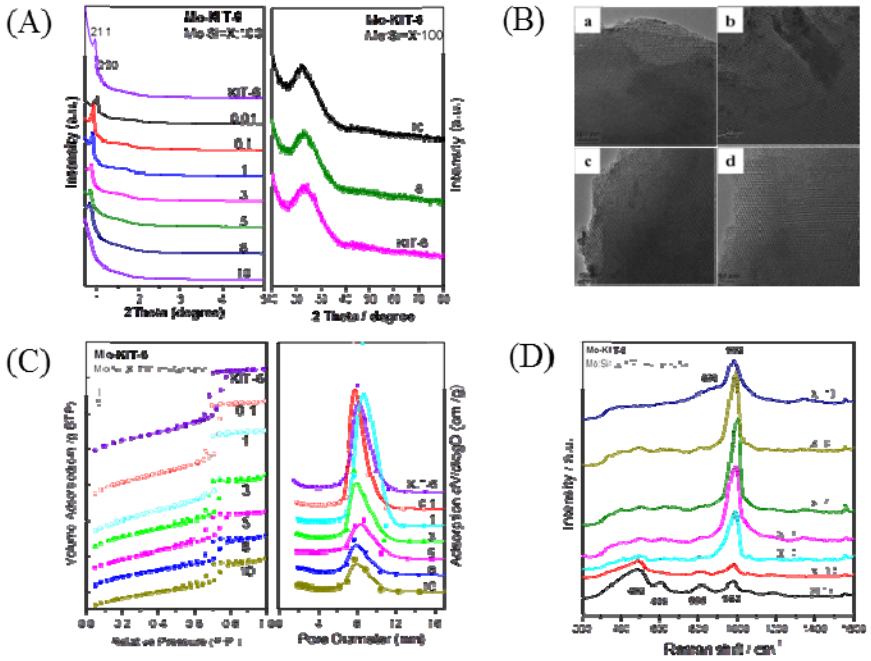

Fig. 1. The characterisations of Mo-KIT-6 catalysts: (A) Low-angle and wide-angle XRD patterns; (B) TEM images, a)0.1Mo-KIT-6, b)5Mo-KIT-6, c)8Mo-KIT-6, d)10Mo-KIT-6; (C) The N_2 adsorption-desorption isotherms and pore-size distribution; (D) Raman spectra

Table 1. The catalytic performances of Mo-KIT-6 catalysts for the selective oxidation of propane

Conv., %	Temp., K	Selectivity [a], %							Yield, %	
		Oxy.			C_3H_6	HC	CO	CO_2	Acr	Olefins+Acr
		Acr	C2	Ace						
76.5	873	25.4	0.9	0.9	20.4	20.4	23.0	7.8	19.4	46.0

[a] Oxy.: oxygenated chemicals; Acr: acrolein; C2: acetaldehyde; Ace: acetone, HC: ethylene and methane

4 Conclusions

A kind of framework-incorporated Mo-KIT-6 mesoporous molecular sieve catalysts with different Mo contents were successfully synthesized by one-spot co-assembly method. It was found that the catalyst was effective for the oxidative conversion of propane to acrolein. Detailed characterizations and catalytic behavior showed that highly dispersed MoO_x species were predominant in the catalysts and the high concentrations of highly dispersed active sites are favorable for enhancing the activity of selective oxidation of propane to acrolein.

Acknowledgements

The National Natural Science Foundation of China (21477164, 21376261, 21173270, 21177160), the 863 Program of China (2013AA065302)

References

[1] K. Soni, B. S. Rana, A. K. Sinha, et al, Appl. Catal. B. 90(2009) 55
[2] Z. Liu, J. Zhou, K. Cao, et al, Appl. Catal. B. 125(2012) 324
[3] H. Wu, A. Duan, Z. Zhao, et al, J. Catal. 317(2014) 303
[4] J. Li, J. Liu, Z. Zhao, Q. Liu, et al, J. Energ. Chem. 23(2014) 609
[5] Y. Lou, H. Wang, Q. Zhang, Y. Wang, J. Catal. 247(2007) 245
[6] K. Chen, S. Xie, E. Iglesia, A. T. Bell, J. Catal. 189 (2000) 421
[7] J. Liu, L. Yu, Z. Zhao, et al, J. Catal. 285(2012) 134
[8] L. Shi, X. Zhu, Y. Su, et al, J. Catal. 307(2013) 316
[9] T. Kim, F. Kleitz, B. Paul, R. Ryoo, J. Am. Chem. Soc. 9(2005) 7601

ISO-PP21

Oxidative Dehydrogenation of Ethane on NiO Supported on Pillared Clays

Solsona B.[1*], Dejoz A.[1], Vazquez M.I.[1], Lopez Nieto J.M.[2], Soriano M.D.[3], Concepcion P.[2], Cecilia J.A.[3], Jimenez Jimenez J.[3], Rodríguez Castellon E.[3]

1 - Universitat de Valencia, Valencia, Spain
2 - ITQ (UPV-CSIC), Valencia, Spain
3 - Universidad de Málaga, Málaga, Spain

* benjamin.solsona@uv.es

Keywords: ethane, ethylene, nickel oxide, pillared clay, dehydrogenation

1 Introduction

Ethylene is the most important raw material in Petrochemistry. It is industrially obtained through a very inefficient process from an energetic viewpoint, which is called "steam reforming". The oxidative dehydrogenation (ODH) of ethane is considered as a viable alternative to "steam reforming" for the industrial manufacture of ethylene. Currently, two catalytic systems are the most promising in the ODH of ethane, those based on MoV oxides and those based in nickel oxide [1]. Nickel oxide alone is highly active but presents a low selectivity towards ethylene. However the addition of an appropriate either support or promoter leads to an enhanced formation of ethylene [2,3]. At the present work, the use of a silica with a pillared structure as support for nickel oxide will be studied for the ODH of ethane and its performance will be compared to that of conventional silica.

2 Experimental/methodology

Supported NiO catalysts were prepared through the evaporation at 60 ºC of a stirred ethanolic solution of nickel(II) nitrate, $Ni(NO_3)_2 \cdot 6H_2O$ (Sigma-Aldrich) and oxalic acid to which the corresponding support (conventional silica, pillared clay silica with columns of silica or silica/titania 5/1) was added. The solids obtained were dried overnight at 120 ºC and calcined for 2 h at 500 ºC. Pillared clays were synthesized according to reference [4].

The catalysts have been characterized by several techniques: XRD, XPS, Nitrogen adsorption, SAED-EDX, TEM, HR-TEM, TPR and Oxygen isotopic-exchange. The catalytic tests for the ODH of ethane were carried using a mixture of ethane/O_2/He with a molar ratio of 3/1/29. The temperature used varied from 300 to 500 ºC. The catalyst weight and total flow was varied to get different pairs selectivity-conversion at a given temperature. Blank runs showed no conversion in the range of reaction temperatures employed. Reactant and products were analyzed by gas chromatography using two packed columns [2].

3 Results and discussion

Table 1 summarizes some catalytic properties in the oxidative dehydrogenation of ethane of NiO based catalysts. NiO supported on conventional silica (5 and 10 wt.% NiO) show low selectivity to ethylene (i.e. 20-30%). A drastic improvement in the catalytic performance takes place for catalysts with the same NiO loading but supported on pillared silica, presenting also higher selectivity to ethylene (i.e. 55-60%). A further increase is also observed for NiO supported on silica/titania pillared material. The use of pillared silica instead of conventional silica has meant a decrease in the NiO crystallite size but also a lower reducibility of Ni-species.

Table 1. Catalytic properties of the catalysts synthesized.[a]

Catalyst	NiO wt.%	Support	Ethane conversion (%)	Selectivity to ethylene (%)	Ethylene productivity[b]
5NiSi	5	SiO_2	4.1	20	27
10NiSi	10	SiO_2	11.2	29	111
5NiPCH	5	PCH-SiO_2	8.1	55	152
10NiPCH	10	PCH-SiO_2	15.4	56	295
5NiPCHTi	5	PCH-TiO_2	10.2	60	210
10NiPCHTi	10	PCH-TiO_2	13.1	64	577

[a] Reaction Temperature = 450ºC and W/F = 8 g_{cat} h / $molC_2$; [b] in g_{C2H4} kg_{cat}^{-1} h^{-1}.

The use of pillared silica with titania columns has led to a further decrease of reducibility. Therefore, the catalytic performance has been inversely related to the reducibility of the nickel species (Figure 1).

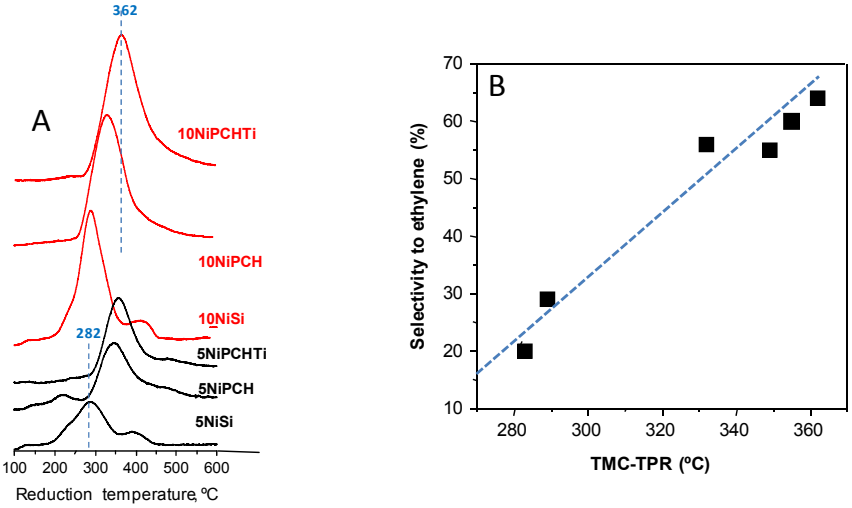

Fig. 1. TPR profiles for supported NiO catalysts (a) and the relationship of the temperature of maximum reductions and the selectivity to ethylene in ethane ODH (b). Note: Selectivity to ethylene at 10% conversion and 450ºC. TMC is the temperature of maximum hydrogen consumption in the TPR experiments.

Accordingly, it can be proposed that highly reducible species activate ethane to give carbon dioxide whereas those less reducible selectively activate ethane. However, no correlation can be established between catalyst reducibility and catalytic activity for ethane conversion.

4 Conclusions

Pillared clays, especially if columns are SiO_2/TiO_2-made, are excellent supports for NiO for the oxidative dehydrogenation of ethane. Selective Ni-species with low reducibility are likely involved in the high ethylene formation.

Acknowledgements

Authors would like to thank the DGICYT in Spain (CTQ2012-37925-C03-01, CTQ2012-37925-C03-02 and CTQ2012-37925-C03-03) for financial support.

References

[1] F. Cavani, N. Ballarini, A. Cericola, *Catal. Today*. 127 (2007) 113.
[2] J.M. López Nieto, B. Solsona, R.K. Grasselli, P. Concepción, *Top. Catal.* 57 (2014) 1248.
[3] I. Popescu, E. Heracleous, Z. Skoufa, A. Lemonidou, I.-C. Marcu, *PCCP* 16 (2014) 4962.
[4] J.A. Cecilia, C. García-Sancho, F. Franco, Micropor. Mesopor. Mater. 176 (2013) 95-102.

ISO-PP22

Gas Phase Hydroxylation of Benzene to Phenol over M (Co, Ni, Cu, Zn)/ZSM-5 Using Nitrous Oxide

Alotaibi M.[1,2*], Kalevaru V.N.[1], Almegren H.[2], Alkinany M.[2], Martin A.[1]

1 - Leibniz Institute for Catalysis at University of Rostock, Rostock, Germany
2 - Petroleum and Petrochemicals Research Institute, King Abdulaziz City for Science and Technology, Riyadh, Saudi Arabia

* Mansour.Alotaibi@catalysis.de

Keywords: benzene hydroxylation, phenol, N_2O, M/ZSM-5 catalysts

1 Introduction

Phenol is very important in chemical industry due to its prevalent use in the fields of agrochemicals, pharmaceuticals etc. It is used for the synthesis of various commercially important chemicals such as caprolactam, bisphenol, chlorophenol [1-2]. Phenol is conventionally produced by a three step processes. A representative example is the cumene process that produces acetone as a major by-product in addition to the desired phenol. In addition, this process also produces an explosive intermediate cumene hydroperoxide. These are some of the drawbacks of this commercial process [3]. On the other hand, direct conversion of benzene to phenol in one step is indeed an attractive alternative method also from the economic and environmental viewpoints. To date, many efforts have been made to synthesise phenol using green oxidising agents such as nitrous oxide, oxygen, and hydrogen peroxide to produce phenol from benzene by means of a gas phase oxidation [e.g. 4]. Fe/ZSM-5 catalysts are widely used for direct synthesis of phenol from benzene [5-6]. In this contribution, we describe the synthesis, characterisation and application of various transition metal doped (e.g. Co, Ni, Cu, Zn) ZSM-5 catalysts towards gas phase hydroxylation of benzene to phenol.

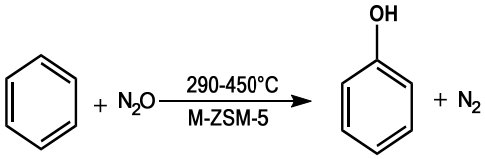

Scheme1. Reaction scheme for benzene to phenol

2 Experimental

Various transition metal doped ZSM-5 catalysts were prepared by impregnation method. A commercial ZSM-5 sample supplied by Zeochem, Germany was used as support for preparing the present catalysts. Required quantities of suitable metal precursors were dissolved in distilled water and then impregnated on to the support. Then the catalysts were dried first and then calcined in a furnace at 500 °C for 6 h in air. The transition metals used were Co, Ni, Cu and Zn and their contents were kept constant at 1 wt% in every case. The solids were characterized by ICP, XRD, N_2 adsorption (BET-SA) etc. Catalytic tests were carried out in a fixed bed stainless steel tubular reactor in the temperature range from 290 to 430 °C. N_2O was used as an oxidant and the catalytic tests were performed under varying reaction conditions. The reactor was filled with 2.0 g of catalyst particles (1-1.25 mm fraction) that were diluted with an equivalent weight of quartz beads of the same size to achieve isothermal operation. The reactant feed mixture was then introduced into the reactor and the reaction was performed at a residence time of 0.9 s (in general). Liquid products were collected for every half-an-hour in an ice-cooled trap and analysed by off-line GC equipped with FID, while gaseous products were detected by TCD.

3 Results and discussion

The BET-surface areas and pore volumes of the catalysts depend upon the nature of the transition metal doped. In general, they varied in the range from 353 to 391 m^2/g and 0.126 to 0.325 cm^3/g, respectively. The metal contents estimated from ICP are in good agreement with those of nominal values (~1 wt%). These materials were also characterised by XRD, but we could not see any crystalline phases corresponding to any of the metals doped. This is due to small loadings of metal and probably their X-ray amorphous nature. Fig. 1 illustrates the catalytic performance of M/ZSM-5 catalysts tested at 410 °C. It is evident from the figure that the yield of phenol obtained is the highest for Zn doped catalysts compared to all others. Among them, Cu-doping gave the lowest yield. Zn/ZSM-5 exhibit acceptably good yield of nearly 9% at a benzene conversion of ca. 20%. The remaining proportion is from the formation of by-products such as catechol, CO, CO_2 etc. Moreover, the catalysts are observed to deactivate gradually with time due to coking.

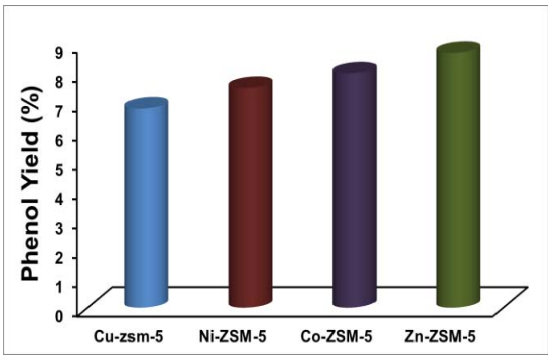

Fig. 1. Phenol yield obtained over different transition metal loaded on ZSM-5 (T=410°C, Benzene: N_2O: N_2 = 1.0: 1.5: 82, 3 Cat: 2 g; GHSV4000 h^{-1})

4 Conclusions

Results revealed that the nature of transition metal has shown considerable influence on the catalytic performance. Among the four different transition metals used, Zn displayed the best performance giving ca. 9% yield of phenol. Coking of catalyst seems to be an important problem of this reaction, which needs to be considered in the future catalyst compositions and catalytic tests.

Acknowledgements

Authors thank King Abdulaziz City for Science and Technology (KACST), Saudi Arabia for financial support.

References

[1] H. Jiang, Fei She, Yan Du, Chinese J.Chem. Eng. 22 (2014) 1199.
[2] H. Yang, H. Yang, J. Li, Catal. Commun. 35 (2013) 101.
[3] M. H. Sayyar, R.J. Wakeman, Chem Eng Res and des 86 (2008) 517.
[4] D.P. Ivanov, L.V. Pirutko, G.I. Panov Appl. Catal A: Gen. 10 (2012) 415.
[5] G.I. Panov, A.K. Uriarte, M.A. Rodkin, Catal. Today 41 (1998) 365.
[6] J. Jia, K. Pillai, W. Sachtler, J.Catal. 221 (2004) 119.

ISO-PP23

DFT Study of the Interaction of CO and O_2 with Gold-Copper Tetrahedral Bimetallic Clusters

Gogol V.V.*, Pichugina D.A., Ku'zmenko N.E.

M.V. Lomonosov Moscow State University, Moscow, Russia

* vl.gogol@gmail.com

Keywords: bimetallic clusters, catalyst, adsorption, density functional theory (DFT), Au, Cu

1 Introduction

The properties of nanoscale materials are usually very different from those of the corresponding bulk materials. The high surface to volume ratio of nanomaterials causes such materials to have frequent contact with the reactants of a targeted chemical reaction and to enhance the catalytic activity. Furthermore, nanoscale materials have a large number of low-coordinated atoms at the surface, which also leads to a high reactivity [1].

The oxidation of carbon monoxide (CO) to carbon dioxide (CO_2) has attracted great interest in recent years because the reaction has many industrial applications such as in catalytic conversion of automobile exhaust and in fuel cells. As we all know, noble metals such as Pt are used as a catalyst for CO oxidation in environment purification and the ORR in fuel cells [2]. However, the high cost of Pt has sparked a search for a Pt substitute or new ways of reducing the quantity of Pt required. For example, in contrast to Au bulk materials, Au nanoparticles can be used in many selective oxidation reactions, particularly in CO oxidation [3]. Also it has been shown that the sub-nano atomic Au_n clusters (n = 2–20) supported on magnesia are the active in CO oxidation [4]. At the same time, some alloyed nanoparticles, including Au–Pd nanoalloys, $MeAu_n$ (Me = W, Pb, Zr, Sc and n = 12–17), Cu-doped Au nanoparticles [5], are more active than pure gold clusters.

In this study we have investigate the CO and O_2 adsorption both on neutral, positively and negatively charged $Au_{20-x}Cu_x$ clusters having the heteroatom on the top, the edge, and the facet of the tetrahedral cluster. The detailed investigation of the cluster structure and electronic properties as well as the possible orientations and activation of the molecular oxygen and carbon monoxide on their surface would allow the further design and modification of the nanoparticles and their application in various processes.

2 Computational methods

Geometry optimizations were performed within the spin-polarized relativistic density functional theory approach using the PBE functional. The Priroda program was used for the all electron calculations within the scalar-relativistic approach, which was based on the full four-component one-electron Dirac equation with separation of the spin–orbit effects. The structures with a Cu atom located on the apex, on the edge and on the facet were obtained by substituting one Au atom with a Cu atom in Au_{20} cluster. Mono-doped copper-rich clusters $Cu_{19}Au$ were constructed from Cu_{20} the same way. The geometries of all generated clusters $Au_{20-x}Cu_x$ were fully optimize in the singlet spin state.

The adsorption energies of CO (or O_2) on the gold-copper clusters are calculated according to the formula:

$$\Delta E_{ad} = E(Cluster - CO) - E(Cluster) - E(CO);$$

where ΔE_{ad} is the CO (or O_2) adsorption energy on cluster; *E(Cluster-CO)* is the total energy of cluster with CO (or O_2) molecule adsorbed, *E(Cluster)* is the total energy of bare cluster and

E(CO) is the total energy of CO (or O_2) free molecule.

3 Results and discussion

The bimetallic clusters are relatively stable and maintained the tetrahedral structure of Au_{20} with slight distortion in the structure. As was expected, Au_{20} weakly interacts with oxygen: O-O bond length changes faintly upon adsorption on Au_{20}. That fact indicates weak oxygen activation. It should be noted, O_2 interacts much easier with negatively charged Au_{20} cluster. The O_2 dissociation is more favourable process on $Au_{20-x}Cu_x$, both molecular and dissociative adsorption take place. For molecular adsorption oxygen prefers bonding on the apex Cu atoms, than both on the edge and facet atoms. In different orientations on $Au_{20-x}Cu_x$ clusters O_2 prefers bonding to copper instead of gold atoms. The same situation we can see in the case of CO adsorption. Compared to the neutral clusters, a charge (negative or positive) on the clusters enhances CO adsorption. Compared with CO reaction on Au_{20} clusters, CO reaction on Cu-doping Au takes place easily, also.

4 Conclusions

To understand how Cu-doping in Au nanoparticles affects atomic-catalytic reactivity, we performed DFT calculations for the CO and O_2 adsorption on Cu-doped tetrahedral Au cluster. These calculations indicate several conclusions, as shown below: (1) CO and/or O_2 molecules are easily adsorbed on $Au_{20-x}Cu_x$ clusters. (2) The charging of $Au_{20-x}Cu_x$ can improve not only O_2 adsorption, but also CO adsorption. (3) The apex atoms in the clusters are more active in the binding of O_2 and CO. The Cu-doped Au nanoparticles are comparable with Au nanoparticles. The $Au_{20-x}Cu_x$ appears to be a good candidate for a CO oxidation catalyst.

Acknowledgements

This research was supported by the Russian Federation Foundation for Fundamental Research through the Projects 13−03−00320, 14-01-00310, and 11−01−00280, and by the Council for Grants of the Russian Federation President Projects MK−92−2013−3 and NSh−3171.2014.3. The reported study was supported by the Supercomputing Center of M.V. Lomonosov Moscow State University.

References

[1] M. Arenz, K.J.J. Mayrhofer, V. Stamenkovic, B.B. Blizanac, T. Tomoyuki, P.N. Ross, N.M. Markovic, *J Am Chem Soc*.127 (2005) 6819–6829.
[2] J.K. Norskov, T. Bligaard, J. Rossmeisl, C.H. Christensen, *NatChem*. 1 (2009) 37.
[3] M. Haruta, T. Kobayashi, H. Sano, N. Yamada, *ChemLett.*16 (1987) 405–408.
[4] S. Chretien, S. Buratto, H. Metiu, *Curr. Opin.Solid State Mater. Sci*. 11 (2007) 62–75.
[5] B. Delley, *J Chem Phys.* 92 (1990) 508–517.

ISO-PP24

Selective Isopropyl Alcohol Oxidation on Palladium and Ruthenium Catalysts Supported on Amphiphilic Hybrid Carbon Nanotubes

Benyounes A.[1,2], Ouanji F.[2], Ziyad M.[3], Kacimi M.[2], Serp P.[1*]

1 - Laboratoire de Chimie de Coordination UPR CNRS 8241, Composante ENSIACET, Université de Toulouse, Toulouse Cedex 4, France

2 - Laboratory of Physical Chemistry of Materials, Catalysis and Environnement (URAC26), Department of Chemistry, Faculty of Science, University of Mohammed V-Agdal, Rabat, Morocco

3 - Hassan II Academy of Science and Technology, Rabat, Morocco

* anas.benyounes@gmail.com

Keywords: oxidation, carbon nanotubes, palladium catalyst, isopropyl alcohol

1 Introduction :

In this study, amphiphilic magnetic hybrid carbon nanotubes (CNTs) are synthesized and used as supports of (2% w/w) ruthenium and palladium supported catalysts, and evaluated for the reaction of decomposition of isopropyl alcohol as probe reaction. These hybrids CNTs interact very well with aqueous media due to the hydrophilic nitrogen doped section, while the undoped hydrophobic part has strong affinity for organic molecules [1].

2 Experimental :

The hybrid carbon nanotubes were synthesized by a catalytic CVD process in a fluidized bed reactor using ethylene as carbon source and acetonitrile as carbon/nitrogen source. Four samples of carbon nanotubes were produced: (a) ethylene alone for 30 min, (b) acetonitrile/N_2 for 30 min, (c) ethylene for 10 min, followed by acetonitrile/N_2 for 20 min, and (d) acetonitrile/N_2 for 20 min followed, by ethylene alone for10 min. The CNTs were purified by a solution of H_2SO_4 (50 vol.%) under reflux for 3 h for the elimination of catalyst particles contained in the nanotubes.

After that, the desired amounts of Pd and Ru precursors were added to an acetone solution containing 0.5 g of the carbon nanotubes supports. After stirring overnight at ambient temperature, the catalysts were filtered, washed with acetone and dried in an oven at 120°C. The catalysts were then reduced at 300°C for 2 hours in a horizontal oven under an Ar-H_2 flow (20 vol% H_2).

3 Results and discussion :

The presence of nitrogen functionalities (pyrrolic, pyridinic and quaternary nitrogen) on the nitrogen doped support induces a high metal dispersion. Figure 1 shows TEM micrographs and particle size distribution for the palladium and shows that the Pd dispersion increases with the nitrogen content in the CNTs for which the mean Pd particle size was 4.4 nm (Pd/CNT) > 1.4 nm (Pd/Amphiphilic-CNT) > 1.2 nm (Pd/N-CNT). For the hybrid structure, for which the nucleation should arise preferentially on the N-doped sections, a much higher density of metallic nanoparticles is noticed on the hydrophilic sections.

Decomposition of isopropyl alcohol on the CNT supports, leads to acetone by dehydrogenation and propene by dehydration. Thus, on hybrid N-CNT, at 210°C as reaction temperature, and in the presence of air as carrier gas, the conversion was higher than on the CNT and nitrogen doped CNT samples. As far as the supported catalysts are concerned, the Pd ones were more active and more selective than the Ru ones. From 90°C, the Pd over hybrid CNT catalysts was 100% selective towards acetone for a conversion of 100%, whereas Ru

catalysts lead to dehydration and dehydrogenation products. The nitrogen doping induces the appearance of redox properties, which appear when oxygen is present in the reaction mixture.

Table 1. Surface and structural characterization of the hybrids CNTs.

Sample	Yield ($g_C\ g_{cat}^{-1}$)	Diam. (nm)	d_{002} (Å)	S_{BET} ($m^2\ g^{-1}$)	Pore vol. ($cm^3\ g^{-1}$)	Pore diam. (nm)	%C (wt.%)	%N (wt.%)
E10A20	1.5	9	3.384	219	1.08	21.9	89.2	1.0
A20E10	1.3	11.5	3.382	206	0.83	18.2	87.5	2.8

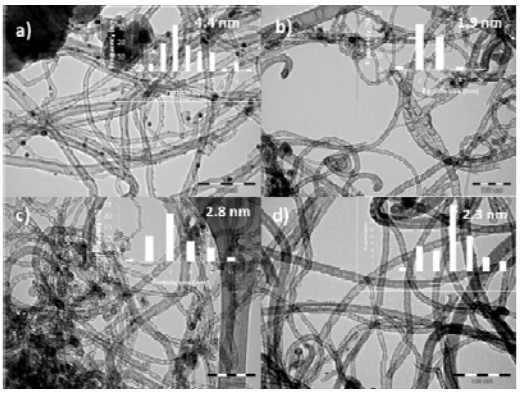

Fig. 1. TEM micrographs and Pd particle size distribution of the fresh Pd catalysts: a) Pd/E30; b) Pd/A30; c) Pd/E10A20; and d) Pd/A20E10.

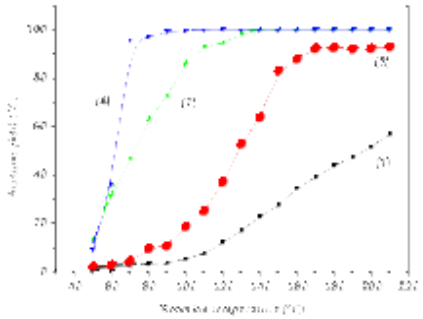

Fig. 2. Acetone yield over Pd/E10A20 catalysts versus reaction temperature in absence (1) and presence (2) of air, and over Pd/A20E10 in absence (3) and in presence (4) of air.

4 Conclusions :

The hybrid carbon nanotubes are very promising for the development of many different applications in catalysis and biphasic processes, other investigations for the recovery of these hybrid nano-structures are in course.

Acknowledgements :

The «Laboratoire de Chimie Moléculaire Maroco-Français» (LIA/LCMMF) is gratefully acknowledged for the grant of A.B. Funding from the (CNRST 2011 2A56) is gratefully acknowledged. The authors also acknowledge Hassan II Academy of Sciences and Technology.

References

[1] A. Benyounes, S. Louisia, R. Axet, M. Mahfoud, M. Kacimi, P. Serp; Catal. Today (2014),

ISO-PP25

Ethanol Transformation over Cu-containing Zirconium Phosphate

Dorofeeva N.V.[1,2*], Vodyankina O.V.[1], Sobolev V.I.[1,3], Koltunov K.Yu.[3,4]

1 - Tomsk State University, Tomsk, Russia
2 - Tomsk Polytechnic University, Tomsk, Russia
3 - Boreskov Institute of Catalysis, SB RAS, Novosibirsk, Russia
4 - Novosibirsk State University, Novosibirsk, Russia

* nv-dorofeeva@yandex.ru

Keywords: zirconium phosphate, copper, phosphate, ethanol, oxidation, dehydrogenation

1 Introduction

Acetaldehyde is used as a raw material for production of many important organic compounds such as acetic acid, acetic anhydride, ethyl acetate, ethylene, crotonaldehyde, etc. As a rule, IB-group metals and transition metal oxides are active towards the oxidation of alcohols to aldehydes [1, 2, 3]. Metal phosphates are considered as catalysts for oxidation, dehydration and dehydrogenation of alcohols [4, 5, 6]. The attention to double metal phosphates is connected with their flexible structure and composition.

In the present work peculiarities of formation of Cu^0 particles in the structure of double copper-zirconium phosphates as well as activity of zirconium phosphate and copper-zirconium phosphate in ethanol transformation were studied.

2 Experimental

The samples of zirconium phosphate (ZP) and copper-zirconium phosphate (CZP) were prepared as previously described [6]. Sols were dried and calcined in air at 700-1000 ^oC during at least 10 h. The CZP sample was pretreated by a flow of H_2/N_2 mixture at 600 ^oC prior to catalytic experiments (CZP-H_2).

The structure of samples was characterized by X-ray diffraction and transmission electron microscopy with high resolution (HRTEM). The interaction of copper cations with the reducing agent was studied by a temperature-programmed reduction-oxidation (TPR/TPO) technique.

The temperature-programmed gas-phase ethanol oxidation reactions were carried out in a quartz tube flow reactor with an internal diameter of 6 mm. The reactor containing the catalyst was fed with the reactive gas mixture EtOH/O_2/He (ODE) or EtOH/He (DE), operating at atmospheric pressure. During the catalytic runs, gas samples were analyzed periodically by integrated online GC with a flame-ionization detector and a thermal conductivity detector.

3 Results and discussion

According to the X-ray phase analysis data of CZP samples calcined at different temperatures, the amount of phases of double copper-zirconium phosphates increased with a rise of sintering temperature, while the amount of pyrophosphate ZrP_2O_7 decreased. Only $Zr_{2.25}(PO_4)_3$ phase was detected for ZP sample. The CZP(700) sample consisted of morphologically homogeneous faceted crystals of $Cu_xZr_y(PO_4)_z$ with sizes about 50 nm. These crystals were combined into mesoporous aggregates with sizes about 100 nm. TEM HR observations of crystal structure showed interplanar distance equal to ≈ 0.7 nm, which related to the frame structure.

TPR profiles of cyclic experiments TPR1/TPO/TPR2 showed thermal instability of double phosphates towards reduction of atmosphere and destruction of original compounds. Treatment of Cu-containing samples (CZP-H_2) by a flow H_2/N_2 mixture at 600 °C led to reduction of copper ions to form Cu^0 (CSR 34 nm) and accompanied by destruction of original double metal phosphates $Cu_{0.5}Zr_2(PO_4)_3$, $CuZr_4(PO_4)_6$. The distribution of Cu^0 particle sizes was in the range from 2 nm to ~1 μm.

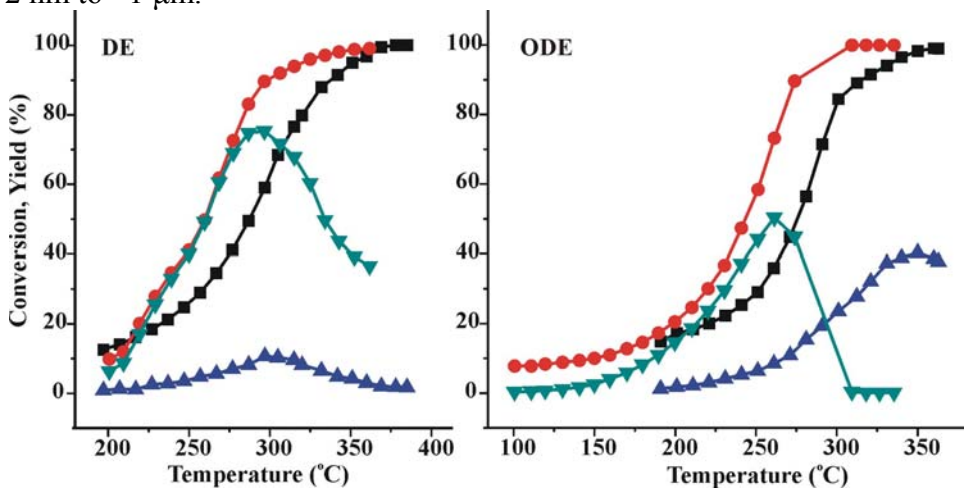

Fig. 1. Catalytic performance of ZP and CZP-H_2 in dehydrogenation (DE) and oxidative dehydrogenation (ODE) of ethanol. Conversion of ethanol over ■ – ZP and ● - CZP-H_2; yields of acetaldehyde over ▲– ZP, ▼ – CZP-H_2.

For both samples conversion of ethanol reached 100% under DE and ODE conditions. Ethanol transformations over the samples led to formation of acetaldehyde, ethylene, COx, diethyl ether and unidentified product. Acetaldehyde was the main product for CZP-H_2 sample in the absence of oxygen (Fig. 1, DE ▼, yield 75 %), while ethylene was the one for ZP sample. Formation of acetaldehyde was also observed over zirconium phosphate in a small amount, 11 % (Fig. 1, DE ▲). The ZP sample was an acid catalyst, and dehydration products were produced above 270 °C resulting in shifting of ethanol conversion curve to higher temperatures (Fig. 1, DE ■).

When oxygen was in the initial feed, the yield of acetaldehyde reached 50 % for CZP-H_2 sample at 260 °C (Fig. 1, ODE ▼). Deep oxidation of ethanol occurred above 260 °C. This was due to formation of Cu_2O on the surface of Cu^0 particles. Ethanol oxidized to acetaldehyde over zirconium phosphate ZP (Fig. 1, ODE ▲) under similar conditions, which can be connected with interaction of oxygen with coordination unsaturated Zr^{4+}.

4 Conclusions

The study on structure, phase composition and catalytic properties of Cu-containing zirconium phosphate and zirconium phosphate in ethanol transformation was carried out. The absence of oxygen in the feed gas favored for dehydrogenation of ethanol to form acetaldehyde over Cu-containing zirconium phosphate: acetaldehyde yield was 75%. Acetaldehyde yield about 40 % was reached for zirconium phosphate in oxygen-containing atmosphere.

References

[1] O. V. Vodyankina, A.S. Blokhina, I.A. Kurzina, V.I. Sobolev, K.Yu. Koltunov, L.N. Chukhlomina, E.S. Dvilis, Catalysis Today. 203 (2013) 127.
[2] O.A. Simakova, V. I. Sobolev, K. Yu. Koltunov, B. Campo, A.-R. Leino, K. Kordas, D. Yu. Murzin, Chem.Cat.Chem. 2 (2010) 1535.
[3] Y. Guan, E.J.M. Hensen, Applied Catalysis A: General. 361 (2009) 49.
[5] I.A. Pylinina, I.I. Mikhalenko, M.M. Ermilova, N.V. Orekhova, V.I. Pet'kov, Russian Journal of Physical Chemistry. 84(2010) 400.
[6] N.V. Dorofeeva, O.V. Vodyankina, O.S. Pavlova, G.V. Mamontov, Studies in Surface Science and Catalysis. 175 (2010) 759.

ISO-PP26

Kinetic Conjugation Effects during C_1-C_2-Hydrocarbon Oxidation in the Conditions of Methane Oxidative Coupling

Lomonosov V.I.[1*], Gordienko Yu.A.[1,2], Usmanov T.R.[1,3], Sinev M.Yu.[1]

1 - Semenov Institute of Chemical Physics, Russian Academy of Sciences, Moscow, Russia
2 - ZAO «SCHAG» Company, Department of Chemical Technology, Moscow, Russia
3 - Lomonosov Moscow University of Fine Chemical Technology, Moscow, Russia

* vlomonosov@mail.ru

Keywords: oxidative coupling of methane, C_1-C_2-hydrocarbon oxidation, heterogeneous-homogeneous processes, kinetic conjugation

1 Introduction

The oxidative coupling of methane (OCM) is a promising one-step process for producing ethylene from methane. One of the factors that hamper its practical implementation is a relatively low per-pass yield of the target products (ethane and ethylene) that is due to their high reactivity as compared to methane. Consequently, the OCM reaction conditions are the subject for optimization based on the reliable kinetic information about the secondary reactions of C_2-hydrocarbons. This work is focused on the detailed study of C_2-hydrocarbon oxidation including the possible reciprocal influence of C_1-C_2 hydrocarbons during their simultaneous oxidation in the presence of OCM catalysts (kinetic conjugation). Some literature data indicate that the presence of methane in the reaction mixture inhibits both ethane and ethylene oxidation in the gas phase [1]. Since all hydrocarbon molecules may undergo activation of the same type via C-H bond capture over typical OCM catalysts, one may expect even more complex conjugation in the conditions of their catalytic oxidation.

2 Experimental/methodology

Separate methane, ethane and ethylene oxidation are studied both in the presence and in the absence of OCM catalyst ($NaWMn/SiO_2$) in a conventional quartz flow micro-reactor at atmospheric pressure with on-line GC analysis. In typical experiments, methane, ethane, ethylene and oxygen partial pressures were 0.5, 0.05, 0.05, and 0.15 atm., respectively (balance – nitrogen). To reveal the reciprocal influence of C_1-C_2 hydrocarbons, we compared the sum of concentrations of different components in the reaction mixture obtained during the oxidation of individual hydrocarbons and their mixtures in the same conditions.

3 Results and discussion

The experimental results demonstrate that in a blank reactor C_2-hydrocarbon oxidation proceeds with a high rate at temperatures above 760°C. Almost total conversion of ethane and ethylene mainly to CO_X is observed at temperature around 840°C (see Fig. 1). In the reactor filled with quartz chips and $NaWMn/SiO_2$ catalyst the rate of conversion of both hydrocarbons significantly drops; in the presence of the catalyst ethane oxidation shifts from non-selective oxidation to oxidative dehydrogenation and ethylene oxidation – from CO to CO_2 formation. These observations suggest that the OCM catalyst surface substantially changes the hydrocarbon transformation pathways and efficiently inhibits unselective gas phase oxidation. The observed inhibitory effect is likely due to the interaction of free radicals responsible for chain branching and propagation with the catalyst active sites. Such radicals can be both generated and captured by the catalysts surface that leads to substantial changes of absolute and relative concentrations of species responsible for the development of chains and formation of different products.

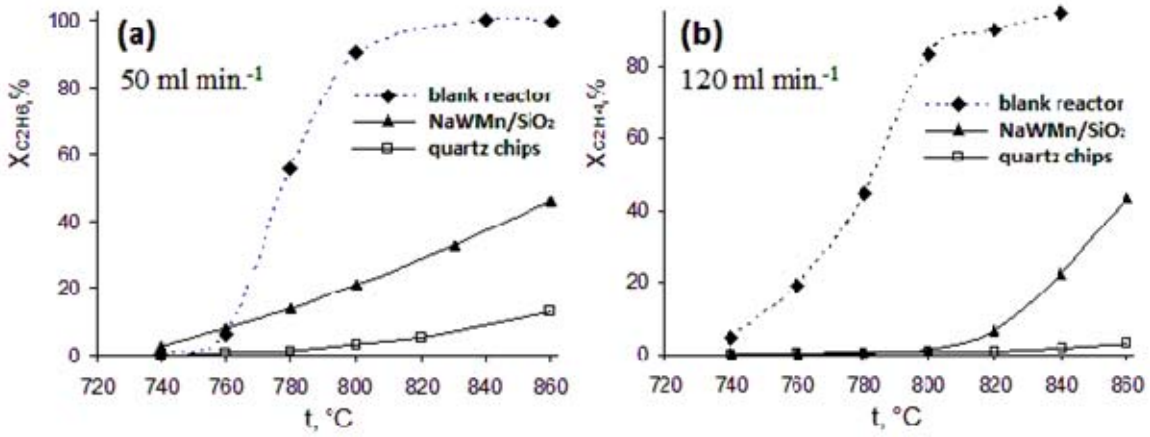

Fig. 1. Ethane (a) and ethylene (b) oxidation in blank reactor and in reactor filled with quartz chips and $NaWMn/SiO_2$ catalyst.

The presence of methane in the initial mixture strongly affects the C_2 hydrocarbon oxidation. In case of ethylene, strong inhibition of its oxidation is observed both in blank reactor and over $NaWMn/SiO_2$ catalyst; the addition of methane also leads to a drastic drop of CO_X concentration and noticeable increase of propylene formation in a good agreement with [1,2]. Based on the results of detailed kinetic modeling of gas phase C_1-C_2 hydrocarbon oxidation [1] it was proposed that high concentrations of methane greatly reduce chain-branching reactions. The newly obtained results demonstrate that such inhibitory effect takes place not only in case of gas phase ethylene oxidation, but in presence of OCM catalysts as well. It is likely that in both cases the observed effects can be explained in the same manner.

A more complex kinetic conjugation is observed during ethane oxidation in presence of methane. In blank reactor, methane acts as the gas-phase oxidation inhibitor (similar to ethylene oxidation). On the contrary, during the methane-ethane mixture oxidation over $NaWMn/SiO_2$ catalyst a strong increase of conversion rates of them both is observed. A possible explanation of observed effect can be likely obtained from the process simulation based on the detailed heterogeneous-homogeneous model [3].

4 Conclusion

C_1-C_2-hydrocarbon oxidation has been studied in conditions of methane oxidative coupling. It is demonstrated that gas phase oxidation of ethane and ethylene proceeds with a high rates at typical OCM temperatures. $NaWMn/SiO_2$ catalyst acts as an efficient inhibitor of gas phase oxidation of C_2-hydrocarbons and substantially changes their reaction pathways. A complex reciprocal influence of C_1-C_2 hydrocarbons during their simultaneous oxidation is demonstrated. Unlike the process in the gas phase, methane and ethane strongly increase the reactivity of each other while oxidized over the OCM catalyst.

Acknowledgements

Authors would like to thank Russian Foundation for Basic Research for financial support of this work (Project No. 13-03-00668 A).

References

[1] J.C. Mackie, J.G. Smith, P.F. Nelson, R.J. Tyler. *Energy Fuels*. 4 (3). 1990.
[2] C.A. Mims, R. Mauti, A.M. Dean, and K.D. Rose. *The Journal of Physical Chemistry*. 98(50). 1994.
[3] M. Sinev and V. Arutyunov. *Adv. Chem. Engng*. 32. 2007.

ISO-PP27

Metal-catalyzed Electrochemical Oxidative Phosphonation of Azoles

Gryaznova T.V.*, Dudkina Y.B., Budnikova Y.H., Sinyshin O.G.

A.E. Arbuzov Institute of Organic and Physical Chemistry, Kazan Scientific Center of Russian Academy of Sciences, Kazan, Russia

* tatyanag@iopc.ru

Keywords: electrooxidation, metal-catalysis phosphonation, azoles, dialkylphosphites

1 Introduction

Aryl phosphonates and their derivatives have found a wide range of applications in medicinal chemistry, catalysis and organic synthesis. Phosphorylated azoles play important role in this field. The first phosphonate derivatives of benzoxazoles were obtained in the 60-s of the last century by Razumov A.I. by heating of o-aminophenol with diethyl diethoxymethyl phosphonate with the distillation of alcohol [1, 2]. Recently, transition metal catalyzed aromatic C–H functionalizations have found increasing applications in the formation of C–heteroatom bonds including scarce catalytic examples of C(sp2)–P bond formation. The first Pd-catalyzed direct phosphonation of azoles with dialkylphosphites has been achieved without addition of base or acid. This method involves the oxidative cleavage of C–H and P(O)–H bonds and represents an atom-efficiency alternative to the classical phosphonation of Ar–X [3]. Electrochemical approach has several advantages over conventional organic synthesis allowing reactions to be carried out under mild conditions without any oxidizing agents. The development of new approaches for selective C-H-functionalization (phosphorylation) of different heteroaromatic substrates under conditions of electrocatalytic generation of palladium or nickel catalysts in high oxidation states is important.

2 Experimental/methodology

Electrochemical approach, which has several advantages over conventional organic synthesis allowing reactions to be carried out under mild conditions without any oxidizing agents, was used. The latter is important for oxidative M(II)-M(III)/M(IV) catalysis that is sensitive to the choice of an oxidant.

3 Results and discussion

The metal-catalyzed electrochemical oxidation (phosphonation) of heteroarylazoles (benzoxazoles, benzothiazole and other) with dialkylphosphite was developed. Palladium and nickel complexes were tested as catalysts.The joint electrochemical oxidation of a mixture of azoles and dialkylphosphite in the presence of palladium acetate Pd(OAc)2 (10 mol %) or (bpy)NiBF4 at room temperature affords the desired ortho C-H substitution product, 2-substituted azoles.

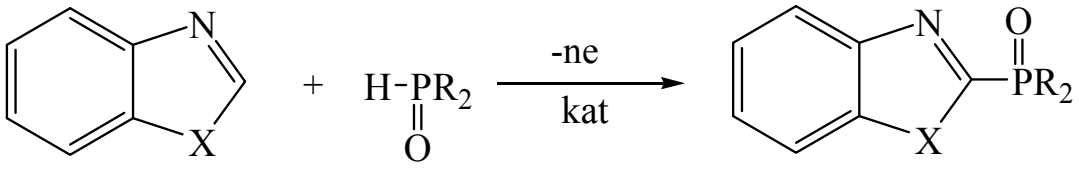

X = O, S, N

R = AlkO, Ph

The structure of the obtained heteroaryl azoles was confirmed by NMR spectroscopy, mass-spectral analysis. To optimize electrochemical synthesis experiments were carried out in different conditions. Metal-catalyzed electrochemical oxidation studied and its mechanism was proposed.

4 Conclusions

Thus a new electrocatalitic approach to C-H phosphonation of heteroarylazoles was developed.

Acknowledgements

This work was supported by a grant from the Russian science Foundation No. 14-23-00016.

References

[1] A.I. Razumov, B.G. Liorber, P.A.Gurevich, *Journal of General Chemistry*.37 (1967) 2782.

[2] A.I. Razumov, P.A.Gurevich,B.G. Liorber, T.D. Borisova, *Journal of General Chemistry*.39 (1969) 392.

[3] Ch. Hou, Yu. Ren, R. Lang, X. Hu, Ch. Xi, F. Li, *Chem. Commun*. 48 (2012), 5181.

Symposium "Education in the field of catalysis"

Advanced Training of Catalysis Experts in Petrochemical and Refining Industries

Zhuravleva M.V.*, Zinnurova O.V., Bashkirtseva N.Yu.

Kazan National Research Technological, University Department of Technology of Basic Organic and Petrochemical Synthesis, Kazan, Russia

* Guravleva0866@mail.ru

Keywords: petrochemistry, oil refining, catalysis, technology, training, personnel

1 Introduction

The priority fields of the economic development of Russia include the sustainable use of energy and natural resources in oil-and-gas production, oil-and-gas processing, and petrochemistry. Their development is supported by solving the problems of effective using and providing the sustainable replenishment of resources for oil producing and processing industries; reducing losses at all stages of operating procedures in oil-and-gas treatment, production, transportation, and processing; deepening oil-and-gas processing; integrated extracting and using all valuable associated and dissolved components, upgrading the existing oil-and-gas processing and petrochemical industries, as well as developing and implementing new technology [1].The efficient solving of the above tasks using catalytic techniques creates a need for highly qualified personnel trained on an advanced basis.

2 Experiment / Methodology

Thus, the primary purpose of the advanced training of catalysis experts in petrochemical and refining industries is educating competent, perspective/innovative-oriented personnel capable of working in the existing productions using known catalytic techniques, as well as in would-be implemented ones, and focusing on the development and research of new catalysts, engineering-ready catalytic productions and their efficient management.

Within the Federal State Budgetary Educational Institution of Higher Professional Education "Kazan National Research Technological University" (FSBEIHPE "KNRTU"), advanced professional training is implemented as an innovative educational process. Its efficiency is determined by integrating science, education and production, by developing and implementing multilevel educational programs, by arranging the professional development of teaching personnel, by developing technical infrastructure, and by developing the methodological support of education.

Integration of science, education and production is promoted within an industry-specific research and education cluster. Within the cluster, the key partners of FSBEIHPE "KNRTU" are:JSCTatneft, JSCKazanorgsintez, OJSCAmmoni, JSCTaneco, and PJSCNizhnekamskneftekhim. Interaction with key employers allows organizing the study of catalytic technology by students in the conditions of real plants: Arranging and equipping catalytic processes, the special features and opportunities of catalysis, analysis of changes in catalysts activity, and the methods of catalyst recovery.

Advanced training in the field of catalysis is supported by implementing the educational programs of multidisciplinary masters course. Within a research masters course, our graduates study advanced catalytic systems, catalytic process chemistry and technology, chemical reaction mechanisms and kinetic models, catalysts manufacturing techniques and research methods, and facilities equipment.

The intensive development of catalytic techniques and their implementation in production create the need for training design engineers. Implementing design engineering master programs covers the need of the complex for catalytic production 3D design experts.

Within a management masters course, future experts are trained to manage chemical and technological processes under the conditions of high integration of modern productions.

Educationis also provided with its advanced nature due to internationally integrated catalysis research and practical studies at Aristotle University of Thessaloniki, Greece, the University of Chemical Technology and Metallurgy – Sofia, Bulgaria, and the Technical University of Denmark, as well as to practical studies at leading companies developing catalytic technologies, such as Hempel Group or HaldorTopsoe (Denmark).

3 Results and discussion

Within the cluster, the key partners of FSBEIHPE "KNRTU" in implementing the advanced training are:JSCTatneft, JSCKazanorgsintez, OJSCAmmoni, JSCTaneco, and PJSCNizhnekamskneftekhim.

When organizing the advanced training, the following programs have been developed and are implemented: In the research masters course – Chemistry and Technology of Basic Organic and Petrochemical Synthesis Products, Chemical Engineering of Manufacturing the Reactants for Oil Extracting/Processing Industries, Catalytic Techniques in Petrochemistry and Oil Processing; in the design masters course – Innovative Petrochemical Synthesis Technology Design, Theoretical Bases and Design of Prospective Chemical Techniques; and in the management masters course – Petrochemical Enterprise Lifecycle Management.

The efficiency of advanced training is confirmed by the increased being in demand of the university's graduates in the industry labor market; professional growth of graduates within 2-3 years on innovative petrochemical enterprises; the students' interest in studying the programs of multidisciplinary masters course; growth in the students' research activities and their participation in innovative project competitions.

4 Conclusions

In training the experts, advanced education, unlike the conventional one, focuses on developing the readiness to get new knowledge and acquire multifunctional skills rather than on a certain professional activity, and enables the professional mobility and competitiveness of a graduate conforming with the demands of the modern and challenging labor market [2].

References

[1] The Energy Strategy of Russia for the period up to 2020 / Supplement to the Energeticheskayapolitika (In Russian. English: Energy Policy) magazine. – 2003. – 136 p.

[2] Novikov P.N. Operezhayushcheyeprofessionalnoyeobrazovaniye (In Russian. English: Advanced Vocational Education): Nauchno-prakticheskoyeposobiye (Academic and research guidebook) / P.N. Novikov, V.M. Zuyev. - M.: RTAiZ, 2000.- 266 p.

Gaining Insight on Catalytic Processes from Molecular Level: Novel Course of Catalysis in KNRTU

Garifzianova G.G.*, Tsyshevsky R.V., Khrapkovskii G.M.

Kazan National Research Technological University, Department of Catalysis, Kazan, Russia

* garifz@kstu.ru

Keywords: catalysis, quantum chemistry, catalytic processes, mechanism and kinetics

1 Introduction

Various traditional courses on catalysis mainly based on available experimental data and consider experimental methods. In addition to these classes, theoretical course "Catalysis and mechanisms of chemical reactions" have been taught in KNRTU over the past five years. This course considers employing of theoretical methods of quantum chemistry, statistical thermodynamics, reactions rate theory for exploration of mechanism and kinetics of the complex multi-stage chemical processes, including catalytic reactions.

2 Methodology

Some methodological features of the course are discussed in this report. First of all, authors believe that gaining skills of using quantum-chemical calculations for exploration of the mechanisms of catalytic reactions is the task of highest priority.

3 Results and discussion

Therefore, the ratio of the time course of lectures and laboratory classes is 1: 3. This course is taught in KNRTU to the students of basic chemical specialties with different level of knowledge and experience in the field of physical chemistry and physics. Hence, it is necessary to spend some time during lectures and laboratory classes for introduction to elements of quantum mechanics and statistical thermodynamics.

The course is taught for bachelors and masters. Classes of chemical compounds and chemical reactions are usually chosen for the undergraduate courses in accordance with students' specialty. Undergraduate students develop skills and acquire basic knowledge for modeling of chemical compounds and determination of the properties of the simulated material. As for the graduated students, selected tasks are usually overlapped with the subject of their master theses. Visiting http://nano-portal.ru/ and www.rusnano.com/ websites is practiced during classes with the purpose to introduce students to latest achievements in the field of catalytic processes.

4 Conclusions

Considerable part of the course and laboratory classes is devoted to the study of the structure of nanocatalysts and their role in catalytic processes at molecular level.

Textbooks and manuals designed and published by the staff of the Department of Catalysis KNRTU are widely used during the course together with existing textbooks.

AUTHORS INDEX

A

B

C

D

E

F

G

H

I

J

K

L

M

N

O

P

Q

R

S

T

U

V

W

X

Y

Z

XII European Congress on Catalysis
"Catalysis: Balancing the use of fossil and renewable resources"

ABSTRACTS

Editors: Professor Valerii I. Bukhtiyarov
Professor Alexander Yu. Stakheev

Most abstract are reproduced as presented camera-ready texts for which the authors bear full responsibility. Some abstracts underwent minor technical editing.

Compiled by: Vasily V. Kaichev, Konstantin P. Bryliakov, Ekaterina A. Kozlova, Lyudmila Ya. Startseva

Computer processing of text: A. Gilmanova, Yu. Klimova, A. Spiridonov

Cover design: E. Melikova

Издатель:
Федеральное государственное бюджетное учреждение науки
Институт катализа им. Г.К. Борескова
Сибирского отделения Российской академии наук
630090, Новосибирск, пр-т Академика Лаврентьева, 5, ИК СО РАН
http://catalysis.ru
E-mail: bic@catalysis.ru Тел. (383) 330-82-69

Электронная версия:
ООО «Мономакс»
E-mail: feedback@monomax.org Тел. (812) 335-20-55
Объём: 72 Мб, 1 CD-R.
Подписано в тираж: 20.08.2015. Тираж: 1000 экз.

Системные требования: i486; Adobe® Reader® (чтение формата PDF)

ISBN 978-5-906376-10-7